Can. J. Chem. Downloaded from www.nrcresearchpress.com by 210.87.254.40 on 09/05/12
For personal use only.

Canadian Journal of Chemistry

Published by
THE NATIONAL RESEARCH COUNCIL OF CANADA

Journal canadien de chimie

Publié par
LE CONSEIL NATIONAL DE RECHERCHES DU CANADA

Volume 53 Number 1 January 1, 1975 Volume 53 numéro 1 1 janvier 1975

The Photochemical Reactivity of Some Benzoylthiophenes. III. The Effect of an Adjacent Methyl Group on the Excited State Reactivity of 2-Benzoylthiophene[1]

D. R. ARNOLD[2] AND B. M. CLARKE, JR.

Photochemistry Unit, Department of Chemistry, University of Western Ontario, London, Ontario N6A 3K7

Received July 31, 1974

D. R. ARNOLD and B. M. CLARKE, JR. Can. J. Chem. **53**, 1 (1975).

The ultraviolet absorption and phosphorescence emission spectra of 2-(2-methylbenzoyl) thiophene (**1**), 2-benzoyl-3-methylthiophene (**2**), 2-benzoyl-4-methylthiophene (**3**), and 2-benzoyl-5-methylthiophene (**4**) are reported and analyzed. Partial energy diagrams are constructed. The lowest triplet is assigned as a π,π^* state of the 2-thienoyl chromophore in every case. Photocycloaddition of isobutylene to the carbonyl group was observed with **1** and **2**. The oxetanes are thermally unstable; olefins 1-(2-thienyl)-1-(2-methylphenyl)-2-methylpropene (from **1**) and 1-phenyl-1-(2-(3-methylthienyl))-2-methylpropene (from **2**) were formed and characterized. Irradiation of **1** and **2** in *O*-deuteromethanol did not lead to incorporation of deuterium; no reaction was observed. These results are discussed in terms of the existing generalizations potentially useful for predicting photochemical reactivity.

D. R. ARNOLD et B. M. CLARKE, JR. Can. J. Chem. **53**, 1 (1975).

On rapporte et analyse les spectres d'absorption ultraviolet et d'émission de phosphorescence des (méthyl-2 benzoyl)-2 thiophène (**1**), benzoyl-2 méthyl-3 thiophène (**2**), benzoyl-2 méthyl-4 thiophène (**3**) et benzoyl-2 méthyl-5 thiophène (**4**). Des diagrammes partiels d'énergie sont rapportés. Dans chaque cas, on assigne l'état triplet le plus bas à un état π,π^* du chromophore thiénoyl. On observe la photocycloaddition de l'isobutylène sur le groupement carbonyle des produits **1** et **2**. Les oxétanes sont thermiquement instables; les oléfines (thiényl-2)-1 (méthyl-2 phényl)-1 méthyl-2 propène (à partir de **1**) et de phényl-1 ((méthyl-3 thiényl)-2)-1 méthyl-2 propène (à partir de **2**) se forment et ont été caractérisées. L'irradiation de **1** et de **2** dans le méthanol-OD ne conduit pas à l'incorporation du deutérium; on n'observe aucune réaction. On discute de ces résultats en termes des généralisations existantes et qui peuvent s'avérer utiles pour prédire la réactivité photochimique. [Traduit par le journal]

Introduction

One photochemical reaction which could be particularly useful for synthesis, if it were general or at least predictable, is that which can formally be viewed as a γ-hydrogen abstraction by the oxygen atom of an α,β-unsaturated carbonyl compound. The resulting intermediate(s), if there is one (are any), may subsequently lead to the cyclobutenol or dienol. These products may be of interest in their own right, or may undergo further reactions.

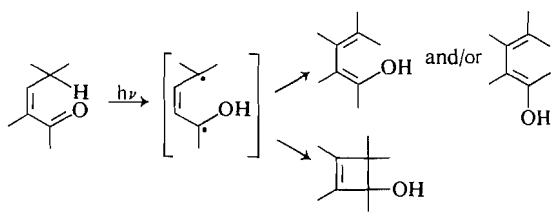

[1]Contribution No. 112 from the Photochemistry Unit.
[2]Alfred P. Sloan Fellow 1972–1974.

Can. J. Chem. Downloaded from www.nrcresearchpress.com by 210.87.254.40 on 09/05/12
For personal use only.

There are now several examples of this type of reaction (1, 2) and a considerable interest in the mechanism(s). There is, to our knowledge, only one example (3) of a planned synthetic sequence which takes advantage of this reactivity.[3] This will probably remain the case, the synthetic utility will not be fully realized, until the generality of the reaction is known and until it is possible to predict when reactions of this type will occur.

An early example of this reaction (4*a*), which has been extensively studied (4), is the irradiation of *o*-methylbenzophenone, where irradiation in benzene solution gave the photoenol which could be trapped with dienophile, ultimately resulting in formation of the naphthalene derivative. The excited state responsible for this reaction has been shown to be the n,π* triplet.

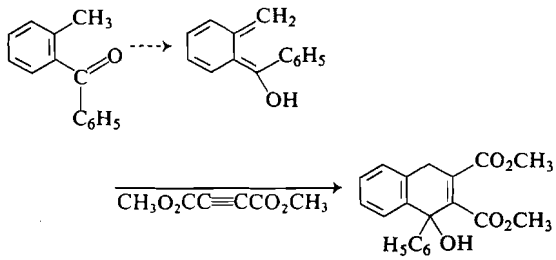

Diagnostic of formation of the photoenol was incorporation of deuterium in the methyl group upon irradiation in *O*-deuteromethanol. This intramolecular hydrogen abstraction from the *o*-methyl group is believed to be the cause of the greatly diminished photochemical reactivity of this compound toward intermolecular hydrogen abstraction leading to pinacol formation, and toward photocycloaddition with olefins to give the oxetane (4*k*). In fact, this ketone has been used as a stabilizer against ultraviolet irradiation in, for example, plastics.

Intramolecular and intermolecular hydrogen abstraction and photocycloaddition to give the oxetane are reactions expected of an n,π* singlet or triplet state. The observed product, following formation of these reactive states, is a function of the relative rates of these competing reactions. With *o*-methylbenzophenone, the intramolecular reaction usually competes favorably. For the general case, therefore, if a carbonyl compound is known to abstract hydrogen intermolecularly, or to undergo photocycloaddition to give an oxetane, it should follow that substitution by an alkyl group (or any other group from which hydrogen could be abstracted) in a position which would allow intramolecular hydrogen abstraction should not only inhibit the intermolecular reactions, but should lead to the photoenol instead. This prediction of course assumes that the substitution by the alkyl group will not significantly alter the nature of the excited states, an assumption which is commonly made, albeit with little justification.

Furthermore, if intermolecular and intramolecular hydrogen abstraction and photocycloaddition to give the oxetane are characteristic of the carbonyl n,π* triplet, one might except a correlation between reactivity in these reactions and the nature of the lowest triplet, as determined by phosphorescence emission studies.

We have recently shown that, although 2-benzoylthiophene emits from a triplet with π,π* character, photocycloaddition of olefins to the carbonyl group does occur (5). We were, therefore, interested in the photochemical reactivity of the methyl substituted 2-benzoylthiophenes, particularly those with the methyl present in the *ortho-* position of the benzoyl group (2-(2-methylbenzoyl)thiophene, **1**) and in the adjacent position of the thiophene (2-benzoyl-3-methylthiophene, **2**).

We ask the following questions:

(*1*) Does the methyl group significantly alter the positioning of the available excited states as determined by a spectroscopic study? While it is sometimes assumed that alkyl substitution does not appreciably (?) influence the excited state(s), this need not be the case. Particularly when the states are close in energy, an upper state in the unsubstituted molecule may become the lowest state upon addition of the alkyl substituent. For this reason we are interested not only in the spectroscopic characterization of the excited states in **1** and **2** but also of 2-benzoyl-4-methylthiophene (**3**) and 2-benzoyl-5-methylthiophene (**4**) as well.

(*2*) Will the adjacent methyl group inhibit the photocycloaddition reaction? Prediction, based on analogy with *o*-methylbenzophenone, would be yes. However, the photocycloaddition reaction with 2-benzoylthiophene may involve a state other than the n,π* state, particularly since the phosphorescence emission spectrum of 2-

[3]Since the absorption spectrum of the photoenol is usually drastically different from that of the ketone, this reaction has received attention as a photochromic system (2).

Can. J. Chem. Downloaded from www.nrcresearchpress.com by 210.87.254.40 on 09/05/12
For personal use only.

benzoylthiophene reveals the lowest triplet has π,π^* character. If some other excited state is involved, perhaps with this state, hydrogen abstraction does not compete with photocycloaddition.

(*3*) Will the photoenol form? If the photoenol of **2** forms, this reaction would afford a convenient route to this reactive intermediate, potentially useful in a wide variety of syntheses.

Answers to these questions might lead to some conclusion with regard to our more general objective, which is to define on what basis photochemical reactivity can be predicted. This may be based on an analogy with the reactivity of related model compounds (*e.g.* benzophenone and *o*-methylbenzophenone); it may be based on the knowledge of the electronic configuration and energy of the lowest excited states gleaned from spectroscopic studies; or extrapolation of one type of "characteristic" photoreactivity to another.

Results

The ketones (**1–4**), required for this study, were prepared by the Friedel–Crafts procedure; **1** has been prepared previously (6), **2–4** are new compounds. The reaction of 3-methylthiophene with benzoyl chloride gave a mixture of two benzoylated products in the ratio 6:1. This mixture was easily separated by preparative vapor phase chromatography. Expectations, based on analogy with other electrophilic substitution reactions of 3-methylthiophene, suggest the major product should have structure **2** (7). This assignment is consistent with the n.m.r. spectra which show the methyl protons in the major product at somewhat lower field than for the minor product, the result of deshielding by the adjacent benzoyl group. Furthermore, the larger coupling observed for the proton in the 5 position of the major product is consistent with **2**, where the coupling results from an adjacent proton.

Confirmation of this structural assignment was provided by alternative synthesis of **2**. Two sequences, involving the Grignard reaction, were utilized: one, using the Grignard reagent from bromobenzene reacting with 3-methyl-2-thiophene carboxaldehyde followed by oxidation of the resulting alcohol; and the other used the reaction of the Grignard reagent from 2-bromo-3-methylthiophene with benzonitrile followed by hydrolysis of the imine. The latter approach gave the better yield of **2**. These reactions are

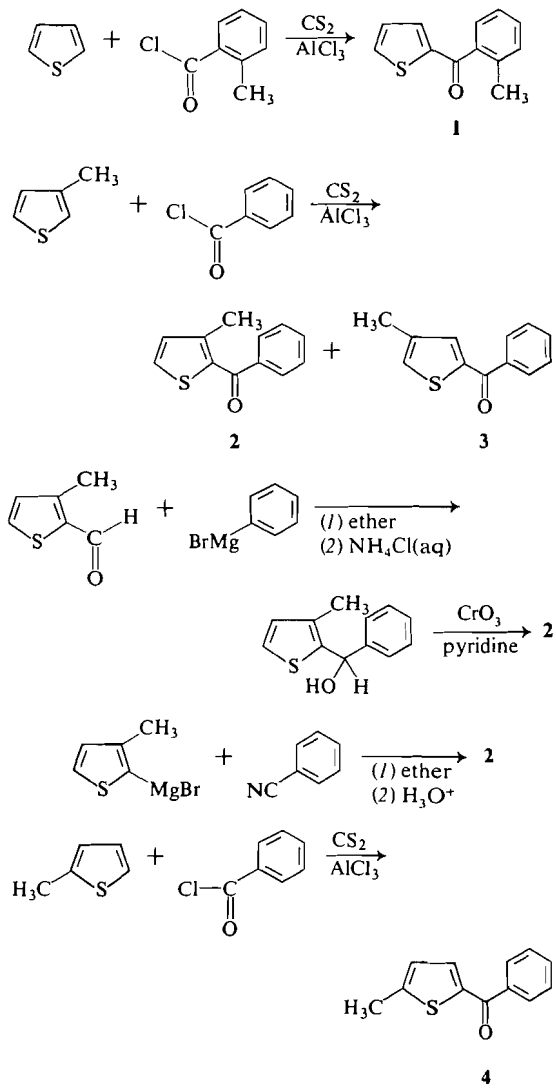

SCHEME I

shown in Scheme 1. The chemical shifts and coupling constants for the protons on the thiophene ring are summarized in Table 1.

The ultraviolet absorption spectra of ketones **1–4** were taken in hexane solution and are shown in Fig. 1. The phosphorescence emission spectra of **1–4** were taken in ethanol:methanol (4:1) glass at 77 °K. The gross vibrational, rotational features of these emission spectra are superficially similar to one another and to that observed from 2-benzoylthiophene (*5a*); however, the O—O band is significantly shifted depending upon the position of the methyl group on the thiophene ring. The triplet energy,

Can. J. Chem. Downloaded from www.nrcresearchpress.com by 210.87.254.40 on 09/05/12
For personal use only.

TABLE 1. Chemical shifts (p.p.m.) and coupling constants (Hz) for the protons on thiophene of some 2-benzoylthiophenes

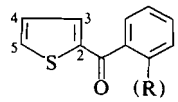

Compound	Chemical shift				Coupling constant		
	H_3	H_4	H_5	R = CH_3‡	$J_{3,4}$	$J_{3,5}$	$J_{4,5}$
5. 2-benzoylthiophene*†	7.59	7.14	7.64	—	4 0	1.5	5.0
1. 2-(2-methylbenzoyl)thiophene†	7.41	7 08	7.68	2.36	4.0	1.5	5.0
2. 2-benzoyl-3-methylthiophene	—	6.94	7.43	2.50	—	—	5.2
3. 2-benzoyl-4-methylthiophene	7.50	—	7.41	2 30	—	1.5	—
4. 2-benzoyl-5-methylthiophene	7.34	6.72	—	2 44	4.0	—	—

*In Table 1 of Part I (*5a*) the chemical shifts and coupling constants assigned to the protons in the 3 and 5 positions were interchanged for both *Ia* and *Ib*.
†See also refs. 14 and 18.
‡The methyl protons of 2-methylbenzophenone are observed at 2.30 p.p.m.

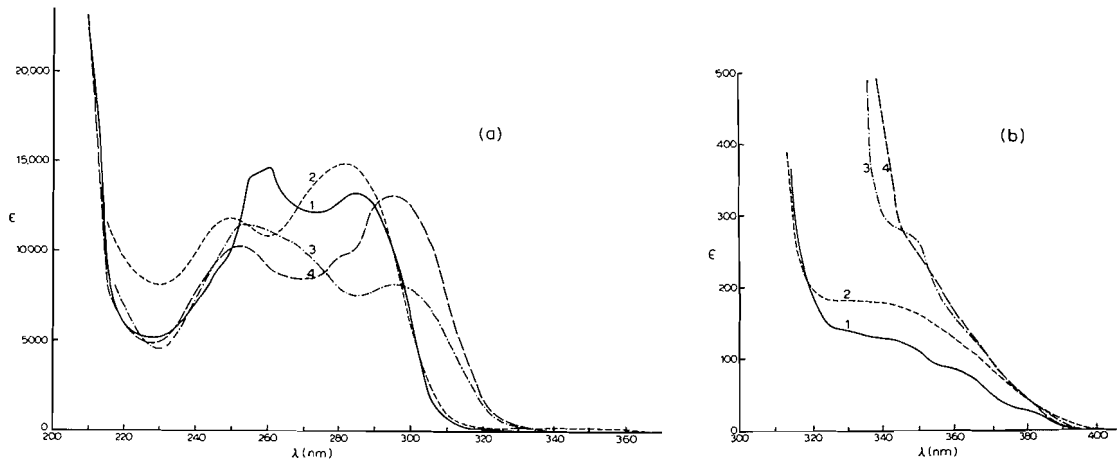

FIG. 1. Ultraviolet absorption spectra of some 2-benzoylthiophenes in hexane.

calculated from the maximum of the short-wavelength band of the emission, and the triplet lifetime, gleaned from the first-order decay of the emission, are summarized in Table 2.

When ketone **1** was irradiated in benzene solution containing isobutylene, cycloaddition of the olefin to the carbonyl group occurred. The resulting oxetane **6** was not detected; but the olefin **7**, formed presumably by loss of formaldehyde from the oxetane, was isolated.

TABLE 2. Triplet energies and phosphorescence lifetimes for some 2-benzoylthiophenes*

Compound	E_T (kcal mol^{-1})	$T \times 10$ (s)
5	63.5 (63.3)†	1.99 (1.41)†
1	63.1	1.60
2	62.5	0.98
3	61.5	1.55
4	60.1	1.40

*Taken in ethanol: methanol (4:1) at 77 °K.
†Taken in diethylether: isopentane: ethanol (5:5:2) glass at 77 °K (*5a*).

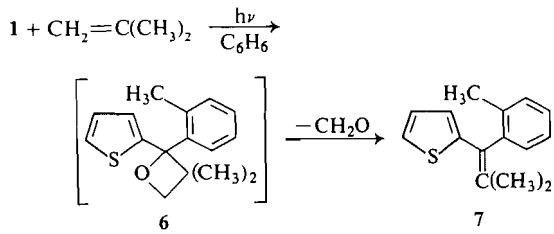

No evidence was obtained for addition of isobutylene to the thiophene ring; however, the material balance indicates considerable starting

Can. J. Chem. Downloaded from www.nrcresearchpress.com by 210.87.254.40 on 09/05/12
For personal use only.

ketone has not been accounted for and the n.m.r. spectrum of the crude reaction mixture suggests several other products form in small amounts. There was no indication of photochemical rearrangement of the starting ketone.

The structure assigned to olefin **7** was suggested by the n.m.r. spectrum which shows methyl protons absorbing at 1.56, 2.08, and 2.11 p.p.m.; the vinyl methyls of 1-phenyl-1-(2-thienyl)-2-methylpropene occur at 1.98 and 1.68 p.p.m. (*5b*). Confirmation of this assignment was obtained by synthesis of the identical material by dehydration of the alcohol prepared by the Grignard reaction of the ketone **1** with isopropylmagnesium bromide.

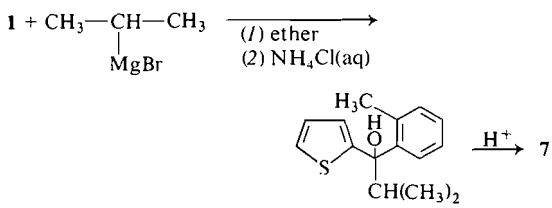

When ketone **2** was irradiated in benzene solution containing isobutylene, the n.m.r. spectrum of the crude reaction mixture gives no indication for the presence of an oxetane; however, peaks at 1.74, 1.85, and 2.09 p.p.m. attributable to olefin **9** are present along with complex absorption due to the formation of other minor products. The olefin **9** was isolated from the crude reaction mixture by column chromatography. The structural assignment was confirmed by synthesizing identical material by dehydrating the alcohol **10** prepared by the Grignard reaction of ketone **2** with isopropylmagnesium bromide or by the Grignard reaction of 3-methyl-2-thienyl magnesium bromide with isobutyrophenone. There was no indication of photochemical rearrangement of the starting ketone **2**.

Ketones **1** and **2** were irradiated in *O*-deuteromethanol. There was no evidence for any photochemical reaction occurring in either case. The starting material could be recovered essentially pure (i.r., n.m.r.) by evaporating the solvent. No isomerization of the thiophene was observed. No deuterium was incorporated in the methyl group since there was no decrease in the integrated n.m.r. signal due to the protons of the methyl. Furthermore, the mass spectra of the recovered starting materials showed no increase in the parent-plus-one mass peak. A control experiment, using *o*-methylbenzophenone, showed rapid incorporation of deuterium in the methyl group, under these conditions.

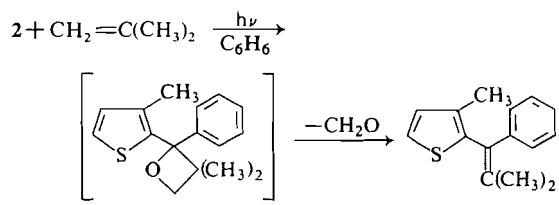

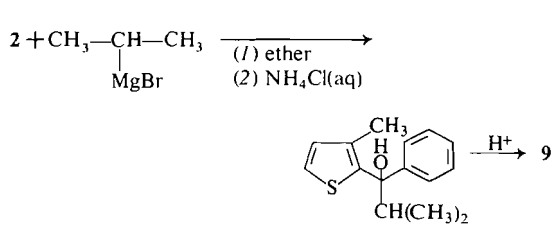

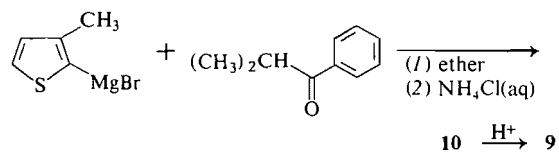

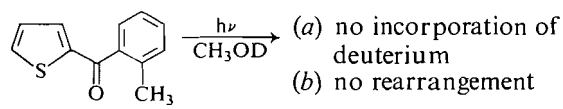

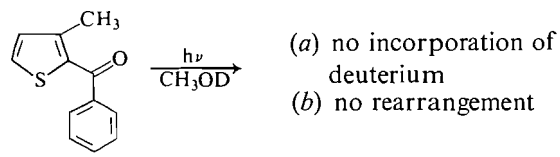

Discussion

Since intermolecular and intramolecular hydrogen abstraction and photocycloaddition to give the oxetane are usually considered to be characteristic reactions of the carbonyl n,π* triplet, and since there frequently is a correlation between photochemical reactivity and the nature of the lowest triplet determined by phosphorescence emission studies,[4] we will first interpret the ultraviolet absorption and phosphorescence emis-

[4]It must be kept in mind that the conditions used in these two types of experiments are very different (*i.e.*, room temperature in fluid solution *vs.* 77 °K in a rigid medium); exceptions are, therefore, not unexpected.

Can. J. Chem. Downloaded from www.nrcresearchpress.com by 210.87.254.40 on 09/05/12
For personal use only.

sion spectra, construct energy diagrams, and discuss the observed reactivity in terms of this generalization.

The ultraviolet absorption spectra of 2-benzoylthiophene (**5**) and several derivatives, mostly substituted in the thiophene 5-position, have been analyzed in some detail (5*a*, 8). The total absorption spectrum is a composite of transitions involving five more or less independent chromophores, Fig. 2. With 2-benzoylthiophene (hexane solution) a maximum occurs at 245 nm which includes transitions of the benzoyl and thienyl chromophores. The $\pi \rightarrow \pi^*$ transition of the 2-thienoyl chromophore causes a maximum at 275 nm. Weak, long wavelength, structured absorption, with a O—O band near 380 nm is due to the carbonyl $n \rightarrow \pi^*$ transition. The gross features of the spectrum of **1** are similar to **5**, with maxima slightly shifted to 261 and 285 nm. The spectra of **1** and **5** are even less different when ethanol is the solvent (λ_{max} 264 and 292 nm for both **1** and **5**) (8).

The absorption spectra of **2** is similar to that of **1** (and **5**); the thienoyl transition at 282 nm is relatively unaffected. This can be taken as evidence that the thienoyl moiety remains essentially planar in spite of the potential increase in steric interaction. The decrease in intensity of the maximum at 250 nm in **2** relative to **5** (ε = 10 800 and 12 300 for **2** and **5** respectively) may in fact result from decreased planarity of the benzoyl moiety because of the methyl group.

The absorption spectra of **3** and **4** show a pronounced bathochromic shift of the band assigned to the thienoyl chromophore; 20 nm relative to that of **5**, a difference in energy of *ca.* 7 kcal mol^{-1}. Obviously, the effect of a methyl group cannot be ignored when predicting the relative positions of the excited states of a molecule.

The 2-thienoyl chromophore has been compared with the α,β- γ,δ-unsaturated carbonyl chromophore. It is therefore interesting to note the similarity of the effect of alkyl substitution on these two systems. The effect of alkyl substitution in the γ or δ position is similar, 18 nm for α,β- γ,δ-unsaturated carbonyl compounds. On the other hand, alkyl substitution in the β-position of the unsaturated carbonyl chromophore (analogous to **2**) causes a much larger effect (12 nm bathochromic) than observed for this transition in **2**.

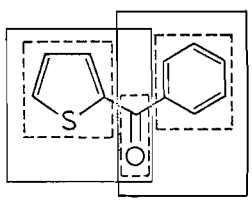

FIG. 2. The ultraviolet absorption spectrum of 2-benzoylthiophene is a composite of transitions involving five, more or less independent chromophores.

The weak absorption at long wave lengths (hexane solution) for **1**–**5** is attributed to the carbonyl $n \rightarrow \pi^*$ transition. It is essentially unaffected (O—O band *ca.* 380 nm) by methyl substitution.

The gross features of the phosphoresence emission spectra from **1**–**4** are similar to one another and to that of **5**. However, the triplet energies, calculated from the position of the short wave length maximum, show significant differences (Table 2). The similarity in the shape of the spectra and the phosphorescence lifetimes (relatively long) indicates the same state is involved in all cases, the π,π^* thienoyl triplet. The progression of triplet energies **1** > **2** > **3** > **4** is interesting. This progression is not observed in the singlet transition (λ_{max}) for this chromophore.

This spectral information is summarized in the partial energy diagrams shown in Fig. 3. The π,π^* singlet energy levels are taken from the maximum of the absorption spectra, they are, therefore, maximum values but are useful for comparison. The n,π^* singlet energies are taken from the O—O band of the absorption spectrum. The π,π^* triplet energies are taken as the O—O band of the emission spectrum and the n,π^* triplet energies are estimated assuming a typical $(n,\pi^*)S$–$(n,\pi^*)T$ separation of 2000 cm^{-1}.

The generalization of photochemical reactivity based upon the nature of the lowest triplet and attributing rapid (and frequently efficient) hydrogen abstraction and photocycloaddition to reactions of the n,π^* triplet would predict **1** and **2** should be unreactive. Thermal equilibration and vibronic mixing of the lower energy π,π^* triplet with the more reactive n,π^* triplet should also be negligible in view of the rather large (>6 kcal mol^{-1}) separation between these states (9). Reaction of the n,π^* singlet is possible; however, the ordering of states, with a π,π^*

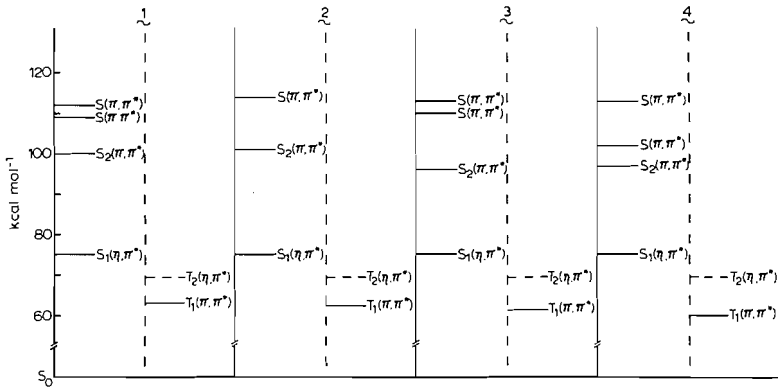

FIG. 3. Partial energy diagrams for some 2-benzoylthiophenes.

triplet below the lowest n,π* singlet, should result in rapid intersystem crossing (10). Therefore, the lack of deuterium exchange in **1** and **2** is predictable based on the knowledge summarized in the partial energy diagrams (Fig. 3). The photocycloaddition is unexpected, not only from the consideration of positioning of the excited states, but, the adjacent methyl does not quench the reaction as it does in the case of *o*-methylbenzophenone.

There is a considerable amount of recent evidence indicating that oxetane formation cannot simply be viewed as requiring the carbonyl n,π* state in a reaction analogous to alkoxy radical addition to an olefin, but that the first step toward oxetane formation is formation of a complex (11). Furthermore, this complex can be formed from either an n,π* or π,π* state and with a rate competitive with intersystem crossing. Obviously several sets of generalizations will be required to predict reactivity in this reaction.

Since it seems unlikely that an n,π* state is involved in the observed photocycloaddition of **1** and **2**, intramolecular hydrogen abstraction does not inhibit this reaction with the state that *is* involved. We cannot, with the information available at this time, assign this reaction to a state; however, we favor the lowest π,π* triplet as the most likely candidate. Sensitization and quenching studies which would make possible an assignment are difficult in this case because of the low yield (the reaction mixture turns dark) and low quantum yield (estimated <0.05).

If generalizations of photochemical reactivity can be based upon characteristic reactivity in different types of reactions, the lack of intramolecular hydrogen abstraction with **1** and **2** is relevant to the question of intermolecular hydrogen abstraction with these ketones and with **5**. The n,π* triplet of *o*-methylbenzophenone can undergo competitive intramolecular and intermolecular hydrogen abstraction. The product obtained following intermolecular hydrogen abstraction from isopropyl alcohol is the pinacol (33% yield) (4*d*). The quantum yield for pinacol formation is low, approximately 0.1 that for pinacol formation from benzophenone, which illustrates the pronounced preference for intramolecular hydrogen abstraction (4*a*, *b*, *d*). Therefore, the prediction can be made that **1** and **2** will not be reduced upon irradiation in isopropyl alcohol. Obviously, the reported (12) reduction of **5**, upon irradiation in isopropanol, which presumed pinacol formation is inconsistent with these results.

We have now turned our attention to the methyl substituted 3-benzoylthiophene derivatives. Since 3-benzoylthiophene emits from an n,π* triplet (5*a*) we predict intramolecular hydrogen abstraction will occur from an adjacent methyl in these cases. The report of this study will constitute Part IV of this series.

Experimental

General

A description of the apparatus used and the general experimental approach was similar to that reported in Parts I and II (5).

Irradiations were carried out using a Hanovia 450-W medium-pressure mercury vapor lamp (679 A36) in a quartz cooling jacket which was immersed in a constant temperature bath at 10°. The samples, contained in sealed quartz or Pyrex tubes (20 mm diameter) having a volume of 40 ml, were arranged around the lamp at a

Can. J. Chem. Downloaded from www.nrcresearchpress.com by 210.87.254.40 on 09/05/12
For personal use only.

Can. J. Chem. Downloaded from www.nrcresearchpress.com by 210.87.254.40 on 09/05/12
For personal use only.

distance of 25 mm; they were not degassed unless stated otherwise.

The n.m.r. spectra were run in 1–2 *M* solutions in deuterochloroform using tetramethylsilane as an internal reference. The spectra were obtained on a Varian HA-100 spectrometer. The chemical shifts are taken as the center of multiplets and the reported coupling constants are the result of first-order analysis. Coupling was confirmed by double irradiation experiments.

The emission spectra were obtained as previously reported (Part I) (*5a*) with the exception that ethanol: methanol (4:1) was used as the solvent instead of diethyl ether:isopentane:ethanol (5:5:2).

Preparative v.p.c. separations were carried out using a F and M Scientific preparative gas chromatograph, Model 776.

Methylthiophene-2 and -3 and 3-methyl-2-thiophenecarboxaldehyde were obtained from Aldrich Chemical Co.

2-(2-Methylbenzoyl) Thiophene(1)

This ketone was prepared by the Friedel–Crafts reaction (6). Treatment of 2-methylbenzoic acid (34.0 g, 0.23 mol) with thionyl chloride (25 ml) at reflux for 1 h gave, after evaporation of excess thionyl chloride, 2-methylbenzoyl chloride (36.4 g, 94%) which was purified by distillation (b.p. 94–96°, 20 mm; lit. (13) 110–111°, 29 mm).

Thiophene (9.0 g, 0.1 mol) and 2-methylbenzoyl chloride (15.4 g, 0.1 mol) were dissolved in carbon disulfide (125 ml) with exclusion of moisture. Anhydrous aluminum chloride (13.2 g, 0.1 mol) was added in 3 g portions over ½ h. This mixture was refluxed 1½ h, cooled, poured into 3 l water, and stirred until the black residue dissolved. The layers were separated, the aqueous layer was extracted (4 × 500 ml) with carbon disulfide, the combined carbon disulfide solutions were washed with 10% aqueous sodium hydroxide (1 × 500 ml) and water (1 × 500 ml) and finally dried over anhydrous sodium sulfate. Filtration, evaporation of the solvent, and distillation gave 2-(2-methylbenzoyl) thiophene (12.5 g, 58%) as a colorless oil (b.p. 101–104°, 0.01 mm). A sample was triply distilled (b.p. 124°, 0.17 mm) for analysis and spectral studies: i.r. ν_{max}^{neat} 1645, 1425, 1315, 1285, 740 cm^{-1}; u.v. λ_{max}^{hexane} 262 nm (ε = 14 600), 283 nm (ε = 13 300).

Anal. Calcd. for $C_{12}H_{10}OS$: C, 71.28; H, 4.99. Found: C, 71.08; H, 5.14.

These physical and spectral properties agree satisfactorily with those reported for this compound (8, 14).

2-Benzoyl-3-methylthiophene (2) and 2-Benzoyl-4-methylthiophene (3) (Friedel–Crafts Reaction)

Treatment of 3-methylthiophene (9.8 g, 0.1 mol) with benzoyl chloride (14.0 g, 0.1 mol) and anhydrous aluminum chloride (26.6 g, 0.2 mol) in carbon disulfide (500 ml), following the same reaction and work-up procedure used for the preparation of 2-(2-methylbenzoyl)thiophene, gave a 6:1 mixture of 2-benzoyl-3-methylthiophene and 2-benzoyl-4-methylthiophene. This mixture was separated by preparative v.p.c. using a 5 ft × 3/4 in. column packed with 5% QF-1 on 60/80 mesh Chromosorb W. Using an injector and column temperature of 150° and a carrier gas (N_2) flow rate of 12 cc/min, the retention time for 2-benzoyl-3-methylthiophene was 1.5 min and for 2-benzoyl-4-methylthiophene, 17.5 min.

2-Benzoyl-3-methylthiophene is a colorless oil: i.r. ν_{max}^{neat} 1630, 1400, 1265, 900 cm^{-1}; u.v. λ_{max}^{hexane} 250 (ε = 10 800), 282 (ε = 14 800).

Anal. Calcd. for $C_{12}H_{10}OS$: C, 71.28; H, 4.99. Found: C, 71.27; H, 5.16.

2-Benzoyl-4-methylthiophene is colorless crystals (m.p. 88–90°, from hexane): i.r. $\nu_{max}^{CCl_4}$ 1641, 1421, 1286, 856, 706 cm^{-1}; u.v. λ_{max}^{hexane} 252 (ε = 11 400), 296 (ε = 8100).

Anal. Calcd. for $C_{12}H_{10}OS$; C, 71.28; H, 4.99. Found: C, 71.00; H, 4.98.

2-Benzoyl-3-methylthiophene (3) (The Grignard Route)

Two different approaches, utilizing the Grignard reaction, were tried; the route from 2-bromo-3-methylthiophene was found to be the best (15).

Via the Aldehyde

A solution of the Grignard reagent prepared from bromobenzene (1.57 g, 10 mmol) and magnesium (240 mg, 1 equivalent) in dry ether (20 ml) was treated dropwise with 3-methyl-2-thiophene carboxaldehyde (1.26 g, 10 mmol). The solution was stirred vigorously during the addition and was then refluxed for 3 h. An aqueous ammonium chloride solution (50 ml, 10%) was added to the reaction mixture. The layers were separated, the aqueous layer extracted with ether (2 × 100 ml) and the combined ether layers were dried over magnesium sulfate. Evaporation of the solvent left a yellow oil (1.76 g, 85%) n.m.r.; δ 2.15 p.p.m. (s, 3H, methyl), 3.25 (broad, 1H, hydroxyl), 5.90 (broad, 1H, benzylic), presumed to be 2-(3-methylthienyl) phenylcarbinol, which was not further purified, but oxidized with Cornforth's reagent (chromium trioxide in pyridine, water) (16).

A pyridine (5.8 ml) solution of chromium trioxide (580 mg) and water (0.58 ml) was prepared and added dropwise to a benzene (20 ml) solution of the carbinol (1.76 g). The resulting mixture was stirred for 3 h and then poured into water/ether. The layers were separated, the aqueous layer was extracted with ether (150 ml) and the combined ether layers were washed with dilute hydrochloric acid (200 ml, 5%), sodium bicarbonate solution (200 ml, 5%), and water. The resulting extract was dried over magnesium sulfate, the ether was evaporated, and the residue chromatographed on alumina. 2-Benzoyl-3-methylthiophene, identical (i.r., n.m.r.) with that obtained from the Friedel–Crafts procedure given above, was eluted from the column using ether. The yield from the crude carbinol was 38% (470 mg).

Via 2-Bromo-3-methylthiophene

To a mixture of magnesium (1.2 g, 1 equivalent) in dry tetrahydrofuran (10 ml, distilled from CaH_2) was added 2-bromo-3-methylthiophene (17) (1 g) and a small crystal of iodine. An exothermic reaction started after approximately 5 min and the mixture began to reflux. The mixture was stirred with a magnetic stirring bar and additional 2-bromo-3-methylthiophene (7.85 g total, 0.05 mol) in 10 ml of dry tetrahydrofuran was added at a rate such that reflux was maintained. After the addition the mixture was heated under reflux for ½ h and then cooled to room temperature. Benzonitrile (5.1 g, 0.05 mol) was added to this solution and the mixture refluxed for 30 h. The resulting mixture was cooled in an ice bath and aqueous hydrochloric acid (20 ml, 10%) was slowly added. The tetrahydrofuran was now removed on a rotary evaporator, the aqueous solution was diluted with

Can. J. Chem. Downloaded from www.nrcresearchpress.com by 210.87.254.40 on 09/05/12
For personal use only.

water (300 ml) and extracted with ether (3 × 200 ml). The combined ether layers were washed with saturated aqueous sodium bicarbonate and dried over magnesium sulfate (anhydrous). Evaporation of the ether followed by vacuum distillation gave a product (b.p. 120°, 0.15 mm; 4.4 g, 45%) which was identified, by spectral analysis, as the imine: i.r. ν_{max}^{neat} 3231, 1591, 1571, 1426, 1341, 1191, 881, 836, 706 cm^{-1}; n.m.r. δ (p.p.m.) 2.05 (s, 3H, methyl protons), 7.75–6.78 (complex, 8H, aromatic protons). The imine was refluxed with a mixture of benzene (20 ml) and aqueous hydrochloric acid (20 ml, 10%) for 10 h. The benzene layer was separated, washed with aqueous sodium bicarbonate solution, dried over sodium sulfate (anhydrous), and the solvent was removed. The resulting orange oil was vacuum distilled to give 2-benzoyl-3-methylthiophene (b.p. 104–108°, 0.05 mm; 3.5 g, 71%) identical (i.r., n.m.r.) with that obtained by the Friedel–Crafts route.

*2-Benzoyl-5-methylthiophene (**4**)*

To a stirred solution of 2-methylthiophene (9.7 g, 0.1 mol) and benzoyl chloride (13.8 g, 0.1 mol) in carbon disulfide (500 ml), anhydrous aluminum chloride (26.4 g, 0.22 mol) was added in portions over 1 h. The resulting mixture was stirred for 3 h and then was poured onto ice (500 g). After the ice melted, the layers were separated, the aqueous layer was extracted with carbon disulfide (500 ml) and the combined carbon disulfide layers were washed with sodium hydroxide (250 ml, 10%) and water (250 ml). This extract was dried over sodium sulfate (anhydrous). The solvent was evaporated and the 2-benzoyl-5-methylthiophene was purified by vacuum distillation (b.p. 130°, 0.06 mm, 16.34 g, 81%). A small sample was bulb-to-bulb distilled prior to spectral analysis: i.r. ν_{max}^{neat} 1630, 1450, 1295, 710 cm^{-1}; λ_{max}^{hexane} 253 (ε = 10 200), 280 (ε = 9650), 295 (ε = 13 000).

Anal. Calcd. for $C_{12}H_{10}OS$: C, 71.28; H, 4.99. Found: C, 71.13; H, 4.86.

*Irradiation of 2-(2-Methylbenzoyl)thiophene (**1**) in the Presence of Isobutylene*

2-(2-Methylbenzoyl)thiophene (2 g) was dissolved in a 25% solution of isobutylene in benzene (35 ml) and was irradiated in a quartz irradiation vessel, sealed with a rubber serum cap, for 190 h. The excess isobutylene and benzene were evaporated and the n.m.r. of the resulting yellow–brown oil was taken. Peaks at δ (p.p.m.) 1.55, 2.05, and 2.10, characteristic of the olefin were observed, along with complex absorption between 0.8–1.85. No absorption was apparent in the region expected for the oxetane methylene protons. This crude reaction mixture was chromatographed on neutral alumina (Shawinigan, activity 1) and a product (58 mg) was eluted, with hexane:benzene (4:1), which was identical (i.r., n.m.r.) with 1-(2-thienyl)-1-(2-methylphenyl)-2-methylpropene (7) prepared by the Grignard method given below. Further elution with benzene gave recovered starting material (1.15 g); so, the yield of olefin was 26%. Similar results were obtained using a Pyrex irradiation vessel.

*Irradiation of 2-Benzoyl-3-methylthiophene (**2**) in the Presence of Isobutylene*

2-Benzoyl-3-methylthiophene (775 mg) was dissolved in a 25% solution of isobutylene in benzene (35 ml) and was irradiated in a Pyrex irradiation vessel, sealed with a rubber serum cap, for 170 h. Evaporation of the excess isobutylene and benzene left a dark oil. The n.m.r. spectra had complex absorption between δ (p.p.m.) 2.2–0.8 including singlets at 2.17, 1.81, and 1.76 characteristic of the olefin and a singlet at 2.42 due to the starting ketone; there was no indication of oxetane being present. The crude reaction mixture was chromatographed on neutral alumina (Shawinigan, activity 1). Elution with hexane:benzene (4:1) gave a product (20 mg) identical (i.r., n.m.r.) with 1-(2-(3-methylthiophene))-1-phenyl-2-methylpropene (**9**) prepared by the Grignard method given below. Further elution with benzene afforded starting material (342 mg); so, the yield of product was 4%. Essentially the same result was obtained when a quartz irradiation vessel was used.

1-(2-Thienyl)-1(2-methylphenyl)-2-methylpropene (7)

To a solution of the Grignard reagent prepared from 2-bromopropane (1.23 g, 0.01 mol) and magnesium (0.24 g, 1 equivalent) in dry ether (10 ml) was added 2-(2-methylbenzoyl)thiophene (0.27 g, 0.023 mol) and the resulting solution was refluxed for 17 h. This reaction mixture was poured into aqueous ammonium chloride (50 ml, 10%), the resulting layers were separated, and the aqueous layer extracted with ether (2 × 50 ml). The combined ether extracts were dried over magnesium sulfate (anhydrous). Evaporation of the solvent left a yellow oil, presumed to contain the alcohol. This oil was dissolved in benzene (25 ml), 4-toluenesulfonic acid (trace) was added, and the solution refluxed for 5 h. The solvent was evaporated, the oil was dissolved in ether and washed with aqueous sodium carbonate (10 ml, 10%), and dried over magnesium sulfate (anhydrous). Evaporation of the solvent left a dark oil which was chromatographed on silica gel (E. M. Reagents, 7733). The product (22 mg, 7.2%) was eluted with 5% hexane in benzene. A sample was distilled, bulb-to-bulb under vacuum, for spectral characterization and analysis: i.r. $\nu_{CHCl_3}^{max}$ 1715, 1595, 1380, 1370, 1280, 905 cm^{-1}; n.m.r. δ (p.p.m.) 1.65(s), 2.13(s), 2.18(s), (methyl protons), 7.35–6.70 (complex), (phenyl and thienyl protons).

Anal. Calcd. for $C_{15}H_{16}S$: C, 78.92; H, 7.06. Found: C, 79.11; H, 7.27.

*1-Phenyl-1-(2-(3-methylthienyl))-2-methylpropene (**9**)*

Two different procedures, involving the Grignard reaction, were used for the preparation of this olefin. The procedure utilizing 2-bromo-3-methylthiophene was found to give the best yields.

The Grignard Reaction of 2-Propyl Magnesium Bromide with 2-Benzoyl-3-methylthiophene

To a solution of the Grignard reagent prepared from 2-bromopropane (280 mg, 0.022 mol) and magnesium (56 mg, 1 equivalent) in anhydrous ether (20 ml) was added 2-benzoyl-3-methylthiophene (470 mg, 0.023 mol) dissolved in ether (20 ml). The reaction was stirred overnight and then was poured into aqueous ammonium chloride (50 ml, 10%). The resulting layers were separated and the aqueous layer extracted with ether (100 ml). The combined ether extract was dried over magnesium sulfate (anhydrous) and the solvent evaporated to obtain a yellow oil. This oil, presumably the alcohol, was not characterized but was dissolved in benzene (25 ml), 4-toluenesulfonic acid (trace) was added, and the resulting

Can. J. Chem. Downloaded from www.nrcresearchpress.com by 210.87.254.40 on 09/05/12
For personal use only.

solution refluxed for 24 h. The resulting mixture was washed with sodium bicarbonate solution (20 ml, 10% aqueous), dried over magnesium sulfate (anhydrous), and the solvent was evaporated to give a dark oil which was chromatographed on neutral alumina (Shawinigan, activity 1). The first fractions, eluting with hexane: benzene, contained the olefin (58 mg, 9%).

Reaction of the Grignard reagent from 2-Bromo-3-methylthiophene with Isobutyrophenone

To a mixture of 2-bromo-3-methylthiophene (17) (1 g) and magnesium turnings (0.324 g, 1 equivalent) in dry tetrahydrofuran (10 ml) a crystal of iodine was added. After several minutes a vigorous reaction started and additional halide (totaling 2.39 g, 0.013 mol) in tetrahydrofuran (20 ml) was added at such a rate as to maintain reflux. The mixture was heated under reflux for 2 h and cooled to room temperature. A solution of isobutyrophenone (2 g, 0.013 mol) in tetrahydrofuran (10 ml) was then added dropwise and the reaction mixture refluxed for 5 h, cooled in an ice bath, and treated with hydrochloric acid (10 ml, 10%). The tetrahydrofuran was removed on a rotary evaporator and replaced by ether. The ether layer was separated and the aqueous layer extracted with ether (2 × 100 ml). The combined ether extracts were dried over magnesium sulfate (anhydrous) and, after removal of the solvent, a dark oil was obtained which, by n.m.r., was approximately half the desired alcohol and the remainder, starting ketone. The alcohol was not further characterized, but was dissolved in benzene (20 ml) with a trace of 4-toluenesulfonic acid and refluxed for 20 h. After evaporation of the solvent the product (1.14 g, 40%, based on unrecovered starting ketone) was obtained by vacuum distillation (b.p. 80–83°, 0.05 mm): i.r. ν_{max}^{neat} 2986, 2912, 2861, 1602, 1496, 1446, 1376, 762, 709 cm^{-1}; n.m.r. δ (p.p.m.) 1.82 (s, 3H, methyl), 1.90 (s, 3H, methyl), 2.12 (s, 3H, methyl), 7.55–6.65 (complex, 7H, aromatic and thienyl).

Anal. Calcd. for $C_{15}H_{16}S$: C, 78.92; H, 7.06. Found: C, 78.93; H, 7.22.

Irradiation of 2-(2-Methylbenzoyl)thiophene (1) in O-Deuteromethanol

A Pyrex n.m.r. tube, containing 2-(2-methylbenzoyl)-thiophene (121 mg) in CH_3OD (3.25 ml) was degassed by three freeze–pump–thaw cycles, sealed, and irradiated for 30 h. Comparison of the integrated area and heights of the n.m.r. peaks due to the methyl group and aromatic protons before and after irradiation indicate little or no deuterium incorporation, (aromatic region/methyl peak, integrated area, calcd. (2.34), observed before irradiation (2.46), observed after irradiation (2.58). Evaporation of the solvent gave recovered starting material which had an essentially identical ratio of $M^+/(M + 1)^+$ peak in the mass spectrum with starting material; starting material, $M^+/(M + 1)^+$ (0.158); recovered starting material (0.161).

A control experiment, using 2-methylbenzophenone under these conditions led to rapid and essentially complete exchange of the methyl protons in a few hours.

Irradiation of 2-Benzoyl-3-methylthiophene (2) in O-Deuteromethanol

A Pyrex n.m.r. tube, containing 2-benzoyl-3-methyl-thiophene (0.1 g) and CH_3OD (1 ml) was degassed by three freeze–pump–thaw cycles, sealed, and irradiated for 45 h. Comparison of the integrated area and heights of the n.m.r. peaks due to the methyl group and aromatic protons before and after irradiation indicate little or no deuterium incorporation (aromatic region/methyl peak, integrated area; calcd. (2.34), observed before irradiation (2.81), observed after irradiation (2.62)). Evaporation of the solvent gave recovered starting material which had an essentially identical ratio of $M^+/(M + 1)^+$ peak in the mass spectrum with starting material; starting material, $M^+/(M + 1)^+$, (0.186); recovered starting material (0.188).

This work was supported by a grant from the National Research Council of Canada. We gratefully acknowledge the assistance of H. Schroeder in obtaining the 100 MHz n.m.r. spectra.

1. P. J. Wagner and G. S. Hammond. Adv. Photochem. **5**, 21 (1968).
2. J. D. Margerum and L. J. Miller. Photochromism. *Edited by* G. H. Brown. Wiley Interscience, New York. 1971. pp. 563–569.
3. (*a*) B. J. Arnold, S. M. Mellows, and P. G. Sammes. J. Chem. Soc. Perkin I, 1266 (1973); (*b*) B. J. Arnold, S. M. Mellows, P. G. Sammes, and T. W. Wallace. J. Chem. Soc. Perkin I, 401 (1974).
4. (*a*) N. C. Yang and C. Rivas. J. Am. Chem. Soc. **83**, 2213 (1961); *In* Reactivity of photoexcited organic molecules. Wiley Interscience, New York. 1967. p. 156; (*b*) A. Beckett and G. Porter. Trans. Faraday Soc. **59**, 2051 (1963); (*c*) J. N. Pitts, Jr., H. W. Johnson, Jr., and T. Kuwana. J. Phys. Chem. **66**, 2456 (1962); (*d*) N. D. Heindel, E. W. Sarver, and M. Pfau. Tetrahedron Lett. 3579 (1968); (*e*) N. D. Heindel, J. Molnar, and M. Pfau. Chem. Commun. 1373 (1970); (*f*) F. Nerdel and W. Brodowski. Chem. Ber. **101**, 1398 (1968); (*g*) E. F. Ullman and K. R. Huffman. Tetrahedron Lett. 1863 (1965); (*h*) G. Porter and M. F. Tchir. J. Chem. Soc. A, 3772 (1971); Chem. Commun. 1372 (1970); (*i*) M. Pfau, E. W. Sarver, and N. D. Heindel. C. R. **268**C, 1167 (1969); (*j*) K. R. Huffman, M. Loy, and E. F. Ullman. J. Am. Chem. Soc. **87**, 5417 (1965), **88**, 601 (1966); (*k*) D. R. Arnold. Adv. Photochem. **6**, 301 (1968); (*l*) E. Block and R. Stevenson. J. Chem. Soc. Perkin I, 308 (1973).
5. (*a*) D. R. Arnold and R. J. Birtwell. J. Am. Chem. Soc. **95**, 4599 (1973); (*b*) D. R. Arnold, R. J. Birtwell, and B. M. Clarke, Jr., Can. J. Chem. **52**, 1681 (1974).
6. W. Steinkopf and M. Bauermeister. Ann. Chem. **403**, 50 (1914).
7. H. D. Hartough and A. I. Kosak. J. Am. Chem. Soc. **69**, 3093 (1947).
8. L. Kaper and T. J. de Boer. Spectrochim. Acta. **26**A, 2161 (1970).
9. (*a*) P. J. Wagner and T. Nakahira. J. Am. Chem. Soc. **95**, 8474 (1973); (*b*) P. J. Wagner, A. E. Kemppainer, and G. N. Schott. J. Am. Chem. Soc. **92**, 5280 (1970); **95**, 5604 (1973).
10. A. A. Lamola. J. Chem. Phys. **47**, 4810 (1967); R. M. Hochstrasser. Acc. Chem. Res. **1**, 266 (1968); M. A. El-Sayed. Acc. Chem. Res. **1**, 8 (1968).
11. (*a*) R. A. Caldwell, G. W. Sovocool, and R. P.

GAJEWSKI. J. Am. Chem. Soc. **95**, 2549 (1973); (*b*) Y. SHIGEMITSU. Y. KATSUHARA, and Y. ODAIRA. Tetrahedron Lett. 2887 (1971); (*c*) S. FARID and S. E. SHEALER. Chem. Commun. 296 (1973).
12. P. TRAYNARD and J. P. BLANCHI. J. Chim. Phys. **69**, 284 (1972).
13. I. HEILBRON and H. M. BUNBURY. Dictionary of organic compounds. Vol. IV. London, Eyre and Spottiswoode. 1953. p. 3074.
14. M. L. MARTIN, C. ANDRIEU, and G. J. MARTIN. Tetrahedron Lett. 921 (1966).
15. P. L. PICKARD and T. L. TOLBERT. J. Org. Chem. **26**, 4886 (1961).
16. R. H. CORNFORTH, J. W. CORNFORTH, and G. POPJAK. Tetrahedron, **18**, 1351 (1962).
17. R. M. KELLOGG, A. P. SCHAAP, E. T. HARPER, and H. WYNBERG. J. Org. Chem. **33**, 2902 (1968).
18. L. KAPER, J. U. VEENLAND, and T. J. DE BOER. Spectrochim. Acta, **23**A, 2605 (1967).

Can. J. Chem. Downloaded from www.nrcresearchpress.com by 210.87.254.40 on 09/05/12
For personal use only.

Hydrothermal Formation of Ferrite Spinels

ALAN ROSS GAINSFORD, MARGARET JOY SISLEY, AND THOMAS WILSON SWADDLE[1]

Department of Chemistry, The University of Calgary, Calgary, Alberta T2N 1N4

AND

PETER BAYLISS

Department of Geology, The University of Calgary, Calgary, Alberta T2N 1N4

Received August 19, 1974

ALAN ROSS GAINSFORD, MARGARET JOY SISLEY, THOMAS WILSON SWADDLE, and PETER BAYLISS. Can. J. Chem. **53**, 12 (1975).

The possibility of forming spinel-type ferrites MFe_2O_4 from $M(OH)_2$ or MO and α-FeO(OH) (goethite) or α-Fe_2O_3 (hematite) under hydrothermal conditions up to 350° has been investigated experimentally for M = Mg, Ca, Mn, Co, Ni, Cu, and Zn. Formation of MFe_2O_4 was observed for M = Mn (jacobsite), Co, Ni (trevorite), and Zn (franklinite), and was in general favored by high temperatures, high p*H*, and the presence of $NaNO_3$ or, especially, NaCl in solution. α-FeO(OH) is more reactive than α-Fe_2O_3, but generally converts to the latter at 220–260°, independently of p*H*, in neutral or alkaline media. Interpretation of the results is complicated by the ion-exchanging properties and varying degrees of crystallinity of $M(OH)_2$, and by the tendency of $M(OH)_2$ to decompose to MO or to be oxidized at the higher temperatures. Nevertheless, the order of reactivity M = Co ≥ Mn > Ni > Zn > (Mg, Ca, Cu) in MFe_2O_4 formation is generally valid. The formation of MFe_2O_4 is limited by kinetic rather than thermodynamic factors for the various M listed (except Cu).

ALAN ROSS GAINSFORD, MARGARET JOY SISLEY, THOMAS WILSON SWADDLE et PETER BAYLISS. Can. J. Chem. **53**, 12 (1975).

On étudie expérimentalement la possibilité de former des ferrites MFe_2O_4 du type spinelle à partir de $M(OH)_2$ ou de MO et de α-FeO(OH) (goethite) ou de α-Fe_2O_3 (hématite) par réaction hydrothermique allant jusqu'à 350°, pour M = Mg, Ca, Mn, Co, Ni, Cu et Zn. On observe la formation de MFe_2O_4 pour M = Mn (jacobsite), Co, Ni (trévorite) et Zn (franklinite); cette réaction est généralement favorisée par de hautes températures, un p*H* élevé et la présence de $NaNO_3$ ou, spécialement NaCl en solution. α-FeO(OH) est plus réactif que α-Fe_2O_3, mais en général, il se transforme en ce dernier à 220–260°, indépendamment du p*H*, en milieu neutre ou alcalin. L'interprétation des résultats se complique à cause des propriétés d'échange d'ions, des degrés variables de cristallinité de $M(OH)_2$, ainsi que de la tendance de $M(OH)_2$ à se décomposer en MO ou à s'oxyder à des températures plus élevées. Néanmoins, l'ordre de la réactivité de M = Co ≥ Mn > Ni > Zn > (Mg, Ca, Cu) pour la formation de MFe_2O_4 est généralement valable. La formation de MFe_2O_4 est limitée par des facteurs cinétiques plutôt que thermodynamiques pour tous les éléments M de la liste à l'exception du Cu. [Traduit par le journal]

Introduction

The heat transfer systems of water-cooled nuclear power reactors are usually operated using liquid H_2O or D_2O under pressure at about 250–300° (523–573 K), with a hydroxide ion concentration of about 3×10^{-4} mol kg^{-1} and an excess pressure of hydrogen so as to minimize corrosion of the structural materials. The chief corrosion product of mild steel under these conditions is magnetite ($Fe^{II}Fe^{III}_2O_4$), which may be regarded as an iron(II) ferrite having the inverse spinel structure. However, if in-core boiling is permitted, oxidizing conditions may develop locally, leading to the formation of hematite (α-Fe_2O_3) and possibly goethite (α-FeO(OH)) rather than lepidocrocite (γ-FeO(OH)) which is the chief constituent of rust formed at ambient temperatures (1).

Replacement of Fe^{2+} by Co^{2+} in the magnetite structure to give $Co_xFe_{3-x}O_4$ ($0 < x \leq 1$) presents a technological problem, since this appears to be the vehicle for the development of strong ^{60}Co radiation fields in certain locations in the coolant circuits outside the reactor core. Nickel(II) is also often present in the corrosion products as $Ni_xFe_{3-x}O_4$. A direct investigation of the mechanism of incorporation of cobalt(II) or nickel(II) into the magnetite lattice would

[1]To whom correspondence should be addressed.

Can. J. Chem. Downloaded from www.nrcresearchpress.com by 210.87.254.5 on 09/05/12
For personal use only.

require strict maintenance and control of a hydrogen pressure, since, at the temperatures and pH values of interest, the $Fe(OH)_2$ produced in the formal reaction

[1] $M(OH)_2 + Fe_3O_4 = MFe_2O_4 + Fe(OH)_2$

would decompose to magnetite and hydrogen (2), the net reaction being

[2] $3M(OH)_2 + 2Fe_3O_4 = 3MFe_2O_4 + 2H_2O + H_2$

In our exploratory studies of hydrothermal spinel-type ferrite formation, we have considered instead the reactions of divalent metal oxides MO or hydroxides $M(OH)_2$ with iron(III) hydroxide, goethite, or hematite in nonreducing conditions, which may have direct relevance to anticipated corrosion-related problems in water-cooled reactors presently under construction which will utilize in-core boiling.

Thermodynamic calculations (3, 4) indicate that the reactions

[3] $MO + \alpha\text{-}Fe_2O_3 \rightarrow MFe_2O_4$

are favored, over the range 25–1000° at least, for M = Mg, Ni, Fe, and Co, the free energy change being increasingly negative in that order and not strongly temperature-dependent. Reference to thermodynamic data for $M(OH)_2$ and MO (5) shows that the corresponding reactions

[4] $M(OH)_2 + \alpha\text{-}Fe_2O_3 \rightarrow MFe_2O_4 + H_2O$

should also proceed spontaneously at 25° for M = Ni, Fe, and Co at least, and presumably this also applies at elevated temperatures. Langmuir (6) has established that goethite is thermodynamically unstable with respect to hematite and liquid water (at its saturation vapor pressure) above 81°, for coarse-grained crystals at least, so that reactions 5 and 6 are also thermodynamically possible under hydrothermal conditions, for M = Ni, Fe, and Co at least.

[5] $MO + 2\alpha\text{-}FeO(OH) \rightarrow MFe_2O_4 + H_2O$

[6] $M(OH)_2 + 2\alpha\text{-}FeO(OH) \rightarrow MFe_2O_4 + 2H_2O$

Ferrites MFe_2O_4 are known to form when iron(III) hydroxide is coprecipitated at 100° with various $M(OH)_2$ by addition of alkali to solutions containing stoichiometric amounts of M(II) and Fe(III) salts (7, 8). The product is too poorly crystalline to be detected by X-ray diffraction unless the suspended precipitate is maintained for many hours at 100° under neutral conditions or for shorter times at pH_{25} 12–14.[2] However, in the present context, we are concerned with the reactions of M(II) and Fe(III) species released into a high-temperature aqueous environment which is already alkaline, and the question arises as to whether iron(III) hydroxide plays a significant role in ferrite formation under hydrothermal conditions. Christensen and co-worker (9, 10) report that the products of decomposition of iron(III) hydroxide suspensions in aqueous alkali at 100–200° are pure goethite at pH_{25} 10.5–10.8, and various mixtures of goethite and hematite between pH_{25} 8.0 and 10.0. However, unpublished preliminary work by Gainsford in our laboratories, using titanium–palladium or stainless steel autoclaves, has shown that while goethite is indeed the sole product at pH_{25} 13–14 up to 100°, hematite is also formed at higher temperatures, comprising 95% of the product after 24 h at 200° (the effective reaction temperature was probably less than this, since the reaction was probably faster than thermal equilibration), and at pH_{25} 10.6 the percentage of hematite recovered rose from 5 at 100° to 95 at 200°. The exact form of the rate law for the conversion of iron(III) hydroxide to goethite at pH_{25} 13–14 at 60–75° depends on the nature of the reaction vessel and the temperature; however, with reference to the reagents and methods used in the present study, it can be said that the time for 50% conversion of iron(III) hydroxide is about 5 h in 1.0 M NaOH at 75°, is roughly proportional to $[OH^-]^2$, and decreases about threefold for a 10° rise in temperature. Thus, the survival time of iron(III) hydroxide is negligible in the conditions of spinel synthesis reported here, especially at $pH_{25} < 13$, and a series of trial experiments showed that direct reaction of iron(III) hydroxide with $M(OH)_2$ is impeded by its decomposition to goethite and particularly hematite at temperatures of the order of 200°.

Accordingly, the present report is concerned primarily with reactions 3–6. Laudise (11) reports some hydrothermal syntheses of $NiFe_2O_4$ and $ZnFe_2O_4$ via reaction 3 under supercritical conditions (470–480° at ~120 MNm^{-2} in 0.5 m NH_4Cl, and ~400° at ~200 MNm^{-2} in ~1.0 m NaOH respectively), but there is little information on the effect of varying the reaction conditions,

[2]In this article, pH values are expressed in terms of measurements at 25°, since the auto-ionization of water is strongly temperature-dependent. Concentrations are expressed on the molal scale (m), mol kg^{-1}.

Can. J. Chem. Downloaded from www.nrcresearchpress.com by 210.87.254.5 on 09/05/12
For personal use only.

Can. J. Chem. Downloaded from www.nrcresearchpress.com by 210.87.254.5 on 09/05/12
For personal use only.

and in any event we are concerned in the present context with subcritical aqueous systems. The interpretation of our results is complicated by the conversion of goethite to hematite, the decomposition of $M(OH)_2$ to MO or M(III) compounds, the ion-exchanging properties of $M(OH)_2$, uncertainties arising from the variable degrees of crystallinity of the reactants, pH changes in the course of reaction, and limitations imposed by the corrosiveness of the hydrothermal media and the lack of a corrosion-proof stirred autoclave. However, several useful generalizations can still be made regarding the effects of pH, temperature, and dissolved electrolytes on the progress of reactions 3–6 under hydrothermal conditions.

Experimental

Apparatus

Except where otherwise indicated, reactions were carried out in unlined 62 cm^3 titanium – 0.2% palladium alloy pressure vessels described previously (2). The interior surfaces of these vessels were preoxidized by autoclaving dilute H_2O_2 in them, and were in general resistant to attack by dilute alkaline solutions under the experimental conditions. However, 1.0 *m* NaOH at temperatures above 200° was found to attack freshly sand-blasted titanium alloy vessels appreciably, forming hydrogen which caused partial reduction of goethite (though not hematite) to magnetite. This was not a serious problem with vessels having well-oxidized interiors, but it does place a limit on the usefulness of this otherwise highly corrosion-resistant alloy, especially since hydrogen embrittles titanium. Autoclaves of type 316 stainless steel are fairly resistant to attack by hot aqueous alkali, but were not widely used because the constituent elements of the steel are among those of the reactants being studied. Silica liners are severely attacked by alkali at high temperatures, and also react hydrothermally with metal hydroxides or oxides to form silicates (12), *e.g.*, α-FeO(OH) in a silica liner with 0.01 *m* NaOH at 230–270° yielded the pyroxene *acmite*, $NaFeSi_2O_6$. Machined Teflon liners are expensive, difficult to clean, and soften above 300°.

Materials

Fisher Certified reagents were used throughout, and distilled water was passed through Barnstead de-ionizer and organic removal cartridges before use. Goethite, free of hematite, was prepared by treating a stirred solution of $Fe(NO_3)_3 \cdot 9H_2O$ (60.6 g) in 1500 cm^3 water with 48 g solid NaOH pelletwise, maintaining the stirred mixture at 75° for 22 h. The product was filtered, then washed with water, 3 *M* HNO_3 (to remove any residual iron(III hydroxide), more water, and finally acetone, and was dried at 70° (13.2 g, 99%).

Procedures

Reaction mixtures were made up as follows.

(a) Hydrothermal Conversion of Goethite to Hematite

Goethite samples (0.444 g, 5.0 mmol) were heated for selected periods in the autoclaves with 40 g water or aqueous NaOH, using a Blue M Conwate CW-160HF-1 forced convection oven ($\pm$ <5°). The goethite–hematite ratios of the dried solid products were determined by X-ray diffractometry from the relative intensities of the goethite *110* (0.418 nm) and hematite *211* (0.366 nm) reflections, with reference to a calibration curve prepared from standard samples.

(b) Reactions of $M(OH)_2$ with Goethite or Hematite in Media Containing Sodium Chloride or Nitrate

Solutions (2 *m*) of MCl_2 or $M(NO_3)_2$ (10.0 mmol) and of NaOH (20.0 mmol) were mixed and made to 40 cm^3 with water or aqueous NaOH to obtain the desired initial pH_{25}, and goethite or hematite (20.0 mmol) was mixed in. The mixtures were sealed in the autoclaves under nitrogen at 0.1 MNm^{-2} pressure and maintained at the desired temperature for 24 h. The pH_{25} of the solution phase was measured before and after each experiment. The solid products were washed with water and acetone, air dried, and identified by X-ray diffractometry with the aid of the JCPDS data files.

(c) Reactions of $M(OH)_2$ with Goethite or Hematite in Media Containing no Solutes other than NaOH

$M(OH)_2$ was made from $M(NO_3)_2$ solution as in (*b*), but was filtered and washed several times with dilute NaOH and then with water before transfer to the autoclave as a slurry in water or NaOH solution of the desired pH. The procedure was then as in (*b*).

Results

The following observations refer to a standard reaction time of 24 h, unless otherwise indicated.

Conversion of Goethite to Hematite

The beginnings of this reaction in a 24 h period were first observed at essentially the same temperature, 220 $\pm$ 10°, whether the initial pH_{25} was 7, 9, 12, or 14, and in all cases the reaction was complete within 24 h at 260°. In a few instances, *e.g.*, one involving pH_{25} 12 at 270°, a small amount of β-$NaFeO_2$ was recovered; the conditions favoring the formation of this compound were not obvious, but seemed to reflect the condition of the vessel wall, *i.e.*, nucleation of β-$NaFeO_2$ crystallization was probably the key factor. In no case was any evidence obtained for the rehydration of hematite to goethite.

The rate of conversion of goethite to hematite was slow initially, but later proceeded rapidly to near-completion. Thus, when samples of goethite were heated at 270° in 1.0 *m* NaOH for various times, the fraction of goethite recovered was still 100% after 70 min and 98% after 80 min, but only 12% after 90 min and progressively less thereafter (the half-time for thermal equilibration in the autoclaves was 7 min).

TABLE 1. Yields (%) of MFe_2O_4 formed in the hydrothermal reactions of $M(OH)_2$ or its derivatives with hematite in 24 h[a]

M	Solute other than NaOH	Initial pH_{25}	Yield (%) at temperature (°C) 100	150	200	250	300	350
Mn	0.5 *m* NaCl	7.0			0[b,c,d]	0[b,c,d]	10[b,e]	10[b,e]
		10.5			0[c,f]	90[c,f]	~100[c,f]	~100[e]
		14.0		0[c]	50[c]	90[c]	~100[c]	~100[c]
	0.5 *m* $NaNO_3$	7.0			0[c,g]	0[c,f]	0[e,f]	0[c,h]
		10.5			0[c,f]	0[c,f]	0[c,f]	0[c,f]
		14.0	0[c]	0[c]	90[c,f]	~100[c]	~100[c]	~100[e]
	None	12.5			0[c]			
		14.0		0[c]	40[c]			
Co	0.5 *m* NaCl	7.0			0[b,i]	0[b,i]	0[b,i]	10[b,e]
		10.5			0[c]	0[e,i]	0[c,i]	<10[c,e]
		14.0	0[c]	80[c]	90[c]	~100[e]	~100[e]	~100[e]
	0.5 *m* $NaNO_3$	7.0			0[b,j]	0[b,j]	0[j]	<10[b,j]
		10.5			0[c,j]	10[e,j]	10[e,j]	20[e,j]
		14.0	0[c]	30[c]	60[c]	60[e]	60[e]	90[e]
	None	7.0					0[j]	<10[j]
		10.5					0[e,j]	10[e,j]
		12.5			0[c]			
		14.0		<10[c]	60[c]			
Ni	0.5 *m* NaCl	7.0			0[i]	0[b,c,i]	20[b,e]	60[b,e]
		10.5			0[i]	0[e,i]	50[e,i]	80[e]
		14.0	0[c]	0[c]	60[c,e]	70[c,e]	80[e]	90[e]
	0.5 *m* $NaNO_3$	7.0			0[b,c]	0[b,c]	0[b,e]	0[b,e]
		10.5			0[c]	0[c]	0[e]	0[e]
		14.0		0[c]	0[c]	0[c,e]	60[e]	70[e]
	None	10.5					0[e]	20[e]
		14.0					<10[e]	20[e]
Zn	0.5 *m* NaCl	7.0			0[e]	50[e]	60[e]	70[e]
		10.5			0[e]	0[e]	20[e]	50[e]
		14.0			0[e]	20[e]	30[e]	60[e]
	0.5 *m* $NaNO_3$	7.0			0[e]	0[e]	0[e]	20[e]
		10.5			0[e]	0[e]	<10[e]	80[e]
		14.0	0[e]	0[e]	0[e]	<10[e]	10[e]	20[e]
	None	7.0					0[e]	20[e]
		10.5					0[e]	60[e]
		14.0				0[e]	<10[e]	

[a]No MFe_2O_4 was detected when M = Cu, Mg, or Ca for any of the reaction conditions covered by Table 1. The species (other than MFe_2O_4 and hematite) detected after each experiment are denoted by footnotes as follows.
[b]$M^{2+}(aq)$.
[c]$M(OH)_2$.
[d]$MnCl_2 \cdot H_2O$.
[e]MO.
[f]γ-Mn_2O_3.
[g]γ-MnO(OH).
[h]α-Mn_2O_3.
[i]$M_2(OH)_3Cl$.
[j]Co_3O_4.

Conversions of $M(OH)_2$ during Spinel Synthesis

The crystallinity of $M(OH)_2$ improved during hydrothermal treatment. However, species other than $M(OH)_2$ and MFe_2O_4 were often detected by X-ray diffractometry after attempted spinel syntheses, and these conversions are outlined in Tables 1 and 2.

Cobalt(II) hydroxide was generally recovered as the pink β-form, which has the brucite structure, but at 250° and above it tends to

Can. J. Chem. Downloaded from www.nrcresearchpress.com by 210.87.254.5 on 09/05/12
For personal use only.

TABLE 2. Yields (%) of MFe_2O_4 formed in the hydrothermal reactions of $M(OH)_2$ or its derivatives with goethite in 24 h[a]

M	Solute other than NaOH	Initial pH_{25}	Yield (%) at temperature (°C) 150	200
Mn	0.5 *m* NaCl	7.0	0[b]	0[b]
		10.5	0[b,c]	80[b]
		12.5	0[b,c]	50[c,d,e]
		14.0	0[d]	>90[e,f]
	0.5 *m* $NaNO_3$	10.5		20[b,c]
		12.5		40[c,d,e]
		14.0		80[c,g]
	None	10.5		20[b,c]
		12.5		20[b,c]
		14.0		50[b,c]
Co	0.5 *m* NaCl	7.0	0[h,i]	0[h,i]
		10.5	0[d,h]	<10[d,h]
		12.5	0[d]	50[d,e]
		14.0	~80[d]	80[b]
	0.5 *m* $NaNO_3$	12.5		50[d,e]
		14.0	50[d]	50[d]
	None	12.5		70[d,e]
		14.0	50[f]	70[d]
Ni	0.5 *m* NaCl	7.0	0[h,i]	0[b,i]
		10.5	0[d,h]	0[d]
		12.5	0[d]	0[d]
		14.0	0[d]	50[d]
	0.5 *m* $NaNO_3$	14.0		30[d,f,j]
	None	14.0		30[d,f,j]

[a]No MFe_2O_4 was detected for M = Mn, Co, or Ni at 100°, or for M = Mg or Zn at 100–200°, for any of the solution compositions listed. The species (other than MFe_2O_4 and goethite) detected after each experiment are denoted by footnotes as follows.
[b]Poorly crystallized $M(OH)_2$ presumed present.
[c]γ-Mn_2O_3.
[d]$M(OH)_2$.
[e]Some hematite recovered as well as goethite.
[f]Unidentified minor product.
[g]γ-MnO(OH).
[h]$M_2(OH)_3Cl$.
[i]M^{2+}(aq).
[j]MO.

dehydrate to CoO. At pH_{25} 7, small amounts of Co^{2+} (more than could be accounted for by the solubility of $Co(OH)_2$ itself) were observed in the solution phase after hydrothermal treatment, which indicates that the freshly precipitated "$Co(OH)_2$" contains some small fraction of Cl^- or NO_3^- in place of hydroxide, so $CoCl_2$ or $Co(NO_3)_2$ is released into solution as hydrothermal recrystallization of the $Co(OH)_2$ proceeds. The tendency of Co(II) to form $Co_2(OH)_3Cl$ (13) in chloride media at pH 7–10.5 is a manifestation of this ion-exchanging property of $Co(OH)_2$. Spontaneous hydrothermal oxidation of Co(II) to Co_3O_4 at near-neutral pH values has been reported previously (12).

The conversions of $Ni(OH)_2$ were closely similar to those of $Co(OH)_2$, except that oxidation to Ni(III) did not occur. The transformation of $Ni(OH)_2$ to NiO (bunsenite) occurred generally at temperatures above 250°, but also at 200° at pH_{25} 14 in several cases. The latter observation shows that Aia's purported phase relationship diagram (14), according to which $Ni(OH)_2$ decomposes to NiO in water at 285 ± 5°, may have kinetic, but no thermodynamic, significance.

The oxidation of $Mn(OH)_2$ presented problems of product identification, since the X-ray diffraction patterns of γ-Mn_2O_3 and γ-Mn_3O_4 (hausmannite) are almost identical (15), while the existence of variously hydrated forms and poly-

Can. J. Chem. Downloaded from www.nrcresearchpress.com by 210.87.254.5 on 09/05/12
For personal use only.

Can. J. Chem. Downloaded from www.nrcresearchpress.com by 210.87.254.5 on 09/05/12
For personal use only.

morphs of MnO(OH), Mn_3O_4, or Mn_2O_3 (16) makes positive identification difficult, especially in mixtures. However, the tentative identification of the Mn(III)-containing products as γ-MnO(OH) (manganite) at the lower temperatures, γ-Mn_2O_3 under most intermediate conditions, and α-Mn_2O_3 (bixbyite) at 350° in one instance follows a logical pattern. The α form of Mn_2O_3 is the more thermodynamically stable, and γ-Mn_2O_3 reverts to it *in vacuo* at 500° in 2 days, or at 25° in about 1 year (15).

Zinc hydroxide invariably decomposed to ZnO (zincite) under hydrothermal conditions, whereas $Mg(OH)_2$ (brucite) and $Ca(OH)_2$ (portlandite) were unchanged. Copper hydroxide was recovered as CuO (tenorite) under all conditions except in chloride media at pH_{25} 7–10.5 at 100–200°, in which circumstances paratacamite ($Cu_2(OH)_3Cl$) was formed instead.

The suppression of the oxidation of $Mn(OH)_2$ and $Co(OH)_2$ at pH_{25} 14 was probably a direct p*H* effect, but there is the possibility that the (II) oxidation state was maintained by the presence of some small amount of hydrogen produced by corrosion of the metal of the autoclave by aqueous alkali or steam (the latter explanation may also explain the reduction of aqueous $CuCl_2$ to CuCl reported previously (12)). However, corrosion of the vessel walls was not extensive, nor was goethite reduced to magnetite in these particular cases, so that the first explanation is to be preferred.

The pH_{25} of the hydrothermal media did not change significantly over the 24 h reaction period when the initial pH_{25} was 7.0 or 14.0. However, a fall of about 1.0 p*H* unit and sometimes more was generally observed for initial pH_{25} 10.5 after 24 *h* of hydrothermal treatment. A similar phenomenon was reported by Christensen and Fregerslev (10) for the hydrothermal decomposition of iron(III) hydroxide. Experiments using Teflon liners showed that this loss of OH^- was not due to corrosion of the titanium alloy of the autoclave walls, but rather to interaction between the fresh $M(OH)_2$ precipitate (and, to a lesser extent, the hematite or goethite) and OH^- in solution. This effect may be attributed to the ion-exchanging properties of the initial $M(OH)_2$ precipitates referred to above; as $M(OH)_2$ becomes more crystalline under hydrothermal treatment, the replacement of residual Cl^- or NO_3^- in the precipitate by OH^- from solution will cause a fall in the pH_{25} toward 7. As little as 0.1% residual Cl^- or NO_3^- in $M(OH)_2$ would account for the observed decreases in p*H*. Nevertheless, the marked differences in the outcome of many experiments run at initial pH_{25} 10.5 relative to those at 7.0 affirm that it is the initial, rather than the final, pH_{25} value that is significant from the standpoint of spinel formation.

Formation of MFe_2O_4

The salient features of these reactions are summarized in Tables 1 and 2. The percentage yields of MFe_2O_4 are rough estimates based upon the intensities of X-ray reflections characterizing MFe_2O_4 and the residual reactants or their derivatives.

Discussion

Although the interpretation of the data of Tables 1 and 2 is complicated by the factors listed in the Introduction, the following generalizations can be made.

(*a*) In the absence of solutes other than NaOH, hydrothermal spinel formation according to reactions 3–6 is negligible in 24 h at pH_{25} 7 over the range 100–350°, and becomes significant for M = Co, Ni, and Zn only at 350° at pH_{25} 10.5. However, at pH_{25} 14, spinel formation via reaction 4 proceeds at a significant rate at 200° or less for M = Co and Mn, though $NiFe_2O_4$ (trevorite) was detected only at 300° and above, and Cu, Mg, and Ca ferrites were not detected under any hydrothermal conditions up to 350°. Since highly alkaline conditions favor MFe_2O_4 formation, it presumably occurs through the solution phase by dissolution of $M(OH)_2$ or MO and goethite or hematite as $M(OH)_3^-$, $Fe(OH)_4^-$, or similar species. The detection of some solid β-$NaFeO_2$ in several instances when the goethite–hematite transformation was being examined at pH_{25} 12 strongly suggests the presence of $Fe(OH)_4^-$ ($\equiv FeO_2^-$) in solution in small concentrations in alkaline media, as proposed by Lengweiler *et al.* (17). The kinetic reactivity sequence M = Co ≥ Mn > Ni ≥ Zn > (Mg, Ca, Cu) parallels the thermodynamic reactivity sequence M = Co > Ni > Mg > Cu for reaction 3 (3, 4). Indeed, $CuFe_2O_4$ is not expected to form by reaction 3 under hydrothermal conditions for thermodynamic reasons (3), and this presumably reflects the Jahn–Teller distortion of the spinel structure originating in the $3d^9$ electronic configuration of Cu^{2+} (18).

Can. J. Chem. Downloaded from www.nrcresearchpress.com by 210.87.254.5 on 09/05/12
For personal use only.

(*b*) The presence of 0.5 *m* chloride or nitrate ion facilitates MFe_2O_4 formation, although high p*H* is still necessary for optimum effect. This may be attributed to solubilization of M(II) or Fe(III) by anion–cation complexing, which becomes increasingly effective in hydrothermal systems as the temperature increases (2, 12, 19). Chloride is more effective than nitrate in catalyzing reactions 3–6, as expected if anion–cation complexing is involved (20). The greater catalytic power of Cl^- was established early in this investigation, so that in many later experiments the effect of NO_3^- was not investigated at temperatures and p*H* values at which chloride-containing systems produced no MFe_2O_4. Nitrate has a disadvantage in that it facilitates the oxidation of Mn(II) and Co(II), whereas chloride, though nonoxidizing, tends to form compounds of the type $M_2(OH)_3Cl$ by reaction with $M(OH)_2$.

(*c*) Reactions 3–6 in hydrothermal conditions are favored by increasing the temperature, as expected for thermodynamically possible processes which are inhibited kinetically. In principle, the relative yields of the various MFe_2O_4 listed in Tables 1 and 2 should provide an index of the relative kinetic reactivities of M in $M(OH)_2$ or MO, since most of these hydroxides and oxides have exactly analogous crystal structures (brucite structure in $M(OH)_2$ where M is Mn, Co, Ni, Mg, or Ca, and halite structure for the corresponding MO (18)), as do the MFe_2O_4 products (spinel structure). However, the picture is confused by the depletion of $M(OH)_2$ reservoir by oxidation or conversion to MO in some cases, by the formation of $M_2(OH)_3Cl$ in chloride media in others, and by the increase in crystallinity of the sundry $M(OH)_2$ to various degrees as the severity of the hydrothermal conditions is increased. A detailed kinetic study of reactions 3–6 would have to take these factors into account, as well as to examine the effect of stirring and to maintain constant p*H*. Nevertheless, the data of Tables 1 and 2 afford a useful qualitative insight into the kinetics and mechanism of ferrite formation.

(*d*) Goethite is markedly more reactive than hematite in the hydrothermal reactions 3–6, as anticipated on thermodynamic grounds (6). The operative factor is probably the solubility or, more specifically, the *rate* of dissolution of goethite and hematite in the hydrothermal media. The conversion of goethite to hematite becomes kinetically significant above about 220° in all cases (and is evidently somewhat catalyzed by $Mn(OH)_2$ and $Co(OH)_2$ at pH_{25} 12.5 at least). In no case was the rehydration of hematite to goethite observed; as Langmuir (6) pointed out, this is thermodynamically possible below 80°, or above this temperature for hematite of very small grain size, but it is unlikely to be observed for kinetic reasons (however, in soils, hematite may be dissolved by complexing and/or reduction by organic anions followed by reprecipitation as goethite (21, 22)). The temperature range found in the present studies for the goethite–hematite conversion agrees with that reported by several other investigators (23–26) for the reaction both in water and in air (which supports our assertion that the reaction does not involve the solution phase), but lower decomposition temperatures have been recorded (1, 27–35). These lower decomposition temperatures could be associated with small particle size, the importance of which was stressed by Langmuir (6), or with the presence of impurities, since we have found that $Co(OH)_2$ and $Mn(OH)_2$ accelerate the reaction significantly. Conversion of goethite to hematite by Tunnell and Posnjak (30) at 100° in 0.1 *M* HCl over several weeks undoubtedly occurred via iron(III) aquo and chloro complexes in solution. Goethite decomposition temperatures of as high as 290–375° have been recorded in differential thermal analysis (35), but in this case the heating rate is an important variable.

(*e*) The position of Ni in the general reactivity order in reactions 3–6 ($M = Co \geq Mn > Ni > Mg$) contrasts with the sequence established (2) for the analogous formation of MCr_2O_4 ($M = Mn > Co > Mg \gg Ni$). An important difference between the chromites and the ferrites is that the former are normal spinels (Cr^{3+} in octahedral sites only, M^{2+} in tetrahedral sites in the face-centered-cubic oxide array) whereas the ferrites considered here are generally inverse spinels (Fe^{3+} in both octahedral and tetrahedral sites, M^{2+} in octahedral sites only) (36). M^{2+} ions in MO with the NaCl structure or in $M(OH)_2$ with the brucite structure are already octahedrally coordinated by oxygen ions, and consequently crystal field effects are not expected to influence the energetics of reactions 3–6 in these cases. However, crystal field stabilization energy losses will be large (8.45 *Dq*, ≡ 100 kJ mol^{-1}) for the $3d^8$ ion Ni^{2+} in the formation of $NiCr_2O_4$ from NiO or $Ni(OH)_2$, relative to Co^{2+} (2.67 Dq), Mn^{2+} (zero), or Mg^{2+} (zero), and these are

reflected in the changes in the reactivity order on going from MFe_2O_4 formation to MCr_2O_4 syntheses.

We thank Atomic Energy of Canada, Ltd., for financial support of this work.

1. G. BUTLER and H. C. K. ISON. J. Chem. Soc. Chem. Commun. 264 (1965).
2. T. W. SWADDLE, J. H. LIPTON, G. GUASTALLA, and P. BAYLISS. Can. J. Chem. **49**, 2433 (1971).
3. T. E. RUMMERY and D. D. MACDONALD. The thermodynamics of selected transition metal ferrites in high temperature aqueous systems. Report No. AECL-4577. Atomic Energy of Canada, Ltd., Pinawa, Manitoba. December, 1973.
4. J. D. TRETJAKOW and H. SCHMALZRIED. Ber. Bunsenges. Phys. Chem. **69**, 396 (1965).
5. D. D. WAGMAN, W. H. EVANS, V. B. PARKER, I. HALOW, S. M. BAILEY, and R. H. SCHUMM. Technical Notes 270–3 (1968) and 270–4 (1969). National Bureau of Standards, Washington, D.C., U.S.A.
6. D. LANGMUIR. Am. J. Sci. **271**, 147 (171).
7. W. J. SCHUELE and V. D. DEETSCREEK. J. Appl. Phys. Suppl. **32**, 235S (1961).
8. T. SATO, C. KURODA, M. SAITO, and M. SUGIHARA. *In* Ferrites. *Edited by* Y. Hoshino, S. Iida, and M. Sugimoto. University Park Press, Baltimore, Md. 1971. p. 72.
9. A. N. CHRISTENSEN. Acta Chem. Scand. **22**, 1487 (1968).
10. A. N. CHRISTENSEN and S. FREGERSLEV. Acta Chem. Scand. **22**, 1043 (1968).
11. R. A. LAUDISE. Prog. Inorg. Chem. **3**, 1 (1962).
12. P. C. KONG, T. W. SWADDLE, and P. BAYLISS. Can. J. Chem. **49**, 2442 (1971).
13. H. B. WEISER and W. O. MILLIGAN. J. Phys. Chem. **36**, 722 (1932).
14. M. A. AIA. J. Electrochem. Soc. **113**, 1045 (1966).
15. T. E. MOORE, M. ELLIS, and P. W. SELWOOD. J. Am. Chem. Soc. **72**, 856 (1950).
16. O. BRICKER. Am. Mineral. **50**, 1296 (1965).
17. H. LENGWEILER, W. BUSER, and W. FEITKNECHT. Helv. Chim. Acta, **44**, 796, 805 (1961).
18. A. F. WELLS. Structural inorganic chemistry. 3rd. ed. Oxford University Press, Oxford. 1962.
19. H. C. HELGESON. Complexing and hydrothermal ore deposition. Pergamon Press, New York, N.Y. 1964.
20. A. E. MARTELL and L. G. SILLÉN. Stability constants of metal ion complexes. Special Publications Nos. 17 (1964) and 25 (1971). The Chemical Society, London.
21. U. SCHWERTMANN. Fortschr. Mineral. **46**, 274 (1969).
22. U. SCHWERTMANN. Nature, **232**, 624 (1971).
23. J. B. POLLACK, D. PITMAN, B. N. KHARE, and C. SAGAN. J. Geophys. Res. **75**, 7480 (1970).
24. M. H. FRANCOMBE and H. P. ROOKSBY. Clay Minerals Bull. **4**, 1 (1959).
25. J. D. BERNAL, D. R. DASGUPTA, and A. L. MACKAY. Nature, **180**, 645 (1957).
26. J. W. GRUNER. Econ. Geol. **26**, 442 (1931).
27. F. G. SMITH and D. J. KIDD. Am. Mineral. **34**, 403 (1949).
28. T. KATSURAI and T. WATANABE. Sci. Pap. Inst. Phys. Chem. Res. Tokyo, **13**, 89 (1930).
29. C. KLINGSBERG and R. ROY. Am. Mineral. **44**, 819 (1959).
30. G. TUNNELL and E. POSNJAK. Econ. Geol. **26**, 337 (1931).
31. R. F. SCHMALZ. Bull. Geol. Soc. Am. **69**, 1939 (1958).
32. H. B. WEISER and W. O. MILLIGAN. J. Phys. Chem. **39**, 25 (1935).
33. E. POSNJAK and H. E. MERWIN. Am. J. Sci. **47**, 311, 339 (1919).
34. L. WALTER-LÉVY and E. QUÉMÉNEUR. Bull. Soc. Chim. Fr. 1947 (1966).
35. W. SCHELLMANN. Chem. Erde, **20**, 104 (1959).
36. J. E. HUHEEY. Inorganic chemistry: principles of structure and reactivity. Harper and Row, New York, N.Y. 1972. pp. 316–319.

Can. J. Chem. Downloaded from www.nrcresearchpress.com by 210.87.254.5 on 09/05/12
For personal use only.

Ring C Functionalized Diterpenoids. Part IV.[1] Minor Products from the Cleavage of the Cyclopropane Ring in Methyl *ent*-Trachyloban-19-oate with Thallic Acetate

HELEN MARGARET CAMPBELL, PATRICK ALISTAIR GUNN, ALAN JAMES MCALEES, AND ROBERT MCCRINDLE[2]

Chemistry Department, University of Guelph, Guelph, Ontario N1G 2W1

Received June 25, 1974

HELEN MARGARET CAMPBELL, PATRICK ALISTAIR GUNN, ALAN JAMES MCALEES, and ROBERT MCCRINDLE. Can. J. Chem. **53**, 20 (1975).

Structures are assigned to seven minor products (**6***b*, **9**, **11***b*, **12***b*, **13***b*, **16**, and **25***b*) obtained from treatment of methyl *ent*-trachyloban-19-oate (**1**) with thallic oxide in acetic acid. The mechanism of the oxidative cleavage is discussed. Formation of the major products, described earlier, and all but one (**25***b*) of the minor products may be rationalized in terms of initial scission of the C_{13}—C_{16} bond.

HELEN MARGARET CAMPBELL, PATRICK ALISTAIR GUNN, ALAN JAMES MCALEES et ROBERT MCCRINDLE. Can. J. Chem. **53**, 20 (1975).

Des structures sont assignées à sept produits mineurs (**6***b*, **9**, **11***b*, **12***b*, **13***b*, **16** et **25***b*) obtenus par la réaction du trachyloban-*ent*-oate-19 de méthyle (**1**) avec l'oxyde thallique dans l'acide acétique. Le mécanisme du clivage oxidant est discuté. La formation des produits majeurs, décrite précédemment, et des produits mineur à l'exception de (**25***b*) peut être rationnalisée en termes d'une scission initiale de la liaison C_{13}—C_{16}. [Traduit par le journal]

In an earlier paper (2) we have assigned structures to the major components (**2**–**5**) of the very complex mixture obtained by oxidative cleavage of the cyclopropane ring in methyl *ent*-trachyloban-19-oate (**1**). The formation of these compounds involves scission of the C_{13}—C_{16} bond in **1**. The present paper is devoted to the minor products of this reaction and a more detailed consideration of the mechanism of the reaction.

Results

Seven new compounds have been isolated, six from the monoacetate fraction (2) and one from the diacetate fraction. Structures have been assigned to the first six on evidence which is outlined below. The structure suggested for the diacetate is tentative and based mainly on mechanistic considerations.

The monoacetate fraction was separated (2) into two parts, the more polar of which consisted largely of the major components **2** and **5**,[3] while the less polar contained a very complex mixture of products. The least polar of these, **6***b*, was isolated only with considerable difficulty. Since the material thus obtained contained residual impurities it was converted into the corresponding alcohol (**6***a*), m.p. 148–150°, which gave n.m.r. resonances attributable to a carbinyl proton (τ 6.43, d), an olefinic proton (τ 4.60, br s), and a methyl group on a double bond (τ 8.31, d). The principal evidence for the structures of **6***a* and *b* is the observation that the former is formed on aqueous treatment of the *p*-toluenesulfonate **7**. The multiplicities of the resonances due to the carbinyl and olefinic protons in **6***a* allowed us to discount the alternative structure **8**. The assignment of the α-orientation to the hydroxy group in **6***a*, which is predicted on both mechanistic (see below) and steric grounds, is supported by the observation that the carbinyl proton shows no appreciable 'W' coupling to αH-11 (3).

The next compound, **9**, m.p. 101–104°, proved to be a ketone, the n.m.r. spectrum of which shows sharp singlets at τ 9.34 (3 H-20), 8.85 (3 H-18), 7.97 (3 H-17), and 7.67 (2 H-15), and a broad singlet at 4.92 (H-12 + H-13). The ready reduction of **9** with sodium borohydride to **10** (probably a mixture of diastereoisomers), m.p. 79°, showed that the signal at

[1]For part III see ref. 1.

[2]To whom correspondence should be addressed.

[3]Substituents designated α or β on the α-bridge of rings C–D refer to orientations *syn* and *anti* to C-20, respectively.

Can. J. Chem. Downloaded from www.nrcresearchpress.com by 210.87.254.42 on 09/05/12
For personal use only.

Can. J. Chem. Downloaded from www.nrcresearchpress.com by 210.87.254.42 on 09/05/12
For personal use only.

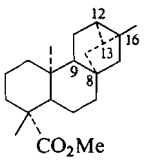

1

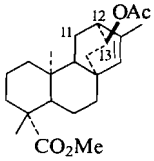

2

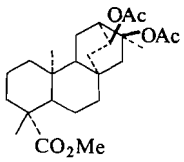

3

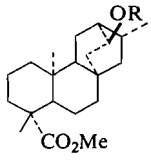

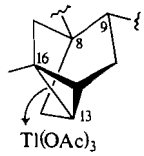

17 18 (1)

a R = H
b R = Ac

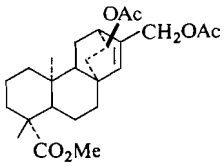

4

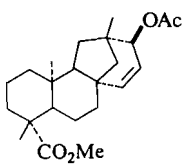

5

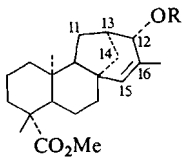

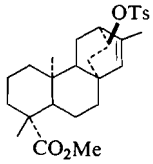

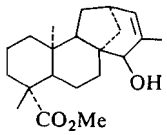

6 7 8

a R = H
b R = Ac

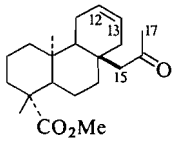

9

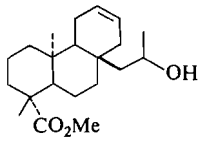

10

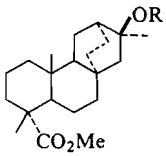

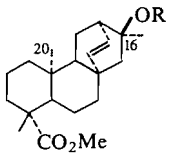

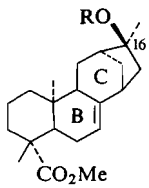

11 12 13

a R = H
b R = Ac

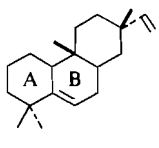

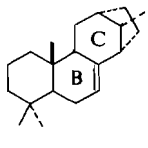

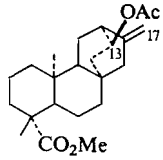

14 15 16

τ 7.97 in **9**, which is replaced by a doublet at τ 8.87, $J = 6$ Hz, in **10**, is due to a methyl ketone rather than an acetate. In addition, integration of the allylic proton region of the n.m.r. spectrum of **10** shows the presence of four allylic protons, thus establishing the position of the double bond in **10** and hence also in **9**.

As further components of the less polar monoacetate fraction could not be separated directly, the remaining mixture was subjected to mild base hydrolysis, which gave the corresponding alcohols without affecting the axial C-19 ester function. Preparative t.l.c. of the alcohols gave three significant fractions. In contrast to our findings for all the other products obtained, the n.m.r. spectrum of the least polar alcohol, **11***a*, m.p. 142–145°, isolated from this mixture showed no resonances attributable to olefinic or carbinyl protons. It did however reveal the presence of three methyl groups, two attached to quaternary carbon atoms and one on a carbon atom which carried a hydroxyl group. This led us to consider that **11***a* was simply the product of acid-promoted opening of the cyclopropane ring in **1**, and indeed, comparison of the physical constants of **11***a* with those published (4) for methyl 16β-hydroxy-*ent*-atisan-19-oate ratified the identity of these two. As anticipated, when **1** was treated with acetic acid alone at 75° for 5 days, it suffered partial conversion into the acetate **11***b*, m.p. 143–144°.

The second alcohol isolated, **12***a*, is also tertiary and has a particularly characteristic n.m.r. spectrum. This reveals the presence of a *cis*-disubstituted double bond, one olefinic proton of which is further coupled to an adjacent methine proton. In addition, the orientation of this double bond is such as to cause a marked shielding of the C-20 methyl group which resonates at τ 9.62. The absence of absorption attributable to OH—π bonding in the i.r.

Can. J. Chem. Downloaded from www.nrcresearchpress.com by 210.87.254.42 on 09/05/12
For personal use only.

spectrum of **12***a* allows assignment of the configuration at C-16 as shown.

The next component is also an olefinic tertiary alcohol, **13***a*, m.p. 120–121°, as evidenced by peaks in the n.m.r. spectrum at τ 4.82 (m, *1* H-7), 8.70 (s, 3 H-17), 8.83 (s, 3 H-18), and 9.36 (s, 3 H-20). The assignment of structure **13***a* to this compound rests largely on the observation of a particularly intense peak in its mass spectrum of *m/e* 146, attributable to a fragment derived by the retro-Diels–Alder fission and dehydration depicted in Fig. 1. The relatively high field position of the C-10 methyl resonance is similar to that observed (5) for rimuene, **14** (τ 9.38) but contrasts with that observed (6, 7) for **15** (τ 9.23, 9.25) although the latter, at first sight, might be expected to provide a closer analogy. However, examination of molecular models suggests that the 16β-substituent in **13***a* interacts sufficiently with H-9 to cause a slight flattening of rings B and C. As a result of this, the C-10 methyl group rotates towards the shielding cone of the C-7 double bond. Flattening of rings A and B in rimuene, **14**, which reduces various nonbonded interactions, could account for the upfield shift of the C-9 methyl resonance. In contrast, flattening of rings B and C in **15** does not lead to a comparable reduction in nonbonded strain.

A further product, **16**, m.p. 128–131°, has been isolated from the more polar monoacetate fraction (2) by preparative t.l.c. over silver nitrate – silica gel. The n.m.r. of **16** shows only two quaternary methyl groups at τ 8.82 (3 H-18) and 9.23 (3 H-20). A broad singlet at τ 5.20, which integrates for three protons, is ascribed to 2 H-17 + H-13. In addition, the hydrogenation of **16** gave a single product **17***b*, which was identical (t.l.c., g.l.c., and n.m.r.) with the single product obtained by hydrogenation of the isomer **2**. Since **17***b* was obtained as an oil which could not be induced to crystallize, final confirmation of its structure was achieved by converting it into the corresponding alcohol, **17***a*, m.p. 134–135°, which had been obtained previously (2).

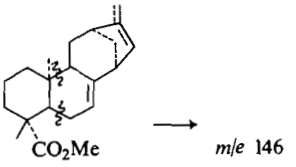

Fig. 1. Mass spectral fragmentation pattern.

Discussion

All but one (discussed below) of the products isolated from the cleavage of **1** with thallic acetate can be most readily envisaged as deriving from initial attack[4] at the C_{13}—C_{16} bond (**18** arrows) with development of considerable carbonium ion character at C-16 (**19**). Preferential cleavage of the C_{13}—C_{16} bond is anticipated on the basis of earlier reports on the cleavage of trachylobanes with acids (8–10).[5] Indeed, it is consistent with the results of cleavage of simple bicyclo[*n*.1.0.] alkanes by thallic acetate (12), where it is found that the relative ease of internal (O bridge) bond cleavage increases with decreasing *n*. The structures of the products isolated suggest that at least three competing processes determine the eventual fate of carbonium ion **19** (Scheme 1).

First, elimination of a proton can give **20** and **21**, from which the olefinic monoacetates **2** and **16** may derive. The stereochemistry of these products requires that the replacement of the —$Tl(OAc)_2$ group with —OAc proceed with retention (2). Migration of the C_{11}—C_{12} bond to C-13 upon heterolysis of the —$Tl(OAc)_2$ group in **21** would produce the allylic cation **22** and thence **6***b*. Diacetate **4** probably results from allylic oxidation of **2** and/or **16**.

Second, attack on the β-face (see below) of **19** by water generated in the formation of $Tl(OAc)_3$ from Tl_2O_3 may produce the tertiary alcohol **23**. This would be expected to fragment as shown (**23** arrows), furnishing the ketone **9**.

Third, attack by solvent (acetic acid) on **19** would give the tertiary acetate **24**, the stereochemistry of which is that expected (12) on the basis of *trans* opening of the cyclopropane ring. It has been suggested (12) that this cleavage involves 'a closely timed sequence in which the addition of metal salt and solvent occur in such a fashion as to preclude loss of stereochemistry.' In the present instance, even if addition of solvent were not concerted with

[4]Since our results do not allow us to draw any conclusions as to the nature of the electrophilic species involved, we have used $Tl(OAc)_3$ in **18** for convenience (*cf.* ref. 13).

[5]The relatively large amounts of beyeranes found in one of these studies (10) are probably obtained by rearrangement of an initially formed atisane carbonium ion (1, 11).

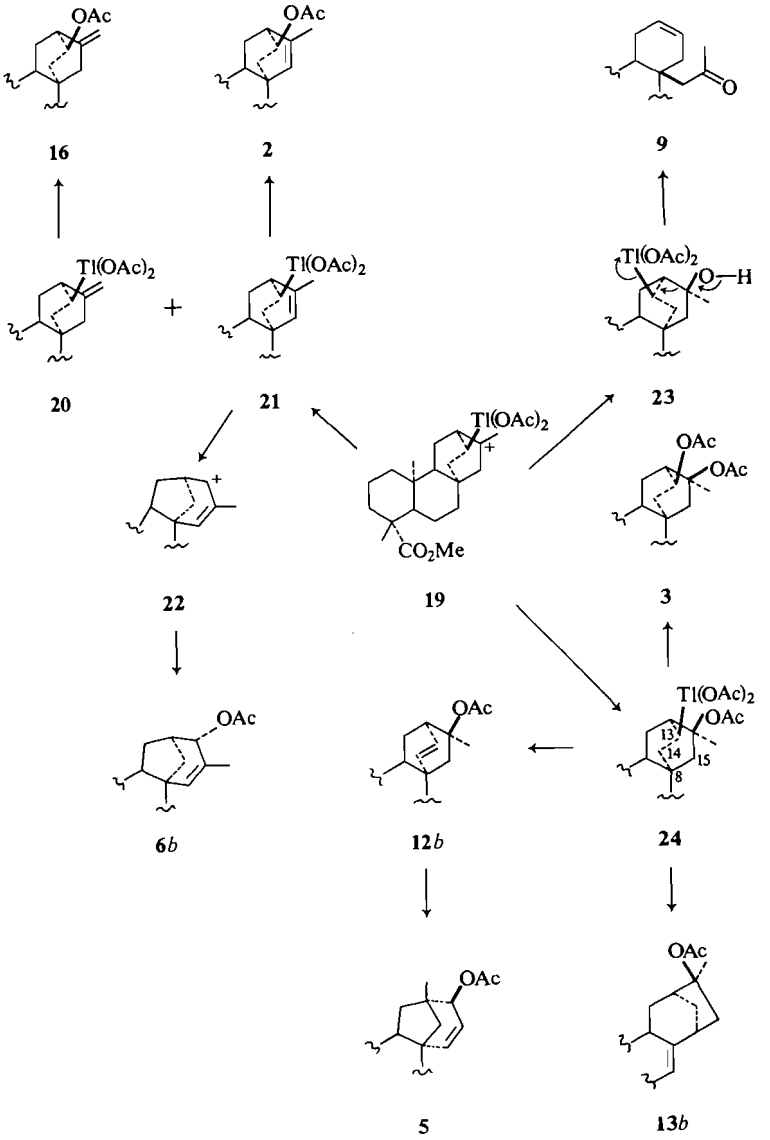

SCHEME 1

ring opening, attack at C-16 would still be expected to take place preferentially on the β-face since α-attack would be severely hindered by the bulky —$Tl(OAc)_2$ substituent at C-13. Several pathways can be invoked to account for the subsequent fate of **24**. Thus, internal nucleophilic substitution gives the diacetate **3**. Alternatively, heterolysis of the —$Tl(OAc)_2$ group with (*a*) loss of a proton from the neighboring carbon (C-14) or (*b*) hydride shift from C-14 to C-13, migration of the C_8—C_{15} bond to C-14, and elimination of a proton from C-7, leads to the olefinic tertiary acetates **12***b* and **13***b*, respectively. The isolation of alcohol **12***a* lends credence to our previous suggestion (2) that **5** might be formed by rearrangement of acetate **12***b*. Ionization of the tertiary acetate function in **12***b* may be assisted by homoallylic participation (14).

Finally, one minor product, the diacetate of intermediate polarity (2) appears to have structure **25***b*. The n.m.r. spectrum shows singlets at τ 9.18 (3 H-20), 8.86 (3 H-18), 8.52 (3 H-17), and 8.12 (6H, 2 —OCOCH_3) and a multiplet

Can. J. Chem. Downloaded from www.nrcresearchpress.com by 210.87.254.42 on 09/05/12
For personal use only.

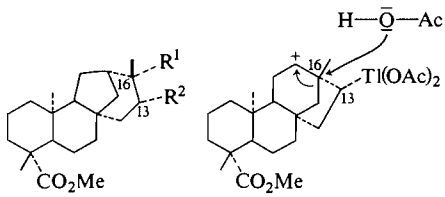

25 **26**

a $R^1 = R^2 = OH$
b $R^1 = R^2 = OAc$
c $R^1 = OAc$; $R^2 = Tl(OAc)_2$

at τ 5.10 (dd, J_{obs} = 3 and 6 Hz). The multiplicity of the last rules out the possibility that the diacetate is a 12α- or β-substituted kaurane or a 13α- or β-substituted atisane since its coupling pattern is very different from theirs (15). This, and the indication from its n.m.r. spectrum that the moiety $H_3C—C—OAc$ (τ 8.52) is present, leads to structures such as **25***b*. Support for structure **25***b* comes from the i.r. absorption of the derived diol, **25***a*, m.p. 195–197°, and a consideration of reaction pathways emanating from **1** which are satisfying on mechanistic grounds. Thus, the diol shows strong hydrogen bonding, $\Delta\nu_{OH} = 95\ cm^{-1}$, a value considerably larger than those recorded for simple cyclohexane vicinal diols but similar to those for certain related bridged systems (16). In addition, the following mechanistic pathway would account for the formation of **25***b*. Attack of the metal salt on the $C_{12}—C_{13}$ bond of **1** and attachment of the thallium substituent to C-13 would give the ion **26**. Wagner–Meerwein rearrangement with transfer of carbonium ion character to C-16 (see **26** arrows) and then capture of solvent at C-16 would give **25***c*. Steric and mechanistic arguments predict capture on the α-face. The diacetate **25***b* would then be generated from **25***c* with retention of stereochemistry (2) at C-13.

Experimental

Melting points were determined on a Kofler hot-stage apparatus and are uncorrected. For normal analytical and preparative t.l.c., chromatoplates were spread with Kieselgel G (Merck), while silver nitrate – silica gel chromatoplates in addition contained 12% of the former. Gas–liquid chromatography was carried out at 200° with a Varian Aerograph 1200 gas chromatograph using a stainless steel column (1/8 in. × 10 ft packed with 5% SE-30) and nitrogen as carrier gas with a flow rate of 25 ml/min. Light petroleum was of b.p. 60–80°. Proton magnetic resonance spectra were run on a Varian Associates A-60A or HA100 spectrometer in carbon tetrachloride unless otherwise stated using approximately 0.3 *M* solutions and tetramethylsilane as internal standard. Infrared spectra were recorded in carbon tetrachloride on a Beckman I.R.12 spectrophotometer. Microanalyses were by Mr. S. McKinnon, Guelph. Routine mass spectra were run on a Varian Associates CH7 instrument and high resolution mass spectra on an AEI MS 902 instrument equipped with a PDP8 computer at the N.T.H., Trondheim, Norway.

Separation of Further Products from the Oxidative Cleavage

The products (3.60 g) from the oxidative cleavage of **1** (3.40 g) were chromatographed over alumina (2). Seven fractions (1.227 g total) were collected using light petroleum – ethyl acetate (24:1) as eluant. The last three of these were combined (556 mg) and a minor component (**16**, 42 mg) separated by preparative t.l.c. over silver nitrate – silica gel (ethyl acetate – light petroleum) before isolation (2) of the alcohols corresponding to **2** and **5** from the rest of this material. This new acetate (**16**) crystallized from light petroleum and had m.p. 128–131°; τ 5.20 (br s, 3H, 2 H-17 + H-13), 7.98 (s, 3H, —OCOCH_3), 8.82 (s, 3 H-18), and 9.23 (s, 3 H-20).

Anal. Calcd. for $C_{23}H_{34}O_4$: C, 73.76; H, 9.15. Found: C, 73.55; H, 9.04.

The other four fractions (of the seven) from the alumina column were also combined (671 mg) and subjected to preparative t.l.c. (ethyl acetate – light petroleum, 3:97, run four times). The fractions obtained by this procedure were then subjected to further preparative t.l.c. this time on silica gel – silver nitrate (ethyl acetate, 3:97, run four times). This yielded a pure sample of **9** (82 mg) and a second component (**6***b*) in almost pure form. The remaining fractions were recombined and hydrolyzed with excess sodium hydroxide (0.5 g) in refluxing aqueous methanol (20 ml, 1:1) for 1 h. The hydrolysis mixture was separated by preparative t.l.c. first on silica gel (ethyl acetate – light petroleum, 1:10, run thrice) and then on silver nitrate – silica gel (ethyl acetate – light petroleum, 1:10, run thrice). This sequence afforded **11***a* (20 mg), **12***a* (74 mg), and **13***a* (41 mg).

Ketone **9** crystallized from light petroleum and had m.p. 101–104°; τ 4.92 (br s, 2H, H-12 + H-13), 7.67 (s, 2 H-15), 7.97 (s, 3 H-17), 8.85 (s, 3 H-18), and 9.34 (s, 3 H-20); *m/e* 332 (M).

Anal. Calcd. for $C_{21}H_{32}O_3$: C, 75.86; H, 9.70. Found: C, 75.88; H, 9.76.

Acetate **6***b*, which had τ 4.58 (br s, 1 H-15), 5.31 (d, 1 H-12, J = 3 Hz), 8.03 (s, 3H, —OCOCH_3), 8.43 (br s, 3 H-17), 8.83 (s, 3 H-18), and 9.36 (s, 3 H-20), failed to crystallize and was hydrolyzed with excess sodium hydroxide (0.1 g) in refluxing aqueous methanol (10 ml, 1:1) for 1 h. The alcohol (**6***a*, 44 mg) was recovered from the reaction mixture by preparative t.l.c. (ethyl acetate – light petroleum, 1:10, run thrice). After crystallization from light petroleum it had m.p. 148–150°; τ 4.60 (br s, 1 H-15), 6.43 (d, 1 H-12, J = 3 Hz), 8.31 (br s, 3 H-17), 8.82 (s, 3 H-18), and 9.31 (s, 3 H-20).

Mol. Wt. Calcd. for $C_{21}H_{32}O_3$: 332.2352. Found (high resolution mass spectrometry): 332.2356.

The known (4) alcohol **11***a* had m.p. 142–145° (lit. (4) m.p. 148°) on crystallization from light petroleum;

Can. J. Chem. Downloaded from www.nrcresearchpress.com by 210.87.254.42 on 09/05/12
For personal use only.

Can. J. Chem. Downloaded from www.nrcresearchpress.com by 210.87.254.42 on 09/05/12
For personal use only.

τ 8.71 (s, 3 H-17), 8.83 (s, 3 H-18), and 9.22 (s, 3 H-20). Alcohol **12***a* was obtained as an oil; τ 3.82 (m, 1 H-14), 4.00 (m, 1 H-13), 8.83 (s, 3 H-18), 8.91 (s, 3 H-17), and 9.62 (s, 3 H-20); in the presence of 0.4 *M* ratio of Eu(DPM)$_3$ to **12***a* τ 2.90 (m, 1 H-14), 3.22 (m, 1 H-13), 6.25 (s, 3 H-17), 8.50 (s, 3 H-18), 8.85 (s, 3 H-20); ν_{max} 3620 and 1740 cm^{-1}.

Mol. Wt. Calcd. for $C_{21}H_{32}O_3$: 332.2352. Found (high resolution mass spectrometry): 332.2353.

Alcohol **13***a* after crystallization from light petroleum had m.p. 120–121°; τ 4.82 (m, 1 H-7), 8.70 (s, 3 H-17), 8.83 (s, 3 H-18), and 9.36 (s, 3 H-20); *m/e* 146 (M − 18 − 168).

Anal. Calcd. for $C_{21}H_{32}O_3$: C, 75.86; H, 9.70. Found: C, 75.88; H, 9.76.

Fractions from the original alumina column eluted with light petroleum – ethyl acetate (23:2) were combined (966 mg total) and subjected to preparative t.l.c. (ethyl acetate – light petroleum, 1:9, run thrice). This yielded (2) **3** and **4** and a compound (**25***b*, 109 mg) of intermediate polarity. The last even after repeated preparative t.l.c. contained traces of **4**. This material (84 mg) which had τ 5.10 (dd, 1 H-13, J_{obs} = 3 and 6 Hz) 8.52 (s, 3 H-17), 8.86 (s, 3 H-18), and 9.18 (s, 3 H-20) was hydrolyzed with sodium hydroxide (0.4 g) in refluxing aqueous methanol (20 ml, 1:1) for 3 h. The product mixture (72 mg) was subjected to preparative t.l.c. (ethyl acetate – light petroleum, 1:4) and afforded substrate (15 mg) and diol **25***a* (26 mg). The latter on crystallization from benzene – light petroleum had m.p. 195–197°; τ ($CDCl_3$) 6.18 (dd, 1 H-13, J_{obs} = 3.5 and 5 Hz), 8.75 (s, 3 H-17), 8.83 (s, 3 H-18), and 9.22 (s, 3 H-20); ν_{OH} (2 mg/ml) 3610, 3515, 3348 cm^{-1}; ν_{OH} (0.5 mg/ml) 3610 and 3515 cm^{-1}.

Anal. Calcd. for $C_{21}H_{34}O_4$: C, 71.96; H, 9.78. Found: C, 71.89; H, 9.69.

Solvolysis of the Tosylate 7

The alcohol (35 mg) derived (2) from **2** was treated with excess *p*-toluenesulfonyl chloride (30 mg) in pyridine (2 ml) overnight. The reaction mixture (one spot on t.l.c., less polar than substrate) was diluted with ether and washed twice with chilled hydrochloric acid (1 *M*) and then water. The product (31 mg, 89%) was purified by preparative t.l.c. (ethyl acetate – light petroleum, 1:9 run twice) and shown to be identical with **6***a* by m.p., mixture m.p., t.l.c., and n.m.r.

*Reduction of the Ketone **9** with Sodium Borohydride*

The ketone **9** (22 mg) was treated with excess sodium borohydride (25 mg) in ethanol (5 ml) at 20° for 3 h. The alcohol **10** formed, was purified by preparative t.l.c. (ethyl acetate – light petroleum, 1:5) and then crystallization from light petroleum. It (16 mg) had m.p. 79°; τ 4.47 (br s, 2H, H-12 + H-13), 7.5–8.15 (m, 4H, 2H-11 + 2H-14), 8.85 (s, 3 H-18), 8.87 (d, 3 H-17, J = 6 Hz), and 9.33 (s, 3 H-20).

Anal. Calcd. for $C_{21}H_{34}O_3$: C, 75.41; H, 10.25. Found: C, 75.53; H, 10.13.

*Hydrogenation of Acetate **16***

Hydrogenation of **16** (25 mg) in ethyl acetate (10 ml) over palladized charcoal (5%, 15 mg) for 30 min afforded a single product which was purified by t.l.c. on silver nitrate – silica gel (ethyl acetate – light petroleum, 1:10, run thrice). This oil (18 mg) was shown by n.m.r., t.l.c., and g.l.c. to be identical with the major product, **17***b*, obtained by hydrogenation of **2**. Hydrolysis of the oil with sodium hydroxide (0.1 g) in refluxing aqueous methanol (10 ml, 1:1) for 3 h yielded **17***a* (14 mg, 88%), which crystallized from ethyl acetate – light petroleum. This alcohol had m.p. 132–134° and was identical (m.p., mixture m.p., t.l.c., and n.m.r.) with an authentic sample (2) of **17***a*.

*Treatment of Methyl ent-Trachyloban-19-oate (**1**) with Acetic Acid*

The ester **1** (100 mg) was heated in 20 ml glacial acetic acid at 75° for 5 days. The solvent was evaporated and the residue separated by preparative t.l.c. (ethyl acetate – light petroleum, 1:5 run thrice). One major product (**11***b*, 23 mg, 19%) was recovered. It crystallized from light petroleum and had m.p. 143–144°; τ 8.05 (s, 3H, —OCO*CH*$_3$), 8.46 (s, 3 H-17), 8.84 (s, 3 H-18), and 9.22 (s, 3 H-20).

Anal. Calcd. for $C_{23}H_{36}O_4$: C, 73.37; H, 9.64. Found: C, 73.34; H, 9.77.

We thank Dr. T. Anthonsen, N. T. H., Trondheim, Norway, for the high resolution mass spectra. The financial support of the National Research Council of Canada and of the Province of Ontario through an operating grant (to R.McC.) and an Ontario Graduate Fellowship (to H.M.C.), respectively, is gratefully acknowledged.

1. J. C. FAIRLIE, A. J. MCALEES, R. MCCRINDLE, and E. NEIDERT. Can. J. Chem. **52**, 706 (1974).
2. H. M. CAMPBELL, P. A. GUNN, A. J. MCALEES, and R. MCCRINDLE. Can. J. Chem. **51**, 4167 (1973).
3. L. M. JACKMAN and S. STERNHELL. Applications of nuclear magnetic resonance spectroscopy in organic chemistry. Pergamon Press, Oxford. 1969. p. 334.
4. R. M. COATES and E. F. BERTRAM. J. Org. Chem. **36**, 2625 (1971).
5. J. D. CONNOLLY, R. MCCRINDLE, R. D. H. MURRAY, and K. H. OVERTON. J. Chem. Soc. (C), 273 (1966).
6. P. A. GUNN, R. MCCRINDLE, and R. G. ROY. J. Chem. Soc. (C), 1018 (1971).
7. K. M. BAKER, L. H. BRIGGS, J. G. ST. C. BUCHANAN, R. C. CAMBIE, B. R. DAVIS, R. C. HAYWARD, G. A. S. LONG, and P. S. RUTLEDGE. J. Chem. Soc. Perkin Trans. 1, 190 (1972).
8. R. A. APPLETON, A. J. MCALEES, A. MCCORMICK, R. MCCRINDLE, and R. D. H. MURRAY. J. Chem. Soc. (C), 2319 (1966).
9. J. ST. PYREK. Tetrahedron, **26**, 5029 (1970).
10. G. HUGEL, L. LODS, J. M. MELLOR, and G. OURISSON. Bull. Soc. Chim. Fr. 2894 (1965).
11. R. M. COATES and E. F. BERTRAM. J. Org. Chem. **36**, 3722 (1971).
12. R. J. OUELLETTE, A. SOUTH, and D. L. SHAW. J. Am. Chem. Soc. **87**, 2602 (1965).
13. A. SOUTH and R. J. OUELLETTE. J. Am. Chem. Soc. **90**, 7064 (1968).
14. J. B. LAMBERT and A. C. HOLCOMB. J. Am. Chem. Soc. **93**, 3952 (1971).
15. A. J. MCALEES and R. MCCRINDLE. To be published.
16. M. TICHY. *In* Advances in organic chemistry. Vol. 5. *Edited by* R. A. Raphael, E. C. Taylor, and H. Wynberg. Interscience, New York. 1965. p. 146.

The Determination of the Preferred Stereochemistry and the Magnitude of the Hydrogen Isotope Effect for 1,3 Elimination in the Locked Norbornyl System Methyl *exo*-2-Bromo-1-norbornanecarboxylate-*endo,endo*-5,6-d_2[1]

NICK HENRY WERSTIUK

Department of Chemistry, McMaster University, Hamilton, Ontario L8S 4M1

Received June 24, 1974

NICK HENRY WERSTIUK. Can. J. Chem. **53**, 26 (1975).

Methyl *exo*-2-bromo-1-norbornanecarboxylate-*endo,endo*-5,6-d_2 (**1***b*) has been prepared and solvolyzed at 112° in 80:20 EtOH-H_2O buffered with NaOAc. The loss of 85–90% of the deuterium available on the front face of **1***b* in the formation of the tricyclic ester **6**D coupled with a novel analysis established that the *endo*:*exo* preference for 1,3 elimination is at least 15:1 to 20:1. A comparison of the solvolytic kinetic isotope effect (1.18 ± 0.04) for **1***b* and the 1,3-elimination kinetic isotope effect (1.45–1.6) with data for 1,2 eliminations indicates that elimination occurs from the classical, perhaps 1,3 hyperconjugatively stabilized carbocation **20**. The *endo*:*exo* preference established in this study is used to reinterpret 1,3-elimination data determined by Collins in the solvolysis of deuteriohydroxyphenyl norbornyl tosylates.

NICK HENRY WERSTIUK. Can. J. Chem. **53**, 26 (1975).

On a préparé et solvolysé l'ester méthylique de bromo-2-*exo* norbornanecarboxylique-1 *endo,endo*-5,6-d_2 (**1***b*) à 112° avec une solution tamponnée de 80:20 EtOh–H_2O avec NaOAc. La perte de 85–90% du deutérium disponible sur la face avant de **1***b* dans la formation de l'ester tricyclique **6**D couplée avec une analyse nouvelle établit que la préférence *endo*:*exo* pour une élimination 1,3 est au moins de 15:1 à 20:1. Une comparaison de l'effet isotopique solvolytique et cinétique (1.18 ± 0.04) pour **1***b* et de l'effet isotopique pour la cinétique de l'élimination 1,3 (1.45–1.6) avec les résultats pour les éliminations 1,2 indique que l'élimination se produit d'une façon classique, peut-être par une carbocation stabilisé par hyperconjugaison 1,3 **20**. La préférence *endo*:*exo* établie dans cette étude est utilisée pour réinterpréter les résultats de l'élimination 1,3 déterminés par Collins dans la solvolyse des tosylates de deutériohydroxyphényl norbonyle.

[Traduit par le journal]

Introduction

The intricacies of the mechanisms of 1,2 (β) elimination have been probed extensively through kinetic and solvent isotope effect studies, through changes in base strength, leaving group and solvent polarity, and studies on stereospecifically deuterium labelled substrates. Many substantial reviews are available presently on this subject (2–9). However, 1,3- and 1,4-elimination reactions have not been studied as extensively, although there is presently activity in the area of 1,3 eliminations, prefaced by the work of Nickon and Werstiuk (*10*).

1,3 Elimination occurs in acyclic and alicyclic systems through E1cb-like, E-2-like, and E-1-like transition states. For example, there are a multitude of three-membered ring-forming reactions both in acyclic and alicyclic systems which involve prior anion formation followed by 1,3 displacement of the leaving group. A recent publication by Bordwell and Jarvis (11) describes some of the latest mechanistic information that has been accumulated on these E1cb-like 1,3 eliminations. An example of a fully concerted E-2-like 1,3 elimination has not yet been documented but studies under selected conditions on 5-*oxo*-*exo*-2-norbornyl derivatives (12) may prove fruitful. There are many examples documented in the literature (12–21) of E-1-like 1,3 elimination especially in bicyclo[2.2.1]heptyl derivatives. However, little mechanistic detail has been established for these 1,3 processes.

This paper describes in detail a study of 1,3 elimination in the norbornyl system methyl *exo*-2-bromo-1-norbornanecarboxylate (**1***a*). The study was undertaken to establish the preferred stereochemistry for the E-1-like 1,3 elimination in this locked norbornyl substrate, where the ubiquitous 1,2 Wagner–Meerwein rearrangement and/or norbornonium ion formation which scrambles C—H stereochemistry at C-6 is precluded or at least diminished. The results of this study would then serve as a basis for the interpretation of the stereochemical preference

[1]For a preliminary account see ref. 1.

Can. J. Chem. Downloaded from www.nrcresearchpress.com by 210.87.254.42 on 09/05/12
For personal use only.

Can. J. Chem. Downloaded from www.nrcresearchpress.com by 210.87.254.42 on 09/05/12
For personal use only.

data for 1,3 elimination in norbornyl systems in general. A specific case that deals with the work of Collins and Benjamin (15) will be discussed subsequently in the text of this paper. Also, the present study would establish both product and solvolysis kinetic isotope effects for the purpose of providing a comparison with those of 1,2 effects. Eventually, it would be desirable to decide through the magnitude of the effects whether or not the *exo* or *endo* C—H bonds at C-6 participate directly in a 1,3 manner in the ionization step during solvolysis. The bromoester **1***a* was chosen for the study because it is a locked system (1) that yields 43% of tricyclic material on solvolysis (13) and the synthesis of the deuterated substrate **1***b* is straightforward.

Preparation of Substrates: Determination of Stereochemical Purity

Compound **1***a* was prepared by the method of Boehme (22, 23). The dideuterated bromoester **1***b* was prepared by using a 1,2 Wagner–Meerwein shift to move *exo* deuterium to the *endo* position (24). Reduction of 5-norbornene-2-carboxylic acid (**2**) (80% *endo*, 20% *exo*) both with dideuteriodimide and deuterium on palladium-on-charcoal gave good yields of a mixture of *exo*-2- and *endo*-2-norbornanecarboxylic-*exo*, *exo*-5, 6-d_2 acid (**3**). Bromination of the acid gave *exo*-2-bromo-1-norbornanecarboxylic-*endo*,*endo*-5,6-d_2 acid (**1***c*) that was esterified with diazomethane. Although the mechanism of the bromination rearrangement sequence for the conversion of **3** → **1***c* has not been established, undoubtedly, the Hell–Volhard–Zelinsky reaction involves enolization of the acid chloride followed by electrophilic attack of bromine on the enol. As charge is developed at C-2, rearrangement occurs to the 1-carboxy system that is captured by bromide ion. Interestingly, a 6,2 hydride (deuteride) shift does not occur significantly in this case. This was established by n.m.r. integration analysis (Fig. 1) of the olefinic region of methyl 1-norbornenecarboxylate-*endo*,*endo*-5,6-d_2 isolated from NaOMe-catalyzed elimination of HBr from **1***b*. Since 1,2 elimination of HBr from **1***b* is specifically *cis-exo* (25) the bromoester, in which a 6,2 deuteride shift has occurred, would give olefin in which a hydrogen at C-3 is replaced by deuterium. From integration analysis an upper limit of 5% is set on the extent of deuteride shift. The presence of a deuteride shifted product,

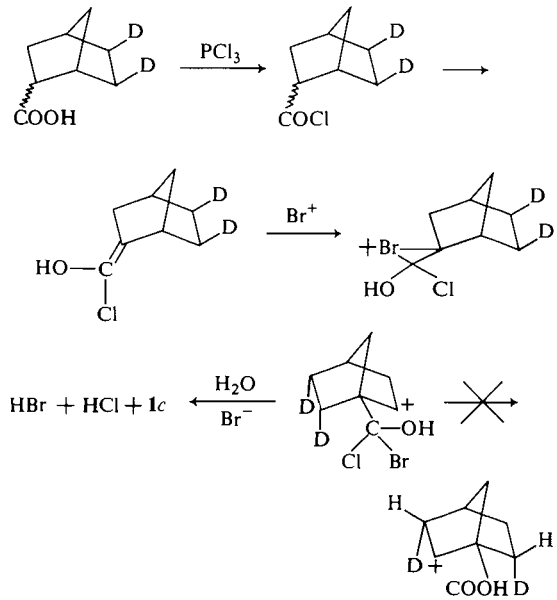

SCHEME I

however, does not affect the interpretation of the stereochemistry studies since the deuterium must necessarily remain 1,3 and *endo* with respect to the bromine.

It is of interest that the 1,2-elimination product is the major component (80%) of the reaction of **1***b* under E-2 conditions. Three other products, listed in order of increasing retention time, were tricyclic ester (8%), unknown (4%), and methyl 2 methoxy-1-norbornanecarboxylate (8%). That methyl 2 methoxy-1-norbornanecarboxylate was one of the minor components (isolated by preparative g.l.p.c.) was established by mass spectrometry which showed a parent ion at *m/e* 186

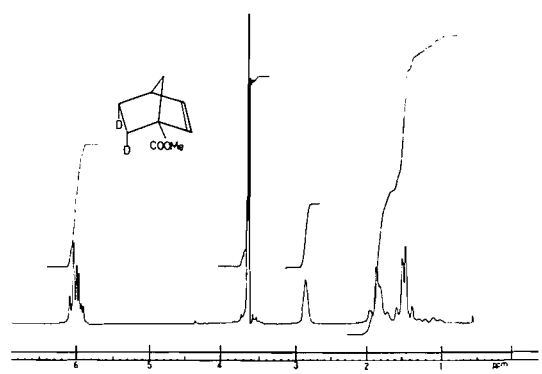

FIG. 1. Nuclear magnetic resonance spectrum (100 MHz; CCl_4) of 4D obtained from NaOMe-catalyzed elimination of HBr from **1***b*.

Can. J. Chem. Downloaded from www.nrcresearchpress.com by 210.87.254.42 on 09/05/12
For personal use only.

($C_{10}H_{14}O_3D_2$) and a fragmentation pattern consistent with the proposed structure. The methoxy group is likely situated *exo* at C-2. That the 1,2-elimination product predominates under E-2 conditions supports our claim that under solvolysis conditions 1,3 elimination is E-1-like and is preceded by ion pair formation. The integration analysis on the olefin **4D** obtained from base-catalyzed elimination also established that the deuterium in the bromoester was at least 95% stereochemically pure *endo* at C-5 and C-6. This reflects the stereospecific *exo* reduction of the norbornenecarboxylic acid which is expected for the system (26). The multiplets centered at 1.8 and 1.5 δ (Fig. 1) are what would be expected for the *exo*-5,6 and C-7 hydrogens, respectively, in the [2.2.1] system (24, 26). The residual of the *endo* hydrogens is centered at around 1.1 δ. Further support for the stereochemistry of the deuterium is obtained from the proton n.m.r. spectrum (Fig. 2) of methyl 2-norbornene-2-carboxylate-*exo*,*exo*-5,6-d_2 (**5***b*) obtained from CH_2N_2 esterification of the product obtained from elimination of HBr from the carboxylic acid **1***c*. Since the rearrangement to **5***a* shifts *endo* deuterium to the *exo* position, the relative intensities of the peaks at around 1.8 and 1.1 δ should interchange. The n.m.r. spectrum (Fig. 2) of **5***b* indicates this to be the case.

Results

Solvolysis of **1***a* and **1***b* in 80:20, v/v, EtOH–H_2O buffered with NaOAc gave the products **4**H, **6**H, **7**H, **8**H, and **4**D, **6**D, **7**D, **8**D respectively as described in Table 1. The deuterium content of both **1***b* and tricyclic material was established by mass spectrometry and n.m.r. spectroscopy

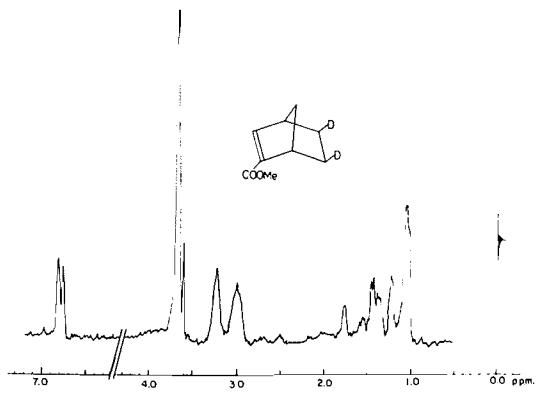

FIG. 2. Nuclear magnetic resonance spectrum (60 MHz; CCl_4) of **5***b*.

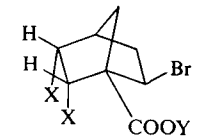

1

a X = H; Y = Me
b X = D; Y = Me
c X = D; Y = H
d X = H; Y = H

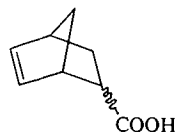

2

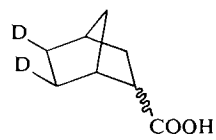

3

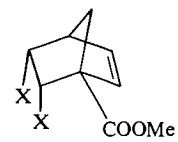

4

H X = H
D X = D

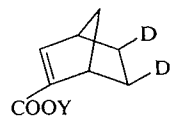

5

a Y = H
b Y = Me

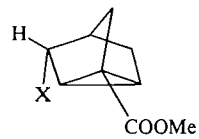

6

H X = H
D X = D

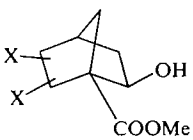

7

H X = H
D X = D

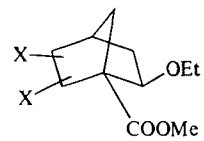

8

H X = H
D X = D

(Fig. 3). As indicated in Table 1 an isotope effect operates in the elimination to decrease the quantity of tricyclic material and increase the amount of the other products. This, coupled with the loss of approximately 90% of the deuterium available on the front face of **1***b*, establishes a large preference for cleavage of the *endo*-C—H bond over the *exo*-C—H bond at C-6 in the 1,3 elimination. The γ-kinetic isotope effect (Table 2) for solvolysis of **1***a* and *b* is 1.18 ± 0.04 in the range of 115°. The data for run 3 is plotted in Fig. 4. The rate constant of 1.04×10^{-5} s^{-1} at 115° for **1***a* (0.03 *M* **1***a*; 0.09 *M* NaOAc) compares favorably with the rate constants of 0.85×10^{-5} s^{-1} (112.6°) and 1.28×10^{-5} s^{-1} (119.5°) reported for **1***a* (0.01–0.04 *M* **1***a*; 0.01–0.04 *M* NaOAc) by Wilt (13). The increased rate

TABLE 1. Product and deuterium loss data for solvolysis of **1***a* and **1***b* in 80:20 EtOH–H_2O

Entry	Substrate	Conditions	Relative % products*					Fractional % loss of one deuterium
				Δ	ROH	ROEt	Other	
1	**1***a*	0.09 *M* **1***a* 0.10 *M* NaOAc 112 ± 2°	7.4	43.0	13.8	31.8	4.0	
2	**1***b*	0.14 *M* **1***b* 0.16 *M* NaOAc 112 ± 2°	9.9	32.0	16.7	38.4	3.0	87†
3	**1***b*	0.07 *M* **1***b* 0.11 *M* NaOAc 112 ± 2°						92‡
4	**1***b*	0.32 *M* **1***b* 0.35 *M* NaOAc 112 ± 2°						86§

*Run consecutively during the same g.l.c. analysis: the average of two analyses integrated electronically.
†A composite of 8.6% d_2, 79.4% d_1, and 12.0% d_0 species (average 0.97 excess D per molecule). Starting **1***b* a composite of 73.7% d_2, 24.5% d_1, and 1.8% d_0 species (average 1.72 excess D per molecule).
‡The 6D a composite of 5.7% d_2, 81.0% d_1, and 13.3% d_0 species (average 0.92 excess D per molecule). Compound **1***b* a composite of 73.7% d_2, 24.5% d_1, and 1.8% d_0 species.
§Compound 6D a composite of 1% d_3, 13.4% d_2, 76.5% d_1, and 9.3% d_0 species (average 1.06 excess D per molecule). Compound **1***b* a composite of 2.3% d_3, 84.2% d_2, 11.2% d_1, and 2.5% d_0 species (average 1.87 excess D per molecule).

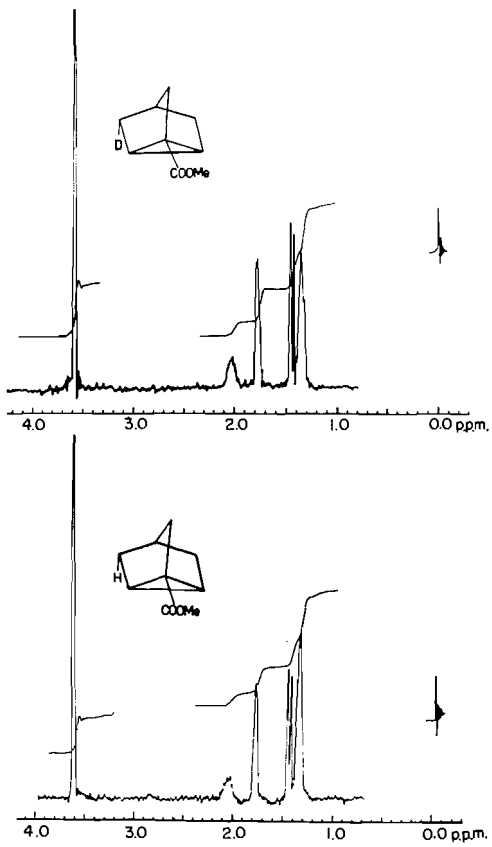

FIG. 3. Nuclear magnetic resonance spectra (60 MHz; CCl_4) of 6H and D obtained from solvolysis of **1***a* and *b*, respectively (entries 1 and 2, Table 1).

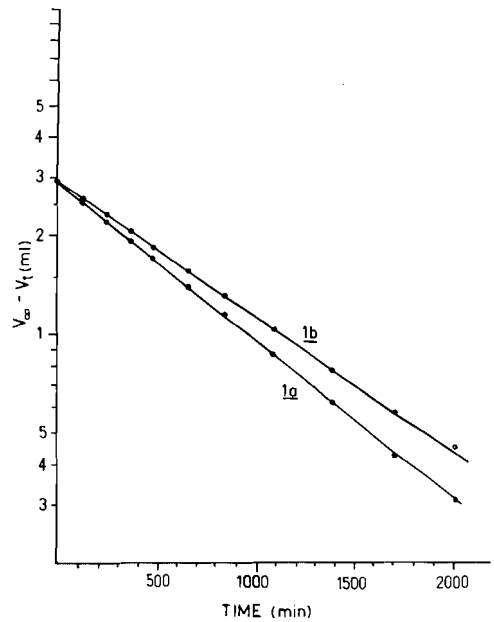

FIG. 4. Semilogarithmic plot of kinetic data for run 3 (Table 2).

constants for runs 2 and 3 likely are a consequence of the higher salt concentration. Nevertheless, the comparison establishes the validity of the kinetic procedure used in this study. The bromoesters used for the kinetic studies were purified by preparative liquid chromatography (l.c.) using a Waters Model 200

Can. J. Chem. Downloaded from www.nrcresearchpress.com by 210.87.254.42 on 09/05/12
For personal use only.

TABLE 2. γ-Kinetic isotope effect for solvolysis of **1***a*,**1***b**

Run	Conditions	$k_H \times 10^5$ (s^{-1})†	$k_D \times 10^5$ (s^{-1})	k_H/k_D
1	0.03 *M* **1***a*,**1***b* 0.09 *M* NaOAc 115.00 ± 0.03°	1.09 ± 0.02	0.92 ± 0.02	1.14 ± 0.04
2	0.05 *M* **1***a*,**1***b* 0.14 *M* NaOAc 116.20 ± 0.03°	1.85 ± 0.02	1.52 ± 0.02	1.21 ± 0.04
3	0.05 *M* **1***a*,**1***b* 0.14 *M* NaOAc 116.10 ± 0.04°	1.86 ± 0.02	1.54 ± 0.02	1.20 ± 0.04
	Mean			1.18 ± 0.04

*Five additional preliminary runs were used to establish the validity of the kinetic procedure. Compounds **1***a* and **1***b* were run simultaneously in the same constant temperature bath and aliquots were removed at the same time.
†The rate constants were obtained by least-squares analysis of the data; the standard deviation of the slope was taken as the error in the slope.

High Pressure Liquid Chromatograph. The solvent system 15–20% $CHCl_3$ – 85–80% hexane (v/v) was used with a 3/8 in. × 3 ft Porasil A column (column volume 34 ml). A flow rate of 0.7 ml/min was used with the pressure being 800 p.s.i. The bromoester was eluted after approximately 80 ml of flow. Although there was some tailing when a 60–70 mg (45 μl neat liquid) sample was injected, careful g.l.p.c. and n.m.r. analysis of the tail fraction showed that no other compound was present. Also, a l.c. analysis of a 4 μl sample showed a symmetrical peak. After a total of 10–12 samples each of **1***a* and *b* were injected and collected, the appropriate fractions were combined and the solvent was taken off on the rotatory evaporator. The residue was distilled under vacuum bulb to bulb twice for final purification. In this case l.c. is far superior to gas chromatography in terms of degree of separation, ease of handling and recovery of materials. This is however offset to some degree by the somewhat lengthy period required to establish conditions.

Discussion

When an ion pair scheme is considered for the solvolysis (Scheme 2) and the formation of products from tight ion pairs (TIP) and solvent separated ion pairs (SSIP) is describable on the basis of pseudo first-order processes, the following analysis can be made.[2] Since it has been established that k_{2S} is negligible in the

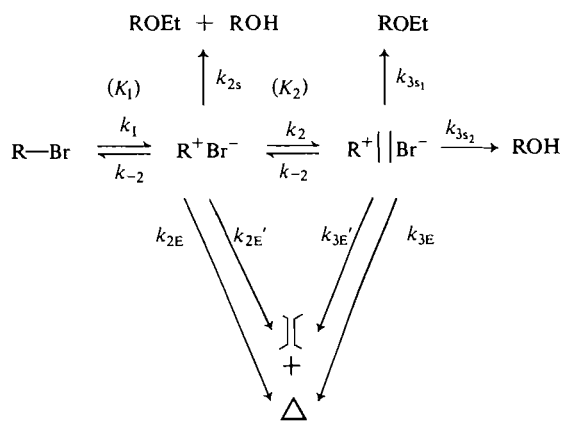

SCHEME 2

[2.2.1] system (27), attack of solvent on TIP to give ether and alcohol products is not important in the solvolysis of **1***a*. If the steady state approximation can be applied in this case, then in the scheme, K_1 would be affected by deuterium substitution but K_2 would not, since k_{2H}/k_{-2H} and k_{2D}/k_{-2D} should remain constant. This is so because the electronic and hybridization changes at C-6 (compared to R_H-Br) in R_H^+ in the $SSIP_H$ should be essentially identical to those in R_H^+ in TIP_H. Also, the changes at C-6 (from R_D-Br) in R_D^+ in $SSIP_D$ should be essentially identical to those for R_D^+ in TIP_D. Therefore, since $[TIP]_H/[SSIP]_H \simeq [TIP]_D/[SSIP]_D \simeq$ constant, the difference in the relative amounts of products from **1***a* and *b* would be governed by the relative magnitudes of the product rate constants and not by a variation in

[2]A hydride shift sequence is omitted from the scheme since the ion which results from an $H^-(D^-)$ shift should exhibit the reactivity of a SSIP even in the case of **1***b*.

Can. J. Chem. Downloaded from www.nrcresearchpress.com by 210.87.254.42 on 09/05/12
For personal use only.

Can. J. Chem. Downloaded from www.nrcresearchpress.com by 210.87.254.42 on 09/05/12
For personal use only.

the magnitude of K_2. This is reasonably important since it is not yet established which of k_{2E} and k_{3E} is most important or whether they both contribute equally to the 1,3 elimination. However, it is likely that for an E-1-like elimination k_{2E} and k_{3E} are of comparable magnitude since the force constant changes in the TIP and SSIP at C-6 should be essentially identical (28). For the same reason, the elimination isotope effects should also be identical for both species. Thus, k_{2E} and k_{3E} (1,3 elimination) are combined into $k_{E\ total}$.[3] Therefore, assuming the equilibrium between TIP and SSIP is fast

$$\frac{k_{HE\ total}}{k_{H3S_1} + k_{H3S_2}} \simeq \frac{6H}{7H + 8H}$$

and

$$\frac{k_{DE\ total}}{k_{D3S_1} + k_{D3S_2}} \simeq \frac{6D}{7D + 8D}$$

On the assumption that the isotope effect for capture of SSIP by solvent is negligible so that $k_{H3S_1} + k_{H3S_2} \simeq k_{D3S_1} + k_{D3S_2}$

$$\frac{k_{HE\ total}}{k_{DE\ total}} \simeq \frac{\dfrac{6H}{7H + 8H}}{\dfrac{6D}{7D + 8D}} \simeq 1.6$$

If an isotope effect does indeed operate on k_{3S} then it is likely inverse (28). Since there is no information available on the magnitude of such a γ-effect, only an estimate is possible presently based on a β-isotope effect. Humski *et al.* (28) have recently reported a value of 0.90 for the β-isotope effect for the collapse of cyclopentyl-*cis*-β-*d* brosylate ion pairs in 80:20 ethanol–water. If this is considered as the maximum value for a collapse isotope effect then $k_{D3S} \simeq 1.10\ k_{H3S}$. Substituting this in the expression for $k_{HE\ (total)}/k_{DE\ (total)}$, a value of 1.45 is obtained for the elimination isotope effect. The value of 1.45–1.60 compares favorably with the values reported for 1,3 elimination in the [2.2.1] system (10).

[3]The sum of k_{3S_1} and k_{3S_2} is used since the elimination process likely also involves both solvent bases. This comparison is an attempt to take into account the pseudo first-order nature of the product steps involving both EtOH and H_2O.

A novel analysis[4] that combines in [1] the initial distribution of deuterated species, the elimination isotope effect (1.6), the stereochemical purity (95–98%), an assumed preference, and the amount of tricyclic material (43%) formed from **1***a*, is used to predict the yield and the distribution of deuterated species of tricyclic material from **1***b*. The data in Table 3 clearly validate the method and establish that for a stereochemical purity of 98–95% there is at least a 15:1 to 20:1 preference for cleavage of the *endo*-C—H bond at C-6.

[4]Described herein is a sample calculation (assumed preference 20:1; isotope effect 1.6) that uses [1] for analysis of *endo vs. exo* cleavage for **1***b* (73.7% d_2, 24.5% d_1, 1.8% d_0) in which the deuterium is taken to be 95% stereochemically pure *endo* and the secondary isotope effect for cleavage of a C—H bond is assumed to be negligible.

endo,endo-5,6-d_2 component

endo cleavage $\left(\frac{73.7}{100}\right)(0.95)\left(\frac{20}{20}\right)\left(\frac{1}{1.6}\right)(43) = 18.80\ d_1$

exo cleavage $\left(\frac{73.7}{100}\right)(0.95)\left(\frac{1}{20}\right)(43) = 1.51\ d_2$

exo,exo-5,6-d_2 component

endo cleavage $\left(\frac{73.7}{100}\right)(0.05)\left(\frac{20}{20}\right)(43) = 1.59\ d_2$

exo cleavage $\left(\frac{73.7}{100}\right)(0.05)\left(\frac{1}{20}\right)\left(\frac{1}{1.6}\right)(43) = 0.05\ d_1$

endo-6-d_1-component

endo cleavage $\left(\frac{\frac{1}{2}\times 24.5}{100}\right)(0.95)\left(\frac{20}{20}\right)\left(\frac{1}{1.6}\right)(43) = 3.12\ d_0$

exo cleavage $\left(\frac{\frac{1}{2}\times 24.5}{100}\right)(0.95)\left(\frac{1}{20}\right)(43) = 0.25\ d_1$

exo-6-d_1 component

endo cleavage $\left(\frac{\frac{1}{2}\times 24.5}{100}\right)(0.05)\left(\frac{20}{20}\right)(43) = 0.25\ d_1$

exo cleavage $\left(\frac{\frac{1}{2}\times 24.5}{100}\right)(0.05)\left(\frac{1}{20}\right)\left(\frac{1}{1.6}\right)(43) =$ Negligible

5-d_1-component

$\left(\frac{\frac{1}{2}\times 24.5}{100}\right)(43) = 5.30\ d_1$

d_0-component

$\left(\frac{1.8}{100}\right)(43) = 0.77\ d_0$

Distribution of species 3.10 d_2 (9.8%), 24.65 d_1 (77.9%), 3.89 d_0 (12.3%); Σ relative yields d_x species = 31.6.

TABLE 3. Relative % yields and distribution of deuterated species: comparison of experimental and calculated values

	Stereochemical purity	*Endo*:*exo* preference	Relative % yield 4D	$\%d_2$	$\%d_1$	$\%d_0$	Excess D remaining per molecule
Experimental*			32	8.6	79.4	12.0	0.97
Calculated using eq.	98%	10:1	33.2	11.1	76.8	12.1	0.99
1 with isotope effect	98%	15:1	31.9	8.2	79.2	12.6	0.96
of 1.6			(34)†	(7.9)	(80.3)	(11.9)	(0.96)
	98%	20:1	31.3	6.8	80.5	12.8	0.94
	95%	10:1	33.5	13.7	74.5	11.7	1.02
	95%	15:1	32.3	11.5	76.4	12.2	0.99
	95%	20:1	31.6	9.8	77.9	12.3	0.97
			(33)†	(9.4)	(78.3)	(12.3)	(0.97)

*Compound 1*b* was a composite of 73.7% d_2, 24.5% d_1, and 1.8% d_0 species; an average of 1.72 excess D per molecule. Deuterium analysis was done mass spectrometrically at low voltage.
†Using an isotope effect of 1.5.

$$\left(\frac{\%\ d_n \text{ species}}{100}\right)\left(\begin{matrix}\text{fractional amount}\\ \text{each stereoisomer}\end{matrix}\right)\left(\begin{matrix}\text{assumed}\\ \text{preference}\end{matrix}\right)\left(\frac{1}{\text{isotope effect}}\right)43 = \text{Relative yield of } d_x \text{ species } (x = 0, 1, 2) \quad [1]$$

$$\text{Relative \% yield of } \mathbf{6D} = \frac{\text{Relative yields of } d_x \text{ species}}{\sum}$$

The *endo* preference for elimination from **1***a* establishes that the semi-U pathway (**A**) (10) is preferred for an E-1-like 1,3 process in locked [2.2.1] systems with $\Delta G^{\ddagger}$ being a *minimum* of 1.5–2 kcal/mol less than that for the semi-W pathway (**B**). Whether or not a symmetrical

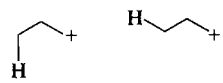

A B

edge-protonated nortricyclane (**9**H, **9**D) is an intermediate from which loss of a proton (deuteron) occurs is a point of interest. This problem is discussed in more detail subsequently in the text. That is, the ion **10**H (**10**D) may be the intermediate and **9**H (**9**D) represents only a transition state for the elimination and $H^-(D^-)$ shift. That a hydride (deuteride) shift does occur during solvolysis of **1***a* (**1***b*) is supported by the following facts. Nuclear magnetic resonance integration analysis of the olefinic region of **4**D, obtained from solvolysis of **1***b*, showed that deuterium was located at C-3 and established that 10–20% of the olefin arises after a deuteride shift occurs. Furthermore, partial collapse of the *endo*-2-C–H multiplet in the n.m.r. spectrum (Fig. 5) of **7**D

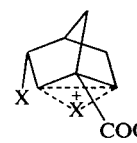

9*H* X = H
9*D* X = D

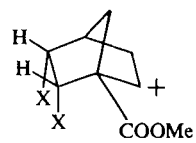

10*H* X = H
10*D* X = D

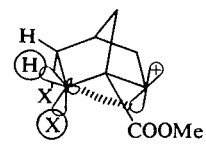

11*H* X = H
11*D* X = D

is consistent with loss of *cis–endo* coupling (29) which would be expected from **12**. That a hydride (deuteride) shift would be expected in this system is supported by Muneyuki's (19) study on the acetolysis of optically active **13** which established that the product acetate racemized partially.

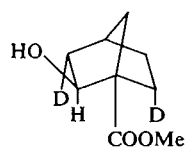

12

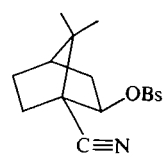

13

The *endo* preference established in this study shows conclusively that the overlap of the back-lobe of *exo*-C-6—H with the p-orbital at C-2 as described in **11**H (**11**D) *does not* play an important role in the stereochemical outcome of an E-1-like 1,3 elimination in the [2.2.1] system.

Can. J. Chem. Downloaded from www.nrcresearchpress.com by 210.87.254.42 on 09/05/12
For personal use only.

Can. J. Chem. Downloaded from www.nrcresearchpress.com by 210.87.254.42 on 09/05/12
For personal use only.

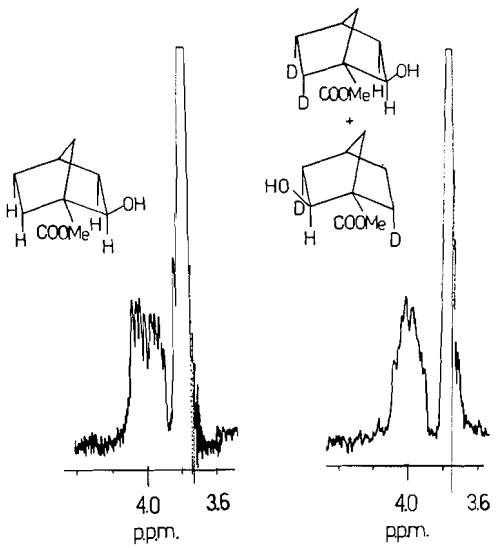

FIG. 5. Nuclear magnetic resonance spectra (60 MHz; $CDCl_3$) (sweep width 250 Hz) of 7H and D obtained from solvolysis of **1***a* and *b*.

This is of interest for two reasons. Farnum and Mehta (30) and Olah and co-workers (31, 32) have reported that this type of overlap operates in the norbornyl system and is the cause of the deshielding of the *exo* over the *endo* proton at C-6 in norbornyl cations generated in strong acids. Apparently, this overlap is not sufficient to preferentially activate *exo*-C—H over *endo*-C—H for 1,3 elimination. Also, *exo* approach of reagents to the [2.2.1] system is preferred, especially for proton transfer in homoenolization and homoketonization (33) processes.

The magnitude (1.45–1.6) of the primary 1,3-elimination isotope effect established in this study parallels closely the few examples documented in the literature (10, 15, 21, 34–38) for E-1 1,2 and 1,3 eliminations (Table 4).

Since the magnitude of the isotope effect for an E-2-like 1,3 elimination has not been determined because there is as yet no experimental support for a concerted 1,3 elimination and no theoretical studies have been carried out on 1,3 processes the usual correlation between the magnitude of the isotope effect and concertedness is difficult to establish in this case. However, the low value observed for **1***b* does fall in the range for 1,2 eliminations and 1,3 eliminations from carbocations (*vide supra*).

The γ-kinetic isotope effect is of interest since the presence of the carbomethoxy group should preclude significant neighboring group (nonvertical) participation of C-1—C-6 bond via **14**. Thus, the γ-effect may arise from any one, or some combination of the three effects. Possibly, 1,3 hyperconjugation to both the *exo*- and *endo*-C—H bonds at C-6 as described by the

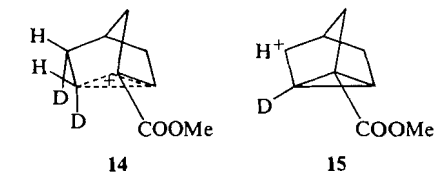

14 **15**

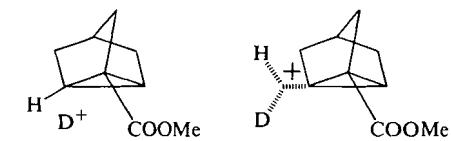

16 **17**

limiting forms **15** and **16** is important in the ionization step. Perhaps the sum of **15** and **16** is equivalent to the H-nortricyclonium ion **17**, the unsubstituted form of which Olah has proposed as a contributor to the structure of the norbornyl cation. Also likely is the direct involvement, as described by **18**, of only the *endo*-C—H(D) bond in the ionization step. Presently, the relative importance of each effect cannot be established although **15** + **16** = **17** may be important in the solvolysis of 7-chloro-*exo*-2-norbornyl- 6-*endo*-*d* and -*exo*,*exo*-5,6-d_2 brosylates (21). Lastly, it is possible that the

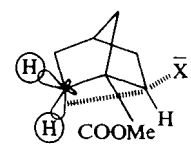

18

kinetic isotope effect is a manifestation of the elimination isotope effects only. If the ion pair scheme (Scheme 2, *vide supra*) is considered and the steady state approximation is applied, then it can be shown that when $k_{2S} = 0$ (27)

$$\left(\frac{k_H}{k_D}\right)_{obs} = \left(\frac{k_{H1}}{k_{D1}}\right)\left(\frac{1 + Y_D}{1 + Y_H}\right) \times \frac{\frac{k_{H2E}}{k_{H2}} + \left[\left(\frac{k_{H3E}}{k_{H3S}} + 1\right)\left(\frac{1}{1 + Z_H}\right)\right]}{\frac{k_{D2E}}{k_{D2}} + \left[\left(\frac{k_{D3E}}{k_{D3S}} + 1\right)\left(\frac{1}{1 + Z_D}\right)\right]} = (IIE)(R)(S)$$

TABLE 4. Tabulation of β-kinetic isotope effects and 1,2 and 1,3 elimination isotope effects for solvolysis reactions

Entry	Deuterated substrate	Conditions	Kinetic isotope effect per D	Primary isotope effect for olefin formation	Reference No.
1	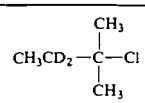	80:20 EtOH–H_2O 25°	1.19	1.8	34
2	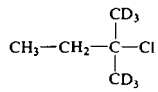	75:25 HOAc–H_2O 57°		2.5–2.8	37
3	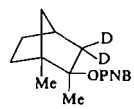	50:50 Dioxane–H_2O 69.3°	1.14* 1.28	1.92	39
4		80:20 EtOH–H_2O 40°	1.18	1.32	28
5	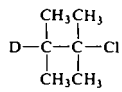	80:20 EtOH–H_2O 55°	1.16	≃1.07†	35
6	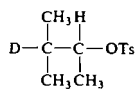	HOAc–NaOAc 75°	1.93	1.2–1.6‡	36
7	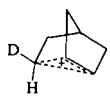	0.054 *M* KO*t*Bu *t*-BuOH 60°		2.1§	10

*The value of 1.14 is based on the *exo* and *endo* effect being identical. The value of 1.28 is the total observed kinetic effect.
†Based on the ratio of olefin fraction from H substrate and D substrate.
‡The value of 1.2 is obtained from the ratio of 2-methylbutene-2 fractions. The value of 1.6 is obtained using the tertiary acetate ratio as well as the olefin ratio in the analysis developed in this paper.
§This is the isotope effect for nortricyclane formation.

where

$$Y = \frac{k_{-1} + k_{2E}}{k_2}$$

and

$$Z = \frac{k_{-2} + k_{3E}}{k_{3S}}$$

If the ionization isotope effect (IIE) $k_{H1}/k_{D1} \simeq 1.0$ then through a consideration of the effect of deuterium substitution on the rate constants k_{2E}, k_2, k_{-2}, k_{3E}, and k_{3S} it is seen that $k_{H2E} > k_{D2E}$, $k_{H2} \simeq k_{D2}$, $k_{H-2} \simeq k_{D-2}$, $k_{H3E} > k_{D3E}$, and $k_{H3S} \simeq k_{D3S}$. Therefore, the R and S terms could control the observed isotope effect but with some mutual attenuation since $1 + Y_D$ is $< 1 + Y_H$ in the R term and the numerator is larger than the denominator in the S term. That the observed kinetic isotope effect can vary with the amount of elimination has been established by Humski (38) through studies on the solvolysis of 1,2-dimethyl-*exo*-2-norbornyl-*p*-nitrobenzoate. This however is not general since in the solvolysis of cyclopentyl brosylate-*trans*-β-*d* in ethanol–water the kinetic isotope effect does not vary significantly with a change in the amount of olefin formed and in fact in trifluoroethanol–water actually increases slightly as the amount of olefin decreases (28).

Nevertheless, 1,3 elimination at some point would involve a transition state which resembles

Can. J. Chem. Downloaded from www.nrcresearchpress.com by 210.87.254.42 on 09/05/12
For personal use only.

Can. J. Chem. Downloaded from www.nrcresearchpress.com by 210.87.254.42 on 09/05/12
For personal use only.

an edge-protonated nortricyclane[5], the overall process being characterized by an isotope effect of 1.45–1.6. If the kinetic isotope effect (1.18 ± 0.04) in fact predominantly reflects the ionization isotope effect then that k_H/k_D (elim) > k_H/k_D (kinetic) indicates that the C—H bonds at C-6 undergo a force constant change during ionization either through **15** + **16** = **17** or **18** or both but the change does not approach that in **9**D. That is, if involvement of the endo-C—D bond at C-6 at ionization approached the extent depicted in **9**D then k_H/k_D (kinetic) > k_H/k_D (elim). There is some support for this concept available in the literature at least for 1,2 eliminations. For example, in Table 4 in entries 1, 3, and 4 where k_H/k_D (obs) > k_H/k_D (elim), elimination is considered to occur from classical species with the β-C—H bonds being perturbed only through hyperconjugation (vertical participation). It must be pointed out here that it is understood that the primary elimination isotope effects are inflated somewhat in entries 1, 2, and 3 because a secondary effect (≃ 1.2) operates in each case as well. However, k_H/k_D (obs) would still be less than k_H/k_D (elim). In the solvolysis of 2-substituted-2,3-dimethylbutanes (entry 5), however, k_H/k_D (obs) > k_H/k_D (elim). In the case of the solvolysis of the tosylate in entry 6, Winstein and Takahashi (36) proposed that neighboring group participation (nonvertical participation) of the C—H(D) leading to an ethonium ion was important. In this case it is reasonable that k_H/k_D (obs) > k_H/k_D (elim) since elimination should now occur from an ethonium ion. The isotope effect for loss of D^+ from such a species would be expected to be less than that for loss of D^+ from a classical ion since the C—H(D) force constants in the former are already lowered substantially. Significantly, Cram and Tadanier (40) proposed that the ethonium ion was formed in the solvolysis of 3-cyclohexyl-2-butyl tosylate where k_H/k_D (obs) is in the order of 1.7–1.8. Unfortunately the olefin ratios were not reported for the deuterated compounds so that an elimination isotope effect cannot be evaluated. However, this author predicts that k_H/k_D (obs) should be greater than k_H/k_D (elim).

Thus from the stereochemical preference data, the relative magnitudes of the kinetic and elimination isotope effects the author proposes that 1,3 elimination in **1***b* occurs from a species which closely resembles the classical ion **20** where the C—H, C—D bonds at C-6 may be involved in 1,3 hyperconjugative stabilization

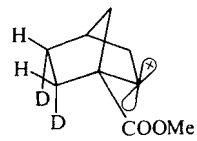

20

but that the transition state for 1,3 elimination and the 6,2 H(D) shift resembles an edge-protonated nortricyclane, the isotope effect for the 1,3 process being around 1.6.

That the semi-U pathway is preferred for E-1-like 1,3 elimination in the [2.2.1] system where rearrangement is precluded provides a basis for the reinterpretation of other 1,3 preference data (15). Collins found that the tosylates **21**H and **22**H gave essentially identical product compositions including the nortricyclanol

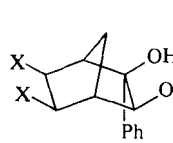

21*H* X = H
21*D* X = D

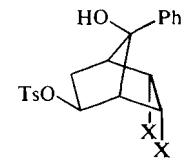

22*H* X = H
22*D* X = D

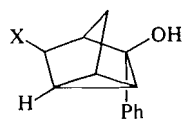

23*H* X = H
23*D* X = D

23H (26%). When **21**D and **22**D were solvolyzed in each case one deuterium atom was lost in the formation of **23**D. That the product composition

[5]E-1-like 1,3 elimination in the [2.2.1] system should be essentially the reverse of the protonation of the appropriately substituted nortricyclane. Although **6**H has not been opened with D^+ to check this, the D^+

opening of nortricyclyl chloride occurs by edge-protonation of bond *a* (39). This correlates very well with the finding that cleavage of *endo*-C—H(D) at C-6 is preferred for 1,3 elimination in solvolysis of the 7-chloro-*exo*-2-norbornyl-6-*endo-d* brosylate (21).

was identical within experimental error from **21**H and **22**H indicated that common intermediates were involved. The authors interpreted the deuterium loss data on the basis of elimination of *exo* deuterium from **21**D and *endo* deuterium from **22**D and stated that the solvolysis results could be accounted for on the basis of either nonclassical or classical ions and that the edge-protonated nortricyclane could be either an intermediate or transition state. On the basis of previous discussion (*vide supra*) the results can be accounted for in the following manner.

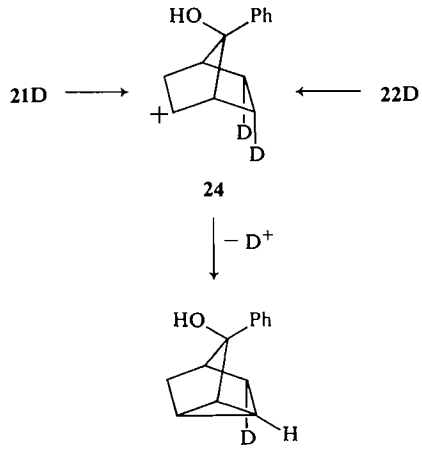

Cleavage of the C—OTs bond in **21**D followed by a 1,2 alkyl shift gives **24**. Solvolysis of **22**D gives **24** directly. In this case the hydroxyl and phenyl groups provide the necessary lock through an inductive effect and perhaps OH-4 participation for the former and an inductive and steric effect for the latter. Ion **24** need be classical and stabilized only through 1,3 hyperconjugation (*vide supra*). Reaction of **24** with an *endo* preference as expected would then lead directly to **23** with a loss of one deuterium in both cases. The point here is that the C—D bond originally *exo* in **21**D is cleaved as an *endo* bond in **24**. That **24** resembles a classical ion and elimination occurs from this species is supported by value of 1.8 for magnitude of the elimination isotope effect which was evaluated from Collins' product data by the method described previously in this paper.

Experimental

General

Melting points were taken on a Kofler hot stage melting point apparatus and are uncorrected. The i.r. spectra were recorded on a Perkin–Elmer Model 337 spectrometer. The n.m.r. spectra were recorded on Varian A-60, T-60 and HA-100 spectrometers on solutions in CCl_4 or $CDCl_3$ with tetramethyl silane as internal standard. Mass spectra were obtained on a Hitachi Model RMU6-A spectrometer. Preparative and analytical gas liquid chromatography was carried out on Varian 90-P-3 and 204 instruments, respectively, with He as carrier gas. High pressure liquid chromatography was accomplished on a Waters Model 200 liquid chromatograph. All solutions were dried over anhydrous Na_2SO_4 or $MgSO_4$.

Dipotassium Azodicarboxylate

To a vigorously stirred solution of 600 ml of 40% KOH maintained at 0–3° was added azodicarbonamide (110 g) portionwise. After the addition was complete the mixture was stirred for 1 h and the salt was filtered through a sintered glass funnel. The salt was washed with 8 l of anhydrous methanol, cooled to 0–5°, and vacuum dried (rotatory pump) for 2 days. The salt that was used for the deuterations was washed with (2 × 50 ml; 1 × 75 ml) MeOD and pumped on for 2 days.

Dideuteriodimide Reduction of Norbornenecarboxylic Acid

Norbornenecarboxylic acid (14 g, 80:20 *endo*:*exo*) was added to a slurry of dipotassium azodicarboxylate (54 g) in MeOD (300 ml, 95%-O-*d*) contained in a three-necked 1-l flask equipped with a condenser, dropping funnel, and stirrer. To the vigorously stirred mixture was added DOAc (26 g, 95–97%-O-*d*) in MeOD (30 ml) over a period of 1 h. After the addition was complete the mixture was stirred for an additional 1.5 h at room temperature. An aliquot was worked up and analyzed by infrared spectroscopy. The absence of an initially strong band at 710 cm^{-1} showed that the reduction was at least 98–99% complete. The MeOD was recovered by distillation through a 14 in. glass helices column to yield a viscous residue of approximately 75 ml. Ether (100 ml) and water (175 ml) were added and after shaking the ether layer was drawn off. The aqueous layer was extracted with additional ether (10 × 50 ml). The combined ethereal layers were washed with water, dried, and the ether was distilled off. Distillation of the residue gave 9 g of the dideuterioacid, b.p. 103–104° (1–8 mm), which solidified to a viscous mass on standing. Nuclear magnetic resonance (60 MHz, $CDCl_3$) δ 11.0 (bs, 1H, COOH), 2.75 (bm, 1H, C-2—*exo*-H), 2.55 and 2.25 (m, 2H, bridgehead C—Hs), 1.8–1.1 (norbornyl envelope, approximately 6H).

Deuteration of Norbornenecarboxylic Acid

Norbornenecarboxylic acid (30 g, 0.218 mol, Aldrich Chemical Co., 80:20 *endo*:*exo*) was dissolved in anhydrous methanol (125 ml) in a 250 ml conical flask. Palladium (10%) on charcoal (4 g) was added and the mixture was connected to a gas burette. The mixture was stirred vigorously while approximately 5 l of D_2 was taken up by the warm solution. The mixture was stirred for 4 h longer and the catalyst was filtered off. The methanol was distilled off through a 12 in. Vigreux column. The residue which remained was distilled under vacuum as above to give 26 g of the dideuteriocarboxylic acid. Nuclear magnetic resonance (60 MHz, CCl_4) δ 12.0 (s, 1H, COOH), 2.88 (m, approximately 1H, C-2—*exo*-H), 2.70 (m, 1H, bridgehead C—H), 2.35 (m, 1H, C-4—H), 1.75 (m, 2H, *syn*- and *anti*-7-H), 1.5 (bs, approximately 4H, norbornyl envelope).

Can. J. Chem. Downloaded from www.nrcresearchpress.com by 210.87.254.42 on 09/05/12
For personal use only.

Can. J. Chem. Downloaded from www.nrcresearchpress.com by 210.87.254.42 on 09/05/12
For personal use only.

Dimide Reduction of Norbornenecarboxylic Acid

To a slurry of dipotassium azodicarboxylate (36 g, freshly prepared) in methanol (distilled from sodium) was added norbornenecarboxylic acid (10 g, 80:20 *endo*:*exo*). To the vigorously stirred solution was added glacial acetic acid (17.5 g, in 20 ml of dry methanol) over a period of 1.5 h. After the addition was complete analysis of an aliquot by i.r. showed the absence of an intense peak at 710 cm^{-1} and indicated that the reduction was complete. Ether was added (700 ml) and the KOAc which precipitated was filtered off. The solvent was distilled off to a volume of 20 ml, then water was added (150 ml) and the solution was extracted with ether (1 × 200 ml; 3 × 50 ml). The ethereal solution was dried and the solvent evaporated. Vacuum distillation of the residue gave 7.6 g of 2-norbornanecarboxylic acid (b.p. 108–109°/2 mm) which solidified to a semi-solid on standing. Nuclear magnetic resonance (60 MHz, $CDCl_3$) δ 12.0 (s, 1H, COOH), 2.75 (bm, < 1H, C-2—*exo*-H), 2.58 (bs, 1H, C-1—H), 2.26 (bs, 1H, C-4—H), 1.45 (norbornyl envelope, 8H). There was no detectable olefinic signal in the n.m.r.

Bromination of 2-Norbornanecarboxylic Acid

The 2-norbornanecarboxylic acid (6.4 g, > 95% pure) was heated on the steam bath with bromine (8.8 g) and PCl_3 (0.1 ml) for 7 h. After the initial time an additional amount of bromine was added (4.0 g) and the mixture was heated for an additional 3 h. The mixture was poured onto water (250 ml) and ether (50 ml). An additional amount of ether was added (100 ml) followed by 6 g of $Na_2S_2O_4$. The ethereal layer was washed with water (50 ml) and dried. The ether was concentrated and the solid mass (5.0 g) was crystallized from toluene to give 3.9 of the bromoacid, m.p. 148–150° (lit. (22, 23) 150–151°).

Bromination of 2-Norbornanecarboxylic-exo,exo-5,6-d_2 Acid

Run 1. The deuteriocarboxylic acid (2.0 g, 0.014 mol), obtained from the dideuteriodimide reduction, was mixed with Br_2 (2.7 g, 0.016 mol) and PCl_3. The mixture was heated on the steam bath for 9 h, then poured into a dilute aqueous solution of $Na_2S_2O_4$, extracted with ether (1 × 100, 2 × 50 ml) and decolorized with charcoal. The residue was recrystallized from toluene to give 1.1 g of the deuterated *exo*-2-bromo-1-norbornanecarboxylic acid, m.p. 148–150°. Nuclear magnetic resonance ($CDCl_3$) δ 11.63 (s, COOH, 1H), 4.19 (m, H—C—Br, 1H), 2.5–1.4 (m, norbornyl envelope, 7.2 H). The n.m.r. showed considerable simplification in the region of 1.5–1.6 δ when compared to that of **1*d***, consistent with the replacement of *endo*-5,6-C—H with deuterium. Mass spectrum (80 eV), *m/e* 218–223 (M^+), 189–192 ($M^+ - C_2H_2D_2$), 139–141 ($M^+ - Br$).

Run 2. The acid (16 g, > 95% pure) prepared by catalytic deuteration of norbornenyl carboxylic acid was heated on the steam bath for 8 h with 1 ml of PCl_3 and 20 g of Br_2 as described previously. An additional 10 g of Br_2 were added and the mixture was heated for an additional 4 h at 75–80°. The reaction mixture was worked up as described previously and recrystallized from toluene to give 6.7 g of the dideuteriobromoacid, m.p. 150–152°.

*Esterification of the Dideuteriobromoacid **1c***

Run 1. The deuterated acid obtained from dideuteriodimide reduction (0.9 g, 0.004 mol, m.p. 148–150°) was dissolved in ether (50 ml) and treated with an ether solution of CH_2N_2 prepared from Diazald. The ether was evaporated and the viscous oil was purified by a bulb-to-bulb distillation at 5 mm to give 0.60 g of the bromoester. Analytical gas chromatography showed the ester to be > 98% pure; n.m.r. ($CDCl_3$) δ 4.18 (m, H—C—Br, 1H) 3.73 (s, —COOMe, 3H), 2.4–1.3 (m, norbornyl envelope, 7.3 H). The n.m.r. showed considerable simplification of the spectrum in the region of 1.7 δ as compared to the nondeuterated ester consistent with the replacement of *endo*-5,6-C—H with deuterium. Mass spectrum (80 eV), *m/e* 232–237 (M^+), 201–206 ($M^+ -$ OMe), 173–178 ($M^+ -$ COOMe), 153–157 ($M^+ - Br$). Analysis of the $M^+ - Br$ peaks at 10 eV showed that the ester was composed of 73.7% d_2, 24.5% d_1, and 1.8% d_0 species, a total of 1.72 excess D per molecule.

Run 2. The bromoacid (3.8 g) obtained from the Pd-on-charcoal reduction was esterified with diazomethane as described previously. Analytical g.l.p.c. on 10 ft × 1/8 in. 10% Carbowax on Chromosorb W at 175° showed the ester to be > 98% pure with two minor components, one (< 1%) of slightly shorter retention time and another (< 1%) of longer retention time. Mass spectrum (14 eV, sample purified by preparative g.l.c.) 2.3% d_3, 84.2% d_2, 11.2% d_1, and 2.5% d_0 species; 1.87 excess D per molecule.

*Esterification of the Bromoacid **1d***

Run 1. The bromoacid (0.14 g) was treated with an ether solution of diazomethane prepared in the usual manner and after work-up gave the methyl ester. Nuclear magnetic resonance ($CDCl_3$) δ 4.20 (m, H—C—Br, 1H), 2.80 (s, COOMe, 3H), 2.5–1.2 (m, norbornyl envelope, 9H). Mass spectrum (80 eV, sample purified by preparative g.l.p.c.) 232–235 (M^+), 201–204 ($M^+ -$ OMe), 173–176 ($M^+ -$ COOMe) 153–154 ($M^+ - Br$). Analysis of $M^+ - Br$ peak at 10 eV established that 153 and 154 were 9.45 and 0.80% of the 152 peak, respectively.

Run 2. The bromoacid (3.5 g, m.p. 148–150°) was esterified as described previously. Gas chromatographic analysis on a 10 ft × 3/8 in. 10% SE-30 on Chromosorb W column at 160° showed the ester to be 95–97% pure with two minor components present.

*Solvolysis of the Dideuteriobromoester **1b***

Run 1. The deuteriobromoester (0.16 g, purified by preparative g.l.p.c.) obtained from dideuteriodimide reduction sequence was dissolved in EtOH (4 ml) and H_2O (1 ml) containing NaOAc (0.065 g) and the mixture was sealed in a tube which was suspended in refluxing toluene (112°) for 4 days. The tube was opened, the contents poured into water (50 ml), and extracted with pentane (1 × 25 ml, 2 × 15 ml). The dried solution was analyzed by analytical g.l.p.c. with electronic area integration on a 5 ft × 1/8 in. 5% SE-30 Chromosorb W column with temperature programming from 100–150° at 80 min. The following product distribution, listed in order of increasing retention time, was established; methyl deuterio-1-norbornenecarboxylate 9.9%, methyl deuterio-1-nortricyclanecarboxylate 32.0%, methyl deuterio-*exo*-2-hydroxynorbornane-1-carboxylate 16.7%, methyl deuterio-*exo*-2-ethoxynorbornane-1-carboxylate 38.4%, unknown 1.6%, unknown 1.4% (entry 2, Table 1). The pentane was distilled off to yield an oily residue which

Can. J. Chem. Downloaded from www.nrcresearchpress.com by 210.87.254.42 on 09/05/12
For personal use only.

was separated into the four major components by preparative gas chromatography on a 5 ft × 1/4 in. 20% SE-30 on Chromosorb W column at 155°. Nuclear magnetic resonance (CCl_4) (Fig. 3) methyl deuterio-1-nortricyclanecarboxylate: δ 3.60 (s, COOMe, 3H), 2.06 (m, C-4—H, 1H), 1.78 (m, C-7, 2H) 1.47 (d, C-2, C-6—H, <2H), 1.37 (m, C-3, C-5—H, >3H). Mass spectrum methyl 1-nortricyclanecarboxylate (10 eV); a composite of 8.6% d_2, 79.4% d_1, and 12.0 d_0 species, corresponding to 0.97 excess D per molecule.

Nuclear magnetic resonance integration analysis (average of two integrations) utilizing the ester methyl and the total of the signals at 1.47 and 1.37 established that essentially only one deuterium remained in the nortricyclane with reduction of the signal at 1.37 being pronounced. A slight decrease in the relative intensity of the signal at 1.78 was consistent with some deuterium positioned on the cyclopropane ring (Fig. 3).

Run 2. The deuteriobromoester (0.080 g) obtained from the dideuteriodimide reduction sequence and purified by preparative g.l.p.c. was dissolved in EtOH (4 ml) and H_2O (1 ml) and anhydrous NaOAc (0.043 g) was added. The mixture was refluxed for 4 days and poured into water (10 ml) and extracted with ether (3 × 10 ml). The ether was distilled off after drying and the oily residue was separated by preparative gas chromatography on a 5 ft × 1/4 in. 20% SE-30 on Chromosorb W column at 140° into the four major products, in the following order of elution; methyl deuterio-1-norbornenecarboxylate, methyl deuterio-1-nortricyclanecarboxylate, methyl deuterio-*exo*-2-hydroxynorbornanecarboxylate, and methyl deuterio-1-*exo*-2-ethoxynorbornanecarboxylate. Mass spectrum methyl deuterio-1-nortricyclanecarboxylate (80 eV): *m/e* 153 (M^+, $C_9H_4O_2D$); analysis at 10 eV of M^+ showed the tricyclic material to be a composite of 5.7% d_2, 81.0% d_1, and 13.3% d_0 species, a total of 0.92 excess D per molecule.

Large Scale Solvolysis of the Dideuteriobromoester 1b

The dideuteriobromoester (1.5 g, >98% pure) prepared by CH_2N_2 esterification of the dideuterio acid obtained by catalytic deuteration was dissolved in 20 ml of 80:20, v/v, EtOH–H_2O (0.35 *M* in NaOAc) and the solution was sealed in a tube and suspended in refluxing toluene. After 14 days the tube was removed and the contents were poured into water (50 ml, saturated with NaCl) and the mixture was extracted with purified pentane (1 × 20 ml, 2 × 10 ml). The aqueous layer was then extracted with ether (1 × 20, 2 × 10 ml). The two solutions were washed with water and dried. Distillation of the solvent in each case through a 2 ft helices packed column gave 1–1.5 ml of residue in each case. The products were isolated by preparative g.l.p.c. (5 ft × 1/4 in., 20% Carbowax on Chromosorb W, 180°). The norbornenyl ester which was difficult to collect because of its volatility was collected with the aid of a collector that contained glass wool in the inlet and $CDCl_3$ in a bulb at the bottom. After every collection the tube was inverted carefully in order to dissolve the collected ester. Compound **4D** n.m.r. (60 MHz, $CDCl_3$) δ 6.18 (m,

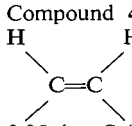

, 1.90 ± 0.10 H), 3.70 (s, —O—Me, 3.0 H), 2.95 (m, C-4—H, 1.0 H) 1.90 (unresolved quartet with fine structure, C-6, C-5 *exo*-H, *ca.* 2.0 H), 1.55 (m, C-7-*syn*- and *anti*-H, 2.0 H). The other products were also collected with a V-tube in which glass wool was placed in the part of the collector that was inserted into the preparative g.l.c. Compound **6D**; n.m.r. (60 MHz, CCl_4) δ 3.72 (s, —OMe, 3.0 H) 2.15 (m, C-4—H, 1.0 H), 1.90 (s, C-2; C-6—H, 1.90 H), 1.58 (d, C-7—H, 2.0 H), 1.45 (s, C-3; C-5—H, approximately 3H). Compound **7D** n.m.r. δ 3.70 (s, COOMe, 3H), 3.5 (m, H—C—O—CH_2—, 3H), 2.5 (m, C-4—H, 1H), 1.6 (m, norbornyl envelope, approximately 6H), 1.10 (t, —CH_3, 3H). Compound **8D** n.m.r. δ 4.0 (m, H—C—OH, 1H), 3.80 (s, COOMe, 3H), 3.0 (bs, —O—H, 1H), 2.30 (m, C-4—H, 1H), 2.0–1.1 (m, norbornyl envelope, approximately 6H). There was considerable simplification of the H—C—OH signal at 4.0 δ (Fig. 5) indicating that a deuteride shift results in the positioning of a deuterium *endo* at C-3. Compound **6D** mass spectrum (14 eV) 1.0% d_3, 13.4% d_2, 76.5% d_1, 9.3% d_0; 1.06 excess D per molecule.

Solvolysis of the Bromoester 1a

Run 1. The bromoester (0.1 g) was mixed with EtOH (4 ml), H_2O (1 ml), and NaOAc (0.040 g) and sealed in a tube. The tube was heated in refluxing toluene (112°) for 4 days and the contents were poured into water (50 ml) and extracted with pentane (1 × 25 ml, 2 × 15 ml). Analytical g.l.p.c. analysis on a 5 ft × 1/8 in. 5% SE-30 on Chromosorb W column with temperature programming (100–150° at 8°/min) and electronic area integration established the product distribution; methyl 1-norbornenecarboxylate 7.4%, methyl 1-nortricyclanecarboxylate 43.0%, unknown 0.2%, methyl *exo*-2-hydroxynorbornane-1-carboxylate 13.8%, methyl *exo*-2-ethoxynorbornane-1-carboxylate 31.8%, unknown 3.0%, unknown 0.6%, unknown 0.2%.

Run 2. The bromoester (1.24 g, 95–97% pure) was dissolved in 30 ml of solvolysis solution (EtOH 80 ml, H_2O 20 ml, NaOAc 1.6 g) and the solution (0.18 *M* ester, 0.2 *M* NaOAc) was sealed in a tube and heated on the steam bath (95°) for 6 days. The contents were poured into water (100 ml) saturated with NaCl and extracted with pentane (2 × 30, 3 × 20 ml). Analytical g.l.p.c. analysis on the 5 ft, 5% SE-30 column showed the four major products and *ca.* 15% starting material. The pentane layers were dried and distilled through a 1.5 ft helices packed column. Preparative g.l.p.c. on a 5 ft × 1/4 in. 20% SE-30 on Chromosorb W column at 165° gave the pure norbornenyl and nortricyclyl esters. The ether and alcohol were collected together then separated on a 10 ft × 3/8 in. 15% Carbowax on Chromosorb W column at 190°. Nuclear magnetic resonance (60 MHz, CCl_4): methylnorbornene-1-carboxylate, δ 6.05 (m,

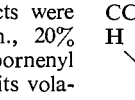

, 2H), 3.70 (s, COOMe, 3H), 2.90 (m, C-4—H, 1H), 1.9 (m, C-5, C-6—*exo*-H, 2H), 1.5 (m, C-7-H, 2H), 1.1 (m, C-5, C-6—*endo*-H, 2H); methyl 1-nortricyclane-1-carboxylate δ 3.70 (s, COOMe, 3H), 2.10 (m, C-4—H, 1H), 1.90 (s, C-2, C-6—H, 2H), 1.5 (d, C-7—H, 2H), 1.20 (s, C-3, C-5-H, 4H); methyl *exo*-2-ethoxynorbornane-1-carboxylate δ 3.70 (s, COOMe, 3H), 3.3 (m, H—C—O—Et, 3H), 2.25 (m, C-4—H, 1H), 2.0–1.2 (m, norbornyl envelope, 8H), 1.10 (t, —O—CH_2—CH_3, 3H); methyl *exo*-2-hydroxynorbornane-1-carboxy-

late δ 4.0 (m, H—C—OH, 1H), 3.0 (bs, —O—H, 1H), 2.30 (m, C-4-H, 1H), 2.1–1.0 (m, norbornyl envelope, 8H).

Methoxide-catalyzed Elimination of HBr from ***1b***

The bromoester obtained via dideuteriodimide reduction (0.23 g, 0.00096 mol) was dissolved in 10 ml of a saturated solution of NaOMe in MeOH and the solution was refluxed for 24 h. The mixture was poured into water (30 ml) and extracted with ether (2 × 30 ml). The aqueous layer was acidified with dilute aqueous HCl and extracted with ether (2 × 30 ml). The ethereal layers were dried and the solvent was taken off on the rotatory evaporator to yield a solid. The solid was taken up in ether and treated with diazomethane. Analytical g.l.p.c. of the solution showed that the product ester had the same retention time as the material obtained from extraction of the basic solution. The two ethereal solutions were combined and the volume was reduced to *ca.* 3 ml by distillation through a 1-ft helices packed column. The methyl deuterionorbornene-1-carboxylate (0.075 g) was isolated by preparative g.l.p.c. In addition to the norbornenyl ester there were three minor products, the deuterionortricyclyl ester < 8%, unknown 4%, and *exo*-2-methoxynorbornyl ester < 8%. The latter product was isolated and its structure inferred from the mass spectrum (80 eV): *m/e* 186 (M^+, $C_{10}H_4O_2D_2$). Compound **4D** (Fig. 1) n.m.r. (100 MHz, CCl_4): δ 6.18 (d, C-2-H, J = 5 Hz), 6.03 (pair of doublets, C-3-H, J = 5.3 Hz), 3.70 (s, COOMe, 3H), 2.95 (m, C-4-H, 1H), 1.87 (A, B quartet with fine structure with higher field position coupled more than low-field position, C-6,C-5—*exo*-H's, respectively, < 2H), 1.5 (A, B quartet with fine structure, C-7-*syn*- and *anti*-H's, 2H), 1.2 (m, C-5, C-6-*endo*-H's < 0.3 H). Area integration analysis of the olefinic and methyl ester protons (average of 8 integrals) showed that there was only 1.95 hydrogens at C-2, C-3. This establishes that a deuteride shift occurs only to the extent of 5% during bromination of the dideuterionorbornylcarboxylic acid.

t-Butoxide-catalyzed Elimination of HBr from ***1c***

The deuteriobromoacid (0.25 g, m.p. 144–146°) was dissolved in a saturated solution of KO*t*Bu in *t*-BuOH (30 ml) and the mixture was refluxed for 7 h. The mixture was poured into water (25 ml) and acidified with dilute aqueous hydrochloric acid and extracted with ether (1 × 50, 2 × 25 ml). The ethereal layer was dried and treated with diazomethane. Analytical g.l.p.c. 5 ft × 1/8 in. 5% SE-30 on Chromosorb W column with temperature programming (100–150°) at 10°/min showed in order of increased retention time, methyl deuterio-2-norbornene-1-carboxylate (20%), unknown < 1%, methyl deuterio-2-norbornene-2-carboxylate 60%, unknown 1%, unknown 10%, unknown 10% as well as 3% of bromoester. The ester **5D** was isolated by preparative g.l.p.c. on a 5 ft × 1/4 in. 20% SE-30 on Chromosorb W column maintained at 160°. The n.m.r. spectrum (60 MHz, CCl_4) showed signals at δ 6.83 (d, 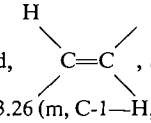 , J = 3.5 Hz, 1H), 3.70 (s, COOMe, 3H), 3.26 (m, C-1—H, 1H), 3.03 (m, C-4—H, 1H), 1.77 (m, C-5,C-6—*exo*-H's, 0.3 H), 1.42 (m, C-7-*syn*-H, 1H), 1.15 (m, C-7—*anti*-H, 1H), 1.09 (m, C-5, C-6—*endo*-H's, 1.86 H). Integration analysis of the methyl ester signal at 3.70 and the signals at 1.77 (*exo*-C—H) and 1.09 (*endo*-C—H) gave ratios which were consistent with the deuterium being 95% stereochemically pure *exo*.

Kinetic Procedure

Sample tubes were made from 10 mm pyrex tubing and washed exhaustively with distilled water and absolute ethanol and dried in an oven. The bromoesters used for the exploratory runs and run 1 (Table 2) were purified by preparative g.l.p.c. on a 5 ft × 1/4 in. 20% SE-30 on Chromosorb W at 170–180°. The bromoesters used in runs 2 and 3 (Table 2) were purified by high pressure liquid chromatography using a Waters Model 200 Chromatograph. The solvent system 15–20% $CHCl_3$ – 85–80% hexane (v/v) was used with a 3/8 in. × 3 ft Porasil A column (column volume 34 ml). At a flow rate of 0.7 ml/min (800 p.s.i.) the bromoester was eluted after approximately 80 ml of flow. After 10–12 injections of 45 μl of neat liquid the appropriate fractions were combined and the solvent was removed on the rotatory evaporator. Final purification was achieved by two bulb-to-bulb vacuum distillations. The 0.09 and 0.135 *M* NaOAc in 80:20 EtOH–H_2O solvolysis solutions were prepared by dissolving 0.68 g of NaOAc·$3H_2O$ and 0.79 g of anhydrous NaOAc, respectively, in 100 ml of 80:20 EtOH–H_2O solution which was 0.04 *M* in NaOAc. The water used in the EtOH–H_2O solution was distilled then doubly distilled from $KMmO_4$. The absolute ethanol was distilled prior to use. In a typical kinetic run 0.10–0.17 g of each ester was dissolved in 15.00 ml of solvolysis solution transferred by means of 10 and 5 ml volumetric pipettes. The solution was mixed and approximately 1.2 ml of the solution of each of the esters was transferred to the ampoules (10–12) which were flushed with dry nitrogen. The ampoules containing the deuterated and non-deuterated esters were sealed and simultaneously submerged completely in a Haake Model NBe bath maintained at around 115.00 ± 0.03° with ethylene glycol as solvent. Both deuterated and nondeuterated aliquots were withdrawn simultaneously at appropriate intervals and stored in the freezer. After the kinetic run was complete and infinity samples were obtained by suspending two samples in refluxing toluene for 1–2 weeks, the samples were removed and equilibrated to room temperature. An exact portion (1.00 ml) was removed from each aliquot, distilled water (1.0 ml), and 6 *N* HOAc (1.0 ml) and 2 drops of 0.1% eosin in 95% EtOH was added and the aliquot was titrated to a pink end point (41) with 0.0100–0.0150 *N* $AgNO_3$ using a 5.00 ml burette. Titers ranged from 0.4 to 3.5 ml. The results were subjected to least-squares analysis. An example of the data is described in Fig. 4.

Financial support by the National Research Council of Canada is gratefully acknowledged.

1. N. H. Werstiuk. Chem. Commun. 1499 (1970).
2. C. K. Ingold. Proc. Chem. Soc. 265 (1962).
3. J. F. Bunnett. Angew. Chem. Int. Ed. Engl. **1**, 228 (1962).
4. J. F. Bunnett. Surv. Prog. Chem. **5**, 53 (1969).
5. J. Hine, R. Wiesboech, and O. B. Ramsay. J. Am. Chem. Soc. **83**, 1222 (1961).

Can. J. Chem. Downloaded from www.nrcresearchpress.com by 210.87.254.42 on 09/05/12
For personal use only.

6. J. CSAPILLA. Chimica, **18** (2), 37 (1964).
7. D. V. BANTHROPE. Reaction mechanisms in organic chemistry. Vol. 2. Elsevier, Amsterdam. 1963.
8. N. A. LEBEL. Advances in alicyclic chemistry. Vol. 3. Academic Press, New York. 1971. p. 195.
9. F. G. BORDWELL. Acc. Chem. Res. **5**, 374 (1972).
10. A. NICKON and N. H. WERSTIUK. J. Am. Chem. Soc. **89**, 3914, 3915, 3917 (1967).
11. F. G. BORDWELL and B. B. JARVIS. J. Am. Chem. Soc. **95**, 3585 (1973).
12. J. C. GREEVER and D. E. GWYNN. Tetrahedron Lett. 813 (1969).
13. J. W. WILT and W. T. WAGNER. J. Am. Chem. Soc. **90**, 135 (1968).
14. R. J. ARHART and J. C. MARTIN. J. Am. Chem. Soc. **94**, 5003 (1972).
15. C. J. COLLINS and B. M. BENJAMIN. J. Am. Chem. Soc. **89**, 1652 (1967).
16. C. J. COLLINS, I. T. GLOVER, M. D. ECKART, V. F. RAAEN, B. M. BENJAMIN, and B. S. BENJAMIN. J. Am. Chem. Soc. **94**, 899 (1971).
17. C. J. COLLINS and B. M. BENJAMIN. J. Org. Chem. **37**, 4358 (1972).
18. N. H. WERSTIUK and I. VANCAS. Can. J. Chem. **48**, 3963 (1970).
19. R. MUNEYUKI and T. YANO. J. Am. Chem. Soc. **92**, 746 (1970).
20. P. G. GASSMAN, J. L. MARSHALL, and J. G. MACMILLAN. J. Am. Chem. Soc. **95**, 6319 (1973).
21. N. H. WERSTIUK, G. TIMMINS, and F. P. CAPPELLI. Can. J. Chem. **51**, 3473 (1973).
22. W. R. BOEHME. J. Am. Chem. Soc. **80**, 4740 (1958).
23. W. R. BOEHME. J. Am. Chem. Soc. **81**, 2762 (1959).
24. N. H. WERSTIUK. Can. J. Chem. **48**, 2310 (1970).
25. N. A. LEBEL, P. D. BERINE, and P. M. SUBRAMANIAN. J. Am. Chem. Soc. **86**, 4144 (1964).
26. B. FRANZUS, N. C. BAIRD, JR., N. F. CHAMBERLAIN, T. HINES, and E. I. SNYDER. J. Am. Chem. Soc. **90**, 3721 (1968).
27. S. WINSTEIN and G. C. ROBINSON. J. Am. Chem. Soc. **80**, 169 (1958).
28. K. HUMSKI, V. SENDIJAREVIĆ, and V. J. SHINER, JR. J. Am. Chem. Soc. **95**, 7722 (1973).
29. A. F. THOMAS and B. WILLHALM. Tetrahedron Lett. 1309 (1965).
30. D. G. FARNUM and G. MEHTA. J. Am. Chem. Soc. **91**, 3256 (1969).
31. G. A. OLAH, A. M. WHITE, J. R. DEMEMBER, A. COMMERYAS, and C. Y. JUI. J. Am. Chem. Soc. **92**, 4627 (1970).
32. G. A. OLAH, J. R. DEMEMBER, C. Y. LUI, and R. D. PORTER. J. Am. Chem. Soc. **93**, 1442 (1971).
33. A. NICKON, J. L. LAMBERT, S. J. R. O. WILLIAMS, and N. H. WERSTIUK. J. Am. Chem. Soc. **88**, 3354 (1966).
34. V. J. SHINER, JR. J. Am. Chem. Soc. **75**, 2925 (1953).
35. V. J. SHINER, JR. J. Am. Chem. Soc. **76**, 1603 (1954).
36. S. WINSTEIN and J. TAKAHASHI. Tetrahedron, **2**, 316 (1958).
37. M. S. SILVER. J. Am. Chem. Soc. **83**, 3487 (1961).
38. K. HUMSKI. Croat. Chem. Acta, **42**, 501 (1970).
39. F. P. CAPPELLI, G. TIMMINS, and N. H. WERSTIUK. Can. J. Chem. **50**, 2163 (1972).
40. D. J. CRAM and J. TADANIER. J. Am. Chem. Soc. **81**, 2737 (1959).
41. T. M. KOLTOFF and E. B. SANDELL. Textbook of quantitative inorganic analysis. 3rd Ed. Macmillan Co., New York. 1952. p. 544.

Can. J. Chem. Downloaded from www.nrcresearchpress.com by 210.87.254.42 on 09/05/12
For personal use only.

Biosynthesis of Lycopodine. The Question of the Intermediacy of Piperidine-2-acetic Acid

W. D. MARSHALL, T. T. NGUYEN, D. B. MACLEAN, AND IAN D. SPENSER
Department of Chemistry, McMaster University, Hamilton, Ontario L8S 4M1
Received August 12, 1974

W. D. MARSHALL, T. T. NGUYEN, D. B. MACLEAN, and IAN D. SPENSER. Can. J. Chem. **53**, 41 (1975).

In *Lycopodium tristachyum* lycopodine is derived from L-lysine whereas pipecolic acid is derived from D-lysine. Malonic acid serves as a specific precurser of the non-lysine derived segments of lycopodine. Piperidine-2-acetic acid is not incorporated into the alkaloid.

W. D. MARSHALL, T. T. NGUYEN, D. B. MACLEAN et IAN D. SPENSER, Can. J. Chem. **53**, 41 (1975).

Dans le *Lycopodium tristachyum*, la lycopodine dérive de la L-lysine alors que l'acide pipécolique dérive de la D-lysine. L'acide malonique sert de précurseur spécifique pour les segments de la lycopodine ne dérivant pas de la lysine. L'acide piperidine-2 acétique n'est pas incorporé dans l'alkaloïde. [Traduit par le journal]

Introduction

In the course of our studies of the biosynthesis of the *Lycopodium* alkaloids (1–6) it was found that acetate (2), lysine (**1**) (1, 2), cadaverine (**2**) (2, 6), Δ^1-piperideine (**3**) (4, 6), and pelletierine (**7**) (3, 4) serve as specific precursors of lycopodine (**8**). Activity from radioactively labelled samples of all these substrates is incorporated nonrandomly into the alkaloid. Radioactivity from all except pelletierine (**7**) is incorporated in such a manner that the two 'halves' of lycopodine, *i.e.*, the C_8 chains, C-1 to -8 and C-9 to -16, respectively, each contain 50% of the label. Pelletierine, which in another plant species is itself derived from lysine, cadaverine, Δ^1-piperideine, and acetate (7–9), enters only one of the 'halves' of lycopodine, the C_8 chain, C-9 to -16 (3, 4), of which it is an obligatory precursor (6). Pelletierine does not enter the C_8 chain, C-1 to -8, of lycopodine. To account for the apparent anomaly that pelletierine enters only one of the 'halves' of the lycopodine molecule whereas lysine, cadaverine, Δ^1-piperideine, and acetate, from which pelletierine is apparently derived, enter both halves, we proposed the biogenetic model outlined in Scheme 1 (6). The salient features of this scheme are that pelletierine (**7**), the precursor of the C_8 chain, C-9 to -16, of lycopodine, is derived from piperidine-2-acetoacetate (**6**) in an irreversible decarboxylation, that the piperidine-2-acetoacetate (or its coenzyme A derivative (**5**)) is the precursor of the C_8 chain, C-1 to -8, of lycopodine, and that a CO_2 unit is expelled from the system at some stage after combination of piperidine-2-acetoacetate with pelletierine. Provided the steady state concentration of pelletierine is small compared to that of its postulated precursor, piperidine-2-acetoacetate, all experimental observations (1–4, 6) are accounted for by this hypothesis (6).

Piperidine-2-acetoacetate (**6**) could, in turn, be derived from Δ^1-piperideine (**3**) by stepwise condensation with two units of malonyl coenzyme A. The coenzyme A derivative (**4**) of piperidine-2-acetate is predicted to be a stage on this proposed route to lycopodine. Since malonyl coenzyme A originates by carboxylation of acetyl coenzyme A (10) and since Δ^1-piperideine is likely to be derived, via cadaverine, from L-lysine (9), the previously observed incorporation pattern (1–4) would be accounted for.

In the present study several aspects of the biogenetic model outlined in Scheme 1 were examined experimentally. It is shown that, as predicted, malonate enters lycopodine. It is demonstrated that, as predicted, lycopodine is derived from L-lysine and not from D-lysine. It is shown that, contrary to prediction, piperidine-2-acetate is not an intermediate in the biosynthesis of lycopodine.

Results and Discussion

In principle, there are a number of ways in which the hypothesis outlined in Scheme 1

Can. J. Chem. Downloaded from www.nrcresearchpress.com by 210.87.254.6 on 09/05/12
For personal use only.

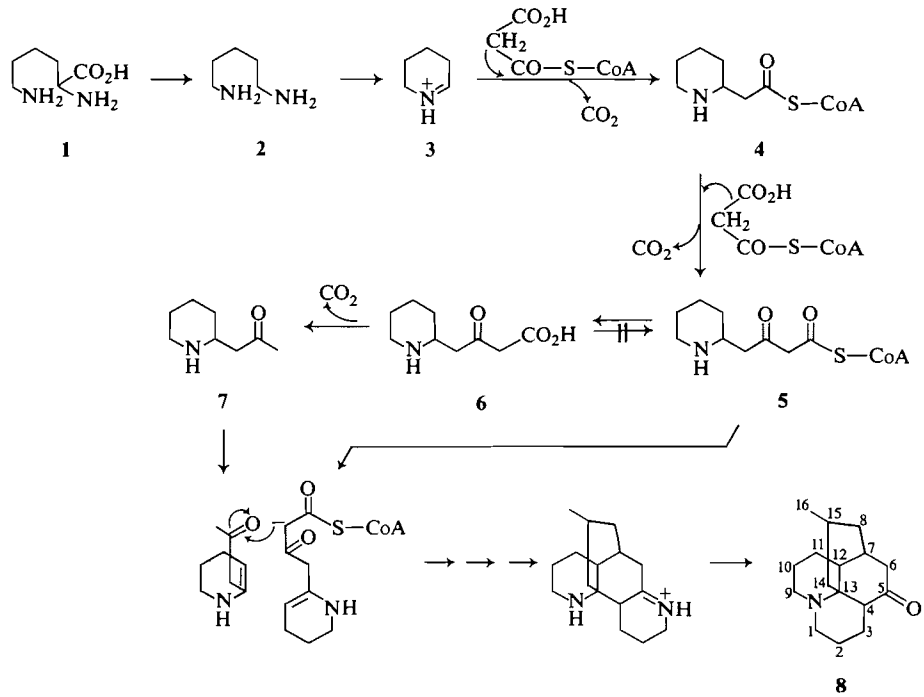

SCHEME 1. The biosynthesis of lycopodine. A hypothetical pathway consistent with published experimental evidence (1–4, 6).

could be tested by means of tracer experiments. The most direct approach, by an experiment with piperidine-2-acetoacetate which is predicted to enter the C_8 unit, C-1 to -8, as well as the pelletierine derived C_8 unit, C-9 to -16, of lycopodine, has not yet been feasible since the required substrate has not been described.[1] Several other approaches were therefore attempted.

Piperidine-2-acetoacetate (**6**) is postulated to arise by condensation of malonyl coenzyme A with piperidine-2-acetyl coenzyme A (**4**) and the latter, in turn, by addition of malonyl coenzyme A to Δ^1-piperideine (**3**), an established intermediate in lycopodine biosynthesis (4, 6).

The present work therefore focussed on testing the intermediacy of malonate and of piperidine-2-acetate in lycopodine biosynthesis.

The first set of the present experiments, aimed at the attempted demonstration that piperidine-2-acetic acid (**13**) serves as a precursor of lycopodine, gave an inconclusive result. Piperidine-2-acetic acid or, more precisely, its coenzyme A ester (**4**), is postulated by the hypothesis to be a precursor of piperidine-2-acetoacetic acid (**6**), and should, like the latter, be incorporated into both 'halves' of lycopodine. It should serve as a source of the C_7 units, C-1 to -7 and C-9 to -15. A sample of (±)-[*carboxyl*-^{14}C]piperidine-2-acetate was prepared in 57% radiochemical yield by the conventional steps, outlined in Scheme 2, which are fully described in the Experimental section. A sample of this compound (100 μCi) was administered to cuttings of *Lycopodium tristachyum* (Experiment 18). The lycopodine which was isolated showed radioactivity but the specific activity of the alkaloid after rigorous purification was too low (approximately 3 d.p.m./mg above background) to permit conclusions to be drawn, since the low activity precluded degradation of the sample.

In another experiment (Experiment 19) a sample of the (±)-[*carboxyl*-^{14}C]piperidine-2-acetate (20 μCi) was administered to *L. tristachyum* cuttings in admixture with DL-[*4*-^3H]-lysine (100 μCi). The lycopodine which was

[1]The ethyl ester of the corresponding carbinol has now been prepared (I. Noguchi and D. B. MacLean, unpublished work, 1973) and the synthesis of a ^{14}C-labelled sample is in hand.

Can. J. Chem. Downloaded from www.nrcresearchpress.com by 210.87.254.6 on 09/05/12
For personal use only.

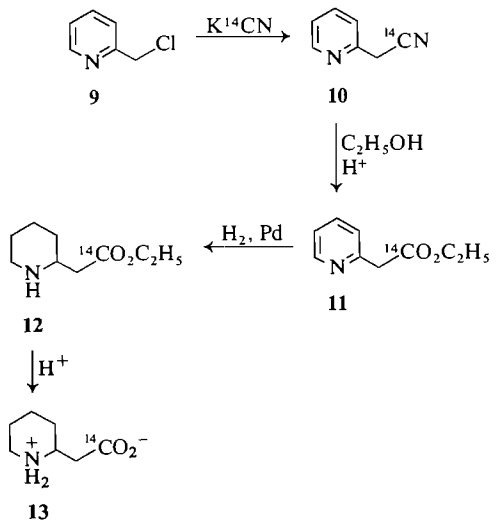

SCHEME 2. Synthesis of [*carboxyl-*^{14}*C*]piperidine-2-acetic acid.

isolated showed a specific activity relative to ^{14}C (approximately 2 d.p.m./mg) not greatly different from that of the sample obtained in the earlier experiment.

The high ^{3}H/^{14}C ratio of the sample of lycopodine (^{3}H/^{14}C = 82 ± 3) indicated that biosynthesis of the alkaloid had taken place during the experiment and that lysine (*i.e.*, ^{3}H) had been incorporated *ca.* 17 times as efficiently as (±)-piperidine-2-acetate (*i.e.*, ^{14}C). This result raised further doubts regarding the intermediacy of this compound.

A second approach to test the hypothesis outlined in Scheme 1 was based on the predicted intermediacy of malonate. If ^{14}C-labelled malonate were incorporated into lycopodine, the labelling pattern to be expected would be identical with that found after administration of correspondingly labelled [^{14}*C*]acetate (2). Activity from [*1-*^{14}*C*]malonate should thus be equally distributed among C-7 and -15 of lycopodine, each of these containing 50% of the total activity of the alkaloid. Activity from [*2-*^{14}*C*]malonate should be equally distributed among C-6, -8, -14, and -16 of lycopodine, each of these containing 25% of the total activity of the alkaloid.

Activity from [*1-*^{14}*C*]malonate was indeed incorporated into lycopodine (Experiment 20). Consistent with prediction, half of this activity was located at C-15 of the lycopodine (Kuhn–Roth acetate (C-15, -16) minus Schmidt methylamine (C-16), Table 3). As in the last experiment, the ^{14}C tracer (250 μCi) was administered in admixture with DL-[*4-*^{3}*H*]lysine (1 mCi).[2] It is of interest that in this experiment it was the malonate (*i.e.*, ^{14}C) which was incorporated into the lycopodine (^{3}H/^{14}C = 0.74 ± 0.01) *ca.* 14 times[3] as efficiently as the lysine (*i.e.*, ^{3}H).

If piperidine-2-acetate were a precursor of lycopodine, its formation from lysine and malonate, at a time when these are incorporated into lycopodine, would be mandatory. It should then be present in the system from which ^{3}H,^{14}C-labelled lycopodine was isolated after administration of a mixture of [^{3}*H*]lysine and [^{14}*C*]malonate, and should, under these conditions, show a ^{3}H/^{14}C ratio identical with that of lycopodine. Piperidine-2-acetic acid was isolated from the plant material from this experiment (Experiment 20) by carrier dilution. After purification by column chromatography (Dowex 50W-X4, H^+) and derivatization by reaction with phenylisothiocyanate, the sample contained tritium (specific activity 3.0 (±0.1) × 10^4 d.p.m./mmol) but no ^{14}C. Even though it appeared to be present in the system,[4] piperidine-2-acetate clearly did not play a part in the biosynthesis of lycopodine, since it did not show a ^{3}H/^{14}C ratio identical with that of the product.

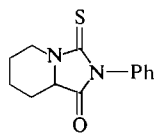

14

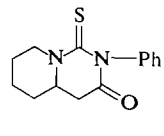

15

[2]Incorporation into lycopodine of tritium from DL-[*4-*^{3}*H*]lysine, without loss relative to C-6 of lysine, was demonstrated by a separate experiment (Experiment 22, *vide infra*).

[3]Since in the course of incorporation one of the carboxyl groups of malonate is expelled, one half of the activity administered as malonate must be lost as carbon dioxide.

[4]Piperidine-2-acetic acid does not appear to have been isolated from natural sources. The natural occurrence of the compound, apparently indicated by the tritium content of the trapped sample of piperidine-2-acetic acid must be regarded as questionable on the basis of the absence of ^{14}C.

It is very likely that tritium activity of the sample was due to contamination by traces of pipecolic acid. The method adopted to re-isolate piperidine-2-acetate from the plant extract to which piperidine-2-acetate had been

Can. J. Chem. Downloaded from www.nrcresearchpress.com by 210.87.254.6 on 09/05/12
For personal use only.

Can. J. Chem. Downloaded from www.nrcresearchpress.com by 210.87.254.6 on 09/05/12
For personal use only.

Having obtained inconclusive results concerning the intermediacy of piperidine-2-acetate in lycopodine biosynthesis by direct feeding experiments (Experiments 18 and 19) and having found strong indication against its involvement by a trapping experiment, we made a further attempt to obtain a conclusive result.

With the demonstration that malonate, like acetate, served as a specific precursor of lycopodine, [2-^{14}C]malonate was employed in this third approach to test the biosynthetic intermediacy of piperidine-2-acetate.

Activity from [2-^{14}C]malonate should enter lycopodine in the same manner as activity from [2-^{14}C]acetate, supplying C-6, -8, -14, and -16, each of which should contain 25% of the activity of intact lycopodine. If piperidine-2-acetate were an intermediate in lycopodine biosynthesis according to Scheme 1, two of these carbon atoms, C-6 and -14, would originate from malonate via the α-methylene group of piperidine-2-acetate. The other two carbon atoms, C-8 and -16, would arise more directly from malonate. It follows that in a tracer experiment with [2-^{14}C]malonate, incorporation of activity into C-6 and -14 of lycopodine but not into C-8 and -16 should be suppressed in the presence of inactive piperidine-2-acetate, if this were an intermediate.

Thus, if piperidine-2-acetate were not an obligatory intermediate, addition of unlabelled piperidine-2-acetate would not affect entry of ^{14}C from [2-^{14}C]malonate into the four carbon atoms, C-6, -8, -14, -16. Each of these would contain one quarter of the label of the intact lycopodine derived from [2-^{14}C]malonate, regardless of whether inactive piperidine-2-acetate were added to the system or not.

However, if piperidine-2-acetate were an obligatory intermediate on the route from malonate into lycopodine, addition of inactive piperidine-2-acetate to the system would suppress entry of label from [2-^{14}C]malonate into the two carbon atoms, C-6 and -14, but not into the two carbon atoms, C-8 and -16. It follows that under these conditions, the four carbon atoms in question, derived from [2-^{14}C]malonate, would no longer be equally labelled.

The two carbon atoms, C-6 and -14, each should contain less activity than the two carbon atoms, C-8 and -16. In the limit, suppression of incorporation of label into C-6 and -14 by carrier piperidine-2-acetate would be complete, so that all activity from [2-^{14}C]malonate would be equally divided between C-8 and -16, each of which would now contain 50% of the activity of intact lycopodine.

Thus, if the lycopodine, derived from an experiment in which [2-^{14}C]malonate were administered in the presence of excess inactive piperidine-2-acetic acid, yielded Kuhn–Roth acetate (C-15, -16) and Schmidt methylamine (C-16), each containing one quarter of the activity of the intact alkaloid, piperidine-2-acetate is not an intermediate of lycopodine biosynthesis. If Kuhn–Roth acetate and Schmidt methylamine were obtained containing more than one quarter and up to one half of the activity of the intact alkaloid, the intermediacy of piperidine-2-acetate would be established.

In the event, lycopodine, isolated from an experiment in which [2-^{14}C]malonate was administered in the presence of inactive piperidine-2-acetic acid (Experiment 21), contained one quarter of its activity at the *C*-methyl group (C-16, methylamine) (Table 3). Thus, piperidine-2-acetate cannot be an intermediate.

A fourth approach which was followed con-

---

added as carrier (see Experimental), is not specific for this compound but is an adaptation of a general method for the isolation of secondary amino acids. Pipecolic acid, among other compounds, is also separated by this procedure.

The two compounds were isolated in the form of their crystalline condensation products with phenylisothiocyanate (**14** and **15**). These can be readily differentiated by physical methods (see Experimental) but persistent attempts to achieve chromatographic separation failed. The presence of contaminating pipecolic acid in the trapped sample of piperidine-2-acetic acid could thus not be detected by radiochromatography. A further trapping experiment strongly suggested that activity was due mainly, if not entirely, to pipecolic acid. An inactive sample of the phenylisothiocyanate adduct of pipecolic acid (**14**) (10 mg) was added to the mother liquors from the crystallization of the ^{3}H-containing sample of the piperidine-2-acetic acid adduct (**15**). The pipecolic acid derivative (**14**) was then re-isolated. After repeated crystallization of the two derivatives, (**14**) and (**15**), the pipecolic acid derivative (**14**) showed a specific activity two orders of magnitude higher (2×10^4 d.p.m./mg) than the derivative of piperidine-2-acetic acid (**15**) (1.1×10^2 d.p.m./mg). It is very likely, therefore, that the activity associated with the sample of piperidine-2-acetic acid found in Experiments 20 was due to contamination with traces of pipecolic acid, and that piperidine-2-acetic acid does not occur naturally in *L. tristachyum*.

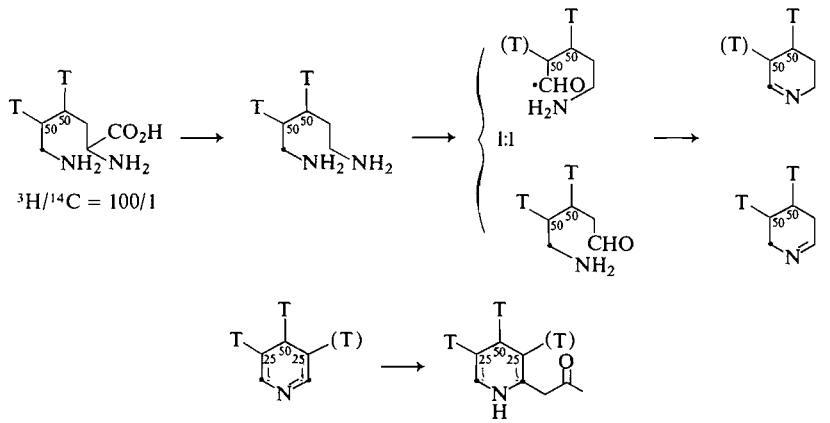

SCHEME 3. Predicted mode of incorporation of [4,5-$^3H_2$,6-^{14}C]lysine into lycopodine (2).

currently with the above experiments to evaluate the hypothesis, that piperidine-2-acetate was an intermediate of lycopodine biosynthesis, was based on stereochemical considerations. Its primary objective was to investigate whether the same enantiomer of lysine was incorporated into both.

It is known that the piperidine nucleus of several piperidine alkaloids is derived from L-lysine whereas pipecolic acid, isolated from the same sources, is derived from D-lysine (8). This was demonstrated by a new technique whereby the chirality of a precursor–product relationship can be determined by tracer experiments with doubly labelled substrate. Provided intact incorporation of ^3H,^{14}C-labelled racemate of a substrate into a product has been shown to take place with maintenance of the $^3H/^{14}C$ ratio, it is possible to determine, by the use of a multiply labelled substrate in which one enantiomer is labelled with tritium while the other is labelled not only with tritium but also with ^{14}C, which of the enantiomers of the substrate is incorporated into the product (8).

Before this technique could be applied to the study of the chirality of the conversion of lysine into lycopodine, incorporation of activity from a ^3H,^{14}C-labelled sample of DL-lysine into lycopodine without change in $^3H/^{14}C$ ratio had to be demonstrated. The entry into lycopodine of an intact C_5 fragment (C-2 to -6 of lysine), derived from lysine by decarboxylation, may be inferred from earlier work on the incorporation of DL-[2-^{14}C]- and DL-[6-^{14}C]-lysine, [1-^{14}C]cadaverine, and [2-^{14}C]- and [6-^{14}C]-Δ^1-piperideine (1, 2, 4, 6).

In an earlier feeding experiment with a doubly labelled sample of lysine, DL-[4,5-$^3H_2$,6-^{14}C]lysine, incorporation into lycopodine was accompanied by 22% loss of tritium, relative to ^{14}C (Experiment 5) (2). A maximum loss of 25% of tritium, relative to ^{14}C, may be accounted for, without breakdown of the carbon skeleton of lysine other than loss of the carboxyl group, by removal of tritium from C-5 of lysine, as shown in Scheme 3 (2).

It can be predicted on the basis of this scheme, that a sample of DL-[4-^3H,6-^{14}C]lysine should enter lycopodine without change in $^3H/^{14}C$-ratio. That this is indeed the case is shown by

Can. J. Chem. Downloaded from www.nrcresearchpress.com by 210.87.254.6 on 09/05/12
For personal use only.

Can. J. Chem. Downloaded from www.nrcresearchpress.com by 210.87.254.6 on 09/05/12
For personal use only.

TABLE 1. Incorporation of labelled compounds into lycopodine

Experiment No.	Compounds administered	Nominal specific activity (mCi/mmol)	Nominal total activity (mCi)	$^3H/^{14}C$ ratio in feeding solution	Date and duration (days)	Weight of dry plant material (g)	Lycopodine		
							Yield (mg)	Specific activity (d.p.m./mmol) (^{14}C)	$^3H/^{14}C$ ratio
18	(±)-[*carboxyl*-^{14}C]Piperidine-2-acetic acid, HCl salt[a]	0.63	0.1	—	July 1972 (2)	60	70	$5.3(\pm0.1)\times10^2$	—
19	(±)-[*carboxyl*-^{14}C]Piperidine-2-acetic acid, HCl salt[a] plus DL-[4-^3H]lysine[b]	0.63 39×10^3	0.02 0.1	4.9 ± 0.6	Aug. 1972 (4)	80	80	$1.6(\pm0.1)\times10^2$	81.8 ± 3.4
20	Sodium [1-^{14}C]malonate[c] plus DL-[4-^3H]lysine[b]	6.9 39×10^3	0.25 1	5.2 ± 0.1	Aug. 1972 (4)	88	63	$1.96(\pm0.02)\times10^6$	0.74 ± 0.01
21	Sodium [2-^{14}C]malonate[c] plus inactive piperidine-2-acetic acid (200 mg)	17	0.13	—	June 1973 (2)	68	37	$2.86(\pm0.03)\times10^6$	—

[a]See Experimental.
[b]Commissariat à l'Énergie Atomique, France.
[c]Amersham-Searle.

TABLE 2. Incorporation of doubly labelled lysine into lycopodine and pipecolic acid

Experiment No.	Compounds administered	Nominal specific activity (mCi/mmol)	Nominal total activity (mCi)	$^3H/^{14}C$ ratio	Date and duration (days)	Weight of dry plant material (g)	Products				
							Lycopodine			Pipecolic acid	
							Yield (mg)	Specific activity (d.p.m./mmol) (^{14}C)	$^3H/^{14}C$ ratio	Specific activity[d] (d.p.m./mmol) (^{14}C)	$^3H/^{14}C$ ratio
5 (Ref. 2)	DL-[4,5-$^3H_2$]Lysine[b] plus DL-[6-^{14}C]lysine[c]	2.9×10^3 9.2	1 0.1	10.7 ± 0.2	Sept. 1967 (2)	430 (fresh weight)	350	$3.66(\pm0.09)\times10^4$	8.4 ± 0.1	Not isolated	
22	DL-[4-^3H]Lysine[e] plus DL-[6-^{14}C]lysine[c]	39×10^3 48	1 0.1	12.5 ± 0.2	Aug. 1972 (4)	85	60	$6.54(\pm0.04)\times10^5$	13.0 ± 0.1	$2.26(\pm0.08)\times10^6$	12.9 ± 0.1
23	DL-[4,5-$^3H_2$]Lysine[b] plus D-[6-^{14}C]lysine[d]	5.4×10^3 48	0.5 0.05	11.1 ± 0.3	July 1971 (3)	31	22	$1.41(\pm0.05)\times10^5$	90.0 ± 1.0	$2.20(\pm0.02)\times10^6$	6.4 ± 0.1
24	L-[4,5-$^3H_2$]Lysine[e] plus DL-[6-^{14}C]lysine[c]	0.25×10^3 48	0.5 0.05	8.5 ± 0.2	July 1971 (3)	29	19	$2.46(\pm0.06)\times10^5$	13.3 ± 0.2	$1.84(\pm0.06)\times10^6$	0.49 ± 0.03

[a]After dilution with inactive pipecolic acid as carrier.
[b]New England Nuclear.
[c]Commissariat à l'Énergie Atomique, France.
[d]See Experimental.
[e]Amersham-Searle.

Can. J. Chem. Downloaded from www.nrcresearchpress.com by 210.87.254.6 on 09/05/12
For personal use only.

the result of Experiment 22 (Table 2) in which a sample of DL-[4-^3H,6-^{14}C]lysine[5] ($^3H/^{14}C$ = 12.5 ± 0.2) was administered to *L. tristachyum* cuttings. The lycopodine ($^3H/^{14}C$ = 13.0 ± 0.1) as well as the pipecolic acid ($^3H/^{14}C$ = 12.9 ± 0.1) which were isolated from this plant material were found to maintain the $^3H/^{14}C$ ratio of the substrate.

This finding confirms the view (2) that the change in the $^3H/^{14}C$ ratio, observed in the earlier experiment with DL-[4,5-$^3H_2$,6-^{14}C]lysine (Experiment 5) (2), was due entirely to loss of tritium from C-5 of lysine in the course of its incorporation into lycopodine.

With the demonstration that DL-[4-^3H,6-^{14}C]-lysine enters lycopodine without change in $^3H/^{14}C$ ratio, together with the earlier evidence on the mode of incorporation of lysine into lycopodine, the necessary conditions have been met to determine the chirality of the precursor–product relationship by means of the tracer method referred to earlier.

Samples of DL-[4,5-$^3H_2$]/D-[6-^{14}C]lysine and of L-[4,5-$^3H_2$]/DL-[6-^{14}C]lysine were administered in separate experiments to cuttings of *L. tristachyum* (Experiments 23 and 24), and lycopodine and pipecolic acid were isolated from the plants (Table 2). Comparison of the $^3H/^{14}C$ ratios of substrate and products[6] (Table 4) clearly indicates that lycopodine is derived from L-lysine whereas pipecolic acid is derived largely, if not exclusively, from D-lysine. These results are analogous to those obtained with other plant species in which piperidine alkaloids are derived entirely from L-lysine while L-pipecolic acid is generated almost totally from D-lysine (8).

[5]That the labelled components of this substrate, [4-^3H]lysine and [6-^{14}C]lysine, used in Experiment 22, were indeed racemates was shown in a separate experiment (8). A mixture of the two labelled samples ($^3H/^{14}C$ = 8.1 ± 0.1) was subjected to the action of L-lysine decarboxylase (*ex Bacillus cadaveris*, Sigma Chemical Co.). The resulting cadaverine ($^3H/^{14}C$ = 7.7 ± 0.1), originating by decarboxylation of L-lysine, and the unreacted D-lysine which was recovered ($^3H/^{14}C$ = 8.1 ± 0.1), each maintained the $^3H/^{14}C$ ratio of the original mixture, within experimental error. This shows that each of the labelled components of the [4-^3H,6-^{14}C]lysine used as the substrate in Experiment 22 had indeed been a racemic mixture.

[6]A correction factor was applied to the observed $^3H/^{14}C$ ratio of lycopodine, to allow for the established loss of ^3H (~22%) in the course of the incorporation of [4,5-$^3H_2$]lysine into lycopodine, now shown to be from C-5 by the results of Experiments 22 and 5.

Since lycopodine is derived exclusively from L-lysine, intermediates of lycopodine biosynthesis must also be derived from L-lysine. It follows that a condition for the intermediacy of piperidine-2-acetate in lycopodine biosynthesis was its derivation from L-lysine. Experiments to test this condition were not attempted when it emerged from the other evidence, described earlier, that piperidine-2-acetate was not an intermediate in the biosynthesis of lycopodine.

It is clear that the hypothesis of lycopodine biosynthesis outlined in Scheme 1 requires modification. If piperidine-2-acetoacetate does serve as an intermediate, its derivation from L-lysine and malonate (or acetate) cannot proceed by way of free piperidine-2-acetate.

Experimental

Labelled Compounds

Sodium [1-^{14}C]malonate (Experiment 20), sodium [2-^{14}C]malonate (Experiment 21), DL-[4-^3H]lysine (Experiments 19, 20, 22), DL-[4,5-$^3H_2$]lysine (Experiment 23), L-[4,5-$^3H_2$]lysine (Experiment 24) and DL-[6-^{14}C]lysine (Experiments 22, 24) were commercial products (see Tables 1 and 2). D-[6-^{14}C]Lysine was prepared from DL-[6-^{14}C]lysine by destruction of the L-enantiomer by means of L-lysine decarboxylase (8). (±)[carboxyl-^{14}C]-Piperidine-2-acetic acid was prepared from potassium [^{14}C]cyanide, as described below. The intermolecularly doubly labelled samples of lysine which were used in Experiments 22–24 were prepared by mixing suitable quantities of the above tracers. Nominal total activities, and the $^3H/^{14}C$ ratios of the doubly labelled samples, determined by liquid scintillation counting, are given in Tables 1 and 2.

*(±)-[carboxyl-^{14}C]Piperidine-2-acetic Acid (**13**)*

*[cyano-^{14}C]Pyridine-2-acetonitrile (**10**) (**11**)*

2-Chloromethylpyridine hydrochloride (**9**) (270 mg) (2-picolyl chloride, Aldrich Chemical Co., recrystallized from ethanol–ether, m.p. 128–130°) was dissolved in a little water, sodium bicarbonate solution (10% w/v) was added and the free base was extracted into chloroform (3 × 5 ml). The chloroform solution was dried (anhydrous sodium sulfate) and filtered, and the solvent was evaporated, leaving 2-chloromethylpyridine (200 mg) as an oily liquid. Potassium cyanide (1.2 mg, nominal total activity 1 mCi, nominal specific activity 54 mCi/mmol, Amersham Searle) was washed into the reaction flask with aqueous ethanol (5 ml, 60% v/v). Nonradioactive potassium cyanide (113 mg) was added as carrier, together with potassium iodide (12 mg). The mixture was refluxed with stirring. A drying tube containing solid potassium hydroxide was attached to the condenser during this operation to absorb any gaseous hydrogen [^{14}C]cyanide which might be liberated. The mixture was kept overnight and was then concentrated with repeated addition of water until all ethanol had been distilled off. Saturated aqueous sodium carbonate (5 ml) was added and the mixture continuously extracted with ether for

Can. J. Chem. Downloaded from www.nrcresearchpress.com by 210.87.254.6 on 09/05/12
For personal use only.

24 h and then for another 24 h with a new portion of ether. The combined ether extract was evaporated with a stream of nitrogen. The residue was distilled at 60° and 10^{-2} mm yielding a liquid whose R_f value (t.l.c., silica gel 0.2 mm, ether–chloroform, 1:1, R_f 0.56) was identical with that of an authentic sample of inactive pyridine-2-acetonitrile (11); n.m.r. spectrum, δ 3.8 (s, 2H), 7.4 p.p.m. (m, 4H); i.r. spectrum, 2230 cm^{-1} (CN).

*Ethyl [carboxyl-^{14}C]Pyridine-2-acetate (**11**) (11)*

The above nitrile was dissolved in ethanol, the solution was cooled to −20° and kept at that temperature with stirring, while a stream of dry hydrogen chloride gas was passed through it. The mixture was refluxed overnight, ethanol was distilled off, the residue was dissolved in water (10 ml), the solution transferred into a liquid–liquid extractor, basified with saturated aqueous sodium carbonate (10 ml) and extracted 2 × 24 h with ether. The ether extract was evaporated in a stream of nitrogen and the residue distilled at 90° and 10^{-2} mm, yielding an oil which was identical on t.l.c. (silica gel 0.2 mm, ether–chloroform, 1:1, R_f 0.60) with an authentic sample of inactive ethyl pyridyl-2-acetate (11); n.m.r. spectrum, δ 3.9 (s, 2H), 7.4 (m, 4H), 1.4 (t, 3H) 4.3 p.p.m. (q, 2H).

*[carboxyl-^{14}C]Piperidine-2-acetic Acid (**13**) (12)*

The above ester was transferred into a 50 ml hydrogenation flask and hydrochloric acid (10%, 10 ml) and Adams' catalyst (40 mg) was added. Hydrogenation was carried out at room temperature and atm. pressure for 15 h. The catalyst was filtered off, rinsed with hydrochloric acid (10%, 20 ml) and the combined filtrate refluxed for 10 h. The solvent was evaporated *in vacuo* and the residue sublimed at 120° and 10^{-2} mm. The sublimate was recrystallized from methanol–ether. [*carboxyl*-^{14}C]-Piperidine-2-acetic acid hydrochloride (158 mg) was obtained as colorless needles. The purity of the product was checked by thin-layer radiochromatography (silica gel, 0.2 mm, 1-butanol – acetic acid – water, 4:2:1). A single radioactive peak, R_f 0.4, appeared which was identical in R_f value with that given by an authentic specimen of the product (*vide infra*). The specific activity of the product was 0.63 mCi/mmol, its total activity 0.57 mCi (57% radiochemical yield).

Piperidine-2-acetic Acid

(*i*) By chromic acid oxidation of 2-(2-piperidine)ethan-1-ol (13): A mixture of chromium trioxide (20 g), concentrated sulfuric acid (40 g) and water (300 ml) was added dropwise with stirring to an ice-cooled solution of 2-(2-piperidine)ethan-1-ol (10 g) (2-piperidineethanol, Aldrich Chemical Co.) in water (10 ml). Addition was completed after 1 h and stirring continued for 3 h at room temperature. The solution was basified with saturated barium hydroxide solution, excess barium precipitated with carbon dioxide and the mixture filtered through celite. The filtrate was evaporated and the residue was dissolved in methanol. On addition of ether the product, (±)-piperidine-2-acetic acid (8 g, 72%) crystallized in colorless needles; m.p. 217–218° (lit. (12) m.p. 212°); (mass spectrum, molecular ion *m/e* 143). A small sample was converted into the *hydrochloride salt* which was purified by sublimation at 120° and 10^{-2} mm; m.p. 180–182° (lit. (13) m.p. 180–182°; (12) 182–185°); i.r. spectrum, 1730 cm^{-1} (C=O), 2800–3300 cm^{-1} (NH_2^+).

(*ii*) By hydrogenation of ethyl pyridine-2-acetate (**11**) (12): Ethyl pyridine-2-acetate (165 mg) was hydrogenated in aqueous hydrochloric acid (10 ml, 6 *M*) in the presence of Adams' catalyst at room temperature and atm. pressure for 10 h. The mixture was filtered, the filtrate neutralized with aqueous sodium bicarbonate and the product extracted into chloroform. The extract was dried (anhydrous sodium sulfate) the solvent evaporated and the residue distilled at 80° and 10^{-2} mm. Ethyl piperidine-2-acetate (**12**) (150 mg, 88%) was obtained as a yellow oil; mass spectrum, molecular ion *m/e* 171; n.m.r. spectrum δ 1.3 (t, 3H), 4.1 (q, 2H), 1.9 p.p.m. (s, 1H); i.r. spectrum, 1730 cm^{-1} (ester). Acid hydrolysis of a small sample of the ester gave piperidine-2-acetic acid (**13**), identical with the sample prepared by method *i*.

Tracer Experiments

In each of the seven feeding experiments radioactive tracer was administered to excised shoots of *Lycopodium tristachyum*. The method has been described in earlier papers (2, 6). The details of the seven experiments are summarized in Tables 1 and 2.

Isolation of Lycopodine, Pipecolic Acid, and Piperidine-2-acetic Acid

The shoots of *L. tristachyum* were dried and ground to a fine powder in a blender. The powder was continuously extracted with methanol for 48 h. Solvent was changed after 24 h. The extract was concentrated to remove all methanol, dilute hydrochloric acid (5%, 200 ml) was added, the mixture stirred for 2 h, and filtered through celite. The filtrate was washed with ether (3 × 50 ml) and was then basified with dilute ammonia and extracted with chloroform (3 × 150 ml). Lycopodine was isolated from the chloroform extract, pipecolic and piperidine-2-acetic acid from the aqueous layer.

Lycopodine (6)

The chloroform extract was dried and evaporated, the residue extracted repeatedly with hexane, the extract was dried (anhydrous sodium sulfate) and evaporated. The residue was dissolved in benzene and applied to a short column of alumina. Lycopodine was eluted with benzene and was purified to constant activity by crystallization from hexane followed by sublimation at 110° and 5 × 10^{-3} mm.

Pipecolic Acid (8)

The basified filtrate from which lycopodine had been removed by chloroform extraction was concentrated on the steam bath after inactive DL-pipecolic acid (100 mg) had been added as carrier. The residue was redissolved in water, a little charcoal was added, the suspension filtered through cotton and the filtrate applied to a column (18 × 1.5 cm) of Dowex 50W-X4 (H^+ form). The column was eluted with water until the eluate no longer contained carbohydrates as detected by the Molisch test (α-naphthol – concentrated sulfuric acid). Amino acids were eluted from the washed column with 1 *M* ammonia (approximately 200 ml). Pipecolic acid, m.p. 280–281°, 15–20 mg, was isolated from the eluate by the nitrosation method described earlier (8).

*Phenylisothiocyanate Condensation Product of Pipecolic Acid (Perhydro-3-oxo-2-phenyl-1-thioimidazo[1,5-a]pyridine) (**14**)*

Pipecolic acid (20 mg) was dissolved in aqueous pyridine (50% v/v, 3 ml) and the p*H* of the mixture adjusted

TABLE 3. Incorporation of malonate into lycopodine

Products	[1-^{14}C]Malonic acid (Exp. 20)		[2-^{14}C]Malonic acid (Exp. 21)	
	SA[a]	RSA[b]	SA[a]	RSA[b]
Lycopodine	4.92 ±0.01[c]	100±0.2	10.40±0.01[c]	100 ±0.1
Acetic acid (C-15, -16)	2.29 ±0.01	47±0.2	2.62±0.01	25.1±0.1
Methylamine (C-16)	0.003±0.006	0±0.3	2.54±0.01	24.4±0.1

[a]Specific activity (d.p.m./mmol) × 10^{-5}.
[b]Relative specific activity: % (lycopodine = 100).
[c]Obtained from the original sample of lycopodine by dilution with inactive lycopodine, followed by crystallization to constant activity.

TABLE 4. Chirality of lysine serving as precursor of lycopodine and pipecolic acid

Experiment 23	$^3H/^{14}C$	% of product derived from D-lysine[a]
Precursor		
DL-[^{3}H]/D-[^{14}C]lysine	11.1±0.3	
Product		
Lycopodine	115±3[c]	4.8±0.2
Pipecolic acid	6.4±0.1	87±3

Experiment 24	$^3H/^{14}C$	% of product derived from L-lysine[b]
Precursor		
L-[^{3}H]/DL-[^{14}C]lysine	8.5±0.2	
Product		
Lycopodine	16.9±0.5[c]	100±4
Pipecolic acid	0.49±0.03	2.9±0.2

[a]See ref. 8. In an experiment with DL-[^{3}H]/D-[^{14}C]substrate, % of product derived from D-substrate = $50 \times \frac{^3H/^{14}C \text{ in substrate}}{^3H/^{14}C \text{ in product}}$.
[b]See ref. 8. In an experiment with L-[^{3}H]/DL-[^{14}C]substrate, % of product derived from L-substrate = $50 \times \frac{^3H/^{14}C \text{ in product}}{^3H/^{14}C \text{ in substrate}}$.
[c]These values for the $^3H/^{14}C$ ratio of lycopodine are the observed values (Table 2), corrected for loss of tritium from C-5 of lysine in the course of its incorporation into lycopodine. The correction factor is (10.7 ± 0.2)/(8.4 ± 0.1) (see Expts. 5 and 22, and footnote 6).

to p*H* 8.6 with sodium carbonate. Freshly distilled phenylisothiocyanate (4 drops) was added and the mixture heated 2 h at 40°. The mixture was acidified with dilute hydrochloric acid and extracted with chloroform (2 × 2 ml). The extract was concentrated, the oily residue dissolved in methanolic hydrochloric acid (1 *M*, 5 ml) and the solution heated 1 h at 80°. Solvent was evaporated and the title product (25–35 mg) crystallized from methanol; m.p. 162–163°; i.r. spectrum, 1740 cm^{-1} (C=O), 1210 cm^{-1}, no absorption above 3100 cm^{-1}; mass spectrum, molecular ion *m/e* 246 (base peak), M − 29, M − 33, M − 111.

Anal. Calcd. for $C_{13}H_{14}N_2OS$: C, 63.4; H, 5.7; N, 11.4. Found: C, 63.3; H, 5.9; N, 11.3.

Piperidine-2-acetic Acid

DL-Piperidine-2-acetic acid (50 mg) was added to the basified aqueous filtrate from the plant extract from which lycopodine had been removed by extraction with chloroform. The re-isolation procedure of piperidine-2-acetic acid was similar to that for the isolation of pipecolic acid. The mixture was concentrated, treated with charcoal, and applied to a column of Dowex 50W-X4 (H^+ form). The column was washed, amino acids eluted with 1 *M* ammonia, the eluate evaporated, the residue acidified with hydrochloric acid (6 *M*, 5 ml) and sodium nitrite (1 g) was added in small portions. After 1 h the solution was extracted with ether (4 × 15 ml), the extract dried (anhydrous sodium sulfate) and evaporated. The residue, containing nitroso derivatives of secondary amino acids, was heated 15 min with concentrated hydrochloric acid (2 ml). The solution was evaporated and the residue applied to a second column (10 × 1 cm) of Dowex 50W-X4 (H^+ form) which was washed with water. The product was eluted with 1 *M* ammonia, eluate being collected until no more radioactivity emerged from the column.

The ammoniacal eluate was evaporated, the residue dissolved in aqueous pyridine (50% v/v, 5 ml) and the p*H* adjusted to 8.6 with sodium carbonate. Freshly distilled

Can. J. Chem. Downloaded from www.nrcresearchpress.com by 210.87.254.6 on 09/05/12
For personal use only.

phenylisothiocyanate (5 drops) was added, the mixture was heated 2 h at 40°, acidified and extracted with chloroform (2 × 2 ml). The extract was dried and evaporated, the residual oil hydrolyzed by heating 1 h at 80° with hydrochloric acid (1 *M*) in aqueous methanol. The solvent was evaporated and the phenylisothiocyanate condensation product of piperidine-2-acetic acid (perhydro-3-oxo-2-phenyl-1-thiopyrido[1,2-*c*]-pyrimidine) (**15**) (7 mg), recrystallized from methanol; m.p. 195–196°; i.r. spectrum 1715 cm^{-1} (C=O), 1210 cm^{-1}, no absorption above 3100 cm^{-1}; mass spectrum: molecular ion *m/e* 260 (base peak), M − 29, M − 43, M − 125.

Mol. Wt. Calcd. for $C_{14}H_{16}N_2OS$: 260.098. Found (high resolution mass spectrum of molecular ion): 260.099.

Anal. Calcd. for $C_{14}H_{16}N_2OS$: C, 64.6; H, 6.2; N, 10.8; S, 12.3. Found: C, 64.6; H, 6.3; N, 10.8; S, 12.2.

Degradation of Lycopodine

Carbons-15 and -16 as Acetic Acid

The Kuhn–Roth oxidation of lycopodine was carried out essentially as described in an earlier paper (2) and the resulting acetic acid converted into acetyl-α-naphthylamide, m.p. 157–159°.

Carbon-16 as Methylamine

The Kuhn–Roth acetate was further degraded to methylamine by the Schmidt reaction, as described in an earlier publication (14). The methylamine so obtained has converted into the β-naphthoyl derivative, m.p. 111–112° (sealed capillary).

Determination of Radioactivity

Radioactivity was determined by liquid scintillation counting (Mark I Liquid Scintillation Computer, Nuclear Chicago Corp., Model 6860). Activity due to ^3H and ^{14}C was determined simultaneously, by external standardization counting with ^{133}Ba.

'Aquasol' (New England Nuclear Corp.) (10 ml) was used as the counting medium. Triplicate samples of each compound were counted under comparable conditions of quenching. Confidence limits shown in the results are standard deviations of the mean. For highly quenched samples the confidence limit of the quench correction curves were ±5%.

We thank Dr. A. I. Meyers, Louisiana State University of New Orleans, for a generous sample of DL-piperidine-2-acetic acid. This work was supported by a grant from the National Research Council of Canada.

1. R. N. GUPTA, M. CASTILLO, D. B. MACLEAN, I. D. SPENSER, and J. T. WROBEL. J. Am. Chem. Soc. **90**, 1360 (1968).
2. M. CASTILLO, R. N. GUPTA, D. B. MACLEAN, and I. D. SPENSER. Can. J. Chem. **48**, 1893 (1970).
3. M. CASTILLO, R. N. GUPTA, Y. K. HO, D. B. MACLEAN, and I. D. SPENSER. J. Am. Chem. Soc. **92**, 1074 (1970).
4. M. CASTILLO, R. N. GUPTA, Y. K. HO, D. B. MACLEAN, and I. D. SPENSER. Can. J. Chem. **48**, 2911 (1970).
5. Y. K. HO, R. N. GUPTA, D. B. MACLEAN, and I. D. SPENSER. Can. J. Chem. **49**, 3352 (1971).
6. J.-C. BRAEKMAN, R. N. GUPTA, D. B. MACLEAN, and I. D. SPENSER. Can. J. Chem. **50**, 2591 (1972).
7. R. N. GUPTA and I. D. SPENSER. Phytochemistry, **8**, 1937 (1969).
8. E. LEISTNER, R. N. GUPTA, and I. D. SPENSER. J. Am. Chem. Soc. **95**, 4040 (1973).
9. E. LEISTNER and I. D. SPENSER. J. Am. Chem. Soc. **95**, 4715 (1973).
10. F. LYNEN and M. TADA. Angew. Chem. **73**, 513 (1961).
11. K. WINTERFELD and K. FLICK. Arch. Pharm. **289**, 448 (1956); Chem. Abstr. **51**, 11346d (1957).
12. F. MOLL. Arch. Pharm. **301**, 230 (1968).
13. W. KOENIGS and G. HAPPE. Ber. **35**, 1343 (1902); **36**, 2904 (1903).
14. H. L. HOLLAND, M. CASTILLO, D. B. MACLEAN, and I. D. SPENSER. Can. J. Chem. **52**, 2818 (1974).

Can. J. Chem. Downloaded from www.nrcresearchpress.com by 210.87.254.6 on 09/05/12
For personal use only.

Infrared Studies of Water in Crystalline Hydrates: $K_2FeCl_5 \cdot H_2O$ (Erythrosiderite) and Related Aquopentachloroferrates(III)[1]

MICHAEL FALK AND CHUNG-HSI HUANG

Atlantic Regional Laboratory, National Research Council of Canada, Halifax, Nova Scotia B3H 3Z1

AND

OSVALD KNOP

Department of Chemistry, Dalhousie University, Halifax, Nova Scotia B3H 4J3

Received July 22, 1974

MICHAEL FALK, CHUNG-HSI HUANG, and OSVALD KNOP. Can. J. Chem. **53**, 51 (1975).

Infrared spectra of $M_2[FeCl_5(H_2O)]$ (M = K, Rb, NH_4) at different degrees of deuteration were recorded, between 4000 and 300 cm^{-1}, at 30 and −160 °C. The spectra of the three compounds were closely similar, as was that of natural $K_2[FeCl_5(H_2O)]$ (*erythrosiderite*). They indicate the existence of only one type of water molecule in the structure. The water molecules are symmetric, well separated from one another, and engage in O—H . . . Cl bonds with O . . . Cl distances of about 3.22 Å, as estimated from the OH and OD stretching frequencies. These conclusions support the structure proposed for $K_2[FeCl_5(H_2O)]$ by Bellanca and lead to approximate location of the H atoms. The observed mixing of the librational and translational modes, which occurs when the frequencies of translational modes are high, may be characteristic of H_2O molecules coordinated to cations of high charge.

MICHAEL FALK, CHUNG-HSI HUANG et OSVALD KNOP. Can. J. Chem. **53**, 51 (1975).

Les spectres infrarouge de $M_2[FeCl_5(H_2O)]$ (M = K, Rb, NH_4) ont été enregistrés, entre 4000 et 300 cm^{-1}, à 30 et −160 °C et à différents degrés de deutération. Ces spectres, comme celui du $K_2[FeCl_5(H_2O)]$ naturel (*érythrosidérite*), se ressemblent d'une manière frappante. Ils indiquent que la structure cristalline ne contient qu'un seul type de molécule d'eau. Les molécules d'eau sont symétriques, bien isolées les unes des autres, et forment des liaisons hydrogène O—H . . . Cl, dont la distance interatomique O . . . Cl, estimée à partir des valeurs des fréquences OH et OD, est proche de 3.22 Å. Ces résultats corroborent la structure proposée pour $K_2[FeCl_5(H_2O)]$ par Bellanca. Ils permettent aussi d'estimer les positions des atomes d'hydrogène. Les modes mixtes de libration et de translation, observés pour ces composés, et qui sont dus à de hautes fréquences des modes de translation, peuvent être charactéristiques de molécules d'eau coordonnées à des cations de charge élevée.

The spectroscopic properties of water molecules strongly coordinated to cations of high charge have received relatively little systematic attention. For example, not much reliable information exists on the effect of cationic size and charge on the strength and geometry of the hydrogen bonds formed by such H_2O molecules (1). To extend our knowledge of the behavior of H_2O in aquocomplexes of this type we have studied the i.r. spectra, between 4000 and 300 cm^{-1}, of polycrystalline $M_2FeCl_5.H_2O$ = $M_2[FeCl_5(H_2O)]$ (M = K,[2] Rb, NH_4) at different temperatures and degrees of deuteration. The low water content and the favorable crystallographic features make these compounds well suited for a detailed investigation. The region below 600 cm^{-1} in the spectra of all three compounds (undeuterated and fully deuterated) was previously investigated by Adams and Lock (2) in the i.r. and by Adams and Newton (3) in the Raman (below 400 cm^{-1}); the Raman spectrum of the NH_4 compound was reported also by Cotton and Gibson (4). However, the frequencies above 600 cm^{-1} do not appear to have been studied in any compounds of the general formula $M_2[XCl_5(H_2O)]$.

Experimental

Ruby-red crystals of $K_2FeCl_5.H_2O$ were obtained by slow evaporation of mixed aqueous solutions of $FeCl_3$ and KCl, acidified with HCl, at about 40 °C.

Anal. Calcd. for $K_2FeCl_5.H_2O$: Fe, 16.96; Cl, 53.83; H_2O, 5.47. Found: Fe, 16.94(5); Cl, 53.50(13); H_2O, 5.43(4).

Deuterated crystals were prepared in a similar manner using mixtures of H_2O and D_2O, or by recrystallization of

[1]NRCC No. 14310.

[2]$K_2FeCl_5.H_2O$ occurs in nature as the mineral *erythrosiderite*.

Can. J. Chem. Downloaded from www.nrcresearchpress.com by 210.87.254.105 on 09/05/12
For personal use only.

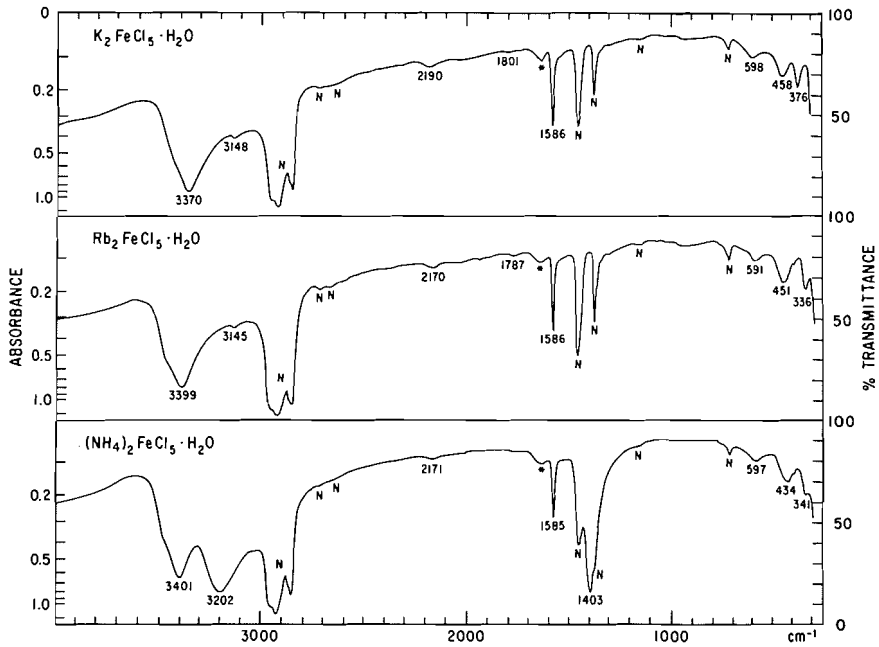

FIG. 1. Survey spectra of undeuterated $M_2FeCl_5.H_2O$ (M = K, Rb, NH_4) at room temperature (Nujol mulls, CsBr windows). *N* denotes Nujol bands, asterisks denote spurious bands.

the undeuterated material from such acidified isotopic mixtures. To obtain the highest degree of deuteration (about 95%), anhydrous $FeCl_3$ was dissolved in D_2O acidified with DCl, and the solution was allowed to crystallize in a stream of dry nitrogen in a dry-box. The Rb and NH_4 compounds were prepared in an analogous manner.

A specimen of natural *erythrosiderite* from the Vesuvius (R 1364, Washington A. Roebling Collection) was obtained from the U.S. National Museum, Washington, D.C.

Infrared spectra of polycrystalline samples were recorded between 4000 and 300 cm^{-1} at 30 and −160 °C on a Perkin–Elmer model 521 spectrophotometer purged with dry N_2. The use of automatic frequency marker and careful calibration made it possible to measure the frequencies of sharp peaks to within 0.5 cm^{-1}. Finely ground sample powders were mulled with Nujol or Fluorolube, and the mulls were mounted between KBr or CsBr plates. Deuterated samples were handled in a dry-box. KCl-pellet technique was also used, but it was found impossible to prevent small amounts of atmospheric moisture from being introduced into the pellets.

Results

The spectra of typical Nujol mulls of undeuterated $K_2FeCl_5.H_2O$ and its Rb and NH_4 analogs at room temperature are shown in Fig. 1 in a form suitable for identification purposes.[3] The frequencies of the major H_2O bands are listed in Table 1. The spectrum gradually sharpened upon cooling to liquid-nitrogen temperature; the frequencies quoted in the following will normally be those obtained from the low-temperature spectra. No evidence of a phase transition on cooling was observed.

A pellet of $K_2FeCl_5.H_2O$ in KCl and a pellet obtained by pressing $FeCl_3$ with a large excess of *nearly* anhydrous KCl (*cf.* ref. 6) produced essentially the same spectra as the mull. The spectrum of the erythrosiderite sample differed only by the presence of additional bands between 1250 and 850 cm^{-1} attributable to an admixture of sulfate.

The frequencies of the major H_2O, HDO, and D_2O bands of $K_2FeCl_5.H_2O$ are listed in Table 2. Figure 2 shows the spectrum in the region of the OH and OD stretching fundamentals at different D contents at liquid-nitrogen temperature. Although in the room-temperature spectrum the two H_2O stretching

[3]The survey spectrum of the undeuterated NH_4 compound at room temperature reproduced in the collection of spectra by Nyquist and Kagel (5) agrees well with ours, but their spectrum of the K compound is of very low quality.

Can. J. Chem. Downloaded from www.nrcresearchpress.com by 210.87.254.105 on 09/05/12
For personal use only.

TABLE 1. Frequencies (cm^{-1}) of the water molecule in $M_2FeCl_5.H_2O$ (M = K, Rb, NH_4)*

	Frequencies (cm^{-1})						
	Erythrosiderite (at 30 °C)	$K_2FeCl_5.H_2O$		$Rb_2FeCl_5.H_2O$		$(NH_4)_2FeCl_5.H_2O$	
		30 °C	−160 °C	30 °C	−160 °C	30 °C	−160 °C
H_2O: Stretch	3367†	3370†	3384 3356	3377†	3416 3375	3400†	3427 3393
2 × bend	3144	3148	3146	3145	3140	—	3121
Bend + libration	2187	2190	2187	2170	2176	2175	2163
Bend + translation	1802	1801	1800	1789	1794	—	—
Bend	1585	1586	1583	1585	1582	1585	1580
Libration {wag	598	598	600	591	593	599	591
Libration {rock	452	458	456	451	447	~440	427
Fe—OH_2 stretch	~375	376	395	336	357	341	359
HDO: OD stretch		2508	2498	2528	2520	2528	2524
Bend		1405	1402	1404	1401	‡	‡
D_2O: Stretch		2560 2477	2538 2468	2589 2492	2568 2487	2588 2491	2579 2490
Bend		1176	1173	1176	1172	1176	1171

*There was no detectable dependence of the frequencies on the D contents of the samples.
†Unresolved doublet.
‡Overlapped by NH_4 bending fundamental.

TABLE 2. Vibrational assignments for water in $K_2FeCl_5.H_2O$*

	Frequencies (cm^{-1})					
	HOH		HOD		DOD	
	30 °C	−160 °C	30 °C	−160 °C	30 °C	−160 °C
OH stretch {ν_3	3370†	3384	3380	3367		
OH stretch {ν_1		3356				
2 × bend	3148	3146	—	2788	2332	2331
OD stretch {ν_3			2508	2498	2560	2538
OD stretch {ν_1					2477	2468
Bend + libration	2190	2187	—	1924	—	1635
Bend + translation	1801	1800				
Bend	1586	1583	1405	1402	1176	1173
Libration {wag	598	600	—	532	—	469
Libration {rock	458	456	—	440	—	~338
Fe—OH_2 stretch	376	395	~369	~389	—	381

*There was no detectable dependence of the frequencies on the D contents of the samples.
†Unresolved doublet.

fundamentals, ν_1 and ν_3, were not resolved (Fig. 1), they were well resolved at liquid-nitrogen temperature. The frequency separation of ν_1 and ν_3, which is about 100 cm^{-1} for the H_2O molecule in the vapor and in inert solvents, tends to decrease when these frequencies shift downward as a consequence of H-bonding (7); its value in $K_2FeCl_5.H_2O$ and in the related hydrates (Table 1) appears to be the smallest on record. The corresponding fundamentals

Can. J. Chem. Downloaded from www.nrcresearchpress.com by 210.87.254.105 on 09/05/12
For personal use only.

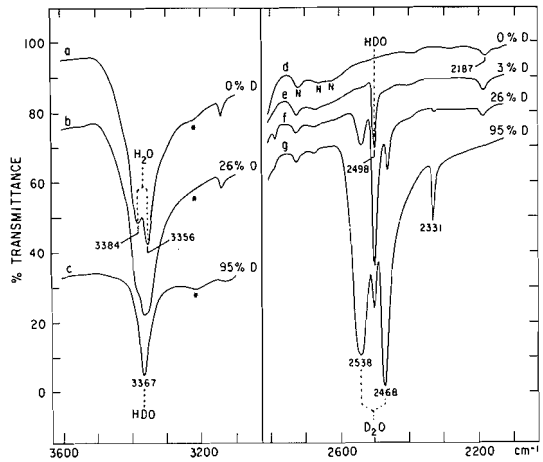

FIG. 2. Spectra of $K_2FeCl_5.H_2O$ at $-160\,°C$ (Nujol mulls, KBr windows): regions of OH and OD stretching fundamentals of water at different degrees of sample deuteration. The vertical scale refers to curves *b* and *f*; the other curves have been displaced for clarity.

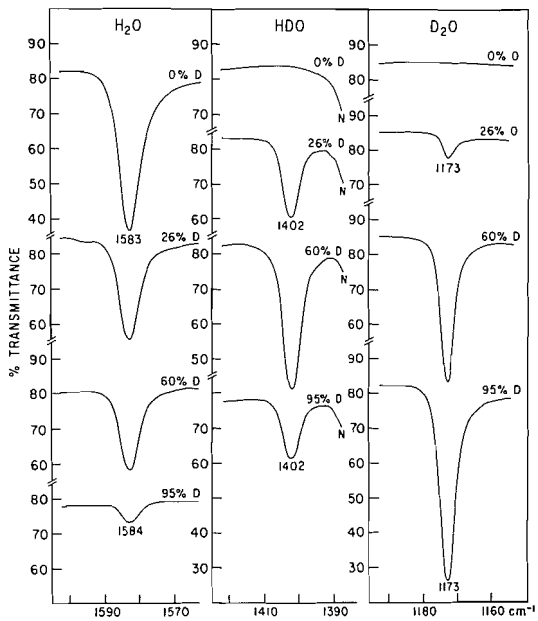

FIG. 3. Spectra of $K_2FeCl_5.H_2O$ at $-160\,°C$ (Nujol mulls, KBr windows): bending fundamentals of H_2O, HDO, and D_2O at different degrees of sample deuteration.

of D_2O were well resolved even at room temperature. This is because of the well-known narrower band width and greater ν_1–ν_3 separation for D_2O. In assigning these two fundamentals we have assumed that $\nu_3 > \nu_1$; this relation generally holds for the water molecule.

The vibrationally isolated OH stretching fundamental of isotopically dilute HDO gives rise to a singlet at 3367 cm^{-1}. The absence, at intermediate D contents, of distinct spectral features arising from pairs of water molecules of the same isotopic species indicates that such pairs vibrate at frequencies approaching those of the isotopically isolated molecules. Vibrational coupling of the stretching fundamentals of neighboring molecules is thus negligible.

The bending fundamentals of H_2O, HDO, and D_2O at liquid-nitrogen temperature were all singlets (Fig. 3). Their frequencies did not change with the D content of the sample, showing that vibrational coupling of the bending fundamentals is also negligible.

Three bands due to H_2O were observed in the region 650 to 300 cm^{-1} (Fig. 4). Their frequencies agree reasonably well with those reported by Adams and Lock (2), who assigned the band at *ca.* 600 cm^{-1} to the wagging libration, the band at *ca.* 456 cm^{-1} to the rocking vibration, and the band at *ca.* 395 cm^{-1} to a translation of the H_2O molecule in the direction of the Fe—OH_2 bond. In this assignment the frequencies of the two librations are reversed from the usual sequence rock > wag (*cf.* ref. 1); the i.r. *intensities* are usually larger for wagging than for rocking (1), and this also is reversed in the spectrum of $K_2FeCl_5.H_2O$. The correctness of the assignment of Adams and Lock is supported by the following consideration based on the present results. Under the site symmetry C_s the Fe—O stretching (A') may, in principle, mix with the wagging libration (A') but not with the rocking libration (A'') (Fig. 5). Values of the H_2O/D_2O frequency ratio of bands believed to correspond to purely librational (unmixed) motions fall in the range 1.35–1.41 (*cf.* for example ref. 8). The ratio for the 456 cm^{-1} band is 456/338 = 1.35, that for the 600 cm^{-1} band is 600/469 = 1.28. Hence the more intense lower-frequency band corresponds to an essentially pure libration and thus to rocking. The reversals may be characteristic of the spectra of water molecules strongly coordinated to one metal atom, as in the aquopentachloroferrates(III).

The twisting libration is expected to be of very low intensity in the i.r. spectrum (1). Bands corresponding to the other two transla-

Can. J. Chem. Downloaded from www.nrcresearchpress.com by 210.87.254.105 on 09/05/12
For personal use only.

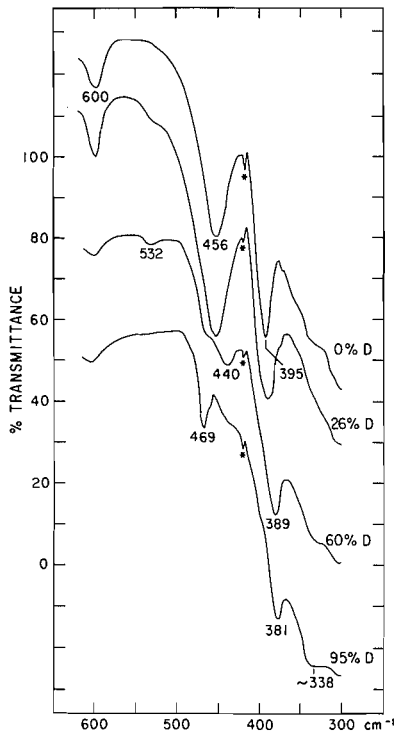

FIG. 4. Spectra of $K_2FeCl_5.H_2O$ at −160 °C (Nujol mulls, KBr windows): bands in the region of libration and translation of water molecules at different degrees of sample deuteration. The vertical scale refers to the curve for 26% D; the other curves have been displaced for clarity.

tions of the water molecule are to be looked for at frequencies lower than 300 cm^{-1}.

Our assignment of the 376 cm^{-1} H_2O band in the room-temperature i.r. spectrum to the Fe—OH_2 stretching is supported by the existence of a corresponding A_g band at 384 cm^{-1} in the Raman spectrum (3). Furthermore, a corresponding band is observed, at 387 cm^{-1}, in the i.r. spectrum of $Cs_2[RhCl_5(H_2O)]$, but it is absent in the spectrum of $Cs_3[RhCl_6].H_2O$ (footnotes 4 and 5 of ref. 9). If the Fe—OH_2 stretching mixed only with the wagging libration, an H_2O/D_2O frequency ratio greater than $(20/18)^{1/2} = 1.054$ (pure translation) could be expected for the stretching. However, the observed value is lower, 395/381 = 1.037.[4] This indicates further mixing of this mode, presumably with vibrations of lower frequencies involving the chlorine atoms.

[4]Low-temperature frequencies.

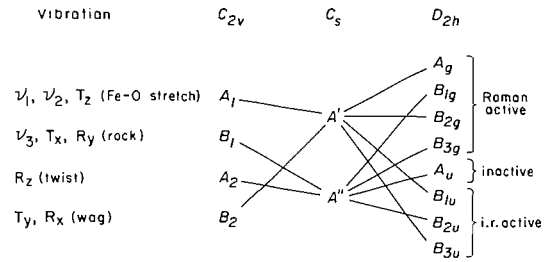

FIG. 5. Correlation of the symmetry species of the molecular group (C_{2v}; $C_2 = z'$, plane containing H_2O = $x'z'$ plane), the site group (C_s; mirror plane = $y'z'$ plane of H_2O || xz plane of the unit cell), and the factor group (D_{2h}). The coordinates x', y', z' are the conventional internal coordinates of the water molecule, while x, y, z are the unit-cell coordinates ($x' = y$, $y'z'$ || 010 (= xz plane); *cf.* Table 3).

No evidence of measurable vibrational coupling was detected for any of the observed fundamentals. For the three internal vibrations (ν_1, ν_2, ν_3) and for the wagging libration there was clear absence of frequency shifts with changing D content of the sample; the severe overlap of the H_2O, HDO, and D_2O absorptions between 500 and 300 cm^{-1} precluded observation of possible shifts for the rocking and the Fe—OH_2 stretching (translation). The doubling of the ν_1, ν_2, wagging and T_z fundamentals, required by the rules of factor-group splitting (Fig. 5), was not observed, and so the magnitude of the splitting must be very small. This can be taken to indicate that at least the ν_1, ν_2, ν_3, and the wagging vibration of each water molecule in this hydrate occur nearly independently of those of its neighbors.

The frequencies of the ammonium compound are very similar to those of the K compound (Table 1), and as the two compounds are isostructural (10), a separate analysis of the spectrum of H_2O in $(NH_4)_2FeCl_5.H_2O$ is not required. The frequencies (in cm^{-1}) of the NH_4 and NH_3D groups are as follows:

Vibration		Frequency (cm^{-1}) 30 °C	−160 °C
NH_4:	NH stretch	3202	3214, 3172
	NH_2 bend	1403	1402
NH_3D:	NH stretch	2352	2370, 2334
	NHD bend	1247	1254, 1243

No crystallographic information is available

Can. J. Chem. Downloaded from www.nrcresearchpress.com by 210.87.254.105 on 09/05/12
For personal use only.

TABLE 3. Positional parameters* and site symmetries of atoms in $K_2FeCl_5.H_2O$ (*Pnma*, No. 62; $Z = 4$) (11)

Atom	Equipoint	Site symmetry	x	y	z
Fe	4(*c*)	*m*	0.111	¼	0.302
K	8(*d*)	*1*	0.356	0.003	0.339
Cl(1)	4(*c*)	*m*	0.004	¼	0.030
Cl(2)	4(*c*)	*m*	0.251	¼	0.071
Cl(3)	4(*c*)	*m*	0.226	¼	0.561
Cl(4)	8(*d*)	*1*	0.111	0.003	0.302
O	4(*c*)	*m*	0.996	¼	0.490

*The unit-cell dimensions quoted by Bellanca (11) are $a = 13.75(2)$ Å, $b = 9.92(2)$ Å, $c = 6.93(2)$ Å. The compounds $(NH_4)_2FeCl_5.H_2O$, $K_2RuCl_5.H_2O$, $Cs_2TlCl_5.H_2O$, $M_2VCl_5.H_2O$ (M = K, Rb, NH_4), and $M_2InCl_5.H_2O$ (M = K, Rb, Cs, Tl, NH_4) have been reported to be isostructural with $K_2FeCl_5.H_2O$ (12–14).

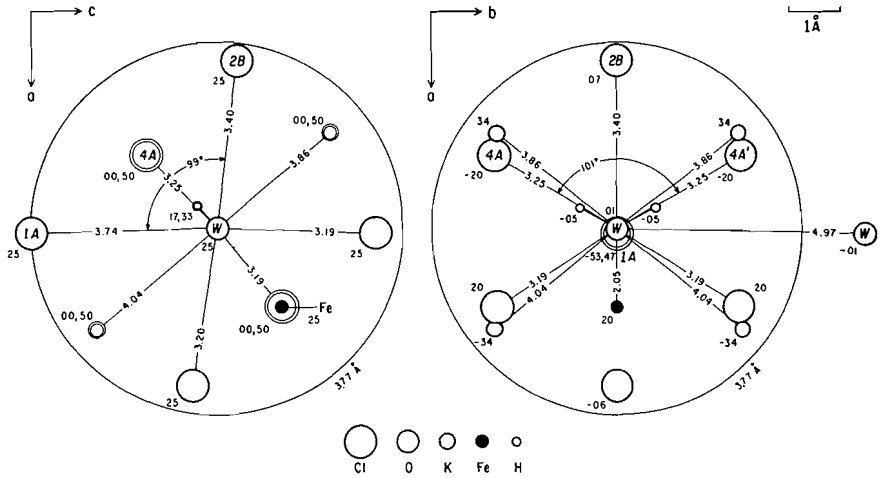

FIG. 6. Immediate environment of an oxygen atom (*W*) in $K_2FeCl_5.H_2O$ according to ref. 11. The fractional coordinates have been multiplied by 100; the interatomic distances are in Å. Double circles represent atoms related by a mirror plane || 010. *Left*, projection on 010; *right*, projection on 001. The hydrogen atoms are placed midway between positions *a* and *b* discussed in text.

for the Rb compound, but as its frequencies are closely similar to those of the ammonium compound (Table 1) and the effective radii of the NH_4^+ and Rb^+ ions are not very different, it is reasonable to assume that the Rb compound too is isostructural with $K_2FeCl_5.H_2O$.

Discussion

In the structure proposed for $K_2[FeCl_5(H_2O)]$ by Bellanca (11) (Table 3) the four oxygen atoms in the unit cell lie on mirror planes parallel to 010 and are all equivalent; the hydrogen atoms were not located. In view of the large separation of the neighboring oxygens, *ca.* 4.97 Å (Fig. 6), hydrogen bonding in this crystal can only be of the O—H. . .Cl type. Each oxygen atom has eight Cl neighbors at distances shorter than 3.77 Å, the upper limit postulated for effective O—H. . .Cl bonding (1). The reported Fe—O distance, 2.05 Å, agrees well with the average Fe^{3+}—OH_2 distance of 2.06 Å in crystalline hydrates (1).

Only two of the orientations of the water molecule that are possible in Bellanca's structure yield acceptable geometries (*cf.* ref. 1):

(*i*) The H_2O molecule is *in* the mirror plane, each H atom belongs to a different 4(*c*) equipoint, and both hydrogen bonds are normal (*i.e.* not bifurcated): $Cl(2)^B$. . .H—O—H′. . .$Cl(1)^A$, corresponding to an O. . .$Cl(2)^B$ distance of 3.40(4) Å, an O. . .$Cl(1)^A$ distance of 3.74(4) Å, and a Cl. . .O. . .Cl angle of *ca.* 99°.

(*ii*) The plane of the water molecule is at right angles to the mirror plane, both H atoms belong to the same equipoint 8(*d*), and only one possibility of hydrogen bonding exists:

Can. J. Chem. Downloaded from www.nrcresearchpress.com by 210.87.254.105 on 09/05/12
For personal use only.

Can. J. Chem. Downloaded from www.nrcresearchpress.com by 210.87.254.105 on 09/05/12
For personal use only.

$Cl(4)^4$. . .H—O—H′. . .$Cl(4)^{4'}$, corresponding to an O. . .Cl distance of 3.25(4) Å and a Cl. . .O. . .Cl angle of *ca.* 101°.

In (*i*) one of the hydrogen bonds is weak and the other very weak; probably only one of the two H atoms is engaged in hydrogen bonding. In (*ii*) the two hydrogen bonds are equivalent and relatively strong.

The essential correctness of Bellanca's structure is supported by evidence from the i.r. spectra to this extent: (*1*) The H_2O (and D_2O) fundamentals are single, hence there is only *one* type of water molecule in the unit cell. (*2*) Coupling of internal vibrations is negligible, hence the water molecules are "far apart" (*cf.* last paragraph of ref. 6).

The i.r. evidence leads further to new information about the water molecule: (*3*) The water molecule is symmetric, as only singlet HDO bands are observed. This eliminates (*i*) and establishes (*ii*) as the correct alternative. (*4*) The value of the stretching frequency (2508 cm^{-1} for isolated OD stretch at room temperature) corresponds to a hydrogen-bonded O. . .Cl distance of 3.22(4) Å (*cf.* the *R*–ν correlation of ref. 1). This is in good agreement with the value calculated from Bellanca's structure for case (*ii*), 3.25(4) Å.

The orientation of the water molecule may be expected to be the result of a compromise between (*a*) a tendency to minimize the H. . .Fe repulsions, which are minimum when the bisector of the HOH angle points along the Fe. . .O direction, and (*b*) a tendency to maximize the H. . .Cl attractions, which are maximum when the H atoms are in the Cl. . .O. . .Cl plane. Since the Fe atom is only about 0.18 Å from this plane, the orientations corresponding to the requirements (*a*) and (*b*) are not very different. Assuming that the internal geometry of the H_2O molecule in $K_2[FeCl_5(H_2O)]$ is the average geometry of H_2O in crystalline hydrates, with OH distances of 0.98 Å and an HOH angle of 108° (1), the approximate fractional coordinates (*cf.* Table 3) of the H atoms are calculated to be (0.036, 0.830, 0.457) for (*a*) and (0.034, 0.830, 0.452) for (*b*) (Fig. 6). The distance between these two positions is only 0.04 Å, which is comparable with the uncertainty in the positions of the Fe, Cl, and O atoms in Bellanca's structure.

The frequencies of the isolated OD stretch in the NH_4 and Rb analogs are about 20 cm^{-1} higher (Table 1), pointing to a small decrease in the H-bond strength with increasing size of the M^+ ion. Discussion of the variation of H-bond strength with *X* in compounds containing the aquo complex $[XCl_5(H_2O)]^{2-}$ is not possible at present, the above three $M_2[FeCl_5(H_2O)]$ compounds being the first of this type in which the H_2O vibrations have been studied in detail.

In hydrates studied so far mixing of librations and translations of the water molecule is rarely evident; translational frequencies lie generally well below 300 cm^{-1}, while librational frequencies usually are found above 450 cm^{-1} for H_2O and above 350 cm^{-1} for D_2O. Mixed modes can be expected when the higher translational modes attain frequencies comparable with the librational frequencies, as in the aquopentachloroferrates(III). This situation is probably characteristic of water molecules strongly coordinated to cations and may be expected of other hydrates in which H_2O is coordinated to cations of high charge.

We wish to thank Professor W. H. Baur for supplying us with a copy of his program CALPHO (Calculation of Hydrogen Positions in Crystal Structures), Dr. John S. White, Jr. for the sample of natural erythrosiderite, and Miss Gwen H. Thomas and Mr. P. F. Seto for assistance with the experimental work.

1. M. Falk and O. Knop. Water: a comprehensive treatise. Vol. 2. *Edited by* F. Franks. Plenum Press, New York. 1973. Chapt. 2.
2. D. M. Adams and P. J. Lock. J. Chem. Soc. A, 2801 (1971).
3. D. M. Adams and D. C. Newton. J. Chem. Soc. Dalton, 681 (1972).
4. S. A. Cotton and J. F. Gibson. J. Chem. Soc. A, 1693 (1971).
5. R. A. Nyquist and R. O. Kagel. Infrared spectra of inorganic compounds. Academic Press, New York. 1971.
6. G. H. Thomas, M. Falk, and O. Knop. Can. J. Chem. **52**, 1029 (1974).
7. J. Schiffer. Ph.D. Thesis. Princeton University, Princeton, N.J. 1963; Diss. Abstr. **25**, 2786 (1964).
8. M. Falk, C.-H. Huang, and O. Knop. Can. J. Chem. **52**, 2380 (1974).
9. C. K. Thomas and J. A. Stanko. J. Coord. Chem. **2**, 231 (1973).
10. I. Lindqvist. Ark. Kemi, **A24**, 1 (1946).
11. A. Bellanca. Period. Mineral. **17**, 59 (1948).
12. R. W. G. Wyckoff. Crystal structures. 2nd ed. Vol. 3. Wiley, New York. 1965.
13. A. W. Atkinson and B. O. Field. J. Inorg. Nucl. Chem. **32**, 2601 (1970).
14. L. P. Podmore and P. W. Smith. Aust. J. Chem. **25**, 2521 (1972).

Synthesis and Crystal and Molecular Structures of the *N,N*-Dimethylethanolaminogallane and *N,N*-Dimethylethanolaminogallium Dimethyl Dimers

STEVEN J. RETTIG, ALAN STORR, AND JAMES TROTTER

Department of Chemistry, University of British Columbia, Vancouver, British Columbia V6T 1W5

Received July 30, 1974

STEVEN J. RETTIG, ALAN STORR, and JAMES TROTTER. Can. J. Chem. **53**, 58 (1975).

Crystals of the *N,N*-dimethylethanolaminogallane dimer **1***a* are monoclinic, $a = 8.540(1)$, $b = 7.0433(7)$, $c = 12.227(6)$ Å, $\beta = 92.94(3)°$, $Z = 2$, space group $P2_1/c$ and crystals of the *N,N*-dimethylethanolaminogallium dimethyl dimer **1***b* are orthorhombic, $a = 15.608(3)$, $b = 11.655(2)$, $c = 10.266(2)$ Å, $Z = 4$, space group *Pccn*. Both structures were determined by Patterson and Fourier syntheses and were refined by full-matrix least-squares procedures to final *R* values of 0.039 and 0.053 for 1062 and 1155 reflections with $I \geq 3\sigma(I)$ respectively. Both structures feature well-separated centrosymmetric dimeric units occurring via the formation of four-membered Ga_2O_2 rings. The five-coordinate gallium atoms have distorted trigonal bipyramidal geometry. Steric interactions between methyl groups in **1***b* are believed responsible for the lengthening of the axial Ga—N distance from 2.279(3) in **1***a* to 2.471(4) Å in **1***b*. Other bond distances are: for **1***a*; Ga—O (axial), 2.053(3), Ga—O, 1.911(3), Ga—H, 1.50(7) and 1.73(5), O—C, 1.369(5), N—C, 1.466–1.485(6), C—C, 1.512(7), and mean C—H, 1.05; for **1***b*; Ga—O (axial), 2.078(3), Ga—O, 1.913(3), Ga—C, 1.936(6) and 1.948(7), O—C, 1.382(7), N—C, 1.452–1.482(7–8), C—C, 1.516(9), and mean C—H, 1.01 Å.

STEVEN J. RETTIG, ALAN STORR et JAMES TROTTER. Can. J. Chem. **53**, 58 (1975).

Les cristaux du dimère du *N,N*-diméthyléthanolaminogallane sont monocliniques, $a = 8.540(1)$, $b = 7.0433(7)$, $c = 12.227(6)$ Å, $\beta = 92.94(3)°$, $Z = 2$, groupe d'espace $P2_1/c$; les cristaux du dimère du *N,N*-diméthyléthanolamino diméthyl gallium sont orthorhombiques, $a = 15.608(3)$, $b = 11.655(2)$, $c = 10.266(2)$ Å, $Z = 4$, groupe d'espace *Pccn*. On détermine les deux structures par les synthèses de Patterson et de Fourier et on procède à un raffinement par la méthode de moindres carrés (matrice complète) pour 1062 et 1155 réflexions jusqu'à des facteurs d'accord *R* de 0.039 et 0.053 avec $I \geq 3\sigma(I)$. Les deux structures sont caractérisées par des unités dimériques centrosymétriques bien séparées qui proviennent de la formation de noyaux Ga_2O_2 à quatre membres. Les atomes de gallium de coordination cinq ont la géométrie d'une bipyramide trigonale déformée. On croit que les interactions stériques entre les groupes méthyles dans **1***b* sont la cause de l'allongement de la distance axiale Ga—N de 2.279(3) dans **1***a* à 2.471(4) Å dans **1***b*. On établit que les autres longueurs de liaisons sont: pour **1***a*; Ga—O (axial), 2.053(3); Ga—O, 1.911(3); Ga—H, 1.50(7) et 1.73(5); O—C, 1.369(5); N—C, 1.466–1.485(6); C—C, 1.512(7) et C—H moyen, 1.05; pour **1***b*; Ga—O(axial), 2.078(3); Ga—O, 1.913(3); Ga—C, 1.936(6) et 1.948(7); O—C, 1.382(7); N—C, 1.452–1.482(7–8); C—C, 1.516(9) et C—H moyen, 1.01 Å.

[Traduit par le journal]

Introduction

A previous report (1) characterized the *N*-methyldiethanolaminogallane dimer, $[MeN(CH_2CH_2O)_2GaH]_2$, as the first crystallographic example of a five-coordinate gallium complex, the gallium atoms having trigonal bipyramidal coordination, with an angle of 151.2° between the axial substituents. It was postulated at that time that similar derivatives employing the *N,N*-dimethylethanolamino, "$Me_2NCH_2CH_2O$", moiety as a ligand might also provide examples of five-coordinate gallium atoms in crystalline samples. The present report deals with the preparations and crystal structures of two such complexes, $[Me_2NCH_2CH_2OGaH_2]_2$ and $[Me_2NCH_2CH_2OGaMe_2]_2$. In both compounds the four-membered Ga_2O_2 ring encountered in the previous work (1) is again the central feature, and in addition coordination of the nitrogen atom is also involved to give the predicted five-coordinate gallium atoms in both structures **1**. Steric interactions in the dimethylgallium derivative (**1***b*) make the Ga—N link weaker than that in the corresponding gallane compound $[Me_2NCH_2CH_2OGaH_2]_2$ (**1***a*). The Ga—H bonds in the latter compound are significantly different and an interaction between one of the hydrogen atoms and the bridging oxygen atom is postulated.

Can. J. Chem. Downloaded from www.nrcresearchpress.com by 210.87.254.5 on 09/05/12
For personal use only.

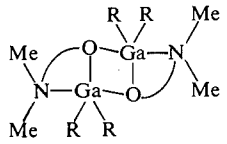

1

a: R = H
b; R = Me

Experimental

Starting Materials

N,N-Dimethylethanolamine was refluxed over anhydrous $CaSO_4$ and distilled prior to use. Trimethylaminegallane (2) and gallium trimethyl (3) were prepared as previously described. All materials were handled in a glove-box filled with dry nitrogen or on a standard high-vacuum line.

N,N-Dimethylethanolaminogallium Dimethyl Dimer, $[Me_2NCH_2CH_2OGaMe_2]_2$

This was prepared by reacting *N,N*-dimethylethanolamine (0.585 g, 5.91 mmol) with gallium trimethyl (0.679 g, 5.91 mmol) in refluxing benzene solvent. After removal of solvent the product was isolated as a moisture-sensitive white solid which was recrystallized from toluene to yield colorless crystals, m.p. 81 °C.

Anal. Calcd. for $[Me_2NCH_2CH_2OGaMe_2]_2$: Ga, 37.1; C, 38.3; H, 8.5; N, 7.5. Mol. wt. 376. Found: Ga, 37.0; C, 38.0; H, 8.6; N, 7.2. Mol. wt. 372.

N,N-Dimethylethanolaminogallane Dimer, $[Me_2NCH_2CH_2OGaH_2]_2$

Trimethylaminegallane (0.440 g, 3.34 mmol) was reacted with *N,N*-dimethylethanolamine (0.297 g, 3.34 mmol) in benzene solvent and the hydrogen evolved measured (75 ml, 3.35 mmol)

$$2Me_3NGaH_3 + 2Me_2NCH_2CH_2OH \rightarrow [Me_2NCH_2CH_2OGaH_2]_2 + 2H_2 + 2Me_3N$$

After removal of solvent the product remained as an air-sensitive white solid which was recrystallized from toluene to give colorless crystals.

Anal. Calcd. for $[Me_2NCH_2CH_2OGaH_2]_2$: Ga, 43.6; hydrol. H, 1.25. Mol. wt. 320. Found: Ga, 43.5; hydrol. H, 1.24. Mol. wt. 315.

Crystallographic Studies of the N,N-Dimethylethanolaminogallane Dimer (1a)

The crystal chosen for study was mounted with c^* parallel to the goniostat axis and had dimensions of *ca.* 0.31 × 0.30 × 0.30 mm. Unit-cell and space group data were obtained from film and diffractometer measurements. The unit-cell parameters were refined by a least-squares treatment of $\sin^2\theta$ values for 26 reflections measured on a diffractometer with CuK_α radiation. Crystal data are:

$C_8H_{24}Ga_2N_2O_2$ f.w. = 319.7

Monoclinic, $a = 8.540(1)$, $b = 7.0433(7)$, $c = 12.227(6)$ Å, $\beta = 92.94(3)°$, $V = 734.5(4)$ Å^3, $Z = 2$, $\rho_c = 1.446(1)$ g cm^{-3}, $F(000) = 328$ (20 °C, CuK_α, $\lambda = 1.5418$ Å, $\mu = 47$ cm^{-1}). Absent reflections: $0k0$, $k \neq 2n$ and $h0l$, $l \neq 2n$ define uniquely the space group $P2_1/c$ (C_{2h}^5, No. 14).

Intensities were measured on a Datex-automated General Electric XRD 6 diffractometer, with a scintillation counter, CuK_α (nickel filter and pulse height analyser), and a θ–2θ scan at 2° min^{-1} over a range of (1.80 + 0.86 tan θ) deg in 2θ, with 20 s background counts being measured at each end of the scan. Data were measured to $2\theta = 145°$ (minimum interplanar spacing 0.81 Å). A check reflection was monitored every 40 reflections throughout the data collection. The r.m.s. deviation of the intensity of the check reflection from its initial value was 2.0% and the final intensity was 1.03 times the initial intensity. Lorentz and polarization corrections were applied, and the structure amplitudes were derived. No absorption correction was made due to irregularities of the crystal surface. Of the 1454 independent reflections measured, 369 had intensities less than $3\sigma(I)$ above background where $\sigma^2(I) = S + B + (0.06S)^2$ with S = scan count and B = time averaged background count. These reflections were given zero weight in the refinement.

The position of the gallium atom was determined from the three-dimensional Patterson function. Two cycles of full-matrix least-squares refinement of the positional and isotropic thermal parameters of the gallium atom gave $R = 0.31$. A difference map at this point revealed the positions of the O, N, and C atoms. Two cycles of refinement with the gallium atom anisotropic and the O, N, and C atoms isotropic followed by two cycles with all non-hydrogen atoms anisotropic gave $R = 0.070$. The positions of all 12 hydrogen atoms were revealed by a difference map at this point. The hydrogen atoms were included in all subsequent refinement with isotropic thermal parameters. The refinement was concluded after four cycles with $R = 0.039$ for 1062 reflections with $I \geq 3\sigma(I)$ (23 planes with $|F_o - F_c| > 3\sigma(F)$ were given zero weight in the final stages of refinement).

The least-squares refinement was based on the minimization of $\Sigma w(F_o - F_c)^2$. The scattering factors of ref. 4 were used for the non-hydrogen atoms and those of ref. 5 for the hydrogen atoms. Anomalous scattering corrections (6) were applied for Ga, O, N, and C atoms. The anisotropic temperature factors employed in the refinement are U_{ij} in the expression

$$f = f^0 \exp[-2\pi^2(U_{11}h^2a^{*2} + U_{22}k^2b^{*2} + U_{33}l^2c^{*2} + 2U_{12}hka^*b^* + 2U_{13}hla^*c^* + 2U_{23}klb^*c^*)]$$

where f^0 is the tabulated scattering factor and f is that corrected for thermal motion. The weighting scheme: $w = 1/\sigma^2(F)$ where $\sigma^2(F)$ is derived from the previously defined $\sigma^2(I)$, gave constant average values of $w(F_o - F_c)^2$ over ranges of $|F_o|$ and was employed in the final stages of refinement. The mean error in an observation of unit weight was 1.04. In the final stages of refinement an extinction parameter was refined, the final value being 8.74×10^{-7}.

On the final cycle of refinement the mean parameter shift was 0.15σ, the largest shift being 1.3σ for the temperature factor of H(1B).

Can. J. Chem. Downloaded from www.nrcresearchpress.com by 210.87.254.5 on 09/05/12
For personal use only.

Can. J. Chem. Downloaded from www.nrcresearchpress.com by 210.87.254.5 on 09/05/12
For personal use only.

Crystallographic Studies of the N,N-Dimethylethanolaminogallium Dimethyl Dimer (1b)

Experimental details for **1b** are the same as for compound **1a** except where noted. Two crystals were used for the data collection. The first crystal was mounted with [011] parallel to the goniostat axis and had dimensions of *ca.* 0.3 × 0.5 × 0.6 mm. The second crystal was mounted with [032] parallel to the goniostat axis and had dimensions of *ca.* 0.4 × 0.4 × 0.7 mm. 20 reflections measured with CuK_α radiation were employed in the refinement of the unit-cell parameters. Crystal data are:

$C_{12}H_{32}Ga_2N_2O_2$ f.w. = 375.8

Orthorhombic, $a = 15.608(3)$, $b = 11.655(2)$, $c = 10.266(2)$ Å, $V = 1867.7(7)$ Å^3, $Z = 4$, $\rho_c = 1.337(1)$ g cm^{-3}, $F(000) = 784$ (20 °C, CuK_α, $\mu = 38$ cm^{-1}). Absent reflections: $0kl$, $l \neq 2n$, $h0l$, $l \neq 2n$, and $hk0$, $h + k \neq 2n$ define uniquely the space group $Pccn$ (D_{2h}^{10}, No. 56).

The r.m.s. deviations of the intensities of the check reflections from their mean values were 0.6% for crystal *1* and 2.2% for crystal *2*. The first 1009 intensities were measured with crystal *1* before it shattered inside the sealed glass capillary tube. The remaining data were collected with the second crystal. Of the 1852 independent reflections measured, 675 had intensities less than $3\sigma(I)$ above background.

The position of the gallium atom was determined from the three-dimensional Patterson function. Two cycles of isotropic refinement gave $R = 0.27$. The positions of the O, N, and C atoms were then taken from a difference map. Two cycles of refinement with the gallium atom anisotropic and the O, N, and C atoms isotropic followed by two cycles with all the non-hydrogen atoms anisotropic gave $R = 0.074$. A difference map at this point gave positions for 15 of the 16 hydrogen atoms, the remaining hydrogen atom was located on a subsequent difference map. The hydrogen atoms were included in the final cycles of refinement with isotropic thermal parameters. The refinement was concluded after six more cycles with $R = 0.053$ for 1155 reflections with $I \geq 3\sigma(I)$ (22 planes with $|F_o - F_c| > 3\sigma(F)$ were given zero weight in the final stages of refinement). The mean error in an observation of unit weight was 1.21 and the final value of the extinction parameter was 3.13×10^{-7}.

On the final cycle of refinement the mean parameter shift was 0.12σ, the largest shift being 0.87σ for the y coordinate of methyl hydrogen atom H (3A).

The final positional parameters for both **1a** and **1b** are given in Table 1 and the thermal parameters in Table 2. Measured and calculated structure factors have been placed in the Depository of Unpublished Data.[1]

The thermal motions of both **1a** and **1b** have been analyzed in terms of the rigid-body modes of translation and libration using the computer program MGTLS (7). The analysis of **1a** was unsuccessful while the thermal motion of the entire dimeric molecule of **1b** was adequately described by the derived rigid-body parameters (r.m.s. $\Delta U_{ij} = 0.0115$ Å^2, r.m.s. $\sigma U_{ij} = 0.0039$ Å^2). The appropriate bond distances for **1b** have been corrected for libration (8, 9) and appear along with the uncorrected distances in Table 3.

[1]The structure factor table is available, at a nominal charge, from the Depository of Unpublished Data, National Science Library, National Research Council of Canada, Ottawa, Canada K1A 0S2.

TABLE 1. Final positional parameters (fractional × 10^4, Ga × 10^5, H × 10^3) with estimated standard deviations in parentheses

Atom	x	y	z
	$[Me_2NCH_2CH_2OGaH_2]_2$		
Ga	67472(5)	52361(8)	46652(4)
O	4993(3)	3566(6)	4463(4)
N	7708(4)	2913(4)	3589(3)
C(1)	4975(7)	2047(8)	3764(5)
C(2)	6278(6)	2259(7)	2981(4)
C(3)	8471(8)	1393(9)	4238(5)
C(4)	8828(8)	3673(10)	2808(5)
H(1)	676(5)	676(8)	356(4)
H(2)	754(8)	543(9)	579(6)
H(1A)	396(7)	202(7)	326(4)
H(1B)	522(7)	137(10)	418(5)
H(2A)	665(5)	101(7)	241(3)
H(2B)	586(5)	368(7)	233(3)
H(3A)	979(5)	197(9)	471(4)
H(3B)	784(7)	95(10)	483(5)
H(3C)	943(8)	66(10)	397(5)
H(4A)	998(9)	381(10)	315(5)
H(4B)	914(7)	279(9)	240(5)
H(4C)	819(7)	475(7)	241(5)
	$[Me_2NCH_2CH_2OGaMe_2]_2$		
Ga	3077(4)	7594(5)	11960(5)
O	604(2)	−608(3)	270(3)
N	1538(2)	−35(4)	2413(3)
C(1)	1277(4)	−1326(5)	586(7)
C(2)	1953(4)	−678(6)	1349(6)
C(3)	1282(6)	−795(10)	3463(8)
C(4)	2161(5)	813(7)	2921(8)
C(5)	912(5)	2138(6)	593(8)
C(6)	−472(5)	652(8)	2672(7)
H(1A)	134(5)	−196(6)	41(7)
H(1B)	101(7)	−200(10)	141(10)
H(2A)	248(4)	−127(4)	172(5)
H(2B)	233(5)	11(6)	87(7)
H(3A)	178(7)	−107(9)	403(10)
H(3B)	113(3)	−13(4)	410(5)
H(3C)	89(5)	−132(6)	308(7)
H(4A)	236(7)	89(8)	220(10)
H(4B)	180(5)	140(6)	361(6)
H(4C)	271(5)	48(6)	332(7)
H(5A)	53(4)	261(7)	23(6)
H(5B)	154(4)	193(5)	24(6)
H(5C)	108(6)	247(8)	130(7)
H(6A)	−60(5)	−16(7)	294(7)
H(6B)	−104(4)	93(5)	246(6)
H(6C)	−37(5)	112(9)	356(10)

Results and Discussion

Two crystallographic examples of pentacoordinate gallium have been reported recently (1, 10). The present X-ray analyses provide

TABLE 2. Final thermal parameters and their estimated standard deviations

(*a*) Anisotropic thermal parameters ($U_{ij} \times 100$ Å^2)

Atom	U_{11}	U_{22}	U_{33}	U_{12}	U_{13}	U_{23}
			$[Me_2NCH_2CH_2OGaH_2]_2$			
Ga	6.04(3)	8.34(4)	7.54(4)	−1.72(2)	0.31(2)	−2.26(2)
O	5.9(2)	11.4(3)	12.3(3)	−3.7(2)	3.4(2)	−8.2(3)
N	7.2(2)	6.7(2)	6.9(2)	0.5(1)	0.4(1)	−0.1(1)
C(1)	8.6(3)	7.8(3)	8.7(3)	−2.3(3)	1.4(3)	−2.5(3)
C(2)	9.0(3)	8.1(3)	8.2(3)	−1.4(2)	0.8(2)	−1.8(2)
C(3)	12.4(5)	10.0(4)	11.4(4)	3.7(4)	1.7(4)	3.2(4)
C(4)	10.0(4)	10.0(4)	8.9(3)	−0.2(3)	2.7(3)	−0.2(3)
			$[Me_2NCH_2CH_2OGaMe_2]_2$			
Ga	7.74(4)	6.52(4)	6.33(6)	−0.27(3)	0.26(3)	−1.16(2)
O	9.1(2)	8.1(2)	7.8(2)	1.8(2)	−2.6(2)	−2.0(2)
N	7.4(2)	8.1(2)	6.3(2)	−0.2(2)	−0.3(2)	0.1(2)
C(1)	11.1(5)	7.7(4)	10.9(4)	2.1(3)	−3.7(4)	−2.1(4)
C(2)	9.2(4)	10.2(4)	10.2(4)	2.2(3)	−1.5(3)	−2.3(3)
C(3)	11.9(6)	15.8(8)	10.0(5)	−2.2(6)	−0.9(4)	5.8(6)
C(4)	9.6(5)	11.6(5)	10.3(4)	−1.1(4)	−1.7(4)	−2.4(4)
C(5)	10.3(5)	8.7(4)	11.8(5)	−0.1(4)	−1.2(4)	1.3(4)
C(6)	9.2(5)	13.4(6)	8.8(4)	−0.1(5)	1.7(3)	−0.8(4)

(*b*) Isotropic thermal parameters

$[Me_2NCH_2CH_2OGaH_2]_2$		$[MeNCH_2CH_2OGaMe_2]_2$	
Atom	B (Å^2)	Atom	B (Å^2)
H(1)	9(1)	H(1A)	11(2)
H(2)	11(2)	H(1B)	20(4)
H(1A)	9(1)	H(2A)	8(1)
H(1B)	12(2)	H(2B)	11(2)
H(2A)	7.0(9)	H(3A)	20(4)
H(2B)	8(1)	H(3B)	7(1)
H(3A)	9(1)	H(3C)	10(2)
H(3B)	9(1)	H(4A)	14(3)
H(3C)	10(2)	H(4B)	11(2)
H(4A)	11(2)	H(4C)	10(2)
H(4B)	10(2)	H(5A)	10(2)
H(4C)	8(1)	H(5B)	9(2)
		H(5C)	16(3)
		H(6A)	10(2)
		H(6B)	8(2)
		H(6C)	15(3)

additional crystallographic examples of this type of coordination and further information on Ga—H bond lengths. The crystallographic numbering schemes and 50% probability thermal ellipsoids for the two molecules are shown in Fig. 1. Figure 2 shows the structure of $[Me_2NCH_2CH_2OGaH_2]_2$ (**1***a*) viewed along *b* and Fig. 3 shows the structure of $[Me_2NCH_2CH_2OGaMe_2]_2$ (**1***b*) viewed along *c*. Bond lengths and angles are given in Tables 3 and 4 respectively. Table 5 gives the intraannular dihedral angles defining the conformations of the five-membered GaOCCN rings and selected inter- and intramolecular non-bonded contacts are listed in Table 6. Throughout the discussion the uncorrected bond lengths for **1***b* will be employed for direct comparison to **1***a* and atoms marked with an asterisk are related to those in Table 1 by the crystallographic center of symmetry.

The molecules exhibit the structures predicted on the basis of the previous study of the dimer, $[MeN(CH_2CH_2O)_2GaH]_2$ (1), and contain gallium atoms with distorted trigonal bipyramidal geometry. The monomer units (containing

Can. J. Chem. Downloaded from www.nrcresearchpress.com by 210.87.254.5 on 09/05/12
For personal use only.

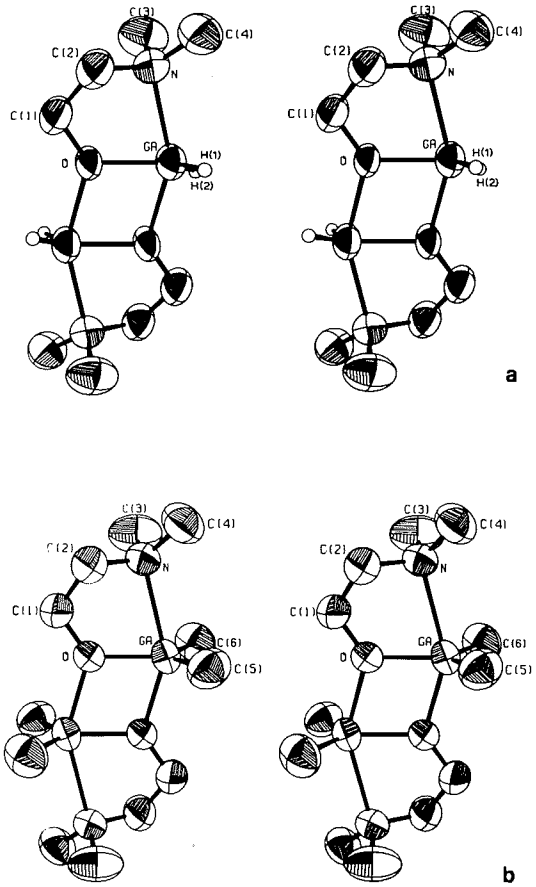

FIG. 1. Stereoscopic views of (*a*) $[Me_2NCH_2CH_2OGaH_2]_2$ (**1***a*) and (*b*) $[Me_2NCH_2CH_2OGaMe_2]_2$ (**1***b*) showing the atom numbering scheme and 50% probability thermal ellipsoids. Methylene and methyl hydrogen atoms have been omitted for clarity.

tetrahedrally coordinated gallium atoms) which might be predicted by comparison with similar boron compounds (11, 12), dimerize via the formation of four-membered Ga_2O_2 rings to form centrosymmetric molecules featuring a system of three fused rings. The $[MeN(CH_2CH_2O)_2GaH]_2$ dimers (1) have C_2 symmetry while the present molecules both have crystallographically imposed $\bar{1}$ (C_i) symmetry. The gallium coordination spheres have nitrogen atoms occupying axial positions and the oxygen atoms occupying an equatorial site on one gallium and an axial position on the second gallium atom. The two remaining equatorial positions are occupied by hydrogen atoms in **1***a* and by methyl groups in **1***b*.

The importance of steric interactions is emphasized by the Ga—N bond distances in the two compounds. In the gallium dimethyl derivative (**1***b*) there is steric interaction between the methyl groups [C(3) ... C(6), C(4) ... C(5)] and as a consequence the Ga—N link is rather long at 2.471(4) Å. In contrast the gallane derivative (**1***a*) experiences much less severe steric interactions and the Ga—N bond length is reduced considerably to 2.279(3) Å, nearer the corresponding mean axial Ga—N distance of 2.193 Å in $[MeN(CH_2CH_2O)_2GaH]_2$.

The rather long and consequently weak Ga—N bond in $[Me_2NCH_2CH_2OGaMe_2]_2$ (**1***b*) may explain the chemical evidence which led to the original prediction of a four-coordinate gallium structure for the dimer, involving the four-membered Ga_2O_2 ring, but lacking any involvement of nitrogen atoms in the gallium coordination sphere. Thus Coates and Hayter (13), on the basis of the formation of a dimethiodide from the reaction of methyl iodide with $[Me_2NCH_2CH_2OGaMe_2]_2$, concluded that the nitrogen atoms were not utilized in the dimer bonding scheme. On the present structural evidence it seems probable that in solution the methyl iodide reagent may quite well break the weak Ga—N link and produce a dimethiodide thus indicating the presence of tercovalent nitrogen atoms in the dimer units.

The equatorial Ga—O bond lengths in **1***a* and **1***b*, 1.911(3) and 1.913(3) Å respectively, are equal within experimental error, while the axial Ga—O bond lengths, 2.053(3) in **1***a* and 2.078(3) Å in **1***b*, are significantly different. These distances also differ from those in $[MeN(CH_2CH_2O)_2GaH]_2$ where the bridging equatorial and axial Ga—O distances are 1.960(8) and 2.018(2) and the "free" equatorial Ga—O distance is 1.847(2) Å. The mean Ga—O distances for tetrahedrally and octahedrally coordinated gallium atoms are both 1.96 Å (14–16). On the basis of hybridization effects alone the equatorial bonds would be expected to be shorter and axial bonds longer than this value which is indeed the case in each of the three five-coordinate structures. In compound **1***a* the two equatorial Ga—H distances are 1.50(7) and 1.73(5) Å while the equatorial Ga—H distance in $[MeN(CH_2CH_2O)_2GaH]_2$ is 1.41(7) Å. There appears to be an interaction of H(2) with O*, the distance O* ... H(2) (2.28(7) Å) being shorter than a normal van der

Can. J. Chem. Downloaded from www.nrcresearchpress.com by 210.87.254.5 on 09/05/12
For personal use only.

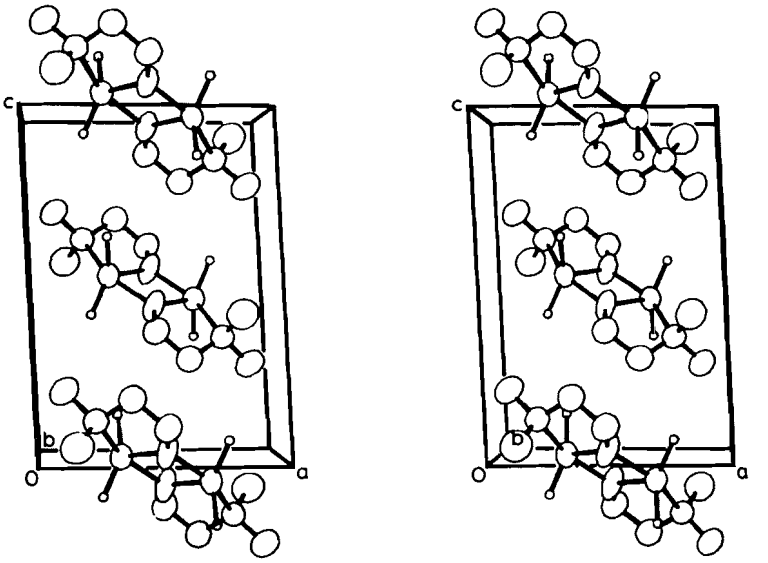

FIG. 2. The structure of $[Me_2NCH_2CH_2OGaH_2]_2$ (1*a*) viewed along *b*.

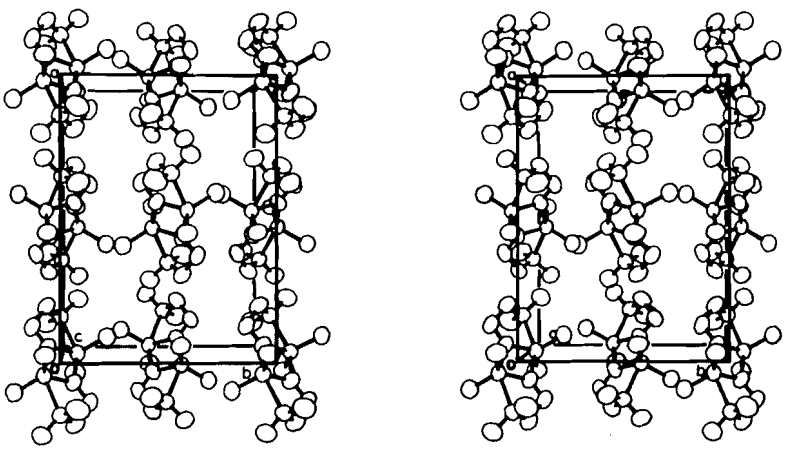

FIG. 3. The structure of $[Me_2NCH_2CH_2OGaMe_2]_2$ (1*b*) viewed along *c*.

Waals contact. The three remaining O ... H contact distances in the gallium coordination sphere range from 2.92–2.96 Å (see Table 6).

The distortion of the trigonal bipyramids occurs as a deformation of the angles between the axial substituents from the ideal value of 180° to 152.4(1) in **1***a* and 150.0(1)° in **1***b*. These values are similar to that of 151.2(4)° for the corresponding angle in $[MeN(CH_2CH_2O)_2GaH]_2$. This deformation appears to result directly from the steric constraints associated with the formation of the four-membered Ga_2O_2 rings in all three compounds. Unlike $[MeN(CH_2CH_2O)_2GaH]_2$, these compounds both have slightly nonplanar equatorial groups. The dihedral angles between normals to the mean planes of the equatorial groups and the planes of the Ga_2O_2 rings are 100.4 in **1***a* and 87.9° in **1***b*. Angular distortions occur in the gallium coordination spheres as a result of steric forces. In both compounds the angles within the equatorial groups as well as the axial–Ga–equatorial angles show some considerable deviations from their "ideal" values (see Table 4).

Can. J. Chem. Downloaded from www.nrcresearchpress.com by 210.87.254.5 on 09/05/12
For personal use only.

TABLE 3. Bond lengths (Å) with estimated standard deviations in parentheses

$[Me_2NCH_2CH_2OGaH_2]_2$		$[Me_2NCH_2CH_2OGaMe_2]_2$		
			Distance	
Bond	Distance (uncorrected)	Bond	Uncorrected	Corrected
Ga—O	1.911(3)	Ga—O	1.913(3)	1.925
Ga—O*	2.053(3)	Ga—O*	2.078(3)	2.083
Ga—N	2.279(3)	Ga—N	2.471(4)	2.479
Ga—H(1)	1.73(5)	Ga—C(5)	1.963(6)	1.971
Ga—H(2)	1.50(7)	Ga—C(6)	1.948(7)	1.951
O—C(1)	1.369(5)	O—C(1)	1.382(7)	1.384
N—C(2)	1.471(5)	N—C(2)	1.475(7)	1.482
N—C(3)	1.466(6)	N—C(3)	1.452(8)	1.454
N—C(4)	1.485(6)	N—C(4)	1.482(7)	1.484
C(1)—C(2)	1.512(7)	C(1)—C(2)	1.516(9)	1.519
Mean C—H	1.05	Mean C—H	1.01	
Range	0.72–1.32(4–7)	Range	0.76–1.23(5–11)	

TABLE 4. Bond angles (degrees) with estimated standard deviations in parentheses

$[Me_2NCH_2CH_2OGaH_2]_2$		$[Me_2NCH_2CH_2OGaMe_2]_2$	
Bonds	Angle	Bonds	Angle
O—Ga—O*	74.7(1)	O—Ga—O*	74.6(1)
O—Ga—N	77.7(1)	O—Ga—N	75.6(1)
O—Ga—H(1)	109(1)	O—Ga—C(5)	114.2(3)
O—Ga—H(2)	119(3)	O—Ga—C(6)	118.9(3)
O*—Ga—N	152.4(1)	O*—Ga—N	150.0(1)
O*—Ga—H(1)	101(2)	O*—Ga—C(5)	99.8(3)
O*—Ga—H(2)	78(3)	O*—Ga—C(6)	97.5(3)
N—Ga—H(1)	89(2)	N—Ga—C(5)	95.4(3)
N—Ga—H(2)	116(3)	N—Ga—C(6)	93.9(3)
H(1)—Ga—H(2)	129(3)	C(5)—Ga—C(6)	126.7(4)
Ga—O—Ga*	105.3(1)	Ga—O—Ga*	105.4(1)
Ga—O—C(1)	123.0(3)	Ga—O—C(1)	124.8(3)
Ga*—O—C(1)	131.3(3)	Ga*—O—C(1)	129.8(3)
Ga—N—C(2)	101.7(2)	Ga—N—C(2)	99.1(3)
Ga—N—C(3)	112.0(3)	Ga—N—C(3)	113.0(4)
Ga—N—C(4)	112.0(3)	Ga—N—C(4)	115.9(4)
C(2)—N—C(3)	112.3(4)	C(2)—N—C(3)	111.1(6)
C(2)—N—C(4)	109.5(4)	C(2)—N—C(4)	108.2(5)
C(3)—N—C(4)	109.2(5)	C(3)—N—C(4)	109.1(6)
O—C(1)—C(2)	109.5(4)	O—C(1)—C(2)	110.5(5)
N—C(1)—C(2)	109.2(5)	N—C(1)—C(2)	109.2(5)
Mean R—C—H	109.4	Mean R—C—H	109.8
Range	95–122(2–5)	Range	90–128(2–7)
Mean H—C—H	107.5	Mean H—C—H	106.5
Range	68–127(3–6)	Range	65–139(5–9)

The four-membered Ga_2O_2 rings are centrosymmetric (and planar) with Ga—O distances of 1.911(3) and 2.053(3) in **1***a* and 1.913(3) and 2.078(3) Å in **1***b*. The angles at Ga and O are 74.7(1) and 105.3(1) in **1***a* and 74.6(1) and 105.4(1) in **1***b*. These values can be compared to Ga—O distances of 1.960(8) and 2.018(2) Å and angles of 76.0(3) at Ga and 100.0(2)° at O in the nonplanar ring with C_2 symmetry in $[MeN(CH_2CH_2O)_2GaH]_2$ showing a smaller difference be-

Can. J. Chem. Downloaded from www.nrcresearchpress.com by 210.87.254.5 on 09/05/12
For personal use only.

TABLE 5. Intra-annular dihedral angles (deg)

	$[Me_2NCH_2CH_2OGaH_2]_2$		$[Me_2NCH_2CH_2OGaMe_2]_2$	
Bond	Observed	Calculated	Observed	Calculated
Ga—O	7.2(3)	7.0	1.7(3)	1.3
O—C(1)	16.4(5)	20.0	23.9(5)	25.0
C(1)—C(2)	−42.8(5)	−39.2	−48.8(5)	−41.6
C(2)—N	44.4(3)	43.4	44.3(4)	42.3
N—Ga	−28.6(2)	−31.2	−26.1(3)	−27.1

TABLE 6.

(*a*) Selected intramolecular contacts

$[Me_2NCH_2CH_2OGaH_2]_2$		$[Me_2NCH_2CH_2OGaMe_2]_2$	
Atoms	Distance	Atoms	Distance
C(1) ... C(3)	3.047(10)	N ... H(1B)	2.65(11)
N ... H(1B)	2.53(6)	C(2) ... H(4A)	2.12(10)
C(2) ... H(4C)	2.52(5)	C(2) ... H(3C)	2.55(7)
C(2) ... H(4B)	2.61(6)	C(2) ... H(4C)	2.70(8)
C(2) ... H(3B)	2.72(6)	C(1) ... H(3C)	2.63(7)
C(3) ... H(4B)	2.55(5)	C(1) ... C(3)	3.018(12)
C(3) ... H(4A)	2.55(7)	C(4) ... H(1A)	2.77(5)
C(3) ... H(2A)	2.67(4)	C(4) ... H(1B)	2.27(7)
C(3) ... H(1B)	2.78(6)	C(4) ... H(3A)	2.55(10)
C(4) ... H(2B)	2.58(4)	C(4) ... H(3B)	2.29(5)
C(4) ... H(3C)	2.59(6)	H(1A) ... H(2A)	2.37(9)
C(4) ... H(2A)	2.67(5)	H(1B) ... H(4A)	1.63(11)
C(4) ... H(3A)	2.70(5)	H(2B) ... H(3C)	1.90(11)
H(1) ... H(4C)	2.38(7)	H(4B) ... H(3B)	2.12(8)
H(1A) ... H(2B)	2.34(7)		
H(1B) ... H(3B)	2.35(9)		
H(3A) ... H(4A)	2.32(8)		

(*b*) Selected intermolecular contacts[a]

$[Me_2NCH_2CH_2OGaH_2]_2$		$[Me_2NCH_2CH_2OGaMe_2]_2$	
Atoms	Distance	Atoms	Distance
C(1) ... H(2B)[1]	2.79(5)	H(2B) ... H(6C)[4]	2.40(15)
H(1) ... H(1A)[2]	2.28(7)	C(6) ... H(2B)[5]	3.01(11)
H(2) ... H(2A)[3]	2.39(8)	C(5) ... H(4B)[6]	3.00(7)

(*c*) Gallium coordination spheres

$[Me_2NCH_2CH_2OGaH_2]_2$		$[Me_2NCH_2CH_2OGaMe_2]_2$	
Atoms	Distance	Atoms	Distance
Ga ... Ga*	3.1524(9)	Ga ... Ga*	3.176(1)
O ... O*	2.408(6)	O ... O*	2.423(6)
O ... N	2.644(4)	O ... N	2.723(5)
O ... H(1)	2.96(5)	O ... C(5)	3.255(8)
O ... H(2)	2.95(6)	O ... C(6)	3.326(8)
O* ... H(1)	2.92(4)	O* ... C(5)	3.092(8)
O* ... H(2)	2.28(7)	O* ... C(6)	3.027(8)
N ... H(1)	2.83(5)	N ... C(5)	3.300(9)
N ... H(2)	3.23(7)	N ... C(6)	3.250(9)
H(1) ... H(2)	2.92(8)	C(5) ... C(6)	3.496(10)

[a]Superscripts refer to atoms at positions: (*1*), $1-x, y-\frac{1}{2}, \frac{1}{2}-z$; (*2*), $1-x, \frac{1}{2}+y, \frac{1}{2}-z$; (*3*), $x, \frac{1}{2}-y, \frac{1}{2}+z$; (*4*), $-x, y-\frac{1}{2}, \frac{1}{2}-z$; (*5*), $-x, \frac{1}{2}+y, \frac{1}{2}-z$; (*6*), $x, \frac{1}{2}-y, z-\frac{1}{2}$.

Can. J. Chem. Downloaded from www.nrcresearchpress.com by 210.87.254.5 on 09/05/12
For personal use only.

Can. J. Chem. Downloaded from www.nrcresearchpress.com by 210.87.254.5 on 09/05/12
For personal use only.

tween axial and equatorial Ga—O distances than in the present structures. The octahedral complex $[Ga_2(OH)_2Cl_2(C_{14}H_{17}N_3)_2]Cl_2 \cdot H_2O$ (15) also exhibits a planar centrosymmetric Ga_2O_2 ring with Ga—O distances of 1.908 and 2.017 Å.

The dihedral angles in the five-membered GaOCCN chelate rings are compared with those obtained from energy minimization calculations (17) in Table 5. The ring conformations in **1***a* and **1***b* are different, that in **1***a* having a conformation closest to that calculated for $\omega_1 = 20°$ and **1***b* nearest to that calculated for $\omega_1 = 25°$. These conformations are similar to that of the "free" (not containing the bridging oxygen atom) chelate rings in $[MeN(CH_2CH_2O)_2GaH]_2$ rather than the corresponding rings containing the bridging oxygen atoms. The mean angles in the five-membered rings of 104.2 for **1***a* and 103.8 for **1***b* compare well with the calculated value of 104.2 (17), values of 104.8 and 103.8 for the "bridging" and "free" rings in $[MeN(CH_2CH_2O)_2GaH]_2$, and values of 104.8 and 104.9° in the BOCCN rings in related compounds $Ph_2BOCH_2CH_2NH_2$ (11) and $(p\text{-}FC_6H_4)_2BOCH_2CH_2NH_2$ (12). The C—O, C—C, and C—N distances in the chelate rings (Table 3), which are sensitive to conformational and electronic differences, are slightly, but not significantly, different in the two compounds. The corresponding C—O, C—C, and C—N distances in related structures are: 1.427(3), 1.507(6), and 1.477(2) in the "bridging" and 1.412(3), 1.534(1), and 1.468(4) Å in the "free" rings of $[MeN(CH_2CH_2O)_2GaH]_2$, and the mean values for the two boron compounds (11, 12) are 1.416(3), 1.500(6), and 1.488(3) Å. The N—C(methyl) distances are as expected. The mean valence angles at the quaternary nitrogen atoms are 109.5 in **1***a* and 109.4 in **1***b* with the smallest angles occurring in the five-membered rings. The geometry involving the hydrogen atoms is as expected.

Both crystal structures (see Figs. 2 and 3) consist of discrete dimeric units separated by normal van der Waals distances, the shortest of which are listed in Table 6. Nonbonded contacts in the gallium coordination spheres and other intramolecular contacts which correspond to steric interactions are also given in Table 6.

The low frequency infrared spectra of the two compounds again display a number of absorptions attributable to "Ga—O", "Ga—N", and ring modes. Compound **1***a* has three bands in this region (530 s, 508 vs, and 420 s) and in addition displays the characteristic Ga—H stretch (at 1830 vs) and Ga—H deformation (at 750 s) modes. Compound **1***b* exhibits three absorption bands in positions close to those in **1***a* (525 s, 507 vs, and 425 s) and in addition a characteristic Ga—C stretch (at 570 s).

Extension of this work on five-coordinate gallium complexes to include other aminoalcohols and related chelating ligands is in progress.

We thank the National Research Council of Canada for financial support and the University of British Columbia Computing Centre for assistance.

1. S. J. Rettig, A. Storr, and J. Trotter. Can. J. Chem. **52**, 2206 (1974).
2. N. N. Greenwood, A. Storr, and M. G. H. Wallbridge. Inorg. Chem. **2**, 1036 (1963).
3. A. Storr and B. S. Thomas. Can. J. Chem. **48**, 3667 (1970).
4. D. T. Cromer and J. B. Mann. Acta Cryst. A**24**, 321 (1968).
5. R. F. Stewart, E. R. Davidson, and W. T. Simpson. J. Chem. Phys. **42**, 3175 (1965).
6. D. T. Cromer and D. Liberman. J. Chem. Phys. **53**, 1891 (1970).
7. V. Schomaker and K. N. Trueblood. Acta Cryst. B**24**, 63 (1968).
8. D. W. J. Cruickshank. Acta Cryst. **9**, 747, 754 (1956).
9. D. W. J. Cruickshank. Acta Cryst. **14**, 896 (1961).
10. K. Dymock and G. J. Palenik. Chem. Commun. 884 (1973).
11. S. J. Rettig and J. Trotter. Can. J. Chem. **51**, 1288 (1973).
12. S. J. Rettig and J. Trotter. Acta Cryst. B**30**, 2139 (1974).
13. G. E. Coates and R. G. Hayter. J. Chem. Soc. 2519 (1953).
14. G. S. Smith and J. L. Hoard. J. Am. Chem. Soc. **81**, 3907 (1959).
15. K. Dymock, G. J. Palenik, and A. J. Carty. Chem. Commun. 1218 (1972).
16. C. H. L. Kennard. Inorg. Chim. Acta, **1**, 347 (1967).
17. J. B. Hendrickson. J. Am. Chem. Soc. **83**, 4537 (1961); **85**, 4059 (1963).

The Synthesis and Pyrolytic Rearrangement of Phthalate Esters of Some Tertiary Silanols. An Attempt to Prepare a Silicon Carbon Double Bond Species

K. G. RUTHERFORD[1] AND R. J. SEIDEWAND[2]

Department of Chemistry, University of Windsor, Windsor, Ontario N9B 3P4

Received November 26, 1973[3]

K. C. RUTHERFORD and R. J. SEIDEWAND. Can. J. Chem. **53**, 67 (1975).

The synthesis and pyrolysis of the methyl phthalate esters of diphenylmethylsilyl, *t*-butylsilyl, benzyldiphenylsilyl, and optically active 2-octanol yielded corresponding silyl ethers and phthalic anhydride. In the case of the latter compound, almost complete retention of configuration was observed about the asymmetric carbon atom. A mechanism is proposed for this rearrangement.

K. G. RUTHERFORD et R. J. SEIDEWAND. Can. J. Chem. **53**, 67 (1975).

La synthèse et la pyrolyse des phtalates de méthyle et de diphénylméthylsilyle, de *t*-butylsilyle, de benzyldiphénylsilyle et de l'octyl-2 optiquement actif conduit aux éthers silylés et à l'anhydridre phtalique. Dans le cas du dernier ester, on a observé une rétention pratiquement complète de la figuration autour du carbone asymétrique. On propose un mécanisme pour ce réarrangement. [Traduit par le journal]

Introduction

Over the past several years, our laboratory has been engaged in an exhaustive study on the pyrolysis of tertiary hydrogen phthalate esters which at abnormally low temperatures (below 150°) decompose to afford near quantitative yields of olefins and phthalic acid (1). Mechanistic studies have shown that the decomposition of such esters occurs through a reversibly formed ion pair with *ortho*-carboxylate hydrogen participation, followed by a kinetically controlled elimination of phthalic acid and olefin (2, 3). A natural extrapolation would be to study the pyrolysis of tertiary silyl hydrogen phthalates which presumably might lead to a stable Si=C system especially if these derivatives decomposed at low temperatures and contained within the compounds resonance and/or steric stabilization.

There is a scarcity of such derivatives in the literature. Gilman and co-workers (4) recorded an unsuccessful attempt at the preparation of a silyl hydrogen phthalate upon reacting triphenylsilanol with phthalic anhydride. A patent reference (5) reports the chloroplatinic acid catalyzed preparation of silyl derivatives of dicarboxylic acids, including phthalic acid, although the report indicates that a mixture of silyl hydrogen phthalate and disilyl ester was produced. We were not successful in obtaining pure monosilyl derivatives from the reaction of potassium phthalate with several tertiary silyl chlorides. The disilyl esters were the predominating products. It is interesting to report that an attempt to prepare the monosilver hydrogen phthalate salt using an obvious exchange reaction of the corresponding monopotassium salt and silver nitrate gave only the disilver salt in quantitative yield. Although silver salts of acids are generally water insoluble, it appears that this salt has sufficient solubility to allow further selective reaction with silver nitrate under more homogeneous conditions. In any event, a preparation of silver hydrogen phthalate does not appear in the literature.

The reaction of phthalic acid with tertiary silyl chlorides (pyridine catalysis) under homogeneous conditions, again lead to mixtures. The procedure of Sommer and co-workers (ref. 6 and references cited therein) which involves the treatment of an organosilicon hydride with an organic acid in the presence of 10% palladium on carbon to yield esters did not prove fruitful with phthalic acid and diphenylmethylsilane. Here again, mixtures were obtained.

---

[1]To whom all correspondence should be addressed.

[2]Present address: Dwight P. Joyce Research Center, Gildden-Durkee Div. SCM Corp., Strongsville, Ohio 44136.

[3]Revision received September 30, 1974.

Can. J. Chem. Downloaded from www.nrcresearchpress.com by 210.87.254.5 on 09/05/12
For personal use only.

Can. J. Chem. Downloaded from www.nrcresearchpress.com by 210.87.254.5 on 09/05/12
For personal use only.

It was decided to prepare *t*-silyl methyl phthalate esters for pyrolytic studies to circumvent the problems previously encountered with the preparation of the monosilyl derivatives. Thus methyldiphenylsilyl, trimethylsilyl, and benzyldiphenylsilyl methyl phthalates (**1**, **2**, and **4**) were prepared in excellent yields from anhydrous potassium methyl phthalate with the appropriate silyl chloride (Scheme 1).

Thermal decomposition of **1** was effected only very slowly at 250° to give phthalic anhydride (**5**) and diphenylmethylmethoxysilane (**6**) as the major products. A more rapid decomposition was realized at 400°. The silyl ester (**2**) decomposed in a similar manner over the temperature range 400–470° to give **5** and methoxytrimethylsilane (**7**). Decomposition of **4** at 400° yielded **5** and benzyldiphenylmethoxysilane (**8**). No silicoolefin nor products which could be construed as arising from such an intermediate were observed.

Isolation of silyl ethers (**6**, **7**, and **8**) from the pyrolysis of **1**, **2**, and **4** contrasts with the pyrolysis of methyl alkyl phthalates which give the appropriate alkene, methanol, and **5** (7). The reaction is postulated to initially involve the formation of alkenes and methyl hydrogen phthalate, followed by decomposition of this acid ester to methanol and **5** (8).

In order to provide some idea of the stereochemical aspects of our results, optically active trimethylsilyl-2-octyl phthalate (**10**) was prepared and subjected to pyrolysis. The synthesis of **10**, the pyrolysis, and proof of retention of configuration about the asymmetric carbon atom is shown in Scheme 2.

It is proposed then that the reaction proceeds in a concerted manner as indicated in Scheme 3 with essentially complete retention of configuration about the asymmetric carbon atom.

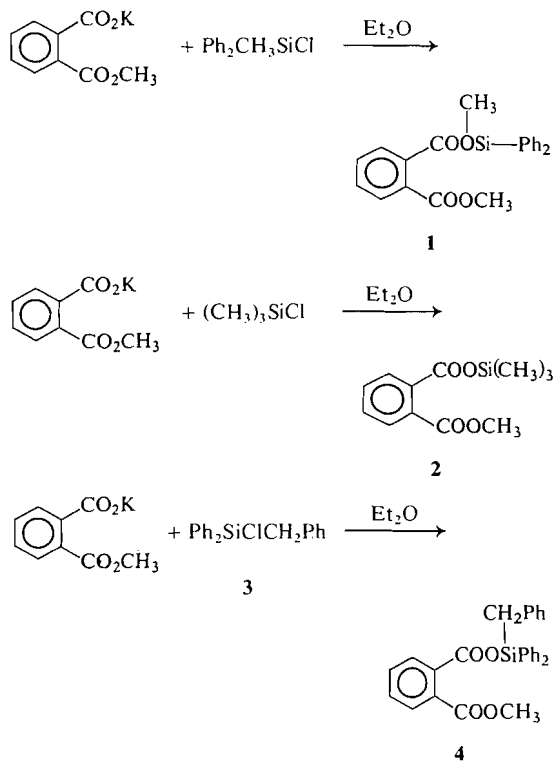

SCHEME 1. Synthesis of diphenylmethylsilyl, trimethylsilyl, and diphenylbenzylsilyl methyl phthalates (**1**, **2**, and **4**).

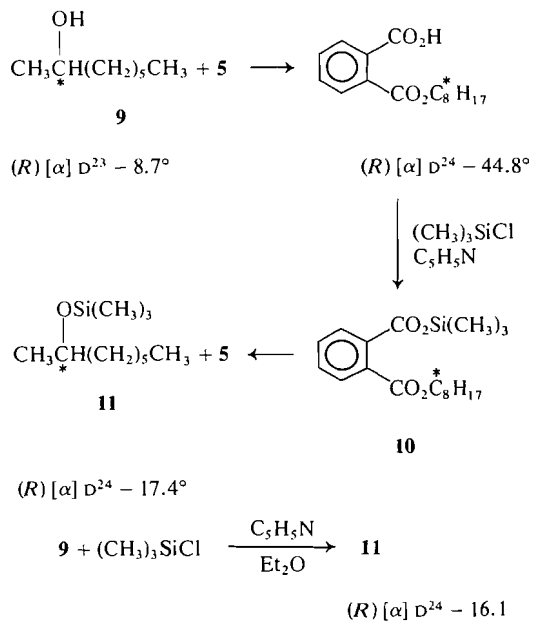

SCHEME 2. Synthesis and pyrolysis of optically active trimethylsilyl-2-octyl phthalate (**10**) and synthesis of optically active trimethylsilyl-2-octanol (**11**)

Experimental

Melting points were determined on a Fisher–Johns apparatus and are uncorrected. Infrared spectra were recorded on Beckman IR-10 and IR-12 spectrometers in chloroform or deuterochloroform solutions unless otherwise noted. Nuclear magnetic resonance spectra were obtained with a Jeolco C-60 HL spectrometer in deuterochloroform with methylene chloride as an internal standard (τ 4.70) unless otherwise specified. Optical rotation measurements were determined with a Rudolph Model 80 polarimeter equipped with a sodium lamp (λ 589 nm) using 2 dm polarimeter tubes. Gas chromatography (g.c.) was performed on Hewlett Packard 720 and 5750 instruments. Columns utilized were as follows: 6 ft × 1/4 in. 10% SE 30 on 60–80 Chromosorb W, 8 ft × 1/4 in. 20% SE 30 on 60–80 Chromosorb W, 8 ft × 3/8 in.

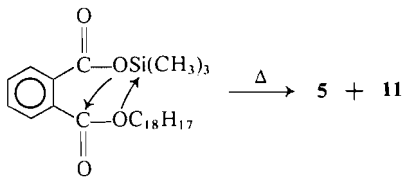

10

SCHEME 3. Postulated thermal decomposition pathway for *t*-silyl alkyl phthalates.

10% SE 30 on 60–80 Chromosorb W, and 6 ft × 1/4 in. 10% Dexsil 300 on 60–80 Chromosorb W. All nonaqueous reactions were run in dried apparatus under an atmosphere of nitrogen and the silyl chlorides utilized were distilled prior to use. All ethereal solvents were purified by distillation from lithium aluminum hydride and pyridine was distilled from calcium hydride. Anhydrous sodium sulfate was used for all drying operations unless otherwise noted. Microanalyses were performed by Schwarzkopf Microanalytical Laboratory, Woodside, N.Y. and A. B. Gygli Microanalyses Laboratory, Toronto, Ontario.

*Methyldiphenylsilyl Methyl Phthalate (**1**)*

To 1.09 g (5 mmol) of potassium methyl phthalate in 50 ml of ether was added 0.83 g (4 mmol) of diphenylmethylsilyl chloride. The resultant heterogeneous mixture was vigorously stirred for 4 h at room temperature and then allowed to stand for an additional 4 h. The mixture was filtered through Super Cel under an atmosphere of nitrogen and concentrated overnight at 35° (1 mm) to give 1.2 g (82%) of **1** as a pale yellow viscous liquid: i.r. 5.78, 5.85, and 8.93 μ (PhSi); n.m.r. 2.4 (m, 14), 6.34 (s, 3, OCH_3), and 8.98 (s, 3, CH_3Si).

Anal. Calcd. for $C_{22}H_{20}O_4Si$: C, 70.18; H, 5.35; Si, 7.46. Found: C, 70.13; H, 5.41; Si, 7.45.

*Trimethylsilyl Methyl Phthalate (**2**)*

To 3.27 g (15 mmol) of potassium methyl phthalate in 80 ml of ether was added 1.53 g (12 mmol) of chlorotrimethylsilane and the mixture was vigorously stirred for 4 h. The mixture was filtered through Super Cel under an atmosphere of nitrogen and concentrated overnight at 40° (0.5 mm) to give 2.4 g (80%) of **2** as a yellow liquid: i.r. 5.78, 5.85, and 11.7 μ (CH_3Si); n.m.r. 2.4 (m, 4), 6.1 (s, 3, OCH_3), and 9.61 (s, 9, CH_3Si).

Anal. Calcd. for $C_{12}H_{16}O_4Si$: C, 57.11; H, 6.39; Si, 11.13. Found: C, 57.48; H, 6.55, Si, 11.21.

*Benzyldiphenylchlorosilane (**3**)*

Benzylmagnesium chloride (200 mmol) in 150 ml of ether and chlorodiphenylsilane (53.2 g, 210 mmol) in 125 ml of ether were stirred for 15 min at 0° and then refluxed for 2 h. Upon cooling, the solution was filtered through Super Cel under a nitrogen atmosphere with the aid of another 150 ml of ether and the filtrate was concentrated *in vacuo*. Methylene chloride (50 ml) was added and the solution was refiltered and concentrated to a pale yellow liquid. Short-path distillation gave 40.9 g (66%) of the chlorosilane: b.p. 147–150° (0.003 mm); m.p. 52–57°; n_D^{25} 1.6085; i.r. 7.0, 8.97, and 19.0 μ (SiCl); n.m.r. 2.7 (m, 15) and 7.2 (s, 2).

Anal. Calcd. for $C_{19}H_{17}SiCl$: C, 73.87; H, 5.54; Cl, 11.47. Found: C, 73.76; H, 5.58; Cl, 11.38.

*Benzyldiphenylsilyl Methyl Phthalate (**4**)*

To 1.09 g (5 mmol) of potassium methyl phthalate in 50 ml of ether was added 1.23 g (4 mmol) of **3** in 1 ml of ether and the mixture was stirred for 4 h and then allowed to stand without stirring for 4 h. The mixture was filtered through Super Cel under an atmosphere of nitrogen and concentrated overnight at 45° (0.3 mm) to give 1.4 g (78%) of **4** as a pale yellow viscous liquid: i.r. 5.78, 5.84, and 8.90 μ (PhSi); n.m.r. 2.6 (m, 19), 6.38 (s, 3, OCH_3), and 6.85 (s, 2, CH_2Ph).

Anal. Calcd. for $C_{28}H_{24}O_4Si$: C, 74.30; H, 5.34; Si, 6.20. Found: C, 74.48; H, 5.45; Si, 5.90.

*(R)-(−)-Trimethylsilyl-2-octyl Phthalate (**10**)*

(*R*)-(−)-2-octanol (**9**), $[\alpha]_D^{23}$ − 8.7° was reacted with **5** according to the procedure of Kenyon (9) to give 26 g (74%) of (*R*)-(−)-2-octyl hydrogen phthalate; m.p. 69–70°; $[\alpha]_D^{24}$ − 44.8° (C 3.4, abs. ethanol) [lit. (7) m.p. 75°; $[\alpha]_D^{24}$ − 48.4°]. The trimethylsilyl derivative **10** was prepared from the potassium salt according to the procedure described for **1** to obtain **10** (72%) as a colorless liquid, i.r. 5.83 and 11.7 μ; n.m.r. ($CDCl_3$–*p*-dioxane), 8.7 (m, 16), and 9.6 (m, 9, CH_3Si).

Anal. Calcd. for $C_{19}H_{30}O_4Si$: C, 65.10; H, 8.62. Found: C, 65.24; H, 8.50.

*(R)-(−)-2-Octyltrimethylsiloxane (**11**)*

This was prepared in 64% yield by the method of Fertig *et al.* (10) using ether as a solvent: b.p. 99.0–99.5° (30 mm); n_D^{20} 1.4124; $[\alpha]_D^{24}$ − 16.1°.

*Diphenylmethylmethoxysilane (**6**)*

Diphenylmethylchlorosilane (**3**) was converted by the procedure of Sommer *et al.* (11) into **6** (53%): b.p. 87–90° (0.075 mm); n_D^{25} 1.5531 [lit. (11) n_D^{25} 1.5510].

*Trimethylmethoxysilane (**7**)*

Chlorotrimethylsilane was converted by the method of Sauer (12) into 7 (18%): b.p. 57.5°; n_D^{20} 1.3675 (lit. (12) b.p. 57°, n_D^{20} 1.3678).

*Benzyldiphenylmethoxysilane (**8**)*

Benzyldiphenylchlorosilane (**3**) (5.17 g) was converted by the method of Sauer (12) into **8** (3.9 g, 76%): b.p. 142–144° (0.005 mm); n_D^{25} 1.5923; i.r. 3.52, 7.0, 8.93, and 9.17 μ; n.m.r. 2.7 (m, 15), 6.42 (s, 3), and 7.24 (s, 2).

Anal. Calcd. for $C_{20}H_{20}OSi$: C, 78.89; H, 6.62, Si, 9.22. Found: C, 78.55; H, 6.78; Si, 8.90.

General Pyrolysis Procedure

The thermal rearrangements were effected by a calibrated variac controlled heating mantle or by the use of a bunsen flame (the results were not altered by this method). The sample was placed in a dried single-necked flask which was attached to a cooled flask for trapping of volatile products. All pyrolyses were conducted under an atmosphere of nitrogen. After the pyrolysis assembly cooled, pentane was added and the insoluble phthalic anhydride was filtered, washed with pentane, dried, and identified by comparison of its infrared spectrum and its melting point with authentic material. The combined pentane fractions were concentrated to yield oils. The components which constituted the oils were identified by i.r., n.m.r., and g.c. (retention time) comparison with authentic material and the relative amounts were calculated by n.m.r. integration.

Can. J. Chem. Downloaded from www.nrcresearchpress.com by 210.87.254.5 on 09/05/12
For personal use only.

Pyrolysis of Diphenylmethylsilyl Methyl Phthalate (1)

Pyrolysis of 1.1 g of **1** with a bunsen flame for 15 min and then for 3 min (0.5 mm) to remove volatile material from the reaction flask gave **5** (0.4 g, 88%) and a yellow oil (0.64 g) which contained four components as indicated by i.r. and n.m.r. inspection. The components were identified as diphenylmethylmethoxysilane (**6**, 85%), sym-tetraphenyldimethyldisiloxane (7%), m.p. 45–46° (lit. (13), m.p. 50°), methyl hydrogen phthalate, and undecomposed **1** (6%). Pyrolysis of **1** at 250° indicated *ca.* 90% decomposition at the end of 6 h.

Pyrolysis of Trimethylsilyl Methyl Phthalate (2)

Pyrolysis of 2.3 g of **2** at 400° and then at 470° (0.5 h) gave **5** (0.75 g, 48%) and methoxytrimethylsilane (**7**) (0.37 g, 38%). The remaining material (0.87 g) from concentration of the pentane layer, was shown by i.r. and n.m.r. inspection to consist of methyl hydrogen phthalate along with small amounts of trimethylsilanol, hexamethyldisiloxane, undecomposed **2** as well as **5**.

Pyrolysis of Benzyldiphenylsilyl Methyl Phthalate (4)

Pyrolysis of 0.96 g of **4** at 400° (1 h) and then with a Bunsen flame for 3 min (0.5 mm) gave **5** (0.28 g, 90%) and a yellow oil (0.24 g) which was identified as **8** along with trace amounts of starting material.

Pyrolysis of (R)-(−)-Trimethylsilyl-2-Octyl Phthalate (10)

Pyrolysis of 5.5 g of **10** at 400° (1.5 h) and then at 470° (0.5 h) gave **5** (2.2 g, 93%) and a colorless volatile liquid (2.6 g) which contained five components by g.c. analysis. The products were separated by preparative g.c. and were identified by spectral comparison and retention time with authentic samples. The first two components were identified as trimethylsilanol (1%) and hexamethyldisiloxane (2%). The third peak (4%) consisted of at least three components tentatively identified as a mixture of octenes by g.c. and spectral comparison with an authentic sample of 1-octene. The fourth component (10%) was identified as 2-octanol (**9**): $[\alpha]_D^{24} - 8.8°$ (C, 1.7, abs. ethanol). The last component (83%) was identified as the (*R*)-(−)-2-octyltrimethylsilyl ether **11**: $[\alpha]_D^{24} - 17.4°$ (C, 3.4, isooctane).

The authors wish to thank Dr. A. G. Brook of the University of Toronto, Toronto, Ontario and Dr. M. Rabin of Wayne State University, Detroit, Michigan, U.S.A. for many helpful discussions during the course of this work. Financial support by the National Research Council of Canada and by the Petroleum Research Fund (Grant No. 1575-A4) administered by the American Chemical Society is gratefully acknowledged.

1. K. G. Rutherford, J. M. Prokipcak, and D. P. C. Fung. J. Org. Chem. **28**, 582 (1963); K. G. Rutherford and D. P. C. Fung. Can. J. Chem. **42**, 2657 (1964).
2. K. G. Rutherford and R. M. Ottenbrite. J. Org. Chem. **45**, 679 (1967).
3. R. M. Ottenbrite, J. M. Brockington, and K. G. Rutherford. J. Org. Chem. **38**, 1186 (1973); S. Wassenar. Ph.D. Thesis, University of Windsor, Windsor, Ontario. 1968; H.H. Holton. Ph.D. Thesis, University of Windsor, Windsor, Ontario, 1971; J. F. Brien. Ph.D. Thesis, University of Windsor, Windsor, Ontario. 1971.
4. H. Gilman and R. Smart. J. Org. Chem. **16**, 424 (1951).
5. Midland Silicones Ltd. British Patent 842, 674 (1960); Chem. Abstr. **55**, 1066 (1961).
6. L. H. Sommer and J. E. Lyons. J. Am. Chem. Soc. **91**, 7061 (1969).
7. W. Nagel and R. H. Abelsdorff. Wiss, Veroff. Siemens-Konz, **5**, 193 (1926); Chem. Abstr. **21**, 1642 (1927).
8. G. P. Shulman, J. H. Bennett, and D. G. Botteron. J. Org. Chem. **27**, 3923 (1962).
9. J. Kenyon. Organic synthesis. Collect. Vol. I. Wiley, New York, N.Y. 1941. p. 418.
10. J. Fertig, W. Gerrard, and H. Herbst. J. Chem. Soc. 1488 (1957).
11. L. H. Sommer, C. L. Frye, G. A. Parker, and K. W. Michal. J. Am. Chem. Soc. **86**, 3271 (1964).
12. R. O. Sauer. J. Am. Chem. Soc. **66**, 1707 (1944).
13. W. H. Daudt and J. F. Hyde. J. Am. Chem. Soc. **74**, 386 (1952).

Can. J. Chem. Downloaded from www.nrcresearchpress.com by 210.87.254.5 on 09/05/12
For personal use only.

The Far Infrared Spectra and X-Ray Powder Diffraction Patterns of the Structure I Hydrates of Cyclopropane and Ethylene Oxide at 100 °K

JOHN E. BERTIE, FRANCES E. BATES, AND DAVID K. HENDRICKSEN
Department of Chemistry, University of Alberta, Edmonton, Alberta T6G 2E1

Received August 19, 1974

JOHN E. BERTIE, FRANCES E. BATES, and DAVID K. HENDRICKSEN. Can. J. Chem. **53**, 71 (1975).

This paper presents the far-infrared spectrum and X-ray powder diffraction pattern of the structure I hydrate of cyclopropane at 100 °K, and the powder diffraction pattern of the isostructural ethylene oxide hydrate at 100 °K. Between 360 and 100 cm^{-1} the absorption by cyclopropane hydrate is essentially identical to that by ethylene oxide hydrate, but is shifted to low frequency by about 2%. This shift is undoubtedly related to the hydrogen bonds being slightly longer in cyclopropane hydrate, whose cubic lattice parameter is 11.98 ± 0.02 Å compared to 11.89 ± 0.02 Å for ethylene oxide hydrate, both at 110 ± 20 °K. The absorption by cyclopropane hydrate below 100 cm^{-1} decreases rapidly with decreasing frequency; this confirms that the absorption plateau observed for ethylene oxide hydrate between 100 and about 50 cm^{-1} is due to primarily rotational vibrations of ethylene oxide. A recent statement, that the orientational disorder of the water molecules need not be invoked to explain the far infrared spectrum of ice 1h, is disputed.

JOHN E. BERTIE, FRANCES E. BATES et DAVID K. HENDRICKSEN. Can. J. Chem. **53**, 71 (1975).

Dans cette publication, on présente les spectres infrarouges lointains et les patrons de diffraction au rayon-X des poudres de l'hydrate de structure I du cyclopropane à 100 °K et les patrons de diffraction des poudres, aussi à 100 °K, de l'hydrate d'oxyde d'éthylène qui lui est isostructural. Entre 360 et 100 cm^{-1}, l'absorption de l'hydrate de cyclopropane est pratiquement identique à celle de l'hydrate d'oxyde d'éthylène mais le spectre est déplacé vers les basses fréquences par environ 2%. Ce déplacement est sans doute relié au fait que les ponts hydrogène sont légèrement plus longs dans l'hydrate de cyclopropane dont les paramètres de mailles cubiques sont de 11.98 ± 0.02 Å comparé à 11.89 ± 0.02 Å pour l'hydrate d'oxyde d'éthylène; les deux à 110 ± 20 °K. L'absorption de l'hydrate de cyclopropane en bas de 100 cm^{-1} diminue rapidement à mesure que la fréquence diminue; ceci confirme que le plateau d'absorption observé dans le cas de l'hydrate de l'oxyde d'éthylène entre 100 et environ 50 cm^{-1} est principalement dû à des vibrations rotationnelles de l'oxyde d'éthylène. On conteste une affirmation récente à l'effet que le désordre dans l'orientation des molécules d'eau n'est pas nécessaire pour expliquer le spectre infrarouge lointain de la glace 1h. [Traduit par le journal]

Introduction

Cyclopropane forms clathrate hydrates with both of the common structures, I and II (1–4). Its structure I hydrate is isostructural with ethylene oxide hydrate (5) but, due to their larger size, cyclopropane molecules only occupy the tetrakaidecahedral cages (2, 4) whereas some ethylene oxide molecules also occupy the smaller dodecahedral cages (5). In both cases the water molecules are orientationally disordered and reorient extremely slowly at about 100 °K (3, 4, 6), while the guest molecules reorient rapidly at this temperature (3, 4, 6, 7). The far-infrared spectrum of ethylene oxide hydrate has been reported (8), and no firm assignment could be made of the absorption below 100 cm^{-1} to vibrations of the water molecules or to those of the ethylene oxide molecules. The intensity of the absorption by the ethylene oxide molecules is undoubtedly mainly due to the molecular dipole moment (8), so a comparison of the spectra of the structure I hydrates of ethylene oxide and the non-dipolar cyclopropane should clarify the assignment.

Experimental

The experimental methods have been described previously (8) except for the preparation of the structure I cyclopropane hydrate. About 3 ml of outgassed distilled water were maintained at 5 °C in contact with the equilibrium vapor pressure of cyclopropane at 5 °C, about 3000 Torr (2). The hydrate usually formed within 10 min sufficiently to prevent a steel rod or ball in the water from rattling, and the apparatus was left for about 2 days at

Can. J. Chem. Downloaded from www.nrcresearchpress.com by 210.87.254.6 on 09/05/12
For personal use only.

TABLE 1. X-Ray powder diffraction patterns of cyclopropane and ethylene oxide structure I hydrates at 110 ± 20 °K

Index	Calculated intensity*	Cyclopropane hydrate			Ethylene oxide hydrate		
		2θ	d (Å)	Intensity†	2θ	d (Å)	Intensity†
110	14	10.39	8.51	25	10.50	8.43	13
200	2	14.72	6.016	6			
210	<0.01						
211	10	18.05	4.913	21	18.27	4.857	14
220	5	20.88	4.253	10	21.14	4.203	8
310	12	23.35	3.810	25	23.68	3.757	15
222	49	25.68	3.468	71	25.95	3.434	58
320	54	26.77	3.330	66	27.02	3.300	53
321	100	27.80	3.206	100	28.08	3.177	100
400	9	29.74	3.004	13	30.00	2.979	10
410	23	30.73	2.909	37	30.97	2.888	21
330, 411	11	31.69	2.823	17	31.97	2.799	11
420	0.7			2‡			2‡
421	10	34.26	2.618	12	34.52	2.598	9
332	5	35.17	2.552	8	35.48	2.530	5
422	0.7			3‡			1‡
430	2.5	37.49	2.399	5			3‡
510, 431	2.3	38.35	2.347	5			2‡
520, 432	8.6	40.53	2.226	12	40.87	2.208	7
521	1.2			2‡			
440	0.04						
433, 530	28	44.10	2.054	34	44.41	2.040	19
531	8.3	44.83	2.022	8			5‡
600, 442	6.4	45.48	1.994	8			4‡
610	2.4						
611, 532	13	46.79	1.942	16	47.11	1.929	8
620	3.0	47.98	1.896	4			3‡
540, 621	2.5	48.77	1.867	4			3‡

*Integrated intensity for flat-plate powder camera, calculated from $I \propto [(1 + \cos^2 2\theta)/\sin^2 \theta \cos \theta] \cos 2\theta p F^2$, where p is the multiplicity factor and F is the observed structure factor taken from ref. 5.
†Relative heights of peaks on microdensitometer trace; precision ~20% of value given.
‡The 2θ values for these features could not be measured reliably.

5 °C to ensure complete formation of the hydrate. The hydrate was cooled to −80 °C and the excess cyclopropane was removed under vacuum, then the hydrate was cooled in liquid nitrogen, transferred to glass storage vials in the dry gas above boiling liquid nitrogen, and was stored under liquid nitrogen. For infrared and X-ray samples, the hydrate was ground by hand, using a stainless steel pestle and mortar at 77 °K, because the mechanical grinding used successfully for ethylene oxide hydrate (8) converted most of the cyclopropane hydrate to ice 1h. In this work the infrared samples were held at 100 ± 10 °K and the X-ray samples at 110 ± 20 °K.

Results and Discussion

The finely ground cyclopropane hydrate used for the infrared samples was shown to be the structure I hydrate, free from ice and solid cyclopropane, by its X-ray powder pattern. This is shown in Table 1 together with the powder pattern of ethylene oxide hydrate at 110 ± 20 °K and the intensities calculated (9), for all of the lines that should be seen, from the structure factors of ethylene oxide hydrate at −25 °C (5). The program DREFINE (10) was used to fit the 2θ values shown in Table 1, and gave a = 11.975 ± 0.004 Å for cyclopropane hydrate and a = 11.891 ± 0.003 Å for ethylene oxide hydrate. The 2θ values varied by ±0.1° for different samples, and the average of at least 6 determinations gave a = 11.98 ± 0.02 Å for cyclopropane hydrate and 11.89 ± 0.03 Å for ethylene oxide hydrate. The flat-plate powder camera was calibrated by comparing the lattice parameters of ice 1h determined as described above with those of Brille and Tippe (11). The parameter determined for ethylene oxide hydrate is about 0.05 Å lower than the probable value extrapolated from the data of McIntyre and Petersen for flash-frozen samples (12). It is clear that the lattice parameter for cyclopropane hydrate is

Can. J. Chem. Downloaded from www.nrcresearchpress.com by 210.87.254.6 on 09/05/12
For personal use only.

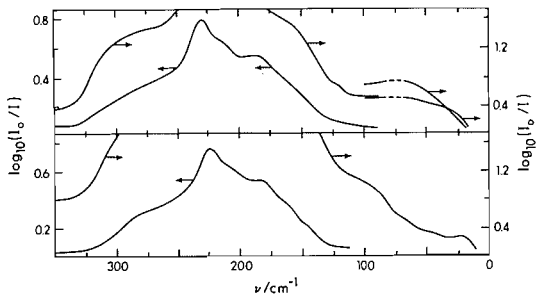

FIG. 1. The far-infrared spectra of the structure I hydrates of cyclopropane (lower box) and ethylene oxide (upper box), mulled in propane, at 100 °K. The arrows indicate the appropriate absorbance scale.

about 0.75% greater than that of ethylene oxide hydrate, which means that the hydrogen-bonded O---O distances are about 0.02 Å longer in cyclopropane hydrate, assuming a proportional lengthening of each hydrogen bond. The lattice parameters of cyclopropane and ethylene oxide hydrates have been given as 12.14 ± 0.1 Å at +5 °C (2, 3) and 12.03 ± 0.01 Å at −25 °C (3, 5), respectively. If the 12.14 Å is taken to be correct, it is also clear that the thermal expansion of both hydrates is considerably greater than that of ice 1h (11). This result is qualitatively consistent with the greater deviation from harmonicity found (8) for the translational vibrations of the water molecules in ethylene oxide hydrate than for those in ice I.

The far infrared spectrum of cyclopropane hydrate at 100 °K is shown in Fig. 1 and the frequencies of the features are given in Table 2. The corresponding data for ethylene oxide hydrate are included for comparison. The absorption above 100 cm^{-1} is very similar to that by ethylene oxide hydrate, which confirms the previous (8) conclusion that it is due to the translational vibrations of the water molecules. It is assigned to the density of vibrational states, modified by an intensity function which very crudely approximates the square of the frequency, through the theory for absorption by translational vibrations in orientationally disordered crystals (13, 14). The density of states curve for cyclopropane hydrate deduced from the spectrum above 100 cm^{-1} is essentially the same as that deduced for ethylene oxide hydrate (8), which is expected since the two water lattices are isostructural, but is shifted to low frequency by about 2%. This shift is undoubtedly related to the longer lattice parameter and, therefore, hydrogen bonds in

TABLE 2. The far-infrared spectra of the structure I hydrates of cyclopropane and ethylene oxide at 100 °K*

Cyclopropane hydrate		Ethylene oxide hydrate†	
ν (cm^{-1})	Description	ν (cm^{-1})	Description
285	sh	~300	sh
224±1	s	229.6±0.9	s
218±2	sh		
205	sh	210	sh
188±2	min	198	min
181±2	ms	184	ms
162	sh		
146±2	sh		
		120	sh
88	sh		
68	sh		
		~60	L
46±2	sh		
23±3	w		

*sh ≡ shoulder, min ≡ minimum, s, ms, w ≡ strong, medium strong, weak, maxima, L ≡ low-frequency edge of plateau.
†From ref. 8.

cyclopropane hydrate. Qualitative support for the density of states curve deduced from the spectra (8) is obtained from an inelastic neutron scattering study of the isostructural sulfur dioxide hydrate at 248 °K (15). The density of water molecule vibrational states obtained in that work shows a broad maximum from 100 to 300 cm^{-1}, with peaks at about 150, 184, and 244 cm^{-1}. The frequency increase on cooling to 100 °K is probably about 20 cm^{-1}, which places the neutron scattering results in fair agreement with the spectroscopic results. However, the vibrations above about 230 cm^{-1} are stronger in the neutron spectra than in the infrared spectra, as has been found for ice 1h (16–18). A more detailed assignment of the spectrum above 100 cm^{-1} must await a calculation of the density of states curve.

The neutron scattering spectra (15) of sulfur dioxide hydrate show that the first maximum in the density of vibrational states of the water molecules lies about 20 cm^{-1} higher than in ice 1h at 248 °K. This places the maximum at 80–85 cm^{-1} at 100 °K (8) if the 20 cm^{-1} difference holds true at this temperature. Further, preliminary calculations of the density of states of the translational vibrations of the water molecules in structure I hydrates have been made (19), using nearest-neighbor O...O stretching and O...O...O angle-bending force constants. They indicate that the same angle-bending force constant that places the first maximum at 60

Can. J. Chem. Downloaded from www.nrcresearchpress.com by 210.87.254.6 on 09/05/12
For personal use only.

Can. J. Chem. Downloaded from www.nrcresearchpress.com by 210.87.254.6 on 09/05/12
For personal use only.

cm^{-1} in ice 1h places it between 80 and 90 cm^{-1} in the hydrate. Thus the broad shoulder at about 88 cm^{-1} in the spectrum of cyclopropane hydrate can be assigned to the first maximum in the density of states of the translational vibrations of the water molecules.

This interpretation of the absorption by translational lattice vibrations in crystals formed by orientationally disordered water molecules has recently been questioned by Zerbi and co-workers (20). These authors deny that the breadth of the features observed for ice 1h (18) is evidence of the influence of the disorder. They prefer to assign the features to vibrations which are infrared-active under the factor group of a fully ordered structure, whose symmetry is reduced from the known diffraction symmetry by placing the hydrogen atoms in ordered positions. We cannot agree with their interpretation for several reasons. As Zerbi and co-workers point out, ice 1h does not have the ordered structure that they assume, but is disordered apart from short-range correlation effects (18). Therefore, since Zerbi and co-workers rely upon the activation of vibrations by the reduction in the diffraction symmetry that they impose by their model, it seems illogical to deny that the much greater reduction in symmetry to the actual structure of ice 1h activates all of the vibrations, which are, thus, activated by the disorder. Further, Zerbi and co-workers predict 7 infrared-active vibrations for ice 1h which they calculate to lie between 47 and 284 cm^{-1}, and one infrared-active vibration for ice 1c which they assign at 225 cm^{-1}. They then say that these predictions account for the identity of the spectra of ices 1h and 1c (18). We cannot agree that they do. Finally, the number of vibrations which are infrared-active under the factor groups of the ordered forms of ice, ices II and IX, exceeds the number predicted for ice 1h under the model of Zerbi and co-workers, yet the far-infrared absorption by ices II and IX consists of sharp discrete lines (21). The only conclusion that we can logically draw from this evidence is that the continuous broad absorption observed for the disordered forms of ice (18, 21, 22) and the clathrate hydrates ((8) and this work) is due to the activation of all of the vibrations by the known disorder.

The absorption by cyclopropane hydrate below 100 cm^{-1} (Fig. 1) decreases rapidly with decreasing frequency, in marked contrast to the absorption plateau between 100 and 50 cm^{-1} observed for ethylene oxide hydrate (8). This plateau must, therefore, be associated with the dipole moment of the guest molecule through the rotational–translational vibrations of the guest. It was noted previously (8) that approximate calculations based on the dielectric constants (3) place the rotational vibrations of ethylene oxide near 35 cm^{-1} at 4 °K, but at 100 °K they clearly influence the absorption up to 100 cm^{-1} and yield broad absorption which is similar to that in liquids (8). Klug and Whalley (23) have shown that similar, but rather more structured, absorption by the structure II hydrate of tetrahydrofuran at 80 °K develops into bands at 25 and 38 cm^{-1} at 17 °K, compared with about 15 and 20 cm^{-1} predicted (3) from the dielectric constants. It is possible that the weak features at 23 and 46 cm^{-1} shown in Fig. 1 are corresponding absorptions in cyclopropane hydrate. A study of the absorption below 100 cm^{-1} by ethylene oxide and cyclopropane hydrates and deuterates between 100 and 4 °K has been initiated, to try to reliably determine the vibrational frequencies of the guest molecules.

We thank the National Research Council of Canada for financial support and for the award of a scholarship to F.E.B. We are grateful to Dr. F. W. Birss for permission to quote unpublished results from his laboratory.

1. A. J. BARDUHN, H. E. TOWLSON, and Y. C. HU. A.I.Chem. Eng. J. **8**, 176 (1962).
2. D. R. HAFEMANN and S. L. MILLER. J. Phys. Chem. **73**, 1392 (1969).
3. D. W. DAVIDSON. *In* Water – a comprehensive treatise, Vol. 2. *Edited by* F. Franks. Chapt. 3.
4. Y. A. MAJID, S. K. GARG, and D. W. DAVIDSON. Can. J. Chem. **47**, 4697 (1969).
5. R. K. MCMULLAN and G. A. JEFFREY. J. Chem. Phys. **42**, 2725 (1965).
6. S. K. GARG, B. MORRIS, and D. W. DAVIDSON. J. Chem. Soc. Faraday Trans. II, **68**, 481 (1972).
7. A. W. K. KHANZADA and C. A. MCDOWELL. J. Mol. Struct. **16**, 1 (1973).
8. J. E. BERTIE and D. A. OTHEN. Can. J. Chem. **50**, 3443 (1972).
9. E. W. NUFFIELD. X-ray diffraction methods. J. Wiley and Sons Inc., New York, 1966. p. 107.
10. K. M. SIMPSON. Ph.D. Thesis. University of Alberta, Edmonton, Alberta. 1972. Available from the National Science Library, Ottawa, Canada.
11. R. BRILLE and A. TIPPE. Acta Cryst. **23**, 343 (1967).
12. J. A. MCINTYRE and D. R. PETERSEN. J. Chem. Phys. **47**, 3850 (1967).

13. E. WHALLEY and J. E. BERTIE. J. Chem. Phys. **46**, 1264 (1967).
14. D. D. KLUG and E. WHALLEY. J. Chem. Phys. **56**, 553 (1972).
15. A. W. NAUMANN and G. J. SAFFORD. J. Chem. Phys. **47**, 867 (1967).
16. H. PRASK, H. BOUTIN, and S. YIP. J. Chem. Phys. **48**, 3367 (1968).
17. E. WHALLEY. *In* Physics and chemistry of ice. *Edited by* E. Whalley, S. J. Jones, and L. W. Gold, R. Soc. Canada, 1973, p. 73, and references cited therein.
18. J. E. BERTIE and E. WHALLEY. J. Chem. Phys. **46**, 1271 (1967).
19. F. W. BIRSS, R. S. GAY, and J. C. NASH. Private communication.
20. P. BOSI, R. TUBINO, and G. ZERBI. J. Chem. Phys. **59**, 4578 (1973).
21. J. E. BERTIE and E. WHALLEY. J. Chem. Phys. **49**, 775 (1968).
22. J. E. BERTIE, H. J. LABBÉ, and E. WHALLEY. J. Chem. Phys. **49**, 2141 (1968).
23. D. D. KLUG and E. WHALLEY. Can. J. Chem. **51**, 4062 (1973).

Can. J. Chem. Downloaded from www.nrcresearchpress.com by 210.87.254.6 on 09/05/12
For personal use only.

Electrochemiluminescence of Phenanthrene-d_{10}: A Possible Case of Efficient Triplet–Triplet Annihilation

N. PERIASAMY AND K. S. V. SANTHANAM

Chemical Physics Group, Tata Institute of Fundamental Research, Homi Bhabha Road, Bombay-400005, India

Received July 11, 1974

N. PERIASAMY and K. S. V. SANTHANAM. Can. J. Chem. **53**, 76 (1975).

Electrochemiluminescence (e.c.l.) of mixed phenanthrene(Ph)-d_{10}-oxidant and Ph-h_{10}–oxidant systems have been studied. Emission from excited singlet state of Ph-d_{10} or Ph-h_{10} is observed. On the basis of energetics of the electron transfer reaction, triplet–triplet annihilation is postulated to give the excited singlet state of Ph. Comparison of these results with photoluminescence of Ph-d_{10}, shows efficient triplet–triplet annihilation occurs in e.c.l.

N. PERIASAMY et K. S. V. SANTHANAM. Can. J. Chem. **53**, 76 (1975).

On étudie l'électrochimiluminescence (e.c.l.) de systèmes mixtes de phénanthrène (Ph)-d_{10}–oxydant et Ph-h_{10}–oxydant. On observe une émission de l'état singulet excité de Ph-d_{10} ou Ph-h_{10}. A partir des énergies de la réaction de transfert d'électrons, on suppose que l'annihilation triplet–triplet donne l'état singulet excité de Ph. La comparaison de ces résultats avec la photoluminescence de Ph-d_{10} montre l'apparition de l'annihilation triplet–triplet efficace en e.c.l. [Traduit par le journal]

Introduction

Although several previous reports of electrochemiluminescence (e.c.l.) systems containing phenanthrene (Ph) alone (1, 2) have appeared, there are no studies reported of mixed Ph-h_{10}–oxidant or Ph-d_{10} (deuterated phenanthrene)–oxidant systems. With mixed systems, it has been possible to choose stable oxidants for the e.c.l. reactions and hence complexity arising from the decomposition products of the oxidant is less with these systems (2); Ph cation used as the oxidant in e.c.l. of Ph is unstable under the conditions employed in e.c.l. We wish to report here a detailed consideration of the energetics of the e.c.l. reactions of the mixed Ph–oxidant systems which suggest that triplet intermediates are involved in the e.c.l. reactions. The observed emission from the excited singlet state of Ph can be most reasonably explained as due to triplet–triplet annihilation. Earlier studies (3, 4) on Ph-d_{10} by photoluminescence indicated the absence of excited singlet state formation via triplet–triplet annihilation (delayed fluoresence) in spite of the triplet formation efficiency, ϕ_t of 0.93. Under similar conditions Ph-h_{10} (ϕ_t = 0.88) is known to give delayed fluorescence (5). The present investigation by e.c.l. suggests efficient triplet–triplet annihilation occuring in both Ph-h_{10} and Ph-d_{10} systems.

Magnetic field has been shown to alter the e.c.l. emission intensity of systems where triplet intermediates are involved in the formation of excited singlet state (6–8). Mixed Ph–oxidant systems show magnetic field enhancement and these results are also presented herewith.

Experimental

Ph-h_{10} (99%) was obtained from GMBH & Co. (Germany). The sample was purified by zone refining. Ph-d_{10} (~98%) (Merck) was zone refined before use. *p*-Phenylenediamine (PPD), and *N'N'*-tetramethyl-*p*-phenylenediamine (TMPD) (BDH), were purified by vacuum sublimation. Tri-*p*-tolylamine (TPTA) used in these studies were obtained from Dr. Zachariasse. Polarographic grade tetra-*n*-butyl ammonium perchlorate (TBAP) (South Western Analytical Chemicals) was used as the supporting electrolyte. The TBAP sample was dried *in vacuo* at 100 °C for 24 h and stored in a desiccator. 1,2-Dimethoxyethane (DME) (Fluka) was purified by distillation after drying it over freshly cut sodium pieces for 24 h. The distillate was vacuum redistilled over $LiAlH_4$ and the middle fraction was stored under vacuum over sodium anthracenide. About 2–3 ml of DME is distilled into the e.c.l. cell from the storage vessel.

Fluorescence and e.c.l. spectra were recorded with Hilger-Watts D-292 monochromators. The procedure for electrochemical measurements and the cells used have been described (9). The i.r. effect in the cyclic voltammetric curves were reduced by a positive feed back in the potentiostatic circuit. Magnetic field experiments were conducted according to the procedure described earlier (8). The field effects were examined on the singlet and excimer components by using Corning filters CS-7-59, CS-3-68, and Ilford 520.

Can. J. Chem. Downloaded from www.nrcresearchpress.com by 210.87.254.42 on 09/05/12
For personal use only.

Can. J. Chem. Downloaded from www.nrcresearchpress.com by 210.87.254.42 on 09/05/12
For personal use only.

Results and Discussion

The oxidants employed in the present e.c.l. studies are the cations of PPD, TMPD, and TPTA. The cyclic voltammetric cathodic peak potentials (E_{pc}) for reduction of Ph-d_{10} or -h_{10} to the anion radical

$$[1] \qquad Ph + e \rightarrow Ph^-$$

has been obtained with solutions containing 1.0 m*M* Ph and 1.0 m*M* PPD or TMPD or TPTA in DME to be -2.63 V *vs.* s.c.e. (practically no shift in E_{pc} was observed between Ph-d_{10} and Ph-h_{10}), while oxidation of PPD or TMPD or TPTA (represented by R) to the cation radical

$$[2] \qquad R - e \rightarrow R^+$$

occurs at $E_{pa} = +0.24$, $+0.22$, or $+0.91$ V. The enthalpies of the radical ion electron transfer reactions, calculated from the relation

$$[3] \qquad \Delta H^0 = E_{\frac{1}{2}(Ph/Ph^-)} - E_{\frac{1}{2}(R/R^+)} + 0.10$$

are 2.71 eV with PPD^+, 2.69 eV with $TMPD^+$, and 3.38 eV with $TPTA^+$. The singlet (E_s) and triplet (E_t) states of Ph-d_{10} are located at 3.60 and 2.69 eV (10). The enthalpies of the electron transfer reactions are thus enough to form the triplet state of Ph-d_{10} but are insufficient to form the singlet state of Ph-d_{10}. A similar argument may be extended to Ph-h_{10} where the singlet and triplet levels are expected to be close to the values of Ph-d_{10} (10). The electron transfer reaction with a typical oxidant like PPD^+ thus leads to

$$[4] \qquad Ph^- + PPD^+ \rightarrow {}^3Ph + PPD$$

The e.c.l. spectrum of Ph (-d_{10} or -h_{10}) has maximum at 25 000 cm^{-1} and agrees with the fluorescence spectrum[1] of Ph. Thus the e.c.l. emission comes from

$$[5] \qquad {}^3Ph + {}^3Ph \rightarrow {}^1Ph^* + Ph$$
$$\swarrow$$
$$Ph + h\nu$$

Consideration of the above energetics shows that the electron transfer reaction cannot produce the excited singlet or triplet states of PPD or TMPD located at $E_s = 3.60$ eV and $E_t = 2.90$ eV, and $E_s = 3.52$ eV and $E_t = 2.83$ eV respectively. The location of $E_s = 3.51$ eV and $E_t = 2.96$ eV for TPTA shows that the enthalpy of the e.c.l. reaction is sufficient to form the triplet state of TPTA directly. The e.c.l. emission spectrum generated with $TPTA^+$ as oxidant has a tailing in the region of fluorescence of TPTA, suggesting the emission is coming from the excited singlet state of TPTA also.

In addition to the emission from the excited singlet state of Ph, a broad structureless emission is observed at longer wavelengths with TPTA (21 500 cm^{-1}) or TMPD (16 700 cm^{-1}). This structureless emission observed with pure Ph system (19 379 cm^{-1}) in e.c.l. is due to the products of decomposition of Ph^+ (2) or emission attributed to triplet of Ph (1). Under the present experimental conditions the cations of TMPD or TPTA are highly stable and emission coming from the decomposition products is absent. The emission coming from Ph triplet in the present studies is unlikely due to differences in emission wavelengths with oxidants. It is suggested that the longer wavelength emission is due to heteroexcimer as proposed by Weller and Zachariasse (11*a*) for chemiluminescent systems. The relative amounts of singlet to excimer components obtained in e.c.l. are presented in Table 1.

No pre-annihilation e.c.l. is observed with either Ph-h_{10}–oxidant or Ph-d_{10}–oxidant systems in the present investigation. Such a pre-annihilation e.c.l. is observed with Ph-h_{10} alone in solvents like *N*,*N*-dimethylformamide (1).

TABLE 1. Electrochemiluminescence data for phenanthrene in DME

System	Emission (%) Singlet*	Excimer†
Ph-h_{10}–PPD	100	—
Ph-d_{10}–PPD	100	—
Ph-h_{10}–TMPD	95	5
Ph-d_{10}–TMPD	12	88
Ph-h_{10}–TPTA	20	80
Ph-d_{10}–TPTA	33	67

*The percentage singlet emission was calculated from the e.c.l. spectrum with maximum at 25 000 cm^{-1} from the total singlet and excimer emissions. Integrated areas have been used in the calculations. Errors in the values reported are ±10%.

†The percentage excimer emission was based on the emission at longer wavelength, from the total singlet and excimer emissions.

[1]The fluorescence spectrum of Ph in ethanol shows maxima at 360, 380, and 400 nm.

Changes occurring in the e.c.l. emission intensity in the external magnetic field has been taken as an indication of the presence of triplet intermediates (6–8). The recorded enhancement of emission intensities in the magnetic field for Ph–oxidant systems are presented in Table 2. These results support the above conclusions of triplet intermediates formed in the e.c.l. reactions involving Ph–oxidant systems. The excimer emission does not show a magnetic field effect. This suggests excimer is formed directly in the electron transfer reaction (11).

The difference in behavior (in terms of relative production of excimer) exhibited by Ph-h_{10} and Ph-d_{10} probably arises from the relative rates of heteroexcimer formation and triplet production and the decomposition of the heteroexcimer in the reaction

$$[6] \qquad Ph^- + TMPD^+ \begin{cases} \nearrow (a)\ {}^1(TMPD^+Ph^-) \\ \searrow (b)\ {}^3Ph + TMPD \end{cases}$$

(for reaction 6*a*, see footnote 1). The heteroexcimer cannot be formed via ^{3}Ph and ^{3}TMPD as indicated by the absence of magnetic field effect on the e.c.l. intensity of the mixed systems.

Absence of delayed fluorescence in Ph-d_{10} was reported (3) during photoluminescence studies. In e.c.l., since the emission from the excited singlet state of Ph-d_{10} is observed via triplet–triplet annihilation it may be possible that efficient production of triplet state of Ph-d_{10} may be the cause for observing emission from the excited singlet state.[2]

[2]Rate of production of triplets in e.c.l. is proportional to concentrations of the free radicals. For a solution with 1.0 mM phenanthrene-d_{10} and 1.0 mM PPD and a rate constant of 10^9 l M^{-1} s^{-1} (12), the rate would be in the range of 1.0–10.0 M l^{-1} s^{-1}. In photoluminescence the rate of production of the triplets is equal to $I_a\phi_t$ where I_a is the rate of light absorption which is in the range of 10^{-5}–10^{-6} einstein l^{-1} s^{-1} and ϕ_t is 0.93. The rate of production of triplets in the latter case is thus small by orders of magnitude.

TABLE 2. Enhancement of intensity in the magnetic field

Field (kG)	Enhancement (%)	
	Ph-h_{10}–TMPD*	Ph-d_{10}–PPD
1.0	8	5
3.0	11	7
8.0	11	9

*The intensity of the excimer component is not affected by the field.

Authors wish to thank Professor Weller and Dr. Zachariasse for the gift of TPTA, Dr. Prasad for Ph-d_{10} and Professor Bard for a preprint of his work on Marcus' theory. We wish to thank Professor B. Venkataraman for helpful discussions and Mrs. Shah for assistance.

1. (*a*) A. ZWEIG, D. L. MARICLE, J. S. BRINEN, and A. H. MAURER. J. Am. Chem. Soc. **89**, 473 (1967); (*b*) D. L. MARICLE, A. ZWEIG, A. H. MAURER, and B. G. ROBERTS. J. Am. Chem. Soc. **90**, 261 (1968); (*c*) D. L. MARICLE, A. ZWEIG, A. H. MAURER, and J. S. BRINEN. Electrochim. Acta, **13**, 1209 (1968).
2. (*a*) A. J. BARD, K. S. V. SANTHANAM, S. A. CRUSER, and L. R. FAULKNER. *In* Fluorescence. *Edited by* G. G. Guilbault. Marcel Dekker, New York. 1967. Chapt. 14; (*b*) R. E. VISCO and E. A. CHANDROSS. Electrochim. Acta. **13**, 1187 (1968); J. Phys. Chem. **72**, 378 (1968); (*c*) N. PERIASAMY, S. J. SHAH, and K. S. V. SANTHANAM. J. Chem. Phys. **58**, 821 (1973).
3. R. E. KELLOGG. J. Chem. Phys. **41**, 3046 (1964).
4. R. G. BENNETT. J. Chem. Phys. **41**, 3048 (1964).
5. C. A. PARKER and C. G. HATCHARD. Proc. Chem. Soc. 147 (1962); Proc. R. Soc. Lond. A, **269**, 574 (1962).
6. L. R. FAULKNER and A. J. BARD. J. Am. Chem. Soc. **91**, 209 (1969).
7. H. TACHIKAWA and A. J. BARD. Chem. Phys. Lett. **19**, 287 (1973).
8. K. S. V. SANTHANAM. Can. J. Chem. **49**, 3577 (1971).
9. N. PERIASAMY, S. J. SHAH, and K. S. V. SANTHANAM. Proc. 14th Seminar on Electrochemistry, Karaikudi. 1973. p. 173.
10. J. B. BIRKS. *In* Photophysics of aromatic molecules. Wiley–Interscience, New York. 1970. pp. 182, 185.
11. (*a*) A. WELLER and K. ZACHARIASSE. Chem. Phys. Lett. **10**, 197, 424 (1971); (*b*) K. ZACHARIASSE. Ph.D. Thesis. Free University, Amsterdam. 1972.
12. H. TACHIKAWA and A. J. BARD. Chem. Phys. Lett. **26**, 246 (1974).

Can. J. Chem. Downloaded from www.nrcresearchpress.com by 210.87.254.42 on 09/05/12
For personal use only.

Pyrophosphates of Tetravalent Elements and a Mössbauer Study of SnP_2O_7

CHUNG-HSI HUANG,[1] OSVALD KNOP, AND DAVID A. OTHEN
Department of Chemistry, Dalhousie University, Halifax, Nova Scotia B3H 4J3
AND
FRANK W. D. WOODHAMS AND R. ALLAN HOWIE
Departments of Natural Philosophy and Chemistry, University of Aberdeen, Aberdeen, Scotland AB9 2UE
Received June 6, 1973[2]

CHUNG-HSI HUANG, OSVALD KNOP, DAVID A. OTHEN, FRANK W. D. WOODHAMS, and R. ALLAN HOWIE. Can. J. Chem. **53**, 79 (1975).

Cubic $M^{4+}P_2O_7$ pyrophosphates of Ti, Zr, Hf, Sn, and Pb have been examined by X-ray powder diffractometry and by infrared, Raman, and Mössbauer ^{119}Sn spectroscopy. The tin compound appeared to be of Chaunac's type *I* (with P_2O_7 groups oriented at random) and could be converted to type *II* (with ordered P_2O_7 groups) by heating to high temperatures. All the other preparations were of Chaunac's type *II*. Evidence from lattice parameters and intensity features of the Raman spectra suggests that the cubic MP_2O_7 pyrophosphates fall in two groups, one containing the compounds of the typical elements (Ge, Sn, Pb) and the other, the compounds of the transition elements. No support has been found for the view that the P—O—P groupings of the pyrophosphate anion in these compounds are linear. The ^{119}Sn chemical shift in SnP_2O_7 is only slightly less negative than the shift in $CuSnF_6.4H_2O$, which makes SnP_2O_7 one of the most ionic compounds of tetravalent tin known. The observed quadrupole splitting in the Mössbauer spectrum of SnP_2O_7 arises largely from the contribution of the valence term to the electric field gradient at the Sn atom.

CHUNG-HSI HUANG, OSVALD KNOP, DAVID A. OTHEN, FRANK W. D. WOODHAMS et R. ALLAN HOWIE. Can. J. Chem. **53**, 79 (1975).

On a examiné les diffractogrammes X de poudre et les spectres infrarouge, Raman et Mössbauer (^{119}Sn) des pyrophosphates $M^{4+}P_2O_7$ cubiques de Ti, Zr, Hf, Sn et Pb. Le composé d'étain, qui était du type Chaunac *I* (à l'orientation aléatoire des groupes P_2O_7), a pu être converti par chauffage à hautes températures en type *II* (à groupes P_2O_7 ordonnés). Les autres préparations étaient du type *II*. Les paramètres de mailles élémentaires et les caractères d'intensité des spectres Raman suggèrent que les pyrophosphates MP_2O_7 cubiques se divisent en deux groupes, l'un contenant les composés des éléments typiques (Ge, Sn, Pb) et l'autre, les composés des éléments de transition. Aucune indication de linearité n'a été trouvée pour les groupements P—O—P des anions $P_2O_7^{4-}$ dans ces composés. La valeur négative du déplacement isomère de ^{119}Sn dans SnP_2O_7 est légèrement inférieure à celle du $CuSnF_6.4H_2O$, ce qui rend SnP_2O_7 un des composés les plus ioniques connus de l'étain quadrivalent. C'est le terme de valence du gradient de champ éléctrique sur l'atome d'étain qui est largement responsable du dédoublement quadrupolaire observé dans le spectre Mössbauer de SnP_2O_7.

The cubic pyrophosphates of tetravalent elements, MP_2O_7, are of interest for several reasons. These refractory compounds span the entire range of tetravalent elements from Si to Th, SiP_2O_7 being one of the few compounds that contain silicon in 6-coordination, but it is not known to what extent they are isostructural. The configuration of the P—O—P group of the $P_2O_7^{4-}$ anion in these phosphates has been the subject of controversy and conjecture (1–12) ever since the appearance of the paper of Levi and Peyronel (13), largely because of the uncertainty as to the true size of the MP_2O_7 unit cells. McGeachin (1) has pointed out that the description of Levi and Peyronel (the "LP cell": $a \sim 8$ Å, $Pa3$, $Z = 4$) would necessitate a *linear* P—O—P group, but this geometry is not encountered in other pyrophosphates. Insight into the complexities of the crystal chemistry of the cubic MP_2O_7 has been gained only recently through the efforts of Chaunac and co-workers (2, 3) and Tillmanns *et al.* (14). Their principal results, which are essential for our dis-

[1]INCO Graduate Research Fellow, 1968–1970. This paper is based in part on the M.Sc. thesis submitted by C.-H. Huang to the Department of Chemistry, Dalhousie University (34). Present address: Department of Chemistry, Memorial University of Newfoundland, St. John's, Newfoundland.

[2]Revision received October 2, 1974.

Can. J. Chem. Downloaded from www.nrcresearchpress.com by 210.87.254.40 on 09/05/12
For personal use only.

Can. J. Chem. Downloaded from www.nrcresearchpress.com by 210.87.254.40 on 09/05/12
For personal use only.

cussion of the problem, can be summarized as follows.

An X-ray and i.r. study of ZrP_2O_7 has enabled Chaunac and co-workers to distinguish three forms, all of cubic symmetry. *Form I* ($a \sim 8.25$ Å; the LP cell) is obtained when ZrO_2 or hydrated Zr oxide is heated with H_3PO_4 to temperatures not exceeding about 250 °C. The P—O—P groups are bent, but their orientations relative to the trigyres containing the P—P pairs are disordered. Averaging the positions of the oxygen atoms over the crystal thus simulates the linear P—O—P groups and the D_{3d} symmetry of the anion demanded by the diffraction symmetry *Pa*3.[3] The orientation disorder is attributed to frozen-in stacking faults produced during the crystal growth at the relatively low temperatures.

Form II is obtained from ZrO_2 or hydrated Zr oxide and H_3PO_4 by heating above *ca.* 250 °C, or directly from *I* by heating to these temperatures; the transformation $I \rightarrow II$ is irreversible. The lattice parameter *a(II)* is three times that of *I*. This large unit cell results from ordering of the P_2O_7 anions. The P—P vectors of the P—O—P groups are no longer required to coincide with the trigyres, and in the absence of constraints imposed by space-group symmetry the P—O—P groups assume their natural bent configurations and their equilibrium orientations in the crystal.

Form III ($a(III) \sim 8.27$–8.28 Å) exists only above 300 °C and has the space-group symmetry *Pa*3. In contrast to *I*, this symmetry is not "statistical" but true. The P—P vectors are on the trigyres, but the oxygen atoms are "thermally disordered", *i.e.* their abnormally high amplitudes of thermal motion result in *dynamic* (time-averaging) simulation of linear P—O—P groupings. The transformation $II \rightarrow III$ is reversible and is confirmed by independent dilatometric evidence (28); the enthalpy change associated with the process between 530 and 575 °K has been estimated as 130 cal/mol (3).

It seems that this polymorphism exists in all the cubic MP_2O_7. Chaunac and co-workers (3; *cf.* also ref. 15) state that TiP_2O_7 behaves in an analogous manner, and X-ray diffraction evidence of the tripled cell has been reported for the Si (15–17), Ge (15, 16), Sn (15), Pb (15), Hf (15), α-U (15, 18), and probably also Ce (15) compounds. Dilatometric evidence of similar transitions in the U and Th compounds has also been reported (19, 20). Independent supporting evidence for the existence of form *III* comes from the relatively weak band at 740 cm^{-1} in the i.r. spectra of $ZrP_2O_7(I)$ and $ZrP_2O_7(II)$. This band, which is absent, or at least extremely weak, in spectra of ZrP_2O_7 at 320 °C (3), was considered to be characteristic of bent X_2O_7 groups by Lazarev *et al.* (4–6), and of diagnostic importance. A weak band at 490 cm^{-1} in the spectrum of $ZrP_2O_7(I)$ seems to be characteristic of form *I* (3).

The structural features postulated by Chaunac for $ZrP_2O_7(II)$ have been reported to exist in $SiP_2O_7(II)$ (or SiP_2O_7AI according to ref. 17). Because of the complexity of the problem (a cubic unit cell having a volume of 11267 $Å^3$), Tillmanns *et al.* (14) generated a trial structure by computer simulation from assumed interatomic distances and bond angles, starting from values that had been obtained by refining the LP substructure in *Pa*3. The trial structure was then refined in *Pa*3, using individual isotropic temperature factors, to an *R* of 30.8%, with more than 50% of the reflections unobserved ($|F_o| = 0$). The 108 P_2O_7 groups in the unit cell fall into six sets of configurations: four of these, each accounting for 24/108 = 22.2% of the total, have bent P—O—P bridges (O_{bridge} in 24(*d*)) and staggered PO_3 groups. The remaining 12/108 = 11.1% contain *linear* P—O—P groupings: one third (= 3.7%) are of symmetry D_{3d} (O_{bridge} in 4(*b*)), while the other two thirds have a *gauche* configuration of symmetry C_3 (O_{bridge} in 8(*c*)). However, the temperature factors of the O_{bridge} atoms in the linear P—O—P groupings were, respectively, about twice and three times the average of the temperature factors of *all* the oxygens in the unit cell, and their estimated standard deviations were 2.5 times those for all the other oxygen atoms; one of the PO_3 oxygens had a *B* of 0.0(2) $Å^2$. In the circumstances the linearity of the 11.1% of the P—O—P groupings cannot be viewed as established. The authors themselves recognize the desirability of an anisotropic temperature factor refinement.

Useful as these results are, they do not indicate which other compounds have properties *strictly* analogous to those of $SiP_2O_7(II)$ and ZrP_2O_7.

[3]Refinement from photographic Weissenberg intensities (2) in both *Pbca* and *Pa*3 gave similar results, with characteristically large thermal parameters and abnormally short P—O distances.

Can. J. Chem. Downloaded from www.nrcresearchpress.com by 210.87.254.40 on 09/05/12
For personal use only.

The Si atom is too small for SiP_2O_7 to be considered a "typical" representative of the cubic MP_2O_7 group (*cf.* the variety of non-cubic polymorphs reported for SiP_2O_7 but not for the other compounds, refs. 17, 21, and 22), and some differences may be expected to occur when going from the small Ge to the large Th atom. The question of isomorphism can be properly answered only when the crystal structures of the individual compounds are known, but it ought to be possible to increase our understanding of these pyrophosphates from lesser evidence. To this end we have prepared the polycrystalline Ti, Zr, Hf, Sn, and Pb compounds and re-examined them by X-ray diffraction and i.r. spectroscopy. The laser Raman spectra of these compounds are being reported here for the first time, as is also the Mössbauer ^{119}Sn spectrum of SnP_2O_7.

Experimental

Chemicals of reagent-grade or better purity were used in the preparations. The phosphoric acid was 85%.

ZrP_2O_7 was prepared in two ways. (*i*) An excess of freshly prepared 10% solution of $(NH_4)_2HPO_4$ was added to a sulfuric acid solution of zirconyl sulfate. The mixed solution was digested at 50 °C, cooled, and filtered. The precipitate was washed with a cold 5% solution of NH_4NO_3 until the excess phosphate was removed, dried in a Pt crucible, and calcined for 12 h at 900 °C. (*ii*) An excess of H_3PO_4 was added slowly to 500 ml of a solution containing 5 g of $ZrO(NO_3)_2$. After decantation the precipitate was transferred to a Pt crucible, calcined at 350 °C for 1 h and quenched in CCl_4. The product was washed with water, filtered and dried, and fired subsequently for 12 h at 900 °C. The X-ray powder patterns of products obtained by (*i*) and (*ii*) were identical.

HfP_2O_7 also was prepared by two methods. (*i*) The precipitate of $HfP_2O_7 \cdot 2H_2O$ prepared from $HfOCl_2 \cdot 8H_2O$ according to ref. 23 was calcined for 3 h at 1200 °C. (*ii*) A mixture of $1HfO_2 + 3H_3PO_4$ was heated for 1 h to 400 °C, cooled, and the resulting solid treated as under (*ii*) for ZrP_2O_7. The product of (*ii*) gave a sharper X-ray powder pattern than that of (*i*), for which the high-angle lines were weak and diffuse.

The Ti, Sn, and Pb pyrophosphates were prepared as under (*ii*) for HfP_2O_7 using TiO_2, $SnCl_4.5H_2O$, and PbO_2 instead of HfO_2 (Table 1).[4] All the pyrophosphates were very fine white powders.

The oxygen contents of the preparations were determined by vacuum fusion. Density of the powders was determined, in duplicate, by double weighing as in ref. 24.

The lattice parameters, oxygen contents, and densities of the products are compared in Table 1 with results reported by other workers.

[4]Copies of Table 1 are available, at a nominal charge, from the Depository of Unpublished Data, National Science Library, National Research Council of Canada, Ottawa, Canada K1A 0S2.

Infrared and Raman Spectra

Infrared spectra were obtained as described in ref. 31. Raman spectra were obtained using the 4880 Å line of a Carson Ar^+ laser in conjunction with a Spex 1401 double monochromator and a SSR photon counter. The instrumental frequencies were calibrated using CCl_4 lines; furthermore, when the exciting line was not filtered, calibration against the argon plasma lines present in the sample spectra was possible (32). The pyrophosphate powders were contained in glass capillaries. The instrumental resolution for the survey spectra shown (Figs. 3 and 4) was better than 5 cm^{-1}, but frequencies were measured from *expanded* spectra taken at 2 cm^{-1} resolution and averaged to give the tabulated results (Table 4).

Both capillaries and pressed powders were used for the Sn compounds, whose Raman spectra were much weaker than those of the other pyrophosphates. With pellets the instrumental resolution was 7 or 9 cm^{-1}. This lower resolution did not affect the spectra; most bands had half-widths of about 10 cm^{-1} and hence the positions of the peak maxima were difficult to ascertain, but the spectra had much better signal-to-noise ratios than when the capillaries were used. The frequencies quoted for the Sn compounds are from the pellet spectra.

For all samples the frequencies of the stronger Raman features are accurate to ± 2 cm^{-1} and of the weaker features, to about ± 5 cm^{-1}.

Mössbauer ^{119}Sn Spectra

The details of apparatus and procedure are described in ref. 35. The chemical shifts δ in Table 5 are quoted with respect to $BaSnO_3$ at room temperature; values relative to β-Sn are obtained by subtracting 2.570 mm/s and to α-Sn, by subtracting 1.92 mm/s (33).

Other Methods

Thermogravimetric (TGA) curves were obtained as described in ref. 31. Typically a 0.5 g sample was placed in a recrystallized-alumina crucible and heated in stagnant air at a rate of 6 °C/min.

Collection of integrated X-ray diffractometer intensities (CuKα) and details of X-ray diffraction are described in ref. 31. As_2O_3 or Si were used as internal standards for Guinier photographs (CuKα and $CuK\alpha_1$). The a_0 values were determined from powder photographs obtained in 114.6 mm diameter cameras except for $a_0(TiP_2O_7)$, which was determined from a Guinier photograph.

Characterization of the Products

The anhydrous Ti, Zr, and Hf compounds did not undergo any change in weight when heated to 1300 °C (TGA in stagnant air), indicating that no significant loss, if any, of P_2O_5 occurred.[5] The slope of the TGA curve of $HfP_2O_7.2H_2O$ prepared by (*i*) was practically zero above 700 °C.

[5]According to ref. 28 ZrP_2O_7 lost P_2O_5 rather readily when heated at 1550 °C for 4 h and was converted to $(ZrO)_2P_2O_7$, the latter being stable to at least 1600 °C. In another paper (18) ZrP_2O_7 is reported to be stable up to 1500 °C, above which temperature $(ZrO)_2P_2O_7$ (stated to be stable up to about 1700 °C) begins to appear.

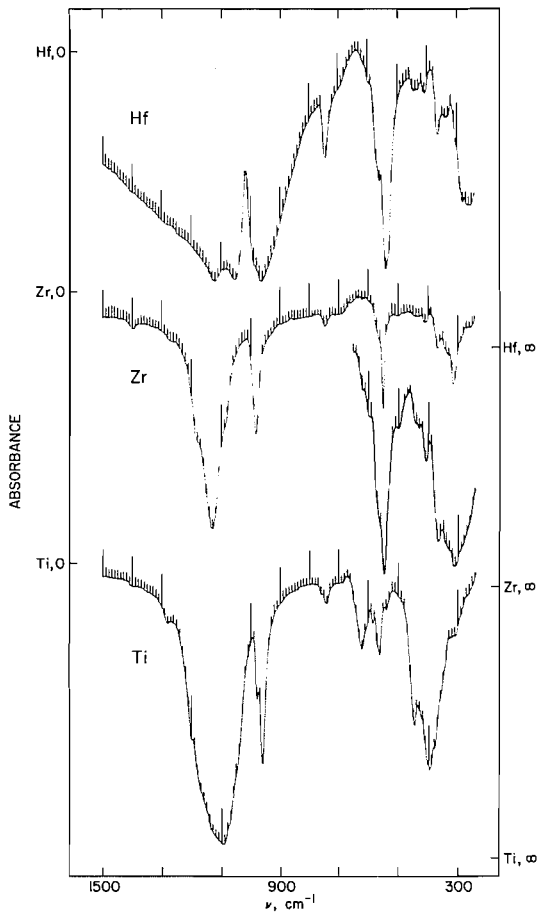

FIG. 1. Infrared spectra of cubic MP_2O_7 (M = Ti, Zr, Hf) pyrophosphates in the region 1500–250 cm^{-1} (compensated KBr pellets). The detail shown is for the Zr compound.

PbP_2O_7 began to lose weight at about 400 °C. The TGA curve quickly reached a plateau extending from *ca.* 580 °C (*cf.* ref. 27). The sample fused to a transparent light-amber-colored glass. The loss of weight, which corresponded to one oxygen per PbP_2O_7, is compatible with the reduction of Pb^{4+} to Pb^{2+} and formation of a Pb^{2+} phosphate (possibly metaphosphate, *cf.* ref. 27). The i.r. spectrum of the glass was quite different from that of PbP_2O_7, although there was absorption in the 740 cm^{-1} region.

The TGA curve obtained with SnP_2O_7 in an alumina crucible indicated progressive loss of weight (34). The loss began to be perceptible in the 550–600 °C range. The sample continued to lose weight up to *ca.* 930 °C, after which the weight remained constant to about 1060 °C. The total weight loss corresponded to about one oxygen per SnP_2O_7. The sample fused to a transparent colorless glass which was not investigated further. It is likely that the glass was formed by reaction with the crucible material. Heating SnP_2O_7 in a Pt crucible to 1200 °C for 1 d followed by quenching in air resulted in a weight loss of *ca.* 16%. The product had the same appearance as the initial material, but small amounts of a colorless glassy material adhered to the crucible where the metal was in contact with the sample powder. The glassy material dissolved in hot water, suggesting that it may have been P_2O_5 or phosphate glass. The powder diffraction photograph of the bulk of the product was almost identical with that of the original SnP_2O_7 except for a small contraction of the unit cell (a_0 = 7.943(2) Å, *i.e.* about 0.4%) and a few very weak extra lines. Compared with the initial material the i.r. spectrum of the product showed significant differences in the 600–300 cm^{-1} region (Fig. 2). In the following the original SnP_2O_7 will be referred to as $SnP_2O_7(1)$ and the product of heating *1* to 1200 °C, as $SnP_2O_7(2)$.

With the exception of SnP_2O_7 the Guinier photographs of the pyrophosphates revealed numerous very weak but mostly well-defined lines which could not be accounted for on the LP cell but were indexable on the 27LP cell. Some of the stronger "extra" lines appeared also in standard powder photographs and in the diffractometer patterns, the 310 line of ZrP_2O_7 being the most clearly visible. The i.r. spectra of *all* these compounds (Figs. 1 and 2) contained the band near 740 cm^{-1} characteristic of bent P—O—P groupings. The products must thus have been of type *II*. The PbP_2O_7 preparation may have contained slight impurity.

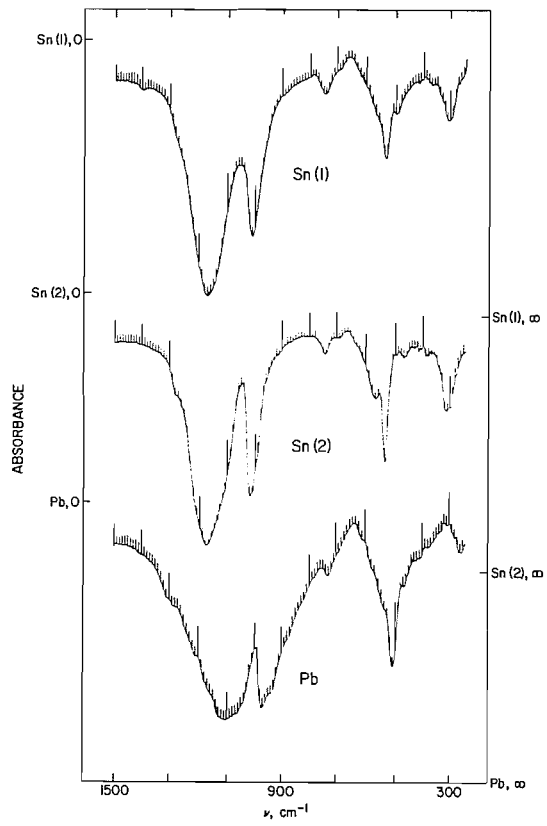

FIG 2. Infrared spectra of cubic MP_2O_7 (M = Sn, Pb) pyrophosphates in the region 1500–250 cm^{-1} (compensated KBr pellets).

Can. J. Chem. Downloaded from www.nrcresearchpress.com by 210.87.254.40 on 09/05/12
For personal use only.

TABLE 2. Refinement of MP_2O_7 structures in *Pa*3 from LP-subcell data (CuKα)

	$ZrP_2O_7(II)$						
Parameter[a]	Reference 13	Reference 16	Reference 2	This work[b]	This work[c]	$SnP_2O_7(I)$ This work[d]	$SiP_2O_7(II)$ Ref. 14
u(P)	0.39	0.395(1)	0.396(1)	0.3933(17)	0.3952(9)	0.3962(13)	0.3833(5)
$x(O_{outer})$	0.394	0.446(4)	0.448(4)	0.443(5)	0.443(2)	0.447(4)	0.441(2)
$y(O_{outer})$	0.218	0.229(4)	0.227(4)	0.223(4)	0.220(2)	0.226(2)	0.202(2)
$z(O_{outer})$	0.458	0.427(4)	0.420(4)	0.438(6)	0.433(3)	0.414(4)	0.408(2)
B(M), Å^2		2.3(1)	1.40(8)	2.2(2)	2.1(11)	2.2(2)	1.8(2)
B(P), Å^2		2.0(2)	1.16(20)	2.6(6)	1.7(3)	1.4(6)	1.4(1)
$B(O_{outer})$, Å^2		6.5(6)	4.92(69)	8.3(14)	5.8(5)	4.2(9)	5.8(4)
$B(O_{bridge})$, Å^2		5.2(14)	7.85(23)	11.2(28)	1.8(15)	7.9(16)	10(2)
R, %		12.8	12.8	3.9[e]			13.7[f]
$D(\Delta I)$, %					7.1[e]	7.3[e]	
$D(I)$					1000[e]	1007[e]	

[a]The xyz coordinates of ref. 2 have been permuted cyclically to match those of ref. 16; those of ref. 13 (obtained from FeKα data) are quoted without change. $D(\Delta I) = 100\,\Sigma|\Delta I|/\Sigma I_o$, $D(I) = 1000\,\Sigma I_c/\Sigma I_o$.
[b]F-refinement of $Zr^{4+}P_2{}^0O_6{}^0O^0$ from 23 out of the 27 single reflections possible in *Pa*3 up to and including 10.2.2+666; weighting scheme W3 of ref. 39.
[c]I-refinement of $Zr^{4+}P_2{}^0O_6{}^0O^0$ from 66 out of the 127 I_0 possible in *Pa*3 up to and including 10.2.2+666; $w(hkl) = \sigma^{-1}[I_o(hkl)]$.
[d]I-refinement of $Sn^{4+}P_2{}^0O_6{}^0O^0$ from 47 out of the 82 I_o (monochromator after the specimen) possible in *Pa*3 up to and including 731+371+553; $w(hkl) = \sigma^{-1}[I_o(hkl)]$.
[e]Includes only reflections used in the refinement.
[f]This R appears to refer to an F^2-refinement (MoKα).

The Guinier photographs of SnP_2O_7 contained only a few, relatively diffuse "extra" lines, and the i.r. spectrum of $SnP_2O_7(I)$ contained an additional band at 499 cm^{-1}. This seemed to correspond to the 490 cm^{-1} band in Chaunac's room-temperature spectrum of $ZrP_2O_7(I)$. On the strength of this evidence $SnP_2O_7(I)$ was taken to be of type *I* and $SnP_2O_7(2)$, of type *II*.

Results

Structure Refinement of $ZrP_2O_7(II)$ and $SnP_2O_7(I)$

The integrated diffractometer LP-subcell intensities were used in full-matrix refinements in *Pa*3 with individual isotropic temperature factors and *ad hoc* programs. A number of models were tried in both *F*- and *I*-refinements employing different combinations of the scattering factors for Zr^{4+} and Sn^{4+} (36); P, O, O^-, and O^{2+} (37); and O^{2-} (38). The results for $Zr^{4+}P_2{}^0O_6{}^-O^0$ and $Sn^{4+}P_2{}^0O_6{}^0O^0$ are shown in Table 2. The refined parameter values are not very accurate, though they compare with those from similar refinements of $ZrP_2O_7(II)$ (16) and $ZrP_2O_7(I)$ (2) from single-crystal data. The largest correlation coefficients were, typically, $B(Zr) - K$ (0.68), $x - z$ (−0.51), and $z - B(O_{outer})$ (0.49); the $x - B(O_{outer})$ and $y - B(O_{outer})$ values were only −0.07 and 0.17 respectively. Refinements designed to determine the effective scattering factors $n_i f_i$ were inconclusive because of the large standard deviations of the refined values of n_i. They indicated, however, a high degree of correlation of n_i and B_i for P, O_{outer}, and O_{bridge}, the $n_i - B_i$ terms in the correlation matrices having values greater than |0.8|.

The results of our *I*-refinements of $ZrP_2O_7(II)$ are quite similar to those obtained for $ZrP_2O_7(I)$ by Chaunac from single-crystal data, in spite of the fact that the assumed structure and the space group *Pa*3 are *statistically correct* for form *I* but only subcell approximations for form *II*. The refinement of $SnP_2O_7(I)$ also gave results strikingly similar to those for $ZrP_2O_7(I)$ of ref. 2. The large B(oxygen) values support Chaunac's model for form *I*. Refinements of form *I* structures cannot thus provide information about the geometry of the P_2O_7 ion.

Infrared Spectra

Infrared spectra of cubic MP_2O_7 have been reported by Steger and Leukroth (26) for M = Ti, Zr, Si, Sn; by Lecomte *et al.* (9) for Zr, Si, Ge; by Haider (40) for Zr; and by Hubin and Tarte (8) for Ti, Zr, Hf, U, Si, Sn, and Pb. There is general agreement between those frequencies that are listed both in Table 2 and in ref. 8; the few values that differ by more than the stated uncertainty are identified in Table 2. However, comparison of the list of Hubin and Tarte with the spectra shown in their paper reveals that the spectra are more complex than the list of frequencies corresponding to the most prominent bands would indicate. This is shown even more clearly in our Figs. 1 and 2, in which the *original* (not redrawn) traces are reproduced. While

Can. J. Chem. Downloaded from www.nrcresearchpress.com by 210.87.254.40 on 09/05/12
For personal use only.

TABLE 3. Infrared spectra of polycrystalline cubic MP_2O_7 pyrophosphates between 250 and 1500 cm^{-1}[a]

Ti	Zr	Hf	Sn(*1*)	Sn(*2*)	Pb
260(12) wS	258(8) w		255(10) wS		
	290(8) wS	258(4) s		299(4) m	
310(10) m	313(4) s	280(2) wS	305(3)[b] s	312(3)[b] s	255(5) s
		~300 vwS			
			330(10) vwS	340(8) wS	280(5) wS
357(5) vwS	340(10) vwS	338(3) vw			
378(3) vwS	368(3) w	365(3)[b] m	368(6)[b] w	382(8)[b] w	305(3) vw
397(3)[b] s	409(2) w	409(4) w			338(10) vwS
			416(5) vw	418(5) vw	389(8)[b] vwS
423(5) vwS	431(3) vwS				
448(2) m	442(3) vwS	445(5) w	469(3) w	469(3) w	408(10)[b] wS
500(4) vwS	500(2) w		499(3) m		468(5) wS
	530(12) vvwS				
539(3) wS	549(2) s	540(3) s	536(4) s	538(2) vs	510(3) s
561(2) m	563(8) vwS	559(2) wS	565(10) vwS	569(3) s	542(10) vwS
583(3) w					580(15) vvwS
600(5) vwS	595(6) vwS	595(5) vwS			
621(2) m	615(10) vwS	612(10) vwS	620(15) vvwS	635(10) vvwS	612(10) vwS
649(5) vwS	658(4)[b] vvw				
690(10) wS	690(10) w	695(5) wS	685(10) wS	690(10) vw	690(10) vwS
741(3) w	746(3) w	742(3)[b] m	743(3) m	745(5) m	733(5) w
759(4) wS					
845(15) vvw	845(15) vvw				
895(15) vwS			885(10) vwS		
	930(15) vwS			915(10) vwS	823(15) vwS
			955(15) vwS	955(15) vwS	875(8) wS
960(2) s	981(2) s	962(2) vs		995(10) vvwS	938(7) wS
979(2) wS		987(10) wS	1010(2) s	1018(5) vs	985(5)[b] s
				1110(20) vwS	1042(10) vwS
1045(15) vwS	1085(5) wS	1051(5) vs	1145(10) vvwS		1062(8) vwS
1075(7) vwS					
1095(5) vs					
1130(15) vwS	1132(3)[b] vs	1120(5) vs	1168(5) vs	1178(3) vs	1118(10) vs
1170(12) vwS	1180(7) wS		1180(10) vwS		1180(15) vwS
1200(7) vwS			1205(15) vvwS	1215(15) vvwS	1208(7) wS
		1240(10) vwS			
1280(7) w	1270(10) w	1280(12) vwS	1280(15) vwS	1280(10) wS	1285(12) wS
					1308(10) vwS
1400(12) vw	1398(5) vw	1405(10) vw	1400(5) vw		1405(10) vw

[a]Compensated KBr pellets. S, shoulder.
[b]This frequency differs from the value quoted in ref. 8 by more than the stated uncertainty.

Table 2 contains the frequencies of all the minor features that can be detected in our spectra with reasonable confidence, many of the band profiles suggest the existence of further, unresolved peaks.

The weak or very weak band or shoulder at *ca.* 690 cm^{-1} was present in all the i.r. spectra of Table 3 but has not been reported by other authors (8, 26). If it is present in the Raman spectra, it must be very weak. The possibility cannot be ruled out that this feature is spurious, although we cannot offer an explanation for its presence.

The strong band at *ca.* 300 cm^{-1} is present in the i.r. spectra of SnP_2O_7 as well as in that of SnO_2 (41). It very likely corresponds to a deformation mode of the SnO_6 octahedron. The very intense SnO_2 band with a maximum at *ca.* 630 cm^{-1} is, however, seen in neither spectrum of SnP_2O_7; the vvw shoulder at *ca.* 635 cm^{-1} in the spectrum of $SnP_2O_7(2)$ occurs in the region of grating change-over of the spectrometer used and may not be real.

The main difference between the i.r. spectra of $SnP_2O_7(1)$ and $SnP_2O_7(2)$ is the sharpening of the bands at *ca.* 536 and 1010 cm^{-1} in *2* and the disappearance, or at least a great weakening, of the 1400 and 499 cm^{-1} bands of *1*. This last

Can. J. Chem. Downloaded from www.nrcresearchpress.com by 210.87.254.40 on 09/05/12
For personal use only.

Can. J. Chem. Downloaded from www.nrcresearchpress.com by 210.87.254.40 on 09/05/12
For personal use only.

difference is less evident in the Raman spectra. The increasing sharpness of the bands may be attributed to an improvement in crystallinity on firing. However, the band at 499 cm^{-1} appears to correspond to the 490 cm^{-1} i.r. band reported in ref. 3 for $ZrP_2O_7(I)$ but absent in the spectra of $ZrP_2O_7(II)$ and $ZrP_2O_7(III)$. While the 740 cm^{-1} band of the $ZrP_2O_7(I)$ spectrum reappears when *III* changes to *II* on cooling, the 490 cm^{-1} band does not, although Chaunac and co-workers (3) mention that the latter has been seen to reappear, partially, on cooling after *I* had been heated *very briefly* to 300 °C. The 490 cm^{-1} band could accordingly be considered to be characteristic of form *I*; its presence in the i.r. spectrum of $SnP_2O_7(1)$ suggests that $SnP_2O_7(1)$ was in fact $SnP_2O_7(I)$. The 469 cm^{-1} band in the i.r. spectrum of $SnP_2O_7(2)$ has its counterpart at 468 cm^{-1} in the spectrum of PbP_2O_7, but a similar band appears to be absent in the i.r. spectra of the Ti, Zr, and Hf compounds. The slight difference in the values of some of the i.r. frequencies of $SnP_2O_7(1)$ and $SnP_2O_7(2)$ (Table 3) may well arise from the better definition of the spectrum of *2*, though for the 1168, 1010, and 305 cm^{-1} bands the differences are probably real.

Raman Spectra

The photographic spectrum of ZrP_2O_7 reported in ref. 26 is grossly incomplete and the band frequencies are inaccurate, largely because of the weak intensities of most of the bands. The laser spectra (Figs. 3 and 4, Table 4) also suffer from the general weakness of the spectrum. Because of this and the uncertainty in the frequencies of weak shoulders and poorly resolved bands, it is difficult to establish with certainty which i.r. and Raman bands correspond and so to determine which modes are active in both spectra. These factors are also responsible for the often unsatisfactory agreement of i.r. and Raman frequencies which otherwise appear to correspond.

A further complication arose with the spectra of the Sn pyrophosphates. It was found that a spectrum of a pellet of $SnP_2O_7(1)$ obtained after the pellet had been exposed to laser light for about 6 h (Fig. 4*B*) differed from that of a freshly prepared, unirradiated pellet (Fig. 4*A*). It resembled more closely that of a freshly prepared pellet of $SnP_2O_7(2)$ (Fig. 4), except that the high scatter associated with sample *1* was still present. These differences are genuine, since the resolution of the sample *1* spectra is higher (7 cm^{-1}) than the resolution of the sample *2* spectrum (9 cm^{-1}). It seems therefore possible that the blue laser light causes a change from form *I* to form *II* on the surface of the pellet. However, the high scatter of spectrum 4*B* probably indicates that the crystallinity of the material was not changed, while the smoother spectrum of sample *2* is indicative of the improved crystallinity on prolonged firing. Further investigation would be required to verify these hypotheses.[6]

The spectra of the Ti, Zr, and Hf compounds (Fig. 3) are dominated by the very strong multiple bands in the 1200–1000 cm^{-1} region generally ascribed to P—O stretching modes. While these bands are prominent in all the spectra, in the spectra of the Sn and Pb compounds (Fig. 4) they are less intense than the band groups at *ca.* 340 cm^{-1} characteristic of MO_6 deformation modes.

Mössbauer ^{119}Sn Spectrum of SnP_2O_7

The spectra of $SnP_2O_7(1)$ appeared to consist of a single resonance absorption in the Sn(IV) velocity region, with no asymmetry or fine structure. There was no change in the appearance of the spectrum on cooling the absorber to 4.2 °K. The spectrum of $SnP_2O_7(2)$ was identical to that of $SnP_2O_7(1)$. No evidence of any Sn(II) absorption was found in spectra taken on a larger velocity scale.

All spectra were fitted to two models, (*a*) a single line and (*b*) a pair of lines of equal widths and intensities. The assumed line-shape was Lorentzian; for details of the fitting see ref. 24. The χ^2 of an acceptable fit was required to lie between the 1 and 99% limits of the χ^2 distribution, *i.e.* between about 150 and 242 for spectra with 194 degrees of freedom.

The Mössbauer parameters are listed in Table 5. The two-line fits (*b*) always gave substantially lower χ^2 than the one-line fits (*a*) and more acceptable values for the line width.[7] Indeed the

[6]It is likely that the small decrease in a_0 on firing $SnP_2O_7(1)$ (see Experimental) also reflects improved crystallinity of $SnP_2O_7(2)$. Shrinkage of the lattice parameters with increased firing temperature or time or both is a well-known occurrence in preparative solid-state reactions at high temperatures.

[7]The χ^2 values for fit (*b*) to the $SnP_2O_7(1)$ spectrum at 77 °K (Table 5) are too high. However, this spectrum was obtained to very high statistics and the untypically high χ^2 values may reflect the inadequacy of fitting to strictly Lorentzian shapes.

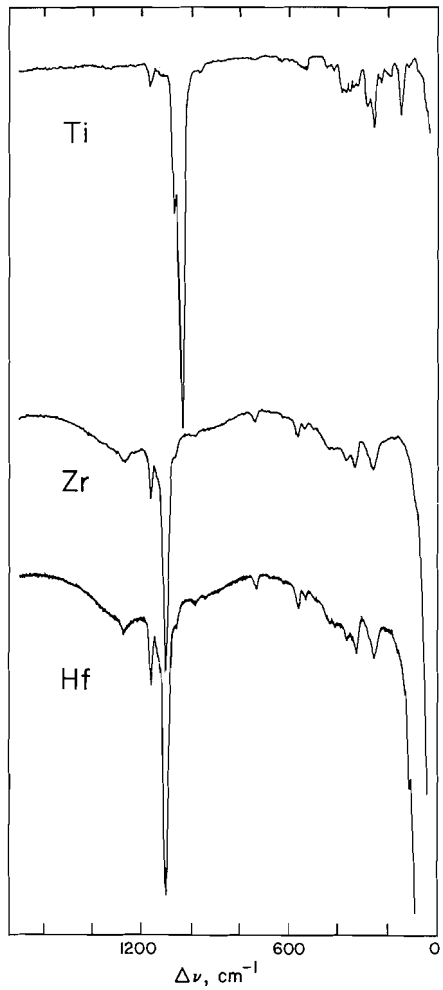

FIG. 3. Raman spectra of cubic MP_2O_7 (M = Ti, Zr, Hf) pyrophosphates in the region 1600–50 cm^{-1} (arbitrary intensity scale).

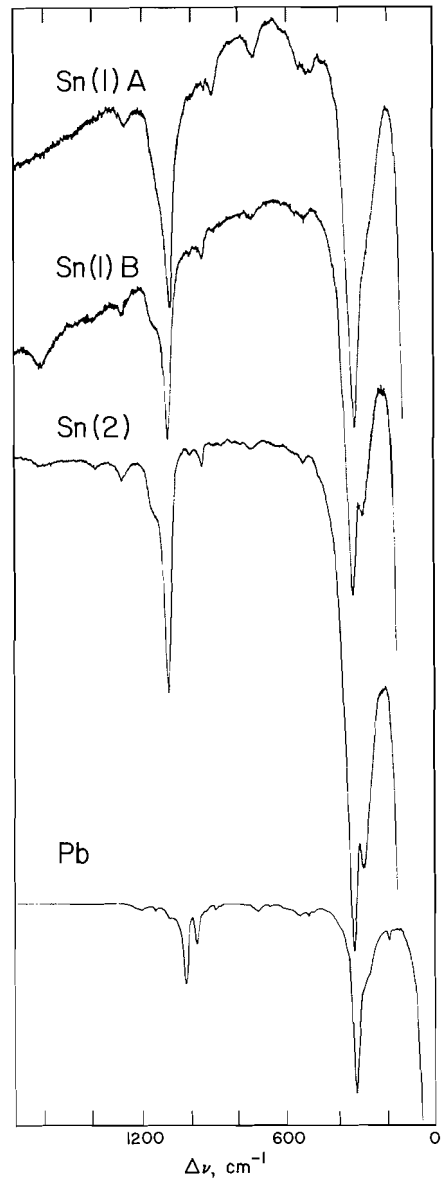

FIG 4. Raman spectra of cubic MP_2O_7 (M = Sn, Pb) pyrophosphates in the region 1600–50 cm^{-1} (arbitrary intensity scale). Sn(*1*)*A*, freshly prepared, unirradiated pellet; Sn(*1*)*B*, spectrum taken after *ca.* 6 h exposure to the laser beam and two months standing.

one-line χ^2 are not statistically acceptable. This may be taken as good evidence that the spectra consist at least of a pair of unresolved lines. The accuracy of the Δ and Γ values does not permit definite conclusions to be made about the effect of temperature lowering.

Discussion

Are the Cubic $M^{4+}P_2O_7$ Isostructural?

Only a complete determination of the individual crystal structures can provide a definitive answer. The crystallographic results will have to explain, or at least be compatible with, (*1*) the observed inconsistencies in the a_0 *vs.* $r^{vi}(M^{4+})$ plot (Fig. 5), and (*2*) the dissimilarities of some of the principal features of the Raman spectra (Figs. 3 and 4).

(*1*) Völlenkle *et al.* (15) accommodated the points of their a_0 *vs.* $r(M^{4+})$ plot on two separate curves, one containing Si, Ge, Sn, Pb and the other, the transition elements. An amended set of the Ahrens radii appears to have been

Can. J. Chem. Downloaded from www.nrcresearchpress.com by 210.87.254.40 on 09/05/12
For personal use only.

TABLE 4. Raman spectra of polycrystalline cubic MP_2O_7 pyrophosphates between 50 and 1600 cm^{-1}[a]

Ti	Zr	Hf	Sn(*1*)[b]	Sn(*2*)	Pb
69 S					
109 w		110 m			111 m
126 w		120 w			
140 m		138 vw			
		148 w	142 S		149 vw
156 vw	164 vw	163 w			170 vvw
183 w		177 vvw		180 vvw?	
195 vw					193 m
222 w		213 vvw?			212 vvw
253 m	254 m	255 m	~265 mBS		246 vvw?
275 w		304 vvw		300 s	~282 S
316 w					
327 w	326 m	329 m			
331 w					332 vs
348 w			341 vs	340 vs	
364 w	363 m	364 m			
371 vwS					376 S
381 w					394 S
416 wD?		413 vw			413 S
432 w	~436 vwD?	435 w	420 wS		
444 w		473 vvw	465 vwB	470 vwS	
	495 ?	495 vvw	507 vwB		499 w
527 vw	533 vw	532 w	525 vwB	522 w	520 m
536 vw					
548 vvw	561 w	560 m	550 vwB		555 w
559 vvwS				570 vvw	
625 vwB		?		637 vvw	613 vvwB
					676 w
737 vvw	737 w	738 w	741 w	741 vw	729 mB
					882 S
			911 w		902 w
	~940 vvw?	951 vvw	950 vwS	954 m	944 w
					960 w
961 vw	~993 vvwB?	998 vvw	998 vvwB	1001 w	984 m
982 vvw	1066 S	~1068 S			
		1104 s			
1038 vs	1106 vs	1109 s	1093 sB	1094 vs	1028 s
		~1140 S			
1070 m	1166 m	1166 m	1148 mS		1096 w
1119 vw					
1135 vvwS	?	?		1144 BS	1154 w
1165 w					
	1272 w	1271 w	1269 w	1272 m	1207 vwB
				1380 w	
				~1600 vvwB	

[a]S, shoulder; B, broad; D, doublet.
[b]Fresh pellet (see text).

used. Replotting the available $a_0(I)$ or $a_0(II)/3$ values (Table 1) against the most recent set of $r^{vi}(M^{4+})$ values (42) produces a less clear-cut result (Fig. 5): the points for Ge, Sn, and Pb are significantly below the straight line defined by the set Si, Ti, Hf, Zr, Pu, Ce, Th and do not fall on a straight line of their own. The spread does not seem to be ascribable to experimental inaccuracies. When more than one a_0 value have been reported for a particular M, the agreement is usually reasonable (Table 1), and the differences between $a_0(I)$ and $a_0(II)/3$ are quite small.

(*2*) The relative intensity of the Raman bands in the 340 cm^{-1} region, characteristic of MO_6 deformation modes, is considerably higher for Sn and Pb than for Ti, Zr, and Hf (Fig. 4), despite the general weakness of the Sn and Pb spectra. The difference, which is not evident in the i.r. spectra, can be explained as due to the greater polarizability of the Sn and Pb ions com-

Can. J. Chem. Downloaded from www.nrcresearchpress.com by 210.87.254.40 on 09/05/12
For personal use only.

TABLE 5. Mössbauer ^{119}Sn parameters of SnP_2O_7[a]

T (°K)	Model	δ	|Δ|	Γ	χ^2
Room temperature	*a*	−0.39(2)		1.14(1)	310, 243
	b	−0.40(2)	0.32(2)	0.99(2)	162, 122
77	*a*	−0.353(2)		1.121(8)	2424, 2635
	b	−0.353(6)	0.320(6)	0.944(8)	513, 673
4.2	*a*	−0.348(2)		1.15(1)	440, 425
	b	−0.349(8)	0.335(8)	0.961(16)	260, 173

[a]δ, chemical shift relative to $BaSnO_3$ at room temperature; |Δ|, quadrupole splitting; Γ, line width. All values are in mm/s. The parameters are the averages of the two mirror-image spectra (see text). The two χ^2 values refer to the spectra accumulated in channels 0–199 and 200–399 respectively.

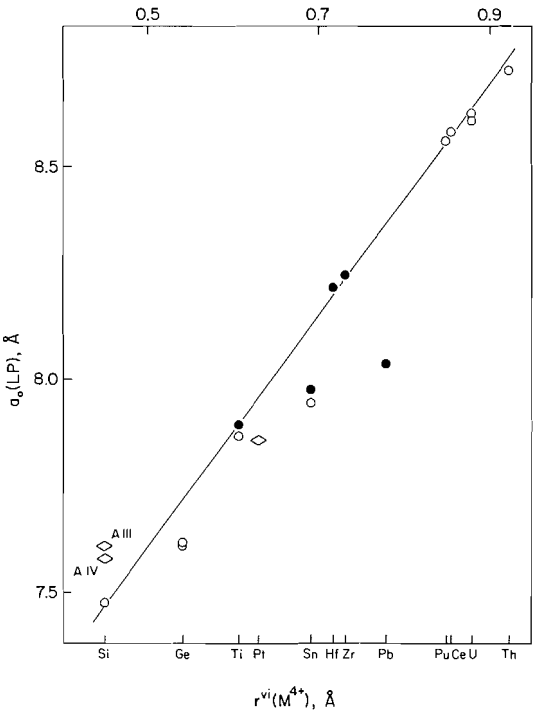

FIG. 5. Lattice parameters a_0(LP) of MP_2O_7 *vs.* empirical ionic radii of M^{4+} for 6-coordination (42). Full circles, this work; open circles, literature values (see Table 1). The $(V_{u.c.})^{1/3}$ values for the monoclinic SiP_2O_7*AIII* (21), SiP_2O_7*AIV* (22), and PtP_2O_7 (43) pyrophosphates are shown for comparison (rhombs).

pared with Ti, Zr, and Hf. Stated differently, it is due to the higher degree of covalency of the M—O bonds in the pyrophosphates of the typical elements (*cf.* also the isomer shift in SnP_2O_7, below). The consequence of increased covalency would be a shortening of the M—O distances, which in turn would be reflected in a reduction of the lattice parameter.

It would appear that the failure of the points for Ge, Sn, and Pb to fall on the straight line of Fig. 5 has some foundation in differences in the electronic configurations of the M^{4+} atoms. Ge, Sn, and Pb have d^{10} configurations, whereas the M^{4+} with points on the straight line do not contain, formally, electrons beyond the inert-gas cores.

Infrared and Raman Spectra

Some of the existing partial, approximate assignments of the i.r. frequencies (7–12) are based on normal-coordinate analysis of the P_2O_7 ion under the symmetry D_{3d} (7) or D_{3h} (in $M_2^{2+}P_2O_7$, *cf.* ref. 10). However, the X-ray evidence leads to the conclusion that forms *I* and *II* contain nonlinear P—O—P groupings and so the spectra must be interpreted on the assumption that the anion has a lower symmetry, *viz.*, C_{2v}, C_s, C_2, or C_1. Even if one accepts that 11% of the P—O—P bridges in SiP_2O_7(*II*) are linear, and assuming that all the MP_2O_7(*II*) are strictly isostructural with SiP_2O_7(*II*), the dominant contribution to the spectrum will be from P_2O_7 having configurations of symmetries other than trigonal.

Since form *I* contains a large number of P_2O_7 rotational orientations about the P—P vectors and these orientations are at random, there will be a quasi-continuous distribution of frequencies about a mean for each vibrational mode of the anion; this will appear as line broadening. The frequency density of such a distribution will be higher than in form *II*, where ideally (assuming analogy with SiP_2O_7(*II*)) only six distinct P_2O_7 configurations and environments would be expected. Comparison of the spectra of SnP_2O_7-(*I*) and SnP_2O_7(*II*) (Fig. 2), however, shows only minor differences between the two. The crystal structure of *I* is in principle indeterminate, except in the statistical (space-averaging) sense. Hence even if the structures of the form *II* com-

Can. J. Chem. Downloaded from www.nrcresearchpress.com by 210.87.254.40 on 09/05/12
For personal use only.

Can. J. Chem. Downloaded from www.nrcresearchpress.com by 210.87.254.40 on 09/05/12
For personal use only.

pounds were known in detail, the possibility of a *detailed* interpretation of the spectra appears remote.

The number of bands between *ca.* 1300 and 400 cm^{-1} in some of the spectra (Ti, Pb; Table 3) is compatible with the symmetries C_2, C_s, and C_1, for which 21 i.r. active fundamentals would be expected; in *all* the spectra it is greater than the number (ten) of i.r. active fundamentals that would be expected if the anion were of symmetry D_3, and the complicated band shapes indicate the existence of unresolvable component bands of closely spaced frequencies.[8] Numerous similarities in the frequency values for the cubic MP_2O_7 and the pyrophosphates of Mg(α), Ca, Sr, and Ba provide further circumstantial support for the anion having a symmetry lower than trigonal, for the anion is known to be bent in α-$Mg_2P_2O_7$ (44). However, the principal band assignments made under symmetry D_{3d} (and also under D_{3h}) do go some way toward an understanding of the spectra in a general way.

In view of the complexity of the structures of *I* and *II* the real nature of Lazarev's "diagnostic" band at 740 cm^{-1} is not clear. Lazarev assigns this band to the symmetric stretching fundamental of the P—O—P group, which should be i.r. inactive if the anion were of symmetry D_{3d} or D_{3h}. Hubin and Tarte (8) interpret this band as arising from the antisymmetric stretching vibration of the P—O—P group, but as pointed out by Chaunac and coworkers (3; *cf.* also ref. 7), this can hardly be correct in view of the temperature dependence of the intensity of this band. Lazarev's assignment, which is consistent with other evidence presented by Mooney and Goldsmith (7), was adopted by these authors in their calculation of force constants of P_2O_7 in cubic MP_2O_7 from the experimental i.r. frequencies of Hubin and Tarte; the assumption of the D_{3d} symmetry for the anion unfortunately renders the calculation unrealistic. If the 740 cm^{-1} band does correspond to the symmetric stretching fundamental, its width should reflect the effect of the distribution of P_2O_7 geometries, but as comparison of the spectra of $SnP_2O_7(I)$ and $SnP_2O_7(II)$ shows, the difference for the two forms is not readily discernible. This is perhaps a manifestation of the relative insensitivity of the frequencies to changes in the geometry of the ion.

[8]Because of their general weakness the Raman spectra (Table 4, Figs. 3 and 4) are less well suited for arguments based on the observed number of bands.

The ^{119}Sn Chemical Shift in SnP_2O_7

The chemical shift in SnP_2O_7 lies, at room temperature as well as at 77 °K (Table 5), between those of Cs_2SnF_6 and $K_2SnF_6.H_2O$ (35). It is close to the most negative δ value reported to date, that for $CuSnF_6.4H_2O$ (35):

	δ value (mm/s)	
Compound	Room temperature	77 °K
Cs_2SnF_6	−0.374(8)	−0.281(10)
$K_2SnF_6.H_2O$	−0.413(8)	−0.390(6)
$CuSnF_6.4H_2O$	−0.456(10)	−0.415(10)

Lees and Flinn (33) regarded the Sn atom in K_2SnF_6 as being close to the ideal Sn^{4+} and used its δ value to define the $4d^{10}$ point in their chemical-shift calibration equation. SCFMO calculations of Greenwood *et al.* (45) have, however, shown that in the SnF_6^{2-} ion there is appreciable occupation of the 5s and 5p orbitals of the Sn atom, *viz.*, ~0.7 and 1.3 electrons respectively. A linear relation between δ and the 5s orbital occupation number was also found. In view of the closeness of the δ values for $SnP_2O_7(I)$ and the hexafluostannates the electron densities at the Sn atom in these structures must then be very similar but quite different from that in SnO_2. This difference is not unexpected. In the SnP_2O_7 structure each tin atom is surrounded by six oxygen neighbors as in SnO_2, but unlike in the oxide each of the oxygen atoms has a phosphorus nearest neighbor. The electron charge density on these oxygens will be reduced owing to formation of a strong covalent bond with the P atom. This in turn will reduce the degree of covalency between the oxygens and the Sn^{4+} ion and lead to a decrease in s-electron density from that in SnO_2, as observed. It is also noted that the chemical shift of Sn(II) pyrophosphate is close to that of SnF_2 (33).

Jørgensen (46) has shown that the nephelauxetic ratio β may be factored into a metal-ion parameter and a ligand parameter *h*. Duffy and Ingram (47) have recently discussed covalency in molten salts and glasses in terms of this *h* factor and shown that a linear relation exists between *h* and the splitting between the s and p levels of the metal ion as measured optically.

Can. J. Chem. Downloaded from www.nrcresearchpress.com by 210.87.254.40 on 09/05/12
For personal use only.

This splitting is expected to decrease with increasing covalency. It is thus reasonable to conclude that there is an approximate correlation between covalency and the h factor. The values of h for phosphate, fluoride, and oxide ligands are ~ 1.0, 0.8, and 2.4 respectively (46), so that the degree of covalency of the pyrophosphate is much closer to that of the fluoride than that of the oxide, as observed. SnP_2O_7 must thus be regarded as one of the most ionic compounds of tetravalent tin known.

Quadrupole Splitting in SnP_2O_7

Mössbauer ^{119}Sn spectra are expected to show quadrupole splitting for Sn atoms in sites of symmetry lower than cubic. This is the situation encountered in $SnP_2O_7(I)$. Because of the random orientations of the P_2O_7 anions the symmetry of the SnO_6 octahedra will be at most $\bar{3}$. If *all* the octahedra were equivalent and of symmetry $\bar{3}$ (the case of the LP structure), the quadrupole-split spectrum would be symmetric and simple, and the observed separation of the components of the doublet would measure the value of the splitting Δ uniquely.[9] However, in $SnP_2O_7(I)$ the majority of the octahedra will have symmetries lower than $\bar{3}$, mostly non-axial, and even octahedra having the same point-group symmetry may be expected to be metrically different. Such a distribution of geometries will be reflected in a distribution of Δ values, and instead of a simple spectrum a composite spectrum consisting of a pair of broadened, possibly non-Lorentzian-shaped lines will be observed. The widths of the lines of model *b* (Table 5), however, are of the same order as those observed in cubic hexafluostannates (35) for comparable absorber thickness. Hence we conclude that the distribution about the mean of electric field gradient (e.f.g.) values arising from the distribution of SnO_6 geometries is too small to give rise to any appreciable line broadening, and so the observed separation, ~ 0.32 mm/s, may be taken to be the unique value of Δ.

This insensitivity of Δ to variations in SnO_6 geometry present in $SnP_2O_7(I)$ is further manifested on comparing the spectra of $SnP_2O_7(I)$ and $SnP_2O_7(II)$: although only a small number of distinct types of SnO_6 octahedra is expected to be present in *II* (six if *II* is isostructural with $SiP_2O_7(II)$) compared with the quasi-continuous distribution in *I*, the spectra are indistinguishable. In these circumstances it is reasonable to attempt an estimate of the relative contributions made to the observed Δ by the two components of the e.f.g. at the Sn atom, $q_{\text{latt.}}$ and $q_{\text{val.}}$. Assuming the symmetry of the SnO_6 octahedron to be $\bar{3}$, $\Delta = \frac{1}{2}e^2qQ$, $a = (1 - R)q_{\text{val.}} + (1 - \gamma_\infty)q_{\text{latt.}}$, where R and γ_∞ are the Sternheimer antishielding factors for the valence (val.) and lattice (latt.) contributions respectively. An estimate of $q_{\text{latt.}}$ can then be obtained from a point-charge model. A calculation using the average positional parameters of the Sn, P, and O atoms as determined from the structure refinement in $Pa3$ (Table 2), and assuming formal charges of 4+, 5+, and 2− respectively, gave $q_{\text{latt.}} = 0.384 \times 10^{14}$ e.s.u./cm^3. Taking $Q(\text{Sn}) = -0.07 \times 10^{-24}$ cm^2 (48) and $\gamma_\infty = -10$ (49) leads to an expected Δ of only about 0.05 mm/s, *i.e.* about six times smaller than the observed value and only about 1/20 the resonance line-width. Covalency and polarization factors will necessitate reduction of the formal charges on the ions which in turn will reduce $q_{\text{latt.}}$ still further. When the computation was repeated for the formal charges of 4+, 1.5+, and 1−, the resulting values were 0.135×10^{14} e.s.u./cm^3 for $q_{\text{latt.}}$ and 0.02 mm/s for Δ. It can thus be argued that a significant, possibly the dominant, contribution to the observed Δ comes from $q_{\text{val.}}$. A nonzero $q_{\text{val.}}$ term implies nonzero occupancy of the valence orbitals on the Sn atom, *i.e.* the "Sn^{4+} ion" is not ideal (*cf.* preceding section). When the symmetry of the Sn site is lowered from $m3m$ to $\bar{3}$, the t_{1u} orbitals, formed from the 5p atomic orbitals of Sn and ligand-group orbitals, are split into a doublet E_u (p_x, p_y character) and a singlet A_u (p_z character). The e.f.g. then arises from differences in p-character of this doublet and singlet. The $q_{\text{val.}}$ term cannot be calculated as the distribution of the valence electrons on the Sn atom is not known.

[9]In principle a distribution of environments of the Sn atom would produce a distribution of chemical shift values, which too might falsify evaluation of Δ from the experimental spectrum. However, in SnP_2O_7 the δ distribution must be completely negligible; in the cubic pyrochlores $Ln_2Sn_2O_7$ (Ln = La to Lu) the progressive distortion of the SnO_6 octahedron of symmetry $\bar{3}m$ increases Δ from ~ 0.42 to ~ 0.80 mm/s, yet δ remains constant (50, 51).

We wish to express our gratitude to Dr. L. D. Calvert for obtaining the Guinier photographs; Dr. J. A. Duffy for many helpful discussions; Dr. M. Falk for the use of

his i.r. spectrometer; Dr. C. R. Masson and Mr. J. Uher for the oxygen analyses by vacuum fusion; Dr. W. G. Parker for obtaining the low-temperature Mössbauer spectra of SnP_2O_7; and Mr. P. F. Seto for obtaining some of the i.r. spectra. Award of an INCO Graduate Research Fellowship to one of the authors is gratefully acknowledged.

This investigation was supported by a grant in aid of research from the National Research Council of Canada.

1. H. McD. McGeachin. Acta Cryst. **14**, 1286 (1961).
2. M. Chaunac. Bull. Soc. Chim. Fr. 424 (1971).
3. R. Pascard, M. Chaunac, and E. Grison. Bull. Soc. Chim. Fr. 429 (1971).
4. A. N. Lazarev and V. S. Aksel'rod. Opt. Spektrosk. **9**, 326 (1960).
5. A. N. Lazarev. Izv. Akad. Nauk. SSSR, Otd. Khim. Nauk. **7**, 1314 (1962).
6. A. N. Lazarev and T. F. Tenisheva. Izv. Akad. Nauk. SSSR, Ser. Khim. **3**, 403 (1964).
7. R. W. Mooney and R. L. Goldsmith. J. Inorg. Nucl. Chem. **31**, 933 (1969).
8. R. Hubin and P. Tarte. Spectrochim. Acta, **23A**, 1815 (1967).
9. J. Lecomte, A. Boullé, C. Dorémieux-Morin, and B. Lelong. C. R. **255**, 621 (1962); **258**[6], 131 (1964).
10. A. Hezel and S. D. Ross. Spectrochim. Acta, **23A**, 1583 (1967).
11. E. Steger and B. Kässner. Z. Anorg. Allg. Chem. **355**, 131 (1967).
12. E. Steger and B. Kässner. Spectrochim. Acta, **24A**, 447 (1968).
13. G. R. Levi and G. Peyronel. Z. Krist. **92A**, 190 (1935).
14. E. Tillmanns, W. Gebert, and W. H. Baur. J. Solid State Chem. **7**, 69 (1973).
15. H. Völlenkle, A. Wittman, and H. Nowotny. Monatsh. Chem. **94**, 956 (1963).
16. L.-O. Hagman and P. Kierkegaard. Acta Chem. Scand. **23**, 327 (1969).
17. F. Liebau, G. Bissert, and N. Köppen. Z. Anorg. Allg. Chem. **359**, 113 (1968).
18. A. Burdese and M. Lucco Borlera. Atti Accad. Sci. Torino, Cl. Sci. Fis. Mat. Nat. **94**, 97 (1959–60).
19. A. Burdese and M. Lucco Borlera. Atti Accad. Sci. Torino, Cl. Sci. Fis. Mat. Nat. **94**, 107 (1959–60); Ric. Sci. **30**, 1343 (1960).
20. A. Burdese and M. Lucco Borlera. Ann. Chim. Rome, **53**, 333 (1963).
21. G. Bissert and F. Liebau. Acta Cryst. B, **26**, 233 (1970).
22. F. Liebau and K.-F. Hesse. Z. Krist. **133**, 213 (1971).
23. G. Hevesy and K. Kimura. J. Am. Chem. Soc. **47**, 2541 (1925).
24. O. Knop, C.-H. Huang, and F. W. D. Woodhams. Am. Miner. **55**, 1115 (1970).
25. M. Lucco Borlera and A. Burdese. Atti Accad. Sci. Torino, Cl. Sci. Fis. Mat. Nat. **94**, 89 (1959–60).
26. E. Steger and G. Leukroth. Z. Anorg. Allg. Chem. **303**, 169 (1960).
27. G. Peyronel. Gazz. Chim. Ital. **69**, 254 (1939).
28. D. E. Harrison, H. A. McKinstry, and F. A. Hummel. J. Am. Ceram. Soc. **37**, 277 (1954).
29. G. Peyronel. Z. Krist. **94A**, 311 (1936).
30. C. W. Bjorklund. J. Am. Chem. Soc. **79**, 6347 (1958).
31. O. Knop, F. Brisse, L. Castelliz, and Sutarno. Can. J. Chem. **43**, 2812 (1965).
32. J. Loader. Basic laser Raman spectroscopy. Heyden and Son Ltd., London, 1970.
33. J. K. Lees and P. A. Flinn. J. Chem. Phys. **48**, 882 (1968).
34. C.-H. Huang. M.Sc. Thesis. Dalhousie University, Halifax, Nova Scotia. 1967.
35. F. W. D. Woodhams, R. A. Howie, and O. Knop. Can. J. Chem. **52**, 1904 (1974).
36. D. T. Cromer and J. T. Waber. Acta Cryst. **18**, 104 (1965).
37. International tables for X-ray crystallography. Vol. 3. The Kynoch Press, Birmingham. 1962.
38. M. Tokonami. Acta Cryst. **19**, 486 (1965).
39. Sutarno, O. Knop, and K. I. G. Reid. Can. J. Chem. **45**, 1391 (1967).
40. S. Z. Haider. Anal. Chim. Acta, **24**, 250 (1961).
41. F. Brisse and O. Knop. Can. J. Chem. **46**, 859 (1968).
42. O. Knop and J. S. Carlow. Can. J. Chem. **52**, 2175 (1974).
43. B. Wellmann and F. Liebau. Acta Cryst. B, **28**, S 59 (1972).
44. C. Calvo. Acta Cryst. **23**, 289 (1967).
45. N. N. Greenwood, P. G. Perkins, and D. H. Wall. Symp. Faraday Soc. **1**, 51 (1967).
46. C. K. Jørgensen. Absorption spectra and chemical bonding in complexes. Pergamon Press, New York. 1962. pp. 138 and 187.
47. J. A. Duffy and M. D. Ingram. J. Chem. Phys. **54**, 443 (1971).
48. A. H. Muir, K. T. Ando, and H. M. Coogan. Mössbauer effect data index, 1958–1965. Interscience, New York. 1967. p. 126.
49. M. Cordey-Hayes. *In* Chemical applications of Mössbauer spectroscopy. *Edited by* V. I. Gol'danskii and R. H. Herber. Academic Press, New York. 1968. p. 322.
50. C. Ayasse. Ph.D. Thesis. Dalhousie University, Halifax, Nova Scotia. 1972.
51. H. M. Loebenstein, R. Zilber, and H. Zmora. Phys. Lett. **33A**, 453 (1970).

Can. J. Chem. Downloaded from www.nrcresearchpress.com by 210.87.254.40 on 09/05/12
For personal use only.

Radiation-sensitized Thermal Cracking of *n*-Butane. II. Ionic Reactions

SHINGO MATSUOKA[1]

Central Research Laboratory, The Furukawa Electric Co., Ltd., 2-9-15, Futaba, Shinagawa-ku, Tokyo, Japan

TAKAAKI TAMURA AND KEICHI OSHIMA

Department of Nuclear Engineering, Faculty of Engineering, University of Tokyo, Bunkyo-ku, Tokyo, Japan

AND

YUNOSUKE OSHIMA

Japan Atomic Energy Research Institute, Takasaki Research Establishment, Watanuki-cho, Takasaki-shi, Gunma-ken, Japan

Received May 1, 1974

SHINGO MATSUOKA, TAKAAKI TAMURA, KEICHI OSHIMA, and YUNOSUKE OSHIMA. Can. J. Chem. **53**, 92 (1975).

Ionic reactions in the radiolysis of *n*-butane were studied at temperatures ranging from 17 to 548 °C. Ionic chain reactions were found for the first time to take part in the radiation-sensitized thermal cracking mechanism of hydrocarbon system.

The isobutane and isobutene yields increased with increasing temperature and at 548 °C their *G*-values reached 31.2 and 12.1, respectively, though they were not formed by the thermal cracking of *n*-butane. The formation was completely suppressed by the addition of 0.15 mol% ammonia. They were produced with high yields irrespective of the kind of wall of the irradiation cells. It was concluded from these results that isobutane and isobutene were formed by homogeneous ionic chain reactions with activation energies. Part of the propane product was also found to have been formed by ionic chain reactions. From the effect of adding *n*-pentane on the yields of the ionic products, $C_4H_9^+$ ion was inferred as the carrier ion.

In the vicinity of room temperature, formation by ionic reactions of polymers with more than 14 carbon atoms was inferred from the material balance of the products from H_2 to C_{14}.

SHINGO MATSUOKA, TAKAAKI TAMURA, KEICHI OSHIMA et YUNOSUKE OSHIMA. Can. J. Chem. **53**, 92 (1975).

On a étudié les réactions ioniques de la radiolyse du *n*-butane dans un intervalle de température de 17 à 548 °C. Les réactions ioniques en chaîne ont été observées pour la première fois dans le mécanisme de craquage thermique, sensibilisé par les radiations, d'un système d'hydrocarbure.

Les rendements pour l'isobutane et l'isobutène augmentent avec l'élévation de température, et à 548 °C les valeurs *G* atteignent respectivement 31.2 et 12.1, même s'ils ne sont pas formés par le craquage thermique du *n*-butane. La formation a été entièrement supprimée par l'addition de 0.15 mol% d'ammoniac. On les a obtenu avec de hauts rendements sans tenir compte de la sorte de paroie des cellules servant à l'irradiation. Ces résultats indiquent que l'isobutane et l'isobutènes sont formés par des réactions ioniques en chaîne homogène ayant des énergies d'activation. On a trouvé qu'une partie de propane s'est formée par des réactions ioniques en chaîne. L'effet produit par addition de *n*-pentane sur les rendements en produits ioniques indique que l'ion $C_4H_9^+$ est impliqué comme ion vecteur.

Au voisinage de la température ambiante, la formation par des réactions ioniques de polymères, ayant plus de 14 atomes de carbone est déduite du bilan matériel des produits de H_2 à C_{14}.

[Traduit par le journal]

Introduction

The radiation-sensitized thermal cracking (r.t.c.) of hydrocarbons has been studied by many workers mainly from the viewpoint of industrial interest (1–6). Its reaction mechanism, however, has not been subjected to close investigation, since a radiation-initiated radical chain mechanism which is similar to the well-known radical chain mechanism for the thermal cracking of hydrocarbons has been taken for granted.

On the other hand, Bansal and Freeman (7) and van der Linde and Freeman (8) carried out a detailed study of the r.t.c. of alcohols, and have discovered that ionic chain reactions take part in the reaction system. These ionic chain

[1]Present address: Japan Atomic Energy Research Institute, Takasaki Research Establishment, Watanuki-cho, Takasaki-shi, Gunma-ken 370-12, Japan.

Can. J. Chem. Downloaded from www.nrcresearchpress.com by 210.87.254.105 on 09/05/12
For personal use only.

Can. J. Chem. Downloaded from www.nrcresearchpress.com by 210.87.254.105 on 09/05/12
For personal use only.

reactions involve formation of a protonated cluster of alcohols and its subsequent thermal decomposition. Nakagawa *et al.* have observed the large yields of benzene ($G = 28.5$) and cyclohexene ($G = 14.0$) in the radiolysis of 1,4-cyclohexadiene vapor at room temperature and a pressure of 42 Torr, and have interpreted these products in terms of an ionic chain mechanism (9, 10).

In a previous paper (11), we reported the behavior of radical products from the r.t.c. of *n*-butane. The present paper is concerned with the behavior of several ionic products and describes especially a participation of ionic chain reactions in the r.t.c. mechanism.

Experimental

The apparatus and techniques used for the experiments were described in detail in the previous paper (11). Experiments were carried out in both static and flow systems. The cylindrical Pyrex irradiation cells with 0.3 mm thick electron admission windows (105 mm long and 16.5 mm i.d.) were used for the static experiments and the copper irradiation cell with a 0.04 mm thick stainless steel window (124 mm long and 17 mm i.d.) for the flow experiments, unless otherwise stated.

Irradiations were performed with a collimated 1.5 MeV electron beam from a Hitachi Cockcroft–Walton type accelerator. The absorbed dose in the static experiments was measured by the ethylene dosimeter assuming $G(H_2) = 1.31$ (12), and in the flow experiments it was determined on the basis of the acetylene yield of $G(C_2H_2) = 2.45$ from the radiolysis of ethylene (11). The product yields from the r.t.c. of *n*-butane-additive mixtures were calculated on the basis of the energy absorbed only in the *n*-butane. The dose rate distribution curve along the length of the cell was shown previously.

The total gas pressure of the samples used in the static experiments was 400 mm Hg at 0 °C, and in the flow experiments it was constant at atmospheric pressure irrespective of reaction temperature.

The reactants *n*-butane, ethylene, propylene, and ammonia were the same as those used before. GR grade *n*-pentane (99.99%) obtained from Tokyo Kagaku Seiki Co. was dried with molecular sieve 3A before use.

The products hydrogen and hydrocarbons from C_1 to C_8 were analyzed by gas chromatography (11). For some samples, the C_9–C_{14} products were also analyzed by gas chromatography, using a 25 m Apiezon-L capillary column (0.25 mm i.d.) at 150 °C.

Results and Discussion

(A) Formation of Isobutane and Isobutene

(i) Effect of Temperature

The yields of isobutane and of isobutene from the radiolysis of *n*-butane were measured at temperatures between 17 and 548 °C. Arrhenius plots of them are shown in Fig. 1.[2] To investigate the effect of the wall of the irradiation cell on these products, several kinds of walls were used. In the static experiments, Pyrex cells and internally silver-coated Pyrex cells were compared under the following reaction conditions: dose rate = 1.17×10^{18} eV/g s, dose[3] = 3.41×10^{20} to 3.10×10^{19} eV/g, conversion of *n*-butane = 0.101 to 2.00%. In the flow experiments, the quartz and the copper cells were used under these conditions: dose rate = 9.3×10^{17} eV/g s for the copper cell, 1.30×10^{18} eV/g s for the quartz cell, contact time = 16.6 to 24.0 s, conversion = 0.055 to 5.0%.

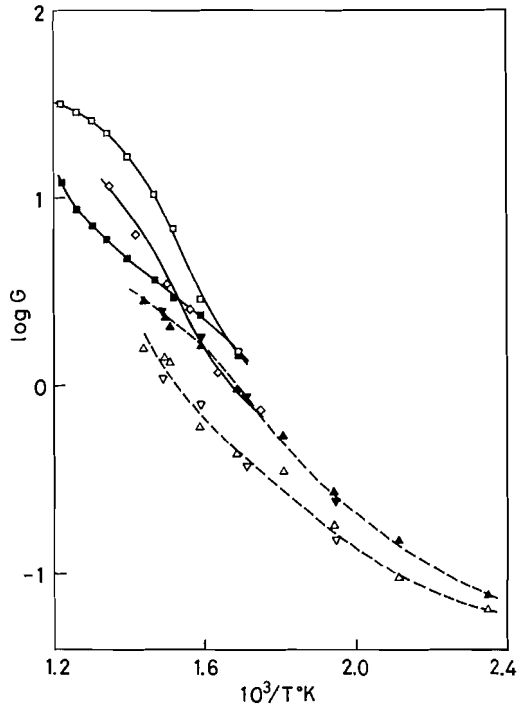

FIG. 1. Arrhenius plots for the formation of isobutane (open points) and of isobutene (filled points) in the various irradiation cells: (△, ▲) Pyrex cell and (▽, ▼) internally silver-coated Pyrex cell, in the static experiments; (◇) quartz cell and (□, ■) copper cell, in the flow experiments.

The *G*-values of isobutane and isobutene

[2]The isobutane yield in the flow system increased, finally reaching the asymptotic value, as the time of passing the feed gas through the flow line became longer. This increase is probably due to the dessication of the flow line (see later). The yields reported were measured after a sufficient aging time of the flow line.

[3]Dose was varied corresponding to reaction temperature.

TABLE 1. Effect of varying amount of ammonia on the yields of several products from the r.t.c. of *n*-butane at 393 °C, in the static experiments with Pyrex cells

Products	G-values with amount of NH_3 (mol%) = 0	0.021	0.146	0.99	2.48	10.1	20.0
$-n$-B	270	276	266	274	273	292	295
Pr	4.7	4.4	3.73	3.27	2.96	2.69	2.30
cyclo-Pr	—	0.0066	0.0045	0.018	0.029	0.048	0.046
iso-B	1.37	0.200	0.120	0.109	0.111	0.117	0.098
iso-B$^=$	2.15	1.31	0.185	0.201	0.142	0.136	0.078
1-B$^=$	1.96	2.25	2.50	2.70	2.45	2.32	1.92
trans-2B$^=$	2.17	2.26	2.25	2.39	2.25	2.27	2.09
cis-2B$^=$	1.37	1.39	1.44	1.43	1.41	1.31	1.22
2M1B$^=$	0.154	0.084	0.055	0.067	0.077	0.074	0.055
2M2B$^=$	0.240	0.208	0.086	0.048	0.045	0.040	0.037
Hexenes	0.39	0.49	0.367	n.d.	0.227	0.217	0.210
Heptenes	0.63	1.44	1.01	n.d.	0.41	0.44	n.d.

*B = butane, B$^=$ = butene, M = methyl, Pr = propane.

increased with increasing temperature and in the copper cell reached 31.2 and 12.1, respectively, at 548 °C. Their yields from the thermal cracking (t.c.) at 548 °C did not amount to even 0.5% of those from the r.t.c., even when the t.c. reaction proceeded to the same conversion as the r.t.c. reaction did. The apparent activation energies for the formation of isobutane and isobutene varied with temperature, and at 400 °C they were about 15 and 8 kcal/mol, respectively.

(ii) Effect of Adding Ammonia

Table 1 shows the effect of ammonia added in varying amounts on the yields of several products related to ionic reactions. The experiments were carried out in the static system under the following conditions: temperature = 393 °C, dose rate = 1.24×10^{18} eV/g s, dose = 3.72×10^{19} eV/g, conversion = 1.1%.

The effect of adding 11.4 mol% ammonia at 449 °C, obtained in the flow system is presented in Table 2. The dose rate was 9.8×10^{17} eV/g s, the contact time 16.2 to 14.5 s, and the conversion 1.2%.

The striking suppression of the formation of isobutane and isobutene, caused by the addition of ammonia is seen from Tables 1 and 2.

(iii) Effect of Adding Propylene

Isobutane and isobutene were formed as minor products; for instance, at 548 °C they constituted only 0.47 and 0.18 mol% of the total products, respectively. We studied the effect of propylene, one of the major products, on the formation of the isomerized C_4 products (in the flow system).

TABLE 2. Effect of ammonia addition on the yields of several products from the r.t.c. of *n*-butane at 449 °C, in the flow experiments with the quartz cell

Products	*G*-values with amount of NH_3 (mol%) = 0	11.4
$-n$-B	800	870
Pr	7.9	4.0
cyclo-Pr	—	0.053
iso-B	8.4	0.097
iso-B$^=$	3.7	0.085
1-B$^=$	5.1	6.0
trans-2B$^=$	5.3	5.6
cis-2B$^=$	3.30	3.48
Higher paraffins	1.58	1.11
Higher olefins	2.00	1.92

The results are given in Fig. 2*A*. The amount of propylene in Fig. 2*A* is the sum of the added propylene and a half of the product propylene. The experimental conditions used were as follows: temperature = 449 °C, dose rate = 9.8×10^{17} eV/g s, contact time = 13.4 to 15.8 s, conversion = 1.17 to 0.24%.

The isobutene formation is seen to be sensitized by propylene and on the contrary the isobutane formation to be suppressed.

(iv) Effect of Adding n-Pentane

Figure 2*B* shows the effect of adding *n*-pentane (0 to 3.6 mol%) on the yields of the isomerized C_4 and C_5 products. The *n*-pentane added contained 2-methylbutane, 2-methyl-1-butene, and 2-methyl-2-butene as impurities, and the yields in Fig. 2*B* were corrected for these

Can. J. Chem. Downloaded from www.nrcresearchpress.com by 210.87.254.105 on 09/05/12
For personal use only.

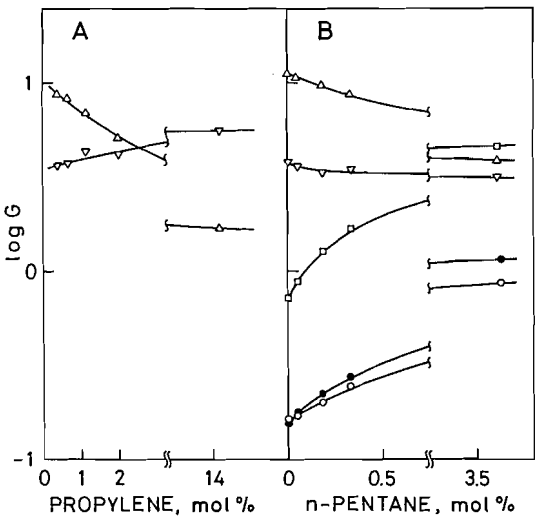

FIG. 2. The effects of the additives on the yields of (△) isobutane, (▽) isobutene, (□) 2-methylbutane, (○) 2-methyl-1-butene, and (●) 2-methyl-2-butene from the r.t.c. of *n*-butane at 449 °C in the flow experiments with the quartz cell.

impurities; the maximum corrections were 2.9, 44, and 44% respectively. The experimental conditions were the same as used in the experiments on the effect of propylene addition.

As seen in Fig. 2*B*, the yields of isobutane and isobutene decreased with increasing *n*-pentane and on the contrary, the yields of 2-methylbutane, 2-methyl-1-butene, and 2-methyl-2-butene, which were not formed by radical reactions, increased.

Formation Mechanism

The following results indicate that isobutane and isobutene were formed by homogeneous ionic chain reactions. (*a*) The *G*-values of isobutane and isobutene both exceeded 10 at high temperatures (Fig. 1). (*b*) They were not formed by the t.c. of *n*-butane and their formation by the r.t.c. was completely inhibited by the addition of ammonia. (*c*) Their formation is not due to the radiation-sensitized wall effect, because they were produced with high yields in all kinds of walls studied. (*d*) At the dose rates used in the present experiments, the ions formed in the gas-phase are considered to react according to homogeneous kinetics (13).

In the present system, the primary ions formed by ionizing radiation change mostly into $C_4H_9^+$ ions by ion–molecule reactions (14, 15). If we assume that the precursor ion for the isomerized C_4 products is $C_4H_9^+$, the decrease of the yields of these products by the addition of *n*-pentane (Fig. 2*B*) is explained by the following hydride ion transfer reaction.

[1] $C_4H_9^+ + n\text{-}C_5H_{12} \rightarrow C_5H_{11}^+ + C_4H_{10}$

The newly formed $C_5H_{11}^+$ ion is probably the precursor of the isomerized C_5 products, in agreement with the experimental observation.

We propose a following mechanism for the isobutene formation.

[2] $s\text{-}C_4H_9^+ + C_3H_6 \rightarrow C_7H_{15}^+$

[3] $C_7H_{15}^+ \rightarrow C_7H_{15}'^+$ (isomerization)

[4] $C_7H_{15}'^+ \rightarrow C_3H_7^+ + \text{iso-}C_4H_{10}$

[5] $C_3H_7^+ + n\text{-}C_4H_{10} \rightarrow s\text{-}C_4H_9^+ + C_3H_8$

The reactant propylene in reaction 2 is produced as a major product of the radical chain reactions (11). Although Abramson and co-worker have reported that reaction 2 did not proceed at 0.005 Torr (16), at higher pressures as in our system this reaction probably proceeds. As shown in Table 1, the heptene yield increased from 0.63 to 1.44 by the addition of 0.021 mol% ammonia, but as more ammonia was added the yield decreased to 0.41. This can be explained by the competitive reactions between reactions 2–8.

[6] $C_3H_7^+ + NH_3 \rightarrow C_3H_6, \ldots .$

[7] $s\text{-}C_4H_9^+ + NH_3 \rightarrow C_4H_8, \ldots .$

[8] $C_7H_{15}^+ + NH_3 \rightarrow C_7H_{14}, \ldots .$

The participation of reaction 2 is also supported by the increase of the isobutene yield by the addition of propylene (Fig. 2*A*).

$C_7H_{15}^+$ or $C_7H_{15}'^+$ ion is much more stable in our system than $C_3H_7^+$ and $s\text{-}C_4H_9^+$ ions, and therefore reaction 3 or 4 competes with the corresponding neutralization reaction. The participation of the stable ion in the chain mechanism explains that only 0.15 mol% ammonia inhibits the isobutene formation, and is also consistent with the result that the isobutene formation has an activation energy.

Ionic chain reactions 2–5 produce propane in addition to isobutene. This is consistent with the results; that is, at temperatures where ionic chain reactions proceeded significantly, the decrement of $G(C_3H_8)$ caused by the addition of 20 mol% ammonia exceeded 1.1 (Tables 1 and 2) which was the decrement at temperatures where ionic chain reactions did not occur.

Can. J. Chem. Downloaded from www.nrcresearchpress.com by 210.87.254.105 on 09/05/12
For personal use only.

Can. J. Chem. Downloaded from www.nrcresearchpress.com by 210.87.254.105 on 09/05/12
For personal use only.

The initial increase and subsequent decrease of the yields of the straight chain butenes with increasing ammonia (Table 1) is also explained by reactions 2–8, and this trend agrees with the results obtained at room temperature (17). As seen in Table 1, the change of the yield of 1-butene is prominent among the straight butenes. This suggests that reaction 7 favorably produces 1-butene.

The inhibition of the isobutane formation by 0.021 mol% ammonia (Table 1) also suggests the participation of a stable ion in the chain mechanism. This stable ion may be scavenged by traces of water existing in the system, analogous to the reaction between $C_3H_7^+$ and H_2O to produce $C_3H_7 \cdot H_2O^+$ (18), explaining the sensitivity of the isobutane yield to the dessication of the flow line.[4]

The isobutane yield, however, decreased by propylene addition. The same decrease was observed by adding the products from the t.c. of *n*-butane instead of adding propylene. Further, as the addition of 11.4 mol% ammonia caused only a slight change of the yields of higher paraffins, higher olefins, and the straight chain butenes (Table 2), the participation of the accumulated products in the chain mechanism of the isobutane formation may be excluded. If we assume that isobutane is formed by a usual hydride ion transfer reaction of $C_4H_9^+$ with *n*-butane molecule, $C_4H_9^+$ must be a protonated methylcyclopropane or isobutyl cation to secure an exothermicity of the reaction (19, 20). However, Lias *et al.* have reported that the isobutyl cation formed as a fragment ion from the radiolysis of isopentane at 27 °C isomerizes promptly to *t*-butyl cation before it undergoes a hydride ion transfer reaction (21). A further study is necessary to construct a mechanism leading to the isobutane formation.

The observed activation energies for the formation of isobutane and isobutene should not be attributed to the increase of the quantity of the accumulated propylene, one of the reactants, with increasing temperature, since the isobutane formation was suppressed by propylene and the isobutene formation was only slightly sensitized by the addition of a large amount of propylene. They should be attributed to the activation energy of elementary reactions such as reactions 3 and 4.

(B) Formation of Polymer (Material Balance of the Products)

In Fig. 3 are given the temperature dependence curves of the ratio of the sum of hydrogen atoms to that of carbon atoms in the products from H_2 to C_8, *H/C*, obtained by the static experiments with and without the addition of 20 mol% ammonia. Also presented are Arrhenius plots of the decomposition *G*-values of *n*-butane calculated on the basis of numbers of C atoms in the products. The *H/C* values obtained from the radiolysis of *n*-butane in the internally silver-coated Pyrex cells and those from the radiolysis of *n*-butane containing 0.72 mol% of 3-methylheptane in the Pyrex cells are also plotted. In some samples, the *G*-values for C_9–C_{14} products were determined; they were all less

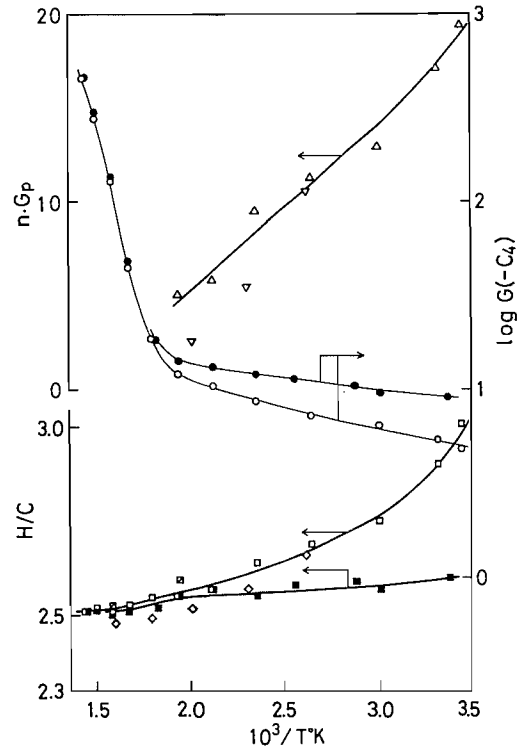

FIG. 3. The temperature dependence curves of (□)*H/C*, (△)$n \cdot G_p$, and (○)$G(-C_4)$ from the r.t.c. of *n*-butane in Pyrex cells; (◪)*H/C* in internally silver-coated Pyrex cells; (◇)*H/C* and (▽)$n \cdot G_p$ from the r.t.c. of *n*-butane containing 0.72 mol% 3-methylheptane in Pyrex cells. Filled marks correspond to the r.t.c. in the presence of 20 mol% ammonia.

[4]The lower yields of isobutane in the static system than in the flow system (Fig. 1) are probably ascribed to the difference in the residual water concentration between the two systems.

Can. J. Chem. Downloaded from www.nrcresearchpress.com by 210.87.254.105 on 09/05/12
For personal use only.

than 0.02. Thus the contribution of the products from C_9 to C_{14} to the H/C is negligible. The experimental conditions are given in $(A)(i)$.

The H/C values from the radiolysis of pure *n*-butane deviated significantly at near room temperature from that of the feed *n*-butane, 2.5. For instance, the H/C was calculated to be 3.0 at 17 °C. Since the same deviation was observed in the experiments with the internally silver-coated Pyrex cells, this cannot be ascribed to the selective adsorption of products by Pyrex wall. The H/C value, however, approached 2.5 by the addition of 20 mol% ammonia. Therefore, this deviation is presumably ascribed to the formation of polymer, having more than 14 carbon atoms, by an ionic mechanism. A slight deviation from 2.5 of the H/C value obtained in the presence of ammonia may be explained by the formation of hydrogen and amines from the ammonia decomposition. The polymer formation has also been reported in the gas-phase radiolysis of methane (22) and in the solid-phase radiolysis of methane, ethane, and propane (23).

Assuming the chemical formula of the polymer to be $(CH_2)_n$ (23) and denoting its G-value by G_p, we can determine the values of nG_p so as to adjust the H/C value to 2.5. The temperature dependence curve of nG_p is also plotted in Fig. 3. The polymer formation has an apparent negative activation energy.

The addition of 0.72 mol% 3-methylheptane caused a slight decrease of the yields of polymer from the radiolysis of *n*-butane (at about 0.1% conversion) and did not change the yield of 3,4-dimethylhexane (one of the major products at temperatures below 280 °C). Considering that the final concentration of the 3,4-dimethylhexane product was less than 150 p.p.m. in our experiments, this result indicates that the consumption of higher paraffin products through hydride ion transfer reaction can be neglected. This suggests that the *n*-butane molecule is one of the reactants for the polymer formation, as in the case of the radiolysis of methane (22, 23).

The authors would like to express their sincere thanks to Professor Yoneho Tabata of the University of Tokyo for his helpful discussions and encouragement. The authors are also deeply indebted to Mr. Keiichi Yotsumoto and Mr. Hiromi Sunaga of Japan Atomic Energy Research Institute for their valuable assistance.

1. P. J. Lucchesi, B. L. Tarmy, R. B. Long, D. L. Baeder, and J. P. Longwell. Ind. Eng. Chem. **50**, 879 (1958).
2. A. V. Topchiev. Radiolysis of hydrocarbons. Elsevier Publ. Co., Amsterdam. 1963. p. 203.
3. K. P. Lavrovskii, M. M. Florentsev, D. V. Makarov, V. B. Titov, Yu. N. Aleksenko, and Yu. L. Fish. Neftekhimiya, **7**, 580 (1967).
4. A. E. Pereverzev, K. S. Polak, and N. Ya. Chernyak. Neftekhimiya, **8**, 537 (1968).
5. S. A. Gabstarova and A. M. Kabakchi. Khim. Vys. Energ. **3**, 126 (1969).
6. G. M. Panchenkov and G. I. Zhurablev. Zh. Fiz. Khim. **46**, 1438 (1972).
7. K. M. Bansal and G. R. Freeman. J. Am. Chem. Soc. **92**, 4173 (1970).
8. H. J. van der Linde and G. R. Freeman. J. Am. Chem. Soc. **92**, 4417 (1970).
9. T. Nakagawa, S. Takamuku, and H. Sakurai. Bull. Chem. Soc. Jap. **40**, 2081 (1967).
10. T. Nakagawa, S. Takamuku, and H. Sakurai. Bull. Chem. Soc. Jap. **40**, 2773 (1967).
11. S. Matsuoka, T. Tamura, K. Ohima, and Y. Oshima. Can. J. Chem. **52**, 2579 (1974).
12. G. G. Meisels. J. Chem. Phys. **41**, 51 (1964).
13. G. R. Freeman. Radiat. Res. Rev. **1**, 1 (1968).
14. M. S. B. Munson, J. L. Franklin, and F. H. Field. J. Phys. Chem. **68**, 3098 (1964).
15. F. H. Field. J. Am. Chem. Soc. **91**, 2827 (1969).
16. F. P. Abramson and J. H. Futrell. J. Phys. Chem. **72**, 1994 (1968).
17. T. Miyazaki and S. Shida. Bull. Chem. Soc. Jap. **38**, 2114 (1965).
18. D. P. Beggs and F. H. Field. J. Am. Chem. Soc. **93**, 1576 (1971).
19. F. P. Lossing and G. P. Semeluk. Can. J. Chem. **48**, 955 (1970).
20. S.-L. Chong and J. L. Franklin. J. Am. Chem. Soc. **94**, 6347 (1972).
21. S. G. Lias, R. E. Rebbert, and P. Ausloos. J. Am. Chem. Soc. **92**, 6340 (1970).
22. L. W. Sieck and R. H. Johnsen. J. Phys. Chem. **67**, 2281 (1963).
23. D. R. Davis, W. F. Libby, and W. G. Meinschein. J. Chem. Phys. **45**, 4481 (1966).

Etude des succinates simples et complexes de cobalt(II)

PATRICK SHARROCK ET THEOPHILE THEOPHANIDES
Département de chimie, Université de Montréal, Montréal, Québec H3C 3V1

Reçu le 22 mai 1974

PATRICK SHARROCK et THEOPHILE THEOPHANIDES. Can. J. Chem. **53**, 98 (1975).

Le succinate de cobalt(II) tétrahydraté, $CoC_4H_4O_4 \cdot 4H_2O$, ainsi que le sel anhydre amorphe et cristallisé ont été préparés et étudiés par spectroscopie i.r., u.v.–visible, susceptibilité magnétique, thermogravimétrie et par diffraction de rayons X. Les sels alcalins du succinate de cobalt $M_2Co_2(C_4H_4O_4)_3$, où $M = K^+$ et NH_4^+ ont été synthétisés pour la première fois. Les conformations, alternée *gauche* et alternée *trans* de l'acide succinique ont été trouvées dans ces complexes. Les succinates du cobalt étudiés ici n'ont pas la structure-cage.

PATRICK SHARROCK and THEOPHILE THEOPHANIDES. Can. J. Chem. **53**, 98 (1975).

Cobalt(II) succinate tetrahydrate, $CoC_4H_4O \cdot 4H_2O$ and anhydrous (amorphous and crystalline) have been prepared and studied by i.r. and u.v.–visible spectroscopy, magnetic susceptibility, thermogravimetry, and by X-ray diffraction. The alkaline salts of cobalt succinate $M_2Co_2(C_4H_4O_4)_3$, where $M = K^+$ and NH_4^+ have also been prepared for the first time. The staggered *gauche* and *trans* conformations of succinic acid have been found to be present in the complexes. The cage-like structure has not been found in any of the Co(II) carboxylates studied here.

Introduction

L'acide succinique est un acide α,ω-dicarboxylique et sa structure cristalline présente de longues chaînes dans lesquelles les molécules sont en conformation *trans* et forment des ponts hydrogènes entre elles (1). L'acide succinique avec les éléments de transition forme des complexes polymères ou des chélates (2). On a trouvé par spectroscopie infrarouge (3) que le succinate de sodium, de symétrie C_{2h} a une conformation alternée *trans* (voir fig. 1).

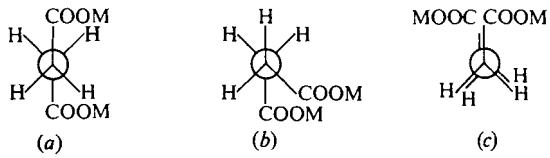

FIG. 1. Les trois rotamères de l'acide succinique complexé. (*a*) Alternée *trans*: $M = H^+$, Na^+, K^+, NH_4^+, Co^{2+}. (*b*) Alternée *gauche*: $M = Co^{2+}$. (*c*) Eclipsée *cis*: $M = Cu^{2+}$, Cr^{2+}.

Les structures des complexes succinates polymères du cuivre(II) et chrome(II) sont connues (4) et leurs spectres infrarouges sont caractéristiques de la conformation éclipsée *cis*. Par contre la conformation alternée *gauche* a été trouvée dans les complexes $M_2[Co_2(\text{succinate})_3]$, où $M = K^+$ et NH_4^+, présentés dans ce travail. Le $K_2[Co_2(\text{succinate})_3]$ a été étudié antérieurement par "hétérométrie" (5). L'acide succinique forme des structures cages (6) avec le Cu(II) et le Cr(II). Par contre, le présent travail n'indique pas la présence de liens métal–métal ou de structures cages pour les succinates de Co(II).

Partie expérimentale

Succinates simples de cobalt(II)

Le succinate de cobalt(II) tétrahydraté a été préparé d'après la méthode publiée précédemment (7). Le succinate de Co(II) anhydre et amorphe est préparé en déshydratant le tétrahydraté dans une étuve à 100 °C à pression atmosphérique. En tirant sous vide et en chauffant entre 280 et 290 °C pendant plus d'une heure, on obtient le succinate de Co(II) anhydre et cristallin. Les réactions procèdent comme suit

$$Co(OH)_2 \cdot 6H_2O + HOOC{-}CH_2CH_2{-}COOH \xrightarrow[H_2O]{\Delta(60\,^\circ C)} CoC_4H_4O_4 \cdot 4H_2O$$

$$CoC_4H_4O_4 \cdot 4H_2O \xrightarrow[1\ atm]{100\,^\circ C} CoC_4H_4O_4\ (\text{amorphe}) \xrightarrow[\text{sous vide}]{285\,^\circ C} CoC_4H_4O_4\ (\text{cristallin})$$

Le succinate de cobalt deutéré, $CoC_4H_4O_4 \cdot 4D_2O$, a été obtenu en recristallisant le produit amorphe dans le D_2O.

Succinates complexes de cobalt (II)

Les sels alcalins de succinates de Co(II) ont été synthétisés pour la première fois en utilisant la méthode suivante.

Le sel d'ammonium-succinate cobalt(II)

A une solution de 5 g de succinate d'ammonium dans 5 ml d'eau on ajoute 30 ml de *t*-butanol qui restent sur

Can. J. Chem. Downloaded from www.nrcresearchpress.com by 210.87.254.5 on 09/05/12
For personal use only.

Can. J. Chem. Downloaded from www.nrcresearchpress.com by 210.87.254.5 on 09/05/12
For personal use only.

une phase supérieure. On ajoute ensuite 15 ml d'une solution de 1.5 g de $CoCl_2 \cdot 6H_2O$ dans l'éthanol à 90%. On mélange vigoureusement sur agitateur magnétique. L'addition de 50 ml de méthanol rend homogène les deux phases et le sel d'ammonium succinate cobalt(II) précipite. Le précipité, lavé avec 5 portions de 75 ml d'un mélange 90% CH_3OH – 10% est rincé au méthanol pur et séché. On obtient 1.4 g de produit bleu (44.5%).

Anal. calc. pour $(NH_4)_2Co_2(C_4H_4O_4)_3$: C, 26.69; H, 4.46; N, 5.22. Trouvée par Chemalytics Inc., Tempe, Arizona: C, 26.51; H, 3.85; N, 5.18.

Le sel d'ammonium succinate cobalt(II) se disproportionne lentement dans le méthanol contenant 10% d'eau pour donner du succinate d'ammonium et du succinate de cobalt, comme suit

$$(NH_4)_2[Co_2(\text{succinate})_3] \xrightarrow{H_2O} 2Co(\text{succinate}) \cdot 4H_2O + (NH_4)_2(\text{succinate})$$

Le sel de potassium succinate cobalt(II)

La présence de deux phases n'est pas nécessaire pour commencer cette préparation. A 50 ml d'une solution saturée de succinate de potassium dans l'éthanol à 90% on ajoute goutte à goutte une solution saturée de $CoCl_2$ dans le même solvant. Il se forme un précipité huileux qui se sépare dans une phase inférieure. Ce précipité se coagule lentement et on arrête l'addition de Co^{2+} lorsqu'une suspension poudreuse est obtenue. On filtre et on lave le précipité de couleur mauve avec 250 ml de méthanol contenant 10% d'eau pour éliminer le chlorure de potassium qui se forme durant la réaction

$$2CoCl_2 \cdot 6H_2O + 3K_2C_4H_4O_4 \xrightarrow{EtOH\ 90\%} K_2Co_2(C_4H_4O_4)_3 + 4KCl + 6H_2O$$

Le produit est rincé au méthanol et séché à l'air.

Anal. calc. pour $K_2Co_2(C_4H_4O_4)_3$: C, 26.48; H, 2.21. Trouvée: C, 26.43; H, 1.73.

Le sel de potassium succinate cobalt(II) se disproportionne dans le méthanol contenant 30% d'eau et semble être plus stable que le sel analogue d'ammonium. Le succinate de lithium réagit, dans les mêmes conditions, pour former un complexe bleu, mais le succinate de sodium n'a pas donné de complexe bleu malgré de nombreuses tentatives. Dans chaque cas, il se formait un précipité rose de succinate de cobalt simple.

Tous les diagrammes de poudres ont été pris dans une caméra Debye–Scherrer (114.56 mm de diamètre) en utilisant les radiations filtrées du cuivre et du chrome (λ $CuK_{\bar{\alpha}}$ = 1.5418 Å et λ $CrK_{\bar{\alpha}}$ = 2.2909 Å). Les échantillons finement broyés ont été introduits dans les capillaires de quartz de 0.3 mm de diamètre. Les intensités des raies ont été estimés visuellement.

Les spectres infrarouges ont été enregistrés avec un spectrophotomètre Perkin–Elmer 621 entre 4000 et 250 cm^{-1}. L'échantillon a été broyé dans le Nujol et son spectre a été enregistré à l'aide d'un compensateur.

Les analyses thermogravimétriques ont été effectuées sur des échantillons de 50 mg environ, dans un panier en aluminium. La température était contrôlée par un programmeur et suivie sur papier graphique à l'aide d'un thermocouple. Le poids a été mesuré par une électrobalance de Cahn enregistré sur le même graphique à l'aide d'une plume Graphispot. Le panier était dans un long tube en verre, qui nous a permis de faire des mesures sous vide.

Résultats et discussion

Les succinates de cobalt(II) simples sont connus depuis quelques temps (7). Les diagrammes thermogravimétriques des échantillons de 60 à 80 mg avec un taux de chauffage de 3.5 °C/min ne révèlent pas de composé hydraté intermédiaire défini. Ceci concorde avec les travaux antérieurs où la perte d'eau, avec chauffage lent sous vide se traduit par un seul pic endothermique dans le diagramme thermodifférentiel (7). La perte observée de 29.12% correspond à celle calculée de 29.18% pour quatre molécules d'eau. Les quatre molécules d'eau du succinate semblent être équivalentes. Dans l'acétate de nickel tétrahydraté, isostructural avec l'acétate du cobalt(II) on trouve deux sortes de molécules d'eau qui diffèrent par leur nombre de liens hydrogènes (8). Ceci explique les spectres infrarouges (9) et les diagrammes thermogravimétriques (10) de l'acétate de cobalt(II) tétrahydraté. Le succinate de cobalt(II) ne se décompose pas comme l'acétate (11), sa stabilité provenant de la structure polymère du composé et de la non volatilité de l'acide succinique. La détermination de sa structure tridimensionnelle serait intéressante pour expliquer l'équivalence des 4 molécules d'eau. Au-dessus de 330 °C, le succinate anhydre se décompose pour donner du CoO (perte de poids calc., 40.4%; obs.; 39.8%).

Les travaux antérieurs ont permis de détecter une forme cristalline du succinate de cobalt(II) anhydre, obtenue en chauffant le composé amorphe sous vide et au-dessus de 280 °C. Les échantillons du produit cristallin ont donné des diagrammes X en bon accord avec ceux obtenus par la radiation $CoK_{\bar{\alpha}}$ et $CrK_{\bar{\alpha}}$ (tableau 1).

Les spectres visibles sont représentés dans la fig. 3. Le succinate tétrahydraté de couleur rose a une bande à λ_{max} = 19 550 cm^{-1} avec un épaulement à 21 300 cm^{-1}, en solution. A l'état solide on a deux bandes à λ_{max} = 19 680 et 21 880 cm^{-1}. Il est analogue au spectre de l'acétate de cobalt tétrahydraté (λ_{max} = 18 900 cm^{-1} avec épaulement à 20 200 cm^{-1}) et vérifie la géométrique octaédrique autour du cobalt (fig. 2*b*). Les molécules d'eau occupent 4 positions de coordination. L'absorption faible (car interdite par symétrie) de la transition $^4T_{1g}(P) \leftarrow {}^4T_{1g}(F)$, est caractéristique de la coordination

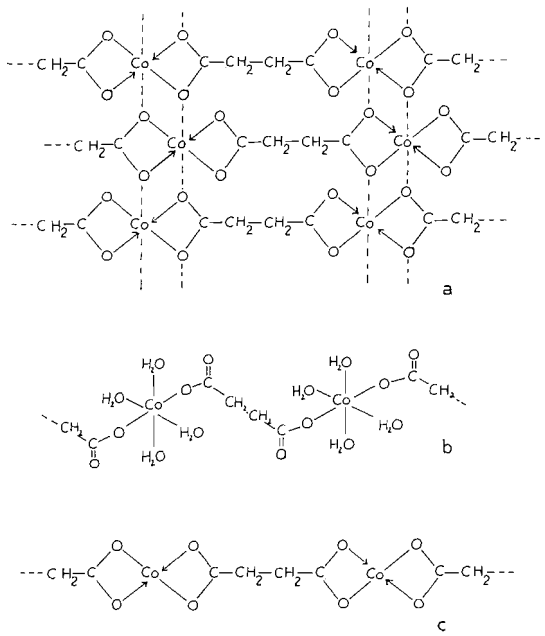

FIG. 2. Structures proposées les succinates de cobalt(II) simples: (*a*) Co(succinate), anhydre cristallin, (*b*) Co(succinate)·$4H_2O$ et (*c*) Co(succinate) anhydre amorphe.

octaédrique et l'épaulement vers les longueurs d'ondes plus courtes est une conséquence du couplage spin–orbite de l'état excité $^4T_{1g}(P)$.

Le succinate de cobalt anhydre et amorphe est bleu. L'absorption intense vers $\lambda_{max} = 18\,525$ cm^{-1} est due à la transition $^4T_1(P) \leftarrow {}^4A_2$. Le couplage spin–orbite dédouble l'état $^4T_1(P)$ et permet à la transition $^2G \leftarrow {}^2F$ (12) d'augmenter en intensité. Le calcul théorique prévoit une absorption près de 18 900 cm^{-1}, mais généralement on observe une bande complexe vers 15 000 cm^{-1}. Le spectre visible du succinate anhydre et amorphe désigne la géométrie tétraédrique proposée dans la fig. 2*c* pour le Co(II). Le succinate anhydre et cristallin a une absorption vers $\lambda_{max} = 21\,010$ cm^{-1} avec un épaulement à 18 875 cm^{-1}.

Le Co(II) de configuration d^7 avec trois électrons célibataires donne un moment magnétique, $\mu = 3.87$ M.B. Cependant, le couplage spin orbite cause un éclatement des états avec différents J de l'ordre de grandeur kT. Le calcul prévoit $\mu = 5.21$ M.B. pour le Co(II) octaédrique (13) et les moments magnétiques généralement observés sont compris entre 4.7 et 5.3 M.B. Les succinates tétrahydratés et cristallins ont respectivement, un moment magnétique à 22 °C de 4.88 et 5.11 M.B. Les mesures de suceptibilité magnétique suggérent aussi les structures déduites à l'aide des spectres visibles. Ces valeurs sont proches de celles observées pour des carboxylates analogues: $Co(CH_3COO)_2(H_2O)$, fraîchement recristallisé, $\mu = 4.84$ M.B. et $\mu = 5.16$ M.B. (14); $Co(CH_3COO)_2(D_2O)_2$, $\mu = 4.906$ M.B. et $Co(C_4H_4O_4)\cdot 4D_2O$, $\mu = 4.90$ M.B.

Lorsque le Co(II) est dans un environnement tétraédrique, le moment magnétique se situe généralement entre 4.4 et 4.8 M.B. Le succinate $CoC_4H_4O_4$ amorphe a un moment assez élevé avec $\mu = 4.89$ M.B. Ceci élimine la possibilité d'avoir une structure plan carré ou tétragonale car dans ces cas μ serait entre 2.4 et 2.8 M.B. (15). Puisque les spectres visibles montrent que le Co a un nombre de coordination de quatre, le succinate amorphe doit être tétraédrique, bien que la mesure de la susceptibilité magnétique soit dans l'intervale ordinaire du Co(II) octaédrique.

Les spectres infrarouges donnent des renseignements surtout sur la conformation adoptée par l'acide succinique dans les complexes. Les fréquences et les attributions sont rassemblées dans le tableau 2. Toutes les absorptions observées (fig. 4) pour le succinate tétrahydraté se retrouvent dans le spectre du succinate de sodium ou d'ammonium. La conformation est

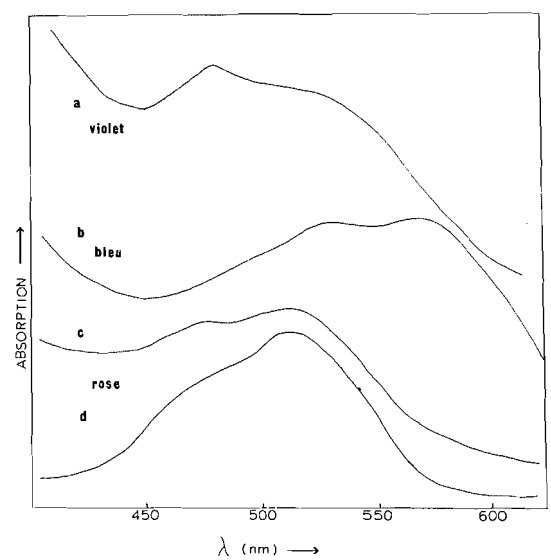

FIG. 3. Spectres visibles des succinates de cobalt(II); (*a*) Co(succinate), anhydre cristallin; (*b*) Co(succinate), anhydre amorphe; (*c*) Co(succinate) tétrahydraté (solide); (*d*) Co(succinate) tétrahydraté (en solution H_2O–CH_3OH).

Can. J. Chem. Downloaded from www.nrcresearchpress.com by 210.87.254.5 on 09/05/12
For personal use only.

TABLEAU 1. Diagrammes de poudre des succinates de cobalt(II) distances reticulaires en Å et intensites en % de la raie la plus forte

	Co(succinate)·4H_2O				Co(succinate)				$K_2Co_2(succ)_3$	
	$CuK_{\bar{\alpha}}$*		$CoK_{\bar{\alpha}}$ (7)		$CuK_{\bar{\alpha}}$*		$CoK_{\bar{\alpha}}$ (7)		$CuK_{\bar{\alpha}}$*	
Raie N°	Intensité	*d*	Intensité	*d*	Intensité	*d*	Intensité	*d*	Intensité	*d*
1	85	7.30	24	7.34	50	9.48	80	9.50	8	10.65
2	5	6.81	3	6.85	100	8.77	100	8.75	5	7.22
3	10	6.51	5	6.55	1	7.55			2	6.78
4			12	5.42	1	5.58			1	5.74
5	75	5.34	21	5.33	2	4.72			60	5.28
6	5	5.18	4	5.20	10	4.614	20	4.61	2	5.03
7	3	4.572			25	4.379	19	4.37	2	4.640
8	100	4.575	100	4.56	10	3.523	20	3.51	2	4.225
9	15	4.153	9	4.17	1	2.939			5	4.040
10	10	4.070	4	4.10	3	2.784	10	2.800	100	3.793
11			4	3.78	2	2.652	10	2.650	20	3.754
12	85	3.700	48	3.70	8	2.552	15	2.554	8	3.637
13	5	3.649	7	3.67	8	2.308	15	2.308	8	3.547
14	5	3.546	2	3.548	1	2.146			5	3.476
15	15	3.439	10	3.440	1	2.102			5	3.376
16	5	3.330	2	3.330	2	2.018			3	3.076
17	10	3.183	2	3.190	1	1.832			10	3.002
18	15	3.106	5	3.113					3	2.959
19	15	3.032	6	3.030					50	2.880
20	50	2.902	31	2.895					5	2.790
21	5	2.752							5	2.752
22	5	2.632	3	2.630					60	2.648
23	10	2.467	10	2.470					20	2.469
24	45	2.410	9	2.414					2	2.407
25	10	2.344	6	2.347					2	2.298
26			2	2.327					10	2.183
27			12	2.275					8	2.146
28	15	2.266	12	2.270					10	2.065
29	10	2.233	5	2.234					8	2.044
30	10	2.185	2	2.190					10	1.936
31	10	2.037	2	2.037					3	1.860
32	10	1.884	3	1.880					2	1.813
33	15	1.869	7	1.874						
34	10	1.253								

*Present travail.

donc alternée *trans* (fig. 1*a*). Le succinate amorphe a des bandes assez larges, comme attendu pour un produit amorphe et les absorptions ν_sCOO et ν_aCOO n'ont pas une structure fine. Par contre, dans le succinate cristallin ces deux bandes sont dédoublées. De plus, quatre bandes caractéristiques ν_{C-C} et CH_2 de la conformation éclipsée *cis* (fig. 1*c*) apparaissent vers 900 et 1050 cm^{-1}. Les bandes de torsion et de balancement hors du plan du CH_2 sont complexes, mais ces massifs ressemblent dans cette région le spectre de l'anhydride succinique (fig. 4). Le sel amorphe a donc une conformation distordue, compatible avec la structure proposée (fig. 2*c*).

Les sels de potassium et d'ammonium du succinate de Co(II) présentent des spectres intéressants qui sont presque identiques. Les bandes ν_sCOO et ν_aCOO sont complexes. Les fréquences en dessous de 1400 cm^{-1} correspondent aux absorptions caractéristiques de la conformation alternée *trans* seulement légèrement déplacées et facilement reconnaissables d'après leur intensité (ces bandes sont indiquées avec des flèches dans la fig. 4). De plus, certaines fréquences typiques de la conformation *cis* sont présentes dans les spectres et sont indiquées par des astériques. Contrairement aux bandes caractéristiques de la conformation alternée *trans*, on ne retrouve pas intégralement toutes les fré-

Can. J. Chem. Downloaded from www.nrcresearchpress.com by 210.87.254.5 on 09/05/12
For personal use only.

TABLEAU 2. Spectres infrarouges des succinates de Co(II) à l'état solide*

Infrarouge (cm^{-1})					
Acide succinique (21)	$Co(C_4H_4O_4 \cdot 4H_2O)$ tétrahydraté	$Co(C_4H_4O_4)$ amorphe	$Co(C_4H_4O_4)$ cristallin	$K_2Co_2(C_4H_4O_4)_3$	Attributions (voir réf. 21)
225		260F		263tf	δ(C′C′C)
				293m	
			340f	312m	Libration
				342m	M—O
388			485f	430tf	δ(CC′O)
545	525f	538f	525m	550m	
575	580tf	580f	580m	573f	π(C=O)
584				595m	
639	670F	665F	670F	682F	δ(OCO)
678	800m	770f	770tf	807mF	δ(O—C=O)
802		807f	775f	820m H_2O	Libration
893	890m	900m	900f	890F	ν_s(C′C)
914			925m	930f	π(OH)
931	970f	970m	970f	957m	ν_a(C′C)
		997m	995m	988m	
1084	1038	1030f	1038tf	1030fL	νC′C′
	1063f	1050f	1055tf		t(CH_2)+ν_aCC
1175	1115f	1110f	1110f		
	1172m	1170m	1177m	1153f	t(CH_2)
		1220m	1198F	1177mF	
1203	1245F		1225m	1227m	w(CH_2)
1289	1287m	1300F	1295F		ν(C—O)
1308	1330F		1303F		
1370	1385F		1385e	1385TF	w(CH_2)
	1402TF	1410TFL	1402TF	1405F	δ‖(OH...O)
1418	1420F		1428TF		
1445	1460m				s(CH_2)
1652					
1690	1547TF	1560TF	1580TF	1568e	
			1610TF	1580TF	ν_a(C=O)
1729				1615TF	
2930		2950m	2920f	2920m	ν_s(CH)
			2965f	2960m	ν_a(CH)
2966			2980m	2970m	
2990					
	3100L				ν(OH)
2997	3520e	3420fl	3420fl		ν(OH)
	3400F				

*r = rocking (balancement); b = bending (déformation); ν = stretching (vibration de valence); t = twisting (torsion de CH_2); w = wagging (balancement hors du plan); π = scissoring (déformation hors du plan); ν_s = vibration de valence symétrique; ν_a = vibration de valence asymétrique; f = faible; m = médium; F = fort; L = large; e = épaulement; T = très.

quences typiques de la conformation *cis*. C'est pourquoi nous proposons que la forme alternée *gauche* est présente dans les sels alcalins de succinate de Co(II) et donne les huit absorptions qui restent, après avoir éliminé celles qui proviennent de la conformation alternée *trans*. Les deux conformations de l'acide succinique sont donc alternées *trans* et *gauche*. La structure proposée pour $M_2[Co_2(\text{succinate})_3]$ est représentée sur la fig. 5. Les ponts simples d'acide succinique alternent avec les ponts doubles. Dans la fig. 5 la conformation alternée *trans* de plus basse énergie correspond aux ponts simples comme dans le cas du succinate tétrahydraté. La conformation alternée *gauche* correspond aux ponts doubles et sera décrite dans la conclusion. La présence des deux conformations dans les sels alcalins de succinate de Co(II) se trouve vérifiée aussi par les trois fréquences ν_{CH} observées. En effet, les succinates de sodium et de cuivre ne présentent que deux bandes chacun dans cette région.

Can. J. Chem. Downloaded from www.nrcresearchpress.com by 210.87.254.5 on 09/05/12
For personal use only.

Can. J. Chem. Downloaded from www.nrcresearchpress.com by 210.87.254.5 on 09/05/12
For personal use only.

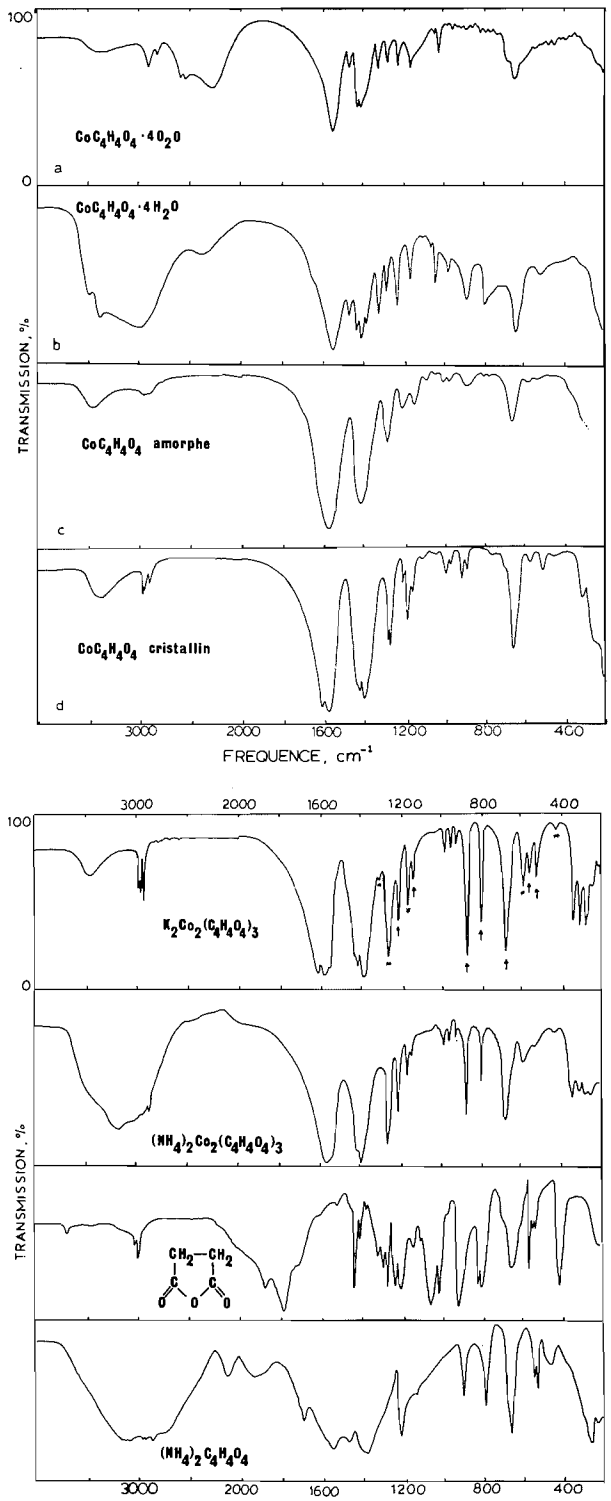

FIG. 4. Spectres infrarouges des succinates de cobalt(II) de l'anhydride succinique et du succinate d'ammonium.

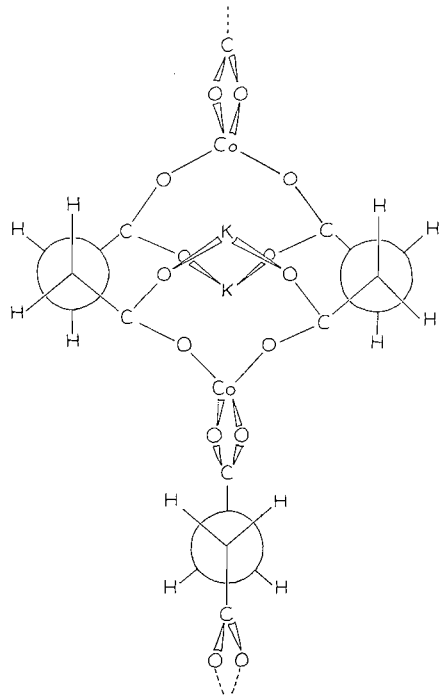

FIG. 5. Structure proposée pour le complexe K_2Co_2-(succinate)$_3$.

Les sels complexes $M_2[Co_2(\text{succinate})_3]$ sont de couleur mauve foncé et ont un spectre visible très simple avec deux absorptions d'intensité à peu près égale: $\lambda_{max} = 558$ et 522 nm pour $M = K^+$ et $\lambda_{max} = 588$ et 520 nm pour $M = NH_4^+$. Ceci appuie la structure proposée, où le métal est dans un environnement tétraédrique. Le moment magnétique observé de 5.36 M.B. pour $K_2[CO_2(\text{succinate})_3]$ est raisonnable et le diagramme X montre des distances réticulaires différentes.

Conclusion

La structure cage n'a été trouvée dans aucune des trois formes de succinate de cobalt(II) dans cette étude. Ceci démontre la tendance du cobalt(II) à former des environnements, soit octaédriques, soit tétraédriques et des polymères sans lien métal–métal. La formation des liens métal–métal n'est pas essentielle pour obtenir la structure cage dans le succinate de cuivre. Cependant, le présent travail indique que la géométrie autour du métal joue un rôle important dans la structure des carboxylates. Ainsi, dans le cas du Cu(II) et du Cr(II), la préférence marquée de la géométrie plan-carré permet le rapprochement des deux métaux et la formation subséquent d'une structure cage. L'influence des ligands en position axiale dans le case des carboxylates dinucléaires du Cu(II) est connue (16). L'étude des structures cages doit inclure, les ligands axiaux, le métal et sa géométrie habituelle, la présence d'un lien métal–métal (17) et les substituants en α des groupes carboxyliques (18). Le seul carboxylate de Co(II) à structure cage est le benzoate de cobalt, stabilisé avec la monoquinoline en position axiale (19).

L'acide succinique donne des complexes polymères stables et permet d'étudier le comportement des groupes carboxyliques et la conformation des chaînes organiques. La conformation alternée *gauche* proposée pour les ponts doubles dans $M_2[Co_2(\text{succinate})_3]$ est trouvée reliée à une structure pseudo-cage, où deux groupes COO forment deux ponts entre un cobalt et un potassium. Dans une vraie structure cage, quatre groupes COO forment quatre ponts entre deux métaux identiques. La structure pseudo-cage est par ce fait plus souple et permet au cobalt d'adopter une géométrie tétraédrique. Il est intéressant de remarquer que les sels alcalins du succinate de cuivre ont la composition $M_2[Cu(\text{succinate})_2]$, qui diffère de celle du $M_2[Co_2(\text{succinate})_3]$. L'acide succinique forme donc avec le cobalt et le potassium, un sel complexe analogue à celui formé avec l'acide acétique de composition $K_2Co_2(CH_3COO)_6 \cdot 4H_2O$ (20).

Nos vifs remerciements vont au Conseil national des recherches du Canada pour l'aide accordée à ce travail.

1. R. G. WYCKOFF. Crystal structures, Vol. 5. Interscience Publishers Inc., New York, 1960. pp. 557–560.
2. (*a*) E. M. BRAININA, M. KH. MINACHEVA, R. KH. FRAIDLINA et A. N. NESMEYANOV. Dokl. Akad. Nauk. SSR **138**, 598 (1961); (*b*) C. BATTISTONI, G. CIULLO, G. MATTOGNO, A. MONACI et F. TARLI. Ann. Chim. Rome, **60**, 661 (1970).
3. C. B. BADDIEL, C. D. CAVENDISH et W. O. GEORGE. J. Mol. Struct. **5**, 263 (1970).
4. (*a*) P. SHARROCK et T. THÉOPHANIDES. Can. J. Chem. **52**, 418 (1974); (*b*) P. SHARROCK, T. THÉOPHANIDES et F. BRISSE. Can. J. Chem. **51**, 2963 (1973).
5. M. BOBTELSKY et I. BAR-GADDA. Bull. Soc. Chim. Fr. 687 (1953).
6. R. CHIDAMBARAM et G. M. BROWN. Cryst. Struct. Commun. **1**, 269 (1972).
7. L. V. MY, G. PÉRINET et R. LAFONT. C. R. série C, **268**, 406 (1969).
8. T. C. DOWNIE, W. HARRISON, E. S. RAPER et M. A. HEPWORTH. Acta Cryst. **B27**, 706 (1971).

Can. J. Chem. Downloaded from www.nrcresearchpress.com by 210.87.254.5 on 09/05/12
For personal use only.

9. K. J. EISENTRAUT. Ph.D. Thesis. Rensselaer Polytechnics Institute, 1964. Analytical 65, 6455 University Microfilms, Inc., Ann Arbor, Michigan.
10. T. KUBO et K. MANABE. J. Chem. Soc. Jap. Ind. Chem. Sect. **68**, 162a (1965).
11. D. A. EDWARDS et R. N. HAYWARD. Can. J. Chem. **46**, 3443 (1968).
12. (*a*) R. L. CARLIN. *Dans* Transition metal chemistry, Vol. 1. M. Dekker, Inc., New York. 1965. Chapt. 1. pp. 6–9. (*b*) J. FERGUSON. J. Chem. Phys. **39**, 116 (1963).
13. B. N. FIGGIS. Introduction to ligand fields. J. Wiley and Sons, Inc., New York. 1966.
14. F. A. COTTON et R. H. HOLM. J. Am. Chem. Soc. **82**, 2983 (1960).
15. F. A. COTTON et G. WILKINSON. Advanced inorganic chemistry. 2nd ed. Interscience Publishers, New York. 1966. p. 873.
16. (*a*) M. A. PORAI-KOSHITS, A. S. ANTSYSHKINA, G. G. SADIKOV et G. A. KUKINA. Sov. Phys. Crystallogr. **16**, 1047 (1972); (*b*) G. DAVEY et F. S. STEPHENS. J. Chem. Soc. A, 2803 (1970); 1917 (1971).
17. (*a*) L. DUBICKI et R. L. MARTIN. Inorg. Chem. **9**, 673 (1970); (*b*) F. A. COTTON et J. G. NORMAN, JR. J. Am. Chem. Soc. **94**, 5697 (1972).
18. M-F. LUDMANN-OBIER, M. DARTIGUENAVE et Y. DARTIGUENAVE. J. Mol. Struct. **18**, 123 (1973).
19. J. DREW, M. B. HURSTHOUSE, P. THORNTON et A. J. WELCH. Chem. Commun. 52 (1973).
20. N. V. MAKHONIN. Chem. Abstr. **73**, 39203 (1970).
21. M. SUZUKI et T. SCHIMANOUCHI. J. Mol. Spectrosc. **28**, 394 (1968).

Can. J. Chem. Downloaded from www.nrcresearchpress.com by 210.87.254.5 on 09/05/12
For personal use only.

The Kinetics and Mechanism of H_2–D_2 Exchange Catalyzed by Hydridochlorotris(triphenylphosphine)ruthenium(II)[1]

GRAEME STRATHDEE AND RUSSELL GIVEN

Research Chemistry Branch, Atomic Energy of Canada Limited, Whiteshell Nuclear Research Establishment, Pinawa, Manitoba R0E 1L0

Received August 15, 1974

GRAEME STRATHDEE and RUSSELL GIVEN. Can J. Chem. **53**, 106 (1975).

The H_2–D_2 exchange reaction is catalyzed extremely efficiently by solutions of hydridochlorotris(triphenylphosphine)ruthenium(II) in benzene between 279 and 298 K. Rates of exchange were partly controlled by the mass transport of hydrogen. A mechanism involving formation of di- and tetrahydride ruthenium species has been employed to explain the rapid H–D exchange without the participation of the original Ru—H bond of $RuHCl(PPh_3)_3$. Nuclear magnetic resonance and infrared experiments showed that the rate of exchange of Ru—H with D_2 was insignificant with respect to the rate of the H_2–D_2 equilibration process.

GRAEME STRATHDEE et RUSSELL GIVEN. Can. J. Chem. **53**, 106 (1975).

La réaction d'échange H_2–D_2 est catalysée d'une façon très efficace par des solutions d'hydridochlorotris (triphénylphosphine) de ruthenium(II) dans le benzène entre 279 K et 298 K. Les vitesses d'échange sont en partie contrôlées par le transport de masse de l'hydrogène. On a utilisé un mécanisme impliquant la formation d'espèces di- et tétrahydrure de ruthénium pour expliquer l'échange rapide H–D sans participation du lien original Ru—H du $RuHCl(PPh_3)_3$. Des expériences de r.m.n. et d'infrarouge montrent que le taux d'échange de Ru—H avec D_2 est très faible par rapport au taux d'équilibration de H_2 avec D_2. [Traduit par le journal]

Introduction

Hydrogen–deuterium exchange between D_2 and metal complexes in aprotic solvents has been used to show that metal hydride complexes can undergo intermolecular H–D transfer. Schunn has reviewed this subject in considerable detail (1). Often, metal complexes which participate in these reactions also catalyze H_2–D_2 equilibration to yield HD. This conversion has unique requirements: hydrido-complexes with one or more labile M—H bonds must have the capability to oxidatively add H_2 and D_2 either sequentially or simultaneously so that H and D scrambling may occur at the metal atom. The former route, sequential oxidative addition to the metal hydride containing an exchangeable metal–hydrogen bond, is probably favored in most cases, for example $RhH(CO)(PPh_3)_3$ (2), $FeH_2[P(O\text{-}i\text{-}C_3H_7)_3]_4$ (3), $CoH_3(PPh_3)_3$ (4), and $IrH_3(CO)(PPh_3)_2$ (5), likely function in this way. Eberhardt and Vaska have suggested that $Ir(CO)Cl(PPh_3)_2$ promotes H_2–D_2 exchange via an eight-coordinate intermediate, that is, by the second mechanism (6). Siegel has compared heterogeneous with homogeneous catalysts for the H_2–D_2 reaction (7). A detailed study of the kinetics of the H_2–D_2 exchange reaction has not been reported in any of these cases.

The possibility that this equilibration occurred extremely rapidly in the presence of $RuHCl(PPh_3)_3$ was suggested by our detailed study of the $RuCl_2(PPh_3)_3$ catalysis of D_2–C_2H_5OH exchange in 1:1 C_6H_6–C_2H_5OH (8). The gas phase composition was determined at all times by K_1 (9) for the reaction

$$[1] \qquad D_2 + H_2 \rightleftarrows 2HD$$

The present study of the kinetics of reaction 1 catalyzed by $RuHCl(PPh_3)_3$ has confirmed this hypothesis. In addition, it has been found that the original Ru—H bond does not participate in the exchange mechanism in C_6H_6 solution. The inplications of this unexpected behavior for other reactions catalyzed by $RuHCl(PPh_3)_3$ are discussed.

Experimental

The monohydrido complex, $RuHCl(PPh_3)_3$, was prepared by reaction of a benzene solution of $RuCl_2(PPh_3)_3$, obtained from Strem Chemicals Inc., with sodium borohydride in water (10). The dihydride, $RuH_2(PPh_3)_4$, was obtained by the method of Levison and Robinson (11).

Benzene was purified by slow percolation through a 0.2 m × 0.03 m column of activated Linde type 4A molecular sieve followed by distillation in a dry nitrogen atmosphere. All materials were stored and handled in a

[1]AECL No. 4890.

Can. J. Chem. Downloaded from www.nrcresearchpress.com by 210.87.254.6 on 09/05/12
For personal use only.

Can. J. Chem. Downloaded from www.nrcresearchpress.com by 210.87.254.6 on 09/05/12
For personal use only.

N_2-filled glove box which was continuously purged with nitrogen containing less than 20 p.p.m. of oxygen.

The H_2–D_2 exchange reactions were always performed with freshly prepared solutions of $RuHCl(PPh_3)_3$. The reaction flask of total volume 93.3 ml was evacuated and filled with an H_2–D_2 mixture obtained from Matheson of Canada Ltd. Mass spectrometric analysis gave (mol %): H_2, 49.4; HD, 0.75; D_2, 49.8. The exchange reaction commenced with the rapid injection of 20.0 ml of the catalyst solution. The gas–liquid dispersion was magnetically stirred at about 2800 r.p.m. and the temperature was controlled to ± 0.1 K. Gas samples (1.0 ml) were removed by syringe and retained in glass bombs for mass spectrometric analysis. No exchange was observed in blank experiments without $RuHCl(PPh_3)_3$. No hydrogenation of C_6H_6 was detected by v.p.c. analysis, therefore no Ru metal was present.

Rates of equilibration are reported as rates of disappearance of D_2

$$[2] \qquad -d[D_2]/dt = \ln [(n_0-n_e)/(n_t-n_e)]A/t$$

where n_0, n_t, and n_e represent the mol% D_2 at $t = 0$, $t = t$ s and at equilibrium, respectively. A is the gas:liquid ratio in mol D_2 per l defined as: total initial D_2 in moles ÷ volume of solution in liter.

Nuclear magnetic resonance spectra were recorded with a Perkin Elmer R12A spectrometer which thermoregulated samples at 311 K.

Results

H_2–D_2 Exchange

Rate Measurements

A typical set of experimental data is shown in Fig. 1. These exchange reactions were extremely rapid even at low temperature in dilute solutions of the catalyst. Half-lives for the disappearance of D_2 (or H_2) were generally 100–300 s. If the reaction was not followed for a sufficiently long period to establish the equilibrium concentration of D_2, then n_e was calculated using the values for the equilibrium constant K for [1] given by Bond (9). There was no detectable change in the atom-fraction of D in the gas phase during these experiments, therefore no significant transfer of D to ligand or solvent C—H bonds occurred.

The dependence of the rate of the H_2–D_2 exchange reaction at 297 K on dissolved deuterium and total ruthenium concentrations is illustrated in Fig. 2. From the slopes of the lines through each data set, it was calculated that

$$[3] \qquad -d[D_2]/dt = k[D_2]^{1.5}\,[Ru]^{0.38}$$

The activation energy for the H_2–D_2 exchange reaction was evaluated from the data presented in Fig. 3. The slope of the line through the data plotted as log (rate) against $1/T$ gave $E_a = 25.9$ kJ/mol.

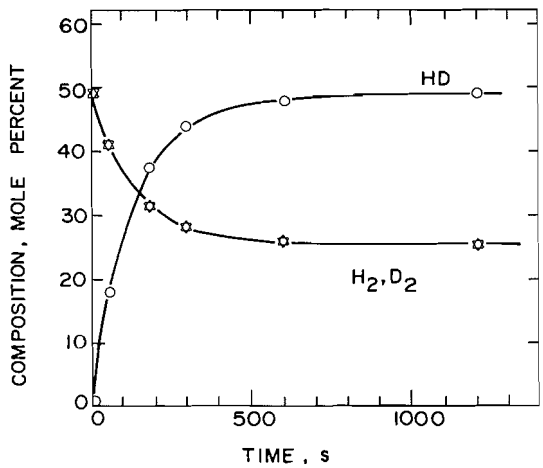

FIG. 1. Typical set of experimental data. △, D_2; ▽, HD; ○, H_2. Conditions: total ruthenium: 1.1×10^{-4} mol/l; initial pressure of D_2: 38.5 kPa; temperature: 278.1 K; solvent: C_6H_6.

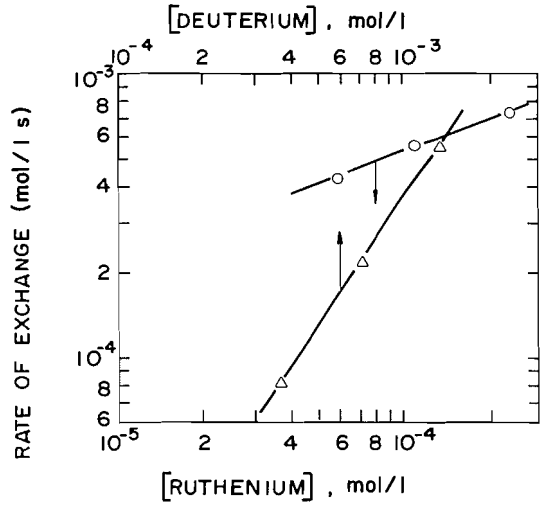

FIG. 2. Dependence of H_2–D_2 exchange rate on the concentrations of deuterium and total ruthenium. Temperature 278.1 K.

It may be seen in Fig. 2 that the rates of these reactions were extremely high: about 5×10^{-3} mol D_2/l s at 10^{-4} mol/l Ru. Since E_a was low, the possibility that the exchange rates were D_2-mass-transport-limited was tested by varying the stirring speed. Reduction in agitation rate by a factor of two decreased the reaction rate by a factor of approximately two, with [Ru] = 10^{-4} mol/l and [D_2] = 1.35×10^{-3} mol/l at 279 K. This suggested that the measured D_2 exchange rates were partly affected by the gas–liquid

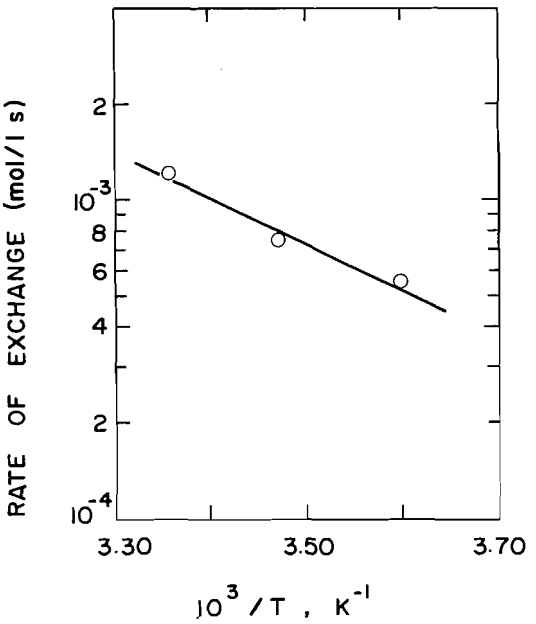

FIG. 3. Effect of temperature on the H_2–D_2 exchange rate.

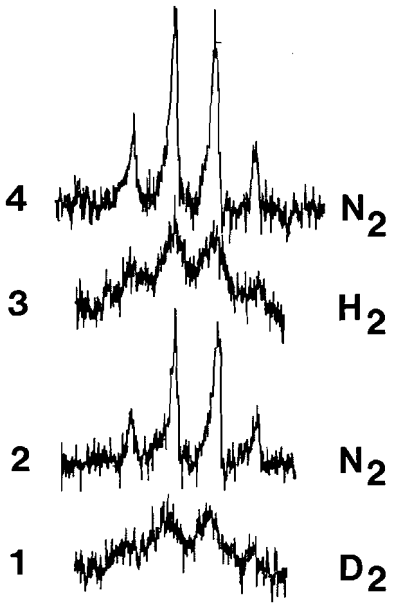

FIG. 4. Nuclear magnetic resonance spectra of a 0.1 *M* solution of $RuHCl(PPh_3)_3$ in $DCCl_3$: *1*, after 5 min D_2 purge; *2*, after 5 min N_2 purge; *3*, after 5 min H_2 purge; *4*, after 2.5 min N_2 purge.

diffusion rate. It was not feasible to increase gas–liquid transfer of D_2, HD, and H_2 by raising the stirring power since cavitation of the stirring bar occurred in the dispersion. Neither was it possible to reduce the temperature below 279 K in benzene (m.p. 278.6 K) nor to further dilute the catalyst solution below 5×10^{-5} mol/l Ru without increasing the effects of trace impurities such as O_2. The effect of partial diffusion control of the reaction rates on the kinetic parameters quoted above is considered in the discussion.

Effect of Added Reagents

PPh_3: Addition of a 5:1 excess to a C_6H_6 solution 1.2×10^{-4} mol/l in $RuHCl(PPh_3)_3$ and 1.3×10^{-3} mol/l in both H_2 and D_2 caused no change in the H_2–D_2 exchange rate. Since PPh_3 did not inhibit this reaction, generation of the catalytically active species did not require dissociation of PPh_3 from the complex.

O_2: Dissolution of $RuHCl(PPh_3)_3$ in C_6H_6 under oxygen yielded an oxidized green solution which was inactive for H_2–D_2 exchange. Since ruthenium metal is known to be an effective catalyst for this reaction, any trace amounts of Ru metal formed during the borohydride reduction of $RuCl_2(PPh_3)_3$ to yield $RuHCl(PPh_3)_3$ would have catalyzed H_2–D_2 exchange at a measurable rate. The lack of activity under O_2 confirmed that no metallic ruthenium had been formed during the preparation of $RuHCl(PPh_3)_3$.

Identification of the Catalytically Active Species

Because the rates of the H_2–D_2 reactions were rapid with respect to the rates of olefin hydrogenation using $RuHCl(PPh_3)_3$ (10), it was essential to establish if this hydrido–ruthenium complex, or another species derived from it, was catalytically active.

Nuclear Magnetic Resonance Analyses

Solutions of $RuHCl(PPh_3)_3$, up to 0.1 mol/l in $DCCl_3$, were purged in succession with D_2, N_2, H_2, and N_2 again. A typical set of spectra in the region of the high-field resonance of Ru—H is shown in Fig. 4. The initial spectrum under N_2 is not shown, but it was a well-defined quartet centered at 27.5 τ *vs.* TMS, with J(P—H) of 26 Hz, due to coupling of Ru—H with three equivalent P nuclei similar to scan 2 in Fig. 4. It may be seen that in either D_2- or H_2-saturated solution, the Ru—H quartet was considerably broadened. In every case, the sharp resonance was restored by purging with N_2. It is also important to note that rapid exchange (comparable to that for the H_2–D_2 reaction) of the Ru—H bond with D_2 did not occur.

Can. J. Chem. Downloaded from www.nrcresearchpress.com by 210.87.254.6 on 09/05/12
For personal use only.

Can. J. Chem. Downloaded from www.nrcresearchpress.com by 210.87.254.6 on 09/05/12
For personal use only.

Addition of 1 mole of anhydrous HCl per mole of $RuHCl(PPh_3)_3$ destroyed the quartet and yielded a broad resonance at 20.5 τ which decreased in intensity with time. This was likely due to production of $RuCl_2(PPh_3)_3$ with release of H_2 from the solution.

These data suggest that there was a fast ligand exchange process at the Ru atom, due either to weak complex formation between $RuHCl(PPh_3)_3$ and H_2 or D_2 without deuterium transfer to the Ru—H bond, or to slight but rapid dissociation of HCl from $RuHCl(PPh_3)_3$ occurring in the presence of H_2 or D_2.

Infrared Spectra

A comparison of the relative intensities of the ν(Ru—H) band at 2015 cm^{-1} (10) with the ν(C—H) band at 3055 cm^{-1} of $RuHCl(PPh_3)_3$ before and after exposure to D_2 gas in C_6H_6 solution for 5 min confirmed the n.m.r. observation that no significant Ru—H exchange with D_2 occurred on this time-scale.

Weak H_2 – Adduct Formation

By using the gas chromatographic H_2-stripping technique developed by us (12) to determine H_2-uptake equilibria with metal complexes, we detected a small but significant absorption of H_2 by a 2.5 mmol/l solution of $RuHCl(PPh_3)_3$ in C_6H_6. The ratio H_2:Ru was 0.056 ± 0.020 (σ). This is direct evidence for a weak interaction between $RuHCl(PPh_3)_3$ and H_2.

Experiments with $RuH_2(PPh_3)_4$

This dihydride was of interest as a potential catalytically active intermediate during H_2–D_2 exchange. The ability of this complex to absorb an additional mole of H_2 has been described by Knoth (13).

A bright yellow benzene solution, 1.1 mmol/l in $RuH_2(PPh_3)_4$, gave an H_2–D_2 exchange rate of only 2×10^{-4} mol D_2/l s at $[D_2] = 1.3$ mmol/l and 279 K. However, after sitting overnight under hydrogen, the solution had turned red. Under identical conditions, the H_2–D_2 exchange rate with this solution was then found to be 7.2×10^{-4} mol D_2/l s, that is, it had increased by a factor of 3.5. This enhanced rate may have been due to the formation of either the potentially more catalytically active $RuH_2(PPh_3)_3$ by loss of one PPh_3 ligand, or the red solvated cationic species $[Ru(PPh_3)_3]^{2+}$ reported by Mitchell *et al.* (14). The improved rate obtained with this $RuH_2(PPh_3)_4$ solution was about half that predicted for $RuHCl(PPh_3)_3$ at 1.1 mmol/l by extrapolation of the data in Fig. 2. Thus, the activities of these two solutions were comparable.

Discussion

Mechanism of the H_2–D_2 Exchange Reaction

Our observations that the specific rate of H_2–D_2 exchange is extremely rapid, and that the exchange of D_2 with the Ru—H bond of $RuHCl(PPh_3)_3$ is slow in comparison, may be accounted for if the following equilibria are considered

$$[4] \quad RuHCl(PPh_3)_3 + D_2 \overset{K_4}{\rightleftarrows} RuD_2(PPh_3)_3 + HCl$$

$$[5] \quad RuD_2(PPh_3)_3 + H_2 \overset{K_5}{\rightleftarrows} RuH_2D_2(PPh_3)_3 \overset{K_5'}{\rightleftarrows} RuHD(PPh_3)_3 + HD$$

$$[6] \quad RuD_2(PPh_3)_3 + N_2 \overset{K_6}{\rightleftarrows} RuD_2(N_2)(PPh_3)_3$$

The dependence of the apparent rate law, eq. 3, on $[D_2]^{1.5}$ and $[Ru]^{0.38}$ may be explained if the rate limiting step is the uptake of a second molecule of hydrogen by $RuD_2(PPh_3)_3$, that is, the forward step of equilibrium 5 with rate constant k_5.

It should be noted that other similar equations may be written by replacement of H by D and D by H as appropriate to take into account the additional possibilities of isotopic substitution. These will not be entirely equivalent expressions since the relative magnitude of the equilibrium constants will depend on different thermodynamic isotope effects (15). However, for the purpose of this discussion, H and D will be regarded as interchangeable and equilibrium H—D isotope effects will be ignored.

In the following discussion, the chemical aspects of H_2–D_2 exchange catalyzed by $RuHCl(PPh_3)_3$ are examined, and derivations of expressions which account for the observed dependence of the equilibration rate on $[D_2]$ and [Ru] are presented. The effect of D_2 and H_2 mass transport control are also discussed.

Chemical Aspects of the H_2–D_2 Exchange Mechanism

The validity of reaction 4 is supported by our n.m.r. and infrared data. It is clear that rapid chemical exchange at the Ru atom does not occur in the absence of H_2 (or D_2). In the presence of D_2, exchange of $RuHCl(PPh_3)_3$ in either $CDCl_3$ or C_6H_6 solution is very slow

Can. J. Chem. Downloaded from www.nrcresearchpress.com by 210.87.254.6 on 09/05/12
For personal use only.

between 279 and 298 K (10). Since the rate of H_2–D_2 exchange catalyzed by C_6H_6 solutions of $RuHCl(PPh_3)_3$ is fast in comparison, then the Ru—H bond cannot participate directly by a route involving alternate oxidative activation of H_2 and D_2, and exchange with, the monohydride. Also, because the atom-fraction of D in the gas-phase did not change during H_2–D_2 exchange experiments with $RuHCl(PPh_3)_3$, no significant transfer of D occurred to other proton pools such as the ortho-protons of the triphenylphosphine ligands.[2] This reaction rate is several orders of magnitude slower than that for the H_2–D_2 exchange discussed here (16, 17).

Dissociation of HCl from $RuHCl(PPh_3)_3$ must occur to allow formation of the di- and tetrahydrido species (reactions 4, 5). Activation of both H_2 and D_2 by $RuHCl(PPh_3)_3$ without loss of HCl or PPh_3 would violate the 16 and 18 electron rule as formulated by Tolman for homogeneous metal catalysts (18), since the potential pentahydrido intermediate would contain 20 valence shell bonding and non-bonding electrons. Our observation that excess PPh_3 did not retard the H_2–D_2 exchange reaction shows that PPh_3 dissociation is not a contributary step in the exchange.

The monohydride, $RuHCl(PPh_3)_3$, is thermodynamically stable with respect to loss of HCl. No $RuH_2(PPh_3)_3$ or $RuH_4(PPh_3)_3$ was evident in the n.m.r. spectrum of $CDCl_3$ solutions of $RuHCl(PPh_3)_3$ under 1 atm of H_2. Also, addition of 1:1 HCl to $RuHCl(PPh_3)_3$ readily yielded $RuCl_2(PPh_3)_3$ with loss of H_2. During this reaction, the high-field Ru—H quartet broadened and shifted to about 20 τ, and decayed with time as H_2 was evolved from solution. The dihydride is also unstable in the presence of HCl (13). The data above suggest that in reaction 4, the dihydrido species concentration is no greater than 5% of $[RuHCl(PPh_3)_3]$. Therefore K_4 is low (≤ 0.08).

The uptake of either H_2 (or D_2) or N_2 by $RuH_2(PPh_3)_3$ is well known (13, 19), although the equilibrium constants for reactions 5 and 6 have not been determined. Harris *et al.* have also shown that the conversion of $RuH_2(PPh_3)_4$ to $RuH_4(PPh_3)_3$ is facile. The reaction of $RuH_2(N_2)(PPh_3)_3$ with H_2 occurs readily as well to yield the tetrahydride (13, 19). Knoth's n.m.r. data (13) suggest that H_2 dissociation occurs from the related tetrahydridotris(tri-*p*-tolyl) phosphine ruthenium complex and the component reactions are rapid, but under 1 atm of H_2 this species appears to be somewhat more stable than the dihydrido adduct. In the hydrogen-saturated C_6H_6 solution of $RuHCl(PPh_3)_3$, the monohydride is thermodynamically the most stable Ru-complex.

Relatively low H_2–D_2 exchange rates were obtained with $RuH_2(PPh_3)_4$ as the catalyst. Presumably, the extent of PPh_3 dissociation from this complex to yield the catalytically active $RuH_2(PPh_3)_3$ is small. This is certainly true for the closely related dihydride $RuH_2(CH_3PPh_2)_4$ (20). A detailed investigation of reaction 7 has not been reported in the literature, but

$$[7] \qquad RuH_2(PPh_3)_4 \rightleftharpoons RuH_2(PPh_3)_3 + PPh_3$$

if this equilibrium is established slowly, and lies well to the left, the enhancement of the H_2–D_2 exchange rate with time (*c.f.* section under Experiments with $RuH_2(PPh_3)_4$) could be explained in terms of an increase in the concentration of the catalytically active dihydride.

H–D Exchange on $RuH_2D_2(PPh_3)_3$

Nuclear magnetic resonance experiments have not exclusively related the broad Ru—H resonance either to rapid chemical exchange of $RuH_4(PPh_3)_3$ with hydrogen or to stereochemical non-rigidity. If mechanism I is correct, then the occurrence of fast H_2–D_2 exchange suggests that either three or four metal–hydrogen bonds are chemically equivalent for at least a fraction of their mutual lifetime on Ru. Also, the tetrahydride must be non-rigid, since addition and dissociation of H_2 and D_2 could otherwise occur without randomization and H_2–D_2 exchange. These criteria may be met if one or more of the Ru—H bonds moves through the plane of the three P atoms, *e.g.*

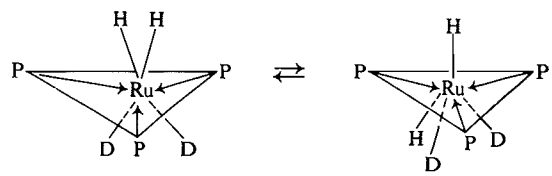

1 **2**

or if a structure similar to **2** is dominant. An equilibrium of this type may also account for the chemical reactivity of 1 mole of H_2 per mole

[2]The deuterium analyses would detect the loss of 5 microequivalents of D from the gas phase.

Can. J. Chem. Downloaded from www.nrcresearchpress.com by 210.87.254.6 on 09/05/12
For personal use only.

of Ru in the tetrahydride (13, 19, 21). In comparison to the free energies of activation for intramolecular rearrangement of dihydrides of the type RuH_2L_4 (L = phosphines, phosphites) which fall in the range 75 ± 9 kJ mol^{-1} (22), the free energies of activation for the proposed intramolecular process of $RuH_4(PPh_3)_3$ must be comparatively small because the overall $E^{\ddagger}$ for H_2–D_2 exchange was found to be only 26 kJ mol^{-1}.

Evaluation of H_2–D_2 Exchange Reaction Mechanisms

Three possible routes are considered, based on reactions 4–6, for which the rate-determining steps are: (*I*) activation of D_2 (or H_2) by $RuH_2(PPh_3)_3$ or $RuD_2(PPh_3)_3$; (*II*) uptake of H_2 by $RuHCl(PPh_3)_3$; and (*III*) activation of H_2 by $Ru(PPh_3)_3$. Mechanism I is favored.

Mechanism I

Assuming that the ruthenium complex species in solution are $RuHCl(PPh_3)_3$, $RuH_2(PPh_3)_3$, $RuH_4(PPh_3)_3$, and $RuH_2(N_2)(PPh_3)_3$ and their deuterated equivalents, and the rate-determining step is

$$[8]\quad (\text{Rate})_0 = -\text{d}[D_2]_0/\text{d}t = k_5[D_2]_0[RuH_2]$$

then initial rates are given by

$$[9]\quad (\text{Rate})_0 = \frac{2k_5K_4[D_2]_0^2[Ru]_0}{([HCl] + K_4[H_2]_T + K_4K_6[H_2]_T[N_2] + K_4K_5[H_2]_T^2)}$$

where $[D_2]$, $[Ru]_0$, and $[H_2]_T$ are the concentrations of initial D_2, total ruthenium, and total hydrogen, *i.e.*, H_2 + HD + D_2 respectively. If $[RuH_2]$, $[RuH_2(N_2)]$, and $[RuH_4]$ (the PPh_3 ligands have been omitted) are small with respect to [RuHCl], then the limiting case of eq. 9 becomes

$$[10]\quad (\text{Rate})_0 = \frac{2k_5K_4[D_2]_0^2[Ru]_0}{[HCl]}$$

But, since $[HCl] \doteqdot (K_4[H_2]_T\ [RuHCl])^{1/2}$ *c.f.* eq. 4, then at constant $[H_2]_T$, [HCl] varies approximately as $[Ru]_0^{1/2}$ and expression 10 yields

$$[11]\quad (\text{Rate})_0 = k_5(2K_4)^{1/2}[D_2]_0^{1.5}[Ru]_0^{0.5}$$

Depending on the magnitudes of constants K_4, K_5, and K_6, it may be seen from eq. 9 that the apparent rate law will have the form

$$[12]\quad (\text{Rate})_0 = (\text{Constant})\,[D_2]_0^{<2}[Ru]_0^{0.5\text{ to }1.0}$$

A rigorous test of eq. 9 could not be made, because it was not clear what effect diffusion had on the observed exchange rates. However, alternative rate-limiting steps based on the equilibria described by reactions 4–6 cannot account for the observed $[D_2]$ and [Ru] dependence, therefore this scheme is preferred.

Mechanism II

If uptake of D_2 by $RuHCl(PPh_3)_3$ is rate-controlling, *i.e.*,

$$[13]\quad (\text{Rate})_0 = -\text{d}[D_2]_0/\text{d}t = k_4[D_2]_0\ [RuHCl(PPh_3)_3]$$

then one may derive the expression

$$[14]\quad (\text{Rate})_0 = \frac{k_4[D_2]_0[Ru]_0[HCl]}{([HCl] + K_4[H_2]_T + K_4K_5[H_2]_T^2 + K_1K_3[H_2]_T[N_2])}$$

Using arguments similar to those presented above, the observable H_2–D_2 exchange reaction orders in $[D_2]_0$ and $[Ru]_0$ would be ≤ 1 and 1, respectively.

Mechanism III

If loss of HCl from $RuHCl(PPh_3)_3$ occurred rapidly and dissociatively to yield a Ru(0) intermediate such as $Ru(PPh_3)_3$

$$[15]\quad RuHCl(PPh_3)_3 \rightleftarrows Ru(PPh_3)_3 + HCl$$

and the rate-determining step was uptake of H_2 (or D_2) by this species

$$[16]\quad Ru(PPh_3)_3 + D_2 \xrightarrow{k_{16}} RuD_2(PPh_3)_3$$

Then one would obtain

$$[17]\quad (\text{Rate})_0 = \frac{k_{16}[D_2]_0[Ru]_0}{\left(\frac{[HCl]}{K_{13}} + 1 + K_{14}[H_2]_T + K_5[H_2]_T^2 + K_5K_6[H_2]_T[N_2]\right)}$$

Can. J. Chem. Downloaded from www.nrcresearchpress.com by 210.87.254.6 on 09/05/12
For personal use only.

In this case, the H_2–D_2 exchange reaction orders in $[D_2]_0$ and $[Ru]_0$ would be ≤ 1 and 0.5 to 1.0 respectively, depending on the magnitudes of K_5, K_6, K_{15}, and K_{16}. The n.m.r. evidence suggests that this route is highly unlikely, because rapid dissociation of HCl from $RuHCl(PPh_3)_3$ is not observed in the absence of H_2 (or D_2).

The Effect of Mass Transfer Resistance

To justify the selection of eq. 9 over eq. 14, it is necessary to consider the possible influence of the interfacial mass transport of hydrogen on the apparent H_2–D_2 exchange reaction kinetics.

Gessner (23) has summarized the rate expressions and reaction orders for four different chemical reaction rate regimes. The two extreme cases are those in which the chemical reaction rate is either extremely fast (his regime I) or very slow (regime IV) with respect to the gas–liquid mass transfer rate. It appears that the present H_2–D_2 exchange system is a regime II case (*i.e.*, moderately fast reaction), since the reaction orders with respect to $[D_2]_0$ and $[Ru]_0$ would be 0 and 1 in regime I (very fast reaction) and 1 and 0 in regime III (slow reaction), respectively. Recall that these orders were found to be 1.5 and 0.38, respectively. In regime II, theory would predict these values to be $(\alpha + 1)/2$ and $\beta/2$ where α and β are the true chemical orders in $[D_2]_0$ and $[Ru]_0$. If $\alpha = 1.5$ and $\beta = 0.5$ as given by eq. 11, then the apparent reaction orders would be $[D_2]_0^{1.25}$ and $[Ru]_0^{0.25}$. In the case of mechanism II, from eq. 13, $\alpha \leq 1 = \beta$, therefore in regime II, the observed dependence would be $[D_2]_0^{\leq 1}$ and $[Ru]_0^{0.5}$. The exponents for mechanism I are closer to the observed values than are those for mechanism II. Extension of these calculations to obtain rate and equilibrium constants cannot be justified in view of the uncertainties associated with the control of deuterium exchange by mass transfer.

Implications of the Present Results for Other Reactions Catalyzed by "$RuHCl(PPh_3)_3$"

Since we have demonstrated that extremely rapid H_2–D_2 exchange can occur in solutions of $RuHCl(PPh_3)_3$ without participation of the original Ru—H bond, the possibility should be considered that this monohydride is also catalytically inactive in other hydrogen-transfer reactions under H_2. These include olefin hydrogenation and isomerization, H–D exchange with olefins, or *ortho*-hydrogens of ligand PPh_3.

Hallman, McGarvey, and Wilkinson proposed that the active catalyst for olefin hydrogenation was $RuHCl(PPh_3)_2$, formed by PPh_3 dissociation (10). However, because of doubt about the independence of their hydrogenation rate data from H_2-mass transfer control, they were unable to directly test their proposed mechanism (insertion of the activated olefin into the Ru—H bond followed by H_2 addition to the alkyl complex and alkane elimination). James has discussed this matter in detail (24). Since Pennella has reported that toluene solutions of $RuH_4(PPh_3)_3$ are highly active for pent-1-ene isomerization and reduction (21, 25), we suggest that this species is also generated and is catalytically active in solutions of $RuHCl(PPh_3)_3$ in the presence of olefins. A pentene-coordinated hydrido-complex $RuH_2(C_5H_{10})(PPh_3)_3$ has been tentatively identified by Pennella (21), although Harris *et al.* detected no adduct formation between C_2H_4 and $RuH_2(PPh_3)_4$ in C_6H_6 under mild conditions (19). Since Hallman *et al.* (10) found that significant $Ru(C_2H_5)Cl(PPh_3)_3$ formation from $RuHCl(PPh_3)_3$ and C_2H_4 required 35 atm pressure, the instability of alkene adducts of the dihydride is not surprising. In the absence of a definitive study of the chemical kinetics of olefin hydrogenation by "$RuHCl(PPh_3)_3$" the currently accepted explanation for the activity of these solutions is questionable. Hydrogenation may equally well proceed via spectroscopically undetectable intermediates of the type $RuH(alkyl)(PPh_3)_3$ or $RuH_3(alkyl)(PPh_3)_3$.

The D_2–$RuHCl(PPh_3)_3$ exchange observed by Schunn (16), which included deuteration of the *ortho*-hydrogens of the both free and complexed PPh_3, may have involved species of the type

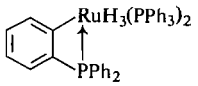

However, those H–D exchange experiments conducted with olefins in the absence of H_2 (or D_2) undoubtedly occurred by the monohydride route (16, 26) because reaction 4 could not occur. Similarly, the polymerization or either ethylene or butadiene catalyzed by solutions of $RuHCl(PPh_3)_3$ in *N,N*-dimethylacetamide (27) must occur via $RuHCl(PPh_3)_2$.

Summary

Solutions of $RuHCl(PPh_3)_3$ in C_6H_6 have been found to promote extremely rapid H_2–D_2 exchange. The rate data were shown to be affected by mass-transfer of hydrogen across the gas–liquid phase boundary. A mechanism involving formation of di- and tetrahydrido ruthenium species was invoked to explain the lack of participation by the Ru—H bond of the precursor of the active catalyst.

The authors wish to thank Dr. N. H. Sagert and M. Tomlinson for useful discussions, and D. Bell, Analytical Science Branch, for the deuterium analyses.

1. R. A. SCHUNN. *In* Transition metal hydrides. *Edited by* E. L. Muetterties. Marcel Dekker, New York. 1971. Chapt. 5.
2. D. EVANS, G. YAGUPSKY, and G. WILKINSON. J. Chem. Soc. (A), 2660 (1968).
3. D. H. GERLACH, W. G. PEET, and E. L. MUETTERTIES. J. Am. Chem. Soc. **94**, 4545 (1972).
4. J. L. HENDRIKSE and J. W. E. COENEN. J. Catal. **30**, 72 (1973).
5. M. G. BURNETT and R. J. MORRISON. J. Chem. Soc. Dalton, 632 (1973).
6. G. G. EBERHARDT and L. VASKA. J. Catal. **8**, 183 (1967).
7. S. SIEGEL. J. Catal. **30**, 139 (1973).
8. G. G. STRATHDEE and R. M. GIVEN. 56th Canadian Chemistry Conference, Montreal. 1973.
9. G. C. BOND. Catalysis by metals. Academic Press, New York. 1962. p. 151.
10. P. S. HALLMAN, B. R. MCGARVEY, and G. WILKINSON. J. Chem. Soc. (A) 3143 (1968).
11. J. J. LEVISON and S. D. ROBINSON. J. Chem. Soc. (A) 639 (1970).
12. G. G. STRATHDEE and R. M. GIVEN. J. Catal. **30**, 30 (1973).
13. W. H. KNOTH. J. Am. Chem. Soc. **94**, 104 (1972).
14. R. W. MITCHELL, A. SPENCER, and G. WILKINSON. J. Chem. Soc. Dalton, 846 (1973).
15. G. G. STRATHDEE and R. M. GIVEN. Can. J. Chem. **52**, 2216 (1974).
16. R. A. SCHUNN. Inorg. Chem. **9**, 2567 (1970).
17. G. W. PARSHALL, W. H. KNOTH, and R. A. SCHUNN. J. Am. Chem. Soc. **91**, 4990 (1969).
18. C. A. TOLMAN. Chem. Soc. Rev. 337 (1972).
19. R. O. HARRIS, N. K. HOTA, L. SADAVOY, and J. M. C. YUEN. J. Organometal. Chem. **54**, 259 (1973).
20. K. C. DEWHIRST, W. KEIM, and C. A. REILLY. Inorg. Chem. **3**, 546 (1968).
21. F. PENNELLA. J. Organometal. Chem. **C17**, 65 (1974).
22. P. MEAKIN, E. L. MEUTTERTIES, and J. P. JESSON. J. Am. Chem. Soc. **95**, 75 (1973).
23. A. W. GESSNER. *In* Homogeneous catalysis. *Edited by* R. F. GOULD. Adv. Chem. Ser. **70**, 35 (1968). Am. Chem. Soc., Washington, D.C.
24. B. R. JAMES. Homogeneous hydrogenation. Wiley-Interscience, New York. 1973. p. 83.
25. F. PENNELLA, R. L. BANKS, and M. R. RYCHECK. Proc. XIVth Intern. Conf. Coordin. Chem. Toronto. 1972. p. 78.
26. B. HUDSON, D. E. WEBSTER, and P. B. WELLS. J. Chem. Soc. Dalton, 1205 (1972).
27. B. R. JAMES and L. D. MARKHAM. J. Catal. **27**, 442 (1972).

Can. J. Chem. Downloaded from www.nrcresearchpress.com by 210.87.254.6 on 09/05/12
For personal use only.

Crystal Structures of K_2MgCl_4 and Cs_2MgCl_4

CYRIL S. GIBBONS,[1] VINCENT C. REINSBOROUGH, AND W. ALEXANDER WHITLA[2]

Department of Chemistry, Mount Allison University, Sackville, New Brunswick E0A 3C0

Received July 10, 1974

CYRIL S. GIBBONS, VINCENT C. REINSBOROUGH, and W. ALEXANDER WHITLA. Can. J. Chem. **53**, 114 (1975).

Supporting evidence for complex ion formation in $MgCl_2$ alkali chloride melts was sought from a single crystal X-ray analysis of the title compounds. Crystals of K_2MgCl_4 are tetragonal, a = 4.94, c = 15.58 Å, Z = 2, space group $I\,4/mmm$. The compound is isostructural with K_2NiF_4, and was determined with MoKα diffractometer data and refined by full-matrix least-squares to R = 0.046 for 180 reflections.

Crystals of Cs_2MgCl_4 are orthorhombic, a = 9.777, b = 7.514, c = 13.234 Å, Z = 4, space group *Pnma*. The compound is isostructural with β-K_2SO_4, and was determined with MoKα diffractometer data and refined by full-matrix least-squares to R = 0.074 for 1084 reflections. The K_2MgCl_4 structure contains an infinite two-dimensional array of $MgCl_6$ octahedra sharing edges. The Cs_2MgCl_4 structure contains discrete $MgCl_4^{2-}$ anions which likely continue to exist in the melt close to the melting point.

CYRIL S. GIBBONS, VINCENT C. REINSBOROUGH et W. ALEXANDER WHITLA. Can. J. Chem. **53**, 114 (1975).

On a cherché par diffraction des rayons-X de cristaux uniques des composés mentionnés dans le titre, l'existence d'ions complexes dans les produits de fusion de $MgCl_2$ avec des chlorures alcalins. Les cristaux de K_2MgCl_4 sont tétragonaux, a = 4.94, c = 15.58 Å, Z = 2, groupe d'espace $I\,4/mmm$. Le composé est isostructural avec K_2NiF_4 et sa structure a été déterminée avec des données du diffractomètre mesurées avec MoKα et affinée par moindres-carrés (matrice complète) jusqu'à une valeur R de 0.046 pour 180 réflexions.

Les cristaux de Cs_2MgCl_4 sont orthorhombiques, a = 9.777, b = 7.514, c = 13.234 Å, Z = 4, groupe d'espace *Pnma*. Le composé est isostructural avec le β-K_2SO_4 et sa structure a été déterminée à l'aide des données diffractomètriques mesurées avec MoKα et affinée par moindres-carrés (matrice complète) jusqu'à une valeur de R de 0.074 pour 1084 réflexions. La structure de K_2MgCl_4 contient un arrangement bidimensionnel infini d'octaèdres $MgCl_6$ liés par deux côtés. La structure de Cs_2MgCl_4 contient des anions $MgCl_4^{2-}$ individuels qui continuent vraisemblablement d'exister près du point de fusion. [Traduit par le journal]

Introduction

The controversy over complex ions in molten salts most often centers upon the binary MCl_2 – alkali metal chloride melts where deviations from additivity or ideality in transport and thermodynamic properties are extreme at stoichiometrically appropriate mole fractions (1, 2). Flood and Urnes (3) were the first to suggest the tetrahedral MCl_4^{2-} as being the principal complex species in these systems and recent calorimetric (4–7) and Raman investigations (8, 9) concur in this assessment. Postulated ions have ranged from the pyramidal MCl_3^- to larger and more highly charged species such as MCl_6^{4-}. Direct evidence for these complex species in melts is difficult to obtain so that mass spectrometric or vapor pressure studies are often performed on the vapors above the melts in hopes of obtaining some hint of what species are in the liquid state (10). As far as is known, the approach from the solid state has never been employed for these binary systems although it has long been recognized that the solid structure is maintained to some extent in the melt (11). Recent Raman work confirms this view (12). In the present work, single crystal X-ray analyses of the compounds K_2MgCl_4 and Cs_2MgCl_4 obtained from melts of the appropriate stoichiometry were undertaken to provide details of the magnesium ion coordination in the solid state.

Experimental

The phase diagrams indicate that both K_2MgCl_4 and Cs_2MgCl_4 are congruently melting compounds (13, 14). To obtain single crystals suitable for X-ray diffraction analysis, a modified Bridgman technique was used in which the ampoule containing a molten mixture

[1]Present address: Department of Materials Chemistry, Ontario Research Foundation, Sheridan Park, Ontario.

[2]To whom correspondence should be addressed.

Can. J. Chem. Downloaded from www.nrcresearchpress.com by 210.87.254.42 on 09/05/12
For personal use only.

Can. J. Chem. Downloaded from www.nrcresearchpress.com by 210.87.254.42 on 09/05/12
For personal use only.

of the salts in the correct stoichiometric proportions was withdrawn at a rate of 3 mm per hour from a Stanton–Redcroft furnace equipped with a Eurotherm temperature controller. All materials were dried prior to use and manipulated in a drybox. Exact stoichiometry was achieved by weighing the sealed container of the salts on an analytical balance and adjusting the weight of the nonhygroscopic salt (CsCl or KCl). The resulting complexes were hygroscopic and were examined under a binocular microscope sealed inside a glove bag. Samples of the appropriate size were chipped from the mass of the solid and sealed inside quartz capillaries for X-ray examination. The fragments did not show any well-defined cleavage planes for either of the compounds studied.

The unit cell parameters and space group were determined from Weissenberg and precession photographs and diffractometer data, the unit cell parameters being refined by the least-squares procedure of the Picker FACS I system for 9 (K_2MgCl_4) and 11 (Cs_2MgCl_4) reflections with MoKα radiation. Crystal data are:

K_2MgCl_4 f.w. = 244.3
Tetragonal, $a = 4.94(1)$, $c = 15.58(4)$ Å, $V = 380.2$ Å^3, $Z = 2$, $\rho_c = 2.13$, $F(000) = 236$. MoKα, $\lambda = 0.7107$ Å, $\mu = 25.7$ cm^{-1}. Space group $I\,4/mmm$.

Cs_2MgCl_4 f.w. = 431.9
Orthorhombic, $a = 9.777(4)$, $b = 7.514(3)$, $c = 13.234(6)$ Å, $V = 972.2$ Å^3, $Z = 4$, $\rho_c = 2.95$, $F(000) = 760$. MoKα, $\lambda = 0.7107$ Å, $\mu = 86.8$ cm^{-1}. Space group *Pnma*.

The intensities of all reflections with $2\theta(\text{MoK}\alpha) \leq 60°$ (minimum interplanar spacing, 0.71 Å) for K_2MgCl_4 and $2\theta(\text{MoK}\alpha) \leq 55°$ (minimum interplanar spacing, 0.77 Å) for Cs_2MgCl_4 were measured on a Picker FACS I diffractometer system with a scintillation counter, approximately monochromatic MoKα radiation (graphite monochromator and pulse-height analyzer), and a θ–2θ scan of 1° min^{-1} in 2θ. Background counts were made at the beginning and end of the scan, and a check reflection was measured every 25 reflections and used to scale the data.

The crystals used for data collection were irregular cleavage fragments of average cross-section 0.3 mm. The K_2MgCl_4 crystal was initially mounted with a parallel to the ϕ axis of the goniostat, but was displaced slightly in ϕ and χ for the data collection. The Cs_2MgCl_4 crystal was similarly displaced from its b axis setting for the data collection. No absorption corrections were made. Lorentz and polarization factors were applied, and the structure amplitudes derived. For K_2MgCl_4, 180 reflections of the 196 measured (92%) were classified as observed, and for Cs_2MgCl_4, 1084 of the 1200 measured (90%) were classified as observed. Reflections were classified as observed if the net count was greater than 7% of the scaled background count. Unobserved reflections were given zero weight in the refinement of the structures.

Differential thermal analyses (Deltatherm model D2000-16) were carried out on both compounds and indicated no major phase changes from room temperature to the melting point. Precession photographs were obtained for K_2MgCl_4 at approximately 250 °C, and were identical to the room temperature photographs, except for a slight expansion of the lattice parameters. Since the DTA apparatus did not allow completely anhydrous conditions, minor deflections below 200 °C on the DTA trace were ascribed to the evolution of adsorbed water. Therefore we are confident that the room temperature structures are maintained up to the melting point.

All crystallographic calculations were made on an IBM 1130 computer using programs written by W.A.W. Standard test data (15) were used to confirm the reliability of the programs.

Structure Analysis

K_2MgCl_4

Consideration of the space group and unit cell data indicated possible isomorphism with the known K_2NiF_4 structure (16, 17), and this was verified by the Patterson function. With the atomic positions of ref. 16, scattering factors from ref. 18, and isotropic temperature factors $B = 1.0$ Å^2, a structure factor calculation gave $R = 0.36$. Two cycles of full-matrix least-squares with unit weights reduced R to 0.16. To complete the refinement, all atoms were assigned anisotropic thermal parameters, and with $\sqrt{w} = 1.0$ for $|F_o| \leq 20$, $\sqrt{w} = 20/|F_o|$ for $|F_o| > 20$, five cycles of refinement resulted in a final R of 0.045 for the 180 observed reflections. The maximum parameter shift in the final cycle was 1.3σ, and a final difference map showed no spurious detail.

Cs_2MgCl_4

The space group and unit cell data indicated that the structure was of the K_2SO_4 type, but initial parameters used were averages of K_2SO_4 and the isomorphous Cs_2CuCl_4 (16), to allow for the differences in ionic size. With these initial coordinates, scattering factors from ref. 18, and isotropic temperature factors $B = 2.0$ Å^2, a structure factor calculation gave $R = 0.42$. A subsequent Fourier map was computed, and the positional coordinates adjusted. At this point, R was 0.32, and two cycles of full-matrix least-squares refinement with unit weights reduced R to 0.17. All atoms were then assigned anisotropic temperature factors, and four further cycles of least-squares refinement with $\sqrt{w} = 1.0$ for $|F_o| \leq 50$, $\sqrt{w} = 50/|F_o|$ for $|F_o| > 50$, gave a final R of 0.074 for the 1084 observed reflections. The maximum parameter shift in the final cycle was 0.09σ, and a final difference map showed only minor peaks around the heavier atoms, probably due to series-termination errors.

Final positional and thermal parameters are listed in Tables 1 and 2, and interatomic distances and angles in Table 3. Figures 1 and 2 show the packing arrangements in K_2MgCl_4 and Cs_2MgCl_4 respectively.

Observed and final calculated structure factors are given in Table 4.[3]

Discussion

The structure of K_2MgCl_4 is of the K_2NiF_4 type (16, 17) and is illustrated in Fig. 1. The two independent Mg—Cl distances are 2.470 and

[3]Photocopies of Table 4 are available upon request, at a nominal charge, from the Depository of Unpublished Data, National Science Library, National Research Council of Canada, Ottawa, Canada K1A 0S2.

TABLE 1. Final positional (fractional) and anisotropic thermal (Å² × 10²) parameters for K_2MgCl_4, with standard deviations in parentheses. (Off diagonal elements of the thermal parameters are zero due to symmetry restrictions.)

Atom	X	Y	Z	U_{11}	U_{12}	U_{33}
K(4*e*)	0	0	0.3567(1)	4.21(7)	4.21(7)	2.34(6)
Mg(2*a*)	0	0	0	1.13(8)	1.13(8)	2.09(11)
Cl(1)(4*c*)	0.5	0	0	1.15(7)	2.85(9)	5.20(10)
Cl(2)(4*e*)	0	0	0.1598(1)	4.55(7)	4.55(7)	1.87(6)

TABLE 2. Final positional (fractional) and anisotropic thermal (Å² × 10²) parameters for Cs_2MgCl_4, with standard deviations in parentheses

Atom	X	Y	Z
Cs(1)	0.6385(1)	0.25	0.4049(1)
Cs(2)	−0.0181(1)	0.25	−0.3178(1)
Mg	0.2287(5)	0.25	0.4230(3)
Cl(1)	−0.0055(4)	0.25	0.4108(4)
Cl(2)	0.3142(4)	0.25	0.5856(3)
Cl(3)	0.3194(3)	0.0025(5)	0.3451(3)

Atom	U_{11}	U_{12}	U_{13}	U_{22}	U_{23}	U_{33}
Cs(1)	2.77(5)	0.0	−0.67(5)	5.06(7)	0.0	8.56(10)
Cs(2)	2.30(4)	0.0	0.12(3)	4.66(6)	0.0	2.85(4)
Mg	1.89(20)	0.0	−0.14(16)	2.38(22)	0.0	2.12(20)
Cl(1)	2.02(17)	0.0	−0.94(16)	8.14(37)	0.0	5.52(26)
Cl(2)	3.63(21)	0.0	−1.03(15)	8.27(36)	0.0	2.48(17)
Cl(3)	4.39(17)	−0.31(15)	2.13(17)	4.29(18)	−3.28(19)	9.14(27)

2.491 Å, and all angles at Mg are constrained to 90° by symmetry. The $MgCl_6$ octahedra share four corners to form infinite layers parallel to (001) separated by $c/2$, with the potassium ions situated in the "valleys" formed by the faces of the octahedra. K ... Cl contacts are 3.331(1) and 3.503(1) Å in the one layer, and 3.071(2) Å to the unshared corner of the octahedron in the next layer.

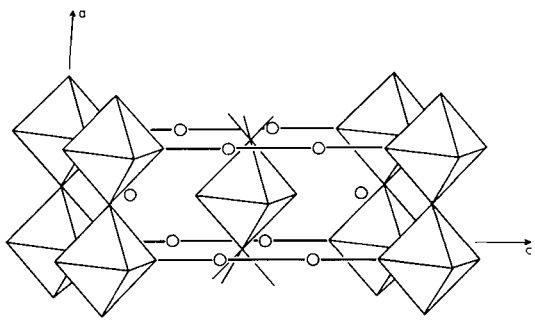

FIG. 1. General view of the unit cell contents of K_2MgCl_4. The circles represent potassium ions.

Cs_2MgCl_4 is isostructural with β-K_2SO_4 (16, 19) and consists of cesium cations and discrete $MgCl_4^{2-}$ tetrahedra (Fig. 2). Distortion of the tetrahedron is only slight as indicated by the bond lengths and angles of Table 3, and compares with that found in Cs_2ZnCl_4 (20). There

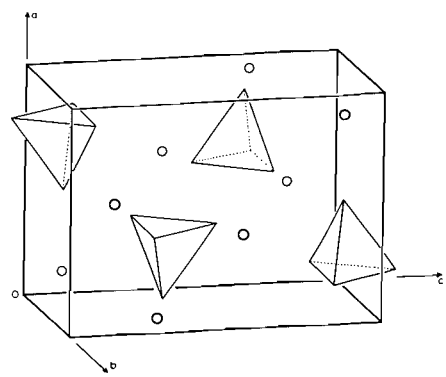

FIG. 2. General view of the unit cell contents of Cs_2MgCl_4. The heavier circles are cesium ions at $\frac{3}{4}b$ while the lighter ones are at $\frac{1}{4}b$.

Can. J. Chem. Downloaded from www.nrcresearchpress.com by 210.87.254.42 on 09/05/12
For personal use only.

TABLE 3. Interatomic distances and angles*

Compound	Bond	Distance (Å)	Bonds	Angle (deg)
K_2MgCl_4				
Mg environment†	Mg—Cl(1)	2.470(2)×4		
	Mg—Cl(2)	2.492(2)×2		
K environment	K—Cl(2)	3.071(2)	Cl(2)—K—Cl(1)	132.12(2)×4
	K—Cl(1)	3.331(2)×4	Cl(1)—K—Cl(1)	63.27(2)×4
	K—Cl′(2)	3.503(1)×4		95.76(4)×2
			Cl(2)—K—Cl′(2)	85.79(4)×4
			Cl(1)—K—Cl′(2)	61.72(2)×8
				124.91(4)×8
			Cl′(2)—K—Cl′(2)	89.69(5)×4
				171.58(6)×2
Cs_2MgCl_4				
Mg environment	Mg—Cl(1)	2.296(6)	Cl(1)—Mg—Cl(3)	110.6(2)×2
	Mg—Cl(3)	2.304(5)×2	Cl(3)—Mg—Cl(3)	107.6(2)
	Mg—Cl(2)	2.308(6)	Cl(2)—Mg—Cl(3)	106.1(2)×2
			Cl(1)—Mg—Cl(2)	115.3(2)
Cs environment	Cs(1)—Cl(1)	3.482(4)	Cl(1)—Cs—Cl(3)	147.5(2)×2
	Cs(1)—Cl(3)	3.717(4)×2	Cl(3)—Cs—Cl(3)	60.0(2)
	Cs(1)—Cl(2)	3.788(1)×2	Cl(1)—Cs—Cl(2)	82.9(2)×2
	Cs(1)—Cl′(3)	3.836(4)×2	Cl(3)—Cs—Cl(2)	67.3(2)×2
	Cs(1)—Cl′(2)	3.971(4)		127.3(2)×2
			Cl(2)—Cs—Cl(2)	165.4(2)
			Cl(1)—Cs—Cl′(3)	82.7(2)×2
			Cl(3)—Cs—Cl′(3)	91.5(2)×2
				121.4(2)×2
			Cl(2)—Cs—Cl′(3)	57.8(2)×2
				116.7(2)×2
			Cl′(3)—Cs—Cl′(3)	59.3(2)
			Cl(1)—Cs—Cl′(2)	141.7(2)
			Cl(3)—Cs—Cl′(2)	57.2(2)×2
			Cl(2)—Cs—Cl′(2)	94.5(2)×2
			Cl′(3)—Cs—Cl′(2)	64.3(2)×2
	Cs(2)—Cl(3)	3.467(4)×2	Cl(3)—Cs(2)—Cl(3)	66.3(2)
	Cs(2)—Cl(2)	3.483(4)	Cl(3)—Cs(2)—Cl(2)	73.5(2)×2
	Cs(2)—Cl′(2)	3.492(4)	Cl(3)—Cs(2)—Cl′(2)	72.9(2)×2
	Cs(2)—Cl′(3)	3.522(3)×2	Cl(2)—Cs(2)—Cl′(2)	139.6(2)
	Cs(2)—Cl(1)	3.595(5)	Cl(3)—Cs(2)—Cl′(3)	103.8(2)×2
	Cs(2)—Cl′(1)	3.961(2)×2		145.8(2)×2
			Cl(2)—Cs(2)—Cl′(3)	72.4(2)×2
			Cl′(2)—Cs(2)—Cl′(3)	137.8(2)×2
			Cl′(3)—Cs(2)—Cl′(3)	65.2(2)
			Cl(3)—Cs(2)—Cl(1)	127.0(2)×2
			Cl(2)—Cs(2)—Cl(1)	153.9(2)
			Cl′(2)—Cs(2)—Cl(1)	66.5(2)
			Cl′(3)—Cs(2)—Cl(1)	85.8(2)×2
			Cl′(1)—Cs(2)—Cl(1)	71.8(2)×2
			Cl(3)—Cs(2)—Cl′(1)	70.0(2)×2
				132.8(2)×2
			Cl(2)—Cs(2)—Cl′(1)	107.6(2)×2
			Cl′(2)—Cs(2)—Cl′(1)	80.3(2)×2
			Cl′(3)—Cs(2)—Cl′(1)	60.4(2)×2
				121.9(2)×2
			Cl′(1)—Cs(2)—Cl′(1)	143.1(2)

*Standard deviations, in parentheses, are for the last figure given. Cell errors are not included. The primes on the atom numbers indicate atoms related by the equivalent positions and translations of the space group. The angles are only for atoms in the distance table.
†All angles constrained by symmetry to 90° or 180°.

Can. J. Chem. Downloaded from www.nrcresearchpress.com by 210.87.254.42 on 09/05/12
For personal use only.

Can. J. Chem. Downloaded from www.nrcresearchpress.com by 210.87.254.42 on 09/05/12
For personal use only.

are two independent cesium ions in the structure with slightly different coordination. Each ion has seven contacts between 3.47 and 3.84 Å with one additional contact at 3.97 Å in this case and two, at 3.96 Å in the other. In both situations, the cesium ions have no unusual features. Further discussion of these structures is unnecessary as many isostructural compounds have already been described in the literature.

To extend these solid state structures to the structure of the melt is necessarily tenuous. The liquid state will not have the long term ordering characteristic of the solid state and thus the K_2MgCl_4 structure, with an infinite array of octahedra sharing corners, probably has little relationship to the liquid state. However, the Cs_2MgCl_4 structure contains the $MgCl_4^{2-}$ anion which can retain its existence in the liquid state and thus it is reasonable to propose that discrete $MgCl_4^{2-}$ anions exist in the liquid cesium salt at least near the melting point.

The crystal structures of the 1:1 complexes $KMgCl_3$ (21) and $CsMgCl_3$ (22) are also known with octahedra sharing edges in the former and octahedra sharing faces in the latter. No discrete anionic complexes have been observed in either, and no conclusions regarding complex species in the corresponding melts can be made. However, it is interesting to note that both the enthalpy and the entropy of fusion for Cs_2MgCl_4 are substantially lower than those for the other three compounds mentioned above (23). This is consistent with a smaller degree of reorganization of the solid on melting for Cs_2MgCl_4 which would occur if the $MgCl_4^{2-}$ ions were essentially unaltered on melting. This does not however preclude the presence of other ions which could exist as well.

It is evident from these two structures that the ionic size and charge density of the alkali metal ion is a factor affecting the coordination of the magnesium ion. From melts of the same stoichiometric ratio, $2KCl{\cdot}MgCl_2$ forms a two dimensional infinite array with the potassium ion coordinated by two adjacent layers, while the cesium compound forms a loosely packed structure containing discrete $MgCl_4^{2-}$ tetrahedra. Also, the potassium ion has a distorted nine coordination by chloride ions whereas the cesium coordination is more regular. The larger, more easily polarized cesium ion must interfere with the tendency in the solid for the magnesium ion to coordinate six ligands. Since potassium is more polarizing than cesium, the ionic size may be the dominant factor in the change. Further studies on related systems are being undertaken to clarify this point.

We thank the National Research Council of Canada for a postdoctoral fellowship to C.S.G.; Mr. C. Cole of the Nova Scotia Technical College for carrying out the differential thermal analyses; the computing centre staff of Mount Allison University for assistance; Dr. H. Lynton for permitting us to use the diffractometer facilities at the University of New Brunswick; and Dr. M. H. Brooker for helpful discussions.

1. M. A. Bredig. *In* Molten salts. *Edited by* G. Mamantov. Marcel Dekker, N.Y. 1969. p. 55.
2. A. D. Pelton. Can. J. Chem. **49**, 3919 (1971).
3. H. Flood and S. Urnes. Z. Elektrochem. **59**, 834 (1955).
4. G. N. Papatheodorou and O. J. Kleppa. J. Inorg. Nucl. Chem. **32**, 889 (1970).
5. G. N. Papatheodorou and O. J. Kleppa. Inorg. Chem. **10**, 873 (1971).
6. G. N. Papatheodorou and O. J. Kleppa. J. Inorg. Nucl. Chem. **33**, 1249 (1971).
7. G. N. Papatheodorou. J. Inorg. Nucl. Chem. **35**, 465 (1973).
8. V. A. Maroni, E. J. Hathaway, and E. J. Cairns. J. Phys. Chem. **75**, 155 (1971).
9. V. A. Maroni. J. Chem. Phys. **55**, 4789 (1971).
10. H. Bloom. *In* The chemistry of molten salts. Benjamin, N.Y. 1967. p. 134.
11. H. Bloom and E. Heymann. Proc. R. Soc. A**188**, 392 (1947).
12. R. J. Capwell. Chem. Phys. Lett. **12**, 443 (1972).
13. K. Grjotheim, J. L. Holm, and M. Rønes. Acta Chem. Scand. **26**, 3802 (1972).
14. E. M. Levin, C. R. Robbins, and H. F. McMurdie. *In* Phase diagrams for ceramists. *Edited by* M. K. Reser. American Ceramic Society, Columbus, Ohio. 1964. p. 371.
15. F. R. Ahmed, D. W. Cruickshank, A. C. Larson, and J. M. Stewart. Acta Cryst. A**28**, 365 (1972).
16. R. W. G. Wyckoff. (*Editor*). Crystal structures. Vol. III. 2nd ed. Interscience. New York. 1963. p. 68.
17. D. Balz and K. Plieth. Z. Elektrochem. **59**, 545 (1955).
18. International tables for X-ray crystallography. Vol. III. Kynoch Press. Birmingham. 1962.
19. J. A. McGinnety. Acta Cryst. B**28**, 2845 (1972).
20. J. A. McGinnety. Inorg. Chem. **13**, 1057 (1974).
21. J. Brynestad, H. L. Yakel, and G. P. Smith. J. Chem. Phys. **45**, 4652 (1966).
22. G. L. McPherson, T. J. Kistenmacher, and G. D. Stucky. J. Chem. Phys. **52**, 815 (1972).
23. J. L. Holm, B. J. Holm, B. Rinnan and F. Grønvold. J. Chem. Thermodyn. **5**, 97 (1973).

Pyrazolo[1,5-*a*]pyrimidine: Synthesis and Regiospecific Electrophilic Substitution in the Pyrazole and/or Pyrimidine Rings[1]

BRIAN MAURICE LYNCH,[2] MISBAHUL AIN KHAN,[3] SURESH CHANDRA SHARMA,[4] AND HUK CHIA TEO[5]

Organic Chemistry Laboratory, Saint Francis Xavier University, Antigonish, Nova Scotia B0H 1C0

Received June 17, 1974

BRIAN MAURICE LYNCH, MISBAHUL AIN KHAN, SURESH CHANDRA SHARMA, and HUK CHIA TEO. Can. J. Chem. **53**, 119 (1975).

A general cyclization route to pyrazolo[1,5-*a*]pyrimidines from 3-aminopyrazole and 1,3-dicarbonyl compounds is applied to synthesis of the parent ring system. In nitration of this species the orientation of substitution is strongly reagent dependent. Mixed nitric and sulfuric acids yield the 3-nitro compound, whereas nitric acid in acetic anhydride yields the 6-nitro compound. Brominations yield 3-bromo and 3,6-dibromo species.

The majority reacting species in the strongly acidic medium is identified as the 1-protonated entity by conjoint use of approximate molecular orbital calculations and the variation of coupling constant patterns accompanying protonation. The molecular orbital calculations predict successive 3- and 6-substitution by electrophiles in pyrazolo[1,5-*a*]pyrimidine and its conjugate acid, and an addition–elimination sequence is proposed to account for the observed 6-nitration.

BRIAN MAURICE LYNCH, MISBAHUL AIN KHAN, SURESH CHANDRA SHARMA et HUK CHIA TEO. Can. J. Chem. **53**, 119 (1975).

Une méthode générale de cyclisation conduisant aux pyrazolo[1,5-*a*]pyrimidines, à partir des amino-3 pyrazole et des composés dicarbonylés 1,3, est appliquée à la synthèse de ces systèmes cycliques fondamentaux. Lors de la nitration de ces espèces, l'orientation de la substitution dépend beaucoup de la nature du réactif. Un mélange d'acides nitrique et sulfurique conduit au composé portant un groupe nitro en position 3 alors que l'acide nitrique dans l'anhydride acétique conduit au composé portant un groupe nitro en position 6. La bromuration conduit aux dérivés bromo-3 et dibromo-3,6.

On a identifié les espèces réagissant d'une façon prédominante dans les milieux fortement acide comme étant les entités protonées en position 1; cette conclusion a été établie par l'utilisation à la fois de calcul d'orbitales moléculaires approché et la variation de patron de constante de couplage accompagnant la protonation. Les calculs d'orbitales moléculaires prédisent des substitutions électrophiles successives en position 3 et 6 pour les pyrazolo [1,5-*a*]pyrimidines et leurs acides conjugués et l'on propose une séquence d'addition et d'élimination pour tenir compte de la nitration observée en position 6. [Traduit par le journal]

Introduction

As part of a systematic synthesis program for fused-ring species derived from pyrazole (1, 2), we communicated in 1970 (1) a brief account of routes to pyrazolo[1,5-*a*]pyrimidine **1** and some 3-substituted derivatives. Patent claims to a similar synthetic route (3) and reports of enzyme-inhibitory activity for 3-substituted 5,7-dimethylpyrazolo[1,5-*a*]pyrimidines (4 and references therein) prompt us to provide details of the synthesis of **1**, and to report and analyze the patterns revealed in its common electrophilic substitutions and in its p.m.r. spectra, using an interpretive framework of π-electron (HMO) and all-valence-electron (CNDO/2) quantum chemical calculations.

Results

The parent species **1** is available in excellent yield by a sequential condensation and electrophilic cyclization, employing 1,1,3,3-tetramethoxypropane (malondialdehyde tetramethylacetal) and 3-aminopyrazole (generated by thermal decarboxylation of the commercially available 3-aminopyrazole-4-carboxylic acid) with zinc chloride in refluxing ethanolic solution. This route is based on related precedents in the Russian literature (5) and we have also applied

[1]This study was assisted by grants-in-aid from the National Cancer Institute of Canada, the National Research Council of Canada, and the Saint Francis Xavier University Council for Research.

[2]Author to whom reprint requests should be addressed.
[3]Postdoctorate research associate, 1967–1970.
[4]Postdoctorate research associate, 1971–1974.
[5]Graduate research assistant, 1969–1971.

Can. J. Chem. Downloaded from www.nrcresearchpress.com by 210.87.254.6 on 09/05/12
For personal use only.

Can. J. Chem. Downloaded from www.nrcresearchpress.com by 210.87.254.6 on 09/05/12
For personal use only.

it to construction of compounds in the isomeric pyrazolo[3,4-*b*]pyridine series (1, 6).

One of our purposes in examining the patterns of electrophilic substitution of **1** was to seek further examples of *reagent-dependent orientation* (as explored previously for brominations and nitrations of arylpyrazoles (7, 8), acetanilides (9), and arylpyrimidines (10)). In considering such substitutions, the actual reacting species could be either the free base **1** or a conjugate acid species, and the favored positions of substitution might differ for attack on each entity. The expectation of reagent-dependent orientation was fulfilled for nitration reactions: treatment of **1** with mixed concentrated nitric and sulfuric acids at 0 ± 5° (standard conditions for mononitration of arylpyrazoles (7, 8)) gave the 3-nitropyrazolo[1,5-*a*]pyrimidine **2***a*, whereas corresponding treatment with nitric acid – acetic anhydride gave the 6-nitropyrazolo-[1,5-*a*]pyrimidine **3***a*, with each reaction being regiospecific.

In contrast, brominations under a variety of conditions (6) provided the 3-bromopyrazolo-[1,5-*a*]pyrimidine **2***b* and/or 3,6-dibromopyrazolo[1,5-*a*]pyrimidine **3***b* but there was no indication of initial 6-substitution.

The formation of **2***a* in nitration of **1** corresponds to the orientation in mononitration of pyrazolo[1,5-*a*]pyridine (2), whereas the 6-nitration to **3***a* has precedent in the nitration of tetrazolo[1,5-*a*]pyridine (11).

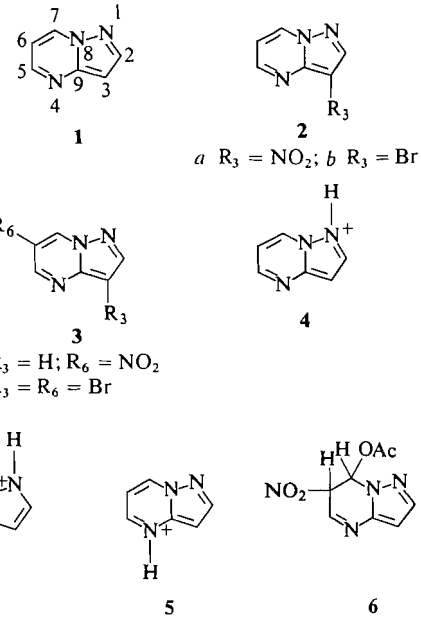

Discussion

Explanation of the Regioselective Nitrations

The remarkable feature of the nitration results is that their sense is opposite to that observed in the nitrations of arylpyrazoles (7, 8) and pyrazolo[1,5-*a*]pyridine (2), where we found that the nitric acid – acetic anhydride reagent favors attack in the pyrazole moiety. A necessary starting point for an explanation is a definition of the majority reacting species in the nitration media. The pK_a of the conjugate acid derived from **1** is 2.30 (determined potentiometrically (6)), suggesting very strongly that the majority species in the mixed acid nitrations of **1** will be this conjugate acid (compare pyrazole and 1-arylpyrazoles, of similar basic strength to **1**, where kinetic proof of nitration via the conjugate acid species has been given (12, 13).

The species **1** could undergo either 1-protonation (to entity **4**) or 4-protonation (to entity **5**) and it is difficult to decide between these potential basic centers (the 1- or the 4-nitrogen). The results of quantum-chemical calculations favor **4**: thus the π-electron distribution from a HMO calculation on **1** (Fig. 1) indicates that position 1 would be protonated first (accepting that a proton would attach itself most readily to the nitrogen atom of highest π-electron density (*cf.* 14), and HMO calculations of the π-electron binding energies of assumed models of **4** and **5** (which give respective values of 13.353 and 13.297 β) indicate that **4** is the more stable entity. The all-valence-

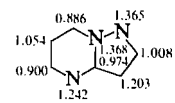

FIG. 1. HMO π-electron densities for species **1**

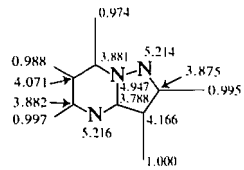

FIG. 2. CNDO/2 electron densities for species **1**.

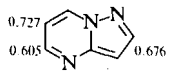

FIG. 3. HMO π-bond orders for species **1**.

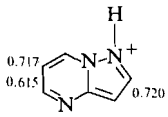

FIG. 4. HMO π-bond orders for species **4**.

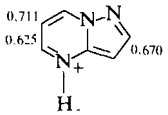

FIG. 5. HMO π-bond orders for species **5**.

electron CNDO/2 calculation for **1** (Fig. 2) yields virtually identical total electron densities (5.214 at nitrogen-1, 5.216 at nitrogen-4) but the 2s electron populations (corresponding to the lone-pair basic center) strongly favor protonation at nitrogen-1 (the 2s electron populations are 1-nitrogen, 1.520; 4-nitrogen, 1.458).

Furthermore, conjoint comparison of the calculated HMO π-bond orders for **1**, **4**, and **5** (see Figs. 3–5) with changes in the magnitudes of interproton couplings accompanying protonation of **1** (as revealed by the comparison of p.m.r. spectra in deuteriochloroform and in trifluoroacetic acid-*d*, see Table 1) favors **4** as majority species. The calculated bond orders for the 2–3 bond in **4** as compared with **1** increase significantly (from 0.676 to 0.720), with but little change in the bond orders on the periphery of the pyrimidine moiety; for the model comparison of **5** with **1**, the bond orders where proton–proton coupling would be detectable are closely similar for each species.

The changes in coupling constants accompanying protonation are confined to an increase in J_{23} from 2.0 to 3.0 Hz, whereas J_{56} and J_{67} are unaffected; in view of previously demonstrated bond order – coupling constant relationships (15, 16), this pattern is consistent with **4** but not with **5**. The increase in bond order between atoms 2 and 3 may be understood in resonance formalism by considering the contribution of structure **4***a*. Related evidence supporting position 1 as the protonation site is provided by the lanthanide-induced shifts of the protons in **1**, where the pattern of shifts indicates almost exclusive complexation at nitrogen-1 (unpublished work with Mr. Philip Smith).

Accepting that the predominant conjugate acid species of **1** is **4**, we have modelled the expected site of electrophilic substitution in **4** by evaluating the HMO localization energies for substitution at positions 3 and 6, taking cation–cation repulsion into account by a summation procedure (17, 18). 3-Substitution is strongly favored (the localization energies are 2.04 β for 3-substitution and 2.39 β for 6-substitution) and although the cation–cation repulsions favor 6- over 3-substitution the difference in repulsions is only *ca.* 20 kJ M^{-1} and is not sufficient to counterbalance the difference in σ-complex energies. Similarly, the higher-level CNDO/2 calculations of the relative binding energies for 3- and 6-proton exchange intermediates (σ-complexes for proton exchange) involving each of the species **1** and **4**, give energy differences of 107 kJ M^{-1} favoring

TABLE 1. Proton magnetic resonance spectra of pyrazolo[1,5-*a*]pyrimidine and derivatives

Species	Solvent	Chemical shifts for protons[a]					Coupling constants (Hz)			
		2	3	5	6	7	J_{23}	J_{56}	J_{67}	J_{57}
1	$CDCl_3$	8.13	6.72	8.69	6.80	8.47	2.0	5.0	7.0	2.0
	$CDCl_3$:DMSO-d_6 (9:1)	8.11	6.65	8.93	6.86	8.50	2.0	4.8	7.0	2.0
	TFA-*d*	8.75	7.32	9.88	7.72	9.20	3.0	5.0	7.0	2.0
2*a*	DMSO-d_6	9.07	—	9.43	7.50	9.03	—	4.0	7.0	2.0
3*a*	DMSO-d_6	8.60	7.02	10.25	—	9.20	2.0	—	—	1.9
2*b*	$CDCl_3$:DMSO-d_6 (9:1)	8.23	—	8.92	7.08	8.65	—	4.0	7.0	2.0
3*b*	$CDCl_3$:DMSO-d_6 (9:1)	8.10	—	8.97	—	8.53	—	—	—	2.0

[a]In p.p.m. downfield from internal tetramethylsilane.

Can. J. Chem. Downloaded from www.nrcresearchpress.com by 210.87.254.6 on 09/05/12
For personal use only.

Can. J. Chem. Downloaded from www.nrcresearchpress.com by 210.87.254.6 on 09/05/12
For personal use only.

3-substitution in species **1** and 35 kJ M^{-1} favoring 3-substitution in species **4**. Both theoretical approaches agree in suggesting that 3-substitution will be the normal pattern for electrophilic substitution in pyrazolo[1,5-*a*]-pyrimidine, for reaction through either the conjugate acid **4** or the free base **1**.

This leads to the conclusion that the 6-nitration observed using the nitric acid – acetic anhydride reagent is not a simple displacement of a proton by nitronium ion. Since it is known that this reagent often adds the elements of nitronium acetate to bonds of high order in olefinic and heteroaromatic species (10, 19), we propose that formation of the 6-nitro compound **3***a* results from rapid addition of nitro and acetate moieties to the 6—7 bond of **1** to yield the adduct **6** (reaction through the free base **1** is suggested since this will be present in significant proportions in the reaction medium); **6** is postulated to yield **3***a* by elimination of acetic acid during work-up. The rate of formation of **6** from pyrazolo[1,5-*a*]pyrimidine is postulated to be faster than the encounter rate of nitronium ion with substrate, in order to account for the absence of 3-nitration. Evidence supporting the postulated intermediacy of **6** is cited in the Experimental section.

Proton Magnetic Resonance Spectra

The data assembled in Table 1 for the various pyrazolo[1,5-*a*]pyrimidines reveal that the 3- and 6-protons in **1** have characteristic chemical shifts and interprotonic couplings: species carrying substituents at these positions lack these characteristic signals. The nitro group in **2***a* and **3***a* exerts the expected deshielding influence on vicinal protons (20), whereas bromo substituents (as in **2***b* and **3***b*) have little effect on the shifts of the remaining protons, again in accord with expectation (20).

The sequence of chemical shifts for the protons of pyrazolo[1,5-*a*]pyrimidine in trifluoroacetic acid-*d* follows the order of calculated HMO π-electron densities for the 1-protonated species **4** if the shifts are corrected for ring-current and anisotropy effects (*cf.* 21): the equation linking these quantities is

$$\delta = 15.31 - 6.92q_\pi$$

$$(n = 5, r = 0.968)$$

and the response in p.p.m./electron is in the range typical of aromatic protons (21).

Experimental

Microanalyses were carried out using a Hewlett-Packard Model 185 Analyzer. Melting points were measured on a Kofler Heizbank and are corrected with reference to standard samples. The p.m.r. spectra were recorded with a Varian A-60D spectrometer, equipped with a V-6040 variable temperature controller. Infrared spectra were obtained on a Beckman Acculab 4 spectrometer.

Synthesis of Pyrazolo[1,5-a]pyrimidine, 1

3-Aminopyrazole-4-carboxylic acid (Aldrich Chemical Co.) (5 g) was decarboxylated by heating at *ca.* 170° until evolution of carbon dioxide ceased. The decarboxylation product was dissolved in ethanol (75 ml) and to this solution was added 10 *M* hydrochloric acid (5 ml) and zinc chloride (2.5 g). The mixture was heated to reflux and a solution of 1,1,3,3-tetramethoxypropane (6.6 g) in ethanol (10 ml) was added; heating under reflux was continued for 1 h. The reaction mixture was poured onto ice water (500 g), neutralized with aqueous ammonia, and extracted with chloroform (4 × 100 ml). Removal of the chloroform under reduced pressure, followed by vacuum sublimation at *ca.* 80°, provided pyrazolo[1,5-*a*]pyrimidine **1**, m.p. 105° (4.0 g, 86% based on 3-aminopyrazole-4-carboxylic acid).

Anal. Calcd. for $C_6H_5N_3$: C, 60.50; H, 4.23; N, 35.27. Found: C, 60.60; H, 4.25; N, 35.15.

Nitrations

To 3-Nitropyrazolo[1,5-a]pyrimidine, 2a

Pyrazolo[1,5-*a*]pyrimidine (1.19 g, 0.01 mol) was dissolved in concentrated sulfuric acid (*d* 1.84, 10 ml) at 20°, cooled to −5°, and treated at this temperature with a mixture of concentrated sulfuric acid and fuming (90%) nitric acids (1:1 v/v; 4 ml). The reaction mixture was kept at 0° for 15 min and at 5° for 15 min, and poured onto ice. The precipitated light yellow solid was collected by filtration, washed with cold water, and crystallized from water, yielding 623 mg 3-nitropyrazolo[1,5-*a*]-pyrimidine **2***a*, m.p. 259–260°.

Anal. Calcd. for $C_6H_4N_4O_2$: C, 43.91; H, 2.45; N, 34.14. Found: C, 43.59; H, 2.36; N, 33.82.

Extraction of the filtrate with chloroform, followed by evaporation of the extract, yielded recovered pyrazolo-[1,5-*a*]pyrimidine (170 mg); the yield of isolated, crystallized product based upon the apparent conversion is 44%. Monitoring of the p.m.r. spectra of model reaction mixtures using deuterated nitrating media indicated no organic species other than the 3-nitro compound **2***a* and unreacted **1**.

To 6-Nitropyrazolo[1,5-a]pyrimidine, 3a

Pyrazolo(1,5-*a*)pyrimidine (510 mg, 0.005 mol) in acetic anhydride (10 ml) was nitrated by dropwise addition of fuming (90%) nitric acid (5 ml) over 1 h at 0–5°. The reaction mixture was poured onto crushed ice and allowed to stand overnight. The precipitate was collected and crystallized from methanol, yielding 6-nitropyrazolo-[1,5-*a*]pyrimidine **3***a*, m.p. 180° (300 mg, 43% of crystallized product).

Anal. Found: C, 43.50; H, 2.71; N, 34.30.

The p.m.r. spectrum of the crude product showed no indication of the presence of the 3-nitro compound **2***a*. Marginally successful efforts were made to demonstrate

Can. J. Chem. Downloaded from www.nrcresearchpress.com by 210.87.254.6 on 09/05/12
For personal use only.

the intermediacy of the addition product **6** in yielding **3***a*, as follows: removal of the volatile materials from an aliquot portion of a reaction mixture by low-temperature vacuum distillation left yellow oily material, which was extracted with chloroform-*d* at 5°; the extract was washed repeatedly with ice-cold aqueous sodium hydrogen carbonate, dried overnight over anhydrous magnesium sulfate at 5°, and concentrated at 5° under reduced pressure. The p.m.r. spectrum of the concentrate was recorded using a probe temperature of 0°; it showed signals of similar intensity at δ 7.90 and 7.84, assigned, respectively, to acetate methyl groups in residual acetic acid (or acetic acid from the decomposition of **6**) and to the species **6** (*cf.* the chemical shift of acetate methyl signals in a related adduct isolated in the acetyl nitrate nitration of 4-phenylpyrimidine (10)). The aromatic region showed 17 signals between 400 and 600 Hz from tetramethylsilane, consistent with the presence of **1**, **3***a*, and **6**; resolution was limited by peak half-widths of 2–3 Hz but subtraction of signals assignable by inspection to **1** and **3***a* (compare Table 1) suggested the following chemical shifts for the protons of **6**: δ 8.4 (2-proton), 7.3 (3-proton) 9.5 (5-proton), 8.0 and 8.2 (6- and 7-protons). After standing overnight, the p.m.r. spectrum of this sample indicated the presence of **1**, **3***a*, and acetic acid. A further portion of the chloroform-*d* concentrate was used to obtain a rapid-scan i.r. spectrum. By comparison with spectra of authentic samples of **1** and **3***a*, it was evident that these were major components but carbonyl absorptions were also present at 1750 (s) and 1700 cm^{-1} (vs); the high-frequency peak is in the region expected (*cf.* (10)) for the *C*-acetate group of **6** (the 1700 cm^{-1} absorption is due to the acetic acid).

Brominations

To 3-Bromopyrazolo[1,5-a]pyrimidine, 2b

Pyrazolo[1,5-*a*]pyrimidine (1.19 g, 0.01 mol) was brominated using a stoichiometric amount of bromine in chloroform at room temperature for 1 h. The reaction mixture was washed with aqueous sodium hydrogen carbonate and the chloroform layer was separated and evaporated, leaving crude 3-bromopyrazolo[1,5-*a*]pyrimidine, which was crystallized from water to give pure **2***b*, m.p. 158–159° (1.00 g, 50%).

Anal. Calcd. for $C_6H_4BrN_3$: C, 36.36; H, 2.02; N, 21.21. Found: C, 36.05; H, 2.05; N, 21.40.

To 3,6-Dibromopyrazolo[1,5-a]pyrimidine, 3b

To a stirred solution of pyrazolo[1,5-*a*]pyrimidine (1.19 g, 0.01 mol) in ethanol (25 ml) was added, dropwise, a saturated aqueous solution of bromine (50 ml). During the addition, nitrogen gas was bubbled slowly through the solution. After addition of the bromine reagent was complete (2 h), the reaction mixture was made basic with aqueous sodium hydroxide, and the precipitated solid was collected. The aqueous filtrate was extracted with chloroform (3 × 100 ml), the chloroform extracts were combined, dried (anhydrous sodium carbonate), and evaporated. The residue was added to the precipitated solid, and the entire material was crystallized from ethanol, yielding 3,6-dibromopyrazolo[1,5-*a*]-pyrimidine **3***b*, m.p. 198–200° (1.40 g, 50%).

Anal. Calcd. for $C_6H_3Br_2N_3$: C, 26.02; H, 1.09; N, 15.18. Found: C, 26.00; H, 1.03; N, 15.09.

Molecular Orbital Calculations

The calculations using the simple Hückel method (HMO) were made using a standard program (10, 21) with an IBM 1130 computer. The electronegativity parameters h for various types of nitrogen were: pyrroloid, $h = 1$; pyridinoid, $h = \frac{1}{2}$. Electrostatic corrections to the localization energies were taken into account as follows (18): the interaction energy between the incoming electrophile and the charge-field of the cationic heterocyclic substrate was calculated for slightly polarized models of the substrate (the Coulomb integral of the carbon under attack was increased from α to $\alpha + \frac{1}{2}\beta$). Corrections were evaluated by summation of the terms q_i/r_i for each atom, using the HMO π-electron densities (q_i is the net charge at a particular atom and r_i its distance from the incoming electrophile, which was assumed to be normal to the aromatic ring plane and 0.3 nm directly above the site of attack).

CNDO/2 calculations were made using a version of Quantum Chemistry Program Exchange Program 91 modified for operation on a Hewlett-Packard 3000 Computer. The bond lengths chosen were as follows: for **1** (bond, bond length) 1—2, 0.132 nm; 2—3, 3—9, 4—9, 4—5, 5—6, 6—7, 0.14 nm; 7—8, 8—9, 0.134 nm; 8—1, 0.145 nm; and for the conjugate acid species **4** and **5**, 1—2, 0.130 nm; 8—1, 0.150 nm; all other ring bonds, 0.140 nm. All aromatic C—H bonds are 0.108 nm; the N—H bond, 0.100 nm. All C—H bonds and the N—H bond bisect the bond angles linking the C or N atoms to the ring system. Bond angles were as follows: for **1** (angle defined by constituent atoms, angle) 9—8—1, 105°; 8—1—2, 112°; 1—2—3, 107°; 2—3—9, 109°; 3—9—8, 109°; 8—4—9, 115°; 9—4—5, 4—5—6, 5—6—7, 6—7—8, 120°; 7—8—9, 125°; and for the conjugate acid species, 9—8—1, 108°, 8—1—2, 106°, 1—2—3, 110°; 2—3—9, 3—9—8, 108°; all other ring angles, 120°.

The σ-complexes from attachment of protons to the 3 or 6 positions of **1** and the conjugate acid **4** were modelled by changing the bond lengths linking the site of proton attachment to the other ring atoms to 0.150 nm, assuming equivalent C—H bonds of length 0.109 nm, and a tetrahedral H—C—H angle; the other angles in the affected ring were adjusted to reform the ring, without variation of bond lengths.

The molecular geometries chosen are based upon those used for a previous study (2) of a closely related condensed pyrazole species, where the choice gave good correspondence with observed dipole moments. Variations for conjugate acid species and for σ-complex models used the standard set of bond lengths and bond angles recommended for the CNDO/2 program.

We thank the following persons for analytical and computational assistance: Messrs. E. Schuegraf and B. A. Dawson, and Mesdames L. Graham and K. von Reubendale. The program of research of which this paper is one part was supported generously by the National Cancer Institute of Canada, the National Research Council of Canada, and the Saint Francis Xavier University Council for Research. We thank Drs. R. K. Robins and D. E. O'Brien (ICN Nucleic Acid Research Institute, Irvine, California) for their courtesy in discussion of unpublished results.

1. M. A. KHAN and B. M. LYNCH. J. Heterocycl. Chem. **7**, 247 (1970).
2. B. M. LYNCH and B. P. LEM. J. Heterocycl. Chem. **11**, 223 (1974).
3. R. K. ROBINS, D. E. O'BRIEN, T. NOVINSON, and R. H. SPRINGER. Ger. Offen. 2,257,547. Chem. Abstr. **79**, 78840 (1973).
4. T. NOVINSON, R. K. ROBINS, and D. E. O'BRIEN. J. Heterocycl. Chem. **10**, 887 (1973); A. H. ALBERT, R. K. ROBINS, and D. E. O'BRIEN. J. Heterocycl. Chem. **10**, 885 (1973).
5. V. G. ZHIRYAKOV and P. I. ABRAMENKO. Chem. Heterocycl. Compd. (U.S.S.R.) **1**, 219 (1965).
6. H. C. TEO. M. Sc. Thesis. St. Francis Xavier University, Antigonish, Nova Scotia. 1971.
7. M. A. KHAN, B. M. LYNCH, and Y. HUNG. Can. J. Chem. **41**, 1540 (1963).
8. B. M. LYNCH and Y. HUNG. Can. J. Chem. **42**, 1605 (1964).
9. B. M. LYNCH, C. M. CHEN, and Y. WIGFIELD. Can. J. Chem. **46**, 1141 (1968).
10. B. M. LYNCH and L. POON. Can. J. Chem. **45**, 1431 (1967).
11. T. SASAKI, K. KANEMATSU, and M. MURATA. Tetrahedron, **27**, 5121 (1971).
12. M. W. AUSTIN, J. R. BLACKBOROW, J. H. RIDD, and B. V. SMITH. J. Chem. Soc. 1051 (1965).
13. M. R. GRIMMETT, S. R. HARTSHORN, K. SCHOFIELD, and J. B. WESTON. J. Chem. Soc. Perkin Transactions II, 1654 (1972).
14. R. D. BROWN. Q. Rev. **6**, 63 (1952).
15. N. JONATHAN, S. GORDON, and B. P. DAILEY. J. Chem. Phys. **36**, 2443 (1961).
16. W. B. SMITH, W. H. WATSON, and S. CHIRANJEEVI. J. Am. Chem. Soc. **89**, 1438 (1967).
17. I. L. FINAR. J. Chem. Soc. B, 725 (1968).
18. B. M. LYNCH. Combined meeting, Am. Chem. Soc.—Chem. Inst. Can. Toronto, May 1970. Abstr. Paper ORGN 26.
19. F. G. BORDWELL and E. W. GARBISCH. J. Am. Chem. Soc. **82**, 3588 (1960).
20. H. SPIESECKE and W. G. SCHNEIDER. J. Chem. Phys. **35**, 731 (1961).
21. B. M. LYNCH, A. J. ROBERTSON, and J. G. K. WEBB. Can. J. Chem. **47**, 1129 (1969).

Can. J. Chem. Downloaded from www.nrcresearchpress.com by 210.87.254.6 on 09/05/12
For personal use only.

A Synthesis of (±)-Cularicine

ISAO NOGUCHI AND DAVID B. MACLEAN

Department of Chemistry, McMaster University, Hamilton, Ontario L8S 4M1

Received July 5, 1974

ISAO NOGUCHI and DAVID B. MACLEAN. Can. J. Chem. **53**, 125 (1975).

A synthesis of (±)-cularicine is reported. 2-(2′-Benzyloxyphenoxy)-4,5-methylenedioxyphenylacetic acid was converted in four steps to 6-benzyloxy-2,3-methylenedioxy-10,11-dihydrodibenz[*b*,*f*]oxepin-10(11*H*)-one. A modified Pomeranz–Fritsch reaction was applied to this ketone to add the two carbon atoms and one nitrogen atom required to complete the carbon skeleton of cularicine. The norcularicine derived from this reaction was *N*-methylated with formaldehyde and sodium borohydride.

ISAO NOGUCHI et DAVID B. MACLEAN. Can. J. Chem. **53**, 125 (1975).

On rapporte une synthèse de la (±)-cularicine. L'acide (benzyloxy-2′ phénoxy)-2 méthylènedioxy-4,5 phénylacétique est transformé en quatre étapes en 11*H*-benzyloxy-6 méthylènedioxy-2,3 dihydro-10,11 dibenz[*b*,*f*]oxepinone-10. On a soumis cette cétone à une forme modifiée de la réaction de Pomeranz–Fritsch. Afin d'ajouter les deux atomes de carbone et l'atome d'azote nécessaire pour compléter le squelette carboné de la cularicine. La norcularicine obtenue par cette réaction a été *N*-méthylée avec de la formaldéhyde et du borohydrure de sodium.

[Traduit par le journal]

(+)-Cularicine (**1**, $C_{18}H_{17}NO_4$), an alkaloid of *Corydalis claviculata* (L.) DC, was isolated by Manske (1, 2), who elucidated its structure (2) by converting it into cularine (**2**), an alkaloid of established structure (3, 4). Besides **1** and **2** only two other alkaloids of this type have been isolated, cularimine (3) and cularidine (4). The absolute configuration of cularine, shown in the accompanying structure, has recently been established by relating it chemically to *S*-laudanosine (5) and by X-ray analysis of its methiodide (6). Since **1**, **3**, and **4** have all been converted to cularine their configuration is also known (3, 4).

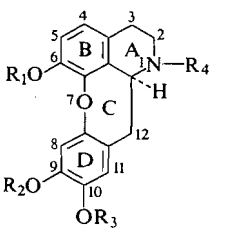

1 (cularicine) $R_1 = H$; $R_2 + R_3 = CH_2$; $R_4 = Me$
2 (cularine) $R_1 = R_2 = R_3 = R_4 = Me$
3 (cularimine) $R_1 = R_2 = R_3 = Me$; $R_4 = H$
4 (cularidine) $R_1 = H$; $R_2 = R_3 = R_4 = Me$

Several successful approaches to the synthesis of cularine have been reported. In two of these the diphenyl ether linkage was formed in an Ullmann reaction in the initial stages of the synthetic scheme and rings A and C were subsequently constructed from the appropriately substituted diphenyl ether (7, 8). In another approach, substituted benzylisoquinolines were synthesized and the diphenyl ether linkage was introduced in a late stage of the synthetic scheme either through oxidative coupling (9–11) or through an intramolecular Ullmann reaction (12, 13). Resolution of synthetic (±)-cularine has been effected (14). Initial attempts to synthesize cularidine (15, 16) led only to derivatives that were not convertible into the racemic phenolic base. More recently, however, the intramolecular Ullmann reaction has been applied to the synthesis of cularidine (17) and of cularicine (18). Here we describe another synthesis of (±)-cularicine by a method that should serve equally well for the synthesis of (±)-cularidine.

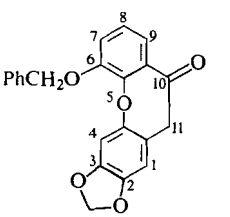

5

Can. J. Chem. Downloaded from www.nrcresearchpress.com by 210.87.254.6 on 09/05/12
For personal use only.

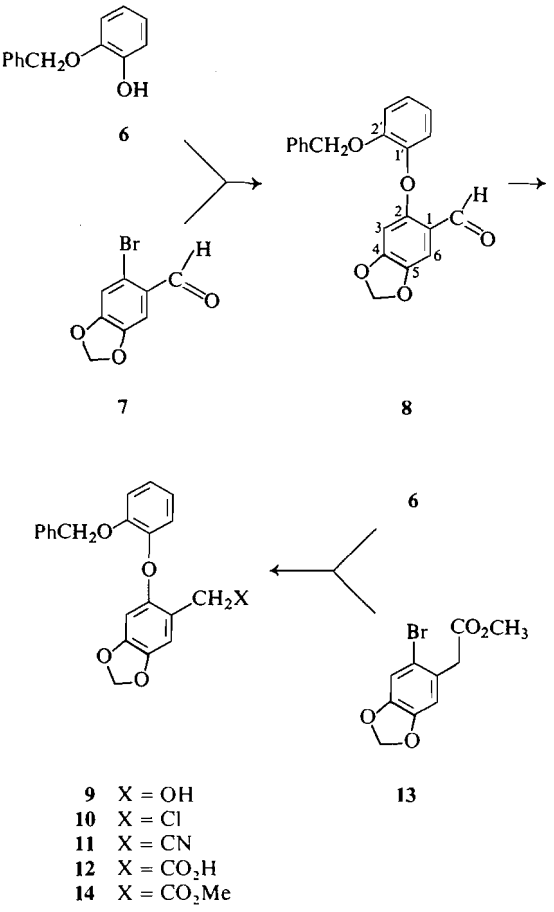

SCHEME 1

The first objective of our synthesis was the oxepinone (**5**) containing three of the four rings of cularicine with the potential phenolic group at C-6 of cularicine suitably protected. The synthesis of **5** was brought about in the manner shown in Schemes 1 and 2. Ullmann condensation of *o*-benzyloxyphenol (**6**) (19) with 6-bromopiperonal (**7**) (20) in the presence of copper and cupric oxide gave the diphenyl ether (**8**), in 53% yield, which was reduced to the alcohol (**9**) in quantitative yield. Treatment of **9** with thionyl chloride yielded the chloride (**10**) that was converted directly to the cyanide (**11**) with sodium cyanide in methyl ethyl ketone. Base-catalyzed hydrolysis of **11** led to the acid **12** in good yield. Compound **12** was also prepared by fusion of **6** with methyl 6-bromohomopiperonylate (**13**) in the presence of copper and cupric oxide at 140° for 8 h. The methyl ester (**14**) so obtained was hydrolyzed directly to the acid (**12**). These experiments are summarized in Scheme 1. Up to this point our synthetic scheme is analogous to that used in the original synthesis of cularine (7).

Attempts to cyclize **12** in various acidic media led to failure. Similarly, cyclization of the acid chloride (**15**) under a variety of Friedel–Crafts conditions gave uncharacterized products apparently resulting from debenzylation of the ether by the Lewis acid catalysts. At length it was found that the amide (**16**) cyclized to the enamine (**17**) on treatment with phosphoryl chloride in a mixture of benzene and toluene at reflux. To our knowledge this method of cyclization is unique. However, it has an analogy in the Bischler–Napieralski cyclization of phenylethyl amides to dihydroisoquinolines. The general utility of this cyclization for the preparation of ketones will be investigated further. The structure of **17** follows from an examination of its spectroscopic properties and from its hydrolysis to the oxepinone (**5**). The spectroscopic properties of **5** are in accord with the structure assigned. These transformations are outlined in Scheme 2.

The introduction of two carbon atoms and a

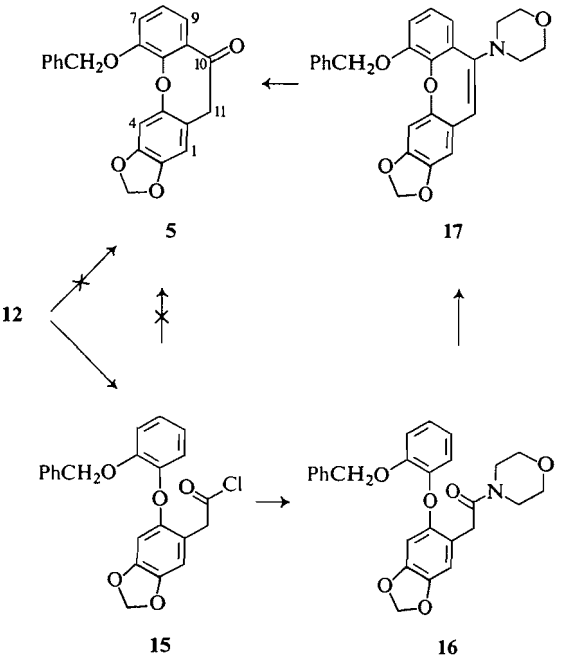

SCHEME 2

Can. J. Chem. Downloaded from www.nrcresearchpress.com by 210.87.254.6 on 09/05/12
For personal use only.

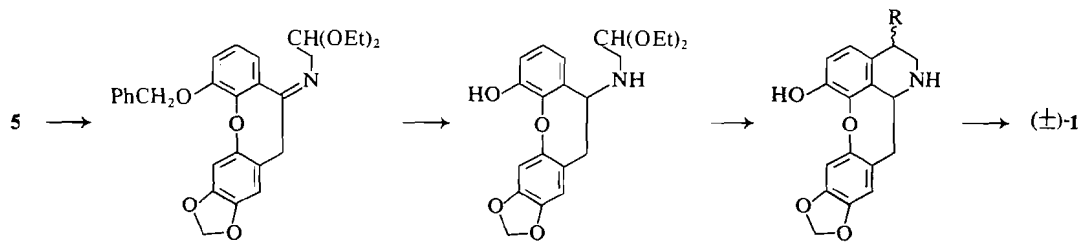

SCHEME 3

nitrogen atom was now necessary to complete the ring system of cularicine. To bring this about, we turned to the modified Pomeranz–Fritsch procedure developed by Bobbitt *et al.* (21) and eventually worked out satisfactory conditions to prepare a Schiff base and to effect the cyclization of its dihydro derivative (Scheme 3).

The oxepinone (**5**) was condensed with aminoacetaldehyde diethyl acetal to the Schiff base (**18**) which was converted directly to the phenolic amino acetal (**19**). The protecting benzyl group was removed by hydrogenolysis simultaneously with the reduction of the carbon–nitrogen double bond. The acetal (**19**) was converted in 6 *N* ethanolic hydrochloric acid into the cyclized compound (**20**). The formation of an ethoxy rather than the usual hydroxy compound in the Bobbit cyclization appears to be without precedent in the literature (22, and references cited therein). The 3-ethoxynorcularicine (**20**) obtained in this reaction represents one of a pair of racemates but its relative configuration was not established. In an analogous reaction Dalton *et al.* (23) also obtained only one of a pair of possible racemates. The ethoxy group of **20** was removed by hydrogenolysis over Pt in ethanolic hydrochloric acid yielding racemic norcularicine (**21**). Treatment of the mother liquor, remaining after the separation of **20**, with hydrogen over Pt also led to the recovery of (±)-norcularicine.

Finally, *N*-methylation was brought about with formaldehyde and sodium borohydride. The product of this reaction, (±)-cularicine, had spectral properties in solution that were identical with those of a sample of natural (+)-cularicine obtained from Professor R. H. F. Manske. The melting point of our product differs from that reported (18) but the spectral properties agree within experimental error.

Experimental

Apparatus, Methods, and Materials

Infrared spectra were recorded on a Beckmann IR-5 spectrometer in KBr, in liquid film or in solution as stated. The data are reported in $\nu\,cm^{-1}$.

Proton magnetic resonance spectra were recorded on Varian HA-100 or A-60 spectrometers. All spectra were recorded at ambient temperature in solution in the solvent specified with tetramethylsilane (TMS) as internal standard. Chemical shifts are reported relative to TMS = 0.0 δ. The symbols s, d, t, m, refer to singlet, doublet, triplet, and multiplet, respectively.

Mass spectra were determined on a C.E.C. 21-110B mass spectrometer. Samples were introduced through a direct inlet system. Relative intensity data were obtained from low resolution spectra recorded under identical conditions at an ionization voltage of 70 eV, a trap current at 140 μA, and at 200 °C or at the source temperature specified. Relative intensities of individual ions are placed in parenthesis after the *m/e* value.

Melting points are uncorrected.

2-(2′-Benzyloxyphenoxy)-4,5-methylenedioxybenzaldehyde (8)

A mixture of *o*-benzyloxyphenol (19) (**6**, 5.0 g), 6-bromopiperonal (20) (**7**, 5.5 g), potassium carbonate (12.0 g), copper powder (10.0 g), cupric oxide (5.0 g) and pyridine (15 ml) was heated at 110–115° with vigorous stirring for 20 h. The product was extracted with chloroform, and the extract was filtered and washed with 10% HCl and 5% NaOH. It was then dried over potassium carbonate and evaporated to leave a dark syrup. Purification was effected by column chromatography on silica gel using chloroform as eluent to give 2-(2′-benzyloxyphenoxy)-4,5-methylenedioxybenzaldehyde (**8**, 4.6 g, 52.9%) as colorless needles melting at 104–105° after recrystallization from ethanol; i.r. (KBr): 1670 (CO), 935 (OCH_2O), 735, 695 (monosubstituted benzene); p.m.r. ($CDCl_3$): 10.14 (1 H, s, —C*H*O), 7.35–6.92 (10 H, m, Ar—H), 6.25 (1 H, s, H-3), 5.92 (2 H, s, OCH_2O), 5.05 (2 H, s, OCH_2Ph).

Anal. Calcd. for $C_{21}H_{16}O_5$: C, 72.40; H, 4.63. Found: C, 72.52; H, 4.74.

2-(2′-Benzyloxyphenoxy)-4,5-methylenedioxybenzyl Alcohol (9)

Sodium borohydride (10.0 g) was added in portions to a stirred solution of the aldehyde (**8**) (20.0 g) in methanol

Can. J. Chem. Downloaded from www.nrcresearchpress.com by 210.87.254.6 on 09/05/12
For personal use only.

Can. J. Chem. Downloaded from www.nrcresearchpress.com by 210.87.254.6 on 09/05/12
For personal use only.

(600 ml) at room temperature. After stirring the mixture for a further 2 h, the solvent was removed to leave a colorless viscous residue which was diluted with water and extracted with benzene. The extract gave on evaporation the alcohol (**9**), (19.4 g, 97%) as colorless needles melting at 84–85° after crystallization from chloroform–hexane; i.r. (KBr): 3250 (OH), 935 (OCH_2O), 745, 695 (monosubstituted benzene); p.m.r. ($CDCl_3$): 7.27 (5 H, s, C_6H_5), 7.15–6.90 (4 H, m, Ar—H), 6.85 (1 H, s, H-6), 6.34 (1 H, s, H-3), 5.83 (2 H, s, OCH_2O), 5.02 (2 H, s, OCH_2Ph), 4.58 (2 H, CH_2OH), 2.48 (1 H, broad s, OH).

Anal. Calcd. for $C_{21}H_{18}O_5$: C, 71.99; H, 5.18. Found: C, 71.99; H, 5.23.

*2-(2′-Benzyloxyphenoxy)-4,5-methylenedioxybenzyl Cyanide (**11**)*

Thionyl chloride (40 ml) was added dropwise to a stirred solution of alcohol (**9**) (20 g) in benzene (300 ml) at 5–10° and the mixture was then heated under reflux for 1 h. Removal of the solvent yielded the chloride (**10**) which was used in the next step without further purification. The chloride (**10**) in benzene (100 ml) was added dropwise to a stirred mixture of methyl ethyl ketone (500 ml), sodium cyanide (20 g), and sodium iodide (15 g) at room temperature. This mixture was warmed to 60–70° and stirred for a further 8 h at the same temperature. Water (100 ml) was then added to the reaction mixture, and the organic layer was separated, washed with a small amount of water, and dried over potassium carbonate. The extract was worked up to give the crude cyanide (**11**) which crystallized from ethanol to afford colorless needles melting at 108–109°; yield, 19.2 g (93.2% based on **9**); i.r. (KBr): 2255 (weak, CN), 935 (OCH_2O), 735, 695 (monosubstituted benzene); p.m.r. ($CDCl_3$): 7.29 (5 H, broad s, C_6H_5), 6.9–7.2 (4 H, m, Ar—H) 6.88 (1 H, s, H-6), 6.34 (1 H, s, H-3), 5.91 (2 H, s, OCH_2O), 5.04 (2 H, s, OCH_2Ph), 3.67 (2 H, s, CH_2CN).

Anal. Calcd. for $C_{22}H_{17}NO_4$: C, 73.53; H, 4.77; N, 3.90. Found: C, 73.74; H, 4.81; N, 3.75.

*2-(2′-Benzyloxyphenoxy)-4,5-methylenedioxyphenylacetic Acid (**12**)*

A mixture of the cyanide (**11**) (19.5 g), ethanol (500 ml), potassium hydroxide (40 g), and water (100 ml) was refluxed for 48 h. After removal of solvent from the mixture, the brown residue was diluted with water, washed with ether, and then acidified with hydrochloric acid to afford a precipitate which was extracted with chloroform. The extract was dried over magnesium sulfate, and evaporated to leave a slightly colored syrup which crystallized from chloroform–hexane yielding the acid (**12**) (14.3 g, 70.0%) as colorless needles melting at 128–129°; i.r. (KBr): 3300–2550 (OH), 1720 (CO), 750, 700 (monosubstituted benzene); p.m.r. ($CDCl_3$): 7.30 (5 H, broad s, C_6H_5), 7.15–6.85 (4 H, m, Ar—H), 6.75 (1 H, s, H-6), 6.37 (1 H, s, H-3), 5.90 (2 H, s, OCH_2O), 5.08 (2 H, s, OCH_2Ph), 3.63 (2 H, s, CH_2COOH).

Anal. Calcd. for $C_{22}H_{18}O_6$: C, 69.83; H, 4.80. Found: C, 69.90; H, 4.66.

*Methyl 2-(2′-Benzyloxyphenoxy)-4,5-methylenedioxyphenylacetate (**14**)*

A mixture of methyl 6-bromohomopiperonylate (24) (**13**, 5.6 g), *o*-benzyloxyphenol (**6**, 6.0 g), potassium carbonate (5.6 g), copper powder (6.0 g), cupric oxide (2.0 g), and pyridine (8 ml) was heated at 140° under vigorous stirring for 8 h. The product was exhaustively extracted with chloroform and the extract was filtered to remove suspended material. The chloroform filtrate was then washed with 10% HCl, dried over magnesium sulfate, and evaporated, yielding a dark colored syrup. Purification of the crude product by column chromatography on silica gel using chloroform as eluent gave the diphenyl ether (**14**) (6.7 g, 58.1%) as a slightly colored syrup; i.r. (liquid film): 1730 (CO), 925 (OCH_2O), 745, 680 (monosubstituted benzene); p.m.r. ($CDCl_3$): 7.33 (5 H, broad s, C_6H_5), 7.15–6.85 (4 H, m, Ar—H), 6.77 (1 H, s, H-6), 6.39 (1 H, s, H-3), 5.89 (2 H, s, OCH_2O), 5.08 (2 H, s, OCH_2Ph), 3.63 (2 H, s, $—CH_2COOCH_3$), 3.57 (3 H, s, OCH_3).

*Hydrolysis of **14***

The methyl ester (**14**) (6.5 g) was dissolved in a mixture of ethanol (150 ml) and 20% NaOH (80 ml) and refluxed for 2 h. The residue obtained after removal of solvent was diluted with water, washed with ether, and acidified with hydrochloric acid to afford a colorless precipitate. Extraction of the precipitate with chloroform gave the phenylacetic acid (**12**) (5.4 g, 96.3%) obtained as colorless needles melting at 128–129.5° after crystallization from chloroform–hexane. This compound was identical with the sample prepared above.

*N-[2-(2′-Benzyloxyphenoxy)-4,5-methylenedioxyphenacetyl]morpholine (**16**)*

Thionyl chloride (60 ml) was added dropwise to a cooled solution of the acid (**12**) (20.0 g) in dry benzene (300 ml) and the mixture was gently refluxed for 1.5 h. Removal of the solvent gave the acid chloride (**15**) which was dissolved in 30 ml of chloroform and used in the next reaction without purification.

To a stirred mixture of triethylamine (24 ml), morpholine (36 g), and chloroform (240 ml) the acid chloride solution, prepared above, was added dropwise at 0–10°. The mixture was stirred for 3.5 h at room temperature and was then washed with 10% NaOH and 10% HCl. The chloroform solution was dried over potassium carbonate and evaporated to yield the amide **16**, (21 g, 88.9%) as a slightly colored syrup; i.r. (liquid film): 1660 (CO), 935 (OCH_2O), 750, 700 (monosubstituted benzene); p.m.r. ($CDCl_3$): 7.33 (5 H, broad s, C_6H_5), 7.10–6.80 (4 H, m, Ar—H), 6.90 (1 H, s, H-6), 6.38 (1 H, s, H-3), 5.92 (2 H, s, OCH_2O), 5.08 (2 H, s, OCH_2Ph), 3.63 (2 H, s, CH_2CON), 3.58–3.23 (8 H, m, morpholine hydrogens).

*10-N-Morpholino-6-benzyloxy-2,3-methylenedioxydibenz[b,f]oxepin (**17**)*

A mixture of the amide (**16**) (20 g), dry toluene (120 ml), dry benzene (60 ml), and phosphoryl chloride (51 ml) was gently refluxed for 3.5 h. The reaction mixture was poured into a large volume of hexane and yielded

Can. J. Chem. Downloaded from www.nrcresearchpress.com by 210.87.254.6 on 09/05/12
For personal use only.

a precipitate which was collected by filtration. The crude product was basified by adding it in portions to a stirred mixture of chloroform and aqueous ammonia. The chloroform layer was separated, and worked up in the usual manner to give a dark colored viscous residue. Purification by column chromatography on silica gel using chloroform gave the enamine (**17**) (3.84 g, 20.0%) as yellow prisms melting at 175–177° after recrystallization from ether; i.r. (KBr): 1630 (weak, C=C), 945 (OCH_2O), 745, 695 (monosubstituted benzene); p.m.r. ($CDCl_3$): 7.65–6.95 (8 H, m, Ar—H), 6.82 (1 H, s, H-1), 6.60 (1 H, s, H-4), 5.93 (1 H, s, H-11), 5.90 (2 H, s, OCH_2O), 5.19 (2 H, s, OCH_2Ph), 3.86 (4 H, t, J = 4.0 Hz, 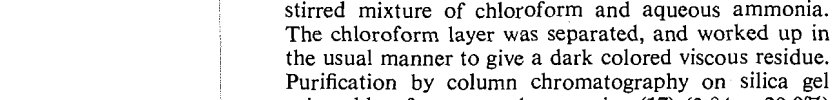), 2.98 (4 H, t, J = 4.0 Hz, 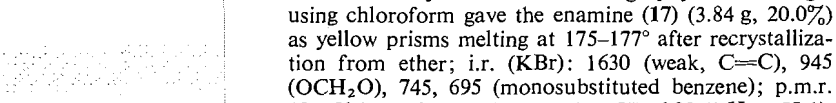); mass spectrum: *m/e* 429 (M^+).

Anal. Calcd. for $C_{26}H_{23}NO_5$: C, 72.71; H, 5.40; N, 3.26. Found: C, 72.77; H, 5.64; N, 3.26.

*6-Benzyloxy-2,3-methylenedioxy-10,11-dihydrodibenz-[b,f]oxepin-10(11H)-one (**5**)*

A stirred solution of the enamine (**17**) (1.5 g) in tetrahydrofuran (43 ml) was treated dropwise with 1 *M* sulfuric acid (50 ml) and the mixture stirred for 4 h at room temperature. The reaction mixture was extracted with chloroform, the extract dried over magnesium sulfate and potassium carbonate, and evaporated to give a brown syrup. Crystallization from ether gave the dihydrodibenzoxepinone (**5**) (0.91 g, 72.2%) as yellow prisms melting at 131–132°; i.r. (KBr); 1680 (CO), 935 (OCH_2O), 735, 700 (monosubstituted benzene); p.m.r. ($CDCl_3$); 7.69 (1 H, pair of doublets, J = 2.5 and 7.5 Hz, H-7 or H-9), 7.55–7.05 (7 H, m, Ar—H), 6.86 (1 H, s, H-1 or H-4), 6.75 (1 H, s, H-4 or H-1), 5.98 (2 H, s, OCH_2O), 5.26 (2 H, s, OCH_2Ph), 4.02 (2H, s, CO-CH_2); mass spectrum; *m/e* 360 (M^+).

Anal. Calcd. for $C_{22}H_{16}O_5$: C, 73.32; H, 4.48. Found: C, 73.43; H, 4.34.

*10-(2′,2′-Diethoxyethylamino)-6-hydroxy-2,3-methylenedioxy-10,11-dihydrodibenz[b,f]oxepin (**19**)*

A mixture of **5** (1.6 g), dry toluene (50 ml), aminoacetaldehyde diethyl acetal (3.5 ml), and pyridine (6 drops) was allowed to stand at room temperature for 10 h and then refluxed using a Dean–Stark apparatus for 20 h. Most of the solvent was removed, fresh toluene (40 ml) and aminoacetaldehyde diethyl acetal (3.5 ml) were added and reflux was continued for a further 8 h. The solvent was removed leaving the Schiff base **18** as a slightly colored syrup. This residue was dissolved in ethanol (100 ml) and hydrogenated over platinum at 20 p.s.i.g. for 15 h. The filtrate, after removal of catalyst, was hydrogenated again in the presence of 10% palladium-on-charcoal at 40 p.s.i.g. for 20 h. The catalyst was filtered off and the solvent was evaporated to give a pale yellow syrup. The residue, dissolved in ether, was treated with ether saturated with dry hydrogen chloride yielding the hydrochloride of **19** (0.91 g). Attempts to crystallize the hydrochloride from ethanol–ether gave only an amorphous material melting at 118° (dec.); i.r. (KBr): 3200 (OH), 2800–2500 ( ), 930 (OCH_2O). Crude **19** was used in the next reaction without purification.

*Cyclization of **19***

A stirred solution of the hydrochloride of **19** (0.85 g) in ethanol (6 ml) was treated dropwise with 6 *N* ethanolic hydrochloric acid solution (40 ml) at 5–10° and the mixture was stirred for 20 h at room temperature. The colorless precipitate, which separated, was collected by filtration, and recrystallized from ethanol–ether to afford 3-ethoxy-norcularicine (**20**) hydrochloride (0.75 g, 88.1%) as colorless needles melting at 236° (dec.); i.r. (KBr): 3200 (OH), 2450 ( ), 925 (OCH_2O); p.m.r. (DMSO-d_6): 6.96, 6.85 (each 1 H, d, J = 8.2 Hz, H-4 and H-5), 6.95, 6.71 (each 1 H, s, H-8 and H-11), 5.92 (2 H, s, OCH_2O), 4.73–4.40 (2 H, m, H-12a and H-3), 3.60–3.00 (7 H, m, 3 × CH_2 and NH), 0.97 (3 H, t, J = 7.0 Hz, CH_2CH_3).

Anal. Calcd. for $C_{19}H_{19}NO_5 \cdot HCl$: C, 60.40; H, 5.33; N, 3.70. Found: C, 60.50; H, 5.36; N, 3.79.

The free base was liberated from the hydrochloride by ammonia. It melted at 176–178° (dec.) after crystallization from chloroform–hexane; i.r. (KBr): 3290 (NH), 930 (OCH_2O); p.m.r. (DMSO-d_6): 7.01, 6.64 (each 1 H, s, H-8 and H-11), 6.91, 6.71 (each 1 H, d, J = 8.2 Hz, H-4 and H-5), 5.92 (2 H, s, OCH_2O), 4.38 (1 H, pair of doublets, J = 10.0 and 7.0 Hz, H-12a), 4.07 (1 H, m, H-3), 3.46 (2 H, m, CH_2CH_3), 3.08–2.85 (4 H, m, 2 × CH_2), 1.08 (3 H, t, J = 7.0 Hz, CH_2CH_3); mass spectrum *m/e*: 341 (M^+, 100), 324 (7), 311 (7), 294 (41), 283 (33), 278 (13).

The mother liquor from the separation of **20** was treated with hydrogen over platinum at 25 p.s.i.g. for 6 h. The filtrate, after removal of catalyst, was concentrated to 5 ml, cooled with ice, carefully basified with ammonia, and then extracted with chloroform. The extract gave on evaporation a brown gum which was purified by preparative thick-layer chromatography on silica gel (chloroform–benzene–methanol, 1:3:1) to give (±)-*N*-norcularicine (**21**) (72 mg, 7.0% based on **19**) as a glass which crystallized from methanol yielding colorless prisms melting at 99° with softening and some decomposition at 92°. The crystals are probably solvated. Mass spectrum (270°), *m/e*: 297 (M^+, 100), 296 (46), 280 (47), 268 (16), 267 (21), 148.5 (M^{2+}, 7), 147 (20); i.r. (KBr): 3400–3300 (NH and OH), 935 (OCH_2O). Compound **21** was recrystallized from acetone yielding colorless needles melting at 96–99°. These crystals were also solvated; i.r. (KBr): 3400–3300 (NH and OH), 935 (OCH_2O), 1710 (acetone carbonyl); p.m.r. (CD_3OD):[1] 6.92, 6.58 (each 1 H, s, H-8 and H-11), 6.74 (2 H, s, H-4 and H-5), 5.90, 5.88 (each 1 H, d, J = 1.0 Hz, O—CH_2—O), 4.33 (1 H, pair of doublets,

[1]The sample for p.m.r. analysis was prepared in the following manner. The crystals obtained from the crystallization in acetone were dissolved in an excess of methanol, the solution evaporated to dryness, and the residue taken up in CD_3OD.

J = 11.0 and 4.0 Hz, H-12a), 3.25–2.60 (6 H, m, 3 × CH_2). Compound **21** formed a picrate as yellow needles melting at 241° (dec.); i.r. (KBr): 3410 (OH), 1570, 1320 (NO_2), 935 (OCH_2O).

Anal. Calcd. for $C_{17}H_{15}NO_4 \cdot C_6H_3N_3O_7$: C, 52.47; H, 3.45; N, 10.64. Found: C, 52.59; H, 3.65; N, 10.41.

Acid-catalyzed Hydrogenolysis of 20

3-Ethoxynorcularicine hydrochloride (**20**, HCl, 320 mg) was dissolved in 3 *N* ethanolic hydrochloric acid solution (60 ml) and treated with hydrogen over platinum at 25 p.s.i.g. for 15 h. The filtrate, after removal of catalyst, was concentrated to 15 ml, basified with ammonia, and extracted with chloroform. The extract was dried over magnesium sulfate, and evaporated to leave a brown residue. This was purified by preparative thick-layer chromatography on silica gel (chloroform–benzene–methanol, 1:3:1) to give (±)-*N*-norcularicine (**21**, 104 mg, 41%) as a colorless glass which crystallized from methanol to give colorless prisms melting at 101°. The mass spectrum of this sample was the same as that described above for **21**. Recrystallization from acetone gave a sample melting at 97–101°. The i.r. spectrum of this sample was superimposable on that described in the preceding section for the sample of (±)-norcularicine crystallized from acetone.

(±)-Cularicine (1)

A mixture of (±)-*N*-norcularicine (**21**) (60 mg), methanol (6 ml), and 37% formalin (1.0 ml) was warmed at 40–45° for 30 min. The mixture was cooled and sodium borohydride (0.7 g) was then added in portions. The solvent was removed *in vacuo* and the residue obtained was treated with water and extracted with chloroform. The extract, after drying over magnesium sulfate, was evaporated to leave a slightly colored syrup which was purified by preparative thick-layer chromatography on silica gel (chloroform–benzene–methanol, 1:3:1) to give (±)-cularicine (**1**, 45 mg, 71%) as a glass which crystallized from methanol yielding solvated crystals melting at 95–96°; i.r. (KBr): 3150 (OH), 935 (OCH_2O); mass spectrum (270°), *m/e*: 311 (M^+, 100), 310 (16), 294 (58), 282 (10), 267 (9), 161 (18), 155.5 (M^{2+}, 5).

Recrystallization of **1** from acetone gave a colorless crystalline mass melting at 81–82°; i.r. (KBr): 3400 (OH), 935 (OCH_2O), 1710 (acetone carbonyl). The presence of acetone of crystallization was also apparent when the mass spectrum of this sample was recorded.

Compound **1**, obtained from acetone, was dissolved in chloroform and evaporated to dryness yielding a glass that was used to measure the i.r. and p.m.r. spectra; p.m.r. ($CDCl_3$): 6.80 (2 H, s, H-4 and H-5), 6.67, 6.53 (each 1 H, s, H-8 and H-11), 5.91, 5.89 (each 1 H, d, J = 1.3 Hz, OCH_2O), 4.23 (1 H, pair of doublets, J = 10.0 and 4.0 Hz, H-12a), 3.20–3.75 (6 H, m, 3 × CH_2), 2.53 (3 H, s, N—CH_3); i.r. ($CHCl_3$): 3550 (OH), 2820 (N—CH_3), 940 (OCH_2O). The i.r. spectrum in chloroform and the p.m.r. spectrum in deuteriochloroform were identical with those of natural (+)-cularicine. When recrystallized from ether racemic **1** gave colorless needles melting at 155–156°. Mass spectrum (270°), *m/e*: 311 (M^+, 100), 310 (21), 294 (65), 282 (12), 268 (5), 267 (11), 174 (10), 161 (24), 155.5 (M^{2+}, 7); t.l.c. of racemic **1** in a variety of solvent systems showed the same behavior as natural (+)-cularicine.

Compound **1** formed a hydrochloride as colorless needles melting at 255–257° (dec.), (MeOH–Et_2O); i.r. (KBr): 3150 (OH), 2750–2400 ($\overset{+}{\underset{/}{\backslash}}$NH, 935 ($OCH_2O$).

Anal. Calcd. for $C_{18}H_{17}NO_4 \cdot HCl$: C, 62.16; H, 5.21; N, 4.02. Found: C, 62.31; H, 5.36; N, 4.02.

We thank the National Research Council of Canada for support of this work and Dr. R. H. F. Manske for a sample of (+)-cularicine.

1. R. H. F. MANSKE. Can. J. Res. **18B**, 97 (1940).
2. R. H. F. MANSKE. Can. J. Chem. **43**, 989 (1965).
3. R. H. F. MANSKE. Alkaloids, **4**, 249.
4. R. H. F. MANSKE. Alkaloids, **10**, 463.
5. J. KUNITOMO, K. MORIMOTO, K. YAMAMOTO, Y. YOSHIKAWA, K. AZUMA, and K. FUJITANI. Chem. Pharm. Bull. **19**, 2197 (1971).
6. T. KAMETANI, T. HONDA, H. SHIMANOUCHI, and Y. SASADA. Chem. Commun. 1072 (1972).
7. T. KAMETANI and K. FUKUMOTO. J. Chem. Soc. 4289 (1963).
8. T. KAMETANI, S. SHIBUYA, S. SEINO, and K. FUKUMOTO. J. Chem. Soc. 4146 (1964).
9. T. KAMETANI, K. FUKUMOTO, and M. FUJIHARA. Chem. Commun. 352 (1971).
10. T. KAMETANI, K. FUKUMOTO, and M. FUJIHARA. Bioorg. Chem. **1**, 40 (1971).
11. A. H. JACKSON and G. W. STEWART. Chem. Commun. 149 (1971).
12. S. ISHIWATA, T. FUJII, N. MIYAJI, Y. SATOH, and K. ITAKURA. Chem. Pharm. Bull. **18**, 1850 (1970).
13. H.-C. HSU, T. KIKUCHI, S. AOYAGI, and H. IIDA. Yakugaku Zasshi, **92**, 1030 (1972).
14. T. KAMETANI and S. SHIBUYA. J. Chem. Soc. 5565 (1965).
15. T. KAMETANI, H. IIDA, and C. KIBAYASHI. J. Heterocycl. Chem. **6**, 61 (1969).
16. T. KAMETANI, H. IIDA, and C. KIBAYASHI. J. Heterocycl. Chem. **7**, 339 (1970).
17. H. IIDA, H.-C. HSU, and T. KIKUCHI. Chem. Pharm. Bull. **21**, 1001 (1973).
18. H. IIDA, H.-C. HSU, T. KIKUCHI, and K. KAWANO. Yakugaku Zasshi, **92**, 1242 (1972).
19. J. DRUEY. Bull. Soc. Chim. **2**, 1737 (1935).
20. (*a*) A. H. PARIS. Thesis, Leiden, Netherlands. 1928; Chem. Abstr. **23**, 4204 (1929). (*b*) H. KONDO, T. IKEDA, and K. TAKEDA. Annual Rep. ITSUU Lab. **1**, 24 (1950); Chem. Abstr. **47**, 7516 (1953).
21. J. M. BOBBITT, J. M. KIELY, K. L. KHANNA, and R. EBERMANN. J. Org. Chem. **30**, 2247 (1965).
22. J. M. BOBBITT. Adv. Heterocycl. Chem. **15**, 99 (1973).
23. D. R. DALTON, S. I. MILLER, C. K. DALTON, and J. K. CRELLING. Tetrahedron Lett. 575 (1971).
24. T. S. STEVENS. J. Chem. Soc. 663 (1935).

Can. J. Chem. Downloaded from www.nrcresearchpress.com by 210.87.254.6 on 09/05/12
For personal use only.

C-Nucleosides and Related Compounds. IV. The Synthesis and Chemistry of D,L-2,5-Anhydroallose Derivatives

GEORGE JUST, ALAIN MARTEL, KARL GROZINGER, AND MOHABIR RAMJEESINGH
Department of Chemistry, McGill University, Montreal, Quebec H3C 3G1

Received July 11, 1974

GEORGE JUST, ALAIN MARTEL, KARL GROZINGER, and MOHABIR RAMJEESINGH. Can. J. Chem. **53**, 131 (1975).

Methyl β-nitroacrylate (**1**) reacted with furan to give the corresponding Diels–Alder adduct, which was converted to D,L-3,4-di-*O*-isopropylidene-2,5-anhydroallose (**9**) in a five-step sequence in 14% yield, based on **1**. The conversion of **9** to its oxime, semicarbazone, and thiosemicarbazone is described, as well as the synthesis of the free aldehyde **15**, and of the Wittig reaction product **14**.

GEORGE JUST, ALAIN MARTEL, KARL GROZINGER et MOHABIR RAMJEESINGH. Can. J. Chem. **53**, 131 (1975).

Le β-nitroacrylate de méthyle (**1**) réagit avec le furanne pour conduire au produit d'addition de Diels–Alder correspondant; ce dernier peut être transformé en cinq étapes, avec un rendement global de 14% basé sur **1**, en D,L-di-*O*-isopropylidène-3,4 anhydro-2,5 allose (**9**). On décrit la transformation de **9** en oxime, semicarbazone et thiosemicarbazone, de même que la synthèse de l'aldéhyde **15** et du produit **14** provenant de la réaction de Wittig. [Traduit par le journal]

In a preliminary communication, we reported (1) on the synthesis of 3,4-isopropylidene-2,5-anhydroallose (**9**). We wish to give a full account of this and related work.

Treatment of methyl β-nitroacrylate (**1**) (2, 3) with an excess of furan at room temperature gave in quantitative yield a mixture of **2***a* and **2***b*, from which *endo*-nitro ester **2***b* could be obtained crystalline, and **2***a* as an oil. This separation allowed the analysis of the n.m.r. spectra of the isomers. However, the stereochemistry of the isomers was assigned based on spectral data of the hydroxylation products **3** and **4**. Hydroxylation of **2***a* or **2***b* with hydrogen peroxide and a catalytic amount of osmium tetroxide gave diols **3** and **4**, respectively. Alternatively, the mixture of **2***a* and *b* was hydroxylated and diols **3** and **4** were separated by crystallization. There is ample precedent for the preferential *exo*-hydroxylation of bicyclo[2.2.1] systems of type **2**, leaving little doubt as to the correctness of the stereochemical assignment of the hydroxy groups (4).

It is known that the coupling constant of *endo*-protons with the bridgehead proton in bicyclo-[2.2.1]heptane derivatives is close to zero (5), whereas the coupling constants of an *exo*-proton with the bridgehead proton and with the adjacent *endo*-proton should be of comparable order of magnitude ($J \cong 4$ Hz, (5)). One would therefore expect that the low-field proton α to nitro group in **3** should appear as a doublet and in **4** as a doublet of doublets or a triplet. The structures of **2***a*, **2***b*, **3**, and **4** have been assigned accordingly. The structure of **2***a* was further confirmed by chemical transformations leading to lactone **17**.[1]

Treatment of **3** and **4** with acetone–dimethoxypropane in the presence of *p*-toluenesulfonic acid for several hours gave a good yield of the corresponding isopropylidene derivatives **3***a* and **4***a*. Elimination of nitrous acid by means of diazabicyclo[5.4.0]undec-5-ene (DBU) in cold or boiling ether or methylene chloride from the *exo*-nitro ester **3***a* proceeded in good yield. A small amount of dimer **7** was also formed in this reaction. In the case of *endo*-nitro ester **4***a*, the dimer became the major product (48%) when the elimination was carried out with DBU in ether at 0°, olefin **6** being produced in 28% yield. By carrying out the reaction under reflux, the desired olefin **6** became the major reaction product.

Dimer **7** is formed by Michael addition of the carbanion generated by abstraction of the proton α to the nitro group of **4** to olefin **6**, followed by elimination of nitrous acid. The structure of dimer **7** was based on its spectral data and those of its dihydro derivative $\mathbf{7}\cdot H_2$ obtained by catalytic hydrogenation.

Olefin **6** was characterized by cleaving the

[1]M. I. Lim and G. Just. Unpublished results.

Can. J. Chem. Downloaded from www.nrcresearchpress.com by 210.87.254.40 on 09/05/12
For personal use only.

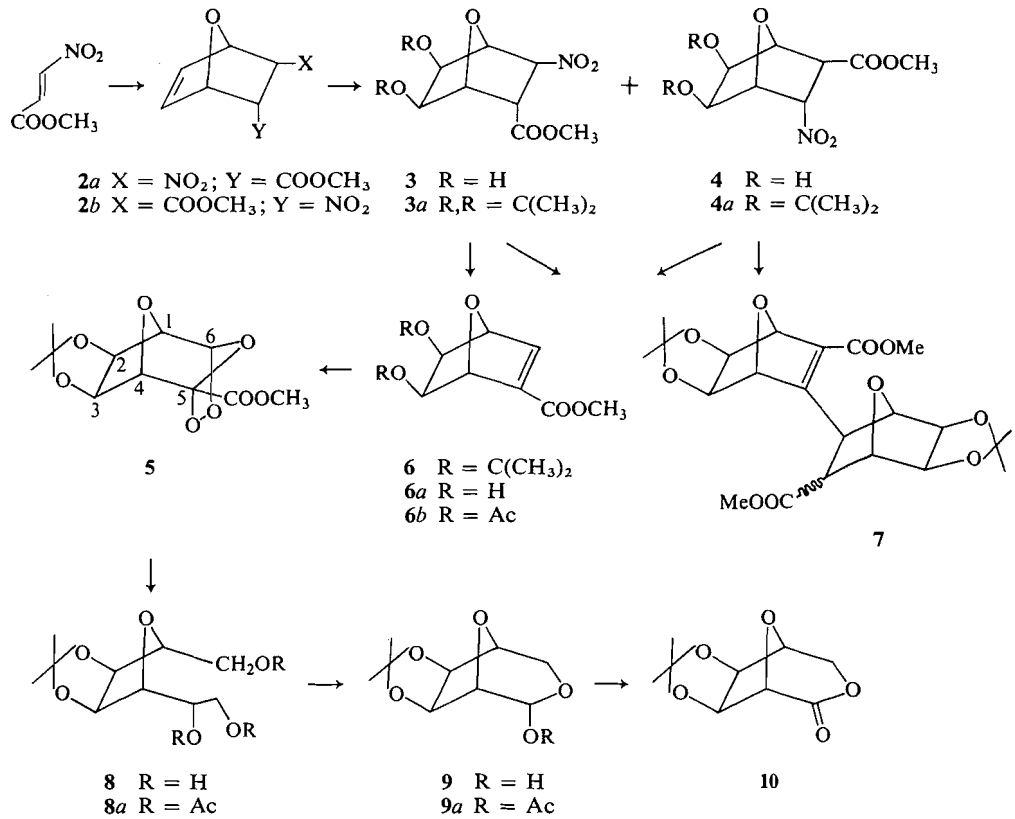

isopropylidene group with aqueous trifluoroacetic acid and acetylating the resulting diol **6***a* to diacetate **6***b*.

Ozonolysis of **6** gave a single oily ozonide, to which structure **5** was assigned, based on the following arguments. Protons H_2 and H_3 appear as a singlet at 5.25 p.p.m., so that the carbomethoxy group does not influence their chemical shift. Proton H_1 is coupled with H_4 (*w*-coupling; $J = 2$ Hz) and with H_6, which appears as a doublet ($J = 5.5$ Hz). Models indicate that in structure **6**, the dihedral angle between H_1 and H_6 is 0°, whereas in the corresponding isomeric ozonide, it is approximately 35°. Comparison with sugar derivatives having a similar degree of substitution (6–9) suggest that a coupling constant of 5.5 Hz is more appropriate for a dihedral angle of 0°, rather than 35°, so that structure **5** is preferred for the ozonide.

Sodium borohydride reduction of ozonide **5** gave triol **8**, in 36% yield. It was characterized as its acetate **8***a*. When the borohydride reduction mixture was evaporated and acetylated *in situ*, triacetate **8***a* was obtained in 79% yield. Reaction of triol **8** with periodate (10) converted it nearly quantitatively to D,L-3,4-isopropylidene-2,5-anhydroallose, **9**, m.p. 185–186°. The sodium borohydride reduction mixture could also be acidified with aqueous acetic acid and the mixture directly submitted to periodate cleavage. In that instance, the yield of the anhydroallose **9**, based on olefin **6**, was 61%. Anhydroallose **9** was characterized by making its 1-*O*-acetyl derivative **9***a* and by oxidizing it to lactone **10** with Fetizon's reagent (11).

Treatment of lactol **9** with semicarbazide gave the crystalline semicarbazone **13***c*, which was further converted to acetate **13***d*. Similarly, a crystalline thiosemicarbazone **13***b* could be obtained from **9**. In each case, only one geometric isomer was obtained. Upon oximation, an oily oxime **13***a* consisting of a mixture of the *syn*- and *anti*-isomer was obtained. Treatment of the oxime **13***a* with *p*-nitrobenzoyl chloride in pyridine gave the crystalline *p*-nitrobenzoate nitrile **16**.

Lactol **9** reacted with carbethoxymethylene triphenylphosphorane to give the α,β-unsaturated

Can. J. Chem. Downloaded from www.nrcresearchpress.com by 210.87.254.40 on 09/05/12
For personal use only.

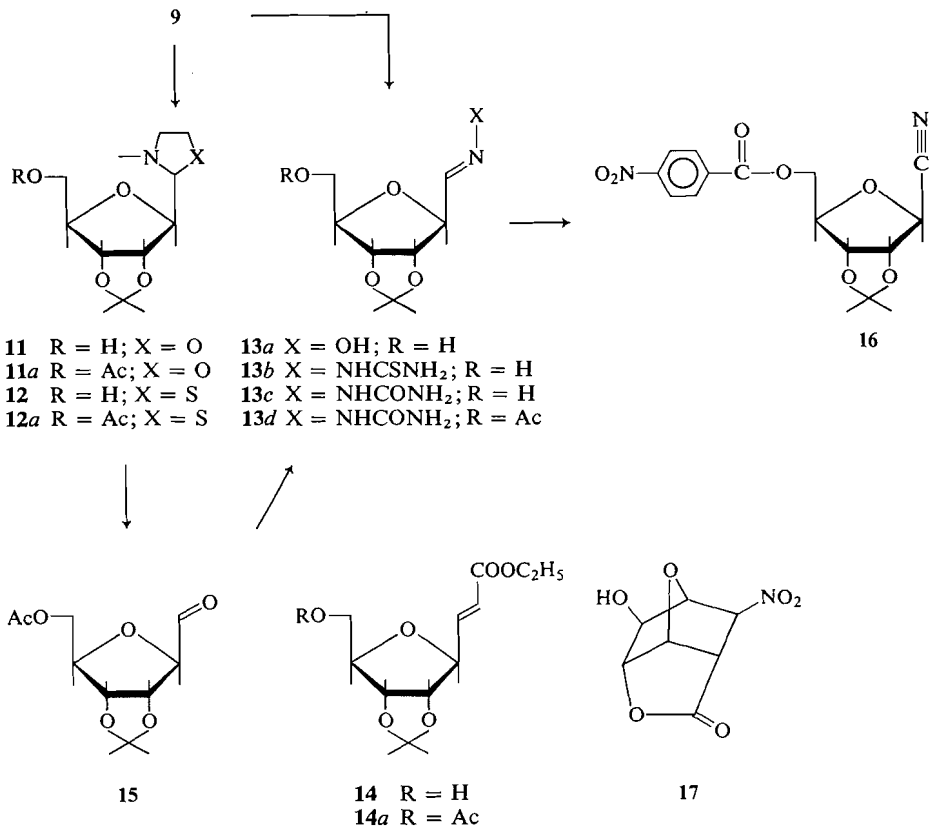

trans-ester **14** in good yield and purity. Acetylation transformed it to **14***a*.

Reaction of lactol **9** with unstabilized Wittig reagents gave starting material only. Since this lack of reactivity severely curtailed the synthetic utility of **9**, free aldehyde **15** was prepared in the following manner. Compound **9** was treated with *N*-methylethanolamine in boiling benzene with continuous removal of water. The resulting oxazolidine **11** could not be purified and was converted to its acetate **11***a*, which was equally unstable to purification by chromatography. Hydrolysis of **11***a* with aqueous acetic acid gave the equally unstable aldehyde **15**. Its semicarbazone proved to be identical to **13***d*, obtained via the sequence **9** → **13***c* → **13***d*. As will be reported later, aldehyde **15** reacted with unstabilized Wittig reagents in the expected manner.

Reaction of **9** with *N*-methylthioethanolamine gave the stable thiazolidine **12**, which was further converted to acetate **12***a*. Since **12***a* is much more stable than **11***a*, it might be the preferred precursor to aldehyde **15**. However, the relative inconvenience of preparing *N*-methylthioethanolamine, coupled with the fact that aldehyde **15** obtained via **11** was of sufficient purity to undergo clean Wittig reactions, made this second pathway relatively unattractive.

Experimental

Melting points were determined on a Gallenkamp block and are uncorrected. Mass spectra were obtained on an AE1-MS-902 mass spectrometer at 70 eV using a direct-insertion probe. Nuclear magnetic resonance spectra were recorded on a Varian Associates T-60 spectrometer. Infrared spectra were obtained on a Unicam SP1000 and a Perkin–Elmer 257 i.r. spectrophotometer. Ultraviolet spectra were determined with a Unicam SP-800 spectrophotometer. Microanalyses were carried out by C. Daessle, Montreal.

Methyl trans-7-Oxabicyclo[2.2.1]hept-5-ene-2(3)-nitro-3(2)-carboxylate (2)

3-Nitroacrylate (**1**, 120 g) and 125 g (2 equiv.) of furan were stirred overnight. During the course of the reaction crystals separated out. After refrigeration, the product was collected and crystallized from ether to give 31 g (17%) of *endo*-nitro compound **2***b*, m.p. 66–67°. Upon evaporation of the filtrate 100 g (55%) of the *exo*-nitro **2***a* isomer was obtained as an oil.

Exo-nitro isomer **2***a*: i.r. (film) 1735 (C=O), 1550 (NO_2), 875 cm^{-1} (C—N); n.m.r. ($CDCl_3$) δ 3.70 (s, 3H),

Can. J. Chem. Downloaded from www.nrcresearchpress.com by 210.87.254.40 on 09/05/12
For personal use only.

Can. J. Chem. Downloaded from www.nrcresearchpress.com by 210.87.254.40 on 09/05/12
For personal use only.

3.90 (dd, 1H), 4.82 (d, J = 3 Hz, 1H), 5.22–5.50 (m, 2H), 6.53 (m, 2H).

Endo-nitro isomer **2***a*: i.r. (KBr) 1730 (C=O), 1540 (NO_2), 870 cm^{-1} (C—N); n.m.r. ($CDCl_3$) δ 3.20 (d, J = 2 Hz, 1H), 3.80 (s, 3H), 5.30 (d, J = 2 Hz, 1H), 5.47–5.60 (m, 2H), 6.35 (dd, $J_{6.5}$ = 6 Hz, $J_{6.1}$ = 2 Hz, 1H), 6.70 (dd, $J_{5.6}$ = 6 Hz, $J_{5.4}$ = 2 Hz).

Anal. Calcd. for $C_8H_9NO_5$: C, 48.24; H, 4.56; N, 7.03. Found: C, 48.33; H, 4.77; N, 7.35.

*Methyl exo-cis-5,6-Dihydroxy-7-oxabicyclo[2.2.1]-heptane-trans-3-endo-nitro-2-carboxylate (**4**)*

The Diels–Alder adduct **2***b* (31 g) was treated with osmium tetroxide (10 ml of a solution made from 1 g of osmium tetroxide in 200 ml of *t*-butanol) and 20 ml of 30% hydrogen peroxide according to the procedure of Daniels and Fischer (4). After refrigeration to 4°, 18.3 g (50.5%) of **4**, m.p. 169–170°, was filtered off. Upon further evaporation, only 3-nitroacrylate could be recovered; i.r. (KBr) 3500–3200 (OH), 3040 (C—H), 1740 (C=O), 1550 cm^{-1} (NO_2); n.m.r. (DMSO-d_6) δ 3.42 (d, J = 5 Hz, 1H), 3.70 (s, 3H), 3.78 (d, J = 6 Hz, 1H), 4.02 (d, J = 6 Hz, 1H), 4.50–4.70 (m, 2H), 5.00 (20H, ex), 5.35 (t, J = 5 Hz, 1H).

*Methyl exo-cis-5,6-Dihydroxy-7-oxabicyclo[2.2.1]-heptane-trans-2-exo-nitro-3-carboxylate (**3**)*

The Diels–Alder adduct **2***a* (25 g) was treated as above with osmium tetroxide to give 12.5 g (42.5%) of **3**, m.p. 145–147°; i.r. (KBr) 3500–3200 (OH), 1735 (C=O), 1560 cm^{-1} (NO_2); n.m.r. (DMSO-d_6) δ 3.70 (s, 3H), 3.80–4.02 (m, 3H), 4.55–4.72 (m, 2H), 5.00 (d, J = 6 Hz, 20H ex), 5.18 (d, J = 5 Hz, 1H); mass spectrum (70 eV) *m/e* 233 (M^+), 215 ($M^+ - H_2O$), 186 ($M^+ - HNO_2$).

Anal. Calcd. for $C_8H_{11}NO_7$: C, 41.20; H, 4.76; N, 6.01. Found: C, 41.14; H, 4.68; N, 6.06.

*Methyl exo-cis-5,6-Dihydroxy-O-isopropylidene-7-oxabicyclo[2.2.1]heptane-trans-3-endo-nitro-2-carboxylate (**4a**)*

Diol **4** (18.3 g) was heated under reflux in a mixture of acetone 150 ml and dimethoxypropane (210 ml) containing *p*-toluenesulfonic acid (10 mg) with a Dean–Stark trap filled with molecular sieves. At the end of the reaction, which was followed by t.l.c., the residue obtained was dissolved in chloroform and washed three times with 15 ml of water. After drying and evaporation of the solvent, the crystalline isopropylidene derivative was obtained in 96% yield, m.p. 90–92°; i.r. (KBr) 1745 (C=O), 1550 (NO_2), 1385, 1360 cm^{-1} (*gem*-dimethyl); n.m.r. ($CDCl_3$) δ 1.30 (s, 3H), 1.47 (s, 3H), 3.35 (d, J = 5 Hz, 1H), 3.82 (s, 3H), 4.42 (q, J = 6 Hz, 2H), 4.82 (s, 1H), 4.87 (d, J = 5 Hz, 1H), 5.40 (t, 1H).

Anal. Calcd. for $C_{11}H_{15}NO_7$: C, 48.35; H, 5.53; N, 5.13. Found: C, 48.59; H, 5.49; N, 5.21.

*Methyl exo-cis-5,6-Dihydroxy-O-isopropylidene-7-oxabicyclo[2.2.1]heptane-trans-2-exo-nitro-3-carboxylate (**3a**)*

Diol **3** (12.7 g) was treated with acetone and dimethoxypropane as above to give 13.0 g (95%) of **3***a*, m.p. 85–87°; i.r. (KBr) 1750 (C=O), 1560 (NO_2), 1385, 1375 cm^{-1} (*gem*-dimethyl); n.m.r. ($CDCl_3$) δ 1.30 (s, 3H), 1.45 (s, 3H), 3.82 (s, 3H), 3.95 (d, 4Hz, 1H), 4.35 (q, J = 6 Hz; 2H), 4.76–5.00 (m, 3H); mass spectrum (70 eV) *m/e* 258 ($M^+ - CH_3$).

Anal. Calcd. for $C_{11}H_{15}NO_7$: C, 48.35; H, 5.53; N, 5.13. Found: C, 48.19; H, 5.58; N, 5.06.

*Methyl exo-cis-5,6-Dihydroxy-O-ixopropylidene-7-oxabicyclo[2.2.1]hept-2-ene-2-carboxylate (**6**)*

To a stirred refluxing mixture of 29.3 g 1,5-diazabicyclo-[5.4.0]undec-5-ene (DBU) in 500 ml ether was added dropwise a solution of **3***a* (26.4 g) in 100 ml anhydrous ether. After addition, the reaction mixture was cooled, filtered, and the filtrate washed with 2 *N* sodium bicarbonate solution. The organic layer was dried over sodium sulfate and the crystalline product obtained on evaporation was crystallized twice from ethyl ether. Yield 15.0 g (80%), m.p. 118–119°; i.r. (KBr) 1720 (C=O), 1610 (C=C), 1380, 1370 (*gem*-dimethyl) 1065 cm^{-1} (C—O—C); n.m.r. ($CDCl_3$) δ 1.32 (s, 3H), 1.50 (s, 3H), 3.75 (s, 3H), 4.42 (s, 2H), 4.90 (m, 1H), 5.00 (s, 1H), 7.05 (d, J = 2 Hz, 1H); mass spectrum (70 eV) *m/e* 211 ($M^+ - CH_3$) 126, 100.

Anal. Calcd. for $C_{11}H_{14}O_5$: C, 58.40; H, 6.24. Found: C, 58.20; H, 6.39.

Elimination of nitrous acid using the *endo*-nitro isomer gave **6** in a 72% yield.

*Dimer **7***

An ether solution of *endo*-nitro ester **4***a* (18.0 g) was treated with 14.5 g DBU at 0° for 1 h. After work-up, the crystalline residue was chromatographed on silicic acid using benzene – ethyl acetate (95:5) as an eluent. The first fraction (4.2 g, 28%) was identified as olefin **6**. The major product, which was eluted later, consisted of colorless plates, m.p. 169–171° (6.8 g) of the dimer **7**.

Using the above reaction conditions on *exo-nitro* ester **3***a*, a mixture of olefin **6** (60%) and dimer **7** (8%) was obtained. The dimer proved to be in all respects identical with the sample obtained from the *endo-nitro* ester **4***a*; i.r. (KBr) 1735, 1720 (C=O), 1640 (C=C), 1370, 1380 (*gem*-dimethyl), 1070, 1075 cm^{-1} (C—O—C); n.m.r. ($CDCl_3$) δ 1.30 (s, 3H), 1.35 (s, 3H), 1.45 (s, 3H), 1.50 (s, 3H), 2.98 (t, J = 6 Hz, 1H), 3.78 (s, 6H), 3.85 (s, H), 4.20 (s, 1H), 4.42 (s, 2H), 4.45 (s, 2H), 4.70 (d, J = 6 Hz, 1H), 4.97 (s, 2H); u.v. λ_{max}(EtOH) 237 nm, ε 5700.

Anal. Calcd. for $C_{22}H_{28}O_{10}$: C, 58.40; H, 6.24. Found: C, 58.66; H, 6.27.

*Hydrogenation of **7***

7 (904.8 mg, 2 mmol) was dissolved in 50 ml of absolute ethanol and hydrogenated at atmospheric pressure over 100 mg of palladium-on-charcoal. After quantitative hydrogen uptake of 1 equiv. in 30 min, the catalyst was filtered off, and the solvent was removed under reduced pressure to leave 900 mg of a crystalline solid. Crystallization from ethanol gave 800 mg (88%) of **8**·H_2, m.p. 188–189°; i.r. (KBr) 1745 (C=O), 1380, 1375 (*gem*-dimethyl), 1060 cm^{-1} (C—O—C); n.m.r. ($CDCl_3$); δ 1.30 (s, 6H), 1.48 (s, 6H), 2.2–3.2 (m, 4H), 3.60 (s, $3H_3$), 3.70 (s, $3H_3$), 4.20 s(11H), 4.42 (s, 2H), 4.5–4.8 (m, 5H).

Anal. Calcd. for $C_{22}H_{30}O_{10}$: C, 58.14; H, 6.65. Found: C, 57.91; H, 6.93.

*Methyl exo-cis-5,6-Diacetoxy-7-oxabicyclo[2.2.1]hept-2-ene-2-carboxylate (**6b**)*

The isopropylidene derivative (**6**, 250 mg) was treated with 5 ml of trifluoroacetic acid and 1 ml of water for 1 h. Evaporation and acetylation of the residue with acetic anhydride and pyridine gave, after separation by

Can. J. Chem. Downloaded from www.nrcresearchpress.com by 210.87.254.40 on 09/05/12
For personal use only.

t.l.c. on silicagel, the oily diacetate **6***b* in 56% yield; i.r. (KBr film) 1755 (C=O), 1735 (C=O) 1625 (C=C), 1255 cm^{-1} (C—O—C); n.m.r. ($CDCl_3$) δ 2.08, 2.10 (2s, 6H), 3.75 (s, 3H), 4.88 (s, 2H), 5.00 (d of d, J = 2 Hz, 1H), 5.08 (d, J = 2 Hz, 1H), 7.07 (d, J = 2 Hz, 1H).

*Ozonide **5** of the Olefin (**6**)*

The olefin **6** (100 mg), dissolved in ethyl acetate, was treated with ozone at −78°. Evaporation of the solvent gave a quantitative yield of pure ozonide **5**; i.r. (KBr film) 1760 (C=O), 1390, 1380 (*gem*-dimethyl), 1020, 1055, 1085 cm^{-1} (ozonide); n.m.r. ($CDCl_3$) δ 1.40 (s, 3H), 1.54 (s, 3H), 4.10 (s, 3H, OCH_3), 4.58 (dd, J_{AM} = 5.5 Hz, J_{MX} 2 Hz, 1H), 4.85 (d, J = 2 Hz, 1H), 5.28 (s, 2H), 6.33 (d, J = 5.5 Hz, 1H).

*3,4-O-Isopropylidene-2β-(1′,2′-dihydroxyethyl)-5β-hydroxymethyl tetrahydrofuran-3α,4α-diol [**8**]*

Ozonide **6**, obtained from olefin **5** (400 mg), was treated with sodium borohydride in refluxing isopropanol for 4 h. To the reaction mixture previously cooled down to 0° was added 50% aqueous acetic acid (6 ml). After evaporation of the solvent, the solid residue was extracted with ethyl acetate to give the triol **8** in 35% yield; i.r. (KBr film) 3500, 3300 (OH), 1390, 1380 (*gem*-dimethyl), 1080, 1050 cm^{-1} (C—O); n.m.r. ($(CD_3)_2CO$) δ 1.31 (s, 3H), 1.48 (s, 3H), 3.70 and 4.00 (10H), 4.72 (b.s., 2H); mass spectrum (70 eV) *m/e* 219 ($M^+ - CH_3$), 189 ($M^+ - CH_3 - CH_2O$).

*3,4-O-Isopropylidene-2β-(1′,2′-diacetoxyethyl)-5β-acetoxymethyltetrahydrofuran-3α,4α-diol (**8***a*)*

To the ozonide **6** (200 mg) in isopropanol (15 ml) was added sodium borohydride (400 mg) and the mixture was then refluxed for 3 h. After acidification of the reaction mixture at 0° and evaporation of the solvent to dryness *in vacuo*, the solid residue was treated with a mixture of acetic anhydride – pyridine (4:6 ml) overnight. After evaporation *in vacuo*, the solid residue was extracted with methylene chloride. The pure acetate **8***a* was obtained in 79% yield; i.r. (KBr film) 1750 (C=O), 1380 (*gem*-dimethyl), 1230 cm^{-1} (CH_3COO); n.m.r. ($CDCl_3$) δ 1.37 (s, 3H), 1.56 (s, 3H), 2.05 and 2.12 (2s, 9H), 4.20 (m, 6H), 4.54 (m, 2H), 5.22 (m, 1H); mass spectrum (70 eV) *m/e* 345 ($M^+ - CH_3$), 303 ($M^+ - CH_3 - CH_2CO$), 285 ($M^+ - CH_3 - CH_3COOH$).

Anal. Calcd. for $C_{16}H_{24}O_9$: C, 53.33; H, 6.71. Found: C, 53.15; H, 6.70.

D,L-*2,5-Anhydro-3,4-O-isopropylideneallose (**9**)*

Ozonide **6** from 550 mg of olefin **5** was treated in isopropanol with sodium borohydride (900 mg) at 0° and then refluxed for 4 h. After cooling, the mixture was stirred for 30 min with 50% aqueous acetic acid (8 ml) and then evaporated down and the residue azeotroped with ethyl alcohol and benzene. The solid residue was then dissolved in 50% aqueous methanol (20 ml), sodium periodate (600 mg) was added and the solution stirred 1 h. The resulting precipitate was filtered off and the filtrate extracted with chloroform. The organic layer was dried over sodium sulfate and evaporated to give 61% yield of **11**, m.p. 185–186°; i.r. (Nujol) 3480, 3420, 3200 (OH), 1095, 1075, 1055 cm^{-1} (C—O); n.m.r. ($(CD_3)_2CO$) δ 1.30 (s, 3H, CH_3), 1.38 (s, 3H, CH_3), 2.76 (s, OH), 3.42 (m, 1H), 4.00 (m, 3H), 4.75 (m + s, 3H); mass spectrum (70 eV) *m/e* 187 ($M^+ - CH_3$) 173.

Anal. Calcd. for $C_9H_{14}O_5$: C, 53.45; H, 6.98. Found: C, 53.86; H, 7.06.

*1-O-acetyl-2,5-anhdro-3,4-O-isopropylidene-*D,L-*allose (**9***a*)*

The hemiacetal **11** (30 mg) was acetylated overnight with 2 ml of acetic anhydride and 3 ml of pyridine. Work-up of the mixture gave a quantitative yield of the crystalline acetate **11***a*, which was recrystallized from a mixture of methanol–acetone–hexane, m.p. 138.5–139.5°; i.r. ($CHCl_3$) 1750 (OAc), 1385 (*gem*-dimethyl), 1230 cm^{-1} (OAc); n.m.r. ($CDCl_3$) δ 1.38 (s, 3H, C—CH_3), 1.51 (s, 3H, C—CH_3), 2.18 (s, 3H, OAc), 3.50 (d, 1H), 4.23 (m, 3H), 4.88 (s, 2H), 5.72 (s, 1H); mass spectrum (70 eV) *m/e* 229 ($M^+ - CH_3$).

D,L-*2,5-Anhydro-3,4-O-isopropylideneallonic Acid Lactone (**10**)*

Fetizon reagent (9 mequiv.) (11) was added to 400 mg (2 mmol) of **9** in 70 ml of dry benzene. The mixture was heated to reflux for 36 h. The solution was then filtered through Celite and evaporated. The crude product (275 mg) was purified by chromatography on a silica gel column (activity I). Elution with benzene–ether (1:1) gave colorless platelets of **10**, m.p. 122–124°, yield 70%; i.r. ($CHCl_3$ solution) 1770 (lactone), 1385 cm^{-1} (*gem*-dimethyl); n.m.r. ($CDCl_3$) δ 1.3 (s, 3H), 1.5 (s, 3H), 4.45 (α, 1H), 4.62 (s, 1H), 4.0–4.7 (m, 2H), 4.85 (s, 2H); mass spectrum (70 eV) *m/e* 185 ($M^+ - CH_3$), 143, 99, 97, 69, 59.

Anal. Calcd. for $C_9H_{12}O_5$: C, 53.99; H, 6.04. Found: C, 53.67; H, 5.85.

*N-Methyl-2(3α,4α-dihydroxy-di-O-isopropylidene-5β-hydroxymethyl-furan-2β-yl)oxazolidine (**11**)*

Anhydroallose (**9**) (202 mg, 1 mmol) was dissolved in 50 ml of dry benzene containing *N*-methylethanolamine (150 mg, 2 mmol). The mixture was refluxed with a Dean–Stark trap filled with molecular sieves (type 3A) for 36 h. The reaction mixture was then evaporated off under high vacuum leaving 275 mg of the crude oily oxazolidine. Attempts at purification by chromatography led to decomposition of the product; i.r. (film) 3500 (O—H), 2810 (N—CH_3), 1470, 1380 cm^{-1} (*gem*-dimethyl); n.m.r. ($CDCl_3$) δ 1.28 (s, 3H), 1.42 (s, 3H), 2.38 (s, 3H), 2.6 (m, 1H), 3.2 (m, 1H), 3.4–4.2 (m's 8H), 4.5 (d, 2H); mass spectrum (70 eV) *m/e* 259 (M^+), 244 ($M^+ - CH_3$), 228 ($M^+ - CH_2OH$), 189, 152, 86.

*6-O-Acetyl-2,5-anhydro-3,4-O-isopropylidene-*D,L-*allose (**15**)*

Oxazolidine **11** (275 mg), was stirred for 14 h with pyridine (5 ml) and acetic anhydride (3 ml). Evaporation of the solution gave the crude acetate which was dissolved in 10 ml of 50% aqueous acetic acid and stirred for 45 min at room temperature. The aqueous solution was extracted with 3 × 15 ml of methylene chloride and the organic layer dried over sodium sulfate and evaporated to give 200 mg of unstable aldehyde **15**; i.r. ($CHCl_3$) 1750 (acetate), 1720 (aldehyde), 1380 cm^{-1} (*gem*-dimethyl); n.m.r. ($CDCl_3$) δ 1.27 (s, 3H), 1.47 (s, 3H), 2.0 (s, 3H), 4.0 (m, 2H), 4.4–4.2 (m's, 2H), 4.45 (m, 1H), 4.7 (m, 1H), 9.22 (2, 1H).

The aldehyde (200 mg) was characterized as the semicarbazone **13***d* (12). It crystallized from the reaction mixture after standing for several days in the refrigerator,

Can. J. Chem. Downloaded from www.nrcresearchpress.com by 210.87.254.40 on 09/05/12
For personal use only.

giving 160 mg of product, m.p. 146–148°. Compound **13***d* was obtained in 55% yield, based on anhydroallose **9**. This compound was identical in every respect to that prepared by the other route.

Anal. Calcd. for $C_{12}H_{19}O_6N_3$: C, 47.83; H, 6.36; N, 13.95. Found: C, 47.56; H, 6.29; N, 13.86.

N-Methyl-2(3α,4α-dihydroxy-di-O-isopropylidene-5β-hydroxymethyl-furan-1β-yl)thiazolidine (12)

Anhydroallose (**9**) (150 mg, 0.75 mmol) was heated to reflux in 20 ml of dry benzene containing *N*-methyl thioethanolamine (182 mg, 2 mmol) with a Dean–Stark condenser containing molecular sieves (type 3A) for 36 h. Evaporation and separation on a 20 × 20 silica gel plate, using ethyl ether as a solvent system, gave 115 mg of **12** as a clear oil (R_f = 0.25), yield 55%; i.r. (film) 3400 (O—H), 2800 (N—CH_3), 1460, 1380 (*gem*-dimethyl), 1215 cm^{-1}; n.m.r. ($CDCl_3$) δ 1.32 (s, 3H), 1.52 (s, 3H), 2.48 (s, 3H), 3.10 (m's, 5H), 3.65 (d, 2H), 3.8–4.2 (m's, 3H), 4.6 (m, 2H); mass spectrum (70 eV) *m/e* 275 (M^+), 274 ($M^+ - 1$), 260 ($M^+ - CH_3$), 228, 200, 168, 102.

Analysis was made on the acetate derivative (**12***a*).

N-Methyl-2(3α,4α-dihydroxy-di-O-isopropylidene-5β-acetoxymethyl-furan-1β-yl)thiazolidine (12a)

The thiazolidine **12** (100 mg, 0.36 mmol), was acetylated with pyridine – acetic anhydride in the usual way. The crude product was chromatographed on a silica gel column (activity III). Elution with ethyl ether gave the acetate derivative as a colorless oil in quantitative yield; i.r. (film) 2600 (N—CH_3), 1760 (acetate), 1385 cm^{-1} (*gem*-dimethyl); n.m.r. ($CDCl_3$) δ 1.25 (s, 3H), 1.45 (s, 3H), 2.05 (s, 3H), 2.35 (s, 3H), 3.0 (m's, 4H), 3.5 (m, 1H), 4.02 (d + m, 2H), 4.18 (broad s, 2H), 4.5 (d, 2H); mass spectrum (70 eV) *m/e* 317 (M^+), 316 ($M^+ - 1$), 302 ($M^+ - CH_3$), 270 ($M^+ - CH_3 - S$), 259, 229, 182, 139, 102.

Anal. Calcd. for $C_{14}H_{23}O_5NS$: C, 52.99; H, 7.31; N, 4.41; S, 10.08. Found: C, 53.36; H, 7.03; N, 4.05; S, 9.87.

*2,5-Anhydro-3,4-O-isopropylidene-*D,L*-allose Oxime (13a)*

Anhydroallose (**9**) (202 mg, 1 mmol) was dissolved in 30 ml of methanol containing hydroxylamine hydrochloride (100 mg, 1.43 mmol) and anhydrous sodium acetate (125 mg, 1.52 mmol). The solution was refluxed for 1 h, cooled, and evaporated to leave a colorless oily oxime as a mixture of *syn*- and *anti*-H isomers in the ratio 3:2. Purification on a silica gel column (activity III) eluting with ethyl ether gave 140 mg of the oxime, yield 65%; i.r. (film) 3350 (O—H), 1720 (C=N ~ OH), 1380 cm^{-1} (*gem*-dimethyl); n.m.r. ($CDCl_3$) δ 1.38 (s, 3H), 1.58 (s, 3H), 3.78 (d, 2H, J = 3 Hz), 4.1 (b.s, 1H), 4.62 and 5.1 (m, 1H), 4.70 (m, 2H), 5.4 to 6.4 (b.s, 2H, O—H), 6.86 (d, J = 6 Hz, *anti*-H), 7.65 (d, J = 4 Hz, *syn*-H); mass spectrum (70 eV) *m/e* 217 (M^+), 202 ($M^+ - CH_3$), 184 ($M^+ - CH_3 - H_2O$), 173, 159, 98, 85.

Anal. Calcd. for $C_9H_{15}O_5N$: C, 49.76; H, 6.96; N, 6.45. Found: C, 49.34; H, 6.79; N, 6.34.

*2,5-Anhydro-3,4-O-isopropylidene-*D,L*-allose Thiosemicarbazone (13b)*

Anhydroallose **9** (202 mg, 1 mmol) was dissolved in 30 ml of methanol containing thiosemicarbazide (101 mg, 1.1 mmol). The solution was refluxed with a Dean–Stark trap containing molecular sieves (type 3A) and the reaction followed by t.l.c. until the disappearance of allose. Evaporation and separation of the residue on 20 × 20 silica gel plates using ethyl ether as a solvent system gave 175 mg of an oil, yield 65%. This oil was dissolved in chloroform and on standing for several days gave crystals, m.p. 156°; i.r. (KBr disc) 3400 (NH_2), 3180 to 3330 (multiple bands, NH_2, NH), 1610, 1530, 1385 (*gem*-dimethyl), 1090, 1065 cm^{-1}; n.m.r. ($CDCl_3$) δ 1.25 (s, 3H), 1.45 (s, 3H), 3.2 (1H, OH), 3.5 (m, 2H), 4.0 (m, 1H), 4.35 (dd, 1H), 4.55 (b.s., 2H), 6.65 (NH_2), 7.15 (d, 1H, J = 5 Hz), 9.68 (NH); mass spectrum (70 eV) *m/e* 275 (M^+), 260 ($M^+ - CH_3$), 216 ($M^+ - CSNH$), 200 ($M^+ - NH_2CSNH$), 201 ($M^+ - CH_3 - CSNH$), 173 ($M^+ - CH{:}NNHCSNH_2$), 102.

Anal. Calcd. for $C_{10}H_{17}O_5N_3$: C, 43.63; H, 6.23; N, 15.27; S, 11.63; Found: C, 43.48; H, 6.03, N, 15.40; S, 11.81.

*2,5-Anhydro-3,4-O-isopropylidene-*D,L*-allose Semicarbazone (13c)*

Anhydroallose **9** (202 mg, 1 mmol) was dissolved in 30 ml of methanol containing semicarbazide (82.5 mg, 1.1 mmol). The solution was refluxed with a Dean–Stark trap for 5 h by which time no allose could be detected by t.l.c. Evaporation and separation of the residue on 20 × 20 silica gel plates using methanol – ethyl acetate (3:7) as a solvent system gave 180 mg of the crystalline product (R_f = 0.65), yield 70%. Recrystallization from acetone – ethyl ether gave small cubic crystals, m.p. 136–137°; i.r. (KBr disc) 3500 to 3200 (multiple bands, NH_2, NH, OH) 1690 (semicarbazone), 1640 (C=N), 1385 cm^{-1} (*gem*-dimethyl); n.m.r. ($(CD_3)_2CO$) δ 1.24 (s, 3H), 1.40 (s, 3H), 2.82 (1H, OH), 3.4 (2H), 3.82 (m's, 2H), 4.20 (dd, J = 6 Hz, J = 3 Hz), 4.5 (m's, 2H), 5.82 (NH_2), 6.8 (d, 1H, J = 6 Hz), 9.05 (1H, NH); mass spectrum (70 eV) *m/e* 259 (M^+), 244 ($M^+ - CH_3$), 201 (244 – CONH), 185 (244 – NH_2CONH), 158 (244 – CH:NNHCONH$_2$), 116, 86.

Anal. Calcd. for $C_{10}H_{17}O_5N_3$: C, 46.32; H, 6.61; N, 16.21. Found: C, 46.11; H, 6.75; N, 16.01.

*6-O-Acetyl-2,5-anhydro-3,4-O-isopropylidene-*D,L*-allose Semi-carbazone (13d)*

The semicarbazone derivative (**13***c*) (100 mg, 0.4 mmol) was dissolved in 3 ml of pyridine and 2 ml of acetic anhydride. The solution was stirred for 10 h. Evaporation of the excess pyridine – acetic anhydride left an oily brown residue which was chromatographed on a 20 × 20 silica gel plate. Elution with methanol–ethyl acetate (1:4) gave 95 mg of colorless oil (R_f = 0.8), yield 90%. The product was crystallized from methanol – petroleum ether, m.p. 148°; i.r. (KBr disc) 3490 (NH), 1760 (acetate), 1700 (amide), 1640 (C=N), 1390 cm^{-1}; n.m.r. ($CDCl_3$) δ 1.40 (s, 3H), 1.60 (s, 3H), 2.05 (s, 3H), 3.50 (1H, OH), 4.28 (b.s, 2H), 4.30 (m, 1H), 4.68 (m, 2H), 4.90 (m, 1H), 5.80 (2H, NH_2), 7.20 (d, 1H, J = 6 Hz), 10.0 (1H, NH); mass spectrum (70 eV) *m/e* 301 (M^+), 286 ($M^+ - CH_3$), 269, 258 ($M^+ - NHCO$), 243, 226, 215, 171, 86, 69.

Anal. Calcd. for $C_{12}H_{19}O_6N_3$: C, 47.83; H, 6.36; N, 13.95. Found: C, 48.04; H, 6.28; N, 13.81.

Ethyl trans-3-(5β-Hydroxymethyl-3α,4α-dihydroxy-di-O-isopropylidene-furan-1β-yl)acrylate (14)

Carbethoxymethylene triphenylphosphorane (600 mg, 1.725 mmol) was added to the anhydroallose (**9**) (300 mg, 1.48 mmol) in 15 ml of dimethylformamide. The solution

Can. J. Chem. Downloaded from www.nrcresearchpress.com by 210.87.254.40 on 09/05/12
For personal use only.

was heated at 95 °C for 6 h, cooled, and stripped of solvent by evaporation under high vacuum. The residue was triturated with ether and the white crystalline material that precipitated was filtered off. The filtrate was evaporated to dryness and chromatographed on 20 × 20 silica gel plates. Elution with methylene chloride – ether (2:3) gave 250 mg of colorless oily product, yield 66%; i.r. (film) 3500 (OH), 1730 (ester), 1670 (C=C), 1380 cm^{-1} (*gem*-dimethyl); n.m.r. ($CDCl_3$) δ 1.20 (t, 3H, J = 7 Hz), 1.30 (s, 3H), 1.52 (s, 3H), 2.02 (s, O—H), 3.5 to 4.52 (m's, 8H), 5.73 (d, 1H, J = 14 Hz), 6.70 (dd, 1H, J = 14 Hz, J = 4 Hz); mass spectrum (70 eV), *m/e* 272 (M^+), 257 ($M^+ - CH_3$), 227 ($M^+ - CH_3 - CH_2O$), 214 ($M^+ - CH_3 - CH_3COO$), 167, 129, 85.

Anal. Calcd. for $C_{13}H_{20}O_6$: C, 57.35; H, 7.35. Found: C, 56.61; H, 7.66.

*Ethyl trans-3-(5β-Acetoxymethyl-3α,4α-dihydroxy-di-O-isopropylidenefuran-1β-yl)acrylate (**14a**)*

Crude or pure ester **14** (200 mg) was acetylated using 5 ml of acetic anhydride in 6 ml of pyridine stirring for 6 h at room temperature. The mixture was then evaporated to dryness under high vacuum. The oil product was purified on a silica gel column (activity III), eluting with ether–hexane (1:1). When intermediate **14** was not isolated, overall yield based on **9** is 80%; i.r. (film) 1745 (acetate), 1725 (ethyl ester), 1660 (C=C), 1380 cm^{-1} (*gem*-dimethyl); n.m.r. ($CDCl_3$) δ 1.24 (t, 3H, J = 7 Hz), 1.33 (s, 3H), 1.55 (s, 3H), 2.10 (s, 3H), 4.0–4.52 (m's, 8H), 6.18 (d, 1H, J = 16 Hz), 6.95 (dd, 1H, J = 16 Hz, J = 5 Hz); mass spectrum (70 eV) *m/e* 314 (M^+), 299 ($M^+ - CH_3$), 256 (299 − CH_3CO), 211, 196, 86.

*9β-Cyano-5β-p-nitrobenzoylmethyl-(3α,4α-dihydroxy-di-O-isopropylidene)furan (**16**)*

The oily oxime **13***a* (150 mg, 0.7 mmol), dissolved in 5 ml of pyridine containing *p*-nitrobenzoyl chloride (400 mg, 2.16 mmol) was stirred for 14 h at room temperature. *p*-Nitrobenzoic acid was then filtered off and the solution evaporated under high vacuum. Chromatography of the oily mixture on 20 × 20 silica gel plates, eluting with ether–hexane (1:1), gave 190 mg of the crystalline nitrile **16** (R_f = 0.45), yield 75%. Recrystallization of the product from chloroform–hexane at room temperature gave small needle-like crystals, m.p. 118–120°; i.r. (Nujol) 2230 (C=N), 1740 (nitro benzoate), 1380 cm^{-1} (*gem*-dimethyl); n.m.r. ($CDCl_3$) δ 1.40 (s, 3H), 1.50 (s, 3H), 4.62 (b.s., 3H), 4.82 (d, 2H, J = 8 Hz), 5.18 (dd, 1H, J = 8 Hz, J = 2 Hz); mass spectrum (70 eV) *m/e* 333 ($M^+ - CH_3$), 303 ($M^+ - CH_3 - NO$), 275 (303 − CO), 226 ($M^+ - C_6H_5NO_2$), 208, 166, 150, 131, 120.

Anal. Calcd. for $C_{16}H_{16}N_2O_7 \cdot H_2O$: C, 52.46; H, 4.95; N, 7.65. Found: C, 52.29; H, 4.47; N, 7.54.

We wish to thank the National Research Council of of Canada for financial support.

1. G. Just and A. Martel. Tetrahedron Lett. 1517 (1973).
2. T. E. Stevens and W. D. Emmons. J. Am. Chem. Soc. **80**, 338 (1958).
3. H. Schechter, F. Conrand, A. L. Daulton, and R. B. Kaplan. J. Am. Chem. Soc. **74**, 3052 (1952).
4. R. Daniels and J. L. Fischer. J. Org. Chem. **28**, 320 (1963).
5. W. L. Nelson and D. R. Allen. J. Heterocycl. Chem. **9**, 561 (1972).
6. D. H. Williams and N. S. Bhacca. J. Am. Chem. Soc. **86**, 2742 (1964).
7. L. D. Hall. Adv. Carbohydr. Chem. **19**, 51 (1964).
8. H. Booth. Tetrahedron Lett. 411 (1965).
9. P. Laszlo and P. von R. Schleyer. J. Am. Chem. Soc. **85**, 2709 (1963).
10. E. J. Reist and P. H. Christie. J. Org. Chem. **35**, 3521 (1970).
11. M. Fetizon, M. Golfier, and J. M. Louis. Chem. Commun. 1118 (1969).
12. R. L. Shriner, R. C. Fuson, and D. Y. Curtin. The systematic identification of organic compounds. John Wiley & Sons, Inc., N.Y. p. 218.

Synthesis of 6-Hydroxyfulvenes. II. Isomerization of 7-Oxanorbornadienes and 3-Oxaquadricyclanes[1]

RAJ KUMAR BANSAL,[2] ARCHIBALD WILSON MCCULLOCH, PAUL WAYNE RASMUSSEN, AND ALISTER GAVIN MCINNES

Atlantic Regional Laboratory, National Research Council of Canada, Halifax, Nova Scotia B3H 3Z1

Received July 24, 1974

RAJ KUMAR BANSAL, ARCHIBALD WILSON MCCULLOCH, PAUL WAYNE RASMUSSEN, and ALISTER GAVIN MCINNES. Can. J. Chem. **53**, 138 (1975).

Substituted 7-oxanorbornadienes (**1***a–e*) isomerize in good yield in the presence of iodine to 6-hydroxyfulvenes (**2***a–e*): the reaction is catalyzed by light. Oxaquadricyclanes having bridgehead methyl substituents (**3***b*, *c*) also undergo slow photoisomerization (2537 Å) to the same fulvenes. Irradiation of the oxanorbornadienes with bridgehead phenyl substituents (**1***d*, *e*) resulted in oxepines (**7***d*, *e*). Phenyl substituted oxaquadricyclanes could not be isolated.

RAJ KUMAR BANSAL, ARCHIBALD WILSON MCCULLOCH, PAUL WAYNE RASMUSSEN et ALISTER GAVIN MCINNES. Can. J. Chem. **53**, 138 (1975).

En présence d'iode, les oxa-7 norbornadiènes substitués (**1***a–e*) s'isomérisent avec de bons rendements pour conduire aux hydroxy-6 fulvènes (**2***a–e*); la réaction est catalysée par la lumière. Les oxaquadricyclanes possédant les substituants méthyles en tête de pont (**3***b*, *c*), subissent aussi une photoisomérisation lente (2537 Å) conduisant aux mêmes fulvènes. L'irradiation d'oxanorbornadiènes possédant des groupements phényles en tête de pont (**1***d*, *e*) fournit les oxépines (**7***d*, *e*). On n'a pas pu isoler d'oxaquadricyclanes substitués par des groupes phényles.

[Traduit par le journal]

Recent reports on the photoisomerization of 7-oxanorbornadienes and the transition metal promoted isomerizations of 7-oxanorbornadienes and 3-oxaquadricyclanes to 6-hydroxyfulvenes (1, 2) have prompted us to report our observations on these systems.

Stusche and Prinzbach have reported that the 6-hydroxyfulvenes **2***a*, *c*, *f* are formed upon direct or sensitized excitation of oxanorbornadienes **1***a*, *c*, *f* or by Cu^{I} or Ag^{I} catalyzed isomerization of the corresponding oxaquadricyclanes **3***a*, *c*, *f* (1). Bruggink and Hogeveen found that **1***a–c* and **3***a–c* are converted under the influence of $[Rh(CO)_2Cl]_2$ to **2***a–c* (2).

We have found that oxanorbornadienes **1***a–e* isomerize rapidly to **2***a–e* in the presence of *iodine*. The reaction is catalyzed by light. With the exception of **2***a* (33%) yields were $\geq 75\%$. The iodine-promoted conversion of **1** to **2** is characterized by a very fast rate and a high degree of regioselectivity. Thus, isomerization of **1***b* affords *two* fulvenes, **2***b* and **4**, but in a molar ratio of 12:1.

The reaction proceeds equally well in ether, benzene, CCl_4, or *n*-heptane. It does not, how-

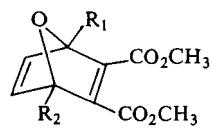

1

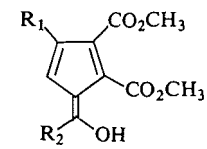

2

a $R_1 = R_2 = H$
b $R_1 = H; R_2 = CH_3$
c $R_1 = R_2 = CH_3$

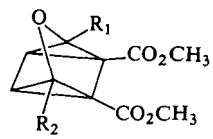

3

d $R_1 = H; R_2 = C_6H_5$
e $R_1 = R_2 = C_6H_5$
f $R_1 = H; R_2 = CH(OEt)_2$

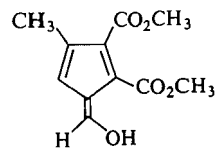

4

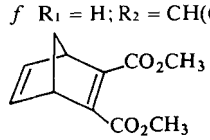

5

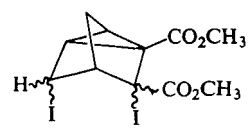

6

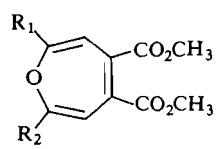

7

[1]Issued as NRCC No. 14296.
[2]NRCC Postdoctorate Fellow, 1968–1970.

Can. J. Chem. Downloaded from www.nrcresearchpress.com by 210.87.254.5 on 09/05/12
For personal use only.

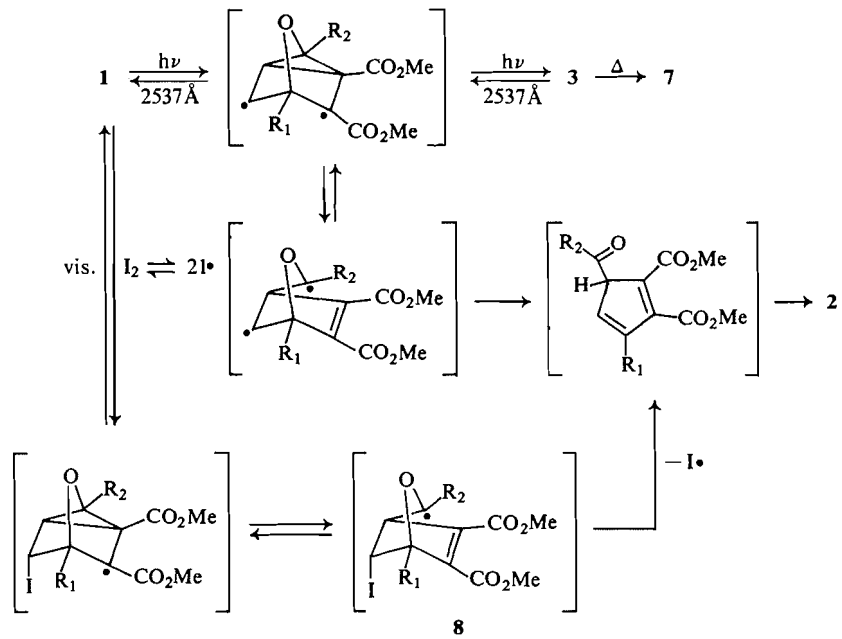

8

a $R_1 = H; R_2 = CH_3$
b $R_1 = CH_3; R_2 = H$

SCHEME 1

ever, appear to be applicable to norbornadienes which lack a bridge heteroatom. Under the same conditions compound **5** was converted to a mixture of stereoisomeric diiodonortricyclenes **6**.[3] The iodine-assisted isomerization is moreover not applicable to the oxaquadricyclane system: under the same conditions **3***b*, *c* rapidly gave complex mixtures of products containing only small amounts of **2***b*, *c*.

Stusche and Prinzbach have observed low-yield photoisomerization of **1** to **2** on direct excitation with light of wavelength >2800 Å (1). We have found that isomerization of **3***b*, *c* (prepared by irradiation of **1** at 3000 Å) to **2***b*, *c* may be achieved slowly (30–40% in 24 h) upon irradiation of the former at 2537 Å. The latter conversions are best explained by the equilibrium (1 ⇆ 3) shown in Scheme 1 (*cf.* 3, 4).

The regioselectivity observed in both the iodine-assisted conversion of **1***b*, and the photoconversion of **3***b*, to **2***b*, is strongly suggestive of closely related pathways. We believe that the iodine-promoted conversion can best be interpreted by a radical pathway. A possible mechanism is outlined in Scheme 1.

[3]A. W. McCulloch, D. G. Smith, J. A. Walter, and A. G. McInnes. Unpublished work.

It is known that tertiary radicals are more stable than secondary by about 4 kcal (5). The observed regioselectivity of the reaction (product ratio **2***b*:**4**, 12:1) can thus be rationalized in terms of the energy difference between the radical intermediates **8***a* and **8***b*. We have derived pseudo first-order rate constants for the conversions of **1***a–c* to **2***a–c* (Table 1). The fact that increasing methyl substitution at the bridgehead positions leads to increasing rates of isomerization is consistent with the proposed mechanism. The iodine-promoted reaction, although slowed by a factor of two or three, proceeds also in the dark, presumably initiated by thermal homolytic fission of the iodine.

We were unable to isolate the phenyl-substituted oxaquadricyclanes **3***d*, *e* since irradia-

TABLE 1. Pseudo first-order rate constants for **1***a–c* → **2***a–c*

	k (s^{-1})	
Conversion	Light reaction	Dark reaction
1*a* → **2***a*	4.65×10^{-4}	1.62×10^{-4}
1*b* → **2***b*	2.59×10^{-3}	9.90×10^{-4}
1*c* → **2***c*	7.16×10^{-3}	3.16×10^{-3}

Can. J. Chem. Downloaded from www.nrcresearchpress.com by 210.87.254.5 on 09/05/12
For personal use only.

TABLE 2. Proton magnetic resonance (60 MHz) data for **1**, **2**, **4**, 7, and **12**

Compound	Chemical shifts, δ		
	$-CO_2CH_3$	—OH	Others
1*d*	3.62 (3H, s), 3.76 (3H, s)		5.84 (1H, q, H-4, $J_{4,5} + J_{4,6} = 2.2$ Hz); 7.2–7.6 (7H, m, H-5, H-6, and aryl)
1*e*	3.62 (6H, s)		7.48 (10H, m, aryl); 7.59 (2H, s, H-5 and H-6)
2*b*	3.86 (3H, s), 3.90 (3H, s)	16.25 (1H, bs)	6.71 (2H, q, H-3 and H-4, $\Delta\nu_{3,4} = 34.9$, $J_{3,4} = 4.8$ Hz); 2.54 (3H, bs)
2*d*	3.88 (3H, s), 3.96 (3H, s)	16.30 (1H, s)	6.62 (2H, q, H-3 and H-4, $\Delta\nu_{3,4} = 20.9$, $J_{3,4} = 4.8$ Hz); 7.3–7.9 (5H, m, aryl)
2*e*	3.83 (3H, s), 3.98 (3H, s)	16.25 (1H, s)	6.90 (1H, s, H-4); 7.2–7.9 (10H, m, aryl)
4	obscured by **2***b*	14.67 (1H, d, $J = 13.1$ Hz)	2.02 (3H, d, $J = 1.1$ Hz, CH_3); 6.52 (1H, d, $J = 1.1$ Hz, H-4); 7.71 (1H, d, $J = 13.1$ Hz, H-6)
7*d*	3.80 (3H, s), 3.83 (3H, s)		6.06* (2H, s, H-6 and H-7); 6.50 (1H, s, H-3); 7.2–7.45 (3H, m, aryl); 7.55–7.8 (2H, m, aryl)
7*e*	3.85 (6H, s)		6.60 (2H, s, H-3 and H-6); 7.2–7.5 (6H, m, aryl); 7.5–7.9 (4H, m, aryl)
10			6.79 (2H, s, H-3 and H-6); 7.15–7.55 (6H, m, aryl); 7.60–7.95 (4H, m, aryl)

*Observed in benzene-d_6 as an AB quartet centered at 5.75 δ ($\Delta\nu_{6,7} = 16.6$, $J_{6,7} = 5.3$ Hz).

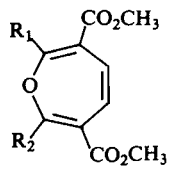

9

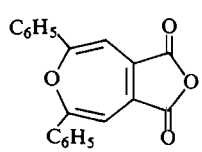

10

d $R_1 = C_6H_5$; $R_2 = H$
e $R_1 = R_2 = C_6H_5$

tion of **1***d*, *e* at 3000 Å led directly to the oxepines 7*d*, *e* (~60% in 24 h at 30°).[4] The thermal instability of oxaquadricyclanes and their isomerization to oxepines is well known (6–8). The latter process is highly dependent on substitution (9); it clearly is favored when aryl substituents occupy the bridgehead positions.

The structures of oxanorbornadienes **1***d*, *e* follow from their mode of formation and comparison of their spectral properties with those of the corresponding ethyl esters (10).

Compounds **2***d* and **2***e* both show infrared absorptions for the strongly bonded hydroxyl (~2950 cm^{-1}) and carbomethoxy carbonyl (~1600 cm^{-1}) groups characteristic of 1-carbomethoxy-6-hydroxyfulvenes. This is confirmed by the low-field shift of the enolic hydroxyl (~16.3 δ). The chemical shifts and multiplicities of the ring hydrogens in these compounds are comparable to those observed for the analogous methylated compounds **2***b* and **2***c*.

Although fulvene **4** could not be isolated, its p.m.r. spectral characteristics provide strong evidence for the assigned structure. The low-field hydroxyl proton and H-6 form a very distinctive AX system ($J = 13.1$ Hz), similar to that observed in the spectrum of **2***a* (2). The coupling between the ring proton and the ring methyl hydrogens is identical to that between H-4 and the *C*-methyl at C-3 in **2***c*.

Compounds 7*d* and 7*e* show infrared absorption for unsaturated ester carbonyl groups near 1720 cm^{-1} and strong ultraviolet maxima (see Experimental) compatible with oxepine structures. Their spectral properties are consistent with either 7*d*, *e* or 9*d*, *e*. Conclusive proof that the carboxylate groupings are located at C-4 and C-5, as in **7**, was provided by facile conversion of 7*e* to the cyclic anhydride **10**, the structure of which could be readily deduced from its mass, i.r., u.v., and p.m.r. spectra. The 3,6-diphenyl isomer of 7*e* has been shown to exist as the benzene oxide tautomer (11). Our p.m.r. data for 7*d*, *e* clearly indicate oxepine structures, at least at ambient temperature. It should be noted that

[4]We did not detect 3*d*, *e* in the products of irradiation at 0° and did not attempt their isolation at even lower temperatures.

Can. J. Chem. Downloaded from www.nrcresearchpress.com by 210.87.254.5 on 09/05/12
For personal use only.

Can. J. Chem. Downloaded from www.nrcresearchpress.com by 210.87.254.5 on 09/05/12
For personal use only.

tautomerism of **7***d*, *e* to the benzene oxide forms would result in decreased conjugation.

Our physical data for **2***a–c* are identical to those previously reported (1, 2, 12). Proton magnetic resonance data for **1***d*, *e*, **2***d*, *e*, **4**, **7***d*, *e*, and **10** are given in Table 2.

Experimental

The p.m.r. spectra were obtained on a Varian A-60A spectrometer equipped with a V-6058 spin-decoupler, using $CDCl_3$ as solvent (unless stated otherwise) and tetramethylsilane as internal standard. Infrared spectra were recorded on a Perkin–Elmer 521 spectrometer, u.v. spectra (in EtOH) on a Unicam SP 8000 instrument, and mass spectra on a Dupont-CEC 21–491 spectrometer. Ultraviolet irradiation experiments were conducted in a Rayonet photochemical reactor. All column chromatography was carried out using Mallinckrodt silicic acid (100–150 mesh); preparative t.l.c. employed Merck silica gel HF-254.

2,3-Dicarbomethoxy-7-oxabicyclo[2.2.1]hepta-2,5-dienes (1a–d)

Adducts **1***a–d* were prepared by conventional thermal Diels–Alder reaction (100°) of the appropriate furan with dimethyl acetylenedicarboxylate (DMAD) and were purified by column chromatography ($CHCl_3$). Adduct **1***d* was obtained as a yellow oil, n_D^{24} 1.5312.

2,3-Dicarbomethoxy-1,4-diphenyl-7-oxabicyclo[2.2.1]hepta-2,5-diene (1e)

A solution of 2,5-diphenylfuran (14.30 g, 0.065 mol) in CH_2Cl_2 (75 ml) was added to a stirred mixture of DMAD (9.24 g, 0.065 mol) and $AlCl_3$ (8.67 g, 0.065 mol) in CH_2Cl_2 (250 ml), both solutions being cooled to −20° before mixing. Stirring was continued for 1 h at −20°. The reaction mixture was then washed with water, dried (Na_2SO_4), and evaporated. Trituration of the residue with ether–petroleum ether gave **1***e* as cream-coloured prisms (3.84 g, 16%), m.p. 120–121°.

Isomerization of 1 to 2

General procedure

An ether solution of the oxanorbornadiene **1** and iodine was irradiated (3000 Å in Rayonet reactor, or exposure to daylight) for 15 min at 25–30°. The mixture was washed with sodium bisulfite solution, then H_2O, dried (Na_2SO_4), and evaporated. The 6-hydroxyfulvene was obtained by purification of the residue.

1,2-Dicarbomethoxy-6-hydroxyfulvene (2a)

The general procedure was modified in that a solution of **1***a* (1.2 g, 0.006 mol) and I_2 (2.89 g, 0.011 mol) in Et_2O (150 ml) was irradiated (3000 Å) for 90 min. Column chromatography of the oily product gave **2***a* as a yellow oil (400 mg, 33%), n_D^{25} 1.6554; molecular ion at *m/e* 210 ($C_{10}H_{10}O_5$ requires 210).

1,2-Dicarbomethoxy-6-methyl-6-hydroxyfulvene (2b) and 1,2-Dicarbomethoxy-3-methyl-6-hydroxyfulvene (4)

Reaction of **1***b* (0.4 g, 0.002 mol) and I_2 (0.045 g, 0.0002 mol) in Et_2O (100 ml) gave a product shown by p.m.r. (see Table 2) to contain **2***b* and **4** in a ratio of 12:1. Crystallization from petroleum ether gave **2***b* as yellow needles (0.31 g, 78%), m.p. 84–85°; molecular ion at *m/e* 224 ($C_{11}H_{12}O_5$ requires 224); ν_{max} (CCl_4) 2955, 1730 cm^{-1}; ν_{max} (KBr) 2955, 1720, 1610 cm^{-1}; λ_{max} (ε) 238 (12 300), 326 nm (21 700). All attempts to isolate **4** by chromatography were unsuccessful.

1,2-Dicarbomethoxy-3,6-dimethyl-6-hydroxyfulvene (2c)

Column chromatography ($CHCl_3$) of the crude product from reaction of **1***c* (4.0 g, 0.017 mol) and I_2 (0.100 g, 0.0004 mol) in Et_2O (400 ml) gave **2***c* as a yellow oil (3.21 g, 80%), identical to the material obtained previously by acid-catalyzed rearrangement of **3***c* (11). The conversion of **1***c* also proceeded readily in benzene, CCl_4, or *n*-heptane.

1,2-Dicarbomethoxy-6-phenyl-6-hydroxyfulvene (2d)

The oily product obtained from reaction of **1***d* (0.6 g, 0.002 mol) and I_2 (0.05 g, 0.0002 mol) in Et_2O (150 ml) was submitted to preparative t.l.c. ($CHCl_3$). This gave **2***d* as a viscous yellow oil (0.45 g, 75%), which slowly crystallized as needles, m.p. 92–94°; molecular ion at *m/e* 286 ($C_{16}H_{14}O_5$ requires 286); ν_{max} (liquid film) 2950, 1715, 1605, 1563 cm^{-1}; λ_{max} (ε) 230 (11 100), 270 (5400), 347 nm (12 000).

1,2-Dicarbomethoxy-3,6-diphenyl-6-hydroxyfulvene (2e)

Crystallization (EtOH) of the crude product from reaction of **1***e* (2.00 g, 0.0055 mol) and I_2 (0.050 g, 0.0002 mol) in Et_2O (300 ml) gave **2***e* as bright orange needles (1.80 g, 90%), m.p. 141–142°; molecular ion at *m/e* 362 ($C_{22}H_{18}O_5$ requires 362); ν_{max} (CCl_4) 2955, 1732 cm^{-1}; ν_{max} (KBr) 2950, 1725, 1620, 1608, 1588, 1567 cm^{-1}; λ_{max} (ε) 237 (15 500), 273 (21 100), 345 nm (14 800).

Rate Studies

Stirred CCl_4 solutions 0.0155 *M* in adduct **1***a*, *b*, or *c*, and 0.00465 *M* in I_2 were allowed to react at 27° in the dark and under illumination from a 15 W bulb filtered through an Ilford F-904 red filter. Disappearance of the adduct was followed by gas chromatography assay (benzophenone internal standard) of aliquots after passage through a column of 8:1 $NaHSO_3$:celite 545. Values of $\log_e A_0/A$, where A_0 = ratio of adduct to benzophenone at zero time, and A = ratio of adduct to benzophenone at time t, were then plotted against time to give in each case over the first 5 min of reaction a straight line from which a pseudo first-order rate constant could be determined (Table 1).

2,3-Dicarbomethoxy-3,6-diiodonortricyclenes (6)

A solution of 2,3-dicarbomethoxybicyclo[2.2.1]hepta-2,5-diene **5** (7.16 g, 0.034 mol) and I_2 (10.13 g, 0.040 mol) in Et_2O (400 ml) was exposed to daylight for 4 h at room temperature, and was then washed with bisulfite, then H_2O, and dried (Na_2SO_4). The residue (13.62 g) obtained on evaporation was shown by n.m.r. studies to be predominantly a mixture of two stereoisomeric nortricyclenes of overall structure **6**.[3]

Oxaquadricyclanes 3b and 3c

These compounds were prepared by irradiation of Et_2O solutions of **1***b* and **1***c* at 3000 Å for 6 h at 30°.

Isomerization of 3 to 2

Reactions of **3***b* or **3***c* with I_2 using the standard procedure employed above for the conversion of **1** to **2** resulted in complex mixtures of products containing only small amounts of **2***b* and **2***c*.

Irradiation of Et_2O solutions of **3***b* or 3*c* at 2537 Å for 24 h at 30° caused 30–40% conversion (p.m.r.) to **2***b* and **2***c*.

Isomerization of 1 to 7

4,5-Dicarbomethoxy-2-phenyloxepine (7d)

A solution of **1***d* (2.00 g) in Et_2O (200 ml) was irradiated at 3000 Å for 24 h at 30°. The residue obtained on evaporation of solvent[5] was chromatographed ($CHCl_3$). Pure **7***d* was collected as a yellow oil (0.36 g, 18%), n_D^{24} = 1.5940; molecular ion at *m/e* 286 ($C_{16}H_{14}O_5$ requires 286); ν_{max} (liquid film) 1723 cm^{-1}; λ_{max} (ε) 249 (14 900), 325 (5100), 345 nm (6100).

4,5-Dicarbomethoxy-2,7-diphenyloxepine (7e)

A solution of **1***e* (2.40 g) in Et_2O (425 ml) was irradiated at 3000 Å for 24 h at 30°. Evaporation of the solvent and crystallization of the residue from EtOH gave **7***e* as bright yellow prisms (1.44 g, 60%), m.p. 113–114°; molecular ion at *m/e* 362 ($C_{22}H_{18}O_5$ requires 362); ν_{max} (KBr) 1716, 1603 cm^{-1}; λ_{max} (ε) 268 (37 500), 325 (8500), 365 nm (8300).

4,5-Dicarbethoxy-2,7-diphenyloxepine, prepared in the same way from 2,3-dicarbethoxy-1,4-diphenyl-7-oxabicyclo[2.2.1]hepta-2,5-diene, crystallized as yellow-orange prisms, m.p. 108.5–109.5°; molecular ion at *m/e* 390.

2,7-Diphenyloxepine-4,5-dicarboxylic Anhydride (10)

A solution of **7***e* (250 mg) in 1 *N* methanolic KOH (15 ml) was refluxed for 75 min. The precipitated salt (bronze coloured leaflets) and supernatant were concentrated and the residue dissolved in H_2O. The yellow aqueous solution was extracted with Et_2O (colourless extract → no material) and then acidified with HCl. The acid solution was extracted with Et_2O until colourless: evaporation of solvent gave crude **10** as an orange solid (225 mg), m.p. 160–167°, which gave no effervescence with bicarbonate. A sample of the pure anhydride was obtained by preparative t.l.c. ($CHCl_3$) as bright orange-red rosettes, m.p. 168–170°; molecular ion at *m/e* 316 ($C_{20}H_{12}O_4$ requires 316); ν_{max} (KBr): 1840, 1815, 1800, 1755, 1297, 1246 cm^{-1}; λ_{max} (ε) 271 (30 200); 326 (5400), 364 nm (5500).

[5]Proton magnetic resonance examination of the crude product indicated a conversion to **7***d* of the order of 50–60%. The low yield after chromatography must be due to partial decomposition of the oxepine on the column.

We thank Mrs. M. G. Flack for her excellent technical assistance and Mr. P. F. Seto for the i.r. spectra.

1. D. Stusche and H. Prinzbach. Chem. Ber. **106**, 3817 (1973).
2. (*a*) A. Bruggink and H. Hogeveen. Tetrahedron Lett. 4961 (1972); (*b*) H. Hogeveen and T. B. Middlekoop. Tetrahedron Lett. 4325 (1973).
3. (*a*) G. Kaupp. Liebig's Ann. Chem. 844 (1973); (*b*) G. Kaupp and H. Prinzbach. Liebig's Ann. Chem. **725**, 52 (1969).
4. G. Kaupp, J. Perreten, R. Leute, and H. Prinzbach. Chem. Ber. **103**, 2288 (1970).
5. C. Walling. Free radicals in solution. Wiley, New York. 1957. p. 50.
6. H. Prinzbach. Rev. Pure and Appl. Chem. **16**, 17 (1968).
7. H. Prinzbach, P. Vogel, and W. Auge. Chimi. **21**, 469 (1967).
8. W. Eberbach, M. Perroud-Arguelles, H. Achenbach, E. Druckrey, and H. Prinzbach. Helv. Chim. Acta, **54**, 2579 (1971).
9. H. Prinzbach and M. Thyes. Chem. Ber. **104**, 2489 (1971).
10. A. W. McCulloch, B. Stanovnik, D. G. Smith, and A. G. McInnes. Can. J. Chem. **47**, 4319 (1969).
11. H. Prinzbach and P. Vogel. Helv. Chim. Acta, **52**, 396 (1969).
12. A. W. McCulloch, B. Stanovnik, D. G. Smith, and A. G. McInnes. Can. J. Chem. **49**, 241 (1971).

Can. J. Chem. Downloaded from www.nrcresearchpress.com by 210.87.254.5 on 09/05/12
For personal use only.

Conversion of Bicyclo[2.2.2]octane Systems into Tricyclo[3.2.1.$0^{2,7}$]octanes: A Third Synthesis of the Diterpenoid Trachylobane

RONALD B. KELLY, BARRY A. BECKETT, JENO EBER, HING-KWOK HUNG, AND JIRI ZAMECNIK

Department of Chemistry, University of New Brunswick, Saint John, New Brunswick

Received August 20, 1974

RONALD B. KELLY, BARRY A. BECKETT, JENO EBER, HING-KWOK HUNG, and JIRI ZAMECNIK. Can. J. Chem. **53**, 143 (1975).

The cyclization of bicyclooctane systems to tricyclooctane systems is discussed with particular reference to stereochemical aspects as encountered during the total syntheses of ishwarane and trachylobane. Of special interest are the homoallylic cyclizations. A third, convenient synthesis of trachylobane via a reductive homoallylic cyclization is reported.

RONALD B. KELLY, BARRY A. BECKETT, JENO EBER, HING-KWOK HUNG et JIRI ZAMECNIK. Can. J. Chem. **53**, 143 (1975).

On discute de la cyclisation des systèmes bicyclooctane en systèmes tricyclooctane; on s'intéresse particulièrement aux aspects stéréochimiques rencontrés durant les synthèses totales de l'ishwarane et du trachylobane. Les cyclisations homoallyliques sont d'un intérêt spécial. On rapporte une troisième synthèse très pratique du trachylobane par l'intermédiaire d'une cyclisation homoallylique réductrice. [Traduit par le journal]

Formerly, we have described a total synthesis of the sesquiterpenoid ishwarane (**1**) (1) and two synthetic routes to the diterpenoid trachylobane (**2**) (2). A novel structural feature common to both of these terpenoids is a tricyclo[3.2.1.$0^{2,7}$]-octane system. Consequently, during our work on the synthesis of ishwarane and trachylobane, we became interested in devising methods for converting bicyclo[2.2.2]octane systems, readily available by synthesis, into tricyclo[3.2.1.$0^{2,7}$]-octane systems.

We have already described (1, 2) two methods for achieving such conversions. We now wish to report the application of yet another method which has resulted in a third, convenient synthesis of trachylobane (**2**). Also, we wish to discuss some recently observed stereochemical aspects of the cyclization of bicyclooctane systems to tricyclooctane systems and to present some experimental details of our work which have not yet been published.

Very recently we were successful in converting the synthetic mesylate **3** directly into trachylobane (**2**) in 60% yield by reduction with lithium aluminum hydride under mild conditions. Since **3** (*2b*) and the corresponding alcohol **4** (*2a*) are intermediates in our previously described syntheses of trachylobane, the conversion **3** → **2** constitutes a third and, so far, the most convenient synthesis of trachylobane.

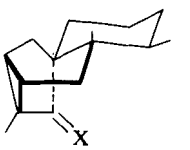

1 X = H,H
8 X = O

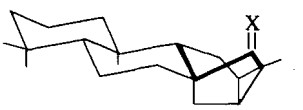

2 X = H,H
10 X = O
16 X = H,OH

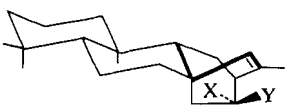

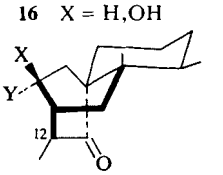

3 X = OMs; Y = H
4 X = OH; Y = H
5 X = H; Y = OMs
6 X = H; Y = OH
7 X = OTs; Y = H
11 X = H; Y = OTs
12 X = O—$\overset{+}{S}(CH_3)_2$; Y = H

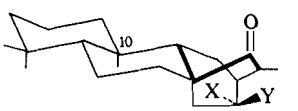

9 X = OTs; Y = H
13 X = H; Y = OTs
14 X = O—$\overset{+}{S}(CH_3)_2$; Y = H
15 X = H; Y = OH

With regard to the conversion **3** → **2** by lithium aluminum hydride, it should be mentioned that there is precedent (3) for such reductive homoallylic cyclizations which are understandable in

Can. J. Chem. Downloaded from www.nrcresearchpress.com by 210.87.254.42 on 09/05/12
For personal use only.

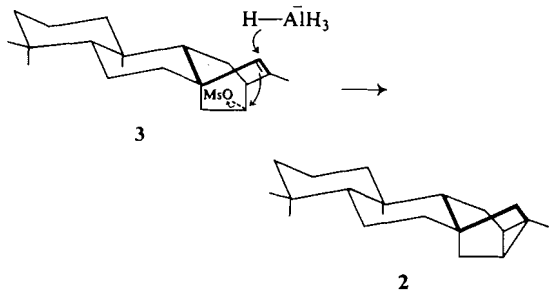

SCHEME 1

terms of the mechanism shown in Scheme 1. As might be expected from precedent (3), treatment of the epimeric *syn*-mesylate **5** of the alcohol **6** (2*a*) with lithium aluminum hydride (as above) produced a mixture of intractable olefinic material possibly containing skeletally rearranged olefin (3).

Our original method for converting bicyclooctane systems into tricyclooctane systems depended on an S_N2i displacement of tosylate by a carbanion as exemplified by the cyclization of **7** to **8** in 70% yield (1) and **9** to **10** in 52% yield (2*a*). These cyclizations, which were achieved by heating the keto tosylates with methylsulfinyl carbanion (4) in dimethyl sulfoxide at 60°, may be regarded as stereochemically unexceptional because, in both instances, the tosylate function is favorably aligned (*anti*) for an S_N2i displacement by the carbanion.

Surprisingly, however, it was found that the *syn*-keto tosylate **11** also cyclized in 60% yield under the same conditions. A mechanism proposed (1) for this cyclization invoked an S_N2 displacement of tosylate by dimethyl sulfoxide to give the intermediate **12** which, being favorably aligned, underwent S_N2i displacement of dimethyl sulfoxide by the carbanion at C-12 to give **8**.

In view of the cyclization of **11**, it was of interest to investigate the behavior of the *syn*-keto tosylate **13** under cyclization conditions identical to those employed in the case of **11** (these conditions were also employed for the cyclizations **7** → **8** and **9** → **10**). In the event, **13** did indeed cyclize to **10** but in only 21% yield. The low yield of **10** suggests that stereochemical factors play an important role in this type of reaction.[1]

A plausible explanation for the low yield of **10** from **13** can be adduced on the basis of stereochemical considerations applied to the proposed double-displacement mechanism (*vide supra*). Thus, models show that the approach of dimethyl sulfoxide during an S_N2 displacement of tosylate in **13** to give the postulated intermediate **14** is hindered by the methyl group at C-10. Consequently, the proposed double-displacement mechanism via the intermediate **14** cannot operate as effectively as in the cyclization **11** → **8**. In the latter the approach of dimethyl sulfoxide required for an S_N2 displacement of tosylate is relatively unhindered. These observations lend support to the proposed double-displacement mechanism.

The key step in our second synthetic route to trachylobane (2*b*) was a homoallylic cyclization of the mesylate **3** of the alcohol **4** (*cf.* ref. 6). Thus, when **3** was heated at 60° in dimethyl sulfoxide containing methylsulfinyl carbanion it was converted to a ketone (60% from **4**) and an alcohol (30% from **4**).

The ketone was identified as the cyclopropyl ketone **10**, the immediate precursor of trachylobane (**2**) in our original synthesis of this diterpenoid (2*a*). The crystalline alcohol possessed properties consistent with structure **16**; the i.r. spectrum showed hydroxyl absorption at 3240 cm^{-1} and the n.m.r. spectrum was devoid of signals attributable to vinylic protons and vinylic methyl but exhibited a singlet (1H) at δ 3.25 due to the *H*—C—OH group. Also consistent with structure **16** was the fact that it could be oxidized in 70% yield with Jones' reagent (5) to the cyclopropyl ketone **10**.

The ketone **10** was also obtained in 70% yield from **4** by direct oxidation of the crude cyclization product with Jones' reagent (5). In our original synthesis of trachylobane (2*a*) the conversion of **4** into **10** required six steps and was accomplished in 14% yield. The conversion of **4** into **10** by the method just described therefore completes a synthesis of trachylobane which is a significant improvement over the original synthesis.

A plausible mechanism for the cyclization of **3** to **10** and **16**, shown in Scheme 2, involves the intermediate **17** which arises by the homoallylic mechanism indicated. Elimination of the proton at C-14 of the intermediate **17** would give the cyclopropyl ketone **10** (*cf.* ref. 7) whereas hydrolysis of **17** would produce the alcohol **16**.

Lately we have subjected the *syn*-mesylate **5**,

[1]The synthesis of the alcohol **15**, corresponding to the tosylate **13** is described in the sequel.

Can. J. Chem. Downloaded from www.nrcresearchpress.com by 210.87.254.42 on 09/05/12
For personal use only.

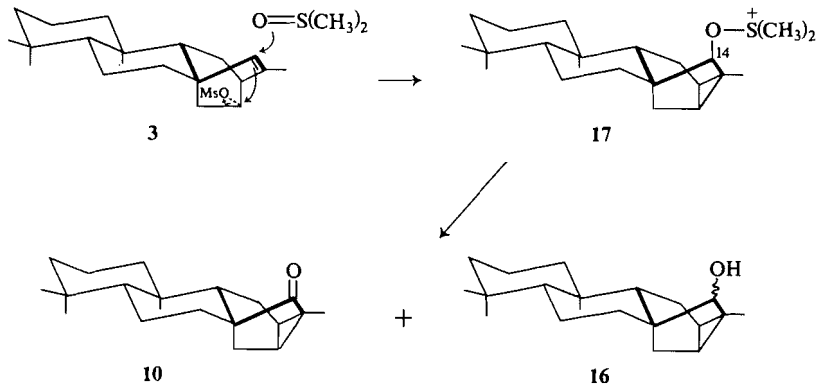

SCHEME 2

epimeric with the mesylate **3** at C-16, to the identical conditions whereby **3** underwent cyclization to **10** and **16**. In contrast with **3**, the mesylate **5** was recovered quantitatively. Thus, it would appear that the stereochemical requirements for homoallylic cyclizations are critical. This is demonstrated by the fact that, whereas **3** underwent reductive homoallylic cyclization to trachylobane **2** (*vide supra*) and cyclized to the cyclopropyl ketone **10** and the cyclopropyl alcohol **16** as just described, the epimeric mesylate failed to cyclize under identical conditions.

The synthesis of the keto alcohol **15** is outlined in Scheme 3. The starting material for this synthesis was the totally synthetic enol **6**, encountered during our original synthesis of trachylobane (*2a*). This was converted in 69% yield to the crystalline benzyl ether **18** which, on hydroboration followed by oxidation with peroxide, afforded the crystalline benzyl ether alcohol **19**. The spectral properties of the hydroboration–oxidation product were consistent with structure **19**; the i.r. spectrum showed hydroxyl absorption at 3490 cm^{-1} and the n.m.r. spectrum showed a singlet (3H) at δ 0.81 and two superimposed singlets (6H) at 0.88 due to tertiary methyl groups, a doublet (3H) at 1.33 due to the secondary methyl, a single-proton doublet at 3.00 due to *H*—C—OH, a multiplet (1H) at 3.64 due to *H*—C—O, a 2-proton multiplet at 4.48 due to benzylic protons and a multiplet (7H) at 7.32 due to aromatic protons.

Oxidation of **19** with the Sarett reagent (8) afforded, in 87% yield, the crystalline keto benzyl ether **20** (i.r. 1705 cm^{-1} (ketone)). Removal of the benzyl group of **20** by hydrogenolysis gave the crystalline keto alcohol **15** in 80% yield (i.r. 3450 cm^{-1} (OH), 1705 cm^{-1} (ketone); n.m.r. δ 4.10 (m, 1H, *H*—C—OH), devoid of signals for aromatic protons).

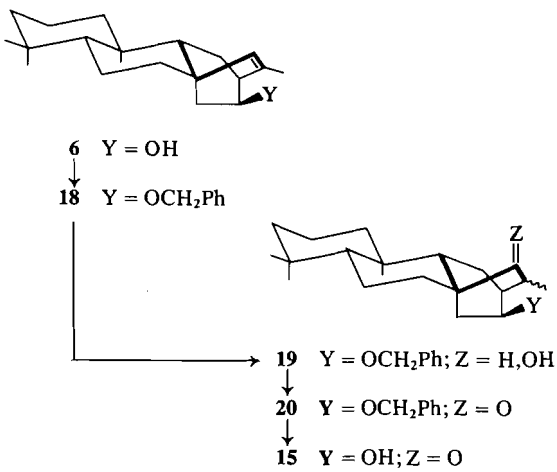

SCHEME 3

Experimental

Instrumentation,[2] *Methods, and Materials*

The n.m.r. chemical shifts are expressed in p.p.m. (δ values) downfield from the signal for tetramethylsilane which is used as an internal standard.

Reaction products were isolated by the following procedure. The product was extracted into the specified solvent and the extract was washed three times with appropriate aqueous solutions as indicated. The original aqueous layer (if any) and the aqueous washings were extracted three times with the solvent and the combined extracts were dried over anhydrous magnesium sulfate, filtered and evaporated *in vacuo* on a rotary evaporator.

[2]Information about instrumentation may be obtained by consulting ref. *2a*.

Can. J. Chem. Downloaded from www.nrcresearchpress.com by 210.87.254.42 on 09/05/12
For personal use only.

Can. J. Chem. Downloaded from www.nrcresearchpress.com by 210.87.254.42 on 09/05/12
For personal use only.

Petroleum ether refers to the fraction with b.p. 30–60°. Brine refers to a saturated solution of sodium chloride.

*Conversion of Mesylate **3** Directly to Trachylobane with Lithium Aluminum Hydride*

A solution of 50 mg of the enol **4** in 3 ml of pyridine was cooled to 0° then treated with 0.1 ml of methanesulfonyl chloride. The solution was left, under nitrogen, at −14° for 62 h then at 10° for a further 10 h. Ice was added to the reaction mixture and the resulting aqueous solution was worked up in the usual manner with cold 1 *N* hydrochloric acid and brine. Evaporation of the dried ether extracts gave 64 mg of mesylate **3** which was used in the next step without further purification.

The following reaction was carried out in a dry nitrogen atmosphere. A solution of 64 mg of the mesylate **3** in 3 ml of ether was added slowly over a period of 30 min to a stirred suspension of 38 mg of lithium aluminum hydride in 3 ml of ether. The mixture was then refluxed for 5 h. The cooled reaction mixture was treated with 0.3 ml of brine, stirred for 5 h, dried with anhydrous sodium sulfate and filtered. Evaporation of the filtrate and purification of the residue by t.l.c. on silica gel with pentane as solvent afforded 28 mg (60%) of (±)-trachylobane. This synthetic sample of trachylobane was identical with a sample of authentic trachylobane obtained from natural sources (i.r. and n.m.r. spectra, a single peak on v.p.c. when coinjected with the authentic sample).[3]

Anal. Calcd. for $C_{20}H_{32}$: C, 88.16; H, 11.84. Found: C, 88.31; H, 12.01.

*Homoallylic Cyclization of Mesylate **3** to Cyclopropyl Ketone **10** and Cyclopropyl Alcohol **16***

The enol **4** (75 mg) was converted to the mesylate **3** by the procedure described in the preceding experiment and the mesylate was treated as follows in a dry nitrogen atmosphere. A solution of 95 mg of **3** in 2.6 ml of dry dimethyl sulfoxide was treated with 0.51 ml of a 0.5 *M* dimethyl sulfoxide solution of methylsulfinyl carbanion (4). The solution was heated at 60° for 1.5 h then cooled and treated with 0.5 ml of water. The reaction solution was worked up with ether, brine, and water in the usual manner. The product, obtained by evaporation of the ether extracts, was separated into two fractions by t.l.c. on silica gel with chloroform as solvent.

Crystallization of the faster moving fraction from petroleum ether afforded 45 mg (60%) of the *cyclopropyl ketone **10***, m.p. 88°; identical (mixture m.p., u.v., i.r., and n.m.r. spectra) with the same cyclopropyl ketone previously obtained by a different method (*2a*).[3]

Anal. Calcd. for $C_{20}H_{30}O$: C, 83.86; H, 10.56. Found: C, 84.20; H, 10.61.

Crystallization of the slower moving fraction from ether – petroleum ether afforded 23 mg (30%) of the *cyclopropyl alcohol **16***, m.p. 118–119°; ν_{max} (Nujol) 3240 cm^{-1} (OH); n.m.r. ($CDCl_3$), *ca.* δ 0.60 (m, 2H, protons on cyclopropane ring), 0.79, 0.83, 0.97, and 1.19 (s, 3H each, tertiary methyls), 3.25 (s, 1H, *H*—C—OH), devoid of signals for vinylic protons and vinylic methyl.

Anal Calcd. for $C_{20}H_{32}O$: C, 83.27; H, 11.25. Found: C, 83.25; H, 11.02.

In a separate experiment, 100 mg of **4** was converted to the mesylate **3** and treated with methylsulfinyl carbanion (4) in dimethyl sulfoxide as above. A solution of the crude cyclization product (120 mg) in 12 ml of ether was cooled on an ice bath and treated dropwise with 8 *N* Jones' reagent (5) until a persistent orange color was observed. After the addition of 1 ml of methanol, the reaction mixture was worked up in the usual manner with ether, sodium carbonate solution and brine. Crystallization of the product from petroleum ether afforded 69 mg (70%) of the *cyclopropyl ketone **10***, m.p. 88°; identical (mixture m.p., u.v., i.r., and n.m.r. spectra) with the cyclopropyl ketone obtained in a preceding section of this experiment.[3]

*Oxidation of the Cyclopropyl Alcohol **16** to the Cyclopropyl Ketone **10***

Oxidation of 117 mg of the cyclopropyl alcohol **16** with Jones' reagent (5) by the procedure described in the preceding experiment afforded 81 mg (70%) of the cyclopropyl ketone **10**, m.p. 88°; identical (mixture m.p., u.v., i.r., and n.m.r. spectra) with the cyclopropyl ketone obtained in the preceding experiment.[3]

*Benzyl Ether **18***

A mixture of 546 mg of the enol **6** (*2a*), 546 mg of sodium hydride and 45 ml of benzene was refluxed under a dry nitrogen atmosphere for 5 h. Benzyl chloride (2.28 ml) was then added and reflux was continued for an additional 17 h. After cooling, the reaction mixture was treated dropwise with 5 ml of methanol then added to 100 ml of water. The benzene layer was separated and the aqueous layer was extracted with ether. The benzene layer and the ether extracts were combined and evaporated *in vacuo*. The residual oil was chromatographed on a column of 90 g of silica gel with 2% of ether in petroleum ether as solvent. The material eluted from the column was rechromatographed on a column of 30 g of silica gel impregnated with 20% of silver nitrate. Elution of the column with 1% of ether in petroleum ether and crystallization of the eluted product from pentane afforded 500 mg (69%) of **18**, m.p. 47°; ν_{max} (smear) 3030–3000, 2000–1600, and 800–680 (multiple bands, aromatic) and 1650 cm^{-1} (olefin); n.m.r. ($CDCl_3$), δ 0.79 (s, 3H, tertiary methyl), 0.84 (s, 6H, superimposed signals for two tertiary methyls), 3.55 (m, 1H, *H*—C—O), 4.47 (s, 2H, benzylic methylene), 5.61 (m, 1H, vinylic proton), 7.27 (m, 5H, aromatic protons).

Anal. Calcd. for $C_{27}H_{38}O$: C, 85.66; H, 10.12. Found: C, 85.82; H, 10.31.

*Benzyl Ether Alcohol **19***

A solution of 188 mg of the benzyl ether **18** in 1.6 ml of dry tetrahydrofuran was treated, while cooled on an ice bath, with 0.62 ml of a 1 *M* tetrahydrofuran solution of borane. The reaction solution was allowed to warm to room temperature and kept under dry nitrogen for 16 h. After the addition of 0.3 ml of water, the reaction solution was treated with 1 ml of 3 *M* sodium hydroxide followed by 1 ml of 30% hydrogen peroxide. The mixture was stirred at 40° for 45 min then worked up in the usual manner with ether and brine. Purification of the product by t.l.c. on silica gel with ether – petroleum ether as solvent followed by crystallization from pentane gave 105 mg (54%) of **19**, m.p. 106–107°; ν_{max} (Nujol) 3490 cm^{-1}; n.m.r. ($CDCl_3$), δ 0.81 (s, 3H, tertiary methyl),

[3]For the spectral properties of trachylobane and the cyclopropyl ketone **10** see ref. *2a*.

0.88 (s, 6H, superimposed signals for two tertiary methyls), 1.33 (d, J = 6.5 Hz, 3H, secondary methyl), 3.00 (d, J = 3.0 Hz, 1H, *H*—C—OH), 3.64 (m, 1H, *H*—C—O), 4.48 (m, 2H, benzylic protons), 7.32 (m, 5H, aromatic protons).

Anal. Calcd. for $C_{27}H_{40}O_2$: C, 81.76; H, 10.17. Found: C, 81.27; H, 10.45.

Keto Benzyl Ether ***20***

A solution of 134 mg of the benzyl ether alcohol **19** in 2.5 ml of pyridine was added to 240 mg of chromic anhydride suspended in 2.5 ml of pyridine. The mixture was stirred in the dark at room temperature for 4 h. The pyridine was evaporated *in vacuo*, the residue suspended in water and the product extracted into ether. The ether extracts were worked up in the usual manner with brine. Crystallization of the product from methylene chloride – ether afforded 116 mg (87%) of **20**, m.p. 154°; ν_{max} (Nujol) 1705 cm^{-1} (ketone); n.m.r. ($CDCl_3$) δ 0.83, 0.86 and 0.96 (s, 3H each, tertiary methyls), 1.31 (d, J = 6.5 Hz, 3H, secondary methyl), 3.78 (m, 1H, *H*—C—O), 4.50 (s, 2H, benzylic protons), 7.27 (m, 5H, aromatic protons).

Anal. Calcd. for $C_{27}H_{38}O_2$: C, 82.18; H, 9.71. Found: C, 82.49; H, 9.66.

Keto Alcohol ***15***

The keto benzyl alcohol **20** in 38 ml of ethanol was hydrogenated at *ca.* 2 atm. pressure over 75 mg of palladium–charcoal catalyst (10% Pd) for 15 h. Removal of the catalyst by filtration, evaporation of the solvent *in vacuo* and crystallization of the residue from ether – petroleum ether afforded 83 mg (80%) of **15**, m.p. 161–162°; ν_{max} (Nujol) 3450 (OH) and 1705 cm^{-1} (ketone); n.m.r. ($CDCl_3$), δ 0.84, 0.87, and 0.97 (s, 3H each, tertiary methyls), 1.30 (d, J = 6.5 Hz, 3H, secondary methyl), 4.10 (m, 1H, *H*—C—OH).

Anal. Calcd. for $C_{20}H_{32}O_2$: C, 78.89; H, 10.60. Found: C, 79.12; H, 10.88.

We are grateful to the National Research Council of Canada for a grant in support of this work.

1. R. B. KELLY, J. ZAMECNIK, and B. A. BECKETT. Can. J. Chem. **50**, 3455 (1972); R. B. KELLY, J. ZAMECNIK, and B. A. BECKETT. Chem. Commun. 479 (1971).
2. (*a*) R. B. KELLY, J. EBER, and H.-K. HUNG. Can. J. Chem. **51**, 2534 (1973); (*b*) R. B. KELLY, J. EBER, and H.-K. HUNG. J. Chem. Soc. Chem. Commun. 689 (1973).
3. R. A. APPLETON, J. C. FAIRLIE, and R. MCCRINDLE. Chem. Commun. 690 (1967).
4. E. J. COREY and M. CHAYKOVSKY. J. Am. Chem. Soc. **87**, 1345 (1965).
5. K. BOWDEN, I. M. HEILBRON, E. R. H. JONES, and B. C. L. WEEDON. J. Chem. Soc. 39 (1946).
6. W. HERZ, R. N. MIRRINGTON, H. YOUNG, and Y. Y. LIN. J. Org. Chem. **33**, 4210 (1968).
7. E. J. COREY and C. U. KIM. J. Am. Chem. Soc. **94**, 7586 (1972).
8. G. I. POOS, G. E. ARTH, R. E. BEYLER, and L. H. SARETT. J. Am. Chem. Soc. **75**, 422 (1953).

Can. J. Chem. Downloaded from www.nrcresearchpress.com by 210.87.254.42 on 09/05/12
For personal use only.

Carbon-13 Fourier Transform Nuclear Magnetic Resonance. IX.[1] Complete Assignments of some Prodigiosins. Bioincorporation of Label

ROBERT J. CUSHLEY,[2] RICHARD J. SYKES, C.-K. SHAW, AND HARRY H. WASSERMAN

Department of Chemistry, Yale University, and Section of Physical Sciences, Yale University School of Medicine, New Haven, Connecticut 06520

Received July 15, 1974

ROBERT J. CUSHLEY, RICHARD J. SYKES, C.-K. SHAW, and HARRY H. WASSERMAN. Can. J. Chem. **53**, 148 (1975).

A comprehensive study has been made of the carbon-13 chemical shifts of substituted pyrroles. The data, together with perdeuteration, single resonance, and off-resonance techniques, formed the basis for the complete interpretation of the carbon-13 spectra of the prodigiosins. Based on these assignments the biosynthetic origin of the prodigiosin carbons was elucidated, with further biosynthetic studies to be reported.

Carbon-13 chemical shifts are shown to be an effective means of determining sites of protonation.

ROBERT J. CUSHLEY, RICHARD J. SYKES, C.-K. SHAW et HARRY H. WASSERMAN. Can. J. Chem. **53**, 148 (1975).

On a fait une étude exhaustive des déplacements chimiques du carbone-13 de pyrroles substitués. Ces données, accompagnées de la perdeutération et des techniques de résonance simple et d'irradiation hors résonance (off-resonance, permettent une interprétation complète du spectre de carbone-13 des prodigiosines. Sur la base de ces attributions, on a élucidé l'origine biosynthétique des carbones de la prodigiosines; on a fait aussi appel à d'autres études biosynthétiques qui seront rapportées.

Les déplacements chimiques en carbone-13 sont des moyens efficaces de déterminer les sites de protonation. [Traduit par le journal]

Introduction

The prodigiosins are red bacterial pigments, unique in nature as the only known polypyrroles that are biosynthetically unrelated to the porphyrins. Six prodigiosins are known, all having in common a methoxybipyrrolepyrrolemethane skeleton. A listing of the recent literature on these pigments was given in the communication of this work (2), which described the biological incorporation of [1-^{13}C]- and [2-^{13}C]-acetate into prodigiosin (**17**).[3]

A number of studies have been published recently on the ^{13}C n.m.r. of porphyrins and corrinoid compounds especially of vitamin B_{12} (3), including studies of samples biosynthetically enriched with ^{13}C (4). Because of the importance attached to the pyrrole moiety, and in order to assign the ^{13}C spectra of several prodigiosins, we have made a systematic study of the ^{13}C chemical shifts of a number of pyrrole derivatives by Fourier transform n.m.r. Unambiguous assignments for the prodigiosins was critical since it formed the basis for biosynthetic studies.

Experimental

Carbon-13 spectra were determined using a computer controlled Fourier transform n.m.r. system consisting of an on-line IBM 1800 computer with 24K of 4 μs core and a 21.5 kGauss Bruker HFX-3 spectrometer (5). The computer is remotely controlled through an 1816 typewriter, interrupts, and digital input at the n.m.r. console. The 1800 is capable of sampling up to 8192 FID double precision or 16 384 single precision data points at rates up to 20 KHz (11 bit ADC for both one- and two-word integers). The r.f. excitation pulse is created at a set of H-P 10514 mixers by logic levels from the IBM 1800 Electronic Contact Operate (ECO). Pulses are amplified using a commercially available power amplifier. After amplification and phase detection, the FID signal is conditioned for the ±5 V input level of the 1800 ADC Multiplexer with an HP-8875A Differential Amplifier followed by a four-pole Tchebyscheff active filter with selectable cutoff frequencies (automatically set by the controlling program) for use at

[1]For Part VIII see ref. 1.

[2]Author to whom inquiries should be addressed. Present address: Department of Chemistry, Simon Fraser University, Burnaby, British Columbia, V5A 1S6, Canada.

[3]C2-Methyl-C3-*n*-amylprodigiosin (**17**) is commonly referred to as prodigiosin.

Can. J. Chem. Downloaded from www.nrcresearchpress.com by 210.87.254.105 on 09/05/12
For personal use only.

Can. J. Chem. Downloaded from www.nrcresearchpress.com by 210.87.254.105 on 09/05/12
For personal use only.

several sampling rates. A 4096 channel hard-wired computer which has been modified to accept digital data serves as an on-line buffered CRT-plotter for data presentation.

Unless otherwise indicated in the text, ^{13}C spectra were run using the following conditions: digitizing rate = 10 KHz; pulse width = 50 μs; receiver skip = 100 μs; ISKIP (5) = 0 s.

When a 4K data set was obtained, chemical shifts are quoted to the nearest tenth ±0.1 p.p.m.; 8K data set quoted to the nearest hundredth ±0.05 p.p.m.

Materials

Compounds **1–8**, **10**, and **11** are commercially available from the Aldrich Chemical Company. Compound **9** was obtained by pyrolysis of **17** (6). Sources for the remaining compounds were: **12–14** (7); **15** (8); **16** (9); **17** (10); **19** (11), and **21** (12).

Perdeuterioprodigiosin (Typical Run)

Prodigiosin hydrochloride (**18** 2.5 g, 7.5 mmol) was dissolved in 100 ml deuteriochloroform in a 300 ml round bottomed flask; 6 *N* DCl in D_2O (25 ml) was added and the flask was shaken vigorously for 48 h. The chloroform layer was filtered and finely powdered sodium carbonate (anhydrous) was added to neutralize the bulk of the excess acid; after a further filtration the chloroform solution was washed with 1 *N* KOH–D_2O until the pigment had been converted to the free base. The chloroform layer was separated and the chloroform removed *in vacuo*. The residue was dissolved in methylene chloride and this solution was washed with 0.1 *N* DCl–D_2O. The methylene chloride was removed on the rotovac and the residue thoroughly dried in high vacuum. A single recrystallization gave clean crystals of perdeuterio **18** (1.8 g, 70% yield). The proton n.m.r. spectrum showed only two aromatic absorptions, both sharp singlets, the high field one of which became a doublet on washing the n.m.r. solution with H_2O: δH 6.19 p.p.m. (A4) and δH 6.71 p.p.m. (1′′).

Biosynthetic Experiments

The bioincorporation experiment consisted of feeding sodium [1-^{13}C]- and [2-^{13}C]-acetate (Prochem Ltd., 62% ^{13}C) in two separate experiments at 10 mmol/l in a Bactopeptone and glycerol medium in agar gel. The ^{13}C Fourier transform spectra of isolated prodigiosin (**17**) showed levels of labeled carbons of ~8 and ~11%, respectively (2).

Results and Discussion

Pyrroles

The ^{13}C spectra of pyrrole (**1**) and two alkyl pyrroles (**3**, **5**) have been published by Grant and co-workers (13) and Roberts and co-workers (14). Lippmaa *et al.* (15) have reported ^{13}C spectra of a number of nitropyrroles. Our list of pyrroles includes some with electron withdrawing and electron donating substituents, and two bipyrroles.

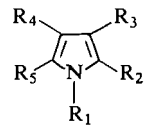

1 R_1–R_5 = H
2 R_1 = CH_3; R_2–R_5 = H
3 R_2 = CH_3; R_1, R_3–R_5 = H
4 R_1, R_2 = CH_3; R_3–R_5 = H
5 R_2, R_5 = CH_3; R_1, R_3, R_4 = H
6 R_1, R_2, R_5 = CH_3; R_3, R_4 = H
7 R_2, R_4 = CH_3; R_1, R_3, R_5 = H
8 R_2, R_4 = CH_3; R_3 = Et; R_1, R_5 = H
9 R_2 = CH_3; R_3 = *n*–Amyl; R_1, R_4, R_5 = H
10 R_2 = CHO; R_1, R_3–R_5 = H
11 R_1 = CH_3; R_2 = CHO; R_3–R_5 = H
12 R_2 = COOMe; R_1, R_3–R_5 = H
13 R_2 = COOEt; R_5 = CH_3; R_1, R_3, R_4 = H
14 R_2 = COOEt; R_3 = OMe; R_5 = CH_3; R_1, R_4 = H

The ^{13}C chemical shift assignments of these pyrroles and bipyrroles are given in Table 1. Spectra were run with 20% solutions of the pyrroles in a $CHCl_3$–C_6F_6–HMDS[4] mixture (3:1:1) with proton noise decoupling. In addition, the normal ^{13}C spectrum of **8** (single resonance spectrum) and off-resonance spectra of **7** and **12** were determined to aid in the assignment and INDOR ^{13}C spectra were measured from the C–H satellites in the proton n.m.r. spectra of **10** and **15**.

The aromatic absorptions of the eight alkyl pyrroles (**2–9**) all fell in the region δ_C 105–135 p.p.m. Assignments were made, in part, by assuming that a free α-carbon should absorb downfield of a free β-carbon, and that a substituted α-carbon would be more deshielded than a substituted β-carbon. Table 2 shows the effect at each aromatic carbon of alkyl substitution at the *N*-, 2-, and 3- positions: the change in chemical shift at each of the four aromatic carbons is approximately additive, as has been noted by Grant and co-workers (13) for 2-methyl and 2,5-dimethyl five-membered heterocycles.

The strong deshielding (~10 p.p.m.) of the directly methylated carbon (Table 2) is frequently observed in ^{13}C n.m.r. (16). *N*-Methylation reduces the magnitude of this effect to about 7 p.p.m. in pyrrole. Upon α-alkylation, the *ortho* β-carbon is shielded by about 2 p.p.m.: similarly on β-alkylation, the *ortho* α-position

[4]Hexamethyldisilane (HMDS) (b.p. 113°) was chosen as the internal reference as TMS (b.p. 27°) evaporated too easily from the sample under noise decoupling conditions; $\delta_{THS} = \delta_{HMDS} - 2.34$ p.p.m.

TABLE 1. ^{13}C chemical shifts of pyrroles[a]

Compound No.		Chemical Shifts (p.p.m.)[b] Aromatic carbons 2	3	4	5	Alkyl carbons	—C=O |
1		120.88	110.73	110.73	120.88		
2		124.34	111.16	111.16	124.34	NMe 38.13	
3		130.42	108.52	110.90	119.20	Py—Me 15.10	
4		131.18	109.28	109.28	123.31	Py—Me 14.02, NMe 35.60	
5		129.20	108.67	108.67	129.20	Py—Me 15.34	
6		130.28	107.70	107.70	130.28	Py—Me 14.80, NMe 36.17	
7		130.42	110.41	121.74	116.78	Py—Me 14.20, 15.26	
8		126.00	120.39	123.30	115.97	Py—Me 12.72, 13.37, Py—$\underline{C}H_2$—CH_3 20.38, Py—CH_2—$\underline{C}H_3$ 18.22	
9		126.6	122.66	111.65	117.58	Py—Me 13.42, 1′ 28.80, 2′ 33.87 3′ 34.73, 4′ 25.45, 5′ 16.61	
10		136.03	124.97	114.02	130.37		182.48
11		135.28	126.43	112.19	134.74	NMe 38.72	181.99
12		125.25	118.24	112.84	126.33	—OMe 53.94	164.95
13		124.00	118.77	111.44	136.60	—OCH_2CH_3 62.78, 17.04, Py—Me 15.42	164.50
14		108.40	156.70	97.95	135.06	—OMe, —$O\underline{C}H_2CH_3$ 60.73, 62.35, —$OCH_2\underline{C}H_3$, Py—Me 16.07, 17.25	164.36
15		129.43	105.99	111.49	120.22		
16	Ring A	126.8	111.6	112.6	123.5		
	Ring B	120.9	161.8	94.5	136.4	—OMe 61.1	175.2

[a]Run as 20% solutions in chloroform–HMDS–C_6F_6 (3:1:1) mixture except **13**, **14**, which were run as 5% solutions, and **15**, **16**, which were run as saturated solutions in DMSO with external C_6F_6.
[b]Chemical shifts downfield from HMDS.[4] Samples run in DMSO; chemical shifts were converted to HMDS scale using $\delta_{HMDS} - \delta_{DMSO} = 43.85$ p.p.m.

is shielded by 2.5–4.5 p.p.m. (while the *ortho* β-carbon is deshielded). This shielding of the *ortho* position has been noted by Roberts and co-workers (14) and by Grant and co-workers (13) for the α-methylation of furan and thiophene, and in the case of the methyl indoles (17). However, while 2-alkylation of pyridines results in a small (1 p.p.m.) shielding of the *ortho* 3-carbon, 3- and 4-alkylation shows a small deshielding of the carbons *ortho* to the site of alkylation (18). This is also the case for substituted benzenes as Lauterbur has reported a 0.2–1.0 p.p.m. deshielding *ortho* to the site of methylation (19).

In both pyridines and benzenes, alkylation generally results in the shielding (2.5–3.0 p.p.m.) of the aromatic carbon *para* to the site of alkylation: in pyrroles there is a 1.0–2.0 p.p.m. shielding of the 5-carbon on alkylation of the 2-carbon.

Methyl groups bonded directly to the pyrrole nucleus absorb in the range δ_C 13–16 p.p.m. This shows a substantial shielding of the methyl groups when compared to methyl groups bonded to benzenes (δ_C 23–25 p.p.m.) (19) and pyridines (δ_C 21–28 p.p.m.) (18, 20) and is in the same region as methyls bonded to the hetero-ring of indole (17).

On the basis of the data available for compounds **8** and **9**, the β and γ effects of pyrrole substitution on an alkane chain fit the pattern observed for most other polar functionalities (16): a deshielding of the β-carbon by 8–10 p.p.m. and a smaller shielding of the γ-carbon by 2–4 p.p.m.

Pyrroles **10–14** all carry carbonyl substituents. The ^{13}C chemical shifts of the three unsubstituted aromatic carbons of pyrrole 2-carboxaldehyde (**10**) were measured by INDOR spectroscopy in order to provide an unam-

Can. J. Chem. Downloaded from www.nrcresearchpress.com by 210.87.254.105 on 09/05/12
For personal use only.

TABLE 2. Effects of alkylation on pyrrole ^{13}C chemical shifts

	Compound[a]	$\Delta\delta_C$ p.p.m. at aromatic carbon[b] 2	3	4	5
2-Substitution					
NH-pyrrole	*2*-Me-pyrrole	−9.5	+2.2	−0.2	+1.7
	2,*5*-DiMe-pyrrole	−10.0	+2.2	−0.2	+1.2
NMe-pyrrole	1,*2*-DiMe-pyrrole	−6.8	+1.9	+1.9	+1.0
	1,*2*,5-TriMe-pyrrole	−7.0	+1.6	+1.7	+0.9
3-Substitution					
	3,5-DiMe-pyrrole[c]	+2.4	−10.0	−1.9	0.0
NH-pyrrole	2,4-DiMe-*3*-Et-pyrrole	+4.4	−10.0	−1.6	+0.8
	2-Me-*3*-Amyl-pyrrole	+4.8	−14.1	−0.8	+1.6
1-Substitution					
	1-Me-pyrrole	−3.5	−0.4	−0.4	−3.5
	1,2,5-TriMe-pyrrole	−1.1	+1.0	+1.0	−1.1
	1,2-DiMe-pyrrole	−0.8	−0.8	+1.6	−4.1

[a]The position of alkylation is indicated in italics. Thus 2.4-diMe-*3*-Et-pyrrole indicates that the data given on that line refers to the effect of placing an ethyl group on the 3-position of 2,4-dimethylpyrrole.
[b]Positive shifts are upfield (shielded) and negative shifts are downfield (deshielded).
[c]For example, 2,4-dimethylpyrrole.

biguous assignment of the Fourier transform spectrum of this key compound.

Compared to free pyrrole, the aldehyde exhibits strong deshielding of carbons 3 and 5 of −14.2 and −9.5 p.p.m., respectively, while carbon 4 is deshielded by only −3.3 p.p.m. A similar phenomenon has been noted in the proton n.m.r. spectra of pyrroles α-substituted with strong electron withdrawing groups (21). It reflects the reduction of π-electron density at positions 3 and 5:

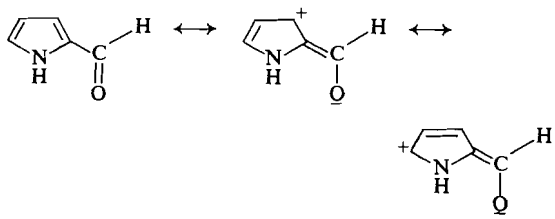

When pyrrole is substituted with a 2-carboxaldehyde group, the deshielding of each of the aromatic ring carbons is substantially greater than the aromatic ring deshielding observed on formation of benzaldehyde (22) or the pyridine carboxaldehydes (20*a*, *b*).

By comparison, 2-carbmethoxypyrrole (**12**) shows a very much smaller deshielding of the 3 and 5 carbons, and an especially small deshielding (only 5 p.p.m. compared to free pyrrole) of the substituted 2-carbon.

The ^{13}C spectrum of 5-methyl-2-carbethoxypyrrole (**13**) includes two substituted carbons at δ_C 124.0 and 136.6 p.p.m. Comparison with the observed α-carbon absorptions in 2-carbmethoxypyrrole (**12**) (δ_C 125.3 and 126.3 p.p.m.) lead to the assignment of the lowest field peak (δ_C 136.6 p.p.m.) to the 5-carbon. The changes in chemical shift between **12** and **13** then fit the established pattern for the effects of 2-alkylation: the substituted carbon is deshielded by 10.7 p.p.m. and the *ortho* β-carbon is shielded by 1.7 p.p.m. (Table 2). Thus, the most deshielded substituted carbon is not the carbon carrying the carbethoxy group but the carbon carrying the methyl group.

Introduction of the 3-methoxyl group into **13** to give **14** radically alters the ^{13}C spectrum. The new low field substituted aromatic carbon (δ_C 156.7 p.p.m.) is assigned to carbon 3 by analogy with the strongly deshielded aromatic carbon of anisole (δ_C 163.4 p.p.m.) (22, 23). The downfield shift reflecting the inductive effect of the oxygen. The one unsubstituted aromatic carbon in **14** (carbon 4) absorbs at δ_C 97.95 p.p.m. suggesting strong mesomeric electron donation from the oxygen lone pair. An *ortho* shielding of similar magnitude (about 14 p.p.m.) is seen when anisole is compared to benzene (22, 23). On this basis, the other *ortho* position, the 2-carbon, was assigned to the high field substituted carbon absorption at δ_C 108.4 p.p.m.: this represents a shielding of about 16 p.p.m. over the analogous position in **13**. The remaining substituted carbon, at position 5, is only very slightly shielded by the methoxyl substituent (1.5 p.p.m.).

Can. J. Chem. Downloaded from www.nrcresearchpress.com by 210.87.254.105 on 09/05/12
For personal use only.

Can. J. Chem. Downloaded from www.nrcresearchpress.com by 210.87.254.105 on 09/05/12
For personal use only.

The carbonyl groups of pyrrole-2-carboxaldehyde (**10**) and its 2-methyl derivative, **11**, show the same shielding effect noted for alkyl substituents (*vida supra*) being 10 p.p.m. to higher field than carbonyls of benzaldehyde (22) or pyridine-2-carboxaldehyde (20*b*). The carbonyl resonance signals of the two carbalkoxy pyrroles **12** and **13** are found 2–5 p.p.m. to higher field than the corresponding benzoate carbonyl (24). Aromatic substitution with a strong electron releasing group (OMe in **14**) has no effect on the carbonyl absorption, in keeping with the results of Stothers and Lauterbur who found a similar effect in *para*-substituted benzaldehydes, acetophenones, and benzoates (25).

Bipyrroles

The ^{13}C n.m.r. spectrum of bipyrrole (**15**) in DMSO showed four absorptions, the lowest field signal (δ_C 129.4 p.p.m.) being due to the substituted carbon. The free α-carbon absorbed at δ_C 120.2 p.p.m. One of the two β-carbons absorbed at relatively high field (δ_C 106.0 p.p.m.) and was assigned as carbon 3, since, from the above discussion, this carbon should be the most sensitive to any mesomeric electron donation by the neighboring α-substituent, a pyrrole ring. The other β-carbon (carbon 4) absorbed at δ_C 111.5 p.p.m.

The ^{13}C n.m.r. spectrum of the 3-methoxybipyrrolecarboxaldehyde **16** was also determined in DMSO. INDOR spectra were measured for carbons A3, A4, A5, and B4: in each case they coincided in the FT spectrum with those absorptions that showed Overhauser enhancements. The B4 position showed the same shift to high field observed in the model methoxy pyrrole **14**. By analogy with the 3-carbon in **14**, the low field absorption at δ_C 161.8 p.p.m. in **16** was assigned to B3.

Comparison of the chemical shifts measured for **10** and **12** indicates that conversion of a 2-carbalkoxy function to a 2-carboxaldehyde function results in a deshielding of the 2-carbon by some 10 p.p.m. and of the 3-carbon by some 7 p.p.m. The chemical shifts observed in bipyrrole (**15**) suggest that the pyrrole ring is similar to the methyl group in its substituent effect on the pyrrole ring, except that the β-carbon *ortho* to the site of substitution is somewhat more strongly shielded. Assuming that an approximate additivity of chemical shifts exists between the pairs of pyrroles **10,12** and **14,16**, then the B2 carbon of **16** is predicted to absorb around δ_C 118 p.p.m., and the B5 carbon of **16** at around δ_C 135 p.p.m. On this basis, the substituted absorption at δ_C 120.9 p.p.m. was assigned to B2 and the substituted absorption at δ_C 126.8 p.p.m. was assigned to A2: this carbon is thus some 2.6 p.p.m. more shielded in **16** than in bipyrrole (**15**).

Long-range ^{13}C–^{1}H Coupling

Both long-range cross-ring and ring to side-chain couplings proved to be of importance in the assignment of the ^{13}C spectra of the prodigiosins. Generally, the limiting resolution (1.2 Hz) of the single resonance spectra determined using an 8K data set proved insufficient to resolve the complex multiplets in the single resonance spectra of the prodigiosins and pyrroles, and hence, half-band widths were measured. While cross-ring coupling has been reported for pyrrole (**1**) and 2,5-dimethylpyrrole (**4**) by Weigert and Roberts (14), no data were reported for side-chain to ring ^{13}C–^{1}H coupling. Therefore, we studied 1,5-dideuterio-2,4-dimethyl-3-ethylpyrrole (**8**-d_2), prepared by acid catalyzed exchange of **8** with D_2O–DCl. Single resonance and proton noise decoupled spectra were determined and the half-band widths are given in Table 3.

The substantial increase in the half-band widths ($\Delta_{1/2}$) of each aromatic carbon upon removal of proton decoupling is firm proof of side-chain to ring coupling in **8**-d_2. The ^{13}C peaks of carbons 2 and 3 of **8**-d_2 were well-defined sextets with splittings of 5.4 Hz. Carbon 4, on the other hand showed extra splittings which we interpret as three, or more, bond coupling of carbon 4 with the protons of the side chains. In addition, carbon 5, which is deuterated and shows an isotope shift of 0.34 ± 0.05 p.p.m., showed substantial broadening in the single resonance spectrum, while $\Delta_{1/2}$ in the proton noise decoupled spectrum was identical with that of the tertiary carbons. This indicates no detectable long-range deuterium coupling, and a coupling of carbon 5 with the alkyl substituent protons three or more bonds away.

Prodigiosins

Prodigiosin hydrochloride (**18**)

Our original report on the biosynthetic incorporation of ^{13}C-enriched acetate into prodigiosin outlined the assignment of the

TABLE 3. Long range ^{13}C–^{1}H coupling in 1,5-dideuterio-2,4-dimethyl-3-ethylpyrrole

Aromatic carbon	^{13}C shift[a] (p.p.m.)	$\Delta_{1/2}$[b] (^{1}H noise decoupled)	$\Delta_{1/2}$[b] (single resonance)
2	125.89	4.0	17.2[c]
3	120.28	4.0	18.2[c]
4	123.52	4.0	19.5
5	115.63	3.0	17.7[d]
$CHCl_3$	80.0	5.0	2.3

[a]From internal HMDS.[4]
[b]$\Delta_{1/2}$ = peak width at half-height in Hz: values are accurate to ± 1.2 Hz (8K data set).
[c]Sextet, splitting 5.4 Hz.
[d]$\Delta_{1/2}$ of each peak of triplet ($J_{^{13}C-^{1}H} = 28$ Hz).

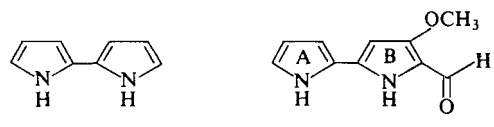

15 16

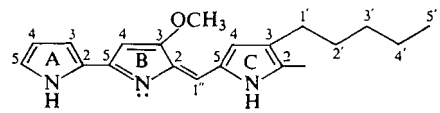

17
18:17–HYDROCHLORIDE

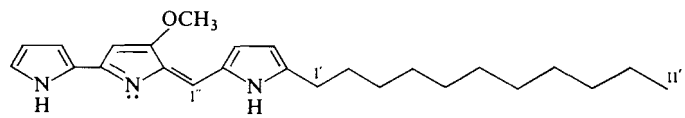

19
20:19–HYDROCHLORIDE

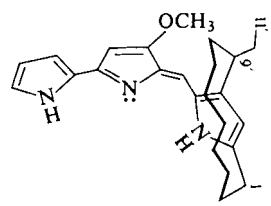

21
22:21–HYDROCHLORIDE

^{13}C n.m.r. spectrum of prodigiosin hydrochloride (**18**) (2). The ^{13}C assignments of **18** are shown in Table 4 referenced to external HMDS.[4] The proton noise-decoupled spectrum of **18** showed seven resonance signals upfield of $CHCl_3$ (δ_C 80.0 p.p.m.). The methoxyl carbon was assigned to the peak at δ_C 61.3 p.p.m. on the basis of chemical shift data. The C2 and 5′ methyls were assigned to the absorptions at δ_C 14.8 and 16.5 p.p.m., respectively, on the basis of INDOR measurements. An off-resonance experiment with the cw decoupling frequency placed at the center of the methylene region delineated carbons 2′, 3′ and 4′, whose ^{13}C absorptions were sharp singlets, from 1′, whose absorption at δ_C 27.8 p.p.m. was a broad triplet, ($\Delta_{1/2}$ 8 Hz). Of the three carbons 2′, 3′, and 4′, carbon 4′ was assigned to the resonance signal at δ_C 25.0 p.p.m. by analogy with the known range of ^{13}C shifts for β-

Can. J. Chem. Downloaded from www.nrcresearchpress.com by 210.87.254.105 on 09/05/12
For personal use only.

TABLE 4. ^{13}C chemical shifts of several prodigiosins[a]

Carbon	Prodigiosin hydrochloride (18)	Prodigiosin (17)	Undecyl-prodigiosin hydrochloride (20)	Undecyl-prodigiosin (19)	Metacyclo-prodigiosin hydrochloride (22)	Metacyclo-prodigiosin (21)
Aromatic						
A2	124.7	131.4	124.8	131.2	125.1	131.6
A3	119.8	115.3	120.7	115.7	119.7	115.0
A4	114.3	112.6	115.0	112.8	114.4	112.6
A5	129.0	125.4	129.8	125.6	129.4	125.0
B2	123.3[b]	140.7	124.1	141.4	123.5	140.4
B3	168.3	171.9	168.9	171.9	168.6	171.7
B4	95.5	98.2	95.7	98.0	95.6	98.1
B5	150.2	162.4	151.4	163.2	150.4	162.1
C2	148.8[b]	139.6	155.3	147.4	156.8	147.2
C3	130.8[c]	126.9	114.6	111.4	115.3	111.9
C4	130.8	123.8	131.7	124.0	152.9	144.0
C5	127.6[c]	130.1	128.7	131.2	128.7	130.2
1''	11.2	118.7	118.8	118.8	116.0	116.1
Alkyl						
—O*CH*$_3$	61.3	61.0	61.5	61.0	61.4	61.0
	(1') 27.8	(1') 28.3	(1') 31.1	(1') 30.1	(1'–7', 10')	(1'–7', 10')
	(2') 32.2	(2') 32.9	(2'–8') 32.3–32.1	(2'–8') 32.4–32.1	32.5 31.6	32.8 30.7
	(3') 34.0	(3') 34.5	(9') 34.8	(9') 34.7	29.9 29.6	30.3 29.4
	(4') 25.0	(4') 25.2	(10') 25.4	(10') 25.4	29.4 28.4	27.9 27.5
	(5') 16.5	(5') 16.7	(11') 16.8	(11') 16.8	27.4 25.6	25.4
	(C2-*Me*) 14.8	(C2-*Me*) 12.7			(11') 15.2	(11') 15.3

[a]Chemical shifts are given relative to HMDS[4] and are calculated from the solvent peak $CHCl_3$ (δ_C 80.0 p.p.m.). Since chloroform does show solvent effects of several tenths of a part per million, all data has been rounded off to the nearest 0.1 p.p.m.
[b]These carbons are reversed from original assignment (2).
[c]These carbons are reversed from original assignment (2).

carbons of straight chain alkanes (δ_C 25.0–26.0 p.p.m.) (1, 26). Carbons 2' and 3' were resolved by studying the ^{13}C n.m.r. spectrum of a sample of **18** biosynthetically enriched with ^{13}C from [1-^{13}C]-acetate (2). Of the alkyl carbons, 4' and *either* 2' or 3' were enriched with ~10% ^{13}C. Hence, the absence of any detectable ^{13}C–^{13}C coupling in the spectrum assigned the absorption at δ_C 32.2 p.p.m. to 2', and the absorption at δ_C 34.0 p.p.m. to 3'.

The 13 aromatic carbons of **18** have only 12 absorptions downfield of chloroform because of the overlap of two absorptions at δ_C 130.8 p.p.m. INDOR measurements assigned the following secondary carbons: A3 at δ_C 119.8; A4 at δ_C 114.3; A5 at δ_C 129.0; B4 at δ_C 95.5; C4 at δ_C 130.8; and 1'' at δ_C 118.2 p.p.m. In the off-resonance experiment, the absorption at δ_C 130.8 p.p.m. became a triplet, indicating the overlap of the absorption of a substituted aromatic carbon with the absorption of the unsubstituted aromatic carbon, C4.

Carbon B3, substituted with —OMe, was assigned the lowest field resonance (δ_C 168.3 p.p.m.) by analogy with the methoxypyrroles **14** and **16**.

A sample of **18** biosynthetically enriched with [1-^{13}C]-acetate gave a spectrum indicating that three aromatic substituted carbons, including B3 were enriched (2). Compound **18** was degraded to **9** (6) which showed enrichment at carbons 3 and 5. Thus, the C3,C5 pair was assigned to the peaks at δ_C 130.8 and 127.6 p.p.m.

Perdeuteration of **18** gave a compound in which only A4 and 1'' of the aromatic carbons remained protonated. A single resonance spectrum of perdeuterio-**18** assigned C3 at δ_C 130.8 p.p.m. (peak broadened due to long range coupling with the alkyl side chain; $\Delta_{1/2}$ = 18.5 Hz), and C5 to δ_C 127.6 p.p.m. (sharp singlet; $\Delta_{1/2}$ = 5 Hz). Carbon A2 was assigned to the narrow doublet at δ_C 124.7 p.p.m. (J = 8 Hz; cross-ring coupling with A4-*H*), while C2 could be assigned to the broad peak at δ_C 148.8 p.p.m. ($\Delta_{1/2}$ = 11.5 Hz, coupling with C2-*Me*). Carbons B2 and B5 both ap-

Can. J. Chem. Downloaded from www.nrcresearchpress.com by 210.87.254.105 on 09/05/12
For personal use only.

peared as sharp singlets ($\Delta_{1/2}$ = 4 Hz), while B3 was broadened ($\Delta_{1/2}$ = 11.5 Hz) by long-range coupling with the methoxyl protons.

Proof of these assignments was obtained in a study of **18** biosynthetically enriched with ^{13}C at 1″ and B2 (23% ^{13}C) (27). An AB pattern (J = 75 Hz) was found for 1″ and B2. As well, the natural abundance signal for B4 showed a coupling of 68 Hz with B5 when the B5 carbon was enriched (28% ^{13}C) (27).

^{13}C Fourier transform n.m.r. studies of samples of **18** biosynthetically enriched with ^{13}C from [1-^{13}C]- and [2-^{13}C]-acetate allowed the first details of the biosynthesis of this pigment to be elucidated (2). Spectra of both samples showed primary incorporation of acetate at five sites in the molecule. Feeding [1-^{13}C]-acetate led to the enrichment of aromatic carbons B3, C3, and C5, and alkyl carbons 2′ and 4′, while feeding [2-^{13}C]-acetate led to the enrichment of two aromatic carbons, B4 and C4, and three carbons in the amyl side chain, 1′, 3′, and 5′ (Fig. 1). Thus, we showed the C ring is constituted from an eight carbon polyacetate chain, while ring B includes one further acetate unit, at B3–B4. No primary incorporation of acetate was found in ring A. Our further studies, using ^{13}C enriched substrates, have elucidated the origin of ring A as proline. As well, the remaining carbons of **18** were shown to be constituted from serine, glycine, and methionine (27). Results of the study on the biosynthetic origin of undecyl **19** and metacyclo **21** have also been completed and form the substance of a separate communication (28).

Prodigiosin (**17**)

The ^{13}C spectrum of the free base of prodigiosin (**17**) was assigned by a very similar approach. The seven alkyl carbons were assigned by analogy with the alkyl carbons of **18**. While C2-*Me* is 2 p.p.m. more shielded in **17** than **18** the remaining alkyl absorptions in **17** are all within 0.5 p.p.m. of the equivalent absorptions of **18**.

INDOR measurements on **17** specifically assigned 1″ (δ_C 118.7 p.p.m.), C4 (δ_C 123.8 p.p.m.), and B4 (δ_C 98.2 p.p.m.), as well as the pair of carbons A3 and A5, whose ^{13}C–^{1}H satellites overlapped. A3 was assigned to the higher field absorption (δ_C 115.3 p.p.m.) and A5 to the lower field absorption (δ_C 125.4 p.p.m.) as the pyrrole α carbon is always found to low field of the pyrrole β carbon (Table 1). The residual couplings in an off-resonance spectrum supported this assignment (A5, J_r = 44 Hz, J = 187.5 Hz; A3, J_r = 41.5 Hz, J = 167.5 Hz). The remaining secondary aromatic carbon, A4, was then assigned to δ_C 112.6 p.p.m.

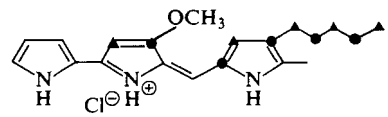

FIG. 1. Pattern of biosynthetic incorporation of ^{13}C label into prodigiosin.

The seven substituted carbons were assigned by exactly the same procedure of perdeuteration and single resonance spectroscopy used to make their assignments in the hydrochloride salt, **18**. The long range couplings measured in **17** were, within experimental error, identical to those measured for **18**.

Undecylprodigiosin Free Base (**19**)

The ^{13}C n.m.r. spectrum of **19**, is shown in Fig. 2. The assigned chemical shifts are listed in Table 4.

Of the alkyl absorptions, 11′ (δ_C 16.8 p.p.m.), 10′ (δ_C 25.4 p.p.m.) and 9′ (δ_C 34.7 p.p.m.) were assigned by analogy with the chemical shifts of the equivalent carbons in *n*-undecane (carbons 11 δ_C 16.1 p.p.m., 10 δ_C 25.0 p.p.m., 9 δ_C 34.3 p.p.m. (26)). 1′ was assigned to the absorption at δ_C 30.1 p.p.m. by comparison with the similarly shielded methylenes of **17** (1′ in **17**, δ_C 28.3 p.p.m.) and the model 2-*n*-undecylpyrrole (δ_C 30.3 p.p.m.). The remaining alkyl methylenes (2′–8′) all absorb in the intense peaks at δ_C 32.4 and δ_C 32.1 p.p.m. The methoxyl carbon is found at δ_C 61.0 p.p.m. (compared with δ_C 61.0 and 61.3 p.p.m. in **17** and **18**, respectively).

Quantitative measurements of the peak intensities in a spectrum of **19**, accomplished using a delay between pulses (ISKIP = 2 s (5), showed that the absorption at δ_C 131.2 p.p.m. was due to two carbons. An off-resonance spectrum showed that the seven protonated aromatic carbons all absorbed upfield of the six substituted aromatic carbons (insert in Fig. 2).

By analogy with previous assignments (pro-

Can. J. Chem. Downloaded from www.nrcresearchpress.com by 210.87.254.105 on 09/05/12
For personal use only.

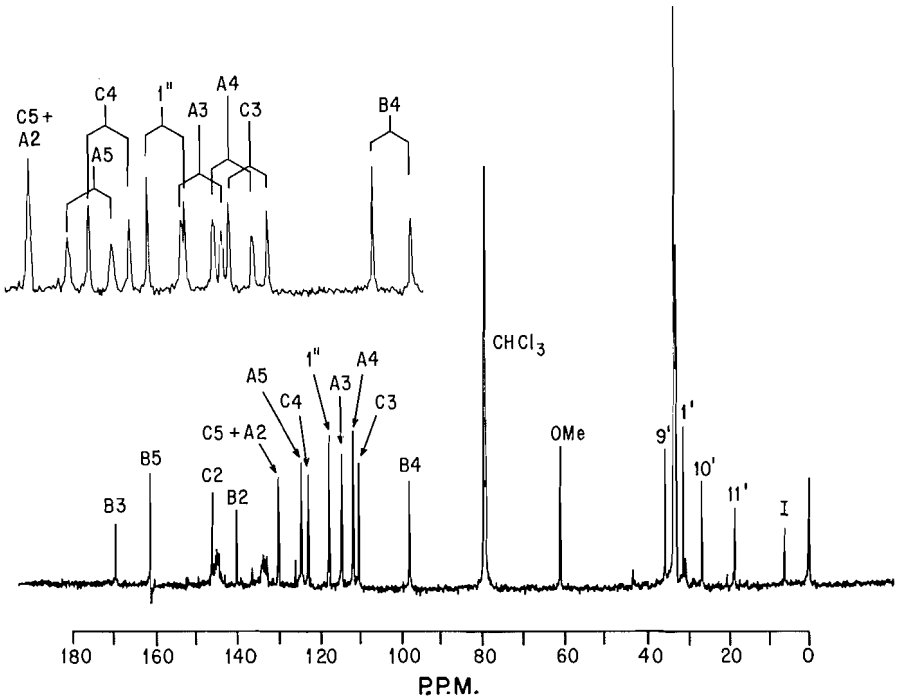

FIG. 2. Proton noise decoupled ^{13}C Fourier transform spectrum of 1 *M* undecylprodigiosin base (**19**) in $CHCl_3$ using an external C_6F_6 lock. Insert: off-resonance spectrum of portion 95.8–133.4 p.p.m. downfield from HMDS.

digiosin **17**, prodigiosin hydrochloride **18**, and two model pyrroles **14** and **15**), B3 (inductively deshielded by the methoxyl substituent) was assigned to the lowest field absorption (δ_C 171.9 p.p.m.), and B4 (mesomerically shielded by the methoxyl group) to the highest field absorption (δ_C 98.4 p.p.m.); B3 and B4 in **19** both absorb within 0.2 p.p.m. of B3 and B4 in **17**. As expected, the change in alkyl substitution in ring C does not affect the chemical shifts in ring B significantly.

Comparison of ring C in **19** with ring C in **17** shows that the gross structural differences are the removal of the *n*-amyl from C3, and extension of the methyl group at C2 into a polymethylene chain. Thus, C3 changes by removal of α (−10 p.p.m., Table 2), β (−9 p.p.m. (26)), and γ (+3 p.p.m. (1, 26))[5] substituent shifts. C2 undergoes a β and γ substituent shift due to extension of C2—CH_3 to C2—$(CH_2)_{10}CH_3$, plus removal of a C3-substituent shift, Table 2. From Table 2, the remote substituent effects are small and this is common to other alkylated aromatics such as benzenes, (19, 24), pyridines (18, 20), and indoles (17). The C-ring chemical shifts fit the predicted shifts closely in both sign and magnitude (number in parenthesis is chemical shift **17** → **19**): C2 δ_C 147.4 p.p.m. (−7.8 p.p.m.); C3 δ_C 111.4 p.p.m. (+15.1 p.p.m.); C4 δ_C 124.0 p.p.m. (+0.2 p.p.m.); C5 δ_C 131.2 p.p.m. (−1.1 p.p.m.).

Perdeuteration of **19** resulted in exchange of all protons except A4-*H*, 1″-*H*, and C4-*H*, thus assigning A4, 1″, and C4. A single resonance experiment confirmed these assignments yielding the following ^{13}C–^{1}H coupling constants: J_{A4-H} = 172.8 Hz, $J_{1''-H}$ = 154.8 Hz and J_{C4-H} = 171.0 Hz. In the single resonance spectrum of perdeuterio-**19**, B2 and B5 are sharp singlets, B3 a broadened singlet ($\Delta_{1/2}$ 9 Hz) due to long-range coupling to —O*C*H_3 and C2 a broad peak ($\Delta_{1/2}$ 19 Hz) due to cross-ring coupling and long-range coupling to the alkyl protons. A2 and C5 remained overlapping doublets ($J \sim 7$ Hz).

Undecylprodigiosin Hydrochloride (**20**)

The hydrochloride was assigned similarly by chemical shift, perdeuteration, and off-resonance techniques. By taking chemical shift

[5]Alkyl carbons are designated: ω, terminal; ω − 1, penultimate; etc.

Can. J. Chem. Downloaded from www.nrcresearchpress.com by 210.87.254.105 on 09/05/12
For personal use only.

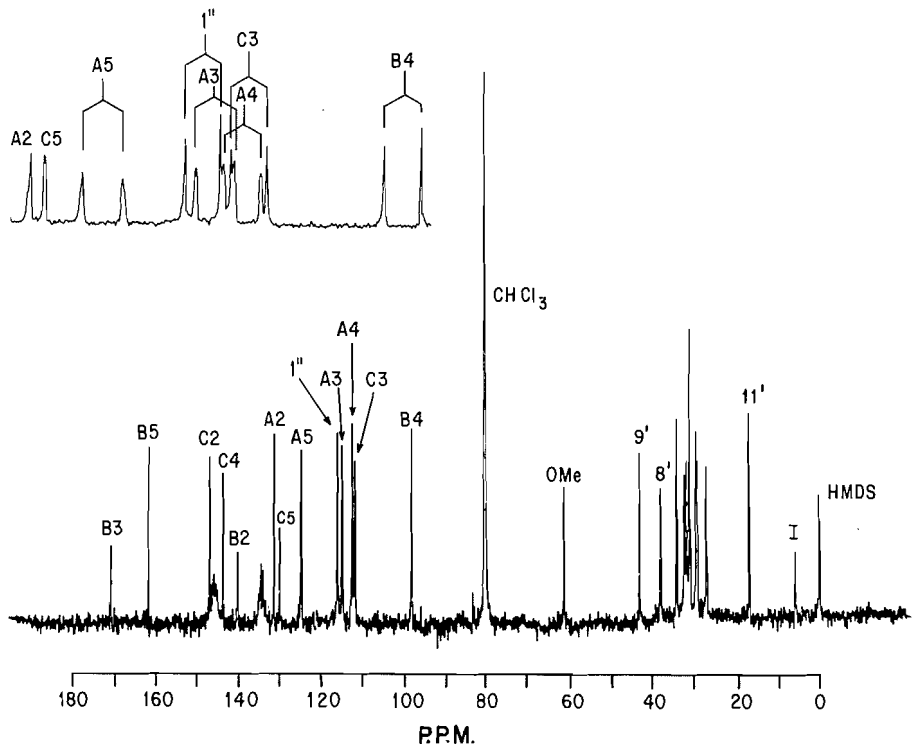

FIG. 3. Proton noise decoupled ^{13}C Fourier transform spectrum of 1 *M* metacycloprodigiosin base (**21**) in $CHCl_3$ (external C_6F_6 lock). Insert: off-resonance spectrum of portion 95.8–133.4 p.p.m. downfield for HMDS.

differences of specific carbons in **18** compared with **17**, the shift differences for the **20**,**19** pair are predicted to within ≤ 0.7 p.p.m. with the exception of C2 (1.3 p.p.m.) (See Table 4).

As found with **18**, B2 undergoes a large upfield shift of 17.3 p.p.m. upon salt formation and was distinguished from A2 (Fig. 4) since the latter is a doublet ($J \sim 7$ Hz) in the single resonance spectrum of perdeuterio-**20**. An interesting case is the shift crossover (Fig. 4) of A5 and C4 on going from base (**19**) to hydrochloride (**20**). Since both A2 and C5 both are identical doublets in the single resonance spectrum of perdeuterio-**20**, they were distinguished by secondary incorporation of ^{13}C when [2-^{13}C]-acetate was used as precursor (28). Such a secondary pathway of ^{13}C incorporation at A2 is consistent with the known biological pathway of acetate to proline.

Metacycloprodigiosin Free Base (**21**)

All 13 aromatic absorptions are resolved in the ^{13}C n.m.r. spectrum of **21**, as are 9 of the 11 carbons of the cyclic alkane chain (Fig. 3). The resolution of alkane absorptions provides a striking contrast with the lack of resolution of the alkane carbons in **19** (Fig. 2).

The alkyl absorption at δ_C 15.3 p.p.m. can be assigned to 11′ as the only alkyl methyl in **21**. Compared to terminal methyl groups of γ-branched alkanes (29), 11′ is somewhat deshielded (the terminal methyl of 3-ethylheptane absorbs at δ_C 12.9 p.p.m.). The low field alkyl absorption at δ_C 42.1 p.p.m. can be assigned to 9′ since it becomes a doublet in off-resonance spectra and the shift is in the range typical for tertiary alkane carbons (the 3-carbon of 3-ethylheptane absorbs at δ_C 43.0 p.p.m. (26)). Similarly, carbons at the $\omega - 3$ position[5] of alkanes which are adjacent to a tertiary center absorb at δ_C 35–39 p.p.m. (26), hence, the resonance at 36.9 p.p.m. was assigned to 8′.

A detailed assignment of the remaining alkyl absorptions is not possible at present. Several factors may help explain the resolution of the cycloalkane carbons. There will be steric (1) and linear electric field (1) interactions between the ethyl sidechain and neighboring

Can. J. Chem. Downloaded from www.nrcresearchpress.com by 210.87.254.105 on 09/05/12
For personal use only.

Can. J. Chem. Downloaded from www.nrcresearchpress.com by 210.87.254.105 on 09/05/12
For personal use only.

carbons. A study of space filling models of **21** shows that the cycloalkane chain is somewhat strained and inflexible, hence, cross-ring effects may be important. Finally, steric and electric field effects (29) due to the unsaturated ring will contribute to the polymethylene carbon shifts.

An interesting effect is seen for the bridgehead carbon, 1″. The 1″ shift for metacyclo compounds is, on the average, 2.6 p.p.m. to higher field than for prodigiosin and undecyl compounds (Table 4). Such an upfield shift can be attributed to γ interaction between 1″ and 9′. The results indicate the stereochemistry about the 1″—B2 bond and the configuration of the 9′-ethyl are substantially as indicated in the structural formula for **21**, shown above.

The six unsubstituted aromatic carbons in **21** were distinguished in an off-resonance spectrum (insert in Fig. 3); as in **17** and **19**, they all absorb upfield of the seven substituted aromatic carbons. B3 (δ_C 171.7 p.p.m.) and B4 (δ_C 98.1 p.p.m.) were assigned as the most deshielded and most shielded aromatic absorptions; they both absorb within 0.2 p.p.m. of the equivalent carbons of **17**. Of the remaining carbons in rings A and B, B5, B2 and A5 can be assigned unambiguously; each absorbs within 0.4 p.p.m. of the equivalent carbon in **17** (see Fig. 4).

The absorption at δ_C 116.1 p.p.m. gave a residual splitting of 71 Hz in the off-resonance spectrum, while the absorption at δ_C 115.0 p.p.m. had a residual splitting of 78 Hz. $J_{^{13}C-^{1}H}$ for 1″, measured in the proton spectrum of **21**, is 156 Hz. Because the proton absorptions for A3-*H* and A5-*H* overlap, $J_{^{13}C-^{1}H}$ cannot be measured exactly for either carbon, but it is greater than 174 Hz and less than 184 Hz. Therefore, since the absorption at δ_C 116.1 p.p.m. shows the smaller residual splitting, it was assigned to 1″, and A3 was assigned to the absorption at δ_C 115.0 p.p.m.

Compound **21** can be regarded as a derivative of **19** in which the *n*-undecyl chain of **19** has been cyclized onto C4. The chief consequence of this should be a very strong deshielding of C4 (since the substituting group is α-branched), C5 should be slightly shielded, and C2 and C3 should be relatively little affected (see Table 2). On this basis, unambiguous assignments can be made for C2 at δ_C 147.2 p.p.m., and C4 at δ_C 144.0 p.p.m. C5 is assigned to δ_C 130.2 p.p.m. (1.0 p.p.m. shielded from C5 in **19**); and A2 can be assigned to δ_C 131.6 p.p.m., which is very similar to the position of absorption of A2 in **19** (δ_C 131.2 p.p.m.) and in **17** (δ_C 131.4 p.p.m.).

Perdeuteration of **21** gave a triprotonated compound (1″-*H*, B4-*H*, and C3-*H*) thus obviating any difficulty due to small shift differences between A4 (112.6 p.p.m.) and C3 (111.9 p.p.m.). The A2-C5 pair (Fig. 4) were distinguished using the bioenrichment scheme outlined above for **20**.

Metacycloprodigiosin Hydrochloride (**22**)

Assignments for **22** were made identical to the methods used for **20** and are listed in Table 4. Of the carbons possible of misassignment, Fig. 4, a clear distinction of A5 from C5 was made possible when a sample of **22** was enriched using [1-^{13}C]-acetate. Sharp singlets were observed for C2, C4, and A5, thus C5 δ_C = 128.7 p.p.m. while A5 δ_C = 129.4 p.p.m. Since the bridgehead, 1″, always has the smallest C–H coupling, it was assigned δ_C 116.0 p.p.m. ($J_{1''-H}$ = 155 Hz) and A4 was therefore assigned δ_C 114.4 p.p.m. (J_{A4-H} = 175.5 Hz).

From Fig. 4 the striking shift continuity in the prodigiosin series is apparent, first, in the comparison of free base – hydrochloride pairs and, second, in the comparisons of series of free bases or series of hydrochlorides. For instance, in the free base series **17**, **19**, and **21** the ring A carbons all absorb within ±0.4 p.p.m. of **17**. Similarly, the ring B carbons absorb within ±0.3 p.p.m. of **17** except for B5 (±0.8 p.p.m.).

Both *in vivo*, and *in vitro*, prodigiosin (**17**) is formed by the condensation of 2-methyl-3-amylpyrrole (**8**) and the 3-methoxybipyrrole-carboxaldehyde (**15**) (30). If the ^{13}C chemical shifts of the aromatic carbons of **8** and **15** are compared with the equivalent carbons of prodigiosin free base (**17**), it is clear that formation of the bipyrropyrromethane system results in a deshielding of every aromatic carbon. The deshielding is most marked at carbons B2 (−21.9 p.p.m.) and B5 (−28.1 p.p.m.).

Protonation of Prodigiosins

Because of the wide dispersion of chemical shifts observed, ^{13}C n.m.r. provides an effective means of determining sites of protonation. In Fig. 4, the ^{13}C chemical shifts of the free base

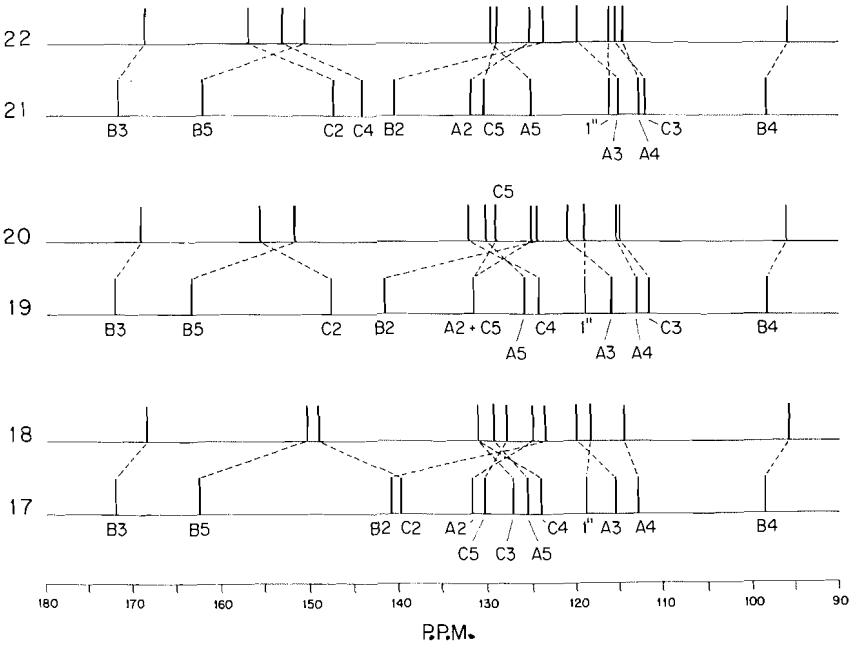

FIG. 4. Comparison of aromatic ^{13}C chemical shifts for the prodigiosin series.

of prodigiosins **17**, **19**, and **21** are compared with the chemical shifts of prodigiosin hydrochlorides **18**, **20**, and **22**. All of the carbons in ring B shift sharply to higher field, while the carbons of ring A (except A2) and ring C (except C5) shift downfield upon protonation.

Pugmire and Grant have reported that carbons α to the nitrogen in various five-membered nitrogen heterocycles are strongly *shielded* on protonation of the nitrogen, by about 9.0 p.p.m. (31). Explanations of this phenomenon differ; Grant has proposed a change in the N—C bond order, while Adam *et al.* have considered changes in the average excitation energy (32). Whatever the explanation, the strong shielding of carbons B2 (+17.4 p.p.m.) and B5 (+12.2 p.p.m.) suggests that the additional positive charge is highly localized in the B ring. The ^{13}C chemical shifts of the A and C rings of the hydrochlorides support this contention.

Work supported by Grants RR 00356, Biotechnology Branch, and AI 04798 of the National Institutes of Health.

1. Part VIII. J. G. BATCHELOR, R. J. CUSHLEY, and J. H. PRESTEGARD. J. Org. Chem. **39**, 1698 (1974). Biosynthesis of Prodigiosin. II.
2. R. J. CUSHLEY, D. R. ANDERSON, S. R. LIPSKY, R. J. SYKES, and H. H. WASSERMAN. J. Am. Chem. Soc. **93**, 6284 (1971).
3. (*a*) D. DODDRELL and A. ALLERHAND. Proc. Nat. Acad. Sci. U.S. **68**, 1083 (1971); Chem. Commun. 728 (1971). (*b*) D. DODDRELL and W. S. CAUGHEY. J. Am. Chem. Soc. **94**, 2510 (1972).
4. (*a*) A. I. SCOTT, C. A. TOWNSEND, K. OKADA, M. KAJIWARA, P. J. WHITMAN, and R. J. CUSHLEY. J. Am. Chem. Soc. **94**, 8267 (1972). (*b*) A. I. SCOTT, C. A. TOWNSEND, K. OKADA, M. KAJIWARA, and R. J. CUSHLEY. J. Am. Chem. Soc. **94**, 8269 (1972). (*c*) A. R. BATTERSBY, J. MORON, E. M. MCDONALD, and J. FEENEY. Chem. Commun. 920 (1972). (*d*) C. E. STROUSE, V. H. KOLLMAN, and N. A. MATWIYOFF. Biochem. Biophys. Res. Commun. **46**, 328 (1972). (*e*) C. E. BROWN, J. J. KATZ, and D. SHEMIN. Proc. Nat. Acad. Sci. U.S. **69**, 2585 (1972). (*f*) J. J. KATZ, T. R. JANSON, A. G. KOSTKA, R. A. UPHAUS, and G. L. CLOSS. J. Am. Chem. Soc. **94**, 2883 (1972). (*g*) A. I. SCOTT, C. A. TOWNSEND, and R. J. CUSHLEY. J. Am. Chem. Soc. **96**, 5759 (1973). (*h*) A. R. BATTERSBY, M. IHARA, E. MCDONALD, J. R. STEPHENSON, and B. T. GOLDING. Chem. Commun. 404 (1973). (*i*) A. R. BATTERSBY, G. L. HODGSON, M. IHARA, E. MCDONALD, and J. SAUNDERS. Chem. Commun. 441, (1973). (*j*) A. R. BATTERSBY, E. HUNT, and E. M. MCDONALD. Chem. Commun. 442 (1973). (*k*) A. R. BATTERSBY, K. H. GIBSON, E. MCDONALD, L. N. MANDOR, J. MORON, and L. N. NIXON. Chem. Commun. 768 (1973). (*l*) C. E. BROWN, D. SHEMIN, and J. J. KATZ. J. Biol. Chem. **248**, 8015 (1973). (*m*) N. A. MATWIYOFF and B. F. BURNHAM. Ann. N.Y. Acad. Sci. **206**, 365 (1973). (*n*) J. J. KATZ and T. R. JANSON, Ann. N.Y. Acad. Sci. **206**, 579 (1973).

Can. J. Chem. Downloaded from www.nrcresearchpress.com by 210.87.254.105 on 09/05/12
For personal use only.

5. R. J. CUSHLEY, D. R. ANDERSON, and S. R. LIPSKY. Anal. Chem. **43**, 1281 (1971).
6. J. E. MCKEON. Ph.D. Thesis, Yale University, New Haven, Connecticut. 1961. p. 51.
7. L. A. WILLIAMS. Unpublished results.
8. C.-K. SHAW. Unpublished results.
9. U. V. SANTER and H. J. VOGEL. Biochim. Biophys. Acta, **19**, 578 (1956).
10. R. J. SYKES. Ph.D. Thesis, Yale University, New Haven, Connecticut. 1973. p. 305.
11. H. H. WASSERMAN, G. C. RODGERS, and D. D. KEITH. J. Am. Chem. Soc. **91**, 1263 (1969).
12. H. H. WASSERMAN, G. C. RODGERS, and D. D. KEITH. Chem. Commun. 825 (1966).
13. T. F. PAGE, JR., T. ALGER, and D. M. GRANT. J. Am. Chem. Soc. **87**, 5333 (1965).
14. F. J. WEIGERT and J. D. ROBERTS. J. Am. Chem. Soc. **90**, 3543 (1968).
15. E. LIPPMAA, M. MAGI, S. S. NOVIKOV, L. I. KHMELNITSKI, A. S. PRIHODKO, O. V. LEBEDEV, and L. V. EPISHINA. Org. Magn. Res. **4**, 153 (1972).
16. G. C. LEVY and G. L. NELSON. Carbon-13 nuclear magnetic resonance for organic chemists. Wiley Interscience. 1972. Chapt. 3–5.
17. R. G. PARKER and J. D. ROBERTS. J. Org. Chem. **35**, 996 (1970).
18. P. LAUTERBUR. J. Chem. Phys. **43**, 360 (1965).
19. P. C. LAUTERBUR. J. Chem. Phys. **38**, 1416, 1432 (1960).
20. (*a*) H. L. RETCOFSKY and R. A. FRIEDEL. J. Phys. Chem. **71**, 3592 (1967). (*b*) H. L. RETCOFSKY and R. A. FRIEDEL. J. Phys. Chem. **72**, 290, 2619 (1968). (*c*) P. LAUTERBUR. Ann. N.Y. Acad. Sci. **70**, 841 (1958).
21. R. J. ABRAHAM and H. J. BERNSTEIN. Can. J. Chem. **39**, 905 (1961).
22. H. SPIESECKE and W. G. SCHNEIDER. J. Chem. Phys. **35**, 731 (1961).
23. P. C. LAUTERBUR. J. Am. Chem. Soc. **83**, 1846 (1961).
24. K. S. DHAMI and J. B. STOTHERS. Can. J. Chem. **45**, 233 (1967).
25. J. B. STOTHERS and P. C. LAUTERBUR. Can. J. Chem. **42**, 1563 (1964).
26. (*a*) D. M. GRANT and E. G. PAUL. J. Am. Chem. Soc. **86**, 2984 (1964). (*b*) L. P. LINDEMAN and J. Q. ADAMS. Anal. Chem. **43**, 1245 (1971).
27. H. H. WASSERMAN, R. J. SYKES, P. PEVERADA, C. K. SHAW, R. J. CUSHLEY, and S. R. LIPSKY. J. Am. Chem. Soc. **95**, 6874 (1973).
28. H. H. WASSERMAN, C. K. SHAW, R. J. SYKES, and R. J. CUSHLEY. Tetrahedron Lett. 2787 (1974).
29. J. G. BATCHELOR, J. H. PRESTEGARD, R. J. CUSHLEY, and S. R. LIPSKY. J. Am. Chem. Soc. **95**, 6358 (1973).
30. H. H. WASSERMAN, J. E. MCKEON, and U. V. SANTER. Biochem. Biophys. Res. Commun. **3**, 146 (1960).
31. R. J. PUGMIRE and D. M. GRANT. J. Am. Chem. Soc. **90**, 4232 (1968).
32. W. ADAM, A. GRIMISON, and G. RODRIGUEZ. J. Chem. Phys. **50**, 645 (1969).

Can. J. Chem. Downloaded from www.nrcresearchpress.com by 210.87.254.105 on 09/05/12
For personal use only.

Can. J. Chem. Downloaded from www.nrcresearchpress.com by 210.87.254.5 on 09/05/12
For personal use only.

Canadian Journal of Chemistry

Published by
THE NATIONAL RESEARCH COUNCIL OF CANADA

Journal canadien de chimie

Publié par
LE CONSEIL NATIONAL DE RECHERCHES DU CANADA

Volume 53 Number 2 January 15, 1975 Volume 53 numéro 2 15 janvier 1975

The Structure of the Dimethylthallium Ion Oriented in a Lyotropic Nematic Phase

YUNKO LEE AND LEONARD W. REEVES

Department of Chemistry, University of Waterloo, Waterloo, Ontario N2L 3G1

Received August 30, 1974

YUNKO LEE and LEONARD W. REEVES. Can. J. Chem. **53**, 161 (1975).

The proton magnetic resonance spectra of dimethylthallium ion has been studied in both anionic and cationic detergent nematic phases. The spectra were analyzed to derive the values of inter- and intramethyl proton–proton dipolar coupling and the intermethyl scalar coupling constants. The degree of orientation of the dimethylthallium cation is much higher in the anionic nematic phase than in the cationic phase. It is proposed that electrostatic interactions play a significant role in the orientation of complex ions in ionic detergent nematic phases.

YUNKO LEE et LEONARD W. REEVES. Can. J. Chem. **53**, 161 (1975).

On a étudié les spectres de résonance magnétique du proton de l'ion diméthylthallium dans des phases nématiques de détergents anionique et cationique. On a analysé les spectres pour déterminer les valeurs des couplages dipolaires proton–proton inter- et intraméthyle et les constantes de couplage scalaire interméthyle. Le degré d'orientation du cation diméthylthallium est beaucoup plus élevé dans la phase nématique anionique que dans la phase cationique. On suggère que les interactions électrostatiques jouent un rôle important dans l'orientation des ions complexes dans des phases nématiques de détergents ioniques. [Traduit par le journal]

Introduction

The techniques to determine relative nuclear positions in relatively small molecules by studying their nuclear magnetic resonance spectra in nematic solutions (1–3) have recently been extended to include structure determinations of complex ions (4, 5). This has been a valuable addition to existing techniques since otherwise only X-ray and neutron diffraction are available for the study of ions. The orientation of complex ions is achieved in lyotropic nematic phases based on detergent/water/alcohol/electrolyte systems. In the original communications a complex ion detergent, anionic or cationic whichever is appropriate for the sign of the charge on the complex ion to be determined, is synthesized and nematic phases prepared. The preparation of the complex ion detergents by several generalized methods have been described and structure studies of methylammonium, dimethylammonium, acetate, and dimethyltin have already been reported (6–9).

The present study is an extension of these methods to include orientation of complex ions without preparation of the complex ion detergent. In this study we shall show that nematic phases can be prepared by using simple monatomic ion salts of detergent acids but substituting a complex ion electrolyte for a simple electrolyte in the phase. Some sacrifice of signal is inevitable but we shall show that a complex cation can be oriented in both anionic and cationic detergent nematic phases. The present study of the structure of the dimethylthallium ion illustrates a departure in technique and reveals some new aspects of electrical double layer phenomena.

Can. J. Chem. Downloaded from www.nrcresearchpress.com by 210.87.254.5 on 09/05/12
For personal use only.

TABLE 1. Analytical results for the spectra of dimethylthallium ion oriented in the lyotropic nematic phases*

Composition, wt.%							D_{11} (Hz)	D_{12} (Hz)	D_{Tl-H} (Hz)		J_{Tl-H} (Hz)		$S_{C\infty}$	$\Delta\nu_D$ of D_2O (Hz)
Cesium decyl sulfate	Decylammonium tetrafluoroborate	D_2O	n-$C_{10}H_{21}OH$	Cs_2SO_4	NH_4BF_4	$Tl(CH_3)_2NO_3$			Experimental	Equation 2	Experimental	Equation 2		
45.58		47.50	3.77	0		3.15	−1399.65±0.05	114.81±0.13	403.4±0.15†	404.10±0.02	−403.4±0.15†	−404.1±0.4‡	6.70×10^{-2}	302
41.56		49.71	3.58	2.23		2.92	−1399.65±0.05	115.26±0.14	403.4±0.15†	404.10±0.02	−403.4±0.15†	−404.1±0.4‡	6.70×10^{-2}	260
	50.48	42.28			3.56	3.68	−23.55±0.03	1.94	7.1±0.2§	6.80±0.10	−403.4±0.4‖	−403.1±0.5‡	1.13×10^{-3}	308
	50.47	45.89			0	3.64	−21.68±0.03	1.78	6.6±0.2§	6.26±0.10	−403.4±0.4‖	−403.1±0.5‡	1.04×10^{-3}	
	50.46	45.58			0	3.86	−19.66±0.03	1.62	5.6±0.2§	5.68±0.10	−403.4±0.4‖	−403.5±0.5‡	9.41×10^{-4}	229
	49.31	46.22			0	4.47	−16.49±0.02	1.36	4.6±0.2	4.76±0.10	−403.4±0.4‖	−403.6±0.5‡	7.90×10^{-4}	237
	48.41	46.23			2.37	2.99	−15.06±0.02	1.24	4.5±0.1§	4.35±0.10	−403.4±0.4‖	−403.3±0.5‡	7.21×10^{-4}	256

*D_{11} = the intramethyl dipole–dipole coupling constant; D_{12} = the intermethyl dipole–dipole coupling constant; D_{Tl-H} = the thallium–proton dipole–dipole coupling; J_{Tl-H} = the thallium–proton spin–spin scalar coupling; $S_{C\infty}$ = the degree of orientation of the C_∞ or C—Tl—C axis; $\Delta\nu_D$ = nuclear quadrupole splitting (doublet separation) of the oriented D_2O in the sample.
†Results obtained from spectrum analysis by the UEA computer program.
‡Calculated from the experimental value of $|D_{Tl-H} + J_{Tl-H}|$ as obtained from the separation of the triplets and the value of D_{Tl-H} obtained from eq. (2).
§Calculated from the experimental values of J_{Tl-H} from isotropic micellar solutions and $|D_{Tl-H} + J_{Tl-H}|$ obtained from the separation of the triplets.
‖Values measured from the isotropic micellar solutions.

Can. J. Chem. Downloaded from www.nrcresearchpress.com by 210.87.254.5 on 09/05/12
For personal use only.

Experimental Section

The proton n.m.r. spectra of the oriented dimethylthallium ion in the lyotropic nematic phases were recorded on a HA-100 spectrometer at 30.6 °C. The HA-100 was operated in the locked mode. The position of the individual peak was obtained by bracketing with frequency difference markers from the lock signal.

Cesium decyl sulfate was prepared by neutralizing cesium carbonate with decyl sulfuric acid, which was prepared by passing sodium decyl sulfate through an acidified chromatographic column containing Dowex 50-H^+. Decylammonium tetrafluoroborate was prepared from the reaction of decylamine and fluoboric acid. Dimethylthallium nitrate was prepared by shaking an equivalent amount of silver nitrate in an aqueous suspension of dimethylthallium bromide. The insoluble silver bromide precipitate was filtered and the solution was concentrated and allowed to stand. Dimethylthallium nitrate was recrystallized from the ethanol–water solvent system and then dried in a desiccator under reduced pressure.

Several lyotropic nematic phases were prepared which were typically birefringent and oriented by the magnetic field used in the n.m.r. experiment. The compositions of typical phases are listed in Table 1.

Results and Discussion

The proton n.m.r. spectra of the dimethylthallium ion oriented in the anionic nematic phases of cesium decyl sulfate, *n*-decanol, and deuterium oxide were recorded. Figure 1 illustrates the typical spectrum of oriented dimethylthallium ion in the lyotropic anionic nematic phases. The spectrum consists of a 1:2:1 triplet and each of which has several components. The central peaks (*a*) of total relative intensity 2 are symmetrically arranged, while at +2058 Hz the upper resonance (*b*) of relative intensity 1 is not a symmetrical arrangement of transitions. The high field signals are always somewhat broader because they are more affected by an heterogeneity in the nematic order of the phase. The two abundant isotopes of thallium are ^{203}Tl (29.52%) and ^{205}Tl (70.48%), both with spin $\frac{1}{2}$. The gyromagnetic ratios of ^{203}Tl and ^{205}Tl differ by only 1% and the differences in dipolar and scalar couplings are too small to resolve peaks associated with each isotopic species. Only one set of triplets was observed and this infers that the value of $|D_{Tl-H} + J_{Tl-H}|$ is very small, *i.e.*, that D and J have opposite signs.

The scalar coupling J_{Tl-H} in isotropic solutions was reported to be −403 Hz and independent of concentration by Maher and Evans (10). Another Tl—H scalar coupling

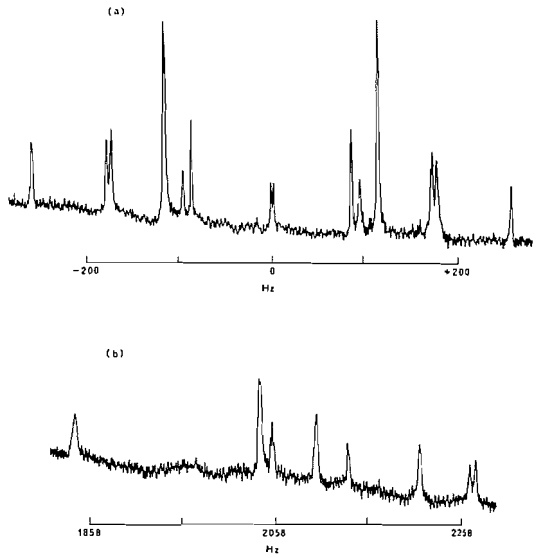

FIG. 1. Proton magnetic resonance spectrum of dimethylthallium ion oriented in a lyotropic phase of cesium decyl sulfate, *n*-decanol, and D_2O. (*a*) Central components of the triplet. (*b*) The high field component which is centered at about 2058 Hz with respect to the symmetric spectrum of the components.

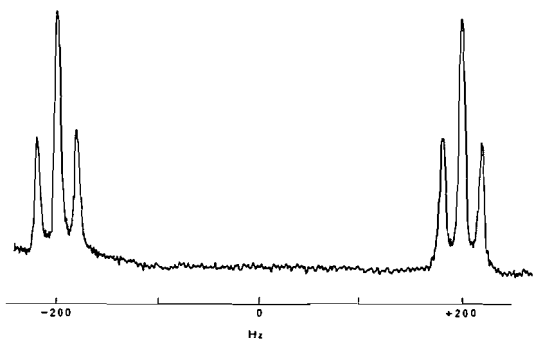

FIG. 2. Proton magnetic resonance spectrum of dimethylthallium ion oriented in a lyotropic nematic phase of decylammonium tetrafluoroborate and D_2O.

constant of 408 Hz was reported by Chan and Reeves from the ^{205}Tl magnetic resonance (11). The environment of an isotropic aqueous solution is sufficiently different from the aqueous part of the nematic phase to warrant investigation of medium effects on J (6). Isotropic concentrated micellar solutions were prepared by adding minimum amounts of deuterium oxide to the nematic phases. The mean value of J_{Tl-H} in the isotropic micellar solutions was found to be 403.4 ± 0.4 Hz.

Can. J. Chem. Downloaded from www.nrcresearchpress.com by 210.87.254.5 on 09/05/12
For personal use only.

The proton n.m.r. spectrum of the oriented dimethylthallium ion is determined by three parameters: The inter- and intramethyl proton–proton dipolar couplings, D_{12} and D_{11}, and the intermethyl scalar coupling J_{12}. These parameters were obtained from the analysis of the spectrum by using a modified UEA computer program (12) with iterative fitting to minimum error in the peak positions. The derived values and the compositions of the nematic phases are tabulated in Table 1.

Several cationic lyotropic nematic phases with about 3 to 4.5% by weight dissolved dimethylthallium nitrate were made from decylammonium tetrafluoroborate and deuterium oxide. The proton n.m.r. spectra of the oriented dimethylthallium ion were taken and Fig. 2 shows a typical spectrum obtained in the cationic nematic phase. In contrast to those obtained in an anionic phase, the proton spectrum of the dimethylthallium ion oriented in the cationic phase shows two sets of well separated triplets. However no fine structure could be resolved for the individual components of the triplet. This is due to the very small intermethyl proton dipolar coupling and the slight difference in ^{203}Tl and ^{205}Tl proton coupling. It is assumed that the dimethylthallium ion has the same structure and geometric parameters in both the anionic and cationic phases. The intermethyl proton–proton dipolar coupling constant D_{12} of the dimethylthallium ion was calculated and kept invariant in the spectrum analysis. Only these transitions near the center of the peaks were selected in the iterative fitting process. The dipolar and scalar coupling constants were also listed in Table 1. The spectral analysis indicates that the enhanced line width obtained derives from the number of closely spaced transitions arising from intermethyl proton–proton dipole–dipole couplings.

The dimethylthallium ion is known to be linear (13) and Fig. 3 depicts the geometric parameters necessary for discussion. Assuming that the methyl groups rotate freely and independently, the ratio of D_{12} to D_{11} is given as (14)

$$[1]\quad \frac{D_{12}}{D_{11}} = \frac{-3\sqrt{3}}{\pi} \times \int_0^{2\pi} \frac{[(\beta - 1) + \cos\phi]}{[(\beta + 2) - 2\cos\phi]^{5/2}}\, d\phi$$

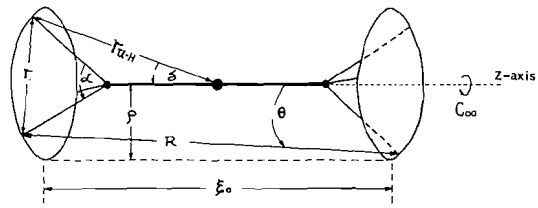

FIG. 3. Geometric parameters appropriate for a discussion of the structure of the dimethylthallium ion. On the n.m.r. time scale the C—Tl—C bond direction is a C_∞ axis, denoted as the z axis. The methyl protons rotate freely on two circles displaced a distance ξ_0. The intramethyl proton–proton distance is r. The instantaneous value of the intermethyl proton–proton distance is designated as R; this axis makes an angle θ with the z axis. ρ is the radius of the two circles swept out by the rotating methyl protons. r_{Tl-H} is the thallium–proton distance and this vector makes an angle δ with the z axis. The C—H—C angles are given the symbol α.

where φ is the relative rotational angle between the two methyl groups and $\beta = (3\xi_0^2/r^2) = (\xi_0^2/\rho^2)$ such that ρ is the distance from the methyl proton to the C_∞ axis of symmetry and ξ_0 is the separation between the two parallel planes containing the three protons of the same methyl groups. The value of β was obtained by numerical computation of the integral in eq. 1. For free rotation the value $\beta = 21.28 \pm 0.05$ was obtained from the experimental values of D_{12} and D_{11}. If we now assume that $\rho = 1.034$ Å (from a tetrahedral carbon and a C—H bond distance of 1.097 Å) the values of other geometric parameters can be evaluated and are listed in Table 2.

The structure of dimethylmercury in a thermotropic solution (15) and that of dimethyltin in a lyotropic nematic phase (6) have been studied. With the same reasonable assumptions

TABLE 2. The structural parameters of the dimethylthallium ion with freely rotating methyl group

Parameter	Value
D_{12}/D_{11}	-0.0822 ± 0.0002
β	21.28 ± 0.05
ρ	1.034 ± 0.005 Å
ξ_0	4.77 ± 0.03 Å
$\sqrt{\langle R^2 \rangle}$	4.88 ± 0.03 Å
θ	$12.23 \pm 0.2°$
δ	$23.44 \pm 0.2°$
r_{Tl-H}	2.019 ± 0.010 Å

TABLE 3. The proton dipolar coupling and degree of orientation of methanol molecule in the nematic phases

Composition, wt. %								
Decylammonium tetrafluoroborate	Cesium decyl sulfate	D_2O	*n*-Decanol	NH_4BF_4	CH_3OH	D_{HH} (Hz)	S_{C_3}	$\Delta\nu_D$ of D_2 (Hz)
48.05		47.54	3.04	0	1.38	177.1	8.53×10^{-3}	307
47.41		41.58	4.59	3.63	2.79	180.3	8.68×10^{-3}	286
45.56		48.85	2.19	1.36	2.02	148.0	7.13×10^{-3}	235
	46.38	47.91	4.42		1.29	150.3	7.24×10^{-3}	341

of linear species and free rotation of the methyl groups, the metal–carbon distances were calculated to be 2.052 Å for r_{Hg-C} and 2.015 Å for r_{Sn-C}. The present calculated value of 2.019 Å for the thallium–carbon distance falls within the same range.

In the linear skeleton of the dimethylthallium ion, the thallium atom is a center of symmetry. The average thallium–proton dipolar coupling constant D_{Tl-H} can be related to the intramethyl proton dipolar coupling constant D_{11} as (15)

$$[2] \quad D_{Tl-H} = \frac{-3\sqrt{3}\gamma_{Tl}}{\gamma_H} \sin^3\delta(2 - 3\sin^2\delta)$$

where γ_{Tl} is the average gyromagnetic ratio of ^{203}Tl and ^{205}Tl. The values of D_{Tl-H} were obtained from the experimental values of D_{11} and were tabulated also in Table 1. With the values of D_{Tl-H} being known, the scalar coupling constant J_{Tl-H} was evaluated from the separation of the triplets. The average value of J_{Tl-H} obtained over the five cationic nematic phases is 403.3 ± 0.4 Hz, which is in good agreement with the value obtained from the isotropic micellar solutions.

The dimethylthallium ion in the nematic phase may be characterized by the degree of orientation of the C_∞ axis. The C_∞ axis is perpendicular to the proton–proton vector in the same methyl group so that (16)

$$[3] \quad D_{11} = -\frac{h\gamma_H^2}{4\pi^2 r^3} S_{C\infty}$$

where γ_H is the proton gyromagnetic ratio and r is the intramethyl proton–proton distance. The values of degree of orientation of the C_∞ axis of the dimethylthallium ion were calculated from the experimental D_{11} values. Table 1 also gives the S_{C_∞} values.

The present results show that the degree of orientation of the dimethylthallium ion is about 60 to 90 times higher in the anionic nematic phase than in the cationic phase. A tentative explanation would be that electrostatic interactions between the positive dimethylthallium ion and the electrical double layer interface play an important role on the orientation of the complex ion. It is proposed that the dimethylthallium ion which achieves orientation in the nematic phase does so in an exchange process in the interface region of the oriented electrical double layer. The proposed exchange process in the interstitial water of the nematic phase and with the electrical double layer interface can be considered somewhat analogous to ion-pair formation at the interface and a free ion environment in water. In the anionic nematic phase the ionic head groups at the electrical double layer interface are negatively charged. The attractive forces between these negatively charged ionic head groups and the positively charged dimethylthallium ions contribute to the latter spending more time in the electrical double layer interface during the exchange process. Therefore a high degree of orientation of the dimethylthallium ion results. On the other hand, in a cationic nematic phase the repulsive forces between the ionic head groups and the dimethylthallium ions (both positively charged) cause the dimethylthallium ions to spend a relatively longer lifetime in less ordered regions of the interstitial water; and hence a smaller degree of orientation of the complex ions is observed.

In order to support the proposal that electrostatic interactions are significant in the orientation of ions in a nematic phase, we have also studied the orientation of the neutral methanol and D_2O molecules in both the anionic and cationic phases. The proton magnetic resonance spectra of the methanol molecules oriented in a lyotropic nematic phase show clearly a triplet expected for the intramethyl proton dipolar

Can. J. Chem. Downloaded from www.nrcresearchpress.com by 210.87.254.5 on 09/05/12
For personal use only.

coupling. The compositions of the nematic phases studied here and the intramethyl dipolar coupling constants of the methanol molecule are given in Table 3. The degree of orientation of the C_3 axis (S_{C_3}) was evaluated by using eq. 3 with the assumption that the interproton distance of the methyl group is 1.795 Å (17). The present results show that the degree of orientation of the neutral methanol molecule has similar values in both cationic and anionic phases. This is the first firm evidence that ionic distribution in the electrical double layer can greatly affect the degree of orientation of counter ions while leaving a neutral molecule such as methanol and D_2O relatively unperturbed. Further studies are continuing in this area.

We thank the National Research Council of Canada and the Defense Research Board of Canada for their financial support of this research.

1. S. MEIBOOM and L. C. SNYDER. Acc. Chem. Res. **4**, 81 (1971).
2. A. SAUPE and G. ENGLERT. Phys. Rev. Lett. **11**, 462 (1963).
3. K. D. LAWSON and T. J. FLAUTT. J. Am. Chem. Soc. **89**, 5489 (1967).
4. L. W. REEVES, J. SANCHES DE CARA, M. SUZUKI, and A. S. TRACEY. Mol. Phys. **25**, 1481 (1973).
5. L. W. REEVES, A. S. TRACEY, and M. M. TRACEY. J. Am. Chem. Soc. **95**, 3799 (1973).
6. L. W. REEVES, M. SUZUKI, A. S. TRACEY, and J. A. VANIN. Inorg. Chem. **13**, 999 (1974).
7. L. W. REEVES and A. S. TRACEY. J. Am. Chem. Soc. **96**, 1198 (1974).
8. L. W. REEVES and A. S. TRACEY. J. Am. Chem. Soc. **96**, 1198 (1974).
9. D. M. CHEN, L. W. REEVES, A. S. TRACEY, and M. M. TRACEY. J. Am. Chem. Soc. **96**, 5349 (1974).
10. J. P. MAHER and D. F. EVANS. J. Chem. Soc. 637 (1965).
11. S. O. CHAN and L. W. REEVES. J. Am. Chem. Soc. **96**, 404 (1974).
12. J. A. FERRETTI, R. K. HARRIS, and R. B. JOHANNESEN. J. Magn. Reson. **3**, 84 (1970).
13. M. G. MILES, J. H. PATTERSON, C. W. HOBBS, M. J. HOPPER, J. OVEREND, and R. S. TOBIAS. Inorg. Chem. **7**, 1721 (1968).
14. G. ENGLERT, A. SAUPE, and J. P. WEBER. Z. Naturforsch. **23a**, 152 (1968).
15. G. ENGLERT. Z. Naturforsch. **24a**, 1074 (1969).
16. P. DIEHL and C. L. KHETRAPAL. NMR basic principles and progress, Vol. 1. Springer–Verlag, New York, Heidelberg, Berlin. 1969.
17. P. DIEHL and C. L. KHETRAPAL. Can. J. Chem. **47**, 1411 (1969).

Can. J. Chem. Downloaded from www.nrcresearchpress.com by 210.87.254.5 on 09/05/12
For personal use only.

Conformational Study of *N*-Alkyl 5,6-Dihydro-7*H*,12*H*-dibenz[*c*,*f*]azocines by Nuclear Magnetic Resonance Spectroscopy[1]

ROBERT R. FRASER AND MOHAMMAD A. RAZA
Department of Chemistry, University of Ottawa, Ottawa, Canada K1N 6N5
AND
ROGER N. RENAUD AND ROBERT B. LAYTON[2]
Chemistry Division, National Research Council of Canada, Ottawa, Canada K1A 0R6
Received August 2, 1974

ROBERT R. FRASER, MOHAMMAD A. RAZA, ROGER N. RENAUD, and ROBERT B. LAYTON. Can. J. Chem. **53**, 167 (1975).

The influence of substituents on the conformational properties of *N*-substituted 5,6-dihydro-7*H*,12*H*-dibenz[*c*,*f*]azocines and their conjugate acids was studied by n.m.r. spectroscopy. The position of the equilibrium between a rigid boat-chair and a flexible twist-boat conformation has been measured. The twist-boat conformation in deuterochloroform increased as the size of the substituent increased. However, the effect was opposite for the series of conjugate acids in trifluoroacetic acid.

A number of inversion barriers for the boat-chair ⇌ twist-boat and the twist-boat ⇌ twist-boat equilibria in $CDCl_3$ and TFA were determined. It was found that all barriers to interconversion were raised on protonation. The barrier to racemization for the twist-boat form of the quaternary methiodide of **1** was found to be > 18 kcal/mol.

ROBERT R. FRASER, MOHAMMAD A. RAZA, ROGER N. RENAUD et ROBERT B. LAYTON. Can. J. Chem. **53**, 167 (1975).

On a étudié, par spectroscopie r.m.n., l'influence des substituants sur les propriétés conformationnelles de dihydro-5,6 7*H*,12*H*-dibenz[*c*,*f*]azocines *N*-substitués et de leurs acides conjugués. On a mesuré la position de l'équilibre entre une conformation rigide bateau-chaise et une conformation flexible bateau-croisé. La conformation bateau-croisé dans le chloroforme deutéré augmente à mesure que la grosseur du substituant augmente. Toutefois l'effet est opposé pour la série des acides conjugués dans l'acide trifluoroacétique.

On a déterminé, dans $CDCl_3$ et dans TFA, un certain nombre de barrières d'inversion pour les équilibres bateau-chaise *vs.* bateau-croisé et bateau-croisé *vs.* bateau-croisé. On a trouvé que toutes les barrières aux interconversions sont augmentées par protonation. La barrière à la racémisation, dans la forme bateau-croisé du sel d'ammonium quaternaire de **1**, est plus grande que 18 kcal/mol. [Traduit par le journal]

We have recently described a study of the conformational properties of *N*-methyl-5,6-dihydro-7*H*,12*H*-dibenz[*c*,*f*]azocine, **1**, by means of proton n.m.r. spectroscopy (1). This compound is of inherent interest as an unexplored medium sized heterocycle, as well as serving as a model for 1,4-cyclooctadiene, for which no experimental evidence has been reported.[3] The azocine was found to possess two stable conformations, the boat-chair (BC) and twist-boat (TB) forms, whose barrier for the TB → BC transformation amounted to 15.3 kcal/mol (1). We wish to report an extension of these studies to include azocines **2**–**6** in which the bulk of substituents at the nitrogen atom varies considerably. In this manner, the influence of the substituent on the conformational properties of the free base and its conjugate acid (in trifluoroacetic acid) can be examined.

[1]NRCC No. 14326.
[2]NRCC Postdoctoral Fellow 1972–1973.
[3]In a recent paper Dunitz and Waser (2*a*) proposed two conformers, the rigid and flexible forms, for 1,4-cyclooctadiene. Subsequently Turner *et al.* (2*b*) suggested the rigid form as being energetically favored. This nomenclature, as pointed out to us by one of the referees, is based upon dynamic rather than static characteristics of each conformer. In spite of our use of the terms "rigid crown" and "flexible" conformers in our previous paper (1) we wish now to change nomenclature. There are two conformers of cyclooctane (3) which closely resemble the two allowed conformations of the azocine ring. These are the boat-chair (BC) and twist-boat (TB) conformers whose names will now be used to designate the rigid crown and flexible forms respectively.

Can. J. Chem. Downloaded from www.nrcresearchpress.com by 210.87.254.40 on 09/05/12
For personal use only.

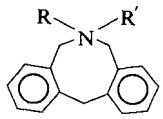

1 R = CH_3, R′ = lone pair
2 R = H, R′ = lone pair
3 R = $CD_2C_6H_5$, R′ = lone pair
4 R = $CH(CH_3)_2$, R′ = lone pair
5 R = $C(CH_3)_3$, R′ = lone pair
6 R = R′ = CH_3, I^-

Conformational Equilibria

For any *N*-substituted azocine, four stable conformations are capable of being populated. These are the BC_a and BC_e forms and the TB_i and TB_o forms where the orientation of the substituent on nitrogen can be described as axial-like or equatorial-like in the BC forms (subscript a or e) and inside or outside in the TB forms (subscript i or o). Scheme 1 depicts the most probable interconversion pathway for these conformations. The BC_e form converts to the TB_o form via rotation about the Ar—CH_2—Ar bonds. Inversion of the ring of TB_o produces TB_i which can invert at the Ar—CH_2—Ar end to produce BC_a. Models suggest that either a $BC_e \rightarrow TB_i$ or $BC_a \rightarrow TB_o$ conversion would have a much greater energy barrier and seem less probable as an alternate pathway. It should be noted that the complete pathway $BC_e \rightarrow TB_o \rightarrow TB_i \rightarrow BC_a$ must be followed to interchange the environment of the ring protons of the BC conformer while $TB_o \rightarrow TB_i$ will result in exchange of the environments of the methylene protons of the TB form (provided *N*-inversion is rapid).

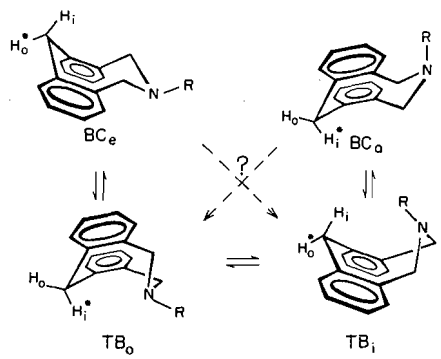

SCHEME 1. The most probable pathway for interconversion of the boat-chair and twist-boat conformations.

Criteria for Conformational Assignments

The elucidation of the conformational properties of **1** was possible as a result of distinctive differences in the n.m.r. spectral properties of the BC and TB species. The following criteria were employed.

(*a*) Temperature dependence of *K* for the BC ⇌ TB equilibrium. By integration of identifiable signals for the two isomers as a function of temperature, values for ΔS were obtainable. Since the TB form could be expected to have the greater entropy, assignment of conformation could be made.

(*b*) ^2J for $(Ar)_2CH_2$ protons. The BC conformation shows a more positive ^2J (−12 to −14 Hz) than does the TB form (−19 Hz). This is in accord with the stereochemical dependence of ^2J on hyperconjugative withdrawal (4).

(*c*) $J_{H-\overset{+}{N}-CH}$ in TFA. In TFA, the conjugate acids of the azocines exhibit vicinal H—$\overset{+}{N}$—C—H coupling constants, which obey a Karplus relation (5). The BC conformer is characterized by a value of zero to one Hz for the H—$\overset{+}{N}$—C—H coupling constant between protons having a 90° dihedral angle between them.

(*d*) Shift equivalence. A further criterion is used in this study. It is seen that, in $CDCl_3$, one of the conformers shows nonequivalent methylenes, while the other has singlet methylene peaks. The only assignment consistent with Scheme 1 is for the TB form to be responsible for the singlet absorptions.

The BC ⇌ TB Equilibrium in $CDCl_3$

Use of the above methods of configurational assignment has allowed determination of the position of the BC to TB equilibrium for azocines **2–6** in $CDCl_3$. Although inversion at nitrogen is rapid in this solvent (6), the ring inversion barrier varies from 15 to 16.5 kcal/mol and results in broadening of all lines at 27 °C. For this reason, integration measurements were made at 0 °C or below, where kinetic broadening is no longer present. The results which are summarized in Table 1 will be briefly described for each derivative.

2 (R = H)

The unsubstituted amine in deuterochloroform gives rise to one extensive broad n.m.r signal in the methylene region (δ 2–5) at ambient temperature, as seen in Fig. 1. As the tempera-

Can. J. Chem. Downloaded from www.nrcresearchpress.com by 210.87.254.40 on 09/05/12
For personal use only.

TABLE 1. BC ⇄ TB equilibria*

Compound R =	Solvent					
	$CDCl_3$			TFA		
	K_{eq} (°C)	ΔG	ΔS	K_{eq} (°C)	ΔG	ΔS
2, H	BC only			0.25 (−17)	+0.7	
1, CH_3	0.053 (0)	+1.6		0.53 (20)	+0.37	
	0.008 (−62)		+7	0.37 (−20)	+0.50	+3
3, $CD_2\phi$	Mainly BC			0.39 (−3)	+0.51	
4, $CH(CH_3)_2$	1.44 (0)	−0.15		0.39 (27)	+0.55	
	0.61 (−51)	+0.22	+8	0.28 (−3)	+0.67	+4
5, $C(CH_3)_3$	8.10 (0)	−1.14		0.099 (−3)	+1.24	
				1.04† (10)		
				0.77† (−10)		+8
6, $(CH_3)_2{}^+I^-$	0.25‡ (27)	+0.82				

*Values for ΔG are given in kcal/mol; for ΔS in entropy units.
†In 93% $CDCl_3$, 7% TFA as solvent.
‡75% $CDCl_3$, 25% DMSO-d_6 as solvent.

ture is lowered to −30 °C, (see insert *A*) this absorption sharpens to reveal two AB quartets in a ratio of 2:1. The lack of any other peaks indicates the presence of a single conformer. This must be the BC form, since (*a*) the methylene protons are nonequivalent and (*b*) a ^2J of −12.7 Hz is found for the CH_2Ar_2 group. Raising the temperature causes coalescence of the central peaks of the N—CH_2 protons at 50 °C (see insert *B*). From this coalescence temperature the barrier to the BC ⇌ BC interconversion is 16.1 kcal/mol.[4]

[4]All barriers quoted in this paper have been derived from measurement of the coalescence temperature or assigning an upper or lower limit to the coalescence temperature. The equations which we used to calculate ΔG^* are those for a two-site exchange and for an AB system, as given by Binsch (7). Normally, determinations of ΔG^* by this method are accurate to ±0.2 kcal/mol. In the values we have measured, there is additional uncertainty in ΔG^* for several reasons: (*a*) in $CDCl_3$, the barrier represents a weighted average of two BC ⇌ two TB conformers, (*b*) in TFA, small quantities of unidentified conformers may be involved in the interconversion pathway, (*c*) overlap of peaks impairs accuracy, and (*d*) line-broadening as a result of a changing rate of relaxation of ^{14}N and concomitant partial decoupling of the ^{14}N—C—H splittings may distort line shapes.

In view of these complications, we have not undertaken accurate determinations of barriers by the more sophisticated complete line shape method. We are restricted by these complexities to obtaining approximate values for the barriers which may be in error by up to 1 kcal/mol.

3 (R = $CD_2\phi$)

The n.m.r. spectrum of this derivative also showed only two AB quartets ascribable to a BC conformation.

4 (R = $CH(CH_3)_2$)

At 0 °C, the spectrum showed two AB quartets characteristic of the BC form and two singlets representing the TB conformer. Integration of the methylene region gave a value of 1.44 for K_{eq} (TB dominant). At −51 °C, this equilibrium constant decreased to 0.61. These data reveal a ΔS of +8 e.u., which confirms the assignment. Retention of the singlet character for the two methylene group absorptions down to −51 °C is a strong indication that ring inversion for the TB conformer of **4** has a barrier of less than 11 kcal/mol. This conclusion is valid, provided that the methylene protons of a slowly inverting TB form are magnetically nonequivalent. Such nonequivalence is extremely probable for **4** in view of its presence for **6** in $CDCl_3$ and **1**, **3**, and **4** in TFA (*vide infra*).

5 (R = $C(CH_3)_3$)

The spectrum of the *N*-*t*-butyl derivative at 0 °C shows the presence of TB and BC forms in a ratio of 8:1 (from integration of the two separated *t*-butyl singlets). Assignments are again based on the appearance of two singlets for the major and two AB quartets for the minor component. In addition, a change in the medium

Can. J. Chem. Downloaded from www.nrcresearchpress.com by 210.87.254.40 on 09/05/12
For personal use only.

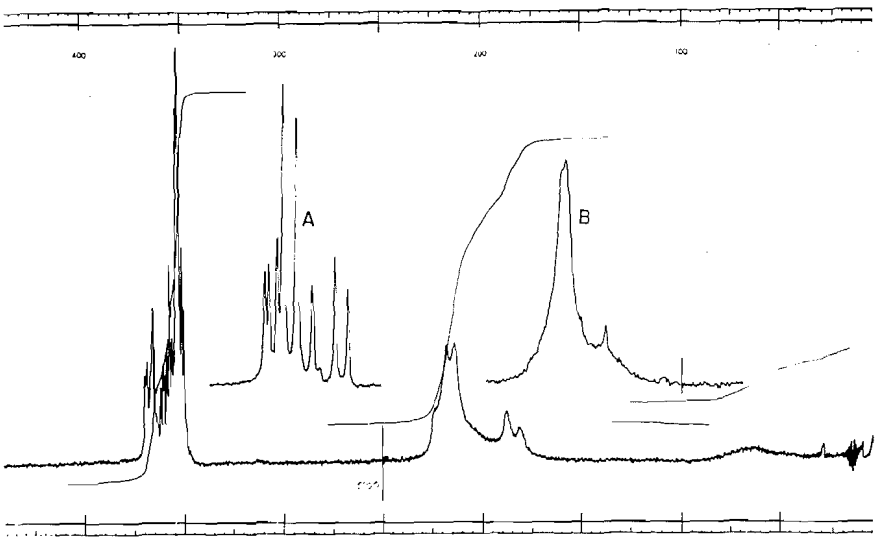

FIG. 1. The 100 MHz p.m.r. spectrum of **2** in $CDCl_3$ at 27 °C. Insert *A* shows the methylene absorption at −30 °C; insert *B* at 48 °C, just below the temperature at which the AB quartet for the NCH_2 protons coalesce.

to a 13:1 mixture of $CDCl_3$:TFA gave approximately equal amounts of the two conformers. It was found that the change in equilibrium distribution from +10° to −10° indicated a ΔS of 8 e.u. consistent with the above assignment. Heating the same solution to 40 °C caused coalescence of the two signals, indicative of a barrier to interconversion of 16.5 kcal/mol.

A final point regarding the spectrum of **5** in $CDCl_3$ was the maintenance of the two singlet absorptions at −60 °C, again indicative of a barrier to inversion of <11 kcal/mol for the TB form.

Studies in TFA Solvent

As reported in our study of **1**, the use of trifluoroacetic acid as solvent gives spectra of the conjugate acids. Perhaps the most important property of this solvent is its ability to completely protonate all basic nitrogen atoms and thereby prevent any nitrogen inversion processes. Previously work by Booth and Little (8) has established the deprotonation of substituted piperidines to be very slow ($t_{1/2}$ > 200 d) in this solvent. We have found that deprotonation is also slow for the azocines used in this study. For example, adding TFA to a solution of **1** in TFA-*d* showed only a gradual change in the singlet character of the $\overset{+}{N}(D)—CH_3$ absorption over a period of a day. The half-life for dedeuteration

$\overset{+}{N}(H)—CH_3$

(producing a $\overset{+}{N}(H)—CH_3$ doublet) was approximately 1.5 days. Similarly, for **5**, the half-life for exchange was found to be >1.5 d. Thus, any kinetic processes leading to line-broadening or coalescences ($\Delta G^{\ddagger} \leq 20$ kcal) cannot involve the intermediacy of free amine and consequent nitrogen inversion processes. In effect, the four diastereomers depicted in Scheme 1 (H or D in place of lone pair) can only interconvert via conformational processes on the n.m.r. time scale.

1 (R = CH_3)

We have now carried out a more detailed examination of the temperature dependence of the equilibrium for **1** in TFA. In this solvent at 27 °C, the spectrum actually shows three $N—CH_3$ group absorptions at δ 2.39, 2.98, and 3.45. The weakest peak at δ 3.45 was not noted in our initial study (1). But as the temperature is lowered, this peak sharpens to a clear doublet (TFA) or singlet (TFA-*d*). This isomer amounts to 4.6% of total mixture at 20 °C. Raising the temperature causes further broadening until, at 45°, it is no longer discernible. At 70°, all peaks in the spectrum have become broadened, indicating the onset of interconversion of all diastereoisomers. In view of the complexity of this

Can. J. Chem. Downloaded from www.nrcresearchpress.com by 210.87.254.40 on 09/05/12
For personal use only.

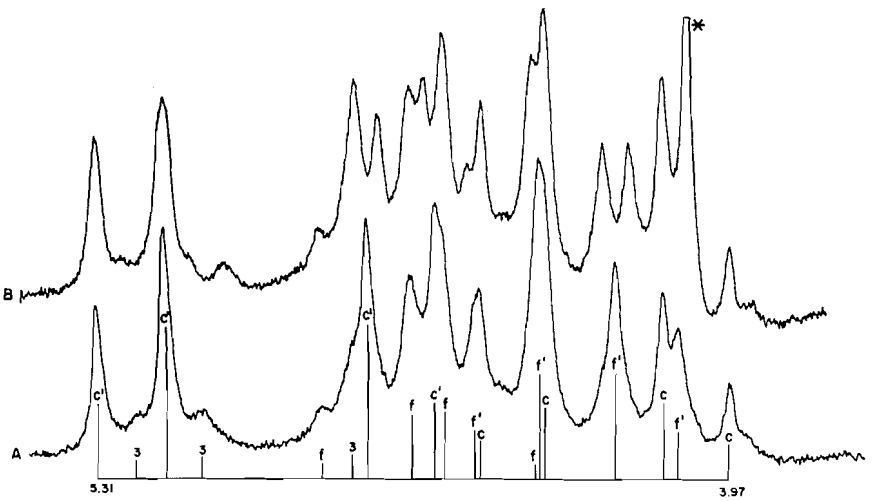

FIG. 2. The complete absorption of all methylene protons in the 100 MHz spectrum of **3**. *A* shows the spectrum in TFA-*d*, *B*, in TFA. The individual assignments are given on the stick spectrum at the bottom where the primed letter is used to denote the N—CH_2 absorption. The two peaks near the extreme left hand side bearing the label 3 likely represent a third conformer. The peak marked with an asterisk in *B* is due to a small amount of water in the solvent.

system, we are limited to the following qualitative conclusion: in order for coalescence of all peaks to occur in the range of 70 to 90 °C, the BC $\rightleftharpoons$ TB and TB $\rightleftharpoons$ TB equilibria must have barriers of 17 to 18 kcal/mol in TFA.

In our initial study, the most abundant isomer was assigned a BC conformation and the next most abundant isomer, a TB conformer, on the basis of geminal and vicinal coupling constants. We have now measured the equilibrium between these isomers by integration of the methyl absorptions at +20 and −20 °C.

From the data shown in Table 1, the less abundant isomer is found to possess the greater entropy, in accord with the previous assignment.

A detailed assignment of all of the peaks in the spectrum of **1** in TFA can be made by comparison with its spectrum in TFA-*d*. The same is true for the spectrum of **3** which shows even fewer overlapping peaks. For this reason, we have chosen **3** to illustrate their spectral characteristics in both solvents.

3 (R = $CD_2\phi$)

Figure 2 shows the absorptions in the methylene region, (*A*) in TFA-*d* and (*B*) in TFA. The proton assignments are indicated by the stick spectra using the nomenclature explained in the legend. In (*B*), three of the four pairs of *N*-methylene protons show vicinal coupling to the proton on nitrogen, while in (*A*), the smaller H—D splitting is not detectable. The lowest field doublet for the *N*-methylene protons of the BC form does not show this splitting, as the dihedral angle is near 90° in this case. Since evidence to be presented later will show that the proton on nitrogen is equatorial in the BC forms of **1** and **3**, these *N*-methylene protons must be pseudo-axial. Previously, several examples of downfield shifts for structurally similar axial-like protons have been described (9–11). It is, therefore, likely that the lower field half of the $ArCH_2Ar$ absorption for BC **1** and **3** also represents pseudo-axial protons. It is not possible to assign configuration to any of the protons of the TB conformers.

A study of the spectrum of **3** in TFA-*d* as a function of temperature, revealed a broadening and coalescence of the α-methylene peaks (δ 4.28) at 60° which indicates a TB $\rightleftharpoons$ TB barrier of 16.5 kcal/mol. The fact that the lines due to the BC conformer remain sharp at this temperature shows that the BC $\rightleftharpoons$ TB barrier is much higher (>17 kcal/mol). It is also clear that the barrier to racemization (see section on **6** for explanation of this process) in the TB conformer must be low. Otherwise, the protons α to nitrogen would appear as two AB quartets.

2 (R = H)

For the azocine **2** in TFA at −17°, the BC form dominates over the TB by a 4:1 ratio. The two sharp singlets representing the TB form show

Can. J. Chem. Downloaded from www.nrcresearchpress.com by 210.87.254.40 on 09/05/12
For personal use only.

that both the TB ⇌ TB inversion and the racemization processes are rapid ($\Delta G^{\ddagger} < 13$ kcal/mol). As the temperature is raised to 45°, all methylene absorptions coalesce. However, insufficient resolution of the peaks prevents an accurate determination of the BC ⇌ TB barrier.

4 ($R = CH(CH_3)_2$)

The only reliable data obtainable from the spectrum of **4** in TFA is the ratio of BC to TB conformers. As Table 1 shows, the BC form dominates at both 27 and −3° and the entropy difference between the two forms is 4 e.u.

5 ($R = C(CH_3)_3$)

Solvent has a marked effect on the BC ⇌ TB equilibrium of **5**. Integration of the signals for the two *t*-butyl groups in TFA gave a BC to TB ratio of 91:9 in contrast to the ratio of 11:89 in $CDCl_3$. As mentioned previously, equal amounts of the two conformers occur when a 13:1 proportion of $CDCl_3$ to TFA is used as solvent. In addition, a third isomer's presence is indicated by a third singlet in the *t*-butyl region. Heating to 50° caused coalescence of the two large peaks ($\Delta G^{\ddagger}_{BC \rightarrow TB} = 16.5$ kcal/mol) but the minor peak only begins to broaden at this temperature. It seems likely that the minor peak is due to a second BC form whose interconversion barrier is >17 kcal/mol, since a TB form with the *t*-butyl group inside would possess considerably more strain energy.

Conformational Properties of the Quaternary Methiodide, 6

The quaternary salt, **6**, provides interesting spectra for comparison with those exhibited by the conjugate acids in TFA. Spectra of **6** were measured using a 3:1 mixture of $CDCl_3$:DMSO-d_6 solvent. Peaks due to both BC (80%) and TB forms (20%) were observed and these remained unchanged over the temperature range of −20 to +60°.[5] Two features of the absorption due to the TB conformer are particularly noteworthy. Both the CH_2Ar_2 and N—CH_3 peaks are sharp singlets, while the α-methylene absorptions give rise to an AB quartet. Assuming the singlets are not the result of fortuitous shift equivalence, these observations show that the TB ⇌ TB ring inversion barrier is low (<14 kcal/mol) but nonequivalence of the

[5]Accurate integration measurements as a function of temperature could not be obtained, due to overlap of peaks.

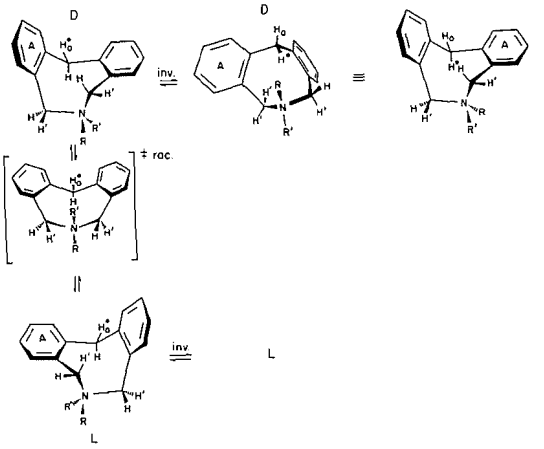

SCHEME 2. Allowed conformational interconversions between twist-boat forms. It is notable that ring inversion (inv.) causes interchange of the environments of the $ArCH_2Ar$ protons since one enantiomer (arbitrarily labelled D in the figure) upon inversion reforms the same enantiomer. Only interconversion of enantiomers (rac.) which can only occur via the symmetrical boat-like form will cause equivalent environments for the N—CH_2 protons.

α-methylenes reveals that an additional conformational barrier exists for **6**. This is the barrier to racemization for the TB conformers. As shown in Scheme 2, the symmetrical boat conformation represents a transition state for this process (severe nonbonded interactions between the inside N—CH_3 and the inside C—H bonds of the CH_2Ar group occur). Only a combination of ring inversion and this racemization process can render the α-methylenes equivalent.

Configuration at Nitrogen in TFA

We have seen that the $BC_e \rightleftharpoons TB_o \rightleftharpoons TB_i \rightleftharpoons BC_a$ equilibria have barriers in the range of 15 to 18 kcal/mol. This means that rapid equilibration of all isomers is occurring at room temperature. It is of interest to assign the con-

TABLE 2. Configurational assignments at nitrogen

Compound	$\overset{+}{N}H$ shift H_a	$\overset{+}{N}H$ shift H_e	Alkyl configuration (BC isomer)
2	6.67	8.17	
1		8.30	ax′
3		8.25	ax′
4	6.50		eq′
5	5.92		eq′

Can. J. Chem. Downloaded from www.nrcresearchpress.com by 210.87.254.40 on 09/05/12
For personal use only.

Can. J. Chem. Downloaded from www.nrcresearchpress.com by 210.87.254.40 on 09/05/12
For personal use only.

TABLE 3. Nuclear magnetic resonance parameters for BC conformers*

Compound R =	$CDCl_3$					TFA					^3J	
	$ArCH_2$		$N—CH_2$		*N*-alkyl	$ArCH_2$		NCH_2		*N*-alkyl		
	a′	e′	a′	e′		a′	e′	a′	e′		a′	e′
2, H†	4.41 (J = 12.7)	3.75	4.34 (J = 14.8)	4.10	—	4.40 (J = 13.7)	4.02	4.95 (J = 14.4)	4.69	—	7.5	<2
1, CH_3	4.47 (J = 12.7)	3.71	4.68 (J = 14.9)	3.92	1.94	4.38 (J = 13.5)	4.02	5.26 (J = 14.3)	4.58	2.39	<1	4.7
3, $CD_2\phi$	4.46 (J = 13.0)	3.66	4.60 (J = 15.0)	3.98	—	4.42 (J = 13.5)	4.04	5.22 (J = 14.2)	4.66	—	<1	4.8
4, $CH(CH_3)_2$	4.54 (J = 13.0)	3.64	4.40 (J = 14.8)	4.04	2.95 1.06 (^3J = 6.6)	4.45 (J = 13.6)	4.01	5.10 (J = 14.1)	4.54	3.64 1.67 (^3J = 6.4)	7.3	0
5, $C(CH_3)_3$	Not identifiable, 3.82		4.21 (J = 14.0)	4.05	1.60	4.53 (J = 13.5)	4.05‡	5.02 (J = 13.8)	4.96‡	1.82	6.0§	<2
6,‖ $(CH_3)_2I^-$	4.73 (J = 13.0)	3.85	5.70 (J = 13.5)	4.71	2.66 3.82							

*All chemical shifts in δ units, ^2J in Hz.
†Data for spectra measured at −51°.
‡Reverse assignment possible.
§From $CDCl_3$–acetone–TFA mixture.
‖3:1 $CDCl_3$:DMSO-d_6.

TABLE 4. Nuclear magnetic resonance parameters for TB conformers*

Compound R =	$CDCl_3$			TFA			
	$ArCH_2$	$N-CH_2$	*N*-alkyl	$ArCH_2$	$N—CH_2$	*N*-alkyl	^3J
2, H	†	†	†	4.56	4.30	—	—
1, CH_3	‡	‡	2.44	4.53, 4.71 (J = 19.0)	4.07, 4.53 (J = 13.5)	2.98	2.5 low f. 4.5 high f.
3, $CD_2\phi$	†	†	†	4.49, 4.71 (J = 19.0)	4.16, 4.42 (J = 13.5)	—	2.5 low f. 5.6 high f.
4, $CH(CH_3)_2$	4.47	3.87	3.11, 1.04 (J = 6.4)	‡	‡, 4.21 (J = 13.6)	1.57	—
5, $C(CH_3)_3$	4.51	3.89	1.12	‡	‡	1.65	
6, $(CH_3)_2\ I^-$	4.56	4.53, 4.27 (J = 12.8)	3.24				

*All chemical shifts in δ units, J in Hz.
†No detectable concentration.
‡Peaks not identifiable due to overlap.

figuration at the protonated nitrogen atom for as many of the species as possible, to ascertain their thermodynamic stabilities.

One reliable criterion for this purpose is the value for the chemical shift of the proton on the nitrogen. In **2**, the two protons of the $\overset{+}{N}H_2$ group differ in chemical shift by 1.5 p.p.m. Such a shift in a BC conformation is readily ascribed to the ring current effects of the two aromatic rings (12) which cause shielding of the quasi-axial proton and deshielding of the quasi-equatorial one. It follows that in alkylated azocines a high-field N—H shift indicates an equatorial alkyl group on nitrogen and *vice versa*.[6] On this basis, the BC forms of the four azocine derivatives are assigned the configurations shown in Table 2. Additional n.m.r. features allow at least a tentative assignment to be made to the TB forms of **1** and **3**. Their TB forms show AB patterns for both types of methylenes consistent with slow inversion and rapid racemization on the n.m.r. time scale. Since slow racemization in **6** most likely results from the presence of an inside $N—CH_3$ group, it is unlikely that either **1** or **3** have the alkyl group inside.

Nuclear Magnetic Resonance Parameters

The chemical shifts and coupling constants for all identified isomers of the series of azocines are summarized in Tables 3 and 4. Assignments have been made on the basis of the many criteria already outlined. As in the case of **3**, corroboration of all shift assignments has been made by studies in TFA-*d* solvent in comparison with TFA as solvent. Additional aid for the identification of the α-methylene absorptions is available from the well-documented downfield shift on protonation (13).

Discussion

The results of this study of compounds **1–6** provide clear evidence that these azocines are capable of existing in two ring conformations as suggested by Dunitz and Waser (2). The stabilities of the BC and TB conformations are basically similar, so that substitutions at nitrogen involving alkyl group size and protonation can significantly alter the position of the conformational equilibrium. In particular, examination of Table 1 shows that an increase in the size of the group on nitrogen increases the proportion of TB conformation in the free base, but has the opposite effect in the series of conjugate acids in TFA. The complete explanation for this contrasting behavior would require knowledge of the configuration at nitrogen in all members of both series of conformations in $CDCl_3$ and TFA.

The configuration at nitrogen is known for the BC forms of the conjugate acids in TFA as indicated in Table 2. However, the only information regarding the BC forms of the free bases comes from an X-ray study of **2**. In the solid state, the methyl group was found to occupy the

[6]Confirmatory evidence for these assignments is found in the data in Table 3. Compounds **1** and **3** show vicinal coupling between the high-field methylene and NH protons, whereas **4** and **5** show coupling between the low-field methylene and N—H protons.

Can. J. Chem. Downloaded from www.nrcresearchpress.com by 210.87.254.40 on 09/05/12
For personal use only.

TABLE 5. Barriers to ring inversion (kcal/mol)

	Solvent				
	$CDCl_3$		Trifluoroacetic acid		
Compound	BC ⇄ TB	TB ⇄ TB	BC ⇄ TB	TB ⇄ TB	Racemization
2	16.1*			<13	<13
1	15.3		17.5	17.5	<15
3				16.5	<15
4		<11			
5	16.5†	<11			
6‡	>18		>18	<14	>18

*This measurement was for the BC ⇄ BC interconversion.
†$CDCl_3$:TFA, 13:1.
‡$CDCl_3$:DMSO-d_6, 3:1.

pseudo-axial position (14). Information regarding TB forms is even more scarce. It would, therefore, be overly speculative to rationalize the effect of substituents on the BC ⇌ TB equilibrium at this time.

Three conformational interconversion processes have been identified from a study of temperature effects on suitable spectra. These are the BC ⇌ TB (A) TB ⇌ TB (B) interconversions and the racemization process for **6** (C). Table 5 summarizes these results. Process A varies from 15 to 16.5 kcal/mol in $CDCl_3$ and is raised to >17 kcal/mol in TFA. Process B shows a marked change from <11 kcal/mol in $CDCl_3$ to up to 17.5 kcal/mol in TFA. A minimum of 18 kcal/mol is found for process C in **6** in contrast to its very low value (undetectable by n.m.r.) for other TB forms. There appears to be a very marked influence of protonation in raising all barriers to interconversion. Since this increase is also produced by quaternization (*e.g.*, **6**), the effects are most logically attributed to bond length changes and increased steric interactions when the nitrogen becomes tetrasubstituted and positively charged. The presence of the racemization barrier in **6** undoubtedly arises from the severe passing interaction between the inside *N*-methyl group and the inside hydrogen of the CH_2Ar_2 methylene group.

These findings constitute the first data on the conformational properties of the dibenzazocine ring and to some extent, it may be anticipated that the results provide an indication of the conformational properties of 1,4-cyclooctadiene.

Experimental

The melting points are all uncorrected. All n.m.r. spectra were recorded on a Varian HA-100 spectrometer. All coupling constants were determined with an accuracy of ±0.1 Hz and chemical shifts are reported on the δ scale. Measurement of the probe temperature was carried out using a methanol thermometer. Such measurements should be accurate to ±2.0 °C.

α-Dideuteriobenzylamine

To a solution of benzonitrile (4.2 g) in 50 ml of dry THF, was added slowly 1.64 g of $LiAlD_4$ and the solution was refluxed for 14 h. Then, the reaction mixture was cooled in ice, and the excess hydride was decomposed with water. After filtration, the solvent was removed *in vacuo* and the residue was dissolved in ether. The ethereal solution was dried with $MgSO_4$, filtered, and distilled. A clear oil (2.0 g, 44%) was obtained. Examination of the product by g.l.c. and n.m.r. showed that the benzylamine has a deuterium content of 98% in the α-position. This amine was converted to **3** (15) whose deuterium content was found to be 97.8% by low voltage mass spectrometry.

*N-Substituted-5,6-dihydro-7H,12H-dibenz[c,f]azocines (**1**, **2**, and **4**)*

The azocines **1**, **2**, and **4** were synthesized as reported in the literature (1, 15).

*N-t-butyl-5,6-dihydro-7H,12H-dibenz[c,f]azocine, **5***

The azocine **5** was synthesized using the general method described by Casadio *et al.* (15, method E).

The crude solid residue obtained from the reaction was purified by sublimation *in vacuo* to give 65% of the azocine melting at 61–62 °C.

Anal. Calcd. for $C_{19}H_{23}N$: C, 85.98; H, 8.74; N, 5.28. Found: C, 85.79; H, 8.84; N, 5.19.

*N-Methyl-5,6-dihydro-7H,12H-dibenz[c,f]azocine Methiodide, **6***

To a solution of the azocine **1** (80 mg) in 8 ml of ethanol was added 80 mg of methyl iodide. The solution was refluxed for 30 min. On cooling to room temperature, the methiodide crystallized into colorless crystals. Most of the solvent was siphoned out. The solid was washed twice with ether and dried in an atmosphere of dry nitrogen.

Anal. Calcd. for $C_{17}H_{20}NI$: C, 55.89; H, 5.48; N, 3.83; I, 34.79. Found: C, 55.90; H, 5.56; N, 3.85; I, 34.58.

The authors thank the National Research Council of Canada for financial support of this work.

Can. J. Chem. Downloaded from www.nrcresearchpress.com by 210.87.254.40 on 09/05/12
For personal use only.

1. R. N. RENAUD, R. B. LAYTON, and R. R. FRASER. Can. J. Chem. **51**, 3380 (1973).
2. (*a*) J. D. DUNITZ and J. WASER. J. Am. Chem. Soc. **94**, 5645 (1972); (*b*) R. B. TURNER, B. J. MALLON, M. TICHY, W. VON E. DOERING, W. R. ROTH, and G. SCHRODER. J. Am. Chem. Soc. **95**, 8605 (1973).
3. J. B. HENDRICKSON. J. Am. Chem. Soc. **89**, 7047 (1967).
4. M. BARFIELD and D. M. GRANT. J. Am. Chem. Soc. **85**, 1899 (1963); J. A. POPLE and A. A. BOTHNER-BY. J. Chem. Phys. **42**, 1339 (1965); R. R. FRASER and R. N. RENAUD. Can. J. Chem. **49**, 755 (1971).
5. R. R. FRASER, R. N. RENAUD, J. K. SAUNDERS, and Y. Y. WIGFIELD. Can. J. Chem. **51**, 2433 (1973).
6. J. B. LAMBERT. Top. Stereochem. **6**, 19 (1971).
7. G. BINSCH. Top. Stereochem. **3**, 164 (1968).
8. H. BOOTH and J. H. LITTLE. J. Chem. Soc. Perkin II, 1846 (1972).
9. R. R. FRASER and R. N. RENAUD. Can. J. Chem. **49**, 746 (1971).
10. R. F. CHILDS and S. WINSTEIN. J. Am. Chem. Soc. **89**, 6348 (1967).
11. J. G. COLSON, P. T. LANSBURY, and F. D. SAEVA. J. Am. Chem. Soc. **89**, 4987 (1967).
12. L. M. JACKMAN and S. STERNHELL. Applications of NMR spectroscopy in organic chemistry. 2nd ed. Pergamon Press, London. 1969. p. 94.
13. J. C. N. MA and E. W. WARNHOFF. Can. J. Chem. **43**, 1849 (1965).
14. A. D. HARDY and F. R. AHMAD. Acta Cryst. B**30**, 1670 (1974).
15. S. CASADIO, G. PALA, E. CRESCENZI, E. MARAZZI-UBERTI, G. COPPI, and C. TURBA. J. Med. Chem. **11**, 97 (1968); G. PALA, A. MANTEGANI, and F. ZUGNA. Tetrahedron, **26**, 1275 (1970).

Can. J. Chem. Downloaded from www.nrcresearchpress.com by 210.87.254.40 on 09/05/12
For personal use only.

Complexes of Cobalt(II), Nickel(II), and Copper Acetates, Perchlorates, and Tetrafluoroborates with Heterocyclic Ligands Containing VA and VIA Group Donor Atoms

C. PRETI AND G. TOSI

Istituto di Chimica Generale ed Inorganica, University of Modena, 41100 Modena, Italy

Received July 10, 1974

C. PRETI and G. TOSI. Can. J. Chem. **53**, 177 (1975).

Cobalt(II), nickel(II), copper(II), and copper(I) acetate, perchlorate, and tetrafluoroborate complexes with thiazolidine-2-thione, thiomorpholin-3-one, and thiomorpholin-3-thione have been prepared. On the basis of infrared and far infrared spectra, electronic spectroscopy, magnetism, and molecular conductance, the stereochemistries of these complexes were identified. Assignments for the metal–ligand modes have also been made. By the use of infrared spectroscopy it has been possible to distinguish whether or not the polyanions present in the complexes are coordinated to the transition metal ion or are present as free ions. Spectroscopic parameters for the complexes have been calculated and compared with similar chromophores containing sulfur, oxygen, and nitrogen donor atoms.

C. PRETI et G. TOSI. Can. J. Chem. **53**, 177 (1975).

On a préparé les complexes des acétates, perchlorates, et tétrafluoroborates de cobalt(II), nickel(II), cuivre(II), et cuivre(I) avec la thiazolidinethione-2, la thiomorpholinone-3, et la thiomorpholinethione-3. En se basant sur les spectres infrarouge et infrarouge lointain, sur la spectrocopie électronique, sur le magnétisme et la conductance moléculaire, on a identifié les stéréochimies des ces complexes. On a aussi fait des attributions pour les mode metal–ligand. En faisant appel à la spectroscopie infrarouge, on a pu déterminer si les polyanions présents dans les complexes sont ou ne sont pas coordonnées à l'ion de métal de transition ou s'ils sont présents sous forme d'ions libres. On a calculé les paramètres spectroscopiques de ces complexes et on les a comparés avec des chromophores similaires contenant des atomes de soufre, d'oxygène et d'azote comme donneur. [Traduit par le journal]

We have reported in previous papers the study of coordination compounds with heterocyclic ligands and transition metal halides (1–3) in order to study the competition between VA and VIA donor atoms in heterocyclic ligands in the coordination to the metals. We now describe the preparation of some new complexes of cobalt(II), nickel(II), copper(II), and copper(I) acetates, perchlorates and tetrafluoroborates with thiazolidine-2-thione

(ttz = S=C—NH—CH_2—CH_2—S),

thiomorpholin-3-one

(tm = O=C—NH—CH_2—CH_2—S—CH_2),

and thiomorpholin-3-thione

(ts = S=C—NH—CH_2—CH_2—S—CH_2)

for comparison purposes in order to check the influence of the anion both on the coordination number of the metal (hence on the stereochemistry of the complex), and on the different behavior in the coordination of the donor atoms of the ligands.

According to the methods reported in the Experimental section we have obtained microcrystalline compounds, soluble in methanol, ethanol, *N*,*N*′-dimethylformamide, and nitromethane.

The metal complexes obtained, analytical data, room temperature magnetic moments, conductivity measurement values, and other physical properties are reported in Table 1. The most important i.r. data are shown in Tables 2, 3, and 4, solid state electronic spectra are reported in Tables 5, 6, and 7.

The cobalt(II) complexes have tetrahedral or octahedral stereochemistries, the nickel(II)-derivatives are tetrahedral, octahedral, or square planar while the copper(II) complexes of tm are hexacoordinated. In the derivatives of ttz and ts the copper is present as copper(I) as demonstrated by magnetic susceptibility measurements. The complex [$Cuttz_3ClO_4$] has been previously reported (4) and we have included it in this paper for comparison purposes only.

As for the infrared spectra, we observe that in the ttz-derivatives (Table 2), ν(NH) appears as a

Can. J. Chem. Downloaded from www.nrcresearchpress.com by 210.87.254.40 on 09/05/12
For personal use only.

Can. J. Chem. Downloaded from www.nrcresearchpress.com by 210.87.254.40 on 09/05/12
For personal use only.

TABLE 1. Analytical data and other physical properties

Compound	Color	Found			Calcd.			μ (B.M.)	Λ_M*	Decomposition point (°C)
		C	H	M	C	H	M			
$[Cotm_2Ac_2]\cdot H_2O$	Pink	33.6	5.2	13.5	33.6	5.2	13.7	5.2	5.9	138–140†
$[Cots_2Ac_2]$	Dark brown	32.0	4.3	13.3	32.5	4.5	13.3	4.1	6.0	110–112†
$[Cottz_4](ClO_4)_2$	Dark green	19.9	3.0	8.2	19.6	2.7	8.0	4.9	139.9	190–195
$[Cotm_6](ClO_4)_2$	Pink	30.5	4.7	6.4	30.0	4.4	6.1	5.5	150.2	230–232†
$[Cots_4](ClO_4)_2$	Dark green	25.1	3.7	7.8	24.3	3.6	7.5	4.4	120.7	110–112†
$[Cottz_4](BF_4)_2$	Green	20.5	2.9	8.3	20.3	2.8	8.3	4.8	126.5	210–212
$[Cotm_6](BF_4)_2$	Pink	31.0	4.9	6.3	30.8	4.5	6.3	4.9	154.8	130–132†
$[Cots_4](BF_4)_2\cdot 4H_2O$	Brown	23.1	4.3	6.8	22.9	4.3	7.0	4.4	126.0	150–152†
$[Nittz_2Ac_2]\cdot 2H_2O$	Brown	26.6	4.4	12.7	26.6	4.5	13.0	dia	6.3	320–322
$[Nitm_2Ac_2]\cdot H_2O$	Yellow–green	33.2	5.2	13.6	33.6	5.2	13.7	2.9	5.7	165–167
$[Nits_2Ac_2]$	Brown	32.5	4.2	13.0	32.5	4.5	13.2	dia	5.8	>350
$[Nittz_4](ClO_4)_2$	Green	19.5	2.4	7.9	19.6	2.7	8.0	3.5	170.8	>350
$[Nitm_6](ClO_4)_2$	Yellow–green	30.5	4.2	6.0	30.0	4.4	6.1	3.3	173.1	165–167†
$[Nits_2(ClO_4)_2]$	Dark green	18.7	3.1	11.2	18.3	2.7	11.3	dia	dec	215–217†
$[Nittz_6](BF_4)_2$	Yellow–green	22.5	3.2	6.0	22.8	3.2	6.2	2.3	120.1	105–107
$[Nitm_6](BF_4)_2$	Yellow–green	30.8	4.4	6.2	30.8	4.5	6.3	3.3	183.8	236–237†
$[Nits_2(BF_4)_2]$	Brown	19.7	3.0	11.7	19.3	2.8	11.8	2.1	dec	190–192†
$[CuttzAc]\cdot 2H_2O$	White	21.8	3.8	22.9	21.6	4.3	22.9	dia	6.6	260–262
$[Cutm_4Ac_2]$	Light blue	36.8	5.1	9.6	36.9	5.3	9.7	1.7	5.9	165–167
$[Cuttz_3ClO_4]$	Yellow	20.9	2.9	11.7	20.8	2.9	12.1	dia	dec	168–170†
$[Cutm_6](ClO_4)_2$	Yellow–green	30.1	4.1	6.5	29.9	4.4	6.6	1.9	183.8	200–202†
$[Cuts_3(ClO_4)]$	Light brown	25.4	4.1	11.2	25.6	3.8	11.3	dia	dec	115–117†
$[Cuttz_3(BF_4)]$	Yellow	21.3	2.9	12.1	21.3	3.0	12.5	dia	—	70–72†
$[Cutm_6](BF_4)_2\cdot 2H_2O$	Light green	29.5	4.7	6.6	29.5	4.8	6.5	1.8	205.5	140–142†
$[Cuts_3(BF_4)]$	Light brown	26.4	3.6	11.4	26.2	3.8	11.5	dia	50.6	180–182†

*For 10^{-3} *M* nitromethane solutions.
†Melting point.

Can. J. Chem. Downloaded from www.nrcresearchpress.com by 210.87.254.40 on 09/05/12
For personal use only.

TABLE 2. Infrared absorption bands of ttz derivatives (cm^{-1})

Compound	ν(NH)	Thioamide I	ν(CS) + δ(NCS)	ν(CS) sym. and asym.	ν(M—L)	Other bands
ttz $CHCl_3$ sol.	3400s	1490s	1288vs	690s,650vs	—	434ms,290m
$[Cottz_4](ClO_4)_2$	3150s	1530vs	1310vs	700m,660ms	252m	[1110vs,935vs,630s],†430ms,300m
$[Cottz_4](BF_4)_2$	3140vs	1530vs	1305vs	700ms,655vs	250m	[1070vs,522s],‡435vs,292ms
$[Nittz_2Ac_2]\cdot 2H_2O$	3100m	1535vs	1310m	695m, —	228m	[1520s,1370m],*445mw,290sh
$[Nittz_4](ClO_4)_2$	3200s	1582vs	1305m	690w,640mw	220m	[1105vs,940m,627ms],†460w,300sh
$[Nittz_6](BF_4)_2$	3100vs	1505vs	1300vs	695s,652s	215m	[1080vs,530ms],‡438s,285w
$[CuttzAc]\cdot 2H_2O$	3200m	1525vs	1310s	720w,680ms	315m	poor spectrum 432m,290vw
$[Cuttz_3(ClO_4)]$	3120s	1500vs	1300vs	690m,650m	322m,310s	[1110vs,1085vs,930s,630m,620s, 460sh],§430ms
$[Cuttz_3(BF_4)]$	3120s	1500vs	1300vs	690m,650m	323m,310s	[1120m,1080vs,1040vs,760m,530m, 520m,354m],§430s

*ν(OCO) sym. and asym.
†Bands for an ionic ClO_4 group.
‡Bands for an ionic BF_4 group.
§Assignments for bonded ClO_4 and BF_4 groups.

TABLE 3. Infrared absorption bands of tm derivatives (cm^{-1})

Compound	ν(NH)	ν(CO)	ν(CS) sym. and asym.	ν(M—L)	Other bands
tm solid	3220s	1620s	692m,643m	—	452s,405vw,350vw
tm $CHCl_3$ sol.	3400s	1660vs	690m,650m	—	
$[Cotm_2Ac_2]\cdot H_2O$	3350vs	1620vs	675ms,645m	438m	[1570vs,1490s],*455s,410m,355m
$[Cotm_6](ClO_4)_2$	3310vs	1630vs	690ms,650ms	431vs	[1120vs,930s,625vs],†470m,400sh,360s
$[Cotm_6](BF_4)_2$	3300vs	1620vs	695m,650ms	432vs	[1080vs,520s],‡470ms,400sh,360ms
$[Nitm_2Ac_2]\cdot H_2O$	3300s	1625vs	680ms,645ms	440m	[1570vs,1490vs],*458s,390sh,358m
$[Nitm_6](ClO_4)_2$	3410vs	1620vs	690ms,650ms	435vs	[1110vs,930s,625vs],†478s,400sh,360ms
$[Nitm_6](BF_4)_2$	3340s	1630vs	685ms,655s	435vs	[1080vs,525s],‡470ms,400sh,362ms
$[Cutm_4Ac_2]$	3400s	1660vs	650ms,630mw	365s	[1620vs,1460ms],*460ms,400sh,350sh
$[Cutm_6](ClO_4)_2$	3300s	1660vs	670sh,630s	371m	[1105vs,945ms,630s],§†460ms,405sh
$[Cutm_6](BF_4)_2\cdot 2H_2O$	3300s	1660vs	675m,640m	358m	[1060vs,530ms],‡460ms,405sh

*ν(OCO) sym. and asym.
†Bands for an ionic ClO_4 group.
‡Bands for an ionic BF_4 group.
§Overlapping ν_{sym}(CS).

Can. J. Chem. Downloaded from www.nrcresearchpress.com by 210.87.254.40 on 09/05/12
For personal use only.

sharp band and shows a negative shift of *ca.* 250 cm^{-1}, having as reference ν(NH) value for the free ligand in chloroform solution. The thioamide I band, the band at 1288 cm^{-1}, attributed to ν(C═S) + δ(NCS), and those due to symmetric and asymmetric ν(CS) show positive shifts suggesting that the sulfur atoms are not involved in the coordination to the metals.

Passing on thiomorpholin-3-one derivatives (Table 3), we observe that ν(NH) falls at 3260–3330 cm^{-1} compared to the value of 3400 cm^{-1} for ν(NH) for the free ligand in chloroform solution. The vibration of the C═O group is shifted towards lower frequencies in the spectra of cobalt(II) and nickel(II) derivatives, while it is the same as in the free ligand in the spectra of copper(II) complexes. The stretching vibrations due to the prevailing contribution of ν(CS) symmetric and asymmetric occur at the same wave numbers or show small positive shifts in the cobalt and nickel derivatives and are shifted towards lower energies in the spectra of the copper complexes.

In the derivatives of thiomorpholin-3-thione (Table 4), we observe that the bands I, II, and III of the —N—C═S group (5) are at about the same wave numbers as in the free ligand spectrum. The ν(NH) in the ts-complexes is shifted towards lower energies of about 200 cm^{-1} using as reference the value of 3380 cm^{-1} for ν(NH) for the free ligand in chloroform solution. The bands due to the prevailing contribution of ν(CS) are at the same wave numbers or show very small negative shifts.

From these facts we can suppose that in tm-complexes the coordination center is the oxygen atom in the derivatives of cobalt and nickel and the sulfur atom in the complexes of copper. In fact the carbonyl stretching frequency is lowered by *ca.* 40 cm^{-1} whenever the oxygen atom is bonded to a metal (6). The small negative shift of ν(NH) in the tm-derivatives spectra could arise from intermolecular hydrogen bonding.

The nitrogen atom clearly is the donor atom in the ttz- and ts-complexes; in fact, when a ligand is *N*-bonded, the ν(NH) occurs as a sharp band near 3100–3200 cm^{-1} (2, 3, 7–12). According to Singh and Rivest (13) a sharp NH band in the metal derivatives is indicative of absence of hydrogen bonding and a comparison of these values with the ν(NH) solution frequency of the ligand could be used to suggest a coordination through the nitrogen atom.

The above conclusions are in accord with most of the observations on the previously reported complexes, furthermore the electronic spectra provide some further evidence to this point.

As for the polyanions present in the complexes, by means of infrared spectroscopy, it is possible to determine whether or not they are coordinated to the transition metals. Coordination lowers the original symmetry of the free ion and results in the splitting of the originally degenerate modes, and in the previously forbidden i.r. modes becoming allowed.

The acetate ion is able to coordinate as a simple unidentate ligand, as a chelate (symmetrical or asymmetrical), and as a bridging group in polymeric complexes. All the acetate derivatives of cobalt, nickel, and copper with the different ligands are nonelectrolytes in nitromethane, Λ lying in the range 6.6–5.7 ohm^{-1} cm^2 mol^{-1} (14). By comparing the infrared spectra of our complexes with those of the acetate ion in compounds of known structure, it has been possible to distinguish between the various types of coordination (15).

In the complexes $[Nittz_2Ac_2]\cdot 2H_2O$, $[Nits_2Ac_2]$, $[Cots_2Ac_2]$, and $[Cutm_4Ac_2]$ the observed carboxy-group frequencies and their separation (150–170 cm^{-1}) are as expected for unidentate coordination.

The position of the carboxy-bands and their separation, 80 cm^{-1}, indicate a symmetric bidentate coordination of the acetate in the complexes $[Cotm_2Ac_2]\cdot H_2O$ and $[Nitm_2Ac_2]\cdot H_2O$.

As for the perchlorate derivatives, monodentate coordination results in a lowering of symmetry, $T_d \rightarrow C_{3v}$. The originally triply-degenerate modes, ν_3 and ν_4 of the free ion, are both split into two bands and the previously forbidden i.r. modes ν_1 and ν_2 of the free ion become i.r. active. In the complexes $[Cuttz_3ClO_4]$, $[Nits_2(ClO_4)_2]$, and $[Cuts_3ClO_4]$ the ν_3 mode is split in two bands in the range 1110–1085 cm^{-1}, while ν_4 is split into two bands between 640–620 cm^{-1}. The ν_1 mode appears at some 950 cm^{-1} while ν_2 lies at 460 cm^{-1} (Tables 2 and 4). The ν_1 mode in $[Cuttz_3ClO_4]$ is combined with a ligand band which is reinforced; in the two remaining complexes one of the two bands of split ν_4 overlaps the —N—C═S first band.

The i.r. values of all the remaining perchlorate derivatives are typical for a nonbonded perchlorate group (16).

In the tetrafluoborato derivatives, when the

Can. J. Chem. Downloaded from www.nrcresearchpress.com by 210.87.254.40 on 09/05/12
For personal use only.

TABLE 4. Infrared absorption bands of ts derivatives (cm^{-1})

Compound	ν(NH)	—N—C=S I	—N—C=S II	—N—C=S III	ν(CS) sym. and asym.	ν(M—L)	Other bands
ts solid	3225s	1590vs,1560vs	1345vs	1100vs	700w,620w	—	395ms,370s,361sh,329s,320sh
ts $CHCl_3$ sol.	3380s	1580vs,1570vs	1335vs	1100vs	— —	—	
$[Cots_2Ac_2]$	3200s	1550vs	1345ms	1120m	675s,*620ms	254m	[1590vs,1420vs],†392ms,366s,329s,320sh
$[Cots_4](ClO_4)_2$	3180s	1568vs	1348s	1090s	695w,640ms	260m	[1105vs,955m,630s],‡397m,375w,360sh,335m,310sh
$[Cots_4](BF_4)_2{\cdot}4H_2O$	3170s	1570vs	1350vs	1105vs	695m,630sh	257m	[1040vs,528ms],§400m,377m,335m
$[Nits_2Ac_2]$	3230m	1570m	1340m	1097s	670w,*610m	218m	[1600w,1440s],†394w,364s,330s
$[Nits_2(ClO_4)_2]$	3160ms	1560vs	1350ms	1110vs	690w,610w	215m	[1090vs,955m,640ms,630ms,465sh],‖390mw,360w,325w
$[Nits_2(BF_4)_2]$	3200vs	1560vs	1350vs	1140s	690ms, —	219m	[1160vs,1090vs,1035vs,750vs,535vs,525vs,350m],‖ 385m,360vs,330sh
$[Cuts_3(ClO_4)]$	3170s	1575vs	1355vs	1110vs	698w, —	327m,313m	[1090vs,960m,640ms,630ms,465sh],‖400w,375m,335m
$[Cuts_3(BF_4)]$	3160vs	1565vs	1355vs	1105vs	695w, —	323m	[1160s,1050vs,1020sh,750s,540ms,528ms,354w],‖ 400m,378ms,335m

*Overlapping the deforming ν(OCO).
†ν(OCO) sym. and asym.
‡Bands for an ionic ClO_4 group.
§Bands for an ionic BF_4 group.
‖Assignments for bonded ClO_4 and BF_4 groups.

TABLE 5. Electronic spectra and ligand field parameters of Co(II) complexes*

Compound	ν_3	ν_2	ν_1†	B'	β	Dq
Tetrahedral	$^4A_1(F) \rightarrow {}^4T_1(P)$	$^4A_2(F) \rightarrow {}^4T_1(F)$	$^4A_2(F) \rightarrow {}^4T_2(F)$			
$[Cottz_4](ClO_4)_2$	14 925	8000	4760	576	0.60	476
$[Cottz_4](BF_4)_2$	15 100	7935	4700	596	0.62	470
$[Cots_2Ac_2]$	15 050	7520	4420	621	0.64	442
$[Cots_4](ClO_4)_2$	14 990	7810	4610	598	0.61	461
$[Cots_4](BF_4)_2{\cdot}4H_2O$	14 930	8165	4870	565	0.58	487
Octahedral	$^4T_{1g}(F) \rightarrow {}^4T_{1g}(P)$	$^4T_{1g}(F) \rightarrow {}^4A_{2g}(F)$	$^4T_{1g}(F) \rightarrow {}^4T_{2g}(F)$			
$[Cotm_2Ac_2]{\cdot}H_2O$	20 500	17 920	8380	885	0.91	954
$[Cotm_6](ClO_4)_2$	20 140	18 200	8530	850	0.88	967
$[Cotm_6](BF_4)_2$	20 015	17 860	8370	851	0.88	949

*B is taken to be 967 cm^{-1} for the Co(II) free ion.
†Calculated values.

Can. J. Chem. Downloaded from www.nrcresearchpress.com by 210.87.254.40 on 09/05/12
For personal use only.

anion is bonded to a transition metal, we observe a similar behavior as in perchlorate group, *i.e.* ν_3 and ν_4 split, ν_1 and ν_2 i.r. active.

The complexes $[Cuttz_3BF_4]$, $[Nits_2(BF_4)_2]$, and $[Cuts_3BF_4]$ have i.r. spectra which suggest an anion coordinated to the metal (17). ν_1 and ν_2 lie in the ranges 760–750 cm^{-1} and 354–350 cm^{-1}; ν_4 and ν_3 split in the ranges 540–525 cm^{-1} and 1160–1020 cm^{-1}, respectively (Tables 2 and 4).

It is further observed that in the other fluoborato derivatives this anion is not bonded to the metal ions.

The conductivity values agree very well with these i.r. results.

The medium absorption bands present in the range 3480–3450 cm^{-1}, ν(OH), in $[Nittz_2Ac_2]\cdot 2H_2O$, $[CuttzAc]\cdot 2H_2O$, $[Cotm_2Ac_2]\cdot H_2O$, $[Nitm_2Ac_2]\cdot H_2O$, $[Cutm_6](BF_4)_2\cdot 2H_2O$, and $[Cots_4](BF_4)_2\cdot 4H_2O$ confirm the presence of water of crystallization. This water is purely lattice water since it is lost near 100 °C. In addition the wagging, the twisting, and the rocking vibrational modes of coordinated water are not present in the expected ranges (18).

Analysis of the electronic spectra of the complexes allows us to determine the mode of bonding.

With cobalt(II), complexes of tetrahedral and octahedral geometries are formed. Their magnetic moments and solid state electronic spectra (Tables 1 and 5) are in accord with those expected for these stereochemistries. As for the tetrahedral derivatives the magnetic moments at room temperature (4.1–4.9 B.M.) and the electronic spectra are consistent with a tetrahedral configuration for high spin cobalt(II) derivatives (Tables 1 and 5). Using the frequencies of ν_3 and ν_2 we have calculated the values of Dq, B', and β (19). The B' values suggest that there is a considerable orbital overlap.

As for the octahedral derivatives of cobalt(II) (μ 4.9–5.5 B.M.), the Dq, B', and β parameters were evaluated using ν_2 and ν_3 (19). Unfortunately, the ν_1 wave number was not identified from the experiments because in the tm free ligand spectrum a medium-strong absorption is present at 8300 cm^{-1}. The calculated ν_1 wave numbers are reported in Table 5.

Passing on to nickel(II) derivatives (Table 6) we have obtained tetrahedral, octahedral, and square planar complexes; the magnetic moments measurements and solid state electronic spectra are in very good agreement with these results.

The complex $[Nittz_4](ClO_4)_2$ (μ 3.5 B.M.) has a spectrum typical of tetrahedral Ni(II) (Table 6) (20, 21); Dq and B' were calculated using only ν_2 and ν_3 values, because of the ambiguous assignment of ν_1.

The reflectance spectra of the nickel complexes of ttz with BF_4 and of tm with Ac, ClO_4, and BF_4 are typical of octahedral nickel(II) (Table 6). A band at 8500 cm^{-1} was identified as a d–d transition only in the ttz-derivative, a medium-strong absorption due to the tm ligand being present at some 8300 cm^{-1}. Dq, B', and β parameters have been calculated from ν_2 and ν_3 only.

The B' values of the tetrahedral complex and of the octahedral derivatives suggest that there is a considerable orbital overlap with a strong covalency in the metal–ligand σ bonds.

The magnetic moments at room temperature lie within the range usually observed for octahedral high spin nickel(II) compounds. The μ value of $[Nittz_6](BF_4)_2$ is lower than expected, probably because of the hygroscopicity of the compound that could strongly interfere.

All the remaining nickel(II) diamagnetic derivatives have a square planar geometry except $[Nits_2(BF_4)_2]$ (μ = 2.1 B.M.).

The assignment of the d–d bands (Table 6) is made by assuming the convention that the metal x and y axes lie between the metal–ligand bonds (22). In the complex $[Nits_2(BF_4)_2]$ shoulders are present in addition to the reported bands, and the $^1A_{1g} \rightarrow {}^1B_{1g}$ transition appears only as a shoulder; we can therefore assign to this compound a distorted structure with a predominantly planar environment.

The above suggested stereochemistries are supported by the absence of electronic transitions below 10 000 cm^{-1}.

By assuming a value of $F_2 = 10F_4 = 800$ cm^{-1} for the Slater–Condon interelectronic repulsion parameters (23), a correction factor of 2800 cm^{-1} gives Δ_1 values, Table 6.

According to the conductivity values (Table 1) and to the solid state electronic spectra (Table 7), the copper(II) derivatives of tm have an octahedral stereochemistry.

The spectral data of cupric acetate – tm complex indicate the presence of octahedrally coordinated copper(II), in spite of the low magnetic

Can. J. Chem. Downloaded from www.nrcresearchpress.com by 210.87.254.40 on 09/05/12
For personal use only.

TABLE 6. Electronic spectra and ligand field parameters of Ni(II) complexes*

Compound	ν_3	ν_2	ν_1†	B'	β	Dq	Δ_1
Tetrahedral	$^3T_1(F) \rightarrow {}^3T_1(P)$	$^3T_1(F) \rightarrow {}^3A_2(F)$	$^3T_1(F) \rightarrow {}^3T_2(F)$				
$[Nittz_4](ClO_4)_2$	14 930	8850	4070	771	0.74	478	
Octahedral	$^3A_{2g}(F) \rightarrow {}^3T_{1g}(P)$	$^3A_{2g}(F) \rightarrow {}^3T_{1g}(F)$	$^3A_{2g}(F) \rightarrow {}^3T_{2g}(F)$				
$[Nittz_6](BF_4)_2$	25 000	14 100	8500	907	0.87	850	
$[Nitm_2Ac_2]\cdot H_2O$	25 125	14 245	8600	905	0.87	860	
$[Nitm_6](ClO_4)_2$	24 630	14 490	8820	844	0.81	882	
$[Nitm_6](BF_4)_2$	24 510	14 285	8690	848	0.81	869	
Square-planar	C.T. or $\rightarrow {}^1A_g$	$^1A_g \rightarrow {}^1B_{3g}$	$^1A_g \rightarrow {}^1B_{1g}$				
$[Nittz_2Ac_2]\cdot 2H_2O$	22 625	20 660	16 670				19 470
$[Nits_2Ac_2]$	22 220	18 520	15 630				18 430
$[Nits_2(ClO_4)_2]$	25 000	19 880	16 400				19 200
$[Nits_2(BF_4)_2]$	25 320 21 500sh	19 600 18 200sh	15 750sh				18 550

*B is taken to be 1041 cm^{-1} for the Ni(II) free ion.
†Calculated values for octahedral and tetrahedral derivatives.

TABLE 7. Electronic spectra of Cu(II) complexes (cm^{-1})

Compound	Frequency (cm^{-1})		
$[Cutm_4Ac_2]$	27 400	14 185	12 270
$[Cutm_6](ClO_4)_2$		14 750	11 975
$[Cutm_6](BF_4)_2 \cdot 2H_2O$		14 600	12 100

moment, 1.7 B.M. and of the presence of a band at 27 400 cm^{-1}.

By comparison of *Dq* values reported for CoL_4^{2+} cations (24) we can see that for CoS_4 chromophores *Dq* lies in the range 316–425 cm^{-1}; the corresponding range for CoN_4 chromophores is 467–538 cm^{-1}. Table 5 shows that *Dq* values of the complexes of the type CoL_4^{2+} are in very good agreement with the literature data for CoN_4 chromophores. The complex $[Cots_2Ac_2]$ shows a *Dq* value that is, using the "law of the average environment", typical of CoN_2O_2 chromophore. This value is obviously lower than those of CoN_4^{2+} complexes.

As for CoL_6^{2+} cations, the *Dq* values for CoS_6 chromophores are in the range 770–860 cm^{-1}, for CoO_6 chromophores in the range 920–980 cm^{-1}, while the values corresponding to CoN_6 chromophores are higher than 1000 cm^{-1} (21, 25). The *Dq* values of our CoL_6^{2+} complexes agree very well with the data for CoL_6^{2+} derivatives containing cobalt–oxygen bonds.

These results strongly support the i.r. conclusions that the cobalt(II) derivatives of ttz and ts are *N*-bonded while the tm-derivatives are *O*-bonded.

Comparison of the electronic spectrum of the complex $[Nittz_4](ClO_4)_2$ with those of derivatives involving Ni—S bonds and Ni—N bonds confirms that this compound is *N*-bonded, since the band energies are at higher values than in *S*-bonded derivatives (2, 21).

As for the octahedral nickel(II) derivatives, the *Dq* values for NiS_6 chromophores and NiO_6 chromophores lie between 770–810 cm^{-1} and 850–930 cm^{-1}, respectively, higher values being expected for NiN_6 groups (21, 25). The derivatives of thiomorpholin-3-one (Table 6), have *Dq* values in accord with the reported data for NiO_6^{2+} cations. The *Dq* value for the ttz-derivative is in the range typical for NiO_6 chromophores, but this ligand contains sulfur and nitrogen donor atoms only.

Taking into account the relative order of the lowest energy band in the square planar nickel complexes increasing in the approximate sequence $NiS_4 < NiN_2O_2 \sim NiN_2X_2 \sim NiO_4 < NiN_4$, we can place ttz and ts in the spectrochemical series of nitrogen donors.

We can conclude that the nickel(II) ion is oxygen-bonded in the tm-derivatives and nitrogen-bonded in the derivatives of ttz and ts.

From these results the bands which appear in the i.r. spectra of the complexes and which are absent in the free ligands spectra, in the range 250–252 cm^{-1} and 215–228 cm^{-1} in both ttz- and ts-complexes of cobalt(II) and nickel(II), can be attributed to ν(Co—N) and ν(Ni—N), respectively (2, 26–28). New medium strong bands appear at 431–440 cm^{-1} in the complexes of tm with cobalt(II) and nickel(II), which could be attributed to a metal–oxygen interaction (29, 30).

In the copper derivatives the coordination center is the sulfur atom in the complexes of tm and the nitrogen atom in the complexes of ttz and ts. The strong band present in the i.r. spectra of the copper–tm derivatives in the range 358–371 cm^{-1} could be attributed to ν(Cu—S), according to literature data (31). This assignment is supported by the noticeable shift of the bands due to the prevailing contribution of C—S bond stretching towards lower wave numbers and by the absence of absorption bands in the range 290–330 cm^{-1} where ν(Cu—N) generally lies. In the copper derivatives of ttz and ts the bands present in the range 310–330 cm^{-1} could be attributed to a ν(Cu—N) stretch (4, 9, 32).

Experimental

Preparation of the Ligands

Thiomorpholin-3-one

tm supplied by Aldrich was purified by extraction with ethyl ether in soxlet apparatus (m.p. 93 °C, lit. 93 °C) (33).

Thiomorpholin-3-thione

ts was prepared by treating thiomorpholin-3-one with an excess of P_4S_{10} slurry in refluxing benzene as previously described (7) (m.p. 141–141.5 °C).

Thiazolidine-2-thione

ttz supplied by Fluka, was twice recrystallized from hot water (m.p. 106–107 °C, lit. 106–107 °C) (34).

Preparation of Complexes

The complexes $[Cotm_2Ac_2] \cdot H_2O$, $[Cots_2Ac_2]$, and $[Nitm_2Ac_2] \cdot H_2O$ have been obtained by reaction of the corresponding metal acetate in a little excess of molten ligands. The compound $[Nittz_2Ac_2] \cdot 2H_2O$ has been obtained by reaction of nickel acetate in refluxing stirred chlorobenzene solution of the ligand. The complexes $[Nits_2Ac_2]$ and $[Cutm_4Ac_2]$ have been prepared by reaction of the corresponding acetate in refluxing stirred chloroform solution of the ligands, while [CuttzAc] has been prepared in a similar way in ethanol solution.

Can. J. Chem. Downloaded from www.nrcresearchpress.com by 210.87.254.40 on 09/05/12
For personal use only.

All the perchlorate derivatives have been prepared by reaction of the corresponding metal perchlorate in ethanol in refluxing stirred chloroform solution of the ligands. When the complexes did not separate out during the reactions, the compounds were obtained by adding petroleum ether.

The tetrafluoborato complexes have been obtained by reaction of the metal tetrafluoborate in molten ligands in the required stoichiometrical ratio.

The complexes have been purified by means of repeated washing with chloroform in the case of ttz-derivatives, with ethyl ether and toluene for tm- and ts-derivatives, respectively.

Infrared Measurements

The i.r. spectra have been recorded in the range 4000–200 cm^{-1} with Perkin–Elmer 457 and 225 spectrophotometers as KBr discs. The far i.r. spectra (400–200 cm^{-1}) were recorded as Nujol mulls between polyethylene sheets.

Ultraviolet–Visible Spectra

Solid state electronic spectra have been recorded with a Shimadzu MPS-50L spectrophotometer by the method of Venanzi and co-workers (35).

Magnetic Susceptibility Measurements

These were carried out by Gouy's method. Molecular susceptibilities were corrected for diamagnetism of the component atoms by use of the Pascal's constants.

Conductivity Measurements

These measurements were carried out with a WTW LBR type conductivity bridge for 10^{-3} M solutions in nitromethane at 25 ± 0.1 °C.

We thank Dr. M. Menozzi for his experimental work and the National Research Council (C.N.R.) of Italy for financial support.

1. C. PRETI, G. TOSI, D. DE FILIPPO, and G. VERANI. J. Inorg. Nucl. Chem. In press.
2. C. PRETI, G. TOSI, D. DE FILIPPO, and G. VERANI. Can. J. Chem. **52**, 2021 (1974).
3. C. PRETI and G. TOSI. Can. J. Chem. **52**, 2845 (1974).
4. D. DE FILIPPO, F. DEVILLANOVA, C. PRETI, E. F. TROGU, G. VERANI, and P. VIGLINO. Can. J. Chem. **51**, 1172 (1973).
5. C. N. R. RAO and R. VENKATARAGHAVAN. Spectrochim. Acta, **18**, 541 (1962).
6. S. C. JAIN and R. RIVEST. J. Inorg. Nucl. Chem. **29**, 2787 (1967).
7. D. DE FILIPPO, A. LAI, C. PRETI, E. F. TROGU, and G. VERANI. J. Inorg. Nucl. Chem. **36**, 73 (1974).
8. I. S. AHUJA. J. Inorg. Nucl. Chem. **29**, 2091 (1967).
9. I. S. AHUJA and P. RASTOGI. Inorg. Nucl. Chem. Lett. **5**, 255 (1969).
10. D. DE FILIPPO, F. DEVILLANOVA, C. PRETI, and G. VERANI. J. Chem. Soc. A, 1465 (1971).
11. E. A. ALLEN, N. P. JOHNSON, D. T. ROSEVEAR, and W. WILKINSON. J. Chem. Soc. A, 2141 (1971).
12. I. S. AHUJA. Inorg. Chim. Acta, **3**, 110 (1969).
13. P. P. SINGH and R. RIVEST. Can. J. Chem. **46**, 2361 (1968).
14. W. J. GEARY. Coord. Chem. Rev. **7**, 81 (1971).
15. N. F. CURTIS. J. Chem. Soc. A, 1579 (1968).
16. B. J. HATHAWAY and A. E. UNDERHILL. J. Chem. Soc. 3091 (1961).
17. B. J. HATHAWAY and D. E. WEBSTER. Proc. Chem. Soc. 14 (1963).
18. K. NAKAMOTO. Infrared spectra of inorganic and coordination compounds. J. Wiley, New York. 1963.
19. A. E. UNDERHILL and D. E. BILLING. Nature, **210**, 834 (1966).
20. W. J. EILBECK, F. HOLMES, C. E. TAYLOR, and A. E. UNDERHILL. J. Chem. Soc. A, 1189 (1968).
21. A. B. P. LEVER. Inorganic electronic spectroscopy. Elsevier, Amsterdam. 1968.
22. O. SIIMANN and J. FRESCO. J. Am. Chem. Soc. **92**, 2652 (1970).
23. A. R. LATHAM, V. ASCALL, and H. B. GRAY. Inorg. Chem. **4**, 788 (1965).
24. B. P. KENNEDY and A. B. P. LEVER. Can. J. Chem. **50**, 3488 (1972).
25. C. K. JORGENSEN. Absorption spectra and chemical bonding in complexes. Pergamon Press, Oxford. 1962.
26. W. J. EILBECK, F. HOLMES, C. E. TAYLOR, and A. E. UNDERHILL. J. Chem. Soc. A, 128 (1968).
27. M. J. M. CAMPBELL, D. W. CARD, R. GRZESKOWIAK, and M. GOLDSTEIN. J. Chem. Soc. Dalton, 1687 (1972).
28. J. REDIJK. Rec. Trav. Chim. **90**, 117 (1971).
29. C. V. BERNEY and J. H. WEBER. Inorg. Chem. **7**, 283 (1968).
30. D. DE FILIPPO, F. DEVILLANOVA, C. PRETI, and G. VERANI. J. Inorg. Nucl. Chem. **36**, 1017 (1974).
31. B. SINGH, LAKSHMI, and U. AGARWALA. Inorg. Chem. **8**, 2341 (1969).
32. D. M. L. GOODGAME, M. GOODGAME, P. J. HAYWARD, and J. W. RAYNER-CANHAM. Inorg. Chem. **7**, 2447 (1968).
33. A. H. SOMMERS and B. W. HORROM. J. Am. Chem. Soc. **76**, 1187 (1954).
34. R. C. WEAST (*Editor*). Handbook of chemistry and physics, 49th Ed. The Chemical Rubber Co., Cleveland, Ohio. 1968–1969. p. C565.
35. G. DYER, J. G. HARTLEY, and L. M. VENANZI. J. Chem. Soc. A, 1293 (1965).

Can. J. Chem. Downloaded from www.nrcresearchpress.com by 210.87.254.40 on 09/05/12
For personal use only.

^{13}C Nuclear Magnetic Resonance Studies of Organometallic Compounds. IX. Phenylaminocarbene Derivatives[1]

HOWARD C. CLARK, JOHN E. H. WARD,[2] AND KATSUTOSHI YASUFUKU
Department of Chemistry, The University of Western Ontario, London, Ontario N6A 3K7

Received July 31, 1974

HOWARD C. CLARK, JOHN E. H. WARD, and KATSUTOSHI YASUFUKU. Can. J. Chem. **53**, 186 (1975).

The ^{13}C nuclear magnetic resonance parameters for a series of transition metal carbene complexes of the type *trans*-$[(CH_3)Pt(As(CH_3)_3)_2(p\text{-}XC_6H_4NH(CH_3)C)]^+PF_6^-$ are presented. Comparisons of the σ^+ substituent constants for —X with the carbene carbon shieldings reveal that both σ and π interactions are occurring between the aromatic rings and the carbene carbons. A quantitative inverse relationship between these carbene carbon shieldings and those of analogous phenylthiocarbene complexes is discussed. The phenyl rings are shown to adopt *cis* orientations with respect to the carbene methyl groups.

HOWARD C. CLARK, JOHN E. H. WARD et KATSUTOSHI YASUFUKU. Can. J. Chem. **53**, 186 (1975).

On présente les paramètres de résonance magnétique nucléaire du carbone 13 d'une série de complexes entre des métaux de transitions et des carbènes du type *trans*-$[(CH_3)Pt(As(CH_3)_3)_2(p\text{-}XC_6H_4NH(CH_3)C]^+PF_6^-$. La comparaison des constantes σ^+ des substituants X avec les valeurs de blindage des carbones du carbènes montre que des interactions σ et π se produisent entre le noyau aromatique et les carbones du carbène. On discute d'une relation quantitative inverse entre ces blindages des carbones des carbènes et ceux de complexes analogues contenant des phénylthiocarbènes. On montre que les noyaux phényles adoptent des orientations *cis* par rapport aux groupes méthyles des carbènes. [Traduit par le journal]

Introduction

In a previous ^{13}C nuclear magnetic resonance spectroscopic study (2), we examined a series of transition metal carbene complexes of the sort $p\text{-}XC_6H_4S(CH_3)CW(CO)_5$, **A**, where X = —OH, —OCH_3, —CH_3, —F, —H, or —Br. Unexpectedly, the ^{13}C n.m.r. data revealed that the carbene carbons were *shielded* as the overall electron withdrawing properties of the *para* substituents *increased*; as expressed in terms of their substituent constants. Thus, a plot of $\sigma_{para}{}^n$ (3) for —X *vs.* the appropriate carbene carbon shielding gave a linear relationship with negative slope. In contrast, a similar plot for σ^+ *vs.* the carbene carbon shieldings of a series of complexes with *para*-substituted phenyl groups directly attached to the carbene carbon, $(R(R')CW(CO)_5$, **B**, where R = $p\text{-}C_6H_4X$, and R′ = —OCH_3) gave a trend with positive slope (2, 4). Thus, for series **B**, a more typical trend is followed where the carbene carbons are *deshielded* as the overall electron withdrawing properties of the *para* substituents increase.

It would appear then, that the presence of the intervening sulfur atom between the carbene carbon and *para*-substituted phenyl group markedly affects the transmission of electron density from the phenyl ring to the carbene carbon. Since nitrogen, which is also a common hetero atom in carbene ligands, may also exhibit unusual electron transmitting or insulating properties, we have synthesized and obtained the ^{13}C and ^1H n.m.r. parameters of a series of platinum(II) phenylamino carbene complexes of the type *trans*-$[(CH_3)Pt(As(CH_3)_3)_2(p\text{-}XC_6H_4NH(CH_3)C]^+PF_6^-$, where —X = —Br, —Cl, —H, —CH_3, and —OCH_3. Here, the effects of varying —X can be studied not only via ^{13}C shieldings, but also by ^{13}C—^{195}Pt coupling constants.

Experimental

The following chemicals were obtained commercially and used without further purification: aniline, *p*-chloroaniline, *p*-bromoaniline, *p*-toluamine, and *p*-anisamine. *trans*-$[(CH_3)Pt(As(CH_3)_3)_2(C(OCH_3)CH_3)]^+PF_6^-$, **1** was prepared by the method of Chisholm and Clark (5).

All reactions and recrystallizations were carried out using spectroscopic grade solvents. Microanalyses were performed by Chemalytics Inc., Tempe, Ariz. Uncorrected

[1]For the previous paper in this series see ref. 1.
[2]To whom correspondence should be addressed.

Can. J. Chem. Downloaded from www.nrcresearchpress.com by 210.87.254.6 on 09/05/12
For personal use only.

TABLE 1. Analytical data for the new phenylaminocarbene complexes *trans*-$[(CH_3)Pt(As(CH_3)_3)_2(p\text{-}XC_6H_4NH(CH_3)C)]^+PF_6^-$, **2–6**

Complex	—X	Reaction time (days)	Calculated (%) C	Calculated (%) H	Found (%) C	Found (%) H	Melting point (°C)*
2	—Br	7	22.7	3.69	22.4	3.81	175
3	—Cl	21	24.1	3.90	24.3	3.91	152–154
4	—H	3	25.2	4.23	25.1	4.15	†
5	$-CH_3$	1	26.4	4.43	26.4	4.48	153–154
6	$-OCH_3$	1	25.8	4.33	25.9	4.46	150–152

*Complex melts with decomposition.
†Complex is an oil.

melting points were determined on a Thomas Hoover unimelt capillary melting point apparatus.

The ^{13}C n.m.r. spectra were measured on a Varian XL-100-15 spectrometer operating in the pulsed Fourier transform mode at 25.2 MHz. All spectra were determined with noise-modulated proton decoupling using 3 s delays between pulses. The spectra were taken on methylene chloride-d_2 solutions in 5 mm sample tubes and were calibrated using the solvent resonances as secondary calibration standards (6).

The ^1H n.m.r. spectra were recorded on a Varian HA-100 spectrometer; the ^1H chemical shifts are reported with TMS as the internal standard.

Preparation of trans-$[(CH_3)Pt(As(CH_3)_3)_2(p\text{-}XC_6H_4NH(CH_3)C)]^+PF_6^-$ *(Compounds 2–6, see Table 1)*

To a solution of *trans*-$[(CH_3)PtAs(CH_3)_3)_2(C(OCH_3)CH_3)]^+PF_6^-$, **1**, (0.15 g, 0.23 mmol) in *ca.* 0.5 ml chloroform was added excess *para*-substituted aniline (*ca.* 1.3 mmol). The reaction was considered to be complete when the methoxyl resonance of **1** in the ^1H n.m.r. spectra of the reaction mixture had disappeared. Next, the reaction mixture was evaporated and the dark brown residue was extracted several times with *ca.* 10 ml 1:1 ether–pentane. The residue was chromatographed through a short Florisil column with methylene chloride. Concentration of the eluted solution, followed by the addition of ether, gave pale brown crystals. These were repurified by crystallization from ether–chloroform.

The aniline carbene complex could not be obtained in the crystalline state. The crude mixture obtained by chromatography with methylene chloride was rechromatographed on a short Florisil column eluting with benzene, 1:1 pentane–chloroform, and chloroform. The colorless oil recovered from the chloroform solution proved to be the desired product.

Analytical data are summarized in Table 1.

Results

Preparation of the Complexes

All the new *para*-substituted phenylaminocarbene complexes **2–6** were prepared by the aminolysis reaction shown in reaction 1 (7, 8).

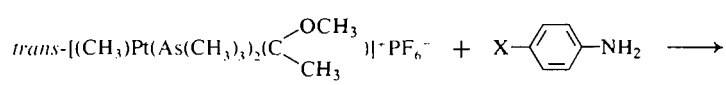

1

[1]

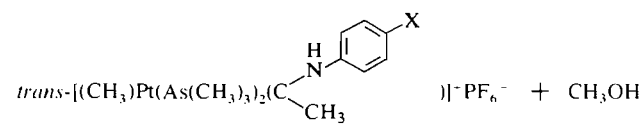

2–6

It is evident from the reaction times in Table 1 that the reaction rates depend markedly on the nature of the *para*-substituent —X, being most rapid for anilines with electron-releasing substituents. This is reminiscent of the observations of Connor and Fischer (8), who prepared complexes of the type $(p\text{-}XC_6H_4NH(CH_3)C)Cr(CO)_5$ by the general method shown in reaction 1.

Our attempts to prepare analogs of **2–6** where —X = —F, $-CF_3$, and $-NO_2$ were unsuccessful. When —X = —F, formation of the phenylaminocarbene complex was observed in solution by ^1H n.m.r. spectroscopy; however, the complex could not be isolated. On the other hand, when —X = $-CF_3$ or $-NO_2$, the phenylaminocarbene complexes were apparently not formed. This is presumably due to the rather

Can. J. Chem. Downloaded from www.nrcresearchpress.com by 210.87.254.6 on 09/05/12
For personal use only.

TABLE 2. Observed (and predicted) ^{13}C shieldings for the new complexes *trans*-$[(CH_3)Pt(As(CH_3)_3)_2(p\text{-}XC_6H_4NH(CH_3)C]^+PF_6^-$, **2–6***

Complex	—X	δCH_3Pt	$\delta As(CH_3)_3$	δC (carbene)	$\delta C(CH_3)$	δC_1	$\delta C_{2,6}$	$\delta C_{3,5}$	δC_4	X
2	—Br	−18.9	9.2	252.0	38.4	140.2 (139.6)	122.4 (122.7)	132.5 (133.0)	121.8 (123.3)	
3	—Cl	−19.0	9.3	252.0	38.4	139.8 (139.3)	122.2 (122.3)	129.5 (130.0)	134.0 (135.0)	
4	—H	−19.3	9.4	250.3	38.4	141.2	121.0	129.6	128.8	
5	—CH_3	−19.3	9.3	248.4	38.2	138.8 (138.3)	120.8 (120.9)	129.9 (130.3)	139.1 (137.7)	δCH_3 20.9
6	—OCH_3	−19.2	9.3	246.2	38.1	134.5 (133.5)	122.3 (122.0)	114.5 (115.2)	159.7 (160.2)	δOCH_3 55.8

*In p.p.m. (±0.1) (downfield positive) from TMS. All spectra were measured on methylene chloride-d_2 solutions. The numbering of the aromatic carbons takes C_1 as directly bonded to the nitrogen atom.

TABLE 3. $^{13}C—^{195}Pt$ coupling constants for the new complexes *trans*-$[(CH_3)Pt(As(CH_3)_3)_2(p\text{-}XC_6H_4NH(CH_3)C)]^+PF_6^-$, **2–6***

Complex	—X	$\lvert^1J_{PtCH_3}\rvert$	$\lvert^2J_{PtAsC}\rvert$	$\lvert^1J_{PtC}$ (carbene)$\rvert$	$\lvert^2J_{PtCC}\rvert$	$\lvert^3J_{PtCNC}\rvert$
2	—Br	377(±1)	50(±1)	686(±2)	45(±1)	20(±2)
3	—Cl	378(±1)	49(±1)	686(±2)	46(±1)	21(±2)
4	—H	374(±1)	50(±1)	686(±3)	48(±1)	†
5	—CH_3	381(±1)	50(±1)	687(±2)	47(±1)	22(±4)
6	—OCH_3	378(±1)	50(±1)	686(±2)	47(±1)	20(±1)

*Coupling constants in Hz. All spectra were measured on methylene chloride-d_2 solutions.
†Coupling not observed.

slow reaction rates for anilines with electron withdrawing *para*-substituents. In such cases, reduction to platinum(0) was observed, as we have noticed in the preparation of related platinum(II) carbene complexes. Finally, we should note that our attempts to prepare bis-(dimethylphenylphosphine) analogs of **2–6** were also unsuccessful; it would appear that the transition states for the aminolysis reaction are sufficiently sterically hindered to preclude phenylaminocarbene formation (7).

Nuclear Magnetic Resonance Results

The ^{13}C n.m.r. shieldings and coupling constants obtained from the spectra of **2–6** are summarized in Tables 2 and 3, respectively. The assignments of the carbon resonances of the platinum-methyl, arsenic-methyl, carbene-methyl and carbene carbons were carried out by comparisons with related derivatives (1, 9). However, the assignments of all the aromatic carbons were not so straightforward. The signals arising from the *quaternary* carbons C_1 and from the *para* carbons C_4 could be distinguished from the *ortho* and *meta* carbons on the basis of their relative intensities. The *quaternary* carbons C_1 were distinguished from the *para* carbons C_4 by their characteristic $^3J_{PtCNC}$ value (*ca.* 20 Hz). (We would not anticipate that $^6J_{PtCNCCCC}$ values would be large, since we have observed that $^nJ_{PtC}$ values generally decrease in magnitude as the number of intervening atoms between the coupling nuclei increases (10, 11).) Each complex gave a signal at *ca.* 121.5 (±1) p.p.m., which was assigned to the 2,6 carbons on the basis of the well-known insensitivity of ^{13}C shieldings of aromatic carbons *meta* to a varied substituent (12). All these assignments were checked by assuming additivity of the individual *para*-substituent effects (12*b*) on the aryl carbon shieldings of **2**, **3**, **5**, and **6**. The average deviation between the observed and predicted shieldings of all the aromatic carbons of those complexes is 0.6 p.p.m.

We have not determined the relative signs of the $^{13}C—^{195}Pt$ coupling constants; thus, the absolute values of those parameters are provided in Table 3. Needless to say, the use of absolute values of the coupling constants is adequate for the arguments we will present later.

Can. J. Chem. Downloaded from www.nrcresearchpress.com by 210.87.254.6 on 09/05/12
For personal use only.

TABLE 4. ^1H chemical shifts*† and coupling constants‡ for the new complexes *trans*-$[(CH_3)Pt(As(CH_3)_3)_2(p\text{-}XC_6H_4NH(CH_3)C)]^+PF_6^-$ **2–6**

Complex	—X	δCH_3Pt	$\lvert^2J_{PtCH}\rvert$	$\delta As(CH_3)_3$	$\lvert^3J_{PtAsCH}\rvert$	δCCH_3	$\lvert^3J_{PtCCH}\rvert$	$\lvert^3J_{HNCH}\rvert$	Other§
2	—Br	0.14	50.0	1.34	24.2	2.71	17.9	1.0	
3	—Cl	0.15	51.9	1.32	24.3	2.69	15.4	1.0	
4	—H	0.12	48.4	1.30	24.4	2.69	15.8	‖	
5	$-CH_3$	0.11	50.3	1.35	24.4	2.70	15.8	1.0	$\delta CH_3 = 2.90$
6	$-OCH_3$	¶	¶	1.33	24.1	2.67	16.4	1.0	$\delta OCH_3 = 3.90$

*In p.p.m. (±0.01) (downfield positive) from TMS.
†The ^1H n.m.r. spectra were measured on methylene chloride solutions.
‡In Hz (±0.5).
§The aromatic protons occur in the usual positions as complex multiplets.
‖Signals too broad to measure this coupling constant.
¶Signals not recorded.

The ^1H n.m.r. data for the new phenylaminocarbene complexes **2–6** are summarized in Table 4. The assignments of the ^1H chemical shifts and J_{PtH} values were based on arguments similar to those used to assign the ^1H n.m.r. parameters of related carbene complexes.

Discussion

The ^{13}C n.m.r. data reveal that with variations in the *para*-substituent —X, characteristic variations in the ^{13}C shieldings and $^{13}C—^{195}Pt$ coupling constants may occur. For example, those parameters for the platinum-methyl (*ca.* −19.1 (±0.2) p.p.m. and *ca.* 318 (±4) Hz), arsenic-methyl (*ca.* 9.3 (±0.1) p.p.m. and *ca.* 50 (±1) Hz, and carbene-methyl (*ca.* 38.2 (0.2) p.p.m. and 46 (2) Hz) carbons are almost invariant. The carbene carbon shieldings are more sensitive and vary from 246.2 to 252.0 p.p.m., over a range of *ca.* 6 p.p.m. In comparison, the carbene carbon shieldings for the related phenylthiocarbene complexes **A** were found to span a range of *ca.* 2.2 p.p.m. (2). The $^1J_{PtC}$ values for the carbene carbons of **2–6**, as well as the $^3J_{PtCNC}$ values for the C_1 aromatic carbons are essentially invariant at *ca.* 686 (±2) and 21 (±1) Hz, respectively. Finally, the shieldings of the aromatic carbons of **2–6** are sensitive to variations in —X, as would be anticipated (12).

Carbene Carbon Shieldings

Our results (2) for the phenylthiocarbenes **A** revealed regular relationships between the σ^+ and σ^n_{para} substituent constants (3) and δ_C (carbene). Accordingly, we have plotted σ^+ *vs.* δ_C (carbene) for the phenylaminocarbene complexes **2–6**, as shown in Fig. 1, and by linear

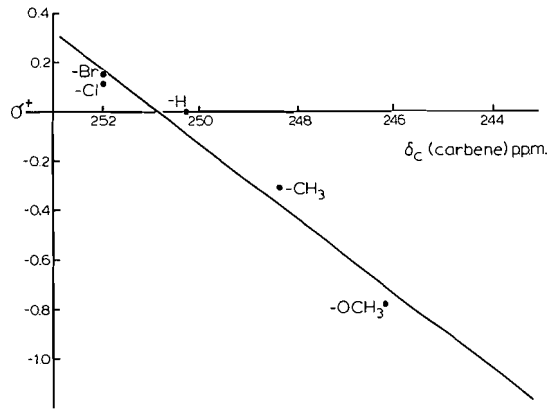

FIG. 1. Plot of σ^+ *vs.* δ_C (carbene) for the phenylaminocarbene complexes **2–6**.

regression analysis obtain eq. 2[3]

$$[2]\quad \sigma^+ = 0.15(\pm 0.01)\delta_C\ (\text{carbene}) - 38.3(\pm 1.5)$$
$$r = 0.983$$

The excellent linear fit indicates that the changes in carbene carbon shieldings are sensitive to the changes in overall ($\sigma + \pi$) electron density induced by variations in the *para*-substituent —X. When the ^{13}C shielding data for the carbene carbons are compared wtih the σ_{para}^n substituent constants, a very similar plot results, except for the point for the methoxyl derivative **6**. For that

[3]The average deviations of the slopes and intercepts for all the linear equations presented here are calculated on the basis of the maximum possible error due to the inherent uncertainty of the experimental measurements. These errors have already been cited in Tables 2 and 3. It is worthwhile noting that these variations represent the maximum error in *precision* and that as such they may be generous estimates.

Can. J. Chem. Downloaded from www.nrcresearchpress.com by 210.87.254.6 on 09/05/12
For personal use only.

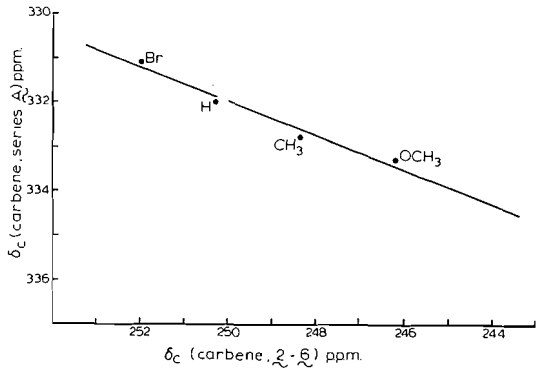

FIG. 2. Plot δ_C (carbene, **A**) *vs.* δ_C (carbene; **2**, **4–6**) for complexes sharing common *para*-substituents —X.

relationship, a poorer linear correlation coefficient ($r = 0.901$) was obtained. Thus, it would appear that the σ^+ parameters provide a better model than the $\sigma_{para}{}^n$ constants for these complexes.

It is particularly interesting to compare the carbene carbon shieldings of analogs of the phenylthio and phenylamino series of complexes. A plot of these data is given in Fig. 2, and eq. 3 provides the linear regression analysis parameters.

$$[3]\quad \delta_C\text{ (carbene, A)} = -0.38(\pm 0.03)\delta_C\text{ (carbene, 2, 4–6)} + 427(\pm 7)$$
$$r = 0.984$$

To our surprise, the carbene carbon shieldings of these series of complexes appear to be *inversely* related. Whereas an increase in the overall electron withdrawing properties of —X causes *shielding* of the carbene carbons in series **A**, it causes a *deshielding* of the carbene carbons in **2–6**. Thus, it would appear that the transmission of electron density through sulfur markedly differs from that through nitrogen, assuming that the change in transition metal and its substituents is of minor importance. We assume that only the degree and not mode of metal–carbene bonding differs between the two series. Since nitrogen can transmit changes in electron density via s and p-orbitals, while sulfur has s, p, and d orbitals available, such a result is not entirely unreasonable. In any event, eq. 3 indicates that both series of complexes regularly reflect changes in electron density at the carbene carbon induced by variations in —X.

In addition, the phenylaminocarbenes carbene carbons follow shielding trends similar, but not identical to the phenylmethoxylcarbenes carbons in **B**. While the slopes of plots of σ^+ *vs.* the shieldings for those carbons of both series are positive, there does not appear to be a relationship between these carbene carbon shieldings for analogous compounds. Thus, the three series of carbene complexes, **A**, **B**, and **2–6**, exhibit markedly different shielding variations at the carbene carbons.

Aryl Carbon Shieldings

Next, we considered the aryl carbon shieldings in order to determine whether any interactions of the carbene carbon with the p-XC_6H_4NH— group were revealed. Thus differences in the bonding of a carbene carbon, which can employ both σ and π bonding, and a proton, which employs only σ bonding, would be reflected in comparisons between the individual aryl carbons of **2–6** and the parent *para*-substituted anilines. The ^{13}C shieldings of those derivatives may be predicted with considerable precision as described in ref. 12*b*. A consideration of the individual substituent effects in the anilines p-$XC_6H_4NH_2$ yields the following shielding data, where C_1 is bound to the NH_2 moiety: —X = —Br, δC_1 145.1, $\delta C_{2,6}$ 117.1, $\delta C_{3,5}$ 133.0, and δC_4 113.4 p.p.m.; —X = —Cl, δC_1 144.8, $\delta C_{2,6}$ 116.7, $\delta C_{3,5}$ 130.0, and δC_4 125.1 p.p.m.; —X, = —H, δC_1 146.7, $\delta C_{2,6}$ 115.4, $\delta C_{3,5}$ 129.6, and δC_4 118.9 p.p.m.; —X = —CH_3, δC_1 143.8, $\delta C_{2,6}$ 115.3, $\delta C_{3,5}$ 130.3, δC_4 127.8 p.p.m.; and —X = —OCH_3, δC_1 139.0, $\delta C_{2,6}$ 116.4, $\delta C_{3,5}$ 115.2, and δC_4 150.3 p.p.m.

First, we note that carbons C_1 of the carbene complexes **2–6** are shielded by an average of *ca.* 5 p.p.m. with respect to the corresponding carbons in the parent *para*-substituted anilines. (Summaries of the qualitative origins of ^{13}C shieldings of aromatic carbons appear in refs. 2 and 10.) Assuming that the neighborhood anisotropies of the nitrogen atoms are similar in both series of compounds, it would appear that there is an appreciable shift of electron density into the aromatic ring from the nitrogen atoms and probably carbene carbon atoms. This may be substantiated by reviewing the shieldings of C_4 in the parent anilines and carbene derivatives.

In contrast, those carbons for **2–6** are *deshielded* by *ca.* 9.5 p.p.m. with respect to the *para*-

Can. J. Chem. Downloaded from www.nrcresearchpress.com by 210.87.254.6 on 09/05/12
For personal use only.

substituted anilines. Thus, it would appear that the assumption that the neighborhood anisotropies of the nitrogen atoms in **2–6** and the *para*-anilines are similar may not be reasonable. In any event, since *para*-carbon shieldings are believed to be mainly governed by resonance effects, it follows that a substantial π-delocalization from the aromatic ring may be occurring. These considerations as well as the correlation described by eq. 2 support the notion that σ and π electron density variations are transmitted from the aromatic ring to the nitrogen and carbene carbon atoms of **2–6**.

Interestingly, the C_1 carbons of the phenylthiocarbene derivatives A are *deshielded* by *ca.* 8 p.p.m. with respect to the parent thiols, in contrast to the C_1 carbons in **2–6** which are *shielded* by *ca.* 5 p.p.m., with respect to the parent anilines. Thus, the two series of complexes again exhibit opposite trends (see eq. 3), presumably arising from the differing electron transmitting properties of the sulfur and nitrogen hetero atoms.

^{13}C—^{195}Pt Coupling Constants

The insensitivity of the ^{13}C—^{195}Pt coupling constants obtained for **2–6**, with regard to variations in the *para*-substituent —X, is quite reasonable when it is noted that the changes in electron density at C_1 and the carbene carbon should arise mainly via changes in π-electron density. Moreover, we have previously shown that many ^{13}C—^{195}Pt coupling constants do not appear to be sensitive to π-bonding in bonds between the coupling nuclei (10, 13), but only to changes in σ-hybridization. Since the changes in σ-electron density at C_1 and the carbene carbon are likely very small, we would anticipate that both $^1J_{PtC}$ (carbene) and $^3J_{PtCNC}$ would be almost invariant, as we observe.

We have previously shown that there exists a marked stereochemical dependence of the $^3J_{PtCNC}$ values in alkylamino carbenes (1). While it is difficult to predict the stereochemical disposition of the *para*-substituted phenyl groups in **2–6** without recourse to further data, the constancy of the $^3J_{PtCNC}$ values at *ca.* 21 (±1) Hz at least indicates that these complexes probably have similar geometries in solution. Fortunately, the ^1H n.m.r. data allows us to determine which isomer about the carbene carbon – nitrogen bond predominates.

^1H Nuclear Magnetic Resonance Parameters

Like their ^{13}C counterparts, the ^1H n.m.r. parameters for the platinum-methyl, arsenic-methyl, and carbene-methyl groups apparently vary randomly within narrow ranges. However, the magnitudes of the $^3J_{HCNH}$ values merit comment. By ^1H n.m.r. studies, Moser and Fischer (14) have shown that analogous complexes of the sort p-$XC_6H_4NH(CH_3)CCr(CO)_5$, **C**, favor the isomer in which the *para*-substituted phenyl ring is *cis* to the carbene methyl group. Those complexes exhibit a $^3J_{HCNH}$ value of 1.0 (±0.1) Hz, identical to those ^1H—^1H coupling constants we have observed for **2–6**. Since the complexes of series **C** provide good n.m.r. models for **2–6** (1), it would appear that the substituted phenyl groups in the latter complexes also adopt *cis* orientations with respect to the carbene-methyl groups.

We thank the National Research Council of Canada for financial support of this project and for an award of an NRCC postdoctoral fellowship to J.E.H.W.

1. M. H. CHISHOLM, H. C. CLARK, J. E. H. WARD, and K. YASUFUKU. Inorg. Chem. In press.
2. C. V. SENOFF and J. E. H. WARD. To be published.
3. L. P. HAMMETT. Physical organic chemistry. McGraw-Hill Book Co., New York, N.Y. 1970. p. 356.
4. G. M. BODNER, J. B. KAHL, K. BORK, B. N. STORHOFF, J. E. WEILLER, and L. J. TODD. Inorg. Chem. **12**, 1071 (1973).
5. M. H. CHISHOLM and H. C. CLARK. Inorg. Chem. **10**, 1711 (1971).
6. G. C. LEVY and J. D. CARGIOLI. J. Magn. Reson. **6**, 143 (1972).
7. M. H. CHISHOLM, H. C. CLARK, W. S. JOHN's, J. E. H. WARD, and K. YASUFUKU. Inorg. Chem. In press.
8. J. A. CONNOR and E. O. FISCHER. J. Chem. Soc. A, 578 (1969).
9. M. H. CHISHOLM, H. C. CLARK, L. E. MANZER, J. B. STOTHERS, and J. E. H. WARD. J. Am. Chem. Soc. **95**, 8574 (1973).
10. H. C. CLARK and J. E. H. WARD. J. Am. Chem. Soc. **96**, 1741 (1974).
11. H. C. CLARK and J. E. H. WARD. Can. J. Chem. **52**, 570 (1974).
12. (*a*) J. B. STOTHERS. Carbon-13 NMR spectroscopy. Academic Press, New York, N.Y. 1972; (*b*) G. C. LEVY and G. L. NELSON. Carbon-13 nuclear magnetic resonance for organic chemists. Wiley–Interscience, New York, N.Y. 1972.
13. M. H. CHISHOLM, H. C. CLARK, L. E. MANZER, J. B. STOTHERS, and J. E. H. WARD. J. Am. Chem. Soc. In press.
14. E. MOSER and E. O. FISCHER. J. Organometal. Chem. **13**, 387 (1968).

Can. J. Chem. Downloaded from www.nrcresearchpress.com by 210.87.254.6 on 09/05/12
For personal use only.

An X-Ray Study of the Synthetic Intermediate 9-Cyano-1,10-dimethyl-6-ethylenedioxy-1-octalin

HARRY LYNTON AND PIK-YUEN SIEW

Department of Chemistry, University of New Brunswick, Fredericton, New Brunswick

Received March 19, 1974

HARRY LYNTON and PIK-YUEN SIEW. Can. J. Chem. **53**, 192 (1975).

The crystal structure of the synthetic intermediate, 9-cyano-1,10-dimethyl-6-ethylenedioxy-1-octalin, $C_{15}H_{21}O_2N$, was solved by direct methods. The compound crystallizes in the space group $P2_1/c$ with cell dimensions $a = 12.282(4)$, $b = 7.144(3)$, $c = 15.619(5)$ Å, $\beta = 104.04(1)°$. Refinement was carried out isotropically for hydrogen and anisotropically for non-hydrogen atoms using full matrix least squares to an R-value of 0.043 for 1669 observed reflections.

This compound, which has a *cis* configuration at the octalin ring junction, is a precursor to a moiety of the alkaloid thelepogine. The *cis* conformation is essential for total synthesis of thelopogine by this route.

HARRY LYNTON et PIK-YUEN SIEW. Can. J. Chem. **53**, 192 (1975).

On a résolu par des méthodes directes la structure cristalline de l'intermédiaire de synthèse, cyano-9 diméthyl-1,10 éthylènedioxy-6 octaline-1, $C_{15}H_{21}N_2O$. Le composé cristallise dans le groupe d'espace $P2_1/c$ avec des dimensions de mailles $a = 12.282(4)$, $b = 7.144(3)$, $c = 15.619(5)$ Å, $\beta = 104.04(1)°$. On a fait un affinement isotropique pour les atomes d'hydrogène et anisotropique pour les autres atomes; on a utilisé la méthode des moindres carrés (matrice complète) jusqu'à une valeur R de 0.043 pour les 1669 réflections observées.

Ce composé qui possède une configuration *cis* à la jonction des cycles de l'octaline, est un précurseur pour une portion de l'alcaloide thélépogine. Cette conformation *cis* est essentielle pour la synthèse de la thélépogine par ce schéma. [Traduit par le journal]

Introduction

Thelepogine, a diterpenoid alkaloid extracted from the grass species *thelepogon elegam* (1, 2), has been identified together with other alkaloids in investigations primarily concerned with the use of a variety of grasses as pasture materials.

Compound **2** represents a moiety of the novel structure found for thelepogine (**1**). It is therefore of interest as a possible intermediate in a total synthesis of the alkaloid. Recently, a total synthesis of compound **2** was completed (3) through the precursor 9-cyano-1,10-dimethyl-6-ethylenedioxy-1-octalin (**3**). Before utilizing compound **2** for further work, it was essential to ensure that the stereochemistry at the octalin ring junction was the same as in the alkaloid (4). Unfortunately, neither the stereochemistry of compound **2** nor any of its precursors could be ascertained with confidence by spectroscopic means. As compound **2** does not itself form crystals suitable for X-ray structure analysis, the precursor compound **3** was chosen. Compound **3** is convertible into compound **2** in four steps by a method which does not affect the stereochemistry at the ring junction.

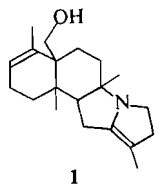

1

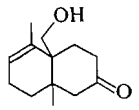

2

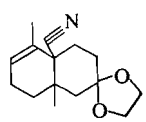

3

Experimental

The crystal data are as follows:

$C_{15}H_{21}O_2N$ m.w. = 237.34

Monoclinic, $a = 12.282(4)$, $b = 7.144(3)$, $c = 15.619(5)$ Å, $\beta = 104.04(1)°$, $V = 1329.45$ Å^3, $Z = 4$, $p_c = 1.34$ g cm^{-3} (22 °C, MoKα_1, $\lambda = 0.7093$ Å).

The unit cell dimensions and their estimated standard deviations (in parentheses) were obtained from a least squares evaluation of the angular settings of 12 independent reflections. The space group is $P2_1/c$ (C_{2h}^5) No. 14 in ref. 5.

The crystals are translucent, stable at room temperature and with respect to prolonged humidity and X-rays.

A crystal of size 0.44 × 0.44 × 0.32 mm^3 was mounted with the a axis along the ϕ direction of the Picker, computer-controlled, four-angle diffractometer. Intensity data were collected with graphite monochromated MoKα_1 radiation and a scintillation detector using a $\theta/2\theta$ scan. Four octants hkl, $h\bar{k}l$, $\bar{h}kl$, and $\bar{h}\bar{k}l$, were explored to a 2θ maximum of 50°. In this region there were 2364 independent reflections of which 1669 were con-

Can. J. Chem. Downloaded from www.nrcresearchpress.com by 210.87.254.40 on 09/05/12
For personal use only.

TABLE 1. Final parameters (e.s.d.) $x,y,z, \times 10^4$, $U_{ij} \times 10^3$ Å^2, T.F. = exp $[-2\pi^2(a^{*2}h^2U_{11} + \ldots + 2b^*c^*klU_{23})]$

Atom	x	y	z	U_{11}	U_{22}	U_{33}	U_{12}	U_{13}	U_{23}
O(1)	1097(1)	4603(2)	2380(1)	73(1)	46(1)	60(1)	5(1)	38(1)	7(1)
O(2)	1346(1)	6409(2)	1257(1)	63(1)	39(1)	43(1)	3(1)	16(1)	6(1)
N	3808(2)	−90(3)	1961(1)	62(1)	70(1)	88(1)	−0(1)	−4(1)	35(1)
C(1)	4100(2)	2715(3)	231(1)	42(1)	38(1)	54(1)	−1(1)	14(1)	−2(1)
C(2)	3697(2)	3225(3)	−599(1)	55(1)	52(1)	49(1)	−1(1)	19(1)	−2(1)
C(3)	2521(2)	3843(3)	−994(1)	60(1)	60(1)	40(1)	−1(1)	8(1)	4(1)
C(4)	1858(2)	4202(3)	−304(1)	45(1)	46(1)	38(1)	2(1)	1(1)	2(1)
C(5)	1387(2)	3064(3)	1105(1)	40(1)	40(1)	48(1)	−2(1)	10(1)	3(1)
C(6)	1715(2)	4719(3)	1715(1)	49(1)	40(1)	42(1)	−1(1)	17(1)	5(1)
C(7)	2959(2)	4758(3)	2137(1)	56(1)	53(1)	39(1)	−2(1)	7(1)	−0(1)
C(8)	3651(2)	4571(3)	1461(1)	41(1)	48(1)	42(1)	−8(1)	4(1)	−2(1)
C(9)	3363(1)	2784(2)	888(1)	36(1)	37(1)	43(1)	−1(1)	4(1)	5(1)
C(10)	2085(1)	2709(1)	424(1)	35(1)	39(1)	42(1)	−3(1)	4(1)	−1(1)
C(11)	5305(2)	2151(3)	584(1)	43(1)	57(1)	76(1)	5(1)	15(1)	−1(1)
C(12)	3629(2)	1150(3)	1490(1)	39(1)	52(1)	56(1)	−1(1)	2(1)	9(1)
C(13)	1757(2)	773(3)	16(1)	50(1)	45(1)	55(1)	−7(1)	8(1)	−6(1)
C(14)	780(2)	6418(3)	2562(2)	117(2)	49(1)	73(2)	14(1)	50(2)	4(1)
C(15)	1098(2)	7664(3)	1893(1)	70(1)	44(1)	52(1)	2(1)	18(1)	−4(1)

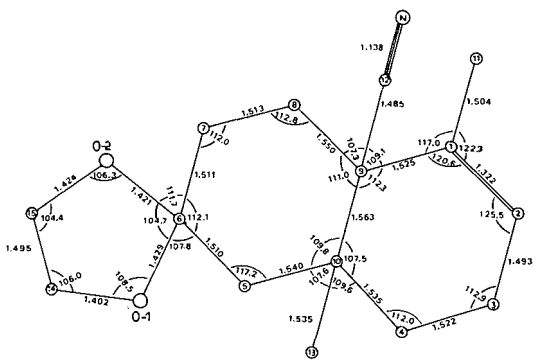

FIG. 1. Bond distances and bond angles of 9-cyano-1,10-dimethyl-6-ethylenedioxy-1-octalin.

sidered observed. The threshold was taken as 10% of the background or 20 counts, whichever was the higher; a scan speed of 1°/min was used with a scan range of 2.2°. The background was measured for 20 s at each end of the range. Data were also corrected against two standard reflections taken at intervals of 25 readings. The linear absorption coefficient for MoKα radiation is 0.872 cm^{-1}. No corrections were made for absorption or extinction.

Structure Analysis

From an E-map computed with phases established by the method of symbolic addition (6), coordinates were obtained for the twelve best defined peaks, all in general positions (4e). Based on the phases using these positions, a Fourier synthesis was computed from which coordinates for the remaining non-hydrogen atoms were established in general positions.

Refinement was carried out isotropically, then anisotropically by full matrix least squares for each of the atoms. The R-value for observed reflections was then 0.103. Scattering factor curves used were those given in ref. 7. The weighting scheme used was $1/w = 1 + [(|F_o| - P_2)/P_1]^2$ with $P_1 = 9.7$ and $P_2 = 19.7$.

From a difference synthesis, coordinates were established for the 21 hydrogen atoms in general positions. Each of these hydrogen atoms was first assigned the isotropic temperature factors of the carbon atoms to which it is attached. Full matrix least squares refinement was then carried out isotropically for hydrogen and anisotropically for non-hydrogen atoms to a final R-value of 0.043. In the final refinement cycle, no parameter shift/estimated standard deviation ratio exceeded 0.44 for hydrogen and 0.27 for other atoms. A final difference synthesis showed no residual peaks greater than 0.1 e Å^{-3}.

A list of the observed and calculated structure factors for the parameters as listed in Tables 1 and 2 has been placed in the Depository of Unpublished Data.[1] Bond distances and angles are given in Fig. 1. The stereochemistry of the molecule is shown in Fig. 2.

Discussion

The decrease in the residual R, obtained by inclusion of the refined hydrogen parameters, is significant by Hamilton's test (8) at the 0.005 (0.5%) level.

The C—H bond lengths range from 0.96–1.02 Å, e.s.d. 0.02 Å, and are comparable with many other values reported in the literature. C(14)—H(18) 1.04(4) Å and C(14)—H(19) 0.92(3) Å are outside this range, but are calculated for atoms with large thermal parameters and are consequently less reliable. H—C—C bond angles range 115–120° for carbon atoms

[1]Complete set of tabular data is available, at a nominal charge, from the Depository of Unpublished Data, National Science Library, National Research Council of Canada, Ottawa, Canada K1A 0S2.

Can. J. Chem. Downloaded from www.nrcresearchpress.com by 210.87.254.40 on 09/05/12
For personal use only.

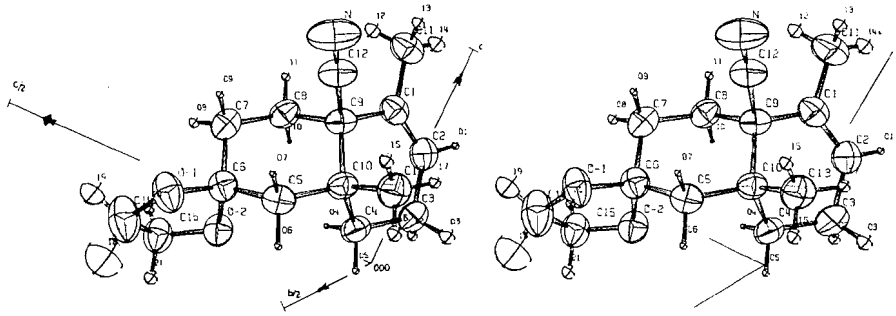

FIG. 2. Stereoscopic view of 9-cyano-1,10-dimethyl-6-ethylenedioxy-1-octalin.

TABLE 2. Hydrogen parameters $x,y,z \times 10^3$, $U \times 10^3$ Å^2

Atom	x	y	z	U
H(1)	419(2)	323(3)	−101(1)	22(5)
H(2)	255(2)	503(3)	−134(1)	34(6)
H(3)	210(2)	290(4)	−144(2)	48(7)
H(4)	207(2)	546(3)	−7(1)	17(5)
H(5)	104(2)	420(3)	−59(1)	22(5)
H(6)	57(2)	321(3)	77(1)	21(5)
H(7)	146(1)	197(3)	149(1)	20(5)
H(8)	312(2)	594(3)	247(1)	33(6)
H(9)	312(2)	373(3)	254(1)	23(5)
H(10)	353(1)	564(2)	106(1)	13(5)
H(11)	445(2)	456(3)	174(1)	27(5)
H(12)	567(2)	292(4)	111(2)	50(7)
H(13)	536(2)	84(3)	81(1)	42(6)
H(14)	580(2)	228(4)	18(2)	54(7)
H(15)	188(2)	−16(3)	47(1)	40(6)
H(16)	94(2)	76(3)	−26(1)	41(6)
H(17)	218(2)	51(3)	−44(1)	34(6)
H(18)	−8(3)	643(5)	252(2)	110(11)
H(19)	112(2)	672(5)	314(2)	74(9)
H(20)	176(2)	839(3)	216(1)	33(6)
H(21)	45(2)	849(4)	158(1)	42(7)

with sp^2 hybridization and 105–114° for sp^3 carbons. Estimated standard deviations are 1–2°. The H(14)—C(11)—C(1) bond angle is exceptionally large, 117°.

All the C—C single bond distances are in the range 1.504–1.563 Å, except for the short C(9)—C(12) 1.483 Å adjacent to the C(12)—N triple bond 1.138 Å, C(2)—C(3) 1.493 Å adjacent to the C(1)—C(2) double bond 1.322 Å and C(14)—C(15) 1.495 Å in the five membered ring. These short bonds probably result from partial transfer of electrons from adjacent multiple bonds, and in the case of C(14)—C(15) distortion in the five membered ring. The C—O bond lengths range from 1.402–1.429 Å. All bond lengths are within the limits reported for other compounds with similar molecular moieties. All non-hydrogen bonds have e.s.d. of 0.003 Å. Bond angles for non-hydrogen atoms range 117.0–125.5° for trigonal situations, 104.4–108.5° for tetrahedral in the five membered ring and 104.7–117.0° elsewhere, e.s.d. being 0.2°. Except where ring strain is present these correspond with expected values of 120° and 109.5°. The C(9)—C(12)—N bond angle is 178.2(4)°, very close to linear.

The three ring system of this structure consists of an octalin fused ring system with an ethylenedioxy moiety at C(6). The cyanide group at C(9) and the methyl group at C(10) are *cis* to each other. This configuration is the same as in the alkaloid thelepogine, and allows the possibility of a total synthesis of the alkaloid by this route.

We wish to thank Dr. R. B. Kelly for the crystals and for suggesting the problem, the National Research Council of Canada for financial support. We also thank Dr. J. M. Stewart of the University of Maryland for use of his computer programs.

1. J. FRIDRICHSONS and H. M. MATHIESON. Tetrahedron Lett. **26**, 18 (1960).
2. W. D. CROW. Aust. J. Chem. **15**, 159 (1962).
3. R. B. KELLY *et al.* In press.
4. J. FRIDRICHSONS and H. M. MATHIESON. Acta Cryst. **16**, 206 (1963).
5. International tables for X-ray crystallography, Vol. 1. The Kynoch Press, Birmingham, England. 1965.
6. J. KARLE and I. L. KARLE. Acta Cryst. **21**, 849 (1966).
7. International tables for X-ray crystallography, Vol. II. The Kynoch Press, Birmingham, England. 1962.
8. W. C. HAMILTON. Acta Cryst. **18**, 502 (1965).

Can. J. Chem. Downloaded from www.nrcresearchpress.com by 210.87.254.40 on 09/05/12
For personal use only.

Reactions of Ketene Acetals. III.[1] A New Synthesis of α-Pyrones. II[2]

ALAIN BÉLANGER AND PAUL BRASSARD
Département de Chimie, Université Laval, Québec, Québec G1K 7P4

Received November 27, 1973[3]

ALAIN BÉLANGER and PAUL BRASSARD. Can. J. Chem. **53**, 195 (1975).

The cycloaddition of chloroketene acetals to α,β-unsaturated aldehydes and ketones gives the corresponding 2,2-dialkoxy-3-chloro-3,4-dihydro-1,2-pyrans. Treatment of these compounds with alkoxides in dimethylsulfoxide or dimethylformamide yields α-pyrones directly. Some intermediates and by-products have been identified and the reaction conditions have been studied.

ALAIN BÉLANGER et PAUL BRASSARD. Can. J. Chem. **53**, 195 (1975).

La cycloaddition des acétals du chlorocétène aux aldéhydes et cétones α,β-insaturés donne les dialcoyloxy-2,2 chloro-3 dihydro-3,4 pyrannes-1,2 correspondants. En présence d'alcoolates dans le diméthylsulfoxyde ou le diméthylformamide, ces substances se transforment directement en α-pyrones. Quelques intermédiaires et sous-produits de la réaction sont identifiés et les conditions expérimentales étudiées.

Can. J. Chem. Downloaded from www.nrcresearchpress.com by 210.87.254.6 on 09/05/12
For personal use only.

The convenient synthesis of dihydropyrans from enals or enones and ketene acetals devised by McElvain *et al.* (1) seemed, with some modification, to provide an interesting basis for a new and simple synthesis of α-pyrones (Scheme 1). 3-Chloro-3,4-dihydro-1,2-pyrans have now been prepared (by the cycloaddition of chloroketen acetals to α,β-unsaturated carbonyl compounds) and are easily converted to the corresponding aldehydo or keto esters. However all attempts to eliminate hydrogen chloride from the latter by various means yielded only starting material, cyclopropanes or complex mixtures of unidentified products. Eventually it was found that the dehydrohalogenation of the chlorodihydropyrans by sodium methoxide in dimethylsulfoxide gave the α-pyrones directly. This paper describes the preparation of a number of alkyl and aryl α-pyrones; the use of β-functionalized enones and a discussion of the mecanism are reported in the companion article.

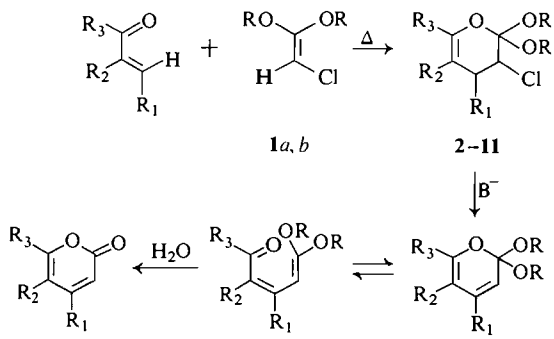

SCHEME 1

The Preparation of 2,2-Dialkoxy-3-chloro-3,4-dihydro-1,2-pyrans

These dihydropyrans were prepared in moderate yields (27–66%) by heating the α,β-unsaturated aldehyde or ketone and an excess of chloroketene dialkyl acetal (1.5 equiv.) at 82–155° for 0.5–105 h, generally in a sealed tube. With the exception of the 4-phenyl and 4,6-diphenyl derivatives, the chlorodihydropyrans are viscous substances; all are relatively unstable, become rapidly discolored, and most do not give satisfactory analyses. The liquid compounds show a slight absorption at about 1740 cm^{-1} in their i.r. spectra, probably due to decomposition products (not detected by n.m.r. spectroscopy) which could not be eliminated by the usual means. After distillation, these were converted directly to the α-pyrones without further purification.

The chlorodihydropyrans can be conveniently characterized by spectroscopic means; they all show an intense band between 1655 and 1700 cm^{-1} due to the enol ether double bond and generally four typical peaks between 1145 and 980 cm^{-1} for the orthoester group. Nuclear magnetic resonance gives characteristic spectra

[1]For parts I and II see refs. 12 and 13.
[2]For a preliminary report and part I see refs. 14 and 13.
[3]Revision received September 30, 1974.

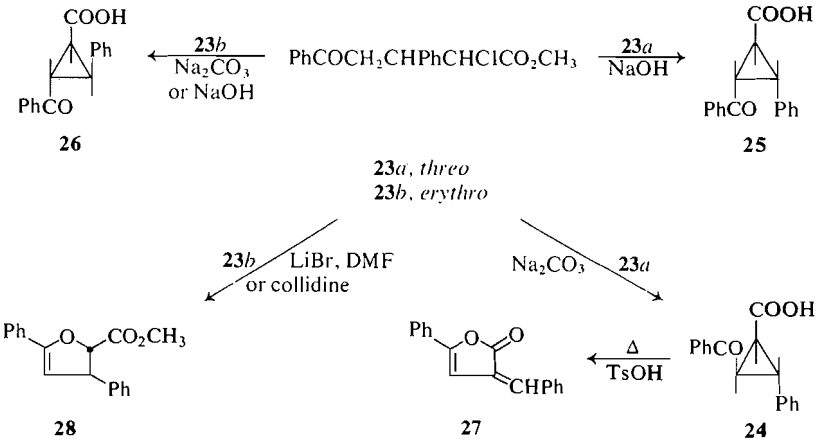

SCHEME 2

for these compounds with signals at δ 4.10–4.55 (3-CH), 2.45–2.70 (4-CH_2), 4.50–5.60 (5-CH), and 6.10–6.45 (6-CH) with the appropriate coupling constants. The compounds substituted in the 4 position can give diastereoisomeric mixtures and these are present for the 4-propyl (**3**, **4**) and 4,6-diphenyl (**7**) derivatives. Only one isomer is observed, however, in the reaction mixtures of products **5** and **6**. In each case, the configurations are assigned on the basis of the expected coupling constants for the most stable conformation. The magnitude of the coupling constants for the protons in positions 3 and 4 (J = 4.5 and 10.5 Hz) seems to indicate, in spite of the limited number of observations, that these substances assume essentially rigid conformations (equatorial 3-CH and pseudo-axial 4-CH for the *cis*-isomers; axial 3-CH and pseudo-axial 4-CH for the *trans*); this also seems confirmed in one case (**7***b*) by the existence of long-range coupling between the protons in the 3 and 5 positions).

The Hydrolysis of Chlorodihydropyrans and the Attempted Dehydrohalogenation of the Corresponding Esters

The acid hydrolysis of 2,2-diethoxy-3,4-dihydro-1,2-pyrans under mild conditions is known to yield the corresponding δ-oxo esters (1). The 3-chloro derivatives have now been found to behave in an analogous way; in particular *cis*- and *trans*-3-chloro-4,6-diphenyl-3,4-dihydro-1,2-pyran give the *erytho*- and *threo*-4-benzoyl-2-chloro-3-phenylbutanoates, respectively. This conclusion is confirmed by n.m.r. data, the relative magnitude of the constants for the coupling between the protons in 3 and 4 ($J_{erythro} > J_{threo}$) being such as predicted (2).

Dehydrohalogenations at this stage were attempted by various means using the *erythro*-ester **23***b*. Silver nitrate in boiling methanol gives several products, none of which seems to be the expected substance. Lithium bromide in dimethylformamide and *s*-collidine at 140° both give a principal product tentatively identified as *trans*-2-carbomethoxy-3,5-diphenyl-3,4-dihydrofuran (ν_{max} 1750 cm^{-1}; δ ($CDCl_3$) 3.79 s (CO_2CH_3), 4.48 dd (J = 3.0, 6.0 Hz) (3-CH), 4.99 d (J = 6.0 Hz) (2-CH), 5.5 d (J = 3.0 Hz) (4-CH) 7.10–7.90 m (aromatic CH)) (3).

Bases such as sodium carbonate and hydroxide produced only cyclopropanecarboxylic acids, the configurations of which are well known (4). Some of these reactions are highly stereospecific; thus the *threo*-ester **23***a* in the presence of carbonate gives *cis*-3-benzoyl-*trans*-2-phenylcyclopropanecarboxylic acid (**24**) while hydroxide yields the epimerized *trans*,*trans*-isomer **25**. As expected, the *erythro*-ester **23***b*, with both reagents forms the same product, the *trans*,*cis*-acid **26** (Scheme 2).

An attempt to rearrange the cyclopropanecarboxylic acid **24** by heating it in the presence of *p*-toluenesulfonic acid gave a product which on spectroscopic and analytical grounds is thought to be α-benzal-γ-phenylcrotonolactone (**27**).

The Preparation of α-Pyrones (Scheme 1)
4-Aryl; 4,6-Diaryl; and 4,5,6-Trialkyl-α-pyrones

The compounds are formed quite straight forwardly from the corresponding chlorodihydro-

Can. J. Chem. Downloaded from www.nrcresearchpress.com by 210.87.254.6 on 09/05/12
For personal use only.

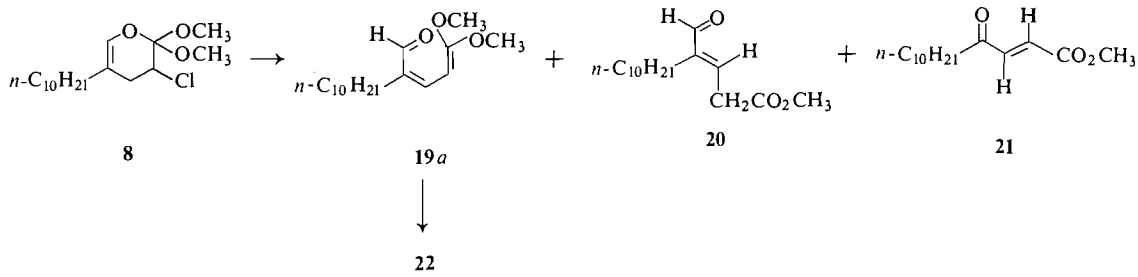

SCHEME 3

pyrans using 4.5 equiv. of sodium methoxide in dimethylsulfoxide. The yields are excellent (72–85%) and no by-products are detected (method A).

4- and 6-Alkyl-α-pyrones

α-Pyrone and the 6-methyl derivative could not be prepared by the foregoing procedure and their intermediates are thought to be unstable under these conditions. The 4-propyldihydropyran **3** was inert to methoxide but potassium *t*-butoxide gave a low yield of the α-pyrone **15** along with a very small quantity of a by-product which probably is one of the corresponding 4-formylbutenoic esters (method B).

6-Aryl-α-pyrones

Under the usual conditions, 6-phenyl-α-pyrone (**11**) is obtained in low yield (15%) and numerous variations of the method were devised in order to improve the efficiency of the reaction and to gain some insight into the nature of the process. Sodium hydroxide was found to be inactive and potassium *t*-butoxide did not raise the yield. By replacing the usual solvent by the lower-melting dimethylformamide and carrying out the reaction at −10°, a good yield of the naturally occurring 6-phenyl-α-pyrone (**18**) was obtained along with appreciable amounts of two esters. The pyrone can be isolated by chromatography on Florisil which retains the by-products. The mixture of esters can be isolated by the use of silica gel activity I with the concomitant decomposition of the pyrone. The by-products appear to be the methyl *trans*-4-benzoylbut-2- and 3-enoates and could not be separated by chromatography (method C).

5-Alkyl-α-pyrones (Scheme 3)

Compounds of this type were considered of particular interest since they have the substitution characteristics of steroidal dienolides. 3-Chloro-5-*n*-decyl-3,4-dihydro-1,2-pyran (**8**), under the usual conditions (4.5 equiv. of methoxide in DMSO at 25°) gave as principal product methyl *trans*-4-formyltetradeca-3-en-1-oate (**20**) and a low yield of the α-pyrone **22**. No reaction is observed when either potassium *t*-butoxide at −5° or sodium methoxide in dimethylformamide at 25° are used.

A slight modification of the work-up process produced an unexpected result. By adding ice to the reaction mixture instead of pouring it into water, the oxidation product **21** is obtained besides the usual aldehydo ester **20**. The use of larger amounts of base (8 equiv.) gives a new type of product in a moderate yield (55%); this was eventually identified as 2-*n*-decyl-5,5-dimethoxypenta-2,4-dien-1-al (**19***a*), an unstable substance which undergoes spontaneous and almost quantitative rearrangement to the α-pyrone (probably in the presence of moisture) (method D).

α-Pyrones from Chlorodiethoxydihydropyrans

The dimethyl acetal of chloroketene was used throughout this investigation in order to simplify the n.m.r. spectra of the reaction mixture which are often complex. Since the diethyl derivative is more readily accessible, an attempt was made to compare the efficiency of both acetals. The analogous chlorodihydropyrans are obtained in comparable yields but seem to be less stable than the dimethoxy derivatives. In the case of the 5-*n*-decyl compound **9**, a similar amount of the pentadienal **19***b* is produced but the rearrangement to the α-pyrone is much less efficient (17%). The same results are observed in the case of the 4-propyl derivatives **4***a*,*b*.

Experimental

The melting points were taken in capillary tubes using a calibrated thermometer (Thomas-Hoover Apparatus). The i.r. spectra were recorded on a Beckman IR-12 instrument, u.v. spectra on a Beckman DK-1A spectropho-

Can. J. Chem. Downloaded from www.nrcresearchpress.com by 210.87.254.6 on 09/05/12
For personal use only.

Can. J. Chem. Downloaded from www.nrcresearchpress.com by 210.87.254.6 on 09/05/12
For personal use only.

tometer and the n.m.r. on a Varian A60 spectrometer with tetramethylsilane as internal standard.

3-Chloro-2,2-dialkoxy-3,4-dihydro-1,2-pyrans

General Method

The α,β-unsaturated aldehyde or ketone, the chloroketen dialkyl acetal **1***a,b* (1.5 equiv.) (5,6), and hydroquinone (1–5 mg) are placed in a glass tube which is flushed with nitrogen, sealed, and heated. The excess acetal and the volatile by-products are then evaporated under vacuum and the dihydropyran is distilled or crystallized from the appropriate solvent. The distilled products contain small amounts of impurities and must be converted immediately to the α-pyrones:

3-Chloro-2,2-dimethoxy-3,4-dihydro-1,2-pyran (**2**) from acrolein (4.0 g) and **1***a* (125°, 3 h), b.p. 90–92°/12 mm (56%); ν_{max} (film) 1665, 1130, 1090, 1050, 1030 cm^{-1}; δ (neat) 2.50 m (4-CH_2), 3.30 and 3.32 2s (2,2-OCH_3) 4.32 t (J = 6.0 Hz) (3-CH), 4.75 dt (J = 3.5, 6.0 Hz) (5-CH), 6.25 dt (J = 2.0, 6.0 Hz) (6-CH).

cis- and *trans*-3-Chloro-2,2-dimethoxy-4-propyl-3,4-dihydro-1,2-pyran (**3***a,b*) from *trans*-hex-2-enal (3.0 g) and **1***a* (145°, 72 h), b.p. 110–130°/7 mm (39%); ν_{max} (film) 1660, 1140, 1090, 1060 cm^{-1}; δ ($CDCl_3$) 0.85–1.10 m (4-$(CH_2)_2CH_3$), 1.30–1.60 m (4-$(CH_2)_2CH_3$), 3.31, 3.32, 3.40, and 3.42 4s (2,2-OCH_3), 4.00–4.25 m (3-CH), 4.50–4.75 m (5-CH), 6.22 dd (J = 3.0, 6.5 Hz) (6-CH).

cis- and *trans*-3-Chloro-2,2-diethoxy-4-propyl-3,4-dihydro-1,2 pyran (**4***a,b*) from *trans*-hex-2-enal (3.0 g) and **1***b* (150°, 72 h), b.p. 105–116°/7 mm (39%); ν_{max} (film) 1660, 1110, 1090, 1050 cm^{-1}; δ ($CDCl_3$) 0.90–1.15 m (2,2-OCH_2CH_3 and 4-$(CH_2)_2CH_3$), 1.15–1.60 m (4-$(CH_2)_2CH_3$), 3.71 q (J = 7.0 Hz) (2,2-OCH_2CH_3), 4.00–4.25 m (3-CH), 4.50–4.80 m (5-CH), 6.24 dd (J = 3.0, 6.0 Hz) (6-CH).

cis-3-Chloro-4-ethyl-2,2-dimethoxy-3,4,5,6,7,8-hexahydro-1,2-benzopyran (**5**) from 2-propylidenecyclohexanone (5.0 g) (b.p. 89–90°/8 mm) (7) and **1***a* (150°, 105 h), b.p. 80–90°/0.01 mm (27%); ν_{max} (film) 1698, 1150, 1120, 1065, 1000 cm^{-1}; δ ($CDCl_3$) 0.95 t (J = 7.0 Hz) (4-CH_2CH_3), 1.50–2.50 m (4-CH_2CH_3 and 5,6-$(CH_2)_4$-, 3.40 and 3.42 2s (2,2-OCH_3), 4.28 d (J = 4.5 Hz) (3-CH). (This product contains a small amount of the *trans*-isomer, δ 4.18 d (J = 9.0 Hz) (3-CH).)

trans-3-Chloro-2,2-dimethoxy-4-phenyl-3,4-dihydro-1,2-pyran (**6**) from cinnamaldehyde (6.0 g) and **1***a* (150°, 72 h), b.p. 95–96°/1.0 mm (43%), m.p. 106–107° (ether); ν_{max} (KBr) 1662, 1610, 1120, 1070, 1040, 1020 cm^{-1}; δ ($CDCl_3$) 3.46 and 3.49 2s (2,2-OCH_3), 3.85 m (4-CH), 4.22 d (J = 10.0 Hz) (3-CH), 4.89 dd (J = 2.5, 6.0 Hz) (5-CH), 6.42 dd (J = 2.5, 6.0 Hz) (6-CH), 7.38 s (4-C_6H_5).

Anal. Calcd. for $C_{13}H_{15}ClO_3$: C, 61.41; H, 5.90. Found: C, 61.31; H, 5.93.

trans-3-Chloro-2,2-dimethoxy-4,6-diphenyl-3,4-dihydro-1,2-pyran (**7***a*) from benzalacetophenone (6.0 g) and **1***a* (150°, 72 h), m.p. 125–126° (ether – petroleum ether, b.p. 30–60°) (36%); ν_{max} (KBr) 1655, 1600, 1580, 1145, 1110, 1005, 980 cm^{-1}; δ ($(CD_3)_2CO$) 3.48 and 3.53 2s (2,2-OCH_3), 3.95 dd (J = 2.5, 10.5 Hz) (4-CH), 4.52 d (J = 10.5 Hz) (3-CH), 5.51 d (J = 2.5 Hz) (5-CH), 7.25–7.85 m and 7.40 s (4,6-C_6H_5).

Anal. Calcd. for $C_{19}H_{19}ClO_3$: C, 69.00; H, 5.74. Found: C, 69.08; H, 5.71.

cis-3-Chloro-2,2-dimethoxy-4,6-diphenyl-3,4-dihydro-1,2-pyran (**7***b*), m.p. 79–80° (ether – petroleum ether, b.p. 30–60°) (21%); ν_{max} (KBr) 1655, 1605, 1115, 1072, 1060, 1025 cm^{-1}; δ ($CDCl_3$) 3.45 and 3.51 2s (2,2-OCH_3), 4.31–4.53 (AB part of an ABX system; J = 1.5, 2.0, 4.5 Hz) (3,4-CH), 5.59 dd (J = 1.5, 2.0 Hz) (5-CH), 7.25–7.90 m and 7.42 s (4,6-C_6H_5).

Anal. found: C, 68.94; H, 5.59.

2-*n*-Decylacrolein. A mixture of lauraldehyde (20.0 g), dimethylamine hydrochloride (14.0 g), and formaldehyde (30 ml of a 37% aqueous solution) is stirred at 75° for 24 h and then steam-distilled. After extraction of the distillate with ether and evaporation of the solvent, the residue is fractionated under vacuum and gives 2-*n*-decylacrolein, b.p. 70–75°/0.1 mm (79%); λ_{max} (ethanol) 218 nm (log ε 4.10); ν_{max} (film) 3090, 2700, 1700, 1630 cm^{-1}; δ ($CDCl_3$) 0.98 (CH_3), 1.32 bs ($(CH_2)_9$), 6.01 s (*trans*-C=CH) 6.28 s (*cis*-C=CH), 9.63 s (CHO). Semicarbazone, m.p. 145–146° (ethanol).

Anal. Calcd. for $C_{14}H_{27}ON_3$: C, 66.36; H, 10.74; N, 16.58. Found: C, 66.25; H, 10.97; N, 16.35.

3-Chloro-5-*n*-decyl-2,2-dimethoxy-3,4-dihydro-1,2-pyran (**8**) from 2-*n*-decylacrolein (10.0 g) and **1***a* (150°, 24 h), b.p. 100–120°/0.01 mm (48%) ν_{max} (film) 1680, 1125, 1070 cm^{-1}; δ ($CDCl_3$) 0.91 ~ t (J = 6.0 Hz) (5-$(CH_2)_9CH_3$), 1.30 s (5-$CH_2(CH_2)_8CH_3$), ~1.90 m (5-$CH_2(CH_2)_8CH_3$), 2.51 m (4-CH_2), 3.38 and 3.43 2s (2,2-OCH_3), 4.32 t (J = 5.5 Hz) (3-CH), 6.13 bs (6-CH).

3-Chloro-5-*n*-decyl-2,2-diethoxy-3,4-dihydro-1,2-pyran (**9**) from 2-*n*-decylacrolein (3.0 g) and **1***b* (155°, 24 h), b.p. 127–137°/0.08 mm (49%); ν_{max} (film) 1670, 1120, 1100, 1050 cm^{-1}; δ ($CDCl_3$) 0.80–1.00 m (2,2-OCH_2CH_3 and 5-$(CH_2)_9CH_3$), 1.27 s (5-$CH_2(CH_2)_8CH_3$), ~ 1.90 m (5-$CH_2(CH_2)_8CH_3$), 2.49 m (4-CH_2), 3.67 and 3.72 2 q (J = 7.0 Hz) (2,2-OCH_2CH_3), 4.27 t (J = 5.5 Hz) (3-CH), 6.10 bs (6-CH).

3-Chloro-2,2-dimethoxy-6-methyl-3,4-dihydro-1,2-pyran (**10**) from methyl vinyl ketone (5.7 g) and **1***a* (82°, 1.5 h), b.p. 72–74°/12 mm (60%); ν_{max} (film) 1670, 1120, 1100, 1040, 1020 cm^{-1}; δ (CCl_4) 1.79 m (6-CH_3), 2.45 m (4-CH_2), 3.32 and 3.37 2s (2,2-OCH_3), 4.22 t (J = 5.5 Hz) (3-CH), 4.52 m (5-CH).

3-Chloro-2,2-dimethoxy-6-phenyl-3,4-dihydro-1,2-pyran (**11**) from acrylophenone (4.8 g) (b.p. 100–105°/10 mm) (8) and **1***a* (150°, 24 h; 100°, 0.5 h), b.p. 122–128°/1.2 mm (66, 58%); ν_{max} (film) 1665, 1600, 1580, 1125, 1095, 1050, 1020 cm^{-1}; δ ($CDCl_3$) 2.69 dt (J = 4.0, 5.5 Hz) (4-CH_2), 3.40 and 3.45 2s (2,2-OCH_3), 4.32 t (J = 5.5 Hz) (3-CH), 5.37 t (J = 4.0 Hz) (5-CH), 7.25–7.75 m (6-C_6H_5).

Hydrolysis of 3-Chloro-2,2-dimethoxy-3,4-dihydro-1,2-pyrans and Attempted Dehydrohalogenation of the Corresponding Esters

Hydrolysis

Methyl threo-4-benzoyl-2-chloro-3-phenylbutanoate (**23***a*). *trans*-3-Chloro-2,2-dimethoxy-4,6-diphenyl-3,4-dihydro-1,2-pyran (**7***a*) (700 mg) in aqueous HCl (20 ml; 1.0 *N*) was heated on a water bath for 2 h. Extraction of the solution with ether gave the *threo*-ester **23***a* (510 mg), m.p. 45–46° (ether – petroleum ether, (b.p. 30–60°); ν_{max} (KBr) 1748, 1685, 1600, 1585 cm^{-1}; δ ($CDCl_3$) 3.58 d (J = 2.5 Hz) (4-CH_2), 3.68 s (CO_2CH_3), 4.20 dd (J = 2.5, 6.0 Hz)

Can. J. Chem. Downloaded from www.nrcresearchpress.com by 210.87.254.6 on 09/05/12
For personal use only.

(3-CH), 4.90 d (J = 6.0 Hz) (2-CH), 7.32 s, ~ 7.55 and ~ 8.00 2 m (aromatic CH).

Anal. Calcd. for $C_{18}H_{17}ClO_3$: C, 68.25; H, 5.37. Found: C, 68.22; H, 5.45.

Methyl erythro-4-benzoyl-2-chloro-3-phenylbutanoate (*23b*). A mixture of the *cis*-isomer 7*b* (300 mg), methanol (5 ml), water (10 ml) and concentrated HCl (1.0 ml) was refluxed for 30 min. On cooling, the *erythro*-acid **23***b* crystallized (215 mg), m.p. 99–100°; ν_{max} (KBr) 1735, 1682, 1600 cm^{-1}; δ ($CDCl_3$) 3.58 s (CO_2CH_3), 3.70 d (J = 3.5 Hz) (4-CH_2), 4.15 dd (J = 3.5, 7.5 Hz) (3-CH), 4.62 d (J = 7.5 Hz) (2-CH), 7.30 s, ~ 7.50 and ~ 7.95 2 m (aromatic CH).

Anal. found: C, 68.17; H, 5.53.

Formation of Cyclopropanecarboxylic Acids

The methyl ester **23***a* or *b* (200 mg) was stirred for 1 h in an aqueous solution (5 ml) of the appropriate base, which was then further diluted with water, extracted with ether, acidified, and again extracted with ether:

cis-3-Benzoyl-*trans*-2-phenylcyclopropanecarboxylic acid (**24**) from **23***a* and Na_2CO_3 (600 mg), m.p. 173–174° (ether – petroleum ether, b.p. 30–60°) (148 mg) (lit. (4) m.p. 174–175°); ν_{max} (KBr) 1695, 1678, 1600, 960 cm^{-1}; δ ($CDCl_3$) 2.58–3.54 (ABC system) (1,2,3-CH), 7.48 s, ~7.60 and ~8.15 2 m (aromatic CH), 10.80 s (COOH).

trans-3-Benzoyl-*trans*-2-phenylcyclopropanecarboxylic acid (**25**) from **23***a* and NaOH (50 mg), m.p. 151–152° (ether – petroleum ether) (77 mg) (lit. (4) m.p. 152–153°); ν_{max} (KBr) 1695, 1670, 1600, 1010 cm^{-1}; δ ($CDCl_3$) 3.08–3.82 (ABC system) (1,2,3-CH), 7.25 s, ~7.45 and ~8.00 2 m (aromatic CH), 11.50 s (COOH).

trans-3-Benzoyl-*cis*-2-phenylcyclopropanecarboxylic acid (**26**) from **23***b* and Na_2CO_3 (600 mg) or NaOH (50 mg), m.p. 134–135° (ether – petroleum ether) (30 and 74 mg) (lit. (4) m.p. 136–137°); ν_{max} (KBr) 1708, 1680, 1600, 1015 cm^{-1}; δ ($CDCl_3$) 2.78 dd (J = 5.0, 10.0 Hz), 3.28 dd (J = 7.0, 10.0 Hz) and 3.80 dd (J = 5.0, 7.0 Hz) (1,2,3-CH), 7.58 s, ~7.60 and ~8.15 2 m (aromatic CH), 10.60 s (COOH).

α-Benzal-γ-phenylcrotonolactone (**27**). A mixture of *cis*-3-benzoyl-*trans*-2-phenylcyclopropanecarboxylic acid (**24**) (190 mg), *p*-toluenesulfonic acid (2 mg) and benzene (40 ml) was refluxed for 3 h, poured in water and extracted with ether. The ethereal phase after extraction with an aqueous solution of $NaHCO_3$ gave **16**, m.p. 149–150° (preparative t.l.c.; benzene) (ether – petroleum ether, b.p. 30–60°) (lit. (9) m.p. 155°); λ_{max} (ethanol) 250, 384 nm (log ε 4.31, 4.37); ν_{max} (KBr) 1790–1785, 1630, 1600, 1590 cm^{-1}; δ ($CDCl_3$) 7.00 s (4-CH), ~ 7.70 m (3-CHC_6H_5 and 5-C_6H_5).

Anal. Calcd. for $C_{17}H_{12}O_2$: C, 82.25; H, 4.85. Found: C, 82.18; H, 4.95.

α-Pyrones

Method A

A solution of the chlorodihydropyran **5**, **6**, or 7*a* and sodium methoxide (4.5 equiv.) in anhydrous dimethylsulfoxide was stirred at room temperature for 24 h under nitrogen, then poured into a mixture of ice and water and extracted with ether.

4-Ethyl-5,6,7,8-tetrahydrocoumarin (**12**) from **5** (1.3 g) (50 ml of DMSO), m.p. 80–81° (ether – petroleum ether, b.p. 30–60°) (the mother liquor from this crystallization was chromatographed on silica gel (30 g) using a mixture of benzene and ether (4:1) as eluant) (78%); λ_{max} (ethanol) 245, 265 (sh) nm (log ε 4.18, 4.12); ν_{max} (KBr) 1705, 1640, 1560 cm^{-1}; δ ($CDCl_3$) 1.21 t (J = 7.5 Hz) (4-CH_2CH_3), 1.70–1.95 m (6,7-CH_2), 2.25–2.70 m (4,5,8-CH_2), 6.05 s (3-CH).

Anal. Calcd. for $C_{11}H_{14}O_2$: C, 74.15; H, 7.92. Found: C, 74.19; H, 7.89.

4-Phenyl-α-pyrone (**13**) from **6** (570 mg), (50 ml of DMSO), m.p. 75–76° (ether – petroleum ether, b.p 30–60°) (85%); λ_{max} (ethanol) 228, 272, 298 (sh) (log ε 4.20, 4.17, 4.07); ν_{max} (KBr) 1705, 1640, 1540, cm^{-1}; δ ($(CD_3)_2CO$) 6.63 m (3-CH), 6.75 dd (J = 2.0, 5.5 Hz) (5-CH), 7.55–8.00 m (4-C_6H_5 and 6-CH).

Anal. Calcd. for $C_{11}H_8O_2$: C, 76.73; H, 4.66. Found: C, 77.03; H, 4.47.

4,6-Diphenyl-α-pyrone (**14**) from 7*a* (430 mg) (60 ml of DMSO), m.p. and mixture m.p. 136–137° (ether – petroleum ether, b.p. 30–60°) (72%) (lit. (10) m.p. 137–138°); λ_{max} (ethanol) 263, 345 nm (log ε 4.35, 4.15); ν_{max} (KBr) 1700, 1630, 1540 cm^{-1}; δ ($CDCl_3$) 6.54 d (J = 1.5 Hz) (3-CH), 7.34 d (J = 1.5 Hz) (5-CH), 7.50–8.10 2 m (4,6-C_6H_5).

Method B

A solution of the chlorodihydropyran **3** or **4** and potassium *t*-butoxide (8 equiv.) in anhydrous dimethylsulfoxide was stirred at room temperature under nitrogen, diluted by addition of ice and extracted with ether.

4-Propyl-α-pyrone (**15**) from **3** (500 mg) (50 ml of DMSO; 6 h), b.p. 100–110°/11 mm (preparative t.l.c.; ether-hexane, 1:1), (43%) and from **4** (600 mg) (40 ml of DMSO; 2 h) (10%); λ_{max} (ethanol) 285 nm (log ε 4.00); ν_{max} (film) 1730, 1645, 1555 cm^{-1}; δ ($CDCl_3$) 0.98 t (J = 7.5 Hz) (4-$CH_2CH_2CH_3$), 1.62 m (4-$CH_2CH_2CH_3$), 2.42 t (J = 7.0 Hz) (4-$CH_2CH_2CH_3$), 6.08–6.22 m (3,5-CH), 7.49 d (J = 6.0 Hz) (6-CH).

Anal. Calcd. for $C_8H_{10}O_2$: C, 69.54; H, 7.30. Found: C, 69.47; H, 7.33.

Method C

A solution of the chlorodihydropyran **11** and sodium methoxide (4.5 equiv.) in anhydrous dimethylformamide is stirred at −10°, then poured in ice water and extracted with ether.

6-Phenyl-α-pyrone (**18**) from **11** (783 mg) (50 ml of DMF; 20 h) (chromatographed on Florisil (50 g); benzene–ether, 97:3), m.p. 64–65° (ether – petroleum ether, b.p. 30–60°) (53%) (lit. (11) m.p. 64–65°); λ_{max} (ethanol) 332 nm (log ε 4.23); ν_{max} (KBr) 1720, 1632, 1549 cm^{-1}; δ ($CDCl_3$) 6.33 d (J = 9.0 Hz) (3-CH), 6.72 d (J = 7.0 Hz) (5-CH), 7.40–8.00 m (4-CH, 6-C_6H_5). When the crude product of a similar reaction is chromatographed on silica gel activity I (benzene–ether, 49:1) an oil is obtained, tentatively identified as a mixture of methyl *trans*-4-benzoyl-2-buten-1-oate (**16**) and methyl *trans*-4-benzoyl-3-buten-1-oate (**17**) (23%); ν_{max} (film) 1750–1710, 1695–1665 cm^{-1}; δ ($CDCl_3$) ~3.40 (AB part of an ABX system) (2-CH_2 of **17**), 3.75 s (CO_2CH_3), ~3.89 (AB part of an ABX system) (4-CH_2 of **16**), 6.00 dt (J = 1.0, 16.0 Hz) (2-CH of **16**), 7.00–8.15 (olefinic and aromatic CH). The α-pyrone **18** and the mixture of esters **17** and **18** can be obtained from the same reaction mixture by chromatography on silica gel activity III.

Method D

A solution of the chlorodihydropyran **8** or **9** and sodium methoxide (8.0 equiv.) in anhydrous dimethylsulfoxide was stirred at room temperature under nitrogen, diluted by addition of ice and extracted with ether.

5-*n*-Decyl-α-pyrone (**22**). 3-Chloro-5-*n*-decyl-3,4-dihydro-1,2-pyran (**8**) (500 mg; 25 ml of DMSO) gives a crude product, the major component of which is 2-*n*-decyl-5,5-dimethoxypenta-2,4-dien-1-al (**19***a*); ν_{max} (film) 1599 cm^{-1}; δ ($CDCl_3$) 3.82 and 3.88 2 s (OCH_3), 4.88 d (J = 11.0 Hz) (4-CH), 7.29 d (J = 11.0 Hz) (3-CH), 9.57 s (CHO). This compound is unstable and is converted within a few hours into the α-pyrone **22**. By the use of preparative t.l.c. (chloroform), the reaction mixture yielded the following substances: methyl trans-4-formyltetradeca-3-en-1-oate (**20**) (10%); λ_{max} (ethanol) 226 nm (log ε 4.41); ν_{max} (film) 2710, 1750, 1700, 1650, 1200, 1180 cm^{-1}; δ ($CDCl_3$) 0.95 (CH_3), 1.30 bs ($(CH_2)_8$), 3.45 d (J = 7.0 Hz) (2-CH_2), 6.78 t (J = 7.0 Hz) (3-CH), 9.60 s (CHO); 5-*n*-decyl-α-pyrone (**22**), m.p. 9.5–11.5° (distilled at 0.1 mm) (52%); λ_{max} (ethanol) 300 nm (log ε 3.77); ν_{max} (film) 1750, 1725, 1648, 1549 cm^{-1}; δ ($CDCl_3$) 0.95 ~ t (5-$(CH_2)_9CH_3$), 1.29 bs (5-$CH_2(CH_2)_8CH_3$), 2.30 ~ t (5-$CH_2(CH_2)_8CH_3$), 6.37 d (J = 10.5 Hz) (3-CH), 7.20–7.45 m (4,6-CH).

Anal. Calcd. for $C_{15}H_{24}O_2$: C, 76.22; H, 10.23. Found: C, 76.30; H, 10.39.

When the reaction was carried out with 5.5 equiv. of the base the following products were isolated:

Compounds **20** (11%) and **22** (31%) and methyl *trans*-tetradec-2-en-4-on-1-oate (**21**), m.p. 61.5–62° (ether–petroleum ether, b.p. 30–60°), (17%); λ_{max} (ethanol) 221 nm (log ε 4.29); ν_{max} (KBr) 3070, 1730, 1670, 1640 cm^{-1}; δ ($CDCl_3$) 0.95 (CH_3), 1.30 bs ($(CH_2)_8$), 2.62 t (J = 7.0 Hz) (5-CH_2), 3.80 s (CO_2CH_3), 6.96 dd (J = 16.0 Hz; Δν = 20.4 Hz) (2,3-CH).

Anal. Calcd. for $C_{15}H_{26}O_3$: C, 70.83; H, 10.30. Found: C, 71.09; H, 10.38.

From the chlorodihydropyran **9** (500 mg; 25 ml of DMSO, 8.0 equiv. of methoxide), the crude product contained 2-*n*-decyl-5,5-diethoxypenta-2,4-dien-1-al (**19***b*); δ ($CDCl_3$) 4.85 d (J = 12.0 Hz) (4-CH), 7.30 d (J = 12.0 Hz) (3-CH), 9.50 s (CHO); and **20**. This mixture was allowed to stand for 24 h, chromatographed as described above and gave the methyl ester **20** (15%) and the α-pyrone **22** (17%).

1. S. M. McElvain, E. R. Degginger, and J. D. Behun. J. Am. Chem. Soc. **76**, 5736 (1954).
2. L. M. Jackman and S. Sternhell. Applications of nuclear magnetic resonance spectroscopy in organic chemistry. Second ed. Pergamon Press, Toronto. 1969. pp. 291–292.
3. L. H. Zalkow and M. Ghosal. J. Chem. Soc. Chem. Commun. 922 (1967).
4. R. Stoermer and F. Schenck. Chem. Ber. **60**, 2566 (1927).
5. S. M. McElvain and M. J. Curry. J. Am. Chem. Soc. **70**, 3781 (1948).
6. A. Magnani and S. M. McElvain. J. Am. Chem. Soc. **60**, 2210 (1938).
7. G. Lardelli, V. Lamberti, W. T. Weller, and A. P. De Jonge. Rec. Trav. Chim. **86**, 481 (1967).
8. F. F. Blicke and J. H. Burckhalter. J. Am. Chem. Soc. **64**, 451 (1942).
9. F. W. Schueler and C. Hanna. J. Am. Chem. Soc. **73**, 3528 (1951).
10. E. P. Kohler. J. Am. Chem. Soc. **44**, 379 (1922).
11. D. Molho and M. Giraud. Bull. Soc. Chim. Fr. 2603 (1968).
12. J. Banville, J.-L. Grandmaison, G. Lang, and P. Brassard. Can. J. Chem. **52**, 80 (1974).
13. A. Bélanger, P. Brassard, G. Dionne, and Ch. R. Engel. Steroids. **24**, 377 (1974).
14. A. Bélanger and P. Brassard. J. Chem. Soc. Chem. Commun. 863 (1972).

Can. J. Chem. Downloaded from www.nrcresearchpress.com by 210.87.254.6 on 09/05/12
For personal use only.

Reactions of Ketene Acetals. IV. A New Synthesis of α-Pyrones. III

ALAIN BÉLANGER AND PAUL BRASSARD
Département de Chimie, Université Laval, Québec, Québec G1K 7P4
Received November 27, 1973[1]

ALAIN BÉLANGER and PAUL BRASSARD. Can. J. Chem. **53**, 201 (1975).

A simple one-step synthesis of α-pyrones and 3-chloro-α-pyrones from β-functionalized α,β-enones and ketene acetals has been devised. The method has also been adapted to the preparation of some 4-methoxy-α-pyrones. Finally the mechanism of the reaction has been investigated.

ALAIN BÉLANGER et PAUL BRASSARD. Can. J. Chem. **53**, 201 (1975).

Une synthèse simple d'α-pyrones et de chloro-3 α-pyrones en une étape à partir d'α,β-énones β-fonctionnalisées a été réalisée. La méthode s'adapte aussi à la préparation de quelques méthoxy-4 α-pyrones. Enfin le mécanisme de la réaction a été étudié.

In a companion paper (1) we described a new synthesis of α-pyrones. This method involved the cycloaddition of chloroketene acetals to α,β-unsaturated carbonyl compounds followed by a dehydrohalogenation which yields α-pyrones. It was then assumed that placing the leaving-group on the enone should facilitate the elimination step, prevent the formation of by-products, and simplify the overall process. This modification uses the more readily accessible ketene dialkyl acetals and produces the α-pyrones directly in moderate to good yields (30–77%) (Scheme 1; R_1 = OAc, OBz, or Cl; R_2 and R_3 = H, alkyl, or aryl). β-Functionalized enals and β-alkylenones are either unreactive or give only exchange reactions.

The great stability of a 2,2,4-trimethoxy-3,4-dihydro-1,2-pyran suggested that the cycloaddition of chloroketene acetals to β-methoxy enones and a subsequent dehydrohalogenation would provide a new synthesis of 4-methoxy-α-pyrones. The 3-chloro-4-methoxy-3,4-dihydro-1,2-pyrans are formed by heating the substrates at about 150° (35–80%) and converted to the expected α-pyrones with yields of 32–90%. (Scheme 2; R_1 = OMe; R_2 = H, R_3 = aryl or styryl; and R_2 = alkyl, R_3 = aryl).

The Reaction of β-Functionalized Enones with Ketene Acetals (Scheme 1)

With β-Acetoxy and β-Benzoyloxy Enones

The β-acetoxy enones **3***a*, **4***a*, **5***a*, and **7***a* react readily with ketene dimethyl acetal (**1**) when heated at about 95° for 3–8 h. Examination of the n.m.r. spectra of the crude product usually reveals the presence of a mixture of the expected 4-acetoxy-2,2-dimethoxy-3,4-dihydro-1,2-pyran and elimination product, the 5,5-dimethoxypentadienone. The magnitude of the coupling constant between the protons in the 2 and 3 positions of the latter (~15 Hz) indicates that the tautomer has the *trans*-configuration (β-acetoxyacrylophenone reacts in 48 h at room temperature and gives only the relatively unstable dihydropyran).

Since all attempts to separate the dihydropyran from the dienone were unsuccessful, the mixture was then heated to 120–130° when a vigorous reaction ensued. The α-pyrone could then be isolated directly by chromatography on Florisil. Most variations of the experimental procedure such as the use of an inert solvent (xylene) or the addition of acetic acid to the reaction mixture produced no appreciable effect; no α-pyrone is obtained when the heating is carried out under vacuum. The use of a benzoyloxy derivative in one case gave analogous results but a somewhat lower yield.

With β-Chloro Enones

The reaction was next attempted with 3-chloroacrylophenone (**5***c*) and produced quite different results. At 95° hydrogen chloride was completely eliminated and the mixture after evaporation consisted essentially of the *trans*-pentadienone and the 1,2-pyran. These isomers could not be separated and their nature was deduced solely from spectral data. By subtracting in the n.m.r. spectrum the signals due to the now familiar pentadienone, the structure of the other

[1]Revision received August 2, 1974.

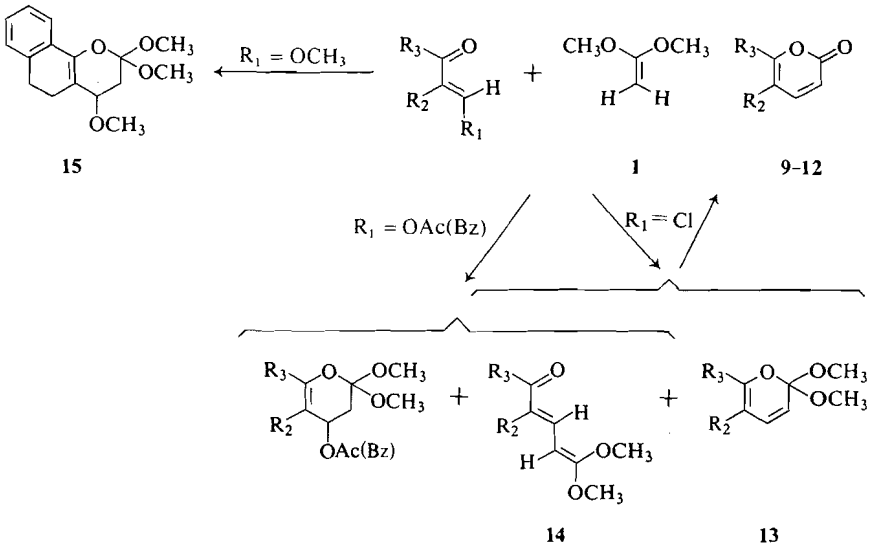

SCHEME 1

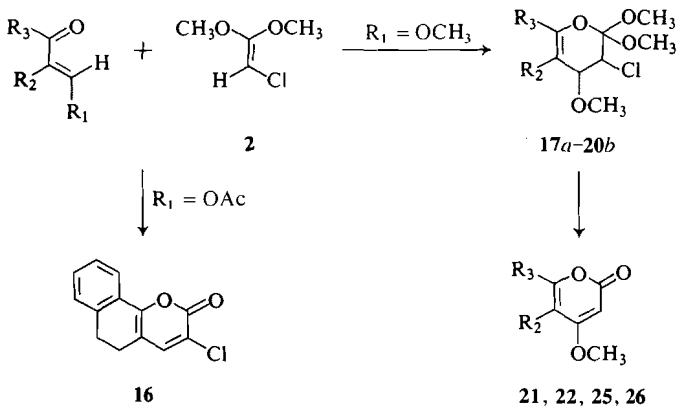

SCHEME 2

isomer, 6-phenyl-1,2-pyran, is readily arrived at (a methoxyl peak at δ 3.40 seems characteristic of cyclic structures (1) and the presence of doublets at 5.45 (J = 9.5 Hz) and 6.00 (J = 6.5 Hz) and of a doublet of doublets at 6.50 confirms the proposed structure, *i.e.* the coupling constants are the same as in the corresponding α-pyrone but the chemical shifts are quite different).

A subsequent heating of the mixture of isomers at 120° resulted in extensive decomposition and in the formation of only a trace of the α-pyrone. Chromatography on silica gel also decomposed these products but the addition of benzoic acid followed by heating at the same temperature gave good yields of 6-phenyl-α-pyrone and methyl benzoate.

With β-Methoxy Enones

These enones were significantly less reactive than the foregoing and the cycloaddition had to be carried out at 135° in a sealed tube. Only the 4-methoxydihydropyran was obtained and heating it progressively to 200° only caused decomposition; moreover it was quite inert to alkoxides under the usual conditions. This negative result suggested that analogous 4-methoxydihydropyrans could be used in the synthesis of 4-methoxy-α-pyrones, many derivatives of which are naturally occurring compounds.

With Chloroketene Dimethyl Acetal (Scheme 2)

When 2-acetoxymethylene-α-tetralone (**4***b*) was heated to 130° for 24 h with chloroketene dimethyl acetal (**2**) an 82% yield of the correspond-

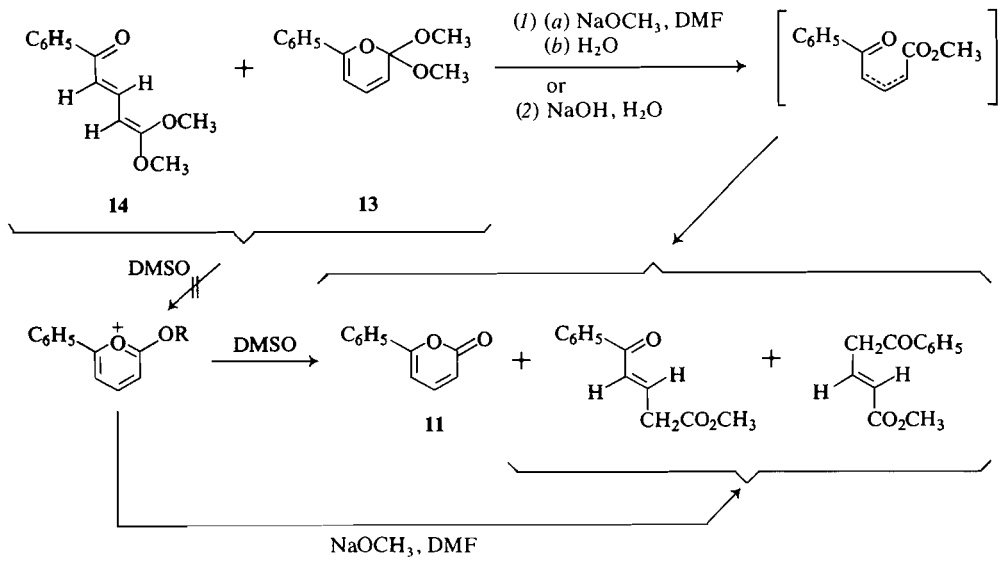

SCHEME 3

ing 3-chloro-α-pyrone **16** was obtained. Although the procedure was not further explored it undoubtedly constitutes an excellent method of preparing certain compounds of this type.

The Reaction of β-Methoxy Enones with Chloroketene Acetals (Scheme 2)

In this procedure 2-methoxymethylene-α-tetralone (**4***b*), 3-methoxyacrylophenone (**5***b*), 2-methoxyvinyl styryl ketone (**7***b*), and 3′,4′-methylenedioxystyryl 2-methoxyvinyl ketone (**8**) were successfully added to chloroketene dimethyl acetal (**2**) at the boiling point of the latter; 2-methoxymethylenecyclohexanone (**3***b*) and 3-methoxy-2-isopropylacrolein were found to be unreactive whereas 2-methoxyvinyl 3′-pyridyl ketone (**6**) gave a variety of products, none of which seemed to be the expected dihydropyran. In most cases, both diastereoisomers were obtained and the *cis*-compounds are thought to be usually predominant; however only the *cis*-isomer **20***a* was observed but the yield was low in this instance and the *trans*-isomer could have remained undetected. These isomers can be partially separated by chromatography on Florisil but, with the exception of those of **17***a* and *b*, the configurations cannot be assigned with certainty since the signals for the protons in positions 3,4 of the dihydropyran system are usually superimposed. The 6-phenyl isomers **18***a* and *b* show very different reaction rates in the presence of sodium methoxide and the more reactive one is assumed to be the *cis*-compound. Other mixtures do not show this characteristic and structures have been tentatively assigned on the basis of small differences in chemical shifts and coupling constants, and of chromatographic behavior.

The dehydrohalogenation of the 3-chloro-2,2,4-trimethoxydihydropyrans was attempted under the usual conditions (4.5 equiv. of methoxide in DMSO). The mixture of isomers **17***a* and *b* gave a 90% yield of the corresponding α-pyrone but a similar reaction with the 6-phenyl compounds **18***a* and *b* showed the rapid disappearance of the *cis*-isomer while a large amount of the *trans*-isomer remained unaffected (a prolonged reaction increases the proportion of by-products) The pure *trans*-compound **18***b* gave a very low yield (14%) which could not be improved but the *cis*-isomer **18***a* at $-10°$ could be converted more efficiently to the α-pyrone (40%). Finally the 6-styryl derivatives **19***a* and *b* and **20***a* reacted readily at low temperatures but provided only moderate yields of the expected products (37–43%).

The Mechanism of the Reaction (Scheme 3)

The conversion of 3- or 4-functionalized dihydropyrans to α-pyrones in the presence of alkoxide or by heating raises a number of mechanistic problems. There seems to be little doubt that an elimination occurs in the first step of the process, that the 1,2-pyran is the initial intermediate, and that an equilibrium then exists between the latter and the oxodienes since all of these are occasionally observed (the fact that

the 1,2-pyran appears only when hydrogen chloride is eliminated by a thermal reaction remains unexplained). We have elucidated two main problems: (*a*) whether the α-pyrones are produced by a nucleophilic attack on the 1,2-pyran-oxodiene mixture or by the formation and subsequent conversion of the corresponding pyrilium salt and (*b*) whether the ketoester by-products are formed during the reaction or by subsequent hydrolysis (these compounds are not observed in the thermal procedure).

It has been shown that 1,2-pyrans exist mainly in the oxodiene form and that substituents capable of enhancing the resonance in this isomer also displace the equilibrium in its favor (2–5). The formation of α-pyrones was thought at first to proceed through the pyrilium salt because of the ease with which 5,5-dimethoxy-2-*n*-decyl-penta-2,4-dienal (1) was converted to such a compound and since the intermediate 1,2-pyrans (orthoesters) were expected to be stable in basic media. The postulate which assumed that pyrilium salts were formed from the 1,2-pyrans and that a lowering of the reaction temperature would increase the concentration of the latter and thence facilitate the formation of the specific intermediate presented certain difficulties at the outset. Indeed there seemed to be no valid reason why the 4-phenyl-, 4-alkyl-, and 4,6-diphenyldihydropyrans should yield α-pyrones quite readily whereas the 6-phenyl and 5-alkyl derivatives having comparable electronic effects behaved abnormally (1). The difficulty in effecting the conversion and the occurrence of appreciable amounts of ketoester by-products in the last instances seemed related rather to steric factors and a greater ease of isomerization (in the case of the 4-methoxy dihydropyrans the ease of isomerization could be due to an electronic effect). It should be noted here that 2-*n*-decyl-pentadienal is only encountered when a large excess of methoxide is used and it is possible that this structure is stabilized by a Michael-type addition and is regenerated during hydrolysis.

The initial assumption that 1,2-pyrans are the first intermediates even in the base-induced reaction was tested by treating the mixtures of isomers **13** and **14** with sodium methoxide in dimethylformamide at $-10°$. Hydrolysis and chromatography of the reaction mixture gave 6-phenyl-α-pyrone (**11**) and a small amount of the usual ketoesters. The next step in the elucidation of the mechanism consisted in determining whether preformed pyrilium salts were capable of undergoing the conversion to α-pyrones under similar conditions. Pirkle and Dines (6) had previously proposed the intermediacy of pyrilium salts in the nitration of α-pyrones and confirmed this possibility by thermally converting the former to dienolides (4-methoxy pyrilium salts are known to be stable under analogous conditions) (7). We prepared 2-ethoxy-6-phenyl-pyrilium fluoroborate (**27**) and dissolved it in dimethylsulfoxide. Examination of the reaction mixture both before hydrolysis (DMSO-d_6) and after revealed efficient conversion to the α-pyrone; when a similar reaction was carried out with the usual amount of methoxide (DMF, $-10°$) only a trace of compound **11** was obtained (the reaction mixture consisted mainly of the ketoester by-products). However, by dissolving the mixture of isomers **13** and **14** in deuterated dimethylsulfoxide, a progressive decomposition of the substrates was observed but neither the pyrilium salt nor the α-pyrone could be detected.

It now seems quite obvious that pyrilium salts must be discounted as intermediates in the new synthesis of α-pyrones that we describe. The latter compounds can only result from the hydrolysis of or the nucleophilic attack on the oxodiene. This was confirmed when hydrolysis of the mixture of isomers **13** and **14** with aqueous sodium hydroxide was found to yield the α-pyrone and the usual ketoesters. The configuration of the oxodiene also seems to enter into consideration. Although it could not be established which isomer was present in the case of the 2-*n*-decylpenta-2,4-dienals, the ease with which they are converted to the α-pyrone seems to indicate a *cis*-configuration; on the other hand some dienones produced at higher temperatures are undoubtedly *trans*. The *cis*-oxodienes are therefore hydrolyzed to a mixture of *cis*- and *trans*-oxopentenoates and the *cis*-esters then cyclize spontaneously to the α-pyrones. The improved yields we have observed at low temperature undoubtedly result from slower rates of isomerization. As to the thermal formation of α-pyrones, McElvain (8) has proposed a mechanism for the conversion of ketene acetals to esters and this seems a plausible process for the transformation we have observed. Indeed the elimination of hydrogen chloride from chlorodihydropyran at 95° prevents the formation of the α-pyrone since the reagent would be

volatilized under these conditions and a similar situation is observed when the corresponding acetoxy compounds are heated under vacuum.

Experimental

The melting points were taken in capillary tubes using a calibrated thermometer (Thomas-Hoover Apparatus). The i.r. spectra were recorded on a Beckman IR-12 instrument, u.v. spectra on a Beckman DK-1A spectrophotometer, and the n.m.r. on a Varian A60 spectrometer with tetramethylsilane as internal standard.

The Preparation of β-Functionalized α,β-Enones

No attempt has been made to determine the configuration of these compounds since (*a*) in most cases only one isomer is obtained, (*b*) the β-hydrogen is not always discernible in the n.m.r. spectrum, and (*c*) compounds of this type are known to isomerize readily under the reaction conditions used. However the chemical shifts, when visible, and the coupling constants of the olefinic protons suggest that the configurations are *cis*.

2-Methoxymethylenecyclohexanone (3b)

A mixture of the sodium salt of 2-hydroxymethylenecyclohexanone (10.0 g) (9), dimethylsulfate (7.0 ml), anhydrous potassium carbonate (10.0 g), and acetone (100 ml) was refluxed for 24 h. The methyl ester **3***b* was isolated in the usual way, b.p. 110–115°/10 mm (34%) (lit. (10) b.p. 85°/3.2 mm); ν_{max} (film) 1685, 1600 cm^{-1}; δ ($CDCl_3$) 1.50–2.50 m ($(CH_2)_4$), 3.90 s (OCH_3), 7.18 t (J = 2.0 Hz) (C=CH).

2-Chloromethylene-α-tetralone (4c)

A solution of 2-hydroxymethylene-α-tetralone (2.6 g) (11), thionyl chloride (1.2 ml), and benzene (10 ml) was refluxed for 4 h. Evaporation of the mixture under vacuum gave the chloro compound **4***c*, m.p. 61–62° (ether – petroleum ether) (90%); λ_{max} (ethanol) 272 nm (log ε 4.29); ν_{max} (KBr) 1670 cm^{-1}; δ ($CDCl_3$) 3.03 s ($(CH_2)_2$), 7.20–7.50 and 7.80–8.40 2 m (aromatic and vinyl CH).

Anal. Calcd. for $C_{11}H_9OCl$: C, 68.57; H, 4.71. Found: C, 68.70; H, 4.81.

3-Methoxyacrylophenone (5b)

A mixture of the sodium salt of 3-hydroxyacrylophenone (15.0 g) (12), dimethylsulfate (8 ml), anhydrous potassium carbonate (10.0 g), and acetone (50 ml) was refluxed for 3 h. The methyl ether **5***b* was isolated in the usual way, b.p. 100–105°/0.1 mm (88%) (lit. (10) b.p. 112°/1.8 mm); λ_{max} (ethanol) 274 nm (log ε 4.12); ν_{max} (film) 1670 cm^{-1}; δ ($CDCl_3$) 3.80 s (OCH_3), 6.43 d (J = 12.5 Hz) (2-CH), 7.40–7.70 and 7.85–8.15 2 m (aromatic CH), 7.90 d (J = 12.5 Hz) (3-CH).

2-Methoxyvinyl 3′-Pyridyl Ketone (6)

A solution of hydrogen chloride (7.8 g) in anhydrous methanol (10 ml) was added dropwise at 0° to a suspension of the sodium salt of 3′-pyridyl 2-hydroxyvinyl ketone (10.0 g) (13) in methanol (10 ml). After allowing the reaction to rest for 1/2 h at the same temperature and evaporating it under vacuum, the methyl ether **6** was obtained by pouring the residue into a 5% solution of sodium carbonate, extracting the latter with ether and distilling the residue over sodium carbonate (50 mg), b.p. 170–175°/0.9 mm, m.p. 74–75° (47%); λ_{max} (ethanol) 240, 278 nm (log ε 4.00, 4.08); ν_{max} (KBr) 1670, 1640 cm^{-1}; δ ($CDCl_3$) 3.89 s (OCH_3) 6.38 d (J = 12.0 Hz) (1-CH), 7.45 dd (J = 4.5, 8.5 Hz) (5′-CH), 7.92 d (J = 12.0 Hz) (2-CH), 8.25 dt (J = 2.0, 8.5 Hz) (4′-CH), 8.82 dd (J = 2.0, 4.5 Hz) (6′-CH), 9.20 d (J = 2.0 Hz) (2′-CH).

Anal. Calcd. for $C_9H_9O_2N$: C, 66.25; H, 5.56; N, 8.58. Found: C, 66.32; H, 5.84; N, 8.32.

2-Methoxyvinyl Styryl Ketone (7b)

A mixture of the sodium salt of 2-hydroxyvinyl styryl ketone (10.0 g) (14), dimethylsulfate (5.5 ml), anhydrous potassium carbonate (6.0 g), and acetone (50 ml) was refluxed for 5 h. The methyl ether 7*b* was isolated in the usual way, b.p. 140–145°/0.2 mm, m.p. 89–90° (ether – petroleum ether) (57%); λ_{max} (ethanol) 226, 309 nm (log ε 4.13, 4.32); ν_{max} (KBr) 1650 cm^{-1}; δ ($CDCl_3$) 3.70 s (OCH_3), 5.95 d (J = 12.5 Hz) (1-CH), 6.92 d (J = 16.0 Hz) (α-styryl CH), 7.25–7.65 m (aromatic CH), 7.74 d (J = 16.0 Hz) (β-styryl CH), 7.86 d (J = 12.5 Hz) (2-CH).

Anal. Calcd. for $C_{12}H_{12}O_2$: C, 76.59; H, 6.43. Found: C, 76.85; H, 6.60.

3′,4′-Methylenedioxystyryl 2-Methoxyvinyl Ketone (8)

A suspension of the sodium salt of 3′,4′-methylenedioxystyryl 2-hydroxyvinyl ketone (4.0 g), dimethylsulfate (2.0 ml), potassium carbonate (2.18 g), and acetone (20 ml) was refluxed for 3 h. The methyl ether **8** was obtained in the usual way, m.p. 90–91° (carbon tetrachloride) (50%); λ_{max} (ethanol) 259, 304, 348 nm (log ε 4.12, 4.20, 4.37); ν_{max} (KBr) 1650 cm^{-1}; δ ($CDCl_3$) 3.82 s (OCH_3), 5.95 d (J = 12.5 Hz) (1-CH), 6.08 s (—OCH_2O—), 6.75 d (J = 16.0 Hz) (α-styryl CH), 6.80–7.35 m) (aromatic CH), 7.65 d (J = 16.0 Hz) (β-styryl CH), 7.86 d (J = 12.5 Hz) (2-CH).

Anal. Calcd. for $C_{13}H_{12}O_4$: C, 67.23; H, 5.21. Found: C, 67.50; H, 5.08.

The Synthesis of α-Pyrones from β-Functionalized α,β-Enones

From β-Acetoxy or β-Benzoyloxy Enones

A mixture of the β-acetoxy or β-benzoyloxy enone and ketene dimethyl acetal (**1**) (3–5 equiv.) (in this procedure (15) benzene was replaced by xylene) was heated under nitrogen. The excess of the acetal and the volatile by-products were evaporated under vacuum and the residue heated at 120–130° for 10–15 min. The following products were obtained.

5,6,7,8-Tetrahydrocoumarin (**9**) from 2-acetoxymethylenecyclohexanone (**3***a*) (3.09 g) (16) (110°; 15 h) was chromatographed on Florisil (107 g) (benzene–ether, 23:2), m.p. 64–65° (ether – petroleum ether) (30%) (lit. (17) m.p. 64.5–65°); λ_{max} (ethanol) 304 nm (log ε 3.88); ν_{max} ($CHCl_3$) 1740, 1720, 1649, 1560 cm^{-1}; δ ($CDCl_3$) 1.50–1.90 m (6,7-CH_2), 2.20–2.60 m (5,8-CH_2) 6.12 d (J = 9.5 Hz) (3-CH), 7.10 d (J = 9.5 Hz) (4-CH).

Anal. Calcd. for $C_9H_{10}O_2$: C, 71.98; H, 6.71. Found: C, 72.36; H, 6.69.

5,6-Dihydro-2-naphtho[1,2-*b*]pyrone (**10**) from 2-acetoxymethylene-α-tetralone (**4***a*) (200 mg) (18) (95°; 8 h) (preparative t.l.c.; benzene – ethyl acetate, 7:3), m.p. 102–103° (ether) (76%) (lit. (19) m.p. 96–97°); λ_{max} (ethanol) 237, 354 nm (log ε 4.15, 4.27); ν_{max} (KBr) 1720, 1630, 1540 cm^{-1}; δ ($CDCl_3$) 2.60–3.10 m (5,6-CH_2), 6.28 d (J = 9.5 Hz) (3-CH), 7.10–7.60 and 7.70–8.20 2 m (3- and aromatic CH).

Anal. Calcd. $C_{13}H_{10}O_2$: C, 78.77; H, 5.09. Found: C, 78.78; H, 5.13.

6-Phenyl-α-pyrone (**11**) from 3-acetoxyacrylophenone (**5***a*) (300 mg) (11) (95°; 2 h) (preparative t.l.c.; benzene – ethyl acetate, 7:3; and filtration on Florisil), m.p. 64–65° (77%) (lit. (20) m.p. 63–64°) and from 3-benzoyloxyacrylophenone (200 mg) (24) (95°; 2 h) (61%).

6-Styryl-α-pyrone (**12**) from 2-acetoxyvinyl styryl ketone (7*a*) (200 mg) (21) (95°; 2 h) (preparative t.l.c.; dichloromethane–benzene, 1:1), m.p. 112.5–113° (ether – petroleum ether) (67%) (lit. (22) m.p. 115–116°); λ_{max} (ethanol) 262, 270, 370 (log ε 4.21, 4.22, 4.29); ν_{max} (KBr) 1730, 1630, 1530 cm^{-1}; δ ($CDCl_3$) 6.19 d (J = 7.0 Hz) (5-CH), 6.23 d (J = 9.0 Hz) (3-CH), 6.68 d (J = 16.0 Hz) (α-styryl CH), 7.20–7.70 m (4-, β-styryl and aromatic CH).

Anal. Calcd. for $C_{13}H_{10}O_2$: C, 78.77; H, 5.09. Found: C, 78.79; H, 5.12.

From β-Chloro Enones

*6-Phenyl-α-pyrone (**11**).* The condensation of 3-chloroacrylophenone (**5***c*) (200 mg) (23) with ketene dimethyl acetal (1.00 g) under nitrogen at 95° for 5 h gave, after evaporation, a mixture of 2,2-dimethoxy-6-phenyl-1,2-pyran (**13**); δ ($CDCl_3$) 3.40 s (OCH_3), 5.45 d (J = 9.5 Hz) (3-CH), 6.00 d (J = 6.5 Hz) (5-CH), 6.52 dd (J = 6.5, 9.5 Hz) (4-CH)) and *trans*-5,5-dimethoxy-1-phenylpenta-2,4-dien-1-one (**14**); δ 3.71 s (OCH_3), 4.80 d (J = 11.5 Hz) (4-CH), 6.79 d (J = 15.0 Hz) (5-CH). After heating this mixture with benzoic acid (180 mg) for 10 min at 120°, 6-phenyl-α-pyrone, m.p. 64–65° (80%) and methyl benzoate (125 mg) were isolated in the usual way.

*5,6-Dihydro-2-naphtho[1,2-b]pyrone (**10**).* This pyrone is obtained as in the preceding paragraph from 2-chloromethylene-α-tetralone (**4***c*) (200 mg), **1** (1.00 g) (95°; 10 h) and benzoic acid (180 mg), m.p. 102–103° (preparative t.l.c.; benzene – ethyl acetate, 7:3) (79%).

From β-Methoxy Enones

*2,2,4-Trimethoxy-3,4,5,6-tetrahydro-2-naphtho[1,2-b]-pyran (**15**).* This pyran **15** was obtained by heating a mixture of 2-methoxymethylene-α-tetralone (**4***b*) (1.0 g) (24) and **1** (1.40 g) for 30 h at 135°, m.p. 68–69° (ether – petroleum ether) (92%); ν_{max} (KBr) 1665, 1120, 1095, 1050 cm^{-1}; δ ($CDCl_3$) 1.80–2.90 m (3,5,6-CH_2) 3.38, 3.43 and 3.48 3s (OCH_3), 4.11 bt (J = ~7.5 Hz) (4-CH), 7.10–7.80 m (aromatic CH).

Anal. Calcd. for $C_{16}H_{20}O_4$: C, 69.54; H, 7.30. Found: C, 69.65; H, 7.52.

From β-Acetoxy Enones and Chloroketene Dimethyl Acetal

A mixture of 2-acetoxymethylene-α-tetralone (**4***a*) (3.6 g) and chloroketen dimethyl acetal (**2**) (7.3 g) (25) was heated at 130° for 24 h, and evaporated under vacuum. The residue gave 3-chloro-5,6-dihydro-2-naphtho[1,2-*b*]-pyrone (**16**), m.p. 142–143° (ether) (82%); λ_{max} (ethanol) 245, 252, 370 (log ε 4.11, 4.17, 4.16); ν_{max} (KBr) 1740, 1720, 1640, 1535 cm^{-1}.

Anal. Calcd. $C_{13}H_9O_2Cl$: C, 67.10; H, 3.89; Cl, 15.22. Found: C, 67.31; H, 3.93; Cl, 15.34.

The Preparation of 3-chloro-2,2,4-trimethoxy-3,4-dihydro-1,2-pyrans

A mixture of the β-methoxy enone and chloroketene dimethyl acetal (**2**) (25) (2–4 equiv.) was heated at 150° under nitrogen. After evaporation of the volatile products under vacuum, the residue was chromatographed on Florisil.

cis- and *trans*-3-Chloro-2,2,4-trimethoxy-3,4,5,6-tetrahydro-2-naphtho[1,2-*b*]pyrans (**17***a* and *b*) were obtained from 2-methoxymethylene-2-tetralone (**4***b*) (900 mg) and **2** (48 h). Chromatography (benzene then benzene–ether 19:1) gave the *trans*-isomer **17***b*, m.p. 107–109° (ether – petroleum ether) (19%); ν_{max} (KBr) 1661, 1130, 1108, 1070, 990 cm^{-1}; δ ($CDCl_3$) 2.30–3.10 2m (5,6-CH_2), 3.49, 3.58 and 3.65 3s (2,2,4-OCH_3), 4.24 bd (J = 8.0 Hz) (4-CH), 4.49 d (J = 8.0 Hz) (3-CH), 7.20–7.70 2m (aromatic CH).

Anal. Calcd. for $C_{16}H_{19}O_4Cl$: C, 61.83; H, 6.16. Found: C, 62.14; H, 6.10.

Later fractions gave a mixture of the *cis-* and *trans*-isomers (8%) and the *cis*-isomer **17***a* (an oil) (53%); ν_{max} (film) 1660, 1135, 1100, 1065, 1055 cm^{-1}; δ ($CDCl_3$) 2.30–3.20 2m (5,6-CH_2), 3.38, 3.55 and 3.59 3s (2,2,4-OCH_3), 4.39 bd (J = 5.0 Hz) (4-CH), 4.62 d (J = 5.0 Hz) (3-CH), 7.20–7.80 2m (aromatic CH).

cis- and *trans*-3-Chloro-2,2,4-trimethoxy 6-phenyl-3,4-dihydro-1,2-pyrans (**18***a* and *b*) were prepared from 3-methoxyacrylophenone (**5***b*) (2.0 g) and **2** (36 h). Chromatography (benzene) gave successively: the *trans*-isomer **18***b* (an oil) (20%); ν_{max} (film) 1665, 1100, 1052, 1025 cm^{-1}; δ ($CDCl_3$) 3.50, 3.56 and 3.58 3s (2,2,4-OCH_3), 4.36 d (J = 1.5 Hz) (3,4-CH), 5.63 t (J = 1.5 Hz) (5-CH), 7.40–7.90 2m (aromatic CH); a mixture of the *cis-* and *trans*-isomers (16%); the *cis*-isomer **18***a* (an oil) (53%); δ ($CDCl_3$) 3.41, 3.52, and 3.58 3s (2,2,4-OCH_3), 4.56 d (J = 2.0 Hz) (3,4-CH), 5.50 t (J = 2.0 Hz) (5-CH), 7.30–7.90 2m (6-C_6H_5).

cis- and *trans*-3-Chloro-2,2,4-trimethoxy-6-styryl-3,4-dihydro-1,2-pyrans (**19***a* and *b*) were obtained from 2-methoxyvinyl styryl ketone (7*b*) (1.0 g) and **2** (48 h). Chromatography (benzene) gave successively: a mixture of the *cis-* and *trans*-isomers (38%); the *cis*-isomer **19***a*, m.p. 109–110° (ether – petroleum ether) (24%); ν_{max} (KBr) 1650, 1130, 1091, 1071, 1050 cm^{-1}; δ ($CDCl_3$) 3.39, 3.49, and 3.54 3s (2,2,4-OCH_3), 4.49 d (J = 2.0 Hz) (3,4-CH), 5.03 t (J = 2.0 Hz) (5-CH), 6.47 d (J = 16.0 Hz) (α-styryl CH), 7.00–7.80 m (β-styryl and aromatic CH).

Anal. Calcd. for $C_{16}H_{19}O_4Cl$: C, 61.83; H, 6.16. Found: C, 62.12; H, 6.28.

cis-3-Chloro-2,2,4-trimethoxy-3′,4′-methylenedioxystyryl-3,4-dihydro-1,2-pyran (**20***a*) was prepared from 2-methoxyvinyl 3′,4′-methylenedioxystyryl ketone (**8**) (1.0 g) and **2** (32 h). Chromatography (benzene) gave only the *cis*-isomer **20***a*, m.p. 124–125° (ether) (35%); ν_{max} 1655, 1120, 1091, 1071, 1050 cm^{-1}; δ ($CDCl_3$) 3.35, 3.46, and 3.52 3s (2,2,4-OCH_3), 4.48 d (J = 2.0 Hz) (3,4-CH), 4.98 t (J = 2.0 Hz) (5-CH), 5.97 s (—OCH_2O—), 6.31 d (J = 16.0 Hz) (α-styryl CH), 6.80–7.40 m (β-styryl and aromatic CH).

Anal. Calcd. for $C_{17}H_{19}O_6Cl$: C, 57.55; H, 5.39. Found: C, 57.79; H, 5.30.

The Synthesis of 4-Methoxy-α-pyrones

A solution of the chlorodihydropyran and sodium methoxide (4.5 equiv.) in the appropriate solvent was stirred under nitrogen, diluted by addition of ice and extracted with ether.

4-Methoxy-5,6-dihydro-2-naphtho[1,2-*b*]pyrone (**21**) was obtained from the mixture of *cis-* and *trans*-pyrans **17***a* and *b* (420 mg) (25 ml of DMSO; 25°; 15 h), m.p. 173–174° (ether) (90%); λ_{max} (ethanol) 222, 228, 260, 270, 330, 340 nm (log ε 4.27, 4.29, 3.81, 3.81, 4.23, 4.23); ν_{max} (KBr) 1705, 1640, 1555 cm^{-1}; δ ($CDCl_3$) 2.40–3.10 m

(5,6-CH_2), 3.86 s (4-OCH_3), 5.58 s (3-CH), 7.10–8.10 2m (5- and aromatic CH).

Anal. Calcd. for $C_{14}H_{12}O_3$: C, 73.66; H, 5.31. Found: C, 73.78; H, 5.21.

4-Methoxy-6-phenyl-α-pyrone (**22**) from the *trans*-pyran **18***b* (640 mg) (50 ml of DMSO; 25°; 24 h) (preparative t.l.c.; chloroform), m.p. 125–126° (ether) (14%) (lit. (26) m.p. 129.5–131.5°); λ_{max} (ethanol) 220, 233, 315 nm (log ε 4.23, 4.21, 4.19); ν_{max} (KBr) 1708, 1645, 1569 cm^{-1}; δ ($CDCl_3$) 3.90 s (4-OCH_3), 5.62 d (J = 2.0 Hz) (3-CH), 6.51 d (J = 2.0 Hz) (5-CH), 7.40–8.10 2m (6-C_6H_5).

Anal. Calcd. for $C_{12}H_{10}O_2$: C, 71.28; H, 4.98. Found: C, 71.08, H, 4.92.

Compound **22** was also obtained from the *cis*-isomer **18***a* (500 mg) (40 ml of DMF; −10°; 12 h), m.p. 125–126° (40%) along with a mixture of the methyl *trans*-4-benzoyl-3-methoxybut-2- and 3-en-1-oates (**23** and **24**) (23%); ν_{max} (film) 1740, 1700, 1665, 1640 cm^{-1}; δ ($CDCl_3$) 3.62, 3.68, 3.75, and 3.83 4s (OCH_3 and CO_2CH_3), 3.95 s (4-CH_2), 4.50 s (2-CH_2), 5.30 s (2-CH), 6.38 s (4-CH), 7.40–7.70 and 7.85–8.20 2m (aromatic CH).

4-Methoxy-6-styryl-α-pyrone (**25**) from the mixture of *cis*- and *trans*-pyrans **18***a* and *b* (207 mg) (30 ml of DMF; −20°; 20 h) (preparative t.l.c.; chloroform), m.p. 136–137° (ether) (43%) (lit. (27) m.p. 138–140°); λ_{max} (ethanol) 226, 233, 255, 343 nm (log ε 4.32, 4.33, 4.28, 4.42); ν_{max} ($CHCl_3$) 1710, 1641, 1560 cm^{-1}; δ ($CDCl_3$) 3.87 s (4-OCH_3), 5.60 d (J = 2.0 Hz) (3-CH), 6.05 d (J = 2.0 Hz) (5-CH), 6.70 d (J = 16.0 Hz) (α-styryl CH), 7.30–7.70 m (β-styryl and aromatic CH).

Anal. Calcd. for $C_{14}H_{12}O_3$: C, 73.66; H, 5.30. Found: C, 73.90; H, 5.35.

6-(3′,4′-Methylenedioxystyryl)-4-methoxy-α-pyrone (**26**) from the *cis*-pyran **20***a* (280 mg) (30 ml of DMF; −20°; 5 h), m.p. 233–234° (ether) (37%) (lit. (28) m.p. 233°); λ_{max} (ethanol) 221, 248, 370 nm (log ε 4.24, 3.91, 4.37); ν_{max} (KBr) 1720, 1640, 1555 cm^{-1}; δ ($(CD_3)_2SO$) 3.88 (4-OCH_3), 5.68 d (J = 2.0 Hz) (3-CH), 6.13 s (—OCH_2O—), 6.32 d (J = 2.0 Hz) (5-CH), 6.63 d (J = 16.0 Hz), 6.90–7.50 m (β-styryl and aromatic CH).

Anal. Calcd. for $C_{15}H_{12}O_5$: C, 66.17; H, 4.44. Found: C, 66.10; H, 4.26.

Miscellaneous Reactions

2-Ethoxy-6-phenylpyrilium Fluoroborate (27)

A mixture of 6-phenyl-α-pyrone (**11**) (240 mg) and of a solution of triethyloxonium fluoroborate (methylene chloride, 0.01 *M*) (1.4 ml) was stirred at room temperature for 48 h, filtered and evaporated. The residue upon crystallization from acrylonitrile – methylene chloride gave 2-ethoxy-6-phenylpyrilium fluoroborate, m.p. 147.5–148° (86%); λ_{max} (ethanol) 238, 332 nm (log ε 4.23, 4.14); ν_{max} (KBr) 1641, 1519 cm^{-1}.

Anal. Calcd. for $C_{13}H_{13}O_2BF_4$: C, 54.20; H, 4.54. Found: C, 54.07; H, 4.41.

Reactions of 2-Ethoxy-6-phenylpyrilium Fluoroborate

With Sodium Methoxide. A solution of 2-ethoxy-6-phenylpyrilium fluoroborate (200 mg) and sodium methoxide (167 mg) in dimethylformamide (20 ml) was stirred for 15 min at −15°. The n.m.r. spectrum of the crude product showed the presence of the corresponding methyl ketoesters. Thin-layer chromatography revealed only a trace of the α-pyrone **11**.

With Dimethylsulfoxide. 2-Ethoxy-6-phenylpyrilium fluoroborate (50 mg) was dissolved in deuterated dimethylsulfoxide (0.8 ml). After 10 min, the n.m.r. spectrum of the reaction mixture revealed mainly 6-phenyl-α-pyrone and the usual working up gave a 90% yield of the pyrone **11**.

With Acetic Acid. A mixture of 2-ethoxy-6-phenylpyrilium fluoroborate (200 mg) and acetic acid (1 ml) was heated at 120° for 10 min, dissolved in ether and washed with water. Evaporation of the solvent gave 6-phenyl-α-pyrone (**11**) (83%).

Reactions of the Mixture of Isomers 13 and 14

With Sodium Methoxide. The mixture of isomers **13** and **14** prepared as before from 3-chloroacrylophenone (**5***c*) (1.0 g) and **1** (1.7 g) was treated with sodium methoxide (280 mg) in dimethylformamide (20 ml) at −10° for 10 min. The reaction medium after dilution by addition of ice gave 6-phenyl-α-pyrone (**11**) (34%) and a mixture of the corresponding ketoesters (7%) (1), (preparative t.l.c.; benzene – methylene chloride – ethyl acetate, 5:4:1). The n.m.r. spectrum of a similar reaction on a small scale in deuterated dimethylsulfoxide shows the presence of the 1,2-pyran **13** and another substance which is probably one of the open-chain dienones.

With Aqueous Base. The mixture of the isomers **13** and **14** obtained as above was dissolved in ether (40 ml) and extracted several times with a 2% aqueous solution of sodium hydroxide. Evaporation of the ethereal layer gave a mixture of the pyrone **11** (78%) and of the corresponding ketoesters (15%).

1. A. BÉLANGER and P. BRASSARD. Can. J. Chem. This issue.
2. P. ROUILLIER, D. GAGNAIRE, and J. DREUX. Bull. Soc. Chim. Fr. 689 (1966).
3. J.-P. LEROUX, G. LETERTRE, P.-L. DESBENE, and J.-J. BASSELIER. Bull. Soc. Chim. Fr. 4059 (1971).
4. A. DUPERRIER and J. DREUX. Tetrahedron Lett. 3127 (1970).
5. E. N. MARVELL, T. CHADWICK, G. CAPLE, T. GOSINK, and G. ZIMMER. J. Org. Chem. **37**, 2992 (1972).
6. W. H. PIRKLE and M. DINES. J. Heterocycl. **6**, 313 (1969).
7. P. BEAK. Tetrahedron, **20**, 831 (1964).
8. S. M. MCELVAIN. Chem. Rev. **45**, 453 (1949).
9. K. v. AUWERS, W. BUSCHMANN, and R. HEIDENREICH. Ann. **435**, 277 (1924).
10. E. E. ROYALS and K. C. BRANNOCK. J. Am. Chem. Soc. **75**, 2050 (1953).
11. K. v. AUWERS and C. WIEGAND. J. Prakt. Chem. **134**, 82 (1932).
12. K. v. AUWERS and W. SCHMIDT. Chem. Ber. **58**, 528 (1925).
13. L. FABBRINI. Il Farmaco (Pavia), Ed. sci. **9**, 603 (1954); Chem. Abstr. **49**, 14762 (1955).
14. G. A. MINA, L. RATEB, and G. SOLIMAN. J. Chem. Soc. 4234 (1962).
15. S. M. MCELVAIN, H. I. ANTHES, and S. H. SHAPIRO. J. Am. Chem. Soc. **64**, 2525 (1942).
16. R. JACQUIER, C. PETRUS, F. PETRUS, and M. VALENTIN. Bull. Soc. Chim. Fr. 2678 (1970).
17. A. S. DREIDING and A. J. TOMASEWSKI. J. Am. Chem. Soc. **76**, 6388 (1954).
18. C. BARAT. J. Indian Chem. Soc. **8**, 801 (1931).

19. L. I. ZAKHARKIN and L. P. SOROKINA. Izv. Akad. Nauk SSSR, Otd. Khim. Nauk, 287 (1962); Chem. Abstr. **57**, 12417 (1962).
20. D. MOLHO and M. GIRAUD. Bull. Soc. Chim. Fr. 2603 (1968).
21. L. RATEB, G. A. MINA, and G. SOLIMAN. J. Chem. Soc. (C), 2137 (1968).
22. A. M. BITTENCOURT, O. R. GOTTLIEB, W. B. MORS, M. TAVEIRA MAGALHAES, S. MAGESWARAN, W. D. OLLIS, and I. O. SUTHERLAND. Tetrahedron, **27**, 1043 (1971).
23. A. N. NESMEYANOV, N. K. KOCHETKOV, and M. I. RYBINSKAYA. Izv. Akad. Nauk SSSR, Otd. Khim. Nauk, 741 (1954); Chem. Abstr. **49**, 10838 (1955).
24. D. NASIPURI and K. K. BIWAS. J. Indian Chem. Soc. **44**, 620 (1967).
25. S. M. MCELVAIN and M. J. CURRY. J. Am. Chem. Soc. **70**, 3781 (1948).
26. D. HERBST, W. B. MORS, O. R. GOTTLIEB, and C. DJERASSI. J. Am. Chem. Soc. **81**, 2427 (1959).
27. O. R. GOTTLIEB and W. B. MORS. J. Org. Chem. **24**, 17 (1959).
28. H. BRINKHOFF. German Patent No. 1,279,683; Chem. Abstr. **70**, 11570 (1969).

A New Thiophene Synthesis

JOHN M. MCINTOSH AND HAMDY KHALIL

Department of Chemistry, University of Windsor, Windsor, Ontario N9B 3P4

Received August 30, 1974

JOHN M. MCINTOSH and HAMDY KHALIL. Can. J. Chem. **53**, 209 (1975).

2,5-Dihydrothiophenes are dehydrogenated to thiophenes in high yield using chloranil in *tert*-butanol or pyridine. The presence of a fully substituted carbon atom blocks the reaction. The method allows a flexible regiospecific synthesis of thiophenes in high yield from readily available starting materials.

JOHN M. MCINTOSH et HAMDY KHALIL. Can. J. Chem. **53**, 209 (1975).

Le chloranil, dans le *tert*-butanol ou la pyridine, permet de déshydrogéner les dihydro-2,5 thiophènes en thiophènes avec de bons rendements. La présence d'un carbone complètement substitué arrête complètement la réaction. La méthode fournit une synthèse flexible et régiospécifique de thiophènes qui s'effectue avec de bons rendements à partir de composés de départ facilement accessibles. [Traduit par le journal]

Because of the importance of their role in biological systems, much attention has been focussed on the synthesis of pyrroles. Consequently, a variety of methods is available for their construction from a number of different types of starting materials (1). However, the methods available for the preparation of the related thiophenes are generally much more classical and not nearly so varied. Several methods are available for formation of the ring (2), perhaps the best known of these being the Hinsberg (3) synthesis utilizing thiodiacetic ester and the sulfide-induced cyclization of 1,4-difunctional compounds (4). Each of the methods suffers from a lack of generality, especially when applied to the synthesis of polyalkylated materials. Furthermore, while direct substitution of the thiophene nucleus occurs very easily at the positions adjacent to sulfur (5), preparation of β-substituted or unsymmetrical trisubstituted compounds can present a complex problem.

We recently published a new synthesis of 2,5-dihydrothiophenes **1** (6, 7) which provides an extremely facile and general route to this type of compound. Unlike most other methods for this synthesis, the method does not require the corresponding thiophene as a starting material (8), but rather involves the condensation of mercaptoaldehydes and ketones with vinylphosphonium salts. The method allows the formation of alkylated products in a completely regiospecific manner.

We have already shown the utility of **1** in the preparation of conjugated dienes (6) and as part

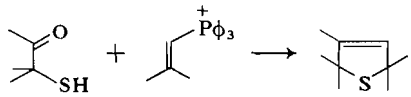

1

of a program to expand the utility of **1** in synthesis, we considered their dehydrogenation to thiophenes. Of the many reagents available for dehydrogenation, we chose to investigate the use of chloranil and we present here the results of that investigation.

2 **3**

Prior to the start of our work, there were some indications of its potential success. Wynberg *et al.* (9) reported the chloranil-induced dehydrogenation of several 2,3-dihydrothiophenes in excellent yields and the stability of the thiophene ring to the reaction conditions has been noted (9, 10).

The use of quinones for dehydrogenation reactions has been reviewed (11). Although chloranil is the least reactive of these materials, we have used it routinely as a matter of economy and convenience. The use of *o*-chloranil does not seem to afford any advantage in the examples cited here.

Results and Discussion

The traditional solvents used for quinone dehydrogenation have been benzene and its chlorinated derivatives. However, we chose to

Can. J. Chem. Downloaded from www.nrcresearchpress.com by 210.87.254.6 on 09/05/12
For personal use only.

TABLE 1. Yields of thiophenes

Dihydrothiophene	R_1	R_2	R_3	Product	Ref.	Yield (%) *tert*-BuOH	Yield (%) Pyridine	Yield (%) Overall[a]
2*a*[b]	Me	Me	Me	3*a*	12	87	83	72
2*b*[c]	Et	H	Me	3*b*	13	82	80	57
2*c*[b]	Me	Et	Me	3*c*	14	73	80	64
2*d*[b]	Me	Et	Et	3*d*		89	82	57
2*e*[d]	$-(CH_2)_4-$		Me	3*e*	15	90	86	82

[a]Yield from vinyl salt.
[b]See footnote 1.
[c]Reference 7.
[d]Reference 6.

use *tert*-butanol or pyridine in order to facilitate the work-up procedure as the separation of the thiophenes from the aromatic solvents caused problems in trial experiments. The quinones are only modestly soluble in *tert*-butanol and since an excess is required for acceptable rates of reaction, the mixture is heterogeneous at all times. However, as can be seen by the yields of products (Table 1) this does not seem to affect the reaction adversely. The unreacted reagent can easily be recovered from the medium.

The ease with which pyridine can be removed by acid extraction prompted an investigation of its use. When chloranil is added to pyridine it dissolves but almost immediately an exothermic reaction occurs with the precipitation of a brown solid. The nature of this has not been determined but it appears to function in the same manner as the quinone. However, the unreacted quinone cannot be recovered from this medium.

As can be seen from inspection of Table 1, the yields from representative 2,5-dihydrothiophenes[1] are generally excellent. However, under our conditions, migration or elimination of alkyl groups from fully substituted centers does not occur and the starting material is recovered in nearly quantitative yields in these cases.

The overall yield of alkylated thiophenes from mercaptocarbonyl compounds is also recorded in Table 1. As can be seen, this route allows a simple regiospecific two-step procedure for the formation of thiophenes under very mild conditions from a set of starting materials which is different from that normally used.

[1]Prepared as outlined in ref. 6. Yields and spectral data on compounds 2*a*, *c*–*e* are incorporated in a manuscript now in preparation.

Experimental

Unless otherwise noted, n.m.r. spectra were obtained on a JEOLCO C60HL spectrometer in deuteriochloroform and are reported in p.p.m. from TMS as internal standard. Gas–liquid chromatography analyses were carried out on an F and M Model 720 gas chromatograph utilizing an 8 ft × 0.375 in. 20% SE30 on Chromosorb W column. The flow rate of the helium carrier gas was 1 ml/s. Chloranil was recrystallized from benzene prior to use. Unless otherwise noted, the drying agent used was anhydrous sodium sulfate and solvents were removed on a rotary evaporator at reduced pressure. Chromatography was performed using Fisher neutral alumina, 80–200 mesh, Brockman activity grade 1. Microanalyses were performed by A. B. Gygli, Microanalysis Laboratory, Toronto, Ontario.

General Procedure

A. Using tert-Butanol as Solvent

A stirred mixture of dihydrothiophene (8 mmol) and chloranil (39 mmol) in *tert*-butanol (60 ml) was heated at reflux for 6 h. Excess chloranil was filtered, the filtrate was added to 600 ml of water and this was extracted with pentane or ether (3 × 150 ml). The organic layer was washed with water (6 × 150 ml), 5% sodium hydroxide (2 × 100 ml) and finally with water until the washings were neutral. The dried solution was evaporated and the residue was chromatographed using pentane as eluant. The thiophene was obtained essentially pure by evaporation of the pentane. Reduction of the reaction time to 3 h afforded incomplete reaction.

B. Using Pyridine as Solvent

Chloranil (39 mmol) was added with stirring to dry pyridine (100 ml). An exothermic reaction occurred immediately and a deep red color developed. After 5 min a deep brown precipitate formed. This mixture was stirred for 15 min and the dihydrothiophene (8 mmol) was added all at once. The mixture was refluxed 6 h, cooled, poured into 600 ml of water, and extracted with ether (4 × 150 ml). The extracts were washed with 10% hydrochloric acid (2 × 100 ml), dried and concentrated. Chromatography as previously outlined gave the thiophene.

Analytical samples were collected from g.l.c. Indices of refraction and n.m.r. spectra are shown in Table 2. Infrared spectra were generally uninformative.

Can. J. Chem. Downloaded from www.nrcresearchpress.com by 210.87.254.6 on 09/05/12
For personal use only.

TABLE 2. Indices of refraction and n.m.r. spectra

Compound	n_D^{25} (lit. (ref.))	Nuclear magnetic resonance data[a,b]
3*a*	1.5121 (1.5131 (12))	6.25 (s, 1), 2.33 (s, 3), 2.23 (s, 3) 1.98 (s, 3).
3*b*	1.5045 (1.5073 (13))	6.68 (m, 2), 2.83 (q, 2, J = 7.5 Hz), 2.47 (s, 3), 1.43 (t, 3, J = 7.5 Hz).
3*c*	1.5073	6.61 (s, 1), 2.52 (q, 2, J = 7.5 Hz) 2.43 (s, 3), 2.29 (s, 3) 1.16 (t, 3, J = 7.5 Hz).
3*d*	1.5093	6.73 (m, 1), 2.80 (q, 2, J = 7.5 Hz) 2.53 (q, 2, J = 7.5 Hz), 2.35 (s, 3), 1.25 (t, 3, J = 7.5 Hz), 1.15 (t, 3, J = 7.5 Hz).
3*e*	1.5432 (1.5452 (15))	6.13 (s, 1), 2.46–1.66 (m, 8), 2.22 (s, 3).

[a]Tabulation follows the order: chemical shift (δ), multiplicity, number of protons, coupling constant.
[b]Spectra run in CCl_4.

3,5-Diethyl-2-methylthiophene (*3d*)

Anal. Calcd. for $C_9H_{14}S$: C, 70.07; H, 9.15. Found: C, 70.36; H, 8.77.

The financial support of the National Research Council of Canada is most gratefully acknowledged.

1. E. BALTAZZI. Chem. Rev. **63**, 511 (1963).
2. (*a*) S. GRONOWITZ. *In* Advance in heterocyclic chemistry. Vol. 1. *Edited by* A. R. Katritzky. Academic Press, New York. 1963. p. 2; (*b*) D. E. WOLF and K. FOLKERS. *In* Organic reactions. Vol. 6. Wiley, New York, N.Y. 1951. p. 410.
3. O. HINSBERG. Chem. Ber. **43**, 901 (1910).
4. L. A. PAQUETTE. Modern heterocyclic chemistry. Benjamin, New York, N.Y. p. 107ff.
5. L. A. PAQUETTE. Modern heterocyclic chemistry. Benjamin, New York, N.Y. p. 115ff.
6. J. M. McINTOSH, H. B. GOODBRAND, and G. M. MASSE. J. Org. Chem. **39**, 202 (1974).
7. J. M. McINTOSH and R. S. STEEVENSZ. Can. J. Chem. **52**, 1934 (1974).
8. S. F. BIRCH and D. T. McALLAN. J. Chem. Soc. 2556 (1951).
9. H. WYNBERG, A. LOGOTHETIS, and D. VERPLOEG. J. Am. Chem. Soc. **79**, 1972 (1957).
10. A. I. KOSAK, R. PALCHAK, W. A. STEELE, and C. M. SELWITZ. J. Am. Chem. Soc. **76**, 4450 (1951).
11. L. M. JACKMAN. *In* Advances in organic chemistry. Vol. 2. *Edited by* R. A. Raphael. Interscience, New York, N.Y. 1960. p. 329ff.
12. W. J. KING and F. F. NORD. J. Org. Chem. **14**, 638 (1949).
13. A. F. SHEPARD. J. Am. Chem. Soc. **54**, 2951 (1932).
14. N. P. BUU-HOI and N. HOAN. Rec. Trav. Chim. **67**, 309 (1948).
15. N. P. BUU-HOI and M. KHENSISSI. Bull Soc. Chim. Fr. **3**, 359 (1958).

Can. J. Chem. Downloaded from www.nrcresearchpress.com by 210.87.254.6 on 09/05/12
For personal use only.

Nuclear Magnetic Resonance Studies. XXVII.[1] Homoenolization of Fenchone. A Mechanistic Study Utilizing ^{13}C and ^{2}H Nuclear Magnetic Resonance

A. L. JOHNSON,[2] J. B. STOTHERS, AND C. T. TAN
Department of Chemistry, University of Western Ontario, London, Ontario
Received August 29, 1974

A. L. JOHNSON, J. B. STOTHERS and C. T. TAN. Can. J. Chem. **53**, 212 (1975).

Deuterium exchange occurs at five β positions in fenchone under homoenolization conditions (t-BuO$^-$–t-BuOD, 185°), C-6 (*exo* and *endo*), C-8, C-9, and C-10. Both ^{13}C and ^{2}H n.m.r. methods were employed to monitor deuterium incorporation and the particular advantages of the latter are illustrated. The relative rates of the five exchange processes were determined directly by ^{2}H n.m.r. in contrast to the earlier homoenolization studies for which the stereoselectivity of exchange was established indirectly. The intermediate homoenolate ion can lead to rearrangement and the rearrangement products have been characterized by ^{13}C n.m.r. as the 3,3,6-trimethylnorcamphors. Homoenolization of this mixture gave further evidence on the stereochemistry of homoenolate formation.

A. L. JOHNSON, J. B. STOTHERS et C. T. TAN. Can. J. Chem. **53**, 212 (1975).

Dans des conditions d'homoénolisation (t-BuO$^-$–t-BuOD, 185°) l'échange de deutérium se produit dans cinq positions β de la fenchone; ces cinq positions sont les positions C-6 (*exo* et *endo*), C-8, C-9 et C-10. Des méthodes impliquant la r.m.n. du ^{13}C et du ^{2}H ont été utilisées pour suivre l'incorporation du deutérium; les avantages particuliers de la dernière méthode sont démontrés. On a déterminé directement par r.m.n. du ^{2}H les vitesses relatives des cinq processus d'échange; ces résultats sont en contraste avec les études antérieures d'homoénolisation pour lesquelles la stéréosélectivité de l'échange n'avait été établit qu'indirectement. L'ion homoélonate intermédiaire peut conduire à des réarrangements; les produits de réarrangements ont été caractérisés par r.m.n. du ^{13}C comme étant les triméthyl-3,3,6 norcamphres. L'homoénolisation de ce mélange peut donner d'autres preuves sur la stéréochimie de la formation de l'homoénolate.

[Traduit par le journal]

Several years ago, Nickon and Lambert (1) presented the first example of base-catalyzed hydrogen abstraction from the β-position of a bicyclic ketone, a process they termed homoenolization. Their initial example was camphenilone (**1**) and through an elegant series of experiments it was unequivocally established that hydrogen–deuterium exchange only occurred at the C-1, C-6, and methyl positions (2). Reaction through the symmetric homoenolate anion **2** leads to deuterium incorporation at C-1 and C-6, equivalent in **2**, and serves to racemize **1** thereby rendering the methyl groups equivalent and thus masking any stereoselectivity which may be involved in the exchange at the *exo* and *endo* methyl positions. To examine the stereochemistry of exchange at C-6 the reverse reaction, homoketonization of 1-acetoxynortricyclene (**3**), was studied (3) and it was found that in alkaline media protonation occurred with high stereoselectivity favoring inversion of configuration, *i.e.* *exo*-protonation.

The synthetic potential of skeletal rearrangement via homoenolate anions to generate systems otherwise difficult to obtain was also demonstrated in the initial investigations of homoenolization by Nickon *et al.* (4). Treatment of brexan-2-one (**4**) with t-BuO$^-$–t-BuOH at 185° gave a 60% yield of brendan-2-one (**5**). A similar rearrangement of longicamphenilone (**6**) was employed by Coates and Chen (5) to generate the *endo*-bridged system **7** as a structural proof for one of the solvolysis products of longicamphenilyl tosylate. Further information on homoenolization in polycyclic systems was provided by Arigoni and co-workers (6) who examined deuterium exchange in longicamphor (**8**) and copacamphor (**9**) under homoenolization conditions. While **8** was found to incorporate up to 3 equiv. of deuterium, only monodeuteration was observed for **9** exclusively at the α-position. Clearly, the additional deuterium incorporation in **8** shows that homoenolization occurred. The lack of more remote exchange in

[1]Part XXV, ref. 27. Part XXVI, ref. 25.

[2]Present address: College of Southern Idaho, Twin Falls, Idaho.

Can. J. Chem. Downloaded from www.nrcresearchpress.com by 210.87.254.42 on 09/05/12
For personal use only.

Can. J. Chem. Downloaded from www.nrcresearchpress.com by 210.87.254.42 on 09/05/12
For personal use only.

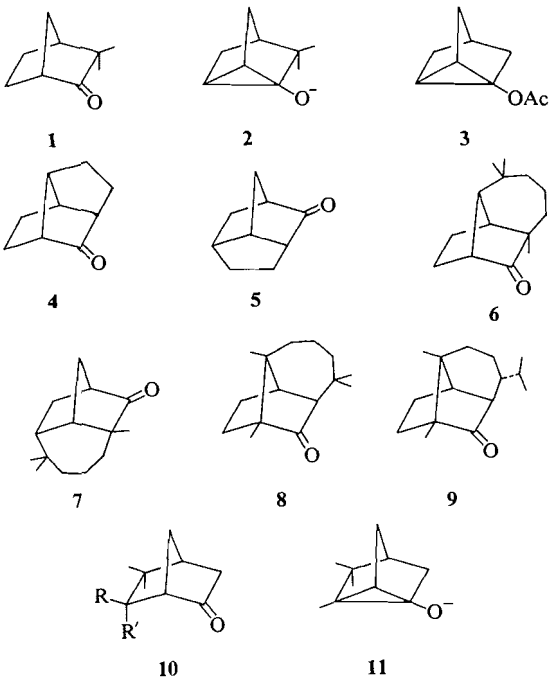

a R = H; R′ = Me
b R = Me; R′ = H

9 was attributed to "the additional strain imposed by the three-membered bridge on the [2.2.1]bicycloheptane system" but it seems somewhat surprising that **9** failed to homoenolize in view of the **4** → **5** conversion; perhaps more vigorous conditions and/or a longer reaction time would cause more extensive deuterium exchange. In addition to these polycyclic examples, homoenolization has been invoked to account for the results in two acyclic examples (7, 8), in one of which ^{13}C labelling experiments afforded evidence for a pathway involving two homoenolate ions (8).

Evidence that homoenolization can occur concurrently with enolization in bridged ketones containing an α-methylene group was recently presented (9). The *endo*- and *exo*-isocamphanones (**10***a* and *b*, respectively) are interconvertible via a common homoenolate ion **11** which could also lead to camphor. The interconversion of **10***a* ⇌ **10***b* gave further evidence for preferential *exo*-protonation of **11** since **10***a* gave only 1.5% of **10***b* whereas, under comparable conditions, **10***b* gave 42% of **10***a*; in these experiments the relative yields of camphor were 58 and 22%, respectively.

Each of the foregoing examples involves proton abstraction from a β-position of the ketone but more remote abstraction should also be possible and has in fact been observed at the *syn*-methyl of camphor (10) and for the half-cage ketone **12** rearranging to **13**. Homoketonization of the bird cage alcohol **14**, expected to be the intermediate alkoxide species, gave the same mixture of **12** and **13** heavily favoring the latter (11).

In the earlier work, a variety of techniques was employed to establish the course of deuterium exchange by homoenolate ions. For example, the details of camphenilone homoenolization were elucidated through a combination of ^{1}H n.m.r., i.r., and mass spectra together with separate synthesis of deuterated analogs (1–3). More recently, we have demonstrated that the same information is more readily available by ^{13}C n.m.r. (9). The characteristic effects produced by ^{2}H-labelled centers in ^{13}C spectra afford a straightforward monitor for deuterium exchange studies in a variety of systems (1, 12). Comparison of the ^{13}C spectrum of the labelled material with that of the unlabelled compound immediately reveals the site(s) of deuterium incorporation and integrated intensity data provide a measure of the ^{2}H content at the individual carbons. In practice, however, meaningful intensity data from ^{13}C spectra require careful selection of the optimum operating conditions, because of variations in relaxation times and nuclear Overhauser enhancements of nonequivalent

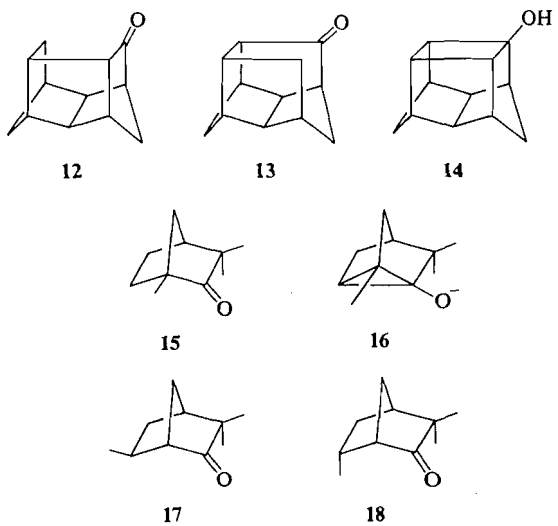

Can. J. Chem. Downloaded from www.nrcresearchpress.com by 210.87.254.42 on 09/05/12
For personal use only.

carbons, and calibration data from spectra of the natural abundance material. In our experience, the precision of quantitative assessments of the ^2H content at individual centers is 3–5% and, thus, lightly labelled centers can be missed. A second deficiency of the ^{13}C method concerns exchange at methylene carbons bearing nonequivalent hydrogens. In general, the ^{13}C absorption pattern will be the same regardless of which hydrogen undergoes exchange. Hence, information on the stereochemistry of exchange at such methylene carbons is unavailable from the ^{13}C spectrum.

The striking advantages of ^2H n.m.r. for mechanism studies have been clearly illustrated (13) and, in the present case, the use of ^2H spectra of the labelled species neatly overcomes the major deficiencies of the ^{13}C method. Since magnetic relaxation of deuterium nuclei is induced entirely by an intramolecular quadrupole mechanism (14) there is no Overhauser enhancement accompanying proton decoupling. In addition, ^2H relaxation times are relatively short (15) which minimizes the possibility of partial saturation. These two features circumvent the major pitfalls associated with ^{13}C spectra and render integrations of ^2H spectra more favorable. Another advantage of ^2H spectroscopy accrues from the low natural abundance of deuterium, 0.015%. Thus, even at low incorporation levels of *ca.* 1%, the n.m.r. signals of ^2H labels will be about two orders of magnitude more intense than the natural abundance signals and one can readily monitor lightly deuterated centers. With proton decoupling and the absence of other magnetic nuclei, deuterium spectra consist of relatively narrow singlets having half-widths of *ca.* 1 Hz for each nonequivalent site. Although the shieldings for ^1H and ^2H in identical environments are the same, on a p.p.m. scale, for observations at the same magnetic field (16), the shift range for ^2H nuclei is reduced by a factor of 6.5 because of the lower magnetogyric ratio and the spectra of compounds containing similar but nonequivalent ^2H nuclei may have heavily overlapping signals. In many cases, this inconvenience may be reduced through the use of lanthanide shift reagents to obtain greater shift dispersion (17). Even with overlapping signals, however, precise integrated intensities may be obtained by computer line-shape fitting rather than the usual electronic integration. Our experience indicates that the line-shape fitting technique permits precisions of the order of 1–2%.

The results of a detailed examination of the behavior of fenchone (**15**) under homoenolization conditions, namely at 185° in *t*-BuO^-–*t*-BuOD are presented in this paper; a preliminary account of part of this work has appeared (9).

Deuterium incorporation was monitored by both ^{13}C and ^2H n.m.r., and from the latter data, the relative rates of exchange were estimated for the *exo*- and *endo*-6-protons and at the three methyl groups. This direct measure of the stereoselectivity is the key advantage of the ^2H n.m.r. method for this study. The intermediate homoenolate ion **16** can lead to rearranged ketones; these have been characterized by ^{13}C n.m.r. and their homoenolization behavior was examined.

Experimental

Materials

Commercial fenchone was employed for these studies. Initially, the camphor present (~5%) was not removed before use but in the later stages this impurity was removed by reaction with 2,4-dinitrophenylhydrazine or by preparative gas chromatography (g.c.) on a 20% SE-30 column. *t*-Butyl alcohol-*O*-d_1 was prepared according to the procedure of Young and Guthrie (18). For the second set of homoenolization runs, the preparation of the alcohol-*O*-d_1 was modified. After the initial hydrolysis of the borate ester, a small amount of potassium metal was added to the wet alcohol and the alcohol was distilled. This was repeated and a third distillation from molecular sieves gave *t*-butyl alcohol-*O*-d_1 which was $<0.005\ M$ in water by Karl Fischer titration.

Homoenolization Experiments

The general procedure followed was essentially as described by Nickon *et al.* (2). Typically, fenchone was added to the base, prepared by dissolving potassium metal in *t*-butyl alcohol, to give a solution containing ketone–*t*-BuO^-–*t*-BuOH(D) in the mole ratio 1:4:60. Aliquots were placed in glass tubes which were sealed after degassing. After heating at 185 ± 3° for varying periods of time, the tubes were opened and the ketonic products isolated by pentane extraction in average yields of 80%. The total product composition was analyzed by g.c. on 20% SE-30 or 10% FFAP columns. In each case a small peak appeared at a slightly longer retention time than fenchone. In the longer runs, this second peak made up 6–7% of the total product. After column chromatography on alumina, the second peak was reduced to *ca.* 5% of the total product, and could be easily separated from fenchone by preparative g.c. on SE-30 columns.

Characterization of the Minor Products

Some larger scale runs were conducted to obtain samples of the second fraction by g.c. on SE-30 columns.

Can. J. Chem. Downloaded from www.nrcresearchpress.com by 210.87.254.42 on 09/05/12
For personal use only.

Infrared spectra of these samples indicated the presence of an alcohol which was readily removed by chromatography on alumina. Its chromatographic (g.c., t.l.c.) behavior was identical to that of fenchol. Gas chromatographic analysis of alcohol-free material on a 15% DEGS column showed this second fraction to contain two partially separated components in a ratio of *ca.* 1:3. The i.r. spectrum exhibited strong carbonyl absorption and its ^{13}C spectrum consisted of 18 signals in the higher field region with 2 additional peaks at low field, 220.0 and 219.3 p.p.m.; the latter, in the ratio of *ca.* 1:3, are typical carbonyl carbon signals. The high field signals formed two sets of nine, having an intensity ratio of *ca.* 1:3. Off-resonance decoupling established that each set contained three methyl, two methylene, three methine, and one quaternary carbon signals. The signal at lowest field in each of these groups, 57.0 and 56.3 p.p.m., arose from a methine carbon, whereas the three at highest field in each group were methyl signals, 21.0, 21.3, and 23.2; 18.1, 20.0, and 23.9 p.p.m., respectively. The remaining signals appeared at: 31.5, 31.7, 30.6, 36.3 (CH_2's); 33.5, 46.6, 33.4, 46.9 (CH's), and 46.0 and 47.7 p.p.m. (quaternary C's); the less intense peaks of the two sets of signals are listed first.

Model experiments showed that the reduction of fenchone with $LiAlH(OMe)_3$ gave fenchol which was >96% *endo*. A sample of the mixture of rearranged ketones was reduced to provide a mixture of the corresponding alcohols which by g.c. on a 10% SE-30 column were present in the ratio of 3:1 but not well resolved. Column chromatography on silica gel gave upon elution with ether–pentane (3:97) a fraction which was essentially a single component and a second fraction enriched in the less abundant isomer; these fractions were examined by ^{13}C n.m.r. The spectrum of the single component contained 10 signals which were shown by off-resonance decoupling to arise from methyl (18.9, 20.1, and 31.2 p.p.m.), methylene (31.8 and 35.5 p.p.m.), methine (33.2, 48.6, 49.5, and 83.9 p.p.m.), and one quaternary carbon at 37.4 p.p.m. The spectrum of the second fraction contained in addition to these signals a set of nine more intense peaks at 19.7, 21.7, and 30.6 (CH_3's); 29.7 and 34.8 (CH_2's); 24.1, 49.3, 51.1, and 80.6 p.p.m. (CH's). From its intensity it was apparent that the 37.4 p.p.m. signal is common to both isomers.

A 400 mg sample of the ketone mixture was subjected to the homoenolization conditions for 200 h and the product was analyzed by g.c. using the 15% DEGS column. This mixture was found to contain 75% of fenchone and 25% of the two ketones in a ratio of 4:1, *i.e.* the relative amount of the more abundant isomer originally present was much reduced.

Spectra

^{13}C spectra were obtained with a Varian XL-100-15 system operating in the Fourier transform mode. To optimize operating conditions for measuring the integrated intensities in the ^{13}C spectra, samples of fenchone in $CDCl_3$ were run under a variety of conditions varying the pulse width and repetition rate using sweep "windows" of 1 kHz or less. Under conditions which gave essentially equal integrals for each nonequivalent protonated carbon in fenchone, the deuterated samples of fenchone-d_x at similar concentrations were examined and the relative intensities of the absorption for each carbon were measured. As a check on these results, mass spectral data were obtained using a Varian M-66 instrument to determine the relative concentrations of the various deuterated species in each sample. The estimates of deuterium content at the individual carbons by ^{13}C n.m.r. were judged to be within $\pm 5\%$ and comparison of the total ^2H content with that from the mass spectra supports this.

Deuterium spectra were obtained at 15.4 MHz with a Varian XL-100-15 system in the Fourier transform mode. A solvent mixture of C_6F_6 and $CHCl_3$ (1:4 v/v) was used and the instrument locked to the ^{19}F signal with noise modulated proton decoupling. Because of the relatively small ^2H shift range, on a frequency scale, and the fact that the signals are ~1 Hz wide, the individual signals of similar deuterium nuclei are heavily overlapped. Greater shift dispersion was obtained through the use of the $Pr(fod)_3$ shift reagent but line broadening accompanies the increased dispersion. Consequently, line-shape fitting by computer, assuming Lorentzian line shapes, was employed to obtain the relative areas of the individual absorption signals. For this purpose a modified version of the BMDX85 program (19) was used. With the total deuterium content, as measured by mass spectrometry, the relative concentrations of deuterium at individual centers was readily calculated and these data are judged to have precisions of 1%. Shift reagent studies of the proton spectra of fenchone, using a Varian HA-100 instrument, were also carried out to confirm the assignments in the ^2H spectra.

Results

^{13}C Nuclear Magnetic Resonance Assessment of Deuterium Incorporation

Initially, the prime reason for examining the behavior of **15** under homoenolization conditions was the need for unequivocal ^{13}C n.m.r. assignments in this bicyclic system. Analogous behavior to that of **1**, which had been studied in detail (1, 2), was expected but the unsymmetrical homoenolate ion **16**, in contrast to **2**, could lead to rearranged product and could reveal stereoselectivity of exchange at the *exo*- and *endo*-methyl carbons, C-8, and C-9. In the first set of experiments, the progress of deuterium incorporation in **15** was monitored with ^{13}C n.m.r. and mass spectrometry. From the ^{13}C spectra, the specific carbons undergoing exchange were readily revealed because of the distinctive spectral changes produced by deuterium incorporation (9, 12); spectra of two samples are shown in Fig. 1. The triplets characteristic of —CHD— and —CH_2D groups were apparent only for the C-6 and *exo*-methyl (C-8) absorptions while isotope shifts for C-1, C-3, and C-5 were also observed. Careful integration of the ^{13}C absorptions for all protonated and partially protonated carbons

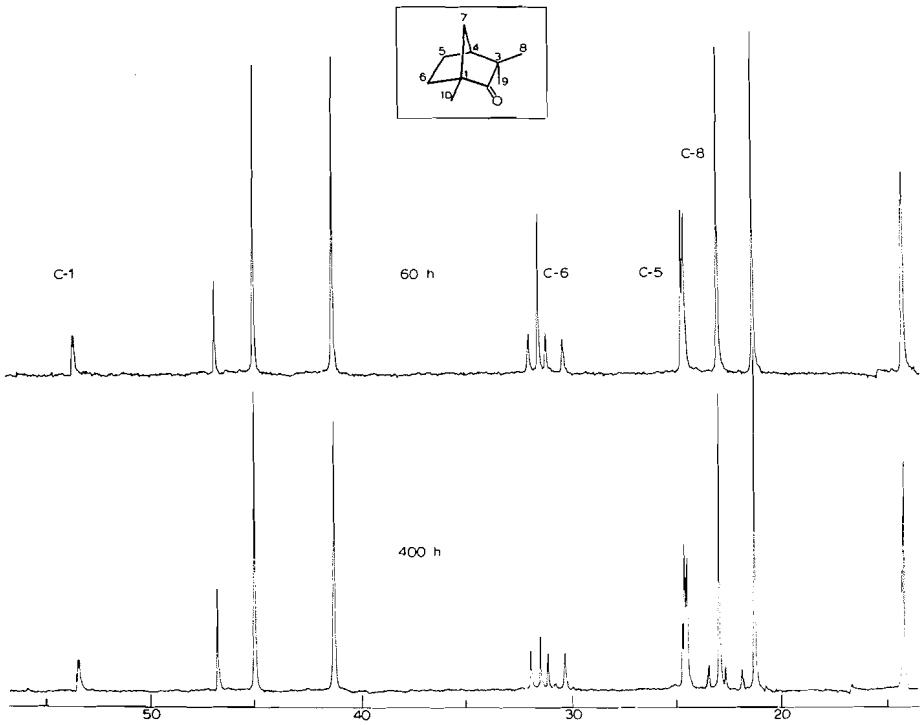

FIG. 1. ^{13}C spectra of **15** after treatment with *t*-BuO$^-$–*t*-BuOD at 185° for the times indicated. The scale is in p.p.m. from TMS.

gave a measure of the ^2H content at C-6 and the *exo*-methyl group. For example, the C-6 absorption consisted of a singlet identical to that in normal fenchone and a CHD triplet, the relative intensity of the latter provides a measure of the extent of monodeuteration at this center. From the intensities of the non-deuterated carbons, a "standard" intensity for a single carbon for each sample was obtained as the average. The difference between this "standard" value and the sum of the —CH_2— and —CHD— intensities gave the relative concentration of the —CD_2— species. As a check on the ^2H assay by ^{13}C n.m.r., each sample was analyzed by mass spectrometry to obtain precise data on the ^2H content. These data for samples which were allowed to react for various times are listed in Table 1. The agreement between the total atoms ^2H/molecule obtained by mass spectrometry and ^{13}C n.m.r.

TABLE 1. Deuteration in fenchone at 185°

Time (h)	^2H content by mass spectrometry[a]							^2H assay by ^{13}C n.m.r.[b]			
	1D	2D	3D	4D	5D	6D	Total atoms ^2H	CHD	CD_2	CH_2D	Total atom ^2H
60	0.468	0.071					0.61	0.42	0.07		0.56
140	0.589	0.188	0.015				1.01	0.59	0.19	0.07	1.04
272	0.381	0.387	0.111	0.015			1.55	0.44	0.42	0.17	1.45
400	0.342	0.404	0.143	0.022	0.005		1.69	0.36	0.50	0.25	1.61
400[c]	0.278	0.497	0.144	0.035	0.009		1.86	0.33	0.68	0.27	1.96
800[d]	0.206	0.457	0.238	0.055	0.009	0.001	2.10_6	[e]	[e]	0.40	—

[a]Atoms ^2H ±0.001.
[b]Atoms ^2H, ±0.05.
[c]**15**-d_x from a 140 h run was treated with fresh *t*-BuO$^-$–*t*-BuOD for 260 h.
[d]**15**-d, from a 400 h run was treated with fresh base for an additional 400 h.
[e]The C-6 absorption was too complex for precise integration (see text).

Can. J. Chem. Downloaded from www.nrcresearchpress.com by 210.87.254.42 on 09/05/12
For personal use only.

Can. J. Chem. Downloaded from www.nrcresearchpress.com by 210.87.254.42 on 09/05/12
For personal use only.

is gratifyingly good, even though the estimated error for the measurement of ^2H content at individual carbons by ^{13}C n.m.r. is *ca.* 5%.

To try to maximize the deuterium content in **15**, one sample recovered after 140 h was treated again with a fresh deuterium pool for 260 h and a sample from a 400 h run was reacted with fresh base for an additional 400 h. From the latter experiment it was apparent that up to 6 deuterium atoms can be incorporated into **15** under homoenolization conditions; this result is in complete accord with some preliminary data obtained by Lambert (10) several years ago. The ^{13}C spectrum of this sample very clearly served to point up some of the deficiencies in the ^{13}C n.m.r. method for deuterium analysis. The presence of species containing more than five ^2H nuclei demands that exchange has occurred at centers in addition to C-6 and C-8, but the ^2H content at the lightly deuterated centers was not observable from the ^{13}C spectrum. In addition the exchange was so extensive at C-6 that the intensity of the "quintet", probably a triplet of triplets, for the $—CD_2—$ containing molecules precluded precise integrations of the $—CH_2—$ and —CHD— absorptions. The intensity of the "quintet" is not meaningful for comparison with the intensities of the signals from protonated carbons, since the former absorption lacks the significant Overhauser enhancement produced by proton decoupling. Another weakness of the ^{13}C analysis is the fact that it is not possible to distinguish between *exo* and *endo* deuteration at C-6, only the total ^2H incorporation at this carbon can be assayed.

Notwithstanding these deficiencies, however, ^{13}C spectra can be valuable for quantitative analysis of deuterium incorporation in a host of systems. In the present case, the major result of the exchange was clearly apparent from the ^{13}C spectra and the total deuterium content was readily assayed for C-6 and C-8.

Identification of the Rearrangement Products

Examination of the recovered material from each run by g.c. on SE-30 columns showed an additional peak, comprising 6–7% of the total product, having a longer retention time than that of fenchone (93–94% of the isolated product). Column chromatography on alumina of the total product decreased the second fraction to *ca.* 5% for products obtained from the longer runs. Since the g.c. retention time corresponded to that of fenchol, there was apparently some reduction (~1%) of the fenchone, presumably by undissolved potassium metal. Some larger scale runs provided larger samples of the second fraction and, after removal of the alcohol, g.c. analysis of these on a DEGS column showed the minor fraction to contain two components in a ratio of *ca.* 1:3, although the peaks were not separately resolved. Infrared spectra and ^{13}C n.m.r. spectra confirmed that these were ketonic and isomeric with fenchone since each contained three methyl, two methylene, three methine and one quaternary carbon signal in the higher field region of the ^{13}C spectrum, besides a typical carbonyl carbon signal near 220 p.p.m. (20). The positions (see Experimental) of the individual resonances corresponded well with those expected for ketones **17** and **18**, the 3,3,6-trimethyl norcamphors, which could arise from homoenolate **16** by cleavage of the bond formed between the original carbonyl carbon and C-1 in **15**. The assignments have been discussed in conjunction with a ^{13}C study of several methyl substituted norcamphors (21).[3] For additional confirmation of the structure of these rearranged ketones, the mixture was reduced to the corresponding *endo*-alcohols with $LiAlH(OMe)_3$. This reagent was chosen since a variety of methyl norcamphors give alcohols which are 96–98% *endo* upon reaction with it; for example, the alcohol formed from fenchone is >96%-*endo*. The product was found to contain two major components in a ratio of *ca.* 1:3 by g.c. analysis on SE-30 columns, but, again, separate bands were not resolved. Column chromatography on silica gel, however, afforded two fractions, one of which was essentially a single alcohol corresponding to the more abundant component of the original mixture, while the second fraction was enriched in the less abundant component (70%) together with the more abundant alcohol (30%). The ^{13}C shielding of these two alcohols (see Experimental) accorded well with those expected for the *endo*-alcohols, corresponding to **17** and **18**; the ^{13}C data for several methyl norbornanols were available (22) since the

[3]In the paper describing the ^{13}C spectra of these norcamphors, there is a typographical error and the shielding of C-3 in fenchone should read 47.1 p.p.m.

norcamphors cited above had been reduced to the alcohols. Thus it can be concluded that the homoenolate ion **16** opened in the two possible modes to produce **15** or a mixture of **17** and **18**. Since the concentration of the minor products never exceeded 5% even in the longest runs, this appears to be the equilibrium amount.

A sample of the mixture of rearranged ketones (**17** and **18** in a ratio of 1:3) was treated with *t*-BuO$^-$–*t*-BuOH at 185° for 200 h and the isolated product was examined by g.c. It was found that the ratio of ketones was 20:5:75 for **17**, **18**, and **15**, respectively, thus **18** is the more reactive of the rearranged ketones.

^2H *Nuclear Magnetic Resonance Assessment of Deuterium Incorporation in* **15**

A number of developments suggested that a second examination of **15** might be valuable. After obtaining the results discussed above, we extended our study of homoenolization to other bicyclic systems and had some difficulty with reproducibility of the rates of deuterium incorporation. We found that a modified drying procedure of the *t*-butyl alcohol-*O*-d_1 eliminated this problem and all subsequent work was done with *t*-butyl alcohol which tested $<0.005\ M$ in water by Karl Fischer titration. The rate-depressing effect of water on *t*-BuO$^-$–*t*-BuOH has been discussed by Cram *et al.* (23). It may be noted that the general precautions regarding the use of *t*-BuO$^-$ have been discussed recently (24); these problems have been circumvented in the present work by generation of the base *in situ*. Recently, the n.m.r. spectrometer was modified to perform ^2H experiments in the Fourier transform mode. The direct examination of deuterated samples by ^2H n.m.r. offered distinct advantages over the ^{13}C approach as noted in the introduction. Consequently, a second set of experiments was carried out for **15** under homoenolization conditions.

A prime reason for this re-examination was to follow the rate of deuterium incorporation at the *exo*- and *endo*-6 protons separately and to check for small extents of incorporation in the remaining two methyl groups (C-9 and C-10): features which could not be discerned by ^{13}C n.m.r. The ^2H spectra of samples of **15**-d_x recovered after treatment with *t*-BuO$^-$–*t*-BuOD consisted of three distinct absorptions at 5.79, 5.98 and 6.32 p.p.m. upfield from the

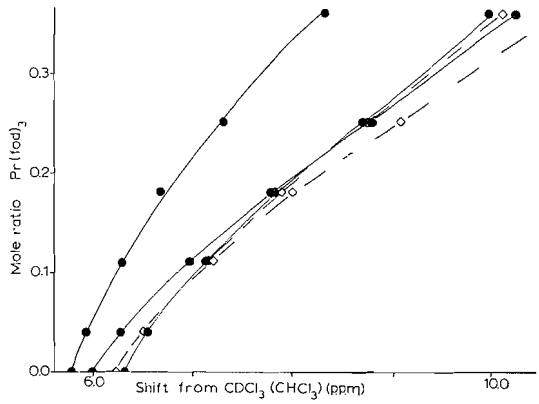

FIG. 2. Effects of Pr(fod)$_3$ on the relative shifts of **15**; ^2H shifts (●) are indicated with full lines, ^1H shifts (○) with dashed lines. Spectra were obtained for $CHCl_3$–C_6F_6 (4:1 v/v) solutions.

absorption of $CDCl_3$. These signals were tentatively assigned to the 6-*exo*-, 6-*endo*-, and C-8-methyl deuterons, respectively. In the ^1H spectrum of **15**, the C-10 methyl group absorbs at 6.22 while the C-8 and C-9 protons are equivalent at 6.32 p.p.m., upfield from $CHCl_3$ in $CHCl_3$–C_6F_6 (4:1) solution. Thus, this medium is inappropriate for the desired measurements, since the ^2H signals had line widths of 1.0–1.2 Hz (0.06–0.08 p.p.m.). To increase the separation of the deuterium resonances as well as to obtain unequivocal proof for the assignments of the C-6 signals, spectra were obtained using Eu(fod)$_3$ and Pr(fod)$_3$ as shift reagents. The results with the latter reagent seemed better for our purposes and the shifts produced in its presence were examined in detail.

Upon addition of Pr(fod)$_3$ to solutions of **15**-d_x in $CHCl_3$–C_6F_6 (4:1 v/v), each of the three signals noted above shifted to higher field with the central peak exhibiting the greatest relative shift. These shifts over the range of 0–0.36 equiv. of Pr(fod)$_3$ are plotted in Fig. 2, together with the corresponding shifts for the remaining methyl protons as observed in ^1H spectra. Decoupling experiments in the ^1H spectra confirmed the tentative assignments noted above for the 6-deuterons. In the more dispersed spectra the methylene proton absorption at highest field was essentially a six-line pattern with repeated spacings of 13, 7 and 2 Hz corresponding in a first-order analysis to the couplings with the *exo*-6, *endo*-5 and *exo*-5

Can. J. Chem. Downloaded from www.nrcresearchpress.com by 210.87.254.42 on 09/05/12
For personal use only.

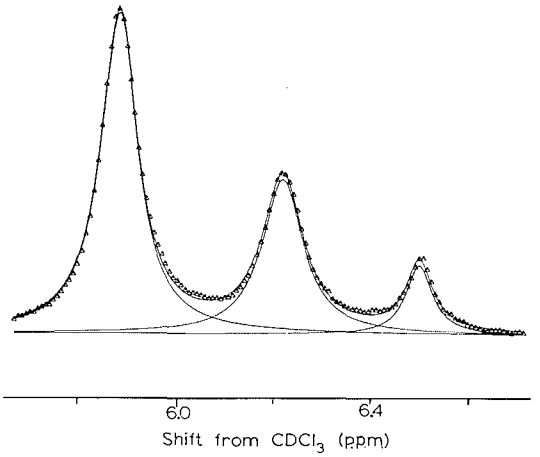

FIG. 3. Observed (△) and computer-fitted (full line) ^2H spectra of **15**-$d_{1,18}$ after treatment for 40 h with *t*-BuO^-–*t*-BuOD at 185°. The spectrum was obtained in $CHCl_3$–C_6F_6 (4:1) containing 0.03 equiv. of $Pr(fod)_3$. The line-shape fitting utilized 130 data points; the individual Lorentzian curves for each absorption are also shown.

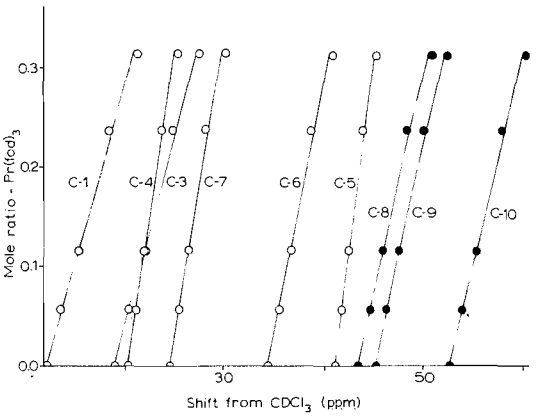

FIG. 4. Effects of $Pr(fod)_3$ on the ^{13}C shieldings of **15**. Spectra were obtained for $CDCl_3$–C_6F_6 (1:4 v/v) solutions.

protons, respectively. Double irradiation at the position of the *exo*-6 proton, as found from the ^2H spectrum, eliminated the larger of these splittings in the high field methylene proton pattern, confirming the assignments for the *exo*- and *endo*-6-deuterium nuclei. For the **15**-d_x samples isolated after reaction with the base for relatively short times, ^2H spectra for solutions containing about 0.05 equiv. of $Pr(fod)_3$ were recorded and the relative intensities of the three absorption signals measured by line-shape fitting by computer. An example is shown in Fig. 3. These data, together with the total ^2H content determined for each sample by mass spectrometry, provided a measure of the relative extent of deuteration at the three positions.

From Fig. 2, it is apparent that the three types of methyl protons show different shifts with added $Pr(fod)_3$ reagent so that, in principle, the ^2H spectra of heavily doped samples should permit the detection of deuterium at C-9 and C-10. In practice, however, the increased line broadening which accompanied the increased shifts produced by the lanthanide reagent gave spectra with insufficient resolution of the closely-lying absorptions for good integrations, although it was apparent for 40, 100, and 300 h samples that some deuteration had occurred at C-9 and C-10. At somewhat lower concentrations of **15** in $CHCl_3$–C_6F_6 (1:4 v/v), the relative shifts are larger for comparable amounts of added $Pr(fod)_3$; this solvent change was serendipitous. With 0.25 equiv. of $Pr(fod)_3$ five resonances were apparent in the ^2H spectrum of the 300 h sample at 8.76, 10.66, 10.82, 11.04, and 11.50 p.p.m. upfield from $CDCl_3$. From the relative intensities and the known effects of added $Pr(fod)_3$ these signals could be assigned to the *exo*-6, C-8, C-9 (or 10), *endo*-6, and C-10 (or 9) deuterons. It remained to distinguish unequivocally between the C-9 and C-10 signals. Since the assignments for the ^{13}C signals for each of the methyl carbons were known (21), ^{13}C spectra of **15** were recorded with added $Pr(fod)_3$ to determine the relative shifts for each. These results are shown in Fig. 4 from which it is apparent that the order of the methyl shieldings is unchanged with added shift reagent. In the ^1H spectrum of solutions containing 0.313 equiv. of $Pr(fod)_3$, the methyl protons absorbed at 10.95, 11.08, and 11.93 p.p.m., upfield from $CHCl_3$. Selective proton decoupling at the highest field methyl protons gave a ^{13}C spectrum in which only the highest field carbon signal was decoupled; selective irradiation at the lowest field methyl protons decoupled only the third highest field ^{13}C signal. Thus, the shieldings of the methyl signals are in the same order in both ^1H and ^{13}C spectra, namely, C-8 < C-9 < C-10, and the assignments were completed for the ^2H spectra.

With the greater relative shift dispersion obtained in $CHCl_3$–C_6F_6 (1:4) solutions, ^2H

Can. J. Chem. Downloaded from www.nrcresearchpress.com by 210.87.254.42 on 09/05/12
For personal use only.

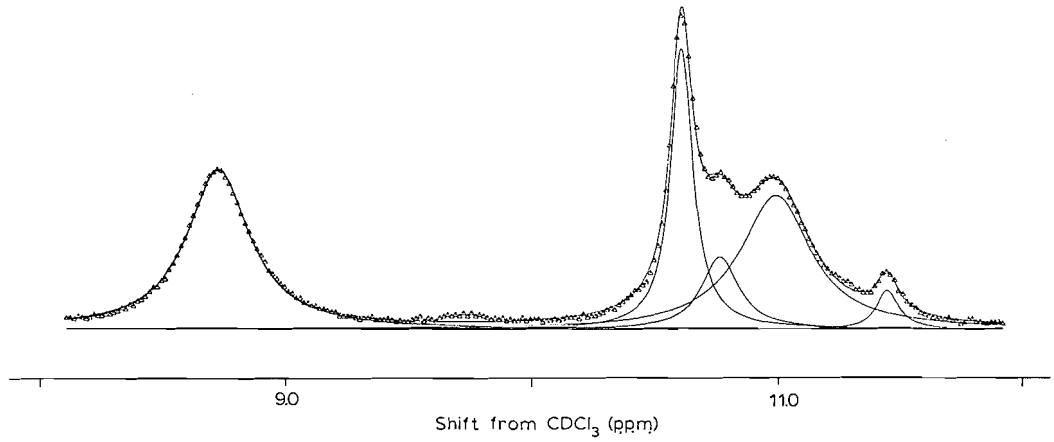

FIG. 5. Experimental (△) and computer-fitted (full line) ^2H spectra of **15**-$d_{1.94}$ after treatment with *t*-BuO^-–*t*-BuOD at 185° for 300 h. The spectrum was obtained in $CHCl_3$–C_6F_6 (1:4) containing 0.26 equiv. of $Pr(fod)_3$. The line-shape fitting was done with 472 data points but, for clarity, every second point is plotted. The individual Lorentzian curves for each signal are also shown.

TABLE 2. Deuterium incorporation in **15** at 185°

	^2H content by mass spectrometry[a]							^2H assay by ^2H n.m.r.[b]					
								C-6		CH_3			
Time (h)	1D	2D	3D	4D	5D	6D	Total atoms ^2H	*Exo*	*Endo*	Total	*Exo*	*Endo*	Bridge
10	0.311	0.025					0.36	0.26	0.08	0.01_8			
20	0.399	0.040					0.48	0.34	0.12	0.02_5			
40	0.551	0.273	0.030				1.18	0.70	0.38	0.10	0.09		0.01
100	0.352	0.444	0.117	0.017			1.66	0.75	0.58	0.33	0.26	0.05	0.01_8
200	0.328	0.433	0.137	0.027	0.007		1.75	0.68	0.68	0.39			
300	0.286	0.370	0.190	0.059	0.014	0.005	1.94	0.65	0.64	0.65	0.42	0.16	0.06

[a]Atoms ^2H, ±0.001.
[b]Atoms ^2H, ±0.02.

spectra for 40, 100, and 300 h samples were recorded and the extent of deuteration at C-6, C-8, C-9, and C-10 determined by line-shape fitting. To illustrate the line-shape fitting, the spectrum of a 300 h sample is reproduced in Fig. 5. The deuterium incorporation data for several samples from this second set of homoenolization experiments are listed in Table 2.

Discussion

A comparison of the results in Tables 1 and 2 readily reveals the significantly faster rates of deuterium incorporation found for the second set of experiments. We attribute the difference to the use of a drier medium for the second set. These results are the more informative with regard to the details of homoenolization of **15** because the stereoselectivity of the exchange could be determined. From the results for the samples from the shorter reaction times in Table 2, one can estimate the first-order rate constants for deuteration at the *exo*-6, *endo*-6, and *exo*-methyl positions as $\sim 7 \times 10^{-6}$, $\sim 2 \times 10^{-6}$, and $\sim 2 \times 10^{-7}\ s^{-1}$, respectively. The pathways available for these processes can be set out as in Scheme 1 and as a test of the relative magnitudes of these estimated rate constants for C-6 and *exo*-methyl exchange, the rate equations for Scheme 1 were numerically integrated using the MIMIC simulation language of the CDC computer, neglecting secondary kinetic isotope effects. The observed and computed ^2H concentrations at the three sites for the 10, 20, and 40 h runs are listed in Table 3, as obtained using $k_X:k_N:k_M$ of 3.5:1.0:0.085. Inclusion of a primary isotope effect of 4–5

Can. J. Chem. Downloaded from www.nrcresearchpress.com by 210.87.254.42 on 09/05/12
For personal use only.

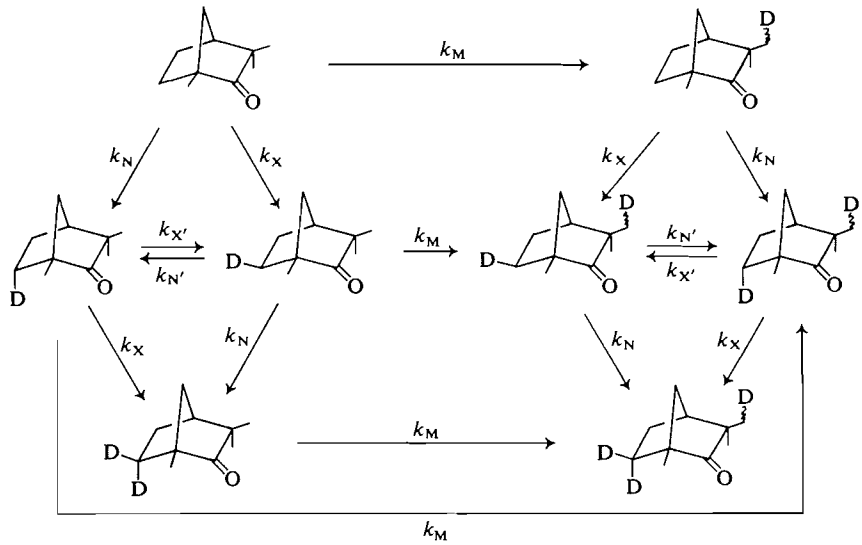

SCHEME I

for the inversion reactions, $k_{N'}$ and $k_{X'}$, led to consistently poorer agreement with experiment indicating that the isotope effect is <2. These inversion reactions represent the formation of the homoenolate ion **16** by abstraction of an *endo*-deuterium and ring opening by *exo*-deuteration, or the reverse. Effectively this partitions the homoenolate ion according to the relative rates k_X and k_N, modified by the isotope effect of deuterium abstraction. Since the standard free energies of formation of *endo*- and *exo*-6-deuteriofenchone are nearly equal, $k_{X'} = k_{N'}$ and assuming the isotope effects for *exo*- and *endo*-deuterium abstraction to be equal it follows that $k_{X'} = k_X k_N/(k_X + k_N) \times k_D/k_H = k_{N'}$.

From the homoenolate ion **16**, formed by abstraction of a C-6 proton in **15**, there are four ways in which the ring opening can occur to give ketones. Cleavage of bond *a* with retention or inversion at C-6 produces *endo*-6-deuterio-**15** or *exo*-6-deuterio-**15**, respectively (arrows N and X indicate *endo*- and *exo*-deuteration). Similarly, cleavage of bond *b* leads to the *exo*-6-methyl derivative **18** (arrow N) or its *endo* isomer **17** (arrow X). From the results cited earlier it is apparent that the bond *a* cleavage is favored by *ca.* 20:1, with *exo*-deuterium attack, *i.e.* inversion at C-6, favored over *endo*-deuteration by a factor of *ca.* 3.5. Since **18** is the more abundant of the two rearrangement products, inversion at the methyl bearing center with cleavage of bond *b* is also the favored pathway. Apparently, the relative rates of *endo* and *exo* attack are similar for both modes of cleavage, *a* or *b*, since **18** and **17** were formed in a ratio of *ca.* 3:1. Since *exo*-deuteration is favored in the ring opening of **16** it follows, by the principle of microscopic reversibility, that *exo*-proton abstraction from

TABLE 3. Observed and computed ^2H incorporation[a] in **15**

Time (h)	Observed			Computed[b]		
	C-6			C-6		
	Exo	*Endo*	C-8	*Exo*	*Endo*	C-8
10	0.26	0.08	0.006	0.24	0.08	0.007
20	0.34	0.12	0.008	0.33	0.12	0.010
40	0.70	0.38	0.033	0.70	0.38	0.032

[a]Given as % ^2H/exchangeable hydrogen.
[b]For Scheme 1, using $k_N = 1.0$, $k_X = 3.5$, $k_{N'} = k_{X'} = 0.78$, $k_M = 0.085$.

Can. J. Chem. Downloaded from www.nrcresearchpress.com by 210.87.254.42 on 09/05/12
For personal use only.

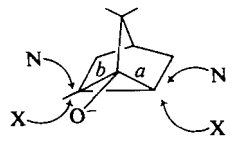

19

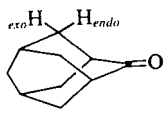

20

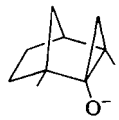

21

C-6 in **15** is the lower energy process. The experiment in which the mixture of **17** and **18** was subjected to homoenolization conditions shows this to be the case since **18** was converted to **15** significantly faster than **17**. Homoenolization of **18** to **16** must involve *exo*-proton abstraction while *endo* abstraction is required for **17** → **16**. Thus, the stereochemistry of homoenolization of **15** is analogous to that of **2** as deduced by Nickon *et al.* (3) from the homoketonization of **3**. The latter in a variety of alkaline media gave *exo*-6-deuterionorcamphor with high stereoselectivity (95–98%). These reactions, however, proceed under much milder conditions and a quantitative comparison of the ΔΔG values for *exo* and *endo* deuteration of the two homoenolate ions is precluded. It may be noted that a recent examination of the homoenolization of adamantanone (**20**) showed that *exo*-deuteration occurred at the β-positions about 15 times faster than *endo*, under conditions comparable to those of the present study (25).

For the samples from the longer reaction times in Table 2 it is apparent that the ^2H content at C-6 passes through a maximum and approaches an equilibrium value because of dilution of the deuterium pool by exchanged protons. The progressive increases in ^2H concentration at C-9 and C-10, therefore, can only provide lower limits for the estimated rates of exchange at these centers. It appears, however, that *endo*-methyl exchange (C-9) is *ca.* twice as fast as bridgehead methyl exchange (C-10) and approximately 25% as fast as exchange at the *exo*-methyl carbon. In any event, the stereoselectivity of methyl exchange is a new observation for homoenolization reactions. From the relative rates, $k^{C\text{-}8} \approx 4k^{C\text{-}9} \approx 10k^{C\text{-}10}$, the activation energies differ by *ca.* 1 kcal/mol. The fact that the rates are different for the three methyl carbons provides evidence for the intermediacy of homoenolate ions such as **21** since the inductive effect of the carbonyl group, as an activating influence for proton abstraction, would be comparable at each methyl carbon. In principle, species such as **21** could lead to ring expanded products but none was isolated or detected. This was not unexpected since cyclopropanols open in base to give the product derived from the more stable carbanion (26) hence **21** → **15** is the favored path. The alternative ring opening of **21** would lead to an enolizable ketone which could undergo condensation reactions. The stereoselectivity of methyl exchange as observed for **15** could be useful for preparing selectively deuterated derivatives for other tracer studies.

We wish to thank the National Research Council of Canada for financial support of this study. We are grateful to Charles S. Peters for his modification of the Varian FT program to generate the experimental line shape data, to Dr. L. L. Coatsworth for his modification of the BMDX85 program for Lorentzian line-shape fitting and to Prof. N. C. Baird for his assistance with several aspects of the data processing. We thank Prof. D. H. Hunter for valuable discussions, Prof. A. Nickon for helpful comments on the manuscript and Inára Grikis for technical assistance.

1. A. Nickon and J. L. Lambert. J. Am. Chem. Soc. **84**, 4604 (1962).
2. A. Nickon and J. L. Lambert. J. Am. Chem. Soc. **88**, 1905 (1966); A. Nickon, J. L. Lambert, and J. E. Oliver. J. Am. Chem. Soc. **88**, 2787 (1966).
3. A. Nickon, J. H. Hammons, J. L. Lambert, and R. O. Williams. J. Am. Chem. Soc. **85**, 3713 (1963); A. Nickon, J. L. Lambert, R. O. Williams, and N. H. Werstiuk. J. Am. Chem. Soc. **88**, 3354 (1966).
4. A. Nickon, H. Kwasnik, T. Swartz, R. O. Williams, and J. B. Di Giorgio. J. Am. Chem. Soc. **87**, 1615 (1965).
5. R. M. Coates and J. P. Chen. Chem. Commun. 1481 (1970).
6. K. W. Turnbull, S. J. Gould, and D. Arigoni. J. Chem. Soc. Chem. Commun. 597 (1972).
7. J. P. Freeman and J. H. Plonka. J. Am. Chem. Soc. **88**, 3662 (1966).
8. M. J. Betts and P. Yates. J. Am. Chem. Soc. **92**, 6982 (1970).
9. D. H. Hunter, A. L. Johnson, J. B. Stothers, A. Nickon, J. L. Lambert, and D. F. Covey. J. Am. Chem. Soc. **94**, 8582 (1972).
10. J. L. Lambert. Ph.D. Thesis, Johns Hopkins University, Baltimore, Maryland. 1963.

Can. J. Chem. Downloaded from www.nrcresearchpress.com by 210.87.254.42 on 09/05/12
For personal use only.

11. R. HOWE and S. WINSTEIN. J. Am. Chem. Soc. **87**, 915 (1965); T. FUKUNAGA. J. Am. Chem. Soc. **87**, 916 (1965).
12. J. B. STOTHERS, C. T. TAN, A. NICKON, F. HUANG, R. SRIDHAR, and R. WEGLEIN. J. Am. Chem. Soc. **94**, 8581 (1972); D. H. HUNTER and J. B. STOTHERS. Can. J. Chem. **51**, 2884 (1973); J. B. STOTHERS. *In* Topics in carbon-13 NMR spectroscopy. Vol. 1. *Edited by* G. C. Levy. J. Wiley, N.Y. 1974. Chapt. 6.
13. W. R. MOORE, P. D. MOGOLESKO, and D. D. TRAFICANTE. J. Am. Chem. Soc. **94**, 4753 (1972).
14. A. ABRAGAM. Principles of nuclear magnetism. Oxford, London. 1961. Chapt. 8.
15. H. H. MANTSCH, H. SAITO, L. C. LEITCH, and I. C. P. SMITH. J. Am. Chem. Soc. **96**, 256 (1974).
16. P. DIEHL and T. LEIPERT. Helv. Chim. Acta, **47**, 545 (1964).
17. A. F. COCKERILL, G. L. O. DAVIES, R. C. HARDEN, and D. M. RACKHAM. Chem. Rev. **73**, 553 (1973).
18. A. T. YOUNG and R. D. GUTHRIE. J. Org. Chem. **35**, 853 (1970).
19. W. J. DIXON (*Editor*). BMDX85 Biomedical computer programs X-series supplement. University of Calif. Press, Berkeley. 1969.
20. J. B. STOTHERS. Carbon-13 NMR spectroscopy. Academic Press, New York. 1972.
21. J. B. STOTHERS, C. T. TAN, and K. C. TEO. Can. J. Chem. **51**, 2893 (1973).
22. J. B. STOTHERS, C. T. TAN, and K. C. TEO. To be published.
23. D. J. CRAM, B. RICKBORN, C. A. KINGSBURY, and P. HABERFIELD. J. Am. Chem. Soc. **83**, 3678 (1961).
24. D. E. PEARSON and C. A. BUEHLER. Chem. Rev. **74**, 45 (1974).
25. J. B. STOTHERS and C. T. TAN. J. Chem. Soc. Chem. Commun. 738 (1974).
26. C. H. DEPUY. Acc. Chem. Res. **1**, 33 (1968); C. H. DEPUY, F. W. BREITBEIL, and K. R. DEBRUIN. J. Am. Chem. Soc. **88**, 3347 (1966).
27. M. GORDON, A. STOESSL, and J. B. STOTHERS. Can. J. Chem. **51**, 748 (1973).

Can. J. Chem. Downloaded from www.nrcresearchpress.com by 210.87.254.42 on 09/05/12
For personal use only.

The Catalysis of Proton Exchange in Creatinine by General Acids and General Bases

R. SRINIVASAN AND ROSS STEWART

Department of Chemistry, University of British Columbia, Vancouver, British Columbia V6T 1W5

Received July 9, 1974

R. SRINIVASAN and ROSS STEWART. Can. J. Chem. **53**, 224 (1975).

The rate of exchange of methylene protons in creatinine has been followed in D_2O by means of proton magnetic resonance spectroscopy over a range of acidity from p*D* 12.22 to $D_A - 4.24$. A plot of the logarithm of the rate against acidity function is in the form of a "W", one wing of which involves reaction of neutral creatinine with hydroxide ion, and the other diprotonated creatinine with water. The central peak represents reaction of protonated creatinine with a molecule of creatinine acting as base. The reaction is subject to catalysis by buffers.

The activation of exchange produced by protonating the substrate is designated *proton activating factor*, p.a.f., and factors affecting its size are discussed in terms of structure.

R. SRINIVASAN et ROSS STEWART. Can. J. Chem. **53**, 224 (1975).

Faisant appel à la résonance magnétique du proton, on a pu suivre la vitesse d'échange des protons méthyléniques de la créatinine dans D_2O, à des acidités allant de p*D* 12.22 à D_A −4.24. Une courbe du logarithme de la vitesse en fonction de l'acidité à la forme d'un "W"; une portion implique la réaction de la créatinine neutre avec l'ion hydroxyde et l'autre celle de la créatinine diprotonée avec l'eau. Le pic central représente la réaction de la créatinine protonée avec une molécule de créatinine agissant comme base. La réaction est sujette à une catalyse par les tampons.

On appelle *facteur d'activation du proton* (p.a.f.) l'activation de l'échange produite par la protonation du substrat; on discute des facteurs influençant sa grosseur en terme de structure.

[Traduit par le journal]

Introduction

Carbon–hydrogen bonds in compounds containing electronegative groups often exhibit measurable rates of ionization in basic media, and, as a consequence, the literature contains many reports of studies of base-catalyzed exchange in such compounds (1). However, there are few examples of general-acid catalyzed exchange in which the base abstracts a proton from the conjugate acid of the substrate. The difficulty in studying general-acid catalyzed exchange is one of finding conditions where the exchange rate and the concentrations of the base and protonated substrate can all be determined. Nitrogen heterocyclic compounds such as creatinine are attractive systems for study in this regard, since their nitrogen atoms are both basic and electronegative.

Though creatinine, which is an end product of nitrogen metabolism in vertebrates, can exist in different tautomeric forms (2) the most stable tautomer has been shown to be 1-methyl-2-amino-2-imidazolin-4-one, **1** (3). The methylene protons are reported to undergo exchange in basic media at rates greater than those for hydrolysis (4). We report herein studies of acid and base catalysis of proton exchange at the 5-position in this compound over a wide range of acidity.

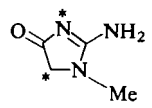

1

Experimental

Measurements of acidity in the aqueous region were made on a Radiometer Model 26 p*H* instrument with an aqueous glass–calomel assembly. The electrode system was calibrated using standard aqueous buffers. The p*D* values were obtained from the relationship p*D* = p*H* reading + 0.40 (5).

Solvents and Reagents

The deuterated solvents D_2O (99.7 atom% D), D_2SO_4, CH_3OD, and aqueous solutions of DCl and NaOD were obtained from Merck, Sharp and Dohme of Canada Limited. Prior to use D_2O was heated to boiling and allowed to cool with a slow stream of nitrogen bubbling through it. The remaining deuterated solvents were used as supplied.

Creatinine was purified by crystallization from aqueous ethanol. *N,N*-Dideuteriocreatinine was obtained by dissolving crystallized creatinine in a consider-

Can. J. Chem. Downloaded from www.nrcresearchpress.com by 210.87.254.105 on 09/05/12
For personal use only.

Can. J. Chem. Downloaded from www.nrcresearchpress.com by 210.87.254.105 on 09/05/12
For personal use only.

able excess of CH_3OD–D_2O and removing the solvent *in vacuo*. Commercial samples of sodium acetate and sodium formate (AR grade) were dried at 140° before use. Sodium pivalate was prepared from pivalic acid and sodium bicarbonate by standard techniques, crystallized from aqueous ethanol, and dried at 140°. The Hammett indicators were purified by crystallization to constant melting point.

1,3-Dimethyl-2-iminoimidazolidin-4-one Hydrochloride (4, X = Cl)

1,3-Dimethyl-2-iminoimidazolidin-4-one hydroiodide (**4**, X = I) was synthesized by the method of Kenyon and Rowley (4), m.p. 212–214° dec; lit. (4) m.p. 213–215.5° dec. The corresponding hydrochloride was prepared by treating a well-stirred hot suspension of lead chloride in water (3.27 g, 11.77 mmol in 50 ml water) with an aqueous solution of the hydriodide (3.0 g, 11.77 mmol in 10 ml water). The mixture was heated and stirred for an hour, cooled, and the lead iodide removed by filtration. The filtrate was concentrated to about 20 ml, cooled, filtered again, and the filtrate evaporated to dryness to give a colorless solid (95% yield), m.p. 232–235° dec. (from ethanol).

Anal. Calcd. for $C_5H_{10}N_3OCl$: C, 36.70; H, 6.11; N, 25.70. Found: C, 36.55; H, 6.10; N, 25.85.

Determination of the Basicity of Creatinine in D_2O (pK')[1]

The acid dissociation constant of creatininium ion, pK', was determined by a standard spectrophotometric procedure (6) in D_2O, at 34.5°, ionic strength 1.2, the conditions under which most of the kinetic experiments were done.

A solution of boric acid in D_2O was prepared, the ionic strength adjusted to 1.2 with sodium chloride, and the pD brought to 9.84 with NaOD. A portion of this solution (3 ml) was transferred to a cuvette and thermostated at 34.5°. A creatinine solution (10 μl, 3.0×10^{-2} M) was injected into this solution and the absorbance at 234 nm (λ_{max} for creatinine) immediately recorded. A buffer solution without creatinine was used as blank. Similar measurements were made in acetic acid – sodium acetate buffer (3.40×10^{-2} M) at pD 4.23, 4.63, 5.01, 5.42, and 5.78. The absorbance of creatininium ion at 234 nm was determined in 0.01 M DCl. In all measurements the ionic strength was held at 1.2 by the addition of sodium chloride. The pK' value determined under these conditions is 5.40 ± 0.05, compared to the thermodynamic pK of 4.72, determined in H_2O at 34.5° (7).

Acidity Measurements

All acidity measurements on solutions employed in kinetic studies were made after the creatinine was dissolved. This is necessary in view of the concentration of creatinine used (0.18 to 1.20 M) and its basicity. The pD values of creatinine solutions were adjusted with DCl or NaOD, both those with, and those without, added buffer. In the sulfuric acid region the acidities of creatinine solutions are determined by standard indicator procedures (8). Since no precise acidity function

[1]The prime indicates the nonthermodynamic character of the pK, caused by the high ionic strength of the medium (1.2).

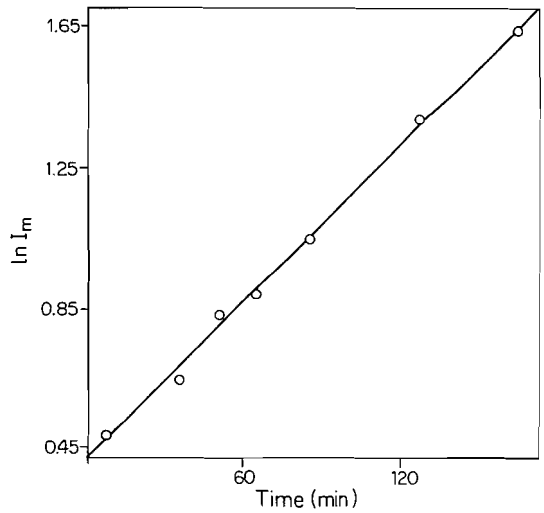

FIG. 1. Exchange kinetics for creatinine in sodium acetate buffer, [NaOAc] = 0.9 M, $[Cr]_a$ = 0.18 M, μ = 1.2, pD = 5.84, T = 34.5°.

governing the process believed to be taking place with creatinine in this region (protonation[2] of creatininium ion in D_2O) is available we have used derived D_A values as an approximation. The D_A function being unknown we have employed standard Hammett indicators (4-chloro-2-nitroaniline, 2,6-dichloro-4-nitroaniline, 2,4-dinitroaniline, 4-chloro-2,6-dinitroaniline, and 2-bromo-4,6-dinitroaniline) to determine the apparent D_0 values for the solution mixtures (8*b*, 8*c*) and have converted these directly to apparent D_A values. It is assumed that the relationship between D_0 and D_A is the same as that between H_0 and H_A.

Kinetic Measurements

The exchange of methylene protons was followed using a Varian T-60 MHz spectrometer at a sweep width of 100 Hz using the general procedure outlined previously (9). The solvent peak (HOD) was used as lock signal. The n.m.r. tube containing the sample was thermostated at 34.5° and periodically introduced into the n.m.r. probe (probe temperature 34.5°). The reaction was usually followed up to 75% completion.

Since the *N*-methyl protons of creatinine did not exchange under the reaction conditions the peak corresponding to these protons was used as reference. The extent of exchange was determined from the ratios of the areas due to methylene and *N*-methyl peaks. The acidity of the medium did not change during the reaction.

The exchange reaction followed first-order kinetics. The observed first-order exchange constant k_{obs} was obtained by plotting the data according to eq. 1.

$$\ln I_m = k_{obs}t \qquad [1]$$

where $I_m = R_t/S_t$, R_t = average area of the *N*-methyl peak, and S_t = average area of the methylene peak,

[2]For the sake of simplicity the term protonation is used for either the addition of a proton or a deuteron.

both at time t. A typical rate plot for the exchange of creatinine is shown in Fig. 1. The reproducibility was within ±10%.

Results

Matsumoto and Rapoport (3) have shown the most stable form of creatinine to be **1**, but some uncertainty exists regarding the structure of creatininium ion. Grzybowski and Datta (7) envisaged two possibilities (**2** and **3**).

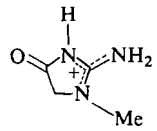

2

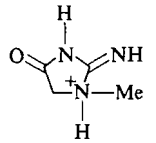

3

Structure **2** would be expected to be more stable than **3** in view of its ability to delocalize the positive charge. Verification of this structure was achieved by comparing the ultraviolet absorption spectrum of creatininium chloride with that of 1,3-dimethyl-2-iminoimidazolidin-4-one hydrochloride, the structure of the corresponding iodide having been established as **4** (X = I) (4). Creatininium chloride and **4** (X = Cl) have very similar absorption spectra (λ_{max}(pH3) = 215 nm, ε = 4940; λ_{max}(0.01 M HCl, EtOH) = 215 nm, ε = 5130 for creatininium

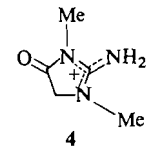

4

chloride (3) and λ_{max}(pH2) = 220 nm, ε = 4880; λ_{max}(0.01 M HCl, EtOH) = 218 nm, ε = 6390 for **4** (X = I)) and we conclude that **2** is the favored structure for the cation.

The exchange of methylene protons of creatinine was investigated over the entire range of acidity accessible to experiment (76% sulfuric acid to pD 12.22). Rate measurements in more acidic solutions were precluded for solubility reasons, while in more basic solutions the exchange was too fast to permit meaningful measurements. The acidity was varied by addition of DCl or NaOD; the results are summarized in Table 1. When log k_{obs} was plotted against the most appropriate acidity functions obtainable (see Experimental section) a "W" shaped curve resulted (Fig. 2). The shape of the curve suggests that the substrate undergoes exchange by both general-acid and general-base catalyzed routes.

The rate of the reaction at a given acidity in the absence of added buffer may be represented by eq. 2.

TABLE 1. Exchange rates for creatinine in aqueous solution (1.2 M) in absence of added buffer

pD	k_{obs} (min^{-1})	pD	k_{obs} (min^{-1})
12.22	0.109	5.60	6.70×10^{-3}
11.67	2.95×10^{-2}	5.11	6.65×10^{-3}
10.92	4.20×10^{-3}	4.57	3.92×10^{-3}
10.15	8.88×10^{-4}	3.50	5.20×10^{-4}
9.55	1.60×10^{-4}	2.75	2.70×10^{-4}
7.60	2.35×10^{-4}	2.06	4.67×10^{-5}
6.50	1.95×10^{-3}	1.12	2.25×10^{-5}
		0.60	2.25×10^{-5}

D_0*	D_A†	k_{obs} (min^{-1})	I‡	pK of I§	log [I]/[IH$^+$]
−0.52	−0.52	5.20×10^{-5}	a	−0.46	0.06
−2.75	−2.10	1.22×10^{-4}	b	−2.96	0.21
−3.06	−2.30	1.47×10^{-4}	b	−2.96	−0.10
−4.17	−2.88	2.17×10^{-4}	b	−2.96	−1.21
−4.50	−3.04	5.33×10^{-4}	c	−5.82	1.32
−5.78	−3.70	7.83×10^{-4}	c	−5.82	0.04
−6.25	−3.94	1.17×10^{-3}	d	−6.48	0.23
−6.85	−4.24	1.80×10^{-3}	d	−6.48	−0.17

*D_0 = pK + log [I]/[IH$^+$].
†Computed from D_0 values (see Experimental).
‡Indicators: a, 4-chloro-2-nitroaniline; b, 2,6-dichloro-4-nitroaniline; c, 4-chloro-2,6-dinitroaniline; d, 2-bromo-4,6-dinitroaniline.
§References 8*b* and 8*c*.

Can. J. Chem. Downloaded from www.nrcresearchpress.com by 210.87.254.105 on 09/05/12
For personal use only.

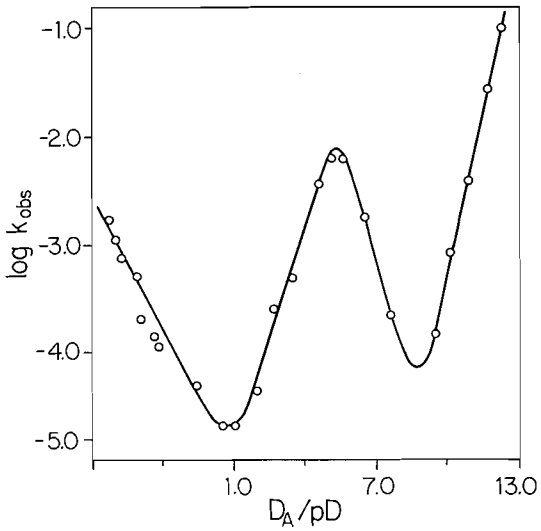

FIG. 2. Effect of acidity on the exchange rate of creatinine at 34.5°, in absence of added buffer; creatinine concentration 0.18 *M* to 1.2 *M*.

$$[2]\quad \frac{-d[Cr]_T}{dt} = k_1[Cr][OD^-] + k_2[CrD^+][OD^-] + k_3[Cr][D_2O] + k_4[CrD^+][D_2O] + k_5[CrD^+][Cr'] + k_6[Cr][Cr']$$

$[Cr]_T$ = total concentration of neutral creatinine and creatininium ion containing methylene proton(s) at time t; $[CrD^+]$ = concentration of creatininium ion containing methylene proton(s) at time t; $[Cr]$ = concentration of neutral creatinine containing methylene proton(s) at time t; $[Cr']$ = total concentration of neutral creatinine. The k's refer to second-order exchange rate constants corresponding to the elementary steps represented by the terms associated with them. The contribution made by each term depends upon the acidity of the medium, the magnitude of k, and the concentration of creatinine. (To simplify the kinetic treatment no distinction has been made between molecules containing two protons and those containing one proton and one deuteron. The conclusions are unaffected by this simplification.)

pD Region 9.55 to 12.22

A satisfactory straight line can be drawn through the points in the log k_{obs} *vs.* p*D* plot (Fig. 2) giving a slope of 1.05. This means that the exchange in this region can be completely accounted for in terms of proton loss by creatinine to OD^-, and eq. 2 reduces to eq. 3

$$[3]\quad \frac{-d[Cr]_T}{dt} = k_1[Cr][OD^-]$$

Since $[Cr] = [Cr]_T$ in this region k_{obs} would be governed by eq. 4

$$[4]\quad k_{obs} = k_1[OD^-]$$

An average value of 36.3 M^{-1} min^{-1} is obtained for k_1, using the first five rate constants shown in Table 1 and using the corresponding p*D* values to calculate $[OD^-]$ ($pK_{D_2O} = 14.8$ (10)).

pD Region 7.60 to 3.50

Creatinine exists mostly as a free base at p$D > 5.4$ and as the conjugate acid at p$D < 5.4$. The shape of the plot suggests that most of the exchange results from abstraction of a methylene proton from creatininium ion by neutral creatinine. If this is so, eq. 2 reduces to eq. 5.

$$[5]\quad \frac{-d[Cr]_T}{dt} = k_5[CrD^+][Cr']$$

Equation 5 can be written in an integratable form as shown by the following sequence of equations

$$[6]\quad [Cr'] = [Cr]_a\frac{K'}{K' + [D^+]}$$

where $[Cr]_a$ is the analytical concentration of added creatinine (usually 1.2 *M*), and $[D^+]$ is calculated from the glass electrode measurements.

$$[7]\quad [CrD^+] = \frac{[D^+]}{K' + [D^+]}[Cr]_T$$

Therefore

$$[8]\quad \frac{-d[Cr]_T}{dt} = k_5\frac{K'[D^+]}{(K' + [D^+])^2}[Cr]_a[Cr]_T$$

Equation 9 gives the value of k_{obs}

$$[9]\quad k_{obs} = \frac{k_5K'[D^+]}{(K' + [D^+])^2}[Cr]_a$$

When k_{obs} was plotted against $K'[D^+]/(K' + [D^+])^2$ a reasonably satisfactory linear relationship was observed (Fig. 3), indicating that indeed, almost all the exchange in this region arises by abstraction of proton from creatininium ion by creatinine. A value of 2.38 ×

Can. J. Chem. Downloaded from www.nrcresearchpress.com by 210.87.254.105 on 09/05/12
For personal use only.

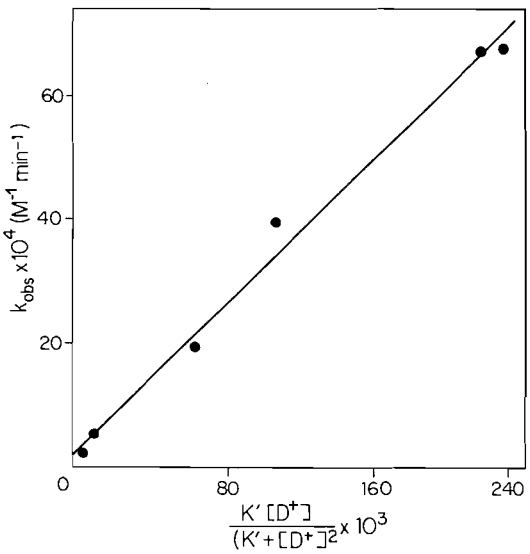

FIG. 3. Plot of k_{obs} *vs.* $K'[D^+]/(K' + [D^+])^2$.

$10^{-2}\ M^{-1}$ min^{-1} is calculated for k_5 from the slope of this plot. Further, the observation that the exchange rate could be adequately represented by eq. 5 at pD 7.60 suggests that the ratio k_5/k_6 must be large, a surprising result in light of the results obtained with carboxylate buffers.

Since the exchange rate constants k_5 and k_6 refer to exchanges by creatininium ion and creatinine respectively (where the substrates differ by a proton) we term the activation due to protonation, p.a.f. (proton activating factor). The blander terms reactivity ratio and discrimination factor were used previously for this quantity (9).

The significance of the maximum in the log k_{obs} *vs.* pD plot (Fig. 2) can be seen by imposing on eq. 9 the following condition, one that must be satisfied by a continuous differentiable function at the maximum.

$$\frac{\mathrm{d} \log k_{obs}}{\mathrm{d}\ \mathrm{p}D} = 0$$

This leads to the conclusion that the pD value at the maximum rate is equal to pK'. The theoretical curve (pD region 7.60 to 3.50 in Fig. 2) in the log k_{obs} *vs.* pD plot was constructed by nonlinear least square fitting of the data according to eq. 9, the pK' and k_5 values being treated as arbitrary parameters. This procedure gives a value of $2.77 \times 10^{-2}\ M^{-1}$ min^{-1} for k_5 and a value of 5.36 for pK', in excellent agreement with the values referred to above ($k_5 = 2.38 \times 10^{-2}\ M^{-1}$ min^{-1} and p$K' = 5.40$).

Sulfuric Acid Region

The exchange in this region follows the D_A acidity function reasonably well, but with a slope much less than unity (0.55) in keeping with a reaction involving attack by water on the conjugate acid of an amide (11–14). Although D_A is probably a satisfactory function to use, it is not the actual function governing the protonation (see Experimental section). Accordingly, we have not attempted a detailed analysis of the sort that leads to information about the role of water in the reaction (11, 12).

Exchange in Presence of Buffers

The rate of exchange in presence of buffer (DA/A^-) may be represented by eq. 11

$$[11] \quad \frac{-\mathrm{d}[Cr]_T}{\mathrm{d}t} = k_{DA}[DA][Cr] + k_{A^-}[A^-][Cr] + v_0$$

where v_0 is the exchange rate in the absence of buffers, the rate of proton abstraction by creatinine from creatininium ion being the major component. The other coefficients are exchange rate constants referring to the species indicated by the subscripts. The magnitudes of k_{DA} and k_{A^-} may be calculated by standard procedures (15). Since rate measurements were made at pD values close to the pK' value, eq. 12 must be inserted into eq. 11 to permit integration.

$$[12] \quad \frac{[Cr]}{[Cr]_T} = \frac{K'}{K' + [D^+]} = \gamma$$

The exchange rates were studied at constant pD but different total buffer concentration $[Buf]_T$, the creatinine concentration being kept as low as possible, in order to minimize v_0. A plot of k_{obs} *vs.* $[Buf]_T$ produces a straight line of slope k_2', defined by eq. 13 (Fig. 4).

$$[13] \quad k_2' = k_{DA}\gamma\{1 - [A^-]/[Buf]_T\} + k_{A^-}\gamma[A^-]/[Buf]_T$$

The magnitudes of k_{A^-} and k_{DA} can be obtained from eq. 13 if k_2' is determined at different pD values. The second-order rate constant for the abstraction of a methylene proton by A^- from creatininium ion, $k_{CrD^+ + A^-}$ is calculated (9) from k_{DA} and pK_{DA}. The second order rate

Can. J. Chem. Downloaded from www.nrcresearchpress.com by 210.87.254.105 on 09/05/12
For personal use only.

TABLE 2. Specific catalytic constants for creatinine exchange at 34.5°[a]

Base, A^-	pK_{DA}[b]	$10^3 k_{Cr+A^-}$ (M^{-1} min^{-1})	k_{DA} (M^{-1} min^{-1})	$10^2 k_{CrD^+ + A^-}$ (M^{-1} min^{-1})	$\frac{k_{CrD^+ + A^-}}{k_{Cr+A^-}}$[f]
Formate	4.21[c]	—	0.22	1.4	—
Acetate	5.31[d]	4.4	0.09	7.4	17
Pivalate	5.56[e]	5.5	0.14	10	36

[a]The specific catalytic constants are subjected to an estimated error of ±25% (see Experimental section).
[b]Refers to D_2O standard state at 35°. For pK_{HA} values referred to aqueous standard state at 35°. See ref. 18.
[c]Calculated from the relation $pK_{DA} = pK_{HA} + 0.45$ (5*a*).
[d]Reference 19.
[e]Calculated from the general relation $pK_{DA} = 0.41 + 1.02\ pK_{HA}$ (20).
[f]An error of ±25% in the specific catalytic constants would introduce an error of ±35% in this ratio (21).

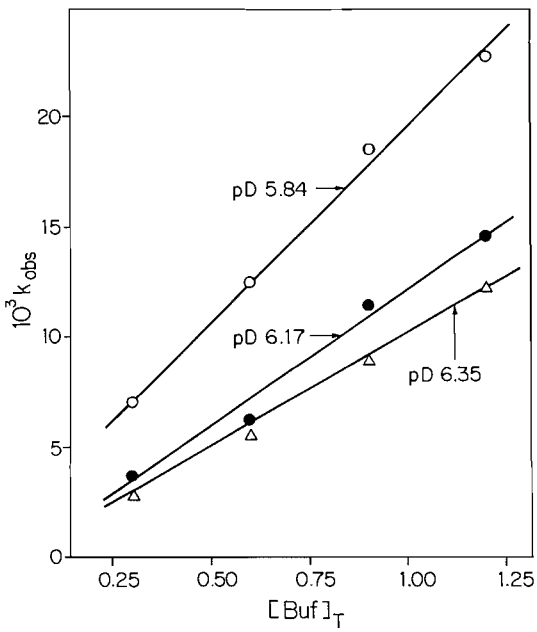

FIG. 4. Plot of k_{obs} *vs.* buffer molarity in acetate buffer solution, $\mu = 1.2$, $T = 34.5°$, $[Cr]_a = 0.18\ M$.

constant k_{Cr+A^-} for proton abstraction from creatinine by A^- is equal to k_{A^-}. The exchange rate constants for the acid- and base-catalyzed reactions were estimated by this procedure in acetate and pivalate buffers.

The kinetics of exchange was investigated in formate buffer at p*D* 4.27 and 4.80. Under these experimental conditions formate-catalyzed exchange of creatinine was not observable. Furthermore, the uncatalyzed exchange rate (v_0) is competitive with the formic acid catalyzed rate to such an extent that the rate constants for formic acid catalysis are, at best, estimates. Similar but less serious difficulties were encountered using acetate and pivalate buffers. The results obtained in buffer solutions are presented in Table 2.

Discussion

The general base- and general acid-catalyzed exchange of creatinine is understandable in terms of the mechanisms shown in Schemes 1 and 2, which are analogous to those generally accepted for other prototropic reactions (1, 9, 16).

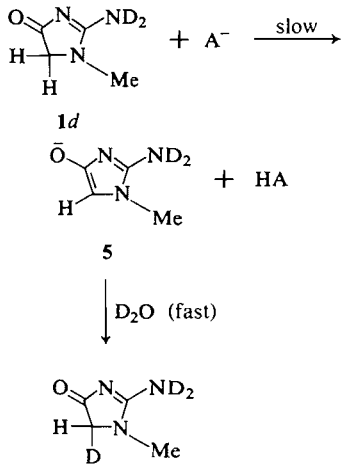

SCHEME 1. General base catalysis.

The acidity of the methylene protons arises chiefly from the presence of electronegative nitrogen atoms in the ring (1*d*, *e*) and from the neighboring carbonyl group. Further, the intermediate **5** resulting from the loss of a methylene proton by creatinine is a substituted imidazole which is aromatic in the sense that imidazole is aromatic. The resulting stabilization of the intermediate undoubtedly provides a considerable driving force towards exchange.

The calculated p.a.f. values for creatinine in acetate and pivalate buffers ($k_{CrD^+ + A^-}/k_{Cr+A^-}$)

Can. J. Chem. Downloaded from www.nrcresearchpress.com by 210.87.254.105 on 09/05/12
For personal use only.

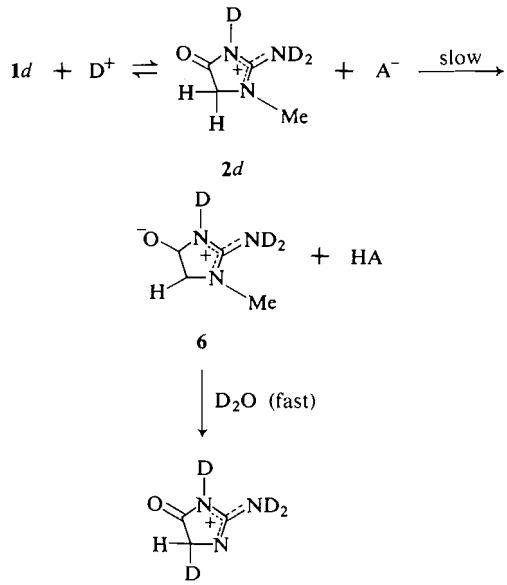

SCHEME 2. General acid catalysis.

are 17 and 36 (Table 2), very low values that seem to have no precedents in the literature. Because of the problem of creatinine self-catalysis these numbers can be considered only as approximate. However, in view of the enormous variation in p.a.f. that results from changes in the structure of the substrate the errors in these quantities are relatively small.

The largest p.a.f., 10^{12}, is observed with acetone (9, 17) while the lowest reported to date, 10^2, is for the exchange of the 7-methyl protons of 6,7,8-trimethyllumazine (9). Stewart and McAndless (9) suggested that large values of p.a.f. might be associated with substrates whose acidity and basicity are very far apart, *e.g.* acetone. Unfortunately, we are not able to determine directly the equilibrium carbon acidity of creatinine. There are, however, some structural features of creatinine that distinguish it sharply from acetone, and hence may account for the very low p.a.f. value that is observed. First, protonation occurs not at the carbonyl group, as in the case of acetone, but at nitrogen.[3] This difference would not be critical *if* the activating positive charge were destroyed in both cases by the subsequent proton loss from carbon. It is destroyed in the case of acetone, but not in the case of creatinine, which goes through the mesoionic intermediate **6**, a much less stable structure.

A second factor that doubtless contributes to the low p.a.f. is the fact that intermediate **5**, being a substituted imidazole, has aromatic character.

An examination of Table 3 shows that the rate of exchange in creatininium ion is quite sensitive to the strength of the attacking base. Unfortunately, a variety of carboxylate buffers could not be used to obtain a Brönsted value because of experimental difficulties associated with the need to use large amounts of substrate in the measurements and the consequent difficulty in detecting catalysis by bases that are much weaker than creatinine itself.

Though the thermodynamic base strength of creatinine is slightly more than that of acetate anion creatinine is much less effective a base in abstracting a proton from creatininium ion than acetate is. We ascribe this effect for the most part to increased steric crowding in the transition state of the creatininium ion – creatinine reaction, a consequence that thermodynamic basicity constants would fail to reflect.

In the sulfuric acid region the results are consistent with doubly charged cation **7** being the intermediate. It is interesting that in this case deprotonation at carbon (presumably by a water molecule acting as base) reduces the charge by a full unit, unlike the case with the monocation **2**. This is consistent with the curve shown in Fig. 1 since it is clear that a high p.a.f. is associated with the path from **2***d* to **7** to **8**.

The degree of activation caused by protonation is clearly related to the sites of protonation and deprotonation within the molecule. It is

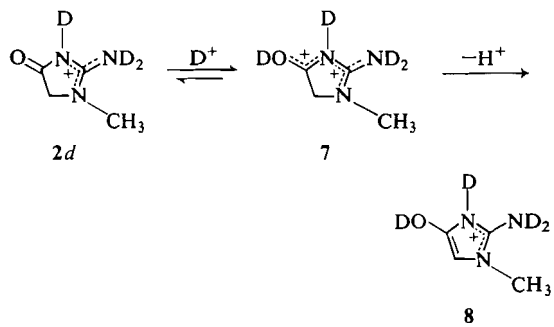

[3]The low p.a.f. values could be accounted for by exchange occurring through the minor component, the O-protonated form. The observation that **2***d* and **4** undergo exchange at comparable rates rules out this possibility. A detailed analysis of this problem will be presented in a subsequent publication.

Can. J. Chem. Downloaded from www.nrcresearchpress.com by 210.87.254.105 on 09/05/12
For personal use only.

obvious that a remote, nonconjugated site will cause only a small degree of activation. Thus, protonation of the amino group will be expected to catalyze the enolization of *p*-aminoacetophenone to only a small degree, there being full charge separation in the intermediate.

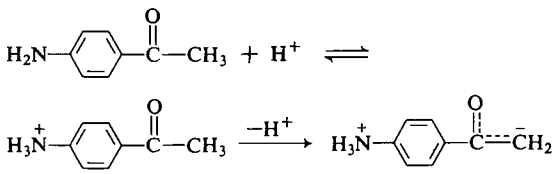

Proximity of the protonation and deprotonation sites does not appear to be the most important factor, however, in determining catalytic effectiveness. These two sites are as close in creatinine as they are in acetone, much closer, indeed, than in 6,7,8-trimethyllumazine (Scheme 3, protonation and deprotonation sites marked by asterisks). However, as we have seen, these two sites are not in conjugation in creatinine, unlike the situation with the other two compounds.

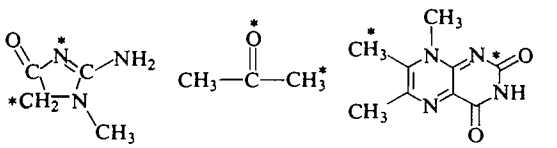

creatinine acetone 6,7,8-trimethyllumazine

SCHEME 3

The financial support of the National Research Council of Canada is gratefully acknowledged.

1. (*a*) D. J. CRAM. Fundamentals of carbanion chemistry. Academic Press, New York. 1965. Chapt. 1; (*b*) M. L. BENDER. Mechanisms of homogeneous catalysis from protons to proteins. Wiley–Interscience, New York. 1971. Chapt. 4; (*c*) R. P. BELL. The proton in chemistry. 2nd ed. Cornell University Press, Ithaca, N.Y. 1973. Chapt. 9; (*d*) P. HAAKE, L. P. BAUSHER, and W. B. MILLER. J. Am. Chem. Soc. **91**, 1113 (1969); (*e*) R. A. OLOFSON, J. M. LANDESBERG, K. N. HOUK, and J. S. MICHELWAN. J. Am. Chem. Soc. **88**, 4265 (1966).
2. C. LEMPERT. Chem. Rev. **59**, 667 (1959).
3. K. MATSUMOTO and H. RAPOPORT. J. Org. Chem. **33**, 552 (1968).
4. G. L. KENYON and G. L. ROWLEY. J. Am. Chem. Soc. **93**, 5552 (1971).
5. (*a*) P. K. GLASOE and F. A. LONG. J. Phys. Chem. **64**, 188 (1960); (*b*) E. MIKKELSEN and S. O. NIELSEN. J. Phys. Chem. **64**, 632 (1960); (*c*) P. SALOMAA, L. SCHALEGER, and F. A. LONG. J. Am. Chem. Soc. **86**, 1 (1964).
6. A. ALBERT and E. P. SERJEANT. Ionization constants of acids and bases. Methuen and Co., Ltd., London. 1962. Chapt. 4.
7. A. K. GRZYBOWSKI and S. P. DATTA. J. Chem. Soc. 187 (1964).
8. (*a*) C. H. ROCHESTER. Acidity functions. Academic Press, London. 1970; (*b*) E. HÖGFELDT and J. BIGELEISEN. J. Am. Chem. Soc. **82**, 15 (1960); (*c*) J. SIERRA, M. OJEDA, and P. A. H. WYATT. J. Chem. Soc. B, 1570 (1970).
9. R. STEWART and J. M. MCANDLESS. J. Chem. Soc. Perkin II, 376 (1972).
10. E. ABEL, E. BRATU, and O. REDLICH, Z. Phys. Chem. A**173**, 353 (1935).
11. K. YATES and J. B. STEVENS. Can. J. Chem. **42**, 1957 (1964).
12. J. F. BUNNETT. J. Am. Chem. Soc. **83**, 4956, 4968, 4973, 4978 (1963).
13. R. B. MOODIE, P. D. WALE, and T. J. WAITE. J. Chem. Soc. 4273 (1963).
14. J. T. EDWARD and S. C. R. MEACOCK. J. Chem. Soc. 2000 (1957).
15. W. P. JENCKS. Catalysis in chemistry and enzymology. McGraw-Hill, New York. 1969. Chapt. 3.
16. J. TOULLEC and J. E. DUBOIS. J. Am. Chem. Soc. **96**, 3524 (1974).
17. G. E. LEINHARD and F. A. ANDERSON. J. Org. Chem. **32**, 2229 (1967).
18. G. KORTÜM, W. VOGEL, and K. ANDRUSSOW. Dissociation constants of organic acids in aqueous solution. Butterworths, London. 1961.
19. R. GARY, R. G. BATES, and R. A. ROBINSON. J. Phys. Chem. **69**, 2750 (1965).
20. A. C. MCDOUGALL and F. A. LONG. J. Phys. Chem. **66**, 429 (1962).
21. P. R. BEVINGTON. Data reduction and error analysis for the physical sciences. McGraw-Hill, New York. 1969. Chapt. 4.

Can. J. Chem. Downloaded from www.nrcresearchpress.com by 210.87.254.105 on 09/05/12
For personal use only.

Isotopic Scrambling and Mass Spectral Fragmentation Studies with 2-Ferrocenylethyl and 2-Ferrocenylethyl-1,1-d_2 Systems

CHOI CHUCK LEE, SHI-CHOW CHEN, AND RONALD G. SUTHERLAND

Department of Chemistry and Chemical Engineering, University of Saskatchewan, Saskatoon, Saskatchewan S7N 0W0

Received July 8, 1974

CHOI CHUCK LEE, SHI-CHOW CHEN, and RONALD G. SUTHERLAND. Can. J. Chem. **53**, 232 (1975).

In a number of reactions including the solvolysis of 2-ferrocenylethyl-1,1-d_2 tosylate (**1**—OTs-1-d_2) in 60% EtOH, HCOOH, or CF_3CH_2OH, the reaction of **1**—OH-1-d_2 with $SOCl_2$ in tetrahydrofuran or toluene, and the treatment of **1**—Cl-1-d_2 with $AlCl_3$ in CH_2Cl_2, no scrambling of the D-label from C-1 to C-2 was observed, indicating the absence of any 1,2-ferrocenyl shifts in any of these S_N1 type of reactions. In the mass spectral fragmentation of **1**—X and **1**—X-1-d_2, where X = OTs, OH, OCHO, OCH_2CF_3 and Cl, a number of common features were observed, including $M^+ \xrightarrow[\text{or } -CD_2X]{-CH_2X} C_5H_5FeC_6H_6^+ \rightarrow C_5H_5Fe^+ \rightarrow Fe^+$ and $M^+ \xrightarrow{-HX} C_5H_5FeC_7H_7^+$ ($C_5H_5FeC_7H_5D_2^+$) $\rightarrow C_7H_7^+$ ($D_7H_5D_2^+$) $\rightarrow C_5H_5^+$ ($C_5H_5^+$, $C_5H_4D^+$, $D_5H_3D_2^+$).

CHOI CHUCK LEE, SHI-CHOW CHEN et RONALD G. SUTHERLAND. Can. J. Chem. **53**, 232 (1975).

On n'observe aucune compétition du deutérium sur le C-1 vers le C-2 pour un grand nombre de réactions de solvolyse du tosylate du ferrocenyl-2 éthyl-1,1-d_2 (**1**—OTs-1-d_2) dans l'éthanol à 60%, l'acide formique ou le trifluoroéthanol ou pour la réaction de **1**—OH-1-d_2 avec $SOCl_2$ dans le tétrahydrofuranne ou le chloroforme et pour le traitement de **1**—Cl-1-d_2 avec $AlCl_3$ dans CH_2Cl_2; ces résultats indiquent qu'il n'y a pas du tout de déplacements 1,2 du groupe ferrocényle dans ces réactions du type S_N1. Lors de la fragmentation en spectrométrie de masse de **1**—X et de **1**—X-1-d_2 où X = OTs, OH, OCHO, OCH_2CF_3 et Cl, on a observé un certain nombre de processus qui sont communs à tous les composés incluants $M^+ \xrightarrow[\text{ou } -CD_2X]{-CH_2X} C_5H_5FeC_6H_6^+ \rightarrow C_5H_5Fe^+ \rightarrow Fe^+$ et $M^+ \xrightarrow{-HX} C_5H_5FeC_7H_7^+$ ($C_5H_5FeC_7H_5D_2^+$) $\rightarrow C_7H_7^+$ ($D_7H_5D_2^+$) $\rightarrow C_5H_5^+$ ($C_5H_5^+$, $C_5H_4D^+$, $D_5H_3D_2^+$).

[Traduit par le journal]

Richards and co-workers (1) have reported that the solvolysis of 2-ferrocenylethyl-1,1-d_2 tosylate (**1**—OTs-1-d_2) in HOAc or 80% acetone resulted in no detectable scrambling of the D-label from C-1 to C-2. Consideration of the kinetic and stereochemical data from **1**—OTs and related systems has led these workers to conclude that solvolyses of β-ferrocenylalkyl tosylates may involve participation of the interannular electrons of the ferrocenyl group (1, 2). Since solvolyses in more ionizing and/or less nucleophilic solvents than HOAc or 80% acetone might give rise to more extensive isotopic scrambling, in the present work, solvolytic reactions with **1**—OTs-1-d_2 were carried out in 60% EtOH, HCOOH, or CF_3CH_2OH. In all of these cases, no scrambling of the label from C-1 to C-2 was detectable by n.m.r. in the reaction products, **1**—OH-1-d_2, **1**—OCHO-1-d_2, and **1**—OCH_2CF_3-1-d_2 (details given in the Experimental section), indicating the absence of any 1,2-ferrocenyl shift. In the trifluoroethanolysis, the yield of **1**—OCH_2CF_3 was low; but when this reaction was effected in the presence of CF_3CH_2ONa, a high yield of product was obtained, presumably via the S_N2 process. An attempt was also made in solvolyzing **1**—OTs in CF_3COOH, but only decomposition resulted. This observation is similar to the finding that the attempted trifluoroacetolysis of 2-(*p*-ferrocenylphenyl)ethyl tosylate resulted only in extensive decomposition (3).

Schlögl and co-workers (4, 5) have reported that the reduction of the oxime of acetylferrocene with $LiAlH_4$ or preferably with $LiAlH_4$—$AlCl_3$ gave *N*-ethylaminoferrocene as one of the products. It was suggested that the formation of this secondary amine resulted from a 1,2-migra-

Can. J. Chem. Downloaded from www.nrcresearchpress.com by 210.87.254.105 on 09/05/12
For personal use only.

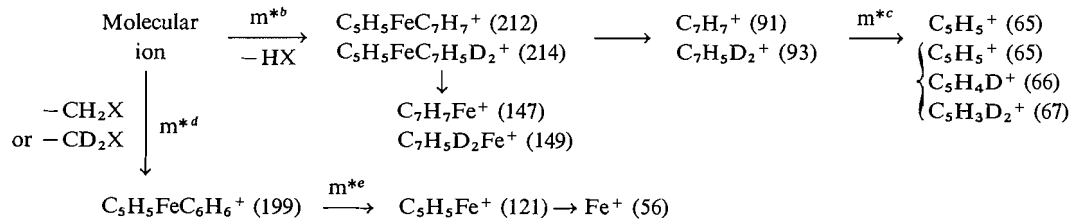

SCHEME 1. Common mass spectral fragmentations for $C_5H_5FeC_5H_4CH_2CH_2X$ and $C_5H_5FeC_5H_4CH_2CD_2X$ (**1**—X and **1**—X-1-d_2)[a]

[a]X = OTs, OH, OCHO, OCH_2CF_3, and Cl; *m/e* given in parentheses.
[b]Metastable peaks observed for 1—OTs, 1—OTs-1-d_2, 1—OH, 1—OH-1-d_2, 1—OCHO, and 1—OCHO-1-d_2.
[c]Metastable peaks observed for 1—OTs, 1—OTs-1-d_2, 1—OH, 1—OH-1-d_2, 1—Cl, and 1—Cl-1-d_2.
[d]Metastable peaks observed for 1—OH, 1—OH-1-d_2, 1—OCH_2CF_3, 1—OCH_2CF_3-1-d_2, 1—Cl, and 1—Cl-1-d_2.
[e]Metastable peaks observed for 1—OH, 1—OH-1-d_2, 1—OCHO, 1—OCHO-1-d_2, 1—OCH_2CF_3, 1—OCH_2CF_3-1-d_2, 1—Cl, and 1—Cl-1-d_2.

tion of the ferrocenyl group to nitrogen. Since $AlCl_3$ is known to have a great propensity for inducing rearrangements, it is of interest to include in the present work a study on the effect of $AlCl_3$ on 2-ferrocenylethyl-1,1-d_2 chloride (**1**—Cl-1-d_2). While the treatment of **1**—OH-1-d_2 with excess $SOCl_2$ resulted in extensive decomposition, **1**—Cl-1-d_2 was prepared without rearrangement from the reaction of **1**—OH-1-d_2 with $SOCl_2$ in tetrahydrofuran or toluene as solvent. The observation that **1**—Cl-1-d_2 was formed without any isotopic scrambling is also of interest since, for example, the reaction of 2-phenylethanol-1-^{14}C with $SOCl_2$ without a solvent gave essentially a complete scrambling of the label between C-1 and C-2 (6), while degenerate rearrangements arising from 1,2-hydride shifts were observed even in a nonpolar solvent such as toluene when 2-butyl chloride was formed from the decomposition of 2-butyl-1-^{14}C chlorosulfite derived from the alcohol and $SOCl_2$ (7). When **1**—Cl-1-d_2 was treated with $AlCl_3$ in CH_2Cl_2, the recovered **1**—Cl-1-d_2 was again isotopically nonrearranged. Thus all the present results show that 1,2-ferrocenyl shifts do not take place in any of the reactions studied, and these findings would tend to suggest the absence of any neighboring carbon group participation in S_N1 type of reactions with the 2-ferrocenylethyl derivatives.

Available from the present work are a number of 2-ferrocenylethyl derivatives including **1**—OTs, **1**—OH, **1**—OCHO, **1**—OCH_2CF_3, **1**—Cl, and the corresponding 1,1-dideuterio analogs. In using mass spectrometry as a means of identifying these compounds, it was noted that their mass spectra show certain fragmentation patterns common to all of these 2-ferrocenylethyl systems as given in Scheme 1. In addition, individual behaviors not common to all of the 5 compounds are given in Scheme 2. The relative abundance of these fragmentation ions are summarized in Table 1.

The mass spectrum of **1**—OH has been reported by Egger (8) and the presently observed mass spectrum of **1**—OH is essentially the same except that the relatively weak peaks for *m/e* 91 and 65 were not reported in the earlier work. The presence of ions at *m/e* 199 and 121 ($C_5H_5FeC_6H_6^+$ and $C_5H_5Fe^+$) as major peaks are well known for monosubstituted ferrocenes (8, 9), and the fragmentation sequence of molecular ion → 199 → 121 → 56 has been noted for a number of methyl or ethyl esters of ω-ferrocenylalkanoic acids (10). From the present work with **1**—X and **1**—X-1-d_2 (X = OTs, OH, OCHO, OCH_2CF_3, or Cl), it is clear that in the frag-

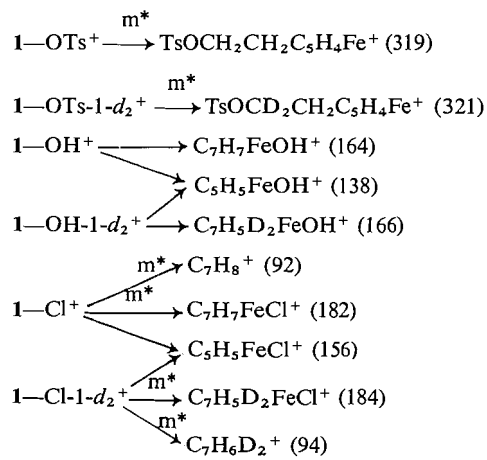

SCHEME 2. Major fragmentations in addition to the processes shown in Scheme 1

Can. J. Chem. Downloaded from www.nrcresearchpress.com by 210.87.254.105 on 09/05/12
For personal use only.

Can. J. Chem. Downloaded from www.nrcresearchpress.com by 210.87.254.105 on 09/05/12
For personal use only.

TABLE 1. Relative abundance of fragmentation ions from 2-ferrocenylethyl and 2-ferrocenylethyl-1,1-d_2 derivatives*

Molecular ion	1—OTs (384)100	1—OTs-1-d_2 (386)100	1—OH (230)100	1—OH-1-d_2 (232)100	1—OCHO (258)100	1—OCHO-1-d_2 (260)100	1—OCH_2CF_3 (312)100	1—OCH_2CF_3-1-d_2 (314)100	1—Cl (248)100 (250)32	1—Cl-1-d_2 (250)100 (252)33
$C_5H_5FeC_7H_7^+$ (212)	74		12		90		10		27	
$C_5H_5FeC_7H_5D_2^+$ (214)		68		12		85		10		20
$FeC_7H_7^+$ (147)	9		9		19		13		25	
$FeC_7H_5D_2^+$ (149)		4		13		14		8		12
$C_7H_7^+$ (91)	39		8		18		45		75	
$C_7H_5D_2^+$ (93)		18		14		14		12		48
$C_5H_5^+$ (65)	8	4	5	2	5	2	10	4	25	4
$C_5H_4D^+$ (66)		2		3		2		3		6
$C_5H_3D_2^+$ (67)		2		2		2		2		5
$C_5H_5FeC_6H_6^+$ (199)	15	12	72	65	23	24	64	77	46	38
$C_5H_5Fe^+$ (121)	35	34	64	59	51	45	50	59	70	33
Fe^+ (56)	18	20	38	25	32	20	20	26	55	38
$FeC_5H_4CH_2CH_2OTs^+$ (319)	22									
$FeC_5H_4CH_2CD_2OTs^+$ (321)		20								
$C_7H_7FeOH^+$ (164)			8							
$C_7H_5D_2FeOH^+$ (166)				19						
$C_5H_5FeOH^+$ (138)			16	10						
$C_7H_7FeCl^+$ (182)									17	
$C_7H_5D_2FeCl^+$ (184)										16
$C_5H_5FeCl^+$ (156)									17	11
$C_7H_8^+$ (92)									50	
$C_7H_6D_2^+$ (94)										45

*Numbers in parentheses are *m/e* values.

Can. J. Chem. Downloaded from www.nrcresearchpress.com by 210.87.254.105 on 09/05/12
For personal use only.

mentation of $C_5H_5FeC_5H_4CH_2CH_2X^+ \rightarrow C_5H_5FeC_6H_6^+$, the C-1 methylene group is lost as CH_2X in the process since **1**—X-1-d_2 also gave rise to the ion with *m/e* 199.

In the formation of $C_5H_5FeC_7H_7^+$ (*m/e* 212) from $C_5H_5FeC_5H_4CH_2CH_2X^+$, HX is lost with the H likely coming from C-2, since in the work with **1**—X-1-d_2, the D-label at C-1 remains intact in the process. The present results as summarized in Schemes 1 and 2 and Table 1 suggest that C_6H_6 and C_7H_7 are energetically favorable structures as ligands in the mass spectral fragmentations of 2-ferrocenylethyl systems. A similar observation has also been made by Roberts *et al.* (10) in their studies with ω-ferrocenylalkanoates. Egger (8) has suggested that the structure of $C_5H_5FeC_6H_6^+$ may be **2**. Analogously, $C_5H_5FeC_7H_7^+$ may be **3**, which could give rise to the tropylium ion, *m/e* 91. Roberts *et al.* (11) have demonstrated with D-labeling that the C_7H_7 ligand bonded to iron in the mass spectra of substituted ferrocences is the symmetrical tropylium species.

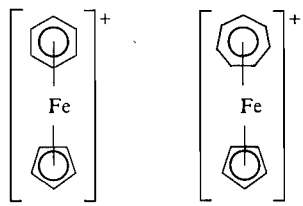

2 **3**

The presence of the tropylium ion is also confirmed by the present work since the decomposition of $C_7H_5D_2^+$ gave rise to $C_5H_5^+$, $C_5H_4D^+$, and $C_5H_3D_2^+$, indicating D-scrambling in $C_7H_5D_2^+$ (Table 1).

Experimental

The n.m.r. spectra of various compounds were recorded on a Varian T-60 or HA-100 spectrometer. The mass spectral studies were carried out using an AEI MS-12 spectrometer at 140° and 70 eV.

2-Ferrocenylethyl and 2-Ferrocenylethyl-1,1-d_2 Tosylates (1—OTs and 1—OTs-1-d_2)

1—OTs and **1**—OTs-1-d_2 were prepared from the reaction of the corresponding alcohol with *p*-toluenesulfonyl chloride in pyridine as reported by Richards and co-workers (1). The yields obtained were considerably better than the reported 24% (1), the difference being probably due to the use of a simpler work-up procedure in the present study. A typical preparation is given below.

To a solution of 1.0 g (4.4 mmol) of 2-ferrocenylethanol (12) in 4.0 ml of dried pyridine, cooled in an ice-bath, was added portionwise, with stirring, 1.0 g (5.2 mmol) of *p*-toluenesulfonyl chloride. The mixture was allowed to stand in the ice-bath for 3 h and the resulting brown solution was poured into 50 g of cracked ice. The material was extracted three times with 50 ml portions of $CHCl_3$. The combined extract was washed successively with a 5% HCl solution, a saturated $NaHCO_3$ solution, and H_2O. After drying over Na_2SO_4, the $CHCl_3$ was removed under reduced pressure. The viscous residue was dissolved in hot *n*-hexane and filtered. On cooling in the refrigerator, 1.31 g (78%) of **1**—OTs was recovered as orange needles, m.p. 77–79° (lit. (1) m.p. 78–79°), n.m.r. ($CDCl_3$) δ 2.43 (s, 3H, $PhCH_3$), 2.70 (t, J = 7 Hz, 2H, $FcCH_2$), 4.07, 410 (overlapping singlets, $C_5H_4FeC_5H_5$), 4.20 (t, J = 7 Hz, partially overlapping with the Fc H's, CH_2OTs), 7.3–7.9 (m, 4H, arom.). For the 1,1-dideuterio analog, **1**—OTs-1-d_2, the n.m.r. spectrum showed that the triplet at 4.20 p.p.m. has disappeared and the triplet at 2.70 p.p.m. has become a broad singlet.

Solvolysis of 1—OTs and 1—OTs-1-d_2 in 60% Ethanol

A solution of 200 mg (0.52 mmol) of **1**—OTs in 10 ml of 60% ethanol – 40% H_2O (v/v) was heated under reflux for 1.5 h. The resultant material was cooled to room temperature, poured into 40 ml of CH_2Cl_2, and washed with a saturated $NaHCO_3$ solution and with H_2O. After drying over Na_2SO_4 and removal of the solvent, the residue was recrystallized from petroleum ether (b.p. 60–70°) to give 105 mg (88%) of 2-ferrocenylethanol (**1**—OH) as orange needles, m.p. 34–35° (lit. (12) m.p. 32.5–33.5°), n.m.r. ($CDCl_3$) δ 1.81 (s, 1H, OH), 2.60 (t, J = 7 Hz, 2H, $FcCH_2$), 3.74 (t, J = 7 Hz, 2H, CH_2OH), 4.10, 4.13 (overlapping singlets, 9H, $C_5H_5FeC_5H_4$). In a similar reaction using **1**—OTs-1-d_2, the product obtained was **1**—OH-1-d_2, the n.m.r. spectrum of which showed that the triplet at 2.60 p.p.m. for the C-2 protons has become a broad singlet, and that there was no detectable absorption at the 3.7 p.p.m. region for the C-1 protons, indicating the absence of any D-scrambling from C-1 to C-2.

Formolysis of 1—OTs and 1—OTs-1-d_2

A solution of 830 mg (2.16 mmol) of **1**—OTs in 6.0 ml of 98–100% HCOOH (BDH analytical reagent) was stirred at room temperature (22°) for 2.5 h. The resultant material was poured into 50 g of cracked ice and then was extracted three times with 50 ml portions of CH_2Cl_2. The combined extract was washed with saturated $NaHCO_3$ solution and with H_2O and then dried over Na_2SO_4. After removal of the solvent, the residue was chromatographed through a silicic acid column, eluting with a 1:1 mixture of hexane–chloroform, to give 500 mg (90%) of 2-ferrocenylethyl formate (**1**—OCHO) which showed only one component on t.l.c. analysis; n.m.r. ($CDCl_3$) δ 2.70 (t, J = 7 Hz, 2H, $FcCH_2$) 4.03, 4.10 (overlapping singlets, $C_5H_4FeC_5H_5$), 4.28 (t, J = 7 Hz, partially overlapping with the Fc H's, CH_2O), 8.00 (s, 1H, CHO). In the presence of a shift reagent (about 0.1 mg $Eu(fod)_3$ and 90 mg sample) the 2-proton triplet at 4.28 p.p.m. for the C-1 protons was shifted downfield to 4.50 p.p.m., clearly separated from the Fc protons at about 4.1 p.p.m. From the analogous reaction with **1**—OTs-1-d_2, the product obtained was **1**—OCHO-1-d_2, the n.m.r. spectrum of which, in the presence of $Eu(fod)_3$, showed a singlet for the C-2 protons at 2.80 p.p.m. and the absence of any absorption at the 4.5 p.p.m. region, indicating no detectable D-scrambling from C-1 to C-2.

Can. J. Chem. Downloaded from www.nrcresearchpress.com by 210.87.254.105 on 09/05/12
For personal use only.

Trifluoroethanolysis of 1—OTs and 1—OTs-1-d_2

A solution of 300 mg (0.78 mmol) of **1**—OTs in 10 ml of CF_3CH_2OH was stirred at room temperature under N_2 for 6 h. At the end of this period, a stream of N_2 was bubbled through the reaction mixture to remove the solvent. Flaked ice was added and the mixture worked up as in the formolysis. Removal of the solvent from the dried CH_2Cl_2 extract gave 160 mg of an oily residue which was found to be a complex mixture by t.l.c. analysis. Chromatographic purification through a silicic acid column, eluting with 10% $CHCl_3$ in *n*-hexane, gave a fraction containing a single component according to t.l.c. and identified as the desired product, 2-ferrocenylethyl trifluoroethyl ether (**1**—OCH_2CF_3), n.m.r. ($CDCl_3$) δ 2.65 (t, J = 7 Hz, 2H, $FcCH_2$), 3.6–4.1 (overlapping t and q, J = 7 and 8.5 Hz, respectively, for the C-1 CH_2 and CH_2CF_3), 4.16 (s, Fc H's). The n.m.r. spectrum of the analogous product from **1**—OTs-1-d_2 showed that the triplet for the C-2 protons at 2.65 p.p.m. has become a singlet and there was a clear quartet of relative intensities of 1:3:3:1 centered at 3.8 p.p.m. for the methylene protons of the trifluoroethyl group. There was no evidence of overlapping of the quartet with any absorption by the C-1 methylene protons indicating no detectable H at C-1 and no scrambling of the D-label.

Since the yield of **1**—OCH_2CF_3 from the above experiment was poor, a much better yield was obtained when the reaction was carried out in the presence of CF_3CH_2ONa. To a solution of 30 mg (1.3 mmol) of Na in 10 ml of CF_3CH_2OH was added 400 mg (1.04 mmol) of **1**—OTs. The mixture was then stirred at room temperature under N_2 for 3 h. The resultant material was poured into ice and worked up the usual way except that the CH_2Cl_2 extract was washed with 5% HCl instead of $NaHCO_3$. Removal of the solvent from the dried extract gave 300 mg (92%) of a residual oil consisting of a single component according to t.l.c. and identified as **1**—OCH_2CF_3 by n.m.r.

Reaction of 1—OH or 1—OH-1-d_2 with $SOCl_2$

To a stirred and cooled (ice-bath) solution of 400 mg (1.74 mmol) of **1**—OH in 25 ml of dried tetrahydrofuran (THF) was added 0.20 ml (2.8 mmol) of $SOCl_2$. Stirring was continued at ice-bath temperature for 1 h and then at room temperature for an additional h. The resultant material was poured into ice and worked up as in the formolysis. Removal of the solvent from the dried CH_2Cl_2 extract gave a residue which on crystallization from *n*-hexane followed by sublimation yielded 180 mg (42%) of orange crystalline 2-ferrocenylethyl chloride, (**1**—Cl), m.p. 52–53° (lit. (13) m.p. 52–54°), n.m.r. (CCl_4) δ 2.80 (t, J = 8 Hz, 2H, $FcCH_2$), 3.55 (t, J = 8 Hz, 2H, CH_2Cl), 4.10 (s, 9H, Fc H's). A similar reaction carried out in toluene instead of THF gave **1**—Cl in 30% yield. When the reaction was carried out with **1**—OH-1-d_2 in either THF or toluene, the product obtained was **1**—Cl-1-d_2, the n.m.r. spectrum of which showed that the triplet at 2.80 p.p.m. has become a singlet and that there was no observable absorption at the 3.5 p.p.m. region, indicating no detectable scrambling of the D-label.

Treatment of 1—Cl or 1—Cl-1-d_2 with $AlCl_3$

In a 100-ml 3-necked round bottom flask equipped with a N_2 inlet, a reflux condenser fitted with a $CaCl_2$ tube and a dropping funnel was placed 110 mg (0.82 mmol) of $AlCl_3$ in 20 ml of CH_2Cl_2. Stirring of the mixture at ice-bath temperature under N_2 for 5 min gave a brownish red solution to which a solution of 100 mg (0.40 mmol) of **1**—Cl in 20 ml of CH_2Cl_2 was added. The reaction mixture was stirred at room temperature under N_2 for 1 h and then poured into ice. More CH_2Cl_2 was added and the mixture was made basic with saturated $NaHCO_3$. The organic layer was separated and the aqueous layer further extracted with CH_2Cl_2. After washing with H_2O, drying over $MgSO_4$, and removal of the CH_2Cl_2, chromatographing the residue through a silicic acid column, eluting with *n*-hexane, gave as a first fraction 15 mg of an unknown yellow liquid and then 40 mg (40%) of recovered **1**—Cl which showed the same n.m.r. spectrum as the starting material.

The unknown fraction, after chromatographing once more through the silicic acid column, still appeared to be impure. Its n.m.r. and mass spectra, however, suggested the probable presence of ethylferrocene as a major component. The n.m.r. spectrum of this unknown showed ferrocenyl absorptions at the 4.10 p.p.m. region and a triplet and quartet, respectively, at 1.16 and 2.30 p.p.m., suggesting an ethyl group, with other absorptions, presumably from impurities, overlapping the triplet and at the 4.0–4.1 region. The mass spectrum of this unknown fraction has as its base peak *m/e* 214 which would fit the molecular ion for ethylferrocene. Other major fragmentation ions were observed at *m/e* 199, 121, and 56, with a metastable peak for 214 → 199 at 185.1.

When **1**—Cl-1-d_2 was treated with $AlCl_3$ in a similar way, 40% **1**—Cl-1-d_2 was recovered which showed the same n.m.r. spectrum as the starting material, indicating the absence of any detectable scrambling of the D-label from C-1 to C-2.

The financial assistance given by the National Research Council of Canada is gratefully acknowledged.

1. M. J. NUGENT, R. E. CARTER, and J. H. RICHARDS. J. Am. Chem. Soc. **91**, 6145 (1969).
2. M. J. NUGENT, R. K. KUMMER, and J. H. RICHARDS. J. Am. Chem. Soc. **91**, 6141 (1969).
3. C. C. LEE, R. G. SUTHERLAND, and B. J. THOMSON. J. Org. Chem. **39**, 406 (1974).
4. K. SCHLÖGL and M. FRIED. Monatsh. Chem. **95**, 558 (1964).
5. K. SCHLÖGL and H. MECHTLER. Monatsh. Chem. **97**, 150 (1966).
6. C. C. LEE and J. W. T. SPINKS. Can. J. Chem. **32**, 1005 (1954).
7. C. C. LEE, J. W. CLAYTON, D. G. LEE, and A. J. FINLAYSON. Tetrahedron, **18**, 1395 (1962).
8. H. EGGER. Monatsh. Chem. **97**, 602 (1966).
9. M. CAIS and M. S. LUPIN. Adv. Organomet. Chem. **8**, 211 (1970).
10. D. T. ROBERTS, JR., W. F. LITTLE, and M. M. BURSEY. J. Am. Chem. Soc. **89**, 6156 (1967).
11. D. T. ROBERTS, JR., W. F. LITTLE, and M. M. BURSEY. J. Am. Chem. Soc. **90**, 973 (1968).
12. D. LEDNICER, J. K. LINDSAY, and C. R. HAUSER. J. Org. Chem. **23**, 653 (1958).
13. K. SCHLÖGL and H. EGGER. Monatsh. Chem. **94**, 376 (1963).

The Synthesis of 4a-Aminoalkyl-1,2,3,4,4a,9-Hexahydrophenanthrenes. Versatile Intermediates for Potential CNS Drugs. I

B. BELLEAU, T. T. CONWAY,[1] T. W. DOYLE, L. MORRIS, AND W. VERBESTEL

Bristol Laboratories of Canada, 100 Industrial Boulevard, Candiac, Quebec J5R 1J1

Received July 12, 1974

B. BELLEAU, T. T. CONWAY, T. W. DOYLE, L. MORRIS, and W. VERBESTEL. Can. J. Chem. **53**, 237 (1975).

The synthesis of 1-aminoalkyl-1-hydroxy-2,2-tetramethylene-1,2,3,4-tetrahydronaphthalenes and their Wagner–Meerwein rearrangements into 4a-aminoalkyl-1,2,3,4,4a,9-hexahydrophenanthrenes are described.

B. BELLEAU, T. T. CONWAY, T. W. DOYLE, L. MORRIS et W. VERBESTEL. Can. J. Chem. **53**, 237 (1975).

On décrit la synthèse d'aminoalkyl-1 hydroxy-1 tétraméthylène-2,2 tétrahydro-1,2,3,4 naphtalènes ainsi que leur réarrangement de Wagner–Meerwein en aminoalkyl-4a hexahydro-1,2,3,4,4a,9 phénanthrènes. [Traduit par le journal]

Introduction

A general, versatile strategy for the synthesis of morphine related compounds was described by one of us several years ago (1). The key intermediates are 1,2,3,4,4a,9-hexahydrophenanthrenes angularly substituted as in **1** thus providing for chemical developments unattainable by the classical Grewe synthesis of morphinans or Gates synthetic approach to morphine (2). The purpose of this communication is to illustrate the applicability of Belleau's approach to morphinan precursors and related structures.

Generally speaking, 2,2-tetramethylene-1-tetralone **2** (R^1 = H or OCH_3) can react with Reformatsky (1), Grignard (1), Wittig or Corey's reagents to give adducts that are especially prone to suffer Wagner–Meerwein arrangements so as to yield 4a-substituted-1,2,3,4,4a,9-hexahydrophenanthrenes (**4**) and/or the isomeric 2,3,4,4a,-9,10-hexahydrophenanthrenes (**6**). The utility of this general strategy as applied to the syntheses of lactone **7** from **3** (R^1 = H, n = 1, Z = CO_2-Et) and of imino ether **8** from **5** (R^1 = H) was reported earlier (1, 3).

The presence of a functional group Z on the substituent at the 4a position in **4** and its (Z's) juxtaposition relative to the Δ10-double bond suggests that cyclization, through a variety of reaction types, to 4a,10-bridged-1,2,3,4,4a,9,10,10a-octahydrophenanthrene systems (**9**) might be achievable. The well known analgesic agent, *N*-methyl-3-hydroxymorphinan (**10**) is one example of a **9**-type system.

It was this possibility, coupled with the anticipated versatility of the approach and the high probability of interesting biological activity in some of the potentially preparable **9**-type systems, that led us into this work.

In this paper we will describe the synthesis of 4a-aminoalkyl-1,2,3,4,4a,9-hexahydrophenanthrenes (**4**) and the methods that have been developed for the synthesis of **3** where Z equals an amino group and n varies from 1 to 3. Later papers will describe the cyclization and related chemistry of some of these **4**-type systems (10). A communication concerning the application of the above described approach has been published recently (9).

Results and Discussion

The syntheses of the 1-aminoalkyl-1-hydroxy-2,2-tetramethylene-1,2,3,4-tetrahydronaphthalenes were carried out as summarized in Scheme 2. The 2,2-tetramethylene-1-tetralones **2** (R^1 = H, OCH_3) were prepared according to the method of Mousseron *et al.* (4). Treatment of ketones **2** (R^1 = H, OCH_3) with excess dimethylsulfonium methylide (*in situ*) in cold DMSO solution produced the epoxides **11** (R^1 = H, OCH_3) in excellent yield. We have found that precautions for excluding moisture and air from this epoxide synthesis are unnecessary in this instance (5). These reactions were commonly run in an open Erlenmeyer flask using commercial reagent grade DMSO.

[1]Author to whom correspondence concerning this paper should be addressed.

Can. J. Chem. Downloaded from www.nrcresearchpress.com by 210.87.254.5 on 09/05/12
For personal use only.

Can. J. Chem. Downloaded from www.nrcresearchpress.com by 210.87.254.5 on 09/05/12
For personal use only.

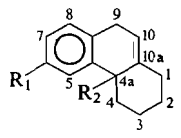

1

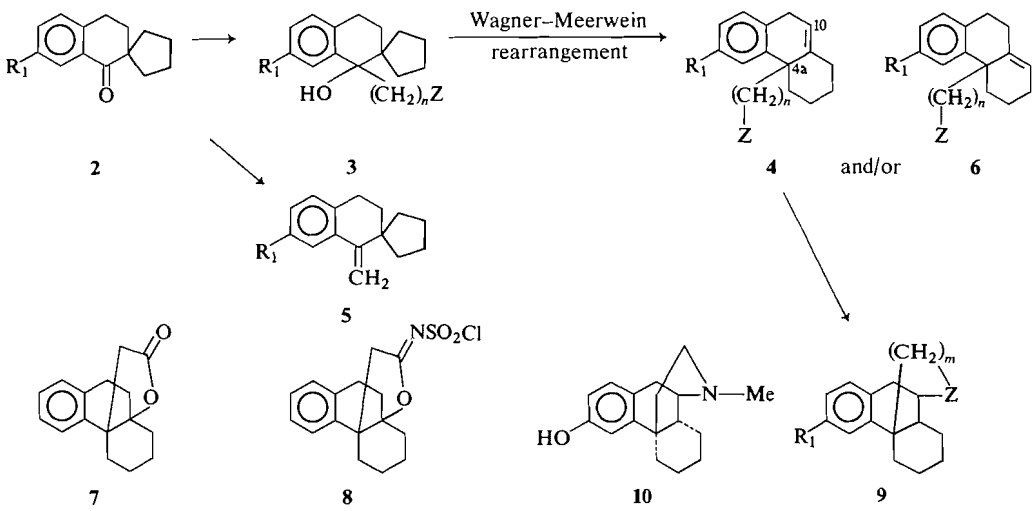

2 3 4 5 6 7 8 9 10

SCHEME 1

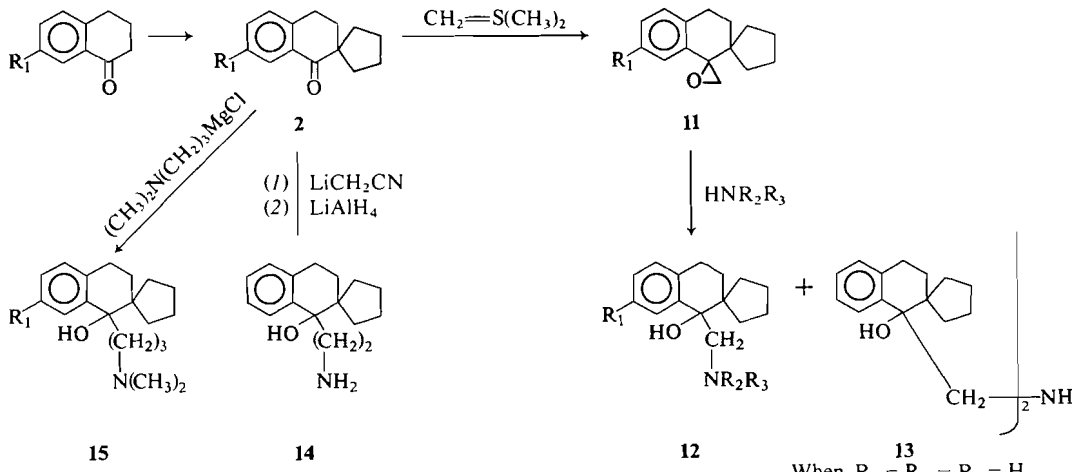

15 14 12 13

When $R_1 = R_2 = R_3 = H$

SCHEME 2

Epoxides **11** (R^1 = H, OCH_3) were converted into the desired amino alcohols **12** (R^1 = H, OCH_3) by heating with an excess of the amine NHR^2R^3 either with or without a solvent. Except in the case of benzylamine, all of these reactions were carried out in a steel pressure bomb at steam bath temperature. The progress of the reactions was followed in some cases by removing aliquots, evaporating off the solvent, and taking the n.m.r. spectrum of the residue. It was usually possible to distinguish clearly the AB pattern of the methylene hydrogens α to

TABLE 1. 1-Substituted-1-hydroxy-2,2-tetramethylene-1,2,3,4-tetrahydronaphthalenes (3)

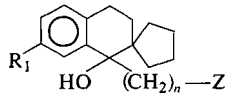

Compound	R_1	n	Z	Yield (%)	Melting point (°C)	Recrystallization[a] solvent	% calculated C	% calculated H	% calculated N	% found C	% found H	% found N
12*a*	H	1	NH_2	98	230–231.5[b]	E	67.27	8.28	5.23	67.24	8.29	5.14
12*b*	H	1	$NHCH_3$	65	216–217[b]	A	68.28	8.58	4.97	68.31	8.68	4.98
12*c*	H	1	$NHCH_2\phi$	65	233[b,c]	B	73.83	7.88	3.91	73.96	8.18	3.83
12*d*	H	1		20	227–228[b]	B	71.51	9.00	4.17	71.42	9.01	4.30
12*e*	H	1		35	226–227[b]	B	67.56	8.06	4.15	67.37	8.24	4.13
12*f*	OCH_3	1	NH_2	90	173–174.5[d]	E	61.52	7.17	3.99	62.01	7.38	3.94
12*g*	OCH_3	1	$NHCH_3$	30	213–213.5[b]	E	65.47	8.40	4.49	65.26	8.41	4.40
12*h*	OCH_3	1	$NHCH_2\phi$	75	202–202.5[b]	B	71.21	7.79	3.61	71.18	7.78	3.68
	H	1	CN	85	60–62.5	F	79.63	7.94	5.80	79.45	8.10	6.20
14	H	2	NH_2	45	166–166.5[b]	D	68.09	8.57	4.97	67.92	8.57	4.88
15*a*	H	3	$N(CH_3)_2$	94	156.5–157[b]	B	70.45	9.34	4.32	70.89	9.18	4.80
15*b*	OCH_3	3	$N(CH_3)_2$	75	174.5–175.5[b]	C	67.87	9.11	5.96	67.77	9.36	3.88

[a]Recrystallization solvents: A, *n*-PrOH–Et_2O; B, MeOH–Et_2O; C, *i*-PrOH–Et_2O; D, EtOH–Et_2O; E, *i*-PrOH; F, benzene – petroleum ether.
[b]Hydrochloride salt.
[c]Decomposition.
[d]Oxalate salt.

oxygen in any unreacted epoxide. If such was the case, the reaction was heated for additional time until it was complete.

The preparation of the primary amine **12** ($R^1 = R^2 = R^3 = H$) gave us some difficulty. Heating mixtures of epoxide with either ammonium hydroxide or liquid ammonia led to a mixture of **12** ($R^1 = R^2 = R^3 = H$) and its dimer **13**. This problem was circumvented by preparing the *N*-benzylamino alcohol **12** ($R^1 = R^2 = H$; $R^3 = CH_2\phi$) and then hydrogenolyzing to the primary amine.

Cyanomethylation (6) of ketone **2** ($R^1 = H$) provided the β-cyanoalcohol in good yield. This was then reduced with lithium aluminum hydride to give compound **14**.

Ketones **2** ($R^1 = H$, OCH_3) were refluxed in ether with the Grignard reagent prepared from magnesium and 3-chloro-*N*,*N*-dimethylpropylamine to provide the desired amino alcohols **15** ($R^1 = H$, OCH_3) in excellent yields.

The physical properties, yields, and analytical data for the 1-aminoalkyl-1-hydroxy-2,2-tetramethylene-1,2,3,4-tetrahydronaphthalenes are summarized in Table 1.

Synthesis of 4a-(Aminoalkyl)-1,2,3,4,4a,9-hexahydrophenanthrenes. The Wagner–Meerwein Rearrangement of 1-(Aminoalkyl)-1-hydroxy-2,2-tetramethylene-1,2,3,4-tetrahydronaphthalenes

Wagner–Meerwein rearrangements of 2,2-tetramethylene-1-cyclohexanol and closely related benzo-fused systems have been the subject of extensive studies by a number of workers (7). The nature of the products produced in such reactions and their rates of formation are determined by a number of factors including the size of each ring in the spiro system, the dehydrating agent, the nature of the carbonium ion generated, the conformation of the leaving group, and the relative thermodynamic stabilities of the products. On the basis of the earlier work one would predict that acid catalyzed dehydration of

Can. J. Chem. Downloaded from www.nrcresearchpress.com by 210.87.254.5 on 09/05/12
For personal use only.

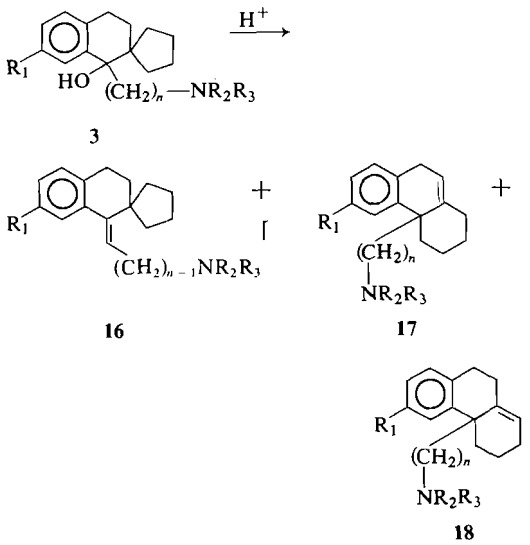

SCHEME 3

systems such as **3** (Scheme 3) would lead to either **16**, **17**, or **18** or mixtures of these three structural types.

When the amino alcohols **12**, **14**, and **15** were treated with concentrated hydrochloric acid we observed the formation of two types of products, **16** and **17** (Scheme 3). We have not observed the formation of the isomeric amine **18**. The relative amounts of these products were found to be related to the concentration and the type of acid used to carry out the rearrangement. Not unexpectedly the reaction temperature and the reaction time are also important determinants in the ratio of **16** to **17**.

A priori one would expect the acid concentration to have an effect on the relative amounts of *exo*-methylene product **16** (proton loss) and the 1–2 alkyl shift product **17**. When the aminomethyl alcohol **12** ($R^1 = R^2 = H$; $R^3 = CH_3$) is heated with $KHSO_4$ at 160° for 1 h, aldehyde **19** is obtained in 80% yield, whereas treatment with concentrated HCl yields solely the 1,2,3,4,-4a,9-hexahydrophenanthrene amine **17**. The n.m.r. spectrum of **19** shows a downfield formyl proton as a doublet ($J = 4.5$ Hz) clearly indicating that the formyl group is attached to a secondary carbon center. We feel that the likeliest origin of aldehyde **19** is from enamine **16** ($n = 1$; $R^1 = R^2 = H$; $R^3 = CH_3$) which is formed by proton loss rather than 1–2 alkyl shift.

Similarly, when the aminoethyl compound **14** is stirred with concentrated hydrochloric acid, a

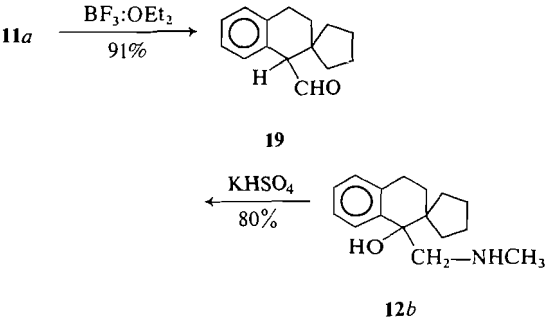

SCHEME 4

smooth rearrangement to the 1–2 alkyl shift product **17** ($R^1 = R^2 = R^3 = H$) occurs in 92.5% yield. If, however, a more dilute ethanolic hydrochloric acid solution is used, a mixture of the **16** and **17** type products is produced.

It was necessary to use formic acid at 98° as the rearrangement condition to obtain the Δ10-amine **17** ($n = 3$; $R^1 = OCH_3$; $R^2 = R^3 = CH_3$) from the *N*,*N*-dimethyl-3-aminopropyl alcohol **6** ($R^1 = OCH_3$). Rearrangement conditions which had been successful in the aminomethyl and aminoethyl cases, namely concentrated hydrochloric acid at reflux and at 25° respectively, failed to yield the Δ10-system for the aminopropyl analog.

The n.m.r. evidence for the production of the 1,2,3,4,4a,9-hexahydrophenanthrene type system **17** is based upon three main points: (*a*) The observed paramagnetic shift of the benzylic methylene signal of the starting materials **3** and the 1,2,3,4,4a,9-hexahydrophenanthrene system **17** (Table 3). (*b*) The presence in **17** of an olefinic signal at *ca.* δ 5.65. (*c*) The obvious coupling of the olefinic hydrogen and the benzylic methylene hydrogens ($J = 4.0$ Hz).

Biological Activity

All the compounds described in this paper were subjected to a routine pharmacological screening procedure which has been described (8). With the exception of amines **14**, **15***a*, and **17***h*, none of these compounds was found to exhibit any significant CNS effects in oral doses of up to 300 mg.

Amino alcohol **14** exhibited "antidepressant" activity in mice at 40 mg/kg. Its related aminoolefin **17***h* produced signs of CNS stimulation at 40 mg/kg. All of these activities were judged to be nontherapeutic and no further work was undertaken.

Can. J. Chem. Downloaded from www.nrcresearchpress.com by 210.87.254.5 on 09/05/12
For personal use only.

Can. J. Chem. Downloaded from www.nrcresearchpress.com by 210.87.254.5 on 09/05/12
For personal use only.

TABLE 2. 4a-Aminoalkyl-1,2,3,4,4a,9-hexahydrophenanthrenes (**17**)

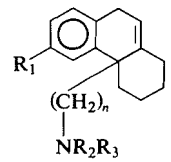

Compound	n	R_1	R_2	R_3	Yield (%)	Melting point (°C)	Recrystallization[a] solvent	% calculated C	% calculated H	% calculated N	% found C	% found H	% found N
17*a*	1	H	H	H	94	223–224[b]	EtOH–Et_2O	74.39	7.80	5.40	74.65	7.82	5.14
17*b*	1	H	H	CH_3	65	277[a,c]	EtOH–Et_2O	72.84	8.41	5.31	72.56	8.63	5.28
17*c*	1	H	H	$CH_2\phi$	53	193–195[a]	2-PrOH–Et_2O	77.74	7.93	4.12	77.63	7.71	4.12
17*d*	1	H	CH_3	CH_3	57	191.5–194[d]	MeOH	55.29	6.55	3.79	55.19	6.61	3.82
17*e*	1	H	—(CH_2—O—(CH_2)—		74	208–211.5[a,e]	EtOH–Et_2O	70.35	8.23	4.32	70.20	8.14	4.64
17*f*	1	OCH_3	H	CH_3	61	160[a,f]	2-PrOH	69.49	8.23	4.77	69.40	8.33	4.71
17*g*	1	OCH_3	H	$CH_2\phi$	61	173–175[a]	2-PrOH	74.68	7.63	3.79	74.46	7.58	3.78
17*h*	2	H	H	H	92	202–205.5(dec.)[a,g]	EtOH–Et_2O	68.19	8.58	4.97	68.30	7.82	4.94
17*i*	3	OCH_3	CH_3	CH_3	70	205–208 (dec.)[a]	2-PrOH	71.51	9.00	4.17	71.53	9.15	4.02

[a]Hydrochloride salt.
[b]Oxalate salt.
[c]Resolidifies and melts 281–282 °C.
[d]Hydroiodide; prepared from monomethylamine **17***b* and methyl iodide.
[e]Contains 0.25 mol water of hydration.
[f]Resolidifies and melts 246.5–7.5 °C.
[g]Contains 1 mol water of hydration.

TABLE 3. Nuclear magnetic resonance spectra of 1-aminoalkyl-1-hydroxy-2,2-tetramethylene-1,2,3,4-tetrahydronaphthalenes and of 4a-aminoalkyl-1,2,3,4,4a,9-hexahydrophenanthrenes (**17**)

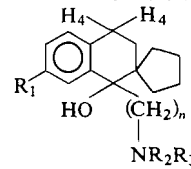

Compound	n	R_1	R_2	R_3	H_4[c]	OCH_3	NR_2R_3	Other
12*a*	1[b]	H	H	H	2.83			
12*b*	1[b]	H	H	CH_3	2.87		2.38 (s)	
12*c*	1[a]	H	H	$CH_2\phi$	2.82		$CH_2\phi$; 3.66 (s)	$CH_2NHCH_2\phi$; 2.73 (s)
12*d*	1[b]	H	—$(CH_2)_5$—		2.83			
12*e*	1[b]	H	—$(CH_2)_2$—O—$(CH_2)_2$—		2.85			CH_2O; 3.64[c]
12*f*	1[b]	OCH_3	H	H	2.80	3.80 (s)		
12*g*	1[b]	OCH_3	H	CH_3	2.82	3.78 (s)	2.38 (s)	
14	2[b]	H	H	H	2.87			
15*a*	3[b]	H	CH_3	CH_3	2.82		2.28 (s)	
15*b*	3[b]	OCH_3	CH_3	CH_3	2.82	3.82 (s)	2.34 (s)	

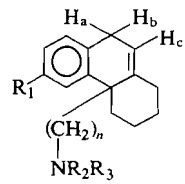

Compound	n	R_1	R_2	R_3	H_aH_b	H_c[d]	OCH_3	NR_2R_3	Other
17*a*	1[b]	H	H	H	3.35 (br s)	5.78			CH_2N; 2.61, 3.22, (dd.; J = 13.0 Hz)
17*b*	1[b]	H	H	CH_3	3.34 (br s)	5.70		2.23 (s)	CH_2N; 2.64, 3.24, (dd.; J = 11.0 Hz)
17*c*	1[b]	H	H	$CH_2\phi$	3.40 (br s)	5.75		$NCH_2\phi$; 3.58 (s)	CH_2N; 2.65, 3.22, (dd.; J = 11.5 Hz)
17*f*	1[a]	CH_3O	H	CH_3	3.30 (br s)	5.68	3.72 (s)	2.22 (s)	CH_2N; 2.62, 3.14, (dd.; J = 12.0 Hz)
17*g*	1[a]	CH_3O	H	$CH_2\phi$	3.34 (br s)	5.71	3.70 (s)	$NCH_2\phi$; 3.58 (s)	CH_2N; 2.60, 3.17, (dd.; J = 11.5 Hz)
17*h*	2[b]	H	H	H	3.35 (br s)	5.65			
17*i*	3[b]	CH_3O	CH_3	CH_3	3.28 (br s)	5.64	3.74 (s)	1.98 (s)	

[a]CCl_4.
[b]$CDCl_3$.
[c]Center of a complex multiplet.
[d]Triplet; J = 4.0 Hz.

Experimental

The i.r. spectra were recorded on a Unicam SP-200G grating i.r. spectrometer. The n.m.r. spectra were determined on a Varian A60-A spectrometer using tetramethyl silane as an internal standard. Melting points are uncorrected and were determined on a Gallenkamp melting point apparatus. The analyses were performed by Micro-Tech Laboratories Inc., Skokie, Illinois.

*1-Oxomethylene-2,2-tetramethylene-1,2,3,4-tetrahydronaphthalene (**11**; R^1 = H)*

Sodium hydride (5.1 g of a 56% mineral oil dispersion; 0.119 mol) was washed twice with dry petroleum ether (30–60°) to remove the mineral oil. Dry DMSO (30 ml) was then added, followed by a solution of trimethylsulfonium iodide (22.4 g; 0.109 mol) in DMSO (120 ml). The solution was magnetically stirred and a mixture of 2,2-tetramethylene-1-tetralone **2** (R^1 = H) (18.4 g; 0.091

Can. J. Chem. Downloaded from www.nrcresearchpress.com by 210.87.254.5 on 09/05/12
For personal use only.

Can. J. Chem. Downloaded from www.nrcresearchpress.com by 210.87.254.5 on 09/05/12
For personal use only.

mol) in DMSO (30 ml) was added slowly over 1 h. The reaction mixture became purple colored after *ca.* 30 min. After stirring at room temperature overnight (19 h) the reaction mixture was poured into cold water (700 ml) and extracted three times with ether. The combined extracts were washed three times with water, dried (Na_2SO_4), and evaporated to dryness *in vacuo*. A residue of 18.1 g (93%) of a yellow oil was obtained, b.p. 123–124°/0.05 mm.

Anal. Calcd. for $C_{15}H_{18}O$: C, 84.07; H, 8.47. Found: C, 83.99; H, 8.51.

*7-Methoxy-1-oxomethylene-2,2-tetramethylene-1,2,3,4-tetrahydronaphthalene (**11**; $R^1 = OCH_3$)*

This was prepared as described above in 90% yield; white needles (95% ethanol) m.p. 96–98°.

Anal. Calcd. for $C_{16}H_{20}O_2$: C, 78.65; H, 8.25. Found: C, 78.58; H, 8.30.

*1-Formyl-2,2-tetramethylene-1,2,3,4-tetrahydronaphthalene (**19**)*

Boron trifluoride etherate (4 ml; 0.032 mol) was added to a solution of epoxide (1.07 g; 5 mmol) in benzene (20 ml). After 12 min at 25° with occasional shaking, the reaction was worked up to give 0.97 g of a brown liquid. Nuclear magnetic resonance indicated that this liquid contained 91% aldehyde **19**. The 2,4-DNP derivative was prepared and recrystallized from acetone–methanol, bright yellow-orange crystals, m.p. 231–232° dec.

Anal. Calcd. for $C_{21}H_{22}N_4O_4$: C, 63.94; H, 5.62; N, 14.21. Found: C, 64.13; H, 5.62; N, 14.48.

*Syntheses of 1-Aminomethyl-1-hydroxy-2,2-tetramethylene-1,2,3,4-tetrahydronaphthalenes (**12***a–h)*

Compounds **12***b*, *d*, *e* and *g* were prepared as in the procedure given for **12***b*. The *N*-benzylamines **12***c* and *h* were prepared as indicated below for **12***h*. The primary amines **12***a* and *f* were prepared as indicated for **12***a*. See Table 1 for the yields, melting points, and analyses of **12***a–h*.

*1-N-methylaminomethyl-1-hydroxy-2,2-tetramethylene-1,2,3,4-tetrahydronaphthalene (**12***b)*

A mixture of **11** (R^1 = H) (1.07 g; 5 mmol), 30–35% aqueous methylamine (5 ml), and dioxane (5 ml) was heated at 98° in a Parr pressure bomb for 20 h. The mixture was then evaporated to dryness *in vacuo*, the residue was dissolved in ether and the HCl salt prepared by bubbling in HCl gas until no further precipitation occurred. The precipitate was filtered off and recrystallized from *n*-propanol–ether to afford 911 mg (65%) of light beige crystals, m.p. 216–217° dec.

*7-Methoxy-1-N-benzylaminomethyl-1-hydroxy-2,2-tetramethylene-1,2,3,4-tetrahydronaphthalene (**12***h)*

A mixture of **11** ($R^1 = OCH_3$) (7.5 g; 30.6 mol) and benzylamine (20 ml) was refluxed under N_2 for 18 h. The excess benzylamine was distilled off at reduced pressure. The distillation residue was dissolved in ether and washed three times with water. Addition of 10% HCl precipitated the hydrochloride salt. This was filtered off, washed with ether, and recrystallized from methanol–ether, m.p. 202–202.5°, 8.80 g (75%).

*1-Aminomethyl-1-hydroxy-2,2-tetramethylene-1,2,3,4-tetrahydronaphthalene (**12***a)*

A mixture of **12***c* (2.0 g; 5.6 mmol), 10% Pd/C (200 mg), and 95% ethanol was hydrogenolyzed in a Parr hydrogenator at room temperature. Hydrogen uptake was complete after 3 h. The catalyst was filtered off and the filtrate was evaporated to dryness *in vacuo* leaving 1.47 g (98%) of a white solid. An analytical sample melted at 230–231.5° (ethanol–ether).

1-Cyanomethyl-1-hydroxy-2,2-tetramethylene-1,2,3,4-tetrahydronaphthalene

To a stirred solution of 23.4 ml (0.055 mol) of 2.35 *M* butyl lithium in hexane at −80° under nitrogen was added 23.4 ml of dry THF and then 2.6 ml (0.05 mol) of acetonitrile dissolved in 10 ml of THF. After stirring for 0.75 h, a solution of ketone **2** (R^1 = H) (10 g; 0.05 mol) in 25 ml of dry THF was added all at once. After stirring for 10 min the cold bath was removed and the reaction stirred for 10 min before it was poured into ice water acidified with hydrochloric acid. The layers were separated and the aqueous phase was extracted three times with ether. The combined organic phases were washed once with brine, dried (Na_2SO_4), and evaporated to dryness *in vacuo* to give 10.25 g (85%) of a light beige colored solid, m.p. 59–62.5°. The analytical sample was recrystallized from benzene – petroleum ether (30–60°), m.p. 60–62.5°, white needles.

Anal. Calcd. for $C_{16}H_{19}NO$: C, 79.63; H, 7.94; N, 5.80. Found: C, 79.45; H, 8.10; N, 6.20.

1-(2-Aminoethyl)-1-hydroxy-2,2-tetramethylene-1,2,3,4-tetrahydronaphthalene

A solution of nitrile (above) (11.24 g, 0.0476 mol) in ether (60 ml) was added as rapidly as possible to a refluxing suspension of LAH (2.6 g; 0.685 mol) in ether (50 ml). The suspension was refluxed with stirring for 24 h. The reaction was worked up in the usual manner to give 9.59 g of a yellow viscous oil. This was dissolved in ether and the hydrochloride salt was prepared by adding ether saturated with HCl gas. This provided 6.1 g (45.5%) of a white solid, m.p. 164–164.5°. An analytical sample was recrystallized from ethanol–ether, m.p. 166–166.5°.

*1-(N,N-Dimethyl-3-aminopropyl)-1-hydroxy-2,2-tetramethylene-1,2,3,4-tetrahydronaphthalene (**15**; R^1 = H)*

To a refluxing mixture of magnesium turnings (3.6 g; 0.15 mol), dry ether (50 ml) and *ca.* 0.02 ml of methyl iodide was added a solution of freshly distilled 3-chloro-*N*,*N*-dimethylpropylamine (18.15 g; 0.15 mol) in 50 ml of dry ether. After refluxing with stirring for 1.5 h a solution of ketone **9** (R^1 = H) (20 g; 0.1 mol) in 50 ml of ether was added. The reaction was refluxed an additional 18 h and then worked up in the usual way to yield 27.0 g of a heavy brown oil (94%) The hydrochloride salt was prepared with ether–HCl and recrystallized from methanol–ether; white solid, m.p. 156.5–157°.

*7-Methoxy-1-(N,N-dimethyl-3-aminopropyl)-1-hydroxy-2,2-tetramethylene-1,2,3,4-tetrahydronaphthalene (**15**; $R^1 = OCH_3$)*

This was prepared as described above in 75% yield. The free base was a crystalline white solid, m.p. 85–86°. An analytical sample of the hydrochloride salt was recrystallized from 2-propanol-ether, m.p. 174.5–175.5°.

Syntheses of 4a-Aminomethyl-1,2,3,4,4a,9-hexahydrophenanthrenes (17a–i)

Compounds **17***a*, *b*, *e*, *f* and *g* were prepared as in the procedure given for **17***c*. See Table 2 for the yields, melting points, and analyses of **17***a–i*.

N-Benzyl-4a-aminomethyl-1,2,3,4,4a,9-hexahydrophenanthrene (17c; $R^1 = R^2 = H$; $R^3 = CH_2\phi$)

N-Benzyl-1-aminomethyl-1-hydroxy-2,2-tetramethylene-1,2,3,4-tetrahydronaphthalene hydrochloride **12***c* (40.0 g; 0.112 mol) was dissolved in 200 ml of hot methanol. This solution was added over 10 min to 800 ml of boiling concentrated hydrochloric acid in a 3-l flask with vigorous stirring (CAUTION! foaming may occur). The solution was refluxed for 10 min then allowed to cool and poured into 600 ml 50% aqueous sodium hydroxide and 1 l of ice. The solution was extracted with five 200-ml portions of ether, the extracts were washed once with brine, dried (Na_2SO_4) and evaporated to dryness *in vacuo*. The resultant oil was taken up in 400 ml of ether and 150 ml of 10% aqueous hydrochloric acid was added with vigorous stirring. A solid separated which was filtered off and recrystallized from 2-propanol–ether to yield 20.0 g (53%) of pure **17***c* as its hydrochloride, m.p. 193–195°.

Wagner–Meerwein Rearrangement of 12b using $KHSO_4$

An intimate mixture of ground, freshly fused $KHSO_4$ (1.09 g; 8 mmol) and 1-*N*-methylaminomethyl-1-hydroxy-2,2-tetramethylene-1,2,3,4-tetrahydronaphthalene hydrochloride (**12***b*) (564 mg; 2 mmol) was put under nitrogen and then immersed in a 200° oil bath for 70 min. Water was added, then 10% aqueous NaOH, and then it was extracted with ether. The ether extract was washed with water, dried (Na_2SO_4), and evaporated *in vacuo* to leave 358 mg of a brown oil. Nuclear magnetic resonance examination of this oil showed >95% aldehyde **19**. A 2,4-DNP derivative was prepared and recrystallized from acetone–methanol, m.p. 225–227° dec. Mixture m.p. with the 2,4-DNP prepared from the BF_3 derived aldehyde was 225–227° (dec.).

4a-N,N-Dimethylaminomethyl-1,2,3,4,4a,9-hexahydrophenanthrene (17d)

A solution of 4a-*N*-methylaminomethyl-1,2,3,4,4a,9-hexahydrophenanthrene **17***b* (2.175 g; 9.5 mmol), methyl iodide (15 ml; excess), and *ca.* 100 ml AR.Et_2O was heated at reflux for 1 h. The reaction mixture was evaporated to dryness *in vacuo* leaving 2.97 g of a cream-colored solid. This was recrystallized from MeOH to yield 1.82 g of white crystals, m.p. 191.5–195° (dec.) (57% yield).

4a-(2-Aminoethyl)-1,2,3,4,4a,9-hexahydrophenanthrene (17h)

Concentrated hydrochloric acid (30 ml) was added slowly and with stirring to 1-(2-aminoethyl)-1-hydroxy-2,2-tetramethylene-1,2,3,4-tetrahydronaphthalene (**14**), (7.84 g; 32 mmol). After stirring at 25° for 0.5 h the reaction mixture had nearly solidified. It was alkalized with 10% sodium hydroxide solution and extracted twice with ether. The ether extract was washed twice with water, dried (Na_2SO_4), and evaporated *in vacuo* to give 6.73 g (92.5%) of **17** ($n = 2$; $R^1 = R^2 = R^3 = H$) as a thick oil which crystallized on standing. Its hydrochloride recrystallized from ethanol–ether as a white solid, m.p. 202–205.5° dec.

6-Methoxy-4a-N,N-dimethyl-3-aminopropyl-1,2,3,4,4a,9-hexahydrophenanthrene (17i)

A solution of 7-methoxy-1-(3-*N*,*N*-dimethylaminopropyl)-1-hydroxy-2,2-tetramethylene-1,2,3,4-tetrahydronaphthalene (**15**) ($R^1 = OCH_3$) (8.85 g; 27.9 mmol) in glacial formic acid (200 ml) was heated on a steam bath at 98° for 19 h. After the solution was cooled to 25° it was alkalized by the careful addition of concentrated NH_4OH and extracted twice with ether. After washing (H_2O) and drying (Na_2SO_4) the ether was removed *in vacuo* leaving 6.48 g of a red-brown oil whose n.m.r. spectrum indicated 90% content of **17***i* (70%). The hydrochloride salt was prepared in the usual manner and recrystallized from isopropanol, white crystals, m.p. 205–208° (dec).

1. B. BELLEAU. J. Am. Chem. Soc. **75**, 1159 (1953).
2. M. GATES and G. TSCHUDI. J. Am. Chem. Soc. **78**, 1380 (1956).
3. T. W. DOYLE and T. T. CONWAY. Tetrahedron Let. 1889 (1969).
4. M. MOUSSERON, R. JACQUIER, and H. CHRISTOL. Bull. Soc. Chim. Fr. 346 (1957).
5. E. J. COREY and M. CHAYKOVSKY. J. Am. Chem. Soc. **87**, 3402 (1965).
6. E. M. KAISER and C. R. HAUSER. J. Org. Chem. **33**, 3402 (1968).
7. W. R. DOLBIER. *In* Mechanisms of molecular migrations. Vol. 3. *Edited by* B. S. Thyagarajan. Wiley-Interscience, New York, London, Sydney, Toronto. 1971. pp. 1–66.
8. E. D. BERGMANN and Z. GOLDSCHMIDT. J. Med. Chem. **11**, 1121 (1968).
9. I. MONKOVIC, T. T. CONWAY, H. WONG, Y. G. PERRON, I. J. PACHTER, and B. BELLEAU. J. Am. Chem. Soc. **95**, 7910 (1973).
10. T. T. CONWAY, T. W. DOYLE, Y. G. PERRON, J. CHAPUIS and B. BELLEAU, Can. J. Chem. This issue.

Can. J. Chem. Downloaded from www.nrcresearchpress.com by 210.87.254.5 on 09/05/12
For personal use only.

Base-catalyzed Rearrangement Reactions of 4a-Aminomethyl-1,2,3,4,4a,9-Hexahydrophenanthrenes. Synthesis of D-Normorphinans

TERRY T. CONWAY,[1] TERRENCE W. DOYLE,[1] YVON G. PERRON, JACQUES CHAPUIS, AND BERNARD BELLEAU

Bristol Laboratories of Canada, Candiac, Quebec J5R 1J1

Received July 12, 1974

TERRY T. CONWAY, TERRENCE W. DOYLE, YVON G. PERRON, JACQUES CHAPUIS, and BERNARD BELLEAU. Can. J. Chem. **53**, 245 (1975).

The syntheses of members of the D-normorphinan system, which is unreported prior to this work, are described. Two methods employing 4a-aminomethyl-1,2,3,4,4a,9-hexahydrophenanthrenes (**1***a–d*) as starting materials were developed. These were the base-catalyzed rearrangement of **1** to the 4a-aminomethyl-4a,10a-*cis*-1,2,3,4,4a,10a-hexahydrophenanthrenes **2** followed by base-catalyzed ring closure of one of these (**2***b*) to *N*-methyl-D-normorphinan (**3**) and the intramolecular cyclization of the chloramine derived from **2***c* to give 10-substituted-*N*-benzyl-D-normorphinans which were transformed into a number of derivatives.

The $Eu(fod)_3$ induced shifts in the n.m.r. spectra of certain of these D-normorphinans are reported and form the basis of a configurational assignment to one of the products obtained on chloramine solvolysis.

TERRY T. CONWAY, TERRENCE W. DOYLE, YVON G. PERRON, JACQUES CHAPUIS et BERNARD BELLEAU. Can. J. Chem. **53**, 245 (1975).

On décrit la synthèse d'un certain nombre de composés contenant le système D-normorphinane; aucune synthèse de ce système n'avait été rapportée avant le présent travail. On a développé deux méthodes faisant appel aux aminométhyl-4a hexahydro-1,2,3,4,4a,9 phénanthrène (**1***a–d*) comme produits de départ. Ces deux méthodes font appel à des réarrangements, catalysés par les bases, des produits **1** en aminométhyl-4 hexahydro-1,2,3,4,4a,10a phénanthrènes **2** de stéréochimie 4a,10a *cis*; la cyclisation catalysée par les bases de **2***b* fournit le *N*-méthyl D-normorphinane **3** et la cyclisation intramoléculaire de la chloramine dérivée de **2***c* fournit les *N*-benzyl D-normorphinanes substitués en position 10 qui sont transformés en un grand nombre de dérivés.

On rapporte les spectres r.m.n. de certain de ces D-normorphinanes lorsqu'ils sont mis en présence du réactif $Eu(fod)_3$; ces spectres forment la base de l'attribution configurationnelle d'un des produits obtenus par la solvolyse de la chloramine. [Traduit par le journal]

In the preceding communication, the synthesis of 4a-alkylamino-1,2,3,4,4a,9-hexahydrophenanthrenes via acid-catalyzed rearrangements of 1-hydroxy-1-aminoalkyl-2,2-tetramethylene-1,2,3,4-tetrahydronaphthalenes was described (1). In this paper we should like to report our results on the base-catalyzed rearrangements of the 4a-aminomethyl-1,2,3,4a,9-hexahydrophenanthrenes to 4a,10a-*cis*-4a-aminomethyl-1,2,3,4,4a,10a-hexahydrophenanthrenes and on the subsequent base-catalyzed ring closure of 4a,10a-*cis*-4a-*N*-methylaminomethyl-1,2,3,4,-4a,10a-hexahydrophenanthrene (**2***b*) to *N*-methyl D-normorphinan (**3**). The results of ring closures of the chloramine derived from 4a,10a-*cis*-4a-*N*-benzylaminomethyl-1,2,3,4,4a,10a-hexahydrophenanthrene (**2***c*) are also discussed.

[1]Authors to whom correspondence concerning this paper should be addressed.

Results and Discussion

The synthesis of *N*-substituted β-phenethylamines via base-catalyzed addition of amines to styrene has been demonstrated by Wegler and Pieper (2*a*) and Falk and co-workers (2*b*). More recently Freter and co-workers have utilized a variation of this method in the synthesis of tetrahydroquinolines (3). The addition of amines to α- and γ-vinylpyridines has been demonstrated by Doering and Weil (4). Recently Gates *et al.* have applied this reaction to the syntheses of cinchona alkaloids (5). These results suggested to us that base catalyzed rearrangement of the readily available 4a-aminomethyl-1,2,3,4,4a,9-hexahydrophenanthrenes to the 4a-aminomethyl-

Can. J. Chem. Downloaded from www.nrcresearchpress.com by 210.87.254.42 on 09/05/12
For personal use only.

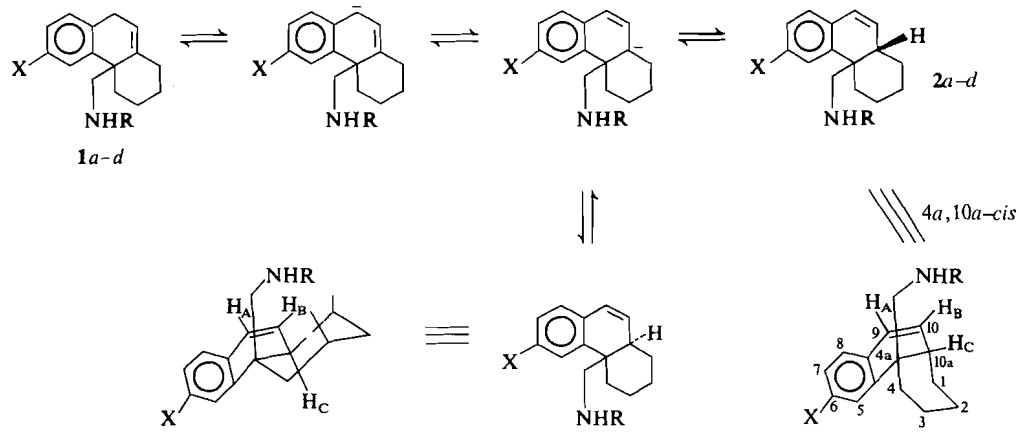

a R = H X = H
b R = Me X = H
c R = $CH_2\phi$ X = H
d R = Me X = OMe

SCHEME 1

1,2,3,4,4a,10a-hexahydrophenanthrenes followed by intramolecular base-catalyzed addition to the styrenoid double bond might provide an entry into the previously unreported D-normorphinan or D-norisomorphinan series (depending on the stereochemistry of the 4a-aminomethyl-1,2,3,4a,-10a-hexahydrophenanthrene produced in the first instance). Consequently the isomerization of 4a-aminomethyl-1,2,3,4,4a,9-hexahydrophenanthrenes (**1***a–d*) has been examined.

The base-catalyzed isomerization of these systems is an allylic proton transfer reaction (6). In recent years it has been found that the use of solvents of high polarity such as dimethylsulfoxide (DMSO) permits rapid isomerizations at low temperatures (6*a*).

Treatment of 4a-aminomethyl-1,2,3,4,4a,9-hexahydrophenanthrene (**1***a*) with potassium *tert*-butoxide in DMSO for 30 min at 25 °C gave 4a-aminomethyl-4a,10a-*cis*-1,2,3,4,4a,10a-hexahydrophenanthrene (**2***a*) in 73% yield (see Scheme 1).[2] The stereochemistry of the product was shown by the n.m.r. spectrum (see Table 1). An examination of Drieding models permits an estimation of the dihedral angles of the 4a,10a-*cis*-1,2,3,4,4a,10a-hexahydrophenanthrene and 4a,10a-*trans*-1,2,3,4,4a,10a-hexahydrophenanthrene systems between H_{10} and H_{10a} (H_B and H_C, respectively, in Table 1). For the 4a,10a-*cis* system $\phi H_B H_C \cong 20°$ and for the 4a,10a-*trans* system $\phi H_B H_C \cong 100°$. The Karplus equation predicts a value of $J_{H_BH_C} \cong 7.0$ Hz for the 4a,10a-*cis* system and $J_{H_BH_C} \cong 0.1$ Hz for the 4a,10a-*trans* system (7). In compounds **2***a–d* and compound **5** $J_{H_BH_C} = 5.9$ Hz thus indicating the *cis* stereochemistry of these compounds. Recently Nelson and co-workers have reported $J_{H_BH_C} = 0$–1 Hz for the parent 4a,10a-*trans*-1,2,3,4,4a,10a-hexahydrophenanthrene (8).

Similarly, treatment of compounds **1***b–d* with potassium *tert*-butoxide in DMSO (either for 30 min or 24 h, see Experimental) produced compounds **2***b–d* (in 52, 89, 65% yields, respectively) of 4a,10a-*cis* stereochemistry. These results are not too surprising in view of the greater thermodynamic stability of the 4a,10a-*cis*-1,2,3,4,4a,10a-hexahydrophenanthrenes relative to the *trans* isomer. An examination of models indicates that in going from 4a,10a-*trans* to 4a,10a-*cis* the molecule is relieved of two *syn* triaxial interactions (4a-aminomethyl substituent and axial hydrogens at C_1 and C_3, see Scheme 1[3]) as well as a *gauche* interaction of H_B and the C_{10a}—C_1 bond. As the reactions are carried our under what might be expected to be equilibrating conditions the exclusive formation of the 4a,10a-*cis*

[2]In addition to the amine approximately 25% of neutral material was isolated which consisted of at least three components which were not identified.

[3]Only one of two possible conformers of the 4a,10a-*cis* systems is illustrated in Scheme 1. The second conformer is expected to be considerably less stable (see Scheme 2).

Can. J. Chem. Downloaded from www.nrcresearchpress.com by 210.87.254.42 on 09/05/12
For personal use only.

TABLE 1. Nuclear magnetic resonance spectra of Δ^9-hexahydrophenanthrene systems[a]

Compounds	Aromatic protons	H_A	H_B	CH_2NHR	CH_2NHR
2*a*	7.3–6.9 (m, 4H)	6.27 (d, 1H) J_{AB} = 9.5 Hz	5.82 (dd, 1H) J_{AB} = 9.5 Hz J_{BC} = 5.9 Hz	2.75 (d, 1H)[b] 2.34 (d, 1H) J = 13 Hz	0.8 (s, 2H)
2*b*	7.3–6.9 (m, 4H)	6.22 (d, 1H) J_{AB} = 9.5 Hz	5.80 (dd, 1H) J_{AB} = 9.5 Hz J_{BC} = 5.9 Hz	2.62 (d, 1H)[b] 2.25 (d, 1H) J = 12 Hz	0.4 (s, 1H)[c]
2*c*	7.3–6.8 (m, 9H)	6.30 (d, 1H) J_{AB} = 9.5 Hz	5.83 (dd, 1H) J_{AB} = 9.5 Hz J_{BC} = 5.9 Hz	2.74 (d, 1H)[b] 2.29 (d, 1H) J = 12 Hz	0.6 (s, 1H)[d]
2*d*	7.2–6.6 (m, 3H)	6.52 (d, 1H) J_{AB} = 9.5 Hz	5.78 (dd, 1H) J_{AB} = 9.5 Hz J_{BC} = 5.9 Hz	2.67 (d, 1H)[b] 2.32 (d, 1H) J = 12 Hz	0.6 (s, 1H)[e]
4[f]	7.4–6.8 (m, 9H)	6.22 (d, 1H) J_{AB} = 9.5 Hz	5.78 (dd, 1H) J_{AB} = 9.5 Hz J_{BC} = 5.9 Hz	3.15 (d, 1H)[b] 2.90 (d, 1H) J = 15 Hz	[g]
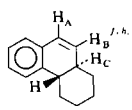	7.20 (m, 4H)	6.55 (dd, 1H) J_{AB} = 10 Hz J_{AC} = 2 Hz	5.85 (d, 1H) J_{AB} = 10 Hz J_{BC} = 0–1 Hz		

[a]All spectra were recorded in CCl_4 unless otherwise stated.
[b]AB quartet.
[c]*N*-methyl protons at 2.20 (s, 3H).
[d]Benzyl methylene at 3.59 (s, 2H).
[e]*N*-Methyl at 2.28 (3H, s) and *O*-methyl at 3.76 (s, 3H).
[f]Recorded in $CDCl_3$.
[g]Benzyl methylene as AB quartet at 3.96 (J = 13.9 Hz) and 3.65 (J = 13.9 Hz).
[h]Ref. 6.

systems is to be expected. The possibility that stereospecific allylic proton transfer is occurring must also be considered. Cram and co-workers have shown that in solvents of high polarity such as DMSO allylic proton transfer may proceed with a high degree of intramolecularity (6*c* and references therein). An examination of a model of **1***a–d* shows that these systems are ideally disposed for such a process (Scheme 2). Stereospecific proton transfer of the axial 9-β-hydrogen in **1***a–d* would lead to the less stable conformer of the 4a,10a-*cis*-1,2,3,4,4a,10a-hexahydrophenanthrene systems which may undergo ring inversion to the more stable conformer. Similarly Nieuwstad and Van Bekkum have postulated that proton transfer in the isomerization of 1,4-dihydronaphthalene to 1,2-dihydronaphthalene occurs in a one-step manner via a transition state involving proton transfer on one face of the molecule (see Scheme 2) (9).

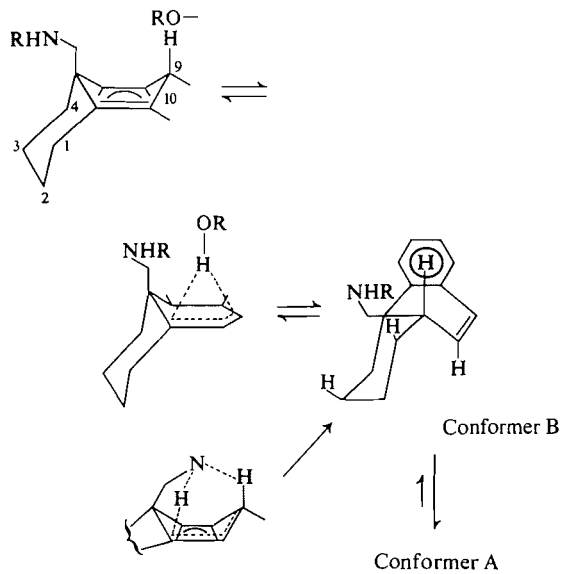

SCHEME 2

With the desired 4a-aminomethyl-4a,10a-*cis*-1,2,3,4,4a,10a-hexahydrophenanthrene systems at hand the conversion of these to the D-normorphinans was studied next. Treatment of *N*-methyl-4a-aminomethyl-4a,10a-*cis*-1,2,3,4,4a,-10a-hexahydrophenanthrene (**2***b*) with lithium diisopropylamide in benzene or of *N*-methyl-4a-aminomethyl - 1,2,3,4,4a,9 - hexahydrophenan - threne (**1***b*) with potassium *tert*-butoxide in DMSO gave *N*-methyl-D-normorphinan (**3**) (in

Can. J. Chem. Downloaded from www.nrcresearchpress.com by 210.87.254.42 on 09/05/12
For personal use only.

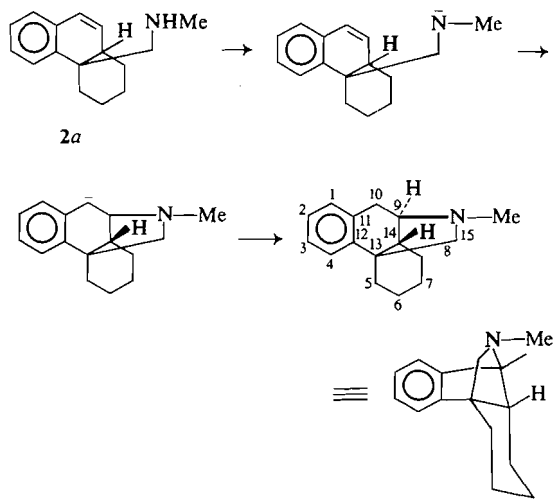

SCHEME 3

71 and 31% yields, respectively). For the purposes of large scale preparations of **3** it was found to be more convenient to use the latter procedure, thus eliminating the necessity of isolating **2***b* in the direct conversion of **1***b* to **3** (see Experimental).

Treatment of compounds **2***a*, *c*, and *d* under the conditions described for the conversion of **2***b* to **3** failed to give any D-normorphinans. The failure of the 6-methoxy derivative **2***d* may be ascribed to destabilization of the presumed intermediate benzyl carbanion (see Scheme 3) by the *p*-methoxyl function. The failure of the primary amine **2***a* to add to the styrenoid double bond might have been expected on the basis of the results of Wegler and Pieper (2*a*), Falk and co-workers (2*b*), and Freter *et al.* (3). The first authors (2*a*) report only moderate yields for the addition of primary amines (methylamine 10%, propylamine 18%, cyclohexyl amine 30%) and ammonia (8%) to styrene. Similarly, Freter *et al.* (3) report only a 10% yield of tetrahydroquinoline from primary amine. The failure of compound **2***c* to cyclize may be due to steric factors, since the transition state leading to addition of the *N*-anion to the double bond would require eclipsing of the C_{15}—N bond thus bringing the bulky benzyl group into proximity with either the fused benzene ring or the protons at C_{14} and C_5.

Attempts to demethylate *N*-methyl-D-normorphinan (**3**) by the usual methods failed to give, for example, the desired parent D-normorphinan **8**. Treatment of **3** with phenyl chloroformate gave the eliminated product **i**.[4] The n.m.r. spectrum of **i** indicated the B/C-*cis* ring juncture shown. The n.m.r. spectrum of **3** (the n.m.r. spectra of all D-normorphinans prepared in this study are recorded in Table 2) confirmed the assigned structure. The proton at C_9 exhibits a doublet of broadened triplets at 3.06 δ $J_{H_9H_{10}}$ = 3 Hz and $J_{H_9H_{14}}$ = 5 Hz. An examination of molecular models permits one to estimate the dihedral angle ϕ $H_9H_{14} \cong 37°$ on the basis of which one may predict a value of $J_{H_9H_{14}} \cong 5$ Hz which corresponds to one of the observed coupling constants. One would predict a coupling constant $J_{H_9H_{14}} < 0.3$ Hz for the corresponding D-norisomorphinan. The predicted values for $J_{H_9H_{10cis}} \cong 0.6$ Hz and $J_{H_9H_{10trans}} \cong 3.1$ Hz which would account for the broadened nature of the observed coupling constant of 3 Hz.

Chloramine Solvolysis

In view of the failure to demethylate *N*-methyl-D-normorphinan (**3**), an alternative approach was explored.

The use of *N*-chloramines in the syntheses of bicyclic amines via intramolecular addition to olefins has received much attention in recent years (10–15). The *N*-chloramine **4** was prepared from *N*-benzyl-4a-aminomethyl-4a,10a-*cis*-1,2,3,4,4a,10a-hexahydrophenanthrene (**2***c*) according to the method of Nakano and Votický (16). Refluxing a solution of **4** in methanol produced 20% of **2***c* and 50% of 10-*trans*-methoxy-*N*-benzyl-D-normorphinan.[5] Compound **5** was the only cyclized product which could be recovered from the reaction. Similarly treatment of **4** in aqueous tetrahydrofuran resulted in **2***c* in 26% yield and the formation of 10-*trans*-hydroxy-*N*-benzyl-D-normorphinan (**9**) in 34% yield.

Two mechanistic possibilities have been proposed to account for the products obtained in unassisted 'solvolyses'. Gassman has proposed the intermediacy of nitrenium ions to account for both the unassisted and silver ion assisted

[4]T. T. Conway, unpublished results. The results of this and related experiments will be published elsewhere.

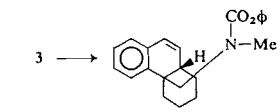

i

[5]The terms *cis* and *trans* in this context indicate the relationship of the 10-substituent and the *N*-alkylamino bridge.

Can. J. Chem. Downloaded from www.nrcresearchpress.com by 210.87.254.42 on 09/05/12
For personal use only.

Can. J. Chem. Downloaded from www.nrcresearchpress.com by 210.87.254.42 on 09/05/12
For personal use only.

TABLE 2. Nuclear magnetic resonance spectra of D-normorphinan systems

Compounds	Aromatic protons	H_9	$H_{10\text{-}trans}$	$H_{10\text{-}cis}$	H_{15}	CH_2-ϕ	Other[a]
3[b]	7.0 (m, 4H)	3.06 (dt, 1H) $J_{H9,H14}$ = 3 Hz $J_{H9,H10}$ = 5 Hz		~2.8 (m, 2H)	2.56 (d, 1H)[c] 2.81 (d, 1H)[c] J = 8.2 Hz		N—CH_3 2.36 (s, 3H)
5[d]	7.3 (m, 9H)	3.28 (1H)[e]		3.96 (d, 1H) $J_{H9,H10}$ = 3 Hz	2.88 (d, 1H)[c] 2.40 (d, 1H)[c] J = 8 Hz	3.83 (s)	OCH_3 3.24 (s, 3H)
6[d]	7.3 (m, 4H)	3.64 (1H)[e]		3.92 (d, 1H) $J_{H9,H10e}$ = 2.5 Hz	2.73 (s, broad)		OCH_3 3.57 (s, 3H)
7[b]	7.2 (m, 9H)	3.32 (dt, 1H) $J_{H9,H14}$ = 5 Hz $J_{H9,H10}$ = 3 Hz		~2.8 (m, 2H)	2.95 (d, 1H)[c] 2.63 (d, 1H)[c] J = 7.5 Hz	3.92 (d, 1H)[c] 3.68 (d, 1H)[c] J = 14 Hz	[f]
8[b]	7.0 (m, 4H)	3.32 (dt, 1H) $J_{H9,H14}$ = 5 Hz $J_{H9,H10}$ = 3 Hz		[g]	[g]		[f]
9	7.3 (m, 1H) 7.2–7.1 (m, 8H)	3.16 (dd, 1H) $J_{H9,H14}$ = 5.0 Hz $J_{H9,H10e}$ = 3.0 Hz		4.34 (d, 1H) $J_{H9,H10e}$ = 3.0 Hz	2.74 (d, 1H)[c] 2.36 (d, 1H)[c] J = 8 Hz	3.80 (s, 2H)	[f,l]
10[d]	7.4 (m, 4H)	3.54 (dd, 1H) $J_{H9,H14}$ = 5.0 Hz $J_{H9,H10e}$ = 3.0 Hz		4.36 (d, 1H) $J_{H9,H10e}$ = 3.0 Hz	2.77 (s, 2H)		[h]
11[d]	8.02 (m, 1H) 7.28 (s) 7.1–7.8 (m)	3.62 (d, 1H) $J_{H9,H14}$ = 5 Hz			3.11 (d, 1H)[c] 2.40 (d, 1H)[c] J = 9 Hz	3.93 (d, 1H)[c] 3.37 (d, 1H)[c] J = 14 Hz	[l]
12[d]	7.44 (m, 1H) 7.3 (m, 8H)	3.20 (dd, 1H) $J_{H9,H14}$ = 6.0 Hz $J_{H9,H10t}$ = 4.0 Hz	4.34 (d, 1H) $J_{H9,H10t}$ = 4.0 Hz		2.91 (d, 1H)[c] 2.30 (d, 1H)[c] J = 9 Hz	4.00 (d, 1H)[c] 3.37 (d, 1H)[c] J = 14 Hz	[f,l]
13[d]	7.6 (m, 1H) 7.3 (m, 3H)	3.49 (dd, 1H) $J_{H9,H14}$ = 5.1 Hz $J_{H9,H10t}$ = 3.5 Hz	4.71 (d, 1H) $J_{H9,H10t}$ = 3.5 Hz		2.83 (s, 2H)		[h]

[a]All compounds exhibited a broad methylene envelope for the protons on C_5—C_8 and on C_{14} from ~0.8–2.2 δ.
[b]Recorded in CCl_4.
[c]One arm of an AB quartet.
[d]Recorded in $CDCl_3$.
[e]H_9 obscured by OCH_3 signal.
[f]One exchangeable H.
[g]These protons appear as a complex pattern between 2.2 and 3.0 δ.
[h]Two exchangeable H.
[l]For a discussion of the 100 Mc spectra and Eu(fod)$_3$ experiments see text.

Can. J. Chem. Downloaded from www.nrcresearchpress.com by 210.87.254.42 on 09/05/12
For personal use only.

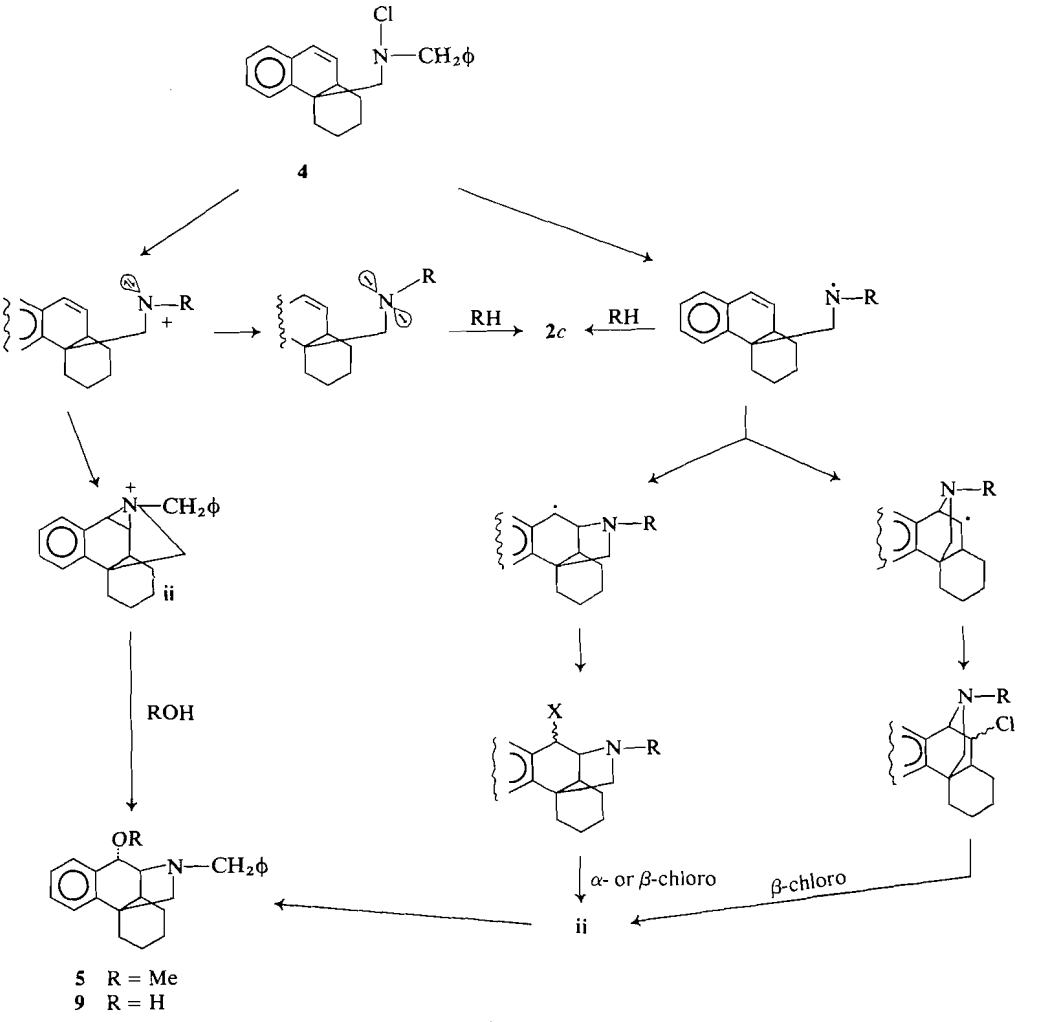

SCHEME 4

solvolyses (10*a*). On the other hand Edwards *et al.* (14*a*) and Hobson and co-workers (14*b*) have presented convincing evidence for a radical chain mechanism in these reactions (see Scheme 4). Either of these mechanisms may account for the products observed in our system.

Hydrogenolysis of compund **5** with Pd/C in acetic acid did not give the desired D-normorphinan **8**, rather, 10-*trans*-methoxy-D-normorphinan (**6**) was isolated in 70% yield. Treatment of **5** with sodium in liquid ammonia gave *N*-benzyl-D-normorphinan (**7**) which on hydrogenolysis with Pd/C in acetic acid gave the desired D-normorphinan (**8**) in 75% yield (Scheme 5). Similarly hydrogenolysis of compound **9** gave 10-*trans*-hydroxy-D-normorphinan (**10**) in 89% yield.

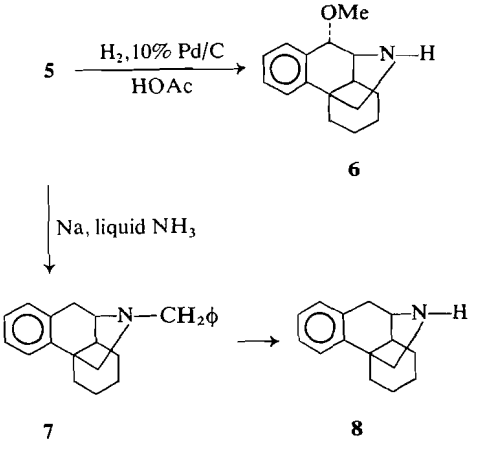

SCHEME 5

Can. J. Chem. Downloaded from www.nrcresearchpress.com by 210.87.254.42 on 09/05/12
For personal use only.

The n.m.r. spectra of *N*-benzyl-D-normorphinan (**7**) and D-normorphinan (**8**) were compatible with the assigned structures showing the same splitting pattern for H_9 as in *N*-methyl-D-normorphinan (**3**) (see Table 2). The hydrogenolysis of the methoxy function in **5** with sodium in liquid ammonia established the position of substitution as C_{10}. The n.m.r. spectra of compounds **5** and **9** were ambiguous with respect to the assignment of the configuration of the methoxy and hydroxy functions relative to the alkylamino bridge. In order to resolve this problem compound **9** was oxidized with chromic acid (17) to 10-keto-*N*-benzyl-D-normorphinan (**11**) in 53% yield (69.5% based on alcohol consumed). The i.r. spectrum of **11** ($CHCl_3$ solution) showed a carbonyl absorption at 1682 cm^{-1} as expected for carbonyl adjacent to an aromatic ring. The n.m.r. spectrum of **11** shows deshielding of H_1 *ortho* to the carbonyl. The coupling constant for $H_9, J_{H_9H_{14}} = 5.0$ Hz, confirming the assignment of B/C-*cis* stereochemistry. Reduction of **11** with lithium aluminum hydride in ether gave a mixture of the 10-*trans*-hydroxy **9** and 10-*cis*-hydroxy-*N*-benzyl-D-normorphinan (**12**) in a ratio of 2:3 (99% yield). The epimeric alcohols were separated by chromatography. Compound **12** was hydrogenolyzed to 10-*cis*-hydroxy-D-normorphinan (**13**) in 82% yield.

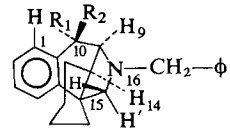

9 $R_1 = OH; R_2 = H$
12 $R_1 = H; R_2 = OH$

FIG. 1

Examination of a model of ketone **11** shows that the approach of hydride from the side opposite the alkylamino bridge might be expected to be slightly less hindered than from the same side leading one to predict that the formation of **12** over **9** should be favored as is the case. The configurational assignments to **9** and **12** have been made on the basis of their 100 MHz n.m.r. spectra and the magnitude of the $Eu(fod)_3$ induced shifts (18).

The 60 MHz n.m.r. spectra of the 10-substituted D-normorphinans are recorded in Table 2. In the spectra of the secondary amines, compounds **6**, **10**, and **13**, the protons on C_{15} appear as broadened singlets. On the other hand in the n.m.r. spectra of the *N*-benzyl substituted compounds **5**, **9**, **11**, and **12** the protons on C_{15} appear as pairs of doublets. An examination of molecular models indicates that in these compounds the benzyl group most likely adopts (for steric reasons) the configuration in which the benzyl group is on the side of the methyl amino bridge opposite the aromatic ring of the D-normorphinans. Consequently, we have assigned the upfield doublet (shielded) to H_{15}' and the downfield doublet to H_{15} (see Fig. 1).

The use of lanthanide shift reagents in the configurational assignment of pairs of isomers has been demonstrated for a number of systems (19) including alcohols (19*a*, *b*, *e*, *f*, and *g*), ethers (19 *g* and *i*), esters (19*h*), sulfoxides (19*c*), and phosphetan oxides (19*d*). A number of authors have shown the utility of lanthanide shift reagents in the analysis of the n.m.r. spectra of bifunctional compounds (20).

On addition of $Eu(fod)_3$ to compounds **9**, **11**, and **12** lanthanide induced shifts (l.i.s.) are

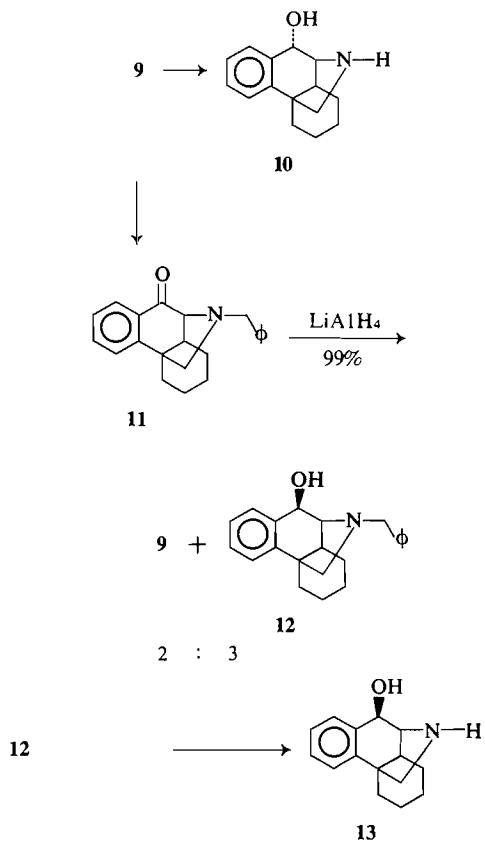

SCHEME 6

TABLE 3. Displacement induced by $Eu(fod)_3$[a]

Compound	H_1	$\Delta\delta$[b] $H_{10\text{-}cis}$	$H_{10\text{-}trans}$	H_9	H_{15}	H_{15}'	H_{16}	H_{16}'
9[c]	2.95	5.56	—	3.42	0.96	0.73	0.53	
12[d]	3.50	—	4.03	4.48	1.64	0.99	0.96	1.13
11[d]	3.48	—	—	4.01	1.24	1.37	2.17	2.48

[a]Mol $Eu(fod)_3$/mol compound = 0.31.
[b]$\Delta\delta = \delta$ Eu = 15 mg $- \delta$Eu = 0 mg expressed in p.p.m.
[c]Product concentration = 4.7×10^{-5} mol in 0.5 ml $CDCl_3$.
[d]Product concentration = 4.7×10^{-5} mol in 0.4 ml $CDCl_3$.

observed (recorded in Table 3). Presumably in the alcohols **9** and **12** the primary sites of coordination of the europium complex are the hydroxyl functions in competition with the tertiary amine. *A priori* one would predict a greater shift for protons on C_{15} in the isomer having the hydroxyl group oriented *cis* to the aminomethyl bridge. The observed l.i.s. for compounds **9** and **12** bear out this prediction. In the *cis* isomer **12** H_{15} and H_{15}' as well as H_9 and 2 H_{16} show considerably greater l.i.s. thus confirming the configurational assignments of compound **9** as the *trans* alcohol and compound **12** as the *cis* alcohol. The greater l.i.s. of H_1 in compound **12** is also to be expected in as much as the hydroxyl group in **12** is oriented in a pseudo equatorial position while that of compound **9** is pseudo axial. This relationship may also be deduced from the 100 MHz n.m.r. spectra of **9** and **12** before the addition of $Eu(fod)_3$. In compound **12** H_1 is more shielded than in compound **9** (7.44 *vs.* 7.30 δ). The possibility that the tertiary amine is the primary site of coordination of the $Eu(fod)_3$ in compounds **9** and **12** may be ruled out since if this were the case one would expect l.i.s. of greater magnitude for H_{15}, H_{15}' and the two H_{16} protons. The same argument would apply if the $Eu(fod)_3$ were to form a complex with the bidentate ligand in compound **12**.[6]

In the ketone **11** the results would seem to indicate a competition of the tertiary amine and keto functions for the $Eu(fod)_3$. While the magnitude of the l.i.s. for the protons at C_{15} and C_{16} is greater than in the alcohols **9** and **12** the relatively greater shifts for H_1 and H_9 indicate that some complex formation with the keto function must be occurring in competition with the amine.

[6]A similar argument has been used by Okutani and co-workers (20*b*) in their configurational assignment to the diastereoisomeric 1-cyclohexyl-2-phenylazetidin-3-ols. They have observed coordination of $Eu(DPM)_3$ to occur exclusively at the hydroxyl function in their compounds.

Experimental

The i.r. spectra were recorded on a Unicam Sp-200G grating i.r. spectrometer. The n.m.r. spectra were determined on a Varian A60-A spectrometer using tetramethyl silane as an internal standard, with the exception of compounds **9**, **11**, and **12** which were recorded at 100 Mc (see below). Melting points are uncorrected and were determined on a Gallenkamp melting point apparatus. The analyses were performed by Micro-Tech Laboratories, Skokie, Illinois. The 100 Mc spectra and $Eu(fod)_3$ experiments were carried out by Mr. R. Vulcano of Bristol Laboratories (Syracuse) whose assistance in this matter is gratefully acknowledged. The i.r. spectra of all compounds were compatible with the assigned structures.

Base-catalyzed Rearrangements of 4a-Aminomethyl-1,2,3,4,4a,9-hexahydrophenanthrenes

4a,10a-cis-4a-Aminomethyl-1,2,3,4a,10a-hexahydrophenanthrene (2a)

To a solution of 400 mg (1.88 mmol) of 4a-aminomethyl-1,2,3,4,4a,9-hexahydrophenanthrene **1***a* in 7 ml dry DMSO was added 400 mg (3.58 mmol) potassium *tert*-butoxide at ambient temperature ($\sim$23 °C). The solution initially turned green, then to deep red-brown and warmed slightly. The solution was stirred 30 min, poured into 50 ml water and extracted into methylene chloride (3 × 25 ml). The aqueous layer was saturated with NaCl and extracted with ether (1 × 25 ml). The organic extracts were washed with water (1 × 25 ml), dried over Na_2SO_4, filtered, and concentrated. The residue was taken up in 50 ml of ether and extracted into 10% HCl (3 × 10 ml). The aqueous phase was neutralized with Na_2CO_3 and extracted with methylene chloride (3 × 25 ml). The extracts were dried over Na_2SO_4, filtered, and evaporated to yield 288.3 mg (73%) of pure (as determined by n.m.r.) 4a,10a-*cis*-4a-aminomethyl-1,2,3,4,4a,10a-hexahydrophenanthrene, b.p. 122–125°/0.01 mm. The amine formed a hygroscopic hydrochloride, m.p. 205–210 °C (dec.) (recrystallized from methanol–ether).

Anal. Calcd. for $C_{15}H_{19}N{\cdot}HCl{\cdot}3/8H_2O$: C, 70.22; H, 8.15; N, 5.46. Found: C, 70.40; H, 8.05; N, 5.59.

N-Methyl-4a,10a-cis-4a-aminomethyl-1,2,3,4,4a,10a-hexahydrophenanthrene (2b)

Treatment of 2.41 g (10.20 mmol) of *N*-methyl-4a-aminomethyl-1,2,3,4,4a,9-hexahydrophenanthrene with 620 mg (5.5 mmol) of potassium *tert*-butoxide in 90 ml dry DMSO for 72 h at ambient temperature gave 1.26

Can. J. Chem. Downloaded from www.nrcresearchpress.com by 210.87.254.42 on 09/05/12
For personal use only.

Can. J. Chem. Downloaded from www.nrcresearchpress.com by 210.87.254.42 on 09/05/12
For personal use only.

g (52%) of *N*-methyl-4a,10a-*cis*-aminomethyl-1,2,3,4,4a,-10a-hexahydrophenanthrene after the usual work-up (see above). The amine formed a crystalline oxalate, m.p. 203–203.5 °C (recrystallized from methanol).

Anal. Calcd. for $C_{16}H_{21}N{\cdot}C_2H_2O_4$: C, 68.12; H, 7.30; N, 4.41. Found: C, 68.31; H, 7.35; N, 4.56.

N-Benzyl-4a-aminomethyl-4a,10a-cis,1,2,3,4,4a,10a-hexahydrophenanthrene (2c)

Method A. To 1.30 g (6.1 mmol) of 4a,10a-*cis*-4a-aminomethyl-1,2,3,4,4a,10a-hexahydrophenanthrene **2a** in 10 ml ethanol was added 0.645 g (6.1 mmol) benzaldehyde. The solution was let stand 1 h at room temperature, 0.29 g (6.1 mmol) sodium borohydride was added, and the solution stirred 1 h at room temperature. The solution was poured into 50 ml water and extracted into methylene chloride (3 × 25 ml), the extracts were dried over Na_2SO_4 and evaporated to yield 1.95 g (quantitative) of *N*-benzyl-4a-aminomethyl-4a,10a-*cis*-1,2,3,4,-4a,10a-hexahydrophenanthrene. The amine formed a hygroscopic hydrochloride, m.p. 243–245 °C (decomposition) (recrystallized from methanol – ethyl acetate).

Anal. Calcd. for $C_{22}H_{25}N{\cdot}HCl{\cdot}1/2H_2O$: C, 75.73; H, 7.79; N, 4.01. Found: C, 75.81; H, 7.75; N, 3.99.

Method B. Treatment of *N*-benzyl-4a-aminomethyl-1,2,3,4,4a,9-hexahydrophenanthrene hydrochloride (16.57 g, 0.049 mol) with 16.0 g (0.141 mol) of potassium *tert*-butoxide in 100 ml dry DMSO at ambient temperature for 30 min gave, after the usual work-up, 15.1 g of an oil. The oil was taken up in 150 ml of ether and the amine hydrochloride was precipitated to yield 14.77 g (89%) of the salt, m.p. 243–245 °C (dec.).

6-Methoxy-N-methyl-4a,10a-cis-4a-aminomethyl-1,2,3,4,4a,10a-hexahydrophenanthrene (2d)

Treatment of 3.40 g (11.5 mmol) of 6-methoxy-*N*-methyl-4*a*-aminomethyl-1,2,3,4,4*a*,9-hexahydrophenanthrene with 3.40 g (30 mmol) of potassium *tert*-butoxide in 25 ml dry DMSO for 24 h at ambient temperature followed by the usual work-up gave 2.05 g of a pale brown oil. The hydrochloride salt was prepared and recrystallized from isopropanol–ether, m.p. 208–209 °C. The salt was treated with 20% Na_2CO_3 and re-extracted into ether. The extract was dried over Na_2SO_4 and evaporated to give 1.80 g (65%) of pure 6-methoxy-*N*-methyl-4a-aminomethyl-4a,10a-*cis*-1,2,3,4,4a,10a-hexahydrophenanthrene b.p. 139–141 °C/0.25 mm. Pure hydrochloride salt was prepared for analysis, m.p. 209–209.5 °C.

Anal. Calcd. for $C_{17}H_{23}NO{\cdot}HCl{\cdot}1/5H_2O$: C, 68.65; H, 8.27; N, 4.71. Found: C, 68.69; H, 8.38; N, 4.55.

N-Methyl-D-normorphinan (3)

Method A

From N-Methyl-4a-aminomethyl-1,2,3,4,4a,10a-hexahydrophenanthrene (2b). A solution of 900 mg (4.0 mmol) of *N*-methyl-4a-aminomethyl-1,2,3,4,4a,10a-hexahydrophenanthrene **2b** in 5 ml of dry benzene was added (under nitrogen and with magnetic stirring) to a solution of lithium diisopropylamide (prepared by adding 0.80 ml of a 5.07 *N* solution of methyl lithium in ether to a mixture of 0.56 ml (4 mmol) diisopropylamine in 15 ml dry benzene at 25 °C). The reaction mixture was refluxed for 4 h, cooled to 25 °C, and an equal volume of water added. The organic phase was separated, washed twice with water (20 ml), dried over Na_2SO_4, filtered, and evaporated at reduced pressure to yield 640 mg (71%) of *N*-methyl-D-normorphinan (**3**). The cyclohexylsulfamate salt of this material was prepared, m.p. 117–118.5 °C (recrystallized from ethanol–ether).

Anal. Calcd. for $C_{16}H_{21}N{\cdot}C_6H_{13}NO_2S$: C, 64.99; H, 8.43; N, 6.89; S, 7.89. Found: C, 64.81; H, 8.54; N, 6.79; S, 7.82.

Method B

From N-Methyl-4a-aminomethyl-1,2,3,4,4a,9-hexahydrophenanthrene (1b)

To a solution of 100.6 g (0.543 mol of *N*-methyl-4a-aminomethyl-1,2,3,4,4a,9-hexahydrophenanthrene in 730 ml of dry DMSO was added 32.0 g (0.286 mol) potassium *tert*-butoxide. The solution was stirred at room temperature for 140 h at which time an additional 13.5 g (0.120 mol) of potassium *tert*-butoxide was added. The solution was heated to 35–38 °C for 20 h, poured into 4 l of ice water, and extracted with ether (3 × 500 ml). The organic phase was extracted with 3 *N* HCl (3 × 100 ml), the aqueous layer made alkaline with 30% NaOH and extracted into ether (3 × 100 ml). The extracts were dried over Na_2SO_4 and concentrated to yield 51.5 g of crude *N*-methyl-D-normorphinan (**3**). The compound was distilled to yield 31.26 g (31%) of pure *N*-methyl-D-normorphinan, b.p. 108–114 °C/0.005 mm. An additional 4.4 g, b.p. 114–125 °C/0.005 mm was also obtained. A small sample was redistilled, b.p. 98–101 °C/0.05 mm (bath 150 °C).

N-Benzyl-N-chloro-4a,10a-cis-4a-aminomethyl-1,2,3,4,4a,10a-hexahydrophenanthrene (4)

To a solution of 9.09 g (30 mmol) of *N*-benzyl-4a,10a-*cis*-4a-aminomethyl-1,2,3,4,4a,10,10a-hexahydrophenanthrene **2c** in 100 ml of dry methylene chloride was added 4.0 g (30 mmol) *N*-chlorosuccinimide (16). The solution was stirred 30 min, washed with water (4 × 25 ml), dried over Na_2SO_4, and concentrated to yield 10.2 g of an oily *N*-chloro derivative. The n.m.r. spectrum of **4** was compatible with the assigned structure.

10-trans-Methoxy-N-benzyl-D-normorphinan (5)

Chloramine **4** (10.11 g, 30 mmol prepared from 9.09 g amine) was placed in 250 ml of dry methanol and boiled at reflux for 18 h. The solvent was removed at reduced pressure, the residue taken up in 50 ml of water, neutralized with Na_2CO_3, and extracted into ether (4 × 25 ml). The extracts were shaken with 25 ml of 10% HCl. A solid separated which was removed by filtration to give 2.0 g of the hydrochloride salt of the starting amine **2c**. The aqueous layer was neutralized with solid Na_2CO_3 and extracted into ether. The extracts were dried over Na_2SO_4 and concentrated to yield 5.12 g of 10-*trans*-methoxy-*N*-benzyl-D-normorphinan (**5**) contaminated with ~5% starting amine. A small sample was chromatographed on Florisil with ϕH–Et_2O (19:1) to give pure **5** as an oil. The amine was converted to its hydrochloride salt which was amorphous.

Anal. Calcd. for $C_{23}H_{27}NO{\cdot}HCl$: C, 74.67; H, 7.62; N, 3.79. Found: C, 74.39; H, 7.83; N, 3.85.

10-trans-Methoxy-D-normorphinan (6)

A mixture of 2.59 g (7.8 mmol) 10-*trans*-methoxy-*N*-benzyl-D-normorphinan and 100 mg 10% Pd/C in 50 ml acetic acid was hydrogenated at atmospheric pressure at 22 °C. When 1 equiv. H_2 had been absorbed, the solution was filtered and evaporated. The residue was taken up in 50 ml of water, neutralized with Na_2CO_3, saturated

Can. J. Chem. Downloaded from www.nrcresearchpress.com by 210.87.254.42 on 09/05/12
For personal use only.

with NaCl, and extracted into methylene chloride (3 × 50 ml). The extracts were dried over Na_2SO_4, filtered, and evaporated to yield 1.68 g of an oil. Trituration with 5 ml ether and filtration gave 1.35 g of pure 10-*trans*-methoxy-D-normorphinan (**6**) as a solid, m.p. 105–107 °C.

Anal. Calcd. for $C_{16}H_{21}NO$: C, 78.97; H, 8.70; N, 5.76. Found: C, 78.67; H, 8.83; N, 5.77.

N-Benzyl-D-normorphinan (7)

To a solution of 0.05 g sodium in 30 ml of liquid ammonia was added 462.3 mg (1.39 mmol) of 10-*trans*-methoxy-*N*-benzyl-D-normorphinan **5** in 20 ml ether over 5 min. The solution was stirred 10 min and 3 ml ethanol added over 1 min to quench the excess sodium. The ammonia was allowed to evaporate and the residue partitioned between water and ether. The ethereal extracts were dried over Na_2SO_4, filtered, and evaporated to yield 274.4 mg crude *N*-benzyl-D-normorphinan (65%). The oil was chromatographed on Florisil (20 g) with benzene–ether (9:1) to give 200 mg (47.5%) pure compound 7 as an oil.[7] Compound 7 formed an amorphous hydrochloride salt.

Anal. Calcd. for $C_{22}H_{25}N{\cdot}HCl{\cdot}3/4H_2O$: C, 74.76; H, 7.84; N, 3.96. Found: C, 74.70; H, 7.95; N, 4.01.

D-*Normorphinan (8)*

Hydrogenation of 464.6 mg (1.53 mmol) of *N*-benzyl-D-normorphinan (7) over 50 mg 10% Pd/C in acetic acid (50 ml) gave after work-up (see preparation of **6**) 243.5 mg (75%) of D-normorphinan (**8**), b.p. 118–120 °C/0.06 mm. On standing in carbon tetrachloride a crystalline carbonate formed, m.p. 98 °C (with gas evolution), which contained carbon tetrachloride.

Anal. Calcd. for $C_{15}H_{19}N{\cdot}H_2CO_3{\cdot}1.25\ CCl_4$: C, 44.30; H, 4.52; N, 2.99. Found: C, 44.47; H, 4.68; N, 3.15.

Careful drying of the sample (below 50 °C) gave the carbonate.

Anal. Calcd. for $C_{15}H_{19}N{\cdot}H_2CO_3$: C, 69.79; H, 7.68; N, 5.08. Found: C, 69.87; H, 8.08; N, 5.46.

10-trans-Hydroxy-N-benzyl-D-normorphinan (9)

A solution of 10.11 g (30 mmol) chloramine **4** in 150 ml THF–H_2O (4:1) was refluxed 18 h. The solution was evaporated and the residue partitioned between ether-saturated $NaHCO_3$ (200–50 ml). The ethereal extract was dried over Na_2SO_4. Evaporation gave 8.63 g of an oil. Thin-layer chromatography (10% EtOAc-ϕH) on alumina indicated the presence of 2 major components one of which was the starting amine. The oil was chromatographed on 650 g of alumina (Act II) via dry-column technique (21) using 20% EtOAc–ϕH as eluting solvent. In this manner 2.33 g pure starting amine (25.6%) was recovered (elutes 1st from the column) and 3.25 g of the desired 10-*trans*-hydroxy-*N*-benzyl-D-normorphinan (34%; 45% conversion) was obtained as a crystalline solid, m.p. 124–125 °C. A small sample was converted to its hydrochloride salt. This salt did not give a sharp m.p. (dec.), 140–160 °C.

Anal. Calcd. for $C_{22}H_{25}NO{\cdot}HCl$: C, 74.24; H, 7.36; N, 3.93. Found: C, 74.52; H, 7.44; N, 3.89.

[7]In larger scale experiments yields as high as 90% of **7** could be obtained. The average yield for four experiments was 71%.

10-trans-Hydroxy-D-normorphinan (10)

Hydrogenation of 2.233 g (7 mmol) of 10-*trans*-hydroxy-*N*-benzyl-D-normorphinan (**9**) over 100 mg 10% Pd/C in 50 ml acetic acid in the usual manner yielded 1.43 g of a gum. On trituration with benzene the gum crystallized. Filtration gave 1.05 g (66%) pure 10-*trans*-hydroxy-D-normorphinan, m.p. 142–143 °C (recrystallized from benzene). The amino alcohol gave an amorphous hydrochloride salt.

Anal. Calcd. for $C_{15}H_{19}NO{\cdot}HCl$: C, 67.78; H, 7.58; N, 5.27. Found: C, 67.62; H, 7.42; N, 5.12.

10-Keto-N-benzyl-D-normorphinan (11)

A solution of chromic acid was prepared according to the method of Brown *et al.* (17). To 10 g (0.033 mol) sodium dichromate dihydrate in 30 ml of water was added 13.6 g sulfuric acid (0.134 mol). The solution was then diluted to 50 ml with water.

To 1.75 g (5.5 mmol) 10-*trans*-hydroxy-*N*-benzyl-D-normorphinan **10** in 20 ml acetone – 10 ml water was added 4 ml of the CrO_3 solution. The resultant solution was stirred 18 h at room temperature (~22 °C). The solution was diluted to 100 ml with water, neutralized with solid sodium carbonate and extracted into ether (5 × 20 ml). The extracts were dried over Na_2SO_4, filtered, and evaporated to yield 1.65 g of an oil. The oil was chromatographed on Alumina (Act III) with benzene: 0.41 g (23%) starting material and 0.94 g (53.5%, 69.5% conversion) of 10-keto-*N*-benzyl-D-normorphinan (**11**) were obtained. Recrystallization of the ketone from benzene gave white needles, m.p. 106–106.5 °C.

Anal. Calcd. for $C_{22}H_{23}NO$: C, 83.24; H, 7.30; N, 4.41. Found: C, 83.34; H, 7.28; N, 4.29.

10-cis-Hydroxy-N-benzyl-D-normorphinan (12)

To a solution of 800 mg (2.52 mmol) 10-keto-*N*-benzyl-D-normorphinan **11** in 25 ml dry ether at 25 °C was added 0.3 ml of a 4 *M* lithium aluminum hydride solution. The solution was stirred 5 min at 25 °C and cooled to 0–5 °C in an ice bath. To this was added 0.05 ml water. The suspension was stirred 5 min at 20 °C and filtered. Evaporation of the filtrate gave 800 mg of a mixture of the 10-*trans*- and 10-*cis*-hydroxy-*N*-benzyl-D-normorphinans **9** and **12**. Trituration of the gum with 25 ml of petroleum ether (30–60°) caused partial crystallization of the 10-*trans* isomer. The mother liquors (enriched in 10-*cis* isomer) were evaporated and chromatographed on 70 g of alumina (Activity III) via dry-column technique using benzene – ethyl acetate (9 l) as the eluting solvent. 10-*cis*-Hydroxy-*N*-benzyl-D-normorphinan **13** was obtained as an oil; 470 mg (59.5%). The 10-*trans*-hydroxy isomer totaled 320 mg (40.5%) (total yield (99%).

The 10-*cis*-hydroxy isomer formed a crystalline hydrochloride, m.p. 276–278 °C (dec.) (recrystallized from methanol – ethyl acetate).

Anal. Calcd. for $C_{22}H_{25}NO{\cdot}HCl$: C, 74.24; H, 7.36; N, 3.94. Found: C, 74.27; H, 7.39; N, 3.83.

10-cis-Hydroxy-D-normorphinan (13)

Hydrogenation of 319 mg (1 mmol) of 10-*cis*-hydroxy-*N*-benzyl-D-normorphinan **12** in 20 ml acetic acid over 100 mg 10% Pd/C in the usual manner gave 251 mg of an oil. Trituration of the oil with 5 ml of ether induced crystallization. Filtration gave 190 mg (82%) of the

desired 10-*cis*-hydroxy-D-normorphinan **13**. The sample was recrystallized from benzene, m.p. 165–166 °C.

Anal. Calcd. for $C_{15}H_{19}NO$: C, 78.57; H, 8.35; N, 6.10. Found: C, 78.72; H, 8.48; N, 5.99.

1. B. BELLEAU, T. T. CONWAY, T. W. DOYLE, L. MORRIS, W. VERBESTEL. Can. J. Chem. This issue.
2. (*a*) R. WEGLER and G. PIEPER. Chem. Ber. **83**, 1 (1950). C.A. **44**, 5321 (1950); (*b*) R. J. SCHLOTT, J. C. FALK, and K. W. NARDUCY. J. Org. Chem. **37**, 4243 (1972).
3. K. FRETER, E. DUBOIS, and A. THOMAS. J. Heterocycl. Chem. **7**, 159 (1970).
4. W. E. DOERING and R. A. N. WEIL. J. Am. Chem. Soc. **69**, 2461 (1971).
5. M. GATES, B. SUGAVANAM, and W. L. SCHREIBER. J. Am. Chem. Soc. **92**, 205 (1970).
6. (*a*) A. HUBERT and H. REIMLINGER. Synthesis, 97 (1969); (*b*) C. D. BROADDUS. Acc. Chem. Res. **1**, 231 (1968); (*c*) D. J. CRAM. Fundamentals of carbanion chemistry. Academic Press, New York and London. 1965. pp. 175–210.
7. (*a*) M. KARPLUS. J. Am. Chem. Soc. **85**, 2870 (1963); (*b*) S. STERNWELL. Q. Rev. **23**, 236 (1969).
8. W. L. NELSON, D. D. MILLER, and E. SHEFTER. J. Org. Chem. **35**, 3433 (1970).
9. T. J. NIEUWSTAD and H. VAN BEKKUM. Recueil, **91**, 1069 (1971).
10. (*a*) P. G. GASSMAN. Acc. Chem. Res. **3**, 26 (1970); (*b*) P. KOVACIC, M. K. LOWERY, and K. W. FIELD. Chem. Rev. **70**, 639 (1970).
11. P. G. GASSMAN and J. H. DYGOS. Tetrahedron Lett. 4745, (1970); 4749 (1970).
12. A. HEUMANN, R. FURSTOSS, and B. WAEGELL. Tetrahedron Lett. 993 (1972).
13. J. M. SURZUR, L. STELLA, and P. TORDO. Tetrahedron Lett. 3107 (1970).
14. (*a*) O. E. EDWARDS, G. BERNATH, J. DIXON, J. M. PATON, and D. VOCELLE. Can. J. Chem. **52**, 2123 (1974); (*b*) J. D. HOBSON and W. D. RIDDELL. Chem. Commun. 1178 (1968). J. W. BASTABLE, J. D. HOBSON, and W. D. RIDDELL. J. Chem. Soc. C, 2205 (1972).
15. R. S. NEALE. Tetrahedron Lett. 483 (1966); J. Org. Chem. **32**, 3263 (1967); R. S. NEALE and N. L. MARCUS. J. Org. Chem. 3273 (1967).
16. T. NAKANO and Z. VOTICKÝ. J. Chem. Soc. C, 590 (1970).
17. H. C. BROWN, C. P. GARG, and K-T. LIU. J. Org. Chem. **36**, 387 (1971).
18. R. E. SIEVERS (*Editor*) Nuclear magnetic resonance shift reagents. Academic Press, New York and London. 1973.
19. (*a*) P. V. DEMARCO, T. K. ELZEY, R. B. LEWIS, and E. WENKERT. J. Am. Chem. Soc. **92**, 5734 (1970); (*b*) J. BRIGGS, F. A. HART, and G. P. MOSS. Chem. Soc. D, 1506 (1970); (*c*) R. R. FRASER and Y. Y. WIGFIELD. J. Chem. Soc. D, 1471 (1970); (*d*) J. R. CORFIELD and S. TRIPPET. J. Chem. Soc. D, 721 (1971); (*e*) P. BELANGER, C. FREPPEL, D. TIZANE, and J. C. RICHER. Can. J. Chem. **49**, 1985 (1971); (*f*) B. L. SHAPIRO, J. R. HLUBUCEK, G. R. SULLIVAN, and L. F. JOHNSON. J. Am. Chem. Soc. **93**, 3281 (1971); (*g*) M. R. WILLCOTT, J. F. M. OTH, J. THIO, G. PLINKE, and G. SCHRODER. Tetrahedron Lett. 1579 (1971); (*h*) L. F. JOHNSON, J. CHAKRAVARTY, R. DASGUPTA, and U. R. GHATAK. Tetrahedron Lett. 1703 (1971); (*i*) J. F. CAPUTO and A. R. MARTIN. Tetrahedron Lett. 4547 (1971).
20. (*a*) G. MONTAUDO and P. FINOCCHIARO. J. Org. Chem. **37**, 3434 (1972); (*b*) T. OKUTANI, A. MORIMOTO, T. KANEKO, and K. MASUDA. Tetrahedron Lett. 1115 (1971).
21. B. LOEV and M. M. GOODMAN. Intra-Science Chem. Rep. **4**, 283 (1970).

Can. J. Chem. Downloaded from www.nrcresearchpress.com by 210.87.254.42 on 09/05/12
For personal use only.

Chemistry of Proximal π-Bond Systems. Part III.[1] Synthesis of Substituted Benzopolycyclic Hydrocarbons

D. N. BUTLER AND R. A. SNOW

Chemistry Department, York University, Toronto, Ontario M3J 1P3

Received August 7, 1974

D. N. BUTLER and R. A. SNOW. Can. J. Chem. **53**, 256 (1975).

A series of 21 bridged, vicinal, exocyclic dimethylene hydrocarbons (**1–21**) have been converted to the related benzopolycyclic dimethyl esters (**C1–C21**) by oxidation of their respective dimethyl acetylenedicarboxylate Diels–Alder adducts (**B1–B21**).

This synthetic sequence represents an excellent, general route to aromatic ring-substituted benzopolycyclic hydrocarbons.

D. N. BUTLER et R. A. SNOW. Can. J. Chem. **53**, 256 (1975).

On a transformé une série de 21 hydrocarbures (**1–21**) pontés comportant des diméthylènes exocycliques vicinaux en esters diméthyliques des dérivés benzopolycycliques correspondants (**C1–C21**); cette conversion s'est effectuée par oxydation des adduits de Diels–Alder (**B1–B21**) provenant de la réaction entre les hydrocarbures **1–21** avec l'acétylènedicarboxylate de méthyle.

Cette séquence synthétique représente une excellente route générale pour conduire à des hydrocarbures benzopolycycliques substitués sur le noyau aromatique.

[Traduit par le journal]

Introduction

The incorporation of benzo anellation into bi- and polycyclic hydrocarbons has been used in recent literature (1) to compare the mechanisms of the thermal, photochemical, or solvolytic rearrangements or isomerisms in these systems with those in the corresponding parents by locating one (or more) of the π-bonds in a benzene ring (or rings). The most general preparative route to these compounds involves benzyne cycloadditions (π^2s and π^4s) to suitable conjugated cyclic dienes (2). However, such syntheses do not easily lend themselves to benzene-ring substituted derivatives and indeed, in most of the examples described herein, only the parent hydrocarbons have been synthesized.

The possibility of exploitation of the well known effects of aromatic substituents (perhaps best illustrated in the work of Tanida *et al.* (3*a*) and Brown and Tritle (3*b*) relating to the benzonorbornane system) in unravelling mechanistic details, as well as the positional labels such substitution affords, make a general synthesis of ring-substituted benzo bi- and polycyclic hydrocarbons desirable. The availability of a series of related vicinal exocyclic dimethylene hydrocarbons (4) has allowed the realization of this synthetic goal.

[1]For Part II see ref. 14.

Results and Discussion

The three dienes **16**, **17**, and **18** have not been described prior to this work. They were respectively prepared via the tosylation – base-catalyzed double elimination route (4) from the corresponding *trans*-bis primary alcohols **22***a*, **23***a*, and **24***a*.

The silver-catalyzed rearrangement (5) of dimethyl pentacyclo[4.2.2.$0^{2,5}$.$0^{3,8}$.$0^{4,7}$]decane-(*trans*)-9,10-dicarboxylate (6) to the dimethyl snoutane dicarboxylate **22***b* provided, after reduction, the intermediate diol **22***a* necessary for diene **16**. For hydrocarbon **17**, dimethyl tetracyclo[4.3.0.$0^{2,4}$.$0^{3,7}$]nonane-(*endo,cis*)-8,9-dicarboxylate (7) was epimerized ($NaOCH_3$–CH_3OH) to the *trans*-diester **23***b*, before reduction ($LiAlH_4$) to the corresponding diol **23***a*. For **18**, the known adduct of indene and maleic anhydride (8) was hydrolyzed and esterified (diazomethane) to the *cis*-dimethyl ester before epimerization to **24***b* and reduction to the *trans*-diol, **24***a*, as above.

The dienes 1–21 were readily characterized as their respective tetracyanoethylene (TCNE) adducts, **A1–A21** (where X and Y represent the corresponding bridge moieties of the hydrocarbon structures **1–21**). In every case these compounds corresponded to the expected 1:1 Diels–Alder adducts as indicated by their respective, predicted parent ions in the mass

Can. J. Chem. Downloaded from www.nrcresearchpress.com by 210.87.254.105 on 09/05/12
For personal use only.

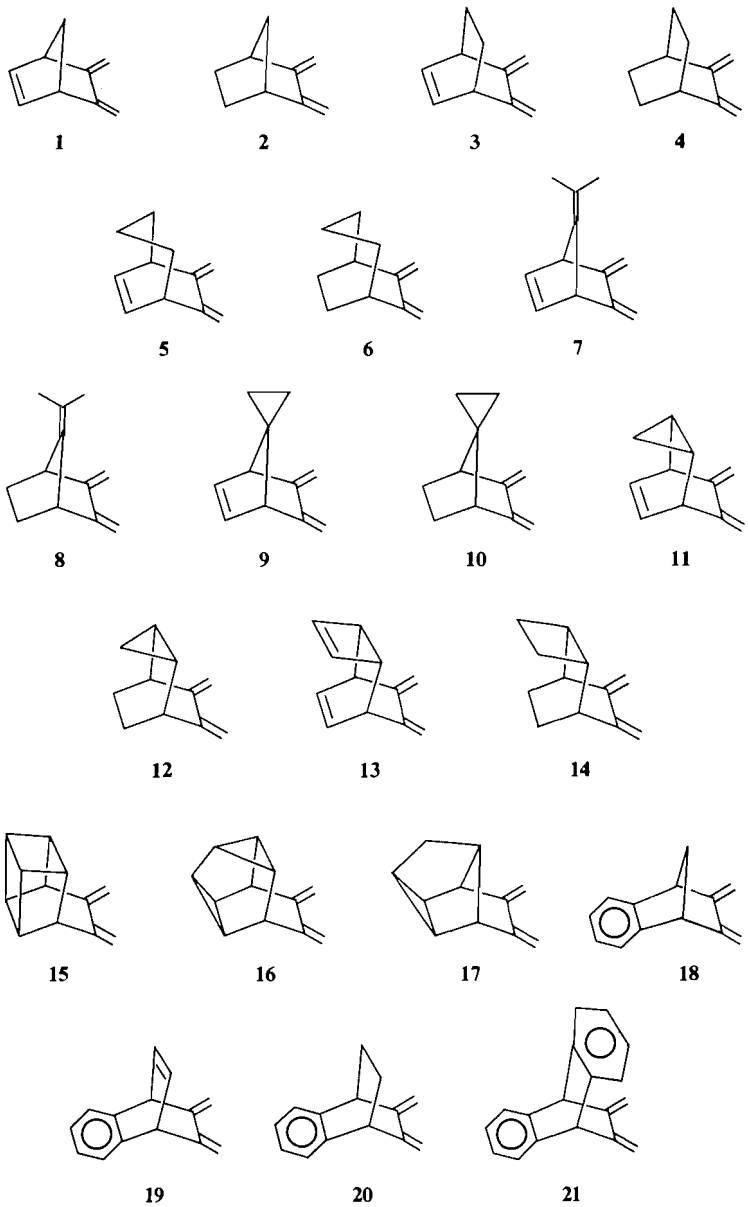

spectra and their consentaneous p.m.r. spectra.[2] The melting points of these adducts are recorded in the Experimental section.

Whereas the TCNE additions to the dienes were very rapid (typically less than 5 min for completion in tetrahydrofuran solvent), the reactions with dimethyl acetylenedicarboxylate (DMAD) in CCl_4 solvent showed considerable rate differences ranging from less than 5 min for **4** (fastest) to 2 days at reflux temperature (75°) for **9** (slowest) for complete reaction. In general, those of the hydrocarbons **1**–**21** containing the diene fragment on a five-membered ring were the slowest to react in spite of the locked *cisoid* conformation of the diene. At present, a quantitative study of the Diels–Alder reaction rates of

[2]Spectroscopic and analytical data have been placed in the Depository of Unpublished Data. Copies of the material in the Depository may be obtained at a nominal charge, from the Depository of Unpublished Data, National Science Library, National Research Council of Canada, Ottawa, Canada K1A 0S2.

Can. J. Chem. Downloaded from www.nrcresearchpress.com by 210.87.254.105 on 09/05/12
For personal use only.

Can. J. Chem. Downloaded from www.nrcresearchpress.com by 210.87.254.105 on 09/05/12
For personal use only.

TABLE 1. DMAD Adducts **B1**–**B21**; physical and spectroscopic data[a]

Adduct	Melting point (°C)	Molecular formula	Observed parent ion *m/e*	Proton magnetic resonance assignments[b]: Vicinal vinyl —C(H)=C(H)—	Bridgehead —C(H)—	Ester —CH_3	Dihydro aromatic —CH_2—	Other proton assignments
B1	57	$C_{15}H_{16}O_4$	260	6.72 (2H)	3.33 (2H)	3.68 (6H)	3.09 (4H)	1.99 (2H)[e]
B2	73.5–74.5[c]	$C_{15}H_{18}O_4$	262	—	2.70 (2H)	3.68 (6H)	3.01 (4H)	0.91–1.80 (6H)[e]
B3	60.5–61.5	$C_{16}H_{18}O_4$	274	6.23 (2H)	3.31 (2H)	3.67 (6H)	3.05 (4H)	1.29 (4H)[e]
B4	60.5–61.5[d]	$C_{16}H_{20}O_4$	276	—	2.29 (2H)	3.70 (6H)	3.04 (4H)	1.15–1.65 (8H)[e]
B5	45 – 46	$C_{17}H_{20}O_4$	288	6.17 (2H)	2.61 (2H)	3.70 (6H)	3.03 (4H)	1.15–1.83 (6H)[e]
B6	26	$C_{17}H_{22}O_4$	290	—	2.13 (2H)	3.69 (6H)	2.96 (4H)	1.31–1.91 (10H)[e]
B7	99.5–101	$C_{18}H_{20}O_4$	300	6.87 (2H)	3.85 (2H)	3.75 (6H)	3.17 (4H)	1.45 (6H) *gem* dimethyl
B8	63 – 64	$C_{18}H_{22}O_4$	300[f]	—	3.04–3.17 (2H)	3.76 (6H)	3.04–3.17 (4H)	0.96–1.73 (4H)[e]; 1.55 (6H) *gem* dimethyl
B9	61.5–62	$C_{17}H_{18}O_4$	286	6.75 (2H)	2.76 (2H)	3.68 (6H)	3.10 (4H)	0.45 (4H) cyclopropyl
B10	87.5–88	$C_{17}H_{20}O_4$	288	—	1.98 (2H)	3.69 (6H)	3.03 (4H)	1.04–1.95 (4H)[e]; 0.20–0.54 (4H) cyclopropyl
B11	80.5–81.5	$C_{17}H_{18}O_4$	286	5.92 (2H)	3.32 (2H)	3.68 (6H)	3.13 (4H)	0.35–1.22 (4H) cyclopropyl
B12	100 –101	$C_{17}H_{20}O_4$	288	—	2.44 (2H)	3.70 (6H)	3.12 (4H)	0.51–1.56 (8H)[e] and cyclopropyl
B13	95 – 96	$C_{18}H_{18}O_4$	298	6.00–6.11 (4H)	3.10–3.24 (2H)	3.76 (6H)	3.10–3.24 (4H)	2.49–2.61 (2H) cyclobutenyl
B14	87.5–88.5	$C_{18}H_{22}O_4$	302	—	→	3.78 (6H)	3.09 (4H)	0.98–1.28 (2H) and 1.80–2.29 (10H)[e] cyclobutyl and bridgehead
B15	89 – 90	$C_{18}H_{18}O_4$	298	—	→	3.78 (6H)	3.19 (4H)	2.79–3.56 (8H) cyclobutyl and bridgehead
B16	138 –139	$C_{18}H_{18}O_4$	298	—	2.96 (2H)	3.73 (6H)	3.20 (4H)	2.09–2.23 (2H) and 1.52–1.68 (4H) cyclopropyl
B17	95 – 96	$C_{17}H_{18}O_4$	286	—	2.43 (2H)	3.67 (6H)	3.06 (4H)	1.28–1.93 (6H)[e]; cyclopropyl and bridgehead
B18	71 – 71.5	$C_{19}H_{18}O_4$	310	—	3.58 (2H)	3.63 (6H)	3.05 (4H)	6.74–7.14 (4H) aromatic; 2.22 (2H)[e]
B19	73.5–74.5	$C_{20}H_{18}O_4$	322	6.74 (2H)	4.48 (2H)	3.67 (6H)	3.18 (4H)	6.66–7.14 (4H) aromatic
B20	104.5–105.5	$C_{20}H_{20}O_4$	324	—	3.65 (2H)	3.75 (6H)	3.17 (4H)	6.86–7.39 (4H) aromatic; 1.23–1.73 (4H)[e]
B21	177 –178	$C_{24}H_{20}O_4$	372	—	4.70 (2H)	3.63 (6H)	3.23 (4H)	6.80–7.24 (8H) aromatic

[a]Analytical data have not been obtained.
[b]δ value, determined in 10% CCl_4 solution using TMS as internal standard; centers of multiplets or ranges indicated.
[c]Literature m.p. 76° (9).
[d]Literature m.p. 65° (10).
[e]Protons in saturated bridge or bridges.
[f]$M^+ - 2$.

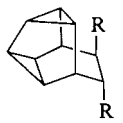

22

a R = —CH_2OH
b R = —$COOCH_3$

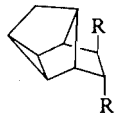

23

a R = —CH_2OH
b R = —$COOCH_3$

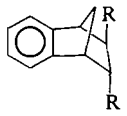

24

a R = —CH_2OH
b R = —$COOCH_3$

certain of these dienes is underway to try to correlate the spectroscopic data with geometric and reactivity parameters. Only two of these DMAD adducts have been described previously (**B2** (9) and **B4** (10)). The Diels–Alder reaction yields were all quantitative as indicated by p.m.r. spectroscopy, although isolation of the crystalline adducts was difficult in many cases and is not necessary if the benzopolycyclics, **C1–C21**, are the synthetic goal.

The spectral evidence supporting the expected adduct structures **B1–B21** is collected in Table 1. No 2:1 or other unexpected products were observed under the equimolar conditions used for these reactions.

Oxidation of these 21 DMAD adducts **B1–B21** in benzene at room temperature with 2,3-dichloro-5,6-dicyanobenzoquinone (DDQ) afforded the benzopolycyclic dimethyl esters **C1–C21**, in quantitative yield. Isolation as crystals was again very difficult in many cases and several of these compounds failed to crystallize. These were hydrolyzed to the corresponding phthalic acids to obtain analytical samples.

The spectroscopic data compiled in Table 2 leave no doubt as to the structures **C1–C21** as shown. One of these bridged benzene diesters, **C2**, is known (11).

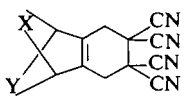

A1–A21

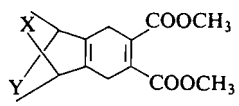

B1–B21

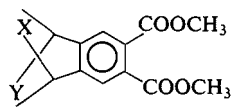

C1–C21

Adduct **B20** lost ethylene on heating at 230° in an oil bath to furnish **25** which was readily oxidized by DDQ to **26**, shown to be identical to the known dimethyl anthracene-2,3-dicarboxylate (12).

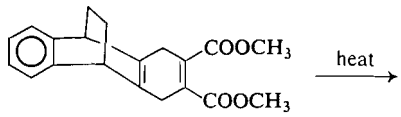

B20

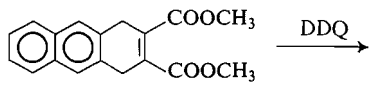

25

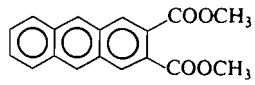

26

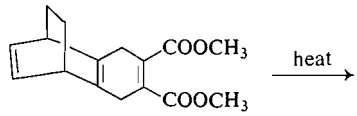

B3

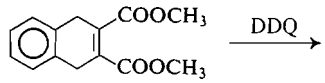

27

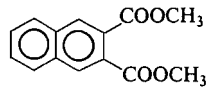

28

Entirely similar chemistry was observed for **B3** with respect to dimethyl 1,4-dihydronaphthalene-2,3-dicarboxylate (**27**) and dimethyl naphthalene-2,3-dicarboxylate (**28**) (13).

In conclusion, these syntheses obviously provide an efficient route into aromatic ring-substituted benzopolycyclic hydrocarbon systems. Other dienophiles such as propiolic esters, mono- and dicyanoacetylene, phenylacetylene, quinones, etc. would obviously extend the utility of the method. One limitation is the unreactivity of certain of the dienes. For example, reaction of **21** with tolan was unsuccessful even at elevated temperatures. DMAD was chosen to

Can. J. Chem. Downloaded from www.nrcresearchpress.com by 210.87.254.105 on 09/05/12
For personal use only.

Can. J. Chem. Downloaded from www.nrcresearchpress.com by 210.87.254.105 on 09/05/12
For personal use only.

TABLE 2. Benzopolycyclic dimethyl esters, **C1–C21**; physical and spectroscopic data[a]

Compound	Melting point (°C)	Molecular formula	Observed parent ion *m/e*	Proton magnetic resonance assignments[b] Aromatic —C—H	Vicinal vinyl —C=C— H H	Bridgehead —C—H	Ester —CH_3	Other proton assignments
C1	[d]	$C_{15}H_{14}O_4$	258	7.43 (2H)	6.66 (2H)	3.86 (2H)	3.76 (6H)	2.18 (1H)[c]; 2.31(1H)[c]
C2	[d,e]	$C_{15}H_{16}O_4$	260	7.43 (2H)	—	3.35 (2H)	3.79 (6H)	1.07–1.87 (6H)[c]
C3	93 – 93.5	$C_{16}H_{16}O_4$	244[f]	7.41 (2H)	6.41 (2H)	3.96 (2H)	3.79 (6H)	1.37–1.54 (4H)[c]
C4	53 – 54	$C_{16}H_{18}O_4$	274	7.43 (2H)	—	3.01 (2H)	3.81 (6H)	1.22–1.97 (8H)[c]
C5	60 – 61	$C_{17}H_{18}O_4$	286	7.40 (2H)	6.32 (2H)	3.44 (2H)	3.81 (6H)	1.10–1.77 (6H)[c]
C6	53.5	$C_{17}H_{20}O_4$	288	7.35 (2H)	—	3.03 (2H)	3.80 (6H)	1.46–2.09 (10H)[c]
C7	103 –104	$C_{18}H_{18}O_4$	298	7.45 (2H)	6.79 (2H)	4.34 (2H)	3.77 (6H)	1.51 (6H) *gem* dimethyl
C8	[d]	$C_{18}H_{20}O_4$	300	7.42 (2H)	—	3.73 (2H)	3.79 (6H)	1.11–1.99 (4H)[c]; 1.58 (6H) *gem* dimethyl
C9	86.5– 87	$C_{17}H_{16}O_4$	284	7.50 (2H)	6.81 (2H)	3.35 (2H)	3.87 (6H)	0.37–0.79 (4H) cyclopropyl
C10	[d]	$C_{17}H_{18}O_4$	286	7.50 (2H)	—	2.70 (2H)	3.88 (6H)	0.48 (4H) cyclopropyl; 1.13–2.24 (4H)[c]
C11	101 –102	$C_{17}H_{16}O_4$	284	7.43 (2H)	6.09 (2H)	4.01 (2H)	3.80 (6H)	0.51–1.36 (4H) cyclopropyl
C12	134 –135	$C_{17}H_{18}O_4$	286	7.45 (2H)	—	3.19 (2H)	3.82 (6H)	0.70–1.87 (8H)[c] and cyclopropyl
C13	75 – 75.5	$C_{18}H_{16}O_4$	296	7.45 (2H)	6.13 (2H) 5.98 (2H)	3.78 (2H)	3.79 (6H)	2.57 (2H) cyclobutenyl
C14	78.5	$C_{18}H_{20}O_4$	300	7.39 (2H)	—	2.94 (2H)	3.80 (6H)	1.06–2.46 (10H)[c] and cyclobutyl
C15	66 – 66.5	$C_{18}H_{16}O_4$	296	7.53 (2H)	—	3.42 (2H)	3.81 (6H)	2.83–4.24 (6H) cyclobutyl
C16	181	$C_{18}H_{16}O_4$	296	7.57 (2H)	—	3.67 (2H)	3.86 (6H)	2.32–3.48 (2H) and 1.61–1.76 (4H) cyclopropyl
C17	105 –106	$C_{17}H_{16}O_4$	284	7.41 (2H)	—	3.03 (2H)	3.77 (6H)	1.26 (2H), 1.83 (1H) cyclopropyl; 1.68 (2H)[c]; 2.33 (1H) bridgehead
C18	94.5– 95	$C_{19}H_{16}O_4$	308	7.52 (2H)	—	4.25 (2H)	3.74 (6H)	2.48 (2H)[c]; 6.79–7.24 (4H) aromatic
C19	136 –137	$C_{20}H_{16}O_4$	320	7.51 (2H)	6.82 (2H)	5.06 (2H)	3.73 (6H)	6.70–7.22 (4H) aromatic
C20	108 –108.5	$C_{20}H_{18}O_4$	322	7.53 (2H)	—	4.29 (2H)	3.77 (6H)	1.58 (4H)[c]; 6.90–7.23 (4H) aromatic
C21	193 –194	$C_{24}H_{18}O_4$	370	7.73 (2H)	—	5.47 (2H)	3.82 (6H)	6.88–7.48 (8H) aromatic

[a]Analytical data has been placed in the Depository of Unpublished Data.[2]
[b]δ value determined in 10% CCl_4 solution using TMS as internal standard; centers of multiplets or ranges indicated.
[c]Protons in saturated bridge or bridges.
[d]Liquid-molecularly distilled at 90°/0.01 mm; hydrolyzed to the diacid for analysis.
[e]Known compound (11).
[f]$M^+ - C_2H_4$.

Can. J. Chem. Downloaded from www.nrcresearchpress.com by 210.87.254.105 on 09/05/12
For personal use only.

illustrate the generality of the synthetic sequence and because we have used this dienophile in our rate studies and thus needed to characterize the products.

Many of these adducts and the bridged phthalic esters contain proximal π- or other thermally reactive and/or photoreactive bonding systems and a study of their thermal chemistry and photochemistry is underway.

Taken collectively, the proton chemical shift data for the dienes **1–21** (4), the TCNE adducts **A1–A21**, the DMAD adducts **B1–B21** and the benzopolycyclic dimethylesters **C1–C21** together with the equivalent data for 2,3-dimethylenebicyclo[2.2.2]octa-5,7-diene (14), provide an extensive field for the critical assessment of anisotropic and geometric effects on chemical shifts in these related, rigid molecules. We are currently analyzing the proton and ^{13}C magnetic resonance data in these terms.

Experimental

All melting points are uncorrected. The i.r. spectra were determined on a Unicam SP1000 spectrophotometer as liquid films or KBr discs. The p.m.r. spectra were recorded on a Varian HA100 instrument in carbon tetrachloride or deuteriochloroform using tetramethylsilane as the internal standard. Mass spectra were taken at 70 eV using a Hitachi-Perkin Elmer RMU-6E instrument. The u.v. spectra were run on a Unicam SP800A spectrophotometer. Microanalyses were obtained from A. B. Gygli, Toronto.

9,10-Dimethylenepentacyclo[4.4.0.0^{2,4}.0^{3,8}.0^{5,7}]decane (16)

Anhydrous silver fluoroborate (0.5 g) was added to a stirred solution of dimethyl pentacyclo[4.2.2.0^{2,5}.0^{3,8}.0^{4,7}]-decane-(*trans*)-9,10-dicarboxylate (8.3 g) (6) in ethanol-free chloroform (50 ml) at room temperature and the stirring continued for 12 h. The dark reaction mixture was passed through a column of alumina (Woelm; activity grade 1; 3 × 15 cm) followed by a chloroform wash (50 ml). The total red eluate was evaporated and vacuum distilled to give a white solid b.p. 140°/0.9 mm, (5.9 g), which was recrystallized from methanol to give pure **22***b* (5.0 g), m.p. 75.5–76°; p.m.r. δ ($CDCl_3$) 1.23–1.91 (m, 6H), 2.83 (m, 2H), 3.24 (m, 2H), 3.73 (s, 6H) p.p.m.; i.r. (CCl_4) $\nu_{C=O}$ 1740 cm^{-1}; *m/e* M$^+$ 248, calcd. 248.

Anal. Calcd. for $C_{14}H_{16}O_4$: C, 67.73; H, 6.50. Found: C, 67.77; H, 6.82.

This material was subjected to the general reduction–tosylation–elimination procedure (4) to secure diene **16**. All the intermediates showed consistent i.r. and p.m.r. spectra for the structures indicated.

9,10-*trans*-Bis(hydroxymethyl)pentacyclo[4.4.0.0^{2,4}.0^{3,8}.0^{5,7}]decane (**22***a*), m.p. 77.5–78° (methanol).

Anal. Calcd. for $C_{12}H_{16}O_2$: C, 74.97; H, 8.39. Found: C, 74.79; H, 8.54.

Di-*p*-toluenesulfonate, m.p. 152–153° (methanol).

Anal. Calcd. for $C_{26}H_{28}O_6S_2$: C, 62.38; H, 5.64. Found: C, 62.38; H, 5.31.

9,10-Dimethylenepentacyclo[4.4.0.0^{2,4}.0^{3,8}.0^{5,7}]decane **16**, m.p. 77° (preheated block: this diene readily polymerized); p.m.r. δ (CCl_4) 1.50 (m, 4H), 1.90 (m, 2H), 2.94 (m, 2H), 4.74 (s, 2H), 5.28 (d, J = 0.9 Hz, 2H) p.p.m.; i.r. (CCl_4) 890, 1315, 1620, 2940, 3050 cm^{-1}; u.v. (cyclohexane) λ_{max} 246 (7490), 254 (7970), and 263 sh (4760) nm; *m/e* M$^+$ 156, calcd. 156.

Anal. Calcd. for $C_{12}H_{12}$: C, 92.26; H, 7.74. Found: C, 91.88; H, 8.01.

8,9-Dimethylenetetracyclo[4.3.0.0^{2,4}.0^{3,7}]nonane (17)

Dimethyl tetracyclo[4.3.0.0^{2,4}.0^{3,7}]nonane-(*endo,cis*)-8,9-dicarboxylate (38 g) (7) was held under reflux for 6 h in methanol (150 ml) containing sodium methoxide (0.3 g). The methanol was evaporated under vacuum and the remaining oil partitioned between solvent ether (200 ml) and 0.1 *N* hydrochloric acid (250 ml). After separation, the aqueous phase was extracted with ether (2 × 75 ml) and the combined ether phases were dried ($MgSO_4$) and evaporated to the colorless oily *trans*-dimethyl ester **23***b* (36.6 g) showing two methoxyl (—OCH_3) absorptions (δ = 4.00 and 4.02 p.p.m.) in the p.m.r. spectrum (CCl_4). This material was subjected directly to the general reduction–tosylation–elimination procedure (4) to secure diene **17**. All the intermediates showed consistent i.r. and p.m.r. spectra for the structures indicated.

8,9-*trans*-Bis(hydroxymethyl)tetracyclo[4.3.0.0^{2,4}.0^{3,7}]-nonane (**23***a*) failed to crystallize.

Di-*p*-toluenesulfonate, m.p. 143–144° (methanol–chloroform).

Anal. Calcd. for $C_{25}H_{28}O_6S_2$: C, 61.50; H, 5.78. Found: C, 61.81; H, 5.61.

8,9-Dimethylenetetracyclo[4.3.0.0^{2,4}.0^{3,7}]nonane (**17**), liquid (vacuum transferred at 120°/0.01 mm); p.m.r. δ (CCl_4) 1.05 (m, 2H), 1.29 (m, 1H), 1.53 (m, 2H), 1.77 (m, 1H), 2.48 (m, 2H), 4.75 (s, 2H), and 5.12 (s, 2H) p.p.m.; i.r. (film) 801, 816, 882, 1078, 1198, 1361, 1657, 2858, 2965 and 3062 cm^{-1}; u.v. (cyclohexane) λ_{max} 204 (2590), 234 (6590), 250 (7315), 265 sh (4700) nm; *m/e* M$^+$ 144, calcd. 144.

Anal. Calcd. for $C_{11}H_{12}$: C, 91.61; H, 8.39. Found: C, 91.58; H, 8.26.

2,3-Dimethylene-1,4-methano-1,2,3,4-tetrahydronaphthalene (18)

Dimethyl 1,4-methano-1,2,3,4-tetrahydronaphthalene-(*trans*)-2,3-dicarboxylate (**24***b*) (8) was subjected to the general reduction–tosylation–elimination procedure (4) to secure diene **18**. All the intermediates showed consistent i.r. and p.m.r. spectra for the structures indicated.

2,3-*trans*-Bis(hydroxymethyl)-1,4-methano-1,2,3,4-tetrahydronaphthalene (**24***a*), m.p. 102–102.5° (benzene).

Anal. Calcd. for $C_{13}H_{16}O_2$: C, 76.44; H, 7.90. Found: C, 76.66; H, 7.78.

Di-*p*-toluenesulfonate, m.p. 159–160° (methanol–chloroform).

Anal. Calcd. for $C_{27}H_{28}O_6S_2$: C, 63.30; H, 5.52. Found: C, 63.34; H, 5.58.

2,3-Dimethylene-1,4-methano-1,2,3,4-tetrahydronaphthalene (**18**), m.p. 83° (sublimed 60°/0.01 mm); p.m.r. δ (CCl_4) 2.00 (q, 2H), 3.75 (m, 2H), 4.98 (s, 2H), 5.10 (s, 2H), and 7.02 (m, 4H) p.p.m.; i.r. (KBr disc) 736,

781, 894, 1461, 1630, 2981, 3070 cm^{-1}; u.v. (cyclohexane) λ_{max} 213 (6845), 232 sh (5780), 239 sh (4895), 246 sh (4365), 273 (1276), and 279 (1235) nm; *m/e* M^+ 168, calcd. 168.

Anal. Calcd. for $C_{13}H_{12}$: C, 92.81; H, 7.19. Found: C, 92.78; H, 7.04.

TCNE Adducts A1–A21

The hydrocarbons **1–21** (0.05 g) were separately mixed with TCNE (1.1 equiv. wt.) dissolved in dry tetrahydrofuran (5 ml) and stirred at room temperature for 1 h. The solvent was evaporated under vacuum, the residue rubbed with a small quantity of dry ether, and the crystalline adducts collected by filtration. These products were either recrystallized from ether or sublimed under vacuum (0.01 mm) to afford the pure adducts.[2] Melting points from hydrocarbon: **1**, 193–194°; **2**, 187–188°; **3**, 163–164°; **4**, 207–208°; **5**, 265°; **6**, 236.5–237°; **7**, 196–197°; **8**, 230–231°; **9**, 153–154°; **10**, 178°; **11**, 217.5–218°; **12**, 205–206°; **13**, 198–199°; **14**, 215.5–216.5°; **15**, 216–217°; **16**, 138–139°; **17**, 173.5–174.5°; **18**, 174.5–175°; **19**, 232–232.5°; **20**, 248–249°; **21**, > 300°.

DMAD Adducts B1–B21

The freshly recrystallized or vacuum transferred dienes **1–21** (1 mmol) were individually mixed with exactly 1 equiv. of freshly vacuum-transferred dimethyl acetylenedicarboxylate in CCl_4 (15 ml) and this mixture was held under reflux until the diene *exo*-methylene proton signals were seen to disappear as indicated by p.m.r. spectroscopy. The times varied from 5 min to 2 days. The reaction mixtures were evaporated under vacuum to quantitatively afford the crude adducts **B1–B21**. Crystallization was wasteful and difficult to effect for some of these adducts; petroleum ether (30–60°) or methanol were the preferred solvents for these recrystallizations. The melting points and some spectroscopic data of these adducts appear in Table 1.

Benzopolycyclic Dimethyl Esters C1–C21

The crude adducts **B1–B21** (1 mmol) were separately dissolved in benzene (5 ml) and DDQ (1.2 mmol) added. The resulting mixtures were stirred magnetically for 24 h, then filtered and eluted with benzene through short beds of neutral alumina (Woelm; activity grade 1; 8 × 1 cm). The colorless eluates were evaporated under vacuum to afford the benzopolycyclic dimethyl esters **C1–C21** (melting points and pertinent spectral data are collected in Table 2). Crystallization was again difficult for many of these adducts, though petroleum ether (30–60°) and methanol were the most useful solvents. Those diesters which failed to crystallize and which were previously unknown compounds (*viz.* **C1**, **C8** and **C10**) were hydrolyzed overnight in aqueous methanolic KOH and the corresponding phthalic acids isolated in the usual way.[2]

C1 diacid, m.p. 178°, preheated block (aqueous methanol); **C8** diacid, m.p. 177–178°, preheated block (aqueous methanol); **C10** diacid, m.p. 118°, preheated block (aqueous methanol).

Dimethyl Anthracene-2,3-dicarboxylate (26)

The adduct **B20** (30 mg) was heated in an oil bath at 230° until gas evolution ceased (15 min) and the residue was recrystallized from methanol to give dimethyl 1,4-dihydroanthracene-2,3-dicarboxylate (**25**), m.p. 120–121°; p.m.r. δ (CCl_4) 3.93 (s, 10H), 7.30–7.77 (m, 6H); *m/e* M^+ 296, calcd. 296.

Anal. Calcd. for $C_{18}H_{16}O_4$: C, 72.96; H, 5.44. Found: C, 73.24; H, 5.38.

This material (18 mg) was oxidized with DDQ as described above to afford dimethyl anthracene-2,3-dicarboxylate (**26**), m.p. 151–152° (lit. (12) 151°); p.m.r. δ (CCl_4) 3.96 (s, 6H), 7.54 (m, 2H), 8.03 (m, 2H), 8.40 (s, 2H), and 8.48 (s, 2H); *m/e* M^+ 294, calcd. 294.

Dimethyl Naphthalene-2,3-dicarboxylate (28)

The adduct **B3** (46 mg) was heated as above to give dimethyl 1,4-dihydronaphthalene-2,3-dicarboxylate (**27**), m.p. 37° (CCl_4); p.m.r. δ (CCl_4) 3.64 (s, 4H), 3.77 (s, 6H) and 7.14 (s, 4H); *m/e* M^+ 246, calcd. 246.

Anal. Calcd. for $C_{14}H_{14}O_4$: C, 68.28; H, 5.73. Found: C, 68.42; H, 5.81.

This material (24 mg) was oxidized with DDQ to afford dimethyl naphthalene-2,3-dicarboxylate (**28**), m.p. 48°, (lit. (13) 47°); p.m.r. δ (CCl_4) 3.88 (s, 6H), 7.44–7.95 (m, 4H), and 8.18 (s, 2H); *m/e* M^+ 244, calcd. 244.

1. (*a*) L. A. PAQUETTE, M. J. KUKLA, and J. C. STOWELL. J. Am. Chem. Soc. **94**, 4920 (1972); (*b*) L. A. PAQUETTE and G. V. MEEHAN. J. Am. Chem. Soc. **92**, 3039 (1970); (*c*) H. E. ZIMMERMAN, R. S. GIVENS, and R. M. PAGNI. J. Am. Chem. Soc. **90**, 6096 (1968).
2. (*a*) L. FRIEDMAN and D. F. LINDOW. J. Am. Chem. Soc. **90**, 2329 (1968); (*b*) J. IPAKTSCHI. Chem. Ber. **103**, 3944 (1970); (*c*) L. A. PAQUETTE and J. C. STOWELL. Tetrahedron Lett. 2259 (1970); (*d*) R. MUNEYUKI and H. TANIDA. J. Org. Chem. **31**, 1988 (1966); (*e*) G. WITTIG and E. KNAUSS. Chem. Ber. **91**, 895 (1958).
3. (*a*) H. TANIDA, T. IRIE, and T. TSUSHIMA. J. Am. Chem. Soc. **92**, 3404 (1970); (*b*) H. C. BROWN and G. L. TRITLE. J. Am. Chem. Soc. **90**, 2689 (1968).
4. D. N. BUTLER and R. A. SNOW. Can. J. Chem. **50**, 795 (1972).
5. L. A. PAQUETTE and J. C. STOWELL. J. Am. Chem. Soc. **93**, 2459 (1971).
6. W. G. DAUBEN and D. L. WHALEN. Tetrahedron Lett. 3743 (1966).
7. G. A. RUSSELL, P. R. WHITTLE, R. G. KESKE, G. HOLLAND, and C. AUBUCHON. J. Am. Chem. Soc. **94**, 1693 (1972).
8. K. ALDER, F. PASCHER, and H. VAGT. Chem. Ber. **75**, 1501 (1942).
9. K. ALDER and A. GRELL. Chem. Ber. **89**, 2198 (1956).
10. K. ALDER and H.-H. MÖLLS. Chem. Ber. **89**, 1960 (1956).
11. G. KAUPP. Chemia, **25**, 230 (1971).
12. J. D. LONDON and A. D. B. SLOAN. J. Chem. Soc. 3262 (1962).
13. E. F. BRADBROOK and R. P. LINSTEAD. J. Chem. Soc. 1739 (1936).
14. D. N. BUTLER and R. A. SNOW. Can. J. Chem. **52**, 447 (1974).

Can. J. Chem. Downloaded from www.nrcresearchpress.com by 210.87.254.105 on 09/05/12
For personal use only.

A Primary Hydrogen–Deuterium Isotope Effect Study on the Carbonyl Elimination Reaction of 9-Fluorenyl Nitrate with Various Bases[1]

PETER JAMES SMITH AND LORRAINE MARION NOBLE

Department of Chemistry and Chemical Engineering, University of Saskatchewan, Saskatoon, Saskatchewan S7N 0W0

Received July 22, 1974

PETER JAMES SMITH and LORRAINE MARION NOBLE. Can. J. Chem. **53**, 263 (1975).

The carbonyl elimination reaction of 9-fluorenyl nitrate with various nitrogen bases in anhydrous ethanol at 0 °C was examined. In all cases fluorenone was formed in 100% yield indicating that there was not any substitution. A reasonable Brønsted plot was obtained for reaction promoted by structurally similar bases with $\beta = 0.84$ which suggests a product-like transition state. As well, deviations from the Brønsted plot are discussed. Primary hydrogen–deuterium isotope effects were measured for reaction promoted by 11 different amine bases. A reasonable correlation was obtained for structurally similar bases when a plot of k^H/k^D *vs.* pK_a was made. The conclusion is reached that when k^H/k^D reaches a maximum, ~9.2 at 0 °C, it remains unchanged and hence is a poor measure of transition state geometry. As well, very poor correlations are found when the abstracting base is tertiary which leads to the conclusion that a comparison of k^H/k^D values is not warranted for structurally different bases.

PETER JAMES SMITH et LORRAINE MARION NOBLE. Can. J. Chem. **53**, 263 (1975).

On examine la réaction d'élimination du carbonyle du nitrate de fluorényl-9 à 0 °C dans l'étanol anhydre en présence de diverses bases azotées. Dans tous les cas, la fluorénone se forme avec un rendement de 100% montrant qu'il n'y a pas de substitution. Une courbe de Brønsted raisonnable a été obtenue pour la réaction catalysée par des bases de structure similaire et la valeur $\beta = 0.84$ suggère un état de transition qui ressemble aux produits. On discute aussi des déviations de la droite de Brønsted. On a mesuré les effets isotopiques primaires de l'hydrogène et du deutérium pour la réaction catalysée par 11 bases azotées différentes. On a obtenu une corrélation raisonnable pour des bases similaires lorsque une courbe de k^H/k^D en fonction du pK_a a été faite. On arrive à la conclusion que lorsque k^H/k^D atteint un maximum, ~9.2 à 0 °C, cette mesure demeure inchangée et devient une mesure imprécise pour la géométrie de l'état de transition. De plus on trouve de mauvaises corrélations quand la base enlevant le proton est tertiaire; ceci conduit à conclure qu'une comparaison des valeurs k^H/k^D ne peut se faire pour des bases qui ont des structures différentes. [Traduit par le journal]

Introduction

The carbonyl elimination reaction ($E_{CO}2$) of 9-fluorenyl nitrate with acetate ion in anhydrous ethanol has been investigated (1). The absence of deuterium exchange between the nitrate ester and ethanol-*O-d* as well as primary nitrogen and hydrogen–deuterium isotope effects of 1.0091 ± 0.0007 and 4.3 ± 0.2, respectively, led the authors to conclude that the reaction was a one-step concerted process.

The degree of carbon–hydrogen bond rupture at the transition state can be determined by measuring the primary hydrogen–deuterium isotope effect. It is now generally assumed that this effect is at a maximum when the proton is one-half transferred to base at the transition state, C—H—B, and that smaller values for the isotope effect are obtained when the proton is more than or less than half transferred (2). Consequently, a systematic increase in the strength of the abstracting base should lead to a more reactant-like transition state (3) and a decrease

Concerted mechanism:

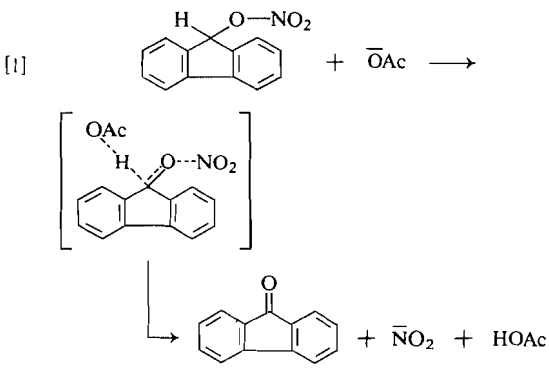

[1]Presented in part at the 56th Canadian Chemical Conference of the Chemical Institute of Canada, Montreal, June, 1973.

Can. J. Chem. Downloaded from www.nrcresearchpress.com by 210.87.254.5 on 09/05/12
For personal use only.

TABLE 1. Rate constants and primary hydrogen–deuterium isotope effects in the $E_{CO}2$ reaction of 9-fluorenyl nitrate and 9-fluorenyl-9-*d* nitrate with various amines in ethanol at 0 °C

Base (number)	9-H(D)	k (l mol^{-1} min^{-1})	k^H/k^D[a]	pK_a
p-Chlorobenzylamine (**1**)	H	0.139 ± 0.001[b]	8.80 ± 0.28	9.18 (7)[c]
	D	0.0158 ± 0.0005		
Benzylamine (**2**)	H	0.192 ± 0.006	9.23 ± 0.30	9.34 (7)
	D	0.0208 ± 0.0002		
1-Phenylethylamine (**3**)	H	0.204 ± 0.002	10.36 ± 0.19	9.45 (9)
	D	0.0197 ± 0.0003		
2-Phenylethylamine (**4**)	H	0.425 ± 0.009	9.32 ± 0.25	9.83 (6)
	D	0.0456 ± 0.0008		
Piperidine (**5**)	H	4.90 ± 0.04	9.14 ± 0.08	11.12 (5)
	D	0.536 ± 0.001		
Pyrrolidine (**6**)	H	8.65 ± 0.32	9.26 ± 0.34	11.27 (5)
	D	0.934 ± 0.006		
Triethanolamine (**7**)	H	0.0446 ± 0.0006	7.61 ± 0.12	7.76 (8)
	D	0.00586 ± 0.00005		
Morpholine (**8**)	H	0.706 ± 0.017	8.54 ± 0.07	8.33 (5)
	D	0.0827 ± 0.0006		
N-Methylbenzylamine (**9**)	H	0.692 ± 0.015	7.96 ± 0.19	9.59 (7)
	D	0.0869 ± 0.0008		
N,*N*-Dimethylbenzylamine (**10**)	H	0.203 ± 0.006	6.25 ± 0.19	8.93 (6)
	D	0.0325 ± 0.0002		
N,*N*-Diethylbenzylamine (**11**)	H	0.0834 ± 0.0024	6.84 ± 0.21	9.48 (6)
	D	0.0122 ± 0.0001		

[a]Ratio of rates of elimination; deviation = $\pm(k^H/k^D)[(r^H/k^H)^2 + (r^D/k^D)^2]^{1/2}$, where r is the standard deviation in k.
[b]Standard deviation.
[c]Reference.

(increase) in the magnitude of k^H/k^D if the proton is less (more) than half transferred.

It is reasonable to expect that the transition state for the reaction of 9-fluorenyl nitrate with base is reactant-like since a nitrogen effect, $k^{14}/k^{15} = 1.0091$, was obtained (1) which indicates a small degree of O—N bond rupture at the transition state for the reaction with acetate ion. Consequently, a small degree of carbon–hydrogen bond rupture is predicted since it has been shown that the degree of carbon–hydrogen and carbon–nitrogen bond rupture is complementary for the E2 reaction of quaternary ammonium ions (4). Accordingly, in the present study, β-deuterium isotope effects have been measured for the $E_{CO}2$ reaction of 9-fluorenyl nitrate with 11 different nitrogen bases in ethanol at 0 °C.

Results

Hydrogen–Deuterium Isotope Effects

The rate constants for the reaction of 9-fluorenyl nitrate and 9-fluorenyl-9-*d* nitrate with the various bases in ethanol are shown in Table 1. The primary hydrogen–deuterium effects calculated from the rate data are also given in this table along with the pK_a of the conjugate acid of the abstracting base in water.

Discussion

Rate Measurements

The second-order rate constants for the reaction of 9-fluorenyl nitrate with various amine bases (**1**–**11**) in ethanol at 0 °C, Table 1, are plotted against the pK_a of the conjugate acid of the abstracting base, Fig. 1. It is seen that a straight line is obtained for the structurally similar bases, the primary amines, and the two heterocycles, amines **1**–**6**, with a slope $\beta = 0.84$. The rate constants covered a range of about 1.8 log units, while pK_a's covered a range of 2 units. One can conclude that the large value for β suggests that the transition state for the proton transfer is product-like; *i.e.*, the proton is more than one-half transferred from carbon to the amine. It is noteworthy, however, that Bordwell and Boyle (10) have shown for the deprotonation of nitroalkanes and ketones that β changed very

Can. J. Chem. Downloaded from www.nrcresearchpress.com by 210.87.254.5 on 09/05/12
For personal use only.

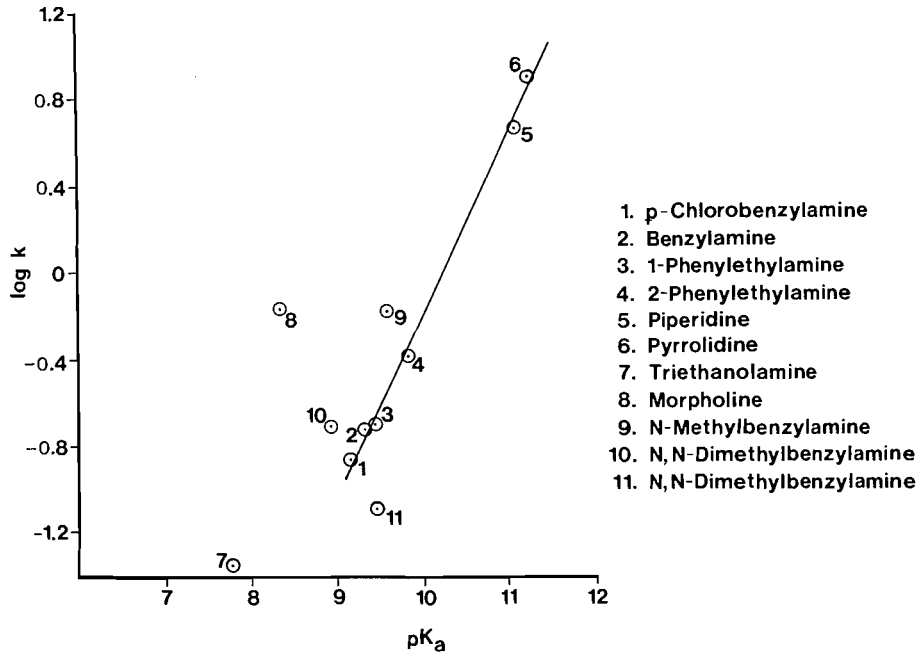

FIG. 1. Plot of log k *vs.* pK_a for the $E_{co}2$ reaction of 9-fluorenyl nitrate with various amine bases in ethanol at 0 °C.

little over a pK_a range of almost 20 units. He concluded that either β is a very poor guide to the extent of proton transfer in the transition state or that transition-state structures for the reactions studied vary to a small extent over wide ΔpK_a ranges.

It is reasonable that points 7 and 8, reaction promoted by triethanolamine and morpholine, fall off the Brønsted plot since such correlations between log k and pK_a are observed only for structurally similar bases. Triethanolamine and morpholine will be solvated to a much greater extent than amines **1–6** due to the oxygen atoms and hence will be less available as bases for steric reasons. As well, points 9–11 also fall off the line, and here reaction is promoted by *N*-methylbenzylamine, *N*,*N*-dimethylbenzylamine, and *N*,*N*-diethylbenzylamine where there is presumably a steric factor associated with the attack of the secondary and two tertiary amines at the 9-hydrogen; the rate constants for reaction promoted by benzylamine and *N*,*N*-diethylbenzylamine are 0.192 and 0.0834 l mol^{-1} min^{-1}, respectively.

Hydrogen–Deuterium Isotope Effects

The rate constant for reaction of 9-fluorenyl nitrate and 9-fluorenyl-9-*d* nitrate with the various amine bases was determined under pseudo first-order conditions with excess base. The second-order rate constants, as shown in Table 1, were obtained from the pseudo first-order by dividing by the concentration of base. In all cases the same base solution was used to measure the rate constants for reaction of the undeuterated and deuterated substrates. As well, for every base used, the optical density at infinity was the same for reaction of the undeuterated and deuterated compounds indicating that the reaction was solely elimination.

The primary hydrogen–deuterium isotope effects obtained for reaction with amines **1–8**; the primary amines as well as piperidine, pyrrolidine, morpholine, and triethanolamine, appear to vary with pK_a. A plot of k^H/k^D versus pK_a for all of the bases studied is shown in Fig. 2. From the plot of the data for amines **1–8**, it can be seen that the smaller the pK_a (the weaker the abstracting base) the smaller is the primary hydrogen–deuterium isotope effect; *i.e.* for triethanolamine pK_a and k^H/k^D are 7.76 and 7.61 while for pyrrolidine they are 11.27 and 9.26, respectively.

Since Thornton[2] has predicted (3) and it has been shown experimentally (4) that for E2 reac-

[2]The Thornton prediction is a particular application of the well-established general principle that the proton in the transition state is nearer the weaker base (11).

Can. J. Chem. Downloaded from www.nrcresearchpress.com by 210.87.254.5 on 09/05/12
For personal use only.

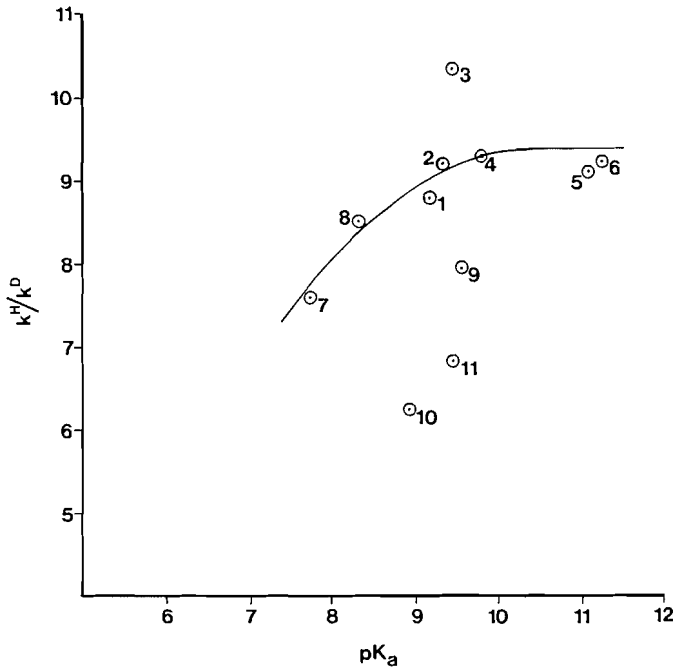

FIG. 2. Plot of k^H/k^D *vs.* pK_a for the $E_{CO}2$ reaction of 9-fluorenyl nitrate with various amine bases in ethanol at 0 °C.

tions the transition state has greater carbon–hydrogen bond rupture when reaction is promoted by weaker bases, then it can be concluded that for the $E_{CO}2$ reaction of 9-fluorenyl nitrate with the amine bases a *decrease* in the magnitude of k^H/k^D indicates *increased* C—H bond weakening with the proton more than one-half transferred to base at the transition state (on the right hand side of Westheimer's curve). Further evidence that the transition state is product-like is given by the large Brønsted β of 0.84.

Furthermore, it appears that the value for the primary hydrogen–deuterium isotope effect levels off at a value of approximately 9.2 for all bases, excluding 1-phenylethylamine, in the series **1–8** with pK_a greater than 9. In other words, it appears that there is a broad maximum in Westheimer's curve with $k^H/k^D \simeq 9.2$ (this value corresponds to the theoretical maximum of $\simeq$ 7.4 at 30° calculated for the loss of a stretching vibration). Consequently, for bases of the series with $pK_a > 9$ one cannot determine the change in transition state geometry since the value of k^H/k^D remains essentially constant. It may be concluded that k^H/k^D is either insensitive to the structure of the transition state or that the activated complex does not change for reaction with bases with pK_a greater than 9.

It appears that the data for triethanolamine and morpholine lie on the plot shown in Fig. 2, whereas the rate constants obtained for reaction with these two bases did not satisfy the Brønsted relationship shown in Fig. 1. It is not unexpected that triethanolamine and morpholine would effect the rate of reaction differently than amines **1–6** due to the presence of the oxygen atoms which would lead to quite different solvation effects. However, when they act as abstracting bases at the transition state, the degree of C—H bond rupture as measured by k^H/k^D should be dependent only on their pK_a and hence the observed correlation.

It should be noted that whereas the rate constant for 1-phenylethylamine falls on the Brønsted plot the value of $k^H/k^D = 10.36$, determined for reaction promoted by this primary amine, is significantly higher than for all other amines. Indeed, the value of 10.36 is greater than expected for the loss of a stretching vibration and may suggest that tunneling is operative in this particular instance. In any event, it appears that it is not reasonable to interpret the value of k^H/k^D obtained for reaction promoted by 1-phenylethylamine and, for example, 2-phenylethylamine in terms of the degree of C—H bond weakening at the transition state.

Can. J. Chem. Downloaded from www.nrcresearchpress.com by 210.87.254.5 on 09/05/12
For personal use only.

Can. J. Chem. Downloaded from www.nrcresearchpress.com by 210.87.254.5 on 09/05/12
For personal use only.

It is of particular interest that the values for the hydrogen–deuterium isotope effect determined for reaction of 9-fluorenyl nitrate with *N*-methylbenzylamine, *N*,*N*-dimethylbenzylamine, and *N*,*N*-diethylbenzylamine, amines **9–11**, do not fall on the plot of k^H/k^D *vs.* pK_a, Fig. 2. In all three cases, the magnitude of k^H/k^D is less than expected for an amine base with their respective pK_a values. This is not unreasonable as it is expected that the ability of the two tertiary amines and the secondary to protonate and to abstract the 9-hydrogen to be quite different whereas the abilities of a primary amine might be similar. Consequently, it is proposed that amines **9–11**, due to steric effects, act as weaker abstracting bases for the $E_{CO}2$ reaction than indicated by their pK_a values. This would lead to the situation where there is a greater extent of C—H bond weakening than expected from the pK_a value with a corresponding decrease in the magnitude of the primary isotope effect as observed.

In conclusion, it must be pointed out that for the reaction investigated great care must be taken in interpreting the magnitude of k^H/k^D in terms of the degree of carbon–hydrogen bond weakening at the transition state because of the great scatter of points on the plot of k^H/k^D *vs.* pK_a. It may be reasonable to compare values obtained for structurally similar bases but even for this situation it appears that, for several bases with different pK_a values, experimentally identical values of k^H/k^D are obtained.

Experimental

Materials

9-Fluorenyl Nitrate

This compound was prepared by the action of silver nitrate on 9-bromofluorene in acetonitrile (12) and was recrystallized from petroleum ether (b.p. 30–60°), m.p. 88–89° (lit. (13) m.p. 88–89°).

9-Fluorenyl-9-d Nitrate

The deuterated compound was prepared by the following reaction sequence: (*a*) reduction of 9-fluorenone to 9-fluorenol-9-*d* with lithium aluminum deuteride; (*b*) conversion of the alcohol into 9-bromofluorene-9-*d* by means of acetyl bromide; and (*c*) reaction of the bromo compound with silver nitrate. The overall yield of 9-fluorenyl-9-*d* nitrate was 70%. The product, recrystallized from petroleum ether, had a melting point of 88.0–89.0° and was at least 99% deuterated in the 9-position, as shown by n.m.r. analysis.

9-Fluorenol-9-d

9-Fluorenone (24.0 g, 0.133 mol) was treated for 8 h with lithium aluminum deuteride (3.0 g, 0.07 mol) in 300 ml of diethyl ether which had been dried by distillation from lithium aluminum hydride. The complex was decomposed by addition of water, the precipitated salts were removed by filtration, and the product was isolated from the ether solution. Recrystallization from benzene gave 22.7 g of 9-fluorenol-9-*d* (93% yield), m.p. 153.5–154.0° (lit. (14) m.p. 156°).

9-Bromofluorene-9-d

Acetyl bromide (16.6 g, 0.135 mol) was added all at once to 9-fluorenol-9-*d* (12.5 g, 0.068 mol) and the flask stoppered. A vigorous reaction set in, and in a short time the mixture solidified. The reaction was completed by warming the mixture on a steam bath, and acetic acid and excess reagents were removed under reduced pressure. The residue was recrystallized from petroleum ether (b.p. 30–60°), giving 12.9 g (77% yield) of 9-bromofluorene-9-*d*, m.p. 98.5–100.0 (lit. (15) m.p. 102–103°).

Amines

All the amines were obtained from commercial sources. Each amine, immediately before use, was fractionally distilled under reduced pressure.

Kinetic Measurements

The reaction rate was followed spectrophotometrically by measuring the optical density of the reaction solutions at 380 nm, the λ_{max} of the elimination product fluorenone. The reaction solution was analyzed for nitrite and nitrate ions by the method of differential reduction to ammonia (16) and no nitrate ion was found. Nitrite ion, from the $E_{CO}2$ reaction, was found in theoretical quantities. Consequently, since a large excess of base was used in the kinetic study, the pseudo first-order rate constant obtained is for the carbonyl elimination reaction as S_N2 displacement and solvolysis are not observed.

A solution of 9-fluorenyl nitrate (0.003–0.009 *M*) and the appropriate amine base (0.04–0.57) in anhydrous ethanol, prepared by mixing temperature-equilibrated solutions of each reactant, was maintained in a constant-temperature bath at ±0.02°. At suitable time intervals 5-ml samples were removed and added to approximately 15 ml of quenching solution. The resulting solution was diluted to 25 ml with ethanol and the optical density of this solution was measured on a Perkin-Elmer Hitachi spectrophotometer. The quenching solution was prepared by mixing 5 ml of an acid solution of 2 ml of concentrated H_2SO_4 in 100 ml of water with 10 ml of 95% ethanol.

The pseudo first-order rate constants for the disappearance of fluorenyl nitrate was determined by plotting log $(OD_\infty - OD_t)$ against time for the equation $kt = 2.303 \log (OD_\infty - OD_0/(OD_\infty - OD_t)$, where OD_0, OD_∞ and OD_t are the optical densities at time zero, infinity, and t, respectively. The best fit of the data was obtained by the method of least squares using a computer program. These constants were converted into second-order constants by dividing by the concentration of the base.

This work was supported by the National Research Council of Canada.

1. P. J. SMITH and A. N. BOURNS. Can. J. Chem. **44**, 2553 (1966).
2. F. H. WESTHEIMER. Chem. Rev. **61**, 265 (1961).
3. E. R. THORNTON. J. Am. Chem. Soc. **89**, 2915 (1967).
4. P. J. SMITH and A. N. BOURNS. Can. J. Chem. **52**, 749 (1974).
5. R. C. WEAST (*Editor*). Handbook of chemistry and physics. 54th Ed. The Chemical Rubber Co., Cleveland, Ohio. 1973. p. D126.
6. N. A. LANGE (*Editor*). Handbook of chemistry. 10th Ed. McGraw-Hill Book Company, Inc., New York. 1961. p. 1203.
7. L. M. LITVINENKO, V. A. DADALI, A. M. VOLOVIN, and E. T. TITOV. Reakt. Sposobnost Org. Soedin., Tartu. Gos. Univ. **3**(3), 75 (1966).
8. D. D. PERRIN. Aust. J. Chem. **17**, 484 (1964).
9. F. KIEFFER. C. R. **238**, 1043 (1954).
10. F. G. BORDWELL and William J. BOYLE, JR. J. Am. Chem. Soc. **93**, 511 (1971).
11. J. R. JONES. Ionization of carbon acids. Academic Press, New York. 1973. p. 124.
12. J. P. FREEMAN. J. Org. Chem. **21**, 471 (1956).
13. G. W. H. CHEESEMAN. J. Chem. Soc. 448 (1959).
14. C. L. ARCUS and J. V. EVANS. J. Chem. Soc. 789 (1958).
15. W. E. BACHMANN and J. C. SHEEHAN. J. Am. Chem. Soc. **62**, 2687 (1940).
16. E. BUNCEL and A. N. BOURNS. Can. J. Chem. **38**, 2457 (1960).

Can. J. Chem. Downloaded from www.nrcresearchpress.com by 210.87.254.5 on 09/05/12
For personal use only.

Photo-oxidation of Iodomethane in Solid Argon[1]

J. F. OGILVIE,[2] VIRGINIA R. SALARES, AND MICHAEL J. NEWLANDS

Department of Chemistry, Memorial University of Newfoundland, St. John's, Newfoundland A1C 5S7

Received June 14, 1973[3]

J. F. OGILVIE, VIRGINIA R. SALARES, and MICHAEL J. NEWLANDS. Can. J. Chem. **53**, 269 (1975).

Photolysis of iodomethane in the presence of oxygen in solid argon near 10 K has yielded several products detected by their vibrational absorption spectra. Isotopic labeling of reactants has proved methanal, water, hydrogen iodide, carbon monoxide, carbon dioxide, and hydroperoxyl radicals to be significant products, and a further set of major absorptions is attributed to hydrogen hypoiodite HOI, hydrogen-bonded to methanal. Other minor vibrational features are discussed, and a possible reaction scheme is briefly outlined.

J. F. OGILVIE, VIRGINIA R. SALARES et MICHAEL J. NEWLANDS. Can. J. Chem. **53**, 269 (1975).

La photolyse de l'iodométhane, en présence d'oxygène dans l'argon solide près de 10 K, conduit à plusieurs produits détectés par leur spectre d'absorption vibrationnelle. Le marquage isotopique des réactifs a prouvé que le méthanal, l'eau, l'iodure d'hydrogène, le monoxyde de carbone, le dioxyde de carbone et des radicaux hypropéroxyles sont des produits importants; on a attribué un autre groupe majeur d'absorptions à de l'hypoiodite d'hydrogène (HOI) lié par pont hydrogène au méthanal. On discute d'autres vibrations mineures et on décrit un schéma réactionnel possible. [Traduit par le journal]

Introduction

In his investigation of photolysis of iodomethane in solid oxygen Roebber (1) postulated that several trapped radicals may have been produced, but lack of isotopically substituted reactants and problems of spectral range and resolution hampered positive identification. Also only a few trapped radicals were at that time characterized by vibrational spectra; even for many pertinent stable substances, reliable absorption spectra were available for neither gas phase nor argon matrix. Now that these conditions no longer prevail, we are able, in performing similar experiments, to identify several products unambiguously, and we have also obtained evidence for a previously undetected molecule which seems to be a major product.

Experimental

The apparatus consisted essentially of a refrigerator (Air Products Displex CS-202) mounted in an infrared spectrophotometer (Perkin–Elmer 225) and connected to both a metal high-vacuum pumping system and a glass manifold for sample preparation. In the conduct of each experiment, after deposition of gases during 5–10 h, frozen samples were irradiated for 10–30 h (low pressure Hg lamp) and 1–2 h (HPK 125 lamp); the extent of photodecomposition of reactants and formation of products was measured by analysis of vibrational absorption spectra recorded before and after each irradiation operation. Flow of gases to the refrigerator was controlled by needle valves in the range 0.1–0.7 μmol s^{-1}, monitored by Penning and Pirani pressure gauges. The gases were frozen on a CsI window in the refrigerator, held at 8–10 K (measured by a Chromel *vs.* 0.07% Fe/Au thermocouple). The irradiation sources were mercury arcs: Philips HPK 125, 125 W operating at a pressure $\sim 8 \times 10^5$ N m^{-2}, or a specially constructed lamp, 8 W operating at a pressure of 1.3×10^3 N m^{-2} so as to emit principally at 39 412 and 54 069 cm^{-1}. A filter transmitting 8 000–14 000 and 24 000–47 000 cm^{-1} was occasionally used with the HPK 125 lamp. Spectral slit widths of the spectrometer varied from 0.3–1.5 cm^{-1} in the range 200–4000 cm^{-1}; wavenumber accuracy and reproducibility were 0.5 cm^{-1} for sharp lines.

Iodomethane ($H_3{}^{12}CI$ from Fisher, $D_3{}^{12}CI$ from Merck, Sharp and Dohme, and $H_3{}^{13}CI$ (86.3% enrichment) from Prochem) was distilled and degassed before use. $^{16}O_2$ was generated from $KMnO_4$; $^{18}O_2$ (94 atomic% enrichment) was obtained from Yeda. Mixtures of $^{16}O_2$, $^{18}O_2$, and $^{16}O^{18}O$ (~40 atomic% ^{18}O randomly distributed, as deduced from ozone byproduct composition) were prepared by electric discharge of $^{16}O_2$ and $^{18}O_2$. Argon (Matheson, 99.998% nominal purity) was used directly from the cylinder. $D_2{}^{12}CO$ was generated from polyoxymethylene-d_2 (Merck, Sharp and Dohme). Mixtures of iodomethane vapor (or $D_2{}^{12}CO$) and argon, or oxygen and argon, were prepared and stored several hours before use.

[1]Presented at XI International Symposium on Free Radicals, Berchtesgaden-Königssee, September, 1973.

[2]To whom correspondence should be addressed.

[3]Revision received September 20, 1974.

Can. J. Chem. Downloaded from www.nrcresearchpress.com by 210.87.254.5 on 09/05/12
For personal use only.

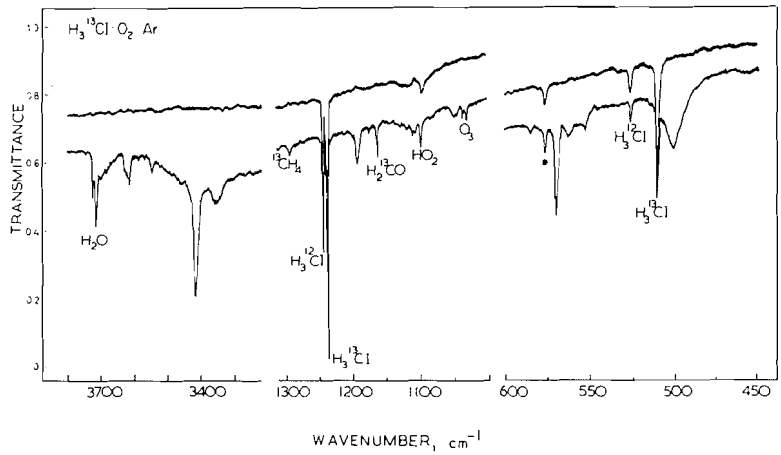

FIG. 1. Selected portions of spectra of $H_3{}^{13}Cl{:}{}^{16}O_2{:}Ar = 1{:}25{:}200$. Upper spectrum, before photolysis; lower trace, sample had been irradiated for 27 h with the low-pressure Hg lamp. * represents background feature.

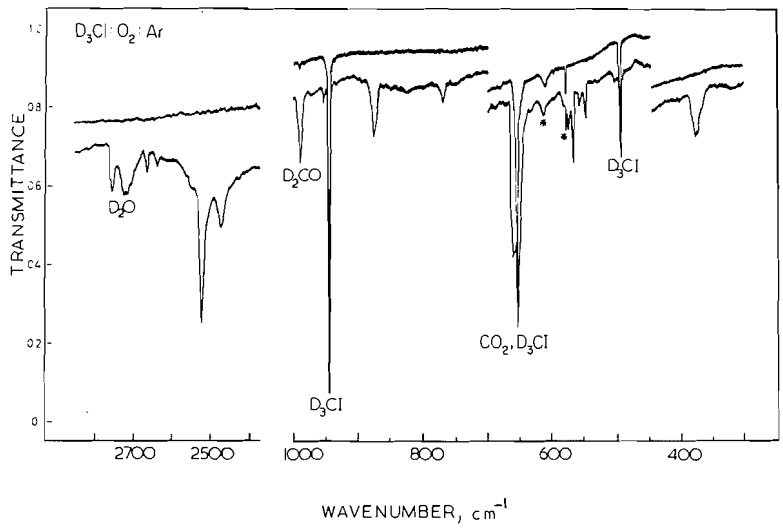

FIG. 2. Selected portions of the spectrum of $D_3{}^{12}Cl{:}{}^{16}O_2{:}Ar = 1{:}20{:}100$. Upper spectrum, before photolysis; lower spectrum, sample had been irradiated for 30 h with the low-pressure Hg lamp and 2 h with the HPK 125 lamp.

Results

Representative spectra recorded before and after irradiation of iodomethane–oxygen–argon mixtures are shown in Fig. 1 and 2. That a reaction had occurred after irradiation was clearly evident from the reduction in intensity of iodomethane lines and appearance of many new absorptions. (In contrast, when only iodomethane–argon mixtures were irradiated, no spectral changes were detected.) Characteristic growth patterns with the two radiation sources were observed for the new absorptions. By comparison of relative intensities during various photolytic operations within particular and between different experiments, lines exhibiting similar intensity patterns were grouped and are now presented in text and tables. Isotopic labeling of reactants permitted identification of produced substances; mixtures of both ^{12}C- and ^{13}C-containing iodomethane or all of $^{16}O_2$, $^{18}O_2$, and $^{16}O^{18}O$ were particularly useful in indicating the number of either carbon or oxygen atoms in carriers of major absorption features. By this method, it was ascertained

Can. J. Chem. Downloaded from www.nrcresearchpress.com by 210.87.254.5 on 09/05/12
For personal use only.

TABLE 1. Absorption lines (cm^{-1}) of water molecules produced after irradiation of specified reactants*

$H_3{}^{12}CI$ $^{16}O_2$	$H_3{}^{12}CI$ $^{18}O_2$	$H_3{}^{13}CI$ $^{16}O_2$	$D_3{}^{12}CI$ $^{16}O_2$	$D_3{}^{12}CI$ $^{18}O_2$
3723.5	3710	3723.5	2756	2742.5
3712.7	3700.4	3714		2733
3700 br	3687 br	3696 br	2718 br	2708 br
3678 br		3678 br		
	3621	3622		
3614	3605	3614.3	2666	2651
			2640	
1615 br	1615 br	1612 br	1183 br	1177 br
1594.5		1595		
1591	1578.6	1591	1176	
1585		1585		

*In this and following tables, br = broad and sh = shoulder.

TABLE 2. Absorption lines (cm^{-1}) of methanal molecules produced after irradiation of specified reactants, with reference lines

$H_3{}^{12}CI$ $^{16}O_2$	$H_2{}^{12}CO$ (ref. 5)	$H_3{}^{12}CI$ $^{18}O_2$	$H_3{}^{13}CI$ $^{16}O_2$	$D_3{}^{12}CI$ $^{16}O_2$	$D_2{}^{12}CO$ (ref. 6)	$D_3{}^{12}CI$ $^{18}O_2$
2882	2862	2865	2862.5	2200	2177	2200
2816.5	2796	2816.5	2812	2084	2069.7	2082.5
1735 sh	1742	1701	1697	1690	1697.8	
1728	1738	1695.5	1691	1682	1691.6	1645
1722.5 sh	1732	1690	1685.5	1677	1687.6	1640
1496	1498	1486	1496.4	1097.5	1099.4	1092.5
1492.5		1481.5	1492			
				990	987.1	982.5
1175.3	1167.5	1173.5	1163.5			

that no carrier of other than weak absorptions contained two or more carbon or oxygen atoms. Varying mole fractions of iodomethane and oxygen by dilution with argon was also helpful, a technique which Roebber (1) did not exploit.

Water, characterized by absorptions listed in Table 1, had both sharp lines at wavenumbers attributed to isolated molecules (2–4), and broad lines attributed to water hydrogen-bonded to other polar molecules within the same cavity bounded by argon and oxygen molecules. During an annealing operation, in which the sample temperature was allowed to rise to 20–30 K before recooling, sharp lines at 3712.7 and 3723.5 cm^{-1} decreased in intensity, lines at 3678 and 3614 cm^{-1} increased, and that at 3700 cm^{-1} was little affected.

Methanal is also readily identified by its characteristic fundamentals, for which wavenumbers are listed in Table 2 and compared with published values (5, 6). Intensity measurements indicated dissimilar rates of iodomethane decomposition and methanal formation during irradiation. Simultaneous destruction of methanal by radiation from the HPK 125 lamp was confirmed in separate experiments with $D_2CO:O_2:Ar$ samples.

Carbon monoxide and dioxide were both easily detected; wavenumbers are listed in Table 3. Atmospheric carbon dioxide hampered quantitative absorbance measurements in the 2350 and 667 cm^{-1} regions, but there is no doubt that rates of carbon dioxide formation and of iodomethane decomposition were dissimilar. In fact, use of the HPK 125 lamp after the low-pressure lamp resulted in a relatively rapid increase of CO_2. This behavior is consistent with its production via a secondary process.

Carbon monoxide lines are generally as previously reported (7–10), with slight variation attributed to matrix environment effects. An

Can. J. Chem. Downloaded from www.nrcresearchpress.com by 210.87.254.5 on 09/05/12
For personal use only.

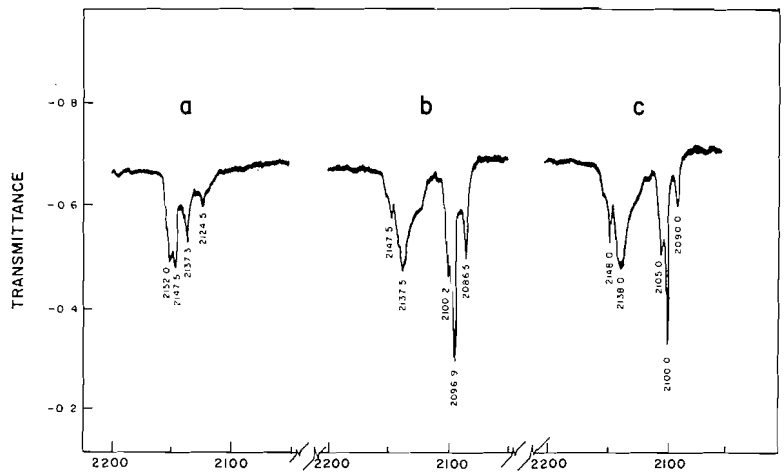

FIG. 3. Absorptions between 2050–2200 cm^{-1} produced by photolysis of: (*a*) $H_3{}^{12}CI:{}^{16}O_2:Ar = 1:25:100$; (*b*) $H_3{}^{12}CI:{}^{18}O_2:Ar = 1:13:110$; (*c*) $H_3{}^{13}CI:{}^{16}O_2:Ar = 1:25:200$.

TABLE 3. Absorption lines (cm^{-1}) of carbon oxide molecules produced after irradiation of specified reactants

	$H_3{}^{12}CI$ $^{16}O_2$	$H_3{}^{12}CI$ $^{18}O_2$	$H_3{}^{13}CI$ $^{16}O_2$	$D_3{}^{12}CI$ $^{16}O_2$	$D_3{}^{12}CI$ $^{18}O_2$
CO_2	2341	2308*	2776.5	2341	2308†
	662	645*	643	662.3	645*
	652.5		635		
CO	2152	2100.2	2105	2152.5	2100
	2147.5	2096.9	2100	2149†	2097.5
	2137.5	2086.5	2090	2137.5	‡

*Overlapped with $C^{18}O_2$ initially present in $^{18}O_2$ sample.
†Obscured by D_3CI line.
‡Obscured by $D_2C^{18}O$ absorption.

TABLE 4. Absorption lines (cm^{-1}) of hydroperoxyl radicals produced after irradiation of specified reactants

$H_3{}^{12}CI$ $^{16}O_2$	$H_3{}^{12}CI$ $^{18}O_2$	$H_3{}^{13}CI$ $^{16}O_2$	$D_3{}^{12}CI$ $^{16}O_2$
1390	1381	1390.0	
1388	1379.2	1388.3	
1100	1039.5	1100.5	1022

intense line at 2149 cm^{-1} has been previously assigned to $^{12}C^{16}O$ adjacent to $H_2{}^{16}O$ (10), although a shoulder at 2152 cm^{-1} has not previously been cited.

Underneath the fairly sharp lines assigned to $^{12}C^{16}O$ was a broad line about 2138 cm^{-1} with an apparent shoulder at 2125 cm^{-1}. As shown in Fig. 3, ^{18}O- or ^{13}C- labeled reactants produced a shift of the CO lines leaving the broad line distinct. On the other hand, when $D_3{}^{12}CI$ was used, this broad line disappeared, but another appeared about 1525 cm^{-1}, also unaffected by ^{18}O-labeled reactant. These observations lead to assignment of the absorbing species as hydrogen iodide (11). The breadth of the lines and shift from the gas-phase band center both indicate extensive hydrogen bonding.

Weak absorptions at wavenumbers noted in Table 4 indicate by their behavior on isotopic labeling that the carrier is the hydroperoxyl radical, consistent with similar wavenumbers measured in different experiments on this apparatus (12). Although lines were also found near the wavenumbers appropriate to OH and OD valence-stretching fundamentals of these radicals, that the peak intensities were anomalously large and that these lines were present when the lines listed in Table 4 were, in some experiments, absent strongly indicate that they belong to a different molecular carrier (*vide infra*).

Can. J. Chem. Downloaded from www.nrcresearchpress.com by 210.87.254.5 on 09/05/12
For personal use only.

TABLE 5. Absorption lines (cm^{-1}) of methanoic acid produced after irradiation of specified reactants, with reference lines

$H_3{}^{12}CI$ $^{16}O_2$	$H^{12}COOH$* (ref. 13)	$H_3{}^{12}CI$ $^{18}O_2$	$H_3{}^{13}CI$ $^{16}O_2$	$H^{13}COOH$* (ref. 13)	$D_3{}^{12}CI$ $^{16}O_2$	$D_3{}^{12}CI$ $^{18}O_2$
1748	1758	1715.5	1708.5	1715	1710	1679.5
1121	1129	1089.5	1111.8	1117		
1118.5		1086	1108.8			

*In carbon monoxide matrix.

TABLE 6. Absorption lines (cm^{-1}) tentatively attributed to hydrogen hypoiodite molecules produced after irradiation of specified reactants

$H_3{}^{12}CI$ $^{16}O_2$	$H_3{}^{12}CI$ $^{18}O_2$	$H_3{}^{13}CI$ $^{16}O_2$	$D_3{}^{12}CI$ $^{16}O_2$	$D_3{}^{12}CI$ $^{18}O_2$
3417	3406	3417	2524.5	2513.5 sh 2508
1193	1191	1193	874.5	868
571.3	543.1	571.3	566.5	539.8

Some weak lines listed in Table 5 appear to be due to the s-transoid rotamer of methanoic acid (HCOOH and DCOOD), by comparison with results obtained for a carbon monoxide matrix (13) and the vapor phase (14).

A weak line at 1304 cm^{-1} in $H_3{}^{12}CI$ experiments which was insensitive to ^{18}O presence but which shifted to 1296 cm^{-1} when $H_3{}^{13}CI$ was used is attributed to methane (15). The lines were relatively most intense when the mole fraction of oxygen in the argon matrix was smallest. Other fundamentals of CH_4 or CD_4 would have been masked by absorptions of H_3CI, D_3CI, or D_2CO present in greater abundance.

Weak lines at 1032 and 1038 cm^{-1}, unaffected by ^{13}C- or D-labeled reactants were observed after irradiation with the low-pressure Hg lamp when oxygen mole fractions were relatively large, and even when iodomethane was absent. Assignment to ozone is consistent with known argon matrix wavenumbers (16).

The remaining lines detected after irradiation are not easily assigned to specific known molecules. One group of these, listed in Table 6, was fairly intense and had similar intensity behavior during various operations and under varied experimental conditions. Selected regions of spectra illustrated in Figs. 1 and 2 show these lines obtained from two sets of isotopically labeled reactants.

Other lines, listed in Table 7, are difficult to assign to particular molecules, but the wavenumber values and isotope shift do provide some clues to the nature of the chromophores.

Discussion

Tentative Identification of Hydrogen Hypoiodite

The lines in Table 6 may be analyzed according to the wavenumber positions and isotope effects as follows. The lines near 3400 and 2500 cm^{-1} are obviously O—H and O—D stretching modes. The lines between 540 and 575 cm^{-1} are suitable for O—I valence-stretching modes; these values are similar both to the mean, 504 cm^{-1}, of wavenumbers of symmetric and antisymmetric stretching modes of IO_2-containing molecules (17), and to the single fundamental of the IO free radical, 673 and 504 cm^{-1}, in its two characterized electronic states (18). The lines near 1190 and 870 cm^{-1} are appropriate to a deformation mode in which most of the amplitude (and kinetic energy) of vibration belongs to the H and D atoms. All lines are insensitive to ^{13}C-labeling, indicative of absence of carbon in the carrier. When ^{16}O- and ^{18}O-reactants, including $^{16}O_2$, $^{18}O_2$, and $^{16}O^{18}O$, were used, no further lines were produced; thus the carrier contains a single oxygen atom. The best estimate of the carrier consistent with these observations is hydrogen hypoiodite HOI. Two further broad lines, near 502 cm^{-1} in H_3CI and 377 cm^{-1} in D_3CI experiments, seem to have similar intensity behavior to the

Can. J. Chem. Downloaded from www.nrcresearchpress.com by 210.87.254.5 on 09/05/12
For personal use only.

TABLE 7. Absorption lines (cm^{-1}) of miscellaneous species produced after irradiation of specified reactants

$H_3{}^{12}CI$ $^{16}O_2$	$H_3{}^{12}CI$ $^{18}O_2$	$H_3{}^{13}CI$ $^{16}O_2$	$D_3{}^{12}CI$ $^{16}O_2$	$D_3{}^{12}CI$ $^{18}O_2$
3544	3532	3544		
3351 br	3338 br	3351 br	2475 br	2462 br
1754	1721	1714		
1050	1049	1050	770	
839.3	795.1	838.4	837	795.7
			835	
801.5	760	801.5	799.8	759.3
587	557	587	573	546
562.3	536.5	563	556	530
553.5		553.8	548	522.3

lines in Table 6, but show no ^{18}O shift, perhaps because of their breadth. The large deuterium isotope shift is appropriate to a H- or D-stretching or, more likely in this wavenumber region, deformation mode. The breadth of these two lines suggests strongly hydrogen-bonded interactions. Because of the line breadth and insensitivity to ^{18}O-labeling, these lines will be assumed not to belong to the same carrier, in the same environment, as the lines in Table 6.

On the basis of assignment of these twelve lines to four isotopic varieties of hydrogen hypoiodite with a common vibrational force field, a complete normal coordinate analysis has been conducted. The results (19) include a fit of these wavenumbers to 0.2% accuracy and a potential energy distribution entirely consistent with the above deductions. Comparison of the force field parameters obtained thus for HOI with those for the other hydrogen hypohalites HOF, HOCl, and HOBr, all with ~0.2% fitting accuracy, shows gradual periodic trends expected for such a family of simple molecules. These results are taken as strong support for the identification of the new carrier as stated.

Other Unidentified Products

Sharp but weak lines between 760 and 840 cm^{-1} (*cf.* Table 7) appeared during irradiation with the low-pressure Hg lamp but disappeared rapidly when the HPK 125 lamp was used. Isotopic shifts are appropriate to either O—O or I=O vibrations. We expect the O—O bond to be much more susceptible to rupture by near ultraviolet radiation, copiously emitted by the HPK 125 lamp, than the I=O bond. $H_3{}^{12}COOH$ and $D_3{}^{12}COOD$ absorb at 820 and 794 cm^{-1} respectively (20); the measured deuterium shifts are much smaller. Other peroxides expected to absorb in this region are the radical H_3COO and its iodide H_3COOI.

Lines near 3350 or 2475 cm^{-1} were relatively broad, presumably indicative of OH or OD groups involved in hydrogen bonding. Two weak lines at 1754 and 1054 cm^{-1} (and their isotopic counterparts) gave measurable absorbances in experiments only with larger oxygen mole fractions (~0.25) but they do not necessarily belong to the same carrier. The former line exhibited shifts appropriate to a carbonyl stretching mode, whereas the broader line at 1050 cm^{-1} seemed to be unaffected by ^{13}C-labeling.

Groups of lines between 500 and 600 cm^{-1} are much more sensitive to ^{18}O-presence than to ^{13}C-labeling, indicative of O—I vibrations for instance, but not C—I. Their carriers may be further iodine oxides or oxyacids, but absorbance effects on annealing do indicate that a few different species are involved.

Mechanism of Photolytic and Oxidation Processes

A full treatment of the reactions must explain the production of the following species definitely detected: H_2O, H_2CO, CO, CO_2, HI, HO_2, O_3; and the probable detection of HOI, HCOOH, CH_4, some peroxide; but the absence of CH_3, OI, HCO, OH, H_2O_2, H_2O_3, H_2O_4, HIO_2, HIO_3, HIO_4. The following set of reactions briefly summarizes a reasonable, but not unique, explanation of the product distribution under the conditions of these experiments:

Can. J. Chem. Downloaded from www.nrcresearchpress.com by 210.87.254.5 on 09/05/12
For personal use only.

Can. J. Chem. Downloaded from www.nrcresearchpress.com by 210.87.254.5 on 09/05/12
For personal use only.

$$[1]\quad H_3CI + O_2 \xrightarrow{h\nu} [CH_3 + O_2 + I \rightarrow \begin{Bmatrix} H_3COO + I \\ \text{or } H_3COOI \end{Bmatrix} \xrightarrow{h\nu}] H_2CO + HOI$$

$$[2]\quad H_2CO \xrightarrow{h\nu} H_2 + CO$$

$$[3]\quad H_2CO + O_2 \rightarrow H_2O + CO_2$$

$$[4]\quad H_3CI + O_2 \xrightarrow{h\nu} [CH_2 + O_2 + HI \rightarrow] HCOOH + HI$$

$$[5]\quad HCOOH \xrightarrow{h\nu} H_2O + CO$$

$$[6]\quad HI \xrightarrow{h\nu} H + I$$
$$H + H_3CI \rightarrow CH_4 + I$$
$$H + O_2 \rightarrow HO_2$$

$$[7]\quad O_2 \xrightarrow{h\nu} O + O$$
$$O + O_2 \rightarrow O_3$$

$$[8]\quad HOI \xrightarrow{h\nu} OH + I$$
$$OH + I + H_2CO \rightarrow H_2O + CO + HI$$
$$\rightarrow HCOOH + HI$$

$$[9]\quad H_3CI \xrightarrow{h\nu} H_3C + I \rightarrow H_3CI \text{ (recombination)}$$

Separate experiments with one of H_3CI, O_2, or D_2CO in argon justify inclusion of reactions 2, 7, and 9, and experiments on D_2CO and O_2 in Ar for [3]. This reaction scheme may be compared with those proposed for the gas phase photo-oxidation of iodomethane (21–23). Whether ozone was produced only directly from oxygen in experiments with iodomethane could not be ascertained.

Evidence exists for the production of both H_2CO and HOI in the same matrix cage in that widths of HOI lines were greater than those of, for instance, ozone, and the shifts of some methanal vibrations from wavenumbers associated with isolated molecules in solid argon (5, 6). These effects suggest a hydrogen-bonded interaction of form

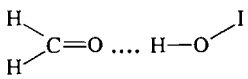

The resulting perturbation of HOI wavenumbers probably does not appreciably affect the force field parameters calculated from these measurements (19).

National Research Council of Canada provided financial support of this work.

1. J. L. Roebber. J. Phys. Chem. **67**, 2391 (1963).
2. R. L. Redington and D. E. Milligan. J. Chem. Phys. **37**, 2162 (1962); **39**, 1276 (1963).
3. K. B. Harvey and H. F. Shurvell. J. Mol. Spectrosc. **25**, 120 (1968).
4. J. F. Ogilvie. Unpublished results.
5. K. B. Harvey and J. F. Ogilvie. Can. J. Chem. **40**, 85 (1962).
6. H. Khoshkoo and E. R. Nixon. Spectrochim. Acta, **29A**, 603 (1973).
7. G. E. Leroi, G. E. Ewing, and G. C. Pimentel. J. Chem. Phys. **40**, 2298 (1964).
8. J. B. Davies and H. E. Hallam. J. Chem. Soc., Faraday Trans. II. **68**, 509 (1972).
9. R. N. Perutz and J. J. Turner. J. Chem. Soc., Faraday Trans. II, **69**, 452 (1973).
10. H. Dubost and L. Abouaf-Marguin. Chem. Phys. Lett. **17**, 269 (1972).
11. A. J. Barnes, J. B. Davies, H. E. Hallam, and J. D. R. Howells. J. Chem. Soc., Faraday Trans. II, **69**, 246 (1973).
12. J. F. Ogilvie. Nature, **243**, 210 (1973).
13. D. E. Milligan and M. E. Jacox. J. Chem. Phys. **54**, 927 (1971).
14. I. C. Hisatsune and J. Heicklen. Can. J. Spectrosc. **18**, 135 (1973).
15. C. D. Bass and G. C. Pimentel. J. Am. Chem. Soc. **83**, 3754 (1961).
16. L. Andrews and R. C. Spiker. J. Phys. Chem. **76**, 3208 (1972).
17. P. M. A. Sherwood and J. J. Turner. Spectrochim. Acta, **26A**, 1975 (1970).
18. R. A. Durie, F. Legay, and D. A. Ramsay. Can. J. Phys. **38**, 444 (1960).
19. J. F. Ogilvie. Can. J. Spectrosc. In press.
20. N. R. Subbaratnam and J. G. Calvert. J. Am. Chem. Soc. **84**, 1113 (1962).
21. J. Heicklen and H. S. Johnston. J. Am. Chem. Soc. **84**, 4030 (1962).
22. M. Barber, J. Farren, and J. W. Linnett. Proc. R. Soc. Lond. **A274**, 306 (1963).
23. J. Farren, J. R. Gilbert, J. W. Linnett, and I. A. Read. Trans. Faraday Soc. **60**, 740 (1964).

The Behavior of Thiochromanone and Isothiochromanone Sulfoxides in the Schmidt Reaction: Isolation of a Novel Azide Product from Thiochromone Sulfone[1]

IAN W. J. STILL, M. THOMAS THOMAS, AND ALAN M. CLISH[2]
Department of Chemistry, University of Toronto, Toronto, Ontario L5L 1C6

Received September 23, 1974

IAN W. J. STILL, M. THOMAS THOMAS, and ALAN M. CLISH. Can. J. Chem. **53**, 276 (1975).

The Schmidt reaction has been carried out on thiochroman-4-one 1-oxide and a number of related sulfoxides. In all cases lactam formation by attack of HN_3 on the carbonyl group of the keto sulfoxide appears to predominate, with no evidence for sulfoximine formation. The question of aryl *vs.* alkyl migration, as in other systems, is dependent on the degree of substitution of the alkyl group. When the Schmidt reaction was carried out upon thiochromone 1,1-dioxide two products, the lactam resulting from preferential vinyl migration and a novel α-azido sulfone resulting from 1,4-addition, were obtained.

IAN W. J. STILL, M. THOMAS THOMAS et ALAN M. CLISH. Can. J. Chem. **53**, 276 (1975).

On a effectué la réaction de Schmidt sur la thiochromanone-4 oxyde-1 et un certain nombre de sulfoxydes qui lui sont apparentés. Dans tous les cas, il y a formation de lactame par attaque de HN_3 sur le groupement carbonyle du céto-sulfoxyde et cette réaction semble prédominante; on n'a trouvé aucune preuve expérimentale pour la formation d'une sulfoxymine. La question de la migration des groupes aryles par opposition à la migration à des groupes alkyles dépend du degré de substitution en accord avec ce qui a été observé dans d'autres systèmes. Lorsque l'on effectue la réaction de Schmidt sur la thiochromonedioxyde-1,1, on obtient deux produits: la lactame résultant de la migration préférentielle du groupe vinyle et une nouvelle α-azido sulfone qui résulte d'une addition-1,4. [Traduit par le journal]

Introduction

The Schmidt reaction of ketones was first reported over fifty years ago and the scope and mechanism of this rearrangement reaction have been extensively reviewed by Smith (1) and, more recently, by Koldobskii *et al.* (2) Interest in this reaction, and the mechanistically related Beckmann rearrangement, remains high, however, as indicated by a number of recent publications (3–6). Some years ago, Evans and Lockhart (7) had studied a series of tetralones **1***a* and contrasted their behavior in the Schmidt reaction with that of the analogous chromanones **1***b*. They concluded that the preference for the formation of cyclic benzamide derivatives (by alkyl rather than aryl migration) in the heterocyclic series could be attributed to the electron-releasing effect of oxygen. It occurred to us that the thiochromanone **1***c* series of compounds would be interesting to study from this point of view as the hetero atom in this series might be expected to show quite different behavior according to whether it was present as the sulfide, sulfoxide, or sulfone functionality. Indeed, Wünsch and co-workers (8) had earlier examined a limited number of thiochromanones and thiochromanone 1,1-dioxides with variable substituents in the aromatic ring only. In addition to completing the series by including the corresponding sulfoxide **2***a* and its derivatives in the present work, we have also attempted to study the effect of variation in the substitution pattern of the heterocyclic ring on the course of the Schmidt rearrangement.

The interesting results obtained recently by Williams and Cram (9) from the reaction of certain keto-sulfoxides with hydrazoic acid, in which attack at both functional groups was observed, and the work already referred to by Hill and Cullison (5) on the fragmentation of isothiochromanone oxime under the conditions of the Beckmann rearrangement provided a further impetus for our study.[3] Our findings in relation to these aspects will also be discussed.

[1]Presented in part at the 57th Canadian Chemical Conference of the Chemical Institute of Canada, Regina, Saskatchewan, June 2–5, 1974.

[2]Undergraduate research participant.

[3]Unless otherwise stated all Schmidt reactions described in this report were conducted with sodium azide in concentrated H_2SO_4 at 25°.

Can. J. Chem. Downloaded from www.nrcresearchpress.com by 210.87.254.105 on 09/05/12
For personal use only.

Can. J. Chem. Downloaded from www.nrcresearchpress.com by 210.87.254.105 on 09/05/12
For personal use only.

Results and Discussion

The product expected from the Schmidt reaction of thiochromanone 1-oxide **2***a* was the lactam 2,3-dihydro-1,5-benzothiazepin-4(5*H*)-one 1-oxide **3**, resulting from preferred aryl migration in the (presumed) intermediate iminodiazonium ion **5***a*. The sole product isolated from the reaction did indeed possess this structure, the proof of which rests mainly on analytical and mass spectral (molecular ion) data, as well as analogy with the earlier work of Wünsch *et al.* (8). Because of the relative insolubility of this compound and the related sulfoxide lactams it was not possible to use n.m.r. data in assigning structure in the manner reported in earlier studies of the Schmidt reaction of some chromanone derivatives (10, 11).

It was found in the mass spectrum of the lactam **3**, for example, that there were no significant amounts of the fragment ions at *m/e* 105 or 153 due to C_7H_5O(benzoyl) and $C_7H_5SO_2$-(benzoyl + SO), whereas in the lactam **6**, resulting from the Schmidt reaction of 3,3-dimethylthiochroman-4-one 1-oxide **2***c*, fragment ions are observed at *m/e* 105 and 153 with intensities of 71 and 75%, respectively. Thus it can be argued from this and several similar considerations of the mass spectra that in the case of lactam **6** both the S=O and the C=O units are directly bonded to the aromatic ring and thus this lactam is a substituted 2,3-dihydro-1,4-benzothiazepin-5-(4*H*)-one 1-oxide. Conversely, the lactam **3** and related lactams (see Table 1) which lack such fragment ions are members of the isomeric 2,3-dihydro-1,5-benzothiazepin-4(5*H*)-one 1-oxide series.

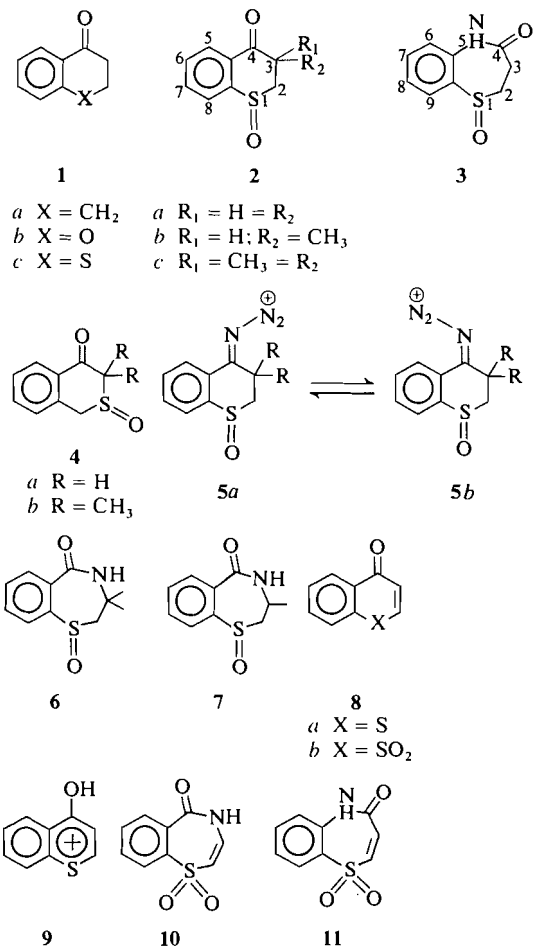

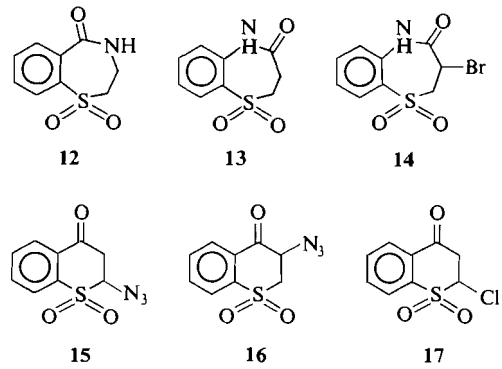

The results of the Schmidt reaction on some simple thiochromanone sulfoxides are summarized in Table 1. In the parent case and in the 8-methyl and 2,2-dimethyl substituted analogs aryl migration is strongly preferred over the alternative primary alkyl migration. In the case of **2***c*, as has been mentioned above, the preference is for tertiary alkyl over aryl migration, leading to the alternative lactam insertion product. Whether this result, however, is a reflection of migratory aptitude or simply involves equilibration of the two possible iminodiazonium ions **5***a* and *b* followed by concerted (*anti*) migration in the sterically more favorable ion **5***b*, is a dilemma posed in a recent review of the Schmidt reaction (12), but unfortunately one not resolved by the present study. Interestingly, in the intermediate case of 3-methylthiochroman-4-one 1-oxide, **2***b*, two isomeric lactams are obtained, in a roughly 3:5 ratio, indicating that both possible modes of migration occur. The major product has been assigned the structure of the 3-methyl derivative of **3**, corresponding to aryl migration,

TABLE 1. Products of Schmidt rearrangement of thiochromanone sulfoxides

Starting sulfoxide	Lactam	Melting point[a] (°C)	Isolated yield (%)
Thiochroman-4-one 1-oxide, **2***a*	**3**	184–185[b]	30
8-Methyl-**2***a*	9-Methyl-**3**	210–211[b]	52
2,2-Dimethyl-**2***a*	2,2-Dimethyl-**3**	201–202[c]	77
3-Methylthiochroman-4-one 1-oxide, **2***b*	3-Methyl-**3**	195–196[c]	45
	7	292–294[b]	27
3,3-Dimethylthiochroman-4-one 1-oxide, **2***c*	**6**	235–236[c]	82
Isothiochromanone 2-oxide, **4***a*	—	—	—
3,3-Dimethylisothiochromanone 2-oxide, **4***b*	—	—	—[d]

[a]All samples melted with decomposition.
[b]Recrystallized from MeOH.
[c]Recrystallized from 95% EtOH.
[d]Starting material recovered in 75% yield.

and the minor product is assigned structure **7** arising from *sec*-alkyl migration.

It is interesting to note in passing that Wünsch and his collaborators (8) had attempted to carry out the Schmidt reaction on 3,3-dimethylthiochroman-4-one but obtained only small amounts of uncharacterizable oils, a not uncommon result with *tert*-alkyl ketones. The reason for the quite different result we have obtained with the analogous sulfoxide is not clear. The rather low isolated yield of the lactam **3** from the parent thiochroman-4-one 1-oxide is probably attributable to the greater solubility of the unsubstituted lactam in water or to formation of water-soluble cleavage products. In the case of 3-methylthiochroman-4-one 1-oxide, where both isomeric lactams are obtained, they were found to have rather similar solubility characteristics in hydroxylic solvents and so we do not feel that there is likely to be any significant amount of the alternative lactam product in the thiochroman-4-one 1-oxide reaction.

Attempts to carry out the Schmidt reaction on isothiochromanone sulfoxide **4***a* (see Table 1) met with no success, due presumably to the much greater likelihood of ring cleavage occurring via carbonium ion intermediates arising from protonation in the strongly acidic media employed. Indeed, charring and decomposition of both **4***a* and of isothiochromanone itself, as indicated by immediate formation of a deep brown color in concentrated sulfuric acid, was evident even before addition of the sodium azide. In contrast, members of the thiochromanone sulfoxide series (and the related sulfides) dissolve in concentrated sulfuric acid with the formation of a very deep red color, which is discharged on dilution with water. The only other sulfide examined, 3,3-dimethylisothiochromanone was likewise decomposed by exposure to concentrated sulfuric acid, although rather surprisingly the corresponding sulfoxide **4***b* was recovered unchanged in the Schmidt reaction.

We have also attempted to carry out the reaction of thiochroman-4-one 1-oxide **2***a* with hydrazoic acid in the presence of chloroform at 45°, conditions used by Whitehead and Bentley (13) for the formation of sulfoximines from simple sulfides, as well as by Williams and Cram (9) for the formation of Schmidt rearranged sulfoximines from acyclic keto sulfoxides structurally rather similar to ours. Although the latter authors found that attack at sulfur was apparently faster than attack on the carbonyl group, our attempts to isolate sulfoximines according to the procedures detailed in the excellent review by Oae *et al.* (14) have been without success. Only lactam formation was observed, but in somewhat lower yield than in the procedure carried out at 25° in the absence of chloroform. Even in the case of the sterically unfavorable 3,3-dimethylthiochroman-4-one 1-oxide, only attack at carbonyl (lactam formation) could be observed under these conditions.

To complete our investigation we attempted to carry out the Schmidt reaction on the unsaturated analogs of thiochromanone, namely thiochromone **8***a* and its 1,1-dioxide **8***b*.[4] Treatment of the former under the conditions of the Schmidt reaction led, not surprisingly, to an almost quantitative recovery of unreacted ketone, presumably because of the initial formation and relative stab-

[4]The third member of this series, the analogous sulfoxide, is at present unknown. Attempts to synthesize this potentially interesting molecule are currently under investigation in our laboratory.

Can. J. Chem. Downloaded from www.nrcresearchpress.com by 210.87.254.105 on 09/05/12
For personal use only.

Can. J. Chem. Downloaded from www.nrcresearchpress.com by 210.87.254.105 on 09/05/12
For personal use only.

ility of the thiapyrylium cation **9**. In the case of the sulfone, however, a more interesting result was the formation of two products, one of which is a lactam arising from 1,2-addition of HN_3 to the carbonyl group, followed by Schmidt rearrangement, and the other is an α-azido sulfone resulting from 1,4-addition of HN_3.

The lactam formed has been assigned structure **10**, *i.e.* the product of vinyl migration, rather than the isomeric lactam structure arising from aryl migration. Some evidence in support of the gross structure of the lactam came from its mass spectrum which had a base peak at *m/e* 209 (molecular ion) and showed evidence of rearrangement to a cyclic sulfinate, followed by consecutive loss of SO, O, and CO leading (presumably) to an indole fragment at *m/e* 117 (< 10%). A second major fragmentation led, by loss of CHO + HCN (or some alternative combination of the same composition), to an ion at *m/e* 153 (11%) and by subsequent loss of O to an ion at *m/e* 137 (6%). Confirmation of the assignment as structure **10**, rather than the isomer **11**, was sought by reducing the unsaturated lactam to the known 2,3-dihydro-1,4-benzothiazepin-5(4*H*)-one 1,1-dioxide, **12**, synthesized by the method of Wünsch *et al.* (15) from 2-mercaptobenzoic acid. Several attempts to reduce the double bond by palladium or platinum catalyzed hydrogenation, at pressures up to 5 atm, were totally unsuccessful, perhaps because of catalyst poisoning by the sulfur and/or nitrogen atom in the substrate. An alternative approach was to synthesize 2,3-dihydro-1,5-benzothiazepin-4(5*H*)-one 1,1-dioxide, **13**, by Schmidt rearrangement of thiochroman-4-one 1,1-dioxide as described in the earlier paper by Wünsch *et al.* (8) and dehydrogenate this to the unsaturated lactam isomer **11** which, of course, should *not* have been identical with our lactam product. Such attempts, using chloranil and 2,3-dichloro-5,6-dicyano-*p*-benzoquinone in refluxing dioxan or xylene were also quite ineffectual. Finally, however, we were able to convert 3-bromothiochroman-4-one 1,1-dioxide by the Schmidt reaction under Wünsch's conditions (8) into the 3-bromo-2,3-dihydro-1,5-benzothiazepin-4(5*H*)-one 1,1-dioxide, **14**, in good yield. Simple dehydrobromination of this compound by heating with pyridine afforded, again in good yield, the unsaturated lactam **11**. This compound was clearly different from, although isomeric with, our original unsaturated lactam.Compound **11**, for example, shows a carbonyl band in the infrared at 1665 cm^{-1} as compared to 1650 cm^{-1} shown by the (benzoyl) carbonyl of **10**. Compound **11** is considerably more soluble in organic solvents than **10** and the n.m.r. spectrum confirmed the presence of both the NH group and the double bond. Finally, the mass spectrum of **11** is exceedingly simple compared to that of **10**. It reveals a molecular ion at *m/e* 209 (14%) but, unlike the isomeric lactam, fragments by a simple mechanism involving loss of first SO_2 to give a peak at *m/e* 145 (36%), followed by loss of CO leading to the indole fragment ion at *m/e* 117 (100%) which, as expected, further fragments almost exclusively by loss of HCN (16).

Although the final confirmation of structure thus did not include the direct comparison with a known compound which we would have liked, we feel that the evidence described establishes the structure of **10** beyond reasonable doubt. It is inconceivable, for example, that in the rearrangement of 3-bromothiochroman-4-one 1,1-dioxide, using the conditions described by Wünsch *et al.* (8) for the rearrangement of the parent thiochromanone sulfone, the lactam formed could be other than that expected from preferred aryl migration *i.e.* **14**.

The second product from the Schmidt reaction of **8***b* could be isolated only by reducing the reaction time and by carefully controlling the p*H* during the work-up procedure. That this product is the simple adduct of thiochromone 1,1-dioxide and HN_3 **15** was shown by analytical, i.r., and n.m.r. data. It is well known from the work of Moore *et al.* (17) that addition of HN_3 to quinones occurs readily, although the initial hydroquinone adducts often undergo disproportionation to aminoquinones accompanied by loss of nitrogen. The Schmidt rearrangement of simple quinones to azepine-2,5-dione derivatives has also been reported by Rickards and Smith (18). In our case, nucleophilic addition of azide ion could, in principle, occur at either the C-2 or C-3 position in **8***b* (or its conjugate acid) leading to either **15** or **16**. Attempts to add azide ion and other nucleophiles to **8***b* under neutral or basic conditions were unsuccessful, and led only to water-soluble cleavage products (presumably sulfinates) by nucleophilic addition at C-2 followed by elimination. This proposition has some support from the work of Nesmeyanov and Rybinskaya (19) on the addition of azide to acyclic β-sulfonyl α,β-unsaturated ketone sys-

Can. J. Chem. Downloaded from www.nrcresearchpress.com by 210.87.254.105 on 09/05/12
For personal use only.

tems and that of Elkaschef *et al.* (20) on the ring opening of thiochromones by the attack of even relatively weak nucleophiles such as amines. This ease of ring opening may be taken as somewhat indirect evidence that C-2 is the preferred site for nucleophilic attack, given the relative leaving group capabilities of $ArC{=}O$ and $ArSO_2^-$.

By the addition of HCl in acetic acid to thiochromone 1,1-dioxide (21) we obtained an excellent yield of 2-chlorothiochroman-4-one 1,1-dioxide, **17**. This compound was clearly distinct from the known 3-chloro isomer and showed a remarkable similarity in the n.m.r. to our HN_3 adduct **15**. Finally, by extending this method to the addition of HN_3 in chloroform to **8***b* we were able to prepare the expected adduct **15** identical in all respects with the product of the Schmidt reaction.

We believe that the α-azido sulfone **15** may be the first representative of this class of compound.[5] A study of its chemical behavior is under way in our laboratory and will be the subject of a separate publication.

Experimental

General

The i.r. spectra (cm^{-1}) were recorded (Nujol mulls unless otherwise stated) on a Perkin-Elmer 337 grating spectrophotometer and the low resolution mass spectra were obtained on a Bell and Howell 21-490 spectrometer. Accurate mass measurements were carried out on the AEI MS-902 instrument. Nuclear magnetic resonance spectra were recorded on a Varian T-60 spectrometer in $CDCl_3$ with TMS as internal standard. Elemental analyses were performed by the Scandinavian Microanalytical Laboratory, Box 25, DK2730 Herlev, Denmark. Column chromatography and thin-layer chromatography (analytical and preparative) were run on silica gel using Fisher A.C.S. grade solvents. All melting points and boiling points are uncorrected.

Thiochromanones

Thiochroman-4-one, 8-methylthiochroman-4-one, 3-methylthiochroman-4-one, and isothiochromanone were prepared as described previously (22). The synthesis of 2,2-dimethylthiochroman-4-one was also reported earlier by us (23). The synthesis of 3,3-dimethylisothiochroman-4-one from isothiochromanone by reaction with methyl iodide and sodium hydride used essentially the method we described recently to prepare 3,3-dimethylthiochroman-4-one from its unsubstituted counterpart (24).

Sulfoxides

The general method, using H_2O_2 – acetic acid, for the conversion of thiochromanones into their corresponding sulfoxides has been described (23). In the case of the isothiochromanone sulfoxides a much shorter reaction time (1–2 h) sufficed. 3,3-Dimethylisothiochromanone 2-oxide could not be obtained crystalline and the liquid, as is usual with such sulfoxides, decomposed on attempted distillation, but n.m.r. and i.r. data for this compound were in accord with the expected structure.

Schmidt Reaction on Thiochroman-4-one 1-Oxide (2a)

The ketone (634 mg) was dissolved in concentrated H_2SO_4 (4 ml). To the stirred solution at 0–5° was added sodium azide (488 mg) in portions over 15 min. After 2 h at 0–5°, the deep red mixture was stirred at 25° for 16 h before pouring rapidly over crushed ice with stirring. The pale brown solid (210 mg) which formed was filtered off from the ice-cold solution and recrystallized from methanol, m.p. 184–185° (dec.) The 2,3-dihydro-1,5-benzothiazepin-4(5*H*)-one 1-oxide **3** so obtained had i.r. bands at 3110, 3180(NH); 1665(C=O); and 1040(S=O) cm^{-1} and the mass spectrum showed a molecular ion peak at *m/e* 195(25%) and major fragment ions at *m/e* 167(10), 149(20), and 147(18).

Anal. Calcd. for $C_9H_9NO_2S$: C, 55.38; H, 4.61; N, 7.18; S, 16.41. Found: C, 55.36; H, 4.75; N, 7.13; S, 16.48.

Schmidt Reaction on 8-Methylthiochroman-4-one 1-Oxide

Using the above procedure the lactam 9-methyl-**3** was obtained as a white solid, m.p. 210–211° (MeOH). Infrared bands were observed at 3100, 3180(NH); 1640, 1690(C=O); and 1035(S=O) cm^{-1}. The mass spectrum showed a molecular ion peak at *m/e* 209(9) and major fragment ions at *m/e* 193(35), 160(18), 150(19), 143(35), and 107(12).

Anal. Calcd. for $C_{10}H_{11}NO_2S$: C, 57.41; H, 5.30; N, 6.70; S, 15.30. Found: C, 57.27; H, 5.30; N, 6.66; S, 15.35.

Schmidt Reaction on 2,2-Dimethylthiochroman-4-one 1-Oxide

The above procedure afforded the lactam 2,2-dimethyl-**3** as a white solid, m.p. 201–202° (95% EtOH). Infrared bands were observed at 3100, 3160(NH); 1640, 1680 (C=O); and 1040(S=O)cm^{-1}. The mass spectrum showed a molecular ion peak at *m/e* 223(11) and major fragment ions at *m/e* 152(14), 141(32), 125(27), and 123(17).

Anal. Calcd. for $C_{11}H_{13}NO_2S$: C, 59.18; H, 5.87; N, 6.28; S, 14.34. Found: C, 59.07; H, 5.84; N, 6.21; S, 14.31.

Schmidt Reaction on 3,3-Dimethylthiochroman-4-one 1-Oxide (2c)

The above procedure afforded 3,3-dimethyl-2,3-dihydro-1,4-benzothiazepin-5(4*H*)-one 1-oxide, **6**, as a white solid, m.p. 235–236° (95% EtOH). Infrared bands appeared at 3180(NH); 1640(C=O); and 1035(S=O) cm^{-1}. The mass spectrum showed a molecular ion peak at *m/e* 223(20) and major fragment ions at *m/e* 166(41), 161(21), 152(75), 146(16), 136(23), 121(21), 118(31), and 105(71).

Anal. Calcd. for $C_{11}H_{13}NO_2S$: C, 59.18; H, 5.87; N, 6.28; S, 14.34. Found: C, 59.11; H, 5.96; N, 6.16; S, 14.44.

Schmidt Reaction on 3-Methylthiochroman-4-one 1-Oxide (2b)

The reaction of **2***b* (582 mg) with sodium azide – concentrated H_2SO_4, conducted under the usual conditions,

[5]NOTE ADDED IN PROOF: Since this work was submitted for publication the preparation of a similar compound has been reported (26).

Can. J. Chem. Downloaded from www.nrcresearchpress.com by 210.87.254.105 on 09/05/12
For personal use only.

was stopped after 3 h at 25°. Only a small amount of precipitate (32 mg) formed on pouring the concentrated H_2SO_4 solution over crushed ice. The cold aqueous filtrate was neutralized with solid sodium hydrogen carbonate and extracted thoroughly with methylene chloride. Evaporation afforded a crude solid product (438 mg). Treatment of the solid with a small quantity of chloroform and filtration of the residual solid gave a white solid (151 mg), identical with the original solid obtained on pouring the reaction mixture over ice. The combined product was recrystallized from methanol, m.p. 292–294° (dec.). This compound had infrared bands at 3150, 3075(NH); 1660(C=O); and 1035(S=O)cm^{-1}. Mass spectral analysis showed the expected molecular ion in accord with structure **7** at *m/e* 209(1) and major fragment ions at *m/e* 153(18), 152(100), 150(17), 136(10), 121(18), and 104(11).

Anal. Calcd. for $C_{10}H_{11}NO_2S$: C, 57.41; H, 5.30; N, 6.70; S, 15.30. Found: C, 57.30; H, 5.43; N, 6.57; S, 15.41.

The chloroform-soluble filtrate obtained by the above procedure was evaporated, affording a white solid (251 mg) further purified by column chromatography and elution with 5% methanol in chloroform. Recrystallization from methanol afforded white prisms of the lactam 3-methyl-**3**, m.p. 195–196°. Infrared $\nu_{max}(CHCl_3)$ 3150, 3100(NH); 1660(C=O); and 1020(S=O)cm^{-1}. Mass spectrum *m/e* 209(100), 193(37), 167(22), 152(28), 150(15), 146(15), 136(45), 123(44), and 106(26). Nuclear magnetic resonance δ 1.2(3H, d, J = 6 Hz); 3.4(3H, m); 7.2–8.0(4H, m); 8.8(1H, br s) p.p.m.

Anal. Calcd. for $C_{10}H_{11}NO_2S$: C, 57.41; H, 5.30; N, 6.70; S, 15.30. Found: C, 57.01; H, 5.25; N, 6.48; S, 15.23.

*Attempted Schmidt Reaction on 3,3-Dimethylisothiochromanone 2-Oxide (**4b**)*

A solution of the keto sulfoxide (416 mg) in concentrated H_2SO_4 (5 ml) was treated in the usual manner at 0–5° with sodium azide (405 mg) and the solution finally maintained at 25° for 18 h. The usual work-up procedure afforded only starting material (315 mg, 75%).

*Schmidt Reaction on Thiochromone 1,1-Dioxide (**8b**)*

Thiochromone sulfone (21, 23) (0.97 g) was dissolved in concentrated H_2SO_4 (10 ml) and cooled to 0–5°. Careful addition of sodium azide (0.39 g) over 1 h was followed by stirring at 0° for 30 min and then at 25° for a further 30 min. The reaction mixture was poured on to ice and the yellow precipitate formed removed at once by filtration. The acidity of the aqueous solution was adjusted to around p*H* 7 by the addition of sodium acetate and the solution then extracted thoroughly with chloroform. Partial evaporation of the chloroform extracts afforded a yellow solid identical with that obtained from the original aqueous solution by filtration and the two fractions were combined (56 mg, 6%) and recrystallized from methanol as yellow needles, m.p. 295–296°. The infrared spectrum showed bands at 3350, 3220(NH); 1650(C=O); 1320 and 1145(SO_2) cm^{-1}. Mass spectral analysis showed the expected molecular ion at *m/e* 209(100) in accord with the lactam structure **10**, and major fragment ions at *m/e* 161(24), 153(11), 152(7), 145(8), 137(6), 121(8), and 104(9).

Anal. Calcd. for $C_9H_7NO_3S$: C, 51.68; H, 3.37; N, 6.70; S, 15.30. Found: C, 51.60; H, 3.43; N, 6.61; S, 15.35.

The chloroform filtrate obtained by isolation of the yellow solid (lactam) described above was evaporated and a pale yellow solid (103 mg, 10%) obtained by crystallization from aqueous alcohol, m.p. 110–111°. That this compound possessed the structure **15** was shown by the following spectral and analytical data. (Mass spectral analysis was unsatisfactory, presumably due to the thermal instability of the azide.) Infrared $\nu_{max}(CHCl_3)$ 2125 (N_3); 1697 (C=O); 1325 and 1140, 1120(SO_2) cm^{-1}; δ 3.5 (2H, doublet of quartets); 5.1 (1H, dd) (J_{AB} = 18 Hz, J_{AX} = 4 Hz, J_{BX} = 5 Hz); 7.7–8.3 (4H, m) p.p.m.

Anal. Calcd. for $C_9H_7N_3O_3S$: C, 45.57; H, 2.98; N, 17.72; S, 13.48. Found: C, 45.62; H, 2.99; N, 17.64; S, 13.65.

*3-Bromo-2,3-dihydro-1,5-benzothiazepin-4(5H)-one 1,1-dioxide (**14**)*

This compound, m.p. 235–237° (dec.) on recrystallization from ethanol–DMF, was prepared by the reaction of HN_3 with 3-bromothiochroman-4-one 1,1-dioxide according to the general procedure described by Wünsch *et al.* (8).

Anal. Calcd. for $C_9H_8BrNO_3S$: C, 37.24; H, 2.76; S, 11.03; Br, 27.58. Found: C, 37.45; H, 2.80; S, 11.51; Br, 27.41.

*1,5-Benzothiazepin-4(5H)-one 1,1-dioxide (**11**)*

The above lactam (200 mg) was heated with dry pyridine (3 ml) until all the solid had dissolved, and then for a further 1–2 min. The unsaturated lactam (128 mg, 89%), had m.p. 214–215° on recrystallization from 95% ethanol. Infrared ν_{max} 3115, 3170(NH); 1665(CO): 1315 and 1140(SO_2)cm^{-1}. Nuclear magnetic resonance δ (acetone-d_6) 5.33 (1H, part of AB quartet); 6.01–6.73 (5H, multiplet); 8.97 (1H, br s) p.p.m. *m/e* 209(14), 145(36), 117(100), 90(43).

Anal. Calcd. for $C_9H_7NO_3S$: C, 51.68; H, 3.37. Found: C, 51.72; H, 3.48.

Addition of HCl to Thiochromone 1,1-Dioxide

Thiochromone 1,1-dioxide (395 mg) was suspended in glacial acetic acid and the mixture saturated with dry HCl gas (21). After 30 min, the reaction mixture was poured into ice water and 2-chlorothiochroman-4-one 1,1-dioxide, **17** (371 mg, 80%) was collected by filtration as a white solid, m.p. 98–100° (hexane–benzene). Infrared $\nu_{max}(CHCl_3)$ 1700(C=O); 1320 and 1140(SO_2) cm^{-1}; δ 3.75 (2H, doublet of quartets); 5.3 (1H, dd) (J_{AB} = 18 Hz, J_{AX} = 4 Hz, J_{BX} = 6 Hz); 7.7–8.3 (4H, m) p.p.m.

Anal. Calcd. for $C_9H_7ClO_3S$: C, 46.85; H, 3.03; Cl, 15.40; S, 13.88. Found: C, 46.96; H, 3.12; Cl, 15.29; S, 13.85.

Addition of HN_3 to Thiochromone 1,1-Dioxide

Thiochromone 1,1-dioxide (388 mg), in chloroform (5 ml) was treated with a solution of hydrazoic acid in chloroform (6 ml; approximately 0.4 M), prepared according to the method of Fieser and Fieser (25). After 15 min at 25°, the solution was evaporated and the product **15** obtained as a pale yellow solid (449 mg, 95%) recrystallized from aqueous alcohol, m.p. 110–112°. This compound was identical (m.p., mixture m.p., i.r., n.m.r.) with the azide obtained in the Schmidt reaction of thiochromone 1,1-dioxide.

We wish to thank Erindale College, Univerity of Toronto, for financial support of this work.

1. P. A. S. SMITH. *In* Molecular rearrangements. Vol. I. *Edited by* P. de Mayo. John Wiley and Sons, Inc., New York. 1963. pp. 507–526.
2. G. I. KOLDOBSKII, G. F. TERESCHENKO, E. S. GERASIMOVA, and L. I. BAGEL. Russ. Chem. Rev. **40**, 835 (1971).
3. H. SINGH, R. K. MALHOTRA, and V. V. PARASHAR. Tetrahedron Lett. 2587 (1973).
4. K. NAGARAJAN and R. K. SHAH. J. Chem. Soc. Chem. Commun. 926 (1973).
5. R. K. HILL and D. A. CULLISON. J. Am. Chem. Soc. **95**, 2923 (1973).
6. P. BEAK and J. A. BARRON. J. Org. Chem. **38**, 2771 (1973).
7. D. EVANS and I. M. LOCKHART. J. Chem. Soc. 4806 (1965).
8. K.-H. WÜNSCH, K.-H. STAHNKE, and A. EHLERS. Chem. Ber. **103**, 2302 (1970).
9. T. R. WILLIAMS and D. J. CRAM. J. Org. Chem. **38**, 20 (1973).
10. G. S. SIDHU, G. THYAGARAJAN, and U. T. BHALERAO. J. Chem. Soc. (C) 969 (1966).
11. S. MINAMI, M. TOMITA, H. TAKAMATSU, and S. UYEO. Chem. Pharm. Bull. **13**, 1084 (1965).
12. D. V. BANTHORPE. *In* The chemistry of the azido group. *Edited by* S. Patai. John Wiley and Sons Ltd., London. 1971. pp. 405–416.
13. J. K. WHITEHEAD and H. R. BENTLEY. J. Chem. Soc. 1572 (1952).
14. S. OAE, K. HARADA, K. TSUJIHARA, and N. FURUKAWA. Int. J. Sulfur Chem. [A], **2**, 49 (1972).
15. K.-H. WÜNSCH, A. EHLERS, and H. BEYER. Chem. Ber. **102**, 1618 (1969).
16. Q. N. PORTER and J. BALDAS. Mass spectrometry of heterocyclic compounds. Wiley-Interscience, New York. 1971. pp. 343–344.
17. H. W. MOORE, H. R. SHELDEN, and D. F. SHELLHAMER. J. Org. Chem. **34**, 1999 (1969); H. W. MOORE, W. WEYLER, JR., and D. S. PEARCE. J. Am. Chem. Soc. **95**, 2603 (1973).
18. R. W. RICKARDS and R. M. SMITH. Tetrahedron Lett. 2361 (1966).
19. A. N. NESMEYANOV and M. I. RYBINSKAYA. Dokl. Akad. Nauk. SSSR, **170**, 600 (1966).
20. M. A.-F. ELKASCHEF, F. M. E. ABDEL-MEGEID, K.-E. M. MOKHTAR, and M. F. ELBARNASHAWI. Ind. J. Chem. **11**, 860 (1973).
21. T. NAMBARA. Yakugaku Zasshi. **78**, 624 (1958); Chem. Abstr. **52**, 18392i (1958).
22. I. W. J. STILL and M. T. THOMAS. J. Org. Chem. **33**, 2730 (1968).
23. M. S. CHAUHAN and I. W. J. STILL. Int. J. Sulfur Chem. In press.
24. I. W. J. STILL, M. S. CHAUHAN, and M. T. THOMAS. Can. J. Chem. **51**, 839 (1973).
25. L. F. FIESER and M. FIESER. Reagents for organic synthesis. Vol. I. John Wiley and Sons, Inc., New York. 1967. p. 446.
26. H. BOEHME and F. ZIEGLER. Justus Liebig's Ann. Chem. 734 (1974).

Can. J. Chem. Downloaded from www.nrcresearchpress.com by 210.87.254.105 on 09/05/12
For personal use only.

Substrate Inhibition in the Hydrolysis of Hippuric Acid Esters by Carboxypeptidase A[1]

JOE MURPHY AND JOHN W. BUNTING

Department of Chemistry, University of Toronto, Toronto, Ontario M5S 1A1

Received July 29, 1974

JOE MURPHY and JOHN W. BUNTING. Can. J. Chem. **53**, 283 (1975).

The dependence of initial velocity upon substrate concentration has been examined in the carboxypeptidase A catalyzed hydrolysis of the following hippuric acid esters (at p*H* 7.5, 25°, ionic strength 0.5): $C_6H_5CONHCH_2CO_2CHRCO_2H$: R = CH_3; CH_2CH_3; $(CH_2)_2CH_3$; $(CH_2)_3CH_3$; $(CH_2)_5CH_3$; $CH(CH_3)_2$; $CH_2CH(CH_3)_2$; C_6H_5; $CH_2C_6H_5$. All of these esters display marked substrate inhibition of their enzymic hydrolyses. With the exception of R = CH_3, the velocity-substrate concentration profiles for each of these esters can be rationalized by the formation of an E.S_2 complex which, independent of the alcohol moiety of the ester, reacts approximately 25 times more slowly than the E.S complex. For most of these esters, the formation of E.S_2 approximates ordered binding of the substrate molecules at the catalytic and inhibitory sites. While binding at the catalytic site is markedly dependent on the nature of the R group, binding of a second substrate molecule to E.S is not significantly affected by the nature of the R side chain. For R = C_6H_5, the D ester is neither a substrate nor a competitive inhibitor of the hydrolysis of the L-ester but can replace the L-ester at the binding site which is responsible for substrate inhibition. The kinetic analysis suggests that this behavior of D- and L-enantiomers is also typical of the other esters examined (except possibly R = CH_3). For R = CH_3 only, substrate activation also seems to occur prior to the onset of substrate inhibition at higher substrate concentrations.

JOE MURPHY et JOHN W. BUNTING. Can. J. Chem. **53**, 283 (1975).

On a examiné la dépendance, sur la concentration du substrat, de la vitesse initiale de l'hydrolyse, catalisée par la carboxypeptidase A, des esters suivants de l'acide hippuriques (à p*H* 7.5, 25°, force ionique de 0.5): $C_6H_5CONHCH_2CO_2CHRCO_2H$: R = CH_3; CH_2CH_3; $(CH_2)_2CH_3$; $(CH_2)_3CH_3$; $(CH_2)_5CH_3$; $CH(CH_3)_2$; $CH_2CH(CH_3)_2$; C_6H_5; $CH_2C_6H_5$. L'hydrolyse enzymatique de tous ces esters montrent une inhibition importante par le substrat. En faisant exception du cas où R = CH_3, tous les profils de la vitesse par rapport à la concentration de substrat, pour chacun de ces esters, peuvent être rationalisés par la formation d'un complexe E.S_2 qui, indépendant de la portion alcoolique de l'ester, réagit environ 25 fois moins rapidement que le complexe E.S. Pour la plupart de ces esters, la formation des complexes E.S_2 est approximativement parallèle avec la liaison ordonnée des molécules de substrat aux sites catalytique et inhibiteur. Alors que la liaison au site catalytique dépend d'une façon importante sur la nature du groupe R, la liaison d'une deuxième molécule de substrat au complexe E.S n'est pas effectée d'une manière importante par la nature de la chaîne latérale R. Pour R = C_6H_5, l'ester D n'est ni un substrat ni un inhibiteur compétitif de l'hydrolyse de l'ester L mais peut remplacer l'ester L au site de liaison qui est responsable pour l'inhibition du substrat. L'analyse de la cinétique suggère que la façon de réagir des énantiomères D et L est aussi typique des autres esters examinés (à l'exception possiblement de R = CH_3). Dans le cas particulier où R = CH_3, l'activation du substrat semble aussi se produire avant l'apparition de l'inhibition du substrat à des concentrations de substrat plus élevées.

[Traduit par le journal]

The hydrolysis of many ester and peptide substrates by bovine carboxypeptidase A is complicated by complex substrate activation and inhibition effects (1–9). Thus, the enzymic hydrolyses of *O*-hippuryl-L-3-phenyllactic acid (**1**: R = $CH_2C_6H_5$) and *O*-hippuryl-L-mandelic acid (**1**: R = C_6H_5) exhibit substrate inhibition at substrate concentrations greater than approximately 10^{-3} *M* (3, 5, 7, 8), whereas for *O*-hippurylglycolic acid (**1**: R = H) substrate activation is observed (4, 9). Complex substrate activation and inhibition effects have also been observed with *N*-hippuryl and *N*-carbobenzoxy-

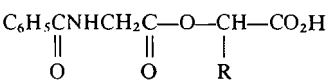

1

[1]For a preliminary communication, see ref. 37.

Can. J. Chem. Downloaded from www.nrcresearchpress.com by 210.87.254.42 on 09/05/12
For personal use only.

Can. J. Chem. Downloaded from www.nrcresearchpress.com by 210.87.254.42 on 09/05/12
For personal use only.

glycyl amino acid substrates (1, 2, 6, 8). On the other hand, a few ester substrates are known for which the enzymic hydrolysis seems to be free of activation and inhibition effects over the experimentally attainable substrate concentration ranges (7, 10–14). Substrate activation and inhibition are also much less pronounced with tripeptide substrates than with their smaller dipeptide analogs (15, 16).

A schematic model has been presented (17) to account qualitatively for substrate activation and inhibition in these reactions. This model assumes multiple sites for the binding of substrate molecules to carboxypeptidase A and also requires that alternative binding modes are possible within one or more of these sites. The model is supported by the X-ray crystallographic study of carboxypeptidase A crystals, which has revealed a relatively "open" active-site region (18–20). Model-building studies indicate (19, 20) that at least two substrate molecules of the size of an *N*-acyl dipeptide can be contained in this active-site region in various orientations which allow reasonable noncovalent bonds (hydrogen bonds, electrostatic interactions, hydrophobic interactions, etc.) between the substrate and enzyme.

A comprehensive quantitative description of the kinetics of hydrolysis in the presence of substrate activation and inhibition has been lacking, and this has hampered the study of the substrate specificity and mechanism of action of this enzyme. Individual attempts have been made to explain the dependence of initial velocity on substrate concentration for **1**: R = C_6H_5 and **1**: R = $CH_2C_6H_5$. Thus, Awazu *et al.* (7) fitted the substrate inhibition of the hydrolysis of **1**: R = C_6H_5 to a relatively simple kinetic scheme which suggested that inhibition arises from the formation of a nonproductive 1:2 enzyme–substrate complex ($E.S_2$). However, McClure *et al.* (3) postulated a much more complex scheme for **1**: R = $CH_2C_6H_5$ that requires either inactive enzyme–substrate complexes containing up to five substrate molecules per enzyme molecule, or alternatively, the existence of four enzyme species having different activities toward this substrate. It seems unlikely that two substrates which are structurally as closely related as **1**: R = C_6H_5 and **1**: R = $CH_2C_6H_5$ would be involved in such kinetically different mechanisms. Substrate inhibition has also been interpreted in terms of an $E.S_4$ complex for the peptide substrate, carbobenzoxyglycylphenylalanine (2), although later studies have suggested (5, 8) that substrate activation, related to the formation of an $E.S_2$ species (6), is also important at lower concentrations of this substrate. These diverse results with a few substrates clearly indicate that a comprehensive systematic study under constant experimental conditions is essential if these phenomena are to be quantitatively understood.

We have recently reported (9) an analysis of substrate activation for three hippuric acid esters (**1**: R = H, **1**: R = *p*-ClC_6H_4 and *O*-hippuryl-2-methyllactic acid) and have shown that in each of these cases substrate activation is consistent with the formation of $E.S_2$ complexes. In a companion investigation, we have now studied the dependence of initial velocity on substrate concentration for the enzymic hydrolysis (p*H* 7.5, 25°, ionic strength 0.5) of a series of nine hippuric acid ester substrates (**1**) for carboxypeptidase A. The purpose of this study was two-fold. Firstly, we felt that it should be possible to quantitatively interpret substrate inhibition for the previously studied **1**: R = C_6H_5 and **1**: R = $CH_2C_6H_5$ and other hippuric acid esters by a common mechanism. Secondly, we hoped to define the specificity of carboxypeptidase A with respect to the alcohol moiety of ester substrates, and compare this specificity with recent studies in our laboratory (21, 22) on the reversible binding of carboxylate anion inhibitors to this enzyme, and with the limited available data on the specificity of this enzyme for peptide substrates.

Experimental

Synthesis of Substrates

All esters, except where indicated below, were prepared as the racemates. The synthesis of *O*-hippuryl-DL-2-hydroxybutanoic acid (**1**: R = C_2H_5) from hippuric acid and benzyl 2-bromobutanoate has been previously described (14).

*O-Hippuryl-*DL*-lactic acid (1: R = CH_3)*: this was similarly prepared; yield 30% from 2-chloropropionic acid, m.p. 169–170°; p.m.r. (CF_3CO_2H): δ 1.71 (3H, d, J = 7 Hz), 4.57 (2H, d, J_{CHNH} = 4 Hz), 5.43 (1H, q, J = 7 Hz), 7.67 (6H, m).

Anal. Calcd. for $C_{12}H_{13}NO_5$: C 57.4; H 5.21; N 5.58. Found: C 57.4; H 5.27; N 5.72.

The remaining esters were synthesized by the following general route: a stirred mixture of hippuryl chloride (23) (4.7 g, 0.024 mol), the 2-hydroxy-acid[2] (RCH(OH)CO_2H,

[2]Usually prepared from the commercially available 2-bromo acids by refluxing in 1 *M* aqueous KOH solution for 18–20 h.

Can. J. Chem. Downloaded from www.nrcresearchpress.com by 210.87.254.42 on 09/05/12
For personal use only.

0.029 mol) and tetrahydrofuran (60 ml) was treated dropwise with pyridine (5 ml, 0.060 mol). The resultant mixture was stirred at room temperature for 15–20 h. Pyridine hydrochloride was filtered off and the solvent removed under vacuum. The viscous yellow residue was redissolved in dichloromethane or chloroform (200 ml) and extracted with 3 *M* hydrochloric acid (35 ml). After drying over anhydrous magnesium sulfate, the organic solvent was removed under vacuum to give the crude ester as a solid or an oil which solidified upon standing. These crude products were recrystallized from acetonitrile–1,2-dichloroethane mixtures.

O-Hippuryl-DL-*2-hydroxyisovaleric acid (1: R = $CH(CH_3)_2$)*: yield 54% from 2-bromoisovaleric acid; m.p. 162–163°; p.m.r. (CF_3CO_2H): δ 1.14 (6H, m), 2.37 (1H, m), 4.60 (2H, d, J_{CHNH} = 4 Hz), 5.23 (1H, d, J = 4 Hz), 7.73 (6H, m).

Anal. Calcd. for $C_{14}H_{17}NO_5$: C 60.2; H 6.14; N. 5.02. Found: C 60.4; H 6.19; N 5.15.

O-Hippuryl-DL-*2-hydroxyvaleric acid (1: R = $(CH_2)_2CH_3$)*: yield 42% from 2-bromovaleric acid; m.p. 137–139°; p.m.r. (CF_3CO_2H): δ 1.07 (3H, t, J = 7 Hz), 1.83 (4H, m), 4.63 (2H, d, J = 4 Hz), 5.40 (1H, t, J = 6 Hz), 7.80 (6H, m).

Anal. Calcd. for $C_{14}H_{17}NO_5$: C 60.2; H 6.14; N 5.02. Found: C 60.35; H 6.29; N 4.94.

O-Hippuryl-DL-*2-hydroxyisocaproic acid (1: R = $CH_2CH(CH_3)_2$)*: yield 49% from 2-bromoisocaproic acid; m.p. 128–129°; p.m.r. (CF_3CO_2H): δ 1.12 (6H, d, J = 6 Hz), 2.00 (3H, m), 4.65 (2H, d, J = 4 Hz), 5.47 (1H, distorted triplet), 7.77 (6H, m).

Anal. Calcd. for $C_{15}H_{19}NO_5$: C 61.4; H 6.54; N 4.77. Found: C 61.3; H 6.79; N 4.89.

O-Hippuryl-DL-*2-hydroxycaproic acid (1: R = $(CH_2)_3CH_3$)*: yield 35% from 2-bromocaproic acid; m.p. 158–159°; p.m.r. (CF_3CO_2H): δ 0.95 (3H, t, J = 6 Hz), 1.48 (4H, m), 2.07 (2H, m), 4.58 (2H, d, J = 4 Hz) 5.32 (1H, t, J = 6 Hz), 7.73 (6H, m).

Anal. Calcd. for $C_{15}H_{19}NO_5$: C 61.4; H 6.54; N 4.77. Found: C 61.2; H 6.47; N 4.76.

O-Hippuryl-DL-*2-hydroxyoctanoic acid (1: R = $(CH_2)_5CH_3$)*: yield 80% from 2-bromooctanoic acid; m.p. 142–143°; p.m.r. (CF_3CO_2H): δ 0.95 (3H, t, J = 6 Hz), 1.42 (8H, m), 2.05 (2H, m), 4.63 (2H, d, J = 4 Hz), 5.38 (1H, t, J = 6 Hz), 7.77 (6H, m).

Anal. Calcd. for $C_{17}H_{23}NO_5$: C 63.5; H 7.21; N 4.36. Found: C 63.0; H 7.34; N 4.30.

O-Hippuryl-DL-*mandelic acid (1: R = C_6H_5)*: yield 77% from hippuryl chloride and DL-mandelic acid; m.p. 151–152°; p.m.r. (CF_3CO_2H): δ 4.68 (2H, d, J_{CHNH} = 4 Hz), 6.32 (1H, s), 7.55–7.73 (11H, m).

Anal. Calcd. for $C_{17}H_{15}NO_5$: C 65.2; H 4.83; N 4.47. Found: C 65.1; H 5.18; N 4.53.

O-Hippuryl-L-*mandelic acid*: yield 63% from hippuryl chloride and L-mandelic acid; m.p. 166–167° (lit. (24) 167–168°); $[\alpha]_D^{24}$ +102° (*c* 3.04, dimethyl formamide) (lit. (24) +104° (*c* 3.14, dimethyl formamide).

O-Hippuryl-D-*mandelic acid*: yield 56% from hippuryl chloride and D-mandelic acid; m.p. 165–166° $[\alpha]_D^{24}$ −102° (*c* 2.94, dimethyl formamide).

O-Hippuryl-DL-*3-phenyllactic Acid (1; R = $CH_2C_6H_5$)*: prepared as the sodium salt as described by McClure (23); m.p. 191–194° after recrystallization from acetone (lit. (23) 125–126°). This product has a satisfactory p.m.r. spectrum and is 50% hydrolyzed by carboxypeptidase A. The difference between the m.p. of this product and the literature value may be due to water of crystallization in the literature product. Commercial samples of this salt frequently contain one (or more) mole of water per mole of sodium salt.

Kinetics

Carboxypeptidase A was obtained as a toluene-preserved suspension from Worthington Biochemical Corporation (Code COA). Stock solutions of this enzyme and of the substrates were prepared as described previously (14).

All hydrolyses (enzymic and nonenzymic) were followed on a Radiometer p*H*-Stat in aqueous solution at 25°, ionic strength 0.5 (substrate + NaCl). The general experimental technique and estimation of the velocities for the enzymic hydrolyses (performed at p*H* 7.5) have been described elsewhere (14). Calculations for the racemic esters are based on the assumption that only the L-ester is hydrolyzed. This has been established for several carboxypeptidase A substrates (3, 5, 11, 25) and was supported by the observation that only 50 ± 2% of each racemic ester had been hydrolyzed by carboxypeptidase A at equilibrium. We also confirmed that *O*-hippuryl-L-mandelic acid is 100% hydrolyzed by carboxypeptidase A, and that the D-enantiomer is not a substrate for this enzyme.

All esters were completely hydrolyzed in aqueous base (p*H* 10–11). Pseudo first-order rate constants for the non-enzymic reactions were obtained from the slopes of linear first-order plots, and in each case the values of k_{OH} were obtained by averaging four runs in the region p*H* 10–11.

Results

The dependence of initial velocity of enzymic hydrolysis on substrate concentration at p*H* 7.5 is shown in Fig. 1 for nine hippuric acid esters: **1**: R = CH_3; CH_2CH_3; $(CH_2)_2CH_3$; $(CH_2)_3CH_3$; $(CH_2)_5CH_3$; $CH(CH_3)_2$; $CH_2CH(CH_3)_2$; C_6H_5; $CH_2C_6H_5$. In each case, substrate inhibition is clearly important at high substrate concentrations. For each ester, Lineweaver–Burk plots at substrate concentrations less than that at which the maximum velocity occurs are linear, and so suggest that in these low substrate concentration ranges the reactions proceed through the formation of an E.S complex. The intercepts of such plots afford estimates of k_{cat} and K_m for each ester (although these parameters are better evaluated as described later), except for the lactic acid derivative, **1**: R = CH_3, for which both intercepts are indistinguishable from zero (Fig. 2) and thus suggest that K_m is relatively large for this ester.

Inspection of Fig. 1 at high substrate concentrations suggests that the velocity does not decrease to zero at very large substrate concentrations, but rather approaches a nonzero limiting

Can. J. Chem. Downloaded from www.nrcresearchpress.com by 210.87.254.42 on 09/05/12
For personal use only.

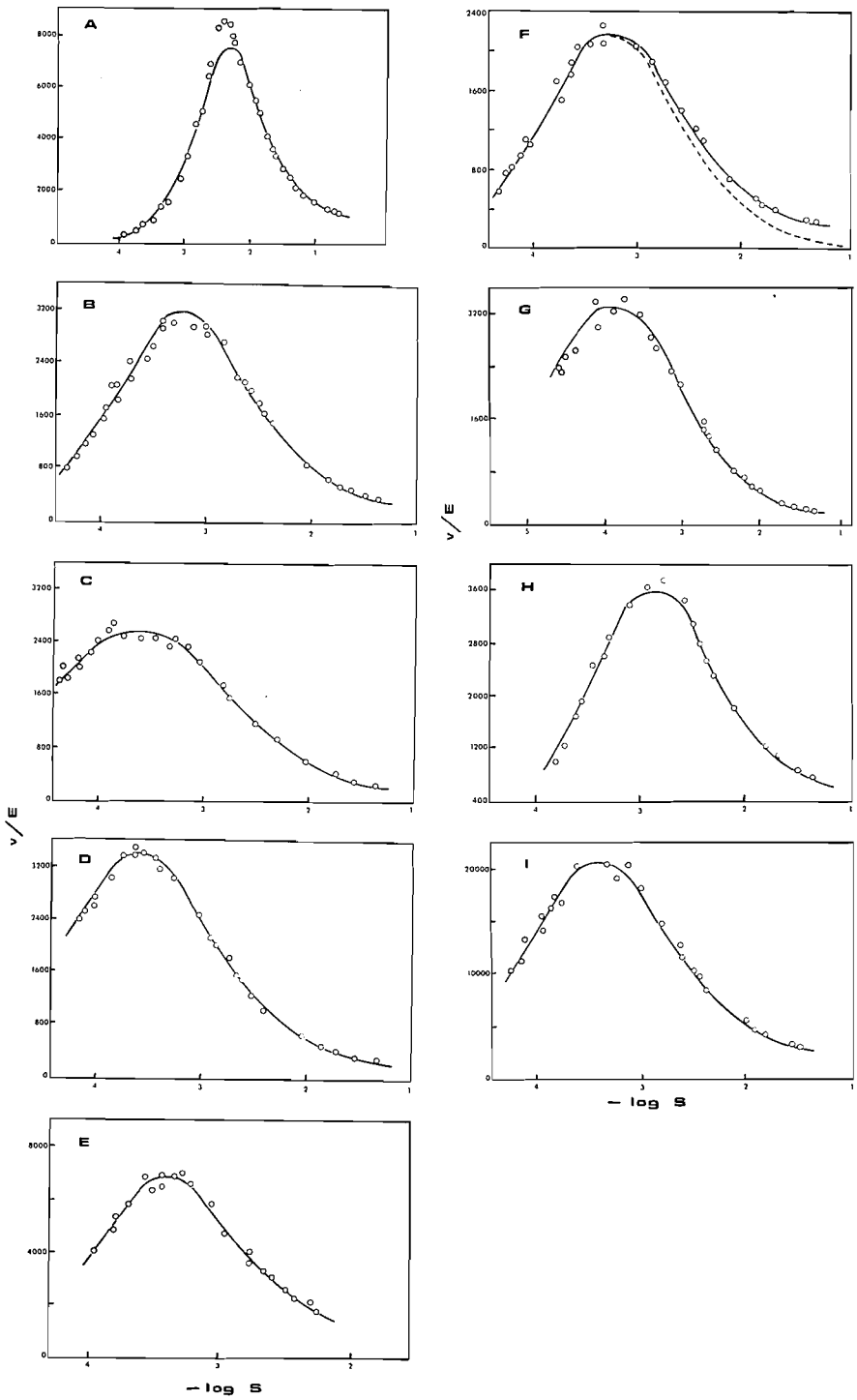

FIG. 1. Dependence of initial velocity (v/E, min^{-1}) on substrate concentration for the hydrolysis of the L-enantiomer (S, mol/l) of racemic esters $C_6H_5CONHCH_2CO_2CHRCO_2H$ by carboxypeptidase A (pH 7.5, 25°, ionic strength 0.5): (*A*) R = CH_3; (*B*) R = CH_2CH_3; (*C*) R = $(CH_2)_2CH_3$; (*D*) R = $(CH_2)_3CH_3$; (*E*) R = $(CH_2)_5CH_3$; (*F*) R = $CH(CH_3)_2$; (*G*) R = $CH_2CH(CH_3)_2$; (*H*) R = C_6H_5; (*I*) R = $CH_2C_6H_5$. Lines indicate the calculated velocities according to eq. 2 and the parameters in Table 1. The broken line is the best fit for $k_3 = 0$.

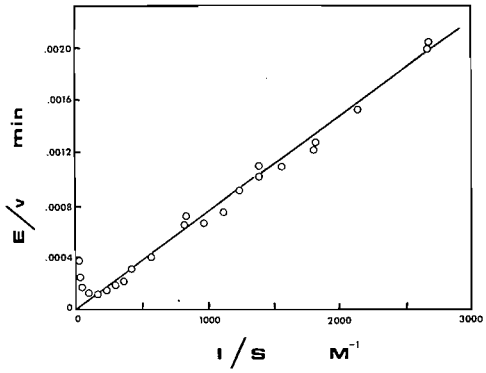

FIG. 2. Lineweaver–Burk plot for the hydrolysis of the L-isomer of the racemate of $C_6H_5CONHCH_2CO_2$-$CH(CH_3)CO_2H$ by carboxypeptidase A (p*H* 7.5, 25°, ionic strength 0.5).

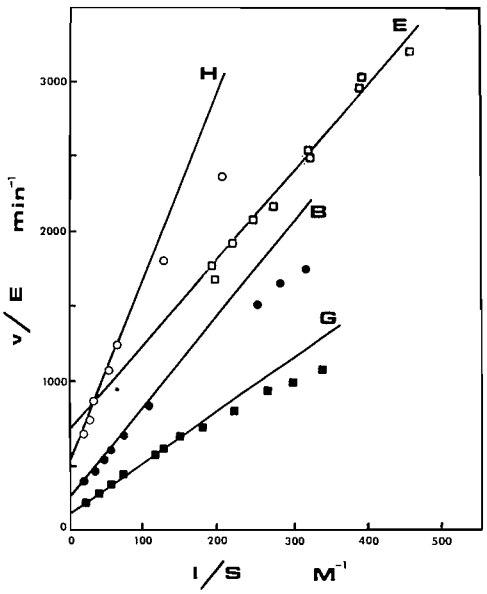

FIG. 3. Dependence of v/E on $1/S$ for some esters in Fig. 1.

value. Support for a nonzero limiting velocity is also provided by plots of v/E *vs.* $1/S$ shown in Fig. 3. For each ester, such plots approach linearity at the highest substrate concentrations and upon extrapolation to $1/S = 0$ it is clear that the limiting velocity (*i.e.* ordinate intercept) is nonzero.

The simplest kinetic scheme that is capable of fitting the observed overall dependence of initial velocity on substrate concentration seems to be that shown in Scheme 1. If it is assumed that the equilibria are established rapidly relative to k_2 and k_3, then Scheme 1 predicts the

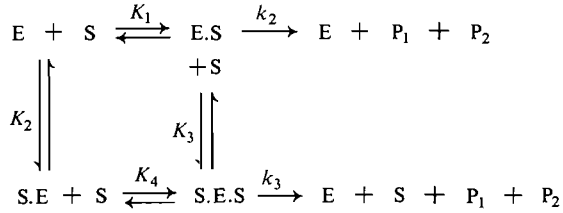

SCHEME 1

velocity dependence in eq. 1, which has the form of eq. 2. Equation 2 has been fitted to the experi-

$$[1]\quad \frac{v}{E} = \frac{\dfrac{k_2 S}{(1 + K_1/K_2)} + \dfrac{k_3 S^2}{K_3(1 + K_1/K_2)}}{\dfrac{K_1}{1 + K_1/K_2} + S + \dfrac{S^2}{K_3(1 + K_1/K_2)}}$$

$$[2]\quad \frac{v}{E} = \frac{k_2^{app} S + k_3 S^2/K_{SS}^{app}}{K_S^{app} + S + S^2/K_{SS}^{app}}$$

mental data for each of the nine esters in Fig. 1 by the iteration technique that we have previously described (26) for second-degree equations of this form. For all esters except **1**: R = CH_3 and **1**: R = $(CH_2)_5CH_3$, unique sets of parameters k_2^{app}, k_3, K_S^{app}, and K_{SS}^{app} were obtained from the iteration and are collected in Table 1; the curves in Fig. 1 are calculated using eq. 2 and these determined parameters, and give an acceptable fit to the experimental data. In agreement with the extrapolations in Fig. 3, the iteration procedure also suggests a nonzero limiting velocity. Modified iterations, in which k_3 was fixed at zero, gave considerably poorer fits to the experimental data in all cases than the fits obtained from the free iterations. An example of the type of velocity–concentration profile obtained for $k_3 = 0$ is shown for **1**: R = $CH(CH_3)_2$ in Fig. 1 (broken line), and it is clear that this assumption forces the velocity to fall off more rapidly at higher substrate concentrations than is actually observed experimentally.

Unlike the cases discussed above, the data for **1**: R = $(CH_2)_5CH_3$ could not be fitted to eq. 2 by a unique set of kinetic parameters. Multiple solutions to eq. 2 were obtained from the iteration technique, each having less than 5% average error between calculated and experimental velocities. In fact, any value for K_{SS}^{app} less than $5 \times 10^{-4}\,M$ (with suitable modification of the other parameters) leads to an acceptable fit to the data for this ester. In an effort to select the physically meaningful solution to eq. 2 for this ester, a combination of graphical and iter-

Can. J. Chem. Downloaded from www.nrcresearchpress.com by 210.87.254.42 on 09/05/12
For personal use only.

TABLE 1. Kinetic parameters for the hydrolysis of $C_6H_5CONHCH_2CO_2CHRCO_2H$ by carboxypeptidase A[a]

R	K_S^{app} (mM)	K_{SS}^{app} (mM)	k_2^{app} (min^{-1})	k_3 (min^{-1})	Average % error[b]	k_2^{app}/k_3
CH_3[c]	27	1.0	8.2×10^4	820	10.1[c]	(100)
CH_2CH_3	0.31	1.2	6.4×10^3	200	5.4	32
$(CH_2)_2CH_3$	0.034	1.6	3.2×10^3	120	4.7	27
$(CH_2)_3CH_3$	0.077	0.79	5.4×10^3	210	3.5	26
$(CH_2)_5CH_3$[d]	0.75	0.20	3.2×10^4	700[d]	4.5	46
$CH(CH_3)_2$	0.24	1.3	4.0×10^3	170	6.9	24
$CH_2CH(CH_3)_2$	0.021	0.78	4.4×10^3	160	5.5	27
C_6H_5	1.2	1.2	1.1×10^4	490	6.5	22
$CH_2C_6H_5$	0.17	0.83	3.8×10^4	2200	6.5	17

[a]Parameters obtained by fitting data of Fig. 1 to eq. 2.
[b]Average % difference between calculated and experimental velocities.
[c]"Best fit" to eq. 2 for this ester; see text.
[d]Parameters obtained by fixing k_3 = 700 min^{-1}; see text.

ative analyses was attempted. Thus, when k_3 was fixed at the limiting value indicated for this ester in Fig. 3 (700 min^{-1}), and the other three parameters were allowed to vary during the iteration to give the best fit to the experimental data, a unique solution was obtained. The parameter values for this solution are included in Table 1. The multiple solutions obtained in the free iteration for this ester seem to be related to the limited substrate concentration range that could be covered ($<5\times10^{-3}$ M) owing to solubility limitations. Unlike the other esters, in this case the approach to the limiting velocity at high substrate concentrations does not seem to be sufficiently well defined to allow a unique fit in the free iteration.

A different problem was encountered in attempting to fit the data for **1**: R = CH_3 to eq. 2. The best fit obtained is shown in Fig. 1 using the parameters in Table 1, and gives an average error of 10.1%. This relatively large error in the difference between calculated and experimental velocities is mainly due to the inability of the calculated curve to afford a satisfactory fit to the data points in the vicinity of the maximum velocity. This negative deviation of eq. 2 in this region was encountered for all sets of parameters which give reasonable fits to the data at both low and high substrate concentrations, and seems to suggest that eq. 2 is not sufficient to represent the experimental data in this case.

The influence of the presence of the D-ester in these racemic substrates has been investigated in the case of *O*-hippurylmandelic acid (**1**: R = C_6H_5). The dependence of the initial velocity of enzymic hydrolysis upon the concentration of the L-isomer is indicated in Fig. 4 for

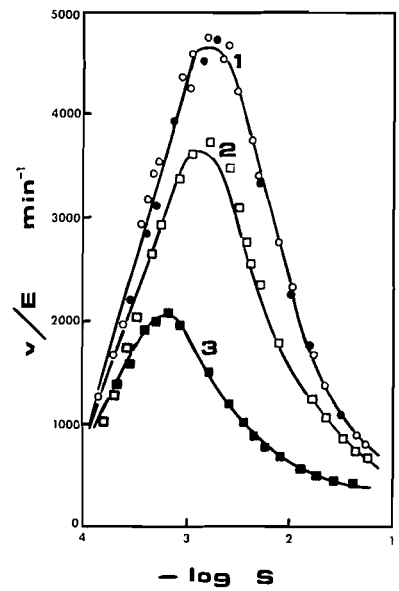

FIG. 4. Dependence of initial velocity on substrate concentration for the hydrolysis of L-$C_6H_5CONHCH_2CO_2CH(C_6H_5)CO_2H$ in: (*1*) the pure L-ester; (*2*) the DL-racemate; (*3*) a 9.2:1 mixture of D- and L-esters. Lines are calculated according to eq. 2 using the parameters in Table 2. Data of ref. 7 for the pure L-ester (●).

the pure L-ester, the racemic ester, and a mixture of the D and L esters in the ratio D/L = 9.2 at all substrate concentrations. The data obtained for the pure L-isomer are in close agreement with those reported previously for this ester by Kaiser and co-workers (7). The data in Fig. 4 clearly indicate that the D-ester is an inhibitor of the hydrolysis of its enantiomer at high substrate concentrations. Each of these three sets of experimental data can be fitted to eq. 2 to give the kinetic parameters in Table 2. The only param-

Can. J. Chem. Downloaded from www.nrcresearchpress.com by 210.87.254.42 on 09/05/12
For personal use only.

TABLE 2. Kinetic parameters for the hydrolysis of mixtures of D- and L-*O*-hippurylmandelic acid[a]

n[b]	K_S^{app} (mM)	K_{SS}^{app} (mM)	k_2^{app} (min^{-1})	k_3^{app} (min^{-1})	Average % error[c]
0	0.98	2.6	1.1×10^4	3.2×10^2	5.2
1	1.2	1.2	1.1×10^4	4.9×10^2	6.5
9.2	1.2	0.27	9.8×10^3	3.6×10^2	3.2

[a]Parameters obtained by fitting data of Fig. 4 to eq. 2.
[b]Ratio of D:L esters.
[c]Average % difference between calculated and experimental velocities.

eter that is significantly affected by the increasing proportions of D-isomer is K_{SS}^{app}, with K_S^{app}, k_2^{app}, and k_3 all being effectively constant within experimental error. The ability of the D-ester to change K_{SS}^{app}, but not k_3, suggests that the nature of the inhibition by the D-isomer is essentially similar to that caused by the L-ester when the latter acts as an inhibitor of its own hydrolysis. Thus the enzyme, L-ester substrate (S) and D-ester inhibitor (I), may combine to form an I.E.S. complex which must then react at about the same rate as for the S.E.S species in Scheme 1, if k_3 is to be independent of inhibitor concentration as is observed.

The rates of the nonenzymic base-catalyzed hydrolysis of some of these hippurate esters have also been measured. Second-order rate constants, k_{OH}, are collected in Table 3, and are compared with k_2^{app} for the enzymic hydrolyses.

Discussion

With the exception of **1**: R = CH_3, the substrate inhibition observed in the enzymic hydrolysis of the eight other hippuric acid esters in the present study appears to be assignable to the binding of two molecules of substrate to the enzyme. Substrate inhibition occurs because the rate of hydrolysis of the $E.S_2$ complex (k_3) is significantly smaller than that of the E.S complex (k_2). As the results of the experiments with *O*-hippuryl-D-mandelic acid show, the role of an L-ester substrate as an inhibitor can also be assumed by the D-ester. The action of carboxypeptidase A on the racemic hippuric acid esters is thus best described in terms of the three complexes E.S, $E.S_2$, and E.S.I, all of which can hydrolyze to form products. The substrate inhibition of the carboxypeptidase A catalyzed hydrolysis of **1**: R = $CH_2C_6H_5$ was ascribed previously by McClure *et al.* (3) to a complex reaction sequence involving two enzyme species and $E.S_5$ complexes. In contrast, the data obtained here for this same ester can be explained by a much simpler scheme, which invokes no more than two molecules of substrate, binding to a single enzyme species.

TABLE 3. Comparison of base-catalyzed and enzymic hydrolyses of $C_6H_5CONHCH_2CO_2CHRCO_2H$

R	$k_{OH}(M^{-1}$ min$^{-1})$[a]	k_2^{app}/k_{OH}
CH_2CH_3	25.1	250
$(CH_2)_2CH_3$	19.5	170
$(CH_2)_5CH_3$	25.7	1250
$CH(CH_3)_2$	9.9	400
C_6H_5	71.4	150
$CH_2C_6H_5$	41.1	920

[a]At 25°, ionic strength 0.5.

The scheme proposed previously by Kaiser and co-workers (7) to account for substrate inhibition in the hydrolysis of *O*-hippuryl-L-mandelic acid by carboxypeptidase A is essentially Scheme 1, but with the additional assumption that $E.S_2$ is nonproductive, *i.e.* $k_3 = 0$. As discussed above, this assumption leads, in general, to a significantly poorer fit between the calculated and experimental velocities for the hippuric acid ester substrates than when k_3 is allowed to assume positive values.

The conclusion that substrate inhibition can be attributed, in general, to the binding of two molecules of substrate to the enzyme is in good agreement with theoretical models proposed previously to account for the phenomenon. Based mainly on kinetic studies, Vallee and co-workers (17, 27) postulated that the hydrolysis of ester and peptide substrates by carboxypeptidase A occurs at two different catalytic sites, each of which can bind but not hydrolyze, *both* types of substrate. They suggested that substrate inhibition (or activation) could arise from the binding of a second molecule of substrate to the "wrong" site. For example, substrate inhibition of ester hydrolysis would result, on the basis of this model, from binding of a second molecule of ester to the peptide catalytic

Can. J. Chem. Downloaded from www.nrcresearchpress.com by 210.87.254.42 on 09/05/12
For personal use only.

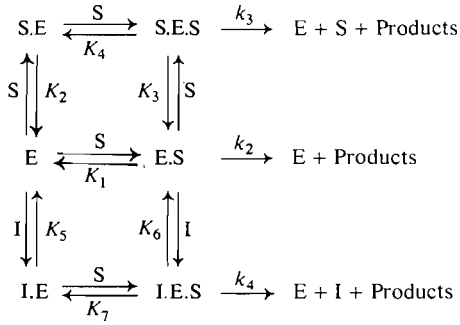

SCHEME 2

site. Subsequently, Lipscomb and co-workers deduced from their X-ray diffraction work (18–20) that the active site of carboxypeptidase A is located at the bottom of a deep cleft in the enzyme. Model building studies indicated that this cleft could accommodate two, but no more than two, *N*-acyl dipeptide (or depsipeptide) molecules. Lipscomb has suggested that binding of two substrate molecules in this manner might account for the observed substrate inhibition and activation phenomena.

In the light of the current observation that the presence of the D-ester can influence the rate of hydrolysis of the L-ester, Scheme 1 must be modified as in Scheme 2 (where I represents the D-ester) which generates the rate eq. 3.

$$[3] \qquad \frac{v}{E} = \frac{k_2 S + (k_3/K_3)S^2 + (k_4/K_6)I.S}{K_1 + (1 + K_1/K_2)S + (K_1/K_5)I + (1/K_3)S^2 + (1/K_6)I.S}$$

For a constant ratio n of the D- to L-isomer, eq. 3 may be transformed to eq. 4

$$[4] \qquad \frac{v}{E} = \frac{k_2 S + [(k_3/K_3) + (nk_4/K_6)]S^2}{K_1 + [1 + (K_1/K_2) + (nK_1/K_5)]S + [(1/K_3) + (n/K_6)]S^2}$$

which may be rearranged to have the same form as eq. 2, but with

$$[5] \qquad K_S^{app} = \frac{K_1}{1 + (K_1/K_2) + (nK_1/K_5)}$$

$$[6] \qquad k_2^{app} = \frac{k_2}{1 + (K_1/K_2) + (nK_1/K_5)}$$

$$[7] \qquad K_{SS}^{app} = \frac{1 + (K_1/K_2) + (nK_1/K_5)}{(1/K_3) + (n/K_6)}$$

$$[8] \qquad k_3^{app} = \frac{(k_3/K_3) + (nk_4/K_6)}{(1/K_3) + (n/K_6)}$$

If the random binding of the substrate and its D-isomer to the enzyme is operative, as in Scheme 2, an increase in the D- to L-isomer ratio, n, should effect a reduction in k_2^{app} and K_S^{app}, little or no change in k_3^{app}, and an unpredictable change in K_{SS}^{app}. The data obtained for the enzymic hydrolysis of mixtures of D- and L-*O*-hippurylmandelic acid demonstrate (Table 2) that increasing the value of n from 0 to 9.2 in this system causes a marked decrease in K_{SS}^{app}, but no significant changes in K_S^{app}, k_2^{app}, and k_3^{app}. These results are inconsistent, apparently, with the behavior predicted for Scheme 2, although the apparent independence of k_3^{app} of n suggests that $k_3 \approx k_4$ for this system. However, if the inequality [9] were to hold, then

$$[9] \qquad nK_1/K_5 < 1 + (K_1/K_2)$$

eqs. 5–8 would reduce to eqs. 10–13

$$[10] \qquad K_S^{app} = \frac{K_1}{1 + (K_1/K_2)}$$

$$[11] \qquad k_2^{app} = \frac{k_2}{1 + (K_1/K_2)}$$

$$[12] \qquad K_{SS}^{app} = \frac{1 + (K_1/K_2)}{(1/K_3) + (n/K_6)}$$

$$[13] \qquad k_3^{app} = \frac{(k_3/K_3) + (nk_4/K_6)}{(1/K_3) + (n/K_6)} = K_3 \text{ (for } k_3 = k_4)$$

which indicate that only K_{SS}^{app} should be dependent on n, which is consistent with the data of Table 2. Equation 12 may be combined with the values of K_{SS}^{app} and n listed in Table 2 to afford $K_3(1 + K_1/K_2) = K_6(1 + K_1/K_2) = 2.6$ mM, *i.e.* $K_3 = K_6$. Thus, the two enantiomers of the ester have equal affinity for the inhibitory site in the E.S complex.

For the enzymic hydrolysis of mixtures of the enantiomers of *O*-hippurylmandelic acid, K_6 cannot be greater than 2.6 mM, while K_1 cannot be less than 1.0 mM (since $K_1 > K_S^{app}$). Thus, when $n = 9.2$, nK_1/K_6 must be greater than 3.3. Clearly, K_5 must be appreciably greater than K_6

Can. J. Chem. Downloaded from www.nrcresearchpress.com by 210.87.254.42 on 09/05/12
For personal use only.

Can. J. Chem. Downloaded from www.nrcresearchpress.com by 210.87.254.42 on 09/05/12
For personal use only.

if the inequality [9] is to remain valid at all values of n investigated.[3] Binding of the D-ester inhibitor to the regulatory site is thus facilitated if an L-ester substrate molecule is already bound to the active site. This type of behavior, involving cooperative interaction between two binding sites, is commonly observed in allosteric enzymes (28).

The inequality [9] also indicates that K_5 must be considerably greater than K_1; *i.e.* the affinity of E for binding of L-ester at the catalytic site, *i.e.* formation of E.S, is much greater than for binding of D-ester at the inhibitory regulatory site (I.E). A special case of $K_5 > K_1$ is obligatory ordered binding of substrate to the catalytic site before inhibitor may bind to the regulatory site (*i.e.* $K_5 = \infty$). Thus, this special case of Scheme 2 cannot be distinguished for this ester from genuine random binding for which the inequality [9] is obeyed. It should also be noted that if K_5 is infinite, then K_2 is also likely to be infinite (since $K_3 = K_6$ is indicated above), and so the data of Table 2 are also consistent with ordered binding of the L-ester to catalytic and inhibitory sites. In fact, the restriction inherent in inequality [9] implies that substrate inhibition via formation of an $E.S_2$ complex approximates ordered binding of the two substrate molecules to the enzyme for this ester.

In a recent report, Lang and co-workers (29) have shown that *O*-hippuryl-D-3-phenyllactic acid inhibits the hydrolysis of its L-enantiomer. Although these workers have not attempted a detailed kinetic analysis of the nature of this inhibition, inspection of their data suggests that the influence of the D-isomer in the racemate on the hydrolysis of the L-isomer of this ester is exactly analogous to our observations on the lower homolog *O*-hippurylmandelic acid (Fig. 4). The actual form of inhibition which is observed for these D-esters with their L-enantiomers as substrates must be construed as mixed inhibition, since from the above discussion it is clear that $K_5 \neq K_6$ and $k_4 \neq k_2$.

All other hippuric acid esters studied in this work are racemic mixtures. If the random binding mechanism of Scheme 2 is applicable to the carboxypeptidase A catalyzed hydrolysis of these esters, the dependence of initial velocity on L-ester substrate concentration should be described by eq. (4) (where $n = 1$) and the apparent kinetic parameters by eqs. 5–8 (with $n = 1$). Inspection of the experimental values for the parameters in Table 1 indicates that K_{SS}^{app} is essentially constant for all seven esters listed, while K_S^{app} depends strongly on the nature of the R side chain. These two observations can be satisfied simultaneously by the eqs. 5–8 ($n = 1$) only if one of the following conditions is valid: (*a*) K_1/K_2 and K_1/K_5 are variable, but K_3 and K_6 vary in such a way that K_{SS}^{app} is always approximately constant; (*b*) K_1/K_2, K_1/K_5, K_3, and K_6 are all constant, but K_1 varies from one ester to another; (*c*) K_3 and K_6 are constant, and for all esters studied, the inequality (14) is valid.

$$[14] \qquad K_1/K_2 + K_1/K_5 \ll 1$$

It seems extremely unlikely that five different equilibrium constants can all vary in such a manner that their combination in K_{SS}^{app} remains unchanged. Thus, condition *a* can probably be ruled out. Condition *b* implies that binding of the ester (D or L) to the regulatory site of the free enzyme should be dependent on the R side chain, whereas binding of the ester to the regulatory site of the E.S complex should be independent of the side-chain. Although not impossible, this does not seem too probable. Condition *c* seems to be the only one capable of explaining the variation of K_S^{app} and constancy of K_{SS}^{app} in a satisfactory manner. The inequality [14] in condition *c* asserts that the L-ester is bound much more strongly to the active site of the free enzyme than either enantiomer is to the regulatory site. This restriction is essentially similar to that required (inequality [9]) in the interpretation of *O*-hippuryl-mandelic acid hydrolysis by a random binding scheme, and so suggests that for each of the esters in Table 1, formation of $E.S_2$ approximates ordered binding. Thus, using condition *c* and $K_3 = K_6$ and $k_3 \approx k_4$ as were established above for the mandelic acid derivative, the eqs. 5–8 (with $n = 1$) simplify to:

$$K_S^{app} = K_1$$
$$k_2^{app} = k_2$$
$$K_{SS}^{app} = K_3/2$$
$$k_3^{app} = k_3$$

Thus, K_S^{app} represents the dissociation constant of the catalytically active E.S complex; k_2^{app} is

[3]This argument assumes that K_2 cannot be considerably smaller than K_1, so that $K_1/K_2 \gg 1$ is not possible. This assumption is supported by the constancy of K_{SS}^{app} for the various hippuric acid esters, as discussed later.

Can. J. Chem. Downloaded from www.nrcresearchpress.com by 210.87.254.42 on 09/05/12
For personal use only.

the specific rate of hydrolysis of E.S; K_{SS}^{app} for racemic esters is half of the dissociation constant for $E.S_2$ to E.S and S; and k_3^{app} is the specific rate of hydrolysis of $E.S_2$.

The effect of the R side chain of the alcohol moiety of the hippuric acid esters **1** on the rate of hydrolysis of the E.S complex may be compared with the effect of R on the alkaline hydrolysis of these esters by consideration of the k_2^{app}/k_{OH} ratios in Table 3. These results suggest that, to a first approximation, the influence of R on the enzymic hydrolysis is not seriously different from the effect of R on the alkaline hydrolysis. Possible exceptions to this behavior are manifested by the enhanced k_2/k_{OH} values for the esters **1**: R = $CH_2C_6H_5$ and **1**: R = $(CH_2)_5CH_3$. The k_2^{app} values for these two esters are clearly larger than one would predict from a comparison of the enzymic and alkaline hydrolysis rates of the other substrates. In these two cases, the labile ester group may possibly be closer to (or better oriented with respect to) the catalytic groups of the enzyme, perhaps because of increased steric interaction between the larger R groups of these substrates and the enzyme.

The values of k_2 and K_1 from Table 1 are both dependent on the nature of the R side chain of the ester; however, there is no apparent relationship between these two parameters. Independent behavior of k_2 and K_1 has also been observed by Auld and Vallee (15, 16) in the hydrolysis of *N*-acyl tripeptides by several metallocarboxypeptidases at various p*H* values. This result is compatible with the assumption that the binding of substrate to the active site is fast relative to the rate of hydrolysis of the E.S complex, since if the rates of equilibration of E and E.S were comparable with k_2, then one would expect an influence of k_2 on K_S^{app}.

Inspection of the values of K_{SS}^{app} ($= K_3/2$) in Table 1 indicates that, with the exception of **1**: R = $(CH_2)_5CH_3$ and **1**: R = CH_3, K_3 is approximately constant for the other esters listed. Thus, the binding of most substrates to the regulatory site of E.S is independent of the size, nature, or hydrophobicity of the R side chain. The constancy of K_{SS}^{app} for the racemic esters also implies that the R group has no significant influence on the binding of D enantiomers of these substrates to the regulatory site. The binding of either enantiomer to the E.S complex must, therefore, involve only the 2-hippuroxyacetate moiety of the ester. These results suggest that the ester molecule is bound to the regulatory site of E.S such that the R side chain does not contact the enzyme molecule. The smaller K_{SS}^{app} and K_3 values for **1**: R = $(CH_2)_5CH_3$ may reflect the onset of an increased interaction between the regulatory site and the side chain when R becomes large, or may be due to the increased relief of solvent entropy when this large hydrophobic moiety is removed from a strictly aqueous environment.

With the possible exception[4] of **1**: R = $(CH_2)_5CH_3$, values of the ratio k_2/k_3 listed in Table 1 appear to be constant within experimental error. Thus, the second ester molecule appears to bind so as to decrease the rate of enzymatic hydrolysis by a constant factor, independent of the nature of R. This could be accomplished if the binding of the ester molecule to the regulatory site were to cause a small but constant conformational change at the active site, such that the distance between (or orientation of) the catalytic groups of the enzyme and the ester bond of the substrate becomes altered. Conformational mobility of the active site region of carboxypeptidase A has been clearly indicated by X-ray diffraction, chemical modification, and spectroscopic studies (19, 20, 30–33). The independence of the proposed conformational change on the R side chain is not too surprising if, as discussed above, the R group of the ester molecule bound to the regulatory site is not in contact with the enzyme.

Unlike K_3, K_{SS}, and k_2/k_3, the parameter K_1 displays a marked dependence on the nature of the R moiety of the hippuric acid esters. Variation of the hydrophobic R group exerts a strong influence, therefore, on the binding of these substrates to the active site of the enzyme. The X-ray crystallographic studies of carboxypeptidase A suggest that the side chain of the substrate *C*-terminal residue is accommodated at the active site by insertion into a hydrophobic pocket of the enzyme (18–20). The influence of R on substrate binding might be ascribed, therefore, to varying degrees of hydrophobic interac-

[4]As discussed in the Results section, the parameters for this ester were obtained by a less satisfactory method than for the other esters listed in Table 1. Consequently, values of k_2/k_{OH} and k_2/k_3 for this ester may be erroneously high. There is no doubt, however, that K_{SS}^{app} for this ester is significantly smaller than the approximately constant value of 1.0 m*M* obtained for the other substrates.

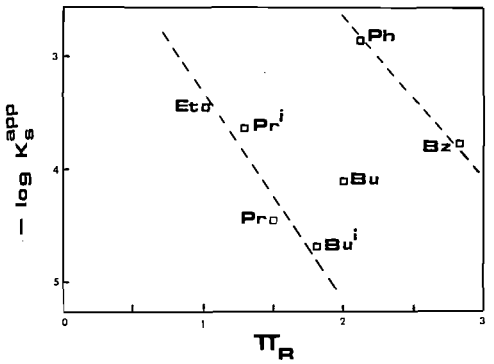

FIG. 5. Dependence of log K_S^{app} on π_R in the hydrolysis of $C_6H_5CONHCH_2CO_2CHRCO_2H$ by carboxypeptidase A. Linear correlations (broken lines) are suggested by inhibition studies (21, 22).

tion between the substrate and the enzyme. The importance of hydrophobic interaction between the enzyme and inhibitor anions has been demonstrated in our laboratory (21, 22) by showing that inhibition constants for the binding of RCO_2^- and $RCH(CO_2^-)_2$ which are competitive inhibitors of the hydrolysis of **1**: R = $CH_2C_6H_5$ by carboxypeptidase A are linearly correlated with Hansch's π parameter (34, 35), provided the hydrophobic moiety of the inhibitor does not become too large.

The dependence of K_1 for the present hippuric acid esters on π is shown in Fig. 5. Although data over only a relatively narrow range of π values is available, two points are clear from this plot. Firstly, increasing the hydrophobic character of R strengthens the binding of substrate to the enzyme only if R is relatively small. Beyond a certain optimum hydrophobicity (π value), binding of substrate is weakened, presumably because the R group is now too large to fit into the hydrophobic pocket in its energetically most favorable conformation. Secondly, substrates with aromatic side chains are bound less strongly to the active site than those with aliphatic side chains of comparable hydrophobicity. Both of these features are also observed in the binding of the above competitive inhibitor carboxylate anions to this enzyme (21, 22) and so there can be little doubt that the hydrophobic side chains of the ester substrates **1** and the carboxylate anion inhibitors previously studied are accommodated by the same hydrophobic region of the enzyme.

The apparent discrimination of aliphatic and aromatic hydrophobic groups by the enzyme is not readily interpreted. Such discrimination does not appear to be present in the binding of peptide substrates for which carbobenzoxyglycylglycyl-L-phenylalanine ($K_m = 2.5 \times 10^{-4}$ *M*) apparently binds about tenfold more strongly to carboxypeptidase A than does carbobenzoxyglycylglycyl-L-leucine ($K_m = 3 \times 10^{-3}$ *M*) (15) in accord with the greater hydrophobicity of the benzyl side chain (π = 2.63) of phenylalanine than of the isobutyl side chain (π = 1.80) of leucine. The data for the analogous hippurate esters, **1**: R = $CH_2C_6H_5$ and **1**: R = $CH_2CH(CH_3)_3$, in Table 1 indicate that the isobutyl side chain appears to be bound approximately eight times more strongly than the benzyl group. This points out a further way in which carboxypeptidase A discriminates between ester and peptide substrates, and is in accord with the now generally accepted view of different productive binding modes to this enzyme for ester and peptide substrates (17, 29, 36, 38).

The inability to fit the maximum velocity observed for the lactic acid derivative (**1**: R = CH_3) with eq. 2 suggests that both substrate activation and substrate inhibition may be occurring to some extent with this ester. In view of our recent observations (9) of substrate activation with the related *O*-hippuryl-2-methyllactic acid and the known substrate activation for *O*-hippurylglycolic acid, the occurrence of substrate activation for **1**: R = CH_3 is not really unexpected. Even in the absence of any interference from substrate activation, one might have predicted that **1**: R = CH_3 could show a different overall set of kinetic parameters for eq. 2 than the other esters investigated here. Thus, the expected large value of K_1 for this ester may lead to the inequalities [9] and [14] not being applicable in this case and so the simplified forms of K_S^{app}, k_2^{app}, and K_{SS}^{app} discussed above may not hold for this ester.

We appreciate the continued support of this work by the National Research Council of Canada and the award of an Ontario Graduate Fellowship to J.M.

1. J. E. SNOKE, G. W. SCHWERT, and H. NEURATH. J. Biol. Chem. **175**, 7 (1948).
2. R. LUMRY, E. L. SMITH, and R. R. GLANTZ. J. Am. Chem. Soc. **73**, 4330 (1951).
3. W. O. MCCLURE, H. NEURATH, and K. A. WALSH. Biochemistry, **3**, 1897 (1964).
4. E. T. KAISER, S. AWAZU, and F. W. CARSON. Biochem. Biophys. Res. Commun. **21**, 444 (1965).
5. J. R. WHITAKER, F. MENGER, and M. L. BENDER. Biochemistry, **5**, 386 (1966).

Can. J. Chem. Downloaded from www.nrcresearchpress.com by 210.87.254.42 on 09/05/12
For personal use only.

6. J. R. WHITAKER. Biochem. Biophys. Res. Commun. **22**, 6 (1966).
7. S. AWAZU, F. A. CARSON, P. L. HALL, and E. T. KAISER. J. Am. Chem. Soc. **89**, 3627 (1967).
8. R. C. DAVIES, J. F. RIORDAN, D. S. AULD, and B. L. VALLEE. Biochemistry, **7**, 1090 (1968).
9. J. MURPHY and W. BUNTING. Can. J. Chem. **52**, 3829 (1974).
10. W. O. MCCLURE and H. NEURATH. Biochemistry, **5**, 1425 (1966).
11. E. T. KAISER and F. W. CARSON. J. Am. Chem. Soc. **86**, 2922 (1964).
12. P. L. HALL, B. L. KAISER, and E. T. KAISER. J. Am. Chem. Soc. **91**, 485 (1969).
13. G. TOMALIN, B. L. KAISER, and E. T. KAISER. J. Am. Chem. Soc. **92**, 6046 (1970).
14. J. BUNTING and J. MURPHY. Can. J. Chem. **52**, 2640 (1974).
15. D. S. AULD and B. L. VALLEE. Biochemistry, **9**, 602 (1969).
16. D. S. AULD and B. L. VALLEE. Biochemistry, **9**, 4352 (1969).
17. B. L. VALLEE, J. F. RIORDAN, J. L. BETHUNE, T. L. COOMBS, D. S. AULD, and M. SOKOLOVSKY. Biochemistry, **7**, 3547 (1968).
18. T. A. STEITZ, M. L. LUDWIG, F. A. QUIOCHO, and W. N. LIPSCOMB. J. Biol. Chem. **242**, 4662 (1967).
19. W. N. LIPSCOMB, G. N. REEKE, JR., J. A. HARTSUCK, F. A. QUIOCHO, P. H. BETHGE, M. L. LUDWIG, T. A. STEITZ, H. MUIRHEAD, and J. C. COPPOLA. Brookhaven Symp. Biol. **21**, 24 (1968).
20. W. N. LIPSCOMB, G. N. REEKE, JR., J. A. HARTSUCK, F. A. QUIOCHO and P. H. BETHGE. Phil. Trans. Roy. Soc. Lond. Ser. B, **257**, 177 (1970).
21. J. W. BUNTING and C. D. MYERS. Can. J. Chem. **51**, 2639 (1973).
22. J. W. BUNTING and C. D. MYERS. Can. J. Chem. **52**, 2053 (1974).
23. W. O. MCCLURE. Biochem. Prep. **11**, 54 (1964).
24. F. W. CARSON and E. T. KAISER. J. Am. Chem. Soc. **88**, 1212 (1966).
25. J. W. SNOKE and H. NEURATH. J. Biol. Chem. **181**, 789 (1949).
26. J. W. BUNTING and J. MURPHY. Can. J. Biochem. **50**, 1369 (1972).
27. B. L. VALLEE and J. F. RIORDAN. Brookhaven Symp. Biol. **21**, 91 (1968).
28. J. MONOD, J. WYMAN, and J.-P. CHANGEUX. J. Mol. Biol. **12**, 98 (1965).
29. L. G. LANG III, D. S. AULD, and J. F. RIORDAN. Biochemistry, **13**, 1983 (1974).
30. H. FUJIOKA and K. IMAHORI. J. Biol. Chem. **237**, 2804 (1962).
31. J. F. RIORDAN, M. SOKOLOVSKY, and B. L. VALLEE. Biochemistry, **6**, 358, 3609 (1967).
32. J. T. JOHANSEN, D. M. LIVINGSTON, and B. L. VALLEE. Biochemistry, **11**, 2584 (1972).
33. W. N. LIPSCOMB. Proc. Nat. Acad. Sci. U.S. **70**, 3797 (1973).
34. C. HANSCH. Acc. Chem. Res. **2**, 232 (1969).
35. A. LEO, C. HANSCH, and D. ELKINS. Chem. Rev. **71**, 525 (1971).
36. J. F. RIORDAN. Biochemistry, **12**, 3915 (1973).
37. J. MURPHY and J. W. BUNTING. Biochem. Biophys. Res. Commun. **48**, 1316 (1972).
38. D. S. AULD and B. HOLMQUIST. Biochemistry, **13**, 4355 (1974).

Can. J. Chem. Downloaded from www.nrcresearchpress.com by 210.87.254.42 on 09/05/12
For personal use only.

An Epitetrathiodioxopiperazine with 3*S*,6*S* Configuration from *Hyalodendron* sp.

GEORGE M. STRUNZ, MASATOSHI KAKUSHIMA, AND MERLYN A. STILLWELL

Canadian Forestry Service, P.O. Box 4000, Fredericton, New Brunswick E3B 5G4

Received July 24, 1974

GEORGE M. STRUNZ, MASATOSHI KAKUSHIMA, and MERLYN A. STILLWELL. Can. J. Chem. **53**, 295 (1975).

(3*S*,6*S*)3-Benzyl-6-hydroxymethyl-1,4-dimethyl-3,6-epitetrathiopiperazine-2,5-dione has been isolated from cultures of *Hyalodendron* sp. The same compound is produced when hyalodendrin is heated with methanol – hydrochloric acid.

GEORGE M. STRUNZ, MASATOSHI KAKUSHIMA et MERLYN A. STILLWELL. Can. J. Chem. **53**, 295 (1975).

La (3*S*,6*S*) 3-Benzyl-6-hydroxyméthyl-1,4-diméthyl-3,6-epitetrathiopiperazine-2,5-dione a été isolé de cultures d'une espèce *d'Hyalodendron*. Le même composé est produit en chauffant l'hyalodendrine avec une solution de méthanol et d'acide chlorhydrique.

The fungitoxic epidithiodioxopiperazine hyalodendrin, **1**, and the corresponding di(methylthio) ether, **2**, both with 3*S*,6*S* configuration have recently been isolated from culture filtrates of *Hyalodendron* sp. (1–3). Metabolites **1** and **2**, and the trisulfide **3**, of undetermined absolute configuration, were obtained from cultures of an unidentified fungus (NRRL 3888) (4). The metabolite **1**, with *R* configuration at positions 3 and 6, and compounds **2** and **4**, evidently belonging to the same stereochemical series, are produced by *Penicillium turbatum* (5). Gliovictin, a metabolite of *Helminthosporium victoriae* also has structure **2** (6) and is likewise enantiomeric (3*R*,6*R*) with the corresponding *Hyalodendron* product.

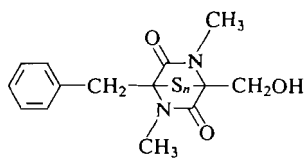

1 $n = 2$
3 $n = 3$
4 $n = 4$

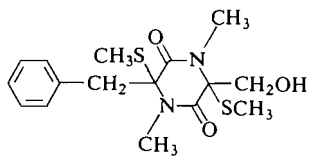

2

We record here some observations made during a study of the 3*S*,6*S* tetrasulfide **4**, isolated from fermentations of *Hyalodendron* sp. This compound, $C_{14}H_{16}N_2O_3S_4$, was present in chloroform extracts of the filtered culture medium in amounts which ranged up to 3% of the yield of pure hyalodendrin. It was slightly more polar than the latter, and could be separated and purified by preparative-layer chromatography, followed by crystallization. Comparison of the spectral characteristics of **4** (see Experimental section) with those of its co-metabolites **1** and **2** leave no doubt as to its constitution. Comparison of the circular dichroism curve of the *Hyalodendron* tetrasulfide (see Experimental section) with that published for the *Penicillium* metabolite (5) establishes that these compounds are enantiomeric at positions 3 and 6. A detailed discussion of the geometry of the tetrasulfide system of **4** is deferred at this stage, although it is noted that the synthetic compound *N*,*N'*-dimethyl-3,6-epitetrathiopiperazine-2,5-dione and sporidesmin G have been shown by X-ray analysis to be structurally similar with respect to the epitetrathiodioxopiperazine moiety (7, 8).

A tetrasulfide, identical in all respects (including c.d. spectrum) with the *Hyalodendron* tetrasulfide, was obtained in modest yield when hyalodendrin was refluxed in methanolic hydrochloric acid until no starting material remained (t.l.c.). By-products from this transformation, depleted in sulfur, resisted preliminary purifica-

Can. J. Chem. Downloaded from www.nrcresearchpress.com by 210.87.254.105 on 09/05/12
For personal use only.

Can. J. Chem. Downloaded from www.nrcresearchpress.com by 210.87.254.105 on 09/05/12
For personal use only.

tion attempts and have not been investigated further at this stage. Tetrasulfide formation was also effected in low yield by shaking a solution of hyalodendrin in the culture medium (3) (initial p*H* 3.5, methanol co-solvent) for a period comparable with the fermentation time. This result raises the possibility that the tetrasulfide isolated could be an artifact, formed from hyalodendrin by a similar acid-catalyzed mechanism. Although such a possibility cannot be excluded at present, the fact that the *P. turbatum* tetrasulfide is produced in a substantially different medium (5), and that sporidesmin G appears to be a true metabolite[1] seems to attest the 'natural' origin of at least part of the *Hyalodendron* tetrasulfide.

Refluxing hyalodendrin in aqueous methanol solution without addition of hydrochloric acid also led to the formation of a tetrasulfide. This transformation occurred more slowly than that in acid solution and the yield of tetrasulfide obtained was substantially higher. The product formed under these conditions was *racemic*.

Conversion of epidithiodioxopiperazines to the corresponding tetrasulfides (with retention of configuration) has previously been effected by the action of dihydrogen disulfide (9, 10). In bioassays, the 3*S*,6*S* tetrasulfide **4** was in general comparable with hyalodendrin (in some cases slightly less effective) in its ability to inhibit the growth of selected test fungi.[2]

Experimental

See refs. 1 and 2 for description of instrumentation, etc.

Isolation of 'Natural' Tetrasulfide 4

The production and isolation of hyalodendrin and bisdethiodi(methylthio) hyalodendrin have been detailed elsewhere (1–3). In a typical isolation sequence, material extracted with chloroform from 37 l of filtered culture medium which had supported growth of *Hyalodendron* sp. for 12 days was chromatographed on a column of silica gel (500 g Kieselgel, 100–200 mesh, Gebr. Herrmann, Köln). The eluates were monitored by t.l.c. Elution with benzene–chloroform (65:35) afforded initially 2 g of hyalodendrin. In the later fractions, the emergence of a second compound, with slightly lower R_f became evident (t.l.c.). Fractions containing the new compound were combined and rechromatographed on a preparative-layer plate of silica gel (benzene–acetone, 9:1, $R_f \sim 0.5$). This separation provided 78 mg of crude tetrasulfide, which gave 60 mg of crystalline material from benzene–cyclohexane. Recrystallization from benzene–cyclohexane afforded colorless crystals, m.p. 133–139° (pulverized crystals, 125–132°); c.d. (*c* 2.81 × 10^{-3} *M* in MeOH, 1 mm cell) λ nm (Δε): 370(0), 328(+0.9), 316(0), 297(−4.4), 287(0), 263(+13.6), 225(inflection +12.1), 230(0), and <220 (−*ve* max); ν_{max}(KBr) *inter alia* 3400, 1666, 1648, 1375, 1060, 742, 735, 701, and 657 cm^{-1}; n.m.r. ($CDCl_3$, 220 MHz) δ 3.03 (3H, s), 3.07 (3H, s) 3.25 (2H, d, $J \sim 15$ Hz), broadened base), 3.83 (1H, d, $J \sim 12$ Hz), 4.02 (1H, d, $J \sim 15$ Hz), 4.20 (1H, d, $J \sim 12$ Hz), 7.09–7.27 (5H, m). The signal for the hydroxyl proton (broad absorption around δ 3.25) disappeared on deuterium exchange. Mass spectrum *inter alia*, *m/e* 260 (base peak) $(M - S_4)^+$, 242 $(M - S_4 - H_2O)^+$, 169 $(M - S_4 - C_7H_7)^+$, and 64.

Anal. Calcd. for $C_{14}H_{16}N_2S_4O_3$: C, 43.27; H, 4.15; N, 7.21; S, 33.01. Found: C, 43.42; H, 4.11; N, 7.20; S, 33.02.

Acid Treatment of Hyalodendrin

Methanol – Hydrochloric Acid

A solution of hyalodendrin (582 mg, 1.79 mmol) in methanol (30 ml) containing 1 *N* aqueous hydrochloric acid (3.0 ml) was heated under reflux for 24 h, when no starting material remained. (Longer reaction times, up to 16 days, did not appear to have much effect on either the yield or c.d. properties of the tetrasulfide product.) After addition of saturated sodium chloride solution, the mixture was extracted thoroughly with chloroform. The extracts were washed with saturated sodium bicarbonate solution, dried ($MgSO_4$), and evaporated *in vacuo*. The tetrasulfide **4** was separated and purified by repeated chromatography on preparative-layer plates of silica gel (benzene–acetone, 94:6). Crystallization from benzene–cyclohexane gave 100 mg (0.257 mmol) of colorless crystals of **4**, m.p. 132–136° (pulverized crystals, 125–132°); mixture melting point with 'natural' **4**: 125–132°; c.d., i.r. (KBr), n.m.r. ($CDCl_3$, 220 MHz), and mass spectra identical with 'natural' **4** (*vide supra*). An analytical sample was prepared by recrystallizations from benzene: colorless prisms, m.p. 135–138°.

Anal. Calcd. for $C_{14}H_{16}N_2S_4O_3$: C, 43.27; H, 4.15; N, 7.21; S, 33.01. Found: C, 43.30; H, 4.16; N, 7.28; S, 32.99.

Culture Medium, pH 3.5 (3)

Because of the low solubility of hyalodendrin in water, methanol was used as co-solvent. An aliquot (1 ml) of a solution of hyalodendrin (2 g) in methanol (40 ml) was added to each of 40 1-l Erlenmeyer flasks, each containing 500 ml of synthetic culture medium at p*H* 3.5 (3). The flasks were stoppered with foam-plastic plugs (as used in fermentation) and shaken on a gyratory shaker at 22° for 14 days (final p*H* ~ 4). Unchanged hyalodendrin and tetrasulfide **4** were recovered from the chloroform extracts by chromatography as described above (isolation of 'natural' tetrasulfide **4**). Recrystallization from benzene–cyclohexane afforded 37 mg of **4** as almost colorless crystals, m.p. 133–142°; c.d. (*c* 2.75 × 10^{-3} *M* in MeOH, 1 mm cell) λ nm (Δε): 370 (0), 330 (+0.9), 318 (0), 298 (−4.2), 288 (0), 264 (+12.8), 254 (inflection + 10.4), 231 (0), and <220 (−*ve* max); i.r. (KBr), and mass spectra identical with those of 'natural' **4**.

Formation of Racemic Tetrasulfide 4

A solution of hyalodendrin (1.0 g, 3.08 mmol) in methanol (40 ml) and water (4 ml) was heated under reflux for 18 days, when no unchanged starting material remained (t.l.c.). A saturated aqueous solution of sodium

[1]Dr. A. Taylor. Personal communication.
[2]M. A. Stillwell. Unpublished data.

chloride was added and the mixture was extracted with chloroform. Material from the chloroform extracts was chromatographed on preparative layer plates of silica gel (benzene–acetone, 9:1), and the product corresponding in R_f with the tetrasulfide **4** was collected. Recrystallization from benzene afforded 410 mg (1.05 mmol, 68% theoretical) of tetrasulfide as almost colorless crystals, m.p. 155–166°; c.d. (c 2.92 × 10^{-3} M in MeOH, 1 mm cell) 600–250 nm, $\Delta\varepsilon = 0$; n.m.r. ($CDCl_3$, 220 MHz) and mass spectra identical with those of 'natural' tetrasulfide **4**. The main peaks in the i.r. (KBr) spectrum were essentially as quoted for 'natural' **4**: minor differences were detectable in the fingerprint region. An analytical sample was prepared by recrystallizations from benzene–chloroform, m.p. 159–166°.

Anal. Calcd. for $C_{14}H_{16}N_2S_4O_3$: C, 43.27; H, 4.15; N, 7.21; S, 33.01; 0, 12.35. Found: C, 43.26; H, 4.20; N, 7.22; S, 32.97; 0, 12.28.

Mol. Wt. Calcd. for $C_{14}H_{16}N_2S_4O_3$: 388.6. Found (osmometer, $CHCl_3$ solvent): 399.

NOTE ADDED IN PROOF: An additional correlation of the *Hyalodendron* tetra- and disulfide has been effected by sodium borohydride reduction of the former, followed by oxidation with iodine–iodide solution (*cf.* ref. 11). This treatment yielded a product, identical in all respects, including c.d. spectrum, with hyalodendrin.

The enantiometric relationship of bisdethiodi(methylthio)hyalodendrin and gliovictin was confirmed by direct comparison of the former with a sample of the latter, kindly provided by Professor Arigoni.

We thank Mr. J. Hoyle, University of Alberta for the circular dichroism measurements and Mrs. M. Austria, University of New Brunswick for the mass spectra.

1. G. M. STRUNZ, M. KAKUSHIMA, M. A. STILLWELL, and C. J. HEISSNER. J. Chem. Soc. Perkin I, 2600 (1973).
2. G. M. STRUNZ, C. J. HEISSNER, M. KAKUSHIMA, and M. A. STILLWELL. Can. J. Chem. **52**, 325 (1973).
3. M. A. STILLWELL, L. P. MAGASI, and G. M. STRUNZ. Can. J. Microbiol. **20**, 759 (1974).
4. R. L. DE VAULT and W. ROSENBROOK, JR. J. Antibiot. (Tokyo) **26**, 532 (1973).
5. K. H. MICHEL, M. O. CHANEY, N. D. JONES, M. M. HOEHN, and R. NAGARAJAN. J. Antibiot. (Tokyo) **27**, 57 (1974).
6. F. DORN and D. ARIGONI. Experientia, **30**, 134 (1974).
7. B. R. DAVIS and I. BERNAL. Proc. Natl. Acad. Sci. U.S.A. **70**, 279 (1973).
8. M. PRZYBYLSKA, E. M. GOPALAKRISHNA, A. TAYLOR, and S. SAFE. Chem. Commun. 554 (1973).
9. S. SAFE and A. TAYLOR. J. Chem. Soc. C, 432 (1970).
10. E. FRANCIS, R. RAHMAN, S. SAFE, and A. TAYLOR. J. Chem. Soc. Perkin I, 470 (1972).
11. E. OHLER, H. POISEL, F. TATARUCH, and U. SCHMIDT. Chem. Ber. **105**, 635 (1972).

Can. J. Chem. Downloaded from www.nrcresearchpress.com by 210.87.254.105 on 09/05/12
For personal use only.

The Adsorption, Desorption, and Exchange Reactions of Oxygen, Hydrogen, and Water on Platinum Surfaces. II. Hydrogen Adsorption, Exchange, and Equilibration

Y. K. PENG AND P. T. DAWSON[1]

Chemistry Department and Institute for Materials Research, McMaster University, Hamilton, Ontario L8S 4M1

Received August 13, 1974

Y. K. PENG and P. T. DAWSON. Can. J. Chem. **53**, 298 (1975).

The adsorption, desorption, exchange, and equilibration reactions of hydrogen and deuterium on a platinum filament have been investigated by thermal desorption mass spectrometry. A surface saturated with hydrogen at 120 °K has a coverage 4.2×10^{14} molecules cm^{-2} and gives desorption spectra with four distinct peaks: β_1(165 °K), β_2(220 °K), β_3(280 °K), and β_4(350 °K). Apparent activation energies and pre-exponential factors were determined for the β_2-, β_3-, and β_4-peaks. For both co-adsorption and sequential adsorption of H_2 and D_2 the mass 2, 3, and 4 desorption spectra have identical shapes and the gas desorbs at equilibrium throughout. It is concluded that hydrogen adsorbs dissociatively. Exchange and equilibration were studied at 120, 210, and 285 °K by determining the surface composition and isotope distribution after varying fractions of preadsorbed H had been replaced. Following exchange at 120 °K the desorption spectra show a higher D content and a lack of equilibrium in the desorbing gas at low temperature. In most other experiments the mass 2, 3, and 4 desorption spectra had identical shapes and the gas desorbed at equilibrium. The results are interpreted by a model which requires that the polycrystalline platinum surface is intrinsically heterogeneous. It appears that different mechanisms are unnecessary to interpret the differences in kinetics observed for exchange and equilibration at low temperatures.

Y. K. PENG et P. T. DAWSON. Can. J. Chem. **53**, 298 (1975).

On a étudié, par spectrométrie de masse impliquant la désorption, les réactions d'équilibre et d'échange de l'hydrogène et du deutérium sur un filament de platine. Une surface saturée avec de l'hydrogène à 120 °K supporte 4.2×10^4 molécules cm^{-2} et conduit à des spectres de désorption contenant 4 pics distincts: β_1(165 °K), β_2(220 °K), β_3(280 °K) et β_4(350 °K). On a déterminé les énergies d'activation apparente et les facteurs pre-exponentiels pour les pics β_2, β_3, et β_4. Pour la co-adsorption et l'adsorption en séquence de H_2 et D_2, les spectres de désorption des masses 2, 3 et 4 ont des formes identiques et le gaz se désorbe à l'équilibre à tout moment. On en conclut que l'hydrogène s'absorbe d'une façon dissociative. On a étudié l'échange et l'équilibre à 120, 210 et 285 °K en déterminant la composition à la surface et la distribution isotopique après que diverses fractions d'hydrogène préadsorbé avaient été remplacées. Après échange à 120 °K, le spectre de désorption montre un contenu en deutérium qui est plus élevé et un manque d'équilibration dans les gaz désorbants à base température. Dans la plupart des expériences, les spectres de désorption des masses 2, 3 et 4 ont des formes identiques et les gaz se désorbent à l'équilibre. On interprète les résultats à l'aide d'un modèle qui demande que la surface polycristalline du platine soit intrinsèquement hétérogène. Il semble qu'il ne soit pas nécessaire de faire appel à différents mécanismes pour interpréter les différences dans les cinétiques observées pour l'échange et l'équilibration à base température. [Traduit par le journal]

Introduction

The adsorption and isotope interchange reactions of hydrogen and deuterium have been studied on many transition metal surfaces (1, 2). The isotope interchange reactions have been classified as either exchange, in which one isotope is preadsorbed

[1] $$D_2(g) + H(a) \rightarrow HD(g) + D(a)$$

or equilibration, for which both isotopes are initially present in the gas phase

[2] $$H_2(g) + D_2(g) \rightleftarrows 2HD(g)$$

Many basic types of mechanism have been proposed for the exchange and equilibration reactions, together with some subtle variants, but the experimental evidence for any mechanism is limited and our understanding of these reactions is still very poor. Of particular interest is the observation that under the same experimental conditions the kinetics of the exchange and equilibration reactions on platinum differ, from

[1]To whom correspondence should be addressed.

Can. J. Chem. Downloaded from www.nrcresearchpress.com by 210.87.254.105 on 09/05/12
For personal use only.

Can. J. Chem. Downloaded from www.nrcresearchpress.com by 210.87.254.105 on 09/05/12
For personal use only.

which it is inferred that these reactions proceed via different mechanisms (3, 4).

In an attempt to gain more information on these reactions, the adsorption, exchange, and equilibration processes have been investigated by thermal desorption mass spectrometry using a platinum filament which has been characterized in earlier studies of oxygen adsorption (5). In the experiments described in this paper the isotopic composition of the surface has been determined at various stages during exchange with and equilibration of the gas phase. This is in contrast with previous studies in which these reactions have been followed by gas phase composition measurement alone.

Experimental Methods

The ultra-high vacuum system used in this work is the same as that described previously (5, 6). The sample filament, a 12 cm length of 0.01 in. diameter platinum (Johnson, Matthey and Mallory, Grade I), equipped with 0.003 in. diameter sensing leads for temperature measurement and control, was spot welded to heavy tungsten leads. This sample was from the same spool and processed in the same way as that described in the first paper of this series (5). In low temperature experiments a filament temperature of 120 °K was obtained by immersing the heavy tungsten leads of the press seal in liquid nitrogen.

Hydrogen and deuterium were purified by diffusion through palladium. Hydrogen and deuterium pressures were monitored with a quadrupole mass spectrometer which was calibrated against an ion gauge attached directly to the reaction vessel. This ion gauge was removed from the system after calibration. The relative sensitivity for H_2 and D_2 was found to be 1.5. However, in contrast with flash experiments in a closed system, the areas under the mass 2 and mass 4 desorption spectra differed by only $\sim 5\%$ since the measured pumping speed for H_2 was greater than that for D_2 by a factor of ~ 1.4. The desorption spectra were obtained with a slow linear heating rate of 5.6 deg s^{-1} using an automated Kelvin double bridge.

Results

Adsorption of Hydrogen on Platinum

Thermal Desorption Spectra

The thermal desorption spectra obtained after exposure of the clean platinum filament to various doses of hydrogen are shown in Fig. 1. The adsorbed phase obtained by saturating the surface at 120 °K with hydrogen at 10^{-4} Torr is unstable at temperatures higher than 140 °K and produces a desorption spectrum, spectrum *e*, with four distinct peaks with peak maxima at 165, 220, 280, and 350 °K, designated the β_1-, β_2-, β_3-, and β_4-peaks, respectively. The saturation coverage obtained under these conditions is 4.2×10^{14} molecules cm^{-2}; this coverage is

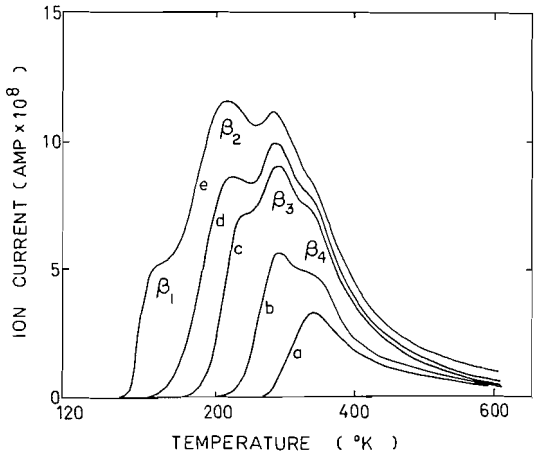

FIG. 1. Thermal desorption spectra obtained after hydrogen adsorption on platinum at 120 °K for (*a*) 2×10^{-7}, (*b*) 6×10^{-7}, (*c*) 3×10^{-6}, (*d*) 2×10^{-5}, and (*e*) 6×10^{-4} Torr s.

unaffected by prolonged pumping at the adsorption temperature. Desorption spectra obtained with increasing exposure, spectra *a–e* reveal that the β-peaks develop successively as the coverage increases. This is most simply interpreted as the population of binding states of steadily decreasing binding energy with increasing coverage; however, account may have to be taken of possible induced heterogeneity in addition to the intrinsic heterogeneity expected for a polycrystalline surface.

At 210 and 285 °K the adsorbed phases produced spectra similar to spectra *c* and *a* respectively of Fig. 1. At 10^{-6} Torr the saturation coverages were 2×10^{14} molecules cm^{-2} at 210 °K and 8×10^{13} molecules cm^{-2} at 285 °K.

Tsuchiya *et al.* (7) also observed four peaks (α, β, γ, and δ) in hydrogen desorption spectra from platinum black. The α and γ peak maximum temperatures correspond closely to those observed in the present work for the β_1- and β_4-peaks respectively and their β falls exactly between the β_2- and β_3-peaks, however, no features analogous to their δ were observed.

Desorption Kinetics

Extensive overlap between the peaks makes it difficult to determine the order for the desorption kinetics. The kinetic parameters for the desorption process have been determined from the variation of the peak maximum temperature, T_m, with heating rate, b, assuming first order kinetics. Plots of $\log (T_m^2/b)$ vs. $1/T_m$ for values

TABLE 1. Activation energies, $E^{\ddagger}$, and pre-exponential factors, ν, for hydrogen desorption from platinum

Desorption peaks	$E^{\ddagger}$(kcal mol^{-1})	ν (s^{-1})
β_2	7.0	1.3×10^6
β_3	9.0	1.6×10^6
β_4	12.4	1×10^7

of b varying from 1.2 to 28 deg s^{-1} were linear. From the slopes of these lines (5, 8) the kinetic parameters for desorption shown in Table 1 were calculated.

Tsuchiya *et al.* only report kinetic parameters for their γ hydrogen for which $E^{\ddagger} = 12$ kcal mol^{-1} and $\nu = 3.8 \times 10^5$ (7); these values compare well with those shown in Table 1 for the β_4-peak which occurs at the same temperature.

Sticking Probability

The initial sticking probability, determined by the flash desorption method, was 0.29 at 120 °K and 0.15 at 285 °K. This temperature dependence suggests a weakly-bound precursor to adsorption in the β-state (9–11) and is in good agreement with that reported by Norton and Richards (4) although the magnitudes they report are slightly smaller. Procop and Völter report a much lower initial sticking probability of $\sim 4 \times 10^{-3}$ (12) and Tsuchiya *et al.* (7) observed the opposite temperature dependence, indicating an activation energy to adsorption.

Adsorption of Hydrogen and Deuterium

Co-adsorption

At 120 °K, the sample was exposed for 10 min to a flowing mixture of H_2 and D_2 in approximately equal amounts at a total pressure of 10^{-8} Torr. The mass 2, 3, and 4 desorption spectra obtained after this co-adsorption are shown in Fig. 2. It should be noted that all the spectra have identical shapes. Furthermore, if f_{H_2}, f_{D_2}, and f_{HD} are the fractions of H_2, D_2, and HD in the desorbing gas, we can define the reaction quotient, Q, for the desorbing gas as

$$[3] \qquad Q = (f_{HD})^2/(f_{H_2})(f_{D_2})$$

It can be seen that the reaction quotient has a magnitude identical with the equilibrium constant, K, for the entire desorption spectrum.

Sequential Adsorption

At 120 °K, the surface was first subjected to a limited 2 min exposure to H_2 gas at 2×10^{-8} Torr and then after pumping the H_2 gas from the system the surface was saturated using D_2 gas at 10^{-5} Torr for a further 3 min. In the time required to saturate the surface very little exchange would occur at 120 °K. The mass 2, 3, and 4 desorption spectra obtained after this sequential adsorption are shown in Fig. 3. As was the case following co-adsorption, the spectra have identical shapes and the values determined for Q are fairly close to the equilibrium values.

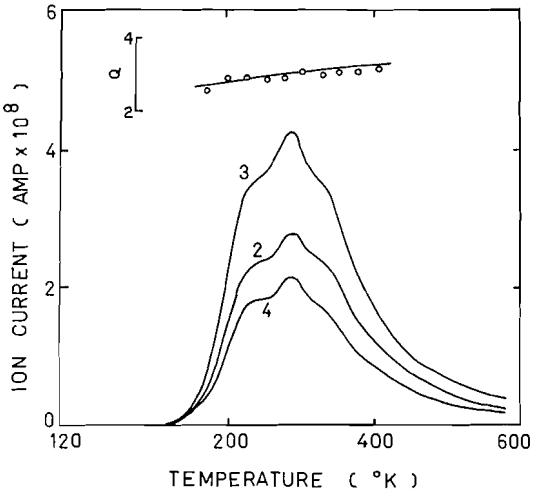

FIG. 2. Mass 2, 3, and 4 desorption spectra obtained after the platinum filament had been exposed at 120 °K to a flowing equimolar mixture of H_2 and D_2 for a total exposure of 5×10^{-6} Torr s. The inset shows the reaction quotient for the desorbing gas, $Q = (f_{HD})^2/(f_{H_2})(f_{D_2})$, as data points compared with its values at equilibrium (curve); $K = 4.24 \exp(-157/RT)$ (25).

These results show that the adsorbed isotopes desorb at equilibrium, *i.e.* no steps leading to equilibrium, such as adatom migration, are slow. Furthermore, they strongly suggest that hydrogen is dissociatively adsorbed in the β-state on platinum. The argument is somewhat tautological in that we are defining adsorption in the atomic state to be adsorption for which complete isotope mixing occurs on desorption. It is perhaps more correct to conclude that hydrogen adsorbs in the β-state in a manner such that the residual interaction between the hydrogen atoms is small and the interaction with the original partner is not appreciably different from that with other hydrogen atoms.

Exchange and Equilibration Reactions

These reactions have been studied at three different temperatures by determining the surface composition and isotope distribution in the

Can. J. Chem. Downloaded from www.nrcresearchpress.com by 210.87.254.105 on 09/05/12
For personal use only.

Can. J. Chem. Downloaded from www.nrcresearchpress.com by 210.87.254.105 on 09/05/12
For personal use only.

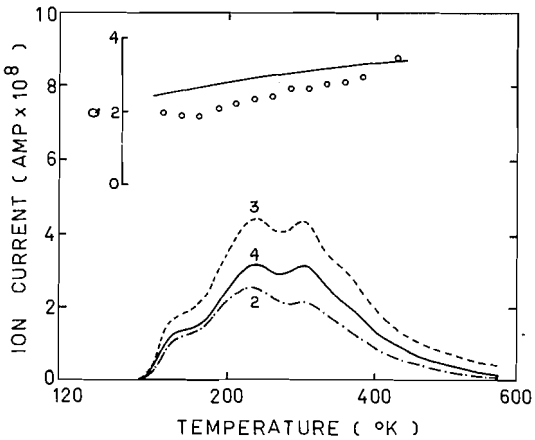

FIG. 3. Mass 2, 3, and 4 desorption spectra obtained after the platinum filament had been exposed at 120 °K, first to H_2 gas up to approximately one-half monolayer coverage and subsequently to D_2 gas up to saturation coverage. The reaction quotient is shown as an inset.

desorption spectra after varying fractions of preadsorbed hydrogen had been replaced.

Exchange at 120 °K

The hydrogen saturated surface (Fig. 1*e*) was exposed to D_2 gas at 10^{-4} Torr in a closed system. After a fraction of the preadsorbed hydrogen had been replaced the isotopic composition of the adlayer was determined from the mass 2, 3, and 4 desorption spectra. Spectra obtained after 28, 48, and 64% of the preadsorbed hydrogen had been replaced are shown in Figs. 4, 5, and 6 respectively; the reaction quotient, Q,

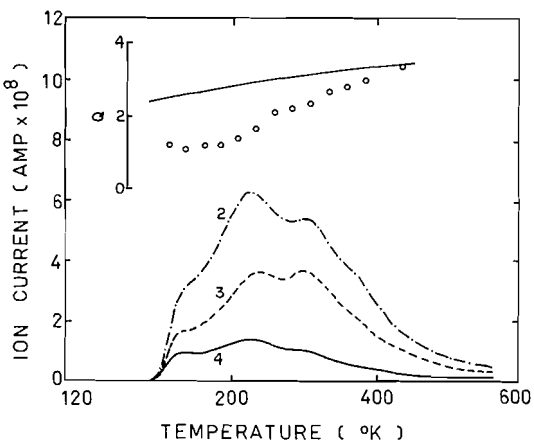

FIG. 4. Mass 2, 3, and 4 desorption spectra obtained after exposing a saturated hydrogen adlayer (Fig. 1*e*) at 120 °K to gas phase deuterium at 10^{-4} Torr for 10 min. At this stage, 28% of the preadsorbed hydrogen has been exchanged.

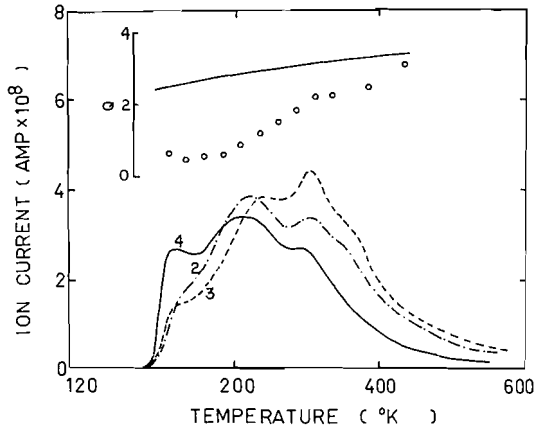

FIG. 5. Mass 2, 3, and 4 desorption spectra obtained after exposing a saturated hydrogen adlayer at 120 °K to gas phase deuterium at 10^{-4} Torr for 50 min. 48% of the preadsorbed hydrogen has been exchanged.

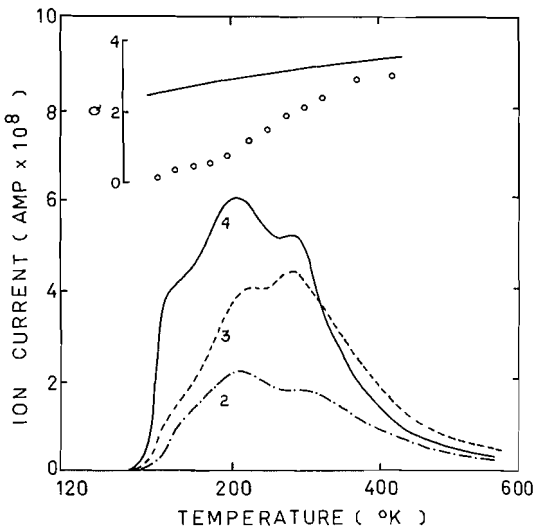

FIG. 6. Mass 2, 3, and 4 desorption spectra obtained after exposing a saturated hydrogen adlayer at 120 °K to gas phase deuterium at 10^{-4} Torr for 120 min. 64% of the preadsorbed hydrogen has been exchanged.

is also recorded. Note that, especially in Figs. 5 and 6, the desorption spectra obtained for the three isotopic species are quite different and the reaction quotient does not correspond to its equilibrium value, particularly below 250 °K where the β_1- and β_2-peaks occur. The exchange reaction is a slow process at 120 °K but 80% of the preadsorbed hydrogen was replaced after a five-hour exposure. This contrasts with the much more limited exchange observed by Tsuchiya *et al.* (3).

Can. J. Chem. Downloaded from www.nrcresearchpress.com by 210.87.254.105 on 09/05/12
For personal use only.

Equilibration at 120 °K

Similar experiments have been carried out to see how the isotopic composition of the surface varies during equilibration of an equimolar gas phase mixture of H_2 and D_2 at 2×10^{-4} Torr on a platinum surface which had been saturated with hydrogen. After only a few minutes the gas phase had equilibrated whereas only a small fraction (~20%) of the preadsorbed hydrogen had been replaced. In a blank experiment, with the platinum filament removed, the equilibration was very slow confirming that the rapid equilibration in the gas phase was taking place on the platinum surface. The observation that exchange is slower than equilibration at low temperatures has been reported previously (3, 4).

The desorption spectra obtained after 20 min, when 28% of the preadsorbed hydrogen had been replaced, are shown in Fig. 7. These spectra are very similar to those shown in Fig. 4 after 28% replacement by exchange. However, after 50 min, when 48% of the hydrogen had been replaced the spectra (Fig. 8) differ from those obtained during exchange (Fig. 5) in that the shapes are identical and $Q \simeq K$ throughout the desorption process. This is to be expected if the whole surface is in equilibrium with an equilibrated gas mixture.

Exchange and Equilibration at 210 and 285 °K

The exchange reaction proceeds rapidly at these temperatures and preadsorbed hydrogen can be completely replaced. Similar desorption spectra were obtained when the hydrogen saturated surface was exposed either to D_2 gas or a mixture of H_2 and D_2; mass 2, 3, and 4 spectra have identical shapes with Q equal to K throughout.

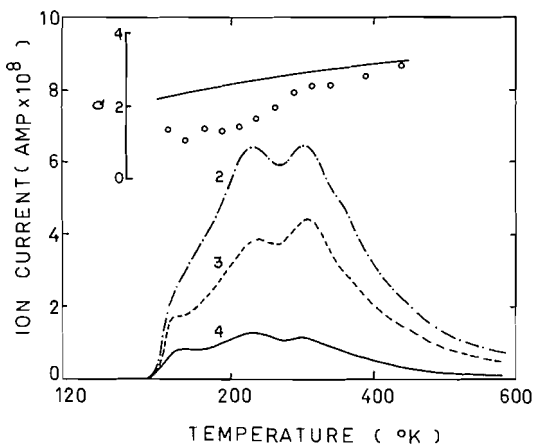

FIG. 7. Mass 2, 3, and 4 desorption spectra obtained after exposing a saturated hydrogen adlayer at 120 °K to an equimolar gas phase mixture of H_2 and D_2 at 2×10^{-4} Torr for 20 min. At this stage 28% of the hydrogen has been replaced.

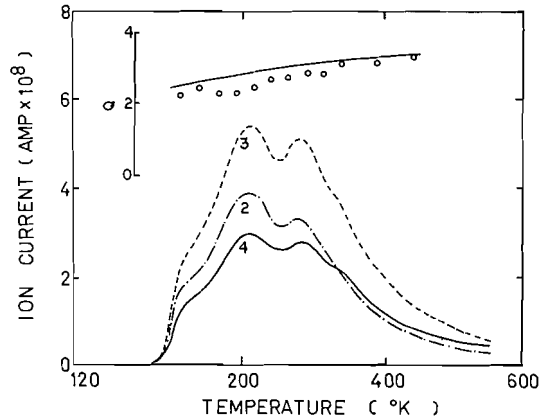

FIG. 8. Mass 2, 3, and 4 desorption spectra obtained after exposing a hydrogen saturated adlayer at 120 °K to an equimolar gas phase mixture of H_2 and D_2 at 2×10^{-4} Torr for 50 min. 48% of the preadsorbed hydrogen has been replaced.

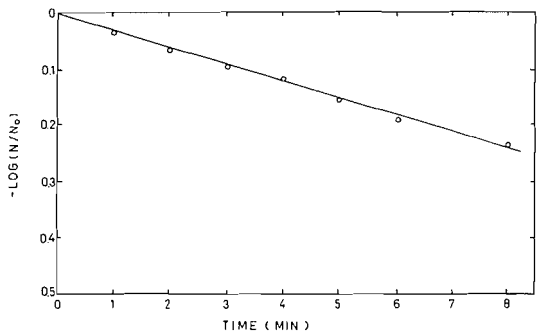

FIG. 9. Variation of the fraction of preadsorbed hydrogen remaining on the surface with time of exposure to gas phase D_2 at 3×10^{-8} Torr. The filament temperature was 210 °K throughout.

Figure 9 shows the variation in the fraction of hydrogen remaining on the surface after it had been saturated at 210 °K and then exposed at 210 °K to D_2 gas at 3×10^{-8} Torr for varying times. The straight line obtained in this semilog plot shows that the rate of exchange is first order with respect to the coverage of adsorbed hydrogen, *i.e.* $\ln (n/n_0) = kt$. This has been reported in studies where the variation in gas phase composition was measured (4) rather than the surface composition. The rate constant, k, determined from the slope of this plot is 5×10^{11}

Can. J. Chem. Downloaded from www.nrcresearchpress.com by 210.87.254.105 on 09/05/12
For personal use only.

molecules cm^{-2} s^{-1} which is about 20 times smaller than the value reported by Norton and Richards (4). However, the gas pressure used in the present work was 400 times smaller, so the difference between the values for k could be attributed to a gas pressure dependence for a pseudo rate constant. The results would agree if the reaction order in D_2 was 0.50 which is the upper limit for the order determined during equilibration at 208 °K (4). Considering the different methods used to follow the reaction, the agreement is satisfactory.

Discussion

The Adsorbed States of Hydrogen on Platinum

The adsorption of hydrogen on platinum surfaces has been studied extensively but the nature of the adsorbed states is not well understood. It is generally accepted that hydrogen is adsorbed in at least two states (13–16). Strongly-bound hydrogen is associated with a negative surface potential whereas weakly-bound hydrogen, present on the surface at higher coverage, has a positive surface potential (13, 15, 16). Strongly and weakly adsorbed hydrogen have infrared absorption bands at 4.86 μ and 4.74 μ respectively (14). Hydrogen in the strongly-bound state is believed to be atomic but there is little agreement concerning the nature of the weakly-bound state, whether it is atomic (14, 17, 18) or molecular (13, 16).

Any reversibly adsorbed species, *i.e.* any species which can be removed by pumping at the adsorption temperature, could not be detected in the present thermal desorption experiments. However, the weakly adsorbed, electropositive, species desorbs into vacuum between 200 and 250 °K (15, 16) and must therefore have been detected in the present work. The complete isotope mixing observed in both co-adsorption and sequential adsorption supports the view that this species is adsorbed atomically, in the sense discussed earlier. The reversibly adsorbed species, probably the precursor to adsorption in the β-state, present when the surface is in equilibrium with gas phase hydrogen is probably molecular. While this even more weakly bound hydrogen undoubtedly plays an important role in the equilibration and exchange reactions, it seems unlikely that these molecules are sufficiently perturbed to effect isotope exchange between molecules within this adlayer.

Desorption Kinetics

The kinetic parameters for desorption of β-hydrogen (Table 1) are characterized by low pre-exponential factors when compared with the value expected for simple first order processes of $\sim 10^{13}$ s^{-1}. This implies a statistically improbable transition state in the desorption mechanism. The calorimetric heat of adsorption of hydrogen extrapolated to zero coverage has been reported as 28 kcal mol^{-1} on supported platinum (19) and 25 kcal mol^{-1} on a platinum filament (20). Thus the measured activation energies (Table 1) are much lower than the heats of adsorption and must be apparent activation energies for desorption, again suggesting that the mechanism is complex. One possibility is a two-step process in which formation of an adsorbed molecular complex represents the first, rate-limiting, step. However, one should not ignore the possibility that the observed kinetic parameters are an artefact of the experimental method. Thus if we assume a value of $\nu = 10^{13}$ s^{-1}, then the calculated $E^{\ddagger}$ for the β_4 desorption would be 21 kcal mol^{-1} in better agreement with the heats of adsorption. The nature and origin of such "slow" desorption processes (21) is worth further investigation.

Heterogeneity of the Surface

The role of intrinsic, as opposed to induced, heterogeneity of platinum surfaces in the binding of hydrogen is uncertain. It has been argued that the surface is homogeneous in one case because the various forms of adsorbed hydrogen seem to be interrelated (7) and in another, the argument is based on the linearity of the first order exchange plots and the completeness of exchange (4). On the other hand the small amount of hydrogen which is exchangeable at low temperature has been taken to indicate a heterogeneous surface (22). However, contamination could reduce the extent of exchange (23).

In sequential adsorption experiments the observation of a memory effect is a strong indication that the surface is heterogeneous. In the sequential adsorption experiment shown in Fig. 3 there is no evidence of such a memory effect but this does not necessarily indicate that the surface is homogeneous as will be discussed later. The desorption spectra observed after exchange of 48 and 64% of the preadsorbed hydrogen, Figs. 5 and 6, have widely differing shapes for the desorbing isotopes. This is very

difficult to understand if the surface were homogeneous. In these experiments the center of the filament was at a higher temperature than the ends which were in good thermal contact with the coolant. Thus it could be claimed that the exchange is faster in the center of the filament and that during desorption the gas desorbs first from this same portion of the filament. The experiments were therefore repeated with the whole reaction vessel and sample filament press seal completely immersed in an isopentane slush at 113 °K. The results were unchanged and therefore the differences in the shapes of the mass 2, 3, and 4 desorption spectra cannot arise from a nonuniform temperature of the sample during exchange. The surface must be heterogeneous.

Model for the Exchange and Equilibration Results

Assuming that β-hydrogen is adsorbed dissociatively on a heterogeneous platinum surface we can interpret the present observations with the following model. For simplicity, consider that only two types of crystal plane, A and B, are present on the surface. The binding energy of hydrogen adatoms on plane A is assumed to be slightly lower than that on plane B.

In the exchange reaction, prior to the introduction of D_2 gas both plane A and B are saturated with β-hydrogen adatoms and every adatom on a given plane is assumed to have the same binding energy. In the presence of D_2 gas exchange will occur more rapidly on plane A where the hydrogen is more weakly bound. After 50% of the preadsorbed hydrogen has been replaced the surface isotope composition will be predominantly D on plane A but still mainly H on plane B, represented schematically in Fig. 10*a*. Isotope mixing on each plane can be expected below 140 °K (16), the temperature where desorption starts, and therefore the isotope composition of the gas desorbing from each plane should be determined by the equilibrium constant for the isotope exchange reaction, *K*. However, desorption from a surface containing planes of type A and B in macroscopic patches and with a surface isotope distribution as shown in Fig. 10*a* would give rise to a desorbing gas with a higher deuterium content at low temperature compared with that desorbing at higher temperatures (Figs. 5 and 6). We assume that the β_1-, β_2-, β_3-, and β_4-peaks arise, at least in part, from the intrinsic heterogeneity of the polycrystalline surface. These desorption features overlap considerably so if, for example, the β_1- and β_3-peaks were attributed to type A planes (two peaks could arise from adatom interactions, *i.e.* induced heterogeneity) whereas the β_2- and β_4-peaks were from type B planes then we would expect an apparent reaction quotient, *Q*, deviating considerably from its equilibrium value, as observed at lower desorption temperatures. At higher temperatures adatom mobility will increase and mixing between different macroscopic planes will produce a statistical distribution of adatoms accounting for the observation that *Q* approaches its equilibrium value at higher desorption temperatures (Figs. 5 and 6). In this way the model successfully interprets the two salient features of the exchange results, the higher mass 4 component at low desorption temperatures and the deviation of *Q* from *K*.

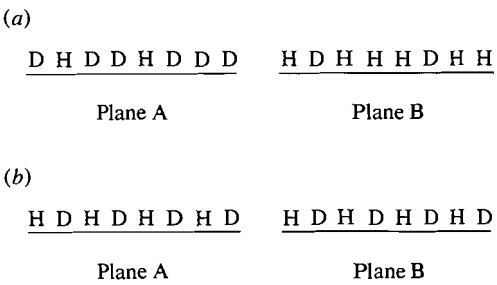

FIG. 10. Schematic diagram showing the distribution of isotopes between type A and B planes after 50% of the preadsorbed hydrogen had been replaced by exposure to (*a*) D_2 gas and (*b*) an equimolar mixture of H_2 and D_2.

In contrast, during equilibration of an equimolar gas phase mixture of H_2 and D_2 the isotope composition of each plane will successively reach the equilibrium value. Figure 10*b* schematically represents the isotope distribution on the surface after 50% of the preadsorbed hydrogen has been replaced. The mass 2, 3, and 4 desorption spectra obtained from the surface represented in Fig. 10*b* should have identical shapes and a reaction quotient, *Q*, close to the equilibrium value, *K*, as observed in Fig. 8.

This model for the exchange and equilibration results makes it unnecessary to invoke different mechanisms to explain the difference in kinetics of exchange and equilibration (3, 4). The equilibration reaction will occur predominantly on plane A, where hydrogen is more weakly bound, until the gas phase is equilibrated whereas in the

Can. J. Chem. Downloaded from www.nrcresearchpress.com by 210.87.254.105 on 09/05/12
For personal use only.

Can. J. Chem. Downloaded from www.nrcresearchpress.com by 210.87.254.105 on 09/05/12
For personal use only.

exchange reaction, after hydrogen on plane A has been replaced further exchange occurs on plane B with a slower rate. Thus the model would predict that both reactions would occur rapidly in the initial stages but the exchange reaction will slow down as the preadsorbed hydrogen concentration decreases. Actually during the initial stage of exchange some of the preadsorbed isotope appears rapidly in the gas phase and this is subtracted before constructing the kinetic plots (4). Though the origin of this desorbing gas is unspecified, it could represent the initial fast exchange reaction on type A planes. However the reason why this appears initially as homonuclear molecules is not clear.

At low temperature a difference in the activation energy for reaction on type A and B planes of as little as 1 kcal mol^{-1} would result in rates differing by a considerable factor, *i.e.* $\sim 10^2$ at 100 °K. At higher temperatures the difference becomes less significant, accounting for the observation that the rates of equilibration and exchange become comparable at higher temperatures (3, 4).

Sequential Adsorption

In the sequential adsorption experiment, Fig. 3, there is no evidence of a memory effect, complete isotope mixing occurs on desorption. Complete mixing does not necessarily indicate that the surface is homogeneous since mixing can occur during desorption or at the adsorption temperature if the adatoms are sufficiently mobile. However since after the exchange reaction (Figs. 5 and 6) the mass 2, 3, and 4 desorption spectra are quite different in shape, the adlayer cannot have sufficient mobility to produce the complete mixing observed following sequential adsorption (Fig. 3). Interpretation of the exchange results requires that the surface be heterogeneous and so some alternative explanation for the complete mixing observed after sequential adsorption must be found. The total sticking probability for hydrogen on polycrystalline platinum is initially high and remains more or less unchanged up to half-coverage and then drops very rapidly (4). Adsorption of gases on single crystal planes shows a similar variation of sticking probability with coverage and, moreover, there is no simple correlation between initial sticking probability and binding energy (24). Thus a similar variation of sticking probability for hydrogen adsorption on type A and B planes of polycrystalline platinum seems likely. In this case, preadsorption of hydrogen up to half-coverage would populate both type A and type B planes and in the subsequent adsorption of deuterium the remaining empty sites on both planes will be occupied. On completion of the sequential adsorption the isotope distribution on the surface would resemble that shown in Fig. 10*b*. Isotope mixing on each plane prior to desorption would result in complete mixing. Since Q does not exactly equal K following sequential adsorption (Fig. 3) we conclude that the distribution of isotopes on different planes is not identical as is suggested in the simple model of Fig. 10*b*.

Exchange and Equilibration Mechanisms

The exchange and equilibration reactions occur rapidly at temperatures below those required for desorption of the binding state investigated in this work, the β-state. Clearly additional adsorbed states which are unstable in the absence of gaseous hydrogen are important in achieving exchange and equilibration. An increase in surface coverage on introducing gas phase hydrogen presumably either reduces the binding energy of the whole adlayer, through adsorbate–adsorbate interactions, permitting exchange with the gas phase, or provides a distinct binding state of intermediate energy between the β-state and the gas phase and therefore a pathway to exchange. The nature of these additional states has not been examined in this work and therefore we can provide no direct evidence for any of the detailed mechanisms proposed for the exchange and equilibration reactions.

Conclusions

The results described in the present paper show that, for polycrystalline platinum surfaces, heterogeneity plays an important role in the exchange and equilibration reactions of hydrogen. It is shown that different mechanisms are not required to interpret differences in the kinetics observed for these reactions. However it is not established that different mechanisms do not exist. Particularly we would stress that different mechanisms may exist at different temperatures; thus, at low temperature exchange may occur between the atomically adsorbed β-state and a (molecularly) adsorbed precursor state whereas at high temperature and low pres-

sure the reactions may occur entirely within an atomically adsorbed β adlayer.

The authors wish to thank Atomic Energy of Canada Limited, Chalk River Nuclear Laboratories, for their support of this research.

1. G. C. BOND. Catalysis by metals. Academic Press, London and New York. 1962.
2. R. P. H. GASSER. Surface and defect properties of solids, Vol. 1. The Chemical Society, London. 1972.
3. S. TSUCHIYA, Y. AMENOMIYA, and R. J. CVETANOVIC. J. Catal. **20**, 1 (1971).
4. P. R. NORTON and P. J. RICHARDS. Surf. Sci. **41**, 293 (1974).
5. Y. K. PENG and P. T. DAWSON. Can. J. Chem. **52**, 3507 (1974).
6. P. T. DAWSON and Y. K. PENG. Surf. Sci. **33**, 565 (1972).
7. S. TSUCHIYA, Y. AMENOMIYA, and R. J. CVETANOVIC. J. Catal. **10**, 245 (1970).
8. P. A. REDHEAD. Vacuum, **12**, 203 (1962).
9. G. EHRLICH. J. Phys. Chem. **59**, 473 (1955).
10. G. EHRLICH. J. Phys. Chem. Solids, **1**, 3 (1956).
11. P. KISLIUK. J. Phys. Chem. Solids, **3**, 95 (1957); **5**, 78 (1958).
12. M. PROCOP and J. VÖLTER. Surf. Sci. **33**, 69 (1972).
13. J. C. P. MIGNOLET. J. Chim. Phys. **54**, 19 (1957).
14. W. A. PLISKIN and R. P. EISCHENS. Z. Phys. Chem. **24**, 11 (1960).
15. W. J. M. ROOTSAERT, L. L. VAN REIJEN, and W. M. H. SACHTLER. J. Catal. **1**, 416 (1962).
16. R. LEWIS and R. GOMER. Surf. Sci. **17**, 333 (1969).
17. T. TOYA. Suppl. Prog. Theor. Phys. **23**, 250 (1962).
18. P. H. LEWIS. J. Phys. Chem. **67**, 2151 (1963).
19. J. M. BASSET, A. THEOLIER, M. PRIMET and M. PRETTRE. Proc. Vth Int. Cong. Catal. Miami Beach, 1972. *Edited by* J. W. Hightower. North-Holland/American Elsevier, Vol. 2, 921 (1973).
20. P. R. NORTON and P. J. RICHARDS. Surf. Sci. **44**, 129 (1974).
21. L. A. PÉTERMANN. Prog. Surf. Sci. **3**, 1 (1972).
22. G. K. BORESKOV and A. O. WASSILJEWITSCH. Dokl. Akad. Nauk SSSR, **127**, 1033 (1959).
23. H. GENTSCH. Z. Phys. Chem. **35**, 69 (1962).
24. L. D. SCHMIDT. Cat. Rev.-Sci. Eng. **9**, 115 (1974).
25. E. A. MOELWYN-HUGHES. Physical chemistry. Pergamon Press, New York. 1957. p. 976.

Can. J. Chem. Downloaded from www.nrcresearchpress.com by 210.87.254.105 on 09/05/12
For personal use only.

^{119}Sn Mössbauer Spectra of Sn–Ni Compounds

G. MICHAEL BANCROFT[1] AND K. DAVID BUTLER[2]

Department of Chemistry, University of Western Ontario, London, Ontario N6A 3K7

Received September 5, 1974

G. MICHAEL BANCROFT and K. DAVID BUTLER. Can. J. Chem. **53**, 307 (1975).

^{119}Sn Mössbauer spectra have been recorded for eleven tin–nickel compounds of the type $Cl_xSn[NiLCp]_{4-x}$ (L = CO, PPh_3; x = 2, 3) and $Cl_3SnNiL_2Cp.S$ (S = solvent molecule). The center shifts are used to distinguish coordinated $SnCl_3$ and uncoordinated ionic $SnCl_3^-$, respectively. In the $SnCl_3^-$ compounds, the Mössbauer parameters indicate that the solvent molecules are not bonded to the Sn atom. In compounds containing Sn—Ni bonds, the center shifts and quadropole splittings show that $Ni(PPh_3)Cp$ is the best donor of the first row transition metal moieties, and that the Sn—Ni bond has the highest Sn s character. Ni(CO)Cp is a slightly poorer donor than $Ni(PPh_3)Cp$, and the Sn—Ni bond has a smaller s character.

G. MICHAEL BANCROFT et K. DAVID BUTLER. Can. J. Chem. **53**, 307 (1975).

On a enregistré les spectres Mössbauer de ^{119}Sn de onze composés étain–nickel du type $Cl_xSn[NiLCp]_{4-x}$ (L = CO, PPh_3; x = 2, 3) et $Cl_3SnNiL_2Cp.S$ (S = une molécule de solvant). Les déplacements de centre ont été utilisés pour distinguer les $SnCl_3$ coordonnés et des espèces des $SnCl_4$ ioniques non coordonnées. Dans les composés $SnCl_3^-$, les paramètres du spectre Mössbauer indiquent que les molécules de solvant ne sont pas liées à l'atome d'étain. Dans les composés contenant des liens Sn—Ni, les c.s. et q.s. montrent que, parmi les groupes contenant des métaux de transition de la première rangée, le $Ni(PPh_3)Cp$ est le meilleur donneur; ces données permettent aussi de conclure que le lien Sn—Ni a le plus grand caractère s pour l'atome Sn. Le complexe Ni(CO)Cp est un plus mauvais donneur que $Ni(PPh_3)Cp$ et le lien Sn—Ni a un caractère s plus petit. [Traduit par le journal]

Introduction

^{119}Sn Mössbauer spectra of compounds containing a Sn—M (M = transition metal) bond have been the subject of a number of recent studies (1–6). The great majority of such compounds have contained $Mn(CO)_5$, $Fe(CO)_2Cp$, or $Co(CO)_4$ moieties or phosphine substituted derivatives. Center shifts and quadrupole splittings have been very useful in distinguishing and explaining differences in the Sn—M bonds, and partial quadrupole splittings (7) have been successfully applied in correlating and predicting quadrupole splittings (1, 2). In addition, ^{119}Sn Mössbauer center shifts have been used to distinguish between coordinated and uncoordinated $SnCl_3$ groups (8–11). Thus, coordinated $SnCl_3$ containing tetravalent Sn normally has center shifts under 2 mm s^{-1}, while uncoordinated $SnCl_3^-$ containing divalent Sn has a center shift of over 3 mm s^{-1}.

A number of Sn compounds containing nickel of the type $Cl_xSn[NiLCp]_{4-x}$ (L = CO, PR_3; x = 2, 3) and $Cl_3SnNiL_2Cp.S$ (S = solvent molecule) have recently been prepared (12–17). Conductivity and mass spectrometric studies in these papers indicated that a Sn—Ni bond was present in the $Cl_xSn[NiLCp]_{4-x}$ compounds. This evidence is substantiated by the covalent Ge—Ni bond shown by X-ray diffraction studies of the Ge analogue $Cl_3GeNi(PPh_3)Cp$ (15). In contrast, the above studies indicated that the $Cl_3SnNiL_2Cp.S$ compounds are ionic and can be formulated as $[CpNiL_2]^+[S.SnCl_3]^-$ although the role of the solvent molecule is unclear. In the original report of the compounds with L = PPh_3 and S = CH_2Cl_2 or $(CH_3)_2CO$ (13), the authors suggested that the solvent molecules were bonded to the Sn on the basis of infrared data and the difficulty with which the solvent molecules are removed. The ν(CO) band of acetone in the acetone complex was at 1705 cm^{-1} compared with 1740 cm^{-1} in gaseous acetone. A similar reduction of 23 cm^{-1} in the (C—Cl) stretching frequency for CH_2Cl_2 was noted (13) in the CH_2Cl_2 compound. The ^{1}H n.m.r. signals due to the solvent molecules were not shifted detectably from those of the free solvent, but this is possibly due to dissociation in solution.

As part of our continuing ^{119}Sn Mössbauer

[1]To whom correspondence should be addressed.

[2]Present address: Analytical Research Division, Imperial Oil Enterprises Ltd., Sarnia, Ontario N7T 7M1.

Can. J. Chem. Downloaded from www.nrcresearchpress.com by 210.87.254.5 on 09/05/12
For personal use only.

studies on Sn metal bonds, we report the ^{119}Sn Mössbauer spectra of a number of Sn—Ni compounds. The Mössbauer spectra are very useful in distinguishing between coordinated and uncoordinated $SnCl_3$, and the role of the solvent molecule is clarified in the $SnCl_3^-$ compounds. The bonding of the NiLCp moiety is compared with the $Mn(CO)_5$, $Fe(CO)_2Cp$, and $Co(CO)_4$ moieties studied earlier.

Experimental

The compounds were synthesized using methods outlined previously (12–17). The identity and purity of all compounds was checked from melting points, infrared, and n.m.r. spectra. Microanalyses were performed by Chemalytics Inc. (Arizona, U.S.A.). All compounds were made and stored under a nitrogen atmosphere and carefully recrystallized from deoxygenated solvents immediately before Mössbauer spectra were run.

The two new solvent analogues $[Cl_3Sn][Ni(PPh_3)_2Cp].S$ (S = CH_3OH, THF) were prepared by recrystallization from the appropriate solvent.

Anal. Calcd. for $[Cl_3Sn][Ni(PPh_3)_2Cp].CH_3OH$: C, 55.7; H, 4.34; Cl, 11.8. Found: C, 55.3; H, 4.09; Cl, 11.2.

Anal. Calcd. for $[Cl_3Sn][Ni(PPh_3)_2Cp].THF$: C, 57.2; H, 4.58; Cl, 11.3. Found: C, 57.2; H, 4.19; Cl, 11.9.

The THF, acetone, and methanol adducts dissociated extensively to $CpNi(PPh_3)Cl$ and $SnCl_2$ in solution (13–15), but the required product recrystallized on cooling overnight at −20 °C.

$[Cl_3Sn][Ni(dppe)Cp]$ was prepared in 60% yield by mixing one mole equivalent each of 1,2-bis(diphenylphosphino)ethane and $[Cl_3Sn][Ni(PPh_3)_2Cp]$ in acetone.

Anal. Calcd. for $[Cl_3Sn][Ni(dppe)Cp]$: C, 49.8; H, 3.91; Cl, 14.2. Found: C, 50.1; H, 3.79; Cl. 15.3.

$[Ni(PPh_3)_2Cp]PF_6$.acetone was synthesized by mixing mole equivalents of $CpNi(PPh_3)Cl$, PPh_3, and $AgPF_6$ in acetone. AgCl was removed by centrifugation and decantation, and the yellow product crystallized when the volume of the acetone was reduced under vacuum (yield 85%).

Infrared spectra were recorded on a Perkin-Elmer 621 spectrometer calibrated with polystyrene. ^1H n.m.r. spectra were measured using a Varian T-60 spectrometer, and the spectra were calibrated with TMS and chloroform. Mössbauer spectra were obtained on an Austin Science Associates spectrometer using a Ba $^{119m}SnO_3$ source at room temperature. Calibration and computation were obtained using methods previously described (18, 19).

Results and Discussion

The Mössbauer parameters for the tin–nickel compounds are given in Table 1. The compounds can immediately be divided into two groups on the basis of their center shifts: compounds **1–7** having center shifts larger than 3 mm s^{-1}, and compounds **8–11** having center shifts less than 2 mm s^{-1}. These results strongly indicate that the first seven compounds contain an anionic $SnCl_3^-$ (divalent tin) species which is not coordinated to the nickel atom. The low center shifts for compounds **8–11** show that a Sn—Ni bond exists in these compounds. These conclusions are entirely consistent with previous assertions (12–17).

The center shifts and quadrupole splittings for the anionic $SnCl_3$ compounds are very similar despite the variation in solvent molecule. This evidence suggests that the solvent molecules are not coordinated to the Sn to give $S.SnCl_3^-$ species as previously suggested (13). Confirmation of this assertion comes from the compound $[CpNi(PPh_3)_2^+][PF_6^-]$.acetone, whose infrared ν(CO) band is a narrow doublet at 1709/1713 cm^{-1}, little different from the position of the band for the corresponding tin-containing compound. In addition, it has been shown (20) from an X-ray diffraction study that the acetone molecule in the metal–metal bonded compound $(Cl_3Sn)Pd(PPh_3)(h^3\text{-}C_3H_5)$ (0.4 acetone) is not bound to any other atom in the molecule. The ν(CO) band for acetone in this compound occurs at 1710 cm^{-1}, close to the values observed here for the acetone-containing compounds. Similarly, the structure of the compound $[Co(dppe)_2Cl^+][SnCl_3^-]$ in solvated form (with C_6H_5Cl) is known from a diffraction study (10). It contains a discrete $SnCl_3^-$ ion, and the C_6H_5Cl molecule is not bonded to either the anion or cation, both of which have very similar geometries to the same ions in the unsolvated form of the compound.

The solvent molecules are surprisingly difficult to remove from the ionic compounds if they are not bonded, acetone and dichloromethane only being removed from compounds **2** and **3** (Table 1) at 85° and 115° respectively under vacuum (13). On the other hand, it is difficult to prevent the spontaneous loss of dichloromethane from the neutral compound **10** at room temperature. The ν(C—Cl) infrared band for the neutral and ionic compounds containing CH_2Cl_2 differ by only 6 cm^{-1}.

Using center shifts and quadrupole splittings, it is interesting to compare the character of the Sn—Ni bond with other Sn transition metal bonds previously studied. It is apparent from Table 2 that $Cl_3SnNi(PPh_3)Cp$ has the largest center shift and quadrupole splitting of the four first row transition metal $SnCl_3$ derivatives. The large center shift indicates that the Sn—Ni bond has the highest s character in the series and the large quadrupole splitting shows that the

Can. J. Chem. Downloaded from www.nrcresearchpress.com by 210.87.254.5 on 09/05/12
For personal use only.

TABLE 1. Mössbauer parameters for Sn—Ni compounds (mm s^{-1})

Compound	Center shift[a]	Quadrupole splitting[a]	$\Gamma_{1,2}$[b]
1, $[Cl_3Sn^-][Ni(PPh_3)_2Cp^+]$	3.15	1.29	1.06, 1.02
2, $[Cl_3Sn^-][Ni(PPh_3)_2Cp^+].1{\cdot}3CH_2Cl_2$	3.18	1.20	1.11, 1.09
3, $[Cl_3Sn^-][Ni(PPh_3)_2Cp^+].(CH_3)_2CO$	3.19	1.24	1.06, 1.06
4, $[Cl_3Sn^-][Ni(PPh_3)_2Cp^+].CH_3OH$	3.21	1.33	1.07, 1.11
5, $[Cl_3Sn^-][Ni(PPh_3)_2Cp^+].THF$	3.11	1.29	1.06, 1.13
6, $[Cl_3Sn^-][Ni(PPh_3)_2Cp^+].\frac{1}{2}C_6H_6$	3.15	1.23	1.01, 0.99
7, $[Cl_3Sn^-][Ni(dppe)Cp^+]$	3.20	1.49	1.06, 1.07
8, $Cl_2Sn[Ni(CO)Cp]_2$	1.87 ± 0.05	2.15 ± 0.05	1.20, 1.27
9, $Cl_3SnNi(PPh_3)Cp$	1.76	2.01	1.06, 1.06
10, $Cl_3SnNi(PPh_3)Cp.CH_2Cl_2$	1.80	2.06	1.06, 1.02
11, $Cl_3SnNi(PPh_3)Cp.(CH_3)_2CO$	1.81	1.97	1.06, 1.01

[a] ± 0.02 unless otherwise shown.
[b] ± 0.05.

TABLE 2. Mössbauer parameters for transition metal $SnCl_3$ and $SnCl_2$ derivatives (mm s^{-1})

Compound	Center shift	Quadrupole splitting	Reference
1, $Cl_3SnMn(CO)_5$	1.65	1.60	21
2, $Cl_3SnFe(CO)_2Cp$	1.75	1.83	21
3, $Cl_3SnCo(CO)_4$	1.42	1.20	2
4, $Cl_3SnNi(PPh_3)Cp$	1.76	2.01	This work
5, $Cl_2Sn[Mn(CO)_5]_2$	1.90	2.10	1, 22
6, $Cl_2Sn[Fe(CO)_2Cp]_2$	1.99	2.39	1, 7
7, $Cl_2Sn[Co(CO)_4]_2$	1.75	1.44	2
8, $Cl_2Sn[Ni(CO)Cp]_2$	1.87	2.15	This work

$Ni(PPh_3)Cp$ moiety is the best donor of the four transition metal moieties (1, 2). This large donor ability of the $Ni(PPh_3)Cp$ group should be reflected in a very large negative partial quadrupole splitting value (> -1.1 mm s^{-1}), but as in previous studies we do not want to assign *pqs* values from distorted $SnCl_3$ derivatives.

In contrast, both the center shift and quadrupole splitting for $Cl_2Sn[Ni(CO)Cp]_2$ are proportionately smaller than their analogues (Table 2, compounds **5**–**8**), indicating that the Ni(CO)Cp group is not as good a donor as $Ni(PPh_3)Cp$, and that the Sn—Ni bond contains less Sn s character for the carbonyl derivative. As predicted by the point charge model, one would expect that the Cl_2SnM_2 compounds should have quadrupole splittings about 15% larger than their Cl_3SnM analogues. An increase of at least this amount is found for M = $Mn(CO)_5$, $Fe(CO)_2Cp$, and $Co(CO)_4$, but an increase in the quadrupole splitting of only 7% is found on going from $Cl_3SnNi(PPh_3)Cp$ to $Cl_2Sn[Ni(CO)Cp]_2$. The weaker donor properties of the carbonyl species are not unexpected because of the excellent acceptor ability of CO relative to PPh_3. Similar effects in the ^{119}Sn Mössbauer parameters are found in the phosphine and phosphite substituted $Cl_xSn[Fe(CO)_2Cp]_{3-x}$ compounds (23, 24).

We thank the National Research Council of Canada for a support grant, and an NRCC scholarship to K.D.B.

1. G. B. BANCROFT, K. D. BUTLER, A. T. RAKE, and B. DALE. J. Chem. Soc. Dalton, 2025 (1972) and refs. 1–16.
2. G. M. BANCROFT and K. D. BUTLER. J. Chem. Soc. Dalton, 1694 (1973).
3. S. ICHIBA, M. KATADA, and H. NEGITA. Bull. Chem. Soc. Jap. **45**, 1679 (1972).
4. B. LIENGME, J. R. SAMS, and J. C. SCOTT. Bull. Chem. Soc. Jap. **45**, 2956 (1972).
5. S. R. A. BIRD, S. CENINI, J. D. DONALDSON, A. F. LEC. HOLDING, and B. RATCLIFF. Inorg. Chim. Acta, **6**, 379 (1972).
6. S. R. A. BIRD, J. D. DONALDSON, A. F. LE C. HOLDING, S. CENINI, and B. RATCLIFF. Inorg. Chim. Acta, **8**, 149 (1974).
7. G. M. BANCROFT and R. H. PLATT. Adv. Inorg. Radiochem. **15**, 59 (1973).
8. D. E. FENTON and J. J. ZUCKERMAN. Inorg. Chem. **8**, 1771 (1969).
9. G. M. BANCROFT and K. D. BUTLER. J. Chem. Soc. Dalton, 1209 (1972).
10. J. K. STALICK, D. W. MEEK, B. Y. K. Ho, and J. J. ZUCKERMAN. Chem. Commun. 630 (1972).
11. M. J. MAYS and P. L. SEARS. J. Chem. Soc. Dalton. In press.
12. D. J. PATMORE and W. A. G. GRAHAM. Inorg. Chem. **5**, 1405 (1966).
13. M. VAN DEN AKKER and F. JELLINEK. J. Organometal. Chem. **10**, 37 (1967).
14. P. A. MCARDLE and A. R. MANNING. Chem. Commun. 417 (1967).

Can. J. Chem. Downloaded from www.nrcresearchpress.com by 210.87.254.5 on 09/05/12
For personal use only.

15. F. GLOCKLING, A. MCGREGOR, M. L. SCHNEIDER, and H. M. M. SHEARER. J. Inorg. Nucl. Chem. **32**, 3101 (1970).
16. F. GLOCKLING and A. MCGREGOR. J. Inorg. Nucl. Chem. **35**, 1481 (1973).
17. R. C. EDMONDSON, E. EISNER, M. J. NEWLANDS, and L. K. THOMPSON. J. Organometal. Chem. **35**, 119 (1972).
18. G. M. BANCROFT and T. K. SHAM. Can. J. Chem. **52**, 1361 (1974).
19. G. M. BANCROFT. Mössbauer spectroscopy: an introduction for inorganic chemists and geochemists. McGraw-Hill, London. 1973.
20. R. MASON, G. B. ROBERTSON, P. O. WHIMP, and D. A. WHITE. Chem. Commun. 1655 (1968); R. MASON and P. O. WHIMP. J. Chem. Soc. (A), 2709 (1969).
21. G. M. BANCROFT, K. D. BUTLER, and A. T. RAKE. J. Organometal. Chem. **34**, 137 (1972).
22. R. V. PARISH. Prog. Inorg. Chem. **15**, 101 (1972).
23. W. R. CULLEN, J. R. SAMS, and J. A. J. THOMPSON. Inorg. Chem. **10**, 843 (1971).
24. G. M. BANCROFT and A. T. RAKE. Inorg. Chim. Acta. In press.

Can. J. Chem. Downloaded from www.nrcresearchpress.com by 210.87.254.5 on 09/05/12
For personal use only.

Canadian Journal of Chemistry

Published by
THE NATIONAL RESEARCH COUNCIL OF CANADA

Journal canadien de chimie

Publié par
LE CONSEIL NATIONAL DE RECHERCHES DU CANADA

Volume 53 Number 3 February 1, 1975

Volume 53 numéro 3 1 février 1975

The Determination of Traces of Nickel(II) by Solid State Spectroscopy

DOUGLAS EARL RYAN AND JIRI HOLZBECHER

Trace Analysis Research Centre, Dalhousie University, Halifax, Nova Scotia B3H 4J1

Received August 28, 1974

DOUGLAS EARL RYAN and JIRI HOLZBECHER. Can. J. Chem. **53**, 311 (1975).

Traces of nickel(II) are determined by measurement of light absorption in the solid state after co-precipitation with a large excess of α-benzildioxime. The detection limit is 0.2 μg Ni and nickel can be recovered even from 1000 ml sample volumes (*i.e.* <1 ng/ml can be determined). Only a few foreign ions interfere.

DOUGLAS EARL RYAN et JIRI HOLZBECHER. Can. J. Chem. **53**, 311 (1975).

On détermine des traces de nickel(II) par mesure d'absorption de la lumière à l'état solide après co-précipitation avec un grand excès d'α-benzildioxime. La limite de la détection est de 0.2 μg de nickel et on peut même récupérer le métal à partir d'échantillons ayant des volumes de 1000 ml (*i.e.* on peut déterminer des quantités <1 ng/ml). Seulement quelques ions étrangers interfèrent dans cette analyse. [Traduit par le journal]

Introduction

In recent communications, methods have been described for the determination of trace metal ions by solid state fluorescence after preconcentration by co-precipitation. Two major principles were used: (*1*) co-precipitation with an inorganic carrier and subsequent activation by ignition to produce a phosphor (1–3); (*2*) co-precipitation of a fluorescent chelate with a large excess of a non-fluorescent, water insoluble chelating agent (4, 5).

While these methods exhibit a high sensitivity, because of the preconcentration effect, they often suffer from interferences. Since color-forming methods in solution are not usually subject to interferences to such a degree as fluorimetric methods, the potential of spectrophotometry in the solid state, based on chelate formation, was studied.

The basic requirements for a suitable chelating agent can be summarized as follows: (*a*) react to form a color with the metal ion of interest, (*b*) be selective, (*c*) have a low solubility in water so that the method would be essentially independent of the sample volume, (*d*) have appreciable solubility in some organic, water miscible solvent.

One of the very selective color and, at the same time, precipitation reactions is that of α-dioximes with nickel(II). Among various dioximes α-benzildioxime shows a very low water solubility, dissolves readily in dimethylsulfoxide, and can be easily synthesized. The present paper describes the determination of nickel(II) at ng/ml levels using co-precipitation of the nickel chelate with α-benzildioxime and subsequent measurement of the light absorption of the precipitate.

Experimental

Apparatus and Reagents

All spectrophotometric measurements were made with a Farrand VIS-UV Chromatogram Analyzer or with a Zeiss Chromatogram Spectrophotometer. The sample cell was an aluminum sheet painted white with drilled holes (diameter 5 mm) and covered with a glass plate. It was packed with a sample powder which was held in place by masking tape; the glass was removed prior to measurement.

A stock solution containing 1000 μg/ml of nickel(II) was prepared from nickel(II) chloride hexahydrate (BDH) and was standardized by EDTA titration using xylenol orange (6). The α-benzildioxime was synthesized according to the procedure given in the monograph by Diehl (7). Benzil (BDH) (40 g) was dissolved in 200 ml of hot methanol; 32 g of hydroxylamine hydrochloride (Baker) were added and the reaction mixture was boiled and stirred for 3 h. After cooling, the precipitate of dioxime was filtered off with suction, washed with hot water and then with 50% ethanol; 12 g of white, crystalline product were obtained after drying. It was used without further purification. The reagent solution was 1% (w/v) in dimethylsulfoxide (Fisher, Certified A.C.S.).

The buffer solution (pH ~ 10) was prepared by mixing 70 g of ammonium chloride with 570 ml of concentrated ammonia and diluting to 1 l with water.

The ammonium tartrate (Baker & Adamson) solution was 1 M.

Procedure

To 100 ml of solution containing 0.2–10.0 μg of nickel add 3 ml of ammonia buffer (pH ~ 10)[1], 1 ml of 1 M ammonium tartrate and, finally, 3 ml of the reagent solution with rapid stirring. Filter the precipitate through a filter crucible, wash with distilled water and dry in a vacuum desiccator for 1 h. Pack the cell (grinding of the powder causes electrostatic charge and thus packing difficulties) and measure the light absorption. Settings of the Farrand instrument: function SIG (single beam), λ, 435 nm (on both monochromators), excitation filter removed, filter 3–73, screen mesh reducer 0.625 and aperture 0.021 in the analyzer leg, range 1.0 (if measurement at 570 nm is desired use aperture 0.062).

Results and Discussion

The reflectance spectrum of the nickel chelate in the solid state (obtained with the Zeiss instrument) exhibits two absorption maxima at 435 and 570 nm, absorption at 435 nm being stronger and thus recommended for measurement. This is in agreement with the spectrum obtained in solution of the nickel chelate in amyl-alcohol.

Typical calibration curves are shown in Fig. 1 (two different runs); A, 0.2–2 μg, B, 1–10 μg Ni. They do not pass through the origin because the plate background was selected as the base line (zero absorption). The relative standard deviation of six determinations of 2 μg Ni/100 ml (20 ng/ml) is ~7%.

Factors Affecting the Method

It is necessary to have the reagent solution as concentrated as possible so that the minimum amount of solvent is introduced, together with the reagent, into the sample solution. The solubility of the resulting precipitate is thus kept low and dependence on the sample volume is minimized. Dimethylsulfoxide has been selected as a solvent since at least a 1% solution of the reagent could be prepared. Three ml of this solution added to 100 ml of water are sufficient to produce enough precipitate (~ 30 mg) to fill a hole in the measuring cell.

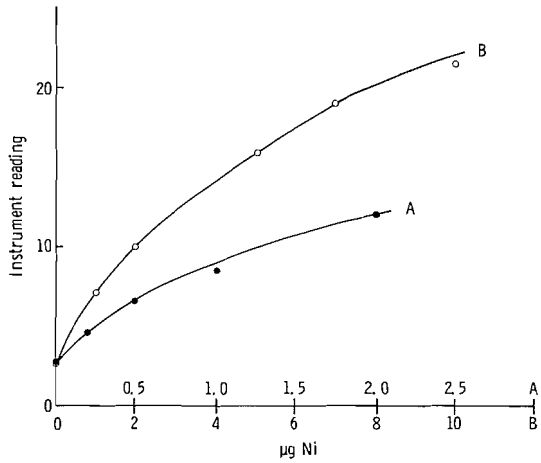

FIG. 1. Calibration curves for nickel. A, 0.2–2.0 μg; B, 1.0–10.0 μg.

While at pH ~ 5 there is virtually no difference in absorption between the precipitates separated from solution containing nickel- and respective blank, the absorption of the precipitates from nickel containing solutions increases sharply with increasing pH up to ~8, and then remains essentially unchanged up to pH ~10. For better masking, pH ~ 10 was selected for further work.

There is no appreciable dependence of light absorption or quality of the precipitate upon the rate of addition of the reagent solution. Essentially the same readings are obtained for precipitates filtered immediately after their precipitation and those allowed to stand for various periods of time (up to 1 h) before filtration.

The light absorption of the powder increases with increasing sample volume (containing 2 μg Ni) from 10 to 100 ml and remains virtually constant with further increase of volume up to 1 l. This fact makes it possible to increase the sensitivity of the method by an order of magnitude if a large volume of sample is available. Lower readings for sample volumes under 100 ml can be attributed to the increased solubility of the precipitate (due to the higher concentration

[1]If the buffer is insufficient, due to the original acidity of the sample solution, adjust pH to ~10 by addition of 1:1 ammonia.

of organic solvent) and thus lower effectiveness of co-precipitation of the nickel chelate.

When the precipitation is performed at elevated temperatures progressively lower readings are obtained. Precipitation at the room temperature is, therefore, recommended.

The presence of 1 mmol of ammonium tartrate in the solution does not have an appreciable effect on the calibration curve. Tartrate is, therefore, included in the procedure to mask some metal ions which would otherwise precipitate in basic medium, particularly iron(III).

The method is independent of many variables: p*H* (within 8–10), volume (100–1000 ml), rate of reagent addition, time of standing before filtration (up to 1 h at least), presence of a large amount of tartrate.

It has been observed that the precipitates become paler in color upon drying. If the light absorption is measured while still wet a stronger signal is obtained making possible the determination of even 0.1 μg Ni/100 ml; however the uncertainty in water content, especially during the measurement in the instrument, results in poorer reproducibility.

At least a 1000-fold weight excess of the following ions is without interference in the determination of 2 μg Ni in 100 ml of water: aluminum(III), bismuth(III), cadmium(II), calcium(II), iron(III), lead(II), magnesium(II), manganese(II), mercury(II), palladium(II), potassium(I), silver(I), sodium(I), tin(IV), zinc(II), acetate, borate, bromide, citrate, fluoride, iodide, nitrate, perchlorate, phosphate, sulfate, sulfide, and thiocyanate. A 50-fold excess of cobalt(II) and a 10-fold excess of chromium(III), copper(II), iron(II), and EDTA are also without interference. Cyanide can be tolerated only at a 1:1 ratio.

Iron(III) does not interfere even at 10 000-fold excess (20 mg Fe) provided 2 mmol of tartrate are present and the p*H* is adjusted to ~ 10 with ammonia. For still higher amounts of iron(III), the higher concentration of tartrate necessary to keep iron in solution results in a decrease of the signal.

Since the detection limit of the method is 0.2 μg Ni, it should be possible to determine 0.2 μg Ni in 20 mg iron. For example, the method was applied to the determination of nickel in a sample of mild steel (British Chemical Standards, #324). After dissolution of the sample in diluted hydrochloric and nitric acids, tartrate was added and the solution was neutralized with concentrated ammonia. Aliquots were taken and, after dilution, the regular precipitation procedure was performed. The average nickel content given was 0.050%, found 0.049%; the results demonstrate the potential of the method in a relatively complex matrix.

The simplicity, sensitivity, and reproducibility of the method should lead to many applications for the determination of very small amounts of nickel.

This work was supported by a grant from the National Research Council of Canada.

1. D. E. RYAN, R. J. PRIME, J. HOLZBECHER, and R. E. YOUNG. Anal. Lett. **6**, 721 (1973).
2. D. E. RYAN, J. HOLZBECHER, and H. ROLLIER. Anal. Chim. Acta, **73**, 49 (1974).
3. D. E. RYAN, H. ROLLIER, and J. HOLZBECHER. Can. J. Chem. **52**, 1942 (1974).
4. D. E. RYAN and H. ROLLIER. Anal. Chim. Acta. In press.
5. D. E. RYAN, M. GRANDA, and M. JANMOHAMMED. Anal. Chim. Acta. In press.
6. G. SCHWARZENBACH and H. FLASCHKA. Complexometric titrations. Methuen, London. 1969. p. 289.
7. H. DIEHL. The applications of the dioximes to analytical chemistry. G. F. Smith, Columbus. 1940. p. 47.

^{13}C Nuclear Magnetic Resonance and ^{14}C Tracer Studies on 1,2-Phenyl Shifts in the Reaction of Labeled Triphenylvinyl Bromide with Acetic Acid and Silver Acetate

FRANZ H. A. RUMMENS AND ROBERT D. GREEN
Department of Chemistry, University of Regina, Regina, Saskatchewan S4S 0A2
AND
ALLAN J. CESSNA, MITSUO OKA, AND CHOI CHUCK LEE
Department of Chemistry and Chemical Engineering, University of Saskatchewan S7N 0W0
Received June 24, 1974

FRANZ H. A. RUMMENS, ROBERT D. GREEN, ALLAN J. CESSNA, MITSUO OKA, and CHOI CHUCK LEE. Can. J. Chem. **53**, 314 (1975).

Reaction of triphenylvinyl bromide, labeled at C-2 with ^{14}C or ^{13}C (**1**—Br-2-^{14}C or **1**—Br-2-^{13}C), with HOAc–AgOAc gave an isotopically rearranged product, **1**—OAc-*x*-^{14}C or **1**—OAc-*x*-^{13}C. After conversion of the product to 1,2,2-triphenylethanol (**2**—*x*-^{14}C or **2**—*x*-^{13}C), ^{14}C assays after degradation to benzophenone, or analyses by FT c.m.r. and by ^{13}C satellites of p.m.r. in the FT or CW mode all gave results that were in reasonable agreement, indicating 6.8 ± 0.9% scrambling of the label from C-2 to C-1. The work shows that while the c.m.r. technique eliminates the need for degradation, the tracer method, with appropriately high specific activities, is capable of giving higher precision.

FRANZ H. A. RUMMENS, ROBERT D. GREEN, ALLAN J. CESSNA, MITSUO OKA et CHOI CHUCK LEE. Can. J. Chem. **53**, 314 (1975).

Le bromure de triphénylvinyle portant un ^{13}C ou un ^{14}C en position 2 (**1**—Br-2-^{13}C ou **1**—Br-2-^{14}C) réagit avec le couple AcOH-AcOAg pour donner un produit qui est isotopiquement réarrangé, **1**—OAc-*x*-^{13}C ou **1**—OAc-*x*-^{14}C. Après conversion du produit un triphényl-1,2,2 éthanol (**2**—*x*-^{13}C ou **2**—*x*-^{14}C), les déterminations de ^{14}C sur le produit dégradé en benzophénone ou une analyse par transformation de Fourier du spectre r.m.c. du ^{13}C et l'analyse des bandes satellites du ^{13}C dans le spectre r.m.c. du proton ont tous donné des résultats qui sont généralement en accord et qui indiquent qu'environ 6.8 ± 0.9% d'isotope migre de la position 2 vers la position 1. Ce travail montre que quoique la technique de la r.m.c. du carbone élimine la nécessité de dégradation, la méthode des marqueurs avec des activités spécifiques elevées est capable de donner une plus grande précision. [Traduit par le journal]

As facilities for ^{13}C n.m.r. become more commonly available, it is of interest to extend the utilization of the c.m.r. technique to quantitative isotopic scrambling studies which have generally been investigated using ^{14}C as tracer. A recent example of such a quantitative application is the work of Vaughan and co-workers (1) who studied the mechanism of the acid-catalyzed racemization of (−)-camphene-8-^{13}C. These workers pointed out the advantage of ^{13}C n.m.r. over the previously employed ^{14}C-labeling since the amount of the ^{13}C-label at the C-8, C-9, and C-10 positions could be measured simultaneously without the necessity of degradation. The data obtained suggested a number of racemization processes including a small, but not quite negligible *endo*-methyl 3,2-migration (1), although this conclusion has recently been questioned (2). Recently, ^{14}C-labeling has been utilized in this laboratory to study the extent of degenerate rearrangement arising from 1,2-phenyl shifts in solvolyses of triphenylvinyl-2-^{14}C triflate (3). In the present work, the extent of isotopic scrambling arising from a similar degenerate 1,2-phenyl shift in the reaction of triphenylvinyl bromide (**1**—Br) with HOAc–AgOAc is investigated. The reactant, **1**—Br, is labeled at the C-2 position with ^{13}C or ^{14}C. Quantitative measurements using ^{13}C n.m.r. are explored and the results are compared with those obtained from the ^{14}C tracer studies.

Treatment of $PhCH_2MgCl$ with $^{14}CO_2$ or $^{13}CO_2$ gave the corresponding labeled phenylacetic acid which was converted to **1**—Br-2-^{14}C or **1**—Br-2-^{13}C by procedures previously described for the preparation of **1**—Br-2-^{14}C (3). Acetolysis of either of these labeled bromides in the presence of AgOAc gave **1**—OAc-*x*-^{14}C or

Can. J. Chem. Downloaded from www.nrcresearchpress.com by 210.87.254.6 on 09/05/12
For personal use only.

TABLE 1. Data from reaction of triphenylvinyl-2-^{14}C bromide (**1**—Br-2-^{14}C) with HOAc–AgOAc

Specific activity*, d.p.m./mmol				Rearrangement from C-2 to C-1 (%)	
$(Ph)_2CHCH(OH)Ph$		PhCOPh†			
Run 1	Run 2	Run 1	Run 2	Run 1	Run 2
2 365 000	1 825 000	2 205 000	1 710 000	6.8	6.3

*Measured by a liquid scintillation counter.
†Assayed as the oxime.

1—OAc-*x*-^{13}C, which was reduced with $LiAlH_4$, again as previously described (3), to give 1,2,2-triphenylethanol-*x*-^{14}C or 1,2,2-triphenylethanol-*x*-^{13}C (**2**—*x*-^{14}C or **2**—*x*-^{13}C). In the ^{14}C tracer work, the scrambling of the label from C-2 to C-1 was determined by oxidation of **2**—*x*-^{14}C to benzophenone (3) and the results are given in Table 1.

In the quantitative measurements using ^{13}C n.m.r., the total amount of ^{13}C enrichment and the distribution of the ^{13}C-label at the C-1 and C-2 positions of the reactant and product molecules, **1**—Br-2-^{13}C and **2**—*x*-^{13}C, have to be

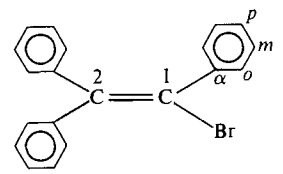

1—Br

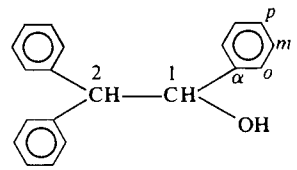

2

ascertained. The product is analyzed as the alcohol, **2**—*x*-^{13}C, rather than as triphenylvinyl acetate (**1**—OAc-*x*-^{13}C) since in **2**, the C-1 and C-2 ^{13}C signals are clearly separated from the aromatic absorptions and these signals are enhanced by the nuclear Overhauser effect (N.O.E.). The unlabeled reactant and product molecules, containing ^{13}C in its natural abundance, are used to establish the effect of relaxation time, T_1, on spectral intensities as well as to determine the relative N.O.E. enhancement factors for the carbon nuclei of interest. The labeled molecules were then used for the remaining measurements.

The ^{1}H-decoupled ^{13}C n.m.r. spectrum of **1**—Br is given in Fig. 1. The C-2 signal appears at 144.2 p.p.m. since in the spectrum of **1**—Br-2-^{13}C this is the strongest peak. From considerations based on the additivity of chemical shifts of related compounds, peaks *b*, *c*, and *d* at 144.2, 141.7, and 122.7 p.p.m. (Fig. 1) are tentatively assigned, respectively, to C-2 and C-α of the ring geminal to Br, the other two C-α, and C-1.[1] The remaining signals are due to the other aromatic carbons, C-*o*, C-*m*, and C-*p* of the three rings. If these assignments are correct, and if the N.O.E. enhancement for the quaternary carbons, peaks *b*, *c*, and *d*, is negligibly small, the ratio of intensities of *b*:*c*:*d* should be 2:2:1. Using the computer integration of these spectral regions and normalizing peak *c* to an intensity of 2.00, from three separate spectra, the average ratio of the intensities of C-2:C-1 was found to be 0.97 ± 0.19. This ratio is certainly unity within the limits of the experimental uncertainty.

The ^{1}H-decoupled ^{13}C n.m.r. spectrum of **2** is shown in Fig. 2. The absorptions at 76.0 and 59.8 p.p.m. are assigned to C-1 and C-2, respectively, since in the product molecule, **2**—*x*-^{13}C, the 59.8 p.p.m. peak is much stronger and this should correspond to C-2 as the ^{14}C tracer work indicated only 6–7% scrambling of the label from C-2 to C-1. The peaks at 140.9, 141.8, and 142.7 p.p.m. may be assigned to the three C-α while the remaining absorptions are due to the other aromatic carbons.

If T_1 for the nuclei of interest were different, the recovery of magnetization of each nucleus between pulses would be different and hence their ratio of intensities might be dependent on the pulse repetition rate. It is, therefore, desirable to test, under the present experimental conditions (HX 90 spectrometer, spectral width 5000 Hz, 4K memory, 4K pulses, pulse repetition rate

[1]In one spectrum only (shown in Fig. 1), peak *b* was found to be resolved into two components separated by approximately 4.5 Hz or 0.2 p.p.m.

Can. J. Chem. Downloaded from www.nrcresearchpress.com by 210.87.254.6 on 09/05/12
For personal use only.

Can. J. Chem. Downloaded from www.nrcresearchpress.com by 210.87.254.6 on 09/05/12
For personal use only.

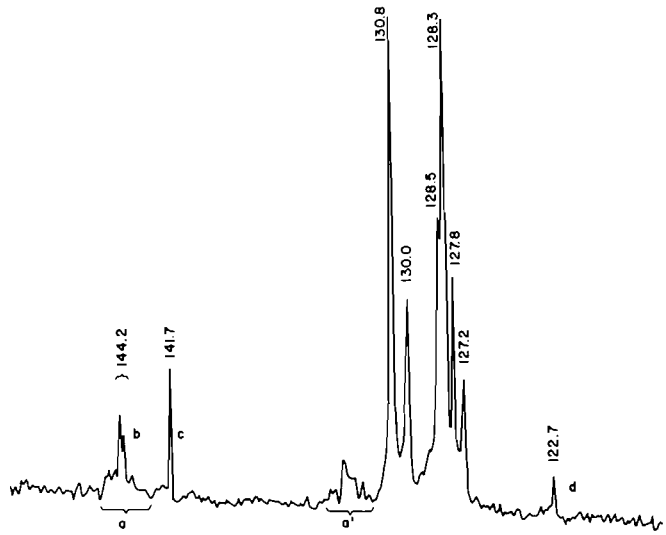

FIG. 1. ^{1}H-decoupled ^{13}C n.m.r. spectrum of triphenylvinyl bromide (**1**—Br). Peak positions are in p.p.m. from tetramethylsilane. C_6F_6, used as the locking compound, gave absorptions in the 144 and 132 p.p.m. regions (*a* and *a'*).

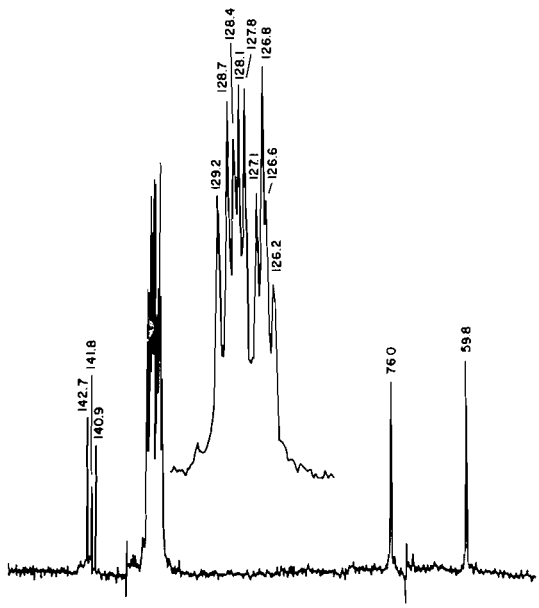

FIG. 2. ^{1}H-decoupled ^{13}C n.m.r. spectrum of 1,2,2-triphenylethanol (**2**). Peak positions are in p.p.m. from tetramethylsilane.

1.0 s), whether the relative intensities of C-1 and C-2 of **2** would vary with different pulse repetition rates. From triplicate spectra obtained with acquisition times of 0.5, 1.0, 2.0, and 4.0 s, the average value of the intensity ratio, I_2/I_1, was found to be 0.99 $\pm$ 0.05 and this ratio did not show any perceptible change with pulse repetition rate.

Using the ratio of intensities of (C-1 + C-2) to (C-*o* + C-*m* + C-*p*) of the unlabeled **2**, to be designated as $(I_1^0 + I_2^0)/I_{arom}$, as a reference standard, the extent of ^{13}C scrambling from C-2 to C-1 in the product molecule, **2**—*x*-^{13}C, derived from the original reactant, **1**—Br-2-^{13}C, can be calculated as illustrated in Appendix 1. The results are summarized in Table 2.

The extents of ^{13}C scrambling obtained from the ^{13}C n.m.r. spectra of **2** and **2**—*x*-^{13}C could be checked by measurements using the ^{13}C satellites of the ^{1}H signals of C-1 and C-2. The ^{1}H n.m.r. spectra of **2** and **2**—*x*-^{13}C, obtained by the FT mode with the HX 90 spectrometer, are shown in Fig. 3. The well separated signals due to the C-1 and C-2 protons (doublets *a* and *b*, respectively, in Fig. 3), and their respective ^{13}C satellites, are readily observable. From the spectrum of **2**—*x*-^{13}C (Fig. 3*B*), using the treatment derived in Appendix 2 and the appropriate integrated intensities, the ^{13}C enrichment and the

TABLE 2. Total ^{13}C enrichment and % ^{13}C scrambling from C-2 to C-1 in 1,2,2-triphenylethanol-*x*-^{13}C (**2**—*x*-^{13}C) calculated from ^{13}C n.m.r.

I_2/I_1	$(I_2 + I_1)I_{arom}$	^{13}C enrichment (%)	^{13}C scrambling from C-2 to C-1 (%)
9.81	2.68	47	7.4
8.86	2.40	42	8.1
10.31	2.61	46	7.2

Can. J. Chem. Downloaded from www.nrcresearchpress.com by 210.87.254.6 on 09/05/12
For personal use only.

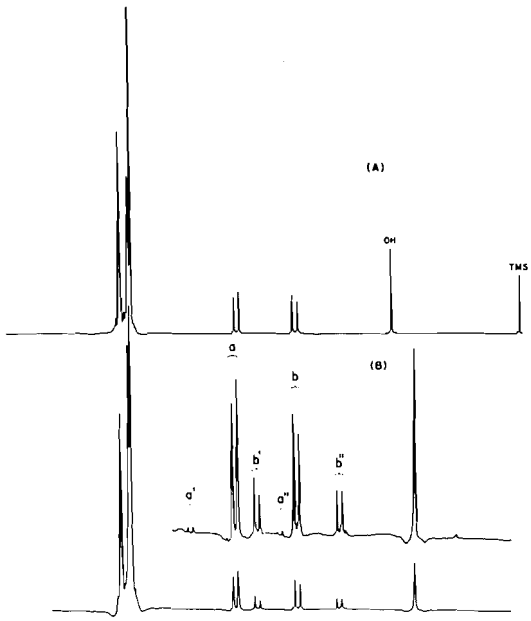

FIG. 3. ^{1}H n.m.r. spectra of 1,2,2-triphenylethanol (**2**) (*A*) and 1,2,2-triphenylethanol-*x*-^{13}C (**2**—*x*-^{13}C) (*B*).

^{13}C scrambling from C-2 and C-1 were calculated. The results are given in Table 3.

Another independent analysis of the extent of ^{13}C scrambling in **2**—*x*-^{13}C was carried out using the intensities of the C-1 and C-2 proton signals and their respective ^{13}C satellites (4). From a set of three spectra obtained with the HA100 spectrometer, the average intensity values were found to be 92, 4.0, 53, and 43, respectively, for the C-1 proton, C-1 satellites, C-2 proton, and C-2 satellites. Calculation from these data as described in the following paper (5) gave a total ^{13}C enrichment of 47% and a scrambling of the label from C-2 to C-1 of 6.6%. This result is in good agreement with those given in Table 3.

It is seen that the results from the n.m.r. work, including c.m.r. (Table 2), ^{13}C satellites of FT p.m.r. (Table 3) and ^{13}C satellites of CW p.m.r. (with HA100 spectrometer) all showed reasonable agreement, the average extent of 1,2-phenyl shift ± standard deviation in the reaction of **1**—Br-2-^{13}C with HOAc–AgOAc being 6.8 ± 0.9%. This value is also in agreement with the results from the ^{14}C tracer studies (Table 1). The present studies thus demonstrate that ^{13}C n.m.r. can be utilized quantitatively in appropriate isotopic scrambling investigations. However, the ^{14}C tracer method, although requiring additional steps involved in the degradation of the reaction product, is not obsolete. An important advantage in the radioactive tracer method that is made apparent from the present work in that the use of reactants of high specific activity is capable of giving results of higher precision and also allows for the use of liberal amounts of inactive carriers in aiding the isolation and purification of the desired products.

TABLE 3. Total ^{13}C enrichment and % ^{13}C scrambling from C-2 to C-1 in 1,2,2-triphenylethanol-*x*-^{13}C (**2**—*x*-^{13}C) calculated from ^{13}C satellites

p	*q*	^{13}C enrichment (%)	^{13}C scrambling from C-2 to C-1 (%)
46.2	11.9	50	6.0
45.9	12.7	50	5.4
44.5	10.2	48	7.0

It is of interest to point out that the 6.8 ± 0.9% 1,2-phenyl shift observed in the present work is, coincidentally, essentially the same as the extent of the analogous isotopic scrambling in the acetolysis of triphenylvinyl-2-^{14}C triflate (**1**—OTf-2-^{14}C) (3). In the solvolyses of **1**—OTf-2-^{14}C (3), it was suggested that the isotopic scrambling arises from a 1,2-phenyl shift across the double bond in the triphenylvinyl cation or ion-pair, the longer the lifetime of the cation or ion-pair, the greater the extent of isotopic rearrangement. Apparently, a similar mechanism operates in the reaction of C-2 labeled **1**—Br with HOAc–AgOAc.

Experimental

*Triphenylvinyl-2-^{14}C Bromide (**1**—Br-2-^{14}C) and Triphenylvinyl-2-^{13}C Bromide (**1**—Br-2-^{13}C)*

1—Br-2-^{14}C was prepared as described previously (3). Carboxyl-labeled phenylacetic acid was prepared by carbonation of $PhCH_2MgCl$ with $^{13}CO_2$ (from $BaCO_3$-^{13}C, 91 atom % ^{13}C, obtained from Merck, Sharp and Dohme of Canada, Ltd. and diluted with about an equal amount of ordinary $BaCO_3$), and then converted to **1**—Br-2-^{13}C by the same series of reactions as used in the preparation of **1**—Br-2-^{14}C (3).

*Reaction of **1**—Br-2-^{14}C or **1**—Br-2-^{13}C with HOAc–AgOAc*

A solution of 2.5 g (7.5 mmol) of **1**—Br-2-^{14}C or **1**—Br-2-^{13}C and 1.4 g (8.3 mmol) of AgOAc in 60 ml of glacial HOAc was refluxed with stirring for 24 h. The reaction mixture was cooled and the HOAc was removed in a rotary evaporator. The residue was dissolved in 100 ml of ether and washed with 10% K_2CO_3 solution and with H_2O. After drying over $MgSO_4$, the ether solution was treated with $LiAlH_4$ as described previously (3) to give 1,2,2-triphenylethanol-*x*-^{14}C or *x*-^{13}C (**2**—*x*-^{14}C or **2**—*x*-^{13}C). In a preparative run using non-labeled material,

20 g of **1**—Br was treated with HOAc–AgOAc in an analogous manner and the product, triphenylvinyl acetate (**1**—OAc), was isolated by the removal of the ether after drying and crystallization of the residue from 95% ethanol to give 16 g (90%) of **1**—OAc, m.p. 103–105° (lit. (6) m.p. 104–105°).

In the ^{14}C work, the alcohol, **2**—x-^{14}C, with added carrier if necessary, was degraded by oxidation to benzophenone (3). In the ^{13}C studies, except for one set of ^{1}H spectra obtained by the HA100 spectrometer for ^{13}C satellite analysis, all other n.m.r. spectra were obtained in CS_2 solution using a Bruker HX 90 spectrometer operating in the FT mode at 90.0 MHz for ^{1}H and at 22.63 MHz for ^{13}C, using a Nicolet 1080 series computer with 12K memory to collect and transform the free induction decays. In most cases, 4K memory was used for data collection.

The financial support given by the National Research Council of Canada and the technical assistance of B. A Davis are gratefully acknowledged.

Appendix 1

^{13}C Scrambling in **2**—x-^{13}C from ^{13}C Nuclear Magnetic Resonance Spectral Intensities

Since **2**—x-^{13}C consists of a mixture of **2**—2-^{13}C and **2**—1-^{13}C, let the integrated intensities of the ^{13}C signals at the C-2 and C-1 positions be I_2 and I_1. As part of the total intensity is due to naturally occurring ^{13}C (1.11%), let this part be designated I_2^0 and I_1^0, and let the part of the intensity due to ^{13}C enrichment be designated I_2^* and I_1^*.

From a typical measurement

$$I_2/I_1 = (I_2^* + I_2^0)/(I_1^* + I_1^0) = 9.81$$

and

$$(I_2 + I_1)/I_{arom} = (I_2^* + I_2^0 + I_1^* + I_1^0)/I_{arom} = 2.68$$

Since for the unenriched **2**,

$$(I_2^0 + I_1^0)/I_{arom} = 0.120$$

$$\frac{I_2^* + I_1^* + I_2^0 + I_1^0}{I_2^0 + I_1^0} = \frac{I_2^* + I_1^*}{I_2^0 + I_1^0} + 1 = \frac{2.68}{0.120} = 23.3$$

Converting the intensities to percentage ^{13}C

$$\frac{I_2^* + I_1^*}{1.11 + 1.11} + 1 = 23.3$$

Therefore $I_2^* + I_1^* = 47.3\%$, and this is the ^{13}C enrichment of the **2**—x-^{13}C.

Since

$$\frac{I_2^* + I_2^0}{I_1^* + I_1^0} = \frac{I_2^* + 1.11}{I_1^* + 1.11} = 9.81$$

and $$I_2^* = 47.3 - I_1^*$$

Hence $$I_1^* = 3.5\%$$

and ^{13}C scrambling from C-2 to C-1

$$(3.5/47.3) \times 100 = 7.4\%$$

Appendix 2

^{13}C Scrambling in **2**—x-^{13}C from ^{13}C Satellite Intensities

Firstly, for the reactant molecule, **1**—Br-2-^{13}C, let I_2 and I_1 be the ^{13}C intensities at C-2 and C-1, and let $I_2/I_1 = p$.

Since ^{13}C is present in natural abundance at C-1

$$I_1 = 1.11\%$$

Therefore

$$I_2 = I_1 p = 1.11p\%$$

The total ^{13}C content would be

$$I_2 + I_1 = 1.11(p + 1)\%$$

and the total ^{13}C enrichment would be

[1] $$I_2 - I_1 = 1.11(p - 1)\%$$

Now consider the product molecule, **2**—x-^{13}C, consisting of **2**—2-^{13}C and **2**—1-^{13}C.

Let I_2 and I_1 be the ^{13}C intensities at C-2 and C-1, and let

$$I_2/I_1 = q$$

it can be shown that the % of ^{13}C

$$\text{at C-1} = I_1/(I_2 + I_1) \times \text{total } ^{13}\text{C content} = 1.11(p + 1)/(q + 1)$$

$$\text{and at C-2} = \%\text{ total } ^{13}\text{C} - \%\ ^{13}\text{C at C-1} = 1.11q(p + 1)/(q + 1)$$

Subtracting the natural ^{13}C abundance of 1.11% would give the % ^{13}C enrichments at C-1 and C-2 (% $^{13}C_1$* and % $^{13}C_2$*) as follows

$$\%\ ^{13}C_1^* = [1.11(p + 1)/(q + 1)] - 1.11 = 1.11(p - q)/(q + 1)$$

$$\%\ ^{13}C_2^* = [1.11q(p + 1)/(q + 1)] - 1.11 = 1.11(pq - 1)/(q + 1)$$

Hence the % ^{13}C scrambling from C-2 to C-1 would be

Can. J. Chem. Downloaded from www.nrcresearchpress.com by 210.87.254.6 on 09/05/12
For personal use only.

$$[2]\quad \frac{\%^{13}C_1^*}{\%^{13}C_1^* + \%^{13}C_2^*} \times 100 = \frac{(p-q)100}{p-q+pq-1}$$

Referring to the peaks of Fig. 3*B*:

$$q = I_2/I_1 = (b' + b'')/(a' + a'')$$

Since

$$\text{The } \%\ ^{13}\text{C at C-2} = [(b' + b'')/(b + b' + b'')] \times 100 = 1.11q(p+1)/(q+1)$$

it can be shown that

$$p = \frac{100\left(\frac{b' + b''}{a' + a''} + 1\right)}{1.11\left(\frac{b' + b''}{a' + a''}\right)\left(1 + \frac{b}{b' + b''}\right)}$$

Thus p and q can be calculated from the integrated intensities of the C-2 proton (doublet b), the C-2 satellites ($b' + b''$), and the C-1 satellites ($a' + a''$). The treatment also eliminates the need for the use of the ratio of the very large doublet a to the very small satellites $a' + a''$. Knowing p and q, the total ^{13}C enrichment and the $\%\ ^{13}C$ scrambling from C-2 to C-1 can be calculated from eqs. 1 and 2.

1. C. W. David, B. W. Everling, R. J. Kilian, J. B. Stothers, and W. R. Vaughan. J. Am. Chem. Soc. **95**, 1265 (1973).
2. C. J. Collins and M. H. Lietzke. J. Am. Chem. Soc. **95**, 6842 (1973).
3. C. C. Lee, A. J. Cessna, B. A. Davis, and M. Oka. Can. J. Chem. **52**, 2679 (1974).
4. M. Oka. Ph.D. Thesis, University of Arkansas, 1973.
5. M. Oka and C. C. Lee. Can. J. Chem. This issue.
6. W. M. Jones and D. D. Maness. J. Am. Chem. Soc. **92**, 5457 (1970).

Can. J. Chem. Downloaded from www.nrcresearchpress.com by 210.87.254.6 on 09/05/12
For personal use only.

Nuclear Magnetic Resonance Studies on the Acetolysis and Trifluoroacetolysis of Trianisylvinyl-2-^{13}C Bromide

MITSUO OKA AND CHOI CHUCK LEE

Department of Chemistry and Chemical Engineering, University of Saskatchewan, Saskatoon, Saskatchewan S7N 0W0

Received June 24, 1974

MITSUO OKA and CHOI CHUCK LEE. Can. J. Chem. **53**, 320 (1975).

The product from the reaction of trianisylvinyl-2-^{13}C bromide (**3**—Br-2-^{13}C) with HOAc–AgOAc or with CF_3COOH–CF_3COOAg was converted to 1,2,2-trianisylethanol-x-^{13}C (**4**—x-^{13}C) and examined for isotopic scrambling by the use of relative intensity ratios in the c.m.r. spectra with the CH_3O absorption as the internal standard, or by the intensities of the ^{13}C satellites in the p.m.r. spectra. About 20 and 50% rearrangements of the ^{13}C-label from C-2 to C-1 were found, respectively, for the acetolysis and trifluoroacetolysis. The results are in accord with the suggestion that there may be a competition between 1,2-aryl shifts in the triarylvinyl cation or ion-pair and the reaction of the ion with solvent to give product.

MITSUO OKA et CHOI CHUCK LEE. Can. J. Chem. **53**, 320 (1975).

Le produit de la réaction du bromure de trianisylvinyl-2-^{13}C (**3**—Br-2-^{13}C) avec AcOH–AcOAg ou avec CF_3COOH–CF_3COOAg a été transformé en trianisyl-1,2,2 éthanol-x-^{13}C (**4**—x-^{13}C). Faisant appel à la résonance magnétique nucléaire du carbone et utilisant l'absorption du OCH_3 comme référence interne, on a pu déterminer la compétition isotopique dans ces produits; une autre méthode d'arriver au même résultat est d'examiner l'intensité des bandes satellites ^{13}C dans le spectre r.m.n. du proton. On a trouvé environ respectivement 20 et 50% de réarrangement du ^{13}C de la position C-2 vers la position C-1 dans les réactions d'acétolyse et de trifluoroacétolyse. Ces résultats concordent avec l'hypothèse qu'il peut y avoir une compétition entre les déplacements 1,2 des groupes aryles dans le cation triarylvinyle ou une paire d'ion et la réaction de l'ion avec le solvant pour donner le produit. [Traduit par le journal]

In the preceding paper (1), the extent of isotopic scrambling in the reaction of triphenylvinyl-2-^{13}C bromide (**1**—Br-2-^{13}C) with HOAc–AgOAc was measured using ^{13}C n.m.r. and the ^{13}C satellites of ^{1}H n.m.r. The results, indicating $6.8 \pm 0.9\%$ rearrangement arising from 1,2-phenyl shifts across the double bond in the triphenylvinyl cation, were found to be in agreement with analogous scrambling data obtained from the same reaction with **1**—Br-2-^{14}C (1). In this work, the reaction product, **1**—OAc-x-^{13}C, was converted to 1,2,2-triphenylethanol-x-^{13}C (**2**—x-^{13}C) and the ^{13}C enrichments in the C-1 and C-2 positions of this product molecule were measured from c.m.r. intensity ratios utilizing the total intensities of the *o*, *m*, and *p*-carbons of the aromatic rings as a reference standard. The present work extends the study on the use of n.m.r. to measure isotopic scrambling in ^{13}C labeled systems. The reactions investigated are those of tri-*p*-methoxyphenylvinyl-2-^{13}C bromide (trianisylvinyl-2-^{13}C bromide, **3**—Br-2-^{13}C) with HOAc–AgOAc and with CF_3COOH–CF_3COOAg. The method (2) is based on measurements of relative intensities in the c.m.r. spectrum with respect to a suitable internal standard, and in the present work, the CH_3O absorption containing ^{13}C in its natural abundance is utilized as such an internal standard.

3—Br-2-^{13}C was prepared in a manner similar to the preparation of **1**—Br-2-^{13}C (1). Reaction of *p*-$CH_3OPhCH_2{}^{13}COOEt$ with *p*-CH_3OPh-MgBr gave 1,1,2-trianisylethanol-1-^{13}C which on treatment with Br_2 in HOAc yielded the desired trianisylvinyl-2-^{13}C bromide (**3**—Br-2-^{13}C). The acetolysis of **3**—Br-2-^{13}C in the presence of AgOAc was carried out at reflux temperature for 2 h as described by Rappoport and Gal (3), while the trifluoroacetolysis in the presence of CF_3COOAg was effected at room temperature for 10 min. The reaction product, **3**—OAc-x-^{13}C or **3**—$OOCCF_3$-x-^{13}C, was reduced twice successively with $LiAlH_4$ (4) to give 1,2,2-trianisylethanol-x-^{13}C (**4**—x-^{13}C) for n.m.r. examination.

The ^{1}H-decoupled ^{13}C n.m.r. spectrum of ordinary **4** with ^{13}C in its natural abundance, in $CDCl_3$ as solvent and as the locking compound, is shown in Fig. 1*A*. The chemical shifts from the c.m.r. spectra as well as data from the p.m.r. spectra of **4** are given in Table 1. From Fig. 1*A*, the intensity ratios for the unenriched **4**, I_1/I_s, I_2/I_s, and I_2/I_1, where I_1, I_2, and I_s are the

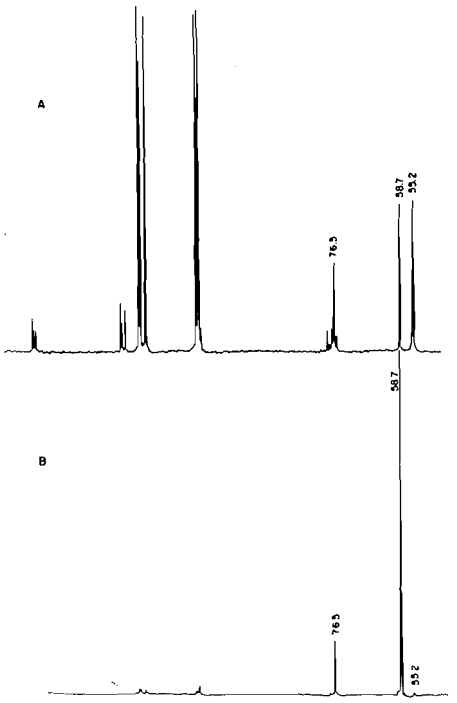

FIG. 1. ^{1}H-decoupled ^{13}C n.m.r. spectra of unenriched 1,2,2-trianisylethanol (**4**) (*A*) and of 1,2,2-trianisylethanol—*x*-^{13}C (**4**—*x*-^{13}C) (*B*) derived from acetolysis of 90% enriched trianisylvinyl-2-^{13}C bromide (**3**—Br-2-^{13}C).

integrated intensities of C-1, C-2, and the $\bar{C}H_3O$ standard, respectively, were measured, and the results are given in Table 2.

Figure 1*B* shows the ^{1}H-decoupled ^{13}C n.m.r. spectrum of **4**—*x*-^{13}C derived from the acetolysis, in the presence of AgOAc, of **3**—Br-2-^{13}C prepared from $BaCO_3$-^{13}C that was commercially designated as 90% enriched. While I_2/I_1 could be measured from Fig. 1*B*, the CH_3O absorption, I_s, was too weak; but with an amplified spectrum, I_1/I_s was obtained (Table 2). A duplicate experiment was carried out using 45% enriched **3**—Br-2-^{13}C, while a third measurement was made by diluting the 90% enriched **4**—*x*-^{13}C with carrier to give 9% enrichment. Using the appropriate intensity ratios and calculations as illustrated in the Experimental section, the scrambling of the label from C-2 to C-1 for the various experiments were obtained. The results, showing about 20 ± 1% rearrangement, are summarized in Table 2. Also included in Table 2 is the result, indicating about 50% rearrangement, calculated from the c.m.r. intensity ratios for the **4**—*x*-^{13}C derived from trifluoroacetolysis, in the presence of CF_3-COOAg, of 45% enriched **3**—Br-2-^{13}C.

The ^{13}C scrambling from C-2 to C-1 was also measured by the ^{13}C satellite intensities in the ^{1}H n.m.r. spectra of **4**—*x*-^{13}C obtained from acetolysis or trifluoroacetolysis of 90% enriched **3**—Br-2-^{13}C. Figure 2 shows a p.m.r. spectrum of **4**—*x*-^{13}C derived from the trifluoroacetolysis. Data on chemical shifts and coupling constants are summarized in Table 1. From the amplified portion of the spectrum, it is seen that the upfield portions of the satellites for the C-1 and C-2 protons, H_a and H_b, are complicated by overlaps. The total satellite intensity is, therefore, taken as twice the integrated area of the downfield half of the H_a and H_b satellites. It may be also noted that the H_b absorption is clearly split by long range coupling with the ^{13}C at C-1 as indicated in Fig. 2. From the intensity values for the C-1 proton, C-1 satellites, C-2 proton, and C-2 satellites, calculations as shown in the Experimental section gave the extents of ^{13}C scrambling from C-2 to C-1 as 21 and 50%, respectively, for the acetolysis and trifluoroacetolysis (Table 2).

1,2-Anisyl shifts across the double bond in the triarylvinyl cation have been observed in the solvolysis of 2,2-dianisyl-1-phenylvinyl bromide (**5**) in HOAc–AgOAc (5) and in CF_3CH_2OH or 60% EtOH (6).[1] Considerations of the kinetics, stereochemistry, and nature of products in reactions of **5** and related triarylvinyl systems (5, 6) have led to the conclusion that such solvolyses proceed via the S_N1 mechanism without β-aryl participation. The rearrangement of the 2,2-dianisyl-1-phenylvinyl cation to the 1,2-dianisyl-2-phenylvinyl cation took place readily since the latter ion, with the anisyl substituent at C-1, is more stable. The present results demonstrate the occurrence of degenerate 1,2-anisyl shifts in the trianisylvinyl cation. As suggested earlier in accounting for the different extents of degenerate 1,2-phenyl shifts in the triphenylvinyl system (4), there may be a competition between 1,2-aryl shift in the triarylvinyl cation or ion-pair and the reaction of the ion with solvent to give product. Thus, a greater extent of rearrangement may be related to a longer lifetime of the cation or ion-pair. In the present work, about 20% 1,2-anisyl shift is

[1]For references to other 1,2-aryl shifts and general reviews on reactions of vinyl cations, see literature cited in ref. 4.

TABLE 1. Carbon-13 and proton n.m.r. of 1,2,2-trianisylethanol (**4**)

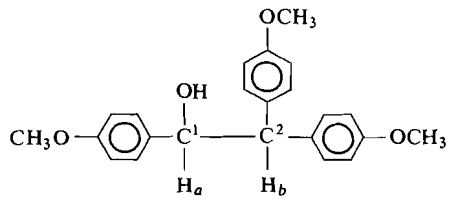

(*a*) Carbon-13 magnetic resonance

C	δ, p.p.m. from TMS in $CDCl_3$	δ, p.p.m. from TMS in Acetone-d_6
C-1	76.5	76.6
C-2	58.7 $J_{^{13}C_1{}^{13}C_2}$ = 38 Hz	59.0
CH_3O	55.2	55.2(55.12, 55.16, 55.24)*
Aromatic carbons	113.4, 113.6, 114.1 128.0, 129.4, 129.8	113.6, 113.9 128.7, 130.2, 130.6
Aromatic quaternary carbons	133.5, 134.3, 134.7 157.7, 158.3, 158.7	135.6, 136.1, 137.1 158.3, 158.7, 159.1

(*b*) Proton magnetic resonance

	Proton	δ ($CDCl_3$), p.p.m. from TMS
OH	1H broad singlet	2.21
OCH_3	9H 3 singlets	3.60, 3.65, 3.68
H_b	1H doublet $J_{H_aH_b}$ = 9 Hz $J_{^{13}CH_b}$ = 128 Hz $J_{^{13}CCH_b}$ = 5 Hz	4.07
H_a	1H doublet $J_{^{13}CH_a}$ = 142 Hz	5.17
Aromatic	12H multiplets	6.50–7.30

*Numbers in parentheses show the three methoxyl absorptions when the spectral width was expanded from 5000 Hz to 1000 Hz.

TABLE 2. ^{13}C scrambling data from the ^{13}C and ^{1}H n.m.r. spectra of 1,2,2-trianisylethanol-*x*-^{13}C (**4**—*x*-^{13}C) derived from acetolysis or trifluoroacetolysis of trianisylvinyl-2-^{13}C bromide (**3**—Br-2-^{13}C)

Designated ^{13}C enrichment (%)*		Intensity ratios†			Calculated ^{13}C enrichment (%)	^{13}C rearrangement from C-2 to C-1 (%)
		I_1/I_s	I_2/I_s	I_2/I_1		
Unenriched **4**		0.586	0.982	1.68		
Acetolysis						
c.m.r.	90	10.4		6.54	91	20
	45	5.43	33.7		46	20
	9	1.49	7.73		9.3	18
p.m.r.	90				87	21
Trifluoroacetolysis						
c.m.r.	45	14.0	23.2		50	50
p.m.r.	90				92	50

*Based on the commercial designation of 90% enrichment without dilution or diluted with carrier by factors of 2 and 10.
†I_1, I_2, and I_s are, respectively, the integrated c.m.r. intensities for C-1, C-2, and the CH_3O internal standard.

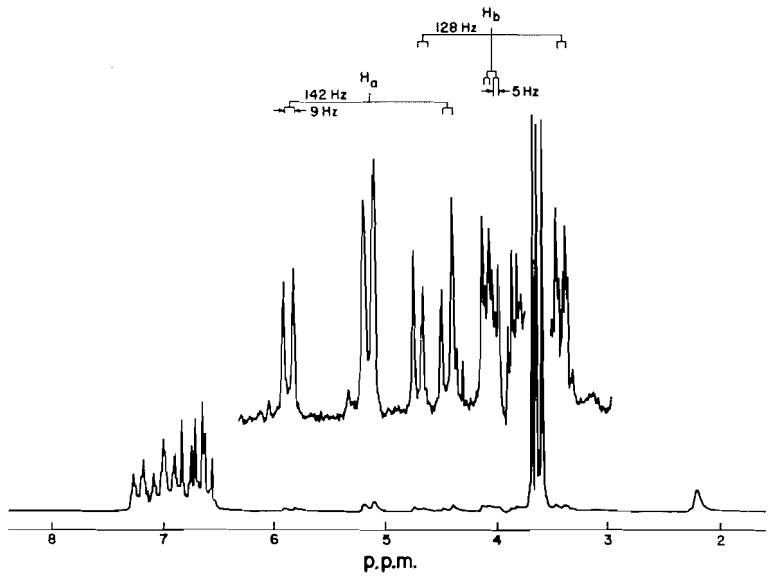

FIG. 2. ^{1}H n.m.r. spectrum of 1,2,2-trianisylethanol—*x*-^{13}C (**4**—*x*-^{13}C) derived from trifluoroacetolysis of 90% enriched trianisylvinyl-2-^{13}C bromide (**3**—Br-2-^{13}C).

found in the reaction of **3**—Br-2-^{13}C with HOAc–AgOAc, and this compares with about 7% rearrangement arising from 1,2-phenyl shifts in the analogous reaction with **1**—Br-2-^{13}C (1). The difference reflects the greater migratory aptitude of the anisyl group and probably also suggests a longer lifetime for the more stable trianisylvinyl cation as compared to the triphenylvinyl cation. For the trifluoroacetolysis, the extremely low nucleophilicity of the solvent (7, 8) allows the 1,2-anisyl shift to compete favorably to give the completely scrambled trianisylvinyl cation with 50% rearrangement, and this is in accord with the previous finding (4) that in solvolytic studies with triphenylvinyl-2-^{14}C triflate, the highest rearrangement was observed in the solvent of lowest nucleophilicity.

Experimental

1,1,2-Trianisylethanol-1-^{13}C

p-Methoxyphenylacetic acid-1-^{13}C was prepared from reaction of *p*-CH_3OPhCH_2MgCl with $^{13}CO_2$ from 90% enriched $Ba^{13}CO_3$ (Merck, Sharp and Dohme of Canada Ltd.) as previously described for the analogous preparation of *p*-$CH_3OPhCH_2{}^{14}COOH$ (9). Esterification of the labeled acid in absolute EtOH in the presence of a catalytic amount of H_2SO_4 gave a 97% yield of the ester, *p*-$CH_3OPhCH_2{}^{13}COOCH_2CH_3$, p.m.r. ($CCl_4$) δ 1.20 ($CH_3$ of Et, t, J = 7 Hz), 3.42 (CH_2, J^{13}_{CCH} = 8 Hz), 3.70 (CH_3O, s), 4.07 (CH_2 of Et, q of d, J^{13}_{CCH} = 4 Hz), 6.67–7.20 (aromatic, m).

To the Grignard reagent prepared from 11.2 g (0.060 mol) of *p*-CH_3OPhBr and 2.0 g (0.082 mol) of Mg in 80 ml of tetrahydrofuran (THF) was added over a period of 1 h a solution of 3.7 g (0.019 mol) of *p*-CH_3OPhCH_2-$^{13}COOC_2H_5$ in 35 ml of THF. The reaction mixture was refluxed for 2 h and then poured into a solution of 20 g NH_4Cl and 4 ml NH_4OH in 200 ml H_2O. The THF layer was separated and the aqueous layer was extracted twice with ether. The combined THF solution and ether extract was washed with H_2O and dried over $MgSO_4$. After removal of the solvent, the residual product was washed with CCl_4 and then recrystallized from EtOH to give 4.4 g (63%) of 1,1,2-trianisylethanol-1-^{13}C, m.p. 129° (lit. (10) m.p. 130–131°), p.m.r. ($CDCl_3$) δ 2.23 (OH, broad s), 3.52 (CH_2, J^{13}_{CCH} = 4 Hz), 3.73, 3.77 (three CH_3O two singlets), 6.60–7.43 (aromatic, m).

Trianisylvinyl-2-^{13}C Bromide (3—Br-2-^{13}C) (4)

A solution of 2.1 g (0.013 mol) of Br_2 in 10 ml of HOAc was added dropwise with stirring to a solution of 4.2 g (0.012 mol) of 1,1,2-trianisylethanol-1-^{13}C in 200 ml of HOAc. The reaction mixture was stirred at room temperature for 7 h and then poured into 250 ml of H_2O containing 1.0 g of $Na_2S_2O_3$. The product was collected by filtration, washed with H_2O, and recrystallized from CH_3OH to give 3.2 g (65%) of **3**—Br-2-^{13}C, m.p. 120–122° (lit. (10) m.p. 119–121°), p.m.r. ($CDCl_3$) δ 3.70, 3.77, 3.80 (three CH_3O, three singlets), 6.53–7.07 (aromatic, m). Comparison of the c.m.r. spectra of the labeled **3**—Br-2-^{13}C and the unlabeled **3**—Br indicated that the ^{13}C enrichment was located only at one quaternary carbon at 141.7 p.p.m. and this absorption was assigned to C-2 of the **3**—Br-2-^{13}C.

Acetolysis of Trianisylvinyl-2-^{13}C Bromide (3—Br-2-^{13}C) (3)

In a typical run, a mixture of 0.90 g (2.1 mmol) of 90% enriched **3**—Br-2-^{13}C, 0.38 g (2.3 mmol) of AgOAc, 13 ml of HOAc, and 1.0 ml of acetic anhydride was heated under reflux for 2 h. The hot solution was filtered,

most of the solvent evaporated off, the residue redissolved in cyclohexane, and the solution was again filtered. After removal of the solvent from the cyclohexane solution, the residual trianisylvinyl-*x*-^{13}C acetate (**3**—OAc-*x*-^{13}C), recovered as an oil, p.m.r. ($CDCl_3$) δ 2.00 (AcO, s), 3.77, 3.82 (three CH_3O, two singlets), 6.67–7.33 (aromatic, m), and was utilized directly for reduction to 1,2,2-trianisylethanol-*x*-^{13}C (**4**—*x*-^{13}C). In preliminary larger scale runs with unlabeled material, **3**—OAc, recrystallized from EtOH, m.p. 97–98° (lit. (3) m.p. 97–98°), was obtained in yields of more than 90% as reported by Rappoport and Gal (3).

Trifluoroacetolysis of Trianisylvinyl-2-^{13}C Bromide (3—Br-2-^{13}C)

When 0.90 g (2.1 mmol) of **3**—Br-2-^{13}C and 0.50 g (2.3 mmol) of CF_3COOAg were added to 13 ml of CF_3COOH, a purple color developed and the mixture was stirred at room temperature for 10 min. The solution was filtered, the solvent removed at room temperature under reduced pressure, the residue redissolved in cyclohexane, and the solution was again filtered. After removal of the solvent from the cyclohexane solution, the residual **3**—$OOCCF_3$-*x*-^{13}C was recovered as an oil, p.m.r. ($CDCl_3$) δ 3.75, 3.78 (three CH_3O, two singlets), 6.67–7.30 (aromatic, m), and was utilized directly for reduction to **4**—*x*-^{13}C. In preliminary runs with unlabeled material, the oily **3**—$OOCCF_3$ was obtained in about 50% yield, the mass spectrum of which show *m/e* 458 as the molecular ion and the base peak.

1,2,2-Trianisylethanol-x-^{13}C (4—x-^{13}C)

The **3**—OAc-*x*-^{13}C and **3**—$OOCCF_3$-*x*-^{13}C, obtained from acetolysis and trifluoroacetolysis, respectively, were reduced successively twice with $LiAlH_4$ to give **4**—*x*-^{13}C (4). The following is a typical experiment.

The **3**—OAc-*x*-^{13}C obtained from the acetolysis of 0.90 g of 90% enriched **3**—Br-2-^{13}C was dissolved in 35 ml of THF and 1.0 g of $LiAlH_4$ was added portionwise. After the reaction mixture was refluxed for 5 h, H_2O was added and the resulting material was extracted 4 times with ether. The combined extract was washed with H_2O, dried over Na_2SO_4, and the ether was removed to give a product, the p.m.r. analysis of which indicated that it was a 30:70 mixture of the ketone, $AnCOCHAn_2$-*x*-^{13}C, and the alcohol, **4**—*x*-^{13}C. The product mixture was redissolved in 40 ml of THF and treated once more with 1.0 g of $LiAlH_4$ as described above. The recovered colorless product was recrystallized from EtOH, giving 0.50 g of pure **4**—*x*-^{13}C, m.p. 113–114°.

Anal. Calcd. for $C_{23}H_{24}O_4$ (90% ^{13}C enriched for one C atom): C, 75.86; H, 6.62. Found: C, 76.09; H, 6.70.

Nuclear Magnetic Resonance Studies

The ^{1}H-decoupled ^{13}C n.m.r. spectra were obtained at 25.2 MHz on a Varian XL-100-15 spectrometer operating in the FT mode. The spectra were collected with 0.4 s acquisition time, a pulse width of 50 μs, for a 5000 Hz spectral width or with 2.0 s acqusition time, a pulse width of 90 μs, for a 1000 Hz spectral width, by a 6201/i computer with 8K memory. The data length for all spectra were 4960 points. The accumulation time was 0.5–2.0 h depending on amounts of sample (0.1–0.5 g) which were examined in 12 mm sample tubes in either $CDCl_3$ or acetone-d_6. The assignments for C-1 and C-2 of 1,2,2-trianisylethanol-*x*-^{13}C (**4**—*x*-^{13}C) (Table 1 and Fig. 1) were confirmed by mass spectrometry in that the fragmentation of **4**—*x*-^{13}C showed that the An_2CH^+ fragment was much more enriched in ^{13}C than the $AnCHOH^+$ fragment. These assignments are also consistent with the corresponding chemical shifts for C-1 and C-2 of 1,2,2-triphenylethanol-*x*-^{13}C (**2**—*x*-^{13}C) which were assigned unambiguously by ^{14}C data (1).

As an illustration of the calculation of the ^{13}C scrambling from C-2 to C-1 in the **4**—*x*-^{13}C using the intensity ratios I_1/I_s, I_2/I_s, and I_2/I_1 (Table 2), take as an example the data from the acetolysis of 90% enriched **3**—Br-2-^{13}C. If we designate I_1^0 and I_1^* as the ^{13}C absorption due to the naturally abundant ^{13}C at C-1 and to the ^{13}C enrichment at C-1, from Table 2, it is seen that

$$I_1^0/I_s = 0.586,$$

and

$$I_1/I_s = (I_1^0 + I_1^*)/I_s = 10.4$$

Hence

$$(I_1^0 + I_1^*)/I_1^0 = 10.4/0.586 = 17.7$$

Converting the intensities to % ^{13}C

$$(1.1 + I_1^*)/1.1 = 17.7$$

Therefore, the ^{13}C enrichment at C-1 = I_1^* = 18%.

Where I_2/I_s is also measured from the c.m.r. spectrum, I_2^* can be calculated in the same way.

In the **4**—*x*-^{13}C from the experiment with 90% enrichment, I_s was too weak in comparison to I_2 for an accurate measurement of I_2/I_s, hence I_2/I_1 was utilized. Since

$$I_2/I_1 = (I_2^0 + I_2^*)/(I_1^0 + I_1^*) = 6.54,$$

and

$$I_2^0/I_1^0 = 1.68$$

$$\frac{(I_2^0 + I_2^*)I_1^0}{(I_1^0 + I_1^*)I_2^0} = 6.54/1.68 = 3.89$$

Converting the intensities to % ^{13}C

$$\frac{(1.1 + I_2^*)1.1}{(1.1 + 18)1.1} = 3.89$$

Therefore,

The ^{13}C enrichment at C-2 = I_2^* = 73%

Hence, the calculated ^{13}C enrichment = 18 + 73 = 91% and the ^{13}C rearrangment from C-2 to C-1 = (18/91) × 100 = 20%.

The p.m.r. spectra were obtained using a Varian HA-100 spectrometer. Determinations of ^{13}C scrambling by satellite intensities were carried out using products derived from acetolysis or trifluoroacetolysis of 90% enriched **3**—Br-2-^{13}C. For the trifluoroacetolysis, from a set of three spectra (an example is given in Fig. 2), the average intensity values for the C-1 proton, C-1 satellites, C-2 proton, and C-2 satellites, respectively, were found to be 49, (2 × 22), 47, and (2 × 21). Hence, the ^{13}C contents at C-1 and C-2, respectively, were [44/(49 + 44)] × 100 = 47% and [42/(47 + 42)] × 100 = 47%. Thus ^{13}C enrichments at each of C-1 and C-2, would be 47 − 1.1 = 46%, giving a total enrichment of 92% and a scrambling of the label from C-2 to C-1 of (46/92) × 100 = 50%. In a similar way, the p.m.r. spectra of the **4**—*x*-^{13}C derived

from the acetolysis of 90% enriched **3**—Br-2-^{13}C gave average intensity values for the C-1 proton, C-1 satellites, C-2 proton, and C-2 satellites of 50, 12, 21, and 48, respectively, and these intensities corresponded to a 21% ^{13}C scrambling from C-2 to C-1.

The financial support given by the National Research Council of Canada and the technical assistance in obtaining the c.m.r. and p.m.r. spectra given by Mr. Mytosk Mazurek of the Prairie Regional Laboratory of the National Research Council are sincerely acknowledged.

1. F. H. A. RUMMENS, R. D. GREEN, ALLAN J. CESSNA, M. OKA, AND C. C. LEE. Can. J. Chem. This issue.
2. M. OKA. Ph.D. Thesis, University of Arkansas, 1973; M. OKA, J. HINTON, T. W. WHALEY, and A. FRY. To be published.
3. Z. RAPPOPORT and A. GAL. J. Am. Chem. Soc. **91**, 5246 (1969).
4. C. C. LEE, A. J. CESSNA, B. A. DAVIS, and M. OKA. Can. J. Chem. **52**, 2679 (1974).
5. Z. RAPPOPORT, A. GAL, and Y. HOUMINER. Tetrahedron Lett. 641 (1973).
6. Z. RAPPOPORT and Y. HOUMINER. J. Chem. Soc. Perkin II, 1506 (1973).
7. P. E. PETERSON and F. J. WALLER. J. Am. Chem. Soc. **94**, 991 (1972).
8. T. W. BENTLEY, F. L. SCHADT, and P. v. R. SCHLEYER. J. Am. Chem. Soc. **94**, 992 (1972).
9. C. C. LEE, D. NEWMAN, and D. P. THORNHILL. Can. J. Chem. **41**, 620 (1963).
10. R. S. SHELTON, M. G. V. CAMPEN, JR., D. F. MEISNER, S. M. PARMERTER, E. R. ANDREWS, R. E. ALLEN, and K. K. WYKOFF. J. Am. Chem. Soc. **75**, 5491 (1953).

Mixed Boron Trihalide Adducts. A Nuclear Magnetic Resonance Study of Halogen Redistribution in Adducts of Trimethylphosphine, Trimethylphosphine Oxide, and Trimethylphosphine Sulfide

MICHAEL J. BULA, J. STEPHEN HARTMAN,[1] AND CHIRAKAL V. RAMAN

Department of Chemistry, Brock University, St. Catharines, Ontario L2S 3A1

Received September 3, 1974

MICHAEL J. BULA, J. STEPHEN HARTMAN and CHIRAKAL V. RAMAN. Can. J. Chem. **53**, 326 (1975).

Halogen redistribution in the sparingly soluble boron trihalide adducts of Me_3P, Me_3PO, and Me_3PS gives mixed boron trihalide adducts of these bases. Only small proportions of the fluorine-containing mixed boron trihalide adducts are present at equilibrium in the Me_3PS adduct system, in accord with previous studies of adducts of other sulfur donors. The effects of the donor on F,Cl and F,Br halogen redistribution are discussed.

MICHAEL J. BULA, J. STEPHEN HARTMAN et CHIRAKAL V. RAMAN. Can. J. Chem. **53**, 326 (1975).

La redistribution des halogènes, dans les adduits peu solubles des halogénures de bore avec Me_3P, Me_3PO et Me_3PS, conduit à des adduits de ces bases avec des trihalogénures mixtes de bore. Seulement une faible portion d'adduit de trihalogénure mixte de bore contenant du fluor est présent à l'équilibre dans le système d'adduits avec Me_3PS; ce résultat concorde avec des études antérieures sur des adduits d'autres dérivés du soufre agissant comme donneurs. On discute des effets du donneur sur la redistribution des halogènes F,Cl et F,Br. [Traduit par le journal]

Introduction

Recent studies have demonstrated that oxygen-donor and sulfur-donor adducts of the boron trihalides show characteristic differences in halogen redistribution equilibria (1–3). Striking deviations from the statistical distribution of halogens among mixed and unmixed boron trihalide adducts were observed when sulfur was the donor and fluorine was one of the halogens (1, 2). We now report a study of adducts of a further series of related Lewis bases, Me_3P, Me_3PO, and Me_3PS, to provide further information about the effects of the donor atom on halogen redistribution in adducts.

Some n.m.r. parameters for boron trihalide adducts of Me_3P have been reported previously (4–6), and the BCl_2Br and $BClBr_2$ adducts of Et_3P and Me_3P have been identified by n.m.r. (7). In the course of the present work, Drake and Rapp reported n.m.r. studies of mixed boron trihalide adducts of PH_3 and CD_3PH_2 (8), as well as n.m.r. parameters of unmixed boron trihalide adducts of related phosphines (9). Also Sisler and co-workers have shown that certain methyldichlorophosphine – boron trihalide adducts undergo halogen redistribution between the phosphorus and boron halogens (10). Nuclear magnetic resonance parameters of the BCl_3, BBr_3, and BI_3 adducts of Me_3PS have recently been reported (11, 12).

[1]To whom all correspondence should be addressed.

Experimental

Trimethylphosphine was prepared from methyl magnesium iodide and phosphorus trichloride in ether, and purified via the silver iodide complex (13). Trimethylphosphine oxide was prepared from phosphorus oxychloride by the method of Burg and McKee (14). Trimethylphosphine sulfide (Maybridge Research Chemicals) was dried under vacuum overnight and used without further purification. ^1H spectra revealed no impurities in any of the bases. The purification of the boron trihalides and methylene chloride has been described previously (3), as has the n.m.r. instrumentation (1, 3).

Nuclear magnetic resonance samples containing Me_3P were prepared entirely on a high-vacuum system. The less volatile compounds Me_3PO and Me_3PS were added to n.m.r. tubes in a dry box. After weighing, solvent, Lewis acids, and n.m.r. reference compounds were condensed in at $-196°$, and the samples were sealed off. The BF_3 adducts of all of the bases were very soluble in methylene chloride but the BCl_3 and especially the BBr_3 adducts were much less soluble, and the low solubility restricted the study. Solubility problems were serious in the mixed-adduct systems as well; insoluble material, which was not further investigated, was present in many samples.

Results

Nuclear magnetic resonance parameters are given in Table 1. All of the adduct and free-base ^1H signals were split into 1:1 doublets by

Can. J. Chem. Downloaded from www.nrcresearchpress.com by 210.87.254.40 on 09/05/12
For personal use only.

TABLE 1. Nuclear magnetic resonance parameters of boron trihalide adducts

Adduct	Chemical shifts*		Coupling constants (Hz)		
	^{1}H	^{19}F	^{1}H–^{31}P	^{11}B–^{19}F	^{19}F–^{31}P
Me_3P†	1.02		1.6		
$Me_3P \cdot BF_3$†	1.47	137.4	12.0	51.5	232.0
$Me_3P \cdot BF_2Cl$	1.53	131.2	12.0	75.2	179.0
$Me_3P \cdot BFCl_2$	1.57		12.0		
$Me_3P \cdot BCl_3$†	1.62		12.0		
$Me_3P \cdot BF_2Br$	1.63	129.7	12.0	84.0	167.0
$Me_3P \cdot BFBr_2$	1.68	135.1	12.0	112.6	125.0
Me_3PO	1.56		13.2		
$Me_3PO \cdot BF_3$	1.95	145.2	13.9		
$Me_3PO \cdot BF_2Cl$	2.05	120.8	13.8		
$Me_3PO \cdot BFCl_2$	2.12	105.2	13.9		
$Me_3PO \cdot BCl_3$	2.19		13.9		
$Me_3PO \cdot BF_2Br$	2.08	117.5	13.9		
$Me_3PO \cdot BFBr_2$	2.19		13.8		
$Me_3PO \cdot BBr_3$	2.26		13.8		
$Me_3PO \cdot BCl_2Br$	2.21		13.7		
$Me_3PO \cdot BClBr_2$	2.24		13.5		
Me_3PS‡	1.83		13.3		
$Me_3PS \cdot BF_3$	2.08§	119.0	14.2§		
$Me_3PS \cdot BF_2Cl$	2.10	102.3	13.8	63.8	
$Me_3PS \cdot BFCl_2$	2.14	98.1	14.0	95.5	
$Me_3PS \cdot BCl_3$‡	2.21		14.2		
$Me_3PS \cdot BF_2Br$	2.11		13.7		
$Me_3PS \cdot BFBr_2$	2.19		13.5		
$Me_3PS \cdot BBr_3$‡	2.27		13.9		

*^{1}H, −90°, p.p.m. to low field of internal tetramethylsilane; ^{19}F, −50°, p.p.m. to high field of internal $CFCl_3$; methylene chloride solution.

†Literature values of ^{1}H chemical shift and $J_{^{1}H-^{31}P}$: Me_3P, 0.97 δ and 2.0 Hz in methylene chloride (23); 0.81 δ and 2.5 Hz in benzene (5). $Me_3P.BF_3$, 0.63 δ and −11.3 Hz in benzene (5); 1.38 δ and 10.6 Hz in acetonitrile (6). ^{19}F chemical shift and ^{11}B—^{19}F coupling constant in acetonitrile: $Me_3P.BF_3$, 139.0 p.p.m. and 51 Hz (6).

‡Literature values of ^{1}H chemical shift and $J_{^{1}H-^{31}P}$: Me_3PS, 1.73 δ, 13.0 Hz; $Me_3PS.BCl_3$, 2.07 δ, 13.5 Hz; $Me_3PS.BBr_3$, 2.14 δ, 13.7 Hz in methylene chloride (11).

§Obtained by plotting the ^{1}H n.m.r. parameter obtained from the averaged (Me_3PS + $Me_3PS.BF_3$) resonance *vs.* BF_3/Me_3PS ratio; the constant value obtained at high ratios was taken to be the BF_3 adduct value.

coupling to ^{31}P. In the Me_3P adduct resonances there was also a pronounced broadening of the doublet components due to unresolved coupling with ^{11}B, so that the closely-spaced mixed-adduct resonances could not be resolved. This problem was overcome by the use of ^{11}B decoupling. Typical ^{1}H spectra with well-resolved mixed-adduct resonances are shown in Fig. 1. It was not possible, except in the Me_3PO system, to resolve the more closely spaced BCl_nBr_{3-n} adduct ^{1}H peaks. In the Me_3PO and Me_3PS mixed-adduct systems the proton chemical shifts showed a dependence of up to 0.15 p.p.m. on sample composition. However relative chemical shifts between successive mixed-halogen adducts in the series (donor).BF_nX_{3-n} (n = 0–3, X = Cl, Br) were constant to within 0.02 p.p.m. in different samples.

In Fig. 1 the contrast is evident between the large proportions of mixed-adduct species present at equilibrium in the Me_3PO adduct sample and the small proportions in the Me_3PS adduct sample. In the Me_3P system there are large proportions of the BF_2Cl adduct but only very small proportions of the $BFCl_2$ adduct.

Pronounced differences in the appearance of the ^{19}F resonances of fluorine-containing adducts of each of the three bases, described below, arise because of different degrees of resolution of ^{11}B–^{19}F and ^{19}F–^{31}P coupling in the different adduct series.

Me_3P Adducts

Separate doublets for $Me_3P.BF_3$ and Me_3P could be observed at −40° in the ^{1}H spectrum, but only averaged signals were observed at room temperature due to rapid chemical exchange (5, 15). Since the BF_2Cl, $BFCl_2$, and BCl_3 adducts under ^{11}B decoupling gave separate sharp doublets at room temperature in

Can. J. Chem. Downloaded from www.nrcresearchpress.com by 210.87.254.40 on 09/05/12
For personal use only.

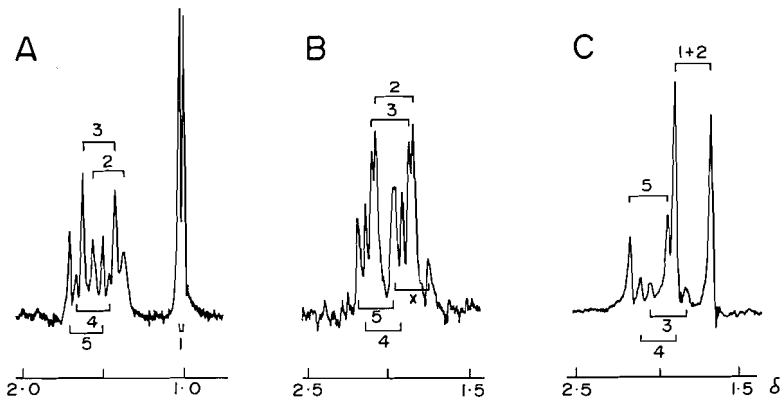

FIG. 1. ^1H n.m.r. spectra of methylene chloride solutions of Lewis base, BF_3, and BCl_3. (*A*) Me_3P, −40°, ^{11}B decoupled; (*B*) Me_3PO, 35°; (*C*) Me_3PS, −90°, 3:1:1 molar ratio. Identification of doublets: *1*, free base; *2*, BF_3 adduct; *3*, BF_2Cl adduct; *4*, $BFCl_2$ adduct; *5*, BCl_3 adduct. An exchange-averaged doublet arising from free Me_3PO and an unknown species is marked X.

the presence of excess Me_3P, exchange of free base with these adducts is much slower than with the BF_3 adduct.

^{19}F spectra of the Me_3P adducts were eight-line multiplets due to coupling to both ^{11}B and ^{31}P. There is an approximate inverse relationship between ^{11}B–^{19}F and ^{19}F–^{31}P coupling constants. The eight-line multiplets of the BF_3 and BF_2Cl adducts overlapped and it was not possible to resolve the low-intensity multiplet arising from the $BFCl_2$ adduct.

Me_3PO Adducts

Separate 1:1 doublets were observed for Me_3PO and its BF_3 adduct at 35° in the ^1H spectrum, showing that chemical exchange is slower than in the Me_3P–BF_3 adduct system. A small doublet arising from an impurity, and appearing at about 0.09 p.p.m. to low field of the BF_3 adduct doublet, was present as well and apparently corresponds to a small second ^{19}F peak observed at 150.3 p.p.m. Me_3PO–BCl_3 samples also gave, in addition to the 1:1 doublets of free base and adduct, a small doublet at lower field.

In the Me_3PO–BF_3–BCl_3 system additional large doublets corresponding to the BF_2Cl and $BFCl_2$ adducts were observed in the ^1H spectrum, indicating that large amounts of the mixed-halogen adducts are present at equilibrium. However, a precipitate formed, and in several samples that should have contained an excess of uncomplexed Me_3PO if only 1:1 adduct were formed, no free-base doublet could be detected. Titration of further Me_3PO into one such solution gave a "free-base" doublet but this had variable chemical shift; as more Me_3PO was added the doublet moved to higher field toward the normal position of the Me_3PO resonance. This is indicative of a very rapid chemical exchange between Me_3PO and a complex. Since no additional doublets could be "frozen out" even at −90°, the exchange would have to be a very rapid process. Protonation of Me_3PO due to the presence of impurity H_2O or HF does not seem likely as a similar effect was not observed in unmixed-halogen samples, and a more plausible explanation is the formation of ionic mixed boron trihalide adducts (16), which exchange rapidly with free base. Low solubilities and an appreciable variation of adduct chemical shifts with solution composition made this system especially difficult to study.

Similar effects were encountered in the Me_3PO–BF_3–BBr_3 system, but not in the Me_3PO–BCl_3–BBr_3 system where the formation of BCl_2Br and $BClBr_2$ adducts was demonstrated by the appearance of large new closely-spaced adduct resonances without any extraneous peaks. The extra complexity when both fluorine and a heavier halogen are present is reminiscent of the tetramethylurea–BF_3–BCl_3 system in which ionic adducts could be formed in large amounts (16), and it seems likely that ionic adducts of low solubility are formed in the present system. If these have structures such as $(Me_3PO)_2BF_2^+$. Cl^-, the anomalies in the spectra could be explained. Slow formation of such species would be consistent with the observation that initially-soluble n.m.r. samples eventually become insoluble after storage and crystallization at −78°.

^{19}F spectra of Me_3PO–BF_3–BCl_3 solutions

Can. J. Chem. Downloaded from www.nrcresearchpress.com by 210.87.254.40 on 09/05/12
For personal use only.

Can. J. Chem. Downloaded from www.nrcresearchpress.com by 210.87.254.40 on 09/05/12
For personal use only.

contained peaks which could be assigned to the BF_3, BF_2Cl, and $BFCl_2$ adducts, and a large additional peak at 138.8 p.p.m. which also appeared in spectra of Me_3PO–BF_3–BBr_3 solutions. The BF_3, BF_2Cl, and $BFCl_2$ adduct peaks were successively more broadened, but no splittings due to spin–spin coupling were resolved. The presence of the additional peak confirms that these systems are complex. The very weak and broad BF_2Br and $BFBr_2$ adduct resonances could not be adequately resolved.

Me_3PS Adducts

The presence of BF_3 causes a pronounced shift of the Me_3PS proton resonance to low field, demonstrating that an adduct is formed. However, separate 1:1 doublets could not be observed for Me_3PS and its BF_3 adduct even at $-100°$, showing that chemical exchange with excess base occurs much more rapidly than in the BF_3 adducts of Me_3P and Me_3PO. Separate doublets due to free and complexed Me_3PS could however be resolved in the Me_3PS–BCl_3 system below $-5°$, and in the Me_3PS–BBr_3 system at room temperature.

In the Me_3PS–BF_3–BCl_3 system separate low-temperature doublets could be observed for all of the BF_nCl_{3-n} adducts except the BF_3 adduct. All of these doublets coalesced with the free-Me_3PS doublet below room temperature to give a single averaged 1:1 doublet due to rapid chemical exchange. Approximate coalescence temperatures are: BF_2Cl adduct, $-70°$; $BFCl_2$ adduct, $-30°$; BCl_3 adduct, $-5°$. The BF_nBr_{3-n} adducts could be formed in the same way and behaved similarly. All of these mixed boron trihalide adducts were present in only small concentrations at equilibrium, compared to the unmixed-halogen adducts. In the Me_3PS–BCl_3–BBr_3 system a single broadened doublet, of chemical shift intermediate between the chemical shifts of the BCl_3 and BBr_3 adducts, indicated but did not prove the presence of the BCl_2Br and $BClBr_2$ adducts.

The ^{19}F spectrum of $Me_3PS.BF_3$ was a broad single peak whereas the BF_2Cl and $BFCl_2$ adducts gave broad 1:1:1:1 quartets due to coupling with ^{11}B; coupling with ^{31}P could not be detected.

Discussion

Effects of the Donor Atom

The Me_3PO and Me_3PS adduct results are in accord with the previously noted pattern of differences between oxygen-donor and sulfur-donor boron trihalide adducts (2), although here the oxygen-donor results are complex as with tetramethylurea (16) rather than simple as with Me_2O (3). Thus at equilibrium only small proportions of mixed F,Cl and F,Br adducts of Me_3PS are present, in contrast to the much larger proportions of these adducts of Me_3PO. Also the BF_3 adduct of Me_3PS, unlike that of Me_3PO, undergoes such rapid exchange with free base that separate free-base and BF_3 adduct peaks cannot be resolved at $-100°$. This very rapid exchange is in accord with a very weak donor–acceptor bond in $Me_3PS.BF_3$, and hence with the inability of Boorman and Potts to isolate this adduct at 0 °C (11). The similarity to the Me_2S system is striking. The $Me_3PS.BF_nCl_{3-n}$ adduct peaks coalesce with the free Me_3PS peak at temperatures that are within 10° of those observed in the coalescence of the corresponding adduct peaks in the $Me_2S.BF_nCl_{3-n}$ adduct system (1), further demonstrating the great similarity between the sulfur-donor systems. The principal difference between them is that the Me_3PS system gives detectable amounts of *both* the BF_nCl_{3-n} and BF_nBr_{3-n} series of mixed adducts; it is the first sulfur donor reported to do so.

In the Me_3P adducts the phosphorus donor does not appear to give rise to unique effects. The rates of donor–acceptor bond breaking are within the range observed for oxygen-donor adducts, slower than with Me_2O and faster than with tetramethylurea as donor. The halogen redistribution equilibrium gives large amounts of $Me_3P.BF_2Cl$ but surprisingly only small amounts of $Me_3P.BFCl_2$. These studies were hampered by low solubilities. It is interesting that when Me_3N is present as well in the system the $Me_3P.BFCl_2$ adduct is present in larger relative proportions (22).

The occurrence of very small or zero amounts of fluorine-containing mixed adducts at equilibrium has also been noted in adducts of certain of the Me_nPH_{3-n} series of bases. Successive methylation of PH_3 gives successively more stable BF_3 adducts (17). PH_3 does not form a BF_3 adduct, whereas the BCl_3 and BBr_3 adducts are quite stable; in this situation no BF_2Cl or $BFCl_2$ adducts could be detected, although the probable presence of BF_2Br and $BFBr_2$ adducts was reported (8). $MePH_2$ forms a weak BF_3 adduct (8, 17) and in this system both the BF_nCl_{3-n} and BF_nBr_{3-n} series of mixed adducts

Can. J. Chem. Downloaded from www.nrcresearchpress.com by 210.87.254.40 on 09/05/12
For personal use only.

were present in sufficient amounts to be detected. The $Me_3P.BF_3$ adduct, which is more stable, gives larger proportions of fluorine-containing mixed boron trihalide adducts. Thus the very nonstatistical redistribution equilibria between fluorine and heavier halogens is neither a specific sulfur-donor effect nor an effect of "soft bases" in general, but seems to occur in systems where there is an anomalously large difference between BF_3 and BCl_3 acceptor strengths. The *cause* of such large differences in basicity towards these superficially similar Lewis acids has not yet been satisfactorily explained.

Nuclear Magnetic Resonance Parameters

^1H complexation shifts of the adducts are as expected from previous work, those of Me_3PS being smaller than those of the corresponding Me_3PO adducts. For each donor, complexation shifts are smallest for the BF_3 adduct and largest for the BBr_3 adduct. The ^1H n.m.r. parameters are consistent with literature values where these are available. It is of interest that Grobe and Möller report a ^1H complexation shift to *high* field in $Me_3P.BF_3$ (5), apparently as a result of a specific solvent–solute interaction. They used benzene as a solvent. To obtain meaningful complexation shifts, anisotropic solvents such as benzene which are capable of strong specific interactions with solute species (18) should be avoided.

Table 1 gives magnitudes and not signs of the coupling constants. Grobe and Möller assign the ^1H–^{31}P coupling constant as positive in free Me_3P and negative in the BF_3 adduct (5). Since the magnitude of this coupling constant varies only slightly among all of the adducts the sign is probably negative in all of these species as well.

^{19}F chemical shifts of BF_nX_{3-n} (n = 1–3, X = Cl, Br) adducts normally move to lower field with increasing substitution of fluorine by a heavier halogen (1–3, 16, 19). This trend is reversed in the Me_3P adducts, where the $BFBr_2$ adduct has a chemical shift intermediate between those of the BF_3 and BF_2Br adducts. This apparent anomaly can be accounted for in terms of "pairwise interaction" parameters, as we have discussed elsewhere (20). ^{19}F pairwise interaction parameters derived from Table 1 can be used to calculate a chemical shift of 134.2 p.p.m. for $Me_3P.BFCl_2$. Thus the low-intensity eight-line ^{19}F multiplet of this adduct occurs approximately midway between the overlapping $Me_3P.BF_3$ and $Me_3P.BF_2Cl$ multiplets and is obscured by them.

Adduct Solubility and Further Reactions

Low solubilities and further reactions of the adducts have prevented studies as detailed as those that we have carried out on boron trihalide adducts of other donors (1–3, 16). Other workers have experienced similar difficulties with these adduct systems (8, 12, 15). Cowley and Mills attributed their phosphine adduct solubility difficulties to reaction with the methylene chloride solvent to give quaternary phosphonium salts (15). BCl_3, PCl_3, and *t*-butyl chloride have been shown to give an ionic product (21). Formation of ionic boron trihalide adducts seems especially likely in the Me_3PO system which may be as complex as the tetramethylurea adduct system (16), and in which the solubility problems are much worse.

We wish to thank the National Research Council of Canada for financial support of this work, Dr. J. M. Miller for help with the ^{11}B decoupling experiments, and the Department of Chemistry, McMaster University, for the use of ^{19}F n.m.r. facilities.

1. M. J. Bula and J. S. Hartman. J. Chem. Soc. Dalton, 1047 (1973).
2. M. J. Bula, J. S. Hartman, and C. V. Raman. J. Chem. Soc. Dalton, 725 (1974).
3. M. J. Bula, D. E. Hamilton, and J. S. Hartman. J. Chem. Soc. Dalton, 1405 (1972).
4. D. E. Young, G. E. McAchran, and S. G. Shore. J. Am. Chem. Soc. **88**, 4390 (1966).
5. J. Grobe and U. Möller. Z. Naturforsch. **26B**, 639 (1971).
6. C. W. Heitsch. Inorg. Chem. **4**, 1019 (1965).
7. G. Jugie, J.-P. Laussac, and J.-P. Laurent. Bull. Soc. Chim. Fr. 2542, 4238 (1970); J.-P. Laussac, G. Jugie, J.-P. Laurent, and F. Gallais. C. R. **276C**, 1497 (1973).
8. J. E. Drake and B. Rapp. J. Chem. Soc. Dalton, 2341 (1972).
9. B. Rapp and J. E. Drake. Inorg. Chem. **12**, 2868 (1973).
10. R. M. Kren, M. A. Mathur, and H. H. Sisler. Inorg. Chem. **13**, 174 (1974).
11. P. M. Boorman and D. Potts. Can. J. Chem. **52**, 2016 (1974).
12. M. L. Denniston and D. R. Martin. J. Inorg. Nucl. Chem. **36**, 1461 (1974).
13. F. G. Mann, A. F. Wells, and D. Purdie. J. Chem. Soc. 1828 (1937); F. G. Mann and A. F. Wells. J. Chem. Soc. 708 (1938).
14. A. B. Burg and W. E. McKee. J. Am. Chem. Soc. **73**, 4590 (1951).
15. A. H. Cowley and J. L. Mills. J. Am. Chem. Soc. **91**, 2911 (1969).

16. J. S. HARTMAN and G. J. SCHROBILGEN. Inorg. Chem. **13**, 874 (1974).
17. H. C. BROWN. J. Chem. Soc. 1248 (1956).
18. L. M. JACKMAN and S. STERNHELL. Applications of nuclear magnetic resonance spectroscopy in organic chemistry. Pergamon Press, Oxford. 1969. pp. 104–113.
19. J. S. HARTMAN and G. J. SCHROBILGEN. Inorg. Chem. **11**, 940 (1972); B. BENTON-JONES, M. E. A. DAVIDSON, J. S. HARTMAN, J. J. KLASSEN, and J. M. MILLER. J. Chem. Soc. Dalton, 2603 (1972).
20. J. S. HARTMAN and J. M. MILLER. Inorg. Chem. **13**, 1467 (1974).
21. J. I. BULLOCK, N. J. TAYLOR, and F. W. PARRETT. J. Chem. Soc. Dalton, 1843 (1972).
22. J. S. HARTMAN and C. V. RAMAN. Unpublished results.
23. F. CALDERAZZO, S. A. LOSI, and B. P. SUSZ. Helv. Chim. Acta, **54**, 1156 (1971).

Can. J. Chem. Downloaded from www.nrcresearchpress.com by 210.87.254.40 on 09/05/12
For personal use only.

The Thermal Rearrangement of α-Substituted Silanes

ALAN R. BASSINDALE, A. G. BROOK, PETER F. JONES, AND JOHN M. LENNON
Department of Chemistry, University of Toronto, Toronto, Ontario M5S 1A1

Received July 15, 1974

ALAN R. BASSINDALE, A. G. BROOK, PETER F. JONES, and JOHN M. LENNON. Can. J. Chem. **53**, 332 (1975).

The thermal rearrangement of α-substituted silanes ($R_3SiCHXR'$), in which there is exchange of X and R between the silicon atom and the adjacent carbon atom, has been studied. Kinetic parameters for two compounds ($Me_3SiCBrPh_2$ and $Ph_3SiCHOAcPh$) have been measured. Migratory aptitudes of both X and R have been examined. A mechanism involving initial migration of X to silicon, to form an "inverse ylid" ($R_3\bar{S}iX—\overset{+}{C}HR'$) is proposed.

ALAN R. BASSINDALE, A. G. BROOK, PETER F. JONES et JOHN M. LENNON. Can. J. Chem. **53**, 332 (1975).

On a étudié le réarrangement thermique de silanes α-substitués ($R_3SiCHXR'$) dans lesquels il y a un échange de X et de R entre l'atome de silicium et l'atome de carbone adjacent. On a mesuré les paramètres cinétiques pour la réaction de deux composés le ($Me_3SiCBrPh_2$ et $Ph_3SiCHOAcPh$). On a examiné les aptitudes migratrices des groupes X et R. On propose un mécanisme impliquant une migration initiale du X vers le silicium formant un "ylide inverse" du type ($R_3\bar{S}iX—\overset{+}{C}HR'$). [Traduit par le journal]

Introduction

We have previously reported, in a brief communication, that certain α-substituted benzyltriphenylsilanes undergo the following thermal rearrangement (1)

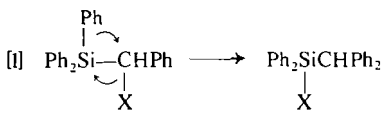

[1] $Ph_2Si(Ph)—CHPh(X) \longrightarrow Ph_2SiCHPh_2(X)$

(X = F, Cl, OAc, OTos)

The present study represents a more detailed examination of this rearrangement together with some extension in its scope.

Other examples of this kind of thermal rearrangement are known. Seyferth and co-worker (2) reported that dimethyldichlorostannane was one of the products of the thermolysis of trimethyl(α,α-dichlorobenzyl)tin at 150° in cyclohexene. The reaction course proposed was

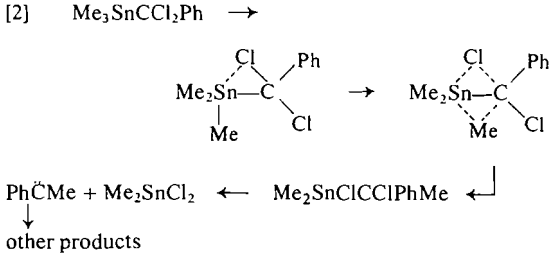

[2] $Me_3SnCCl_2Ph \rightarrow Me_2Sn(Cl)(Ph)—C(Me)(Cl) \rightarrow Me_2Sn(Cl)—C(Ph)(Me)(Cl)$

$Me_2SnClCClPhMe \rightarrow PhCMe + Me_2SnCl_2$ (other products)

Haszeldine and co-workers (3, 4) have described a similar rearrangement involving halogen exchange between the adjacent carbon and silicon atoms

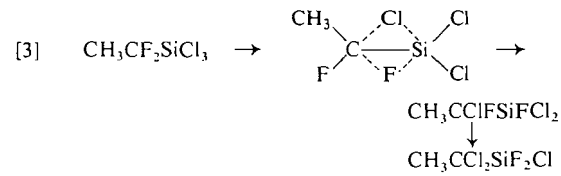

[3] $CH_3CF_2SiCl_3 \rightarrow CH_3(Cl)(Cl)C(F)(F)—Si(Cl)(Cl) \rightarrow CH_3CClFSiFCl_2 \rightarrow CH_3CCl_2SiF_2Cl$

which they considered to involve a cyclic transition state of the type shown. Such a doubly-bridged transition state is of the type encountered in a symmetry-allowed, type-I dyotropic rearrangement (5); however, at present there is no unambiguous mechanistic evidence for a simultaneous double σ-shift. It was, therefore, of considerable importance to determine the activation parameters E_a, $\Delta S^{\ddagger}$, and A for the thermal rearrangement of these α-substituted silanes and we have measured these for two representative examples. As an additional aid to the interpretation of the mechanism the relative migratory aptitudes of a variety of groups on both silicon and the α-carbon have been studied.

Results and Discussion

A series of α-substituted silanes, $R_3SiCHXR'$ (R = Ph, Me; X = F, Cl, Br, OTos, OAc;

Can. J. Chem. Downloaded from www.nrcresearchpress.com by 210.87.254.5 on 09/05/12
For personal use only.

TABLE 1. Thermal rearrangement of α-substituted silanes

Starting material	Product	Yield*	Temperature	Time (min)
$Ph_3SiCHFPh$	$Ph_2SiFCHPh_2$	100	145	6
$Ph_3SiCHOTosPh$	$Ph_2SiOTosCHPh_2$	100	150	10
		17	145	6
$Ph_3SiCHOAcPh$	$Ph_2SiOAcCHPh_2$	100	255	60
		58	230	60
		8	200	60
Ph_3SiCH_2OAc	$Ph_2SiOAcCH_2Ph$	33	254	60
		37	277	60
		0	200	60
$Ph_3SiCHCH_3OAc$	$Ph_2SiOAcCHCH_3Ph$	100	277	60
$Ph_3SiCHClPh$	$Ph_2SiClCHPh_2$	45	253	52
$Ph_3SiCHBrPh$	$Ph_2SiBrCHPh_2$	24	250	60
		23	230	270
Ph_3SiCH_2Cl	$Ph_2SiClCH_2Ph$	16	330	65
$Ph_3GeCHClPh$	$Ph_2GeClCHPh_2$	25	285	90
$Me_3SiCBrPh_2$	$Me_2SiBrCMePh_2$	100	220	27
$Et_3SiCBrPh_2$	$Et_2SiBrCEtPh_2$	100	220	2
$Ph_3SiCBrPh_2$	$Ph_2SiBrCPh_3$	95†	240	30
$Ph_2MeSiCBrPh_2$	$PhMeBrSiCPh_3$	100	240	30

*By n.m.r.
†Isolated product.

R′ = Ph, Me, H), $R_3SiCBrPh_2$ (R = Ph, Me, Et) and chlorobenzyltriphenylgermane were heated in sealed, flame dried Pyrex ampoules under a variety of conditions. The products obtained, the conditions, and the extent of reaction are given in Table 1. The reactions observed are summarized below

[4] $R_3SiCHXR' \rightarrow R_2SiXCHRR'$

[5] $R_3SiCBrPh_2 \rightarrow R_2SiBrCPh_2R$

[6] $Ph_3GeCHClPh \rightarrow Ph_2GeClCHPh_2$

The kinetics of the rearrangement of bromobenzyhydryltrimethylsilane (**1**) and acetoxybenzyltriphenylsilane (**2**) were studied. Both reactions were first-order in reactant to at least 90% completion.

The results, as shown in Table 2, are inconsistent with a highly-ordered doubly-bridged transition state which would be expected to have a very large, negative $\Delta S^{\ddagger}$. The near-zero value of $\Delta S^{\ddagger}$ (−1.3 e.u.) for **1** is indicative of a relatively open transition state. Thus, the results in Table 1 are consistent with and strongly support the following mechanism

[7] $R_3SiCHXR' \rightarrow R_3\bar{S}i\text{—}\overset{+}{C}HR' \rightarrow R_2SiXCHR'R$
(X)

3

The "inverse ylid", **3**, may be either a transition state or a discrete intermediate but our results do not allow a distinction to be made. However, the first, and rate-determining, step indicated by the study of relative migratory aptitudes appears to be the formation of the "inverse ylid" by migration of X from carbon to silicon. The transition state for this step should resemble a singly-bridged species, **4**,

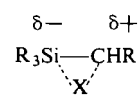

4

with a considerably less negative value of $\Delta S^{\ddagger}$ than expected for a doubly-bridged transition state. An acetoxy group, unlike a bromine atom, should migrate through a five-centered species, **5**,

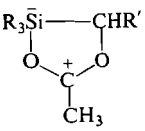

5

and the value of −20 e.u. for $\Delta S^{\ddagger}$ for **2** is consistent with this interpretation. With this alternative mode of migration the rearrangement of **2** relative to **1** should have a lower activation

Can. J. Chem. Downloaded from www.nrcresearchpress.com by 210.87.254.5 on 09/05/12
For personal use only.

TABLE 2. Kinetic data for the thermal rearrangement of bromobenzhydryltrimethylsilane and acetoxybenzyltriphenylsilane

T (°C)	$k_1 \times 10^3$ (min^{-1})	E_A (kcal mol^{-1})	$\Delta S^{\ddagger}$ *(e.u.)	$\log_{10} A$ (s)
$Me_3SiCBrPh_2$				
164	1.44 ± 0.14	37 ± 3	− 1.3 ± 3	13.9
184	7.61 ± 0.5			
200	30.3 ± 1.0			
220	185 ± 15			
$Ph_3SiCHOAcPh$				
210	5.9 ± 0.4	30 ± 3	−20 ± 4	9.1
220	10.6 ± 1			
230	19 ± 1			
242	41.8 ± 0.4			

*500 °K.

energy, a more negative $\Delta S^{\ddagger}$ and a smaller A value. These trends are clearly illustrated by the data in Table 2, where comparison shows lowering of the activation energy from 37 to 30 kcal mol^{-1}, change of $\Delta S^{\ddagger}$ from −1.3 to −20 e.u., and lowering $\log_{10} A$ from 13.9 to 9.1, for **2** relative to **1**. The comparison must be qualitative rather than quantitative since R and R′ differ in the two compounds but the kinetic parameters indicate that a dyotropic mechanism is most unlikely, and the transition state is not significantly bridged but resembles the "inverse ylid" **3**.

Recently O'Brien and co-worker (6) have obtained good kinetic evidence for the intermediacy of an "inverse ylid" in the SbF_5-catalyzed rearrangement of 2-chloro-2-trimethylsilylpropane

[8] 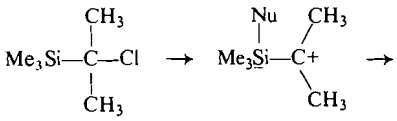

Products (Nu = nucleophile)

This is, of course, the catalyzed equivalent of the present rearrangement and is well known in organosilicon chemistry. The aluminum chloride catalyzed isomerization of (chloromethyl)trimethylsilane to chlorodimethylethylsilane was reported by Sommer and co-workers in 1947 (7).

Based on the results given in Table 1 the relative ease of migration of X from carbon to silicon appears to decrease in the following order: F > OTos > OAc > Cl > Br ≫ OMe. This coincides with the expected order of stabilization of a penta-coordinated silicon atom, based on bond energies, and the electronegativities of X, with the exception that since alkoxy compounds do not thermally rearrange, other factors not yet fully understood must be involved at least in these cases.

The ease of migration of R from silicon to carbon decreased in the order Ph > Me, Et. Thus bromobenzhydryldiphenylmethylsilane on heating rearranged to triphenylmethylphenylmethylbromosilane as a result of exclusive phenyl migration

[9] $Ph_2MeSiCBrPh_2 \rightarrow PhMeSiBrCPh_3$

After 1 h at 253° a sample of bromobenzyltrimethylsilane contained no 1-phenylethyldimethylbromosilane (although the n.m.r. spectrum did show a substantial amount of benzyltrimethylsilane, presumably due to redistribution[1]). Under the same conditions bromobenzyltriphenylsilane rearranged to benzhydryldiphenylbromosilane to the extent of 30%. (Redistribution products were also present.) The migration of a phenyl group to a carbonium ion center is generally faster than alkyl migration (8). If the inverse ylid was a true intermediate formed in the rate determining step then the rate of

[1]The rate of rearrangement of α-bromo compounds was difficult to duplicate. In addition they sometimes underwent redistribution reactions concurrently with rearrangement, according to the reaction

$$R_3SiCHBrR' \rightarrow R_2SiBrCHRR' + R_3SiCH_2R' + R_3SiCBr_2R'$$

The extent of redistribution was variable and may have been catalyzed by traces of unknown impurities. However, a sample of bromobenzyltriphenylsilane containing 5% by weight of dibenzoyl peroxide rearranged at the same rate to give the same product mixture as a sample without added peroxide. Therefore, free radical intermediates in either rearrangement or redistribution reactions appear unlikely.

Can. J. Chem. Downloaded from www.nrcresearchpress.com by 210.87.254.5 on 09/05/12
For personal use only.

Can. J. Chem. Downloaded from www.nrcresearchpress.com by 210.87.254.5 on 09/05/12
For personal use only.

migration of R from silicon to carbon would be relatively fast and should not affect the overall reaction rate. Therefore the reactivity series observed does not necessarily reflect migratory aptitudes of aliphatic and aromatic moieties, but rather the ability of R to stabilize the ylid through delocalization of the positive charge on the carbon atom.

With changes in R′ the ease of rearrangement decreases in the order Ph > Me > H. This order is consistent with a build up of positive charge on the α-carbon and reflects the ability of the groups to stabilize a carbonium ion.

Finally it was observed that α-chlorobenzyltriphenylsilane rearranged faster than the analogous germanium compound. This probably reflects the greater bond energy of Si—X compounds and the lower energy of the silicon d orbitals.

As a further test of the proposed mechanism equimolar solutions of α-fluorobenzyltriphenysilane (**6**) in $CDCl_3$ and DMSO-d_6 were heated to 140° for 4½ h. The solution in DMSO-d_6 was 32% rearranged to benzhydryldiphenylfluorosilane (**7**), the remaining material being unreacted **6**. The solution in $CDCl_3$ contained only unreacted **6**. The faster reaction in polar solvents is evidence of substantial charge separation in the transition state.

In summary, the available evidence strongly supports the open-chain mechanism for rearrangement of α-substituted silanes, where Si—X bond formation is significantly developed in the transition state. The transition state thus resembles an inverse ylid.

Experimental

Experiments involving reactive organometallic reagents were carried out under nitrogen using dried, purified solvents. Infrared spectra were recorded on a Perkin–Elmer 237B instrument. Nuclear magnetic resonance spectra were determined using Varian T-60 or A-60 spectrometers. Melting points were measured on a Fisher–Johns apparatus and are recorded uncorrected. Analyses were carried out by A. B. Gygli, Toronto.

Preparation of Starting Materials

Known compounds were prepared by the standard literature preparations. All benzyltriphenylsilyl derivatives were prepared by the action of HX on phenyltriphenylsilydiazomethane (1). The general method is given below and the results of individual preparations are given in Table 3.

The experimental procedure was as follows. A solution of diazoalkane and excess acid in an organic solvent was allowed to stand at ambient temperature, in the dark, until the color of the diazoalkane was completely discharged. With HCl the gas was bubbled through the reaction mixture until decolorization occurred. The workup procedure involved washing the reaction mixture several times with water, drying the organic layer over $MgSO_4$, removing the solvent on a rotary evaporator, and then recrystallizing the product. Reaction conditions and other information are given in Table 3. The n.m.r. spectra of starting materials and products are shown in Table 4.

Rearrangement Studies

Samples of the α-substituted silanes were sealed in carefully flame-dried Pyrex ampoules which were then immersed in an oil bath. After a given time, the sample was removed and the contents analyzed. The results are given in Table 1.

Synthesis of Previously Unknown Rearrangement Products

Acetoxybenzhydryltriphenylsilane

A mixture of benzhydryldiphenylchlorosilane (5 g, 13 mmol) and silver acetate (2.16 g, 13 mmol) in benzene (50 ml) was stirred for 16 h at ambient temperature, filtered, and the filtrate was evaporated to dryness. The residue was recrystallized from pentane to yield acetoxybenzhydryldiphenylchlorosilane 2.55 g (48%), m.p. 113–115°.

Anal. Calcd. for $C_{27}H_{24}O_2Si$: C, 79.37; H, 5.92. Found: C, 79.70; H, 6.03.

Tosyloxybenzhydryldiphenylsilane

A mixture of benzhydryldiphenylchlorosilane (5 g, 13 mmol) and silver tosylate (3.62 g, 13 mmol) in benzene (50 ml) was stirred for 16 h at ambient temperature, filtered, and the filtrate was evaporated to dryness. The residue was recrystallized from pentane to afford tosyloxybenzhydryldiphenylsilane 2.65 g (40%), m.p. 162–163°.

Anal. Calcd. for $C_{33}H_{28}O_3SSi$: C, 74.40; H, 5.30. Found: C, 74.27; H, 5.49.

(Triphenylmethyl)diphenylbromosilane

Bromobenzhydryltriphenylsilane (4 g, 7.9 mmol) was sealed in a glass ampoule and heated at 240° for 1 h. A black solid was obtained which was dissolved in benzene, clarified with activated charcoal, and recrystallized from hexane to yield pure (triphenylmethyl)diphenylbromosilane, m.p. 214–215°.

Anal. Calcd. for $C_{31}H_{25}BrSi$: C, 73.64; H, 5.05; Br, 15.81. Found: C, 73.51; H, 4.98; Br, 15.83.

(Triphenylmethyl)phenylmethylbromosilane

Bromobenzhydryldiphenylmethylsilane (4 g, 9 mmol) was sealed in a glass ampoule and heated at 240° for 1 h. The brown solid obtained was dissolved in benzene, clarified with activated charcoal, and recrystallized from hexane to afford (triphenylmethyl)phenylmethylbromosilane, m.p. 133–135°.

Anal. Calcd. for $C_{26}H_{33}BrSi$: C, 70.42; H, 5.24; Br, 18.01. Found: C, 70.51; H, 5.12; Br, 17.82.

Methylbenzhydryldimethylbromosilane

Bromobenzhydryltrimethylsilane (2 g) was heated at 240° for 22 h. After this time, the brown liquid was flash-distilled under aspirator pressure in a Kugelröhr apparatus. The resulting clear liquid, methylbenzhydryldimethylbromosilane was analyzed immediately.

Can. J. Chem. Downloaded from www.nrcresearchpress.com by 210.87.254.5 on 09/05/12
For personal use only.

TABLE 3. Reaction of Ph_3MCN_2Ph with HX (M = Si, Ge; X = F, Cl, Br, OTos, OAc) at ambient temperature

							Analytical data (%)			
							Calculated		Found	
Diazoalkane	HX	Product	Solvent	Time	Yield (%)	Melting point (°C)	C	H	C	H
Ph_3GeCN_2Ph	HCl	$Ph_3GeCHClPh$	Toluene	1 min	88	131–132*	69.90	4.93	70.14	5.30
Ph_3SiCN_2Ph	HCl	$Ph_3SiCHClPh$	Ether	1 min	94	136–138*§				
Ph_3SiCN_2Ph	HF	$Ph_3SiCHFPh$	Toluene	45 min	82	120–122*	81.49	5.75	81.04	5.93
Ph_3SiCN_2Ph	AcOH	$Ph_3SiCHOAcPh$	AcOH/toluene	90 min	89	154–155†	79.37	5.92	79.71	5.83
Ph_3SiCN_2Ph	TosOH	$Ph_3SiCHOTosPh$	Toluene	15 h	80	138–141‡	73.82	5.42	74.50	5.47
Ph_3SiCN_2Ph	HBr	$Ph_3SiCHBrPh$	Benzene	2 h	92	147–148*§				

*From MeOH.
†From EtOH.
‡From hexane.
§Mixed m.p. with authentic sample undepressed.

TABLE 4. Nuclear magnetic resonance data for α-substituted silanes (δ(CCl_4) p.p.m.)

Compound	Nuclear magnetic resonance data (p.p.m.)			
$Ph_3SiCHPhF$	6.65–7.7	(m,* 20H, aromatic)	6.13	(d, 1H, J_{FH} = 45 Hz, C*H*F)
$Ph_3SiCHPhCl$	6.85–7.75	(m, 20H, aromatic)	4.94	(s, 1H, CHCl)
$Ph_3SiCHPhBr$	7.0 –7.6	(m, 20H, aromatic)	4.88	(s, 1H, CHBr)
$Ph_3SiCHPhOAc$	6.8 –7.5	(m, 20H, aromatic)	6.41	(s, 1H, C*H*OAc) 1.90 (s, 3H, $OCOCH_3$)
$Ph_3SiCHPhOTos$	6.5 –7.5	(m, 24H, aromatic)	6.00	(s, 1H, C*H*OTos) 2.21 (s, 3H, $ArCH_3$)
$Ph_3SiCHPhOMe$	6.8 –7.7	(m, 20H, aromatic)	4.70	(s, 1H, C*H*OCH_3) 3.32 (s, 3H, OCH_3)
Ph_3SiCH_2Cl	7.2 –7.7	(m, 15H, aromatic)	3.43	(s, 2H, CH_2Cl)
Ph_3SiCH_2OAc	7.2 –7.7	(m, 15H, aromatic)	4.48	(s, 2H, C*H*$_2$OAc) 1.89 (s, 3H, $OCOCH_3$)
$Ph_3SiCHMeOAc$	7.2 –7.7	(m, 15H, aromatic)	5.58	(q, 1H, *J* = 7 Hz, C*H*Me) 1.84 (s, 3H, $OCOCH_3$) 1.41 (d, 3H, *J* = 7 Hz CH*Me*)
$Ph_3SiCBrPh_2$	6.6 –7.7	(m, aromatic)		
$Ph_2MeSiCBrPh_2$	7.0 –7.65	(m, 20H, aromatic)	0.76	(s, 3H, CH_3Si)
$Me_3SiCBrPh_2$	7.2 –7.6	(m, 10H, aromatic)	0.71	(s, 9H, CH_3Si)
$Et_3SiCBrPh_2$	7.0 –7.5	(m, 10H, aromatic)	0.90	(broad s, 15H, EtSi)
$Ph_3GeCHClPh$	6.6 –7.7	(m, 20H, aromatic)	5.08	(s, 1H, CHCl)

*It was possible to differentiate between C-phenyl protons and Si-phenyl protons, the former being shielded by *ca.* 0.4 p.p.m. relative to the latter.

TABLE 5. Nuclear magnetic resonance data for the products of rearrangement of α-substituted silanes (δ(CCl_4) p.p.m.)

Compound	Nuclear magnetic resonance data (p.p.m.)			
$Ph_2SiFCHPh_2$	7.1 –7.3	(2 singlets, 20H, aromatic)	4.10	(d, 1H, *J* = 7 Hz $CHPh_2$)
$Ph_2SiClCHPh_2$	7.1 –7.5	(m, 20H, aromatic)	4.25	(s, 1H, $CHPh_2$)
$Ph_2SiBrCHPh_2$	7.1 –7.5	(m, 20H, aromatic)	4.34	(s, 1H, $CHPh_2$)
$Ph_2SiOAcCHPh_2$	7.05–7.5	(m, 20H, aromatic)	4.78	(s, 1H, $CHPh_2$) 1.81 (s, 3H, $OCOCH_3$)
$Ph_2SiOTosCHPh_2$	6.8 –7.5	(m, 24H, aromatic)	4.64	(s, 1H, $CHPh_2$) 2.30 (s, 3H, ArMe)
$Ph_2SiClCH_2Ph$	6.8 –7.7	(m, 15H, aromatic)	2.77	(s, 2H, CH_2Ph)
$Ph_2SiOAcCH_2Ph$	6.7 –7.7	(m, 15H, aromatic)	2.90	(s, 2H, CH_2Ph) 1.97 (s, 3H, $OCOCH_3$)
$Ph_2SiOAcCHMePh$	6.7 –7.7	(m, 15H, aromatic)	3.38	(q, 1H, *J* = 7 Hz CHPh) 1.94 (s, 3H, $OCOCH_3$) 1.41 (d, 3H, *J* = 7 Hz CH*Me*)
$Ph_2SiBrCPh_3$	6.6 –7.7	(m, aromatic)		
$Me_2BrSiCMePh_2$	7.0 –7.33	(m, 10H, aromatic)	1.76	(s, 3H, CCH_3) 0.46 (s, 6H, $SiCH_3$)
$Et_2BrSiCEtPh_2$	7.0 –7.5	(m, 10H, aromatic)	2.33	(q, 2H, *J* = 10.5 Hz, C*H*$_2$$CH_3$)
			0.37–1.27	(m, 13H, SiEt, CCH_2CH_3)
$Ph_2ClGeCHPh_2$	6.6 –7.7	(m, 20H, aromatic)	4.51	(s, 1H, C*H*Ph_2)

Anal. Calcd. for $C_{16}H_{19}BrSi$: C, 60.18; H, 6.00; Br, 25.03. Found: C, 60.33; H, 5.98; Br, 24.82.

Kinetic Studies

In a typical run, ten or more aliquots of the α-substituted silane in sealed tubes were simultaneously immersed in an oil bath whose temperature was constant to within ±1°. The ampoules were removed periodically and the extent of reaction was measured by integration of suitable signals in the n.m.r. spectrum. A plot of log [reagent] *vs.* time gave a good straight line and first order rate constants were obtained with an accuracy of better than ±10%. Several runs were carried out at each temperature. The results are given in Table 2.

This research was supported by the National Research Council of Canada.

1. A. G. BROOK and P. F. JONES. Chem. Commun. 1324 (1969).
2. D. SEYFERTH and F. M. ARMBRECHT, JR. J. Am. Chem. Soc. **91**, 2616 (1969).
3. W. I. BEVAN, R. N. HASZELDINE, J. MIDDLETON, and A. E. TIPPING. *In* New pathways in inorganic chemistry. *Edited by* E. A. V. Ebsworth, A. G. Maddock, and A. G. Sharpe. Cambridge University Press, London. 1968. p. 130.
4. W. I. BEVAN, R. N. HASZELDINE, J. MIDDLETON, and A. E. TIPPING. J. Organomet. Chem. **23**, C 17 (1970).
5. M. T. REETZ. Tetrahedron, **29**, 2189 (1973).
6. T. J. HAIRSTON and D. H. O'BRIEN. J. Organomet. Chem. **29**, 79 (1971).
7. F. C. WHITMORE, L. H. SOMMER, and J. R. GOULD. J. Am. Chem. Soc. **69**, 1976 (1947).
8. Y. POCKER. *In* Molecular rearrangements, Vol I. *Edited by* P. de Mayo. Interscience, New York, N.Y. 1963.

Can. J. Chem. Downloaded from www.nrcresearchpress.com by 210.87.254.5 on 09/05/12
For personal use only.

Carbon-13 Spin–Lattice Relaxation Times for Selected Steroids

JOHN W. APSIMON
Chemistry Department, Carleton University, Ottawa, Canada K1S 5B6
AND
HELMUT BEIERBECK AND JOHN K. SAUNDERS
Département de Chimie, Université de Sherbrooke, Sherbrooke, Québec J1K 2R1

Received July 10, 1974

JOHN W. APSIMON, HELMUT BEIERBECK, and JOHN K. SAUNDERS. Can. J. Chem. **53**, 338 (1975).

The spin–lattice relaxation time (T_1) data for a number of androstane and cholestane derivatives is presented. The NT_1 value of carbon-3 in several of the compounds is found to be shorter than the average NT_1 value for the other ring carbons which is interpreted in terms of anisotropic motion with the long steroid axis being the preferred axis of rotation. As this effect is only observed for carbon-3, an effective molecular correlation time can be calculated from the average NT_1 value for all other CH and CH_2 carbons. The correlation time (τ_i) for internal rotation of a methyl group is shown to depend on the number of 1,3 diaxial methyl group – hydrogen interactions. Thus τ_i(C-19) is shorter than τ_i(C-18) for androstane, τ_i(C-19) is shorter for *trans*-cholestanol than for either *cis*-cholestanol or cholesterol. The effects of substituents and conformational changes on τ_i as well as the effect of solvent on T_1 are discussed.

JOHN W. APSIMON, HELMUT BEIERBECK et JOHN K. SAUNDERS. Can. J. Chem. **53**, 338 (1975).

Nous avons mesuré les temps de relaxation spin–milieu (T_1) pour un nombre des dérivés de l'androstane et du cholestane. Dans plusieurs de ces composés, on trouve que la valeur de NT_1 pour le carbone-3 est plus court que la moyenne obtenue pour les autres carbones CH et CH_2 cycliques; ce résultat est interprété en termes de mouvements anisotropiques dont l'axe préféré de rotation est l'axe le plus long du stéroide. Comme on observe cet effet seulement pour le carbone-3, on peut utiliser la moyenne des autres carbones CH et CH_2 rigide pour calculer la valeur du temps de correlation effectif de la molécule. Il est démontré que le temps de correlation (τ_i) pour la rotation interne d'un groupement méthyle dépend du nombre des interactions 1,3 diaxiales méthyle – hydrogène. Ainsi, τ_i(C-19) est moins long que τ_i(C-18) pour l'androstane, τ_i(C-19) est plus court dans *trans*-cholestanol que dans le *cis*-cholestanol ou le cholestérol. L'effet des substituents et le changement de conformation sur τ_i, ainsi que l'effet du solvant sur T_1, sont discutés. [Traduit par le journal]

The advent of the Fourier transform technique has not only made the recording of natural abundance C-13 spectra routine but has also made feasible the recording of spin–lattice relaxation time (T_1) data. A number of reports (1, 2) have appeared in which the strategies employed are presented and possible application quoted. However, to date, little evidence has been given to the possibility of using T_1 data for structural conformational analysis. In order to explore this possibility we have recorded the C-13 T_1 values for a number of monosubstituted androstanes as well as for several cholestane derivatives. The results are given in Tables 1 and 2 together with the values recorded by Allerhand *et al.* (2) for cholesteryl chloride. Rather than give the T_1 values for each carbon of each compound, we have shown in Fig. 1 the complete set of values recorded for cholesterol and androstan-4β-ol and then in the tables quoted the average NT_1 values of all rigid CH and CH_2 carbons, with the exception of C-3, as these were always within experimental error of the average.

In the limit of extreme narrowing ($\omega^2\tau_c^2 \ll 1$), the T_1 value for a protonated carbon is given by eq. 1 (1) provided the molecule is undergoing isotropic motion. The symbol N represents the

$$\frac{1}{T_1} = \frac{N\hbar^2\gamma_C^2\gamma_H^2}{(r_{C-H})^6}\tau_c \qquad [1]$$

number of protons attached to the observed carbon, r_{C-H} is the C—H bond length, and τ_c is the rotational correlation time which can be expressed as in eq. 2 with η being the viscosity and $4\pi a^3/3$ the effective molecular volume. From eq. 1, it is evident that for isotropic motion T_1

$$\tau_c = \frac{4\pi\eta a^3}{3\hbar T} \qquad [2]$$

Can. J. Chem. Downloaded from www.nrcresearchpress.com by 210.87.254.40 on 09/05/12
For personal use only.

Can. J. Chem. Downloaded from www.nrcresearchpress.com by 210.87.254.40 on 09/05/12
For personal use only.

TABLE 1. Carbon-13 NT_1 data for selected androstane derivatives[a]

Substituent	α[b]	C-3	C-18	C-19	τ_i(C-18)[c]	τ_i(C-19)
2 βOH	2.0	1.7	7.7	8.3	1.7	1.5
2 C=O	2.0	2.1	7.3	8.6	1.9	1.4
3 βOH	2.2	2.0	9.0	13.2	1.5	0.5
3 αOH	2.1	1.5	8.0	12.0	1.7	0.6
3 C=O	2.7	—	9.6	12.6	1.5	0.8
4 αOH	2.5	1.6	8.6	12.7	1.7	0.7
4 βOH	2.0	1.5	7.7	7.8	1.8	1.7
4 C=O	2.2	1.4	8.1	8.7	1.7	1.5
4 C=O[d]	2.1	—	8.4	8.4	1.5	1.5
11 C=O	2.3	1.9	5.4	13.8	4.7	0.5
16 C=O	2.1	1.3	4.5	11.8	7.2	0.6
17 C=O	2.45	1.6	8.8	13.8	1.7	0.6
Δ^5 ene	2.4	1.9	8.4	6.8	1.8	2.9

[a]1 *M* in $CDCl_3$.
[b]α refers to the average value of ring CH_2 and CH carbons.
[c]$\times 10^{-12}$ s.
[d]1 *M* in CCl_4 with 3–5% benzene-d_6.

TABLE 2. Carbon-13 NT_1 data for some cholestane derivatives[a]

Carbon	Cholesterol $CDCl_3$	Cholesterol CCl_4	Cholesteryl chloride[b] (CCl_4)	*trans*(5α-)-Cholestanol ($CDCl_3$)	*cis*(5β-)-Cholestanol ($CDCl_3$)
α[c]	0.60	0.23	0.5	0.63	0.73
3	0.55	0.21	0.5	0.65	0.61
18	3.3	2.2	4.5	3.6	4.2
19	3.0	2.1	4.5	5.1	3.0
20	0.54	0.20	0.49	0.64	
21	2.2	1.7	4.5	2.3	2.7
22	0.68			0.62	0.7
23	0.92	0.34	0.84	0.62	0.8
24	1.3	0.62	1.3	1.40	1.4
25	1.7	1.1	1.8	2.0	2.1
26	4.7	3.7	6.0	3.5	4.8
27	4.9	4.0	6.3	4.8	5.1
C-18/α	5.5	9.4	9	5.7	5.7
ρ(C-18)[e]	34			37	37
τ_i(C-18)[e]	2.3			2.0	1.8
19/α	5.0	9	9	8.1	4.1
ρ(C-19)	26				16
τ_i(C-19)	3.0				4.9

[a]Estimated error ± 10%.
[b]Reference 1.
[c]α refers to the average value of ring CH and CH_2 carbons.
[d]$\rho(\text{C-18} \equiv \tau_G/\tau_G$ for carbon 18.
[e]$\times 10^{-12}$ s.

(CH) = $2T_1$ (CH_2) ≪ T_1 (C) and this can be used to assign the various carbons as either C, CH, or CH_2 (4, 5). In Fig. 1, the T_1 values for the carbons of the ring system of cholesterol can be seen to follow this type of behavior. The CH_3 groups and side chain carbons have at least one extra degree of freedom and thus their T_1 values cannot be expressed in terms of eq. 1. The correlation time of these carbons is a combination of two correlation times, namely τ_c and the time for internal reorientation τ_i. Its cross-correlational effects are negligible and provided the motion is isotropic, T_1 is expressed by eq. 3 (2) where the constants *A*, *B*, and *C* depend on the angle between the axis of rotation and the C—H bond vector. If σ is the angle between the C—H bond

$$[3]\quad \frac{1}{T_1} = \frac{N\hbar^2\gamma_H{}^2\gamma_C{}^2}{r_{C-H}{}^6}\tau_c \times \left[A + B\frac{6\tau_i}{6\tau_i + \tau_c} + C\frac{3\tau_i}{3\tau_i + 2\tau_c}\right]$$

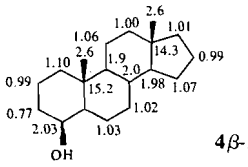

4β-Androstanol

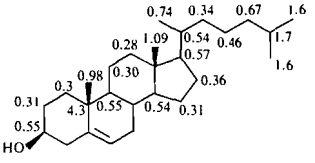

Cholesterol

FIG. 1. Carbon-13 spin–lattice relaxation times for 4-β-androstanol and cholesterol.

vector and the axis of internal rotation, then $A = \frac{1}{3}(\cos^2\sigma - 1)$; $B = 3\sin^2\sigma\cos^2\sigma$, and $C = \frac{3}{4}\sin^4\sigma$ which gives for a tetrahedral carbon $A = 1/9$, $B = 8/27$, and $C = 16/27$ (5). The value of T_1 for a CH_3 group or a side chain with one degree of freedom, relative to a rigid CH carbon, is given by eq. 4 where α is for the rigid CH carbon, β refers to carbons with internal motion, and $\rho = \tau_{c/\tau_i}$.[1] In the limit of very slow internal

$$[4]\quad \frac{T_1^{\alpha}}{N^{\beta}T_1^{\beta}} = \frac{1}{9}\left[1 + \frac{16}{6+\rho} + \frac{16}{3+2\rho}\right]$$

reorientation, $\rho \to 0$ and $N^{\beta}T_1^{\beta} = T_1^{\alpha}$ whereas in the limit of very rapid rotation, $\rho \to \infty$ and $9\,T_1^{\alpha} = N^{\beta}T_1^{\beta}$. Thus, for example, T_1 for a CH_3 group can vary from $\frac{1}{3}T_1$ (CH) to $3T_1$ (CH). In the case of cholesterol in CCl_4 as was the case of cholesteryl chloride, $3T_1$ (CH) = T_1 (CH_3) *i.e.* the limit of rapid rotation. As can be observed, $2T_1$ (CH_2) = T_1 (CH) for all ring carbons in the cholestane derivatives. From this Allerhand *et al.* (2) concluded that cholesteryl chloride is undergoing isotropic motion. However, in the androstane examples, NT_1 (C-3) is, in many compounds, less than that observed for other ring carbons. In steroids the long steroidal axis passes through or very close to C-3 as shown below and intuitively we expect rotation about this axis to be more rapid than about any other axis. In T_1 determinations, we are measuring the

[1]Strictly speaking $\rho = D_2/D_1$ *i.e.* the ratio of the diffusion rates.

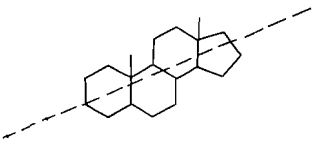

motion of the C—H bond vector of the proton causing relaxation. If this vector resides on a preferred axis of rotation, then obviously its molecular motion will be less than that for C—H bonds that are not on the axis. Levy *et al.* (1) have shown for monosubstituted aromatic compounds that T_1 (*para*) < T_1 (*ortho*) = T_1 (*meta*) as the preferred axis of rotation is coincident with the *para* C—H bond. Examination of Table 1 shows that for androstan-3β-ol, T_1 (C-3) is within experimental error of other NT_1 values whereas for androstan-3α-ol, T_1 (C-3) is significantly less than the average NT_1 value. For the 3β-OH compound, H-3 is axial and thus rotation about the long axis will cause motion of the C—H bond whereas for the 3α-OH, H-3 is equatorial and the C—H bond will approach coincidence with the long steroid axis thus significantly reducing the motion of this bond. This effect of anisotropic motion in the androstan-3α-ol as well as several other derivatives is observed only for C-3 as all other ring CH and CH_2 carbons exhibit values with experimental error of the average value. This apparent anomaly from comparison with much simpler molecules (6) is a result of complex molecular motion as well as the experimental error.

This explanation has, of necessity, been qualitative as the theory of anisotropic motion developed to date requires high symmetry restriction (6) and is thus inapplicable in the steroids. Thus, observation of identical NT_1 values for rigid carbons does not necessarily indicate that the molecule is undergoing isotropic motion. However, eq. 1 can be used at least to a first approximation in order to obtain correlation time data although the correlation time so obtained is not the isotropic correlation time but an effective correlation time (7). From this, the internal reorientation time can be calculated as has been performed in the tables.

Inspection of the τ_G data for the androstane derivative leads to a number of interesting substituent effects. The value of τ_i for C-18 is $1.7 \pm 0.2 \times 10^{-12}$ s for all ring A or B substituted compounds and for the 17 ketone. For C-19, τ_i for the 3α, 3β, and 4α alcohols as well as the 11, 16, and 17 ketones is $0.6 \pm 0.1 \times 10^{-12}$

Can. J. Chem. Downloaded from www.nrcresearchpress.com by 210.87.254.40 on 09/05/12
For personal use only.

Can. J. Chem. Downloaded from www.nrcresearchpress.com by 210.87.254.40 on 09/05/12
For personal use only.

s. The other values vary significantly (greater than 25%) from these. The rotation rate, $1/\tau_i$, is a measure of the energy difference between the energy of the preferred conformation of the CH_3 group and the transition state to rotation. In ethane, the barrier to rotation is 3.6 kcal/mol which corresponds to a correlation time of 8×10^{-11} s. The τ_i value in these compounds is of the order of 10^{-12} s and consequently the barrier to rotation is significantly less than that of ethane. It is instructive in order to explain the effect of substituents on T_1 to compare the value of C-19 in the 17-keto and the Δ^5 compounds. The preferred conformation for the 17 ketone will be as shown in **a** below in which the CH_3 group has 1,3 diaxial interactions with the axial protons of carbons 2, 4, 6, 8, and 11. For the Δ^5 compound, one of these interactions has been removed and the interaction with two others has become less severe. The energy of the preferred

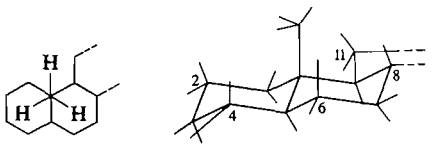

a

conformation of the CH_3 group is thus less in the 5-ene than in the 17 ketone. For both compounds, the transition state for rotation is when the C—H bonds of the CH_3 eclipse the C—C bonds and hence the energy difference of this state between the two compounds will be less. The barrier to rotation for the 5-ene will thus be higher resulting in a slower rotation rate and a shorter T_1. The same argument is true for the replacement of a β axial proton by a keto group although the effect is somewhat smaller. It is of interest to note that for C-18 an 11 or 16-keto group causes a significant change in T_1 whereas the 17 ketone shows values in line with the ring A substituted compounds.

The compounds with a β axial hydroxyl group would be, at first sight, expected to cause an increase in the rotation rate of the C-19 methyl group. However, ring A is quite flexible and studies on 2β and 4β alkyl substituted steroids (8) have shown that ring A in the compounds is distorted. A reasonable twist-boat conformation can be obtained[2] in which the internuclear distance between the CH_3 and the OH is at or greater than the sum of their respective van der Waal's radii. The net effect of such a distortion is to remove one 1,3 CH_3 – hydrogen interaction and to slightly alleviate another. Thus the rotation rate of the CH_3 group in these compounds would be less than that of the 17 ketone as the energy of the preferred conformation has been decreased whereas the energy of the transition state is only slightly affected. Evidence for this distortion is also observed in the chemical shift of C-6 for the 4α and 4β compounds. In the former, δ for C-6 is 20.4 p.p.m. whereas in the latter it is 25.4 p.p.m., both of which are shielded relative to the unsubstituted value of 28.4 p.p.m. Thus a significant variation of T_1 as a result of conformational change has been observed.

The various cholestane derivatives exhibit similar behavior to that of the androstane derivative. For *cis*-cholestanol, τ_G for C-19 is longer than in the *trans*-compound as the CH_3 group is now axial to one ring and equatorial to the other thus decreasing the number of 1,3 diaxial interactions. As expected, the values of τ_G calculated for cholesterol and androst-5-ene agree within experimental error even though the effective correlation times of the ring carbons are significantly different and one compound exhibits evidence for anisotropic motion whereas the other does not.

The effect of solvent can be seen from the values quoted for cholesterol and androstan-4-one in CCl_4 and $CDCl_3$. For the former a large difference is observed whereas for the latter, T_1 is independent of solvent within experimental error. In both cases the difference in viscosity is similar to the viscosity difference between the two pure solvents. Combining eq. 1 and 2 for a specific carbon gives T_1 in terms of the macroviscosity η as shown in eq. 5 and thus, provided *a*

$$[5] \qquad \frac{1}{T_1} = \frac{K\eta a^3}{T}$$

is constant, $1/T_1$ at constant temperature should be proportional to the viscosity. That this is not the case is evident as cholesterol exhibits a difference in T_1 which is larger than the difference in viscosities whereas for 4-androstanone the difference is negligible. Also the values for cholesterol are approximately half of that recorded for cholesteryl chloride (2) in the same solvent. A portion but not all of this difference

[2]We wish to thank Professor Hart for helpful discussion in this area.

is due to a difference in temperature, 30 °C compared to 42 °C. It has been shown (9) for 1-decanol that the motion of the CH_2 attached to the OH is restricted relative to the CH_2 attached to the CH_3 group because of the interaction between the OH group and CCl_4. In the steroid, a similar effect is present and the variation is explicable qualitatively by consideration of solvation of the functional group as CCl_4 can form H bonds with the OH group but not with a keto nor a chloro group whereas $CDCl_3$ can form hydrogen bonds with both hydroxyl and carbonyl groups. This demonstrates that for n.m.r. relaxation data we are concerned with microviscosity rather than macroviscosity as determined by normal viscosity measurements.

It is apparent from this work that T_1 data can be a useful aid in structural and conformational analysis. Evidence for anisotropic motion has been presented but, provided the preferred axis of rotation is not close to coincidence with the C—H bond vector of the proton causing relaxation, values of an effective molecular correlation time and hence the internal reorientation time for the CH_3 groups can be calculated. The value of τ_i depends on the number of 1,3 diaxial CH_3 group – H interactions. Thus τ_i will depend on the configuration of the CH_3 group as seen from the difference for C-19 between *trans*- and *cis*-cholestanol with the τ_i value for an equatorial CH_3 being longer than that in *cis*-cholestanol. The CH_3 group C-19 has more 1,3 diaxial interactions than C-18 and thus its τ_i is shorter than τ_i (C-18) in androstane. A ketone group in the molecule will affect the T_1 value observed if it removes one β axial proton and thus we can distinguish, for example, between the 2-keto and 3-keto compound but not between the 2- and 4-ketones from τ_i for C-19. From a conformational standpoint, the effect on C-19 of β hydroxyls at C-2 and C-4 illustrates the possibility of use of T_1 data for conformational analysis as in these compounds where ring A is distorted, a significant effect on T_1 was observed.

Experimental

All steroids used in this study were available in the laboratory. The T_1 values were recorded on 0.8–1.0 *M* solutions, generally at 35 °C. In all cases 1 ml of solution in 10 mm tubes was used. Approximate viscosities were measured using standard techniques.

The equipment consisted of a Bruker HX-90 spectrometer operating in the single coil mode and a Nicolet 1083 computer. A 90° pulse corresponded to a pulse width of 20 μs and thus sweep widths up to 4000 Hz could be used. In order to check the values obtained when using a 4 kHz sweep width, the T_1 values were determined with the pulse at both the high and low frequency ends of the spectrum. The values for all carbons were independent of which end of the spectrum the pulse was placed. Normally, spectral widths of 2000 or 2500 Hz were used. The T_1 values were obtained from the standard (180–τ–90–$5T_1$) pulse sequence (1) using at least 10 τ values for the CH_2 carbons and 14–20 τ values for CH and CH_3 carbons. A least-squares plot of ln $(M_\infty - M_z)$ *vs.* τ was used to obtain the values of T_1. The values in the tables are quoted to ±10% even though the standard deviation from the least squares plot is of the order of 2%. This difference is added in order to account for errors in M_∞ (generally three to six values recorded), long term drift and errors that result when two peaks of unequal T_1 are close together.

We gratefully acknowledge generous financial assistance from the National Research Council of Canada.

1. G. C. LEVY, J. D. CARGIOLI, and F. A. L. ANET. J. Am. Chem. Soc. **95**, 1528 (1973).
2. A. ALLERHAND, D. DODDRELL, and R. KOMOROSKI. J. Chem. Phys. **55**, 189 (1971).
3. G. C. LEVY. Acc. Chem. Res. **6**, 161 (1973).
4. K. NAKANISHI, V. P. GULLO, I. MIURA, T. GOVINDACHARI, and N. VISAWANATHAN. J. Am. Chem. Soc. **95**, 6473 (1973).
5. R. FREEMAN, H. D. W. HILL, and R. KAPTAIN. J. Magn. Res. **7**, 82 (1972).
6. D. M. GRANT, R. J. PUGMIRE, E. P. BLACK, and K. A. CHRISTENSEN. J. Am. Chem. Soc. **95**, 8465 (1973).
7. D. E. WOESSNER, B. S. SNOWDEN, and G. H. MEYER. J. Chem. Phys. **50**, 719 (1969).
8. C. DJERASSI, O. HALPERN, V. HALPERN, and B. RINIKER. J. Am. Chem. Soc. **80**, 4001 (1958).
9. D. DODDRELL and A. ALLERHAND. J. Am. Chem. Soc. **93**, 1558 (1971).

Can. J. Chem. Downloaded from www.nrcresearchpress.com by 210.87.254.40 on 09/05/12
For personal use only.

6*H*-Dibenzo[*b*,*d*]pyrans. I. Synthesis

JOHN P. DEVLIN
Pharma Research Canada Ltd., Pointe Claire, Quebec H9R 1G8
Received August 28. 1974

JOHN P. DEVLIN. Can. J. Chem. **53**, 343 (1975).

The preparation of 2′,4′-dihydroxy- and 2′,6′-dihydroxybiphenyl-2-carboxylic acid lactones (**3** and **4**) is described. Grignard addition to or direct boron trifluoride etherate – sodium borohydride reduction of these lactones yields respectively these 6,6-substituted (*e.g.* **6**) or the 6,6-unsubstituted (**13***a*) 6*H*-dibenzo[*b*,*d*]pyrans. Evidence that the reductive route proceeds without ring cleavage is presented.

JOHN P. DEVLIN. Can. J. Chem. **53**, 343 (1975).

On décrit la synthèse des lactones des acides dihydroxy-2′,4′ et dihydroxy-2′,6′ biphenylcarboxylique-2. Par addition de Grignard ces lactones donnent des 6*H*-dibenzo[*b*,*d*]pyrans substitués en 6,6 (*e.g.* **6**). Par réduction avec le borohydrure de sodium – éthérate de fluorure de bore elles fournissent des 6*H*-dibenzo[*b*,*d*]pyrans non substitués en 6,6 (**13***a*). On présente la preuve que cette réduction procède sans ouverture du cycle.

Can. J. Chem. Downloaded from www.nrcresearchpress.com by 210.87.254.40 on 09/05/12
For personal use only.

We have investigated the effects of the inclusion of the 6*H*-dibenzo[*b*,*d*]pyran ring system in a variety of pharmacologically active molecules (1). The synthesis of the basic nucleus is herein reviewed and a novel preparation of the 6,6-unsubstituted members is described.

2′-Hydroxybiphenyl-2-carboxylic acid lactones were invariably the synthetic precursors to the compounds prepared in this study. In the earlier literature the copper-catalyzed condensation of the diazonium salt of an anthranilic acid and the appropriate phenol (2, 3) or of the corresponding phenyl anthranilate (4, 5) was frequently employed although the yields were generally very low. More recently the oxidative cyclization (6–10) of biphenyl-2-carboxylic acids and the decomposition of the corresponding peroxides (5, 8, 11–14) have been investigated. The intramolecular condensation of 2′-nitrobiphenyl-2-carboxylic acid **1** (15), the photoacylation of ethyl 2-biphenylyl carbonate **2** (16), and the Baeyer–Villiger oxidation of 9-fluorenones (17, 18) offer interesting and novel approaches.

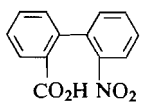

1

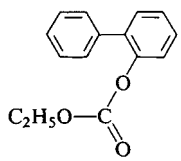

2

2′,4′Dihydroxybiphenyl-2-carboxylic acid lactones of the general formula **3** (R_3 = H) are most conveniently prepared by the condensation of the appropriate 2-bromobenzoic acid with resorcinol or a 2-substituted resorcinol in the manner described by Hurtley (19). Under these conditions no trace of the alternate condensation product **4** (R_3 = H) was found; however, when

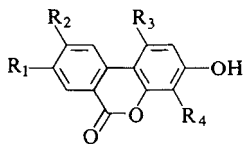

3

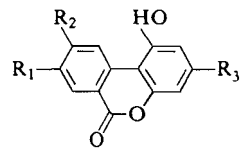

4

the condensation of 2-bromobenzoic acid was effected with 5-methyl- and with 5-methoxyresorcinol the isomers **4** (R_3 = CH_3 and R_3 = OCH_3) were also formed in yields of 0.4 and 12%, respectively, of the total crude products. The separation of these isomers was more conveniently accomplished by chromatography of the dimethyl derivatives, the preparation of which are described below. The lactones which have been prepared in this study are described in Table 1.

The reaction of 2′-hydroxybiphenyl-2-carboxylic acid lactones with excess methyl magnesium iodide and the thermal dehydration of the intermediary dimethyl carbinols (*e.g.* **5**) to 6,6-dimethyl-6*H*-dibenzo[*b*,*d*]pyrans (*e.g.* **6**) has been described (3, 20). We have applied this procedure to the preparation of the dimethyl derivatives which are described in Table 2, with the modification that the dimethyl carbinols (**5**) were

TABLE 1. 2′,4′-Dihydroxybiphenyl-2-carboxylic acid lactones

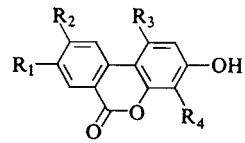

Compound	R_1	R_2	R_3	R_4	Yield (%)	Melting point (°C)	Found (%) C	Found (%) H	Calculated (%) C	Calculated (%) H
3a	H	H	H	H	61	234–236 (lit. (20) m.p. 232)	—	—	—	—
3b	Cl	H	H	H	55	298–302	63.22	3.09	63.30	2.86
3c	H	Cl	H	H	43	305–308	63.17	2.78	63.30	2.86
3d	F	H	H	H	47	270–275	67.95	2.99	67.82	3.06
3e	OCH_3	H	H	H	72	271–280	69.30	4.08	69.42	4.16
3f	H	H	H	OCH_3	36	160–162	69.61	4.36	69.42	4.16
3g	H	H	CH_3	H	30*	304–306 (lit. (22) m.p. 313)	—	—	—	—
3h	H	H	OCH_3	H	29*	290–294	69.25	4.18	69.42	4.16

*A second isomer is also formed; see text.

TABLE 2. 3-Hydroxy-6,6-dimethyl-6H-dibenzo[*b*,*d*]pyrans

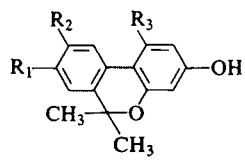

Compound	R_1	R_2	R_3	Yield (%)	Melting point (°C)	Found (%) C	Found (%) H	Calculated (%) C	Calculated (%) H
6a	H	H	H	66	130–132 (lit. (22) m.p. 128)	—	—	—	—
6b	Cl	H	H	77	91– 93	69.00	5.21	69.10	5.03
6c	H	Cl	H	40	151–153	69.17	5.49	69.10	5.03
6d	F	H	H	85	132–136	73.91	5.49	73.75	5.36
6e	OCH_3	H	H	64	115–116	74.96	6.21	74.98	6.29
7	H	H	CH_3	63	144–145 (lit. (22) m.p. 144)	—	—	—	—
9	H	H	OCH_3	70	146–148	75.20	6.29	74.98	6.29

dehydrated by brief treatment at room temperature with boron trifluoride in benzene.

The separation of the dimethyl derivatives (**7** and **8**) of the two isomers obtained from the condensation of 2-bromobenzoic acid and orcinol, as indicated above, was effected by chromatography of the crude reaction product. The constitution of **7** is well established (20) and therefore the identity of **8** was obvious. The n.m.r. spectra ($CDCl_3$) of these two isomers (Table 3) were distinct. The anisotropic effect of the hydroxyl at C-1 in compound **8** produced a downfield shift ($\Delta\delta$ 0.77) of the C-10 proton over that observed for compound **7**. Similarly, the methyl protons at C-1 in compound **7** were deshielded by the neighboring aromatic ring and were found at δ 2.57 whereas the methyl protons in compound **8** occurred at δ 2.25. These n.m.r. variations were particularly useful for the identification of compounds **9** and **10** as described below.

The isomers **9** and **10** obtained by the methylation of the lactone mixture from the condensation of 2-bromobenzoic acid and 5-methoxyresorcinol, were separated by chromatography and identified by a comparison of their n.m.r. spectra ($CDCl_3$). As would be anticipated, the difference between the chemical shifts of the C-10

Can. J. Chem. Downloaded from www.nrcresearchpress.com by 210.87.254.40 on 09/05/12
For personal use only.

TABLE 3. Chemical shifts (δ) of compounds **7** to **10** ($CDCl_3$)

Compound	$(CH_3)_2C$	X—CH_3	Protons at C-2 + C-4	Protons at C-10
7	1.58(s)	2.57(s)	6.37(s)	7.63(m)
8	1.60(s)	2.25(s)	6.27(d)*, 6.43(d)*	8.40(m)
9	1.60(s)	3.83(s)	6.15(s)	8.31(m)
10	1.62(s)	3.68(s)	6.02(d)†, 6.22(d)†	8.37(m)

*J = 1 Hz.
†J = 2.5 Hz.

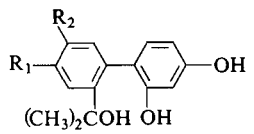

5

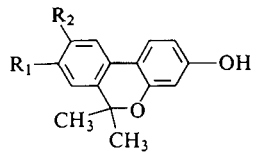

6

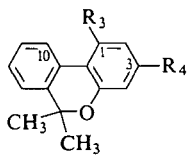

7 $R_3 = CH_3$; $R_4 = OH$
8 $R_3 = OH$; $R_4 = CH_3$
9 $R_3 = OCH_3$; $R_4 = OH$
10 $R_3 = OH$; $R_4 = OCH_3$

proton of **9** and that of **10** was not as pronounced as in the foregoing examples. Nevertheless, a slight difference (Δδ 0.06) did occur (see Table 3) and the assignments which were made received support from the downfield shift (Δδ 0.15) of the methoxyl protons at C-1 (**9**) over that at C-3 (**10**). The latter effect parallels that observed for the dimethyl ether of *N*-acetylapocrotonosine (21). Further evidence for these assignments was provided by a comparison of the n.m.r. spectra (CD_3SOCD_3) of compound **9** with that of the precursor, **11***a* (see Table 4). Molecular models demonstrate that in this substance the bulky dimethylcarbinol (at C-2), the methoxy (at C-6′), and the hydroxy (at C-2′) groupings maintain rings A and B almost perpendicular to each other and permit shielding of the methoxy- and the dimethylcarbinol protons by rings A and B, respectively. If the structural assignments of compounds **9** and **10** were reversed then the precursor to **9** would have the constitution **11***b* and the shielding effect on the methoxyl would not be observed. The n.m.r. spectrum of the dimethyl ether (**11***c*) supported this observation in that the protons of both shielded methoxyls resonated at δ 3.61 (compare **11***a*) while the protons of the methoxyl at C-4′ were found at δ 3.83.

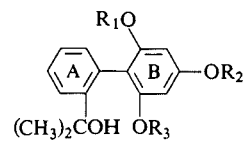

11

a $R_1 = CH_3$; $R_2 = R_3 = H$
b $R_2 = CH_3$; $R_1 = R_3 = H$
c $R_1 = R_2 = R_3 = CH_3$

The lithium aluminum hydride reduction of **12***a* to **14***a* has been described (22). Substitution of the benzylic hydroxyl with bromine via

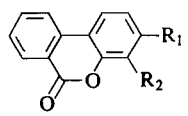

12

a $R_1 = R_2 = H$
b $R_1 = OH$; $R_2 = H$
c $R_1 = OH$; $R_2 = OCH_3$
d $R_1 = NO_2$; $R_2 = H$

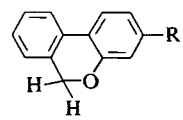

13

a $R_1 = R_2 = H$
b $R_1 = OH$; $R_2 = H$
c $R_1 = OH$; $R_2 = OCH_3$
d $R_1 = NO_2$; $R_2 = H$

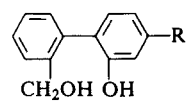

14

a R = H
b R = OH

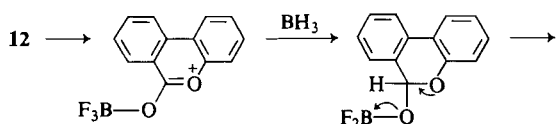

15 **16**

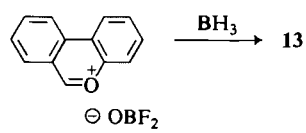

17

Can. J. Chem. Downloaded from www.nrcresearchpress.com by 210.87.254.40 on 09/05/12
For personal use only.

TABLE 4. Chemical shifts (δ) of compounds **9** to **11** (CD_3SOCD_3)

Compound	$(CH_2)_2C$	OCH_3	Protons at C-2 + C-4	Protons at C-10
9	1.56(s)	3.88(s)	6.07(d),* 6.26(d)*	8.28(m)
10	1.57(s)	3.77(s)	6.03(d),* 6.20(d)*	8.53(m)
			C-3′ + C-5′	C-3
11*a*	1.20(s), 1.25(s)	3.54(s)	5.96(d),† 6.06(d)†	7.85(m)
11*c*	1.15(s)	3.61(s,6H), 3.83(s,3H)	6.30(s)	7.87(m)

*J = 2.5 Hz.
†J = 2.0 Hz.

hydrogen bromide, followed by dehydrohalogenation yielded 6*H*-dibenzo[*b*,*d*]pyran (**13***a*). For our purposes a direct reductive route (**12** → **13**) was certainly more attractive, and to this end we investigated the utilization of the sodium borohydride – boron trifluoride combination which had been developed by Petitt and co-workers (23–26). This reagent has been shown (23, 24) to effectively reduce aliphatic esters and lactones to the corresponding ethers; however, when either the alcohol or acid moiety was aromatic, ethers were not formed and only the corresponding alcohols were obtained (25, 26). Nevertheless, we have applied this technique to the reduction of the 2′-hydroxybiphenyl-2-carboxylic acid lactones (**12***a–d*) and have obtained only the corresponding 6*H*-dibenzo[*b*,*d*]pyrans (**13***a–d*) in high yield. It may be considered that reduction initially occurs to the phenolic alcohol **14** with subsequent dehydration to the ether by boron trifluoride; a dehydration possibly encouraged by the close proximity of the interacting groups. In order to determine whether this 'two step' mechanism was involved, compound **14***b* was prepared by lithium aluminum hydride reduction of **12***b* and treated with boron trifluoride etherate in tetrahydrofuran under the same reaction conditions employed in the reduction procedure. No significant amount of compound **13***b* was detected. When **14***b* was heated at 250°, however, dehydration did occur and **13***b* was obtained in a moderate yield.

The foregoing evidence supports a reductive mechanism not involving ring cleavage. The sequence (12 → 15 → 16 → 17 → 13) may be considered as a likely pathway and is analogous to that which has been suggested (24) for the mechanism involved in the boron trifluoride – sodium borohydride reduction of aliphatic esters. The inherent stability of the oxonium ions **15** and **17** provides a logical explanation for the absence of ring cleavage products.

Experimental

Melting points were determined on a Reichert Kofler Micro Heating Stage and are uncorrected. Ultraviolet spectra were recorded in ethanol solution on a Bausch and Lomb Spectronic 505 and i.r. spectra on a Perkin Elmer 237B spectrophotometer. Nuclear magnetic resonance spectra were taken on a Varian T-60 spectrometer. Tetramethylsilane was used as an internal standard. Elemental analyses were determined at Microanalysis Laboratories Limited, Toronto.

2′4′-Dihydroxy-biphenyl-2-carboxylic Acid Lactones (3a–f)

The following procedure (19) was used in the preparation of compounds **3***a–f*, the physical properties of which are described in Table 1.

A solution of the appropriate 2-bromobenzoic acid (0.05 mol), resorcinol (0.1 mol), and sodium hydroxide (0.1 mol) in water (30 ml) was heated under reflux for 30 min. A 10% aqueous solution of copper sulfate (5 ml) was then added whereupon a slightly exothermic reaction ensued. The resulting mixture was heated under reflux for an additional 10 min and then cooled to 20°. The insoluble product was collected, washed well with water and dried. This material was of sufficient purity to be used as such for the preparations of the 6*H*-dibenzo[*b*,*d*]pyrans which are described below. Analytical samples were recrystallized to constant melting point (Table 1).

2′,4′-Dihydroxy-6′methylbiphenyl-2-carboxylic Acid Lactone (3g)

This compound was prepared by the copper-catalyzed condensation of 2-bromobenzoic acid (44.3 g, 0.22 mol) and orcinol (50.2 g, 0.40 mol) in aqueous 1.5 *N* sodium hydroxide solution (270 ml) in the general manner described above, with the exception that the reaction mixture was heated under reflux for 1 h following the addition of the copper sulfate solution. The crude product (16.7 g, 34%) was recrystallized from glacial acetic acid to provide **3***g* (14.7 g, 30%; see Table 1).

2′,4′-Dihydroxy-6-methoxybiphenyl-2-carboxylic Acid Lactone (3h)

This compound was prepared by the copper-catalyzed condensation of 2-bromobenzoic acid (22.1 g, 0.11 mol) and 5-methoxyresorcinol (25 g, 0.21 mol) in aqueous 1 *N*

Can. J. Chem. Downloaded from www.nrcresearchpress.com by 210.87.254.40 on 09/05/12
For personal use only.

Can. J. Chem. Downloaded from www.nrcresearchpress.com by 210.87.254.40 on 09/05/12
For personal use only.

sodium hydroxide solution (220 ml) in the general manner described above, with the exception that the reaction mixture was heated under reflux for 30 min following the addition of the copper sulfate solution. The crude product (15 g, 56%) was crystallized from methanol and from acetonitrile to provide **3*h*** (7.7 g, 29%; see Table 1).

3-Hydroxy-6,6-dimethyl-6H-dibenzo[b,d]pyrans

The following procedure was used in the preparation of all compounds listed in Table 2.

A suspension of the appropriate 2′,4′-dihydroxybiphenyl-2-carboxylic acid lactone (0.15 mol) in benzene (750 ml) was added over 15 min to a solution of methyl magnesium iodide prepared from magnesium turnings (24.3 g, 1 mol) and methyl iodide (130 g, 0.9 mol) in ether (400 ml). The ether was removed by distillation and the resulting mixture was heated under reflux for 3 h. The reaction mixture was cooled and poured into a mixture of concentrated sulfuric acid (40 ml) and ice (600 g) with vigorous stirring. The insoluble solid was collected and dried. The benzene phase was removed, dried over sodium sulfate, and evaporated. The residue was combined with the foregoing insoluble solid and the resulting mixture was suspended in benzene (300 ml). Boron trifluoride was bubbled in at a moderate rate at room temperature until a uniform solution was formed (15 min to 1 h). The reaction mixture was then poured into 2 *N* sodium hydroxide solution (300 ml) with vigorous stirring. The benzene was removed, and the aqueous phase was neutralized with 2 *N* hydrochloric acid and extracted with ether (3 × 100 ml). The ether extracts were combined with the benzene phase, dried over sodium sulfate, and evaporated. The crude product so obtained was crystallized to constant melting point (see Table 2).

*1-Hydroxy-3,6,6-trimethyl-6H-dibenzo[b,d]pyran (**8**) and 3-Hydroxy-1,6,6-trimethyl-6H-dibenzo[b,d]pyran (7)*

2-Bromobenzoic acid (88.4 g, 0.44 mol) was condensed with orcinol (99.2 g, 0.80 mol) in the manner described above for **3*g***. The crude product (29.5 g) was not purified further but was reacted in the general manner, described above, with excess methyl magnesium iodide, prepared from magnesium (24.3 g) and methyl iodide (130 g) in ether (220 ml). The crude product was similarly dehydrated with boron trifluoride and then twice chromatographed on silica (chloroform). Compound **8** (70 mg, 0.07% overall) was thereby obtained as a beige solid (m.p. 160–163°) which on sublimation (120°/0.05 mm) yielded colorless prisms, m.p. 162–165°; λ_{max} 275 (sh, log ε 4.19), 282 nm (log ε 4.21); n.m.r.: see text.

Anal. Calcd. for $C_{16}H_{16}O_2$: C, 79.97; H, 6.71. Found: C, 79.64; H, 6.82.

Later column fractions provided compound 7 (15.9 g, 15.1% overall; see also Table 2) m.p. 143–144° (lit. (22) m.p. 144°); λ_{max} 272 nm (sh log ε 4.10), 276 (log ε 4.13), 305 nm (log ε 3.98); n.m.r.: see text.

*1-Hydroxy-3-methoxy-6,6-dimethyl-6H-dibenzo[b,d]-pyran (**10**) and 3-Hydroxy-1-methoxy-6,6-dimethyl-6H-di-benzo[b,d]pyran (**9**)*

2-Bromobenzoic acid (8.4 g, 0.042 mol) was condensed with 5-methoxyresorcinol (9.5 g, 0.08 mol) in the manner described above for **3*h***. The crude product (5.8 g, 60%) was not purified further but was reacted, in the general manner described above, with excess methyl magnesium iodide prepared from magnesium (3.5 g) and methyl iodide (18 g) in ether (30 ml). The crude intermediate was similarly dehydrated with boron trifluoride and then chromatographed on silica (chloroform). Compound **10** (410 mg, 3.8% overall) was thereby obtained as a pale yellow oil which on further purification by short path distillation (200°/0.3 mm) and crystallization from toluene–hexane provided colorless prisms, m.p. 124–125°; λ_{max} 287 (log ε 4.21), 302 nm (sh, log ε 4.08); n.m.r.: see text.

Anal. Calcd. for $C_{16}H_{16}O_3$: C, 74.98; H, 6.29. Found: C, 75.00; H, 6.42.

Later column fractions provided compound **9** (3.1 g, 29% overall; see also Table 2), which on recrystallization from toluene yielded colorless prisms, m.p. 146–148°; λ_{max} 288 (log ε 4.21), 303 nm (sh, log ε 4.07); n.m.r.: see text.

*2-(1-Hydroxyisopropyl)-2′,4′-dihydroxy-6′methoxybi-phenyl (**11*a*)***

A suspension of **3*h*** (35 g, 0.145 mol) in benzene (400 ml) was added over 15 min to a solution of methyl magnesium iodide prepared from magnesium (18 g, 0.74 mol) and methyl iodide (100 g, 0.7 mol) in ether (100 ml) and heated under reflux for 4 h. The reaction mixture was cooled then poured into 1 *M* KH_2PO_4 (1000 ml) containing ice (500 g). The benzene–ether layer was removed, dried over sodium sulfate, and applied directly to a short column (15 cm × 15 cm) of silica gel (1 kg) and eluted with ether. Earlier fractions provided **9** (12.8 g, 35%) followed by the title compound (**11*a***, 5.8 g, 15%). Recrystallization from ether–hexane provided colorless needles, m.p. 99–110° (dec.); n.m.r.: see text.

Anal. Calcd.[1] for $C_{16}H_{18}O_4 \cdot \frac{1}{2}(C_2H_5)_2O$: C, 69.43; H, 7.45. Found: C, 69.92; H, 7.38.

*2-(1-Hydroxyisopropyl)-2′,4′,6′-trimethoxybiphenyl (**11*c*)***

A solution of **11*a*** (1.8 g, 0.0066 mol) in dimethyl sulfoxide (35 ml) was treated with methyl iodide (12 g, 0.084 mol) and powdered anhydrous potassium carbonate (12 g, 0.087 mol). The mixture was stirred at room temperature for 24 h and then diluted with water (100 ml). The crude product was extracted with ether (2 × 50 ml) and the combined extracts washed with water (3 × 20 ml), dried over sodium sulfate and evaporated. The residue upon chromatography (chloroform–silica) provided the title compound (**11*c***, 0.51 g, 26%) as a white solid. Recrystallization from hexane – carbon tetrachloride yielded colorless prisms, m.p. 119–121°; n.m.r.: see text.

Anal. Calcd. for $C_{18}H_{22}O_4$: C, 71.50; H, 7.53. Found: C, 71.82; H, 7.40.

*6H-Dibenzo[b,d]pyran (**13*a*)***

A cooled solution of 2′-hydroxybiphenyl-2-carboxylic acid lactone (37.3 g, 0.19 mol) in a mixture of boron trifluoride etherate (500 ml) and tetrahydrofuran (1 l) was added over 15 min to a suspension of sodium borohydride (25 g, 0.66 mol) in tetrahydrofuran (500 ml) under dry nitrogen while maintaining the reaction temperature below 10°. The reaction mixture was then raised within 30 min to the reflux temperature, kept under reflux for 1 h, and then cooled to −3°. Ice cold aqueous 2 *N* hydro-

[1]The presence of ½ mol of ether was confirmed in the n.m.r. spectrum of this substance. It was not expelled by drying at room temperature for 48 h; higher temperatures dehydrated **11*a*** to **9**.

Can. J. Chem. Downloaded from www.nrcresearchpress.com by 210.87.254.40 on 09/05/12
For personal use only.

chloric acid (800 ml) was then cautiously added and the temperature was allowed to increase to 25°. Water (4000 ml) was added and the reaction mixture was extracted with chloroform (3 × 500 ml). The combined extracts were evaporated and the oily residue was heated at 80° with aqueous 2 *N* sodium hydroxide solution (800 ml) for 20 min. The resulting mixture was cooled and extracted with ether (4 × 100 ml). The ether extracts were combined, dried over sodium sulfate, and evaporated. The resulting violet oil (33.6 g) was distilled to provide the title compound (29.1 g, 84%) as a clear colorless oil, b.p. 122–123°/0.2 mm (lit. (21) b.p. 108–110°/0.2 mm); λ_{max} 263 (log ε 4.12), 270 (log ε 4.13), 291 (sh, log ε 3.66), and 310 nm (log ε 3.85); n.m.r. ($CDCl_3$): δ 5.07 (s, 2H, $-CH_2O-$).

Anal. Calcd. for $C_{13}H_{10}O$: C, 85.69; H, 5.53. Found: C, 85.54; H, 5.32.

*3-Hydroxy-6H-dibenzo[b,d]pyran (**13b**)*

This substance was prepared in a manner analogous to that described above for compound **13***a* with the following modification. The crude product dissolved on treatment with hot aqueous 2 *N* sodium hydroxide solution. The ether extracts were discarded and the free phenol was precipitated with 4 *N* hydrochloric acid, dried, and recrystallized from carbon tetrachloride to provide the title compound as colorless needles (88%), m.p. 108–110°; λ_{max} 280 (log ε 4.08), 297 (sh, log ε 3.98), and 319 nm (log ε 4.01); n.m.r. ($CDCl_3$): δ 5.02 (s, 2H, $-CH_2O-$).

Anal. Calcd. for $C_{13}H_{10}O_2$: C, 78.77; H, 5.09. Found: C, 79.15; H, 5.17.

*3-Hydroxy-4-methoxy-6H-dibenzo[b,d]pyran (**13c**)*

This substance was prepared in a manner analogous to that described for compound **13***b*. The crude product was recrystallized from ethanol and provided the title compound as colorless plates (70%), m.p. 143–145°; λ_{max} 282 (log ε 4.17), 308 nm (sh, log ε 3.85); n.m.r. (CD_3SOCD_3): δ 3.77 (s, 3H, $-OCH_3$), 5.13 (s, 2H, $-CH_2O-$).

Anal. Calcd. for $C_{14}H_{12}O_3$: C, 73.67; H, 5.30. Found: C, 73.48; H, 5.44.

*3-Nitro-6H-dibenzo[b,d]pyran (**13d**)*

This substance was prepared in a manner analogous to that described for compound **13***a*. The crude product was recrystallized from ethanol and provided the title compound as yellow needles (67%), m.p. 118–119°, λ_{max} 252 (log ε 3.82), 308 (log ε 3.91), and 354 nm (log ε 3.94); n.m.r.: (CD_3SOCD_3): δ 5.35 (s, 2H, $-CH_2O-$).

Anal. Calcd. for $C_{13}H_9NO_3$: C, 68.72; H, 3.99; N, 6.17. Found: C, 68.55; H, 3.95; N, 6.25.

*2-Hydroxymethyl-2′,4′-dihydroxybiphenyl (**14a**)*

A suspension of **5***a* (2.1 g, 0.01 mol) in tetrahydrofuran (500 ml) was added over 5 min to a stirred solution of lithium aluminum hydride (1 g, 0.026 mol) in tetrahydrofuran (50 ml) at room temperature. The reaction mixture was heated under reflux for 1 h and then cooled to 10°. Ethyl acetate (50 ml) was cautiously added over 10 min followed by aqueous 6 *N* sodium hydroxide solution (75 ml). The tetrahydrofuran – ethyl acetate phase was removed and discarded. The aqueous alkaline solution was cooled by the addition of ice (100 g), acidified with 4 *N* hydrochloric acid, and extracted with ether (2 × 100 ml). The ether extracts were combined and evaporated. The residual oil upon crystallization from water provided **14***a* (1.4 g, 65%) as a beige solid, m.p. 136°. One recrystallization from benzene yielded colorless needles, m.p. 138–139°; n.m.r. (CD_3SOCD_3): δ 4.37 (s, 2H, $-CH_2OH$).

Anal. Calcd. for $C_{13}H_{12}O_3$: C, 72.21; H, 5.59. Found: C, 72.46; H, 5.50.

*Attempted BF_3 Dehydration of **14b***

A solution of **14***b* (800 mg) in a mixture of boron trifluoride etherate (15 ml) and tetrahydrofuran (60 ml) was heated under reflux for 90 min. The reaction mixture was cooled and aqueous 2 *N* hydrochloric acid (15 ml) was added followed by water (80 ml). The resulting mixture was extracted with chloroform (3 × 50 ml). The extracts were combined and evaporated and the residue was heated at 80° with aqueous 2 *N* sodium hydroxide solution (15 ml) for 20 min. The red solution was extracted with ether (2 × 20 ml). The ether extracts were discarded and the aqueous phase was acidified with 4 *N* hydrochloric acid and extracted with ether (3 × 50 ml). This extract was dried over sodium sulfate and evaporated. The residue was crystallized from water to provide **14***b* (450 mg, 56% recovery) as a beige crystalline solid, m.p. 136°, identical in all respects with the starting material. The mother liquor was examined by t.l.c. (silica gel, 10% methanol–chloroform) but failed to indicate any trace of compound **13***b*.

*Thermal Dehydration of **14b***

A test tube containing compound **14***b* (400 mg) was immersed in an oil bath preheated to 250° and maintained at this temperature for 30 min. The melt, so obtained, was cooled, dissolved in ether (10 ml), filtered, and evaporated. The residue was dissolved in methanol (2 ml) and water (8 ml) and extracted with hot carbon tetrachloride (4 × 5 ml). The extracts were combined, dried over magnesium sulfate, and evaporated. The residue was triturated with cold carbon tetrachloride and the insoluble solid (180 mg, 49%) was collected, dried, and identified as compound **13***b*, m.p. 102–106°, by t.l.c. and spectral comparisons.

The author gratefully acknowledges the technical assistance of Mrs. I. Guse and Mr. U. Rothenbühler.

1. J. P. Devlin, K. R. Freter, and P. B. Stewart. 167th American Chemical Society National Meeting, Los Angeles, 1974. Abstr. No. MEDI-43; P. B. Stewart, J. P. Devlin and K. R. Freter. Federation Proc. **33**, 762 (1974).
2. W. Borsche. Ann. **312**, 225 (1900).
3. R. S. Cahn. J. Chem. Soc. 1400 (1933).
4. H. L. Rule and E. Bretscher. J. Chem. Soc. 925 (1927).
5. R. A. Heacock and D. H. Hey. J. Chem. Soc. 2481 (1954).
6. G. W. Kenner, M. A. Murray, and C. M. B. Taylor. Tetrahedron, **1**, 259 (1957).
7. W. R. Moore and H. Arzoumanian. J. Org. Chem. **27**, 4667 (1962).
8. D. I. Davies and C. Waring. J. Chem. Soc. (C), 1639 (1967).
9. P. M. Brown, J. Russell, R. H. Thomson, and A. G. Wylie. J. Chem. Soc. (C), 842 (1968).

10. D. J. CHALMERS and R. H. THOMSON. J. Chem. Soc. (C), 848 (1968).
11. D. B. DENNEY and P. P. KLEMCHUCK. J. Am. Chem. Soc. **80**, 3289 (1958).
12. F. D. GREENE, G. R. VAN NORMAN, J. C. CANTRILL, and R. D. GILLIOM. J. Org. Chem. **25**, 1790 (1960).
13. D. F. DETAR and CHIN-CHIUN CHU. J. Am. Chem. Soc. **82**, 4969 (1960).
14. J. K. KOCHI and R. D. GILLIOM. J. Am. Chem. Soc. **86**, 5251 (1964).
15. D. H. HEY, J. A. LEONARD, and C. W. REES. J. Chem. Soc. 4579 (1962).
16. N. C. YANG, A. SHANI, and G. R. LENZ. J. Am. Chem. Soc. **88**, 5369 (1966).
17. A GRINGAUZ and E. TASK. Org. Prep. Proc. (New York), **2**, 185 (1970).
18. W. v. E. DOERING and L. SPEERS. J. Am. Chem. Soc. **72**, 5515 (1950).
19. W. R. H. HURTLEY. J. Chem. Soc. 1870 (1929).
20. R. ADAMS, D. C. PEASE, J. H. CLARK, and B. R. BAKER. J. Am. Chem. Soc. **62**, 2197 (1940).
21. L. J. HAYNES and K. L. STUART. J. Chem. Soc. 1789 (1963).
22. Y. INUBUSHI. J. Pharm. Soc. Jap. **72**, 656 (1952); Chem. Abstr. **47**, 2173e (1953).
23. G. R. PETTIT, U. R. GHATAK, B. GREEN, T. R. KASTURI, and D. M. PIATAK. J. Org. Chem. **26**, 1685 (1961).
24. G. R. PETTIT and T. R. KASTURI. J. Org. Chem. **26**, 4557 (1961).
25. G. R. PETTIT and D. M. PIATAK. J. Org. Chem. **27**, 2127 (1962).
26. G. R. PETTIT, B. GREEN, G. L. DUNN, P. HOFER, and W. J. EVERS. Can. J. Chem. **44**, 1283 (1966).

Can. J. Chem. Downloaded from www.nrcresearchpress.com by 210.87.254.40 on 09/05/12
For personal use only.

6*H*-Dibenzo[*b*,*d*]pyrans. II. Boron Trifluoride Catalyzed Acylation of Hydroxy-6*H*-dibenzo[*b*,*d*]pyrans

JOHN P. DEVLIN
Pharma Research Canada Ltd., Pointe Claire, Quebec H9R 1G8

Received August 28, 1974

JOHN P. DEVLIN. Can. J. Chem. **53**, 350 (1975).

The Friedel–Crafts acetylation of 3-hydroxy-6*H*-dibenzo[*b*,*d*]pyrans (**1**) with acetic acid in the presence of boron trifluoride is described. Representatives unsubstituted at C-1 acylate exclusively at C-2. A methyl or methoxyl substituent at C-1 directs acylation to the C-4 position. The identities of the individual isomers are established primarily on the basis of n.m.r. spectral interpretations.

JOHN P. DEVLIN. Can. J. Chem. **53**, 350 (1975).

On décrit l'acylation selon Friedel–Crafts des hydroxy-3 6*H*-dibenzo[*b*,*d*]pyrans par l'acide acétique en présence de trifluorure de bore. Pour les composés non substitués en C-1, l'acylation se fait exclusivement en C-2. Un substituant méthyle ou méthoxy en C-1 dirige l'acylation en C-4. Il est possible d'identifier les différents isomères principalement au moyen de leur spectre r.m.n.

We have investigated the pharmacological effects of the inclusion of the 6*H*-dibenzo[*b*,*d*]-pyran ring system in a variety of biologically active molecules.

The *o*-acetyl derivatives of hydroxy-6*H*-dibenzo[*b*,*d*]pyrans were of particular interest in relation to our investigations of the anti-allergic activities of benzopyranobenzopyran carboxylic acids (*e.g.* PR-D-92, **2**) (2). Unfortunately, the reactions of dibenzo[*b*,*d*]pyrans have received scant attention in the literature and no reports were available in relation to the introduction and orientation of acyl groups in the monohydroxy representatives (*e.g.* **1** and **7**). We have investigated the Friedel–Crafts acylation of these compounds and have found the method of choice to be that of direct condensation with the appropriate acid in the presence of boron trifluoride (3–5). This preparative route was preferred on the basis of the convenience of the reaction, the ease of work-up and the high yields obtained. The use of aluminum trichloride was discouraged by the facile rearrangement of C-1 unsubstituted 6,6-dimethyldibenzo[*b*,*d*]pyrans in the presence of this Lewis acid to the corresponding 4-hydroxy-9,9-dimethylfluorene. This rearrangement, which is herein represented by the conversion of **3** to **4**, will be described in greater detail in a forthcoming paper.

3-Hydroxy-6*H*-dibenzo[*b*,*d*]pyrans without substitution at C-1 (**1**) rapidly condensed at room temperature with acetic acid in benzene solution in the presence of boron trifluoride and provided exclusively the 2-acetyl derivatives (**5**) in high yields (Table 1). In one instance (**1***c*) an increase in the reaction temperature resulted in the formation of a small amount of the 4-acetyl derivative (**6**) although the overall yield of monoacetylated product was reduced. The individual identities of these isomers were established by n.m.r. spectroscopy. In **5***c* the C-1 and C-4 protons, in $CDCl_3$ solution, occur as sharp singlets at δ 8.01 and 6.47, respectively, whereas in **6** the C-1 and C-2 protons are observed as **a** pair of doublets (J = 9 Hz) centered at δ 7.76 and 6.64, respectively.

3-Hydroxy-6*H*-benzo[*b*,*d*]pyrans with substitution at C-1 (**7**) behave somewhat differently than the unsubstituted series. The 1-methyl representative (**7**, R = CH_3) under the acetylation conditions described above yielded both isomers **8** and **9** in yields of 34 and 17%, respectively. The individual structural assignments in this instance are based primarily upon the deshielding effect of the acetyl carbonyl on the chemical shift of the C-1 methyl protons in isomer **8** (δ 2.82) relative to that in **9** (δ 2.56). This shift (Δδ 0.26) parallels that observed (Δδ 0.24) for the methyl protons in the n.m.r. spectra (6) of *o*-tolualdehyde (δ 2.65) and *p*-tolualdehyde (δ 2.41).

The main product from the boron trifluoride catalyzed acetylation of 1-methoxy-3-hydroxy-6,6-dimethyl-6*H*-dibenzo[*b*,*d*]pyran (**7**, R = OCH_3) was identified by n.m.r. spectroscopy as a monoacetyl derivative having the constitu-

Can. J. Chem. Downloaded from www.nrcresearchpress.com by 210.87.254.105 on 09/05/12
For personal use only.

Can. J. Chem. Downloaded from www.nrcresearchpress.com by 210.87.254.105 on 09/05/12
For personal use only.

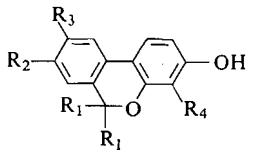

1

a $R_1 = R_2 = R_3 = R_4 = H$
b $R_1 = R_2 = R_3 = H; R_4 = OCH_3$
c $R_1 = CH_3; R_2 = R_3 = R_4 = H$
d $R_1 = CH_3; R_2 = OCH_3; R_3 = R_4 = H$
e $R_1 = CH_3; R_2 = Cl; R_3 = R_4 = H$
f $R_1 = CH_3; R_2 = R_4 = H; R_3 = Cl$
g $R_1 = CH_3; R_2 = F; R_3 = R_4 = H$

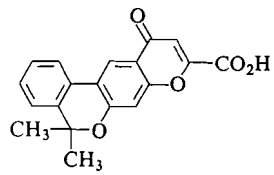

2

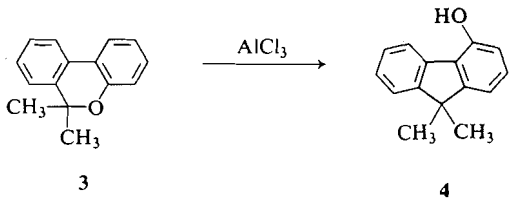

3 4

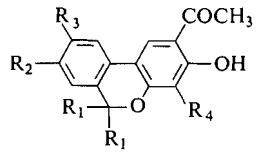

5

a $R_1 = R_2 = R_3 = R_4 = H$
b $R_1 = R_2 = R_3 = H; R_4 = OCH_3$
c $R_1 = CH_3; R_2 = R_3 = R_4 = H$
d $R_1 = CH_3; R_2 = OCH_3; R_3 = R_4 = H$
e $R_1 = CH_3; R_2 = Cl; R_3 = R_4 = H$
f $R_1 = CH_3; R_2 = R_4 = H; R_3 = Cl$
g $R_1 = CH_3; R_2 = F; R_3 = R_4 = H$

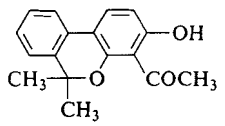

6

tion **10** or **11**. It was not possible to determine which assignment was correct by spectral methods and therefore the following proof of structure was devised. The acetylation of 1-hydroxy-3-methoxy-6,6-dimethyl-6*H*-dibenzo-

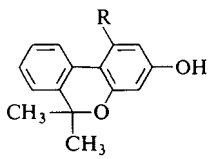

7

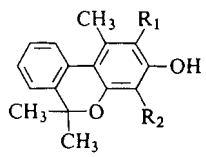

8 $R_1 = COCH_3; R_2 = H$
9 $R_1 = H; R_2 = COCH_3$

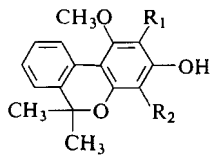

10 $R_1 = COCH_3; R_2 = H$
11 $R_1 = H; R_2 = COCH_3$

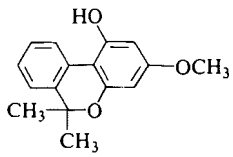

12

[*b*,*d*]pyran (**12**) (1) provided the 2-acetyl derivative (**13**). The identity of this product was established by the dark blue coloration with ferric chloride solution, the sharp low-field n.m.r. signal for the bound hydroxyl proton (δ 15.33) and finally by the facile conversion with diethyl oxalate to the tetracyclic carboxylic acid (**14**).

Methylation of **13** provided **15**. If the acetyl derivative of **7** (R = OCH_3) had the constitution **10**, methylation in the same manner should also provide **15**. This was not the case and the methylation product was, by elimination, assigned the constitution **16**. The monoacetyl derivative of **7** (R = OCH_3) were thereby identified as **11**. An attempt to demethylate **15** and **16** with hydriodic acid – acetic acid resulted in cleavage of the acetyl group as well, so that in both instances only the phenol, **17**, was obtained.

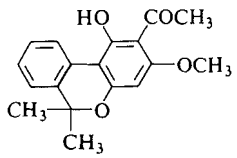

13

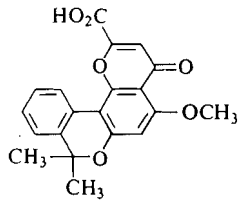

14

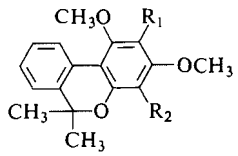

15 $R_1 = COCH_3; R_2 = H$
16 $R_1 = H; R_2 = COCH_3$

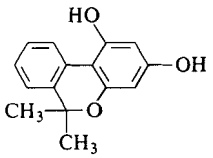

17

Can. J. Chem. Downloaded from www.nrcresearchpress.com by 210.87.254.105 on 09/05/12
For personal use only.

TABLE 1. 2-Acetyl-3-hydroxy-6*H*-dibenzo[*b*,*d*]pyrans (**5**)

Compound	Melting point (°C)	Yield (%)	Calculated (%)		Found (%)		Nuclear magnetic resonance chemical shifts (δ values in $CDCl_3$) protons at				
			C	H	C	H	C-1	C-4	C-10	$COCH_3$	OH
5*a*	131–132	77	74.99	5.03	74.57	5.27	7.95	6.47	7.57	2.57	12.50
5*b*	138–139	32	71.10	5.22	71.02	5.32	8.15*		7.95*	2.72*	12.60*
5*c*	108–109	73	76.10	6.01	76.16	6.16	8.01	6.47	7.60	2.57	12.66
5*d*	128–129	65	72.46	6.08	72.31	5.97	7.97	6.50	7.60	2.60	12.63
5*e*	205–206	73	67.44	4.99	67.00	4.75	8.05	6.52	7.62	2.65	12.62
5*f*	173–176	60	67.44	4.99	67.56	4.81	8.47*	6.40*	8.13*	2.75*	12.70*
5*g*	169–173	72	71.32	5.28	71.34	5.14	8.07	6.56	7.70	2.65	12.60

*In CD_3SOCD_3 solution.

Can. J. Chem. Downloaded from www.nrcresearchpress.com by 210.87.254.105 on 09/05/12
For personal use only.

The specific orientation of the acetyl group to the C-2 position of the phenols (**1**) in the boron trifluoride catalyzed acylation herein described, parallels that observed for the Friedel–Crafts acylation of 3-alkoxyphenols (3). That the introduction of a substituent at C-1 results in partial (**7**, R = CH_3) or predominant (**7**, R = OCH_3) acylation at C-4, may be accounted for on the basis of steric crowding at C-2 and in the case of **7** (R = OCH_3), additional electronic direction to this position.

Experimental

Melting points were determined on a Reichert Kofler Micro Heating Stage and are uncorrected. Ultraviolet spectra were recorded in ethanol solution on a Bausch and Lomb Spectronic 505 and i.r. spectra (KBr pellet) on a Perkin Elmer 237B spectrophotometer. Nuclear magnetic resonance spectra were taken on a Varian T-60 spectrometer. Tetramethysilane was used as an internal standard. Elemental analyses were determined at Microanalysis Laboratories Limited, Toronto.

*The Rearrangement of 6,6-Dimethyl-6H-dibenzo[b,d]-pyran (**3**) to 4-Hydroxy-9,9-dimethylfluorene (**4**)*

Aluminum trichloride (1.4 g, 0.011 mol) was added at once to a solution of 6,6-dimethyl-6*H*-dibenzo[*b*,*d*]pyran (2.1 g, 0.01 mol) in ethylene dichloride (100 ml). The reaction mixture was stirred at room temperature for 15 min and then poured into 2 *N* hydrochloric acid (100 ml). The organic phase was removed, washed with water (50 ml), dried over sodium sulfate, and evaporated. The residue was crystallized from hexane and provided **4** (1.85 g, 88%) as colorless prisms m.p. 91–94° (lit. (7) m.p. 90–91°); λ_{max} 262 (log ε 4.11), 270 (log ε 4.13), 286 (log ε 3.92), 294 (log ε 3.92), 305 nm (log ε 3.67); n.m.r. ($CDCl_3$): δ 1.47 (s, 6H, $(CH_3)_2C$), 5.15 (broad s, 1H, —OH).

*2-Acetyl-3-hydroxy-6H-dibenzo[b,d]pyrans (**5a–g**)*

Boron trifluoride was bubbled, at a moderate rate (*ca.* 100 ml/min) for 1 h, into a solution of the 3-hydroxy-6*H*-dibenzo[*b*,*d*]pyran (**1**, 0.05 mol) in benzene (200 ml) containing acetic acid (0.06 mol) at room temperature. The reaction mixture was stirred at room temperature for 16 h and then poured into 2 *N* sodium hydroxide solution (500 ml) with vigorous stirring. After 5 min the mixture was acidified with 4 *N* hydrochloric acid and the benzene layer was removed. The aqueous phase was extracted with ether (2 × 200 ml). The ether extracts were combined with the benzene portion, dried over sodium sulfate, and evaporated. The 2-acetyl derivatives so obtained were recrystallized to constant melting point. These derivatives are described in Table 1.

*4-Acetyl-3-hydroxy-6,6-dimethyl-6H-dibenzo[b,d]pyran (**6**)*

Boron trifluoride was bubbled, at a moderate rate (*ca.* 100 ml/min), into a solution of **1***c* (19 g, 0.085 mol) and acetic acid (8.4 g, 0.14 mol) in benzene (260 ml) under reflux. After 3 h the reaction mixture was cooled and poured into aqueous 2 *N* sodium hydroxide solution (230 ml) with vigorous stirring. The mixture was acidified with 4 *N* hydrochloric acid and the benzene layer was removed. The aqueous phase was extracted with benzene (3 × 100 ml). The extracts were combined with the former benzene portion, dried over sodium sulfate, and evaporated. The residue was recrystallized from hexane and provided **5***c* (7.8 g). The mother liquor was evaporated and upon chromatography on silica ($CHCl_3$–hexane) provided the title compound (0.27 g, 1.2%) as yellow prisms m.p. 139–141°; λ_{max} 2.72 (log ε 4.31), 298 (sh log ε 4.06), 364 nm (log ε 3.33); ν_{max} 1627, 1605, 1593, 1570 cm^{-1}; n.m.r. ($CDCl_3$): δ 1.70 (s, 6H, —$(CH_3)_2$-CO—), 2.77 (s, 3H, —$COCH_3$), 6.64 (d, J = 9 Hz, 1H, C-2-H), δ 7.76 (d, J = 9 Hz, 1H, C-1-H).

Anal. Calcd. for $C_{17}H_{16}O_3$: C, 76.10; H, 6.01. Found: C, 76.30; H, 6.03.

Later fractions yielded a further amount (1.2 g) of **5***c* (total yield 9 g, 40%; compare Table 1). Recrystallization from hexane yielded colorless plates m.p. 108–109°; λ_{max} 260 (log ε 4.33), 289 (sh, log ε 4.02), 299 (sh log ε 3.83), 347 nm (log ε 3.67); ν_{max} 1642, 1610, 1574 cm^{-1}; n.m.r.: see Table 1.

*2-Acetyl-3-hydroxy-1,6,6-trimethyl-6H-dibenzo[b,d]pyran (**8**) and 4-Acetyl-3-hydroxy-1,6,6-trimethyl-6H-dibenzo[b,d]pyran (**9**)*

A solution of **7** (R = CH_3) (6.8 g, 0.028 mol) and acetic acid (1.9 g, 0.031 mol) in benzene (100 ml) was treated with boron trifluoride for 30 min in the manner described above for the preparation of compounds (**5***a–g*). After 72 h at room temperature the reaction mixture was similarly worked up and the crude product was chromatographed on silica ($CHCl_3$). The first fraction yielded **8** (1.36 g, 11%) as a pale yellow oil. Distillation (110°/0.1 mm) and recrystallization from hexane provided yellow prisms m.p. 74–75°; λ_{max} 274 (log ε 4.34), 298 (sh log ε 3.88), 362 nm (log ε 3.19); ν_{max} 1612, 1590, 1560 cm^{-1}; n.m.r. ($CDCl_3$): δ 1.63 (s, 6H, —$(CH_3)_2CO$—), 2.56 (s, 3H, CH_3-Ar), 2.68 (s, 3H, $COCH_3$), 6.65 (s, 1H, C-2-H), 14.5 (s, 1H, —OH).

Anal. Calcd. for $C_{18}H_{18}O_3$: C, 76.57; H, 6.43. Found: C, 76.59; H, 6.49.

Later column fractions yielded **8** (2.67 g, 34%) which on recrystallization from heptane provided pale yellow prisms, m.p. 110–111°; λ_{max} 263 (log ε 4.25), 285 (sh, log ε 3.98), 313 nm (log ε 3.65); ν_{max} 1642, 1610, 1574 cm^{-1}; n.m.r. ($CDCl_3$): δ 1.60 (s, 6H, —$(CH_3)_2CO$—), 2.68 (s, 3H, $COCH_3$), 2.82 (s, 3H, $ArCH_3$), 6.50 (s, 1H, C-4-H), 14.1 (s, 1H, OH).

Anal. Calcd. for $C_{18}H_{18}O_3$: C, 76.57; H, 6.43. Found: C, 76.75, H, 6.49.

*4-Acetyl-1-methoxy-3-hydroxy-6,6-dimethyl-6H-dibenzo[b,d]pyran (**11**)*

A solution of **7** (R = OCH_3) (8.3 g, 0.032 mol) and acetic acid (2.93 g, 0.049 mol) in benzene (250 ml) was treated with boron trifluoride in the manner described above for the preparation of compound (**5***a–g*). After 2 days at room temperature the reaction mixture was similarly worked up and the crude product was chromatographed on silica ($CHCl_3$). The title compound was obtained as a colorless oil which crystallized from benzene–hexane and provided pale yellow crystals (5.7 g, 59%), m.p. 89–90°; λ_{max} 275 (log ε 4.33), 286 (sh log ε 4.29), 345 nm (log ε 3.11); ν_{max} 1630, 1590, 1573 cm^{-1};

Can. J. Chem. Downloaded from www.nrcresearchpress.com by 210.87.254.105 on 09/05/12
For personal use only.

n.m.r. (CCl_4): δ 1.65 (s, 6H, —$(CH_3)_2CO$—), 2.62 (s, 3H, CH_3CO), 3.92 (s, 3H, OCH_3), 6.05 (s, 1H, C-2-H), 8.10 (m, 1H, C-10-H), 13.67 (s, 1H, OH).

Anal. Calcd. for $C_{18}H_{18}O_4$: C, 72.46; H, 6.08. Found: C, 72.69; H, 6.21.

*2-Acetyl-1-hydroxy-3-methoxy-6,6-dimethyl-6H-dibenzo[b,d]pyran (**13**)*

A solution of **12** (21 g, 0.082 mol) and acetic acid (7.2 g, 0.12 mol) in benzene (250 ml) was treated with boron trifluoride in the manner described above. After 10 days at room temperature, although the reaction was still incomplete, the mixture was worked up in the usual way. The crude product was chromatographed on silica and provided the title compound (9.1 g, 37%) which on recrystallization from hexane yielded pale yellow needles, m.p. 172–174°; λ_{max} 277 (log ε 4.44), 292 (log ε 4.43), 348 nm (log ε 3.31); ν_{max} 1615, 1585, 1565 cm^{-1}; n.m.r. (CCl_4): δ 1.63 (s, 6H, —$(CH_3)_2CO$—), 2.64 (s, 3H, —$COCH_3$), 3.86 (s, 3H, —OCH_3), 5.93 (s, 1H, C-4-H), 8.60 (m, 1H, C-10-H).

Anal. Calcd. for $C_{18}H_{18}O_4$: C, 72.46; H, 6.08. Found: C, 72.45; H, 5.91.

*4-Oxo-5-methoxy-8,8-dimethyl-4H,8H-(2)benzopyrano(3,4-h)-(1)-benzopyran-2-carboxylic Acid (**14**)*

A suspension of **13** (1.0 g, 0.0034 mol) in ethanol (15 ml) containing diethyl oxalate (0.9 g, 0.0062 mol) was added at once to a solution of sodium (0.69 g, 0.03 mol) in ethanol (15 ml) at the reflux temperature. The reaction mixture was heated under reflux for 45 min, cooled to 10°, and acidified with 4 *N* hydrochloric acid. Water (50 ml) was then added and the resulting mixture was extracted with ether (3 × 50 ml). The combined extracts were dried over sodium sulfate and evaporated. The residue was treated with a mixture of acetic acid (10 ml) and concentrated hydrochloric acid (5 ml) under reflux for 2 h. The reaction mixture was then diluted with water (100 ml) and extracted with chloroform (5 × 80 ml). The combined chloroform extracts were dried over sodium sulfate and evaporated. The residue was crystallized from ethyl acetate and provided the title compound (0.35 g, 30%). Recrystallization from acetonitrile yielded pale yellow prisms, m.p. 242–248° (dec.); λ_{max} 276 (log ε 4.42), 304 (sh, log ε 3.57), 334 nm (log ε 3.32); ν_{max} 1718, 1660, 1620, 1608, 1598, 1585, 1562 cm^{-1}; n.m.r. (CD_3SOCD_3): δ 1.63 (s, 6H, —$(CH_3)_2CO$—), 3.88 (s, 3H, OCH_3), 6.65 (s, 1H, C-6-H), 6.72 (s, 1H, C-3-H), 8.65 (m, 1H, C-12-H).

Anal. Calcd. for $C_{20}H_{16}O_6$: C, 68.17; H, 4.57. Found: C, 68.14; H, 4.57.

*2-Acetyl-1,3-dimethoxy-6,6-dimethyl-6H-dibenzo[b,d]pyran (**15**)*

A solution of compound **13** (1 g, 0.0034 mol) and methyl iodide (2.3 g, 0.016 mol) in acetone (50 ml) was heated under reflux in the presence of powdered anhydrous potassium carbonate (2.3 g, 0.015 mol) for 15 h. The reaction mixture was cooled, filtered, and evaporated. The residue was dissolved in toluene (30 ml), filtered and evaporated. The residue was crystallized from toluene–hexane to provide compound **15** (0.9 g, 85%) as colorless prisms, m.p. 121–122°; λ_{max} 259 (log ε 4.19), 281 (log ε 4.08), 301 (log ε 3.91), 310 nm (log ε 3.84); ν_{max} 1695, 1605, 1585, 1565 cm^{-1}; n.m.r. (CD_3SOCD_3): δ 1.58 (s, 6H, —$(CH_3)_2CO$—), 2.45 (s, 3H, —$COCH_3$), 3.64 (s, 3H, —OCH_3), 3.82 (s, 3H, —OCH_3), 6.55 (s, 1H, C-4-H), 8.17 (m, 1H, C-10-H).

Anal. Calcd. for $C_{19}H_{20}O_4$: C, 73.06, H; 6.45. Found: C, 73.09; H, 6.38.

*4-Acetyl-1,3-dimethoxy-6,6-dimethyl-6H-dibenzo-[b,d]pyran (**16**)*

Compound **11** (1 g, 0.0034 mol) was methylated in the manner described above for the preparation of compound **15**. The crude product was similarly crystallized from toluene–hexane and provided compound **16** (0.85 g, 81%) as colorless needles, m.p. 152–153°; λ_{max} 276 (log ε 4.24), 287 (log ε 4.25) 301 nm (sh, log ε 3.84); ν_{max} 1700, 1613, 1600, 1590, 1580 cm^{-1}; n.m.r. (CD_3SOCD_3): δ 1.57 (s, 6H, —$(CH_3)_2CO$—), 2.42 (s, 3H, —$COCH_3$), 3.90 (s, 3H, —OCH_3) 4.03 (s, 3H, —OCH_3), 6.55 (s, 1H, C-2-H), 8.34 (m, 1H, C-10-H).

Anal. Calcd. for $C_{19}H_{20}O_4$: C, 73.06; H, 6.45. Found: C, 73.47; H, 6.72.

*1,3-Dihydroxy-6,6-dimethyl-6H-dibenzo[b,d]pyran (**17**)*

(*a*) Compound **15** (300 mg, 1.2 mmol) was heated under reflux in a mixture of acetic acid (2.5 ml) and hydriodic acid (57%, 2.5 ml) for 45 min. The reaction mixture was cooled, diluted with water (50 ml), and extracted with chloroform (2 × 50 ml). The extracts were combined, dried over sodium sulfate, and evaporated. The residue was purified by thick-layer chromatography (2-mm 20 × 20 cm silica gel plate, 7% methanol – 93% chloroform) and on recrystallization from toluene provided compound **17** (180 mg, 77%) as colorless needles m.p. 147–148°; λ_{max} 288 (log ε 4.21), 300 nm (log ε 4.08); n.m.r. (CD_3SOCD_3): δ 1.53 (s, 6H, —$(CH_3)_2CO$—), 5.88 (d, J = 2.5 Hz, 1H, C-2- or C-4-H), 6.12 (d, J = 2.5 Hz, 1H, C-4- or C-2-H), 8.40 (m, 1H, C-10-H), 9.47 (broad s, 1H, C-3-OH), δ 9.90 (s, 1H, C-1-OH).

Anal. Calcd. for $C_{15}H_{14}O_3$: C, 74.36; H, 5.82. Found: C, 74.54; H, 5.68.

(*b*) Compound **16** (300 mg, 1.2 mmol) was also treated with acetic acid – hydriodic acid and in a similar manner the crude product provided compound **17** (170 mg, 73%) m.p. 147–148°, identical with that obtained in (*a*).

The author gratefully acknowledges the technical assistance of Mrs I. Guse and Mr. U. Rothenbühler.

1. J. P. DEVLIN. Can. J. Chem. This issue, preceding paper.
2. J. P. DEVLIN, K. R. FRETER, and P. B. STEWART. 167th American Chemical Society National Meeting, Los Angeles, 1974. Abstr. No. MEDI-43; P. B. Stewart, J. P. Devlin, and K. R. Freter. Federation Proc. **33**, 762 (1974).
3. P. H. GORE. *In* Friedel–Crafts and related reactions. *Edited by* G. A. Olah. Interscience Publishers, New York. 1964. Vol. 3, p. 1.
4. D. KÄSTNER. *In* Neuere Methoden der präparativen organischen Chemie. *Edited by* W. Foerst. Verlag Chemie, Weinheim. 1963. Vol. 1, p. 413.
5. N. P. BUU-HOÏ and J. SEAILLES. J. Org. Chem. **20**, 606 (1955).
6. SADTLER STANDARD SPECTRA. Sadtler Research Laboratories, Philadelphia. Spectra Nos. 3936M and 6900M.
7. M. ANCHEL and A. H. BLATT. J. Am. Chem. Soc. **63**, 1948 (1941).

A 2-Azapentadienyl Carbanion: a Nonstereospecific Electrocyclization

D. H. HUNTER AND R. P. STEINER
Department of Chemistry, University of Western Ontario, London, Ontario N6A 3K7

Received August 21, 1974

D. H. HUNTER and R. P. STEINER. Can. J. Chem. **53**: 355 (1975).

Treatment of 1,3,5-triphenyl-4-aza-1,3-pentadiene under selected basic conditions leads to either isomerization among the azapentadienes or to cyclization. Analysis of the products from reaction under aprotic conditions (LiTMP in THF) suggested that the open-chain delocalized carbanion exists in both the W and sickle forms. The open-chain anions were observed to electrocyclize in a nonstereospecific manner to produce a 1:1 mixture of *cis*- and *trans*-2,4,5-triphenyl-1-pyrrolines. Reaction in protic media (methanol and *tert*-butyl alcohol) produced a 1,5-proton transfer as well as cyclization. The details of the 1,5-proton transfer reaction were elucidated using methanol-*O-d* and the collapse preferences and intramolecularity in this medium were determined.

D. H. HUNTER et R. P. STEINER. Can. J. Chem. **53**, 355 (1975).

Le traitement du triphényl-1,3,5 aza-4 pentadiène-1,3, dans des conditions basiques choisies, conduit soit à une isomérisation entre les azapentadiènes soit à une cyclisation. L'analyse des produits formés par la réaction dans des conditions aprotiques (LiTMP dans THF) suggère qu'un carbanion délocalisé sur une chaîne ouverte existe dans la forme W et dans la falsiforme. On a observé que les anions en chaîne ouverte s'électrolisent d'une façon non-stéréospécifique pour conduire à un mélange 50:50 des triphényl-2,4,5 pyrrolines-1 *cis* et *trans*. La réaction dans des milieux protiques (méthanol ou *tert*-butanol) conduit à un transfert-1,5 de proton de même qu'à une cyclisation. On a élucidé les détails de la réaction de transfert-1,5 de proton en faisant appel à du méthanol-*O-d*; on a déterminé la nature des effondrements préférentiels et la nature intramoléculaire de la réaction dans ce milieu. [Traduit par le journal]

Introduction

We have previously reported (1) the remarkably rapid and stereoselective electrocyclization of a 2,4-diazapentadienyl anion. This stands in contrast to the lack of reactivity of the pentadienyl anion (2). We have now studied a 2-azapentadienyl anion since its propensity for cyclization might be expected to lie between the other two systems. This in fact was the case and as a consequence information has been obtained about open-chain anion stabilities and geometries. A striking effect of aza-substitution on the electrocyclization rate and stereochemistry has been observed.

In order to make a direct comparison with our earlier work on the 1,3,5-triphenyl-2,4-diazapentadienyl anion **5**, the particular system chosen for study was the 1,3,5-triphenyl-2-azapentadienyl anion **4**.

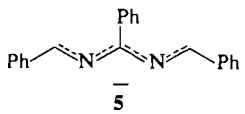

5

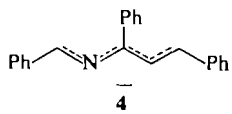

4

Results

Preparation and Characterization of Substrates

1,3,5-Triphenyl-4-aza-1,3-pentadiene

From a synthetic viewpoint, of the three carbon acid precursors to the 1,3,5-triphenyl-2-azapentadienyl anions, 1,3,5-triphenyl-4-aza-1,3-pentadiene **1** appeared to be the most attractive substrate. Synthesis of **1** was accomplished by condensation of chalcone and benzylamine yielding a 3:1 mixture of geometrical isomers of **1**. On the basis of the magnitude of the proton–proton coupling constant between the vinyl protons ($J \approx 17$ Hz), the carbon–carbon double bond in **1** was assigned the *trans*-geometry in both isomers. Thus apparently the two isomers of **1** differ by being *syn* or *anti* at the carbon–nitrogen double bond. The major equilibrium isomer was obtained in a pure state by recrystallization. However, it is not known whether this isolated isomer of **1** corresponds to the *syn* or *anti* possibility. The *syn–anti* interconversion rates of **1** are sufficiently slow to permit characterization but are accelerated by base.

Can. J. Chem. Downloaded from www.nrcresearchpress.com by 210.87.254.5 on 09/05/12
For personal use only.

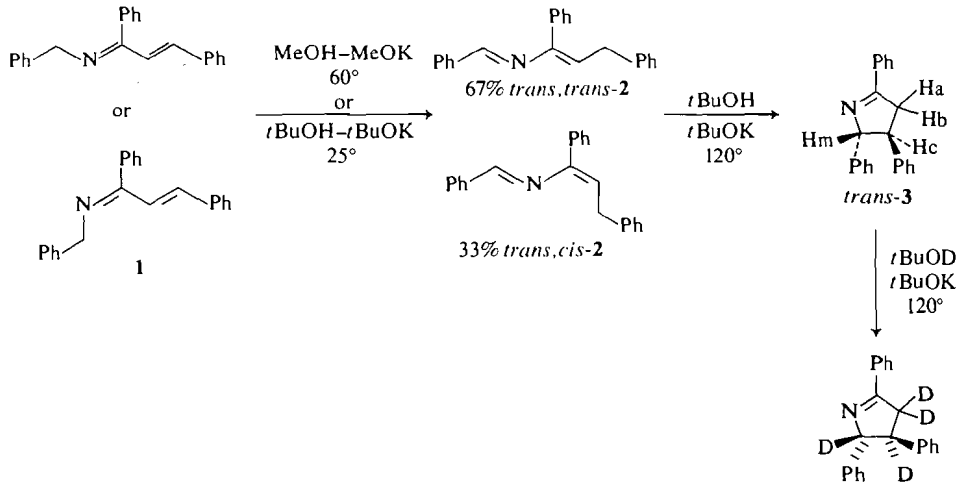

1,3,5-Triphenyl-2-aza-1,3-pentadiene

The 1,3,5-triphenyl-2-aza-1,3-pentadienes **2** were prepared by base-catalyzed isomerization of **1** and the appropriate data are gathered in Table 1. As indicated in runs 4 and 5, when **1** was reacted in 0.22 *M* potassium methoxide – methanol at 60° the fastest reaction was equilibration of the *syn* and *anti* forms of **1** to provide a 3.2:1 mixture of unassigned geometry. More slowly a mixture of geometrical isomers of **2** was produced in a time-dependent ratio. At low percentages of conversion (run 4) *trans,cis*-**2** was preferred by about 3:1, whereas at apparent equilibrium (run 5) *trans,trans*-**2** was favored by 2:1 and no **1** was observed.

The major isomer from run 5 (assigned the *trans,trans* geometry as described below) was isolated by t.l.c., purified, and characterized by n.m.r., i.r., and mass spectrometry. The minor isomer could not be isolated due to hydrolysis on silica gel.[1] Instead, its structure was assigned on the basis of its n.m.r. spectrum in the mixture of the two isomers of **2**.

The geometries of the isomers of **2** were assigned on two counts. First, the geometry of the carbon–nitrogen double bond was assumed to be *trans*(*syn*) since geometrical isomerization around this bond ought to be rapid at ambient temperature (3) and thermodynamics should certainly favor the *syn*-isomer. Second, the geometry at the carbon–carbon double bond was assigned on the basis of relative reactivity of the two isomers of **2** with 4-phenyl-1,2,4-triazoline-3,5-dione to form a Diels–Alder type product. The relative reactivity was assessed by n.m.r. monitoring of the changes in the ratio of the two isomers of **2** in a mixture upon successive addition of aliquots of the triazolinedione. The major isomer of run 5 reacted at least five times faster than the minor isomer. This reactivity ratio is a minimum because the increasing signals of the product partially overlapped those of **2**.

The more reactive isomer (the major isomer of run 5) was assigned the *trans,trans*-**2** structure since it is anticipated that it will more readily adopt the *S-cis* conformation necessary for Diels–Alder reactivity. The product of the reaction of *trans,trans*-**2** with the triazolinedione was isolated by t.l.c. and characterized by n.m.r., i.r., and mass spectrometry. These data were consistent with the product of a Diels–Alder reaction.

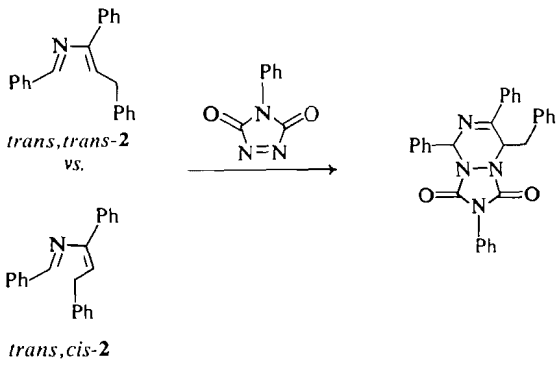

[1]The major isomer also underwent some hydrolysis during t.l.c. yielding β-phenylpropiophenone.

Can. J. Chem. Downloaded from www.nrcresearchpress.com by 210.87.254.5 on 09/05/12
For personal use only.

TABLE 1. Results of base-catalyzed isomerization of **1** to **2**

Run	Base-solvent[b]	T,°C	Time, min	Products[a] % **1**[c]	% *trans,trans*-**2**	% *trans,cis*-**2**
1	$KOC(CH_3)$–$HOC(CH_3)_3$	25	20	0	67	33
2	$KOC(CH_3)_3$–$HOC(CH_3)_3$	25	120	0	67	33
3	$LiOC(CH_3)_3$–$HOC(CH_3)_3$	60	60	60	10	30
4	$KOCH_3$–$HOCH_3$	60	60	60	10	30
5	$KOCH_3$–$HOCH_3$	60	4300	0	67	33
6	$KOCH_3$–$DOCH_3$[d]	60	7	60[e]	10[f]	30[f]
7	$KOCH_3$–$DOCH_3$[d]	40	20	80[g]	≤5	15[h]
8	$KOCH_3$–$DOCH_3$[d]	40	60	65[i]	10	25
9	LiTMP–THF	−78	300	25	50	25
10	LiTMP–THF	−10 to −20	180	25	50	25

[a]Yields are based upon n.m.r. integration; 0% means not detected by n.m.r. or t.l.c.
[b]See Experimental for concentrations and procedures.
[c]Recovered **1** was a 3.2:1 mixture of *syn* and *anti* isomers.
[d]Contains 10 vol. % THF.
[e]0.8 atoms D/molecule by n.m.r.
[f]Analysis of hydrolyzed material yielded d_0, 10.5%, d_1, 78%, d_2, 12% by mass spectrum.
[g]0.35 atoms D/molecule by n.m.r.
[h]d_0, 10.5%, d_1, 85%, d_2, 4.5% by mass spectral analysis of hydrolysis product.
[i]0.7 atoms D/molecule by n.m.r.

TABLE 2. Results of base-catalyzed cylization and exchange of **1** and **3**

Run	Substrate: Nature	Concn., *M*	Base-solvent[a]	T,°C	Time, min	Products % **2**[b]	% *cis*-**3**[c]	% *trans*-**3**
11	**1**	0.5	$KOC(CH_3)_3$–$HOC(CH_3)_3$	120	30	12	0	70
12	*cis*-**3**	0.5	$KOC(CH_3)_3$–$HOC(CH_3)_3$	120	30	0	0	88
13	*trans*-**3**	0.25	$KOC(CH_3)_3$–$DOC(CH_3)_3$	120	30	0	0	[d]
14	**1**	0.07	LiTMP–THF	0–5	30	15	35	29[e]
15	**1**	0.07	LiTMP–THF	25	180	0	21	26[f]

[a]See Experimental for concentrations.
[b]Based upon recovered β-phenylpropiophenone from hydrolysis of 2.
[c]Yields are based upon isolated purified materials. 0% means not detected by n.m.r. or t.l.c.
[d]Four atoms D/molecule in the pyrroline ring.
[e]5% of 2,3,5-triphenylpyrrole.
[f]11% of 2,3,5-triphenylpyrrole.

trans-2,4,5-Triphenyl-1-pyrroline (trans-3)

Treatment of **1** under more basic conditions, *tert*-butyl alcohol – potassium *tert*-butoxide, first at 25° led to isomerization to **2** (runs 1 and 2 of Table 1) and then at 120° to *trans*-**3** (run 11 of Table 2) as the only observed product in good yield. This product was shown to be isomeric with **1** and **2** by mass spectrometry but unlike **1** and *trans,trans*-**2**, *trans*-**3** yielded the five-membered ring oxidation product, 2,3,5-triphenylpyrrole, upon oxidation with 2,3-dichloro-5,6-dicyano-1,4-benzoquinone (DDQ).

The presence of a carbon–nitrogen double bond in *trans*-**3** was verified by i.r. with observation of a band due to C=N and absence of an N—H bond. The analysis of the 100 MHz proton n.m.r. spectrum as an ABCM pattern, with assistance of the LAOCOON III program, was consistent with placement of the carbon–nitrogen double bond as in *trans*-**3** and is inconsistent with the other possibility. The proton–proton coupling constant for the 4 and 5 hydrogens, $J = 6.7$ Hz, was consistent with but did not require a *trans* configuration.

The *trans* configuration was assigned by establishing that this material had the thermodynamically preferred configuration at positions 4 and 5. This was done in two ways. First, treatment of *trans*-**3** with potassium *tert*-butyl alcohol-*O*-*d* at 120° (run 13) which is the condition required for its formation from **1** (run 11) yielded *trans*-**3** back again but having incorporated **4** atoms D/molecule in the pyrroline ring. This indicates that the conditions of run 11 are more than sufficient to ensure formation of the thermodynamically more stable isomer or *trans* phenyl groups. More convincingly when *cis*-**3**, whose preparation is discussed below, was treated un-

Can. J. Chem. Downloaded from www.nrcresearchpress.com by 210.87.254.5 on 09/05/12
For personal use only.

der the same conditions (run 12), *trans*-**3** was observed as the only reaction product and in good yield.

cis-2,4,5-Triphenyl-1-pyrroline (cis-3)

When **1** was treated with lithium 2,2,6,6-tetramethylpiperidide (LiTMP) in tetrahydrofuran (THF) and the resultant blue solutions were quenched with acetic acid, a new product distribution was observed. As indicated in runs 9 and 10 of Table 1, if the temperature was kept below $-10°$ only **1** and **2** were obtained. However upon warming the solutions to 0° and above (runs 14 and 15) cyclized materials became the major products. In contrast to *tert*-butoxide in *tert*-butyl alcohol (run 11), both *cis*-**3** and *trans*-**3** were produced and in similar amounts. The two cyclized products could be separated by t.l.c. The structure assignment for *cis*-**3** was analogous to that for *trans*-**3**.

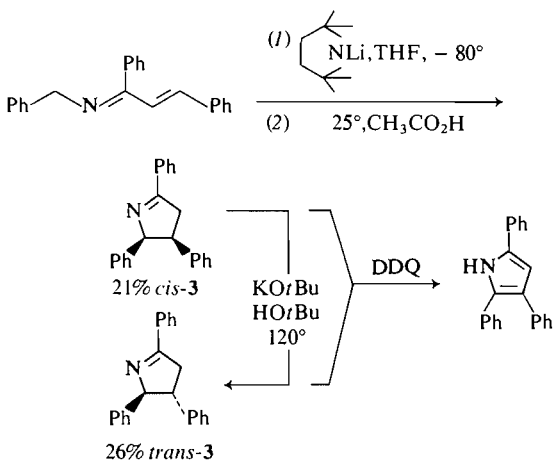

Mass spectrometry confirmed its isomeric nature to **1**, **2**, and *trans*-**3**, and oxidation with DDQ yielded 2,3,5-triphenylpyrrole. The presence of C=N was shown by i.r., and n.m.r. was consistent with the structure indicated. As mentioned above, evidence for the *cis* assignment lies in its conversion to *trans*-**3** upon treatment with potassium *tert*-butoxide in *tert*-butyl alcohol at 120° (run 12).

Discussion

As described in the Results section, the reaction of **1** under selected basic conditions can lead to specific types of isomerization. Under mildly basic conditions interconversion between open-chain isomers can be observed both in protic media (potassium methoxide in methanol or lithium *tert*-butoxide in *tert*-butyl alcohol at 60° and potassium *tert*-butoxide in *tert*-butyl alcohol at 25°) and aprotic media (LiTMP in THF below $-10°$). Under more vigorous basic conditions conversion to cyclic isomers occurs also in protic media (potassium *tert*-butoxide in *tert*-butyl alcohol at 120°) and aprotic media (LiTMP in THF above 0°). This differing reactivity between open-chain isomerization and cyclization has made it possible to obtain information on the role of the 1,3,5-triphenyl-2-aza-pentadienyl anion **4** in both processes.

The discussion of the properties of the 1,3,5-triphenyl-2-azapentadienyl anion **4** will first center on the geometries of the open-chain anion, then its electrocyclization reaction, both rate and stereochemistry, and then on its behavior as a short-lived species in protic solvent with emphasis on stability, collapse ratio, and intramolecularity.

Anion Geometries

In an attempt to ascertain the geometry that anion **4** prefers to adopt, quenching of the lithium salt of **4** in THF with acetic acid was investigated. When pure **1** was treated with a slight excess of LiTMP in THF at $-78°$, a deep blue color resulted. As indicated in runs 9 and 10 of Table 1, addition to this of an equivalent of acetic acid at either $-78°$ or $-15°$ led to the same mixture of four open-chain isomers. That these isomers had arisen from quenching of **4** was established using CH_3CO_2D. The n.m.r. spectrum of the reaction mixture was qualitatively consistent with incorporation of 1 atom D/molecule. In spite of the sensitivity of **1** to geometrical isomerization a control experiment verified that the isolated isomer of **1** survived the work-up conditions unchanged. The 3:1 geometrical isomer ratio for **1** is then both the kinetic and thermodynamic mixture.

The observation of four geometrical isomers of **1** and **2** requires that anion **4** exist in more than one geometry. The interconversion between anion geometries must be reasonably facile since equilibration occurs within 300 min at $-78°$ (run 9). Rapid interconversion rates are not unexpected since allyl and pentadienyllithiums show coalescence phenomena in their proton n.m.r. spectra consistent with fairly rapid geometrical interconversions (4).

The 2-azapentadienyl anion can, in principle, adopt four different geometries; a W shape, two

Can. J. Chem. Downloaded from www.nrcresearchpress.com by 210.87.254.5 on 09/05/12
For personal use only.

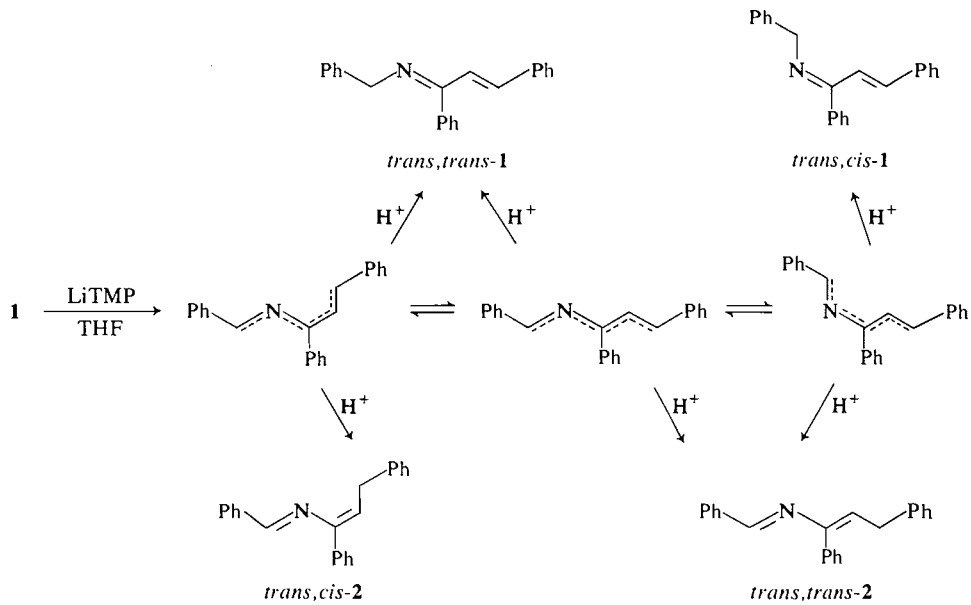

FIG. 1. Geometries anticipated for **4** and products of quenching.

sickle shapes, and a U shape. Of these, the U shape should be the least favored and n.m.r. results for pentadienyllithiums (2) support this contention. If phenyl rings are placed at the 1,3, and 5 positions of the W and two sickle shapes so as to minimize nonbonded interactions (5), the anions shown in Fig. 1 are obtained. Figure 1 also indicates the four products that could arise upon quenching of these anions. Since all four products are observed and occur in similar amounts, it would appear that the three geometries of anions do exist and in similar amounts. A direct calculation of anion populations from product distribution was not achieved since all three anions can form two products.

However, it can be concluded that anion **4** exists in a W shape and in two sickle shapes. These shapes can interconvert fairly rapidly and at equilibrium they exist in similar amounts.

The Electrocyclization Reaction

As mentioned above, under more vigorous conditions cyclization was observed in both protic and aprotic media and information was gathered on both the rates and stereochemistry of the cyclization reaction.

Rate of Cyclization

Information on the propensity of anion **4** for electrocyclization has been obtained in both protic and aprotic media and can be compared with the earlier results (1) for the 1,3,5-triphenyl-2,4-diazapentadienyl anion **5**. As is indicated in runs 9, 10 and 14, 15, while anion **4** may be generated at $-78°$ in THF, electrocyclization is not observed until above 0°. This is in contrast with **5** which electrocyclizes competitively with its formation at $-78°$ in THF.

This same phenomenon is illustrated for protic solvents in runs 1–5 and 11. Both potassium methoxide in methanol and lithium *tert*-butoxide in *tert*-butyl alcohol at 60° are sufficiently basic to convert **1** to **2**, presumably through the short-lived anion **4**. However, potassium *tert*-butoxide in *tert*-butyl alcohol, a kinetically much stronger base, at 120° must be used to produce electrocyclization. A rate ratio of at least 10^6 between the rate of anion formation and the rate of electrocyclization can be deduced.[2]

The results in both protic and aprotic media correspond to a reaction profile where a more rapidly formed open-chain anion **4** slowly electrocyclizes in the rate-determining step. This should be contrasted with the results obtained

[2]Potassium *tert*-butoxide in *tert*-butyl alcohol is a kinetically stronger (6) base than potassium methoxide in methanol by about 10^6. The 60° temperature difference (120° *vs.* 60°) should correspond to an additional rate ratio depending upon the activation energy (an unknown).

Can. J. Chem. Downloaded from www.nrcresearchpress.com by 210.87.254.5 on 09/05/12
For personal use only.

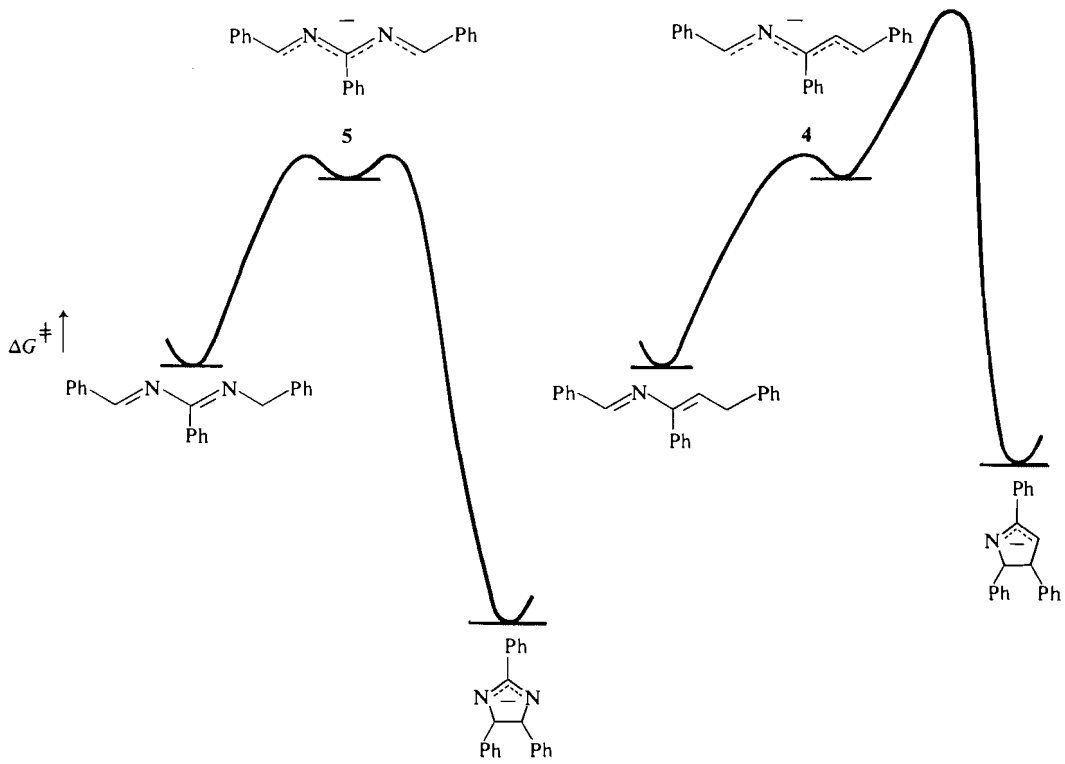

FIG. 2. Free energy profiles for formation and electrocyclization of anions **4** and **5**.

for the 2,4-diazapentadienyl anion **5**. In this earlier study (1) it was found that while formation of **5** seemed to occur at a rate comparable to **4** in both protic and aprotic media, the rate of electrocyclization of **5** was significantly faster. Electrocyclization and anion formation occurred at competitive rates with **5**. The difference in behavior in the two systems is summarized in the energy profiles of Fig. 2. The difference in ease of electrocyclization is presumably a reflection of the difference in the stability of the cyclized forms of the anions. The negative charge should reside primarily on the termini of the three atom system coincident with the position of the nitrogen.

Stereochemistry of Electrocyclization

When a solution of the lithium salt of **4** in THF was allowed to warm to 0–5° for 30 min and then quenched with acetic acid (run 14) significant amounts of cyclization were observed and cyclization was complete at 180 min and 25° (run 15). Under these conditions both *cis*-**3** and *trans*-**3** were isolated as the major products and in similar amounts (a *cis–trans* ratio of 1.2 in run 14 and 0.8 in run 15) along with minor amounts of the oxidation product, 2,3,5-triphenyl-pyrrole. It is likely that the observed *cis*-**3**:*trans*-**3** of *ca.* 1 is close to the actual kinetic product distribution on two counts. First, base-catalyzed equilibration of *cis*-**3** (run 12) and *trans*-**3** (run 13) yields just *trans*-**3** in analogy to the diaza-system (1). Second, if there is *cis–trans* equilibrium in THF, it must be slow as shown by the slight, if real, change in the *cis*-**3**:*trans*-**3** ratio with a significant change in reaction conditions (runs 14 and 15).

In contrast to the kinetic distribution in the aprotic medium, the conditions necessary to produce electrocyclization in protic media are also sufficient to equilibrate any cyclized products. As shown in run 11, reaction of **1** in a potassium *tert*-butoxide – *tert*-butyl alcohol solution at 120° for 30 min is necessary to produce significant cyclization and only *trans*-**3** is observed. As mentioned earlier, reaction of *cis*-**3** under the same conditions (run 12) results in complete conversion to *trans*-**3**. That *trans*-**3** is probably

Can. J. Chem. Downloaded from www.nrcresearchpress.com by 210.87.254.5 on 09/05/12
For personal use only.

Can. J. Chem. Downloaded from www.nrcresearchpress.com by 210.87.254.5 on 09/05/12
For personal use only.

the thermodynamically most stable of the possible, 2,3,5-triphenylpyrrolines is shown by the base-catalyzed exchange results of run 13 with *trans*-**3**; *trans*-**3** was recovered as the only product of run 13 and had completely exchanged the pyrroline ring (4 atoms D/molecule). Thus apparently all centers within the pyrroline ring had an opportunity to epimerize and *trans*-**3** remained the sole product. Thus the results in *tert*-butyl alcohol do not also allow determination of the kinetic ratio of *cis*-**3** and *trans*-**3** from electrocyclization of **4** but provide the equilibrium product.

A comparison (Fig. 3) with the stereochemical behavior of the 2,4-diazapentadienyl anion **5** is revealing since **5** produced exclusively the cyclized material with *cis*-phenyl groups ($\geq$ 99.7%). This change in stereoselectivity corresponds to a change in the *cis–trans* product ratio of $\geq$300 on aza-substitution. This marked sensitivity of stereochemistry to aza-substitution deserves some mechanistic comment, as does the observation of a nonstereospecific electrocyclization.

One mechanistic scheme invokes the same U-shaped geometry of anion (as in Fig. 3) for electrocyclization of both the diazapentadienyl anion **5** and the monoazapentadienyl anion **4**. In this scheme the change in product distribution would reflect a change in the relative rates of the conrotatory and disrotatory modes of electrocyclization. In the symmetrical anion **5** the expected disrotatory mode (7) is exclusively involved. However, in the unsymmetrical anion **4** the conrotatory and disrotatory modes are competitive. This change in stereoselectivity could be a result of changes in orbital symmetry demands accompanying loss of molecular symmetry (8).

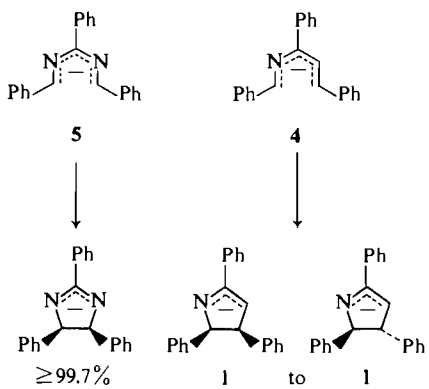

FIG. 3. Comparison of the stereochemistry of electrocyclization of anions **4** and **5**.

A second and similarly unprecedented scheme assumes the same disrotatory mode of electrocyclization for both **4** and **5**. The different product stereochemistries are then a consequence of reaction from different anion geometries. Both U and W shaped anions would lead to cyclized material with *cis*-phenyl rings and the 'sickle' shaped anion would produce *trans*-product. Such differing stereochemistries could then arise if the highly reactive diazapentadienyl anion **5** were produced initially in the W shape and electrocyclized before or while geometrical interconversions occurred.

The much less reactive azapentadienyl anion **4**, in contrast, is observed to undergo geometrical interconversions much faster than electrocyclization. Analogous mechanistic schemes in which both **4** and **5** undergo equilibration of geometries before electrocyclization suffer from the disadvantage of having to postulate either different distributions of geometries or differing geometry reactivities as a result of aza-substitution. While these remain as possibilities, they prove difficult to rationalize convincingly.

These two contrasting mechanisms correspond to cases where the changes in product stereochemistry are attributed to changes, first, in reaction pathway or second, in reactant structure (geometry). The data gathered in this study are insufficient to distinguish between these mechanistic possibilities but a more complete analysis will be reported in a subsequent paper on the all-carbon system.

Relative Stability of the Azapentadienes

The relative thermodynamic stabilities of some of the isomers of **1** and **2** can be deduced from the isomerization results of runs 1–6 of Table 1. Analysis of the reaction mixture of runs 3, 4, 6, 7, and 8 in which unreacted **1** was present revealed a facile base-catalyzed *syn–anti* isomerization which provided a 3:1 mixture of **1**. The results of equilibration of **1** (runs 1, 2, and 5) showed that only **2** is present at equilibrium between **1** and **2** and *trans,trans*-**2** predominates over *trans,cis*-**2** by a factor of 2. Although there is no direct evidence bearing on the point, by analogy with **2**, it is likely that the isolated and major equilibrium isomer of **1** also has the *trans,trans* structure. While *trans,trans*-**2** is predominant at equilibrium, it is *trans,cis*-**2** that is

Can. J. Chem. Downloaded from www.nrcresearchpress.com by 210.87.254.5 on 09/05/12
For personal use only.

the kinetically preferred product (runs 3, 4, 6, 7, and 8). This occurs whether the reaction involves ion-pairs ($LiOC(CH_3)_3$ in $HOC(CH_3)_3$; run 3) or dissociated ions ($KOCH_3$ in $HOCH_3$; run 4). If the initial product distribution reflects the intermediate anion stability, the sickle shaped anion would appear to be the most stable.

While it is not surprising that none of the 2-aza-1,4-pentadienes were present upon equilibration of **1** and **2**, the exclusive formation of **2** was unexpected. Simple Hückel molecular orbital calculations predict the reverse. Although the generality of this observation has not been demonstrated, base-catalyzed isomerization of 2-aza-2,4-pentadienes to 2-aza-1,3-pentadienes may be a satisfactory synthetic route to some examples of this unique functionality, *i.e.* vinylimines.

Intramolecularity

Since examples of base-catalyzed 1,5-proton transfer reactions are few, an attempt was made to further characterize the intermediate anion by comparing isomerization and hydrogen–deuterium exchange (runs 6, 7, and 8). The extent of involvement of an intramolecular component in the 1,5-proton shift was estimated from the percentage of d_0 material found in *trans,trans*-**2** and *trans,cis*-**2** produced from **1** after short reaction times in CH_3OD (runs 6 and 7). The geometrical isomers of **2** were not analyzed directly but the combined hydrolysis product, β-phenylpropiophenone, was analyzed by mass spectrometry and showed 0.9 atoms D/molecule. Although this 10% intramolecular component should be a lower limit, due to concurrent exchange of both **1** and **2**, model calculations indicate corrections should be minor.

Although the observed 1,5-proton shift could actually be the result of two consecutive 1,3 shifts, this is unlikely. The anion **5** produced by proton abstraction from the central carbon of the analogous 2,4-diazapentadienyl system, hydrobenzamide, was found to protonate exclusively at the terminal position. The 1,3-proton shift via **5** occurred with 14% intramolecularity in CH_3OD. The only other examples of base-catalyzed 1,5-proton shifts involves tautomers of triphenylmethane (9) (Fig. 4). Only one of these systems has been studied in methanol-*O*-*d* but comparable results are available for *tert*-butyl alcohol-O-*d* and these systems show consistently higher intramolecular components (~50%) than the open-chain systems (~10%). While the geometries differ between these two types of substrates, the difference in pK_a between substrate and solvent has also changed. The pK_a's of the aza-substituted pentadienes are estimated from kinetic acidity to be ~24 and triphenylmethane has been assigned a pK_a of 32.5 on the MSAD scale (6). It is surprising that in comparison to the large change in substrate pK_a's, the change in intramolecularity is quite small. However, the actual intramolecularity will be less than 10% if significant amounts of protium are introduced from the protons in solvent reinforced by an isotope effect on protonation.

Collapse Ratios

The exchange data of runs 6, 7, and 8 also can be used to determine the preferred positions of protonation of the intermediate anions **4**. The percentage of isotopic exchange in recovered **1** gives a measure of the acts of carbanion formation that have occurred but with deuteration at the 1-position. The percentage of **2** observed gives a measure of carbanion formation from **1** but with collapse at the 5-position. The extent of isotopic exchange in **1** does not give a true measure of collapse at the 1-position since there is a small intramolecular component (see above) but the correction is small.

The results of runs 6, 7, and 8 were simulated by numerical integration of the corresponding reaction scheme using the MIMIC language of the CDC computer. As is qualitatively evident from the isotopic exchange results and as borne out more quantitatively ($k_{-1}/k_{-5} = 1.6$), there is only a slight preference for deuteration of anion **4** at the 1-position. A comparison of these results with the quenching results of runs 9 and 10 shows that again there is a close competition between reaction at each end of anion **4** but under quenching conditions, reaction at the 5-position predominates ($k_{-1}/k_{-5} = 0.3$). Although several factors could be involved, the products do indicate that different ratios of anion geometries are present and different geometries may show different collapse ratios.

The overall picture from both these studies indicates that in spite of apparently large differences in the thermodynamic stability of the two products of anion collapse (**1** and **2**), there is only slight selectivity in the collapse ratio. The observed collapse ratio is consistent with an anion whose positional reactivity is little affected

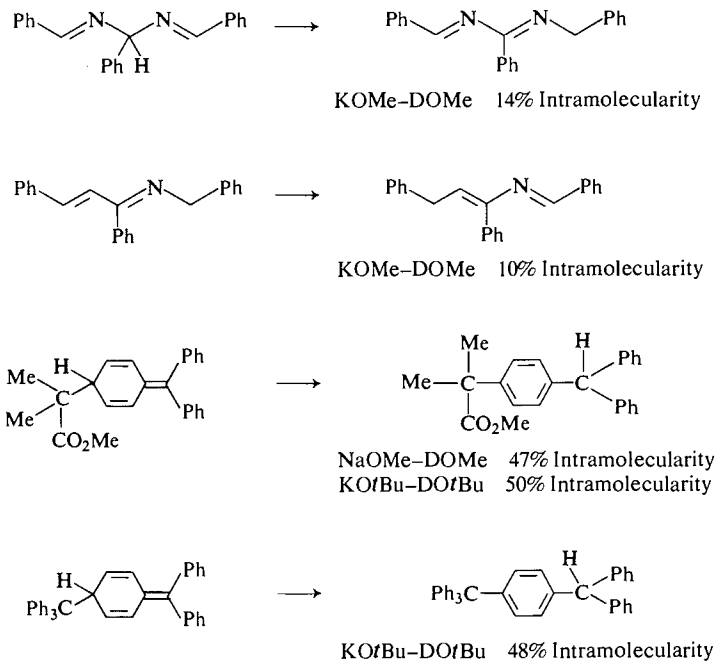

FIG. 4. Examples of reactions involving 1,5-proton shifts of pentadienyl anions and the observed intramolecularity.

by product stability but may reflect similar steric demands. The absence of quenching products due to reaction in the middle (the 3-position) would also seem to support this hypothesis. The charge distribution in **4** may also be important (10) but its contribution is not readily evaluated in the present system.

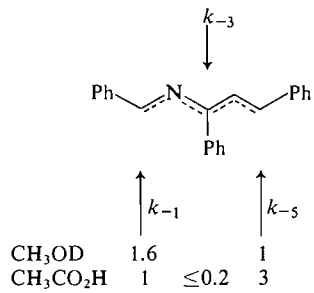

Experimental

Solvent and Bases

The methanol was distilled from magnesium and the *tert*-butyl alcohol was distilled from calcium hydride. The potassium *tert*-butoxide in *tert*-butyl alcohol (0.53, 0.03 *M* in H_2O) and the potassium methoxide in methanol (0.22, 0.05 *M* in H_2O) were prepared by the reaction of the alcohol with freshly cleaned potassium and were stored under argon. The methanol-*O-d* was prepared from dimethyl carbonate (11) and the base solution was prepared as above (0.59, 0.08 *M* in D_2O). The *tert*-butyl alcohol-*O-d* (12) was similarly reacted with potassium to produce a base solution (0.53 *M*).

Tetrahydrofuran (THF) was freshly distilled from lithium aluminum hydride before use. Solutions of lithium 2,2,6,6-tetramethylpiperidide in THF (1.0–2.0 *M*) were prepared by adding an equivalent of *n*-butyllithium (Alfa Inorganics) to a cooled solution (~−20°) of 2,2,6,6-tetramethylpiperidine in THF followed by stirring for 1 h from cold up to ambient temperature.

1,3,5-Triphenyl-1-4-azapenta-1,3-diene (1)

A mixture of chalcone (5.0 g, 23.3 mmol) and benzylamine (2.5 g, 23.3 mmol) in 150 ml of hexane (freshly distilled from calcium hydride) was refluxed 8 h over 50 g of 5A molecular sieves using a Barrett water trap. After filtration and solvent removal, the crude oil crystallized upon refrigeration. Recrystallization from hexane yielded 2.6 g (30%) of product, m.p. 83–85°. It is imperative that the crystals be grown slowly.

Mass spectrum: *m/e* 297, molecular ion. The n.m.r. spectrum (CCl_4) showed a 2 hydrogen singlet at δ = 4.40, and one hydrogen doublet at δ = 6.35 (*J* = 17 Hz), and a 16 hydrogen multiplet in the region δ = 6.96–7.53. The i.r. spectrum ($CHCl_3$) showed C=N at 1598 cm^{-1}.

A second geometrical isomer was present in the crude oil but was not isolated. The n.m.r. (CCl_4) of the second component in the mixture showed a 2 hydrogen singlet at δ = 4.80, a 1 hydrogen doublet at δ = 6.67 (*J* = 17 Hz), and an apparent 16 hydrogen multiplet at δ = 6.96–7.53 as obtained by difference.

1,3,5-Triphenyl-2-azapenta-1,3-diene (2)

A degassed solution of **1** (0.1 g, 0.34 mmol) in 0.64 ml of 0.53 *M* potassium *tert*-butoxide in *tert*-butoxide in

Can. J. Chem. Downloaded from www.nrcresearchpress.com by 210.87.254.5 on 09/05/12
For personal use only.

Can. J. Chem. Downloaded from www.nrcresearchpress.com by 210.87.254.5 on 09/05/12
For personal use only.

tert-butyl alcohol was stirred at ambient temperature for 0.5 h. The reaction mixture was extracted using ether and water. After the ether layer was washed once with water, once with saturated sodium chloride, and dried with magnesium sulfate, the solvent was removed under reduced pressure. An n.m.r. of the residual oil indicated a 3:1 ratio of *trans,trans*-**2** to *trans,cis*-**2**.

Thin-layer chromatography (silica gel, 10% ether-in-hexane) resulted in isolation of β-phenylpropiophenone (66% yield, m.p. 68–69°) and *trans,trans*-**2** (28%, m.p. 44–46°). Mass spectrum: *m/e* 297 for molecular ion. The n.m.r. spectrum (CCl_4) showed a 2 hydrogen doublet at $\delta = 3.72$ ($J = 7.5$ Hz), a 1 hydrogen triplet at $\delta = 5.60$ ($J = 7.5$ Hz), a 15 hydrogen multiplet in the region $\delta =$ 6.82–7.78, and a 1 hydrogen singlet at $\delta = 8.09$.

The i.r. spectrum ($CHCl_3$) showed C=N at 1630 cm^{-1}.

The geometrical isomer, *trans,cis*-**2** was not isolated but was characterized from its n.m.r. spectrum (CCl_4) in the mixture before t.l.c.; a 2 hydrogen doublet at $\delta =$ 3.36 ($J = 8$ Hz), a 1 hydrogen triplet at $\delta = 6.01$ ($J =$ 8 Hz), a 1 hydrogen singlet at $\delta = 7.86$, and a 15 hydrogen multiplet at the region $\delta =$ 6.82–7.78 as obtained by difference.

Diels–Alder Reaction of trans,trans-2 and trans,cis-2 with 4-Phenyl-1,2,4-triazoline-3,5-dione

The relative rates of reaction of a 2:1 mixture of *trans,cis*-**2** and *trans,trans*-**2** (0.1 g, 0.34 mmol in 0.5 ml CCl_4) were followed by n.m.r. monitoring of the doublets at $\delta = 3.36$ and 3.72 as aliquots (3 mg, 0.017 mmol) of 4-phenyl-1,2,4-triazoline-3,5-dione were added. The final ratio of doublets was 8:1 before the upfield doublet disappeared into the other increasing signals. After solvent removal, the crude oil was separated by t.l.c. (silica gel, chloroform) yielding the Diels–Alder adduct (45 mg, 33%) as the major product (m.p. 105–107° from hexane–benzene). Mass spectrum: $m/e = 472.7$ for molecular ion. The n.m.r. spectrum ($CDCl_3$) showed a 2 hydrogen AB part of an ABX at $\delta = 3.05$–3.65 ($\nu_a = 3.16$, $\nu_b = 3.50$ and $J_{ab} = 14$ Hz, $J_{ax} = 5$ Hz, and $J_{bx} = 6$ Hz), the 1 hydrogen X part at $\delta = 5.72$, a 1 hydrogen singlet at $\delta =$ 6.46, and a 20 hydrogen multiplet at $\delta = 6.86$–8.06. The i.r. spectrum ($CHCl_3$) showed carbonyl bands at 1780 and 1720 cm^{-1}.

trans-2,4,5-Triphenyl-1-pyrroline (trans-3)

A degassed solution of **1** (0.1 g, 0.34 mmol) in 0.68 ml of 0.53 *M* potassium *tert*-butoxide in *tert*-butyl alcohol in a sealed evacuated tube was heated for 30 min at 120°. The reaction mixture was extracted using ether, and washed with water, with saturated sodium chloride and dried with magnesium sulfate. After ether removal, the residue was separated by t.l.c. (10% ether in hexane) and the main band yielded 68 mg (68%) of material (m.p. 89.5–91, from hexane). Mass spectrum: $m/e = 297$ for molecular ion.

The n.m.r. spectrum ($CDCl_3$) showed a 2 hydrogen multiplet $\delta = 7.61$–8.02 and a 13 hydrogen multiplet $\delta = 6.94$–7.50. The remaining 4 hydrogen pattern was analyzed as an ABCM with the assistance of the LAOCOON III program: $\nu_a = 3.16$, $\nu_c = 3.40$, $\nu_b = 3.58$, $\nu_m = 5.30$ and $J_{ab} = -16.8$ Hz, $J_{ac} = 7.6$ Hz, $J_{bc} = 9.3$, $J_{am} = 2.0$ Hz, $J_{bm} = 2.2$ Hz, and $J_{cm} = 6.7$ Hz. The i.r. spectrum ($CHCl_3$) showed no N—H absorption and C=N at 1602 cm^{-1}.

cis-2,4,5-Triphenyl-1-Pyrroline (cis-3)

A solution of **1** (0.1 g, 0.34 mmol) in a minimum of THF was added by syringe to a solution of 0.5 mmol lithium 2,2,6,6-tetramethylpiperidide in 5 ml of THF held at −78° under an argon atmosphere. After stirring for 30 min at 0–6°, the dark blue solution was treated with an excess of acetic acid. The reaction mixture was treated with water and ether and the ether layer was washed twice with water, once with saturated sodium chloride solution, dried, filtered, and solvent removed. Nuclear magnetic resonance of the residual oil indicated 85% conversion to cyclic materials. Silica gel t.l.c. (10% ether in hexane) yielded 29% *trans*-**3** and 35% *cis*-**3** plus 5% of 2,3,5-triphenylpyrrole. Compound *cis*-**3** (m.p. 88–90°) depressed the m.p. of *trans*-**3** and was recovered unchanged after melting. Mass spectrum: *m/e*-297 for molecular ion. The n.m.r. spectrum (CCl_4) showed a 2 hydrogen multiplet $\delta = 7.82$–8.15, a 13 hydrogen multiplet $\delta = 6.60$–7.58, 1 hydrogen multiplet 5.43–5.64, 1 hydrogen multiplet 3.79–4.21, 2 hydrogen multiplet 3.18–3.48. The i.r. spectrum ($CHCl_3$) showed no N—H absorption and C=N at 1611 cm^{-1}.

2,3,5-Triphenylpyrrole

Both *cis*-**3** and *trans*-**3** (94 mg, 0.32 mmol) were oxidized separately in 5 ml of benzene at reflux under an argon atmosphere using 2,3-dichloro-5,6-dicyano-1,4-benzoquinone (72 mg, 0.32 mmol). After 1 h at reflux, the solution was concentrated and the product purified by t.l.c. (silica gel, 10% ether in benzene) yielded 63 mg (67%) of material (m.p. 138–140°, undepressed by admixture with an authentic sample) (13).

Isotopic Exchange of trans-3

A degassed solution of *trans*-**3** (75 mg, 0.25 mmol) in 1 ml of 0.24 *N* potassium *tert*-butoxide in *tert*-butyl alchol-*O-d* in a sealed evacuated tube was heated at 120° for 30 min. After cooling, the reaction mixture was extracted using ether and water. After drying and solvent removal, the residue was purified by t.l.c. (silica gel, 10% ether–hexane). After recrystallization from hexane, mixture m.p. with *trans*-**3** showed no depression and both the n.m.r. and mass spectra showed incorporation of 4 atoms D/molecule into the pyrroline ring.

Isomerization of cis-3

A degassed solution of *cis*-**3** (100 mg, 0.34 mmol) in 0.68 ml of 0.54 *M* potassium *tert*-butoxide in *tert*-butyl alcohol in a sealed evacuated tube was heated at 120° for 30 min. After the usual work-up, the residue recrystallized from hexane yielded 88% of material of m.p. 89–91° (undepressed by admixture with an authentic sample of *trans*-**3**).

Isomerization and Exchange of 1

To the stirred degassed potassium methoxide in methanol (methanol-*O-d*) solution held at constant temperature and under an argon atmosphere was added solid **1**. At the reported time the reaction was poured into water and ether. The ether layer was washed twice with water, once with saturated sodium chloride solution, dried over magnesium sulfate and solvent removed on a rotary evaporator. The residual oils were analyzed by n.m.r. and separated by t.l.c. (silica gel, 10% ether in hexane).

The deuterium content of **1** was determined by analyzing (mass spectroscopy) the β-phenylpropiophenone obtained by hydrolysis on silica gel.

Isomerization of 1 with Lithium 2,2,6,6-Tetramethylpiperidide

To a stirred degassed solution of LiTMP in THF under argon at the reported temperature, was added solid **1**. After stirring for the reported time, the reaction was quenched with water and extracted with ether *vs.* water. The ether layer was further extracted twice with water, once with saturated sodium chloride solution, dried over magnesium sulfate, filtered, and the solvent removed with a rotary evaporator. The residual oils were separated by silica gel t.l.c. (10% ether in hexane) and analyzed by n.m.r.

The authors wish to thank the National Research Council of Canada for financial support.

1. D. H. HUNTER and S. K. SIM. J. Am. Chem. Soc. **91**, 6202 (1969); Can. J. Chem. **50**, 669, 678 (1972).
2. R. B. BATES, D. N. GOSSELINK, and J. A. KACZYNSKI. Tetrahedron Lett. 205 (1967); G. J. HEIZWOLF and H. KLOOSTERZIEL. Rec. Trav. Chim. Pays-Bas, **86**, 807 (1967); W. T. FORD and M. NEWCOMB. J. Am. Chem. Soc. **96**, 309 (1974).
3. C. G. MCCARTY. *In* The chemistry of the carbon–nitrogen double bond. Interscience, New York, N.Y. 1970. pp. 364–373; H.-O. KALINOWSKI and H. KESSLER. *In* Topics in stereochemistry. Vol. 7. Interscience, New York, N.Y. 1973. p. 295.
4. L. D. MCKEEVER. *In* Ions and ion pairs in organic reactions. Vol. 1. Wiley-Interscience, New York, N.Y. 1972. p. 263.
5. D. H. HUNTER. *In* Isotopes in organic chemistry. Vol. 1. Elsevier, Amsterdam. 1975. In press.
6. D. J. CRAM. Fundamentals of carbanion chemistry. Academic Press, New York, N.Y. 1965.
7. R. B. WOODWARD and R. HOFFMANN. The conservation of orbital symmetry. Academic Press, Germany. 1971.
8. J. P. SNYDER. Private communication; N. P. EPIOTIS. J. Am. Chem. Soc. **95**, 1200 (1973).
9. D. J. CRAM, F. WILLEY, H. P. FISCHER, and D. A. SCOTT. J. Am. Chem. Soc. **86**, 5370 (1964); D. J. CRAM, F. WILLEY, H. P. FISCHER, H. M. RELLES, and D. A. SCOTT. J. Am. Chem. Soc. **88**, 2759 (1966); R. D. GUTHRIE and G. R. WEISMAN. Chem. Commun. 1316 (1969).
10. R. B. BATES, S. BRENNER, C. M. COLÉ, E. W. DAVIDSON, G. D. FORSYTHE, D. A. MCCOMBS, and A. S. ROTH. J. Am. Chem. Soc. **95**, 926 (1973); R. J. BUSHBY and G. L. FERBER. Chem. Commun. 407 (1973).
11. A. E. STREITWIESER, L. VERBIT, and P. STANG. J. Org. Chem. **29**, 3706 (1964).
12. A. T. YOUNG and R. D. GUTHRIE. J. Org. Chem. **35**, 853 (1970).
13. J. M. PATTERSON and S. SOEDIGDO. J. Org. Chem. **33**, 2057 (1968).

Can. J. Chem. Downloaded from www.nrcresearchpress.com by 210.87.254.5 on 09/05/12
For personal use only.

A Nuclear Magnetic Resonance Study of the Conformation of Six-membered Chelate Rings in Four-coordinate Complexes

WILLIAM R. CULLEN, LAURANCE D. HALL, JOHN T. PRICE, AND GREGORY SPENDJIAN

Chemistry Department, University of British Columbia, Vancouver, British Columbia V6T 1W5

Received July 15, 1974

WILLIAM R. CULLEN, LAURANCE D. HALL, JOHN T. PRICE, and GREGORY SPENDJIAN. Can. J. Chem. **53**, 366 (1975).

The ditertiary arsine $(CH_3)_2AsCH_2CH(C(CH_3)_3)CD_2As(CH_3)_2$ (L–L) forms 'tetrahedral' (L–L)Ni(CO)$_2$ and square planar (L–L)NiOC(CF$_3$)$_2$C(CF$_3$)$_2$O. In both complexes the conformations of the chelate rings are locked with the *t*-butyl groups equatorial. The dihedral angles are very similar in spite of the anticipated differences in angles at the central atom. The square planar complexes (L–L)′PtbipyCl$_2$ and (L–L)$_2$′PtCl$_2$ and their palladium analogs ((L–L)′ = $H_2NCH_2CH(C(CH_3)_3)CD_2NH_2$) also have their chelate rings in locked chair conformations. This results in the identification of isomers in the case of (L–L)$_2$′M^{2+}. The $^3J_{H-H}$ couplings indicate that the dihedral angles are similar in the group VIII complexes with a degree of puckering which could be less than in related complexes of L–L. The $^3J_{Pt-H}$ couplings indicate changes in the puckering about the N...N axis.

WILLIAM R. CULLEN, LAURANCE D. HALL, JOHN T. PRICE et GREGORY SPENDJIAN. Can. J. Chem. **53**, 366 (1975).

L'arsine ditertiaire $(CH_3)_2AsCH_2CH(C(CH_3)_3)CD_2As(CH_3)_2$(L–L) forme des complexes (L–L)Ni(CO)$_2$ tétraédrique et (L–L)NiOC(CF$_3$)$_2$C(CF$_3$)$_2$O plan carré. Dans chacun de ces complexes, les conformations des cycles des ligands sont bloquées avec les groupements *t*-butyles en positions équatoriales. Les angles dièdres sont très semblables malgré les différences que l'on aurait pu anticiper pour les angles vers l'atome central. Dans les complexes plan carré (L–L)′PtbipyCl$_2$ et (L–L)$_2$′PtCl$_2$ de même que dans leurs analogues avec du palladium ((L–L)′ = $H_2NCH_2CH(C(CH_3)_3)CD_2NH_2$), les cycles des ligands sont aussi bloqués dans des conformations chaises. Ceci conduit à l'identification d'isomères dans le cas des complexes (L–L)$_2$′M^{2+}. Les constantes de couplage $^3J_{H-H}$ indiquent que les angles dièdres sont similaires dans les complexes du groupe VIII avec un degré de plissement qui pourrait être plus faible que dans les complexes apparentés contenant les groupes (L–L). Les constantes de couplage $^3J_{Pt-H}$ montrent qu'il y a un changement dans le degré de plissement autour de l'axe N...N.

[Traduit par le journal]

Introduction

In earlier publications (1–5) we have discussed the conformation of five- and six-membered chelate rings in the octahedral metal carbonyl complexes (L–L)M(CO)$_4$ and (L–L)M′(CO)$_3$X, (M = Cr, Mo, W; M′ = Mn, X = Cl, Br, I). The ligands, L–L, were specially prepared to allow studies by high resolution n.m.r. techniques and in particular were of the type $(CH_3)_2AsCH_2$-$CHRCH_2As(CH_3)_2$ (R = H, **1**; R = CH_3, **2**; R = $C(CH_3)_3$, **3**) for the studies on the six-membered chelate rings (4, 5). We were able to show that complexes of **1** with the group VI carbonyls undergo fast conformational chair $\rightleftharpoons$ chair interconversion while the similar complexes of **3** have locked chair configurations with the *t*-butyl group in an equatorial position. Similarly the Mn(CO)$_3$X complexes of **3** were locked allowing the characterization of two isomers **A** and **B**, X = halogen. R = *t*-butyl. The preferred isomers have the same chair configuration as the

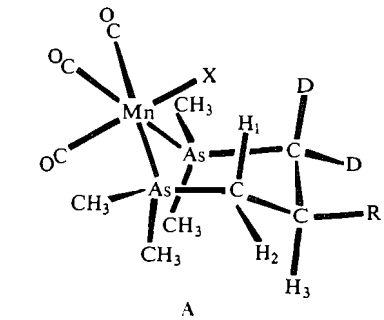

A

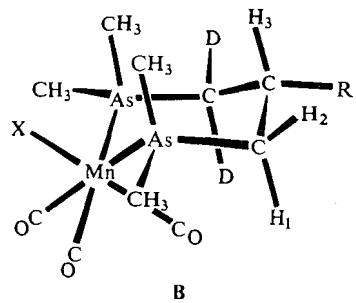

B

Can. J. Chem. Downloaded from www.nrcresearchpress.com by 210.87.254.6 on 09/05/12
For personal use only.

Can. J. Chem. Downloaded from www.nrcresearchpress.com by 210.87.254.6 on 09/05/12
For personal use only.

analogous complexes of **1** (**A**, R = H) which, surprisingly, are also locked (5). This preferred configuration is the one that minimizes the interaction between the arsenic methyl groups and the axial halogen atom (6). Conformational calculations (7, 8) predict that the six-membered rings would be puckered chairs as we have found in solution (4, 5) and as others have found in the solid state (*e.g.* 6, 9–11).

The present work extends our n.m.r. and conformational study of six-membered chelate ring systems to four-coordinate complexes of Ni, Pd, and Pt. Ligand **3** and the analogous diamine ligand ($NH_2CH_2CH(C(CH_3)_3)CH_2NH_2$, **4**) were used as chelating agents. Selectively deuterated ligands, **3**-d_2 and **4**-d_2 $(CH_3)_2AsCH_2CH(C(CH_3)_3$-$CD_2As(CH_3)_2$ and $NH_2CH_2CH(C(CH_3)_3)$-CD_2NH_2, were prepared in order to simplify the n.m.r. spectra of the chelate complexes.

Experimental

Infrared spectra were recorded on a Perkin-Elmer 457 instrument. The n.m.r. spectra were run on an extensively modified Varian HA-100 instrument (12). The final refined n.m.r. parameters were obtained using the LAOCOON III program modified for use on the U.B.C. IBM 300-67 computer. Microanalyses were done by Mr. Peter Borda of this department.

Preparation of Ligands

The preparation of ligands **3** and **3**-d_2 has been described previously (4). The preparation of 1,3-diamino-2-*t*-butylpropane, ligand **4**, is described below. This and the analogous deuterated compound **4**-d_2 were prepared in a similar manner starting with the appropriate diol, $HOCH_2CH(C(CH_3)_3)CH_2OH$ or $HOCD_2CH(C(CH_3)_3)CH_2OH$, which were prepared as previously reported (4). Perfluoropinacol (PFP) was prepared according to published procedures (13).

The Preparation of 2-t-Butyl-1,3-propanediol Ditosylate

2-*t*-Butyl-1,3-propanediol (15 g) was added slowly to tosyl chloride (50 g) in pyridine (200 ml) and the resulting solution stirred for 16 h at 5°. Water (100 ml) was added and the mixture maintained at a temperature of 5° for an additional hour before additional water (1 l) was added. The resulting precipitate was filtered to give a crude yield of 40 g (82%). The compound was recrystallized from ethanol and its n.m.r. spectrum measured on a sample dissolved in $CDCl_3$. Resonance signals centered at 7.6 (area 8), 4.2 (area 4), 2.5 (area 6), 1.8 (area 1), and 0.96 (area 9) p.p.m. correspond to the aryl, methylene, methyl, methyne, and *t*-butyl protons, respectively.

The Preparation of 1,3-Diamino-2-t-butylpropane

Sodium azide (35 g) was added to a solution of 2-*t*-butyl-1,3-propanediol ditosylate (35 g) in dimethylformamide (300 ml). The temperature of the suspension was raised to 130–140° and stirred continuously for 4 h. The cooled mixture was diluted with ether (300 ml) and then extracted with eight (100 ml) portions of water. The remaining ether layer was dried over anhydrous sodium sulfate for 2 h, filtered, and reduced in volume (to 50 ml). The resulting azide solution was diluted with anhydrous THF (50 ml) and added slowly to a suspension of excess $LiAlH_4$ (15 g) in anhydrous THF (50 ml) and stirred at room temperature for 2 h and at 50° for an additional 8 h. The THF suspension was cooled and treated with water (15 ml), 15% sodium hydroxide solution (15 ml), and again with water (45 ml). The resulting suspension was filtered and the filtrate dried over anhydrous sodium sulfate, filtered, then evaporated to leave a pale yellow liquid (6.3 g) (yield 60%).

The 1,1-dideutero-2-*t*-butyl-1,3-diaminopropane was prepared in a similar manner. This ligand's n.m.r. spectrum ($CDCl_3$ solution) shows resonance multiplets centered at 2.9 (area 2), 2.1 (area 4), 1.3 (area 1), and 1.0 (area 9) p.p.m. from TMS and represent the methylene, amine, methyne, and *t*-butyl protons, respectively. Upon the addition of D_2O, the signal at 2.1 p.p.m. disappeared while a new signal appeared at 4.7 p.p.m. attributable to the formation of HOD. The i.r. spectrum (liquid film) had adsorptions at 3370 (s), 3280 (s), 2960 (s), 2860 (s), 2200 (w), 2090 (w), 1595 (s), 1475 (s), 1395 (m), 1365 (m), and 900 (m) cm^{-1}. The bands at 2200 and 2090 cm^{-1} are attributed to the C—D stretching absorptions and are not the result of an azide impurity. The diamine was used directly for complex formation without further purification.

Preparation of Complexes

The Preparation of $(CO)_2NiAs(CH_3)_2CH_2CH$-$((CH_3)_3)CH_2As(CH_3)_2$

1,3-Bis(dimethylarsino)-2-*t*-butylpropane (0.5 g) was added to a stirred solution of nickel carbonyl in benzene and was maintained under a nitrogen atmosphere. After heating the mixture to 40° for 30 min, the resulting yellow solution was filtered and evaporated to dryness. The residue was sublimed (80° at 0.01 mm) to yield a cream-colored solid (0.55 g, 81%) m.p. 135°. The i.r. spectrum of a sample dissolved in cyclohexane had two carbonyl stretching vibrations at 2005 (s) and 1944 (vs) cm^{-1}.

Anal. Calcd. for $C_{13}H_{26}As_2NiO_2$: C, 36.7; H, 6.12. Found: C, 36.6; H, 6.29.

The Preparation of $O(CF_3)_2CC(CF_3)_2ONiAs(CH_3)_2$-$CH_2CH(C(CH_3)_3)CH_2As(CH_3)_2$

Upon the addition of ligand **3** to a solution of potassium bis(perfluoropinacolato)nickel(II) in benzene (30 ml) at 40° under a nitrogen atmosphere a change in color from violet to orange was observed. The orange solution was extracted with two portions of water (10 ml), dried over anhydrous sodium sulfate, filtered, and evaporated to dryness. The orange residue was recrystallized from CH_2Cl_2 – petroleum ether to give orange crystals, m.p. 245° (yield 80%). The ^{19}F n.m.r. spectrum of the complex measured in $CHCl_2$ solution showed a sharp resonance at 73.0 p.p.m. upfield from $CFCl_3$.

Anal. Calcd. for $C_{17}H_{26}As_2F_{12}NiO_2$: C, 29.1; H, 3.70. Found: C, 29.0; H, 3.70.

The Preparation of $NH_2CH_2CH(C(CH_3)_3)CH_2NH_2$-$MCl_2$ (M = Pd or Pt)

An equimolar quantity of the diamine ligand (0.2 g) was added to an aqueous solution of K_2MCl_4 and stirred at 50° for 2–3 min. The precipitate of complex chloride was filtered and washed with water until no chloride ion could be detected by silver nitrate solution. This almost colorless material was used directly for further syntheses.

The Preparation of $(NH_2CH_2CH(C(CH_3)_3)CH_2NH_2)_2MCl_2$

The diamine ligand was added to an equimolar quantity of $(NH_2CH_2CH(C(CH_3)_3)CH_2NH_2)MCl_2$ in water (15 ml), then stirred and heated (80°) until most of the insoluble material had dissolved. The solution was filtered and the filtrate reduced in volume (1 ml). The white product was precipitated by the addition of acetone, then recrystallized from concentrated solutions of water (5°) (yield ~85%).

Anal. Calcd. for $C_{14}H_{36}Cl_2N_4Pt$: C, 31.9; H, 6.8; N, 10.6. Found: C, 31.8; H, 7.0; N, 10.9.

Anal. Calcd. for $C_{14}H_{36}Cl_2N_4Pd$: C, 38.4; H, 8.3; N, 12.8. Found: C, 38.4; H, 9.0; N, 12.9.

The deuterated analogs were prepared similarly.

The Preparation of $[(bipy)MNH_2CH_2CH(C(CH_3)_3)CH_2NH_2]Cl_2$

α,α′-Dipyridyl (0.2 g) was added to an equimolar quantity of $NH_2CH_2CH(C(CH_3)_3)CH_2NH_2MCl_2$ in water (20 ml) then stirred and heated (90°) for 1 h under an atmosphere of nitrogen. The resulting solution was filtered, then reduced in volume (1 ml) before acetone was added to precipitate the product. The pure (yellow) products were obtained by recrystallizing twice from concentrated solutions of acetone–water at 5° (yield 80%).

Anal. Calcd. for $C_{17}H_{26}Cl_2N_4Pd.2H_2O$: C, 40.9; H, 6.0; N, 11.2. Found: C, 40.5; H, 6.2; N, 11.0.

Anal. Calcd. for $C_{17}H_{26}Cl_2N_4Pt.2H_2O$: C, 34.6; H, 5.1; N, 9.5. Found: C, 34.2; H, 5.6; N, 9.4.

The n.m.r. spectra of the Pd and Pt complexes have signals attributed to the dipyridyl group at 8.21 and 8.75 p.p.m. and 8.14 and 8.75 p.p.m., respectively, from external TMS. The signals attributed to the six-membered ring protons are summarized in Table 1.

Results and Discussion

The new ligand 1,3-diamino-2-*t*-butylpropane, **4**, was prepared from the appropriate diol via the azide (Scheme 1). Althought the method is not original (14, 15) it is given in detail since deviations result in diminished yields.

The n.m.r. spectrum of the amine was as expected and, although it was not subjected to microanalysis, the complete characterization of its complexes leaves no doubt that it is formulated correctly.

The bis dimethylarsino analog **3** reacts with nickel tetracarbonyl to afford the expected chelate complex $(L\text{–}L)Ni(CO)_2$ (L–L = **3**). This complex which contains nickel in the zero oxidation state is probably pseudo tetrahedral. The diamagnetic square planar complex (L–L)Ni(PFP) (L–L = **3**, PFP = $^-O—C(CF_3)_2—C(CF_3)_2—O^-$) which contains nickel(II) was also prepared.

In order to simplify the n.m.r. spectra the complex $(L\text{–}L)Ni(CO)_2$ (L–L = **3**-d_2) was measured in a saturated benzene solution (the complex decomposes in $CHCl_3$). The spectrum of the ring protons is of the ABX type. The downfield

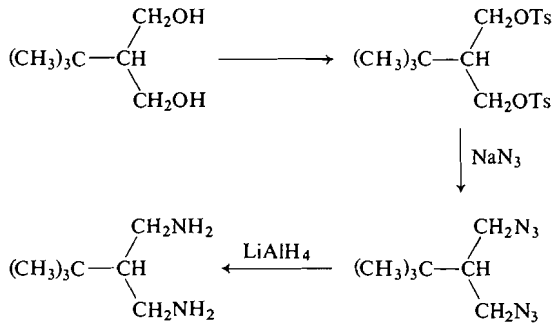

SCHEME 1

portion of the spectrum is deceptively simple and is seen as a doublet which is sharpened only slightly when the sample is deuterium decoupled. The AB portion of the spectrum is partly hidden by the arsenic methyl signal but it is considerably sharpened when the sample is deuterium decoupled. The AB portion of the spectrum is, therefore, associated with the axial proton on the ring carbon adjacent to the arsenic atom and the axial proton on the central carbon atom. Similarly the n.m.r. spectrum of $PFPNiAs(CH_3)_2\text{-}CH_2CH(C(CH_3)_3)CD_2As(CH_3)_2$ (measured in CH_2Cl_2) is also of the deceptively simple ABX type and is similar in appearance to the spectra of the analogous group VIB complexes $(L\text{–}L)M(CO)_4$ (4). The downfield X portion of the spectrum sharpened only slightly upon deuterium decoupling when compared with the upfield AB portion which indicates the two protons on the carbon adjacent to the arsenic atoms have quite different chemical shifts; the upfield one is near the chemical shift of the proton on the central carbon atom. All the derived n.m.r. parameters are listed in Table 1.

Both nickel complexes have vicinal coupling constants for the protons on the ring carbons with values of approximately 12 and 1 Hz (Table 1). The former value is representative of an axial–axial interaction between the two vicinal protons and indicates that the *t*-butyl group occupies an equatorial position with respect to the 'locked' ring. The values are comparable to those found in the analogous group VIB complexes which are thought to have puckered chair configurations (4). The $^3J_{H_{ax}-H_{eq}}$ coupling (~1 Hz) for these nickel complexes are slightly smaller than they are for the analogous manganese tricarbonyl halides (~2 Hz) (5) and may indicate that the nickel compounds are slightly

Can. J. Chem. Downloaded from www.nrcresearchpress.com by 210.87.254.6 on 09/05/12
For personal use only.

Can. J. Chem. Downloaded from www.nrcresearchpress.com by 210.87.254.6 on 09/05/12
For personal use only.

TABLE 1. Selected n.m.r. parameters of complexes[a]

	δ					J_{H-H}			J_{Pt-H}	
				—CH_2As(N)		Vicinal		Geminal		
	As$(CH_3)_2$		—C$(CH_3)_3$	—C*H*R—	H_{ax}	H_{eq}	J_{ax-eq}	J_{ax-ax}	J	$J_{Pt-H_{eq}}$	$J_{Pt-H_{ax}}$
$(CO)_2NiAs(CH_3)_2CH_2CH(C(CH_3)_3)CD_2As(CH_3)_2$	1.01	1.02	0.71	0.94	0.70	1.66	0.9	11.7	−12.4		
$PFPNiAs(CH_3)_2CH_2CH(C(CH_3)_3)CD_2As(CH_3)_2$	1.34	1.39	0.88	1.07	1.04	1.78	1.2	12.3	−12.9		
$Cl_2Pt[NH_2CH_2CH(C(CH_3)_3)CD_2NH_3]_2$ A isomer			1.352	1.94	2.99	3.48	2.9	11.2	−12.5	62.0	22.0
B isomer			1.352	1.94	2.96	3.48	2.9	11.3	−12.5	62.0	22.0
$Cl_2Pd[NH_2CH_2CH(C(CH_3)_3)CD_2NH_2]_2$ A isomer			1.354	1.88	2.87	3.39	2.9	11.2	−12.7		
B isomer			1.354	1.88	2.85	3.39	2.9	11.2	−12.7		
$bipyPt[NH_2CH_2CH(C(CH_3)_3)CD_2NH_2]$			1.40	2.23	3.17	3.54	3.5	10.9	−12.8	54.5	30.5
$bipyPd[NH_2CH_2CH(C(CH_3)_3)CD_2NH_2]$			1.41	2.12	2.96	3.46	3.13	11.0	−12.8		

[a]Chemical shifts are given downfield from external TMS in p.p.m. The couplings involving platinum were measured from spectra obtained from a Varian XL-100 spectrometer using Fourier transform techniques. Couplings are given in Hz.

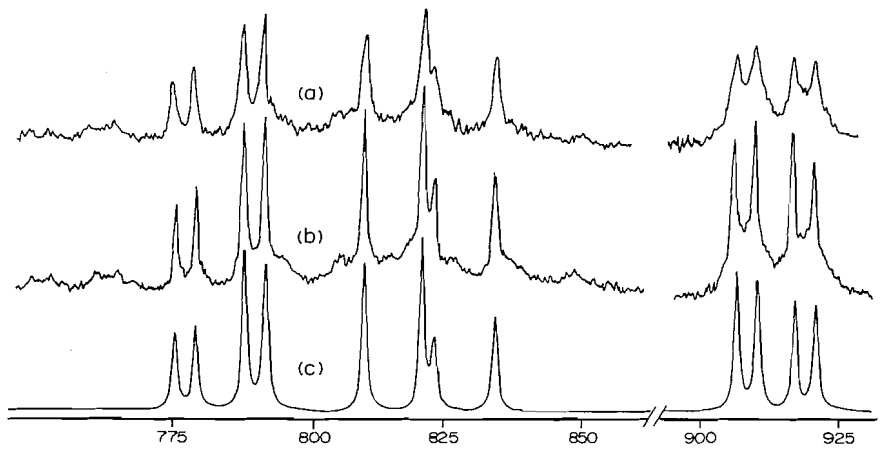

FIG. 1. The bridge proton region of the n.m.r. spectrum of $[bipyPtNH_2CH_2CH(C(CH_3)_3)CD_2NH_2]Cl_2$ in D_2O: (*a*) is the normal spectrum, (*b*) is the same region run with deuterium decoupling, (*c*) is the computer simulated spectrum using the parameters listed in Table 1.

more puckered. The small differences, however, may be caused by inductive effects and not by conformational distortions. It is not surprising to find that the conformation of the chelate ring in the octahedral and square planar complexes is very similar since the As—M—As angle is expected to be ~90° and this, together with the As—M distance is expected to have the greatest effect on ring conformations (2, 7). The 'tetrahedral' nickel complex $(L–L)Ni(CO)_2$ could be expected to have a different degree of puckering because the As—Ni—As could be greater than 90° but it seems that the angle subtended by a ligand at a metal is more a function of of the ligand than the metal. For example the P—Fe—P angle in the isoelectronic complex $(C_6H_5)_2PC{=}CP(C_6H_5)_2CF_2CF_2CF_2Fe(NO)_2$ is 87° (16).

The n.m.r. spectra of the nickel complexes were not measured in the same solvents as the analogous $M(CO)_4$ and $M(CO)_3X$ complexes because of solubility and stability problems. This makes it difficult to make a detailed comparison of the chemical shifts of the ring protons. It is probably significant that H_{ax} is considerably upfield of H_{eq} in the $—CH_2—$ group as is the case for the $(L–L)M(CO)_4$ complexes of ligands **1** and **3** (4). However in the 'locked' $(L–L)M'(CO)_3X$ complexes of ligand **1**, H_{ax} (2.24 p.p.m.) is downfield of H_{eq} (1.77 p.p.m.) (values are for X = Br) and the same trend is seen in the isomer of the $(L–L)M'(CO)_3X$ complex of ligand **3** which has the same conformation (**A**, R = H or *t*-butyl). In the case where X = Br, H_{ax} is at 1.86 p.p.m. and H_{eq} at 1.91 p.p.m. This downfield shift for H_{ax} when it is adjacent to an axial halogen on the metal may indicate some interaction between the two.

The diamine **4** reacts with MCl_4^- (M = Pt, Pd) to afford the insoluble MCl_2 derivatives which were not suitable for n.m.r. studies. Fortunately further reaction of **4** afforded the ionic $(L–L)_2M^{2+}2Cl^-$ which could be investigated in aqueous solution. In order to obtain a complex with only one ligand **4** chelated to the group VIII metal, the insoluble MCl_2 derivatives were treated with α,α′-dipyridyl to afford the water soluble $(L–L)M(bipy)^{2+}$ $2Cl^-$ complexes.

Figure 1 shows the n.m.r. spectrum of the ring protons of the platinum–bipy complex dissolved in D_2O. The upfield (X) portion of this ABX spectrum is considerably sharpened when the sample is deuterium decoupled and is associated with the proton on the central ring carbon. The AB portion of the spectrum is assigned to the protons on the ring carbon atom that is adjacent to a nitrogen atom. The equatorial proton has a chemical shift at lower field than the axial proton on the same carbon. The magnitudes of the coupling constants (Table 1) indicates an axial–axial interaction between protons 2 and 3, **A** which requires the *t*-butyl group to have taken an equatorial position and effectively locked the six membered ring. The n.m.r. spectrum of the diamine metal complexes definitely eliminates the possibility of any existence of skew-boat con-

Can. J. Chem. Downloaded from www.nrcresearchpress.com by 210.87.254.6 on 09/05/12
For personal use only.

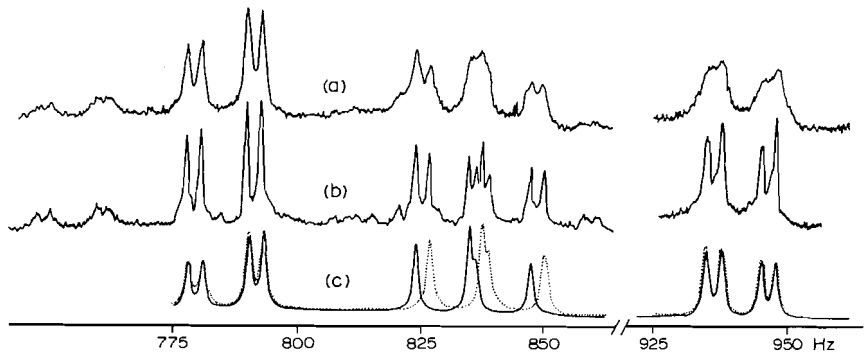

FIG. 2. The bridge proton region of the n.m.r. spectrum of $[Pt(NH_2CH_2CH(C(CH_3)_3)CD_2NH_2)_2]Cl_2$ in D_2O: (*a*) is the normal spectrum, (*b*) is the same region run with deuterium decoupling, (*c*) is the computer simulated spectrum using the parameters listed in Table 1, both isomers are included — and ... lines, but Pt–H couplings are not.

formers because a locked configuration of this type would lead to two conformers (depending upon the positions of the $-CD_2-$ and $-CH_2-$ groups relative to the ring). The $^3J_{Pt-H}$ couplings also provide evidence for a locked chair configuration as will be described below.

The parameters from the analogous palladium complex indicate a very similar structure in solution.

The n.m.r. spectrum of the ion $(L-L)_2Pt^{2+}$ (L–L = **4**) is shown in Fig. 2. Analysis of the spectrum shows that two isomers are present in solution in equal amounts. The derived parameters for the two isomers are nearly identical indicating both isomers have their six-membered rings locked in chair configurations with the *t*-butyl group equatorial (for the same reasons as those given for the dipyridyl complexes). The two isomers undoubtedly have the structures shown in Fig. 3 where both rings are locked with the *t*-butyl groups equatorial. The chemical shifts of the axial protons on the $N-CH_2-$ group differ slightly for each isomer and examination of Fig. 3 shows that these are the protons whose magnetic environment changes most in the two isomers. The palladium analog shows the same isomer distribution and the n.m.r. parameters indicate identical structures in solution. In a similar study of $(L-L)_2M^{2+}$ complexes Appleton and Hall (17, 18) isolated isomeric compounds for L–L = *meso*-$H_2NCH(CH_3)CH_2CH(CH_3)NH_2$. These are probably related as in Fig. 3 with the equatorial methyl groups providing the locking force. However the 60 MHz n.m.r. spectra did not reveal the difference. Their vicinal $^3J_{H-H}$ couplings of 2.5 Hz (ax–eq) and 11.0 Hz (ax–ax)

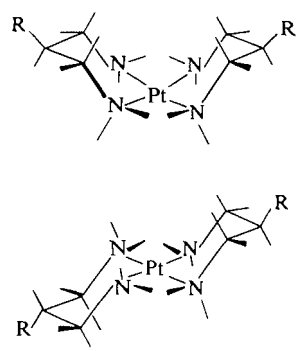

FIG. 3. Structures of the two isomers of $[Pt(NH_2CH_2CHRCH_2NH_2)_2]^{2+}$.

are similar to those obtained in the present investigation. In another paper (19) n.m.r. evidence for geometric isomerism was obtained by these workers when L–L is $H_2NCH_2CHOHCH_2NH_2$.

It seems that $^3J_{Pt-H}$ couplings follow a Karplus type relationship where the *trans* coupling is expected to be ~90 Hz and the *gauche*, ~31 Hz from amino acid derivatives (20) or ~65 and ~15 Hz, respectively, from diamine complexes (19, 21). In the platinum complexes of **4** both isomers of $(L-L)_2Pt^{2+}$ have the same values indicating that there is little steric interaction between the two halves of the ion. Furthermore the ratio $^3J_{Pt-H_{eq}}/^3J_{Pt-H_{ax}}$ is ~3. This indicates that the very similar values obtained by Appleton and Hall do indicate locked six-membered rings in the complexes of $H_2NCH_2CHXCH_2NH_2$ (X = Cl, OH) (19). In the dipyridyl complex of **4** the $^3J_{Pt-H}$ couplings are considerably changed

Can. J. Chem. Downloaded from www.nrcresearchpress.com by 210.87.254.6 on 09/05/12
For personal use only.

although their sum (54.5 + 30.5) Hz is much the same as in the $(L\text{–}L)_2Pt^{2+}$ complexes of the same ligand. This suggests that a conformational change involving the N—Pt—N and CNNC planes, has taken place since the $^3J_{H-H}$ are invarient.

Although it is difficult to compare coupling constants obtained from different compounds in different solvents, it seems that the ditertiary arsine complexes have slightly larger $^3J_{H_{ax}-H_{ax}}$ and smaller $^3J_{H_{ax}-H_{eq}}$ values than the diamine complexes. This could indicate that the diamine complexes are less puckered.

Our study indicates that the chemical shift of protons attached to ring carbons bonded to nitrogen are at lower field than those bonded to the central ring carbon and agreee with the results of Appleton and Hall (17, 19, 21). For a pair of geminal protons, the axial proton is as usual (22, 23) at higher field than the equatorial proton. In the arsenic complexes investigated the protons on the carbon bonded to arsenic are at much higher field than in the nitrogen complexes. This is presumably caused by the more electropositive nature of the arsenic atom relative to nitrogen.

The authors wish to thank the National Research Council of Canada for financial support of this work in the form of operating grants (to W.R.C. and L.D.H.) and Postdoctorate Fellowships (to J.T.P. and G.S.). We also thank Mr. R. B. Malcolm for helpful discussions.

1. W. R. CULLEN, L. D. HALL, and J. E. H. WARD. J. Am. Chem. Soc. **94**, 5702 (1972).
2. W. R. CULLEN, L. D. HALL, and J. E. H. WARD. J. Am. Chem. Soc. **96**, 3422 (1974).
3. W. R. CULLEN, L. D. HALL, and J. E. H. WARD. J. Am. Chem. Soc. **96**, 3431 (1974).
4. W. R. CULLEN, L. D. HALL, J. T. PRICE, and G. SPENDJIAN. J. Am. Chem. Soc. **96**, 410 (1974).
5. W. R. CULLEN, L. D. HALL, J. T. PRICE, and G. SPENDJIAN. Inorg. Chem. **13**, 2130 (1974).
6. C. A. BEAR and J. TROTTER. J. Chem. Soc. Dalton, 673 (1973).
7. J. R. GOLLOGLY and C. J. HAWKINS. Inorg. Chem. **8**, 1168 (1969).
8. L. J. DE HAYES and D. H. BUSCH. Inorg. Chem. **12**, 1505 (1973).
9. K. MATSUMOTO, S. OOI, and H. KUROYO. Bull. Chem. Soc. Jap. **43**, 1903 (1970).
10. Y. SAITO, T. NOMURA, and F. MARUMO. Bull. Chem. Soc. Jap. **41**, 530 (1968).
11. A. PAJUNIEN. Suom. Kemistilehti B, **41**, 232 (1968).
12. R. BURTON and L. D. HALL. Can. J. Chem. **48**, 59 (1970).
13. N. P. GAMBARYAN, Y. A. CHEBURKOV, and I. L. KNUNYANTS. Izv. Akad. Nauk SSSR. Ser. Khim. 1526 (1964).
14. E. B. FLEISCHER, A. E. GEBALA, A. LEVEY, and P. A. TASKER. J. Org. Chem. **36**, 3042 (1971).
15. M. S. NEWMAN, D. H. BUSCH, G. E. CHENEY, and C. R. GUSTAFSON. Inorg. Chem. **11**, 2890 (1972).
16. W. HARRISON and J. TROTTER. J. Chem. Soc. A, 1542 (1971).
17. T. G. APPLETON and J. R. HALL. Inorg. Chem. **9**, 1807 (1970).
18. T. G. APPLETON and J. R. HALL. Inorg. Chem. **9**, 1800 (1970).
19. T. G. APPLETON and J. R. HALL. Inorg. Chem. **11**, 117 (1972).
20. L. E. ERICKSON, M. D. ERICKSON, and B. L. SMITH. Inorg. Chem. **12**, 412 (1973).
21. T. G. APPLETON and J. R. HALL. Inorg. Chem. **10**, 1717 (1971).
22. F. A. BOVEY. Nuclear magnetic resonance spectroscopy. Academic Press, New York. 1969. p. 364.
23. W. J. KASOWSKI and J. C. BAILAR. J. Am. Chem. Soc. **91**, 3212 (1969).

Can. J. Chem. Downloaded from www.nrcresearchpress.com by 210.87.254.6 on 09/05/12
For personal use only.

Investigations of Substituent Effects by Nuclear Magnetic Resonance Spectroscopy and All-valence Electron Molecular Orbital Calculations. IV. 4-Substituted Phenylacetylenes[1]

DANIEL A. DAWSON[2] AND WILLIAM F. REYNOLDS
Department of Chemistry, University of Toronto, Toronto, Ontario M5S 1A1

Received July 15, 1974

DANIEL A. DAWSON and WILLIAM F. REYNOLDS. Can. J. Chem. **53**, 373 (1975).

^{13}C and ^{1}H spectra have been determined for 18 4-substituted phenylacetylenes and carbon charge densities have been estimated by CNDO/2 molecular orbital calculations. Correlations of these parameters with σ_I and σ_R^0 indicate that the important mechanisms of transmission of substituent effects are field, resonance, and π polarization effects, as previously noted for 4-substituted styrenes. Evidence is presented that demonstrates that both ^{1}H and ^{13}C chemical shifts for these compounds reflect ground state charge densities. CNDO/2 calculations on a variety of aromatic derivatives suggest that the σ_I dependence of ^{19}F chemical shifts in these derivatives may primarily be due to π polarization.

DANIEL A. DAWSON et WILLIAM F. REYNOLDS. Can. J. Chem. **53**, 373 (1975).

On a déterminé les spectres r.m.n. du ^{1}H et du ^{13}C de 18 phénylacétylènes substitués en position 4 et on a estimé les densités de charge au carbone par des calculs d'orbitales moléculaires CNDO/2. Les corrélations de ces paramètres avec σ_I et σ_R° montrent que les mécanismes important de transmission des effets des substituants sont des effets de champ de résonance et de polarisation π tel que noté antérieurement pour des styrènes substitués en position 4. Les données sont présentées pour démontrer que les déplacements chimiques du proton et du carbone 13 pour ces composés réflètent les densités de charges à l'état fondamental. Les calculs CNDO/2 sur un grand nombre de dérivés aromatiques suggèrent que la dépendance des déplacements chimiques du ^{19}F sur σ_I dans ces dérivés peut être due principalement à une polarisation π.
[Traduit par le journal]

Introduction

We recently utilized n.m.r. spectral parameters (measured under inert conditions) and all-valence electron molecular orbital calculations to determine mechanisms of transmission of substituent effects in a series of 4-substituted styrenes and α-alkylstyrenes (1, 2). It was concluded that field effects, resonance effects, and π inductive (polarization) effects are all important in determining electronic distributions in these molecules.

Classical electric field calculations (3), CNDO/2 molecular orbital calculations (4), and correlations of ^{1}H and ^{13}C chemical shifts with field (F) and resonance (R) divided substituent parameters (DSP) (5) were used to determine mechanisms of transmission of substituent effects in styrenes. If chemical shift – DSP correlations are valid (see refs. 6 and 7 for objections to the approach), then the weighting factors for closely related systems should vary in a manner which is consistent with the proposed mechanisms of transmission of substituent effects (1). This has been partially tested by comparing results for nonplanar α-alkylstyrenes with those for planar styrenes (2).

As a further test, it was decided to carry out a similar investigation of 4-substituted phenylacetylenes. The only previous systematic investigation of this system was by Cook and Danyluk who measured ^{1}H chemical shifts of eight 4-substituted phenylacetylenes at infinite dilution in CCl_4 (8). Since CCl_4 is not an inert solvent for ^{1}H chemical shifts (9), this prevented a meaningful comparison with the styrene data which were determined in C_6H_{12} (1). In addition, it has been suggested that a minimum of 10 substituents should be included in an investigation of this type (6, 10). Consequently, a more detailed investigation seemed necessary. ^{13}C and ^{1}H chemical shifts have been measured (under inert conditions) for 18 4-substituted phenylacetylenes. Results are reported below.

Results and Discussion

^{1}H and ^{13}C chemical shifts and ^{13}C–^{1}H coupling constants are given in Table 1. In most

[1]For part III see ref. 24.

[2]Walter P. Sumner Memorial Fellowship holder, 1972–1974.

Can. J. Chem. Downloaded from www.nrcresearchpress.com by 210.87.254.5 on 09/05/12
For personal use only.

TABLE 1. ^1H and ^{13}C chemical shifts (in p.p.m. to low field of internal tetramethylsilane) and ^{13}C–^1H coupling constants (in Hz) for 4-substituted phenylacetylenes

Substituent	δ_H	$\delta_{C(\beta)}$	$\delta_{C(\alpha)}$	$\delta_{C(1)}$	$\delta_{C(2,6)}$	$\delta_{C(3,5)}$	$\delta_{C(4)}$	$J_{C(\beta)-H}$
H	2.7883	77.06	83.52	122.52	131.96	127.94	128.24	250.9
NH_2	2.6336	74.77	84.20	111.94	133.21	114.09	146.38	249.3
$N(CH_3)_2$	2.6413	74.78	84.52	109.81	132.86	111.51	149.85	248.9
OCH_3	2.6928	75.67	83.52	114.57	133.25	113.61	159.68	249.8
$C(CH_3)_3$	2.7298	76.36	83.62	119.54	131.71	124.81	151.09	249.9
CH_3	2.7302	76.36	83.62	119.54	131.86	128.67	137.67	249.9
OC_6H_5	2.7430	76.41	83.12	116.81	—[a]	—	—	250.8
F	2.7735	76.82	82.43	118.42	133.79	115.36	162.60	251.1
SCH_3	2.7796	77.07	83.28	118.60	132.07	125.60	139.67	250.7
$Si(CH_3)_3$	2.7960	77.37	83.63	122.68	131.02	132.70	140.67	250.5
$CH=CH_2$	2.8194	77.66	83.43	121.68	132.06	125.80	137.58	251.0
Cl	2.8391	78.03	82.36	120.75	133.04	128.40	134.77	251.6
C_6H_5	2.8398	77.62	83.43	121.14	—[a]	—	—	250.8
Br	2.8566	78.21	82.38	121.14	133.21	131.32	122.93	251.7
C≡C—H	2.8910	78.85	82.92	122.59	131.70	131.70	122.59	251.4
CF_3	2.9475	79.49	82.08	126.02	132.16	125.05	130.79	252.5
C≡N	3.0394	81.08	81.83	126.55	132.36	131.57	113.28	253.1
NO_2	3.0907	81.74	81.59	128.39	132.52	123.26	147.58	253.6

[a]Chemical shifts not assigned due to complexity of the spectrum.

cases, infinite dilution ^1H chemical shifts in C_6D_{12} were estimated from least-squares plots of ^1H chemical shift *vs.* concentration in the range 0.5–3 mol%. In those cases where solubility precluded dilution studies (see Experimental), infinite dilution shifts were taken as the chemical shift of a single solution of <0.25 mol%. It is estimated that infinite dilution chemical shifts are accurate to ±0.002 p.p.m. Repeated experimental measurements with different concentrations, spectral widths, etc. suggested that ^{13}C chemical shifts were accurate to ± 0.04 p.p.m. and ^{13}C–^1H coupling constants to ±0.2 Hz.

Hydrogen and carbon charge densities estimated by CNDO/2 molecular orbital calculations are summarized in Table 2.

(a) ^1H and ^{13}C Chemical Shifts and Mechanisms of Transmission of Substituent Effects

In order to compare mechanisms of substituent effects in 4-substituted styrenes and phenylacetylenes, it is particularly instructive to compare substituent-induced ^1H chemical shifts for the *trans* vinyl proton, H_c, in styrene and the ethynyl proton in phenylacetylene. For example, the $N(CH_3)_2$ group induces smaller chemical shifts in phenylacetylene than in styrene (−0.147 p.p.m. compared to −0.250 p.p.m.) whereas the NO_2 group induces larger shifts (+0.302 p.p.m. compared to +0.249 p.p.m.). One possible explanation for these observations is that field–inductive effects are enhanced in phenylacetylene relative to styrene while resonance effects are reduced (since NO_2 and $N(CH_3)_2$ groups respectively have dominant field and resonance effects (5, 11)).

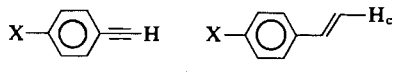

1 2

To test this explanation, it was originally intended to correlate ethynyl ^1H and ^{13}C chemical shifts with F and R (5), just as in the case of styrene (1). However, it was noted that many substituents whose F and R values seemed doubtful to us (*e.g.* $Si(CH_3)_3$, CF_3, NH_2, CH_3CO, C_6H_5O (1)), appeared to have more reasonable σ_I and σ_R values (11). Consequently, ^{13}C and ^1H chemical shifts for both 4-substituted phenylacetylenes and styrenes were correlated with σ_I and σ_R^0.[3] Twelve substituents

$$[1] \qquad \delta = \delta^0 + \rho_I\sigma_I + \rho_R\sigma_R^0$$

were chosen for the correlations which were common to both families and for which σ_I and σ_R^0 values were available (see Table 3). Halogens were omitted for reasons previously discussed (1), while a correction was applied for the magnetic

[3]σ_R^0 gave more precise correlations than the other σ_R scales of Taft and co-workers (11).

Can. J. Chem. Downloaded from www.nrcresearchpress.com by 210.87.254.5 on 09/05/12
For personal use only.

Can. J. Chem. Downloaded from www.nrcresearchpress.com by 210.87.254.5 on 09/05/12
For personal use only.

TABLE 2. (*A*) Calculated (CNDO/2) excess charge densities for carbons and ethynyl hydrogen of 4-substituted phenylacetylenes relative to unsubstituted phenylacetylene ($\times 10^4$)

Substituent	H	C(β)	C(α)	C(1)	C(2,6)	C(3,5)	C(4)
NH_2[a]	−19[e]	−88	+26	−285	+203	−535	+1333
$N(CH_3)_2$	−26	−100	+18	−370	+242	−648	+1447
OCH_3	−9	−45	+6	−275	+209	−617	+1829
$C(CH_3)_3$	−11	−29	−4	−150	+80	−254	+344
CH_3	−8	−32	+8	−99	+57	−177	+376
OC_6H_5[b]	−7	−43	+11	−252	+198	−591	+1852
F	+14	+7	+11	−164	+199	−556	+2243
SCH_3	+2	−9	+6	−94	+91	−182	+642
$Si(CH_3)_3$	−5	−12	−1	−10	−6	+92	−1240
$CH{=}CH_2$	−2	−10	+3	−48	+27	−135	+349
Cl	+20	+50	−13	−75	+110	−240	+1289
C_6H_5[c]	−4	−4	−10	−80	+35	−157	+269
$C{\equiv}C{-}H$	+6	+14	−3	−28	+19	−62	+484
CF_3	+43	+124	−24	+167	−31	+229	−583
$C{\equiv}N$	+24	+76	−22	+43	−7	+48	+333
$(C{\equiv}N)$[d]		(+93)	(+27)	(+52)			
NO_2	+67	+204	−46	+217	−23	+157	+239
(NO_2)[d]		(+161)	(−36)	(+171)			

(*B*) Calculated valence electron density for unsubstituted phenylacetylene

H	C(β)	C(α)	C(1)	C(2,6)	C(3,5)	C(4)
0.9381	4.1124	4.0048	3.9465	4.0006	3.9925	3.9977

[a]Pyramidal geometry for NH_2 group (34).
[b]Both phenyl groups twisted 37° from C—O—C plane (35).
[c]Dihedral angle between phenyl groups of 21° (34, 36).
[d]Charge densities for $C{\equiv}N$ and NO_2 derivatives scaled by ratios of experimental and calculated dipole moments for benzonitrile and nitrobenzene. Charge densities were scaled because CNDO/2 calculations respectively underestimate and overestimate electronic effects of $C{\equiv}N$ and NO_2 groups in aromatic derivatives (1, 37). Scaled charge densities were used for correlations in Table 3 and eqs. 2 and 3.
[e]Negative sign represents increased electron density.

anisotropy effect of the phenyl substituent. Correlations of both chemical shifts and carbon charge densities with σ_I and σ_R^0 are given in Table 3.

λ values ($\lambda = \rho_R/\rho_I$) for δ_H, $\delta_{C(\beta)}$, and $q_{C(\beta)}$ correlations all indicate decreased resonance/field effects for phenylacetylenes relative to styrenes. The δ_H and $q_{C(\beta)}$ correlations both support the postulate of increased field effects and decreased resonance effects. By contrast, ρ_I for the $\delta_{C(\beta)}$ correlation shows only a slight increase while ρ_R shows a marked decrease from styrene to phenylacetylene. However, correlations of $\delta_{C(\beta)}$ *vs.* $q_{C(\beta)}$ provide an explanation for this apparent anomaly since they indicate that ethynyl ^{13}C chemical shifts are less sensitive than vinyl ^{13}C chemical shifts to carbon charge density changes. Thus the nearly equal field

[2] $\delta_{C(\beta)}$ (styrene) $= \delta^0 + 3.6 \times 10^2 q_{C(\beta)}$ ($r = 0.967$)

[3] $\delta_{C(\beta)}$ (phenylacetylene $= \delta^0 + 2.7 \times 10^2 q_{C(\beta)}$ ($r = 0.974$)

dependence for $\delta_{C(\beta)}$ in styrene and phenylacetylene can be attributed to a trade-off between larger field-induced charge density changes for ethynyl carbons and lower sensitivity of the chemical shifts of these carbons to charge density changes.[4] Similarly, the large decrease in ρ_R can be attributed to a combination of the latter factor plus smaller resonance-induced changes in carbon charge density for phenylacetylenes.

δ_H in phenylacetylene should be slightly less sensitive to through-space field effects than

[4]This explanation has been advanced by Cushley and co-workers (12) to account for their observation that ^{13}C chemical shifts in alkynes and alkenes show similar sensitivities to field effects. Further evidence is provided in section *b*.

Can. J. Chem. Downloaded from www.nrcresearchpress.com by 210.87.254.5 on 09/05/12
For personal use only.

TABLE 3. (*A*) Correlations of ^1H and ^{13}C chemical shifts and carbon charge densities for 4-substituted phenylacetylenes[a] and (in parentheses) 4-substituted styrenes[a] with σ_I and σ_R^0

Parameter	ρ_I[b]	ρ_R[b]	r[c]	λ[d]
δ_H[e]	0.332±0.026 (0.265±0.018)	0.396±0.027 (0.482±0.019)	0.992 (0.996)	1.19 (1.82)
$\delta_{C(\beta)}$	4.92±0.43 (4.69±0.43)	6.20±0.45 (8.88±0.31)	0.990 (0.997)	1.26 (1.89)
$\delta_{C(1)}$	4.29±0.95 (4.14±0.72)	22.00±0.99 (19.58±0.75)	0.993 (0.995)	5.1 (4.7)
$q_{C(\beta)}$	0.0182±0.0020 (0.0132±0.0023)	0.0214±0.0021 (0.0228±0.0023)	0.983 (0.977)	1.18 (1.73)
$q_{C(1)}$	0.0150±0.0059 (0.0155±0.0053)	0.0625±0.0061 (0.0609±0.0056)	0.968 (0.972)	4.2 (3.9)
$J_{C(\beta)-H}$	3.54±0.18	3.85±0.19	0.996	1.09

(*B*) Corresponding correlations with F and R for same derivatives

Parameter	f[f]	r[f]	r[c]
δ_H[e]	0.193±0.018 (0.161±0.010)	0.332±0.028 (0.402±0.016)	0.988 (0.997)
$\delta_{C(\beta)}$	2.86±0.27 (2.83±0.15)	5.23±0.43 (7.45±0.23)	0.988 (0.998)
$\delta_{C(1)}$	2.93±0.64 (2.75±0.49)	18.60±1.02 (16.59±0.77)	0.990 (0.993)

[a]Correlations for the following phenylacetylene and styrene derivatives: $N(CH_3)_2$, NH_2, CH_3, $C(CH_3)_3$, OCH_3, $Si(CH_3)_3$, SCH_3, H, C_6H_5, CF_3, C≡N, NO_2. ^1H chemical shifts for C_6H_5 derivatives were corrected for the magnetic anisotropy of the phenyl group using Johnson–Bovey (38) calculations. Corrected values were $\delta_{H(C)} = 5.0907$ for 4-vinylbiphenyl (1) and $\delta_H = 2.8060$ for 4-ethynylbiphenyl.
[b]Weighting factors in equation: $\delta = \delta^0 + \rho_I\sigma_I + \rho_R\sigma_R^0$ (11).
[c]r = correlation coefficient (corrected for number of degrees of freedom).
[d]$\lambda = \rho_R/\rho_I$.
[e]Styrene correlations in brackets.
[f]Weighting factors in equation: $\delta = \delta^0 + fF + rR$ (5).

$\delta_{H(C)}$ in styrene (see Table 4).[5] However, the increased field dependence of both δ_H and $q_{C(\beta)}$ can be attributed to increased π polarization of the ethynyl group by polar substituents. This is

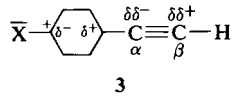

3

the expected result since the ethynyl C≡C bond is significantly more polarizable than the vinyl C=C bond.

($\alpha^{\parallel}_{C\equiv C} = 35.4 \times 10^{-25}$ cm^3, $\alpha^{\parallel}_{C=C} = 28.6 \times 10^{-25}$ cm^3 (15))

Concomitant with the decreased resonance effect at $C_{(\beta)}$ in phenylacetylene is an increased resonance effect for C(1), relative to styrene. This suggests an increased localization of substituent resonance effects in the phenyl group of phenylacetylene, *i.e.* a decreased contribution of resonance hybrid **5***c* relative to **4***c*.

A similar localization of resonance effects in

TABLE 4. Calculated chemical shift components upon δ_H in phenylacetylene and $\delta_{H(C)}$ in styrene due to the electric field of a polar substituent in the 4 position

Parameter	E (e.s.u.)[a]	δ_H[b] (p.p.m.)
δ_H (phenylacetylene)	6.14×10^3	0.021
$\delta_{H(C)}$ (Styrene), $\alpha^c = 120°$	7.01×10^3	0.025
$\delta_{H(C)}$ (Styrene), $\alpha = 130°$	6.37×10^3	0.023

[a]Electric field component acting along C—H bond. The field component is evaluated half way along the C—H bond (13). The electric field is that due to an axially symmetric substituent dipole of dipole moment 1 Debye, located 0.9 Å from C(4), along the C(4)—X bond.
[b]Electric field estimated by the Buckingham equation (3), $\delta = \delta^0 + A.E_z$, assuming an average value for A of 3.5×10^{-12} (1).
[c]α = C(1)—C(α)—C(β) valence angle (1).

[5]This assumes that the A constant in the Buckingham eq. 3 is identical for C(sp^2)—H and C(sp)—H bonds. The evidence on this point is contradictory (13, 14).

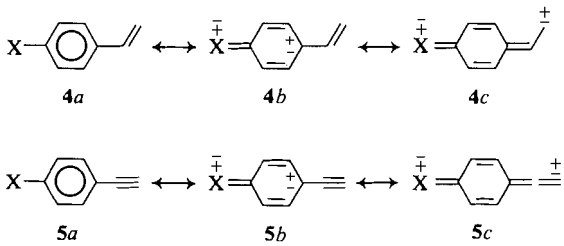

4a 4b 4c

5a 5b 5c

the phenyl group was noted for α-*t*-butylstyrenes where steric hindrance minimizes phenyl–vinyl conjugation (2). On the basis of i.r. spectroscopic evidence, Katritzky and co-workers have recently concluded that the ethynyl group in substituted phenylacetylenes can be an electron donor or acceptor by resonance, depending on the nature of the substituent (16). This also holds for the vinyl group in styrene (1, 17). Katritzky and co-workers have also summarized evidence that the ethynyl group is less susceptible to resonance interactions than the vinyl group (16), in agreement with our results. Thus the increased field dependence and the decreased resonance dependence for $\delta_{C(\beta)}$ and δ_H in 4-substituted phenylacetylenes can be reasonably accounted for in terms of increased π polarization effects and increased localization of resonance interactions in the phenyl group. Correlations of phenylacetylene chemical shifts with F and R reproduce the trends from the σ_I, σ_R^0 correlations. Therefore, we conclude that δ–DSP correlations for styrenes and phenylacetylenes show trends which are consistent with the proposed mechanisms of transmission of substituent effects.

(b) Evidence that ^1H and ^{13}C Chemical Shifts Reflect Intramolecular Electronic Effects

Implicit in the above discussion is the assumption that substituent-induced changes in δ_H and $\delta_{C(\beta)}$ in phenylacetylene reflect intramolecular electronic effects with insignificant contributions from solvent and magnetic anisotropy effects. This investigation has provided evidence that this is a valid assumption. λ is nearly equal for δ_H (λ = 1.19) and $\delta_{C(\beta)}$ (λ = 1.26). In a specific case like this, a cross correlation of the two chemical shifts should be linear, provided that intramolecular electronic effects are dominant. On the other hand, if there are significant contributions from magnetic anisotropy effects and solvent–solute interactions (6) or if λ is not equal for the two nuclei (10), then a δ–δ plot should be

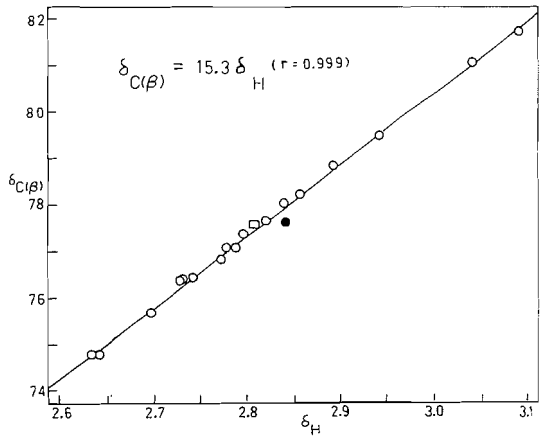

FIG. 1. Plot of β ^{13}C chemical shifts *vs.* ^1H chemical shifts for 4-substituted phenylacetylenes. Filled circle is point for 4-ethylbiphenyl while square is point for the same derivative corrected for the anisotropic magnetic susceptibility of the phenyl substituent.

nonlinear. In fact the δ_H–$\delta_{C(\beta)}$ plot for phenylacetylene is linear (Fig. 1). Only the phenyl derivative shows a significant deviation, due to the ring current effect of the phenyl substituent. The $\delta_{H(C)}$–$\delta_{C(\beta)}$ correlation for styrene is also linear:

$$[4] \qquad \delta_{C(\beta)} = 18.2\delta_{H(\beta)} \quad (r = 0.996)$$

By constrast, $\delta_{H(B)}$ for styrene gives a poorer correlation with $\delta_{C(\beta)}$ (r = 0.957), as expected since $\delta_{H(B)}$ is relatively less sensitive to field effects (λ = 3.1) than $\delta_{C(\beta)}$ (λ = 1.9) and $\delta_{H(C)}$ (λ = 1.8).

The δ–δ correlations and the $\delta_{C(\beta)}$–$q_{C(\beta)}$ correlations (eqs. 2 and 3) illustrate that both β ^{13}C and ^1H chemical shifts in styrenes and phenylacetylenes are dominated by changes in C(β) charge density. Changes in carbon π charge density alter ^1H chemical shifts by polarizing the C—H bond (13, 18). Unit change in π charge density for an sp^2 carbon should respectively induce ^{13}C and ^1H chemical shifts of 160–200 p.p.m. (19, 20) and 10 p.p.m. (13, 21). Thus the expected slope for eq. 4 is 16–20, in quantitative agreement with the observed value. The smaller slope for the phenylacetylene δ–δ plot indicates that ^{13}C chemical shifts for sp carbons are less sensitive to charge density changes than ^{13}C chemical shifts for sp^2 carbons (see part *a*).

We have concluded that ^1H chemical shifts in styrenes and phenylacetylenes are sensitive to resonance, π polarization, and field effects. The

Can. J. Chem. Downloaded from www.nrcresearchpress.com by 210.87.254.5 on 09/05/12
For personal use only.

Can. J. Chem. Downloaded from www.nrcresearchpress.com by 210.87.254.5 on 09/05/12
For personal use only.

first two mechanisms alter ^1H chemical shifts as a result of changes in carbon π charge density while the third mechanism acts by through-space polarization of the C—H bond. Therefore, one might expect that δ_H for phenylacetylene would show a proportionately larger σ_I dependence than $\delta_{C(\beta)}$, due to through-space field effects. However, field induced C—C σ bond polarization leads to a field effect upon ^{13}C chemical shifts which is an order of magnitude greater than field effects on ^1H chemical shifts (22). This is further enhanced by the closer proximity of $C_{(\beta)}$ (since field effects vary as $1/r^3$ (4)). Thus the relative sensitivity of $\delta_{C(\beta)}$ and δ_H to through-space field effects should be similar to their relative sensitivity to all electronic effects (*ca.* 15, see Fig. 1), leaving λ almost unaltered. Similarly, $\delta_{H(C)}$ for styrene shows a similar field dependence ($\lambda = 1.8$) as $\delta_{C(\beta)}$ ($\lambda = 1.9$). By contrast, $\delta_{H(\beta)}$ (where through-space field effects are negligibly small (1)) shows a smaller field dependence ($\lambda = 3.1$).

(c) The Validity of δ–DSP Correlations and the Evidence for π Polarization Effects

There have been two recent criticisms of δ–DSP correlations for aromatic derivatives from quite different viewpoints (6, 7). These criticisms will be considered in turn.

Wiley and Miller have argued that these correlations are theoretically unsound and that ^1H chemical shifts in particular are sensitive to many factors other than intramolecular electronic effects (6). We have already discussed this criticism in some detail (10). The results presented above support our previous conclusions that these correlations are meaningful when chemical shifts are measured for a large number of substituents under inert conditions (1, 2, 10). They also confirm that these chemical shifts reflect intramolecular electronic effects.

While Wiley and Miller reject δ–σ correlations, Mitchell and Phillips claim that substituent-induced chemical shifts in a large variety of systems (including 4-substituted styrenes) are linearly related to σ_p (7). They conclude that 'the statistical superiority of DSP correlations should not be used as a reason for proposing unusual mechanisms of transmission of substituent effects' and suggest that these apparent mechanisms may simply be artifacts of the correlation (7).

While a limited number of families may correlate with σ_p, this approach should not be of general validity since different systems will often have different resonance–field ratios (10). Even for compounds of type **6**, where Mitchell and Phillips claim that ^{19}F chemical shifts adequately correlate with σ_p (7), recent results on further families of this type show that λ varies by more than 2 as G is changed (23). Perhaps the most compelling evidence for the necessity of DSP treatment of chemical shifts is provided by our results for 4-substituted styrenes (1). Correlations of $\delta_{H(B)}$ and $\delta_{H(C)}$ with σ_p give different slopes but do not identify the origin of the difference (7). However, correlations with F and R demonstrated that the difference is due to through-space field effects (1). The evidence is not based on statistical arguments but rather on the observation that DSP correlations, classical electric field calculations, and molecular orbital calculations of charge density provide a consistent picture of field effects (1). Similarly, the conclusions concerning resonance and π polarization effects in styrenes and phenylacetylenes are based on the pattern of weighting factors (f and r or ρ_I and ρ_R) and the fact that these factors vary in a reasonable manner on going from styrene to α-*t*-butylstyrene or phenylacetylene.

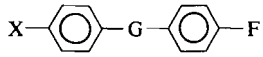

6

Since Mitchell and Phillips specifically cast doubt on the existence of π effects which depend on σ_I (or F) (7), the evidence for these effects will be considered in greater detail. In addition to our DSP correlations, ^{13}C chemical shifts and calculated charge densities for both trimethylammonio styrene derivatives (2) and α-, β-, and γ-substituted phenylalkanes (24) provide evidence for phenyl π polarization. In the latter compounds, the degree of polarization depends upon both the polarizing ability of the substituent and its distance from the phenyl group (23).

Stock and co-workers noted an increased σ_I dependence of ^{19}F chemical shifts on going from

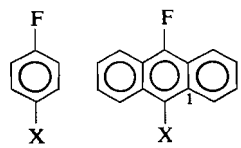

7 **8**

Can. J. Chem. Downloaded from www.nrcresearchpress.com by 210.87.254.5 on 09/05/12
For personal use only.

7 to **8** (25). This was attributed to an increased π inductive effect in **7**. Taft and co-workers have also noted a σ_I dependence of ^{19}F chemical shifts in compounds of type **6** which they attributed to π inductive effects (23, 26).

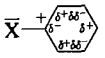

9

Both sets of results could be due to π polarization effects. Alternatively they could be due to a π inductive effect in which the polar C—X bond induces a π charge density change at the bonded carbon, with this perturbation inducing π charge density changes at other carbons similar to that due to a resonance effect (27, 28). The basic difference between the two mechanisms is the magnitude of charge density change at the *ortho* carbons.

In an attempt to distinguish between the two possible mechanisms, CNDO/2 calculations were performed for ammonio derivatives of benzene, anthracene, diphenylmethane, and stilbene. Ammonio derivatives were chosen because this group has a large positive field–inductive effect and a zero (5) or small negative (29) resonance effect. The calculated π charge densities (see Fig. 2) indicate a substantial π inductive effect in each case and correctly reproduce the experimental observations of enhanced

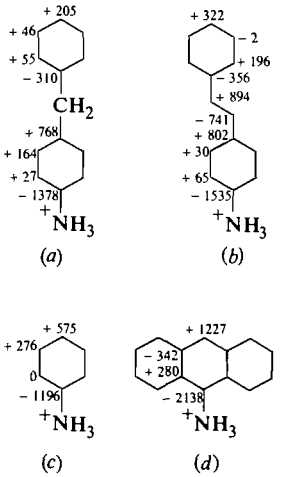

FIG. 2. Changes in π charge densities for aromatic derivatives induced by an ammonio group (positive charge density corresponds to decreased electron density): (*a*) diphenylmethane, (*b*) *trans*-stilbene, (*c*) benzene, (*d*) anthracene. Charge densities × 10^4.

π inductive effects for anthracene relative to benzene (25) and stilbene relative to diphenylmethane (23, 26). The patterns of π charge density generally resemble **3** more than **9**, *i.e.* basically a π polarization effect. Just as in the case of styrene (2), calculations for diphenylmethane and stilbene indicate that π polarization can be transmitted through space but is enhanced in a planar conjugated system.

Calculations were also performed for the corresponding fluoro derivatives (**6**, **7**, and **8**) with X = H, NH_3^+. Calculated changes in F $2p_z$ (π) charge density due to the ammonio group (respectively +0.0029, +0.0042, +0.0097, and +0.0154 for diphenylmethane, stilbene, benzene, and anthracene derivatives) parallel the σ_I values for ^{19}F chemical shifts for the same families of compounds (respectively −1.95, −2.84, −8.13, and −13.08 in CCl_4 (23)).[6]

In summary, there is a considerable body of evidence indicating the presence of a π inductive effect in aromatic derivatives which follows the σ_I or F order. The evidence is based not only on weighting factors in chemical shift – DSP correlations but also on chemical shifts and charge densities for individual compounds where resonance effects are minimized. The evidence is not based on statistical arguments but rather on the consistent pattern of results for a large variety of compounds. In addition, δ–δ plots for styrenes and phenylacetylenes provide further evidence that ^{13}C and ^1H chemical shifts (measured under inert conditions) can be used to probe electronic effects of remote substituents.

(d) Substituent Effects on Ethynyl ^{13}C–^1H Coupling Constants

The directly bonded ethynyl ^{13}C–^1H coupling constant has a similar relative sensitivity to reasonance-field effects ($\lambda = 1.09$) as $\delta_H(\lambda = 1.19)$. In fact, the two parameters are linearly related:

[6]The experimental σ_I value for diphenylmethane is taken from the correlation for triphenylmethane derivatives (23). There should be little difference between the two series. The calculations predict a smaller relative change from stilbene to benzene than noted experimentally. This is presumably due to solvent effects on the experimental chemical shifts since Dayal and Taft (23) have noted that solvent effects decrease σ_I dependence of ^{19}F chemical shifts for triphenylmethane and stilbene derivatives while increasing the σ_I dependence for benzene and anthracene derivatives.

TABLE 5. Methods of synthesis and physical properties of 4-substituted phenylacetylenes which were synthesized for this investigation

Substituent	Synthetic method	Melting or boiling point	
		This work	Literature
CH_3	[a]	59.5–60°/15mm	52–53°/11mm (40)
$C(CH_3)_3$	[a]	70°/2mm	67°/1.7mm (45)
F	[a]	74–75°/20mm	34–35°/10mm (40)
Cl	[a]	71.5–72.5°/18mm	62–63°/13mm (40)
Br	[a]	62.5–63°	62–63°
CF_3	[a]	47–48°/20mm	(46)[g]
OCH_3	[b]	73–74°/2mm	86°/9mm (40)
NO_2	[b]	149–150°	149–150° (40)
$N(CH_3)_2$	[b]	51–52°	52–53° (47)
C_6H_5	[c]	79–80°	80–81° (48), 86–87° (49)
C≡N	[c]	154–155°	153° (50)
NH_2	[d]	99–100°	99–100° (40)
C≡C—H	[e]	93–94°	95° (43)
$Si(CH_3)_3$	[f]	64–65°/2mm	65–66°/2.5mm (44)

[a]Reaction of corresponding acetophenone with PCl_5 to yield α-chlorostyrene followed by dehydrohalogenation with strong base to yield phenylacetylene (39).
[b]Bromination of corresponding cinnamic acid followed by treatment with base to yield phenylacetylene (40).
[c]Pyrolysis of corresponding selenadiazole to yield phenylacetylene (31, 41) (see text for detailed description of synthesis of SCH_3 derivative.)
[d]Reduction of 4-nitrophenylacetylene with Zn/NH_4Cl (42).
[e]Bromination of *para*-divinylbenzene followed by dehydrobromination with strong base (43).
[f]Synthesized from 4-bromophenylacetylene using the method of Eaborn *et al.* (44).
[g]No physical properties given.

$$[5] \qquad \Delta J_{C-H} = 10.0\Delta\delta_H \quad (r = 0.991))$$

The fact that this relationship exists suggests that the substituent dependence of J_{CH} is also due to polarization of the C—H bond, either by field effects or π charge density changes at C(β). Since J_{CH} is insensitive to magnetic anisotropy effects, eq. 5 also provides further evidence that δ_H reflects intramolecular electronic effects.

To summarize, correlations of ethynyl ^1H and ^{13}C chemical shifts and carbon charge densities for 4-substituted phenylacetylenes with σ_I and σ_R^0 indicate that field – inductive substituent effects are enhanced and resonance effects are inhibited, relative to 4-substituted styrenes. This is attributed to increased π polarization of the ethynyl group and increased localization of resonance effects within the phenyl group. Both styrene and phenylacetylene chemical shifts can be interpreted in terms of field, resonance, and π polarization effects. There is a linear relationship between the ^1H chemical shifts and ^{13}C–^1H coupling constants, suggesting that the substituent dependence of the coupling constant arises from C—H bond polarization.

Linear cross correlations of β ^{13}C and ^1H chemical shifts for both phenylacetylenes and styrenes confirm that these substituent-induced chemical shifts are reflecting ground state electron density changes. The dominant factor appears to be carbon π electron density changes. Both the phenylacetylene results and comparisons of calculated electron distributions for benzene, anthracene, stilbene, and diphenylmethanes with previously reported ^{19}F chemical shifts indicate that π polarization effects are important in these derivatives.

The above results support our previous conclusions that: (*i*) ^1H and ^{13}C chemical shifts measured at infinite dilution in a noninteracting solvent can be used to monitor changes in ground state electron distributions in aromatic derivatives and (*ii*) correlations of substituent-induced chemical shifts with divided substituent parameters (F and R or σ_I and σ_R) can be used to deduce mechanisms of transmission of electronic effects.

Experimental

Synthesis of Compounds

The parent phenylacetylene was obtained commercially, 4-phenoxyphenylacetylene was supplied by Professor G. H. Schmid, University of Toronto and 4-vinylphenylacetylene was supplied by Dr. G. K. Hamer, University of Toronto. All of the other phenylacetylenes except 4-methylmercaptophenylacetylene were known compounds and were synthesized by previously reported methods. Details of synthesis and physical properties are

Can. J. Chem. Downloaded from www.nrcresearchpress.com by 210.87.254.5 on 09/05/12
For personal use only.

Can. J. Chem. Downloaded from www.nrcresearchpress.com by 210.87.254.5 on 09/05/12
For personal use only.

summarized in Table 5. Purities of compounds were checked by their n.m.r. spectra.

4-Methylmercaptophenylacetylene

4-Methylmercaptoacetophenone (m.p. 81–82°), prepared by Friedel–Crafts acylation of thioanisole with acetyl chloride and aluminum chloride in chloroform (30), was stirred with semicarbazide hydrochloride and sodium acetate in 50:50 ethanol–water. The resulting semicarbazone (m.p. 216–217°) was filtered off, washed with water, ethanol, and ether, and dried. The semicarbazone was suspended in 10 times its weight of glacial acetic acid and powdered selenium dioxide was added slowly (31). The solution was heated on a water bath (70°) and stirred overnight. After cooling, the precipitate was collected, washed with water, and dried. The crude selenadiazole was a reddish brown solid (m.p. 124–126° dec.). It was pyrolyzed over sand to give 4-methylmercaptophenylacetylene (b.p. 83°/0.6 mm).

Anal. Calcd. for C_9H_8S: C, 72.93; H, 5.44; S, 21.63. Found: C, 72.90; H, 5.35; S, 21.57.

Recording of Spectra

^1H spectra were recorded on a Varian HA-100 spectrometer operating in frequency sweep mode at 27 °C. Spectra were recorded in forward and reverse directions (6–8 spectra per solution) at a sweep rate of 0.05 Hz/s. Internal tetramethylsilane (3 mol%) was used as a lock and reference signal. In most cases, spectra were measured for three phenylacetylene solutions with concentrations (in C_6D_{12}) between 0.5 and 3.0 mol%. For NH_2, NO_2, C≡C—H, and C≡N derivatives, limited solubility made this procedure impossible and spectra were recorded for single solutions of <0.25 mol%.

^{13}C spectra were recorded on a Varian XL-100-15 (with 16K 620i computer) operating in pulsed Fourier transform mode at a probe temperature of 32 °C. Proton-decoupled spectra were recorded for 0.4 *M* solutions of phenylacetylene in CCl_4 with 8 mol% C_6D_{12} as a lock signal. Spectra were recorded with a spectral width of 5000 Hz and acquisition time of 0.8 s.

^{13}C–^1H couplings were determined from proton-coupled ^{13}C spectra with a spectral width of 500 Hz and acqusition time of 8 s. ^{13}C–^1H couplings are estimated to be accurate to within ±0.2 Hz.

Molecular Orbital Calculations

CNDO/2 molecular orbital calculations were carried out on an IBM 370 computer, using a standard CNINDO program (32). Standard bond lengths and angles were used for phenylacetylene (33). Substituent bond lengths and angles are tabulated elsewhere (34).

Financial support from the National Research Council of Canada is gratefully acknowledged. D.A.D. thanks the Walter C. Sumner Foundation for a fellowship.

1. G. K. Hamer, I. R. Peat, and W. F. Reynolds. Can. J. Chem. **51**, 897 (1973).
2. G. K. Hamer, I. R. Peat, and W. F. Reynolds. Can. J. Chem. **51**, 915 (1973).
3. A. D. Buckingham. Can. J. Chem. **38**, 300 (1960).
4. J. A. Pople and G. A. Segal. J. Chem. Phys. **43**, 3289 (1966).
5. C. G. Swain and E. C. Lupton. J. Am. Chem. Soc. **90**, 4328 (1968).
6. G. R. Wiley and S. I. Miller. J. Org. Chem. **37**, 767 (1972).
7. P. J. Mitchell and L. Phillips. J. Chem. Soc. Perkin II, 109 (1974).
8. C. D. Cook and S. S. Danyluk. Tetrahedron, **19**, 177 (1963).
9. P. Laszlo. Progress in N.M.R. spectroscopy. Vol. 2. *Edited by* J. W. Emsley, J. Feeney, and L. H. Sutcliffe. Pergamon Press, Oxford. 1967, Chapt. 6.
10. D. A. Dawson, G. K. Hamer, and W. F. Reynolds. Can. J. Chem. **52**, 39 (1974).
11. S. Ehrenson, R. T. C. Brownlee, and R. W. Taft. Progress in physical organic chemistry. Vol. 10. *Edited by* A. Streitwieser and R. W. Taft. Interscience, New York. 1973. Chapt. 1.
12. J. G. Batchelor, R. J. Cushley, and J. H. Prestegard. J. Org. Chem. **39**, 1698 (1974).
13. J. I. Musher. J. Chem. Phys. **37**, 34 (1962).
14. R. Aminova and R. Z. Gubaidullina. Zh. Strukt. Khim, **10**, 236 (1969).
15. K. G. Denbigh. Trans. Faraday Soc. **36**, 936 (1940).
16. T. B. Grindley, K. F. Johnson, A. R. Katritzky, H. J. Keogh, and R. D. Topsom. J. Chem. Soc. Perkin II, 273 (1974).
17. K. S. Dhami and J. B. Stothers. Can. J. Chem. **43**, 510 (1965).
18. G. K. Fraenkel, R. E. Carter, A. McLachlan, and J. H. Richards. J. Am. Chem. Soc. **82**, 5846 (1960).
19. P. C. Lauterbur. J. Am. Chem. Soc. **83**, 1838 (1961).
20. H. Spiesecke and W. G. Schneider. Tetrahedron Lett. 468 (1961).
21. T. Schaefer and W. G. Schneider. Can. J. Chem. **41**, 966 (1963).
22. J. G. Batchelor, J. H. Prestegard, R. J. Cushley, and S. R. Lipsky. J. Am. Chem. Soc. **95**, 6358 (1973).
23. S. K. Dayal and R. W. Taft. J. Am. Chem. Soc. **94**, 9113 (1972).
24. W. F. Reynolds, I. R. Peat, M. H. Freedman, and J. R. Lyerla, Jr. Can. J. Chem. **51**, 1857 (1973).
25. G. L. Anderson, R. C. Parish, and L. M. Stock. J. Am. Chem. Soc. **93**, 6984 (1971).
26. S. K. Dayal, S. Ehrenson, and R. W. Taft. J. Am. Chem. Soc. **94**, 9113 (1972).
27. P. R. Wells, S. Ehrenson, and R. W. Taft. Progress in physical organic chemistry. Vol. 6. *Edited by* A. Streitwieser and R. W. Taft. Interscience, New York. 1968. Chapt. 4.
28. M. J. S. Dewar. J. Am. Chem. Soc. **74**, 3350 (1952).
29. P. J. Q. English, A. R. Katritzky, T. T. Tidwell, and R. D. Topsom. J. Am. Chem. Soc. **90**, 1767 (1968).
30. R. A. Cutler, R. J. Stenger, and C. M. Suter. J. Am. Chem. Soc. **74**, 5475 (1952).
31. I. Lalezari, A. Shafiee, and M. Yalpani. J. Org. Chem. **36**, 2836 (1971).
32. Quantum Chemistry Program Exchange Program, 141.
33. D. L. Beveridge and J. A. Pople. Approximate molecular orbital theory. McGraw-Hill, New York. 1970.
34. G. K. Hamer. PhD Thesis, University of Toronto, Toronto, Ontario, 1973.

35. R. J. W. LeFevre and J. D. Saxby. J. Chem. Soc. B, 1064 (1966).
36. H. Suzuki. Electronic absorption spectra and geometry of organic molecules. Academic Press, New York. 1967. p. 269.
37. R. T. C. Brownlee and R. W. Taft. J. Am. Chem. Soc. **92**, 7007 (1970).
38. C. E. Johnson and F. A. Bovey. J. Chem. Phys. **29**, 1012 (1958).
39. T. L. Jacobs. Org. React. **5**, 1 (1949).
40. C. D. Cook. PhD Thesis, University of Toronto, Toronto, Ontario, 1962.
41. J. Lalezari, A. Shafiee, and M. Yalpani. Angew. Chem. Int. Ed. 464 (1970).
42. J. H. Boyer and H. Alul. J. Am. Chem. Soc. **81**, 2136 (1959).
43. A. S. Hay. J. Org. Chem. **25**, 637 (1960).
44. C. Eaborn, A. R. Thompson, and D. R. M. Walton. J. Chem. Soc. C, 1364 (1967).
45. R. W. Bott, C. Eaborn, and D. R. M. Walton. J. Chem. Soc. 384 (1965).
46. R. E. Dessy, Y. Okuzumi, and A. Chen. J. Am. Chem. Soc. **84**, 2899 (1962).
47. P. Barbieri. C. R. **231**, 57 (1950).
48. W. Ried and V. B. Saxena. Justus Liebigs Ann. Chem. **739**, 159 (1970).
49. T. L. Jacobs and D. Danker. J. Org. Chem. **22**, 1424 (1957).
50. Y. Yukawa and H. Yamada. Nippon Kagaku Zasshi, **85**, 501 (1964).

Can. J. Chem. Downloaded from www.nrcresearchpress.com by 210.87.254.5 on 09/05/12
For personal use only.

The Reactivity of Tungsten Halides with Organic Sulfides: S-Dealkylation and Reductive Elimination Reactions[1]

P. MICHAEL BOORMAN,[2] TRISTRAM CHIVERS, AND KALABEERAPPA N. MAHADEV

Department of Chemistry, University of Calgary, Calgary, Alberta T2N 1N4

Received September 9, 1974

P. MICHAEL BOORMAN, TRISTRAM CHIVERS, and KALABEERAPPA N. MAHADEV. Can. J. Chem. **53**, 383 (1975).

Tungsten hexa- or pentachloride reacts with alkyl sulfides to give $(R_3S)_2[WCl_6]$. The reactions involve S-dealkylation followed by reductive elimination of R_2S_2. Alkylation of R_2S by RCl probably occurs at the tungsten site through the intermediacy of $WCl_4(R_2S)_2$. The latter compounds have been shown to be unstable with respect to displacement of the sulfide ligands by halide ions or neutral donors and therefore form excellent intermediates for W(IV) synthetic chemistry.

P. MICHAEL BOORMAN, TRISTRAM CHIVERS et KALABEERAPPA N. MAHADEV. Can. J. Chem. **53**, 383 (1975).

Les penta- et hexa-chlorures de tungstène réagissent avec les sulfures d'alkyle pour donner des $(R_3S)_2[WCl_6]$. Les réactions impliquent une S-déalkylation suivie par une élimination réductrice de R_2S_2. L'alkylation de R_2S par RCl se produit principalement sur le tungstène par l'intermédiaire de $WCl_4(R_2S)_2$. On a démontré que les ligands sulfures de ces derniers composés peuvent être facilement déplacés par les ions halogénures ou par des donneurs neutres et qu'ils forment par conséquent d'excellents intermédiaires pour la chimie de synthèse impliquant le W(IV). [Traduit par le journal]

Introduction

The coordination chemistry of heavy metals with sulfur donor ligands is of potential importance in the context of metalloenzyme chemistry and industrial catalysis. The reactivity of tungsten-halides towards alkyl sulfides has been discussed in two previous reports (2, 3). Simple adducts of WCl_6 and WCl_5 with alkyl sulfides result from the reaction of the component species in dilute carbon tetrachloride solution (2). Schaeffer-King and McCarley (3) reported that $WCl_4(tht)_2$ and $WCl_4(Et_2S)_2$ (tht = tetrahydrothiophene) may be prepared from the normally unreactive WCl_4 by refluxing with the neat ligands.

In this paper we discuss the direct reactions of organic sulfides with tungsten(VI) and tungsten(V) chlorides which yielded the unexpected products, $(R_3S)_2[WCl_6]$. Evidence will be presented concerning the mechanism of reaction which must involve both dealkylation and alkylation of sulfur as well as a metal–sulfur redox reaction. The identity of the products has been confirmed by spectroscopic studies, alternative syntheses, and by a full X-ray crystallographic study of the compound $(Et_3S)_2[WCl_6]$.

[1]A preliminary account of this work has appeared previously (1).

[2]To whom correspondence should be addressed.

Experimental

General Procedures

All handling procedures were carried out in a dry nitrogen-filled glove box. Alkyl sulfides were obtained from Aldrich Chemicals, dried with calcium hydride, and redistilled under nitrogen before use. Alkylthiotrimethylsilanes were prepared by published methods (4). Tungsten hexachloride was obtained from Alfa Inorganics and resublimed *in vacuo* before use. Conversion of WCl_6 to WCl_5 was effected by red phosphorus reduction (5), followed by resublimation. Tungsten was analyzed by ignition to the oxide, and chloride potentiometrically. Other analyses were carried out by Chemalytics and Alfred Bernhardt Laboratories. Infrared spectra were recorded as Nujol mulls between CsI plates using a Beckman IR 20-A spectrometer. Visible spectra were recorded in the solid state as Nujol mulls with a Cary 16 spectrophotometer and magnetic data were obtained using a standard Gouy technique, at 22°. The susceptibilities were corrected for the diamagnetism of the ligands using Pascal's constants. Nuclear magnetic resonance spectra were recorded with a Varian A-60 spectrometer.

Syntheses of $(R_3S)_2WCl_6$

The reactions of WCl_5 and WCl_6 with sulfides were carried out in evacuated sealed Pyrex glass tubes. The halides were loaded in the glove box, and the alkyl sulfides were condensed on *in vacuo*, at liquid nitrogen temperature. The sealed tubes were allowed to warm up to room temperature, but exothermic reactions occurred

Can. J. Chem. Downloaded from www.nrcresearchpress.com by 210.87.254.6 on 09/05/12
For personal use only.

Can. J. Chem. Downloaded from www.nrcresearchpress.com by 210.87.254.6 on 09/05/12
For personal use only.

immediately upon melting of the R_2S. Orange-brown crystalline products were slowly deposited. Characterization of these products as the $(R_3S)_2WCl_6$ complexes is discussed in the Results section.

Synthesis of $WCl_4(Me_2S)_2$

The complex was prepared from WCl_4 and Me_2S in a similar way to the ethyl sulfide adduct previously reported (3).

Anal. Calcd. for $WCl_4(Me_2S)_2$: W, 40.9; Cl, 31.5; C, 10.6; H, 2.7. Found: W, 41.0; Cl, 31.9; C, 10.1; H, 2.7.

Molecular weight determinations, carried out cryoscopically in nitrobenzene, gave values of 120 ± 15 for $WCl_4(Me_2S)_2$, 150 ± 20 for $WCl_4(Et_2S)_2$; ($WCl_4(Me_2S)_2$ = 450; $WCl_4(Et_2S)_2$ = 506). In each case the solutions showed electrical conductance behavior well below that expected for 1:1 electrolytes, inferring that the low molecular weight values were due primarily to loss of coordinated sulfide ligand in the $PhNO_2$ solvent. Subsequent reactions were carried out to check the reactivity towards ligand displacement.

Reaction of $WCl_4(Me_2S)_2$

With Neutral Ligands

Dissolution of $WCl_4(Me_2S)_2$ in dioxane, followed by pumping off volatiles, yielded $WCl_4(Me_2S)$ (dioxane).

Anal. Calcd. for $WCl_4(Me_2S)$: W, 38.6; Cl, 29.8. Found: W, 39.0; Cl, 29.1.

The addition of 2 mol of stronger donors such as Ph_3P and Me_2PhP to the dioxane solutions of $WCl_4(Me_2S)_2$, followed by removal of volatiles, yielded the known adducts $WCl_4(Ph_3P)_2$ (3, 6) and $WCl_4(PMe_2Ph)_2$ (7). With an excess of $PhMe_2P$ the seven coordinate adduct $WCl_4(PPhMe_2)_3$ was readily formed, as reported previously (7). These compounds were identified on the basis of i.r. spectra and physical appearance.

With Chloride Ion

Two molar quantities of tetraethylammonium chloride displaced the alkyl sulfide to form $(Et_4N)_2WCl_6$, when solid Et_4NCl was shaken with a CCl_4 solution of $WCl_4(Me_2S)_2$.

Anal. Calcd. for $(Et_4N)_2WCl_6$: W, 28.0. Found: W, 27.6.

The i.r. spectrum showed the presence of Et_4N^+ ions and the absence of Me_2S. The same product could also be precipitated from CH_2Cl_2 solution of the two reagents.

Reaction of Me_3SCl (solid) with a CCl_4 solution of $WCl_4(Me_2S)_2$ yielded $(Me_3S)_2WCl_6$, identified by its i.r. spectrum which was identical to that of the product obtained from the $WCl_{5/6}/Me_2S$ reactions.

Anal. Calcd. for $(Me_3S)_2WCl_6$: W, 33.4. Found: W, 33.2.

With Alkyl Chlorides

Direct reaction of $WCl_4(Me_2S)_2$ with methyl chloride was accomplished by cold distilling MeCl onto the complex contained in a thick-walled glass tube. On warming, reaction ensued to yield $(Me_3S)_2WCl_6$ (identified by i.r. spectrum and solubility properties), but there was a severe explosion hazard. Reaction of $WCl_4(Me_2S)_2$ with ethyl chloride would only occur in the presence of ethyl sulfide, at 50°, whereupon $(Et_3S)_2WCl_6$ was produced.

Results and Discussion

Characterization of the Compounds $(R_3S)_2WCl_6$

Analytical data (Table 1) show that major products from the reaction of WCl_5 or WCl_6 with R_2S are identical. Physical and spectroscopic properties of the respective products were also invariant with respect to sample origin. Infrared spectra are consistent with the presence of both R_3S^+ cations and WCl_6^{2-} anions. The essential features with suitable reference spectra are presented in Table 2. The compounds were so insoluble that no solution spectra could be obtained. However, the solid state electronic spectra of the $(R_3S)_2WCl_6$ complexes were recorded as mulls in the transmission mode. Since the electronic spectrum of the WCl_6^{2-} ion appears to be cation dependent (10, 11), it does not provide a good diagnosis of the presence of the ion. Not surprisingly therefore, as shown in Table 3, although the charge-transfer bands for our compounds are similar to those previously reported, there is some variation in the ligand-field regions of the spectra.

The magnetic moments for $(R_3S)_2WCl_6$ were 1.45 B.M., well within the range of 1.43–1.47 B.M. reported by Peacock and co-worker (10) for alkali metal hexachlorotungstates (IV).

The ultimate proof of the identity of our compounds has been obtained through a full crystal structure of $(Et_3S)_2WCl_6$.[3] This compound crystallizes in the space group $C\bar{1}$ with two WCl_6^{2-} ions located on nonequivalent centers of symmetry. A pair of $(C_2H_5)_3S^+$ ions is centrosymmetrically associated with each WCl_6^{2-} ion.

Discussion of Reaction Mechanism

Reduction of transition metal halides by sulfur compounds has been reported previously (12), but the oxidation products of the sulfides have not been identified. In addition, the formation of hexachlorotungstate(IV) ions by reaction of amines with WCl_6 has been described (13), but again, no experimental evidence for the mechanism was reported.

In the present work the reactions are of potentially broad interest, since they involve S-dealkylation, S-alkylation, and a redox reaction, under relatively mild conditions. We have therefore obtained a considerable body of experimental evidence to support the mechanisms described in Schemes 1 and 2 for the reactions between R_2S and WCl_6 and WCl_5 respectively. Schemes 1 and 2 can be broken down into four

[3]We thank Kerr and Durley for a preliminary communication of their results (17).

TABLE 1. Analytical data for the compounds $(R_3S)_2WCl_6$

Product from	Analysis (%) C	H	S	W	Cl	Yield (%)
$WCl_5 + Me_2S$	13.1	3.3	11.6	33.7	38.6	50
$WCl_6 + Me_2S$	13.2	3.2	11.6	33.5	38.6	~75
Calculated for $(Me_3S)_2WCl_6$	13.1	3.3	11.6	33.4	38.6	
$WCl_5 + Et_2S$	22.7	5.1	10.1	28.6	33.1	50
$WCl_6 + Et_2S$	22.5	4.9	10.2	28.9	33.2	~75
Calculated for $(Et_3S)_2WCl_6$	22.7	4.8	10.1	28.9	33.5	

TABLE 2. Infrared spectra of the compounds $(R_3S)_2[WCl_6]$ and reference compounds

Compound	ν(C—S) bands*			ν(W—Cl) bands (ν_3 in O_h)*
$(Me_3S)_2[WCl_6]$	728 (m)	717 (m)	652 (w)	285 vs br
$(Et_3S)_2[WCl_6]$	760 (m)	720 (w)	673 (vw)	285 vs br
Me_3SCl (8)	728 (m)	724 (m)	667 (msh) 652 (w)	
Me_3SHgI_3 (8)	725 (m)	648 (m)		
Et_3SI (9)	774 (sh)	673 (w)		
Et_3SHgI_3 (9)	759 (w)	673 (w)		
K_2WCl_6 (10)				324
Cs_2WCl_6 (10)				308

*Intensities: s, strong; m, medium; w, weak; v, very; br, broad; sh, shoulder.

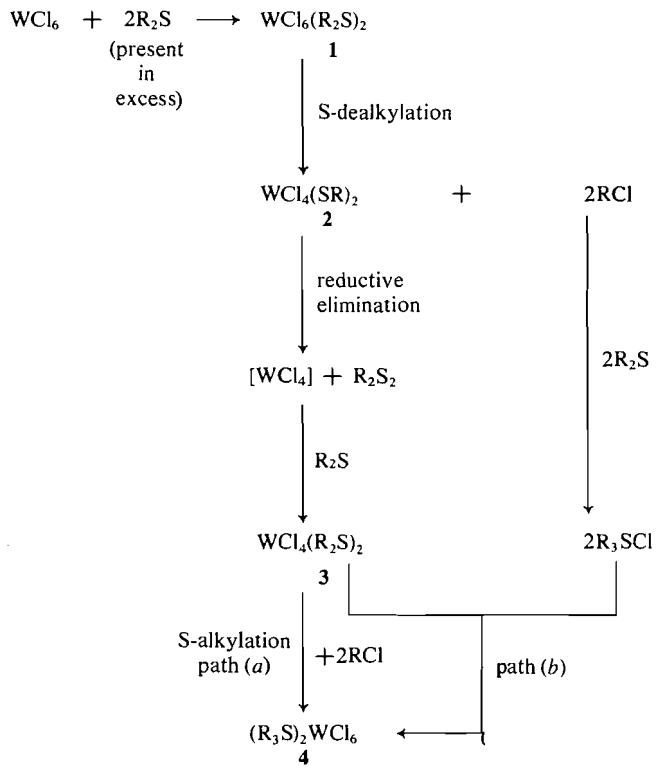

SCHEME 1

Can. J. Chem. Downloaded from www.nrcresearchpress.com by 210.87.254.6 on 09/05/12
For personal use only.

TABLE 3. Solid state electronic spectra of compounds containing the hexachlorotungstate (IV) anion

Compound	Bands observed (cm^{-1})					
$(Et_3S)_2WCl_6$	—	29 000	31 500	35 100	38 400	—
$(Me_3S)_2WCl_6$	21 400	29 400	32 800	35 100	—	—
Rb_2WCl_6 (10)	18 200	—	31 100	35 100	38 500	42 600
WCl_6^{2-}* (11)	19 230	—	31 750	35 300	39 400	42 600

*Cation not specified.

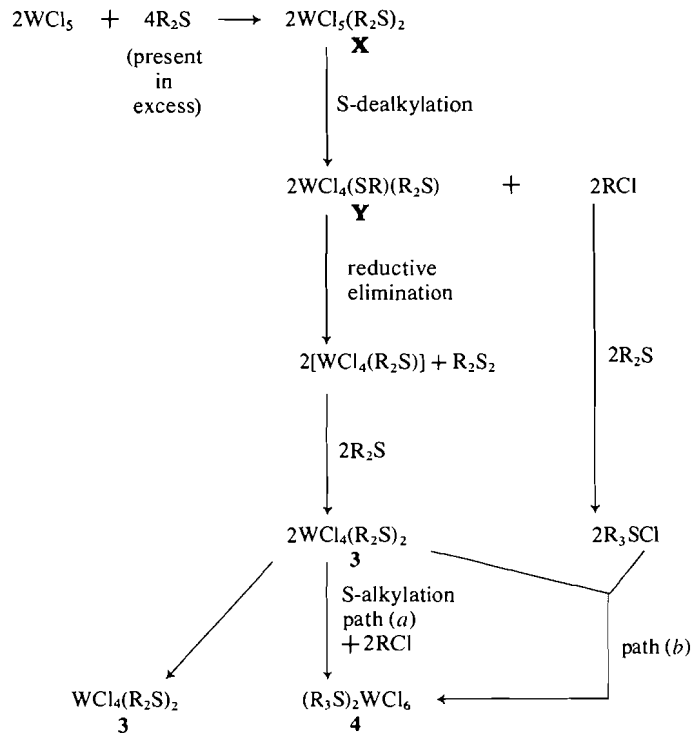

SCHEME 2

steps, and experimental evidence will be presented to support the plausibility of each.

(1) Uptake of R_2S by WCl_x ($x = 5, 6$)

Previous work (2) has shown that adducts such as WCl_6L_2, WCl_6L, and WCl_5L_2 can readily be formed with sulfur donors. In dilute solution in CCl_4 the reaction terminates at this stage, since no other products could be isolated, and no evidence was obtained for reduction occurring.

(2) Dealkylation of Sulfur

Dealkylation of sulfides has been reported in several instances, although relatively high boiling solvents have usually been involved. Such dealkylation reactions may be temperature sensitive (14). In the specific case of tungsten halides, Fowles and co-workers (15) showed that $WSeCl_4$ will dealkylate dimethoxyethane to yield $WSeCl_3$ (OCH_2CH_2OMe), but no instance of S-dealkylation by tungsten has been reported. In the case of direct reaction with the higher tungsten halides, the exothermicity of the coordination reaction is probably responsible for the difference in behavior between the "neat" ligand reactions and those done in dilute solution.

(3) Reductive Elimination of R_2S_2

The key reaction is the reduction of W(VI) and W(V) to W(IV) which would result in the formation of dialkyldisulfides.

Can. J. Chem. Downloaded from www.nrcresearchpress.com by 210.87.254.6 on 09/05/12
For personal use only.

$$W(VI) + 2S^{2-} \rightarrow W(IV) + S_2^{2-}$$

$$2W(V) + 2S^{2-} \rightarrow 2W(IV) + S_2^{2-}$$

It has been confirmed that in both the WCl_5 and WCl_6 reactions, R_2S_2 is formed. For example in the case of $WCl_6 + Me_2S$ the distilled solvent shows n.m.r. signals due to Me_2S ($\tau = 7.92$) which is present in excess, and Me_2S_2 ($\tau = 7.61$). Although this result confirms the oxidation product is R_2S_2, it does not conclusively prove that W—SR moieties were involved. Evidence in favor of the latter was obtained by reaction of tungsten chlorides with the thioalkylation reagents Me_3SiSR (16). In CS_2 solvent the tungsten products are complex, and depend upon the stoichiometry of the reaction, but simple replacement of Cl by —SR was invariably followed by reduction of W(VI) and W(V) and production of R_2S_2 identified by the n.m.r. spectrum of the distillate. These reactions in fact lead to some interesting low-valent polynuclear tungsten compounds which will be described in a later paper, but the reaction can be simplified by carrying it out in the presence of R_2S. The following reaction was shown to occur, which verifies the possible steps from **2** to **3** in Scheme 1.

$$WCl_6 + 2Me_3SiSEt + Et_2S \xrightarrow{CS_2} WCl_4(Et_2S)_2 + Et_2S_2 + 2Me_3SiCl \text{ (excess } Et_2S, \sim 5 \text{ mol)}$$

The presence of excess Et_2S thus prevents the complication of polymerization reactions occurring. Alkylthiolato-groups are clearly unstable with respect to oxidation by W(V) and W(VI).

(4) Reactivity of $WCl_4(R_2S)_2$ as an Intermediate

The above reaction with Me_3SiSEt and Et_2S gives support to the possible synthesis of $WCl_4(R_2S)_2$ (**3**) complexes as intermediates. Further studies were undertaken to investigate whether in the presence of RCl, RCl and R_2S, or R_3SCl, **3** could be converted to the eventual product **4**.

Although the synthesis, vibrational spectra, and magnetic properties of the complexes $WCl_4(Et_2S)_2$ and $WCl_4(tht)_2$ were reported by McCarley and co-worker (3), relatively little has been done to investigate their reactivity. We have found that these complexes, and in particular the new compound $WCl_4(Me_2S)_2$, are extremely reactive. Molecular weight measurements in nitrobenzene show that loss of ligand is a facile reaction even in this relatively poor donor solvent. Displacement of sulfide by other donors is such that this type of compound is potentially of even more value than $WCl_4(RCN)_2$ (6) as an intermediate in tungsten(IV) synthetic chemistry. The low boiling point Me_2S is particularly easy to remove from the system. The following reactions are typical examples[4]

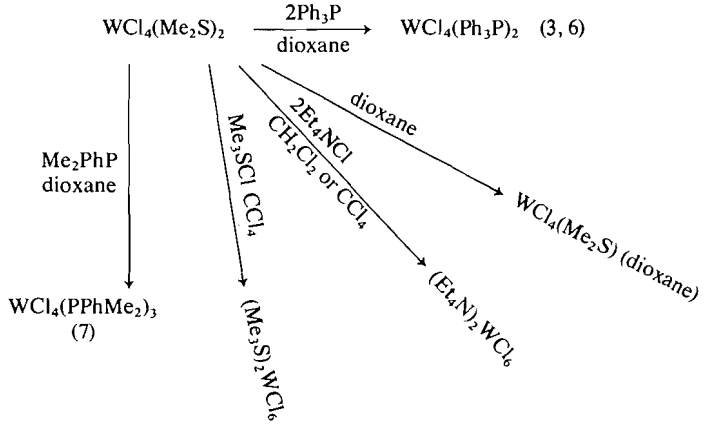

Thus reaction of $WCl_4(Me_2S)_2$ with Me_3SCl can definitely yield **4** in Schemes 1 or 2, making path (*b*) viable, if Me_3SCl could be formed from Me_2S and MeCl in the reaction mixture. Separate experiments showed that direct reaction of R_2S and RCl required relatively vigorous conditions, which would suggest that path (*a*) may be a more likely alternative. Accordingly it was found that sealed tube reactions of MeCl with $WCl_4(Me_2S)_2$

[4]References indicate previous reports of these complexes.

Can. J. Chem. Downloaded from www.nrcresearchpress.com by 210.87.254.6 on 09/05/12
For personal use only.

readily yielded $(Me_3S)_2[WCl_6]$ at room temperature, and although EtCl would not easily react alone it did so readily in the presence of Et_2S at $\sim 50°$, yielding $(Et_3S)_2[WCl_6]$. Since RCl cannot be identified in the reaction mixture it is probably rapidly converted into product **4** at the tungsten site.

As final evidence, it will be observed that in Scheme 2, for every mole of **4** formed an equimolar quantity of **3** would also result, since there is inadequate RCl or R_3SCl for complete conversion to **4**. As shown in Table 1 only 50% of the WCl_5 could be converted into **4**. An equimolar amount of **3** was also produced, as expected. In the WCl_6 reactions yields of at least 75% of the $(R_3S)_2WCl_6$ products could be obtained, and no $WCl_4(R_2S)_2$ was identified as a product.

In summary, therefore, there is a large body of evidence which supports Schemes 1 and 2. To our knowledge this is the first example of the reductive elimination of R_2S_2 from a metal center, and is the first fully documented report of the mechanism of reduction of higher halides of tungsten by neutral ligands.

We thank the National Research Council of Canada for financial support.

1. P. M. Boorman, T. Chivers, and K. N. Mahadev. J. Chem. Soc. Chem. Commun. 502 (1974).
2. P. M. Boorman, M. Islip, M. M. Reimer, and K. J. Reimer. J. Chem. Soc. Dalton, 890 (1972).
3. M. A. Schaeffer-King and R. E. McCarley. Inorg. Chem. **12**, 1972 (1973).
4. E. W. Abel. J. Chem. Soc. 4406 (1960).
5. G. I. Novikov, N. V. Andreeva, and D. G. Polyachenok. Zhur. Neorg. Khim. **6**, 1990 (1961).
6. D. G. Blight, D. L. Kepert, R. Mandyczewsky, and K. R. Trigwell. J. Chem. Soc. Dalton, 313 (1972).
7. J. R. Moss and B. C. Shaw. J. Chem. Soc. Dalton, 595 (1970).
8. J. A. Creighton, J. H. S. Green, D. J. Harrison, and S. M. Waller. Spectrochim. Acta, **23A**, 2973 (1967).
9. W. O. George, J. H. S. Green, and D. J. Harrison. Spectrochim. Acta, **24A**, 367 (1968).
10. C. D. Kennedy and R. D. Peacock. J. Chem. Soc. 3392 (1963).
11. J. M. Horner and S. Y. Tyree. Inorg. Nucl. Chem. Lett. **1**, 43 (1966).
12. (*a*) J. Chatt, G. J. Leigh, and A. P. Storace. J. Chem. Soc. A, 1380 (1971); (*b*) P. M. Boorman and K. J. Reimer. Can. J. Chem. **49**, 2926 (1971).
13. B. J. Brisdon, G. W. A. Fowles, and B. P. Osborne. J. Chem. Soc. 1330 (1962).
14. C. A. McAuliffe. Inorg. Chem. **12**, 2477 (1973).
15. D. Britnell, M. G. B. Drew, G. W. A. Fowles, and D. A. Rice. Inorg. Nucl. Chem. Lett. **9**, 415 (1973).
16. E. W. Abel and D. A. Armitage. Adv. Organomet. Chem. **5**, 1 (1967).
17. K. A. Kerr and R. Durley. To be published.

Can. J. Chem. Downloaded from www.nrcresearchpress.com by 210.87.254.6 on 09/05/12
For personal use only.

Electrochemical Behavior of the Lead Electrode in HCl and NaCl Aqueous Electrolytes

REMIGIO GERMANO BARRADAS, KEITH BELINKO, AND JOHN AMBROSE[1]

Department of Chemistry, Carleton University, Ottawa, Canada K1S 5B6

Received June 14, 1974

REMIGIO GERMANO BARRADAS, KEITH BELINKO, and JOHN AMBROSE. Can. J. Chem. **53**, 389 (1975).

The electrochemical properties of lead electrodes in aqueous chloride solutions were experimentally investigated over a range of 0.1 to 6.0 *M* HCl with the aim of extending previous work carried out only at 1.0 *M* HCl concentration. Experimental results using the rotating disc electrode technique, cyclic voltammetry, galvanostatic and potentiostatic charging conditions were employed in conjunction with spectroscopic studies of the electrolyte and X-ray powder diffraction analyses of electrode surface products. Experiments were also carried out in simulated sea water (3% NaCl) at different p*H* and compared with results obtained using HCl at the same molar concentration. At all chloride concentrations the overall reaction led to the formation of $PbCl_2$ on the electrode surface, with the exception that in NaCl solutions where p*H* $\geq$ 6.5, Pb(OH)Cl was found to be one of the products. For concentrations of less than 0.4 *M* HCl, our results indicated that the diffusion of chloride ions to the electrode surface was the limiting factor in the formation of a passivating $PbCl_2$ layer. At concentrations of about 0.7 *M* HCl, the electrochemical behavior showed a pattern of results which were interpreted in terms of a "passivation–dissolution" competitive mechanism consistent with the solubility minimum of $PbCl_2$ in aqueous chloride solutions.

REMIGIO GERMANO BARRADAS, KEITH BELINKO et JOHN AMBROSE. Can. J. Chem. **53**, 389 (1975).

On a étudié expérimentalement les propriétés électrochimiques d'électrodes de plomb dans des solutions aqueuses de chlorure entre 0.1 et 6.0 *M* en HCl; le but en était d'étendre un travail précédent qui n'avait été effectué que jusqu'à 1.0 *M* en HCl. Les résultats expérimentaux obtenus (en utilisant la technique de l'électrode à disque tournant, de la voltamétrie cyclique et de la charge galvanostatique et potentiostatique) ont été utilisés en conjonction avec des données spectroscopiques de l'électrolyte et des diagrammes de rayons-X des poudres des produits de surface des électrodes. On a aussi effectué des expériences dans de l'eau de mer artificielle (3% de NaCl) à différents p*H* et on a comparé les résultats avec ceux obtenus en utilisant du HCl à la même concentration molaire. A toutes les concentrations de chlorure, la réaction globale conduit à la formation de $PbCl_2$ à la surface de l'électrode. Il y a toutefois une exception pour les cas de solutions de NaCl à p*H* $\geq$ 6.5 où Pb(OH)Cl est l'un des produits formés. A des concentrations plus basses que 0.4 *M* en HCl, nos résultats indiquent que la diffusion des ions chlorures vers la surface de l'électrode est le facteur contrôlant la formation d'une couche passivante de $PbCl_2$. A des concentrations de l'ordre de 0.7 *M* en HCl, le comportement électrochimique montre un ensemble de résultats qui a été interprété comme résultant d'un mécanisme compétitif "passivation–dissolution" en accord avec les minima de solubilité de $PbCl_2$ dans des solutions aqueuses de chlorure. [Traduit par le journal]

Introduction

Recent interest (1–5) has been focused on the possibility of the $Pb/PbCl_2$ electrode as an economical substitute for the Ag/AgCl electrode in sea water activated batteries which employ a Mg alloy anode. The $Pb/PbCl_2$ electrodes have been made by a number of procedures of which the hot-pressing method has been found to be convenient and satisfactory (3). The discharge characteristics of these electrodes have been studied (1–5), but there has been relatively little fundamental electrochemistry of Pb in aqueous chloride solutions reported in the literature (5–8).

Our studies in 1 *M* HCl have already been reported (9) and in the present paper further experimental studies are extended to other HCl concentrations ranging from 0.1 to 6 *M*. In addition results for simulated sea water (3% NaCl) at various p*H* will be presented and correlated with data for HCl at the same concentration (0.5 *M*).

[1]Present address: International Nickel Co. of Canada Ltd., J. Roy Gordon Laboratory, Sheridan Park, Mississauga, Ontario L5K 1Z9.

Can. J. Chem. Downloaded from www.nrcresearchpress.com by 210.87.254.42 on 09/05/12
For personal use only.

Can. J. Chem. Downloaded from www.nrcresearchpress.com by 210.87.254.42 on 09/05/12
For personal use only.

Experimental

The apparatus for electrochemical measurements, cells and rotating disc assembly were as described before (9). In addition a PAR model 170 electrochemistry system was used for some of the measurements. p*H* changes during the electrolysis of simulated sea water (3% NaCl) were monitored by a glass electrode contained in a side tube in the working compartment of the three compartment cell. The reference electrode was saturated calomel and all potentials unless stated otherwise refer to this electrode.

Pb of 99.999% purity (Alfa Inorganics Inc.) was made into discs and embedded in Teflon. The surface was cleaned with hydrogen peroxide – acetic acid mixture and finally rubbed with microcloth (Buehler Ltd.).

AnalaR chemicals were employed and solutions made up with triply distilled water. NaCl solutions of various p*H* were prepared by the addition of the requisite amount of HCl. Galvanostatic formation of $PbCl_2$ on Pb in aqueous 0.1 *M* HCl, its discharge characteristics, the effects of temperature, and presaturation of the electrolyte with $PbCl_2$ were carried out with rectangular shaped electrodes with an apparent surface area of 2 cm^2 prepared from Pb foil (99.99% purity supplied by A.D. MacKay Inc.). In these studies the reference electrode used was Ag/AgCl and the potentials in Figs. 1 and 2 refer to this electrode.

Results and Discussion

(a) Galvanostatic Work

Galvanostatic charging curves of Pb in 0.1 *M* HCl as shown in Fig. 1*a* and *b* consisted of two parts designated as regions I and II. The potential in region I was always found to be steady whereas the potential in region II was found to be time dependent.

The potential in region II was found to rise with time (as Fig. 1*a*) for $PbCl_2$ presaturated electrolytes, and also in 0.1 *M* HCl for current densities greater than 5 mA/cm^2 at temperatures $\leqslant$15 °C. In 0.1 *M* HCl at 25 °C the potential in region II fell at first as a function of time (Fig. 1*b*) for current densities in excess of 3 mA/cm^2 for the rectangular shaped electrode. However, for disc electrodes the same effect did not occur until about 5 mA/cm^2. It is difficult to establish an exact current density for the change in behavior due to uncertainties of surface roughness. When the electrolyte was stirred by bubbling with N_2 gas over the rectangular electrode, or by rotating the disc electrode, falling potentials in region II were observed at $\leqslant$15 °C. In $PbCl_2$ presaturated solutions, stirring had no effect on the potential behavior in region II.

Products taken from the electrode surface in the course of both potential regions I and II were found by X-ray powder diffraction analysis to be $PbCl_2$; no other species were detected. This is suggestive that there is only one distinct electrochemical step occurring during the galvanostatic electrolyses, which may be represented by the overall reaction

[1] $$Pb + 2Cl^- \rightarrow PbCl_2 + 2e$$

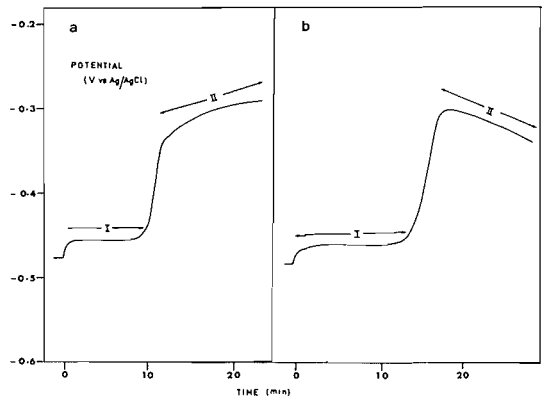

FIG. 1. Polarization curves of Pb at 25 °C and 4 mA/cm^2. (*a*) 0.1 *M* HCl solution presaturated with $PbCl_2$; (*b*) 0.1 *M* HCl.

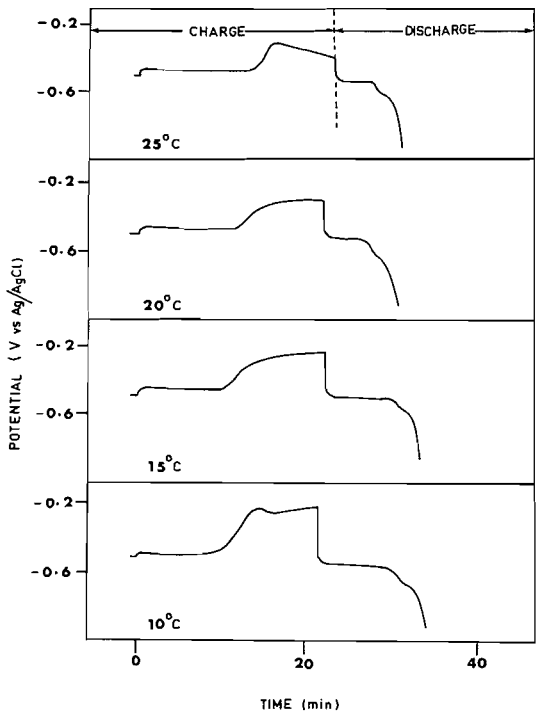

FIG. 2. Polarization curves of Pb in 0.1 *M* HCl at 4 mA/cm^2 for different temperatures.

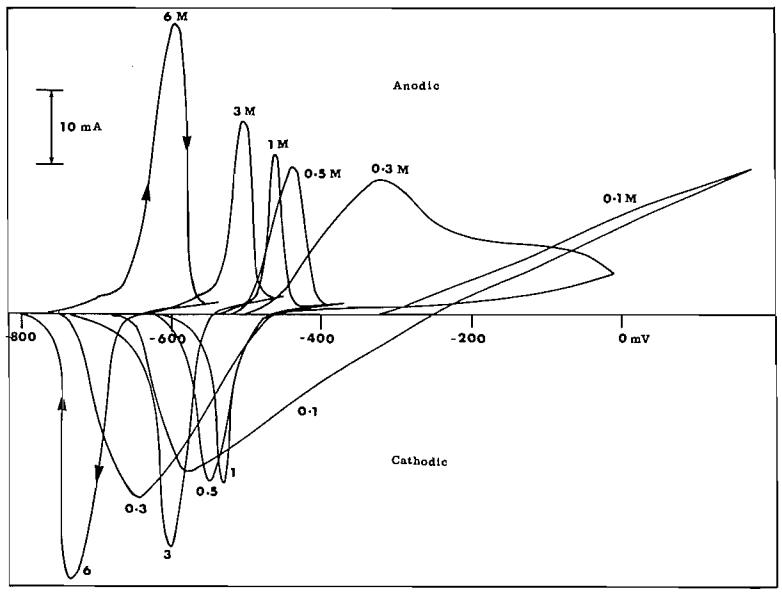

FIG. 3. Cyclic voltammograms recorded with a sweep rate of 10 mV/s in various HCl concentrations.

Complementary evidence concerning the formation of $PbCl_2$ was obtained from open circuit potential measurements. In all instances the potential of the electrode fell to a value of approximately -484 mV at 25 °C in 0.1 *M* HCl, Fig. 1, which agrees rather well with the value calculated from E^0 given by Parsons for $Pb/PbCl_2$ (10).

The rise in potential between regions I and II (Fig. 1) can therefore be due to the formation of a passivating layer of $PbCl_2$. The subsequent behavior in region II can be explained in the following way. In presaturated $PbCl_2$ solutions and at temperatures $\leqslant 15$ °C the dissolution of the passivating layer of $PbCl_2$ is inhibited, and therefore, increases in thickness with time at sufficiently high c.d., thereby causing the potential in region II to increase. At 25 °C the dissolution of the $PbCl_2$ layer is enhanced and the converse effect in thickness and potential behavior are apparent, except at low current densities. The behavior of the electrode on stirring the electrolyte is consistent with the above interpretations.

Charge and discharge curves are depicted in Fig. 2 for different temperatures. It is noteworthy to mention that two potential arrests were observed on discharge, as has been observed in previous work (2) on hot pressed $PbCl_2$ plates. During the course of the second potential arrest the formation of dendritic lead, confirmed by X-ray powder diffraction analysis, was observed on the electrode, especially in $PbCl_2$ presaturated solutions where the second arrest was considerably larger. It may be concluded that the Pb is formed by reduction of soluble Pb(II) species.

Further insight into the nature of the first cathodic arrest may be gained by considering the ratio of the charge represented by this arrest, Q_c (*i.e.*, the first plateau on the cathodic side of Fig. 2), to the charge represented by the first anodic plateau, Q_a, from Fig. 2. The ratio Q_c/Q_a varies from 0.3 at 25 °C to 0.9 at 10 °C at a current density of 4 mA/cm^2. Q_c/Q_a was also sensitive to changes in applied current density, *e.g.* changing from 0.08 at 3 mA/cm^2 to 0.5 at 5 mA/cm^2 at 25 °C. In $PbCl_2$ saturated HCl the cathodic arrests are poorly separated and an accurate estimation of Q_c is difficult. However, Q_c/Q_a approximates to unity and is temperature independent under these conditions. From the variable nature of Q_c/Q_a in 0.1 *M* HCl without presaturation of $PbCl_2$, it could be inferred that the first cathodic arrest is in all likelihood due to the reduction of surface $PbCl_2$ as represented by the reverse of reaction 1.

(b) Cyclic Voltammetry

Voltammograms for Pb in various concentra-

Can. J. Chem. Downloaded from www.nrcresearchpress.com by 210.87.254.42 on 09/05/12
For personal use only.

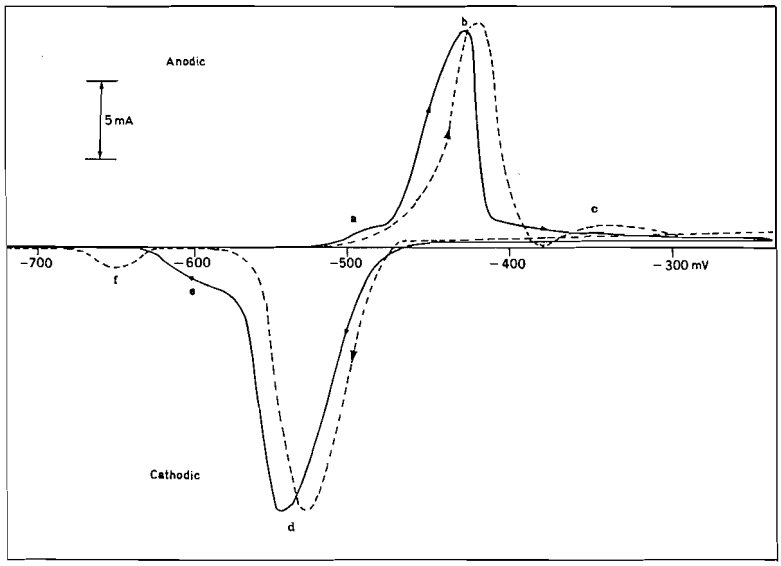

FIG. 4. (—) Cyclic voltammogram in 0.5 M HCl at v = 10 mV/s. (---) Cyclic voltammogram recorded in 3% NaCl at v = 10 mV/s.

tions of HCl and also 3% NaCl (simulated sea water) at a sweep rate of 10 mV/s are shown in Figs. 3 and 4, respectively. For concentrations above 0.5 M HCl they are divided into five regions, Fig. 4: (*a*) a pre-peak region, (*b*) an anodic passivation peak, (*c*) a reactivation region, (*d*) a cathodic peak, and (*e*) a shoulder at more negative potentials which appears only in HCl solutions.

The two cathodic processes (*d*) and (*e*) seen in HCl can be correlated with the two plateaux seen in the galvanostatic reduction of $PbCl_2$ plates (2). The shoulder is increased in size with the addition of $PbCl_2$ to the electrolyte. Since Pb dendrites, identified by X-ray powder diffraction, only begin to appear in this voltage region this shoulder may be correlated with the second cathodic arrest reported in part (*a*), and is probably therefore due to the reduction of soluble Pb(II) species.

The voltammogram changes considerably with Cl^- ion concentration Fig. 3, but very little with pH, Fig. 4. For all concentrations of Cl^- ion, i_p (current at the peak on a voltammogram) was found to be linear with $v^{1/2}$ (v = sweep rate). For a solution diffusion controlled process (22),

$$[2] \qquad i_p = 3.67 \times 10^5 n^{3/2} A c_0^{\,b} D^{1/2} v^{1/2}$$

where n = number of electrons, A = electrode surface area, $c_0^{\,b}$ = bulk concentration of Cl^- ion, D = diffusion coefficient. From [2] it is possible to calculate diffusion coefficients, D. Data for the various HCl concentrations using the values taken from peak (*b*) are shown in Table 1.

The total charge under the anodic passivation

TABLE 1. Peak current *vs.* sweep rate data (stationary electrode)

HCl concentration (mol/l)	Sweep rate range (mV/s)	Diffusion coefficient (cm^2/s)
0.1	1–20	4×10^{-5}
0.3	5–200	1.7×10^{-6}
0.5	2–200	7.6×10^{-7}
0.7	7.5–200	1.6×10^{-7}
1.0	5–200	8.0×10^{-8}
3.0	7.5–200	4.0×10^{-8}
6.0	10–500	1.0×10^{-8}

Can. J. Chem. Downloaded from www.nrcresearchpress.com by 210.87.254.42 on 09/05/12
For personal use only.

TABLE 2. Q_A (to point of passivation) *vs.* sweep rate data

Sweep rate (mV/s)	Q_A (mC); under stationary conditions						
	3 *M*	1 *M*	0.8 *M*	0.7 *M*	0.6 *M*	0.5 *M*	0.2 *M**
500	41	31	21	18	20	51	
200	51	39	27	25	28	70	
100	60	44	32	31	34	87	164
50	68	50	36	36	40	99	183
20	87	62	48	45	50	123	183
10	110	71	51	52	58	138	193
5	135	77	60	60	66	164	

*ω = 25 Hz.

peak (*b*), Q_A, was obtained by integrating the curve to the point of passivation. Q_A for different sweep rates and HCl concentrations is given in Table 2. The variation of Q_A with sweep rate suggests some degree of dependence on the extent of oxidation with time spent in the anodic region. The value of Q_A was also found to be dependent on HCl concentration displaying a minimum at 0.7 *M*. The implications of this trend in behavior will be discussed under section (*c*) on a comparative basis with the results of rotating disc experiments.

As in 1.0 *M* HCl (9), i_p was found to be proportional to E_p, the potential at the peak on a voltammogram. The slopes of i_p *vs.* E_p plots, which represent a resistance, possibly that of a surface layer, were approximately 1 $\pm$ 0.5 ohm cm^2 for all concentrations studied except 0.1 *M* HCl, where the "resistance" appears unexpectedly to be approximately ten times higher; an observation which is not easy to interpret.

For low Cl^- ion concentrations (0.1 to 0.3 *M*) voltammograms of stationary discs were somewhat irreproducible and cannot be divided into three anodic regions. At sweep rates of the order of 10 mV/s the first anodic peak is poorly defined, and extends over a wide potential region. This is especially noticeable in the case of 0.1 *M* HCl where a very broad peak was observed over a potential region of at least 1 V, but at no point were currents small enough to indicate passivation. On repeated cycling, *i.e.* forming and reducing the surface layer several times, current oscillations were observed. A plot of the peak current i_p *vs.* $v^{1/2}$ for the sweep rate range 1 to 20 mV/s was found to be linear, and the diffusion coefficient calculated from eq. 2 and given in Table 1 is of the same order of magnitude as the diffusion coefficient of HCl (3×10^{-5} cm^2/s) (11), which suggests that Cl^- ion diffusion is the limiting process.

In 0.3 *M* HCl the broad anodic peak is followed by a flat portion with the electrode finally passivating at about 0 mV, Fig. 3. Again reproducibility is irregular and electrodes which have been previously cycled show rising currents after the anodic peak instead of a flat portion, and larger cathodic peaks were observed. Plots of i_p *vs.* $v^{1/2}$ were also linear, and the diffusion coefficient calculated (see Table 1) is now much lower than that for 0.1 *M* HCl, so that solution diffusion of Cl^- is no longer limiting. It seems clear that surface growth on the electrode is becoming an important process as the HCl concentration is increased from 0.1 to 0.3 *M* as evidenced by progressive cycling in 0.3 *M*. Although cathodic peaks are observed when the anodic scan extends only as far as the rising portion of the curve in both concentrations under quiescent conditions, the hysteresis on the return sweep is higher in 0.3 than 0.1 *M*. In addition the cathodic peaks persist in 0.3 *M* even upon rotating the electrode.

When a concentration of 0.5 *M* HCl is reached, surface growth is the predominant part of the anodic process. Previous work in 1.0 *M* HCl (9) has shown that a reversible dissolution

TABLE 3. Diffusion coefficients of Cl^- in 3% NaCl from i_p *vs.* $v^{1/2}$ data

p*H*	Diffusion coefficient (10^7 cm^2/s)
0.3 (0.5 *M* HCl)	7.6
3.0	3.9
4.0	3.7
5.0	2.0
6.5	1.4

Can. J. Chem. Downloaded from www.nrcresearchpress.com by 210.87.254.42 on 09/05/12
For personal use only.

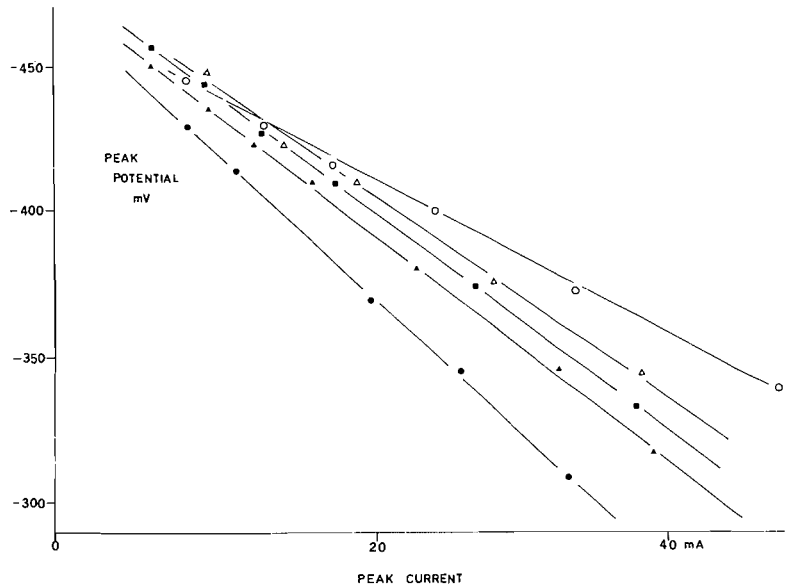

FIG. 5. Peak potential as a function of peak current for the anodic process in 3% NaCl at pH: ●, 6.5; ▲, 5; ■, 4; △, 3; and in 0.5 M HCl, ○.

step is taking place in region (*a*) and the main peak (*b*) is due to surface formation of $PbCl_2$. At 0.5 M HCl and higher concentrations, values of D are down to 10^{-7} cm^2/s (Table 1), so that solute diffusion of Cl^- is again not a limiting factor. Such values of calculated diffusion coefficient from eq. 2 are meaningless in 0.5 M Cl^-, because eq. 2 applies only for a solution diffusion limiting process. They only serve to show that there is a trend in changing values of D as calculated from eq. 2 with pH as shown in Table 3. The role of pH changes is also reflected by the slopes of E_p *vs.* i_p plots which were found to increase as the pH decreased, Fig. 5. Such changes in electrochemical behavior with pH are possibly associated with changes in surface structure, as might be expected, for example, from the observed formation of species such as Pb(OH)Cl at higher pH. This speculation is supported by X-ray powder diffraction evidence of precipitate of Pb(OH)Cl from $PbCl_2$ solutions at high pH (7.0). In the voltammogram at pH 6.5, Fig. 4, two new peaks marked (*c*) and (*f*) were observed. Peak (*c*) shifts to more negative potentials with decreasing pH values and eventually disappears in 0.5 M HCl. It is noteworthy to mention that peak (*c*) is very reproducible, but that peak (*f*) is far less reproducible by comparison, thereby making it difficult to correlate these two peaks. Despite the identification of Pb(OH)Cl, and the probability that it may be one of the species which is changing the surface structure of the electrode, the experimental evidence about the behavior of peak (*c*) shifting to more cathodic potentials with decreasing pH values cannot be used as evidence that only Pb(OH)Cl forms at the electrode. One would expect that the reverse behavior of peak (*c*) as a function of pH and potential must occur if only Pb(OH)Cl was the new surface product. Peak (*c*) must therefore represent some undeterminable species occurring through localized hydrolysis other than just Pb(OH)Cl. In essence, it is impossible to characterize the nature of peak (*c*) on the basis of the experimental results obtained.

For HCl concentrations greater than 0.5 M, the current falls rapidly after the main anodic peak to a very small value, and thereafter, rises linearly but very slowly with increasing potential. The rate of rise also increases with sweep rate. A voltammogram (extended to more positive potentials) in 0.7 M HCl showed that the small current was maintained as far as +2.4 V when irregular oscillation in currents occurred due to O_2 evolution. On reverse of the sweep, the linear dependence of current upon potential was maintained until reduction of the surface layer took place.

Can. J. Chem. Downloaded from www.nrcresearchpress.com by 210.87.254.42 on 09/05/12
For personal use only.

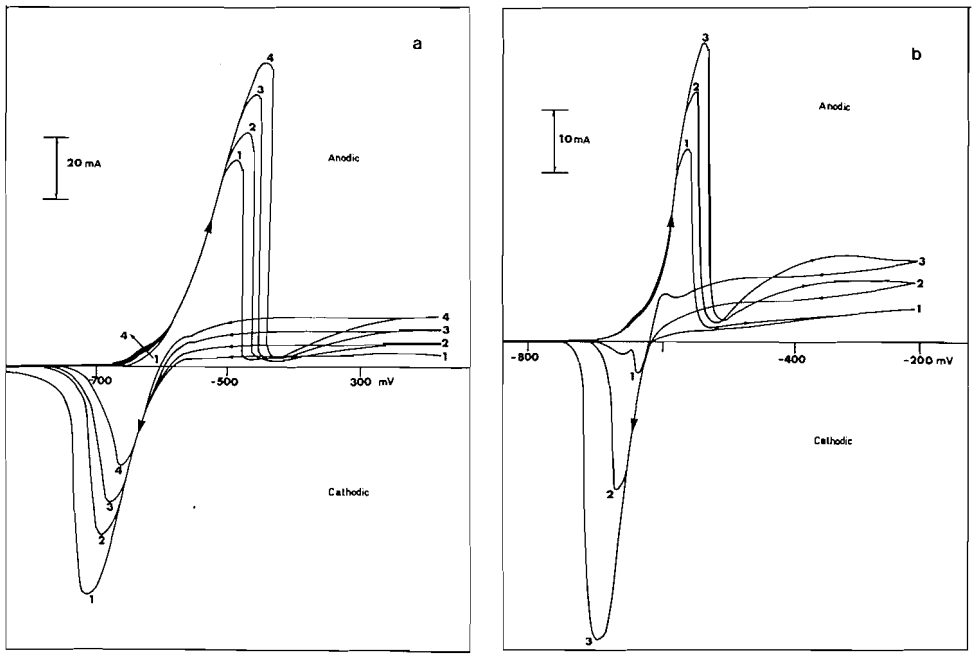

FIG. 6. Cyclic voltammograms recorded in 6 *M* HCl. (*a*) v = 50 mV/s; (*1*) 0, (*2*) 9, (*3*) 25, and (*4*) 49 Hz. (*b*) v = 10 mV/s; (*1*) 0, (*2*) 9, (*3*) 16 Hz.

Voltammograms in 3.0 and 6.0 *M* HCl were morphologically the same as in 0.5 *M*. The fall in current after the first anodic peak was much faster than in 0.5 *M* HCl, and for slow sweep rates it was almost vertical in 6.0 *M*. As in 1.0 *M* HCl (9), the observed currents were dependent upon sweep rate in the pre-peak region, but during the rest of the rising portion the current became sweep rate independent. The potential at which the current becomes sweep rate independent determines the beginning of the formation of the surface layer. In section (*d*) it will be shown that this observation correlates well with the rotating disc progressive cycling experiments, which do not show appreciable cathodic peaks when the anodic sweep extends only as far as the pre-peak region.

The behavior on the cathodic side of the voltammograms can be correlated to the anodic behavior. In 3.0 and 6.0 *M* HCl, the main cathodic peak has a linear section which has a slope equal to the slope of the rising section of the anodic side. The shoulder on the cathodic side of the peak appears only in $\leqslant 1$ *M* HCl, and then only at the lower sweep rates. Two cathodic peaks appear on some of the runs, and a consistent pattern in their behavior is seen only on the rotating electrode. These results are discussed below where further details on the nature of the surface growth are investigated.

(c) Cyclic Voltammetry using the Rotating Disc Electrode Technique

Behavior in Concentrations Greater than 0.4 M HCl

The rotating Pb disc was used in all concentrations, and except for the two lowest concentrations (0.1 and 0.3 *M*), an increase in currents compared with the stationary disc was observed. Although peak currents were generally proportional to $\omega^{1/2}$ (ω is the electrode angular velocity), the behavior in the reactivation region was more complicated, and depended simultaneously on HCl concentration and sweep rate. This made it difficult to analyze the data quantitatively.

In 6.0 *M* HCl currents in the reactivation region rose to steady value at 50 mV/s which increased with increasing rotation speed. On reversing the sweep in the reactivation region the current fell slowly, so that over a limited range of potentials, currents were higher on the reverse than on the forward sweep, Fig. 6*a*. At 10 mV/s there was evidence of a broad peak in the reacti-

Can. J. Chem. Downloaded from www.nrcresearchpress.com by 210.87.254.42 on 09/05/12
For personal use only.

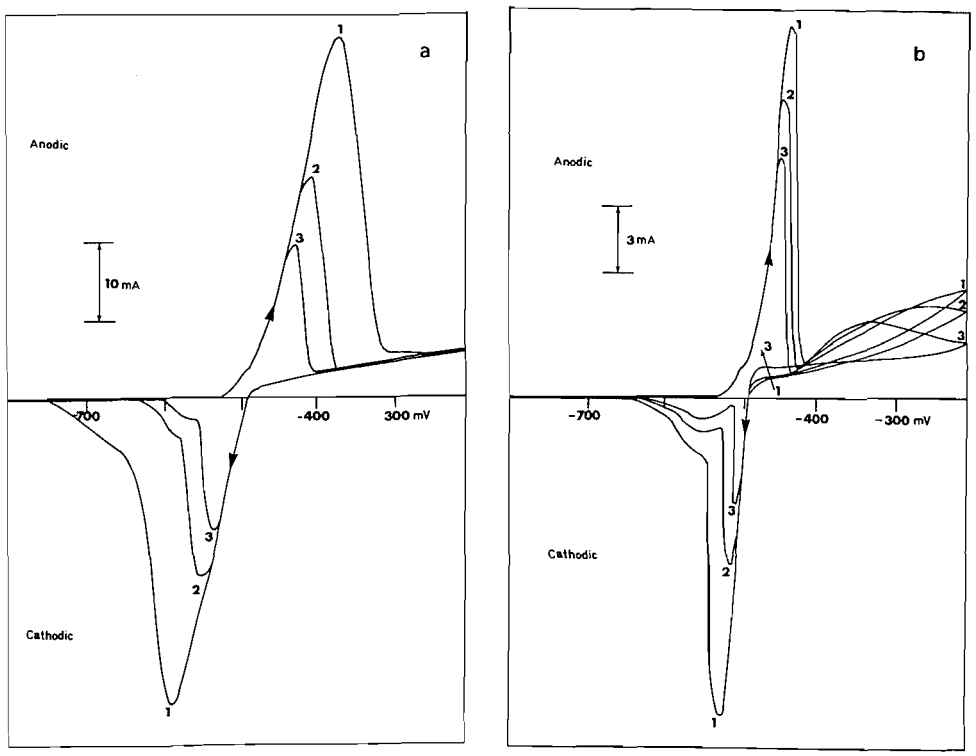

FIG. 7. Cyclic voltammograms for Pb is 0.7 *M* HCl; ω = 25 Hz. (*a*) (*1*) *v* = 200 mV/s, (*2*) 60 mV/s, (*3*) 20 mV/s. (*b*) (*1*) *v* = 10 mV/s, (*2*) 6 mV/s, (*3*) 3 mV/s.

vation region, Fig. 6*b*. In all cases, the current observed at the point of sweep reversal was maintained on the reverse sweep with only a slight fall which occurred about 100 mV prior to the reduction of the surface layer, irrespective of whether the current at the point of sweep reversal was rising or falling.

In other concentrations the behavior in the reactivation region is similar to that shown in Fig. 6*a* and *b*. At sweep rates below about 10 mV/s, the current passes through a maximum just after passivation and then attains a potential independent value, although sometimes oscillations in current are observed before the steady value is reached, Fig. 7*a* and *b*. An extended voltammogram in 0.7 *M* HCl showed that this steady value was maintained until oxygen evolution occurred at about +2 V, and was indicated by a gradual rise in current and the appearance of small bubbles on the electrode. This behavior is contrasted with that under quiescent conditions where a very gradual rise in current with increasing potential occurred. The current can be attributed to a thickening of the surface layer, because on the cathodic sweep, the cathodic peak was very much greater than for smaller anodic excursions. At sweep rates above 10 mV/s the behavior was similar to the stationary case, *i.e.*, a linear rise to a potential independent value, except that the rate of rise was greater. On the reverse sweep linearity was maintained until reduction of the surface layer took place, and as under quiescent conditions the current–potential slope during reduction was similar to that on oxidation. In the case where the current passed through a maximum in the reactivation region, the current on the reverse part of the cycle depended on the point of reversal. If the point of reversal occurred during the rising part of the peak, then currents on the reverse were the same or higher than that on the forward sweep. If reversal happened after the maximum, then reverse currents were lower. This is illustrated in Fig. 8 where a sweep rate of 8.3 mV/s was used in 0.7 *M* HCl. It was found that *i vs.* $\omega^{1/2}$ was linear for all points within the reactivation region.

The use of HCl solutions saturated with $PbCl_2$

Can. J. Chem. Downloaded from www.nrcresearchpress.com by 210.87.254.42 on 09/05/12
For personal use only.

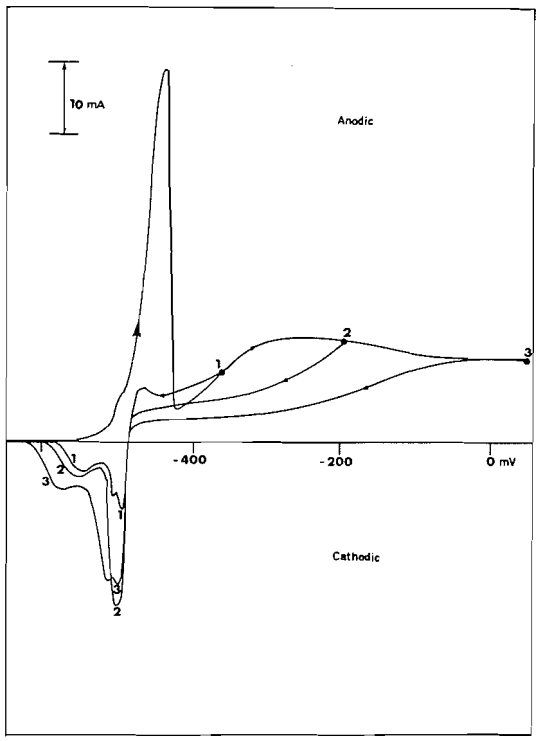

FIG. 8. Progressive cycling experiments in 0.7 *M* HCl; v = 8.3 mV/s; ω = 49 Hz; 1–3 are points of sweep reversal.

removed the reactivation effect, but changes in i_p with ω were unaffected. This shows that the reactivation process is dependent on the concentration of $PbCl_2$ in solution. However, the observation that i_p remains unaffected suggests that the main anodic peak is caused by a different reaction mechanism in the process of passivating the lead electrode, and this need not necessarily depend on any specific concentration of lead chloride in solution. Therefore, one surmises that the reactivation region is associated with the formation of soluble lead species subsequent to the passivating step.

Small changes in E_p with rotation speed, ω, were observed as might be expected from a dissolution–precipitation mechanism (9), but the behavior of the electrode depended greatly on its previous history, such as whether the electrode surface was freshly prepared or had undergone one or more oxidation–reduction cycles. The peak height increases and appears at more positive potentials with successive cycles until generally about the fifth cycle after which the peaks are reproducible. Therefore, in all these experiments the electrode was precycled about 5 times while being rotated at different speeds before actual measurements were made. In carrying out a series of runs starting at ω = 25 Hz and increasing in steps of $\omega^{1/2} = 1$ up to ω = 100 Hz, and then decreasing again in steps of $\omega^{1/2} = 1$, appreciable hysteresis in E_p were observed, but there were no significant perturbations in the values of i_p. The cycles were extended just past the point of passivation. It was found that the width of the hysteresis in E_p depended on the rotation speed used during the precycling.

The hysteresis effect is summarized in Table 4 where ΔE_p is the peak potential difference between the run where ω is increasing, and where it is decreasing. It is not possible at present to give a very satisfactory explanation of the results, but the cause may in part be due to the effects of changes in surface roughness which occur during an experiment. It had been formerly stated (9) that formation and reduction of a surface layer of $PbCl_2$ would cause roughening of the Pb surface, and dissolution would tend to smooth the surface. The discs have been observed to appear brighter after a voltammogram on a rotating electrode than on a stationary electrode, although etch pits appear when appreciable dissolution takes place. The occurrence of surface roughening or smoothing is probably very sensitive to hydrodynamic conditions, and quantitative treatments are not possible with

TABLE 4. Hysteresis in peak potential, sweep rate: 5 mV/s

0.5 *M* HCl		1.0 *M* HCl		3.0 *M* HCl	
ΔE_p (mV)	Precycling (Hz)	ΔE_p (mV)	Precycling (Hz)	ΔE_p (mV)	Precycling (Hz)
4	10	2.5	0	1.5	49
2	36	7.4	25	0.5	81
1	64	6.8	36	0	100
0	100				

Can. J. Chem. Downloaded from www.nrcresearchpress.com by 210.87.254.42 on 09/05/12
For personal use only.

TABLE 5. Q_C/Q_A data for different sweep rates and rotation speeds

Sweep rate (mV/s)	Rotation speed (Hz)	Q_C/Q_A at [HCl] = 3 *M*	1 *M*	0.7 *M*	0.5 *M*	0.2 *M*
200	0	0.97	0.95	0.92	0.95	0.70
	25	0.82	0.73	0.92	0.88	
	64	0.60	0.69	0.77	0.64	0.57
100	0	0.98	0.96	0.94	0.95	0.65
	25	0.73	0.66	0.91	0.81	0.58
	64	0.50	0.50	0.71	0.50	0.43
	0	0.98	0.93	0.96	0.96	0.65
	25	0.62	0.55	0.89	0.78	0.49
	64	0.32	0.36	0.60	0.41	0.27
20	0	0.99	0.91	0.97	0.96	0.64
	25	0.42	0.42	0.81	0.64	0.39
	64	0.25	0.26	0.45	0.24	0.10
5	0	0.94	0.94	0.88	0.97	0.66
	25	0.26	0.31	0.52	0.28	0.32*
	64	0.16*	0.15	0.17	0.09	0.05

*10 mV/s.

the available data. If the major reaction is dissolution, then currents would be expected to be higher where the Pb surface is initially rough. Consideration of a surface growth mechanism is much more complicated, because a nucleation and growth process would be very sensitive to surface asperities; alternatively a dissolution–precipitation mechanism would be equally sensitive to the hydrodynamic conditions near the electrode.

The cathodic side of the voltammograms in all concentrations shows the large amount of electrode dissolution that occurs. Data for voltammograms which extend only a short way into the reactivation region are given in Table 5. The ratio of cathodic charge to anodic charge, Q_C/Q_A is dependent upon rotation speed and HCl concentration (Q_A and Q_C are charges consumed in the anodic and cathodic reactions, respectively). The ratio approaches values closest to 1 at zero rotational speed, in all concentrations (with the exception of 0.2 *M* HCl) and at all sweep rates. Because the values are so close to unity, distinction between different sweep rates and concentrations is not possible until the electrode is rotated. The ratio reaches a maximum value at the highest sweep rate studied, and at 0.7 *M* HCl. In addition the ratio is larger at $\omega = 25$ than at $\omega = 64$ Hz. These results are consistent with the trend in the shape of voltammograms recorded in different HCl concentrations (Fig. 3) and the data of Q_A shown in Table 2. With respect to Fig. 3, since these voltammograms were all recorded with the same sweep rate, the half-width of the main anodic peak is indicative of the time required for the electrode to passivate. A minimum in the half-width occurs at about 0.7 *M* HCl. A similar result is shown in Table 2, where a minimum in Q_A, the charge under the main anodic peak (*cf.* Fig. 4, peak (*b*)), is observed at 0.7 *M* HCl. A minimum in Q_A was again found at approximately 0.7 *M* HCl under rotating conditions.

This trend in behavior is apparently consistent with solubility considerations which predict least dissolution when mass transport of products away from the electrode surface is minimal (at zero or low rotation speeds), when the Cl^- concentration is near the minimum in the solubility curve for lead chloride, and when surface/solution contact time is shortest (highest sweep rate).

Behavior at Concentrations Less than 0.4 M HCl

In 0.4 *M* HCl and lower concentrations, the stationary and rotating electrodes show different behavior. The difference is most pronounced in 0.1 *M* HCl (*cf.* Fig. 3 and Fig. 9). The stationary electrode gives increasing currents with potential over a very wide potential range and this is accompanied by appreciable loss of Pb. On

Can. J. Chem. Downloaded from www.nrcresearchpress.com by 210.87.254.42 on 09/05/12
For personal use only.

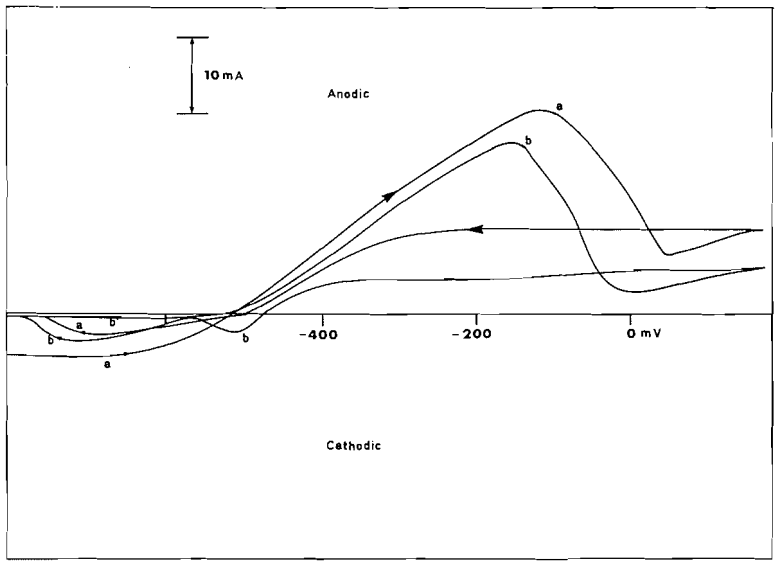

FIG. 9. Cycling voltammogram recorded in 0.1 *M* HCl at 8 mV/s. (*a*) $\omega = 64$ Hz, (*b*) $\omega = 16$ Hz.

rotation, the voltammogram is similar to the voltammograms of the stationary Pb electrode in concentrations above 0.4 *M*. The transition from one type of behavior to the other could be clearly seen under certain conditions. For example, in 0.4 *M* for varying sweep rates two anodic peaks were observed, the more positive of which increased with decreasing sweep rate and the other decreased (see Fig. 10). The second peak disappears upon rotation. In 0.3 *M* HCl cycling with changing rotation speed showed that the anodic peak has approximately the same type of shape (Fig. 11, curve 1), except for small changes in peak potential and peak height similar to those discussed earlier for higher HCl concentrations. If the rotation is stopped, but the cycling continued, the peak changes as depicted by curves 2 to 5, Fig. 11. This change in profile which indicates a delay in attaining passivation must be attributed to surface growth becoming increasingly difficult. It therefore follows that because of its dependence upon Cl^- ion concentration and hydrodynamic conditions, surface growth is dependent upon a solution diffusion of Cl^- ions.

The cathodic peaks were found to increase in size when the rotation of the electrode was stopped, Fig. 11. It is, however, not possible to determine whether the process is a reduction of a surface layer only. Reduction of soluble species may likely be a concurrent reaction.

It is of interest to note that the reactivation of the electrode on rotation in these low concentrations is similar to those in higher concentrations.

(d) Progressive Cycling Experiments

Progressive cycling of the electrode with and without rotation were carried out. Results in 0.5 *M* HCl, at a sweep rate of 5 mV/s at $\omega = 0$ and $\omega = 36$ are shown in Fig. 12*a* and *b*, respectively. Results at higher rotation speed are substantially the same as those for $\omega = 36$.

In the stationary case the cathodic peak grows steadily as the anodic scan extends along the rising portion of the anodic peak. There is an appearance of a small shoulder on the forward side of the cathodic peak. The size of the cathodic peak continues to grow until passivation is reached on the anodic side.

In the experiments carried out with a rotating electrode (Fig. 12*b*) the same qualitative trend of results was observed on the early rising portion of the main peak where forward and backward sweeps have the same current. This may be ascribed to a dissolution process unhindered by surface growth as had been shown previously (9), (*cf.* section (*e*)). By the time curve 2 is reached a cathodic peak appears which increases in size up to curve 4. In run 6 where the electrode on the anodic side is being swept as far as the reactivation region, the cathodic peak shifts about 10 mV to a more positive value. The shoulder increases

Can. J. Chem. Downloaded from www.nrcresearchpress.com by 210.87.254.42 on 09/05/12
For personal use only.

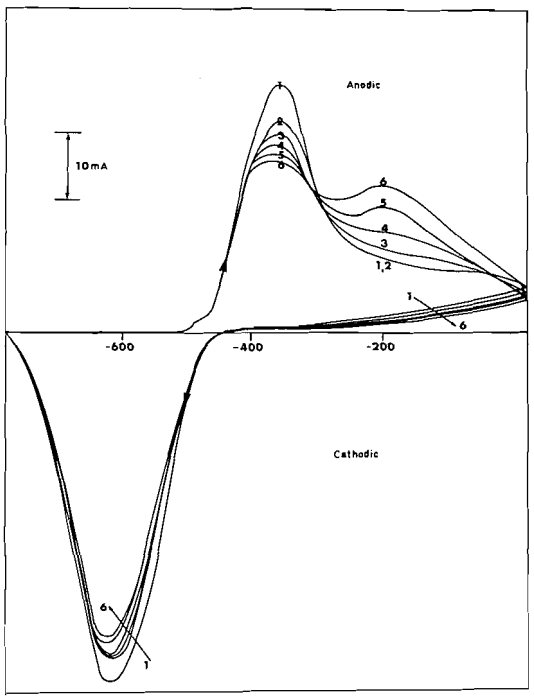

FIG. 10. Cycling voltammograms for Pb in 0.4 *M* HCl at different sweep rates; (*1*) 40, (*2*) 26.6, (*3*) 20, (*4*) 16, (*5*) 13.3, (*6*) 11.5 mV/s.

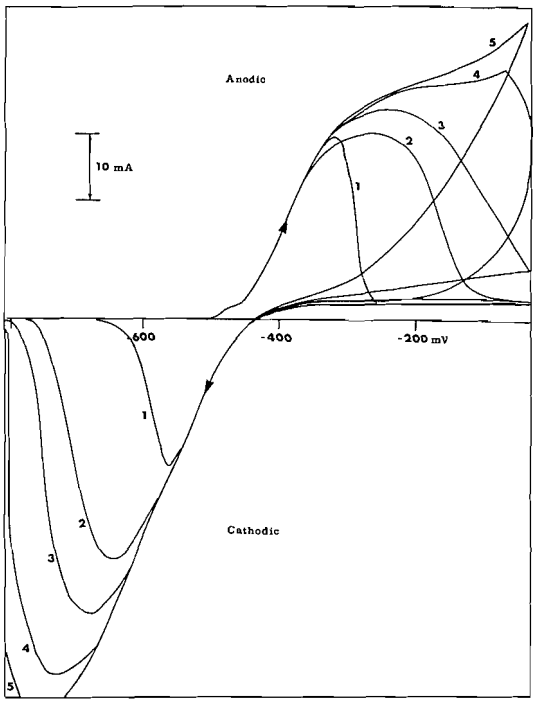

FIG. 11. Cycling voltammograms for Pb in 0.3 *M* HCl at $v = 40$ mV/s; $\omega = 25$ Hz for (*1*); (*2*)–(*5*) are subsequent voltammograms recorded under stationary conditions.

commensurately in size. Experiments in 0.7 *M* HCl where the anodic excursion was extended to higher overpotentials the cathodic peak was found to increase, while the shoulder remained practically unchanged. It appears that a large proportion of the residual current observed in the reactivation region is used in building up the surface layer. For a particular anodic excursion the cathodic peak current, but not the shoulder current depends on ω.

In some situations, *e.g.*, 1.0 *M* HCl, the cathodic peak is split in two with the more negative peak decreasing, and the positive peak increasing as the anodic sweep extends through the point of passivation (9). In order to establish the sequence of cathodic peak formation, an extended series of new experiments in 1.0 *M* HCl was carried out in which anodic sweeps to a particular potential were made with the electrode being either held at the selected potential, or placed on open circuit for varying lengths of time before the reverse sweep was performed. In all cases a sweep rate of 5 mV/s, and a rotation speed of 25 Hz was employed. The holding potentials were (*i*) −460 mV which is at the peak maximum, (*ii*) −450 mV which is at the peak maximum, (*iii*) −440 mV which is the point of passivation, and (*iv*) −390 mV which is well into the reactivation region. At all these potentials passivation was reached on holding the potential.

In the experiments where the current was not interrupted, three peaks were observed (I) −510 to −515 mV, (II) −525 to −530 mV, and a third broad peak (III) from −545 mV to more cathodic values. The latter was about twice as broad as peaks (I) and (II), Fig. 13. Data for peak heights with different hold times are given in Table 6, and from inspection peak (I) is seen to increase in height with increasing potential of hold.

When the electrode was allowed to remain on open circuit, different results were obtained. Over the whole range of hold times peak (I) was practically constant in size, while peak (II) decreased with length of holding time. Peak (I) was larger when the sweep extended to a less anodic potential. Although the maximum currents of peak (III) did not change, the peak increased in

Can. J. Chem. Downloaded from www.nrcresearchpress.com by 210.87.254.42 on 09/05/12
For personal use only.

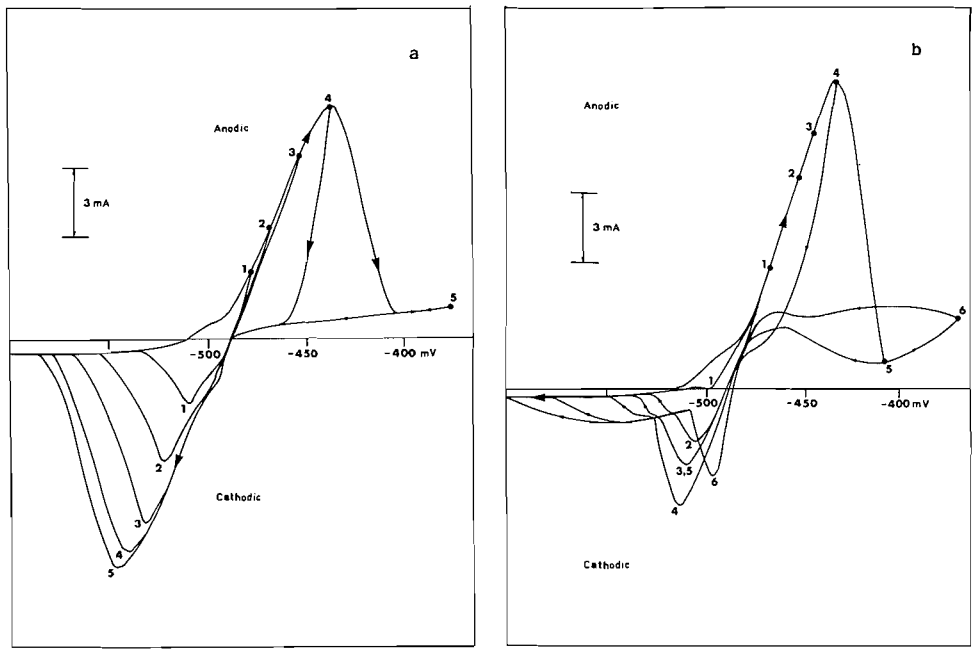

FIG. 12. (*a*) Progressive cycling experiments recorded in 0.5 *M* HCl at $v = 5$ mV/s and $\omega = 0$ Hz; 1–5 are points of sweep reversal. (*b*) Progressive cycling experiments recorded in 0.5 *M* HCl at $v = 5$ mV/s and $\omega = 36$ Hz; 1–6 are points of sweep reversal.

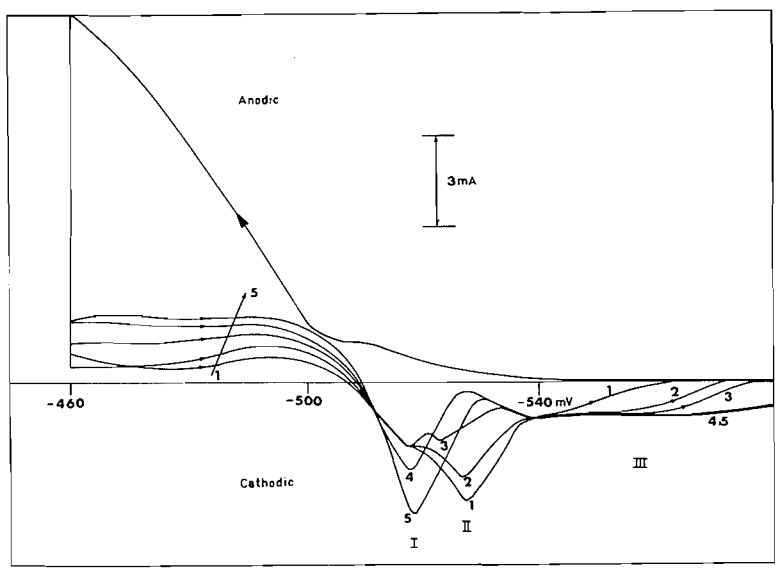

FIG. 13. Holding experiments conducted in 1.0 *M* HCl at $v = 5$ mV/s and $\omega = 36$ Hz. (Current on) (*1*) no holding, (*2*) 5 s, (*3*) 10 s, (*4*) 30 s, (*5*) 90 s.

width with increasing time of hold during passage of current. When the current was switched off during the hold period, this third peak was unaffected by length of holding time.

The above data is complicated by the fact that the cathodic peaks arise not only from the forward sweep in which surface growth and accompanying dissolution take place, but also

Can. J. Chem. Downloaded from www.nrcresearchpress.com by 210.87.254.42 on 09/05/12
For personal use only.

TABLE 6. Sweep and hold experiments in 1.0 *M* HCl*

Anodic excursion limit (mV)	Hold time (s)	i_{pII} (mA)	i_{pI} (mA)
Current on (ω = 25)			
−460	0	6.6	0
	15	6.6	1.5
	30	4.8	2.1
	100	1.5	2.6
−450	0	6.6	0
	10	4.5	2.4
	30	3.6	3.6
	60	3.0	5.3
−440	0	5.7	0.1
	10	4.7	3.6
	20	4.2	4.2
	40	1.5	5.7
	80	0	7.2
−390	0	4.8	4.8
	10	4.8	5.7
	20	3.0	6.6
	60	0	8.4
Current off (ω = 36)			
−470	0	6.0	0
	10	3.3	3.0
	30	0	3.5
	60	0	3.5
	120	0	3.5
−460	0	5.7	2.3
	5	2.1	2.5
	10	1.2	2.5
	30	0	2.5
	60	0	2.5
	120	0	2.5

*i_{pI}: −510 to −515 mV; i_{pII}: −525 to −530 mV.

from the reverse part of the sweep where enhanced surface growth can take place.

By comparison of anodic and cathodic charges, it was apparent that dissolution of the surface layer was very great with Q_C/Q_A usually less than 0.5. Furthermore the anodic charge consumed during the sweep reversal after holding was similar to the cathodic charge of peaks (I) and (II). This implies that the cathodic peaks could both have been formed entirely during the sweep reversal. These suppositions were confirmed by starting the reversal sweep at −510 mV instead of any of the selected holding potentials shown in Table 6. The combined cathodic charges were reduced to a very small value, and both peaks (I) and (II) disappeared when the electrode was allowed to stand for any length of time on open circuit. If the sweep reversal was performed immediately then only peak (II) remained. It is plausible that the species being reduced in the potential region represented by peak (I) is formed during the sweep reversal and its formation may be related to the small anodic peak observed just before reduction.

Peak (II) disappears on holding the potential either with the current being on or off. The species undergoing reduction at the originally formed peak (II) potential is not formed in the reverse sweep. Although the peak (II) height decreases in the reactivation region, it is not certain whether the species are removed electrochemically in the reactivation reaction or just dissolved away from the electrode.

The shape of peak (III) suggests a reduction of a soluble species of Pb(II). It occurs at the same potential as the shoulder (*e*) discussed in section (*b*) of this paper.

Progressive cycling experiments in 1.0 *M* HCl show peak (III) to appear when the potential of the electrode is swept into the rising portion of the main oxidation peak, but the charge under the peak only begins to increase after passivation has occurred. This is true where passivation is reached either by holding the potential, or by extending the anodic scan to some appropriate anodic value. Thus in cases where the electrode is still active at the point of sweep reversal, *e.g.*, holding at −470 mV, peak (III) is small. Where the anodic scan extended far into the reactivation region, peak (III) was eventually obscured by peak (II).

It seems likely that peak (II) is representative of a surface layer produced by dissolution–precipitation (9, 23), since the charge shown by peak (II) passes through a maximum when anodic sweeps are extended just to the point of passivation, and that it is not formed on the reverse sweep. This proposed surface layer may be sufficiently soluble to render the Pb surface liable to further oxidation. This would then give rise to the reactivation behavior and the formation of another surface layer whose reduction is observed as peak (I). The reduction of this secondary layer can be expected to occur at a somewhat different potential from the dissolution–precipitation product, since the modes of formation of the two layers are different. Formation of the layer represented by peak (I) can only occur on the reverse part of the sweep if the reaction causing dissolution of the surface layer

Can. J. Chem. Downloaded from www.nrcresearchpress.com by 210.87.254.42 on 09/05/12
For personal use only.

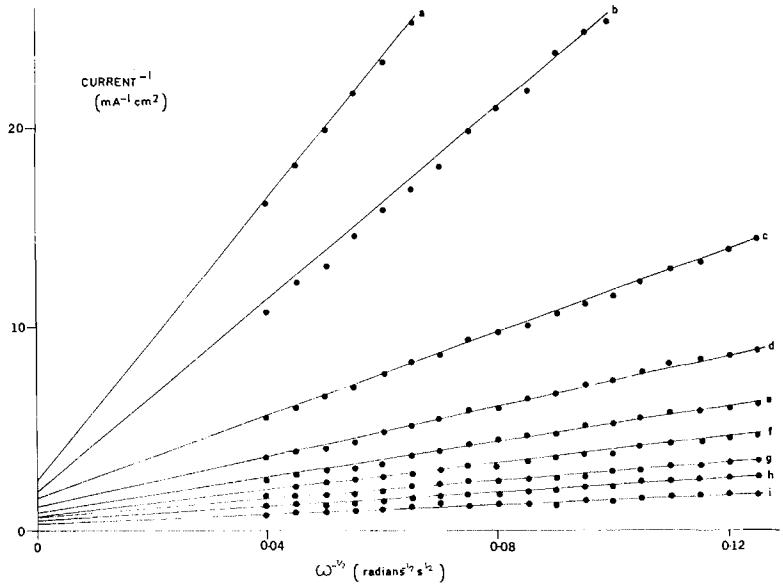

FIG. 14. Plot of data recorded at the rotating disc electrode in 0.5 *M* HCl for various constant potential values: (*a*) −530, (*b*) −525, (*c*) −520, (*d*) −515 (*e*) −510, (*f*) −505, (*g*) −500, (*h*) −495, (*i*) −490 mV.

TABLE 7. Dissolution step: i^{-1} *vs.* $\omega^{-1/2}$ data

HCl concentration (mol/l)	*E vs.* log slope (mV)	*E vs.* log i_∞ (mV)
6.0	29.1	Intercept 0
3.0	30	Intercept 0
1.0	30	Intercept 0
0.5	36	60
0.4	29.5	Intercept 0
0.3	28.5	Intercept 0
0.1	20–55*	40–125*

*Change in slope at −450 mV.

is somewhat lessened. This may explain the anodic currents observed under the main peak region in the reverse part of the sweep.

Anodic sweeps, under quiescent conditions, which were completed by holding the electrode for various times at different potentials in the reactivation region, were followed by sweeps which began at a potential just positive to peak (I) (about −510 mV). The cathodic sweeps showed only peak (II), which decreased sharply with increasing hold times in the reactivation region. When the hold times were long the

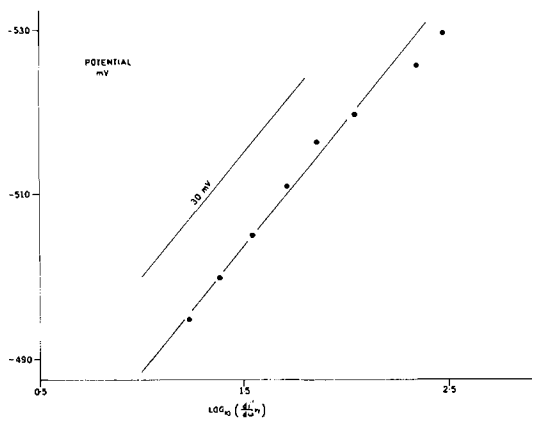

FIG. 15. The slopes of the plots of Fig. 14 as a function of potential.

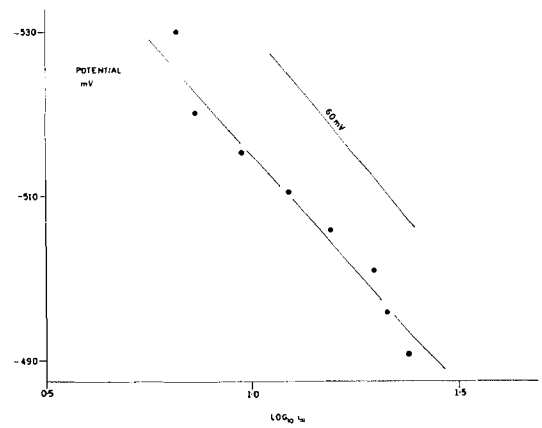

FIG. 16. Plot of log i_∞ obtained from Fig. 14 as a function of potential.

Can. J. Chem. Downloaded from www.nrcresearchpress.com by 210.87.254.42 on 09/05/12
For personal use only.

cathodic charge became small and, it is consistent with the longer periods that the electrode surface film could dissolve accordingly. If a normal voltammogram had been conducted, this effect would have been obscured because surface growth occurs during the reverse part of the sweep.

(e) Rotating Disc at Constant Potential

At low overpotentials it was found that constant anodic currents were dependent on ω. As in the case of 1.0 *M* HCl (9) an analysis of the dissolution reaction mechanism was carried out on the basis of the current being limited by diffusion away from the electrode of a soluble Pb species. Plots of i^{-1} *vs.* $\omega^{-1/2}$ were made, and it was found that straight lines were obtained for all the HCl concentrations studied. Figure 14 exemplifies this general observation. The data obtained for dependence of log slope and log i_∞ upon potential are given in Table 7, and illustrated in Figs. 15 and 16 for 0.5 *M* HCl (i_∞ = current minus contribution from diffusion).

It should be noted that except for 0.1 and 0.5 *M* HCl intercepts were near zero indicative of i_∞ to be large. This corresponds to a large exchange current. The Nernstian slope of about 30 mV for all the concentrations except for the case of 0.1 *M* HCl supports the conclusion that the overall reaction involves a two electron step.

The change in slope in 0.1 *M* HCl is possibly due to the relatively dilute concentration of the electrolyte which could cause a change in the nature of the dissolution mechanism. This hypothesis is supported by the finding that in 0.1 *M* HCl a much wider range of potentials could be studied before the slopes of i^{-1} *vs.* $\omega^{-1/2}$ became independent of potential, contrary to the other HCl concentrations.

(f) Potentiostatic Transients

In view of the complexity of the surface growth process, as evidenced by our earlier experimental results, interpretation of the *i–t* transients was found to be just as difficult. A series of transients at different potentials in 6.0 *M*, Fig. 17, and previously published results in 1.0 *M* HCl under stationary and rotating conditions (9), show that the current in all cases passes through a maximum. At lower overpotentials where passivation does not occur the currents were found to attain a steady value. At larger times (*i.e.*, after passivation), under rotating conditions, the currents began to rise again towards a steady value, and these steady values had a linear dependence upon $\omega^{1/2}$. In $PbCl_2$ saturated solution no final rise in currents were observed.

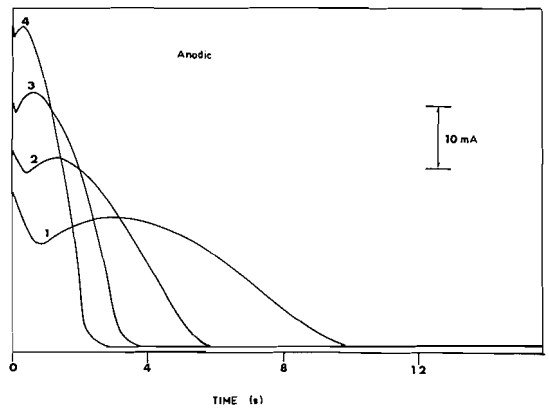

FIG. 17. Anodic current – time transients in 6.0 *M* HCl recorded at (*1*) −610, (*2*) −600, (*3*) −590 (*4*) −580 mV.

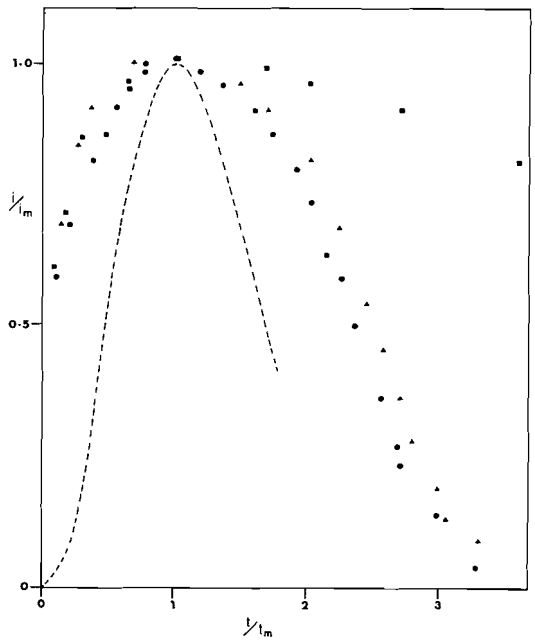

FIG. 18. Reduced variable plots (i/i_m *vs.* t/t_m) for instantaneous nucleation (---). ●, 6.0 *M* HCl; $E = -580$ mV; $\omega = 0$ Hz; ■, 1.0 *M* HCl; $E = -480$ mV; $\omega = 0$ Hz; ▲, 1.0 *M* HCl; $E = -480$ mV; $\omega = 25$ Hz. (i_m = current value at transient maximum, t_m = time at transient maximum.)

Can. J. Chem. Downloaded from www.nrcresearchpress.com by 210.87.254.42 on 09/05/12
For personal use only.

Can. J. Chem. Downloaded from www.nrcresearchpress.com by 210.87.254.42 on 09/05/12
For personal use only.

It is not possible to reconcile the appearance of a current maximum with a previously proposed dissolution–precipitation process (9, 23). Our present results could not be adequately used to fit any surface nucleation models proposed by other workers (12–15). For example, a comparison of the data for 1.0 and 6.0 *M* HCl with the theoretical reduced variable plot for instantaneous nucleation (12, 13) is shown in Fig. 18. The fit is extremely poor, but seems to be slightly improved for the higher HCl concentration, and also by rotating the electrode. In 6.0 *M* HCl there was no significant change in the reduced variable plot upon rotation of the electrode.

Preliminary work based on very different experimental conditions where surface roughness is minimized gave results which seem to indicate that some pattern of surface nucleation may possibly be operative. However, considerable amount of additional work appears to be necessary, before any firm conclusion can be made in terms of models and quantitative theory.

(g) Spectral Studies

The solubility curve for $PbCl_2$ in aqueous chloride solutions exhibits a minimum (16–18) suggestive of complexation of the Pb^{2+} ion by chloride. The ligand-to-metal charge-transfer bands for $PbCl_n^{2-n}$ complexes have been studied by u.v.-absorption (16–18). Since charge-transfer bands generally shift to longer wavelength with greater complexation, it is possible to establish spectroscopically which species predominate in solution for different Cl^- ion concentrations.

Spectral studies were carried out for Pb^{2+} (formed electrochemically under potentiostatic conditions) in various HCl concentrations and in 3% NaCl at different p*H*. For the complex $PbCl_n^{2-n}$, the value of n increases correspondingly with the increase of chloride ion concentration. For example in 0.1 *M* HCl, $PbCl^+$ is the predominant species and only traces of $PbCl_2$ are detected. At 0.5 *M* HCl concentration, the amount of $PbCl_2$ present in solution far exceeds those of $PbCl^+$ and $PbCl_3^-$. When more HCl is present (*e.g.*, between 0.5 to 3.0 *M*) the main complex is $PbCl_3^-$, whereas at concentrations in excess of 3.0 *M*, the predominant species is $PbCl_4^{2-}$. The results reported in the literature (16–18) were obtained under a constant ionic strength of 4.0 *M*. Under conditions of higher ionic strength the tendency is obviously towards the formation of higher charged complex species. It should be emphasized that our spectral data of solutions obtained after electrolytic conditions at varying concentrations are not unexpectedly somewhat different from those published by other workers (16–18). Nonetheless the general trends of complex species formation in our experiments are in reasonable agreement with those reported in the literature.

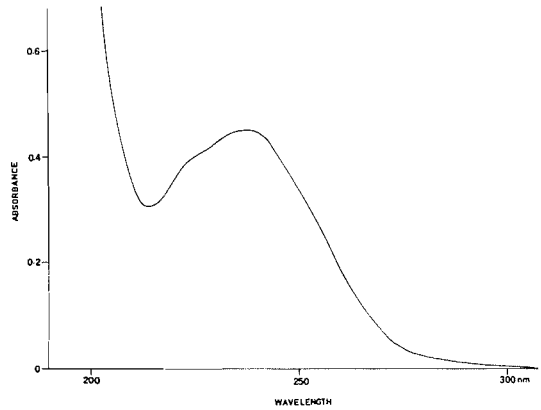

FIG. 19. Ultraviolet-absorption spectrum of 10^{-4} *M* $PbCl_2$ in 0.5 *M* HCl. Absorption band for $PbCl^+$ occurs at 225 nm. Absorption band for $PbCl_2$ occurs at 242 nm.

The spectrum for $PbCl_2$ in 3% NaCl is identical to that obtained for $PbCl_2$ in 0.5 *M* HCl under normal chemical conditions, Fig. 19. The spectrum changes little with p*H* up to p*H* 7 above which precipitation of Pb(OH)Cl, identified by X-ray diffraction, occurs. The formation of Pb(OH)Cl leads to a decrease in the intensities of the $PbCl^+$ and $PbCl_2$ spectral bands proportionally. Although the formation of Pb(OH)Cl at high p*H* as a surface layer is likely, there is no spectral evidence for the presence of such a species in solution. Perhaps it absorbs at too short a wavelength, or is only so very slightly soluble to the extent that no significant spectral band arises.

Conclusions

There was a noticeable transition in the electrochemical behavior of Pb in aqueous chloride solutions occurring at approximately 0.4 *M* HCl. At concentrations lower than 0.4 *M* HCl, where the solubility of $PbCl_2$ is relatively high (16), and where surface growth is limited by diffusion of Cl^- ion, passivation of the electrode was somewhat inhibited. This implied that the rate of surface growth was low compared to the

rate of dissolution. Although rotation of the electrode increased the amount of dissolution, transport of Cl^- ion to the electrode surface was found to be enhanced, and hence passivation occurred more readily. At Cl^- ion concentrations greater than 1.0 *M*, the solubility of $PbCl_2$ is again relatively high (16), but since there is now no limitation by diffusion of Cl^- to the surface of the electrode, passivation of the electrode was easily attained.

The competition between surface growth and dissolution as demonstrated by our experimental data gave rise to another noticeable transition in the trend of the electrochemical behavior at about 0.7 *M* HCl, which approximately coincides with the minimum in the solubility curve for $PbCl_2$ in chloride solutions. This led us to conclude that chemical dissolution of the surface $PbCl_2$ played an important role in the passivation mechanism.

Dissolution of the $PbCl_2$ layer after passivation also appeared to be a significant factor. This was indicated by the large reactivation currents observed in the voltammograms and potentiostatic transients under rotating conditions. This reactivation behavior had been postulated previously to be caused by the rupture of the surface layer of $PbCl_2$ by Cl^- ion (7), and in other electrochemical systems not involving Pb electrodes (19–21). The dissolution reaction of the passivated layer may be expressed as follows

$$PbCl_{2(surf.)} + nCl^- \rightarrow PbCl_{n+2}^{n-}$$

Financial support from grants awarded by the Defence Research Board and the National Research Council of Canada are gratefully acknowledged. We are indebted to Dr. D. W. Shoesmith for helpful discussions. We also wish to thank Dr. G. Y. Chao of Carleton University's Department of Geology for technical assistance in X-ray Powder Diffraction Analyses. One of us (K.B.) is grateful for the award of a National Research Council Studentship.

1. A. A. Vyselkov and G. Rogova. Chem. Abstr. **52**, 1077 (1958); U.S.S.R. Patent 109, 345, Feb. 23, 1958.
2. J. R. Coleman. J. Appl. Electrochem. **1**, 65 (1971).
3. J. R. Coleman. 8th Int. Power Sources Conf., Brighton, England. 1968.
4. A. A. Vyselkov, I. Y. Kop'Yev, and V. A. Naumenko. Electrotekhnika, **12**, 50 (1969).
5. H. Nomura, M. Takeuchi, and H. Abe. G.S. News, **26**, 47 (1967).
6. E. L. Littauer and L. L. Shreir. 1st Int. Congr. Met. Corros. London, England. 1961.
7. G. W. D. Briggs and W. F. K. Wynne-Jones. J. Chem. Soc. 2966 (1956).
8. J. Mindowicz and S. Biallozor. Electrochim. Acta, **9**, 1129 (1964).
9. J. Ambrose, R. G. Barradas, K. Belinko, and D. W. Shoesmith. J. Colloid Interface Sci. **47**, 441 (1974).
10. R. Parsons. Handbook of electrochemical constants. Butterworths, London. 1954. p. 69.
11. R. A. Robinson and R. H. Stokes. Electrolyte solutions. Butterworths, London. 1970. p. 515.
12. R. D. Armstrong, M. Fleishmann, and H. R. Thirsk. J. Electroanal. Chem. **11**, 3128 (1966).
13. R. D. Armstrong, M. Fleishmann, and H. R. Thirsk. J. Electroanal. Chem. **11**, 208 (1966).
14. A. Bewick, M. Fleishmann, and H. R. Thirsk. Trans. Faraday Soc. **58**, 2200 (1962).
15. M. F. Bell and J. A. Harrison. J. Electroanal. Chem. **43**, 305 (1973).
16. G. P. Haight, Jr. and J. R. Peterson. Inorg. Chem. **4**, 1073 (1965).
17. F. Vierling, G. Scarsch, and J. Bye. Rev. Chim. Minér. **3**, 875 (1966).
18. F. Vierling. Bull. Soc. Chim. **22**, 25 (1971).
19. A. K. Vijh. Corros. Sci. **11**, 161 (1971).
20. K. W. Mao and J. P. Hoare. Corros. Sci. **13**, 799 (1973).
21. N. Sato. Electrochim. Acta, **16**, 1683 (1971).
22. P. Delahay. New instrumental methods in electrochemistry. Interscience Publishers, New York. 1954.
23. J. O'M. Bockris and A. K. N. Reddy. Modern electrochemistry. Plenum Press, New York. 1970. p. 1321.

Can. J. Chem. Downloaded from www.nrcresearchpress.com by 210.87.254.42 on 09/05/12
For personal use only.

Rotating Ring-disc Electrode Studies of Lead in HCl and NaCl Solutions

REMIGIO GERMANO BARRADAS, KEITH BELINKO, AND ELENA GHIBAUDI
Department of Chemistry, Carleton University, Ottawa, Canada K1S 5B6

Received July 22, 1974

REMIGIO GERMANO BARRADAS, KEITH BELINKO, and ELENA GHIBAUDI. Can. J. Chem. **53**, 407 (1975).

The rotating ring-disc electrode technique was used to investigate the nature of the dissolution reactions that take place during the anodic charging of a Pb electrode in aqueous chloride electrolytes. Chemical dissolution of the $PbCl_2$ film formed on the disc was found to be an important process which occurred prior to and after passivation of the disc electrode. A ring current due to the electrochemical dissolution of the Pb disc was only observed at low disc currents during galvanostatic charging experiments, or at low disc overpotentials in potentiostatic and voltammetric studies. Observations of anodic ring current excursions under potentiostatically cathodic conditions hitherto not reported in the literature are described.

REMIGIO GERMANO BARRADAS, KEITH BELINKO et ELENA GHIBAUDI. Can. J. Chem. **53**, 407 (1975).

On a utilisé la technique de l'électrode à disque tournant annulaire pour étudier la nature des réactions de dissolution qui ont lieu durant la charge anodique d'une électrode de Pb dans des électrolytes de chlorures aqueux. On a trouvé que la dissolution chimique, du film de $PbCl_2$ formé sur le disque, est un processus important qui a lieu avant et après la passivation de l'électrode. On a observé un courant d'anneau dû à la dissolution électrochimique du disque de Pb uniquement à des bas courants de disque durant les experiences de charges galvanostatiques ou à des bas niveaux de surtension du disque dans des études potentiostatique et voltamétrique. On décrit l'observation de courant d'anneau anodique sous des conditions potentiostatiquement cathodiques; aucune observation de ce genre n'avait été rapportée dans la littérature jusqu'à maintenant.
[Traduit par le journal]

Introduction

Recent investigations on the electrochemical nature of lead in aqueous chloride solutions have been reported elsewhere (1, 2). The purpose of the present work is to characterize the dissolution reactions that occur prior to and after passivation of the lead electrode. This may be accomplished by using a rotating ring-disc electrode (3, 4), since a potentiostatically controlled ring acts as a probe for the detection of soluble species discharged by the disc. If the collection efficiency (5) of the ring-disc system is known it is possible to establish what fraction of the anodic disc current is due to the dissolution reaction.

Experimental

Lead of 99.999% purity was obtained from Alfa Inorganics, Inc. Ring-disc measurements were made on both a rotating Pb ring – Pb disc electrode (RPbR–PbDE), and a rotating Pt ring – Pb disc electrode (RPtR–PbDE). The disc and ring were embedded in Teflon. When a Teflon separator alone was used to separate the disc and ring, a 20 kohm resistance was observed between the two electrodes. Electrical contact was presumably occurring as a result of fine lead particles depositing within the pores of the Teflon separator. This problem was eliminated by using a 0.07 mm PVC sleeve (Ideal-Hellerman (Canada) Ltd.) around the disc for additional insulation. This arrangement gave a resistance better than 10^3 Mohms between the ring and disc electrodes.

The disc, internal ring, and external ring radii of the RPbR–PbDE were 0.302, 0.354, and 0.416 cm, respectively. The corresponding dimensions for the RPtR–PbDE were 0.296, 0.347, and 0.407 cm, respectively. The calculated collection efficiency, N, was 0.29 for the RPbR–PbDE and 0.28 for the RPtR–PbDE. Smaller ring-disc gap separation resulted with shorting between the ring and disc due to plating out of lead. Experimentally, the collection efficiency was generally found to be 0.28 ± 0.04. A higher value of N than that predicted by theory is explained by a change in ring-disc geometry resulting as a consequence of the large amounts of lead depositing on the ring. Since the lead preferentially deposited on the innermost part of the ring, the gap separation between the ring and disc was constantly changing, and unless the electrode was cleaned periodically, collection efficiencies of the order of 0.45 were obtained. An added complication was encountered when using the RPtR–PbDE. Since the hydrogen overpotential is different on Pt and Pb, it was hard to obtain reproducible results once Pb started depositing on the Pt ring. Hence, unless otherwise stated, most experiments described in this paper involved the use of the RPbR–PbDE. The RPtR–PbDE was only used in order to verify certain experimental findings obtained with the RPbR–PbDE.

The mounted ring-disc electrode was rotated with a

Can. J. Chem. Downloaded from www.nrcresearchpress.com by 210.87.254.6 on 09/05/12
For personal use only.

Can. J. Chem. Downloaded from www.nrcresearchpress.com by 210.87.254.6 on 09/05/12
For personal use only.

Beckman variable drive assembly Model No. 188501. The lead surface was cleaned with a hydrogen peroxide–acetic acid mixture (6), and finally rubbed with microcloth (Buehler Limited). Electropolishing resulted with preferential dissolution around the edges of the disc giving rise to a hemispherical surface, and was consequently not used.

AnalaR reagent grade chemicals were employed and solutions made up with triply distilled water. NaCl solutions of various p*H* were prepared by addition of the requisite amount of HCl in some experiments. Nitrogen gas was passed through the solution prior to electrolysis and maintained with a slight pressure over the solution during an experiment. All experiments were conducted at room temperature.

A PAR model 170 Electrochemistry System was used for most disc electrode measurements. The potential at the ring was maintained by a second floating-ground potentiostat (Wenking type 70 HP10) using another counter electrode, as described elsewhere (7). A Shielded Line Isolator (Berkleonics, Inc.) was also employed to ensure isolation of the two instruments; however, this gave the same results obtained by simply floating one of the instruments. In order to verify that no coupling was occurring between the ring and disc electrodes, a Wenking Potentiometer (type PPT69) was used to test the constancy of the ring potential during an experiment. At no time did the ring potential change by more than ± 0.1 mV from its potentiostatted value. Ring currents were monitored on a Honeywell type 530 XY recorder. A Wenking Model 61RH Potentiostat was also used for some measurements.

The reference electrode was saturated calomel, and all potentials mentioned in this paper refer to this electrode. The thin Luggin capillary was mounted at 1–2 mm below the center of the disc electrode throughout all the experiments.

Results and Discussion

(a) Ring Polarograms and Titration Curves (11)

A ring polarogram for the RPbR–PbDE in 3% NaCl[1] is shown in Fig. 1. Curve (*a*) represents the residual ring current, while curve (*b*) is the ring polarogram obtained by holding the disc potential at -480 mV. The disc current was constant at 0.95 mA. A collection efficiency of about 0.29 was observed for the entire potential range shown. This suggests that the ring current was limited by diffusion of soluble Pb^{2+} species to the surface of the ring within this range of potentials.

Ring-disc titration curves for the RPbR–PbDE in 3% NaCl and 0.5 *M* HCl, at electrode rotation speed $\omega = 25$ Hz, were attempted. The disc current was galvanostatically controlled and the ring currents were corrected for the residual current. In 0.5 *M* HCl, the collection efficiency was found to be about 0.28 for the whole range of disc currents shown (Fig. 2). However, in 3% NaCl, the collection efficiencies were significantly lower than 0.28 for low disc currents (<5 mA), but they eventually approached the theoretical value at higher disc currents. Therefore the data for NaCl were not plotted in Fig. 2, because such a graphical representation does not depict what is commonly known as a ring-disc titration curve (11). The observations in 3% NaCl can be explained by the removal of a small concentration of soluble Pb^{2+} species. Since the p*H* of a 3% NaCl solution is about 6.5, the formation of PbOHCl in the vicinity of the disc is not unlikely (2). The inability to detect PbOHCl at the ring may be due to the insolubility of lead hydroxychloride.

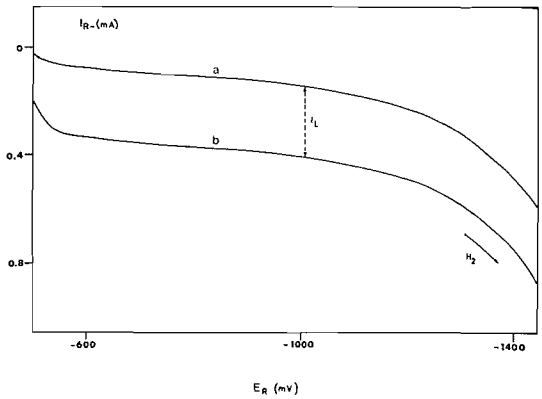

FIG. 1. Ring polarograms for the RPbR–PbDE in 3% NaCl; $\omega = 25$ Hz; $E_R = -700$ mV. Curve (*a*), residual current; curve (*b*), $E_D = -480$ mV; $i_D = 0.95$ mA.

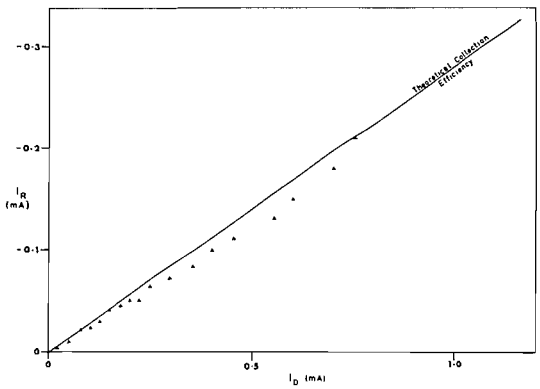

FIG. 2. Titration curve for the RPbR–PbDE at $\omega = 25$ Hz; $E_R = -700$ mV. ▲, 0.5 *M* HCl.

[1]3% NaCl in normal scientific units corresponds to approximately 0.5 mol dm^{-3}.

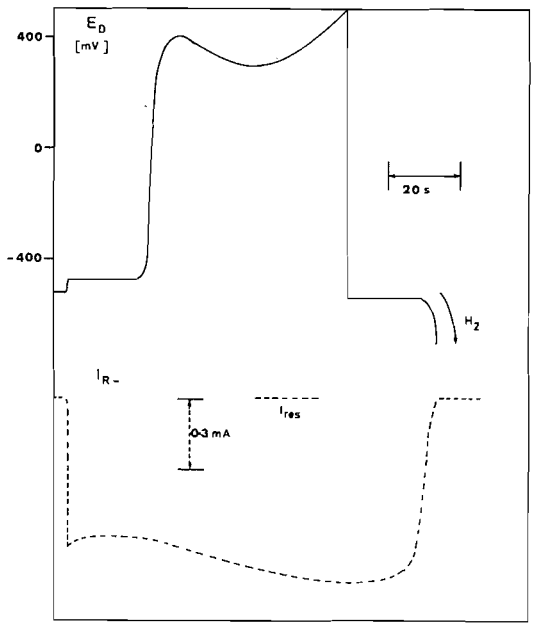

FIG. 3. Galvanostatic charging curve for the Pb disc electrode in 0.5 *M* HCl at 13 mA/cm^2; ω = 25 Hz (—). Corresponding ring current – time profile; E_R = −700 mV (---).

(b) Galvanostatic Studies

Constant current charging curves for Pb in aqueous chloride solutions were characterized by two anodic potential regions (2). X-Ray powder diffraction analysis of the products taken from the electrode surface in the course of both oxidation stages indicated the presence of $PbCl_2$ only. Figure 3 shows a galvanostatic transient for Pb in 0.5 *M* HCl at 13 mA/cm^2, and at ω = 25 Hz. The corresponding ring current – time profile is also shown; the ring was held at a cathodic potential of −700 mV. The ring current remained essentially constant for the duration of the first anodic plateau at the disc. The value of the ring current during this first disc potential region was about 0.57 mA. From the collection efficiency of the ring-disc electrode (0.29), one can calculate that only 50% of the total disc current was utilized in building up a passivating layer of $PbCl_2$. It is difficult to postulate whether the Pb^{2+} species reduced at the ring originated from a simple electrochemical dissolution step

[1] $$Pb \rightarrow Pb^{2+} + 2e^-$$

or from a chemical dissolution of the $PbCl_2$ layer being formed.

TABLE 1. Q_D and Q_R *vs.* ω data for galvanostatic studies

ω (Hz)	Q_D (mC)	Q_R (mC)	% of total charge due to dissolution
4	52	43	17
9	56	44	21
16	76	61	20
25	110	63	43
36	168	67	60
49	216	68	69

During the second disc potential region (*i.e.*, after passivation of the disc), the ring current increased slightly and finally levelled off to a steady value, despite the fact that the disc potential continued to increase. The ring current was observed to remain constant regardless of whether the disc was subsequently reduced or placed on open circuit. The constancy in ring current is highly indicative of chemical dissolution at the disc, possibly caused by a chemical breakdown of the passivating $PbCl_2$ layer. This reaction may be represented by

[2] $$PbCl_{2(surf)} + nCl^- \rightarrow PbCl_{2+n}^{n-}$$

Chemical breakdown of this nature has been previously postulated (1, 2, 8).

From experimental knowledge of the chemical dissolution of the passivating $PbCl_2$ layer, it was possible to estimate the charge associated with passivating the Pb disc electrode. This was accomplished by first allowing the disc to passivate at a current density of 13 mA/cm^2, and followed immediately by switching the disc current off. The ring current was then recorded as a function of time until all the $PbCl_2$ present on the surface of the disc had dissolved. Table 1 gives the total charge required to passivate the disc for different rotation speeds:

[3] $$Q_D = \tau i_D$$

where τ = time required to passivate the disc electrode under galvanostatic charging conditions, i_D = disc current. The charge accumulated by the ring after the disc current was turned off is given by

[4] $$Q_R = \int_{t=0}^{t=t_f} i_R' \, dt$$

where Q_R = charge corresponding to the passivating layer on the disc, and t_f is the time required to completely dissolve the passivating layer and

[5] $$i_R' = (i_R - i_{res})/N$$

Can. J. Chem. Downloaded from www.nrcresearchpress.com by 210.87.254.6 on 09/05/12
For personal use only.

Can. J. Chem. Downloaded from www.nrcresearchpress.com by 210.87.254.6 on 09/05/12
For personal use only.

where i_R = ring current, i_{res} = residual current at the ring, and N = collection efficiency.

Table 1 shows that the amount of charge lost due to dissolution during surface formation of $PbCl_2$ is large and increases with increasing rotation speed. It has been previously mentioned that the collection efficiency changes during the course of such an experiment owing to changes in geometric configuration brought about by the plating of Pb on the ring. The large variations indicated by the data regarding Q_R as a function of rotation speed may possibly be associated with the changes in collection efficiency.

By assuming the total charge required to passivate the disc to be about 45 mC, and taking the density of $PbCl_2$ as 5.9 g/cm^3, the thickness of the passivating layer was estimated to be about 4000 Å.

(c) Potentiostatic Experiments

Disc current – time measurements at low overpotentials (less than 70 mV) showed typical steady currents under controlled rotation conditions. The ring held at a reducing potential of −700 mV maintained a steady cathodic current. Ring to disc current ratios were generally within 0.02 of the theoretical collection efficiency.

A potentiostatic transient for a Pb disc in 3% NaCl, under rotating conditions, and at an oxidizing potential of −380 mV is shown in Fig. 4. A growth transient is displayed and a reactivation of the electrode occurs subsequent to passivation. The cathodic transient was recorded at a disc potential of −550 mV. The corresponding ring current – time profile is also shown for a ring potential of −700 mV. Except for the small initial dissolution part of the anodic disc transient, the ring current was found to be constant and independent of disc passivation or reactivation. Also, at any chosen rotation speed, the value of the ring current was independent of the potential applied to the disc, when the potential was sufficiently anodic to give rise to a growth transient. As with the galvanostatic studies, the same ring current was observed if the disc current was suddenly switched off. This suggests that the reduction step at the ring is diffusion control due to the release of soluble Pb^{2+} species by a chemical dissolution reaction at the surface of the disc. Under these conditions the limiting ring current is given by

$$[6] \qquad i_R = (nNFAc_0D)/\delta$$

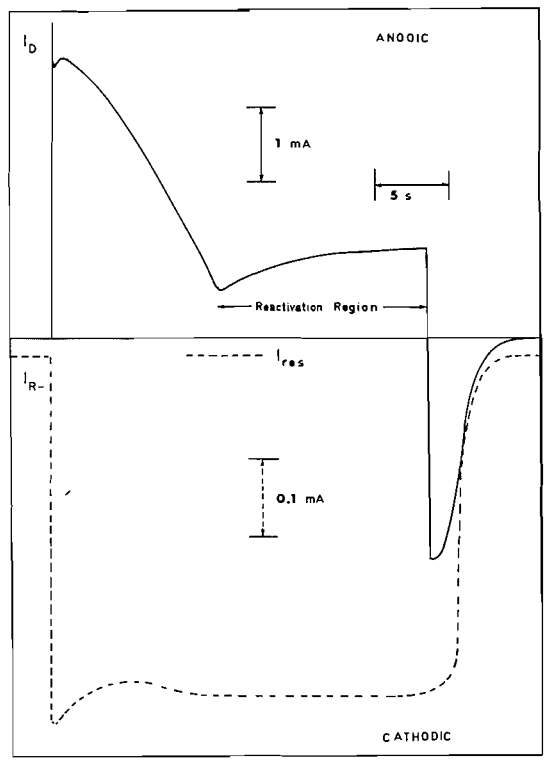

FIG. 4. Current – time transients for the Pb disc recorded potentiostatically in 3% NaCl. Potential stepped to −380 mV; reducing potential, −550 mV (—). Current *vs.* time curve for the Pb ring; E_R = −700 mV (---).

where n = number of electrons, F = Faraday constant, A = disc electrode surface area, c_0 = the concentration of soluble Pb^{2+} species in equilibrium with the disc, D = diffusion coefficient, and δ = diffusion layer thickness. The collection efficiency N, in eq. 6 corrects for the actual amount of current measured at the ring (i_R). From Levich (9), the thickness of the diffusion layer is

$$[7] \qquad \delta = 1.62\, D^{1/3}\nu^{1/6}\omega^{-1/2}$$

where ν = kinematic viscosity. Combining eqs. 6 and 7 gives

$$[8] \qquad i_R = (nFNAc_0D^{2/3}\omega^{1/2})/1.62\nu^{1/6}$$

A plot of i_R *vs.* $\omega^{1/2}$ for Pb in 3% NaCl is shown in Fig. 5. As stated *vide supra* the value of the oxidizing potential at the disc is immaterial. The data presented in Fig. 5 was taken after $PbCl_2$ had been formed and the disc placed on open circuit (see Fig. 6). If the diffusion coeffi-

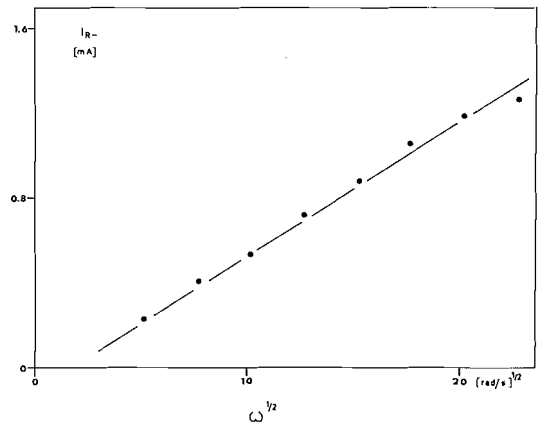

FIG. 5. Plot of i_R *vs.* $\omega^{1/2}$ for the Pb ring electrode in 3% NaCl showing chemical dissolution at the disc.

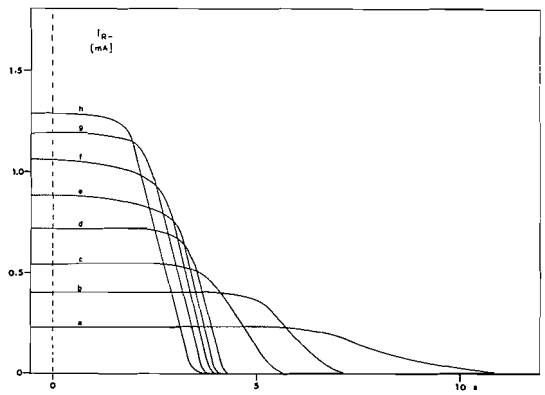

FIG. 6. Ring current – time transients recorded subsequent to passivation at the disc; $E_R = -700$ mV. The dotted line refers to the point at which the disc was switched off. (*a*) $\omega = 4$ Hz, (*b*) 9 Hz, (*c*) 16 Hz, (*d*) 25 Hz, (*e*) 36 Hz, (*f*) 49 Hz, (*g*) 64 Hz, (*h*) 81 Hz.

cient for the soluble Pb^{2+} species is assumed to be 10^{-5} cm^2/s in eq. 8, the concentration of soluble Pb^{2+} in equilibrium with the disc can be estimated to be 5×10^{-3} *M*, which compares reasonably well with the calculated value of 6.73×10^{-3} *M* using the solubility data of Table I in a paper published by Lewin (10).

Similar to the galvanostatic studies, it was possible to estimate an approximate thickness of the passivating layer. A series of ring current – time transients at different ω is shown in Fig. 6. The point at which the disc was switched off is indicated. These experiments were conducted with a RPbD–PbRE in 3% NaCl; the disc was stepped to -350 mV and allowed to passivate while the ring current was monitored with a reducing potential of -700 mV. Q_R as defined by eq. 4 for different ω is presented in Table 2. The charges were generally found to be significantly smaller than those associated with passivating the disc under galvanostatic conditions. Table 2 also gives the percent of the total charge lost due to dissolution during the formation of the passivating $PbCl_2$ layer. These values show fair agreement with the corresponding results obtained under constant current conditions. Based on an average value of Q_R in Table 2, the thickness of the passivating layer under potentiostatic conditions was estimated to be about 700 Å. A slight change in Q_R (about 3 mC) was observed when the disc was stepped to another anodic potential (-300 mV); such a small change in Q_R is not sufficiently reliable to draw any significant conclusion about the system under investigation.

TABLE 2. Q_R from potentiostatic studies as a function of ω

ω (Hz)	Q_R (mC)	% of total charge due to dissolution
4	7.2	19
9	7.2	27
16	7.5	36
25	7.8	43
36	8.2	49
49	8.8	53
64	9.4	54
81	10.2	60

(d) Cyclic Voltammetry

Figure 7 shows a rotating ring disc experiment conducted in 3% NaCl at p*H* 2.2. The ring electrode was held constant at -700 mV, while the disc was subjected to a linear potential sweep. Only at the very beginning of the rise of the disc current did the reduction current at the ring show corresponding changes due to an electrochemical dissolution of the Pb disc. Once the electrochemical dissolution step was replaced by the formation of a surface film, the ring currents were found to be steady, and independent of disc potential, with the exception of a slight change in ring current at about the point of disc passivation.

Chemical dissolution of the electrode surface layer of $PbCl_2$ was experimentally verified by switching off the disc current after passivation. The ring current fell steadily, eventually reaching the residual current value, demonstrating that

Can. J. Chem. Downloaded from www.nrcresearchpress.com by 210.87.254.6 on 09/05/12
For personal use only.

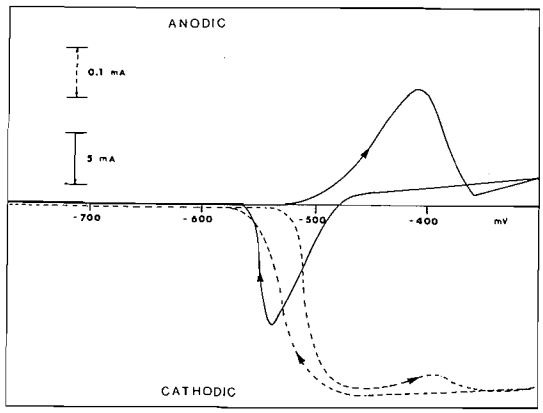

FIG. 7. Ring-disc experiment in 3% NaCl at pH 2.2; ω = 25 Hz. Disc potential swept at v = 20 mV/s; E_R = −700 mV. (---) i_R, (—) i_D.

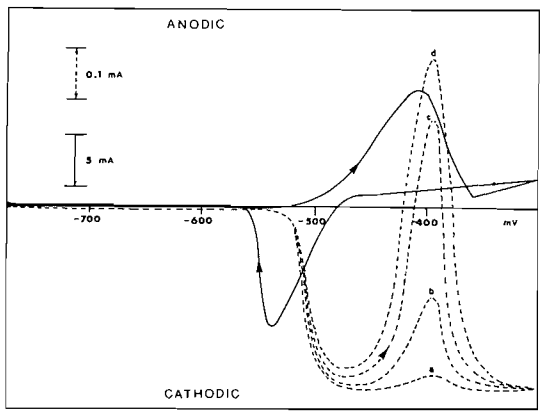

FIG. 8. Ring-disc experiment in 3% NaCl at pH 2.2; ω = 25 Hz. Disc potential swept at v = 20 mV/s. E_R held constant at (*a*) −700 mV, (*b*) −650 mV, (*c*) −600 mV, (*d*) −550 mV. (---) i_R, (—) i_D.

the surface layer on the disc had completely dissolved.

(e) Some Apparently Unusual Observations

The ring-disc results presented so far have involved monitoring the ring current at a ring potential of −700 mV. When a lower cathodic overpotential was applied to the ring an unexpected behavior in i_R was observed. Figure 8 shows a series of ring-disc experiments conducted in 3% NaCl at pH 2.2. As in Fig. 7, the Pb disc electrode was subjected to a voltammetric sweep while the ring current was monitored. However, a number of different ring potentials were used. Curve (*a*) corresponds to a reducing potential of −700 mV, curve (*b*) −650 mV, curve (*c*) −600 mV, and curve (*d*) −550 mV. When the disc began to passivate the ring current showed a sudden excursion in the anodic direction, and if the ring potential was less cathodic (curves (*c*) and (*d*)), the ring current actually became anodic. This result was found to be independent of pH (values $\leqslant$6.5) of the solution. It was quite sensitive to rotation speed by displaying increasing positive ring currents with faster rotation speeds. These investigations have also shown a dependence on Cl^- ion concentration. The effect appears to decrease somewhat with increasing Cl^- ion concentration (from 0.5 to 3.0 M), but the anodic ring current excursion persists. Potentiostatic transient studies showed similar effects. The results obtained under galvanostatic studies, on the other hand, were not well defined. Although there was a tendency for ring currents to show a slightly smaller cathodic value at the point of passivation, with corresponding decreasing cathodic overpotentials; no anodic currents were ever observed.

As mentioned in the Experimental section, the ring potential was monitored with a potentiometer, and at no time was coupling observed between the two potentiostats. The result observed is not an experimental artifact (12) because it has been checked often under varying conditions by three independent workers. The behavior may possibly be due to a concurrent anodic process occurring together with the reduction of soluble Pb^{2+} species. The formation of an unstable species such as Pb^+ at the disc seems unlikely in view of the magnitudes of currents and times involved. A plausible explanation could involve oxidation of the Pb at the ring. This speculation is possible only if the value of the reversible potential for the Pb/Pb^{2+} couple changes so as to make what was initially a cathodic overpotential to an anodic overpotential at the point of passivation.

Open circuit measurements of the Pb electrode as a function of $PbCl_2$ concentration have confirmed that a Nernstian behavior is followed according to the relation

$$[9] \qquad E_{Pb/Pb^{2+}} = E^0 + \frac{RT}{2F} \ln a_{Pb^{2+}}$$

where $E_{Pb/Pb^{2+}}$ is the reversible potential for the Pb/Pb^{2+} couple. If at the point of passivation the concentration of soluble Pb^{2+} species arriving at the ring is considerably lessened, the

Can. J. Chem. Downloaded from www.nrcresearchpress.com by 210.87.254.6 on 09/05/12
For personal use only.

reversible potential of the ring should shift to a more negative value according to eq. 9. When this happens the overpotential at the ring (defined as $E_{\text{Potentiostatted}} - E_{Pb/Pb^{2+}}$) will decrease accordingly. In view of the reversible nature of this system (1), even a small change in $E_{Pb/Pb^{2+}}$ at the point of disc passivation may be sufficient to give rise to an anodic ring overpotential, which can qualitatively account for the observed anodic excursions in ring current.

Some indirect corroborative experiments to support the above-mentioned tentative explanation may be offered. If a $PbCl_2$ layer was allowed to form on the disc, and subsequently the disc current was switched off while the open circuit potential at the ring was monitored, the ring potential then remained steady for a short period of time and later slowly decreased to a more negative value before finally levelling off. This experiment was essentially the same as those previously described except that now the ring open circuit potential was monitored instead of the ring current. The change in rest potential at the ring from the time the disc current was switched off to the time when all the $PbCl_2$ on the disc had dissolved was about 60 mV. Although it is not possible to measure directly the rest potential at the ring during an experiment when the disc was under an applied potential, changes in the reversible potential of the Pb ring cannot be discounted.

It would indeed be highly desirable to offer at least an empirical semiquantitative treatment to fit the given explanation of the anodic excursion, say for example, to predict some shape of a curve or model in order to calculate the concentration of Pb^{2+} which corresponds to the observed anodic currents. However, it does not seem possible at present to make any quantitative estimates of the reversible potential at the ring at any time during the experiment, because the entire process is a dynamic one. Experimentally we could not conceive any viable way to measure the reversible potential at the ring during a potentiodynamic sweep at the disc electrode used in this work.

This work has been financially supported by grants from the Defence Research Board (Grant No. 5480-34) and the National Research Council of Canada. One of us (K.B.) is grateful for the award of a National Research Council Studentship.

1. J. AMBROSE, R. G. BARRADAS, K. BELINKO, and D. W. SHOESMITH. J. Colloid Interface Sci. **47**, 441 (1974).
2. R. G. BARRADAS, K. BELINKO, and J. AMBROSE. Can. J. Chem. This issue.
3. A. N. FRUMKIN, L. N. NEKRASOV, V. LEVICH, and JU. IVANOV. J. Electroanal. Chem. **1**, 84 (1959).
4. A. N. FRUMKIN and L. N. NEKRASOV. Dokl. Akad. Nauk. SSSR, **126**, 115 (1959).
5. W. J. ALBERY and S. BRUCKENSTEIN. Trans. Faraday Soc. **62**, 1920 (1966).
6. W. J. MCG. TEGART. The electrolytic and chemical polishing of metals. Pergamon Press, New York. 1959.
7. C. ARCHDALE and J. A. HARRISON. J. Electroanal. Chem. **39**, 357 (1972).
8. G. W. D. BRIGGS and W. F. K. WYNNE-JONES. J. Chem. Soc. 2966 (1956).
9. V. G. LEVICH. Physicochemical hydrodynamics. Prentice-Hall, Englewood Cliff, New Jersey. 1966. Chapt. VI.
10. S. Z. LEWIN. J. Phys. Chem. **59**, 1030 (1955).
11. W. J. ALBERY and M. L. HITCHMAN. Ring-disc electrodes. Oxford University Press, Oxford, 1971.
12. M. SHABRANG and S. BRUCKENSTEIN. J. Electrochem. Soc. **121**, 1439 (1974).

Can. J. Chem. Downloaded from www.nrcresearchpress.com by 210.87.254.6 on 09/05/12
For personal use only.

Nuclear Magnetic Resonance Evidence for High Barrier of Conformational Inversion in Hexahydro-3,3,7,7-tetramethyl-1,2-oxazepine-5-one

RODERICK E. WASYLISHEN,[1] KENNER C. RICE, AND ULRICH WEISS

Laboratory of Chemical Physics, National Institute of Arthritis, Metabolism, and Digestive Diseases, National Institutes of Health, Bethesda, Maryland 20014

Received July 8, 1974

RODERICK E. WASYLISHEN, KENNER C. RICE, and ULRICH WEISS. Can. J. Chem. **53**, 414 (1975).

Variable temperature proton n.m.r. spectra indicate an activation energy of 19.0 ± 0.5 kcal/mol for conformational equilibration in hexahydro-3,3,7,7-tetramethyl-1,2-oxazepine-5-one. It is suggested that the rate process involves slow conformational interconversion of the seven-membered ring and not slow inversion at the nitrogen atom. The synthesis of several related 1,2-oxazepines is described.

RODERICK E. WASYLISHEN, KENNER C. RICE et ULRICH WEISS. Can. J. Chem. **53**, 414 (1975).

Les spectres r.m.n. du proton, à température variable, indiquent que l'énergie d'activation pour l'équilibre conformationnel de l'hexahydrotétraméthyl-3,3,7,7 oxazépinone-1,2,5 est de 19.0 ± 0.5 kcal/mol. On suggère que le processus dynamique implique une interconversion conformationnelle lente du cycle à sept membres qu'une inversion lente autour de l'atome d'azote. On décrit la synthèse de plusieurs oxazépines-1,2 reliées au produit principal.

[Traduit par le journal]

In an earlier publication (1) the synthesis of hexahydro-3,3,7,7-tetramethyl-1,2-oxazepine-5-one (**1***a*) and two of its derivatives (**1***b* and *c*) was described.

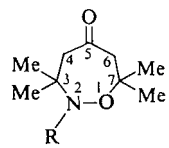

1

a R = H
b R = COC_6H_5
c R = Me

Here we wish to discuss the observed (1) magnetic nonequivalence of the four methylene hydrogens and the four methyl groups in the 60 MHz proton n.m.r. spectra of **1***a*, *b*, and *c* at room temperature. Above room temperature, the proton n.m.r. spectra of the methylene and methyl groups of **1** first show broadening characteristic of intermediate exchange rates (2, 3). Finally, at temperatures above 150 °C, the resonances of the four methylene hydrogens simplify to two relatively sharp resonances (one each for the two hydrogen atoms on C_4 and C_6, respectively), while the four resonances observed for the four nonequivalent methyl groups at room temperature collapse into two resonances (one for the two methyl groups at C_3 and one for the two at C_7).

By a careful study of the methyl resonances at several temperatures it has now been possible to obtain an estimate of T_c, the coalescence temperature, and thus an estimate of the free energy of activation at this temperature, using the expression (4):

$$\Delta G_c^{\ddagger} = 4.57\, T_c(9.97 + \log_{10} T_c/\Delta\nu)$$

The observed chemical shift differences, $\Delta\nu$, when the rate of exchange is slow, the observed coalescence temperature, and the calculated $\Delta G_c^{\ddagger}$ values are listed in Table 1, which also gives the experimental details. It will be seen that all three compounds show exceptionally high coalescence temperatures and energy barriers.

Several influences could be responsible, singly or in combination, for the large energy barriers; the most obvious of these are steric interactions between the two pairs of *gem*-methyl groups leading to slow conformational inversion of the seven-membered ring, and pyramidal inversion of the nitrogen which would also be slow on the n.m.r. time scale. Of these, the possibility of slow nitrogen inversion can be eliminated. Barriers to

[1]National Research Council of Canada Postdoctorate Fellow, 1972–1974. Present address: Department of Chemistry, University of Winnipeg, Winnipeg, Manitoba R3B 2E9.

Can. J. Chem. Downloaded from www.nrcresearchpress.com by 210.87.254.105 on 09/05/12
For personal use only.

TABLE 1. Spectral data and activation parameters for compounds **1***a*, *b* and *c*

Compound	Solvent[a]	Δν (Hz)[b]	T_c (°K)[c]	$\Delta G_c^{\ddagger}$ (kcal/mol)[d]
1*a*	DMF-d_7	8.5	359	19.0
		4.1	350	19.0
	Toluene-d_8	19.5	374	19.2
1*b*	DMF-d_7	22.5	388	19.9
		10.5	377	19.9
	Toluene-d_8	21.4	395	20.3
		17.6	391	20.2
1*c*	DMF	9.1	407	21.6

[a]The concentration of all samples was approximately 5 mol% in dimethylformamide-d_7 (DMF) or toluene-d_8. A small amount of tetramethylsilane (TMS) was added and each sample was thoroughly degassed by the freeze–thaw technique and sealed under vacuum.
[b]All n.m.r. spectra were measured at a sweep width of 1 or 2 Hz/cm as a function of temperature on a Varian A-60 spectrometer. All Δν values refer to methyl resonances and were obtained at approximately 308 °K.
[c]Temperatures were measured using the standard ethylene glycol samples.
[d]Errors in $\Delta G^{\ddagger}$ are probably less than 0.2 kcal/mol.
[e]The coalescence temperature was not reached at the b.p. of toluene-d_8.

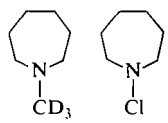

2*a* **2***b*

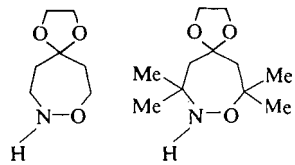

3*a* **3***b*

nitrogen inversion in saturated compounds with seven-membered rings seldom exceed 10 kcal/mol (5); *cf.* the value of 6.4 kcal/mol found for **2***a* (6). It is well known (5) that direct bonding of the nitrogen to an electronegative group increases the barrier to inversion but the observed energies (*e.g.*, 8.4 kcal/mol for **2***b* (6)) fall far short of those needed to explain our findings on **1***a–c*. Furthermore, the presence of bulky substituents on or close to a pyramidal nitrogen generally results in lowering of barriers to nitrogen inversion (5), while we found the barrier in **1***c* even higher than that in **1***a* or *b*.

To examine the influence of the *gem*-methyl groups on the energy barriers we have observed for **1***a*, *b*, and *c*, we have prepared and investigated compounds **3***a* and **3***b*.[2] For a 10 mol% solution of **3***b* in DMF-d_7 the coalescence temperature for one set of methyl groups (Δν = 18.5 Hz) was 88 °C and $\Delta G^{\ddagger}$ = 18.6 kcal/mol, not very different from the value obtained for **1***a*. On the other hand, room-temperature spectra of a 5 mol% solution of **3***a* in toluene-d_8, taken at 60, 100, and 220 MHz, show that the pairs of protons at C-3, C-4, C-6, and C-7 each have equivalent chemical shifts. At temperatures below −60°, these signals begin to show broadening but it has so far not been possible to obtain analyzable spectra in the region of slow exchange. However, because T_c is less than −60 °C, it is unlikely that $\Delta G^{\ddagger}$ should be greater than 12 kcal/mol.

Since the activation energy for site exchange in **3***b* seems at least 6 kcal/mol larger than that in **3***a*, our results suggest that the large barrier in **1***a–c* is due to slow conformational inversion of the seven-membered ring and that the methyl groups play a role. However, they cannot be the only influence responsible. The $\Delta G^{\ddagger}$ values for **1***a–c* listed in Table 1 are more than 10 kcal/mol larger than the ones reported recently by Borgen (7) for the geometrically similar compound, 3,3,6,6-tetramethylcycloheptanone (**4**). In contrast to the results for **1***a–c*, magnetic nonequivalence of the methyl and methylene protons

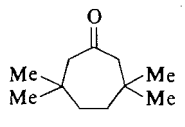

4

[2]Initial attempts to prepare hexahydro-1,2-oxazepine-5-one, the parent ketone of **3***a*, have been unsuccessful so far.

Can. J. Chem. Downloaded from www.nrcresearchpress.com by 210.87.254.105 on 09/05/12
For personal use only.

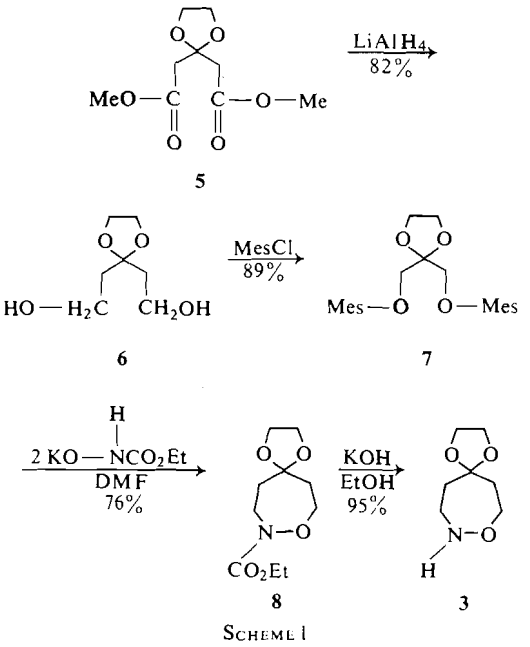

SCHEME 1

of **4** is only observed at temperatures below −80 °C. From the coalescence temperature, an activation energy of 8.5 kcal/mol was calculated for site exchange in **4**. The nature of this inversion barrier has been discussed in detail by Borgen and Dale (8).

The large barriers for **1** compared with those observed for **4** may involve a partial rotation of the N—O bond which entails eclipsing of the lone pairs on nitrogen and oxygen. There is now considerable experimental evidence that lone-pair electrons on adjacent atoms in a ring increase the barrier to rotation about the bond joining them, and thus increase the barrier to ring inversion. (See ref. 9 and references therein.) Also, recent *ab initio* calculations by Radom *et al.* (10) predict a barrier to rotation of approximately 11.7 kcal/mol in hydroxylamine. The corresponding barrier in ethane is only 2.928 ± 0.025 kcal/mol (11). In the case of **3***a*, eclipsing of lone pairs on nitrogen and oxygen may not be necessary for conformational inversion of the seven-membered ring. Thus our results indicate that motion about the various ring skeleton bonds in **1***a–c* and about **3***b* is strongly influenced by the presence of the methyl groups at C_3 and C_7.

Synthesis of 3a and 3b

The synthetic sequence shown in Scheme 1 was used to prepare **3***a*; it is similar to one employed by Pifferi and Consonni (12) for the preparation of hexahydro-1,2-oxazepine. Reduction of **5** to **6** was improved over that given in the literature (13) by using tetrahydrofuran as the solvent and alkali (14) for working up the reaction mixture. The remaining steps in the sequence proceeded smoothly and require no comment.

Attempted ketalization of 3,3,7,7-tetramethyl-1,2-oxazepine-5-one (**1***a*) to **3***b* by standard ketalization procedures with ethylene glycol and an acid catalyst under azeotropic removal of water was unsuccessful, as was transketalization (15) using dimethylformamide ethylene ketal and acetic or methanesulfonic acid as catalysts. Transketalization of **1** to **3***b* was accomplished, however, using 2-ethyl-2-methyl-1,3-dioxolane and a catalytic amount of *p*-toluenesulfonic acid according to the method of Dauben (16).

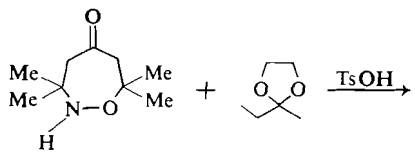

1*a*

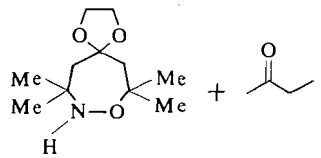

3*b*

Experimental

Boiling points and *melting points* (hot stage) are uncorrected. The i.r. spectra were recorded on a Perkin-Elmer model 257 instrument; for proton n.m.r. spectra either a Varian A-60, HA-100, or HR-220 spectrometer was used. Line positions are given using the δ scale, with tetramethylsilane as internal standard. The multiplicity, integrated peak areas, and coupling constants are indicated in parentheses. The mass spectra were obtained using a Hitachi-Perkin-Elmer RMU 6E instrument. Microanalyses were performed by the Analytical Section, National Institutes of Health.

2,2-Bis(2-hydroxyethyl)-1,3-dioxolane (6)

This material was prepared using a modification of the method previously described (13). 2,2-Biscarbomethoxymethyl-1,3-dioxolane (17) (**5**) (91.5 g, 0.42 m) in dry tetrahydrofuran (300 ml) was added dropwise to a slurry of lithium aluminum hydride (26.6 g, 0.7 m) in dry tetrahydrofuran (1500 ml). After the addition was complete, the reaction mixture was refluxed for 45 min, cooled, and water (27.0 ml) in dry tetrahydrofuran was added dropwise, followed by the dropwise addition of 15% aqueous sodium hydroxide (27.0 ml). After stirring for 15 min,

Can. J. Chem. Downloaded from www.nrcresearchpress.com by 210.87.254.105 on 09/05/12
For personal use only.

Can. J. Chem. Downloaded from www.nrcresearchpress.com by 210.87.254.105 on 09/05/12
For personal use only.

water (81 ml) in tetrahydrofuran (150 ml) was added dropwise, and stirring was continued for 30 min. The solids were then filtered, and washed well with tetrahydrofuran. The filtrate and washings were combined and evaporated *in vacuo*. Distillation of the residue in high vacuum gave 56.1 g (82%) of 2,2-bis(2-hydroxyethyl)-1,3-dioxolane (**6**); b.p. 126–128°/0.12 mm (lit. (13) b.p. 105–110°/0.01 mm., 53% yield); n.m.r. (60 MHz, $DCCl_3$) δ 1.92 (triplet, 4H, J = 6.0), 3.46 (singlet, 2H, exchanges with D_2O), 3.56 (triplet, 4H, J = 6.0), and 4.01 (singlet, 4H).

2,2-Bis(2-mesyloxyethyl)-1,3-dioxolane (7)

To a stirred solution of 2,2-bis(2-hydroxyethyl)-1,3-dioxolane (**6**) (25.0 g, 0.154 m) dissolved in dry pyridine (200 ml), mesyl chloride (45.0 g, 0.394 m) was added dropwise, keeping the temperature between 20 and 25° (ice bath). After the addition was complete, stirring was continued for 1 h. The reaction mixture was next poured onto ice, stirred for 15 min, and extracted with chloroform (3 × 150 ml). The combined chloroform extracts were backwashed with sufficient ice-cold 10% hydrochloric acid to remove the pyridine, dried with anhydrous magnesium sulfate, filtered, and the chloroform was evaporated under reduced pressure (bath temperature < 30°). The crystalline residue was recrystallized from 95% ethanol to give 43.6 g (89%) of slightly colored 2,2-bis-(2-mesyloxyethyl)-1,3-dioxolane (**7**), m.p. 85–88° (dec.). Recrystallization from methanol (charcoal) gave white material, m.p. 89–91° (dec.). The compound slowly decomposed on standing at room temperature but could be kept for several weeks at −5°; n.m.r. (60 MHz, $DCCl_3$) δ 2.17 (triplet, 4H, J = 7.0 Hz), 3.05 (singlet, 6H), 4.0 (singlet, 4H), and 4.36 (triplet, 4H, J = 7.0 Hz); i.r. (chloroform) 1340 and 1358 cm^{-1} among others.

Anal. Calcd. for $C_9H_{18}S_2O_8$: S, 20.14. Found: S, 19.93.

Potassium N-Hydroxyurethane

Potassium metal (9.15 g, 0.228 m) was dissolved in a mixture of absolute ethanol (200 ml) and dry ether (300 ml). *N*-Hydroxyurethane (24.0 g, 0.228 m) in dry ether (100 ml) was added dropwise with stirring. Absolute ether (400 ml) was next added during 15 min. After stirring for 15 min, the solid was filtered, washed with ether, and dried *in vacuo* to give 30.6 g (93%) of light yellow potassium *N*-hydroxyurethane.

Hexahydro-2-carbethoxy-1,2-oxazepine-5-one Ethylene Ketal (8)

To dry dimethylformamide (1.0 l) which had been preheated to 85°, were added in one portion the bismesylate (**7**) (10.3 g, 0.033 m) and potassium hydroxyurethane (10.0 g, 0.0694 m) while stirring. After 10 min, another addition of **7** (10.3 g, 0.033 m) and potassium hydroxyurethane (10.0 g, 0.0694 m) was carried out. Fifteen minutes later final portions of **7** (10.3 g, 0.033 m) and potassium hydroxyurethane (17.4 g, 0.121 m) were added. The reaction mixture was then heated with stirring at 90–100° for 1 h. At the end of this time the batch was cooled, filtered, and the solids were washed with chloroform (50 ml). The combined filtrate and washings were evaporated *in vacuo*; the residue was taken up in chloroform (350 ml) and washed with water (4 × 50 ml). The chloroform solution was dried (anhydrous magnesium sulfate), filtered, and the chloroform evaporated *in vacuo*. The distillation of the residue *in vacuo* gave hexahydro-2-carbethoxy-1,2-oxazepine-5-one ethylene ketal (**8**) (17.17 g, 76%), b.p. 125–127°/0.45 mm; n.m.r. (60 MHz, $DCCl_3$) δ 1.28 (triplet, 3H, J = 7.0 Hz), 1.98 (2 triplets, 4H, $J \sim 6.5$ Hz), 3.67 (triplet, 2H, $J \sim 6.5$ Hz), 3.96 (singlet, 4H), 4.03 (triplet, 2H, $J \sim 6.5$ Hz) and 4.20 (quartet, 2H, J = 7.0 Hz). Mass spectrum, M^+ 231; i.r. (liquid film) 1700 cm^{-1} (C=O).

Anal. Calcd. for $C_{10}H_{17}NO_5$: N, 6.05. Found: N, 6.24.

Hexahydro-1,2-oxazepine-5-one Ethylene Ketal (3a)

Hexahydro-2-carbethoxy-1,2-oxazepine-5-one ethylene ketal (9.25 g, 0.04 m) was added to a solution of potassium hydroxide (6.6 g of 85%, 0.1 m) in 125 ml of absolute ethanol and the reaction mixture was refluxed for 1.5 h. It was then cooled, and the potassium carbonate that had precipitated during the reflux period was filtered and washed with ethanol (25 ml). The combined ethanol filtrate and washings were evaporated *in vacuo* to a syrup, water (35 ml) was added, and the p*H* of the mixture adjusted to 10 with acetic acid. After saturating with salt, the aqueous solution was extracted with chloroform (4 × 50 ml). The combined chloroform extracts were dried (anhydrous magnesium sulfate), filtered, and evaporated *in vacuo*. The residual oil was distilled in high vacuum to yield 6.02 g (95%) of hexahydro-1,2-oxazepine-5-one ethylene ketal (**8**), b.p. 53–55°/0.06 mm; n.m.r. (60 MHz, $DCCl_3$) δ 1.78 (broad triplet, 2H, $J \sim 6$ Hz), 2.00 (triplet, 2H, J = 6.5 Hz), 3.70 (triplet, 2H, J = 6.5 Hz), 3.88 (singlet, 4H), and 5.55 (broad singlet, 1H). Mass spectrum M^+ 159, i.r. (liquid film) 3280, 1290, 1150 and 1075 cm^{-1} among others.

Anal. Calcd. for $C_7H_{13}NO_3$: N, 8.80. Found: N, 8.86.

3,3,7,7-Tetramethyl-1,2-oxazepine-5-one Ethylene Ketal (3b)

3,3,7,7-Tetramethyl-1,2-oxazepine-5-one (5.0 g) (**1a**) and *p*-toluenesulfonic acid monohydrate (500 mg) were added to 2-ethyl-2-methyl-1,3-dioxolane (44 g). The solution was refluxed while the 2-butanone formed was removed by slow distillation through a packed column. After 8 h, t.l.c. (silica gel 60 F 254, 30% ethyl acetate in hexane, 2,4-dinitrophenylhydrazine spray) showed essentially complete conversion to the ketal. The dark reaction mixture was evaporated to a syrup, taken up in hexane (200 ml), treated with Norite, and filtered. The hexane was evaporated *in vacuo* and the residue distilled in high vacuum. This gave 3.52 g (56%) of compound (**3b**), b.p. 53–57°/0.07 mm. For analysis the material was crystallized from hexane at −70° (m.p. ~ 29–31°) and redistilled *in vacuo*, b.p. 100–101°/5.0 mm; n.m.r. (220 MHz, $DCCl_3$) δ 0.95 (3H, singlet), 1.22 (6H, singlet), 1.32 (3H, singlet), 1.62–1.76 (3H, multiplet), 2.22 (1H, doublet, J = 14.0 Hz), 4.06–4.16 (2H, multiplet), 4.18–4.28 (2H, multiplet), and 4.65 (1H, broad, exchanges with D_2O). Mass spectrum, M^+ 215; i.r. (liquid film) 3260, 1359, 1208, 1088, 1030, and 970 cm^{-1} among others.

Anal. Calcd. for $C_{11}H_{21}NO_3$: N, 6.51. Found: N, 6.51.

The authors would like to thank Drs. Edwin D. Becker, Ira Levin, and Ted Schaefer for helpful discussions concerning this work. R. E. W. thanks the National Research Council of Canada for the postdoctoral fellowship.

1. K. C. Rice and U. Weiss. Tetrahedron Lett. 1615 (1973).
2. H. Kessler. Angew Chem. Int. Ed. **9**, 219 (1970).

3. G. BINSCH. *In* Topics in stereochemistry. *Edited by* N. L. Allinger and E. L. Eliel. Vol. 3. Wiley-Interscience, New York. 1968. p. 146.
4. J. M. LEHN and J. WAGNER. Tetrahedron, **26**, 4227 (1970).
5. (*a*) J. M. LEHN. Fortschritte der Chemischen Forschung, **15**, 311 (1970); (*b*) J. B. LAMBERT. *In* Topics in stereochemistry. *Edited by* N. L. Allinger and E. L. Eliel. Vol. 6. Wiley-Interscience, New York. 1971. p. 19; (*c*) A. RAUK, L. C. ALLEN, and K. MISLOW. Angew Chem. Int. Ed. **9**, 400 (1970).
6. J. M. LEHN and J. WAGNER. Chem. Commun. 414 (1970).
7. G. BORGEN. Acta Chem. Scand. **26**, 1738 (1972).
8. G. BORGEN and J. DALE. Acta Chem. Scand. **26**, 3593 (1972).
9. G. WOOD, R. M. SRIVASTAVA, and B. ADLAM. Can. J. Chem. **51**, 1200 (1973).
10. L. RADOM, W. J. HEHRE, and J. A. POPLE. J. Am. Chem. Soc. **94**, 2371 (1972).
11. S. WEISS and G. E. LEROI. J. Chem. Phys. **48**, 962 (1968).
12. G. PIFFERI and P. CONSONNI. J. Heterocycl. Chem. **6**, 111 (1969).
13. M. VISCONTINI and C. EBNÖTHER. Helv. Chim. Acta, **34**, 116 (1951).
14. V. M. MIĆOVIĆ and M. L. J. MIHAILOVIĆ. J. Org. Chem. **18**, 1190 (1953).
15. H. VORBRUEGGEN. Steroids, **1**, 45 (1963).
16. H. G. DAUBEN et al. J. Am. Chem. Soc. **76**, 1359 (1953).
17. M. KUHN. J. Pract. Chem. **156**, 103 (1940).

Can. J. Chem. Downloaded from www.nrcresearchpress.com by 210.87.254.105 on 09/05/12
For personal use only.

The Photolyses of Chloropentammine and Chloropentakis(alkylamine) Chromium(III) Complexes in Acetone/Water Mixtures

C. F. C. WONG AND A. D. KIRK

Department of Chemistry, University of Victoria, Victoria, British Columbia V8W 2Y2

Received August 8, 1974

Can. J. Chem. Downloaded from www.nrcresearchpress.com by 210.87.254.40 on 09/05/12
For personal use only.

C. F. C. WONG and A. D. KIRK. Can. J. Chem. **53**, 419 (1975).

The photochemistry of the $[Cr(RNH_2)_5Cl]^{2+}$ ions where R = H, CH_3, C_2H_5, *n*-C_3H_7, *n*-C_4H_9 has been investigated in water and in acetone/water solutions at p*H* 3. In water and in 33 w/w% acetone/water, the predominant reaction for each ion was found to be amine aquation to give predominantly *cis*-$[Cr(RNH_2)_4(H_2O)Cl]^{2+}$. Photolysis of $[Cr(CH_3NH_2)_5Cl]^{2+}$ in acidified acetone yielded a solvent substituted product $[Cr(CH_3NH_2)_4(S)Cl]^{2+}$ which has predominantly the *cis*-configuration but the extents of water and acetone substitution were not established. The amine quantum yields are almost solvent independent, only slightly wavelength dependent, and they decrease significantly in going from R = H to R = *n*-C_4H_9. The chloride quantum yields, which are of the order of 10^{-4} at 565 nm, are about an order of magnitude smaller than had been previously reported for $[Cr(NH_3)_5Cl]^{2+}$; they are several times larger at 401 nm. The chloride quantum yields show a significant decrease upon changing the solvent from water to 33% acetone/water.

The solvent independence of the main photochemical reaction suggests that the reaction is determined primarily by the photophysical properties of the reacting excited state. The different wavelength and solvent dependences of the amine and chloride quantum yields suggest that the two reactions do not originate from the same excited state. In addition the relative constancy of chloride yields as the ligand field strength of the ligands varies supports the idea that the reponsible state is not a ligand field state. Together with the increase in chloride quantum yield at shorter wavelengths, it suggests that the chloride originates from an excited state partaking of ligand to metal charge transfer character.

C. F. C. WONG et A. D. KIRK. Can. J. Chem. **53**, 419 (1975).

On a examiné, dans l'eau et dans des solutions aqueuses d'acétone à p*H* 3, la photochimie des ions $[Cr(RNH_2)_5Cl]^{2+}$ dans lesquels R = H, CH_3, C_2H_5, *n*-C_3H_7, *n*-C_4H_9. Dans l'eau et dans l'acétone aqueuse à 33% p/p, on a trouvé que la réaction principale pour chaque ion est l'hydratation de l'amine pour donner principalement le *cis*-$[Cr(RHN_2)_4(H_2O)Cl]^{2+}$. La photolyse de $[Cr(CH_3NH_2)_5Cl]^{2+}$, dans de l'acétone acidifiée conduit à un produit où il y a eu substitution par le solvant, $[Cr(CH_3NH_2)_4(S)Cl]^{2+}$ et ce complexe a principalement la configuration *cis*; on n'a toutefois pas établi les pourcentages de substitution par l'eau ou l'acétone. Les rendements quantiques de l'amine sont pratiquement indépendants du solvant, dépendent légèrement de la longueur d'onde et diminuent d'une façon importante lorsque l'on passe de R = H à R = *n*-C_4H_9. Les rendements quantiques en chlorure, qui sont de l'ordre de 10^{-4} à 565 nm, sont pratiquement 10 fois plus petits que ceux rapportés précédemment pour le $[Cr(NH_3)_5Cl]^{2+}$; ils sont beaucoup plus grands à 401 nm. Le rendement en chlorure diminue d'une façon importante lorsque le solvant passe de l'eau pure à de l'acétone à 33% dans l'eau.

Le fait que la réaction photochimique principale soit indépendante du solvant suggère que le cours de la réaction est déterminé principalement par les propriétés photophysiques des états excités réactionnels. La variation des rendements quantiques en amine et en chlorure suivant la longueur d'onde et le solvant indique que les deux réactions ne procèdent pas par le même état excité. De plus, le fait que les rendements quantiques du chlorure sont relativement constants lorsque le champ de force du ligand varie supporte l'idée que l'état excité responsable pour la réaction n'est pas un état rattaché au champ du ligand. Ces résultats, couplés avec le fait que le rendement quantique en chlorure augmente à basse longueur d'onde, suggèrent que le chlorure provient d'un état excité qui est attaché au transfert de charge entre le métal et le ligand.

[Traduit par le journal]

Introduction

The proposal by Adamson (1) seven years ago that the mode of photoaquation of mixed ligand "non-octahedral" chromium(III) complexes could be predicted as preferential loss of the strong field ligand on the weak field axis served to stimulate a large number of studies. As a consequence the photochemical behavior of such compounds

Can. J. Chem. Downloaded from www.nrcresearchpress.com by 210.87.254.40 on 09/05/12
For personal use only.

when irradiated in acidic aqueous solution is now much better characterized (2). It has emerged that the situation is more complicated than suggested by the above proposal. Many complexes do not follow the simple rule (3) and in addition the stereochemistry of the photoaquation process may be complex (2, 4). It now appears, however, that if the relative σ and π donating capabilities of the particular ligands in the complex are known (5), and if the relative extents of axial (d_{z^2}) and equatorial ($d_{x^2-y^2}$) labelization can be estimated (6), a reasonable prediction may be made of the mode of reaction (2) and perhaps even of the quantum yields (7). However, some aspects of the stereochemistry (4, 8), and the question of whether the reactions are essentially dissociative or associative in nature, remain unclear. All of the above refers to what is known about photolysis in aqueous solution.

This study of $[Cr(RNH_2)_5Cl]^{2+}$ complexes was undertaken to explore the effects of change of solvent on the photolysis modes and quantum yields, and in addition to explore for these compounds any trends in quantum yield with wavelength, temperature, and the nature of the group R. Underlying this was the question of whether the reaction modes would alter dramatically or not, whether this would lead to useful conclusions about the nature of the excited states involved, and whether the solvent played a role in determining the solution quantum yields.

A survey of the literature shows that very few studies of the photolysis of chromium(III) complexes have been undertaken in solvents other than water (1, 9). In addition most of the existing work has been concerned with quenching and energy transfer effects and has not brought to bear on the questions posed at the outset of this study. Two exceptions are a study by Wasgestian (10) which showed that hexacyanochromate exhibits essentially the same quantum yield for photosolvation in water and DMF, and the work of Langford and Tipping (11) which had similar objectives to those outlined here. The latter authors investigated the photolysis of $[Cr(NH_3)_6]^{2+}$, $[Cr(NH_3)_5Cl]^{2+}$, $[Cr(CH_3NH_2)_5Cl]^{2+}$, and $[Cr(CH_3CH_2NH_2)Cl]^{2+}$ in water and dimethyl sulfoxide. They did not investigate the nature of the products however and in some aspects their numerical data and trends were in disagreement with ours, as are some of the conclusions drawn.

The choice of the solvent system to be compared with water was one important consideration. It would be of great interest to compare photolysis of complexes in water and in a strong ligand solvent such as ammonia or an alkyl amine. We were inhibited from so choosing, however, by the rapidity of the competing thermal reactions in such solvents together with the difficulties of purification, handling, p*H* control, and analysis. We therefore chose to begin with the simpler acetone/water system because of its good solubility properties, the poor coordinating ability of acetone which might be expected to amplify any solvent effects, the ease of its purification, and the stability of its perchloric acid solutions. The work has led to some useful conclusions about the role of the solvent in chromium(III) photochemistry.

Experimental

Preparation of Complexes

$[Cr(NH_3)_5Cl]Cl_2$ was obtained as a by-product from the preparation of μ-hydroxo-bis{pentamminechromium(III)} chloride as described by Linhard and Weigel (12).

$[Cr(NH_3)_5Cl](ClO_4)_2$ was obtained from the chloride by reprecipitation with sodium perchlorate and twice recrystallized. The purity of the product was confirmed spectrophotometrically and by ion exchange chromatography.

$[Cr(RNH_2)_5Cl](ClO_4)_2$, R = CH_3, C_2H_5, n-C_3H_7, and n-C_4H_9 were prepared as described by Parris and Wallace (13).

Complex	Calculated (%)				Found (%)			
	Cr	C	H	N	Cr	C	H	N
$[Cr(CH_3NH_2)_5Cl](ClO_4)_2$	11.8	13.6	5.7	15.9	11.8	13.6	5.6	15.5
$[Cr(C_2H_5NH_2)_5Cl](ClO_4)_2$	10.2	23.5	6.9	13.7	10.0	23.7	7.0	13.3
$[Cr(n\text{-}C_3H_7NH_2)_5Cl](ClO_4)_2$	8.9	31.0	7.9	12.0	9.1	31.1	7.9	12.1
$[Cr(n\text{-}C_4H_9NH_2)_5Cl](ClO_4)_2$	8.0	36.8	8.5	10.7	7.8	36.8	8.5	10.3

TABLE 1. Spectral data for starting complexes and photolysis products

Complex	Q_1* $\lambda_{max}(\varepsilon_{max})$	Minimum* $\lambda_{min}(\varepsilon_{min})$	Q_2* $\lambda_{max}(\varepsilon_{max})$	$\lambda_{min}(\varepsilon_{min})$	$\lambda_{max}(\varepsilon_{max})$
$[Cr(NH_3)_5Cl]^{2+}$	376(38.2)	426(10.0)	513(36.5)		
trans-$[Cr(NH_3)_4H_2OCl]^{2+}$	383(39.2)	436(13.6)	467(17.3)	507(14.0)	555(18.8)
cis-$[Cr(NH_3)_4H_2OCl]^{2+}$†	383(34.0)	439(9.2)	519(38.6)		
cis-$[Cr(NH_3)_4H_2OCl]^{2+}$‡	385(32.7)	439(8.7)	518(39.6)		
cis-$[Cr(NH_3)_4H_2OCl]^{2+}$§	384(33.3)	439(9.0)	518(40.4)		
$[Cr(NH_3)_5Cl]^{2+}$ photo-product	384(35.8)	439(9.9)	517(42.2)		
$[Cr(CH_3NH_2)_5Cl]^{2+}$	386(55.1)	438(15.9)	524(49.1)		
$[Cr(CH_3NH_2Cl]^{2+}$ photo-product	389(46.8)	477(15.2)	523(52.2)		
$[Cr(C_2H_5NH_2)_5Cl]^{2+}$	388(62.4)	440(16.5)	528(55.4)		
$[Cr(C_2H_5NH_2)_5Cl]^{2+}$ photo-product	392(48.7)	448(14.2)	526(56.8)		
$[Cr(C_3H_7NH_2)_5Cl]^{2+}$	389(67.8)	442(18.2)	530(62.0)		
$[Cr(C_3H_7NH_2)_5Cl]^{2+}$ photo-product	395(55.1)	453(17.1)	530(61.7)		
$[Cr(C_4H_9NH_2)_5Cl]^{2+}$	390(72.5)	443(25.1)	531(65.4)		
$[Cr(C_4H_9NH_2)_5Cl]^{2+}$ photo-product	396(60.6)	458(23.8)	527(63.9)		
$[Cr(CH_3NH_2)_5Cl]^{2+}$ in acetone	390(51.3)	445(14.0)	530(47.6)		
$[Cr(CH_3NH_2)_5Cl]^{2+}$ photo-product in acetone	394(46.8)	456(17.5)	532(49.7)		

*Q_2 gives the low energy ligand field band maxima, Q_1 the next higher, corresponding to $^4T_{2g}$ and $^4T_{1g}$ respectively in O_h symmetry, and minimum indicates the intervening minimum.
†Our measurement.
‡Reference 25.
§Reference 24.

Photolysis Apparatus and Actinometry

Monochromatic light at 401, 479, and 565 nm was obtained by means of Balzers' interference filters (Rolyn Corp., Filtraflex B20) with half widths of 7, 8, and 6 nm respectively. Actinometry was based on 8×10^{-3} *M* solutions of $KCr(NH_3)_2(NCS)_4$ (potassium reineckate) (14). Two procedures were used. In the first an actinometer cell placed directly behind the photolysis cell was used to integrate the total transmitted light flux, F_A. The effective transmittance T_u of the front solution over the transmission band of the interference filter was then calculated (this was made easier by the fact that the transmittance spectrum of the complexes was close to linear over the narrow band of the filter) and the integrated flux absorbed in the photolysis solution calculated as

$$F_u = F_A(1 - T_u)$$

The technique required that the light beam be parallel, a continuous water film be between the two cells, the cell edges be masked, and that the front solution have a transmittance in the range of 30 → 70% for good precision. The advantage of the technique lay in its precision. Several runs with $KCr(NH_3)_2(NCS)_4$ in both cells gave light fluxes calculated from the two cells agreeing to better than 2%.

The second actinometric technique, of advantage at low temperature where the reineckate quantum yield was not known, was to calibrate a photocell which observed the reflected light from a beam-splitter (8%), using reineckate at room temperature, and then continuously monitor, and integrate, the photocell output during a run. This technique had a precision better than 5%.

Difference Spectrophotometry and Product Spectra[1]

The difference spectra used to calculate the product spectral data in Table 1 were obtained by photolyzing to about 10% conversion, stirred 2×10^{-2} *M* solutions of complex in the appropriate acidified solvent system. The difference spectrum was then obtained by running the spectrum of the photolyzed solution *vs.* the same path length of the unphotolyzed solution as reference (Cary 17 spectrophotometer, 0 → 0.2 expanded adsorbance scale).

The extent of conversion was measured precisely by means of the p*H* change in the solution, and the resultant solution composition, together with the starting spectrum and the difference spectrum after photolysis, was used to calculate point by point the spectrum of the total photolysis product.

pH and Chloride Determinations

Solutions, about 10^{-2} *M* in complex, were made up with one of three solutions listed in the second footnote of Table 2. Each photolysis sample was accompanied by a sample kept in the dark.

All p*H* measurements were made at 20 °C with a combination micro glass electrode (Metrohm AG 1900 Herisau) coupled to a Metrohm Compensator E388 potentiometer/p*H* meter. For the quantitative work in aqueous solutions, the proton uptake was determined by measuring the p*H* of the photolyzed and dark solutions

[1]Copies of the spectra of the complexes and of their photoproducts have been lodged with the Depository of Unpublished Data. Photocopies may be obtained, at a nominal charge, from the Depository of Unpublished Data, National Science Library, National Research Council of Canada, Ottawa, Canada K1A 0S2.

Can. J. Chem. Downloaded from www.nrcresearchpress.com by 210.87.254.40 on 09/05/12
For personal use only.

TABLE 2. Amine and chloride quantum yields in photolysis of $[Cr(RNH_2)_5Cl]^{2+}$*

R	Solvent†	Wavelength of irradiation	Quantum yield of amine (Temperature,°C)	Quantum yield of chloride at 13 °C
NH_3	Water	401	0.37_6 (20)	$(2 \pm 3) \times 10^{-4}$
		479	0.39_9 (20)	
		565	0.42_3 (20), 0.36_6 (8)	$(0 \pm 3) \times 10^{-4}$
	33% acetone	565	0.41_4 (20)	
CH_3NH_2	Water	401	0.34_5 (20)	1.4×10^{-3}
		479	0.36_7 (20)	
		565	0.37_4 (20), 0.37_7 (20)‡ 0.36_0 (11.5), 0.33_8 (5)	2.1×10^{-4}
	33% acetone	401	0.35_1 (20)	7×10^{-4}
		479	0.39_1 (20)	
		565	0.39_3 (20), 0.37_2 (8)	4×10^{-4}
	100% acetone	565	0.41 (20)‖	
$C_2H_5NH_2$	Water	401	0.20_3 (20)	7×10^{-4}
		479	0.26_3 (20)	
		565	0.24_8 (20), 0.22_9 (13) 0.22_2 (8), 0.21_7 (6)	8×10^{-5}
	33% acetone	401	0.22_9 (20)	3×10^{-4}
		479	0.24_6 (20)	
		565	0.23_7 (20), 0.20_7 (8)	
n-C_3H_7	33% acetone	401	0.20_2 (20)	5×10^{-4}
		479	0.21_6 (20)	
		565	0.21_2 (20), 0.19_9§ (16) 0.19_6§ (12), 0.18_2§ (9.5) 0.17_9§ (5.5)	1.1×10^{-4}
n-C_4H_9	33% acetone	401	0.17_0 (20)	
		479	0.19_2 (20)	
		565	0.17_6 (20)	

*For the amine yield determinations the concentrations used were: R = NH_3, CH_3NH_2, 1.0×10^{-2} *M*; R = $C_2H_5NH_2$, 0.9×10^{-2} *M*; R = n-$C_3H_7NH_2$, n-$C_4H_9NH_2$, 0.8×10^{-2} *M*; for the chloride yield determinations the concentrations used were: R = NH_3, CH_3NH_2, 2×10^{-2} *M*; R = $C_2H_5NH_2$, n-$C_3H_7NH_2$, 1.0×10^{-2} *M*.

†Water = 0.05 *M* $KClO_4$, 10^{-3} *M* $HClO_4$; 33% acetone = 0.02 *M* $KClO_4$, 10^{-3} *M* $HClO_4$; 100% acetone = 10^{-3} *M* $HClO_4$ in molecular sieve dried and distilled acetone (Spectra analyzed, Fisher Scientific).

‡Determined titrimetrically.

§Single runs.

‖Individual values 0.38 and 0.43.

and using the ΔpH method (15). With 33 w/w% acetone/water solutions, the proton uptake was also determined by back titration with standard base until the starting p*H* was reached. The titrimetric and ΔpH methods were found to be equivalent and so the latter, being quicker and simpler, was used almost exclusively. For work with pure acetone solutions, the final exposed and dark solutions were diluted with water to give solutions which were approximately 33 w/w% acetone and the ΔpH method was used.

Free chloride was determined using a concentration cell without transference (16), the silver/silver chloride electrodes used being masked to avoid photovoltaic effects. The photolysis cell used was a modified 1.0 cm quartz spectrophotometer cell. With an internal reference containing an aqueous solution 4.0×10^{-4} *M* in KCl and 0.050 *M* in $KClO_4$, the apparatus was calibrated over the range of chloride concentrations 1.25×10^{-5} to 4.0×10^{-4} *M* in water (all solutions supported by 0.050 *M* $KClO_4$) and 5.0×10^{-6} to 4.0×10^{-4} *M* in 33 w/w% acetone/water solutions supported by 0.020 *M* $KClO_4$. During photolysis runs, the solution was continuously mixed with a magnetic stirrer and the chloride concentration was continuously measured.

Results and Discussion

Studies of the thermal reaction (13) of the chloropentakis(alkylamine)chromium(III) complexes have shown that they exclusively lose chloride, with rate constants that increase as the size of the alkyl group increases. Thus their thermal reaction mode is a close parallel to the behavior of chloropentammine chromium(III) ion. One would expect a similar parallel in the photochemical reaction modes. Three photoinduced processes are conceivable, photoreduction, solvent substitution of amine and of chloride. Studies of chloropentammine have shown the main photoreaction to be "antithermal" (17), that is, loss of ammonia with chloride loss being

Can. J. Chem. Downloaded from www.nrcresearchpress.com by 210.87.254.40 on 09/05/12
For personal use only.

Can. J. Chem. Downloaded from www.nrcresearchpress.com by 210.87.254.40 on 09/05/12
For personal use only.

minor, while photoreduction appears not to occur at wavelengths of irradiation down to 250 nm (15). The product of amine photoaquation has been shown (17*b*, 18) to be predominantly *cis*-$[Cr(NH_3)_4H_2OCl]^{2+}$.

Our preliminary investigations of these systems therefore occasioned no surprise in that the main photoreaction mode observed in all cases at our irradiation wavelengths both in water and acetone/water mixtures was loss of amine with only minor contributions from chloride loss. We did find, however that the actual chloride quantum yields were significantly lower than reported earlier (16). The quantum yield data are presented and discussed later.

One of the questions of interest in this work was whether the stereochemistry of the photoreaction would alter throughout the series of complexes or with change of solvent. Investigation of this question requires isomeric analysis of the chloroaquotetrakisalkylamino product, which in this work presented difficulties. Ion-exchange chromatography fails to separate *cis* and *trans* chloroaquotetrammine isomers and little better success can be expected with the alkyl–amine analogs. One is therefore forced to use u.v./visible spectroscopic methods and this is made uncertain by the fact that the spectral information for the product isomers is not available as they have not been prepared. Such preparations can be quite difficult and time consuming and were not attempted. Fortunately the spectral differences between *cis* and *trans* isomers of this type are quite large (18) (Table 1) so it was our view that quite a reasonable assessment of the isomeric nature of the product could be made in the absence of the exact spectral data.

Table 1 lists three sets of spectral data for *cis*-$[Cr(NH_3)_4(H_2O)Cl]^{2+}$ together with the spectrum of the photolysis product of $[Cr(NH_3)_5Cl]^{2+}$, derived by the procedure described in the experimental section. Table 1 also presents spectra of the starting complexes and photolysis products of $[Cr(n\text{-}C_4H_9NH_2)_5Cl]^{2+}$, $[Cr(C_2H_5NH_2)_5Cl]^{2+}$, $[Cr(n\text{-}C_3H_7NH_2)_5Cl]^{2+}$, and $[Cr(n\text{-}C_4H_9NH_2)_5Cl]^{2+}$, derived by the same procedure. The data for chloropentammine chromium(III) photolysis in water, where the product is already known to be almost pure *cis*-chloroaquotetrammine, is presented to inspire some confidence that product spectra can be obtained reasonably precisely by this procedure. It can be seen that the spectrum obtained matches well in λ_{max} values although the ε_{max} of the bands are somewhat larger than our directly measured values. It will be noted that there is some disagreement in the literature data for *cis*-$(Cr(NH_3)_4H_2OCl]^{2+}$ and it may be that the photochemically derived molar absorptivities of Table 1 are more precise than those in the literature as impurities likely to occur in the complex will lead to lowered molar absorptivities. The chloride quantum yields, discussed later, are sufficiently small that aquopentammine does not interfere.

Comparison of the spectra of the photolysis products of the chloropentakis(alkylamino)-chromium(III) complexes with their starting complexes, and with *cis*- and *trans*-$[Cr(NH_3)_4(H_2O)Cl]^{2+}$, indicates that in each case the product appears to be predominantly *cis*. Close examination reveals some anomalies; for each product/reactant pair the red shift of λ_{max} and decrease in ε_{max} of the second ligand field band parallels the ammine case, but in contrast λ_{max} of the first ligand field band seems slightly blue shifted, and ε_{max} for the *cis*(*?*)-$[Cr(n\text{-}C_3H_7NH_2)_4H_2OCl]^{2+}$ and *cis*(*?*)-$[Cr(n\text{-}C_4H_9NH_2)H_2OCl]^{2+}$ are lower than the corresponding reactants. We believe these differences are real, and are not due to admixture of *trans* material, but are due to influences of steric hindrance on ligand field strengths of the ligands. Table 3 shows some relevant spectral data for Cr(III) complexes. Whereas CH_3NH_2 is a better base, and presumably a better σ donor than NH_3, nevertheless $\Delta[Cr(NH_3)_5Cl]^{2+} > \Delta[Cr(CH_3NH_2)_5Cl]^{2+}$. That this is due to steric crowding in the pentakis(alkylamino) complex is supported by the other data in Table 3, which show that $[Cr(ibn)_3]^{3+}$ (ibn = isobutylenediamine) where steric hindrance can be seen from models to occur, has Δ smaller than $[Cr(en)_3]^{3+}$ and $[Cr(pn)_3]^{3+}$, and $[Cr(CH_3NH_2)_6]^{2+}$ has Δ smaller than $[Cr(NH_3)_6]^{3+}$ by the same extent. Thus we believe that the blue shift of the first ligand field band upon water substitution to go from $[Cr(RNH_2)_5Cl]^{2+}$ to *cis*(*?*)-$[Cr(RNH_2)_4H_2OCl]^{2+}$ can be explained in terms of relief of steric strain, allowing shorter Cr—N bonds and larger Δ for the remaining alkylamine ligands, in the aquoproduct, with this factor overwhelming the influence of substitution of one amine by water.

Table 1 also gives the product spectrum for

TABLE 3. Spectral data for some chromium(III) complexes

Complex	$\lambda_{max}(4T_{1g})$ (nm)	$\lambda_{max}(4T_{2g})$ (nm)	$\Delta = \bar{\nu}_{max}(4T_{2g})$ cm^{-1} × 10^{-3}
$[Cr(NH_3)_6]^{3+}$	350	464	21.55
$[Cr(CH_3NH_2)_6]^{3+}$	361	474	21.1
$[Cr(en)_3]^{3+}$	351	456	21.93
$[Cr(pn)_3]^{3+}$	350	457	21.88
$[Cr(ibn)_3]^{3+}$	359	474	21.1
$[Cr(NH_3)_5Cl]^{2+}$	376	513	19.49*
$[Cr(CH_3NH_2)_5Cl]^{2+}$	386	524	19.08*
$[Cr(C_2H_5NH_2)_5Cl]^{2+}$	388	528	18.94*
$[Cr(n\text{-}C_3H_7NH_2)_5Cl]^{3+}$	389	530	18.87*
$[Cr(n\text{-}C_4H_9NH_2)_5Cl]^{2+}$	390	531	18.83*

*No attempt has been made to allow for splitting to yield $^4E_2$ and $^4B_2$ bands in these C_{4v} complexes. The value given merely indicates the approximate overall ligand field strength.

photolysis of $[Cr(CH_3NH_2)_5Cl]^{2+}$ in pure acetone. In this solvent, although up to three water molecules are present in the solvation sphere (due to the water added in making up the perchloric acid solutions) it may be that some acetone substitution occurs. Again, however, the product spectrum is typical of that expected for a *cis* product.

In the absence of accurate spectral data for the product complexes it would be foolish to try to make quantitative estimations of the proportion of *cis* isomer in the product. However it is reasonable to conclude that all the complexes studied photolyze to give mainly the *cis* solvated product, whether in acetone or water or acetone/water mixtures. Thus any rules for the stereochemistry of photoreactions may be more solvent independent than for the thermal reactions, where it is found that the stereoretentivity observed in water does not necessarily apply in dimethylformamide, dimethylsulfoxide (19), or in liquid ammonia (7, 8).

The quantum yield data obtained in this work is summarized in Table 2, where in the case of the amine yields the results quoted are generally the mean of at least two determinations agreeing to better than 3%. The quantum yields for chloride are significantly less precise, as discussed elsewhere (16), and are probably subject to some systematic errors.

The quantum yield for amine release shows a general decrease in going through the series from chloropentammine to the butylamine homolog. The question of whether there is a general relationship between overall photolysis quantum yields and the average ligand field strength (or the roughly equivalent quantity ΔE, the spacing of the maxima of the lowest quartet and lowest doublet absorption bands) has often been addressed. The relationship applies roughly for a number of octahedral complexes (20), and has been shown to apply equally roughly in series of mixed ligand complexes (3*c*). The present investigation reveals another series of closely related complexes which show such a crude relationship between quantum yield and ligand field strength. There is not a good quantitative relationship, however, as the large drop in Δ lies between ammine and methylamino, while the largest drop in quantum yield of amine release lies between methylamino and ethylamino.

It now appears fairly certain that the main photoreaction of complexes of this type arises from the quartet state (9, 10, 21) and in the following attempt to rationalize the ligand field strength/quantum yield relationship this will be assumed. It also has been shown that the complex trisethylenediaminechromium(III) has a return intersystem crossing efficiency close to one at room temperature in aqueous solution (21). Since complexes of the type studied here do not phosphoresce in aqueous solution at room temperature, and since their lowest quartet/doublet spacing is less than for $[Cr(en)_3]^{3+}$ it can be reasonably expected that return intersystem crossing is also efficient under the photolysis conditions. The quantum yield for reaction would then be given simply by

$$[1] \qquad \phi_{reaction} = \frac{k_R}{k_2 + k_3 + k_R}$$

where k_2, k_3, and k_R are respectively the first order rate constants for fluorescence, internal

Can. J. Chem. Downloaded from www.nrcresearchpress.com by 210.87.254.40 on 09/05/12
For personal use only.

Can. J. Chem. Downloaded from www.nrcresearchpress.com by 210.87.254.40 on 09/05/12
For personal use only.

conversion to the ground state, and reaction. Since these complexes do not fluoresce in solution and since the quantum yield of reaction is less than one, $k_2 \ll k_3 + k_R$ so that

$$[2] \qquad \phi_R \approx \frac{k_R}{k_3 + k_R}$$

If this analysis is correct it becomes clear that the decrease in amine quantum yield in the series might reside either in an increase in k_3 with alkylamine bulk or a decrease in k_R, or both. The internal conversion rate constant can be expected to depend on the energy above the ground state of the thermally equilibrated quartet excited state, the degree of distortion, and the density of states available for crossover. Moving to the bulkier, weaker field amine certainly decreases the energy spacing, might lead to less distortion, and would increase the density of states, so it is quite reasonable to expect k_3 to increase in the series $[Cr(NH_3)_5Cl]^{2+}$ to $[Cr(n\text{-}C_4H_9NH_2)_5Cl]^{2+}$.

If the explanation of the trend is not photophysical due to changes in internal conversion rate constant in the series, it could reside in a decrease in k_R in the series. If so it would be supportive of an associative mechanism of photosubstitution. Thus, for an associative mechanism, the bulkier amine complexes would be expected to react more slowly due to steric hindrance of the entering solvent molecules. In contrast a dissociative reaction would be expected to show the reverse trend, due to the strain present in the reactant molecule, and its consequent relief upon dissociation of an amine ligand. It is clear that not enough information is yet available to decide which of these explanations is correct or even valid, but it does point out the need for further photophysical studies of the effect of structure on the rate constants for intersystem crossing, and if possible, internal conversion.

The solvent dependence data, which is most complete for $[Cr(CH_3NH_2)_5Cl]^{2+}$ shows that the amine quantum yield increases only by about 10% in going from water to pure acetone. In contrast the quantum yields for chloride seem to decrease by a factor of about two in going from water to 33% acetone (Table 2 lists one reversal of this trend, but this probably reflects varying systematic errors in the chloride yields). The two reaction modes therefore show different solvent effects. The constancy of the amine quantum yield with solvent composition is again suggestive that it is determined largely by purely photophysical factors. The result further implies that the mechanism is either dissociative, or, if associative must involve a water molecule already in the coordination sphere, even in the "100%" acetone solution, as the writers would not expect substitution of acetone in an associative process to occur as fast as water substitution.

Table 2 also shows different wavelength dependencies for the amine and chloride yields, chloride increasing at the shorter wavelength, amine decreasing slightly. Together with the facts that the amine quantum yield is sensitive to the overall ligand field strength of the ligands, while chloride is not, and that amine release increases only slightly in acetone, while chloride decreases significantly, the data overall is suggestive that the two modes of reaction arise from different excited states. Whereas analogy to earlier studies suggests the lowest quartet excited state is responsible for the amine photolysis, the observations on chloride release support reaction through a solvated state having charge transfer character of the type represented by $Cr(II)(RNH_2)_5 \cdot Cl$, as has been earlier suggested (15). Thus at shorter wavelength of irradiation the participation of such a state would be favored, it would show a yield of successful chloride release that was sensitive to the preference of chloride for the solvent, and the tendency to form such a state would be relatively independent of the amine ligand field strength, depending mainly on the redox properties of Cr(III) and Cl^-.

Based on sensitization experiments other workers (22) have suggested that production of chloride arises from the doublet state; this is not necessarily in conflict with our proposal, as both types of excited state could exist and would be expected to release chloride. However it seems to us unlikely that the chloride yields formed here, increasing to shorter wavelength, arise from the doublet state. Langford and Tipping (11) have suggested that chloride arises from the same quartet state as releases amine; this however would fail to explain the different wavelength dependencies of the two processes.

Table 4 shows apparent activation energies for amine loss; no large temperature dependence exists. Following the analysis of Chen (23), based on eq. 2 and its underlying assumptions, one can easily derive the equation

TABLE 4. Activation energies for amine release in $[Cr(RNH_2)_5Cl]^{2+}$ photolyses at 565 nm

Complex	E_{app}(kcal mol^{-1})	$E_3 - E_R$(kcal mol^{-1})	Solvent
$[Cr(NH_3)_5Cl]^{2+}$	2.1 ± 0.4	3.5 ± 0.6	Water
$[Cr(CH_3NH_2)Cl]^{2+}$	1.2 ± 0.3	1.9 ± 0.5	Water
	0.8 ± 0.4	1.2 ± 0.6	33% acetone
$[Cr(C_2H_5NH_2)Cl]^{2+}$	1.5 ± 0.3	2.0 ± 0.4	Water
	1.8 ± 0.4	2.4 ± 0.5	33% acetone
$[Cr(n\text{-}C_3H_7NH_2)Cl]^{2+}$	1.9 ± 0.4	2.4 ± 0.4	33% acetone

[3] $$\log\left(\frac{1}{\phi} - 1\right) = \frac{E_R - E_3}{RT}$$

Plots of log $(1/\phi - 1)$ *vs.* $1/T$ are linear and lead to the values for $E_R - E_3$ shown also in Table 4. Since E_3 is certain to be positive, one may conclude that the reaction of the excited state has a small but appreciable activation energy. However, there appears to be no significant influence of solvent or amine bulk on these values within the precision limits of this data.

The authors thank the National Research Council of Canada and the University of Victoria Faculty Research Fund for financial support. C.F.C.W. wishes to thank the University of Victoria Graduate Faculty for the award of a Graduate Scholarship.

1. A. W. ADAMSON. J. Phys. Chem. **71**, 798 (1967).
2. A. D. KIRK. Mol. Photochem. **5**, 127 (1973).
3. (*a*) S. C. PYKE and R. G. LINCK. J. Am. Chem. Soc. **93**, 5281 (1971); (*b*) G. WIRTH and R. G. LINCK. J. Am. Chem. Soc. **95**, 5913 (1973); (*c*) A. D. KIRK, K. C. MOSS, and J. C. VALENTIN. **49**, 375 (1971); (*d*) C. KUTAL and A. W. ADAMSON. J. Am. Chem. Soc. **93**, 5581 (1971).
4. C. BIFANO and R. G. LINCK. Inorg. Chem. **13**, 609 (1974).
5. (*a*) W. W. FEE and J. N. MACB. HARROWFIELD. Aust. J. Chem. **23**, 1049 (1969); (*b*) D. A. ROWLEY. Inorg. Chem. **10**, 397 (1971).
6. (*a*) M. WRIGHTON, H. B. GRAY, and G. S. HAMMOND. Mol. Photochem. **5**, 165 (1973); (*b*) J. I. ZINK. Inorg. Chem. **12**, 1957 (1973).
7. E. ZINATO, P. RICCIERI, and A. W. ADAMSON. J. Am. Chem. Soc. **96**, 375 (1974).
8. A. D. KIRK and T. L. KELLY. Inorg. Chem. **13**, 1613 (1974).
9. S. N. CHEN and G. B. PORTER. Chem. Phys. Lett. **6**, 41 (1970).
10. H. F. WASGESTIAN. J. Phys. Chem. **76**, 1947 (1972).
11. C. H. LANGFORD and L. TIPPING. Can. J. Chem. **50**, 887 (1972).
12. M. LINHARD and M. WEIGEL. Z. Anorg. Allg. Chem. **299**, 15 (1959).
13. M. PARRIS and W. O. WALLACE. Can. J. Chem. **47**, 2257 (1969).
14. E. E. WEGNER and A. W. ADAMSON. J. Am. Chem. Soc. **88**, 394 (1966).
15. H. F. WASGESTIAN and H. L. SCHLÄFER. Z. Phys. Chem. Frankfurt, **62**, 127 (1968).
16. C. F. C. WONG and A. D. KIRK. Can. J. Chem. In press.
17. (*a*) L. MOGGI, F. BOLLETTA, and V. BALZANI. Ric. Sci. 1228 (1966); (*b*) H. F. WASGESTIAN and H. L. SCHLÄFER. Z. Phys. Chem. Frankfurt, **57**, 282 (1968).
18. M. F. MANFRIN, L. MOGGI, and V. BALZANI. Inorg. Chem. **10**, 207 (1971).
19. D. A. PALMER and D. W. WATTS. Inorg. Chim. Acta, **6**, 197 (1972) and references therein.
20. H. L. SCHLÄFER. J. Phys. Chem. **69**, 2201 (1965).
21. R. BALLARDINI, G. VARANI, H. F. WASGESTIAN, L. MOGGI, and V. BALZANI. J. Phys. Chem. **77**, 2947 (1973).
22. E. L. WEHRY. J. Am. Chem. Soc. **95**, 2137 (1973).
23. S. N. CHEN. Thesis, University of British Columbia, Vancouver, British Columbia. 1970.
24. D. W. HOPPENJANS and J. B. HUNT. Inorg. Chem. **8**, 505 (1969).
25. V. BALZANI. Private communication.

Can. J. Chem. Downloaded from www.nrcresearchpress.com by 210.87.254.40 on 09/05/12
For personal use only.

A Raman Spectral Study of the Kinetics of Hydrolysis of Acetonitrile Catalyzed by Hg(II)[1]

YU-KEUNG SZE[2] AND DONALD E. IRISH[3]

Department of Chemistry, University of Waterloo, Waterloo, Ontario N2L 3G1

Received August 7, 1974

YU-KEUNG SZE and DONALD E. IRISH. Can. J. Chem. **53**, 427 (1975).

Raman spectroscopy has been employed to follow the relatively slow rate of hydrolysis of acetonitrile, catalyzed by mercury(II). Raman lines at 2275 and 2305 cm^{-1} are characteristic of CH_3CN bound to Hg^{2+}, and are distinct from lines of bulk solvent. The intensities of these new lines decrease with time. From the intensities, concentrations of bound acetonitrile, $[CH_3CN]_B$ were calculated for a time span of 400 min. The data fit a second order rate law: Rate = $k[CH_3CN]_B[H_2O]$. The specific rate constant, k, obtained from four sets of data for the system $Hg(ClO_4)_2$–CH_3CN–H_2O equals $1.05 \pm 0.06 \times 10^{-4}$ mol^{-1} l min^{-1} at 25 °C. The energy of activation is 18.9 kcal mol^{-1}. In the proposed mechanism water molecules attack acetonitrile molecules which are bound to Hg^{2+} and form a mercury(II)–acetamide complex. Raman lines characteristic of this species are observed. This species slowly converts to mercury(II) ammine complexes and acetic acid. Anions which coordinate with Hg^{2+} more strongly than CH_3CN, such as nitrate or acetate, slow or prevent the hydrolysis reaction.

YU-KEUNG SZE et DONALD E. IRISH. Can. J. Chem. **53**, 427 (1975).

On a utilisé la spectroscopie Raman pour suivre l'hydrolyse, relativement lente de l'acétonitrile, catalysée par le mercure(II). Les lignes Raman à 2275 et 2305 cm^{-1} sont caractéristiques du CH_3CN lié au Hg^{2+} et se distinguent facilement des lignes du solvant. Les intensités de ces lignes diminuent avec le temps. A partir des intensités, les concentrations d'acétonitrile lié, $[CH_3CN]_B$ ont pu être déterminées pour une période de 400 min. Les données suivent une équation de vitesse du deuxième ordre; la vitesse est égale $k[CH_3CN]_B[H_2O]$. La constante de vitesse spécifique, k, est obtenue à partir de quatre séries de données pour le système $Hg(ClO_4)_2$–CH_3CN–H_2O et cette valeur est égale à $1.05 \pm 0.06 \times 10^{-4}$ mol^{-1} l min^{-1} à 25 °C. L'énergie d'activation est de 18.9 kcal mol^{-1}. Dans le mécanisme proposé, des molécules d'eau attaquent des molécules d'acétonitriles qui sont complexés au Hg^{2+} et forment des complexes mercure (II)-acétamide. On observe les lignes Raman caractéristiques de ces espèces. Cette espèce se transforme lentement en complexe amino mercurique et en acide acétique. Les anions qui se coordonnent avec le Hg^{2+} d'une façon plus forte que le CH_3CN, tels que les nitrates et les acétates, ralentissent ou empêchent la réaction d'hydrolyse. [Traduit par le journal]

Introduction

Mixtures of water and acetonitrile are stable at room temperature and are frequently used as mixed solvents for electrolyte studies. Under strongly acidic or basic conditions and at higher temperatures acetonitrile hydrolyses to give acetamide and subsequently acetic acid (1). Several substances, namely boron halides (2), 100% sulfuric acid (3), manganese dioxide (4), and alkaline hydrogen peroxide (5), accelerate the hydrolysis of acetonitrile at room temperature. The catalytic action of nickel (6), $ZnCl_2$ (7), and cation exchange resins containing Cu^+, Zn^{2+}, Ag^+, and Cd^{2+} (8) have been reported at higher temperatures. The effect of mercuric salts on the rate of hydrolysis of acetonitrile in 3 *N* acid media in the temperature range from 70–95 °C was studied by Travagli (9–13). He reported that HgO in acidic media accelerates the action of acids. The reaction was followed by analysis for NH_3, evolved from aliquots removed periodically and cooled, and was found to be first order with respect to CH_3CN both in the presence and absence of HgO. The rate of the mercury-catalyzed reaction was found to be dependent on the acids used and decreased in the order $H_2SO_4 > HClO_4 > HNO_3 > HCl$.

The hydrolysis of acetamide in acid media is much faster than that of acetonitrile (by approxi-

[1]Presented in part at the Twentieth Canadian Spectroscopy Symposium, Toronto, Ontario, Oct. 29, 1973 and the Fourth International Conference on Raman Spectroscopy, Brunswick, Maine, Aug. 25, 1974.

[2]Present address: Inland Waters Directorate, Environment Canada, 562 Booth St., Ottawa, Canada K1A 0E7.

[3]To whom correspondence should be addressed.

Can. J. Chem. Downloaded from www.nrcresearchpress.com by 210.87.254.5 on 09/05/12
For personal use only.

Can. J. Chem. Downloaded from www.nrcresearchpress.com by 210.87.254.5 on 09/05/12
For personal use only.

mately 350 times in 4 *M* acid) unless the concentration of the acid is very high (14). Under the conditions used by Travagli the formation of acetamide was not revealed but its existence was not excluded. The hydrolysis of acetamide is also faster than acetonitrile in aqueous NaOH solution (15).

The rate of hydrolysis, catalyzed by Hg^{2+} at room temperature, is sufficiently slow that it has been possible to follow the reaction with Raman spectroscopy using a conventional system. The observation of Raman lines from the reacting species and their products provides unique information about the intermediates and their role in the mechanism. Anion effects have also been investigated.

Experimental

Solutions of $Hg(ClO_4)_2$ were prepared from HgO (Fisher Certified Reagent) and $HClO_4$ (~70%, Baker Analyzed Reagent). Appropriate amounts of the $Hg(ClO_4)_2$ solution and water were mixed and kept at 25 ± 0.05 °C in a water bath together with a bottle of CH_3CN (Matheson, Coleman, and Bell, Spectroquality). After thermal equilibrium was achieved, CH_3CN was added to the $Hg(ClO_4)_2$ solution to the 25 ml mark. Since CH_3CN has a lower density, two liquid layers occur with very little mixing. Immediately after a timer was started, the solution was shaken well. The solution showed a small volume contraction. A few drops of CH_3CN were added to bring the volume to the mark. The solution was mixed well and the total amount of CH_3CN determined by weighing.

Raman spectra were obtained as previously described (16). A portion of the solution was poured into the sample cell thermostatted at 25 ± 0.05 °C. The spectrum from 2150 to 2400 cm^{-1} was scanned. Readings of the timer were marked on the spectrum. The time of scanning 2290 cm^{-1} (a point midway between the two bands at 2275 and 2305 cm^{-1} used for analysis) was interpolated and was taken as the reaction time. The scanning of this region required 4 min. The time lapse is negligible since the reaction is slow. The reaction causes a decrease in the volume of the solution by a few percent. To correct for this change, the remaining portion of the solution (also thermostatted at 25 °C) was used for density measurements. A correction curve, density–time, was obtained.

Other solutions for the kinetic measurements were prepared by the same procedures. Most of the kinetic measurements were carried out in duplicate.

Results and Discussion

Spectral Changes of $HgA_2/H_2O/CH_3CN$ Systems with Time, where $A = ClO_4^-$, NO_3^-, OAc^-

Raman and infrared spectra of solutions $Hg(ClO_4)_2/CH_3CN/H_2O$ (or $Hg(NO_3)_2/CH_3CN/H_2O$) show features which are very different from those reported in studies of other electrolytes dissolved in CH_3CN–H_2O (17–20). A number of new lines were observed, the positions of which do not depend on time or the ratios of the three components: $Hg(ClO_4)_2$ (or $Hg(NO_3)_2$), CH_3CN, and H_2O. The intensities of these new lines increase with time. The intensities of a set of lines which can be assigned to acetonitrile decrease with time.

For solutions containing acid and the mixed solvent of acetonitrile and water, reaction is very slow at room temperature. For example, after a period of two weeks, for the solution with composition 4.7 mol $HClO_4$, 21.8 mol H_2O, and 7.7 mol CH_3CN per l, at room temperature CH_3CN is only diminished by approximately 4% as measured from decrease in the intensity of the bands of acetonitrile. Solutions containing nitric acid and acetic acid behave similarly. It is reasonable to assume that under the reaction conditions (25 °C; acid concentration usually equal to 0.15 *M*, and at most 0.5 *M*) for the solutions containing mercury salts, catalysis of the reaction by acid is negligible.

Figures 1 and 2 show spectra recorded at different times for the solution with composition 1.7 mol $Hg(ClO_4)_2$, 19.7 mol H_2O, 9.8 mol CH_3CN, and 0.15 mol $HClO_4$ per l. Positions of bands of acetonitrile are listed in Table 1. The bands at 2275 and 2305 cm^{-1} were not observed in pure acetonitrile or its aqueous solutions. The intensities of these bands decrease with time. It is reasonable to assign these bands to acetonitrile bound to mercury. The 2275 cm^{-1} band was also observed by Addison *et al.* (21) for $Hg(NO_3)_2$ in pure acetontrile. A band at 2270 cm^{-1} is characteristic of CH_3CN bound to Ag^+ (17, 22, 23).

In systems containing $Hg(ClO_4)_2$, the anion gives four bands at 460, 625, 930, and 1110 cm^{-1}. The first two bands are symmetrical (Fig. 1). The band at 930 cm^{-1} overlaps seriously with the 931 cm^{-1} line of acetonitrile. The band at 1110 cm^{-1} appears to be asymmetric. The asymmetry is partly due to overlapping with the 1040 cm^{-1} band of acetonitrile. The contour of this band appears to be practically independent of the concentration of the salt. Raman studies of a large number of perchlorate solutions indicate that in the near-saturated solutions (24) and concentrated solutions (25) of $Hg(ClO_4)_2$ association between the cation and ClO_4^- does not occur, at least to a significant extent.

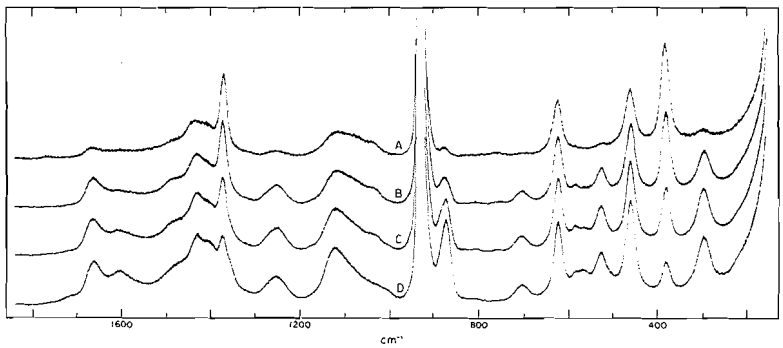

FIG. 1. Raman spectra in the 160–1840 cm^{-1} region for the 2/1 solution (1.70 mol $Hg(ClO_4)_2$, 19.7 mol H_2O, 9.8 mol CH_3CN, 0.15 mol $HClO_4$ per l) as a function of time. (*A*) 164.4–215.8 min; (*B*) 518.7–658.7 min; (*C*) 1191.7–1331.7 min; (*D*) 2989.2–3129.2 min.

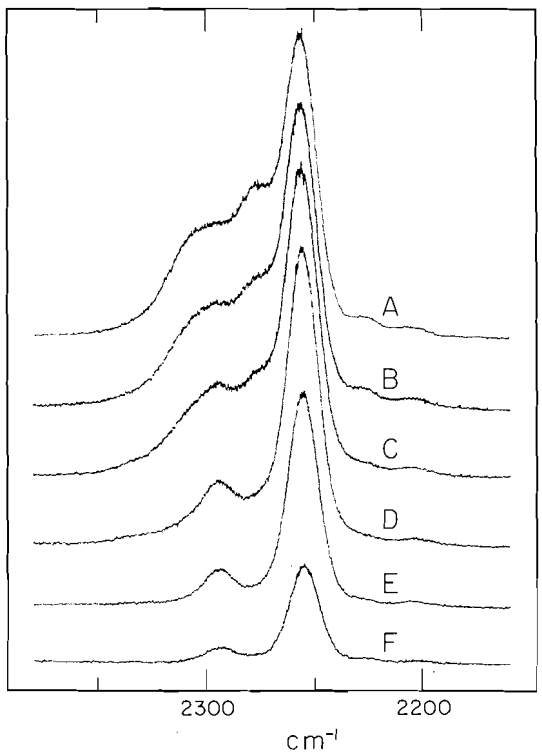

FIG. 2. Raman spectra in the 2160–2380 cm^{-1} region for the 2/1 solution as a function of time. (*A*) 46.7 min; (*B*) 146.5 min; (*C*) 256.7 min; (*D*) 504.8 min; (*E*) 1107.1 min; (*F*) 3187.6 min.

Solutions containing $Hg(NO_3)_2$ in the mixed solvents of acetonitrile and water give bands at 716, 740, 1030, and 1045 cm^{-1} (Fig. 3); bands in the 1200–1600 cm^{-1} region overlap with the acetonitrile bands. These bands compare reasonably well in position with results for aqueous solutions and can be assigned to solvated nitrate (716 and 1045 cm^{-1}) and nitrate bound to mercuric ion (740 and 1030 cm^{-1}). Intensity analysis of the spectra recorded a few hours after preparation indicated that the degree of association of mercuric nitrate is larger in the mixed solvent system of CH_3CN/H_2O than in its aqueous solution. The degree of association of $Hg(NO_3)_2$, however is a function of time (Fig. 3). It decreases as more acetonitrile is hydrolyzed.

Systems of $Hg(OAc)_2/H_2O/CH_3CN$ give no indication of reaction. No new bands were observed in spectra recorded approximately 24 h after the preparation of the solutions. Mercuric acetate gives rise to the following bands in the mixed solvents: 275, 498, 691, 890, 939, 1017, and 2943 cm^{-1}; the bands in the 1400 cm^{-1} region are weak and obscured by the bands due to acetonitrile. For aqueous solutions of $Hg(OAc)_2$, the band positions are identical (± 1 to 2 cm^{-1}) to those observed for $Hg(OAc)_2$ in the mixed solvents. A sodium acetate solution (2 *M*), on the other hand, gives the following bands: 476, 618, 653, 927, 1348, 1414, 1760, 2935, 2985 cm^{-1}. The 275 cm^{-1} band of mercuric acetate is fairly strong and polarized. This band can reasonably be assigned to the mercury–acetate stretching vibration. The appearance of this band together with the difference in band positions between the $Hg(OAc)_2$ and NaOAc solutions strongly suggests that $Hg(OAc)_2$ is highly associated. This is in agreement with the very large value of the association constant, β_2 ($\sim 10^9$) for $Hg(OAc)_2$ obtained by two different methods (26, 27). The absence of the bands at 2275 and 2305 cm^{-1} in the $Hg(OAc)_2/H_2O/CH_3CN$ solutions which can be ascribed to bound acetonitrile indicates that there is no

Can. J. Chem. Downloaded from www.nrcresearchpress.com by 210.87.254.5 on 09/05/12
For personal use only.

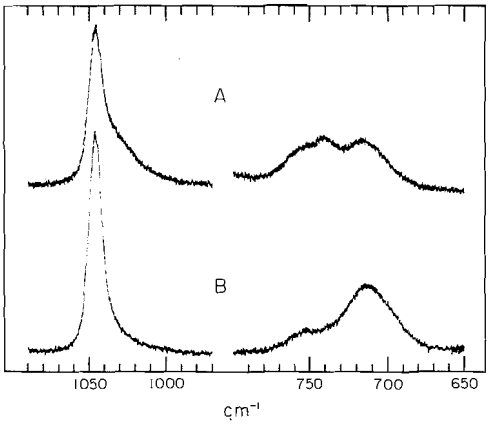

FIG. 3. Raman spectra in the 650–800 cm^{-1} and 960–1090 cm^{-1} regions for the solution with composition: 1 mol $Hg(NO_3)_2$, 21 mol H_2O, 12 mol CH_3CN, and 0.2 mol HNO_3 per litre. (*A*) ≈12 h; (*B*) ≈36 h after the solution was prepared. Spectral slit widths for the 650–800 cm^{-1} region: 10 cm^{-1} and 960–1090 cm^{-1} region: 5 cm^{-1}.

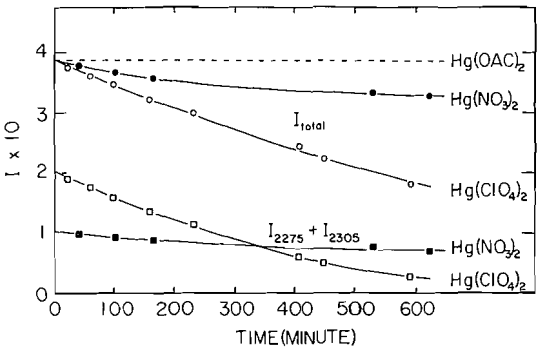

FIG. 4. Intensity in the 2150–2400 cm^{-1} region as a function of time for solutions containing different mercuric salts.

complex formation between Hg^{2+} and CH_3CN and further supports the fact that $Hg(OAc)_2$ exists in its molecular form in solutions.

A comparison of the effect of the three salts on the rate of the hydrolysis of acetonitrile is shown in Fig. 4. The intensities of the total C≡N stretching region, as well as the intensities of lines ascribed to CH_3CN bound to Hg^{2+} (*i.e.*, 2275 + 2305 cm^{-1}) are plotted against time. Since in solutions of $Hg(OAc)_2/H_2O/CH_3CN$, no evidence of hydrolysis was observed, a dashed horizontal line is shown. The compositions of the $Hg(ClO_4)_2$ and $Hg(NO_3)_2$ solutions are similar: 1.69 mol $Hg(ClO_4)_2$, 25.2 mol H_2O, 7.78 mol CH_3CN, 0.15 mol $HClO_4$, and 1.70 mol $Hg(NO_3)_2$, 26.3 mol H_2O, 8.22 mol CH_3CN, 0.48 mol HNO_3 per l. It is apparent that $Hg(ClO_4)_2$ affects a faster reaction than $Hg(NO_3)_2$. This is attributed to a higher concentration of solvated Hg^{2+} in the $Hg(ClO_4)_2$ system which in turn results in a larger intensity ($I_{2275} + I_{2305}$).

Interaction Between Hg(II) and CH_3CN

The intense bands at 2275 and 2305 cm^{-1} (Fig. 2) indicate that the affinity of mercury for acetonitrile is large, in the absence of competition from stronger ligands like halides or acetate. As will be seen later, the $\bar{n}$ value, defined as the average number of acetonitrile molecules bound

TABLE 1. Raman frequencies (cm^{-1}) of acetonitrile, both pure and as a component of several solutions

Pure CH_3CN	33.8 *M* H_2O + 6.8 *M* CH_3CN	$Hg(ClO_4)_2/H_2O/CH_3CN$	$Hg(NO_3)_2/H_2O/CH_3CN$	$Hg(OAc)_2/H_2O/CH_3CN$
379	383	382	383	382
751	755	756	756	755
921	923	—*	923	922
1040	1040	1040	—*	1040
1375	1375	1370	1375	1374
1412	1410	1410	—*	—*
1449	1442	1438	—*	—*
2254	2258	2257	2257	2256
		2275	2275	
2294	2297	2295	2295	2296
		2305	2305	
3945	2945	2944	2944	2945
3004	3005	3005	3005	3005

*Obscured by bands due to the solute.

Can. J. Chem. Downloaded from www.nrcresearchpress.com by 210.87.254.5 on 09/05/12
For personal use only.

Can. J. Chem. Downloaded from www.nrcresearchpress.com by 210.87.254.5 on 09/05/12
For personal use only.

to one mercuric ion, can exceed 3.5, which indicates that $HgCH_3CN^{2+}$, $Hg(CH_3CN)_2^{2+}$, $Hg(CH_3CN)_3^{2+}$, $Hg(CH_3CN)_4^{2+}$ or even higher complexes can exist. Based on Raman spectral results, the following order is inferred for the degree of formation of mercury complexes: $ClO_4^- < H_2O < CH_3CN < NO_3^- \ll (Cl^-, Br^-, OAc^-)$. This observation, together with the fact that the rate of the hydrolysis reaction is closely related to the concentration of the bound acetonitrile concentration, accounts for the results of Travagli: *viz.* that the catalytic effect of a mercury salt decreased in the order $ClO_4^- > NO_3^- \gg Cl^-$ (12).

Spectral Data for Possible Products of the Reaction

The frequencies of the new lines with intensities which increase with time were compared with those of a large number of compounds (28).[4] Acetic acid is one of the products. Its bands are, however, not evident until the reaction time exceeds 1800 min. Band positions characteristic of mercuric acetate and sodium acetate are not observable in spectra of the reaction mixture when products predominate.

The final product containing the nitrogen atom can probably be NH_4^+ or $Hg(NH_3)_x^{2+}$. The species $Hg(NH_2)_x^{-(x-2)}$ is excluded at once by comparison with the known infrared spectra (29, 30), The NH_4^+ ion is not easily distinguished from other products. The lines of mercury-ammine complexes, on the other hand, are clearly observed in the spectra. Their existence is consistent with the very high values of their stability constants in aqueous solutions (31).

Complexes of the formula $[HgCH_3CONH]^+$ and $Hg(CH_3CONH)_2$ exist in dilute aqueous solutions of mercuric chloride and CH_3CONH_2 (32). Their stability constants have been measured by p*H* titration methods. Although these stability constants are very high ($\log K_1 = 8.15$ and $\log K_2 = 7.54$) the concentrations of the complexes are limited by the very low dissociation constant of acetamide, $\log K_a = -15.1$, where $K_a = [CH_3CONH^-][H_3O^+]/[CH_3CONH_2]$(33). A comparison between the infrared results of the compound $Hg(CH_3CONH)_2$ and the spectra for the hydrolysis products indicates that the concentration of $Hg(CH_3CONH)_2$, if it is present, must be very low.

Acetamide and its complex with mercury are difficult to distinguish spectroscopically. It is probable that they both exist in the solutions. $AcNH_2$ reacts with $Hg(NO_3)_2$ (34) and $HgCl_2$ (35), in aqueous solution to form adducts of the formulae $Hg(NO_3)_2 \cdot 2AcNH_2$ and $HgCl_2 \cdot AcNH_2$. No water of crystallization is bound in these compounds. The existence of the acetamide–mercury complex in aqueous solution is indicated by the presence of a strong and polarized band at 300 cm^{-1} which can reasonably be assigned to a Hg–ligand stretching vibration of $Hg(AcNH_2)_x^{2+}$. Indirect evidence supports this association. For solutions containing $Hg(NO_3)_2/CH_3CN/H_2O$, the concentration of nitrate bound to Hg^{2+} decreases as inferred by the decrease in intensity of the bands at 740 and 1030 cm^{-1} (Fig. 3), which indicates that NO_3^- is displaced by a ligand with greater affinity for Hg^{2+}.

The above discussion suggests that the products of the hydrolysis are acetamide and/or its complexes with mercury, mercury ammine complexes, and acetic acid. In general, coordination of the oxygen atom of an amide to a metal ion results in a shift of the C=O stretching mode to a lower frequency and the C—N stretching mode to a higher frequency (36–39). This we did not observe. Acetamide is probably bound to Hg via the N atom as in crystalline mercury(II) acetamide (40, 41). This feature is peculiar as compared with other acetamide complexes such as Ni (42, 43), Cu (44, 45), and H^+ (46), in which the oxygen atom is bound to the cation. The Hg—N bond in the Hg–acetamide complex is a reflection of the great affinity of mercury for nitrogen ligands. Positions of all the bands observed for the products, the polarization data, and the assignments are listed in Table 2.

Quantitative Measurements

In this section, results of experiments designed to obtain the rate law for the reaction are presented. Four solutions with different H_2O/CH_3CN molar ratios were prepared. These solutions will be identified by their molar ratios hereafter. The concentration of $Hg(ClO_4)_2$ was fixed at 1.7 *M* in all four runs to maintain essentially constant the influence of the salt. The intensities of bands in the 2150–2400 cm^{-1}

[4]Tables of data not included in this paper can be found in this source.

TABLE 2. Raman and infrared frequencies (cm^{-1}) and assignments of products of the hydrolysis reaction

		Assignments*		
Raman	Infrared†	$Hg(AcNH_2)$	HOAc	$Hg(NH_3)_x^{2+}$
300 p	—‡	Hg—N st.		
460 dp	458	C—C—N bend	C—C—O bend	
524 p	528		C=O bend	Hg—N st.
570 dp	573		COO out-of-plane bend?	
585 dp	588	NH_2 wag		
624 dp	624		COO bend	
704 dp	707	NH_2 twist		NH_3 rock
870 p	870	C—C st.		
890 p	889		C—C st.	
1020 dp	1013	CH_3 rock	CH_3 rock	
1122 p	1125	C—N st.		
1250 p	—	NH_2 rock		NH_3 sym. bend
1270 p	1270		C—O st.	
1360 p	1345		CH_3 sym. bend	
1400 p	1400	CH_3 sym. bend		
1430 dp	1430		CH_3 asym. bend	
1485 dp	1487	CH_3 asym. bend		
1604 p	1604	NH_2 sym. bend		NH_3 asym. bend
1664 p	1668	C=O st.		
1720 p	1720		C=O st.	
2945 —‡	—‡	CH_3 sym. st.	CH_3 sym. st.	
2990 —	—	CH_3 asym. st.		
3020 —	—		CH_3 asym. st.	
3368 —	—	NH_2 st.		NH_3 st.

*Assignments are consistent with results of polarization studies and intensity changes with time. Assignments are inferred from the literature but there is considerable disagreement concerning assignments of the skeletal deformation modes.
†Observed for the solution with the composition = 1.7 mol $Hg(NO_3)_2$, 26.3 mol H_2O, 8.2 mol CH_3CN, 0.48 mol HNO_3 per l, 12 h after preparation.
‡Not investigated.

region have been measured at appropriate time intervals. Typical spectra in this region were shown in Fig. 2.

Spectral data in the 2150–2400 cm^{-1} region were obtained for the 1.3/1 solution, recorded at intervals of time up to 4414.9 min (28). The *ca.* 2275 and 2305 cm^{-1} bands have been assigned to acetonitrile bound to mercury(II) ion; the intensity ratio of these two bands appears to be a constant (1.23 ± 0.20) independent of time until the intensities are very low and thus of lower accuracy. This constancy suggests that Fermi resonance occurs between these two bands as discussed elsewhere for the $Zn(NO_3)_2/CH_3CN/H_2O$ system (28). For other $Hg(ClO_4)_2$ or $Hg(NO_3)_2/H_2O/CH_3CN$ solutions similar results were obtained. Small differences exist between the zinc and mercury systems. For acetonitrile bound to Hg^{2+} the combination occurs at (923 + 1370) or 2293 cm^{-1}. On Fermi resonance with the fundamental the two lines 2275 and 2305 cm^{-1} are observed; the 2305 cm^{-1} line has a lower peak height but greater integrated intensity because of its width. For the zinc case, the combination occurs at (937 + 1370) or 2307 cm^{-1}, the observed pair of lines occur at 2290 and 2315 cm^{-1} and the intensity at 2315 cm^{-1} is less than the intensity at 2290 cm^{-1}. This comparison (both position and intensity) suggests that (ν_f^b − 2293) for the mercury–acetonitrile complex is smaller than the (ν_f^b − 2307) for the zinc–acetonitrile complex, where ν_f^b is the fundamental ascribed to the bound form of CH_3CN, in the absence of Fermi resonance.

The intensity–time data were interpreted as follows. The intensities at $t = 0$ were obtained by extrapolation. The molar intensity of acetonitrile, J, defined as the total intensity at $t = 0$ divided by the stoichiometric concentration of acetonitrile, does not change appreciably as the solution compositions change. At 25 °C, the J values for the 1.3/1, 2/1, 3.2/1, and 5.2/1 solutions are 48.5, 51.1, 49.2, and 51.6 mol^{-1} l

Can. J. Chem. Downloaded from www.nrcresearchpress.com by 210.87.254.5 on 09/05/12
For personal use only.

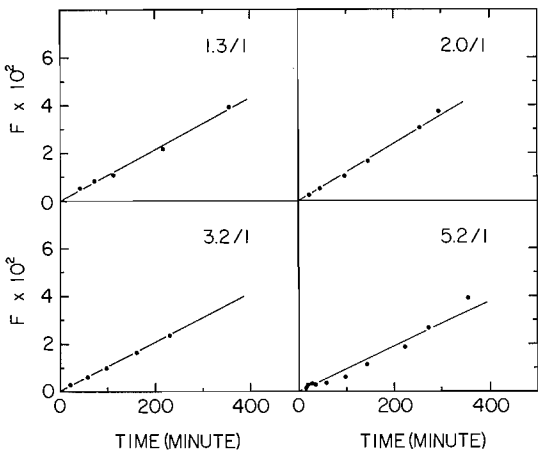

FIG. 5. F against time for the four solutions of $Hg(ClO_4)_2$–H_2O–CH_3CN.

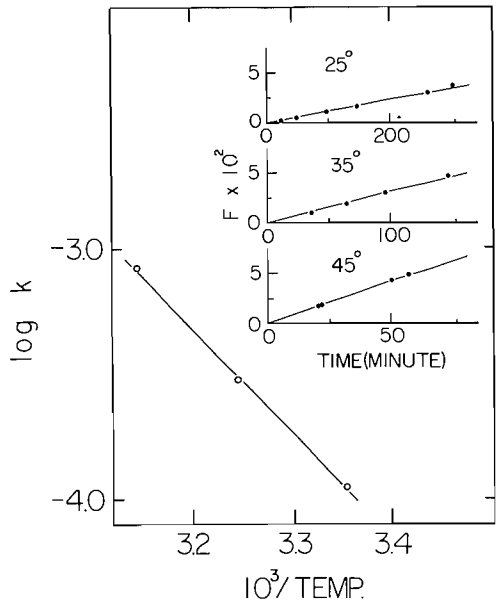

FIG. 6. F against time for the 2/1 solutions at different temperatures, and the logarithm of the rate constant, log k, against the reciprocal of temperature (K).

respectively. For the solution 1.7 mol $Hg(NO_3)_2$, 26.25 mol H_2O, 8.22 mol CH_3CN, 0.48 mol HNO_3 per l, the composition of which is similar to the 3.2/1 solution, the J value is 47.2 mol^{-1} l. Thus it is reasonable to assume that the molar intensities of both the bound and bulk acetonitrile are equal within experimental error. Similar results have been observed in our previous study (28) of $Zn(NO_3)_2/H_2O/CH_3CN$ and have been reported by others (17).

The concentrations of acetonitrile bound to mercury at time t, $[CH_3CN]_B$, were calculated by dividing $(I_{2275} + I_{2305})$ by the molar intensity, J. By dividing $[CH_3CN]_B$ at $t = 0$ by the stoichiometric concentrations of mercury in the solutions, the average numbers of acetonitrile molecules bound to one mercuric ion, $\bar{n}$, can be calculated. They are 3.58, 3.05, 2.44, and 1.84 for the 1.3/1, 2/1, 3.2/1, and 5.2/1 solutions respectively. Presumably all the mercuric ions are bound to at least one acetonitrile molecule in these solutions.

The $[CH_3CN]_B$–time data are consistent with a second order rate expression. For 1.7 M $Hg(ClO_4)_2$ solutions

$$\text{Rate} = k[CH_3CN]_{B,t}[H_2O]_t$$

Plots of $\{[H_2O]_0 - [CH_3CN]_{B,0}\}^{-1} \cdot \ln\{[CH_3CN]_{B,0}[H_2O]_t/[H_2O]_0[CH_3CN]_{B,t}\}$, called F, against time (Fig. 5) are linear with slopes k of 1.08, 1.12, 1.03, and 0.95 $\times$ 10^{-4} mol^{-1} l min^{-1} for the 1.3/1, 2/1, 3.2/1, and 5.2/1 solutions respectively. An average value of 1.05 $\pm$ 0.06 $\times$ 10^{-4} mol^{-1} l min^{-1} is obtained for k. The value of $[H_2O]_t$ is given by $[H_2O]_0 - \{[CH_3CN]_{B,0} - [CH_3CN]_{B,t}\}$. It was found that the data are not consistent with a first order rate law in $[CH_3CN]_B$ nor with a reaction first order in $[CH_3CN]_B$ and second order in $[H_2O]$. To avoid complications from subsequent reactions only the data obtained in the first 400 min have been tested. Note that the concentrations have been corrected for volume changes which occur during the course of reaction.

Although $(I_{2275} + I_{2305})$ decreases monotonically with time, $(I_{2255} + I_{2295})$, assigned to bulk or unbound acetonitrile, increases or remains almost constant over the first 400 min. This observation will be explained later.

Data for the 2/1 solution have also been obtained at 35 and 45 °C. The energy of activation, E_a, for the reaction was found from the log k against $1/T$ plot (Fig. 6) to be 18.9 kcal mol^{-1}. Travagli reported a value of 21.8 kcal mol^{-1} for the reaction catalyzed by Hg(II) in 3 N $HClO_4$ solution (12). Because he worked at high temperatures with a high concentration of acid and low concentrations of mercury salt, the catalytic effect of the acid is significant. As he noted, the activation energy for the Hg(II) catalyzed reaction alone is obtainable by reducing k by the

Can. J. Chem. Downloaded from www.nrcresearchpress.com by 210.87.254.5 on 09/05/12
For personal use only.

amount contributed by the acid (11). This yields a value of 19.3 kcal which is in good agreement with the results obtained from Raman data, considering different experimental conditions.

Mechanism for the Hydrolysis Reaction

It is assumed that virtually all of the Hg^{2+} is initially solvated by acetonitrile; this species $(CH_3CN)_xHg^{2+}$ undergoes reaction as follows

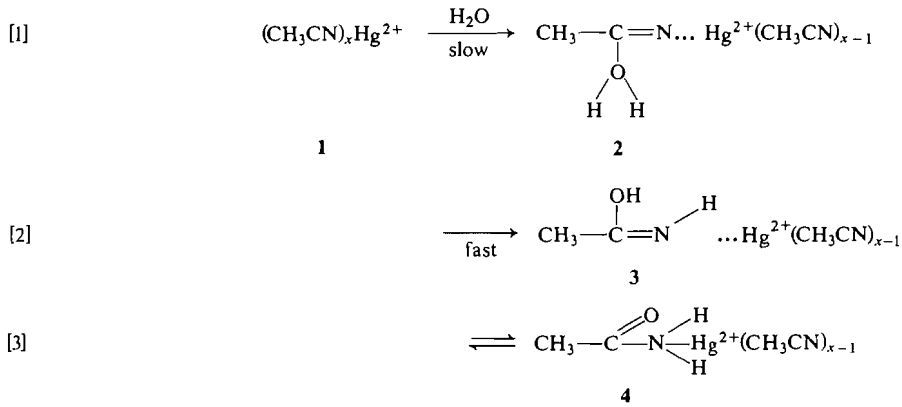

Subsequent slow reaction gives

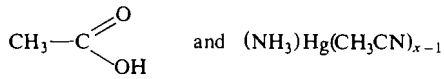

Water attacks species **1** slowly giving intermediate **2**, which is transformed by proton transfer to species **3** and **4**. Species **5** and **6** are significant only after the reaction has progressed for a very long time. A final mercury(II) species is believed to be $Hg(NH_3)_n^{2+}$. However, prior to its formation a species such as **6** which could recycle through steps 1 to 4 is possible. Species **1**, **4**, **5**, and a form of **6** are spectroscopically observable. Species **1** is presumably an ion–dipole complex which is very stable. No Raman frequency attributable to the metal–nitrogen stretch has been observed and thus substantial covalence is excluded. However, the shift in the position of the C≡N stretch is clear indication of the solvation of the cation by acetonitrile and parallels the observations for Zn^{2+} (28) and Ag^+ (23). Observation of lines identical to those of pure acetamide provides support for species **4**; in addition an intense line at 300 cm^{-1} ascribed to the Hg^{2+}—N stretch suggests that the acetamide is associated with the mercury ion. In species **1** to **4** it is not clear what value should be assigned to x. Because more than one molecule of acetonitrile in the solvation sphere of Hg^{2+} is hydrolyzable, the constancy of the line intensity of bulk acetonitrile (2255 + 2295 cm^{-1}) over the first 400 min of reaction is rationalized. The apparent increase in intensity of the 2255 + 2295 cm^{-1} lines over this time span, even after correction for volume changes, may suggest some displacement of CH_3CN from the first coordination sphere of Hg^{2+} in steps such as 1–3.

In the four solutions the mercury(II) concentrations were identical but different amounts of CH_3CN were bound to Hg^{2+}. Presumably remaining sites in the primary coordination sphere are occupied by water molecules; the amount of bound water increases as the H_2O/CH_3CN ratio increases, judging from the $\bar{n}$ data quoted earlier. But the reactivity of all acetonitrile molecules in the primary coordination spheres must be the same and independent of the number or nature of other ligands bound to Hg^{2+} for the rate law to be as observed. The fact that rate depends on total water concentration, despite the wide variation in the amount of bound water over the four solutions, suggests that both unbound and possibly bound water are reactive species. The reaction thus involves acetonitrile in the primary solvation sphere of Hg^{2+} reacting with water while in a medium of acetonitrile (bulk) and water. Apparently the differences in the solvent compositions of the four solutions also do not affect the reactivity of the bound acetonitrile. This behavior does not appear to be widespread although it is difficult to find comparable studies in the literature.

Can. J. Chem. Downloaded from www.nrcresearchpress.com by 210.87.254.5 on 09/05/12
For personal use only.

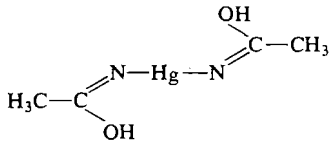

A structure similar to **2** has been proposed for mercury(II) acetamide from X-ray studies (40). According to n.m.r. data, however, the proton is probably bonded to the nitrogen atom (41). These results support the conclusion that the acetamide anion acts as a monodentate N-bonded ligand and that the CN bond is of extensive double bond character. The ability of mercury to form stable bonds with nitrogen accounts for a relatively low activation energy (18.9 kcal compared with 24–26 kcal for acids (14)) and the failure of most other metals to catalyze the reaction at room temperature.

Mercury acetamide complexes appear to be much more stable than mercury acetonitrile towards hydrolysis reactions. The fact mentioned earlier that $Hg(AcNH_2)_2(NO_3)_2$ and $HgAcNH_2Cl_2$ can be prepared from aqueous solutions supports this conclusion. For the 2/1 solution in this study the time for half of the acetonitrile to be hydrolyzed is 650 min (for solutions with higher H_2O/CH_3CN ratios, this period is shorter) as estimated from the intensity variation in the 2150–2400 cm^{-1} region. It is apparent from spectra of this solution that the principal species after this time interval is acetamide. Even when 75% of the acetonitrile is converted (at approximately 1800 min) only a very small amount of acetamide is converted to acetic acid as judged from the bands characteristic of acetic acid and the ammine complexes.

The merit of using mercury(II) to catalyze the reaction is that it is one of very few substances which cause conversion of acetonitrile to acetamide, only mild conditions are required, and the product forms with high yield and purity according to the spectra. Reaction is slower with MnO_2 (4) and side reactions are more numerous with nickel catalysts (6). In suitable cases the use of a mercury(II) catalyst may be advantageous.

The support of the National Research Council of Canada is gratefully acknowledged. We also thank G. L. Rempel, R. S. Tobias, and A. Viste for helpful discussions and Mrs. G. Scoles for translating the works of G. Travagli. Y-K.S. acknowledges with thanks N.R.C.C. postgraduate scholarships, 1970–1973.

1. A. I. Vogel. A text-book of practical organic chemistry, 3rd ed. Longmans, London. 1956. p. 1075.
2. J. R. Blackborow. J. Chem. Soc. C, 739 (1969).
3. M. Liler and Dj. Kosanović. J. Chem. Soc. 1084 (1958).
4. M. J. Cook, E. J. Forbes, and G. M. Khan. Chem. Commun. 121 (1966).
5. K. B. Wiberg. J. Am. Chem. Soc. **77**, 2519 (1953).
6. K. Watanabe and K. Sakai. Bull. Chem. Soc. Jap. **39**, 8 (1966).
7. F. Gesmundo, P. Nanni, and V. Lorenzelli. Atti Accad. Naz. Lincei, Rend. Cl. Sci. Fis. Mat. Nat. **42**, 218 (1967).
8. E. F. Schoenbrunn and V. T. Sinha. U. S. 3 674 848. Chem. Abstr. **77**, 102411s (1972).
9. G. Travagli. Gazz. Chim. Ital. **82**, 528 (1952).
10. G. Travagli. Gazz. Chim. Ital. **87**, 673 (1957).
11. G. Travagli. Gazz. Chim. Ital. **87**, 682 (1957).
12. G. Travagli. Gazz. Chim. Ital. **87**, 830 (1957).
13. G. Travagli. Gazz. Chim. Ital. **88**, 1129 (1958).
14. B. S. Rabinovitch and C. A. Winkler. Can. J. Res. **20B**, 221 (1942).
15. S. Wideqvist. Ark. Kemi, **10**, 265 (1956); Chem. Abstr. **51**, 4107e (1957).
16. H. Chen and D. E. Irish. J. Phys. Chem. **74**, 3796 (1970).
17. B. G. Oliver and G. J. Janz. J. Phys. Chem. **74**, 3819 (1970).
18. J. C. Evans and Y.-S. Lo. Spectrochim. Acta, **21**, 1033 (1965).
19. M.-H. Baron and C. deLoze. J. Chim. Phys. **68**, 1293 (1971).
20. J.-P. Roche and P. M. Huong. J. Chim. Phys. **67**, 211 (1970).
21. C. C. Addison, D. W. Amos, and D. Sutton. J. Chem. Soc. A, 2285 (1968).
22. Z. Kęcki and J. Witanowski. Rocz. Chem. **38**, 691 (1964).
23. T. G. Chang and D. E. Irish. J. Solution Chem. **3**, 161 (1974).
24. R. E. Hester and R. A. Plane. Inorg. Chem. **3**, 768 (1964).
25. M. M. Jones, E. A. Jones, D. F. Harmon, and R. T. Semmes. J. Am. Chem. Soc. **83**, 2038 (1961).
26. P. Mahapatra, S. Aditya, and B. Prasad. J. Indian Chem. Soc. **30**, 509 (1953).
27. D. Banerjea and I. P. Singh. Z. Anorg. Allg. Chem. **331**, 225 (1964).
28. Y.-K. Sze. Ph.D. Thesis, University of Waterloo, Waterloo, Ontario. 1973.
29. S. Mizushima, I. Nakagawa, and D. M. Sweeny. J. Chem. Phys. **25**, 1006 (1956).
30. I. Nakagawa, R. B. Penland, S. Mizushima, T. J. Lane, and J. V. Quagliano. Spectrochim. Acta, **9**, 199 (1957).
31. J. Bjerrum. Chem. Rev. **46**, 381 (1950).
32. R. O. Gould and H. M. Sutton. J. Chem. Soc. A, 1184 (1970).
33. G. E. K. Branch and J. O. Clayton. J. Am. Chem. Soc. **50**, 1680 (1928).
34. A. D. Dzhunusov, B. I. Imanakunov, M. K. Kydynov, and P. T. Yun. Izv. Akad. Nauk Kirg. S.S.R. 67 (1967). Chem. Abstr. **69**, 92482j (1968).
35. B. Imanakunov, S. Baichalova, P. Yun, and A.

Can. J. Chem. Downloaded from www.nrcresearchpress.com by 210.87.254.5 on 09/05/12
For personal use only.

DZHUNUSOV. Mater. Nauch Konf., Posvyashch. 100-[sto] Letiyu Period. Zakona D. I. MENDELEEVA, 15 (1969); Chem. Abstr. **76**, 41417d (1972).
36. G. VICENTINI and R. NAJJAR. J. Inorg. Nucl. Chem. **30**, 2771 (1968).
37. G. VICENTINI and C. AIROLDI. J. Inorg. Nucl. Chem. **33**, 1733 (1971).
38. J. M. GIORIA and B. P. SUSZ. Helv. Chim. Acta, **54**, 2251 (1971).
39. M.-H. BARON, J. CORSET, C. DELOZÉ, and M. L. JOSIEN. C. R. **274**C, 1321 (1972).
40. B. KAMENAR and D. GRDENIC. Inorg. Chem. Acta, **3**, 25 (1969).
41. D. B. BROWN and M. B. ROBIN. Inorg. Chim. Acta, **3**, 644 (1969).
42. M. E. STONE, B. E. ROBERTSON, and E. STANLEY. J. Chem. Soc. A, 3632 (1971).
43. M. A. A. BEG and M. R. FAROOQUI. Pak. J. Sci. Ind. Res. **14**, 336 (1971). Chem. Abstr. **77**, 28326*z* (1972).
44. M. A. A. BEG and M. A. HASHMI. Pak. J. Sci. Ind. Res. **14**, 458 (1971). Chem. Abstr. **77**, 54373*g* (1972).
45. A. S. TAHOUN. U.A.R.J. Chem. **14**, 133 (1971). Chem. Abstr. **77**, 93218*e* (1972).
46. G. WADA and T. TAKENAKA. Bull. Chem. Soc. Jap. **44**, 2877 (1971).

Can. J. Chem. Downloaded from www.nrcresearchpress.com by 210.87.254.5 on 09/05/12
For personal use only.

Determination of 3 × 3 Harmonic Force Field of Planar X_2YZ Molecules[1]

J. C. D. Brand and Ch. V. S. Ramachandra Rao
Department of Chemistry, University of Western Ontario, London, Ontario N6A 3K7

Received July 12, 1974

J. C. D. Brand and Ch. V. S. Ramachandra Rao. Can. J. Chem. **53**, 437 (1975).
The problem of multiple solutions encountered during the determination of a 3 × 3 General Harmonic Force Field is analyzed. The A_1 force fields of the planar molecules $COCl_2$, NO_2F, and H_2CO, are considered and formaldehyde is treated in some detail as illustration.

J. C. D. Brand et Ch. V. S. Ramachandra Rao. Can. J. Chem. **53**, 437 (1975).
On analyse le problème des solutions multiples rencontrées durant la détermination d'un champ de force harmonique général de 3 × 3. Le champ de force A_1 des molécules planaires $COCl_2$, NO_2F et H_2CO sont considérées et on traite, en détail à titre exemple, la molécule de formaldéhyde. [Traduit par le journal]

Introduction

During the least-squares refinement of the force constants of a polyatomic molecule, it is quite common to encounter a situation where several distinct solutions to the force field fit the available data equally well even when the data are in excess. Multiple solutions to the force field result from the fact that force constants are essentially determined from the data as the solutions of a set of polynomial equations of varying degrees. An illuminating discussion of this problem in the case of the 2 × 2 E species force field of XY_3 molecules was given by Hoy, Stone, and Watson (1). McKean and Duncan (2) have given an extensive survey of the problem of multiple solutions for several 2 × 2 and 3 × 3 cases. By analyzing the equations to be solved, Moule and Rao (3) have discussed the uniqueness of the force field of the CH_3F molecule whose vibrations are divided into $3A_1 + 3E$ and found that it is easier to treat the problem in the compliance scheme rather than the force constant scheme.

It is one thing to determine a set of force constants from given data by a least-squares technique and another to establish the uniqueness or otherwise of such a set. In fact, the latter problem has been considered in only a few cases. It is not uncommon either to ignore the existence of alternative physically-reasonable sets of solutions or to discriminate between them on empirical grounds. In this note, we shall discuss a method of establishing the uniqueness of a 3 × 3 force field of A_1 species determined using a variety of data taking $COCl_2$, NO_2F, and H_2CO as illustrations. Force fields of these molecules have of course been determined but an analysis of their uniqueness problem is lacking. We assume that the following data are given for the three molecules: (*i*) $COCl_2$ (frequencies and centrifugal distortion constants) (4); (*ii*) NO_2F (frequencies and centrifugal distortion constants) and $^{15}NO_2F$ (frequencies) (5); (*iii*) H_2CO, D_2CO, HDCO, and $H_2{}^{13}CO$ (frequencies) (2, 6). It is shown that the combination of data represented by (*i*) does not yield a unique solution to the force field whereas the data in (*ii*) and (*iii*) are capable of doing so. In each case we are concerned with the uniqueness, not the actual calculation, of the force field.

[1]Contribution No. 117 of the Photochemistry Unit.

The Method

With the standard notation, the symmetry coordinates for the five in-plane vibrations are taken as (6)

$$\left.\begin{aligned} S_1 &= \frac{1}{\sqrt{2}}(\Delta r_1 + \Delta r_2) \\ S_2 &= \Delta R \\ S_3 &= \frac{1}{\sqrt{6}}(2\Delta\alpha - \Delta\beta_1 - \Delta\beta_2) \end{aligned}\right\} A_1 \text{ species}$$

and

$$\left.\begin{aligned} S_5 &= \frac{1}{\sqrt{2}}(\Delta r_1 - \Delta r_2) \\ S_6 &= \frac{1}{\sqrt{2}}(\Delta\beta_1 - \Delta\beta_2) \end{aligned}\right\} B_2 \text{ species}$$

Can. J. Chem. Downloaded from www.nrcresearchpress.com by 210.87.254.5 on 09/05/12
For personal use only.

Can. J. Chem. Downloaded from www.nrcresearchpress.com by 210.87.254.5 on 09/05/12
For personal use only.

The secular equation in the compliance scheme, in terms of "symmetry forces", is given by (7)

$$[1] \qquad (\mathbf{G}^{-1}\mathbf{C})\mathbf{N} = \mathbf{N}\mathbf{\Lambda}^{-1}$$

Using $\mathbf{K} = \mathbf{G}^{-1}$ and $\mathbf{\Phi} = \mathbf{\Lambda}^{-1}$, the above equation is written as

$$[2] \qquad (\mathbf{KC})\mathbf{N} = \mathbf{N}\mathbf{\Phi}$$

This can be expanded as an algebraic equation for the three vibrations of the A_1 species into linear (L), quadratic (Q), and cubic ($\mathscr{C}$) parts, (3):

$$[3] \qquad L(C_{ij}) = \phi_1 + \phi_2 + \phi_3$$

$$[4] \qquad Q(C_{ij}) = 0$$

and

$$[5] \qquad \mathscr{C}(C_{ij}) = 0$$

For the B_2 species, the corresponding equations are

$$[6] \qquad K_{55}C_{55} + K_{66}C_{66} + 2K_{56}C_{56} = \phi_5 + \phi_6$$

and

$$[7] \qquad (K_{55}K_{66} - K_{56}^2)(C_{55}C_{66} - C_{56}^2) = \phi_5\phi_6$$

The centrifugal distortion constants $\tau_{\alpha\beta\gamma\delta}$ are related to the compliance constants C_{ij} linearly (7, 8)

$$[8] \qquad \frac{-112.9615 \times 10^{-4}}{I_\alpha^e I_\beta^e I_\gamma^e I_\delta^e} \sum_{i,j} J_{\alpha\beta}{}^i J_{\gamma\delta}{}^j C_{ij} = \tau_{\alpha\beta\gamma\delta}$$

$J_{\alpha\beta}{}^i = (\partial I_{\alpha\beta}/\partial S_i)_e$. The τ values are in cm^{-1}, when masses are expressed in a.m.u., internuclear distances in Å, and the stretching, stretch–bend, and bending compliance constants in Å $mdyn^{-1}$, $mdyn^{-1}$, and $(mdyn\ Å)^{-1}$ respectively. Of the four independent τ values, τ_{aaaa}, τ_{bbbb} and τ_{aabb} depend only on the force constants of the A_1 species while τ_{abab} depends only on those of the B_2 species. The set of eqs. 3–8 can now be seen to determine in a simple way the uniqueness or otherwise of the force field.

$COCl_2$ (ν and τ)

Mirri *et al.* (4) have tried to determine the nine force constants of $COCl_2$ for the A_1 and B_2 species using five frequencies and four τ values. As can be seen from the linear nature of eq. 8 connecting τ_{abab} and C_{ij}, one finds from eqs. 6–8, that *two and only two* discrete sets of compliance constants (hence force constants) can be obtained for the B_2 species.[2] This fact does not appear to have been realized (4).

For the A_1 species, Mirri *et al.* (4) noted that it was not possible to determine a unique set of force constants. They obtained several sets corresponding to the range of variation of two chosen force constants F_{12} and F_{23}. We note initially that for the given data, eqs. 3–5 and 8 give rise to four independent linear equations, a quadratic, and a cubic equation in terms of the six compliance constants. From Bézout's theorem (9), the number of mathematically possible solutions is given by the product of the degrees of all the equations. Thus in the present case, we have $2 \times 3 = 6$ sets of solutions for the A_1 species force field. In principle, Bézout's or Sylvester's eliminant may be used to reduce the system of equations to a polynomial equation of degree six in each one of the unknowns, in turn, after which the equation is solved numerically for each of the six values of that unknown. Since the physical solution should correspond to real values of C_{ij} and complex roots occur in pairs, we should obtain a minimum of two and a maximum of six real solutions. Thus with the given data, the force field is *not* unique.

$^{14}NO_2F$ (ν and τ) and $^{15}NO_2F$ (ν)

Mirri *et al.* (5) have obtained the force constants of NO_2F for the A_1 and B_2 species using the ten frequencies of $^{14}NO_2F$ and $^{15}NO_2F$ as well as the four τ values of $^{14}NO_2F$. This essentially means supplementing the type of data of the previous problem with the isotopic shifts.

For the B_2 species, it is now obvious that the solution is unique since the two B_2 frequencies of $^{15}NO_2F$ provide one more independent linear equation from eq. 6 in terms of the three compliance constants C_{55}, C_{66}, and C_{56}. This eliminates one of the two possible sets making the solution to the B_2 force field unique.

For the A_1 species we have five independent linear equations, in terms of the six compliance constants, coming from [3] and [8], and two quadratic equations coming from [4] for the two molecules. These are easily seen to be adequate

[2]For a 2×2 case, even in the force constant scheme, the equation analogous to [8] is linear. Since $|\mathbf{F}| = \lambda_5\lambda_6/|\mathbf{G}|$, we have

$$\tau_{abab} = -2(I_a^e I_b^e I_c^e I_d^e)\tau_{abab}$$
$$= |\mathbf{G}|/\lambda_5\lambda_6[(J_{ab}{}^5)^2 F_{66} + (J_{ab}{}^6)^2 F_{55} - 2(J_{ab}{}^5 \cdot J_{ab}{}^6)F_{56}]$$

Can. J. Chem. Downloaded from www.nrcresearchpress.com by 210.87.254.5 on 09/05/12
For personal use only.

to establish the uniqueness of the A_1 species force field.

H_2CO, D_2CO, HDCO, and $H_2{}^{13}CO$ (Frequencies)

Formaldehyde provides one of the most illuminating examples illustrating the occurrence of two indistinguishable sets of force constants (2). We shall therefore treat this case in a little more detail.

Duncan and Mallinson (6) have obtained the best set of force constants for formaldehyde using all the available data. They have noted that the physically-reasonable alternative set of A_1 species force constants determined from the frequency data of H_2CO, D_2CO, and HDCO (2) is incompatible with the ^{13}C frequency shifts. We now show that these frequency shifts provide the *minimum* extra data necessary to make the force field unique. We assume that the given data consist of the frequencies of all the four molecules[3] and note that the B_2 species force field is uniquely determined. The nine data of H_2CO, D_2CO, and $H_2{}^{13}CO$ give rise to nine equations in terms of the six compliance constants C_{ij}: three linear, three quadratic, and three cubic coming from eqs. 3, 4, and 5 respectively.

For HDCO, the secular equation being of order five ($5A' \leftarrow 3A_1 + 2B_2$) gives rise to five polynomial equations of degrees 1 to 5. Since the B_2 force field is known, the fifth degree equation reduces to a cubic equation $\mathscr{C}_3 = 0$ in terms of the six compliance constants of the A_1 species. As a result, the cubic and quartic equations reduce to quadratic equations in six variables. These equations are somewhat tedious to form and since it is not necessary to consider them in the present context we shall ignore them.

The four linear equations are given by

$$[9]\quad L_i \equiv K_{11}{}^iC_{11} + K_{22}{}^iC_{22} + 2K_{33}{}^iC_{33} + 2K_{12}{}^iC_{12} + 2K_{13}{}^iC_{13} + 2K_{23}{}^iC_{23} = \mu_i$$

where $i = 1, 2, 3$, and 4 indexes the isotopes H_2CO, D_2CO, HDCO, and $H_2{}^{13}CO$ respectively. μ_i consists of given data and for HDCO includes additional terms involving C_{55}, C_{66}, and C_{56} which are known. The advantage of analyzing the uniqueness problem in the compliance scheme lies in the fact that the above four equations are completely independent unlike in the force constant scheme (10). Solving them for C_{11}, C_{22}, C_{33}, and C_{12} in terms of $x = C_{13}$ and $y = C_{23}$ and substituting in [4] and [5], we have

$$[10]\quad Q_i(x, y) \equiv A_ix^2 + 2H_ixy + B_iy^2 + 2U_ix + 2V_iy + W_i = 0$$

for $i = 1, 2, 3, 4$ and

$$[11a]\quad \mathscr{C}_1(x, y) \equiv C_{22}x^2 - 2C_{12}xy + C_{11}y^2 + [\lambda_1\lambda_2\lambda_3/|\mathbf{G}^{-1}| - C_{33}(C_{11}C_{22} - C_{12}{}^2)] = 0$$

$$[11b]\quad \equiv a_{30}x^3 + a_{21}x^2y + a_{12}xy^2 + a_{03}y^3 + a_{20}x^2 + a_{11}xy + a_{02}y^2 + a_{10}x + a_{01}y + a_0$$

The remaining three cubic equations are not independent of $\mathscr{C}_1 = 0$ and lead to three product rule relations. The coefficients in eqs. 10 and 11*b* are functions of K_{ij} and ϕ_i. For given values of C_{11}, C_{22}, C_{33}, and C_{12}, eq. 11*a* becomes a quadratic equation in x and y.

The force constants of formaldehyde for the A_1 and B_2 species obtained by Duncan and Mallinson (6), along with the corresponding compliance constants, are given in Table 1. When the minimum number of algebraic equations is used, as in the above, the calculated compliance (force) constants are extremely sensitive to the data used. Thus for the sake of consistency, we take as data the calculated values obtained by using the best and unique set of force constants (6).

It is instructive to solve the above equations in a graphical form. Equation 10 in general represents an ellipse, a parabola, or a hyperbola depending upon whether $H_i^2 - A_iB_i$ is negative, zero, or positive, respectively. In the present case, all the four eqs. 10 are found to represent ellipses, the values of $H_i^2 - A_iB_i$ ($i = 1, 2, 3, 4$) being -14.36, -105.34, -42.19, and -15.11. These were drawn to scale using a CalComp plotter under the control of a PDP-11 computing system. Figure 1 shows the two ellipses $Q_1 = 0$ and $Q_2 = 0$ representing H_2CO and D_2CO molecules. $Q_1(x, y) = 0$ and $Q_2(x, y) = 0$ which in general have four common points of intersection can be seen to be intersecting at two real points ($x_1 = -0.037$, $y_1 = 0.059$) and ($x_2 = -0.047$, $y_2 = 0.044$) which are close to each other. The remaining two points correspond to complex roots. The two sets of compliance con-

[3]Even though only one of the isotopic shifts, $\Delta\nu_2(^{12}C—^{13}C)$, is known experimentally at present, it does not in any way vitiate the method of analysis presented here.

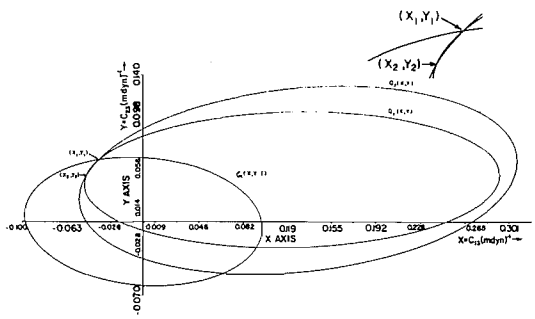

FIG. 1. Ellipses $Q_1 = 0$, $Q_2 = 0$, and $\mathscr{C}_1(I) = 0$ (see eqs. 10 and 11*a*) representing H_2CO, D_2CO, and H_2CO, respectively. Their common point of intersection corresponding to the unique solution to the force field gives the compliance constants $C_{13} = -0.037$ and $C_{23} = 0.059$ in units of mdyn^{-1}. The inset shows the points of intersection.

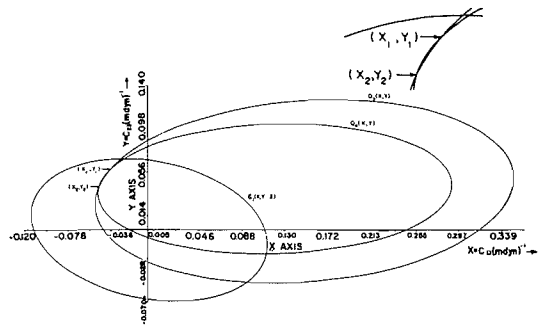

FIG. 2. Ellipses $Q_3 = 0$ and $Q_4 = 0$ (see eq. 10) representing HDCO and $H_2{}^{13}CO$ respectively. They intersect in the same two points (x_1,y_1) and (x_2,y_2) as do $Q_1 = 0$ and $Q_2 = 0$ (see Fig. 1). $\mathscr{C}_1(II) = 0$ representing H_2CO (see eq. 11*a*) can be seen to be incompatible with both the points. The inset shows the points of intersection.

stants C_{11}, C_{22}, C_{33}, and C_{12} corresponding to (x_1,y_1) and (x_2,y_2) are now obtained using the four linear eqs. 9. These values are also given in Table 1 as Sets I and II.

Ellipses $Q_3 = 0$ and $Q_4 = 0$, shown in Fig. 2, representing HDCO and $H_2{}^{13}CO$ are found to intersect at exactly the same two points (x_1,y_1) and (x_2,y_2). Thus these two equations are of no help in determining a unique solution.

Now a simple way to demonstrate that the cubic equation $\mathscr{C}_1 = 0$ weeds out Set II is by considering eq. 11*a* instead of [11*b*]. For the two sets of C_{11}, C_{22}, C_{33}, and C_{12} values corresponding to the two points of intersection (x_1,y_1) and (x_2,y_2), we have two quadratic equations $\mathscr{C}_1(x,y:I) = 0$ and $\mathscr{C}_1(x,y:II) = 0$ in x and y which are again found to represent ellipses. These were drawn in Figs. 1 and 2. While $\mathscr{C}_1(I) = 0$ in Fig. 1 is found to eliminate (x_2,y_2), retaining Set I as the unique solution to the force field, $\mathscr{C}_1(II) = 0$ in Fig. 2 can be seen to be incompatible with both the sets. Incidentally the method also suggests that we have effectively used seven data in obtaining a unique set of six compliance constants. The best set of potential constants is of course obtained by the least-squares refinement procedure employing all the data (6).

Conclusions

In this paper it is shown that the uniqueness of a 3 × 3 harmonic force field can be established more easily than has been thought possible hitherto. A similar analysis wherever possible

TABLE 1. The A_1 and B_2 species force field of formaldehyde (6)

Species	Force constant*	Value	Compliance constant*	Value	Compliance constants Set I	Compliance constants Set II
A_1	F_{11}	4.963	C_{11}	0.2040	0.2039	0.2171
	F_{22}	12.903	C_{22}	0.0801	0.0801	0.0801
	F_{33}	0.570	C_{33}	1.8016	1.8019	1.7698
	F_{12}	0.739	C_{12}	−0.0128	−0.0126	−0.0282
	F_{13}	0.077	C_{13}	−0.0367	−0.0366	−0.0469
	F_{23}	−0.408	C_{23}	0.0591	0.0593	0.0443
B_2	F_{55}	4.852	C_{55}	0.2076		
	F_{66}	0.833	C_{66}	1.2092		
	F_{56}	0.171	C_{56}	−0.0426		

*Units of F_{ij} are mdyn Å^{-1} for stretching, mdyn for stretch–bend and mdyn Å for bending force constants; units of C_{ij} are Å mdyn^{-1} for stretching, mdyn^{-1} for stretch–bend and (mdyn Å)$^{-1}$ for bending compliance constants.

Can. J. Chem. Downloaded from www.nrcresearchpress.com by 210.87.254.5 on 09/05/12
For personal use only.

can be carried out for several molecules, with a variety of data, involving 3 × 3 force fields. It may be noted that the simplified nature of the analysis is a consequence of choosing the compliance scheme.

We thank Dr. G. D. Zeiss for his help in plotting the curves shown in Figs. 1 and 2. This work was supported by the National Research Council of Canada.

1. A. R. Hoy, J. M. R. Stone, and J. K. G. Watson. J. Mol. Spectrosc. **42**, 393 (1972).
2. D. C. McKean and J. L. Duncan. Spectrochim. Acta, **27**A, 1879 (1971).
3. D. C. Moule and Ch. V. S. Rao. J. Mol. Spectrosc. **48**, 560 (1973).
4. A. M. Mirri, L. Ferretti, and P. Forti. Spectrochim. Acta, **27**A, 937 (1971).
5. A. M. Mirri, G. Cazzoli, and L. Ferretti. J. Chem. Phys. **49**, 2775 (1968).
6. J. L. Duncan and P. D. Mallinson. Chem. Phys. Lett. **23**, 597 (1973).
7. J. C. Decius. J. Chem. Phys. **38**, 241 (1963).
8. D. Kivelson and E. B. Wilson, Jr. J. Chem. Phys. **21**, 1229 (1953).
9. J. L. Coolidge. A treatise on algebraic plane curves. Dover Publications, Inc., New York. 1959. p. 10.
10. J. Wright and Ch. V. S. Rao. J. Mol. Spectrosc. **51**, 520 (1974).

Can. J. Chem. Downloaded from www.nrcresearchpress.com by 210.87.254.5 on 09/05/12
For personal use only.

Protonation du *N,N*-diméthylformamide: étude par spectrométries vibrationnelle et électronique

P. COMBELAS, M. COSTES ET C. GARRIGOU-LAGRANGE
Centre de Recherches Paul Pascal, Domaine Universitaire, 33405 – Talence, France

Reçu le 27 juin 1974

P. COMBELAS, M. COSTES et C. GARRIGOU-LAGRANGE. Can. J. Chem. **53**, 442 (1975).

Les spectres infrarouges et Raman du diméthylformamide en solution aqueuse acide (chlorhydrique ou sulfurique) montrent l'existence d'un seul équilibre de protonation

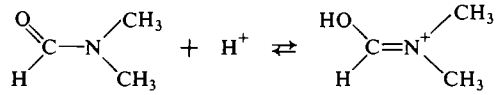

Le pK correspondant, déterminé par spectroscopie ultraviolette, est égal à -1.35 ± 0.05; par spectroscopie Raman, une valeur moins précise (-1.1 ± 0.5) a été obtenue. Ces résultats infirment certaines conclusions précédentes tendant à mettre en évidence l'existence de deux équilibres d'ionisation du diméthylformamide.

P. COMBELAS, M. COSTES, and C. GARRIGOU-LAGRANGE. Can. J. Chem. **53**, 442 (1975).

Infrared and Raman spectra of acidic (hydrochloric or sulfuric) aqueous solutions of dimethylformamide indicate the existence of a single protonation equilibrium.

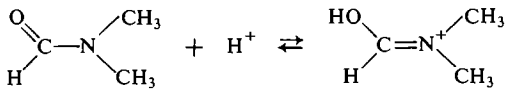

The pK for this reaction was evaluated as -1.35 ± 0.05 from u.v. spectra; a less precise value (-1.1 ± 0.5) was obtained from Raman spectra. This result disagrees with earlier conclusions which favored the existence of two ionization equilibria for dimethylformamide.

[Journal translation]

Parmi les composés organiques, les amides possèdent des propriétés basiques relativement importantes. Leur protonation par les acides minéraux ou organiques a fait l'objet d'un très grand nombre de travaux à la fois qualitatifs (localisation du site de protonation) et quantitatifs (détermination des pK).

Il résulte de ces études que le proton se fixe préférentiellement sur l'oxygène (1), et que les pK sont proches de zéro (2). Toutefois certains travaux récents effectués par r.m.n. montrent qu'on ne peut pas éliminer une faible protonation sur l'azote (3). Certains auteurs interprètent d'ailleurs leurs résultats obtenus par spectrométrie ultraviolette par l'existence de deux valeurs de pK (4), interprétation contestée par d'autres auteurs (5).

La spectrométrie de vibration doit permettre de montrer s'il existe une ou deux espèces protonées. Jusqu'à présent, à notre connaissance, peu d'études de ce type ont été faites. Spinner (6) analysant les spectres infrarouges et Raman du *N,N*-dimethylformamide (DMF) en solution aqueuse chlorhydrique ou sulfurique et à l'état de chlorhydrate solide, conclut à la présence de la forme ionique classique

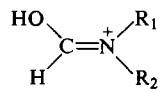

1

et, en outre, d'une forme pouvant avoir l'une des structures (**2**) ou (**3**) selon le milieu considéré

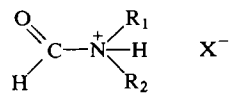

2

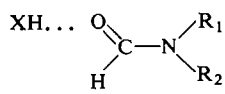

3

Can. J. Chem. Downloaded from www.nrcresearchpress.com by 210.87.254.40 on 09/05/12
For personal use only.

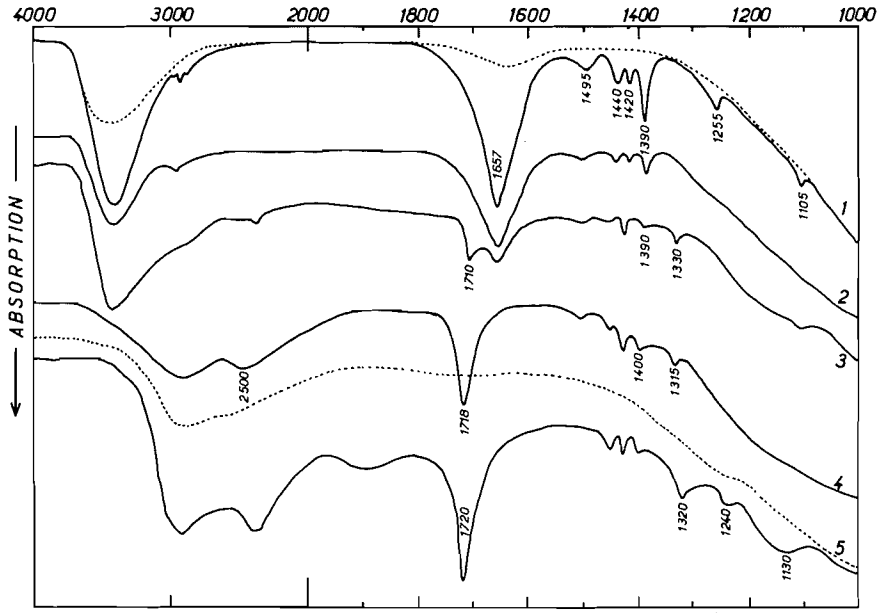

FIG. 1. Spectres infrarouges entre 4000 et 1000 cm^{-1} du DMF (5 *M*) dans des solutions aqueuses sulfuriques à différentes concentrations (*X M*) en acide sulfurique. *1*, $X = 0$; *2*, $X = 4$; *3*, $X = 8$; *4*, $X = 18.5$, DMF = 7.5 *M*. Courbes en pointillés: spectre du solvant en l'absence d'amide. Conditions experimentales: spectromètre Perkin–Elmer 225, cellule CaF_2 de quelques microns d'épaisseur.

Une étude de l'hydratation et de la protonation du *N,N*-diméthylacétamide (DMA) (7) nous avait permis de conclure à l'existence des équilibres suivants

[1] $$B + H_2O \rightleftarrows B \ldots H_2O$$

[2] $$B \ldots H_2O + H^+ \rightleftarrows BH^+ \ldots H_2O$$

excluant toute autre forme d'interaction amide–acide. Il nous a semblé intéressant de reprendre ce type de travail dans le cas du DMF et d'y adjoindre la mesure du (ou des) p*K* en utilisant plusieurs techniques complémentaires: les spectrométries ultraviolette, infrarouge et Raman.

Dans une première partie, nous analyserons les spectres de vibration du DMF en solution aqueuse chlorhydrique ou sulfurique, tandis que, dans la seconde partie, nous déterminerons le p*K* du DMF dans ces solutions.

Analyse des spectres de vibration du DMF en solution aqueuse acide

Sur les figs. 1, 2 et 3 sont représentés les spectres infrarouges et Raman du DMF en solution aqueuse à diverses concentrations d'acide sulfurique (figs. 1, 3) ou chlorhydrique (fig. 2).

Les variations spectrales les plus nettes que l'on peut observer se situent dans le domaine 1600–1800 cm^{-1} où se trouve la bande de vibration de valence νC=O de l'amide. En l'absence d'acide, la fréquence de cette bande est de 1657 cm^{-1} environ. Elle correspond à l'amide neutre dont les groupements carbonyle sont liés à l'eau

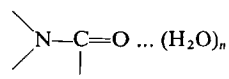

4

une ou deux liaisons hydrogène pouvant s'établir sur l'atome d'oxygène de ce groupe amide (7). Par additions d'acide chlorhydrique ou sulfurique, cette bande tend à disparaître progressivement au profit d'une bande de plus haute fréquence entre 1700 et 1720 cm^{-1} qui subsiste seule dans les spectres des solutions les plus acides. Ceci semble correspondre à un équilibre entre deux formes amide, l'une neutre (**4**), l'autre (**1**) résultant de l'interaction avec l'acide. Par analogie avec nos précédents résultats (7, 8), cette deuxième forme est attribuée aux espèces protonées

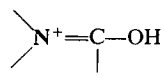

1

probablement liées à l'eau.

Can. J. Chem. Downloaded from www.nrcresearchpress.com by 210.87.254.40 on 09/05/12
For personal use only.

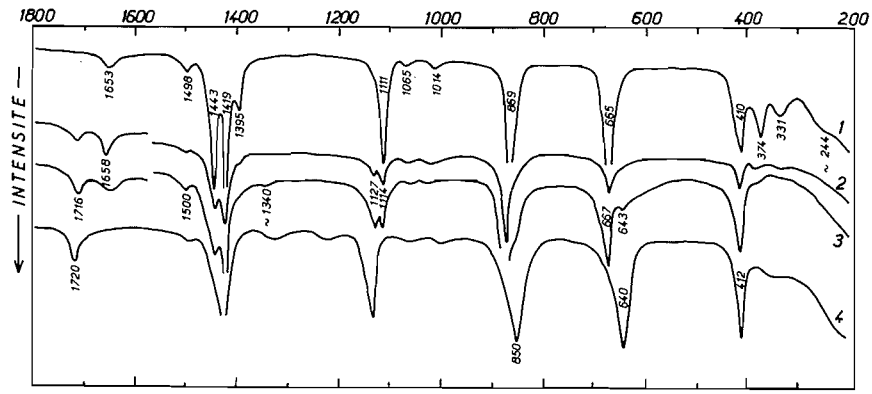

FIG. 2. Spectres Raman entre 1800 et 200 cm^{-1} du DMF (2.5 *M*) dans des solutions aqueuses chlorhydriques à différentes concentrations (*X M*) en acide chlorhydrique. Spectromètre Coderg PHl. Laser He–Ne. *1*, $X = 0$; *2*, $X = 4.2$; *3*, $X = 6.3$; *4*, $X = 12.6$.

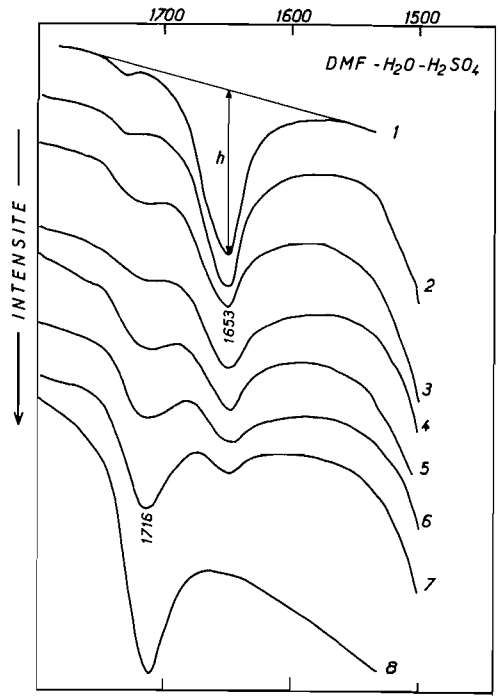

FIG. 3. Spectres Raman entre 1800 et 1500 cm^{-1} du DMF dans des solutions aqueuses sulfuriques à différents pourcentages *P* en acide sulfurique. Concentrations en DMF: *cf.* tableau 1. Spectromètre Coderg PHl. Laser He–Ne Spectra Physics modèle 125(63 mW). Température voisine de 22 °C. *1*, $P = 1.5$; *2*, $P = 6$; *3*, $P = 12$; *4*, $P = 18$; *5*, $P = 24$; *6*, $P = 27$; *7*, $P = 35$; *8*, $P = 46.5$.

La bande intense à $\simeq 1700\,cm^{-1}$ caractéristique de la protonation n'a pas encore été attribuée de manière indiscutable dans les sels d'amide. Nous la faisons correspondre comme dans le cas du DMA (7) à la vibration $\nu C{=}N^+$. Sa fréquence varie quelque peu avec l'acidité (figs. 1–3) ce qui peut être relié à une influence du milieu sur les ions.

On note par ailleurs, d'une part, l'apparition d'une absorption large vers 2500 cm^{-1} (fig. 1) qui peut correspondre à la vibration νOH des cations amidium (**1**) (7) et d'autre part une faible bande à environ 1340 cm^{-1} (figs. 1 et 2) qui peut résulter du couplage entre les vibrations νCO et δOH du DMF protoné (7).

Cette interprétation qualitative des spectres ne conduit donc à envisager, contrairement à Spinner (6), qu'un seul type d'équilibre entre deux formes: amide neutre et amide protoné, cette dernière ayant la structure classique (**1**). Il apparaît difficile d'introduire une autre espèce de type ionique (**2**) ou non-ionique (**3**) caractérisée par une bande $\nu C{=}O$ de fréquence identique à celle de l'amide neutre associé à l'eau (**4**) et qui n'existerait que dans le cas de l'acide chlorhydrique ou du chlorhydrate solide. En effet nos résultats sont très comparables d'un acide à l'autre, en infrarouge et en Raman, seules les concentrations d'acide et d'amide utilisées pouvant perturber l'allure des spectres en modifiant le nombre de chaque espèce.

Spinner (6) appuyait son raisonnement sur une valeur du p*K* du DMF proche de 0 à −0.5 par comparaison avec le résultat trouvé par Huisgen *et coll.* (9) dans un mélange acide perchlorique – acide acétique glacial, aucune mesure n'ayant été faite en milieu aqueux.

Nous avons donc déterminé le p*K* du DMF dans les solutions d'acide chlorhydrique et sulfurique.

Can. J. Chem. Downloaded from www.nrcresearchpress.com by 210.87.254.40 on 09/05/12
For personal use only.

Can. J. Chem. Downloaded from www.nrcresearchpress.com by 210.87.254.40 on 09/05/12
For personal use only.

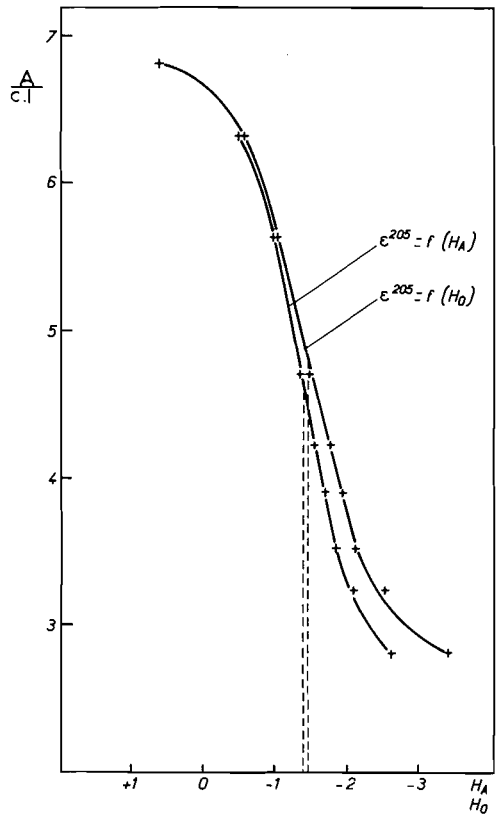

FIG. 4. Variation de l'absorbance à 205 mμ de différentes solutions de DMF–H_2O–H_2SO_4 en fonction de H_0 et de H_A. Spectromètre Cary 16 purgé à l'azote. Température voisine de 22 °C. Cellule de quartz d'épaisseur 2 mm. Concentration du DMF: 10^{-3} *M*.

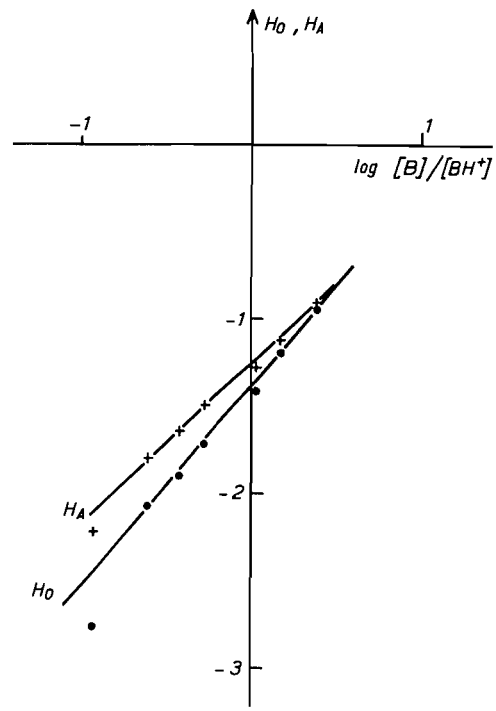

FIG. 5. Evolution du rapport log |B|/|BH^+| du DMF mesuré par spectrométrie ultraviolette en fonction de H_0 et H_A pour H_2SO_4.

Détermination du p*K* du DMF en solution aqueuse acide

Dans le cas de la protonation d'une base faible par un acide fort, il n'est pas possible d'utiliser l'échelle habituelle des p*H*. La concentration en acide demandée pour les réactions étant souvent très importante, il est impossible de faire l'approximation de la solution idéale et il faut tenir compte des coefficients d'activité. La détermination de ces coefficients étant longue et difficile, Hammett (10*a*) a établi empiriquement une fonction d'acidité H_0 définie par la relation 3

$$[3] \qquad H_0 = \mathrm{p}K_{\mathrm{BH}^+} + \log \frac{|\mathrm{B}|}{|\mathrm{BH}^+|}$$

|B| et |BH^+| étant les molarités des formes libres et protonées et il a dressé des tables de valeurs H_0 pour un certain nombre d'acides forts.

Pour déterminer les molarités |B| et |BH^+|, deux techniques ont été utilisées: la spectrométrie ultraviolette, méthode classique de mesure (10*b*), et la spectrométrie Raman, technique plus délicate en raison des sources d'erreurs expérimentales.

Mesures effectuées par spectroscopie ultraviolette

Nous avons étudié la région 180–230 mμ caractéristique de l'absorption du DMF. La fig. 4 montre la variation de l'absorbance à 205 mμ avec les fonctions H_0 et H_A, cette dernière étant plus spécialement adaptée aux amides (11). Ces deux courbes présentent un point d'inflexion qui donne la valeur du p*K* au point de demi-neutralisation, soit: p$K \simeq -1.4$.

L'application de la relation (3) aux résultats obtenus pour chaque fonction d'acidité est représentée sur la fig. 5. Les droites ainsi tracées ont des pentes voisines de 1 (0.95 et 1.20) et leur ordonnée à l'origine conduit à une valeur moyenne du p*K* de -1.35 ± 0.05. Elle est en accord avec un résultat r.m.n. (12) (p$K = -1.34$) publié au cours de ce travail, mais non pas avec les mesures cryoscopiques (13) et potentio-

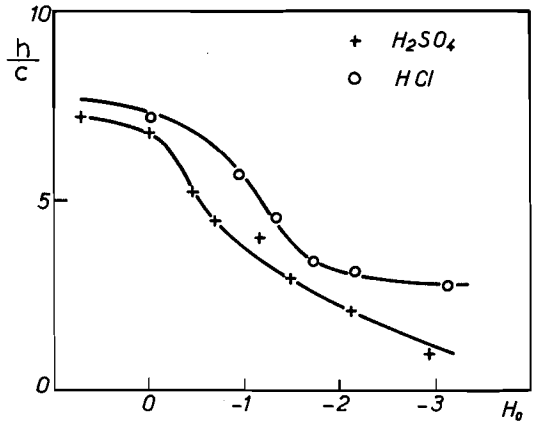

FIG. 6. Variation de l'intensité diffusée à 1650 cm^{-1} du DMF en solution aqueuse sulfurique ou chlorhydrique en fonction de H_0.

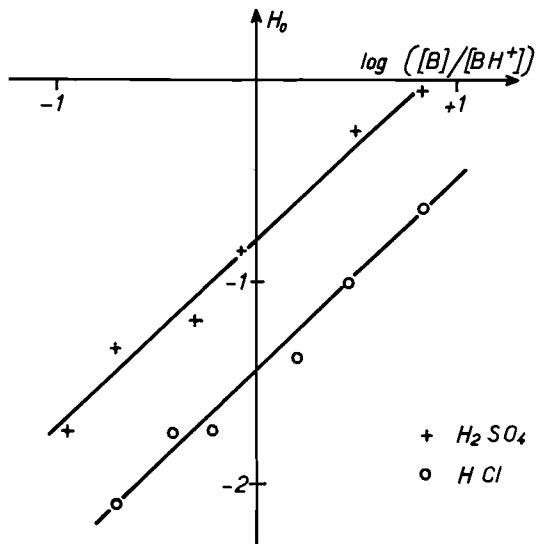

FIG. 7. Evolution du rapport log $|B|/|BH^+|$ du DMF mesuré par spectrométrie Raman en fonction de l'acidité H_0 pour H_2SO_4 et HCl.

métriques (9) ($pK \simeq 0$), relatives à d'autres milieux.

Mesures effectuées par spectrométrie Raman

Peu de travaux de ce type ont été réalisés jusqu'à maintenant. On note les résultats de Deno et Wisotsky (14) sur différentes molécules: acétamide, méthanol, dioxane, acétone et acétonitrile. De nombreux paramètres plus ou moins contrôlables affectent la précision de telles mesures (diffusion parasite, dépoussiérage des

TABLEAU 1. Protonation du DMF par l'acide sulfurique

DMF (mol/l)	H_2SO_4 (%)	$H_0(16)$	α^{1650}
3.86	0		8.2
3.84	1.5	0.70	7.2
3.84	6	0	6.8
3.90	12	−0.55	5.2
3.88	18	−0.90	4.4
3.76	24	−1.35	4.0
3.74	27	−1.55	2.9
3.88	35	−2.10	2.1
3.86	46.5	−2.95	1.0

TABLEAU 2. Protonation du DMF par l'acide chlorhydrique

DMF (mol/l)	HCl (%)	$H_0(15)$	α^{1650}
3.84	2.3	0	7.2
3.93	8.7	−0.90	5.7
3.85	12.9	−1.35	4.5
3.82	16.7	−1.75	3.4
3.85	20.5	−2.15	3.2
3.76	28.1	−3.1	2.8

solutions, stabilité de la source laser, fluorescence éventuelle, etc.). Par ailleurs, la faible intensité des bandes intéressantes conduit à étudier des solutions nettement plus concentrées en amide que lors des expériences précédentes ($\simeq 3$ M au lieu de 10^{-3} M). Ces concentrations étant très élevées, il faudrait pour être exact utiliser les coefficients d'activité.

Une étude préalable de mélanges binaires DMF–eau de diverses concentrations en amide permet de vérifier la loi de diffusion $h = \alpha_v C$ avec h = hauteur de la bande déterminée comme l'indique la fig. 3; C = molarité du DMF; α_v = coefficient de diffusion englobant tous les autres paramètres.

Cette loi testée sur les bandes ν(C=O) à 1650 cm^{-1} et ν(CH) à 2950 cm^{-1} donne,[1] dans le domaine des concentrations utilisées, de très bonnes relations linéaires $h = \alpha_v C$. Celle qui est obtenue pour la vibration de valence carbonyle peut en outre servir de courbe étalon pour les mélanges ternaires acides et donner ainsi les quantités $|B|$ et $|BH^+|$ à l'équilibre.

[1]L'intensité de cette dernière bande a été utilisée par la suite comme référence.

Can. J. Chem. Downloaded from www.nrcresearchpress.com by 210.87.254.40 on 09/05/12
For personal use only.

Dans le cas des solutions acides, toutes précautions ont été prises afin de limiter au maximum les risques d'hydrolyse du DMF (solutions refroidies lors de leur préparation, enregistrement immédiat des spectres). On ne constate ainsi aucune modification sensible des spectres dans un délai de 30 min.

Les résultats obtenus pour H_2SO_4 et HCl sont rassemblés dans les tableaux 1 et 2 et sur les figs. 6 et 7. Les valeurs des pK obtenues en utilisant la fonction H_0 (figs. 6, 7) sont p$K \simeq -0.9$ pour H_2SO_4 et p$K \simeq -1.3$ pour HCl.

On est conduit à prendre une valeur moyenne de l'ordre de -1.1 ± 0.5 qui, compte tenu du manque de précision de cette technique, semble en assez bon accord avec les mesures u.v. et r.m.n. Ceci est intéressant à noter étant donné la grande différence de concentration en amide qui existe entre ces diverses mesures.

Ces études quantitatives u.v. et Raman mettent ainsi en évidence une valeur unique du pK d'ionisation contrairement aux conclusions de divers auteurs (4, 6). Elles sont cohérentes avec l'interprétation qualitative des spectres de vibration que nous avons proposée dans la première partie. Nous pensons que les phénomènes secondaires pouvant parfois être observés sur les spectres (déplacement de fréquences des bandes, apparente variation du pK) doivent s'interpréter, comme l'ont suggéré certains auteurs (5, 11) par des effets du milieu sur les ions.

Nous remercions Mademoiselle H. Richard de l'aide qu'elle nous a apportée pour l'enregistrement et l'étude des spectres ultraviolets.

1. W. E. Stewart et T. H. Siddall, III. Chem. Rev. **70**, 517 (1970).
2. E. M. Arnett. Progress in physical organic chemistry, Vol. 1. 1963. p. 223.
3. B. G. Cox. J. Chem. Soc. B, 1780 (1970).
4. A. R. Goldfarb, A. Mele et N. Gutstein. J. Am. Chem. Soc. **77**, 6194 (1955).
5. J. T. Edward et I. C. Wang. Can. J. Chem. **40**, 966 (1962).
6. E. Spinner. Aust. J. Chem. **19**, 2091 (1966).
7. C. de Lozé, P. Combelas, P. Bacelon et C. Garrigou-Lagrange. J. Chim. Phys. **69**, 397 (1972).
8. P. Combelas, F. Cruege, J. Lascombe, C. Quivoron et M. Rey-Lafon. J. Chim. Phys. **66**, 668 (1969).
9. R. Huisgen et H. Brade. Chem. Ber. **90**, 1432 (1957).
10. (*a*) C. P. Hammett. Physical organic chemistry. McGraw-Hill Book Co., New York, N.Y. 1940. p. 267; (*b*) H. M. Irving, H. S. Rossotti, and G. Harris. Analyst, **80**, 83 (1955).
11. K. Yates et J. Stevens. Can. J. Chem. **43**, 529 (1965).
12. M. Liler. J. Chem. Soc. B, 334 (1971).
13. R. Schaal. J. Chim. Phys. **52**, 719 (1955).
14. N. C. Deno et M. J. Wisotsky. J. Am. Chem. Soc. **85**, 1735 (1963).
15. K. Yates et J. C. Riordan. Can. J. Chem. **43**, 2328 (1965).
16. W. A. Paul et F. A. Long. Chem. Rev. **57**, 1 (1957).

Can. J. Chem. Downloaded from www.nrcresearchpress.com by 210.87.254.40 on 09/05/12
For personal use only.

Kinetics of Environmental Averaging, and the Stereochemistry of $(CH_3)ClGe(C_5H_7O_2)_2$. A Case of a Second Order Kinetic Process

KEN A. HERSH AND NICK SERPONE[1]

Department of Chemistry, Sir George Williams Campus, Concordia University, Montreal, Quebec H3G 1M8

Received September 3, 1974

KEN A. HERSH, and NICK SERPONE. Can. J. Chem. **53**, 448 (1975).

Dynamic n.m.r. studies on the stereochemistry of $(CH_3)ClGe(C_5H_7O_2)_2$ (acac = $C_5H_7O_2^-$), indicate that the complex adopts the *cis* configuration in $CDCl_3$–CCl_4 solutions. Kinetics of environmental averaging of the acac ring proton (—CH=) and acac methyl groups between the respective nonequivalent sites in the C_1 isomer have been investigated in the temperature range −31.0 to 23.1° by line-broadening techniques. Kinetics of the averaging process are second order in complex concentration. Activation parameters are: $E_a = 6.0 \pm 0.3$ kcal/mol, $\Delta S^* = -30 \pm 1$ e.u., and $k_{25} = 1.6 \times 10^2\ M^{-1}\ s^{-1}$. Rearrangements are viewed as occurring via a germanium–oxygen bond rupture as a first step to yield a five-coordinate intermediate. The rate-determining sequence is thought to involve proper orientation of two five-coordinate species prior to formation of a bis-acac bridged dimer.

KEN A. HERSH et NICK SERPONE. Can. J. Chem. **53**, 448 (1975).

Des études de r.m.n. dynamique sur la stéréochimie du $(CH_3)ClGe(C_5H_7O_2)_2$ (acac = $C_5H_7O_2^-$), indiquent que le complexe adopte une configuration *cis* en solution dans $CDCl_3$–CCl_4. On a étudié, à des températures allant de −31.0° à 23.1° et en faisant appel aux techniques des élargissements de bandes, la cinétique de la répartition moyenne de l'environnement des protons du noyau acac (—CH=) et des groupes méthyles acac le tout entre les différents sites non équivalent dans l'isomère C_1. La cinétique de ces processus est du second ordre en concentration du complexe. Les paramètres d'activation sont $E_a = 6.0 \pm 0.3$ kcal/mol, $\Delta S^* = 30 \pm 1$ e.u., et $k_{25} = 1.6 \times 10^2\ M^{-1}\ s^{-1}$. On imagine que les réarrangements se produisent par l'intermédiaire de la rupture d'un lien germanium–oxygène dans une première étape ce qui conduirait à un intermédiaire penta-coordonné. On croit que l'étape déterminante de la réaction implique l'orientation correcte des deux espèces penta-coordonnées avant la formation d'un dimère ponté impliquant un bis-acac. [Traduit par le journal]

Introduction

Recent publications (1–3) from this laboratory have reported on dynamic n.m.r. studies on the stereochemistry of, and on the kinetics and mechanism(s) of environmental averaging processes in the six-coordinate complexes $R_2Sn(acac)_2$ (1, 2), $RClSn(acac)_2$ (1, 2) (R = C_6H_5, CH_3; acac = $C_5H_7O_2^-$, anion of acetylacetone), and $(C_6H_5)ClM(acac)_2$ (3) (M = Ge, Si). It was established that these complexes adopt predominantly the *cis* structure in solution with $\lesssim 5\%$ of the *trans* form present in the $RClM(acac)_2$ chelates. Intramolecular, first-order environmental averaging of methyl groups in the C_2 diphenyltin compound, and of acac ring protons and acac methyl groups in the C_1 monochloro complexes was identified as occurring via a twist mechanism (see, for example, ref. 4 and references therein) if rearrangements proceed by a sole reaction pathway. We now wish to report our findings on the stereochemical nature, and on the configurational rearrangement processes in the six-coordinate $(CH_3)ClGe(acac)_2$ complex in chloroform-*d* – carbon tetrachloride solutions.

Similar studies (5, 6) on several dihalobis(β-ketoenolato)germanium(IV) complexes (halogen = chlorine, bromine, iodine; β-ketoenol = acetylacetone, pivaloylacetone, dipivaloylmethane (dpm)) have also been carried out. It was shown (5, 6) that the dichloro chelates are mainly *cis* in solution with about 15–20% of the *trans* isomer present (5). Aging a mixture of crystals of the two geometrical isomers of $Cl_2Ge(dpm)_2$, yielded the *trans* isomer (6). Also, on the basis of the kinetic data, a one Ge—O bond rupture was favored over a twisting, nonbond-rupture mechanism for the first order exchange of methyl groups between the two nonequivalent sites of the *cis* C_2 complexes (6).

[1]To whom all correspondence should be addressed.

Can. J. Chem. Downloaded from www.nrcresearchpress.com by 210.87.254.40 on 09/05/12
For personal use only.

Can. J. Chem. Downloaded from www.nrcresearchpress.com by 210.87.254.40 on 09/05/12
For personal use only.

Experimental

Methyltrichlorogermane was purchased from Alfa Inorganics and used as received. Acetylacetone (2,4-pentanedione) was Fisher Certified Reagent. Reagent grade carbon tetrachloride (Anachemia) and dichloromethane (Fisher) were dried by refluxing over calcium hydride chips (Fisher) and distilled therefrom prior to use. Chloroform-*d* was prepared as reported elsewhere (6, 7). Thallium(I) acetylacetonate was prepared by allowing excess acetylacetone to react with a suspension of thallous carbonate in 95% alcohol.

Melting points were determined with a Gallenkamp melting point apparatus (Model MF-370), and are uncorrected. Capillaries were sealed with modelling clay under dry nitrogen in a glove bag. Elemental analyses were performed by Galbraith Laboratories, Knoxville, Tenn.

Methylchlorobis(2,4-pentanedionato)germanium(IV)

The synthesis of this product is similar to that of the phenylchloro analogue (3). Thus reaction of thallous acetylacetonate (6.15 g, 21.3 mmol) with a 75-ml dry dichloromethane solution of methyltrichlorogermane (2.29 g, 11.8 mmol) gave a yield of 32% (1.20 g) of the desired white compound which was recrystallized from dichloromethane–hexane solution. M.p. 128–132° (dec.), lit. 128–132°.[2]

Anal. Calcd. for $C_{11}H_{17}O_4ClGe$: C, 41.12; H, 5.33. Analyses on two separate samples gave: C, 25.98, 15.98; H, 3.98, 3.13.

A gravimetric determination of chlorine on a freshly prepared sample in this laboratory gave 11.0% (calcd. 11.04).

This compound decomposes within 2–3 days. Purity of freshly prepared products was checked by infrared and n.m.r. spectra. Neither O—H stretching bands nor C—O stretching bands above 1600 cm^{-1} were observed. N.m.r. chemical shifts in $CDCl_3$–CCl_4/TMS (17.6 g/100 ml; ~31°), −1.11 p.p.m. (Ge—CH_3), −2.07 p.p.m. (acac—CH_3), and −5.57 p.p.m. (acac—CH=).

Nuclear Magnetic Resonance Spectra

Owing to the rapid decomposition of this complex, solutions were prepared under rigorous anhydrous conditions in a dry nitrogen atmosphere in a glove bag just prior to recording n.m.r. spectra. N.m.r. samples were flamesealed *in vacuo* after degassing. Solvent used consisted of a mixture (54.5/45.6 w/w) of chloroform-*d* and carbon tetrachloride to which was added TMS as an internal standard. Such mixture permitted spectra to be recorded down to temperatures of *ca.* −80° (8).

Proton chemical shifts (±0.02 p.p.m.) and variable temperature spectra were recorded in the frequency-sweep mode on a Varian HA-100 high-resolution n.m.r. spectrometer operating at 100.00 MHz and equipped with a V-6040 variable temperature controller and a V-4343 variable temperature probe accessories.

Probe temperatures were calculated with the Van Geet equations (9) and were measured as described earlier (1). Possible experimental errors, consequential in the accuracy of the results, have also been described elsewhere (1).

Determination of Residence Times

Residence times of a —CH= proton in a particular site were obtained from n.m.r. spectra recorded in the temperature range −31.0 to 23.1°. Selected n.m.r. lineshape parameters were: $W_{1/4}$, $W_{1/2}$, and $W_{3/4}$, the full linewidths at one-quarter, one-half, and three-quarters of maximum amplitude; $\delta\nu_e$, the chemical shift separation during exchange; and R, the ratio of maximum intensity to minimum central intensity at $(\nu_a + \nu_b)/2$. Average values of these parameters for five spectral scans are tabulated in Table 1. Mean residence times, $\tau = \tau_a\tau_b/(\tau_a + \tau_b)$, for exchange of ring protons were estimated by comparing experimental lineshape parameters with those from calculated spectra using the Gutowsky-Holm (10) total lineshape equation for two-site exchange. Procedures of the calculation have been detailed earlier (1, 11). The chemical shift separation, $\delta\nu$, is temperature dependent (see Fig. 1 of ref. 3);[3] transverse relaxation times, T_2, are also temperature dependent as evidenced from differences in $W_{1/2}$ of the —CH= proton resonances in the slow and fast exchange regions; *e.g.* $W_{1/2}$ at 55.6° is 0.74 Hz, while at −70.2° $W_{1/2}$ is 2.32 Hz (low field line) and 2.54 Hz (high field line), and at −80.7° the corresponding values are 8.58 and 9.33 Hz. Values in Hz for $\delta\nu_e$ at slow exchange are: 16.02 (−80.7°), 15.76 (−78.4°), 15.62 (−76.1°), 15.39 (−73.0°), 15.29 (−70.2°), 14.70 (−61.7°), 14.18 (−53.5°), 13.75 (−46.2°), and 12.98 (−36.8°); others are collected in Table 1. Values of the transverse relaxation times, $T_{2a} = T_{2b}$, were estimated from line-widths of the acetylacetonate —CH= proton signal of $(CH_3)_2Sn(acac)_2$ in $CDCl_3$–CCl_4/TMS (12).

Below coalescence (−13.3°), mean lifetimes were extracted from a comparison of R, $\delta\nu_e$, $W_{1/4}$, $W_{1/2}$, and $W_{3/4}$. At and above coalescence, τ values were determined by comparing experimental and calculated values of $W_{1/4}$, $W_{1/2}$, and $W_{3/4}$. Mean residence times (Table 1) are average values in which $\delta\nu_e$ was given a weighting factor of two.

The order of the kinetics of environmental averaging of —CH= protons was ascertained by determining mean lifetimes at four different concentrations in the range 0.27–0.52 M at −31.5° and −2.2°. These lifetimes were obtained by digitizing n.m.r. spectra point by point as intensity *vs.* frequency in Hz. Digitization and computer fitting of the spectra were accomplished as described elsewhere (14).

Results and Discussion

Stereochemistry

The stereochemistry of methylchlorobis(2,4-pentanedionato)germanium(IV), $(CH_3)ClGe$-

[2]While our studies were underway we learned that the stereochemistry of this complex and others was being investigated. We thank Professor D. W. Thompson for communicating his unpublished results to us.

[3]The parameter $\delta\nu$ was obtained at each temperature (below coalescence) from differences in chemical shifts (in Hz; 50 Hz spectra) of the resonances corresponding to the *a* and *b* sites of an AB uncoupled system for the acac—CH= proton. Values so obtained were plotted against temperature, and the linear portion of the plot extrapolated to get $\delta\nu$ values above coalescence.

Can. J. Chem. Downloaded from www.nrcresearchpress.com by 210.87.254.40 on 09/05/12
For personal use only.

TABLE 1. Variable temperature n.m.r. data for a 0.548 *M* solution of $(CH_3)ClGe(acac)_2$ in $CDCl_3$–CCl_4

Temperature (°C)	*R*		$\delta\nu_e$ (Hz)	Linewidth (Hz)					$\tau \times 10^2$ (s)
					$W_{1/2}$		$W_{3/4}$		
	Low field	High field		$W_{1/4}$	Low field	High field	Low field	High field	
−31.0	3.54	3.43	12.83[a]	—	4.02	4.23	2.14	2.26	6.03±0.32[b]
−23.0	1.96	1.93	11.45[a]	—		—	3.48	3.55	3.89±0.07
−18.0	1.20	1.20	9.05	—		—		—	2.94±0.26
−13.3(T_c)		—	—	19.61[a]		15.02[a]		11.36	2.57
−5.5		—	—	15.76		9.67		5.92	1.85±0.26
3.4		—	—	10.84		6.22		3.56	1.32±0.07
13.6		—	—	6.53		3.65		2.08	0.86±0.03
23.1		—	—	4.63		2.39		1.32	0.56±0.07

[a]Not used to evaluate τ values.
[b]Standard deviation.

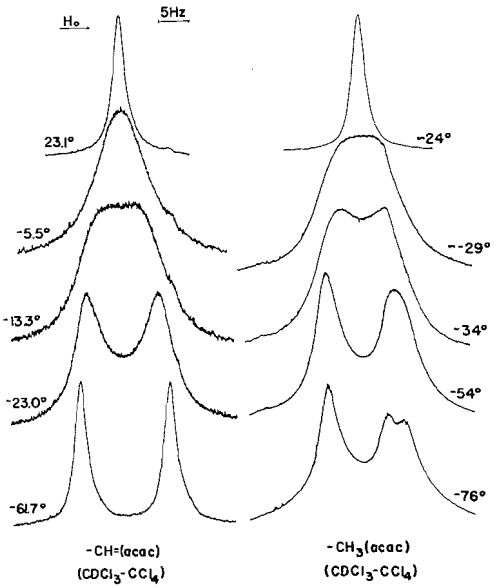

FIG. 1. Acetylacetonate ring proton and methyl proton n.m.r. spectra as a function of temperature for $(CH_3)ClGe(acac)_2$ in $CDCl_3$–CCl_4/TMS solutions.

$(acac)_2$, in solution may be inferred from proton n.m.r. spectra. Two diastereomeric forms are possible for this six-coordinate chelate: one with methyl and chloro groups in *cis* positions, and the other with the monodentate ligands *trans* to each other. The *cis* diastereomer (point group C_1) has no symmetry and, therefore, may give rise to four acetylacetonate methyl and two ring proton resonances. The *trans* form (C_{2v}) should reveal one acetylacetonate methyl and one —CH= proton resonance signal. Proton n.m.r. spectra at several selected temperatures between 23 and −76° are reproduced in Fig. 1. At ambient temperatures the proton spectrum consists of single, sharp ring proton ($W_{1/2}$ = 0.74 Hz) and methyl proton resonances. Below room temperature, line broadening is observed. The methyl resonance begins to split into two lines at *ca.* −29°, and at *ca.* −54° the upfield line splits again to give a total of four lines in the low temperature region (the downfield doublet is unresolved probably owing to chemical shift degeneracy of the two components). The ring proton spectrum reveals a doublet at −61.7°; with increasing temperature the two components broaden and collapse at −13.3°. Line broadening is ascribed to an environmental averaging process which exchanges ring protons and methyl groups between the respective two and four nonequivalent sites of the *cis* diastereomer. An additional observation in the —CH= proton spectrum is a slightly perceptible resonance on the high field side of the upfield component. This resonance is attributed (1, 3) to a small amount (probably not more than 5%) of the *trans* isomer; the corresponding methyl signal is apparently masked by the more intense signals of the *cis* diastereomer.

Kinetics of Environmental Averaging

In the present case, Fig. 1 shows that resonance lines due to nonequivalent nuclei (two —CH= protons and four CH_3 groups) simultaneously broaden and then merge into a single ring proton and a single methyl resonance. These spectra imply simultaneous time-averaging of the four methyl group environments and of the two ring proton environments. Six, independent, first-order rate constants are needed to describe the four-site exchange process. Such an analysis is complicated even with the availability of fast digital computers, and to make matters worse, relaxation times T_2 appear to be temperature dependent (see Experimental section). We have chosen, instead, to study the environmental averaging process by means of the two-site exchange of ring protons owing to its greater simplicity; only one first-order rate constant is required. Mean lifetimes (Table 1) for a —CH= proton in a particular site were obtained from comparisons of experimental spectra with those computed by the Gutowsky–Holm (10) method. In Fig. 2a are illustrated experimental spectra at −2.2° for several concentrations; Fig. 2b shows the comparison between the experimental spectra (solid circles) and the computer-fitted spectra (solid triangles; open circles represent good fit).

Concentration dependence of the mean residence times, summarized in Table 2, indicates that environmental averaging of proton resonances in $(CH_3)ClGe(acac)_2$ is concentration dependent and is second order. This dependence is also pictured in Fig. 3 which shows linear plots of τ_A *vs.* $[(CH_3)ClGe(acac)_2]^{-1}$ at −31.5° and −2.2°. Thus, the rate of environmental averaging may be written as Rate = $k[(CH_3)ClGe(acac)_2]^2$ since

Can. J. Chem. Downloaded from www.nrcresearchpress.com by 210.87.254.40 on 09/05/12
For personal use only.

Can. J. Chem. Downloaded from www.nrcresearchpress.com by 210.87.254.40 on 09/05/12
For personal use only.

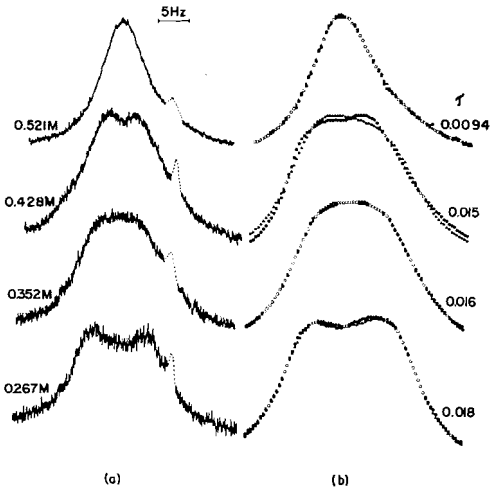

FIG. 2. Acetylacetonate ring proton n.m.r. spectra as a function of concentration of $(CH_3)ClGe(acac)_2$ in $CDCl_3$–CCl_3/TMS solutions at −2.2°: (*a*) experimental spectra; (*b*) comparison of experimental and calculated n.m.r. spectra; solid circles represent experimental points, solid triangles represent calculated points, and open circles denote perfect fit of experimental and calculated points.

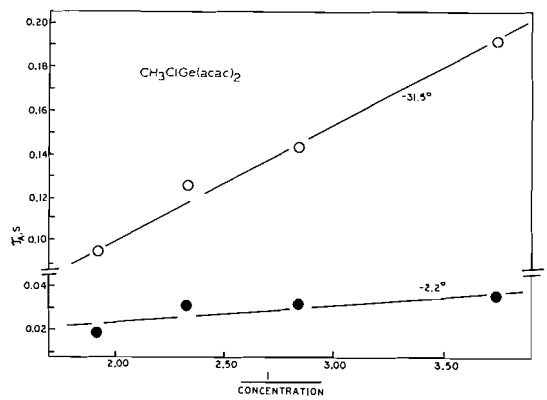

FIG. 3. Plots of the mean lifetime τ_A as a function of $[(CH_3)ClGe(acac)_2]^{-1}$ at the indicated temperatures.

TABLE 2. Concentration dependence of mean residence times for —CH= protons of $(CH_3)ClGe(acac)_2$ in $CDCl_3$–CCl_4/TMS solutions

Concentration (*M*)	$\tau_{(-31.5)} \times 10^2$ (s)	$\tau_{(-2.2)} \times 10^3$ (s)
0.521	4.8	9.4
0.428	6.3	15
0.352	7.2	16
0.267	9.7	18

$$\tau_A^{-1} = [(CH_3)ClGe(acac)]^{-1}\text{Rate}$$
$$= k[(CH_3)ClGe(acac)_2]$$

From the slope of the linear plot at −31.5° of Fig. 3, $k = 19\ M^{-1}\ s^{-1}$ in good agreement with $k = 16\ M^{-1}\ s^{-1}$ obtained from the log k *vs.* $1/T$ plot (Fig. 4 of ref. 3).

Arrhenius activation energy, E_a, and frequency factors, A, were computed from the slope and intercept, respectively, of the least-squares straight line plot of log k *vs.* $1/T$ (see Fig. 4 of ref. 3), where k is the second-order rate constant for the exchange process. The entropy of activation was determined from the relation

$$\Delta S^{\ddagger} = R[\ln A - \ln RT/Nh] - R$$

Arrhenius and Eyring activation parameters for intermolecular exchange of —CH= protons in $(CH_3)ClGe(acac)_2$ are

$$E_a = 6.0 \pm 0.3 \text{ kcal/mol}$$
$$\log A = 6.65 \pm 0.28$$
$$\Delta H_{25}^{\ddagger} = 5.5 \pm 0.3 \text{ kcal/mol}$$
$$\Delta S_{25}^{\ddagger} = -30 \pm 1 \text{ e.u.}$$
$$\Delta G_{25}^{\ddagger} = 14.43 \pm 0.05 \text{ kcal/mol}$$
$$k_{25} = 1.6 \times 10^2\ M^{-1}\ s^{-1}$$

(concentration = 0.548 *M*). The reported random errors were estimated at the 95% confidence level. These errors represent scatter in the data and not systematic errors which may be larger (1) owing to the temperature dependence of the transverse relaxation time, T_2.

It is instructive to compare the above activation parameters with those from exchange processes in analogous phenylchlorotin, -germanium, and methylchlorotin acetylacetonate complexes. It was shown earlier (3) that rearrangements in $(C_6H_5)ClM(acac)_2$ complexes, where M is Sn(IV) and Ge(IV), have nearly identical activation parameters; *e.g.* E_a = 12.8 kcal/mol (M = Ge) and 12.7 kcal/mol (M = Sn). Therefore it does not seem unreasonable to expect both $(CH_3)ClSn(acac)_2$ and $(CH_3)ClGe(acac)_2$ to have similar activation parameters. In the case of the former complex, the activation energy is 8.6 kcal/mol greater (1). This difference cannot be attributed to differences in electronic effects of the metal in view of similarities in the data (3) on phenyl-

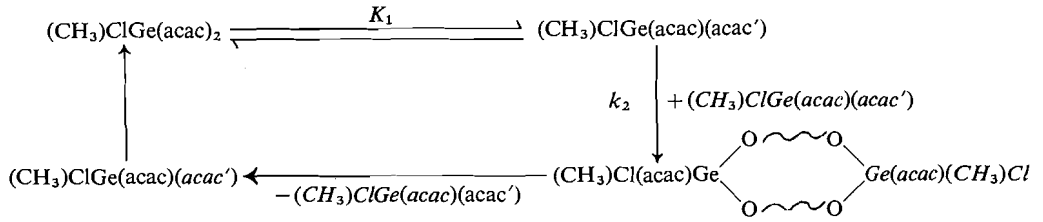

chloro complexes; however it is not unexpected since rearrangements in the tin complexes are intramolecular but intermolecular in the methylchloro germanium chelate.

Mechanisms for the Exchange Process

Stereochemical rearrangements for a complex of the type *cis*-M(chel)$_2$XY via a dissociative S_N1 process have been discussed in some detail before (4). We immediately discount dissociation of the methyl group in $(CH_3)ClGe(acac)_2$ in a medium such as chloroform-*d* – carbon tetrachloride. Although a chloride dissociative process through a square pyramidal intermediate (methyl group basal, and attack by Cl^- at the methyl group) would explain the observed simultaneous time-averaging of acetylacetonate methyl and ring proton environments, it is not considered as a likely path in the present case for the following reasons. First, analogous studies in $M(acac)_2X_2$ complexes (6, 11, 14) (M = Ti, Sn, and Ge; X = F, Cl, or Br) have demonstrated that rearrangements are independent of the nature of the halogen. Second, chloride (^{36}Cl) exchange between tetraethylammonium chloride and $Sn(acac)_2Cl_2$ is slow ($k_2 = 0.0018$ M^{-1} s^{-1} at 15° in $CHCl_3$) (15). Finally, we note that the rate of environmental averaging is second order in the concentration of $(CH_3)ClGe(acac)_2$; a halide dissociative path would be expected to be first order in the concentration of the complex.[4] In addition, the entropy of activation, -30 ± 1 e.u., discourages a dissociative process. Brown (16) has pointed out that $\Delta S^{\ddagger}$ should be positive for a dissociative mechanism and negative for an associative one, in the absence of strong solvent effects. The latter effects probably amount to no more than about 10 e.u. for halogenated organic solvents (13). For the above reasons, complete dissociation of an $acac^-$ ligand is also not considered likely.

A tentative pathway[5] involves the intermolecular exchange of an acetylacetonate ligand. The process is viewed in the scheme below where the primed ligand, acac', represents a dangling unidentate ligand.

The equilibrium defined by K_1 must be shifted largely toward the six-coordinate species as we observed no n.m.r. resonances attributable to the five-coordinate germanium species. The rate-determining sequence, k_2, is thought to involve formation of the bis-acac bridged dimeric species, but prior to this, the five-coordinate species would have to be in the correct orientation (the slow step) for attack by the dangling acetylacetonate ligand end onto the "vacant" coordination site (the "vacant" site may be occupied by a solvent molecule). The rate expression from the proposed mechanism is $R = k_2K_1[(CH_3)ClGe(acac)_2]^2$ consistent with our observations.

Partial support from the National Research Council of Canada is gratefully appreciated.

[4]Consideration of several pathways involving a metal–chlorine bond breaking as a first step reveals no rate expression that contains second order dependence on the concentration of the complex. In all the cases we have looked at the rate law was always first order with respect to [complex].

[5]A referee has suggested that the proposed mechanism would predict that configurational rearrangements in a mixture of $(CH_3)ClGe(dik)_2$ and $(CH_3)ClGe(dik')_2$ (where dik and dik' denote two different β-diketonate ligands) should be accompanied by intermolecular exchange of dik and dik'. Although this possibility is not unexpected, it has not been tested for the present system; but we note however that mixtures of $Ti(dik)_2X_2$ and $Ti(dik')_2X_2$ do yield a mixed complex $Ti(dik)(dik')X_2$ (see *e.g.* ref. 17 and references therein). Also, the mechanism would predict that intermolecular exchange between $(CH_3)ClGe(acac)_2$ and free Hacac may be accompanied by configurational rearrangements, but not necessarily at the same rate. These possibilities are presently being investigated for the corresponding organotin chelates for which a mechanism for ligand exchange has been proposed (see ref. 13). The case for $(CH_3)ClGe(acac)_2$ will be the subject of a further study.

Can. J. Chem. Downloaded from www.nrcresearchpress.com by 210.87.254.40 on 09/05/12
For personal use only.

1. N. SERPONE and K. A. HERSH. Inorg. Chem. **13**, 2901 (1974).
2. D. G. BICKLEY and N. SERPONE. Inorg. Chem. **13**, 2908 (1974).
3. N. SERPONE and K. A. HERSH. J. Organometal. Chem. In press.
4. N. SERPONE and D. G. BICKLEY. Progr. Inorg. Chem. **17**, 391 (1972).
5. T. J. PINNAVAIA, L. J. MATIENZO, and Y. A. PETERS. Inorg. Chem. **9**, 993 (1970).
6. R. W. JONES. Ph.D. Thesis, Cornell University, Ithaca, New York 1971; *Dissertation Abstracts*, 71-25, 160 (1971).
7. P. J. PAULSEN and D. W. COOKE. Anal. Chem. **35**, 1560 (1963).
8. J. TIMMERMANS. The physico-chemical constants of binary systems in concentrated solutions. Vol. 1. Interscience Publishers Incorporated. New York. 1959.
9. A. L. VAN GEET. Anal. Chem. **40**, 2227 (1968); **42**, 679 (1970).
10. H. S. GUTOWSKY and C. H. HOLM. J. Chem. Phys. **25**, 1228 (1956).
11. R. W. JONES, JR. and R. C. FAY. Inorg. Chem. **12**, 2599 (1973).
12. K. A. HERSH and N. SERPONE. Unpublished results.
13. N. SERPONE and R. ISHAYEK. Inorg. Chem. **13**, 52 (1974).
14. R. C. FAY and R. N. LOWRY. Inorg. Chem. **6**, 1512 (1967).
15. J. M. BULL, M. J. FRAZER, L. I. B. HAINES, and J. MEASURES. Abstracts, Chemical Society (London) Autumn Meeting, Southampton. 1969. p. A14.
16. T. L. BROWN. Accounts Chem. Res. **1**, 23 (1968).
17. R. N. LOWRY and R. C. FAY, Inorg. Chem. **13**, 1309 (1974).

Can. J. Chem. Downloaded from www.nrcresearchpress.com by 210.87.254.40 on 09/05/12
For personal use only.

$\Delta G^\theta, \Delta H^\theta, \Delta S^\theta$ de transfert de H_2O et du couple H^+, OH^- de l'eau à ses mélanges contenant jusqu'à 40% de EtOH, *tert*-BuOH, DMSO, acétone et urée à 25°C

HENRI GILLET, LÉVON AVÉDIKIAN ET JEAN-PIERRE MOREL

Laboratoire d'Etude des Interactions Solutés–Solvants, Groupe de Chimie Physique, Université de Clermont, Les Cézeaux, B.P. 45, 63170 Aubière, France

Reçu le 30 juillet 1974

HENRI GILLET, LÉVON AVÉDIKIAN et JEAN-PIERRE MOREL. Can. J. Chem. **53**, 455 (1975).

Nous avons mesuré les enthalpies de neutralisation de HCl en solution diluée dans les mélanges hydroorganiques contenant jusqu'à 40% en poids de *t*-BuOH, DMSO, acétone et urée d'une part, et les constantes d'autoprotolyse de mélanges eau–DMSO et eau–urée d'autre part. Nous avons ainsi pu obtenir les grandeurs thermodynamiques normales ΔG^θ, ΔH^θ et ΔS^θ de la réaction de dissociation de l'eau dans ces milieux. Les résultats relatifs aux mélanges eau–urée doivent être interprétés avec prudence compte-tenu du fait que la dissociation propre de l'urée n'est pas négligeable devant celle de l'eau. A partir de différentes données de la littérature nous avons calculé les valeurs de l'enthalpie libre et de l'enthalpie de transfert de la molécule H_2O du liquide pur aux mélanges ci-dessus. (Nous avons également calculé pour ces mélanges, les coefficients de dilatation isobare et les coefficients de variation de la constante diélectrique avec la température.) Par suite, les grandeurs relatives au tranfert du couple d'ions H^+, OH^- ont été évaluées (ainsi que celles de l'eau aux mélanges eau–EtOH); elles sont comparées à celles déjà connues pour HCl et les halogénures alcalins; leurs différentes variations ne permettent pas d'établir de corrélation simple avec les propriétés structurales habituellement admises pour les milieux considérés.

HENRI GILLET, LÉVON AVÉDIKIAN, and JEAN-PIERRE MOREL. Can. J. Chem. **53**, 455 (1975).

We have measured the heat of neutralization of dilute solutions of HCl in aqueous–organic mixtures containing up to 40% by weight of *t*-BuOH, DMSO, acetone, and urea; autoprotolysis constants of the mixtures H_2O–DMSO and H_2O–urea also were determined. Thus the usual thermodynamic quantities ΔG^θ, ΔH^θ, and ΔS^θ could be determined for the dissociation of water in these mixtures. The results for the H_2O–urea mixtures must be accepted with caution because the dissociation of urea itself is not negligible compared to that of water. Using various literature data we have calculated values of the Gibbs free energy and the enthalpy for the transfer of a molecule of water from the pure liquid to the mixtures noted above. (We also have calculated for these mixtures the coefficients of isobaric expansion and those for the variation with temperature of the dielectric constant.) In addition, the values for the transfer of the ion pair H^+,OH^- have been determined as well as those for the transfer from water to H_2O–EtOH mixtures. These are compared to those already known for HCl and the alkali halides. It is not possible to establish a simple correlation between the differing variations of these quantities with the structural properties usually considered to exist in the media studied. [Journal translation]

Introduction

Pour calculer l'enthalpie de la réaction de dissociation d'un acide faible en milieu hydro-organique, il est nécessaire de connaître l'enthalpie de neutralisation d'une acide fort par une base forte dans ces solvants. Nous avons déjà effectué de telles déterminations expérimentales (1, 2).

L'étude de nouveaux mélanges à l'aide d'un appareillage plus précis nous conduit à proposer aujourd'hui la grandeur ΔH_n, enthalpie de neutralisation de l'acide chlorhydrique par la soude dans les mélanges riches en eau contenant jusqu'à 40% en poids d'alcool *t*-butylique, d'acétone, de diméthylsulfoxyde et d'urée. Les produits d'autoprotolyse de ces milieux, nécessaires au calcul des entropies de réaction, ont été déterminés ou pris dans la littérature.

Nous donnons les valeurs du coefficient de dilatation isobare et du coefficient de variation avec la température de la constante diélectrique des mélanges, calculées à partir des données de la littérature; elles nous permettent de corriger les enthalpies expérimentales au moyen d'une relation dérivant de la théorie de Debye–Hückel–Bjerrum, et d'accéder aux grandeurs normales de la réaction de dissociation de l'eau.

De même, à l'aide des données de la littérature, nous pouvons calculer les variations de l'enthalpie libre et de l'enthalpie molaire partielle de l'eau lors du transfert du liquide pur aux

Can. J. Chem. Downloaded from www.nrcresearchpress.com by 210.87.254.42 on 09/05/12
For personal use only.

Can. J. Chem. Downloaded from www.nrcresearchpress.com by 210.87.254.42 on 09/05/12
For personal use only.

mélanges. Il est alors possible de séparer les grandeurs de transfert relatives au couple d'ions H^+,OH^-; celles-ci pourront être comparées aux grandeurs de transfert des halogénures alcalins et de HCl lorsqu'elles sont connues. Il sera intéressant d'examiner la modification de solvatation, causée par l'addition d'un cosolvant, des ions provenant de la dissociation propre de l'eau.

Partie theorique

Produit d'autoprotolyse. Enthalpie libre

L'expérience donne $K_i^c = \underset{c \to 0}{\text{limite}} ([H^+][S^-])$

où $[H^+]$ est la concentration en protons, mesurée à l'électrode de verre, et $[S^-]$ celle des ions lyates de toute nature (OH^-, RO^-, ...), concentration déterminée par la quantité d'une base forte (NaOH) ajoutée dans le milieu. Cette définition de la constante thermodynamique d'équilibre dans l'échelle molaire (désignée par l'exposant c) implique le choix d'une activité égale à l'unité pour le solvant qui est donc pris comme état de référence.

Dans l'eau

$$\Delta G_d^{0c}(H_2O) = -RT \ln K_i^c$$

est l'enthalpie libre normale de la réaction de dissociation de l'eau

$$H_2O = {}^wH^+ + {}^wOH^-$$

(où l'exposant w indique la phase solvant, ici l'eau).

Les états de référence sont l'eau pure à gauche, et les solutions idéales de molarité unité des ions dans l'eau à droite. Si, dans un mélange hydroorganique, on néglige les ions lyates autres que OH^- (en particulier les ions RO^- provenant des alcools ROH), la valeur de K_i permet de calculer l'enthalpie libre normale de la réaction de dissociation dans le solvant hydroorganique s

$${}^sH_2O = {}^sH^+ + {}^sOH^-$$

Cette approximation est justifiée pour les mélanges contenant de l'alcool *t*-butylique de faible produit d'autoprotolyse et, *a fortiori*, pour ceux d'eau et de solvant aprotique (acétone, DMSO). Elle est naturellement plus discutable pour l'urée dont la dissociation propre entre en concurrence avec celle de l'eau (3, 4).

Remarquons que dans le cas d'un mélange, l'état de référence d'activité unité est l'eau dans ce mélange s à gauche; l'enthalpie libre normale de transfert de la réaction de dissociation de l'eau, de l'eau au mélange hydroorganique, est alors

$$\begin{aligned} {}^s\delta\Delta G_d^{0c}(H_2O) &= RT \ln 10^{s\delta}pK_i^c \\ &= {}^s\delta\mu^{0c}(H^+) + {}^s\delta\mu^{0c}(OH^-) \\ &\quad - {}^s\delta\mu(H_2O) \end{aligned}$$

où les opérateurs ${}^s\delta$ symbolisent les différences des grandeurs concernées entre le solvant s et l'eau, c'est-à-dire les grandeurs de transfert.

La variation du potentiel chimique de l'eau peut se calculer à l'aide des pressions de vapeur de l'eau dans les mélanges

$${}^s\delta\mu(H_2O) = RT \ln \frac{{}^sp(H_2O)}{{}^wp(H_2O)}$$

On peut ainsi accéder à la somme des grandeurs de transfert des ions H^+ et OH^-.

Enthalpies de neutralisation

L'expérience donne la chaleur mise en jeu lors de la neutralisation d'une solution diluée d'acide fort ($c = 5 \times 10^{-3}$ *M*) par la soude.

$$Cl^-,H^+(c) + OH^-,Na^+(c) = H_2O + Na^+,Cl^-(c)$$

L'enthalpie normale de la réaction de dissociation peut être obtenue si l'on connait l'enthalpie de dilution des ions. Nous avons proposé une relation (5) permettant d'évaluer celle-ci dans le domaine d'application de la deuxième loi de Debye–Hückel–Bjerrum pour des électrolytes dont l'association est négligeable

$$\log f_\pm = \frac{-A\sqrt{c}}{1 + A \ln 10 \sqrt{c}}$$

soit

$$\begin{aligned} \Phi_L = -\Delta H_{\text{dilution}} &= \frac{A_H B_H + C_H}{B_H^2} \\ &- 2\frac{A_H B_H + 2C_H}{B_H^3}\frac{1}{\sqrt{m}} + \frac{2C_H}{B_H^4}\frac{1}{m(1 + B_H\sqrt{m})} \\ &+ 2\frac{A_H B_H + 3C_H}{B_H^4 m}\ln(1 + B_H\sqrt{m}) - \frac{2C_H}{B_H^4}\frac{1}{m} \end{aligned}$$

où m est la molalité et

$$A_H = -uv$$

$$B_H = v$$

$$C_H = uv^2$$

avec

$$u = 3RT^2\left(\frac{1}{T} + \frac{\partial \ln D}{\partial T} + \frac{\alpha}{3}\right)$$

$$v = A \ln 10 \sqrt{\rho_0}$$

Can. J. Chem. Downloaded from www.nrcresearchpress.com by 210.87.254.42 on 09/05/12
For personal use only.

D, α, ρ_0 étant respectivement, la constante diélectrique, le coefficient de dilatation isobare et la masse volumique du solvant pur.

Dans le cadre de la théorie de Bjerrum, qui se révèle plus satisfaisante que celle classique où intervient le paramètre d'approche $\hat{a}$ des ions pour claculer Φ_L (5), cette grandeur ne dépend pas de la nature de l'électrolyte si l'on peut négliger son association. Les mesures d'enthalpie de neutralisation étant effectuées en solution diluée ($c = 5 \times 10^{-3}$ M) nous utiliserons donc ces valeurs calculées de Φ_L pour accéder à la grandeur normale

$$\Delta H_d^0(H_2O) = -\Delta H_n^0 = -\Delta H_n - \Phi_L$$

En milieu hydroorganique, cette grandeur s'écrit:

$$\Delta H_d^0(H_2O) = {}^s\overline{H}^0(H^+) + {}^s\overline{H}^0(OH^-) - {}^s\overline{H}(H_2O)$$

On voit que l'enthalpie de transfert du couple H^+,OH^- de l'eau au solvant s peut être calculée si l'on connait l'enthalpie molaire partielle de l'eau dans ce solvant.

Partie expérimentale

Solvants

L'eau, tridistillée dans un appareil en quartz, a été dégazée sous vide juste avant la préparation des mélanges.

L'alcool *t*-butylique a été purifié suivant la technique décrite dans un précédent mémoire (6).

Le DMSO provenant de la S.N.P.A. a été purifié par une double distillation sous pression réduite en présence de charbon activé après avoir séjourné pendant plusieurs jours sur chaux vive (E.b.$_{2mm}$ = 46–47 °C).

L'acétone, un produit Prolabo pur, a été distillée deux fois après avoir séjourné plusieurs jours sur Sikkon Fluka.

L'urée, un produit Prolabo R.P.p.a., a été utilisé sans autre purification.

Détermination des enthalpies de neutralisation

Les mesures ont été réalisées à l'aide d'un calorimètre L.K.B. à titration type 8700, à 25 °C. Nous avons utilisé une cellule contenant 100 cm^3 d'acide chlorhydrique. Les solutions acides, environ 5×10^{-3} M, dans chaque milieu étudié, ont été préparées à partir de solutions aqueuses, environ 0.1 M, titrées à l'aide de carbonate de sodium et de borax.

Nous avons neutralisé l'acide par une solution aqueuse de soude de concentration 2.5 M ajoutée à l'aide d'une burette à piston Tacussel, type électroburap, à la vitesse de 0.2 cm^3 min^{-1}. Des précautions ont été prises pour éviter au maximum la carbonatation de la soude.

Dans un premier temps, nous avons procédé à un étalonnage électrique sur la solution d'acide, puis dans un deuxième à la réaction de neutralisation. Les effets thermiques correspondants, ont été enregistrés. Les longueurs l, proportionnelles aux énergies mises en jeu, ont été mesurées au temps $t/2$, t désignant la durée de l'effet thermique. Cette détermination graphique permet d'éliminer l'influence des phénomènes thermiques secondaires: agitation, fuites thermiques, dilution de la soude, etc. (7).

Les mesures ont été faites à des pourcentages en solvant organique déterminés par l'évolution des ΔH_n. Nous avons fait de trois à six essais pour chaque mélange.

Dans le cas des mélanges eau–acétone, l'excès de soude ajouté après neutralisation totale provoque une réaction parasite exothermique mettant en jeu le solvant, sans doute une cétolisation, qui perturbe la partie finale des courbes (absence de linéarité) et conduit à une précision plus faible des déterminations. L'importance de la perturbation croît avec la teneur en acétone.

L'urée, en solution dans l'eau, se décompose suivant la réaction

$$CO(NH_2)_2 \rightarrow CNO^- + NH_4^+$$

A 25 °C, cette réaction est peu rapide (8) mais les mélanges ne doivent quand même pas être conservés longtemps.

En milieu basique, la réaction de décomposition est catalysée par les ions OH^- (9) et les ions ammonium sont transformés en ammoniac

$$NH_4^+ + OH^- \rightarrow NH_3 + H_2O$$

En milieu acide, les ions cyanate sont quantitativement détruits par la réaction (8)

$$CNO^- + 2H^+ + 2H_2O \rightarrow NH_4^+ + H_2CO_3$$

Il y a donc consommation d'ions H^+ et le titre des solutions acides diminue au cours du temps, ce qui conduit à des résultats erronés pour les ΔH_n. A faible concentration en acide, la réaction est relativement lente et l'on obtient des résultats reproductibles si l'acide est ajouté au mélange juste avant la mesure.

Détermination des pK_i

Nous avons étudié les cellules galvaniques suivantes:

(I) électrode de verre/HCl(m_1), solvant (s)/AgCl, Ag

(II) électrode de verre/NaOH(m_2), KCl(m_3), solvant (s)/AgCl, Ag

m représente la molalité.

Dans le solvant s les tensions réversibles peuvent s'écrire

$${}^sU(I) = {}^sU^0(I) + k \text{ og } \{{}^sa_1(H^+) \cdot {}^sa_1(Cl^-)\}$$

$${}^sU(II) = {}^sU^0(II) + k \log \{{}^sa_2(H^+) \cdot {}^sa_2(Cl^-)\}$$

Les relations équivalentes dans l'eau sont obtenues, en remplaçant les indices supérieurs s par w. a représente l'activité.

Sachant que $K_i = a(H^+) \cdot a(OH^-)$ on peut écrire

$${}^s\delta U^\theta = {}^s\delta U(I) - 2k\left(\log \frac{{}^sm_1}{{}^wm_1} + \frac{{}^wA\sqrt{{}^w\rho\,{}^wm_1}}{1 + {}^wB\,{}^wq\sqrt{{}^w\rho\,{}^wm_1}} - \frac{{}^sA\sqrt{{}^s\rho\,{}^sm_1}}{1 + {}^sB\,{}^sq\sqrt{{}^s\rho\,{}^sm_1}}\right)$$

et

$${}^s\delta U^\theta - k\,{}^s\delta pK_i = {}^s\delta U(II) - k \log \frac{{}^sm_3\,{}^wm_2}{{}^wm_3\,{}^sm_2}$$

Can. J. Chem. Downloaded from www.nrcresearchpress.com by 210.87.254.42 on 09/05/12
For personal use only.

Pour l'étude des mélanges eau–urée, nous avons placé dans la cellule une masse connue de solution aqueuse de HCl, puis ajouté les masses d'urée nécessaires pour obtenir des mélanges à 10, 20, 30 et 40% en poids de substance organique. Une lecture de U(I) a été faite dans chaque milieu. Nous avons exploré une gamme de six concentrations comprises entre 3×10^{-3} et 10^{-2} M. Les valeurs de ${}^{s}\delta U^{0}$ obtenues concordent parfaitement.

Nous avons opéré de la même façon pour la cellule II mais avec des concentrations plus élevées en soude (10^{-1} à 2.5×10^{-2} M) et en KCl (10^{-1} à 5×10^{-2} M). Si la diminution de la concentration en soude n'a pas d'influence sur le résultat, il n'en est pas de même de la diminution de la concentration en KCl. En effet les valeurs de pK_i, qui demeurent constantes dans la gamme de concentrations indiquée ci-dessus, décroissent lorsque la concentration en KCl devient inférieure à 5×10^{-2} M. Ceci a été attribué à la présence, en milieu alcalin, d'ions cyanate qui perturbent le fonctionnement de l'électrode AgCl, Ag lorsque la concentration en ions chlorure est faible.

Pour chaque teneur en urée, nous avons calculé, à partir des mesures de tensions réversibles, les termes ${}^{s}\delta U^{0}$ et ${}^{s}\delta U^{0} - k{}^{s}\delta \mathrm{p}K_i$, et nous en avons déduit pK_i.

Pour l'étude des mélanges eau–DMSO, nous avons employé la même méthode de mesure; mais nous avons pu utiliser, dans la cellule II, des concentrations en soude et en KCl comprises entre 3×10^{-3} et 10^{-2} M. En effet, dans ce cas, la valeur de la concentration en KCl n'a pas d'influence sur le pK_i.

Les mesures potentiométriques ont été effectuées, soit avec un potentiomètre Radiometer 4, soit avec un millivoltmètre Tacussel Aries 10000. Les électrodes AgCl, Ag étaient des électrodes Tacussel Ag/AgCl 1 et l'électrode de verre de la même marque, type TB/HA. La cellule de mesure était maintenue à température constante (25.0 ± 0.1 °C) par une circulation d'eau thermorégulée.

Résultats

Produits d'autoprotolyse

On trouve dans la littérature les valeurs de pK_i des mélanges aqueux de EtOH, *t*-BuOH, acétone (10) que nous utilisons pour les calculs. Dans le cas des mélanges eau–DMSO, les valeurs que nous avons obtenues, à 25 °C, sont en accord avec celles données par différents auteurs (11, 4, 12) et conformes à celles déterminées à 20 °C (13). Par contre, pour les mélanges eau–urée, on observe un écart croissant avec le pourcentage en urée entre nos valeurs et celles données par Woolley et Hepler (4); les remarques formulées dans la partie expérimentale peuvent expliquer cet écart.

Nous avons rassemblé dans le tableau 1 les valeurs de pK_i ramenées à l'échelle molaire en retranchant le terme $2 \log {}^{s}\rho$ et déduites, pour les compositions particulières indiquées, de la courbe de variation $\mathrm{p}K_i = f(X)$.

Enthalpies de neutralisation. Grandeurs de transfert

Les valeurs des enthalpies de neutralisation regroupées dans le tableau 2 correspondent aux résultats expérimentaux. Elles sont déterminées à 200 J mol^{-1} près.

Certaines des mesures dont nous présentons ici les résultats (systèmes H_2O–*t*-BuOH et H_2O–acétone) avaient été précédemment réalisées par l'un d'entre nous à l'aide d'un autre appareillage (1 et 2): si l'allure des variations et les écarts relatifs restent identiques pour les deux séries de résultats, il est à noter que les valeurs obtenues présentent parfois des écarts sensibles. Les déterminations déjà effectuées dans les mélanges eau–DMSO (14) ne permettent pas une définition précise des variations dans la zone riche en eau.

Nous avons déduit des résultats précédents les grandeurs de transfert dont les valeurs sont rassemblées dans le tableau 3. Pour effectuer les calculs, nous avons utilisé les valeurs des enthalpies de neutralisation lissées et corrigées du terme de dilution pour obtenir les grandeurs normales. Dans le domaine de concentrations étudié, ce terme est en général faible (123 J mol^{-1} dans l'eau); il permet cependant de mieux préciser l'allure des courbes de variation et peut atteindre 530 J mol^{-1} dans le mélange contenant 40% de *t*-BuOH. Dans le cas du système H_2O–EtOH, les valeurs de $\Delta H_d^0(H_2O)$ utilisées sont celles obtenues en prenant la moyenne des valeurs proposées par Hepler *et coll.* (15) et par l'un de nous (16).

Propriétés des solvants

Nous avons consigné dans le tableau 4 les valeurs des enthalpies libres et des enthalpies

TABLEAU 1. Produits d'autoprotolyse des mélanges eau–urée et eau–DMSO à 25 °C (pK dans l'échelle molaire)

X*	H_2O–urée†	H_2O–DMSO†
0	14.00	14.00
5.0	(13.73)	(14.07)
10.0	13.53	14.16
15.0	(13.40)	(14.27)
20.0	13.31	14.39
25.0	(13.24)	(14.55)
30.0	13.19	14.71
35.0	(13.16)	(14.88)
40.0	13.14	15.07

*% en poids du constituant organique.
†Valeurs entre parenthèses obtenues par interpolation graphique.

TABLEAU 2. Enthalpies de neutralisation de HCl 5×10^{-3} *M* par NaOH dans les mélanges hydroorganiques ($-\Delta H_n$ en kJ mol^{-1}) à 25 °C*

X	H_2O–*t*-BuOH	H_2O–acétone†	H_2O–DMSO	H_2O–urée†
3.0	56.9	—	—	—
5.0	57.5	56.4	57.0	(55.3)
10.0	58.9	56.7	57.6	54.5
13.0	60.4	—	—	—
15.0	61.2	(57.2)	58.2	(53.8)
17.0	62.4	—	—	—
20.0	63.1	57.9	58.8	53.1
22.0	63.7	—	—	—
25.0	63.6	(58.4)	59.6	(52.5)
30.0	62.9	58.6	60.5	51.7
35.0	62.3	(58.6)	61.3	(50.9)
40.0	61.7	58.4	63.2	49.8
50.0	—	58.0	—	—

*Valeur dans l'eau, dans les mêmes conditions, $\Delta H_n = -56.2$ kJ mol^{-1}.
†Valeurs entre parenthèses obtenues par interpolation graphique.

TABLEAU 3. Enthalpies et entropies (échelle molaire) normales de transfert de la réaction de dissociation de l'eau dans les mélanges hydroorganiques à 25 °C*

	H_2O–EtOH		H_2O–*t*-BuOH		H_2O–acétone		H_2O–DMSO		H_2O–urée	
X	*1*	*2*	*1*	*2*	*1*	*2*	*1*	*2*	*1*	*2*
5.0	0.61	−0.2	1.23	1.1	0.20	−2.2	0.84	1.5	−0.87	3.4
10.0	0.98	−1.1	2.87	3.7	0.51	−4.0	1.38	1.6	−1.65	5.4
15.0	1.12	−2.4	4.89	8.0	1.01	−5.4	2.01	1.6	−2.40	6.3
20.0	1.03	−4.2	6.99	12.7	1.62	−6.6	2.68	1.1	−3.10	7.0
25.0	0.62	−7.1	7.23	11.2	2.11	−8.2	3.39	0.9	−3.67	7.4
30.0	−0.25	−11.5	6.49	6.8	2.34	−10.9	4.23	0.6	−4.38	6.9
35.0	−1.59	−17.4	5.75	2.2	2.28	−14.6	5.24	0.7	−5.25	5.7
40.0	−3.47	−25.2	5.07	−2.5	2.13	−18.9	6.95	2.8	−6.25	4.1

*Dans l'eau ΔH_d^θ (H_2O) = 56.07 kJ mol^{-1}. Colonnes *1*: $^S\delta\Delta H_d^\theta(H_2O)$ en kJ mol^{-1}. Colonnes *2*: $^S\delta\Delta S_d^\theta(H_2O)$ en J mol^{-1} K^{-1}.

molaires partielles de l'eau dans les différents mélanges. Le tableau 5 contient, pour ces mêmes mélanges, les valeurs des coefficients de dilatation isobare et des variations de la constante diélectrique avec la température. Toutes ces grandeurs ont été soit trouvées dans la littérature, soit calculées à partir de données de la littérature.

Discussion

Nous avons d'abord tracé, fig. 1, les variations de l'entropie molaire partielle de l'eau dans les différents mélanges étudiés ici; notons que celles de la grandeur d'excès ($\bar{S}^E = \bar{S} + R \ln x$) sont semblables quoique déplacées vers les valeurs négatives. Il n'est naturellement pas possible de déduire de cette quantité molaire partielle, l'évolution de la structure de la phase aqueuse lors de l'addition de cosolvant. Notons cependant que pour l'urée, composé réputé briseur, on observe une augmentation de $\bar{S}(H_2O)$; au contraire, pour les alcools que l'on admet être des promoteurs de la structure de l'eau, c'est une diminution de $\bar{S}(H_2O)$ qui apparaît. Dans le cas de l'alcool *t*-butylique, on observe sur la courbe un point d'inflexion pour un pourcentage en poids de l'ordre de 17% (fraction molaire égale à environ 0.05); on retrouve ici une composition caractéristique de ce mélange qui pourrait correspondre à un maximum de structure (39).

Examinons maintenant, fig. 2, les variations du potentiel chimique du couple d'ions H^+,OH^-, et comparons les en particulier à celles de H^+,Cl^-: dans les deux cas, on observe une diminution en milieu eau–urée (40) et des augmentations pour les quatre autres mélanges (41, 42); l'augmentation est toujours plus rapide (en fonction de l'addition de cosolvant) pour le couple H^+,OH^- que pour H^+,Cl^-

Can. J. Chem. Downloaded from www.nrcresearchpress.com by 210.87.254.42 on 09/05/12
For personal use only.

TABLEAU 4. Enthalpies libres et enthalpies molaires partielles de l'eau dans les mélanges hydroorganiques à 25 °C. (état de référence: eau liquide à 25 °C)*

	H_2O–EtOH		H_2O–*t*-BuOH		H_2O–DMSO		H_2O–acétone		H_2O–urée	
X	*1*[a]	*2*[b]	*1*[c]	*2*[d]	*1*[e]	*2*[f]	*1*[g]	*2*[h]	*1*[i]	*2*[j]
0	0	0	0	0	0	0	0	0	0	0
5	47	6	31	8	40	50	37	10	37	−5
10	101	57	63	96	93	110	78	40	78	−16
15	151	158	85	243	156	175	117	90	119	−37
20	201	302	106	506	228	255	159	160	164	−64
25	250	483	128	636	306	345	199	249	215	−97
30	293	682	139	703	391	450	239	354	269	−135
35	341	823	161	736	483	575	278	474	331	−180
40	384	907	173	761	575	720	317	603	403	−234

*Colonnes *1*: $-\mu(H_2O)$ en J mol^{-1}. Colonnes *2*: $-\bar{H}(H_2O)$ en J mol^{-1}.
[a]Calculées à partir des pressions de vapeur données par Dobson (17).
[b]Interpolées d'après les valeurs fournies par Bertrand *et al.* (15).
[c]Calculées à partir des pressions de vapeur données par Brown et Ives (18).
[d]Interpolées d'après les valeurs données par Kenttamaa *et al.* (19).
[e]Calculées à partir des activités de l'eau dans les mélanges obtenues par interpolation d'après les valeurs de Das et Kundu (11).
[f]Interpolées d'après les valeurs données par Rallo *et al.* (20).
[g]Valeurs obtenues à partir des coefficients d'activité calculés par l'équation de Van Laar dont les coefficients sont donnés par Perry *et al.* (21).
[h]Calculées d'après le polynome proposé par Kister et Waldman (22) pour représenter l'enthalpie relative molale des mélanges eau–acétone en utilisant la relation $\bar{L}_1 = \bar{L} - x\partial\bar{L}/\partial x$ (x = fraction molaire en acétone).
[i]Calculées à partir de la formule $\ln {}^{s}a(H_2O) \simeq -18.015\Phi m/1000$ en évaluant les coefficients osmotiques Φ grâce à la formule donnée par Stokes (23).
[j]Interpolées d'après les valeurs données par Egan et Luff (24), ces valeurs sont en bon accord avec les valeurs calculées à partir du polynome donné par Gucker et Pickard (25) pour représenter Φ_L, par la formule:

$$\bar{L}_1 = -\frac{m^2}{55.5}\left(\frac{\partial\phi_L}{\partial m}\right)$$

TABLEAU 5. Coefficient de dilatation isobare et variation avec la température de la constante diélectrique des mélanges hydroorganiques à 25 °C*

	H_2O–EtOH		H_2O–*t*-BuOH[c]		H_2O–DMSO		H_2O–acétone		H_2O–urée	
X	*1*[a]	*2*[b]	*1*	*2*	*1*[d]	*2*[e]	*1*[f]	*2*[g]	*1*[h]	*2*[i]
0	4.57[j]	2.57[j]	4.57	2.57	4.57	2.57	4.57	2.57	4.57	2.57
5	4.7	2.78	4.7	2.66	4.57	3.08	4.6	3.23	4.5	3.04
10	4.9	3.15	4.9	3.45	4.57	3.56	4.7	3.92	4.5	3.46
15	5.0	3.89	5.1	4.54	4.57	4.04	4.8	4.66	4.4	3.82
20	5.2	4.84	5.3	5.93	4.57	4.51	4.8	5.45	4.4	4.14
25	5.3	5.83	5.5	7.14	4.57	4.97	4.9	6.24	4.3	4.43
30	5.5	6.75	5.7	7.86	4.57	5.38	5.0	7.02	4.3	4.68
35	5.6	7.43	5.9	8.25	4.57	5.75	5.0	7.81	4.2	4.89
40	5.7	8.05	6.1	8.56	4.57	6.09	5.1	8.60	4.1	5.08

*Colonnes *1*: $-10^3\,(\partial \ln D/\partial T)_p$ en K^{-1}. Colonnes *2*: $10^4\,\alpha$ en K^{-1}.
[a]Déterminées d'après les valeurs de D à différentes températures données par Wyman (26).
[b]Déterminées d'après les masses volumiques à différentes températures données par Osborn *et al.* (27).
[c]Données par Pointud *et al.* (6).
[d]Les valeurs déterminées d'après les contantes diélectriques à différentes températures données par Douheret (28) montrent que ce terme reste sensiblement égal à sa valeur dans l'eau.
[e]Déterminées à partir des masses volumiques à différentes températures données par Schichman et Amey (29) et Sears *et al.* (30). Nous avons nous-mêmes mesuré quelques masses volumiques sur un densimètre Anton Paar.
[f]Déterminées d'après les constantes diélectriques à différentes températures données par Akerlöf (31).
[g]Déterminées à partir des masses volumiques à différentes températures données par Schwers (32).
[h]Déterminées à partir des constantes diélectriques à différentes températures données par Wyman (33*a*).
[i]Donnés par Desrosiers *et al.* (33*b*).
[j]Valeurs dans l'eau pure: $\partial \ln D/\partial T$ moyenne des valeurs données par (34, 35, 36 et 37). α valeur donnée par (38).

(par exemple, à 40% en poids de *t*-BuOH, on atteind ~6.6 kJ pour le premier contre ~3.8 kJ pour le second). L'addition de cosolvant à l'eau diminue donc beaucoup plus fortement la solvatation de l'ion OH^- que celle de l'ion Cl^-. L'effet est particulièrement spectaculaire dans les mélanges eau–DMSO où, à 40%, l'enthalpie libre de transfert de H^+,Cl^- est sensiblement nulle alors que celle de H^+,OH^- atteind ~5.5 kJ. Dans les mélanges eau–*t*-BuOH, où nous avons mesuré ces grandeurs pour les chlorures alcalins (43), on peut voir que le comportement

Can. J. Chem. Downloaded from www.nrcresearchpress.com by 210.87.254.42 on 09/05/12
For personal use only.

Can. J. Chem. Downloaded from www.nrcresearchpress.com by 210.87.254.42 on 09/05/12
For personal use only.

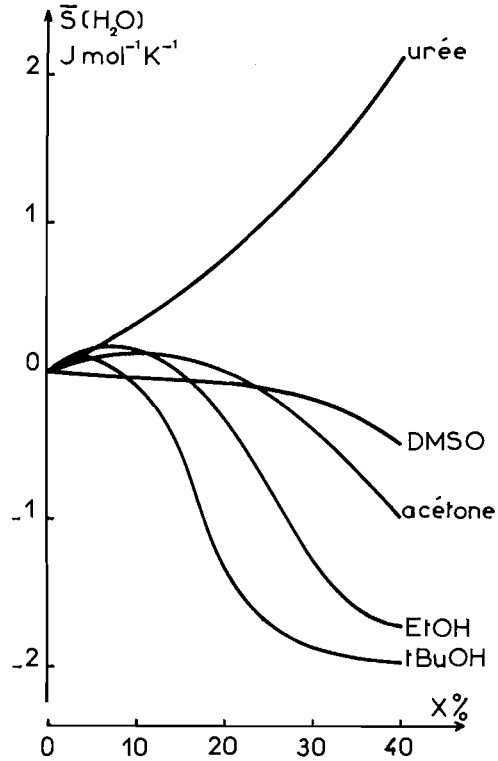

FIG. 1. Entropie molaire partielle de l'eau dans les mélanges hydroorganiques à 25 °C (état de référence: eau liquide à 25 °C).

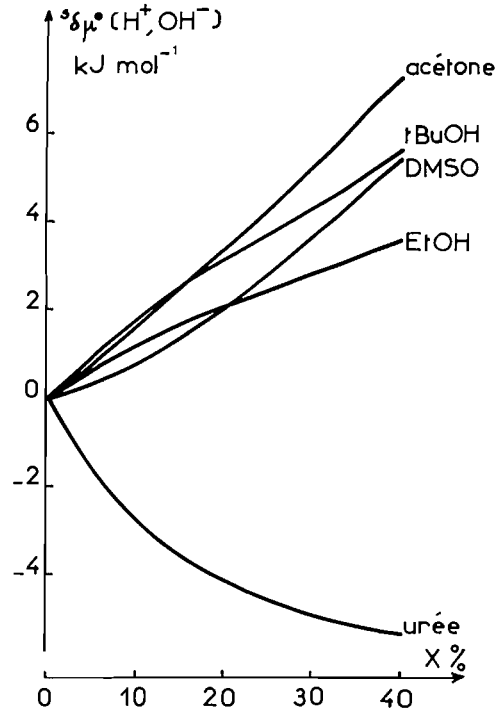

FIG. 2. Potentiel chimique normal (échelle molaire) de transfert du couple H^+,OH^- de l'eau aux mélanges hydroorganiques à 25 °C.

de H^+,OH^- est intermédiaire entre celui de H^+,Cl^- (variations les moins importantes) et celui des chlorures alcalins.

Pour les enthalpies de transfert, fig. 3, on observe un maximum endothermique bien marqué dans les mélanges eau–*t*-BuOH, comme nous en avions observé un pour les chlorures alcalins (6): celui-ci, situé dans les deux cas vers 25% en poids d'alcool, est moins important dans le cas du couple H^+,OH^- (~6.5 kJ) que pour les chlorures alcalins (~10 kJ pour NaCl). Dans les mélanges eau–urée, on observe un transfert exothermique régulièrement croissant attribuable à la basicité de l'urée vis-à-vis du proton. Par contre, dans eau–DMSO, malgré le caractère basique également marqué de la molécule de cosolvant, c'est un effet endothermique qui est observé: ceci laisse supposer que le transfert de l'ion OH^- est très fortement endothermique. Si l'on regarde maintenant les entropies de transfert (fig. 4) deux constatations s'imposent: les deux alcools, EtOH et *t*-BuOH, donnent lieu à des variations opposées dans la zone riche en eau; d'autre

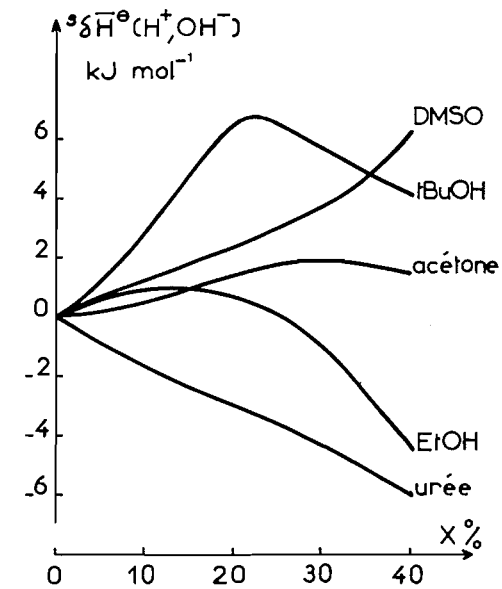

FIG. 3. Enthalpie normale de transfert du couple H^+,OH^- de l'eau aux mélanges hydroorganiques à 25 °C.

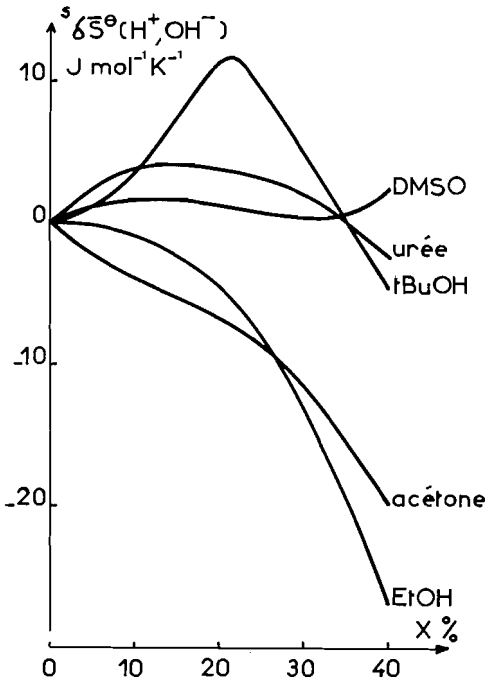

FIG. 4. Entropie normale de transfert (échelle molaire) du couple H^+,OH^- de l'eau aux mélanges hydroorganiques à 25 °C.

part, les entropies de transfert sont positives aussi bien dans eau–*t*-BuOH, milieu réputé plus structuré que l'eau pure jusqu'à environ 15% en poids, que dans le mélange eau–urée réputé moins structuré. En résumé, le potentiel chimique de transfert du couple H^+,OH^- entre l'eau et les mélanges à 20% en poids de cosolvant est contrôlé par l'enthalpie de transfert pour le DMSO et aussi bien pour l'alcool *t*-butylique que pour l'urée; c'est au contraire la contribution entropique qui prévaut pour l'éthanol et l'acétone. Par suite, il n'apparaît pas clairement au vu des grandeurs thermodynamiques que les caractéristiques structurales du milieu soient déterminantes pour expliquer le transfert de ces ions.

1. L. AVEDIKIAN. Bull. Soc. Chim. Fr. **8**, 2832 (1971).
2. L. AVEDIKIAN et J.-P. MOREL. J. Chim. Phys. **68**, 1201 (1971).
3. H. LEMAIRE ET M. J. LUCAS. J. Am. Chem. Soc. **73**, 5198 (1951).
4. E. M. WOOLLEY et L. G. HEPLER. Anal. Chem. **44**, 1520 (1972).
5. J. JUILLARD et J.-P. MOREL. C. R. Acad. Sci. Fr. Série C **277**, 825 (1973).
6. Y. POINTUD, J. JUILLARD, L. AVEDIKIAN, J.-P. MOREL et M. DUCROS. Thermochim. Acta, **8**, 423 (1974).
7. L. AVEDIKIAN. Bull. Soc. Chim. Fr. **8**, 2570 (1966).
8. W. H. R. SHAW et J. J. BORDEAUX. J. Am. Chem. Soc. **77**, 4729 (1955).
9. K. R. LYNN. J. Phys. Chem. **69**, 687 (1965).
10. E. M. WOOLLEY, D. G. HURKOT et L. G. HEPLER. J. Phys. Chem. **74**, 3908 (1970).
11. A. K. DAS et K. K. KUNDU. J. Chem. Soc. Faraday Trans. **69**, 730 (1973).
12. P. FIORDIPONTI, F. RALLO et F. RODANTE. Z. Phys. Chem. N.F. **88**, 149 (1974).
13. J. C. HALLE, R. GABORIAUD et R. SCHAAL. Bull. Soc. Chim. Fr. **6**, 1851 (1969).
14. F. RODANTE, F. RALLO et P. FIORDIPONTI. Thermochim. Acta, **6**, 369 (1973).
15. G. L. BERTRAND, F. J. MILLERO, C. H. WU et L. G. HEPLER. J. Phys. Chem. **70**, 699 (1966).
16. L. AVEDIKIAN et N. DOLLET. Bull. Soc. Chim. Fr. **12**, 4551 (1967).
17. H. J. E. DOBSON. J. Chem. Soc. **127**, 2866 (1925).
18. A. C. BROWN et D. J. G. IVES. J. Chem. Soc. 1608 (1962).
19. J. KENTTAMAA, E. TOMMILA et M. MARTTI. Ann. Acad. Sci. Fenn. AII, **93**, 3 (1959).
20. F. RALLO, F. RODANTE et P. SILVERSTRONI. Thermochim. Acta, **1**, 311 (1970).
21. R. H. PERRY, C. H. CHILTON et S. D. KIRKPATRICK. Perry's chemical engineers' handbook. Vol. 13, 4 ed. McGraw Hill, New York. 1963. p. 7.
22. A. T. KISTER et D. C. WALDMAN. J. Phys. Chem. **62**, 245 (1958).
23. R. H. STOKES. Aust. J. Chem. **20**, 2087 (1967).
24. E. P. EGAN, JR. et B. B. LUFF. J. Chem. Eng. Data, **11**, 192 (1966).
25. F. T. GUCKER, JR. et H. B. PICKARD. J. Am. Chem. Soc. **62**, 1464 (1940).
26. J. WYMAN, JR. J. Am. Chem. Soc. **53**, 3292 (1931).
27. N. S. OSBORN, E. M. MACKELOY et H. W. BEARCE. J. Res. **9**, 327 (1913).
28. G. DOUHERET. Bull. Soc. Chim. Fr. 3122 (1968).
29. S. A. SCHICHMAN et R. L. AMEY. J. Phys. Chem. **75**, 98 (1971).
30. P. G. SEARS, G. R. JURCH, JR. et D. E. SANDS. Trans. Ky. Acad. Sci. **28**, 10 (1967).
31. G. AKERLÖF. J. Am. Chem. Soc. **54**, 4125 (1932).
32. F. SCHWERS. J. Chim. Phys. **9**, 15 (1911).
33. (*a*) J. WYMAN, JR. J. Am. Chem. Soc. **55**, 4116 (1933); (*b*) N. DESROSIERS, G. PERRON et J. E. DESNOYERS. Resultats non-publiés; N. DESROSIERS, G. PERRON, J. G. MATHIESON et J. E. DESNOYERS. J. Solution Chem. **3**, 789 (1974).
34. C. G. MALMBERG et A. A. MARYOTT. J. Res. Natl. Bur. Stand. **56**, 1 (1956).
35. B. B. OWEN, R. C. MILLER, C. E. MILNER et H. L. COGAN. J. Phys. Chem. **65**, 2065 (1961).
36. E. W. RUSCHE et W. B. GOOD. J. Chem. Phys. **45**, 4667 (1966).
37. R. L. KAY, G. A. VIDULICH et K. S. PRIBADI. J. Phys. Chem. **73**, 445 (1969).
38. G. S. KELL. J. Chem. Eng. Data, **12**, 66 (1967).
39. J. JUILLARD, J.-P. MOREL et L. AVEDIKIAN. J. Chim. Phys. **69**, 787 (1972).
40. K. K. KUNDU et K. MAZUMDAR. J. Chem. Soc. Faraday Trans. **69**, 806 (1973).
41. J.-P. MOREL. Bull. Soc. Chim. Fr. 1405 (1967).
42. J.-P. MOREL et J. MORIN. J. Chim. Phys. **67**, 2018 (1970).
43. Y. POINTUD, J. JUILLARD, J.-P. MOREL et L. AVEDIKIAN. Electrochim. Acta, **19**, 229 (1974).

Can. J. Chem. Downloaded from www.nrcresearchpress.com by 210.87.254.42 on 09/05/12
For personal use only.

Can. J. Chem. Downloaded from www.nrcresearchpress.com by 210.87.254.6 on 09/05/12
For personal use only.

A Photochemical Route to *N*-Acyl Imines[1,2]

WILLIAM A. COURT,[3] OLIVER E. EDWARDS,[4] CIRO GRIECO,[5] WERNER RANK,[3] AND TAKEHIRO SANO[3]

Division of Biological Sciences, National Research Council of Canada, Ottawa, Canada K1A 0R6

Received October 24, 1974

WILLIAM A. COURT, OLIVER E. EDWARDS, CIRO GRIECO, WERNER RANK, and TAKEHINO SANO. Can. J. Chem. **53**, 463 (1975).

Irradiation of two steroidal α-azido ketones gave *N*-acyl imines by formal acyl migration onto nitrogen. Spectroscopic characteristics (u.v., i.r., ^{1}H n.m.r., and ^{13}C n.m.r.) and chemistry of these is described. Similarly an α-azido γ-lactone gave a 5,6-dihydro-1,3-oxazin-2-one which added methanol readily to give a 4-methoxytetrahydro-1,3-oxazine-2-one. Possible mechanisms are considered for the observed rearrangements.

WILLIAM A. COURT, OLIVER E. EDWARDS, CIRO GRIECO, WERNER RANK et TAKEHIRO SANO. Can. J. Chem. **53**, 463 (1975).

L'irradiation de deux cétones stéoridales portant chacun un groupe azido en α conduit aux *N*-acylimines provenant d'une façon formelle d'une migration acyle vers l'azote. On décrit les caractéristiques spectroscopiques (u.v., i.r., ^{1}H r.m.n. et ^{13}C r.m.n.) et la chimie de ces composés. De la même manière une α-azido γ-lactone conduit à une dihydro-5,6 oxazinone-1,3,2 qui peut additionner facilement du méthanol pour donner une méthoxy-4 tétrahydro-oxazinone-1,3,2. On considère divers mécanismes possibles pour les réarrangements observés.
[Traduit par le journal]

We wish to record what we believe to be the first examples of photochemical generation of *N*-acyl imines.

Irradiation[6] of methylene chloride solutions of 3β,20β-diacetoxy-12α-azido-5β-pregnan-11-one **1** (1) containing *ca.* 0.1 molar-equiv. of dry pyridine or triethylamine, at 5° or lower, gave as major product (60% isolated) the acyl imine **2**. This had m.p. 192°; $[\alpha]_D$ +184° (*c* 0.13, 95% ethanol); λ_{max} (ethanol) 288 nm (ε 1080); ν_{max} (CCl_4) 1742, 1715, and 1662 cm^{-1}. Its ^{1}H n.m.r. spectrum had a one-proton signal at δ 7.95 (N=CH—) and its ^{13}C n.m.r. spectrum in C_6D_6 had signals at 189.1 (CO—N) and 169.2 p.p.m. (N=CH—). On alumina compound **2** was partially hydrated to **3** (R = H). The hydration was more efficient if a solution of **2** in aqueous dioxane was stirred in the presence of a sulfonic acid ion-exchange resin. The hydroxy lactam **3** (R = H) had ν_{max} ($CHCl_3$) 3520, 3405, 1730, and 1680 cm^{-1}. Treatment of **2** or **3** with anhydrous *p*-toluene sulfonic acid or acidic ion-exchange resin in methanol gave **3** (R = CH_3). This had m.p. 209°; $[\alpha]_D$ +144° (95% ethanol); ν_{max} (CCl_4) 3230, 1740, and 1670 cm^{-1}. In addition to a 1H doublet at δ 6.0 (NH) its ^{1}H n.m.r. spectrum contained a doublet (^{1}H) at δ 4.23. The NH doublet disappeared on shaking with D_2O while the doublet at δ 4.23 collapsed to a singlet. Irradiation of **1** in methanol gave **3** (R = CH_3) directly. That this was probably a two-step process was shown by irradiation of **2** in methanol. The resulting solvation of the imino double bond in **2**, giving rise to **3**, was of comparable speed to the direct photoconversion of **1** to **3**.

Catalytic reduction of **2** gave the saturated lactam **4** as a glass which distilled at 180°, 1×10^{-4} Torr. This had $[\alpha]_D$ +49° (95% ethanol); ν_{max} (CCl_4) 3230, 1740, and 1670 cm^{-1}. In its ^{1}H n.m.r. spectrum, a 2H multiplet at δ 3.3

[1]Issued as NRCC No. 14424.

[2]Presented in part at the Symposium on Heterocyclic Chemistry, Poznan, July 24–26, 1972.

[3]NRCC Postdoctorate Fellow.

[4]To whom correspondence should be addressed.

[5]NATO Fellow from the Dept. of Pharmaceutical Chemistry, Universita degli Studi di Napoli.

[6]A high-pressure Hanovia 100 W mercury lamp was used, with a Pyrex filter. The photolysis of **1** was slower using a Rayonet reactor with lamps with peak emission at 350 nm.

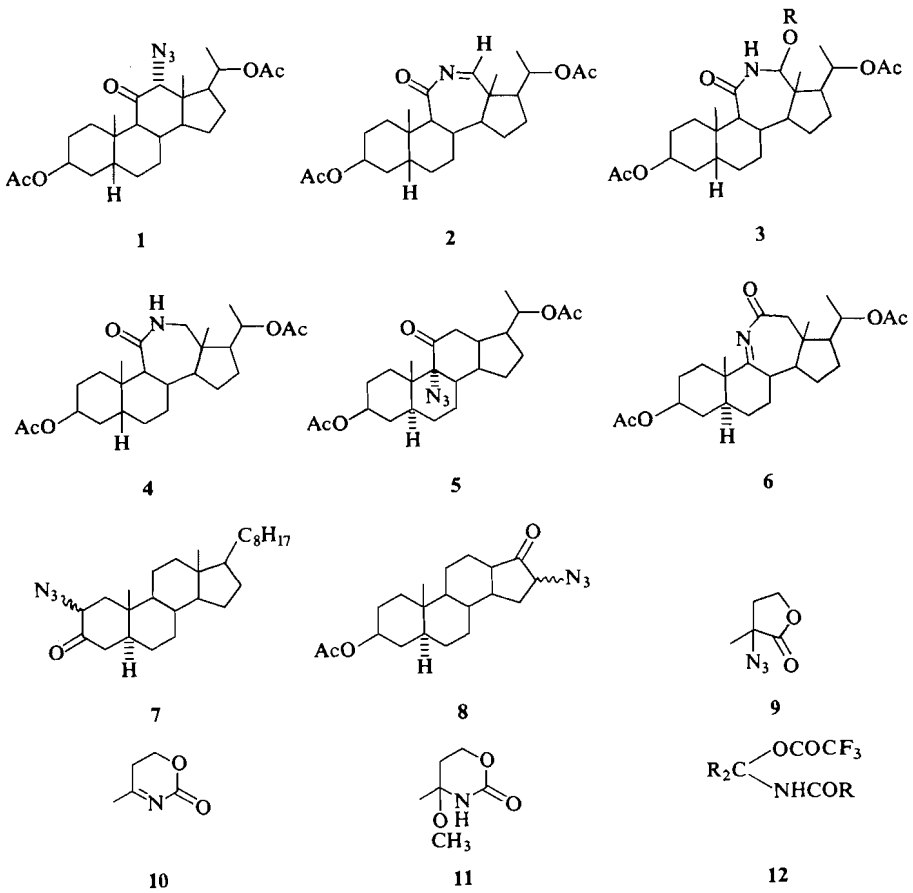

became a quartet when acidified D_2O was added, consistent with its assignment to the system —$CONHCH_2C$—. In refluxing dry dimethylaniline **1** was converted slowly (14 h) into a mixture rich in **2** (50% isolated).

When a methanol solution of 3β,20β-diacetoxy-9α-azido-5α-pregnane-11-one (**5**) (1) was irradiated[6] with wavelengths greater than 300 nm at 5° it gave a 38% yield of the *N*-acyl imine **6**, m.p. 223°; $[\alpha]_D$ +31°; λ_{max} (ethanol) 278 nm (ε 500); ν_{max} (CCl_4) 1737, 1698, and 1668 cm^{-1}. A 2H quartet in its ^1H n.m.r. spectrum centered at δ 2.8 could be attributed to the hydrogens on C-12. Its ^{13}C n.m.r. spectrum in C_6D_6 had signals at 174 (N=C) and 180 p.p.m. (11-carbonyl). Other products[7] from the photolysis of **5** will be described in the full paper. In contrast to the behavior of **1** and **5**, irradiation of methanol solutions of 2α- or 2β-azidocholestan-3-one (**7**) and 16α- and 16β-azido-3-acetoxyandrostan-17-one (**8**) gave complex mixtures containing little, if any, of the desired methoxylactams. On the basis of these observations we suggest that for conformationally rigid α-azido ketones an axial orientation of the azide group (as in **1** and **5**) is necessary for efficient formation of *N*-acyl imine.

Interest in generation of the nitrogen heterocycle present in the ansa macrolide maytansine (2) prompted us to photolyse the α-azido lactone **9** (3). Irradiation of **9** in methanol using a Hanovia 100 W lamp and Vycor filter for 7 h at *ca.* −25° gave a mixture of *N*-acyl imine **10** (4-methyl-5,6-dihydro-1,3-oxazin-2-one) and methoxy urethane **11** (4-methoxy-4-methyltetrahydro-1,3-oxazine-2-one) in the ratio 2.5:1. Further irradiation of this mixture for 3 h at 5° converted it into a 1.5:1 mixture of the two products. The solvation of **10** could also be induced by acid catalysis.

Irradiation of **9** in methylene chloride at −25°

[7]J. L. Douglas and D. C. Horwell, unpublished results.

Can. J. Chem. Downloaded from www.nrcresearchpress.com by 210.87.254.6 on 09/05/12
For personal use only.

[1]

[2] 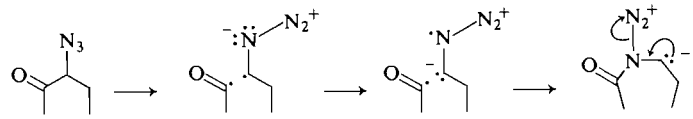

gave a product which from its n.m.r. spectrum and reactions was nearly pure acylimine **10** which had ν_{max} (CH_2Cl_2) 1735 and 1645 cm^{-1} and λ_{max} (dioxane) 262 nm (ε 1060). Its n.m.r. spectrum had signals at δ 2.27 (t, J = 1.8 Hz, 3H), 3.77 (m, 2H), and 4.40 (t, J = 5.5 Hz, 2H). The methoxy urethane **11** had m.p. 89°; ν_{max} ($CHCl_3$) 3430, 3250, 3130, and 1710 cm^{-1}. It gave ^1H n.m.r. signals at δ 1.50 (3H), 1.99 (m, 2H), 3.30 (s, 3H) 4.38 (m, 2H), and 7.88 (broad, NH).

In contrast to the results with **1**, **5**, and **9**, both Millership and Suschitzky (4) and Margaretha and Steffen (5) were unable to detect acyl migration onto nitrogen during photolysis of α-azido lactam and an α-azido ketone, respectively.

The above formal 1,3-acyl migrations onto nitrogen are probably initiated by nitrene formation (Eq. 1). However the long wavelengths that are effective in producing the acyl imines leaves open a second alternative for the photochemical reaction involving Norrish type 1 cleavage of the cyclic ketone (Eq. 2).

N-acyl imines are probable transient intermediates in numerous reactions (6–15). Their possible importance in biosynthesis has been recognized (16). Meyers and Shaw (17) have recently described the synthesis of an analog of **11** in which an acyl imine may be an intermediate. Two acyl imines which have been isolated arose from thermal analogs of the above 1,3-acyl migration (4, 18). Tsuda and Hayatsu described the preparation in low yield of a steroidal *N*-acyl imine produced by rearrangement of an enamide (19) and recently *N*-acyl imines have been produced by elimination of trifluoroacetic acid from compounds of type **12** (20).

Preparation of the other steroid analogs of **3** and **6**, and of compounds related to **10** and **11** which may be useful in synthesis of maytansine, are being explored.

1. O. E. Edwards and T. Sano. Can. J. Chem. **47**, 3489 (1969).
2. S. M. Kupchan, Y. Komoda, W. A. Court, G. J. Thomas, R. M. Smith, A. Karim, C. J. Gilmore, R. C. Haltiwanger, and R. F. Bryan. J. Am. Chem. Soc. **94**, 1354 (1972).
3. O. E. Edwards and C. Grieco. Can. J. Chem. **52**, 3561 (1974).
4. J. S. Millership and H. Suschitzky. Chem. Commun. 1496 (1971).
5. P. Margaretha and H. Steffen. Chimia, **27**, 479 (1973).
6. M. Toda, H. Niwa, K. Ienaga, and Y. Hirata. Tetrahedron Lett. 335 (1972).
7. J. E. Baldwin, F. J. Urban, R. D. G. Cooper, and F. L. Jose. J. Am. Chem. Soc. **95**, 2401 (1973).
8. G. A. Koppel and R. E. Koehler. J. Am. Chem. Soc. **95**, 2403 (1973).
9. H. L. Ammon, P. H. Mazzocchi, W. J. Kopecky, Jr., H. J. Tamburin, and P. H. Watts, Jr. J. Am. Chem. Soc. **95**, 1968 (1973).
10. W. von E. Doering and M. J. Goldstein. Tetrahedron, **5**, 53 (1959).
11. J. E. Baldwin, S. B. Haber, and J. Kitchin. Chem. Commun. 790 (1973).
12. R. A. Firestone and B. G. Christensen. J. Org. Chem. **38**, 1436 (1973).
13. R. B. Morin, E. M. Gordon, T. McGrath, and R. Shuman. Tetrahedron Lett. 2159 (1973).
14. R. B. Morin, E. M. Gordon, and J. R. Lake. Tetrahedon Lett. 5213 (1973).
15. R. B. Morin, J. R. Lake, and E. M. Gordon. Tetrahedron Lett. 2979 (1974).
16. B. W. Bycroft. Nature, **224**, 595 (1969).
17. A. I. Meyers and C.-C. Shaw. Tetrahedron Lett. 717 (1974).
18. H. W. Moore and D. S. Pearce. Tetrahedron Lett. 1621 (1971).
19. K. Tsuda and R. Hayatsu. J. Am. Chem. Soc. **78**, 4107 (1956).
20. W. Steglich, K. Burger, M. Durr, and E. Burgis. Chem. Ber. **107**, 1488 (1974).

Can. J. Chem. Downloaded from www.nrcresearchpress.com by 210.87.254.6 on 09/05/12
For personal use only.

Can. J. Chem. Downloaded from www.nrcresearchpress.com by 210.87.254.42 on 09/05/12
For personal use only.

Canadian Journal of Chemistry

Published by
THE NATIONAL RESEARCH COUNCIL OF CANADA

Journal canadien de chimie

Publié par
LE CONSEIL NATIONAL DE RECHERCHES DU CANADA

Volume 53 Number 4 February 15, 1975 Volume 53 numéro 4 15 février 1975

Silyl-, Germyl-, and Stannyl-pentacarbonylmetalates of Chromium, Molybdenum, and Tungsten[1]

E. E. ISAACS AND W. A. G. GRAHAM

Department of Chemistry, University of Alberta, Edmonton, Alberta T6G 2E1

Received September 3, 1974

E. E. ISAACS and W. A. G. GRAHAM. Can. J. Chem. **53**, 467 (1975).

The new anions $[R_3M'M(CO)_5]^-$ (R_3M' = Ph_3Si, $MePh_2Si$, Ph_3Ge, Ph_3Sn, Me_3Sn, and Ph_3Pb; M = Cr, Mo, W) have been prepared as tetraethylammonium salts by reaction of $R_3M'Li$ with $[Et_4N(ClM(CO)_5]$. The redistribution reaction between $[Ph_3SnW(CO)_5]^-$ and $[Cl_3SnW(CO)_5]^-$ affords $[PhCl_2SnW(CO)_5]^-$ or $[Ph_2ClSnW(CO)_5]^-$. Anhydrous HCl reacts with $[Ph_3SiW(CO)_5]^-$ and $[Ph_3GeW(CO)_5]^-$ to form $[ClW(CO)_5]^-$ but with $[Ph_3SnW(CO)_5]^-$ to form $[Cl_3SnW(CO)_5]^-$. An insertion reaction of $SnBr_2$ with $[BrW(CO)_5]^-$ forms the new anion $[Br_3SnW(CO)_5]^-$ while $SnCl_2$ and $GeCl_2$ (from $HGeCl_3$) react with $[ClM(CO)_5]^-$ to produce the known species $[Cl_3M'M(CO)_5]^-$ (M' = Ge, Sn; M = Cr, Mo, W). Infrared spectra in the carbonyl stretching region are reported for all anions.

E. E. ISAACS et W. A. G. GRAHAM. Can. J. Chem. **53**, 467 (1975).

On a préparé, par réaction de $R_3M'Li$ avec $Et_4N[ClM(CO)_5]$, les nouveaux anions $[R_3M'M(CO)_5]^-$ (R_3M' = Ph_3Si, $MePh_2Si$, Ph_3Ge, Ph_3Sn, Me_3Sn et Ph_3Pb; M = Cr, Mo, W) sous forme de sels de tétraéthylammonium. La réaction de redistribution entre $[Ph_3SnW(CO)_5]^-$ et $[Cl_3SnW(CO)_5]^-$ conduit à $[PhCl_2SnW(CO)_5]^-$ ou $[Ph_2ClSnW(CO)_5]^-$. Le HCl anhydre réagit avec $[Ph_3SiW(CO)_5]^-$ et $[Ph_3GeW(CO)_5]^-$ pour conduire à $[ClW(CO)_5]^-$ mais HCl anhydre réagit avec $[Ph_3SnW(CO)_5]^-$ pour former $[Cl_3SnW(CO)_5]^-$. Une réaction d'insertion du $SnBr_2$ avec du $[BrW(CO)_5]^-$ conduit au nouvel anion $[Br_3SnW(CO)_5]^-$ alors que $SnCl_2$ et $GeCl_2$ (obtenu à partir de $HGeCl_3$) réagissent avec $[ClM(CO)_5]^-$ pour conduire aux espèceş connues $[Cl_3M'M(CO)_5]^-$ (M' = Ge, Sn; M = Cr, Mo, W). On rapporte les spectres infrarouges, dans la région de l'élongation du carbonyle, de tous les anions

[Traduit par le journal]

Introduction

The synthesis and study of bonds between transition metals and the elements below carbon in the fourth main group has attracted wide interest (1–3). Most of the reported compounds are neutral molecules, and the chemistry of anionic complexes containing these bonds is much less well developed. The inherent interest of such complex ions, as well as their probable synthetic value, prompted the present work.

The first anionic, mononuclear derivatives of the hexacarbonyls of chromium, molybdenum, and tungsten to contain ligands of the fourth main group other than carbon were the six compounds $[Ph_4As]^+[Cl_3M'M(CO)_5]^-$ (M' = Ge, Sn; M = Cr, Mo, W) (4). They were prepared by the displacement of carbon monoxide from $M(CO)_6$, under ultraviolet irradiation, by the anions $[Cl_3Ge]^-$ and $[Cl_3Sn]^-$ as the tetraphenylarsonium salts. More recently, the anions $[X_3M'M(CO)_5]^-$ (X = Cl, Br, I) have been prepared by reaction of halide ion with the claimed neutral complexes $[X_2M'M(CO)_5]$ (5).

[1]Organometallic Compounds Having Metal–Metal Bonds, Part XXII. For Part XXI, see ref. 20.

Can. J. Chem. Downloaded from www.nrcresearchpress.com by 210.87.254.42 on 09/05/12
For personal use only.

TABLE 1. Yields, melting points, and microanalytical data of the new anions

Compound	Yield (%)	Melting point (°C)	Calculated (%)				Found (%)			
			C	H	N	Cl	C	H	N	Cl
$Et_4N^+[Ph_3SiCr(CO)_5]^-$	82	181–185	64.05	6.07	2.41	—	63.59	5.90	2.41	—
$Et_4N^+[MePh_2SiCr(CO)_5]^-$	91	139–141	60.00	6.40	2.70	—	59.92	6.33	2.93	—
$Et_4N^+[Cl_3GeCr(CO)_5]^-$	78	185–187	31.15	4.02	2.79	21.29	30.87	4.12	2.86	21.72
$Et_4N^+[Ph_3GeCr(CO)_5]^-$	59	175–177 dec.	59.46	5.63	2.24	—	58.99	5.65	2.42	—
$Et_4N^+[Cl_3SnCr(CO)_5]^-$	96	135–138 dec.	28.53	3.68	2.56	19.43	28.37	3.82	2.64	19.56
$Et_4N^+[Ph_3SnCr(CO)_5]^-$	75	164–166 dec.	55.41	5.25	2.10	—	55.10	5.25	2.10	—
$Et_4N^+[Me_3SnCr(CO)_5]^-$	64	~160 dec.	39.53	6.01	2.88	—	39.68	5.95	3.39	—
$Et_4N^+[Ph_3PbCr(CO)_5]^-$	45	87–93	48.94	4.64	1.84	—	47.97	4.75	1.95	—
$Et_4N^+[Ph_3SiMo(CO)_5]^-$	73	150–154	59.51	5.64	2.24	—	58.80	5.71	2.25	—
$Et_4N^+[MePh_2SiMo(CO)_5]^-$	71	130–131	55.41	5.90	2.48	—	54.77	5.80	2.49	—
$Et_4N^+[Cl_3GeMo(CO)_5]^-$	74	~180 dec.	28.64	3.70	2.57	19.51	28.54	3.88	2.61	19.68
$Et_4N^+[Ph_3GeMo(CO)_5]^-$	57	150–153	55.56	5.26	2.09	—	54.79	5.44	2.04	—
$Et_4N^+[Cl_3SnMo(CO)_5]^-$	38	82–85	26.41	3.41	2.37	17.99	26.43	3.76	2.61	18.98
$Et_4N^+[Ph_3SnMo(CO)_5]^-$	58	139	51.98	4.92	1.96	—	51.62	5.06	2.18	—
$Et_4N^+[Me_3SnMo(CO)_5]^-$	58	>220	36.26	5.51	2.64	—	35.52	5.54	3.39	—
$Et_4N^+[Ph_3PbMo(CO)_5]^-$	43	129–131	46.27	4.38	1.74	—	45.81	4.33	1.92	—
$Et_4N^+[Ph_3SiW(CO)_5]^-$	85	165	52.18	4.94	1.96	—	51.70	5.00	1.86	—
$Et_4N^+[MePh_2SiW(CO)_5]^-$	91	132–135 dec.	47.93	5.10	2.15	—	47.28	5.14	2.25	—
$Et_4N^+[Cl_3GeW(CO)_5]^-$	100	174 dec.	24.66	3.18	2.21	16.70	24.74	3.29	2.18	17.37
$Et_4N^+[Ph_3GeW(CO)_5]^-$	55	163–165	49.12	4.65	1.85	—	49.05	4.42	1.95	—
$Et_4N^+[Br_3SnW(CO)_5]^-$	42	138–140	19.22	2.48	1.72	29.50*	19.38	2.39	1.68	29.32*
$Et_4N^+[Cl_3SnW(CO)_5]^-$	90	130 dec.	22.99	2.97	2.06	15.66	22.99	2.97	2.37	14.39
$Et_4N^+[Cl_2PhSnW(CO)_5]^-$	88	95–96	31.66	3.50	1.94	9.84	31.59	4.01	2.06	10.83
$Et_4N^+[ClPh_2SnW(CO)_5]^-$	61	100–104	39.38	3.97	1.84	4.65	38.84	4.10	1.53	5.14
$Et_4N^+[Ph_3SnW(CO)_5]^-$	72	142 dec.	46.30	4.37	1.74	—	46.51	4.45	2.31	—
$Et_4N^+[Me_3SnW(CO)_5]^-$	87	181	31.10	4.73	2.27	—	30.86	4.70	3.13	—
$Et_4N^+[Ph_3PbW(CO)_5]^-$	59	140–144 dec.	41.71	3.95	1.57	—	41.25	3.94	1.45	—

*Bromine.

TABLE 2. Carbonyl stretching frequencies,[a] assignments, and nuclear magnetic resonance data[b] for the new anions

Compound	Frequencies (cm^{-1})[a]			
	$A_1^{(2)}$	$A_1^{(1)}$	B_1	E
$Et_4N^+[Ph_3SiCr(CO)_5]^-$	2014.5	1877	1928	1894
$Et_4N^+[MePh_2SiCr(CO)_5]^-$[c]	2010.5	1872	1922	1888
$Et_4N^+[Cl_3GeCr(CO)_5]^-$	2059	1930	(1966)	1945
$Et_4N^+[Ph_3GeCr(CO)_5]^-$	2017.5	1872.5	1934	1898
$Et_4N^+[Cl_3SnCr(CO)_5]^-$	2056	(1927)	(1960)	1942
$Et_4N^+[Ph_3SnCr(CO)_5]^-$	2014.5	1877	1930.5	1897
$Et_4N^+[Me_3SnCr(CO)_5]^-$[d]	2002.5	1867	1913	1884
$Et_4N^+[Ph_3PbCr(CO)_5]^-$	2020	1879	1940	1907
$Et_4N^+[Ph_3SiMo(CO)_5]^-$	2031	1880	1943	1904.5
$Et_4N^+[MePh_2SiMo(CO)_5]^-$[e]	2026	1876	1936	1899
$Et_4N^+[Cl_3GeMo(CO)_5]^-$	2069	1925		1947
$Et_4N^+[Ph_3GeMo(CO)_5]^-$	2034	1878	1946	1908
$Et_4N^+[Cl_3SnMo(CO)_5]^-$[f]	2068			1938
$Et_4N^+[Ph_3SnMo(CO)_5]^-$	2033	1884	1946	1910
$Et_4N^+[Me_3SnMo(CO)_5]^-$[g]	2021	1871	1930	1896
$Et_4N^+[Ph_3PbMo(CO)_5]^-$	2039	1883.5	1954	1918
$Et_4N^+[Ph_3SiW(CO)_5]^-$	2030.5	1875	1936	1899
$Et_4N^+[MePh_2SiW(CO)_5]^-$[h]	2026	1871	1928	1894
$Et_4N^+[Cl_3GeW(CO)_5]^-$	2066.5	1919	(1966)	1938
$Et_4N^+[Ph_3GeW(CO)_5]^-$	2033.5	1873	1939	1902
$Et_4N^+[Br_3SnW(CO)_5]^-$	2065	1915	(1958)	1940.5
$Et_4N^+[Cl_3SnW(CO)_5]^-$	2069	1929	(1985)	1942
$Et_4N^+[Cl_2PhSnW(CO)_5]^-$	2058	1915	(1970)	1930
$Et_4N^+[ClPh_2SnW(CO)_5]^-$	2045	1897		1916
$Et_4N^+[Ph_3SnW(CO)_5]^-$	2032	1878	1939	1903
$Et_4N^+[Me_3SnW(CO)_5]^-$[i]	2020.5	1868	1924	1891
$Et_4N^+[Ph_3PbW(CO)_5]^-$	2037.5	1879	1947	1909.5

[a]Infrared spectra in tetrahydrofuran except as noted. Bands in parentheses were too broad for accurate measurement.
[b]The τ value quoted in footnotes refers to the methyl group of the compound in question.
[c]τ 9.25 in acetone-d_6.
[d]τ 9.96; $^2J(Sn—CH_3)$ = 37 Hz (^{117}Sn and ^{119}Sn coupling not resolved); acetone-d_6.
[e]τ 9.28; $^2J(^{29}Si—CH_3)$ = 5.2 Hz; CD_3CN.
[f]Infrared in CH_2Cl_2; unstable in tetrahydrofuran.
[g]τ 10.0; $^2J(Sn—CH_3)$ = 33 Hz (^{117}Sn and ^{119}Sn coupling not resolved); acetone-d_6.
[h]τ 9.12; $^2J(^{29}Si—CH_3)$ = 5.4 Hz; CD_3CN.
[i]τ 9.90; $^2J(^{117}Sn—CH_3)$ = 35.5 Hz; $^2J(^{119}Sn—CH_3)$ = 37.0 Hz; CD_3CN.

Although the present work is restricted to anions in which a single carbonyl ligand is replaced by an X_3M' or R_3M' group, it is of interest to note that more than one such replacement is possible. Thus, Ruff (4) in his original report isolated $[Ph_4As]_2^+[(Cl_3Ge)_2Mo(CO)_4]^{2-}$, and obtained spectroscopic evidence for several other disubstituted products. More recently, displacement of benzene from π-$C_6H_6M(CO)_3$ and $(\pi$-$C_6H_6)_2M$ by $[SnCl_3]^-$ has been reported to form the ions $[(Cl_3Sn)_3M(CO)_3]^{3-}$ and $[(Cl_3Sn)_6M]^{6-}$ respectively (6).

Experimental

Melting points were determined using a Kofler hot-stage microscope. Analytical results (Table 1) were obtained by the Microanalytical Laboratory of this department. Infrared spectra of the carbonyl stretching region were measured by means of a Perkin–Elmer Model 337 spectrometer at a scanning rate of 39 cm^{-1} min^{-1}, and recorded in expanded form (1 cm of chart ≈ 10 cm^{-1}) on an external recorder. Spectra were calibrated with bands of gaseous CO and DBr, and are considered accurate to ±1 cm^{-1}. Band positions quoted in Table 2 refer to the midpoint at half-height.

Table 2 lists as footnotes selected n.m.r. data for the $MePh_2Si$ and Me_3Sn derivatives. The phenyl substituents appeared as a complex multiplet at τ 2.2–2.8, and the characteristic τ 8.6 triplet – 6.4 quartet due to $[Et_4N]^+$ was observed in all spectra.

Solvents and Reagents

Tetrahydrofuran for use in reactions was dried over calcium hydride; that used as infrared solvent was also distilled from potassium benzophenone under nitrogen. Dichloromethane was dried over phosphorus pentoxide, and *n*-pentane over calcium hydride. All solvents were purged with nitrogen before use.

Chromium, molybdenum, and tungsten hexacarbonyls

Can. J. Chem. Downloaded from www.nrcresearchpress.com by 210.87.254.42 on 09/05/12
For personal use only.

Can. J. Chem. Downloaded from www.nrcresearchpress.com by 210.87.254.42 on 09/05/12
For personal use only.

were purchased from Strem Chemicals, Inc. Triphenyltin chloride and Sn_2Me_6 were obtained from M & T Chemicals Inc. Triphenylchlorosilane and $MePh_2SiCl$ were obtained from Pierce Chemical Company, Ph_3PbCl from PCR Inc., and $HGeCl_3$ from Alfa Products Division of Ventron Corp. The literature method (7) was used to prepare $[Et_4N][XM(CO)_5]$ (M = Cr, Mo, W; X = Cl, Br). Lithium metal was obtained from Alfa Products as 3.2 mm wire; high-sodium (1.0% Na) and low-sodium (0.01%) grades were equally satisfactory.

All reactions and crystallizations were carried out under a nitrogen atmosphere, and details of representative preparations are given below.

Preparation of $[Et_4N][Ph_3SiCr(CO)_5]$

Lithium wire (*ca.* 6 cm, excess) was wrapped in a piece of polyethylene, pounded with a hammer, cut into small pieces, and dropped into a solution of Ph_3SiCl (3.5 g, 11.9 mmol) in 25 ml tetrahydrofuran. The solution was magnetically stirred for 3–4 h, by which time it had become deep red. It was then transferred by means of a 50 ml syringe, taking care to leave any excess lithium behind, and added slowly to a solution of $[Et_4N][Cr(CO)_5Cl]$ (3.3 g, 9.2 mmol) in 50 ml tetrahydrofuran. The reaction mixture was stirred at room temperature for 1 h and then the solvent was removed under reduced pressure. The sticky solid residue was extracted with *ca.* 120 ml dichloromethane, the extract was filtered through Celite, and ether was added to the filtrate to precipitate a white solid. The analytical sample was recrystallized twice from dichloromethane–ether to afford 4.4 g (82% yield) of flaky white crystals.

Preparation of $[Et_4N][Cl_3GeCr(CO)_5]$

Trichlorogermane (1.5 ml, 2.7 g, 15.0 mmol) was added to a magnetically stirred solution of $[Et_4N][Cr(CO)_5Cl]$ (3.0 g, 8.4 mmol) in 80 ml dichloromethane. The solution was heated to reflux for 15 min and then filtered through Celite. Addition of ether precipitated a pale yellow compound which was collected and shaken with a methanol–water (1:1) solution to remove yellow adsorbed impurities. The solid was filtered, dried, and recrystallized from dichloromethane–ether to give 3.3 g (78% yield) of white crystals.

Preparation of $[Et_4N][Cl_3SnMo(CO)_5]$

Tin(II) chloride (2.0 g, 10.6 mmol) and $[Et_4N][ClMo(CO)_5]$ (3.0 g, 7.5 mmol) were refluxed in 80 ml dichloromethane for 1 h. The yellow solution became pale orange and was filtered through Celite. Addition of ether to the filtrate precipitated an oil; the solvents were decanted and the oil washed with ether and with *n*-pentane. The remaining oil was then extracted with 60 ml dichloromethane, 40 ml ether was added, and the solution was filtered leaving behind an orange solid residue. An additional 20 ml of ether was added to the colorless filtrate, which upon cooling at 0° overnight afforded the white crystalline product (1.7 g, 38% yield).

Preparation of $[Et_4N][Me_3SnMo(CO)_5]$

To a solution of hexamethylditin (1.8 g, 8.6 mmol) in 25 ml tetrahydrofuran, lithium clippings (excess) were added and the solution stirred for 1 h. The deep red solution was added to a solution of $[Et_4N][Mo(CO)_5Cl]$ (3.1 g, 7.7 mmol) in tetrahydrofuran (100 ml) and the reaction mixture stirred for 1 h. The solvent was removed and the solid residue extracted with dichloromethane and filtered through a 10 cm column packed with aluminum oxide. Addition of ether precipitated an oil which gave a pale yellow solid after pumping overnight in high vacuum. Two careful recrystallizations from dichloromethane–ether–pentane afforded the analytical sample (2.4 g, 58% yield).

Preparation of $[Et_4N][Ph_3PbMo(CO)_5]$

Lithium clippings (excess, from 6 cm wire) were added to a solution of Ph_3PbCl in tetrahydrofuran (25 ml). The reaction was slightly exothermic, and the mixture turned black after *ca.* 3 h stirring. The organolithium solution was then added to a solution of $[Et_4N][Mo(CO)_5Cl]$ (3.6 g, 9.0 mmol) in 100 ml tetrahydrofuran and the reaction mixture was stirred for an additional 0.5 h. After removal of solvent under reduced pressure, the solid residue was extracted with dichloromethane and filtered through Celite. The filtrate was concentrated and ether was added in 5 ml portions until the solution became cloudy. During cooling overnight, white crystals formed which were collected (3.1 g, 43% yield). The sample was sufficiently pure for further reaction. The analytical sample was obtained by two further recrystallizations from dichloromethane–ether.

Preparation of $[Et_4N][Ph_3GeW(CO)_5]$

Hexaphenyldigermane (3.5 g, 6.5 mmol) or alternatively Ph_3GeCl (3.2 g, 10.6 mmol) in 20 ml tetrahydrofuran was stirred with excess lithium wire. The reaction was slightly exothermic and a milky precipitate appeared. The disappearance of the white precipitate was followed by color changes from deep yellow through dark green to a deep red color over a period of 4 to 6 h (3 h for Ph_3GeCl). This reaction mixture was added slowly to a solution of $[Et_4N][W(CO)_5Cl]$ (4.5 g, 9.3 mmol) in 100 ml tetrahydrofuran and stirred for 0.5 h. Solvent was then removed under reduced pressure. The residue was extracted with dichloromethane, filtered through Celite, and the filtrate concentrated under a stream of nitrogen. On cooling at 0° overnight, fluffy white crystals formed (4.5 g, 55% yield).

Preparation of $[Et_4N][Ph_2ClSnW(CO)_5]$

A mixture of $[Et_4N][Ph_3SnW(CO)_5]$ (2.38 g, 2.96 mmol) and $[Et_4N][Cl_3SnW(CO)_5]$ (1.00 g, 1.47 mmol) was heated at 150° in the absence of solvent. The progress of the reaction was followed by the removal of samples at short intervals and recording their spectra in dichloromethane. After 1 h the mixture was cooled to room temperature and the crude product extracted with dichloromethane. Solvent was removed from the extract, leaving an oil which solidified on pumping overnight at 60°. Three recrystallizations from dichloromethane–ether afforded the analytical sample (2.0 g, 88% yield). Trace amounts of starting materials were difficult to eliminate.

Under similar conditions using $[Et_4N][Ph_3SnW(CO)_5]$ and $[Et_4N][Cl_3SnW(CO)_5]$ in 1:2 molar ratio, $[Et_4N][PhCl_2SnW(CO)_5]$ was obtained.

Reactions of Anions with Hydrogen Chloride

An ethereal HCl solution was prepared by bubbling gaseous HCl (Matheson of Canada Ltd.) through 200–250 ml of diethyl ether for 30 min. The flask was capped by means of a rubber septum and the molarity of the solution

Can. J. Chem. Downloaded from www.nrcresearchpress.com by 210.87.254.42 on 09/05/12
For personal use only.

determined by titrating 10 ml aliquots, placed in water, against a standard NaOH solution.

An aliquot of ethereal HCl (0.4 ml, 1.3 mmol HCl) was added to a solution of $[Et_4N][Ph_3GeW(CO)_5]$ (0.6 g, 0.8 mmol) in tetrahydrofuran (15 ml). The initially colorless solution turned yellow at once. The infrared spectrum showed the disappearance of starting material and new bands at 2065 (w), 1916(s), and 1857(m), which were identical with those of an authentic sample of $[Et_4N][ClW(CO)_5]$. Reaction of $[Et_4N][Ph_3SiW(CO)_5]$ under the same conditions afforded the same product in an equally rapid reaction. When gaseous HCl was passed over a stirred dichloromethane solution of $[Et_4N][Ph_3SiW(CO)_5]$, the same product was formed.

A sample of $[Et_4N][Ph_3SnW(CO)_5]$ in tetrahydrofuran reacted rapidly and completely with ethereal HCl under the above conditions forming $[Et_4N][Cl_3SnW(CO)_5]$, recognized by its infrared spectrum (Table 2). The product was stable to further treatment with excess ethereal HCl. In dichloromethane, gaseous HCl formed the same product.

Results and Discussion

Synthesis

As noted above, the previously reported group IV ligands in the pentacarbonylmetalates of chromium, molybdenum, and tungsten have been restricted to X_3Ge and X_3Sn (X = Cl, Br, I). We have prepared and characterized a number of new complexes of this type in which the group IV ligand is Ph_3Si, $MePh_2Si$, Ph_3Ge, Ph_3Sn, Me_3Sn, and Ph_3Pb. The reaction is a displacement using the well-known lithio derivatives $R_3M'Li$, in which the preferred starting material is the chloropentacarbonyl anion (7).

$$[ClM(CO)_5]^- + R_3M'Li \xrightarrow{\text{tetrahydrofuran}} [R_3M'M(CO)_5]^- + LiCl$$

Use of the tetraethylammonium salt of $[ClM(CO)_5]^-$ affords the product as the tetraethylammonium salt as well. The progress of the reaction could be monitored, and excess $R_3M'Li$ avoided, by following the disappearance of the highest carbonyl stretching band of $[ClM(CO)_5]^-$. Reactions took place smoothly at room temperature in about 1 h, affording the product in yields ranging from 40 to 90%.

Tetraethylammonium salts of the new anions reported here form colorless crystals,[2] soluble in polar solvents such as dichloromethane, acetone, and tetrahydrofuran, but not in ether or in hydrocarbon solvents. The compounds are stable in the solid state in air for long periods. Most are stable for periods of days in solution under a nitrogen atmosphere, but $[Et_4N][Cl_3SnW(CO)_5]$ decomposed in tetrahydrofuran solution in a few minutes.

An interesting and perhaps advantageous alternative route to certain of the trihalogeno derivatives was discovered involving insertion of $SnCl_2$, $SnBr_2$, and $GeCl_2$ into the metal–halogen bond of $[XM(CO)_5]^-$ anions.[3]

$$[ClM(CO)_5] \xrightarrow{SnCl_2,\ 40°,\ CH_2Cl_2} [Cl_3SnM(CO)_5]^-$$

$$[ClM(CO)_5] \xrightarrow{HGeCl_3,^{(3)}\ 40°,\ CH_2Cl_2} [Cl_3GeM(CO)_5]^-$$

$$[BrM(CO)_5] \xrightarrow{SnBr_2,\ 40°,\ CH_2Cl_2} [Br_3SnM(CO)_5]^- \quad (M = Cr, Mo, W)$$

The insertion reactions were complete within a few minutes and yields were high. Subsequent to our work, we learned that $[Cl_3SnM(CO)_5]^-$ (M = Cr, Mo, W) had been prepared independently by this route.[4]

Chemical Reactions

A reaction of some interest and considerable synthetic value is that of redistribution. Thus, mixed organohalogenotin complexes were obtained by the following reactions at 150° without solvent.

$$2[Et_4N][Ph_3SnW(CO)_5] + [Et_4N][Cl_3SnW(CO)_5] \rightarrow 3[Et_4N][Ph_2ClSnW(CO)_5]$$

Use of 1:2 molar ratio afforded $[Et_4N][PhSnCl_2W(CO)_5]$. Such a redistribution is familiar in organotin chemistry, and was first applied by Gorsich to tin transition metal derivatives (8). In the present work, only the reaction between $[Ph_3SnW(CO)_5]^-$ and $[Cl_3SnW(CO)_5]^-$ was investigated, so its generality has not been established.

Reactions of $[Ph_3M'W(CO)_5]^-$ (M' = Si, Ge, Sn) with hydrogen chloride in ether–tetrahydrofuran were investigated. For the triphenylsilyl and triphenylgermyl derivatives, very rapid cleavage of the metal–metalloid bond occurred.

$$[Et_4N][Ph_3M'W(CO)_5] + HCl \xrightarrow[\text{tetrahydrofuran}]{\text{ether}} [Et_4N][ClW(CO)_5] + (HM'Ph_3)$$

[2]In a few cases the crystals were pale yellow in appearance, presumably due to adsorbed impurities. The yellow color was removed by shaking the crystals with water–methanol (1:1).

[3]Trichlorogermane is presumed to serve as a source of $GeCl_2$ in this reaction.

[4]Unpublished results of H. Behrens and H. P. Burkon, quoted in footnote 11 of ref. 5.

Can. J. Chem. Downloaded from www.nrcresearchpress.com by 210.87.254.42 on 09/05/12
For personal use only.

Formation of $[ClW(CO)_5]^-$ was indicated by infrared spectroscopy. The hydride $HM'Ph_3$ is written in parentheses since it is the other presumed product of the reaction.

On the other hand, the tin-tungsten anion reacted under similar conditions to cleave the phenyl-tin bond.

$$[Et_4N][Ph_3SnW(CO)_5] + 3HCl \xrightarrow[\text{tetrahydrofuran}]{\text{ether}} [Et_4N][Cl_3SnW(CO)_5] + 3PhH$$

In this reaction, the behavior of $[Ph_3SnW(CO)_5]^-$ parallels that of the neutral, isoelectronic $Ph_3SnRe(CO)_5$, where the reaction product is $Cl_3SnRe(CO)_5$ (9, 10).[5] The different character of the cleavage reaction with silicon and germanium on the one hand, and tin on the other is not understood, but may be the consequence of the relative rate of Ph—M′ cleavage, which would be greater for tin.

Protonation of $[Et_4N][Ph_3SnW(CO)_5]$ and $[Et_4N][Cl_3GeMo(CO)_5]$ using a pentane – 85% H_3PO_4 mixture[6] afforded only the corresponding hexacarbonyl. The intent in this reaction was to prepare the hypothetical neutral seven-coordinate hydrides, *e.g.*, $Ph_3SnW(H)(CO)_5$, but no direct evidence for their formation was obtained. The products of the phosphoric acid reactions can readily be interpreted in terms of initial formation of the hydrido species, which would rapidly undergo reductive elimination of Ph_3SnH to form coordinatively unsaturated $M(CO)_5$; partial decomposition of the latter would provide carbon monoxide for conversion of the balance to $M(CO)_6$.[7] This process would be analogous to the elimination of Ph_3SiH from π-$C_5H_5Mn(CO)_2HSiPh_3$ (12).

In a further attempt to prepare a seven-coordinate neutral derivative, $[Ph_3GeW(CO)_5]^-$ was reacted in tetrahydrofuran with Ph_3PAuCl; the Ph_3PAu ligand is considered to have a small steric requirement. However, the reaction product (established by infrared spectroscopy) was $[ClW(CO)_5]^-$. Again, one could speculate that $[Ph_3GeW(CO)_5AuPPh_3]$ was formed as an intermediate, followed by elimination of $Ph_3GeAuPPh_3$ and attack of chloride ion on the $W(CO)_5$ moiety.

A further comparison of the reactivity of these anions with that of neutral trihalogeno derivatives is provided by their reaction with $AgBF_4$. Reaction of $[Et_4N][Cl_3SnW(CO)_5]$ with $AgBF_4$ in acetonitrile solvent afforded $[CH_3CNW(CO)_5]$, recognized by infrared and mass spectroscopy. Neutral trichlorotin compounds are normally converted to the trifluoro analogs (13).

Reactions of several anions $[Ph_3M'M(CO)_5]^-$ with triphenylphosphine were attempted, but the carbonyl groups were inert to substitution; for example, there was no reaction when $[Et_4N][Ph_3SnMo(CO)_5]$ was stirred overnight in dichloromethane solution with excess triphenylphosphine. Under similar conditions $[Cl_3SnMo(CO)_5]^-$ reacted to form *cis*-$Mo(CO)_4(PPh_3)_2$ in almost quantitative yield (4); this trend is consistent with the expected stronger σ-donor ability of the organotin ligands (14). Under ultraviolet irradiation, $[Et_4N][Ph_3SnMo(CO)_5]$ and PPh_3 in dichloromethane reacted to form a product with carbonyl stretching bands at 2021(ms), 1920(sh), 1902(vs), and 1887(m) cm^{-1}, although a satisfactory analysis could not be obtained to confirm that the product was the anticipated $[Ph_3SnMo(CO)_4PPh_3]^-$.

Infrared Spectra

Free anions of the type $[R_3M'M(CO)_5]^-$ are expected to have idealized C_{4v} symmetry, under which three infrared-active carbonyl stretching fundamentals are expected ($2A_1 + E$). In addition, the B_1 mode is often observed as a weak band in the infrared, since the symmetry is not strictly C_{4v} (15). All of these bands are observed in the typical spectrum shown in Fig. 1*a*, which is that of $[Et_4N][Ph_3SiMo(CO)_5]^-$ in tetrahydrofuran. In addition all of these ions show a weak shoulder on the low frequency side of the higher A_1 band, which is an A' vibration of the radially mono-^{13}CO substituted species present in natural abundance (16). Since this latter weak band invariably falls 6–9 cm^{-1} below the $A_1^{(2)}$ band, it is not listed in Table 2.

[5]Reactions with $Ph_3SnRe(CO)_5$ were carried out in CCl_4 (9) or CH_2Cl_2 (10) rather than ether–tetrahydrofuran, but we have shown that for the Si—W and Sn—W anions, the product is the same in CH_2Cl_2, without ether.

[6]These conditions are well-suited to the preparation of neutral hydrides of low stability (11).

[7]A similar scheme would account for the cleavage of Si—W and Ge—W bonds by hydrogen chloride, in which case chloride ion would attack the coordinatively unsaturated intermediate forming $[ClW(CO)_5]^-$.

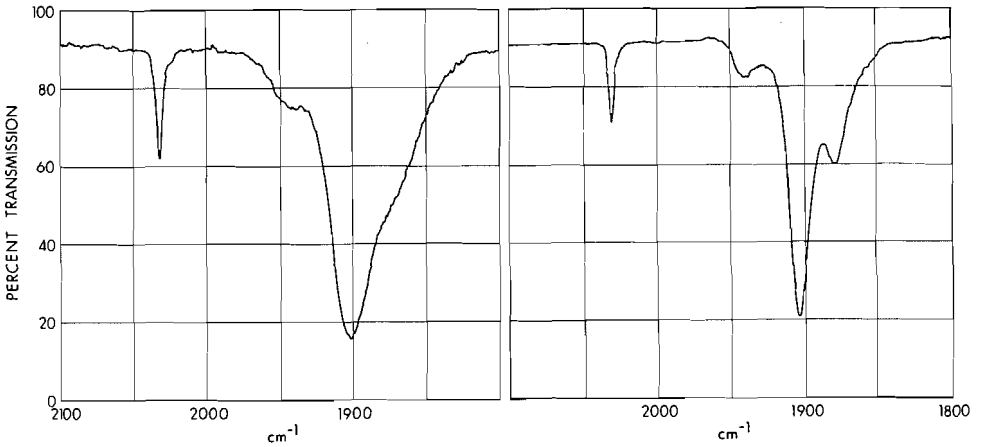

FIG. 1. Infrared spectra of $[Et_4N][Ph_3SiMo(CO)_5]$ in dichloromethane (left) and tetrahydrofuran (right) illustrating superior band sharpness in the latter. Band positions and assignments in the right hand spectrum are 2031 cm^{-1} ($A_1^{(2)}$), 1943 cm^{-1} (B_1), 1905 cm^{-1} (E), and 1880 cm^{-1} ($A_1^{(1)}$).

Carbonyl bands have previously been reported in dichloromethane solution for the trichlorogermanium and trichlorotin derivatives (4). We have observed that the bands are less broad in tetrahydrofuran, so that, for example, the E and $A_1^{(1)}$ bands are clearly resolved. This solvent effect is illustrated in Fig. 1. There is no significant frequency shift between the two solvents.

In general, the band positions are shifted to lower frequency by 40–70 cm^{-1} as compared to the corresponding neutral, isolectronic complexes $R_3PM(CO)_5$, (M = Cr, Mo, W) (17), and by 80–130 cm^{-1} compared to $R_3M'M''(CO)_5$ (M′ = Si, Ge, Sn; M″ = Mn, Re) complexes (18). This shift is consistent with the higher electron density on the metal in the anionic compound which leads to increased back donation. Carbonyl stretching force constants using the Cotton–Kraihanzel (15) approximation have been evaluated and discussed for all the compounds of Table 2 (19). Since these derived parameters are available in a rather straightforward way from the given frequencies, they will not be reported here. The force constants range from 14.24 to 15.38 mdyn $Å^{-1}$ for k_1 and 14.90 to 15.91 for k_2, lower by 1–1.5 mdyn $Å^{-1}$ than in the neutral, isoelectronic derivatives.

We thank the National Research Council of Canada for financial support and for a postgraduate scholarship to E.E.I.

1. J. F. YOUNG. Adv. Inorg. Chem. Radiochem. **11**, 91 (1968).
2. E. H. BROOKS and R. J. CROSS. Organomet. Chem. Rev. A, **6**, 227 (1970).
3. C. S. CUNDY, B. M. KINGSTON, and M. F. LAPPERT. Adv. Organomet. Chem. **11**, 253 (1973).
4. J. K. RUFF. Inorg. Chem. **6**, 1502 (1967).
5. D. UHLIG, H. BEHRENS, and E. LINDNER. Z. Anorg. Allg. Chem. **401**, 233 (1973).
6. T. KRUCK and H. BREUER. Chem. Ber. **107**, 263 (1974).
7. E. W. ABEL, I. S. BUTLER, and J. G. REID. J. Chem. Soc. 2068 (1963).
8. R. D. GORSICH. J. Am. Chem. Soc. **84**, 2486 (1962).
9. A. N. NESMEYANOV, K. N. ANISIMOV, N. E. KOLOBOVA, and V. N. KHANDOZHKO. Proc. Acad. Sci. U.S.S.R., Chem. Sect. **156**, 502 (1964).
10. J. A. J. THOMPSON. Ph.D. Thesis, University of Alberta, Edmonton, Alberta. 1968.
11. A. S. FOUST, W. A. G. GRAHAM, and R. P. STEWART, JR. J. Organomet. Chem. **54**, C22 (1973).
12. A. J. HART-DAVIS and W. A. G. GRAHAM. J. Am. Chem. Soc. **93**, 4388 (1971).
13. T. J. MARKS and A. M. SEYAM. J. Organomet. Chem. **31**, C62 (1971).
14. W. A. G. GRAHAM. Inorg. Chem. **7**, 315 (1968).
15. F. A. COTTON and C. S. KRAIHANZEL. J. Am. Chem. Soc. **84**, 4432 (1962).
16. H. D. KAESZ, R. BAU, D. HENDRICKSON, and J. M. SMITH. J. Am. Chem. Soc. **89**, 2844 (1967).
17. F. A. COTTON. Inorg. Chem. **3**, 702 (1964).
18. W. JETZ, P. B. SIMONS, J. A. J. THOMPSON, and W. A. G. GRAHAM. Inorg. Chem. **5**, 2217 (1966).
19. E. E. ISAACS. Ph.D. Thesis, University of Alberta, Edmonton, Alberta. 1974.
20. L. Y. Y. CHAN and W. A. G. GRAHAM. To be published.

Can. J. Chem. Downloaded from www.nrcresearchpress.com by 210.87.254.42 on 09/05/12
For personal use only.

Déroulement anormal d'une réaction de Michaelis–Becker: caractère ambident de l'anion diéthylphosphonate $(C_2H_5O)_2PO^-$; stéréochimie de la réaction de Michaelis–Becker

CLAUDE BENEZRA ET JEAN-LOUIS BRAVET
Département de Chimie, Université d'Ottawa, Ottawa, Canada K1N 6N5

Reçu le 28 juin 1974

CLAUDE BENEZRA et JEAN-LOUIS BRAVET. Can. J. Chem. **53**, 474 (1975).

La réaction du phosphonate diéthylique monosodique $NaOP(OC_2H_5)_2$ avec les mésylates des *cis* et *trans*-*t*-butyl-4 cyclohexanols a été étudiée dans le toluène, le dioxanne et la diméthylformamide (DMF). A côté des produits attendus de la réaction (élimination et P-alcoylation), se forment des produits provenant de l'attaque par l'oxygène du groupe phosphonate. Cette attaque est en compétition avec la P-alcoylation (réaction de Michaelis–Becker normale) et correspond à la seule réaction de substitution dans la DMF. Une interprétation des résultats est proposée qui fait intervenir la théorie des acides et bases durs et mous et également la solvatation préferentielle. Le caractère S_N2 de la réaction de Michaelis–Becker est confirmé.

CLAUDE BENEZRA and JEAN-LOUIS BRAVET. Can. J. Chem. **53**, 474 (1975).

The reaction of sodium diethylphosphonate $NaOP(OC_2H_5)_2$ with the mesylates of *cis* and *trans*-4-*t*-butyl cyclohexanols has been studied in toluene, dioxane, and dimethylformamide (DMF). Beside the products expected from the reaction (elimination and P-alkylation products originating from initial O-attack have been isolated. This latter reaction competes with P-alkylation (normal Michaelis–Becker reaction) and is the only substitution reaction in DMF. Results are interpreted in terms of the HSAB (Hard and Soft Acids and Bases) theory and by preferential solvation. Since the substitution products are of inverted configuration, the S_N2 mechanism seems to be well substantiated.

Parmi les méthodes de synthèse de liaison carbone–phosphore les plus utilisées, la réaction de Michaelis–Becker (1) est une des plus anciennes. Dans cette réaction, un sel alcalin d'un phosphonate dialcoylique, $HP(O)(OR)_2$, réagit avec un halogénure (1) ou un pseudo-halogénure ($X = OSO_2R'$) (2) pour donner un phosphonate

$$(RO)_2P{-}O^-M^+ + R'X \rightarrow R'P(O)(OR)_2 + MX$$

Cette réaction comporte deux aspects encore mal connus: d'une part, bien qu'il soit généralement admis (3), le caractère S_N2 du mécanisme n'a pas été démontré; d'autre part, l'anion phosphonate est *ambident*

$$(RO)_2P{-}O^- \leftrightarrow (RO)_2\bar{P}{=}O$$

et peut théoriquement attaquer soit par l'oxygène, soit par le phosphore. Il n'y a, à notre connaissance aucun exemple, dans la littérature, de phosphonate alcalin réagissant par l'oxygène (O-alcoylation). Le seul exemple qui se rapproche d'une réaction de Michaelis–Becker avec O-alcoylation est celui du sel d'*argent* du phosphonate diéthylique qui réagit avec les chlorures de triarylméthyle pour donner des produits d'O- et de P-alcoylation (4).

En étudiant la réaction de phosphonate diéthylique monosodique avec les méthanesulfonates (mésylates, Ms) des *cis* et *trans*-*t*-butyl-4 cyclohexanols, nous avons découvert que, d'une part, l'anion phosphonate $(EtO)_2PO^-$ pouvait réagir par l'oxygène et que, d'autre part, les réactions de substitution se déroulaient avec *inversion* de configuration, apportant ainsi une confirmation du mécanisme S_N2 postulé. Les résultats de cette étude conduite avec trois solvants (dioxanne, toluène, diméthylformamide) sont décrits dans cet article.

Résultats

Les réactions ont été réalisées sur chacun des deux épimères purs **1***b* et **2***b* dans trois solvants différents dans des conditions identiques de concentration. L'anion du phosphonate diéthylique a été préparé *in situ* par réaction du sodium métallique sur $HP(O)(OC_2H_5)_2$, sous azote. Après obtention d'une solution claire du sel de sodium, le mésylate dissous dans un solvant approprié a été rajouté sous azote et le mélange réactionnel chauffé à la température indiquée dans les tableaux 1 et 2, suivant un temps variable. Le tableau 3 résume les résultats.

Can. J. Chem. Downloaded from www.nrcresearchpress.com by 210.87.254.40 on 09/05/12
For personal use only.

TABLEAU 1. Résultats obtenus à partir du mésylate *axial* **1***b*

Poids (g) de mésylate (mmol)	Solvant	Durée (h) de réaction température	Produits de réaction: g (mmol)*					
			5	**1***b*	**2***a*	**2***d*	**1***e*	**4**
5.00(21)	Dioxanne	168 h (reflux)	0.94 (6.8)	0.74 (3.3)	0.12 (0.74)	0.42 (1.4)	0.10 (0.4)	0.79 (2.9)
5.00(21)	Toluène	168 h (reflux)	1.39 (10.1)	0.37 (1.6)	0	0.28 (0.97)	0.18 (0.69)	0.77 (2.8)
4.03(17)	DMF	40 h (140 °C)	1.81 (13.1)	0.03 (0.1)	0.09 (0.6)	0.12 (0.4)	0.02 (0.06)	0

*Les produits sont indiqués par ordre d'élution (**5** élué en premier, **4** en dernier).

TABLEAU 2. Résultats obtenus à partir du mésylate *équatorial* **2***b*

Poids en g du mésylate de départ (mmol)	Solvant	Durée (h) de réaction et température	Produits de réactions: g (mmol)*				
			5	**2***b*	**1***a*	**1***d*	**3**
5.00(21)	Dioxanne	168 h (reflux)	0.28 (2.0)	2.63 (11.3)	0.15 (0.96)	0.34 (1.2)	0.87 (3.1)
3.00(13)	Toluène	168 h (reflux)	0.40 (2.9)	0.74 (3.2)	0	0.39 (1.3)	0.75 (2.7)
5.00(21)	DMF	24 h (140°)	1.63 (11.8)	0	0.30 (1.9)	0.54 (1.9)	0

*Classés par ordre d'élution (**5** est élué en premier, **3** en dernier).

TABLEAU 3. Résultats d'ensemble

Produit de départ	Solvant	Nature de la réaction			Attaque‡	Par
		Elimination*	Substitution*	Autres*†	P	O
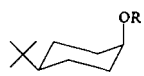 **1** (R = SO_2CH_3)	Dioxanne	56	42	2	57	43
	Toluène	70	26	4	73	27
	DMF	91	9	0	0	100
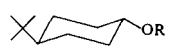 **2** (R = SO_2CH_3)	Dioxanne	27	73	0	59	41
	Toluène	42	58	0	67	33
	DMF	75	25	0	0	100

*% Elimination + % substitution + % "autres" = 100%.
†Produits avec rétention de la configuration: **1***e*.
‡% attaque par P + % attaque par O = 100%.

Tout d'abord quelques remarques générales s'imposent; la réaction est la plus rapide dans la diméthylformamide (DMF); 24 à 48 h sont suffisantes pour que tout le mésylate de départ soit consommé. Dans les autres solvants étudiés, le temps de réaction est beaucoup plus long (1 semaine) et le mésylate de départ n'a pas entièrement réagi. Après réaction et isolement du mélange réactionnel (voir Partie expérimentale), les produits ont été séparés sur colonne de silice.

Structure et configuration des composés obtenus

Le *t*-butyl-4 cyclohexène **5** a été identifié par spectroscopie (i.r. et r.m.n.) et par chromatographie sur couche mince (c.c.m.) à un échantillon authentique. On récupère dans la plupart des cas (sauf pour les réactions dans le toluène) l'alcool de configuration *inverse* de celle du mésylate de départ. Les alcools *axial* **1***a* et *équatorial* **2***a* ainsi obtenus, ont été identifiés (i.r., r.m.n., c.c.m.) à des échantillons authentiques.

On isole également des *phosphates* **1***d* et **2***d* à

Can. J. Chem. Downloaded from www.nrcresearchpress.com by 210.87.254.40 on 09/05/12
For personal use only.

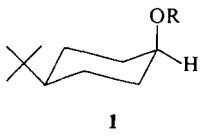

1

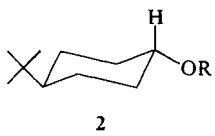

2

a; R = H
b; R = OSO_2CH_3
c; R = $P(OC_2H_5)_2$
d; R = $P(O)(OC_2H_5)_2$
e; R = $PH(O)(OC_2H_5)$

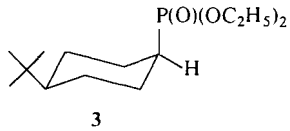

3

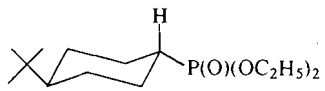

4

5

la place des phosphites **1***c* et **2***c*, produits d'une O-alcoylation. Ces phosphates sont très vraisemblablement des artefacts provenant de l'oxydation lors de l'isolement des phosphites correspondants. Nous reviendrons sur ce point important lors de la discussion. Les phosphates ainsi obtenus ont été identifiés (i.r., r.m.n., c.c.m.) à des échantillons authentiques préparés par phosphorylation des alcools correspondants (5). L'aspect en r.m.n. du signal du proton H-1 permet d'ailleurs l'attribution non équivoque de la configuration *axiale* ou *équatoriale*. Il est bien connu, en effet, que dans le cyclohexane, un hydrogène *axial* donne un signal en r.m.n. considérablement plus étendu qu'un hydrogène équatorial (6).

La réaction avec le mésylate *axial* offre une particularité par rapport à celle avec le mésylate *équatorial*. Dans le premier cas, en effet, on obtient toujours, un hydrogène phosphonate éthylique **1***e* de configuration *identique* (axiale) à celle du mésylate de départ. Cette *rétention* de configuration ne peut s'expliquer que par une attaque directe de l'anion phosphonate sur le soufre du groupement mésylate et transestérification. Ce point sera traité plus en détail dans la discussion. La détermination de la structure de l'hydrogène phosphonate mono-éthylique découle de l'analyse centésimale et des propriétés spectroscopiques: la liaison P—H est visible en infrarouge (2420 cm^{-1}) et l'hydrogène attaché au phosphore apparaît en r.m.n. sous forme d'un doublet avec une forte constante de couplage J_{P-H} = 721 Hz. La configuration *axiale* du groupe $PH(O)(OC_2H_5)$ est prouvée par l'aspect en r.m.n. de l'hydrogène H-1 (multiplet étroit, compatible avec un hydrogène équatorial). D'autre part, les deux hydrogènes phosphonates **1***e* et **2***e* ont été préparés[1] à partir du mélange commercial (Aldrich) des *t*-butyl-4 cyclohexanols et de PCl_3 et d'EtOH (7). Ils ont été séparés par chromatographie sur colonne de silice.

La configurations des *t*-butyl-4 cyclohexylphosphonates diéthyliques **3** et **4** a été plus difficile à établir. Les analyses centésimales et les propriétés spectrales (i.r. et r.m.n.) sont compatibles avec les structures attribuées. D'autre part, nous leur attribuons une configuration *inverse* de celle du mésylate de départ, ce qui est compatible avec un mécanisme S_N2 pour la réaction de Michaelis–Becker.

Les structures sont essentiellement fondées sur la spectrométrie de masse. Comme c'est généralement le cas pour des épimères (8), notamment des dérivés organophosphorés (9), les spectres des deux épimères **3** et **4** sont très semblables, notamment, ils montrent tous les deux un pic de masse à *m/e* 276 et un pic de base à *m/e* 219, correspondant à la perte du radical $[(CH_3)_3C\cdot]$. La différence essentielle entre les deux spectres est l'intensité du pic à *m/e* 220, correspondant à la perte d'isobutylène. Par rapport au pic de base, ce pic représente 27% dans l'isomère auquel nous attribuons la configuration équatoriale **4** alors qu'il représente 98% du pic de base dans l'isomère *axial* **3**. Ceci peut s'expliquer par une élimination plus facile lorsque les groupes *t*-butyle et $P(O)(OC_2H_5)_2$ sont *cis* [1].

[1]

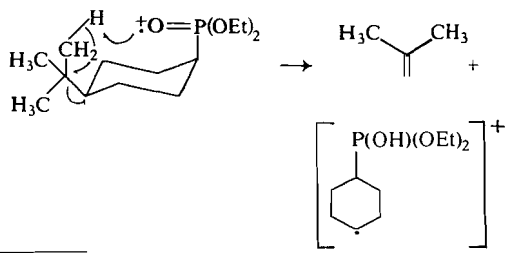

[1]Cette synthèse aurait dû normalement donner les phosphites mixtes (*t*-butyl-4 cyclohexyl-1) $P(OC_2H_5)_2$. L'obtention des hydrogènes phosphonates **1***e* et **2***e*, peut s'expliquer par l'hydrolyse d'un intermédiaire tel que (*t*-butyl-4 cyclohexyl-1) $P(OC_2H_5)$ (Cl) → (*t*-butyl-4 cyclohexyl-1) $P(OC_2H_5)(OH)$ qui est sous forme hydrogène phosphonate.

Can. J. Chem. Downloaded from www.nrcresearchpress.com by 210.87.254.40 on 09/05/12
For personal use only.

Can. J. Chem. Downloaded from www.nrcresearchpress.com by 210.87.254.40 on 09/05/12
For personal use only.

Ces attributions sont confirmées par l'utilisation des complexes de terres rares [Eu(dpm)$_3$] en r.m.n.: l'effet de l'addition d'Eu(dpm)$_2$ sur le déplacement chimique du *t*-butyle est considérable pour l'isomère *cis* ou *axial* **3** (l'addition de 0.50 équivalent d'Eu^{III} fait passer le déplacement chimique du *t*-Bu de 0.88[2] à 1.2. p.p.m. soit ($\Delta\delta$ = 0.33 p.p.m.) alors que l'effet de l'Eu^{III} sur l'isomère *trans* (où les groupes *t*-Bu et P(O)(OC$_2$H$_5$)$_2$, *trans*, sont plus éloignés) est faible ($\Delta\delta$ = 0.09 p.p.m.). Bien que l'effet des complexes de terres rares dépende non seulement de la distance au centre considéré, mais aussi de l'angle de contact Φ (10), l'effet le plus important est celui qu'on attendrait avec la configuration attribuée: l'Eu^{III} complexe l'oxygène du groupe P=O (11).

La réaction de Michaelis–Becker étudiée ici est stéréospécifique: avec le mésylate *axial* **1***b*, aucune trace du phosphonate *axial* **3** ou du phosphate *axial* **1***d* n'a pu être décelée, avec le mésylate *équatorial* **2***b*, ni **4** ni **2***d* n'étaient présents.[3]

Discussion

Des résultats résumés dans les tableaux 1, 2 et 3, deux constatations intéressantes sont à faire: (*a*) La réaction de Michaelis–Becker est stéréosélective et donne des produits avec *inversion complète* de configuration (avec l'exception des produits secondaires **1***e*, obtenus avec l'isomère *axial*); le caractère S_N2 (tout au moins en ce qui concerne le cours stéréochimique de la réaction) semble donc bien établi. (*b*) Le caractère *ambident* de l'anion phosphonate (EtO)$_2$P$^{\cdots}$O$^-$ a été démontré par l'isolement de phosphites (oxydés en phosphates) et d'alcools de configuration inverse du mésylate de départ (et provenant donc de l'attaque par l'oxygène).

Si l'on fait le bilan des produits obtenus, on s'aperçoit qu'il faut considérer trois types de réaction: (1) élimination (obtention de *t*-butyl-4 cyclohexène); (2) substitution par le phosphore (produits normaux de Michaelis–Becker) et (3) substitution par l'oxygène (produits anormaux). Considérons successivement ces trois points.

Il faut tout d'abord noter le fort pourcentage d'élimination (obtention du *t*-butyl-4 cyclohexène **5**): celle-ci varie de 56 à 91% du total de la réaction[4] pour le mésylate axial **1***b* et de 27 à 75% pour l'équatorial **2***b*. Si l'élimination de type E_2 est attendue avec l'isomère **1***b* à cause de l'orientation favorable (*trans*-diaxiale) des groupes H et MsO, elle est plus difficile à expliquer dans le cas de l'isomère équatorial. Ce résultat est cependant loin d'être unique puisque Winstein *et al.* (12) ont déjà décrit 10 à 40% d'élimination dans le cas de la réaction de BrLi et ClLi avec les tosylates **1** et **2** (R = SO$_2$C$_6$H$_4$-CH$_3$). Pour expliquer l'élimination dans le cas de l'isomère équatorial **2**, malgré un arrangement stéréoélectronique défavorable, ils ont proposé un mécanisme baptisé "merged bimolecular substitution and elimination" (12) dans lequel l'état de transition classique pour une S_N2 est remplacé par un intermédiaire **6**

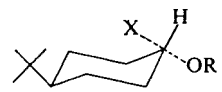

6

qui peut évoluer soit vers une élimination, soit vers une substitution. Le fort pourcentage d'élimination qui a été observé avec les mésylates est à rapprocher de l'étude par Roudier (13) de la réaction de Michaelis–Becker de NaOP(OC$_4$H$_9$)$_2$ avec l'iodure de cyclohexyle; le seul produit obtenu est le cyclohexène. Comme on pouvait s'y attendre (14), le pourcentage d'élimination augmente avec la température de la réaction (c'est avec la DMF qu'il est le plus élevé).

En ce qui concerne les produits de substitution, les produits normaux de Michaelis–Becker (les phosphonates **3** et **4**, produits de P-alcoylation), le tableau 3 montre que la meilleure façon de les obtenir consiste à faire la réaction dans le toluène. En termes de théorie des acides et bases "durs" et "mous" de Pearson *et coll.* (15), les composés de P-alcoylation correspondent à l'attaque d'une base "molle" (P) sur un centre "mou" (*C*—OMs). Néanmoins ce centre C est beaucoup plus "dur" que lors de la réaction de

[2]En unités δ, par rapport au TMS, référence interne.

[3]Les isomères **3** et **4** ont, en c.c.m., le même R_f (éluant: acétate d'éthyl – hexane 1:1) après une élution; ils ont cependant des R_f nettement différents, et il devient facile de les distinguer, après 3 élutions successives dans le même mélange de solvants. En solution dans CDCl$_3$, le signal du groupe *t*-butyle se trouve au même endroit (0.87 p.p.m.) dans les deux épimères; en solution benzènique, cependant, le déplacement chimique du *t*-butyle est de 0.86 p.p.m. pour **3** et de 0.75 p.p.m. pour **4**.

[4]Calculé par rapport au mésylate qui a réagi.

Can. J. Chem. Downloaded from www.nrcresearchpress.com by 210.87.254.40 on 09/05/12
For personal use only.

TABLEAU 4. Analyse, propriétés physiques et spectrales des produits nouveaux

Composés[a]	Analyse Calc.	Analyse Tr.	Infrarouge (cm^{-1})[b]	Resonance magnetique nucleaire[c]	Masse[d]
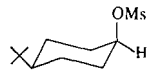 **1b** (p.f. 71°)	C 56.39 H 9.47 S 13.66	56.60 9.57 13.62	1170(OSO_2)	0.90(s, 9H, *t*-Bu); 3.03(s, 3H, CH_3SO_2) 5.00 (m étroit, 1H, —C*H*OMs, $W_{1/2}$ = 8)	
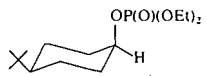 **1d** (huile; p.é. 66–71° 0.05 Torr)	C 57.62 H 10.00 P 10.51	58.01 9.97 10.81	1260(P=O) 1170(POEt) ~1000(POC)	0.90(s, 9H, *t*-Bu); 1.37(t, 6H, CH_3CH_2OP, J_{HH} = 7.3); 4.12 (d de q, CH_3CH_2OP, $J_{HH} = J_{PH}$ = 7.3); 4.70(m, 1H, —C*H*OP, $W_{1/2}$ = 14)	155(100), 127(23), 99(31), 81(10), 67(10), 57(25), 55(10), 54(6)
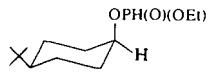 **1e** (huile; p.é. 70° 0.05 Torr)	C 58.04 H 10.15 P 12.47	57.78 10.21 12.29	2420(P—H) 1230(P=O) 1180(POEt) ~980(POC)	0.89(s, 9H, *t*-Bu); 1.37(t, 3H, CH_3CH_2OP, J_{HH} = 7.1) 4.12(d de q, 2H, CH_3CH_2OP, J_{HH} 7.1, J_{PH} 9.1); 4.77(d, de m, 1H, —C*H*OP, J_{PH} ~ 8.0) 6.56(d, 1H, P*H*, J_{PH} = 721)	155(13), 111(100), 83(54), 82(7), 81(13), 67(19), 65(9), 57(42), 55(14), 56(8)
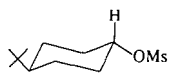 **2b** (p.f 91°)	C 56.39 H 9.47 S 13.66	56.55 9.47 13.53	1150(OSO_2)	0.89(s, 9H, *t*-Bu); 2.97(s, 3H, CH_3SO_2); 4.53(m élargi, 1H, —CH OMs, $W_{1/2}$ = 21)	
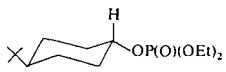 **2d** (huile; p.é. 70° 0.05 Torr)	C 57.62 H 10.00	57.67 10.31	1250(P=O)	0.90(s, 9H, *t*-Bu); 1.33(t, 6H, CH_3CH_2OP, J_{HH} = 7.2); 4.10(d de 9, 4H, CH_3CH_2OP, J_{HH} = 7.2 ≃ J_{PH})	155(100), 127(25), 111(64), 99(33), 83(27), 81(14), 67(14), 57(42), 56(9), 55(10)

Can. J. Chem. Downloaded from www.nrcresearchpress.com by 210.87.254.40 on 09/05/12
For personal use only.

TABLEAU 4. (*Concluded*)

Composés[a]	Analyse Calc.	Analyse Tr.	Infrarouge (cm^{-1})[b]	Resonance magnetique nucleaire[c]	Masse[d]
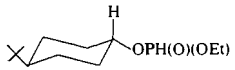 **2***e* (huile; p.é. 75° 0.05 Torr)	C 58.04 H 10.15 P 12.47	57.88 10.41 12.25	2420(P—H) 1260(P=O) 1170(POEt) ~1000(POC)	0.89(s, 9H, *t*-Bu); 1.37(t, 3H, CH_3CH_2OP, J_{HH} = 7.1); 4.13(d de q, 2H, $CH_3CH_2OP^-$, J_{HH} = 7.1 ≃ J_{PH}) 6.57(d, 1H, P—*H*, J_{PH} =	155(13), 111(100), 83(58), 81(19), 69(13), 67(19), 58(10), 57(54), 56(19), 55(26)
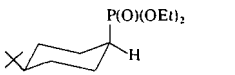 **3** (huile; p.é. 70–73° 0.05 Torr)	C 58.04 H 10.15 P 12.47	57.88 10.41 12.25	2420(P—H) 1260(P=O) 1170(POEt) ~1000(POC)	0.87(s, 9H, *t*-Bu); 1.30(t, 6H, CH_3CH_2OP, J_{HH} = 7.2); 4.12(d de q, 4H, CH_3CH_2OP, J_{HH} = 7.2 ≃ J_{PH})	276(M^+, 19), 220(98), 219(100), 155(24), 139(24), 138(54), 111(29), 81(53), 57(45), 55(22)
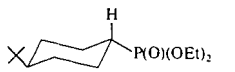 **4** (huile; p.é. 65–70° 0.05 Torr)	C 60.85 H 10.58 P 11.21	[e] 10.94	~1250(P=O) ~1000(POC)	0.87(s, 9H, *t*-Bu); 1.31(t, 6H, CH_3CH_2OP, J_{HH} = 7.2); 4.11(d de q, 4H, CH_2CH_2OP, J_{HH} = 7.2 ≃ J_{PH})	276(M^+, 48), 220(27), 219(100), 139(70), 138(54), 111(44), 81(75), 67(44), 57(95), 55(54), 54(37)

[a]p.f. ou huile (p.é.)
[b]Spectres pris sur Beckman IR-20 en liquide pur ou en suspension dans le Nujol.
[c]Spectres pris dans $CDCl_3$ sur un appareil Varian T-60; déplacements chimiques en unités δ p.p.m. par rapport au TMS, référence interne; entre parenthèse la forme du signal d = doublet, t = triplet etc. et le couplage en Hz.
[d]Spectres de masses pris sur Hitachi Perkin-Elmer RMU-6D; les pics les plus importants sont indiqués (pourcentage du pic de base); les phosphates **1***d* et **2***d*, et les hydrogènes phosphonates **1***e* et **2***e* ne donnent pas de pic de masse.
[e]La détermination de la masse exacte de cet échantillon a été réalisée sur un appareil MS-902-S à haute résolution; masse calculée pour $C_{14}H_{29}O_3P$:276.185; masse trouvée: 276.19 ± 0.01.

Can. J. Chem. Downloaded from www.nrcresearchpress.com by 210.87.254.40 on 09/05/12
For personal use only.

Michaelis–Becker ordinaire avec des halogénures comme groupes partants, ce qui explique l'obtention de produits correspondant à une O-alcoylation: phosphites (puis phosphates) et alcools.

L'O-alcoylation est importante; elle représente, pour le composé *axial* **1***b*, 27% (toluène), 43% (dioxanne) et 100% (DMF), pour le composé *équatorial*, **2***b*, 33% (toluène), 41% (dioxanne) et 100% (DMF). Il y a deux sortes de produits provenant d'une attaque par l'oxygène, les phosphates **1***d* et **2***d* et les alcools **1***a* et **2***a*. Ces derniers proviennent très certainement de l'hydrolyse *in situ* des phosphites correspondants. En effet à partir du mésylate *axial* **1***b* on obtient l'alcool *équatorial* **2***a* et à partir de **2***b*, on obtient l'alcool **1***a*; il y a donc *inversion* de configuration.

L'obtention des phosphates **1***d* et **2***d* au lieu des phosphites attendus **1***c* et **2***c* s'explique sans doute par une oxydation lors de l'isolement de ces phosphites. En effet, bien que la réaction ait été effectuée sous azote, on aurait pu concevoir une oxydation préalable de l'anion phosphonate en anion phosphate et attaque nucléophile de l'anion phosphate sur le carbone porteur du groupe OMs.

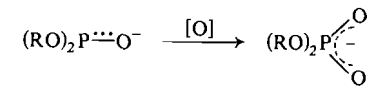

Cette hypothèse a été écartée de la façon suivante: le mésylate équatorial **2***b* en solution dans la DMF a été traité par une quantité stoéchiométrique du sel de sodium du phosphate diéthylique $(NaO)P(O)(OC_2H_5)_2$ et chauffé pendant 24 h. Le seul produit formé a été le *t*-butylcyclohexène. D'ailleurs il est connu (16) que l'anion phosphate $(C_2H_5O)_2PO_2^-$ n'est que faiblement nucléophile.

Un résultat du tableau 3 est frappant, si le % d'O-alcoylation est comparable dans le toluène et le dioxanne en revanche, il y a 100% d'attaque par l'oxygène dans la DMF. Si, avec Hudson (17), on admet que dans un ion ambident on peut traiter les deux centres nucléophiles indépendamment, on peut concevoir que la DMF, qui solvate préferentiellement les "gros" anions (18) (ici le P), rendrait ainsi l'oxygène plus disponible pour une attaque nucléophile. D'ailleurs le fait d'obtenir 91 et 75% d'élimination à partir des isomères *axial* **1***b* et *équatorial* **2***b*, respectivement, dans la DMF pourrait être interprété non seulement comme résultant d'une température plus élevée (favorisant donc l'élimination au détriment de la substitution (14), mais aussi comme étant le résultat de l'attaque d'une base "dure" (1′O^- de P—O^-) sur un acide "dur" (1′H en β du groupe MsO: [2]).

[2] 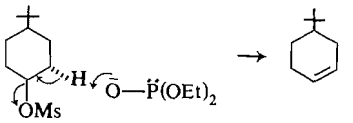

Les résultats décrits ici suggèrent que le diéthylphosphonate de sodium se retrouve sous forme de paire d'ions intimes: $(C_2H_5O)_2P—O^- \ldots Na^+$, dans le dioxanne et la toluène (favorisant l'attaque par le phosphore) et sous forme d'ions séparés (et solvatés) dans le DMF.[5] Dans ce dernier cas, la charge négative serait, probablement, plutôt sur l'oxygène, rendant compte ainsi du pourcentage élevé d'O-alcoylation.

La rareté des O-alcoylations dans les conditions de Michaelis–Becker s'explique bien par la théorie des acides et bases "durs" et "mous" (15); le centre d'attaque (le carbone C—X) est "mou" quand X est un halogène (et donc est attaqué préférentiellement par la base "molle", le P de P⋯O^-) et "dur" quand X = OTs ou OMs (et donc l'attaque par l'oxygène de P⋯O^-, base dure, devient compétitive). En répétant l'expérience de Myers *et al.* (2) sur le tosylate de cyclohexyle, nous avons pu mettre en évidence la formation, à côté du phosphonate de cyclohexyle attendu, de composés à liaison O—P (phosphites ou phosphates).

La réactivité des centres dans un ion ambident dépend du substrat, du solvant et du cation (19). Lorsque le milieu est homogène c'est l'atome nucléophile de plus forte densité électronique qui réagit sur le centre positif (C—X). Ainsi peut-on expliquer l'exemple d'Arbuzov et Kaziljnikova (4) dans lequel le sel d'argent du phosphonate diisopropylique donne des *phosphites* avec des chlorures de triarylméthyle.

$$Ar_3CCl + AgOP(O—iso\text{-}Pr)_2 \rightarrow Ar_3COP(O—iso\text{-}Pr)_2$$

Cet exemple diffère cependant des conditions de Michaelis–Becker; en effet en raison de la catalyse électrophile de l'ion Ag^+ la réaction a un caractère S_N1 plus prononcé et on observe

[5]Nous remercions un rapporteur d'avoir suggéré cette interprétation complémentaire.

Can. J. Chem. Downloaded from www.nrcresearchpress.com by 210.87.254.40 on 09/05/12
For personal use only.

une attaque par l'atome de plus forte électronégativité (19).

La nature homogène ou hétérogène du milieu réactionnel, dans les réactions avec les ions ambident a également son importance (20); avec les ions phénolates, par exemple, on observe plus de C-alcoylation en milieu hétérogène, plus d'O-alcoylation en milieu homogène. Dans le cas des réactions étudiées ici, la réaction, homogène pendant un certain temps, devient hétérogène à cause de la précipitation de NaOMs.

Enfin, il est intéressant de constater la formation (bien qu'en faible quantité) dans le cas du mésylate *axial* **1***b*, d'hydrogène phosphonate *axial* **1***e* donc, avec rétention de configuration. On ne peut expliquer l'obtention de ces produits que par une attaque directe sur le soufre du groupe mésylate (laissant donc intacte la liaison C—O *axiale*) et transestérification de l'anion phosphonate sur l'alcool axial ainsi obtenu. Nous n'avons pas, pour l'instant, d'explication pour le fait que le composé equivalent (**2***e*) ne se forme pas dans le cas du mésylate équatorial.

En conclusion, cette étude a montré d'une part le caractère S_N2 de la réaction de Michaelis–Becker (obtention des produits avec *inversion* de configuration) d'autre part, un des rares exemples de réactivité à l'oxygène de l'anion phosphonate $Na^{+-}OP(OC_2H_5)_2$. En contrôlant le groupe portant et le solvant, il devient donc possible d'orienter la réaction de Michaelis–Becker vers une O- ou vers une P-alcoylation.

Partie expérimentale

Indications générales

Le dioxanne a été purifié de la façon suivante: après une nuit sur du CaH_2, il a été reflué 2 h puis distillé. La diméthylformamide (DMF) a été distillé puis passé sur une colonne d'alumine basique Woelm cation–otropique, activité I, de Waters Associates Inc. pour le débarrasser de l'eau résiduelle. Le toluène a été distillé et conservé sur sodium. Le phosphonate diéthylique, d'Aldrich, a été distillé avant réaction.

Séparation des isomères axial et équatorial du t-butyl-4 cyclohexanol

Le produit commercial, d'Aldrich, contient un mélange 2:1 des isomères équatorial et axial (on peut évaluer les proportions par r.m.n. en intégrant l'hydrogène-C*H*OH). Le mélange d'épimère (35.0 g) est chromatographié sur 1000 g d'oxyde d'aluminium Shawinigan de McArthur Chemical (Montréal). Au mélange éther de pétrole – éther (1:1) on élue 10.46 g d'isomère *axial* pur **1***a*, puis 6.07 g d'un mélange des deux alcools et enfin à l'éther pur sont élués 16.04 g d'isomère *équatorial* pur **2***a*.

Préparation des mésylates **1***b et* **2***b*

(*a*) A une solution refroidie dans la glace d'alcool axial **1***a* (5.00 g, 320 mmol) dans du chlorure de méthylène (60 ml) contenant du CH_3SO_2Cl (4.22 g, 36.8 mmol), on ajoute goutte à goutte une solution de triéthylamine (3.72 g, 36.8 mmol) dans du chlorure de méthylène (6.0 ml). Après addition, on laisse réagir à température ambiante pendant 10 min et on ajoute 60 ml d'eau. La phase organique est séparée, puis la phase aqueuse est extraite du chlorure de méthylène. Les phases organiques réunies sont réunies, lavées à l'eau, séchées sur Na_2SO_4 et évaporées à sec; on obtient ainsi 7.59 g de mésylate *axial* **1***b* pur. On purifie en recristallisant dans l'éther de pétrole (30–60°).

(*b*) Le même mode opératoire est suivi pour l'alcool équatorial on utilise 6.70 g (4.30 mmol) d'alcool + 80 ml CH_2Cl_2 + 5.16 g (45.0 mmol) de CH_3SO_2Cl + 4.56 g (45 mmol) de triéthylamine + 7.0 ml CH_2Cl_2. On obtient 10.0 g d'un *mélange* d'alcool de départ et de mésylate équatorial **2***b* (1:4) que l'on sépare sur colonne de silice. On obtient ainsi 7.77 g de mésylate équatorial **2***b* pur. (Rendement 75%.)

Procédé général (réaction de Michaelis–Becker)

A l'aide d'une ampoule à addition munie d'un égalisateur de pression, on ajoute pendant environ vingt minutes, sous azote, goutte à goutte une solution de 1.25 n millimoles (mmol) de $HP(O)(OEt)_2$ dans 0.33 n ml de solvant, à une suspension de 1.15 n atome-g de sodium dans 0.75 n ml de solvant. A la fin de l'addition, on chauffe le mélange à 100° jusqu'à disparition complète du sodium (environ 1 à 2 h). On ajoute ensuite, toujours sous azote, n mmoles de mésylate dissoutes dans n ml de solvant, goutte à goutte, pendant 30 min. Le mélange est alors chauffé à reflux pendant le temps indiqué sur les tableaux 1 et 2.

Isolement et séparation du mélange

(*a*) *Toluène*: On filtre le précipité de $NaOSO_2CH_3$ et on évapore à sec le toluène. Le mélange est alors mis sur une colonne de silice (40 fois le poids du brut).

(*b*) *DMF et dioxanne*: On ajoute 3 n ml d'éther au mélange réactionnel et on ajoute n ml d'eau. On extrait 3 fois à l'éther de la manière habituelle, puis les fractions éthérées sont lavées à l'eau jusqu'à neutralité, séchées sur sulfate de sodium et évaporées à sec.

Les produits sont élués à l'éther pur puis avec des mélanges éther–méthanol contenant des quantités croissantes de méthanol. Les résultats sont consignés dans les tableaux 1 et 2.

Synthèse des phosphates de t-butylcyclohexyle et de diéthyle **1***d et* **2***d*.

A un mélange de *trans-t*-butyl-4 cyclohexanol **1***a* (0.50 g, 3.2 mmol), d'$HP(O)(OC_2H_5)_2$ (0.43 g, 3.0 mmol) et de (CCl_4 0.94 g, 6.1 mmol), on ajoute goutte à goutte 0.34 g (3.4 mmol) de triéthylamine. On chauffe a reflux 4 h puis le mélange refroidi est filtré et le précipité lavé à l'éther. Les filtrats mis ensemble sont séchés sur Na_2SO_4, évaporés à sec et chromatographiés sur silice. On recueille l'alcool qui n'a pas réagi et le phosphate de *t*-butyle et de diethyle **1***d* (0.15 g, 0.51 mmol) que l'on identifie (i.r., r.m.n., c.c.m.) au produit **1***d* obtenu directement dans la réaction de Michaelis–Becker.

Le même mode opératoire (5) est suivi pour préparé le phosphate équatorial **2***d*; à partir de 0.84 g de $HP(O)(OC_2H_5)_2$, on obtient ainsi 0.51 g (1.8 mmol) de composé

2*d* identifié au produit de la réaction de Michaelis–Becker (i.r., r.m.n., c.c.m.).

Synthèse des hydrogènes phosphonates ***1e*** *et* ***2e*** *selon (7)*

A un mélange refroidi à 0 °C de PCl_3 (6.85 g, 50 mmol) et d'éther anhydre (10 ml), on ajoute goutte à goutte pendant 1 h un mélange des *t*-butyl-4 cyclohexanols d'Aldrich (7.80 g, 50 mmol) et de *N,N*-diméthylaniline (6.05 g, 50 mmol) dans 10 ml d'éther anhydre. On rajoute ensuite, pendant 2 h, un mélange d'éthanol anhydre (4.6 g, 100 mmol) et de *N,N*-diméthylaniline (12.1 g, 100 mmol). A la fin de la réaction, on rajoute 25 ml d'éther anhydre, on filtre lave le précipité à l'éther anhydre et évapore à sec; 11.56 g de résidu sont chromatographiés sur colonne de silice; on recueille les alcools qui n'ont pas réagi, puis les hydrogènes phosphonates; **2***e* (2.51 g, 10.1 mmol), un mélange de **2***e* + **1***e* (1.00 g, 4.0 mmol) puis **1***e* pur (1.00 g, 4.3 mmol).

Nous remercions Madame Danielle Landry pour son aide technique très appréciable et le Conseil national de la recherche du Canada pour son aide financière (octroi A-5496).

1. A. Michaelis et T. Becker. Chem. Ber. **30**, 1003 (1897).
2. T. C. Myers, S. Preis et E. V. Jensen. J. Am. Chem. Soc. **76**, 4172 (1954).
3. R. G. Harvey et E. De Sombre. *Dans* Topics in organophosphorus chemistry. Vol. 1. *Rédigé par* M. Grayson and E. J. Griffith. Interscience Publishers, New York. 1964. p. 61.
4. A. E. Arbuzov et E. A. Kasiljnikova. Izv. Akad. Nauk. S.S.S.R. Otdel. Khim. Nauk. 30 (1959); Abstr. **53**, 14982 (1959).
5. G. M. Sternberg. J. Org. Chem. **15**, 637 (1950).
6. L. M. Jackman et S. Sternhell. Applications of NMR spectroscopy in organic chemistry. 2eme ed. Pergamon Press, Oxford. 1969. p. 288.
7. S. R. Laudauer et H. N. Rydon. J. Am. Chem. Soc. 2224 (1953).
8. D. C. DeJongh et S. R. Shrader. J. Am. Chem. Soc. **88**, 3881 (1966).
9. H. J. Callot et C. Benezra. Org. Mass. Spectrom. **5**, 343 (1971).
10. F. Lefèvre et M. L. Martin. Org. Magn. Reson. **4**, 732 (1972).
11. K. C. Yee et W. G. Bentrude. Tetrahedron Lett. 2775 (1971).
12. S. Winstein, D. Darwish et N. J. Holness. J. Am. Chem. Soc. **78**, 2915 (1956).
13. L. Roudier. C. R. **245**, 2296 (1956).
14. K. A. Cooper, E. D. Hughes, C. K. Ingold, G. A. Maw et B. J. MacNulty. J. Chem. Soc. 2049 (1968).
15. R. G. Pearson et J. Songstad. J. Am. Chem. Soc. **89**, 1827 (1967).
16. A. J. Kirby and S. G. Warren. The organic chemistry of phosphorus. Elsevier, Amsterdam. 1967. p. 221.
17. R. F. Hudson. Structure and mechanism in organophosphorus chemistry. Academic Press, London. 1965. p. 116.
18. A. J. Parker. Q. Rev. **16**, 163 (1962).
19. N. Kornblum, R. A. Smiley, R. K. Blackwooe et D. C. Iffland. J. Am. Chem. Soc. **77**, 6269 (1955); R. Gompper. Angew. Chem. Int. Ed. Engl. **3**, 560 (1964).
20. N. Kornblum et A. P. Lurie. J. Am. Chem. Soc. **81**, 2705 (1959).

Can. J. Chem. Downloaded from www.nrcresearchpress.com by 210.87.254.40 on 09/05/12
For personal use only.

La photolyse du sulfure de méthyle et de vinyle

GILLES LEDUC ET YVES ROUSSEAU

Département de Chimie, Université de Montréal, C.P. 6210, Montréal, Québec H3C 3V1

Reçu le 3 juin 1974

GILLES LEDUC et YVES ROUSSEAU. Can. J. Chem. **53**, 483 (1975).

La photolyse du sulfure de méthyle et de vinyle dans la région 230–270 nm donne des produits dont la formation s'explique par les deux scissions primaires suivantes.

$$CH_3—S—CH=CH_2 + h\nu \rightarrow CH_3^{\cdot} + {}^{\cdot}S—CH=CH_2$$

$$CH_3—S—CH=CH_2 + h\nu \rightarrow CH_3S^{\cdot} + {}^{\cdot}CH=CH_2$$

L'addition de méthanethiol (10 à 15%) permet de doser les radicaux méthyles et vinyles formés.

$$R^{\cdot} + CH_3SH \rightarrow RH + CH_3S^{\cdot}$$

La somme des rendements quantiques en méthane et en éthylène tend alors vers l'unité pour des temps d'irradiation courts.

GILLES LEDUC and YVES ROUSSEAU. Can. J. Chem. **53**, 483 (1975).

The photolysis of methylvinylsulfide in the 230–270 nm region yields products which can be explained by the following primary reactions.

$$CH_3—S—CH=CH_2 + h\nu \rightarrow CH_3^{\cdot} + {}^{\cdot}S—CH=CH_2$$

$$CH_3—S—CH=CH_2 + h\nu \rightarrow CH_3S^{\cdot} + {}^{\cdot}CH=CH_2$$

The methyl and vinyl radicals are titrated by the addition of methyl mercaptan to the system.

$$R^{\cdot} + CH_3SH \rightarrow RH + CH_3S^{\cdot}$$

At short photolysis time, the sum of the methane and ethylene quantum yields is near unity.

Introduction

L'étude de la photolyse du sulfure de méthyle et de vinyle (SMV) a été entreprise pour déterminer les processus primaires et les produits qui en résultent. Castonguay et Rousseau (1) ont démontré que la décomposition photosensibilisé au mercure (Hg 6^3P_1) du méthylvinyléther (MVE), homologue oxygéné du SMV, s'explique principalement par une scission du lien CH_3—O [1].

[1] $CH_3OCHCH_2 + Hg\,(^3P_1) \rightarrow CH_3^{\cdot} + {}^{\cdot}O—CH=CH_2 + Hg\,(^1S_0)$

Il a été également souligné que l'éthylène formé provient d'un processus intramoléculaire et il semble que le taux de réaction des radicaux primaires avec la molécule de départ est faible.

L'étude de la photolyse de sulfures d'alkyle par Knight et coll. (2–4) a démontré que le processus primaire de décomposition est une scission du lien C—S,

[2] $R—S—R + h\nu \rightarrow R^{\cdot} + {}^{\cdot}S—R$

De plus, les radicaux méthyles formés lors de la photolyse du sulfure de méthyle semblent posséder un surplus d'énergie.

La présente étude permet d'établir certains mécanismes de réaction et de comparer le comportement du SMV avec celui des molécules ci-haut mentionnées.

Partie expérimentale

Le SMV est obtenu de la Compagnie K & K et purifié par chromatographie en phase gazeuse (colonne 10 pd × 1/4 po remplie avec 30% d'huile DC-200 sur chromosorb W). Le produit est ensuite introduit dans une rampe à vide, distillé pour éliminer l'eau et le CO_2, et, gardé dans un ballon fermé par une valve au mercure. Le méthanethiol (CH_3SD) obtenu de la Compagnie Merck Sharp et Dohme et le perfluoropropane obtenu de la Compagnie Matheson sont utilisés tels quels.

La décomposition photolytique du produit se fait dans une cellule cylindrique en quartz (5 cm de diamètre × 9.4 cm de longueur) irradiée par une lampe de pression moyenne au mercure (Hanovia "Utility Lamp"). Un filtre de Vycor est placé entre la lampe et la cellule.

Le spectre u.v. du produit est pris sur un spectromètre Cary 17 (fig. 1). La photolyse du SMV se fait donc entre 230 et 270 nm (limites imposées par le filtre de Vycor et la capacité d'absorption du produit).

L'actinométrie est faite dans la même cellule (remplie

Can. J. Chem. Downloaded from www.nrcresearchpress.com by 210.87.254.6 on 09/05/12
For personal use only.

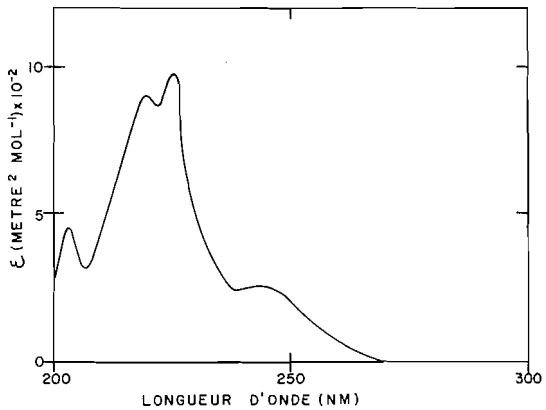

FIG. 1. Spectre u.v. du sulfure de méthyle et de vinyle.

grâce à un systême sans mercure) en utilisant une lampe de basse pression au mercure (Hanovia "Flat Spiral" Z1500-203) et l'actinomètre utilisé est un mélange N_2O–butane (5).

Les produits les plus volatils sont analysés après distillations à différentes températures grâce à une burette à gaz et un chromatographe en phase gazeuse (colonne 10 pd × 1/4 po remplie de "Porapak Q") couplé au système à vide pour permettre une injection directe des produits à analyser. Les composés lourds sont injectés à la seringue sur la même colonne utilisée pour purifier le SMV. L'analyse qualitative des produits de réaction est effectuée à l'aide des temps de rétention sur les colonnes lors des chromatographies et d'un spectromètre de masse (CEC 21-104) après avoir recueilli ces derniers à la sortie de la colonne.

Résultats et discussions

L'analyse des produits plus volatils que le SMV permet d'identifier les composés suivant, CH_4, C_2H_4, C_2H_6, $CH_3CH{=}CH_2$, $C_2H_3{-}C_2H_3$, CH_3SH et CH_3SCH_3. Le taux de formation des principaux produits en fonction du temps d'irradiation est donné à la fig. 2 pour une pression de SMV de 6.7 kPa.

Ces résultats démontrent qu'il y a formation, lors de la photolyse du SMV, de radicaux $CH_3{\cdot}$ (CH_4 et C_2H_6) et de radicaux $C_2H_3{\cdot}$ (C_2H_4 et butadiène-1,3). L'absorption d'un photon par le SMV produit une molécule excitée SMV* qui, ensuite, subit une scission homolytique. Les processus primaires peuvent se décrire ainsi,

[3] $SMV + h\nu \rightarrow SMV^*$

[4] $SMV^* \rightarrow CH_2{\cdot} + {\cdot}SCH{=}CH_2$

[5] $SMV^* \rightarrow CH_3S{\cdot} + {\cdot}CH{=}CH_2$

Le comportement du radical $C_2H_3S{\cdot}$ ne peut être établi à partir des produits identifiés mais il

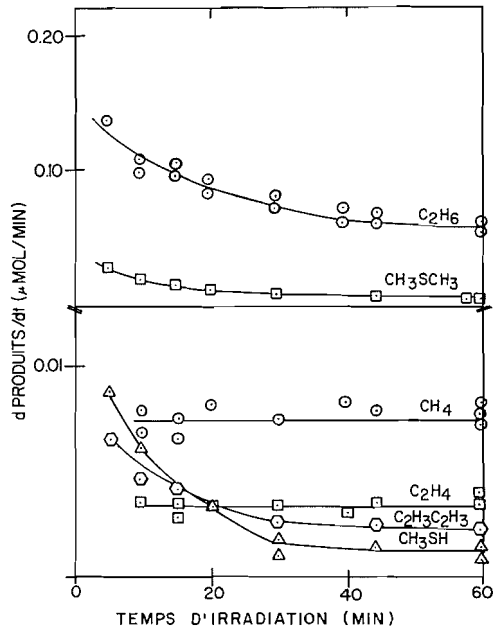

FIG. 2. Taux de formation des principaux produits en fonction du temps d'irradiation.

pourrait être responsable de la formation du dépôt blanchâtre présent sur les parois à la fin d'une photolyse. Les autres radicaux primaires formés lors des scissions [4] et [5] peuvent réagir entre eux pour former les composés analysés.

[6] $CH_3{\cdot} + CH_3{\cdot} + M \rightarrow C_2H_6 + M$

[7] $CH_3{\cdot} + C_2H_3{\cdot} \rightarrow CH_3CHCH_2$

[8] $CH_3{\cdot} + CH_3S{\cdot} \rightarrow CH_3SCH_3$

[9] $C_2H_3{\cdot} + C_2H_3{\cdot} \rightarrow C_2H_3{-}C_2H_3$

[10] $CH_3S{\cdot} + CH_3S{\cdot} \rightarrow CH_3SSCH_3$

Addition de NO

L'addition de 0.5 kPa de NO dans une cellule contenant 6.7 kPa de SMV inhibe la production de C_2H_6, diminue le taux de formation d'éthylène ($T_{C_2H_4}$) et la quantité de méthane obtenue est alors très faible (tableau 1).

La formation d'éthylène, malgré la présence de NO dans le système, peut s'expliquer par un processus intramoléculaire.

[11] $SMV^* \rightarrow C_2H_4 + CH_2S$

La réaction 8, impliquant deux radicaux ne peut être responsable de la formation de sulfure de méthyle en présence de NO. Par contre le sulfure de méthyle pourrait être formé directe-

Can. J. Chem. Downloaded from www.nrcresearchpress.com by 210.87.254.6 on 09/05/12
For personal use only.

Can. J. Chem. Downloaded from www.nrcresearchpress.com by 210.87.254.6 on 09/05/12
For personal use only.

TABLEAU 1. Taux de formation de CH_4, C_2H_4 et C_2H_6 (μmol/min) en fonction de la pression de NO (kPa) pour un temps d'irradiation de 60 min

P_{NO}	dCH_4/dt	dC_2H_4/dt	dC_2H_6/dt
0	0.0075	0.0035	0.060
4	<0.0002	0.0011	Nil

ment par réaction de radicaux méthyles sur le substrat.

[12] $CH_3^{\cdot} + CH_3{-}SCH{=}CH_2 \rightarrow CH_3SCH_3 + C_2H_3^{\cdot}$

Addition de CH_3SD. Effet de l'energie des photons incidents

Pour doser les radicaux primaires ($CH_3^{\cdot}$ et $C_2H_3^{\cdot}$), l'addition de CH_3SD à 6.7 kPa de SMV s'avère efficace. Les taux de formation de méthane, d'éthylène et d'éthane en fonction du CH_3SD ajouté (fig. 3) démontrent cette efficacité. Il faut remarquer que lors des expériences effectuées avec le CH_3SD, CH_4 signifie en réalité CH_4 et CH_3D et de même C_2H_4 signifie C_2H_4 et C_2H_3D. La capacité d'absorption du CH_3SD est telle que même dans les conditions expérimentales les plus défavorables utilisées ici (15% CH_3SD – 85% SMV) le méthanethiol absorbe

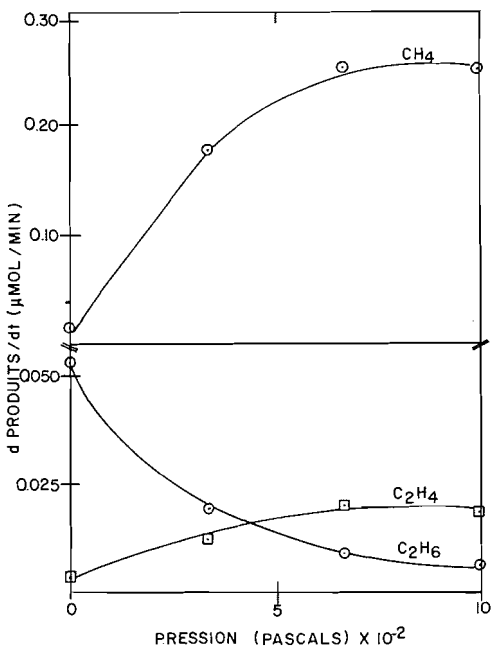

FIG. 3. Taux de formation de CH_4 (CH_4 + CH_3D), C_2H_4 (C_2H_4 + C_2H_3D) et C_2H_6 en fonction de la pression de CH_3SD ajouté.

moins de 1% de la lumière incidente totale. Les réactions 13 et 14 permettent le dosage de ces radicaux.

[13] $CH_3^{\cdot} + CH_3SD \rightarrow CH_3D + CH_3S^{\cdot}$

[14] $C_2H_3^{\cdot} + CH_3SD \rightarrow C_2H_3D + CH_3S^{\cdot}$

L'enrichissement isotopique du méthane et de l'éthylène analysés au spectromètre de masse confirme ces réactions. En calculant le taux total (T_T) de formation de ces radicaux comme étant

[15] $$T_T = T_{CH_4} + T_{C_2H_4} + 2T_{C_2H_6}$$

on trouve un rendement quantique total ($\phi_T = T_T/I_a$) s'approchant de l'unité pour les temps de réaction courts. Les processus primaires semblent bien décrits par les réactions 3, 4, 5 et 11.

L'analyse qualitative des produits lourds apporte d'autres précisions. Ainsi en absence de CH_3SD la formation de ces produits s'explique par la réaction de radicaux méthyles avec la molécule de départ:

[16] $CH_3^{\cdot} + SMV \rightarrow CH_3{-}S{-}\underset{\displaystyle CH_3}{\underset{|}{CH}}{-}{}^{\cdot}CH_2$

[17] $CH_3^{\cdot} + SMV \rightarrow CH_3{-}S{-}\dot{C}H{-}C_2H_5$

[18] $CH_3{-}S{-}(C_3H_6)^{\cdot} + C_2H_3S^{\cdot} \rightarrow CH_3{-}S{-}(C_3H_7) + C_2H_2S$

[19] $CH_3{-}S{-}(C_3H_6)^{\cdot} + C_2H_3S^{\cdot} \rightarrow CH_3{-}S{-}(C_3H_5) + C_2H_4S$

Aucun produit ne permet d'affirmer la contribution des radicaux $C_2H_3S^{\cdot}$ aux réactions 18 et 19. Cependant le taux de formation du radical thiovinyl étant le même que celui des radicaux méthyles (réaction 4) cette hypothèse est fort plausible.

Les produits lourds identifiés sont les suivants, $CH_3{-}S{-}CH_2CH_2CH_3$, $CH_3{-}S{-}CH{=}CHCH_3$, $CH_3{-}S{-}\underset{\displaystyle CH_3}{\underset{|}{C}}{=}CH$, $CH_3{-}S{-}\underset{\displaystyle CH_3}{\underset{|}{CH}}{-}C_2H_5$, $CH_3{-}S{-}\underset{\displaystyle CH_3}{\underset{|}{C}}{=}C{-}CH_3$ et $CH_3{-}S{-}S{-}CH_3$ [10].

Le sulfure d'isopropyle et de méthyle n'a pas été identifié mais il est probable que sa présence est voilée par le SMV lors de l'analyse au chromatographe. La formation des autres produits lourds peut s'expliquer ainsi:

Can. J. Chem. Downloaded from www.nrcresearchpress.com by 210.87.254.6 on 09/05/12
For personal use only.

TABLEAU 2. Variation du rapport k_5/k_4 en fonction de la source utilisée

Source	Energie moyenne (kJ)	Temps photolyse (min)	k_5/k_4
Lampe de pression moyenne avec filtre en Vycor	<471	60	6.8/93.2
		30	7.0/93
		5	7.5/92.5
		2	7.3/92.7
Lampe de basse pression	471	30	12.2/87.8
		20	12.5/87.5
		5	12.4/87.6
		1	12.5/87.5
Lampe de pression moyenne sans filtre	>471	60	17.7/82.3

TABLEAU 3. Taux de formation de différents produits (μmol/min) en fonction de la pression du substrat (kPa)

Pression	dCH_4/dt	dC_2H_4/dt	dC_2H_6/dt	dSM/dt	$dBTD/dt$	dC_3H_6/dt
3.3	0.0079	0.0028	0.070	0.0024	0.0036	0.0015
6.7	0.0075	0.0035	0.058	0.0045	0.0017	0.0013
10.0	0.0064	0.0044	0.050	0.0045	0.0016	0.0012
13.3	0.0064	0.0064	0.042	0.0053	0.0012	0.0012
16.7	0.0052	0.0065	0.054	0.0058	0.0013	0.0012

[20] $CH_3^{\cdot} + CH_3—S—(C_3H_6)^{\cdot} \rightarrow CH_3—S—\underset{\displaystyle CH_3}{\underset{|}{CH}}—CH_2—CH_3$

[21] $CH_3^{\cdot} + CH_3—S—(C_3H_5) \rightarrow CH_3—S—(C_4H_8)^{\cdot}$

[22] $CH_3—S—(C_4H_8)^{\cdot} + C_2H_3S^{\cdot} \rightarrow CH_3S—\underset{\displaystyle CH_3}{\underset{|}{C}}=CHCH_3 + C_2H_4S$

En présence de CH_3SD seul le sulfure de méthyle et de propyle (en plus du disulfure de méthyle) est détecté.

[23] $CH_3—S—\dot{C}H—C_2H_5 + CH_3SD \rightarrow CH_3—S—CHD—C_2H_5 + CH_3S^{\cdot}$

L'analyse au spectromètre de masse montre un enrichissement en deutérium pour ce produit. La réaction 17 est donc suffisamment rapide pour permettre la formation de $CH_3—S—\dot{C}HC_2H_5$ même en présence de CH_3SD.

L'addition de 1.0 kPa de CH_3SD à 6.7 kPa de SMV permet également de remarquer la variation du rapport 24 en fonction de la source lumineuse utilisée:

$$[24] \qquad \frac{k_5}{k_4} = \frac{T_{C_2H_4}}{T_{CH_4} + 2T_{C_2H_6}}$$

Ce rapport tient compte uniquement des réactions 4, 5, 6, 13 et 14 mais dans les conditions expérimentales précitées ce sont les plus importantes.

La variation de ce rapport (tableau 2) démontre que plus l'énergie moyenne des photons incidents augmente, plus ce rapport augmente.

Variation de la pression du substrat

Une étude du taux de formation de différents composés en fonction de la pression de SMV (tableau 3) montre une augmentation de ce taux pour l'éthylène, et le sulfure de méthyle, et, une diminution pour les produits de réactions interradicalaires. Un accroissement du taux de formation des produits résultant de réactions entre les radicaux méthyles et le SMV est également remarquée.

La réaction 12 explique l'augmentation de $T_{C_2H_4}$ et de $T_{CH_3SCH_3}$. Les radicaux $C_2H_3^{\cdot}$ formés réagissent ensuite pour donner de l'éthylène.

[25] $C_2H_3^{\cdot} + SMV \rightarrow C_2H_4 + R^{\cdot}$

[26] $C_2H_3^{\cdot} + C_2H_3S^{\cdot} \rightarrow C_2H_4 + C_2H_2S$

Can. J. Chem. Downloaded from www.nrcresearchpress.com by 210.87.254.6 on 09/05/12
For personal use only.

Une réaction semblable entre radicaux méthyles et thiovinyles explique la formation du méthane et la diminution de T_{CH_4} en fonction de la pression du substrat.

[27] $CH_3^{\cdot} + C_2H_3S^{\cdot} \rightarrow CH_4 + C_2H_2S$

Une pression plus élevée de SMV favorise les réactions radicaux–molécules au détriment des réactions inter-radicalaires. L'augmentation du taux de formation de C_2H_4 nous porte à croire que la réaction d'abstraction du radical $C_2H_3^{\cdot}$ [25] sur le SMV est plus importante qu'une réaction de dismutation avec un autre radical alors que pour le méthane c'est le cas contraire qui se produit.

On remarque pour le $T_{C_2H_6}$ une remontée pour une pression de 16.6 kPa et la même tendance semble s'amorcer pour le butadiène-1,3. L'augmentation locale de la concentration des radicaux à plus haute pression (*i.e.* l'absorption de la lumière se fait dans un espace plus restreint) explique ce phénomène. Egalement, pour l'éthane, une pression totale plus élevée signifie une plus grande facilité de désactivation (réaction 6).

Addition de C_3F_8

L'addition de C_3F_8 au milieu réactionnel permet de mettre en évidence un intermédiare excité qui peut être désactivé par collision.

[28] $SMV^* + C_3F_8 \rightarrow SMV + C_3F_8$

Deux séries d'expériences (tableau 4) indiquent la présence d'un tel intermédiaire. Dans une première série la cellule est remplie de 6.7 kPa de SMV et de diverses pressions de C_3F_8. Dans la deuxième série on ajoute également 1.0 kPa de CH_3SD.

Aux basses pressions (<40.0 kPa) il y a augmentation du taux de formation de l'éthane (première série) et du méthane (deuxième série) en fonction de la pression. La désactivation de radicaux méthyles chauds par le C_3F_8 peut expliquer un tel comportement.

[29] $CH_3^{\cdot *} + C_3F_8 \rightarrow CH_3^{\cdot} + C_3F_8$

Un calcul de l'enthalpie de la réaction 4 (tableau 5) donne un ΔH de -238 kJ/mol. Lors de l'irradiation environ 460 kJ/mol sont transferrés au SMV. Il est donc fort probable que les radicaux méthyles soient formés avec un surplus d'énergie. Cependant la désactivation de ces radicaux $CH_3^{\cdot *}$ par le C_3F_8 rend ces derniers moins réactifs avec le SMV et ainsi il y a un plus grand nombre de radicaux disponibles pour former du méthane ou de l'éthane.

TABLEAU 4. Taux de formation de produits (μmol/min) en fonction de la pression de C_3F_8 (kPa)

	Expérience 1*	Expérience 2*	
$P_{C_3F_8}$	dC_2H_6/dt	dCH_4/dt	dC_2H_4/dt
0	0.0670	0.225	0.020
20.0	0.0692	0.248	
40.0	0.0720	0.257	0.021
80.0	0.0669	0.252	0.024
113.3	0.0633	0.248	0.027
153.2	0.0588	0.240	0.25

*Expérience 1: sans CH_3SD; expérience 2: avec 1.0 kPa.

TABLEAU 5. Calcul des enthalpies de réactions (6, 7)

Réaction	ΔH (kJ/mol)
$CH_3SCH{=}CH_2 \rightarrow CH_3^{\cdot} + {}^{\cdot}SCH{=}CH_2$	238
$CH_3SCH{=}CH_2 \rightarrow CH_3S^{\cdot} + CH_2CH^{\cdot}$	347
$CH_3OCH{=}CH_2 \rightarrow CH_3^{\cdot} + {}^{\cdot}OCH{=}CH_2$	268
$CH_3OCH{=}CH_2 \rightarrow CH_3O^{\cdot} + CH_2CH^{\cdot}$	381

La présence d'un troisième corps (réaction 6) pour désactiver la molécule nouvellement formée contribue également à l'augmentation de la quantité de C_2H_6 mesurée à pression plus élevée.

Aux plus hautes pression de C_3F_8 (>40.0 kPa) la diminution de T_{CH_4} et $T_{C_2H_6}$ est due à la désactivation subie par l'intermédiaire excité SMV*.

En portant sur un graphique $(dCH_4/dt)^{-1}$ *vs.* $P_{C_3F_8}$ (fig. 4) les résultats obtenus à 80.0,113 et

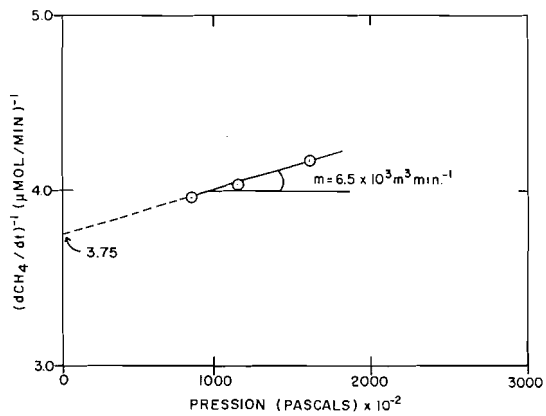

FIG. 4. Inverse du taux de formation du méthane en fonction de la pression de C_3F_8.

153 kPa de C_3F_8 on obtient une droite. Considérant les réactions 3, 4, 5, 13 et 28 comme les seules importantes, on trouve l'équation:

$$[30] \quad \frac{dCH_4}{dt} = \frac{1}{I_a}\left(1 + \frac{k_5}{k_4}\right) + \frac{1}{I_a}\frac{k_{28}[PFP]}{k_4}$$

où [PFP] est la concentration de C_3F_8 ajouté dans la cellule.

En prenant comme valeur de $k_5/k_4 = 7.3/92.7$ pour la lampe utilisée on trouve alors que $k_{28}/k_4 = 1.9 \times 10^3$ m^3 mol^{-1}. En estimant le diamètre de collision entre le C_3F_8 et le SMV à 0.5 nm et en supposant que chaque collision dissipe suffisamment d'énergie pour empêcher toute scission subséquente, on évalue alors k_{28} à 1.63×10^8 m^3 mol^{-1} s^{-1} et de là $k_4 = 8.6 \times 10^{10}$ s^{-1}. Le temps de vie τ du SMV* est donc de 1.2×10^{-11} s. La constante k_5 est alors calculée comme étant 6.8×10^9 s^{-1}.

L'augmentation du taux de formation de l'éthylène (pour des pressions de C_3F_8 allant de 0 à 113.3 kPa) pourrait s'expliquer par la réaction 17 suivie des réactions 31 et 32.

$$[31] \quad CH_3S\dot{C}HCH_2CH_3 + M \rightarrow (CH_3SMV)^{\cdot *} + M$$

$$[32] \quad (CH_3SMV)^{\cdot *} \rightarrow C_2H_4 + \dot{C}H_2SCH_3$$

Ces réactions peuvent expliquer également la hausse du taux de formation de l'éthylène lorsqu'on augmente la pression de SMV et contribuer à la formation de l'éthylène malgré l'addition de NO au mélange réactionnel.

En conclusion, la photolyse du SMV permet donc de mettre en évidence un intermédiaire excité dont le temps de vie est 1.2×10^{-11} s. Castonguay (8) a trouvé un temps de vie de 1.4×10^{-10} s pour le MVE.

L'énergie fournie à la molécule de SMV est inférieure à 471 kJ/mol (lampe de pression moyenne avec filtre Vycor) alors que celle fournie au MVE est de 471 kJ/mol (lampe de basse pression, 1). Malgré cela le temps de vie du SMV est plus court. De même le SMV est promu à un singulet lors de l'excitation (photolyse directe) alors que le MVE est promu à un triplet (réaction photosensibilisée, 1). Cette différence dans le mode d'excitation peut se traduire par une différence dans la réactivité. Cependant l'équation bien connue (9)

$$[33] \quad k_i = v_i\left(\frac{E - E_a}{E}\right)^N$$

qui peut s'appliquer pour une scission homolytique comme celles considérées ci-haut permet d'expliquer cette différence dans les temps de vie. En effet on remarque que l'énergie nécessaire pour briser le lien CH_3—S dans le SMV est plus faible que celle pour briser le lien CH_3—O dans le MVE (tableau 4). Donc E_a est plus élevée pour le MVE que pour le SMV d'où une constante k_i plus grande pour le SMV. De même la liaison vinyl – S est suffisamment faible pour en permettre la scission (compétition entre les réactions 4 et 5) alors que la liaison vinyl – O est plus forte et aucun clivage de celle-ci n'a été mis en évidence. Considérant l'équation 33, il est normal qu'un accroissement de l'énergie E augmente la probabilité de la scission du lien le plus fort relativement au bris de la liaison plus faible et c'est ce qui se produit lorsqu'on accroit l'énergie des photons incidents (tableau 1).

Une autre explication nous vient à l'esprit lorsqu'on considère le spectre électronique du SMV. Il y a chevauchement de deux transitions électroniques dans la région où s'effectue la photolyse. La première bande plus faible correspond à une transition $4S \leftarrow \Pi$ et la seconde à une transition $\Pi^* \leftarrow \Pi$ (10). Une augmentation de l'énergie des photons se traduirait par une importance accrue de l'absorption dans la bande $\Pi\Pi^*$

$$[34] \quad (\Pi,\Pi^*) \rightarrow \dot{C}_2H_3 + CH_3S^{\cdot}$$

$$[35] \quad (\Pi,4S) \rightarrow CH_3^{\cdot} + C_2H_3S^{\cdot}$$

Donc un déplacement hypsochrome de la région d'irradiation augmenterait la possibilité de formation du radical vinyl.

La mise en évidence d'un intermédiaire excité nous porte à croire cependant que la molécule a le temps de redistribuer son énergie électronique en énergie vibrationnelle et ainsi l'énergie totale fournie à la molécule lors de l'absorption d'un photon est plus importante que le type de transition électronique subie par cette même molécule.

Les auteurs remercient le Conseil National de Recherches du Canada pour l'aide apportée sous forme de bourses et de subvention. Ils remercient également les Ministère de l'Education de la Province de Québec pour les subventions accordées pour ce projet.

Can. J. Chem. Downloaded from www.nrcresearchpress.com by 210.87.254.6 on 09/05/12
For personal use only.

1. J. CASTONGUAY et Y. ROUSSEAU. Can. J. Chem. **49**, 2125 (1971).
2. P. M. RAO et A. R. KNIGHT. Can. J. Chem. **50**, 844 (1972).
3. D. R. TYCHOLEZ et A. R. KNIGHT. Can. J. Chem. **50**, 1734 (1972).
4. C. S. SMITH et A. R. KNIGHT. Can. J. Chem. **51**, 780 (1973).
5. Y. ROUSSEAU et H. E. GUNNING. Can. J. Chem. **41**, 465 (1963).
6. J. L. FRANKLIN. J. Chem. Phys. **21**, 2029 (1953).
7. S. W. BENSON, F. R. CRUIKSHANK, D. M. GOLDEN, G. R. HAUGEN, H. E. O'NEAL, A. S. RODGERS, R. SHAW et R. WALSH. Chem. Rev. **69**, 279 (1969).
8. J. CASTONGUAY. Thèse de doctorat, Université de Montréal, Montréal, Québec, 1972.
9. R. W. KISER. Introduction to mass spectrometry and its applications. Prentice-Hall, Inc., New Jersey. 1965.
10. ADRIEN PLANKAERT. Thèse de doctorat, Université de Montréal, Montréal, Québec. 1974.

Can. J. Chem. Downloaded from www.nrcresearchpress.com by 210.87.254.6 on 09/05/12
For personal use only.

Mise en évidence des tautomères énoliques des hydroxypyridines dans la source du spectromètre de masse

A. MAQUESTIAU, Y. VAN HAVERBEKE ET C. DE MEYER
Université de l'Etat, Faculté des Sciences, Service de Chimie Organique, Mons, Belgique
ET
A. R. KATRITZKY, M. J. COOK ET A. D. PAGE
University of East Anglia, School of Chemical Sciences, Norwich, England
Reçu le 6 juin, 1974

A. MAQUESTIAU, Y. VAN HAVERBEKE, C. DE MEYER, A. R. KATRITZKY, M. J. COOK et A. D. PAGE. Can. J. Chem. **53**, 490 (1975).

L'utilisation de mélanges approximativement équimolaires d'hydroxypyridines et de DO-pyridines permet la mise en évidence sur la perte de CO, d'un effet isotopique, identique en ce qui concerne les isomères 3 et 4. Ce résultat suggère que les tautomères énoliques constituent essentiellement la phase gazeuse, comme le confirme d'ailleurs une étude des rapports d'abondance métastable au niveau d'ions fragments hydroxypyridine et sur les mêmes ions créés par ionisation directe. La 2-hydroxypyridine exhibe également un effet isotopique quoique plus faible ainsi que le confirme l'étude de mélanges équimolaires 2-éthoxy et 2-éthoxy-d_5-pyridines. La mise en évidence du tautomère énolique est également invoquée pour cet isomère.

A. MAQUESTIAU, Y. VAN HAVERBEKE, C. DE MEYER, A. R. KATRITZKY, M. J. COOK, and A. D. PAGE. Can. J. Chem. **53**, 490 (1975).

3- and 4-Hydroxypyridines exist in their enolic form, in the gas phase, as evidenced by the similarity of the deuterium isotope effects on the loss of CO, calculated on nearly equimolar mixtures of HO- and DO-pyridines. This is confirmed by analysis of metastable ratios evaluated on hydroxypyridine fragment ions and on the same ions produced by direct ionization. 2-Hydroxypyridine shows a weaker isotope effect for the same reaction and this is confirmed by the study of an equimolar mixture of 2-ethoxy- and 2-ethoxy-d_5-pyridines. It is shown that 2-hydroxypyridine also exists as its enolic form, in the gas phase.

Introduction

Les 2-, 3- et 4-hydroxypyridines (**1**, **2** et **3**) étant des composés susceptibles de participer à un équilibre protomère du type énol–cétone ont fait l'objet de nombreuses recherches tant à l'état solide qu'en solution. Les résultats des études spectroscopiques et physico-chimiques établissent que les 2- et 4-hydroxypyridines existent presque exclusivement sous forme pyridone à l'état cristallin et en solution; par contre, l'isomère 3-hydroxy se présente comme tel à l'état condensé et dans les solvants de faible constante diélectrique (1) (schéma 1). En phase gazeuse, au contraire, quelques données récentes de la littérature indiquent une plus grande stabilité des tautomères énoliques. Ainsi, Grønneberg et Undheim (2), par des mesures de potentiels d'ionisation, concluent à la présence unique des molécules 2-, 3- et 4-hydroxypyridines. La prépondérance de l'isomère énolique a encore été confirmée par spectroscopie u.v.: à 120–140 °C en phase vapeur, le dérivé 2-hydroxylé existe en tant que tel à raison de 65 ± 15% (3).

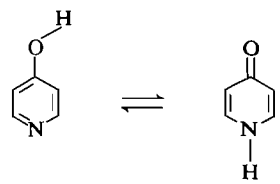

4-Hydroxypyridine Forme énolique-(OH) — 4-Pyridone Forme pyridone-(NH)

SCHÉMA 1

Nous nous proposons dans le présent travail, de confirmer l'existence prépondérante des formes énoliques des hydroxypyridines dans la source du spectromètre de masse par la mise en évidence d'effets isotopiques primaires mesurés au niveau des ions de fragmentation directe et métastables. La manifestation de tels effets a d'ailleurs déjà permis d'apporter de précieux renseignements mécanistiques (4–6).

Can. J. Chem. Downloaded from www.nrcresearchpress.com by 210.87.254.42 on 09/05/12
For personal use only.

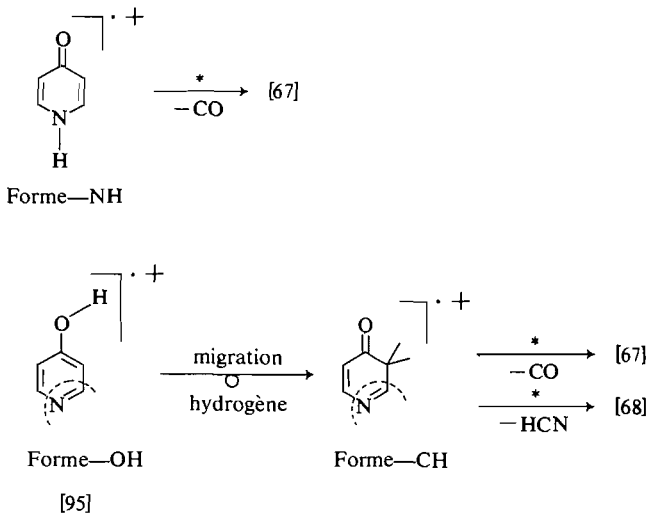

SCHÉMA 2

Résultats expérimentaux et discussion

Les spectres de masse des 3- et 4-hydroxypyridines mentionnés dans la littérature (7, 8) révèlent une élimination compétitive de HCN et de CO au départ des ions moléculaires; par contre, le dérivé 2-hydroxy perd quasi spécifiquement une molécule de CO. Pour **2** et **3**, dont on a remplacé l'hydrogène tautomérisable par du deutérium, nous observons l'expulsion de cyanure d'hydrogène quasi spécifiquement sous forme DCN. Ce phénomène n'a trouvé, jusqu'à présent, aucune explication pleinement satisfaisante.

Toutes ces éliminations sont appuyées par des transitions métastables, qui dans le cas de l'expulsion de CO présentent un sommet concave, traduisant une libération d'énergie cinétique.

La perte de HNC ne se conçoit pas aisément au départ d'une forme NH (2-pyridone ou 4-pyridone). Il faut d'ailleurs remarquer que l'élimination de HCN, observée au départ de l'isomère 3-hydroxypyridine, incapable de présenter une forme pyridone, accrédite cette suggestion. Par contre, l'élimination de CO peut être envisagée aussi bien à partir d'une forme lactame qu'au départ d'un ion de type CH obtenu par migration de l'hydrogène hydroxylique de l'énol (schéma 2).

De telles migrations d'hydrogène ont déjà été invoquées pour expliquer, notamment, la dégradation du phénol et de l'aniline (réf. 8, p. 116 et réf. 9). Si un tel réarrangement, uniquement concevable au départ d'une forme énolique, constitue l'étape déterminante, le marquage au deutérium de l'hydrogène hydroxylique modifie les probabilités de rupture des liaisons O—H et O—D. Il en résulte une diminution de l'intensité de l'ion fille ou métastable associé à l'élimination de CO. La manifestation de tels effets isotopiques correspondrait donc à la mise en évidence de tautomères énoliques.

La mesure de ces effets n'est toutefois pas simple, car les dérivés monodeutériés des 3- et 4-hydroxypyridines éliminent une molécule de DCN. Les pics correspondants se confondent avec ceux provenant de la perte de CO et il est nécessaire pour les distinguer de travailler à haute résolution. Dans ces conditions, afin d'augmenter la précision de la mesure, seules les valeurs relatives i du rapport des intensités $([M - CO]^{\cdot+})/(M^{\cdot+})$ sont déterminées et ce sur des mélanges approximativement équimoléculaires en produits mono- et non deutériés.

$$i = \frac{\left|\frac{[M - CO]^{\cdot+}}{M^{\cdot+}}\right|_{HO-Py}}{\left|\frac{[M - CO]^{\cdot+}}{M^{\cdot+}}\right|_{DO-Py}}$$

Les résultats expérimentaux sont repris au tableau 1.

Les valeurs pour les pics métastables ne peuvent bien entendu pas être déterminées à cause de la superposition mentionnée ci-dessus. Pour des raisons identiques, il n'est pas possible

Can. J. Chem. Downloaded from www.nrcresearchpress.com by 210.87.254.42 on 09/05/12
For personal use only.

			masses précises	m^*
	$\xrightarrow{-CO}$	[67]	67.042	47.25
HO-Pyridine				
[95]	$\xrightarrow{-HCN}$	[68]	68.026	48.67
+	$\xrightarrow{-CO}$	[68]	68.048	48.16
DO-Pyridine				
[96]	$\xrightarrow{-DCN}$	[68]	68.026	48.16

SCHÉMA 3

TABLEAU 1. Valeurs de i des mélanges équimoléculaires des hydroxypyridines non- et monodeutériées

Pyridine	i
2-Hydroxy (**1**)	1.04
3-Hydroxy (**2**)	1.47
4-Hydroxy (**3**)	1.41

NOTE: HO-Py ≃ 50% + DO-Py ≃ 50%.

d'évaluer l'effet isotopique éventuel sur la perte de H(D)CN et ce aussi bien au niveau des ions de fragmentation directe et métastables comme illustré ci-après (schéma 3). Les valeurs mesurées des effets isotopiques primaires (i) rapportées au tableau 1 sont de l'ordre de grandeur de celles auxquelles on pouvait s'attendre au vu des données de la littérature (10, 11), du moins pour les dérivés 3- and 4-hydroxylés.[1]

Comme, d'une part la 3-hydroxypyridine existe entièrement sous forme OH, et comme d'autre part, on peut *a priori* admettre un même effet isotopique pour une rupture O—H d'un hydroxyle fixé en position 3 ou 4, la quasi égalité de i pour **2** et **3** laisse présumer que la 4-hydroxypyridine se trouve au moins de façon largement prédominante, sous forme OH en phase gazeuse. Ces résultats sont en parfait accord avec les conclusions du travail de Grønneberg et Undheim (2). La valeur de i de 1.04 pour la 2-hydroxypyridine ne permet par contre pas, à ce stade, de tirer de conclusions. Cependant, comme cette substance n'élimine pas de HCN, il n'y a pas superposition des pics relatifs à la perte de CO et DCN dans la molécule deutériée. Il est donc possible ici, de mesurer l'effet isotopique i^* au niveau des transitions métastables (première région libre de champ).

$$i^* = \frac{[m^*(M - CO)]_{2HO-Py}}{[m^*(M - CO)]_{2DO-Py}}$$

Les valeurs de i et i^* mesurées à basse résolution sur un mélange équimoléculaire de 2-hydroxypyridine non et monodeutériés sont reprises au tableau 2. Comme on peut le remarquer, le faible effet isotopique (i) mesuré à basse résolution (1.07, tableau 2)[2] est quasi identique à celui obtenu à haute résolution (1.04, tableau 1). Ce résultat confirme la précision des valeurs renseignées au tableau 1. La faible valeur de i mesurée au niveau d'ions de fragmentation directe, pour la 2-hydroxypyridine, permet de douter de l'existence d'un effet isotopique réel et partant exclut à ce stade toute conclusion quant à la composition de la phase gazeuse. Il est dès lors apparu plus intéressant de confirmer la manifestation de l'effet isotopique au niveau de transition métastable de première région libre de champ. Il est en effet bien établi que l'effet isotopique augmente avec la diminution de l'énergie moyenne interne de l'ion précurseur (10), et ce pour un même mécanisme de réarrangement. L'observation de la valeur de i^* de 1.8, au niveau métastable, (tableau 2), permet de conclure à la présence, au moins partielle, du tautomère énolique de la 2-hydroxypyridine en phase gazeuse. En effet, la diminution de l'intensité du métastable correspondant à l'élimination de CO suite à la substitution isotopique implique une migration préalable de l'hydrogène

[1]Bien que des effets isotopiques secondaires de l'ordre de deux aient été rapportés par Neeter et Nibbering (11), il faut remarquer qu'il est difficile de chiffrer indépendemment un effet isotopique primaire et secondaire pour de tels processus de réarrangement prototropique; en général, la seule considération des effets isotopiques primaires est appliquée (4, 5, 6, 10).

[2]Valeur corrigée pour la contribution en ^{13}C.

Can. J. Chem. Downloaded from www.nrcresearchpress.com by 210.87.254.42 on 09/05/12
For personal use only.

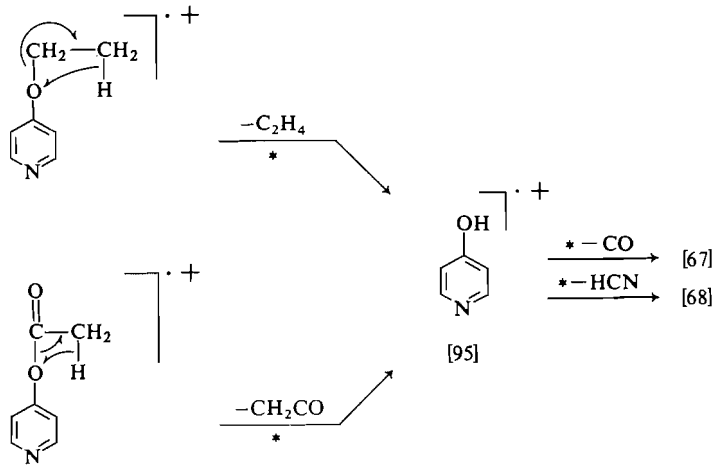

SCHÉMA 4

hydroxylique au cours d'une étape déterminante. Une forme 2-pyridone pouvant éliminer directement CO, n'aurait conduit par conséquent à aucune modification d'intensité suite au marquage au deutérium, aussi bien au niveau d'ions de fragmentation directe que métastable, tout au moins si l'on exclut l'effet isotopique secondaire. Le bien-fondé d'une telle hypothèse de travail sera d'ailleurs confirmé plus loin par l'étude d'un mélange 2-éthoxy et 2-éthoxy-d_5-pyridines.

TABLEAU 2. Valeurs de i et i^* d'un mélange equimoléculaire de 2-hydroxypyridine non- et monodeutériées

	i^*	i
OC_2H_5 + OC_2D_5 (50% / 50%)		
$-C_2H_4$ / $-C_2D_4$		
OH / OD [95] / [96]	1.7	1.09
$-CO$ / $-CO$ [67] / [68]		
OH + OD (50% / 50%)	1.8	1.07
$-CO$ / $-CO$		

Créations d'ions "in situ"

Les substituants éthyle ou acétyle fixés sur un hétéroélément tel l'azote ou l'oxygène éliminent par un mécanisme unique à quatre centres, respectivement de l'éthylène et du cétène (4, 5, 12, 13). A partir des 3- et 4-éthoxy ou acétoxypyridines, il est donc, en principe, possible de créer un ion fragment identique en structure à celui d'un ion moléculaire de type OH (schéma 4).

Les rapports d'abondance métastables pour la perte de HCN et de CO, mesurés au départ des ions fragments $M - \overline{CH_2CO}^{\cdot +}$ et $M - \overline{C_2H_4}^{\cdot +}$ issus respectivement des substrats acétoxy et éthoxypyridines, et ceux mesurés sur les ions moléculaires hydroxypyridines correspondants sont renseignés au tableau 3. La similitude dans les rapports d'abondance pour les dérivés substitués en 3 (Tableau 3) implique l'identité de structure des ions fragments $M - \overline{CH_2CO}^{\cdot +}$ et $M - \overline{C_2H_4}^{\cdot +}$ et de l'ion moléculaire de la 3-hydroxypyridine (14, 15, 16). Comme on sait de manière non ambiguë que cette substance existe sous forme OH, ce résultat confirme l'élimination de cétène ou d'éthylène par un mécanisme à quatre centres. Un même schéma de fragmentation s'appliquant en toute logique aux dérivés 4 substitués, la quasi égalité des valeurs renseignées pour **3**, **6** et **7** (tableau 3) démontre à nouveau l'existence de la 4-hydroxypyridine, en phase vapeur dans le spectromètre de masse, sous forme énolique.

La création "*in situ*" de la 4-pyridone, espérée au départ de la *N*-éthyl-4-pyridone n'a

Can. J. Chem. Downloaded from www.nrcresearchpress.com by 210.87.254.42 on 09/05/12
For personal use only.

TABLEAU 3. Rapports d'abondance métastable (seconde région) pour la perte de HCN et de CO

	Y	Composé	$\left\lvert\frac{[m^*(-HCN)]}{[m^*(-CO)]}\right\rvert_{m/e=95}$
	OH	**2**	1.28
	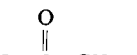	**4**	1.27
	OEt	**5**	1.24
	OH	**3**	2.22
	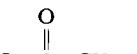	**6**	2.48
	OEt	**7**	2.50

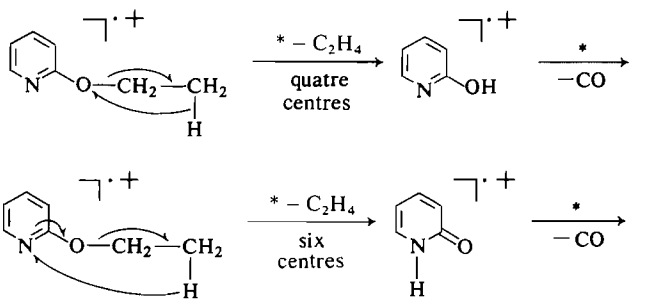

SCHÉMA 5

pu malheureusement être réalisée, celle-ci se dégradant presque exclusivement par une perte de monoxyde de carbone au départ de l'ion moléculaire, excluant ainsi une confirmation supplémentaire de nos résultats.

L'absence d'élimination compétitive de HCN et de CO dans le cas de la 2-hydroxypyridine ne permet pas une analyse semblable à celle mentionnée au tableau 3. Néanmoins, les 2-éthoxypyridines donnent naissance sous l'impact électronique, du moins partiellement, à des ions fragments de type 2-hydroxy (*vide infra*).

Il est donc possible d'évaluer des effets isotopiques pour **1** ou pour des ions correspondants formés *in situ* au départ de spectres relevés sur des mélanges 50:50 en produits deutérié et non deutérié (tableau 2). La quasi égalité des valeurs de i, d'une part, et de i^*, d'autre part, confirme l'existence en phase gazeuse du tautomère énolique pour **1**; une telle égalité observée à la fois sur les transitions métastables et ordinaires, correspondant à l'élimination de CO (tableau 2), pourrait même suggérer l'existence unique de la forme 2-hydroxypyridine, résultat déjà avancé par Grønneberg et Undheim (2). En effet, un mélange, à l'état gazeux, de 2-pyridone/2-hydroxypyridine aurait conduit à des effets isotopiques plus petits que 1.09[3] et 1.7 obtenus au départ d'éthoxypyridine à moins que cette dernière ne se dégrade aussi via un mécanisme à six centres pour donner le même mélange, ce qui paraît totalement improbable (schéma 5). Il peut toutefois sembler surprenant que la 2-hydroxypyridine, contrairement aux deux autres isomères, ne perde pas de molécule de HCN. Ceci pourrait toutefois s'expliquer par

[3]Valeur corrigée pour la contribution du ^{13}C.

Can. J. Chem. Downloaded from www.nrcresearchpress.com by 210.87.254.42 on 09/05/12
For personal use only.

Can. J. Chem. Downloaded from www.nrcresearchpress.com by 210.87.254.42 on 09/05/12
For personal use only.

l'intervention d'un effet *ortho*, exercé par l'azote pyridinique qui faciliterait le transfert de l'hydrogène hydroxylique et accréditerait d'ailleurs par la même occasion notre hypothèse selon laquelle une forme 2-pyridone élimine difficilement HNC. L'abaissement notable de l'énergie d'activation correspondant à l'élimination de CO, éclipserait par voie de conséquence toute possibilité de perte de HCN. L'intervention de cet effet *ortho* pourrait expliquer la petite valeur de l'effet isotopique observé sur la 2-hydroxypyridine et d'autre part certaines fragmentations propres aux pyridines substituées en position 2, comme la perte intense d'un radical hydrogène et méthyle au départ des substrats 2-méthoxy- et 2-éthoxypyridines, conduisant probablement à la quaternisation de l'azote. De tels effets *ortho* exercés par l'azote pyridinique ont été mentionnés dans la littérature (réf. 7, pp. 427, 465 et 471; 17).

Conclusions

L'étude de mélanges OH- et OD-pyridines révèle une diminution de l'intensité de l'ion fille et de l'ion métastable correspondant à l'élimination de CO, suite au marquage isotopique. Cette observation suggère que les tautomères énoliques constituent principalement la phase gazeuse. En effet, dans ce cas, l'expulsion de CO ne peut se concevoir que suite à la migration de l'hydrogène hydroxylique et ceci dans une étape déterminante. Par contre, les formes lactames, pouvant éliminer directement CO sans réarrangement, ne présenteront pas un tel effet isotopique primaire.

L'égalité dans les effets isotopiques primaires et secondaires, relatifs à la perte de CO, au départ des substrats 3- et 4-hydroxypyridines, vérifie le bien-fondé de nos hypothèses. L'analogie dans les rapports d'abondances métastables, calculés d'une part au niveau d'ions fragments hydroxypyridines, et d'autre part au niveau des mêmes ions, résultant d'une ionisation directe, confirme également nos résultats. L'isomère 2-hydroxypyridine présente aussi un effet isotopique, beaucoup plus faible certes mais réel, sur la perte de CO. Celui-ci se retrouve exactement sur les ions fragments 2-hydroxypyridines, créés via une élimination d'éthylène au départ de 2-éthoxypyridine. Si cette élimination procède suivant le mécanisme conventionnel à quatre centres, cette égalité dans les effets isotopiques suggère que le tautomère énolique constitue quasi uniquement la phase gazeuse.

Partie expérimentale

Tous les spectres ont été relevés sur un spectromètre A.E.I. MS 902, soit par introduction dans la source (Intr. dir.), soit via le système en verre (Intr. liq.), travaillant à 70 eV (100 μA, 8 kV).

Les valeurs d'effet isotopique ainsi que les rapports d'abondance mentionnés constituent la moyenne de plusieurs balayages, effectués dans les mêmes conditions expérimentales. La comparaison des transitions métastables de première région libre de champ est réalisée par la technique de refocalisation d'ions (18, 19) (4 kV) en maintenant constante la tension du multiplicateur d'électrons.

La réalisation de mélanges équimolaires en produits hydrogéné et monodeutérié est réalisée par échange direct dans la source du spectromètre grâce à l'admission contrôlée de D_2O via le système d'introduction des gaz. L'évolution du taux de deutériation est suivie au moyen de l'oscilloscope de l'appareil et l'admission de D_2O est coupée dès que l'on obtient un mélange équimolaire. Les expériences en haute résolution (environ 10.000) ont été réalisées avec la perfluorotributylamine, comme substance de référence. Les intensités relatives rapportées ci-après sont résumées par rapport au pic de base. Seuls sont mentionnés les fragments dont l'intensité est supérieure à 3%.

2-Hydroxypyridine: [95] Intr. dir.; Produit Aldrich; *m/e* 96(6), 95(100), 68(5), 67(31), 66(7), 51(5), 50(4), 41(13), 40(11, 5), 39(23).

3-Hydroxypyridine: [95] Intr. dir.; Produit Aldrich; *m/e* 96(6), 95(100), 68(8), 67(4), 66(3), 55(4), 42(4), 41(7), 40(8), 39(15).

4-Hydroxypyridine: [95] Intr. Dir.; Produit Aldrich; *m/e* 96(6), 95(100), 94(4), 68(15, 5), 67(9), 66(3, 5), 55(6), 53(3, 5), 51(4), 50(3, 5), 42(4), 41(11), 40(8), 39(14), 38(4).

2-Ethoxypyridine: [123] Intr. Liq.; p.é. 40–41°/18 mm (litt. (20) 156°/760 mm); *m/e* 123(42), 122(7), 108(100), 96(4), 95(52), 79(89), 78(32), 67(70), 66(8), 52(14), 51(18), 50(5, 5), 41(9), 40(9), 39(25, 5), 38(8).

2-Ethoxy d_5-pyridine: [128] Intr. Liq. (20); *m/e* 128(30), 126(5), 110(100), 97(4), 96(61), 82(10), 81(6), 80(96), 79(5), 78(23), 69(5), 68(91), 67(5), 66(6), 53(5), 52(13), 51(16), 50(6, 5), 42(10), 41(7), 40(10), 39(39), 38(13).

3-Ethoxypyridine: [123] Intr. Liq.; p.é. 78–80°/15 mm (21); *m/e* 123(52), 96(6), 95(100), 78(6), 68(6, 5), 67(8), 66(4), 55(3), 51(8), 50(3), 41(5), 40(7), 39(24), 38(6).

4-Ethoxypyridine: [123] Intr. Liq.; p.é. 98–100°/17 mm (litt. (22) 94°/14 mm); *m/e* 123(91), 108(3), 96(7), 95(100), 78(14), 68(19), 67(16, 5), 66(3), 55(5), 53(3), 52(4), 51(19), 50(7), 41(11), 40(9), 39(14), 38(3, 5).

N-Ethyl-4-pyridone: [123] Intr. Dir.; p.é. 170°/0.5 mm (23) (litt. (24) 180–195°/1.3 mm); *m/e* 123(100), 122(4), 108(28, 5), 96(5), 95(19), 94(4), 82(14, 5), 81(3, 5), 80(55), 68(6), 67(17, 5), 66(4), 54(6), 53(8), 52(5, 5), 51(3), 43(3, 5), 42(8), 41(12, 5), 40(11), 39(19), 38(5).

3-Acétoxypyridine: [137] Intr. Liq.; p.é. 98–100°/15 mm (litt. (25) 210°); *m/e* 137(14), 109(5), 96(7), 95(100), 68(4), 67(7, 5), 66(5), 51(4), 50(3), 43(83), 42(3), 41(3), 40(6), 39(22).

4-Acétoxypyridine: [137] Intr. Dir.; p.f. 135° (litt. (26) 140–150°); *m/e* 137(30), 109(19), 96(5), 95(78), 68(11, 5), 67(17), 66(3), 60(3), 55(3), 53(3), 52(3), 51(7), 50(5), 45(4), 43(100), 42(10), 41(40), 40(10), 39(15).

1. A. R. KATRITZKY et I. M. LAGOWSKI. *Dans* Advances in heterocyclic chemistry. *Edité par* A. R. Katritzky. Vol. 1. Academic Press, London. (1963) p. 339.
2. T. GRØNNEBERG et K. UNDHEIM. Org. Mass Spectrom. **6**, 823 (1972).
3. P. BEAK et F. S. FRY. J. Am. Chem. Soc. **95**, 1700 (1973).
4. I. HOWE et D. H. WILLIAMS. Chem. Commun. 1195 (1971).
5. N. A. UCCELLA, I. HOWE et D. H. WILLIAMS. Org. Mass Spectrom. **6**, 229 (1972).
6. I. HOWE, N. A. UCCELLA et D. H. WILLIAMS. J. Chem. Soc. (Perkin II), 76 (1973).
7. Q. N. PORTER et J. BALDAS. *Dans* Mass spectrometry of heterocyclic compounds. *Edité par* A. Weissberger et E. C. Taylor. Wiley-Interscience, New-York. 1971. p. 385.
8. H. BUDZIKIEWICZ, C. DJERASSI et D. H. WILLIAMS. *Dans* Mass spectrometry of organic compounds. Holden Day Inc., San Francisco. (1967). p. 571.
9. J. H. BEYNON, G. R. LESTER et A. E. WILLIAMS. J. Phys. Chem. **63**, 1861 (1959).
10. I. HOWE et F. W. MCLAFFERTY. J. Am. Chem. Soc. **93**, 99 (1971).
11. R. NEETER et N. M. M. NIBBERING. Org. Mass Spectrom. **7**, 1091 (1973).
12. H. NAKATA et A. TATEMATSU. Org. Mass Spectrom. **5**, 1343 (1971).
13. N. M. M. NIBBERING. Tetrahedron, **29**, 385 (1973).
14. T. W. SHANNON et F. W. MCLAFFERTY. J. Am. Chem. Soc. **88**, 5021 (1966).
15. J. L. OCCOLOWITZ. J. Am. Chem. Soc. **91**, 5202 (1969).
16. I. HOWE. *Dans* Mass spectrometry specialist periodical reports. *Edité par* D. H. Williams. Vol. 1. The Chemical Society, London. (1971) p. 44; et Vol. 2. London. (1973). p. 33.
17. D. M. CLUGSTON et D. B. MACLEAN. Can. J. Chem. **44**, 781 (1966).
18. K. R. JENNINGS. J. Chem. Phys. **43**, 4176 (1965).
19. M. BARBER et R. M. ELLIOTT. American Society for mass spectrometry, 12th Annual Conference on Mass spectrometry and allied topics, Montreal, Quebec. 1964.
20. G. C. HOPKINS, J. P. JONAK, H. J. MINNEMEYER et H. TIECKELMANN. J. Org. Chem. **32**, 4040 (1967).
21. H. J. DEN HERTOG, C. JOUWERSMA, A. A. VAN DER WAL et E. C. C. WILLEBRANDS-SCHOGT. Rec. Trav. Chim. **8**, 275 (1949).
22. K. CLARKE et K. ROTHWELL. J. Chem. Soc. II, 1885 (1960).
23. D. G. MARKEES. J. Org. Chem. **23**, 1030 (1958).
24. S. B. COAN, B. JAFFE et D. PAPA. J. Am. Chem. Soc. **78**, 3701 (1956).
25. O. FISHER et E. RENOUF. Ber. **17**, 1896 (1884).
26. F. ARDNT et A. KALISCHEK. Ber. **63**, 587 (1930).

Can. J. Chem. Downloaded from www.nrcresearchpress.com by 210.87.254.42 on 09/05/12
For personal use only.

Sulfur-free Penicillin Derivatives. V. Preparation, Hydrolysis, and Oxidative Rearrangement of Fused Oxazoline–Azetidinones[1]

SAUL WOLFE, SHUI-LUNG LEE, JEAN-BERNARD DUCEP, GÉRARD KANNENGIESSER, AND WHA SUK LEE

Department of Chemistry, Queen's University, Kingston, Ontario K7L 3N6

Received September 30, 1974

SAUL WOLFE, SHUI LUNG LEE, JEAN-BERNARD DUCEP, GÉRARD KANNENGIESSER, and WHA SUK LEE. Can. J. Chem. **53**, 497 (1975).

Chlorinolysis of an anhydropenicillin affords a 2-(2′-chloro-3′*S*-amino, -acylamino or -phthalimido-4′-oxo)azetidinyl-3-methyl-2-butenoyl chloride, as a mixture of 2′*R* (*cis*) and 2′*S* (*trans*) epimers in which the 2′*R* epimer usually predominates. Hydrolysis of the acid chloride and treatment of the carboxylic acid with aqueous bicarbonate causes cyclization, in the case of a 3′-acylamino substituent, to a 2*R*-6-(1′-carboxy-2′-methyl-prop-1′-enyl)-1-oxa-3,6-diaza-4*S*,5*R*-bicyclo[3,2,0]hept-2-ene-7-one. The mechanisms of these transformations are discussed, and alternative routes to such fused oxazoline–azetidinones are also presented.

The oxazolines undergo ready hydrolysis to sulfonic acid salts of 2-(2′*R*-acyloxy-3′*S*-amino-4′-oxo)azetidinyl-3-methyl-2-butenoates upon treatment with the hydrate of a sulfonic acid in acetone solvent. Neutralization of these salts proceeds without O → N acyl transfer, because acylation yields a diacylated azetidinone in which the new acyl substituent is attached to nitrogen. Monobromination of the allylic methyl groups of these salts, followed by treatment with 2 molar-equiv. of triethylamine, leads to a deep-seated rearrangement, in high yield, to an oxazinone. The mechanism of this rearrangement and, in particular, the role of acylimines in this and related reactions, including the biosynthesis of penicillin, are discussed.

SAUL WOLFE, SHUI LUNG LEE, JEAN-BERNARD DUCEP, GÉRARD KANNENGIESSER et WHA SUK LEE, Can. J. Chem. **53**, 497 (1975).

La chlorolyse d'un anhydropénicilline conduit au chlorure de (chloro-2′ *S*-amino, acylamino ou phtalimido-3′ oxo-4′)-2 azétidinyl méthyl-3 butène-2 oyle sous forme de mélange d'épimères 2′*R* (*cis*) et 2′*S* (*trans*) dans lequel l'épimère 2′*R* prédomine d'une façon générale. Lorsque le substituant en 3′ est un groupe acylamino, l'hydrolyse du chlorure d'acide et le traitement de l'acide carboxylique avec une solution aqueuse de bicarbonate amènent une cyclisation conduisant à la 2*R* (carboxy-1′ méthyl-2′ propène-1′ yl)-6 oxa-1 diaza-3,6 4*S*,5*R*-bicyclo[3,2,0] heptène-2 one-7. On discute des mécanismes de ces transformation et on présente aussi des méthodes alternatives pouvant conduire à de telles oxazoline–azétidinones condensées.

Les oxazolines, traitées par l'hydrate de l'acide sulfonique dans de l'acétone, s'hydrolisent facilement et conduisent aux sels sulfoniques des (*R*-acyloxy-2′ *S*-amino-3′ oxo-4′)-2 azétidinyl méthyl-3 butene-2 oates. La neutralisation de ces sels se fait sans transfert des groupes acyles de O → N; ce résultat est dû au fait que l'acylation conduit à une azétidinone diacylée dans laquelle le nouveau groupement acyle est attaché à l'azote. La monobromuration des groupes méthyles allyliques de ces sels, suivi par le traitement avec deux moles de triéthylamine, conduit, avec un bon rendement et par l'intermédiaire d'un réarrangement important, à une oxazinone. On discute du mécanisme de ce réarrangement et en particulier du rôle des acylimines dans cette réaction et dans d'autres réactions qui lui sont reliées incluant la biosynthèse de la pénicilline.

[Traduit par le journal]

Introduction

Penicillins are *N*-acylated derivatives of 6-aminopenicillanic acid (**1**, 6-APA) (1). Their chemical and biological properties were elucidated following intensive effort by British and American chemists during the Second World War. As a result of this (2) and later (3) work, it was believed for some time that antibacterial activity was associated uniquely with compounds containing the fused β-lactam thiazolidine ring system found in 6-APA. The investigations of Abraham and Newton and their collaborators into the structure and biological properties of Cephalosporin C (**2**) and its derivatives (4) therefore constituted not only a major therapeutic advance but also a psychological breakthrough

[1]Portions of this work were presented at the Canadian Chemical Conference of the Chemical Institute of Canada, Quebec City, June, 1972, and at the 9th IUPAC Symposium on the Chemistry of Natural Products, Ottawa, June, 1974.

Can. J. Chem. Downloaded from www.nrcresearchpress.com by 210.87.254.42 on 09/05/12
For personal use only.

Can. J. Chem. Downloaded from www.nrcresearchpress.com by 210.87.254.42 on 09/05/12
For personal use only.

because, through this work, it was demonstrated that the five-membered thiazolidine ring is not essential for activity. The later discovery of the cephamycin antibiotics (**3**) revealed (5) that structural modification in the azetidinone ring is also possible. In recent years, the fused thiazolidine β-lactam **4**, known as Woodward's intermediate (6), and its functional equivalents (7) have been employed as starting materials for the synthesis of unnatural bicyclic azetidinones possessing antibacterial activity. In addition, a number of elegant and efficient total syntheses of penicillin and cephalosporin derivatives have appeared (6, 8). The effect of all of this work is that Alexander Fleming's forecast[2] of the future of β-lactam antibiotics research (9*a*) continues to be correct; and it does not seem unduly optimistic to predict that clinically useful azetidinones with structures quite different from those of the natural products will eventually become available (9*b–d*).

In a series of communications (10) we have described the transformation of anhydropenicillins **5** (11) into a variety of sulfur-free monocyclic and bicyclic azetidinones. The purpose of the present paper is to present details of the preparation of the fused oxazoline azetidinones **6**. Some novel reactions of the compound **6** (R_1 = $PhCH_2$; R_2 = CH_3, $PhCH_2$) are also discussed.

Results and Discussion

The Anhydropenicillin Route to Oxazolines

The conversion of a penicillin into an oxazoline of type **6** involves the elimination of H_2S from the nucleus and, is, formally, an oxidative rearrangement. Sheehan (12), Barton *et al.* (13), and Stoodley and Whitehouse (14) have reported on the synthesis of such oxazolines employing *t*-BuOCl (12), $PhICl_2$ (13), and $Hg(OAc)_2$ (14) as the oxidizing agents.

The key step in the present work is the chlorinolysis of an anhydropenicillin. Treatment of **5** (R = *p*-TsOH·H_2N) with excess chlorine in methylene chloride solvent at 0 °C, followed by evaporation of the solvent, afforded a quantitative yield of **7** as a 4:1 mixture of 2*R*(*cis*):2*S*(*trans*) epimers. The mechanism of this reaction has not been investigated but is believed to proceed via attack at sulfur, with subsequent rupture of the C5—S bond of the chlorosulfonium intermediate, as depicted in **8** (R = *p*-TsOH·H_2N). In agreement with this view is the spectroscopic characterization of the compound **9** (R = phthalimido) following the reaction of **5** (R = phthalimido) with a limited amount of chlorine, and the conversion of this compound, on standing, to **10** (R = phthalimido) (15). An analogous mechanism has been suggested by Kukolja (16) for the chlorine-promoted fission of the C5—S bond of penicillin itself.

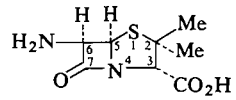

1

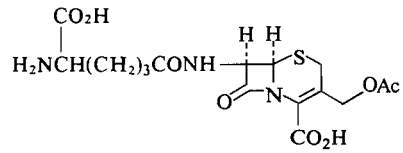

2

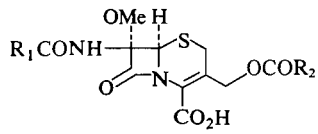

3

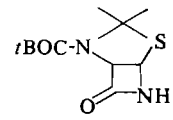

4

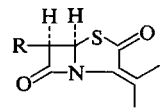

5

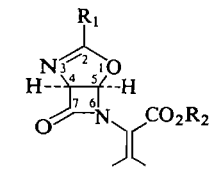

6

At 0 °C, hydrolysis of **7** to the carboxylic acid **11** was complete in 3 h in aqueous tetrahydrofuran or aqueous acetone. Neutralization of these reaction mixtures with a slight excess of sodium bicarbonate yielded the amino acid salt **12**, which could be converted into acylaminoazetidinones **13**. Alternatively, the same compounds could be obtained from anhydropenicillins **5** (R = RCONH) by a chlorination–hydrolysis sequence.

Dissolution of the azetidinone **13** (R = $PhCH_2$) in 5% bicarbonate, followed by acidification of the solution, afforded the oxazoline **6** (R_1 = $PhCH_2$; R_2 = H) in 53% overall yield from anhydrobenzylpenicillin. The methyl and benzyl

[2]And we are not at the end of the penicillin story. Perhaps we are only just at the beginning.

Can. J. Chem. Downloaded from www.nrcresearchpress.com by 210.87.254.42 on 09/05/12
For personal use only.

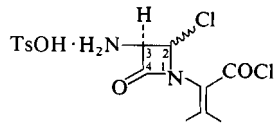

7

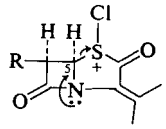

8

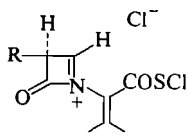

9

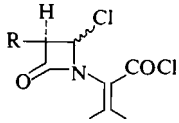

10

esters of this compound (**6**, $R_2 = CH_3$ or CH_2Ph) were prepared without difficulty using diazomethane and phenyldiazomethane, respectively. Since **13** is a mixture of epimers at C2, in which the compound having the *R* configuration (*cis*) predominates, and cyclization to an oxazoline affords a compound which also has the *R* configuration at the same asymmetric center, it is evident that the new C—O bond is formed with net retention of configuration.

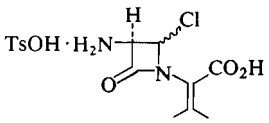

11

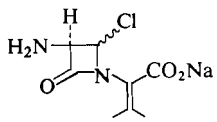

12

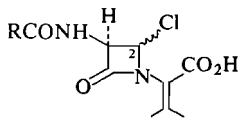

13

Two mechanistic paths can be considered to account for this result. In the first, cyclization may generate the *oxa*anhydropenicillin **14** (R = $PhCH_2$), with inversion of configuration at C2. Then the new C—O bond may undergo a displacement, also with inversion, by the acylamino oxygen. Two kinds of observations lend credence to this proposal: (*i*) the oxaanhydropenicillin **14** (R = $PhCH_2O$) could be isolated in 48% yield following bicarbonate treatment of the azetidinone **13** (R = $PhCH_2O$), which has a less nucleophilic carbonyl group in the side chain; (*ii*) the *trans*-disubstituted azetidinone **16** could be characterized spectroscopically following phenylacetylation of **15**, but it underwent rapid and spontaneous cyclization to the oxazoline **6** ($R_1 = PhCH_2$; $R_2 = CH_3$). In contrast, **17**, the

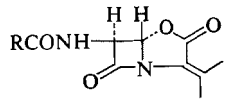

14

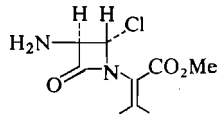

15

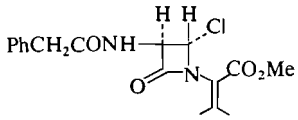

16

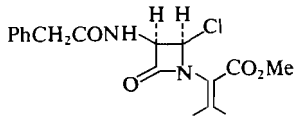

17

C2 epimer of **16**, could be isolated and characterized fully. This latter compound, however, also cyclized to **6** ($R_1 = PhCH_2$; $R_2 = CH_3$) during chromatography on silica gel or alumina.

A second mechanism for oxazoline formation involves the intervention of the unsaturated azetidinone **18** when **13** (R = $PhCH_2$) is dissolved in aqueous bicarbonate; in this case, cyclization to the oxazoline must generate the *R* configuration at the new asymmetric center, because the *trans*-fused bicyclic system is sterically impossible. Although, as discussed earlier, unsaturated azetidinones are hypothesized but not proven intermediates in the chlorinolysis, their formation in other types of reactions seems more secure. Thus, Corbett and Stoodley (17) have found that the oxazoline **19** is converted into *trans*-disubstituted azetidinones **20***a* upon treatment with alcohols in the presence of trace amounts of *p*-toluenesulfonic acid, or with various carboxylic acids and thioacids. More recently, the same workers (18) have observed that alkanethiols react with **19** to give mixtures of **20***a* and **20***b*. *Cis–trans* mixtures of 2-alkyloxy or acyloxyazetidinones were also obtained following reaction of either epimer of **21** with alcohols or carboxylic acids in the presence of Lewis acid catalysts (10*d*). It is evident that, under solvolytic conditions, there is a significant driving force for

Can. J. Chem. Downloaded from www.nrcresearchpress.com by 210.87.254.42 on 09/05/12
For personal use only.

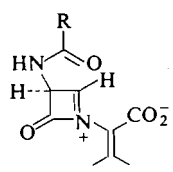

18

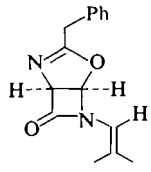

19

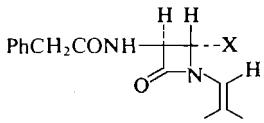

20*a*

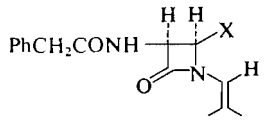

20*b*

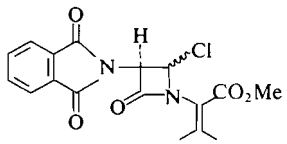

21

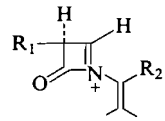

22

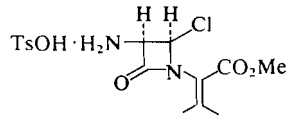

23

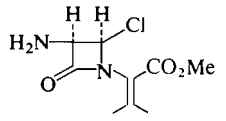

24

the cleavage of the C—O or C—Cl bonds of these azetidinones to form the cations **22**.

The conversion of **13** (R = $PhCH_2$) to **6** (R_1 = $PhCH_2$; R_2 = H) is performed in aqueous bicarbonate, a medium in which solvolytic cleavage of the C2—Cl bond is expected to be facilitated. The oxaanhydropenicillin **14** (R = $PhCH_2$) cannot be detected among the products of this reaction, even after a 1 min reaction time, at which point **13** has disappeared. We therefore consider that the cyclization of **13** (R = $PhCH_2$) to **6** (R_1 = $PhCH_2$; R_2 = H) proceeds via an unsaturated azetidinone intermediate. The cyclization of **17** on silica gel or alumina columns requires an analogous explanation, because oxaanhydropenicillin formation is precluded in the absence of a free carboxyl group.

Compound **17** was synthesized either from **13** (R = $PhCH_2$) by methylation, or from **7** in three steps: (*i*) reaction with methanol at 0° to give **23** (67% from **5** (R = *p*-TsOH·H_2N)); (*ii*) bicarbonate (**23** → **24**); (*iii*) phenylacetylation of the free base (80%). The *trans*-2-chloro-3-aminoazetidinone **15** was obtained as the predominant epimer (5:1–6:1 by n.m.r.) following equilibration of **23** or **24** in chloroform solvent in the presence of excess tetramethylguanidinium chloride (**24** ⇄ **15**).

Four mechanisms can be considered for this and similar epimerizations (10*a*). Since what is actually observed by n.m.r. is not necessarily the interconversion of **15** and **24** but, rather, the interconversion of geometrical isomers, and C6 epimerization of penicillin (corresponding to C3 of these azetidinones) is well known (19), the reaction may, in principle, proceed by epimerization either at C2 or C3. Further, since unsaturated azetidinones of type **25** are also known (20), an elimination–addition sequence is also possible. However, **25** is achiral in this case and its intervention would lead to optically inactive products; this is not observed. Both the *cis* and *trans* isomers resulting from the epimerization reactions are optically active and have the same rotation as the materials prepared by chlorinolysis of the anhydropenicillins. This latter observation also rules out *cis–trans* isomerization by epimerization at C3. A third epimerization mechanism involves the unsaturated azetidinone **22**. In this case, however, generation of the cation **22** in the presence of a second nucleophile would be expected to afford two pairs of *cis–trans* isomers (10*d*). This is also not observed. Reaction of **15** with tetramethylguanidinium *azide* (21) leads smoothly to **26**, and **24** reacts similarly to give **27**.

It must be concluded, therefore, that, in methylene chloride or chloroform solvents, epimerization and nucleophilic substitution at C2 of these 2-chloroazetidinones proceeds by an S_N2 mechanism, with inversion of configuration. It thus appears likely that, depending upon the experimental conditions, either stereospecific or nonstereospecific substitution can be achieved at the C2 position of these azetidinones.

Hydrolytic Opening of the Oxazoline Ring

As noted above, Corbett and Stoodley (17) have found that treatment of **19** with *p*-toluenesulfonic acid in chloroform, alcohol, carboxylic

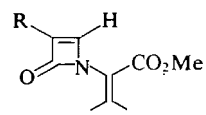

25

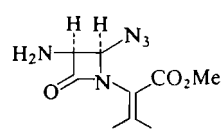

26

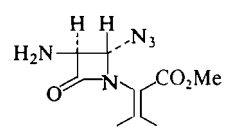

27

Can. J. Chem. Downloaded from www.nrcresearchpress.com by 210.87.254.42 on 09/05/12
For personal use only.

acid, or thioacid solvents leads to opening of the five-membered ring at the C5—O bond. We find that, in acetone solvent, the reaction takes a different course. As noted by Koe (22), the fact that *p*-toluenesulfonic acid is a monohydrate allows ready hydrolysis of acid-labile groups simply by addition of this reagent to the substrate *in acetone solvent* (11*b*). We considered that the analogous reaction in the case of **6** would consist of acid-promoted hydration of the imino group. In deuteroacetone solvent, the n.m.r. spectrum of **6** (R_1 = $PhCH_2$; R_2 = CH_3) shows, among other peaks (see Experimental), two doublets (J = 3.8 Hz) at 5.20 and 5.98 p.p.m. The doublet at 5.20 is assigned to the azetidinone proton geminal to nitrogen because it is coupled further (J = 0.5 Hz) to the methylene protons of the benzyl group. The doublet at 5.98 is assigned to the azetidinone proton geminal to oxygen. Addition of 1 molar-equiv. of *p*-toluenesulfonic acid monohydrate to this solution causes an immediate (< 1 min) change in the n.m.r. spectrum, characterized most noticeably by a downfield shift of the azetidinone proton geminal to oxygen. This new spectrum is not that of the *p*-toluenesulfonic acid salt of the oxazoline because neutralization of the solution does not regenerate this compound.

For preparative work, the oxazolines **6** (R_1 = $PhCH_2$; R_2 = CH_3 or CH_2Ph) were allowed to react with *p*-toluenesulfonic acid hydrate in dry acetone, and the solvent was then removed. In each case, a crystalline residue was obtained; recrystallization from acetone–hexane afforded the azetidinone **28** (R = CH_3) in 60% yield, and the azetidinone **28** (R = CH_2Ph) in quantitative yield. The compounds were identified by their spectroscopic properties (see Experimental) and by their chemical reactions, discussed below. Hydrogenolysis of **28** (R = CH_2Ph) produced the amino acid salt **28** (R = H). This novel procedure for hydrolytic ring opening of an oxazoline is presumed to involve the intermediate formation of the hydroxyoxazolidinium cation **29**, with the positive charge on nitrogen then directing the cleavage of the C—N bond, as shown.

Neutralization of **28** (R = CH_3) and acylation of the free base **30** with benzoyl chloride or phenylacetyl chloride gave the diacylated azetidinones **31** (R = Ph, $PhCH_2$). It is known (23) that neutralization of the salt of a β-acyloxyethylamine does not lead to a β-acyloxyethylamine

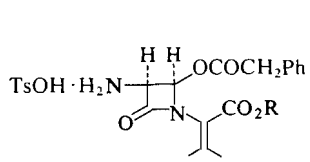

28

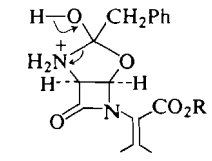

29

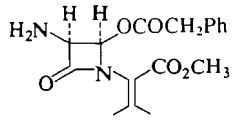

30

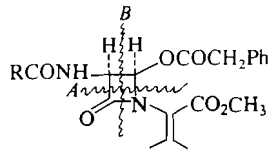

31

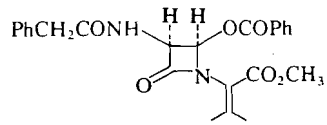

32

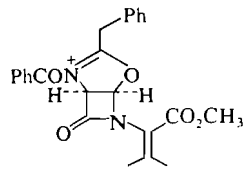

33

but, rather, to a β-acylaminoethanol. The O → N acyl transfer is intramolecular and proceeds via the cyclic hydroxyoxazolidine, so that the rate of the process in any given case depends upon the ease of formation of the five-membered ring intermediate. The structure of **31** (R = $PhCH_2$) is, therefore, secure, but it was necessary to prove that the benzoylation of **30** had given the *N*-benzoyl derivative **31** (R = Ph) and not its *O*-benzoyl isomer **32**. The spectroscopic properties of the compound were ambiguous; in particular, in the mass spectrum, fragmentation occurred principally by path *A* to give a parent ion of mass 281 which retains both acyl groups. The alternative fragmentation, by path *B*, was not observed. However, benzoylation of **6** (R_1 = $PhCH_2$; R_2 = CH_3), followed by hydrolysis of the *N*-benzoyloxazolinium salt **33** (24), afforded an *N*-benzoyl compound which was identical in all respects with the material prepared from **30**.

The neutralization of **28** (R = CH_3) thus proceeds without O → N acyl transfer. This is not

Can. J. Chem. Downloaded from www.nrcresearchpress.com by 210.87.254.42 on 09/05/12
For personal use only.

surprising; the acyl transfer is expected to be slow in this case because the reaction must take place via an intermediate hydroxyoxazolidine which is fused to the four-membered azetidinone ring. Indeed, delaying the benzoylation step for periods up to 5 h following the generation of **30** did not cause a change in the course of the reaction.

Oxidation and Rearrangement of ***28***

The methyl groups of azetidinones derived from **10** can be functionalized with *N*-bromosuccinimide (NBS) (10*b*). Either dibromo compounds (**34**) or approximately 1:1 mixtures of monobromo compounds (**35** and **36**) are obtained, depending on whether 2 molar-equiv. or 1 molar-equiv. of the reagent is employed. The azetidinones **28** were found to exhibit similar behaviour but some difficulty was experienced initially with the stoichiometry because the functionalization of the methyl group of the toluenesulfonate anion proceeded preferentially. Thus, 2 molar-equiv. of NBS were needed to generate the mixture **37** + **38** (R = *p*-$BrCH_2C_6H_4SO_3H$) and 3 molar-equiv. of NBS were needed to generate **39** (R = *p*-$BrCH_2C_6H_4SO_3H$). Although this result does not cause problems with the subsequent reactions of these compounds, alternative routes to these systems were sought. One consisted of bromination of the oxazoline **6** prior to the hydrolytic ring opening. However, although the allylic methyl groups were functionalized, the alpha carbon atom of the C2 substituent (*i.e.*, R_1) underwent substitution at the same time. A second and more successful alternative consisted of bromination of *benzenesulfonic* acid salts (**28**, $PhSO_3H$ in place of *p*-TsOH). These latter compounds could be prepared either from **30** or by reaction of **6** with the hydrate of benzenesulfonic acid in dry acetone.

Exposure of the mixture **37** + **38** to 2 molar-equiv. of triethylamine in methylene chloride solvent caused a rapid and deep-seated rearrangement to a crystalline compound $C_{17}H_{18}N_2O_5$, to which structure **40** is assigned. The i.r. and n.m.r. spectra of the crude product, obtained in 94% yield, were identical to those of the crystalline material isolated in 64% yield following chromatography. The compound is optically inactive, shows amide and ester absorption in the i.r., and the n.m.r. spectrum in deuteriochloroform displays two broad one-

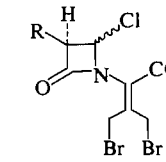

34

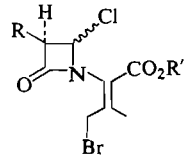

35

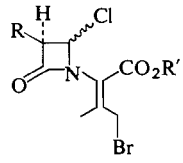

36

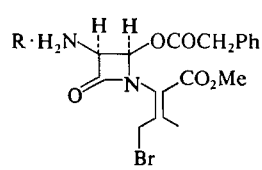

37

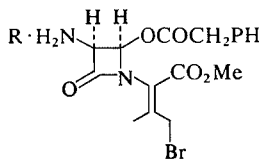

38

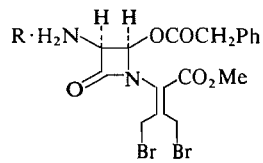

39

proton singlets at 6.80 and 7.43 p.p.m. which exchange with D_2O. The n.m.r. spectrum also contains, in addition to phenylacetyl and methoxycarbonyl signals, a one-proton singlet at 8.24 and a slightly broadened two-proton doublet at 5.21 and 5.26 coupled to a slightly broadened three-proton singlet at 1.84 p.p.m. The compound is stable to the action of excess acetyl chloride, indicating the absence of hydroxyl groups, and it affords a dihydro derivative **41** upon catalytic hydrogenation. The n.m.r. spectrum of this latter compound reveals the presence of an isopropyl group while retaining the phenylacetyl and methyl peaks and the one-proton singlet at low field. Consequently **40** must contain an isopropenyl group, a methoxycarbonyl group, a phenyl*acetamido* group, and an additional amide proton. The structure shown is consistent with all of these data.

Since the 1:1 mixture of **37** + **38** affords **40** in greater than 50% yield, it follows that both geometrical isomers have rearranged to the same compound, presumably via a common intermediate. It is also evident that the rearrangement proceeds with O → N acyl transfer. Scheme 1 illustrates, for the *E* isomer **37**, the mechanism proposed for this reaction, and for the analogous result in the benzyl ester series, which affords the

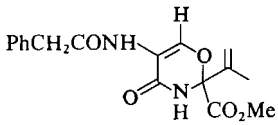

40

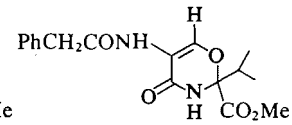

41

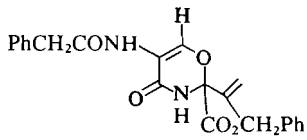

42

oxazinone **42**. Neutralization of **37** gives the free base **43** which, *in contrast to the unbrominated base 30*, undergoes acyl transfer to yield **44**; the second equivalent of triethylamine now induces fragmentation of this carbinolamide (25) to give the aldehyde **45**, which eliminates bromide ion to form the dehydroacylimine **46**. Application of the same reaction sequence to the *Z* isomer **38** also leads to **46**, which cyclizes to **40** via the enol tautomer **47**.

There is precedent for the sequences just proposed in the behaviour of the unsaturated sulfenic acids **48** (26), which are intermediates (27) in the Morin reaction. Among the products of this rearrangement are the isothiazolone **49**

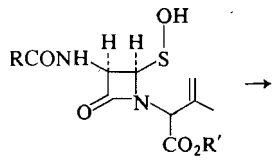

48

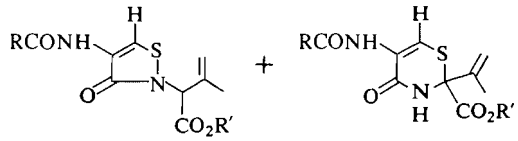

49 50

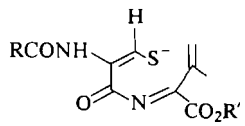

51

and the thiazinone **50**, the sulfur analog of the oxazinone **40**. The isothiazolone rearranges to **50** upon treatment with base (28) and the intermediate proposed for this rearrangement is the acylimine **51**, the sulfur analog of **47**.

Acylimines have recently been the subject of much discussion, in connection with partial

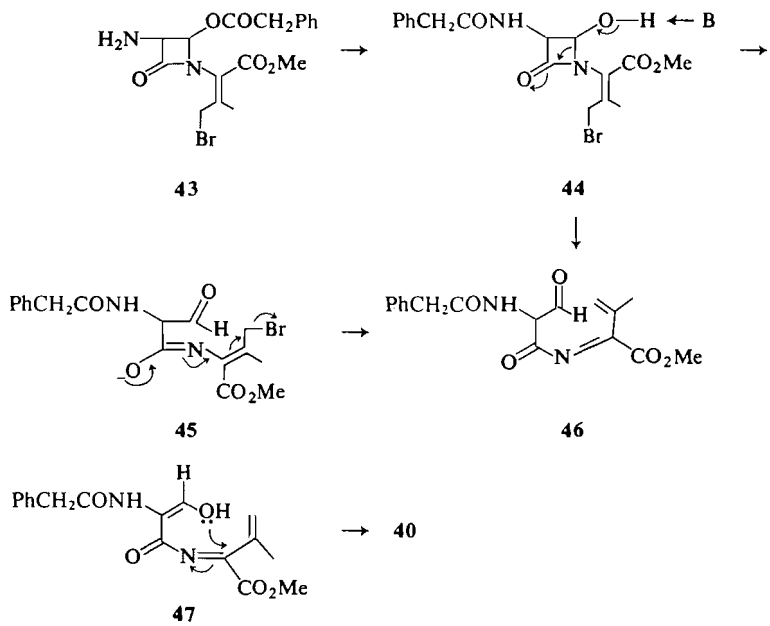

43 44 45 46 47 → 40

SCHEME 1

Can. J. Chem. Downloaded from www.nrcresearchpress.com by 210.87.254.42 on 09/05/12
For personal use only.

Can. J. Chem. Downloaded from www.nrcresearchpress.com by 210.87.254.42 on 09/05/12
For personal use only.

syntheses of cephamycin derivatives (29), and as the hypothetical intermediates in penicillin biosynthesis (30, 31). The present work, in conjunction with the studies of Morin *et al.* (26, 28, 30*a*, 32) and Baldwin *et al.* (30*b*), may permit the development of rational procedures for the study of these compounds under non-enzymatic conditions.

Experimental

Melting points were obtained on Fisher-Johns or Mel-Temp equipment and are uncorrected. Nuclear magnetic resonance (n.m.r.) spectra were recorded on Varian A60 or T60 or Bruker HX60 spectrometers; TMS and TSS were employed as internal standards, and all spectra were obtained in $CDCl_3$ or D_2O, unless stated otherwise. Chemical shifts are reported as p.p.m. downfield from the internal standard. Infrared (i.r.) spectra were recorded on Beckman 5A or Perkin Elmer 180 spectrometers; data from the Beckman instrument are reported in microns, and those from the Perkin Elmer instrument are reported in cm^{-1}. Column chromatography was performed on Woelm alumina (neutral, Activity II), or on Silica Gel 60, obtained from Brinkmann Instruments. Thin-layer chromatography was performed on Eastman Chromatoplates; preparative-layer chromatography (p.l.c.) was performed on Merck precoated t.l.c. plates having a 0.25 mm layer thickness. Optical rotations were measured on a Perkin Elmer Model No. 141 Polarimeter.

Chlorination of **5** *(R = p-TsOH·H_2N)*

The salt (328 mg, 0.89 mmol) was suspended in methylene chloride (30 ml), the mixture cooled to 0°, and gaseous chlorine was introduced for 15 s. Dry nitrogen was passed through the resulting yellow solution for 15 min to remove excess chlorine and the solution was evaporated to dryness. Trituration of the residue with dry ether afforded a quantitative yield of **7**. This material was a stable (below 20°) white powder, m.p. 148–149° dec. The i.r. spectrum showed peaks at 5.55 and 5.62 μ. The 2′*R* isomer (formed in 80% yield) showed n.m.r. absorption ($CDCl_3$) at 7.80 (2H, d), 7.20 (2H, d) 5.98 (1 H, d, 4.2 Hz), 5.18 (1 H, d, 4.2 Hz), 2.37 (3 H), 2.20 (3 H), 2.00 (3 H). (The NH_2 protons were not observed.) The 2′*S* isomer (formed in 20% yield) showed n.m.r. absorption at 7.80 (2 H, d), 7.20 (2 H, d), 5.18 (2 H, m), 2.37 (3 H), 2.17 (3 H), 2.00 (3 H).

Chlorination of anhydro-6-tritylamino penicillin, the precursor of the *p*-toluenesulfonic acid salt, was unsuccessful using Cl_2, SO_2Cl_2, pyrrolidone hydrotrichloride, pyridinium trichloride, PCl_5, and $(C_6H_5O)_3PCl$. In each case a reaction of the desired type occurred but the trityl group was then lost and the product decomposed.

Hydrolysis of **7** *to* **11**

The salt (200 mg) was chlorinated as described above and, after removal of the solvent, the residue was maintained under high vacuum for 30 min. It was then dissolved in a mixture of D_2O (2 ml) and CD_3COCD_3 (2 ml), cooled to 0°, and the n.m.r. spectrum was recorded at intervals. Hydrolysis was complete after 3 h, and the solvent was, therefore, removed by lyophilization. The resulting foam was redissolved in D_2O. The n.m.r. spectrum of this solution indicated that quantitative conversion to a 4:1 mixture of 2′*R*:2′*S* chloro acids had been achieved. The 2*R*-chloro acid showed n.m.r. absorptions at 7.63 (2H, d), 7.22 (2H, d), 6.22 (1H, d, 4.0 Hz), 5.07 (1H, d, 4.0 Hz), 2.23 (3H), 2.12 (3H), 1.91 (3H). The epimeric 2′*S*-chloro acid had n.m.r. absorption at 7.63 (2H, d), 7.22 (2H, d), 5.47 (1H, d, 2.0 Hz), 5.43 (1H, d, 2.0 Hz), 2.23 (3H), 2.02 (3H), 1.76 (3H).

Phenylacetylation of **11**

The *p*-toluenesulfonic acid salt of anhydro-6-amino penicillin (242 mg, 0.65 mmol) was chlorinated and the product hydrolyzed in aqueous acetone as already described. To the resulting solution (volume 20 ml) at 0° was added in portions sodium bicarbonate (275 mg, 3.27 mmol) followed by a solution of phenylacetyl chloride (152 mg, 0.98 mmol) in acetone (5 ml) in one portion. The mixture was stirred for 30 min and then diluted with water and extracted with methylene chloride; this extract was discarded. The aqueous phase was brought to p*H* 3 and extracted with methylene chloride. This extract was dried over anhydrous magnesium sulfate and evaporated to give **13** (R = $PhCH_2$).

Conversion of **7** *to the Methyl Ester* **23**

The anhydropenicillin salt **5** (3.80 g, 10.3 mmol) was suspended in methylene chloride (150 ml), the mixture was cooled to −5°, and a slow stream of dry nitrogen was passed through it. Gaseous chlorine was passed into the mixture for 30 s and the nitrogen stream was then continued for 15 min. Methanol (75 ml) was added and the resulting yellow solution was swept with nitrogen at 0 °C for 20 min. The cooling bath was then removed and, after 15 min, the solvent was removed under reduced pressure at 25°. The residue was treated with 5 ml of methylene chloride and the resulting solution was re-evaporated; this procedure was repeated three times and at this point the pale yellow foam had no odor of chlorine or HCl. The foam was dissolved in dry acetone, the orange solution was filtered to remove a small amount of insoluble material, and petroleum ether (30–60°) was added to the cloud point. A few drops of acetone were then added to clarify the solution and crystallization was allowed to proceed at 10 °C. The white crystals thus obtained were washed with cold 1:1 acetone – petroleum ether and dried in vacuo. The yield was 2.7 g (67%), m.p. 125–130° dec.

Anal. Calcd. for $C_{16}H_{21}N_2O_6Cl$: C, 47.48; H, 5.23. Found: C, 47.62; H, 5.54.

The n.m.r. spectrum shows peaks at 7.78 (2H, d), 7.10 (2H, d), 5.98 (1H, d, 4.0 Hz), 5.13 (1H, d, 4.0 Hz), 3.52 (3H), 2.35 (3H), 2.22 (3H), 1.85 (3H).

Neutralization of **23**

The methyl ester, in methylene chloride (50 ml), was shaken with ice-cold sodium bicarbonate solution. Evaporation of the methylene chloride layer gave the free base, a crystalline compound, m.p. 67–70° dec. The compound was not stable in the solid state and darkened perceptibly after 10 min at room temperature.

The n.m.r. spectrum of the compound has peaks at 6.03 (1H, d, 4.1 Hz), 4.62 (1H, d, 4.1 Hz), 3.78 (3H), 2.30 (3H), 2.00 (3H). The position of the NH_2 protons varies with time; although these peaks shift, no other changes occur in the spectrum. The i.r. spectrum of the com-

Can. J. Chem. Downloaded from www.nrcresearchpress.com by 210.87.254.42 on 09/05/12
For personal use only.

pound has peaks at 2.94, 5.60, 5.80, 6.12 μ which (in CH_2Cl_2) do not change with time.

Chlorination of Anhydrobenzylpenicillin (5, R = $PhCH_2CONH$)

Anhydropenicillin G (176 mg, 0.56 mmol) was dissolved in methylene chloride (7 ml) and the solution was chlorinated at room temperature for 30 s with a strong sweep of chlorine. The solvent was then removed immediately at 20° under reduced pressure to give a pale yellow foam. The i.r. spectrum of this foam showed peaks at 2.92, 5.5, 5.95 μ. The n.m.r. spectrum showed that the product was a 4:1 mixture of 2-(2′*R*-chloro-3′*S*-phenylacetamido-4′-oxo)azetidinyl-3-methyl-2-butenoyl chloride and its 2′*S* epimer. The major isomer has the following n.m.r. spectrum: 7.29 (5H), 6.93 (1H, d, 9 Hz), 6.03 (1H, d, 4.5 Hz), 5.48 (1H, q, 4.5, 9 Hz), 3.63 (2H), 2.22 (3H), 2.08 (3H). The minor isomer has peaks at: 7.29 (5H), 6.93 (1H, d, 9 Hz), 5.88 (1H, d, 2 Hz), 4.83 (1H, q, 2, 9 Hz), 3.56 (2H), 2.22 (6H).

Synthesis of 13 (R = $PhCH_2$) from Anhydrobenzylpenicillin

The above-mentioned mixture of dichlorides (from 176 mg of anhydropenicillin) was dissolved in acetone (6 ml) and water (4 ml) was added followed, at 0°, by excess sodium bicarbonate. The mixture was stirred for 2.3 h and then diluted with water (50 ml) and extracted thrice with methylene chloride and once with ether. Acidification of the aqueous phase to p*H* 2.5, extraction with methylene chloride and evaporation of the dried methylene chloride extract afforded 36 mg of an oil whose i.r. and n.m.r. spectra indicated it to consist mainly of unhydrolyzed acid chloride.

In a second experiment anhydropenicillin G (105 mg) was chlorinated; the resulting white foam was dissolved in ice-cold tetrahydrofuran (3 ml), and cold water (1 ml) was added. The clear yellow solution was maintained at 0° for 2 h and then poured into a mixture of water and ice, and extracted with methylene chloride. Evaporation of the dried methylene chloride extract afforded 113 mg (98%) of a chloro acid whose i.r. and n.m.r. spectra showed it to have structure **13**, R = $PhCH_2$. The i.r. spectrum showed peaks at 3.05, 5.62, 5.90, 5.95 μ. The n.m.r. spectrum showed peaks at 7.28 (5H), 6.90 (1H, d, 8 Hz), 6.07 (1H, d, 4.5 Hz), 5.58 (1H, q, 4.5, 8 Hz), 3.68 (2H), 2.28 (3H), 1.99 (3H).

In a third experiment, the chloro acid from 333 mg of anhydropenicillin G was treated in ether with an excess of ethereal diazomethane. The solution was stirred for 2 h at room temperature and then evaporated to dryness. The residue was left in the refrigerator overnight and then, in methylene chloride, shaken with 5% bicarbonate, dried and evaporated. The residue was chromatographed on silica gel; elution with 1:1 petroleum ether – ethyl acetate afforded 189 mg (51%, m.p 110.5–111°) of the methyl ester and 40 mg (12%) of the oxazoline **6** (R_1 = $PhCH_2$; R_2 = CH_3).

Chlorination of Anhydrocarbobenzoxypenicillin (5, R = $PhCH_2OCONH$)

The anhydropenicillin (470 mg, 1.47 mmol) was chlorinated in methylene chloride for 15 s. After an additional 30 s the solvent was removed to give a white foam which consisted of a 77:23 mixture of dichlorides, the compound having the 2′*R*-chloro configuration predominating. The n.m.r. spectrum of this compound has peaks at 7.31 (5H), 6.86 (1H, d, 9 Hz), 6.07 (1H, d, 4 Hz), 5.25 (1H, q, 4.9 Hz), 5.17 (2H), 2.20 (3H), 2.10 (3H). The minor isomer has peaks at 7.31 (5H), 6.86 (1H, d, 9 Hz), 5.90 (1H, d, 2 Hz), 5.16 (2H), 4.83 (1H, d, 2 Hz), 2.20 (6H).

Hydrolysis of the Anhydrocarbobenzoxypenicillin Chlorination Product

The dichloride (a 77:23 2′*R*:2′*S* mixture from 470 mg of the anhydropencillin) was dissolved in cold tetrahydrofuran (10 ml), and ice-cold water (1 ml) was added. The mixture was left for 3 h at 0° and then added to ice-cold saturated sodium chloride solution. Extraction with methylene chloride and evaporation of the dried methylene chloride extract afforded 535 mg of the chloro acids. The major isomer has peaks at 7.32 (5H), 6.37 (1H, d, 10 Hz) 6.13 (1H, d, 4 Hz), 5.45 (1H, q, 4, 10 Hz), 5.17 (2H), 2.28 (3H), 2.02 (3H).

Chlorination of Anhydro-6-phthalimidopenicillin (5, R = phthalimido)

Chlorine gas was passed at room temperature into a solution of anhydro-6-phthalimidopenicillin (500 mg, 1.52 mmol) in methylene chloride (15 ml). The gas introduction was terminated after 3 min and, after an additional 5 min, the yellow solution was evaporated to dryness. The resulting white foam was crystallized from a mixture of chloroform and petroleum ether to give a total of 250 mg (32%) of material in two crops, m.p. 210° dec. The i.r. spectrum of the residual mother liquor was identical to that of the crystalline material, summarized below.

Anal. Calcd. for $C_{16}H_{12}N_2O_4Cl_2$: C, 52.3; H, 3.31; N, 7.69; Cl, 19.4. Found: C, 52.03; H, 2.96; N, 7.76; Cl, 19.53.

The i.r. spectrum shows peaks in the carbonyl region at 5.48, 5.55, 5.62, and 5.79 μ. The n.m.r. spectrum shows peaks at 7.87 (4H), 6.22 (1H, d, J = 4.2 Hz), 5.76 (1H, d, J = 4.2 Hz), 2.40 (3H), 2.31 (3H). The u.v. spectrum shows λ_{max}(EtOH) 242 (10 000).

Hydrolysis of the Anhydrophthalimidopenicillin Chlorination Product

The dichloride (500 mg, 1.36 mmol), in dimethyl sulfoxide, (500 ml) was treated, dropwise at 0°, with 50 ml of a p*H* 7.95 buffer (prepared by diluting 50 ml of 0.1 *M* boric acid and 2.6 ml of 0.1 *M* NaOH to 100 ml). At the end of the addition, the p*H* of the reaction mixture was 6.8. This mixture was allowed to warm to room temperature, and stirring was continued for 3.25 h. Then ice-cold water (300 ml) was added, the mixture brought to p*H* 3 with ice-cold *N* HCl, and extracted with five 100 ml portions of methylene chloride. The combined extracts were washed twice with water (100-ml portions) and dried over anhydrous sodium sulfate. Evaporation under reduced pressure at 40° afforded a mobile liquid which contained a considerable amount of DMSO. This was redissolved in chloroform (60 ml) and the solution washed 10 times with water (10-ml portions). After drying and evaporation there was obtained from the chloroform phase 0.59 g of a crystalline white solid. This was recrystallized from a mixture of chloroform and petroleum ether giving a total of 350 mg (73%) of short white needles, m.p. 168–174° dec.

Anal. Calcd. for $C_{16}H_{13}N_2O_5Cl$: C, 55.05; H, 3.76; N, 8.02; Cl, 10.02. Found: C, 54.65; H, 3.79; N, 8.46; Cl, 10.53.

Can. J. Chem. Downloaded from www.nrcresearchpress.com by 210.87.254.42 on 09/05/12
For personal use only.

The i.r. spectrum shows peaks in the carbonyl region at 5.52, 5.60, 5.80, and 5.85 μ. The n.m.r. spectrum shows peaks at 7.87 (4H), 6.22 (1H, d, J = 4.1 Hz), 5.71 (1H, d, J = 4.1 Hz), 2.33 (3H), 2.31 (3H). The u.v. spectrum shows λ_{max}(EtOH) 236 (7400), 296 (1800).

Conversion of the Acid to the Methyl Ester

The acid (200 mg, 0.57 mmol) was dissolved in 30 ml of a 1:1 mixture of methylene chloride and ether. The solution was cooled and treated with excess ethereal diazomethane. The solution which resulted was stirred for 0.5 h, allowed to warm to room temperature during an additional 1 h, and then evaporated at 40° to a white crystalline residue. Recrystallization from a mixture of chloroform and petroleum ether gave 0.20 g (97%) of colorless fine needles, m.p. 178–180° dec.

Conversion of the Acid Chloride to the Methyl Ester

The crystalline acid chloride (500 mg, 1.43 mmol) was dissolved in methylene chloride (10 ml) and absolute methanol (10 ml) was added. The mixture was stirred at room temperature for 30 min, then diluted with methylene chloride (50 ml) and washed successively with ice-cold 5% bicarbonate solution (10 ml) and water. After drying over anhydrous magnesium sulfate and removal of the solvent a crystalline residue was obtained. This was recrystallized from methylene chloride – petroleum ether to give 463 mg (93%) of methyl ester identical to that described above.

Anal. Calcd. for $C_{17}H_{15}N_2O_5Cl$: C, 56.3; H, 4.16; N, 7.71; Cl, 9.78. Found: C, 56.58; H, 4.37; N, 7.55; Cl, 9.82.

The n.m.r. spectrum shows peaks at 7.90 (m, 4H), 6.23 (1H, d, J = 4.1 Hz), 5.77 (1H, d, J = 4.1 Hz), 3.82 (3H), 2.43 (3H), 2.34 (3H).

Direct Conversion of Anhydro-6-phthalimidopenicillin into a Mixture of Methyl 2-(2′R-Chloro-3′S-phthalimido-4′-oxo)azetidinyl-3-methyl-2-butenoate and its 2′S Epimer

Chlorine gas was passed at room temperature into a solution of anhydro-6-phthalimidopenicillin (1.0 g, 3.04 mmol) in methylene chloride (30 ml). After 3 min the gas introduction was terminated and, after an additional 5 min, the solvent was removed under reduced pressure at 30°. The solid residue was redissolved in methylene chloride (20 ml) and absolute methanol (20 ml) was added. This solution was stirred at room temperature for 30 min and then evaporated to dryness under reduced pressure at 40°. The residue was crystallized from chloroform – petroleum ether to give 600 mg (55%) of the ester having the 2′*R*-chloro configuration. The mother liquor was chromatographed on a 1.5 × 14 cm column of alumina (Woelm, grade II). Elution with 1:1 methylene chloride – benzene afforded 202 mg (18%) of a new compound in the first 25 ml, followed by 93 mg of a mixture of the 2′*R* ester and the new compound in the next 25 ml. Elution with methylene chloride (40 ml) then afforded an additional 68 mg of the 2′*R* ester.

The new compound was crystallized from methylene chloride – petroleum ether to give the ester having the 2′*S*-chloro configuration, m.p. 192–194°.

Anal. Calcd. for $C_{17}H_{15}N_2O_5Cl$: C, 56.3; H, 4.16; N, 7.71; Cl, 9.78. Found: C, 56.42; H, 4.43; N, 7.68; Cl, 9.60.

The n.m.r. spectrum shows peaks at 7.83 (4H, m), 6.23 (1H, d, J = 2.0 Hz), 5.60 (1H, d, J = 2.0 Hz), 3.83 (3H), 2.30 (3H), 2.08 (3H).

When chlorination was performed for 10 s with a slow stream of chlorine, and the mixture then immediately evaporated to dryness, a single new compound was obtained. The n.m.r. spectrum of this new compound showed peaks at ($CDCl_3$) 7.9 (4H, d), 5.99 (2H, s), 2.40 (3H), 2.36 (3H). In CD_3COCD_3 the two-proton singlet at 5.99 showed slight splitting to a doublet. The compound is assigned structure **9**. That it is an intermediate in the chlorination of the anhydropenicillin was shown by its conversion, on standing, to the 2′*R* and 2′*S* dichlorides.

Equilibration of Methyl 2-(2′R-Chloro-3′S-phthalimido-4′-oxo)azetidinyl-3-methyl-2-butenoate and its 2′S Epimer

Starting with the 2′R Isomer

The pure 2′*R* ester (100 mg, 0.28 mmol) was added to a warm solution of tetraethylammonium chloride (95.2 mg, 0.57 mmol; 2 molar-equiv.) in acetone (15 ml). The solution was refluxed for 2 h, and then cooled to room temperature and poured onto a mixture of water and ice. Extraction with methylene chloride, followed by washing of the extract with water, drying over anhydrous magnesium sulfate, and evaporation afforded a crystalline residue. The n.m.r. spectrum of this residue was identical to that of the starting material except for the appearance of a weak doublet at 5.6 (J = 2 Hz). The substance was therefore redissolved in acetone containing tetraethylammonium chloride (95.2 mg), and refluxing was continued for an additional 14 h. Isolation in the same manner as described above afforded a residue whose n.m.r. spectrum showed it to be a 1:1 mixture of 2′*R* and 2′*S* esters.

The experiment was repeated with 100 mg (0.28 mmol) of the pure 2′*R* ester and 238 mg (5 molar-equiv.) of tetraethylammonium chloride in methyl ethyl ketone (10 ml). After 4 h of refluxing the product was isolated and found to be a 3:2 mixture of 2′*R* and 2′*S* esters. This ratio did not change when the material was refluxed for a further 8.5 h in methyl ethyl ketone containing 5 molar-equiv. of tetraethylammonium chloride.

The experiment was repeated with 100 mg of the pure 2′*R* ester in acetone (15 ml) containing 5 molar-equiv. of tetraethylammonium chloride. After 12 h and after 24 h refluxing a 3:2 2′*S*:2′*R* ratio of esters was observed. The product of a 12 h reaction was chromatographed on alumina (Woelm, grade II). Elution with benzene – methylene chloride (1:1), as already described, afforded 40 mg of the 2′*R* compound in the first 25 ml followed by 34 mg of the 2′*S* compound in the next 45 ml of eluate.

After 6 h in refluxing chloroform (30 ml) containing 5 molar-equiv. of tetraethylammonium chloride, the 2′*R* ester (430 mg) was converted into a 2:1 2′*R*:2′*S* mixture.

Starting with the 2′S Isomer

The 2′*S* ester (40 mg) was refluxed for 12 h in a mixture of acetone (10 ml) and methylene chloride (5 ml) containing 2 molar-equiv. of tetraethylammonium chloride. The product was a 1:2 2′*R*:2′*S* mixture.

Conversion of Methyl 2-(2′R-Chloro-3′S-phthalimido-4′-oxo)azetidinyl-3-methyl-2-butenoate into Methyl 2-(2′S-Azido-3′S-phthalimido-4′-oxo)azetidinyl-3-methyl-2-butenoate

Sodium azide (10.1 mg, 0.16 mmol) was dissolved in DMF (15 ml) by brief warming on the steam bath and to

Can. J. Chem. Downloaded from www.nrcresearchpress.com by 210.87.254.42 on 09/05/12
For personal use only.

this solution was added the methyl ester having the 2′*R*-chloro configuration (50 mg, 0.14 mmol). The resulting solution was stirred at room temperature for 24 h and then diluted with water and extracted with methylene chloride. The methylene chloride extract was washed thoroughly with water, dried over anhydrous magnesium sulfate, and evaporated to dryness. The resulting white crystalline solid was recrystallized from chloroform – petroleum ether to give 42 mg of unreacted 2′*R* ester.

In a second experiment the reaction mixture was heated on the steam bath for 5 h, by which time the color had become a deep yellowish-orange. Isolation of the product as described above afforded 38 mg of a solid residue whose i.r. spectrum showed azide absorption at 4.7 μ and carbonyl peaks at 5.58, 5.62, 5.79, and 5.82 μ. The n.m.r. spectrum showed, in the β-lactam region, one-proton absorptions at 5.78 and 5.29 (d, J = 2.0 Hz).

In a third experiment, sodium azide (20.2 mg, 0.31 mmol) was dissolved in 10 ml of freshly distilled DMF, the 2′*R* ester (100 mg, 0.28 mmol) was added, and the solution was heated for 5 h on the steam bath. The product was isolated in the usual manner and was crystallized from 2-butanone–ethanol to give 25 mg of 2′*S*-azido ester (first crop), m.p. 142–144°.

Anal. Calcd. for $C_{17}H_{15}N_5O_5$: C, 55.29; H, 4.09; N, 18.97. Found: C, 55.45; H, 4.02; N, 18.68.

The n.m.r. spectrum shows peaks at 7.78 (4H, d), 5.78 (1H, d, J = 2.0 Hz), 5.29 (1H, d, J = 2.0 Hz), 3.83 (3H), 2.30 (3H), 2.09 (3H).

In a further experiment sodium azide (20.2 mg, 0.28 mmol) was dissolved in freshly distilled DMF (10 ml) by heating on the steam bath for 0.5 h. Then the 2′*R*-chloro ester (100 mg, 0.28 mmol) was added, followed by an additional 20.2 mg of sodium azide. The resulting mixture was heated at 90° for 3 h, with stirring. Isolation as described above yielded a semi-solid residue which weighed 68.2 mg (67%) and whose n.m.r. spectrum was identical to that described above. Chromatography on a 1 × 2 cm column of alumina (Woelm, grade II) and elution with methylene chloride afforded 62 mg of crystalline material. Recrystallization from methylene chloride – petroleum ether afforded 38 mg in the first crop, m.p. 144–145° (colorless prisms).

Conversion of Methyl 2-(2′S-Chloro-3′S-phthalimido-4′-oxo)azetidinyl-3-methyl-2-butenoate into Methyl 2-(2′R-Azido-3′S-phthalimido-4′-oxo)azetidinyl-3-methyl-2-butenoate

The pure 2′*S*-chloro ester (100 mg, 0.28 mmol) was reacted with sodium azide (2 molar-equiv.) in DMF (10 ml) as in the last experiment described above. Isolation in the same manner afforded 52.2 mg of material. This material was chromatographed on a 4.5 × 1 cm column of alumina (Woelm, activity II). Elution with methylene chloride afforded no material in the first 10 ml followed by 13.0 and 11.1 mg of crystalline material in each of the next 10 ml. Both residues had the same n.m.r. spectrum. They were therefore combined and recrystallized from chloroform – petroleum ether to give 19 mg of colorless needles, m.p. 183–187° dec.

The n.m.r. spectrum shows peaks at 7.90 (4H, d), 5.82 (1H, d, 4.0 Hz), 5.67 (1H, d, 4.0 Hz), 3.90 (3H), 2.53 (6H).

Anal. Calcd. for $C_{17}H_{15}N_5O_5$: C, 55.29; H, 4.09; N, 18.97. Found: C, 55.06; H, 4.25; N, 19.10.

Conversion of ***23*** *into* ***15***

The 2′*R*-chloro-3′*S*-aminotosylate (440 mg, 1.09 mmol) and tetramethylguanidinium chloride (1.387 g, 9.1 mmol, 9 molar-equiv.) were refluxed in spectroscopic grade chloroform (9 ml) for 4.5 h. The solution was then cooled to 0°, washed with ice-cold 5% bicarbonate solution, dried over anhydrous magnesium sulfate, and evaporated to dryness under reduced pressure at 25°. The n.m.r. spectrum of the residue indicated it to be a 5:1 mixture of the 2′*S* and 2′*R* epimers, the predominant isomer being the 2′*S* compound. The n.m.r. spectrum of this compound shows peaks at 5.55 (1H, d, 1.8 Hz), 4.37 (1H, d, 1.8 Hz), 3.82 (3H), 2.30 (3H), 2.00 (3H). The position of the NH_2 protons depends upon the age of the solution.

Complete separation of the two epimers could be achieved by alumina chromatography and elution with 1:1 benzene – ethyl acetate. However, because of the instability of these compounds it was usually more convenient to separate at a later stage.

Conversion of ***23*** *into* ***27***

The crystalline methyl ester having the 2′*R*-chloro-3′*S*-TsOH·H_2N configuration (448 mg, 1.1 mmol) and tetramethylguanidinium azide (347 mg, 2.2 mmol, 2 molar-equiv.) were refluxed for 75 min in 20 ml of anhydrous chloroform. The solution was allowed to cool and excess anhydrous ether was added to precipitate tetramethyl guanidinium chloride, which was removed by filtration. The resulting material, after removal of the solvent, was the desired 2′*S*-azido-3′*S*-amino ester (237 mg, 90%) which appeared pure by t.l.c. and n.m.r. The n.m.r. spectrum had peaks at 5.03 (1H, d, 1.8 Hz), 4.13 (1H, d, 1.8 Hz), 3.80 (3H), 3.00 (2H), 2.28 (3H), 1.98 (3H).

The compound could also be isolated by washing the chloroform reaction mixture with cold water, drying, and evaporating. Tetraethylammonium azide (in various solvents) and sodium azide (in DMF) were less effective for this reaction.

Conversion of ***15*** *into* ***26***

A 4:1 mixture of 2′*S*- and 2′*R*-chloro-3′*S*-amino esters from an epimerization of the 2′*R*-chloro compound (532 mg, 2.29 mmol), and tetramethylguanidinium azide (500 mg, 3.2 mmol), was refluxed in pure chloroform (10 ml) for 4.5 h. The mixture was then washed with ice-cold 5% bicarbonate solution, dried over anhydrous magnesium sulfate, and evaporated to give 465 mg (85%) of a 3.3:1 mixture of 2′*R*- and 2′*S*-azido-3′*S*-amino methyl esters. This mixture was separated by chromatography on neutral alumina (Woelm, activity II). Elution with benzene – ethyl acetate (2:3) afforded the pure 2′*R*-azido-3′*S*-amino ester as a crystalline compound. Recrystallization from chloroform – petroleum ether gave long needles, m.p. 116–117°.

Anal. Calcd. for $C_9H_{13}N_5O_3$: C, 45.19; H, 5.48; N, 29.28. Found: C, 45.42; H, 5.24; N, 28.81.

The i.r. spectrum has peaks at 4.72, 5.62 and 5.80 μ. The n.m.r. spectrum shows peaks at 6.03 (1H, d, 4.1 Hz), 5.62 (1H, d, 4.1 Hz), 3.78 (3H), 2.40 (2H), 2.30 (3H), 2.00 (3H).

Conversion of ***13*** *to the Oxazoline* ***6*** *(R_1 = $PhCH_2$; R_2 = H)*

The chloro acid prepared from 640 mg of anhydropenicillin G was dissolved in 5% bicarbonate solution. This was extracted with methylene chloride and then

Can. J. Chem. Downloaded from www.nrcresearchpress.com by 210.87.254.42 on 09/05/12
For personal use only.

acidified to p*H* 2. Extraction with methylene chloride and evaporation of the dried extract afforded a crystalline residue. Recrystallization from ethyl acetate gave 320 mg (53%) of the oxazoline carboxylic acid, m.p. 119–122° dec. The i.r. spectrum shows a broad peak at 4 μ, as well as peaks at 5.64, 5.92, 6.1 μ, consistent with the zwitterionic structure

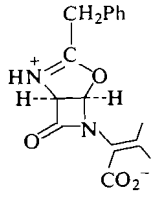

The n.m.r. spectrum (in D_2O) shows peaks at 7.33 (5H), 6.12 (1H, d, 3.8 Hz), 5.25 (1H, d, 3.8 Hz), 3.75 (2H), 1.91 (3H), 1.31 (3H).

Anal. Calcd. for $C_{16}H_{16}N_2O_4$: C, 63.99; H, 5.37; N, 9.33. Found: C, 64.26; H, 4.89; N, 9.54.

Phenylacetylation of ***24***

The free 2′*R*-chloro-3′*S*-amino ester, obtained from 722 mg (1.78 mmol) of the *p*-toluenesulfonic acid salt, was dissolved in methylene chloride (15 ml) and phenylacetic acid (242 mg, 1.78 mmol) was added. This solution was treated, dropwise with stirring, with a solution of dicyclohexylcarbodiimide (405 mg, 1.96 mmol) in methylene chloride (5 ml). Precipitation of dicyclohexylurea commenced before the addition was complete. The reaction mixture was allowed to stand at room temperature for 3 h, by which time no free amine remained (by t.l.c.). Most of the urea was then removed by filtration and the filtrate was washed with ice-cold 5% bicarbonate solution. After drying over anhydrous magnesium sulfate, the organic phase was evaporated to give a solid residue. This was dissolved in boiling chloroform and an equal volume of petroleum ether (30–60°) was added, whereupon crystallization occurred. The crude product weighed 700 mg. One more recrystallization from the same solvent mixture gave 500 mg (80%) of methyl 2-(2′*R*-chloro-3′*S*-phenylacetamido-4′-oxo)azetidinyl-3-methyl-2-butenoate, m.p. 111–115° dec. The n.m.r. spectrum of this compound shows peaks at 7.38 (5H), 6.90 (1H, d, 10 Hz), 6.06 (1H, d, 4.2 Hz), 5.66 (1H, q, 4.2, 10 Hz), 3.78 (3H), 3.69 (2H), 2.30 (3H), 1.98 (3H). The same compound could be obtained, but in slightly lower yield, using diisopropylcarbodiimide or phenylacetyl chloride and triethylamine.

Phenylacetylation of ***15***

The *p*-toluenesulfonic acid salt **23** (651 mg, 1.6 mmol) and tetramethylguanidinium chloride (1.210 g, 5 molar-equiv.) were refluxed in spectroscopic grade chloroform (9 ml) for 4.5 h. The resulting solution was cooled, washed successively with ice-cold 5% bicarbonate, ice-cold saturated sodium chloride, dried over anhydrous magnesium sulfate, and then used immediately for the next step (previous experiments had indicated that the above procedure leads to a 5:1 or 6:1 excess of the 2′*S*-chloro-3′*S*-amino compound over the 2′*R*-chloro-3′*S*-amino compound). To the solution were added phenylacetic acid (228 mg, 1.7 mmol), diisopropylcarbodiimide (222 mg, 1.8 mmol), and methylene chloride (20 ml) and this solution was refluxed for 1 h. Removal of the solvent gave a residue whose n.m.r. spectrum showed peaks at 7.27 (phenyl), 5.28 (d, 1.9 Hz), 4.67 (d, 1.9 Hz), 3.70 (OCH_3), 3.53 (CH_2), 2.20 (CH_3), 1.95 (CH_3), corresponding to the amide **16**.

The spectrum also showed peaks at 5.98 (d, 3.8 Hz), 5.20 (d, 3.8 Hz), 3.67, 2.17, 1.57. This is the spectrum of **6**, *i.e.*, 2-benzyl-6-(1′-methoxycarbonyl-2′-methylprop-1′-enyl)-1-oxa-3,6-diaza-4*S*,5*R*-bicyclo[3,2,0]hept-2-en-7-one, which is formed by intramolecular cyclization of the preceding compound. The cyclization occurs on standing, but is facilitated by heating of a solution of the chloro compound, by shaking with bicarbonate, or by chromatography on alumina or silica gel of either epimeric 2′-chloro-3′-acylamino ester, as will be described below.

Chromatography of the above mixture on silica gel and elution with petroleum ether – ethyl acetate (1:1) afforded the oxazoline. Recrystallization from ethyl acetate gave 240 mg (49% from the *p*-toluenesulfonic acid salt), m.p 126.5–127°.

The n.m.r. spectrum of the pure compound shows peaks at 7.27 (5H), 5.98 (1H, d, 3.8 Hz), 5.20 (1H, d, 3.8 Hz), 3.70 (3H), 3.67 (2H), 2.17 (3H), 1.57 (3H).

Conversion of ***17*** *to the Oxazoline*

The crystalline *cis* compound (100 mg) was chromatographed on alumina (Woelm, grade II). Elution with carbon tetrachloride – benzene (1:1) gave 38 mg of the oxazoline in the first fractions, followed by uncyclized *cis* compound.

In a second experiment, the *cis* compound (1.0 g) was chromatographed on 37 g of silica gel, elution being performed with 1:1 petroleum ether (30–60°) – ethyl acetate. There were obtained in successive fractions 450 mg of recovered *cis* compound, 140 mg of a mixture of the *cis* compound and oxazoline, and 210 mg of oxazoline.

In a third experiment the crystalline methyl ester **24** (157 mg, 0.68 mmol), in dry methylene chloride (8 ml), was treated successively with phenylacetic acid (92 mg, 0.68 mmol) and diisopropylcarbodiimide (93 mg, 0.74 mmol). The solution was stirred at room temperature for 22 h, and the precipitated diisopropylurea was then collected by filtration. Addition of ether to the mother liquor completed the precipitation of the urea. Evaporation of the filtrate, followed by chromatography on a 1.0 × 7 cm column of alumina (activity II) gave, with 1:1 benzene – methylene chloride, 83 mg of crystalline material. This was found, by n.m.r. and t.l.c., to be a mixture of oxazoline and **17**.

Conversion of the Mixture ***15*** *+* ***24*** *to Oxazoline and* ***31*** *(R = PhCH₂)*

The *p*-toluenesulfonic acid salt **23** (4.428 g, 10.9 mmol) and 8.260 g (54.5 mmol) of freshly prepared tetramethylguanidinium chloride were refluxed for 2 h in spectroscopic grade chloroform (65 ml). The cooled solution was washed successively with ice-cold 5% bicarbonate solution, ice-cold saturated sodium chloride solution, and then dried over anhydrous magnesium sulfate. Then a solution of phenylacetic acid (1.490 g, 11 mmol) and diisopropylcarbodiimide (1.500 g, 11.9 mmol) in methylene chloride (25 ml) was added, and the mixture was refluxed

Can. J. Chem. Downloaded from www.nrcresearchpress.com by 210.87.254.42 on 09/05/12
For personal use only.

for 2 h. The n.m.r. spectrum of the reaction product showed only a small amount of the oxazoline (based on the peaks at 2.17 and 1.57). The solution was then washed with ice-cold 5% bicarbonate, dried over anhydrous magnesium sulfate, and evaporated. The n.m.r. spectrum of this residue now showed oxazoline as the major product. Thus, washing with bicarbonate had caused cyclization. The product was left at 10° overnight, then redissolved in methylene chloride and shaken again with bicarbonate solution. After drying and evaporation of the organic layer the n.m.r. spectrum of the residue was redetermined; it now indicated that the mixture contained 70% of oxazoline. The mixture, in 1:1 ethyl acetate – petroleum ether, was filtered through 50 g of silica gel and then chromatographed carefully on 110 g of silica gel. Elution was performed with graded mixtures of petroleum ether and ethyl acetate (250 ml of 20% ethyl acetate, followed by 200 ml of 30% ethyl acetate, followed by 200 ml of 35% ethyl acetate, followed by 200 ml of 45% ethyl acetate, followed by 50% ethyl acetate); 40-ml fractions were collected. Fractions 1–3 afforded 100 mg of **17**. Fractions 5–12 afforded 1.475 g of oxazoline. Fractions 13–15 were rechromatographed and yielded, besides an additional 150 mg of oxazoline (total 1.625 g, 48%), 240 mg of **31** (R = $PhCH_2$; see below).

*Preparation of **14** (R = $PhCH_2O$)*

The chloro acid from 470 mg of the anhydropenicillin, in acetone (5 ml), was added to a solution of sodium bicarbonate (247 mg, 2.94 mmol) in water (10 ml). After 1 min, crystallization began. The mixture was stirred for 15 min and then diluted with saturated sodium chloride solution (20 ml) and extracted twice with methylene chloride (10 ml each) and once with ether (10 ml). The combined organic extracts were dried over anhydrous magnesium sulfate and evaporated. The crystalline residue weighed 216 mg. Chromatography on silica gel afforded 185 mg of material which was recrystallized to give **14** (R = $PhCH_2O$), m.p. 170–172° dec., $[\alpha]_D^{25}$ −64.5° (*c* 0.45, $CHCl_3$). Anhydrocarbobenzoxypenicillin has $[\alpha]_D^{25}$ +259° (*c* 1, $CHCl_3$). The 5-epioxaanhydropenicillin has i.r. absorption at 2.98, 5.55, 5.65, 5.88, and 6.51 μ. The n.m.r. spectrum has peaks at 7.56 (6H), 5.86 (1H, d, 1.8 Hz), 5.18 (2H), 5.02 (1H, q, 1.8, 8 Hz), 2.18 (3H), 2.12 (3H). The mass spectrum shows the molecular ion at *m/e* 316.

Anal. Calcd. for $C_{16}H_{16}N_2O_5$: C, 60.75; H, 5.10; N, 8.86. Found: C, 60.67; H, 5.20; N, 8.99.

*Preparation of **28** (R = CH_3)*

The oxazoline (500 mg, 1.6 mmol) and *p*-toluenesulfonic acid monohydrate (300 mg, 1.6 mmol) were stirred in dry acetone (20 ml) for 30 min. The solvent was then removed below 40° to give a colorless foam which was crystallized from acetone–hexane to give 480 mg (60%) of methyl 2-(2′*R*-phenylacetoxy-3′*S*-amino-4′-oxo)azetidinyl-3-methyl-2-butenoate *p*-toluene-sulfonate as colorless fine needles, after washing with cold ethyl acetate, m.p., 145–146°, $[\alpha]_D^{EtOH}$ +40.1 (*c* 0.17).

Anal. Calcd. for $C_{24}H_{28}N_2O_8S$: C, 57.14; H, 5.56. Found: C, 56.75; H, 5.85.

The n.m.r. spectrum has peaks at 7.83 (2H, d, 9 Hz), 7.06 (5H, s) 7.06 (2H, d, 9 Hz), 6.30 (1H, d, 4.0 Hz), 4.90 (1H, d, 4.0 Hz), 3.62 (3H, s), 3.52 (2H, s), 2.30 (3H, s), 2.03 (3H, s), 1.88 (3H, s). In KBr, the i.r. spectrum has peaks at 1800, 1776, 1728, 1690 cm^{-1}.

*Preparation of **28** (R = CH_2Ph)*

The oxazoline **6** (R_1 = $PhCH_2$; R_2 = H) (1.0 g, 3.33 mmol), in ether (50 ml), was treated dropwise with stirring with a solution of phenyldiazomethane in ether. The pink color of the phenyldiazomethane disappeared immediately, and a gas was evolved. When a permanent pink solution was obtained, the mixture was stirred for an additional hour and then evaporated to dryness to give a pale orange oil. This was chromatographed on silica gel and the column eluted with graded mixtures of petroleum ether – ethyl acetate. The fractions obtained with a 60:40 solvent mixture afforded 1.21 g (93%) of **6** (R_1 = $PhCH_2$, R_2 = CH_2Ph); n.m.r.: 7.33 (5H, s), 7.27 (5H, s), 5.88 (1H, d, 4 Hz), 5.17 (2H, s), 5.07 (1H, d, 4 Hz), 3.57 (2H, s), 2.17 (3H, s), 1.55 (3H, s). The benzyl ester (1.1 g, 2.8 mmol) and *p*-toluenesulfonic acid monohydrate (532 mg, 2.8 mmol) were stirred in dry acetone (50 ml) for 30 min. Removal of the solvent afforded a quantitative yield of **28** (R = CH_2Ph), m.p., 128–130° dec., after crystallization from ethyl acetate – petroleum ether. The n.m.r. spectrum has peaks at 7.68 (2H, d, 8 Hz), 7.15 (5H, s), 6.97 (5H, s), 6.93 (2H, d, 8 Hz), 6.23 (1H, d, 4 Hz), 5.02 (s, 2H), 4.73 (br d, 4 Hz), 3.43 (2H, s), 2.23 (3H, s), 1.97 (3H, s), 1.50 (3H, s). The ester (100 mg) was hydrogenated at 15 p.s.i. in absolute ethanol (20 ml) containing 5% palladium-on-charcoal (10 mg) to give **28** (R = H). The n.m.r. spectrum has peaks at 7.67 (2H, d, 8 Hz), 7.17 (5H, s), 7.00 (2H, d, 8 Hz), 6.35 (1H, d, 4 Hz), 4.97 (1H, d, 4 Hz), 3.47 (2H, s), 2.23 (3H, s), 2.00 (3H, s), 1.58 (3H, s).

*Preparation of Diacylated Azetidinones **31** from **28** (R = CH_3)*

The salt (500 mg, 1.0 mmol) in CH_2Cl_2 (40 ml), cooled to 0°, was shaken vigorously for 30 min in an ice-bath with an ice cold solution of sodium bicarbonate (263 mg, 3.0 mmol) in water (20 ml). Then a solution of benzoyl chloride (280 mg, 2.0 mmol) in CH_2Cl_2 (10 ml) was added dropwise during 5 min and stirring was continued at 0° for an additional 2 h. The layers were then separated and the aqueous layer extracted twice with CH_2Cl_2. Evaporation of the combined dried CH_2Cl_2 layers afforded 550 mg of a colorless solid. Recrystallization from CH_2Cl_2 – petroleum ether gave 330 mg (75.5%) of **31** (R = Ph) as colorless prisms, m.p. 139–141°. The i.r. spectrum (KBr) has peaks at 1777, 1722, 1669 cm^{-1}. The n.m.r. spectrum has peaks at 7.78–6.97 (6H, m), 7.13 (5H, s), 6.37 (1H, d, 4 Hz), 5.58 (1H, q, 2, 8 Hz), 3.73 (3H, s), 3.57 (2H, s), 2.18 (3H, s), 1.83 (3H, s).

To prove the structure of this compound, **6** (R_1 = $PhCH_2$; R_2 = CH_3) was converted directly into the same material. The oxazoline (100 mg, 0.3 mmol) and benzoyl chloride (140 mg, 1 mmol) were stirred in tetrahydrofuran (5 ml) at room temperature for 24 h. Then water (2 ml) and sodium bicarbonate (100 mg, 1.2 mmol) were added, and stirring continued for a further 30 min. The mixture was then diluted with water and extracted with CH_2Cl_2. After drying of this extract, evaporation yielded 140 mg of a yellow oil, whose n.m.r. spectrum showed it to be a mixture of oxazoline and the above-mentioned *N*-benzoyl compound. This latter material was isolated by p.l.c. on silica gel (elution with 1:2 ethyl acetate – hexane) and crystallized from ethyl acetate – hexane. Its i.r., n.m.r. spectra, m.p., and mixture melting point with the *N*-benzoyl compound showed the two to be identical.

The diacylated azetidinone **31** (R = $PhCH_2$), prepared

Can. J. Chem. Downloaded from www.nrcresearchpress.com by 210.87.254.42 on 09/05/12
For personal use only.

from **28** as described above has i.r. absorption at 2.9, 3.0, 5.60, 5.70, 5.80, 5.98, 6.06, 6.65 μ. The n.m.r. spectrum has peaks at 7.35–7.25 (10H, m), 6.74 (1H, d, 9.5 Hz), 6.32 (1H, d, 4.1 Hz), 5.47 (q, 4.1, 9.5 Hz), 3.73 (3H), 3.57 (2H), 3.46 (2H), 2.18 (3H), 1.72 (3H). The mass spectrum shows a molecular ion at *m/e* 450.

Allylic Bromination of Methyl 2-(2'R-Chloro-3'S-phthalimido-4'-oxo)azetidinyl-3-methyl-2-butenoate

To a suspension of the methyl ester (100 mg, 0.276 mmol) in carbon tetrachloride (7.5 ml) were added *N*-bromosuccinimide (108 mg, 0.61 mmol) and benzoyl peroxide (2 mg). When this mixture was brought to reflux, the ester dissolved; the heat source was then replaced by a 100 W Photoflood No. 2 lamp and reflector mounted close to the reaction flask and stirring was continued until the reaction was complete (10 min). The resulting suspension was cooled, diluted with a small amount of chloroform, and the precipitated succinimide was removed by filtration. Evaporation of the filtrate gave a white crystalline solid residue whose n.m.r. spectrum showed no absorption in the region of the allylic methyl groups (2.5 to 2.0), but did show succinimide absorption at 2.8. This was removed, in part, by trituration with carbon tetrachloride and methylene chloride, and the total product was then chromatographed on neutral alumina (Woelm, activity II). Elution with methylene chloride afforded a crystalline dibromo compound which, after recrystallization from carbon tetrachloride – petroleum ether, melted at 65°–70° dec. and weighed 116 mg (80%).

Anal. Calcd. for $C_{17}H_{13}N_2O_5ClBr_2$: C, 39.22; H, 2.52; N, 5.38. Found: C, 38.95; H, 2.36; N, 5.40.

The n.m.r. spectrum has peaks at 7.87 (4H), 6.20 (1H, d, 4.2 Hz), 5.79 (1H, d, 4.2 Hz), 4.93 (1H, d, 10.2 Hz), 4.77 (1H, d, 10.9 Hz), 4.73 (1H, d, 10.2 Hz), 4.67 (1H, d, 10.9 Hz), 3.89 (3H). The spectrum appears unusually complex because one of the $-CH_2Br$ groups is *cis* to the methoxycarbonyl substituent and the other is *trans*; and, in each $-CH_2Br$ group, the methylene protons are magnetically nonequivalent. The i.r. spectrum has peaks at 5.55, 5.62, and 5.79 μ.

Allylic Bromination of Methyl 2-(2'S-Chloro-3'S-phthalimido-4'-oxo)azetidinyl-3-methyl-2-butenoate

The compound (100 mg) was reacted with 2 molar-equiv. of *N*-bromosuccinimide in exactly the same manner as described above. Chromatography on alumina (Woelm, activity II) and elution with methylene chloride afforded 122 mg (84%) of the desired compound, m.p. 164–167 °C. The n.m.r. spectrum shows peaks at 7.92 (4H), 6.38 (1H, d, 1.7 Hz), 5.73 (1H, d, 1.7 Hz), 4.95 (1H, d, 10.0 Hz), 4.64 (1H, d, 10.0 Hz), 4.62 (1H, d, 11.0 Hz), 4.43 (1H, d, 11.0 Hz), 3.96 (3H).

Reaction of Methyl 2-(2'R-Chloro-3'S-phthalimido-4'-oxo)azetidinyl-3-methyl-2-butenoate with One Molar-equiv. of N-Bromosuccinimide

A suspension of the *cis* compound (75 mg, 0.207 mmol), *N*-bromosuccinimide (36.9 mg, 0.207 mmol), and benzoyl peroxide (1.5 mg) in carbon tetrachloride (5 ml) was heated to reflux until a clear solution resulted. The heat source was then removed and the mixture was stirred while being illuminated with a 100 W Photoflood No. 2 lamp. After 10 min the reaction was terminated and the mixture was cooled to room temperature and filtered to give succinimide (17 mg, 85% of the theoretical amount), identified by its melting point and i.r. spectrum. The filtrate was evaporated to dryness to give a white solid residue which, on the basis of its n.m.r. spectrum contained a small amount of succinimide and an exactly 1:1 mixture of the two possible monobrominated compounds. The solid was chromatographed on alumina to remove the succinimide. Elution with methylene chloride afforded the 1:1 mixture of monobrominated compounds as a white foam (87.5 mg, 96%). The n.m.r. spectrum of this mixture shows peaks at 7.80 (4H), 6.17 (0.5H, d, 4.2 Hz), 6.13 (0.5H, d, 4.2 Hz), 5.72 (0.5H, d, 4.2 Hz), 5.68 (0.5H, d, 4.2 Hz), 4.90–4.12 (2H, m, overlapping AB quartets), 3.85 (1.5H), 3.83 (1.5H), 2.45 (3H).

Reaction of Methyl 2-(2'S-Chloro-3'S-phthalimido-4'-oxo)azetidinyl-3-methyl-2-butenoate with One Molar-equiv. of N-Bromosuccinimide

A mixture of the pure *trans* methyl ester (165 mg, 0.455 mmol), *N*-bromosuccinimide (81 mg, 0.455 mmol), and benzoyl peroxide (4 mg), in carbon tetrachloride (12 ml), was brought to reflux. The heat source was then removed and replaced with a 100 W Photoflood No. 2 lamp. Illumination of the stirred reaction mixture was maintained for 15 min. The suspension was then cooled, filtered, and the filtrate evaporated to a white foam. This was chromatographed on a 0.5 × 13 cm column of 3.0 g of neutral alumina (Woelm, activity II). Elution with methylene chloride afforded 206 mg of a 60:40 mixture of monobromo compounds. The n.m.r. spectrum of this mixture has peaks at 7.83 (4H), 6.27 (1H, d, 2 Hz), 5.63 (1H, d, 2 Hz), 4.73–4.35 (2H, m, two overlapping AB quartets), 3.85 (3H), 2.41 (1.2H), 2.18 (1.8H).

*Oxidative Rearrangement of **28** ($R = CH_3$) to **40***

The toluenesulfonic acid salt (504 mg, 1 mmol) was brominated for 15 min in CCl_4 (50 ml) with NBS (356 mg, 2 mmol). The product was dissolved in CH_2Cl_2 (30 ml) containing triethylamine (202 mg, 2 mmol) and this solution was stirred at room temperature for 1 h and then evaporated to dryness. The residue was triturated with methylene chloride and water and the dried methylene chloride phase was evaporated to give 310 mg of a white foam. The n.m.r. spectrum of this foam was identical to that of crystalline material, m.p. 151–152°, obtained as follows. The crude product was chromatographed on silica gel and eluted with 1:1 petroleum ether – ethyl acetate. Crystallization from petroleum ether – CH_2Cl_2 afforded 210 mg of the dehydrooxazinone.

Mass Calcd. for $C_{17}H_{18}N_2O_5$ (M + 1): 330.1205. Found: 330.1216.

Anal. Calcd. for $C_{17}H_{18}N_2O_5$: C, 61.81; H, 5.49; N, 8.48. Found: C, 61.76; H, 5.52; N, 8.45.

The n.m.r. spectrum has peaks at 8.04 (1H, s), 7.30 (5H, s), 5.24 (2H, d), 3.74 (3H, s), 3.66 (2H, s), 1.81 (3H, s) at 100 MHz in DMSO-d_6 containing a drop of D_2O.

The compound gave a dihydro derivative, m.p. 178–180° upon hydrogenation in ethanol over 5% palladium-on-charcoal. Its n.m.r. spectrum shows the following peaks: 8.28 (1H, s), 7.38 (1H), 7.23 (5H), 7.18 (1H), 3.76 (3H), 3.63 (2H), 2.24 (1H, m), 1.00 (3H, d, 7 Hz), 0.94 (3H, d, 7 Hz).

Oxidative Rearrangement of 28 ($R = CH_2Ph$) to 42

The *p*-toluenesulfonic acid salt (100 mg, 0.17 mmol) was suspended in CCl_4 (spectroscopic grade, 20 ml) containing *N*-bromosuccinimide (62 mg, 0.35 mmol) and benzoyl peroxide (2 mg). The mixture was heated to reflux with mechanical stirring. After 2 min, the heat source was removed and the stirred mixture was irradiated with a 100 W Photoflood No. 2 lamp for 8 min. Irradiation was then discontinued and the reaction mixture was evaporated to dryness. The residue was dissolved in methylene chloride (15 ml) and triethylamine (35 mg) was added. This solution was stirred at 20° for 1.5 h and then evaporated. The residue was dissolved in methylene chloride, and this solution was washed with water, dried, and evaporated. The 42 mg of material thus obtained was chromatographed on silica gel. Elution with graded mixtures of petroleum ether and ethyl acetate afforded 7 mg of material with the 1:1 mixture. This material crystallized when triturated with ether. Recrystallization from methylene chloride – petroleum ether afforded 2-isopropenyl-2-benzyloxycarbonyl-5-phenylacetamido-5,6-dehydrooxazine-4-one, m.p. 162–163°. The n.m.r. spectrum shows peaks at 8.33 (1H, s), 7.53 (10H, s), 5.50 (4H, br s), 3.93 (2H, s), 1.98 (3H, s). The i.r. spectrum shows carbonyl absorptions at 1725, 1690, and 1642 cm^{-1}.

We thank the National Research Council of Canada and Bristol Laboratories for financial support of this research, and Drs. G. N. Knaus, Queen's University, and P. A. Hart, School of Pharmacy, University of Wisconsin-Madison, for assistance with some of the experimental work. Numerous discussions with Dr. R. B. Morin concerning the structure of the oxazinone **40** and the role of acylimines in penicillin biosynthesis are also gratefully acknowledged.

1. K. KATO. J. Antibiot. Tokyo Ser. A, **6**, 130, 184 (1953); F. R. BATCHELOR, F. P. DOYLE, J. C. NAYLER, and G. N. ROLINSON. Nature, **183**, 257 (1959).
2. H. T. CLARKE, J. R. JOHNSON, and R. ROBINSON. The chemistry of penicillin. Princeton University Press, Princeton, New Jersey. 1949.
3. G. T. STEWART. The penicillin group of drugs. Elsevier, New York. 1965.
4. E. P. ABRAHAM and G. G. F. NEWTON. Biochem. J. **79**, 377 (1961).
5. (*a*) E. O. STAPLEY, D. HENDLIN, S. HERNANDEZ, M. JACKSON, J. M. MATA, A. K. MILLER, H. B. WOODRUFF, T. W. MILLER, G. ALBERS-SCHONBERG, B. H. ARISON, and J. L. SMITH. XIth International Conference on Antimicrobial Agents and Chemotherapy, Atlantic City, New Jersey. 1971. Abstr. p. 8; (*b*) R. NAGARAJAN, L. D. BOECK, M. GORMAN, R. L. HAMILL, C. E. HIGGENS, M. M. HOEHN, W. M. STARK, and J. G. WHITNEY. J. Am. Chem. Soc. **93**, 2308 (1971).
6. R. B. WOODWARD, K. HEUSLER, J. GOSTELI, P. NAEGELI, W. OPPOLZER, R. RAMAGE, S. RANGANATHAN, and H. VORBRÜGGEN. J. Am. Chem. Soc. **88**, 852 (1966).
7. R. D. G. COOPER and D. O. SPRY. *In* Cephalosporins and penicillins. Chemistry and biology. *Edited by* E. H. Flynn. Academic Press, New York. 1972. Chapt. 5.
8. (*a*) J. E. DOLFINI, J. SCHWARTZ, and F. WEISENBORN. J. Org. Chem. **34**, 1582 (1968); (*b*) D. M. BRUNWIN, G. LOWE, and J. PARKER. J. Chem. Soc. C, 3756 (1971); (*c*) N. GIROTA and N. WENDLER. Tetrahedron Lett. 5301 (1972); (*d*) G. LOWE and M. V. J. RAMSAY. J. Chem. Soc. Perkin I, 479 (1973); (*e*) G. LOWE and D. D. RIDLEY. J. Chem. Soc. Chem. Commun. 328 (1973); (*f*) R. HEYMES, G. AMIARD, and G. NOMINÉ. Bull. Soc. Chim. Fr. 2343 (1973); (*g*) R. W. RATCLIFFE and B. G. CHRISTENSEN. Tetrahedron Lett. 4645, 4649, 4653 (1973); (*h*) J. A. EDWARDS, A. GUZMAN, R. JOHNSON, P. J. BEEBY, and J. H. FRIED. Tetrahedron Lett. 2031 (1974).
9. (*a*) A. FLEMING. Nobel lectures. Physiology or medicine. 1942–1962. Elsevier, Amsterdam. 1964. p. 83; (*b*) R. R. CHAUVETTE and P. A. PENNINGTON. J. Am. Chem. Soc. **96**, 4986 (1974); (*c*) L. D. CAMA and B. G. CHRISTENSEN. J. Am. Chem. Soc. **96**, 7582 (1974); (*d*) R. N. GUTHIKONDA, L. D. CAMA, and B. G. CHRISTENSEN. J. Am. Chem. Soc. **96**, 7584 (1974).
10. (*a*) S. WOLFE, W. S. LEE, G. KANNENGIESSER, and J. B. DUCEP. Can. J. Chem. **50**, 2894 (1972); (*b*) S. WOLFE, W. S. LEE, J. B. DUCEP, and G. KANNENGIESSER. Can. J. Chem. **50**, 2898 (1972); (*c*) S. WOLFE, J. B. DUCEP, G. KANNENGIESSER, and W. S. LEE. Can. J. Chem. **50**, 2902 (1972); (*d*) S. WOLFE and M. P. GOELDNER. Tetrahedron Lett. 5131 (1973).
11. (*a*) S. WOLFE, J. C. GODFREY, C. T. HOLDREGE, and Y. G. PERRON. Can. J. Chem. **46**, 2549 (1968); (*b*) S. WOLFE. Can. J. Chem. **46**, 459 (1968).
12. J. C. SHEEHAN. *In* Molecular modification in drug design. *Edited by* R. F. Gould. Advances in chemistry series. No. 45. American Chemical Society, Washington, D.C. 1964. p. 15.
13. D. H. R. BARTON, F. COMER, D. G. T. GREIG, P. G. SAMMES, C. M. COOPER, G. HEWITT, and W. G. E. UNDERWOOD. J. Chem. Soc. C, 3540 (1971).
14. R. J. STOODLEY and N. R. WHITEHOUSE. J. Chem. Soc. Perkin I, 181 (1974).
15. S. WOLFE and B. G. RAMSAY. Unpublished results.
16. S. KUKOLJA. J. Am. Chem. Soc. **93**, 6267 (1971).
17. D. F. CORBETT and R. J. STOODLEY. J. Chem. Soc. Perkin I, 185 (1974).
18. D. F. CORBETT and R. J. STOODLEY. J. Chem. Soc. Chem. Commun. 417 (1974).
19. (*a*) S. WOLFE and W. S. LEE. Chem. Commun. 242 (1968); (*b*) D. A. JOHNSON, D. MANIA, C. A. PANETTA, and H. H. SILVESTRI. Tetrahedron Lett. 1903 (1968); (*c*) R. A. FIRESTONE, N. S. MACIEJEWICZ, R. W. RATCLIFFE, and B. G. CHRISTENSEN. J. Org. Chem. **39**, 437 (1974).
20. Ö. K. J. KOVACS, B. EKSTRÖM, and B. SJÖBERG. Tetrahedron Lett. 1863 (1969); S. WOLFE, W. S. LEE, and R. MISRA. Chem. Commun. 1067 (1970).
21. A. J. PAPA. J. Org. Chem. **31**, 1426 (1966).
22. B. K. KOE. Nature, **195**, 1200 (1962).
23. L. V. PAVLOVA and F. YU. RACHINSKII. Russ. Chem. Rev. **37**, 587 (1968).
24. E. M. FRY. J. Org. Chem. **15**, 802 (1950).
25. (*a*) S. KUKOLJA, R. D. G. COOPER, and R. B. MORIN. Tetrahedron Lett. 3381 (1969); (*b*) K. HEUSLER. Helv. Chim. Acta, **55**, 388 (1972).
26. R. B. MORIN, B. G. JACKSON, R. A. MUELLER, E. R. LAVAGNINO, W. B. SCANLON, and S. L. ANDREWS, J. Am. Chem. Soc. **91**, 1401 (1969).

Can. J. Chem. Downloaded from www.nrcresearchpress.com by 210.87.254.42 on 09/05/12
For personal use only.

27. T. S. CHOU, J. R. BURGTORF, A. L. ELLIS, S. R. LAMMERT, and S. P. KUKOLJA. J. Am. Chem. Soc. **96**, 1609 (1974).
28. R. B. MORIN, E. M. GORDON, T. MCGRATH, and R. SHUMAN. Tetrahedron Lett. 2159 (1973).
29. (*a*) J. E. BALDWIN, F. J. URBAN, R. D. G. COOPER, and F. L. JOSÉ. J. Am. Chem. Soc. **95**, 2401 (1973); (*b*) G. A. KOPPEL and R. E. KOEHLER. J. Am. Chem. Soc. **95**, 2403 (1973); (*c*) R. A. FIRESTONE and B. G. CHRISTENSEN. J. Org. Chem. **38**, 1436 (1973).
30. (*a*) R. B. MORIN, E. M. GORDON, and J. R. LAKE. Tetrahedron Lett. 5213 (1973); (*b*) J. E. BALDWIN, S. B. HABER, and J. KITCHIN. J. Chem. Soc. Chem. Commun. 790 (1973).
31. B. W. BYCROFT. Nature, **224**, 595 (1969).
32. R. B. MORIN, J. R. LAKE, and E. M. GORDON. Tetrahedron Lett. 2979 (1974).

Can. J. Chem. Downloaded from www.nrcresearchpress.com by 210.87.254.42 on 09/05/12
For personal use only.

Deacylation of Fluorine-substituted *trans*-Cinnamoyl-α-chymotrypsins[1]

J. T. GERIG AND R. S. MCLEOD

Department of Chemistry, University of California, Santa Barbara, Santa Barbara, California 93106

Received July 23, 1974

J. T. GERIG and R. S. MCLEOD. Can. J. Chem. **53**, 513 (1975).

Deacylation of unsubstituted and of *o*-F-, *m*-F, *p*-F, α-F, pentafluoro-, *p*-methyl-, and *p*-trifluoromethyl-substituted *trans*-cinnamoyl-α-chymotrypsins has been studied from p*H* 4 to 8. The deacylation rate constants were found to depend upon the ionization state of a group on the enzyme with an apparent p*K* in the range 6.3–7.3. The hydrolysis rates of the correspondingly substituted *p*-nitrophenylcinnamate esters were determined at p*H* 10.6. Correlation of the data for these model reactions with the corresponding rates of enzyme deacylation suggests that the *p*-methyl-substituted acylenzyme is about an order of magnitude more reactive than expected while *p*-trifluoromethyl substitution results in deacylation at a rate 10 times slower than expected. The remaining substituents exert about the anticipated rate effect on deacylation.

J. T. GERIG et R. S. MCLEOD. Can. J. Chem. **53**, 513 (1975).

On a étudié, entre les p*H* 4 et 8, la réaction de déacylation de *trans*-cinnamoyl-α-chymotrypsines non-substitués et substitués par des groupes *o*-F, *m*-F, α-F, pentafluoro, *p*-méthyle et *p*-trifluorométhyle. Les constantes de vitesse de déacylation dépendent de l'état d'ionisation d'un groupe de l'enzyme ayant un p*K* apparent entre 6.3 et 7.3. On a déterminé, à p*H* de 10.6, les vitesses d'hydrolyse des esters *p*-nitrophénylcinnamates substitués d'une façon correspondantes. La corrélation des données pour les réactions de ces modèles avec les vitesses des réactions de déacylation correspondantes catalysées par les enzyme suggère que l'acyle-enzyme substitué par un groupe *p*-méthyle est environ 10 fois plus réactif que l'on aurait pu l'attendre alors que la substitution par un groupe *p*-trifluorométhyle conduit à des résultats de déacylation qui sont environ 10 fois plus lent que prévu. Les autres substituants exercent sur la déacylation les effets anticipés. [Traduit par le journal]

Numerous studies have been carried out to elucidate the properties as well as the catalytic mechanism of the proteolytic enzyme, α-chymotrypsin (1–5). Equation 1 represents the minimal features of this mechanism in which enzyme (E) and substrate (S) first combine to form a Michaelis complex (ES). The substrate is pre-

$$[1] \quad E + S \rightleftarrows ES \rightarrow ES' \rightarrow EP_2 \rightleftarrows E + P_2 + P_1$$

sumed to consist of an alcohol, amine, or thiol moiety symbolized P_1 which is present as a derivative of a carboxylic acid (P_2). A large body of evidence points to the appearance of a covalent enzyme–substrate intermediate (ES′) along the reaction pathway, likely one in which the acyl group of the substrate is attached to serine-195 of the enzyme (6, 7). Generally, nonspecific substrates produce acylchymotrypsins that are relatively stable and, in several studies, these species have been directly observed or isolated (8–12). Acylenzymes have also been detected in the reactions of specific ester substrates but more rarely or under unusual conditions (13, 14). Hydrolysis of the intermediate enzyme–ester gives initially an enzyme–acid product complex (EP_2) which, upon dissociation, regenerates the native enzyme.

The goal of a program in our laboratory is to compare the structures of acylenzyme intermediates with the structures of the corresponding enzyme–P_2 complexes. Fluorine n.m.r. spectroscopy should be useful in such studies since fluorine chemical shift and relaxation time data can provide information about the local environment of the fluorine 'reporter' nuclei (15, 16).

The purpose of the present work was to determine the stabilities of various fluorine-substituted cinnamoyl-α-chymotrypsins in the hope that some of these acylenzymes would prove amenable to study by fluorine n.m.r.; experiments

[1]The authors gratefully acknowledge the support of the National Cancer Institute (Grant CA-11220) for this work. J. T. G. is a PHS Research Career Development awardee (Grant GM-70373 from the National Institute of General Medical Sciences).

Can. J. Chem. Downloaded from www.nrcresearchpress.com by 210.87.254.5 on 09/05/12
For personal use only.

Can. J. Chem. Downloaded from www.nrcresearchpress.com by 210.87.254.5 on 09/05/12
For personal use only.

with the corresponding cinnamate–enzyme complexes are already underway (17). Previous kinetic investigations have shown that the electronic nature of the acyl group as well as its size are important in determining the rate of deacylation of the corresponding acylenzyme (11*a*, 18–20). In some cases unexpectedly large or small rates are observed, especially if fluorine substituents are present (20*b*). A second thrust of this work, then, was to compare the rates of deacylation of the fluorinated derivatives to their nonfluorinated analogs; such comparisons may give some indication of how representative of the nonfluorinated acylenzymes are the fluorine-containing ones.

Experimental

Materials

trans-Cinnamic acid (Matheson, Coleman and Bell), α-fluorocinnamic acid (Aldrich), and 4-methylcinnamic acid (Aldrich) were obtained commercially.

The other substituted cinnamic acids were prepared by heating at reflux the appropriate benzaldehyde (0.02 mol) and malonic acid (0.022 mol) in a solvent composed of pyridine (0.6 ml) and ethanol (0.4 ml). Upon heating, the malonic acid slowly dissolves; as the product forms, it precipitates from the solution until the mixture is pasty. At this point a few additional drops of ethanol can be added to maintain fluidity. Typical reaction times were 5–6 h. The cinnamic acids so produced were recrystallized from ethanol–water. Table 1 gives yields and melting points for these materials. Proton magnetic resonance spectra of these compounds uniformly showed a coupling constant between the vinyl protons of 15–17 Hz indicating a *trans* double bond.

The corresponding cinnamoyl chlorides were prepared by treating the appropriate cinnamic acid (0.03 mol) with thionyl chloride (0.11 mol, *ca.* 8 ml). After heating at reflux for 2 h and removal of excess thionyl chloride at atmospheric pressure, the products were distilled under vacuum. Table 1 records the boiling points and yields observed in these preparations.

p-Nitrophenylcinnamates were synthesized by dissolving the desired cinnamoyl chloride (0.006 mol) in dry benzene (25 ml) containing pyridine (1.2 ml). *p*-Nitrophenol (0.84 g, 0.006 mol) was added and the mixture heated at reflux for 1 h. Upon cooling the reaction mixture was washed five times with 5% potassium carbonate solution and then with water. (Addition of a small amount of ether was helpful when emulsion formation was a problem during these extractions.) After drying over anhydrous sodium sulfate, the solvent was stripped off *in vacuo* and the crystalline residue recrystallized from chloroform–cyclohexane. Data regarding yield, melting point, and microanalyses of these esters are given in Table 1.

The α-chymotrypsin used was a Worthington three-times crystallized product. Matheson spectroquality acetonitrile was used as co-solvent. Buffers were 0.05 *M* in buffer salts and contained 0.1 *M* KCl. Potassium phosphate was used at p*H* 6–8; at p*H* values lower than 6, acetate was used.

Kinetic Methods

Except for pentafluorocinnamoylchymotrypsin, the rates of deacylation of the various substituted cinnamoyl-enzymes were followed by monitoring the disappearance of the acylenzyme (12) at the wavelength indicated in Table 2 with a Beckman Model DUR spectrophotometer equipped with a Gilford 2000 recorder accessory. The temperature in the cell compartment was maintained at 30.2° by circulating thermostated water (±0.05°) through spacers on each side of the cell compartment. Stock solutions of the *p*-nitrophenyl esters at 0.54 m*M* were prepared

TABLE 1. Synthesis of substituted cinnamic acids and derivatives

					p-Nitrophenyl ester					
							Analysis[g]			
	Cinnamic acid		Cinnamoyl chloride				Calcd.		Found	
Substituent	Yield (%)	m.p. (lit.)	Yield (%)	b.p./mm Hg	Yield (%)[e]	m.p.	C	H	C	H
None	Commercial	132 —	94	87/0.1	68	145–146[f]	—		—	
o-F	88	178 (172[a])	88	84/0.2	70	154–155	62.72	3.51	62.39	3.12
m-F	95	161 (166[b])	39	84/0.05	52	149–150	62.72	3.51	62.42	3.04
p-F	78	208 (209[b])	90	90/0.15	53	148–149	62.72	3.51	62.51	3.16
α-F	Commercial	157 —	60	79/0.5	39	151–152	62.72	3.51	62.20	3.51
Pentafluoro	30	151 (153[c])	66	74/0.05	36	99–100	50.16	1.68	50.19	1.63
p-CH_3	Commercial	196 —	74	128/0.3	51	133–134	67.84	4.63	67.50	4.44
p-CF_3	88	229 (230[d])	82	90/0.1	55	110–111	56.98	2.99	57.53	2.84

[a]See ref. 30.
[b]See ref. 31.
[c]See ref. 32.
[d]See ref. 33.
[e]After three recrystallizations.
[f]Literature (34) m.p. 146°.
[g]Microanalyses by Chemalytics, Inc., Tempe, Arizona.

TABLE 2. Deacylation of substituted *trans*-cinnamoyl-α-chymotrypsins[a]

Substituent	Observed rate constant (k_ψ) × 10^5 s^{-1} (wavelength, nm)[b]				
	p*H* 7.99	p*H* 7.15	p*H* 6.13	p*H* 5.04	p*H* 4.13
None	1360 (310)	766 (305)	135 (304)	14.9 (304)	2.54 (305)
o-F	2170 (310)	1110 (306)	194 (306)	21.4 (306)	4.20 (307)
m-F	3660 (310)	1830 (303)	326 (303)	32.8 (303)	5.84 (303)
p-F	2450 (310)	1320 (307)	242 (306)	26.8 (306)	4.70 (307)
α-F	[c]	[c]	12100 (300)	1410 (300)	230 (300)
Pentafluoro	[c]	[c]	7220[d]	921[d]	[c]
p-CH_3	12300 (310)	5540 (310)	992 (310)	91.4 (310)	16.2 (315)
p-CF_3	436 (300)	265 (300)	64.4 (300)	7.75 (300)	2.25 (300)

[a]In water at 30.2°, 6.25% acetonitrile.
[b]Wavelength used to follow deacylation reaction by direct observation of acylenzyme.
[c]Could not be determined under these conditions.
[d]Dye-displacement technique.

in acetonitrile. An α-chymotrypsin stock solution at 1.37 m*M*, p*H* 3, was prepared assuming a molecular weight of 25 200 (21). An aliquot of the enzyme stock solution (0.4 ml) was diluted to 10 ml with the appropriate buffer solution; 3-ml aliquots of this solution were added to each cuvette, including the reference cell; 0.2 ml of acetonitrile was also added to the reference cell. The contents of the cells were allowed to reach thermal equilibrium at 30.2°. To initiate a reaction 0.2 ml of ester stock solution was added to a sample cuvette. The final reaction mixture thus had a total volume of 3.2 ml and was 0.034 m*M* in substrate, 0.051 m*M* in enzyme, and 6.25% in acetonitrile. Depending upon p*H* an initial change in absorbance due to acylation was noted followed by a slower exponential loss of absorbance as a result of deacylation.

Plots of ln ($A_\infty - A_t$), where A_∞ is the observed absorbance at infinite time and A_t is the observed absorbance at time t, *vs.* t were linear; least squares analysis of the data, using a program prepared for a Hewlett-Packard 9820A calculator, gave correlation coefficients in excess of 0.999. The slope of such a plot gives the apparent first-order rate constant, k_ψ, for deacylation.

Deacylation of the pentafluoro derivative was followed by a dye displacement technique (11*b*) using the dye Biebrich scarlet (22). Reaction conditions identical to those described above were used except that the dye was present in the reaction mixture and reference cell at a concentration of 5.96×10^{-5} *M*. With this technique no enzyme was added to the reference cuvette and the reappearance of the enzyme–dye complex as deacylation proceeded was followed at 550 nm.

The kinetics of base-catalyzed hydrolysis of the *p*-nitrophenyl esters were carried out as follows. Twenty milliliters of acetonitrile was diluted to 100 ml with 0.05 *M* potassium carbonate buffer. A 3-ml aliquot of this solution was placed in a cuvette and allowed to equilibrate at 30.2 °C. To start the reaction a 0.2-ml aliquot of the ester stock solution described above was added (because of decreased solubility, with the *p*-methyl compound 0.1 ml of stock solution and 0.1 ml of acetonitrile was used); an equivalent amount of acetonitrile was added to the reference cell. Total acetonitrile in the reaction system was 25%. The evolution of *p*-nitrophenol was followed at 400 nm and was strictly first order. The measured p*H* of the reaction medium was 10.59 and the pseudo first-order rate constants obtained were thus divided by $[OH^-] = 3.89 \times 10^{-4}$ *M* to obtain the second-order rate constant, k_{OH}, for hydroxide reaction.

Results

The kinetics of deacylation of *o*-fluoro-, *m*-fluoro-, *p*-fluoro-, α-fluoro-, *p*-methyl-, *p*-trifluoromethyl-substituted and unsubstituted cinnamoyl-α-chymotrypsins have been studied by direct spectrophotometric observation over the p*H* range 4–8. The α-fluoro derivative was examined only from p*H* 4 to 6 because the reaction is too rapid at higher p*H* values to be followed by the present techniques. An appropriate wavelength at which to observe the pentafluoro-substituted cinnamoylenzyme could not be found and a dye displacement method was used in this case. Deacylation in this system was also too rapid to be measured above p*H* 6 and at p*H* values below 5 the dye displacement technique was not usable because the dye precipitates from solution under these conditions. The results of these kinetic experiments are assembled in Table 2.

As expected, the deacylation reactions with all groups were found to be p*H* dependent. A mechanism of the form shown in eq. 2 was assumed where EH^+A and EA represent forms of the acylenzyme in which a critical group is proton-

$$\begin{array}{ccc} EA & \xrightarrow{k_3} & E + A \\ K \Big\| & & \\ EH^+A & \xrightarrow{k_3'} & EH^+ + A \end{array} \qquad [2]$$

Can. J. Chem. Downloaded from www.nrcresearchpress.com by 210.87.254.5 on 09/05/12
For personal use only.

Can. J. Chem. Downloaded from www.nrcresearchpress.com by 210.87.254.5 on 09/05/12
For personal use only.

ated or not protonated, respectively. For this mechanism, the observed first-order rate constant k_ψ is given by eq. 3*a*.

$$[3a] \qquad k_\psi = \frac{k_3 + \frac{k_3'[H^+]}{K}}{1 + \frac{[H^+]}{K}}$$

$$[3b] \qquad k_\psi = k_3 + \frac{k_3'}{K}[H^+] - \frac{k_\psi[H^+]}{K}$$

The available rate data were used to calculate the parameters k_3, k_3', and K which characterize the assumed mechanism by a least-squares technique using the rearranged form, eq. 3*b*. With the pentafluoro-substituted acylenzyme, data at only two pH values were available. In this case, k_3' was assumed to be zero in order to obtain an estimate of the equilibrium constant K and the first-order rate constant for deacylation, k_3. Table 3 presents the parameters found to describe the reaction of each cinnamoylchymotrypsin; these values for k_3, k_3', and K reproduce the experimentally observed rate constants well, usually with an accuracy of 5% or better. It should be noted that the accuracy of k_3' depends critically upon the accuracy of K (*cf.* eq. 3*b*).

The rates of hydroxide ion catalyzed hydrolysis of the *p*-nitrophenyl esters of the cinnamic acids used in this work were determined. At pH 10.59, these reactions are pseudo first-order with hydroxide ion in large excess concentration over the ester substrate. The second-order rate constants obtained from these experiments are recorded in Table 3.

Discussion

An unexpected aspect of our results in this work is the apparently substantial contribution reaction of the protonated form of the enzyme (EH^+A in eq. 2) makes to the overall deacylation process. While the rate constant, k_3', for this step is very small relative to k_3, at pH values below 6 this pathway for deacylation appears to generate an appreciable fraction of the total reaction observed. Although others have included steps analogous to the one defined by k_3' in eq. 2 in discussions of the chymotrypsin mechanism (23) we are unaware of estimates for the relative magnitudes of k_3 and k_3' from previous work. Rather, the usual assumption appears to be that $k_3' = 0$. Our results suggest that this assumption should be made with caution. However, it is possible that the complete mechanism for deacylation under our conditions is inadequately represented by eq. 1 and that additional terms perhaps involving the buffer components or other ionization constants may become necessary in a more refined description of this reaction.

The rate constants k_3 and k_3' for deacylation define steps in the mechanism that are essentially ester hydrolyses. A linear free energy relation between k_3, for example, and the rate constant for attack of hydroxide on a corresponding simple ester analog of the acylenzyme is expected and has been observed in a number of cases (18, 19). Substantial deviations from the regression line in these correlations can be taken to indicate interactions between an acyl group and the protein structure which significantly affect the enzyme reaction; previous work has shown that remote fluorine substitution can have an accelerating, a decelerating or no effect on the hydrolysis of acylchymotrypsins (20*b*).

Figure 1 shows a plot of the logarithm of k_3 for substituted cinnamoylchymotrypsin deacylation *vs.* the logarithm of k_{OH}, the rate constant for basic hydrolysis of the corresponding *p*-nitro-

TABLE 3. pH independent rate parameters for deacylation of substituted cinnamoylchymotrypsins[a]

Substitutent	pK	$k_3' \times 10^5$ s^{-1}	$k_3 \times 10^2$ s^{-1}	k_{OH}[b] l mol^{-1} s^{-1}
None	7.09	0.94	1.48	0.87
o-F	7.15	2.0	2.36	1.42
m-F	7.18	2.3	4.05	1.59
p-F	7.09	1.9	2.61	0.90
α-F	6.50	59	40.1	50.4
Pentafluoro	~6.3[c]	—	~18[c]	8.15
p-CH_3	7.23	5.4	13.5	0.57
p-CF_3	6.90	1.5	0.45	2.47

[a]At 30.2°, 6.25% acetonitrile.
[b]At 30.2°, 25% acetonitrile.
[c]Estimates based upon the reasonable assumption that k_3' is negligibly small.

Can. J. Chem. Downloaded from www.nrcresearchpress.com by 210.87.254.5 on 09/05/12
For personal use only.

phenylcinnamate esters. Excepting the data points for the methyl and trifluoromethyl derivatives, a reasonably linear relationship is found. This indicates that the steric and electronic effects of the other various fluorine substituents on the cinnamoyl group are being felt in both types of ester hydrolyses to about the same extent. The kinetics of deacylation of the various monofluorine substituted and the pentafluorinated cinnamoylchymotrypsins thus appear to be 'normal' by this criterion.

Placement at the *para* position of the cinnamoyl group of a methyl or trifluoromethyl group has unexpected kinetic consequences. Using the correlation shown in Fig. 1 as a guide, it appears that the *p*-methyl compound deacylates about a factor of 10 more rapidly than anticipated on the basis of the model reaction while the *p*-trifluoromethyl derivative reacts about a factor of 10 more slowly than expected. These results may be related in some way to the prior observation that a *p*-trimethylammonium substituent greatly retards the rate of deacylation (24), although there is no evidence that the acyl groups of these three *para*-substituted cinnamoylchymotrypsins are in similar environments at the enzyme active site.

A plot of the logarithm of k_3' against the logarithm of k_{OH} gives a plot similar to Fig. 1. The points for the *p*-methyl- and *p*-trifluoromethyl-substituted compounds again lie off the correlation line but the deviations are not so large as those in Fig. 1.

p*H*-reactivity studies of the action of α-chymotrypsin have repeatedly implicated a group on the enzyme with a p*K* of approximately 7 in the catalytic mechanism (4, 23). This group, which controls the rate of deacylation, has usually been assigned to histidine-57 (25, 26) although more recent evidence indicates that the buried carboxyl group of aspartate-102 may be this group (27). Interestingly, the apparent p*K* of the group involved in enzyme deacylation (determined kinetically) changes with the structure of the acyl group (11, 18, 23, 29). Bernhard *et al.* have indicated, for a variety of acyl groups, that this p*K* is linearly related to the p*K* of the corresponding free acid: the more acidic is the free acid, the lower is the p*K* observed in the deacylation reaction of the corresponding acylenzyme (11). Although we do not have available p*K* data for the acids employed in this study under our experimental conditions, the data in Table 3 are qualitatively consistent with the observations of

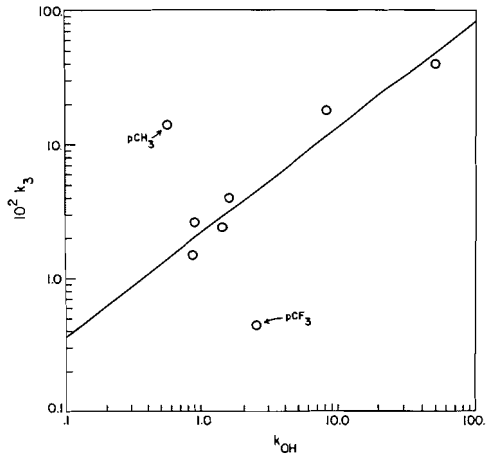

FIG. 1. Correlation of the rate of basic hydrolyses of various cinnamate *p*-nitrophenyl esters (k_{OH}) with the rate of deacylation of the corresponding acylchymotrypsin (k_3) (data from Table 3).

the Bernhard group. The pentafluoro- and α-fluorocinnamic acids are expected to be the most acidic of the group studied here because of the inductive effects of the fluorine atoms; in each of these cases the observed p*K* which determines the kinetics of deacylation of the corresponding acylenzyme is low. Similarly, the observed p*K*'s for the remaining cinnamoyl systems correlate reasonably well with Hammett's σ parameters.

There is little indication from this work that single substitution of fluorine atoms on the carbons of the double bond or the aromatic ring of the cinnamoyl group produce any special enzyme–cinnamoyl interaction that has kinetic consequences. In these cases, except for their electronic effect, fluorine atoms appear to be able to masquerade as hydrogen atoms. Substituents at the *para* position more bulky than a single fluorine do have an unexplained influence on the rate of deacylation; a methyl group in this location has an accelerating effect but if the hydrogen atoms of the methyl group are replaced by fluorine atoms, a substantial slowing of the deacylation reaction results. It seems likely, therefore, that contacts between the enzyme and the aromatic end of the cinnamoyl group are sufficient to significantly modify the positions of the atoms at the site of reaction for these cases. The abnormally low reactivity of the *p*-trifluoromethyl cinnamoyl enzyme warns that spectroscopic investigations of this protein by u.v. or magnetic resonance techniques may

not provide data that are particularly relevant to the nature of the other acylenzymes examined in this work. We hope that fluorine n.m.r. experiments in progress will illuminate this point.

1. E. ZEFFREN and P. L. HALL. The study of enzyme mechanisms. Wiley, New York. 1973. p. 168.
2. G. P. HESS. *In* The enzymes. Vol. 3. *Edited by* P. D. Boyer. Academic, New York. 1971. Chapt. 7.
3. W. P. JENCKS. Catalysis in chemistry and enzymology. McGraw-Hill, New York. 1969. p. 218.
4. T. C. BRUICE and S. J. BENKOVIC. Bioorganic mechanisms. Vol. 1. Benjamin, New York. 1966. p. 212.
5. M. L. BENDER and F. J. KEZDY. Ann. Rev. Biochem. **34**, 49 (1965).
6. M. L. BENDER. Chem. Rev. **60**, 53 (1960).
7. R. HENDERSON. J. Mol. Biol. **54**, 341 (1970).
8. C.-C. WANG and E. SHAW. Arch. Biochem. Biophys. **150**, 259 (1972).
9. J. E. C. HUTCHINS and T. H. FIFE. J. Am. Chem. Soc. **94**, 8848 (1972).
10. K. BROCKLEHURST and K. WILLIAMSON. Biochem. Biophys. Res. Commun. **26**, 175 (1967).
11. (*a*) S. A. BERNHARD, E. HERSHBERGER, and J. KEIZER. Biochemistry, **5**, 4120 (1966); (*b*) S. A. BERNHARD, B. F. LEE, and Z. H. TASHJIAN. J. Mol. Biol. **18**, 405 (1966).
12. M. L. BENDER, G. R. SCHONBAUM, and B. ZERNER. J. Am. Chem. Soc. **84**, 2540 (1962).
13. C. G. MILLER and M. L. BENDER. J. Am. Chem. Soc. **90**, 6850 (1968).
14. A. L. FINK. Biochemistry, **12**, 1736 (1973).
15. W. A. HUESTIS and M. A. RAFTERY. Biochemistry, **11**, 1648 (1972).
16. E. W. BITTNER and J. T. GERIG. J. Am. Chem. Soc. **92**, 5001 (1970).
17. (*a*) J. T. GERIG and J. D. REINHEIMER. J. Am. Chem. Soc. **92**, 3146 (1970); (*b*) J. T. GERIG, B. A. HALLEY, C. E. ORTIZ, and J. A. REIMER. Work in progress.
18. M. CAPLOW and W. P. JENCKS. Biochemistry, **1**, 833 (1962).
19. A. WILLIAMS and G. SALVADORI. J. Chem. Soc. (B), 2401 (1971).
20. (*a*) T. H. FIFE and J. B. MILSTEIN. Biochemistry, **6**, 2901 (1967); (*b*) P. M. ENRIQUEZ and J. T. GERIG. Biochemistry, **8**, 3156 (1969).
21. K. C. AUNE and S. N. TIMASHEFF. Biochemistry, **10**, 1609 (1971).
22. (*a*) A. N. GLAZER. J. Biol. Chem. **242**, 4528 (1967); (*b*) J. T. GERIG and D. C. ROE. J. Am. Chem. Soc. **96**, 233 (1974).
23. A. R. FERSHT and Y. REQUENA. J. Am. Chem. Soc. **93**, 7079 (1971).
24. J. R. KNOWLES and J. M. PRESTON. Biochim. Biophys. Acta, **151**, 290 (1968).
25. G. SCHOELLMANN and E. SHAW. Biochemistry, **2**, 252 (1963).
26. W. H. CRUICKSHANK and H. KAPLAN. Biochem. J. **130**, 1125 (1972).
27. M. W. HUNKAPILER, S. H. SMALLCOMBE, D. R. WHITTAKER, and J. H. RICHARDS. Biochemistry, **12**, 4732 (1973).
28. R. L. VANDLEN and A. TULINSKY. Biochemistry, **12**, 4193 (1973).
29. J. L. MARINI and M. CAPLOW. J. Am. Chem. Soc. **93**, 5560 (1971).
30. M. M. KOTON, E. P. MOSKVINA, and F. S. FLORINSKII. Zhur. Obshchei Khim. **21**, 1843 (1951).
31. D. S. RITTER and S. I. MILLER. J. Am. Chem. Soc. **86**, 1507 (1964).
32. A. K. BARBOUR, M. W. BUXTON, P. L. COE, R. STEPHENS, and J. C. TATLOW. J. Chem. Soc. 808 (1961).
33. T. A. WITTSTRUCK and E. N. TRACHTENBERG. J. Am. Chem. Soc. **89**, 3803 (1967).
34. R. ANSCHÜTZ. Ber. **60**, 1320 (1927).

Can. J. Chem. Downloaded from www.nrcresearchpress.com by 210.87.254.5 on 09/05/12
For personal use only.

Sodium Borohydride Reduction of 1-Acyl-1,2(1*H*)-diazepines and their Iron Tricarbonyl Complexes. Some Reactions of 2,3-Dihydro-1,2(1*H*)-diazepines

TAKASHI TSUCHIYA[1] AND VICTOR SNIECKUS

Department of Chemistry, University of Waterloo, Waterloo, Ontario N2L 3G1

Received August 13, 1974

Can. J. Chem. Downloaded from www.nrcresearchpress.com by 210.87.254.40 on 09/05/12
For personal use only.

TAKASHI TSUCHIYA and VICTOR SNIECKUS. Can. J. Chem. **53**, 519 (1975).

Sodium borohydride reduction of the 1,2(1*H*)-diazepines **1***a–e* and **7**, and the 1,2(1*H*)-diazepine iron tricarbonyl complexes **4***a–b* provides the 2,3-dihydro-1,2(1*H*)-diazepines **2***a–e* and **8**, and the (2,3-dihydro-1,2(1*H*)-diazepine)$Fe(CO)_3$ derivatives **5***a–b*, respectively. $Fe(CO)_3$ complexes **5***a* and **6***a* may be also directly obtained from the 1,2(1*H*)-diazepines **2***a* and **3***a*, respectively. A number of diacylated compounds (**3***a–c*, **6***a–b*, and **9**) are prepared some of which (**2***a*, **3***a*, **8**, and **9**) are readily converted into their corresponding $(4 + 2)\pi$ cycloadducts (**14***a–d*). Treatment of the borohydride reduction products **2***a–c* with sodium methoxide in methanol gives the 3,4-dihydro-1,2(2*H*)-diazepines **15***a–c*. Acetylation of **15***a* affords the 2-acetyl derivative **16***a* which may also be prepared by sodium methoxide deacetylation of either **3***a* or **9**. 2-Tosyl-3,4-dihydro-1,2(2*H*)-diazepine (**18**) is obtained from **2***a* by a similar tosylation and deacetylation sequence. When either **2***a* or **3***a* are subjected to sodium methoxide in methanol-*O-d*, compounds **15***a* and **16***a*, respectively, are produced which show high deuterium incorporation at C_4 and C_6 (n.m.r. analysis). Photolysis of the 2,3-dihydro-1,2(1*H*)-diazepines **2***a*, **3***a*, **8**, and **9** and the 3,4-dihydro-1,2(2*H*)-diazepine **16***a* affords the unstable 2,3-diazabicyclo[3.2.0]hept-6-ene **23***a*, **23***b*, **25***a*, and **25***b* and 1,2-diazabicyclo[3.2.0]hept-6-ene **27** derivatives, respectively. Treatment of either **25***a* or **25***b* with sodium methoxide results cleanly in N_2-deacylation to give compound **26**.

TAKASHI TSUCHIYA et VICTOR SNIECKUS. Can. J. Chem. **53**, 519 (1975).

La réduction des (1*H*)-diazépines-1,2 (**1***a–e* et **7**) de même que les complexes fer-tricarbonyl des (1*H*)-diazépines-1,2 (**4***a* et **4***b*), par le borohydrure de sodium, conduit dans le premier cas aux dihydro-2,3(1*H*)-diazépines-1,2 (**2***a–e* et **8**) et dans le deuxième cas aux complexes fer-tricarbonyl des dihydro-2,3 (1*H*) diazépines-1,2 (**5***a–b*). Les complexes fer-tricarbonyl de **5***a* et de **6***a* peuvent aussi tre obtenus d'une façon directe à partir des (1*H*)-diazépines-1,2, **2***a* et **3***a*. On a préparé un certain nombre de dérives diacétylés (**3***a–c*, **6***a–b* et **9**); la cycloaddition $(4 + 2)\pi$ des composés **2***a*, **3***a*, **8** et **9** conduit facilement aux produits (**14***a–d*) correspondants. Le traitement, des produits **2***a–c* par le méthylate de sodium dans le méthanol conduit aux dihydro-3,4 (2*H*)-diazépines-1,2 (**15***a–c*). L'acétylation de **15***a* conduit à **16***a*, acétylé en position 2; ce dérivé peut aussi être préparé par la déacétylation, à l'aide du méthylate de sodium, soit de **3***a* ou de **9**. On obtient la tosyl-2 dihydro-3,4 (2*H*) diazépine-1,2 (**18**) en soumettant **2***a* à une réaction de tosylation puis une réaction de déacétylation. Quand ont soumet soit **2***a* soit **3***a* à l'action du méthylate de sodium dans le méthanol-*O-d*, il y a production respectivement de **15***A* et de **16***a* dans lesquels il y a (d'après l'analyse par r.m.n.) une forte incorporation de deutérium en C_4 et en C_6. La photolyse des dihydro-2,3 (1*H*)-diazépines-1,2 (**2***a*, **3***a*, **8** et **9**) ainsi que celle de la dihydro-3,4 (2*H*)-diazépine-1,2 (**16***a*) fournit d'une part les diaza-2,3 bicyclo[3.2.0] heptènes-6 (**23***a*, **23***b*, **25***a* et **25***b*) qui sont instables et d'autre part le diaza-1,2 bicyclo[3.2.0] heptène-6 (**27**). Le traitement soit de **25***a* ou de **25***b* avec le méthylate de sodium conduit à une N_2 déacylation conduisant au composé **26**.

[Traduit par le journal]

As part of our continuing investigation of the organic (1) and organometallic (2) chemistry of 1,2(1*H*)-diazepines, we have studied the sodium borohydride reduction of the 1-acetyl- and 1-carbethoxy-1,2(1*H*)-diazepines (**1***a–e* and **7**) and the corresponding iron tricarbonyl derivatives (**4***a–b*). This reaction has provided the 2,3-dihydro-1,2(1*H*)-diazepines (**2***a–e*, **5**, and **8**) (Scheme 1), some of which by base treatment have given rise to 3,4-dihydro-1,2(2*H*)-diazepine derivatives (**15***a–c*) (Scheme 3). These results together with the photochemical (Scheme 4) and Diels–Alder (Scheme 2) reactivity of several

[1]On leave of absence from The School of Pharmaceutical Sciences, Showa University, Tokyo, Japan.

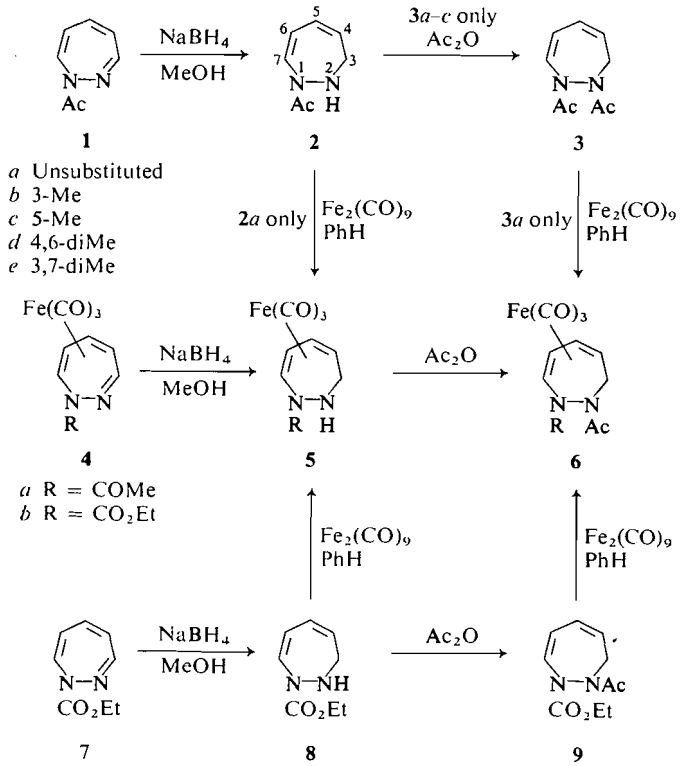

SCHEME 1

examples of both dihydro series constitute the present report.[2] Previous work has dealt with acid- (4, 5) and base- (4, 6) catalyzed, thermolytic (1*b*, 4, 6, 7), photochemical (1*b*, 6), and cycloaddition (5, 8, 9) reactions of simple and aryl substituted 1,2(1*H*)-diazepine derivatives. In comparison to the extensive studies on the 1,2-diazepin-4-one system by Moore and coworkers (10), the chemistry of the 1,2(1*H*)-diazepines is in the initial stages of exploration.

Sodium Borohydride Reduction

Sodium borohydride reduction of 1-acetyl-1,2(1*H*)-diazepine (**1***a*) in methanol solution gave, after chromatography, a single compound (75–80%) whose analytical and spectral data are consistent with 2,3-dihydro-1,2(1*H*)-diazepine formulation **2***a* (Scheme 1). The i.r. spectrum showed absorption at 3300 (NH) and 1660 (C=O) cm^{-1} while the 90 MHz n.m.r. spectrum exhibited signals as indicated aside the structural formula below. Assignments were made by reference to the n.m.r. spectrum of *1a* (11) and coupling constants were confirmed by decoupling experiments. The n.m.r. information in particular speaks against the alternate dihydro structures **10** (R = H) and **11** (R = H) in which coupling of the low field signal (C_3—H in both strucutes) with NH would have been expected. Due to some uncertainty of this spectral analysis, it was necessary to obtain chemical evidence in order to eliminate the alternate structures from further consideration. Towards this end, the methyl substituted 1,2(1*H*)-diazepines **1***b* and *c* were analogously reduced to give single products in high yields which showed, *inter alia*, methyl resonances at τ 1.21 (d, 3H, J = 7 Hz) and τ 1.87 (s, 3H), respectively. These data are consistent with the assignment of structures **2***b* and *c*, respectively, for the two products and not with alternate respective formulations, **10** (R = Me) and **11**

[2]During the preparation of the manuscript, a report appeared on the diborane and diisobutylaluminum hydride reduction of 1,2(1*H*)-diazepine derivatives (3). Our results, although partially complementary, are more extensive and overlap only in the obtainment of two compounds (**8** and **23***b*).

Can. J. Chem. Downloaded from www.nrcresearchpress.com by 210.87.254.40 on 09/05/12
For personal use only.

Can. J. Chem. Downloaded from www.nrcresearchpress.com by 210.87.254.40 on 09/05/12
For personal use only.

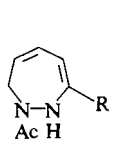

10

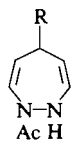

11

(R = Me). Additional data for compounds **2***b* and *c* as well as complete analytical, physical, and spectral information on the borohydride reduction products **2***d*, **2***e*, and **8** are collected in Table 1.[3] Spectral data for **8** are in good agreement with those reported by Streith and Willig for this compound obtained by diborane reduction of **7** (3).

Thus the 1-acyl-1,2(1*H*)-diazepine ring system (**1**) shows normal reactivity towards sodium borohydride in that the C=N function is reduced. The remaining *N*-acyl dienamine moiety in the product (**2**) is not susceptible to further reduction under the mild conditions of the reaction.

Reduction of the iron tricarbonyl 1,2(1*H*)-diazepine complexes **4***a* (2*a*) and **4***b* (4) provided the dihydro derivatives **5***a* (45%) and **5***b*, respectively (Scheme 1). In agreement with the structural assignment, compound **5***a* showed i.r. absorption at 3420 (NH), 2040, 1970, and 1950 (C≡O), 1655 (C=O), and 1635 and 1600 (C=C) cm^{-1} and n.m.r. parameters indicated aside the structural formula below. The $Fe(CO)_3$ complexes **5***a* and *b* could also be obtained from the reaction of compounds **2***a* and **8** with nonacarbonyldiiron(0). The instability of **5***b* precluded its characterization; therefore, it was immediately converted into its stable acetyl derivative (**6***b*) (65%). Complete analytical, physical, and spectral data for **5***a*, **6***a*, and **6***b* are recorded in Table 2.[3]

In fact, most of the other dihydro 1,2(1*H*)-diazepine derivatives (**2***a–c*, **5***a*, **8**) were found to be somewhat unstable under ordinary laboratory conditions. Therefore these compounds were also transformed into their stable acetyl derivatives (**3***a–c*, **6***a*, and **9**) (Scheme 1). Analytical and spectral data are summarized in Tables 1 and 2.[3] It is of interest to compare the n.m.r. spectra of compounds **3***a* and **6***a* with their corresponding

[3]Tables 1–5 are placed in the Depository of Unpublished Data and are available, at a nominal charge, from the National Science Library, National Research Council of Canada, Ottawa, Canada K1A 0S2.

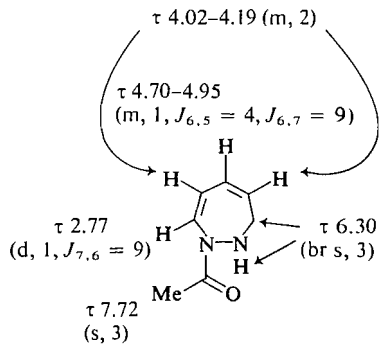

2*a*

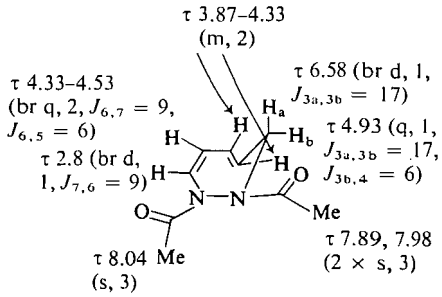

3*a* ≡ **13**

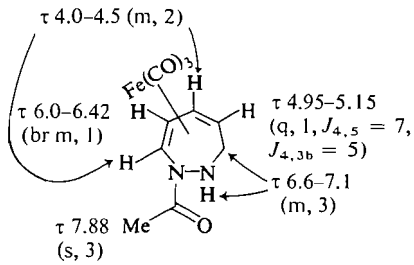

5*a*

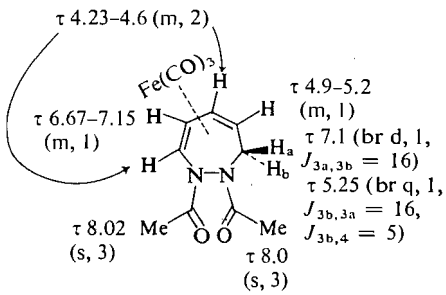

6*a*

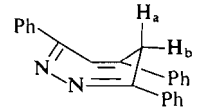

12

Can. J. Chem. Downloaded from www.nrcresearchpress.com by 210.87.254.40 on 09/05/12
For personal use only.

immediate precursors, **2***a* and **5***a*, respectively (see structures above). Whereas the C_3-methylene protons in **2***a* and **5***a* appeared as broad singlets at τ 6.30 and 6.6–7.1, respectively, these protons in the corresponding acetyl derivatives **3***a* and **6***a* were observed at chemical shift separations Δ p.p.m. $\approx$1.6 and 1.85, respectively. The behavior of **3***a* and **6***a* is reminiscent of 3,5,7-triphenyl-1,2(4*H*)-diazepines (**12**) and their corresponding diazepinium salts in which similar large chemical shift differences could be attributed to anisotropic effects on the methylene protons (H_a and H_b in **12**) (1*a*, 12). Similar behavior has been noted in some closely related 1,2-diazepin-4-one derivatives (13).[4] In the case of **3***a*, n.m.r. parameters for the C_3-methylene protons argue in favor of representation **13** for the predominant conformation. In this conformation, the anisotropic effects of the quasiequatorial N_2—Ac function are clearly more pronounced on H_b than on H_a in agreement with the assignments labelled on the structure. However, the n.m.r. spectrum of **3***a* at room temperature also shows the presence of a minor contributing conformational isomer (<5%). Thus these assignments are tentative pending a detailed temperature variable n.m.r. spectral (including line shape) analysis.[5] Another point of interest is the complicated N—Ac methyl absorptions in the n.m.r. spectra of **3***a* as well as the other acyl derivatives **3***b* and **3***c*. In sharp contrast to the corresponding NH systems (**2***a–c*), compounds **3***a–c* showed at least three N—Ac methyl signals at ambient temperature. For example, **3***a* shows two major singlets at τ 7.89 and 8.04 and a minor peak at τ 7.98. Most probably, these observations indicate the occurrence of N—Ac hindered rotation and/or inversion phenomena (13, 14) which, as a result of their apparent complexity, require a more detailed analysis.[5]

Several of the 2,3-dihydro-1,2(1*H*)-diazepines (**2***a*, **3***a*, **8**, and **9**) were converted into the (4 + 2)π cycloaddition products **14***a–d* with 4-phenyl-1,2,4-triazoline-3,5-dione (Scheme 2). Sasaki and his co-workers have previously shown that 1,2(1*H*)-diazepines exhibit this type of behavior with this reactive dienophile as well as with tetracyanoethylene (TCNE) (8). Furthermore, Streith and Willig have obtained some [4 + 2]π cycloadducts from the reaction of 2,3-dihydro-1,2(1*H*)-diazepines with TCNE and have offered a possible explanation for the much higher reactivity of the dihydrodiazepines in comparison to their fully unsaturated counterparts (3). The adducts **14***a–d* were also obtained in high yield under mild conditions. The collected analytical, physical, and spectral data (Table 3)[3] are in agreement with the normal Diels–Alder formulations **14***a–d* for the structures of these products. The n.m.r. spectral assignments (*e.g.* for **14***a* and *b* below) were derived by comparison with those of similar adducts of 1,2-diazepine (8) and dihydro-1,2-diazepine (3) systems and by effecting appropriate decoupling experiments. Contrary to the 1,2(1*H*)-diazepine–TCNE and -triazoline–dione adducts which undergo predominant mass spectral fragmentation by a retro-Diels–Alder reaction (8), the adducts **14***a–d* show a major common peak at *m/e* 227 corresponding to the loss of the —N_2—N_3—C_4— bridge. Common fragments are also observed at *m/e* 119 and 80 which may correspond to PhNCO and pyridazine, respectively, and may be derived

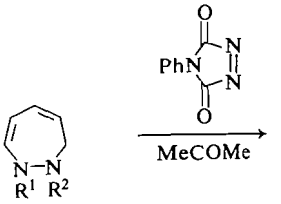

2*a* R^1 = COMe; R^2 = H
3*a* R^1 = R^2 = COMe
8 R^1 = CO_2Et; R^2 = H
9 R^1 = CO_2Et; R^2 = COMe

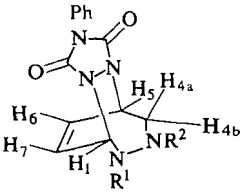

14

a R^1 = COMe; R^2 = H
b R^1 = R^2 = COMe
c R^1 = CO_2Et; R^2 = H
d R^1 = CO_2Et; R_2 = COMe

SCHEME 2

[4]We thank a referee for drawing our attention to this report.

[5]T. E. Gough, D. J. Harris, and V. Snieckus, in preparation.

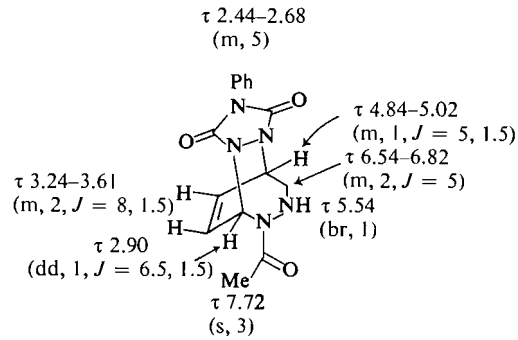

14*a*

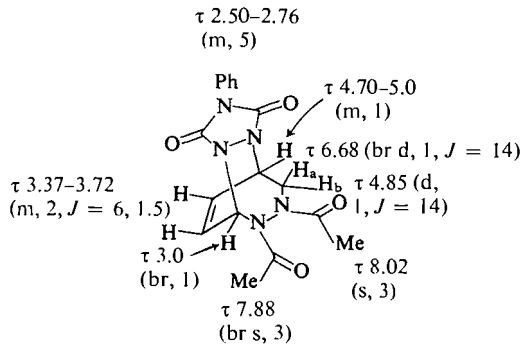

14*b*

from the *m/e* 227 fragment. Minor H_2 loss from **14*a*** and *c* and major CH_2CO loss from **14*b*** and *d* are also evident.

Base-catalyzed Deacylation

Treatment of 1-acetyl-2-3-dihydro-1,2(1*H*)-diazepine (**2*a***) with an excess of sodium methoxide in methanol at room temperature gave the unstable 3,4-dihydro-1,2(2*H*)-diazepine (**15*a***) (Scheme 3). Of the three mechanistically reasonable dihydro-diazepines which may have been formed, the spectral data are consistent only with structure **15*a***. The available data also eliminate less plausible diazabicyclo[3.2.0]heptane derivatives which require *a priori* consideration in view of the past history of diverse ring contractions and rearrangements in the related 1,2-diazepin-4-one series (10). Compound **15*a*** shows i.r. absorption at 3300 (NH) and 1660 (C=N) cm^{-1} and u.v. (max) at 238 (3600) and 303 (3330) nm, the latter indicating extended conjugation. Its n.m.r. spectrum (indicated on structural formula **15*a***) also provides strong evidence for the structural assignment. As a consequence of its instability, **15*a*** was converted to the N_2—Ac derivative **16*a*** which could also be obtained by deacetylation of **3*a*** or decarbethoxylation of **9** under basic conditions. The transformation **9** → **16*a*** as well as the deacetylation of the N_2—Ts derivative **17** (obtained from **2*a*** by treatment with tosyl chloride and pyridine) to **18** offers clear evidence that N_2 is the common site of base-catalyzed deacylation.[6] The i.r. spectrum of **16*a*** shows absorption at 1670 (C=O) cm^{-1} and its u.v. and n.m.r. spectra (u.v. (max) 237 (3150) and 299 (4150) nm; n.m.r. indicated in structural formula **16*a*** below) are, as expected, very similar to those of **15*a***. Moreover, the close similarity of the n.m.r. spectrum of **15*a*** with that observed for the analogous compound, 2-benzoyl-7-phenyl-3,4-dihydro-1,2(2*H*)- diazepine may be noted (15).

The transformation **15*a*** → **16*a*** is of some interest in connection with the similar reaction of the 2,3-dihydro-1,2-diazepin-4-one **19** which, depending on conditions, gives either seven-membered ring (**20**) or bicyclic (**21**) tosyl or acyl derivatives (16, 17). The end result appears to depend on whether or not the N_2-anion of **19** is generated under the conditions of the tosylation or acylation reactions. Attempts to determine if similar behavior would be observed for compound **15*a*** have not been fruitful. Thus using Moore's experiments as a basis (16, 17), tosylation (TsCl, pyridine or NaH, TsCl, glyme) and acylation (MeCOCl, $PhNMe_2$, pyridine, or Et_3N) at a variety of temperatures were carried out to give reaction mixtures which underwent decomposition to red polymeric material upon attempted work-up.[7] In the case of **19**, it is possible that the course of the reaction and stability of the products are strongly influenced by the presence of the carbonyl function.

Compounds **2*b*** and **2*c*** were similarly deacetylated to give **15*b*** and **15*c***, respectively (Scheme 3). The spectral data (Table 4)[3] of **15*b*** and **15*c*** as well as of the N_2—Ac derivative (**16*c***) of the latter are also consistent with the 3,4-dihydro-1,2(2*H*)-diazepine representation and provide firm evidence against 1,2-diazabicyclo[3.2.0]heptane formulations for these products. The reaction undoubtedly involves the intermediacy of the N_1-

[6]Attempts to directly decarbethoxylate **8** with sodium methoxide gave mainly the corresponding carbomethoxy derivative by ester exchange together with a small amount of **15*a*** (see Experimental).

[7]We thank D. J. Harris for these experimental results.

Can. J. Chem. Downloaded from www.nrcresearchpress.com by 210.87.254.40 on 09/05/12
For personal use only.

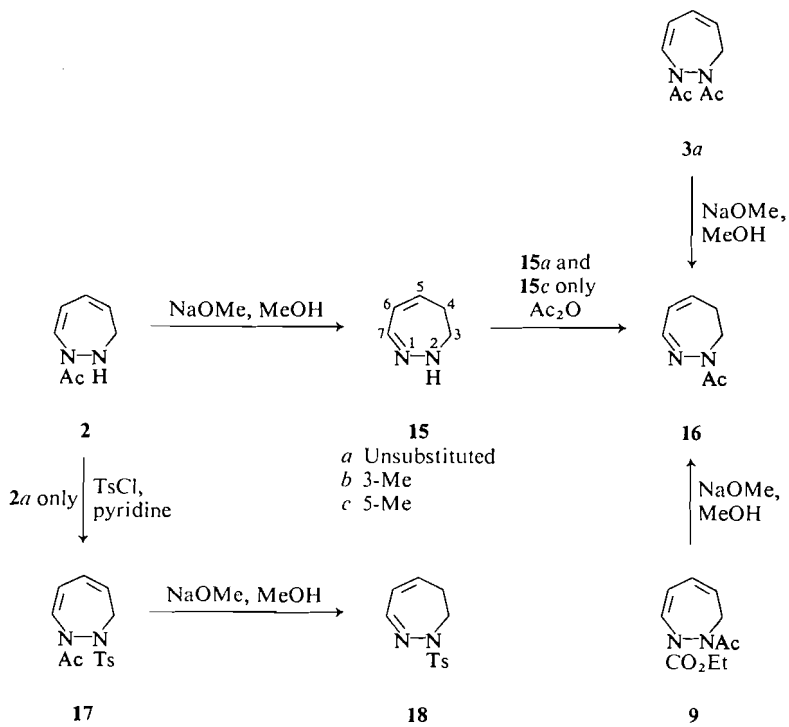

SCHEME 3

anion **22** since deacetylation of **2***a* and **3***a* using sodium methoxide in methanol-*O*-*d* gave, respectively, compounds **15***a* and **16***a* deuterated at C_4 and C_6 as evidenced by n.m.r. analysis (see Experimental). Protonation of the anion **22** then occurs at C_4 rather than at N_1 to generate the

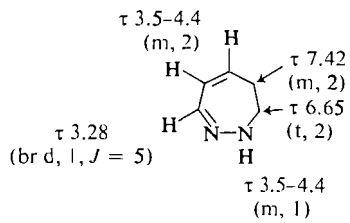

15*a*

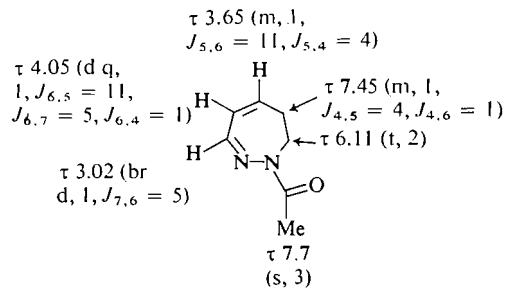

16*a*

thermodynamically more stable ene-hydrazine **15***a* or **16***a* as has been well established in other systems (18).

Photocyclization

Photolysis of the 2,3-dihydro-1,2(1*H*)-diazepines **2***a*, **3***a*, **8**, and **9** gave the 2,3-diazabicyclo-[3.2.0]hept-6-ene derivatives **23***a–b* and **25***a–b* whereas irradiation of the 3,4-dihydro-1,2(2*H*)-diazepine **16***a*[8] yielded the 1,2-diazabicyclo-[3.2.0]hept-6-ene **27** (Scheme 4). Unsaturated and more highly substituted derivatives of both bicyclic systems have been previously obtained by photolysis (1*b*, 6, 19). The NH compounds **23***a* and *b* were highly unstable but they were readily converted into the N—Ac derivatives **25***a* and *b* which were found to be identical with the photoproducts obtained directly from **3***a* and **9**, respectively. An N—Ts derivative **24** was also prepared for additional characterization purposes.

The structures of the bicyclic compounds **23–25** and **27** rest on their analytical and spectral data (Table 5).[3] Comparison of their n.m.r.

[8]Irradiation of the corresponding deacetyl compound **15***a* led only to decomposition.

Can. J. Chem. Downloaded from www.nrcresearchpress.com by 210.87.254.40 on 09/05/12
For personal use only.

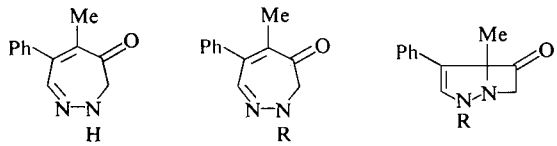

19 20 21

R = Ts or COR′

22

R = H or Ac

spectra with those reported previously for other derivatives of these ring systems (6, 19) was helpful in the proton assignments. Nuclear magnetic resonance parameters for selected examples (**23***a*, **25***a*, and **27**) are given in the structural formulae below. Compound **23***b* was likewise obtained by Streith and Willig (3); our spectral data and theirs show close correspondence. *Cis* ring juncture stereochemistry is assigned to all compounds on the basis of the expected disrotatory mode of the photochemical electrocyclic reaction.

Finally, treatment of **25***a* or *b* with sodium methoxide in refluxing methanol cleanly gave compound **26**. Presumably the steric compression between the N_2-acetyl function and the C_1-hydrogen is responsible for the preferential N_2-deacetylation leading to the anion **28**. The interesting possibility that stabilization by homoconjugation with the C_6—C_7 double bond in **28** is in part responsible for the exclusive N_2-deacetylation was tested by subjecting compound **25***a* to the conditions of sodium methoxide in methanol-*O*-*d*. No incorporation of deuterium at C_6 was found (n.m.r. analysis) thus excluding this possibility.

The chemistry of a number of the dihydro-1,2-diazepine derivatives described in the present report is being explored.

Experimental

Melting points were determined on a Fisher-Johns apparatus and are uncorrected. Analyses were performed by A. B. Gygli, Toronto, Ontario and by Microanalytical Laboratories, Showa University, Tokyo, Japan. The i.r. spectra were recorded on Beckman IR-5A and -10 instruments in chloroform solution unless otherwise

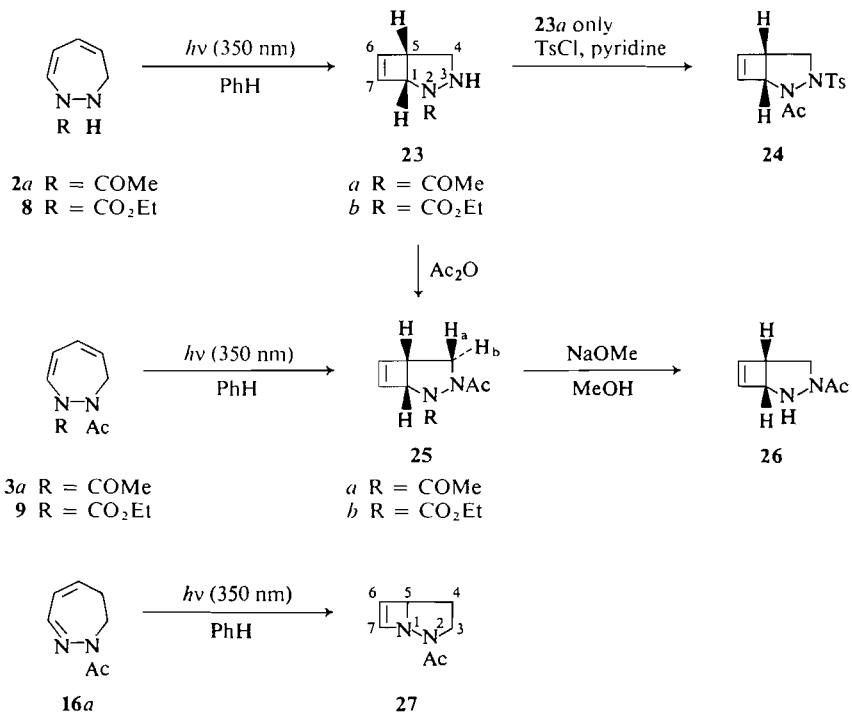

SCHEME 4

Can. J. Chem. Downloaded from www.nrcresearchpress.com by 210.87.254.40 on 09/05/12
For personal use only.

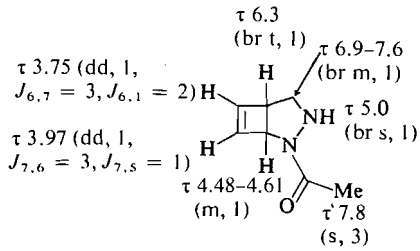

23a

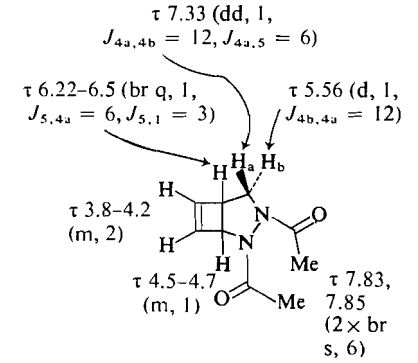

25a

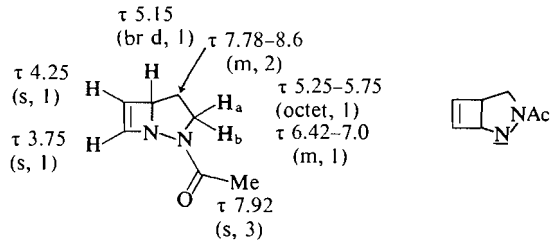

27 **28**

noted. The u.v. spectra were measured on a Beckman DB-G spectrophotometer in ethanol solution. The n.m.r. spectra were recorded on Varian T-60 and HA-100 and Perkin Elmer-Hitachi 90 MHz spectrometers in deuteriochloroform solution using TMS as internal standard. In spectral tabulations, abbreviations for multiplicity are given as follows: br = broad, s = singlet, d = doublet, t = triplet, q = quartet, and m = multiplet. Mass spectra were determined with Hitachi-Perkin Elmer RMU-6E and AE1 MS-30 spectrometers. Thin-layer, preparative-thick-layer, and column chromatography were performed with silica gel specified for these purposes and obtained from Brinkmann (Canada) Ltd. Photolyses were carried out in a Rayonet Type RS Photochemical Reactor equipped with 3500-Å lamps using a Pyrex vessel cooled internally to 10–20° by a cold finger.

1-Acetyl-1,21(*H*)-diazepines (**1***a–e*, and **7**) and the irontricarbonyl complexes (**4***a* and *b*) were prepared by previously described methods (2*b*, 6, 11).

*Preparation of 2,3-Dihydro-1,2(1H)-diazepines (**2***a–e* **5***a–b*, **8**) (General Procedure)*

To a solution of the 1-acyl-1,2(1*H*)-diazepine (**1***a–e* and **7**) (0.2–0.3 g) in absolute methanol (30–40 ml) was added solid sodium borohydride (0.2–0.3 g) in small portions with stirring at room temperature. The solution was stirred further at room temperature for 5–6 h and then was evaporated to dryness *in vacuo* below 30°. The residue was cooled in an ice bath and treated with ice-water (10–15 ml). The resulting aqueous mixture was extracted with methylene chloride (2 × 50 ml). The organic extract was dried ($MgSO_4$) and evaporated to dryness to yield a yellow oil which, upon column chromatography (C_6H_6–CH_2Cl_2, 1:1 or CH_2Cl_2 eluents) gave the 2,3-dihydro-1,2(1*H*)-diazepines **2***a–e* and **8**.

The reduction of the irontricarbonyl complexes (**4***a–b*) to yield the corresponding dihydro complexes **5***a–b* was carried out similarly except that the reactions were effected under nitrogen and ethyl acetate was used as the eluent in chromatography.

The yields as well as full analytical, physical, and spectral data for compounds **2***a–e*, **5***a–b*, and **8** are collected in Table 1.[3]

*Formation of 2-Acetyl-2,3-dihydro-1,2(1H)-diazepines (**3***a–c*, **6***a–b*, and **9**) (General Procedure)*

A solution of the 2,3-dihydro-1,2(1*H*)-diazepine (**2***a–c*, **5***a–b*, and **8**) (*ca.* 100 mg) in acetic anhydride (4–5 ml) was allowed to stand at room temperature for 12–16 h. Excess acetic anhydride was evaporated *in vacuo* and the resulting residue was subjected to column chromatography (eluent: for **3***a–c* and **9**: C_6H_6–CH_2Cl_2, 1:1; for **6***a–b*: C_6H_6–EtOAc) to yield the pure compounds.

The yields as well as analytical, physical, and spectral data are presented in Table 1.[3]

*Reaction of 2,3-Dihydro-1,2(1H)-diazepines (**2***a*, **3***a*, **8**, and **9**) with $Fe_2(CO)_9$. Formation of $Fe(CO)_3$ Complexes (**5***a–b*, **6***a–b*) (General Procedure)*

To a solution of the ligand (**2***a*, **3***a*, **8**, and **9**) (0.2 g) in dry, degassed benzene (50 ml) was added an excess of $Fe_2(CO)_9$ (0.6 g) and the mixture was stirred in the dark at room temperature under nitrogen for 2 days. Solid material was removed by filtration and the filtrate was evaporated to dryness *in vacuo*. The resulting residue was dissolved in a small amount of benzene and subjected to column chromatography. Elution with C_6H_6–EtOAc (1:1) gave the yellow crystalline $Fe(CO)_3$ complex (**5***a*, **6***a–b*).

Complex **5***a*, obtained by the above method, was shown to be identical with the product of sodium borohydride reduction of **4***a* by m.p. and mixture m.p. determination. Likewise, complex **6***a* was shown to be identical with the acetylation product of **5***a*. Complex **5***b* could not be obtained in pure form due to extreme instability; it was therefore immediately acetylated (acetic anhydride, room temperature, overnight) to give complex **6***b*. Complex **6***b* thus obtained was found to be identical with the product of reaction between **9** and $Fe_2(CO)_9$ by m.p. and mixture m.p. determination.

Complete data for compounds **5***a* and **6***a–b* are given in Table 2.[3]

Can. J. Chem. Downloaded from www.nrcresearchpress.com by 210.87.254.40 on 09/05/12
For personal use only.

Can. J. Chem. Downloaded from www.nrcresearchpress.com by 210.87.254.40 on 09/05/12
For personal use only.

[4 + 2]π Cycloaddition Reaction of Compounds **2a**, **3a**, **8**, *and* **9** *with 4-Phenyl-1,2,4-triazoline-3,5-dione. Formation of Adducts* **14a–d** *(General Procedure)*

To a solution of the 2,3-dihydro-1,2(1*H*)-diazepine (**2a**, **3a**, **8**, and **9**) (100–200 mg) in dry acetone (5–10 ml) was added slowly with stirring at room temperature a solution of 4-phenyl-1,2,4-triazoline-3,5-dione (1.1 equiv.) in dry acetone (5 ml). The deep red color of the added reagent was discharged instantaneously. The solution was allowed to stand at room temperature for 2–3 h and was then evaporated to dryness *in vacuo*. The resulting residue was triturated with methanol to yield a solid which was collected by filtration and recrystallized from benzene or acetone to give colorless crystals of adducts (**14a–d**) (80–90%) whose analytical, physical, and spectral data are given in Table 3.[3]

Reaction of 1-Acyl-2-3-dihydro-1,2(1H)-diazepines **2a–c**, **3a**, **9**, *and* **17** *with Sodium Methoxide. Formation of 3,4-Dihydro-1,2(2H)-diazepines* **15a–c**, **16a**, *and* **18** *(General Procedure)*

To a solution of the 1-acyl-2,3-dihydro-1,2(1*H*)-diazepines (**2a–c**, **3a**, **9**, and **17**) (0.2–0.3 g) in methanol (30–40 ml) was added excess sodium methoxide (0.3 g) and the reaction was allowed to proceed at room temperature for the following duration depending on compound: **2a–c** (8–12 h), **3a** (32 h or 6–7 h at reflux), **9** (48 h), **17** (21 h). The pale yellow solution was evaporated to dryness *in vacuo* and the resulting residue was extracted with methylene chloride (2 × 50 ml). Column chromatography (CH_2Cl_2–MeOH, 95:5 eluent) gave the 3,4-dihydro-1,2(2*H*)-diazepines (**15a–c** (40–60%), **16a** (80%), and **18** (70%)). With the exception of **18**, all compounds were unstable yellow oils. Method of purification and complete data are presented in Table 4.[3]

Formation of 1-Carbomethoxy-2,3-dihydro-1,2(1H)-diazepine (Compound **i**, *Table 1)*[3] *from Compound* **8**

To a solution of **8** (0.28 g) in methanol (40 ml) was added sodium methoxide (0.3 g) and the mixture was stirred at room temperature for 24 h. Work-up followed by chromatography as described in the general procedure above gave 170 mg (65%) of 1-carbomethoxy-2,3-dihydro-1,2(1*H*)-diazepine (eluted with CH_2Cl_2) and 25 mg (15%) of compound **15a** (eluted with CH_2Cl_2–MeOH, 95:5). The former compound was characterized by analytical and spectral data (Table 1)[3] while the latter (**15a**) was found to be identical (t.l.c., i.r., n.m.r.) with the sample obtained by deacetylation of **2a**.

Reaction of Compounds **2a** *and* **3a** *with Sodium Methoxide in Methanol-O-d*

Treatment of compounds **2a** and **3a** with sodium methoxide in methanol-*O*-*d* under conditions described for the deacetylation reaction above (general procedure) gave after chromatography deuterated **15a** and **16a** respectively as yellow oils. The relative integrated intensities of the appropriate peaks in the n.m.r. spectra showed the following amounts (±10%) of deuterium incorporation: **15a**: C_5—H (35%), C_4—H_2 (40%); **16a**: C_5—H (80%), C_4—H_2 (70%), N_2—$COCH_3$ (70%). The mass spectrum of deuterated **16a** showed (*m/e*, % relative intensity): 144 (M^+ for $C_7H_4D_6N_2O$, 22), 143 (17), 100 (53), 99 (37), 98 (22), 72 (36), 71 (33), 70 (100), 69 (35).

*1-Acetyl-2-(p-toluenesulfonyl)-2,3-dihydro-1,2(1H)-diazepine (***17***)*

A mixture of **2a** (250 mg), tosyl chloride (350 mg) and dry pyridine (5 ml) was allowed to stand at room temperature overnight. The reaction mixture was evaporated to dryness *in vacuo* and the residue was dissolved in a small amount of benzene and chromatographed. Elution with methylene chloride gave yellow crystals of **17** whose analytical, physical, and spectral properties are given in Table 1.[3]

Photolysis Experiments

*Formation of 2,3-Diazabicyclo[3.2.0]hept-6-enes (***23a–b**, **25a–b***) (General Procedure)*

A solution of the 2,3-dihydro-1,2(1*H*)-diazepine (**2a**, **3a**, **8**, and **9**) (150–200 mg) in dry benzene (100 ml) was irradiated for 12–15 h under a nitrogen atmosphere. The solvent was removed *in vacuo* and the resulting residue was chromatographed (C_6H_6–CH_2Cl_2, 1:1 eluent) to give the bicyclic compound (**23a–b** and **25a–b**) as an unstable yellow oil in 70–80% yield. Analytical, physical, and spectral data are summarized in Table 5.[3]

Treatment of **23a** and *b* with a large excess of acetic anhydride at room temperature overnight followed by evaporation *in vacuo* and chromatography (CH_2Cl_2 eluent) gave compounds **25a** and *b* in 80–85% yields which were shown to be identical (i.r., n.m.r.) with the products obtained by photolysis of **3a** and **9** respectively.

*Formation of 2-Acetyl-1,2-diazabicyclo[3.2.0]hept-6-ene (***27***)*

A solution of **16a** (200 mg) in dry benzene (100 ml) was photolyzed for 12 h under nitrogen. Evaporation of solvent *in vacuo* followed by chromatography (C_6H_6–CH_2Cl_2, 1:2 eluent) gave 130 mg (65%) of compound **27** as a pale yellow oil for which complete data are given in Table 5.[3]

*2-Acetyl-3-(p-toluenesulfonyl)-2,3-diazabicyclo[3.2.0]hept-6-ene (***24***)*

A solution of **23a** (50 mg) and tosyl chloride (60 mg) in dry pyridine (5 ml) was allowed to react overnight at room temperature. Evaporation to dryness *in vacuo* followed by chromatography (CH_2Cl_2 eluent) afforded 73 mg (69%) of **24** as pale yellow crystals for which complete data are given in Table 5.[3]

*Formation of 3-Acetyl-2,3-diaza[3.2.0]bicyclohept-6-ene (***26***) from Either Compound* **25a** *or* **25b**

To a solution of the diacyl bicyclic derivative (**25a** or *b*) (90–100 mg) in absolute methanol (30 ml) was added excess sodium methoxide (200 mg) and the mixture was stirred at room temperature for 2 days or refluxed for 8 h. The reaction mixture was evaporated to dryness and the resulting residue was extracted with methylene chloride. The organic extract was dried ($MgSO_4$) and evaporated to dryness to yield a dark oil which upon chromatography (CH_2Cl_2 eluent) gave the same compound **26** (yellow oil, ~80% from either **25a** or **25b**) as shown by i.r. and n.m.r. spectral comparison. Analytical, physical, and spectral data are collected in Table 5.[3]

When the diacetyl derivative **25a** was treated with sodium methoxide in methanol-*O*-*d* under comparable conditions there was obtained, after chromatography,

compound **26** whose n.m.r. spectrum showed that deuterium incorporation had occurred only at the N_2–$COCH_3$ function (~75% by relative integrated intensity) during the deacetylation reaction.

We are grateful to the National Research Council of Canada and Bristol Laboratories for financial support of this work. We thank Dr. J. M. Miller, Brock University for fast and efficient mass spectral service under contract by our department. Professor D. Mackay kindly provided a large sample of 1-phenyl-1,2,4-triazoline-3,5-dione. Generous samples of pyridine derivatives were made available by the Reilly Tar and Chemical Corp.

1. (*a*) M. T. THOMAS, V. SNIECKUS, and E. KLINGSBERG. Chem. Commun. 504 (1972); D. J. HARRIS, M. T. THOMAS, V. SNIECKUS, and E. KLINGSBERG. Can. J. Chem. **52**, 2805 (1974); (*b*) G. KAN, M. T. THOMAS, and V. SNIECKUS. Chem. Commun. 1022 (1971).
2. (*a*) A. J. CARTY, R. F. HOBSON, H. A. PATEL, and V. SNIECKUS. J. Am. Chem. Soc. **95**, 6835 (1973); (*b*) A. J. CARTY, G. KAN, D. P. MADDEN, V. SNIECKUS, M. STANTON, and T. BIRCHALL. J. Organomet. Chem. **32**, 241 (1971).
3. J. STREITH and B. WILLIG. Bull. Soc. Chim. Fr. 2847 (1973).
4. J. STREITH and J.-M. CASSAL. Bull. Soc. Chim. Fr. 2175 (1969).
5. B. WILLIG and J. STREITH. Tetrahedron Lett. 4167 (1973).
6. J. STREITH, J. P. LUTTRINGER, and M. NASTASI. J. Org. Chem. **36**, 2962 (1971).
7. M. NASTASI and J. STREITH. Bull. Soc. Chim. Fr. 635 (1973).
8. T. SASAKI, K. KANEMATSU, A. KAHEKI, I. ICHIKAWA, and K. HAYAKAWA. J. Org. Chem. **35**, 426 (1970); T. SASAKI, K. KANEMATSU, and K. HAYAKAWA. J. Chem. Soc. (C), 2142 (1971).
9. J. P. LUTTRINGER and J. STREITH. Tetrahedron Lett. 4163 (1973); G. TAURAND and J. STREITH. Tetrahedron Lett. 3575 (1972).
10. J. A. MOORE and E. MITCHELL. *In* Heterocyclic compounds. Vol. 9. *Edited by* R. C. Elderfield. Wiley, New York. 1967. p. 224. A. NABEYA, K. KURITA, and J. A. MOORE. J. Org. Chem. **38**, 2954 (1973) and previous papers in the series.
11. V. SNIECKUS. Chem. Commun. 831 (1969).
12. O. BUCHARDT, C. L. PEDERSEN, U. SVANHOLM, A. M. DUFFIELD, and A. T. BALABAN. Acta Chem. Scand. **23**, 3125 (1969); U. SVANHOLM. Acta Chem. Scand. **25**, 640 (1971).
13. R. L. WINEHOLT, E. WYSS, and J. A. MOORE. J. Org. Chem. **31**, 48 (1966).
14. A. RAUK, L. C. ALLEN, and K. MISLOW. Angew. Chem. Int. Ed. **9**, 400 (1970); H. KESSLER. Angew. Chem. Int. Ed. **9**, 219 (1970); W. E. STEWART and T. H. SIDDALL, III. Chem. Rev. **70**, 517 (1970).
15. J.-J. KOENIG and C.-G. WERMUTH. Tetrahedron Lett. 603 (1973).
16. J. A. MOORE, W. J. FREEMAN, K. KURITA, and M. G. PLEISS. J. Org. Chem. **38**, 2939 (1973).
17. J. A. MOORE, E. J. VOLKER, and C. M. KOPAY. J. Org. Chem. **36**, 1676 (1971) and references therein.
18. P. A. S. SMITH. The chemistry of open-chain organic nitrogen compounds. Vol. II. W. A. Benjamin, Inc., New York. 1966 p. 151.
19. J.-L. DEROCQUE, W. J. THEUER, and J. A. MOORE. J. Org. Chem. **33**, 4381 (1968).

Can. J. Chem. Downloaded from www.nrcresearchpress.com by 210.87.254.40 on 09/05/12
For personal use only.

Electrochemical Oxidation of Trifluoroacetic Acid in an Organic Substrate. III. In the Presence of Substituted Malonic Acid Half Esters and Unsaturated Carboxylic Acid Esters[1,2]

ROGER N. RENAUD AND PHILIPPE J. CHAMPAGNE[3]

Division of Chemistry, National Research Council of Canada, Ottawa, Canada K1A 0R6

Received September 26, 1974

ROGER N. RENAUD and PHILIPPE J. CHAMPAGNE. Can. J. Chem. **53**, 529 (1975).

The electrochemical oxidation of substituted malonic acid half-esters was studied in the presence of trifluoroacetic acid. Some 'crossed' Kolbe products were obtained together with some unsaturated carboalkoxy compounds, trifluoromethylated adducts to the double bond, and trifluoromethylated dimers.

The electrolysis of trifluoroacetic acid in the presence of olefinic carboalkoxy compounds was also studied.

ROGER N. RENAUD et PHILIPPE J. CHAMPAGNE. Can. J. Chem. **53**, 529 (1975).

On a étudié, en présence d'acide trifluoroacétique, l'oxydation électrochimique de monoester d'acides maloniques substitués. On a obtenu avec des produits de Kolbe croisés, quelques composés alkoxycarbonylés, des produits provenant de l'addition de groupe trifluorométhyles sur une double liaison de même que des dimères trifluorométhylés.

On a aussi étudié l'électrolyse de l'acide trifluoroacétique en présence de composés alkoxycarbonylés oléfiniques. [Traduit par le journal]

Introduction

The electrochemical oxidation of trifluoroacetic acid (TFA) has been shown to be a good source of trifluoromethyl radicals (1, 2) which, under appropriate conditions can be made to react with organic substrates to form new trifluoromethylated compounds. It is reported in a previous communication (2) that no 'crossed' Kolbe product was formed during the electrolysis of propionic acid in the presence of trifluoroacetic acid. This was due to the fact that an ethyl radical decomposes to ethylene at a faster rate than its condensation with a CF_3 radical. The aim of this work (part III of the series) was to study the effect of a carboalkoxy group on the formation of 'crossed' Kolbe products from the electrolysis of a mixture of substituted malonic acid half-ester and trifluoroacetic acid.

Since relatively important quantities of products deriving from unsaturated carboalkoxy intermediates were formed when the substituent on the malonic acid ester was a methyl group, the electrolysis of TFA in the presence of unsaturated carboxylic acid esters is also included in this study.[4]

Experimental

All starting materials were commercially available (or easily accessible) and were used without further purification. All melting points and boiling points are uncorrected. The electrolytic apparatus has been described elsewhere (1, 2).

Gas–liquid chromatographic analyses and separations were performed on an Aerograph Autoprep Model A-700 using the following columns: column A, 20 ft × 3/8 in., 20% Carbowax 20 M on 45–80 mesh Chromosorb P; column B, 20 ft × 3/8 in., 10% diethyleneglycol succinate on 45–60 mesh Chromosorb G (AW-DMCS).

The general pattern of the mass spectra is nearly the same for all the trifluoromethylated compounds obtained in this work. Therefore, only one spectrum will be shown (Fig. 1) and will serve as a typical model for the other compounds.

Electrolysis of Malonic Acid Monoester in the Presence of TFA

A solution of trifluoroacetic acid (3.4 g, 30 mmol) in water (6 ml) was added at a rate of 1 drop/10 s to an electrolyzed solution of malonic acid monoethyl ester (30 ml) and potassium hydroxide (2.2 g, 40 mmol) in water (40 ml). The electrolysis was carried out at a current density of 0.7 A/cm^2 at 20 °C and was continued for 1 h after the addition of TFA.

The cell was then attached to a vacuum manifold and

[1]NRCC No. 14405.

[2]Presented at the 57th Canadian Chemical Conference of the Chemical Institute of Canada, Regina, Saskatchewan, June 1974.

[3]NRCC summer student 1974.

[4]While this paper was being prepared for publication, a communication appeared in the literature (3) on electrolysis of TFA in the presence of unsaturated esters.

Can. J. Chem. Downloaded from www.nrcresearchpress.com by 210.87.254.40 on 09/05/12
For personal use only.

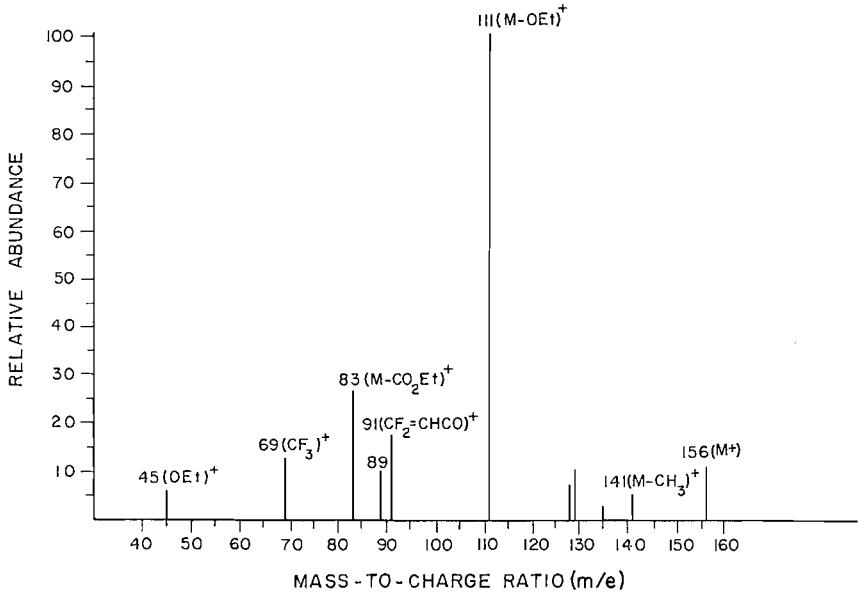

FIG. 1. Mass spectrum of methyl trifluoromethylacrylate (run 1) at 70 eV.

the organic material was collected together with some water in a cold trap (≈10 ml). The heavy oil (2 g, 46%) which separated from the water was nearly pure ethyl trifluoromethylacetate. Further purification can be made by fractional distillation at atmospheric pressure using a semimicro distilling apparatus. The main fraction, boiling at 107 °C (lit. (4) 50 °C/12 mm), showed only one triplet in the ^{19}F n.m.r. spectrum. The mass spectrum is shown in Fig. 1.

Anal. Calcd. for $C_5H_7O_2F_3$: C, 38.46; H, 4.49. Found: C, 38.10; H, 4.49.

Electrolysis of Methyl- and Dimethylmalonic Acid Monoester in the Presence of TFA

Using the same procedure as described above, methyl- and dimethylmalonic acid monoesters were electrolyzed in methanol due to the low solubility of the esters in water. The reaction mixture was poured into water (1l). The heavy oil that separated was washed with a solution of Na_2CO_3 (5%) and distilled in a vacuum manifold. The high vapor pressure (h.v.p.) fraction (>0.1 mm pressure) was collected in a cold trap and the low vapor pressure (l.v.p.) fraction was distilled in a Späth bulb. Both fractions were fractionated separately by preparative g.l.c. and each fraction analyzed by mass spectrometry and ^{19}F n.m.r. spectroscopy. The results are shown in Scheme 1 and Table 1.

Electrolysis of TFA in the Presence of Unsaturated Carboxylic Acid Esters

A solution of the ester (0.04 mol), sodium acetate (or sodium methoxide) (0.03 mol), and TFA (19 g) in acetic acid (or in methanol) (50 ml) was electrolyzed at a current density of 0.07–0.14 A/cm² until a 50% excess of current was used. The solution was then poured into water (1 l). The heavy oil that separated from the water was treated as described above. The results are reported in Table 2 and Scheme 2.

Results and Discussion

The electrochemical oxidation of malonic acid monoethyl ester in the presence of TFA gave ethyl trifluoromethylacetate in 46% yield (Table 1). The compound was easily obtained pure by only a vacuum line distillation. The synthesis of this compound has been described in the literature (4) in a yield of 40% by the Arrnt–Eistert reaction from trifluoroacetic acid. However, the best yields obtained by us by this method were ≈10%. The electrolysis of methyl- and dimethylmalonic monoester in presence of TFA gave some mixed Kolbe product **2** (Scheme 1). However, probably because of the low concentration of trifluoromethyl radicals in the medium, the possibility of the ethyl propionate radical **1** losing a hydrogen radical[5] to form the olefinic compound **3** must be relatively high. Therefore, the formation of compounds **4**, **5**, and **7** can be explained by the addition of two CF_3 radicals across the double bond of compound **3**, by the addition of two CF_3 radicals followed by a hydrogen abstraction, and by the crossed condensation of ethyl β-trifluoromethyl-

[5]By disproportionation or any other mechanisms.

Can. J. Chem. Downloaded from www.nrcresearchpress.com by 210.87.254.40 on 09/05/12
For personal use only.

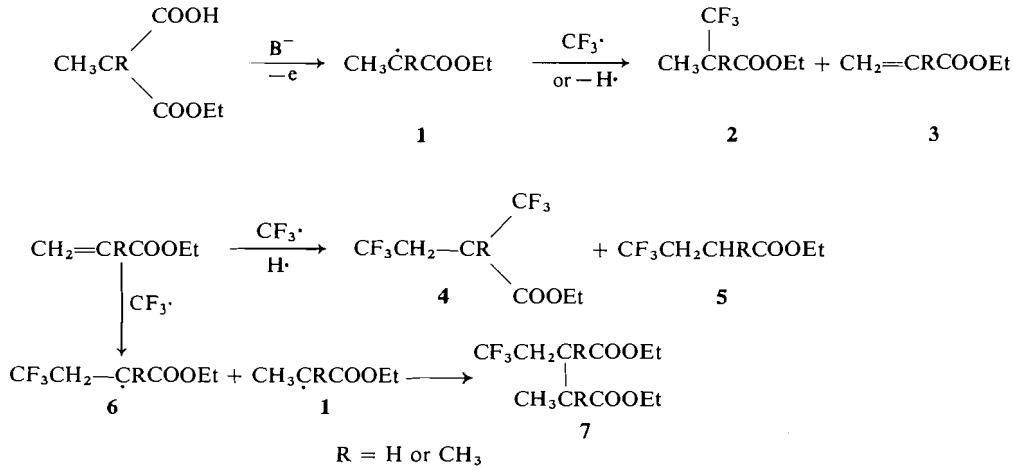

SCHEME I

TABLE 1. Electrochemical oxidation of $RR'C(COOEt)_2$ in presence of CF_3COO^-

Run	Substituent R	Substituent R′	Products† (Scheme 2)	Yield (%)	Boiling point (°C/mm)	^{19}F n.m.r.*	Principal ions in the 70 eV mass spectra (m/e) M^+	$(M - OEt)^+$	$(M - CO_2Et)^+$
1	H	H	$CF_3CH_2CO_2Et$	46	107–108/760	1t	156	111	83
2	H	CH_3	**2**	8.7	—	1d	170	125	97
			4	—	—	1d,1t	238	193	165
			5	0.6	—	1t	170	125	97
			7	5.5	—	1t	270	225	197
3	CH_3	CH_3	**2**	6.2	—	1s	184	139	111
			4	—	—	m	252	207	179
			7	5.2	58–60/0.02	1t	366	321	293

*The symbols s, d, t, and m denote singlet, doublet, triplet, and multiplet, respectively.
†The purity of all the compounds in runs 2 and 3 was over 95%.

propionate radical **6** and ethyl propionate radical **1**, respectively. It is worth noticing that the radical **1** is always present in relatively large quantity in the medium. In addition, a small quantity of the dimer of radical **6** was also formed.

The results obtained from the electrooxidation of substituted malonic acid monoesters prompted us to examine the electrolysis of trifluoroacetic acid in the presence of unsaturated carboalkoxy compounds. The reaction was carried out in either acetic acid or methanol. The advantage of the acetic acid solvent, aside from its ability to dissolve the esters, is that the medium is kept acidic: an important condition in the electrolysis of fluorinated acids, since a basic solution favors the formation of fluoride ions which can ruin the cell. As the pK value for acetic acid is much higher than the value for TFA, only a small concentration of acetate anions is present in the medium. Furthermore, a methanolic solution decreases the overall yield of products and favors the formation of some dark polymeric solids.

The result observed for the electrolysis of TFA in the presence of methyl acrylate is

Can. J. Chem. Downloaded from www.nrcresearchpress.com by 210.87.254.40 on 09/05/12
For personal use only.

Can. J. Chem. Downloaded from www.nrcresearchpress.com by 210.87.254.40 on 09/05/12
For personal use only.

TABLE 2. Electrochemical oxidation of CF_3COO^- in the presence of unsaturated carboalkoxy compounds ($R'CH{=}C(R'')(CH_2)_nCO_2R$)*

Run	Substituent n	Substituent R′	Substituent R″	Products (Scheme 3)	Yield (%)	Boiling (melting) point (°C)	^{19}F n.m.r.†	Elemental analyses (%)‡ C Found	C Calcd.	H Found	H Calcd.
4	0	H	H	**9**	16.5	105–106	1d,1t	32.87	32.15	2.85	2.68
				10	—	—	1t	—	—	—	—
				11	1.9	—	1m	—	—	—	—
				12§	14.3	(44–46)	1t	38.05	38.71	3.87	3.87
				12§	13.8	(82–83)	1t	38.52	38.71	3.93	3.87
5	0	CH_3	H	**9**	18.8	—	4d‖	37.97	38.10	3.97	3.97
				10	6.7	—	1d	—	—	—	—
				12	8.7	—	1d	46.18	45.90	5.57	5.46
6	0	H	CH_3	**12**§	4.6	(65–66)	1t	42.41	42.31	4.64	4.73
				12§	5.2	(60–62)	1t	42.28	42.31	4.66	4.73
7	1	H	H	**9**	14.0	—	2d,2t‖	38.01	38.10	4.03	3.97
				11	5.1	—	m	—	—	—	—
				12	9.1	(52–54)	1t	46.24	45.90	5.42	5.46

*R = CH_3 or C_2H_5.
†The symbols s, d, t, and m denote singlet, doublet, triplet, and multiplet, respectively.
‡The purity of all the compounds was all over 95% but only the elemental analyses of the pure materials are reported.
§Most likely the *dl* and the *meso* forms.
‖This indicates most probably the presence of two stereoisomers in a ratio of 1:1.

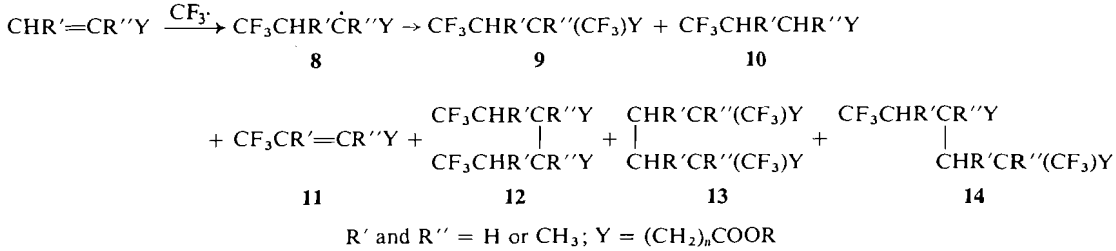

R′ and R″ = H or CH_3; Y = $(CH_2)_nCOOR$

SCHEME 2

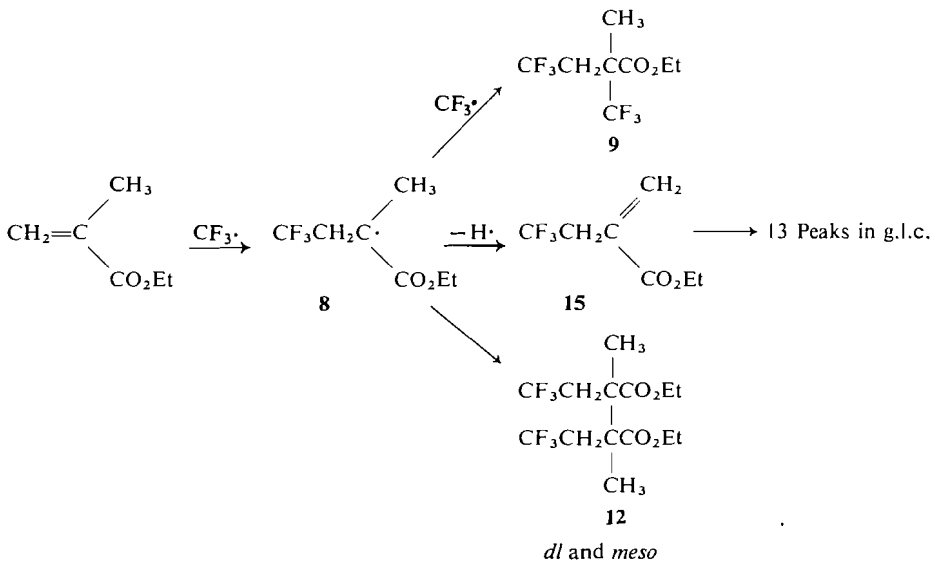

SCHEME 3

shown in Scheme 2 and in Table 2, run 4. The addition of two CF_3 radicals across the double bond to give **9** is the main product in the h.v.p. fraction. Some proton abstraction product (**10**) and proton loss product (**11**) were also observed. The dimerization of radical **8** is also important in this reaction. The dimer **12** was separated into the *dl* and *meso* forms in a ratio of $\approx 1:1$. The structure determination of **12** is based on its mass spectrum and on the fact that the ^{19}F n.m.r. spectrum of **12** showed only one triplet. Isomers **13** and **14** would show either a doublet or a doublet and a triplet respectively. Therefore, the attack of the first CF_3 radical occurs mainly, if not exclusively, on the β-carbon of the α,β-unsaturated carboalkoxy molecule.

Essentially the same result was observed for ethyl crotonate (run 5) as for methyl acrylate (run 4). However, the addition of a methyl group to the α-carbon of methyl acrylate (run 6) leads to a much more complicated reaction mixture than when the methyl group is on the β-position (run 5). In the case of substitution at the α-carbon, the radical **8** (Scheme 3), formed after the first addition of a CF_3 radical on the β-carbon, can condense with another CF_3 radical to give **9**, lose a hydrogen radical to form **15**, or dimerize to **12**. The increased complexity of the reaction mixture (besides the compounds mentioned, 13 other peaks were obtained in the g.l.c. in the h.v.p. fraction and 2 other unidentified peaks in the l.v.p. fraction) is due to the fact that the radicals **8** and CF_3 are in the presence of the starting material and compound **15**.

An electrolysis of TFA was also done in the presence of ethyl vinylacetate in order to study

Can. J. Chem. Downloaded from www.nrcresearchpress.com by 210.87.254.40 on 09/05/12
For personal use only.

the mechanism of the reaction on a non-conjugated system. Five compounds of the h.v.p. fraction were isolated by g.l.c. but only two were identified (compounds **9** and **11** in Table 2, run 7). The main fraction was that due to the addition of two CF_3 radicals across the double bond. The g.l.c. showed that the l.v.p. fraction contained five compounds. The elemental analysis and the mass spectrum of the crude mixture showed that these were all isomers of **12**. The ^{19}F n.m.r. of the main fraction indicates that the compound is most likely diethyl 3,4-bis(β-trifluoroethyl)adipate. Therefore, the attack of the CF_3 radical seems to favor the terminal carbon.

It can be concluded from this work that the electrochemical oxidation of malonic acid ester in the presence of TFA to give the 'crossed' Kolbe product has some limitation. The reaction becomes very complex for α-methylated malonic acid monoesters due to the formation of unsaturated intermediates. However, the addition of CF_3 radicals across a double bond of unsaturated carboalkoxy substrate can be useful for the synthesis of bistrifluoromethylated compounds which could be difficult to synthesize otherwise. Also, because of the fact that the attack of the first CF_3 radical occurs almost exclusively on the terminal carbon, the products of dimerization are limited to only few compounds; otherwise the reaction mixture would have been very complex.

A study was made on controlled concentrations of either the CF_3 radical or the methyl acrylate substrate in order to improve the formation of either the monomeric or the dimeric products, but no significant improvements resulted.

We wish to acknowledge Messrs. H. Séguin and R. Pilon for the elemental analyses and the mass spectral determinations and Dr. S. Brownstein and Mr. J. Bornais for the ^{19}F n.m.r. spectra.

1. R. N. Renaud and D. E. Sullivan. Can. J. Chem. **50**, 3084 (1972).
2. R. N. Renaud and D. E. Sullivan. Can. J. Chem. **51**, 772 (1973).
3. C. J. Brookes, P. L. Coe, D. M. Owen, A. E. Pedler, and J. C. Tatlow. J. Chem. Soc. Chem. Commun. 323 (1974).
4. F. Brown and W. K. R. Musgrove. J. Chem. Soc. 2087 (1953).

Can. J. Chem. Downloaded from www.nrcresearchpress.com by 210.87.254.40 on 09/05/12
For personal use only.

Substituent Effects in the Thermal Isomerization of 1,2-Dicarbonyl Derivatives of 3,6-Bridged 1,2,3,6-Tetrahydropyridazines

JOHN A. CAMPBELL, IAN HARRIS, DONALD MACKAY, AND TIMOTHY D. SAUER

Department of Chemistry, University of Waterloo, Waterloo, Ontario N2L 3G1

Received Agust 12, 1974

JOHN A. CAMPBELL, IAN HARRIS, DONALD MACKAY, and TIMOTHY D. SAUER. Can. J. Chem. **53**, 535 (1975).

The Diels–Alder adducts of cyclopentadiene and azodiacyls or azodiaroyls isomerize to 1,3,4-oxadiazines at rates which show a trend qualitatively related to the rotation rates of the corresponding *N,N*-dimethylamides. The isomerizations probably occur by a cyclic concerted mechanism.

The ring substituents in the adducts of 1,4-dimethyl-2,3-diphenylcyclopentadiene and azodibenzoyl or azodiacetyl accelerate the isomerization; the kinetic evidence supports a cyclic intermediate in the reaction in isooctane as solvent but is more consistent with a dipolar intermediate in aqueous ethanol.

Some generalizations about the effect of substituents on the isomerization are presented on the basis of these and earlier experiments.

JOHN A. CAMPBELL, IAN HARRIS, DONALD MACKAY et TIMOTHY D. SAUER. Can. J. Chem. **53**, 535 (1975).

Les produits d'addition de Diels–Alder entre le cyclopentadiène et les azodiacyles et les azodiaroyles s'isomérisent en oxadiazines-1,3,4 à des vitesses qui indiquent une tendance reliée qualitativement aux vitesses de rotation des *N,N*-diméthylamides correspondantes. Les isomérisations se produisent probablement par un mécanisme cyclique concerté.

Les substituants sur les cycles dans les produits d'addition du diméthyl-1,4 diphényl-2,3 cyclopentadiène avec l'azodibenzoyle ou l'azodiacétyle ont comme effet d'accélérer la vitesse d'isomérisation. Les données cinétiques sont en accord avec un intermédiaire cyclique lorsque la réaction est effectuée dans l'isooctane alors qu'en milieu éthanol aqueux, le mécanisme impliquerait probablement un intermédiaire dipolaire. On présente quelques généralisations sur l'effet des substituants sur de telles isomérisations en se basant sur ces expériences et d'autres rapportées antérieurement. [Traduit par le journal]

Introduction

For some time we have been studying the generalized isomerization of the bridged pyridazine **1** to the *cis*-fused 1,3,4-oxadiazine system **2** and have shown that its rate is highly dependent on the nature of X, R, R_1, and R_2. Our experiments have concentrated on the [2.2.1] system with a one-carbon bridge, in particular the azodicarbonyl adducts **3** of cyclopentadiene (1, 2) and those, **5**, of 2,5-dimethyl-3,4-diphenylcyclopentadienone (3).

In the series **3** → **4** the participation of acyl groups in the isomerization showed a marked steric acceleration, with a rate order of R = CMe_3 > Ph > Me, and, in the phenyl case at least (1), appeared to involve a concerted cyclic mechanism (transition state **7**). Ester groups however, *e.g.* in **3** (R = OEt), did not participate.

The cyclone-derived substituents in the adducts **5** had a powerful accelerating effect. Thus the azodibenzoyl adduct **5***a* could only be transiently detected, the isomeric 1,3,4-oxadiazine **6***a* being the isolated product, whereas adducts of azo esters, *e.g.* **5***c*, though stable enough for isolation, could be isomerized readily and reversibly to **6***c* (3).[1] Detailed kinetic studies were not carried out but the mechanism for the isomerization of **5***c* was most reasonably interpreted as involving the doubly ambident dipolar intermediate **8**.

We wish now to discuss in more detail the effect of the group R in **3**, especially in the substituted phenyl series **3***d–h*, and of ring substituents in the presence of a methylene rather than a keto bridge, *viz.* the adducts **9** in contrast with **5**. We also present in summary some

[1]Both **5***c* and **6***c* isomerized irreversibly to the isomeric 1,2-diazetidine which was thus the end product (3). The mode of fusion of the oxadiazine ring in compounds **6** (oxygen to benzylic carbon) and the stereochemistry follow by mechanistic analogy with the formation of **4**, from their spectra (3), and, in the case of **6***c*, by its chemical reactions (4).

Can. J. Chem. Downloaded from www.nrcresearchpress.com by 210.87.254.6 on 09/05/12
For personal use only.

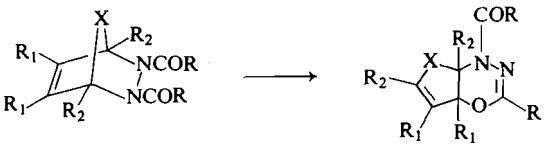

1 2

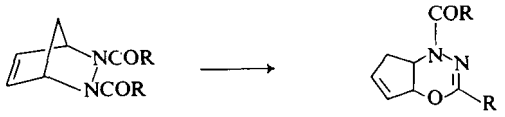

3 4

a R = Ph; *b* R = Me; *c* R = CMe_3; *d* R = *p*-BrC_6H_4; *e* R = *p*-$NO_2C_6H_4$; *f* R = *p*-$MeOC_6H_4$; *g* R = *m*-$NO_2C_6H_4$; *h* R = *o*-$MeOC_6H_4$

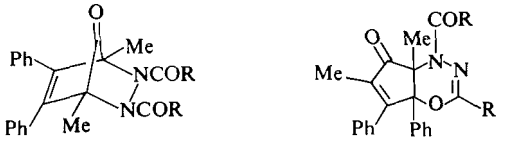

5 6

a R = Ph
b R = Me
c R = OMe

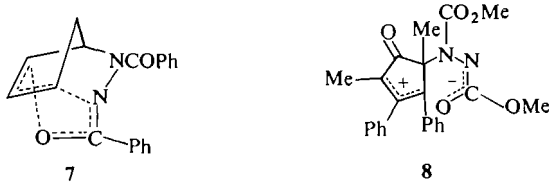

7 8

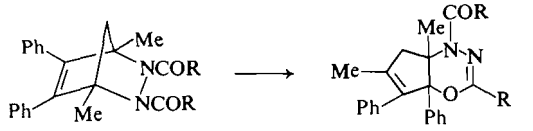

9 10

a = Ph; *b* = Me

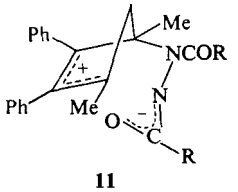

11

generalizations about the influence of X, R, R_1, and R_2 on the isomerization **1** → **2**.

Results and Discussion

All the substituted benzoyl derivatives in the series **3** → **4** have been described earlier (1, 2) except **3***g* and *h* and **4***g* and *h*. Compounds **9***a* and *b* and **10***a* and *b* have been used before in unrelated work (5) but their synthesis and properties are described here for the first time.

Azodi-*m*-nitrobenzoyl, m.p. 159–161°, rapidly gave labile crystalline **3***g* with cyclopentadiene. The hindered azodi-*o*-methoxybenzoyl was too unstable for isolation; it reacted slowly with cyclopentadiene to give the stable but amorphous **3***h*, purified by silica gel chromatography. The very labile (1) **9***a* was prepared in benzene at room temperature and purified by precipitation with pentane. The adduct **9***b*, obtained similarly, was more stable except in hydroxylic solvents. The melting points of **9***a* and *b* depended on the rate and time of exposure to heating. The oxadiazines related to these adducts were obtained by heating the latter in inert solvents at suitable temperatures. Their identities followed unequivocally from their spectra.

Kinetic analyses of the isomerizations were carried out by u.v. spectrophotometry as described before (1, 2, 6).

The first-order rate constants for the isomerization of **3***a–f* at 77° in 71% aqueous ethanol have been given earlier but, except for **3***b*, have now been determined for all of them over a range of temperatures. The Arrhenius activation energy and the entropy of activation are given in Table 1, along with the rate constants at 77°. The rate constants for **3***g* and *h* were determined only at 77° and are also given in Table 1.

From the similarity of the activation parameters to those of **3***a* it seems reasonable that all the isomerizations **3***b–f* go through a concerted cyclic transition state.

The isomerizations of the *p*-substituted benzoyl adducts, **3***d–f*, are clearly not subject to any simple linear free energy correlation (unlike the mechanistically related *ortho*-Claisen rearrangement where the rate data correlated well with σ_p^* constants (7, 8)) since all substituents are rate enhancing, though the effect is small except for the nitro group.

A rationalization of the substituent trends

Can. J. Chem. Downloaded from www.nrcresearchpress.com by 210.87.254.6 on 09/05/12
For personal use only.

TABLE 1. Rate constants at 77 °C and activation parameters for isomerization of adducts 3 in 71% aqueous ethanol

Compound	R	$10^4 k$ (s^{-1})	E_a (kcal mol^{-1})	No. of runs (range, °C)	$\Delta S^{\ddagger}$ at 77 °C (cal deg^{-1})	$\Delta G^{\ddagger}$, $RCONMe_2$ rotation[d] (kcal mol^{-1}) (temperature, °C)
3*a*	Ph	2.42	23.3±1.2	6 (69–84)	−5.5±1.8	15.3 (3–17)[e]; 15.0 (77)[f]
3*b*	Me	0.21[a]				18.1 (70–83)[e]; 17.5 (77)[f]
3*c*	CMe_3	74.5	21.3±0.8[b]	7 (61–79)	−5.0±1.2	11–13[g]
3*d*	*p*-BrC_6H_4	6.77	20.1±1.7	5 (69–80)	−9.0±2.5	
3*e*	*p*-$NO_2C_6H_4$	17.5	20.5±0.6	4 (66–78)	−7.6±0.9	
3*f*	*p*-$MeOC_6H_4$	2.64	23.1±0.6	7 (67–79)	−5.6±0.9	
3*g*	*m*-$NO_2C_6H_4$	30.2	[c]			16 (16)[h]
3*h*	*o*-$MeOC_6H_4$	0.21	[c]			19 (87)[h]

[a]From the value at 79.5 °C and an assumed E_a of 22 kcal mol^{-1}.
[b]Only one run in aqueous ethanol; activation data refer to runs in isooctane.
[c]Only one run.
[d]Data from refs. 9*a* and *b*.
[e]Average of values listed in ref. 9*a*, in the temperature range shown.
[f]Highly reliable values calculated from data of ref. 9*b*.
[g]Estimate at unspecified temperature by authors of ref. 9*a*.
[h]Notable inhibitory *ortho* effect (9*a*): $\Delta G^{\ddagger}$ for *o*-nitro compound, 20 kcal mol^{-1} (102°); for *m*-methoxy compound 15 kcal mol^{-1} (1°).

must explain both the most notable trend, the sensitivity to steric assistance shown in the sequence CMe_3 > aryl > Me, and, within the aryl series, the retarding effect of an *ortho* group (surprising in view of the steric effect of CMe_3) and the slight accelerating effect of a *meta* one.

The transition state for isomerization (*e.g.* 7), in which oxygen to carbon bond formation occurs, requires a well developed pyramidal geometry at nitrogen. A large portion of the free energy of activation must involve the energy difference between the planar amide (with sp^2 nitrogen) in the ground state adduct and the nonplanar amide (with sp^3 nitrogen) in the transition state.[2] This difference is simply the conformational energy barrier for amide rotation. A correlation might thus be expected between the latter and the activation energies for isomerization. The barrier heights ($\Delta G_{rot}^{\ddagger}$) for some of the related *N*,*N*-dimethylamides are also given in Table 1. They correspond to rotation rate constants which show, qualitatively at least, the trend found for the isomerization rates.[3]

The interpretation of the effect of R on the isomerization is thus probably the one applicable to amide rotation (9*a*). Bulky alkyl groups (*e.g.* R = CMe_3) are rate enhancing since they destabilize the ground state more than the transition state and aryl groups (phenyl, *m*- or *p*-substituted phenyl) are more effective than simple alkyl groups (*e.g.* R = Me) since ring resonance competes against amide ground state resonance. *o*-Substituted groups, however, create a retardation, ring twisting inhibiting this competing resonance and steric interaction being less severe in the ground state than in the transition state (9*a*). Thus the *o*-methoxy compound 3*h* reacts more slowly than the *p*-isomer 3*f*.

[2]The other contributions to the activation energy of the isomerization, involving changes in bonding type over the six centers, may be much less sensitive to the nature of R. Changes in bonding type, however, must be the dominant factor when R is an alkoxy group, since the cyclopentadiene adducts of azo esters are extremely stable, even though the rotational energy barriers in urethanes are 2–3 kcal mol^{-1} *lower* than in the corresponding amides (9*a*).

[3]Only the value for 3*g* is seriously out of line. Many early data on rotation barriers, however, are of limited reliability (*cf.* ref. 9*b*).

In each of the adducts 3 the group R has an identical neighbor at the adjacent amide link. A more accurate correlation might be observed if there was a common but nonparticipating neighbor throughout the series, as, for example, in the adducts of $RCON{=}NCO_2Et$.

The substituent effect is electronic to some extent as shown by the rate constants for 3*d*–*f*, in which steric effects are presumably negligible. Not enough reliable data are available on the rotational energy barriers of *p*-substituted benzamides to say whether they too are subject to the same electronic effects.

Can. J. Chem. Downloaded from www.nrcresearchpress.com by 210.87.254.6 on 09/05/12
For personal use only.

Can. J. Chem. Downloaded from www.nrcresearchpress.com by 210.87.254.6 on 09/05/12
For personal use only.

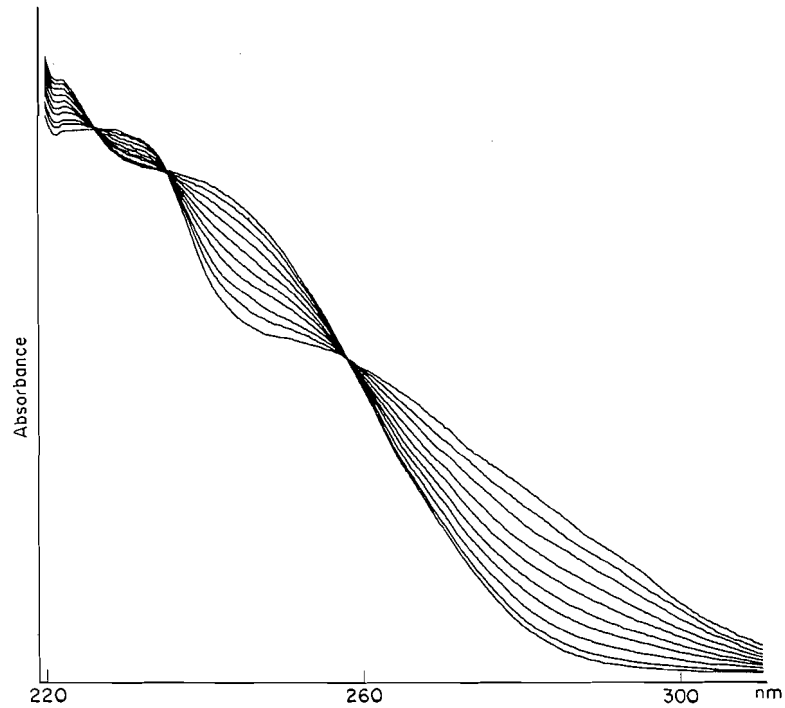

FIG. 1. Isomerization of **9***b* in isooctane at 79.5°. The absorbance decreases with time above 260 nm.

The slightly greater reactivity of **3***g* than **3***e* suggests that the nitro group sterically assists the reaction without causing significant ring twisting. An alternative explanation is that the rate enhancing ring resonance which must put positive charge at *ortho* and *para* carbon atoms would be more effective with the electronegative nitro group in the *meta* rather than the *para* position.

Known values of other amide rotation barriers (9*a*) permit the prediction that, for example, **3** (R = trichloromethyl) would isomerize very rapidly but **3** (R = 2,4,6-trimethylphenyl) would be very stable.

Isomerization studies on the adducts **9***a* and *b*, in which the degree of ring substitution is intermediate between that in the series **3** and **5**, were done in both isooctane and 71% aqueous ethanol. Clean first-order kinetics (see *e.g.* Fig. 1) were obtained in every case. The rates at 69.5° and the activation parameters are given in Table 2, together with the related data for the unsubstituted counterparts **3***a* and *b*. A remarkable solvent effect is observed.

The ring substituents in **9***a* and *b* are strongly rate enhancing in isooctane though the effect (compared with **3***a* and *b*[4]) is less pronounced for the benzoyl (37-fold) than the acetyl (220-fold) case. The rate ratio of $k_{9a}/k_{9b} = 35$ is again indicative of the greater conformational stability of the *N*-acetyl linkage.

In aqueous ethanol both **9***a* and *b* isomerize extremely rapidly at 69.5° (half lives < 30 s) and *at almost the same rate* in contrast with the 35-fold rate factor in isooctane. The high rates[5] and the levelling effect of the solvent suggest a mechanistic difference in the two solvent systems with the intervention of an intermediate whose formation is not dependent on activation to pyramidal

[4]The rate constant for **3***b* was obtained by extrapolation from the value in refluxing isooctane (99°) using an assumed Arrhenius activation energy of 24 kcal mol^{-1} (*cf.* other E_a values in isooctane from Table 2). It is probably a reasonable estimate.

[5]The ring substituent effect in aqueous ethanol is especially striking for the azodiacetyl adducts with $k_{9b}/k_{3b} = 2500$. Large rate factors with solvent change are not in themselves proof of a change in mechanism. Thus the linear plot of $\Delta H^{\ddagger}$ *vs.* $\Delta S^{\ddagger}$ (isokinetic relationship) in the *ortho*-Claisen reaction of allyl *p*-tolyl ether in a wide range of solvents is indicative of a common mechanism in all of them despite a very large rate spread (10).

TABLE 2. Solvent effect on rate constants at 69.5 °C and activation parameters for isomerization of *3a* and *b* and **9***a* and *b*

Compound	Solvent	$10^4 k$ (s^{-1})	E_a (kcal mol^{-1})	No. of runs (range, °C)	$\Delta S^{\ddagger}$ at 69.5 °C (cal deg^{-1})
3*a*	Isooctane	0.75	26.7±1.0	4 (69–84)	−0.8±1.5
	Aqueous ethanol	1.17	23.3±1.2	6 (69–84)	−5.6±1.8
3*b*	Isooctane	0.0036[a]			
	Aqueous ethanol	0.10[b]			
9*a*	Isooctane	27.4	23.3±0.4	7 (55–69)	−4.5±1.3
	Aqueous ethanol	267	19.1±0.5	9 (40–70)	−12.2±1.6
9*b*	Isooctane	0.79	25.5±0.8	6 (72–86)	−5.2±2.2
	Aqueous ethanol	253	17.9±0.3	7 (40–67)	−16.0±0.8

[a]Estimated from the value at the b.p. (99 °C) and an assumed E_a of 24 kcal mol^{-1}.
[b]See Table 1, footnote [a].

nitrogen. A plausible species is the dipole **11**, with a rigid (tight ion pair) rather than a freely rotating (about C—N) structure, a requirement implied by the negative entropy of activation[6] and the exclusive formation of a diasteromerically pure oxadiazine in the reaction. Stabilization of **11** would be provided by the substituents in the allylic cation portion, especially the electron releasing methyl group, and by the solvent polarity.

In our earlier work with the keto bridged compounds **5** we failed to isolate **5***a* from the reaction of azodibenzoyl and the cyclone, though its intermediacy in the formation of **6***a* in benzene solution could be detected by n.m.r. spectroscopy. We repeated the reaction with azodiacetyl in the hope that we might isolate **5***b*, provided the stabilizing effect of the acetyl group in nonpolar solvents still persisted in the presence of the keto bridge. However our efforts were vitiated by our inability to obtain a sufficiently concentrated solution of the azo compound (2) and the rather high temperature necessary to generate the cyclone from its dimer, factors which prevented the bimolecular formation of the adduct from being competitive with its unimolecular isomerization. Though there was evidence (n.m.r. spectroscopy) for the presence of **5***b* in small amounts during the reaction only the oxadiazine **10***b* (5) could be finally isolated.

[6]A negative contribution to $\Delta S^{\ddagger}$ could also come from a highly ordered solvation of the dipole. Other interpretations of the value of $\Delta S^{\ddagger}$ cannot be discounted. The transition state may be cyclic and have highly polarized bonding (positive in diene, negative in azodicarbonyl portion) without C—N rupture.

To conclude, the results in this and previous papers have established that the effectiveness of X, R, R_1, and R_2 in promoting the isomerization **1** → **2** decreases according to the following rules, other substituent variables being kept constant in each case:

(*i*) for R = alkyl or aryl rates appear to decrease roughly in the order of the rotation rates of the NCOR groups;

(*ii*) R = alkyl or aryl > R = alkoxy or aryloxy;

(*iii*) for $X = (CH_2)_n$, $n = 1 > n = 2 > n = 3 > n = 4$ (11);

(*iv*) X = CO, R_1 = Ph, R_2 = Me > X = CH_2, R_1 = Ph, R_2 = Me > X = CH_2, $R_1 = R_2$ = H.

Experimental

The following spectrometers were used: for i.r. a Beckman IR 10; for n.m.r. a Varian T60; for mass spectrometry an AE 1 MS 30; for u.v. a Coleman EPS-3T Hitachi. Details for the use of the latter in the variable temperature kinetic analyses have been given earlier (2, 6).

The isomerization of **3***h* was followed by the repeated scan technique as was that of **9***b* in isooctane at 79.5° (Fig. 1); others were followed by continuous external recording (Beckman Ten-Inch Linear Recorder) of the increase or decrease in absorbance at a suitable fixed wavelength: **3***g* at 305 nm (increase); **9***a* at 295 nm (increase); and **9***b* at 285 nm (decrease). The isomerization of **3***b* → **4***b* provides no suitable chromophore for u.v. analysis and was followed by refluxing solutions of **3***b* in isooctane (99°) or in 71% aqueous ethanol (79.5°) and by evaporating aliquots at intervals for analysis by n.m.r. spectrometry.

In the variable temperature experiments rate constants were determined at several temperatures over a convenient range (see Tables 1 and 2) and the Arrhenius activation energy calculated from a least-squares plot. The temperature range was limited at the lower end by the impracticality of very long reaction times, during which recorder drift or other instrumental variation might become significant. An upper limit was imposed by the risk of

Can. J. Chem. Downloaded from www.nrcresearchpress.com by 210.87.254.6 on 09/05/12
For personal use only.

Can. J. Chem. Downloaded from www.nrcresearchpress.com by 210.87.254.6 on 09/05/12
For personal use only.

damage to the u.v. cells by maintaining them at temperatures too close to the solvent boiling point.

The isooctane used was of spectrophotometric grade and was dried over sodium. The 71% aqueous ethanol was made by diluting 95% ethanol with one third of its volume of water. Anhydrous magnesium sulfate was used for drying organic solutions. Melting points are uncorrected.

*2,3-Di-m-nitrobenzoyl-2,3-diazabicyclo[2.2.1]hept-5-ene (**3g**)*

1,2-Di-*m*-nitrobenzoylhydrazine, m.p. 246–247° (lit. (12) m.p. 240–242°), was converted into its mercury(II) salt and reacted with bromine in methylene chloride as described for previous azo compounds. Concentration of the filtered solution and addition of carbon tetrachloride gave crude product (60%) which was recrystallized from methylene chloride – carbon tetrachloride (1:2) as orange crystals, m.p. 159–161°; ν (Nujol) 1743 cm^{-1} (C=O); λ_{max} ($CHCl_3$) 485 nm (ε 14).

Addition of cyclopentadiene (20 ml) to a solution of the azo compound (1.0 g, 3.05 mmol) in benzene (120 ml) caused the amber color to fade to pale yellow in 5 min. Evaporation and addition of pentane to the yellow residue gave a colorless precipitate which crystallized as prisms (50%), m.p. 196–198°, from benzene–cyclohexane; ν (Nujol) 1695, 1638 cm^{-1} (C=O); λ_{max} (EtOH) 268 nm; τ ($CDCl_3$) 1.1–2.7 (8 phenyl H, complex multiplet), 3.28 (2 vinyl H, closely spaced triplet), 4.56 (2 tertiary H, closely spaced triplet) 7.78, 8.02 p.p.m. (2 methylene H, AB quartet, J = 9.5 Hz).

Anal. Calcd. for $C_{19}H_{14}N_4O_6$: C, 57.87; H, 3.58; N, 14.21. Found: C, 57.74; H, 3.86; N, 14.26.

*cis-4-m-Nitrobenzoyl-4,4a,5,7a-tetrahydro-2-m-nitrophenylcyclopenta-1,3,4-oxadiazine (**4g**)*

Refluxing a solution of **3g** in chloroform for 6 h gave the oxadiazine quantitatively; it was crystallized from methanol as needles, m.p. 206–208°; ν (Nujol) 1650, 1620 cm^{-1} (C=O, C=N); λ_{max} (EtOH) 265 (ε 22 000), sh 295 nm (ε 16 000); τ ($CDCl_3$) 0.7–2.7 (8 phenyl H, complex multiplet), 3.54 (2 vinyl H), 4.5–5.0 (2 tertiary H), 6.72, 7.48 p.p.m. (2 methylene H, AB quartet with further splittings, J_{AB} = 18 Hz).

Anal. Calcd. for $C_{19}H_{14}N_4O_6$: C, 57.87; H, 3.58; N, 14.21. Found: C, 57.64; H, 3.67; N, 13.98.

*2,3-Di-o-methoxybenzoyl-2,3-diazabicyclo[2.2.1]hept-5-ene (**3h**)*

Lead tetraacetate oxidation of 1,2-di-*o*-methoxybenzoyl hydrazine, m.p. 197–199° (lit. (13) m.p. 202–203°), gave more consistent results than reaction of the mercury(II) salt with bromine.

To a stirred suspension of the hydrazide (1.5 g, 5.0 mmol) in methylene chloride (50 ml) at 0° was added, in portions, lead tetraacetate (2.5 g, 5.6 mmol) followed by cyclopentadiene (20 ml). The initial orange-red color faded over 1 h and the mixture was then kept at 5° for 12 h and filtered. The solution was washed in turn with water and aqueous sodium bicarbonate, and then dried and evaporated to a residue (2.4 g) whose n.m.r. spectrum showed the presence of the expected adduct as well as many methoxy containing impurities. The crude material was treated with cold benzene (10 ml), a small amount of insoluble hydrazide was filtered off, and the solution was chromatographed on silica gel. The use of increasing amounts of ether caused the elution of some of the impurities and then with 20% ether the adduct **3h** (1.35 g, 75%) as a glassy solid. It was purified from chloroform solution (5 ml) by adding hexane (75 ml) with stirring and chilling. The colorless adduct had ν (film) 1660–1700 cm^{-1}, broad (C=O); λ_{max} (EtOH) 284 nm (ε 6100); τ (CCl_4) 2.5–3.4 (8 phenyl H), 3.61 (2 vinyl H), 5.00 (2 tertiary H), 6.22 (6 methoxy methyl, sharp singlet), 7.98, 8.40 p.p.m. (2 methylene H, AB quartet, J_{AB} = 8 Hz); *m/e* 364 (P^+, 17%), 135 (o-$CH_3OC_6H_4CO^+$, 100%).

*cis-4-o-Methoxybenzoyl-4,4a,5,7a-tetrahydro-2-o-methoxyphenylcyclopenta-1,3,4-oxadiazine (**4h**)*

A solution of **3h** (1.0 g) was refluxed in tetrachloroethylene (20 ml) for 2 h and evaporated. The slightly brown residue was twice crystallized from benzene–cyclohexane to give dense colorless prisms of **4h**, a metastable polymorph which softened between 90 and 100°, resolidified, and then had m.p. 148–149° (its i.r. spectrum in Nujol showed minor differences from that of the high melting form). Heating at 100° for 3 h gave stable crystals, m.p. 148.5–149.5°; ν (Nujol) 1653, shs 1647, 1636 cm^{-1} (C=O, C=N); λ_{max} (EtOH) sh 278, 284 nm (ε 9900); τ ($CDCl_3$) 2.3–3.3 (8 phenyl H), 3.71 (2 vinyl H), 4.6–5.2 (2 tertiary H), 6.15 (3 methoxy methyl, sharp singlet), 6.33 (3 methoxy methyl, sharp singlet), 6.82, 7.44 p.p.m. (2 methylene H, AB quartet with further splittings, J_{AB} = 16 Hz).

Anal. Calcd. for $C_{21}H_{20}N_2O_4$: C, 69.22; H, 5.53; N, 7.69. Found: C, 68.93; H, 5.37; N, 7.44.

*2,3-Dibenzoyl-1,4-dimethyl-5,6-diphenyl-2,3-diazabicyclo[2.2.1]hept-5-ene (**9a**)*

A solution of azodibenzoyl (238 mg, 1 mmol) and 1,4-dimethyl-2,3-diphenylcyclopentadiene (246 mg, 1 mmol) in benzene (2 ml) at room temperature slowly faded in color and deposited crystals. After 40 min pentane (10 ml) was added slowly and the colorless product (400 mg, 82%) collected and washed with pentane (a longer reaction time led to some isomerization). Crystallization was effected by dissolving it in benzene – methylene chloride, evaporating till crystallization just began (20 ml), and adding pentane–cyclohexane (1:1, 50 ml) with stirring. The crystalline powder had a m.p. dependent on the rate and time of exposure to heating, *e.g.* 109–111° if raised from room temperature in 15 min (if heating was continued slowly above the m.p. the melt solidified and remelted at 162–163°, the m.p. of the pure isomer); ν (Nujol) 1680, 1629 cm^{-1} (C=O); λ_{max} (EtOH) 233, 270 nm; τ ($CDCl_3$) 2.2–3.1 (20 phenyl H), 7.56, 7.83 (2 methylene H, AB quartet, J_{AB} = 9.2 Hz), 8.32 p.p.m. (6 methyl H, sharp singlet).

*cis-4-Benzoyl-4,4a,5,7a-tetrahydryo-4a,6-dimethyl-2,7,7a-triphenylcyclopenta-1,3,4-oxadiazine (**10a**)*

Heating **9a** above its m.p. as described above, or for 10 min in refluxing benzene, gave the oxadiazine quantitatively. It formed fine prisms from 95% ethanol, m.p. 162.5–163.5°; ν (Nujol) 1655, 1640 cm^{-1} (C=O, C=N); λ_{max} (EtOH) 295 nm (12 100); τ ($CDCl_3$) 2.0–3.2 (20 phenyl H) 6.07, 7.40 (2 methylene H, AX quartet, J = 17 Hz), 8.01 (3 vinyl methyl H, sharp singlet), 8.60 p.p.m. (3 tertiary methyl H, sharp singlet).

Can. J. Chem. Downloaded from www.nrcresearchpress.com by 210.87.254.6 on 09/05/12
For personal use only.

Anal. Calcd. for $C_{33}H_{28}N_2O_2$: C, 81.79; H, 5.82; N, 5.78. Found: C, 81.55; H, 6.05; N, 5.75.

*2,3-Diacetyl-1,4-dimethyl-5,6-diphenyl-2,3-diazabicyclo-[2.2.1]hept-5-ene (**9b**)*

Azodiacetyl was prepared in benzene and the solution evaporated, as described earlier (2), to a concentration of 0.27 *M* (determined by n.m.r. spectrometry against the methyl peak in methyl benzoate as standard). To 15 ml of this solution was added 1,4-dimethyl-2,3-diphenylcyclopentadiene (1.00 g, 1.00 equiv.), and after 2 h at room temperature the yellow solution was evaporated to near dryness and pentane (30 ml) added with trituration and chilling. The colorless product (1.2 g, 82%) was recrystallized by dissolving it in cold benzene and adding a 1:1 solution of cyclohexane–pentane with stirring to give colorless prisms, m.p. 115–116°, if inserted at 110° at a heating rate of 2°/min; ν (Nujol) 1693, 1645 cm^{-1} (C=O); λ_{max} (EtOH) 235 (ε 17 600), 252 nm (ε 14 800); τ ($CDCl_3$—CCl_4) 2.5–3.2 (10 phenyl H), 7.6–8.3 (14 H, including slightly broadened 6 acetyl methyl H at 7.94 and 6 sharp tertiary methyl H at 8.04 p.p.m.).

Anal. Calcd. for $C_{23}H_{24}N_2O_2$: C, 76.64; H, 6.71; N, 7.77. Found: C, 76.33; H, 6.75; N, 7.95.

*cis-4-Acetyl-4,4a,5,7a-tetrahydro-2,4a,6-trimethyl-7,7a-diphenylcyclopenta-1,3,4-oxadiazine (**10b**)*

A sample of **9b** (300 mg) was kept at room temperature overnight in methanol (20 ml). Evaporation followed by two crystallizations of the residue from aqueous methanol gave the oxadiazine as large prisms, m.p. 160–161°; ν (Nujol) 1686, 1655 cm^{-1} (C=O, C=N); λ_{max} (EtOH) 243 nm (ε 21 000); τ ($CDCl_3$—CCl_4) 2.3–3.2 (10 phenyl H), 6.27, 7.60 (2 methylene H, AX quartet, J = 17 Hz), 7.70 (3 acetimidoyl methyl H, sharp singlet), 8.03 (3 acetyl methyl H, slightly broadened singlet), 8.48 (3 vinyl methyl H, sharp singlet), 8.80 p.p.m. (3 tertiary methyl H, sharp singlet).

Anal. Calcd. for $C_{23}H_{24}N_2O_2$: C, 76.64; H, 6.71; N, 7.77. Found: C, 76.86, H, 6.68; N, 8.08.

*cis-4-Acetyl-4,4a,5,7a-tetrahydro-2,4a,6-trimethyl-7,7a-diphenylcyclopenta-1,3,4-oxadiazin-5-one (**6b**)*

A solution of the dimer of 2,5-dimethyl-3,4-diphenylcyclopentadienone (1.30 g, 5 mmol cyclone monomer) in tetrachloroethylene (64 ml) containing azodiacetyl (6.7 mmol) failed to react on standing at room temperature for 20 h. When the temperature was raised to 40° n.m.r. spectrometry showed in the methyl region the four peaks of the dimer and the four peaks (two coincident) of the oxadiazine **6b** but also two other singlets at 7.80 and 7.98 τ, attributable to the adduct **5b**. After 3 days the estimated percentage composition was **5b**:**6b**:cyclone = 13:25:62, the proportion of **5b** not being exceeded thereafter.

At 85° reaction was complete in 12 h. Evaporation of the solvent and trituration of the residue with pentane gave the oxadiazine (1.77 g, 94%) which formed prisms from cyclohexane, m.p. 168–169°; ν (Nujol) 1730, 1678, 1664 cm^{-1} (keto and amide C=O, C=N); λ_{max} (EtOH) 242 (ε 15 600), 283 nm (ε 12 600); τ (CCl_4) 2.5–3.1 (10 phenyl H), 7.87 (3 acetimidoyl and 3 acetyl H, coincident, sharp singlet), 8.23 (3 vinyl methyl H, sharp singlet), 9.03 p.p.m. (3 tertiary methyl H, sharp singlet), but all four methyl peaks separated in benzene at 7.76, 7.96, 8.49, and 8.81 p.p.m. (assignments in order as before).

Anal. Calcd. for $C_{23}H_{22}N_2O_3$: C, 73.78; H, 5.92; N, 7.48. Found: C, 73.55; H, 5.90; N, 7.69.

We thank the National Research Council of Canada and the University of Waterloo for financial assistance.

1. D. MACKAY, J. A. CAMPBELL, and C. P. R. JENNISON. Can. J. Chem. **48**, 81 (1970).
2. J. A. CAMPBELL, D. MACKAY, and T. D. SAUER. Can. J. Chem. **50**, 371 (1972).
3. D. MACKAY, C. W. PILGER, and L. L. WONG. J. Org. Chem. **38**, 2043 (1973).
4. D. MACKAY and C. W. PILGER. Can. J. Chem. **52**, 1114 (1974).
5. C. P. R. JENNISON and D. MACKAY. Can. J. Chem. **51**, 3726 (1973).
6. C.Y-J. CHUNG, D. MACKAY, and T. D. SAUER. Can. J. Chem. **50**, 1568 (1972).
7. H. L. GOERING and R. R. JACOBSON. J. Am. Chem. Soc. **80**, 3277 (1958).
8. W. N. WHITE and C. D. SLATER. J. Org. Chem. **27**, 2908 (1962).
9. (*a*) W. E. STEWART and T. H. SIDDALL, III. Chem. Rev. **70**, 517 (1970); (*b*) L. W. REEVES, R. C. SHADDICK, and K. N. SHAW. Can. J. Chem. **49**, 3683 (1971).
10. W. N. WHITE and E. F. WOLFARTH. J. Org. Chem. **35**, 2196 (1970).
11. C.Y.-J. CHUNG, D. MACKAY, and T. D. SAUER. Can. J. Chem. **50**, 3315 (1972).
12. H. H. STRAIN. J. Am. Chem. Soc. **57**, 758 (1935).
13. P. A. S. SMITH. J. Am. Chem. Soc. **76**, 436 (1954).

Water-soluble Lysine-containing Polypeptides. II. The Interaction of Several Sequential Lysine–Glycine Polypeptides with DNA. A Circular Dichroism Study of DNA Conformation in Annealed Complexes[1]

ROSS E. WILLIAMS[2] and SANDRA L. KIELLAND

Division of Biological Sciences, National Research Council of Canada, Ottawa, Canada K1A 0R6

Received August 6, 1974

ROSS E. WILLIAMS and SANDRA L. KIELLAND. Can. J. Chem. **53**, 542 (1975).

To serve as models of protein–nucleic acid complexes, annealed complexes of several sequential lysine–glycine polypeptides with DNA have been formed. Circular dichroic spectra of the DNA contained in the complexes indicates that several discrete conformations of DNA can exist when complexed.

ROSS E. WILLIAMS et SANDRA L. KIELLAND. Can. J. Chem. **53**, 542 (1975).

Comme modèles des complexes entre les protéines et les acides nucléiques, nous avons préparé plusieurs complexes entre quelques polypeptides lysine–glycine de séquence régulière et l'ADN par une méthode de rassemblement spécifique. A partir d'une étude des spectres de dichroisme circulaire, nous avons observé quelques conformations différentes de l'ADN dans ces complexes.

Can. J. Chem. Downloaded from www.nrcresearchpress.com by 210.87.254.5 on 09/05/12
For personal use only.

Protein – nucleic acid interactions play an important role in maintaining the structural integrity of such complex biological structure as ribosomes, gene repressor–operator complexes, and nuclei in eukaryotic cells. Simplification of the structure of the individual components of these complex structures has been one of the experimental tools adopted in order to reduce the number of variables normally found in experiments on the native systems. This reduction has eased, to a certain extent, the interpretation of experiments designed to determine what factors are influential in determining the three-dimensional structure and stability of such complexes. Amongst these factors hydrophobic and electrostatic forces play an important role. Investigation of the role played by electrostatic forces has led to simplification of the protein portion of such complexes and the use of poly-(L-lysine) (**I**) as a model of the proteins involved in the complexes (see refs. 1–8 for leading references to previous work). Although many studies have investigated the interaction of poly-(L-lysine) with deoxyribonucleic acids (DNA) little work has been done on determining the importance of several of the factors controlling the structure and stability of poly-(L-lysine)–DNA complexes. Little work, for example, has been done to investigate the effect which the sequence of lysines within the polypeptide chain might have upon the structure of the complex as a whole and, more specifically, upon the structure of the deoxyribonucleic acid within complex.

Recently several sequential polypeptides containing lysine (lys) and glycine (gly), **II**, **III**, and **IV**, have been synthesized (9) so that studies can be made of the influence of sequence on the structure of DNA in complexes.

poly-(L-lysgly)$_n$ (**II**) = *lys*-gly-*lys*-gly-*lys*-gly

poly-(L-lysglygly)$_n$ (**III**) = *lys*-gly-gly-*lys*-gly-gly

poly-(gly-L-lysglygly)$_n$ (**IV**) = *lys*-gly-gly-gly-*lys*-gly

In this communication the results of a study of the conformation of DNA in annealed complexes of these polypeptides and calf thymus DNA are presented.

Experimental

Reagent-grade chemicals used for buffer preparation were purchased from commercial sources and used without further preparation. Cacodylic acid (dimethyl arsenate) was obtained from Fisher Scientific (Canada).

Dialysis tubing (Spectrapor 3), with nominal cut-off molecular weight 3500, was obtained from Science Essentials, Anaheim, California. This tubing was pre-

[1]NRCC No. 14381.

[2]To whom correspondence should be addressed.

Can. J. Chem. Downloaded from www.nrcresearchpress.com by 210.87.254.5 on 09/05/12
For personal use only.

pared for use as directed (sodium sulfide and dilute sulfuric acid treatments). Leakage from and absorption by sacs prepared from this tubing was checked by amino acid hydrolysis of an aliquot of the polypeptide solution before and after 12 h dialysis against at least 50 vol of 0.15 *M* sodium chloride, sodium cacodylate, p*H* 7.0, and losses were found to be less that 3%. Similarly, DNA losses were found to be negligible as assayed by losses in u.v. absorption at 260 nm.

Polypeptides were prepared and characterized as previously described (9). Stock solutions of polypeptides (approximately 4×10^{-3} *M* lysine) were prepared in sodium cacodylate buffer 0.01 *M*, p*H* 7.0. An aliquot was analyzed for lysine concentration by hydrolysis in 6 *N* HCl and amino acid analysis (Beckman model 120C).

Highly polymerized DNA (Worthington Biochemicals, Freehold, N.J.) was treated as previously described (A260/A230 = 2.20) (10). Stock solutions of DNA (3×10^{-3} *M* phosphate) were prepared by dialysis against 0.01 *M* sodium cacodylate p*H* 7.0 overnight at 4 °C and dilution to the appropriate concentration. DNA-phosphate concentration was determined by absorbance at 260 nm (DNA-phosphate, ε_{260} 6600 (11)).

Circular dichroic spectra were taken in quartz cells (1 cm path) at 26 ± 1 °C on a Cary spectropolarimeter, model 61. No correction for sample turbidity was made. The spectropolarimeter was calibrated with purified, anhydrous *d*-10-camphorsulfonic acid (using $\varepsilon_L - \varepsilon_R$ (290 nm) = 2.36 (12)), $[\alpha]_D$ +21.6° (*c* 4.3, H_2O) (lit. (13) $[\alpha]_D$ +22.1° (*c* 1.0, H_2O)), m.p. (dec.) 198–199 °C (uncorr.).

Anal. Calcd. for $C_{10}H_{16}O_4S$: C, 51.7; H, 6.94. Found: C, 51.5; H, 7.08.

Ultraviolet absortion spectra were taken in quartz cells (1 cm path) at 22 ± 2 °C on a Cary spectrophotometer, model 14. Turbidity of each sample was measured and expressed as $dA^{400} = A_{com}{}^{400} - A_0{}^{400}$ where A_{com} is the absorbance at 400 nm of the complexed DNA solution and $A_0{}^{400}$ is the absorbance at 400 nm of the equivalent uncomplexed DNA solution.

Back Dialysis Experiments

A series of solutions were prepared as follows: 200 µl of DNA stock solution (3×10^{-3} *M* phosphate) was added to a 3.0 ml solution of sodium chloride, 1.5 *M*, sodium cacodylate, 0.001 *M*, p*H* 7.0. The solutions were mixed and an aliquot of polypeptide stock solution ($0 \rightarrow 200$ µl) was added to each in order to provide separate solutions with increasing lysine/DNA-phosphate ratios. The solutions were mixed again and transferred to separate dialysis sacs. Each of the sacs was placed in a 500-ml solution of sodium chloride, 1.5 *M*, sodium cacodylate, 0.001 *M*, p*H* 7.0, and back dialyzed at 4 °C to sodium chloride, 0.15 *M*, sodium cacodylate, 0.001 *M*, p*H* 7.0, according to the previously published procedure (14). The solutions were finally dialyzed against a fresh solution of the final buffer for 2 h at 4 °C before measurement of the c.d. spectra. For calculating the lysine/DNA-phosphate ratios, DNA-phosphate concentration was determined using a sample containing no polypeptide which had been back dialyzed under conditions identical to those used to prepare the complexes. Lysine concentration was taken as the input concentration since bag losses were negligible.

Although absorption readings at 260 nm on complexes with lysine/phosphate ratios around 0.5 indicated no changes in the DNA concentration through specific absorption of complexes by the dialysis sacs used, samples were taken from dialysis sacs containing DNA-poly-(L-lysine) complexes with lysine/phosphate ratios between 0.5 and 1.0. They were then resolubilized in 2 *M* sodium chloride (18). In all cases readings at 260 were taken relative to a DNA sample which had the same initial concentration before complex formation and which was dialyzed under the same conditions used to form the complexes. Only minor losses of DNA (less than 5%) were detected.

Results

Circular dichroic (c.d.) spectra have been proven to be quite useful in the investigation of changes in the conformation of DNA and other polynucleotides (15). Spectra have been taken on the native molecules, not only in solution, but also when they are complexed with various natural and synthetic polypeptides (16, 17). Circular dichroic spectra of the DNA complexed with the polypeptides **II–IV** should provide useful information on the effect the polypeptides have on the conformation of DNA.

Recently, annealed complexes between poly-L-lysine (**I**) and DNA were formed under physiological conditions (0.15 *M* NaCl, p*H* 7.0) by the back dialysis in a linear sodium chloride gradient of complexes formed at high salt concentrations (18). It was reported that the resulting c.d. spectra were reproducible as to type and amount of DNA distortion observed (18). Repetition of the experimental conditions necessary to form this type of complex with poly-L-lysine (**I**) (M_w 10 250 (9)) gave the c.d. spectra of DNA in Fig. 1. The spectra are similar to those previously reported. In general, at lysine/DNA-phosphate ratios less than 0.2 it was readily apparent that spectral alterations in the normal solution spectrum of DNA were occurring. Further increases in the lysine/DNA-phosphate ratio resulted in progressive loss of ellipticity at 275 nm and the formation of a single broad negative band at 280 nm. As the lysine/DNA-phosphate ratio passed above 0.8 apparent loss of distortion occurred, *i.e.* the intensity at 275 nm became less. Above this ratio however turbidity problems were acute as assayed by u.v. absorption spectra ($dA^{400} > 0.3$) and precipitation was occurring. These results are qualitatively similar to those found previously with the same system (18). The differences in the intensity of the ellipticity noted could be the result of

Can. J. Chem. Downloaded from www.nrcresearchpress.com by 210.87.254.5 on 09/05/12
For personal use only.

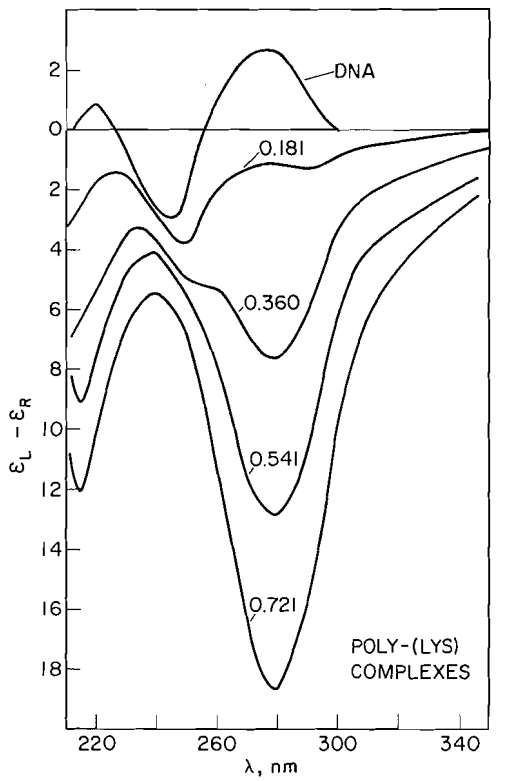

FIG. 1. Circular dichroic spectra of poly-L-lysine–DNA complexes. Variation of spectra with increasing lysine/DNA-phosphate ratios (given as fractional values). Ellipticity calculations were based on the nucleotide phosphate concentration. Repetition of experiments in triplicate indicated that errors in ellipticity values amounted to approximately 5% of the measured value. Turbidity, in all cases, as measured by dA^{400} was less than 0.28. No corrections for sample turbidity have been made. Experimental conditions: DNA-phosphate concentration 1.76×10^{-4} *M*; sodium chloride, 0.15 *M*, sodium cacodylate, 0.001 *M*, p*H* 7.0.

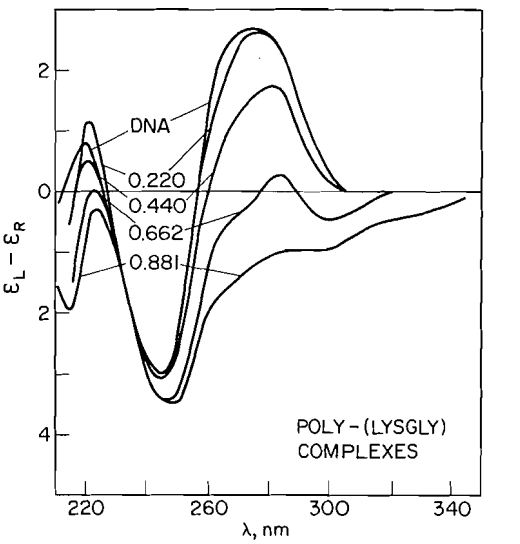

FIG. 2. Circular dichroic spectra of poly-(L-lysylglycine)–DNA complexes. Variation of spectra with increasing lysine/DNA-phosphate ratios. Other details as for Fig. 1. Experimental conditions: DNA-phosphate concentration 1.76×10^{-4} *M*; sodium chloride, 0.15 *M*, sodium phosphate, 0.001 *M*, p*H* 7.0.

differences in the molecular weight of the polylysine samples used. An estimate of the reproducibility of the experimental results was obtained from three repetitions of the complex formation and indicated that spectral intensities were reproducible to within ±5%.

Using the same experimental conditions complexes were formed between the sequential lysine-glycine polypeptides **II**, **III**, and **IV**. The c.d. spectra of the accessible u.v. region of the spectrum are presented in Figs. 2–4.

Several general observations can be made. At lysine/DNA-phosphate ratios less than 0.2 smaller alterations of the normal DNA spectrum occurred than were observed in the polylysine complexes, and within the group, variable amounts of distortion were noted. For example, poly-(L-lysylglycylglycine), **III**, (Fig. 3) seemed to be causing more distortion of the DNA spectrum than either of the other lysine–glycine polypeptides.

At lysine/DNA-phosphate ratios of approximately 0.5 it was noted that in each case the DNA portion of the spectrum was reminiscent of spectra seen in chromatin isolated from various sources (19–29). That is, the single band at 275 nm in the spectrum of the native DNA shifted over to a smaller positive band at approximately 282 nm upon complex formation with polymers **III** and **IV** (Figs. 3 and 4). The origin of this 282 nm band might be connected with the more rapid loss of one of the two bands recently suggested to be present in this spectral region of the calf thymus DNA c.d. spectrum (30). Poly-(L-lysylglycine) (**II**) (Fig. 2) complexes at this ratio (0.5), on the other hand, were reminiscent of spectra taken of DNA in C-type conformation (31). In addition to these changes in the DNA portion of the spectrum little or no increase in ellipticity below 246 nm occurred and seemed to indicate that little long-range ordering, *e.g.* helix formation in the polypeptide, was resulting from complex formation.

Can. J. Chem. Downloaded from www.nrcresearchpress.com by 210.87.254.5 on 09/05/12
For personal use only.

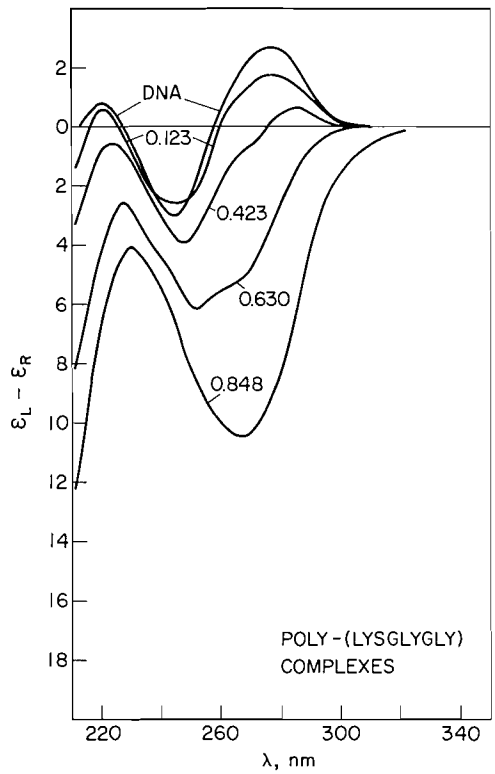

FIG. 3. Circular dichroic spectra of poly-(L-lysyl-glycylglycine)–DNA complexes. Variation of spectra with increasing lysine – DNA-phosphate ratios. Other details as for Fig. 1. Experimental conditions: DNA-phosphate concentration 1.76×10^{-4} *M*; sodium chloride, 0.15 *M*, sodium cacodylate, 0.001 *M*, p*H* 7.0.

Above lysine/DNA-phosphate ratios of 0.5 major differences in complex formation amongst the polylysine–glycine polypeptides became readily apparent. Polypeptides **III** and **IV** (Figs. 3 and 4) caused the formation of distorted c.d. spectra similar to those seen with polylysine (**I**) (Fig. 1), albeit of slightly reduced intensity at similar lysine/DNA-phosphate ratios. In appearance these spectra were like those seen in unoriented dehydrated films of DNA (31), in complexes formed between DNA and poly-(L-alanyl-L-lysyl-L-proline) (32), in complexes formed between calf thymus DNA and the lysine-rich histone f-1 (33–37) and in complexes of polyethylene oxide or sodium polyacrylate and DNA (38). Poly-(L-lysylglycine) (**II**) (Fig. 2) caused the formation of only slightly more distorted spectra than those observed at lower lysine/phosphate ratios; the resulting spectra being very similar to those of c.d. spectra of DNA in high salt concentrations (39–41).

The similarities and differences amongst annealed complexes formed between the polypeptides and DNA are further illustrated in Fig. 5 where changes in ellipticity at 275 nm with changes of lysine/DNA-phosphate ratio are plotted. From this plot it is readily apparent that in the case of polylysine complexes maximal distortion of the DNA spectrum occurred at lysine/DNA-phosphate ratios around 0.7 whereas in the case of the lysine–glycine polypeptide maximal distortion occurred at lysine/DNA-phosphate ratios around 1.5. Finally, within the group of lysine–glycine polypeptides, poly-(L-lysylglycine) (**II**) seemed to cause the least amount of distortion to the DNA spectrum at all lysine/DNA-phosphate ratios.

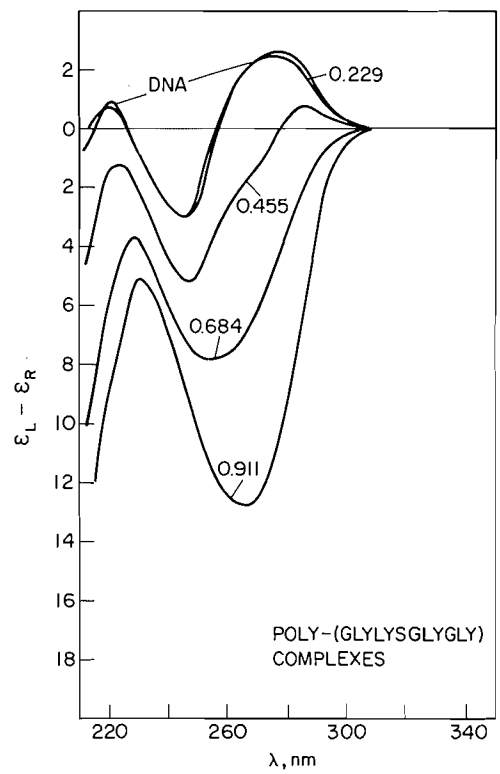

FIG. 4. Circular dichroic spectra of poly-(glycyl-L-lysylglycylglycine)–DNA complexes. Variation of spectra with increasing lysine/DNA-phosphate ratios. Other details as for Fig. 1. Experimental conditions: DNA-phosphate concentration 1.76×10^{-4} *M*; sodium chloride, 0.15 *M*, sodium cacodylate, 0.001 *M*, p*H* 7.0.

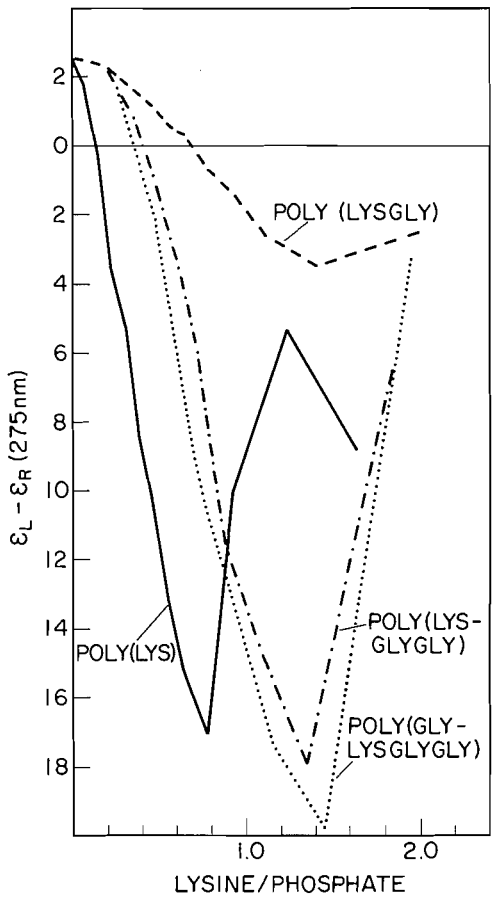

FIG. 5. Variation of molar ellipticity ($\varepsilon_L - \varepsilon_R$) at 275 nm with lysine/DNA-phosphate ratio in complexes between the lysine and lysine/glycine polypeptides and DNA. No corrections for sample turbidity have been made. Experimental conditions: DNA-phosphate concentration: 1.48×10^{-4} *M*; sodium chloride, 0.15 *M*, sodium cacodylate, 0.001 *M*, p*H* 7.0.

Discussion

The results indicate that, in the case of each of the polypeptides, changes in the original solution c.d. spectrum of DNA occur upon increasing the lysine/phosphate (L/P) ratio. These changes, as manifest in changes in the ellipticity at 275 nm (Fig. 5), seem to be of either large or small magnitude relative to the original c.d. spectrum of DNA. Large magnitude changes in the c.d. spectrum, for example those seen in Figs. 1, 3, and 4 at L/P ratios above 0.5, have been suggested to be the result of at least three different, but not unrelated, causes: (*i*) long-range order has been introduced into the DNA (18, 33, 37); (*ii*) solvent surrounding the DNA has been excluded (18, 33, 37); (*iii*) an increase in interhelix interactions caused by aggregation of the DNA has taken place (33, 37, 38). Small magnitude changes in the c.d. spectra, for example, those seen in Figs. 3 and 4 at L/P ratios below 0.5 and in Fig. 2 at all L/P ratios, could be the result, again, of at least three different, but not unrelated, causes: (*i*) the conformation of DNA has changed from that of the B-type to that of the C-type (31, 33); (*ii*) the charge shielding of the DNA sugar–phosphate backbone has been altered (39–41); (*iii*) the interhelix interactions in the aggregated state of the DNA have been reduced (33, 38).

The results also indicate that, even though the observed c.d. spectra are a mix of the spectra of complexed and uncomplexed DNA, differences in the abilities of the polypeptides to cause large or small magnitude changes in the DNA c.d. spectrum exist. These differences are unlikely to be caused by differences in the molecular weight of the polypeptides since each has very similar molecular weights and distributions of molecular weights (9).

The differences noted in the L/P ratio where maximal distortion of the DNA c.d. spectrum occurs (Fig. 5) could be attributed to either one of two different, but not unrelated, causes: (*i*) the poly-(L-lysine) and the lysine–glycine polypeptides adopt different conformations in the final complex; (*ii*) the state of aggregation of the DNA in the two types of complexes differs.

The differences might be related to differences in the abilities of the polypeptides to adopt discrete conformations. This, thereby, would influence the type of conformation the polypeptide could adopt in the final complex. The differences in conformational flexibility might be related to the fact that the polypeptides seem to possess different abilities to adopt several discrete conformations in solution. Poly-(L-lysine), as assessed by changes in its solution optical rotatory dispersion (o.r.d.) and c.d. spectrum, has been shown to have the ability to adopt several discrete conformations, dependent upon conditions of p*H*, ionic strength, and temperature (42–49). In contrast, the constancy of the c.d. spectrum of the lysine–glycine polypeptides upon changes in p*H* and ionic strength (9) as well as the presence of the helix-breaking amino acid, glycine (50), strongly suggest that they are unable to adopt radically different conformations in solution.

Can. J. Chem. Downloaded from www.nrcresearchpress.com by 210.87.254.5 on 09/05/12
For personal use only.

Can. J. Chem. Downloaded from www.nrcresearchpress.com by 210.87.254.5 on 09/05/12
For personal use only.

On the other hand, the differences might be related to differences in the state of aggregation of the DNA in the complexes. The presence or absence of an uncharged amino acid in the polypeptide, in this instance, glycine might be expected to influence DNA interhelix interactions through changes in the balance between electrostatic and hydrophobic forces in the complex. These changes in interhelix interactions might lead to changes in the compacting of the polypeptide–DNA structure and thus, to differences in the ordering of the DNA (18, 37, 38).

At present, the information is insufficient for a choice to be made between these two possible causes and further work in this area will be required before such a choice can be made.

The differences noted in the type of DNA c.d. spectrum seen at L/P ratios where maximal distortion of the c.d. spectrum occurs (Figs. 1–4) could be related to either one of two different, but not unrelated, causes: (*i*) the polypeptides possess different primary sequences; (*ii*) different states of interhelix interactions occur because of different states of DNA aggregation.

Differences in the polypeptide sequences might result in differences in the juxtaposition of charged groups within the complexes. Based on the predominance of simple electrostatic interactions between the polypeptides and the DNA it was recently suggested (9), after modification of a previous proposal (51), that juxtaposition of the positively-charged side chain of the lysine-containing peptides and the negatively-charged phosphates of one strand of the DNA would account for the differences observed in the abilities of the polypeptides to precipitate DNA from solution (9).

Where direct juxtaposition of charged groups would result, the polypeptide would be expected to have little influence on the overall DNA structure, save that of diminishing the electrostatic charges of the phosphate groups. This would offer a plausible explanation of the observations made on the poly-(L-lysylglycine)–DNA complexes (Fig. 2).

Where direct juxtaposition of charged groups would not be possible, thwarted either by primary sequence dictates or by polypeptide chain flexibility, much more extensive influence on the overall DNA structure might be expected. Primary sequence dictates would offer a plausible explanation of the observations made on the poly-(L-lysine)- –and poly-(L-lysylglycylglycine)–DNA complexes (Figs. 1 and 3, respectively). Polypeptide chain flexibility and a resulting lack of cooperativity in aligning charges would offer a plausible explanation of the observations made on the poly-(glycyl-L-lysylglycylglycine)–DNA complexes (Fig. 4).

Differences in type of c.d. spectra might also be related to the states of interhelix interactions which might result from differences in the states of aggregation caused by the polypeptides. This would require that the complexes formed by poly-(L-lysylglycine) and DNA (Fig. 2) be quite different from those of the others (Figs. 1, 3, and 4). The reason for this unique difference is not absolutely clear at present although it could be related simply to the presence of a series of positive charges along the polypeptide backbone which are in phase with the negatively charged phosphates of the DNA. Obviously more structural information would be required to ascertain if, indeed, the complexes of poly-(L-lysylglycine) and DNA did differ fundamentally from those of the others.

The authors wish to thank M. Hector Séguin for elemental analyses, M. A. E. Castagne for amino acid analyses.

1. D. E. Olins, A. L. Olins, and P. H. von Hippel. J. Mol. Biol. **33**, 265 (1968).
2. S. Inoue and T. Ando. Biochem. Biophys. Res. Commun. **32**, 501 (1968).
3. J. T. Shapiro, M. Leng, and G. Felsenfeld. Biochemistry, **8**, 3219 (1969).
4. S. Inoue and T. Ando. Biochemistry, **9**, 395 (1970).
5. M. Haynes, R. A. Garrett, and W. B. Gratzer. Biochemistry, **9**, 4410 (1970).
6. M. Zama and S. Ichimura. Biochem. Biophys. Res. Commun. **44**, 936 (1971).
7. M. Zama and S. Ichimura. Biochim. Biophys. Acta, **294**, 214 (1973).
8. C. Chang, M. Weiskopf, and H. J. Li. Biochemistry, **12**, 3028 (1973).
9. J. Brown, J. R. Langlois, D. R. Lauren, B. K. Stoochnoff, and R. E. Williams. Can. J. Chem. **52**, 3140 (1974).
10. R. E. Williams and V. L. Seligy. Can. J. Biochem. **52**, 281 (1974).
11. H. R. Mahler, B. Kleine, and B. D. Mehrotra. J. Mol. Biol. **9**, 801 (1964).
12. D. F. Detar. Anal. Chem. **41**, 1406 (1969).
13. W. C. Kreuger and L. M. Pschigoda. Anal. Chem. **43**, 675 (1971).
14. D. Carroll. Anal. Biochem. **44**, 496 (1971).
15. J. Brahms and S. Brahms. *In* Fine structure of proteins and nucleic acids. *Edited by* G. D. Fasman and S. N. Timasheff. M. Dekker, New York. 1970. p. 191.
16. I. Tinoco, Jr. and C. R. Cantor. *In* Methods of

biochemical analysis. Vol. 18. *Edited by* D. Glick. Interscience, New York. 1970. p. 81.
17. S. Beycock. Ann. Rev. Biochem. **37**, 437 (1968).
18. D. Carroll. Biochemistry, **11**, 421 (1972).
19. T. Y. Shih and G. D. Fasman. J. Mol. Biol. **52**, 125 (1970).
20. V. I. Permagorov, V. G. Debabov, J. A. Slakkova, and B. A. Rebentish. Biochim. Biophys. Acta, **199**, 556 (1970).
21. P. Henson and I. O. Walker. Eur. J. Biochem. **16**, 524 (1970).
22. F. X. Wilhelm, M. H. Champagne, and M. P. Daune. Eur. J. Biochem. **15**, 321 (1970).
23. T. Wagner and T. C. Spelsberg. Biochemistry, **10**, 259 (1971).
24. I. Fric and J. Sponar. Biopolymers, **16**, 1525 (1971).
25. A. Matsuyama, T. Tagashira, and C. Nagata. Biochim. Biophys. Acta, **240**, 181 (1971).
26. E. I. Ramm, V. I. Vorobev, T. M. Birshtein, I. A. Bolotina, and M. V. Volkenshtein. Eur. J. Biochem. **25**, 245 (1972).
27. R. E. Williams, P. F. Lurquin, and V. L. Seligy. Eur. J. Biochem. **29**, 426 (1972).
28. R. S. Johnson, A. Chan, and S. Hanlon. Biochemistry, **11**, 4347 (1972).
29. S. Hanlon, R. S. Johnson, B. Wolf, and A. Chan. Proc. Natl. Acad. Sci. U.S. **69**, 3263 (1972).
30. B. D. Wells and J. T. Yang. Biochemistry, **13**, 1317 (1974).
31. M. J. B. Tunis-Schneider and M. F. Maestre. J. Mol. Biol. **52**, 521 (1970).
32. J. Sponar, S. Stokova, I. Koruna, and K. Blaha. Coll. Czech. Chem. Commun. **39**, 1625 (1974).
33. G. D. Fasman, B. Schaffhausen, L. Goldsmith, and A. Adler. Biochemistry, **9**, 2814 (1970).
34. A. J. Adler and G. D. Fasman. J. Phys. Chem. **75**, 1516 (1971).
35. T. Y. Shih and G. D. Fasman. Biochemistry, **11**, 398 (1972).
36. J. M. Gottesfeld, M. Calvin, R. D. Cole, D. M. Igdaloff, V. Moses, and W. Vaughan. Biochemistry, **11**, 1422 (1972).
37. J. Sponar and I. Fric. Biopolymers, **11**, 2317 (1972).
38. C. F. Jordan, L. S. Lerman, and J. H. Venable, Jr. Nature (New Biol.), **236**, 67 (1972).
39. D. S. Studdert, M. Patroni, and R. C. Davis. Biopolymers, **11**, 761 (1972).
40. C. Zimmer and G. Luck. Biochim. Biophys. Acta, **312**, 215 (1973).
41. V. I. Ivanov, L. E. Minchenkova, A. K. Schyolkina, and A. I. Poletayev. Biopolymers, **12**, 89 (1973).
42. G. Holzworth and P. Doty. J. Am. Chem. Soc. **87**, 218 (1965).
43. P. Sarkar and P. Doty. Proc. Natl. Acad. Sci. U.S. **55**, 981 (1965).
44. B. Davidson, N. Tooney, and G. D. Fasman. Biochem. Biophys. Res. Commun. **23**, 156 (1966).
45. R. Townend, T. F. Kumosinski. S. N. Timasheff, G. D. Fasman, and B. Davidson. Biochem. Biophys. Res. Commun. **23**, 163 (1966).
46. B. Davidson and G. D. Fasman. Biochemistry, **6**, 1616 (1967).
47. M. L. Tiffany and S. Krimm. Biopolymers, **8**, 347 (1969).
48. D. G. Dearborn and D. B. Wetlaufer. Biochem. Biophys. Res. Commun. **39**, 314 (1970).
49. M. L. Tiffany and S. Krimm. Biopolymers, **11**, 2309 (1972).
50. V. S. Ananthanarayanan, R. H. Andreatta, D. Poland, and H. A. Sheraga. Macromolecules, **4**, 417 (1972).
51. M. H. F. Wilkins. Cold Spring Harb. Symp. Quant. Biol. **21**, 75 (1956).

Can. J. Chem. Downloaded from www.nrcresearchpress.com by 210.87.254.5 on 09/05/12
For personal use only.

Allowed and Forbidden Reaction Paths for the $H_2 + D_2$ Exchange Reaction

JAMES S. WRIGHT

Department of Chemistry, Carleton University, Ottawa, Canada K1S 5B6

JAMES S. WRIGHT. Can J. Chem. **53**, 549 (1975).

Symmetry arguments and *ab initio* s.c.f. calculations (double-zeta basis set) are used to show that the exchange reaction $H_2 + D_2 \rightarrow 2HD$ could proceed in a concerted fashion through a six-center transition state. The computed barrier height of 90 kcal/mol for this process lies below the experimental dissociation energy of H_2 (but above the computed dissociation energy) and also below the energy required for exchange through a four-center transition state. Either the termolecular (2+2+2) or bimolecular (4+2) cycloadditions are thermally allowed. The presence of a transition metal would allow the reaction to proceed through a four-center geometry, leading to the formation of a possibly stable metal-H_4 complex.

JAMES S. WRIGHT. Can. J. Chem. **53**, 549 (1975).

On utilise des arguments de symétrie et des calculs *ab initio* s.c.f. (ensemble double zeta) pour démontrer que la réaction d'échange $H_2+D_2 \rightarrow 2HD$ peut se produire d'une façon concertée par l'intermédiaire d'un état de transition à 6 centres. La barrière d'énergie calculée, 90 kcal/mol, pour ce processus est de beaucoup plus basse que l'énergie de dissociation déterminée expérimentalement pour H_2 (mais toutefois au dessus de la valeur calculée pour cette énergie de dissociation) et aussi plus basse que l'énergie requise pour un état de transition impliquant 4 centres. Les cycloadditions thermoléculaires (2+2+2) ou bimoléculaire (4+2) sont thermiquement permises. La présence d'un métal de transition permettrait à la réaction de se produire par l'intermédiaire d'une géométrie à 4 centres conduisant à la formation possible d'un complexe stable métal-H_4. [Traduit par le journal]

Introduction

The mechanism of the simplest bimolecular reaction, $H_2 + D_2 \rightarrow 2HD$ is of continuing interest because of the apparent disagreement between theory and experiment. In the original experiment of Bauer and Ossa (1), H_2, D_2, and argon were heated to temperatures between 1060–1420 °K in a shock tube. HD was observed as a product, and the following kinetic parameters were obtained: overall order = 2.04 ± 0.05; order with respect to H_2 = 0.38 ± 0.02; order with respect to D_2 = 0.66 ± 0.02; order with respect to argon = 0.98 ± 0.03; activation energy = 42 kcal/mol. In order to explain the argon dependence, the asymmetry in the H_2–D_2 dependence, and the low activation energy, a vibrational excitation mechanism was proposed (1). According to this mechanism, preexcitation of H_2 (D_2) to a critical level is necessary before exchange can occur, which then proceeds via a four-center transition state. Other shock tube studies by Burcat and Lifshitz (2) and Kern and Nika (3) gave similar kinetic results.

The importance of vibrational energy in reactants was proven in a subsequent study by Bauer and co-workers (4), where vibrationally hot but translationally cold molecules were shown to be reactive at room temperature. The possibility of an atomic exchange mechanism, *i.e.* $H_2 \rightarrow 2H$ followed by $H + D_2 \rightarrow HD + H$ has been considered to be ruled out (1) both because of the observed low activation energy and on kinetic grounds; the expected amounts of atoms present were far too low to account for the amount of HD produced.

These experiments have stimulated theoretical searches for low-lying four-center transition states through which exchange could occur. These studies, which have increased both in number and in sophistication, are summarized in the recent extensive *ab initio* search of Silver and Stevens (5). These authors use a double-zeta basis set with full configuration interaction, and are in agreement with the results of previous studies in their failure to find any four-center transition state below the dissociation energy of H_2, 109 kcal/mol (classical limit). To avoid searching the full six-dimensional hyperspace of four atoms these studies have of necessity been restricted to configurations possessing a certain amount of symmetry; however, it appears increasingly unlikely that a low activation energy four-center transition state will be found (5, 6).

This apparent conflict between theory and experiment led the author to propose the possibility of a six-center exchange pathway and

Can. J. Chem. Downloaded from www.nrcresearchpress.com by 210.87.254.105 on 09/05/12
For personal use only.

Can. J. Chem. Downloaded from www.nrcresearchpress.com by 210.87.254.105 on 09/05/12
For personal use only.

to demonstrate the low energy of a hexagonal transition state (7). In the present paper we consider the orbital symmetry requirements along various possible paths leading to exchange, and supplement the discussion with *ab initio* calculations where appropriate.

Four-center Reaction Paths

It was shown by Hoffmann (8), using arguments based on the conservation of orbital symmetry (9), that the coplanar path proceeding through a square transition state is thermally forbidden. An approximate energy barrier for the process is that amount of energy necessary to raise two electrons from the bonding σ_g orbital in H_2 up to a non-bonding hydrogen 1s level, or 119 kcal/mole.[1] This very crude estimate is in reasonable agreement with the figure 142 kcal/mol obtained from quantum-mechanical calculations (10, 5).

Approaches other than coplanar may also be studied, and this has been done by several authors (5, 6, 10, 11, 20, 21). Two paths are particularly interesting: the orthogonal approach passing through a tetrahedron, and the linear approach (6). A correlation diagram for the orthogonal approach is shown in Fig. 1. Reactants pass through a tetrahedral transition state and the path is again thermally forbidden. The tetrahedral H_4 is a high-energy species (5, 6). Thus a resemblance to the allowed (2s + 2a) orthogonal path discussed by Woodward and Hoffman (9) for hydrocarbons is only superficial, due to the absence in this case of p-orbitals with their characteristic nodal properties.

A reaction path of particular interest to this study is the linear approach. A correlation diagram for this approach (also discussed by Gimarc (11)) is shown in Fig. 2. The occupied orbitals of $H_2 + H_2$ correlate directly with those of linear H_4 so the approach is thermally allowed. Indeed, linear equidistant H_4 has been shown to have the very low energy of about 45 kcal/mol relative to $H_2 + H_2$ (5, 12). However, as has been pointed out repeatedly, linear H_4 cannot serve as a transition state for exchange without bond breaking, as in

$$H—H + D—D \rightarrow H \ldots H \ldots D \ldots D \rightarrow H + HD + D$$

and subsequent high energy cost. Other paths have been considered, including the kite, Y, trapezoid, and rhombus geometries (6) and an allowed path suggested by Gimarc (11) passing

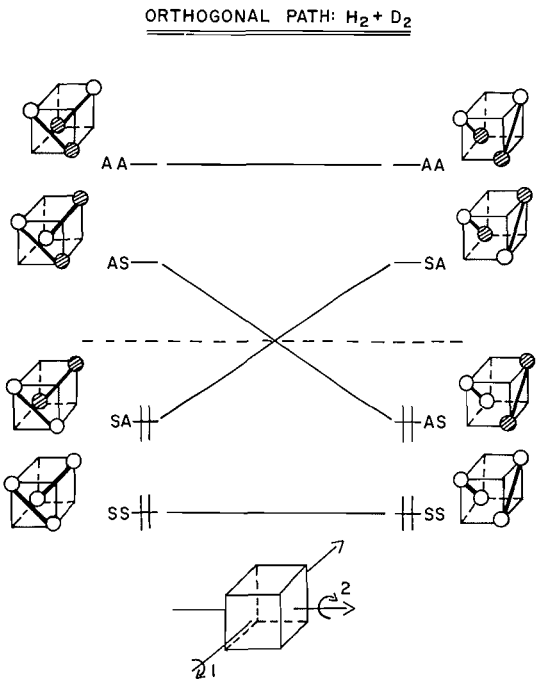

FIG. 1. Orthogonal four-center correlation diagram (thermally forbidden).

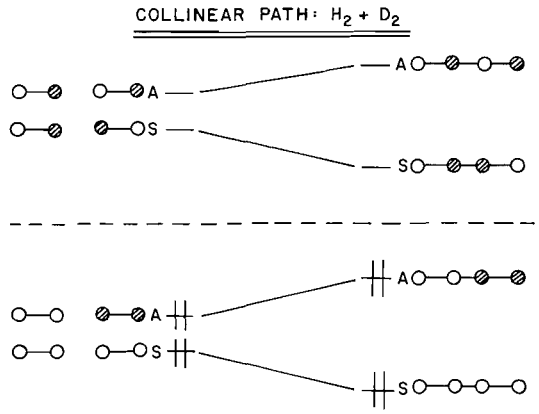

FIG. 2. Linear four-center correlation diagram (thermally allowed).

[1]A double-zeta calculation for H_2 at $r = 1.40$ bohr, $\xi_1 = 1.20$, $\xi_2 = 0.90$ gives -0.595 hartree as the energy of the σ_g orbital. The energy of the 1s orbital in the H atom is taken to be its exact value, -0.500 hartree. Since two electrons are raised to the non-bonding level, the total change is 119 kcal/mol.

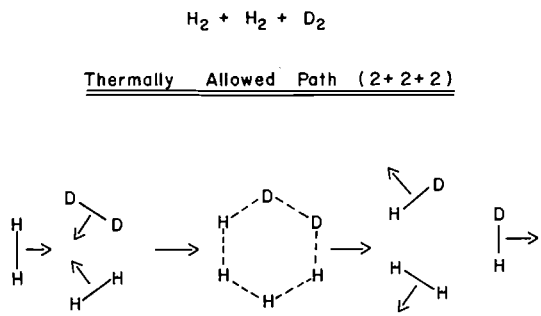

FIG. 3. The (2+2+2) termolecular cycloaddition, proceeding through a hexagonal transition state.

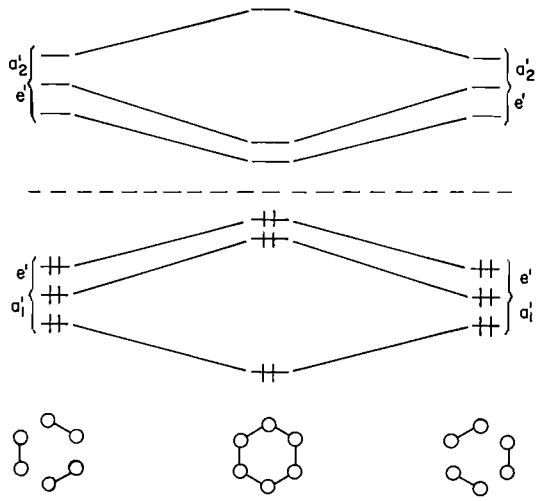

FIG. 4. Correlation diagram for termolecular exchange (thermally allowed).

through T- and Y-shaped transition states; however, it appears that these also are unfavorable energetically (5).

Application of the orbital phase continuity principle (21) has led to the prediction that *no* four-center pathway is of low energy. Thus, the theoretical attempts to find a low-lying four-center reaction path have not been successful, and we must consider alternative mechanisms.

Six-center Reaction Paths

Since (2+2+2) cycloadditions are in general thermally allowed (9), consider first a termolecular reaction, shown in Fig. 3. Along this path a three-fold axis of symmetry is preserved. Because of the C_3 axis and the resulting orbital degeneracy the S,A notation of Woodward and Hoffmann (9) breaks down, and it is necessary to return to group-theoretical notation and treat the conservation of molecular orbital configuration (13).[2] The symmetry combinations and their D_{3h} notation are shown in Fig. 4, which gives an orbital correlation diagram for the reaction passing through a hexagonal transition state. The occupied orbitals of like symmetry correlate directly, and the reaction is seen to be thermally allowed. The "aromatic" character of hexagonal H_6 should contribute to its stabilization (14), and a double-zeta s.c.f. calculation (7) showed hexagonal H_6 to lie only 90 kcal/mol above the energy of three molecules of H_2, *which is below the* (experimental) *energy required to dissociate* H_2. For comparison, the energy of $2H_2 + 2H$ obtained from the double-zeta calculation, and using the exact value of -0.500 hartree for the H atom (obtainable from a single basis orbital) would give an energy of $+80.5$ kcal/mol relative to $3H_2$. However, the fact that an exact result is obtained for H but not for H_2 skews this result, so that it is probably more meaningful to invoke the experimental dissociation energy of H_2 when comparing the energy of H_6, $3H_2$ and $2H_2 + 2H$. Assuming no additional barrier to be surmounted in the formation and decomposition of H_6 (as will be demonstrated), and neglecting zero point energy, an estimated activation energy for the formation of HD is 90 kcal/mol.

To establish whether hexagonal H_6 is a transition state or a potential minimum, a double-zeta calculation with the same exponents was used. The optimum hexagon at $r = 1.87$ bohr was allowed to distort along various possible paths, as shown in Fig. 5. The H_6 energy was studied as a function of increasing distortion. Figure 5*a* shows a "straight pull" path, where the optimum hexagonal distance was maintained at the internuclear distance of the separating H_2 molecules. After an initial flat region (energy constant to 0.001 hartree), the energy smoothly lowered toward that of three molecules of H_2 (at 1.87 bohr). H_6 thus is a transition state for this path, which is downhill toward product H_2. The B_{2u} normal mode for distortion is shown in Fig. 5*b*. Not surprisingly, the path from H_6 is more abruptly downhill, since H_2 can quickly ap-

[2]Alternative approaches include the generalized Woodward–Hoffman rules (9), or orbital phase continuity principle (21).

Can. J. Chem. Downloaded from www.nrcresearchpress.com by 210.87.254.105 on 09/05/12
For personal use only.

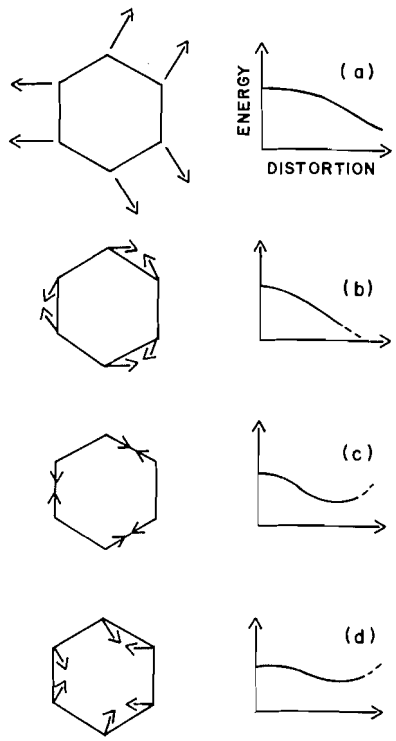

FIG. 5. Decomposition paths for hexagonal H_6. (*a*) Straight pull path. (*b*) B_{2u} distortion path. (*c*) Bond alternation path. (*d*) Implosion path.

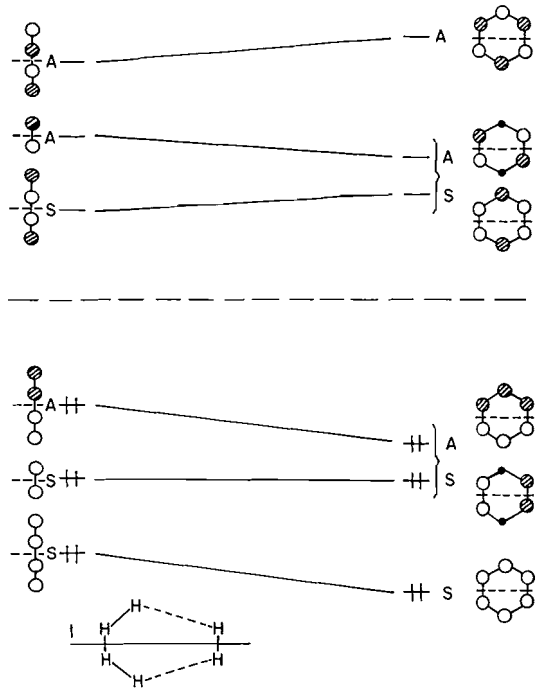

FIG. 6. Correlation diagram for the bimolecular (4+2) cycloaddition (thermally allowed).

proach its preferred distance. Figure 5*c* shows that the hexagon is unstable with respect to bond alternation, again apparently due to the driving force toward formation of H_2 at its optimum bond length. The hexagon is even unstable towards "implosion", as shown in Fig. 5*d*. H_6 is thus far from aromatic in any ordinary sense, although it certainly owes whatever stability it possesses to its benzene-like pattern and occupancy of molecular orbitals (14).

A Symmetry-allowed Biomolecular Path

A straightforward extension of the Woodward–Hoffmann rules to hydrogen systems suggest that a 4+2 cycloaddition, involving 6 electrons, is thermally allowed. As proposed earlier (7), we

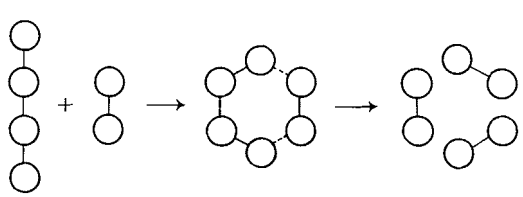

imagine a linear H_4 approached by D_2 in the manner shown below, collapse to the hexagon, and subsequent formation of $2HD + H_2$. The decomposition of the hexagon occurs with no additional activation energy, as already shown. Since the formation of linear H_4 has been shown to be thermally allowed, we need consider only the formation of hexagonal H_6 from linear $H_4 + H_2$. Figure 6 shows that the bonding orbitals of $H_4 + H_2$ do correlate directly with those of H_6. The reaction is allowed, but finding the activation energy for this approach is difficult, due to the number of geometric degrees of freedom available.

Geometric variables defining the (4+2) approach are shown in Fig. 7. Here R_1 is the distance of the approaching H_2, R_2 the (unique) distance in linear equidistant H_4, D the separation between opposite sides of the (incipient) hexagon, and α the bending angle in H_4. Starting from the optimum hexagon at 1.87 bohr, and using the geometric variables defined in Fig. 7, the results of a DZ calculation for the (4+2) decomposition are shown in Table 1. The important result is that there is *no* barrier

Can. J. Chem. Downloaded from www.nrcresearchpress.com by 210.87.254.105 on 09/05/12
For personal use only.

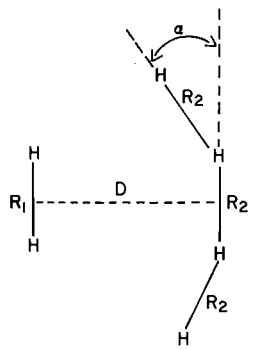

FIG. 7. Geometric variables used to define the (4+2) reaction path.

to be overcome along this path, which is smoothly downhill toward linear equidistant H_4 and H_2, the products of this reaction path. Further, it is seen that at large separation ($D = 4.00$) the energy of the H_6 system is correctly converging toward that of the separated products. The allowed nature of the reaction, and the closed-shell character of H_2, H_4, and H_6 makes this possible in a single determinant calculation.

Although the (4+2) path has the advantage of being a two-step process which is bimolecular at each step, there remains a serious objection to this mechanism. From the work of Silver and Stevens (5), it appears that linear H_4 does not represent a metastable state, even though it is of low energy. This makes it less likely that such a species could participate in a subsequent step, interaction with H_2 to form the hexagon. On the other hand, the only objection to the (2+2+2) path is the termolecular nature of the reaction. As will be discussed, related reactions now show that this sort of process can in fact occur.

TABLE 1. (4+2) decomposition path for hexagonal H_6[a]

R_1 (bohr)	R_2 (bohr)	α (deg)	D (bohr)	E (hartree)
Hexagon				
1.870	1.870	60	3.2389	−3.24086
1.850	1.865	59	3.2439	−3.24087
1.830	1.860	58	3.2489	−3.24094
1.790	1.850	56	3.2589	−3.24137
1.670	1.820	50	3.2889	−3.24567
1.550	1.740	30	3.5000	−3.27208
1.40	1.66	0	4.0000	−3.30188
Separated products				
1.40	1.66	0	∞	−3.3080[b]

[a]DZ basis set, exponents 0.90, 1.20.
[b]Optimum R_1 and R_2 for separated products.

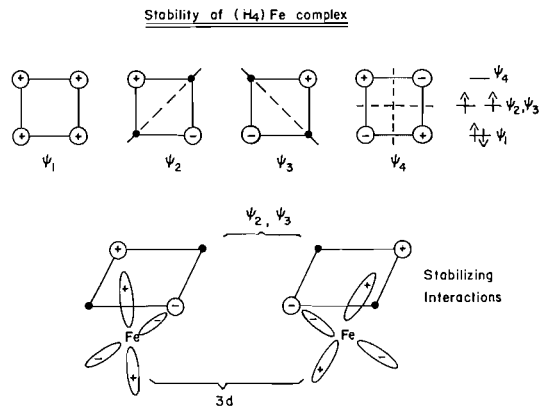

FIG. 8. Stabilizing interactions between non-bonding H_4 orbitals and metal d-orbitals.

Metal Catalysis

As shown by Mango and Schachtschneider (15), reactions which are symmetry forbidden can become allowed by interaction with the d-orbitals of a transition metal. These authors have discussed in detail the case of the addition of two ethylene molecules to give cyclobutane (16). The argument proceeds in a similar fashion for the $H_2 + D_2$ exchange reaction. As in (16), assume a degenerate pair of metal d-orbitals (d_{xy},d_{yz}) having AS and SA symmetry, respectively, and containing a total of 2 electrons. These orbitals can interact with the "ligand" $H_2 + D_2$ orbitals of the same symmetry. Since the non-bonding H_{1s} level at −0.5 hartree lies somewhat below the orbital energy of the metal d-orbital, the AS ligand orbital lies close to the d-orbital energy, and thus experiences a greater interaction with the AS d-orbital. Figure 8 shows these interactions depicted for square planar H_4 interacting with the metal. The net result is that non-bonding orbitals in H_4 and metal have become bonding, with a potentially significant lowering of the activation energy. A correlation diagram for the entire process is shown in Fig. 9 where it is to be understood that the metal orbitals lie underneath H_4 in such a way as to have the required overlap (*i.e.* the d-orbitals are shown in top view). SS and AA ligand orbitals are not included in the correlation diagram since their interaction with the metal is expected to be less significant. The reaction has become thermally allowed, since reactants correlate directly with products. The magnitude of the remaining activation energy is difficult to

Can. J. Chem. Downloaded from www.nrcresearchpress.com by 210.87.254.105 on 09/05/12
For personal use only.

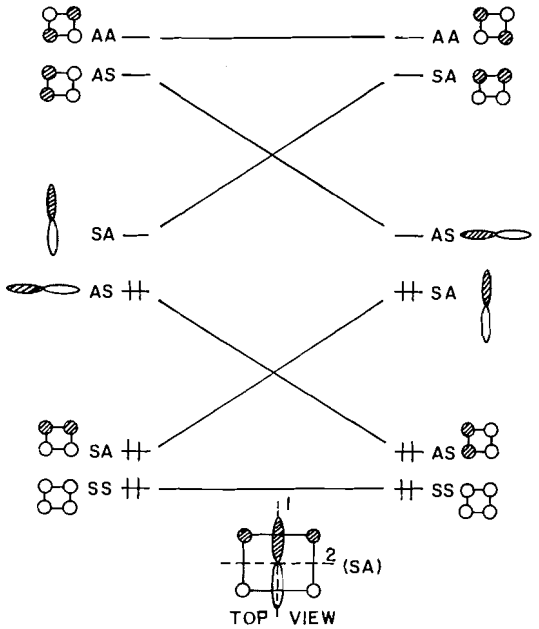

FIG. 9. Correlation diagram for the metal catalyzed 4-center reaction path (thermally allowed).

estimate, since it depends on the strength of the metal–ligand interaction in the region of the transition state. It is not difficult to imagine a stabilization in excess of 30 kcal/mol, which is the amount necessary to bring the energy of H_4 below that of $H_2 + 2H$.

We have so far assumed that the metal–H_4 complex would be a low-lying transition state along the exchange pathway. However, the formal similarity of the orbital energy pattern of square planar H_4 to that of the π-system in square planar cyclobutadiene (14) suggests that a *metastable* H_4–metal species might be isolable. The system iron–cyclobutadiene was predicted to be stable by Longuet-Higgins and Orgel (17) on theoretical grounds, and subsequently synthesized by Pettit and co-workers (18). The same theoretical argument applies to H_4: the degenerate non-bonding orbital containing two electrons can interact in a stabilizing way with the partially occupied metal d-orbitals, as shown previously in Fig. 8. The synthesis of a structure of type $H_4Fe(X)_3$, where X is a two-electron donor and H_4 is situated as described, would of course be of considerable interest.

Discussion

All the four-center reaction paths calculated to date, using *ab initio* techniques, are of unacceptably high activation energy to explain the mechanism of the $H_2 + D_2$ exchange reaction. It is therefore of interest to reexamine the experimental data to see whether, for example, the six-center path can be definitely ruled out.[3] Questions of mechanism have also been reviewed by Bauer and co-workers (4).

The possibility of a molecular exchange reaction proceeding through a six-center transition state has recently been proposed by King *et al.* (19). They studied the halogen exchange reactions $Cl_2 + Br_2$ and $Cl_2 + HI$ in crossed molecular beams. Analysis of the scattering data led to the conclusion that the reaction leading to formation of BrCl was termolecular and six-center. The same was true for the production of ICl. The authors stress the general nature of such a scheme. One reactant which is easily produced under their experimental conditions is a dimer of chlorine, $(Cl_2)_2$, considered to be a weakly bound "van der Waals molecule". By analogy $(H_2)_2$ would have a small van der Waals minimum, which would help to make the linear H_4 complex somewhat more "sticky".

In support of the four-center exchange mechanism the observed partial orders with respect to argon, H_2 and D_2 play a dominant role. As pointed out previously, the overall order is second, argon is strongly involved, and there is an asymmetry in the order between H_2 and D_2. These data have been successfully reconciled in the four-center mechanism with vibrational excitation (1). From the point of view of potential surface calculations, however, the resolution of a four-center transition state proceeds rather independently from these kinetic results. Argon is obviously not involved in the transition state, and the asymmetry in H_2, D_2 dependence seems best ascribed to dynamic effects. One is left with the question of how these results could be interpreted, even given a four-center potential surface of reasonable activation energy. It is the low experimental activation energy which has been the principal target of previous theoretical searches, and in this respect the exchange reaction proceeding through a six-center transition state is certainly promising. The inclusion of configuration interaction in the computation as well as correction for zero-point energy should lead to a lowering

[3]The author is grateful to Professor S. H. Bauer for a critical evaluation of the six-center mechanism from an experimental viewpoint.

Can. J. Chem. Downloaded from www.nrcresearchpress.com by 210.87.254.105 on 09/05/12
For personal use only.

of the energy of H_6 relative to $3H_2$. Such calculations are currently in progress (22).

The author would like to thank S. H. Bauer, D. R. Herschbach, and K. J. Laidler for helpful discussions, and the National Research Council of Canada for financial support.

1. S. H. Bauer and E. Ossa. J. Chem. Phys. **45**, 434 (1966).
2. A Burcat and A. Lifshitz. J. Chem. Phys. **47**, 3079 (1967).
3. R. D. Kern and G. G. Nika. J. Phys. Chem. **75**, 1615 (1971); **75**, 2541 (1971).
4. S. H. Bauer, D. M. Lederman, E. L. Resler, Jr., and E. R. Fisher. Int. J. Chem. Kin. **5**, 93 (1973).
5. D. M. Silver and R. M. Stevens. J. Chem. Phys. **59**, 3378 (1973) and references therein.
6. C. W. Wilson, Jr. and W. A. Goddard III. J. Chem. Phys. **51**, 716 (1969); **56**, 5913 (1972).
7. J. S. Wright. Chem. Phys. Lett. **6**, 476 (1970).
8. R. Hoffmann. J. Chem. Phys. **49**, 3739 (1968).
9. R. B. Woodward and R. Hoffmann. The conservation of orbital symmetry. Verlag Chemie, Gmbh. Weinheim. 1970.
10. M. Rubenstein and I. Shavitt. J. Chem. Phys. **51**, 2014 (1969).
11. B. M. Gimarc. J. Chem. Phys. **53**, 1623 (1970).
12. C. F. Bender and H. F. Schaefer III. J. Chem. Phys. **57**, 217 (1972).
13. L. C. Cusachs, M. Krieger, and C. W. McCurdy, Jr. Int. J. Quant. Chem. **35**, 67 (1969).
14. J. S. Wright. Theor. Chim. Acta. To be published.
15. F. D. Mango and J. H. Schachtschneider. J. Am. Chem. Soc. **89**, 2484 (1967).
16. F. D. Mango and J. H. Schachtschneider. *In* Transition metals in homogeneous catalysis. *Edited by* G. N. Schrauzer. Marcel Dekker. Inc., N.Y. 1971.
17. H. C. Longuet-Higgins and L. E. Orgel. J. Chem. Soc. (London) 1969 (1956).
18. J. D. Fitzpatrick, L. Watts, G. F. Emerson, and R. Pettit. J. Am. Chem. Soc. **87**, 3254 (1965).
19. D. L. King, D. A. Dixon, and D. R. Herschbach. J. Am. Chem. Soc. **96**, 3379 (1974); D. A. Dixon, D. L. King, and D. R. Herschbach. Faraday Discuss. Chem. Soc. **55**, 360 (1973).
20. D. M. Silver. Chem. Phys. Lett. **14**, 105 (1972).
21. W. A. Goddard III. J. Am. Chem. Soc. **94**, 793 (1972).
22. D. R. Herschbach. Private communication.

Can. J. Chem. Downloaded from www.nrcresearchpress.com by 210.87.254.105 on 09/05/12
For personal use only.

Synthèse et propriétés des *tert*-butyl-5 triméthyl-2,3,3 cyclohexanols[1]

JEAN-CLAUDE RICHER ET CLAUDE LAMARRE[2]

Département de Chimie, Université de Montréal, B.P. 6210, Montréal, Québec H3C 3V1

Reçu le 26 juillet 1974

JEAN-CLAUDE RICHER et CLAUDE LAMARRE. Can. J. Chem. **53**, 556 (1975).

On rapporte la synthèse des quatre *tert*-butyl-5 triméthyl-2,3,3 cyclohexanols. On compare les propriétés de ces alcools secondaires avec celles des alcools tertiaires obtenus précédemment lors de la réduction des époxydes dérivés du *tert*-butyl-5 triméthyl-2,3,3 cyclohexène; on peut confirmer que lors de la réduction de ces époxydes il ne se forme pas d'alcools secondaires. On discute de la stéréochimie de la réduction, par $LiAlH_4$, des *tert*-butyl-5 triméthyl-2,3,3 cyclohexanones.

JEAN-CLAUDE RICHER and CLAUDE LAMARRE. Can. J. Chem. **53**, 556 (1975).

The synthesis of the four 5-*tert*-butyl-2,3,3-trimethylcyclohexanols is reported and the properties of these secondary alcohols are compared with those of the tertiary alcohols obtained earlier from the reduction of 5-*tert*-butyl-2,3,3-trimethylcyclohexene epoxides. It is confirmed that secondary alcohols are not formed during the reduction of these epoxides. The stereochemistry of the $LiAlH_4$ reduction of the 5-*tert*-butyl-2,3,3-trimethylcyclohexanones is discussed.

[Journal translation]

Introduction

Nous avons rapporté (1) que la réduction des époxydes **1***a* conduit uniquement aux alcools tertiaires du type **2***a*; par ailleurs la réduction de **1***b* trans[3] conduit selon LeBel et Ecke (2*a*) ainsi que Murphy *et al.* (2*b*) à un mélange contenant seulement *ca.* 31% de l'alcool tertiaire **2***b trans* avec environ 62% d'alcool secondaire **3***b* et 7% d'alcool secondaire **4***b*. La publication de nos résultats a inquiété un certain nombre de collègues et soulevé des questions de la part d'un arbitre. Afin de lever toutes ambiguités concernant nos données, nous avons synthétisé et caractérisé les quatres *tert*-butyl-5 triméthyl-2,3,3 cyclohexanols **3***a*, **4***a*, **5***a* et **6***a* pouvant être formés lors de l'ouverture "anormale" des époxydes **1***a*. Ce sont les résultats stéréochimiques obtenus au cours de cette étude qui font l'objet de la présente note.

Résultats et discussion

L'hydroboration de l'alcène **7***a* effectuée dans le tétrahydrofuranne suivant la technique décrite par Brown et Zweifel (3) conduit, après oxydation des organoboranes intermédiaires par l'eau oxygénée alcaline, à un mélange 83:17 des alcools **4***a* et **5***a*. La chromatographie d'adsorption sur alumine et en phase gazeuse préparative permet d'isoler les deux alcools **4***a* et **5***a* à l'état pur. Leurs propriétés physiques sont résumées dans le tableau 1.

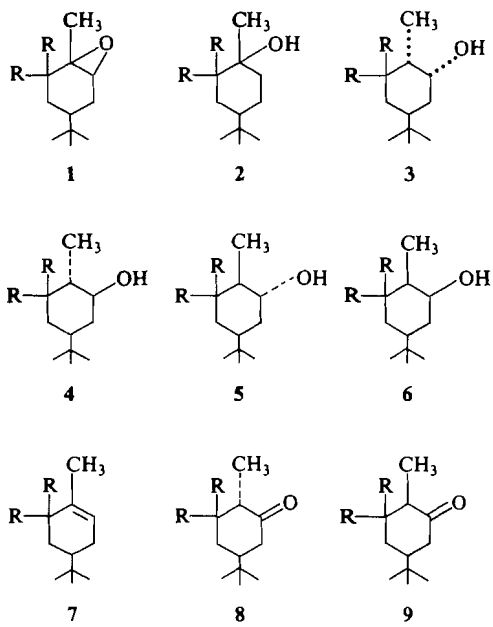

Série *a* R = CH_3; *b* R = H

[1]Les résultats rapportés dans cette note sont tirés en partie de la thèse présentée par Claude Lamarre à la Faculté des Sciences de l'Université de Montréal en vue de l'obtention du grade de Ph.D.

[2]Adresse actuelle: Institut de Recherche de l'Hydro-Québec à Varennes.

[3]La stéréochimie *cis* ou *trans* se réfère à la position relative des fonctions oxygénées par rapport au groupe *tert*-butyle.

Can. J. Chem. Downloaded from www.nrcresearchpress.com by 210.87.254.105 on 09/05/12
For personal use only.

TABLEAU 1. Caractéristiques des alcools **2***a* à **6***a*

Composé	Résonance magnétique nucléaire (CCl_4)		Infrarouge (CCl_4)	Chromatographie en phase gazeuse‡	Point de fusion (°C)
	δ*	$\Delta_H^{1/2}$†	C—O (cm^{-1})	T_r (min)	
3*a*	229.3(231.5)	6.75	980	16.25	§
4*a*	192(190)	18.75	1020	24	99
5*a*	228.6(224.5)	6.37	995	21	86
6*a*	231(229.5)	20.0	—	27	—
2*a cis*				3	
2*a trans*				3.5	

*Déplacement chimique (en Hz) du proton carbinolique *H*—COH. La valeur entre parenthèse est la valeur calculée pour ce déplacement selon la méthode d'Eliel (6).
†Largeur à la demi-hauteur du proton carbinolique *H*—C—OH en Hz.
‡Conditions: voir hyprose dans partie expérimentale.
§Point d'ébullion 105 °C/9 mm Hg; $n_D^{23.5}$ 1.4680.

L'oxydation de ce mélange par une solution d'acide chromique dans l'éther (4) conduit, avec un rendement de 50%, à un mélange des cétones **8***a* et **9***a*. Sous l'influence de l'hydrure de lithium et d'aluminium, ces cétones fournissent un mélange de quatre alcools **3***a*, **4***a*, **5***a* et **6***a* dans les proportions 82.4:8.0:6.8:2.8. La chromatographie en phase gazeuse préparative permet d'isoler **3***a* à l'état pur; ses propriétés sont consignées dans le tableau 1.

La réduction du mélange des cétones **8***a* et **9***a* par le sodium dans l'éthanol conduit aux alcools **4***a* et **6***a* dans un rapport de 89.8:10.2; les propriétés de l'alcool **6***a* sont rapportées au tableau 1.

Il découle d'un examen du tableau 1, dans lequel les propriétés des alcools **2***a cis* et *trans* ont été aussi ajoutées pour fins de comparaison, que les temps de rétention des divers alcools secondaires **3***a* à **6***a* sont très différents de ceux des alcools tertiaires épimères **2***a* et que l'on peut maintenant affirmer d'une façon catégorique que la réduction de l'époxyde **1***a trans*, par opposition à l'époxyde **1***b trans*, conduit uniquement à l'alcool tertiaire **2***a trans* sans traces d'alcools secondaires **3***a* et **4***a*.

Ces résultats signifient qu'une attaque de l'hydrure sur le carbone tertiaire de l'epoxyde **1***a trans* est défavorisée en partie par l'effet du méthyle en position 1 et principalement par le passage par un état de transition chaise déstabilisée par l'interaction 1,3 diaxiale entre le volumineux substituant oxyaluminate et le groupe méthyle; en effet ce processus impliquerait une énergie d'activation tellement élevée qu'il favoriserait plutôt l'attaque de l'hydrure sur le carbone secondaire de l'époxyde **1***a trans* conduisant ainsi à un état de transition ayant une conformation sous la forme croisée et ensuite, après hydrolyse, à l'alcool tertiaire **2***a trans*. (Voir schéma 1.)

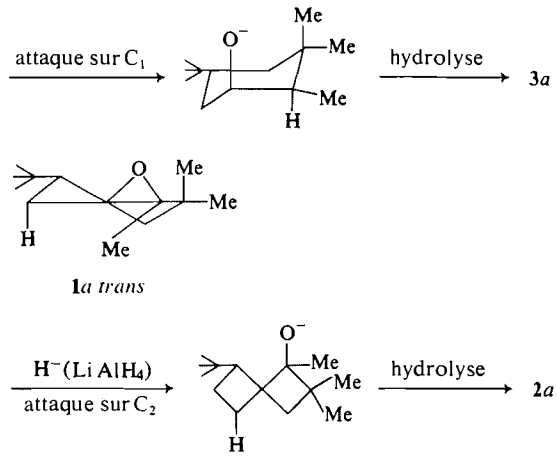

SCHÉMA 1

Les quantités importantes d'alcools axiaux par rapport aux alcools équatoriaux 82.4:8.0 et 6.8:2.8, obtenus lors de la réduction des cétones **8***a* et **9***a* par $LiAlH_4$, indiquent que la stéréochimie de ces réductions est affectée principalement par la présence d'un groupe méthyle axial en position 3 par rapport au groupement carbonyle.

Les pourcentages normalisés d'alcools équatoriaux **4***a* et **6***a* formés lors de la réduction par $LiAlH_4$ des cétones **8***a* et **9***a* sont respectivement de 9 et 30%. Ces résultats montrent d'une façon non ambigüe l'influence du groupe méthyle axial en position 2 de la cétone **9***a* qui contrebalance l'influence du groupe méthyle axial en position 3. Ces résultats tendent à supporter

Can. J. Chem. Downloaded from www.nrcresearchpress.com by 210.87.254.105 on 09/05/12
For personal use only.

Can. J. Chem. Downloaded from www.nrcresearchpress.com by 210.87.254.105 on 09/05/12
For personal use only.

l'hypothèse complètement stérique proposée (5) pour expliquer la stéreochimie des additions d'hydrure sur les cétones.

Partie expérimentale

Les spectres i.r. ont été pris sur un spectrophotomètre Beckman modèle IR-8 à double réseau. Les spectres de masse ont été enregistrés sur un spectromètre de masse Hitachi Perkin Elmer modèle RMU6-D et l'énergie du faisceau d'électrons ionisants était de 70 eV. Les spectres r.m.n. ont été déterminés sur un spectromètre modèle C-60 H de la Compagnie JeolCo. Le tétraméthylsilane est utilisé comme référence interne. Les points de fusion ont été pris sur un "hot stage apparatus" de la Compagnie Reichert et ne sont pas corrigés. Les indices de réfraction ont été déterminés à l'aide d'un réfractomètre de type Abbe de la Compagnie Karl Zeiss. Les analyses par chromatographie en phase gazeuse ont été effectuées à l'aide d'un appareil à détection thermique Microtek utilisant une colonne de 10 pieds par 1/4 de pouce contenant du chromosorb P 30–60 sur lequel 15% d'hyprose a été déposé. Les séparations par chromatographie en phase gazeuse préparative ont été effectuées sur un appareil Varian modèle 705 dans les conditions suivantes: colonne en aluminium de 20 pieds sur 3/8 de pouce de diamètre remplie de chromosorb P 30–60 sur lequel 20% d'hyprose a été déposé. Température de la colonne 160°, du collecteur 135°, du détecteur 255°, de l'injection 225°; le gaz porteur est l'azote et son débit est de 165 ml par min.

Hydroboration du tert-*butyl-4 triméthyl-1,6,6 cyclohexène* **7***a*

Le borane est préparé par addition, sur une période de 1½ h, de 3.6 g d'éthérate de trifluorure de bore fraîchement distillé à une solution de 1.3 g d'hydrure de bore et de sodium dans 50 ml de tétrahydrofuranne porté à reflux. Le borane ainsi formé est entraîné par un courant d'azote dans un ballon refroidi à 0 °C contenant 3.6 g d'alcène **7***a* en solution dans 25 ml de tétrahydrofuranne. Le traitement à la manière habituelle conduit à 3.9 g (rendement brut de 98%) d'un solide blanc qui par analyse en phase gazeuse sur hyprose à 160 °C, débit d'hélium de 75 ml/min, indique la présence de deux pics dans les proportions relatives suivantes: 17% de *tert*-butyl-5 triméthyl-2,3,3 cyclohexanol-1 (*trans* **5***a*), temps de retention 21 min, et 83% de *tert*-butyl-5 triméthyl-2,3,3 cyclohexanol-1 (*cis* **4***a*), temps de retention 24 min. La chromatographie de 6.6 g de ce mélange sur 700 g d'alumine Woelm neutre activité 1 permet d'isoler 5.6 g d'un mélange des deux alcools et 1 g de l'alcool **4***a* à l'état pur. La chromatographie en phase gazeuse préparative de 5.6 g de mélange permet d'isoler 100 mg de l'alcool secondaire **5***a* à l'état pur. Les caractéristiques de ces alcools sont décrites dans le Tableau 1.

Oxydation des alcools secondaires **4***a et* **5***a en cétones* **8***a et* **9***a*

L'oxydation de 9.5 g du mélange des alcools secondaires par 46 g de bichromate de sodium, selon la méthode de Brown et Garg (4), conduit après les extractions à la manière habituelle à 4.7 g (50% de rendement) du mélange des cétones de **8***a* et **9***a* qui n'ont pas pu être obtenues stéréochimiquement pures. Ces cétones ont un point d'ébullition de 114–118/12 mm Hg et présentent une bande à 1700 cm^{-1} dans l'infrarouge; l'indice de réfraction à 24 °C est 1.4609 et leur spectre de masse montre un ion moléculaire à *m/e* de 196.

Réduction des cétones **8***a et* **9***a par l'hydrure de lithium et d'aluminium*

La réduction de 2 g des cétones **8***a* et **9***a* par 1 g d'hydrure de lithium et d'aluminium dans l'éther anhydre conduit avec un rendement quantitatif au mélange des quatre alcools **3***a*, **4***a*, **5***a* et **6***a*; ce mélange peut être analysé par chromatographie en phase gazeuse sur hyprose à 160 °C avec un débit d'hélium de 75 ml/min. La chromatographie en phase gazeuse préparative sur hyprose de 2 g des alcools en solution dans 20 ml de méthanol permet d'obtenir 641 mg de l'alcool **3***a* à l'état pur. Les propriétés de cet alcool sont rapportées dans le Tableau 1.

La réduction par le sodium dans l'éthanol des cétones **8***a et* **9***a*

La réduction de 330 mg des cétones **8***a* et **9***a* par 5.5 g de sodium dans 55 ml d'éthanol absolu conduit à 287 mg (87% de rendement) d'un mélange des alcools **4***a* et **6***a* qui peuvent être séparés par chromatographie en phase gazeuse sur hyprose à 160 °C, débit d'hélium de 75 ml/min.

Les auteurs remercient vivement le Conseil national de recherche du Canada et le Ministère de l'Education de la Province de Québec pour l'aide financière apportée sous forme d'octroi de recherches (CNR A-1295) et de bourse de perfectionnement (C.L. 1966–1969).

1. J. C. Richer et C. Lamarre. Can. J. Chem. **47**, 2349 (1969).
2. (*a*) N. A. LeBel et G. G. Ecke. J. Org. Chem. **30**, 4316 (1965). (*b*) D. K. Murphy, R. L. Alumbaugh et B. Rickborn. J. Am. Chem. Soc. **91**, 2649 (1969).
3. H. C. Brown et G. Zweifel. J. Am. Chem. Soc. **83**, 2544 (1961).
4. H. C. Brown et C. P. Garg. J. Am. Chem. Soc. **83**, 2952 (1961).
5. J. C. Richer. J. Org. Chem. **30**, 324 (1965).
6. E. L. Eliel, M. H. Gianni, Th. W. Williams et J. B. Stothers. Tetrahedron Lett. 741, (1962).

The Reaction of Hydroperoxides with Triphenylarsine and Triphenylstibine

R. HIATT, CHRISTINE MCCOLEMAN, AND G. R. HOWE

Department of Chemistry, Brock University, St. Catharines, Ontario L2S 3A1

Received September 3, 1974

R. HIATT, CHRISTINE MCCOLEMAN, and G. R. HOWE. Can. J. Chem. **53**, 559 (1975).

Triphenylstibine reduced t-BuO_2H to t-BuOH almost as fast as Ph_3P does, while triphenylarsine reacts only 1/60 as fast. Both reductions are first-order in each component; in ethanol k_2 for Ph_3Sb and Ph_3As are $10^{6.7}e^{-9.7/RT}$ and $10^{9.1}e^{-15.7/RT}$, respectively. The reductions are not very sensitive to choice of solvent, but are strongly catalyzed by compounds of molybdenum and vanadium.

The relative rate order $PH_3P \geq Ph_3Sb > Ph_3As$ is ascribed to two conflicting trends, availability of d-orbitals for π-bonding with peroxidic oxygen, and the Group VB to oxygen bond strength.

R. HIATT, CHRISTINE MCCOLEMAN et G. R. HOWE. Can. J. Chem. **53**, 559 (1975).

La triphénylstibine réduit le t-BuO_2H en t-BuOH presqu'aussi rapidement que le fait Ph_3P; par ailleurs la triphénylarsine réagit environ 60 fois moins rapidement. Chacune des réductions est du premier ordre en chacun des réactifs; dans l'éthanol, les valeurs de k_2 pour Ph_3Sb et Ph_3As sont respectivement de $10^{6.7}e^{-9.7/RT}$ et $10^{9.1}e^{-15.7/RT}$. Les réductions ne sont pas sensibles au choix du solvant mais sont fortement catalysées par des composés du molybdène et du vanadium.

L'ordre relatif des vitesses $Ph_3P \geq Ph_3Sb > Ph_3As$ est attribué à deux tendances contradictoires soit la disponibilité d'orbitales pour former des liens π avec l'oxygène du peroxyde et la force de la liaison de l'oxygène avec les éléments du groupe VB. [Traduit par le journal]

Introduction

Not long ago we reported (1, 2) a kinetic study of the reduction of hydroperoxides by triphenylphosphine. This facile reaction, chiefly useful as an analytical tool (3, 4), was found to obey a simple relationship (1)

$$[1] \qquad \text{Rate} = k[RO_2H][Ph_3P]$$

and more importantly, although very rapid itself, to be catalyzed by compounds of vanadium and molybdenum (2). Thus the phosphines were placed squarely in the family of nucleophiles whose other members include olefins (5), organic sulfides, sulfoxides (6), and amines (7, 8) which stoichiometrically reduce hydroperoxides under the influence of these catalysts.

$$[2] \qquad RO_2H + N: \xrightarrow{\text{V or Mo}} ROH + N{\rightarrow}O$$

Phosphorous is unique, however, in giving clean reduction in the absence of catalyst, and may be contrasted particularly with nitrogen; amines take the alternate route of one electron reduction, free radical formation, and chain reaction unless catalyzed.

Accordingly it seemed desirable to investigate the other members of Group VA, arsenic, antimony, and bismuth. Horner and Jürgens had found earlier (3) that triphenylarsine reduced hydroperoxides (as well as acyl peroxides and peroxy acids) stoichiometrically and quantitatively, but did not comment on the rate of the reaction. The reduction of hydroperoxides by triphenylstibine has also been noted (8).

We here describe studies of the reactions of t-BuO_2H with Ph_3As and Ph_3Sb. Preliminary experiments on the reactions between Ph_3Bi and t-BuO_2H indicated a complexity which relegated that investigation to the area of future work.

Experimental

Triphenylarsine (Aldrich) and triphenylstibine (Eastman) were recrystallized from ethanol. t-Butyl hydroperoxide (*i.e.*, Lucidol) was generally used as received, as a 90% aqueous solution. Solvents were reagent grade, generally used without further purification.

To discover whether small amounts of water had any effect, some kinetic experiments were carried out with peroxide purified to greater than 99.5% by vacuum distillation and ethanol dried by distillation from magnesium. Also traces of water equal to that already present were added to reactions of unpurified hydroperoxide in undried ethanol. None of these measures had a noticeable effect on rates.

Rates of reaction were determined by monitoring the disappearance of the u.v. absorption characteristic of Ph_3M: Ph_3As, $\lambda_{max} = 240$ nm; Ph_3Sb, $\lambda_{max} = 255$ nm. Typically, a solution of each reactant in the solvent of choice was freshly prepared, aliquots were mixed and

Can. J. Chem. Downloaded from www.nrcresearchpress.com by 210.87.254.42 on 09/05/12
For personal use only.

Can. J. Chem. Downloaded from www.nrcresearchpress.com by 210.87.254.42 on 09/05/12
For personal use only.

rapidly decanted into a 1 cc thermostated u.v. cell. Concentrations were chosen to give at very least a 25-fold excess of t-BuO_2H over Ph_3M so that peroxide concentration was approximately constant over the course of any run.

For both Ph_3As and Ph_3Sb plots of log $[Ph_3M]$ *vs.* time gave good straight lines. For the Ph_3As runs, pseudo-first-order rate constants were determined using the Newton–Raphson method (9) applied to the equation $A_t - A_\infty = \exp(C + k_1 t)$, where the symbols have their usual meaning and both k_1 and A_∞ are treated as unknowns. A full description and a copy of the Fortran 4 subroutine have been deposited with the International Quantum Chemistry Program Exchange, Dept. of Chemistry, Indiana University, Bloomington, Indiana. For subsequent work with Ph_3Sb a less sophisticated but probably more accurate method was adopted. A large number of runs under identical conditions might differ by as much as 5%, but second order rate constants based on 9 or more determinations seemed reasonably reliable.

Results and Discussion

Products

Reactions on a preparative scale, *i.e.* ~0.1 *M* reactants, between t-BuO_2H and Ph_3As in ethanol confirmed the finding of Horner and Jürgens (3) that the reduction was stoichiometric, yielding only t-BuOH and Ph_3AsO. Crystalline Ph_3AsO was isolated and shown by mass spectrometric analysis to be identical to the product obtained from permanganate oxidation of Ph_3As (10).

Similarly reduction of t-BuO_2H with Ph_3Sb gave only t-BuOH and a crystalline antimony product having the same characteristics as that produced by oxidation of Ph_3Sb by H_2O_2 (11). This has been shown to be a polymeric material (12) and not the monomeric Ph_3SbO prepared by McEwen *et al.* (13).

Kinetics

In ethanol solvent both Ph_3As and Ph_3Sb exhibited first order disappearance in the presence of a large excess of t-BuO_2H, with pseudo first-order rate constants independent of $[Ph_3M]_0$, (Tables 1 and 2). These k_1 were directly proportional to $[t\text{-}BuO_2H]_0$, (varied by a factor of 4 for Ph_3As and a factor of 10 for Ph_3Sb). Dividing k_1 by $[t\text{-}BuO_2H]_0$ gave the second order rate constants (Tables 1 and 2).

$$[3] \qquad \text{Rate} = k_2[Ph_3M][t\text{-}BuO_2H]$$

Qualitatively both reactions are fast, but Ph_3Sb reacts about 60 times faster than Ph_3As and almost as fast as Ph_3P. Table 3 which compares the three reagents shows that the relative slowness of the Ph_3As–t-BuO_2H reaction is due to a higher activation energy.

Reactions in Other Solvents

Both Ph_3Sb and Ph_3As exhibited moderately faster reactions in ethanol–water mixtures than in ethanol (Table 4) and both reacted faster in hexane than in ethanol. This rate increase both when the solvent is made more polar and when it is made less polar, also found with Ph_3P (2) probably has a simple explanation. More acidic solvents facilitate the required proton transfer (2). However, both RO_2H and Ph_3M are dipoles

[4] 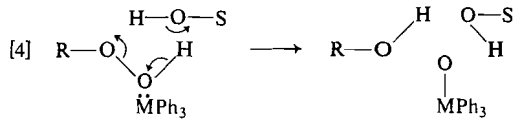

TABLE 1. Reduction of t-BuO_2H by triphenylstibine in ethanol

$[Ph_3Sb]_0$ (10^4 *M*/l)	$[t\text{-}BuO_2H]_0$ (10^3 *M*/l)	*T* (°C)	k_1 ($10^2\ s^{-1}$)	k_2 ($M^{-1}\ s^{-1}$)
0.50	13.9	25	0.376	0.307
1.00	13.9	25	0.385	0.307
2.00	13.9	25	0.393	0.307
1.00	5.55	25	0.174	0.307
1.00	27.8	25	0.867	0.307
1.00	55.5	25	1.83	0.307
1.00	2.58	35	0.146	0.569
1.00	5.16	35	0.282	0.569
1.00	13.9	35	0.707	0.569
1.00	25.8	35	1.44	0.569
1.00	51.6	35	2.89	0.569
1.00	2.58	45	0.237	0.924
1.00	5.16	45	0.495	0.924
1.00	25.8	45	2.31	0.924

Can. J. Chem. Downloaded from www.nrcresearchpress.com by 210.87.254.42 on 09/05/12
For personal use only.

TABLE 2. Reduction of t-BuO_2H by triphenylarsine in ethanol

$[Ph_3As]_0$ (10^4 M/l)	$[t\text{-}BuO_2H]_0$ (10^3 M/l)	T (°C)	k_1 (10^5 s^{-1})	k_2 (M^{-1} s^{-1})
0.351	4.4	41.7	7.6 ± 0.03	0.0173
0.676	4.4	41.7	7.7 ± 0.03	0.0175
0.676	6.6	41.7	12.3 ± 0.02	0.0186
0.676	1.25	41.7	20.5 ± 0.09	0.0164
0.676	1.78	41.7	29.7 ± 0.2	0.0166
0.676	1.78	33.5	15.1 ± 0.08	0.0085
0.676	1.78	37.1	19.6 ± 0.07	0.0101
0.676	1.78	39.2	25.7 ± 0.09	0.0144
0.676	1.78	44.4	35.8 ± 0.03	0.0201

TABLE 3. Constants for the reduction of t-BuO_2H by R_3M*
(Rate = $[RO_2H]\{k_2[R_3M] + k_3[R_3M][V_{naphth}]\}$)

R_3M	k_2, 35 °C (M^{-1} s^{-1})	$\log A_2$	E_{a2} (kcal/mol)	10^{-4} k_3 (°C) (M^{-2} s^{-1})
$PhNH_2$	†	—	—	0.000024 (66)‡
Ph_3P	0.72	7.8	11.2 0.2	1.0 (25)
Ph_3As	0.0093	9.1	15.7 0.7	0.42 (35)
Ph_3Sb	0.57	6.7	9.7 0.4	2.7 (25)

*In ethanol unless otherwise noted.
†Not measurable.
‡In benzene, calculated from ref. 7*b* assuming a third order reaction.

TABLE 4. Reduction of t-BuOH by triphenylstibine and triphenylarsine in various solvents

Solvent	T(°C)	$[t\text{-}BuO_2H]_0$	k_2 (M s^{-1})
$[Ph_3Sb]_0 = 1.00 \times 10^{-4}$ M			
EtOH + trace H_2O	25	21.0	0.314
95% EtOH/H_2O v/v	25	19.6	0.384
90% EtOH/H_2O v/v	25	18.0	0.47
n-Hexane	25	9.40	0.35
$[Ph_3As]_0 = 1.00 \times 10^{-4}$ M			
95% EtOH/H_2O v/v	35	49.0–98.0	0.0152
90% EtOH/H_2O v/v	35	45.0–90.0	0.0205
n-Hexane	35	94.0	0.043

and it is not unreasonable to expect that the transition state would permit a wider distribution of partial charge.

Catalysis by Metal Ions

Most of the molybdenum and vanadium catalysts at our disposal exhibited too great an absorption in the 240–260 nm region to be used in conjunction with the analytical method. However, trace quantities of vanadium naphthenate or $Mo(CO)_6$ could be used and their strong catalytic effect is shown in Table 5.

Plots of k_2 *vs.* $[V_{naphth}]$ intercepted nicely at k_2 measured in the absence of catalyst, leading to the equation

[5] Rate = $[Ph_3M][t\text{-}BuO_2H](k_2 + k_3[V_{naphth}])$

A similar plot for $Mo(CO)_6$ did not intercept at the uncatalyzed rate; this may have been due to the formation of $Mo(CO)_5SbPh_3$ and $Mo(CO)_4(SbPh_3)_2$ during the course of the reaction.

Relative Reactivities

The order of reactivity with t-BuO_2H (Table 3); $PhNH_2 \ll Ph_3As < Ph_3Sb \leq Ph_3P$, is surprising in two respects; the transposition of As

TABLE 5. Catalysis of the reaction between t-BuO_2H and Ph_3M in ethanol

Catalyst	Concentration (10^5 g/ml)	M	T(°C)	k_2 (M^{-1} s^{-1})
V^{III} naphthenate	1.02	As	35	0.034
V^{III} naphthenate	2.50	As	35	0.071
V^{III} naphthenate	0.32	Sb	25	0.30
V^{III} naphthenate	1.60	Sb	25	0.56
V^{III} naphthenate	3.20	Sb	25	0.81
$Mo(CO)_6$	0.055	Sb	25	0.46
$Mo(CO)_6$	0.225	Sb	25	1.49

TABLE 6. Second order rate constants for nucleophilic substitutions at O—O compared to other subtrates

	k_2 (M^{-1} s^{-1})		
Nucleophile	H_2O_2*	$Pt(py)_2Cl_2$†	CH_3I§
$PhNH_2$		0.43	0.052
Ph_3P	(0.72)‡	249 000	1.29
Ph_3As	(0.0093)‡	2320	0.0075
Ph_3Sb	(0.57)‡	1810	Very slow
CN^-	0.001	4000	0.65
I^-	0.011	107	3.42
OH^-	1×10^{-7}		(0.25)§

*In H_2O at 25 °C, ref. 17.
†In H_2O at 25 °C, ref. 15.
‡t-BuO_2H in ethanol at 35 °C.
§MeO^-.

and Sb, and the virtual equality of Sb and P. That is, a series of nucleophilic attacks on a soft electrophile is expected to follow $N \ll Sb < As < P$ (14, 15) and this order has been found in rate studies of ligand substitution reactions (15, 16) (Table 6). It is also the order of the M to oxygen bond strength (14).

[6] $TX_lY_m + MPh_3 \rightarrow TX_lY_{m-1}(MPh_3) + Y$

where T is a transition metal and X and Y are the original ligands.

But as Pearson *et al.* have warned (15) it is fruitless to make too close correlations between apparently similar nucleophilic substitutions. To point out some anomalies, Table 6 compares displacements on peroxidic O—O (17) with those on $Pt(py)_2Cl_2$ and on CH_3I; values for H_2O_2 with MPh_3 are not available, but those from Table 3 for t-BuO_2H can be transposed with some confidence that orders of magnitude errors are not involved (17). While it is evident that reactivities of Ph_3M with O—O do not parallel their reactivities with $Pt(py)_2Cl$ or with methyl iodide, it is equally true that CN^- and OH^- do not parallel I^-. The low nucleophilicity of OH^- and CN^- for 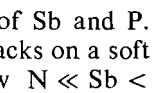 , as compared to 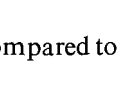 has been explained in terms of nonbonded electron pair repulsions in the transition state. Conversely nucleophiles having low-energy unoccupied orbitals may minimize this repulsion through back-bonding (17, 18).

If the availability of the d orbitals for π-bonding increases monotonically in $Ph_3P \rightarrow Ph_3Sb$, for which there is some evidence (19), the nucleophilicity for oxygen should increase similarly if this were the only important effect. However, the strength of the M-to-oxygen bond being formed must be considered as well. Both As—O and Sb—O bonds are weak while the P—O bond is very strong (19). The combination of these factors satisfactorily accounts for the trend we have observed.

Finally, the relative rates for the vanadium-catalyzed reduction (Table 3), Sb > P > As, fit this hypothesis nicely. Catalysis as well as lowering the activation energy and exerting a general leveling effect would tend to move the transition state forward on the reaction coordinate, making

Can. J. Chem. Downloaded from www.nrcresearchpress.com by 210.87.254.42 on 09/05/12
For personal use only.

it less product-like. The effect of P—O bond strength is diminished, and Ph_3Sb reacts faster than Ph_3P.

The authors gratefully acknowledge financial support received from the National Research Council of Canada.

1. R. HIATT, R. J. SMYTHE, and C. MCCOLEMAN. Can. J. Chem. **49**, 1707 (1971).
2. R. HIATT and C. MCCOLEMAN. Can. J. Chem. **49**, 1712 (1971).
3. L. HORNER and E. JÜRGENS. Angew Chem. **70**, 266 (1958).
4. R. D. MAIR and R. T. HALL. Organic peroxides. Vol. 2. *Edited by* D. Swern. Wiley, New York. 1971. Chapt. 6.
5. (*a*) N. M. SHENG and J. G. ZAJACEK. Adv. Chem. Ser. No. 75, Am. Chem. Soc., Washington, D.C. 1968; (*b*) G. R. HOWE and R. HIATT. J. Org. Chem. **36**, 2493 (1971).
6. VON F. LIST and L. KUHNEN. Erdol Kohle Erdgas Petrochem. 192 (1967).
7. (*a*) N. M. SHENG and J. G. ZAJACEK. J. Org. Chem. **33**, 588 (1968); (*b*) G. R. HOWE and R. HIATT. J. Org. Chem. **35**, 4007 (1970).
8. G. A. RAZUVAEV, T. G. KRILKINA, E. V. KASIL'NIKOVA, T. I. ZINOV'EVA, and A. I. FILIMONOV. J. Organometal. Chem. **40**, 151 (1972).
9. G. R. HOWE. J. Phys. Chem. **75**, 1319 (1971).
10. A. W. JOHNSON. J. Org. Chem. **25**, 183 (1960).
11. G. O. DOAK and L. D. FREEDMAN. Organometallic compounds of arsenic, antimony and bismuth. Wiley, New York. 1970. p. 303.
12. D. L. VENEZKY, C. W. SINK, B. A. NEVETT, and W. F. FORTESCUE. J. Organometal. Chem. **35**, 131 (1971).
13. W. E. MCEWEN, G. H. RILES, and D. N. SCHULTZ. Phosphorous, **2**, 147 (1972).
14. C. S. G. PHILLIPS and R. J. P. WILLIAMS. Inorganic chemistry. Vol. 1. Oxford University Press, New York. 1965. pp. 628–632.
15. R. G. PEARSON, H. SOBEL, and J. SONGSTAD. J. Am. Chem. Soc. **90**, 319 (1968).
16. G. CARDOCI, A. FOFFANI, G. DISTEFANO, and G. INNORTA. Inorg. Chem. Acta, **1**, 340 (1967).
17. R. CURCI and J. O. EDWARDS. Organic peroxides. Vol. 1. *Edited by* D. Swern. Wiley, New York. 1970. Chapt. 4.
18. J. O. EDWARDS and R. G. PEARSON. J. Am. Chem. Soc. **84**, 16 (1962).
19. N. P. BORISOVA and L. N. PETROV. Zhur Strukt. Khim. **13**, 701 (1972).

Can. J. Chem. Downloaded from www.nrcresearchpress.com by 210.87.254.42 on 09/05/12
For personal use only.

A New Method for Determining Individual Rate Constants for Specific Non-chromophoric Substrates of Proteolytic Enzymes

LEWIS J. BRUBACHER

Department of Chemistry, University of Waterloo, Waterloo, Ontario N2L 3G1

Received July 9, 1973[1]

LEWIS J. BRUBACHER. Can. J. Chem. **53**, 564 (1975).

Equations are developed for the pre-steady state kinetics of the proteolytic enzyme-catalyzed hydrolysis of a substrate A in the presence of a monitoring substrate (or covalent inhibitor) S of known properties. A two-intermediate acyl–enzyme mechanism is assumed in which the first intermediate is in instantaneous equilibrium with enzyme and substrate. The appearance of the first product of substrate S is characterized by two relaxation rate constants. From these constants it is possible to determine the dissociation constant and the acylation and deacylation rate constants of substrate A. Criteria are also developed for using the steady state rate parameters of A to establish conditions for which the slower relaxation process is equivalent to the deacylation rate constant of A. The technique of premixing enzyme with substrate A has certain advantages in this approach.

LEWIS J. BRUBACHER. Can. J. Chem. **53**, 564 (1975).

On a développé des équations pour calculer la cinétique intervenant avant l'état stationnaire lors de l'hydrolyse protéolitique, catalisée par les enzymes, d'un substrat A en présence d'un substrat de contrôle (ou un inhibiteur covalent) S de propriétés connues. On fait l'hypothèse qu'un mécanisme à deux intermédiaires acyle–enzyme prévaut et que le premier intermédiaire est un équilibre instantané entre l'enzyme et le substrat. L'apparution du premier produit provenant du substrat S est caractérisé par deux constantes de vitesse de relaxation. A partir de ces données il est possible de déterminer la constante de dissociation et les constantes de vitesse d'acylation et de déacylation du substrat A. On a aussi développé des critères pour l'utilisation des paramètres de vitesse de l'état stationnaire A afin d'établir les conditions dans lesquelles le processus de relaxation le plus lent est équivalent à la constante de vitesse de déacylation de A. La technique de mélange préalable de l'enzyme avec le substrat A a certains avantages dans cette approche. [Traduit par le journal]

Introduction

It is generally accepted (1) that reaction 1 is the minimal mechanism of action of the serine proteinases and cysteine proteinases. The steady state rate equation and rate parameters are given in eqs. 2–5, where K_a is the substrate constant.

$$[1] \qquad E + A \rightleftharpoons EA \overset{k_2}{\rightarrow} EA' \overset{k_3}{\rightarrow} E + Q_2 + Q_1$$

$$[2] \qquad v = k_{cat,a}[E][A]/([A] + K_m)$$

$$[3] \qquad k_{cat,a} = k_2k_3/(k_2 + k_3)$$

$$[4] \qquad K_{m,a} = k_3K_a/(k_2 + k_3)$$

$$[5] \qquad K_a = (k_{-1} + k_2)/k_1$$

Measurement of the acylation and deacylation rate constants, k_2 and k_3, respectively, is important to the study of the nature of the catalysis associated with each step. Pre-steady state kinetic studies provide such information (2, 3), but many good substrates do not have convenient physical properties for rapidly determining their concentrations. Consequently, many indirect methods have been used. One such approach is the argument that the deacylation step is rate-determining if a series of derivatives of the same amino acid have the same value of $k_{cat,a}$. It is claimed that this approach is sometimes misleading (4).

This paper describes a general method, which is well adapted to spectrophotometric fast reaction techniques, by which k_2, k_3, and K_a may be determined for non-chromophoric substrates. A very good substrate with convenient spectrophotometric properties is used as a monitoring substrate in a manner similar to an approach described earlier (5) and used in a variety of ways (6, 7). This paper lays the mathematical basis for an extension of that approach to the case where the acyl–enzyme is too labile to be isolated.

[1]Revision received October 15, 1974.

Can. J. Chem. Downloaded from www.nrcresearchpress.com by 210.87.254.105 on 09/05/12
For personal use only.

Can. J. Chem. Downloaded from www.nrcresearchpress.com by 210.87.254.105 on 09/05/12
For personal use only.

Theory

Two experimental procedures will be considered. In Type I experiments, substrate A and enzyme are pre-mixed. After the steady state is attained, a second substrate, S, is added at time zero at a sufficiently high concentration that in the new steady state, most of the enzyme is involved in catalyzing the hydrolysis of S. The kinetics of the approach to this new steady state are followed. In the second case, the enzyme is added to a solution containing both A and S. The derivation of the rate of appearance of P_1 is common to both procedures. The only difference is in the initial conditions which are needed to evaluate certain constants of integration.

The mechanism is given in reaction 6.

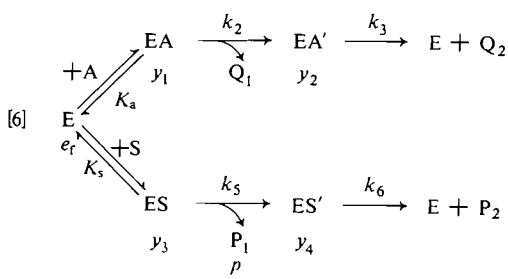

Three assumptions are made about the complete system. (*1*) The species EA, E, and ES are in instantaneous equilibrium with each other through the substrate dissociation constants K_a ($=k_{-1}/k_1$) and K_s ($=k_{-4}/k_4$), *i.e.*, $k_{-1} \gg k_2$ and $k_{-4} \gg k_5$. (*2*) The two substrates, A and S, are maintained at constant concentrations a_0 and s_0, respectively, during the interval of time in which the appearance of P_1 is observed. (*3*) The enzyme concentration, e_0, is much less than a_0 and s_0. The molar concentrations of E, EA, EA′, ES, ES′, and P_1 are defined as e_f, y_1, y_2, y_3, y_4, and p, respectively.

Integrated Rate Equation for P_1

From the definitions for the substrate dissociation constants we may write $e_f + y_1 + y_3 = by_3K_s/s_0$ where b is defined in eq. 7. The differential rate equation for the sum of the

$$[7] \qquad b = 1 + \frac{a_0}{K_a} + \frac{s_0}{K_s}$$

concentrations of E, EA, and ES is $\dot{y}_3 = (k_3y_2 + k_6y_4 - k_2y_1 - k_5y_3)s_0/bK_s$. Eliminating y_4 by use of the enzyme conservation equation, $e_0 = e_f + y_1 + y_2 + y_3 + y_4$, leads to

$$[8] \qquad \dot{y}_3 = \frac{k_6e_0s_0}{bK_s} + \frac{s_0}{bK_s}(k_3 - k_6)y_2 - (k_2' + k_5' + k_6)y_3$$

where

$$[9] \qquad k_2' = k_2a_0/bK_a$$

$$[10] \qquad k_5' = k_5s_0/bK_s$$

Also, from reaction 6

$$[11] \qquad \dot{y}_2 = -k_3y_2 + (k_2a_0K_s/s_0K_a)y_3$$

Combining eqs. 8 and 11, utilizing the operator method (8), gives

$$[12] \qquad \ddot{y}_3 + P\dot{y}_3 + Qy_3 = k_3k_6e_0s_0/bK_s$$

where

$$[13] \qquad P = k_2' + k_3 + k_5' + k_6$$

$$[14] \qquad Q = k_2'k_6 + k_3k_5' + k_3k_6$$

Following standard methods (8), eq. 12 may be solved to give

$$[15] \qquad y_3 = (e_0s_0/bmK_s)(1 + Me^{-Ft} + Ne^{-Gt})$$

where M and N are constants of integration, and

$$[16] \qquad F = (P - \sqrt{P^2 - 4Q})/2$$

$$[17] \qquad G = (P + \sqrt{P^2 - 4Q})/2$$

$$[18] \qquad m = 1 + k_2'/k_3 + k_5'/k_6$$

The parameter m is a convenient composite function of acylation and deacylation rate constant ratios for both substrates. Substituting eq. 15 into $\dot{p} = k_5y_3$ (from reaction 6) and integrating, taking $p = 0$ at $t = 0$, gives

$$[19] \qquad \frac{p}{e_0} = \frac{s_0k_{cat,s}}{s_0 + K_m}\left(t + \frac{M}{F}(1 - e^{-Ft}) + \frac{N}{G}(1 - e^{-Gt})\right)$$

where

$$[20] \qquad k_{cat,s} = k_5k_6/(k_5 + k_6)$$

$$[21] \qquad K_m = K_{m,s}(1 + a_0/K_{m,a})$$

$$[22] \qquad K_{m,s} = k_5K_s/(k_5 + k_6)$$

The first term on the right hand side in eq. 19 represents the steady state hydrolysis of substrate S in the presence of species A acting as a competitive inhibitor.

Evaluation of M and N

Expressions are needed for y_3 and $\dot{y}_3$ at time

Can. J. Chem. Downloaded from www.nrcresearchpress.com by 210.87.254.105 on 09/05/12
For personal use only.

zero, *i.e.*, $y_{3,0}$, and $\dot{y}_{3,0}$. These expressions depend on the order of mixing E, A, and S.

Type I (Premixed E and A)

Experimentally, two solutions are mixed at the defined zero time: solution 1 contains enzyme and substrate A already reacting under steady state conditions; solution 2 contains only substrate S. Equal volumes of both solutions are mixed at time zero to give solution 3. (This is the most convenient mixing ratio if a stopped-flow apparatus is used. Obviously, for slow reactions the solutions may be mixed manually. Other mixing ratios are considered in the Discussion.) Thus, in solution 1 the concentrations of total enzyme and substrate are defined as $2e_0$ and $2a_0$, respectively, and the enzyme conservation equation is $2e_0 = e_{f,ss} + y_{1,ss} + y_{2,ss}$. (The subscript ss denotes steady state concentrations.) Applying the steady state approximation to the upper pathway of reaction 6 leads to an expression for $y_{2,ss}$. Upon mixing the two solutions, the concentration of EA′ in solution 3 at $t = 0$ is

$$[23] \quad y_{2,0} = y_{2,ss}/2 = e_0 \Big/ \left(1 + \frac{k_3}{k_2} + \frac{k_3 K_a}{2k_2 a_0}\right)$$

Also at $t = 0$, that portion of the enzyme which was previously in the form of E and EA in solution 1 is instantaneously re-equilibrated in solution 3 to yield some ES as well. Since $y_{4,0} = 0$ in solution 3, substituting eq. 23 into the enzyme conservation equation at $t = 0$ leads to

$$[24] \quad y_{3,0} = e_0 s_0 (\tfrac{1}{2} + a_0/K_a)/[bK_s(\tfrac{1}{2} + a_0/K_{m,a})]$$

At $t = 0$, eq. 8, along with eqs. 23 and 24, becomes

$$[25] \quad \dot{y}_{3,0} = \frac{e_0 s_0 \left[k_2' \left(\frac{1}{2} + \frac{s_0}{K_s}\right) - k_5' \left(\frac{1}{2} + \frac{a_0}{K_a}\right)\right]}{[bK_s(\tfrac{1}{2} + a_0/K_{m,a})]}$$

When the boundary conditions of eqs. 23 to 25 are applied to eq. 15, the solutions for M and N are

$$[26] \quad M = \frac{\left[k_2' \left(\frac{1}{2} + \frac{s_0}{K_s}\right)\left(m - \frac{G}{k_3}\right) - k_5' \left(\frac{1}{2} + \frac{a_0}{K_a}\right)\left(m - \frac{G}{k_6}\right)\right]}{\left[(G - F)\left(\frac{1}{2} + \frac{a_0}{K_{m,a}}\right)\right]}$$

$$[27] \quad N = \frac{\left[-k_2' \left(\frac{1}{2} + \frac{s_0}{K_s}\right)\left(m - \frac{F}{k_3}\right) + k_5' \left(\frac{1}{2} + \frac{a_0}{K_a}\right)\left(m - \frac{F}{k_6}\right)\right]}{\left[(G - F)\left(\frac{1}{2} + \frac{a_0}{K_{m,a}}\right)\right]}$$

Type II (Premixed A and S)

In this procedure solution 1 contains enzyme only, solution 2, the two substrates. When these two solutions are mixed at $t = 0$ to give solution 3, there is no pre-existing EA′ as there was in the Type I procedure, *i.e.*, $y_{2,0} = y_{4,0} = 0$. From the enzyme conservation equation it follows that $y_{3,0} = e_0 s_0/bK_s$, and from eq. 8, $\dot{y}_{3,0} = -(k_2' + k_5')e_0 s_0/bK_s$. When these boundary conditions are applied to eq. 15, the solutions for M and N are

$$[28] \quad M = [k_2'(G/k_3 - m) + k_5'(G/k_6 - m)]/(G - F)$$

$$[29] \quad N = [k_2'(m - F/k_3) + k_5'(m - F/k_6)]/(G - F)$$

Special Case when $k_6 = 0$

When ES′ does not deacylate, S is a monitoring covalent inhibitor which releases a species P_1.[2] In this case the derivation is analogous to the previous case except that the terms containing k_6 in eqs. 8, 12, 13, and 14 vanish. The resulting expression for p/e_0 is given in Table 1. For both Type I and Type II experiments, the boundary conditions are the same as in the previous case. They lead to the expressions for M and N given in Table 1.

Discussion

The case for S as a substrate (*i.e.*, $k_6 > 0$) is considered first.

[2]Hijazi and Laidler (9) have considered the case of a competitive inhibitor, *i.e.*, $k_5 = 0$ in reaction 6.

Can. J. Chem. Downloaded from www.nrcresearchpress.com by 210.87.254.105 on 09/05/12
For personal use only.

TABLE 1. Equation and parameters for the case of a monitoring covalent inhibitor

$$\frac{p}{e_0} = \frac{k_5'M}{F}(1 - e^{-Ft}) + \frac{k_5'N}{G}(1 - e^{-Gt})$$

$$F = (P - \sqrt{P^2 - 4Q})/2$$

$$G = (P + \sqrt{P^2 - 4Q})/2$$

$$P = k_2' + k_3 + k_5'$$

$$Q = k_3k_5'$$

Type I

$$M = \frac{k_2a_0/K_a + (k_3 - F)(\frac{1}{2} + a_0/K_a)}{(G - F)(\frac{1}{2} + a_0/K_{m,a})}$$

$$N = \frac{-k_2a_0/K_a + (G - k_3)(\frac{1}{2} + a_0/K_a)}{(G - F)(\frac{1}{2} + a_0/K_{m,a})}$$

Type II

$$M = (k_3 - F)/(G - F)$$

$$N = (G - k_3)/(G - F)$$

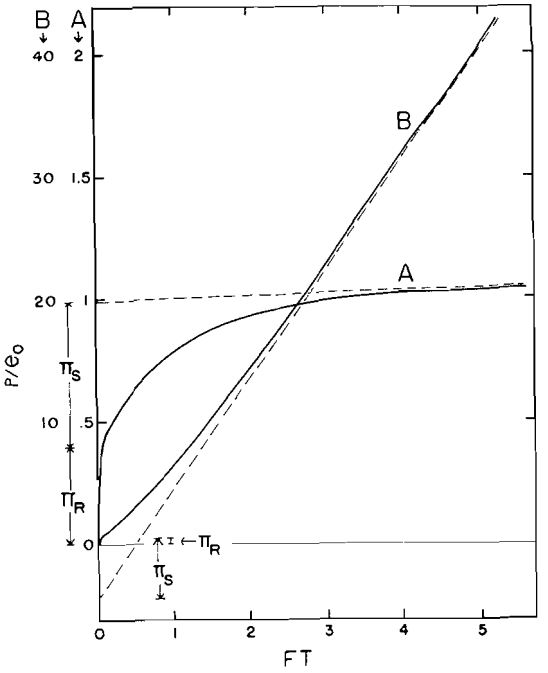

FIG. 1. Normalized plot for the production of P_1 as a function of time according to eq. 19. For both curves, $k_2 = 110$, $k_3 = 11$, $k_5 = 10{,}000$, $s_0/K_s = 10$, $a_0/K_{m,a} = 1$. Curve *A*, $k_6 = 0.1$; curve *B*, $k_6 = 100$. At $Ft = 5$, $e^{-Ft} < 0.01$, and the steady state has been attained.

General Analysis[3]

In Fig. 1 are plotted the general forms of eq. 19 for a Type I experiment. Curve A occurs for $k_3 > k_6$, curve B for $k_6 > k_3$. The rate parameters G and F may be evaluated from such curves by standard methods, either graphically (9, 10) or by data-fitting to an equation having the form of eq. 19. Since the sum and product of G and F are P and Q, respectively (9, 11), combining eqs. 9, 10, 16, and 17, along with the relationship $h = (1 + s_0/K_s)$, leads to

$$[30]\quad G + F = k_3 + k_6 + \frac{k_5s_0}{s_0 + K_s} + \left(k_2 - \frac{k_5s_0}{s_0 + K_s}\right)\left(\frac{a_0}{a_0 + hK_a}\right)$$

$$[31]\quad G \times F = k_3\left(k_6 + \frac{k_5s_0}{s_0 + K_s}\right) + \left(k_2k_6 - \frac{k_3k_5s_0}{s_0 + K_s}\right)\left(\frac{a_0}{a_0 + hK_a}\right)$$

In principle, the constants k_5, k_6, and K_s are independently available from pre-steady state studies on S alone (2, 3). Thus, experimental data obtained at constant s_0 and varying a_0 may be fitted to either eq. 30 or 31 to obtain k_2, k_3, and K_a. Alternatively, if the maximum a_0 is much smaller than $hK_{m,a}$ ($\leqslant hK_a$), eqs. 30 and 31 become linear in a_0, and k_3 may be determined from the intercept of data plotted according to either equation. (Another method for determining k_3 is discussed below.) Once k_3 is known, a plot of $1/[G + F - k_3 - k_6 - k_5s_0/(s_0 + K_s)]$ *vs.* $1/a_0$ according to the rearranged form of eq. 30 (or the analogous form derived from eq. 31) yields slope and intercept values from which k_2 and K_a may be determined.

The ability to observe the two relaxation processes depends upon the magnitude of the rapid and slow bursts (see Fig. 1), which are given by $\pi_r = k_{cat,s}s_0N/[G(s_0 + K_m)]$ and $\pi_s = k_{cat,s}s_0M/[F(s_0 + K_m)]$, respectively. Since the expressions for M and N contain unknown quantities, it is impossible to state general criteria which guarantee that π_r and π_s would be large enough to be observable in either Type I or Type II experiments. However, it is advisable to choose S such that k_6 is quite different from k_3. When k_6 equals k_3 (and one or both of k_2' and k_5' is greater than k_6), M vanishes for both types

[3]While this manuscript was under revision, an extensive series of papers on related topics has been published by Laidler's group (9, 16, 22–25). The revised paper reflects the influence of this series in the inclusion of a general analysis section, and the consideration of Type II experiments. The latter point was also suggested by a referee.

Can. J. Chem. Downloaded from www.nrcresearchpress.com by 210.87.254.105 on 09/05/12
For personal use only.

of experiment. Since k_3 is not known in advance, the safest choice is $k_6 < k_{cat,a}$.

Deacylation Monitoring, a Special Case

The preceding analysis may not always be applicable. The parameter G may be too large to measure. Decreasing G to bring it into the measurable range, by adjusting substrate concentrations, may make it difficult to separate G and F with sufficient precision. Thus, it is useful to consider conditions for which a knowledge of the smaller constant, F, and the steady state rate parameters, $k_{cat,a}$ and $K_{m,a}$, is sufficient to determine k_3 and in some cases k_2 and K_a as well.

The key to this analysis lies in the recognition that if k_5' is much greater than all of the terms k_6, k_2', k_6k_2'/k_3, and k_3, then F equals k_3 (see the exact expression for F in eq. 32).

$$[32] \quad F = \frac{Q}{P - F} = k_3\left(\frac{k_5' + k_6 + k_6k_2'/k_3}{k_5' + k_6 + k_2' + k_3 - F}\right)$$

From eqs. 3, 4, and 9 it follows that $k_2' = k_{cat,a}a_0/bK_{m,a}$, and $k_6k_2'/k_3 \ll k_6a_0/bK_{m,a}$. It will be demonstrated below that there is no advantage in having $a_0/K_{m,a}$ much larger than unity. Thus, the first three inequalities are met if the monitoring substrate S is chosen such that k_5s_0/K_s is much greater than k_6 and $k_{cat,a}$, and a_0 is made approximately equal to $K_{m,a}$. The latter restriction, along with $s_0 \geqslant K_s$, ensures that k_5' approaches its maximum value of k_5. The k_5'/k_3 ratio is not known in advance, but can be decided after the fact. If an experimentally determined value of F is much smaller than k_5 ($\simeq k_5'$), then it equals k_3 according to eq. 32, *i.e.*, $k_5'/k_3 \gg 1$, as required. On the other hand, if the experimental value of F is comparable to k_5, a monitoring substrate with a larger k_5 needs to be used.

The above conditions also ensure that $G \simeq k_5' \gg F$, and hence F may be measured readily from the experimental trace.

In Table 2 are compiled values of G and F which were calculated from the defining equations for Type I experiments using arbitrary values for k_5, k_6, and $k_{cat,a}$. Two pairs of k_2 and k_3 values are considered for each of two values of k_6, one pair having $k_2 \gg k_3$, the other, $k_2 \ll k_3$. The agreement between F and k_3 is generally excellent for a wide range of s_0/K_s and $a_0/K_{m,a}$ values, except when $s_0 \ll K_s$ and $a_0 \gg K_{m,a}$, in accord with the previous discussion.

Once k_3 (*i.e.*, F) is known, both k_2 and K_a can be evaluated from the steady state parameters $k_{cat,a}$ and $K_{m,a}$, provided $k_{cat,a}$ is not dominated by k_3. In effect this approach is limited to cases for which $k_2/k_3 \gtrsim 1$. Even if k_2 and K_a cannot be determined, a firm value of k_3 is always valuable information.

Under the same conditions for which F equals k_3 it may be shown that $k_2'(m - G/k_3) \simeq -k_5'(m - G/k_6) \simeq k_2'k_5'(k_3 - k_6)/k_3k_6$. For Type I experiments, substitution of eq. 26 into the definition for the slow burst, π_s (see above), gives

$$[33] \quad \pi_s \simeq \frac{k_2(k_3 - k_6)}{(k_2 + k_3)k_3} \cdot \frac{s_0}{s_0 + K_m} \cdot \frac{a_0}{K_{m,a}/2 + a_0}$$

Values of π_s given by eq. 33 agree well with the exact values in Tables 2 and 3, except when $s_0 \ll K_s$ and $a_0 \gg K_{m,a}$. Type II experiments are ruled out since $M \simeq 0$ in this case (see eq. 28). The relative slow burst, $\pi_{s,rel}$, is arbitrarily defined as

$$[34] \quad \pi_{s,rel} = |\pi_s|/[(p/e_0)_{5/F} - \pi_r]$$

where $(p/e_0)_{5/F}$ is the amount of P_1 produced (as a multiple of e_0) at a time ($t = 5/F$) when the term e^{-Ft} has decayed to less than 0.01. In Fig. 1, $\pi_{s,rel}$ is 93.6% for curve *A* and 12.1% for curve *B*.

In general π_s and $\pi_{s,rel}$ should be as large as possible so the curvature due to the decay of e^{-Ft} is observable in the P_1 trace. Tables 2 and 3 present exact values of F, G, π_s, and $\pi_{s,rel}$ for selected pairs of values of k_2 and k_3 consistent with $k_{cat,a} = 10$. These data illustrate the following criteria for maximizing π_s, which can be derived from eq. 33: $s_0 \gg K_m$; $a_0 \gg K_{m,a}$; and $k_6 \gg k_3$ or $k_6 \ll k_3$. In view of the previous restriction on a_0 ($\gtrsim K_{m,a}$), a compromise of $a_0 \simeq 2K_{m,a}$ is satisfactory. The k_3/k_6 ratio affects π_s and $\pi_{s,rel}$ in several ways. When $k_3 > k_6$, π_s is positive and cannot exceed $k_2/(k_2 + k_3)$. This case has three advantages over the reverse inequality: it can be confidently attained by choosing a substrate S with $k_6 < k_{cat,a}$; the P_1 *vs.* t curve shape (Fig. 1, curve *A*) permits a more precise determination of F; and $\pi_{s,rel}$ is essentially independent of the k_2/k_3 ratio (see Table 3). The major advantage of choosing $k_6 > k_3$ is that π_s can attain values considerably greater than unity (see Tables 2*A* and 3*A*). This multiplying effect may be useful if other factors demand that e_0 be small. Since k_3 is not known, the only guideline in this case is to choose S such that $k_6 > k_{cat,a}$. Such a choice, which may be dictated

TABLE 2. Dependence of the parameters of eq. 19 on s_0 and a_0 for $k_5 = 10\,000$ and $k_{cat,a} = 10$

		$\frac{s_0}{K_s}$	$\frac{a_0}{K_{m,a}}$	F	G	π_s	$100\pi_{s,rel}(\%)$
A		10	10	11.09	8505	−6.80	18.2
		10	1	11.01	9117	−4.84	12.1
	$k_2 = 110$	10	0.1	11.00	9183	−1.21	2.8
		1	10	11.86	3571	−5.69	17.8
	$k_3 = 11$	1	1	11.09	4887	−4.70	12.0
		1	0.1	11.01	5078	−1.20	2.8
	$k_6 = 100$	0.1	10	18.04	640	−1.73	15.1
		0.1	1	11.80	947	−3.61	11.5
		0.1	0.1	11.08	1002	−1.05	2.7
B	$k_2 = 11.11$						
	$k_3 = 100$	All	All				
	$k_6 = 100$	values	values	100.00	Varies	0	0
C		10	10	10.99	8405	0.859	95.5
		10	1	11.00	9017	0.601	93.6
		10	0.1	11.00	9084	0.150	77.2
	$k_2 = 110$	1	10	10.89	3472	0.862	95.6
	$k_3 = 11$	1	1	10.99	4788	0.602	93.6
	$k_6 = 0.1$	1	0.1	11.00	4978	0.151	77.2
		0.1	10	9.99	549	0.884	95.3
		0.1	1	10.89	848	0.612	93.6
		0.1	0.1	10.99	903	0.153	77.5
D		10	10	99.90	5005	0.098	95.8
		10	1	99.99	8404	0.067	93.7
		10	0.1	100.00	9017	0.017	77.5
	$k_2 = 11.11$	1	10	98.89	919	0.118	96.5
	$k_3 = 100$	1	1	99.90	3452	0.070	93.9
	$k_6 = 0.1$	1	0.1	99.99	4785	0.017	77.8
		0.1	10	72.73	136	0.731	99.7
		0.1	1	98.77	506	0.097	95.6
		0.1	0.1	99.89	841	0.020	80.5

by the need to have $k_5 \gg k_{cat,a}$ (see above), could result in a coincidental equality of k_3 and k_6 (see Table 3*A*). If no burst is observed, a second monitoring substrate with a quite different k_6 value should be used.

It should be noted that the *p*-nitrophenyl ester derivatives of specific amino acid or peptide substrates will generally satisfy the criteria established for substrate S, both for deacylation monitoring and for the general approach.

The Monitoring Covalent Inhibitor Case

When k_6 equals zero, the relationships for the rate of appearance of P_1 are summarized in Table 1. The two relaxations predicted are characterized by rate constants G and F whose sum and product may be expressed as

$$[35]\quad G + F = k_3 + \frac{k_5 s_0}{s_0 + K_s} + \left(k_2 - \frac{k_5 s_0}{s_0 + K_s}\right)\left(\frac{a_0}{a_0 + hK_a}\right)$$

$$[36]\quad G \times F = \frac{k_3 k_5 s_0}{s_0 + K_s} - \frac{k_3 k_5 s_0}{s_0 + K_s}\left(\frac{a_0}{a_0 + hK_a}\right)$$

where $h = (1 + s_0/K_s)$. As discussed above, data obtained at constant s_0 and varying a_0 may be used to determine k_2, k_3, and K_a.

For many covalent inhibitors, it is likely that $K_s \gg s_0$, *i.e.*, no saturation occurs. In this case h is unity and $k_5 s_0/(s_0 + K_s)$ reduces to $k_5 s_0/K_s$, which may be defined as k_i, the pseudo first-order rate constant for inhibition of the enzyme. Also, k_5' becomes $k_i a_0/(a_0 + K_a)$.

By much the same arguments as before, the parameter F reduces to k_3 when $k_5' \gg k_2', k_3$. The first requirement is safely assured when $k_i \gg k_{cat,a} a_0/K_{m,a}$; the latter is demonstrated experimentally if F is found to be much smaller than k_5'. For these same conditions, the slow burst ($\pi_s = k_5' M/F$, see Table 1) is zero for Type II experiments, but is given by $k_2 a_0/[(k_2 + k_3)(K_{m,a}/2 + a_0)]$ for Type I experiments. In the

Can. J. Chem. Downloaded from www.nrcresearchpress.com by 210.87.254.105 on 09/05/12
For personal use only.

TABLE 3. Dependence of the parameters of eq. 19 on the k_2/k_3 ratio under various conditions for $k_{cat,a} = 10$

		k_2	k_3	F	G	π_s	$100\pi_{s,rel}(\%)$
A	$k_6 = 100$	1010	10.1	10.11	9184	−5.80	13.5
	$k_5 = 10^4$	110	11	11.01	9117	−4.84	12.1
	$s_0/K_s = 10$	20	20	20.01	8797	−1.32	5.6
		11.11	100	100.00	8504	0	0
	$a_0/K_{m,a} = 1$	10.34	300	299.98	8457	0.02	0.9
B	$k_6 = 1$	1010	10.1	10.10	9085	0.595	54.8
	$k_5 = 10^4$	110	11	11.00	9018	0.552	55.0
	$s_0/K_s = 10$	20	20	20.00	8698	0.317	56.2
		11.11	100	99.99	8405	0.067	57.4
	$a_0/K_{m,a} = 1$	10.34	300	299.97	8358	0.023	58.3
C	$k_6 = 0.1$	1010	10.1	10.10	9084	0.654	93.6
	$k_5 = 10^4$	110	11	11.00	9017	0.601	93.6
	$s_0/K_s = 10$	20	20	20.00	8697	0.332	93.6
		11.11	100	99.99	8404	0.067	93.7
	$a_0/K_{m,a} = 1$	10.34	300	299.97	8358	0.023	93.9
D	$k_6 = 0.1$	1010	10.1	10.09	909	0.661	93.6
	$k_5 = 10^3$	110	11	10.99	903	0.608	93.6
	$s_0/K_s = 10$	20	20	19.98	871	0.340	93.7
		11.11	100	99.89	841	0.077	94.6
	$a_0/K_{m,a} = 1$	10.34	300	299.53	837	0.037	96.3
E	$k_6 = 0.1$	1010	10.1	10.09	909	0.166	77.4
	$k_5 = 10^4$	110	11	10.99	903	0.153	77.5
	$s_0/K_s = 0.1$	20	20	19.98	871	0.086	77.8
		11.11	100	99.89	841	0.020	80.5
	$a_0/K_{m,a} = 0.1$	10.34	300	299.53	837	0.011	87.4

latter case, the condition, $a_0 \gtrsim K_{m,a}$, ensures that the slow burst is close to maximal. Since there is no steady state reaction, the relative slow burst is equivalent to π_s.

The method of using a monitoring covalent inhibitor is most likely to be useful with enzymes such as the sulfhydryl proteases which have an essential catalytic group that is highly reactive.

Choice of e_0

The enzyme concentration has to be chosen as a compromise between the need to have an observable slow burst (large e_0), and the need to maintain s_0 constant[4] and to avoid too rapid hydrolysis of A in solution 1 of Type I experiments (small e_0). The latter problem may be minimized by using a three-syringe mixing device.

Mixing Ratio

In Type I experiments it was previously assumed that equal volumes of solutions 1 and 2 were mixed at $t = 0$. For any volumes, V_1 of solution 1 and V_2 of solution 2, it may be shown that the factor of $\frac{1}{2}$, which appears in three places in each of eq. 26 (for M) and eq. 27 (for N), should be replaced by $V_2/(V_1 + V_2)$ in the first numerator term, and by $V_1/(V_1 + V_2)$ in the denominator and second numerator terms. The latter replacement also applies to the denominator of eq. 33 (for π_s), and to both terms in the Type I values of M and N in Table 1. Possible advantages in using $V_1 < V_2$ are that, as V_1/V_2 is decreased, π_s increases for a given a_0 value, and temperature control of solution 1 is less critical.

Adequacy of the Mechanism

The steady state definitions of the substrate constants for A and S are $K_a = (k_{-1} + k_2)/k_1$ and $K_s = (k_{-4} + k_5)/k_4$. In this paper it has been assumed that $k_{-1} \gg k_2$ and $k_{-4} \gg k_5$. Although this approximation is not valid in some cases, *e.g.*, the peroxidases (12), it seems appropriate for the common amide, ester, and peptide substrates of the proteolytic enzymes. Association rate constants of 2×10^7 and 1×10^8 M^{-1} s^{-1} (which are typical of many enzyme:ligand associations (13)) have been measured for the

[4]In the deacylation monitoring approach, the only term of eq. 15 which depends significantly on s_0 is s_0/bmK_s $(=s_0k_{cat,s}/[k_5(s_0 + K_m)])$. Thus, a varying s_0 can be accommodated to a good approximation by replacing s_0 in this term with $(s_0 - p)$ before performing the integration of $p = k_5y_3$.

Can. J. Chem. Downloaded from www.nrcresearchpress.com by 210.87.254.105 on 09/05/12
For personal use only.

Can. J. Chem. Downloaded from www.nrcresearchpress.com by 210.87.254.105 on 09/05/12
For personal use only.

reaction between papain and a competitive peptide inhibitor (26) and between α-chymotrypsin and proflavin (11), respectively. Since substrate constants of 10^{-3} to 10^{-2} M are typical for the proteolytic enzymes (14), it follows that $(k_{-1} + k_2)$ is of the order of 10^5 s^{-1}, which is nearly 10-fold greater than the largest recorded k_2 value of α-chymotrpysin (15). It is possible to analyze the mechanism of reaction 1 without making the equilibrium assumption, in which case four relaxation processes are predicted (16). However, since the equations are exceedingly complex, it is useful to have available the simpler equations given in this paper.

It has been suggested (17, 18) that the mechanism of reaction 1 needs to be expanded to include an additional intermediate in the productive pathway. If that is so, in spite of the reported failure (19) to confirm one of these claims, the basic approach reported in this paper is still applicable. The integrated equation corresponding to eq. 19 would then contain an additional exponential term and somewhat more complex coefficients. Indeed the observation of more than two relaxation processes would constitute evidence for additional intermediate species on the reaction pathway (20), provided the equilibrium assumption is valid. As the number of intermediate species increases, it becomes less likely that a single rate constant in the mechanism could be identified with a particular relaxation process. However, a careful analysis of individual cases might prove fruitful.

The existence of additional enzyme:substrate complexes, such as nonproductive complexes (21), which are in rapid equilibrium with free enzyme, would not affect the form of eq. 19. Only the meaning of k_2, K_a, k_5, and K_s would be changed (27).

It has been observed (6) that *N*-acetyl-L-tyrosine ethyl ester causes a five-fold acceleration of the deacylation of acetyl-α-chymotrypsin. This was attributed to an interaction between the specific substrate and the acyl-enzyme where the acyl group (acetyl) was derived from an "incomplete" substrate. When A is a specific substrate, such an effect is less likely. To check this point an experiment may be performed with $s_0 < K_s$, a condition for which S is not likely to bind to EA′ since it does not bind significantly to E. If these results agree with those using $s_0 > K_s$, one may conclude that S does not bind to EA′. Table 3*E* illustrates that with proper choice of S and a_0, there is good separation of G and F, F equals k_3, and the relative slow burst is adequate for the case of $s_0 < K_s$.

This work was supported by a grant from the National Research Council of Canada.

1. M. L. BENDER and F. J. KÉZDY. Ann. Rev. Biochem. **34**, 49 (1965).
2. L. OUELLET and K. J. LAIDLER. Can. J. Chem. **34**, 146 (1956).
3. H. GUTFREUND and J. M. STURTEVANT. Proc. Natl. Acad. Sci. U.S. **42**, 719 (1956).
4. L. A. AE. SLUYTERMAN. Biochim. Biophys. Acta, **151**, 178 (1968).
5. G. H. DIXON and H. NEURATH. J. Biol. Chem. **225**, 1049 (1957).
6. M. L. BENDER, F. J. KÉZDY, and C. R. GUNTER. J. Am. Chem. Soc. **86**, 3714 (1964).
7. (*a*) M. L. BENDER, M. L. BEGUÉ-CANTÓN, R. L. BLAKELEY, L. J. BRUBACHER, J. FEDER, C. R. GUNTER, F. J. KÉZDY, J. V. KILLHEFFER, T. H. MARSHALL, C. G. MILLER, R. W. ROESKE, and J. K. STOOPS. J. Am. Chem. Soc. **88**, 5890 (1966); (*b*) L. J. BRUBACHER. Ph.D. Thesis, Northwestern University, Evanston, Illinois. 1966.
8. L. M. KELLS. Elementary differential equations. 6th ed. McGraw-Hill Book Co., New York. 1965. pp. 126–160.
9. N. H. HIJAZI and K. J. LAIDLER. Can. J. Biochem. **51**, 822 (1973).
10. F. J. KÉZDY and M. L. BENDER. Biochemistry, **1**, 1097 (1962).
11. B. HAVSTEEN. J. Biol. Chem. **242**, 769 (1967).
12. B. CHANCE. Adv. Enzymol. **12**, 153 (1951).
13. M. EIGEN and G. G. HAMMES. Adv. Enzymol. **25**, 1 (1963).
14. B. ZERNER and M. L. BENDER. J. Am. Chem. Soc. **86**, 3669 (1964).
15. B. ZERNER, R. P. M. BOND, and M. L. BENDER. J. Am. Chem. Soc. **86**, 3674 (1964).
16. R. J. MAGUIRE, N. H. HIJAZI, and K. J. LAIDLER. Biochim. Biophys. Acta, **341**, 1 (1974).
17. T. E. BARMAN and H. GUTFREUND. Biochem. J. **101**, 411 (1966).
18. M. R. HOLLOWAY and M. J. HARDMAN. Eur. J. Biochem. **32**, 537 (1973).
19. A. A. KORTT, J. A. HINDS, and B. ZERNER. Biochemistry, **13**, 2029 (1974).
20. M. EIGEN and L. DEMAYER. *In* Techniques of organic chemistry, Vol. 8, pt. 2. *Edited by* A. Wiessberger. Interscience Publishers, New York. 1963. Chapt. XVIII.
21. G. E. HEIN and C. NIEMANN. J. Am. Chem. Soc. **84**, 4495 (1962).
22. N. H. HIJAZI and K. J. LAIDLER. Can. J. Biochem. **51**, 806 (1973).
23. N. H. HIJAZI and K. J. LAIDLER. Can. J. Biochem. **51**, 815 (1973).
24. N. H. HIJAZI and K. J. LAIDLER. Can. J. Biochem. **51**, 832 (1973).
25. N. H. HIJAZI and K. J. LAIDLER. Biochim. Biophys. Acta, **315**, 209 (1973).
26. L. J. BRUBACHER. Unpublished results.
27. L. J. BRUBACHER and B. R. GLICK. Unpublished results.

Complexes of the Early Transition Metals with *o*-Mercaptophenol and 1,2-Dihydroxybenzene

JOEL L. MARTIN AND JOSEF TAKATS

The Department of Chemistry, University of Alberta, Edmonton, Alberta T6G 2E1

Received June 4, 1974

JOEL L. MARTIN and JOSEF TAKATS. Can. J. Chem. **53**, 572 (1975).

A novel synthetic approach, based on the reactivity of amido derivatives of the transition metals, $M(NR_2)_x$, towards protic reagents, for the synthesis of complexes of Ti, Zr, Hf, Nb, and Ta with *o*-mercaptophenol and 1,2-dihydroxybenzene is reported. The complexes, isolated as their tetraalkylammonium and tetraphenylarsonium salts, are moderately air stable, well behaved 2:1 (Ti, Zr, Hf) and 1:1 (Nb, Ta) electrolytes. The u.v.–visible spectra of the complexes, which are somewhat reminiscent of the corresponding benzene-1,2-dithiolates, are dominated by ligand-to-metal charge transfer bands. The band positions change in the expected manner, hypsochromic shifts in the order $C_6H_4S_2^{2-} < C_6H_4SO^{2-} < C_6H_4O_2^{2-}$ for a given metal and Ti < Zr ~ Hf, Nb < Ta, Nb < Zr for a given ligand. It is argued that these spectral resemblances could be a possible indication of variations in coordination geometry of the reported complexes similar to the ones found in compounds of benzene-1,2-dithiol.

JOEL L. MARTIN et JOSEF TAKATS. Can. J. Chem. **53**, 572 (1975).

On décrit une nouvelle synthèse pour la préparation des composés du Ti, Zr, Hf, Nb et Ta avec l'*o*-mercaptophénol et le benzène dihydroxy-1,2. La synthèse utilize la réactivité des amidures des métaux de transition, $M(NR_2)_x$, vis à vis les ligands contenant des protons acidiques. Les composés, obtenus sous forme de sels d'ammonium et d'arsonium quarternaires, sont modérément stable à l'air et se comportent en solution commes des électrolytes 2:1 (Ti, Zr, Hf) et 1:1 (Nb, Ta). Les spectres u.v.–visibles, qui sont dominés par des bandes de transfert de charge, ressemblent à ceux des composés correspondants avec le benzène-1,2-dithiolene. La position des bandes change d'une manière prévisible; les déplacements hyposochromes sont dans l'ordre $C_6H_4S_2^{2-} < C_6H_4OS^{2-} < C_6H_4O_2^{2-}$ pour un metal donné et dans l'ordre Ti < Zr ~ Hf, Nb < Ta et Nb < Zr pour un ligand donné. On discute la possibilité que les ressemblances spectrales indiquent une variation dans la géometrie de coordination similaire à celle trouvée dans le cas des composés avec le benzène dithiol-1,2.

Introduction

In the course of our investigation on the chemistry of benzene-1,2- and toluene-3,4-dithiol complexes of the early transition metals we have devised a convenient new synthetic procedure for the preparation of such complexes (ref. 1 and refs. therein). The method involved the reaction of a metal amide, $M(NR_2)_x$, with a mixture of the dithiol and its sodium salt in tetrahydrofuran and subsequent replacement of the sodium ions by a bulky organic cation. The application of our method to the synthesis of other complexes with ligands of type **1**, where

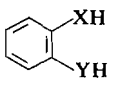

1

X and Y are S,O and O,O, was a logical extension of our previous study. Thus, we report here the preparation and characterization of the following complexes: $[R_4E]_{6-x}[M(XYC_6H_4)_3]$ where M = Ti, Zr, and Hf, $x = 4$, $R_4E = (C_2H_5)_4N$, X = O, and Y = S (also for Ti and Hf X = Y = O); where M = Nb and Ta, $x = 5$, $R_4E = (C_6H_5)_4As$, X = O, and Y = S.

The impetus to extend our studies to these complexes was twofold. First, the complexes are related to the corresponding transition metal benzene-1,2-dithiolates and as such might provide additional information to our understanding of the unusual chemical properties (facile one-electron transfer reactions, trigonal prismatic coordination geometry) of this class of compounds. Second, only a few reports of transition metal complexes where X = O and Y = S have appeared in the chemical literature (2–4) and

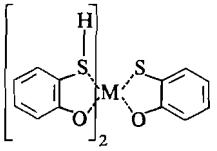

2

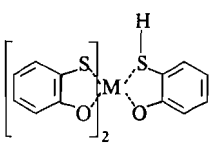

3

Can. J. Chem. Downloaded from www.nrcresearchpress.com by 210.87.254.6 on 09/05/12
For personal use only.

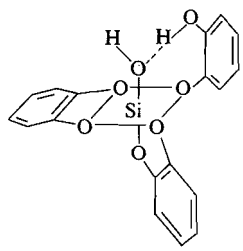

4

only in the case of Nb, Ta, and W were well behaved tris-*o*-mercaptophenolates isolated (4). Furthermore, with the exception of W, all the tris complexes contain ionizable hydrogens, present as SH or OH groups on the ligands (5–11), *i.e.* structures **2** (M = Ti, Zr) and **3** (M = Nb, Ta). The effect of ionizable hydrogens on the structure of this type of complexes produced a mild controversy. It was argued that for complexes of Si(IV), containing water of crystallization, instead of the simple tris-chelated octahedral geometry, a structure like **4** would be observed (12). However a recent single crystal X-ray structure determination of the anhydrous $(C_5H_6N)_2[Si(O_2C_6H_4)_3]$ (C_5H_6N = pyridinium) complex (13) disproved the above postulate and established the occurrence of the tris-chelated octahedral geometry, a similar result was also obtained for a P(V) complex, $[(C_2H_5)_3NH][P(O_2C_6H_4)_3]$ ($(C_2H_5)_3NH$ = triethylammonium) (14). Whether the implications of these studies can be applied to complexes of the transition metals is not yet known since there is a total absence of structural work in this area. Nevertheless the present synthetic method provides a way of avoiding this potential problem when necessary.[1]

Experimental

All operations were carried out under nitrogen atmosphere in Schlenk type apparatus using dry solvents as previously described (1). Metal amides were prepared by known procedures (15–18) and sodium cyclopentadienide was prepared by standard methods. 1,2-Dihydroxybenzene was obtained commercially and sublimed before use. *o*-Mercaptophenol was prepared according to U.S. patent 3,468,961 by permission of Hooker Chemical Corp., which was found to be a much more convenient method for the preparation of this ligand than the previously preferred method (19). Tetraethylammonium chloride was purchased as a monohydrate and dehydrated at 80–90° and 0.05 mm Hg. The anhydrous salt was then dissolved in CH_3CN and stored under nitrogen in a buret with a large reservoir attached to it. The CH_3CN solution was standardized by precipitation of Cl^- as AgCl. Analyses were performed by the analytical services of the University of Alberta.

Preparation of the Compounds

$[(C_2H_5)_4N]_2[Ti(OSC_6H_4)_3]$

Sodium cyclopentadienide, 0.330 g (0.00375 mol), in 20 ml of THF was added to 0.00563 mol of *o*-mercaptophenol in 20 ml of THF. Next 0.00188 mol of $Ti[N(C_2H_5)_2]_4$ in 20 ml of THF was added and after stirring 48 h, 13.8 ml of 0.272 *M* tetraethylammonium chloride in CH_3CN was added. This mixture was stirred for 2 h and then the solvent was removed under vacuum and replaced by 50 ml of CH_3CN. After stirring overnight the solution was filtered to remove NaCl. Addition of 55 ml of ether with vigorous stirring, followed by allowing the solution to stand, produced large black crystals. The reaction mixture was cooled in a freezer for 24 h and the black crystals were filtered off.

All other compounds were prepared in a similar manner with the following modifications.

$[(C_6H_5)_4As][Nb(OSC_6H_4)_3]$

This complex was isolated by adding solid tetraphenyl arsonium chloride to the THF reaction mixture. The THF was removed under vacuum after 2 h and replaced by 50 ml of CH_2Cl_2 and after 2 h the solution was filtered. Addition of ether and cooling produced black crystals in 60% yield which gave poor analysis. The product was recrystallized from hot CH_3CN.

$[(C_2H_5)_4N]_2[Ti(O_2C_6H_4)_3]$

This compound was prepared in the same manner as the corresponding *o*-mercaptophenol complex except that diglyme was used as solvent instead of THF. After several recrystallizations from CH_3CN and ether mixtures orange crystals of suitable purity were obtained.

$[(C_6H_5)_4As][Nb(OC_6H_4(SH))_2Cl_4]$

To 0.840 g (0.00665 mol) of *o*-mercaptophenol in 50 ml of THF was added 0.00229 mol of sodium cyclopentadienide in 12 ml of THF. Solid $NbCl_5$ was then added and the reaction mixture immediately turned dark brown. The reaction mixture was stirred for 96 h after which 0.96 g of tetraphenyl arsonium chloride was added. After stirring for 1 h the solvent was removed under vacuum and was replaced by 50 ml of CH_2Cl_2. After stirring 1 h the mixture was filtered and 20 ml of ether was added resulting in the formation of a dark brown oil. The supernatant was decanted off and the oil was dried under vacuum but could not be characterized. An additional 20 ml of ether was added to the supernatant causing more of the oil to form. This time the reaction mixture was allowed to stand for 1 week at room temperature and the oil disappeared leaving black crystals. The i.r. of the product was very similar to $[(C_6H_5)_4As][Nb(OSC_6H_4)_3]$ except for an additional peak at 800 cm^{-1} and loss of a peak at 270 cm^{-1}. The physical properties and analytical results of the synthesized complexes can be found in Table 1.

[1]It is worth pointing out that the previous synthesis (4) of $H_2[M(OSC_6H_4)_3]$, M = Ti and Zr, produced polymeric, insoluble, materials, clearly undesirable from the synthetic point of view and not too appealing for structural work either.

Can. J. Chem. Downloaded from www.nrcresearchpress.com by 210.87.254.6 on 09/05/12
For personal use only.

Can. J. Chem. Downloaded from www.nrcresearchpress.com by 210.87.254.6 on 09/05/12
For personal use only.

TABLE 1. Physical properties and analytical results of the reported complexes

Compound	Color	Yield (%)	Melting point* (°C)	Analysis (%) C Theoretical	C Observed	H Theoretical	H Observed	N Theoretical	N Observed	S Theoretical	S Observed
$[(C_2H_5)_4N]_2[Ti(OSC_6H_4)_3]$	Black	40	218–220	59.98	59.83, 60.07	7.70	7.64, 7.74	4.11	4.42, 4.24	14.13	14.55, 14.59
$[(C_2H_5)_4N]_2[Zr(OSC_6H_4)_3]$	Pale yellow	30	218	56.39	56.40, 56.47	7.24	7.21, 7.56	3.87	4.00, 4.12	13.28	13.46, 13.18
$[(C_2H_5)_4N]_2[Hf(OSC_6H_4)_3]$	White	77	214–215	50.32	50.86, 50.81	6.46	6.75, 6.72	3.45	3.40, 3.61	11.85	11.58, 11.79
$[(C_2H_5)_4N]_2[Hf(O_2C_6H_4)_3]$	White	34		53.50	53.40	6.87	6.49	3.67	4.01		
$[(C_6H_5)_4As][Nb(OSC_6H_4)_3]$	Black	24		59.44	59.40	3.80	4.29			11.33	11.28
$[(C_6H_5)_4As][Ta(OSC_6H_4)_3]$	Red-orange	18		53.88	53.38, 53.86	3.45	3.49, 3.58			10.27	10.04, 9.88
$[(C_2H_5)_4N]_2[Ti(O_2C_6H_4)_3]$	Orange			64.55	64.03	8.28	7.80				
$[(C_6H_5)_4As][Nb(OC_6H_4(SH))_2Cl_4]$	Black	19	196–198	49.79	50.39, 49.88	3.48	3.54, 3.48			7.38	7.06, 7.13

*Uncorrected.
†Chlorine analysis: theoretical, 16.33; observed, 16.82, 16.87.

TABLE 2. Conductivity measurements and u.v. and visible spectra

	Λ_m*	Maxima, cm^{-1} (ε)
$[(C_2H_5)_4N]_2[Ti(OSC_6H_4)_3]$	251	24 300(9330); 33 300(36 700)
$[(C_2H_5)_4N]_2[Zr(OSC_6H_4)_3]$	242	32 300(19 000)
$[(C_2H_5)_4N]_2[Hf(OSC_6H_4)_3]$	250	32 500(20 500)
$[(C_6H_5)_4As][Nb(OSC_6H_4)_3]$	92	23 900(9190)sh†; 27 800(13 400); 36 100(36 400)
$[(C_6H_5)_4As][Ta(OSC_6H_4)_3]$	—	32 300(16 400); 40 000(39 500)
$[(C_2H_5)_4N]_2[Ti(O_2C_6H_4)_3]$	226	26 700(12 300); 37 000(12 600)
$[(C_2H_5)_4N]_2[Hf(O_2C_6H_4)_3]$	221	33 900(19 700)

*Molar conductivity, Ω^{-1} cm^2 mol^{-1}.
†sh, shoulder.

Physical Measurements

Infrared spectra were recorded as KBr pellets in the region 4000–250 cm^{-1} on a Perkin–Elmer 457. Visible and u.v. spectra were obtained in the region of 10 000–40 000 cm^{-1} on a Cary 14 using various path lengths and solutions which were 10^{-4} *M* in CH_3CN. Polarographic measurements were made as previously described (1). ^1H n.m.r. spectra were recorded on a Varian Associates A 60 and conductivity measurements were made using a Philips PR9500 conductivity bridge and a cell designed for measurements under an inert atmosphere.

Results and Discussion

Sodium salts of the desired complexes can be prepared as THF solutions according to the following equation.

$$M(NR_2)_x + (6 - x)NaXC_6H_4(YH) + (x - 3)(HX)C_6H_4(YH) \rightarrow Na_{(6-x)}M(XYC_6H_4)_3$$

where $x = 4$ for Ti, Zr, and Hf and $x = 5$ for Nb and Ta. In our previous report on the synthesis of complexes of benzene-1,2-dithiol, we isolated the complexes as tetraphenylarsonium or tetraalkylammonium salts by exchange with the appropriate halide salt in CH_3CN or CH_2Cl_2. We have found that, in the synthesis of complexes of *o*-mercaptophenol and 1,2-dihydroxybenzene, one must use a chloride and not a bromide or iodide. It seems that in the latter two cases, exchange of cations is never complete due to the higher solubility of NaBr and NaI. This does not cause a problem in the case of benzene-1,2-dithiol complexes which have lower solubility than the *o*-mercaptophenol and 1,2-dihydroxybenzene complexes. These latter complexes require more drastic conditions to effect precipitation and as a result of this tetraalkylammonium bromide or iodide also precipitates. Therefore, we recommend the use of chlorides in order to avoid such problems. Although most tetraalkylammonium chlorides are hygroscopic, we have found that they may be easily dehydrated under vacuum and subsequently used as standardized CH_3CN solutions.

Alternatively, we have attempted direct synthesis of the sodium salt of the Nb complex with *o*-mercaptophenol by reacting $NbCl_5$ with a mixture of *o*-mercaptophenol and its sodium salt in refluxing THF for 44 h. Under these conditions no characterizable compounds could be isolated but by doing the same reaction at room temperature for 96 h, black crystals were finally obtained from the work-up which appear to be a mixed complex of *o*-mercaptophenol and chloride ions of the formula

$$[(C_6H_5)_4As]Nb[OC_6H_4(SH)]_2Cl_4.$$

With the exception of the *o*-mercaptophenol complexes of Zr and Hf, the complexes reported here appear to be air stable, and all have reasonable solubility in polar solvents such as CH_3CN and CH_2Cl_2.

The u.v. and visible spectra of the synthesized complexes have been recorded in acetonitrile at 10^{-4} *M* concentration. The band positions with the corresponding extinction coefficients are shown in Table 2. Table 2 also lists the molar conductivities of the complexes. The values are consistent with the proposed formulations.

Since all the complexes contain transition metal ions in the d^0 electronic configuration the observed bands must be due to charge–transfer and (or) internal ligand type electronic transitions. The low energy bands observed in the Ti (24 300 cm^{-1}) and Nb (23 900 and 27 800 cm^{-1}) complexes are clearly inconsistent with ligand transitions since they occur at substantially lower energy than the bands observed in the

Can. J. Chem. Downloaded from www.nrcresearchpress.com by 210.87.254.6 on 09/05/12
For personal use only.

TABLE 3. Comparison of the u.v. and visible spectra of $M(S_2C_6H_4)_3$ and $M(OSC_6H_4)_3$ type complexes

	Maxima, cm^{-1} (ε)			
$W(S_2C_6H_4)_3$	12 900(1300)Sh	16 060(20 000)	23 200(2000)	26 140(16 500)
$W(OSC_6H_4)_3$	15 400(3450)	21 800(7780)	24 400(7810)	30 000(7000)
	36 800(14 800)			
$Nb(S_2C_6H_4)_3^-$	17 700(10 700)	27 200(13 800)	30 700(9120)Sh	
$Nb(OSC_6H_4)_3^-$	23 900(9190)Sh	27 800(13 400)	36 100(36 400)	
$Ta(S_2C_6H_4)_3^-$	22 300(4900)	28 700(14 500)	33 900(18 100)	

ligand themselves,[2] therefore they are assigned to charge–transfer transitions. The high energy bands which most assuredly contain ligand based transitions, must also have some charge–transfer character since their positions are shifting when changes are made in the central transition metal ions. Although the exact make-up and assignment of the bands cannot be made, it is nevertheless interesting to note that similar charge–transfer bands played an important role in the spectra of the corresponding benzene-1,2-dithiolate complexes (1). Furthermore the hypsochromic shifts in the band positions are also the same as those previously observed (1) in the dithiol complexes, *i.e.* Ti < Zr < Hf, Nb < Ta, and W < Ta < Hf. This order is consistent with the order of increasing metal d orbital energies[3] (see ref. 21 for the most recent tabulation of ionization potentials of the elements) and hence identifies the nature of the charge–transfer bands as being ligand-to-metal. Consistent with the above idea is the ligand dependence of the band positions. The anticipated trend of hypsochromic shift with increased stability of ligand orbitals is exactly met by the observed order $S_2C_6H_4^{2-} < OSC_6H_4^{2-} < O_2C_6H_4^{2-}$ (3).

Polarographic studies on the W and Nb *o*-mercaptophenol complexes were made in CH_2Cl_2 and the Ti 1,2-dihydroxybenzene complex was studied in both CH_2Cl_2 and CH_3CN, but in no case was either oxidation or reduction observed. The absence of oxidation waves is not surprising considering that the ligand orbitals are more stable than in benzene-1,2-dithiol, and no oxidation waves were observed for complexes of this ligand and the early transition metals (1). Such reasoning assumes that the HOMO has substantial ligand character, as suggested by the visible spectra. However, if the LUMO has any ligand character, reduction of the complexes of *o*-mercaptophenol and 1,2-dihydroxybenzene should fall at more positive potentials than the corresponding benzene-1,2-dithiol complexes. The puzzling absence of any reduction waves for the former ligands remains unexplained at the present time.

Finally, we would like to comment on possible structural similarities between the reported complexes and those of the corresponding 1,2-benzenedithiols. It was shown previously (1) that, at least as far as the second and third row transition metals are concerned, the u.v. and visible spectra of the trisdithiolates can be successfully used to predict qualitatively the co-ordination geometry of the complexes in question. Indeed the prediction of trigonal prismatic geometry of the $Nb(S_2C_6H_4)_3^-$ and the distortion therefrom in the case of $Ta(S_2C_6H_4)_3^-$, were both verified by X-ray crystallographic work (22). It is then interesting to note that spectral similarities do exist between some of the reported complexes and the corresponding trisbenzendithiolates. As can be seen in Table 3 the spectrum of $W(OSC_6H_4)_3$ closely resembles that of $W(S_2C_6H_4)_3$ and there exists a good correlation between the spectra of $Nb(OSC_6H_4)_3^-$ and $Ta(S_2C_6H_4)_3^-$. Are these spectral similarities an indication of similar structures in the solid state? Based on the observation with trisdithiolates, it is tempting to say yes. However, more realistically, a definite answer to the question must await the results of structural studies on some of these complexes.

[2]Ligand spectrum in acetonitrile, maxima cm^{-1} (ε): *o*-mercaptophenol, 31 700(2000) and 35 300(9800); 1,2-dihydroxybenzene, 36 400(2900), this is in good agreement with the previously reported value of 36 000(2630) by Sandorfy and co-workers (20).

[3]S. Fraga. Personal communication.

We thank the National Research Council of Canada, the Research Corporation and the University of Alberta for financial support of this work. We also thank

Can. J. Chem. Downloaded from www.nrcresearchpress.com by 210.87.254.6 on 09/05/12
For personal use only.

Professors J. A. Plambeck and B. Kratochvil for the use of their polarographic apparatus. The useful comments provided by the Hooker Chemical Corp. toward the synthesis of *o*-mercaptophenol are also acknowledged.

1. J. L. MARTIN and J. TAKATS. Inorg. Chem. In press.
2. R. F. HECK. Inorg. Chem. **7**, 1513 (1968).
3. A. L. BALCH. J. Am. Chem. Soc. **91**, 1948 (1969).
4. K. ANDRÄ and W. ROLLKA. Z. Anorg. Allg. Chem. **391**, 19 (1972).
5. A. ROSENHEIM, B. RAIBMANN, and G. SCHENDEL. Z. Anorg. Allg. Chem. **196**, 160 (1931).
6. A. ROSENHEIM and O. SORGE. Chem. Ber. **53**, 932 (1920).
7. C. GOPINATHAN and J. GUPTA. Indian J. Chem. **3**, 470 (1965).
8. A. ROSENHEIM and E. ROEHRICH. Z. Anorg. Allg. Chem. **204**, 442 (1932).
9. R. N. KAPOOR, S. PRAKASH, and P. N. KAPOOR. Z. Anorg. Allg. Chem. **353**, 109 (1967).
10. H. FUNK, W. WEISS, and K. P. ROETHE. Z. Anorg. Allg. Chem. **301**, 271 (1959).
11. R. P. HENRY, P. C. H. MITCHELL, and J. E. PRUE. J. Chem. Soc. A, 3392 (1971).
12. D. W. BARNUM. Inorg. Chem. **11**, 1424 (1972).
13. H. R. ALLCOCK and E. C. BISSELL. J. Am. Chem. Soc. **95**, 3154 (1973).
14. J. J. FLYNN and F. BOER. J. Am. Chem. Soc. **91**, 5756 (1969).
15. D. C. BRADLEY and I. M. THOMAS. J. Chem. Soc. 3857 (1960).
16. D. C. BRADLEY and I. M. THOMAS. Can. J. Chem. **40**, 449, 1355 (1962).
17. D. C. BRADLEY and M. H. GITLITZ. J. Chem. Soc. A, 980 (1969).
18. G. CHANDRA and M. F. LAPPERT. J. Chem. Soc. A, 1940 (1968).
19. D. GREENWOOD and H. A. STEVENSON. J. Chem. Soc. 1514 (1953); P. FRIEDLANDER and F. MAUTHNER. Zeit. Farb. Text. Ind. **3**, 333 (1904).
20. A. KISS, J. MOLNAR, and C. SANDORFY. Bull. Soc. Chem. Fr. **16**, 275 (1949).
21. Astrophysical Quantities 3rd Ed. C. W. Allen, University of London, The Athlone Press. 1973. pp. 36–40.
22. M. J. BENNETT, M. COWIE, J. L. MARTIN, and J. TAKATS. J. Am. Chem. Soc. **95**, 7504 (1973); J. L. MARTIN and J. TAKATS. Inorg. Chem. In press.

Can. J. Chem. Downloaded from www.nrcresearchpress.com by 210.87.254.6 on 09/05/12
For personal use only.

Electric Dipole Moments of a Series of $\Delta^{8\,(14)}$ Cholestenyl Esters

J. M. POCHAN, J. E. KUDER, J. Y. C. CHU, D. WYCHICK, AND D. F. HINMAN

Xerox Corporation, 800 Phillips Road, Webster, New York 14580

Received June 10, 1974

J. M. POCHAN, J. E. KUDER, J. Y. C. CHU, D. WYCHICK, and D. F. HINMAN. Can. J. Chem. **53**, 578 (1975).

Dipole moments of a series of $\Delta^{8(14)}$ cholestenyl esters have been measured. These are isomeric with the cholesteryl alkanoates. There appears to be a limited correlation between crystal melting point and dipole moment. No correlation of dipole moment and mesomorphic tendency is observed.

J. M. POCHAN, J. E. KUDER, J. Y. C. CHU, D. WYCHICK et D. F. HINMAN. Can. J. Chem. **53**, 578 (1975).

On a mesuré les moments dipolaires d'une série d'esters du $\Delta^{8(14)}$ cholestényle. Ces composés sont des isomères des alkanoates de cholestéryle. Il semble y avoir une corrélation limitée entre le point de fusion du cristal et son moment dipolaire. On n'a observé aucune corrélation entre le moment dipolaire et la tendance mesomorphique. [Traduit par le journal]

Introduction

Odd–even effects of the number of carbon atoms in the alkyl chain of the ester group of cholesteryl esters have been reported (1–3) for a variety of physical properties. More recently Chadra and Bahadur (4) have shown these same effects with dipole moments and have noted that there is a correlation between the measured dipole moment and the crystal melting points of the materials.

Recently, one of us (5) has synthesized a series of esters based on $\Delta^{8(14)}$-*cholestenol*. These esters exhibit lower crystal melting points than their cholesteryl counterparts (10–40 °C) and many of them, in particular the C_8 through C_{13} series, exhibit large mesomorphic temperature ranges with low melting points.

It is the purpose of this study to see if a direct correlation exists between crystal melting and/or mesomorphic range and the measured dipole moments of these materials.

Experimental

Measurements

Dielectric and refractive index measurements were performed in reagent grade benzene (Baker) that was washed in succession with concentrated H_2SO_4, water, aqueous Na_2CO_3, and water, then dried over 5A molecular sieves, distilled, and stored in dark bottles over sodium. As no effect of nonpolar solvent was noted in measuring the dipole moments of other cholesteryl compounds (6), only benzene was used in these experiments (6).

Solution dielectric measurements (3 terminal method) were performed at 25.00 ± 0.02 °C with a General Radio 1615-A capacitance bridge at frequencies of 1 and 10 kHz, and within the limits of error, were constant for all solution concentrations. A constant temperature stainless steel cell through which regulated water from a Haake constant temperature bath circulated was fabricated for the measurement. Because of material scarcity, the continuous flow method of measurement was not used. The cell was repeatedly filled with fresh solution (at a given concentration) until three consecutive sets of data differing less than one part in 10^4 were obtained. The concentration range for all the systems studied was 1×10^{-6}–1×10^{-5} mol/l. The dielectric constant (ε) of the solution was measured by the substitution technique with an air reference. The cell gap was set by a Teflon^R spacer. A 1 in. diameter electrode was used in all experiments. Refractive indices (n) were measured with a Bausch and Lomb Precision Refractometer at 25.00 ± 0.02 °C.

The molecular dipole moments were obtained via the Guggenheim method (7) in which the quantity $(\varepsilon - n^2)/(\varepsilon + 2)(n^2 + 2)$ is plotted against concentration. The slope (S) of the best linear regression fit produces the dipole moment by the following equation

$$[1] \qquad \mu = [S(27/4)kT/\pi N]^{1/2}$$

where k = Boltzmann constant and N = Avogadro's number.

Plots of ε and n^2 against concentration were linear indicating that association does not occur in the concentration range considered.

Results and Discussion

Results of the dipole moment (μ) calculations as well as crystal melting points (T_m) (5) for the

Can. J. Chem. Downloaded from www.nrcresearchpress.com by 210.87.254.5 on 09/05/12
For personal use only.

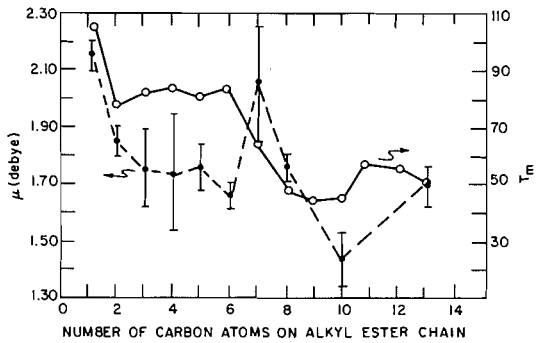

FIG. 1. Crystal melting point and molecular dipole moment (for $\Delta^{8(14)}$ cholestenyl esters) *vs.* cholestenyl ester chain length.

compounds are shown in Fig. 1. It is evident that a similarity exists between μ and T_m; however, a direct correlation is, at most, limited.

Structures for the esters of $\Delta^{8(14)}$ cholestenol (**1**) as well as the cholesteryl esters (**2**) are shown below

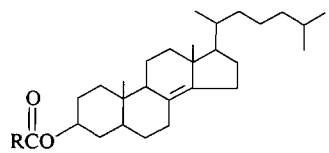

1

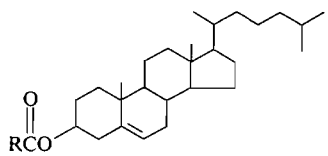

2

The compounds are isomeric and any changes in dipole moment must be due to differences in the electronic charge distribution in each system. Of importance is the fact that, in general, the $\Delta^{8(14)}$ compounds have lower dipole moments (especially those of C_{10} or lower) than their cholesteryl counterparts and exhibit much lower crystalline melting points. Because they are isomeric, this finding indicates that dipolar forces could be important in determining these materials melting points.

Another explanation exists, though; the differences in molecular conformations of the systems. The differences in isomeric series T_m as well as the data shown in Fig. 1 must be considered in light of this.

There is no reason to expect that molecular conformation in the solid and in solution would be identical. The cholesteryl moiety would probably not differ very much, but the ester conformation could change radically. At short ester chain lengths a direct correlation between T_m and μ might be expected, such as the large change in μ and T_m in going from C_1 to C_2. (See Fig. 1.) At longer chain lengths, the direct correlation would not be expected as the longer esters could assume different conformations. The C_2 through C_6 series exhibit an almost inverse relationship, but are only changing slightly. These subtle changes are probably more due to the ester conformation in the solid than the actual dipole moment. If any general conclusion were to be drawn in this region, it would be that solid state molecular conformation (rather than dipole moment) controls the relative melting temperature of this portion of the series. Between C_6 and C_7 of the ester chain, both T_m and μ exhibit large changes. These types of discontinuous changes have been observed in T_m of other liquid crystal systems and are not unique (8). Although all dipoles between C_7 and C_{13} in the series have not been measured, it appears that a general correlation exists in the data. The discontinuity could be an indication of a conformational change in the cholesteryl structure. For instance, a *cis–trans* isomerization of the type shown below may take place, or be the difference between solid and solution conformation.

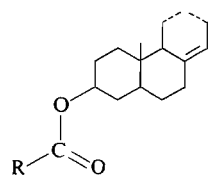

cis

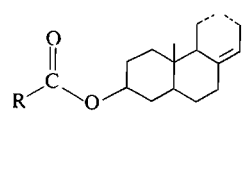

trans

In conclusion, we feel that a limited correlation is observed between the molecular dipole moment, as measured in solution, and the crystal melting point of the cholesteryl esters. For point dipoles, where intermolecular interaction forces might be proportional to the dipole moment, a direct correlation should exist. For true molecules the added complication of dipoles not being point charges, steric restraints (molecu-

Can. J. Chem. Downloaded from www.nrcresearchpress.com by 210.87.254.5 on 09/05/12
For personal use only.

lar packing), conformation, and weak (Van der Walls) interactions should affect such a μ–T_m correlation. We feel steric constraints and variances in solution *vs.* solid state conformation are the most important of these and must conclude that the observed correlation is either fortuitous, or that solution and solid state conformation are similar enough to permit dipolar forces to control interaction energies in the solid state. Without experimental evidence on the molecular conformation a choice can not be made. Also, no correlation is observed between the mesomorphic temperature range, or mesophase, of the cholestenyl compounds, and the measured dipole moment.

1. G. W. GRAY. Molecular structure and properties of liquid crystals. Academic Press, Inc., New York. 1962.
2. G. J. DAVIS, R. S. PORTER, and E. M. BARRALL, II. Mol. Cryst. Liquid Cryst. **10**, 1 (1970).
3. H. ARNOLD, D. DEMUS, M. J. KOCH, A. NELLES, and H. SACKMAN. Zeit. Phys. Chem. **240**, 185 (1969).
4. S. CHANDRA and B. BAHADUR. J. Chem. Phys. **70**, 4 (1973).
5. J. Y. C. CHU. J. Chem. Soc. Chem. Commun. 374 (1974); J. Y. C. CHU. J. Phys. Chem. In press.
6. C. U. S. S. V. GOLALAKRISHNA, C. HARANDH, and C. R. K. MURTZ. Trans. Faraday Soc. **63**, 1953 (1967).
7. E. A. GUGGENHEIM. Trans. Faraday Soc. **45**, 714 (1949).
8. E. M. BARRALL, II. *In* Ordered fluids and liquid crystals. *Edited by* F. Saeva, J. Phys. Chem. To be published.

Can. J. Chem. Downloaded from www.nrcresearchpress.com by 210.87.254.5 on 09/05/12
For personal use only.

^{13}C Nuclear Magnetic Resonance Studies. 45.[1] The ^{13}C Spectra of Some β,γ Unsaturated Polycyclic Ketones

J. B. STOTHERS, J. R. SWENSON, AND C. T. TAN
Department of Chemistry, University of Western Ontario, London, Ontario N6A 5B7

Received August 26, 1974

J. B. STOTHERS, J. R. SWENSON, and C. T. TAN. Can. J. Chem. **53**, 581 (1975).

The ^{13}C spectra of several β,γ unsaturated polycyclic ketones have been recorded to examine the shielding differences for all carbons relative to those for their saturated analogs and the parent olefins. The variations of the sp^2 carbon shieldings provide qualitative evidence for the existence of homoconjugative interactions between the olefinic and carbonyl groups in the ground state. Similar evidence of interaction between γ,δ double bonds and carbonyl groups was found from spectra for a few examples. A simple interpretation of the shielding trends entirely in terms of charge density variations arising from through space polarization is shown to be inadequate, thereby emphasizing the existence of other major shielding contributions.

J. B. STOTHERS, J. R. SWENSON et C. T. TAN. Can. J. Chem. **53**, 581 (1975).

On a enregistré les spectres r.m.n. du ^{13}C de plusieurs cétones polycycliques β,γ insaturées; ces expériences ont été réalisées afin de déterminer les différences de blindage de tous les carbones par rapport à ceux des analogues saturés et des oléfines apparentées. Les variations dans les blindages des carbones sp^2 fournissent une indication qualitative pour l'existence d'interactions homoconjugatives entre les doubles liaisons et les groupements carbonyles dans l'état fondamental. Des indications semblables pour des interactions entre les doubles liaisons γ,δ et les groupements carbonyles ont déjà été trouvées à partir des spectres de quelques exemples. On démontre qu'une interprétation simple des tendances dans les blindages qui dépendent entièrement des variations dans les densités de charge provenant d'une polarisation à travers l'espace est inadéquate et qu'il faut faire appel à d'autres contributions majeures de blindage.
[Traduit par le journal]

Introduction

Some years ago, the carbonyl carbon shieldings for a number of β,γ unsaturated bicyclic ketones were measured to investigate the possibility of detecting homoconjugative interactions between olefinic and carbonyl π systems (1). At that time instrumental limitations precluded definitive detection and assignments for the remaining carbon signals but the carbonyl data indicated an interaction between the β,γ double bond and carbonyl group since the carbonyl carbons were shielded relative to their absorption positions for the saturated analogs. Since it had been established (2) that conjugation significantly increases the shielding of carbonyl carbons, the shift in the β,γ unsaturated systems was ascribed to homoconjugation. The observed dependence of the magnitude of the shift on the relative orientation of the double bond and carbonyl group was also in agreement with this interpretation. Confirmatory evidence should be provided, however, by the variations in shieldings of the olefinic carbons and other closely neighboring centers. For this purpose the data for the β,γ unsaturated ketones were compared with those for the corresponding olefins and saturated ketones. In this report we wish to present these results which tend to support our original conclusions but only in a qualitative fashion. A detailed examination of the shielding variations clearly shows that factors in addition to charge density must make significant contributions to the observed shieldings. In addition the results for some ketones containing γ,δ double bonds were assessed in a similar fashion.

[1]For part 44, see ref. 23.

Experimental

Materials

The compounds employed in this study have been described in the literature and samples were prepared having essentially the same physical constants. Infrared and proton spectra were determined for each to ensure their identities. Compounds **1–10**, **23**, and **24** were available from earlier studies (1, 3, 4) whereas the remaining bicyclo[3.2.1]octane derivatives were obtained utilizing the reaction of dibromocarbene with **4** and with bicyclo-

Can. J. Chem. Downloaded from www.nrcresearchpress.com by 210.87.254.6 on 09/05/12
For personal use only.

Can. J. Chem. Downloaded from www.nrcresearchpress.com by 210.87.254.6 on 09/05/12
For personal use only.

heptadiene. The reaction with **4** gave 2,3-dibromobicyclo-[3.2.1]oct-3-ene (5), which upon reduction with $LiAlH_4$ gave **35** (5) and upon hydrolysis with $AgNO_3$ in aqueous acetone gave 3-bromobicyclo[3.2.1]oct-3-en-2-ol (6). Reduction of the latter with $Na–NH_3$ gave the unsaturated alcohol which was oxidized using CrO_3 in CH_2Cl_2–pyridine (7) to **13** (8) and subsequently reduced catalytically to **12**; compound **12** was also obtained by catalytic hydrogenation of the unsaturated alcohol over PtO_2 in ether followed by CrO_3 oxidation (7). Treatment of **35** with concentrated H_2SO_4 gave **19** (5) whereas reduction of **35** with $Na–NH_3$ gave **22** (5) from which **11** was obtained by catalytic hydrogenation (5). The reaction of dibromocarbene with bicyclo[2.2.1]heptadiene gave an epimeric mixture of 2,3-dibromobicyclo[3.2.1]octa-3,6-dienes (9) from which **29** was obtained by $LiAlH_4$ reduction (9) while hydrolysis with $AgNO_3$ – aqueous acetone (6) gave a mixture of **31** and **32**. Oxidation of this mixture with CrO_3 in CH_2Cl_2–pyridine furnished a sample of **30**. Reduction of **30** with $Na–NH_3$ (10) gave **16** which was converted to **17** by the Wolff–Kishner reduction (11). Treatment of **31** and **32** with $Na–NH_3$ gave a corresponding mixture of **33** and **34** which was oxidized (7) to **14**. Diene **15** was obtained from **29** by $Na–NH_3$ reduction (9). Formolysis (9, 12) of **29** led to the formation of *exo*-6-formyloxy-3-bromobicyclo[3.2.1]oct-3-ene which was converted to bicyclo[3.2.1]oct-3-en-6-ol by reduction with $Na–NH_3$ (12) and to bicyclo[3.2.1]octan-6-ol by catalytic hydrogenation over Pd–C in THF–NaOH (9). Oxidation of each of these alcohols afforded samples of **21** (12) and **20** (9), respectively. Ketone **18** was prepared following the method of LeBel and Maxwell (13) from *anti*-8-bromotricyclo[3.2.1.$0^{2,7}$]octan-3-one which was available from **29** (14). The preparation of **26** and **28** has been described by Haywood-Farmer *et al.* (15), who kindly provided us with samples of each of these ketones. Catalytic hydrogenation of these furnished samples of **25** and **27**, respectively.

Nuclear Magnetic Resonance Spectra

The ^{13}C spectra were obtained with a Varian XL-100-15 system operating in the Fourier transform mode. Samples were examined as 10–15% (w/v) solutions in deuteriochloroform using 5-mm sample tubes. Off-resonance decoupling experiments served to distinguish methylene from methine signals while selective decoupling experiments were employed to assign the olefinic carbons unequivocally. In these experiments the decoupler was operated in the low power mode (108–112 dB) and carefully adjusted to the resonance frequency of an individual olefinic proton to determine the specific olefinic carbon signal affected. To determine the appropriate proton resonance frequencies, spectra were obtained with a Varian HA-100 spectrometer and the individual proton assignments followed readily from the observed splitting patterns together with proton–proton spin decoupling experiments. In most cases the bridgehead proton signals were distinct and double irradiation at these positions uniquely defined the nearer of the two olefinic protons on a given double bond. Decoupling was not essential for the bicyclo[3.2.1]oct-3-ene derivatives since the vicinal coupling of H-4 with the bridgehead proton is relatively large, ~6.5 Hz, and therefore characteristic. In one case, bicyclo[3.2.1]oct-3-en-6-one (**21**) the olefinic protons are nearly equivalent giving rise to a deceptively simple pattern and consequently solutions containing the shift reagent, $Eu(fod)_3$, were employed to enhance their nonequivalence. In the presence of 0.185 equiv. of $Eu(fod)_3$, the olefinic protons differ by 0.56 p.p.m. and the coupling patterns readily identified each center. The ^{13}C shieldings have precisions of better than 0.1 p.p.m.

Results

The ^{13}C shielding data for the polycyclic ketones, olefins, and hydrocarbons are collected in Table 1; for comparison with the more extensive data now available, our earlier results (3, 4) for norbornen-2-one (**1–4**) and bicyclo[2.2.2]-octenone (**7–10**) derivatives have been included. In each case, the carbonyl signals were readily identified from their low field positions. Off-resonance decoupling experiments readily distinguished methylene and methine sp^3 carbons and the latter were easily assignable since, in the unsymmetrical cases, the methine carbon lying closer to the carbonyl group is the more deshielded of the pair in each spectrum. The methylene assignments for the 7-oxonorbornenes (**5** and **6**) as well as the 3-oxo- and Δ^6-bicyclo-[3.2.1]octanes (**17–19**) were straightforward from

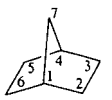

1

2 2-Oxo
3 2-Oxo-Δ^5
4 Δ^5
5 7-Oxo-Δ^5
6 7-Oxo

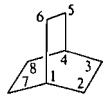

7

8 2-Oxo
9 2-Oxo-Δ^5
10 Δ^5

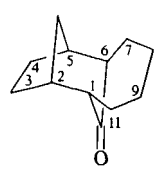

25

26 11-Oxo-Δ^3
27 11-Oxo-Δ^7,Δ^9
28 11-Oxo-Δ^3,Δ^7,Δ^9

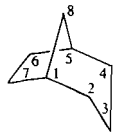

11

12 2-Oxo
13 2-Oxo-Δ^3
14 2-Oxo-Δ^3,Δ^6
15 Δ^3,Δ^6
16 2-Oxo-Δ^6
17 Δ^6
18 3-Oxo-Δ^6
19 3-Oxo
20 6-Oxo
21 6-Oxo-Δ^3
22 Δ^3
23 8-Oxo-Δ^3
24 8-Oxo
29 3-Br-Δ^3,Δ^6
30 2-Oxo-3-Br-Δ^3,Δ^6
31 *exo*-2-OH-3-Br-Δ^3,Δ^6
32 *endo*-2-OH-3-Br-Δ^3,Δ^6
33 *exo*-2-OH-Δ^3,Δ^6
34 *endo*-2-OH-Δ^3,Δ^6
35 3-Br-Δ^3

Can. J. Chem. Downloaded from www.nrcresearchpress.com by 210.87.254.6 on 09/05/12
For personal use only.

TABLE 1. ^{13}C shieldings[a] of several polycyclic derivatives

Compound	Skeleton	Substitution[b]	C-1	C-2	C-3	C-4	C-5	C-6	C-7	C-8	C-11	C-12
1	[2.2.1]	Nil	36.3	29.6	29.6	36.3	29.6	29.6	38.3			
2		2-Oxo	49.7	217.4	45.1	35.3	27.1	24.2	37.6			
			(49.8)	(214.8)	(45.0)	(35.4)	(27.3)	(24.3)	(37.5)			
3		2-Oxo-Δ^5	55.8	214.7	37.1	40.0	142.7	130.4	50.8			
			(57.7)	(212.7)	(37.1)	(40.3)	(142.7)	(131.0)	(50.8)			
4		"Δ^5"	41.8	24.6	24.6	41.8	135.2	135.2	48.5			
5		"7-Oxo-Δ^5"	45.3	21.0	21.0	45.3	133.2	133.2	205.3			
			(45.6)	(21.1)	(21.1)	(45.6)	(133.6)	(133.6)	(204.1)			
6		7-Oxo	37.8	24.2	24.2	37.8	24.2	24.2	216.8			
			(38.0)	(24.4)	(24.4)	(38.0)	(24.4)	(24.4)	(214.5)			
7	[2.2.2]	Nil	24.0	26.1	26.1	24.0	26.1	26.1	26.1	26.1		
8		2-Oxo	42.3	216.7	44.6	27.9	24.8	23.4	23.4	24.8		
9		2-Oxo-Δ^5	48.6	212.4	40.4	32.4	136.8	128.3	22.5	24.3		
10		"Δ^5"	29.5	25.8	25.8	29.5	134.1	134.1	25.8	25.8		
11	[3.2.1]	Nil	35.2	32.8	19.1	32.8	35.2	28.9	28.9	39.7		
12		2-Oxo	51.2	214.0	34.7	32.1	34.1	[28.1]	[28.0]	38.3		
13		2-Oxo-Δ^3	50.6	203.2	127.2[c]	156.5[c]	37.4	29.4	24.5	40.2		
14		2-Oxo-Δ^3,Δ^6	57.1	198.8	123.6[c]	154.9[c]	42.1	143.3[c]	131.8[c]	52.0		
15		Δ^3,Δ^6	[38.7]	28.7	123.8[c]	134.1[c]	[38.3]	139.7[c]	130.2[c]	40.7		
16		2-Oxo-Δ^6	55.9	210.0	34.5	25.2	38.7	137.8[c]	131.7[c]	42.1		
17		Δ^6	39.5	25.2	18.7	25.2	39.5	132.1	132.1	45.1		
18		3-Oxo-Δ^6	38.3	46.4	210.1	46.4	38.3	135.3	135.3	41.8		
19		3-Oxo	35.3	50.3	211.9	50.3	35.3	29.3	29.3	37.8		
20		6-Oxo	32.2	[30.5]	18.9	[30.7]	46.2	221.4	43.5	37.2		
			(32.3)	(30.5)	(19.0)	(30.8)	(45.9)	(218.2)	(43.3)	(37.1)		
21		6-Oxo-Δ^3	30.2	31.9	128.0[d]	126.0[d]	46.7	212.4	43.7	34.3		
22		"Δ^3"	33.6	37.5	123.8[c]	134.7[c]	35.6	35.5	30.6	35.5		
23		"8-Oxo-Δ^3"	42.5	43.1	125.5[c]	132.7[c]	45.2	30.2	25.6	217.9		
			(42.6)	(43.0)	(126.9)	(133.2)	(45.2)	(25.7)	(30.3)	(216.0)		
24		8-Oxo	44.8	37.0	17.4	37.0	44.8	22.7	22.7	222.0		
			(44.9)	(36.8)	(17.5)	(36.8)	(44.9)	(22.8)	(22.8)	(219.0)		
25	[4.4.1.1^{2,5}]	11-Oxo	57.3	42.2	29.2	29.2	42.2	57.3	[28.4]	[26.9]	216.5	30.2
26		11-Oxo-Δ^3	52.8	45.1	137.0	137.0	45.1	52.8	[28.9]	[27.1]	213.2	33.9
27		11-Oxo-Δ^7,Δ^9	62.1	45.2	30.0	30.0	45.2	62.1	[127.3]	[126.3]	210.9	29.4
28		11-Oxo-Δ^3,Δ^7,Δ^9	57.9	48.7	135.4	135.4	48.7	57.9	[128.3]	[126.8]	208.0	33.3

[a]In p.p.m. from internal TMS for $CDCl_3$ and C_6D_6 solutions; the latter values are given in parentheses. Values in square brackets may be interchanged.
[b]For ease of comparisons within the table, some of the monoolefinic compounds are numbered in an unconventional manner: bicyclo[2.2.1]hept-5-ene, bicyclo[2.2.1]hept-5-en-7-one, bicyclo-[2.2.2]oct-5-ene, bicyclo[3.2.1]oct-3-ene and bicyclo[3.2.1]oct-3-en-8-one; the substitution is listed in quotation marks.
[c]Assigned by selective proton decoupling (see text).
[d]Assigned by selective proton decoupling of solutions containing $Eu(fod)_3$ (see text).

TABLE 2. ^{13}C shieldings[a] of some bicyclo[3.2.1]octene derivatives

Compound	Substitution	C-1	C-2	C-3	C-4	C-5	C-6	C-7	C-8
29	3-Br-Δ^3,Δ^6	(40.6)	38.5	120.1	134.3	(40.1)	139.2	130.8	40.3
30	2-Oxo-3-Br-Δ^3,Δ^6	56.8	206.4	118.2	154.6	44.4	143.2	131.7	51.4
31	*exo*-2-OH-3-Br-Δ^3,Δ^6	46.8	71.9	123.7	144.1	41.6	139.5	130.5	37.6
32	*endo*-2-OH-3-Br-Δ^3,Δ^6	47.3	71.9	124.8	143.6	41.6	138.7	130.5	44.3
33	*exo*-2-OH-Δ^3,Δ^6	46.0	66.2	126.3	144.5	39.5	138.2	130.3	37.9
34	*endo*-2-OH-Δ^3,Δ^6	47.2	67.1	127.1	144.1	38.9	137.1	129.8	44.7
35	3-Br-Δ^3	35.2	46.9	120.6	135.6	37.5	34.8	30.2	34.8

[a]In p.p.m. from internal TMS for $CDCl_3$ solutions. Values in parentheses may be interchanged.

the relative intensities and the strong deshielding effect exerted by the carbonyl group at the α carbons. The sp^3 assignments for bicyclo[3.2.1]-octa-3,6-dien-2-one (**14**) were also straightforward and led to the assignments for the corresponding diene. For most of the remaining [3.2.1] derivatives, however, the methylene assignments are not unequivocal but a consistent set was obtained by comparison within the series and with the results for the synthetic precursors **29–35** whose data are listed in Table 2.

The results for **14**, **15**, **29**, and **30** show that C-8 is only slightly affected by the 3-bromo group whereas C-2 in **29** is deshielded by *ca.* 10 p.p.m. relative to **15**. The data for **31–34** indicate that an *exo*-2-hydroxyl shields C-8 while its *endo* counterpart deshields C-8 relative to hydrocarbon **15** and its 3-bromo derivative **29**. The lone methylene signal in **30–34** renders this assignment unambiguous. The methylene shieldings of **22** and its 3-bromo derivative **35** together with the data for **15** and **29** indicated that the most deshielded methylene carbon is C-2; thus, C-8 was assigned the value near 35 p.p.m. for **22** and **35**. The two strong methylene signals for **11**, the parent hydrocarbon, were most appropriately assigned as 32.8 (C-2, -4) and 28.9 p.p.m. (C-6, -7) by comparison with the corresponding centers in **19**. From this it appeared that C-6 would be deshielded relative to C-7 in **22** and **35** because introduction of the double bond at C-3,-4 eliminates a steric interaction between the *endo* protons at C-4 and C-6 in hydrocarbon **11**. From these assignments for **11** and **22** the more intense CH_2 signals in **24** were assigned and those for the methylene signals of **23** followed on the same basis. From the data for **17** and the expected α effect of the carbonyl group, the methylene assignments for **16** were made. By comparison with **11**, the signal near 43.5 p.p.m. was assigned to C-7 in each of **20** and **21**, while

TABLE 3. Olefinic proton shieldings[a] in some bicyclo[3.2.1]octenones

Compound	3-H	4-H	6-H	7-H
13	5.81	7.25		
14	5.41	7.32	6.66	6.15
15	5.21	6.03	6.23	5.71
16			6.21	6.00
17			5.82	5.82
18			6.01	6.01
21	~5.65[b]	~5.75[b]		
	6.35[c]	6.91[c]		
22	5.34	5.86		
23	5.55	5.86		

[a]In p.p.m. from internal TMS for $CDCl_3$ solutions.
[b]Assignments uncertain (see text).
[c]Solution containing 0.2 equiv. $Eu(fod)_3$.

those near 30.5 p.p.m. for **20** were assigned to C-2 and C-4 and that at 32.0 p.p.m. for **21** was ascribed to C-2. These assignments for **20** agree with those made on the basis of the data for the 7-methyl and 7,7-dimethyl derivatives (16). The *exo*-3-methyl and 3,3-dimethyl derivatives of **12** were also available from another project (16) and the assignment in Table 1 was made by comparison with these data. Finally the methylene assignments listed for **13** appear to agree best with the trends found throughout the series. For ketones **25–28**, the assignments were essentially straightforward with the exception of those for C-7(-10) and C-8(-9) which were not unequivocally distinguished.

Individual assignments for the olefinic carbons in the unsymmetrical unsaturated compounds **13–16** and **21–23** were obtained by selectively irradiating each olefinic multiplet at its proton resonance frequency to determine the specific carbon associated therewith. The olefinic proton shieldings for these compounds and the symmetrical systems are listed in Table 3, from which it can be seen that the relatively large separations between nonequivalent protons in each case

Can. J. Chem. Downloaded from www.nrcresearchpress.com by 210.87.254.6 on 09/05/12
For personal use only.

TABLE 4. ^{13}C carbonyl shieldings[a] in several polycyclic ketones

Compound	Skeleton	Carbonyl position	δ_C	Compound	Double bond(s)	δ_C	$\Delta\delta_C$[b]
2	[2.2.1]	2	217.4(214.8)	**3**	Δ^5	214.7(212.7)	−2.7(−2.1)
6		7	216.8(214.5)	**5**	Δ^2	205.3(204.1)	−11.5(−10.4)
8	[2.2.2]	2	216.7	**9**	Δ^5	212.4	−4.3
12	[3.2.1]	2	214.0	**13**	Δ^3	203.2	
				14	Δ^3,Δ^6	198.8	−4.4
				16	Δ^6	210.0	−4.0
19		3	211.9	**18**	Δ^6	210.1	−1.8[c]
20		6	221.4(218.2)	**21**	Δ^3	212.4	−9.0
24		8	222.0(219.0)	**23**	Δ^3	217.9(216.0)	−4.1(−3.0)
25	[4.4.1.$1^{2,5}$]	11	216.5	**26**	Δ^3	213.2	−3.3[c]
				27	Δ^7,Δ^9	210.9	−5.6
				28	$\Delta^3,\Delta^7,\Delta^9$	208.0	−2.9[c,d]

[a]In p.p.m. from internal TMS. Measured in $CDCl_3$ and C_6D_6; the latter values given in parentheses.
[b]The effect of a β,γ double bond unless otherwise indicated.
[c]The effect of the γ,δ double bond.
[d]Compound **28** relative to **27**.

rendered selective decoupling particularly easy. For **21**, however, the olefinic pattern was deceptively simple but with the addition of 0.185 equiv. of $Eu(fod)_3$ these protons were well separated and readily identified, whereupon selective decoupling readily distinguished the olefinic carbons bonded to each.

Some of the ketones were also examined in C_6D_6 solutions to investigate the solvent effect on these shieldings briefly. These data are included in Table 1.

Discussion

In our earlier study of homoconjugated bicyclic ketones (1), attention was focussed entirely on the carbonyl shieldings for which it was found that β,γ unsaturation tended to increase the carbonyl shielding relative to that observed for the saturated analog. The present data, summarized in Table 4, show that this trend is general and that **9** is not anomalous as originally concluded. Previously we had compared our value for **9** with that reported for **8** (17) but apparently the solvent difference masked the shift, now found to be −4.3 p.p.m. in $CDCl_3$. A brief examination of solvent effects for a few examples showed that the shieldings are lower in $CDCl_3$ than in C_6D_6 (Table 4) presumably because of hydrogen bonding in the former, a feature known to deshield carbonyl carbons (18). It is interesting that the $\Delta\delta_C$ values in Table 4 are somewhat less for C_6D_6 solutions. As found earlier, the magnitude of the shift caused by the β,γ double bond depends on the relative orientation of the olefinic and carbonyl bonds, ranging from −2.7 to −11.5 p.p.m. (in $CDCl_3$) for this series. The larger shifts for **5** and **21** are comparable to those found for conjugated systems (1), as illustrated by one bicyclic example, **13**, included in this series, for which $\Delta\delta_C = -10.8$ p.p.m. relative to **12**. Although the marked effect of the β,γ olefinic bond in **5** was well known (1, 17) it seemed somewhat surprising that **21** exhibited a shift of −9.0 p.p.m. since ketones **9**, **16**, and **23** show shifts near −4 p.p.m. although all four ketones appear to be very closely related in terms of the relative orientations of their olefinic and carbonyl bonds. On the basis of the carbonyl shifts for these homoconjugated ketones relative to their saturated analogs, the extent of homoconjugative interaction between the π systems appears to decrease in the order: **5** > **21** > **9** ≈ **23** ≈ **16** > **3**.

A comparison of **27** with **25** indicates that the homoconjugated diene system in **27** shields the carbonyl carbon by −5.6 p.p.m. It is also interesting that the carbonyl shift for **14** *vs.* **13**, −4.4 p.p.m., is comparable to that for **16** *vs.* **12**, −4.0 p.p.m. indicating that the 6,7 double bond is homoconjugated with the carbonyl group in each. The increased carbonyl shielding of **14** relative to **13** is analogous to that found for a number of cross-conjugated ketones (18). Additional evidence for a homoconjugative interaction in **14** is provided by the olefinic shieldings since C-6 is shifted 4.6 p.p.m. downfield from its

Can. J. Chem. Downloaded from www.nrcresearchpress.com by 210.87.254.6 on 09/05/12
For personal use only.

TABLE 5. Shielding effects[a] of the carbonyl group at the olefinic and α carbon positions in unsaturated bicyclic ketones

			Olefinic nuclei				α carbons	
Skeleton	A	B	β-C	γ-C	β-H	γ-H	CH_2	CH
[2.2.1]	1	2					15.5	13.4
		6					—	1.5
	4	3	−4.8	+7.5	−0.03	+0.43	12.5	14.0
		5	−2.0[b]	−2.0[b]	+0.48[b]	+0.48[b]	—	3.5
[2.2.2]	7	8					18.5	18.3
	10	9	−5.8	+2.7	−0.07	+0.22	14.6	19.1
[3.2.1]	11	20					14.6	11.0
	22	21	−8.7	+4.2	−0.10	+0.31	13.1	11.1
	11	12					15.6	16.0
	17	16	−0.4	+5.7	+0.18	+0.39	15.8	16.4
	11	19					17.5	—
	17	18	—	+3.2	—	+0.19	21.2	—
	11	24					—	9.6
	22	23	−2.0	+1.7	0.0	+0.21	—	9.6, 8.9
	22	13	+21.8[c]		+1.91[c]		—	17.0
	15	14	+20.8[c]	+3.6	+1.29[c]	+0.43	—	18.4
			+1.6		+0.44			

[a]The individual values represent ($\delta_C^B - \delta_C^A$) for the compounds listed in columns 2 and 3.
[b]Because of the symmetry of 5 these positions are both β and γ with respect to the carbonyl group.
[c]β position on the conjugated double bond, *i.e.* C-4.

position in **15** and C-3 is essentially the same in both. The latter observation indicates a significant reduction in the α effect of the carbonyl group in **14** relative to that, for example, found for **13**.

A few ketones having γ,δ double bonds were included in this series and the results indicate that there is an interaction between the olefinic and carbonyl groups which is dependent on geometry. For **18** *vs.* **19** the carbonyl shift is −1.8 p.p.m. while for **26** *vs.* **25** the change is −3.3 p.p.m. In **18** and **26**, the relative orientations of the carbonyl and olefinic bonds must be similar since substitution of a tetramethylene chain between C-2 and C-4 in **18** gives **26**. The additional ring, however, must reduce the flexibility of **26** in the neighborhood of the carbonyl group and serve to hold the latter somewhat closer to the γ,δ double bond as the carbonyl shielding data indicate. Since $\Delta\delta_C$ for **28** *vs.* **27** is −2.9 p.p.m., which is comparable to that for **26** *vs.* **25**, the effect of the γ,δ olefinic bond appears to be approximately additive.

Homoconjugation between a double bond and a carbonyl group would be expected to alter the polarization of the olefinic carbons and, therefore, to be reflected in their ^{13}C shieldings relative to the values exhibited by the corresponding olefins. This appears to be the case and the appropriate data are collected in Table 5 including the proton shieldings. In each unsymmetrical β,γ unsaturated ketone the γ olefinic carbon absorbs downfield from its position in the olefin whereas the β carbons are generally shielded. A similar trend emerges for the β and γ olefinic protons. Thus the observed trends for the olefinic centers are qualitatively consistent with the carbonyl shifts but the relative magnitudes of the shielding changes would suggest a quite different order for the relative extents of homoconjugation throughout this series from that indicated by the carbonyl data, namely, **3** > **16** > **21** > **9** > **23**. Another trend could be anticipated to emerge from the shielding variations for the α carbons since homoconjugative interaction of an olefinic bond with a carbonyl group may be expected to reduce its inductive effect, thereby reducing the deshielding effect of the carbonyl carbon at the α positions. The appropriate data are listed in Table 5 to show that the expected trend is found for α-methylene carbons in the β,γ unsaturated cases but the opposite tendency is exhibited by the α-methine (bridgehead) carbons. Clearly, interpretation of the observed trends simply in terms of polarization changes arising from homoconjugative interactions is inadequate.

Recently, the shielding differences observed for

Can. J. Chem. Downloaded from www.nrcresearchpress.com by 210.87.254.6 on 09/05/12
For personal use only.

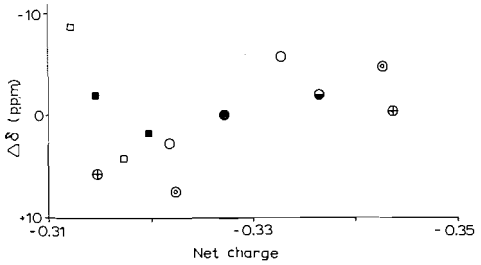

FIG. 1. A plot of the net charges on olefinic carbons as given by '4-31G' m.o. calculations for some β,γ unsaturated ketones *vs.* the observed shifts (Δδ) relative to the corresponding bicyclic olefins: **3** (⊙), **5** (○), **9** (○), **16** (⊗), **21** (□), **23** (■).

olefinic carbons in a series of acyclic unsaturated esters have been ascribed to through-space polarization arising from an electric field effect of the carbonyl group (19). As a test for this sort of contribution to the olefinic shieldings of the bicyclic β,γ unsaturated ketones some model '4–31G' *ab initio* molecular orbital calculations (20) were carried out. To simulate the bicyclic ketone system, the polarization of an ethylene double bond by an electric dipole field of a carbonyl group, defined by point charges 1.20 Å apart having the charges adjusted to simulate the dipole moment of a carbonyl group, was examined. Using the COORD program (21), the positions of the constituent atoms of a specific ketone were determined. With the point charges placed at the geometrical coordinates of the carbonyl C and O, the net charges at the olefinic carbons, represented by ethylene, were calculated using a carbonyl dipole moment of 2.84 D, the value for acetone. In this way the net charges on the olefinic carbons in **3**, **5**, **9**, **16**, **21**, and **23** were computed and the results are shown in Fig. 1. The calculated net charges are plotted against Δδ values representing the ^{13}C shielding difference for the olefinic carbons in the β,γ unsaturated ketone and the parent olefin. For those systems having the olefinic carbons in a two-carbon bridge there appears to be a rough linear trend having a slope of *ca.* 300 p.p.m./unit charge but the β carbons in the ketones having the olefinic bond in a three-carbon bridge, **21** and **23**, are significantly shielded relative to their counterparts in two-carbon bridges. Clearly the notion of a dominant shielding contribution arising from through space polarization by the carbonyl electric dipole field is inadequate to account for the observed trends. It may be noted that, for the present series, the separation between the olefinic bond and the carbonyl group is very much less than that in the acyclic esters for which the electric field effect contributions appeared to dominate the shielding variations.

The basic assumption inherent in an interpretation of the shielding differences in these unsaturated ketones in terms of homoconjugative interactions is that the observed shieldings are dominated by variations in electron density. While there seems little doubt that electron density is a major factor it is not the sole contributor, and it has been shown that variations in bonding parameters can make major contributions. These bicyclic systems undoubtedly differ in strain energy and therefore in the nature of the bonding parameters associated with the constituent carbons. Grant and his coworkers (22) have recently demonstrated for some simple systems that the bonding contribution to ^{13}C shieldings depends strongly on the σ and π character of the orbitals, their orientation, symmetry properties, and the energy gap between ground and excited states. From the variations observed in the present systems it would appear, therefore, that while the trends for the sp^2 carbons are qualitatively in accord with the existence of a homoconjugative polarization, interpretation solely in terms of charge density variations is a grossly simplified and inadequate view. These results underscore the dangers associated with such a simple interpretation and re-emphasize the fact that ^{13}C shieldings are dependent on additional factors. We conclude that homoconjugative interactions are observable by ^{13}C shielding variations but quantitative assessments of the relative extent of these interactions must await further theoretical developments.

We wish to thank the National Research Council of Canada for financial support of this work and we are especially grateful to Prof. N. C. Baird for discussions of the theoretical aspects. We wish to thank Prof. J. Haywood-Farmer for kindly providing generous samples of **26** and **28**.

1. GURUDATA and J. B. STOTHERS. Can. J. Chem. **47**, 3601 (1969).
2. D. H. MARR and J. B. STOTHERS. Can. J. Chem. **43**, 596 (1965); **45**, 225 (1967); K. S. DHAMI and J. B. STOTHERS. Can. J. Chem. **43**, 479, 498 (1965).
3. J. B. STOTHERS, C. T. TAN, and K. C. TEO. Can. J. Chem. **51**, 2893 (1973).
4. K. R. STEPHENS, J. B. STOTHERS, and C. T. TAN. *In* Mass spectrometry and NMR spectroscopy in pesticide chemistry. *Edited by* R. Hague and F. J. Biros. Plenum Press, New York. 1974. pp. 179–196.

Can. J. Chem. Downloaded from www.nrcresearchpress.com by 210.87.254.6 on 09/05/12
For personal use only.

5. W. R. MOORE, W. R. MOSER, and J. E. LAPRADE. J. Org. Chem. **28**, 2200 (1963).
6. A. F. DIAZ, D. L. HARRIS, M. SAKAI, and S. WINSTEIN. Tetrahedron Lett. 343 (1971).
7. R. RATCLIFFE and R. RODEHURST. J. Org. Chem. **35**, 4000 (1970).
8. H. L. GOERING, R. W. GREINER, and M. F. SLOAN. J. Am. Chem. Soc. **83**, 1391 (1961).
9. K. B. WIBERG and B. A. HESS. J. Org. Chem. **31**, 2250 (1966).
10. G. STORK, P. ROSEN, N. GOLDMAN, R. V. COOMBS, and J. TSUJI. J. Am. Chem. Soc. **87**, 275 (1965).
11. HUANG-MINLON. J. Am. Chem. Soc. **71**, 3301 (1949).
12. R. R. SAUERS, J. A. BEISLER, and H. FEILICH. J. Org. Chem. **32**, 569 (1967).
13. N. A. LEBEL and R. J. MAXWELL. J. Am. Chem. Soc. **91**, 2307 (1969).
14. N. A. LEBEL and R. N. LIESEMER. J. Am. Chem. Soc. **87**, 4301 (1965).
15. J. HAYWOOD-FARMER, B. T. FRIEDLANDER, and L. A. HAMMOND. J. Org. Chem. **38**, 3145 (1973).
16. J. B. STOTHERS and C. T. TAN. Unpublished data.
17. G. B. SAVITSKY, K. NAMIKAWA, and G. ZWEIFEL. J. Phys. Chem. **69**, 3105 (1965).
18. J. B. STOTHERS. Carbon-13 NMR spectroscopy. Academic Press, New York. 1972. pp. 493–499.
19. J. G. BATCHELOR, J. H. PRESTEGARD, R. J. CUSHLEY, and S. R. LIPSKY. J. Am. Chem. Soc. **95**, 6358 (1973).
20. R. DITCHFIELD, W. J. HEHRE, and J. A. POPLE. J. Chem. Phys. **54**, 724 (1971).
21. M. J. S. DEWAR and N. C. BAIRD. COORD, Program 136, QCPE, Indiana Univ., Bloomington, Md.
22. A. B. STRONG, D. IKENBERRY, and D. M. GRANT. J. Magn. Res. **9**, 145 (1973).
23. M. H. CHISHOLM, H. C. CLARK, L. E. MANZER, J. B. STOTHERS, and J. E. H. WARD. J. Am. Chem. Soc. In Press.

Can. J. Chem. Downloaded from www.nrcresearchpress.com by 210.87.254.6 on 09/05/12
For personal use only.

^{13}C Nuclear Magnetic Resonance Studies. 47. ^{13}C Spectra of some *exo*-Methylenecycloalkanes and -norbornanes[1]

S. H. GROVER[2] AND J. B. STOTHERS

Department of Chemistry, University of Western Ontario, London, Ontario N6A 3K7

Received September 3, 1974

S. H. GROVER and J. B. STOTHERS. Can. J. Chem. **53**, 589 (1975).

The shielding effects of the *exo*-methylene group on neighboring carbons in several cycloalkanes, methylcyclohexanes, and in the norbornane ring system have been characterized by ^{13}C n.m.r. examination of 28 compounds. The results are compared with those for the carbonyl group and the utility of these data for structural elucidations is discussed. The more distinctive trends exhibited by the methyl carbons in these systems are compared with those for cyclohexanes, cyclohexanones, norbornanes, and norcamphors.

S. H. GROVER et J. B. STOTHERS. Can. J. Chem. **53**, 589 (1975).

On a caractérisé, en examinant les spectres r.m.n. du ^{13}C de 28 composés, les effets de blindage du groupe *exo*-méthylène sur les carbones voisins dans des cycloalkanes, des méthylcyclohexanes et des norbornanes. On compare ces résultats avec ceux obtenus pour le groupement carbonyle et on discute de l'utilité de ces données pour des élucidations de structure. On compare les tendances les plus caractéristiques des carbones des méthyles de ces systèmes avec ceux des cyclohexanes, cyclohexanones, norbornanes et norcamphres.

[Traduit par le journal]

Introduction

In ^{13}C n.m.r. spectra it is generally found that various substituents exert shielding effects which are additive within families of compounds. As a result, the positions of ^{13}C signals for closely related materials may often be predicted with good precision in a wide variety of systems (1). These trends are of special interest in "fixed" systems, as opposed to freely rotating cases, since the shielding effects of a variety of substituents exhibit marked geometrical dependencies (2). This sensitivity to stereochemistry can be useful both for signal assignments in complex spectra and for stereochemical assignments for groups within a molecule; several examples have been discussed in detail (2). Because of the relatively common appearance of the *exo*-methylene group in terpenes and other natural products, it was of interest to examine the variation of the shieldings of these olefinic carbons as a function of structure in some alicyclic model systems and to determine the substituent effects of this group on the neighboring carbons. Further, it has been known for some years that the shieldings of carbonyl carbons in alicyclic systems are remarkably dependent on ring size (1, 3) although an interpretation of the variation has been lacking. It seemed that the results for the corresponding carbon of the *exo*-methylene group in the series of methylenecycloalkanes could possibly aid our understanding of the trends exhibited in the ketone series. For these reasons we have prepared a series of *exo*-methylene substituted alicyclic compounds and recorded their ^{13}C n.m.r. spectra. The methylenecycloalkanes ranged from the 4- to the 12-membered ring examples. Series of methyl substituted cyclohexanes and norbornanes were also examined to compare the effects of methyl substitution in these ring systems with those established for the corresponding hydrocarbons (4) and ketones (5, 6).

Experimental

Materials

Apart from methylenecyclobutane and camphene, which were commercially available, the *exo*-methylene derivatives were prepared from the corresponding ketones using the Wittig reaction. For many cases the procedure described by Corey and co-workers (7) was quite satisfactory although with the hindered ketones and higher molecular weight cases, the procedure of Seyferth and Singh (8) gave better results. The samples were examined as 10–25% (v/v) solutions in dioxane, benzene, and/or deuteriochloroform.

Spectra

The ^{13}C spectra in dioxane and benzene solutions were obtained with a Varian HA-type instrument as previously

[1]For part 46, see ref. 16

[2]Holder of NRCC Scholarships, 1968–1971.

Can. J. Chem. Downloaded from www.nrcresearchpress.com by 210.87.254.40 on 09/05/12
For personal use only.

TABLE 1. ^{13}C shieldings of some methylenecycloalkanes[a] and cycloalkanes

Ring size	*exo*-Methylene CH_2	*exo*-Methylene C	α-C	β-C[b]	Other	C_nH_{2n}[d]
4	105.1	150.3	32.2	16.9		23.3
5	104.9	153.1	33.3	26.9		26.5
6	106.9	149.8	35.7	28.7	26.8	
	106.6[c]	150.1[c]	35.6[c]	28.5[c]	26.6[c]	27.8
7	110.8	151.9	36.5	(29.8)	(28.8)	29.4
8	111.4	152.1	35.7	(28.0)	(27.3), 26.6 (δ)	27.8
	110.9[c]	151.9[c]	35.4[c]	(27.7)[c]	(26.9)[c], 26.1[c] (δ)	
9	112.7	151.6	36.3	(26.6)	(26.2, 26.0)	27.0
10	111.5	149.0	35.0	(25.5)	(25.5, 24.9), 25.0 (ε)	26.2
11	111.4	149.8	35.6	(27.1)	(26.5, 26.2, 25.8)	26.6
12	110.4[c]	147.1[c]	33.1[c]	(24.6)[c]	(24.3[c], 23.9[c], 23.4[c]) 22.8[c](C-7)	24.4

[a]For dioxane solutions unless otherwise indicated (25%, v/v) in p.p.m. from TMS.
[b]Values in parentheses indicate uncertain assignments.
[c]In $CDCl_3$ solution.
[d]From ref. 10; values observed for neat liquids or CS_2 solutions and converted to the TMS scale using the factor, 193.7 p.p.m.

TABLE 2. ^{13}C shieldings for some *exo*-methylenecyclohexanes[a]

Substitution	*exo*-Methylene CH_2	*exo*-Methylene C	C-2	C-3	C-4	C-5	C-6
Nil	106.6	150.1	35.6	28.5	26.6	28.5	35.6
2-Me	104.1	153.7	37.7	36.8	26.0	28.8	36.1
3-Me	106.6	149.3	43.6	34.2	34.6	27.1	34.7
4-Me	106.6	149.4	36.5	34.7	32.3	34.7	36.5
2,2-Me_2	104.8	156.5	36.3	41.6	22.7	28.8	33.2
cis-2,5-Me_2	101.1	158.0	38.4	37.4	26.5	37.4	38.4
trans-2,6-Me_2	103.9		35.5	35.6	21.1	35.6	35.5
2,2,6-Me_3	102.3	160.5	37.1	42.1	22.6	37.8	33.7
2,2,6,6-Me_4	106.1	163.3	36.4	41.5	19.1	41.5	36.4
3,3,5-Me_3	108.2	147.2	48.3	32.5	48.1	29.7	43.5
3,3,5,5-Me_4	109.7	146.5	48.5	33.2	52.5	33.2	48.5

[a]In p.p.m. from TMS for 10–25% (v/v) solutions in $CDCl_3$.

described (9) while the deuteriochloroform solutions were examined using a Varian XL-100-15 system operating in the Fourier transform mode. In the latter case, the solutions were contained in 10-mm tubes which were placed in a 12-mm sample tube containing D_2O, the signal of which was used as the lock. For the dioxane and benzene solutions, the proton decoupled solvent signal served as the lock.

All peak positions are reported relative to internal tetramethylsilane, a few drops of which were added to the $CDCl_3$ solutions; in benzene and dioxane the signal positions were measured relative to the solvent peak and then converted to the TMS scale with the factors 128.7 (C_6H_6) and 67.4 p.p.m. ($C_4H_8O_2$). The precision of these measurements is better than 0.1 p.p.m.

Results

The shielding data for the methylenecycloalkanes examined are listed in Table 1. For this series, the assignments for the methylene carbons more remote than one bond from the olefinic group are equivocal for the compounds with seven-membered or larger rings except for the unique methylene in the 8-, 10-, and 12-ring cases. The olefinic and α carbons, however, were readily assigned for this series. The shielding data for the methyl substituted *exo*-methylenecyclohexanes and norbornanes are collected in Tables 2 and 3. In the spectra of the cyclohexane derivatives, the olefinic, α-methylene, methyl, and methine carbons were readily identified by off-resonance decoupling and their line positions. The remaining methylene carbons were assigned from their relative intensities in the symmetrical cases and from the shielding effects of the methyl substituents at neighboring centers as shown by

Can. J. Chem. Downloaded from www.nrcresearchpress.com by 210.87.254.40 on 09/05/12
For personal use only.

TABLE 3. ^{13}C shieldings of the skeletal carbons in some 2-*exo*-methylenenorbornanes[a]

Substitution	Solvent[b]	*exo*-Methylene		C-1	C-3	C-4	C-5	C-6	C-7
		CH_2	C						
Nil	D	102.2	155.3	46.0	39.4	37.3	28.8	30.2	38.7
	B	102.2	155.2	46.3	39.6	37.5	28.9	30.3	38.8
	C	101.8	155.3	45.7	39.1	37.0	28.5	29.9	38.4
1-Me	D	100.3	158.1	49.1	40.0	36.2	30.5	37.0	46.5
	B	100.5	158.0	49.2	40.2	36.5	30.7	37.2	46.6
	C	99.8	158.3	48.7	39.6	35.9	30.2	36.7	46.0
exo-3-Me	C	100.9	161.8	45.9	43.2	42.7	(29.0)	(28.9)	35.4
endo-3-Me	C	100.4	161.3	46.5	42.3	41.3	21.4	30.7	39.4
3,3-Me_2	D	99.8	165.7	47.4	42.0	48.7	24.2	29.2	37.8
	C	99.2	165.9	46.9	41.7	48.1	23.8	28.9	37.4
1,3,3-Me_3	D	97.6	168.8	50.2	43.1	47.8	25.8	35.8	44.5
	B	97.8	168.9	50.3	43.1	48.0	25.9	36.0	44.7
7,7-Me_2	D	103.4	156.2	54.0	37.7	45.2	(29.0)	(28.7)	46.2
	B	103.5	156.3	54.2	37.7	45.4	(28.9)	(28.7)	46.1
1,7,7-Me_3	D	101.6	159.3	51.7	37.2	45.2	28.3	35.4	47.5
	B	101.7	159.1	51.7	37.3	45.2	28.2	35.4	47.4
Δ^5	C	103.2	150.7	50.8	33.5	41.9	(134.1)	(136.2)	50.0

[a]In p.p.m. from TMS for 10–20% (v/v) solutions.
[b]D = dioxane, B = benzene, C = $CDCl_3$.

the symmetrical examples. Assignments for the norbornane derivatives followed from the results of off-resonance decoupled spectra together with the expected trends for methyl substitution which had been characterized for the methylnorbornanes (11) and methylnorcamphors (5, 11). In this way, consistent assignments were accomplished for the norbornane series. The shieldings for some of the compounds were determined in more than one solvent, since two instruments with different locking capabilities were employed. For these cases, the data for different solvents are tabulated to illustrate the effect of solvent on the observed shieldings.

Discussion

Skeletal Carbons

From Table 1 it is apparent that the shieldings measured in dioxane and chloroform solutions are very similar, having differences <0.5 p.p.m. (average 0.3 p.p.m.) with those in $CDCl_3$ tending toward higher field. There seem to be no distinctive changes with ring size, in contrast to the results for the carbonyl carbons in the cycloalkanones (3, 12) although the *exo*-methylene carbon is somewhat more deshielded in the larger rings while the fully substituted olefinic carbon is slightly shielded. In contrast, carbonyl carbons in the eight-, and nine-, and, especially, the five-membered rings are significantly deshielded (5–10 p.p.m.) with respect to the others. To examine the substituent effects of the olefinic bond, the methylene shieldings may be compared with the results for the cycloalkanes (10) which are included in Table 1. Although definitive assignments are only available for the α-methylene and the most remote carbons in the even-membered rings for the larger systems, comparison with the effects of the carbonyl group indicates some interesting differences. In view of the difference in polarity of the carbonyl and *exo*-methylene bonds one would expect the α-methylene carbons to be less affected by the latter since the inductive effect of a substituent tends to dominate the α effect (1). The α effect in the cyclobutane derivatives is 8.9 and 23.6 p.p.m. for the olefin and ketone, respectively, whereas for the others the α effects are in the ranges 6.8–9.3 and 10.5–15.4 p.p.m., respectively. The much larger difference for the four-membered ring clearly indicates that factors other than the inductive effect are also important. It may be noted that the β carbon (C-3) in these derivatives is markedly shielded, -6.7 and -14.3 p.p.m., in the olefin and ketone, respectively, in contrast to the rest of the series for which the β effect in the

Can. J. Chem. Downloaded from www.nrcresearchpress.com by 210.87.254.40 on 09/05/12
For personal use only.

TABLE 4. Methyl substituent effects[a] in cyclohexane (**1**)[b], methylenecyclohexane (**2**), and cyclohexanone (**3**)[c]

		Effects on sp^3 carbons[d]				Effects on sp^2 carbons	
Substitution	Compound	α	β	γ	δ	>C=	=CH_2
2-Me	**2**	2.1	8.3	−0.6, 0.5	0.3	3.6	−2.5
	3	3.4	9.1	0.2, −0.1	0.9	1.2	
3-Me	**2**	5.7	8.0	−1.4	−0.9	−0.8	0.0
	3	7.0	8.0, 8.3	−1.8	−1.3	−0.5	
Equatorial methyl	**1**	6.0	9.0	0.1	−0.2		
Axial methyl	**1**	1.4	5.4	−6.4	−0.1		
2-Me	**2**	2.5	6.0	−5.6, −5.7	0.4	2.7	1.0
	3	3.6	6.0	−5.9, −6.2	−0.5	3.6	
3-Me	**2**	3.5	6.9, 6.8	−5.1	0.8	−1.0	1.5
	3	5.7	5.9	−5.7	−0.3	0.5	

[a]In p.p.m.
[b]Results from ref. 4.
[c]Results from ref. 6.
[d]Where two values are given, the order follows the carbon numbering.

cycloalkanones is +0.3 to −4.2 p.p.m. (1, 12). The β effect in these olefins is only known with certainty for the five- and six-membered rings, 0.4 and 0.9 p.p.m., respectively, but in any event the β effects cannot exceed −1.3 p.p.m. for any of the examples. Thus, the β effect of the carbonyl group appears to be more shielding than that of the *exo*-cyclic double bond. It is interesting that both groups tend to shield the most remote methylene carbons in the even-membered rings and, again, the effect of the carbonyl group appears to be larger. This ω effect may have a conformational origin as has been suggested earlier (12) but a detailed interpretation of the trends cannot be presented. This difficulty is compounded by the findings for other olefinic systems. For example, the α effect of a double bond varies widely in different olefins. The effects in the methylene cycloalkanes are much larger than those in acyclic systems (1, 13) and those in cyclohexene, cycloheptene, and *cis*-cyclooctene (13) but the α effects in cyclobutene, cyclopentene, and *cis*-cyclododecene (13) are comparable to the corresponding 4-, 5-, and 12-membered methylenecycloalkanes. Presumably, small differences in the bonding parameters associated with the double bond have marked influences on the observed shieldings. It is also apparent from Table 1 that the shieldings for the olefinic *exo*-methylene carbons will be of limited utility for structural elucidations since the effect of ring size is not pronounced, although the methylene carbon in the derivatives having seven-membered or larger rings is deshielded by *ca.* 5 p.p.m. relative to those in the four-, five- and six-ring systems.

The series of methyl substituted methylenecyclohexanes was examined to compare the effects of the methyl substituents with those found for cyclohexane (4) and cyclohexanone (6). From Table 2 it is apparent that an α-methyl group alters the shieldings of the olefinic carbons in a distinctive, and expected, fashion whereas monomethyl substitution at C-3 and C-4 has little effect. Since the monomethyl derivatives exist predominantly in chair conformations with equatorial methyl groups, a set of substituent effects for the latter can be obtained by comparison of the observed shieldings for each carbon with those for the corresponding carbon in methylenecyclohexane. This sort of analysis is the same as that described for the methylcyclohexanones (6) and the data for the di-, tri-, and tetramethyl derivatives permit one to obtain substituent effects for axial methyl groups at C-2 and C-3 as described previously (6). To compare the results for cyclohexane (**1**), methylenecyclohexane (**2**), and cyclohexanone (**3**), the methyl substituent effects for the three systems are summarized in Table 4. From these data it is apparent that with a couple of exceptions the trends for the substituent effects of axial and

Can. J. Chem. Downloaded from www.nrcresearchpress.com by 210.87.254.40 on 09/05/12
For personal use only.

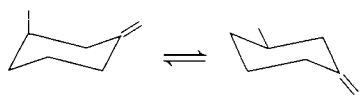

4

equatorial methyl groups are similar for the sp^3 carbons in the three systems. The most distinctive exception is the γ effect of the 3-equatorial methyl groups in the unsaturated cases. However, the conformational equilibrium for 3-methylmethylenecyclohexane (**4**) and the corresponding cyclohexanone is less heavily biased toward the equatorial conformer than 3-methylcyclohexane (**5**) because one *syn*-axial methyl–proton interaction has been eliminated. A recent determination of the equilibrium constant for **4** gave $K = 10$, an order of magnitude less than that for **5** (14). Thus, the 3-methyl group in **4** would be expected to shield the γ carbon through the well known γ *gauche* effect (1, 2). It is interesting, however, that the effect is as large as −1.5 p.p.m. since those found for axial 2- and 3-methyl groups are only −5 to −6 p.p.m. Clearly, the trend is qualitatively as anticipated but the quantitative discrepancy indicates the existence of additional contributing factors. The second notable exception is the magnitude of many of the δ effects which tend to be more pronounced in both unsaturated systems but an explanation is difficult. The β effects are moderately consistent for all cases with the somewhat smaller values for axial methyl groups attributable to the γ *gauche* interactions experienced by these substituents. It is established that all carbons in the fragment involved in a γ *gauche* interaction are shielded relative to the corresponding fragment lacking this interaction (2). This tendency can account also for the attenuated α effects of equatorial 2-methyl groups which are γ to the carbonyl oxygen or *exo*-methylene carbon. Supporting evidence for this interpretation seems to be given by the 2.5 p.p.m. upfield shift exhibited by the *exo*-methylene carbon but the remaining substituent effects on the olefinic centers show that this view may be oversimplified. Axial 2- and 3-methyl groups deshield the *exo*-methylene carbon and shield the fully substituted sp^2 carbon more than the equatorial groups, while the latter trend is reversed for the ketones. There are, however, important differences in the γ interactions of the α-methyl groups with these two substituents; the steric interaction of the methyl protons involves the lone pair on oxygen for the ketones and the nearer of the *exo*-methylene proton for the olefins. Furthermore the carbonyl bond is shorter than an olefinic bond so that the steric perturbation for an equatorial methyl group may be larger in the ketones. This will account for the observed trends if the γ interaction of the methyl with the carbonyl oxygen is greater than the *syn*-axial methyl–proton (in C-4 and C-6) interactions. The methyl shieldings, as discussed later, offer further support for this interpretation. Inspection of the shieldings for the *exo*-methylene carbons in the polymethyl substituted methylenecyclohexanes indicates that the substituent effects of the methyl groups at these centers (Table 4) are approximately additive. The same conclusion follows from a comparison of the monomethyl effects in the norbornane derivatives with those found for the di- and trimethyl substituted compounds. An interesting feature of these methyl substituent effects is the deshielding influence at the *exo*-methylene carbon produced by an axial 3-methyl group in the methylenecyclohexanes and the 7-methyl in the methylenenorbornanes. These can be regarded as δ effects and it has been found that methyl carbons lying close to δ carbons or δ oxygen functions experience significant deshielding (6, 15). In the present cases, the interaction must involve the methyl protons and the π cloud of the olefinic bond.

The sp^3 carbons of the methylenenorbornane derivatives are affected by methyl substitution in much the same way as the corresponding carbons in the norcamphor derivatives (6). The overall average deviations between the two cases is <1 p.p.m. for all cases with the greatest differences (2 p.p.m.) found for the 1,3,3-trimethyl derivatives. Perhaps this indicates slight differences in skeletal twist for the two compounds but in any event there are no major differences in the methyl substituent effects for the two systems.

Methyl Carbons

The methyl shieldings for the *exo*-methylene derivatives are collected in Table 5 together with the corresponding data for the cyclohexanes, cyclohexanones, norbornanes, and norcamphors. Without exception, the α-methyl carbons are more shielded in the ketones than in the *exo*-methylene derivatives and the latter are more shielded than those in the parent hydrocarbons. It is apparent, therefore, that an α-methyl group

Can. J. Chem. Downloaded from www.nrcresearchpress.com by 210.87.254.40 on 09/05/12
For personal use only.

TABLE 5. Methyl shieldings[a] for methyl derivatives of **1**, **2**, **3**, norbornane (**6**), methylenenorbornane (**7**), and norcamphor (**8**)

Substitution[b]	**1**[c]	**2**	**3**[d]	Substitution	**6**[e]	**7**	**8**[f]
2-Me	23.3	18.6	14.7	1-Me	21.0	17.5	13.8
cis-2,6-Me_2	23.4	18.5	14.6	*exo*-3-Me	22.3	20.0	14.1
trans-2,6-Me_2	21.1	18.9	16.0	*endo*-3-Me	17.4	15.1	10.7
2,2-Me_2	29.4	27.7	25.2	3,3-Me_2	27.2(*endo*) 31.6(*exo*)	25.8(*endo*) 29.4(*exo*)	21.4(*endo*) 23.2(*exo*)
2,2,6-Me_3	23.7(3-Me) 25.5(ax) 34.3(eq) 1-Me	19.4(6-Me) 26.7 30.0(2-Me)	15.0(6-Me) 25.2 25.6(2-Me)	1,3,3-Me_3		18.4(1-Me) 26.2(*endo*) 29.6(*exo*)	14.6(1-Me) 21.6(*endo*) 23.3(*exo*)
2,2,6,6-Me_4		31.5	27.6				
3-Me	23.3	22.1	22.0	7,7-Me_2		20.8(*anti*) 21.8(*syn*)	20.7(*anti*) 21.6(*syn*)
3,3,5-Me_3	23.7(3-Me) 25.5(ax) 34.3(eq)	22.6(5-Me) 25.0(ax) 32.4(eq)	22.4(5-Me) 25.7(ax) 32.0(eq)	1,7,7-Me_3	15.8(1-Me) 19.2 19.2	12.6(1-Me) 19.0(*anti*) 19.7(*syn*)	9.3(1-Me) 19.1(*anti*) 19.7(*syn*)
3,3,5,5-Me_4		30.8	31.3				
4-Me	23.3	21.9	22.0				

[a]In p.p.m. from TMS.
[b]For **1** the 2,6- and 3,5-derivatives denote 1,3 substitution to simplify the Table.
[c]From ref. 4.
[d]From ref. 6.
[e]From ref. 11.
[f]From ref. 5.

in the ketones experiences a significant γ interaction with the carbonyl oxygen which is greater than that with an *exo*-methylene carbon. It is also interesting that an equatorial methyl at C-4 in the unsaturated cyclohexanes is slightly shielded relative to that of methylcyclohexane. This may arise from the flattening of the ring from a perfect chair conformation produced by the carbonyl and olefinic groups. The same trend for the 3-methyl group must arise partly from a significant contribution of the axial conformer because of the smaller equilibrium constant for **4** as discussed above. The somewhat greater deshielding of the isolated equatorial 5-methyl carbon in the 3,3,5-trimethyl derivatives is consistent with this notion. In contrast to the cyclohexanes, axial 2-methyl carbons in cyclohexanone and *exo*-methylenecyclohexane are deshielded relative to their equatorial counterparts; shieldings for the axial methyls can be estimated from the observed shieldings for the *trans*-2,6-dimethyl derivatives since these compounds exist as 1:1 mixtures of enantiomers each with one axial and one equatorial methyl group. In this way axial α-methyl shieldings are found to be 19.3 and 17.4 p.p.m. for the ketone and olefin derivatives, respectively, whereas an axial methyl on a cyclohexane ring absorbs at 18.9 p.p.m., from the results for the *trans*-1,3-dimethyl derivative. In all cases these axial methyls experience two *syn*-axial interactions with γ protons, γ *gauche* effects, but the enhanced shielding of the axial methyl for the ketone indicates that a γ interaction with the carbonyl oxygen also contributes while the corresponding effect in the olefin is negligible.

As noted earlier for the cyclohexanones (**6**), the averaged methyl shielding observed for each of the tetramethyl derivatives is at lower field than the values estimated by simply averaging the *gem*-dimethyl shieldings in the trimethyl derivatives. This is clear evidence for the deshielding *syn*-axial δ effect already noted in the cyclohexanones (**6**) and a variety of other systems (15). Since it is known that *both* methyl shieldings of a pair of geminal methyls are affected by the *syn*-axial interaction of one of them (15) it is not possible to estimate the axial and equatorial shieldings for the tetramethyl derivatives.

The α-methyl shieldings for the norbornane derivatives follow the same trends as those found for the cyclohexanes but the 7,7-dimethyl

Can. J. Chem. Downloaded from www.nrcresearchpress.com by 210.87.254.40 on 09/05/12
For personal use only.

systems show an interesting difference in that these methyl carbons appear to be equivalent in the *exo*-methylene and norcamphor derivatives. Although the assignments for the former were not established unambiguously as were those for the ketones (5), it appears that the *syn*-methyl is slightly deshielded by the unsaturated function, which can be regarded as a δ effect. As found for the corresponding ketones (5, 6), it seems that the methyl carbon shieldings undergo the most distinctive changes with molecular geometry and thus will probably be the more informative for structural elucidations in related systems.

We wish to thank the National Research Council of Canada for financial support of this study.

1. (*a*) G. C. LEVY and G. L. NELSON. ^{13}C nuclear magnetic resonance for organic chemists. Wiley-Interscience, New York. 1972; (*b*) J. B. STOTHERS. Carbon-13 NMR spectroscopy. Academic Press, New York. 1972.
2. N. K. WILSON and J. B. STOTHERS. *In* Topics in stereochemistry. Vol. 8. *Edited by* E. L. Eliel and N. L. Allinger. Wiley-Interscience, New York. 1974. Chapt. 1.
3. J. B. STOTHERS and P. C. LAUTERBUR. Can. J. Chem. **42**, 1563 (1964).
4. D. K. DALLING and D. M. GRANT. J. Am. Chem. Soc. **89**, 6612 (1967); **94**, 5318 (1972).
5. J. B. STOTHERS, C. T. TAN, and K. C. TEO. Can. J. Chem. **51**, 2893 (1973).
6. J. B. STOTHERS and C. T. TAN. Can. J. Chem. **52**, 308 (1974).
7. R. GREENWALD, M. CHAYKOVSKY, and E. J. COREY. J. Org. Chem. **28**, 1128 (1963).
8. D. SEYFERTH and G. SINGH. J. Am. Chem. Soc. **87**, 4156 (1965).
9. M. GORDON, S. H. GROVER, and J. B. STOTHERS. Can. J. Chem. **51**, 2092 (1973).
10. J. J. BURKE and P. C. LAUTERBUR. J. Am. Chem. Soc. **86**, 1870 (1964).
11. J. B. GRUTZNER, M. JAUTELAT, J. B. DENCE, R. A. SMITH, and J. D. ROBERTS. J. Am. Chem. Soc. **92**, 7107 (1970).
12. F. J. WEIGERT and J. D. ROBERTS. J. Am. Chem. Soc. **92**, 1347 (1970).
13. D. E. DORMAN, M. JAUTELAT, and J. D. ROBERTS. J. Org. Chem. **36**, 2757 (1971).
14. J. B. LAMBERT, R. E. CLIKEMAN, and E. S. MAGYAR. J. Am. Chem. Soc. **96**, 2265 (1974).
15. S. H. GROVER, J. P. GUTHRIE, J. B. STOTHERS, and C. T. TAN. J. Magn. Res. **10**, 227 (1973); S. H. GROVER and J. B. STOTHERS. Can. J. Chem. **52**, 870 (1974).
16. D. M. HUDYMA, J. B. STOTHERS, and C. T. TAN. Org. Magn. Res. In press.

Can. J. Chem. Downloaded from www.nrcresearchpress.com by 210.87.254.40 on 09/05/12
For personal use only.

Nuclear Magnetic Resonance Chemical Shifts of some Monosubstituted Isothiazoles

RODERICK E. WASYLISHEN,[1] THOMAS R. CLEM, AND EDWIN D. BECKER
National Institutes of Health, Bethesda, Maryland 20014

Received September 13, 1974

RODERICK E. WASYLISHEN, THOMAS R. CLEM, and EDWIN D. BECKER. Can. J. Chem. **53**, 596 (1975).

Carbon-13 and proton chemical shifts have been measured for several monosubstituted isothiazoles. Substituent effects upon these chemical shifts are compared with those observed for monosubstituted benzenes, pyridines, and thiophenes. In general the observed substituent effects in the isothiazoles and thiophenes closely parallel one another. Correlations between the observed carbon-13 chemical shifts and CNDO/2 calculated charge densities are examined.

RODERICK E. WASYLISHEN, THOMAS R. CLEM et EDWIN D. BECKER. Can. J. Chem. **53**, 596 (1975).

On a mesuré les déplacements chimiques du ^{13}C et du proton de plusieurs isothiazoles monosubstitués. On a comparé les effets des substituants sur ces déplacements chimiques avec ceux observés dans des dérivés monosubstitués du benzène, de la pyridine et du thiophène. D'une façon générale, les effets de substituants qui sont observés dans les isothiazoles et dans les thiophènes sont parallèles. On a examiné les corrélations qui existent entre les déplacements chimiques observés pour le ^{13}C et les calculs CNDO/2 pour les densités de charge.
[Traduit par le journal]

Introduction

Substituent effects on the carbon-13 n.m.r. chemical shifts of monosubstituted benzenes have been thoroughly investigated (1–3). The shielding effects induced by the substituents have been correlated with several different parameters which reflect the electronic nature of the substituent. For example, Levy *et al.* (3) have shown that carbon-13 chemical shifts at the *para* position are linearly related to the total calculated charge densities at this position and to the Hammett σ^* constants of the substituents.

There exist a few systematic studies of substituent effects on carbon-13 n.m.r. chemical shifts in aromatic systems containing one hetero atom. For example, substituent effects on the ring-carbon shielding in monosubstituted pyridines (4–8) have been compared with those observed for the corresponding benzenes. For a series of 3-substituted pyridines (6) substituent effects on the ring carbons usually lie within ± 1.3 p.p.m. of those found for the benzenes. The substituent effects in the 2-pyridine derivatives (7), where electronic interactions between the substituent and nitrogen are often significant, display differences from those in benzene derivatives that range up to 21 p.p.m. for the C_2 carbon in 2-fluoropyridine. The shielding effects in a number of 2- and 3-substituted thiophenes have been measured (9).

Here we report and discuss substituent effects on the carbon-13 and proton n.m.r. chemical shifts of several 4-substituted isothiazoles (**1**), aromatic systems containing two different hetero atoms.

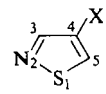

1

Experimental

The ester of isothiazole-4-carboxylic acid was prepared by treatment of the acid with dimethyl sulfate – anhydrous potassium carbonate in dimethylformamide. All other compounds were obtained from Raylo Chemical Company, Edmonton, Alberta, and were used without further purification.

Carbon-13 Spectra

Natural abundance ^{13}C n.m.r. spectra were measured in 5-mm sample tubes with a homemade pulse spectrometer operating at 55.3 MHz. This spectrometer was used with the superconducting magnet of a Varian HR-220, and the data were accumulated and Fourier transformed with a Varian 620L computer. This computer is limited to 8K data points, which transform to 4K real points (10). We used spectral widths of 8–10 kHz; the resulting spectra consisted of data points at 2–2.5 Hz intervals,

[1]NRCC Postdoctorate Fellow, 1972–1974. Present address: Department of Chemistry, University of Winnipeg, Winnipeg, Manitoba R3B 2E9.

Can. J. Chem. Downloaded from www.nrcresearchpress.com by 210.87.254.105 on 09/05/12
For personal use only.

TABLE 1. Carbon-13 chemical shifts in some 4-substituted isothiazoles[a]

X	C_3	C_4	C_5	Other
CH_3	158.6	133.8	144.0	11.2 (CH_3)
$CH_2\phi$	158.0	138.3	144.5	32.4 (CH_2)
		or 139.7		
Br	157.9	107.0	147.0	—
H	157.1	123.4	148.6	—
NO_2	152.8	146.8	151.9	—
CO_2CH_3	157.5	130.7	154.9	161.0 (CO_2CH_3)
				51.5 (CO_2CH_3)
CO_2H	158.4	132.7	154.9	162.4 (CO_2H)
CN	158.3	108.1	158.7	112.7 (CN)
		or 112.7		or 108.1

[a]All chemical shifts are relative to TMS.

which at 55 MHz is adequate to insure that measurements of chemical shifts are accurate to 0.1 p.p.m. All measurements were made on approximately 3 *M* solutions of the isothiazoles in DMSO at 65 ± 5 °C. All carbon-13 chemical shifts were initially measured relative to DMSO ($^{13}CH_3SOCH_3$) and were then converted to the TMS scale by adding 40.48 p.p.m. (11) to the initial values. The 220 MHz circuitry of the HR-220 spectrometer was used to optimize magnetic field homogeneity with a strong proton resonance prior to each ^{13}C run. The HR-220 also served as the source of proton decoupling frequencies. A suitable homemade noise modulator and r.f. amplifier were used to obtain complete proton decoupling (or in some experiments off-resonance decoupling).

Proton Chemical Shifts

All proton chemical shifts were obtained for dilute solutions of the 4-substituted isothiazoles in carbon tetrachloride (approximately 10 mg/ml of CCl_4).[2] Measurements were made at 20 ± 1 °C on a Varian HR-220 spectrometer and a 620-L computer in the FT mode.

Results and Discussion

The general theory of chemical shifts is given in several texts (13–17). Following Saika and Slichter (18) the shielding constant for a nucleus A is usually divided into three components,

$$[1] \qquad \sigma^A = \sigma_d{}^A + \sigma_p{}^A + \sigma'$$

where $\sigma_d{}^A$ is the local diamagnetic contribution, $\sigma_p{}^A$ is the local paramagnetic term, and σ' is the contribution from other atoms. Variation in carbon-13 shieldings for a series of closely related molecules can usually be accounted for by consideration of the paramagnetic term alone (12, 19). The approximate expression for $\sigma_p{}^A$ given by Karplus and Pople (20) is

$$[2] \qquad \sigma_p{}^A = -\frac{e^2\hbar^2}{2mc^2}\langle r^{-3}\rangle_{2p}(\Delta E)^{-1}\sum Q$$

where $\langle r^{-3}\rangle_{2p}$ is the mean cube inverse distance of a 2p electron from the nucleus (there is no contribution from s electrons), ΔE represents a mean excitation energy, and $\sum Q$ is defined in terms of the elements of the charge-density and bond-order matrix. Increasing electron density in a 2p orbital of carbon atom A causes an expansion of the electron cloud, a decrease in $\langle r^{-3}\rangle_{2p}$ and an increase in shielding (high field shift). Since the ΔE and $\sum Q$ terms in eq. 2 are often taken as constants along a series of closely related molecules, one expects carbon-13 chemical shifts to be linearly related to 2p orbital electron densities.

In the discussion to follow, we compare the substituent effects on the carbon-13 shifts of the isothiazoles with those observed for benzenes (1–3, 21), pyridines (5–8), and thiophenes (9). In addition, we correlate variations in the carbon-13 shifts with electron densities obtained from all-valence-electron SCF molecular orbital calculations at the CNDO/2 level of approximation (22).

Carbon-13 Chemical Shifts of some 4-Substituted Isothiazoles

The carbon-13 chemical shifts for a series of 4-substituted isothiazoles are given in Table 1. Assignments were made on the basis of selective decoupling (23) and of off-resonance decoupling (24–37). First-order analysis of the proton coupled carbon-13 spectrum of the unsubstituted isothiazole gives the one-bond coupling constants $^1J(^{13}C,H_3) = 183.6$ Hz, $^1J(^{13}C,H_4) =$

[2]This concentration corresponds to less than 1 mol% for all of the substituted isothiazoles.

Can. J. Chem. Downloaded from www.nrcresearchpress.com by 210.87.254.105 on 09/05/12
For personal use only.

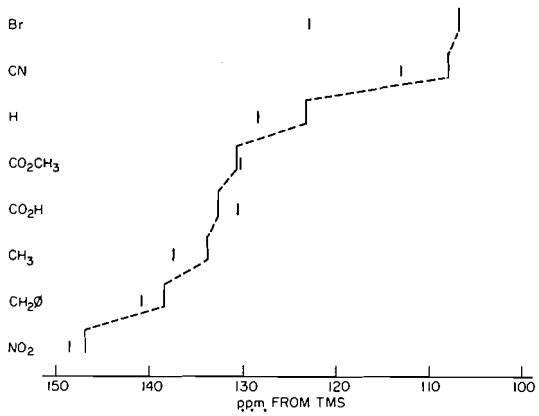

FIG. 1. Carbon-13 chemical shifts of C_4 in some 4-monosubstituted isothiazoles and C_1 in the corresponding monosubstituted benzenes. The dashed lines join vertical bars which indicate carbon-13 chemical shifts of C_4 in the substituted isothiazoles. Data for the benzenes (indicated by the smaller unconnected vertical bars) were taken from ref. 1, except for X = CO_2CH_3 (21) and X = $CH_2\phi$ (present study).

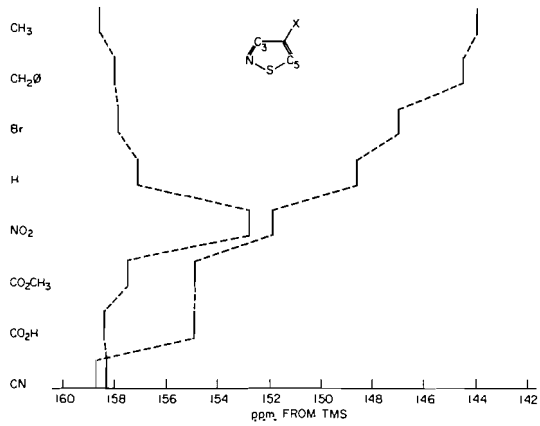

FIG. 2. Carbon-13 chemical shifts of C_3 and C_5 in some 4-monosubstituted isothiazoles; C_5 is to high field of C_3 in all cases except for X = CN.

173.3 Hz, and $^1J(^{13}C,H_5)$ = 187.2 Hz. We have not determined the other $^{13}C,H$ couplings.

Chemical Shift of C_4

The shift of C_4 in isothiazole itself is 123.4 p.p.m., close to the shifts of the analogous carbons, C_3, in both pyridine (124.5 p.p.m.) and thiophene (127.2 p.p.m.). The relative carbon-13 chemical shifts for C_4 in the 4-substituted isothiazoles (**1**) roughly parallel those of C_1 in the monosubstituted benzenes (**2**) as illustrated in Fig. 1. The greatest departure is found for

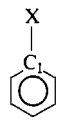

2

X = Br, where C_4 in **1** lies 16 p.p.m. to high field of the corresponding value of C_1 in **2**. It is interesting to note that a similar large upfield shift is observed in 3-bromothiophene but not in 3-bromopyridine. The numbers give shifts relative to the parent molecules. The origin of this large upfield shift in the sulfur heterocyclics is not clear.

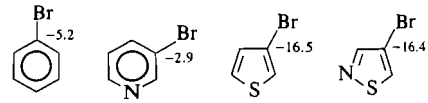

Chemical Shift of C_3 and C_5

The C_3 carbon of isothiazole resonates at 157.1 p.p.m., approximately 6.5 p.p.m. to low field of C_2 in pyridine, whereas the C_5 absorption is 13.2 p.p.m. to low field of the C_2 resonance in thiophene.

One of the striking features of the data in Table 1 is the relative sensitivity of the C_3 and C_5 chemical shifts to the various substituents at C_4. The shifts of C_5 vary over a range of 14.7 p.p.m. whereas those of C_3 vary over a range of only 5.8 p.p.m.; in fact, except for the NO_2 derivative they are virtually constant (see Fig. 2). A similar observation has been made for a series of 3-substituted thiophenes (**3**) where the ranges

3

for C_2 and C_4 were 40.4 and 16.0 p.p.m., respectively (9). However, in a series of 3-substituted pyridines (**4**) the range of shifts for C_2 and C_4 was not significantly different: 7.6 and 9.3 p.p.m., respectively (6).

4

CNDO/2 Calculations

As an aid to understanding the factors responsible for carbon-13 chemical shifts in isothiazoles,

Can. J. Chem. Downloaded from www.nrcresearchpress.com by 210.87.254.105 on 09/05/12
For personal use only.

TABLE 2. CNDO/2 results for some nitrogen- and sulfur-containing heterocyclics

	Total charge density ($\times 10^3$ electrons)		μ		
	S	N	Calculated	Observed	Reference
	−61	—	1.21	0.53	29
	+46	−132	2.30	1.57	30
	−57	−48	3.00	3.28	31
	−61	−114	1.34	1.66	32
	+1	−155	2.87	2.44	33, 34

TABLE 3. Calculated π and total 2p orbital electron densities for some 4-substituted isothiazoles*

	C_3		C_4		C_5	
X	π	2p (total)	π	2p (total)	π	2p (total)
CH_3	0.936	2.867	0.952	2.952	1.028	2.974
H	0.913	2.849	0.990	2.971	0.975	2.944
NO_2	0.903	2.840	1.066	2.965	0.904	2.909
COOH	0.902	2.835	1.028	3.037	0.925	2.908
CN	0.921	2.848	0.989	2.976	0.976	2.940
Range	0.034		0.114		0.124	

*The geometry of the isothiazole ring was assumed unchanged for all substituted isothiazoles. Standard geometries (given on p. 110 of ref. 22) were used for the substituents.

we carried out CNDO/2 calculations. For related nitrogen and oxygen heterocyclics Bloor and Breen (28) found reasonably good correlations between total CNDO/2 charge densities and carbon-13 shifts. They found also that the CNDO/2 method predicted dipole moments in excellent agreement with experimental values. To assess the reliability of the CNDO/2 method for isothiazoles and related molecules we carried out calculations of charge densities and dipole moments for several five-membered nitrogen-sulfur heterocyclics. The calculated dipole moments, as indicated in Table 2, are in only fair quantitative agreement with experiment but their relative magnitudes correlate well with the observed order.[3]

The values of 2p and π electron densities, as obtained from CNDO/2 calculations, are given in Table 3, while the total charge densities are presented in Table 4. With the *assumption* that 2p orbital charge densities are linearly related to carbon-13 chemical shifts, the CNDO/2 cal-

[3]References to observed dipole moments and the geometries or coordinates used for these calculations are given in Table 2.

Can. J. Chem. Downloaded from www.nrcresearchpress.com by 210.87.254.105 on 09/05/12
For personal use only.

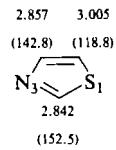

2p orbital densities (chemical shifts)

5

culations predict C_4 in isothiazole itself at highest field and C_3 at lowest field, in agreement with experiment. The calculations also predict the correct relative carbon-13 shifts in thiazole (**5**) (21, 35). It should be noted that π electron densities also predict the correct order of chemical shifts in isothiazole and thiazole but total electron densities (Table 4) are not in agreement with experiment.

For the 4-substituted isothiazoles, there is no apparent correlation between observed chemical shifts at C_4 and the 2p orbital, π or total electron densities.[4]

On the other hand, all three measures of electron density do predict the greater range of chemical shifts observed for C_5 relative to C_3. The range of charge densities calculated for C_5 is approximately double the range calculated for C_3.[5] Also C_5 is calculated to be at highest field for $X = CH_3 > H > NO_2 > CO_2H$, in agreement with experiment.

The relative sensitivity to substituents of the observed shifts at C_5 and C_3 is also compatible with the importance of the following valence bond structures.

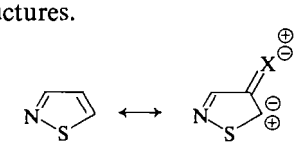

For example, when $X = CH_3$ the most important valence bond structures would be

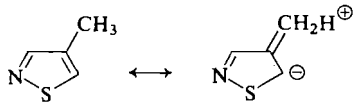

[4]Corrections for substituents containing double and triple bonds, as suggested by Nelson *et al.* (1), for substituted benzenes, might be of some value but their use would be unwarranted with the limited number of data here.

[5]CNDO/2 calculations were also carried out for other 4-X-isothiazoles (X = F, Cl, OH, and NH_2). The total charge densities at C_3 varied over a range of 0.064 electrons while those at C_5 varied over 0.134 electrons.

with C_5 to high field of its value in the parent compound, in agreement with experiment.[6] By analogous argument one would expect low field shifts for C_5 in 4-isothiazole carboxylic acid:

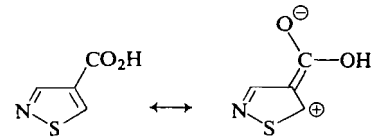

Similar valence structures have been invoked to account for the relative sensitivity of proton (36) and carbon (9) chemical shifts at C_2 and C_4 in a series of 3-monosubstituted thiophenes (**3**).

Proton Chemical Shifts of the 4-Substituted Isothiazoles

The proton chemical shifts measured as dilute solutions in carbon tetrachloride are given in Table 5. All spectra were first order because $10\,J_{35} \ll (\nu_3 - \nu_5)$.

Table 6 gives the changes with substituent in the proton chemical shifts of several 3-substituted thiophenes (36) and 4-substituted isothiazoles. It is apparent that the shift of the proton adjacent to the sulfur atom (H_2 in the thiophenes and H_5 in the isothiazoles) varies over a much larger range than do H_4 of the 3-substituted thiophenes and H_3 of the 4-substituted isothiazoles. Gronowitz and Hoffman (36) have explained this behavior for the thiophenes in terms of inductive effects and simple resonance theory as discussed in the previous section.

Finally it is interesting to note that there is a correlation between the calculated proton charge densities (Table 4) and the substituent effects observed for the proton chemical shifts.

Carbon-13 Chemical Shifts of other Monosubstituted Isothiazoles

Methylisothiazoles

The carbon-13 chemical shifts of the three monomethylisothiazoles have been obtained. The chemical shifts, *relative* to isothiazole itself, are shown below.

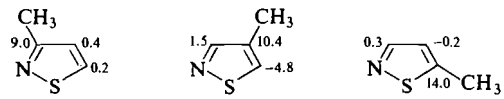

[6]Here it is assumed that carbon-13 chemical shifts are directly related to charge densities.

Can. J. Chem. Downloaded from www.nrcresearchpress.com by 210.87.254.105 on 09/05/12
For personal use only.

Can. J. Chem. Downloaded from www.nrcresearchpress.com by 210.87.254.105 on 09/05/12
For personal use only.

TABLE 4. Calculated total charge densities ($\times 10^3$) for some 4-substituted isothiazoles

X	S_1	N_2	C_3	C_4	C_5	H_3	H_5
CH_3	−3	−153	98	60	−43	8	18
H	1	−155	117	14	−14	10	20
NO_2	53	−138	124	43	8	43	55
COOH	12	−152	130	−21	13	25	29
CN	15	−158	119	58	−12	18	28
Range	56	20	32	81	56	35	37

TABLE 5. Chemical shifts (p.p.m.) of the ring protons in 4-substituted isothiazoles relative to TMS*†

X	H_3	H_5	Other
NO_2	9.00	9.42	—
CO_2Me	8.80	9.19	3.88 (CH_3)
CN	8.69	9.17	—
H	8.47	8.63	7.24 (H_4)
Br	8.33	8.57	—
CH_3	8.20	8.14	2.35 (CH_3)

*Measurements are accurate to ±0.01 p.p.m.
†Proton chemical shifts for three of these compounds have been reported elsewhere (37).

(A positive number refers to a shift to higher frequency, or lower field, upon substitution of the parent molecule.) In 3-methylisothiazole the 9.0 p.p.m. shift of C_3 is quite similar to that of the substituted carbon in toluene, 8.9 p.p.m. (1), and in 2-methylpyridine, 9.3 p.p.m. (7). For 4-methylisothiazole the shifts of 10.4 p.p.m. for C_4 and −4.8 p.p.m. for C_5 compare closely with those of 3-methylthiophene, 10.6 p.p.m. and −4.8 p.p.m. (9), and in 5-methylisothiazole the 14.0 p.p.m. shift of C_5 is almost identical with that of the analogous carbon in 2-methylthiophene, 13.9 p.p.m. (9, 38).

Isothiazole Carboxylic Acids

The carbon-13 chemical shifts of the three carboxylic acids of isothiazole have been obtained, and the observed substituent effects relative to isothiazole are shown below.

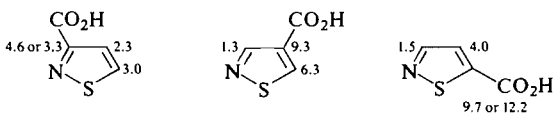

Carbon-13 chemical shift data are not available for carboxylic acids of thiophene and pyridine; however, data are available for 2- and 3-methoxycarboxyl derivatives of thiophene (9). Data are also available for benzoic acid (1) and methyl benzoate (21). The —COOH substituent effect on the carbon-13 chemical shifts for the 3-carboxylic acid is relatively small compared with that observed in the 4- and 5-carboxylic acids. The latter show substituent effects which are similar to those in the 2- and 3-methoxycarboxyl derivatives of thiophene (9):

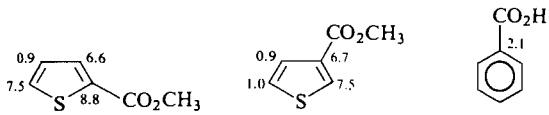

5-Formylisothiazole

The substituent effects of the CHO group on the carbon-13 chemical shifts of isothiazole, thiophene (9), and the benzene ring (1) are compared below; in addition the chemical shifts of the carbonyl carbons are given relative to TMS.

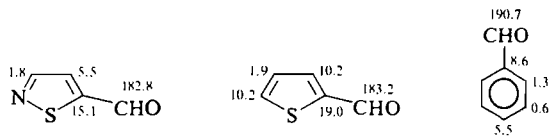

Two points are apparent: (*i*) the carbon-13 chemical shift of the carbonyl carbon in 2-formylisothiazole and 2-formylthiophene appears to be shifted approximately 7 p.p.m. to high field of the values observed for benzaldehyde; (*ii*) the carbonyl group induces a much larger downfield shift of the directly-bonded ring carbon in the case of isothiazole and thiophene than in the case of benzene.

We have no explanation for these differences between the sulfur-containing heterocyclics and benzene at present. It may be important to note, however, that in the case of the sulfur-containing heterocyclics the conformation of the carbonyl group is *s-trans* (39–41).

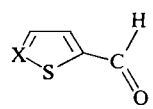

TABLE 6. Proton chemical shifts (p.p.m.) of 4-substituted isothiazoles and 3-substituted thiophenes (9) relative to the α-hydrogens in the parent compounds*

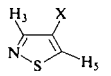
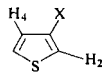

X	H_3	H_5	H_4	H_2
NO_2	0.53	0.79	0.60	0.95
CO_2CH_3	0.33	0.56	0.47	0.78
CN	0.22	0.54	0.20	0.63
H	0.00	0.00	0.00	0.00
Br	−0.14	−0.06	−0.08	−0.12
CH_3	−0.27	−0.49	−0.22	−0.45
Range	0.80	1.28	0.88	1.40

*A positive number refers to a shift to higher frequency, or lower field, with substitution.

To conclude, substituent effects on both proton and carbon-13 chemical shifts of the isothiazoles studied here are quite similar to those in the analogous thiophenes. CNDO/2 charge densities do not correlate well with carbon-13 shifts in general, but some trends are rather well reproduced. For example, the large variation with substituents in both proton and carbon-13 chemical shifts at the 5-position is paralleled by a large change in both total and 2p charge density.

The authors would like to thank Mr. Robert Bradley and Mrs. Val Wasylishen for technical assistance, Dr. Ken Rice for preparing 4-carbomethoxyisothiazole, and Drs. Ted Schaefer and Stan Sojka for helpful discussions.

R.W. is grateful to the National Research Council of Canada for the postdoctoral fellowship.

1. G. L. NELSON, G. C. LEVY, and J. D. CARGIOLI. J. Am. Chem. Soc. **94**, 3089 (1972).
2. J. B. STOTHERS. Carbon-13 NMR spectroscopy. Academic Press, New York. 1972.
3. G. C. LEVY and G. L. NELSON. Carbon-13 nuclear magnetic resonance for organic chemists. Wiley-Interscience, New York. 1972.
4. P. C. LAUTERBUR. J. Chem. Phys. **43**, 360 (1965).
5. H. L. RETCOFSKY and R. A. FRIEDEL. J. Phys. Chem. **71**, 3592 (1967).
6. H. L. RETCOFSKY and R. A. FRIEDEL. J. Phys. Chem. **72**, 290 (1968).
7. H. L. RETCOFSKY and R. A. FRIEDEL. J. Phys. Chem. **72**, 2619 (1968).
8. H. L. RETCOFSKY and F. R. MCDONALD. Tetrahedron Lett. 2575 (1968).
9. K. TAKAHASKI, T. STONE, and K. FUJIEDA. J. Phys. Chem. **74**, 2765 (1970).
10. T. C. FARRAR and E. D. BECKER. Pulse and Fourier transform NMR. Academic Press, New York. 1971.
11. G. C. LEVY and J. D. CARGIOLI. J. Magn. Res. **6**, 143 (1972).
12. W. T. RAYNES. *In* Nuclear magnetic resonance (Specialist Periodical Reports). *Edited by* R. K. Harris. The Chemical Society, London. Vol. 1. 1972. p. 1. Vol. 2. 1973. p. 1.
13. J. D. MEMORY. Quantum theory of magnetic resonance parameters. McGraw-Hill Book Company, New York. 1968.
14. C. P. SLICHTER. Principles of magnetic resonance. Harper and Row, New York. 1963.
15. D. E. O'REILLY. *In* Progress in nuclear magnetic resonance spectroscopy. Vol. 2. *Edited by* J. W. Emsley, J. Feeney, and L. H. Sutcliffe. Pergamon Press. 1967. p. 1.
16. W. L. LIPSCOMB. *In* Advances in magnetic resonance. Vol. 2. *Edited by* J. S. Waugh. 1966. p. 138.
17. J. N. MURRELL and A. J. HARGET. Semi-empirical self-consistent-field molecular-orbital theory of molecules. Wiley-Interscience, 1972.
18. A. SAIKA and C. P. SLICHTER. J. Chem. Phys. **22**, 26 (1954).
19. W. F. REYNOLDS, I. R. PEAT, M. H. FREEDMAN, and J. R. LYERLA, JR. Can. J. Chem. **51**, 1857 (1973).
20. M. KARPLUS and J. A. POPLE. J. Chem. Phys. **38**, 2803 (1963).
21. L. F. JOHNSON and W. C. JANKOWSKI. Carbon-13 NMR spectra. Wiley-Interscience, New York. 1972.
22. J. A. POPLE and D. L. BEVERIDGE. Approximate molecular orbital theory. McGraw-Hill Book Company, New York. 1970.
23. R. FREEMAN and W. A. ANDERSON. J. Chem. Phys. **37**, 2053 (1962).
24. D. SHAW. *In* Nuclear magnetic resonance. Vol. 2. (Specialist Periodical Reports). *Edited by* R. K. Harris. The Chemical Society, London, 1973. p. 269.
25. R. R. ERNST. J. Chem. Phys. **45**, 3845 (1966).
26. B. BIRDSALL and J. FEENEY. J. Chem. Soc. Perkin II, 1643 (1973).
27. K. G. R. PACHLER. J. Magn. Res. **7**, 442 (1972).
28. J. E. BLOOR and D. L. BREEN. J. Am. Chem. Soc. **89**, 6835 (1967).
29. B. BAK, D. CHRISTENSEN, L. HANSEN-NYGAARD, and J. RASTRUP-ANDERSEN. J. Mol. Spectrosc. **7**, 58 (1961).
30. S. V. DOBYNS and L. PIERCE. J. Am. Chem. Soc. **85**, 3553 (1963).

Can. J. Chem. Downloaded from www.nrcresearchpress.com by 210.87.254.105 on 09/05/12
For personal use only.

31. L. NYGAARD, R. L. HANSEN, and G. O. SØRENSEN. J. Mol. Structure, **9**, 163 (1971).
32. L. NYGAARD, E. ASMUSSEN, J. H. HØG, R. C. MAHESHWARI, C. H. NIELSEN, I. B. PATERSEN, J. RASTRUP-ANDERSEN, and G. O. SØRENSEN. J. Mol. Structure, **8**, 225 (1971).
33. J.-L. MEYER, G. DAVIDOVICS, J. CHOUTEAU, J.-C. POITE, and J. ROGGERO. Can. J. Chem. **49**, 2254 (1971).
34. J. H. GRIFFITHS, A. WARDLEY, V. E. WILLIAMS, N. L. OWEN, and J. SHERIDAN. Nature, **216**, 1301 (1967).
35. R. GARNIER, R. FAURE, A. BABADJAMIAN, and E. J. VINCENT. Bull. Soc. Chim. Fr. 1040 (1972).
36. S. GRONOWITZ and R. A. HOFFMAN. Arkiv. Kemi, **16**, 539 (1960).
37. (*a*) R. E. WASYLISHEN, J. B. ROWBOTHAM, and T. SCHAEFER. Can. J. Chem. **52**, 833 (1974); (*b*) H. A. STAAB and A. MANNSCHRECK. Chem. Ber. **98**, 1111 (1965).
38. T. F. PAGE, JR., T. ALGER, and D. M. GRANT. J. Am. Chem. Soc. **87**, 5333 (1965).
39. S. NAGATA, T. YAMABE, K. YOSHIKAWA, and H. KATO. Tetrahedron, **29**, 2545 (1973).
40. L. KAPER and TH.J. DE BOER. Rec. Trav. Chim. **89**, 825 (1970).
41. R. E. WASYLISHEN. Unpublished results.

Can. J. Chem. Downloaded from www.nrcresearchpress.com by 210.87.254.105 on 09/05/12
For personal use only.

Etude par spectrométrie infrarouge de la complexation entre les *N,N*-diméthyl-*N'*-phénylformamidines et quelques donneurs de proton

J. VAES, F. FOUBERT ET TH. ZEEGERS-HUYSKENS

Département de Chimie, Université de Louvain K.U.L., Celestijnenlaan 200-F, 3030-Heverlee-Belgique

Reçu le 11 juillet 1974

J. VAES, F. FOUBERT et TH. ZEEGERS-HUYSKENS. Can. J. Chem. **53**, 604 (1975).

Les constantes de stabilité de complexes formés entre l'éthanol et des phénols avec quelques dérivés de la *N,N*-diméthyl-*N'*-phénylformamidine sont déterminées par spectrométrie i.r. L'application des relations de Hammett montre l'existence, outre des termes du premier degré dépendant de la somme des paramètres de substitution du donneur ($\sum\sigma_a$) et de l'accepteur de proton ($\sum\sigma_b$), d'un terme croisé dépendant du produit $\sum\sigma_a\sum\sigma_b$. Les différents paramètres sont discutés en fonction des propriétés acido–basiques des molécules. Les résultats suggèrent que la formation du pont d'hydrogène s'effectue sur l'atome imino de l'amidine. La constante de stabilité des complexes de stoechiométrie 2:1 est calculée; dans celui-ci, la deuxième molécule de phénol se fixe préférentiellement sur l'atome d'oxygène de la première plutôt que sur l'atome d'azote amino.

J. VAES, F. FOUBERT, and TH. ZEEGERS-HUYSKENS. Can. J. Chem. **53**, 604 (1975).

The stability constants of complexes formed between ethanol and phenols with some *N,N*-dimethyl-*N'*-phenylformamidine derivatives are determined by i.r. spectrometry. The application of the Hammett relation shows the existence, in addition to the first degree terms depending on the substitution parameters of the proton donor ($\sum\sigma_a$) and the proton acceptor ($\sum\sigma_b$), of a crossed term depending on the $\sum\sigma_a\sum\sigma_b$ product. The different parameters are discussed as a function of the acid–base properties of the molecules. The results suggest that the formation of the hydrogen bond takes place on the imino nitrogen atom. The stability constant of the complexes of 2:1 stoichiometry is calculated; in this complex the second molecule of phenol seems to be preferentially bonded to the oxygen atom of the first molecule rather than to the amino nitrogen atom.

Introduction

Les amidines sont des molécules caractérisées par la présence de deux centres basiques: l'atome d'azote amino N_1 et l'atome d'azote imino N_2 implantés sur le même atome de carbone, et subissant le phénomène de mésomérie suivant le schéma suivant:

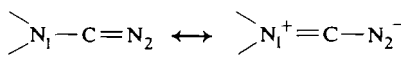

Le caractère de double liaison du lien N_1—C est cependant moins accentué que dans les amides pour lesquels la barrière de rotation autour de ce lien vaut en moyenne 20 kcal par mole alors qu'elle se situe entre 13 à 16 kcal pour les amidines (1–5).

Dans le cadre de recherches effectuées sur la structure et la complexation de molécules organiques, l'on étudie dans ce travail la complexation par pont d'hydrogène de quelques donneurs de proton (éthanol et dérivés phénoliques) avec comme accepteurs de proton, des dérivés de la *N,N*-diméthyl-*N'*-phénylformamidine (DMPF) de formule

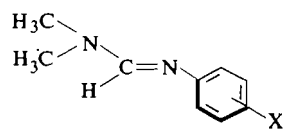

où X = 4-CH_3, H, 4-Cl, 3-Cl et 3,5-diCl.

Comme les benzamidines (6, 7), les amidines adoptent par rapport à la liaison C=N la configuration *trans*. Il est possible que les atomes C—N_1—C=N_2 soient localisés approximativement dans le même plan à cause de la forte conjugaison existant entre le doublet électronique de l'atome d'azote amino et les électrons π de la double liaison C=N (8). Par contre, le cycle aromatique adopterait une configuration non planaire par rapport au reste de la molécule; celle-ci proviendrait de la conjugaison existant entre les électrons non appariés de l'atome

Can. J. Chem. Downloaded from www.nrcresearchpress.com by 210.87.254.40 on 09/05/12
For personal use only.

Can. J. Chem. Downloaded from www.nrcresearchpress.com by 210.87.254.40 on 09/05/12
For personal use only.

d'azote imino et les électrons π du noyau aromatique (9); la conjugaison serait cependant moins accentuée que dans l'aniline. Ces caractéristiques structurales ont été étudiées récemment par la méthode des moments dipolaires (10).

Partie expérimentale

Les amidines ont été synthétisées par la méthode de Bredereck *et al.* (11) à partir de diméthylformamide et d'aniline en présence d'oxychlorure de phosphore. La pureté de celles-ci a été vérifiée par leur spectre r.m.n. et par chromatographie.

Les phénols sont des produits commerciaux (Aldrich, Fluka) purifiés par cristallisation. Le cyclohexane (Fluka pour spectroscopie) a été sèché sur tamis moléculaire 4 Å.

Les spectres i.r. ont été enregistrés à l'aide du spectrophotomètre P.E. 325 dont l'épaisseur de fente spectrale est de 1.07 cm^{-1} à 3000 cm^{-1}. Les cellules munies de fenêtres en KBr sont étalonnées par la méthode des franges d'interférence.

La constante de complexation K est définie par le rapport

$$K = C_{ab}/C_aC_b$$

où C_{ab}, C_a et C_b représentent respectivement les concentrations en complexe, en donneur et en accepteur de proton libres. Cette constante est déterminée à partir de la mesure de l'absorbance de la vibration 1 ν_{OH} du dérivé hydroxylique libre située vers 3600 cm^{-1}; pour chacun de ces dérivés on a effectué une courbe d'étalonnage en fonction de la concentration; celle-ci varie de 0.010 à 0.020 mol dm^{-3}. Les concentrations en amidine sont de l'ordre de 0.010 à 0.030 mol dm^{-3}. Dans ce domaine limité de concentrations, la constante K calculée pour un complexe de stoechiométrie 1:1 reste stable.

Les mesures ont été effectuées dans le cyclohexane ou le tétrachlorure de carbone à la température de 30 ± 0.5 °C.

Résultats expérimentaux et discussion

A. Complexes de stoechiométrie 1:1

La figure 1 indique à titre d'exemple, le spectre i.r. de 3800 à 3000 cm^{-1} de l'éthanol libre et complexé à la DMPF dans lequel le large massif observé à 3383 cm^{-1} correspond au vibrateur $\nu_{OH...N}$. Le tableau 1 rassemble les valeurs de la constante de stabilité K et du glissement de fréquence $\Delta\nu_{OH...N}$ pour les complexes de l'éthanol et des DMPF substituées. Ce tableau reprend également les valeurs du pK_a déterminé dans l'eau à 25 °C par la méthode potentiométrique (10).

L'ensemble de ces résultats montre que les valeurs de K et $\Delta\nu_{OH}$ sont d'autant plus élevées que la basicité de l'amidine est plus accentuée. L'influence du substituant implanté sur le noyau aromatique peut se traduire par la relation de Hammett dans laquelle les valeurs du coefficient

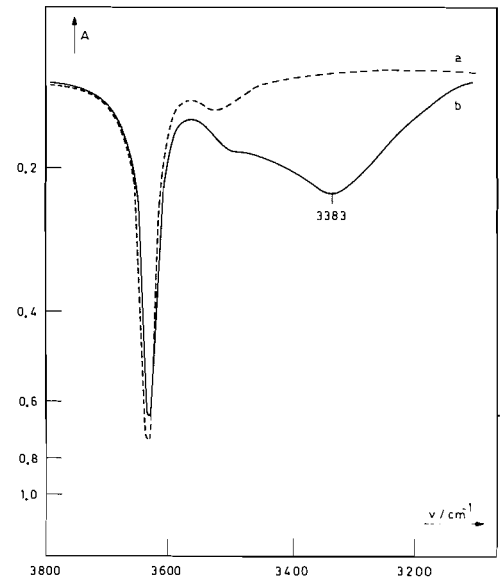

FIG. 1. Spectre i.r. (3800–3000 cm^{-1}); (*a*) éthanol (C = 0.08 mol dm^3); (*b*) éthanol (C = 0.08 mol dm^3) + DMPF (C = 0.12 mol dm^3); solvant = CCl_4.

ρ et de l'ordonnée à l'origine ont été calculées par la méthode des moindres carrés.

[1] $\log K = 0.74 - 0.48\sum\sigma \quad (r = 0.98)$

[2] $\Delta\nu_{OH} = 300 - 53.7\sum\sigma \quad (r = 0.96)$

La figure 2 indique la variation de $\Delta\nu_{OH}$ en fonction de la somme des paramètres de substitution de l'amidine.

Les valeurs de K obtenues pour les complexes de l'éthanol avec les DMPF sont du même ordre de grandeur que celle obtenue pour le même alcool complexé par la triéthylamine (K = 4.5 (12)) dont le caractère basique est cependant plus accentué (pK_a = 10.7). Cet effet peut s'expliquer par l'encombrement stérique important

TABLEAU 1. Valeurs de K (dm^3 mol^{-1}), $\Delta\nu_{OH}$(cm^{-1}) des complexes éthanol–DMPF (solvant = CCl_4, T^0 = 25 °C)

DMPF	K	$\Delta\nu_{OH}$*	pK_a
4-CH_3	6.4±0.3	308	8.45
4-OCH_3	6.5±0.3	316	—
H	6.1±0.3	293	8.15
4-Cl	3.7±0.2	286	7.54
3-Cl	3.6±0.2	276	7.10
3,4-diCl	2.7±0.3	271	6.60
3,5-diCl	2.5±0.2	261	5.13

*Précision sur la mesure = 2 cm^{-1}.

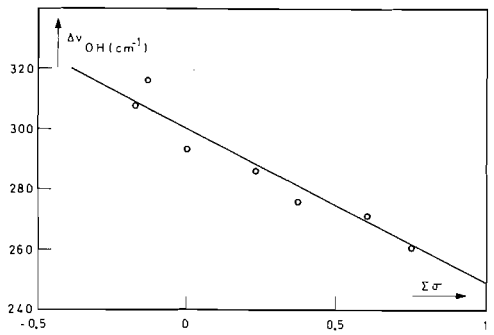

FIG. 2. $\Delta\nu_{OH}(cm^{-1})$ en fonction de $\Sigma\sigma$ pour les complexes éthanol–DMPF substituées.

provoqué par l'accumulation de trois groupements éthyles au niveau du centre réactionnel. Par contre la valeur de $\Delta\nu_{OH}$ reste sensiblement plus élevée pour les complexes des amines aliphatiques tertiaires ($\Delta\nu_{OH} = 427\ cm^{-1}$ pour le complexe éthanol–triéthylamine). En général, les effets stériques semblent influencer les valeurs des constantes de stabilité en diminuant le nombre de configurations favorables à la formation du pont d'hydrogène mais se répercutent moins sur les valeurs de $\Delta\nu_{OH}$ proportionnelles pour une même famille de complexes à l'enthalpie de complexation (17). Par contre, bien que les amidines soient caractérisées par un pK_a nettement plus élevé que la pyridine, les valeurs de K et de $\Delta\nu_{OH}$ sont très semblables (13); cet effet s'explique par la structure de la pyridine dans laquelle l'approche de l'atome d'azote endocyclique est peu limitée par des facteurs stériques.

Le tableau 2 indique les valeurs des constantes de stabilité relatives aux complexes formés de dérivés phénoliques et de DMPF substituées; dans le cas de ceux-ci, il n'est pas possible de déterminer avec précision la position de la vibration $\nu_{OH...N}$ qui se situe aux environs de $3000\ cm^{-1}$ et coïncide avec les vibrations ν_{CH}. Les résultats permettent de préciser l'influence d'un substituant implanté sur le donneur ou sur l'accepteur de proton vis-à-vis de l'équilibre de complexation. En effet, si l'on considère une amidine complexée par la série de dérivés phénoliques mentionnés, la relation de Hammett peut s'écrire:

$$[3] \qquad \log K = \log K^0 + \rho_a \Sigma\sigma_a$$

où K^0 représente la constante d'équilibre du complexe non substitué dans la famille considérée et $\Sigma\sigma_a$ la somme des paramètres de substitution du donneur de proton. L'ensemble de ces relations est illustré dans la fig. 3; par la méthode des moindres carrés, les valeurs suivantes ont été calculées.

DMPF	$\log K^0 + \rho_a \Sigma\sigma_a$
4-CH_3	$2.02+1.25\ \Sigma\sigma_a$
H	$1.96+1.18\ \Sigma\sigma_a$
4-Cl	$1.70+1.09\ \Sigma\sigma_a$
3,4-diCl	$1.52+0.79\ \Sigma\sigma_a$
3,5-diCl	$1.38+0.75\ \Sigma\sigma_a$

La valeur de la pente ρ_a est d'autant plus élevée que l'accepteur de proton est plus basique; la fig. 4 montre qu'il existe une relation approximativement linéaire entre celle-ci et la somme des paramètres de substitution de la base:

$$[4] \qquad \rho_a = \rho_a^0 + B\Sigma\sigma_b$$

De même, l'influence du substituant implanté sur l'amidine peut se traduire par la relation:

$$[5] \qquad \log K = \log K^0 + \rho_b \Sigma\sigma_b$$

dont on a calculé pour chaque dérivé phénolique les valeurs de la pente et de l'ordonnée à l'origine.

TABLEAU 2. Valeurs de K ($dm^3\ mol^{-1}$) pour les complexes des DMPF avec les phénols substitués (solvant = cyclohexane; $T^0 = 30\ °C$)

	Phénol				
DMPF	4-CH_3	H	4-Cl	3-Cl	3,5-diCl
4-CH_3	72 ± 3	98 ± 3	230 ± 5	330 ± 13	803 ± 23
H	58 ± 1	77 ± 2	199 ± 6	288 ± 11	595 ± 18
4-Cl	30 ± 1	56 ± 2	93 ± 2	121 ± 4	334 ± 9
3,4-diCl	24 ± 1	38 ± 1	44 ± 1	60 ± 2	137 ± 3
3,5-diCl	19 ± 1	25 ± 1	30 ± 2	42 ± 1	97 ± 2

Can. J. Chem. Downloaded from www.nrcresearchpress.com by 210.87.254.40 on 09/05/12
For personal use only.

Can. J. Chem. Downloaded from www.nrcresearchpress.com by 210.87.254.40 on 09/05/12
For personal use only.

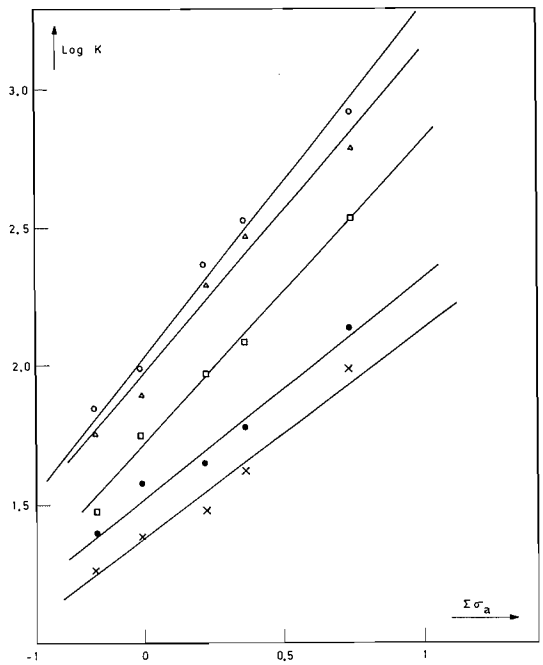

FIG. 3. Log K en fonction de $\Sigma\sigma_a$; ○, 4-CH_3 DMPF; △, DMPF; □, 4-Cl DMPF; ●, 3,4-diCl DMPF; ×, 3,5-diCl DMPF.

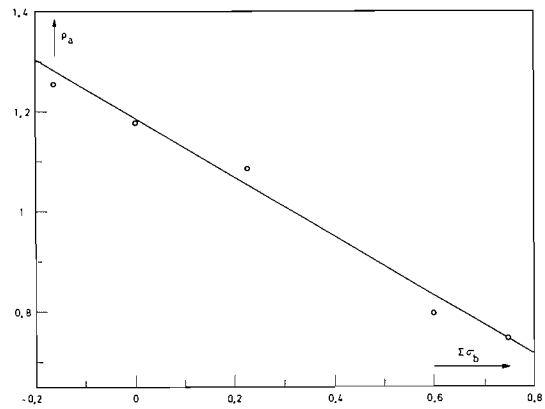

FIG. 4. Variation de ρ_a en fonction de $\Sigma\sigma_b$.

Phénol	$\log K^0 + \rho_b \Sigma\sigma_b$
4-CH_3	$1.71 - 0.64\,\Sigma\sigma_b$
H	$1.89 - 0.66\,\Sigma\sigma_b$
4-Cl	$2.23 - 0.99\,\Sigma\sigma_b$
3-Cl	$2.37 - 1.01\,\Sigma\sigma_b$
3,5-diCl	$2.74 - 1.03\,\Sigma\sigma_b$

La dépendance constatée entre ρ_b et l'acidité du phénol permet d'écrire:

$$[6] \qquad \rho_b = \rho_b^0 + B\Sigma\sigma_a$$

La comparaison des éqs. 3, 4, 5 et 6 fournit la relation:

$$[7] \quad \log K = \log K_o^0 + \rho_a^0\Sigma\sigma_a + \rho_b^0\Sigma\sigma_b + B\Sigma\sigma_a\Sigma\sigma_b$$

où K_o^0 représente la constante d'équilibre relative au complexe non substitué phénol–DMPF. Pour les complexes où la substitution porte à la fois sur le donneur et sur l'accepteur de proton, la constante K dépend donc, en plus des termes du premier degré, d'un terme croisé $B\Sigma\sigma_a\Sigma\sigma_b$ dans lequel la constante B peut être considérée comme une constante réactionnelle supplémentaire. Sa valeur négative (-0.6) montre qu'une augmentation d'acidité du phénol ($\Sigma\sigma_a > 0$) renforce les effets de substitution sur l'amidine. D'un point de vue moléculaire, ce terme croisé peut s'expliquer par une variation de la structure électronique provoquée par l'implantation d'un substituant de part et d'autre dans le complexe; ce changement de distance provoque une variation de l'interaction dipolaire et de l'énergie de polarisation effets qui sont d'autant plus importants que la liaison hydrogène se trouve condensée dans un espace plus réduit. L'existence de ce terme d'interaction peut être également lié aux effets de résonance existant dans le noyau aromatique, effets qui peuvent être perturbés par l'introduction de part et d'autre d'un substituant et qui entraînent une légère modification de l'hybridation de l'atome d'azote (14).

En remplacant dans l'éq. 7 les coefficients ρ et B par leurs valeurs numériques, on obtient l'expression:

$$[8] \quad \log K = 1.90 + 1.18\Sigma\sigma_a - 0.66\Sigma\sigma_b - 0.6\Sigma\sigma_a\Sigma\sigma_b$$

Celle-ci peut se comparer à l'équation obtenue pour les complexes phénol–aniline (15) dans le tétrachlorure de carbone dont la polarité diffère peu de celle du cyclohexane:

$$[9] \quad \log K = 0.61 + 0.67\Sigma\sigma_a - 0.70\Sigma\sigma_b - 1.30\Sigma\sigma_a\Sigma\sigma_b$$

et les complexes phénol–pyridine (16)

$$[10] \quad \log K = 1.76 + 1.08\Sigma\sigma_a - 1.30\Sigma\sigma_b - 0.6\Sigma\sigma_a\Sigma\sigma_b$$

La comparaison de ces expressions indique que les valeurs de K_o^0 et de ρ_a^0 sont d'autant plus

TABLEAU 3. Valeurs de K_2 (dm^3 mol^{-1}) pour quelques complexes phénol–DMF (solvant = cyclohexane; T^0 = 30 °C)

Complexe	K_2	Complexe	K_2
4-CH_3 Phénol – 4-CH_3 DMPF	13±2	Phénol–DMPF	15±2
4-CH_3 Phénol – DMPF	14±2	Phénol – 4-Cl DMPF	15±2
Phénol – 4 CH_3 DMPF	19±2	4-Cl Phénol – 4-Cl DMPF	13±2

élevées que le caractère basique de l'accepteur de proton et l'enthalpie de complexation sont élevés. Celle-ci vaut en effet −5.10 (17), −6.5 (18) et −9 (10) kcal par mole.

Par contre la valeur de ρ_b^0 mesurant l'effet de substitution sur la molécule basique est nettement plus élevée pour la pyridine que pour l'aniline ou l'amidine; celle-ci dépend en général de la structure de la base et notamment du nombre de liaisons séparant le noyau aromatique du centre réactionnel. Cet effet se retrouve également pour l'ionisation de ces bases où le paramètre ρ_i mesurant l'effet de substitution sur l'équilibre d'ionisation dans l'eau est nettement plus élevé pour les pyridines ($\rho_i = -6.4$) (19) que pour les anilines ($\rho_i = -2.89$) (20) ou les amidines ($\rho_i = -2.66$) (10).

D'autre part, la valeur de ρ_b^0 est très proche pour les complexes des amidines et des anilines; cette similitude suggère que la formation du pont d'hydrogène s'effectue sur l'atome d'azote imino. La formation du complexe sur l'atome d'azote amino entraînerait des valeurs de ρ beaucoup plus faibles, les effets du substituant devant se transmettre à travers le squelette N—C=N—. L'étude des moments dipolaires des complexes phénols–formamidines permet d'arriver à une conclusion semblable (10). De même, la comparaison des valeurs de ρ_i des anilines et des amidines indique que la protonation s'effectue également sur la fonction imino; cette déduction est en accord avec les conclusions formulées à partir du spectre i.r. (21), u.v. (22) et de résonance magnétique nucléaire (5) de molécules semblables. De plus, l'étude théorique effectuée sur les aminoazirines caractérisées par un système N=C—N fortement conjugué, montre que la protonation s'effectue préférentiellement sur la paire électronique σ de l'atome d'azote endocyclique (23).

B. Complexes de stoechiométrie 2:1

Si les résultats précédents suggèrent que la formation d'un pont d'hydrogène s'effectue sur l'atome d'azote imino et non sur l'atome d'azote amino, dont le caractère basique semble fortement atténué par la délocalisation électronique, les complexes de stoechiométrie 2:1 formés de deux molécules de phénol et d'une molécule d'amidine peuvent être caractérisés par deux structures possibles: la deuxième molécule de phénol se fixe sur la première (structure **1**) ou forme un pont d'hydrogène avec l'atome d'azote-amino (structure **2**)

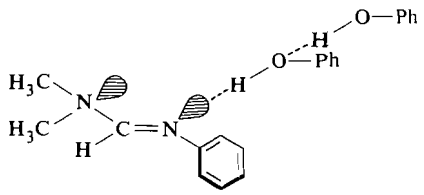

1

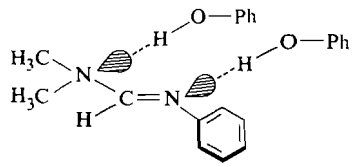

2

La constante de greffage K_2 d'une deuxième molécule de phénol sur le complexe 1:1 se définit par la relation

[11] $$K_2 = C_{a_2b}/C_{ab}C_a$$

dans laquelle C_{a_2b}, C_{ab} et C_a représentent respectivement les concentrations en complexe 2:1, en complexe 1:1 et en phénol libre. Cette constante a été déterminée par spectrométrie i.r. à partir de l'absorbance de la vibration ν_{OH} libre, par une méthode décrite précédemment (24, 25). Celle-ci se base sur la variation d'une constante apparente, K_{app}, calculée sur la base d'un complexe de stoechiométrie 1:1 en fonction de la concentration en phénol libre, C_a. On peut facilement montrer que

Can. J. Chem. Downloaded from www.nrcresearchpress.com by 210.87.254.40 on 09/05/12
For personal use only.

$$[12] \quad \frac{1}{2C_a + K_{app}C_a^2} = \frac{1}{K}\left(\frac{K_{app}}{2C_a + K_{app}C_a^2} - K_2\right)$$

Cette équation permet de calculer K et K_2 séparément. Pour chaque complexe étudié, les résultats énumérés dans le tableau 3 résultent d'une dizaine de points expérimentaux.

Ces résultats montrent qu'il n'existe pas de corrélation entre les propriétés acido–basiques de l'accepteur de proton et les valeurs de K_2. La même constatation s'applique aux constantes de dimérisation K_d des dérivés phénoliques dont la valeur oscille entre 4 à 5 $dm^3\ mol^{-1}$, quel que soit le substituant. Ce fait suggère que le complexe adopte préférentiellement la structure **1**; l'existence de la structure **2** entraînerait en effet une augmentation sensible de K_2 lorsque le phénol devient plus acide. La valeur plus élevée de K_2 vis-à-vis de K_d peut s'expliquer par le transfert de charge ayant lieu du doublet électronique libre de l'atome d'azote vers l'orbitale σ^*(O—H) de la première molécule de phénol; cet effet rend le caractère accepteur de proton de celle-ci vis-à-vis d'une deuxième molécule de phénol, plus élevé. Le spectre i.r. (fig. 1) confirme cet effet; le dimère du phénol absorbe vers 3520 cm^{-1} (vibration $\nu_{OH...O}$) tandis que dans le complexe de stoechiométrie 2:1, cette même vibration s'observe à des nombres d'onde de 20 à 30 cm^{-1} inférieurs. Les valeurs de K_2 relatives aux complexes des phénols substitués avec la triéthylamine où il n'existe qu'un seul centre basique, sont plus élevées (24). Ceci peut s'expliquer par le caractère basique nettement plus élevé de l'amine aliphatique; le transfert de charge dans la chaîne N...H—O...H—O doit par conséquent être plus important.

Les auteurs remercient le N.F.W.O. pour les subsides accordés au laboratoire ainsi que l'I.W.O.N.L. pour la bourse de spécialisation de deux d'entre eux (J.V. et F.F.).

1. D. J. Bertelli et J. T. Gerig. Tetrahedron Lett. 2481 (1967).
2. Y. Shvo. Tetrahedron Lett. 3259 (1967).
3. A. Mannschrek et U. Koelle. Tetrahedron Lett. 863 (1967).
4. D. L. Harris et M. Wellman. Tetrahedron Lett. 5225 (1968).
5. M. Rens. Thèse de doctorat. Louvain 1973.
6. V. I. Minkin. Tetrahedron, **23**, 3651 (1967).
7. H. Lumbroso et G. Pifferi. Bull. Soc. Chim. Fr. **10**, 3401 (1969).
8. D. C. Prevorsek. J. Phys. Chem. **66**, 769 (1962).
9. J. A. Smith et H. Taylor. J. Chem. Soc. B66 (1969).
10. F. Foubert. Thèse. Louvain 1974.
11. H. Bredereck, R. Gomper, K. Klemm et H. Rempfer. Berichte, **92**, 834 (1959).
12. Th. Zeegers-Huyskens, L. Lamberts et P. Huyskens. J. Chim. Phys. **59**, 521 (1962).
13. A. M. Dierckx, P. Huyskens et Th. Zeegers-Huyskens. J. Chim. Phys. **62**, 336 (1965).
14. G. Lichtfus et Th. Zeegers-Huyskens. Spectrochim. Acta, **28A**, 2081 (1972).
15. G. Lichtfus, F. Lemaire et Th. Zeegers-Huyskens. Spectrochim. Acta, **28A**, 2069 (1972).
16. D. Clotman, J. P. Muller et Th. Zeegers-Huyskens. Bull. Soc. Chim. Belges, **79**, 689 (1970).
17. D. Neerinck. Thèse de doctorat. Louvain 1968.
18. D. Neerinck et L. Lamberts. Bull. Soc. Chim. Belges, **75**, 473 (1966).
19. A. Bryson. J. Am. Chem. Soc. **82**, 4871 (1960).
20. A. Bryson. J. Am. Chem. Soc. **82**, 4858 (1960).
21. J. C. Grivas et A. Taurins. Can. J. Chem. **37**, 1260 (1959).
22. Z. B. Kiro, Y. A. Teterin, L. N. Nikolenko et B. I. Stepanov. Zh. Org. Kh. **8**, 2573 (1972).
23. J. M. André et J. Delhalle. Communication personnelle.
24. D. Clotman, D. Van Lerberghe et Th. Zeegers-Huyskens. Spectrochim. Acta, **26A**, 1621 (1970).
25. J. P. Muller, G. Vercruysse et Th. Zeegers-Huyskens. J. Chim. Phys. **69**, 1439 (1972).

Can. J. Chem. Downloaded from www.nrcresearchpress.com by 210.87.254.40 on 09/05/12
For personal use only.

The Structure of Isothiosemicarbazones

CHIJI YAMAZAKI

Department of Chemistry, School of Hygienic Sciences, Kitasato University, 1 Asamizodai, Sagamihara-shi, Japan

Received July 22, 1974

CHIJI YAMAZAKI. Can. J. Chem. **53**, 610 (1975).

Isothiosemicarbazones, except N^2-substituted ones, were found to exist exclusively in the amino structure by means of i.r. and n.m.r. spectroscopy. The *cis* configuration (N^1 *cis* to N^4 about the N^2=C bond) with intramolecular hydrogen bonding was proposed as the predominant structure for N^4-unsubstituted isothiosemicarbazones on the basis of the i.r. spectra from the partially deuterated compounds. The *trans* configuration (N^1 *trans* to N^4 about the N^2=C bond) was identified in all N^4-monsubstituted and in a few N^4-unsubstituted isothiosemicarbazones. The *cis*/*trans* ratios for the former varied depending on the solvent used.

CHIJI YAMAZAKI. Can. J. Chem. **53**, 610 (1975).

Utilisant la spectroscopie i.r. et la r.m.n., on a démontré que les isothiosemicarbazones, à l'exception de celles substituées sur N^2, existent exclusivement sous la forme amino. On propose, comme structure principale pour les isothiosemicarbazones non-substituées en position N^4, une configuration *cis* (N^1 *cis* par rapport à N^4 autour de la liaison N^2=C) impliquant une liaison hydrogène intramoléculaire; cette conclusion dérive des spectres infrarouges de quelques composés partiellement deutérés. On a identifié une configuration *trans* (N^1 *trans* par rapport à N^4 autour du lien N^2=C) dans toutes les isothiosemicarbazones mono-substituées en N^4 et dans quelques cas où il n'y a pas de substituant en N^4. Le rapport d'isomère *cis* à *trans* dans le premier cas varie suivant le solvant utilisé. [Traduit par le journal]

Introduction

Isothiosemicarbazones are potentially tautomeric systems and have long been depicted in either an amino form $>C{=}\overset{1}{N}{-}\overset{2}{N}{=}\overset{3}{C}(SR)\overset{4}{N}H_2$ or an imino form $>C{=}\overset{1}{N}{-}\overset{2}{N}H{-}\overset{3}{C}(SR){=}\overset{4}{N}H$. Shagidullin and co-workers (1) proposed an amino form for methylation products (R = Me) of certain thiosemicarbazones but detailed interpretations are not available as to tautomeric and configurational assignments. Partial deuteration technique in conjunction with n.m.r. spectroscopy now gives some information with respect to the structural classification as well as the conformational and configurational assignments.

Experimental

All melting points are uncorrected. The i.r. spectra were recorded on a Hitachi EPI-G2 grating spectrophotometer. Spectra of carbon tetrachloride solutions were obtained in 1- and 5-mm KRS-5 cells and those of solid samples taken using KBr discs. The frequencies reported in Tables 1–4 were determined by direct calibration against the standard frequencies of indene which were measured in a 0.1-mm KBr cell immediately after each compound was examined, whereas those from KBr discs were calibrated using the 3060 cm^{-1} band of polystyrene. The n.m.r. spectra were recorded at a probe temperature of 36° on a Nichiden-Varian T-60 spectrometer and a Hitachi R-24 spectrometer, both operating at 60 MHz. Chemical shifts were reported in parts per million downfield from internal tetramethylsilane (δ p.p.m.).

Partial deuteration was carried out as follows. A solution of the compound (5 mmol) to be investigated in methanol-d_1 (0.5 ml) was heated in a glass-stoppered flask at 80° for a few minutes and then evaporated *in vacuo*. The deuterated product thus obtained contained sufficient unchanged protium to give spectra as required.

Preparation of Acetophenone S-Methylisothiosemicarbazone (3)

A mixture of *S*-methylisothiosemicarbazide hydriodide (7.0 g, 0.03 mol), acetophenone (3.6 g, 0.03 mol), and 2-propanol (30 ml) was heated at 70° for 3 h. The crystals formed (9.15 g, 91%; m.p. 204.5°) were recrystallized from ethanol (80 ml) to give pure hydriodide (5.9 g) as white prisms, m.p. 206–207°. A portion of the hydriodide was converted to the free base which was then recrystallized twice from 2-propanol to give the product as colorless lustrous prisms, m.p. 94–95°.

Anal. Calcd. for $C_{10}H_{13}N_3S$: C, 57.96; H, 6.32; N, 20.28. Found: C, 58.18; H, 6.40; N, 20.07.

The following isothiosemicarbazones were prepared similarly.

Benzaldehyde S-Methylisothiosemicarbazone (1): colorless prisms (from hexane, and then isopropyl ether), m.p. 80–81° (lit. (2) m.p. 82°).

Benzaldehyde S-Benzylisothiosemicarbazone (2): faintly yellow plates (from 2-propanol), m.p. 113.5–114°. The hydrochloride melted at 191.5° (lit. (3) m.p. 190°).

Anisaldehyde S-Methylisothiosemicarbazone (5): white needles (from 2-propanol), m.p. 98–99° (lit. (2) m.p. 97°).

Can. J. Chem. Downloaded from www.nrcresearchpress.com by 210.87.254.5 on 09/05/12
For personal use only.

TABLE 1. The N—H stretching frequencies of N^4-unsubstituted isothiosemicarbazones, $R^1R^2C{=}N{-}N{=}C(SR^3)NH_2$, in carbon tetrachloride (cm^{-1})

Compound	R^1	R^2	R^3	νNH	
1	C_6H_5	H	CH_3	3500	3380
2	C_6H_5	H	$CH_2C_6H_5$	3498	3380
3	C_6H_5	CH_3	CH_3	3498	3372
4	C_6H_5	CH_3	$CH_2C_6H_5$	3497	3378
5	*p*-$CH_3OC_6H_4$	H	CH_3	3500	3379
6	*p*-$CH_3OC_6H_4$	H	$CH_2C_6H_5$	3501	3380
7	*p*-$CH_3OC_6H_4$	CH_3	CH_3	3496	3373
8	*p*-$CH_3OC_6H_4$	CH_3	$CH_2C_6H_5$	3499	3378
9	*p*-$CH_3OC_6H_4$	H	$CH_2CH{=}CH_2$	3499	3380
10	*p*-$CH_3OC_6H_4$	H	$CH_2CH_2CH_3$	3500	3380
11	*n*-C_3H_7	H	CH_3	3499	3378
12	CH_3	CH_3	CH_3	3500	3375
13	$(CH_2)_5$		CH_3	3496	3369
14	CH_3	CH_3	$CH_2C_6H_5$	3496	3371

TABLE 2. The N—H stretching frequencies of N^4-substituted isothiosemicarbazones, $R^1R^2C{=}N{-}N{=}C(SR^3)NHCH_3$, in carbon tetrachloride (cm^{-1})

Compound	R^1	R^2	R^3	νNH	
15	C_6H_5	H	CH_3	3485w	3382
16	C_6H_5	H	$CH_2C_6H_5$	3455w	3380
17	C_6H_5	CH_3	$CH_2C_6H_5$	3455w	3380
18	*p*-$CH_3OC_6H_4$	H	CH_3	3480w	3380
19	$(CH_2)_5$		CH_3	3480w	3380

*p-Methoxyacetophenone S-Methylisothiosemicarbazone (**7**)*: colorless needles (from 2-propanol), m.p. 83–84°.

Anal. Calcd. for $C_{11}H_{15}N_3OS$: C, 55.68; H, 6.37; N, 17.71. Found: C, 56.00; H, 6.47; N, 17.75.

*p-Methoxyacetophenone S-Benzylisothiosemicarbazone (**8**)*: colorless flat needles (from ethanol), m.p. 125–126°.

Anal. Calcd. for $C_{17}H_{19}N_3OS$: C, 65.16; H, 6.11; N, 13.41. Found: C, 65.31; H, 6.24; N, 13.22.

*Preparation of Anisaldehyde S-Allylisothiosemicarbazone (**9**)*

A suspension of finely divided thiosemicarbazide (18.2 g, 0.2 mol) and 3-bromo-1-propene (24.2 g, 0.2 mol) in 2-propanol (80 ml) was stirred at 70° for 1 h, during which time all the solids dissolved. To this hot solution was added anisaldehyde (27.2 g, 0.2 mol) and the reaction mixture was refluxed for 2 h. The isothiosemicarbazone hydrobromide (57.4 g, 87%) crystallized out as yellow plates with m.p. 157–159° from the cooled reaction mixture. A portion of the hydrobromide was converted to the free base which was then purified by two recrystallizations from 2-propanol, yielding the desired product as faintly yellow prisms, m.p. 100–100.5°.

Anal. Calcd. for $C_{12}H_{15}N_3OS$: C, 57.82; H, 6.07; N, 16.86. Found: C, 57.89; H, 6.06; N, 17.04.

In the same manner as the preparation of **9**, but with some appropriate modifications, the following isothiosemicarbazones were prepared.

*Acetophenone S-Benzylisothiosemicarbazone (**4**)*: colorless needles (from hexane – isopropyl ether), m.p. 68–69°.

Anal. Calcd. for $C_{16}H_{17}N_3S$: C, 67.82; H, 6.05; N, 14.83. Found: C, 67.63; H, 6.13; N, 14.90.

*Anisaldehyde S-Benzylisothiosemicarbazone (**6**)*: almost colorless plates (from 2-propanol), m.p. 103–104°.

Anal. Calcd. for $C_{16}H_{17}N_3OS$: C, 64.20; H, 5.72; N, 14.04. Found: C, 64.31; H, 5.79; N, 13.91.

*Anisaldehyde S-Propylisothiosemicarbazone (**10**)*: white prisms (from hexane – isopropyl ether), m.p. 54–55°.

Anal. Calcd. for $C_{12}H_{17}N_3OS$: C, 57.35; H, 6.82; N, 16.72. Found: C, 57.54; H, 7.01; N, 16.52.

*Butyraldehyde S-Methylisothiosemicarbazone (**11**)*: white needles (from isopropyl ether), m.p. 67–68°.

Anal. Calcd. for $C_6H_{13}N_3S$: C, 45.27; H, 8.23; N, 26.40. Found: C, 45.52; H, 8.01; N, 26.38.

*Acetone S-Methylisothiosemicarbazone (**12**)*: faintly yellow plates (from hexane), m.p. 64.5–66°. The hydriodide melted at 182.5–183° (lit. (4) m.p. 178–180°).

*Cyclohexanone S-Methylisothiosemicarbazone (**13**)*: pale yellow prisms (from 2-propanol), m.p. 79.5–80.5°.

Anal. Calcd. for $C_8H_{15}N_3S$: C, 51.87; H, 8.16; N, 22.69. Found: C, 52.05; H, 8.08; N, 22.78.

*Acetone S-Benzylisothiosemicarbazone (**14**)*: white needles (from isopropyl ether), m.p. 72–73° (lit. (4) m.p. 72–73°).

*Benzaldehyde 4,S-Dimethylisothiosemicarbazone (**15**)*: pale yellow prisms (from ethyl ether – 2-propanol), m.p. 65.5–66.5° (lit. (5) m.p. 66°).

Can. J. Chem. Downloaded from www.nrcresearchpress.com by 210.87.254.5 on 09/05/12
For personal use only.

Can. J. Chem. Downloaded from www.nrcresearchpress.com by 210.87.254.5 on 09/05/12
For personal use only.

TABLE 3. The N—H stretching frequencies of N^2-substituted isothiosemicarbazones and N^4-substituted thiosemicarbazones, $R^1R^2C{=}N{-}(X){-}C(=Y)(Z)$, in carbon tetrachloride (cm^{-1})

Compound	R^1	R^2	X	Y	Z	vNH
20	C_6H_5	H	NCH_3	NH	SCH_3	3375
21	p-$CH_3OC_6H_4$	H	NCH_3	NH	SCH_3	3374
23	p-$C_{10}H_{21}OC_6H_4$	CH_3	NH	S	$NHCH_3$	3383
24	C_6H_5	CH_3	NH	S	$NHCH_3$	3385
25	C_6H_5	H	NH	S	$N(CH_3)_2$	3323

TABLE 4. The N—H and N—D stretching frequencies of partially deuterated N^4-unsubstituted isothiosemicarbazones (cm^{-1}) (0.02 *M* in carbon tetrachloride)

Compound	vNH				Δν	vND			
1	3500	3470	3420	3380	50*	2620	2555	2527	2474
2	3498	3470	3420	3380	50	2624	2555	2526	2468
3	3498	3472	3416	3372	56	2622	2556	2520	2472
4	3496	3468	3407	3378	61	2619	2553	2518	2467
5	3500	3465	3417	3379	48	2619	2554	2525	2470
6	3501	3467	3419	3380	48	2624	2557	2525	2473
7	3496	3467	3410	3373	57	2619	2553	2520	2469
8	3499	3465	3408	3378	57	2620	2555	2522	2469
9	3499	3467	3418	3380	49	2622	2554	2525	2472
10	3500	3467	3419	3380	48	2623	2558	2528	2475
11	3499	3464	3415	3378	49	2620	2558	2525	2470
12	3500	3466	3408	3375	58	2619	2552	2517	2468
13	3497	3466	3404	3370	62	2619	2554	2521	2467
14	3496	3466	3405	3372	61	2619	2554	2517	2468

*3470–3420 = 50 cm^{-1}.

*Benzaldehyde S-Benzyl-4-methylisothiosemicarbazone (**16**)*: pale yellow prisms (from isopropyl ether), m.p. 100–101°.

Anal. Calcd. for $C_{16}H_{17}N_3S$: C, 67.82; H, 6.05; N, 14.83. Found: C, 67.78; H, 6.06; N, 14.62.

*Acetophenone S-Benzyl-4-methylisothiosemicarbazone (**17**)*: pale yellow viscous oil. The hydrochloride monohydrate crystallized as faintly yellow needles from methanol and melted at 170–172° with loss of the water of crystallization at about 130°.

Anal. Calcd. for $C_{17}H_{22}ClN_3OS$: C, 58.03; H, 6.30; N, 11.94. Found: C, 58.29; H, 6.28; N, 12.10.

*Anisaldehyde 4,S-Dimethylisothiosemicarbazone (**18**)*: colorless needles (from 2-propanol), m.p. 84–85.5°.

Anal. Calcd. for $C_{11}H_{15}N_3OS$: C, 55.68; H, 6.37; N, 17.71. Found: C, 55.90; H, 6.38; N, 17.80.

*Cyclohexanone 4,S-Dimethylisothiosemicarbazone (**19**)*: colorless prisms (from isopropyl ether), m.p. 71–73°.

Anal. Calcd. for $C_9H_{17}N_3S$: C, 54.25; H, 8.60; N, 21.09. Found: C, 54.61; H, 8.70; N, 20.83.

*Preparation of Benzaldehyde 2,S-Dimethylisothiosemicarbazone (**20**)*

A solution of **1** (3.86 g, 0.02 mol) and methyl iodide (3.12 g, 0.022 mol) in 2-propanol (35 ml) was heated in a sealed glass tube at 80–86° for 10 h and the resulting solid (2.81 g, 42%) was crystallized from water to give the hydriodide as white needles, m.p. 187–188° (lit. (6) m.p. 187°). It was converted to the free base, m.p. 65–67°; n.m.r. ($CDCl_3$) δ 2.26 (s, 3H, SCH_3), 3.52 (s, 3H, NCH_3), 6.80 (br s, 1H, NH), 7.25–7.75 (m, 5H, C_6H_5), 7.52 (s, 1H, CH=N).

*Anisaldehyde 2,S-Dimethylisothiosemicarbazone (**21**)*

This was obtained similarly as pale yellow plates (from ethanol), m.p. 108–109.5°. The hydriodide melted at 199° (lit. (6) m.p. 195°); n.m.r. ($CDCl_3$) δ 2.26 (s, 3H, SCH_3), 3.49 (s, 3H, NCH_3), 3.82 (s, 3H, OCH_3), 5.75 (br s, 1H, NH), 6.87 (d, J = 9.0 Hz, 2H, ring protons), 7.58 (d, J = 9.0 Hz, 2H, ring protons), 7.50 (s, 1H, CH=N).

Anal. Calcd. for $C_{11}H_{15}N_3OS$: C, 55.68; H, 6.37; N, 17.71. Found: C, 55.81; H, 6.36; N, 17.45.

*Preparation of Benzaldehyde 4,4,S-Trimethylisothiosemicarbazone (**22**)*

A mixture of **25** (0.41 g, 2 mmol), methyl iodide (0.31 g, 2.2 mmol), and 2-propanol (4 ml) was heated at 60° for 2 h and the resulting hydriodide (0.63 g, 91.4%), m.p. 153.5–155°, was converted to the free base, a yellow glass; n.m.r. ($CDCl_3$) δ 2.50 (s, 3H, SCH_3), 3.12 (s, 6H, $N(CH_3)_2$), 7.22–7.83 (m, 5H, C_6H_5), 8.30 (s, 1H, CH=N).

Anal. Calcd. for $C_{11}H_{15}N_3S$: C, 59.71; H, 6.83; N, 18.99. Found: C, 60.00; H, 6.98; N, 18.82.

*Preparation of Acetophenone 4-Methylthiosemicarbazone (**24**)*

A mixture of acetophenone (0.6 g, 5 mmol), 4-methylthiosemicarbazide (0.53 g, 5 mmol), glacial acetic acid (0.5 ml), and ethanol (10 ml) was refluxed for 1 h. The

separated crystals (0.51 g, 53%) were recrystallized from ethanol to give the product as faintly yellow needles with m.p. 140–140.5° (lit. (7) m.p. 135°).

Anal. Calcd. for $C_{10}H_{13}N_3S$: C, 57.96; H, 6.32; N, 20.28. Found: C, 57.92; H, 6.29; N, 20.02.

Similarly, *p-decyloxyacetophenone 4-methylthiosemicarbazone* (**23**), m.p. 114–114.5°, and *benzaldehyde 4,4-dimethylthiosemicarbazone* (**25**), m.p. 167–168° (lit. (8) m.p. 161–162°), were prepared and gave satisfactory elemental analyses.

Results and Discussion

Infrared Spectra

The asymmetric and symmetric NH_2 stretching modes were observed in N^4-unsubstituted isothiosemicarbazones (**1–14**) as two sharp bands near 3500 and 3380 cm^{-1} in carbon tetrachloride at a concentration of 0.02 *M* (Table 1). In this concentration and even at 0.15–0.2 *M*, no bands due to associated species in the N—H stretching region were observed. If the N^4-unsubstituted isothiosemicarbazones were in the imino form, there would be a νN^4—H absorption near 3375 cm^{-1} as observed for the N^2-methyl compounds **20** and **21** and a νN^2—H absorption near 3380 cm^{-1} or lower as observed in the thiosemicarbazones **23–25** (Table 3). Consequently the much higher absorptions of 3501–3496 cm^{-1} exhibited by the compounds **1–14** could not be explained by an imino structure. The N^4-unsubstituted isothiosemicarbazones should thus exist predominantly in the amino structure in solution. With a few exceptions (**11–13**), they showed two to four bands in the N—H stretching region in the solid state of which at least one band appeared at frequencies higher than 3412 cm^{-1}. By analogy with the vibrational behavior of thiosemicarbazones (9), the N^4-unsubstituted isothiosemicarbazones also exist predominantly or exclusively in the amino structure in the solid state taking into account their sharp melting points. The absence of any band higher than 3345 cm^{-1} in **11–13** may be ascribed to strong intermolecular bonding rather than their existence in the imino form, in view of a general tendency (9*a*, 10) that the terminal NH_2 group of lower aliphatic thiosemicarbazones absorbs at relatively lower frequencies than those of aromatic series.

Two N—H bands (Table 4, columns 2 and 3) between the original bands (Table 4, columns 1 and 4) and four N—D bands were observed in the spectra of partially deuterated N^4-unsubstituted isothiosemicarbazones. If the original bands had been due to hydrogen attached to different nitrogen atoms, partial deuteration

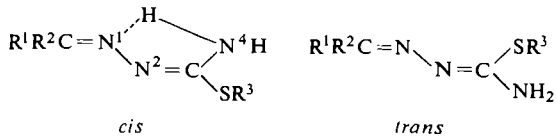

FIG. 1. *Cis* and *trans* isothiosemicarbazones.

would not give rise to such intermediate N—H bands (11). Thus the new N—H bands and the corresponding two N—D bands (Table 4, columns 7 and 8) could unambiguously be assigned to the NHD group. The remaining two N—D bands (Table 4, columns 6 and 9) increased in intensity at higher degrees of deuteration and were assigned to the vas and vs of ND_2 group, respectively. The two N—H bands arising from the NHD group indicate that the original amino group comprises nonequivalent N—H bonds, and from the magnitude of 48–62 cm^{-1} of the band separations ($\Delta\nu$) it may be deduced that the nonequivalency is ascribed to intramolecular hydrogen bonding (12). Thus the *cis* structure may be proposed for the predominant species of N^4-unsubstituted isothiosemicarbazones (Fig. 1). A *trans* form, which cannot hydrogen bond internally is expected to have equivalent N^4—H bonds and therefore a single absorption due to the NHD group at the mean of the vas and vs of the original NH_2 group. Such a band, however, was too weak to identify in the present spectra and in n.m.r. spectroscopy on the N^4-unsubstituted series, only **1**, **4**, and **7** showed two peaks of methylthio or methylenethio protons corresponding to the *cis* and *trans* structures in carbon tetrachloride (Table 5). In **11** and **13** the *trans* methyl peaks could not be identified because the region overlapped other proton resonances.

Proton Magnetic Resonance Spectra

4-Methyl isothiosemicarbazones **15–19** showed two sets of n.m.r. signals. The *N*-methyl protons appeared as two doublets at δ 2.39–2.53 (J = 5.2–5.6 Hz) and at 2.64–2.79 (J = 4.5–4.6 Hz) in benzene or at δ 2.86–2.92 (J = 5.4–5.8 Hz) and at 3.03–3.15 (J = 4.6–5.1 Hz) in pyridine while the methylthio or methylenethio protons appeared as two singlets corresponding to the *N*-methyl doublets in intensity ratio. Because each *N*-methyl doublet collapsed to a singlet on addition of deuterium oxide, the 4-methyl compounds exist essentially in the amino form and two molecular species having an $NHCH_3$ grouping should be present in solution. The

Can. J. Chem. Downloaded from www.nrcresearchpress.com by 210.87.254.5 on 09/05/12
For personal use only.

TABLE 5. Chemical shifts of isothiosemicarbazones (δ p.p.m. from TMS)

					SCH_3		SCH_2		NCH_3	
Compound	R^1	R^2	R^3	Solvent	*Cis*	*Trans*	*Cis*	*Trans*	*Cis*	*Trans*
1	C_6H_5	H	CH_3	$CDCl_3$	2.47	—	—	—	—	—
				CCl_4	2.44	2.28	—	—	—	—
				C_6H_6	2.30	1.70	—	—	—	—
3	C_6H_5	CH_3	CH_3	$CDCl_3$	2.49	—	—	—	—	—
				CCl_4	2.46	?	—	—	—	—
				C_6H_6	2.36	1.62	—	—	—	—
15	C_6H_5	H	CH_3	$CDCl_3$	2.50	2.32	—	—	2.95	3.00
				CCl_4	2.50	2.29	—	—	2.97	2.97
				C_6H_6	2.36	1.70	—	—	2.49	2.74
5	*p*-$CH_3OC_6H_4$	H	CH_3	$CDCl_3$	2.47	—	—	—	—	—
				CCl_4	2.42	—	—	—	—	—
				C_6H_6	2.30	1.68	—	—	—	—
7	*p*-$CH_3OC_6H_4$	CH_3	CH_3	$CDCl_3$	2.53	—	—	—	—	—
				CCl_4	2.46	2.29	—	—	—	—
				C_6H_6	2.43	1.73	—	—	—	—
18	*p*-$CH_3OC_6H_4$	H	CH_3	$CDCl_3$	2.48	2.31	—	—	2.94	2.98
				CCl_4	2.43	2.30	—	—	2.93	2.93
				C_6H_6	2.39	1.76	—	—	2.53	2.79
2	C_6H_5	H	$CH_2C_6H_5$	$CDCl_3$	—	—	4.37	—	—	—
16	C_6H_5	H	$CH_2C_6H_5$	$CDCl_3$	—	—	4.38	4.08	2.89	2.89
				CCl_4	—	—	4.33	4.02	2.85	2.85
				C_6H_6	—	—	4.50	3.73	2.44	2.67
4	C_6H_5	CH_3	$CH_2C_6H_5$	$CDCl_3$	—	—	4.39	4.09	—	—
				CCl_4	—	—	4.28	3.92	—	—
				C_6H_6	—	—	4.33	3.62	—	—
17	C_6H_5	CH_3	$CH_2C_6H_5$	$CDCl_3$	—	—	4.44	4.07	2.89	2.89
				CCl_4	—	—	4.34	3.98	2.88	2.88
				C_6H_6	—	—	4.42	3.49	2.39	2.64

appearance of the α-methyl protons of **17** as a sharp singlet precludes the possibility of *syn–anti*[1] isomerism about the C=N[1] double bond in view of the fact that the two methyl groups of **12** and **14** appeared as two singlets separated by 2.0 Hz. The aldehydic protons (R^2 = H) of 4-methyl compounds were frequently found to be accompanied by a small peak about 1–3 Hz apart, which values are much smaller than those expected from *syn–anti* isomerism as in acetaldehyde semicarbazone and thiosemicarbazone (13). In carbon tetrachloride and chloroform-*d*, the differences in chemical shifts for the two peaks of methylthio or methylenethio protons are much larger than those[2] of the *N*-methyl protons (Table 5), suggesting that the isomerism will be about the N^2=C bond. In benzene, the methylthio or methylenethio proton resonances for a *trans* form exhibit a greater upfield shift than those for a *cis* form, whereas the upfield shift of the *N*-methyl proton signals is larger for the *cis* form (Table 5). As has been discussed by many investigators (14), these solvent shift effects may be explained by the structure of a collision complex in which the lone electron pair on the N^2 atom[3] is as far away from the center of the benzene ring as possible in both configurations about the N^2=C bond. Although the ^{13}C—H coupling constant (15) of 139 Hz obtained for the N—CH_3 protons of benzaldehyde 4,4,*S*-trimethylisothiosemicarbazone (**22**) could offer

[1]The terms *syn* and *anti* are used in this paper to designate the relationship between R^1 (or R^2) and N^2 about the C=N^1 double bond.

[2]In these solvents, the two doublets almost completely overlap to form an apparently single doublet, so that the differences in chemical shifts are equal to zero.

[3]The N^2 atom was believed to be most nucleophilic as shown by the preferential methylation of **1** and **5** with methyl iodide at this position to give **20** and **21**, respectively.

Can. J. Chem. Downloaded from www.nrcresearchpress.com by 210.87.254.5 on 09/05/12
For personal use only.

Can. J. Chem. Downloaded from www.nrcresearchpress.com by 210.87.254.5 on 09/05/12
For personal use only.

a possibility of observable hindered rotation about the C—N^4 bond, the protons gave rise to only a single resonance signal at the same probe temperature. This indicates rapid rotation about the C—N^4 bond at that temperature because the two conformationally different positions for the *N*-methyl groups should be magnetically non-equivalent. The preferred form of 4-methyl series, however, will predominantly involve a conformation stabilized by internal hydrogen bonding. Thus the *cis–trans* isomerism about the N^2=C double bond should account for the existence of two molecular species for isothiosemicarbazones and all the isothiosemicarbazones examined may probably exist in only one isomeric form in terms of *syn–anti* isomerism about the C=N^1 double bond.

Of the two signals from the methylthio or methylenethio protons observed in the n.m.r. spectra of compounds **1–18** (Table 5), the resonances at lower magnetic fields appeared at chemical shifts agreeing essentially with those of the corresponding N^4-unsubstituted compounds which exist substantially in the *cis* configuration, and therefore are reasonably assigned to those from the *cis* form while the signals at higher magnetic fields were assigned to the *trans* configuration. The assignment of the *N*-methyl signals is based on the peak intensity. Further strength for this assignment comes from observations that 4-methyl compounds absorb in the infrared at two different N—H stretching frequencies in a dilute carbon tetrachloride solution (Table 2) and that two NH proton resonances occurred at δ 6.20–6.50 and at δ 4.14–4.33 in chloroform-*d*, with respective peak intensities being approximately in accord with the relative intensity of the two methylthio or methylenethio proton peaks. The NH absorption at higher frequencies and the upfield resonance of the NH protons are unambiguously responsible for the unbonded NH group in the *trans* configuration, whereas the NH absorption at lower frequencies and the downfield resonance of the NH protons are responsible for the internally bonded NH group in the *cis* structure. The *cis*/*trans* ratio was strongly solvent dependent, with a ratio of 90:10 in carbon tetrachloride, 77:23 in chloroform-*d*, 49:51 in pyridine, or 30:70 in dimethylsulfoxide-d_6 being observed in compound **15**. In solution the equilibration is reached rapidly, with each peak intensity of a freshly prepared solution being identical to that of the solution after 24 h at ordinary temperature.

To conclude, the following information has been extracted from the i.r. and n.m.r. spectra of a number of aromatic and aliphatic isothiosemicarbazones. (*i*) Isothiosemicarbazones, except N^2-substituted ones, exist exclusively in the amino structure. (*ii*) N^4-Unsubstituted isothiosemicarbazones predominantly have the configuration in which N^1 lies *cis* to N^4 about the N^2=C double bond with intramolecular hydrogen bonding. (*iii*) N^4-Monosubstituted isothiosemicarbazones exist invariably in two configurations in which N^1 lies either *cis* or *trans* to N^4 about the N^2=C bond, with the *cis*/*trans* ratios varying in dependence of the solvent used.

The author wishes to thank Miss Masako Megata for her technical assistance.

1. R. R. Shagidullin, F. K. Sattarova, G. K. Budnikov, and Vu.P. Kitaev. Izu. Akad. Nauk. SSSR. Ser. Fiz. **26**, 1301 (1962).
2. E. Hoggarth. J. Chem. Soc. 1160 (1949).
3. F. J. Wilson and R. Burns. J. Chem. Soc. 121, 870 (1922).
4. F. Kurzer and K. Douraghi-Zadeh. J. Chem. Soc. 932 (1965).
5. B. A. Gingras, R. L. Somorjai, and C. H. Bayley. Can. J. Chem. **39**, 973 (1961).
6. E. Cattelain. Bull. Soc. Chim. Fr. **12**, 39 (1945).
7. J. McLean and F. J. Wilson. J. Chem. Soc. 1048 (1939).
8. E. Lieber, C. N. Pillai, and R. D. Hites. Can. J. Chem. **35**, 832 (1957).
9. (*a*) B. A. Gingras, R. W. Hornal, and C. H. Bayley. Can. J. Chem. **38**, 712 (1960); (*b*) D. M. Wiles and T. Suprunchuk. Can. J. Chem. **47**, 1087 (1969).
10. P. W. Sadler. J. Chem. Soc. 957 (1961).
11. (*a*) N. Bacon, A. J. Boulton, R. T. C. Brownlee, A. R. Katritzky, and R. D. Topsom. J. Chem. Soc. B, 5230 (1965); (*b*) A. J. Boulton and A. R. Katritzky. Tetrahedron, **12**, 51 (1961).
12. (*a*) A. G. Moritz. Spectrochim. Acta, **18**, 671 (1962); (*b*) L. J. Bellamy and R. J. Pace. Spectrochim. Acta, **28**A, 1869 (1972).
13. G. J. Karabatsos, F. M. Vane, R. A. Taller, and N. Hsi. J. Am. Chem. Soc. **86**, 3351 (1964).
14. (*a*) J. V. Hatton and R. E. Richards. Mol. Phys. **3**, 253 (1960); (*b*) L. A. LaPlanche and M. T. Rogers. J. Am. Chem. Soc. **86**, 337 (1964); (*c*) J. Ronayne and D. H. Williams. Chem. Commun. 712 (1966); J. Chem. Soc. B, 540 (1967); (*d*) G. J. Karabatsos and K. L. Krumel. Tetrahedron, **23**, 1097 (1967); (*e*) J. Sandstroem and B. Uppstroem. Acta Chem. Scand. **21**, 2254 (1967); (*f*) G. J. Karabatsos and R. A. Taller. Tetrahedron, **24**, 3923 (1968); (*g*) T. Yonezawa, I. Morishima, and K. Fukuta. Bull. Chem. Soc. Jap. **41**, 2297 (1968).
15. R. C. Neuman, Jr., and L. B. Young. J. Phys. Chem. **69**, 2570 (1965).

Can. J. Chem. Downloaded from www.nrcresearchpress.com by 210.87.254.42 on 09/05/12
For personal use only.

Catalyzed Orientation Reversals in Diels–Alder Reactions

ŽARKO STOJANAC, ROBERT A. DICKINSON, NADA STOJANAC, RONALD J. WOZNOW, AND ZDENEK VALENTA

Department of Chemistry, University of New Brunswick, Fredericton, New Brunswick, E3B 5A3

Received November 29, 1974

ŽARKO STOJANAC, ROBERT A. DICKINSON, NADA STOJANAC, RONALD J. WOZNOW, and ZDENEK VALENTA. Can. J. Chem. **53**, 616 (1975).

Lewis acid catalysts cause an orientation reversal in the Diels–Alder additions of 2,6-dimethyl-1,4-quinone (**1**) and toluquinone (**12**) to 1-substituted 1,3-butadienes and to 1,2- and 1,3-dialkyl dienes. These results are explained by the preferential formation of one reactive quinone – Lewis acid salt.

ŽARKO STOJANAC, ROBERT A. DICKINSON, NADA STOJANAC, RONALD J. WOZNOW et ZDENEK VALENTA. Can. J. Chem. **53**, 616 (1975).

L'addition d'acides de Lewis comme catalyseurs cause un renversement de l'orientation lors des réactions d'addition de Diels–Alder entre d'une part la diméthyl-2,6 quinone-1,4 (**1**) et la toluquinone (**12**) et d'autre part des butadiènes-1,3 substitués en position 1 et des dialkyl-1,2 et -1,3 diènes. On explique ces résultats par la formation préférentielle d'un sel entre une quinone réactive et l'acide de Lewis. [Traduit par le journal]

We wish to report several cases of an efficient Lewis acid catalyzed (1, 2) orientation reversal in Diels–Alder reactions using alkylated 1,4-quinones as dienophiles. These results suggest that a closer attention to catalysis (or other substituent activation) will enlarge the synthetic utility of the Diels–Alder reaction (3–5) in certain cases; they are also relevant to the incompletely resolved question of the causes for preferred orientation (5–7).

Table 1 summarizes some of our most extreme cases. In all five additions listed, quinone (**1**) in the presence of Lewis acid (usually 1 mol/mol quinone) adds exclusively as indicated, while all five combinations of diene and dienophile give exclusively the expected 'normal' adducts of type **9** (4, 5) in a thermal addition in boiling benzene or toluene.[1] Thus, the catalyst achieves a complete orientation reversal in all five cases. The yields of pure products in these catalyzed additions are uniformly higher than 80%.[2]

Quinone (**1**) can thus be used for the preparation of adducts of either structural orientation. The simplest explanation of these results is the assumption that **1** complexes with the Lewis acid exclusively as indicated in **10** and that this activation then leads to the orientation shown.[3] In the thermal reactions, the generally observed dominance of the '*ortho*-rule' (4, 5) is followed and indicated in **11**. Thus, it is postulated that the cause of the reversal is simply a change of the dienophile to a more reactive

[1]Additional examples performed in this laboratory include a complete catalyzed reversal in addition of **1** to 2-methyl-1,3-pentadiene and a partial one in the total synthesis of ring-A aromatic steroids (8).

[2]In most cases lower temperatures than those listed can be used. Diene polymerization (with the exception of alkoxydienes) is slower than the addition under these conditions. Extraction of the acid with ice-water or ice-cold sodium bicarbonate does not epimerize the *cis* ring-juncture in the products. Configuration at C* of all products (*endo* addition) follows rigorously from synthetic studies in this laboratory.

[3]In frontier orbital reasoning (6, 7), it is plausible that, in combination (**10**), the bigger coefficient would be at * of the LU orbital of the complexed dienophile (7) and at * of the HO orbital of the diene (6).

TABLE 1. Catalyzed additions of 1,3-butadienes to 2,6-dimethyl-1,4-quinone

Diene	Dienophile	Catalyst	Temperature (°C)	Solvent	Product
	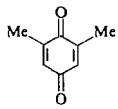 **1**	$BF_3 \cdot Et_2O$	0	Ether	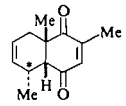 **2** (b.p. 88–90°/ 0.35 mm Hg
	1	$BF_3 \cdot Et_2O$	10	C_6H_6	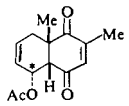 **3** (m.p. 98–100°)
	1	$BF_3 \cdot Et_2O$	20	CH_2Cl_2	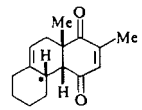 **4** (m.p. 85–87°)
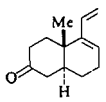 **5**	**1**	$AlCl_3$	−78	CH_2Cl_2	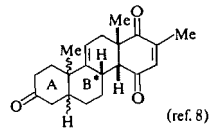 (ref. 8) **6** (m.p. 185–188°, 158–159°) (mixture of two diastereoisomers with A/B *trans* juncture)
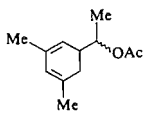 **7** (mixture of two diastereoisomers)	**1**	$BF_3 \cdot Et_2O$	20	Ether	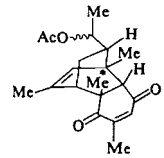 **8** (m.p. 123–126°, 155–156°) (mixture of two diastereoisomers)

TABLE 2. Reactions of toluquinone with *trans*-1,3-pentadiene

Temperature (°C)	Solvent	Catalyst	Ratio **14/13**	Reference
60–70	Dioxane	—	~1	10
0	Toluene	—	2.3	
24	Toluene	—	2.3	
111	Toluene	—	1.8	
24	Acetone	—	2.1	
0	Toluene	$BF_3 \cdot Et_2O$	0.45	

Can. J. Chem. Downloaded from www.nrcresearchpress.com by 210.87.254.42 on 09/05/12
For personal use only.

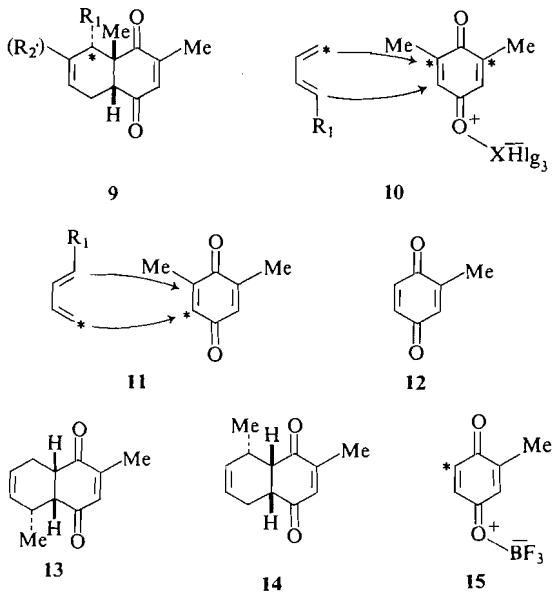

species (1, 2, 9) with a very different electronic distribution.

Synthetically, the above results are directly applicable only to the rather specialized 2,6-dialkylated quinones. Monoalkylated quinones obviously have wider applicability. It has been reported (10) that toluquinone (**12**) in dioxane reacts with *trans*-1,3-pentadiene to give two products, **13** and **14**, in an approximate 1:1 ratio.[4] Table 2 shows the results of our study of this addition. In toluene and acetone, **14** is the predominant thermal product, whereas **13** predominates on catalysis so that either adduct can be obtained in yields up to 60–70%.[5] Following the reasoning applied for additions in Table 1, it can be postulated that complex **15** is the predominant, but in this case not exclusive, reactive species. The result with toluquinone is thus in general accord with the results of Table 1 and indicates that improved yields of adducts of type **13** can be obtained by catalyzing additions of monoalkylated 1,4-quinones and 1-substituted butadienes.

The above results invite many extrapolations. It can, for example, be predicted that 2-substituted 1,3-butadienes will add to **1** (and similar quinones) giving '*meta*' adducts in a catalyzed reaction (see **16**); furthermore, replacement of the appropriate carbonyl group in an unsymmetrically substituted quinone by an imine

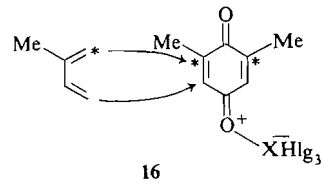

should lead to high regiospecificity in the desired direction in an acid-catalyzed reaction. Finally, it should be possible to use simple aliphatic dienophiles of type XCH=CHY and XCR=CHY, in which X and Y are conjugating and electron-withdrawing substituents, in a regioselective way by a drastic change in the electron demand of X or Y.

The support of this work by the National Research Council, Canada, in the form of an operating grant and a generous gift of a large quantity of **1** by the Hoffmann – La Roche Co., Nutley, N.J., are gratefully acknowledged. We thank Mr. M. S. Phang, a senior student at this University, for his experimental contribution to the toluquinone results.

1. P. YATES and P. EATON. J. Am. Chem. Soc. **82**, 4436 (1960).
2. G. I. FRAY and R. ROBINSON. J. Am. Chem. Soc. **83**, 249 (1961).
3. YU. A. TITOV. USSR Chem. Rev. **31**, 267 (1962).
4. A. S. ONISHCHENKO. Diene synthesis. Israel Program of Scientific Translations, Jerusalem. 1964.
5. J. SAUER. Angew. Chem. Int. Ed. Engl. **6**, 16 (1967).
6. K. N. HOUK. J. Am. Chem. Soc. **95**, 4092 (1973).
7. K. N. HOUK and R. W. STROZIER. J. Am. Chem. Soc. **95**, 4094 (1973).
8. R. A. DICKINSON, R. KUBELA, G. A. MACALPINE, Z. STOJANAC, and Z. VALENTA. Can. J. Chem. **50**, 2377 (1972).
9. J. SAUER, D. LANG, and H. WIEST. Chem. Ber. **97**, 3208 (1964); E. F. LUTZ and G. M. BAILEY. J. Am. Chem. Soc. **86**, 3899 (1964); T. YNUKAI and M. KASAI. J. Org. Chem. **30**, 3567 (1965).
10. M. TISHLER, L. F. FIESER, and N. L. WENDLER. J. Am. Chem. Soc. **62**, 2866 (1940).
11. M. F. ANSELL, G. C. CULLING, B. W. NASH, D. A. WILSON, and J. W. LOWN. Proc. Chem. Soc. 405 (1960).

[4]Unless the substituent is strongly electron withdrawing (11), monosubstituted quinones add exclusively at their unsubstituted side.

[5]The mixtures were analyzed by aromatizing the adducts, converting the resulting mixture of hydroquinones into disilyl ethers and analysing these by g.l.c. Pure **14** was also obtained by fractional crystallization (m.p. 98–99°) (10) and subjected separately to the aromatization sequence.

Can. J. Chem. Downloaded from www.nrcresearchpress.com by 210.87.254.42 on 09/05/12
For personal use only.

A Synthetic Approach to Quassin. Introduction of Functionality and Stereochemistry by a Diels–Alder Reaction

NADA STOJANAC, ASHWANI SOOD, ŽARKO STOJANAC, AND ZDENEK VALENTA
Department of Chemistry, University of New Brunswick, Fredericton, New Brunswick E3B 5A3

Received December 5, 1974

NADA STOJANAC, ASHWANI SOOD, ŽARKO STOJANAC, and ZDENEK VALENTA. Can. J. Chem. **53**, 619 (1975).

Using a Lewis acid catalyzed Diels–Alder reaction as the key step, the crystalline synthetic intermediate (**17**) has been prepared. Compound **17** contains all C-atoms of quassin (**1**) and stereochemistry and 0-functionality suitable for the conversion into **1**.

NADA STOJANAC, ASHWANI SOOD, ŽARKO STOJANAC et ZDENEK VALENTA. Can. J. Chem. **53**, 619 (1975).

On a préparé l'intermédiaire synthétique cristallin (**17**) en faisant appel dans l'étape déterminante à une réaction de Diels–Alder catalysée par un acide de Lewis. Le composé **17** contient tous les atomes de carbone de la quassine (**1**) de même qu'une stéréochimie et une fonctionnalisation sur l'oxygène susceptibles d'amener sa transformation en **1**.

[Traduit par le journal]

Can. J. Chem. Downloaded from www.nrcresearchpress.com by 210.87.254.40 on 09/05/12
For personal use only.

An efficient total synthesis of quassin (**1**) (1–3), the bitter principle of *Quassia amara*, should clearly involve a planned introduction of its oxygen functionality as well as a simple solution of its relatively complex stereochemistry. Of the seven chiral centers present, those marked * in formula **1** are particularly crucial synthetically. The remaining three, marked •, can be established in later stages of the synthesis since neoquassin (**2**) has been found to deuterate at these positions in base without epimerization (1, 2). We now wish to report a synthetic strategy which illustrates the use of a catalytic orientation reversal in Diels–Alder reactions (4), solves the stereochemistry at the four C*'s, and provides for the development of the desired oxygen functionality.

A reaction of diene (**3**)[1] with quinone (**4**) and boron trifluoride etherate (1:1:1) in ether at room temperature gives two crystalline compounds (**5**), m.p.'s 123–124° and 155–156°, respectively, in over 80% yield.[2] These are epimeric only at C—OAc, since acetate hydrolysis and oxidation of both of them gives the same methyl ketone. A rigorous proof of structure and stereochemistry of **5** is given below. It should be noted that the catalyst has directed the addition exclusively *against* the well-established "*ortho* and *para* rules" of diene addition (5, 6). Thermal reaction of **3** and **4** gives two different adducts in a very low yield (<10%) and no trace of **5**.

Reaction of **5** (m.p. 123–124°) with zinc in acetic acid reduces the conjugated double bond to give **6**, m.p. 138–152°.[3] Reduction of **6** with sodium borohydride in ethanol and water at 5° then gives ketoalcohol (**7**), m.p. 100–101°, which on continued reduction at room temperature yields diol (**8**). Without purification, **8** is con-

[1]Compound **3** is prepared by the addition of methyl vinyl ketone to 2-methylpenta-1,3-diene, epimerization in base, reduction with sodium borohydride, acetylation, bromination with Br_2, and dehydrobromination with collidine. The resulting diene is a mixture containing about 40% of the desired **3** (as a mixture of the two possible diastereoisomers) and 60% of dienes containing an exocyclic double bond (n.m.r. analysis). Separation proved impractical because of diene instability. Only cisoid diene (**3**) reacts in the Diels–Alder reaction; no adducts in addition to **5** are found on extensive chromatography.

[2]Yield is based on estimated content of **3** in the diene mixture. Compound **5** and all its transformation products reported here give the expected analytical and spectral data. All reported synthetic compounds are racemic.

[3]This and all subsequent reactions have been performed separately on the two epimers of **5** as well as on their mixture. For simplicity, only one (the major one), of the two epimeric series is given. It should be noted that the two series join at stage **12**.

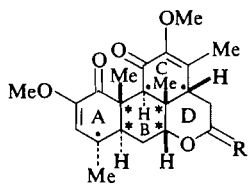

1 R = O
2 R = H,OH

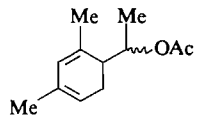

3

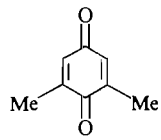

4

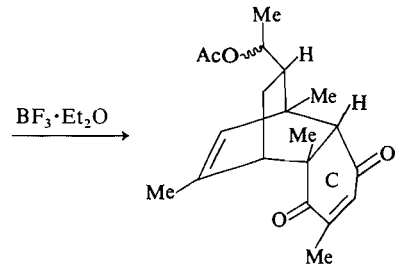

5

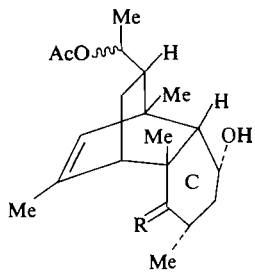

7 R = O

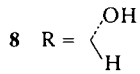

8

verted into cyclic ether (**9**) with *N*-bromosuccinimide in +-butanol and sulfuric acid. The three new chiral centers in ring C of **8** and **9** are formed stereospecifically and their configuration follows from n.m.r. analysis and subsequent reactions.[4] Oxidation of crude **9** with Collins' reagent (7) gives ketone (**10**), m.p. 157–158°,

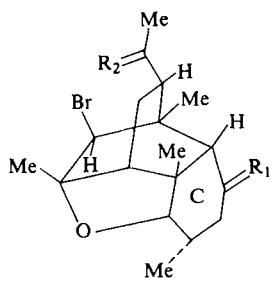

9

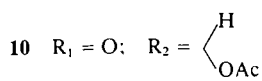

10

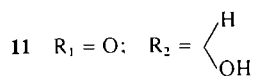

11

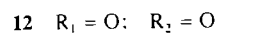

12

which on prolonged treatment with hydrochloric acid in methanol yields alcohol (**11**), m.p. 138–139°. Oxidation of **11** with Collins' reagent (7) leads to the diketone (**12**), m.p. 120–122°, which is also obtained in the same way from the second epimer of **5** and which undergoes a quantitative epimerization to diketone (**13**), m.p. 136–138°, on treatment with potassium carbonate in methanol at room temperature. The overall yield of the seven steps leading from adduct (**5**) to diketone (**13**) is 30%.

Ethoxyethynyl magnesium bromide attacks the methyl ketone of **13** preferentially to give **14**, m.p. 150–152° (dec.), which rearranges on treatment with oxalic acid to the oily ester (**15**). Hydrogenation of **15** with platinum in ethanol then leads to the desired saturated ester **16**. Treatment of **16** with zinc powder in boiling methanol cleanly reforms the original double bond to give **17**, m.p. 96–97°.[5]

It should now be noted that **17** and its derivatives are related to compounds of type **18** by a simple double-bond cleavage[6] and that **18** contains all C-atoms of quassin, the correct stereochemistry at all four C*'s, as well as suitable functionality to complete the synthesis of **1**.

The following cyclization, retro-Michael reaction sequence rigorously establishes the structure of **5**. Treatment of ketone (**10**) (mixture

[4]On treatment of **9** with sodium hydride in benzene, for instance, a pentacyclic compound is formed by a displacement of bromine by the secondary hydroxyl group. Thus, both OH groups in **8** must be *endo* and the ether ring in **9** must be five membered.

[5]Both possible geometric isomers of **15** and C—CH_3 diastereoisomers of **16** are obtained, one in very small quantity. The minor epimer is removed in recrystallization of **17**.

[6]Preliminary study in this laboratory has shown that the ozonolysis of the isolated double bond in compounds related to **7** and **17** is very facile.

Can. J. Chem. Downloaded from www.nrcresearchpress.com by 210.87.254.40 on 09/05/12
For personal use only.

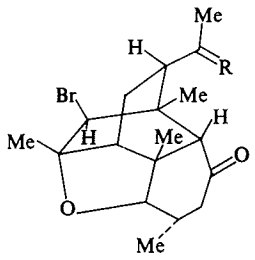

13 R = O

14 R =

15 R = CH—COOEt

16 R = 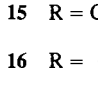

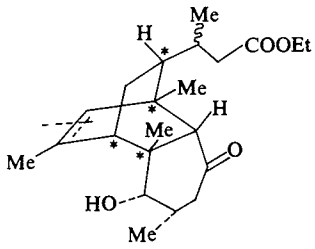

17

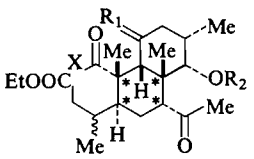

18 X = H or OR
R_1 = O or blocked O

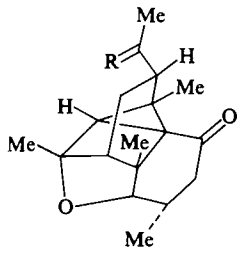

19 R = 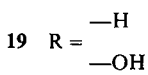

20 R = O

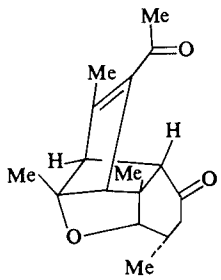

21

of epimers) with sodium hydroxide in aqueous methanol gives a high yield of cyclopropyl ketone (**19**), m.p. of one epimer 176–177°; i.r.$_{max}$ ($CHCl_3$) 1700 cm^{-1}; λ_{max} 212 nm (ε 2100); n.m.r. two low-field H's at τ 5.70 (1H, q), 6.37 (1H, unresolved d). Collins' oxidation of **19** yields diketone (**20**), m.p. 111–112°; λ_{max} 211 nm (ε 1950), which on treatment with potassium carbonate in hot methanol gives diketone (**21**), m.p. 123–124°; λ_{max} 258 nm (ε 6480); n.m.r. ($CDCl_3$) no olefinic H, signals at τ 6.25 (1H, d), 7.75 (3H, s), 8.02 (3H, narrow t), 8.65 (3H, s), 8.88 (3H, d), 8.95 (3H, s).

The geometry of ring C in **5** (*endo*-addition) follows from the formation of cyclic ethers **9–16** and from the fact that the expected cage cyclobutane is formed on exposure of **5** to u.v. light (8). The geometry of attachment of the acetoxyethyl side chain in **5** follows from n.m.r. data which show that the secondary methyl group is shielded by the isolated double bond and from the quantitative epimerization **12** → **13**.

Support of this work by the National Research Council of Canada, Ottawa, and a generous gift of quinone (**4**) by the Hoffmann-LaRoche Co., Nutley, N.J., are gratefully acknowledged.

1. Z. Valenta, S. Papadopoulos, and C. Podešva. Tetrahedron, **15**, 100 (1961).
2. Z. Valenta, A. H. Gray, D. E. Orr, S. Papadopoulos, and C. Podešva. Tetrahedron, **18**, 1433 (1962).
3. R. M. Carman and A. D. Ward. Tetrahedron Lett. 317 (1961); Aust. J. Chem. **15**, 807 (1962).
4. R. A. Dickinson, R. Kubela, G. A. MacAlpine, Z. Stojanac, and Z. Valenta. Can. J. Chem. **50**, 2377 (1972).
5. J. Sauer. Angew. Chem. Int. Ed. Engl. **6**, 16 (1967).
6. A. S. Onishchenko. Diene synthesis. Israel Program of Scientific Translations, Jerusalem. 1964.
7. J. C. Collins, W. W. Hess, and F. J. Frank. Tetrahedron Lett. 3363 (1968).
8. R. C. Cookson, E. Crundwell, and J. Hudec. Chem. Ind. 1003 (1958).

Can. J. Chem. Downloaded from www.nrcresearchpress.com by 210.87.254.40 on 09/05/12
For personal use only.

Can. J. Chem. Downloaded from www.nrcresearchpress.com by 210.87.254.6 on 09/05/12
For personal use only.

Canadian Journal of Chemistry

Published by
THE NATIONAL RESEARCH COUNCIL OF CANADA

Journal canadien de chimie

Publié par
LE CONSEIL NATIONAL DE RECHERCHES DU CANADA

Volume 53 Number 5 March 1, 1975 Volume 53 numéro 5 1 mars 1975

A Kinetic Electron Spin Resonance Study of the Transfer of a Hydrogen Atom from α-Tetralin Hydroperoxide to a Tertiary Alkylperoxy Radical[1]

J. H. B. CHENIER AND J. A. HOWARD

Division of Chemistry, National Research Council Canada, Ottawa, Canada K1A 0R9

Received September 16, 1974

J. H. B. CHENIER and J. A. HOWARD. Can. J. Chem. **53**, 623 (1975).

A kinetic electron spin resonance spectroscopic study of the reaction of tertiary alkylperoxy radicals with α-tetralin hydroperoxide is reported. The absolute rate constants for this hydrogen atom transfer process (k_1) are given by the equation $\log (k_1/M^{-1}\,s^{-1}) = (6.0 \pm 0.5) - (4.5 \pm 0.5)/\theta$, where $\theta = 2.303\,RT$ kcal mol^{-1}.

A significant isotope effect is obtained when the hydroperoxidic hydrogen is replaced by deuterium, *e.g.* k_1^H/k_1^D at 21° = 9.

Other alkyl hydroperoxides, *e.g.* triphenylmethyl, *s*-butyl, and 9,10-dihydro-9-anthracyl have approximately the same reactivity to *t*-ROO· as α-$C_{10}H_{11}$ OOH.

J. H. B. CHENIER et J. A. HOWARD. Can. J. Chem. **53**, 623 (1975).

On rapporte une étude cinétique, effectuée par résonance paramagnétique électronique, de la réaction des radicaux alkylperoxy tertiaires avec l'hydroperoxyde de l'α-tétraline. Les constantes de vitesse absolues pour ce transfert d'atome d'hydrogène (k_1) sont représentées par l'équation $\log(k_1/M^{-1}\,s^{-1}) = (6.0 \pm 0.5) - (4.5 \pm 0.5)/\theta$, où $\theta = 2.303\,RT$ en kcal/mol^{-1}.

On obtient un effet isotopique important quand l'hydrogène de l'hydroperoxyde est remplacé par un deutérium; la valeur de k_1^H/k_1^D à 21° = 9.

D'autres hydroperoxydes en série alkylée, *e.g.* triphénylméthyle, *s*-butyle et dihydro-9,10 anthracyle-9 ont approximativement la même réactivité que l'α-$C_{10}H_{11}$ OOH vis à vis le radical *t*-ROO·.

[Traduit par le journal]

Introduction

Several investigations (1–8) have shown that the preexponential factors and activation energies for endothermic and thermoneutral H-atom transfer reactions between two oxyl radicals are significantly smaller[2] than the Arrhenius parameters that are usually associated with bimolecular reactions (10). A reaction of this class, for which there is little reliable kinetic data, is the nearly thermoneutral transfer of an H-atom from an alkyl hydroperoxide to an alkylperoxy radical. In order to rectify this situation we report in this paper the results of a kinetic electron spin resonance spectroscopic study of the reaction of α-tetralin hydroperoxide with tertiary alkylperoxy radicals, *t*-ROO·.

[1] *t*-ROO· + 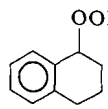 $\xrightarrow{k_1}$ *t*-ROOH + 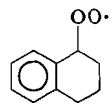

[1]NRCC No. 14379.

[2]The only exception would appear to be the exchange reaction between di-*t*-butyliminoxy and di-*t*-butyloxime (9).

Can. J. Chem. Downloaded from www.nrcresearchpress.com by 210.87.254.6 on 09/05/12
For personal use only.

Experimental Section

Materials

α-Tetralin hydroperoxide (11) and 9,10-dihydro-9-hydroperoxyanthracene (12) were prepared by atmospheric autoxidation of tetralin and 9,10-dihydroanthracene and were purified by repeated recrystallization from hexane and toluene, respectively. *s*-Butyl hydroperoxide was prepared by the method of Williams and Mosher (13) and triphenylmethyl hydroperoxide by the method of Bissing *et al.* (14). All the hydroperoxides were close to 100% pure by iodometric titration.

Kinetic Procedure

t-Butylperoxy radicals were generated by photolysis of 2,2′-azoisobutane (0.02 *M*) in oxygen saturated isopentane and 2-ethyl-2-propylperoxy radicals were produced by photolysis of di-*t*-butyl peroxide (5%) in oxygen saturated isopentane. Photolyses were carried out in the presence of an alkyl hydroperoxide (0.0001–0.005 *M*) from −83 to +25 °C. The radical concentration was followed with respect to time, after the initiating light was shuttered, by kinetic electron spin resonance spectroscopy (15). In a few experiments at −80° the hydroperoxide was added after the radicals had been generated and the light switched off. In these cases radical decays were followed after complete mixing of the reactants had been achieved by bubbling oxygen through the solution. Stoichiometric factors, *n*, (*i.e.*, the number of radicals destroyed by each molecule of hydroperoxide) were determined by a similar technique except that a fraction (Δ[*t*-ROO·]) of a known concentration of *t*-alkylperoxy radicals was destroyed by a known concentration of hydroperoxide, [ROOH] ($n = \Delta$[*t*-ROO·]/[ROOH]).

Results and Discussion

The characteristic e.s.r. spectrum of an alkylperoxy radical was obtained when 2,2′-azoisobutane was photolyzed in the presence of α-tetralin hydroperoxide in an oxygen saturated solvent (usually isopentane or isopentane–trichlorofluoromethane 1:1 by volume) from −83 to +25 °C (broad singlet at $g = 2.015$). The steady state radical concentration ($[ROO\cdot]_{ss}$) was shown to be proportional to the first power of the intensity of the light (and consequently proportional to the first power of the rate of radical production, R_i,) and inversely proportional to the first power of the concentration of α-$C_{10}H_{10}OOH$, *i.e.*,

$$[ROO^{\cdot}]_{ss} \propto \frac{R_i}{[\alpha\text{-}C_{10}H_{11}OOH]}$$

This indicates that the alkylperoxy radical detected in this system was *t*-butylperoxy and not α-tetralylperoxy or a mixture of these two radicals. This is not unexpected as the termination rate constant for self-reaction of $(CH_3)_3COO^{\cdot}$ is $\sim 10^3$ times smaller than the rate constant for self-reaction of α-$C_{10}H_{11}OO^{\cdot}$ and the expected cross-termination rate constant for these two radicals (16).

Rates of disappearance of $(CH_3)_3COO^{\cdot}$ were exactly first-order with respect to the radical concentration and bimolecular rate constants were independent of the concentration of α-$C_{10}H_{11}OOH$. Two peroxy radicals were destroyed by each molecule of hydroperoxide.[3] The following rate law was, therefore, strictly obeyed.

$$[2] \quad \frac{-d[(CH_3)_3COO^{\cdot}]}{dt} = 2k_1[(CH_3)_3COO^{\cdot}][\alpha\text{-}C_{10}H_{11}OOH]$$

Rates of disappearance of the 2-ethyl-2-propylperoxy radical also obeyed eq. 2 and values of k_1 for this radical were identical to the values obtained for $(CH_3)_3COO^{\cdot}$.

Absolute values of the pseudo first-order rate constant k_ψ obtained at different hydroperoxide concentrations at −76 and +22 °C are listed in Table 1 while average values of the bimolecular rate constant k_1 obtained from −83 to +25 °C are summarized in Table 2. The plot of log $(k_1/M^{-1}\ s^{-1})$ against the reciprocal of the absolute temperature is shown in Fig. 1 and yielded the Arrhenius equation

$$[3] \quad \log (k_1/M^{-1}\ s^{-1}) = (6.0 \pm 0.5) - (4.5 \pm 0.5)/\theta$$

where $\theta = 2.303\ RT$ kcal mol^{-1}.[4]

It is conceivable that the reactivity of α-$C_{10}H_{11}OOH$ could be influenced by self-association, particularly at the lower temperatures; E_1 would then be overestimated. If it is assumed that the thermodynamic parameters for self-association of α-$C_{10}H_{11}OOH$ are similar to the values reported by Walling and Heaton (17) for $(CH_3)_3COOH$ ($-\Delta H^0 = 5.95$ kcal mol^{-1} and $-\Delta S^0 = 18.4$ e.u.), α-$C_{10}H_{11}OOH$ should be significantly self-associated at for example −76°. The invariance of k_1 from 0.0025 to 0.025 *M* hydroperoxide at this temperature implies, however, that our values of k_1 are not seriously affected by self-association of α-$C_{10}H_{11}OOH$.

[3]A stoichiometric factor of 2.0 indicates that the α-tetralylperoxy radical formed in reaction 1 is removed by reaction with a *t*-butylperoxy radical.

[4]Rate constants at any one temperature were reproducible to within a factor of 2 over a range of hydroperoxide concentrations. The maximum errors for the activation energy and preexponential factor are 0.5 kcal mol^{-1} and 0.5 log units, respectively.

TABLE 1. Kinetic data for reaction of $(CH_3)_3COO^{\cdot}$ with α-tetralin hydroperoxide

Temperature (°C)	10^3[α-$C_{10}H_{11}$ OOH] (M)	k_ψ (s^{-1})	$\frac{k_\psi}{[\alpha\text{-}C_{10}H_{11}OOH]}$ ($M^{-1}\,s^{-1}$)
−76	2.5	0.09	36
−76	5.0	0.27	54
−76	12	0.59	49
−76	25	0.77	31
25	0.29	0.38	1300
25	0.77	1.15	1500

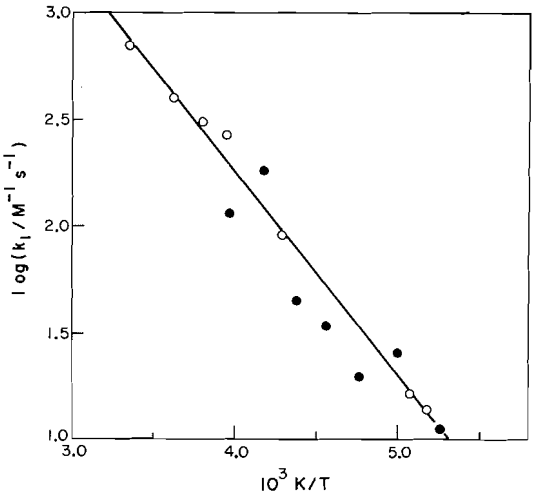

FIG. 1. A plot of log ($k_1/M^{-1}\,s^{-1}$) *vs.* the reciprocal of the absolute temperature for reaction of $(CH_3)_3COO^{\cdot}$ (●) and $C_2H_5C(CH_3)_2OO^{\cdot}$ (○) with α-$C_{10}H_{11}$ OOH.

TABLE 2. Absolute rate constants for reaction of $CH_3COO^{\cdot}$ and $C_2H_5C(CH_3)_2OO^{\cdot}$ with α-tetralin hydroperoxide in isopentane

Temperature (°C)	k_1 ($M^{-1}\,s^{-1}$)
25	700[b]
3	400[b]
−10	310[b]
−20	270[b]
−21	116[a]
−33	183[a]
−40	90[b]
−43	45[a]
−54	34[a]
−63	20[a]
−73	26[a]
−76	21[a]
−76	16.5[b]
−80	14[b]
−83	11.2[a]

[a]With $(CH_3)_3COO^{\cdot}$.
[b]With $C_2H_5C(CH_3)_2OO^{\cdot}$.

Rate constants for reaction of *t*-ROO· with α-$C_{10}H_{11}$OOH at 30° (k_1 = 568 $M^{-1}\,s^{-1}$) and 56° (k_1 = 1025 $M^{-1}\,s^{-1}$) calculated from eq. 3 are in excellent agreement with the rate constants that have been reported (18) for reaction of the cumylperoxy radical (which is also a tertiary alkylperoxy radical) with α-$C_{10}H_{11}$ OOH at these temperatures (600 and 1100 $M^{-1}\,s^{-1}$).

The *A*-factor for reaction of *t*-ROO· with α-$C_{10}H_{11}$OOH is slightly smaller than the *A*-factors that have been reported for the almost thermoneutral abstractions of an H-atom from phenol, log ($A/M^{-1}\,s^{-1}$) = 7.2 (8) and toluene, log (A per active H/$M^{-1}\,s^{-1}$) = 6.1 (19) by *t*-ROO·. Furthermore, the activation energy E_1 is slightly smaller than the activation energy for abstraction of H-atom from phenol (ΔE = 0.7 kcal mol^{-1}) (8) and significantly smaller than the activation energy for abstraction of an H-atom from toluene[5] (ΔE = 6.5 kcal mol^{-1}) (19).

The low Arrhenius parameters for reaction of phenols with *t*-ROO· and the differences in the parameters between hindered and nonhindered phenols can be partially attributed to the involvement of a hydrogen bonded peroxy radical phenol complex in the transition state. A contribution to the low Arrhenius parameters for α-$C_{10}H_{11}$ OOH can also be attributed to this mechanism. This is because alkyl hydroperoxides can probably form an H-bonded complex with *t*-ROO· since they form an H-bonded complex with a Lewis base, such as tetrahydrofuran, with about the same heat of formation as phenol.[6]

[5]The *A*-factor per active hydrogen and the activation energy for reaction of *t*-ROO· with toluene have been assumed to be the same as the values for *p*-xylene (19).

[6]We find that K at 25° for the formation of an H-bond complex between an alkyl hydroperoxide and tetrahydrofuran = 3.0 M^{-1}, with no detectable enthalpy of activation. At this temperature K for phenol is 13.6 M^{-1} with $-\Delta S^0$ = 8.0 e.u. and $-\Delta H^0$ = 4.0 kcal mol^{-1} (20). If we assume that ΔS^0 for phenol and an alkyl hydroperoxide are of similar magnitude, $-\Delta H^0$ for an alkyl hydroperoxide should be about 3 kcal mol^{-1}.

Can. J. Chem. Downloaded from www.nrcresearchpress.com by 210.87.254.6 on 09/05/12
For personal use only.

TABLE 3. Absolute rate constants for reaction of t-ROO$^{\cdot}$ with deuterated α-tetralin hydroperoxide, α-$C_{10}H_{10}OOD$, in isopentane

Temperature (°C)	k_1^D (M^{-1} s^{-1})	k_1^H/k_1^D
21	70	9
−34	~20	~10
−83	~0.5	~20

TABLE 4. Rate constants for reaction of t-ROO$^{\cdot}$ with some alkyl hydroperoxides at 21°

Hydroperoxide	k (M^{-1} s^{-1})
9,10-Dihydro-9-anthracyl	740
s-Butyl	485
Triphenylmethyl	700

α-$C_{10}H_{10}OOD$

Rates of disappearance of tertiary alkylperoxy radicals were significantly slower in the presence of α-$C_{10}H_{10}OOD$ than in the presence of α-$C_{10}H_{11}$ OOH. Reaction 1, therefore, exhibits an isotope effect when the hydroperoxidic hydrogen is replaced by deuterium. Absolute values of k_1^D at the lowest, highest, and an intermediate temperature are summarized in Table 3 and the ratio of rate constants k_1^H/k_1^D at these temperatures are given in the last column. Unfortunately, these rate constants were not of sufficient accuracy to justify their presentation in the form of an Arrhenius equation.

We have previously reported (18) an isotope effect of approximately 30 for reaction of cumylperoxy radicals with α-$C_{10}H_{11}$ OOH at 30°. Based on the present results this rather indirectly determined isotope effect must have been overestimated.

Related Hydroperoxides

9,10-Dihydro-9-hydroperoxyanthracene, s-butyl hydroperoxide, and triphenylmethyl hydroperoxide react rapidly with t-ROO$^{\cdot}$ and rates of radical decay obeyed rate laws analogous to eq. 2. Absolute values of k_1 for these compounds are summarized in Table 4 and it would appear from these data that the nature of the alkyl moiety associated with the hydroperoxide has little influence on reactivity to an alkylperoxy radical.

Conclusions

The ease with which the hydroperoxidic hydrogen is transferred from an alkyl hydroperoxide to an alkylperoxy radical is the reason why the hydroperoxide method has proved to be so successful for determining absolute rate constants for reaction of alkylperoxy radicals with organic compounds (18, 19, 21–28). The facility of this reaction is the result of a low activation energy overshadowing a preexponential factor that is slightly smaller than the normal value for a bimolecular reaction. This H-atom transfer between two peroxy radicals is, therefore, analogous to most H-atom transfers between oxy radicals in that the activation energy falls in the range 0 to 5 kcal mol^{-1}. Both Mahoney (29) and Zavitsas (30) have suggested that BEBO and modified BEBO calculations predict these low activation energies; we eagerly await a full report of their work.

1. R. W. KREILICK and S. I. WEISSMAN. J. Am. Chem. Soc. **84**, 306 (1962).
2. R. W. KREILICK and S. I. WEISSMAN. J. Am. Chem. Soc. **88**, 2645 (1966).
3. M. R. AUCK and S. I. WEISSMAN. J. Am. Chem. Soc. **90**, 1654 (1968).
4. L. R. MAHONEY and M. A. DAROOGE. J. Am. Chem. Soc. **92**, 890 (1970).
5. L. R. MAHONEY and M. A. DAROOGE. J. Am. Chem. Soc. **94**, 7002 (1972).
6. D. GRILLER and K. U. INGOLD. J. Am. Chem. Soc. **96**, 630 (1974).
7. J. A. HOWARD and E. FURIMSKY. Can. J. Chem. **51**, 3738 (1973).
8. J. H. B. CHENIER, E. FURIMSKY, and J. A. HOWARD. Can. J. Chem. **52**, 3682 (1974).
9. G. D. MENDENHALL and K. U. INGOLD. J. Am. Chem. Soc. **95**, 627 (1973).
10. S. W. BENSON. Thermochemical kinetics. Wiley, New York, N.Y. 1968.
11. H. B. KNIGHT and D. SWERN. Org. Synth. **34**, 90 (1954).
12. A. F. BICKEL and E. C. KOOYMAN. J. Chem. Soc. 2215 (1956).
13. H. R. WILLIAMS and H. S. MOSHER. J. Am. Chem. Soc. **76**, 2987 (1954).
14. D. E. BISSING, C. A. MATURAK, and W. E. MCEWAN. J. Am. Chem. Soc. **86**, 3824 (1964).
15. E. FURIMSKY and J. A. HOWARD. J. Am. Chem. Soc. **95**, 369 (1973).
16. J. A. HOWARD. Adv. Free Radical Chem. **4**, 49 (1972).
17. C. WALLING and L. HEATON. J. Am. Chem. Soc. **87**, 48 (1965).
18. J. A. HOWARD, W. J. SCHWALM, and K. U. INGOLD. Adv. Chem. Ser. No. 75, 6 (1968).
19. S. KORCEK, J. H. B. CHENIER, J. A. HOWARD, and K. U. INGOLD. Can. J. Chem. **50**, 2285 (1972).

Can. J. Chem. Downloaded from www.nrcresearchpress.com by 210.87.254.6 on 09/05/12
For personal use only.

20. S. SINGH and C. N. R. RAO. J. Am. Chem. Soc. **88**, 2142 (1966).
21. J. A. HOWARD, K. U. INGOLD, and M. SYMONS. Can. J. Chem. **46**, 1017 (1968).
22. J. A. HOWARD and K. U. INGOLD. Can. J. Chem. **46**, 2655, 2661 (1968).
23. J. A. HOWARD and K. U. INGOLD. Can. J. Chem. **48**, 873 (1970).
24. J. A. HOWARD and S. KORCEK. Can. J. Chem. **48**, 2165 (1970).
25. J. A. HOWARD and S. KORCEK. Can. J. Chem. **49**, 2178 (1971).
26. J. A. HOWARD. Can. J. Chem. **50**, 2298 (1972).
27. J. A. HOWARD and J. H. B. CHENIER. J. Am. Chem. Soc. **95**, 3054 (1973).
28. J. A. HOWARD and J. H. B. CHENIER. Int. J. Chem. Kinet. **6**, 527 (1974).
29. L. R. MAHONEY. Private communication.
30. A. A. ZAVITSAS. Private communication.

Can. J. Chem. Downloaded from www.nrcresearchpress.com by 210.87.254.6 on 09/05/12
For personal use only.

Mass Spectrometric Studies of the Ionization and Thermal Decomposition of Tungsten π-Cyclopentadienyl Tricarbonyl Dimer

J. R. KRAUSE[1] AND D. R. BIDINOSTI

Department of Chemistry, University of Western Ontario, London, Ontario N6A 3B7

Received September 6, 1974

J. R. KRAUSE and D. R. BIDINOSTI. Can. J. Chem. **53**, 628 (1975).

The ionization and thermal decomposition of tungsten π-cyclopentadienyl tricarbonyl dimer $[WC_5H_5(CO)_3]_2$ was investigated using a mass spectrometer fitted with single and double cell molecular flow inlet systems.

The electron impact mass spectrum and appearance potentials for the principle ions in the spectrum have been measured and recorded.

The enthalpy change for the dissociation

$$[WC_5H_5(CO)_3]_2 = 2WC_5H_5(CO)_3$$

obtained from van't Hoff plots of the temperature dependence of the equilibrium constant was found to be 234.4 ± 3.8 kJ/mol. This result was substantiated by an electron impact value of 221.0 ± 20.1 kJ/mol based on an ionization potential for $\cdot WC_5H_5(CO)_3$ of 7.66 ± 0.05 eV measured in the high temperature studies.

J. R. KRAUSE et D. R. BIDINOSTI. Can. J. Chem. **53**, 628 (1975).

On a examiné, en faisant appel à un spectromètre de masse adapté avec des systèmes d'introduction comportant des cellules simples et doubles d'écoulement moléculaire, l'ionisation et la décomposition thermique du dimère $[WC_5H_5(CO)_3]_2$. On a mesuré et enregistré le spectre de masse sous impact électronique et les potentiels d'apparition des principaux ions du spectre. Le changement d'enthalpie pour la dissociation

$$[WC_5H_5(CO)_3]_2 = 2WC_5H_5(CO)_3$$

obtenu à partir d'une courbe de van't Hoff pour la dépendance sur la température des constantes d'équilibre, est de 234.4 ± 3.8 kJ/mol. On a confirmé ce résultat par une valeur de 221.0 ± 20.1 kJ/mol provenant d'impact électronique en se basant sur un potentiel d'ionisation pour $\cdot WC_5H_5(CO)_3$ de 7.66 ± 0.05 eV tel que mesuré dans des études à haute température.

[Traduit par le journal]

Introduction

In the current investigation of tungsten π-cyclopentadienyl tricarbonyl dimer, $[WC_5H_5(CO)_3]_2$, the salient features of some previous Knudsen cell studies from this laboratory (1–4) have been combined and extended. As in the case of the binary metal carbonyls (1), the fragmentation pattern and appearance potentials of the major ions from $[WC_5H_5(CO_3]_2$ have been obtained from electron impact analysis of the molecular beam effusing from a single Knudsen cell adjacent to the ion source. High temperature pyrolysis studies, similar to those on cobalt octacarbonyl (2) and manganese carbonyl (3) were also carried out, but this time using a double Knudsen cell arrangement because of the lower volatility of the tungsten compound. In this way it was possible to study not only the ionization efficiency of thermally produced organotungsten free radicals, but also the enthalpy change accompanying the dissociation process occurring in the reactor chamber of the double oven inlet system.

Experimental

The mass spectrometer used in this work is a medium resolution, 38.2 cm radius, 90° magnetic sector instrument constructed in this laboratory. This new instrument is very similar to our other mass spectrometer (1) with the exception that the ion analyzer now lies in the horizontal plane.

For mass spectral and ion energetic investigations, an effusion cell – ion source arrangement similar to that shown in Fig. 2 ref. 1 has been retained. To minimize the filament temperature the emitter area of the rhenium filaments was covered with a thin layer of a mixture 99% LaB_6 – 1% $LaNO_3$ (5) so that under normal operating conditions (5 μA trap current) the resulting equilibrium ion chamber temperature was 100 ± 10 °C.

Thermal dissociation studies were carried out using the double oven arrangement shown in Fig. 1. The sample, contained in the lower of the two cells, was kept at the

[1]Present address: Abteilung Strahlenchemie, Max Planck Institute, Muehlheim (Ruhr), Federal Republic of Germany.

Can. J. Chem. Downloaded from www.nrcresearchpress.com by 210.87.254.6 on 09/05/12
For personal use only.

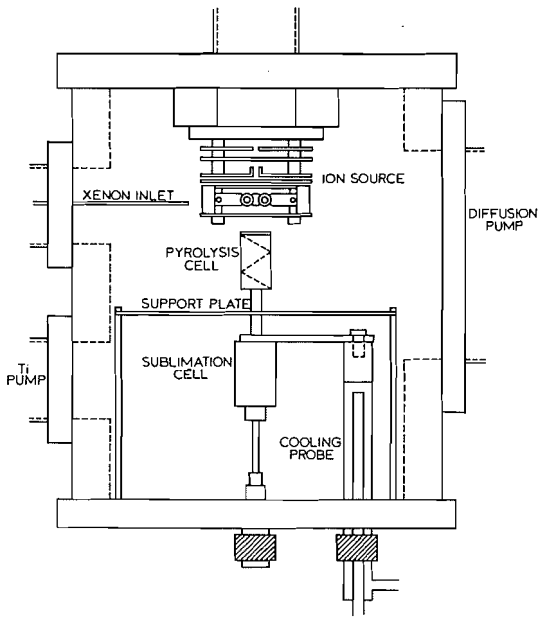

FIG. 1. Knudsen double oven diffusion cell arrangement.

constant temperature just needed to sublime the sample into the gas phase. The vapor so produced passed through a stainless steel connecting pipe into the top cell where it struck a stainless steel baffle. After obtaining thermal equilibrium through numerous collisions with the cell walls, the gas effused through a 0.076 cm orifice into the ion source where a fraction of the beam was ionized and mass analyzed.

During operation, the temperature of the lower cell was fixed by passing a known current from a regulated constant-current power supply through Thermocoax windings (not shown) wrapped around the cell (4). Concurrently, the temperature of the upper cell could be varied systematically by means of a separate regulated supply coupled to that cell's twenty-turn Thermocoax helical heater. Transfer of heat from the upper to the lower cell was effectively prevented by circulating either cold water or cold flowing nitrogen gas through the body of a cold probe connected through a copper bar to the top of the lower cell. The maximum upper cell temperature obtainable was 800 °C and regulation after thermal equilibration was ±2 °C. A sublimation cell temperature of approximately 110 °C gave a suitable pressure for both electron impact and thermal decomposition studies.

The volume about the effusion cells was evacuated by a titanium sublimation pump (1500 l max/s) and the ion source region was pumped by a liquid nitrogen trapped 600 l/s diffusion pump. A separate 150 l/s liquid nitrogen trapped diffusion pump was used to pump the analyzer tube and collector chamber.

Ion detection was with a 15-stage electron multiplier, followed by a Cary model 401 VRE operated in the integration mode.

The $[WC_5H_5(CO)_3]_2$ was prepared according to literature methods (6) and purified by vacuum sublimation before use in the mass spectrometer.

TABLE 1. Mass spectrum and appearance potentials for the ions from $[WC_5H_5(CO)_3]_2$

Ion	Relative intensity, 50 eV	Appearance potential eV
$W_2(C_5H_5)_2(CO)_6^+$	22.2	6.65±0.05
$W_2(C_5H_5)_2(CO)_5^+$	10.3	7.70±0.05
$W_2(C_5H_5)_2(CO)_4^+$	31.7	8.61±0.05
$W_2(C_5H_5)_2(CO)_3^+$	31.7	11.00±0.20
$W_2(C_5H_5)_2(CO)_2^+$	23.4	12.89±0.10
$W_2(C_5H_5)_2(CO)^+$	22.2	13.85±0.10
$W_2(C_5H_5)_2^+$	100.0	15.5 ±0.5
$W_2C_5H_5(C_3H_3)^+$	24.6	25.0 ±1.0
$W_2(C_3H_3)_2^+$	10.0	29.0 ±1.0
$WC_5H_5(CO)_3^+$	26.2	10.05±0.2
$WC_5H_5(CO)_2^+$	42.0	12.3 ±0.2
$WC_5H_5(CO)^+$	28.5	13.2 ±1.0
$WC_5H_5^+$	42.0	14.5 ±0.5
$W(C_3H_3)^+$	10.3	20.1 ±1.0
$C_5H_6^+$	33.0	
$C_3H_3^+$	44.4	

The relative abundances of "monoisotopic" species were calculated by standard procedures (7). All appearance and ionization potentials were measured relative to xenon (i.p. = 12.13 eV) (8) using Warren's method (9). Xenon was introduced into the ion source simultaneously with the effusing beam by means of an independent auxillary inlet system.

Results and Discussion

Single Effusion Cell Studies

The 50 eV mass spectrum and the appearance potentials of the major ions in the spectrum are given in Table 1.

In the mass spectrum, the molecular ion and ions of the type $W_2(C_5H_5)_2(CO)_n^+$ (n = 0–5) due to successive losses of carbon monoxide were found in high abundance. The remainder of the spectrum was composed of monometallic ions of the type $WC_5H_5(CO)_m^+$ (m = 0–3) together with ions formed by the loss of acetylene (C_2H_2) from π-cyclopentadienyl ligands. No ions due to the scission of carbon–oxygen bonds in the carbonyl ligands nor any rearrangement ions were observed.

From the energetics data, Table 1, it can be seen that the ionization potential of the molecular ion is much lower than the ionization potential of the carbonyl and π-cyclopentadienyl ligands (14.01 and 8.69 eV respectively) (8) and is closer to the ionization potential of the central tungsten atoms (7.98 eV) (8) suggesting that the primary ionization process involves removal of

Can. J. Chem. Downloaded from www.nrcresearchpress.com by 210.87.254.6 on 09/05/12
For personal use only.

Can. J. Chem. Downloaded from www.nrcresearchpress.com by 210.87.254.6 on 09/05/12
For personal use only.

TABLE 2. Ionic tungsten–carbon bond dissociation energies (eV)

n	$D(W_2^+(C_5H_5)_2(CO)_{n-1}—CO)$
6	1.05
5	0.91
4	2.39
3	1.89
2	0.96
1	1.65

an electron associated with an essentially nonbonding molecular orbital with prevailing metal character (10).

The energy required to break the first bond in the molecular ion is often different from the average metal–carbon bond energy since there is a variation in the energy necessary to break each successive bond (11). Using eq. 3 (1)

[1] Av. *ionic* metal–carbon bond energy =

$$1/6[\text{a.p.}(W_2(C_5H_5)_2^+) - \text{i.p.}(W_2(C_5H_5)_2(CO)_6)]$$

a value of 1.48 eV was calculated for the mean ionic tungsten–carbon bond dissociation energy. This can be compared with $\bar{D}(W^+—CO) = 2.09$ eV in $W(CO)_6$ (1). The ionic tungsten–carbon dissociation energies are given in Table 2.

The *ionic* tungsten–tungsten bond dissociation energy was calculated from eq. 2 using the appropriate ionization and appearance potentials from Table 1.

[2] $D((CO)_3C_5H_5W—WC_5H_5(CO)_3)$

$$= \text{a.p. } WC_5H_5(CO)_3^+ - \text{i.p. } W_2(C_5H_5)_2(CO)_6^+$$

$$= 10.05 - 6.65$$

$$= 3.40 \text{ eV} = 328 \text{ kJ/mol}$$

This value of the *ionic* tungsten–tungsten bond dissociation energy together with those of the average *ionic* metal–carbon bond dissociation energies help one to rationalize the mass spectrum observed. Since the average activation energy for the splitting of a carbon monoxide fragment from the molecular ion is much smaller than that for metal–metal bond breaking and since the A factors for both fragmentation processes should be similar, it is expected that the excited parent ion will decompose preferentially by carbon monoxide splitting. This in fact is what is observed in the mass spectrum of $[WC_5H_5(CO)_3]_2$.

Double Effusion Cell Studies

When the temperature of the upper cell of a double cell arrangement was the same as the lower cell, the ionic abundances recorded at 50 eV were those of the mass spectrum, Table 1. As the temperature of the upper cell was raised to approximately 460 °K, $WC_5H_5(CO)_3^+$ was observed at electron impact energies below the appearance potential of $WC_5H_5(CO)_3^+$ from $[WC_5H_5(CO)_3]_2$. In addition, with increasing upper cell temperature the relative intensities of ions containing a single tungsten atom remained constant whereas the ratio $I_{WC_5H_5(CO)_3^+}/I_{[WC_5H_5(CO)_3]_2^+}$ increased almost exponentially. This was taken as evidence for the production of $WC_5H_5(CO)_3$ from the dissociation process

[3] $$[WC_5H_5(CO)_3]_2 = 2 \cdot WC_5H_5(CO)_3$$

taking place in the upper cell.

Under conditions of molecular flow, the partial pressure P_i of a gaseous species i in a reactor cell is related to the observed ion current I_i^+ by

[4] $$P_i = C_i I_i^+ T$$

where T is the temperature of the gas in the reactor (13). The constant C_i contains a number of terms which depend on the geometry of both the reactor and ion source, the ion transmission characteristics of the mass spectrometer, the electron multiplier detection efficiency for the ion i^+, and the partial ionization cross section of the ith molecular species. Throughout each experiment, all the terms can be kept constant except the last which is assumed to be temperature independent.

The van't Hoff equation for the process [3] may be written in terms of ion intensities using eq. 4

[5] $$\log \frac{(I_{WC_5H_5(CO)_3^+})^2 T}{I_{[WC_5H_5(CO)_3]_2^+}} = \frac{\Delta H^0}{2.30RT} + C$$

where C is a temperature independent constant.

Van't Hoff plots of ion currents taken at 10 eV for three different reactor pressures are given in Fig. 2.

The least squares fitted analysis of the data (14) gives a value of

[6] $$\Delta H^\circ = 234.4 \pm 3.8 \text{ kJ/mol}$$

for the tungsten–tungsten bond dissociation process.

Can. J. Chem. Downloaded from www.nrcresearchpress.com by 210.87.254.6 on 09/05/12
For personal use only.

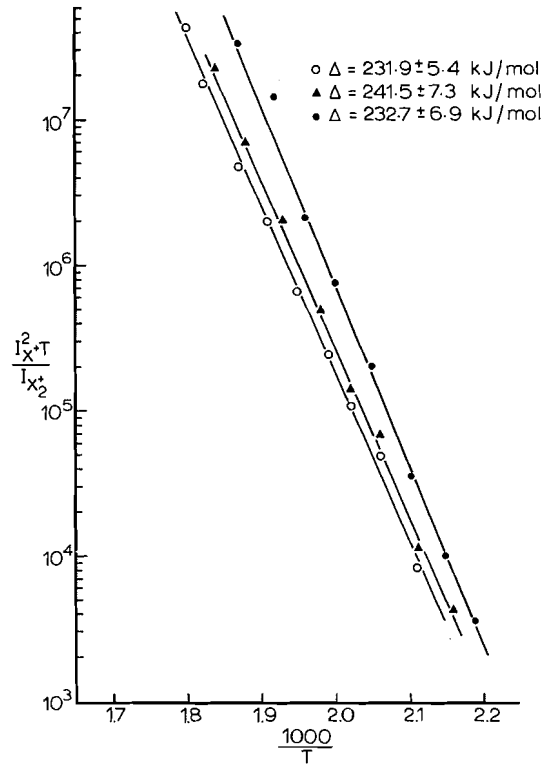

FIG. 2. Van't Hoff plots $[WC_5H_5(CO)_3]_2 = 2WC_5H_5(CO)_3$.

The ionization potential of the radical $WC_5H_5(CO)_3$ from

[7] $WC_5H_5(CO)_3 + e^- \rightarrow WC_5H_5(CO)_3^+ + 2e^-$

was found to be 7.66 ± 0.05 eV from six determinations taken at various times during the different high temperature runs.

From the appearance potential data of Table 1 the minimum energy for the process

[8] $[WC_5H_5(CO)_3]_2 + e^- \rightarrow WC_5H_5(CO)_3^+ + \cdot WC_5H_5(CO)_3 + 2e^-$

is 10.05 ± 0.2 eV.

If the ions produced in [8] and [7] are assumed to be energetically the same then the algebraic difference between them is just reaction 3 for which

[9] $D((CO)_3C_5H_5W—WC_5H_5(CO)_3)$
$= \text{a.p. } WC_5H_5(CO)_3^+ - \text{i.p. } \cdot WC_5H_5(CO)_3$
$= 10.05 - 7.66 \text{ eV}$
$= 2.39 \text{ eV}$
$= 221.0 \pm 20.1 \text{ kJ/mol}$

The agreement between this electron impact bond dissociation energy determination and that from the second-law studies [6] is excellent. It has been pointed out elsewhere (15) that measurements of bond dissociation energies based on the energetics of ions arising from complex organometallic molecules are very dependent on the temperature of the sample inlet system and on ion source temperatures. In this work gaseous samples entered the ion source as well defined molecular beams effusing from Knudsen cells whose temperatures were rigidly fixed and maintained. By using very thin rhenium ribbon cathodes treated with LaB_6 the temperature of the ion source itself was kept low and constant at about 100 °C. Moreover, the "open source" used in this work was designed in such a way that the molecular beam passed directly into the flux of ionizing electrons and any molecules not ionized were quickly pumped away before collisions with the walls led to appreciable decomposition products. It was felt that electron impact data and subsequent bond dissociation energies found under these conditions are more reproducible and dependable than those made using commercial instruments with undefined heated probe inlet and ion source temperatures. The results appear to substantiate these conclusions.

Two factors should be mentioned when viewing the results of the van't Hoff studies. First and foremost the method requires only a relative value of the equilibrium constants, K_i, determined at the various temperatures; absolute values, in contrast to third-law methods, are not necessary (13). With the van't Hoff equation written in the form

$$[10] \qquad \Delta H^0 = \frac{RT_1T_2}{T_1 - T_2} \ln (K_1/K_2)$$

it has been shown that, if $T_1 - T_2$ is 50 °K centered about 500 °K, then a 10% uncertainty in K_1 and K_2 each contribute ±4.2 kJ/mol to ΔH^0 for a total uncertainty given by their vector sum of ±5.9 kJ/mol (16). Secondly, errors in temperature measurement tend to become important when the relative error $2\,\delta T/\Delta T$, where δT is the error in temperature measurement and ΔT is the temperature interval covered, becomes large (13). At the limit, the relative error for temperature measurement in these experiments is at most 4%. Hence the experimental values of the bond dissociation energy determined by our second-law analysis, Fig. 2, are reasonably

defined and at the same time must be said to possess a high degree of precision considering their reproducibility at three different reactor pressures.

The tungsten–tungsten bond energy in tungsten π-cyclopentadienyl tricarbonyl dimer is thus best given as 234.4 ± 3.8 kJ/mol.

The authors gratefully acknowledge financial assistance from the National Research Council of Canada.

1. D. R. BIDINOSTI and N. S. MCINTYRE. Can. J. Chem. **45**, 641 (1967).
2. D. R. BIDINOSTI and N. S. MCINTYRE. Chem. Commun. 1 (1967).
3. D. R. BIDINOSTI and N. S. MCINTYRE. Chem. Commun. 555 (1966).
4. D. R. BIDINOSTI and N. S. MCINTYRE. Can. J. Chem. **48**, 595 (1970).
5. J. D. BIRMINGHAM. Brit. J. Appl. Phys. **16**, 1821 (1965).
6. R. B. KING. Inorg. Synth. **7**, 104 (1963).
7. J. H. BEYNON. *In* Mass spectrometry and its application to organic chemistry. Elsevier, London. 1960.
8. R. W. KISER. *In* Introduction to mass spectrometry and its applications. Prentice Hall Inc., Engelwood Cliffs, N.J. 1965. Appendix IV.
9. J. W. WARREN. Nature, **165**, 811 (1950).
10. A. FOFFANI, S. PIGNATARO, B. CANTONE, and F. GRASSO. Z. Phys. Chem. N.F. **45**, 79 (1965).
11. G. A. JUNK and H. J. SVEC. J. Chem. Soc. A, 2102 (1970).
12. G. A. JUNK, H. J. SVEC, and R. J. ANGELICI. J. Am. Chem. Soc. **90**, 5758 (1968).
13. P. GOLDFINGER. *In* Mass spectrometry. *Edited by* R. I. Reed. Academic Press Inc., London. 1965. p. 265 ff.
14. P. R. BEVINGTON. Data reduction and error analysis for the physical sciences. McGraw-Hill Inc., New York. 1969.
15. H. J. SVEC and G. A. JUNK. Inorg. Chem. **8**, 1688 (1968).
16. S. W. BENSON. J. Chem. Educ. **42**, 502 (1965).

Can. J. Chem. Downloaded from www.nrcresearchpress.com by 210.87.254.6 on 09/05/12
For personal use only.

The Structure and Stability of Ni(II) Complexes of Thiourea and Related Ligands

D. R. EATON AND K. ZAW

Department of Chemistry, McMaster University, Hamilton, Ontario L8S 4M1

Received July 30, 1974

D. R. EATON and K. ZAW. Can. J. Chem. **53**, 633 (1975).

A number of Ni(II) complexes of thiourea, *N*-methylthiourea, *N,N'*-dimethylthiourea, *N*-naphthylthiourea, *N,N'*-diethylthiourea, and ethylene thiourea have been studied in acetone solution by proton magnetic resonance, magnetic susceptibility measurements, and conductivity measurements. In solution these complexes have tetrahedral, square planar, and octahedral geometries. In many cases equilibria between compounds with different geometries exist. Such equilibria have been studied as a function of temperature. The factors determining the relative stability of Ni(II) compounds with different geometries are discussed. In the present series of compounds it is concluded that the charge on the metal ion has the predominant influence in determining geometry. Some qualitative results on ligand exchange rates and mechanisms are also reported.

D. R. EATON et K. ZAW. Can. J. Chem. **53**, 633 (1975).

On a étudié, en solution dans l'acétone, par résonance magnétique nucléaire du proton, par des mesures de susceptibilité magnétique et par des mesures de conductivité, une série de complexes du Ni(II) avec la thiourée, la *N*-méthylthiourée, la *N,N'*-diméthylthiourée, la *N*-naphtylthiourée, la *N,N'*-diéthylthiourée et l'éthylène thiourée. En solution, ces complexes ont des géométries tétraédrique, plan carré et octaédrique. Dans plusieurs cas, des équilibres existent entre des composés ayant des géométries différentes. On a étudié de tels équilibres en fonction de la température. On discute des facteurs déterminant la stabilité relative de composés du Ni(II) avec différentes géométries. Dans la série de composés présentés dans cette communication, on conclut que la charge sur l'ion métallique a une influence prépondérante dans la détermination de la géométrie. On rapporte aussi quelques résultats qualitatifs sur les vitesses d'échanges des ligands et sur les mécanismes de ces échanges. [Traduit par le journal]

Thiourea and substituted thioureas form complexes with most of the transition metal ions in the first period (1). These complexes are generally labile in solution and often partly solvolyzed. They therefore constitute a suitable series for systematic study of the kinetics and mechanisms of rapid ligand exchange reactions. We have previously reported some solution studies of the Co(II) compounds (2). These latter complexes are uniformly tetrahedral in nonaqueous solution. The situation for the analogous Ni(II) compounds is more complicated. Octahedral, square planar, and tetrahedral geometries are all plausible and in the case of thiourea complexes all occur. In a preliminary communication (3) we suggested that the relative stabilities of Ni(II) thiourea complexes with different geometries were determined by electronic rather than steric factors. In the present paper we report the n.m.r. and magnetic susceptibility results that support this conclusion and will also discuss some aspects of the ligand exchange processes.

A substantial number of papers have been published on the synthesis and characterization of nickel thiourea complexes (1, 4–7). The majority of structural studies have concentrated on the solid complexes. The geometric information from these studies is not necessarily pertinent to the solution structures. It has however been concluded from infrared and crystallographic work that the thiourea is always bonded through the sulfur and this conclusion appears to hold in solution. Two papers contain information pertaining to the structure of Ni thiourea complexes in solution. Holt and Carlin (8) reported the magnetic susceptibilities, conductivities, and electronic spectra of a number of complexes involving ethylene thiourea, *N*-naphthylthiourea, and *N,N'*-diethylthiourea. Data on solutions in acetone and nitromethane at room temperature only were presented. They concluded that the compounds $Ni(nptu)_2Br_2$ and $Ni(nptu)_2I_2$ (nptu ≡ *N*-naphthylthiourea) are undissociated and tetrahedral in solution. $Ni(nptu)_4Cl_2$ loses thiourea ligands in solution to give a similar tetrahedral complex. The complexes $Ni(etu)_6$-

Can. J. Chem. Downloaded from www.nrcresearchpress.com by 210.87.254.105 on 09/05/12
For personal use only.

Can. J. Chem. Downloaded from www.nrcresearchpress.com by 210.87.254.105 on 09/05/12
For personal use only.

$(ClO_4)_2$ and $Ni(detu)_6(ClO_4)_2$ (etu ≡ ethylene thiourea, detu ≡ *N,N'*-diethylthiourea) are partly dissociated in solution to give equilibrium mixtures of octahedral and square planar complexes. $Ni(etu)_4(NO_3)_2$ loses thiourea ligands in solution but remains octahedral and is a nonelectrolyte. The NO_3^- ligands may be bidentate or solvent molecules may be involved in the first coordination sphere. They also concluded that $Ni(etu)_4X_2$ and $Ni(detu)_4X_2$ ($X = Cl^-, Br^-, I^-$) give tetrahedral species in solution. This information is supplemented by the work of Basso *et al.* (9). These authors examined the complexes $Ni(tu)_6X_2$ (tu ≡ thiourea, $X = NO_3^-$, ClO_4^-, and BF_4^-) in acetone and concluded that the nitrate was octahedral with coordinated anion but found the perchlorate and fluoroborates to be electrolytes and to show evidence of a square planar – octahedral equilibrium.

Our results agree with the conclusions of the above papers but we have been able to clarify the situation by combining n.m.r., magnetic susceptibility, and conductivity measurements and by studying the various equilibria over a range of temperatures.

Magnetic susceptibility measurements immediately distinguish square planar (diamagnetic) complexes from octahedral and tetrahedral (paramagnetic) compounds. In favorable circumstances they will also distinguish octahedral and tetrahedral compounds. Octahedral Ni^{2+} compounds have a nonorbitally degenerate ground state ($^3A_{2g}$) and they are therefore expected to have magnetic moments close to the spin only value. In practice a range of 2.8–3.3 B.M. is found. Tetrahedral compounds on the other hand have an orbitally degenerate ground state ($^3T_1$) and a moment of up to 4.1 B.M. can be anticipated. However, relatively modest distortions from T_d symmetry can remove the orbital degeneracy and produce a magnetic moment in the octahedral range. A high moment (> 3.4 B.M.) is therefore diagnostic for tetrahedral geometry but a low moment (< 3.4 B.M.) is inconclusive. In the latter case the electronic spectra provide a more useful probe.

The n.m.r. spectra of the paramagnetic complexes are expected to show large isotropic shifts from the usual diamagnetic positions of the resonances (10). In the case of a thiourea ligand (structure 1) restricted rotation about the C—N bond leads to separate resonances for the protons *cis* to the S ("outside") and those *trans* to the S

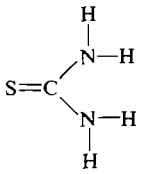

1

("inside") (2). There are analogous possibilities for substituted thioureas. Addition of free ligand immediately determines whether the ligand exchange is fast on the n.m.r. time scale (the spectrum shows a single resonance shifted towards the free ligand position) or slow on the n.m.r. time scale (the complexed ligand resonance is unshifted and a new line appears at the free ligand position). In the absence of equilibria between different geometric forms or of a transition from rapid to slow exchange the isotropic shifts of the complexed protons will approximately increase inversely with the temperature (Curie law). Equilibria between diamagnetic and paramagnetic forms are made apparent by pronounced curvature, often with a change in sign of the slope, of the $1/T$ plots. Transition from fast to slow exchange is manifested by broadening and disappearance of the resonance followed by the reappearance at a lower temperature of a complexed resonance in a different position. Thus the n.m.r. spectra provide information on both the geometric equilibria and the ligand exchange processes. If characteristically similar chemical shifts are observed for a series of compounds the n.m.r. can also be used to identify the geometries present.

$Ni(tu)_4Cl_2$

In the solid state this compound has been shown to have octahedral geometry (4). Acetone solutions show no conductivity at any temperature indicating no dissociation of chloride ion. Data in Table 1 show that the magnetic moment varies from 3.5 B.M. at 37 °C to 3.9 B.M. at −80 °C. The n.m.r. spectrum shows separate resonances for the "inside" and "outside" protons (Table 2). The solubility of this compound is rather low and addition of excess thiourea causes precipitation. At room temperature the two NH signals are of equal intensity. At −50 °C the low field signal becomes very broad but has become relatively sharp again at −84 °C. The high field line remains sharp throughout but

Can. J. Chem. Downloaded from www.nrcresearchpress.com by 210.87.254.105 on 09/05/12
For personal use only.

TABLE 1. Magnetic moments of nickel thiourea halides*

$Nitu_4Cl_2$		$Nitu_6Br_2$		$Nitu_6I_2$	
T (°C)	μ (B.M.)	T (°C)	μ (B.M.)	T (°C)	μ (B.M.)
37	3.5	36	3.6	31	3.5
−14	3.6	−15	3.7	−14	3.0
−25	3.6	−36	3.7	−39	2.5
−37	3.6	−46	3.5	−42	2.3
−45	3.7	−56	3.4	−55	1.6
−50	3.7	−63	3.1	−64	0.9
−61	3.7	−77	2.4	−77	0.8
−75	3.9	−80	2.4	−80	0.6
−79	3.9	−87	2.0	−87	1.1
−94	3.8	−95	1.2	−94	1.4

*Measurements in acetone solution. Estimated errors ±0.1 B.M.

TABLE 2. Nuclear magnetic resonance data on nickel thiourea chloride solutions*

T (°C)	NH	NH′	T (°C)	NH	NH′
27	−2307	−57	−65	−5057	−245
−20	−3020	−95	−75	−5308	−245
−35	−3651	−75	−84	−5499	−287
−50	−4214	−180	−92	−5529	−286

*Solvent acetone-d_6. Shifts in Hz at 56.4 MHz relative to free ligand position. NH and NH′ are the "inside" and "outside" thiourea protons. Estimated errors; low field lines ±30 Hz, high field lines ±5 Hz.

at −84 °C is approximately three times more intense than the low field line. The observed shift of this latter line at −84 °C is approximately one-third of that of the corresponding line of $Nitu_6Br_2$ (see below) for which there is slow exchange at this temperature. The temperature dependence of the low field line is shown in Fig. 1. There is no change in the color of the solution between room temperature and −90 °C.

The above observations are consistent with the complete dissociation of $Nitu_4Cl_2$ to give tetrahedral $Nitu_2Cl_2$ as suggested by Holt and Carlin on the basis of optical spectra for analogous substituted thiourea halide complexes. The high magnetic moment is strongly suggestive of this geometry. The rate of ligand exchange is such that the large shift (~ −4200 Hz) is frozen out at −50 °C but an average resonance is still observed for the smaller shifted complexed resonance (~ −600 Hz) and free ligand at −90 °C. There is no evidence for geometries other than tetrahedral.

$Nitu_6Br_2$

This compound is more soluble in acetone than the chloride. The magnetic moment of the

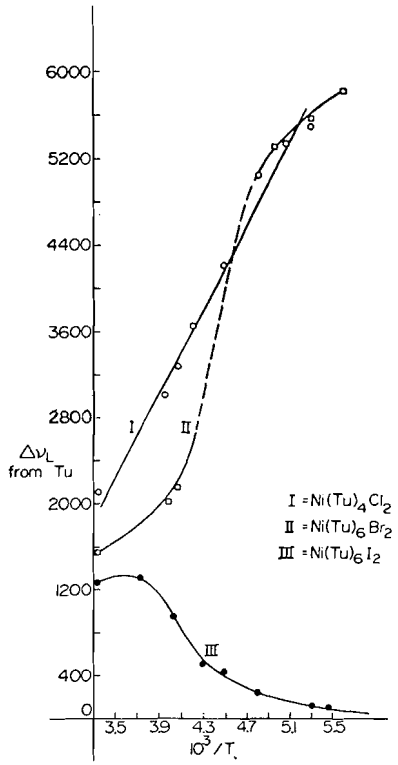

FIG. 1. Temperature dependence of the isotropic shifts of the low field NH resonances of nickel thiourea halides. Shifts in Hz from free ligands.

solution varies from 3.6 B.M. at 27 °C to 1.2 B.M. at −94 °C (Table 1). Acetone solutions give a small conductivity at room temperature which increases at low temperatures. At room temperature the n.m.r. spectrum is quite similar to that of the chloride. Addition of free ligand indicates rapid ligand exchange. A large excess of added thiourea leads to averaging of the inside and outside NH protons due to rapid rotation about the C—N bond in the free ligand. On cooling solutions of the complex the low field resonance commences to broaden at −25 °C and reappears as a complexed ligand resonance at −60 °C. At −93 °C the spectrum shows four resonances. Two at −6219 and −1138 Hz correspond to the frequencies found for the inside and outside protons of tetrahedral $Nitu_2Cl_2$ and a third is at the free ligand position and increases in intensity with the addition of excess free ligand. The fourth resonance comprises a doublet with 20 Hz splitting at −500 Hz and is assigned to a diamagnetic complex. The n.m.r. data is presented in Table 3 and the temperature dependence of the downfield

TABLE 3. Nuclear magnetic resonance data on nickel thiourea bromide solutions*

T (°C)	NH	NH′	NH″	T (°C)	NH	NH′	NH″
27	−1557	−152	—	−75	−5320	−470	−120
−22	−2020	−170	—	−84	−5669	−644	−120
−35	—	−178	—	−93	−5839	−758	−145
−50	—	−184	—				−120
−62	−5239	—	−144				

*Solvent acetone-d_6. Shifts in Hz at 56.4 MHz relative to free ligand position. NH and NH′ are the "inside" and "outside" thiourea protons. NH″ is the resonance from the diamagnetic square planar complex. Estimated errors; low field lines ±30 Hz, high field lines ±5 Hz.

line illustrated in Fig. 1. Addition of tetramethyl ammonium bromide decreases the concentration of the diamagnetic complex relative to the paramagnetic complex.

In this case there is clearly an equilibrium between a paramagnetic and a diamagnetic complex. The high value of the magnetic moment at high temperature (3.7 B.M.) and the similarity of its chemical shifts at low temperature to those of $Nitu_2Cl_2$ suggest the paramagnetic species is tetrahedral $Nitu_2Br_2$. The diamagnetic compound must involve dissociation of bromide ion since its formation is repressed by the addition of tetramethyl ammonium bromide and the drop in susceptibility at low temperatures is paralleled by an increase in conductivity. It could therefore be square planar $Nitu_4^{2+}$ or $Nitu_3Br^+$. However studies of $Nitu_6(ClO_4)_2$ (see below) show that in the presence of 2 mol of excess thiourea at −90 °C $Nitu_4^{2+}$ is completely converted to octahedral $Nitu_6^{2+}$. We deduce therefore that the diamagnetic species in the present case is $Nitu_3Br^+$.

$Nitu_6I_2$

The magnetic moment of $Nitu_6I_2$ in acetone is 3.5 B.M. at 31 °C. The moment falls steadily with decreasing temperature and reaches a minimum of 0.6 B.M. at −80 °C but rises thereafter to 1.4 B.M. at −94 °C. This data is shown in Table 1. The conductivity of these solutions also increases with decreasing temperature and is greater than that of the bromide compound at all temperatures. The solution shows a color change from brown at room temperature to blue at −90 °C. At 27 °C the n.m.r. spectrum shows two lines, one shifted 1261 Hz downfield from the free ligand and the second shifted 95 Hz downfield from the free ligand. On cooling to −5 °C these resonances broaden and become unobservable. On further cooling they reappear and shift steadily upfield. At −90 °C the spectrum shows two lines, one at a position corresponding to free ligand and one at a position corresponding to a diamagnetic square planar complex. The n.m.r. data is given in Table 4 and the temperature dependence of the low field line is plotted in Fig. 1. No lines corresponding to a paramagnetic species are observed at −90 °C. Addition of tetramethyl ammonium iodide to solutions in the high temperature region shifts the lines to low field indicating that the equilibrium is disturbed with the formation of the paramagnetic species.

We infer from these results that at room temperature tetrahedral $Nitu_2I_2$ is the most important species. On cooling diamagnetic square planar $Nitu_3I^+$ is formed. At around −5 °C the equilibrium between square planar and tetrahedral forms becomes slow enough to cause line broadening. The ligand exchange reactions involving both forms remain fast but the proportion of tetrahedral diminishes with decreasing temperature. At −90 °C the square planar ligand exchange has been frozen out. The increase in magnetic moment at very low temperatures is attributed to further ionization to give the doubly charged cation which is stable as octahedral $Nitu_6^{2+}$ at these temperatures. Results with $Nitu_6(ClO_4)_2$ (see below) indicate that the n.m.r. resonances of $Nitu_6^{2+}$ are too broad to observe at −90 °C.

TABLE 4. Nuclear magnetic resonance data on nickel thiourea iodide solutions*

T (°C)	NH	NH′	T (°C)	NH	NH′
27	−1261	−95	−50	−438	−95
−5	−1307	−95	−65	−242	−89
−25	−977	−110	−85	−120	−80
−40	−509	−98	−90	−114	−51

*Solvent acetone-d_6. Shifts in Hz at 56.4 MHz relative to free ligand position. NH and NH′ are the "inside" and "outside" thiourea protons. Estimated errors ±20 Hz.

Can. J. Chem. Downloaded from www.nrcresearchpress.com by 210.87.254.105 on 09/05/12
For personal use only.

Can. J. Chem. Downloaded from www.nrcresearchpress.com by 210.87.254.105 on 09/05/12
For personal use only.

$Ni(nptu)_2Br_2$ and $Ni(nptu)_2I_2$

Both of these compounds were reported to have tetrahedral geometry in solution at room temperature by Holt and Carlin (8). The temperature dependence of the magnetic susceptibility of the bromide shows a constant value of 3.2–3.3 B.M. from 37 to −60 °C followed by a steady drop to 2.5 B.M. at −93 °C. The behavior of the iodide is similar except that the fall off in moment commences at a rather higher temperature (−40 °C) and reaches a value of 2.3 B.M. at −94 °C. The n.m.r. spectra show relatively small shifts for the aromatic protons of the naphthyl groups. At room temperature only two NH resonances appear but below zero three can be distinguished. Steric considerations will favor the configuration

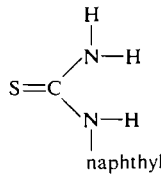

for the ligand which gives three different N—H protons. The shifts are rather greater than those for the thiourea complexes, *e.g.* at −70 °C $Ni(nptu)_2Br_2$ has lines at −6081, −1743, and −1081 Hz compared to −5700 and −880 Hz for $Nitu_6Br_2$. The temperature dependence of the lines follows Curie law rather closely.

Although the magnetic moments of these compounds are rather lower than those of the thiourea complexes we see no reason to doubt the conclusion of Holt and Carlin that at room temperature they have tetrahedral geometry. This is confirmed by the similarity of the n.m.r. shifts to those of the compounds discussed above. The small drop in susceptibility at low temperature suggests some formation of square planar diamagnetic isomers.

Perchlorate and Tetrafluoroborate Complexes

Six complexes in this class have been examined. They all behave in a very similar fashion. Holt and Carlin (8) found the magnetic moment of $Ni(detu)_6(ClO_4)_2$ in acetone solution to be 2.0 B.M. at room temperature. It shows a strong band at 17 000 – 18 000 cm^{-1} which they attributed to a square planar species. Basso *et al.* (9) found similar electronic spectra for other perchlorate and borofluoride complexes. All the complexes are 2:1 electrolytes. On the basis of this evidence a square-planar octahedral equilibrium was suggested.

The variation of magnetic moment with temperature for the six complexes $Nitu_6(ClO_4)_2$, $Ni(dmtu)_6(ClO_4)_2$, $Ni(detu)_6(ClO_4)_2$, $Ni(etu)_6(ClO_4)_2$, $Ni(tu)_6(BF_4)_2$, and $Ni(detu)_6(BF_4)_2$ is shown in Table 5. This behavior is markedly different from the examples discussed above in that the moment *increases* with decreasing temperature. In each case the limiting value is 3.2–3.3 B.M. which is in excellent agreement with the value expected for an octahedral complex. A square planar – octahedral equilibrium is clearly indicated. It appears that the square planar form slightly increases in stability in the series tu < dmtu < detu. There is no significant difference between similar compounds with perchlorate or borofluoride anions.

At room temperature $Nitu_6(ClO_4)_2$ shows a single n.m.r. line at −880 Hz from TMS. At −30 °C there are two lines at −1552 and −394 Hz attributable to inside and outside NH protons. These broaden and disappear at lower temperatures presumably due to slowing of the ligand exchange reaction and no spectrum is observable at −90 °C. $Ni(dmtu)_6(ClO_4)_2$ shows a single NH and a single CH_3 resonance at room temperature. Two CH_3 resonances appear at −18 °C; exchange between the inside and outside positions is no longer fast. On further cooling the CH_3 broaden at around −30 °C and the NH at around −60 °C due to slowing of the ligand exchange process. At low temperature (−104 °C) two CH_3 resonances and one NH all shifted from the free ligand position are observed and this may be taken as the spectrum of the octahedral compound. Nuclear magnetic resonance spectra of $Ni(dmtu)_6(ClO_4)_2$ are shown in Fig. 2. Other alkyl thiourea complexes in this class behave very similarly. Some of the n.m.r. shifts are gathered together in Table 6.

Nitrate Complexes

$Nitu_6(NO_3)_2$ has been reported to be a non-electrolyte in acetone solution and to have octahedral geometry at room temperature. We have examined the magnetic susceptibilities of $Nitu_6(NO_3)_2$, $Ni(dmtu)_6(NO_3)_2$, and $Ni(detu)_6(NO_3)_2$ and find that in each case the moment is 2.8 B.M. at room temperature and increases slowly to 3.3 B.M. at −90 °C. These values are consistent with an octahedral species. The n.m.r. spectra are quite similar to those of the per-

Can. J. Chem. Downloaded from www.nrcresearchpress.com by 210.87.254.105 on 09/05/12
For personal use only.

TABLE 5. Magnetic moments of nickel thiourea perchlorates and borofluorides*

$Nitu_6(ClO_4)_2$		$Nidmtu_6(ClO_4)_2$		$Nidetu_6(ClO_4)_2$		$Nietu_6(ClO_4)_2$		$Nitu_6(BF_4)_2$		$Nidetu_6(BF_4)_2$	
T (°C)	μ (B.M.)	T (°C)	μ (B.M.)	T (°C)	μ (B.M.)	T (°C)	μ (B.M.)	T (°C)	μ (B.M.)	T (°C)	μ (B.M.)
49	2.3	37	2.0	37	1.7	47	2.0	30	2.1	37	1.5
32	2.3	27	2.1	−16	1.7	35	2.1	4	2.1	9	1.5
9	2.1	−11	2.2	−23	1.6	30	2.2	−9	2.1	−4	2.0
−4	2.1	−19	2.6	−33	2.4	13	2.5	−16	2.0	−17	2.0
−11	2.1	−35	2.8	−41	2.8	−7	2.6	−25	2.1	−24	2.7
−38	2.3	−42	2.9	−49	2.9	−23	2.8	−34	2.2	−33	2.8
−50	2.4	−51	3.0	−58	3.1	−31	2.9	−42	2.4	−53	2.9
−62	2.7	−57	3.0	−64	3.2	−52	3.1	−50	2.5	−62	3.0
−71	2.8	−64	3.1	−77	3.2	−74	3.1	−58	2.7	−68	3.1
−90	3.1	−71	3.2	−84	3.3	−83	3.2	−66	2.8	−72	3.3
−99	3.2	−88	3.3	−102	3.3	−89	3.3	−81	3.0	−81	3.3
						−102	3.3	−89	3.1	−87	3.2
										−93	3.3

*Measurements in acetone solution. Estimated errors ±0.1 B.M.

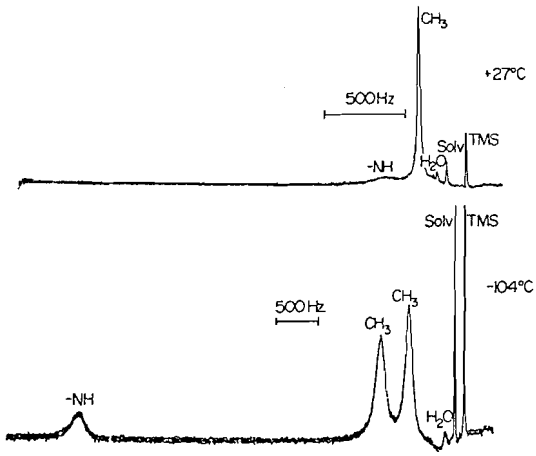

FIG. 2. ^{1}H n.m.r. spectra of $Ni(dmtu)_6(ClO_4)_2$. Solvent acetone-d_6, 56.4 MHz.

chlorates and borofluorides except that the ligand exchange is significantly slower. Thus for $Nitu_6(NO_3)_2$ the NH resonance broadens at -30 °C and reappears as a complexed resonance at -45 °C. For $Ni(detu)_2(NO_3)_2$ the slow exchange limit has been reached at -15 °C. $Ni(dmtu)_6(NO_3)_2$ and $Ni(detu)_6(NO_3)_2$ both show several resonances at low temperature. For example at -100 °C $Ni(dmtu)_6(NO_3)_2$ shows NH lines at -5764, -5125, and -3819 Hz and CH_3 resonances at -1375, -1175, and -736 Hz as well as the free ligand resonances. Other NH lines are probably hidden by the CH_3 lines. This multiplicity of lines could arise from a combination of *cis* and *trans* isomers of $Ni(dmtu)_4(NO_3)_2$ and restricted rotation about the C—N bond. Addition of excess dmtu to this solution leads to a spectrum of $Ni(dmtu)_6^{2+}$ identical to that obtained from the perchlorate indicating replacement of complexed nitrate. It is apparent that these complexes are octahedral at all temperatures.

π-Allyl and π-Crotyl Complexes

We have examined the n.m.r. spectra of the following complexes: (π-allyl)$Ni(tu)_2Br$, (π-allyl)-$Ni(nptu)_2Br$, (π-allyl)$Ni(mtu)_2Br$, (π-crotyl)-$Nitu_2Br$, (π-allyl)$Ni(dmtu)_2Br$, (π-crotyl)-$Ni(dmtu)_2Br$. The thiourea compounds have been reported previously (11). They are reported to be diamagnetic and ionized in solution (11). A crystal structure has shown that the (π-allyl)-$Nitu_2^+$ ion has a planar geometry (12). They are also efficient catalysts for the synthesis of hexadienoic esters from allylic halides, acetylene, carbon monoxide, and alcohols (11). It is therefore of interest to compare the ligand exchange rates with those of noncatalytic thiourea complexes. All n.m.r. spectra were obtained in acetone-d_6 solution for comparison with other thiourea complexes. The π-allyl and π-crotyl resonances are very similar to those reported for analogous complexes (13, 14). Data on the thiourea resonances is given in Table 7. All the lines occur in positions corresponding to diamagnetic complexes. The chemical shifts are slightly temperature dependent and the lines are found 20–70 Hz to low field of the free ligand positions. At room temperature only a single NH resonance is observed but at lower temperatures there are separate lines for the inside and outside positions. The coalescence temperature for this exchange process increases in the series $RNitu_2Br$ (-35 °C) < $RNi(mtu)_2Br$ (-23 °C) < $RNi(dmtu)_2Br$ (-17 °C) < $RNi(nptu)_2Br$ (-10 °C). These temperatures are higher than those of the corresponding ligands. Addition of free ligand demonstrates that the ligand exchange remains fast on the n.m.r. time scale even down to -90 °C. There is no indication of any paramagnetic tetrahedral species in the nptu complex or of the formation of an octahedral species at low temperature on the addition of excess ligand

TABLE 6. Nuclear magnetic resonance chemical shifts of nickel dimethylthiourea perchlorate*

T (°C)	NH	CH_3	CH_3'	T (°C)	NH	CH_3	CH_3'
27	−345	−132	−132	−57	−1247	−243	−180
−18	−372	−210	−102	−66	—	−578	−406
−28	−474	−178	−114	−85	−4179	−781	−434
−33	−643	—	−129	−95	−4328	−858	−511
−35	−645	−136	−117	−104	−4477	—	—
−43	−886	−180	−148				

*Solvent acetone-d_6. Shifts in Hz from free ligand at 56.4 MHz. Estimated errors NH lines ±30 Hz, CH_3 lines ±10 Hz.

Can. J. Chem. Downloaded from www.nrcresearchpress.com by 210.87.254.105 on 09/05/12
For personal use only.

TABLE 7. Chemical shifts of nickel π-allyl and π-crotyl thiourea complexes*

Compound	T(°C)	NH	NH′	CH_3	CH_3'
$(\pi C_3H_5)Nitu_2Br$	−35	−473	−448	—	—
$(\pi C_3H_5)Nidmtu_2Br$	−17	−509	−439	−170	−158
$(\pi C_3H_5)Ninptu_2Br$	−10	−593 −477	−362	—	—
$(\pi CH_3C_3H_4)Nitu_2Br$	−30	−474	−446	—	—
$(\pi CH_3C_3H_4)Nidmtu_2Br$	−22	−511	−419	−172	−156

*Shifts in Hz at 56.4 MHz from TMS. Solvent acetone-d_6. Estimated errors ±2 Hz.

to the tu, mtu, or dmtu compounds. The compounds remain square planar and diamagnetic throughout.

Structural Equilibria

In cases where there is an equilibrium between a diamagnetic and a paramagnetic species it is possible to find the enthalpy and entropy change of the reaction either from the temperature dependence of the n.m.r. shifts or from the temperature dependence of the magnetic susceptibility. There are some difficulties associated with each of these methods. In the n.m.r. method it is necessary to know the shift of the fully paramagnetic species at each temperature. In these nickel complexes there is some displacement of thiourea by solvent acetone as was found for the analogous cobalt compounds (2). The extent of this solvolysis can be found from the concentration dependence of the n.m.r. chemical shifts. For $Nitu_2Cl_2$ equilibrium constants similar to those reported for $Cotu_2Cl_2$ are found. The analysis of the data becomes uncertain though when both solvolysis and a structural equilibrium occur and we have therefore preferred to use the magnetic susceptibility data to obtain equilibrium constants for the structural equilibria. To use this method it is necessary to estimate the moment of the fully paramagnetic species (μ_∞) and then find the fraction of this species at each temperature. There is some error in estimating μ_∞ and the measurement of susceptibility is inherently less accurate than the measurement of chemical shifts. Values of ΔH and ΔS obtained from the susceptibilities are given in Table 8. The quoted errors are from least squares fits of the data and do not include systematic errors arising from incorrect assignment of μ_∞.

For the tetrahedral – square planar equilibria ΔH varies from +2 to +6 kcal/mol and ΔS from +12 to +25 cal/deg mol. These values may be compared with those reported for the tetrahedral – square planar equilibrium in Ni aminotroponeimineates (15) (ΔH, +2 to +4 kcal/mol; ΔS, +8 to +12 cal/deg mol). In both cases the square planar species is favored by the enthalpy and the tetrahedral species by the entropy term. The rather higher values found for ΔS in the present case are consistent with greater solvation of the positively charged square planar form. For the octahedral – square planar equilibria we obtain ΔH −2 to −4 kcal/mol and ΔS −15 to −22 cal/deg mol. The negative signs are consistent with the formation of additional bonds. The magnitudes of ΔH and ΔS are comparable to those reported for octahedral – square planar equilibria in other Ni(II) systems (16).

TABLE 8. Thermodynamic parameters for equilibria

Compound	ΔH (kcal/mol^{-1})	ΔS (cal °K^{-1} mol^{-1})
$Nitu_6Br_2$*	+5.0 ± 0.4	+25 ± 2
$Nitu_6I_2$*	+5.9 ± 0.4	+24 ± 2
$Ninptu_2Br_2$*	+2.4 ± 0.4	+13 ± 2
$Ninptu_2I_2$*	+2.5 ± 0.4	+12 ± 2
$Nitu_6(ClO_4)_2$†	−2.6 ± 0.6	−15 ± 3
$Nidmtu_6(ClO_4)_2$†	−3.4 ± 0.6	−17 ± 3
$Nidetu_6(ClO_4)_2$†	−4.4 ± 0.6	−22 ± 3
$Nietu_6(ClO_4)_2$†	−3.4 ± 0.4	−16 ± 2
$Nitu_6(BF_4)_2$†	−2.0 ± 0.4	−10 ± 2
$Nidetu_6(BF_4)_2$†	−3.4 ± 0.4	−18 ± 2

*Square planar ⇌ tetrahedral equilibrium.
†Square planar ⇌ octahedral equilibrium.

Ligand Exchange Processes

The existence of equilibria between different geometric isomers of these nickel complexes limits the utility of n.m.r. in obtaining information on the kinetics and mechanism of the ligand exchange processes. Some qualitative information is however available. It is possible to distinguish between an associative and a dissociative mechanism for ligand exchange by examining the dependence of the line width of a complexed

Can. J. Chem. Downloaded from www.nrcresearchpress.com by 210.87.254.105 on 09/05/12
For personal use only.

Can. J. Chem. Downloaded from www.nrcresearchpress.com by 210.87.254.105 on 09/05/12
For personal use only.

ligand resonance with the addition of free ligand in the slow exchange region (2). $Nitu_2Br_2$ and $Ni(dmtu)_6(ClO_4)_2$ give spectra suitable for this experiment. Not unexpectedly the former shows an associative process and the latter a dissociative process. We have also examined the line widths of mixtures of $Nitu_2Br_2$ and excess ligand in the fast exchange region (+27 to −8 °C) and using the standard approximations (17) for line widths in this region have analyzed the data to obtain $\Delta H^{\ddagger} = 4.6 \pm 0.6$ kcal/mol and $\Delta S^{\ddagger} = -15 \pm 3$ cal/mol. These results are not particularly reliable since the calculations do not take account of the square planar – tetrahedral equilibrium but it is noteworthy that the values of $\Delta H^{\ddagger}$ and $\Delta S^{\ddagger}$ are quite similar to those obtained for $Cotu_2Br_2$ ($\Delta H^{\ddagger} = 2.9 \pm 0.6$ kcal/mol, $\Delta S^{\ddagger} = -24 \pm 2$ cal/deg mol) (18). From data on $Ni(dmtu)_6^{2+}$ in the slow exchange region we obtain $\Delta H^{\ddagger} = 14 \pm 1$ kcal/mol and $\Delta S^{\ddagger} = +32 \pm 5$ cal/deg mol. The significant point here is the positive value of $\Delta S^{\ddagger}$ is indicative of a true dissociative mechanism.

For the remaining complexes we merely note some trends in ligand exchange rates deduced from coalescence temperatures. It is apparent that in the tetrahedral complexes the rates decrease in the order $Nitu_2Cl_2 > Nitu_2Br_2$. The iodide is apparently slower than the bromide but the presence of the square planar compound obscures the ligand exchange coalescence. This order is observed in the analogous cobalt complexes (2) and also in nickel triphenylphosphine halide complexes (19). For the square planar complexes although the difference is not great it appears that $Nitu_3I^+ > Nitu_3Br^+$. Thus separate lines can be observed for the bromide and excess ligand at −90 °C whereas under the same conditions a single line is observed for the iodide solutions. For the octahedral complexes the rates increase in the order $Ni(detu)_6^{2+} < Ni(dmtu)_6^{2+} < Nitu_6^{2+}$. This behavior also parallels that of cobalt thiourea perchlorate complexes (2). It is interesting to note that the catalytically active π-allyl complexes clearly undergo very rapid ligand exchange.

Discussion

The factors which determine the geometric preferences of Ni(II) complexes have been extensively discussed (20, 21) but not as yet clearly delineated. Thus Holt and Carlin (8) concluded from their study of the geometry of nickel thiourea complexes "we believe that this work on complexes of nickel with substituted thioureas has raised more questions than provided answers in this respect". In the present studies we have found cases where only the tetrahedral form occurs ($Nitu_2Cl_2$), where only the octahedral form occurs (nitrate complexes), where only the square planar form occurs (π-allyl complexes), where there is an equilibrium between tetrahedral and square planar forms ($Nitu_2Br_2$ and $Nitu_3Br^+$), and where there is an equilibrium between square planar and octahedral forms ($Nitu_4^{2+}$ and $Nitu_6^{2+}$). It therefore seems appropriate to ask whether these data throw any new light on the factors determining the relative stability of different geometries.

Thus far the possibility of five coordinate geometries has not been mentioned. Five coordination, although less common than four or six coordination, is well recognized in the chemistry of divalent nickel (22). The majority of examples involve multidentate ligands. With donor atoms such as sulfur they are nearly always diamagnetic. The most plausible possibility is therefore that the diamagnetic compounds which we have formulated as square planar $Nitu_4^{2+}$ and $Nitu_3X^+$ could be five coordinate $Nitu_5^{2+}$ or $Nitu_4X^+$. We do not favor this possibility. The electronic spectra obtained from perchlorate solutions have been satisfactorily assigned to square planar compounds. On lowering the temperature the magnetic susceptibility measurements indicate that a paramagnetic octahedral compound is formed rather than a diamagnetic five coordinate compound. No five coordination has been reported in solid state studies of nickel thiourea complexes. Finally, measurements of the relative intensities of the free ligand and diamagnetic complex lines at −90 °C are more consistent with the formulation $Nitu_3X^+$ than $Nitu_4X^+$. None of these arguments are unequivocal but nevertheless they incline to be against postulating five coordination.

The factors influencing the choice between tetrahedral, square planar, and octahedral geometries may be classified as either steric or electronic. Steric factors clearly operate to give diminishing stability in the order tetrahedral > square planar > octahedral. It would appear that steric factors are *not* dominant for the compounds under discussion. Thus for the compounds $Nitu_2X_2$ and $Nitu_3X^+$ the latter square planar

Can. J. Chem. Downloaded from www.nrcresearchpress.com by 210.87.254.105 on 09/05/12
For personal use only.

compound becomes increasingly more stable in the series Cl < Br < I. This is clearly the opposite of the order expected from the size of the halide ions. In the perchlorate series even the bulky detu ligand forms an octahedral complex but not a tetrahedral one. $Ni(nptu)_2Br_2$ is predominantly tetrahedral but $Ni(nptu)_2(\pi\ allyl)^+$ is square planar. The bulk of the naphthylthiourea ligand does not therefore seem to be the determining factor. We must therefore look to electronic factors to provide a rational interpretation of the observations.

Perhaps the most significant result is that under identical conditions of solvent (acetone) and temperature (−90 °C) the stable neutral molecule $Nitu_2X_2$ is tetrahedral, the stable singly charged species $Nitu_3X^+$ is square planar, and the stable doubly charged species $Nitu_6^{2+}$ is octahedral. This suggests that the geometry is determined primarily by the charge on the metal atom. A rationalization of this result is that the geometric preference depends on a competition between energy gained by bond formation and energy lost through interelectronic repulsion between bonding electrons. The greater the charge on the metal atom the greater will be the gain in bonding energy for either covalent or ionic bonding. Total bonding energy will increase in the series tetrahedral < square planar < octahedral. Total repulsion energy between the bonding electrons will increase in the same order. For a high positive charge on the metal the gain in bonding energy will outweigh the loss due to interelectronic repulsion and an octahedral complex will result. For a low positive charge on the metal the gain in bonding energy on passing from tetrahedral to octahedral will be insufficient to compensate for the increased interelectron repulsion between the bonding electrons and the tetrahedral geometry will be preferred. For intermediate charge on the metal atom an optimum balance is attained with square planar geometry. Competition between ligand field stabilization energy (which on the molecular orbital picture is closely related to bonding energy) and interelectron repulsion between d electrons is a dominant theme in ligand field theory. The role of interelectronic repulsion between bonding electrons and lone pairs in determining the geometry of nontransition metal compounds has long been advocated (23). Application of the idea of balancing bonding energy and interelectron repulsion energy to the problem of the geometries of transition metal complexes therefore seems quite reasonable.

Most of the observations reported above fit this pattern quite well. *N,N'*-diethylthiourea might be expected to be a slightly better donor than thiourea decreasing the positive charge on the metal and slightly favoring a square planar complex over an octahedral complex. The nitrate ion is a rather poor ligand forming essentially ionic bonds thus leaving a high positive charge on the metal favoring octahedral geometry. The π-allyl ligand is a much better π acceptor than a halide ion; hence the positive charge on the metal in the π-allyl complex is relatively high and it assumes a square planar geometry whereas $Nitu_2Br_2$ is tetrahedral. Other examples may be found in the literature. Thus *N,N'*-diphenylaminotroponeimineates of Ni(II) show equilibria between square planar and tetrahedral geometries (15). Electron withdrawing substituents on the phenyl ring, which would increase the positive charge on the metal, favor the square planar form whereas electron donating substituents favor the tetrahedral form.

Finally it should be noted that the above discussion is not intended to imply that electronic effects always dominate steric effects in determining the geometry of Ni(II) complexes. Thus Ni(II) *N,N*-dimethylaminotroponeimineate is predominantly square planar whereas the most stable form of Ni(II) *N,N'*-diethylaminotroponeimineate is tetrahedral. This must clearly be ascribed to the difference in size of a methyl and an ethyl group.

Experimental

Halide, perchlorate, borofluoride, and nitrate complexes of Ni(II) with thiourea and substituted thiourea were synthesized following methods described in the literature (1, 6, 8, 9). Typically mixtures of the appropriate nickel salt and thiourea in the correct stoichiometric proportions were dissolved in *n*-butanol and heated on a water bath until the presence of solid was noticeable. Products separated on cooling. They were then filtered, washed with ether, dried under vacuum, and recrystallized from the solvent used in the preparation. All compounds were characterized by melting points, visible and infrared spectra. All melting points agree to within 2 °C with literature values. The n.m.r. spectra provide a further check on purity since diamagnetic impurities are readily identified. These complexes are stable compounds and may be stored without decomposition. The perchlorates and borofluorides are somewhat deliquescent. All compounds were routinely dried over P_4O_{10} before obtaining spectral or magnetic data.

π-Allyl and π-crotyl complexes were prepared by reaction of the appropriate thiourea with π-allyl nickel

bromide dimer (11). The latter can be obtained by reaction of allyl bromide with nickel tetracarbonyl (24). Typically methanolic solutions of π-allyl nickel bromide dimer and thiourea in the ratio of 1 to 4 mol were mixed at −5 °C under nitrogen. On cooling to −78 °C the required complexes separated as orange red solids and were removed by filtration. All of these compounds are air sensitive materials and must be stored under nitrogen or argon. They were handled in a gas line. The n.m.r. spectra showed a small resonance assigned to benzene (used as a solvent in the synthesis) in addition to the lines due to the complex and to the solvent (acetone-d_5). These spectra served to identify the complex without ambiguity.

Conductivity measurements at 25 and −78 °C were made in a glass cell immersed in either an oil bath maintained at 25 °C or in Dry Ice – acetone mixture. The solvent used was dry acetone and the conductance of solutions was measured with a Wayne–Kerr bridge operating at 1000 Hz. Magnetic susceptibilities were measured in carefully dried acetone using the n.m.r. method suggested by Evans (25). Diamagnetic corrections were made using Pascals constants. It is known that acetone can complex to the metal ion. However, careful measurements revealed no appreciable shift of the solvent resonance relative to TMS in the presence of nickel thiourea complexes. Bulk susceptibility shifts of the solvent resonance can therefore be used to determine the magnetic susceptibility.

Nuclear magnetic resonance spectra were obtained with a Varian DP 60 spectrometer operating at 56.4 MHz. TMS was used as an internal reference throughout.

We are indebted to the National Research Council of Canada for financial support of this research and to the Canadian International Development Agency for a scholarship to one of us (K.Z.).

1. A. Rosenheim and V. J. Meyer. Z. Anorg. Chem. **49**, 20 (1906); F. A. Cotton, C. D. Faut, and J. J. Mague. Inorg. Chem. **3**, 17 (1964); C. D. Flint and M. Goodgame. J. Chem. Soc. A, 744 (1966).
2. D. R. Eaton and K. Zaw. Can. J. Chem. **49**, 3315 (1971).
3. D. R. Eaton and K. Zaw. J. Am. Chem. Soc. **94**, 4394 (1972).
4. A. Lopez-Castro and M. R. Truter. J. Chem. Soc. 1309 (1963).
5. M. Nardelli, G. Gasparri, G. Battistini, and P. Domiano. Acta Cryst. **20**, 349 (1966).
6. R. W. Ollif. J. Chem. Soc. 2036 (1965).
7. A. Yamaguchi, R. B. Penland, S. Mizushima, J. J. Lane, C. Curran, and J. V. Quagliano. J. Am. Chem. Soc. **80**, 527 (1958).
8. S. L. Holt and R. L. Carlin. J. Am. Chem. Soc. **86**, 3017 (1964).
9. S. Basso, J. A. Costamagna, and R. Levitus. J. Inorg. Nucl. Chem. **31**, 1797 (1969).
10. D. R. Eaton and W. D. Phillips. Adv. Magn. Reson. **1**, 103 (1965).
11. F. Guerrieri. Chem. Commun. 983 (1968).
12. A. Sirigu. J. Chem. Soc. D, 256 (1969).
13. M. I. Lobach, B. D. Babitskii, and V. A. Kromer. Russ. Chem. Rev. **36**, 476 (1967).
14. F. Sato, K. Iida, and M. Sato. J. Organomet. Chem. **39**, 197 (1972).
15. D. R. Eaton, W. D. Phillips, and D. J. Caldwell. J. Am. Chem. Soc. **85**, 397 (1963).
16. J. P. Fackler and F. A. Cotton. J. Am. Chem. Soc. **83**, 3775 (1961).
17. J. A. Pople, W. G. Schneider, and H. J. Bernstein. High resolution nuclear magnetic resonance. McGraw-Hill, New York. 1959. p. 222.
18. D. R. Eaton and K. Zaw. To be published.
19. E. A. LaLancette and D. R. Eaton. J. Am. Chem. Soc. **86**, 5145 (1964); W. D. Horrocks and L. H. Pignolet. J. Am. Chem. Soc. **88**, 5929 (1966).
20. L. Venanzi. J. Inorg. Nucl. Chem. **8**, 137 (1958).
21. L. Sacconi. Transition Met. Chem. **4**, 199 (1968).
22. E. L. Muetterties and R. A. Schunn. Qt. Rev. Chem. Soc. **20**, 245 (1966).
23. R. J. Gillespie. Angew. Chem. Int. Ed. **6**, 819 (1967).
24. E. O. Fischer and G. Burger. Z. Naturforsch. **16b**, 77 (1961).
25. D. F. Evans. J. Chem. Soc. 2003 (1959).

Can. J. Chem. Downloaded from www.nrcresearchpress.com by 210.87.254.105 on 09/05/12
For personal use only.

The Kinetics of the Catalyzed Reaction between Two Substrates in a Special Case

JAROSLAV RYBICKY[1]

Welwyn Canada Limited, London, Ontario N5W 2C2

Received July 29, 1974

Can. J. Chem. Downloaded from www.nrcresearchpress.com by 210.87.254.40 on 09/05/12
For personal use only.

JAROSLAV RYBICKY. Can. J. Chem. **53**, 644 (1975).

The kinetics of the catalyzed reaction between two substrates is dealt with for the special case in which the product associated with the catalyst cannot be distinguished from the product dissociated from the catalyst. The rate equation in which the yield is a sum of products both associated with and dissociated from the catalyst is derived and its applicability is assessed with respect to the kinetic and concentration conditions. It was found that under steady-state conditions and fast preequilibrium condition a twenty-fold excess of the substrates over the catalyst is enough for the yield of reaction to be represented by the equation derived with less than 1% relative error, and even for a five-fold excess the equation remains a fairly good approximation. Under such conditions the rate equation can find practical utility.

JAROSLAV RYBICKY. Can. J. Chem. **53**, 644 (1975).

On traite la cinétique de la réaction catalysée impliquant deux substrats comme un cas spécial dans lequel le produit associé avec le catalyseur ne peut pas être distingué du produit dissocié du catalyseur. L'équation de vitesse dans laquelle le rendement est une somme de produits associés et dissociés du catalyseur est déduite et son champ d'application est évalué par rapport à la cinétique et aux conditions de concentration. On a trouvé que dans des conditions d'état d'équilibre et dans des conditions où il y a un prééquilibre rapide, un excès de 20 fois de substrat par rapport au catalyseur est suffisant pour que le rendement de la réaction puisse être représenté par l'équation dérivée avec moins de 1% d'erreur et même pour un excès de 5 fois, l'équation demeure une assez bonne approximation. Dans de telles conditions l'équation de vitesse peut avoir une utilité pratique.

[Traduit par le journal]

Introduction

The yield of a catalyzed reaction is generally represented by the reaction product which has dissociated from the catalyst. The product of the reaction that is still associated with the catalyst is considered an intermediate in the overall reaction mechanism, and it does not form any part of the yield of the reaction (1). In a special case, however, it may be impossible or undesirable to discriminate between the ultimate and penultimate products of a reaction scheme. An example could be found in the polymerization of a ternary complex among a donor-monomer, an acceptor-monomer, and a complexing agent via a mechanism suggested by Gaylord (2). On precipitation the polymer comes out of the solution irrespective of the presence or absence of the catalyst on the macromolecule. For such cases it is necessary to employ kinetics which would consider the yield to be a sum of the products associated with and those dissociated from the catalyst. This paper derives and appraises a rate equation for cases of such nature.

The investigated reaction scheme is identical with the ordered ternary complex mechanism for enzyme systems. Recently, the rate equation for this system was derived (3) by use of the Laplace–Carson transformation and, consequently, the result is quite complex. It would be useful to have a simpler kinetic equation and the analysis of the conditions for which it is valid. This work employs the steady-state and equilibrium approximations to derive the combined transient-state and steady-state rate equation for the scheme.

Derivation of the Rate Equation

The derivation is based on the following scheme.

[1]

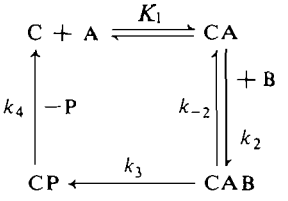

[1]Present address: 1255 Brydges Street, P.O. Box 2484, Terminal A, London, Ontario N5W 2C2.

Can. J. Chem. Downloaded from www.nrcresearchpress.com by 210.87.254.40 on 09/05/12
For personal use only.

In the foregoing reactions: C is a catalyst; A is a substrate able to complex with catalyst C; CA is a binary complex between catalyst C and substrate A; B is a substrate unable to complex with catalyst C, and able to complex with CA; CAB is a ternary complex among catalyst C, substrate A, and substrate B; CP is a product associated with catalyst C; P is a product dissociated from catalyst C; K_1 is an equilibrium constant; and k_i are rate constants for corresponding reactions. In the scheme, reaction 1 is a fast preequilibrium which controls the concentration of CA at any instant.

The yield of the reaction, Y, is defined by eq. 2.

$$[2] \qquad [Y] = [CP] + [P]$$

Two approximations had to be made in order to derive the rate equation. First, the steady-state treatment was applied to the concentration of the ternary complex, as is shown by eqs. 3 and 4.

$$[3] \quad d[CAB]/dt = k_2[CA][B] - (k_{-2} + k_3)[CAB] = 0$$

$$[4] \qquad [CAB] = k_2[CA][B]/(k_{-2} + k_3)$$

Second, the concentrations of the substrates, A and B, were treated as constants equal to the initial concentrations. In practice it means that the two components are in concentration excess over the catalyst.

$$[A]_0, [B]_0 \gg [C]_0$$

so that

$$[5] \qquad [A] \simeq [A]_0 \text{ and } [B] \simeq [B]_0$$

Both approximations are assessed in the following chapters and the kinetic and concentration conditions under which the final rate equation is valid are discussed.

The rate equation is derived as follows. Combining the conservation equation for the catalyst

$$[6] \quad [C]_0 = [C] + [CA] + [CAB] + [CP]$$

with the equilibrium constant K_1

$$[7] \qquad K_1 = [CA]/[C][A]$$

and eq. 4 (under condition 5), the instantaneous concentration of CAB can be expressed by the following form.

$$[8] \qquad [CAB] = R([C]_0 - [CP])$$

where

$$[9] \quad R = QK_1[A]_0/(1 + K_1[A]_0 + QK_1[A]_0)$$

and

$$[10] \qquad Q = [B]_0 k_2/(k_{-2} + k_3)$$

In order to find [CAB] as a function of time, [CP] must be expressed as a function of time.

$$[11] \qquad d[CP]/dt = k_3[CAB] - k_4[CP]$$

Substitution for [CAB] from eq. 8 into eq. 11 yields

$$[12] \quad d[CP]/dt = k_3R[C]_0 - (k_3R + k_4)[CP]$$

Equation 12 may be integrated to give

$$[13] \qquad [CP] = [1 - \exp(-G_2t)]G_1/G_2$$

where

$$[14] \qquad G_1 = k_3R[C]_0$$

$$[15] \qquad G_2 = k_3R + k_4$$

From eq. 2 it follows that

$$[16] \qquad d[Y]/dt = d[CP]/dt + d[P]/dt$$

and

$$[17] \qquad d[Y]/dt = k_3[CAB]$$

Combination of eqs. 8, 13, and 17 leads to

$$[18] \quad d[Y]/dt = k_3R[C]_0 - k_3RG_1/G_2 + k_3R\exp(-G_2t)G_1/G_2$$

This integrates to a rate equation

$$[19] \qquad [Y] = Et + F(1 - \exp(-G_2t))$$

where

$$[20] \qquad E = k_3R([C]_0 - G_1/G_2)$$

$$[21] \qquad F = k_3R\,G_1/G_2^2$$

It should be pointed out that eq. 19 has been derived for a low concentration of catalyst, for the first order conversion of CAB into CP, and that the steady-state approximation was applied.

Assessment of the Approximations in the Kinetics

The mathematical solution of the reaction scheme is based on the approximation of a steady-state concentration of CAB and the applicability of initial concentrations of the two substrates over a range of conversion. The limits imposed on the validity of the solution by the approximations will now be investigated.

A pair of yield/time curves was constructed

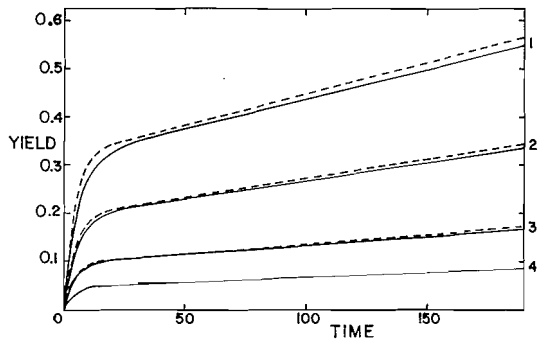

FIG. 1. Effect of conversion on applicability of eq. 19. (---) eq. 19; (—) exact solution: (1) $[C]_0/[A]_0 = 1/3$; (2) 1/5; (3) 1/10; (4) 1/20. Calculated for $[A]_0 = 1$, $[B]_0 = 1$, $k_1 = 8$, $k_{-1} = 4$; $k_2 = 0.4$, $k_{-2} = 0.4$, $k_3 = 4$, $k_4 = 0.004$.

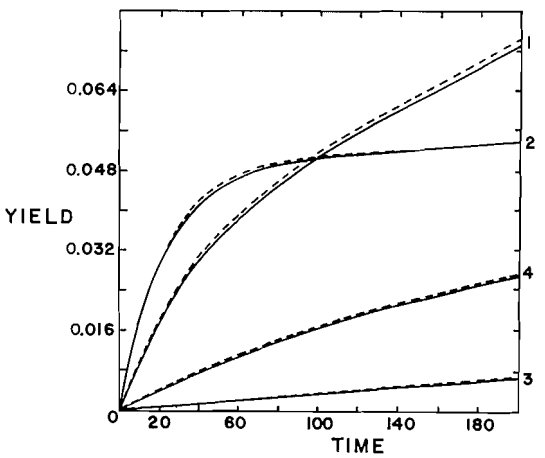

FIG. 2. Effect of relative magnitudes of k_2, k_{-2}, and k_3 on applicability of eq. 19. (---) eq. 19; (—) exact solution. See Table 1.

from a simulated set of concentration and rate parameters. One curve of the pair was calculated by means of eq. 19. The other curve was calculated by means of a fourth order Runge–Kutta numerical method (4) from a set of differential equations describing the reaction scheme and it does not involve any of the approximations.

The effect of the extent of conversion on the validity of results obtained by eq. 19 is demonstrated by Fig. 1. The reading from, *e.g.*, curve 4 shows a relative error of 7% at conversion of 2.3% B, and less than 1% error at conversion of 4.6% B.

Various ratios of the component concentrations were employed as these are also expected

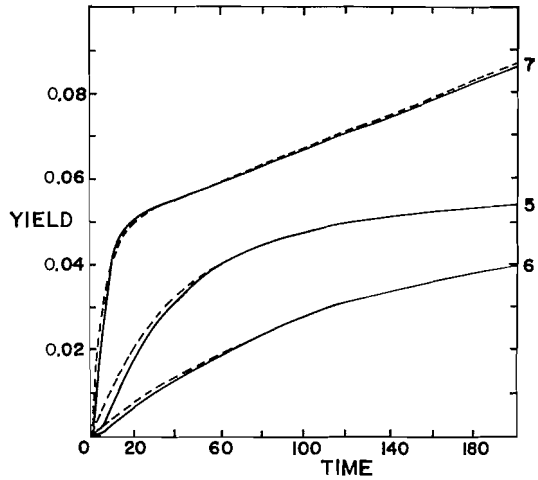

FIG. 3. Effect of relative magnitudes of k_2, k_{-2}, and k_3 on applicability of eq. 19. (---) eq. 19; (—) exact solution. See Table 1.

to affect the constancy of [A] and [B] during reaction. At conversion of 5% B, a ratio 1/3 of $[C]_0/[A]_0$ yields a relative error of 44.0%, 1/5 yields 24.2% error, 1/10 gives 8.1% error, and 1/20 yields 0.5% relative error. (The rate constants used in the simulation of the curves were chosen to satisfy the steady-state approximation and therefore eliminate any deviation due to the late attainment of a steady-state concentration of CAB. The constants also satisfied the assumed rapid attainment of equilibrium 1.)

The effect of the kinetic conditions on the validity of results is demonstrated in Figs. 2 and 3. The approximate and exact solutions were simulated for the following combinations of rate constants (L and S are large and small numbers, respectively; the ratio L/S is 100).

Combination	k_2	k_{-2}	k_3
1	S	L	L
2	S	S	L
3	S	L	S
4	L	L	S
5	S	S	S
6	L	S	S
7	L	S	L

Although other parameters may influence the rate of reaction, these three rate constants are sufficient to define the attainment of the steady state. The constants and concentrations employed

Can. J. Chem. Downloaded from www.nrcresearchpress.com by 210.87.254.40 on 09/05/12
For personal use only.

TABLE 1. Parameters used in the simulation*

Code	k_1	k_{-1}	k_2	k_{-2}	k_3	k_4
1	5	0.5	0.05	5	5	0.005
2	5	0.5	0.05	0.05	5	0.0005
3	8	0.8	0.08	8	0.08	0.0008
4	8	4	1	1	0.01	0.0001
5	8	0.8	0.08	0.08	0.08	0.0008
6	8	4	0.8	0.008	0.008	0.0008
7	8	4	0.4	0.004	0.4	0.004

*$[C]_0 = 0.05$; $[A]_0 = 1$; $[B]_0 = 1$.

for the simulation of the curves are summarized in Table 1. The number of the curve indicates an *L–S* combination for k_2, k_{-2}, and k_3, as listed above. Combinations 1, 2, and 3 (Fig. 2, lines 1, 2, and 3, respectively) satisfy the steady-state approximation and, as expected, the approximated and exact solutions are in good accord. Although the conversion region covered by line 3 is small, the calculations indicate good agreement as a non-steady state phenomenon would have been indicated at the beginning of the reaction. Similarly, a good fit is found for the fourth combination of rate constants, the fast pre-equilibrium condition (line 4). However, for the other three possible conditions, 5, 6, and 7 (Fig. 3, lines 5, 6, and 7) a discrepancy is evident at low conversion.

Conclusion

The reaction scheme for the special case of a catalyzed reaction in which the ultimate and penultimate products cannot be discriminated can be investigated kinetically best when the substrates are in a concentration excess over the catalyst. When the kinetic conditions are such that the steady-state approximation is justified, a twenty-fold excess of the substrates over the catalyst appears to be enough for the yield of reaction to be represented by eq. 19 with less than 1% relative error when the conversion of the substrates has attained 4.6%. However, even for $[C]_0/[A]_0$ ratios as large as 1/5 the kinetic equation derived remains a fairly good approximation.

I wish to thank Dr. B. L. Funt for his constructive and stimulating comments on this work. The helpful suggestions of one of the referees of this article also are gratefully acknowledged.

1. C. CAPELLOS and B. H. J. BIELSKI. Kinetics systems. Wiley-Interscience, a Division of John Wiley and Sons, Inc., New York, 1972.
2. N. G. GAYLORD. J. Polym. Sci. C, **31**, 247 (1970).
3. N. H. HIJAZI and K. J. LAIDLER. Can. J. Biochem. **51**, 832 (1973).
4. P. W. WILLIAMS. Numerical computation. Thomas Nelsons and Sons Ltd., London, Great Britain. 1972. p. 91.

Can. J. Chem. Downloaded from www.nrcresearchpress.com by 210.87.254.40 on 09/05/12
For personal use only.

^{1}H, ^{13}C, ^{14}N, ^{19}F Nuclear Magnetic Resonance Contact Shifts and Electron Spin Distribution in Aniline and Fluoroanilines – Ni(II) Acetylacetonate Complexes

C. CHACHATY, A. FORCHIONI, AND J. VIRLET

Service de Chimie Physique, CEN de Saclay, B.P. n°2, 91190, Gif-sur-Yvette, France

Received July 4, 1974

C. CHACHATY, A. FORCHIONI, and J. VIRLET. Can. J. Chem. **53**, 648 (1975).

The contact shifts of ^{1}H, ^{13}C, ^{14}N, and ^{19}F in chloroform solutions of Ni(II) acetylacetonate – aniline and fluoraniline complexes have been studied by high resolution n.m.r. The unpaired electron spin distribution in these ligands is compared to that calculated by the INDO method for the corresponding aniline cation radicals. The ratio of the hyperfine coupling constants a_{NH}^{H}/a_{N} suggests that in these aniline complexes the $C_1—N\langle^{H}_{H}$ fragment is pyramidal with an angle of 13–15° between the perpendicular of the C—N bond and the axis of the p like orbital centered on nitrogen. The electron spin distribution between the NH_2 group and the phenyl ring may be partially accounted for by assuming an internal rotation about the C—N bond. The ^{13}C relaxation indicates a N—Ni distance of the order of 2 Å for aniline and 2 fluoraniline complexes and an electron spin–lattice relaxation time of $\sim 5 \times 10^{-10}$ s at 300 °K.

C. CHACHATY, A. FORCHIONI et J. VIRLET. Can. J. Chem. **53**, 648 (1975).

Les déplacements de contact de ^{1}H, ^{13}C, ^{14}N et ^{19}F dans les complexes d'acétylacétonate de nickel avec l'aniline et les fluoranilines en solution dans $CHCl_3$, ont été étudiés par r.m.n. haute résolution. La répartition de la densité de spin dans ces ligands est comparée à celle calculée par la méthode INDO pour les radicaux cations correspondants. Le rapport des constantes de couplage a_{NH}^{H}/a_{N} suggère que dans ces complexes d'anilines, le fragment $C_1—N\langle^{H}_{H}$ est pyramidal avec un angle de 13 à 15° entre la normale à la liaison C—N et l'axe de l'orbitale p centrée sur l'azote. La répartition de la densité de spin entre le groupe NH_2 et le cycle aromatique peut être expliquée en partie par une rotation interne autour de la liaison C—N. La relaxation des carbones 13 indique une distance azote–nickel de l'ordre de 2 Å pour l'aniline et la 2 fluoraniline ainsi qu'un temps de relaxation électronique voisin de 5×10^{-10} s à 300 °K.

Introduction

In some coordination complexes of paramagnetic transition ions, the delocalization of the unpaired spin into the ligand σ and π orbitals may be determined from n.m.r. contact shifts if the pseudocontact contribution is negligible (1, 2). It is generally assumed that this condition is fulfilled in the case of Ni(II) aminotroponeiminate (3, 4) and for Ni(II) acetylacetonate ($Ni(AA)_2$) complexes with pyridine like compounds (5–7) and aliphatic (7, 8) or aromatic (6, 8–10) amines. The $Ni(AA)_2$ aniline complex has been studied by proton (9, 10), ^{14}N (8) and ^{13}C (6) n.m.r. spectroscopy. It has been shown that the unpaired spin density is delocalized into the aniline π system and that its distribution on the phenyl ring is somewhat similar to that observed in the case of the benzyl radical, isoelectronic with the $C_6H_5—\dot{N}H_2^{+}$ cation radical (6). The similarity between the electronic structure of the ligand part of some coordination complexes and that of related free radicals which may be studied by electron spin resonance (e.s.r.) is interesting since subsidiary information may be provided by n.m.r., particularly the sign and magnitude of the hyperfine coupling parameters. The Fourier transform n.m.r. is also very convenient for the observation of ^{13}C in natural abundance and the study of its hyperfine coupling, which is difficult to determine by e.s.r., unless a well resolved spectrum is obtained with a high signal-to-noise ratio.

In this work we intend to study the correlation between the contact shifts of the different nuclei (^{13}C, ^{1}H, ^{14}N, ^{19}F) of aniline and its fluorinated homologs, complexed with Ni(II) acetylace-

Can. J. Chem. Downloaded from www.nrcresearchpress.com by 210.87.254.105 on 09/05/12
For personal use only.

Can. J. Chem. Downloaded from www.nrcresearchpress.com by 210.87.254.105 on 09/05/12
For personal use only.

tonate in order to determine the spin density distribution in these ligands and to obtain some information about the hybridization state of nitrogen in the amino group. For that purpose, the experimental data will be compared to the theoretical ones calculated by the INDO method (11) for several possible configurations of the aniline radical cation chosen as a model. This work will be completed by a ^{13}C relaxation time study of the complex aniline and 2F-aniline with $Ni(AA)_2$ and the ligand-to-metal distance will be estimated.

Experimental

The ^1H n.m.r. measurements have been carried out at 250 MHz with a Cameca TSN 250 spectrometer, with some experiments at 60 MHz (Varian T60 or NV14). The ^{13}C and ^{19}F spectra were recorded with a Varian XL 100 12-WG spectrometer operating at 25.15 MHz (^{13}C in Fourier transform) or 94.1 MHz (^{19}F). The ^{13}C spin–lattice relaxation time was measured by the inversion recovery method using the pulse sequences . . . 90° ∞, $T \gg T_1$, 180°, t, 90° . . . (12). ^{14}N contact shift measurements were carried out with a pulsed n.m.r. spectrometer, operating at 4.35 MHz, designed by one of us (J.V.). Solutions of anilines in $CDCl_3$ (20 to 50% v/v) were dried on molecular sieve before addition of $Ni(AA)_2$. The contact shifts were measured for $[Ni(AA)_2]/[aniline]$ ratios of 0.001 to 0.01. In this range the shift variation is linear, indicating a complete complexation of $Ni(AA)_2$ by aniline.

The electron g value for $Ni(AA)_2$, $(aniline)_2$ complexes was determined from relative paramagnetic susceptibility measurements by n.m.r. The shift of the solvent peak ($CHCl_3$) in the presence of the complexes, with respect to TMS contained in a coaxial tube was compared to the shift observed with a known concentration of a reference paramagnetic compound such as diphenylpicrylhydrazyl ($g = 2.0036$, $S = \frac{1}{2}$) and copper diethylthiocarbamate ($g = 2.0486$, $S = \frac{1}{2}$). The g value of the complex was given by the ratio

$$[1] \qquad \frac{\vartheta - \vartheta_0}{\vartheta_{ref} - \vartheta_0} = \frac{C_{complex}}{C_{ref}} \frac{S'(S'+1)g_{complex}^2}{S(S+1)g_{ref}^2}$$

where ϑ and ϑ_{ref} are the shift observed in the presence of a paramagnetic solute, ϑ_0 the solvent shift, C the solute concentration, S' the total electron spin = 1 for the Ni(II) complexes in question.

Results and Discussion

Hyperfine Coupling Constants and Spin Densities

The relationship between the hyperfine coupling of a nucleus i and its contact shift is (13, 14)

$$[2] \qquad \frac{\Delta H}{H_0} = -a_i \frac{g_e^2 \beta_e^2 S(S+1)}{g_i \beta_n 3kT} pq$$

where a_i is expressed in G, g_e and g_i being the electron and nuclear g factor, β_e the Bohr magneton, and β_n the nuclear magneton. For $Ni(AA)_2$, $(aniline)_2$ complexes the total electron spin is $S = 1$ and $g_e = 2.2 \pm 0.1$. p is the ratio $[Ni(AA)_2]/[aniline]$ and q the number of coordinated anilines equal to 2. For all nuclei under study $g_i > 0$ and a downfield or upfield contact shift will be observed according to a_i being positive or negative.

Assuming that in the ligand the unpaired electron spin is delocalized through the π orbitals of the phenyl ring, the spin density on the carbon of a C—H fragment will be given by

$$[3] \qquad a_{CH}^H = \tfrac{1}{2} Q_{CH}^H \rho_C^\pi$$

with $Q_{CH}^H = -27$ G as in the case of benzyl type radicals. In this equation and the following ones, the factor $\frac{1}{2}$ corresponds to $S = 1$ (ref. 2, chapt. III, pp. 93 and 97).

The hyperfine coupling constants of atoms bearing a fraction of the π spin density, such as ^{13}C, ^{14}N, or ^{19}F are given by the general relation of Karplus and Fraenkel (15) which may be represented in the simplified form

$$[4] \qquad a_i^x = \tfrac{1}{2}\left(Q_1^x \rho_{x_i}^\pi + \sum_j Q_2^y \rho_{y_j}^\pi \right)$$

where y_j is a nucleus adjacent to x_i. The parameter Q_1^x may be dependent on the nature of y_j. For a C···C···C fragment (with H on the central C), the constants $Q_1^C = +35.6$ G and $Q_2^C = -13.9$ G given in ref. 15 are often used.

A great deal of work has been carried out on the problem of fluorine hyperfine coupling in π electron radicals and several values have been proposed for the relevant σ–π parameters (16) in eq. 4. It seems however that the ^{19}F hyperfine coupling constant may be given with sufficient accuracy by the simple equation (16*f*)

$$[5] \qquad a^F = \tfrac{1}{2} Q_{eff}^F \rho_C^\pi$$

which may be useful to determine the spin density on carbons in the case of highly fluorine substituted radicals or ligands. In the present work, Q_{eff}^F will be deduced from ρ_C^π values given by eq. 4. The hyperfine coupling constant of nitrogen depends on its hybridization state and is given by the relation (17, 18)

$$[6] \qquad a_N = \tfrac{1}{2}[Q_N^0 + 550 \times 2\mathrm{tg}^2 \varphi]\rho_N^\pi$$

where φ represents the angle between the perpendicular to the C_1—N bond and the axis of

TABLE 1. Hyperfine coupling constants[a]

									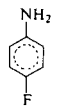			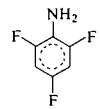			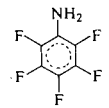	
Amino group	N	H	N	H		N	H		N	H		N	H		N	H
	3.0	−0.84	2.4	−0.79		2.3	−0.65		2.5	−0.74		1.24	−0.38		0.83	−0.22
Ring	C	H	C	H	F	C	H	F	C	H	F	C	H	F	C	F
1	−0.278	—	−0.201	—		−0.222	—		−0.290	—		−0.165			−0.100	
2	0.171	−0.083	0.115	—	0.101	0.135	−0.073		0.174	−0.073		0.102	—	0.093	0.053	0.059
3	−0.107	0.023	−0.071	0.021		−0.083	—	−0.035	−0.093	0.029		−0.066	0.007	—	−0.043	−0.023
4	0.135	−0.09	0.091	−0.051		0.107	−0.084		0.174	—	0.227	0.083	—	0.110	0.061	0.064
5	−0.107	0.023	−0.081	0.021		−0.084	0.030		−0.093	0.029		−0.066	0.007	—	−0.043	−0.023
6	0.171	−0.083	0.101	−0.057		0.139	−0.072		0.174	−0.073		0.102	—	0.093	0.053	0.059

[a]In G, calculated for $g_e = 2.2$.

Can. J. Chem. Downloaded from www.nrcresearchpress.com by 210.87.254.105 on 09/05/12
For personal use only.

TABLE 2. ^{13}C chemical shifts in fluorinated anilines (in p.p.m. from TMS, in $CDCl_3$ at 30 °C)

Compound	Chemical shift					
	C_1	C_2	C_3	C_4	C_5	C_6
2 fluoraniline	134.8	151.9	115.3	118.6	124.6	117.1
3 fluoraniline	148.7	101.8	163.8	104.6	130.4	110.7
4 fluoraniline	142.7	115.9	115.4	156.2	115.4	115.9
2-4-6 trifluoraniline	120.9	151.9	100.0	154.2	100.0	151.9
Pentafluoraniline	122.5	137.2	138.4	133.8	138.4	137.2

the p like orbital centered on nitrogen. Q_N^0 has been taken equal to +35 G in analogy with nitrogen containing cation radicals (19). The ratio a_{NH}^H/a_N depends linearly upon φ between 4 and 16° and is given in this range, by the relation

$$[7] \qquad a_{NH}^H/a_N = -1.32 + 0.072\,\varphi$$

This equation has been derived from INDO calculations on the aniline cation radical using the internuclear distances given in ref. 11. For the two limiting cases $\varphi = 0$ (sp^2 nitrogen) and $\varphi = 19.5°$ (sp^3 nitrogen) where eq. 7 is not valid, INDO calculations give respectively $a_{NH}^H/a_N = -1.14$ in good agreement with e.s.r. data (19) and $a_{NH}^H/a_N = -0.02$.

It will be shown that the spin density on carbon 1 is much smaller in absolute value than ρ_N^π so that its contribution by spin polarization to a_N (relation 4) and by hyperconjugation to a_{NH}^H may be neglected.

The hyperfine coupling constants measured from contact shifts are given in Table 1. The analysis of the proton magnetic resonance of 2, 3, and 4 fluoranilines, giving the chemical shifts of free ligands has been published elsewhere (20). The ^{13}C chemical shifts of fluoranilines under study are given in Table 2.

The ^{13}C hyperfine coupling parameters for complexed aniline and 2 fluoraniline, which include at least four successive —CH— fragments have been calculated from the system

$$[8] \qquad a_3^C = \tfrac{1}{2}[Q_1\,\rho_3 + Q_2\,(\rho_2 + \rho_4)]$$
$$a_4^C = \tfrac{1}{2}[Q_1\,\rho_4 + Q_2\,(\rho_3 + \rho_5)]$$

ρ_2 or ρ_6, ρ_3 or ρ_5, and ρ_4 being given by the corresponding value of a_{CH}^H (relation 3). Thus we get $Q_1 = 34.6$ G, $Q_2 = -12.0$ G for aniline, $Q_1 = 37.4$ G, $Q_2 = -12.8$ G for 2 fluoraniline, in close agreement with the values given in ref. 15, which will be used throughout this work for the calculations of spin densities from ^{13}C contact shifts. This result suggests that the delocalization of the electron spin occurs only through the ring π system and that the contribution of the ligand or metal centered pseudocontact shift is negligible for the ^{13}C.

The agreement between the spin densities calculated from several relations derived from eqs. 3 and 4 may be appraised on the example of the 2-fluoraniline complex (Table 3). It may be expected that relations 19 and 20 of table 3 providing a straightforward determination of ρ_C^π will give the most accurate results, but their use is restricted to a carbon bound to a proton or to a —CH=CH=CH— fragment.

The determination of ρ_1, may be done only by relation 21 since the value of the parameter Q_2^y of eq. 4 relative to the nitrogen is not accurately known. The discrepancy between the ρ_2 value deduced from eqs. 20′ and 21 may also be pointed out in Table 3. The value $\rho_2 = 0.0043$ seems the most likely since it is close to ρ_6 as expected from INDO calculation on the cation radical

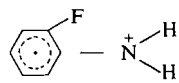

The parameter Q_{eff}^F of eq. 5 has been estimated for the $Ni(AA)_2$ fluoraniline complexes, from the ratio $2a^F/\rho_C^\pi$, ρ_C^π being given by one of the relations of Table 3. It has been found that $Q_{eff}^F = 51 \pm 3$ G, in satisfactory agreement with the value previously determined by e.s.r. fluoroaromatic radicals which are in the range of 53 to 57 G (16*e*, *f*, *g*). It may be seen on the example of 2- and 3-fluoraniline complexes that the substitution of a proton by fluorine does not introduce a noticeable change in the spin density on the adjacent carbon (Table 4) and that $Q_{eff}^F \sim -2Q_{CH}^H$. On the other hand the total spin density on each aniline of the $Ni(AA)_2$-$(aniline)_2$ complex decreases almost linearly with

Can. J. Chem. Downloaded from www.nrcresearchpress.com by 210.87.254.105 on 09/05/12
For personal use only.

Can. J. Chem. Downloaded from www.nrcresearchpress.com by 210.87.254.105 on 09/05/12
For personal use only.

TABLE 3. Different determinations of the spin densities in 2-fluoraniline complexed by $Ni(AA)_2$

Number	Equation	Spin density					
		1	2	3	4	5	6
19	$a_i^{H} = \frac{1}{2}Q_H\rho_i$	—	—	−0.0015	0.0038	−0.0016	0.0042
20	$a_i^{C} = \frac{1}{2}\left[Q_1\rho_i + \frac{2Q_2}{Q_H}(a_{i-1}^{H} + a_i^{H}\right]$	—	—	—	0.0039	−0.0014	—
20′	$a_i^{C} = \frac{1}{2}\left[Q_1\rho_i + 2\left(a_{i-2}^{C} - \frac{Q_1}{Q_H}a_{i-2}^{H} - \frac{Q_2}{Q_H}a_{i-3}^{H} + \frac{Q_2}{Q_H}a_{i+1}^{H}\right)\right]$	—	0.0043	—	—	—	
21	$a_{i+1}{}^{C} = \frac{1}{2}\left[2Q_1\frac{a_{i+1}^{H}}{Q_H} + Q_2\left(\rho_i + \frac{2a_{i+2}^{H}}{Q_H}\right)\right]$	−0.0023	0.0025	−0.0019	0.0034	−0.0019	0.0038
22	$a_i^{C} = \frac{1}{2}[Q_1\rho_i + Q_2(\rho_{i-1} + 2a_{i+1}^{H}/Q_H)]$ $a_{i+1}{}^{C} = \frac{1}{2}[Q_1\rho_{i-1} + Q_2(\rho_i + 2a_{i+2}^{H}/Q_H)]$	—	—	—	0.0039	−0.0017	—

Can. J. Chem. Downloaded from www.nrcresearchpress.com by 210.87.254.105 on 09/05/12
For personal use only.

TABLE 4. π spin density distribution in aniline ligands

(*a*) Experimental spin densities

	Spin densities											
	Aniline		2F-aniline		3F-aniline		4F-aniline		2,4,6-F-aniline		Pentafluoraniline	
	Actual	Normalized to 1	Actual	Normalized to 1	Actual	Normalized to 1	Actual	Normalized to 1	Actual	Normalized to 1	Actual	Normalized to 1
N	0.055	0.870	0.047	0.872	0.043	0.835	0.047	0.888	0.024	0.792	0.015	0.769
C_1	−0.0074	−0.117	−0.0023	−0.043	−0.0049	−0.095	−0.0091	−0.172	−0.0046	−0.150	−0.0010	−0.051
C_2	0.0061	0.097	0.0043	0.080	0.0054	0.105	−0.0054	0.102	0.0038	0.125	0.0023	0.118
C_3	−0.0016	−0.026	−0.0015	−0.028	−0.0015	−0.029	−0.0021	−0.040	−0.0005	−0.017	−0.0008	−0.041
C_4	0.0066	0.105	0.0038	0.071	0.0063	0.122	0.0084	0.160	0.0043	0.142	0.0025	0.128
C_5	−0.0016	−0.026	−0.0016	−0.029	−0.0021	−0.041	−0.0021	−0.040	−0.0005	−0.017	−0.0008	−0.041
C_6	0.0061	0.097	0.0042	0.078	0.0053	0.0103	0.0054	0.102	0.0038	0.125	0.0023	0.118
$\Sigma \rho_i^{\pi}$	0.0632		0.0539		0.0515		0.0529		0.0303		0.0195	
φ	14.4°		13.7°		14.5°		14.2°		14.1°		14.7°	
Q_{eff}^F	—		47		48		54		55		(51)[a]	
Q_{NC}^C	−2.3		−4.3		−2.9		−2.4		−2.6		−6.6	

(*b*) INDO calculated spin densities with $\varphi = 15°$

	N	C_1	$C_{2,6}$	$F_{2,6}$	$C_{3,5}$	$F_{3,5}$	C_4	F_4
$C_6H_5\dot{N}H_2^+$	0.533	0.010	0.171	—	−0.089	—	0.234	—
$C_6F_5\dot{N}H_2^+$	0.505	0.035	0.143	0.025	−0.089	−0.008	0.216	0.040

[a]Average value of Q_{eff}^F used in the calculation of ρ_i^{π}.

Can. J. Chem. Downloaded from www.nrcresearchpress.com by 210.87.254.105 on 09/05/12
For personal use only.

the number of fluorines showing an important effect of this substituent on the electron donor properties of aniline with respect to $Ni(AA)_2$ (Table 4). The Q_1 and Q_2 parameters of eq. 4, which have been given above for a C═CH═C fragment may be different for a C═CF═C fragment. Equation 8, together with $Q_{eff}^F = 51$ G, gives $Q_1 = 41.1$ G, $Q_2 = -10.1$ G for the penta fluoraniline complex, not so different therefore from the values determined for aniline and 2-fluoraniline in the case of a C═CH═C fragment ($Q_1 = 36$ G, $Q_2 = -12.4$ G).

The large downfield shifts observed for ^{14}N might be due in part to the pseudocontact effect arising from the vicinity of the metal ion or from the spin density in the nitrogen centered p like orbital (21). Such a contribution seems difficult to estimate without a precise knowledge of the geometry and electronic configuration of the whole complex. We shall therefore consider tentatively that the observed shifts result mainly from the Fermi contact interaction and verify the likelihood of this assumption.

The ratios a_{NH}^H/a_N of all the anilines under study (Table 1) fall between -0.2 and -0.3 and correspond therefore to an angle φ of the order of 14–16° (eq. 7).

It has been shown by microwave spectroscopy (22) (see also (23)) that for aniline, the angle φ is approximately equal to 13° in good agreement with our estimate from a_{NH}^H/a_N, suggesting that its configuration remains almost unchanged upon complexation. This conclusion may likely be extended to the fluoranilines under study. The differences between the values given in Table 4 for this angle are not very significant owing to the moderate accuracy of ^{14}N shift measurements ($\pm 10\%$).

The spin densities on nitrogen given in Table 4 have been calculated from eqs. 6 and 7 assuming only an isotropic contact shift. A contribution of the dipolar shift would lead to an overestimate of a_N and then to a smaller actual value of φ in the range of 0 to 15°. However, without knowing this angle, ρ_N^π may still be estimated from a_{NH}^H only, with a proportionality constant Q_{NH}^H between -32 and -42 G. These calculations show that 80–90% of the π spin density in complexed anilines is localized on nitrogen. The different experimental values obtained for ρ_N^π, ρ_{1C}^π and a_1^C indicate also that the parameter Q_2^N of eq. 3 (or Q_{NC}^C in the original notation (15) is equal to -3.5 ± 1.7 G).

On the other hand, INDO calculations, carried out on $C_6H_5\dot{N}H_2^+$ and its fluorinated homologs indicate that only 50–60% of the spin density is located on nitrogen in the sp^3 or sp^2 configuration, this last being energetically favorable. A recent e.s.r. work on $C_6H_5\dot{N}H_2^+$ (24) shows that this radical is actually planar with an almost equal distribution of the spin density between C_6H_5 and NH_2. The model of a radical anion, which could be alternatively considered (25), leads to a spin distribution completely inconsistent with our experimental data. The same is likely true for an hybrid of cation and anion radicals (26).

The contribution of metal orbitals (26), although difficult to estimate, could eventually account for the large difference observed between the spin densities localized on the two moities of the ligand. It may be pointed out however that the INDO calculations performed on the aniline cation radical, assuming the configuration of the amino group to be nearly the same as that in free aniline, gives a reasonable agreement with the experimental value of a_{NH}^H/a_N and with the spin distribution in the phenyl ring. We may therefore tentatively assume that the sharing of the spin density between the amino and phenyl groups results at least in part from an internal rotation about the C—N bond restricting the conjugation between these two fragments, as suggested by the example of the *p*-aminophenoxy radical reported by Stone and Carrington (27). The corresponding potential barrier calculated by INDO for $C_6H_5\dot{N}H_2^+$ is 17 kcal/mol against 6 kcal/mol for free aniline. Table 4 shows that in the complex, each aniline ligand bears less than 5% of the total spin density so that its configuration may be compared to free aniline rather than to the cation radical. This point is supported also by the estimate from eq. 7, of the configuration of the amino group in the complex, and the internal rotation about C—N seems therefore likely.

The influence of an internal rotation about C—N on the nitrogen and proton hyperfine couplings has been calculated by INDO for several values of the angle φ, on the example of C_6H_5—$\dot{N}H_2^+$. Figure 2 shows that the ratio a_{NH}^H/a_N is not very dependent upon the twist angle θ around this bond so that a_{NH}^H remains nearly proportional to ρ_N^π. It may be assumed likewise that $\sum a_{CH}^H$ is proportional to the total π spin density on the ring so that the ratio

Can. J. Chem. Downloaded from www.nrcresearchpress.com by 210.87.254.105 on 09/05/12
For personal use only.

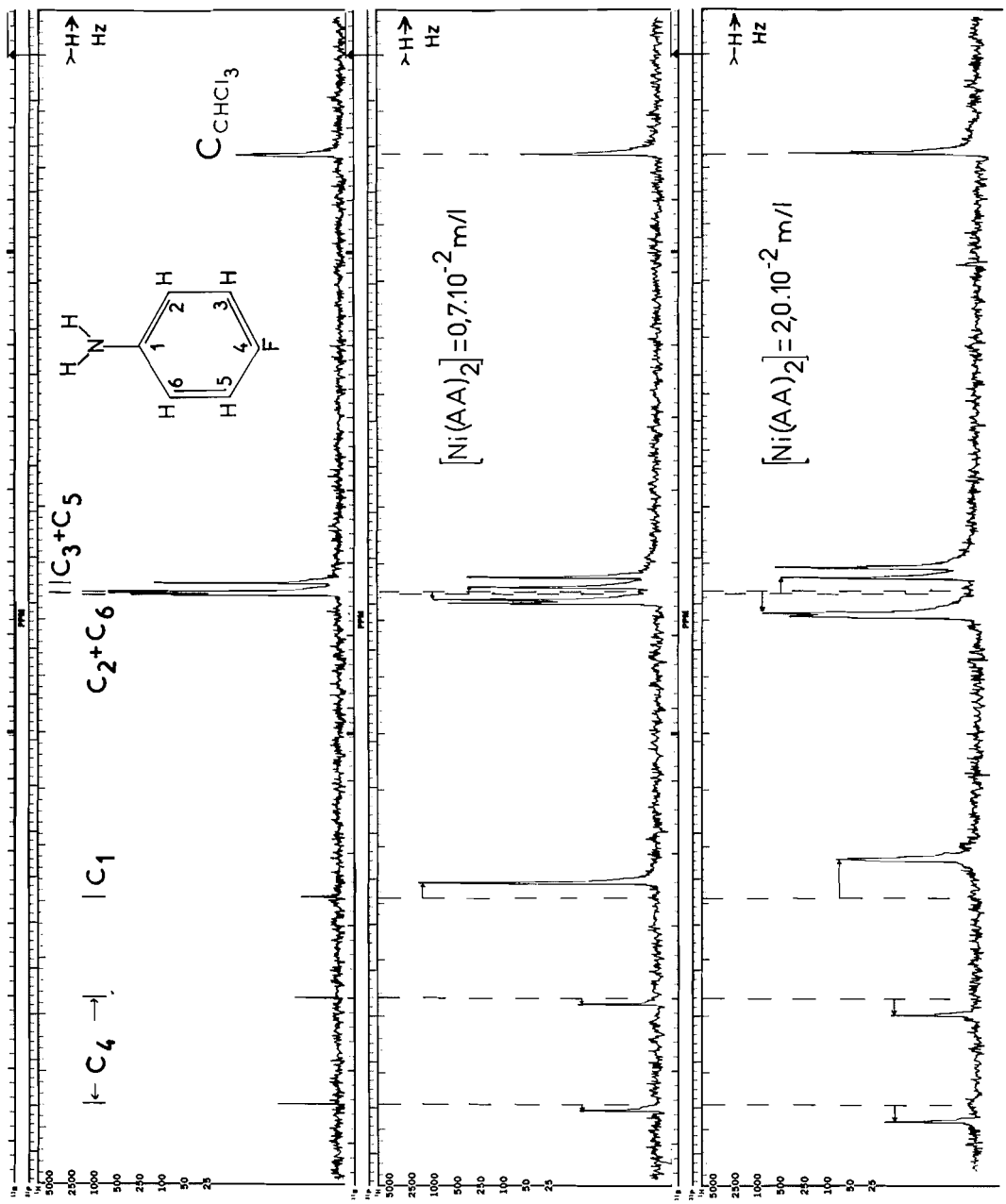

FIG. 1. Influence of the $Ni(AA)_2$ concentration upon the ^{13}C n.m.r. spectrum of a 30% chloroform solution of 4-fluoraniline.

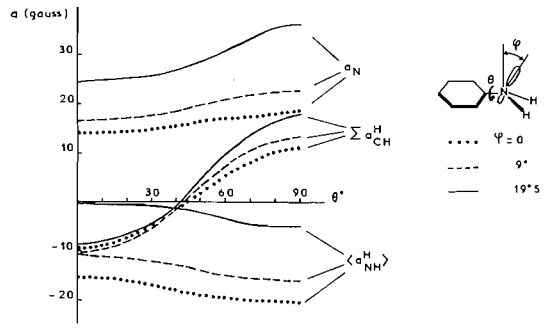

FIG. 2. Dependence of proton and nitrogen hyperfine coupling constants upon the twist angle θ around the C—N bond in the aniline cation radical, computed by INDO for different configuration of the amino group.

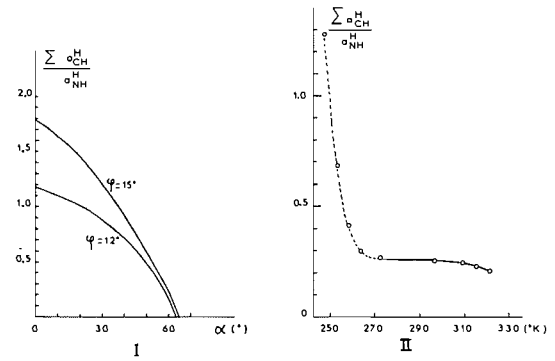

FIG. 3. (*I*) Computed dependence of $\Sigma a_{CH}{}^H/a_{NH}{}^H$ upon an internal harmonic oscillation of amplitude α, about the CN bond of $C_6H_5\dot{N}\overset{+}{H}_2$ for two possible configurations of the amino group. (*II*) Observed temperature dependence of this ratio in the case of the $Ni(AA)_2$, $(aniline)_2$ complex. The dotted line corresponds to the intermediate and slow exchange of the ligand.

$\Sigma a_{CH}{}^H/a_{NH}{}^H$ is a good criterion to estimate the spin density distribution between the ring and amino group in complexed anilines. The average of this ratio, calculated as a function of the amplitude α of an internal harmonic oscillation about $\theta = 0$ for the two boundary values expected for the angle φ (Fig. 3*I*) has been compared with the experimental data. In the temperature range of 275 to 320 °K the ratio $a_{NH}{}^H/a_N$ obtained with the aniline complex is consistent with an oscillation amplitude of 50–60° (Fig. 3*II*). Below 273 °K this ratio increases beyond the limits expected from INDO calculations. This apparent discrepancy may be attributed to a decrease of the exchange rate between the complex and the free ligand, since the contact shift of ring protons diminishes in turn below 240–250 °K to cancel out at ~230 °K (Fig. 4). The variation of $a_{NH}{}^H$ with temperature shows three characteristic domains according to the value of the exchange rate $1/\tau_h$ with respect to the difference $\Delta\omega_M$ in the resonance frequencies of the free ligand and the complex; above 280 °K, in the fast exchange region ($1/\tau_h \gg \Delta\omega_M$), the contact shifts varies as $1/T$. In the slow exchange region ($1/\tau_h \ll \Delta\omega_M$), below 240 °K, the resonance of the free ligand and that of the complex should be observed separately, but this last is undetectable on account of the low concentration of the complex and the line broadening. In the intermediate region (240 to 270 °K) $1/\tau_h$ becomes the same order of magnitude as $\Delta\omega_M$ and the linewidth passes through a maximum. Under these last conditions, the exchange rate may be calculated from eq. 9 (28):

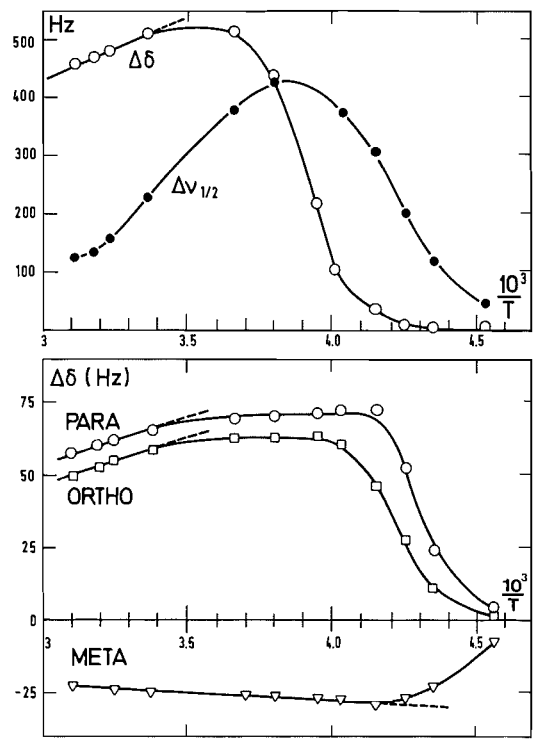

FIG. 4. Temperature dependence of the contact shift of NH_2 protons (upper diagram) and ring protons (lower diagram) for a ratio $[Ni(AA)_2]/[aniline]$ of $\sim 5 \times 10^{-3}$. $\Delta\nu_{1/2}$ is the linewidth of the resonance of NH_2 protons. The upfield shifts are counted positive on the vertical scale.

Can. J. Chem. Downloaded from www.nrcresearchpress.com by 210.87.254.105 on 09/05/12
For personal use only.

Can. J. Chem. Downloaded from www.nrcresearchpress.com by 210.87.254.105 on 09/05/12
For personal use only.

$$[9]\quad \Delta\omega = pq\frac{\Delta\omega_M}{\tau_h^2\left[\left(\frac{1}{T_{2M}}+\frac{1}{\tau_h}\right)^2+\Delta\omega_M^2\right]}$$

where $\Delta\omega$ is the observed shift and T_{2M} the nuclear transverse relaxation time in the complex, deduced from the linewidth ($1/T_{2M} = \pi\Delta\nu/pq$). $\Delta\omega_M$ is determined in the fast exchange region and introduced in eq. 9 after correction from Curie's law. In the temperature range of 240 to 320 °K, the exchange rate varies from 10^5 to 10^7 s^{-1} with an activation enthalpy $\Delta H^{\neq} = 12$ kcal/mol and an activation free energy $\Delta G^{\neq} = 9$ kcal/mol (Fig. 5).

^{13}C Relaxation

The T_1 and T_2 nuclear relaxation times in paramagnetic complexes are dependent upon the contact (29) and dipolar (30) hyperfine interactions. This last results from the local spin density and from the spin density localized on the metal giving therefore information on the internuclear distances. These two relaxation times are given by the relations (31):

$$[10a]\quad \frac{1}{T_{1M}} = \frac{2}{15}S(S+1)B^2\left(3\tau_c+\frac{7\tau_c}{1+\omega_e^2\tau_c^2}\right)+\frac{2}{3}S(S+1)A^2\frac{\tau_e}{1+\omega_e^2\tau_e^2}$$

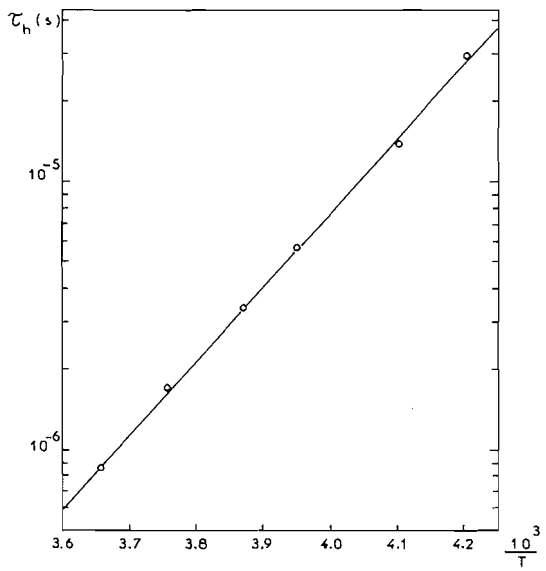

FIG. 5. Arrhenius plot of the residence time τ_h of aniline in the Ni(II) coordination sphere.

$$[10b]\quad \frac{1}{T_{2M}} = \frac{1}{15}S(S+1)B^2\left(7\tau_c+\frac{13\tau_c}{1+\omega_e^2\tau_c^2}\right)+\frac{1}{3}S(S+1)A^2\left(\tau_e+\frac{\tau_e}{1+\omega_e^2\tau_e^2}\right)$$

where T_{1M} and T_{2M} are the spin–lattice and spin–spin ^{13}C relaxation times in the complex, ω_e the Larmor frequency of the electron (4.54×10^{11} rad s^{-1} for a magnetic field of 23.5 kG and $g_e = 2.2$). A and B are the contact and dipolar hyperfine couplings in radians s^{-1}. T_{1M} and T_{2M} are deduced from the observed relaxation times by

$$[11]\quad \frac{1}{T_{1exp}} = (1-pq)\frac{1}{T_{1L}}+pq\frac{1}{T_{1M}}$$

or the similar expression for T_{2exp} which is given by the linewidth, T_{1L} or T_{2L} being the relaxation times of the free ligands. The second term of eq. 11 is predominant and we have actually observed a linear dependence of the relaxation rates on the ratio [Ni(AA)$_2$]/[aniline]. The correlation times τ_c and τ_e related respectively to the dipolar and scalar couplings are given by

$$[12]\quad \tau_c^{-1} = \tau_R^{-1}+\tau_h^{-1}+T_{1e}^{-1}$$

$$[13]\quad \tau_e^{-1} = \tau_h^{-1}+T_{1e}^{-1}$$

τ_R is the reorientation correlation time of the complex, τ_h the residence time of the ligand in the Ni(II) coordination sphere, of the order of 10^{-7} s at 300 °K as it has been shown above, and T_{1e} the electron spin lattice relaxation time. It may be assumed that $\tau_h \gg T_{1e}, \tau_c$, so that the contribution of exchange rate may be neglected in eqs. 12 and 13. If T_{1e} is not smaller than 10^{-11} s, we have $\omega_e^2\tau_c^2$ and $\omega_e^2\tau_e^2 \gg 1$, τ_R being likely of the order of 5×10^{-11} to 5×10^{-10} s. The large difference observed between experimental values of T_{1M}^{-1} and T_{2M}^{-1} suggests that the contact term is negligible compared to the dipolar term in eq. 10*a* but not in eq. 10*b*, so that we may use the simplified expressions

$$[14a]\quad 1/T_{1M} = (4/5)B^2\tau_c$$

$$[14b]\quad 1/T_{2M} = (14/15)B^2\tau_c+(2/3)A^2\tau_e$$

A^2 is given by the coupling constants of Table 2. B^2 is the sum of the contribution of the dipolar

coupling between the spin density localized on Ni(II) and a carbon i located at the distance r_i

$$[15] \qquad B_1^2 = \frac{g_e^2 \beta_e^2 g_n^2 \beta_n^2}{\hbar^2 r_i^6}$$

and the contribution of the π spin density localized on C_i which for $S = 1$

$$[16] \qquad B_2^2 = \frac{b^2}{4}(\rho_i^{\pi})^2$$

b being the ^{13}C dipolar coupling constant for $\rho_c^{\pi} = 1$ estimated to 4.1×10^8 rad s^{-1} (32). The ρ_i^{π} are given in Table 4. Knowing the geometry of the ligand, the carbon-to-metal distances r_i and r_j may be calculated from the ratio

$$[17] \qquad \frac{(B_1^2 + B_2^2)_i}{(B_1^2 + B_2^2)_j} = \frac{(T_{1M})_j}{(T_{1M})_i}$$

r_i and r_j being expressed as a function of d(N—Ni) which is adjusted in order to satisfy eq. 17.

A more simple way is to seek for nitrogen-to-metal distance which gives the minimum standard deviation between the values of τ_c derived from the spin–lattice relaxation times of the different carbons (eqs. 14*a* and 14*b*). These calculations have been carried out assuming (*i*) that the nickel ion occupies an average position in the ring plane, (*ii*) that it is located along the axis of the lone pair atomic orbital centered on nitrogen as expected for a σ bonding (10), the angle φ defined above being taken equal to 14.5°, (*iii*) the same as (*ii*) with an harmonic oscillation of amplitude 60° of the ring around the C_1—N bond.

The plot of $\Delta\tau_c/\bar{\tau}_c$ against d(N—Ni) shown in Fig. 6, indicates that assumption (*i*) is the most convenient, giving moreover nitrogen-to-metal distances of 2.0 and 2.3 Å for aniline and 2 for fluoraniline respectively, consistent with X-ray studies of nickel–amine complexes (see for instance refs. 33 and 34).

The electron spin relaxation time T_{1e} deduced from eqs. 14*a* and 14*b* is of the order of 2×10^{-10} to 5×10^{-10} s at 300 °K and the reorientation correlation time $\tau_R = (\tau_c^{-1} - T_{1e}^{-1})^{-1}$ is found to be $\sim 3 \times 10^{-11}$ s for both ligands (Table 5). For a rigid structure of the complex, τ_R may be estimated from the Stokes–Einstein relation

$$[18] \qquad \tau_R = \frac{4\pi\eta R^3}{3kT}$$

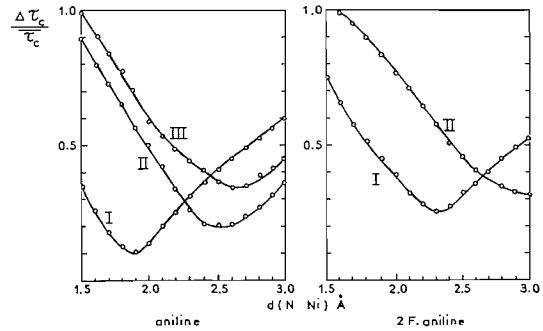

FIG. 6. Determination of the N—Ni distance from the relative deviation of τ_c deduced from the T_1 relaxation times of ring carbons curves *I*, *II*, and *III* correspond to the different assumption on the position of nickel relative to the phenyl ring.

which may be considered as valid for the complexes under study the molecular weights of which are nearly four times that of the solvent molecules (see for instance ref. 35).

For $\eta = 1.1 \times 10^{-2}$ P at 300 °K, a ratio aniline/chloroform of 1 v/v and a radius R of the equivalent sphere of the order of 5 Å, τ_R may be estimated to *ca.* 10^{-10} s. The much smaller experimental value of τ_R suggests that an additional motion of the ligand occurs in the nickel coordination sphere, which averages its position with respect to the ring plane, possibly the inversion of the C_1—N(H)(H) pyramid. A study in progress on other substituted anilines gives very similar results.

Conclusions

The hyperfine coupling parameters of ^{13}C and ^{19}F deduced from contact shift measurements an $Ni(AA)_2(aniline)_2$ complexes are found to be in close agreement with those provided by e.s.r., confirming that the delocalization of the unpaired spin on the phenyl ring may be safely compared to the case of aromatic π electron radicals. The measurement of the ratio of ^1H and ^{14}N hyperfine coupling constants in the amino group appears as a simple method to determine the hybridization state of nitrogen. This seems virtually unchanged upon complexation so that Ni(II) could provide valuable information on the conformation of other nitrogen containing molecules.

The study by Yonezawa *et al.* (36) of the ^1H

Can. J. Chem. Downloaded from www.nrcresearchpress.com by 210.87.254.105 on 09/05/12
For personal use only.

TABLE 5. ^{13}C relaxation data[a]

	Aniline		2-Fluoraniline	
	T_{1M}(s)	T_{2M}(s)	T_{1M}	T_{2M}
C_1	2.4×10^{-3}	3.7×10^{-4}	4.2×10^{-3}	3.8×10^{-4}
$C_{2,6}$	1.0×10^{-2}	5.7×10^{-4}	1.9×10^{-2}	5.2×10^{-4}
$C_{3,5}$	1.8×10^{-2}	1.2×10^{-3}	3.2×10^{-2}	9.3×10^{-4}
C_4	1.8×10^{-2}	7.2×10^{-4}	3.6×10^{-2}	5.8×10^{-4}

	Value	
Parameter	Aniline	2-Fluoraniline
T_{1_e}(s)	$(2.0 \pm 1) \times 10^{-10}$	$(5.7 \pm 2.5) \times 10^{-10}$
τ_{C_I}(s)	$(2.8 \pm 0.3) \times 10^{-11}$	$(3.5 \pm 0.9) \times 10^{-10}$
$\tau_{C_{II}}$(s)	$(2.1 \pm 0.4) \times 10^{-11}$	
τ_{R_I}(s)	3.3×10^{-11}	3.7×10^{-11}
$\tau_{R_{II}}$(s)	2.3×10^{-11}	
d(N—Ni)$_I$ (Å)	1.9	2.3
d(N—Ni)$_{II}$ (Å)	2.5	
d(N—Ni)$_{III}$ (Å)	2.6	

[a]Subscripts I, II, and III refer to the different assumption on the position of nickel relative to the ring plane.

pseudocontact shift in aniline – cobalt acetylacetonate complexes gave also a distance d(N—Co) ~ 2 Å and indicated a pyramidal conformation of the $C_1—N\begin{smallmatrix}H\\H\end{smallmatrix}$ in agreement with our study of ^{14}N and ^{1}H contact shifts in the amino group. The apparent discrepancy between the conclusions drawn from paramagnetic shift measurements and those derived from ^{13}C relaxation may be due to the fact that the former give information about the instantaneous metal and ligand relative positions whereas the latter gives the same information averaged over a long time interval, T_{1M} or T_{2M}, compared to the reorientation correlation time of the ligand in the coordination sphere. This interpretation is only tentative, ^{13}C relaxation measurements on aniline complexes with Gd $(DPM)_3$ are presently being carried out to verify this point.

1. G. A. WEBB. Annual report on NMR spectroscopy, Vol. 3. 1970. p. 211.
2. G. N. LA MAR, W. D. W. HORROCKS, and R. H. HOLM. (*Editors.*) NMR of paramagnetic molecules. Academic Press, N.Y. 1973.
3. D. R. EATON, A. D. JOSEY, W. D. PHILLIPS, and R. E. BENSON. Mol. Phys. **5**, 407 (1962).
4. D. DODDRELL and J. D. ROBERTS. J. Am. Chem. Soc. **92**, 4484 (1970).
5. W. D. HORROCKS, R. C. TAYLOR, and G. N. LA MAR. J. Am. Chem. Soc. **86**, 3031 (1964).
6. I. MORISHIMA, T. YONEZAWA, and K. GOTO. J. Am. Chem. Soc. **92**, 6651 (1970).
7. YU. N. MOLIN and E. E. ZAEV. J. Strukt. Khim. **8**, 167 (1967).
8. YU. N. MOLIN. J. Strukt. Khim. **10**, 932 (1969).
9. J. W. RAKSHYS. Inorg. Chem. **9**, 1521 (1970).
10. R. W. KLUIBER and W. D. W. HORROCKS. Inorg. Chem. **6**, 431 (1967).
11. J. A. POPLE, D. L. BEVERIDGE, and P. A. DOBOSH. J. Am. Chem. Soc. **90**, 4201 (1968).
12. R. FREEMAN and H. D. W. HILL. J. Chem. Phys. **54**, 3367 (1970).
13. H. M. MCCONNELL and D. B. CHESNUT. J. Chem. Phys. **28**, 107 (1958).
14. N. BLOEMBERGEN. J. Chem. Phys. **27**, 595 (1957).
15. M. KARPLUS and G. K. FRAENKEL. J. Chem. Phys. **35**, 1312 (1961).
16. (*a*) A. HINCHLIFFE and J. N. MURRELL. Mol. Phys. **14**, 147 (1968); (*b*) A. CARRINGTON, A. HUDSON, and H. C. LONGUET-HIGGINS. Mol. Phys. **9**, 377 (1965); (*c*) S. V. KULKARNI and C. TRAPP. J. Am. Chem. Soc. **92**, 4801 (1970); J. Am. Chem. Soc. **92**, 4809 (1970); (*d*) A. HUDSON and J. E. LEWIS. **19**, 241 (1970); (*e*) A. MAKI and D. H. GESKE. J. Am. Chem. Soc. **83**, 1852 (1961); (*f*) J. SINCLAIR and D. KIVELSON. J. Am. Chem. Soc. **90**, 5074 (1968); (*g*) P. NETA and R. H. SCHULER. J. Phys. Chem. **77**, 1368 (1973).
17. R. W. FESSENDEN. J. Phys. Chem. **71**, 74 (1967).
18. R. POUPKO, A. LOEWENSTEIN, and B. L. SILVER. J. Am. Chem. Soc. **93**, 580 (1971).
19. J. R. BOLTON, A. CARRINGTON, and J. DOS SANTOS VEIGA. Mol. Phys. **5**, 465 (1962).

Can. J. Chem. Downloaded from www.nrcresearchpress.com by 210.87.254.105 on 09/05/12
For personal use only.

20. A. FORCHIONI and C. CHACHATY. Org. Magn. Reson. **6**, 267 (1974).
21. R. J. KURLAND and B. R. MCGARVEY. J. Magn. Reson. **2**, 286 (1970).
22. D. G. LISTER and J. K. TYLER. Chem. Commun. 152 (1966).
23. R. E. WASYLISHEN and T. SCHAEFFER. Can. J. Chem. **51**, 3087 (1973).
24. F. A. NEUGEBAUER, S. BAMBERGER, and W. R. GROH. Tetrahedron Lett. **25**, 2247 (1973).
25. M. J. SCARLETT, A. T. CASEY, and R. A. CRAIG. Aust. J. Chem. **23**, 1333 (1970).
26. M. J. SCARLETT, A. T. CASEY, and R. A. CRAIG. Aust. J. Chem. **74**, 31 (1971).
27. A. J. STONE and A. CARRINGTON. Trans. Faraday Soc. **84**, 2593 (1965).
28. T. J. SWIFT and R. E. CONNICK. J. Chem. Phys. **37**, 307 (1962).
29. N. BLOEMBERGEN. J. Chem. Phys. **27**, 572 (1957).
30. I. SOLOMON. Phys. Rev. **99**, 559 (1955).
31. N. BLOEMBERGEN and L. O. MORGAN. J. Chem. Phys. **34**, 842 (1961).
32. M. BARFIELD. J. Chem. Phys. **53**, 3836 (1973).
33. L. KH. MINACHEVA, A. S. ANTISHKINA, M. A. PORAI-KOSHITS, and A. E. SHELASHVILI. Zh. Strukt. Khim. **11**, 936 (1970).
34. G. BOMBIERI, E. FORSELLI, R. GRAZIANI, and E. TONDELLO. J. Chem. Soc. A, 3349 (1970).
35. R. J. MEAKINS. Trans. Faraday Soc. **54**, 1160 (1958).
36. T. YONEZAWA, I. MORISHIMA, Y. AKANA, and Z. FUKUTA. Bull. Chem. Soc. Jap. **43**, 379 (1970).

Can. J. Chem. Downloaded from www.nrcresearchpress.com by 210.87.254.105 on 09/05/12
For personal use only.

The Application of a Simple Chemical Model of Natural Waters to Metal Fixation in Particulate Matter

ROBERT D. GUY, C. L. CHAKRABARTI,[1] AND LAURIER L. SCHRAMM

Department of Chemistry, Carleton University, Ottawa, Ontario K1S 5B6

Received August 15, 1974

ROBERT D. GUY, C. L. CHAKRABARTI, and LAURIER L. SCHRAMM. Can. J. Chem. **53**, 661 (1975).

A simple chemical model was used to investigate the mechanisms controlling the distribution of metals between soluble and particulate fractions in natural waters. The model particulates used were potassium bentonite, hydrous MnO_2, and solid humic acid. The soluble species in natural waters were modelled by soluble humic acid, tannic acid, and bicarbonate. The sorption curves for Cu(II), Cd(II), and Zn(II) onto humic acid and MnO_2 obeyed Langmuir adsorption isotherms whereas the sorption of the above ions onto bentonite followed a Freundlich isotherm. Chemical analysis of the total model using atomic absorption spectroscopy and differential pulse anodic stripping voltammetry indicated that copper distribution depends on the p*H* of the suspension: above p*H* 6.0, 50% of the copper is sorbed onto the particulates whereas the copper in solution is in a complexed form; between p*H* 6 and 3.8 the soluble copper is distributed between organic complexes and "free" copper ion; between p*H* 4.2 to 2.5 copper is being desorbed from the particulates; and below p*H* 2.5 all the copper is present in solution as "free" copper ion.

ROBERT D. GUY, C. L. CHAKRABARTI et LAURIER L. SCHRAMM. Can. J. Chem. **53**, 661 (1975).

On a utilisé un modèle chimique simple pour étudier les mécanismes contrôlant la distribution des métaux entre les fractions solubles et particulaires des eaux naturelles. On a utilisé le bentonite de potassium, le MnO_2 hydraté et l'acide humique solide comme modèles de particule. Les espèces solubles dans les eaux naturelles étaient représentées par l'acide humique soluble, l'acide tannique et le bicarbonate. Les courbes de sorption du Cu(II), Cd(II) et Zn(II) sur l'acide humique et le MnO_2 obéissent aux isothermes d'adsorption de Langmuir alors que la sorption des ions mentionnés plus haut sur la bentonite suit une isotherme de Freundlich. L'analyse chimique du modèle total, utilisant la spectroscopie d'absorption atomique et la redissolution anodique par impulsions différentielles indique que la distribution du cuivre dépend du p*H* de la suspension: au dessus d'un p*H* de 6.0, 50% du cuivre est absorbé par les particules alors que le cuivre en solution est sous forme complexée; entre les p*H* de 3.8 et de 6, le cuivre soluble se distribue entre les complexes organiques et des ions cuivre "libres"; entre des p*H* de 2.5 et de 4.2, le cuivre est désorbé des particules; aux p*H* plus bas que 2.5, tout le cuivre est présent en solution sous forme d'ions cuivre "libres". [Traduit par le journal]

Introduction

A natural water sample can be divided into several physico-chemical states, the most important being the particulate and soluble fractions. In the chemical analysis of water samples an operational definition has been employed for distinguishing between the suspended and soluble trace elements. An element is defined as soluble if it can pass through a 0.45 μ pore size membrane filter. Using this definition, several workers (1–3) have reported the analysis of fresh waters with specific reference to the distribution of trace metals between particulate and soluble fractions. Stiff (1), for example, found that the fraction of total copper in particulate form varied from 43 to 87% depending on the river water under study. The distribution ratio has been found to vary with the trace element (3); for example, 8, 21, and 79% of silver, selenium, and cobalt respectively were found in the particulate phase.

The variation in distribution ratio with both the trace element and water system prompted a study into the metal control processes prevalent in the aquatic environment. To date, most of the information on metal control processes has been derived from analysis of sediments and suspended material for major and minor metal content and, from the trends observed, various control mechanisms have been proposed. An example of this approach is a study by Leland *et al.* (4) on the factors controlling lead distribution in Lake Michigan sediments. Regression analysis on the sediment compositions indicated that trace elements were associated with the

[1]To whom correspondence should be addressed.

Can. J. Chem. Downloaded from www.nrcresearchpress.com by 210.87.254.105 on 09/05/12
For personal use only.

Can. J. Chem. Downloaded from www.nrcresearchpress.com by 210.87.254.105 on 09/05/12
For personal use only.

organic and iron oxide components of the sediment. Studies by Rashid (5) indicate that humic acids can complex from 3.4 to 216.6 mg of metal per g of organic material and, since humic acids form colloids with clay minerals (6, 7), the organic matter associated with clays has been proposed as a possible mechanism in metal control. Jenne (8) has compared several possible metal control processes including metal chelation by organic matter, ion exchange reactions with clays, surface sorption or precipitation onto carbonates, and precipitation as the oxide or hydroxide. Jenne (8) proposed one additional control, metal sorption onto hydrous oxides of manganese and iron.

The dissolved components of natural waters can also act as metal control agents. Soluble species include inorganic anions such as bicarbonate, chloride, and sulfate as well as large organic molecules such as humic acids and amino acids (1). Studies by Matson (9), Chau (10), and Schindler *et al.* (11) indicate that the humic compounds can complex metal ions and keep them in solution. The organic compounds can solubilize metals by two possible mechanisms, they can form metal–ligand complexes with sorption characteristics different from those of the free metal ion or they could solubilize the iron and manganese oxides (12–14) thus releasing the sorbed trace elements.

In summary, the literature survey indicates the possible interactions responsible for metal control are as follows: (*1*) metal–clay colloid ion exchange reactions; (*2*) metal sorption onto hydrous oxides; (*3*) metal sorption onto humic acid – clay colloids; (*4*) metal – inorganic anion complexes such as soluble $CuCO_3^0$, $ZnSO_4^0$, and $CdCl^+$ (15); (*5*) metal – organic ligand complexes.

The above mechanisms were suggested from studies on complete natural water systems containing all possible components. Natural water samples are difficult to characterize fully, and in studies using them all the variables that may determine the metal distribution cannot be controlled. In order to obtain definitive conclusions about the metal control processes it is necessary to study simpler model systems that can be characterized more fully. Such a simpler model system was developed in this study, and was composed of: (*1*) potassium bentonite; (*2*) hydrous MnO_2; (*3*) solid humic acid (to represent humic colloids); (*4*) soluble humic acid and tannic acid to represent soluble organic molecules; (*5*) bicarbonate ion to represent inorganic anions. Each particulate was studied separately to determine its metal sorption characteristics as a function of p*H* and sorbing metal concentration. The components were then combined to simulate a natural water sample. This paper describes the behavior of the model system and, using the information obtained from this study, discusses the kind of information that is provided by the analytical techniques used to characterize natural waters.

Experimental

Apparatus

A Princeton Applied Research Polarographic Analyzer, Model 174 A equipped with a Metrohm, Microfeed hanging mercury drop electrode E410 and a magnetic stirrer (Model E405) was used for all anodic stripping voltammetry experiments. A Varian Techtron atomic absorption spectrophotometer, Model AA-4, equipped with an air–acetylene premix atomizer-burner was used for flame atomic absorption measurements, and a Perkin–Elmer atomic absorption spectrophotometer, Model 503, equipped with a Heated Graphite Atomizer 2000 was used for nonflame atomic absorption experiments.

Reagents

The hydrous MnO_2 was prepared *in situ* by adding a solution of $MnSO_4$ to a basic solution of $KMnO_4$ (16)

$$3Mn^{2+} + 2MnO_4^- + 2H_2O \rightarrow 5MnO_2 + 4H^+$$

The brown suspensions of MnO_2 were used in further studies after a 15 min stabilization period. Acid washed bentonite (Fisher Scientific Co.) was converted to the potassium form using the procedure of van Olphen (17). The potassium bentonite thus prepared has a cation exchange capacity of 0.59 meq/g of clay at a p*H* of 5.2 (this cation exchange capacity was measured by the ammonium acetate method). Solid humic acid (Aldrich Chemical Co.) was used after it had been leached with 0.01 *M* HNO_3 to remove metal impurities. Ultrapure water of resistivity 18.3 megohm cm was obtained from a Milli-Q2 system (Millipore Co.). All solutions of metals were prepared from pure metal (of 99.9% purity) by dissolving them in nitric acid. All other solutions were prepared from reagent-grade chemicals.

Procedure

The sorption of copper, cadmium, and zinc onto the separate particulates was studied by adding known weights of MnO_2, bentonite, or solid humic acid to metal ion solutions having initial metal concentrations of 0–15 μg/ml. The solutions were buffered to p*H* 5.0 with a potassium acetate buffer (1×10^{-3} *M*) and allowed to equilibrate for 18 h. The suspensions were filtered through a 0.45 μ pore size membrane filter (Millipore Co.) and the soluble metal concentration was determined by flame atomic absorption spectroscopy. The weight of metal sorbed onto the particulate equalled the difference between the initial and final metal concentrations.

Can. J. Chem. Downloaded from www.nrcresearchpress.com by 210.87.254.105 on 09/05/12
For personal use only.

The effect of pH on the sorption of metal onto the particulates was studied by preparing suspensions of MnO_2, humic acid, or bentonite and 10 μg/ml in copper and allowing them to equilibrate for 18 h at different pH between 1 and 6 (set by HNO_3 or potassium acetate buffer). The suspensions were all 1×10^{-3} M in K^+. The suspensions were filtered and the equilibrium metal concentrations were determined by flame atomic absorption spectroscopy.

The soluble metal fraction of the model system was studied by differential pulse anodic stripping voltammetry (d.p.a.s.v.). The anodic stripping voltammetry (a.s.v.) technique involves two steps (18), the first a plating step in which metals are reduced to an amalgam. The second step is stripping the metal out of the amalgam back into the solution. In this study, the plating step was done at an applied potential of −0.800 V (*vs.* a Ag/AgCl (1 N KCl) reference electrode) into a hanging mercury drop electrode. The plating step was 90 s long. The metal was stripped out of the electrode at a rate of 2 mV/s. In all d.p.a.s.v. studies a 0.01 M potassium acetate electrolyte was used.

Model systems of 10 mg bentonite, 10 mg humic acid, 3.5 mg MnO_2, 5×10^{-5} M tannic acid, 1×10^{-3} M $NaHCO_3$, and 1×10^{-6} M in Cu^{2+} were prepared in 200 ml of ultrapure water and equilibrated for 18 h. The amount of soluble copper in the suspension as a function of pH was determined by both d.p.a.s.v. and nonflame atomic absorption spectroscopy.

Results and Discussion

The sorption of Cu(II), Zn(II), and Cd(II) onto the model particulates was studied with metal concentrations 10–100 times greater than those of natural water levels in order to permit their determination by flame atomic absorption spectroscopy and to study the limiting sorption characteristics of the model particulates. Figure 1 presents the sorption behavior of copper onto MnO_2 and humic acid. The curves are characteristic Langmuir isotherms

$$X = \frac{X_m C}{1 + bC}$$

where X is the amount of metal sorbed per unit weight of solvent, X_m the limiting value of X, C the equilibrium metal concentration in solution, and b is a constant. The sorption isotherm of copper onto potassium bentonite is presented in Fig. 2. Figure 2 shows that copper is preferentially sorbed over K^+ onto the clay. Metal sorption onto the potassium bentonite was found to obey Freundlich isotherms

$$X = kC^n$$

where X is the amount of metal sorbed per g of clay, C is the equilibrium concentration of metal in solution, and k and n are empirical constants.

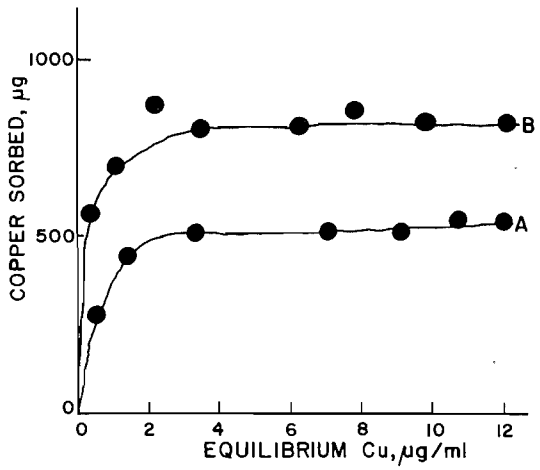

FIG. 1. Copper sorption isotherms at pH 7.5: (*A*) 10 mg humic acid; (*B*) 10 mg humic acid and 3 mg MnO_2.

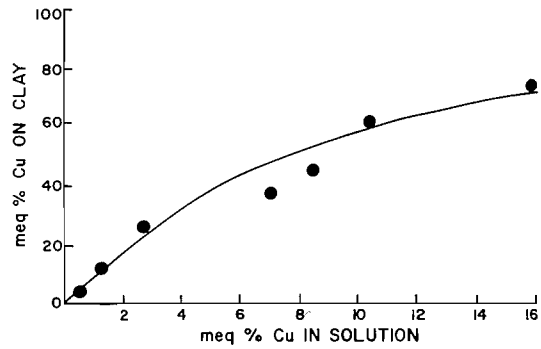

FIG. 2. Copper sorption isotherm onto potassium bentonite at pH 5.5.

TABLE 1. Freundlich isotherm constants for clay bentonite*

Metal ion	k	n
Cu^{2+}	2.96	0.65
Zn^{2+}	1.98	0.60
Cd^{2+}	2.25	0.64

*Determined at pH 5 in the presence of 1×10^{-3} M potassium acetate. Experimental uncertainties in k and n values are ± 10%. The constants are valid when X is in mg metal/g clay and C is in mg metal/ml solution.

Table 1 presents the values of k and n for copper, zinc, and cadmium sorption onto potassium bentonite.

Figure 3 presents the amount of copper sorbed onto the particulate as a function of pH. Each particulate has a characteristic pH below which copper is fully desorbed into solution: bentonite

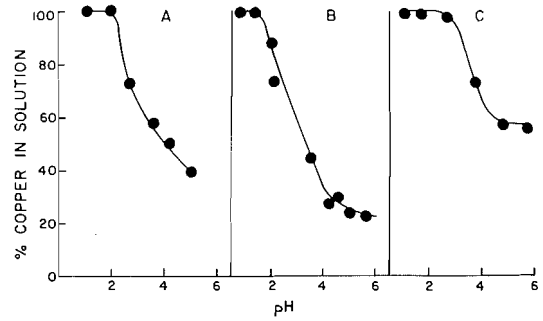

FIG. 3. Copper sorption as a function of pH: (A) potassium bentonite; (B) MnO_2; (C) humic acid.

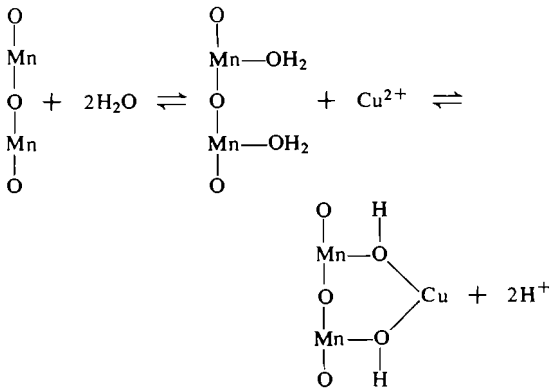

FIG. 4. Mechanism for sorption of copper onto MnO_2 surface.

pH < 1.8, MnO_2 pH < 1.5, and humic acid pH < 3.0.

The sorption characteristics of the metal ions onto the model particulates can be explained by examining the surface and complexing properties of the compounds.

MnO_2

Manganese dioxide crystals can interact with water at the solid–solution interface to form hydrous oxides (19). The polarized water molecule can then dissociate to form a negatively charged surface (16, 20). Metal ions can then interact with the negatively charged particle in two ways: (i) formation of a counter-ion layer. This occurs for both the alkali metal and heavy metal ions; (ii) specific sorption of ions onto the surface (as shown for copper in Fig. 4). The equilibrium responsible for formation of the surface charge

$$2H^+ + MO^- \rightleftharpoons MOH_2^+$$

(where MO^- and MOH_2^+ represent negative and positive surface sites respectively), indicates that H^+ ions are potential-determining. At a sufficiently low pH, the particulate surface would become positively charged and metal ions would be desorbed into solution. The above concept of the MnO_2 particulate leads to the following conclusions:

(i) The amount of metal sorbed will be proportional to the surface area of the particulate. The surface area of a dried, ground MnO_2 sample was 147 m^2/g (B.E.T. measurement using N_2 as the sorbing gas). The sorption of copper onto MnO_2 as a function of weight of MnO_2 prepared *in situ* is compared with a dried sample

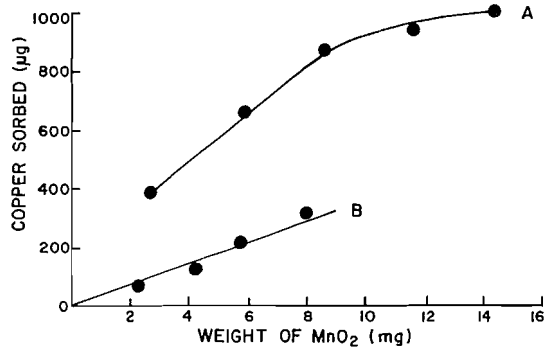

FIG. 5. Sorption of copper onto MnO_2 at pH 5.0 as a function of weight of MnO_2: (A) *in situ* MnO_2; (B) ground, dried MnO_2.

TABLE 2. Sorption characteristics* of humic acid, MnO_2, and bentonite

Metal	X_m (mmol metal / g MnO_2)	X_m (mmol metal / g humic acid)	Distribution coefficient for clay
Copper	1.95	0.42	9.0
Zinc	0.96	0.21	4.3
Cadmium	1.10	0.22	4.8

*These values were for pH 5.0 ± 0.1. The ionic strength was set with 1.0×10^{-3} M potassium acetate. The experimental uncertainties in X_m and the distribution coefficient for clay were ± 3% and ± 10%, respectively.

Can. J. Chem. Downloaded from www.nrcresearchpress.com by 210.87.254.105 on 09/05/12
For personal use only.

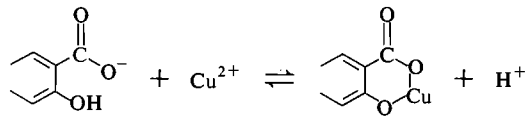

FIG. 6. Mechanism for sorption of copper onto humic acid particulate.

of MnO_2 in Fig. 5. It is evident that the surface area of MnO_2 generated *in situ* was much greater than that of the dried, finely ground sample.

(*ii*) The amount of metal sorbed will depend on the effective charge of the ion (ionic charge/hydrated ionic radius). Table 2 presents the sorption characteristics of humic acid, MnO_2, and potassium bentonite. The order of sorption (Cu > Zn ~ Cd) parallels the order of decreasing effective ionic charge.

Humic Acid

Schnitzer and Khan (7) propose that humic substances are phenolic and benzene carboxylic acids joined by hydrogen bonding to form large molecular structures. Humic acid particulates would have acidic functional groups at the water–solid interface which can chelate metal ions (Fig. 6). This sorption mechanism is consistent with the following conclusions: (*i*) the amount of metal sorbed would be proportional to the number of available complexing sites leading to a limiting sorption value; (*ii*) the relative affinity of different metal ions for humic acid will be a function of the ability of those ions to form metal chelates. The maximum sorption values, X_m, (Table 2) parallels the order of stability of metal humic acid complexes (7) ($Cu^{2+} > Zn^{2+} \sim Cd^{2+} > Ca^{2+}$); (*iii*) since conditional stability constants of the metal complex decrease in magnitude with p*H*, at low p*H* the complex is destabilized and the metal is desorbed into solution.

Clay Particulates

Clays are aluminum and magnesium silicates with layer-like structures. Isomorphous substitution of Al(III) for Si(IV) in the tetrahedral layers and of Fe(II), Zn(II), etc. for the Al(III) in the octahedral layers results in the crystals having a net negative charge. Counter-ions such as K^+ and Ca^{2+} can undergo ion-exchange with heavy metals in solution

$$2K\text{–clay} + Cu^{2+}(aq) \rightleftharpoons Cu\text{–clay}_2 + 2K^+(aq)$$

The exchange reaction can be characterized by a true equilibrium constant K_{eq} (21)

$$K_{eq} = \left[\frac{(C_{K^+})^2}{C_{Cu^{2+}}}\right]_{aq} \Big/ \left[\frac{(C_{K^+})^2}{C_{Cu^{2+}}}\right]_{clay}$$

or by a selectivity coefficient (22)

$$K_s = \frac{\text{meq\% } Cu^{2+} \text{ on clay} \times \text{meq\% } K^+ \text{ in solution}}{\text{meq\% } K^+ \text{ on clay} \times \text{meq\% } Cu^{2+} \text{ in solution}}$$

where

$$\text{meq\% } Cu^{2+} \text{ on clay} = \frac{\text{meq } Cu^{2+} \text{ on clay}}{\text{meq } Cu^{2+} \text{ on clay} + \text{meq } K^+ \text{ on clay}} \times 100$$

The selectivity coefficient is not a constant but is dependent on: (*i*) the size and charge of the exchangeable ions; (*ii*) the total concentration as well as the concentration ratio of existing ions. For the studies of sorption onto the potassium bentonite, the concentration of K^+ was 1×10^{-3} *M*. From inspection of the sorption isotherm (Fig. 2) it is evident that at low copper concentrations $K^+/Cu^{2+} > 50$ the plot is a straight line and the slope is equal to a distribution coefficient.

The distribution coefficient is defined as follows

$$\text{Distribution coefficient} = \frac{\text{meq\% } Cu^{2+} \text{ on clay}}{\text{meq\% } Cu^{2+} \text{ in solution}}$$

In general, the counter-ion concentration in natural waters is much greater than the heavy metal concentrations; therefore, distribution coefficients are reported instead of selectivity or equilibrium constants in Table 2.

The ion-exchange properties of the clays are consistent with the following conclusions: (*i*) the equilibrium constants (K_{eq}) are a function of the effective charge on the ion, the greater the effective charge on the heavy metal ion, the greater the equilibrium constant; (*ii*) the p*H* effects on clay sorption result from a mass action effect of the protons at low p*H*.

Table 2 summarizes the information obtained about the metal particulate interactions. Inspection of the table indicates that: (*1*) the order of sorption capacity of the particulates is MnO_2 > humic acid > clay (at the metal concentration equal to 8 μg/ml); (*2*) the order of metal sorption is $Cu^{2+} > Zn^{2+} \sim Cd^{2+} > K^+$.

As mentioned earlier, the three different partic-

Can. J. Chem. Downloaded from www.nrcresearchpress.com by 210.87.254.105 on 09/05/12
For personal use only.

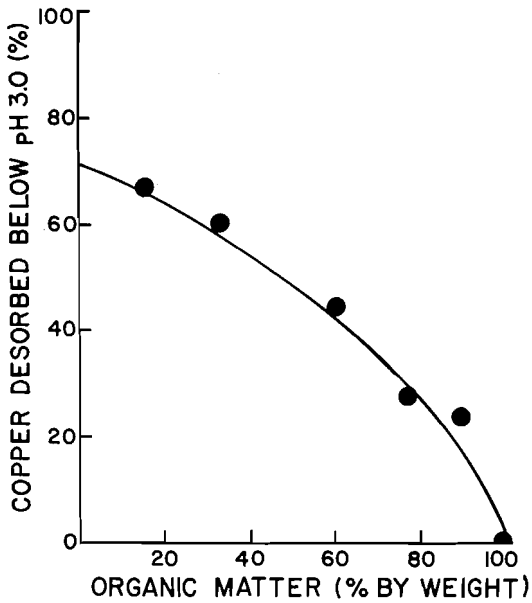

FIG. 7. Percentage of sorbed copper released below pH 3 as a function of humic acid content of suspension.

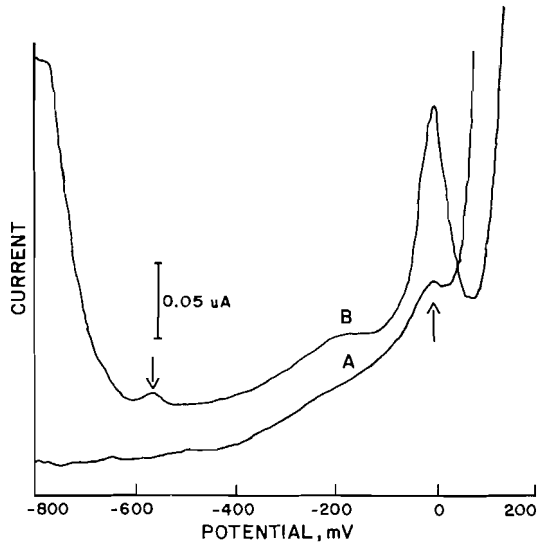

FIG. 8. Differential pulse anodic stripping voltammetry of natural waters in potassium acetate buffer: (*A*) pH 7.8; (*B*) pH 1.0.

ulates studied fully desorb copper at characteristic pH values. It is possible that, by comparing the amount of copper desorbed below pH 3 with the amount desorbed above pH 3, a qualitative differentiation between particulates can be made. The relationship between the amount of copper desorbed below pH 3.0 and the organic content of the suspension (Fig. 7) indicates that the percentage of copper desorbed below pH 3.0 decreases with increasing percentage organic content.

Studies on Soluble Metals

Figure 8 presents stripping voltammograms for a water sample from the Rideau River at two pH values. The stripping curve at pH 8 shows no significant stripping peaks whereas at pH 2 a lead stripping peak at -0.576 V and a copper stripping peak at -0.015 V are observed. Matson (9), Chau and co-worker (23), and Zirino and Healy (24) have observed similar pH-dependence of stripping curves for zinc, cadmium, lead, and copper in both fresh and saline waters. Both Matson (9) and Chau and coworker (23) have attributed this pH dependence to the lability of the metal–ligand complexes in natural water. Matson (9) has defined lability in terms of a relative cell constant; the cell constant, k_c, is related to the total amount of reduced species in the electrode, Q, the volume of the cell, v, the initial concentration of the species, C_0^0, and the time of electrolysis, t, by the equation

$$Q = nFvC_0^0tk_c$$

A metal complex Cu—L was termed nonlabile if k[CuL] $\ll k_c$, where k is the rate constant of the dissociation reaction

$$\text{Cu—L} \xrightarrow{k} \text{Cu}^{2+} + \text{L}$$

and [CuL] is molar concentration of the complex Cu—L.

Metal complexes are generally characterized by stability constants and rate constants of formation and dissociation. The relationship between these constants and the term nonlabile (as it applies to a.s.v. experiments) can be obtained by carefully considering the two steps of the a.s.v. procedure.

The first step is the reduction of metal ions in solution to form an amalgam. If the metal ion is present in the form of a complex and if the complex is not reducible then the plating step involves a chemical reaction before the metal is reduced at the electrode. Nicholson and Shain (25) have investigated the stationary-electrode polarography of kinetically controlled systems using fast, linear-sweep voltammetry. For a homogeneous first-order chemical reaction preceding a reversible charge transfer:

Can. J. Chem. Downloaded from www.nrcresearchpress.com by 210.87.254.105 on 09/05/12
For personal use only.

Can. J. Chem. Downloaded from www.nrcresearchpress.com by 210.87.254.105 on 09/05/12
For personal use only.

[1] $$Z \underset{k_b}{\overset{k_f}{\rightleftarrows}} O$$

$$K = [0]/[Z]$$

[2] $$O + ne^- \rightleftarrows R$$

where K is the equilibrium constant for reaction 1, it is found that when the scan rate exceeds the rate of conversion of $Z \rightarrow O$, the cathodic current is dependent on the equilibrium constant of reaction 1. If K is small then the current is determined by the equilibrium concentration of O denoted by C_0

$$C_0 = \frac{K}{K + 1} C^*$$

where C^* is the stoichiometric concentration of O. If the complex dissociation reaction is taken as a necessary step prior to metal reduction then the small stripping currents in natural water can be accounted for by assuming:

(*i*) That the natural water complexes are not reduced at the plating potential used in this study. If the complex is reducible, enough metal is reduced to give significant stripping peaks and the complex would be termed labile.

(*ii*) That the rate of dissociation of the metal complex is so slow that little metal is converted to an electroactive form in the time of the plating step (if longer plating times are employed more complex will dissociate and larger stripping currents will be observed, this condition is equivalent to Matson's (9) definition of nonlabile).

(*iii*) That the stability constant of the metal complex is large enough to reduce the equilibrium free metal concentration to a very low value. If one assumes a stability constant of 10^7 and [metal]/[ligand] = 10^{-1}, then for [ligand] = 10^{-6} M the equilibrium metal concentration would be 1×10^{-8} M. No appreciable copper stripping peak was observed at this copper concentration under the experimental conditions used in this study. The values for stability constants, metal/ligand ratio, and ligand concentration used in the above example are realistic values for natural waters (10, 23).

(*iv*) As the pH of a natural water sample is lowered, the conditional stability constants of the complexes would be lowered. Under these conditions, the equilibrium metal concentration increases and the stripping currents increase. If the example noted above is extended to include the equilibrium

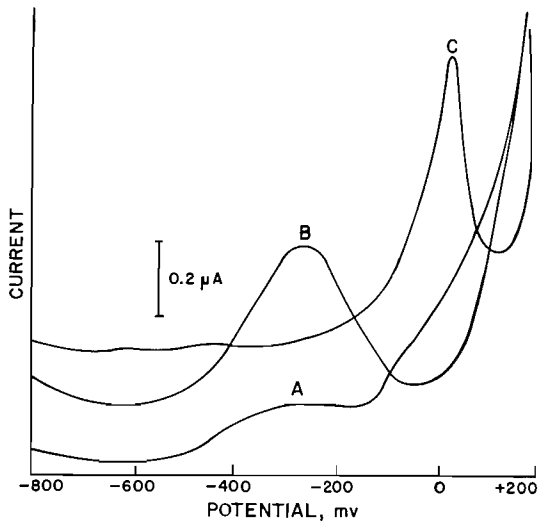

FIG. 9. Differential pulse anodic stripping voltammetry of humic acid – copper solutions as a function of pH: (*A*) pH 8.0; (*B*) pH 6.1; (*C*) pH 2.8.

$$LH \rightleftharpoons H^+ + L^-$$

$$K' = \frac{[H^+][L^-]}{[HL]}$$

and if K' is assumed to be 10^{-6}, then using conditional formation constants (26) one obtains that at pH 8, 9%; pH 4, 91%; and at pH 3, 100% of the total copper is present as uncomplexed copper.

Two model acids, tannic and humic acids, were used to simulate natural water organics. Stripping voltammograms of an 11.4 μg/ml humic acid and 1×10^{-6} M copper at pH 8, 6.1, and 2.0 are presented in Fig. 9. The voltammograms show a copper stripping peak cathodic to the normal copper stripping potential. Bradford (27) notes that such cathodic stripping peaks result from formation of metal–anion complexes only if the rate of formation of the complex is greater than the rate of oxidation of the metal out of the amalgam. The differences between the stripping curves of natural water and the model system arise from the appreciable dissociation of the model copper – humic acid complex during the time of the experiment and the rate of formation of complex being large enough to permit a cathodic stripping peak. The conditions under which a.s.v. will be valuable in distinguishing between soluble metal species is summarized as follows.

Case 1

The metal complexes are reduced at the elec-

Can. J. Chem. Downloaded from www.nrcresearchpress.com by 210.87.254.105 on 09/05/12
For personal use only.

trode during the plating step or they dissociate to an appreciable extent during the time of the experiment. The complexes are called labile. Two different situations can be identified as follows: (*a*) If the rate of complex formation is faster than the rate of oxidation of the amalgam, the stripping peak occurs at a potential cathodic to the normal copper potential. Differentiation of species is possible. (*b*) If the stripping peak occurs at the normal copper potential, the metal complex can not be distinguished from the free copper.

Case 2

The rate of dissociation of metal complex is slow; therefore, the complexes are not dissociated during the time of the experiment. The complexes are called nonlabile. The following observations can be made. (*a*) The magnitude of stripping current is determined by the stability constant of the complex. (*b*) Lowering the solution p*H* to 1 permits the determination of the total concentration of the nonlabile complex.

Anodic stripping voltammetry was used to determine the distribution of copper between free metal and complexed metal for humic acid and tannic acid. The distribution curves are shown in Fig. 10. Complete dissociation of the metal complexes for tannic and humic acid occurs at p*H* 3.2 and 3.3, respectively.

The results of analysis of the total model system as a function of p*H* are presented in Fig. 11. Comparison of the atomic absorption spectroscopy and d.p.a.s.v. results indicated: (*1*) 50% of the total copper was found in the soluble form; (*2*) d.p.a.s.v. indicated that above p*H* 6 all of the soluble copper was in a complexed form and below p*H* 3.6 all soluble copper was in an uncomplexed form; (*3*) below p*H* 2.5 all the copper in the system was in a soluble form. Table 3 is a complete summary of the results.

The total model system indicated that most of the copper was desorbed above p*H* 3.0 which meant that most of the copper was sorbed onto the organic particulate (*cf.* Fig. 7). The filtered model system was light green in color whereas a 5×10^{-5} *M* tannic acid solution was normally colorless. Further studies indicated that the tannic acid can solubilize MnO_2. This agrees with the findings of Hem (13). It appears that the solubilization of MnO_2 by tannic acid can release copper into the solution. The mechanism

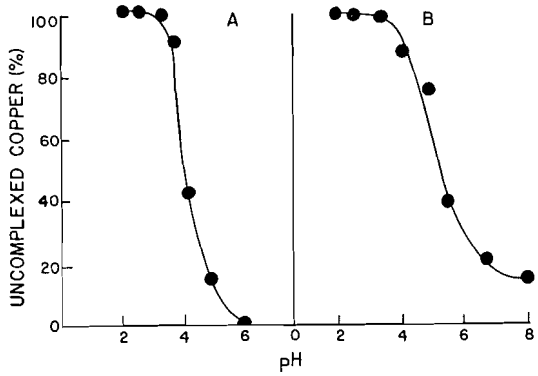

FIG. 10. Distribution of soluble copper as a function of p*H*: (*A*) copper – tannic acid solution; (*B*) copper – humic acid solution.

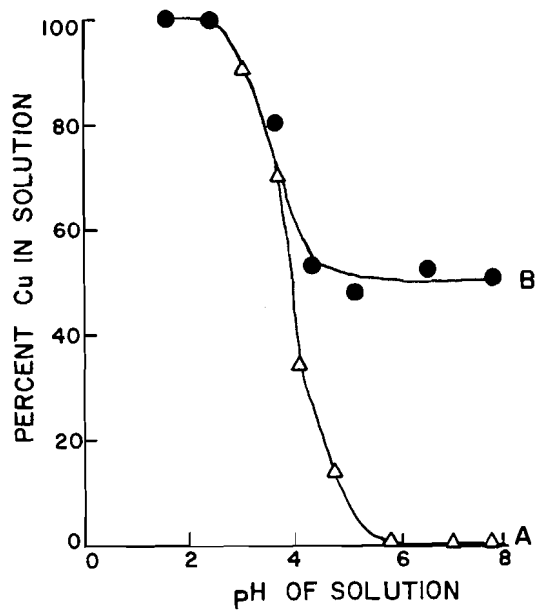

FIG. 11. Determination of copper in the total model system as a function of p*H*: (*A*) d.p.a.s.v. determination of copper; (*B*) Atomic-absorption-spectroscopic determination of copper.

TABLE 3. Copper distribution in the model system

p*H*	Particulate (%)	Compound (%)	Free (%)
8.0	50	50	0
6.0	50	50	0
5.0	50	41	9
4.0	38	22	40
3.0	10	0	90
2.0	0	0	100

of the solubilization and its effect on metal distribution ratio is currently under study.

Conclusions

Studies on the interactions of metal ions with the model compounds bentonite, MnO_2, humic acid (solid and soluble), and tannic acid permitted metal distribution ratios to be explained in terms of coordination chemistry. The combination of the model compounds into a synthetic representation of a natural water sample indicated that the model was at least in qualitative agreement with the reported behavior of natural waters. Further studies using model systems may permit more definitive conclusions regarding the relative contributions of possible control mechanisms.

Anodic stripping voltammetry permits a more definitive characterization of a water sample than nonflame atomic absorption spectroscopy. Anodic stripping voltammetry permits the classification of the metal content of a water sample into several categories: (*1*) metal sorbed onto particulates; (*2*) soluble metal present in complexes and as free metal ion; (*3*) the p*H* titration (*cf.* Fig. 11) may be used as a possible "fingerprint" of natural waters (28).

The authors are grateful to the National Research Council of Canada for financial support of this research.

1. M. J. STIFF. Water Res. **5**, 585 (1971).
2. J. KUBOTA, E. L. MILLS, and R. T. OGLESBY. Environ. Sci. Technol. **8**, 243 (1972).
3. D. P. KHARKAR, K. K. TUREKIAN, and K. K. BERTINE. Geochim. Cosmochim. Acta, **32**, 285 (1968).
4. H. V. LELAND, S. S. SHUKLA, and N. F. SHIMP. *In* Trace metals and metal–organic interactions in natural waters. *Edited by* P. C. Singer. Ann Arbor Science, Ann Arbor, Michigan. 1973. p. 89.
5. M. A. RASHID. Soil Sci. **111**, 298 (1971).
6. M. A. RASHID, D. E. BUCKLEY, and K. R. ROBERTSON. Geoderma, **8**, 11 (1972).
7. M. SCHNITZER and S. U. KHAN. Humic substances in the environment. Marcel Dekker, New York. 1972. p. 253.
8. E. A. JENNE. *In* Trace inorganics in water. *Edited by* Robert F. Gould. Adv. Chem. No. 73, Washington, D.C. 1968. p. 389.
9. W. R. MATSON. Ph.D. Thesis. Massachusetts Institute of Technology, Boston, Massachusetts. 1968.
10. Y. K. CHAU. J. Chromatog. Sci. **11**, 579 (1973).
11. J. E. SCHINDLER, J. J. ALBERTS, and K. R. HONICK. Limnol. Oceanogr. **17**, 952 (1972).
12. M. SZILAGYI. Soil Sci. **111**, 233 (1971).
13. J. D. HEM. Reduction and complexing of manganese by gallic acids, Geological Survey Water Supply Paper 1667-D, 1964.
14. T. L. THEIS and P. C. SINGER. Environ. Sci. Technol. **8**, 569 (1974).
15. A. ZIRINO and S. YAMAMOTO. Limnol. Oceanogr. **17**, 661 (1972).
16. H. S. POSSELT, F. J. ANDERSON, and W. J. WEBER. Environ. Sci. Technol. **2**, 1087 (1968).
17. H. VAN OLPHEN. An introduction to clay colloid chemistry. Interscience, New York. 1963.
18. E. BARENDRICHT. *In* Electroanalytical chemistry, Vol. 2. *Edited by* A. J. Bard. Marcel Dekker, Inc., New York. 1967. p. 53.
19. T. W. HEALY, A. P. HERRING, and D. W. FUERSTENAU. J. Colloid Interfacial Sci. **21**, 435 (1966).
20. J. P. GABANO, P. ETIENNE, and J. F. LAURENT. Electrochim. Acta, **10**, 947 (1965).
21. T. R. E. KRESSMAN and J. A. KITCHENER. J. Chem. Soc. Lond. 1201 (1949).
22. KONRAD DORFNER. Ion exchangers: properties and applications. Ann Arbor Science, Ann Arbor. 1972. p. 44.
23. Y. K. CHAU and K. LUM-SHUE-CHAN. Water Res. **8**, 383 (1974).
24. A. ZIRINO and M. L. HEALY. Limnol. Oceanogr. **16**, 773 (1971).
25. R. S. NICHOLSON and I. SHAIN. Anal. Chem. **36**, 706 (1964).
26. D. A. SKOOG and D. M. WEST. Fundamentals of analytical chemistry. 2nd ed. Holt, Rinehart and Winston, New York. 1969. p. 346.
27. W. L. BRADFORD. Limnol. Oceanogr. **18**, 757 (1973).
28. A. PIRO, M. BERNHARD, M. BRANICA, and M. VERZI. *In* Radioactive contamination of marine environment. I. A. E. A., Vienna. 1973. p. 29.

Can. J. Chem. Downloaded from www.nrcresearchpress.com by 210.87.254.105 on 09/05/12
For personal use only.

Concerning the Problem of Stereospecific Glycosylation. Synthesis and Methanolysis of some 2-*O*-Benzylated D-Galactopyranosyl and D-Galactofuranosyl Halides[1]

JEAN M. J. FRÉCHET AND HANS H. BAER

Department of Chemistry, University of Ottawa, Ottawa, Canada K1N 6N5

Received October 7, 1974

JEAN M. J. FRÉCHET and HANS H. BAER. Can. J. Chem. **53**, 670 (1975).

Acetolysis of 1,6-anhydro-2,3,4-tri-*O*-benzyl-β-D-galactopyranose (**3**) followed by de-*O*-acetylation and *p*-nitrobenzoylation gave 2,3,4-tri-*O*-benzyl-1,6-di-*O*-*p*-nitrobenzoyl-β-D-galactopyranose (**4**) which was converted into 2,3,4-tri-*O*-benzyl-6-*O*-*p*-nitrobenzoyl-α-D-galactopyranosyl bromide (**5**). Benzylation of methyl 4,6-*O*-benzylidene-α-D-galactopyranoside (**6**) gave the 2,3-dibenzyl ether (**7**) which was hydrolyzed to 2,3-di-*O*-benzyl-D-galactose (**8**). *p*-Nitrobenzoylation of **8** furnished 2,3-di-*O*-benzyl-1,5,6-tri-*O*-*p*-nitrobenzoyl-β-D-galactofuranose (**9**) and an isomer, presumably a β-pyranose derivative (**10**). Compound **9** was converted into 2,3-di-*O*-benzyl-5,6-di-*O*-*p*-nitrobenzoyl-β-D-galactofuranosyl bromide (**11**) and chloride (**12**). The new halides **5**, **11**, and **12** as well as known 2,3,4,6-tetra-*O*-benzyl-α-D-galactopyranosyl bromide (**1**) and chloride (**2**) were subjected to methanolysis in dichloromethane solution in the presence of methanol alone and in the presence of tetrabutylammonium bromide, mercuric cyanide, and silver tetrafluoroborate, respectively, and the ratios of anomeric glycosides produced were examined by n.m.r. spectroscopy. Factors influencing stereoselectivity in these reactions are discussed. The new methyl α- and β-glycosides derived from **5** (**13** and **14**) and the methyl α-glycoside (**15**) produced from **11** and **12** were isolated, and methyl 2,3,5,6-tetra-*O*-benzyl-α-D-galactofuranoside (**16**) was prepared for the first time.

JEAN M. J. FRÉCHET et HANS H. BAER. Can. J. Chem. **53**, 670 (1975).

Par acétolyse du 1,6-anhydro-2,3,4-tri-*O*-benzyl-β-D-galactopyranose (**3**) suivie de désacétylation et de *p*-nitrobenzoylation, on a obtenu le 2,3,4-tri-*O*-benzyl-1,6-di-*O*-*p*-nitrobenzoyl-β-D-galactopyranose (**4**) qui est converti en bromure de 2,3,4-tri-*O*-benzyl-6-*O*-*p*-nitrobenzoyl-α-D-galactopyranosyle (**5**). La benzylation du méthyl 4,6-*O*-benzylidène-α-D-galactopyranoside (**6**) a donné l'éther 2,3-dibenzylique (**7**) qui, par hydrolyse, a produit le 2,3-di-*O*-benzyl-D-galactose (**8**). Par *p*-nitrobenzoylation de **8**, on a obtenu le 2,3-di-*O*-benzyl-1,5,6-tri-*O*-*p*-nitrobenzoyl-β-D-galactofuranose (**9**) et un isomère, sans doute le dérivé pyranosique (**10**). Le composé **9** a été transformé en bromure (**11**) et en chlorure (**12**) de 2,3-di-*O*-benzyl-5,6-di-*O*-*p*-nitrobenzoyl-β-D-galactofuranosyle. Ces nouveaux halogénures **5**, **11** et **12**, ainsi que le bromure de 2,3,4,6-tétra-*O*-benzyl-α-D-galactopyranosyle (**1**) et le chlorure correspondant (**2**) qui étaient déja connus, ont été soumis à des réactions de méthanolyse en solution dans le dichlorométhane en présence de méthanol seul, et en présence de bromure d'ammonium tétrabutylé, de cyanure de mercure et de tétrafluoroborate d'argent respectivement. Les quantités de glycosides anomères formées ont été analysées par spectroscopie de r.m.n. Les facteurs qui influencent la stéreosélectivité de ces réactions sont examinés. Les nouveaux méthyl α- et β-glycosides dérivés de **5** (**13** et **14**) et le méthyl α-glycoside (**15**) produit à partir de **11** et **12** ont été isolés; le méthyl 2,3,5,6-tétra-*O*-benzyl-α-D-galactofuranoside (**16**) a été préparé pour la première fois.

Introduction

As groundwork for a long-range project in glycoside and oligosaccharide synthesis we have commenced with the preparation of some new sugar derivatives which, it is hoped, may serve as suitable building stones in syntheses of certain compounds having biological significance, and we have undertaken some studies pertaining to the general problem of stereospecificity in glycoside formation. The present article deals with derivatives of D-galactose. This sugar occurs widely in nature in both α- and β-glycosidic linkage; it is one of the prominent structural units of such important natural products as, for example, gangliosides and other glycolipids, blood group determinants and related glycopeptides, human milk oligosaccharides, immunospecific bacterial polysaccharides, and a great variety of plant hemicelluloses, gums, and mucilages.

The methods most widely used and endowed

[1]Presented in part before the 166th National Meeting of the American Chemical Society, Chicago, Illinois, August, 1973.

Can. J. Chem. Downloaded from www.nrcresearchpress.com by 210.87.254.40 on 09/05/12
For personal use only.

Can. J. Chem. Downloaded from www.nrcresearchpress.com by 210.87.254.40 on 09/05/12
For personal use only.

with broad generality for the synthesis of both simple glycosides and more complex oligosaccharides were, at least until recently, the classical Koenigs–Knorr condensation and its newer variants in which a blocked glycosyl halide is condensed with an alcoholic component. However, control of the anomeric configuration in the glycoside thus generated has long been a major problem and is remaining a current concern despite recent progress (1). Whereas the readily available per-*O*-acylated bromides and chlorides of galactose and other sugars having the same C-2 configuration (*e.g.*, glucose and xylose) normally give β-glycosides (1,2-*trans*) with a high degree of stereospecificity, the controlled synthesis of α-glycosides (1,2-*cis*) of these particular sugars is a far more complicated proposition and continues to draw much attention. With the notable exception of the novel, highly promising α-glycoside synthesis of Lemieux and co-workers (2) which in the key step involves addition of alcohol to an intermediate 2-nitrosoglycal, most approaches were aimed at influencing the stereochemical course of nucleophilic substitution at the anomeric center in glycosyl halides. Success in varying measure was achieved over the years by modifying the reaction conditions (such as solvent and choice of acid acceptor) in Koenigs–Knorr type reactions and by employing glycosyl halides that bear a nonparticipating group at C-2, frequently the benzyloxy function (1, 3). Of particular relevancy in this connection was the discovery by Lemieux and co-workers (4), that stable α-glycosyl halides anomerize by halide ion catalysis to give their more highly reactive β-anomers, albeit in low concentration, a phenomenon which can be utilized in α-glycoside synthesis (5–7). It was found, furthermore, that certain specific groups present in positions other than C-2 may influence reaction rates and have a directive effect which can be enlisted for making 1,2-*cis* glycosides (5, 8–14), and such glycosides have also been obtained from reactive glycosyl derivatives possessing an electropositive leaving group (15). Nevertheless, the scope of some of these approaches is still uncertain and a lack of predictability exists. For example, in our syntheses of several stereoisomeric disaccharides by mercuric cyanide-promoted condensation of per-*O*-benzyl-α-D-glucopyranosyl bromide, the type of linkage produced was found to depend strikingly upon the molecular configuration of the alcoholic monosaccharide component, a factor which apparently has received little attention hitherto (16). In extending their work (14, 17) on the stereoselective methanolysis of D-glucopyranosyl sulfonates, Schuerch and co-workers observed unexpected differences when analogous D-galactose derivatives were used (18).

In order to augment special knowledge in glycoside-forming reactions in the D-galactose series, we have now synthesized three new halides in addition to the previously-described 2,3,4,6-tetra-*O*-benzyl-α-D-galactopyranosyl bromide (**1**) (16) and the corresponding chloride **2** (19), namely, 2,3,4-tri-*O*-benzyl-6-*O*-*p*-nitrobenzoyl-β-D-galactopyranosyl bromide (**5**), 2,3-di-*O*-benzyl-5,6-di-*O*-*p*-nitrobenzyl-β-D-galactofuranosyl bromide (**11**), and 2,3-di-*O*-benzyl-5,6-di-*O*-*p*-nitrobenzoyl-β-D-galactofuranosyl chloride (**12**). With these five compounds we then made a comparative study of the steric course of glycoside formation with methanol under a variety of conditions.

Synthesis of Glycosyl Halides

The synthesis of the 6-*p*-nitrobenzoate **5** departed from 1,6-anhydro-2,3,4-tri-*O*-benzyl-β-D-galactopyranose (**3**) which, by acetolysis and subsequent de-*O*-acetylation and *p*-nitrobenzoylation of the product, was converted into 2,3,4-tri-*O*-benzyl-1,6-di-*O*-*p*-nitrobenzoyl-β-D-galactopyranose (**4**). The bromide **5** was then obtained from **4** by application of the elegant method, first recommended by Fletcher and co-workers (refs. 5 and 20; for further examples see refs. 11–14 and 16) which consists of a facile, quantitative displacement of the C-1 acyloxy function by means of anhydrous hydrogen bromide in dichloromethane solution. Although it seems plausible enough that a β-ester reacts with inversion to yield the stable α-bromide, we shall return to this point for further comment at the end of this section.

The blocked β-D-galactofuranosyl halides **11** and **12** were obtained as follows. Methyl 4,6-*O*-benzylidene-α-D-galactopyranoside (**6**) was benzylated to furnish its crystalline 2,3-dibenzyl ether (**7**). Acid hydrolysis of **7** gave 2,3-di-*O*-benzyl-D-galactose (**8**). This free sugar crystallized in a weakly dextrorotatory form ($[\alpha]_D$ +5.3° in chloroform) but the anomeric configuration and the ring structure of the crystalline material were not established, nor was it possible to assess the proportions of tautomeric forms present in solution. However, **8** must to a high degree exist in, or be especially prone to reaction through, a

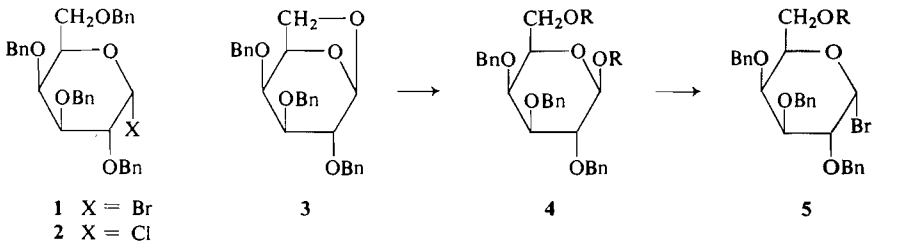

1 X = Br
2 X = Cl

3 **4** **5**

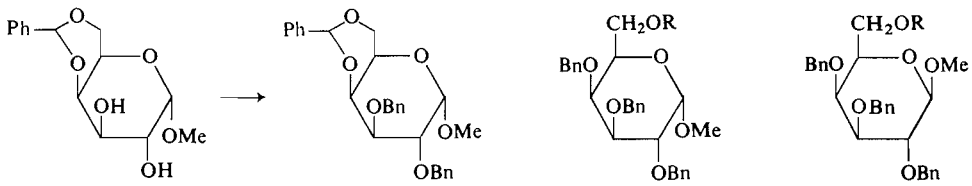

6 **7** **13** **14**

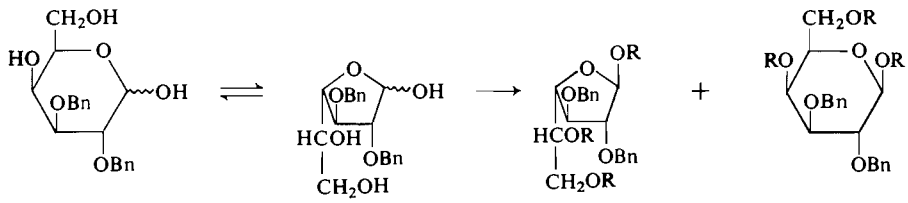

8 **9** **10**

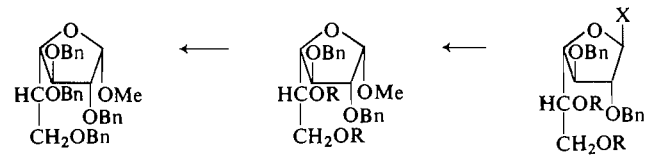

16 **15** **11** X = Br
12 X = Cl

Bn = $PhCH_2^-$; R = p-$NO_2C_6H_4CO^-$

Can. J. Chem. Downloaded from www.nrcresearchpress.com by 210.87.254.40 on 09/05/12
For personal use only.

Can. J. Chem. Downloaded from www.nrcresearchpress.com by 210.87.254.40 on 09/05/12
For personal use only.

furanose form as *p*-nitrobenzoylation afforded two isomeric triesters, each in 40% yield,[2] of which one showing $[\alpha]_D$ −5.5° was revealed to be 2,3-di-*O*-benzyl-1,5,6-tri-*O*-*p*-nitrobenzoyl-β-D-galactofuranose (**9**) (for proof see later). The other isomer also showed low levorotation ($[\alpha]_D$ −9.1°) and was on this basis tentatively judged to be the corresponding β-pyranose 1,4,6-tri-*p*-nitrobenzoate (**10**). It is known that acylation of galactose tends to give mixtures containing substantial amounts of furanose besides pyranose derivatives (21). Treatment of **9** with anhydrous hydrogen bromide and chloride, respectively, produced the substituted β-D-galactofuranosyl halides **11** and **12** as amorphous solids which exhibited strong levorotation but did not mutarotate. As is also the case with alkyl β-D-galactofuranosides (22), these β-halides are expected to be the thermodynamically more stable anomers because they are free from the unfavorable, 1,2-*cis* substituent interaction which exists in the α-anomers; therefore α-halides, if initially formed from **9**, would be liable to rapid anomerization during the reaction. The triester presumed to have structure **10** gave a dextrorotatory bromo sugar, but further examination of this product was postponed.[3]

We now wish to comment upon the isolation of compound **5**, a stable α-pyranosyl bromide, as the sole reaction product obtained from the β-ester **4**. Neither an n.m.r. spectrum nor the optical rotation, both taken prior to work-up as soon as the precipitation of *p*-nitrobenzoic acid was complete, gave any indication for transitory presence of the (expectedly labile) β-bromide. Similarly, 2,3,4,6-tetra-*O*-benzyl-1-*O*-*p*-nitrobenzoyl-β-D-galactopyranose had given (16) a stable α-bromide exclusively. In the absence of a participating group at C-2, such displacement with simple inversion leading directly to the stable halide would normally be no surprise. However, our findings stand in contrast to results of Ishikawa and Fletcher (5) who obtained crystalline β-bromides from the β-D-*gluco* isomer of **4** and from the corresponding 1,4,6-tri-*p*-nitrobenzoate. These and two other β-bromides (that arose, less surprisingly, from α-esters) all anomerized to their more stable α-anomers but seemed to differ in their tendencies to do so. Thus, the β-D-*gluco* isomer of **5** had a half-life of more than 2 h in dry dichloromethane solution, and stability in the series appeared to increase with the number of *p*-nitrobenzoyl groups present, a phenomenon which the authors (5) ascribed to a long-range effect of that functionality.[4] It might be argued that our β-D-galactopyranose esters may have formed intermediary β-bromides which went undetected owing to very fast anomerization.[5] However, this would still leave open the question by what mechanism labile bromides could arise, with retention of configuration. It has been speculated (5) that probably the steric requirement of the bulky bromide ion in its approach to the glucosyl carbonium ion is involved. An alternative possibility, namely participation by the 2-benzyloxy group, has been regarded both as unlikely (5) and as likely (6). Neither hypothesis readily accounts for the fact that Fréchet and Schuerch (11) obtained only α-bromides when they applied the same method to several 1,6-di-*O*-acyl-2,3,4-tri-*O*-benzyl-β-D-glucopyranosides wherein acyl was benzoyl and *p*-methoxy-, *p*-methyl-, *p*-cyano-, 3,5-dinitro-, and 2,4-dinitrobenzoyl.

Solvolysis of Glycosyl Halides

The halides **1**, **2**, **5**, **11**, and **12** were allowed to react with a 70–90 molar excess of methanol in dichloromethane solution at room temperature unless otherwise stated. The conditions were varied as follows: *A*, without any further addition; *B*, with addition of 4 mol-equiv. of tetrabutylammonium bromide; *C*, with addition of 1 mol-equiv. of mercuric cyanide; *D*, with addition of 1 mol-equiv. of silver tetrafluoroborate at −78°. Reactions according to *A* and *B* were followed polarimetrically and plots of optical rotation *vs.* time yielded first-order rate constants from the expression

[2]In addition, a di-*p*-nitrobenzoate resulting from incomplete acylation was isolated in 10% yield.

[3]Preliminary experiments of methanolysis led to mixtures of glycosides which were difficult to analyze and did not promise easy interpretation.

[4]Glaudemans and Fletcher suggested earlier (8) that the strongly electron-withdrawing character of the *p*-nitrobenzoyloxy group renders C-5 electron deficient so that destabilization of an incipient glucosyl carboxonium ion results in strengthening of the C-1—halogen bond. By the same token, β-D-glucopyranosyl halides are stabilized when a strongly electronegative substituent is present at C-2 (3*a*).

[5]In reactions implicating glycosyl carbonium ion intermediates, D-galactopyranose derivatives are generally more reactive than their D-*gluco* isomers. For example, the rates of acid hydrolysis of the pairs of methyl α- and β-pyranosides differ by factors of 5 and 4, respectively (3*b*). Larger factors could possibly apply to halide anomerizations.

TABLE 1. Methanolysis of 2,3,4,6-tetra-*O*-benzyl-α-D-galactopyranosyl bromide (**1**) and chloride (**2**)

Halide	Salt added	$t_{1/2}$ (min)	k (ln, s^{-1})	Ratio of methyl glycosides formed (α:β)
1	—	15	7.6×10^{-4}	35:65
1	*n*-Bu_4NBr	3.25	3.8×10^{-3}	75:25
1	$Hg(CN)_2$			2:98
1	$AgBF_4$ (−78°)			3:97
2	—	240	4.8×10^{-5}	37:63
2	$AgBF_4$ (−78°)			5:95

$$k = (1/t) \ln [(\alpha_0 - \alpha_\infty)/(\alpha_t - \alpha_\infty)]$$

Upon completion of the methanolyses, the anomeric composition of the mixture of methyl glycosides formed was determined by measuring the intensity ratio of the methoxyl proton peaks in n.m.r. spectra (11). In those cases where methoxyl peaks were superimposed on a background due to ring protons, adjustment was made by subtraction of the background intensity as obtained from the spectrum of a separate run that was performed with methanol-d_4.

The results obtained with the perbenzylated halides **1** and **2** are shown in Table 1. In line with expectations the bromide **1** was methanolyzed more rapidly than the chloride **2**. The preponderant product formed in both cases in the absence of an additive was the β-glycoside, which is due to direct displacement with inversion in the bulk of reactant. Halide ion liberated during the reaction catalyzes (4) a continuous anomerization of unreacted α-glycosyl halide to its more highly reactive β-anomer which is constantly and rapidly consumed by methanol, also with inversion. This accounts for the considerable proportion of α-glycoside produced. Increasing the halide ion concentration at the outset by addition of tetrabutylammonium bromide promotes anomerization of the glycosyl halide (4), and consequently the α-glycoside becomes the predominant product. The observed enhancement in the rate of methanolysis is consistent with this view. Thus far, the results parallel those obtained (5) with the D-*gluco* isomer of **1** and support the mechanistic picture which has evolved for this type of reaction (4–6, 11, 14, 23). It is important to note, though, that **1** solvolyzed more rapidly than its D-*gluco* isomer; with methanol alone, the rate was twice as large, and addition of bromide ion caused a fivefold increase in **1** and only a twofold increase in the isomer.[5]

The solvolyses performed in the presence of mercuric cyanide or silver tetrafluoroborate almost exclusively gave the β-glycoside. They proceeded extremely fast so that rates could not conveniently be measured. It is reasonable to assume that the rate increase is due to a 'push-pull' mechanism, a concerted process in which the halogen atom is attracted by the metal while the nucleophile attacks C-1 from the back (14, 24). The abstracted halide ion is bound by the metal and therefore unable to cause anomerization in any temporarily surviving glycosyl halide. The minor proportion of α-glycoside that arises nevertheless may perhaps originate from methanol attack on 'free' glycosyl carbonium ion, an event which could occur when from time to time a halide ion is abstracted without the benefit of simultaneous nucleophilic push.

The observations made on the 6-*O*-*p*-nitrobenzoylglycosyl bromide **5** (Table 2) were quite analogous although the ester group present at C-6 evidently caused the methanolyses with and without added tetrabutylammonium bromide to be slower than those of **1**. One experiment was conducted without additive at low temperature (−20°), with the result that the ratio of α-glycoside (**13**) to β-glycoside (**14**) was shifted slightly in favor of the latter, suggesting that temperature dependence of anomerization is somewhat greater than that of solvolysis. The reactions promoted by metal salts again exhibited a high degree of stereoselectivity, giving nearly exclusively the β-glycoside (**14**). Compounds **13** and **14**, which were previously unknown, were isolated in crystalline condition from runs containing tetrabutylammonium bromide and mercuric cyanide, respectively.

Comparison of Tables 1 and 2 shows that replacement of the 6-*O*-benzyl group by the *p*-nitrobenzoate function had a negligible influence upon the steric outcome of all the reactions here inves-

Can. J. Chem. Downloaded from www.nrcresearchpress.com by 210.87.254.40 on 09/05/12
For personal use only.

TABLE 2. Methanolysis of 2,3,4-tri-*O*-benzyl-6-*O*-*p*-nitrobenzoyl-α-D-galactopyranosyl bromide (**5**)

Salt added	$t_{1/2}$ (min)	k (ln, s^{-1})	Ratio of methyl glycosides formed (α:β)
—	42.5	2.4×10^{-4}	31:69
— (−20°)			24:76
n-Bu_4NBr	14	8.2×10^{-4}	70:30
$Hg(CN)_2$			3:97
$AgBF_4$			5:95

tigated. As far as the methanolyses with and without added bromide ion are concerned, this contrasts sharply with the behavior of the corresponding D-*gluco* derivatives where remarkable shifts in the anomeric product ratio were observed as the nature of the C-6 substituent was varied. Thus, the D-*gluco* isomer of **5** gave 90–96% α-glucoside (5, 11) whereas the corresponding 6-*p*-methoxybenzoate gave 93% β-glucoside (11); other C-6 substituents led to intermediate α/β ratios (11). In related studies, Schuerch and coworkers noted similar, wide ranges of stereoselectivity in diversely 6-substituted D-glucopyranosyl derivatives but at the same time, they observed directive effects of solvent (14, 17). In the D-*galacto* series, on the other hand, selectivity was greatly reduced and certain solvent effects were opposite (18). The results obtained in the D-*gluco* series have been rationalized in terms of a sensitive balance between two competing, key reactions whose rates are of similar order of magnitude but variable depending on the medium and the structure of the substrate; namely, the methanolysis of α-halide to give β-glycoside, and the anomerization of α-halide to form β-halide which subsequently reacts very rapidly to yield α-glycoside (14, 17).[6] Elaborating on this concept (4–6) with regard to the *galacto* series we suggest that both processes are affected, but not necessarily in equal manner, by inductive variation in the electron density at C-5, which should influence the stability and character of intermediary C-1 carbonium ion or ion-pair (*cf.* footnote 4), and also by the dipolar effect of axial O-4. The latter, probably, supplements the anomeric effect in opposing equatorial placement of electronegative groups at C-1, with halogen atoms being opposed more strongly than the methoxyl group. Thus α → β halide anomerization may be retarded and consequently, high proportions of α-pyranosides are less readily obtained in the *galacto* series than in the *gluco* series.

The results of methanolyses of the β-furanosyl halides **11** and **12** are given in Table 3. It is seen that the reactions both with methanol alone and with added tetrabutylammonium bromide were completely stereospecific as far as could be judged from n.m.r. spectra, the product being the methyl α-furanoside **15**. Evidently the methanolysis proceeds with inversion as in the preceding cases, but there is no prior anomerization in part of the glycosyl halide, not even in the presence of excess bromide ion which has no influence on the product composition and merely causes a slight increase in the reaction rate (probably a kinetic salt effect). Compared with its pyranoid counterparts **1** and **4**, the furanoid bromide **11** was considerably more reactive. The pair of chlorides **2** and **12** exhibited the same trend but their rate difference was relatively small. Two opposing factors appear to operate, namely, the generally recognized greater reactivity of furanosyl halides originating from conformational features, and inductive stabilization by the *p*-nitrobenzoyl groups (8). The first factor seems more important in the bromides, and the second factor, in the chlorides. Absence of halide anomerization in both **11** and **12** can be explained by assuming that, in generating the sterically unfavorable furanoid 1,2-*cis* arrangement, halide ions are at a serious disadvantage in competition with methanol molecules. An additional factor could possibly arise from hydrogen bonding of the ether oxygen atom at C-2 with the incoming methanol, assisting in its approach from the α-side of the ring, whereas a halogen ion on the same path would find no such assistance.

Also characterized by complete stereospecificity were the metal salt-assisted reactions of **12**, whereas selectivity was slightly lower in those of **11** (Table 3).

[6]Nonbonded interaction between the C-6 acyl carbonyl group and the anomeric center, as proposed earlier (11), does not satisfactorily explain the more recent findings.

Can. J. Chem. Downloaded from www.nrcresearchpress.com by 210.87.254.40 on 09/05/12
For personal use only.

TABLE 3. Methanolysis of 2,3-di-*O*-benzyl-5,6-di-*O*-*p*-nitrobenzoyl-β-D-galactofuranosyl bromide (**11**) and chloride (**12**)

Halide	Salt added	$t_{1/2}$ (min)	k (ln, s^{-1})	Ratio of methyl glycosides formed (α:β)
11	—	2.8	4.2×10^{-3}	100:0
11	n-Bu_4NBr	1.8	6.3×10^{-3}	100:0
11	$Hg(CN)_2$			96:4
11	$AgBF_4$ (−78°)			95:5
12	—	145	6.2×10^{-5}	100:0
12	n-Bu_4NBr			100:0
12	$Hg(CN)_2$			100:0
12	$AgBF_4$ (−78°)			100:0

The methyl α-furanoside **15** was isolated in crystalline condition. Proof of structure was provided by its treatment with benzyl chloride and potassium hydroxide which replaced the *p*-nitrobenzoyl groups by benzyl groups to give methyl 2,3,5,6-tetra-*O*-benzyl-α-D-galactofuranoside (**16**). The n.m.r. spectrum of this new compound was superimposable on that of an identical product obtained by benzylation of authentic methyl α-D-galactofuranoside but differed clearly from the spectra of perbenzylated methyl β-D-galactofuranoside and methyl α- and β-D-galactopyranosides.

Experimental

Optical rotations were measured at approximately 25° in a Perkin-Elmer 141 automatic polarimeter. The n.m.r. data were obtained with a Varian HA 100 instrument using tetramethylsilane as internal standard.

Preparation of Fully Benzylated Methyl D-*Galactosides*

Samples of the fully benzylated methyl α- and -β-D-galactopyranosides and -furanosides were required as standards for identification of methanolysis products. They were prepared as follows.

Glycosidation of D-*Galactose*

D-Galactose was converted into a mixture of methyl glycosides and the (known) products were separated chromatographically by use of the procedure of Baddiley and co-workers (25), with minor modifications. A suspension of the sugar (5 g) in absolute methanol (40 ml) containing 0.4 ml sulfuric acid was refluxed for 2 h. The cooled solution was neutralized with calcium carbonate, filtered, and evaporated to give a syrup which, with a small amount of added water, was placed on a column containing approximately 200 g of anion exchange resin AG1-X2 (OH^-) of Bio-Rad Laboratories, Richmond, Calif. Elution was performed with carbon dioxide-free, distilled water and monitored by polarimetry of all fractions (8 ml). It yielded methyl α-D-galactopyranoside (fractions 16–20, 1.2 g), methyl β-D-galactopyranoside (fractions 24–32, ~0.1 g), methyl α-D-galactofuranoside (fractions 36–53, 0.66 g), and methyl β-D-galactofuranoside (fractions 85–180, 2.17 g). Intermediate, mixed fractions were discarded.

*Methyl 2,3,4,6-Tetra-O-benzyl-α- and -β-*D-*galactopyranosides*

Methyl α- and β-D-galactopyranoside, respectively, were benzylated with benzyl chloride and potassium hydroxide as described (19), or by use of the method (26) detailed in the next paragraph. The OCH_3 signal of the benzylated α-pyranoside was at δ 3.35, and that of the β-pyranoside at δ 3.51 (in $CDCl_3$).

*Methyl 2,3,5,6-Tetra-O-benzyl-α-*D-*galactofuranoside (16) and its β-Anomer*

To a solution of sodium hydride (0.55 g; oil dispersion, 55% pure) in dimethyl sulfoxide (3 ml) was added dropwise a solution of methyl α-D-galactofuranoside (0.45 g) in dimethyl sulfoxide (3 ml). The mixture was stirred for 30 min, after which benzyl chloride (3 ml) was added dropwise and stirring was continued for another 2.5 h. The reaction mixture was then poured into ice water (50 ml) which was extracted three times with chloroform. The dried ($MgSO_4$) extract was evaporated at 2 mm Hg, leaving an oil which was passed through a small column of silica gel (20 g) by means of benzene–ether (99:1). Compound **16** was obtained as a colorless oil (965 mg, 75%) showing $[\alpha]_D$ +20° (*c* 2, $CHCl_3$). The OCH_3 signal occurred at δ 3.29 (in $CDCl_3$).

Anal. Calcd. for $C_{35}H_{38}O_6$ (554.7): C, 75.79; H, 6.91. Found: C, 75.54; H, 7.01.

The same procedure applied to methyl β-D-galactofuranoside furnished the β-anomer of **16**, $[\alpha]_D$ −49° (*c* 2, $CHCl_3$), as reported (26). Its OCH_3 signal occurred at δ 3.33, and its pattern of ring proton signals was distinctively different from that of **16**.

*2,3,4,6-Tetra-O-benzyl-α-*D-*galactopyranosyl Bromide (1) and Chloride (2)*

Preparation of the bromide **1** via the corresponding 1-*p*-nitrobenzoate has been described (16). The chloride **2** was obtained in analogous fashion (11, 14, 20). Dry hydrogen chloride gas was passed through a solution of the 1-*p*-nitrobenzoate (1 g of crystalline β-anomer) in dry dichloromethane (50 ml), with exclusion of moisture and at room temperature. After 20 min, *p*-nitrobenzoic acid began to precipitate, the gas stream was stopped, and the tightly stoppered vessel was placed in a refrigerator for 3 days. The mixture was then filtered to remove *p*-nitrobenzoic acid (239 mg, 97%) and the filtrate was evaporated *in vacuo* at room temperature. Several portions of added dichloromethane were evaporated from the remaining, faintly yellow syrup of **2** which showed $[\alpha]_D$ +146.5°

Can. J. Chem. Downloaded from www.nrcresearchpress.com by 210.87.254.40 on 09/05/12
For personal use only.

Can. J. Chem. Downloaded from www.nrcresearchpress.com by 210.87.254.40 on 09/05/12
For personal use only.

(*c* 1.6, benzene). Reported (19) for **2** obtained from 2,3,4,6-tetra-*O*-benzyl-D-galactose and thionyl chloride, $[\alpha]_D$ +147° (*c* 2, benzene). The n.m.r. spectrum of **2** showed a doublet for H-1 at δ 6.14 ($J_{1,2}$ = 3.5 Hz).

2,3,4-Tri-O-benzyl-1,6-di-O-p-nitrobenzoyl-β-D-galactopyranose (4)

A solution of 10.3 g of 1,6-anhydro-2,3,4-tri-*O*-benzyl-β-D-galactopyranose (**3**) (27) in warm acetic anhydride (100 ml) was cooled in an ice water bath and mixed with a chilled solution of concentrated sulfuric acid (0.1 ml) in acetic anhydride (5 ml). After 3 min the mixture was poured into, and stirred with, ice water (600 ml) whereby the product of acetolysis separated as an oil. After 45 min the aqueous phase was decanted and replaced by fresh water (600 ml) which was removed after 24 h. The oily product was then dissolved in chloroform and washed with 5% sodium bicarbonate solution and water. After drying, the solvent was evaporated and the nearly colorless product (12 g) was deacetylated overnight, at room temperature, in methanol containing a small amount of sodium methoxide. The methanol was evaporated after neutralization with acetic acid and the product was dissolved in pyridine (100 ml) and allowed to react overnight at 25° with *p*-nitrobenzoyl chloride (15 g). The reaction mixture was treated with ice water and the precipitated product was taken up in chloroform. The solution was washed successively with water, sodium bicarbonate solution and water, then dried and evaporated to give a residue which was crystallized from ethyl acetate – petroleum ether (b.p. 30–60°). The yield was 8.2 g (49%) of **4**, m.p. 152–153°, $[\alpha]_D$ −6.6° (*c* 2, $CHCl_3$). The n.m.r. spectrum showed a doublet at δ 5.94 (H-1, $J_{1,2}$ = 7.5 Hz) indicative of the β-anomeric configuration.

Anal. Calcd. for $C_{41}H_{36}N_2O_{12}$ (748.9): C, 65.77; H, 4.85; N, 3.74. Found: C, 65.62; H, 4.85; N, 3.78.

2,3,4-Tri-O-benzyl-6-O-p-nitrobenzoyl-α-D-galactopyranosyl Bromide (5)

Compound **4** (1 g) was dissolved in dry dichloromethane (25 ml) saturated with hydrogen bromide gas, at room temperature. After 2 min, *p*-nitrobenzoic acid started to precipitate, and after 10 min it was collected by filtration (214 mg, 96%). The filtrate was evaporated to yield a nearly colorless heavy oil from which several portions of added dichloromethane were evaporated *in vacuo*. The product could not be crystallized. It had $[\alpha]_D$ +100° (*c* 2.6, CH_2Cl_2), and its n.m.r. spectrum showed a doublet at δ 6.53 (H-1, $J_{1,2}$ = 1.4 Hz).

Methyl 2,3-Di-O-benzyl-4,6-O-benzylidene-α-D-galactopyranoside (7)

A mixture of 11 g of methyl 4,6-*O*-benzylidene-α-D-galactopyranoside (**6**) (28), powdered potassium hydroxide (20 g), and benzyl chloride (120 ml) was stirred at 105° for 6 h. After cooling, the mixture was shaken with water (150 ml) and chloroform (150 ml). The organic phase was separated, washed with water, and dried over magnesium sulfate. Chloroform was evaporated and remnant benzyl chloride was removed partially by evaporation at 2 mm Hg and finally by steam distillation. The product **7** was then crystallized from ethanol as white plates, m.p. 174–175°, in a yield of 13.8 g (76%). Recrystallization from petroleum ether gave long needles; m.p. 176–177°, $[\alpha]_D$ +77° (*c* 2.4, $CHCl_3$).

Anal. Calcd. for $C_{28}H_{30}O_6$ (462.6): C, 72.71; H, 6.54. Found: C, 72.81; H, 6.63.

2,3-Di-O-benzyl-D-galactose (8)

A solution of 7 (12.5 g) in dioxane (300 ml) and 2 *N* sulfuric acid (90 ml) was refluxed for 3 days. The cooled solution was neutralized with barium carbonate, filtered, and evaporated to give a syrup which was extracted with petroleum ether for removal of benzaldehyde. The remaining material was chromatographed in a column of silica gel (250 g). Elution with benzene–ether (97:3) produced, first, several fractions containing incompletely hydrolyzed material (3.6 g), then a noncrystallizable oil (0.4 g) having $[\alpha]_D$ +43°, and finally, compound **8** (4.1 g, 42%) which crystallized from ether and showed m.p. 74–76°, $[\alpha]_D$ +5.3° (*c* 2, $CHCl_3$).

Anal. Calcd. for $C_{20}H_{24}O_6$ (360.4): C, 66.65; H, 6.71. Found: C, 66.50; H, 6.68.

2,3-Di-O-benzyl-1,5,6-tri-O-p-nitrobenzoyl-β-D-galactofuranose (9) and Isomer (10)

To compound **8** (3.95 g) in dry pyridine (40 ml) was added *p*-nitrobenzoyl chloride (8 g) at 0°. The reaction mixture was then stirred overnight at ambient temperature and processed with ice water (600 ml) in the usual manner. The solid product was washed thoroughly with water and then briefly with ice cold, 0.6 *N* hydrochloric acid. It was dissolved in dichloromethane, the solution was washed repeatedly with sodium bicarbonate solution and then with water, and after drying ($MgSO_4$) the solvent was removed again. The residue upon drying in high vacuum weighed 8.69 g, and t.l.c. revealed that it contained three products besides a small amount of *p*-nitrobenzoic acid. The crude material was passed through a column of silica gel (270 g) by means of benzene–ether (98:2). The fastest-moving component (**9**) was obtained as an amorphous powder (3.5 g, 40%) exhibiting $[\alpha]_D$ −5.5° (*c* 2, $CHCl_3$). It could not be crystallized but was homogeneous in t.l.c. (benzene–ether 7:1).

Anal. Calcd. for $C_{41}H_{33}N_3O_{15}$ (807.7): C, 60.97; H, 4.12; N, 5.20. Found: C, 61.02; H, 4.20 N, 5.19.

The second compound eluted from the column was also an amorphous, chromatographically homogeneous powder (3.5 g, 40%). It showed $[\alpha]_D$ −9.1° (*c* 2.5, $CHCl_3$) and was tentatively assumed to be 2,3-di-*O*-benzyl-1,4,6-tri-*O*-*p*-nitrobenzoyl-β-D-galactopyranose (**10**).

Anal. Calcd. for $C_{41}H_{33}N_3O_{15}$ (807.7): C, 60.97; H, 4.12; N, 5.20. Found: C, 60.80; H, 4.21; N, 5.27.

Finally, after a mixed fraction which was discarded, the most slowly moving component was eluted (952 mg); $[\alpha]_D$ −2° (*c* 1.5, $CHCl_3$). According to n.m.r. and i.r. spectra it contained a hydroxyl group and only two *p*-nitrobenzoyl groups.

2,3-Di-O-benzyl-5,6-di-O-p-nitrobenzoyl-β-D-galactofuranosyl Bromide (11)

Compound **9** (680 mg) was treated with anhydrous hydrogen bromide in dichloromethane as described above for the preparation of **5**. The *p*-nitrobenzoic acid collected weighed 133 mg (95%). The bromide **11** was obtained as a slightly colored, amorphous solid, $[\alpha]_D$ −59.4° (*c* 1.2, CH_2Cl_2).

Anal. Calcd. for $C_{34}H_{29}BrN_2O_{11}$ (721.5): C, 56.60; H, 4.05; Br, 11.08; N, 3.88. Found: C, 56.42; H, 4.17; Br, 10.87; N, 4.12.

Can. J. Chem. Downloaded from www.nrcresearchpress.com by 210.87.254.40 on 09/05/12
For personal use only.

2,3-Di-O-benzyl-5,6-di-O-p-nitrobenzoyl-β-D-galactofuranosyl Chloride (12)

Compound **9** (1.364 g) dissolved in a minimum amount of dichloromethane was added at room temperature to a saturated solution of anhydrous hydrogen chloride in dichloromethane (50 ml). Hydrogen chloride was passed through the solution continuously for 3 h and the closed vessel was then left standing for 36 h, after which t.l.c. indicated the reaction to be complete. By partial evaporation, the major part of *p*-nitrobenzoic acid precipitated (226 mg, 80%). The filtrate therefrom was rapidly washed with an ice cold sodium bicarbonate solution and with water. The dried ($MgSO_4$) solution was then treated with activated charcoal, filtered through Celite, and evaporated to furnish **12** (1.036 g, 90.6%) as an almost colorless solid; $[\alpha]_D$ −31.4° (*c* 2.3, CH_2Cl_2).

Methyl 2,3,4-Tri-O-benzyl-6-O-p-nitrobenzoyl-α-D-galactopyranoside (13)

The product obtained upon work-up of a methanolysis of **5** in the presence of tetrabutylammonium bromide (see a subsequent section) was crystallized from ethyl acetate – petroleum ether and recrystallized from anhydrous ether. It had m.p. 115–117° and $[\alpha]_D$ −3.5° (*c* 2, $CHCl_3$). The OCH_3 signal was at δ 3.34.

Anal. Calcd. for $C_{35}H_{35}NO_9$ (613.6): C, 68.50; H, 5.75; N, 2.28. Found: C, 68.62; H, 5.94; N, 2.36.

Methyl 2,3,4-Tri-O-benzyl-6-O-p-nitrobenzoyl-β-D-galactopyranoside (14)

The product obtained upon work-up of a methanolysis of **5** in the presence of mercuric cyanide was crystallized from ether and recrystallized from ethyl acetate – petroleum ether. It had m.p. 135–137° and $[\alpha]_D$ −33.5° (*c* 2.5, $CHCl_3$). The OCH_3 signal was at δ 3.53.

Anal. Calcd. for $C_{35}H_{35}NO_9$ (613.6): C, 68.50; H, 5.75; N, 2.28. Found: C, 68.61; H, 5.78; N, 2.47.

Methyl 2,3-Di-O-benzyl-5,6-di-O-p-nitrobenzoyl-α-D-galactofuranoside (15)

The product obtained by methanolysis of **11** in the presence of tetrabutylammonium bromide (see a subsequent section) was **15**. Recrystallized from ethyl acetate – petroleum ether it showed m.p. 116–118°, $[\alpha]_D$ +55.7° (*c* 2, $CHCl_3$).

Anal. Calcd. for $C_{35}H_{32}N_2O_{12}$ (672.6): C, 62.50; H, 4.80; N, 4.16. Found: C, 62.43; H, 4.72; N, 4.34.

A sample of **15** (350 mg) was treated with benzyl chloride (12 ml) and powdered potassium hydroxide (1 g) at 105° for 5 h. The reaction mixture was partitioned between chloroform and water. The dried chloroform phase was evaporated, eventually at 2 mm Hg to remove excess benzyl chloride. The oily residue was purified by passage through a silica gel column (30 g) with benzene containing 0.5% ether. There was obtained 167 mg (58%) of **16** whose n.m.r. spectrum was identical in every detail with that of **16** obtained from methyl α-D-galactofuranoside.

Methanolyses

(A) With Methanol Alone

A sample of glycosyl halide (approximately 100 mg, 0.14–0.18 mmol) was accurately weighed in a 5-ml volumetric flask and dissolved in dry dichloromethane (4.4 ml). Methanol (0.50 ml, 12.7 mmol) was added, and the volume was made up to 5 ml with dichloromethane. The change in optical rotation with time was recorded, a 1-dm tube being used. The first recording was usually made after 1 min. When the rotation had become constant, the solution was diluted with dichloromethane, washed once with aqueous sodium bicarbonate and once with water, dried over magnesium sulfate, and evaporated with eventual addition of several portions of carbon tetrachloride. The ratio of anomeric glycosides in the residue was then determined by integration of the OCH_3 signals of the n.m.r. spectrum in $CDCl_3$, at 250 Hz sweep width.

(B) In the Presence of Tetrabutylammonium Bromide

The procedure was the same as in *A* except that 200 mg of $(n\text{-}C_4H_9)_4NBr$ was added immediately prior to the addition of methanol and that, in work-up, two sodium bicarbonate and three water washings were included.

(C) In the Presence of Mercuric Cyanide

The procedure was the same as in *A* exeept that 40 mg (0.16 mmol) of $Hg(CN)_2$ was added prior to the addition of methanol. The reactions were too fast for polarimetric rate determination, and the runs were processed after one to several hours as convenient.

(D) In the Presence of Silver Tetrafluoroborate

In a typical experiment, a solution of glycosyl halide (160 mg) in dichloromethane (10 ml) was cooled to −78°, and approximately 95 mg of $AgBF_4$ was quickly introduced. (The reagent is very hygroscopic; rapid handling is more important than accurate weighing.) The mixture was first stirred in the dark for 10 min, methanol (0.5 ml) was then added, and stirring was continued for 1 h. The reaction mixture was filtered through Celite and then processed as in *A*.

Financial support of this work by the National Research Council of Canada is gratefully acknowledged. Miss Geneviève Pellé is thanked for technical assistance.

1. N. K. KOCHETKOV, O. S. CHISHOV, and A. F. BOCHKOV. MTP Int. Rev. Sci., Org. Chem. Ser. I, **7**, 147 (1973). C. SCHUERCH. Acc. Chem. Res. **6**, 184 (1973). G. WULFF and G. RÖHLE. Angew. Chem. **86**, 173 (1974).
2. R. U. LEMIEUX, T. L. NAGABHUSHAN, and S. W. GUNNER. Can. J. Chem. **46**, 405 (1968). R. U. LEMIEUX, Y. ITO, K. JAMES, and T. L. NAGABHUSHAN. Can. J. Chem. **51**, 7 (1973). R. U. LEMIEUX, T. L. NAGABHUSHAN, K. J. CLEMETSON, and L. C. N. TUCKER. Can. J. Chem. **51**, 53 (1973).
3. (*a*) M. L. WOLFROM and W. A. SZAREK. *In* The carbohydrates. Vol. IA. *Edited by* W. Pigman and D. Horton. Academic Press, Inc., New York, N.Y. 1972. p. 239. (*b*) W. G. OVEREND. *In* The carbohydrates. Vol. IA. *Edited by* W. Pigman and D. Horton. Academic Press, Inc., New York, N.Y. 1972. p. 279.
4. R. U. LEMIEUX and J. HAYAMI. Can. J. Chem. **43**, 2162 (1965). R. U. LEMIEUX and A. R. MORGAN. Can. J. Chem. **43**, 2199, 2214 (1965).
5. T. ISHIKAWA and H. G. FLETCHER, JR. J. Org. Chem. **34**, 563 (1969).
6. R. U. LEMIEUX and T. L. NAGABHUSHAN. Methods Carbohydr. Chem. **6**, 487 (1972). R. U. LEMIEUX, K. B. HENDRIKS, R. V. STICK, and K. JAMES. Personal communication.

7. P. A. GENT and R. GIGG. J. Chem. Soc. Perkin I, 1446 (1974).
8. C. P. J. GLAUDEMANS and H. G. FLETCHER, JR. J. Am. Chem. Soc. **87**, 4643 (1965).
9. P. F. LLOYD, B. EVANS, and R. J. FIELDER. Carbohydr. Res. **22**, 111 (1972). P. F. LLOYD and G. P. ROBERTS. J. Chem. Soc. 2962 (1963); 6910 (1965).
10. H. M. FLOWERS. Carbohydr. Res. **18**, 211 (1971). M. DEJTER-JUSZYNSKI and H. M. FLOWERS. Carbohydr. Res. **18**, 219 (1971).
11. J. M. FRÉCHET and C. SCHUERCH. J. Am. Chem. Soc. **94**, 604 (1972).
12. J. M. FRÉCHET and C. SCHUERCH. Carbohydr. Res. **22**, 399 (1972).
13. M. DEJTER-JUSZYNSKI and H. M. FLOWERS. Carbohydr. Res. **23**, 41 (1972); **28**, 61 (1973).
14. F. J. KRONZER and C. SCHUERCH. Carbohydr. Res. **27**, 379 (1973).
15. A. C. WEST and C. SCHUERCH. J. Am. Chem. Soc. **95**, 1333 (1973); F. J. KRONZER and C. SCHUERCH. Carbohydr. Res. **33**, 273 (1974).
16. H. H. BAER, J. M. J. FRÉCHET, and U. WILLIAMS. Can. J. Chem. **52**, 3337 (1974).
17. R. EBY and C. SCHUERCH. Carbohydr. Res. **34**, 79 (1974).
18. T. J. LUCAS and C. SCHUERCH. Personal communication.
19. P. W. AUSTIN, F. E. HARDY, J. G. BUCHANAN, and J. BADDILEY. J. Chem. Soc. 1419 (1965).
20. C. P. J. GLAUDEMANS and H. G. FLETCHER, JR. J. Org. Chem. **28**, 3004 (1963).
21. C. S. HUDSON. J. Am. Chem. Soc. **37**, 1591 (1915). R. K. NESS, H. G. FLETCHER, JR., and C. S. HUDSON. J. Am. Chem. Soc. **73**, 3742 (1951).
22. V. SMIRNYAGIN and C. T. BISHOP. Can. J. Chem. **46**, 3085 (1968). R. H. PATER, R. A. COELHO, and D. F. MOWERY, JR. J. Org. Chem. **38**, 3272 (1973).
23. A. J. RHIND-TUTT and C. A. VERNON. J. Chem. Soc. 4637 (1960).
24. Y. POCKER and D. N. KEVILL. J. Am. Chem. Soc. **87**, 4760, 4771, 4778, 5060 (1965).
25. P. W. AUSTIN, F. E. HARDY, J. G. BUCHANAN, and J. BADDILEY. J. Chem. Soc. 5350 (1963).
26. T. IWASHIGE and H. SAEKI. Chem. Pharm. Bull. (Japan), **15**, 1803 (1967).
27. T. URYU, H. LIBERT, J. ZACHOVAL, and C. SCHUERCH. Macromolecules, **3**, 345 (1970).
28. G. J. ROBERSTSON and R. A. LAMB. J. Chem. Soc. 1321 (1934).

Can. J. Chem. Downloaded from www.nrcresearchpress.com by 210.87.254.40 on 09/05/12
For personal use only.

Réactions des ions moléculaires cyclohexane en phase gazeuse[1]

GUY J. COLLIN
Département des Sciences Pures, Université du Québec à Chicoutimi, Chicoutimi, Québec G7H 2B1
ET
PIERRE AUSLOOS
Radiation Chemistry Section, National Bureau of Standards, Washington, D.C. 20234
Received October 9, 1974

GUY J. COLLIN et PIERRE AUSLOOS. Can. J. Chem. **53**, 680 (1975).

Les ions cy-$C_6H_{12}^+$ produits dans la photoionisation du cyclohexane (raies de résonance de l'argon: 11.6–11.8 eV) réagissent avec les composés insaturés et cycliques (C_3 et C_4) par transfert d'une molécule d'hydrogène. La réaction est quantitative avec le propène, l'isobutène, le butène-1, le pentène-1 et le butadiène-1,3. Avec les oléfines le transfert observé a lieu seulement si la double liaison est en bout de chaîne. Avec les petits cycles en C_3 et en C_4 il y a ouverture du cycle. Il y a également transfert d'un atome d'hydrogène entre l'ion cy-$C_6H_{12}^+$ et divers additifs et la structure du radical ainsi formé a été déterminée par analyse chimique. Avec le *cis*-butène-2 il y a seulement transfert de charge.

GUY J. COLLIN and PIERRE AUSLOOS. Can. J. Chem. **53**, 680 (1975).

The cy-$C_6H_{12}^+$ ions formed in the photoionization of cyclohexane (resonance lines of argon: 11.6–11.8 eV) react with cyclic (C_3 and C_4) and unsaturated hydrocarbons by H_2 transfer. This reaction is quantitative with propene, 1-butene, 1-pentene, 1,3-butadiene, and isobutene. This transfer is efficient only if there is a terminal double bond. There is ring opening with the C_3 and C_4 hydrocarbons. H atom transfer reactions are also observed between cy-$C_6H_{12}^+$ ions and several compounds and the structure of the radical formed in such a reaction is determined by chemical analysis. With *cis*-2-butene, there is only charge transfer reaction.

Introduction

Dans une étude récente, Ausloos et ses collaborateurs ont montré que les ions moléculaires cyclohexane (cy-$C_6H_{12}^+$) issus de la photoionisation du cyclohexane réagissent beaucoup plus vite avec le propène qu'avec le cyclohexane (1):

[1] $$cy\text{-}C_6H_{12}^+ + C_3H_6 \rightarrow C_3H_8 + C_6H_{10}^+$$

Lorsque la concentration de propène varie de 1 à 7%, le rendement en propane est pratiquement inaltéré. Dans le cas de la radiolyse, une variation de 1 à 87% n'affecte pas le rendement en propane (2): c'est dire que le cyclohexane est pratiquement inerte vis-à-vis des ions cy-$C_6H_{12}^+$, ou que s'il y a réaction, la constante de vitesse de celle-ci est très faible: $k \simeq 5 \times 10^{-14}$ cm^3 mol^{-1} s^{-1} (3). Il est donc intéressant d'utiliser ce système pour étudier certains aspects de la chimie des ions cy-$C_6H_{12}^+$. Il suffit, *à priori*, d'ajouter quelques pourcents d'un intercepteur convenablement choisi pour faire cette étude. Cette dernière s'inscrit dans notre programme d'études de la stabilité des hydrocarbures sous rayonnement et fait suite à d'autres travaux (4).

Nous ne démontrerons pas ici que globalement tout se passe comme s'il y avait un transfert d'une molécule d'hydrogène de l'ion cy-$C_6H_{12}^+$ vers l'additif, plus précisément de part et d'autre de la double liaison.

[2] $$cy\text{-}C_6H_{12}^+ + M \rightarrow C_6H_{10}^+ + MH_2$$

Nous mettrons plutôt l'accent vers les efficacités relatives de ce transfert et des réactions concurrentes possibles comme la réaction de transfert d'un atome d'hydrogène:

[3] $$cy\text{-}C_6H_{12}^+ + M \rightarrow cy\text{-}C_6H_{11}^+ + MH$$

Partie expérimentale

Le cyclohexane et les additifs sont le plus souvent des produits A.P.I. et sont employés sans autre purification. Les autres additifs sont le plus souvent purifiés par chromatographie en phase gazeuse. Les irradiations sont faites à l'aide d'une lampe à argon: 1066 Å (60%) –

[1]Une partie de ce travail a été subventionné par la U.S. Atomic Energy Commission et réalisé au Bureau National des Standards, Washington, D.C. L'autre partie a été réalisée grâce à l'aide reçue du Conseil national de recherches du Canada et de l'Université du Québec à Chicoutimi.

Can. J. Chem. Downloaded from www.nrcresearchpress.com by 210.87.254.6 on 09/05/12
For personal use only.

Can. J. Chem. Downloaded from www.nrcresearchpress.com by 210.87.254.6 on 09/05/12
For personal use only.

1048 Å (40%). Cette lampe a déjà été décrite ainsi que ses caractéristiques (5). La pression du cyclohexane est de 10 Torr (1330 N m^{-2}) sauf dans les cas indiqués. Les analyses ont été faites par introduction d'une fraction de l'échantillon irradié dans un chromatographe à gaz. Dans le cas du mélange cyclohexane:acétylène-d_2, l'éthylène formé est analysé par spectrométrie de masse (6). Chaque expérience est irradiée en présence de 5 ± 2% d'oxygène sauf dans les cas indiqués. Quelques expériences ont été réalisées dans un appareil de résonance cyclotronique ionique pulsé (i.c.r.). La durée de l'impulsion était de 5 ms; l'énergie des électrons était de 15 eV et la pression du cyclohexane était comprise entre 10^{-7} et 10^{-6} Torr.

Résultats

Ceux-ci sont consignés dans les tableaux accompagnant le texte. Les rendements sont indiqués comme étant le nombre de molécules produites (M) divisé par le nombre d'ions cyclohexane formés par le rayonnement (Ni). La quantification de ces rendements, M/Ni, est faite en utilisant la formation de l'éthylène (M/Ni = 0.95) ou le butadiène-1,3 (M/Ni = 0.33) dans la photolyse directe (1) du cyclohexane pourvu que la photolyse directe des additifs ne participe pas à la formation de produits mesurés, ce qui est le cas avec les faibles pourcentages de ceux-ci ajoutés (fig. 1).

La photolyse du cyclohexane pur produit des atomes d'hydrogène (1). En présence d'oléfine, ceux-ci conduisent aux radicaux alkyles susceptibles de former les produits MH et MH_2 par voie radicalaire. Afin d'éviter cette complication, on a ajouté de l'oxygène dans la majorité des systèmes étudiés. Par contre, il est connu que l'ion *cy*-$C_6H_{12}^+$ ne réagit pas avec l'oxygène (2).

Dans tous les cas, une variation de la proportion de l'additif entre 2 et 10% a peu d'effet sur le rendement des produits attribués à la réaction 2 (fig. 1). La variation de la pression totale dans le réacteur n'a pas non plus d'effet appréciable: (*i*) un accroissement de la pression totale de 5 à 20 Torr du système *cy*-C_6H_{12}:CH_3-*cy*-C_3H_5:O_2 (1.0:0.04:0.05) n'a pas d'effet sur le rendement en butane normal; (*ii*) l'addition de 500 Torr de xénon au mélange *cy*-C_6H_{12}:*cy*-C_3H_6:O_2 (1.0:0.04:0.05) n'a pas d'effet sur le rendement en propane; (*iii*) en outre, l'addition de 630 Torr de xénon au mélange *cy*-C_6H_{12}:C_4H_6-1,2:O_2 (10.0:0.3:0.5 Torr) ne change pas les rendements en *cis*- et *trans*-butène-2.

Le changement de l'éthylène-d_2 par l'éthylène-d_4 ne change pas le rendement en éthane. Enfin, aucun transfert du groupe H_2 n'a pu être mesuré avec l'isoprène, les pentadiènes-1,3 et -1,4, le pentène-2 et le méthyl-2-butène-2.

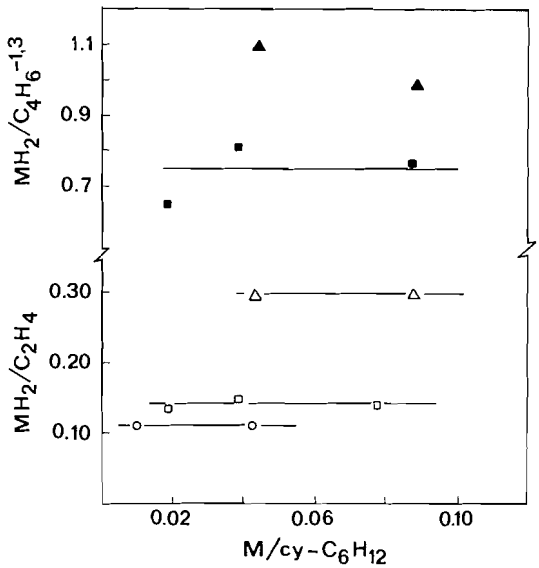

FIG. 1. Photolyse du cyclohexane (10.0 Torr) en présence d'additif M. Rendements relatifs MH_2/C_2H_4, points blancs; MH_2/C_4H_6-1,3, points noirs; ○: M = *cy*-C_3H_6; □, ■: M = *cy*-C_4H_8; △, ▲: M = CH_3-*cy*-C_3H_5.

Un certain nombre d'expériences ont été faites afin de déterminer la structure radical MH formé dans la réaction 3. A cette fin on a utilisé l'éthylène comme intercepteur radicalaire. L'addition des atomes d'hydrogène sur l'éthylène forment les radicaux éthyles. Une partie de ceux-ci se combinent aux autres radicaux présents dans le système pour former des produits caractéristiques. Les observations suivantes ont été notées: (*i*) l'addition de 4% de cyclopropane au mélange *cy*-C_6H_{12}:C_2D_4 (1.0:0.01) forme du *n*-$C_5D_4H_8$ (M/Ni = 0.19); on n'observe pas dans ce cas de formation d'isopentane (M/Ni < 0.01); (*ii*) l'addition de méthylcyclopropane produit du méthyl-3-pentane. On n'a pas observé de formation de *n*-hexane; (*iii*) l'addition de 4% de cyclobutane au mélange *cy*-C_6H_{12}:C_2D_4 (1.0:0.05) produit du *n*-$C_6D_4H_{10}$ tandis que l'on n'observe pas la formation d'hexanes ramifiés.

D'autres expériences utilisant des molécules partiellement ou complètement deutérées ont été faites afin d'obtenir la position dans la molécule de laquelle ou vers laquelle les atomes

TABLEAU 1. Photoionisation à 11.6–11.8 eV du mélange *cy*-C_6H_{12}:M:O_2 (10.0:0.5:0.5). Efficacité relative de la réaction 2

Additif (M)	Potential d'ionisation de M (eV)	Produits mesurés	
		MH_2	M/Ni (MH_2)
C≡C	11.41[d]	C=C	0.13±0.01[a]
C=C	10.51[d]	C—C	0.21±0.01
C≡C—C	10.36[d]	C=C—C	0.32±0.03
C≡C—C—C	10.18[c]	C=C—C—C	0.49±0.04
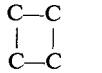	10.06[c]	C—C—C—C	0.22
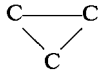	9.93[c]	C—C—C	0.15±0.01
cy-C_6	9.88[d]	Pas de réaction, voir texte	
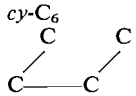	9.77[d]	C—C—C—C—C	0.00
		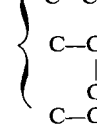	0.00
C=C—C	9.72[c]	C—C—C	1.00±0.02
C=C=C	9.62[c]	C=C—C	0.30±0.02
C=C—C—C	9.58[c]	C—C—C—C	1.00
C=C=C—C	9.57[d]	C=C—C—C	0.01
		C—C=C—C (*trans*)	0.075
		C—C=C—C (*cis*)	0.10
C—C≡C—C	9.56[c]	C=C—C—C	<0.02±0.02
		C—C=C—C (*trans*)	<0.02±0.02
		C—C=C—C (*cis*)	<0.02±0.02
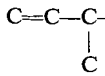	9.52[c]	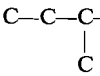	0.16±0.01
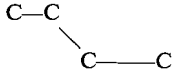	9.50[c]	C—C—C—C—C	0.11
		C—C—C—C	0.00
		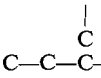	
C=C—C—C—C—C	9.48[c]	C—C—C—C—C	1.00
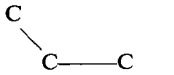	9.46[c]	C—C—C—C	0.32
		C—C—C	0.00
		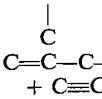	
C=C=C—C—C	9.42[d]	C=C—C—C—C	
		+ C≡C—C—C—C	0.066
		C—C=C—C—C (*trans*)	0.085
		C—C=C—C—C (*cis*)	0.064
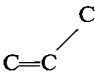	9.19[c]		1.00
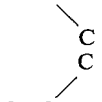	9.12[c]	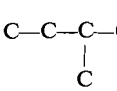	0.41±0.02
C—C=C—C (*cis*)	9.10[c]	C—C—C—C	0.00±0.02
C=C—C=C	9.07[d]	C=C—C—C	1.00

[a]Lorsqu'une incertitude est donnée, il y a eu plus de deux expériences de faites.
[c]Référence 21.
[d]Référence 22.

Can. J. Chem. Downloaded from www.nrcresearchpress.com by 210.87.254.6 on 09/05/12
For personal use only.

Can. J. Chem. Downloaded from www.nrcresearchpress.com by 210.87.254.6 on 09/05/12
For personal use only.

d'hydrogène sont transférés: (*i*) au moins 90% du butane formé dans l'irradiation du mélange *cy*-C_6D_{12}:CH_3-*cy*-C_3H_6:O_2 (100:2:2) consiste de $CH_3CHDCH_2CH_2D$; (*ii*) la photoionisation du mélange méthyl-3-pentane-3-d_1:CH_3-*cy*-C_3H_5:O_2 (100:2:5) produit du *n*-butane dont 81 ± 5% sont constitués de $CH_3CH_2CH_2$-CH_2D, le reste étant formé de C_4H_{10} (5%), $CH_3CH_2CHDCH_3$ (7%) et de $C_4H_8D_2$ (7%); (*iii*) le *n*-butane analysé après l'irradiation du mélange *cy*-C_6H_{12}:*cy*-C_4H_8:CD_3-*cy*-C_5D_9:O_2 (100:5:2:2) consiste de C_4H_{10} (80%), CH_3CHD-$CHDCH_3$ (10%) et de C_4D_{10} (10%); (*iv*) environ 80% du *n*-butane formé dans l'irradiation des mélanges *cy*-C_6D_{12}:*cy*-C_4H_8:O_2 et *cy*-C_6H_{12}:*cy*-C_4D_8:O_2 (100:5:5) consistent en $CH_2DCH_2CH_2CH_2D$ et $CD_2HCD_2CD_2CD_2H$ respectivement.

Les irradiations faites dans l'appareil de résonance cyclotronique ionique des mélanges *cy*-C_6H_{12}:M (100:4) ont montré que l'ion *cy*-$C_6H_{12}^+$ transmet sa charge électrique très rapidement sur l'additif M lorsque celui-ci est soit le *cis*-butène-2, soit l'un des trois méthylbutènes. La constante de vitesse de ces réactions de transfert de charge a été déterminée comme étant voisine de 8×10^{-10} cm^3 mol^{-1} s^{-1}.

Discussion

Transfert de H_2

Il existe plusieurs possibilités de produire l'ion *cy*-$C_6H_{12}^+$. Une méthode simple consiste à photolyser le cyclohexane avec les raies de résonance de l'argon. Le potentiel d'ionisation du cyclohexane est de 9.88 eV et aux raies de résonance de l'argon (11.6–11.8 eV) le rendement quantique ionique est: $\eta = 0.49$ pour le cyclohexane et 0.50 pour le cyclohexane-d_{12}. Même si l'énergie disponible aux raies de résonance de l'argon est suffisante, l'ion parent ne se fragmente pas pourvu que la pression totale du système soit supérieure à 10 Torr (1, 3).

Les résultats indiqués dans le tableau 1 montrent la généralité de la réaction 2. Celle-ci a lieu avec les oléfines simples, conjuguées, les alcynes et les hydrocarbures cycliques en C_3 et en C_4. Thermodynamiquement toutes les réactions envisagées sont exothermiques par environ 1.5 ± 0.6 eV mol^{-1} dépendant de l'additif envisagé. Déjà la radiolyse du cyclohexane et du cyclopentane en phase gazeuse (2, 7) ont montré que la réaction 2 est en fait un exemple d'une réaction plus générale également observée en phase liquide (8).

[4] $\quad cy\text{-}C_nH_{2n}^+ + M \rightarrow C_nH_{2n-2}^+ + MH_2$

Cas des oléfines

Avec les oléfines simples, linéaires ayant la double liaison en bout de chaîne, le transfert d'un groupe H_2 est quantitatif sauf pour l'éthylène. La différence vient probablement du fait que l'éthylène a un potentiel d'ionisation supérieur à celui du cyclohexane. Récemment Lias et Ausloos ont discuté de la réaction de transfert d'un groupe H_2 (9). Tout d'abord, il y a déplacement de la charge électrique vers l'additif si son potentiel d'ionisation est plus bas que celui du cyclohexane. Concurremment il y a un accroissement de l'énergie interne du complexe réactionnel favorisant le transfert de particules de la partie cyclohexane vers la partie additif. Ce n'est pas le cas avec l'éthylène puisque son potentiel d'ionisation est plus élevé que celui du cyclohexane (10). Ensuite, le transfert des deux particules H, dont la première est chargée négativement (sauf dans

TABLEAU 2. Réactions de l'ion *cy*-$C_6H_{12}^+$

Additif (M)	Produit (MH)	k_3/k_2 Ce travail	k_3/k_2 Autres travaux		ΔH ([3])[d] (eV)
C_2H_2	C_2H_3	≤6.7	7±2[a]	4.0[b,c]	−0.05
C_2H_4	C_2H_5	≤3.75	6±2[a]	2.0[b]	−0.43
C_3H_6	CH_3CHCH_3	0.0	1±1[a]	0.11[b]	−0.4
cy-C_3H_6	$CH_3CH_2CH_2$	≃5.65	8±2[a]	5.0[b]	−0.6
n-C_4H_8-1	$CH_3CHCH_2CH_3$	0.0	0±1[a]	≤0.05[b]	−0.6
CH_3-*cy*-C_3H_5	$CH_3CHCH_2CH_3$	≤2.12	—	—	—
cy-C_4H_8	$CH_3CH_2CH_2CH_2$	≤3.55	—	0.0[e]	—

[a]Référence 12; rapports obtenus en extrapolant à 0.0 eV l'énergie des ions dans le spectromètre de masse 'tandemm'. Voir aussi la fig. 4 dans la réf. 23.
[b]Référence 11.
[c]Il y a aussi transfert d'un groupe H_3, réf. 11.
[d]Référence 9.
[e]Référence 19.

Can. J. Chem. Downloaded from www.nrcresearchpress.com by 210.87.254.6 on 09/05/12
For personal use only.

le cas de l'éthylène) se fait d'une façon successive. Le deuxième transfert n'est possible que si le temps de vie du complexe réactionnel est suffisamment long en regard de ce transfert. Dans le cas de l'éthylène l'énergie interne du complexe réactionnel étant moindre que celle des autres complexes, le transfert de la deuxième particule devient moins probable (tableau 2) (11).

[5] $cy\text{-}C_6H_{12}^+ + C_2H_4 \rightarrow (C_2H_5\text{-}cy\text{-}C_6H_{11})^+$

[5a] $(C_2H_5\text{-}cy\text{-}C_6H_{11})^+ \rightarrow C_2H_5 + cy\text{-}C_6H_{11}^+$

[5b] $(C_2H_5\text{-}cy\text{-}C_6H_{11})^+ \rightarrow C_2H_6 + cy\text{-}C_6H_{10}^+$

Lorsque la double liaison se trouve à l'intérieur de la chaîne, il y a d'abord transfert de la charge positive. Le transfert de la première particule, ici l'ion hydride H^-, n'est pas possible car la réaction est endothermique (9). Il s'ensuit qu'aucun transfert d'atome d'hydrogène n'est observable. C'est le cas du butène-2, pentène-2 et du méthyl-2-butène-2 (voir tableau 1).

[6] $cy\text{-}C_6H_{12}^+ + cis\text{-}C_4H_8\text{-}2 \rightarrow C_4H_8\text{-}2^+ + cy\text{-}C_6H_{12}$
$\Delta H = -0.7$ eV

[7] $C_4H_8\text{-}2^+ + cy\text{-}C_6H_{12} \rightarrow cy\text{-}C_6H_{11}^+ + s\text{-}C_4H_9$
$\Delta H = +0.2$ eV

La deuxième étape du transfert ne peut se réaliser bien que globalement le transfert d'un groupe H_2^- soit exothermique. L'absence

[8] $cy\text{-}C_6H_{12} + C_4H_8^+ \rightarrow cy\text{-}C_6H_{10}^+ + n\text{-}C_4H_{10}$
$\Delta H = -0.45$ eV

de transfert d'un atome d'hydrogène est mis en évidence dans l'irradiation du mélange $cy\text{-}C_6H_{12}$:$cis\text{-}C_4H_8$-2 (voir tableau 3). La formation des radicaux butyles secondaires est mis en évidence à travers la formation du *n*-butane

TABLEAU 3. Photoionisation du cyclohexane à 11.6–11.8 eV: mélange $cy\text{-}C_6H_{12}$:$cis\text{-}C_4H_8$-2 (10.0:0.35 Torr)

Produits	Rendements M/Ni
$trans\text{-}C_4H_8$-2	0.17 ± 0.03
$n\text{-}C_4H_{10}$[a]	0.090
iso-C_5H_{12}[a]	0.089
C_2H_6[a]	0.08

[a]En présence de 0.4 Torr d'oxygène, ces produits ne sont pas formés: M/Ni < 0.01.

et de l'isopentane (produits qui ne sont pas formés en présence d'oxygène). Cependant, l'analyse complète de ces résultats montre que ces radicaux sont formés en quantité juste suffisante pour expliquer la capture des atomes d'hydrogène libérés dans la photolyse directe du cyclohexane par le *cis*-butène-2. Le transfert de charge (réaction 6) est mis en évidence par la formation du *trans*-butène-2 même en présence d'oxygène (tableau 2). Il est connu que la photoionisation directe du *cis*-butène-2 conduit à la formation de ce produit à travers l'ion $cis\text{-}C_4H_8^+$ (12) avec un rendement M/Ni de l'ordre de 0.20. La réaction de transfert de charge (réaction 6) a été confirmée par les irradiations dans l'appareil i.c.r. (13). Ceci est enfin en accord avec le fait que l'ion $C_4H_8\text{-}2^+$ ne réagit pas, ou très lentement avec le cyclohexane (14, 15) contrairement aux ions $C_4H_8\text{-}1^+$ et iso-$C_4H_8^+$ (2).

Tout comme avec le *cis*-butène-2, on observe l'isomérisation de chacun des trois méthylbutènes (tableau 4). Récemment Collin et ses collaborateurs ont montré que la photoionisation de chacun des méthylbutènes conduit à cette isomérisation probablement par voie ionique (6, 16–18). L'explication la plus simple

TABLEAU 4. Photoionisation du cyclohexane à 11.6–11.8 eV; additifs: méthylbutène et oxygène

Mélanges irradiés			Rendements M/Ni		
Cyclohexane	Méthylbutène	Oxygène	M3B1[b]	M2B2[c]	M2B1[d]
3.2[a]	M3B1[b], 0.18	0.18[a]	—	0.38	0.08
10.0	M3B1, 0.40	0.43	—	0.32	0.17
10.5	M2B2[c], 0.38	0.50	0.025	—	0.10
9.9	M2B2, 0.40	0.35	0.01	—	0.08
10.1	M2B1[d], 0.70	0.24	0.08	3.2	—
10.0	M2B1, 0.38	0.33	0.32	1.2	—

[a]En Torr.
[b]Méthyl-3-butène-1.
[c]Méthyl-2-butène-2.
[d]Méthyl-2-butène-1.

TABLEAU 5. Photolyse à 11.6–11.8 eV du mélange cyclohexane:cyclopropane:ethylène (20:0.86:0.12)[a]

Produits	Rendements M/Ni
Butadiène-1,3	0.33[b]
n-Butane	0.10
Isobutane	0.00
Isopentane	0.00
n-Pentane	0.19
n-Hexane	0.26
n-1-Pentène	0.04

[a]En Torr.
[b]Pris comme référence pour le calcul des rendements.

serait d'admettre ici un transfert de charge entre l'ion cyclohexane et chacun des méthylbutènes, systèmes alors analogues à celui du *cis*-butène-2 (réactions confirmées par l'appareil i.c.r. (voir Résultats)). Cependant, l'isomérisation observée dans la photoionisation du méthyl-3-butène-1 est sensible à la pression contrairement à ce qui semble être observé ici. Ces observations sont pour l'instant mal comprises et d'autres travaux sont en cours pour essayer de clarifier ce point.

Cas des dioléfines

Alors que le transfert est quantitatif avec le butadiène-1,3, aucun transfert n'est observé avec les pentadiène-1,4 et -1,3 et l'isoprène. Par contre avec l'allène, le butadiène-1,2 et le pentadiène-1,2 un transfert est observé même s'il est très inférieur à l'unité. Il est remarquable que ce transfert a essentiellement lieu sur la double liaison terminale. La formation de pentène-1 (ou de pentyne-1) en présence de pentadiène-1,2 peut sembler être une exception à cette règle, bien que cette formation puisse être attribuable à d'autres processus réactionnels. Les rapports *cis*:*trans* des butènes-2 et des pentènes-2 formés en présence de butadiène-1,2 et de pentadiène-1,2, sont pour le moment incompris. Il faut noter que l'addition de xénon (voir Résultats) ne change pas ce rapport dans le cas du butadiène-1,2.

Cas des alcynes

L'efficacité du transfert de groupe H_2 augmente quand le potentiel d'ionisation de l'alcyne décroît conformément à l'observation déjà faite pour les oléfines linéaires. Il faut noter cependant que dans aucun des cas étudiés le rendement est quantitatif. D'autres réactions interviennent comme le transfert d'un atome d'hydrogène (tableau 2). On a même observé le transfert d'un groupe H_3 entre l'ion *cy*-$C_6H_{12}^+$ et l'acétylène (11). Dans le cas du butyne-2, on n'observe pas ou peu de transfert du groupe H_2.

Cas des cycles en C_3

Le transfert de groupe H_2 se fait avec ouverture du cycle, mais il n'est pas quantitatif. Avec le cyclopropane-d_6 il y a formation de $CD_2HCD_2CD_2H$ (7). L'irradiation du mélange *cy*-C_6H_{12}:*cy*-C_3H_6:C_2H_4 (tableau 5) dans lequel l'éthylène sert d'intercepteur radicalaire, il y a formation des *n*-butane, *n*-pentane et *n*-hexane. Il n'y a formation d'alkanes ramifiés. L'analyse complète de cette irradiation montre qu'il y a formation de radicaux *n*-propyles avec un rendement tel que M/Ni(n-$CH_3CH_2CH_2$) $\simeq 0.85 \pm 0.05$. Le rapport des efficacités des transferts des groupes H et H_2 est ainsi de l'ordre de 5.65 comparativement à 5 déterminé dans un spectromètre de masse (11). Avec le méthylcyclopropane (MCP), il a d'abord transfert de charge (11). L'ion MCP^+ ainsi formé semble réagir avec le cyclohexane pour former le propane (transfert d'un groupe H_2) ou un radical propyle (transfert d'un atome d'hydrogène) contrairement à l'observation faite dans le spectromètre de masse où il ne semble pas y avoir de réaction (11). Dans le présent système, la liaison C—C qui est brisée se trouve en position α du carbone substitué, c'est-à-dire là où la liaison est la plus fragile. Ainsi, la réaction de transfert du groupe D_2^- du cyclohexane vers l'ion MCP^+ se fait avec formation du $CH_3CHDCH_2CH_2D$ (voir Résultats).

[9] *cy*-C_6D_{12} + MCP^+ → *cy*-$C_6D_{10}^+$ + $CH_3CHDCH_2CH_2D$

Lorsque le transfert se limite à un ion hydrure, on observe la formation que du radical butyle secondaire. Ainsi, l'irradiation du mélange *cy*-C_6H_{12}:MCP:C_2H_4 (voir Résultats) conduit à la formation du méthyl-3-pentane et non de l'hexane normal. Le premier transfert de l'ion

[10] MCP^+ + *cy*-C_6H_{12} → $CH_3CHCH_2CH_3$ + *cy*-$C_6H_{11}^+$

[11] $CH_3CHCH_2CH_3 + C_2H_5 \rightarrow C_2H_5CH(CH_3)C_2H_5$

H^- a donc lieu vers le carbone terminal de la chaîne $CH_3CHCHC_2CH_2$ provenant de la

Can. J. Chem. Downloaded from www.nrcresearchpress.com by 210.87.254.6 on 09/05/12
For personal use only.

scission de la liaison C—C en position α dans le MCP. En d'autres termes, c'est le carbone situé en bout de chaîne qui attaque un atome d'hydrogène sur la molécule cyclohexane comme dans le cas des oléfines à double liaison terminale (9). Le mécanisme réactionnel est encore plus en évidence dans la photoionisation du mélange méthyl-3-pentane-d_1:MCP:O_2 (voir Résultats). Dans ce cas le *n*-butane formé est essentiellement constitué de $CH_3CH_2CH_2CH_2D$.

[12] 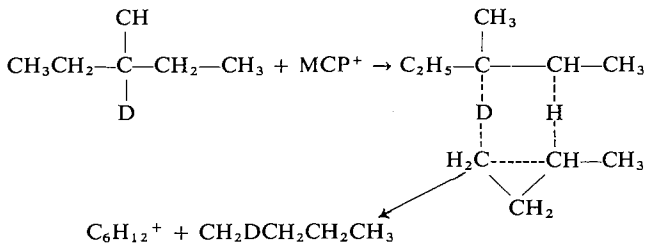

Avec l'éthylpentane, il y a aussi formation de *n*-pentane et non d'isopentane. Là aussi la liaison qui se scinde est située en position α du carbone substitué. Avec le diméthyl-1,2-cyclopropane on n'observe pas de transfert de groupe H_2. La règle précédente voudrait que la liaison qui se scinde soit située entre les deux carbones substitués. Ainsi, cette molécule se comporte comme une oléfine avec la double liaison à l'intérieur de la chaîne.

Cas du cyclobutane

On observe aussi ici transfert d'un groupe H_2 avec ouverture du cycle. La formation du $CH_2DCH_2CH_2CH_2D$ (voir Résultats) en présence du cyclohexane perdeutéré donne une idée de ce que peut être la structure du complexe réactionnel. Ce résultat est cependant en opposition avec les résultats obtenus par spectrométrie de masse à basse pression (0–100 mTorr) (19). On y observe bien le transfert

[13] 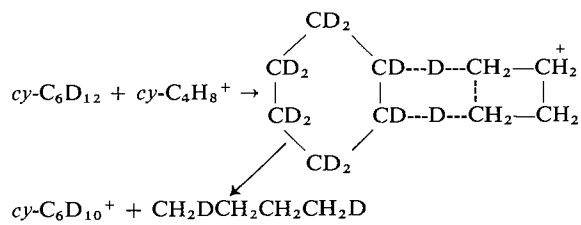

de charge. Cependant, cette réaction est endo-

[14] $cy\text{-}C_6H_{12}^+ + cy\text{-}C_4H_8 \rightarrow C_4H_8^+ + cy\text{-}C_6H_{12}$

thermique et l'endothermicité ne peut-être évitée que par l'ouverture simultanée du cycle. La structure de l'ion $C_4H_8^+$ ainsi formé ne peut-être identique aux ions $C_4H_8^+$ obtenus dans la photoionisation directe des butènes correspondants. L'ion C_4H_8-2^+ ne réagit pas (ou très lentement) avec le cyclohexane. Les ions C_4H_8-1^+ et iso-$C_4H_8^+$ forment le CH_2-$DCHDCH_2CH_3$ et l'isobutane respectivement avec le cyclohexane-d_{12} (2). D'autre part la photoionisation directe du cyclobutane produit des ions $C_4H_8^+$ dont la structure semble être C_4H_8-2^+ (80%) et iso-$C_4H_8^+$ (20%) (19, 20). Les ions $C_4H_8^+$ formés par transfert de charge du cyclohexane vers le cyclobutane semblent donc différents de ceux formés dans la photoionisation directe du cyclobutane. Ainsi, l'irradiation du mélange $cy\text{-}C_6H_{12}$:$cy\text{-}C_4H_8$:CD_3–$cy\text{-}C_5D_9$:O_2 (voir Résultats) forme du *n*-C_4H_{10} (80%) contrairement à celui formé dans l'irradiation du mélange $cy\text{-}C_4H_8$:CD_3 – cy-C_5D_9:O_2 (20.0:0.6:1.0 Torr) constitué de $CH_3CHDCHDCH_3$ (80%) et de CH_2DCD-$(CH_3)_2$ (20%) (19).

On observe également le transfert d'une particule H. L'usage de l'éthylène comme intercepteur radicalaire (voir Résultats) montre la formation de *n*-hexane. Il y aurait donc formation de radicaux *n*-butyles par transfert d'un

Can. J. Chem. Downloaded from www.nrcresearchpress.com by 210.87.254.6 on 09/05/12
For personal use only.

atome d'hydrogène à une extrémité de la liaison C—C brisée.

1. P. AUSLOOS, R. E. REBBERT et S. G. LIAS. J. Phys. Chem. **72**, 3904 (1968).
2. P. AUSLOOS et S. G. LIAS. J. Chem. Phys. **43**, 127 (1965).
3. L. W. SIECK, S. K. SEARLES, R. E. REBBERT et P. AUSLOOS. J. Phys. Chem. **74**, 3829 (1970).
4. R. D. DOEPKER et P. AUSLOOS. J. Chem. Phys. **42**, 3746 (1965).
5. R. GORDEN, JR., R. E. REBBERT et P. AUSLOOS. NBS-Tech. Note 496 (1969).
6. S. G. LIAS, G. J. COLLIN, R. E. REBBERT et P. AUSLOOS. J. Chem. Phys. **52**, 1841 (1970).
7. P. AUSLOOS. Progr. React. Kinet. **5**, 113 (1969).
8. J. W. F. INZEN et W. A. CRAMER. Trans. Faraday Soc. **66**, 857 (1970).
9. S. G. LIAS et P. AUSLOOS. *Dans* Ion-molecule reactions and their role in radiation chemistry. Chap. 6. Amer. Chem. Soc., à paraître en 1975.
10. F. P. ABRAMSON et J. H. FUTRELL. J. Phys. Chem. **71**, 3791 (1967).
11. L. W. SIECK et S. K. SEARLES. J. Am. Chem. Soc. **92**, 2937 (1970).
12. L. W. SIECK, S. G. LIAS, L. HELLNER et P. AUSLOOS. J. Res. Nat. Bur. Stand. **76**A, 115 (1972).
13. P. AUSLOOS. Résultats non publiés.
14. F. P. ABRAMSON et J. H. FUTRELL. J. Phys. Chem. **71**, 1233 (1967).
15. S. G. LIAS et P. AUSLOOS. J. Am. Chem. Soc. **92**, 1840 (1970).
16. H. GAGNON, G. J. COLLIN et C. BERTRAND. J. Phys. Chem. **78**, 98 (1974).
17. G. J. COLLIN et C. M. GAUCHER. Can. J. Chem. **52**, 34 (1974).
18. G. J. COLLIN et C. BERTRAND. J. Photochem. **3**, 123 (1974).
19. L. W. SIECK, S. K. SEARLES et P. AUSLOOS. J. Am. Chem. Soc. **91**, 7627 (1969).
20. S. G. LIAS et P. AUSLOOS. J. Res. Natl. Bur. Stand. **75**A, 591 (1971).
21. F. P. LOSSING. Can. J. Chem. **50**, 3973 (1972).
22. J. L. FRANKLIN, J. G. DILLARD, H. M. ROSENSTOCK, J. T. HERRON, K. DRAXL et F. H. FIELD. NSRDS-NBS 26 (1969).
23. P. AUSLOOS et S. G. LIAS. *Dans* Ion-molecule reactions. *Redigé par* J. Franklin. Plenum Press, New York. 1972.

Can. J. Chem. Downloaded from www.nrcresearchpress.com by 210.87.254.6 on 09/05/12
For personal use only.

Photoreactions of Simple Halonaphthalenes in Solution

LUIS OCTAVIO RUZO, NIGEL J. BUNCE, AND S. SAFE
Department of Chemistry, University of Guelph, Guelph, Ontario N1G 2W1
Received August 22, 1974

LUIS OCTAVIO RUZO, NIGEL J. BUNCE, and S. SAFE. Can. J. Chem. **53**, 688 (1975).

The photolysis products and reaction quantum yields from a number of simple halonaphthalenes have been determined. Fluoronaphthalenes react from a singlet state to yield substitution products in nucleophilic solvents. Chloronaphthalenes and 1-bromonaphthalene afford mainly radical products (naphthalene and binaphthyls) through a triplet state, though some photonucleophilic substitution occurs with chloronaphthalene. Attempts at quenching lead to abnormal behavior, in that enhanced quantum yields for reaction are found with several potential triplet quenchers. Electron transfer processes are proposed to rationalize the observed products.

LUIS OCTAVIO RUZO, NIGEL J. BUNCE et S. SAFE. Can. J. Chem. **53**, 688 (1975).

On a déterminé les produits de photolyse et les rendements quantiques des réactions d'un certain nombre d'halonaphtalènes simples. Les fluoronaphtalènes réagissent à partir d'un état singulet pour conduire, dans les solvants nucléophiles, aux produits de substitutions. Les chloronaphtalènes et le bromo-1 naphtalène fournissent principalement des produits radicalaires (naphtalène et binaphtyls) par l'intermédiaire d'un état triplet; toutefois quelques produits de substitution photonucléophile se produisent avec le chloronaphtalène. Des essais de piégage ont conduit à des réactions anormales; en effet, on observe des rendements quantiques augmentés lorsque l'on utilise divers pièges d'états triplets. Afin de rationaliser la nature des produits obtenus, on fait appel à des transferts d'électrons. [Traduit par le journal]

In contrast with the photochemistry of halogenated benzenes, which has received considerable attention (1–4), little is known about the photochemical reactions of halonaphthalenes. Polychlorinated naphthalenes (Halowaxes, PCNs) are industrial compounds with properties and uses similar to polychlorinated biphenyls (PCBs) and in addition the former compounds have also been identified in commercial PCB preparations (5, 6). Polychlorinated naphthalenes are thus potential environmental pollutants so it is of interest to examine their photochemistry in considering their means of removal from the environment. Because the Halowaxes are complex mixtures, this paper examines the photoreactions of some simple halonaphthalenes with a view to establishing the main processes undergone by them, in terms of products and mechanisms.

Simple naphthalene derivatives exhibit moderate u.v. absorption near 300 nm due to a π–π^* transition. Interaction of the lone pair electrons of the halogen with the aromatic system leads to an excited state with some C—X antibonding character (7) so that bond fission might be expected for all but the fluoronaphthalenes where the C—F bond dissociation energy is greater than that of the incident radiation (8). Correspondingly, the only photoreaction previously observed in the fluoronaphthalene system has been reduction to a 1,4-dihydrofluoronaphthalene by a mechanism involving electron transfer (9).

Chloronaphthalenes have been found to undergo photochemical fragmentations. Chloride ion formation has been observed in the photolysis of 1-chloronaphthalene in ethanol (10); irradiation of the same compound in benzene afforded small amounts of 1-phenylnaphthalene (1). Kulis *et al.* (11) observed photoreduction of 1-chloronaphthalene to naphthalene in the presence of KOH–methanol, and found the quantum yield to be dependent on the concentration of base, suggesting an electron transfer mechanism. Similar photoreductions in the presence of bases have also been observed for 1-bromonaphthalene (12) and for bromoquinolines (13). Mamedov and Nasibov photolyzed the isomeric monochloronaphthalenes in hexane (14); they observed dechlorination but also claimed that there was photoisomerization of the α to the β isomer.

Results and Discussion

Irradiations were carried out at 300 nm, using as solvents methanol, cyclohexane, and aceto-

Can. J. Chem. Downloaded from www.nrcresearchpress.com by 210.87.254.42 on 09/05/12
For personal use only.

TABLE 1. Distribution of photoproducts and quantum yields for reaction of simple halonaphthalenes

Substituent	Solvent	ϕ_r[a]	Dehalogenation[b]	Binaphthyls	Substitution	Other
1-F	CH_3OH	0.018			>99	
1-F	$(C_2H_5)_2NH$				16	84[c]
2-F	CH_3OH	0.010			>99	
2-F	$(C_2H_5)_2NH$				45	55[c]
1-Cl	CH_3OH[e]	0.005	74	25		<1[d]
1-Cl	CH_3OH–O_2	0.002	76	23		<1[d]
1-Cl	CH_3OH–HBr		88	12		
1-Cl	C_6H_{12}		88	12		
1-Cl	CH_3CN–H_2O		<1	94	5	<1[d]
2-Cl	CH_3OH[e]	0.007	58	38	4	
2-Cl	CH_3OH–benzophenone	0.007	2	97	1	
2-Cl	C_6H_{12}		72	28		
2-Cl	CH_3CN–H_2O		2	94	4	
1,2-Cl_2	CH_3OH	0.012	32	66	2	
1,2-Cl_2	CH_3OH–benzophenone	0.014	28	68	4	
1-Br	CH_3OH	0.170	52	48		

[a]Degassed solutions, 20–60 h irradiations.
[b]Yields were estimated as percentage of total product formation by comparison with standard concentrations of naphthalene and binaphthyl.
[c]Photoreduction to hydronaphthalenes.
[d]Chlorination.
[e]The material balance on naphthyl residues was >95% in early stages of the reaction (6 h).

nitrile–water (4:1). The photoproducts are summarized in Table 1, and are seen to be a combination of dehalogenation, arylation, substitution of the halogen by solvent, and in the case of chloronaphthalenes, further chlorination.

Fluoronaphthalenes

Photolysis of each isomer in methanol gave only the corresponding methoxynaphthalenes. This suggests a photonucleophilic substitution, such as has been previously observed for fluorobenzene (15). The absence of quenching with oxygen and the failure of benzophenone to sensitize this reaction point to the involvement of a singlet excited state in the photosubstitution. Like fluorobenzene, both isomers also undergo substitution by diethylamine, affording *N,N*-diethylaminonaphthalenes, together with unstable neutral compounds, presumably dihydronaphthalene derivatives (9).

Chloronaphthalenes in Anhydrous Media

In cyclohexane solution, naphthalene and binaphthyl were the major products. Photolysis in methanol gave additional products of which methoxynaphthalene and dichloronaphthalene are the most notable, together with methoxy- and chlorobinaphthyls. However, we were unable to find any evidence for isomerisation of 1-chloronaphthalene to its isomer as previously claimed (14). The quantum yield for reaction was reduced by a factor of three in the presence of atmospheric amounts of oxygen, while in the presence of benzophenone approximately the same quantum yield was observed, suggesting that a triplet state is the principal precursor of both methoxylated and free radical products, as has been found in the chlorobiphenyl series (16). The predominance of the triplet-derived products is reasonable in view of the high phosphorescence/fluorescence ratio of 5.2 which has been observed in 1-chloronaphthalene (17), compared with 0.09 for the corresponding ratio in naphthalene itself. Such a pronounced heavy atom effect is not unusual for a π–π^* transition in an aromatic system of high symmetry (18).

Quantum yields for the reaction of both 1- and 2-chloronaphthalene are comparable, suggesting a similar lability for the chlorine atom in both environments. This is also true for 1,2-dichloronaphthalene, photolysis of which gave approximately equal yields of both monochloronaphthalenes and only small amounts of binaphthyls upon irradiation to low conversion in methanol.

The major organic products suggest that free radical intermediates are involved; however, simple homolytic fission according to eq. 1 seems unlikely because this reaction would be so endothermic. (Triplet energies of chloronaphthalenes are ~58 kcal/mol (17, 19) whereas

Can. J. Chem. Downloaded from www.nrcresearchpress.com by 210.87.254.42 on 09/05/12
For personal use only.

TABLE 2. Relative rates of halonaphthalene photolysis in methanol with potential quenchers

Substituent[a]	Quencher[b]	k_{diss}[c]	Dechlorination[c]
1-Cl	1,3-Cyclohexadiene	2.5	6.4
1-Cl	Biacetyl	1.3	1.8
2-Cl	1,3-Cyclohexadiene	2.4	6.2
2-Cl	Biacetyl	1.1	1.8
2-Cl	*trans*-Stilbene	1.2	1.2
1,2-Cl_2	Biacetyl	1.2	1.2
1-Br	1,3-Cyclohexadiene	0.9	1.4
1-Br	Biacetyl	0.7	1.3

[a]Halonaphthalene concentrations were $0.1–1.0 \times 10^{-2}$ *M*.
[b]Quencher concentrations were: biacetyl and *trans*-stilbene, 10^{-2} *M*; cyclohexadiene, 5×10^{-3} *M*.
[c]Rate of starting material disappearance (k_{diss}) and of naphthalene formation relative to solutions where the quencher was omitted.

typical Ar—Cl bond dissociation energies are ~85 kcal/mol (20).)

[1] $$^3ArCl \rightarrow Ar\cdot + Cl\cdot$$

By analogy with previous observations on aryl halides (11–13, 21) some kind of electron-transfer process seems likely (eq. 2) and this postulate is supported by the observation that the quantum yield for disappearance of 1-chloronaphthalene increases eightfold in the presence of triethylamine, a known electron donor (9, 21; *cf. a* and *b* of ref. 22).

[2] $$^3ArCl + X \rightarrow Ar\cdot + X^{\cdot+} + Cl^-$$

Chloronaphthalenes in an Aqueous Medium

In aqueous acetonitrile, a solvent which can be considered a suitable model system for the environmental photochemistry, the main photoproducts from 1-chloronaphthalene were chlorobinaphthyl, 1-naphthol, and a hydroxylated dimer. In the presence of oxygen the dimers were largely suppressed. An additional product was detected in trace amounts showing *m/e* 104 by g.l.c. – mass spectrometry but could not be identified owing to its low yield and the difficulty of its separation from starting material. Polycyclic biaryls are thus formed but in the presence of oxygen 1-naphthol is the preponderant product; hydroxylated compounds are also known to arise from the metabolism of chloroaromatics (23). Photosubstitution to give the naphthol may be compared with similar observations by Crosby and Tutass (24) in the photolysis of the herbicide 2,4-dichlorophenoxyacetic acid.

1-Bromonaphthalene

The quantum yield for photolysis of this compound in methanol is considerably higher than those for the chloro compounds, presumably because of the lower C—X bond dissociation energy (65–70 kcal/mol). Naphthalene appears to be the major product; it is possible that HBr present in the solution upon photolysis acts as such a good source of hydrogen abstraction for the naphthyl radicals that arylation does not compete. That this may be the case is suggested by the observation that photolysis of 1-chloronaphthalene in the presence of small amounts of HBr also leads to an increase in the ratio of naphthalene to binaphthyls.

Quenching Experiments

An attempt was made to determine the triplet lifetimes of the isomeric chloronaphthalenes in methanol by quenching experiments (Table 2). 1,3-Cyclohexadiene was initially chosen for this purpose since its triplet energy ($E_T \sim 50$ kcal/mol) is considerably lower than those of the chloronaphthalenes ($E_T > 58$ kcal/mol). The most singular observation was made that the 'quencher' enhanced the rate of both disappearance of the chloronaphthalene and formation of naphthalene, though not to the same extent. Similar rate enhancements were observed when biacetyl ($E_T = 55$ kcal/mol) and *trans*-stilbene ($E_T = 50$ kcal/mol) were tried as quenchers, though as noted already, the reaction is quenched by oxygen. Some small amount of quenching was noted with 1-bromonaphthalene, but even here, the rate of naphthalene formation increased. These increases in the chemical yield of naphthelene apparently result from suppression of binaphthyls and higher arylation products. Either energy transfer does not occur in these systems, despite its energetic favorability, or it is in competition with some chemical pro-

Can. J. Chem. Downloaded from www.nrcresearchpress.com by 210.87.254.42 on 09/05/12
For personal use only.

Can. J. Chem. Downloaded from www.nrcresearchpress.com by 210.87.254.42 on 09/05/12
For personal use only.

cess by which the decomposition of the remaining unquenched molecules is enhanced. Certainly, energy transfer seems to be very inefficient, for the phosphorescence spectrum of 1-chloronaphthalene (5×10^{-2} *M*, EtOH, 77 °K) is quenched only 40% by piperylene concentrations as high as 0.12 *M*. A possible rate-enhancing reaction might be exciplex formation, followed by electron transfer (eq. 2, X = quencher). Whatever the mechanism behind the lack of quenching, its observation seems important because the quenching method is customarily used to determine triplet lifetimes in solution. Failure of the method may thus require reevaluation of the reliability of triplet lifetimes so determined, especially in reactions where ϕ_r is small, for example, other chloroaromatics (16, 25), since only a small intrusion from a rate enhancement process would be necessary to exert a significant effect in such cases.

Routes to Products from Monochloronaphthalenes

The photoreactions of the chloronaphthalenes are similar to those of other chlorinated aromatics. Reductive photodechlorination is well known (16, 26) and has been studied extensively for compounds of environmental importance (25, 27–29). Most of these investigations have been concerned exclusively with product identification; however, we may compare our results on the chloronaphthalenes with recent observations by Ruzo *et al.* (16) on the photolysis of the tetrachlorobiphenyls. Quantum yields for reaction (ϕ_r) for the tetrachlorobiphenyls are also low, in the 10^{-3} range for five of the six compounds studied. The phosphorescence lifetimes of chlorobiphenyls and chloronaphthalenes in rigid glasses are also comparable (1–10 s) (17, 19, 30).

The major products in our study, naphthalene and binaphthyls, clearly result from C—Cl fission, though as argued earlier, this is more likely to involve electron transfer than direct homolytic fission. Formation of the binaphthyl derivatives seems to result from arylation rather than radical coupling. This is apparent from the formation of chloro- and methoxy-substituted binaphthyls as well as the parent compound and by analogy with the production of 1-phenylnaphthalene on photolysis of 1-chloronaphthalene in benzene (1).

We have rationalized the products in the context of the reactions of Scheme 1, in which NpCl is chloronaphthalene, ArH is any naphthyl derivative (including NpCl) and Q is quencher.

[3] $\mathrm{NpCl^* + ArH \rightarrow Np^{\cdot} + Cl^- + ArH^{\cdot +}}$

[4] $\mathrm{Np^{\cdot} + RH \rightarrow NpH + R^{\cdot}}$

[5] $\mathrm{NpCl + Q \rightarrow Np^{\cdot} + Cl^- + Q^{\cdot +}}$

[6] $\mathrm{Np^{\cdot} + ArH \rightarrow \rightarrow Np{-}Ar}$

[7] $\mathrm{Ar^{\cdot +} + ArH \rightarrow \rightarrow Ar{-}Ar}$

[8] $\mathrm{Ar^{\cdot +} + CH_3OH \rightarrow \rightarrow Ar{-}OCH_3}$

SCHEME 1

Observations suggesting a role for chloronaphthalene and its derivatives as electron donors (eq. 3) are the suppression of biaryls in the presence of quencher, when presumably reaction 5 intervenes successfully. The electron transfer complex (exciplex) NpCl·ArH may correspond to the 'π-dimer' of chlorobenzene recently postulated by Fox *et al.* (31) in the photoreactions of chlorobenzene. Whether a monomeric π species corresponding to their π-chlorobenzene (a chlorinating agent) could account for the further chlorination of monochloronaphthalenes is unknown. We observed that photolysis of a solution of chlorine and 1-chloronaphthalene in methanol increased the rate of chlorination by 30% over the dark reaction, and in benzene the rate enhancement was 20-fold. It is possible that the chloronaphthalene undergoes attack by chlorine atoms whose selectivity has been increased by some kind of complexation. Other chloroaromatics have been observed to yield products of enhanced chlorine content upon photolysis (32).

Further experiments are currently in progress to try to substantiate these proposals. One interesting but unexplained observation is that the quantum yield for reaction of the monochloronaphthalenes is the same whether or not benzophenone is present, yet reactions conducted in the presence of benzophenone give substantially more binaphthyls and less naphthalene than those unsensitized, even though the conversion of chloronaphthalene is essentially unchanged. One possibility is that electron transfer is important here too, *e.g.* $\mathrm{NpCl + Ph_2CO^* \rightarrow NpCl^{+\cdot} + Ph_2CO^{-\cdot}}$ (*cf.* ref. 22) but to date we have no evidence to support such a proposal.

Experimental

Materials

Solvents were analytical grade materials that were

Can. J. Chem. Downloaded from www.nrcresearchpress.com by 210.87.254.42 on 09/05/12
For personal use only.

dried and distilled before use. Acetonitrile was purified by successive distillations from sodium hydride and phosphorus pentoxide (33). 1-Fluoronapthalene was obtained in 42% yield by the Schiemann reaction from 1-naphthylamine (34); 2-fluoronaphthalene (Columbia Organic Chemicals) was recrystallized from methanol. 1-Chloronaphthalene (Eastman) was distilled repeatedly until no impurities were present by g.l.c. 2-Chloronaphthalene (Eastman) was twice recrystallized from ethanol. 1,2-Dichloronaphthalene (Chemical Procurement Labs.), benzophenone, naphthalene, and 1-bromonaphthalene (all J. T. Baker) were used as supplied. 1,3-Cyclohexadiene and biacetyl for use as quenchers were Aldrich materials, distilled before use. 1,1′-Binaphthyl was prepared by copper coupling of 1-bromonaphthalene in dimethylformamide (35). All these compounds were authenticated by mass spectrometry and their purity checked by g.l.c. before use. The methoxynaphthalenes were prepared in solution by methylation of the appropriate naphthol with diazomethane but were not isolated.

Photochemical Procedures

Irradiations were conducted in a Rayonet Reactor equipped with RUL 3000 lamps having a maximum output at 300 nm. The chamber temperature was approximately 30°. Equal illumination of samples being photolysed simultaneously was assured by use of a 'merry-go-round' apparatus. Reactions in the presence of oxygen were carried out in screw cap vials; other irradiation mixtures were degassed by four freeze–pump–thaw cycles using liquid nitrogen and sealed *in vacuo*. For calculation of quantum yields, conversions were limited to $< 10\%$ to minimize light absorption and reaction of products. The light intensity was calculated using the modified ferrioxalate actinometer (36).

Analytical Procedures

The gas chromatograph was a Hewlett-Packard model 5710A equipped with a 6 ft × 1/8 in. i.d. glass column packed with 3% SE30 on 80–100 mesh Chromosorb W. This column was operated isothermally at 160° using helium (30 ml/min) as carrier gas. Detection of products was by flame ionization, with injector and detector maintained at 300°. This column separated all the necessary compounds except 1- and 2-chloronaphthalenes, which were partially resolved using a 25% 1,2,3-tris(cyanoethoxy)propane on Gas Chrom Q, 20 ft × 1/16 in. i.d., column operated isothermally at 90° and 30 ml/min helium flow. For product identification, retention times and mass spectra were compared with those of authentic samples. For mass spectrometric analysis a Varian Associates Model 1700 gas chromatograph was interfaced directly to a Varian MAT Model CH7 mass spectrometer operated at 70 eV ionizing voltage.

Irradiation of Simple Halonaphthalenes in Cyclohexane and Methanol

Irradiations of 10^{-2} *M* solutions were carried out from 20 to 60 h for degassed samples and up to 120 h for aerated ones. After photolysis the amount reacted was measured by g.l.c., solutions were then concentrated and analyzed for products.

Irradiation of 1-Chloronaphthalene in Acetonitrile–Water (4:1)

Solutions (10^{-2} *M*) were either degassed by nitrogen flushing or aerated. After 60-h photolysis the samples were evaporated and the residue extracted with ether until the aqueous layer showed no absorption at 250 nm, then concentrated and analyzed by g.l.c.–m.s. Sensitized reactions were 5×10^{-2} *M* in benzophenone and 2×10^{-3} *M* in chloronaphthalene. After photolysis the products were extracted as described.

Irradiation of 1- and 2-Fluoronaphthalenes with Diethylamine

These irradiations were carried out semipreparatively. The appropriate fluoronaphthalene (2.0 g) and diethylamine (100 ml) were irradiated with the unfiltered light of a 450 W medium pressure mercury arc for 7 h. After evaporation of the solvent, basic and neutral extracts were made. From the neutral extract were recovered starting material and unstable compounds presumed to be dihydronaphthalenes (9); chromatography of the basic material over silica gel afforded the isomeric *N,N*-diethylaminonaphthalenes, which were identical with samples prepared for comparison by the action of ethyl iodide on the naphthylamines. *N,N*-Diethyl-1-naphthylamine: oil (0.23 g); n.m.r. (CCl_4): δ 1.02 (triplet, J = 7 Hz, 6H), 3.16 (quartet, J = 7 Hz, 4H), 7.0–8.4 (multiplet, 7H).

Anal. Calcd. for $C_{14}H_{17}N$: C, 84.4; H, 8.5; N, 7.0. Found: C, 84.4; H, 8.1; N, 7.2.

N,N-Diethyl-2-naphthylamine: oil (0.16 g), n.m.r. (CCl_4): δ 1.19 (triplet, J = 7 Hz, 6H), 3.40 (quartet, J = 7 Hz, 4H), 6.6–7.7 (multiplet, 7H).

Anal. Found: C, 84.2; H, 8.3; N, 7.3.

We thank the National Research Council of Canada for financial support.

1. G. E. Robinson and J. M. Vernon. J. Chem. Soc. (C), 3363 (1971).
2. T. Ichimura and Y. Mori. J. Chem. Phys. **58**, 288 (1973).
3. A. Basinsky and E. Latowska. Rocz. Chem. **40**, 1747 (1966).
4. J. A. Barltrop and D. Bradbury. J. Am. Chem. Soc. **95**, 5085 (1973).
5. D. Stalling and J. N. Huckins. J. Ass. Offic. Anal. Chem. **56**, 367 (1973).
6. J. G. deVos, H. H. Koeman, H. L. van der Maas, M. S. ten Noever de Brauu, and R. H. de Vos. Food Cosmet. Toxicol. **8**, 625 (1970).
7. R. J. Majer and J. P. Simmons. Adv. Photochem. **2**, 137 (1964).
8. J. G. Calvert and J. N. Pitts. Photochemistry. J. Wiley and Sons, New York. 1966. p. 824.
9. J. A. Barltrop and R. J. Owers. J. Chem. Soc. (D), 1462 (1970). J. A. Barltrop. Pure and Appl. Chem. **33**, 179 (1973).
10. J. Szychlinski. Rocz. Chem. **34**, 941 (1960).
11. Y. Y. Kulis, I. Y. Poletaeva, and M. G. Kuz'min. J. Org. Chem. USSR (Engl. Transl.), **9**, 1242 (1973).
12. M. G. Kuz'min, Y. A. Mikleev, and L. N. Guseva. Dokl. Akad. Nauk. SSSR, **176**, 368 (1967).

13. C. PÁRKÁNY and Y. J. LEE. Tetrahedron Lett. 1115, (1974).
14. K. I. MAMEDOV and I. K. NASIBOV. Zh. Prikl. Spectrosk. **11**, 859 (1969).
15. J. A. BARLTROP, N. J. BUNCE, and A. THOMSON. J. Chem. Soc. (C), 1142 (1967).
16. L. O. RUZO, M. J. ZABIK, and R. D. SCHUETZ. J. Am. Chem. **96**, 3809 (1974).
17. V. L. ERMOLAEV. Sov. Phys. Uspekhi, 333 (1963).
18. M. A. EL-SAYED. J. Chem. Phys. **41**, 2462 (1964).
19. L. G. THOMPSON and S. E. WEBBER. J. Phys. Chem. **76**, 221 (1972).
20. S. W. BENSON. The foundations of chemical kinetics. McGraw-Hill Book Co. Inc., New York, 1960. p. 670.
21. M. OHASHI, K. TSUJIMOTO, and K. SEKI. J. Chem. Soc. Chem. Commun. 384 (1973).
22. (*a*) B. STEVENS. Advan. Photochem. **8**, 161 (1971); (*b*) S. G. COHEN and N. M. STEIN. J. Am. Chem. Soc. **93**, 6542 (1971).
23. O. HUTZINGER, S. SAFE, D. M. NASH, R. J. NORSTROM, and V. ZITKO. Science, **178**, 312 (1972).
24. D. G. CROSBY and H. O. TUTASS. J. Agr. Food Chem. **14**, 596 (1966).
25. L. O. RUZO, M. ZABIK, and R. D. SCHUETZ. Bull. Environ. Contam. Toxicol. **8**, 217 (1972); G. D. NORDBLOM and L. L. MILLER. J. Agr. Food Chem. **22**, 57 (1974).
26. J. T. PINHEY and R. D. G. RIGBY. Tetrahedron Lett. 1267 (1969).
27. D. G. CROSBY and E. LEITIS. J. Agr. Food Chem. **17**, 1033 (1969); D. G. CROSBY and C. S. TANG. J. Agr. Food Chem. **17**, 1041 (1969).
28. D. G. CROSBY and N. HAMADMAD. J. Agr. Food Chem. **19**, 1171 (1971); K. W. MOILANEN and D. G. CROSBY. J. Agr. Food Chem. **20**, 950 (1972).
29. S. SAFE and O. HUTZINGER. Nature, **232**, 641 (1971); D. D. BILLS, E. J. HANNAN, and J. L. HERRING. Bull. Environ. Contam. Toxicol. **8**, 153 (1972).
30. G. N. LEWIS and M. KASHA. J. Am. Chem. Soc. **66**, 2100 (1944); C. M. O'DONNELL, K. F. HARBAUGH, R. P. FISHER, and J. D. WINEFORDNER. Anal. Chem. **45**, 609 (1973); C. M. O'DONNELL, K. F. HARBAUGH, and J. D. WINEFORDNER. Spectrochim. Acta, **A29**, 753 (1973).
31. M. A. FOX, W. C. NICHOLS, and D. M. LEMAL. J. Am. Chem. Soc. **95**, 8164 (1973).
32. O. HUTZINGER, S. SAFE, B. R. WENTZELL, and V. ZITKO, Environmental Health Perspective. Sept. 1973. p. 267.
33. G. A. FORCIER and J. W. OLVER. Anal. Chem. **37**, 1447 (1965).
34. C. ROE. Org. React. **5**, 193 (1949).
35. N. KORNBLUM. J. Am. Chem. Soc. **74**, 5782 (1952).
36. K. C. KURIEN. J. Chem. Soc. (B), 2081 (1971).

Can. J. Chem. Downloaded from www.nrcresearchpress.com by 210.87.254.42 on 09/05/12
For personal use only.

The Reaction of Hydrogen Atoms with Palladium and its Alloys

W. A. OATES[1] AND TED B. FLANAGAN

Chemistry Department, University of Vermont, Burlington, Vermont 05401

Received September 16, 1974

W. A. OATES and TED B. FLANAGAN. Can. J. Chem. **53**, 694 (1975).

H atoms, which have been generated in the gas phase, have been allowed to interact with palladium metal and several of its substitutional f.c.c. alloys. It has been found that quite high concentrations of interstitial hydrogen can be introduced in this manner even in the absence of poisons such as H_2S. The kinetics of hydrogen uptake have been followed as a function of the hydrogen content of the palladium. The kinetics of the subsequent loss of hydrogen from the palladium have been investigated. Mechanisms for the surface reactions of hydrogen on palladium are discussed.

W. A. OATES et TED B. FLANAGAN. Can. J. Chem. **53**, 694 (1975).

On a permis à des atomes d'hydrogène qui ont été générés en phase vapeur d'interagir avec du palladium sous forme métallique et plusieurs de ses alliages f.c.c. On a trouvé qu'on peut introduire des concentrations importantes d'hydrogène interstitiel de cette manière, même en l'absence de poisons tel que H_2S. On a déterminé la cinétique de l'absorption d'hydrogène comme une fonction du contenu en hydrogène du palladium. On a examiné la cinétique de la perte subséquente d'hydrogène à partir du palladium. On discute des mécanismes des réactions de l'hydrogène sur le palladium. [Traduit par le journal]

Introduction

The attainment of large concentrations of interstitial hydrogen in palladium and its substitutional alloys is very desirable for several reasons. These systems become superconductive at high hydrogen contents; *e.g.*, pure palladium is a superconductor at H-to-Pd (atomic ratio) > 0.83 (1). Another reason is that values for limiting hydrogen contents are needed for theoretical models of these systems; *i.e.*, is the limiting hydrogen content in a f.c.c. substitutional alloy equal to the fraction of palladium or is it greater or less than this for a particular alloy system (2–4)? In palladium it is known that the hydrogen atoms occupy octahedral interstices about the palladium atoms (5). On geometric grounds, therefore, the limiting hydrogen content should be H-to-Pd (atom ratio) = 1. The attainment of this limiting ratio constitutes a scientific challenge.

Baranowski and colleagues in Poland (6) have pioneered in the use of high pressures of gaseous hydrogen for obtaining very high hydrogen contents in palladium. They have recently obtained hydrogen pressures as great as 30 000 atm (298 K) (6). One disadvantage of this direct high pressure technique has been that, so far, it has not been possible to determine the hydrogen contents of the samples *in situ*. For analysis of the hydrogen contents the high pressure apparatus has been cooled, the pressure released, and the samples have been subsequently analyzed. Hydrogen may escape during this process. For pure palladium they have obtained with this cooling procedure an H-to-Pd (atom ratio) of 0.96 (7). The high pressure method has the advantage that equilibrium is obtained and the hydrogen should be uniformly distributed throughout the sample; on the other hand, it has the drawback that it is experimentally very demanding.

The most commonly employed technique for introducing large hydrogen contents into palladium and its alloys has been electrolysis (8). In this method hydrogen atoms are produced at the surface of the metal by making it cathodic, generally in a poisoned electrolytic solution. The presence of the poison, *e.g.* H_2S, inhibits the desorption of hydrogen. With this technique in acidified methanol (195 K) an H-to-Pd ratio of 1.0 has been recently reported (9).

Using ion implantation at liquid helium temperatures Stritzer and Buckel (10) have succeeded in introducing very large concentrations of hydrogen (deuterium) in palladium and its alloys. They have reported a remarkably high superconductive temperature of 16 K for a deuterium-charged Ag/Pd alloy (11). Ion im-

[1]Permanent address: Department of Metallurgy, University of Newcastle, Newcastle, N.S.W., Australia.

Can. J. Chem. Downloaded from www.nrcresearchpress.com by 210.87.254.42 on 09/05/12
For personal use only.

Can. J. Chem. Downloaded from www.nrcresearchpress.com by 210.87.254.42 on 09/05/12
For personal use only.

plantation has the disadvantage that the hydrogen is not uniformly distributed throughout the sample. For the purpose of superconductivity experiments this is not a handicap because the superconductive current follows the path of lowest resistance, but non-uniform distributions of hydrogen may cause difficulties for other experiments.

In the method explored here, reaction of metals with gaseous hydrogen atoms, the equipment requirements are modest. Data relating to the introduction of hydrogen into transition metals by means of atomic hydrogen are scant and conflicting (12). The authors have reported in a brief note (13) that the method was a success for producing very high hydrogen contents in palladium. A value of H-to-Pd = 0.99 $\pm$ 0.01 was found and this was the closest value to the stoichiometric ratio of 1 where a direct and unambiguous method of analysis has been used. Other workers had reported values close to this, or even in excess of the stoichiometric ratio, but in all cases these reports had been based on indirect evidence. For example, arguing from the electrical resistance *vs.* fugacity relationships, Baranowski and co-workers (14) suggested that values in excess of unity may be formed. Suhrman and co-workers (15) reported an H-to-Pd ratio of 1.8 at 95 K on a palladium film but chemisorption could have been a factor. Buckel and Stritzer (16) have reported values in excess of 1 but the uncertain distribution of the implanted hydrogen could introduce sizable errors into their estimated ratios of H-to-Pd. It seems important to stress that the errors introduced into the analysis of the hydrogen contents must be carefully considered. Since our preliminary report (13), Harper has reported an H-to-Pd ratio of "about 1.0" (9) obtained by electrolysis and subsequently analyzed by weighing and by degassing. Values for the uncertainty in the ratio were not reported but it can be estimated for the 5 mm diameter, 25 μ palladium foil, which he employed, the expected error in the gravimetric determination, $\pm 2 \times 10^{-6}$ g, would lead to a minimum uncertainty in the atomic ratio of ± 0.025.

This paper reports the details of the absorption of hydrogen by palladium up to atom ratios near unity via the reaction of the metal with H atoms and additional experiments connected with the introduction of hydrogen into hydrogen-absorbing metals.

Experimental

Palladium metal (> 99.9% purity) was used in the form of thin wire (0.027 cm diameter). The samples were generally flame-annealed prior to insertion into the apparatus. The apparatus was a conventional high vacuum system employing stopcocks, mercury diffusion, and mechanical pumps. Gold-foil separated the sample vessel from mercury but no special precautions were taken to protect the samples from contamination by stopcock grease. Various types of reaction vessels were used depending upon the motive of the particular experiment and whether H-atoms were generated by an electrodeless discharge or by a hot-tungsten filament. For the latter method a tungsten filament from an incandescent light bulb (60 W) was heated (70 V) to approximately 2000 K. The reaction vessels were standard pyrex ones which were used without special pre-treatment. The use of H_3PO_4 to coat the walls of the vessel did not appear to help in the efficiency of loading the sample. (H_3PO_4 is believed to suppress the H–H recombination reaction (17).) After prolonged use, the efficiency of a bulb declined and it was either replaced or washed with HF and distilled water prior to re-use. Both static and flow systems were employed for H atoms generated either with a hot tungsten filament or with an electrodeless r.f. discharge.

In the static experiments the hydrogen absorbed by the sample was monitored by the pressure changes. The accuracy of pressure measurement is critical, especially during the final degassing analysis of the hydrogen content. The following gauges were available: a Pirani gauge (LKB), a McLeod gauge, a narrow-bore manometer (~0.4 cm). a diaphragm gauge (Data-metrics), and a wide-bore mercury manometer (> 1.0 cm). The wide-bore manometer, which was read with a cathetometer, was used to calibrate the diaphragm gauge and to make an independent measurement of the pressure of the evolved hydrogen in one experiment. The Pirani gauge was calibrated by the McLeod gauge.

The most effective procedure for the introduction of large interstitial hydrogen concentrations into palladium was a static one using a hot tungsten filament. The wire was flamed in air, weighed, and placed on the bottom of the reaction flask so as to maximize thermal contact. The wire (~1 g) was generally cut into 1 cm pieces, helping to insure thermal contact. About 1 mm Hg of hydrogen was introduced into the reaction vessel and a pressure change was not noted until the filament was turned-on. The pressure fall was then quite dramatic for an initially hydrogen-free sample and when the pressure fell to a low value, a further dose was introduced. This process was repeated until absorption became sluggish, *i.e.*, when H-to-Pd ~ 0.9. The sample vessel was then cooled to 195 K and the process repeated. The approximate H-to-Pd ratio could be monitored from the pressure changes. This was not very accurate because the temperature of the reaction vessel was not uniform. After absorption via H atoms had apparently stopped, the sample vessel was evacuated (195 K), and the sample gently heated by a flame on the outside of the reaction vessel. The evolved hydrogen was then measured whilst the measuring volume was at a uniform temperature. The Pyrex reaction flask had been repeatedly heated prior to the run at temperatures greater than the degassing temperature of the sample, and it was determined with blank

runs that negligible gas was evolved from the walls of the vessel during this heating. The temperature of the reaction flask during the degassing was only slightly above 500 K. Typical pressures evolved during the degassing of the samples were in the range 3 to 10 mm Hg.

In an attempt to introduce hydrogen more efficiently into palladium, the reaction vessel was cooled to 77 K after introducing hydrogen at 195 K. At 77 K water was produced whereas it was not at 195 K. The H–H recombination reaction is apparently very efficient on the pyrex walls at $\geqslant$195 K but at 77 K it is slow enough for the H atoms to linger on the walls and to react with oxygen atoms of the pyrex. Temperatures between 77 and 195 K were not attempted.

The Pirani gauge was used for the first series of runs and these indicated that large interstitial hydrogen contents were being formed. In order to insure that these results were indeed the case, a diaphragm gauge was installed and this confirmed the observation of values of H-to-Pd close to unity. The diaphragm gauge was then calibrated with a wide-bore mercury manometer. In the range between 3 and 10 mm Hg (the usual range of pressures found after evolution of the hydrogen) a standard deviation of $\pm$0.083 mm Hg was found between the readings of the manometer (corrected for the expansion of mercury) and the diaphragm gauge. The volume of the reaction vessel was determined by filling it with water and weighing. A typical volume for the reaction vessel-was 1225 cm^3. It was used to calibrate the remainder of the system into which the hydrogen evolved. The total volume for a representative reaction flask and the measuring system was 1885 $\pm$ 5 cm^3. The metal samples were weighed to $\pm$0.0001 g.

When H atoms were produced by the electrodeless discharge either a static or flow system was employed. A flow system was also tried for the hot tungsten filament generated H atoms. The pressure was maintained at approximately 1 mm Hg during the flow. The hydrogen was ultra-pure from a cylinder. The flow systems suffered from the disadvantage that the hydrogen contents of the samples could not be monitored by pressure changes. Electrical resistance measurements were used for this purpose.

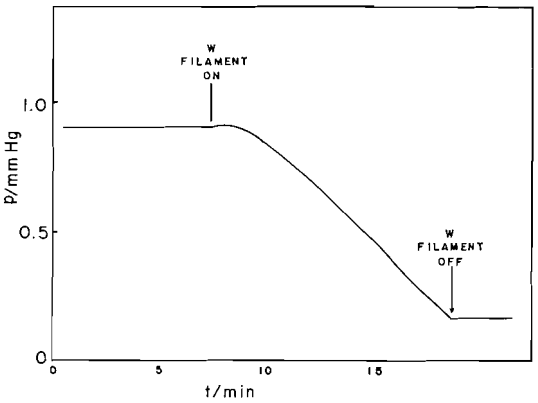

FIG. 1. Recording trace of typical run (273 K) of absorption into hydrogen-free palladium via atomic hydrogen generated by a hot tungsten filament.

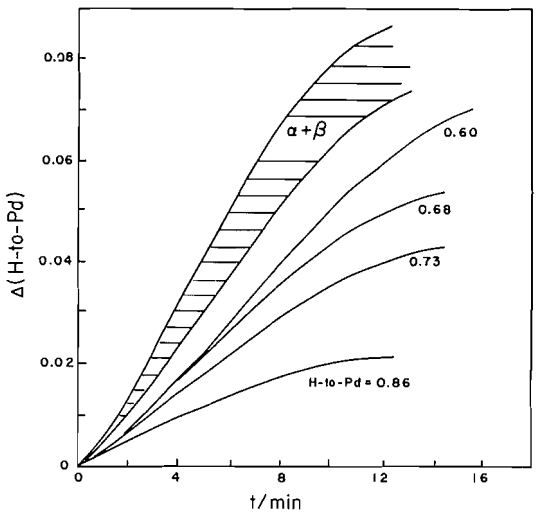

FIG. 2. Typical recording tracings of hydrogen uptake by palladium (273 K) via H-atoms generated by a hot tungsten filament.

Results

Kinetics for H atom Absorption and Subsequent Hydrogen Loss

A typical absorption run, where hydrogen was introduced via gaseous H atoms from a hot tungsten filament is shown in Fig. 1 (273 K). Hydrogen was admitted at 0.9 mm Hg and there were no pressure changes for as long as the pressure was monitored with a strip chart recorder. This finding is in accord with earlier observations; *i.e.*, hydrogen does not equilibrate with palladium in a conventional high vacuum system if possibilities exist for contamination by, for example, stopcock grease (18). On the other hand, equilibrium is fairly rapidly established between bulk palladium and hydrogen, although still controlled by surface steps, if a grease- and mercury-free system is employed (19, 20). When the filament was turned-on, the pressure dropped rapidly (Fig. 1). When it was turned-off again, the pressure did not change. The hydrogen rapidly enters the sample via H atoms and is retained. It has been shown elsewhere that hot tungsten filaments are effective H atom generators (21). It should be noted that the inhibition of the $H_2 \rightarrow 2[H]$ reaction, where [H] represents interstitially absorbed hydrogen, and its reverse, arises from traces of contaminants in the system and not from added poisons such as H_2S. Oxygen is not a poison because chemi-

Can. J. Chem. Downloaded from www.nrcresearchpress.com by 210.87.254.42 on 09/05/12
For personal use only.

Can. J. Chem. Downloaded from www.nrcresearchpress.com by 210.87.254.42 on 09/05/12
For personal use only.

sorbed oxygen is rapidly removed by hydrogen (22). Further doses of hydrogen were added to the reaction vessel and the process repeated. A typical series of recording tracings during absorption (273 K) is shown in Fig. 2. It can be seen that in the two-phase region, the rate of hydrogen uptake is closely constant. Hydrogen-saturated palladium (α) and a non-stoichiometric hydride (β) phase coexist in the palladium/H_2 system at 273 K with the respective compositions H-to-Pd (atom ratio) = 0.009 (α) and 0.6 (β) (8). At ratios greater than 0.6, hydrogen dissolves in the non-stoichiometric hydride phase. Across the two-phase region, although the overall hydrogen content of the sample increases with the proportion of β to α, the surface composition is invariant and the rate of hydrogen uptake via H atoms is constant. At H-to-Pd ratios greater than 0.6, the rate of uptake gradually diminishes as the hydrogen content increases (Fig. 2). If a run was made with another sample, the absolute rates were found to be somewhat different but the general sequence of events is unaffected. When the rate of uptake became very slow at 273 K, the sample was cooled to 195 K, and the process repeated until no further hydrogen was absorbed. Generally at this point the sample vessel was evacuated (195 K) and the final hydrogen content of the sample was determined by degassing the sample *in situ* by gentle heating.

For the study of the kinetics of desorption of hydrogen from a palladium sample which had attained a high hydrogen content the reaction vessel was evacuated at 195 K and then gradually heated whilst monitoring the pressure as a function of temperature. A silicone oil bath was used to gradually heat the bottom of the reaction vessel. With a heating rate of 5° per min, the accumulated pressure against temperature relationship shown in Fig. 3 was obtained. This particular sample originally contained an H-to-Pd (atom ratio) of 0.99. It can be seen that hydrogen is slowly lost from the sample at ~393 K, and the rate of loss is greatest at 473 K where all of the hydrogen is lost. This same behavior was observed with other samples which were charged to ratios near unity and it agrees with the finding that absorption via molecular hydrogen is only established above about 393 K (18); *i.e.*, Everett and Nordon (18) observed that the forward reaction takes place only above about 393 K, and it was observed here that the reverse

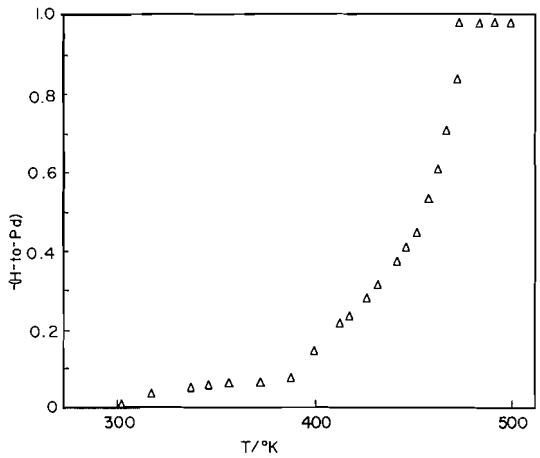

FIG. 3. Typical run showing hydrogen evolution from a palladium sample with an initial H-to-Pd ratio of 0.99. −(H-to-Pd) indicates loss of hydrogen from the sample expressed as the ratio.

reaction takes place at about the same temperature and, therefore, equilibrium cannot be established until the temperature is >393 K. This inhibition of the absorption and desorption of molecular hydrogen in a slightly contaminated system is, of course, a great convenience because it allowed the preparation and analysis of palladium containing large amounts of interstitial hydrogen.

Attainment of Interstitial Hydrogen Contents in Palladium Approaching Unity

Hydrogen to palladium ratios close to unity were obtained by progressive loading of the sample using H atoms generated from hot tungsten filaments in a static system first at 273 and then at 195 K. Typically 15 separate doses were required in order that the optimum pressure range could be employed for the hot tungsten-generated H atoms. The entire process required 4 to 5 h. Results are shown in Table 1. The probable error in the H-to-Pd ratios at large hydrogen contents, *i.e.* H-to-Pd > 0.9, can be estimated as ± 0.005 for the one sample whose evolved hydrogen was measured directly with the wide-bore mercury manometer and ± 0.01 for the majority of the samples which were measured with the diaphragm gauge. The errors in the ratios of the first series of samples run, whose hydrogen analyses were based on the Pirani gauge (calibrated with the McLeod gauge), are probably somewhat greater than ± 0.01. It is of interest that for a sample with a

TABLE 1. Hydrogen contents obtained by H-atom interaction with various metals and alloys

Run No.	Sample	Method	Method of analysis (pressure gauge or other method)	H-to-metal (atom ratio)
1	Pd (wire)	W-filament (static)	Pirani + gravimetric	0.90
2	Pd (wire)	W-filament (static)	Diaphragm	0.96
3	Pd (wire)	W-filament (static)	Pirani	0.96
4	Pd (wire)	W-filament (static)	Diaphragm	0.97
5	Pd (wire)	W-filament (static)	Diaphragm	0.99
6	Pd (wire)	W-filament (static)	Diaphragm + manometer (Hg)	0.99
7	Pd (wire)	W-filament (static)	Diaphragm	1.01
8	Pd (wire)	W-filament (static)	Diaphragm	0.98
9	Pd (wire)	r.f. (static)	Diaphragm	0.99
10	V($X_V = 0.06$)/Pd (wire)	W-filament (flow)	Diaphragm	0.21 (0.22 H/Pd)
11	V($X_V = 0.1$)/Pd (wire)	W-filament (flow)	Diaphragm	0.38 (0.40 H/Pd)
12	Ag($X_{Ag} = 0.35$)/Pd (foil)	W-filament (static)	Diaphragm	0.39 (0.60 H/Pd)
13	Ag($X_{Ag} = 0.55$)/Pd (foil)	W-filament (static)	Diaphragm	0.24 (0.53 H/Pd)
14	Ni (foil)	W-filament (static)	Diaphragm	0.03
15	Rh (foil)	W-filament (static)	Diaphragm	0.00
16	Au (foil)	W-filament (static)	Diaphragm	0.00

lower hydrogen content (run No. 1), H-to-Pd = 0.90, a gravimetric determination of its hydrogen content agreed quite well with the subsequent degassing analysis via the Pirani gauge. (For this sample, at least, hydrogen was not lost upon exposure to air.) The hydrogen contents monitored during absorption of hydrogen were generally not as accurate as the final analysis by degassing; however, they generally agreed to within an uncertainty in the ratio of ± 0.02.

It should be emphasized that the reported ratios of H-to-Pd in Table 1 do not represent an experimental scatter about some maximum value but reflect rather the degree of success of the loading procedure. The more successful runs were performed after experience had been gained and these generally gave values for H-to-Pd = 0.99 ± 0.01, *e.g.*, runs 5 through 8. The report of H-to-Pd $\cong$ 1.0 via electrolysis (9) may certainly be correct but it would be more strongly supported if the errors in the analysis procedure had been fully reported.

The degree of agreement amongst the various analyses using different pressure gauges and the repeated attainment of H-to-Pd ratios of 0.99 ± 0.01 leaves no doubt that such ratios were indeed obtained via reaction of palladium with H atoms. There is still, however, a large degree of art connected with this method. The pre-treatment of the reaction vessel and metal surface and the geometry of the hot tungsten filament relative to the sample are all rather poorly understood variables.

Burch (4) has suggested that for Ag/Pd substitutional alloys the maximum hydrogen contents which can be achieved can be predicted from the relationship H-to-Pd (max) = $1 - CX_{Ag}/X_{Pd}$, where $C = 0.525$. He based this upon his analysis of pressure–composition–temperature data for the H/Ag/Pd system (3) which includes data up to $X_{Ag} = 0.4$. An attempt has been made to charge several Ag/Pd alloys up to their maximum hydrogen contents via H-atoms. For the Ag($X_{Ag} = 0.55$)/Pd a value of H-to-Pd = 0.53 (Table 1) has been found which is in excess of Burch's predicted value of 0.35.

In a recent investigation of the substitutional f.c.c. alloy system V/Pd it was found that only small amounts of substituted vanadium reduced the solubility of hydrogen at 1 atm (298 K) to very small values (23). For example, for an alloy with $X_V = 0.06$ the solubility of hydrogen was only H-to-metal = 0.06 (1 atm, 298 K). With the introduction of hydrogen via H atoms an H-to-metal ratio of 0.22 was found and an even greater ratio for the V($X_V = 0.1$)/Pd alloy (Table 1); this alloy absorbed negligible hydrogen at 1 atm. This suggests that the low one-atmosphere solubility in these alloys is due to energetic reasons and not because vanadium is excluding many adjacent interstitial sites.

Using the hot tungsten filament method for the generation of H-atoms it was found that hydrogen can be readily absorbed by nickel (Table 1). Ratajczykowa and Polczewska (24) have also reported that nickel hydride can be

Can. J. Chem. Downloaded from www.nrcresearchpress.com by 210.87.254.42 on 09/05/12
For personal use only.

Can. J. Chem. Downloaded from www.nrcresearchpress.com by 210.87.254.42 on 09/05/12
For personal use only.

prepared in this manner, in the presence of H_2S in their case. Nickel hydride can be prepared with gaseous H_2 at a pressure of approximately 7000 atm (298 K) (6). The low H-to-Ni ratio observed in this work (Table 1) may be due to the fact that nickel hydride has been observed to penetrate into the nickel substrate only to small depths (6).

There has been evidence presented in the literature that rhodium may form a hydride phase (25). This was based on the extrapolation of the behavior of Rh/Pd alloys to high pressure. The estimated conditions necessary for the formation of rhodium hydride are 35 000 atm (298 K). Attempts to prepare a rhodium hydride via the H atom method were unsuccessful. In one set of experiments a bright palladium layer was electroplated onto the surface of the rhodium but this was also unsuccessful.

The electrodeless discharge (r.f.) method of generating H-atoms also worked for the introduction of large interstitial hydrogen contents into palladium but was not employed as extensively as the simpler hot tungsten filament method. The electrodeless discharge technique was used for the determination of relationships between the relative electrical resistance of palladium (R/R_0, where R is the electrical resistance at any hydrogen content and R_0 is the hydrogen-free resistance) and its hydrogen content. In several experiments the increase of relative resistance with hydrogen content was followed up to a maximum value of 1.73 (273 K) and then past the maximum to values down to 1.2 at H-to-Pd = 0.9. We were not able to increase the hydrogen content so that the resistance fell to its hydrogen-free value and the method was not pursued. Relationships between R/R_0 and H-to-Pd have been obtained over a larger range of hydrogen contents using other methods for introduction of hydrogen (8). The heating effect from the recombination reaction on the electrical leads may have been a problem.

Discussion

Some conclusions may be drawn about the mechanism of hydrogen absorption and recombination on palladium (slightly poisoned surfaces) from these results. In their investigation of the reaction of H atoms with metallic sodium Anderson and Ritchie (26) found that the rate of reaction fell above 0.1 mm Hg; they attributed this to collisional deactivation of excited H_2 species which they suggest can react with the metal. By contrast, in the present study pressures near 1 mm Hg were the most effective for hydrogen uptake and for this reason we do not believe that excited H_2 species contribute. Hydrogen molecules are absorbed by palladium in two consecutive steps:

$$[1] \qquad \tfrac{1}{2}H_2 \rightarrow \underset{*}{H}$$

$$[2] \qquad \underset{*}{H} \rightarrow [H]$$

where $\underset{*}{H}$ and [H] represent chemisorbed and absorbed hydrogen, respectively. Step 1 is believed to be the slow step even for clean surfaces of palladium (bulk) (20). When absorption occurs via H atoms, the dissociation process is not needed and instead the following two steps obtain:

$$[1'] \qquad H\cdot \rightarrow \underset{*}{H}$$

$$[2] \qquad \underset{*}{H} \rightarrow [H]$$

Step 2 and its reverse are believed to be rapid enough for the equilibrium of chemisorbed and absorbed hydrogen (20). Step 1 is extremely slow on slightly poisoned samples as shown by the fact that it does not occur at 298 K or below (these studies) or 393 K (18) and the reverse process was not observed until the temperature was above 393 K (Fig. 3).

Palladium has a very high efficiency for the H–H recombination reaction (27). Approximately 1 out of every 5 atoms which collide with the surface undergo recombination. (The hydrogen content of the palladium was not noted during this study (27) and the efficiency may increase as the hydrogen content increases since the surface coverage increases with the bulk content.) Because of the rapid absorption which takes place via H atom generation it can be concluded that a significant fraction of the hydrogen atoms do not recombine but undergo the transition to the absorbed state.

Since it has been established here that the $2\underset{*}{H} \rightarrow H_2$ reaction is very slow at temperatures below 393 K, it is clear that recombination cannot proceed by this mechanism. The probable mechanism for the recombination reaction is $H\cdot + \underset{*}{H} \rightarrow H_2$. Bond (28) has also suggested this mechanism on the basis of the expected full

Can. J. Chem. Downloaded from www.nrcresearchpress.com by 210.87.254.42 on 09/05/12
For personal use only.

coverage by chemisorbed hydrogen on transition metals. Bond's argument may no longer be generally valid, however, because it has been shown, for example, that on platinum single crystals the coverage with hydrogen is not complete even at rather large pressures (29).

Absorption of hydrogen via H atoms probably occurs by collision with a favorable empty surface site; *i.e.*, a surface interstitial site followed by rapid transition to the absorbed state. The fall-off in the rate of hydrogen uptake (Fig. 2) occurs only at quite high hydrogen contents because only then does the surface coverage start to approach completion.

There are two research papers concerning the kinetics of hydrogen (H_2) absorption by palladium (20, 30). Wicke and Mayer (30) employed a palladium black surface whereas Auer and Grabke (20) used bright palladium. The latter research is, therefore, more relevant to the present situation. They have found that the dissociation of the hydrogen molecule is rate-determining, the reaction step occurs on only one site on the surface, and at least one of the atoms from the dissociation process is incorporated into the lattice.

The chemisorption → absorption equilibrium has been recently investigated (31) and it was proposed that there may be two different hydrogen-binding sites on palladium. On one site strong chemisorption occurs and on the other, which is postulated to be between the surface palladium atoms (a surface interstitial site), weak chemisorption takes place. The hydrogen chemisorbed on the latter site is in equilibrium with absorbed hydrogen. These sites were found to be only incompletely occupied at relatively high pressures, *e.g.*, 10 mm Hg, 298 K.

Auer and Grabke (20) have found an activation energy for the absorption of hydrogen by palladium of 28.6 kJ/mol H_2. It would be expected that the activation energy for the absorption via H atoms would be negligible. It is not clear why reaction step 1 is readily poisoned whereas step 1′ is not affected, if absorption proceeds at the same surface sites. If the atomic hydrogen removes the poison which blocked these sites, absorption could then occur readily through the surface interstitial sites. If this were the correct mechanism, then the poison would have to reblock these sites after cessation of the H atom production. On the other hand, it seems more likely that two adjacent surface interstitial sites are needed for step 1 but only one site for step 1′. If a poison occupied two adjacent surface sites, then there would be few free adjacent surface sites but some vacant single sites for step 1′.

This exploratory study of a complex phenomenon indicates that the interaction of those transition metals capable of absorbing large amounts of hydrogen with H atoms is both useful and mechanistically interesting.

We wish to thank Mr. T. Curran for experimental assistance. The National Science Foundation is thanked for supporting W. A. Oates as a Visiting Foreign Scientist.

1. T. Skoskiewicz, A. Szafranski, W. Bujnowski, and B. Baranowski. J. Phys. In press.
2. K. Allard, A. Maeland, J. Simons, and T. B. Flanagan. J. Phys. Chem. **72**, 136 (1968).
3. H. Brodowsky and E. Poeschel. Zeit. Phys. Chem. N.F. **44**, 143 (1965).
4. R. Burch. Solid State Commun. **7**, 1313 (1969).
5. H. Bergsma and J. A. Goedkoop. Physica, **26**, 744 (1960).
6. B. Baranowski. Ber. Bunsenges. Phys. Chem. **76**, 714 (1972).
7. B. Baranowski, S. Majchrzak, and T. B. Flanagan. J. Phys. F: Metal Phys. **1**, 258 (1971).
8. F. A. Lewis. The palladium hydrogen system. Academic Press, New York, N.Y. 1967.
9. J. M. E. Harper. Phys. Lett. **47A**, 69 (1974).
10. B. Stritzer and W. Buckel. Z. Phys. **257**, 1 (1972).
11. B. Stritzer and W. Buckel. Phys. Lett. **43A**, 403 (1973).
12. B. Siegel. J. Chem. Ed. **38**, 496 (1961).
13. W. A. Oates and T. B. Flanagan. Nature, **231**, 19 (1971).
14. B. Baranowski and R. Wisniewdki. Phys. Stat. Solidi, **35**, 53 (1969).
15. R. Suhrmann, G. Wedler, and G. Schumicki. Structure and properties of thin films. John Wiley, New York. 1959. p. 278.
16. W. Buckel and B. Stritzer. Applications of ion beams to metals. *Edited by* S. T. Pieraux, E. P. Eernisse, and F. L. Vook. Plenum Press, New York. 1974.
17. B. Bak and J. Rastrup-Andersen. Acta Chem. Scand. **16**, 111 (1962).
18. D. Everett and P. Nordon. Proc. Roy. Soc. **259A**, 341 (1960).
19. J. Clewley, T. Curran, T. B. Flanagan, and W. A. Oates. J. Chem. Soc., Faraday Trans. I, **69**, 449 (1973).
20. W. Auer and H. Garbke. Ber. Bunsenges. Phys. Chem. **78**, 58 (1974).
21. V. Ponec, Z. Knor, and S. Cerny. 3rd Int. Congress Cat., Amsterdam. 1968. p. 353.
22. P. A. Sermon. J. Catal. **24**, 460 (1972).

23. D. ARTMAN and T. B. FLANAGAN. To be published.
24. I. RATAJCZYKOWA and W. POLCZEWSKA. Bull. Acad. Pol. Sci. Ser. Chem. **14**, 673 (1966).
25. B. BARANOWSKI, S. MAJCHRZAK, and T. B. FLANAGAN. J. Phys. Chem. **77**, 35 (1973).
26. J. R. ANDERSON and I. M. RITCHIE. J. Phys. Chem. **70**, 3681 (1966).
27. B. WOOD and H. WISE. J. Chem. Phys. **29**, 1476 (1959).
28. G. C. BOND. Catalysis by metals. Academic Press, New York. 1962.
29. M. PROCOP and J. VÖLTER. Surface Sci. **33**, 69 (1973).
30. E. WICKE and K. MAYER. Zeit. Phys. Chem. N.F. **64**, 225 (1969).
31. J. LYNCH and T. B. FLANAGAN. J. Phys. Chem. **77**, 2628 (1973).

Can. J. Chem. Downloaded from www.nrcresearchpress.com by 210.87.254.42 on 09/05/12
For personal use only.

Solvent Effects on Solvent Exchange Reactions at Nickel(II) Centers[1]

COOPER H. LANGFORD[2] AND JAMES P. K. TONG
Department of Chemistry, Carleton University, Ottawa, Canada K1S 5B6
AND
ANDRÉ MERBACH
Institut de Chimie Minérale et Analytique, Université de Lausanne, Lausanne, Suisse

Received June 26, 1974

COOPER H. LANGFORD, JAMES P. K. TONG, and ANDRÉ MERBACH. Can. J. Chem. **53**, 702 (1975).

Several recent correlations relating kinetics of Ni(II) complex formation and solvent exchange to solvent properties are examined after collection of literature and new experiments on solvent exchange kinetics at Ni(II) when *only the solvent* is varied (entering group, leaving group, and nonlabile ligands held constant). The results indicate solvent exchange is remarkably insensitive to bulk solvent. It is suggested that this implies that the interesting correlations of complex formation rates with solvents introduced by Bennetto and Caldin provide a means to study the solvent dependence of the encounter equilibria between a Ni(II) complex and a ligand L. The linear relationship between enthalpies and entropies of activation for reactions at Ni(II) in different media is attributed to the changes in the ligands bound to the Ni(II) center but not undergoing substitution in the reaction observed.

COOPER H. LANGFORD, JAMES P. K. TONG et ANDRÉ MERBACH. Can. J. Chem. **53**, 702 (1975).

On passe en revue plusieurs corrélations récentes reliant les propriétés des solvants avec la cinétique de formation des complexes du Ni(II) et la cinétique de leur échange avec les solvants. On compare les données compilées dans la littérature avec les résultats obtenus lors de nouvelles expériences sur des cinétiques d'échanges avec les solvants au niveau du Ni(II) quand *seule la nature du solvant varie* (on maintient constant le nucléophile, le nucléofuge et les ligands non labiles). Les résultats indiquent que l'échange du solvant est d'une façon remarquable insensible à la nature du solvant comme milieu réactionnel. On suggère que ces résultats impliquent que les corrélations intéressantes, introduites par Bennetto et Caldin, et reliant les vitesses de formation des complexes et les solvants fournissent un moyen d'étudier la dépendance sur le solvant de l'équilibre de formation de complexes externes entre un complexe de Ni(II) et un ligand L. La relation linéaire entre les enthalpies et les entropies de réaction pour la réaction du Ni(II) dans différents milieux est attribuée à des changements dans les ligands, liés au Ni(II) central, qui ne sont pas impliqués dans les réactions de substitutions des réactions observées.

[Traduit par le journal]

Introduction

The model currently accepted for ligand substitution (complex formation) at Ni(II) centers in water as solvent is an I_d path (1) usually called the Eigen–Wilkins (2) mechanism, and written as shown in reaction 1.[3]

$$[I]\quad NiS_6 + L \underset{\text{Encounter or outer sphere complex}}{\overset{K_E}{\rightleftharpoons} L,NiS_6} \overset{k_1}{\rightarrow} \underset{\text{Activated complex}}{L...NiS_5...S} \rightarrow NiLS_5 + S$$

K_E is the equilibrium constant for encounter between NiS_6 and L or, in other words, the constant for transfer of L from bulk solvent to the outer sphere of NiS_6 with a corresponding *reverse transfer of S*. The reaction is designated dissociative (d) because k_1 is insensitive to the specific nature of L and differs from the solvent exchange first order rate constant only by a statistical factor first identified by Langford and Muir (3). Under usual (low concentration) experimental conditions, an observed complex formation reaction is found to be second order, first order in NiS_6 and first order in L. Such a second order constant, k_L, has the interpretation under mechanism 1 that $k_L = K_E k_1$. Such K_E should depend primarily on charge type. The fact that k_L has been seen to vary 20-fold for neutral ligands reacting with $Ni(OH_2)_6^{2+}$ (4) (diamines excluded for the reason of the special

[1]We thank the National Research Council of Canada for financial support. The Brüker spectrometer was bought with a grant of the Fonds National Suisse de la Recherche Scientifique (No. 2.456.71).

[2]To whom correspondence should be addressed.

[3]Charge notations are deliberately omitted for clarity. "S" and "L" stand for solvent and ligand molecules respectively.

mechanism discussed by Wilkins (2)) indicates that there are some problems for a simple account via an I_d mechanism and reaction 1. Caldin and Bennetto have developed a very interesting mechanistic picture which seeks to take solvent effects explicitly into account (4, 5). This picture is applied to reactions in nonaqueous solvents as well as water. A critical, but sympathetic, appraisal of the Caldin–Bennetto viewpoint has been given by Chattopadhyay and Coetzee (6) and the same viewpoint has been taken up for discussion of reactions at Mg(II) centers by Crea *et al.* (7). However, despite the active interest in the Caldin–Bennetto viewpoint, an alternative account of the factors which determine complex formation and solvent exchange (especially solvent exchange) reactivity when the solvent is changed has been developed (8, 9).

The Caldin–Bennetto Model and Reaction 1

The postulates underlying the Caldin–Bennetto model of solvent effects may be summarized as follows (4). (*1*) Solutions of metal ions in nonaqueous polar solvents can be represented by a model similar to the Frank and Wen (10) model for aqueous solutions. (*2*) The kinetics of complex formation are controlled partly by the energy required to dissociate the Ni—S bond and *partly by interaction of the leaving S* molecule with the *bulk solvent* into which it passes. The correlated movement of L or S out of the bulk solvent into the first coordination sphere seems to be less important. (*3*) The *structural* properties of the solvent are modified locally by the presence of L molecules, an effect related to solute–solvent intermolecular forces between L and S. The consequences of these postulates are worked out by consideration of the effects relating to transferring molecules from a "bulk solvent structure" region through a "disordered solvation region"[4] to the primary coordination shell of Ni^{2+} which is identified with the "ordered solvation shell" of Frank (4, 10). In particular, correlations of kinetic parameters with solvent *fluidity*, (viscosity/density) as defined by Bennetto and Caldin (4, 5), and *enthalpy of vaporization* of solvent are emphasized.

The object of the present paper is to consider the kinetics of reaction 1 and their implications for solvent effects. Reaction 1 implies in the case of Ni(II) complexes (where k_1 is of the order of $10^4\ s^{-1}$) that the distribution of L or S between the bulk solvent and the encounter sphere (second coordination sphere or outer sphere) of NiS_6 is governed by a pseudo *equilibrium* which adjusts *rapidly* to any changes in the primary coordination sphere. The effect of bulk solvent structure should then be found in the modification of K_E for L's that interact differently with solvent. Reaction 1 seems to imply the contrary of postulate 2 of Caldin and Bennetto in that the equation emphasized the role of bulk solvent in the transfer of L from bulk to the encounter region prior to any inner–outer sphere exchanges and *neglects* the interaction of the leaving S molecule "with the bulk solvent into which it passes". In the case of solvent exchange in the pure solvent, reaction 1 simplifies. The equilibrium for S between bulk and encounter sites is *trivial*. All sites of both types will be occupied by S at all times. As long as exchange between the two sites remains fast (diffusion is fast compared to k_1 as in all solvents studied except glycerol (11)), the rate of solvent exchange is *independent of bulk solvent structure*. This again sets interpretation according to reaction 1 in contrast with the second postulate above. Another way of looking at this contrast is to observe that solvent is always in encounter with NiS_6 and that solvent exchange is an *inherently* first order process and *not* a pseudo-first order "bimolecular" process (12).

Our purpose here will be to explore the evidence for the claim in postulate 2 of the Caldin–Bennetto model that "... interaction of the leaving S molecule with the bulk solvent into which it passes" is the important factor. We do this by exploring the effect on solvent exchange rates of modification of bulk solvent structure by introducing noncoordinating electrolytes or salts. Our reference point for this is the first approximation suggestion of reaction (1) that *solvent exchange rates are independent of bulk solvent structure* (and activity)!

Relevant Literature

We note that the work of Caldin and Bennetto, Chattopadhyay and Coetzee, and Crea,

[4]It may be noted that the implication that the secondary coordination sphere of a metal complex is "disordered" is valid if order is identified with bulk solvent order. However, various experimental techniques have suggested that the metal ion and primary coordination sphere impose order on the secondary coordination sphere. The degree of ordering in the secondary solvation shell is an unresolved issue.

TABLE 1. Relevant literature studies

Reaction	$k^{25°}$ (s^{-1})[a]	$\Delta H^{\ddagger}$(kcal mol^{-1})	Reference
$Ni(OH_2)_6^{2+}$ + H_2O in			
H_2O	$(4.4 \pm 0.2) \times 10^4$	10.3 ± 0.5	13
6.5 *m* (4.6 *M*) $LiClO_4$	$(4.1 \pm 0.5) \times 10^4$	9.6 ± 1	13
$Ni(DMSO)_6^{2+}$ + DMSO in			
DMSO	3.2×10^3	13.0	15
$DMSO/CH_3NO_2$ to 0.6 *M* DMSO	3.2×10^3	13.0	15
$Ni(NH_3)_6^{2+}$ + NH_3 in[b]			
NH_3(l)	4.7×10^4	10 ± 1	14
Aqueous $NH_3 \sim 15$ *M*	5.6×10^4	9.5 ± 1.1	14
$Co(NH_3)_5DMSO$ + H_2O in			
H_2O	2.83×10^{-4}	—	16
17 mol% CH_3OH	2.60×10^{-4}	—	16
50 mol% C_3H_7OH	2.60×10^{-4}	—	16
90 mol% dioxane	1.14×10^{-4}	—	16

[a]All rate constants are presented as first order exchange rates per coordination site at the metal ion. In some sources, ref. 13*a* for instance, rate constants are given as overall rates of solvent exchange at per molal metal ion, which then must be divided by a factor of 6 as was done by the same author in ref. 13*b*.
[b]Other experiments with added electrolytes revealed no effects on rates.

Lincoln, and West cited above involves change of more than bulk solvent. In those studies, when solvent is changed, so is the nature of the leaving group at the metal center and also the other five ligands attached to the metal center. Contemporaneously, a considerable amount of literature has accumulated in which the bulk solvent was the *only* variable. The main thrust of the present paper is to compare the two types of studies. We add in limited fashion to the experimental documentation by the new experiments reported. The literature we discuss has simply not yet compared the two types of studies. The reactions of the second type previously described are solvent exchange of $Ni(OH_2)_6^{2+}$ studied by $^{17}OH_2$ n.m.r. in water and $>6\,m$ $LiClO_4$ (13), study of solvent exchange of $Ni(NH_3)_6^{2+}$ with NH_3 in NH_3 and aqueous ammonia (14), the effect of the addition of CH_3NO_2 as an unreactive solvent component on the rate of dimethylsulfoxide (DMSO) exchange at $Ni(DMSO)_6^{2+}$ (15), and the addition of large mole fraction of inert solvent on the solvolytic replacement of DMSO by H_2O at $Co(NH_3)_5DMSO^{3+}$ (16). These results are collected in Table 1.

All these results tend to support the conclusion that solvent effects are small. Such changes in solvent exchange rates when the reactive solvent is "diluted" by a second solvent component or a salt are consistent with the idea that a few encounter sites have been denied to the reactive solvent molecules and that the rate is down somewhat for essentially statistical reasons. Even without specific data on viscosities or enthalpies of evaporation, it is clear that the examples represent cases of large change in bulk solvent structural parameters and yet fail to exhibit correspondingly significant changes in either k (which may be insensitive due to cancellation of $\Delta\Delta H^{\ddagger}$ and $\Delta\Delta S^{\ddagger}$) and/or $\Delta H^{\ddagger}$. The extreme is the first example. In water, bulk structure is important. In 6.5 *m* $LiClO_4$ an average of only 4.27 water molecules are associated with each ion. *There is no bulk*, and the co-sphere is also ill-defined. All water is in ion solvation shells. The effect is startlingly small viewed from the perspective of any model.

Results

In imitation of the first entry in Table 1, the present experiments concern the modification of the solvent by addition of salts. The first studies are dimethylformamide (DMF) exchange at $Ni(DMF)_6^{2+}$ in the presence of several concentrations of *n*-Bu_4NClO_4 and $LiClO_4$ studied with the ^1H n.m.r. T_2 of the formyl proton. The results are collected in Fig. 1 and Table 2. The second studies concerned water exchange at $Ni(OH_2)_6^{2+}$ studied by ^{17}O n.m.r. with the addition of tetra-*n*-butylammonium nitrate. The salt was chosen because it produces large changes in water viscosity. The viscosities of the solutions were measured. Temperature depen-

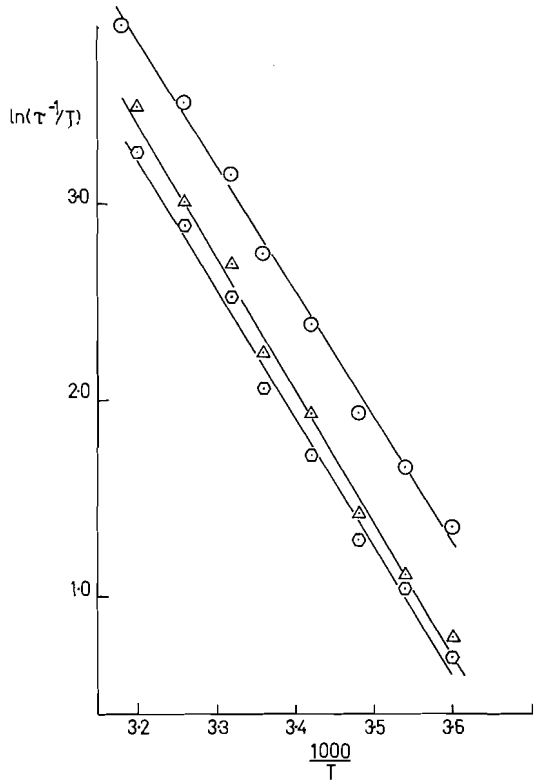

FIG. 1. Temperature dependence of DMF exchange at Ni(II) in: neat DMF ○; 0.528 *m* *n*-Bu_4NClO_4 DMF solution △; 1.077 *m* $LiClO_4$ DMF solution ○.

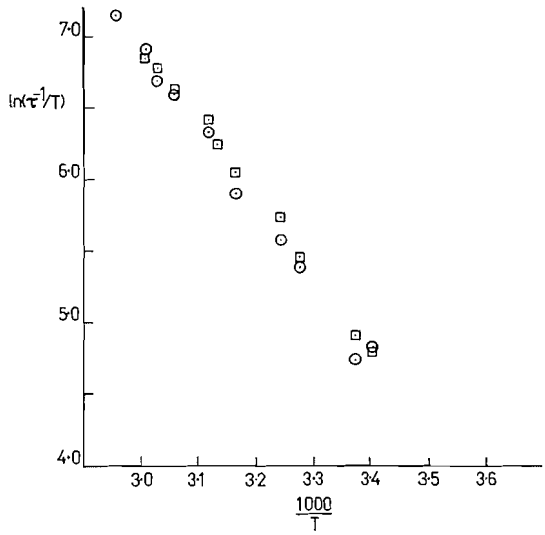

FIG. 2. Temperature dependence of water exchange at Ni(II) in: neat water ○; 0.322 *m* *n*-Bu_4NNO_3 aqueous solution □.

dence of observed rate parameters are shown in Fig. 2. Table 3 collects kinetic parameters and Table 4 reports the viscosities.

Discussion

Role of Solvent in Solvent Exchange Reactions

In the introduction, the concepts of effect of solvent structure on rate introduced by Caldin and Bennetto were outlined. These propositions were based on two kinds of *experimental* evidence. The first kind of evidence from experiments depended on correlation of bulk solvent properties with a parameter n based on eq. 2

$$[2] \qquad n = k_L/K_E k_{ex}$$

where k_L is the second order rate constant for complex formation by a ligand L in a solvent, K_E is the encounter equilibrium constant for that ligand with the solvocomplex and k_{ex} is the solvent exchange rate constant in the solvent. The correlation was between n and the solvent structure related parameters, or between $\Delta H_L^{\ddagger} - \Delta H_{ex}^{\ddagger}$ (where the subscripts L and ex assign the activation enthalpies to k_L and k_{ex} processes) and the solvent parameters. The second line of experimental evidence (5, 6) followed from interpretation of a correlation between enthalpy of activation and entropy of activation including both solvent exchange and complex formation reactions and common to several metal ion centers if correction for ligand field contributions to enthalpy were made.

The limits of the first line of evidence have already been tested by Chattopadhyay and Coetzee (6). Their work establishes that n (and $\Delta H_L^{\ddagger} - \Delta H_{ex}^{\ddagger}$) is a moderately sensitive function of the choice of L. Moreover, the ordering of solvents with respect to the magnitude of n is not constant as L varies. This points to n as a parameter of *ligand* solvent interaction. Such a conclusion accords with the view presented in this paper.

Postulate 2 of the Caldin–Bennetto model requires that change of the bulk solvent structure, dynamics, and activity should change the interaction of the leaving S with bulk solvent and hence the free energy of the transition state. Postulate 2 was introduced to account for variations of n over more than an order of magnitude and substantial changes in $\Delta H_L^{\ddagger} - \Delta H_{ex}^{\ddagger}$. Results in Tables 1 and 2 do not reveal any variations of corresponding magnitude. Most alterations of bulk solvent recorded there leave either

TABLE 2. DMF exchange at Ni(II) ion (n.m.r. line-broadening studies)

Nuclear magnetic resonance probe	$[Ni^{2+}]$ (m)	Anion	Added electrolyte	$\Delta H^{\ddagger}$ (kcal mol^{-1})	k_{ex} (25 °C) (s^{-1})	Reference
^{17}O	0.01–0.1	ClO_4^-	Nil	9.4	7.7×10^3	19
^1H	0.01–0.04	ClO_4^-	Nil	15.0	3.8×10^3	17
	0.01–0.04	ClO_4^-	Nil	10	3.7×10^3	18
	0.0334	ClO_4^-	Nil	12.7 ± 0.5	5.1×10^3	This work
	0.0259	ClO_4^-	0.528 m n-Bu_4NClO_4	13.6 ± 0.5	3.2×10^3	This work
	0.0232	ClO_4^-	1.077 m $LiClO_4$	13.0 ± 0.5	2.7×10^3	This work

TABLE 3. Water exchange at Ni(II) ion. (^{17}O n.m.r. studies)

$[Ni^{2+}]$ (m)	Anion	Added electrolyte	$\Delta H^{\ddagger}$ (kcal mol^{-1})	k_{ex} (25 °C) (s^{-1})	Reference
0.0504	NO_3^-	Nil	10.8 ± 0.5	4.3×10^4	This work
0.0539	NO_3^-	0.322 m n-Bu_4NNO_3	10.6 ± 0.5	4.7×10^4	This work
0.025 and 0.057	NO_3^-	($\mu = 0.5$) ($pH \simeq 6$)	10.3 ± 0.5	4.4×10^4	20

TABLE 4. Viscosities of aqueous tetra-n-butylammonium nitrate solutions*

Salt concentration (m)	Viscosity, η, 25 °C (cp)	Viscosity ratio (η/η^0)
0	0.9016 (η^0)	1.0000
0.122	1.0053	1.1150
0.264	1.1897	1.3195
0.407	1.3839	1.5349
0.567	1.5978	1.7722
0.746	1.8771	2.0820

*Jones–Dole coefficients (21): $A = -0.29 \pm 0.02$, $B = 1.78 \pm 0.03$.

k_{ex} or $\Delta H_{ex}^{\ddagger}$ unaltered within experimental error.

The present paper also bears on the significance of the $\Delta H^{\ddagger}$–$\Delta S^{\ddagger}$ correlation and the role of the dynamic parameter, viscosity. If it is true that the correlation exists over a wide range of reactions in a wide range of solvents because it reflects solvent structure effects (5, 6), it should be possible to alter $\Delta H^{\ddagger}$, $\Delta S^{\ddagger}$, and perhaps k_{ex} by altering solvent structure. Table 1 collects literature data (not refuted by the new experiments) bearing on this question in a way different from the earlier correlations (6). Here the focus is on the effects of *altering solvent* and *solvent structure* while maintaining a *constant* reaction system. If the activation parameters for exchange of, say, DMSO between $Ni(DMSO)_6^{2+}$ and bulk DMSO are compared to those for exchange of water between $Ni(OH_2)_6^{2+}$ and bulk H_2O, at least the following relevant features have been varied: (*1*) the nature of the leaving group, (*2*) the nature of the other ligands bound to the reactive center, (*3*) the nature of the entering group, and (*4*) the solvent. Evidence exists that all of these factors may be important except (*3*).

If the $\Delta H^{\ddagger}$–$\Delta S^{\ddagger}$ correlation is to be interpreted, (*1*) and (*2*) must be considered as well as (*4*). One may begin with the observation that the fundamental significance of a $\Delta H^{\ddagger}$–$\Delta S^{\ddagger}$ correlation is that the reactions have a common mechanism (23). In terms of factor (*1*), the assumption of a dominantly dissociative mechanism suggests variations in $\Delta H^{\ddagger}$ with the enthalpy of the bond to be broken but only small variations in $\Delta S^{\ddagger}$. Factor (*1*) then implies a very large value of the isokinetic temperature in a $\Delta H^{\ddagger}$–$\Delta S^{\ddagger}$ correlation. This is not observed. In

terms of factor (*2*), the $\Delta H^{\ddagger}$–$\Delta S^{\ddagger}$ correlation requires a more negative $\Delta S^{\ddagger}$ as the five ligands which do not leave become more favorable to substitution. There are two points to note. First, the nonlabile ligands do change $\Delta H^{\ddagger}$ for water substitution at Ni(II) significantly (13). Second, a ligand which is strongly bound itself contributes to labilization of another (9). A dissociative transition state will be stabilized (lower $\Delta H^{\ddagger}$) if the five remaining ligands rearrange to bind more strongly to the center of reduced coordination number. This process puts restrictions on the five ligands which are expected to be reflected in lower $\Delta S^{\ddagger}$. It emerges that the $\Delta H^{\ddagger}$–$\Delta S^{\ddagger}$ correlation could be explained, at least in part, by factor (*2*) in a manner consistent with the observed isokinetic temperature. Of course, factor (*4*) can explain the correlation also.

The choice between emphasis on factor (*2*) and factor (*4*) as the major contributor to the $\Delta H^{\ddagger}$–$\Delta S^{\ddagger}$ correlation depends on examination of the behavior of $\Delta H^{\ddagger}$ (or $\Delta S^{\ddagger}$) when one of the factors (*2*) or (*4*) is changed and the other is held constant. The substantial changes in $\Delta H^{\ddagger}$ as nonlabile ligand is changed (factor (*2*)) with solvent (factor (*4*)) held constant, have been reviewed elsewhere in some detail (13). This paper concerns circumstances in which *factor (2) is invariant and factor (4) is varied.*

In aqueous solutions, we see that bulk solvent structure may be "destroyed" with little effect on $\Delta H^{\ddagger}$. A 6.5 *m* solution of $LiClO_4$ allows, on the modest estimate of 4 waters each as nearest neighbors of Li^+ and ClO_4^-, less than 7 mol of water to form secondary solvation shells intervening. Ionic co-spheres strongly overlap. The values of k_{ex} and $\Delta H_{ex}^{\ddagger}$ speak for themselves (Table 1). The impact of the more recent work on other salt containing media is consistent with this striking example. Adding salts to the lower dielectric constant solvent, DMF, resulted in $\Delta H^{\ddagger}$ parameters which could not be reliably distinguished in the presence or absence of salt (Table 2, Fig. 1). In this case, at maximum salt concentration, assumption of four solvent molecules each per cation and anion leaves ~6 mol of solvent outside contact layers. The average distance between two neighboring ions is ~2 solvent molecules. Ionic co-spheres do overlap. The new experiment in water bears on the emphasis on dynamic coupling in Bennetto and Caldin's postulate 2. In water dynamically altered by the significantly structure-making ion $(n\text{-but})_4N^+$ it was impossible to distinguish experimentally between the kinetic parameters in the presence or absence of the salt (Table 3, Fig. 2). The dynamic modification of water structure by the salt is attested by the increase in water viscosity by 40% (Table 4).

Similar results are seen for variation of factor (*4*) in the limited class of cases where solvent mixtures may be examined without alteration of the reactive systems. Frankel's results (15) for mixtures of DMSO with nitromethane, for example, were all represented on the same linewidth–temperature curve without regard to the nitromethane content. Liquid NH_3 and aqueous NH_3 are nearly equivalent and not experimentally distinguishable (14). The remaining examples are for rate constants only but the small variations suggest slight change in activation parameters.

The present critique of the solvent structure interpretation of the $\Delta H^{\ddagger}$–$\Delta S^{\ddagger}$ correlation also leads to the *conclusion that the I_d, Eigen–Wilkins, model has the advantage over the dynamic solvent coupling model of Caldin and Bennetto in that it is capable of explaining a lack of sensitivity of solvent exchange to bulk solvent modification.* In solvent exchange the encounter equilibria are trivial ($\Delta G^0 = 0$) and cannot be altered by alteration of the bulk alone. It remains to be shown that the I_d, Eigen–Wilkins, model can be adapted to the explanation of the solvent effects discovered by Caldin and Bennetto with respect to *complex formation* reactions.

Role of Solvent in Complex Formation Reactions

According to reaction 1, the I_d or Eigen–Wilkins model, the second order rate constant for complex formation, k_L, may be equated to $K_E k_1$ where $k_1 = sk_{ex}$ (*s* is a statistical factor). The role of the statistical factor can be seen in the new experiments in DMF (Table 2, Fig. 1). It can be seen that perchlorate ion can reduce the rate of solvent exchange without measurably changing the value of $\Delta H^{\ddagger}$. In light of the extensive pairing of $Ni(DMF)_6^{2+}$ with ClO_4^- expected in DMF, this is comprehensible. It is plausible to assume that the ClO_4^- ions occupy some outer sphere sites making them unavailable to participate as sites for solvent exchange. As a consequence, this may affect $\Delta S_{ex}^{\ddagger}$, and hence k_{ex}, but not to any significant extent $\Delta H_{ex}^{\ddagger}$.

The parameters for correlation with bulk solvent properties introduced by Caldin and Bennetto, ln *n* and $\Delta\Delta H$, can be interpreted

using the Eigen–Wilkins model. According to Bennetto and Caldin (4)

$$[3] \qquad n = k_L/0.1k_{ex}$$

and

$$[4] \qquad \Delta\Delta H^{\ddagger} = \Delta H_L{}^{\ddagger} - \Delta H_{ex}{}^{\ddagger}$$

In eq. 3, k_L is the observed second order rate constant; and 0.1 is the uniformly assigned value of K_E; refer to eq. 2 of Caldin and Bennetto (4, 5) in their critique of the Eigen–Wilkins model. Using the assumption that K_E is constant or may be calculated from the Fuoss–Eigen electrostatic equation (2, 8, 12) and making the substitution of the original formulation of k_L, due to the Eigen–Wilkins model, into eq. 3, one obtains

$$[5] \qquad n = \frac{K_E s k_{ex}}{0.1k_{ex}} = (s/0.1)K_E$$

It follows that the parameter, ln n, may be interpreted as

$$[6] \qquad \ln n = -\frac{\Delta H_E{}^0}{RT} + \left(\frac{\Delta S_E{}^0}{T} + \ln\frac{s}{0.1}\right)$$

where $\Delta H_E{}^0$ and $\Delta S_E{}^0$ are the free energy, enthalpy, and entropy of formation of the outer sphere complex, $NiS_6.L$. In eq. 4, $\Delta H_L{}^{\ddagger}$ is the observed enthalpy of activation for the ligand substitution process, and can be given as $(\Delta H_E{}^0 + \Delta H_{ex}{}^{\ddagger})$ according to the Eigen–Wilkins model. With this substitution for $\Delta H_L{}^{\ddagger}$, eq. 4 will then read

$$[7] \qquad \Delta\Delta H^{\ddagger} = (\Delta H_E{}^0 + \Delta H_{ex}{}^{\ddagger}) - \Delta H_{ex}{}^{\ddagger} = \Delta H_E{}^0$$

It is quite important to recognize that these parameters, $\Delta H_E{}^0$ and $\Delta S_E{}^0$ of the encounter equilibrium are solvent sensitive.

So far, only a few weak encounter equilibria have proved susceptible to direct experimental examination. Two recent n.m.r. studies are important (24, 25). They show that K_E values for neutral molecule neutral complex encounters vary over more than a factor of ten and are solvent sensitive. We believe that the Bennetto–Caldin parameters $\Delta\Delta H^{\ddagger}$ and n provide the widest ranging and most general method for exploration of the factors controlling K_E that is experimentally available.

Experimental

N,N-Dimethylformamide (DMF) line-broadening experiments were done on a Varian XL-100 n.m.r. spectrometer in 5 mm n.m.r. tubes. By locking on the methyl protons of DMF, the formyl proton absorption line was recorded. Linewidths at the half-height were measured. The probe temperature was calibrated by a copper–constantine thermocouple, and was kept constant to ±0.5 °C.

The ^{17}O n.m.r. line-broadening experiments for water were done on a Brüker HX-90 n.m.r. spectrometer in 8 mm n.m.r. tubes. The differential mode of the resonance signal was recorded. The peak-to-peak separations were measured. Modulation broadening was carefully avoided by minimizing the modulation amplitude and correcting for the residual (26). The sample temperatures were determined by direct insertion of a thermometer into the sample tube while it was still inside the probe.

Viscosity measurements were made by an Ostwald's viscometer which calibrated at 25.0 °C by four pure solvents, namely: water, acetone, methanol and ethanol, with reference to literature values (22).

Aldrich spectrograde DMF was dried over BaO and distilled under reduced pressure. 5% ^{17}O enriched water was obtained from YEDA Research and Development, Rehovoth, Israel,[5] which was then diluted to 2.5% enrichment.

$Ni(DMF)_6.(ClO_4)_2$ was prepared according to the procedure described by Babiec *et al.* (19). $Ni(H_2O)_6.(NO_3)_2$ was obtained from Merck as analytical grade reagent, and was used without further purification.

Tetrabutylammonium perchlorate (n-Bu_4NClO_4) was prepared by adding dilute perchloric acid to a dilute aqueous solution of tetrabutylammonium bromide (Eastman Kodak) solution. The precipitated n-Bu_4NClO_4 was recrystallized from methanol by adding ether. The crystals were dried under vacuum.

Tetrabutylammonium nitrate (n-Bu_4NNO_3) was prepared by mixing equimolar tetrabutylammonium bromide and silver nitrate solutions (with an extremely slight excess of $AgNO_3$) where the silver bromide precipitate was filtered off. The filtrate was used as the stock solution whose concentration was calculated through the reactant solution weights and molalities.

Treatment of Data

The treatment of data follows that reviewed by Stengle and Langford (27) utilizing the slow exchange region where

$$\tau_M{}^{-1} \simeq \frac{1}{P_M}\left(\frac{1}{T_2} - \frac{1}{T_{2A}}\right)$$

and

$$\tau_M{}^{-1} = \frac{kT}{h}\exp\left(-\frac{\Delta H^{\ddagger}}{RT} + \frac{\Delta S^{\ddagger}}{R}\right)$$

where the symbols carry their usual meanings (27). The spin–spin relaxation times, T_2, are related to the linewidths at half-height, $\Delta\nu_{1/2}$, by

$$\frac{1}{T_2} = \pi\Delta\nu_{1/2}$$

and to the peak-to-peak separation, Δ_p, of the differential mode of the absorption signal by

[5]We thank Dr. D. R. Wiles for providing this sample.

$$\frac{1}{T_2} = \sqrt{3}\pi\Delta_p$$

The activation parameters, $\Delta H^{\ddagger}$ and $\Delta S^{\ddagger}$, are obtainable from the slope and intercept of a plot of $\ln(\tau_M^{-1}/T)$ *vs.* $(1/T)$ respectively.

1. C. H. LANGFORD and H. B. GRAY. Ligand substitution processes. W. A. Benjamin, New York. 1966. Chapt. 1.
2. R. G. WILKINS. Acc. Chem. Res. **3**, 408 (1970).
3. C. H. LANGFORD and W. R. MUIR. J. Am. Chem. Soc. **89**, 3141 (1967).
4. E. F. CALDIN and H. P. BENNETTO. J. Sol. Chem. **2**, 217 (1973).
5. H. P. BENNETTO and E. F. CALDIN. J. Chem. Soc. A, 2198 (1971).
6. P. K. CHATTOPADHYAY and J. F. COETZEE. Inorg. Chem. **12**, 113 (1973).
7. J. CREA, S. F. LINCOLN, and R. J. WEST. Aust. J. Chem. **26**, 1227, (1973).
8. C. H. LANGFORD and T. R. STENGLE. Ann. Rev. Phys. Chem. **19**, 193 (1968).
9. C. H. LANGFORD. Can. J. Chem. **49**, 1497 (1971).
10. H. S. FRANK and W. Y. WEN. Discuss. Faraday Soc. **24**, 133 (1957).
11. E. F. CALDIN and M. W. GRANT. J. Chem. Soc. Faraday Trans. I, **69**, 1648 (1973).
12. C. H. LANGFORD. J. Chem. Educ. **46**, 557 (1969).
13. (*a*) S. F. LINCOLN, F. APRILE, H. W. DODGEN, and J. P. HUNT. Inorg. Chem. **7**, 929 (1968); (*b*) J. P. HUNT. Coord. Chem. Rev. **7**, 1 (1971).
14. J. P. HUNT, H. W. DODGEN, and F. KLEMBERG. Inorg. Chem. **2**, 478 (1963).
15. L. S. FRANKEL. Chem. Commun. 1254 (1969).
16. W. L. REYNOLDS, S. ASPERGER, and M. BIRUS. J. Chem. Soc. Chem. Commun. 822 (1973).
17. N. A. MATWIYOFF. Inorg. Chem. **5**, 788 (1966).
18. R. G. LITTLE. Private communication.
19. J. S. BABIEC, C. H. LANGFORD, and T. R. STENGLE. Inorg. Chem. **5**, 1362 (1966).
20. A. G. DESAI, H. W. DODGEN, and J. P. HUNT. J. Am. Chem. Soc. **91**, 5001 (1969).
21. R. W. GURNEY. Ionic processes in solution, Dover, New York. 1962. Chapts. 9 and 10.
22. R. A. ROBINSON and R. H. STOKES. Electrolyte solutions, 2nd ed., Butterworth, London. 1968.
23. J. LEFFLER and E. GRUNWALD. Kinetics and equilibria of organic reactions. J. Wiley and Sons, New York. 1963.
24. D. R. EATON and K. L. CHUA. Can. J. Chem. **51**, 4137 (1973).
25. G. C. LEVY and R. A. KOMOROSKI. J. Am. Chem. Soc. **96**, 678 (1974).
26. H. WAHLQUIST. J. Chem. Phys. **35**, 1708 (1961).
27. T. R. STENGLE and C. H. LANGFORD. Coord. Chem. Rev. **2**, 349 (1967).

Kinetic Studies of Copper(II)-exchange from L-Histidine to Human Serum Albumin and Diglycyl-L-histidine, a Peptide Mimicking the Copper(II)-transport Site of Albumin

SHOW-JY LAU AND BIBUDHENDRA SARKAR

Division of Biochemistry, The Research Institute, The Hospital for Sick Children, Toronto, Ontario M5G 1X8 and The Department of Biochemistry, University of Toronto, Toronto, Ontario M5S 1A8

Received May 1, 1974

SHOW-JY LAU and BIBUDHENDRA SARKAR. Can. J. Chem. **53**, 710 (1975).

The Cu(II)-exchange reactions of L-histidine with human serum albumin and diglycyl-L-histidine were studied at p*H* 7.53 in 0.1 *M* *N*-ethylmorpholine–HCl buffer. The exchange rates from L-histidine to albumin and peptide were determined as 0.67 and 0.42 s^{-1} respectively. Those from albumin and peptide to L-histidine were obtained as 0.04 and 0.07 s^{-1} respectively. This result is in accord with the earlier observations of the equilibrium study that the peptide has about half the Cu(II)-binding affinity as compared to albumin. The difference in the Cu(II)-exchange rates of albumin and peptide may reflect the influence of either the COOH-terminal free carboxyl group of the peptide or the side-chain residues of the Cu(II)-binding site in the native protein or both. An exchange mechanism is proposed in which the ternary complexes are shown to play the important role in the rate-determining step in the Cu(II)-exchange between a macromolecule and a small substance.

SHOW-JY LAU et BIBUDHENDRA SARKAR. Can. J. Chem. **53**, 710 (1975).

On a étudié les réactions d'échange du Cu(II) de la L-histidine avec l'albumine du sérum humain et la diglycyl L-histidine; ces études ont été effectuées à un p*H* de 7.53 dans un tampon de 0.1 *M* de *N*-éthylmorpholine sous forme chlorhydrate. Les taux d'échanges de la L-histidine à l'albumine et au peptide sont respectivement de 0.67 et 0.42 s^{-1}. Ceux de l'albumine et du peptide à la L-histidine sont respectivement de 0.04 et de 0.07 s^{-1}. Ce résultat concorde avec les observations faites antérieurement et selon lesquelles l'affinité du peptide pour le cuivre est environ la moitié de celle de l'albumine. La différence dans les taux d'échanges du Cu(II) de l'albumine et du peptide peut réfléter l'influence soit du groupe COOH terminal libre du peptide soit des résidus des chaines latérales du site fixant le Cu(II) dans la protéine libre ou les deux. On propose un mécanisme d'échange dans lequel on montre que les complexes ternaires jouent un rôle important dans l'étape déterminante dans l'échange du Cu(II) entre une macromolécule et une petite substance. [Traduit par le journal]

Introduction

It is known that metal ions may mediate the binding of small molecules to proteins. The formation of the intermediary ternary complexes has been suggested to play an important role in the exchange and transport of trace metals (1–3). In the case of serum Cu(II), it is the albumin- and the amino acid-bound fraction of Cu(II) which is in rapid equilibrium with Cu(II) in tissues (4–6). The ternary complex such as L-histidine–Cu(II)–albumin is considered to be essential in the exchange of Cu(II) between the macromolecule albumin and the low molecular weight amino acid L-histidine which, in turn, can readily be transported across the biological membrane (3). The tripeptide, diglycyl-L-histidine, which was designed to mimic the specific Cu(II)-transport site of human albumin has been shown to provide the same Cu(II)-binding geometry and specificity as that of albumin (7–10). The ligands involved in the binding are exactly identical to that found in albumin (11, 12) as being α-amino nitrogen, two intervening peptide nitrogens, and the imidazole nitrogen of the histidine in the third position. The four nitrogen atoms are arranged in a nearly square planar configuration around the Cu(II) ion. However, the Cu(II)-binding affinity of this peptide was found to be lower than that for albumin (10). In order to understand the nature of this functional deviation, that is, what effect the secondary and tertiary structures of the protein has on the complex, kinetic studies in regard to the Cu(II)-exchange of this tripeptide with L-histidine, as compared to albumin, were carried out. No such studies have previously been undertaken with either albumin or any histidine-containing peptides. The significance

Can. J. Chem. Downloaded from www.nrcresearchpress.com by 210.87.254.105 on 09/05/12
For personal use only.

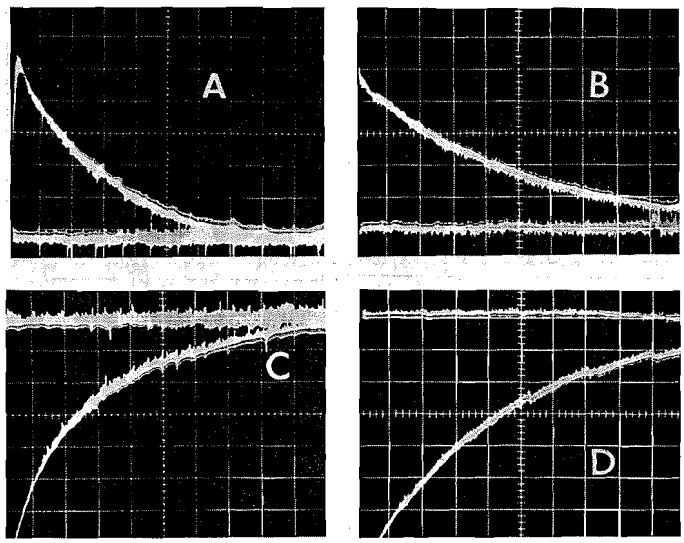

FIG. 1. Oscilloscope traces showing the reactions of Cu(II)-L-histidine$_2$ with albumin or peptide at 20° and p*H* 7.53, 0.1 *M* *N*-ethylmorpholine–HCl buffer. The traces indicate the changes of absorbance at 640 and 525 nm with time. The initial concentrations prior to mixing: Cu(II)-L-histidine$_2$, 2.90×10^{-3} *M*; albumin, 2.60×10^{-4} *M*, (*A*) and (*C*), 1 s per large division; and peptide, 2.54×10^{-4} *M*, (*B*) and (*D*), 2 s per large division.

of the observations as regard to molecular design (7–10) as well as the probable mechanism for the exchange reaction is discussed.

Experimental Section

Materials

Crystalline albumin was purchased from Hoechst Pharmaceutical Company, and further purified to obtain the Cu(II)-free monomeric form (10). Diglycyl-L-histidine was synthesized in our laboratory according to the procedure described elsewhere (10). The purity was checked by thin-layer chromatography and by electrophoresis at different p*H* values. The concentration of the peptide was established by titration and by quantitative analysis with Pauli's reagent. L-Histidine free base ($[\alpha]_D^{20}$ +39.9 ± 0.5°) was obtained from Nutritional Biochemicals. The purity was tested by chromatography. All other reagents were of analytical grade and the water was deionized.

Preparation of Solutions for Exchange Reactions

The $CuCl_2$ stock solution was prepared in 10^{-3} *M* HCl. The Cu(II)-L-histidine$_2$ solution was prepared just before the kinetic runs by mixing a microliter quantity of $CuCl_2$ with L-histidine solution in 0.1 *M* *N*-ethylmorpholine–HCl buffer at p*H* 7.53 and ionic strength 0.16 in a 1:2 molar ratio. The Cu(II)-albumin and Cu(II)-diglycyl-L-histidine solutions were prepared in the same manner except for the equimolar ratio.

Kinetic Experiments

The Cu(II)-exchange reactions were studied under pseudo-first-order conditions in the same buffer. The faster reaction, observed by mixing Cu(II)-L-histidine$_2$ and albumin or diglycyl-L-histidine solutions, was carried out on a Durrum–Gibson stopped-flow spectrophotometer at 20°. The slower reaction, observed by mixing Cu(II)-albumin or Cu(II)-diglycyl-L-histidine with L-histidine, was carried out on a Cary model 15 recording spectrophotometer at 25°. The changes of absorption were followed at both 640 nm, λ_{max} for Cu(II)-L-histidine$_2$ (13) and 525 nm, λ_{max} for Cu(II)-albumin (14) or Cu(II)-diglycyl-L-histidine (10) complexes. The pseudo-first-order rates were calculated accordingly.

Results and Discussion

Comparison of the Rates of Copper(II)-exchange from L-Histidine to Albumin and the Synthetic Site

The faster reaction, observed by mixing Cu(II)-L-histidine$_2$ with albumin or diglycyl-L-histidine solutions, was followed on a stopped-flow spectrophotometer with excess of Cu(II)-L-histidine$_2$. Typical oscilloscope traces, displayed in Fig. 1, show the changes of absorption at wavelengths 640 and 525 nm as the reaction proceeds. The slower reaction was observed from mixing Cu(II)-albumin or Cu(II)-diglycyl-L-histidine with excess of L-histidine solution and followed at both wavelengths. The initial first-order rates obtained at 640 nm corresponding to the change of Cu(II)-L-histidine$_2$ were found to be identical to that obtained at 525 nm for the change of Cu(II)-albumin or Cu(II)-diglycyl-L-histidine complexes for the reactions in both directions. The results of the observed Cu(II)-exchange rates of albumin and diglycyl-L-histi-

Can. J. Chem. Downloaded from www.nrcresearchpress.com by 210.87.254.105 on 09/05/12
For personal use only.

dine with L-histidine are compared in Tables 1 and 2. Due to the relative low molar absorption of the Cu(II)-complexes, it was difficult to obtain reliable rates at the lower concentration regions of either Cu(II)-L-histidine$_2$ or L-histidine. However, in the reactions involving either albumin or the peptide, the rates increased as the Cu(II)-L-histidine$_2$ concentration was increased and began to approach maximum when it was about 30-fold excess. The saturation phenomenon was also observed in the exchange reaction between Cu(II)-albumin and excess L-histidine. In the reaction involving Cu(II)-diglycyl-L-histidine and L-histidine, the rates kept increasing as the concentration of L-histidine increased up to the solubility limit. These observations, together with the results obtained from potentiometric titration and spectral analyses (15), could be accounted for by assuming the pathways described in the following scheme:

$$\begin{array}{ccc} \text{Cu(II)-L-histidine}_2 + \text{albumin} & \underset{k_{-1}}{\overset{k_1}{\rightleftarrows}} & \text{L-histidine-Cu(II)-albumin} + \text{L-histidine} \\ & & \mathbf{1} \\ & & k_{ra} \uparrow\downarrow k_{-ra} \\ \text{Cu(II)-albumin} + \text{L-histidine} & \underset{k_2}{\overset{k_{-2}}{\rightleftarrows}} & \text{L-histidine-Cu(II)-albumin} \\ & & \mathbf{2} \end{array}$$

When mixing the solutions of Cu(II)-L-histidine$_2$ with albumin, there is the rapid formation of the intermediate **1**, followed by a rate-determining conversion to another intermediate **2** (presumably both **1** and **2** are identical to the thermodynamically stable ternary complexes L-histidine-Cu(II)-albumin (15)) through structural rearrangement which is then dissociated to the products, and *vice versa*. Due to the very similar spectral properties of Cu(II)-L-histidine$_2$ and **1**, Cu(II)-albumin and **2**, and also the Cu(II)-complexes of the peptide (3, 10, 14, 15), it is rather difficult to distinguish them in the reactions. Nonetheless, the experimentally determined initial rates are

$$[1]\quad v_f = -\frac{d[\text{albumin}]}{dt} = k_1[\text{Cu(II)-L-histidine}_2][\text{albumin}] - k_{-1}[\mathbf{1}][\text{L-histidine}] = k_{ra}[\mathbf{1}]$$

and

$$[2]\quad v_r = -\frac{d[\text{Cu(II)-albumin}]}{dt} = k_{-2}[\text{Cu(II)-albumin}][\text{L-histidine}] - k_2[\mathbf{2}] = k_{-ra}[\mathbf{2}]$$

By assuming steady-state concentrations of intermediate **1** for the forward direction and also of intermediate **2** for the reverse direction, the following equations may be derived.

$$[3]\quad v_f = k_{f,obs}[\text{albumin}]_0 = \frac{k_{ra}[\text{Cu(II)-L-histidine}_2][\text{albumin}]_0}{K_{Mf} + [\text{Cu(II)-L-histidine}_2]}$$

and

$$[4]\quad v_r = k_{r,obs}[\text{Cu(II)-albumin}]_0 = \frac{k_{-ra}[\text{L-histidine}][\text{Cu(II)-albumin}]_0}{K_{Mr} + [\text{L-histidine}]}$$

where

$$[5]\quad K_{Mf} = \frac{k_{-1}[\text{L-histidine}] + k_{ra}}{k_1}$$

and

$$[6]\quad K_{Mr} = \frac{k_2 + k_{-ra}}{k_{-2}}$$

TABLE 1. Comparison of the initial first-order rates for the reactions between excess Cu(II)-L-histidine$_2$ and albumin or peptide. The concentrations of albumin and peptide were constant throughout the studies. Conditions were the same as described in Fig. 1

[Cu(II)-L-histidine$_2$]$_0$ (10^3 M)	k_{obs} (s^{-1})*	
	Albumin	Peptide
1.45	0.35±0.01	0.12±0.02
2.17	0.43±0.02	0.16±0.01
2.89	0.48±0.01	0.19±0.01
4.03	0.51±0.01	0.25±0.02
5.79	0.52±0.02	0.26±0.01

*The numbers given are the average from at least five runs.

Can. J. Chem. Downloaded from www.nrcresearchpress.com by 210.87.254.105 on 09/05/12
For personal use only.

Can. J. Chem. Downloaded from www.nrcresearchpress.com by 210.87.254.105 on 09/05/12
For personal use only.

TABLE 2. Comparison of the initial first-order rates for the reactions of Cu(II)-albumin or Cu(II)-peptide with excess L-histidine*

$[L\text{-Histidine}]_o$ (10^3 M)	k_{obs} (10^2 s^{-1})†	
	Albumin	Peptide
3.28	2.45±0.01	0.34±0.02
6.45	2.89±0.04	0.64±0.02
9.53	3.34±0.02	—
12.50	3.40±0.01	1.11±0.03
28.55	3.76±0.02	2.29±0.01
38.70	—	2.67±0.01
48.40	—	3.36±0.03
64.50	—	3.99±0.04

*Conditions: pH 7.53 in 0.1 M N-ethylmorpholine–HCl buffer and 25°. Both the concentrations of Cu(II)-albumin and Cu(II)-peptide were 2.90×10^{-4} M.
†The numbers given are the average from three runs.

The double-reciprocal plots of k_{obs} *vs.* appropriate concentrations, as shown in Fig. 2*A* and *B*, yield straight lines. Obviously, during the initial part of the reaction, the term k_{-1}[L-histidine] is much smaller than k_{ra} as to be negligible, and K_{Mf} is thus reduced to k_{ra}/k_1 to become constant in eq. 3. Both kinetic parameters k_{ra}, k_{-ra} and K_{Mf}, K_{Mr} could be calculated from the slopes and intercepts of the reciprocal plots. The values of k_{ra} were obtained as 0.67 and 0.42 s^{-1}, and k_{-ra} were 0.04 and 0.07 s^{-1} for albumin and peptide respectively. The respective values of K_{Mf} were 1.38×10^{-3} and 3.47×10^{-3} M, and K_{Mr} were 2.11×10^{-3} and 6.74×10^{-3} M. The values of k_1 could also be obtained as 4.85×10^2 M^{-1} s^{-1} and 1.21×10^2 M^{-1} s^{-1} for albumin and peptide respectively. The higher values of k_{ra} than k_{-ra} are consistent with the equilibrium result that in the ternary system having equal molar concentration of Cu(II)-L-histidine$_2$ and albumin, the major amount of Cu(II) is in the form of Cu(II)-albumin (3), indicating the relatively higher affinity of Cu(II) for albumin over L-histidine. The ratio of the k_{ra} values for the exchange reactions involving albumin and diglycyl-L-histidine is about 1.7, just the reciprocal of the ratio of the k_{-ra} values. This is in accord with the observation of almost the double Cu(II)-binding strength of albumin over peptide, as a consequence of the kinetic effect (10). In addition, the equilibrium distribution of the quaternary system having Cu(II), L-histidine, albumin, and the peptide has shown the relatively higher binding affinity of the ternary complex L-histidine-Cu(II)-diglycyl-L-histidine than that of the other existing Cu(II)-complexes (10). This is also reflected from the kinetic observation of lacking saturation in the reverse reaction involving Cu(II)-diglycyl-L-histidine.

It is interesting to relate the difference in exchange rates to the different sequence of the peptide and the Cu(II)-binding site of albumin. The amino acid sequence at the native Cu(II)-binding site of human albumin is Asp-Ala-His. Obviously, the COOH-terminal carboxyl group of diglycyl-L-histidine has some influence on the exchange.[1] Also, the β-carboxyl group of the aspartyl residue in albumin could exert an inductive effect causing further change in the exchange rate. Interestingly enough, examination of the Kendrew model indicates that the β-carboxyl group of the aspartic acid residue can easily form an intramolecular hydrogen-bond with the imidazole moiety of the histidine residue. Due to this hydrogen-bond formation, the α-carbon of the NH_2-terminal aspartyl residue is rotated about 70° (ψ angle) and the α-amino nitrogen as a consequence is brought closer toward the plane for Cu(II) coordination.

Mechanism of Copper(II) Exchange

The physiological significance of the ternary complex L-histidine-Cu(II)–albumin in the biological transport of Cu(II) has previously been discussed (3). The present findings indeed demonstrate the rate-controlling role played by the ternary complex in the exchange of Cu(II) between albumin and L-histidine in order to maintain the equilibrium concentrations. A postulated scheme of the exchange pathways is illustrated in Fig. 3. It was derived taking into account both the known interaction of Cu(II) with several oligopeptides (16, 17) and the known structural features of several ternary complexes including those of L-histidine-Cu(II)-diglycyl-L-histidine (15, 18, 19). In the formation of the ternary complex C (involving either albumin or diglycyl-L-histidine) from Cu(II)-L-histidine$_2$ (A), the first step presumably involves the fast

[1]Both diglycyl-L-histamine and the N-methyl amide derivative of diglycyl-L-histidine have the same Cu(II)-exchange rate of 0.56 s^{-1} from L-histidine to the peptides under the same experimental conditions: 20°, pH 7.53 in 0.1 M N-ethylmorpholine–HCl buffer (21).

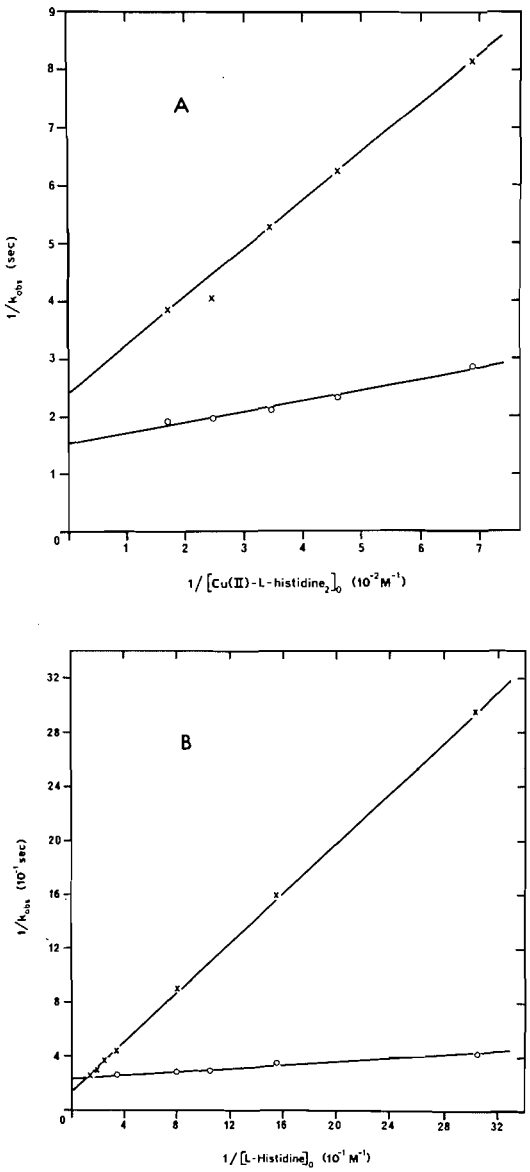

FIG. 2. The reciprocal plots of the initial first-order rates of the Cu(II)-exchange reactions as a function of concentration. The reactions are: (*A*) albumin (○) or peptide (×) with Cu(II)-L-histidine$_2$, (*B*) L-histidine with Cu(II)-albumin (○) or Cu(II)-peptide (×). Conditions are as described in Fig. 1 and Table 2.

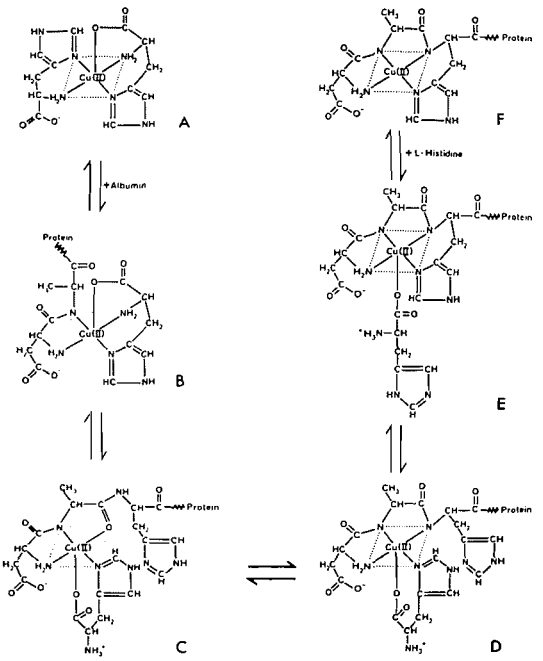

FIG. 3. The proposed reaction paths for the Cu(II)-exchange from L-histidine to albumin and peptide.

dissociation of one histidine molecule to form Cu(II)-L-histidine$^+$ (13), and allow the N-terminal amino nitrogen and the first peptide nitrogen of the protein or the peptide to enter as an anchoring point to form the intermediate B (16, 17). This is followed with the displacement of the amino nitrogen of the remaining histidine by the second carbonyl oxygen of the protein or the peptide to form the ternary complex C (18, 19), which is then converted to another ternary complex D through structural rearrangement. Since both ternary complexes C and D are thermodynamically favorable, this latter process would be expected to be rather sluggish. Once the ternary complex D is formed, three coordination sites of Cu(II) are occupied by the groups from the peptide or albumin, the displacement of the imidazole nitrogen of histidine by the imidazole nitrogen of the peptide or albumin from the histidine in the third position (E and F) would seem to be much more facilitated due to both the chelation and steric effects involved. In the reverse reaction, the same rationale is also implied. There is the facile attachment of the carboxyl group of L-histidine onto the Cu(II)-complex to start with, and followed exactly by the above-mentioned processes in the opposite direction to form the product. Because of the complexity caused by the different Cu(II)-binding species of the binary and ternary complexes as the p*H* varies (15, 20), the present data do not permit any rationale as far as the proton transfer is concerned.

Can. J. Chem. Downloaded from www.nrcresearchpress.com by 210.87.254.105 on 09/05/12
For personal use only.

The designed peptide diglycyl-L-histidine has been shown to possess the same Cu(II)-binding geometry and specificity and compete for Cu(II) with only about half the strength as that of albumin as a kinetic consequence. It is unlikely the conformation of the native protein exerts any effect on the Cu(II)-binding and exchange, although it remains to be solved. However, the present findings do indicate the possible significance of certain groups in the binding and exchange reactions which may shed light on further investigations to bring about the required specificity and affinity of the synthetic site analog. This approach of designing a small molecule to mimic certain functions of a macromolecule seems promising and may have important biomedical applications.

We are grateful to Dr. S. I. Kandel for use of the stopped-flow spectrophotometer. We also wish to thank Dr. J. T. Wong for helpful discussions on the exchange reactions. This work was supported by a grant from the Medical Research Council of Canada.

1. B. SARKAR and Y. WIGFIELD. Can. J. Biochem. **46**, 601 (1968).
2. B. SARKAR. Can. J. Biochem. **48**, 1339 (1970).
3. S. LAU and B. SARKAR. J. Biol. Chem. **246**, 5938 (1971).
4. B. SARKAR and T. P. A. KRUCK. *In* Biochemistry of copper. *Edited by* J. Peisach, P. Aisen, and W. E. Blumberg. Academic Press, New York. 1966. p. 183.
5. P. Z. NEUMAN and A. SASS-KORTSAK. J. Clin. Invest. **46**, 646 (1967).
6. A. G. BEARN and H. G. KUNKEL. Proc. Soc. Exp. Biol. Med. **85**, 44 (1954).
7. B. SARKAR. Can. Fed. Biol. Soc. **15**, 659 (1972).
8. B. SARKAR. Proceedings of the 9th international congress of biochemistry. Stockholm, Sweden. 1973. p. 122.
9. B. SARKAR, T. P. A. KRUCK, and S. LAU. Proceedings of the XVth international conference on coordination chemistry. Moscow, U.S.S.R. 1973. p. 472.
10. S. LAU, T. P. A. KRUCK, and B. SARKAR. J. Biol. Chem. **249**, 5878 (1974).
11. T. PETERS, JR. and F. A. BLUMENSTOCK. J. Biol. Chem. **242**, 1574 (1967).
12. W. T. SHEARER, R. A. BRADSHAW, F. R. N. GURD, and T. PETERS, JR. J. Biol. Chem. **242**, 5451 (1967).
13. T. P. A. KRUCK and B. SARKAR. Can. J. Chem. **51**, 3563 (1973).
14. D. W. APPLETON and B. SARKAR. J. Biol. Chem. **246**, 5040 (1971).
15. T. P. A. KRUCK and B. SARKAR. To be published.
16. G. R. DUKES and D. W. MARGERUM. Inorg. Chem. **11**, 2952 (1972).
17. G. R. DUKES and D. W. MARGERUM. J. Am. Chem. Soc. **94**, 8414 (1972).
18. R.-P. MARTIN, L. MOSONI, and B. SARKAR. J. Biol. Chem. **246**, 5944 (1971).
19. H. C. FREEMAN, J. M. GUSS, M. J. HEALY, R.-P. MARTIN, C. E. NOCCHOLDS, and B. SARKAR. Chem. Commun. 225 (1969).
20. T. P. A. KRUCK and B. SARKAR. Can. J. Chem. **51**, 3549 (1973).
21. S. LAU and B. SARKAR. Unpublished results.

Can. J. Chem. Downloaded from www.nrcresearchpress.com by 210.87.254.105 on 09/05/12
For personal use only.

Thermodynamic Properties of Aqueous Organic Solutes in Relation to their Structure. Part II. Apparent Molal Volumes and Heat Capacities of *c*-Alkylamine Hydrobromides in Water[1]

CARMEL JOLICOEUR, JEANINE BOILEAU, SERGE BAZINET, AND PATRICK PICKER

Département de Chimie, Université de Sherbrooke, Sherbrooke, Québec J1K 2R1

Received September 9, 1974

CARMEL JOLICOEUR, JEANINE BOILEAU, SERGE BAZINET, and PATRICK PICKER. Can. J. Chem. **53**, 716 (1975).

The density and specific heat of aqueous solutions of various *c*-alkylamine hydrobromides, and of *n*-dodecylammonium bromide, have been measured at 25 °C. The limiting apparent molal volumes ϕ_v^0 and heat capacities ϕ_c^0, derived from these data, are compared to the corresponding quantities for *n*-alkylammonium and immonium salts. The methylene group contribution to ϕ_v^0 and ϕ_c^0 of the cyclic compounds is generally lower than that of the linear homologs; this group contribution is also found to depend markedly on ring size, in contrast to monotonous variations found in the series of the linear compounds. The difference is suggested to originate in solvation effects in which geometrical factors (solvent structure and solute geometry) play a significant role.

CARMEL JOLICOEUR, JEANINE BOILEAU, SERGE BAZINET et PATRICK PICKER. Can. J. Chem. **53**, 716 (1975).

Nous avons mesuré la densité et la chaleur spécifique de solutions aqueuses des bromhydrates de diverses *c*-alkylamines et de la *n*-dodecylamine à 25 °C. Les volumes, ϕ_v^0, et les capacités calorifiques, ϕ_c^0, molaires apparents obtenus de ces mesures sont comparés avec les valeurs correspondantes des bromhydrates d'imines et de *n*-alkylamines. Dans ces séries homologues, la contribution d'un groupe —CH_2— à ϕ_v^0 et à ϕ_c^0 est systématiquement plus élevée pour les dérivés linéaires que pour les dérivés cycliques. Pour ces derniers, les valeurs de $\Delta\phi_v^0(CH_2)$ et $\Delta\phi_c^0(CH_2)$ varient selon le nombre d'atomes compris dans le cycle, alors qu'elles atteignent une valeur constante dans la série des homologues linéaires. Nous interprétons ces effets en termes d'une solvatation spécifique, où les facteurs géométriques (structure du solvant et structure du soluté) jouent un rôle significatif.

Introduction

In the first part of this work (1), we reported measurements of the deuterium solvent isotope effect on the chemical potential of various hydrophobic ketones in water. The solutes differed mainly in the size and shape of their hydrocarbon group, and the $H_2O \rightarrow D_2O$ transfer functions were found to be rather sensitive to such differences. The main correlation which emerged from the data showed that linear hydrocarbon groups are more easily accommodated in D_2O than in H_2O, while the opposite seemed generally true for highly branched hydrocarbons. While the interpretation of solvent isotope effects rests on assumption which may be questionable, either from the remaining uncertainties as to the actual structural differences between water and heavy water (2), or from the results of simple calculations which consider both solvents as hard-sphere fluids (3), the previous data strongly suggested that liquid water exhibits preferences in the geometry or shape of the hydrocarbon solutes that it will dissolve.

In the hope of confirming the proposed concept of a relationship between the geometry of a hydrophobic solute and its thermodynamic properties in water, we have carried out other types of measurements which should give a different insight into the question. In this report, we present apparent molal volume and heat capacity data for a number of homologous *c*-alkylamine hydrobromides in water. Comparison with similar data available for the corresponding linear salts (4, 5) again suggests some specificity in the interaction of a hydrocarbon group with liquid water.

Experimental

The salts used in this study were prepared by reacting the amines with concentrated aqueous HBr in anhydrous ethanol; the products were recuperated upon evaporation

[1]Work presented in part at the Third International Conference on Chemical Thermodynamics, Baden, Austria, 1973.

Can. J. Chem. Downloaded from www.nrcresearchpress.com by 210.87.254.6 on 09/05/12
For personal use only.

TABLE 1. Apparent molal volume and heat capacity of several alkylamine hydrobromides in water at 25 °C

Solute	ϕ_v^0 ($cm^3\ mol^{-1}$)	B_v	ϕ_c^0 ($J\ K^{-1}\ mol^{-1}$)	B_c
c-$C_3H_5NH_3Br$	84.72	−0.98	135.0	−18.6
c-$C_5H_9NH_3Br$	113.30	−1.65	263.4	−23.1
c-$C_6H_{11}NH_3Br$	128.21	−1.90	335.7	−33.6
c-$C_7H_{13}NH_3Br$	141.79	−2.39	392.2	−40.8
c-$C_8H_{15}NH_3Br$	155.08	−2.75	455.7	−33.8
c-$C_{12}H_{23}NH_3Br$	214.4	*	702.	*
n-$C_{12}H_{25}NH_3Br$	240.8	*	1003	*
	243.4†		(976)†	

*Because of the limited concentration range accessible, the slopes obtained are not meaningful.
†Values calculated from data on n-OctNH_3Br assuming additivity of methylene groups contribution.

of the solvent and recrystallized in anhydrous ethanol – ether mixtures. The amines were purchased from Aldrich and distilled before use; their purity was found to be at least 99% from gas – liquid chromatographic runs carried out with a Hewlett–Packard (Model HP-5750) chromatograph using a Carbowax-20M on Chromosorb-W column. Conductometric analysis of the bromide content yielded results agreeing within less than 1% of the theoretical content. In the specific cases of the salts of c-pentyl, c-hexyl, and c-heptylamines, for which the analysis were carefully repeated, the deviations on the bromide content were respectively as follows: −0.2%, −0.5%, −0.3%. c-Heptylamine hydrobromide was also prepared from Fluka purum c-heptylamine; its bromide analysis showed −0.1% from the expected value, and the thermodynamic results obtained with this material were, within experimental error, identical to those obtained with previous preparations.

All solutions were prepared by weight using de-ionized water. The density measurements were performed on a flow digital densimeter reported previously (6) capable of 2 p.p.m. precision. The specific heats of the solutions were obtained with a differential flow microcalorimeter described recently by Picker *et al.* (7); the precision attainable on the specific heat increments was 0.3%, with a differential resolution limit of 2×10^{-5}. All measurements were carried out at a temperature of 25.00 ± 0.02 °C; the latter is the mean temperature in the case of specific heat measurement during which the temperature rise of the flowing liquids was 1.80 °C. The required temperature stability (±0.0005 °C) of the instruments was achieved with a closed-loop thermostat similar to the one described by Picker *et al.* (8).

Results

The apparent molal volumes ϕ_v were calculated from the solution densities d using the equation

$$[1] \qquad \phi_v = \frac{M}{d} + \frac{1000\,(d_0 - d)}{mdd_0}$$

where d_0 is the density of water at 25 °C (0.997047 g cm^{-3} (9)), M, the molecular weight of the solute, and m, its molal concentration. The molal concentrations were converted into molarities as required. The apparent molal heat capacities ϕ_c were computed from the measured volumetric specific heat σ ($J\ K^{-1}\ cm^{-3}$) of the solutions and the equation

$$[2] \qquad \phi_c = Mc_p + \frac{1000\,(c_p - c_p^0)}{m}$$

with

$$[3] \qquad \frac{c_p}{c_p^0} = \left(\frac{\sigma - \sigma_0}{\sigma_0}\right)\frac{d_0}{d}$$

In these equations, c_p is the weight specific heat ($J\ K^{-1}\ g^{-1}$) and the zero subscripts again refer to pure water; c_p^0 was taken as 4.1793 $J\ K^{-1}\ g^{-1}$ (10).

The derived quantities ϕ_v and ϕ_c were fitted by least-square methods to the following equations

$$[4] \qquad \phi_v = \phi_v^0 + 1.86c^{1/2} + B_v c$$

$$[5] \qquad \phi_c = \phi_c^0 + 28.99c^{1/2} + B_c c$$

The coefficients in $c^{1/2}$ represent the term given by the Debye–Hückel limiting law (11). The other coefficients ϕ^0 and B, for the systems studied, are collected in Table 1. The complete experimental data sets can be obtained elsewhere,[2] but we illustrate in Figs. 1 and 2 the concentration ranges investigated and the scattering found in the ϕ_v and ϕ_c values. It is obvious from these data that the results for the compounds containing dodecyl groups bear

[2]Values of d, c_p, ϕ_c, ϕ_v for various compounds have been lodged with the Depository of Unpublished Data, National Science Library, National Research Council of Canada, Ottawa, K1A 0S2. Photocopies may be obtained, upon request, at a nominal charge.

Can. J. Chem. Downloaded from www.nrcresearchpress.com by 210.87.254.6 on 09/05/12
For personal use only.

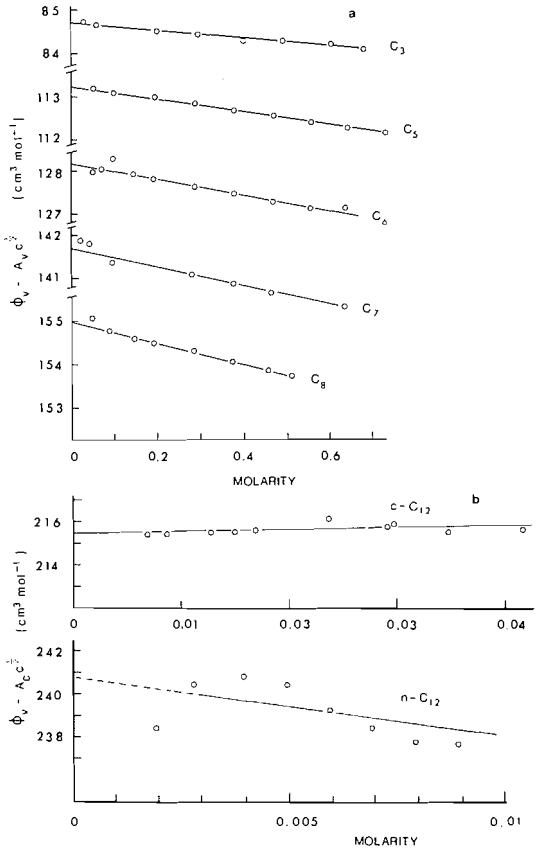

FIG. 1. Apparent molal volumes, corrected for the Debye–Hückel limiting law, of alkylammonium hydrobromides in water at 25 °C. (*a*) Data for *c*-RNH_3Br, R = C_3H_5, $C_5H_9 \rightarrow C_8H_{15}$; (*b*) data for *c*- and *n*-dodecylammonium bromides.

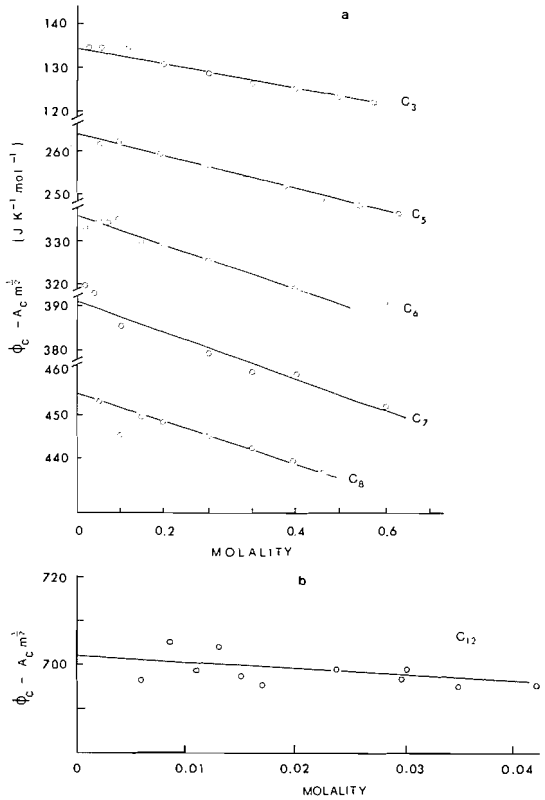

FIG. 2. Apparent molal heat capacities, corrected for the Debye–Hückel limiting law, of alkylammonium hydrobromides in water at 25 °C. (The results are shown here as a function of molality, but are given on the molarity scale in Table 1). (*a*) Data for *c*-RNH_3Br, R = C_3H_5, $C_5H_9 \rightarrow C_8H_{15}$, (*b*) data for *c*-dodecylammonium bromide.

large uncertainties. This is particularly so for *n*-dodecylamine hydrobromide, for which micelle formation limited the measurements to concentrations lower than 0.01 *m*. For the other compounds, the uncertainty on ϕ_v^0 and ϕ_c^0 is respectively ± 0.1 cm^3 mol^{-1} and ± 1.5 J K^{-1} mol^{-1}.

Discussion

(a) Limiting Apparent Molal Volumes and Heat Capacities

From the data in Table 1, it is readily seen that the limiting apparent molal volume and heat capacity of the homologous *c*-alkylamine salts increase in an approximately linear fashion with the number of carbon atoms in the alkyl substituents. The average increment in ϕ_v^0 per methylene group, $\Delta\phi_v^0(CH_2)$, is roughly 14 cm^3 mol^{-1}, compared to 15.9 cm^3 mol^{-1} for the corresponding contribution found within the homologous series bearing *n*-alkyl groups (4). This average difference has also been observed with various organic solutes by Cabani and coworkers (12–14), and it now appears quite general that $\Delta\phi_v^0(CH_2)$ is $\sim 10\%$ smaller for cyclic compounds than for linear compounds of analogous composition. This has been interpreted as resulting from a better packing of the cyclic alkyl group into the water hydrogen-bonded networks (12).

Effects similar to those mentioned above are also found in the ϕ_c^0 data for the linear and cyclic alkylamine salts. The methylene group contribution to ϕ_c^0 in the two homologous series is again quite different; the average $\Delta\phi_c^0(CH_2)$ is 88 ± 3 J K^{-1} mol^{-1} with the *n*-alkylamine

Can. J. Chem. Downloaded from www.nrcresearchpress.com by 210.87.254.6 on 09/05/12
For personal use only.

Can. J. Chem. Downloaded from www.nrcresearchpress.com by 210.87.254.6 on 09/05/12
For personal use only.

hydrobromides (5), whereas the corresponding quantity in the cyclic homologs is in the range of 60–70 J K^{-1} mol^{-1}.

The lower $\Delta\phi_c^0(CH_2)$ for cyclic molecules reported recently by Cabani *et al.* (14) from data on amines, imines and their hydrochloride salts, has been attributed mainly to the larger hydrophobic surface area of the linear alkyl group, rather than to differences in the intrinsic heat capacity of the solute molecules.[3]

The available ϕ_v^0 and ϕ_c^0 data on the hydrochlorides of imines (12, 13, 15) can be converted to the same scale as the present data for the hydrobromides using the following differences

$$\phi_v^0(Br^-) - \phi_v^0(Cl^-) = 6.9 \text{ cm}^3 \text{ mol}^{-1} \quad (16)$$

and

$$\phi_c^0(Br^-) - \phi_c^0(Cl^-) = -4 \text{ J K}^{-1} \text{ mol}^{-1} \quad (17)$$

Comparison of the results then shows that the ϕ_v^0 of *c*-alkylammonium and immonium ions, having the same number of carbon atoms, are very nearly identical. Since it is generally expected (13, 18, 19) that the hydration of a charged nitrogen center depends upon the degree of alkyl substitution, and also in view of the specific effects discussed below, this similarity must be fortuitous. Within the limited values available for imine hydrochlorides, the ϕ_c^0 of immonium and *c*-alkylammonium ions of same carbon content differ by $\sim 10\%$.

(b) Variations of the Methylene Group Contributions to ϕ_v^0 and ϕ_c^0

To examine the variations in the methylene group contributions to ϕ_v^0 and ϕ_c^0, we plot in Figs. 3 and 4, the $\Delta\phi^0(CH_2)$ values calculated as

$$\Delta\phi^0(CH_2) = \frac{\phi^0(n_i) - \phi^0(n_j)}{n_i - n_j}$$

where n_i and n_j are the number of carbon atoms in the homologous pairs considered. In Fig. 3, we illustrate the $\Delta\phi_v^0(CH_2)$ obtained from the *n*-alkyl and *c*-alkylammonium and immonium salts as function of $(n_i + n_j)/2$. Within the *n*-alkyl homologs, the methylene group contribution levels-off for alkyl groups larger than C_4H_9 (4); in this series, it might be expected that $\Delta\phi_v^0(CH_2)$ will remain constant for all higher homologs, though coiling of long alkyl chains could provide deviations to this behavior. In the case of cyclic compounds, the $\Delta\phi_v^0(CH_2)$ shows marked variations, much larger than the experimental uncertainties. It is noteworthy that if we use the number of ring atoms rather than the number of carbon atoms, the two dotted curves shown in Fig. 3 would exhibit their extrema at the same position.[4] It is thus apparent that the ring size is a key factor in fitting these types of ions into the solvent water,

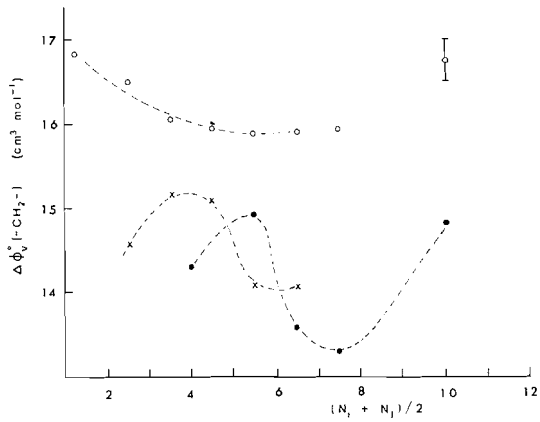

FIG. 3. Methylene group contribution to limiting apparent molal volumes from data on: ○, *n*-alkylamine hydrobromides; ●, *c*-alkylamine hydrobromides; ×, imine hydrochlorides.

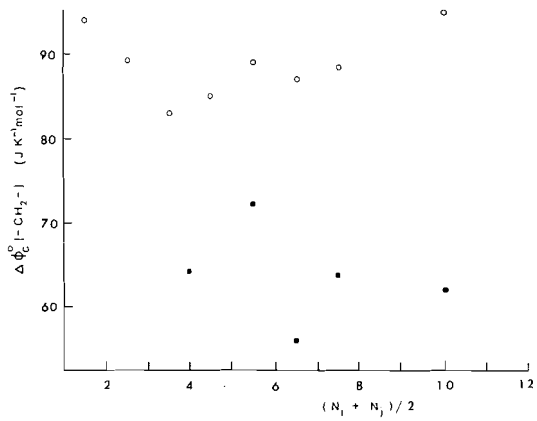

FIG. 4. Methylene group contribution to limiting apparent molal heat capacities from data on: ○, *n*-alkylamine hydrobromides; ●, *c*-alkylamine hydrobromides.

[3]We use here the terms imine and immonium to designate the 1-azacycloalkanes and their corresponding ammonium ions.

[4]A similar plot drawn for $\Delta\phi_v^0(CH_2)$ of imines (12) also exhibits a shallow minimum for the 6 and 7 membered-ring.

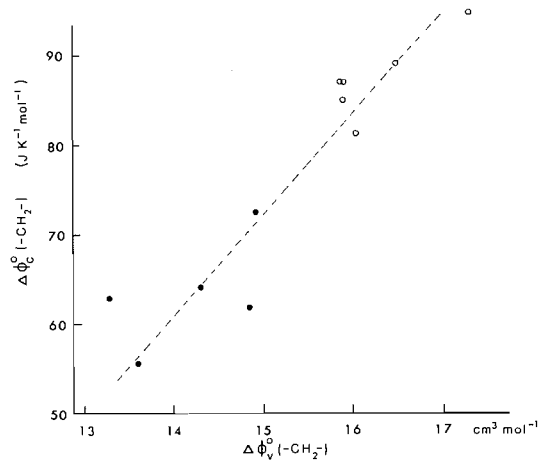

FIG. 5. Correlation plot of methylene group contributions to ϕ_v^0 and ϕ_c^0.

and the data indicate an optimum fit with 7- or 8-membered rings. Measurements on each cyclic homolog between C_8 and C_{12} may yield further details in the variation of $\Delta\phi_v^0(CH_2)$, though it seems probable that for very large rings, $\Delta\phi_v^0(CH_2)$ will be similar to that found with the linear homologs; the effect resulting from the addition of a $—CH_2—$ group to an infinitely long chain should be independent of whether or not the ends of the chain are tied.

The $\Delta\phi_c^0(CH_2)$ values plotted in Fig. 4 again exhibit a rather monotonous behavior in the *n*-alkylammonium homologs, while large variations are observed in the series of the *c*-alkyl compounds. In the latter, the extrema appear for the same ring sizes which were found to give maximum variations in $\Delta\phi_v^0(CH_2)$. In Fig. 5, we correlate the methylene group contributions to ϕ_v^0 and ϕ_c^0, as obtained from the homologous series of *n*- and *c*-alkylammonium salts; indeed we find that $\Delta\phi_c^0(CH_2)$ increases in a roughly linear fashion with $\Delta\phi_v^0(CH_2)$.

It may be pointed out immediately that, from the current views on solvent structural effects induced by hydrocarbon groups,[5] the correlation shown in Fig. 5 would have been expected with a negative slope, *i.e.*, the hydrocarbon group which exhibits the best packing in the solvent structure (minimum volume) would also exhibit the maximum heat capacity (after taking into account the intrinsic contributions of the solutes). In other words, for the data shown in Figs. 3 and 4, we would have anticipated that, corresponding to the minimum $\Delta\phi_v^0(CH_2)$ value, we would observe a maximum in $\Delta\phi_c^0(CH_2)$. Thus, explaining the variations in $\Delta\phi_v^0(CH_2)$ and $\Delta\phi_c^0(CH_2)$, as well as the relationship between these quantities, will require more details than a straightforward extension of the current interpretation of volume and heat capacity effects in the solvation of hydrocarbons. Amongst the various effects which could lead to specificity in the properties of the cyclic homologs studied here, we should first envisage those resulting from the intrinsic properties of the hydrocarbon groups.

While it is difficult to predict quantitatively how the addition of a $—CH_2—$ group will increase the intrinsic volume of a cyclic hydrocarbon, scale molecular models suggest that the $—CH_2—$ contribution to the effective volume should increase with ring size, for hydrocarbons between C_5 and C_{12}. For the latter molecules, the volume of the cavity in the ring center increases with ring size, while remaining excluded to the solvent molecules. Such an effect obviously could not account for the ring-size dependence shown in Fig. 3.

For the heat capacity, judging from earlier data on liquid *n*- and *c*-hydrocarbons, the intrinsic contribution for each methylene group, $\Delta C_{p,1}(CH_2)$, is lower for the cyclic homologs than for the linear ones by 10–20 J K^{-1} mol^{-1} (22). As pointed out by Cabani *et al.* (15) this only accounts for part of the difference in $\Delta\phi_c^0(CH_2)$ observed between the linear and cyclic homologs. Likewise, since $\Delta C_{p,1}(CH_2)$ for the cyclic hydrocarbons is ~30 J K^{-1} mol^{-1}, it seems improbable that variation in this quantity could account for the observed changes in the $\Delta\phi_c^0(CH_2)$ with ring size (see Addendum at the end of the article).

If it can be assumed that the contribution to ϕ_v^0 and ϕ_c^0 of the $—\overset{+}{N}H_3$ group, as well as solvation effects on this group, remain constant in the series of *c*-alkylammonium, we would have reasonable grounds for assigning the ring-size specificity in the $\Delta\phi_v^0(CH_2)$ and

[5]The dissolution of a hydrocarbon group in water is believed to occur with a stabilization of hydrogen-bonded structures in the solvent (20); the increase in volume expected from this effect (by analogy to freezing) would be more than compensated by the volume decrease when the hydrocarbon can be fitted in the structural cavities of water (4, 21). It is this water structure stabilization which is thought to be responsible for the large heat capacities of aqueous solutes containing significant hydrocarbon groups (20).

Can. J. Chem. Downloaded from www.nrcresearchpress.com by 210.87.254.6 on 09/05/12
For personal use only.

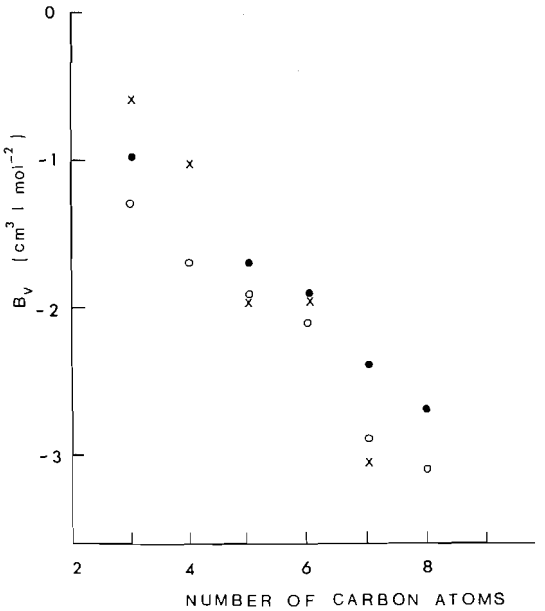

FIG. 6. B_v coefficients (eq. 5) for the various ammonium salts; the symbols are the same as those used in Fig. 3.

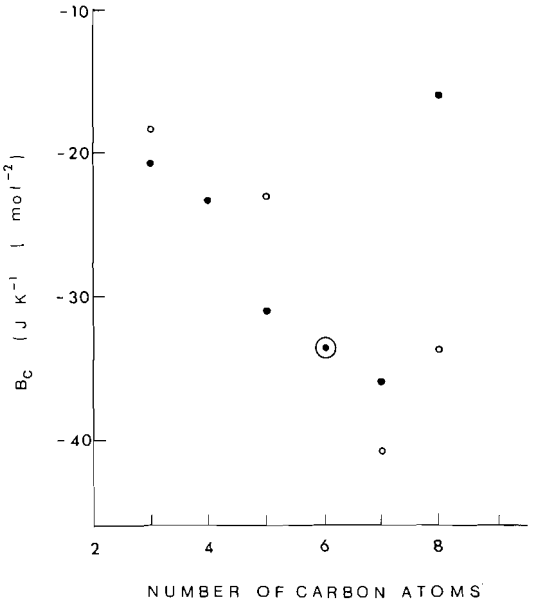

FIG. 7. B_c coefficients (eq. 6) for hydrobromides of *n*- and *c*-alkylamines; the symbols are the same as those in Fig. 4.

$\Delta\phi_c^0(CH_2)$ values to hydrocarbon–water interactions which depend on the structure of the solute. Until similar measurements are carried out in other solvents, however, it can only be suggested that this ring-size dependence is, in fact, a result of solvent structural effects which are responsive to the geometry of the solute.

(c) Excess Functions

We illustrate in Figs. 6 and 7, the deviations of ϕ_v and ϕ_c to the Debye–Hückel limiting law observed for the linear and cyclic ammonium salts. It is striking that the excess functions B_v and B_c, representing the effect of solute–solute interactions other than the limiting electrostatic contribution, appear rather insensitive to the nature of the hydrocarbon substituent on the cation. Except for the B_c coefficients of the *n*- and *c*-octylammonium salts, the other B_v and B_c coefficients are mostly a function of solute volume.[6] Thus any solvation specificity, which might be reflected in ϕ_v^0 and ϕ_c^0 of the homologous compounds, does not seem to play a major role in solute–solute interactions, in the concentration range investigated.

[6]Substantial variations in the magnitude of the B_c coefficients for large organic ions have been found in other systems and discussed elsewhere (23).

Conclusion

The investigation of the partial molal volumes and heat capacities of various homologous series of alkylammonium salts brings out some significant ring-size dependence in the limiting properties of the cyclic compounds. This we tentatively assign to geometrical aspects of the solvation, involving both the structure in the solvent and the structure of the hydrophobic solute. Further evidence will be required to assess the relationship between solute geometry and solvent structural effects, but additional work seems largely warranted if it may help to establish that part of the discriminating behavior observed in biochemical or biological systems, originate in such specific solvation effects.

Addendum

To evaluate the importance of changes in the intrinsic properties (volume and heat capacity) of the hydrocarbon group as function of ring-size, we have measured the density and specific heat of four cyclic hydrocarbons in the pure liquid state. The materials were purchased from Chemical Samples Co. and were quoted of the following purity: *c*-pentane, 99.9%; *c*-hexane, 99.9%; *c*-heptane, 99%; and *c*-octane, 99%. As the reference liquid, we chose *c*-hexane, for

Can. J. Chem. Downloaded from www.nrcresearchpress.com by 210.87.254.6 on 09/05/12
For personal use only.

which molar volume and heat capacity are known as: $V_1^0 = 108.758$ cm^3 mol^{-1} and $C_{p,1}^0 = 156.2_0$ J K^{-1} mol^{-1} (25). The results including the data for *c*-hexane are tabulated below.

Compound	V_1^0 (cm^3 mol^{-1})	$\Delta V_1^0(CH_2)$ (cm^3 mol^{-1})	$C_{p,1}^0$ (J K^{-1} mol^{-1})	$\Delta C_{p,1}^0(CH_2)$ (J K^{-1} mol^{-1})
c-Pentane	97.72		127.28	
		14.04		28.9
c-Hexane	108.76		156.20	
		12.99		24.3
c-Heptane	121.75		180.4_7	
		13.13		33.8
c-Octane	134.88		214.2_4	

These results add a considerable amount of new information on this problem, illustrating that the methylene group contribution to V_1^0 is of the same order as $\Delta\phi_v^0(CH_2)$ observed in water with the *c*-alkylammonium ions; furthermore, it also exhibits a shallow minimum at the seven carbon homolog. Both of these observations were totally unexpected from packing effects, which ought to be rather different in the two situations compared here, *i.e.* pure liquid hydrocarbons and aqueous solutions. The methylene group contribution to $C_{p,1}^0$ is much lower than $\Delta\phi_c^0(CH_2)$ found in aqueous solutions of the cyclic organic ions, and though it also exhibits a minimum near the seven-membered ring, the amplitude of the variations are less than those observed in $\Delta\phi_c^0(CH_2)$.

Clearly, further work will be required to identify, in detail, the origin of the variations in methylene group contributions and the extent to which hydration effects may either enhance such variations or compensate for them.

Financial support of this work by the National Research Council of Canada is gratefully acknowledged.

1. C. JOLICOEUR et G. LACROIX. Can. J. Chem. **51**, 3051 (1973).
2. A. HOLTZER and M F. EMMERSON. J. Phys. Chem. **73**, 26 (1969).
3. P. PHILIP and C. JOLICOEUR. J. Solution Chem. **4**, 3 (1975).
4. J. E. DESNOYERS and M. AREL. Can. J. Chem. **43**, 359 (1967).
5. P. A. LEDUC, J. L. FORTIER, and J. E. DESNOYERS. J. Phys. Chem. **78**, 1217 (1974).
6. P. PICKER, E. TREMBLAY, and C. JOLICOEUR. J. Solution Chem. **3**, 377 (1974).
7. P. PICKER, P. A. LEDUC, P. R. PHILIP, and J. E. DESNOYERS. J. Chem. Thermodyn. **3**, 631 (1971).
8. P. PICKER, C. JOLICOEUR, and J. E. DESNOYERS. J. Chem. Ed. **45**, 614 (1968).
9. G. S. KELL. J. Chem. Eng. Data, **12**, 66 (1967).
10. A. EUCKEN and M. EIGEN. Z. Elektrochem. Dtsch. **55**, 343 (1951).
11. O. REDLICH and D. M. MEYER. Chem. Rev. **64**, 221 (1964); P. R. PHILIP and J. E. DESNOYERS. J. Solution Chem. **4**, 353 (1972).
12. S. CABANI, G. CONTI, and L. LEPORI. J. Phys. Chem. **76**, 1338 (1972).
13. S. CABANI, G. CONTI, L. LEPORI, and G. LEVA. J. Phys. Chem. **76**, 1343 (1972).
14. S. CABANI, G. CONTI, and L. LEPORI. J. Phys. Chem. **78**, 1030 (1974).
15. S. CABANI, G. CONTI, A. MARTINELLI, and E. MATTEOLI. J. Chem. Soc. Faraday Trans. I, **69**, 2112 (1973).
16. J. E. DESNOYERS, M. AREL, G. PERRON, and C. JOLICOEUR. J. Phys. Chem. **73**, 3346 (1969).
17. J. L. FORTIER, P. A. LEDUC, and J. E. DESNOYERS. J. Solution Chem. **3**, 323 (1974).
18. B. E. CONWAY and L. H. LALIBERTÉ. Hydrogen bonded solvent systems. *Edited by* A. K. Covington and P. Jones. Taylor and Francis, London. 1968. p. 139.
19. C. V. KRISHNAN and H. L. FRIEDMAN. J. Phys. Chem. **74**, 3900 (1970).
20. H. S. FRANK and W. Y. WEN. Discuss. Faraday Soc. **24**, 133 (1957); G. NEMETHY and H. A. SCHERAGA. J. Chem. Phys. **36**, 3401 (1962).
21. M. FRIEDMAN and H. A. SCHERAGA. J. Phys. Chem. **69**, 3795 (1965); D. N. GLEW. J. Phys. Chem. **66**, 605 (1962; F. FRANKS and D. J. IVES. Q. Rev. Lond. **20**, 1 (1966).
22. R. SHAW. J. Chem. Eng. Data, **14**, 461 (1969); R. W. GALLANT. Physical properties of hydrocarbons. Gulf Publishing Co., Houston, Texas. 1968. chapt. 15 and 41.
23. C. JOLICOEUR and J. BOILEAU. J. Solution Chem. **3**, 889 (1974).
24. J. L. FORTIER and G. C. BENSON. Private communication.

Can. J. Chem. Downloaded from www.nrcresearchpress.com by 210.87.254.6 on 09/05/12
For personal use only.

Preparation of the Piperazine- and Triethylenediamine–Monoborane Adducts of BH_3, BH_2F, BHF_2, and BF_3

J. M. VANPAASSCHEN AND R. A. GEANANGEL

Department of Chemistry, University of Houston, Houston, Texas 77004

Received August 9, 1974

J. M. VANPAASSCHEN and R. A. GEANANGEL. Can. J. Chem. **53**, 723 (1975).

The new compounds, triethylenediamine–BH_2F, –BHF_2, –BF_3 and piperazine–BH_2F, –BHF_2, –BF_3 have been isolated and characterized from the base displacement reactions involving the diamine and the trimethylamine–fluoroboranes. By this method only the monoborane adducts of the difunctional amines are formed. The stability of these monoborane adducts is rationalized from a mechanistic point of view. The proton and boron-11 n.m.r. and i.r. spectra are presented with the analytical results.

J. M. VANPAASSCHEN et R. A. GEANANGEL. Can. J. Chem. **53**, 723 (1975).

On a isolé et caractérisé les nouveaux composés triéthylènediamine–BH_2F, –BHF_2, –BF_3, pipérazine–BH_2F, –BHF_2 et –BF_3; ces complexes sont obtenus en faisant réagir les diamines appropriées sur le complexe triméthylamine–fluoroborane. L'utilisation de cette méthode conduit uniquement aux adduits du monoborane sur les amines difonctionnelles. On rationnalise la stabilité de ces adduits de monoborane en se basant sur un point de vue mécanistique. En plus des données analytiques, on rapporte les spectres r.m.n. du proton et du bore 11 et les spectres i.r.

[Traduit par le journal]

Introduction

We have recently reported (1) the preparation of the new compounds $(CH_3)_3NBH_2F$ and $(CH_3)_3NBHF_2$ by the reaction of trimethylamine–borane with anhydrous hydrogen fluoride. The preparation of trimethylamine–difluoroborane by another method has been reported by other investigators (2). The synthesis of *t*-butylamine–fluoroboranes by the reaction of anhydrous hydrogen fluoride with *t*-butylamine–borane is reported elsewhere (3).

In this paper we wish to describe some new fluoroborane adducts of diamines which were prepared by base displacement reactions of the diamines on trimethylamine–borane and trimethylamine–fluoroboranes.

Experimental

Nuclear magnetic resonance spectra for boron (32.1 MHz) were obtained on a Varian HA-100 instrument. Chemical shifts are reported in p.p.m. relative to external trimethylborate. Proton n.m.r. spectra were taken on a Varian T-60 instrument. Chemical shifts are given in p.p.m. from internal tetramethylsilane. Infrared spectra were obtained as KBr pellets on a Perkin-Elmer Model 700 spectrophotometer. Melting points were obtained in sealed capillaries on a heated block and are uncorrected. Solvents (Matheson Co.) were dried (4) and stored under vacuum. The ethylenediamine, piperazine, and triethylenediamine (1,4-diazabicyclo[2.2.2]octane) were obtained from Eastman Organic Chemicals. The solids were sublimed and ethylenediamine was distilled before use. Analyses for boron and hydrolyzable hydrogen were carried out by standard methods. Carbon and hydrogen analyses were performed by Chemalytics, Inc., Tempe, Arizona.

Generally the monoborane adducts of the difunctional amines were prepared by displacement reactions starting with a diamine and the appropriate trimethylamine–borane adduct in equimolar quantities. In a typical reaction, 10 mmol of trimethylamine–borane (or –fluoroborane) and an equimolar amount of difunctional base were placed in a 50-ml round-bottom flask which was then evacuated. About 7 ml of dry benzene was condensed into the flask and the reaction was allowed to stir at room temperature for 48 h. The volatile components of the reaction were then fractionated and the quantity of trimethylamine measured. The trimethylamine was discarded and the benzene was condensed back into the reaction vessel. The reaction was then allowed to run for another 48 h after which time the volatile contents were again fractionated and the amount of trimethylamine measured. This procedure was continued until the evolution of trimethylamine had stopped. The benzene was vapor transferred from the reaction vessel. The nonvolatile portion of each reaction was removed from the vessel, purified, and analyzed. The yield at the first equilibration was calculated from the quantity of $(CH_3)_3N$ freed after the first 48 h, while the final yield was calculated from the amount of product isolated.

Triethylenediamine–monoborane, $N(CH_2CH_2)_3N:BH_3$, is a white crystalline sublimable solid which melts at 165–167 °C (lit. (5) 167–170 °C). The solid residue from the reaction between triethylenediamine and trimethylamine–borane was dissolved in a small amount of C_6H_6, then petroleum ether was added until precipitation occurred. The solid was filtered and held under dynamic

Can. J. Chem. Downloaded from www.nrcresearchpress.com by 210.87.254.6 on 09/05/12
For personal use only.

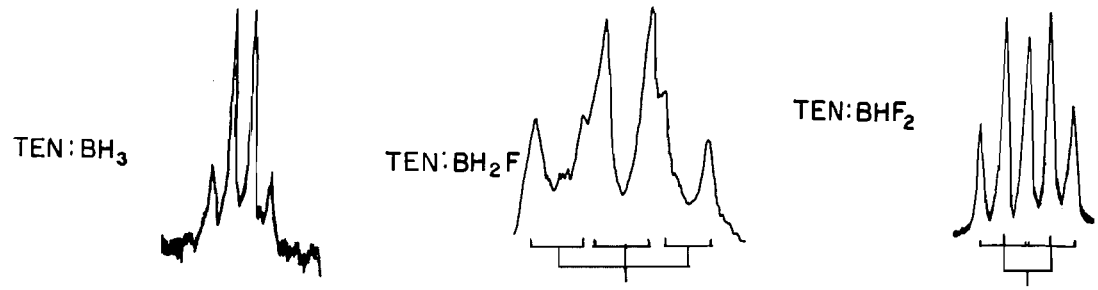

FIG. 1. Boron-11 n.m.r. spectra of triethylenediamine–monofluoroborane, –difluoroborane, and –borane.

vacuum for 24 h. The yield at the first equilibration was 87%, while the final yield was 89%. The resulting solid, which was soluble in C_6H_6, CH_2Cl_2, and CH_3CN, had an i.r. spectrum which matched that reported by Gatti and Wartik (5) for triethylenediamine–monoborane. The only observed proton resonance occurred at δ 2.86. The boron-11 resonance consisted of a 1:3:3:1 quartet (J_{BH} = 103 Hz) observed at +29.6 p.p.m. (Fig. 1).

Triethylenediamine–monofluoromonoborane, $N(CH_2CH_2)_3N:BH_2F$, is a white crystalline sublimable solid which melted in the range 162–164 °C. The solid residue from the reaction between triethylenediamine and $(CH_3)_3NBH_2F$ was dissolved in CH_2Cl_2, filtered, and the solvent removed from the filtrate by vacuum transfer. The crude solid was sublimed, giving a final yield of 83% and a first equilibration yield of 80%. The purified compound was found to be soluble in CH_2Cl_2 and CH_3CN and slightly soluble in C_6H_6. Its i.r. spectrum has bands at 3400(br), 2940(s), 2880(s), 2360(sh), 2310(s), 2260(s), 2190(m), 1460(s), 1445(s), 1305(s), 1270(w), 1205(s), 1180(s), 1150(s), 1110(s), 1040(s), 990(s), 950(s), 905(s), 840(sh), 830(s), and 780(m) cm^{-1}. The methylene proton resonance occurs at δ 2.90 and the ^{11}B resonance is observed at +14.0 p.p.m. (Fig. 1). The measured coupling constants are J_{BH} = 116 Hz and J_{BF} = 87 Hz.

Anal. Calcd. for $C_6H_{14}BFN_2$: B, 7.64; H(neg), 1.39; N, 19.45. Found: B, 7.55; H(neg), 1.43; N, 19.09.

Triethylenediamine–difluoromonoborane, $N(CH_2CH_2)_3N:BHF_2$, is a white crystalline solid which melts in the range 170–171 °C. The reaction between triethylenediamine and $(CH_3)_3NBHF_2$ gave essentially a 100% yield of trimethylamine at the first equilibration and a final yield of 95%. The solid did not sublime up to 130 °C. The solid was analyzed without further purification.

Anal. Calcd. for $C_6H_{13}BF_2N_2$: B, 6.79; H(neg), 0.62; N, 17.25. Found: B, 6.88; H(neg), 0.70; N, 17.33.

The compound has i.r. bands at 3400(br), 2950(m), 2890(m), 2330(m), 2275(m), 1450(m), 1315(m), 1210(s), 1190(s), 1170(s), 1120(s), 1060(s), 990(m), 960(m), 940(w), 910(s), 850(s), 840(s), and 780(vw) cm^{-1}. The methylene proton resonance consists of a doublet (J = 2 Hz) occurring at δ 2.93. The ^{11}B resonance is observed at +14.6 p.p.m. (Fig. 1) with coupling constants of 142 and 65 Hz for J_{BH} and J_{BF}, respectively.

Triethylenediamine–trifluoromonoborane, $N(CH_2CH_2)_3N:BF_3$, is a white crystalline solid with a melting ranging of 199–203 °C, isolated from the reaction of triethylenediamine and $(CH_3)_3NBF_3$, which gave a yield of essentially 100% of the theoretical amount of trimethylamine. The solid residue was washed with benzene and sublimed *in vacuo*, giving a final yield of 90%.

Anal. Calcd. for $C_6H_{12}BN_2F_3$: B, 6.11; N, 15.55. Found: B, 5.99; N, 15.64.

The i.r. spectrum (KBr pellet) contains bands at 3400(br), 2950(m), 2900(m), 1460(s), 1320(s), 1190(s), 1160(sh), 1120(s), 1050(s), 990(s), 930(s), 900(s), 840(s), and 790(m) cm^{-1}. The methylene proton resonance was observed at δ 2.97 and the boron-11 resonance was a singlet at +18.0 p.p.m.

Piperazine–monoborane is a white solid isolated from the reaction of piperazine and trimethylamineborane which yielded 77% of the possible trimethylamine when carried out as a batch reaction. The solid was purified by washing with CH_2Cl_2, after which the melting range was 171–172 °C.

Anal. Calcd. for $C_4H_{13}BN_2$: B, 10.8; H(neg), 3.0. Found: B, 11.0; H(neg), 3.2.

The solubility of piperazine–monoborane in C_6H_6, CH_2Cl_2, CH_3CN, and tetrahydrofuran was negligible; the solid dissolves readily in water with slow hydrolysis accompanied by gas evolution. The i.r. spectrum showed bands at 3400(br), 3300(m), 3075(m), 2900(s), 2850(s), 2325(vs), 2275(vs), 1450(m), 1370(w), 1350(w), 1310(w), 1270(m), 1180(vs), 1140(m), 1100(s), 1070(m), 1040(w), 940(m), 880(s), 840(s), and 740(vw) cm^{-1}. No n.m.r. spectra were obtained because of the low solubility of the solid product.

Piperazine–monofluoromonoborane and –difluoromonoborane are white solids which are insoluble in CH_2Cl_2, C_6H_6, CH_3CN, and THF. They were prepared by the reaction of piperazine with $(CH_3)_3NBH_2F$ and with $(CH_3)_3NBHF_2$ but no effective method was found to purify the solid products. This problem prevented a proper characterization of the adducts except by analogy with the other adducts reported here. When a sample of the solid believed to be piperazine–BHF_2 was heated until the evolution of hydrogen was complete, the ratio of moles of hydrogen to moles of compound was 0.9 to 1.0. This is in reasonable agreement with the amount of hydrogen elimination expected for aminoborane formation.

$$HN(CH_2CH_2)_2NH:BHF_2 \rightarrow HN(CH_2CH_2)_2NBF_2 + H_2$$

The compounds do not sublime and begin to decompose near their melting points (PIP:BH_2F, 106–107 °C; PIP:BHF_2, 133 °C). The yield of trimethylamine for the monofluoro adduct was 81% and for the difluoro adduct 72%. The final yields were not calculated due to the lack of purity in the products.

Piperazine–trifluoromonoborane, PIP:BF_3, is a white crystalline solid insoluble in CH_2Cl_2, CH_3CN and C_6H_6.

Can. J. Chem. Downloaded from www.nrcresearchpress.com by 210.87.254.6 on 09/05/12
For personal use only.

Can. J. Chem. Downloaded from www.nrcresearchpress.com by 210.87.254.6 on 09/05/12
For personal use only.

The reaction of piperazine with an equimolar quantity of trimethylamine–trifluoroborane yielded 66% of the possible trimethylamine and a white solid residue which, after being washed with CH_2Cl_2, melted in the range 142–145 °C.

The i.r. spectrum of the solid has bands at 3400(br, sh), 3310(w), 2625(m), 2500(w), 1450(m), 1410(m), 1370(w), 1320(vw), 1310(vw), 1260(w), 1180(s), 1140(s), 1100(s), 1040(s), 1020(w), 950(s), 880(m), 870(s), 830(m), and 740(w) cm^{-1}.

Anal. Calcd. for $C_4H_{10}BN_2F_3$: B, 7.14. Found: B, 7.39.

Ethylenediamine–boranes. Ethylenediamine displaces some trimethylamine from the trimethylamine-boranes in the formation of the ethylenediamine adducts, but p.m.r. indicates the products are mixtures. We were unable to separate and purify the components of these mixtures. The products were water- and air-sensitive oils similar to those described by Kelly and Edwards (6). The reaction involving $(CH_3)_3NBF_3$ gave a white solid which turned to an oil on exposure to air (7).

Results and Discussion

In principle a displacement reaction with a diamine acting upon an amine–borane (1:1 molar stoichiometry) could produce either a mono- or bisborane adduct of the diamine. One might expect the initial product of the displacement to be the monoborane adduct which could then react further or disproportionate to give the bis adduct with two acid molecules per diamine. There are relatively few reported cases of monoborane adducts of diamines which are stable towards disproportionation at room temperature (5).

Gatti and Wartik (5) reported that triethylenediamine–borane is stable at room temperature but disproportionates above its melting point (167–170 °C). They also found that the monoborane adduct of *N,N'*-dimethylpiperazine had disproportionated after 18 h at room temperature. Other monoborane adducts were even less stable; $(CH_3)_2NCH_2CH_2N(CH_3)_2{:}BH_3$ converted to the bisborane adduct after 1 h (8).

In this study ethylenediamine (EN), piperazine (PIP), and triethylenediamine (TEN) were reacted with $(CH_3)_3NBH_3$, $(CH_3)_3NBH_2F$, $(CH_3)_3NBHF_2$, and $(CH_3)_3NBF_3$. All the products which could be characterized were found to be monoborane adducts. The new monoborane adducts isolated and characterized in this work are $TEN{:}BH_2F$, $TEN{:}BHF_2$, and $TEN{:}BF_3$. These are solids which show no observable tendency to disproportionate at room temperature. They were characterized by elemental analysis and ^{11}B n.m.r. spectra (Fig. 1) which strongly resembled those of the corresponding trimethylamine adducts (1).

The piperazine adducts, $PIP{:}BH_3$, $PIP{:}BH_2F$, $PIP{:}BHF_2$, and $PIP{:}BF_3$, are less well characterized because of their low solubilities and decomposition above room temperature. Melting ranges were not especially good criteria of purity because of disproportionation. The elemental analysis obtained on these compounds suggests some impurity but is more consistent with monoborane adducts than bisborane adducts.

The products of the ethylenediamine displacement reactions were intractable oils which we were unable to purify and characterize. Kelly and Edwards (6) obtained an oil when attempting to prepare the monoborane adduct of ethylenediamine. Also an oil was obtained (7) when crude $H_2NCH_2CH_2NH_2{:}BF_3$ was exposed to air. Generally ethylenediamine displaced less trimethylamine than either of the other diamines, making isolation and purification of products more difficult.

The factors which determine the relative stabilities of monoadducts and diadducts of this type have not been rigorously investigated, but two effects have been discussed. Nöth (9) suggested that more efficient solid state packing of symmetrical bis adducts may favor their formation. Also, hydrolysis studies (7) of bis(trifluoroborane) adducts of ethylenediamine and hexamethylenediamine suggested that the former is more reactive (less stable adduct) because of the inductive effect transmitted through the shorter ethylene chain. The inductive effect tends to lower the base strength of the free amine group of the diamine and, in the absence of other factors, this should stabilize the monoborane with respect to the bisborane adduct. In reactions as carried out here with equimolar proportions of amine–borane and diamine, disproportion of the monoborane adduct to bisborane and free diamine is the most likely way that the bisborane adduct might be formed.

Two routes by which disproportionation might occur are [1] dissociative, where one mono adduct dissociates and the freed borane moiety bonds to another mono adduct giving one bisborane and one free diamine, and [2] by displacement, where the free amine end of one mono adduct attacks the borane portion of another displacing free diamine and leaving a bisborane adduct. The principal driving force for both (reversible) reactions is probably the

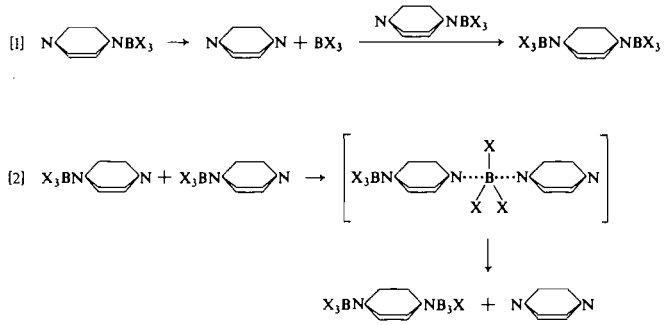

differences in coordinate (B—N) bond energies. Because of the inductive effect of one borane adduct on the other amine in a diamine we must suppose that the B—N bond energies would favor the monoborane adducts (of the diamines considered here) in the disproportionation. We would expect to see the bisborane adducts only when other factors, such as solvation energies or solid state effects which favored the more symmetrical adducts, are active.

The authors gratefully acknowledge the support of this work by the Robert A. Welch Foundation.

1. J. M. VANPAASSCHEN and R. A. GEANANGEL. J. Am. Chem. Soc. **94**, 2680 (1972).
2. H. MONGEOT, J. DAZORD, and J. P. TUCHAGUES. J. Inorg. Nucl. Chem. **34**(3), 825 (1972).
3. J. M. VANPAASSCHEN, M. GRACE HU, L. ALAN PEACOCK, and R. A. GEANANGEL. Syn. React. Inorg. Metal-Org. Chem. **4**(1), 11 (1974).
4. W. L. JOLLY. The synthesis and characterization of inorganic compounds. Prentice Hall, Englewood, New Jersey. 1970.
5. A. R. GATTI and T. WARTIK. Inorg. Chem. **5**, 2075 (1966).
6. H. C. KELLY and J. O. EDWARDS. J. Am. Chem. Soc. **82**, 4842 (1960).
7. C. A. BROWN, E. L. MUETTERTIES, and E. G. ROCHOW. J. Am. Chem. Soc. **76**, 2537 (1954).
8. A. R. GATTI and T. WARTIK. Inorg. Chem. **5**, 329 (1966).
9. H. NÖTH. Prog. Boron Chem. **3**, 215 (1970).

Can. J. Chem. Downloaded from www.nrcresearchpress.com by 210.87.254.6 on 09/05/12
For personal use only.

Can. J. Chem. Downloaded from www.nrcresearchpress.com by 210.87.254.40 on 09/05/12
For personal use only.

The Chemistry of Cochliodinol, a Metabolite of *Chaetomium* spp.[1]

W. A. JERRAM, A. G. MCINNES, W. S. G. MAASS, D. G. SMITH, A. TAYLOR, AND J. A. WALTER

Atlantic Regional Laboratory, National Research Council of Canada, Halifax, Nova Scotia B3H 3Z1

Received November 11, 1974

W. A. JERRAM, A. G. MCINNES, W. S. G. MAASS, D. G. SMITH, A. TAYLOR, and J. A. WALTER. Can. J. Chem. **53**, 727 (1975).

Chemical and spectroscopic (u.v., i.r., ^{1}H and ^{13}C n.m.r., and mass) data are reported which suggest that cochliodinol is 2,5-dihydroxy-3,6-di(5′-(2″-methylbut-$\Delta^{2''}$-ene)-indolyl-3′)-cyclohexadiene-1,4-dione (**1***a*).

W. A. JERRAM, A. G. MCINNES, W. S. G. MAASS, D. G. SMITH, A. TAYLOR et J. A. WALTER. Can. J. Chem. **53**, 727 (1975).

On rapporte des données chimiques et spectroscopiques (u.v., i.r., r.m.n. du proton et du ^{13}C et spectrométrie de masse), qui suggèrent que le cochliodinol est la dihydroxy-2,5 di(méthyl-2″ butène-2″)-5′ indolyl-3′)-3,6 cyclohexadiène-dione-1,4 (**1***a*). [Traduit par le journal]

Introduction

The isolation of the purple antibiotic metabolite cochliodinol (**1***a*; λ_{max} 475 nm) from cultures of *Chaetomium globosum* and *C. cochliodes* has been reported previously (1, 2). The metabolite readily formed dimethyl (**1***d*; λ_{max} 475 nm) and diacetyl (**1***c*; λ_{max} 498 nm) derivatives. Of these compounds only **1***a* was acidic (pK_a 6.7); it gave stable green crystalline salts with strong bases (3). All three compounds (**1***a*, **1***d*, **1***c*) were highly colored, and were readily reduced with hydrogen sulfide in methanol to give colorless (λ_{max} 295 nm) crystalline phenols (**2***a*, **2***f*, **2***g*), which were easily oxidized by oxygen to yield the parent compounds. Such behavior is common among quinones in general and with vat dyestuffs in particular. The phenols were acetylated readily (**2***a* → **2***b*; **2***f* → **2***e*; **2***g* → **2***b*) and the i.r. spectra of the esters (*e.g.*, **2***e*, ν_{max} 1760 cm^{-1}) no longer contained the original carbonyl bands observed at 1640 cm^{-1} for **1***a* and **1***d*, or at 1660 cm^{-1} for **1***c*. Moreover, the phenolic esters (**2***b*, **2***e*) were colorless (λ_{max} 295 nm) and were readily reconverted (**2***b* → **1***a*; **2***e* → **1***d*) to cochliodinol or its dimethyl derivative on hydrolysis in acid or basic solution. These results imply that the products of hydrolysis, **2***a* and **2***f*, had been oxidized by air during the hydrolysis and/or isolation procedures. It is clear that the carbon skeleton of **1***a* and **1***d* remains intact during these interconversions.

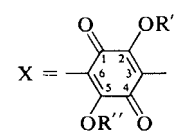

1

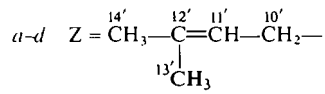

a–d Z = CH_3—C(13′CH_3)=CH—CH_2—

a R = R′ = R″ = H
b R = R′ = H; R″ = CH_3CO
c R = H; R′ = R″ = CH_3CO
d R = H; R′ = R″ = CH_3

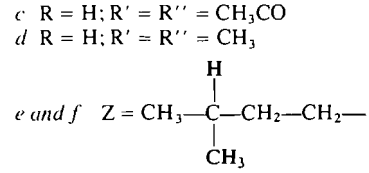

e and f Z = CH_3—C(H)(CH_3)—CH_2—CH_2—

e R = R′ = R″ = H
f R = H; R′ = R″ = CH_3CO

Elemental and mass spectral analysis indicated that **2***b* had a molecular formula of $C_{40}H_{40}N_2O_8$ but the ^{1}H n.m.r. spectrum (see Table 1) only gave a ratio of 1:4:1:2:6:6 for NH, aromatic, olefinic, methylene, methyl (two which are chemically nonequivalent), and acetoxyl methyl (two which are chemically equivalent) hydrogens. All resonances of **2***b* therefore originate from a quartet (acetoxyl methyl) or pairs of chemically equivalent groups of hydrogen(s) due to symmetry in the molecule. This equivalence was unaffected by changing solvent polarity or the magnetic field (60, 100, 220 MHz). The above signals were also present

[1]NRCC No. 14378.

Can. J. Chem. Downloaded from www.nrcresearchpress.com by 210.87.254.40 on 09/05/12
For personal use only.

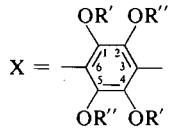

2

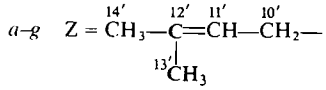

a R = R′ = R″ = H
b R = H; R′ = R″ = CH_3CO
c R = R′ = R″ = CH_3CO
d R = CHO; R′ = R″ = CH_3CO
e R = H; R′ = CH_3; R″ = CH_3CO
f R = R′ = H; R″ = CH_3
g R = R′ = H; R″ = CH_3CO

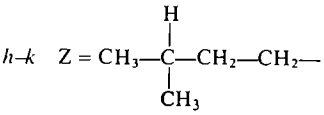

h R = R′ = R″ = H
i R = R′ = H; R″ = CH_3CO
j R = H; R′ = R″ = CH_3CO
k R = R′ = R″ = CH_3CO

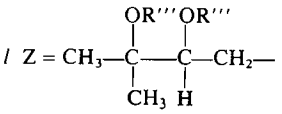

R = H; R′ = R″ = R‴ = CH_3CO

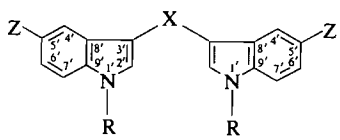

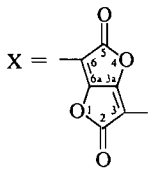

3

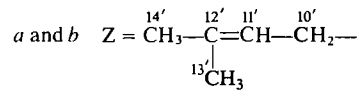

a R = H
b R = CH_3CO

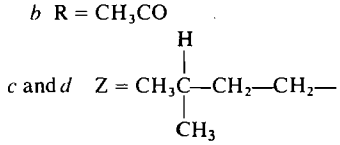

c R = H
d R = CH_3CO

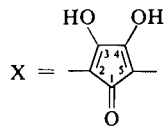

4

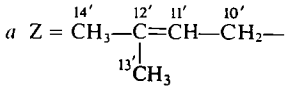

R = H

in the spectrum of **1***c* with a corresponding ratio of 1:4:1:2:6:3, whereas for **1***a*, which contained a broad hydroxyl resonance, but no acetoxyl signal, the same hydrogens bonded to nitrogen or carbon had a ratio of 1:4:1:2:6. Finally, a monoacetate **1***b* was obtained whose proton spectrum (see Experimental) contained the same types of hydrogens as in **2***b* and **1***c* in the ratio of 2:8:2:4:12:3. From the above observation it can be concluded that **1***a* and **1***c*, like **2***b*, are symmetrical molecules and contain double the number of hydrogens indicated by intensity measurements of their ^1H n.m.r. spectra. As **2***b* contains four acetoxyl groups it follows that the basic carbon skeleton of **1***a* has 32 carbons and its conversion to **1***c* implies that **1***a* has two hydroxyl groups. Thus, **1***a* probably has a molecular formula of $C_{32}H_{30}N_2O_4$ and **1***c* of $C_{36}H_{34}N_2O_6$. Similarly, **1***d* has a probable molecular formula of $C_{34}H_{34}N_2O_4$.

As previously reported (1) the ion of greatest mass in the mass spectrum of cochliodinyl diacetate (**1***c*) had *m/e* 592.2032, in agreement with the molecular formula $C_{36}H_{36}N_2O_6$, and similar precise mass measurements of the ions of greatest molecular weight in the spectra of **1***a* and **1***d* also indicated molecular formulae two mass units greater than the formulae deduced from the n.m.r. data, (the elemental analysis also fitted a H_{30} formula better than an H_{32}). When the mass spectrum of the diacetate was measured in the presence of deuterium (4) the ion of greatest mass had *m/e* 594 indicating exchange of two protons but in the presence of deuterium oxide the ion of greatest mass had *m/e* 596. Finally, the apparent molecular ion in the spectrum of the di(trideuterioacetyl) derivative had *m/e* 600. These results indicate that the mass spectra of cochliodinol and its derivatives are anomalous. It was shown recently (5) that the apparent molecular ion in the spectrum of

Can. J. Chem. Downloaded from www.nrcresearchpress.com by 210.87.254.40 on 09/05/12
For personal use only.

TABLE 1. Proton magnetic resonance data (100 MHz) for cochliodinol and some derivatives* in THF-d_8 with TMS as internal reference

	δ†										$J_{p,q}$ (Hz)						
Compound	H-1′§	H-2′	H-4′	H-6′,7′‡	H-10′	H-11′	H-13′	H-14′	OH§	CH_3CO_2	1′,2′	4′,6′	4′,7′	6′,7′	10′,11′	11′,13′	11′,14′
1*a*	10.30 (bd)	7.51 (d)	7.43 (bs)	7.07 (m)	3.41 (bd)	5.39 (m)	1.71 (d)	or 1.73 (d)	9.8 (bs)		2.6	1.6	0.4	8.4	7.0	1.3	or 1.5
1*c*	10.80	7.62	7.47	7.14	3.47	5.41	1.73	or 1.75		2.07 (s)	2.8	1.6	0.6	8.3	7.2	1.3	or 1.4
2*b*	10.18	7.22	7.38	7.07	3.40	5.40	1.72	or 1.75		1.86 (s)	2.6	1.6	0.5	8.3	7.1	1.3	1.3
3*a*	10.76	8.18	8.12	7.13	3.49	5.43	1.82 (bdd)				2.8	1.6	0.5	8.3	7.5		

*Proton magnetic resonance data (60 or 100 MHz; $DCCl_3$ or acetone-d_6) for other derivatives (**1***b*, *d*, *e*, and **2***c*, *k*, *l*) which are not discussed in detail are included in the Experimental.
†b = broad, d = doublet, m = multiplet, s = singlet. Multiplicities remain the same for corresponding resonances in all compounds, except for H-13′,14′ in **3***a* which appear as a broad doublet of doublets.
‡Chemical shifts refer to centroid of the multiplet which was analyzed as an AB system with first order coupling to H-4′. $\Delta_{\nu_{6',7'}} = 28.5$ Hz (**1***a*), 27.7 (**1***c*), 28.2 (**2***b*), 23.8 (**3***a*).
§Protons exchangeable with deuterium.

Can. J. Chem. Downloaded from www.nrcresearchpress.com by 210.87.254.40 on 09/05/12
For personal use only.

TABLE 2. ^{13}C n.m.r. data (25.16 MHz) for cochliodinol and some derivatives in THF-d_8*

	δ_C TMS ($^1J_{CH}$, Hz)†																	
Compound	C-1,4	C-2,5	C-3,6	C-2′	C-3′	C-4′	C-5′	C-6′	C-7′	C-8′	C-9′	C-10′	C-11′	C-12′	C-13′	C-14′	CH_3CO_2	CH_3CO_2
1*a*	168.5 (s)	168.5 (s)	112.1 (s)	128.4 (d)	105.5 (s)	122.8 (d)	127.9 (s)	122.0 (d)	111.5 (d)	132.7 (s)	135.8 (s)	35.6 (t)	126.2 (d)	131.0 (s)	17.9 (q)	25.9 (q)		
1*c*	180.5	145.5	129.4	131.5	104.8	123.7	127.3	121.4	112.1	134.3	136.0	35.4	125.7	131.5	17.9	25.9	167.9 (s)	20.2 (q)
2*b*	140.5	140.5	123.9	126.1	106.7	123.0	127.1	120.4	111.5	133.1	135.6	35.2	125.7	131.0	17.9	25.9	167.3	19.9
2*k*	140.5	140.5	124.0	125.9	106.7	123.0	127.1	120.2	111.5	134.2	135.5	34.7	42.6	28.4	22.9	22.9	167.3	19.9
2*k*‡	140.6	140.6	124.0	125.8 (183.4)	106.8	123.3 (158.6)	127.1	120.3 (160.0)	111.3 (158.6)	134.8	135.2	34.3 (124.6)	42.3 (125.2) (t)	28.2 (c)	22.8	22.8	167.7	19.7 (130.1)
2*k*§	140.3	140.3	124.0	125.5 (184.9)	106.4	123.8	126.3	120.0 (157.8)	111.5 (160.1)	134.9	135.4	34.3 (124.9)	42.3 (128.0) (t)	28.2 (127.1) (d)	22.8 (126.0)	22.8	168.3	20.4 (130.2)
	C-2,5	C-3a,6a	C-3,6															
3*a*	168.0	151.9	98.6	128.4 (187.5)	105.2	124.7 (158)	126.7	120.4 (159.3)	112.1 (160.0)	134.9	136.2	35.2 (125.4)	124.9 (158)	132.5	17.9 (125.0)	26.0 (125.3)		

*Pulse Fourier transform, 8K, sweep width 5K Hz, data accuracy ±0.6 Hz.
†d = doublet, q = quartet, s = singlet, t = triplet. Multiplicities (single frequency off-resonance decoupled spectra) remain the same for corresponding resonances in all compounds, except for C-11′ and C-12′ in 2*k* which appear as indicated.
‡Spectra recorded in dioxane-d_8.
§Spectra recorded in methylene dichloride-d_2.

Can. J. Chem. Downloaded from www.nrcresearchpress.com by 210.87.254.40 on 09/05/12
For personal use only.

polyporyl diacetate (M = 376; $C_{22}H_{16}O_6$) had m/e 378 and in the presence of deuterium oxide m/e 380, whilst the di(trideuterioacetate) had m/e 386. These results are clearly analogous to those in the cochliodinol series and suggest that the latter compounds are also derivatives of 2,5-dihydroxy-1,4-benzoquinone.

Cochliodinol can be converted by chemical means (see below) to cochliodinone **3***a* ($C_{32}H_{28}N_2O_4$; λ_{max} 470 nm), an orange fluorescent metabolite reported previously (1). The ^1H and proton noise decoupled (p.n.d.) ^{13}C n.m.r. spectra of **3***a* only contained resonances for half the expected number of hydrogens and carbons (see Tables 1 and 2), and the proton resonances were the same as those observed for **1***a*, **1***c*, and **2***b* except for the absence of acetoxyl methyl and hydroxyl groups. Symmetry considerations therefore make it highly probable that all resonances for **3***a* arise from pairs of chemically equivalent groups of nuclei. The high resolution ^{13}C n.m.r. spectrum of **3***a* excluded the possibility of fortuitous chemical equivalence of resonances originating from quaternary carbons and carbons bonded to hydrogen, and the multiplicities of eight of the resonances accounted for half the expected number of hydrogens in accord with the above chemical equivalence and symmetry conclusions. Furthermore, eight carbon resonances had chemical shifts, $^1J_{CH}$ values, and multiplicities consistent with the presence of a 3,5-disubstituted indole residue, and five others indicated the presence of a 2-methyl-but-Δ^2-enyl substituent; symmetry considerations therefore require that **3***a* possess two residues of each type. The latter conclusions were supported by the ^1H n.m.r. data (see Table 1). The 13 resonances associated with these molecular fragments in **3***a* have their counterparts (similar chemical shifts, identical multiplicities) in the ^{13}C n.m.r. spectra of **1***a*, **1***c*, and **2***b*. It should be noted that the four acetoxyl groups in **2***b* and the two corresponding groups in **1***c* only give rise to two characteristic signals at about δ_C 20 (acetoxyl methyl carbon) and δ_C 167 (acetoxyl carbonyl carbon), thereby emphasizing molecular symmetry. This analysis accounts for 26 carbons; the remaining resonances in the pnd ^{13}C n.m.r. spectra of these compounds must arise from six carbons. It follows therefore that the three remaining signals of **1***c* (δ_C 180, 145, and 129) and **3***a* (δ_C 168, 152, and 99) are due to pairs of equivalent carbons, whereas in **1***a* (δ_C 168, 112) and **2***b* (δ_C 140, 124) one signal arises from four chemically equivalent carbons and the other from two. At this stage molecular formula considerations leave unaccounted the fragments $C_6H_2O_4$ for **1***a*, $C_{10}H_6O_6$ (two acetoxyls account for $C_4H_6O_4$) for **1***c*, $C_{14}H_{12}O_8$ (four acetoxyls account for $C_8H_{12}O_8$) for **2***b*, and C_6O_4 for **3***a*. The structural elucidation of **1***a*, **1***c*, **2***b*, and **3***a* therefore reduces to establishing the nature of the unknown fragments and how the three components in each molecule are bonded.

Treatment of **1***a* with dimethyl sulfoxide in the presence of acetic anhydride converted it to **3***a*. Under these conditions it is known that 2,5-dihydroxybenzoquinones undergo oxidative rearrangements to dilactones; *e.g.*, polyporic acid is converted in high yield to pulvinic acid dilactone (6). If a similar conversion has occurred in the reaction **1***a* → **3***a* characteristic signals for the dilactone moiety should be observed in the ^{13}C n.m.r. spectrum of **3***a*. For the reasons outlined above the relevant resonances are those occurring at δ_C 168.0, 151.9, and 98.6, and these are indeed very similar to those observed for the carbons of the dilactone moiety of *o*-methoxypulvinlactone (C-2, C-5, δ_C 167.7, 166.9; C-3a, C-6a, δ_C 159.3, 160.2; C-3, C-6, δ_C 99.8, 101.4: numbering system is the same as for the dilactone residue of **3***a*).

Acetylation of **3***a* gave a di-*N*-acetate **3***b* ($C_{36}H_{32}N_2O_6$), while catalytic reduction provided a tetrahydro derivative, **3***c*, having the same chromophore (λ_{max} 476 nm); no colorless intermediates were observed. All of these compounds were very sensitive to base. For example when **3***a* in methanol solution was treated with a trace of 0.02 *N* sodium hydroxide, the solution had λ_{max} 350 nm, whereas the solution on acidification had λ_{max} 408 nm. Such spectroscopic changes are consistent with the opening of a lactone ring. The i.r. spectrum of **3***b* also contained an absorption band at 1820 cm^{-1} in close agreement with that observed for pulvinic acid dilactone (ν_{max} 1825 cm^{-1}). Oxidation of **1***a* with manganese dioxide also gave a product $C_{31}H_{30}N_2O_3$ which was not a lactone and appeared to be analogous to the cyclopentadiene derivative **4***a* (7). These results provide convincing evidence that **3***a* is indeed an analog of pulvinic acid lactone and the reaction used for the interconversion **1***a* → **3***a* implies that **1***a* is a 2,5-dihydroxybenzoquinone. It is clear that the

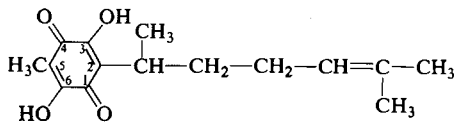

5

carbons giving rise to the two resonances at δ_C 168.5 and 112.1 in **1***a* are the origin of the three pairs of equivalent carbons which appear at δ_C 168.0, 151.9, and 98.6 in the corresponding spectrum of **3***a* as all other spectral features are virtually identical. Moreover, of the above two signals in **1***a* the one at lowest field was a broad singlet whereas the one at highest field was a sharp singlet, and these two signals correspond to six carbons. This is reminiscent of the behavior of carbons in the 2,5-dihydroxyquinone ring system of hydroxyperezone **5** (8). In the pnd ^{13}C n.m.r. spectrum of this compound C-1, C-3, C-4, and C-6 appear as a broad resonance at δ_C 168.5, whereas the other quinone carbons bearing substituents resonate at δ_C 118.7 (C-2) and 111.2 (C-5). The almost complete chemical equivalence of the carbonyl carbons and carbons bearing hydroxyl substituents was attributed to the rapid interconversion of two equivalent tautomeric forms of the 2,5-dihydroxyquinone ring system, which results in the chemical shifts of the four carbons being averaged. If, as indicated by the above results, **1***a* is a symmetrically substituted 2,5-dihydroxybenzoquinone, acetylation to form **1***c* should eliminate chemical equivalences arising from tautomeric interconversions. Indeed in the spectrum of **1***c* the two resonances present at δ_C 168.5 and 112.1 are replaced by three resonances for three equivalent pairs of carbons at δ_C 180.5, 145.5, and 129.4, and are in close agreement with the chemical shifts observed for carbons bearing acetoxyl (δ_C 149.1), phenyl (δ_C 129.6), and carbonyl carbons (δ_C 180.1) in the p.n.d. ^{13}C n.m.r. spectrum of polyporic acid diacetate. The p.n.d. ^{13}C n.m.r. spectrum of **2***b* (which is formed from **1***a* by reduction followed by acetylation) does not possess any of the three characteristic signals of **1***c* given above but instead has two signals at δ_C 140.5 and 123.9. Clearly **2***b* contains a symmetrically substituted benzene ring containing four equivalent carbons bearing acetoxyl substituents (δ_C 140.5) and two others (δ_C 123.9) bearing substituents (ref. 9, p. 197). It can be concluded therefore that **1***a*, **1***c*, and **3***a* are analogs of polyporic acid, polyporic acid diacetate, and pulvinic acid dilactone, respectively, and that **2***b* is a symmetrically substituted 1,2,4,5-tetraacetoxy benzene.

The presence of 2-methyl-but-Δ^2-enyl substituents in **1***a*, **1***c*, **2***b*, and **3***a* was established by the following evidence. Abundant ions at m/e = 69.7040 were ubiquitously present in their mass spectra, as were metastable ions, indicating the loss of a neutral fragment of mass 69. In addition the ^1H n.m.r. spectra of these compounds (see Table 1) established that the two chemically equivalent olefinic hydrogens (H-11′) at δ 5.4 were allylic coupled to the hydrogens of the methyl groups at *ca.* δ 1.7 and vicinally coupled to the hydrogens of the chemically equivalent methylene groups (H-10′) at δ 3.4. Catalytic reduction of **1***a* and **1***c* resulted in the absorption of 3 mol of hydrogen per mole of compound to form hexahydrocochliodinol (**2***h*) and hexahydrocochliodinol diacetate (isolated as the tetraacetate, **2***j*) (**2***i*), respectively, whereas the di-*N*-acetyl derivative **2***c* formed by acetylation of **2***b*, reacted with only 2 mol of hydrogen to form di-*N*-acetyl hexahydrocochliodinol tetraacetate (**2***k*); in the case of **2***c* reduction occurred only under forcing conditions (70°; 100 atm; Pt; AcOH). The ^1H n.m.r. spectra of **2***j* and **2***k* (see Experimental) showed that the alkene substituents had been reduced to isopentyl residues. In addition, autoxidation or catalytic oxidation of hexahydrocochliodinol and hexahydrocochliodinol diacetate gave tetrahydrocochliodinol (**1***e*) ($C_{32}H_{34}N_2O_4$) and tetrahydrocochliodinol diacetate (**1***f*) ($C_{36}H_{38}N_2O_6$), respectively, and all four compounds had the same u.v. and visible absorption spectra. Hence the olefinic bonds in the alkene substituents were not conjugated with the chromopores giving rise to the absorption maxima 475 or 498 nm in **1***a* and **1***c*. The off-resonance decoupled spectrum of **2***b* contained signals with chemical shifts and multiplicities characteristic of methyl groups (δ_C 17.9 and 25.9), a methylene group (δ_C 35.2), a =CH group (δ_C 125.7), and a quaternary olefinic carbon at δ_C 131.0. The corresponding ^{13}C n.m.r. spectrum of hexahydrocochliodinol tetraacetate (**2***j*) was similar to that of **2***b* except that the five signals discussed above were absent and instead the spectrum contained a single methyl resonance (δ_C 22.9), two methylene resonances (δ_C 34.7, 42.6), and a methine resonance at δ_C 28.4. These observations are only consistent with the reduc-

Can. J. Chem. Downloaded from www.nrcresearchpress.com by 210.87.254.40 on 09/05/12
For personal use only.

TABLE 3. Radioactivity of cochliodinol (**1***a*) (and derivatives prepared therefrom) and cochliodinone (**3***a*), isolated from cultures of *C. globosum* fed ^{14}C-labelled precursors

	Metabolites				Derivatives		
	1*a*		**3***a*		**1***c*	**2***g*	**3***a*
Precursor	μCi/mmol	Yield (%)	μCi/mmol	Yield (%)	μCi/mmol	μCi/mmol	μCi/mmol
Bz-U-^{14}C-Tryptophan	15.9	3.6	16.1	0.05	15.8	17.1	16.1
2-^{14}C-Tryptophan	0.22	4.3	0.18	0.003	0.22		0.20
2-^{14}C-Tryptophan	0.56	2.9					
2-^{14}C-Mevalonolactone	0.09	0.15				0.08	

tion of 2-methyl-but-Δ^2-enyl substituents to isopentyl groups during the reduction of **2***b* to hexahydrocochliodinol tetraacetate. Supporting evidence for the nature of the alkene substituents was also obtained when **1***c* reacted smoothly with osmium tetroxide to give a black osmic ester which was readily reduced with hydrogen sulfide (10) to provide (after acetylation) a colorless product $C_{48}H_{52}N_2O_{16}$ whose i.r. spectrum had absorption bands at 1775 and 1740 cm^{-1} plausibly assigned to phenolic and alkyl acetate functions (suggested structure **2***l*). Finally, 2-^{14}C-mevalonolactone was incorporated into cochliodinol (see Table 3) by cultures of *C. globosum*, thus providing further evidence for the presence of such substituents.

An n.O.e. study on **2***b* gave the following results (irradiated protons in parentheses): H-4′ (H-10′) 17.1%; H-6′ (H-10′) 10.5%; H-7′ (H-10′) 0%; H-2′ (H-10′) 0%; H-11′ (H-10′) 12.4%; H-2′ (NH) 24.6%; H-7′ (NH) 13.4%; H-6′ (NH) 0%; H-4′ (NH) 0%; H-2′ (CH_3CO) 5.4%; H-4′ (CH_3CO) 8.5%; H-6′ (CH_3CO) 0%; H-7′ (CH_3CO) 0%. In addition the spin–spin coupling data in Table 1 indicates that the NH hydrogens are spin–spin coupled to H-2′ and that H-7′ is *ortho* coupled to H-6′ and *para* coupled to H-4′, while the latter is also coupled to H-6′. These results establish the relative positions of the NH and aromatic hydrogens in **2***b* (and therefore also in **1***a*, **1***c*, and **3***a*), and the enhancements observed for H-4′ and H-6′, but not H-2′, when H-4″ is irradiated require that the 2-methyl-but-Δ^2-enyl substituents be on C-5′. Moreover, in the ^{1}H n.m.r. spectra of di-*N*-acetyl derivatives **2***c* and **2***k* (see Experimental) H-7′ exhibits a downfield shift, a behavior characteristic of *N*-acyl indoles (11). The ^{1}H and ^{13}C n.m.r. spectra were also correlated by off-resonance decoupling experiments. Thus all signals for carbons bearing hydrogens were readily assigned. The $^1J_{CH}$ value obtained from high resolution spectra (**3***a* and **2***j*) or calculated from off-resonance decoupled spectra (**1***a*, **1***c*, and **2***b*) indicated that spin–spin coupling between C-2′ and H-2′ was greater than 180 Hz; the corresponding value for indole derivatives was 182 Hz. The four remaining quaternary aromatic carbons (at about δ_C 106, 128, 133, and 136) in all of the latter compounds have chemical shifts consistent with those expected for C-3, C-5, C-8, and C-9 of a 3,5-disubstituted indole (ref. 9, pp. 266 and 267); the shielding of C-3′ (δ_C 106) is greater than expected and is probably due to hydrogen bonding of the NH groups in all compounds with the oxygen of THF-d_8, thus increasing the electron density on nitrogen and the shielding of C-3′.

The u.v. spectrum of cochliodinol was similar to that reported (12) for 3,6-di-(2′methylindolyl-3′)-1,4-benzoquinone. The tetraacetate (**2***b*) did not give an Ehrlich compound with aldehydes but with ethyl orthoformate gave the di-*N*-formyl derivative (**2***d*). These observations are consistent with a linkage of two indole residues through a benzoquinone moiety. Finally, DL-tryptophan unspecifically labelled in the benzene ring with ^{14}C was incorporated by the fungus into cochliodinol in about 3% yield and in a similar experiment using DL-2-^{14}C-tryptophan the label was incorporated to about the same extent (Table 3).

The combined evidence therefore is consistent with structure **1***a* for cochliodinol and structure **3***a* for cochliodinone.

Experimental

A Perkin-Elmer 237 spectrophotometer was used to determine i.r. spectra. The u.v. spectra were measured on Cary 14 and Beckman DK-2 instruments. The n.m.r.

Can. J. Chem. Downloaded from www.nrcresearchpress.com by 210.87.254.40 on 09/05/12
For personal use only.

Can. J. Chem. Downloaded from www.nrcresearchpress.com by 210.87.254.40 on 09/05/12
For personal use only.

spectra were recorded on Varian A-60A (V-6058A spin decoupler), HA-100, and XL-100-15 spectrometers; the latter was equipped (VFT-100 data system) for Fourier transform operation. Chemical shifts are reported downfield using TMS as an internal standard. Mass spectra were obtained by direct introduction of samples into the source of a DuPont 110-B instrument at about 260°. Precise masses were measured by the peak matching method using an ion in the spectrum of perfluorokerosene as a standard. Radioactivity measurements were obtained using a Nuclear Chicago Mark I scintillation counter. Samples were dissolved in a solution (15 ml) of 2,5-diphenyloxazole (60 mg) in toluene. All fermentation experiments were carried out using *C. globosum* (HLX 707)[2] as described by Jerram and co-workers (1). Radioactive precursors were added aseptically to the cultures after 3.5 days growth. All cultures were harvested at 7 days and the antibiotics extracted from the lyophilized mycelium as previously described (1). Melting points are uncorrected.

*Cochliodinol (**1a**)*

(*a*) Cochliodinol diacetate (50 mg) in methanol (10 ml) was treated with hydrogen chloride at 25° and the solution kept for 18 h. The solution was evaporated, the residue absorbed from benzene on silica gel (30 g), and cochliodinol (40 mg, m.p. 206°) eluted with ether–benzene (1:9).

(*b*) The diacetate (50 mg) was dissolved in ethanol (10 ml) and treated with sodium hydroxide solution (2 *N*, 0.5 ml) and the green suspension immediately acidified, extracted with chloroform, and the cochliodinol (35 mg; m.p. 206°; λ_{max} (0.01 *N* NaOH) 295 nm (log ε 4.32); λ_{max} (after acidification) 278, 475 nm (log ε 4.38, 3.45)) purified as described.

*Cochliodinol Diacetate (**1c**)*

This compound was prepared as previously described (1); *m/e* 592.2573 (M + 2) ($C_{36}H_{36}N_2O_6$ requires 592.2573), 550 (*m** ≃ 511; 592 → 550 + 42), 534, 508 (*m** ≃ 470; 550 → 508 + 42), 492, 439 (m* ≃ 380; 508 → 439 + 69), 371.1043 ($C_{22}H_{15}N_2O_4$ requires 371.1032), 170, 154, 142, 130, 107, 101, 91, 69.0701 (C_5H_9 requires 69.0704); λ_{max} (MeOH) 278, 498 nm (log ε 4.48, 3.93); λ_{max} (0.01 *N* NaOH) 279, 400 nm (log ε 4.19, 3.61); ν_{max} (CCl_4) 3480, 3030, 2970, 2915, 2855, 1775, 1660, (KBr) 1660, 1600, 1520, 1430, 1280, 1190, 1150, 1030, 800, 730 cm^{-1}; n.m.r. Tables 1 and 2.

Cochliodinol Di(trideuterioacetate)

Cochliodinol (0.5 g) was treated with pyridine (0.2 ml) and trideuterioacetic anhydride (Merck, Sharpe and Dohme, 99.9 atom% [^{2}H]; 5 ml) and the solution kept at 4° for 18 h. The *ester* separated from benzene – light petroleum (b.p. 40–60°) as purple needles, m.p. 201°; 0.55 g.

Anal. Calcd. for $C_{36}[^2H]_6H_{28}N_2O_6$: C, 72.4; N, 4.7; O, 16.1. Found: C, 71.7; N, 4.75; O, 16.0.

[2]Accession number to the collection of fungi held at this laboratory.

*Cochliodinol Monoacetate (**1b**) (by-product of methylation reaction)*

Cochliodinol diacetate (0.5 g) in methanol (50 ml) was treated at room temperature with hydrogen sulfide until the solution was colorless (≃ 3 h). The solution was evaporated with a stream of carbon dioxide and potassium *t*-butoxide (0.5 g), methyl iodide (9 ml), and tetrahydrofuran (100 ml) were added to the residue while an atmosphere of carbon dioxide was maintained. The reaction mixture was stirred for 24 h, evaporated, the residue taken up in benzene, the solution washed with dilute hydrochloric acid and water, and dried (Na_2SO_4). The solution was concentrated to 10 ml, run onto a silica gel (30 g) column which was eluted with benzene (500 ml), and then ether–benzene (1:9). The first 200 ml of the ether–benzene eluate was discarded and the purple band collected in the next 400 ml gave *cochliodinol monoacetate* as almost black prisms from petroleum ether (b.p. 40–60°) – benzene (1:1), m.p. 183–184°; *m/e* 550, 548; λ_{max} (MeOH) 274, 480 nm (log ε 4.45, 3.69); ν_{max} (KBr) 1775, 1650, 1605 cm^{-1}; p.m.r. (60 MHz; $CDCl_3$) δ 8.57 (bs, 1H, exchanged with D_2O, NH), 8.43 (bs, 1H, exchanged with D_2O, NH), 7.45 (bs, 4H, H-2′ and -4′), 7.15 (AB, 4H, H-7′ and -6′, $\Delta\nu_{AB} \simeq 10.5$ Hz, $J_{AB} \simeq 8.5$ Hz, signals broadened by *meta* and *para* coupling of H-6′ and -7′ with H-4′), 5.42 (bt, 2H, H-11′, $J_{11',10'} \simeq 7.5$ Hz, broadened by allylic coupling with H-13′ and -14′), 3.45 (bd, 4H, H-10′), 2.12 (s, 3H, O_2CCH_3), 1.75 (bs, 12H, H-13′ and -14′, vinylic CH_3′s).

Anal. Calcd. for $C_{34}H_{32}N_2O_5$: C, 74.45; H, 5.8; N, 5.1; O, 14.6. Found: C, 74.5; H, 5.7; N, 5.1; O, 14.5.

*Dimethylcochliodinol (**1d**)*

Cochliodinol (2 g) in ether (500 ml) was stirred and treated at room temperature with a solution of diazomethane (0.8 g) in ether. When no further nitrogen was evolved the reaction mixture was evaporated and the residue, on recrystallization from methanol gave *dimethylcochliodinol* as purple needles, m.p. 208–210° (dec.); *m/e* 536.2666 (M + 2) ($C_{34}H_{36}N_2O_4$ requires 536.2675); λ_{max} (MeOH) 276, 475 nm (log ε 4.45, 3.66), (0.2 *N* NaOH) 278, 478 nm (log ε 4.43, 3.59); ν_{max} (KBr) 3350, 2980, 2920, 2850, 1640, 1585, 1575, 1300, 1145, 1060, 790 cm^{-1}; p.m.r. (60 MHz; acetone-d_6) δ 9.8 (bs, 2H, exchanged with D_2O, H-1′, NH), 7.65 (d, 2H, H-2′, coupled to NH, $J_{1',2'} = 2.8$ Hz), 7.37 (bs, 2H, H-4′), 7.20 (AB, 4H, H-7′ and -6′, $\Delta\nu_{AB} \simeq 22$ Hz, $J_{AB} \simeq 8.5$ Hz, $J_{4',6'} \simeq 1.5$, $J_{4',7'} \simeq 0.5$), 5.43 (bt, 2H, H-11′, $J_{11',10'} \simeq 7.5$ Hz, broadened by allylic coupling > 1 Hz with H-13′ and -14′), 3.87 (s, 6H, OCH_3), 3.45 (d, 4H, H-10′), 1.75 (bs, 12H, H-13′ and -14′, vinylic CH_3′s).

Anal. Calcd. for $C_{34}H_{34}N_2O_4$: C, 76.4; H, 6.4; N, 5.2; O, 12.0; OMe, 11.6. Found: C, 76.4; H, 6.5; N, 5.4; O, 11.9; OMe, 11.8.

*Tetrahydrocochliodinol (**1e**)*

(*a*) Cochliodinol (0.5 g) in acetic acid (100 ml) was shaken with hydrogen and platinum oxide (10 mg) until 70 ml of hydrogen had been taken up. The colorless precipitate (λ_{max} (MeOH) 295 nm (log ε 4.25)) was then shaken with oxygen and platinum (5 mg) when 25 ml were absorbed and a brown solution was obtained. The solution was filtered, the filtrate evaporated, and the residue absorbed from benzene on silica gel (30 g). A purple zone was eluted with ether–benzene (1:9) which

Can. J. Chem. Downloaded from www.nrcresearchpress.com by 210.87.254.40 on 09/05/12
For personal use only.

after evaporation and recrystallization from methanol gave *tetrahydrocochliodinol*, m.p. 220–223°; *m/e* 512, 510, 496, 482, (m^* ~ 456; 510 → 482 + 28), 454 (m^* ~ 405; 510 → 454 + 56), 425, 325, 267, 130; λ_{max} (MeOH) 278, 471 nm (log ε 4.49, 3.55); ν_{max} (KBr) 3410, 3330, 2960, 2930, 2860, 1630, 1330, 985, 800 cm^{-1}; p.m.r. (60 MHz; acetone-d_6) δ 10.4 (bs, 2H, exchanged with D_2O, H-1′, NH), 7.63 (d, 2H, H-2′, coupled to NH, $J_{2',1'} = 2.8$ Hz), 7.48 (bs, 2H, H-4′), 7.18 (AB, 4H, H-7′ and -6′, $\Delta\nu_{AB}$ = 20.4 Hz, $J_{AB} = 8.4$ Hz, $J_{4',6'} = 1.6$, $J_{4',7'} \simeq 0.7$), 2.72 (m, 4H, H-10′), 1.2–1.9 (m, 6H, H-11′ (methylene) and -12′ (methine) coupled to signals at 2.72 and 0.96 (double resonance)), 0.96 (d, 12H, $J \simeq 5$ Hz, H-13′ and -14′, isopentyl CH_3's).

Anal. Calcd. for $C_{32}H_{34}N_2O_4$: C, 75.3; H, 6.7; N, 5.5. Found: C, 74.9; H, 6.5; N, 5.1.

(*b*) A solution of hexahydrocochliodinol tetraacetate (see below; 65 mg) in methanol (30 ml) under an atmosphere of argon, was saturated with hydrogen chloride. After 18 h the purple-brown solution (λ_{max} 471 nm) was evaporated, the residue absorbed from benzene on silica gel, and tetrahydrocochliodinol (45 mg, m.p. 220°) eluted from the column with ether–benzene (1:9). The ester (50 mg) was also hydrolyzed under alkaline conditions and gave *tetrahydrocochliodinol* (m.p. 220°; 35 mg).

Tetrahydrocochliodinol Diacetate (1f)

(*a*) Cochliodinol diacetate (0.3 g) in acetic acid (60 ml) was shaken with platinum oxide (5 mg) and hydrogen at room temperature and pressure until 90 ml was absorbed. The hydrogen was replaced when 20 ml of the gas were taken up in 30 min. The filtered solution was evaporated and the residue chromatographed as usual on silica gel. *Tetrahydrocochliodinol diacetate* separated from methanol as purple needles, m.p. 207–209° (dec.); λ_{max} (MeOH) 278, 498 nm (log ε 4.47, 3.93); ν_{max} (KBr) 3340, 2960, 2930, 2870, 1770, 1660, 1600, 1520, 1425, 1280, 1190, 1145, 1030, 800 cm^{-1}; *m/e* 596, 554, 538, 512, 496.

Anal. Calcd. for $C_{36}H_{38}N_2O_6$: C, 72.7; H, 6.4; N, 4.7; O, 16.2. Found: C, 72.9; H, 6.9; N, 4.1; O, 16.1.

(*b*) Tetrahydrocochliodinol (50 mg) in acetic anhydride (5 ml) was treated with pyridine (0.1 ml). The mixture was shaken until a distinct color change (brown-magenta) was noticed, when the solution was poured onto ice and the precipitated diacetate (50 mg; m.p. 207°) recrystallized from methanol.

Dihydrocochliodinol Tetraacetate (2b)

Cochliodinol (3 g) was dissolved in methanol (250 ml) and the solution treated with hydrogen sulfide as described above until a colorless solution was obtained. The solution was evaporated, the crystalline residue (λ_{max} (MeOH) 295 nm; ν_{max} 1780, 1760 cm^{-1}) was taken up in acetic anhydride (200 ml) and pyridine (3 ml) added. The almost colorless solution was kept for 24 h, methanol (1.5 l) added, and the solution heated under reflux for 1 h. The solution was concentrated to 50 ml, water (200 ml) added, and the colorless precipitate collected. *Dihydrocochliodinol tetraacetate* separated from ethanol as colorless needles, m.p. 225°; *m/e* 676.2778 (M) ($C_{40}H_{40}N_2O_8$ requires 676.2785), 371.1028 ($C_{22}H_{15}N_2O_4$ requires 371.1032); n.m.r. Tables 1 and 2.

Anal. Calcd. for $C_{40}H_{40}N_2O_8$: C, 71.0; H, 5.9; O, 18.9. Found: C, 70.4; H, 5.7; O, 18.8.

Di-N-acetyldihydrocochliodinol Tetraacetate (2c)

The tetra-*O*-acetate (1 g) was dissolved in acetic anhydride (50 ml) and anhydrous sodium acetate (4 g) added. The mixture was stirred and heated under reflux for 5 h, kept overnight, water (150 ml) added at 0°, and the mixture stirred until a colorless precipitate was obtained. *Di-N-acetyldihydrocochliodinol tetraacetate* separated from acetic acid as colorless prisms, m.p. 271°; *m/e* 760.2996 (M) ($C_{44}H_{44}N_2O_{10}$ requires 760.2996; $C_{42}H_{42}N_5O_9$ requires 760.2983); ν_{max} (KBr) 1780, 1720, 1350, 1230, 1125 cm^{-1}; p.m.r. (100 MHz; $CDCl_3$) δ 7.78 (AB, 4H, H-7′ and -6′, $\Delta\nu_{AB}$ = 113.0 Hz, $J_{AB} = 8.3$ Hz, $J_{4',6'} \simeq 1.5$, $J_{4',7'} < 0.5$), 7.47 (s, 2H, H-2′), 7.30 (bs, 2H, H-4′), 5.35 (bt, 2H, H-11′, $J_{11',10'} \simeq 7.0$ Hz, broadened by allylic coupling >1 Hz with H-13′ and -14′), 3.42 (d, 4H, H-10′), 2.61 (s, 6H, $NCOCH_3$), 1.88 (s, 12H, O_2CCH_3), 1.74 (bs, 12H, H-13′ and -14′, vinylic CH_3's).

Anal. Calcd. for $C_{44}H_{44}N_2O_{10}\cdot\frac{1}{2}H_2O$: C, 68.7; H, 5.85; N, 3.6; O, 21.8. Found: C, 68.6; H, 5.6; N, 3.8 ;O, 21.8.

Di-N-formyldihydrocochliodinol Tetraacetate (2d)

The tetra-*O*-acetate (150 mg) was suspended in acetic anhydride (10 ml) and ethyl orthoformate (4 ml) added. The colorless solution was heated under reflux for 18 h, diluted with methanol (100 ml), heated to boiling, and when the exothermic reaction ceased, concentrated to 5 ml. Water (10 ml) was added and the precipitate (160 mg) collected. The *diformyl* derivative separated from 1-ethoxy-2-hydroxyethane as prisms, m.p. 275–277°; *m/e* 732.2679 (M) ($C_{42}H_{40}N_2O_{10}$ requires 732.2683); ν_{max} (KBr) 1780, 1720, 740 cm^{-1}.

Anal. Calcd. for $C_{42}H_{40}N_2O_{10}\cdot\frac{1}{2}H_2O$: C, 68.0; H, 5.5; N, 3.8; O, 22.7. Found: C, 68.1; H, 5.6; N, 3.7; O, 22.4.

Dimethyldihydrocochliodinol Diacetate (2e)

Dimethylcochliodinol (0.4 g) was dissolved in methanol (100 ml) and was reduced with hydrogen sulfide as described for the diacetate. The colorless solution was evaporated and the residue (λ_{max} (MeOH) 293 nm) dissolved in a solution of pyridine (0.5 ml) in acetic anhydride (20 ml). The solution was kept for 24 h, was diluted with methanol (100 ml), heated under reflux for 1 h, and evaporated. Water (50 ml) was added and the colorless precipitate recrystallized from ethanol gave *dimethyldihydrocochliodinol diacetate* as parallelograms, m.p. 241°; *m/e* 620; λ_{max} (MeOH) 225, 290 nm (log ε 4.91, 4.39); ν_{max} (KBr) 3390, 1760, 1200, 790 cm^{-1}.

Anal. Calcd. for $C_{38}H_{40}N_2O_6\cdot\frac{1}{2}H_2O$: C, 72.7; H, 6.2; N, 4.5; O, 16.6. Found: C, 72.9; H, 6.6; N, 4.5; O, 15.8.

Hexahydrocochliodinol Tetraacetate (2j)

(*a*) Cochliodinol (1 g) in acetic acid (150 ml) was shaken with hydrogen and platinum (10 mg) in a flask fitted with a side arm equipped with a sintered disc, stopcock, and female ground-glass joint in this order, the disc being proximal to the flask. When the reaction mixture was colorless the flask was evacuated and a solution (30 ml) of pyridine (5 ml) in acetic anhydride was sucked into the reaction vessel through the stopcock and sintered disc. After 2 h the mixture was filtered, concentrated to 50 ml, and methanol (200 ml) added. The colorless solution was heated under reflux for 1 h, evaporated, the residue

Can. J. Chem. Downloaded from www.nrcresearchpress.com by 210.87.254.40 on 09/05/12
For personal use only.

triturated with water (100 ml), and the precipitate collected. The *tetraacetate* separated from ethanol (charcoal) as colorless needles, m.p. 258–260°; λ_{max} (MeOH) 220, 298 nm (log ε 4.85, 4.38); ν_{max} (CCl_4) 3390, 2955, 2925, 2860, 1770, 1750, (KBr) 1365, 1190, 1180, 1020, 990, 800 cm^{-1}; *m/e* 680.3079 (M) ($C_{40}H_{44}N_2O_8$ requires 680.3098), 638, (*m** ~ 602; 680 → 638 + 42), 596 (*m** ~ 557; 638 → 596 + 42), 554 (*m** ~ 517; 596 → 554 + 42), 512.2660 ($C_{32}H_{36}N_2O_4$ requires 512.2675; *m** ~ 473; 554 → 512 + 42), 69; p.m.r. (100 MHz; acetone-d_6) δ 10.42 (bs, 2H, exchanged with D_2O, NH), 7.37 (bs, 2H, H-4′), 7.35 (d, 2H, H-2′, coupled to NH, $J_{2',1'} \simeq$ 2.6 Hz), 7.20 (AB, 4H, H-7′ and -6′, $\Delta_{\nu_{AB}} = 33.6$ Hz, $J_{AB} = 8.4$ Hz, $J_{4',6'} = 1.6$, $J_{4',7'} = 0.6$), 2.70 (m, 4H, H-10′), 1.88 (s, 12H, O_2CCH_3), 1.2–1.9 (m, 6H, H-11′ (methylene) and -12′(methine) coupled to signals at 2.70 and 0.96 (double resonance)), 0.96 (d, 12H, coupled to H-12′, $J \simeq 5$ Hz, isopentyl CH_3's).

Anal. Calcd. for $C_{40}H_{44}N_2O_8$: C, 70.6; H, 6.5; N, 4.1; O, 18.8. Found: C, 70.7; H, 6.6; N, 4.1; O, 18.3.

(*b*) When cochliodinol diacetate (0.25 g) was treated as described above for cochliodinol, the tetraacetate (0.24 g; m.p. 258°) was obtained.

(*c*) Tetrahydrocochliodinol (50 mg) gave this tetraacetate (m.p. 258–260°; 35 mg) when reduced and acetylated as described in *a*.

(*d*) Similarly, tetrahydrocochliodinol diacetate (50 mg) gave the tetraacetate, (m.p. 258°; 35 mg) under the same reaction conditions.

Di-N-acetylhexahydrocochliodinol Tetraacetate (2k)

(*a*) Hexahydrocochliodinol tetraacetate (60 mg), acetic anhydride (15 ml), and anhydrous sodium acetate (0.5 g) were heated together under reflux for 5 h. The mixture was diluted with water at 0° and the colorless precipitate collected. *Di-N-acetylhexahydrocochliodinol tetraacetate* separated from *n*-butyl alcohol as colorless parallelograms, m.p. 276°; *m/e* 764.3317 (M) ($C_{44}H_{48}N_2O_{10}$ requires 764.3309); λ_{max} (MeOH) 235, 304 nm (log ε 4.16, 3.93); ν_{max} (KBr) 1760, 1715 cm^{-1}; p.m.r. (60 MHz, $CDCl_3$), δ 7.78 (AB, 4H, H-7′ and -6′, $\Delta_{\nu_{AB}} = 67.0$ Hz, $J_{AB} \simeq 8.2$ Hz, H-6′ and -7′ broadened by *meta* and *para* coupling with H-4′), 7.47 (s, 2H, H-2′), 7.30 (bs, 2H, H-4′), 2.70 (m, 4H, H-10′), 2.62 (s, 6H, $NCOCH_3$), 1.88 (s, 12H, O_2CCH_3), 1.2–1.9 (m, 6H, H-11′ (methylene) and -12′ (methine), irradiation of this multiplet causes signals at 2.70(m) and 0.94(d) to collapse to broad singlets), 0.94 (d, 12H, coupled to H-12′, $J \simeq 5$ Hz, H-13′ and -14′, isopentyl CH_3's).

Anal. Calcd. for $C_{44}H_{48}N_2O_{10}$: C, 69.1; H, 6.2; N, 3.7; O, 20.9. Found: C, 69.1; H, 6.2; N, 3.7; O, 21.2.

(*b*) Di-*N*-acetyldihydrocochliodinol tetraacetate (1 g) in acetic acid (400 ml) was stirred with platinum (50 mg) and hydrogen at 70°/100 atm for 48 h. The hot solution was filtered and the precipitate washed with ethyl acetate. The filtrate and washings were evaporated and the residue (1 g; m.p. 276°) recrystallized from *n*-butyl alcohol.

Hexahydrocochliodinol Octaacetate (2l)

Cochliodinol diacetate (0.58 g) in benzene (50 ml) was treated with a solution of osmium tetroxide (0.5 g) in benzene (50 ml). The mixture was stirred at room temperature for 48 h when the crystalline black osmic ester was collected, dissolved in methanol (200 ml), and the stirred mixture treated with hydrogen sulfide for 18 h. The osmic sulfide was collected and the filtrate evaporated. The residue was dissolved in acetic anhydride (100 ml) and pyridine (10 ml) added. The solution was kept at 4° for 48 h, when the colorless crystalline precipitate (0.5 g; m.p. 265–267°) was collected. *Hexahydrocochliodinol octaacetate* separated from 1-ethoxy-2-hydroxyethane as minute blunt colorless needles, m.p. 266°; *m/e* 912; ν_{max} (KBr) 3350, 1775, 1740, 1370 cm^{-1}.

Anal. Calcd. for $C_{48}H_{52}N_2O_{16}$: C, 63.2; H, 5.8; N, 3.1; O, 28.1. Found: C, 63.0; H, 5.9; N, 2.8; O, 28.2.

Oxidation of Cochliodinol with Manganese Dioxide and Silver Oxide

Cochliodinol (1 g) was dissolved in toluene (300 ml) and stirred with manganese dioxide (13) (0.3 g) and freshly prepared silver oxide (0.1 g). The stirred mixture was heated under reflux for 3 h when the hot solution was filtered and the metal oxides washed with boiling toluene until the washings were colorless. The combined filtrate and washings were concentrated to 50 ml and the hot solution applied to the top of a silica gel (30 × 4 cm) column. The column was eluted with toluene until the red-orange band was completely eluted. The fluorescent solution was concentrated to 50 ml and then kept at 4° for 24 h. *Cochliodinone* (*3a*) (0.2 g, 25% allowing for recovered cochliodinol; see below) separated from toluene as red-orange needles, m.p. 275–276° (depending on the rate of heating); *m/e* 504.2032 (M) ($C_{32}H_{28}N_2O_4$ requires 504.2049), 475, 462, 448.2150 ($C_{30}H_{28}N_2O_2$ requires 448.2151), 407, 393, 392, 337, 253, 196.1123 ($C_{14}H_{14}N$ requires 196.1126), 69.0706 (C_5H_9 requires 69.0704); λ_{max} (MeOH) 272, 293, 352, 470 nm (log ε 4.06, 4.05, 3.76, 4.35); λ_{max} (excitation) 470 nm (log ε 4.27); λ_{max} (emission, MeOH) 567 nm; λ_{max} (0.02 *N* NaOH) 281, 350 nm (log ε 4.16, 4.29); λ_{max} (after acidification) 272, 408 nm; ν_{max} (CCl_4) 3490, 1730, (KBr) 3430, 3415, 2960, 2850, 1785, 1760, 1660, 1500, 1420, 1100, 855 cm^{-1}; ^1H n.m.r. Table 1, ^{13}C n.m.r. Table 2.

Anal. Calcd. for $C_{32}H_{28}N_2O_4$: C, 76.2; H, 5.55; N, 5.55; O, 12.7. Found: C, 76.7; H, 5.6; N, 5.4; O, 12.3.

This compound was identical with the 'orange fluorescent pigment' previously described (1). Further elution of the column with toluene separated two purple bands and when these were completely separated (15 l) the band of greatest R_F was eluted with ether–toluene (1:19). That of lowest R_F was collected with ether–toluene (1:9) and gave cochliodinol (0.2 g, m.p. 204°) after evaporation. The band of greatest R_F was rechromatographed on a silica gel column (30 × 2 cm) made up with a solution (100 ml) of acetic acid (0.4 ml) in benzene. The column was washed with the same solvent (150 ml) and then the band of greatest R_F was applied to the top. The column was developed with 0.4% (v/v) acetic acid in benzene and the purple band of greatest R_F was collected, concentrated, and the precipitate gave a deoxocochliodinol *e.g.* (*4a*) (77 mg, 10% allowing for the recovered cochliodinol), as purple needles from benzene–petroleum ether (b.p. 40–60°), m.p. 215–220°; *M* (by measurement of depression of vapor pressure) 550; λ_{max} (MeOH) 263, 315 (sh), 475 nm (log ε 4.51, 4.18, 3.88); λ_{max} (0.02 *N* NaOH (MeOH–H_2O, 4:1)) 445 nm (log ε 3.81); λ_{max} (after acidification) 475 nm (log ε 3.88); ν_{max} (CS_2) 3465, 3440 (KBr) 1645, 1600, 1475, 1390, 1340, 1285, 1110, 800 cm^{-1}.

Can. J. Chem. Downloaded from www.nrcresearchpress.com by 210.87.254.40 on 09/05/12
For personal use only.

Anal. Calcd. for $C_{31}H_{30}N_2O_3 \cdot C_6H_6$: C, 79.9; H, 6.5; N, 5.0; O, 8.6. Found: C, 79.9; H, 6.0; N, 5.3; O, 8.8.

Oxidation of Cochliodinol with Dimethyl Sulfoxide

Cochliodinol (0.1 g) was dissolved in dimethyl sulfoxide (20 g) and acetic anhydride (10 g) added. The solution was heated on the steam bath for 30 min, kept overnight at room temperature, diluted with methanol (50 ml), and the solution heated under reflux for 1 h. The solution was evaporated, the residue absorbed from benzene on silica gel and the orange band eluted with benzene gave cochliodinone (m.p. 276°; 20 mg) after evaporation.

N-Acetylcochliodinone (3b)

Cochliodinone (0.1 g), acetic anhydride (20 ml), and anhydrous sodium acetate (0.5 g) were heated together under reflux. A complete solution was obtained from which orange needles were slowly precipitated. After 1.5 h the precipitate was collected. *N-Acetylcochliodinone* separated from acetic anhydride as yellow needles m.p. > 350°; ν_{max} (KBr) 1820, 1780, 1720, 1530, 1225, 1010 cm^{-1}.

Anal. Calcd. for $C_{36}H_{32}N_2O_6$: C, 73.5; H, 5.4; N, 4.8; O, 16.3. Found: C, 73.2; H, 5.2; N, 4.6; O, 16.8.

Tetrahydrocochliodinone (3c)

(*a*) Cochliodinone (0.3 g) in acetic acid (100 ml) was shaken with platinum (10 mg) and hydrogen at room temperature and pressure. A yellow precipitate separated slowly; at no time was a colorless solution obtained. After 30 ml (theory, 29.1 ml) had been absorbed, tetrahydrofuran (50 ml) was added until all the crystalline precipitate had dissolved when the mixture was filtered and evaporated. *Tetrahydrocochliodinone* separated from toluene as yellow needles, m.p. 310°; *m/e* 508.2351 (M) ($C_{32}H_{32}N_2O_4$ requires 508.2361); λ_{max} (MeOH) 230, 274, 298, 475 nm (log ε 4.77, 4.22, 4.22, 4.56); ν_{max} (KBr) 3410, 1795, 1770, 1675, 1510, 1430, 1105, 1040, 865, 805, 780 cm^{-1}.

Anal. Calcd. for $C_{32}H_{32}N_2O_4$: C, 75.6; H, 6.3; N, 5.5; O, 12.6. Found: C, 76.1; H, 6.3; N, 5.4; O, 12.2.

(*b*) Tetrahydrocochliodinol (30 mg) and manganese dioxide ((13), 10 mg) were stirred together in toluene (10 ml) and heated under reflux for 3 h. The mixture was filtered, the manganese salts washed with hot toluene until the washings were colorless, the filtrate and washings combined, concentrated, and absorbed on silica gel (30 × 2 cm). The red band, eluted with benzene, gave tetrahydrocochliodinone (m.p. 310°; 6 mg) on evaporation. The product was yellow in contact with benzene and orange-red when dry.

Di-N-acetyltetrahydrocochliodinone (3d)

Tetrahydrocochliodinone (20 mg), acetic anhydride (10 ml), and anhydrous sodium acetate (20 mg) were heated together under reflux for 1 h. Water (20 ml) was added and the yellow needles (22 mg; m.p. 305°) that separated were collected. *Di-N-acetyltetrahydrocochliodinone* separated from toluene as long yellow needles, m.p. 321°; *m/e* 592, 550 ($m^* \sim 511$; $592 \rightarrow 550 + 42$), 508 ($m^* \sim 469$; $550 \rightarrow 508 + 42$); λ_{max} (tetrahydrofuran) 300, 430 nm (log ε 4.21, 4.46).

Anal. Calcd. for $C_{36}H_{36}N_2O_6$: C, 73.0; H, 6.1; N, 4.7; O, 16.2. Found: C, 73.2; H, 5.7; N, 4.8; O, 16.4.

1. D. BREWER, W. A. JERRAM, and A. TAYLOR. Can. J. Microbiol. **14**, 861 (1968).
2. D. MEILER and A. TAYLOR. Can. J. Microbiol. **17**, 83 (1971).
3. D. BREWER, W. A. JERRAM, D. MEILER, and A. TAYLOR. Can. J. Microbiol. **16**, 433 (1970).
4. J. S. SHANNON. Tetrahedron Lett. 801 (1963).
5. R. GRIGSBY, W. D. JAMIESON, A. G. MCINNES, W. S. G. MAASS, and A. TAYLOR. Can. J. Chem. **52**, 4117 (1974).
6. H. W. MOORE and R. J. WIKHOLM. Tetrahedron Lett. 5049 (1968).
7. H. BESL, A. BRESINSKY, W. STEGLICH, and K. ZIPFEL. Chem. Ber. **106**, 3223 (1973).
8. P. JOSEPH-NATHAN, MA. P. GONZÁLEZ, L. F. JOHNSON, and J. N. SHOOLERY. Org. Magn. Resonance, **3**, 23 (1971).
9. J. B. STOTHERS. Carbon-13 NMR spectroscopy. Academic Press, Inc., New York. 1972.
10. D. H. R. BARTON and D. ELAD. J. Chem. Soc. 2085 (1956).
11. K. NAGARAJAN, M. D. NAIR, and P. M. PILLAI. Tetrahedron, **23**, 1683 (1967).
12. J. D. BU'LOCK and J. HARLEY-MASON. J. Chem. Soc. 703 (1951).
13. O. MANCERA, G. ROSENKRANZ, and F. SONDHEIMER. J. Chem. Soc. 2189 (1953).

Isomérisation d'époxydes d'acétates d'énols en série pinanique

YVONNE BESSIÈRE, MOHAMED MONCEF EL GAÏED ET GINETTE BOUSSAC

Laboratoire de Chimie de l'Ecole Normale Supérieure, 24, rue Lhomond, 75231 Paris Cédex 05, France[1]

Reçu le 7 décembre 1973[2]

YVONNE BESSIÈRE, MOHAMED MONCEF EL GAÏED et GINETTE BOUSSAC. Can. J. Chem. **53**, **53**, 738 (1975)

L'isomérisation d'époxydes d'acétates d'énols par le bromure de zinc conduit à des cétoacétates avec rétention de configuration. L'isomérisation thermique conduit à un cétoacétate avec inversion de configuration (mécanisme concerté) lorsque l'oxiranne ne porte pas d'atome d'hydrogène. Dans le cas d'un oxiranne portant un atome d'hydrogène, le mécanisme concerté est fortement concurrencé par un mécanisme de type 'acide,' celui-ci conduisant au cétoacétate avec rétention de configuration. Cet isomère résultant de la rétention n'est pas le plus stable.

YVONNE BESSIÈRE, MOHAMED MONCEF EL GAÏED, and GINETTE BOUSSAC. Can. J. Chem. **53**, 738 (1975)

The isomerization of enol acetate epoxides by zinc bromide leads to ketoacetates with retention of configuration. Thermal isomerization yields a ketoacetate with inversion of the configuration by a concerted mechanism if the oxirane does not contain a hydrogen atom. In the case of an oxirane containing hydrogen, an 'acid' type mechanism competes favorably with the concerted mechanism; the former yields a ketoacetate with retention of configuration. The isomer in which the configuration is retained is not the most stable. [Journal translation]

Les époxydes d'acétates d'énols I s'isomérisent selon les cas en α-cétoacétates avec inversion, **II**, ou rétention de configuration, **III**, au niveau du carbone β.

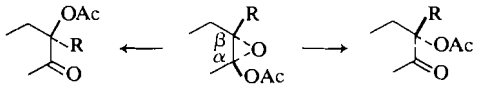

II I III

Une interprétation de ces transpositions a été proposée par Leeds *et coll* (1): les mécanismes A ou B pourraient intervenir quelles que soient les conditions expérimentales. Par contre, d'après Williamson *et coll.* (2, 3), ces conditions détermineraient la formation de l'un ou l'autre des isomères, plusieurs mécanismes étant proposés pour la transposition directe de **I** en **III** en milieu acide, le mécanisme concerté agissant pour la transposition thermique **I** → **II**.

Les observations que nous avons faites sur deux acétates d'énols en série pinanique, doivent, par comparaison avec des résultats décrits dans la littérature, apporter des précisions pour l'élucidation de ces mécanismes.

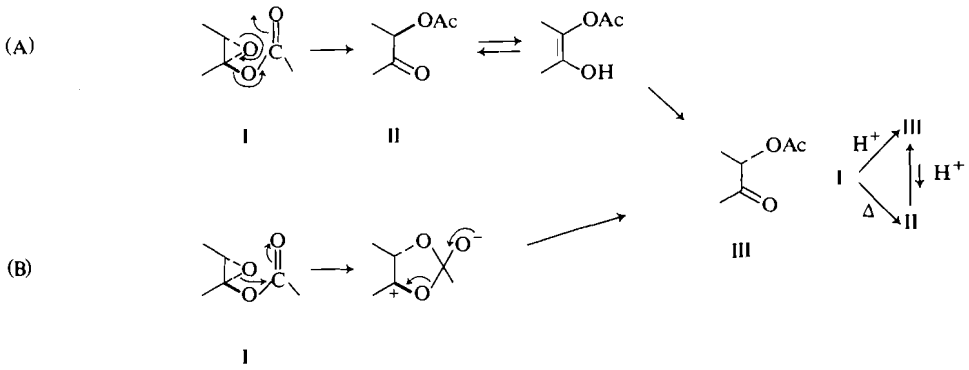

[1]Laboratoire de Réactions sélectives associé au CNRS.

[2]Révision reçue le 9 septembre, 1974.

Can. J. Chem. Downloaded from www.nrcresearchpress.com by 84.22.46.98 on 09/08/12
For personal use only.

Can. J. Chem. Downloaded from www.nrcresearchpress.com by 84.22.46.98 on 09/08/12
For personal use only.

Résultats

La nopinone **1***a* et la *cis*-méthyl-3 nopinone[3] **1***b* traitées en milieu acide par l'acétate d'isopropényle conduisent aux acétates d'énols **2***a* (4) et **2***b*, oxydés en **3***a* et **3***b* par l'acide *p*-nitroper-

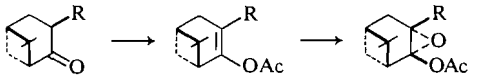

1 **2** **3**

a R = H
b R = CH_3

benzoïque (pour des raisons stériques connues en série pinanique, l'oxygène de l'oxiranne est *trans*). En vue de l'identification de produits secondaires, nous avons également préparé l'acétate d'énol **5** de l'isonopinone **4** puis son époxyde **6**. Il faut noter une difficulté spéciale pour obtenir **5** avec de bons rendements (voir partie expérimentale).

On étudie le comportement des époxyacétates **3***a* et **3***b* en présence de bromure de zinc et thermiquement. Les produits des réactions sont séparés par chromatographie en phase gazeuse (c.p.v.) sur colonne de DEGS.[4]

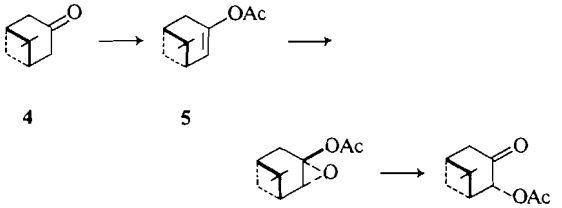

4 **5** **6** **8**

Action du bromure de zinc

Sous l'action du bromure de zinc, **3***a* donne principalement le cétoacétate **7***at* (85%) accompagné d'une petite quantité de **7***ac* (~10%) et d'un autre cétoacétate (d'après les spectres i.r. et r.m.n. du produit isolé en c.p.v.) identique au produit **8** obtenu par traitement de **6** dans les mêmes conditions (~5%).

Avec **3***b*, on obtient également de façon prépondérante le cétoacétate **7***bt* attendu. Cependant la c.p.v. indique la formation de produits légers (10% environ du total). Le composé **7***bt* constitue 70% du mélange des produits lourds; on identifie 5% du cétoacétate **7***bc* et 25% de cétol **9***bt*.

Traitement thermique

L'évolution thermique des époxyacétates est plus complexe. Mise à part la formation de 5%

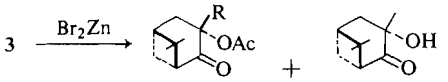

7*t* **9***bt*

c OH, OAc *cis*
t OH, OAc *trans*

environ de produits légers et 2 à 3% de **8**, l'époxyde **3***a* donne un mélange des cétoacétates **7***a cis* et *trans*. A 190–195 °C, en 15 min, la transformation est complète; les proportions sont 25 et 75% respectivement. Si le chauffage est arrêté après 2 min, il reste (d'après la r.m.n.) la moitié d'époxyde non transformé, mais les deux cétoacétates sont présents dans le même rapport que lorsque la transformation est complète. A 255 °C par contre, en 15 min, les proportions sont inversées: on obtient 65% de **7***ac* et 35% de **7***at*.[5]

On observe par ailleurs une lente transformation thermique de **7***at*: le mélange 25% **7***ac* + 75% **7***at* obtenu précédemment donne 40–60 en 2 h à 200 °C; l'échantillon **7***at* (obtenu avec Br_2Zn) donne 30% de **7***ac* et 70% de **7***at* en 2 h à 185 °C, mais la transformation n'est pas sensible en 15 min à 195 °C. Notons enfin que, dans les conditions "acides" (Br_2Zn), un mélange **7***ac* + **7***at* n'est pas transformé.

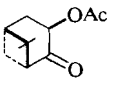

7*ac*

+ **7***at* ⟵ **3***a*

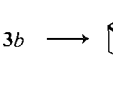

7*bc*

3*b* ⟶ + **9***bt*

[3] *Cis* ou *trans* sont exprimés par rapport au pont *gem*-diméthylé.

[4] Les époxydes d'acétates d'énols, **3***a*, **3***b* et **6**, sont très fragiles en c.p.v. Si l'injecteur n'est pas nettoyé préalablement avec du diéthylaminoéthanol les époxydes s'isomérisent de la même façon qu'avec le bromure de zinc. Ils s'isomérisent de toute façon sur la colonne de DEGS. Les spectres de r.m.n. des mélanges réactionnels permettent de vérifier l'absence de produit de départ après le traitement d'isomérisation.

[5] A température plus élevée, le produit brunit trop et charbonne.

Can. J. Chem. Downloaded from www.nrcresearchpress.com by 84.22.46.98 on 09/08/12
For personal use only.

La transformation de **3***b* est également complète à 195 °C en 15 min. On observe la formation de produits légers (environ 5% du total). Le cétoacétate **7***bc* représente 82% des produits lourds. Il est accompagné de 3% de son isomère **7***bt* et de 15% de cétol **9***bt*. Dans les mêmes conditions, **7***bc* et **7***bt* sont stables.

Si l'on chauffe l'époxyde **3***b* 30 min à 250 °C, il se forme beaucoup de produits légers (parmi lesquels, d'après la r.m.n. et la c.p.v., on identifie la méthylène-3 nopinone **15**), mais les quantités relatives de cétoacétate et de cétol sont les mêmes.

Interprétation des résultats

Nous traiterons d'abord les résultats essentiels, formation des cétoacétates **7**, puis des produits secondaires **8** et **9***bt*.

Action du bromure de zinc

Les résultats essentiels obtenus dans l'action du bromure de zinc sont en accord avec le travail de Williamson *et coll.* (3); le mécanisme de type A (**I** → **II** → **III**) est ainsi exclu, dans le cas de **7***b* du moins où la forme énolique est impossible; il l'est aussi dans le cas de **7***a* puisque nous avons noté l'absence de transformation de **7***ac* dans les conditions "acides." Le mécanisme B intervient: la formation d'un cation tel que **IV** conduisant au cétoacétate, est ici favorisée par rapport à la transformation du squelette qui accompagne généralement la présence d'un carbocation sur le carbone 2.

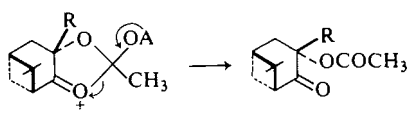

IV 7*t*

Traitement thermique

Dans l'isomérisation thermique, **7***bc* se forme par le mécanisme concerté A (**I** → **II**). Signalons que Carlson et Pierce (6) indiquent une isomérisation difficile pour **10**; ils obtiennent 45% de **11** à 265°, et invoquent des effets stériques pour expliquer cette difficulté.

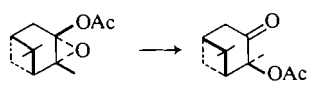

10 **11**

La transformation de **3***a* conduit aux isomères **7***ac* et **7***at* par deux voies différentes: en effet, dans la transformation incomplète, les deux cétoacétates sont présents dans les mêmes proportions que lorsque la transformation est complète (75% de **7***at*). (*a*) On peut exclure le passage **7***ac* → **7***at* (**II** → **III**) puisque le chauffage prolongé de **7***at* (obtenu par Br_2Zn) donne au contraire un mélange **7***ac* + **7***at*; dans le mélange d'isomérisation thermique de **3***a*, la proportion de **7***ac* croît si l'on prolonge le chauffage. (*b*) Pour une très grande part du moins, on peut exclure la formation de **7***ac* par **7***at* → **7***ac*, car la transformation de **7***at* est lente et peu sensible dans les conditions d'isomérisation de **3***a* (15 min à 190 °C). Même à 290 °C en 10 min, **7***at* ne s'isomérise pas. Le mécanisme concerté (type A) serait responsable de la formation de **7***ac* (inversion), d'autant plus que la température est plus élevée et **7***at* (rétention) serait formé par un mécanisme de "type acide" (type B).

Pourquoi l'époxyde **3***a* subit-il de préférence l'ouverture de "type acide" ? Si l'on examine les modèles moléculaires, on voit que pour **3***a* et **3***b* l'état de transition pour le mécanisme concerté (A) est gêné par le méthyle-9. Par contre, la conformation qui doit être adoptée dans un mécanisme de type B est nettement plus difficile à atteindre lorsque R = CH_3, **3***b*, que lorsque R = H, **3***a*. Ceci expliquerait donc que la transformation de type B soit relativement favorisée lorsque R = H, **3***a*, et que l'isomérisation de **3***b*, R = CH_3, soit plus lente en présence de bromure de zinc (il reste en effet 30% d'époxyde **3***b* non transformé après 3 h de reflux dans du benzène, alors que dans les mêmes conditions, la transformation de **3***a* est complète).

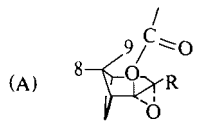

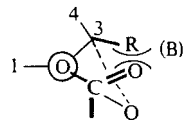

Cette interprétation est en accord avec l'examen des résultats décrits dans la littérature, pour l'isomérisation thermique d'époxyacétates ayant un atome d'hydrogène sur l'oxiranne. Lorsqu'il n'y a pas d'inversion (1), ou bien si l'inversion est partielle au niveau du carbone β (7) (formation de **III**), on observe des interactions stériques pour l'intervention du mécanisme concerté (A). En l'absence de ces interactions (2, 8) l'inversion est normalement observée.[6]

[6]Nous remercions tout particulièrement l'un des rapporteurs pour toutes les suggestions et discussions au sujet de ce paragraphe.

Can. J. Chem. Downloaded from www.nrcresearchpress.com by 84.22.46.98 on 09/08/12
For personal use only.

Produits secondaires

Avec **3***a*, la formation du produit secondaire **8** peut s'expliquer à partir du cation **IV**, par passage à une forme dérivée d'ène diol (5), ou même par simple isomérisation de l'époxyde.

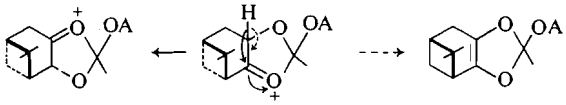

IV

Quant à la formation du cétol **9***bt* dans tous les traitements de **3***b*, on l'explique par les difficultés rencontrées dans l'une et l'autre des transformations, par suite des contraintes stériques. On fait intervenir alors un troisième mécanisme, dans lequel l'oxygène de l'oxiranne attaque un proton de l'acétyle, avec élimination de cétène.[7]

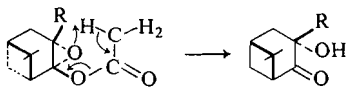

Détermination de la stéréochimie des produits obtenus

Série b

Les cétoacétates **7***b* sont réduits par l'aluminohydrure de lithium et les diols obtenus sont comparés avec des échantillons authentiques préparés comme suit.

L'époxyde **12** du méthylène-3 *trans*-nopinol (9) est réduit en diol **13***b* qui donne un dioxolanne **14***b*. Pour éliminer, dans le spectre r.m.n. de **13***b*, l'ambiguité dans l'attribution des signaux des méthyles 9 et 10, la réduction de **12** a également été effectuée avec $LiAlD_4$.

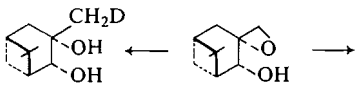

13′*b* **12**

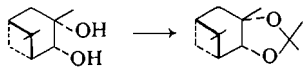

13*b* **14*b***

Le méthylène-3 *cis*-nopinol **16** peut être isolé à l'état cristallisé du mélange de réduction de la méthylène-3 nopinone **15** (10) par $LiAlH_4$. L'époxyde correspondant **17** est réduit en diol **18***b* dont l'oxydation (CrO_3–pyridine) fournit le cétol **9***bt*. Ce cétol ne peut être obtenu pur par oxydation de **13***b* car il y a en même temps rupture du cycle.

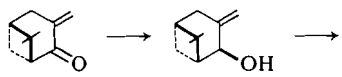

15 **16**

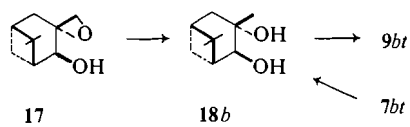

17 **18*b***

Enfin, du mélange **19***t* + **19***c* des époxydes de la méthylène-3 nopinone, on a séparé par c.p.v. l'époxyde *trans* **19***t* le plus abondant (11). Sa réduction par $LiAlH_4$ donne en quantités égales les diols **18***b* et **13***b*.

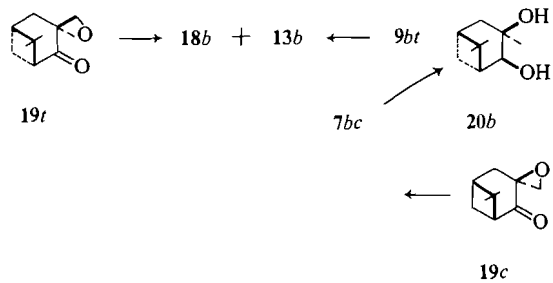

19*t* **7*bc*** **20*b***

19*c*

Un échantillon de **19***t* + **19***c* (2:1), donne les trois diols **18***b*, **13***b* et **20***b* dans des proportions pratiquement équivalentes.

On peut maintenant identifier à **18***b* le diol de réduction de **7***bt* et à **20***b* celui provenant de la réduction de **7***bc*. Ce dernier donne d'ailleurs un dioxolanne **21***b*, ce qui confirme la position *syn* des deux hydroxyles.

Si le cétoacétate **7***bc* est saponifié, on obtient le cétol **9***bc* dont le spectre r.m.n. possède les mêmes déplacements chimiques que celui du produit décrit dans (6). Sa réduction conduit au diol **20***b*, alors que la réduction du cétol **9***bt* est moins sélective (72% de **18***b* et 28% de **13***b*) que celle de l'acétate correspondant **7***bt*. Ces observations sont en accord avec celles de Carlson et Pierce d'une part (6), et Hirata d'autre part (12) sur la réduction de cétols et cétoacétates dans cette série.

On pouvait également effectuer la réduction de l'époxyacétate **3***b* par $LiAlH_4$ pour préparer

[7]A ce sujet, il faut noter un rapport M − 42/M beaucoup plus grand dans le spectre de masse de **3***b* que dans celui de **3***a*.

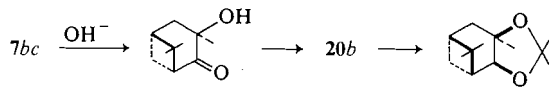

9*bc* 21*b*

le diol **18***b*. La littérature indique en effet la formation d'un seul diol dans la réduction d'époxyacétates (1, 13). En fait, la sélectivité n'est pas totale: on obtient 87% de **18***b* et 13% de **13***b*, soit des proportions légèrement différentes de celles obtenues dans la réduction du cétol **9***bt* dans les mêmes conditions (72 et 28%). On constate, que si l'on effectue la réduction à basse température, avec une quantité limitée d'hydrure, on obtient, après hydrolyse, un mélange réactionnel très riche en cétol **9***bt* (composé de plus d'une petite quantité de produit de départ et de diols de réduction complète). La réduction de l'époxyacétate passe donc par un alcoolate intermédiaire dont l'hydrolyse donne le cétol **9***bt*.

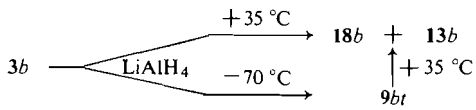

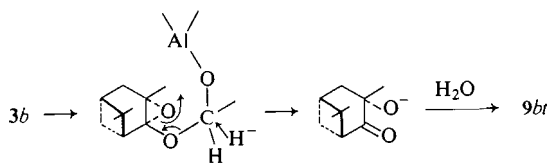

Série a

Le cétoacétate **7***at* a le même temps de rétention en c.p.v. et le même spectre r.m.n. que le produit que nous avons obtenu selon (6) par ozonolyse de l'acétate du *trans*-pinocarvéol **22**.

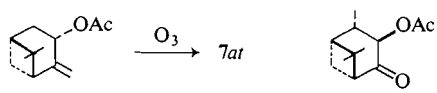

22 23

Le cétoacétate **7***ac* est obtenu pur par c.p.v. (DEGS) du mélange d'isomérisation thermique de **3***a*. En r.m.n., les déplacements chimiques pour les méthyles 9 et 8 (0.82 et 1.37) sont très proches de ceux (0.81 et 1.38) du cétoacétate **23**, pratiquement de même conformation (12).

Le composé **7***ac* est traité par l'iodure de méthylmagnésium. Le diol obtenu de façon prépondérante a les mêmes déplacements chimiques en r.m.n. que **24** décrit dans la littérature (6).

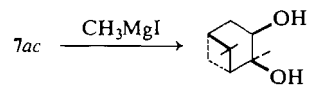

24

Par réduction avec $LiAlH_4$, le cétoacétate **7***at* donne un diol cristallisé pratiquement pur, auquel nous attribuons la structure **18***a* par comparaison avec la réduction de **7***bt* et par analogie des déplacements chimiques pour les méthyles 8 et 9 dans les spectres r.m.n. de **18***a* et **18***b*.

Dans cette série également, la réduction de l'époxyacétate **3***a*, qui aurait pu nous donner le diol **18***a*, n'est pas sélective. Par réduction complète, on obtient deux diols en quantités pratiquement équivalents, **18***a* et **13***a*, ce dernier formant un dioxolanne **14***a*. A basse température, par une réduction incomplète, on observe la formation du cétol **9***at*: dans les mêmes conditions que celles utilisées avec **3***b*, on obtient un mélange de 20% de produit de départ, 40% de cétol **9***at* et 20% de chacun des diols **18***a* et **13***a* (r.m.n.).

Résonance magnétique nucléaire

Il faut faire quelques remarques au sujet des spectres r.m.n. Il est connu que dans la série pinanique, les méthyles 8 et 9 ont des déplacements chimiques très distincts et que celui du méthyle 9 est très influencé par la présence de substituants oxygénés sur les carbones 2, 3 ou 4 (—OH, —OAc, —OTs, oxygène d'oxiranne) (14, 15, 16). Lorsque la fonction est *cis*, le signal est déplacé vers les champs faibles par rapport à l'isomère qui possède la même fonction en *trans*. Cette règle reste valable lorsque deux de ces fonctions sont présentes (6, 12 et, dans ce travail, comparer **13***a* et **18***a*, **13***b*, **18***b* et **20***b*).

Par contre lorsqu'il y a, en plus de la fonction oxygénée à liaison simple, une fonction carbonyle, cette règle n'est plus applicable sans restriction. S'il n'y a pas de différence notable de conformation entre les deux isomères (17), l'observation est la même (6, et ce travail: **7***bt* et **7***bc*, **9***bt* et **9***bc*). L'observation est différente lorsque la conformation varie d'un épimère à l'autre (12, et ce travail **7***at* et **7***ac*).

En conclusion, les époxydes d'acétates d'énols s'isomérisent selon deux schémas: l'isomérisation en milieu acide se fait régulièrement avec rétention de configuration; par action de la chaleur, l'isomérisation se fait avec inversion de configuration selon le mécanisme concerté, si

Can. J. Chem. Downloaded from www.nrcresearchpress.com by 84.22.46.98 on 09/08/12
For personal use only.

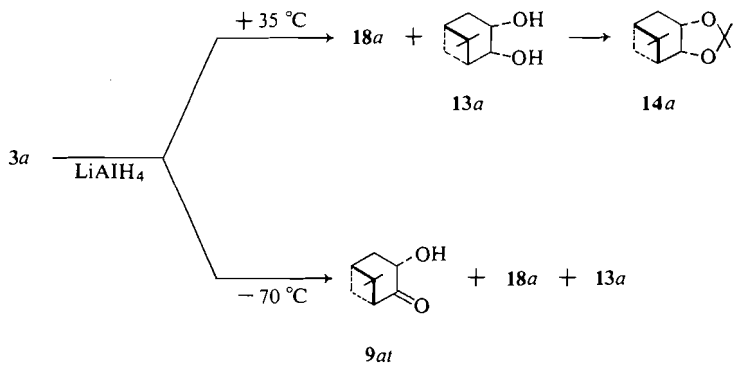

l'oxiranne ne porte pas d'hydrogène; dans le cas contraire, si le mécanisme concerté est empêché stériquement, un mécanisme de "type acide" entre en concurrence. Dans le cas particulier d'un oxiranne entièrement substitué, pour lequel les deux mécanismes rencontrent des empêchements stériques, on observe, à côté de l'isomérisation en cétoacétate, un arrachement d'hydrogène, avec départ probable de cétène et formation de cétol.

Partie expérimentale

Sauf indications particulières, les pouvoirs rotatoires sont mesurés sur un appareil Perkin–Elmer 141, à 589 nm, à 21 °C, la concentration étant 5 g pour 100 cm³ dans le cyclohexane; les spectres de r.m.n. sont effectués sur les appareils Varian A 60 et Jeol C-60 H, dans le deutériochloroforme, le tétraméthylsilane servant de référence interne; les déplacements chimiques sont exprimés en unité δ (p.p.m.). Les spectres i.r. sont enregistrés sur un Perkin–Elmer 457 et effectués sans solvant pour les liquides, dans le Nujol pour les produits cristallisés. Le spectrographe de masse est un Varian MAT CH 7, 70 eV; on opère avec introduction directe sans chauffage pour les produits solides (dir), et vers 160 °C pour les liquides (160); les fragments sont exprimés en *m/e* (% du fragment le plus abondant), et l'absence d'ion parent est indiquée s'il y a lieu. Les chromatographies en phase gazeuse préparatives et analytiques sont effectuées à l'aide d'un Varian Aerograph Autoprep.

Modes opératoires

Les caractéristiques de tous les produits obtenus seront groupés dans un même paragraphe, à la suite des modes opératoires.

Acétates d'énols

Dans un ballon muni d'un réfrigérant, on met une solution de 0.06 mol de cétone dans 120 cm³ d'acétate d'isopropényle; on ajoute 10 cm³ d'acétate d'isopropényle contenant 0.2 cm³ d'acide sulfurique concentré. On laisse à reflux pendant 48 h, puis on concentre à la moitié du volume. La solution est refroidie et diluée avec de l'éther, lavée avec une solution de carbonate de sodium et à l'eau. On sèche et distille.

Acétate d'énol 2b: à partir de 9.2 g de *cis*-méthyl-3 nopinone **1***b*, on distille 9.5 g de **2***b* (82%).

Acétate d'énol 2a: à partir de 8.3 g de nopinone **1***a*, on distille 9.3 g de **2***a* (85%). Pour effectuer la mesure de $[\alpha]_D$, un échantillon est séparé par c.p.v. sur colonne de silicone SE 54 à 1% sur Chromosorb G, diamètre 1/4 po., longueur 3 m, à 110 °C.

Acétate d'énol 5: la mode opératoire est le même, mais il faut laisser le mélange réactionnel à reflux pendant une semaine. A partir de 4 g d'isonopinone **4**, on distille 4.5 g de **5** (85%).

Epoxydation des acétates d'énols

Une solution de 15 mmol d'acétate d'énol dans 20 cm³ d'éther anhydre est ajoutée goutte à goutte, à 0 °C, à une solution de 18 mmol d'acide *p*-nitroperbenzoïque dans 40 cm³ d'éther anhydre. On laisse avec agitation pendant 1 nuit à température ordinaire. L'acide *p*-nitrobenzoïque est essoré; la solution éthérée est lavée avec de la soude 1.5 *N*. Après séchage, on évapore le solvant et on distille.

Epoxyde 3b: 2.8 g d'acétate d'énol **2***b* (0.013 mol) donnent 2.55 g d'époxyde **3***b* cristallisé (80%).

Epoxyde 3a: 8.1 g d'acétate d'énol **2***a* (0.041 mol) donnent 8.5 g d'époxyde **3***a* cristallisé (95%).

Epoxyde 6: 2.5 g d'acétate d'énol **5** donnent 2.5 g d'époxyde **6** (90%).

Isomérisation des époxydes d'acétates d'énols par le bromure de zinc

A une suspension de 50 mg de bromure de zinc fraîchement fondu, dans 5 cm³ de benzène anhydre, on ajoute goutte à goutte une solution de 5.7 mmol d'époxyde dans 5 cm³ de benzène. On porte à reflux, on refroidit ensuite la solution et on lave à l'eau. Après séchage de la phase organique sur sulfate de sodium, on évapore le solvant et on distille (distillation moléculaire, bain vers 80 °C/ 0.05 mm Hg). Le produit est examiné en c.p.v. avant la distillation, sur colonne de DEGS, 15% sur Chromosorb P, diamètre ¼ po., longueur 3 m, à 145 °C. Les séparations par c.p.v. sont effectuées à l'aide d'une colonne de DEGS, 15% sur Chromosorb W NAW, diamètre 3/8 po., longueur 3 m, à 145 °C.

Isomérisation de 3b: une solution de 1.2 g de **3***b* (5.7 mmol) est laissée une nuit à reflux. Après les opérations décrites ci-dessus, on distille 1 g d'un mélange dans lequel on identifie après c.p.v. préparative (dans l'ordre d'élution): le cétol **9***bt* (25%), le cétoacétate **7***bt* (70%) et le cétoacétate **7***bc* (5%).

Isomérisation de 3a: une solution de 2 g (10.2 mmol) de **3***a* est laissé 3 h à reflux dans les conditions indiquées. En fin d'opération, on distille 1.7 g de produit (85%) dans lequel on identifie, après c.p.v. préparative (dans l'ordre d'élution): le *trans*-acétoxy-2 one-3 **8** (ci-dessous) (7%),

Can. J. Chem. Downloaded from www.nrcresearchpress.com by 84.22.46.98 on 09/08/12
For personal use only.

Can. J. Chem. Downloaded from www.nrcresearchpress.com by 84.22.46.98 on 09/08/12
For personal use only.

le *trans*-acétoxy-3 one-2 **7***at* (80%) et le *cis*-acétoxy-3 one-2 **7***ac* (13%).

Isomérisation de **6**: la solution de 1 g (5 mmol) de **6** est laissée à reflux 5 h. On distille 850 mg de produit (85%) dans lequel le *trans*-acétoxy-2 one-3 **8** est le constituant principal.

Traitement thermique

Un ballon de 50 cm³ est chauffé à 195 °C sous un léger courant d'azote. On introduit 2 g d'époxyacétate en on chauffe à la même température pendant 15 min. Le ballon est choisi suffisamment grand par rapport à la masse de produit utilisée pour permettre une équilibration relativement rapide de la température au sein du liquide. Les conditions de c.p.v. sont les mêmes que pour l'isomérisation par le bromure de zinc.

Isomérisation de **3***b*: après le chauffage, on analyse le produit réactionnel par c.p.v.; outre quelques produits légers, on identifie 15% de cétol **9***bt*, 3% de cétoacétate **7***bt* et 82% de cétoacétate **7***bc*. A partir de 2 g de **3***b*, on distille 1.7 g de mélange (85%).

Isomérisation de **3***a*: à partir de 2 g de **3***a*, on distille 1.7 g de produit (85%) contenant essentiellement le *trans*-acétoxy-3 one-2 **7***at* et le *cis*-acétoxy-3 one-2 **7***ac*, dans le rapport 75/25, d'après les intégrations du spectre r.m.n. La c.p.v. préparative permet d'isoler les deux constituants purs.

Réduction des cétoacétates **7** *par l'aluminohydrure de lithium*

On ajoute, à 0 °C, le cétoacétate dissous dans l'éther anhydre, à la solution d'une quantité équimoléculaire de $LiAlH_4$ dans l'éther anhydre. On porte à reflux pendant 1 h après l'addition. Après refroidissement, on hydrolyse avec le minimum d'eau. On filtre et on évapore le solvant.

Réduction de **7***bt*: 840 mg de cétoacétate **7***bt* dissous dans 10 cm³ d'éther sont traités par 150 mg de $LiAlH_4$ dissous dans 10 cm³ d'éther. On obtient 650 mg de diol **18***b* (95%).

Réduction de **7***bc*: 1.35 g d'un échantillon contenant environ 15% de cétol **9***bt* (d'après la c.p.v. et la r.m.n.), dans 25 cm³ d'éther, sont traités avec 300 mg de $LiAlH_4$ dans 20 cm³ d'éther. On obtient 1 g (90%) de diols: 85% de **20***b* et 15% de **18***b* + **13***b* (3:1) provenant de la réduction du cétol **9***bt*. L'évaluation est faite d'après le spectre de r.m.n. et par comparaison avec le spectre du mélange de réduction de **9***bt* (voir plus loin).

Réduction de **7***at*: 200 mg de cétoacétate **7***at* dans 10 cm³ d'éther sont traités par 50 mg de $LiAlH_4$ dans 5 cm³ d'éther. On obtient presque quantitativement le diol **18***a* cristallisé.

Réduction de la méthylène-3 nopinone **15**

Lorsque la réduction de la méthylène-3 nopinone **15** est effectuée avec un excès d'aluminohydrure de lithium dans l'éther à reflux, ou de borohydrure de sodium dans le méthanol à température ordinaire, on obtient des mélanges contenant la *cis*-méthyl-3 nopinone **1***b*, le *cis*-méthyl-3 *cis*-nopinol et le méthylène-3 *cis*-nopinol **16** en quantités variables. Les deux alcools sont difficiles à séparer par c.p.v. Avec le mode opératoire suivant, le produit réactionnel contient uniquement la cétone **1***b* et l'alcool cherché **16**.

A une solution de 1.3 g de méthylène-3 nopinone **15** dans 25 cm³ d'éther anhydre, à 0 °C, on ajoute goutte à goutte assez rapidement, 50 cm³ d'une solution 0.39 *N* de $LiAlH_4$ dans l'éther anhydre (soit environ 2 équiv). On laisse revenir à température ambiante pendant 1/4 h. Puis on hydrolyse avec le minimum de glace, en refroidissant à nouveau le mélange réactionnel. On essore le précipité.

La c.p.v. préparative est effectuée sur une colonne de FFAP 20% sur Chromosorb A NAW, diamètre 3/8 po., longueur 3 m à 110 °C. Le mélange contient, par ordre d'élution, 65% de *cis*-méthyl-3 nopinone **1***b* et 35% de méthylène-3 *cis*-nopinol **16**.

Epoxydation des méthylène-3 nopinols cis et trans

Le mode opératoire est le même que pour l'époxydation des acétates d'énols.

Epoxyde du méthylène-3 cis-nopinol **17**: après réaction de 3.4 g (22 mmol) d'alcool **16** avec 4.6 g (24.5 mmol) d'acide *p*-nitroperbenzoïque, on distille 3 g d'époxyalcool **17** (80%).

Epoxyde du méthylène-3 trans-nopinol **12**: après réaction de 7.6 g (50 mmol) d'alcool avec 11 g (60 mmol) d'acide *p*-nitroperbenzoïque, on distille 6.9 g d'époxyalcool **12** (82%).

Réduction des époxyalcools

On ajoute, à 0 °C, l'époxyalcool dissous dans l'éther anhydre à la solution d'une quantité équimoléculaire de $LiAlH_4$ dans l'éther anhydre. On porte à reflux pendant 1 h après l'addition. Après refroidissement, on hydrolyse avec le minimum d'eau. On essore le précipité et on évapore le solvant.

Réduction de **17**: 840 mg (5 mmol) d'époxyalcool **17** dans 10 cm³ d'éther sont traités par 190 mg de $LiAlH_4$ (5 mmol) dissous dans 10 cm³ d'éther. On obtient 845 mg de produit brut cristallisé **18***b*.

Réduction de **12**: (*a*) avec $LiAlH_4$, 380 mg (10 mmol) dans 20 cm³ d'éther; la réduction de 1.69 g de **12** (10 mmol) dans 20 cm³ d'éther, donne 1.7 g de diol **13***b*; (*b*) avec $LiAlD_4$, 210 mg (5 mmol) dans 10 cm³ d'éther; la réduction de 840 mg de **12** (5 mmol) dans 10 cm³ d'éther conduit à 800 mg de **13***'b* (95%).

Réduction des époxycétones **19***c et* **19***t*

Le mode opératoire est le même que celui décrit ci-dessus pour les époxyalcools.

Réduction de **19***t*: 280 mg de **19***i* (1.68 mmol) dans 5 cm³ d'éther sont réduits par 60 mg de $LiAlH_4$ (1.6 mmol) dans 10 cm³ d'éther. On obtient 240 mg du mélange **18***b* + **13***b* dans des proportions pratiquement équivalentes d'après la r.m.n. Le composé **18***b* cristallise dans le mélange.

Réduction de **19***c* + **19***t* (1:2): 3.32 g (20 mmol) de cétones dans 25 cm³ d'éther sont traités par 0.760 g de $LiAlH_4$ (20 mmol) dans 50 cm³ d'éther. On obtient 3.3 g de trois diols en proportions pratiquement équivalentes (r.m.n. dans CCl_4 et pyridine): **20***b*, *cis*-OH-2 *cis*-OH-3 (réduction de l'époxyde **19***c*); **18***b*, *cis*-OH-2 *trans*-OH-3; et **13***b*, *trans*-OH-2 *trans*-OH-3 (réduction de l'époxyde **19***t*, voir ci-dessus). Le mélange réactionnel est dissous dans 10 cm³ de chloroforme: on laisse à 0 °C, on essore 1 g de **18***b*. La phase liquide contient alors essentiellement **13***b* et **20***b* en quantités équivalentes (spectres r.m.n. pris dans CCl_4 et dans la pyridine).

Préparation des cétols **9***bc et* **9***bt*

Composé **9***bc par saponification du cétoacétate* **7***bc*: dans un ballon de 50 cm³ muni d'un réfrigérant, on met

Can. J. Chem. Downloaded from www.nrcresearchpress.com by 84.22.46.98 on 09/08/12
For personal use only.

la solution de 500 mg de **7***bc* dans 10 cm³ de méthanol; on ajoute la solution de 300 mg de potasse dans un minimum d'eau et 10 cm³ de méthanol. On laisse à reflux pendant 2 h. On évapore le méthanol sous pression réduite. On dilue avec 10 cm³ d'eau et on extrait plusieurs fois à l'éther. On sèche la solution éthérée, on évapore le solvant et distille (distillation moléculaire, bain vers 95 °C/0.05 mm Hg) 320 mg de cétol **9***bc* (80%).

*Composé **9***bt par oxydation du diol **18***b par le complexe anhydride chromique – pyridine*: 500 mg de diol **18***b* (réduction des époxycétones **19**) (3 mmol) dans 10 cm³ de pyridine anhydre sont ajoutés goutte à goutte au complexe formé par l'addition de 1.2 g d'anhydride chromique (12 mmol) à 20 cm³ de pyridine anhydre, à −20 °C. On laisse agiter une nuit à température ambiante. On ajoute 50 cm³ d'eau et on extrait à l'éther. La phase organique est lavée avec une solution diluée d'acide chlorhydrique, une solution de bicarbonate de sodium et à l'eau. On sèche et on évapore le solvant. On obtient 380 mg de cétol **9***bt* (80%).

Réduction des cétols

*Réduction de **9***bc*: on ajoute, à 0 °C, la solution de 300 mg de cétol **9***bc* (1.8 mmol) dans 5 cm³ d'éther anhydre, à la solution de 80 mg (2 mmol) de $LiAlH_4$ dans 10 cm³ d'éther anhydre. Après addition, on porte à reflux pendant 1 h. Après refroidissement, on hydrolyse avec le minimum d'eau, on essore le précipité et on évapore le solvant. On distille (distillation moléculaire, bain vers 110 °C/0.05 mm H) 260 mg de diol **20***b*, *cis*-OH-2 *cis*-OH-3 (87%).

*Réduction de **9***bt*: dans les mêmes conditions, on traite une solution de 360 mg de cétol **9***bt* dans 10 cm³ d'éther, par une solution de 120 mg de $LiAlH_4$ dans 20 cm³ d'éther. On recueille 350 mg de produit brut (95%) contenant les diols **18***b*, *cis*-OH-2 *trans*-OH-3, et **13***b*, *trans*-OH-2 *trans*-OH-3, dans le rapport 72/28 (évaluation faite d'après le spectre de r.m.n.).

Réduction complète des époxydes d'acétates d'énols

On opère dans les mêmes conditions que pour les cétols.

*Réduction de **3***b*: la solution de 1.05 g de **3***b* (20 mmol) dans 20 cm³ d'éther est traitée par la solution de 190 mg de $LiAlH_4$ dans 20 cm³ d'éther. On obtient 0.82 g (95%) de **18***b* + **13***b*, 87:13 d'après la r.m.n. (comparer avec les réductions de l'époxycétone **19***t*, du cétol **9***bt* et du cétatoacétate **7***bt*).

*Réduction de **3***a*: 100 mg de **3***a* (0.5 mmol) dissous dans 5 cm³ d'éther sont ajoutés à la solution de 95 mg de $LiAlH_4$ (2.5 mmol) dans 10 cm³ d'éther. On obtient 72 mg (92%) des diols **18***a* + **13***a* (45:55 d'après le spectre de r.m.n.).

Réduction incomplète des époxydes d'acétates d'énols

On porte à ébullition pendant 30 min la suspension de 420 mg de $LiAlH_4$ dans 40 cm³ d'éther anhydre. On laisse refroidir et décanter et on prélève 10 cm³ de la solution environ 1 *N* (2.5 mmol) que l'on ajoute lentement à la solution de 5 mmol d'époxyacétate dans 10 cm³ d'éther anhydre, refroidie à −70 °C. On laisse agiter pendant 30 min à cette température. Puis on hydrolyse toujours à −70 °C, successivement avec une solution de méthanol dans l'éther anhydre, du méthanol, de l'éther saturé d'eau; on ajoute enfin 10 cm³ d'eau. On essore le précipité, on extrait à l'éther, on sèche et distille.

*Réduction de **3***b*: 1.05 g de **3***b* (5 mmol) est traité par 10 cm³ de solution de $LiAlH_4$. On distille 0.80 g de produit (94%), contenant (d'après le spectre de r.m.n.) le cétol **9***bt* (70%), accompagné de produit de départ (10%) et de diols de réduction totale (20%).

*Réduction de **3***a*: on traite 0.50 g (2.5 mmol) par 5 cm³ de la solution de $LiAlH_4$. On obtient 0.4 g de produit contenant: 25% de produit de départ, 50% de cétol **9***at*, 25% de diol **18***a* et 25% de diol **13***a* (r.m.n.).

*Préparation du diol **24***

L'iodure de méthylmagnésium est préparé à partir de 0.22 g de magnésium (9 mmol) et de 1.3 g d'iodure de méthyle (9 mmol) dans 10 cm³ d'éther anhydre. On ajoute, à 0 °C, 300 mg de cétoacétate **7***ac* (séparé de **7***at* par c.p.v.) (1.5 mmol) dans 10 cm³ d'éther anhydre. On porte à reflux pendant 3 h. On hydrolyse avec une solution saturée de chlorure d'ammonium. On extrait plusieurs fois la phase aqueuse à l'éther. On sèche, on évapore le solvant et on obtient 260 mg de produit brut riche en diol **24** dont la r.m.n. correspond à ce qui est décrit dans (6).

Préparation des dioxolannes

Une portion (2.5 mmol) de diol est dissoutes dans 10 cm³ de diéthoxy-2,2 propane; on ajoute 1 à 2 mg d'acide *p*-toluène sulfonique et on laisse 3 h à température ambiante. On lave avec une solution de carbonate de sodium et à l'eau. On sèche et distille (distillation moléculaire, bain vers 80 °C/0.05 mm Hg).

*Dioxolanne **14***b*: 400 mg de diol **13***b* donnent 400 mg de **14***b* (80%).

*Dioxolanne **21***b*: 200 mg de diol **20***b* donnent 200 mg de **21***b* (80%).

*Dioxolanne **14***a*: à partir de 300 mg du mélange des diols **18***a* + **13***a*, (1:1, voir partie théorique), on distille 180 mg (90%) de dioxolanne **14***a*. Le résidu de la distillation est riche en **18***a*.

Caractéristiques des produits obtenus

Acétates d'énols

*De la cis-méthyl-3 nopinone **2***b*: p.é. 45 °C/0.05 mm Hg; $[\alpha]_D$ −21.5°; i.r.: 1760 (C=O) et 1700 cm⁻¹ (C=C); r.m.n.: 0.90 (CH_3-9), 1.30 (CH_3-8), 1.44 (d, J = 9 Hz, H-7α), 1.56 (CH_3—C=), 2.09 (CH_3—CO); spectre de masse (160): 194 (5), 152 (50), 137 (20), 119 (10), 109 (100), 108 (25), 97 (30), 83 (25), 55 (15), 43 (45).

*De la nopinone **2***a*: p.é. 85 °C/13 mm Hg; $[\alpha]_D^{25}$ (*c* 5.25, $CHCl_3$) −35° (litt. (4) *c* 1.05, $CHCl_3$ −18.6°); i.r.: 1760 (C=O) et 1670 cm⁻¹ (C=CH); r.m.n. 0.95 (CH_3-9), 1.30 (CH_3-8), 1.44 (d, J = 9 Hz (H-7α)), 2.06 (CH_3—CO), 5.16, (septuplet (CH=)). Spectre de masse (160): 180 (5), 138 (90), 123 (45), 109 (12), 105 (18), 95 (100), 83 (60), 55 (30), 43 (90).

*De l'isonopinone **5***: p.é. 98 °C/18 mm Hg; i.r.: 1758 (C=O) et 1668 cm⁻¹ (C=CH); r.m.n.: 1.02 (CH_3-9), 1.30 (CH_3-8), 1.31 (d, J = 8.5 Hz (H-7α)), 2.09 (CH_3—CO), 5.72 (multiplet (CH=)).

Epoxydes des acétates d'énols

*De la méthylnopinone **3***b*: p.f. 60–62 °C (après séchage sur plaque poreuse; recristallise difficilement dans l'éther); $[\alpha]_D$ −21.5°; i.r.: 1752 cm⁻¹ (C=O); r.m.n.: 0.93 (CH_3-9), 1.29 (CH_3-8), 1.42 (CH_3-10), 2 (CH_3—CO); (pyridine: 0.94, 1.21 et 1.48). Spectre de masse (dir):

Can. J. Chem. Downloaded from www.nrcresearchpress.com by 84.22.46.98 on 09/08/12
For personal use only.

210 (trace), 168 (18), 126 (30), 123 (35), 95 (25), 83 (45), 81 (25), 55 (60), 43 (100).

De la nopinone ***3a***: p.f. 59–60 °C (après séchage sur plaque poreuse; recristallise très lentement dans l'éther); $[\alpha]_D$ −69°; i.r.: 1755 cm^{-1} (C=O); r.m.n.: 1.02 (CH_3-9), 1.33 (CH_3-8), 2.04 (CH_3—CO), 3.46 (multiplet (CH—O)). Spectre de masse (dir): 196 (trace), 154 (3), 126 (35), 121 (13), 109 (23), 95 (20), 93 (10), 83 (100), 81 (30), 55 (75), 43 (80).

De l'isonopinone ***6***: p.é. 55–60 °C/0.05 mm Hg; i.r.: 1760 cm^{-1} (C=O); r.m.n.: 1.02 (CH_3-9), 1.30 (CH_3-8), 2.08 (CH_3—CO), 3.45 (d, J = 4.2 Hz (CH—O)). Spectre de masse (160): 196 (trace), 154 (3), 138 (4), 136 (7), 127 (20), 95 (18), 85 (55), 69 (37), 55 (12), 43 (100).

Cétoacétates (OAc trans)

Diméthyl(6,6) trans-acétoxy-3 cis-méthyl-3 norpinanone-2 ***7bt***: i.r.: 1725 cm^{-1}, bande large (C=O); r.m.n.: 0.74 (CH_3-9), 1.37 (CH_3-8), 1.66 (CH_3-10), 1.96 (CH_3—CO). Spectre de masse (160): 210 (trace), 167 (2), 150 (7), 135 (10), 123 (10), 109 (4), 107 (8), 95 (10), 83 (15), 55 (20), 43 (100).

Diméthyl(6,6) trans-acétoxy-3 norpinanone-2 ***7at***: i.r.: 1750 et 1730 cm^{-1} (C=O); r.m.n.: 0.90 (CH_3-9), 1.37 (CH_3-8), 2.07 (CH_3—CO), 5.28 (d de d, J_{cis} = 9 et J_{trans} = 3 Hz (CH—OAc)). Spectre de masse (160): 196 (trace), 154 (10), 136 (10), 121 (28), 95 (25), 83 (50), 55 (30), 43 (100).

Diméthyl(6,6) trans-acétoxy-2 norpinanone-3 ***8***: i.r.: 1753 et 1730 cm^{-1} (C=O); r.m.n.: 1 (CH_3-9), 1.39 (CH_3-8), 2.07 (CH_3—CO), 5.37 (petits couplages (CH—OAc)). Spectre de masse: 196 (trace), 154, 136, 127, 85 (pic de base), 69, 43.

Cétoacétates (OAc cis)

Diméthyl(6,6) cis-acétoxy-3 trans-méthyl-3 norpinanone-2 ***7bc***: i.r.: 1730 cm^{-1} (C=O); r.m.n.: 0.91 (CH_3-9), 1.37 (CH_3-8), 1.78 (CH_3-10), 2.05 (CH_3—CO). Spectre de masse (160): 210 (trace), 168 (2), 167 (3), 150 (8), 135 (8), 125 (6), 123 (13), 109 (6), 107 (6), 95 (13), 83 (20), 55 (30), 43 (100).

Diméthyl(6,6) cis-acétoxy-3 norpinanone-2 ***7ac***: r.m.n.: 0.82 (CH_3-9), 1.37 (CH_3-8), 2.13 (CH_3—CO), 5.62 (d de d, J_{cis} = 10, J_{trans} = 7 Hz (CH—OAc)). Spectre de masse (160): 196 (trace), 154 (10), 136 (7), 121 (25), 95 (25), 83 (50), 55 (50), 43 (100).

Cétols (OH trans)

trans-Hydroxy-3 cis-méthyl-3 one-2 ***9bt***: i.r.: 3350 (OH) et 1715 cm^{-1} (C=O); r.m.n.: 0.77 (CH_3-9), 1.37 (CH_3-8), 1.43 (CH_3-10). Spectre de masse (160): 168 (5), 150 (15), 135 (2), 113 (2), 110 (3), 107 (5), 95 (25), 85 (30), 84 (35), 71 (20), 67 (25), 55 (10), 43 (100).

trans-Hydroxy-3 one-2 ***9at***: i.r.: 3400 (OH) et 1710 cm^{-1} (C=O); r.m.n.: 0.89 (CH_3-9), 1.39 (CH_3-8).

Cétol (OH cis)

cis-Hydroxy-3 trans-méthyl-3 one-2 ***9bc*** (6): i.r.: 3480, bande large (OH) et 1710 cm^{-1} (C=O); r.m.n.: 0.94 (CH_3-9), 1.40 (CH_3-8), 1.50 (CH_3-10); (CCl_4: 0.94, 1.40 et 1.45).

Diols (cis-hydroxy-2 trans-hydroxy-3)

cis-Méthyl-3 ***18b***: p.f. 145–146° (sublimation); $[\alpha]_D$ +25° (*c* 5, éthanol); i.r.: 3330 cm^{-1}, bande large (OH); r.m.n.: 0.96 (CH_3-9), 1.26 (CH_3-8), 1.42 (CH_3-10), 4 (d, J = 3.5 Hz (C*H*OH)); (pyridine: 1.23, 1.28, 1.73 et 4.55). Spectre de masse (dir): 170 (trace), 155, 153 et 152 (trace), 137 (2), 113 (5), 112 (8), 109 (5), 101 (8), 97 (17), 94 (10), 85 (20), 84 (13), 83 (15), 70 (18), 56 (13), 55 (15), 43 (100).

18a: p.f. 95–96 °C (benzène – éther de pétrole) (litt. (18) 99–100°); i.r.: 3350 cm^{-1} bande large (OH); r.m.n.: 1 (CH_3-9), 1.27 (CH_3-8), vers 4.2, massif complexe (2 C*H*OH). Spectre de masse (dir): 156 (1), 138 (2), 123 (4), 112 (5), 99 (15), 97 (17), 95 (20), 86 (60), 85 (100), 81 (40), 55 (25), 43 (30).

Diols (cis-hydroxy-2 cis-hydroxy-3)

trans-Méthyl-3 ***20b***: r.m.n.: 1.09 (CH_3-9), 1.22 (CH_3-8), 1.42 (CH_3-10), 3.75 (d, J = 3 Hz (C*H*OH)); (pyridine: 1.19, 1.23, 1.42 et 3.92).

trans-Méthyl-2 ***23*** (6): r.m.n.: 1.05 (CH_3-9), 1.22 (CH_3-8 et CH_3-10), 3.86 (aspect de triplet, 15 Hz entre les deux pics extrêmes (C*H*OH)).

Diols (trans-hydroxy-2 trans-hydroxy-3)

cis-Méthyl-3 ***13b***: i.r.: 3370 cm^{-1} (OH); r.m.n.: 0.79 (CH_3-9), 1.26 (CH_3-8), 1.32 (CH_3-10), 1.95 (signal d'intensité 6H), 3.80 (C*H*OH); (pyridine: 0.80, 1.22, 1.47 et 4). Spectre de masse (dir): 170 (<0.5), 153 (0.6), 152 (0.5), 137 (1), 112 (11), 97 (18), 85 (30), 56 (15), 55 (15), 43 (100).

cis-Deutériométhyl-3 ***13'b***: i.r.: 3370 bande large (OH) et 2180 cm^{-1} (C—D); r.m.n.: 0.79 (CH_3-9), 1.26 (CH_3-8), massif vers 1.32 (CH_2D), 3.8 (s large (C*H*OH)); (pyridine: 0.8, 1.22, 1.47 et 4). Spectre de masse (dir): 171 (3), 154 (1.5), 153 (2), 138 (3), 112 (30), 97 (40), 86 (45), 85 (45), 56 (25), 44 (100).

13a: r.m.n.: 0.8 (CH_3-9), 1.27 (CH_3-8), vers 4.15 (C*H*OH).

Méthylène-3 cis-nopinol ***16***

Point de fusion 61 °C (après c.p.v., voir modes opératoires); i.r.: 3450 cm^{-1} bande large (OH), 3080, 1640 et 900 cm^{-1} (C=CH_2), 1060 cm^{-1} (C—O); r.m.n.: 1.05 (CH_3-9), 1.3 (CH_3-8), 4.43 (large (C*H*OH)), 5.15 et 5.44 (larges (CH_2=)).

Epoxyde du méthylène-3 cis-nopinol ***17***

Point d'ébullition 60 °C/0.1 mm Hg; r.m.n. (CCl_4): 1.05 (CH_3-9), 1.26 (CH_3-8), 2.85 (système AB, 2d, $\Delta\nu$ = 0.62, J = 5.5 Hz (CH_2-O)), 3.83, (d J = 3 Hz (C*H*OH)).

Epoxyde du méthylène-3 trans-nopinol ***12***

Point d'ébullition: 53 °C/0.05 mm Hg; i.r.: 3500 cm^{-1} (OH), bandes intenses vers 1040–1070 cm^{-1} (C—O); r.m.n.: 0.91 (CH_3-9), 1.29 (CH_3-8), 2.76 (système AB, 2d, $\Delta\nu$ = 0.10, J = 5 Hz (CH_2—O)), 4.11, (large (C*H*OH)); (pyridine: 0.83, 1.21 et 2.71, (2d, $\Delta\nu$ = 0.18)). Spectre de masse (140): 168 (1), 153 (2), 150 (5), 135 (12), 109 (20), 107 (15), 95 (35), 93 (15), 91 (20), 85 (100), 83 (50), 79 (40), 67 (40), 55 (50), 43 (70).

Dioxolannes

14b *(cis-Méthyl-3 dioxolanne-trans)*: i.r.: 1178 et 1140, 1068 et 1042 cm^{-1}, très intenses, (C—O—C—O—C); r.m.n.: 0.83 (CH_3-9), 1.26 (CH_3-8), 1.45 (CH_3-10), 1.45 et 1.56 (2 CH_3), 4.3 (forme de t, J = 2 Hz (CH—O)). Spectre de masse (160): ion parent non visible, 195 (20), 153 (2), 135 (18), 126 (9), 111 (25), 95 (15), 93 (40), 85 (15), 83 (13), 69 (13), 67 (19), 59 (12), 55 (18), 53 (12), 43 (100).

14a *(dioxolanne-trans)*: i.r.: 1075, 1050 et 1020 cm^{-1}

(C—O—C—O—C); r.m.n.: 0.82 (CH_3-9), 1.30 (CH_3-8), 1.35 et 1.50 (2 CH_3), 4.5 (2 CH—O). Spectre de masse (150): ion parent non visible, 181 (100), 139 (2), 126 (70), 121 (90), 111 (80), 97 (25), 95 (40), 93 (30), 79 (60), 69 (45), 67 (40), 59 (30), 43 (85).

21b (trans-méthyl-3 dioxolanne-cis): i.r.: 1035, 1065, 1090 et 1200 cm^{-1}; r.m.n.: 1.07 (CH_3-9), 1.21 (CH_3-8), 1.40, 1.50 et 1.52 (3 CH_3), 4.27 (d, J = 3.8 Hz (CH—O)). Spectre de masse (170): ion parent non visible, 195 (25), 153 (7), 141 (15), 137 (10), 135 (15), 126 (20), 111 (40), 95 (60), 83 (55), 69 (15), 67 (20), 59 (10), 55 (25), 53 (13), 43 (100).

1. N. S. Leeds, D. K. Fukushima et T. F. Gallagher. J. Am. Chem. Soc. **76**, 2943 (1954).
2. K. L. Williamson et W. S. Johnson. J. Org. Chem. **26**, 4563 (1961).
3. K. L. Williamson, J. I. Coburn et M. F. Herr. J. Org. Chem. **32**, 3934 (1967).
4. J. M. Coxon, R. P. Garland et M. P. Hartshorn. Aust. J. Chem. **23**, 1069 (1970).
5. J. J. Riehl, J. M. Lehn et F. Hemmert. Bull. Soc. Chim. Fr. 224 (1963); J. B. Stothers, I. S. Y. Wang, D. Ouchi et E. W. Warnhoff. J. Am. Chem. Soc. **93**, 6702 (1971).
6. R. G. Carlson et J. K. Pierce. J. Org. Chem. **36**, 2319 (1971).
7. J. A. Marshall et G. M. Cohen. J. Org. Chem. **36**, 877 (1971).
8. R. B. Warneboldt et L. Weiler. Tetrahedron Lett. 3413 (1971).
9. Y. Bessière-Chrétien et J. P. Bras. C.R. Acad. Sc. (C), **271**, 200 (1970).
10. Y. Bessière-Chrétien et B. Meklati. C.R. Acad. Sc. (C), **269**, 1315 (1969).
11. S. Meklati et Y. Bessière-Chrétien. Bull. Soc. Chim. Fr. 3133 (1972).
12. T. Hirata. Bull. Chem. Soc. Japan, **45**, 599 (1972).
13. T. Aoki, H. Yamamura, K. Takai et H. Mori. Chem. Pharm. Bull. Japan, **12**, 808 (1964).
14. Y. Bessière-Chrétien et B. Meklati. Bull. Soc. Chim. Fr. 2591 (1971).
15. A. J. Baretta, C. W. Jefford et B. Waegell. Bull. Soc. Chim. Fr. 3985 (1970).
16. J. M. Coxon, E. Dansted, M. P. Hartshorn et K. E. Richards. Tetrahedron Lett. 1149 (1969).
17. Y. Bessière-Chrétien et C. Grison. Bull. Soc. Chim. Fr. 3103 (1970).
18. J. P. Monthéard. Thèse de Doctorat d'Etat, Paris, 3 juin 1966.

Can. J. Chem. Downloaded from www.nrcresearchpress.com by 84.22.46.98 on 09/08/12
For personal use only.

Aril Azines. II.[1] Hydrogenation of *p*-Tolil Monoazine

PETER YATES AND E. M. LEVI

Lash Miller Chemical Laboratories, University of Toronto, Toronto, Ontario M5S 1A1

Received September 23, 1974

PETER YATES and E. M. LEVI. Can. J. Chem. **53**, 748 (1975).

Hydrogenation of *p*-tolil monoazine (**1***b*) over palladium-on-charcoal gives as the major product 4,5-dihydro-5-(*p*-toluyl)-3,4,5-tri-(*p*-tolyl)-1*H*-pyrazol-4-ol (**2***b*), which has previously been obtained by treatment of **1***b* with sodium methoxide. Several minor products are formed, which include *p*-tolualdehyde, *p*-toluic acid, and *p*-toluamide, *p*-tolunitrile, *p*-tolualazine, and 3,4,5-tri-(*p*-tolyl)-4*H*-pyrazol-4-ol (**9**). The structure of the last compound, which is also formed on reduction of **1***b* with sodium borohydride, was established by its independent synthesis from 1,2,3-tri-(*p*-tolyl)-1,3-propanedione by oxidation with lead tetraacetate followed by treatment with hydrazine. It is suggested that **2***b* arises via reduction of a C=N bond of **1***b* and aldol ring closure. The minor hydrogenation products are of interest in that their formation involves C—C hydrogenolysis; it is suggested that this is initiated by addition of a hydrogen atom to a carbonyl carbon atom of **1***b*.

PETER YATES et E. M. LEVI. Can. J. Chem. **53**, 748 (1975).

L'hydrogénation de la *p*-tolil monoazine (**1***b*) sur du palladium-sur-charbon conduit comme produit majeur au dihydro-4,5 *p*-toluyl-5 tri-*p*-tolyl-3,4,5 1*H*-pyrazolol-4 (**2***b*) qui avait été obtenu précédemment en traitant **1***b* par le méthylate de sodium. Plusieurs produits mineurs sont formés parmi lesquels on remarque la *p*-tolualdéhyde, l'acide *p*-toluique, la *p*-toluamide, la *p*-tolunitrile, la *p*-tolualazine et le tri-*p*-tolyl-3,4,5 4*H*-pyrazolol-4 (**9**). On a établi la structure du dernier composé, qui se forme aussi lors de la réduction de **1***b* par le borohydrure de sodium, par une synthèse non ambigue impliquant l'oxydation de la tri-*p*-tolyl-1,2,3 propanedione-1,3 par du tétraacétate de plomb et le traitement du produit obtenu avec l'hydrazine. On suggère que **2***b* provient de **1***b* par la réduction du lien C=N suivi d'une cyclisation aldolique. Les produits mineurs d'hydrogénation présentent de l'intérêt dû au fait qu'ils proviennent d'une hydrogénolyse d'un lien C—C; on suggère que cette réaction débute par l'addition d'un atome d'hydrogène sur l'atome de carbone du carbonyle de la molécule **1***b*. [Traduit par le journal]

Prolonged treatment of aril monoazines (**1**) with sodium methoxide has been shown to give phototropic products of type **2** (1). These products, which are dihydro derivatives of the azines, are formed in low yield (<25%). In order to obtain increased yields of these products we have investigated alternative methods of reduction of the azines. In preliminary experimentation it was found that benzil monoazine (**1***a*) is reduced to **2***a* by hydrogenation over palladium-on-charcoal.[2] We now report on an investigation of the hydrogenation of *p*-tolil monoazine (**1***b*).

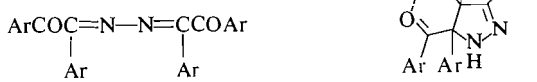

1

a Ar = C_6H_5
b Ar = *p*-$CH_3C_6H_4$

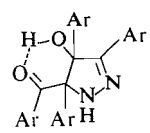

2

a Ar = C_6H_5
b Ar = *p*-$CH_3C_6H_4$

Hydrogenation of **1***b* in benzene over 10% palladium-on-charcoal proceeded slowly with the uptake of *ca.* 4 molar-equiv. of hydrogen in *ca.* 30 h and gave as the major product the dihydro compound **2***b* in 56% yield.[3] This method is thus considerably more efficient and convenient than that involving treatment with sodium methoxide for the conversion of **1***b* to **2***b*.[4]

The hydrogenation of **2***b* also formed a number of other products in low yield. Several of these were compounds of known structure and were identified by direct comparison with authentic samples as *p*-tolualdehyde (**3**), *p*-toluic acid (**4**), *p*-toluamide (**5**), *p*-tolunitrile (**6**), and *p*-tolualazine (**7**). A crystalline product, m.p. 258–259°, isolated in too low a yield for full characterization is tentatively assigned structure

[1]For part I see ref. 1.

[2]We thank Dr. J. A. Weisbach for carrying out these experiments.

[3]The yield of this product was reduced if the hydrogenation was carried out for shorter periods.

[4]It has subsequently been found that the reduction of **1***b*–**2***b* is best effected by sodium in tetrahydrofuran (J. G. Smith and E. M. Levi, unpublished results).

Can. J. Chem. Downloaded from www.nrcresearchpress.com by 210.87.254.5 on 09/05/12
For personal use only.

Can. J. Chem. Downloaded from www.nrcresearchpress.com by 210.87.254.5 on 09/05/12
For personal use only.

8 on the basis of its spectra (see Experimental).

p-$CH_3C_6H_4COX$

3 X = H

4 X = OH

5 X = NH_2

p-$CH_3C_6H_4CN$

6

p-$CH_3C_6H_4CH{=}N{-}N{=}CHC_6H_4CH_3$-$p$

7

p-$CH_3C_6H_4COCHNHCOC_6H_4CH_3$-$p$

$C_6H_4CH_3$-p

8

A pale green crystalline product, $C_{24}H_{22}N_2O$, isolated in 4% yield, is of particular interest since it is also formed by treatment of the pyrazoline **2***b* with sodium borohydride. Its i.r. spectrum shows a band at *ca.* 3.0 μ, but no band in the carbonyl-stretching region, and its u.v. spectrum has a maximum at 342 nm (log ε 4.35). Structure **9** is assigned to this compound on the basis of these data and the observation that it is reduced by zinc and acetic acid to 3,4,5-tri-(p-tolyl)pyrazole (**10**), a product that is formed in addition to **9** in the reduction of **2***b* with sodium borohydride. Treatment of **9** with hot methanolic hydrochloric acid gave an isomeric yellow crystalline product in high yield that is considered to be the pyrazolone **11** formed by migration of a p-tolyl group.

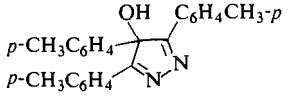

9

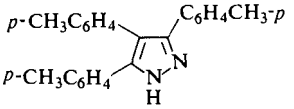

10

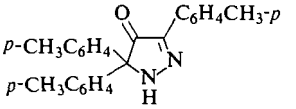

11

The structural assignment **9** was confirmed by an independent synthesis of this compound by the route shown in Scheme 1. Treatment of deoxy-p-toluoin (**12**) with sodium amide followed by p-toluyl chloride gave the 1,3-diketone **13** as the major product, accompanied by the *O*-acylation product **14** and the diacylation product **15**. Oxidation of **13** with lead tetraacetate in acetic acid gave the acetoxylation product **16**, which on treatment with hydrazine gave compounds **9** and **10**; the latter could arise via reduction of the former by hydrazine.

The catalytic hydrogenation of the azines of monocarbonyl compounds has been investigated extensively previously (2). Depending on the reaction conditions, reaction may involve saturation of one or both of the C=N bonds and hydrogenolysis of the N—N bond. In the present case the formation of the major product can be interpreted as proceeding via saturation of one of the C=N bonds of **1***b* to give **17** followed by an intramolecular aldol reaction to give **2***b* (Scheme 2, Ar = p-$CH_3C_6H_4$).

The minor products isolated from the hydrogenation reaction mixture are of interest in that their formation involves hydrogenolysis of one or more C—C single bonds. The formation of several of them can be rationalized in terms of a common radicaloid intermediate **18**, as shown in Scheme 3 (Ar = p-$CH_3C_6H_4$).[5] Others may arise via secondary reactions during work-up; *e.g.*, p-toluic acid (**4**) by air-oxidation of p-tolualdehyde and p-toluamide (**5**) by hydrolysis of p-tolunitrile.

The postulated hydrogenolysis of **1***b* to give the aldehyde **3** and the azines **19** and **7** finds some analogy in the C—C hydrogenolysis of β-diketones over Raney nickel to give aldehydes and ketones (3).

Experimental

Hydrogenation of p-Tolil Monoazine (1b)

A solution of p-tolil monoazine (2.15 g) in hot dry benzene (thiophene free; 175 ml) was added to 10% palladium-on-charcoal (1.8 g) suspended in benzene (thiophene free; 20–40 ml) in an aluminum-foil-wrapped hydrogenation flask. Hydrogenation at atmospheric pressure led to the uptake of 500 ml (4.5 molar-equiv.) of hydrogen, which was complete in 34 h. The catalyst was removed at night under subdued light by filtration through sintered glass and the benzene solution was evaporated to give a red oil. This was taken up in ether (20 ml) and the solution was concentrated at room temperature to *ca.* 10 ml, giving crystalline compound **2***b*, m.p. 173–175° (dec.) (1.20 g; 56%), which was shown by i.r. and ^{1}H n.m.r. spectral comparison to be identical with the product obtained by treatment of **1***b* with sodium methoxide (1).

The residues (7.28 g) from four such hydrogenations of p-tolil monoazine (14.25 g) over 10% palladium-on-charcoal (12.41 g) with uptake of 3150 ml of hydrogen

[5]The radical species involved in this scheme are not considered to be free radicals but are viewed as remaining associated with the catalyst.

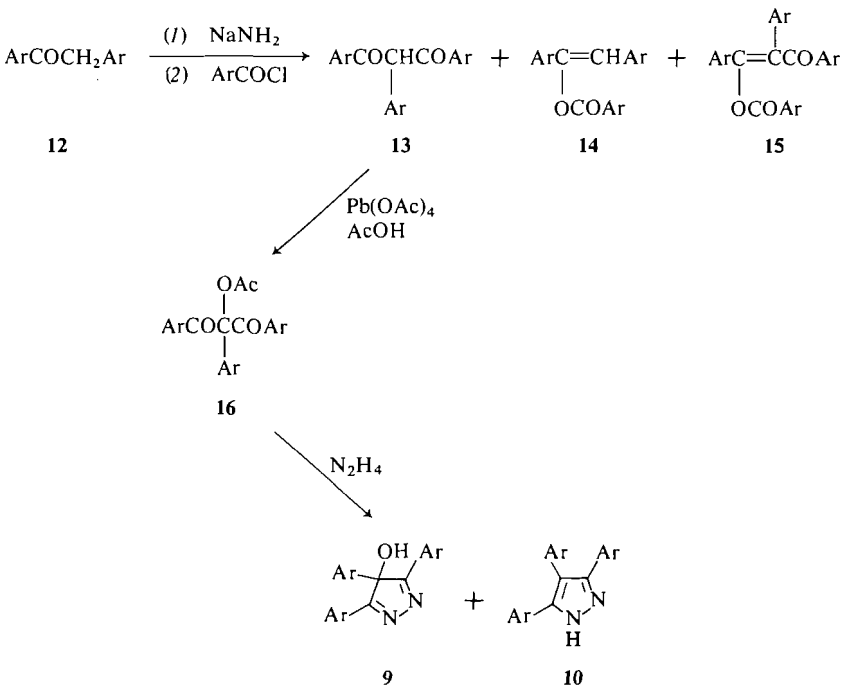

SCHEME 1

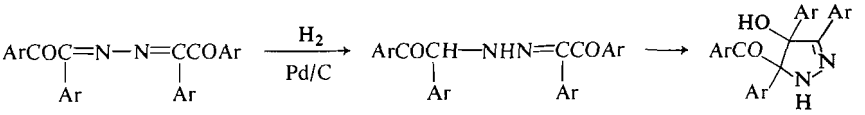

SCHEME 2

were combined after crystallization of compound **2b** (7.27 g) and chromatographed on silica gel (540 g).

Elution with benzene – petroleum ether mixtures gave fractions containing less than 30 mg of material. Elution with benzene gave a semisolid fraction (30 mg), whose i.r. spectrum, with a band at 4.47 μ, showed it to contain *p*-tolunitrile.

Elution with ether–benzene (0.5:99.5) gave *p*-tolil monoazine (330 mg), followed by fractions containing *p*-tolil monoazine and *p*-tolualdehyde (940 mg), identified by i.r. spectroscopy. The formation of *p*-tolualdehyde was confirmed by examination of a fresh hydrogenation residue by v.p.c. and comparison of this chromatogram with a chromatogram of a mixture of this residue with authentic *p*-tolualdehyde. Further elution with the above solvent mixture gave *p*-tolil monoazine (160 mg) and fractions containing *p*-tolil monoazine and *p*-tolualazine (110 mg).

Elution with ether–benzene (1:99 and 2:98) gave an oil (470 mg) from which *p*-tolualazine (220 mg), m.p. 154–155.5° (lit. (4) m.p. 157–158°), crystallized from ethanol, after filtration of some *p*-tolil monoazine. It had λ_{max} ($CHCl_3$) 6.17, 6.23 μ; δ ($CDCl_3$) 2.35 (s, 6H), 7.20 (d, J = 8 Hz, 4H), 7.72 (d, J = 8 Hz, 4H), 8.62 (s, 2H). A mixture m.p. with an authentic sample, m.p. 157–158°, was 157–158°; the spectra of the two samples were indistinguishable.

Elution with ether–benzene (1:24 and 2:23) gave an oil (720 mg), which crystallized from ethanol–benzene to give a white solid (57 mg), m.p. 258–259°; λ_{max} ($CHCl_3$) 2.92, 5.85, 6.03 μ; *m/e*(%) 357(1), 341(2), 238(54), 221(36), 119(100). This product is tentatively assigned structure **8**.

Elution with ether–benzene (3:7 and 1:1) gave a semi-solid mixture (1.52 g), which was triturated with benzene to give a greenish tinged solid (470 mg), m.p. 206–208° (dec.). Recrystallization from methanol gave material, m.p. 209–211° (dec.), which was shown to be 3,4,5-*tri*-(*p*-tolyl)-4*H*-pyrazol-4-ol (**9**) (*vide infra*) by mixture m.p. and i.r. spectral comparison. Extraction of the benzene solution with aqueous sodium bicarbonate followed by acidification of the aqueous solution and extraction gave *p*-toluic acid (510 mg).

Can. J. Chem. Downloaded from www.nrcresearchpress.com by 210.87.254.5 on 09/05/12
For personal use only.

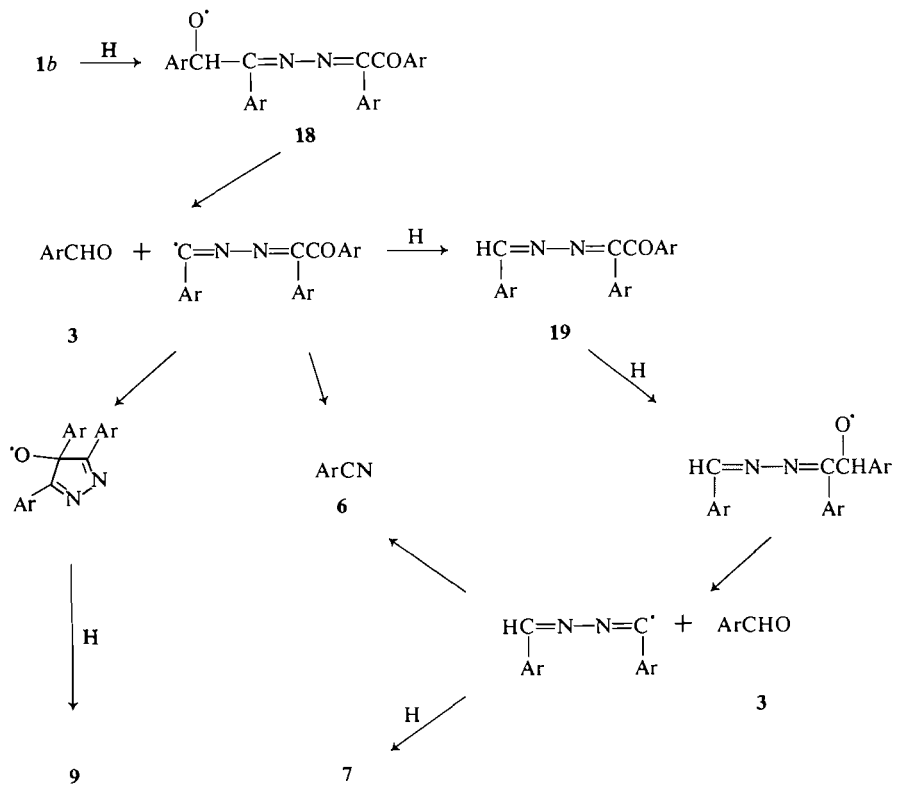

SCHEME 3

Elution with methanol–chloroform mixtures gave a white crystalline solid, m.p. 157–158°; λ_{max} ($CHCl_3$) 2.87, 2.98, 6.02 μ; *m/e*(%) 135(92), 119(100). This was identified as *p*-toluamide by mixture m.p. 158–160° with an authentic sample, m.p. 158.5–160°.

Reduction of **9** *with Zinc in Acetic Acid*

Compound **9** (20 mg) and zinc dust (148 mg) in acetic acid (30 ml) were heated under reflux with stirring until the original yellow color faded (3 h). The solution was filtered from unreacted zinc dust and the solvent was evaporated. The residue was taken up in hot methanol (*ca.* 3 ml), aqueous 10% sodium bicarbonate (4 drops) was added, and the solution was chilled to −20°. The crystalline product, m.p. 244–248°, had an i.r. spectrum indistinguishable from that of 3,4,5-tri-(*p*-tolyl)pyrazole (**10**) (1).

Acid-catalyzed Rearrangement of **9**

Compound **9** (104 mg) was added to a mixture of concentrated hydrochloric acid (3 ml) and methanol (50 ml) to give a dark yellow solution. This was heated under reflux for 1 day, cooled, and evaporated. The residue was taken up in chloroform and chromatographed on a silica gel t.l.c. plate (20 × 20 cm, 1 mm) developed with carbon tetrachloride. The major, deep yellow band (of seven) was extracted from the silica gel with chloroform. The residue obtained on evaporation of the extract was crystallized twice from aqueous methanol to give yellow needles, m.p. 151.5–153° (dec.); λ_{max} ($CHCl_3$) 2.98, 5.78, 5.87 μ; λ_{max} (EtOH) 250 nm (sh, log ε 4.10), 266 nm (log ε 4.16), 362 nm (sh, log ε 3.62), 393 nm (log ε 3.72); δ ($CDCl_3$) 2.27 (s, 6H), 2.33 (s, 3H), 7.0–7.2 (m, 10H), 7.45 (s, 1H, absent after D_2O treatment), 8.01 (d, J = 8 Hz, 2H); *m/e*(%) 354(3), 309(1), 219(50), 194(26), 140(62), 97(100).

Anal. Calcd. for $C_{24}H_{22}N_2O$: C, 81.32; H, 6.26; N, 7.90. Found C, 81.29; H, 6.55; N, 7.95.

*1,2,3-Tri-(p-tolyl)-1,3-propanedione (***13***)*

A crystal of ferric nitrate nonahydrate and sodium (4.4 g) were added to liquid ammonia (*ca.* 100 ml) in a three-necked flask, fitted with a Dry-Ice condenser, a double surface ether condenser, and a gas inlet tube. The solution was stirred for 30 min. Dry ether (100 ml) was added after removal of the Dry-Ice condenser and the flask was allowed to come to room temperature, the excess ammonia being removed by a stream of dry nitrogen. The ethereal suspension was heated under reflux for 5 min. A suspension of deoxy-*p*-toluoin (11.2 g) in dry ether (250 ml) was added and the mixture was heated under reflux for 6 h, cooled, and forced by nitrogen pressure into a pressure-equalized dropping funnel, whence it was added to a rapidly stirred solution of *p*-toluyl chloride (7.78 g) in dry ether (50 ml). The reaction mixture was stirred overnight and then treated with dilute hydrochloric acid (*ca.* 5%; 200 ml). The ethereal solution

Can. J. Chem. Downloaded from www.nrcresearchpress.com by 210.87.254.5 on 09/05/12
For personal use only.

Can. J. Chem. Downloaded from www.nrcresearchpress.com by 210.87.254.5 on 09/05/12
For personal use only.

was separated and the aqueous solution was extracted with fresh ether (200 ml). The ethereal solution was dried and evaporated. The residue was crystallized from absolute ethanol (500 ml) to give a white crystalline solid, m.p. 170–190°. This was treated with hot absolute ethanol to give a solution which upon cooling deposited a white crystalline solid (2.16 g), m.p. 168–170°. The residue (1.54 g) had m.p. 189–194°.

The solid, m.p. 168–170°, was recrystallized twice from absolute ethanol to give 1-(*p*-toluyloxy)-1,2-di-(*p*-tolyl)ethylene (**14**), m.p. 171–172°; λ_{max} ($CHCl_3$) 5.79, 6.06 μ (w); δ ($CDCl_3$) 2.24 (s, 3H), 2.30 (s, 3H), 2.40 (s, 3H), 6.72 (s, 1H), 7.0–7.6 (m, 10H), 8.12 (d, J = 8 Hz, 2H); *m/e*(%) 342(2), 341(7), 119(100).

Anal. Calcd. for $C_{24}H_{22}O_2$: C, 84.17; H, 6.47. Found: C, 84.08; H, 6.59.

The solid, m.p. 189–194°, was twice recrystallized from absolute ethanol to give 3-(*p*-toluyloxy)-1,2,3-tri-(*p*-tolyl)-2-propen-1-one (**15**), m.p. 194–195°; λ_{max} ($CHCl_3$) 5.79, 6.02 μ; δ ($CDCl_3$) 2.24 (s, 6H), 2.28 (s, 6H), 6.9–7.4 (m, 12H), 7.68 (d, J = 8 Hz, 2H), 7.97 (d, J = 8 Hz, 2H); *m/e*(%) 460(9), 341(1), 119(100).

Anal. Calcd. for $C_{32}H_{28}O_3$: C, 83.45; H, 6.13. Found: C, 83.36; H, 6.25.

The original ethanolic mother liquor was concentrated to 75 ml and cooled. A white crystalline product (7.38 g), m.p. 130–145°, was isolated. Seven crystallizations from ethanol gave 1,2,3-tri-(*p*-tolyl)-1,3-propanedione (**13**), m.p. 147–148°; λ_{max} ($CHCl_3$) 5.90, 5.99 μ; δ ($CDCl_3$) 2.27 (s, 3H), 2.32 (s, 6H), 6.54 (s, 1H), 7.0–7.6 (m, 8H), 7.90 (d, J = 8 Hz, 4H); *m/e*(%) 342(18), 119(100).

Anal. Calcd. for $C_{24}H_{22}O_2$: C, 84.17; H, 6.47. Found: C, 84.07; H, 6.32.

3,4,5-Tri-(p-tolyl)-4H-pyrazol-4-ol (9)

1,2,3-Tri-(*p*-tolyl)-1,3-propanedione (**13**; 2.06 g) and lead tetraacetate (9.5 g) were stirred in glacial acetic acid (80 ml) for 6 days. The reaction mixture was poured into water. The solid that precipitated was separated by filtration through sintered glass and washed well with water. The filter cake was extracted with chloroform and these extracts were dried, filtered, and evaporated. The product, a yellow oil (2.49 g), was taken up in benzene and the solution was chromatographed on silica gel (100 g). Elution with ether–benzene (1:99 and 3:97) gave 2-acetoxy-1,2,3-tri-(*p*-tolyl)-1,3-propanedione (**16**) as a yellow oil (1.24 g); λ_{max} (CCl_4) 5.76, 5.98, 8.1–8.2 μ; δ (CCl_4) 1.92 (s, 3H), 2.22 (s, 9H), 6.85–7.15 (m, 6H), 7.33 (d, J = 8 Hz, 2H), 7.63 (d, J = 8 Hz, 4H).

Compound **16** (830 mg), without further purification, and hydrazine (95+%; 300 mg) were stirred in benzene solution (50 ml), containing acetic acid (2 drops) at room temperature. After 3 h crystals appeared in the solution; stirring was continued for 3 days. The crystalline product (230 mg) was filtered; m.p. 198–200° (dec.). Two recrystallizations from methanol gave 3,4,5-tri-(*p*-tolyl)-4*H*-pyrazol-4-ol (**9**), m.p. 211.5–212° (dec.); λ_{max} (KBr) 3.0, 6.22, 6.62 μ; λ_{max} (EtOH) 342 nm (log ε 4.35); *m/e*(%) 354(13), 338(9), 326(4), 237(17), 194(14), 119(25), 118(100), 91(19).

Anal. Calcd. for $C_{24}H_{22}N_2O$: C, 81.52; H, 6.26; N, 7.90. Found: C, 81.05; H, 6.27; N, 8.30.

Evaporation of the benzene filtrate and crystallization of the residue from methanol gave 3,4,5-tri-(*p*-tolyl)pyrazole (**10**) (50 mg), m.p. 232–237°. Two recrystallizations from methanol gave material, m.p. 252–252.5°; mixture m.p. 252.5–253° with an authentic sample, m.p. 253.5–254° (1).

Reduction of 2b with Sodium Borohydride

Compound **2***b* (1.00 g) and sodium borohydride (196 mg) were stirred in tetrahydrofuran–water (9:1; 100 ml) for 12 h. The aqueous layer was separated and the organic layer was dried. Acetyl chloride (2 ml) was added, and the solution was stirred for a few minutes and then poured into water. The aqueous layer was separated and extracted with ether. The ethereal and tetrahydrofuran solutions were combined, dried, and evaporated to give a yellow oil (834 mg), which was taken up in benzene and chromatographed on silica gel (40 g).

Elution with benzene gave 3,4,5-tri-(*p*-tolyl)-4H-pyrazol-4-ol (**9**) (110 mg) as a green tinged solid; crystallization from methanol gave needles, m.p. 209–211° (dec.); mixture m.p. 211–212° (dec.) with an authentic sample, m.p. 211.5–212° (dec.) (*vide supra*).

Elution with ether–benzene (1:4) gave 3,4,5-tri-(*p*-tolyl)pyrazole (**10**) (50 mg), m.p. 243–249°, identified by i.r. spectral comparison.

We thank Mr. G. Koves for technical assistance and the National Research Council of Canada for financial support.

1. P. Yates, E. M. Levi, and B. L. Shapiro. Can. J. Chem. **52**, 3343 (1974).
2. A. N. Kost and I. I. Grandberg. Usp. Khim. **28**, 921 (1959); D. V. Sokol'skii. Hydrogenation in solutions. Israel Program for Scientific Translations, Jerusalem. 1964. pp. 16–23.
3. J. M. Sprague and H. Adkins. J. Am. Chem. Soc. **56**, 2669 (1934).
4. T. Curtius and H. Melsbach. J. Prakt. Chem. [2], **81**, 541 (1909); V. Hanzlik and A. Bianchi. Chem. Ber. **32**, 1285 (1899).

Crystal and Molecular Structure of a Novel Polycyclic Ga, O, N Cage Compound: $(GaH)_6(GaH_2)_2(\mu_3\text{-}O)_2(\mu_3\text{-}NCH_2CH_2NMe_2)_4(\mu\text{-}NHCH_2CH_2NMe_2)_2$

STEVEN J. RETTIG, ALAN STORR, AND JAMES TROTTER

Department of Chemistry, University of British Columbia, Vancouver, British Columbia V6T 1W5

Received September 6, 1974

STEVEN J. RETTIG, ALAN STORR, and JAMES TROTTER. Can. J. Chem. **53**, 753 (1975).

Crystals of 11*H*,22*H*-10,10,21,21-tetramethyl-3,5,14,16-tetra(*N*,*N*-dimethyl-2-aminoethyl)-1,12-dioxonia-3,5,7,10,14,16,18,21-octaazonia-2,4,6,11,13,15,17,22-octagallanata-nonacyclo-[13.7.0.0^{2,7}.0^{3,22}.0^{4,12}.0^{7,11}.0^{11,14}.0^{13,18}.0^{18,22}]docosane are triclinic, $a = 13.358(1)$, $b = 9.300(1)$, $c = 9.545(1)$ Å, $\alpha = 92.16(2)$, $\beta = 107.49(1)$, $\gamma = 89.23(2)°$, $Z = 1$, space group $P\bar{1}$. The structure was solved by Patterson and Fourier syntheses and was refined by full-matrix least-squares procedures to a final R of 0.038 for 3393 reflections with $I \geq 4\sigma(I)$. The bond lengths involving nonhydrogen atoms have been corrected for thermal motion. The molecular structure features a novel Ga, O, N cage structure which includes the first crystallographic examples of four-membered Ga_2NO and six-membered Ga_3N_2O rings. Three of the four crystallographically independent gallium atoms are tetrahedrally four-coordinate with bond lengths: Ga—O, 1.869 and 1.879(2), Ga—N, 1.945–2.001(3), and Ga—H, 1.40–1.52(4–5) Å. The remaining gallium atom is five-coordinate with distorted trigonal bipyramidal geometry (Ga—O(ax), 1.960(3), Ga—N(ax), 2.779(3), Ga—N(eq), 1.949 and 1.999(3), and Ga—H(eq), 1.49(5) Å). Other bond lengths in the molecule are: N—C, 1.449–1.493(4–10), C—C, 1.486–1.528(6–7), N—H, 0.85(5), and mean C—H, 1.03 Å. The errors quoted above are those arising from the least-squares analysis and do not reflect uncertainties introduced by the thermal analysis.

STEVEN J. RETTIG, ALAN STORR et JAMES TROTTER. Can. J. Chem. **53**, 753 (1975).

Les cristaux du 11*H*,22*H* tétraméthyl-10,10,21,21 tétra(*N*,*N*-diméthyl-amino-2 éthyle)-3,5,14,16 dioxonia-1,12 octaazonia-3,5,7,10,14,16,18,21 octagallanata-2,4,6,11,13,15,17,22 nonacyclo[13.7.0.0^{2,7}.0^{3,22}.0^{4,12}.0^{7,11}.0^{11,14}.0^{13,18}.0^{18,22}] docosane sont tricliniques, $a = 13.358(1)$, $b = 9.300(1)$, $c = 9.545(1)$ Å, $\alpha = 92.16(2)$, $\beta = 107.49(1)$, $\gamma = 89.23(2)°$, $Z = 1$, groupe d'espace $P\bar{1}$. On a résolu la structure par une synthèse de Patterson et Fourier et on l'a raffinée par la méthode des moindres carrés (matrice complète) jusqu'à une valeur finale R de 0.038 pour 3393 réflections avec $I \geq 4\sigma(I)$. On a corrigé les longueurs de liaison impliquant les atomes qui ne sont pas des hydrogènes pour les mouvements thermiques. La structure moléculaire implique une nouvelle structure en cage du Ga, O, N qui implique les premiers exemples cristallographiques de cycles à quatre membres du Ga_2NO et à six membres du Ga_3N_2O. Trois des quatres atomes de gallium, qui sont cristallographiquement indépendants, sont coordonnés d'une façon tétraédrique avec des longueurs de liaison de: Ga—O, 1.869 et 1.879(2), Ga—N, 1.945–2.001(3) et Ga—H, 1.40–1.52(4–5) Å. L'autre atome de gallium est penta-coordonné avec une géométrie bipyramide trigonale déformée (Ga—O(ax), 1.960(3), Ga—N(ax), 2.779(3), Ga—N(eq), 1.949 et 1.999(3) et Ga—H(eq), 1.49(5) Å). Les autres longueurs de liaison dans la molécule sont: N—C, 1.449–1.493(4–10), C—C, 1.486–1.528(6–7), N—H, 0.85(5), et la valeur moyenne du C—H est de 1.03 Å. Les erreurs mentionnées plus haut sont celles qui dérivent de l'analyse par la méthode de moindres carrés et ne sont pas un reflet des incertitudes introduits par l'analyse thermique. [Traduit par le journal]

Introduction

Two previous papers (1, 2) have presented crystallographic examples of five-coordinate gallium compounds which involve fused ring systems. In an attempt to extend our studies in this area the reaction of *N*,*N*-dimethylethylenediamine with trimethylamine-gallane has been investigated. The reaction predicted on the basis of previous results (3) was

$$Me_2NCH_2CH_2NH_2 + Me_3NGaH_3 \rightarrow Me_2NCH_2CH_2NHGaH_2 + Me_3N + H_2$$

It was then expected that the monomeric unit, $Me_2NCH_2CH_2NHGaH_2$, would either trimerize, $[—HN(CH_2CH_2NMe_2)GaH_2—]_3$, with non-involvement of the "Me_2N" groups, or that, more probably, these would become involved in the oligomerization process to yield another example of five-coordinate gallium atoms.

The novel Ga, O, N cage structure which is reported here was unexpected, and chance has played a large part in its discovery. The structure does provide a further crystallographic example of five-coordinate gallium atoms, but, more

Can. J. Chem. Downloaded from www.nrcresearchpress.com by 210.87.254.5 on 09/05/12
For personal use only.

importantly, presents the first example of an extensive cage structure involving Ga, N, and O atoms.

Experimental

The present compound was deposited as colorless crystals from a benzene solution of the products from the reaction

$$Me_2NCH_2CH_2NH_2 + Me_3NGaH_3 \rightarrow \text{products}$$

The crystals deposited from the solution over a period of years and it is presumed that the oxygen atoms incorporated into the cage structure entered the reaction sphere as water molecules, via the poor seal of the n.m.r. tube, and that these reacted with the initial product of the reaction to eliminate more hydrogen and incorporate the oxygen atoms into the structure. The small amount of crystalline material available did not enable chemical analyses to be obtained. The air-sensitive sample was positioned in a Lindemann glass capillary tube under nitrogen atmosphere and the tube was then flame-sealed. The instability of the compound precluded an experimental determination of the density.

The crystal chosen for study was mounted with b^* parallel to the goniostat axis and had dimensions of *ca.* 0.3 × 0.4 × 0.3 mm. Unit-cell and space group data were obtained from film and diffractometer measurements. The unit-cell parameters were refined by a least-squares treatment of $\sin^2\theta$ values for 18 reflections measured on a diffractometer with CuK_α radiation. Crystal data are:

$C_{24}H_{72}Ga_8N_{12}O_2$ f.w. = 1118.7

Triclinic, $a = 13.358(1)$, $b = 9.300(1)$, $c = 9.545(1)$ Å, $\alpha = 92.16(2)$, $\beta = 107.49(1)$, $\gamma = 89.23(2)°$, $V = 1130.1(3)$ Å^3, $Z = 1$, $\rho_c = 1.644(1)$ g cm^{-3}, $F(000) = 564$ (23 °C, CuK_α, $\lambda = 1.5418$ Å, $\mu = 60$ cm^{-1}). Space group $P\bar{1}$ (C_i^1, No. 2) from structure analysis. Intensities were measured on a Datex-automated General Electric XRD 6 diffractometer, with a scintillation counter, CuK_α (nickel filter and pulse height analyzer), and a θ–2θ scan at 2° min^{-1} over a range of $(1.80 + 0.86 \tan\theta)$ degrees in 2θ, with 10 s background counts being measured at each end of the scan. Data were measured to $2\theta = 145°$ (minimum interplanar spacing 0.81 Å). The intensity of the check reflection, measured every 40 reflections throughout the data collection, decreased slowly to a final value which was 0.87 times the initial value. Lorentz and polarization corrections and check reflection scaling were applied, and the structure amplitudes were derived. No absorption correction was made due to irregularity of the crystal surface. Of the 4474 independent reflections measured, 1019 had intensities less than $4\sigma(I)$ above background where $\sigma^2(I) = S + B + (0.06S)^2$ with S = scan count and B = time averaged background count. These reflections were given zero weight in the refinement but were included in the structure factor calculations. The criterion of 4σ, rather than $3\sigma(I)$, was used to limit the number of reflections to be included in the refinement and thereby reduce the computing costs. (There are 9.6 reflections included in the refinement for each variable for the 4σ cutoff.)

Structure Analysis

The positions of the gallium atoms were determined from the three-dimensional Patterson function, which indicated four instead of the three heavy atoms which were initially anticipated on the basis of two [—NH(CH_2-CH_2NMe_2)GaH_2—]$_3$ trimers per unit-cell. Two cycles of full-matrix least-squares refinement of the positional and isotropic thermal parameters of the gallium atoms gave $R = 0.24$. A difference map then revealed the positions of the C, N, and O atoms which were refined isotropically and the gallium atoms anisotropically for two cycles, reducing R to 0.082. The oxygen atom, which had been refined as a nitrogen atom up to this point, was characterized by an anomalously low isotropic temperature factor and by the Ga—O bond lengths which were too short to be Ga—N interactions. The nonhydrogen atoms were then refined anisotropically for two cycles giving $R = 0.070$. A difference map then gave positions for 32 of the 36 hydrogen atoms (those not located were associated with the C(11) and C(12) methyl groups). The remaining hydrogen atom positions were calculated and separate cycles of refinement of the nonhydrogen and then the hydrogen atoms reduced R to 0.043. The entire structure, including the hydrogen atoms with isotropic temperature factors (353 variables) was refined for three cycles giving a final R of 0.038 for 3393 reflections with $I \geq 4\sigma(I)$ (62 reflections which had $|F_o - F_c| > 3\sigma(F)$ were removed from the data set in the final stages of refinement due to suspected errors arising from absorption, instrument malfunction, and extinction).

The least-squares refinement was based on the minimization of $\Sigma w(F_o - F_c)^2$. The scattering factors of ref. 4 were used for the nonhydrogen atoms and those of ref. 5 for the hydrogen atoms. Anomalous scattering factors from ref. 6 were used for the nonhydrogen atoms. The anisotropic thermal parameters employed in the refinement are U_{ij} in the expression

$$f = f^0 \exp[-2\pi^2(U_{11}h^2a^{*2} + U_{22}k^2b^{*2} + U_{33}l^2c^{*2} + 2U_{12}hka^*b^* + 2U_{13}hla^*c^* + 2U_{23}klb^*c^*)]$$

where f^0 is the tabulated scattering factor and f is that corrected for thermal motion. The weighting scheme $w = 1/\sigma^2(F)$ where $\sigma^2(F)$ is derived from the previously defined $\sigma^2(I)$ gave uniform average values of $w(F_o - F_c)^2$ over ranges of $|F_o|$ and was employed in the final stages of refinement. The mean error in an observation of unit weight was 1.05. In the latter stages of refinement an extinction parameter, e (where $F_c = F_c^o/(1 + e \times I_u)$ with I_u the uncorrected intensity), was refined, the final value being 9.74×10^{-7}.

On the final cycle of refinement the mean parameter shift was 0.22σ; the largest shifts (up to 3σ) were associated with the C(11) and C(12) methyl group hydrogen atoms and presumably result from the large degree of thermal motion experienced by these groups. A final difference map showed maximum fluctuations of ±0.9 e Å^{-3} in the vicinity of the gallium atoms and ±0.2 e Å^{-3} elsewhere. The final positional and thermal parameters appear in Tables 1 and 2 respectively. Measured and calculated structure factors have been placed in the Depository of Unpublished Data.[1]

[1]The structure factor table is available, at a nominal charge, from the Depository of Unpublished Data, National Science Library, National Research Council of Canada, Ottawa, Canada K1A 0S2.

Can. J. Chem. Downloaded from www.nrcresearchpress.com by 210.87.254.5 on 09/05/12
For personal use only.

Can. J. Chem. Downloaded from www.nrcresearchpress.com by 210.87.254.5 on 09/05/12
For personal use only.

TABLE 1. Final positional parameters (fractional × 10^4, Ga × 10^5, H × 10^3) with estimated standard deviations in parentheses

Atom	x	y	z
Ga(1)	41556(3)	63529(5)	60649(4)
Ga(2)	36056(3)	31231(5)	48560(5)
Ga(3)	42472(3)	56578(5)	27929(4)
Ga(4)	20207(3)	58720(6)	35142(6)
O	4403(2)	3788(3)	3711(2)
N(1)	4187(2)	4321(3)	6618(3)
N(2)	3478(2)	6645(3)	3982(3)
N(3)	2220(2)	3772(4)	3606(3)
N(4)	2041(3)	3094(5)	6707(4)
N(5)	4043(3)	8401(4)	1686(4)
N(6)	305(3)	2102(5)	2519(5)
C(1)	3846(3)	4043(6)	7920(4)
C(2)	2677(3)	4194(6)	7704(5)
C(3)	932(4)	3479(11)	6326(9)
C(4)	2191(6)	1660(9)	7274(10)
C(5)	3344(4)	8214(4)	3782(5)
C(6)	3110(3)	8616(5)	2180(5)
C(7)	3735(5)	8242(7)	83(5)
C(8)	4749(5)	9641(7)	2148(7)
C(9)	1933(4)	2993(6)	2147(5)
C(10)	781(4)	2790(8)	1514(7)
C(11)	−829(5)	2193(13)	1995(14)
C(12)	628(8)	612(10)	2734(13)
H(1)	387(3)	739(4)	699(5)
H(2)	356(4)	150(5)	493(5)
H(3)	361(4)	525(5)	126(5)
H(4)	168(4)	663(6)	474(6)
H(5)	136(3)	614(4)	210(4)
H(n)	179(4)	361(6)	408(6)
H(1*a*)	419(4)	464(5)	868(5)
H(1*b*)	401(3)	323(5)	835(5)
H(2*a*)	260(4)	397(5)	880(5)
H(2*b*)	240(3)	527(4)	735(4)
H(3*a*)	80(4)	359(6)	718(6)
H(3*b*)	59(4)	448(6)	561(6)
H(3*c*)	49(6)	285(7)	578(7)
H(4*a*)	209(5)	161(6)	816(6)
H(4*b*)	169(5)	107(7)	648(7)
H(4*c*)	293(5)	117(6)	763(6)
H(5*a*)	411(4)	877(5)	435(5)
H(5*b*)	273(4)	854(5)	424(5)
H(6*a*)	292(3)	965(4)	210(4)
H(6*b*)	240(3)	798(4)	163(4)
H(7*a*)	347(5)	908(6)	−29(6)
H(7*b*)	443(5)	811(7)	−26(7)
H(7*c*)	328(3)	736(4)	−37(4)
H(8*a*)	437(4)	1052(6)	167(6)
H(8*b*)	507(4)	964(5)	323(6)
H(8*c*)	554(7)	937(8)	181(8)
H(9*a*)	226(4)	216(6)	226(6)
H(9*b*)	220(5)	372(7)	147(7)
H(10*a*)	63(5)	228(7)	42(7)
H(10*b*)	25(6)	388(9)	136(8)
H(11*a*)	−117(6)	161(9)	62(9)
H(11*b*)	−111(7)	142(9)	296(9)
H(11*c*)	−80(6)	331(9)	155(8)
H(12*a*)	−1(6)	−18(9)	136(9)
H(12*b*)	155(7)	67(8)	354(8)
H(12*c*)	26(7)	14(10)	321(9)

Thermal Motion and Correction of Molecular Geometry

The ellipsoids of thermal motion for the non-hydrogen atoms are shown in Fig. 1. The thermal motion has been analyzed in terms of the rigid-body modes of translation (**T**), libration (**L**), and screw (**S**) motion (7) using the computer program MGTLS. The r.m.s. standard deviation in the temperature factors U_{ij} is 0.0031 Å^2 indicating that the molecule as a whole (r.m.s. ΔU_{ij} = 0.0106 Å^2) is not a good rigid-body. The thermal motion of the 16 inner cage atoms (8Ga, 6N, 2O) is well described by the rigid-body thermal parameters given in Table 3 (r.m.s. ΔU_{ij} = 0.0025 Å^2). The **S** tensor is constrained to be identically equal to zero by the crystallographic center of symmetry. The indicated modes of motion are physically reasonable; the largest principal axis of libration being nearly coincident with the long axis of the molecule.

The appropriate bond distances and angles have been corrected for libration (8, 9), using shape parameters q^2 of 0.08 for all atoms involved. The corrected bond distances appear in Table 4. No bond angles changed by more than 0.04° so the corrected bond angles are not reported. Riding motion corrections based on the ΔU_{ij} (10, 11) have been applied to bonds outside the 16-atom molecular core.

Results and Discussion

Bond angles in the compound are given in Table 5 and intraannular dihedral angles in the polycyclic cage are listed in Table 6. Important intramolecular nonbonded contacts and details of the hydrogen-bonding scheme are given in Table 7. Ga—O, Ga—N, and Ga—H bond distances for several different structures are compared in Table 8.

A number of crystallographic examples of pentacoordinate gallium have been reported recently (1, 2, 12, 13). The present X-ray analysis provides an additional crystallographic example of this type of coordination and further information on Ga—H bond lengths. More importantly, the structure determination is the first one reported for this type of cage structure involving Ga, O, and N atoms. A similar, but less extensive, cage structure involving Al and N atoms has been recently reported (14) for the heptameric compound $[MeNAlMe]_7$, the structure being made up from four-membered, $(AlN)_2$, and six-membered, $(AlN)_3$, rings. The present framework

TABLE 2. Final thermal parameters and their estimated standard deviations

(*a*) Anisotropic thermal parameters ($U_{ij} \times 100$ Å^2)

Atom	U_{11}	U_{22}	U_{33}	U_{12}	U_{13}	U_{23}
Ga(1)	3.67(2)	4.92(3)	3.71(2)	−0.20(2)	1.35(2)	−0.30(2)
Ga(2)	3.62(2)	4.67(3)	4.29(3)	−0.83(2)	0.95(2)	0.06(2)
Ga(3)	3.25(2)	5.54(3)	3.36(2)	−0.41(2)	0.91(2)	−0.24(2)
Ga(4)	3.22(2)	6.56(3)	6.13(3)	0.06(2)	1.16(2)	0.84(2)
O	3.5(1)	5.2(1)	3.9(1)	−0.7(1)	1.1(1)	−0.2(1)
N(1)	3.5(1)	6.0(2)	3.3(1)	−0.2(1)	1.4(1)	0.1(1)
N(2)	3.7(1)	4.5(2)	4.5(2)	−0.1(1)	1.3(1)	0.2(1)
N(3)	3.3(1)	6.7(2)	4.5(2)	−1.1(1)	1.1(1)	−0.2(1)
N(4)	5.3(2)	9.7(3)	6.8(2)	−1.2(2)	2.7(2)	0.9(2)
N(5)	4.8(2)	6.6(2)	4.8(2)	−0.5(1)	1.2(1)	0.8(1)
N(6)	4.7(2)	9.0(3)	9.6(3)	−1.5(2)	1.8(2)	−0.7(2)
C(1)	4.3(2)	7.7(3)	3.8(2)	−0.6(2)	1.8(2)	0.7(2)
C(2)	4.8(2)	9.6(4)	6.0(3)	−0.2(2)	2.9(2)	0.5(2)
C(3)	4.7(3)	16.2(7)	9.0(5)	−1.6(4)	2.2(3)	1.5(5)
C(4)	7.7(4)	10.8(5)	11.4(6)	−1.8(4)	3.2(4)	3.2(5)
C(5)	6.4(3)	4.8(2)	5.8(2)	0.5(2)	2.6(2)	0.7(2)
C(6)	5.3(2)	6.1(3)	6.6(3)	1.2(2)	2.2(2)	1.9(2)
C(7)	9.2(4)	8.1(4)	5.1(3)	0.4(3)	1.9(3)	1.8(3)
C(8)	7.1(3)	7.7(3)	8.5(4)	−1.8(3)	2.2(3)	1.9(3)
C(9)	5.3(2)	7.5(3)	5.3(3)	−1.2(2)	0.9(2)	−1.3(2)
C(10)	6.3(3)	10.8(5)	8.2(4)	−1.5(3)	0.1(3)	−1.7(4)
C(11)	5.9(4)	15.4(9)	17.7(10)	−1.8(4)	1.7(5)	−1.8(8)
C(12)	11.6(6)	11.7(6)	17.7(9)	−0.5(5)	4.9(7)	2.8(6)

(*b*) Isotropic thermal parameters ($U \times 100$)

Atom	U(Å^2)	Atom	U(Å^2)	Atom	U(Å^2)
H(1)	6(1)	H(3*c*)	13(2)	H(8*b*)	10(2)
H(2)	9(2)	H(4*a*)	8(2)	H(8*c*)	13(3)
H(3)	8(1)	H(4*b*)	11(2)	H(9*a*)	9(2)
H(4)	10(2)	H(4*c*)	10(2)	H(9*b*)	9(2)
H(5)	5(1)	H(5*a*)	7(1)	H(10*a*)	11(2)
H(n)	10(2)	H(5*b*)	8(1)	H(10*b*)	22(3)
H(1*a*)	5(1)	H(6*a*)	4(1)	H(11*a*)	21(3)
H(1*b*)	6(1)	H(6*b*)	4(1)	H(11*b*)	26(3)
H(2*a*)	8(1)	H(7*a*)	8(2)	H(11*c*)	15(3)
H(2*b*)	5(1)	H(7*b*)	9(2)	H(12*a*)	17(3)
H(3*a*)	9(2)	H(7*c*)	5(1)	H(12*b*)	19(3)
H(3*b*)	7(2)	H(8*a*)	9(2)	H(12*c*)	12(3)

structure of Ga, O, and N atoms (see Fig. 1) is comprised of 8 six-membered rings with distorted "boat" conformations (six Ga_3N_2O rings and two Ga_3N_3 rings) and 2 four-membered Ga_2NO rings. In addition there are 2 five-membered GaNCCN rings in the centrosymmetric structure.

To produce the cage structure a total of 14 hydrogen molecules have been eliminated. Thus of the 24 hydrogen atoms originally associated with the 8 gallium atoms, 14 have been removed. This number is matched by the 10 hydrogen atoms lost from the 6 $Me_2NCH_2CH_2NH_2$ ligands plus the 4 hydrogen atoms lost from the two water molecules deemed to have entered the reaction sphere to provide the pair of oxygen atoms incorporated in the cage.

Each of the four crystallographically independent gallium atoms in the structure is unique. The bridgehead atom Ga(3) is five-coordinate with distorted trigonal bipyramidal geometry and is part of 3 six-membered rings, a five-membered ring, and a four-membered ring. The three remaining gallium atoms are each tetrahedrally four-coordinate. Two of these atoms, Ga(1) and Ga(2), are also bridgehead atoms, each coordinated to two nitrogen atoms, an oxygen atom, and a hydrogen atom. The difference

Can. J. Chem. Downloaded from www.nrcresearchpress.com by 210.87.254.5 on 09/05/12
For personal use only.

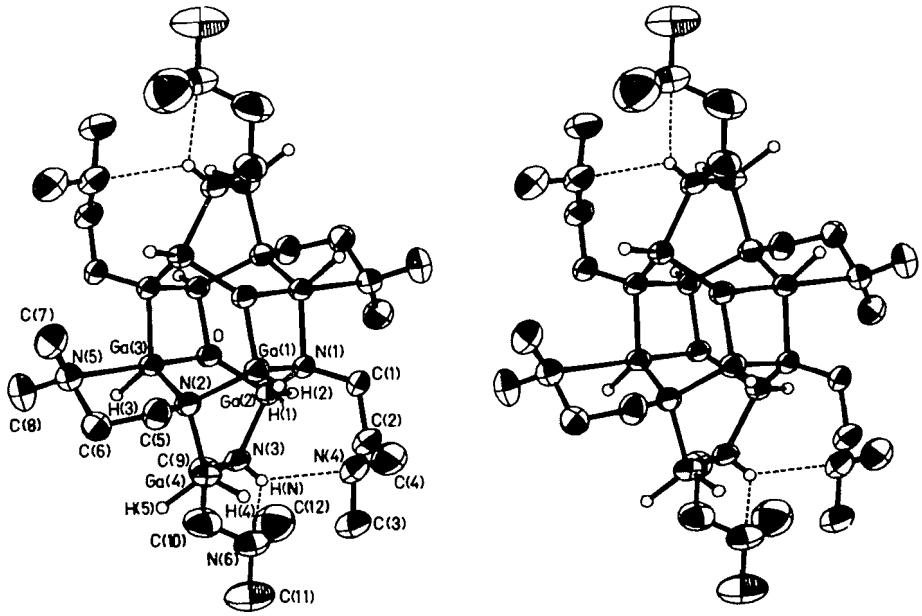

FIG. 1. Stereoscopic view of the $(GaH)_6(GaH_2)_2(\mu_3\text{-}O)_2(\mu_3\text{-}NCH_2CH_2NMe_2)_4(\mu\text{-}NHCH_2CH_2NMe_2)_2$ molecule showing the atom numbering scheme and 50% probability thermal ellipsoids for the nonhydrogen atoms. Broken lines indicate hydrogen bonds. The methylene and methyl hydrogen atoms have been omitted for the sake of clarity.

TABLE 3. Rigid-body thermal parameters of $Ga_8O_2N_6$ molecular core*

(*a*) **L**($\times 10$ deg^2)

$$\begin{pmatrix} 94(12) & 18(4) & 12(6) \\ & 49(4) & -8(4) \\ & & 54(6) \end{pmatrix}$$

(*b*) Principal axes of **L**

R.m.s. amplitude	Direction cosines ($\times 10^3$)		
3.2°	938	304	167
2.4	23	−567	824
1.9	345	−776	−528

(*c*) Principal axes of **T**

R.m.s. amplitude	Direction cosines ($\times 10^3$)		
0.21 Å	−168	957	−235
0.18	−161	−261	−952
0.17	−973	−123	196

*Axes of reference are orthogonal angstrom axes. Estimated standard deviations of components of **L** are given in parentheses in units of the last places shown. R.m.s. $\Delta U_{ij} = 0.0025$ Å^2.

between Ga(1) and Ga(2) arises from the fact that Ga(2) is contained in three six-membered rings while Ga(1) is part of two six-membered rings and a four-membered ring. The other gallium atom, Ga(4), does not occupy a bridgehead position in the polycyclic cage and is coordinated to two nitrogen atoms and two hydrogen atoms.

The tetrahedral Ga—O distances, Ga(1)—O′, 1.879(2) and Ga(2)—O, 1.869(2) Å, are significantly different. This small but significant difference is not surprising since one of these bonds, Ga—O′, is part of a four-membered ring while the other is in a six-membered ring. These bond lengths are considerably shorter than the values of 1.94–1.99 Å in $[Me_2GaOH]_4$ (15). It should be noted that in $[Me_2GaOH]_4$ there are Ga—OH—Ga bridges while in the present structure we are dealing with a Ga—O(Ga)—Ga system. The mean bond angle about the three-coordinate O atom, 117.1°, indicates that there may be some d_π–p_π bonding taking place in this structure. A similar interaction appears to take place in the β-Ga_2O_3 structure (16), which contains two trigonally coordinated O atoms each bonded to three Ga atoms with mean valence angles of 116 and 119° and Ga—O distances ranging from 1.80–1.83 Å. The Ga_2O_3 structure also features a tetrahedrally coordinated O atom bonded to one tetrahedral Ga atom (Ga—O = 1.85 Å) and three octahedral gallium atoms. In light of this information the tetra-

Can. J. Chem. Downloaded from www.nrcresearchpress.com by 210.87.254.5 on 09/05/12
For personal use only.

TABLE 4. Bond lengths (Å) with estimated standard deviations in parentheses

(*a*) Nonhydrogen atoms

Bond	Distance		Bond	Distance	
	Uncorrected	Corrected		Uncorrected	Corrected
Ga(1)—O′	1.876(2)	1.879	N(3)—C(9)	1.490(5)	1.493*
Ga(2)—O	1.866(2)	1.869	N(4)—C(2)	1.462(6)	1.464
Ga(3)—O	1.957(3)	1.960	N(4)—C(3)	1.459(7)	1.461*
Ga(1)—N(1)	1.978(3)	1.982	N(4)—C(4)	1.447(8)	1.449*
Ga(1)—N(2)	1.949(3)	1.953	N(5)—C(6)	1.468(5)	1.470
Ga(2)—N(2)	1.942(3)	1.945	N(5)—C(7)	1.463(6)	1.464
Ga(2)—N(3)	1.978(3)	1.980	N(5)—C(8)	1.467(6)	1.468
Ga(3)—N(1)′	1.996(3)	1.999	N(6)—C(10)	1.469(8)	1.470
Ga(3)—N(2)	1.945(3)	1.949	N(6)—C(11)	1.449(8)	1.451*
Ga(3)—N(5)	2.778(3)	2.779	N(6)—C(12)	1.450(10)	1.454*
Ga(4)—N(2)	1.999(3)	2.001	C(1)—C(2)	1.518(6)	1.519
Ga(4)—N(3)	1.970(3)	1.973	C(5)—C(6)	1.527(6)	1.528
N(1)—C(1)	1.479(4)	1.480	C(9)—C(10)	1.486(7)	1.487*
N(2)—C(5)	1.480(5)	1.480			

(*b*) Bonds involving hydrogen atoms

Bond	Distance	Bond	Distance
Ga(1)—H(1)	1.41(4)	C(6)—H(6*a*)	0.99(4)
Ga(2)—H(2)	1.52(5)	C(6)—H(6*b*)	1.10(4)
Ga(3)—H(3)	1.49(5)	C(7)—H(7*a*)	0.90(6)
Ga(4)—H(4)	1.52(5)	C(7)—H(7*b*)	1.09(6)
Ga(4)—H(5)	1.40(4)	C(7)—H(7*c*)	1.03(4)
N(4)—H(n)	0.85(5)	C(8)—H(8*a*)	1.00(6)
C(1)—H(1*a*)	0.91(5)	C(8)—H(8*b*)	1.00(5)
C(1)—H(1*b*)	0.87(5)	C(8)—H(8*c*)	1.21(8)
C(2)—H(2*a*)	1.11(5)	C(9)—H(9*a*)	0.88(5)
C(2)—H(2*b*)	1.10(4)	C(9)—H(9*b*)	1.09(7)
C(3)—H(3*a*)	0.88(5)	C(10)—H(10*a*)	1.09(6)
C(3)—H(3*b*)	1.18(5)	C(10)—H(10*b*)	1.22(8)
C(3)—H(3*c*)	0.88(7)	C(11)—H(11*a*)	1.35(8)
C(4)—H(4*a*)	0.89(6)	C(11)—H(11*b*)	1.34(8)
C(4)—H(4*b*)	1.00(6)	C(11)—H(11*c*)	1.14(8)
C(4)—H(4*c*)	1.05(6)	C(12)—H(12*a*)	1.51(8)
C(5)—H(5*a*)	1.12(5)	C(12)—H(12*b*)	1.24(8)
C(5)—H(5*b*)	1.08(5)	C(12)—H(12*c*)	0.90(9)

*These bond lengths have been corrected for independent motion as well as libration (see text).

hedral Ga—O distances in this structure appear to be slightly long relative to the similar bonds in Ga_2O_3 while the axial Ga(3)—O bond, 1.960(3) Å, is correspondingly shorter than any other axial Ga—O bond yet observed (see Table 8).

The six unique tetrahedral Ga—N bond lengths range from 1.945(3) to 2.001(3) Å and have a mean value of 1.972 Å. The mean distance is shorter than the value of 1.982 Å for tetrahedral Ga—N bonds given in Table 8 but all of the individual distances in the present structure fall within the observed range of 1.930–2.009 Å. There are highly significant variations between the individual values. The two bonds involving the singly bridging nitrogen atom N(3) (Ga(2)—N(3), 1.980(3), and Ga(4)—N(3), 1.973(4) Å) are neither significantly different from each other nor from the mean value of 1.982 Å from Table 8. The four other tetrahedral Ga—N bonds involve the μ_3 nitrogen atoms N(1) and N(2). Three of these bonds are in the highly constrained six-membered Ga(1)—N(1)—Ga(2)—O—Ga(3)—N(2) ring and divide into two relatively short bonds (Ga(1)—N(2), 1.953(3), and Ga(2)—N(1), 1.945(3) Å) and one "normal" bond (Ga(4)—N(2), 1.982(3) Å), the latter differing from the two others in that it also is one side of a four-membered ring. The last tetrahedral Ga—N bond

Can. J. Chem. Downloaded from www.nrcresearchpress.com by 210.87.254.5 on 09/05/12
For personal use only.

TABLE 5. Bond angles (deg) with estimated standard deviations in parentheses

(*a*) Nonhydrogen atoms

Bonds	Angle (deg)	Bonds	Angle (deg)
O′—Ga(1)—N(1)	88.4(1)	Ga(3)—N(2)—Ga(4)	111.0(1)
O′—Ga(1)—N(2)	105.9(1)	Ga(3)—N(2)—C(5)	115.3(2)
N(1)—Ga(1)—N(2)	113.8(1)	Ga(4)—N(2)—C(5)	105.1(2)
O—Ga(2)—N(1)	99.2(1)	Ga(2)—N(3)—Ga(4)	115.4(1)
O—Ga(2)—N(3)	97.4(1)	Ga(2)—N(3)—C(9)	110.6(3)
N(1)—Ga(2)—N(3)	114.1(1)	Ga(4)—N(3)—C(9)	114.6(3)
O—Ga(3)—N(1)′	85.7(1)	C(2)—N(4)—C(3)	110.2(5)
O—Ga(3)—N(2)	98.2(1)	C(2)—N(4)—C(4)	114.0(5)
O—Ga(3)—N(5)	175.9(1)	C(3)—N(4)—C(4)	109.5(5)
N(1)′—Ga(3)—N(2)	121.5(1)	Ga(3)—N(5)—C(6)	88.8(2)
N(1)′—Ga(3)—N(5)	94.0(1)	Ga(3)—N(5)—C(7)	107.5(3)
N(2)—Ga(3)—N(5)	78.5(1)	Ga(3)—N(5)—C(8)	129.4(3)
N(2)—Ga(4)—N(3)	104.0(1)	C(6)—N(5)—C(7)	110.0(4)
Ga(1)′—O—Ga(2)	131.1(1)	C(6)—N(5)—C(8)	110.3(4)
Ga(1)′—O—Ga(3)	94.2(1)	C(7)—N(5)—C(8)	108.6(4)
Ga(2)—O—Ga(3)	125.9(1)	C(10)—N(6)—C(11)	111.2(7)
Ga(1)—N(1)—Ga(2)	109.0(1)	C(10)—N(6)—C(12)	111.7(6)
Ga(1)—N(1)—Ga(3)′	89.9(1)	C(11)—N(6)—C(12)	109.9(7)
Ga(1)—N(1)—C(1)	116.1(3)	N(1)—C(1)—C(2)	115.6(3)
Ga(2)—N(1)—Ga(3)′	111.3(1)	C(1)—C(2)—N(4)	113.8(4)
Ga(2)—N(1)—C(1)	117.9(3)	N(2)—C(5)—C(6)	112.7(3)
Ga(3)′—N(1)—C(1)	109.1(2)	C(5)—C(6)—N(5)	110.6(3)
Ga(1)—N(2)—Ga(3)	110.7(1)	N(3)—C(9)—C(10)	112.4(4)
Ga(1)—N(2)—Ga(4)	106.7(1)	C(9)—C(10)—N(6)	113.0(5)
Ga(1)—N(2)—C(5)	107.6(2)		

(*b*) Angles involving hydrogen atoms

Bonds	Angle (deg)	Bonds	Angle (deg)
O′—Ga(1)—H(1)	115(2)	C(6)—C(5)—H(5*a*)	104(2)
N(1)—Ga(1)—H(1)	117(2)	C(6)—C(5)—H(5*b*)	113(2)
N(2)—Ga(1)—H(1)	113(2)	H(5*a*)—C(5)—H(5*b*)	112(3)
O—Ga(2)—H(2)	115(2)	N(5)—C(6)—H(6*a*)	108(2)
N(1)—Ga(2)—H(2)	121(2)	N(5)—C(6)—H(6*b*)	119(2)
N(3)—Ga(2)—H(2)	107(2)	C(5)—C(6)—H(6*a*)	109(2)
O—Ga(3)—H(3)	101(2)	C(5)—C(6)—H(6*b*)	102(2)
N(1)′—Ga(3)—H(3)	121(2)	H(6*a*)—C(6)—H(6*b*)	109(3)
N(2)—Ga(3)—H(3)	115(2)	N(5)—C(7)—H(7*a*)	109(4)
N(5)—Ga(3)—H(3)	83(2)	N(5)—C(7)—H(7*b*)	109(3)
N(2)—Ga(4)—H(4)	100(2)	N(5)—C(7)—H(7*c*)	116(2)
N(2)—Ga(4)—H(5)	115(2)	H(7*a*)—C(7)—H(7*b*)	103(5)
N(3)—Ga(4)—H(4)	117(2)	H(7*a*)—C(7)—H(7*c*)	114(4)
N(3)—Ga(4)—H(5)	107(2)	H(7*b*)—C(7)—H(7*c*)	104(4)
H(4)—Ga(4)—H(5)	114(3)	N(5)—C(8)—H(8*a*)	109(3)
Ga(2)—N(3)—H(n)	106(4)	N(5)—C(8)—H(8*b*)	109(3)
Ga(4)—N(3)—H(n)	97(4)	N(5)—C(8)—H(8*c*)	108(4)
C(9)—N(3)—H(n)	112(4)	H(8*a*)—C(8)—H(8*b*)	121(5)
N(1)—C(1)—H(1*a*)	110(3)	H(8*a*)—C(8)—H(8*c*)	113(5)
N(1)—C(1)—H(1*b*)	119(3)	H(8*b*)—C(8)—H(8*c*)	98(4)
C(2)—C(1)—H(1*a*)	108(3)	N(3)—C(9)—H(9*a*)	108(4)
C(2)—C(1)—H(1*b*)	104(3)	N(3)—C(9)—H(9*b*)	103(4)
H(1*a*)—C(1)—H(1*b*)	98(4)	C(10)—C(9)—H(9*a*)	111(4)
N(4)—C(2)—H(2*a*)	105(2)	C(10)—C(9)—H(9*b*)	109(3)
N(4)—C(2)—H(2*b*)	111(2)	H(9*a*)—C(9)—H(9*b*)	114(5)
C(1)—C(2)—H(2*a*)	104(2)	N(6)—C(10)—H(10*a*)	117(4)
C(1)—C(2)—H(2*b*)	111(2)	N(6)—C(10)—H(10*b*)	97(4)
H(2*a*)—C(2)—H(2*b*)	112(3)	C(9)—C(10)—H(10*a*)	108(3)

Can. J. Chem. Downloaded from www.nrcresearchpress.com by 210.87.254.5 on 09/05/12
For personal use only.

TABLE 5. (*Concluded*)

(*b*) Angles involving hydrogen atoms

Bonds	Angle (deg)	Bonds	Angle (deg)
N(4)—C(3)—H(3*a*)	105(4)	C(9)—C(10)—H(10*b*)	116(4)
N(4)—C(3)—H(3*b*)	122(3)	H(10*a*)—C(10)—H(10*b*)	106(5)
N(4)—C(3)—H(3*c*)	117(5)	N(6)—C(11)—H(11*a*)	110(4)
H(3*a*)—C(3)—H(3*b*)	109(5)	N(6)—C(11)—H(11*b*)	103(4)
H(3*a*)—C(3)—H(3*c*)	109(6)	N(6)—C(11)—H(11*c*)	93(4)
H(3*b*)—C(3)—H(3*c*)	96(5)	H(11*a*)—C(11)—H(11*b*)	111(5)
N(4)—C(4)—H(4*a*)	113(4)	H(11*a*)—C(11)—H(11*c*)	91(5)
N(4)—C(4)—H(4*b*)	103(3)	H(11*b*)—C(11)—H(11*c*)	145(6)
N(4)—C(4)—H(4*c*)	122(3)	N(6)—C(12)—H(12*a*)	105(3)
H(4*a*)—C(4)—H(4*b*)	114(5)	N(6)—C(12)—H(12*b*)	105(4)
H(4*a*)—C(4)—H(4*c*)	93(5)	N(6)—C(12)—H(12*c*)	113(6)
H(4*b*)—C(4)—H(4*c*)	112(5)	H(12*a*)—C(12)—H(12*b*)	139(5)
N(2)—C(5)—H(5*a*)	109(2)	H(12*a*)—C(12)—H(12*c*)	86(6)
N(2)—C(5)—H(5*b*)	106(3)	H(12*b*)—C(12)—H(12*c*)	107(7)

TABLE 6. Intraannular dihedral angles (deg)

(*a*) Six-membered rings

Bond	Angle (deg)	Bond	Angle (deg)
Ga(1)—N(2)	−32.3(1)	Ga(1)—N(2)	63.1(1)
N(2)—Ga(3)	41.7(2)	N(2)—Ga(3)	−48.3(1)
Ga(3)—N(1)′	3.7(2)	Ga(3)—O	−18.7(1)
N(1)′—Ga(2)′	−46.6(1)	O—Ga(2)	72.6(1)
Ga(2)′—O′	66.2(1)	Ga(2)—N(1)	−51.1(1)
O′—Ga(1)	−23.0(1)	N(1)—Ga(1)	−4.1(1)
Ga(4)—N(3)	−24.8(1)	Ga(4)—N(3)	−24.8(1)
N(3)—Ga(2)	67.3(1)	N(3)—Ga(2)	−36.3(2)
Ga(2)—O	−43.4(1)	Ga(2)—N(1)	51.3(1)
O—Ga(3)	−18.7(1)	N(1)—Ga(1)	−4.1(1)
Ga(3)—N(2)	70.0(1)	Ga(1)—N(2)	−57.8(1)
N(2)—Ga(4)	−49.5(1)	N(2)—Ga(4)	71.1(1)

(*b*) Five and four-membered rings

Bond	Angle (deg)	Bond	Angle (deg)
Ga(3)—N(2)	6.9(2)	Ga(1)—O′	10.3(1)
N(2)—C(5)	−39.9(3)	O′—Ga(3)′	−10.3(1)
C(5)—C(6)	70.6(4)	Ga(3)′—N(1)	9.7(1)
C(6)—N(5)	−50.0(3)	N(1)—Ga(1)	−10.0(1)
N(5)—Ga(3)	24.8(2)		

(Ga(4)—N(2), 2.001(3) Å) is relatively long, but balances the two short Ga—N bonds involving N(2).

The bond lengths (Ga(3)—N(1)′, 1.999(3), and Ga(3)—N(2), 1.949(3) Å) are the first equatorial Ga—N distances reported. As expected, their mean value (1.974 Å) is shorter than the mean tetrahedral Ga—N distance of 1.982 Å. The longer of these bonds is in the four-membered Ga_2NO ring while the shorter one is in the same Ga_3N_2O ring which contains the short tetrahedral Ga—N bonds. The rather long axial Ga(3)—N(5) distance of 2.779(3) Å must be interpreted as a very weak interaction and further demonstrates the importance of steric forces (2) in the marked variation of axial Ga—N distances (see Table 8). The primary steric constraint in this case is the essentially fixed conformation of the five-membered Ga(3)—N(2)—C(5)—C(6)—N(5) ring, two of whose members are bridgehead atoms of the polycyclic cage. A shortening of the Ga(3)—N(5) bond would result

Can. J. Chem. Downloaded from www.nrcresearchpress.com by 210.87.254.5 on 09/05/12
For personal use only.

Can. J. Chem. Downloaded from www.nrcresearchpress.com by 210.87.254.5 on 09/05/12
For personal use only.

TABLE 7

(*a*) Selected intramolecular contacts

Atoms	Distance (Å)	Atoms	Distance (Å)
Ga(1)...Ga(3)′	2.8081(6)	C(3)...H(2*b*)	2.53(4)
Ga(1)...Ga(4)	3.1683(6)	C(4)...H(2*a*)	2.52(5)
Ga(1)...Ga(2)	3.1909(6)	C(4)...H(3*a*)	2.54(5)
Ga(1)...Ga(3)	3.2035(6)	C(4)...H(3*c*)	2.56(7)
Ga(1)...Ga(2)′	3.4066(6)	C(6)...H(7*a*)	2.60(6)
Ga(1)...O	3.297(2)	C(6)...H(8*a*)	2.62(6)
Ga(2)...Ga(3)′	3.2517(6)	C(7)...H(6*b*)	2.65(4)
Ga(2)...Ga(4)	3.3361(7)	C(7)...H(8*a*)	2.55(6)
Ga(2)...Ga(3)	3.4041(6)	C(8)...H(6*a*)	2.42(4)
Ga(2)...N(4)	3.117(4)	C(8)...H(7*a*)	2.49(6)
Ga(3)...Ga(4)	3.2501(6)	C(8)...H(7*b*)	2.59(6)
Ga(3)...O′	3.306(2)	C(8)...H(5*a*)	2.65(5)
O...O′	3.317(5)	C(10)...H(11*c*)	2.19(7)
N(1)...N(4)	3.125(4)	C(10)...H(n)	2.51(5)
C(1)...C(4)	3.064(8)	C(11)...H(10*b*)	2.36(8)
C(5)...C(8)	3.115(7)	C(11)...H(12*a*)	2.49(9)
C(9)...C(12)	3.006(11)	C(12)...H(11*b*)	2.52(9)
Ga(2)...H(9*a*)	2.72(5)	H(1*b*)...H(2*a*)	2.15(6)
Ga(4)...H(5*b*)	2.66(5)	H(4*c*)...H(8*c*)′	2.01(9)
N(5)...H(5*a*)	2.52(5)	H(5*a*)...H(8*b*)	2.08(7)
C(2)...H(3*a*)	2.47(5)	H(10*b*)...H(11*c*)	1.59(10)
C(3)...H(4*b*)	2.43(6)		

(*b*) Gallium coordination spheres

Atoms	Distance (Å)	Atoms	Distance (Å)
O′...N(1)	2.688(4)	O...H(3)	2.67(5)
O′...N(2)	3.052(4)	N(1)′...N(2)	3.439(4)
O′...H(1)	2.79(4)	N(1)′...N(5)	3.530(5)
N(1)...N(2)	3.290(4)	N(1)′...H(3)	3.05(5)
N(1)...H(1)	2.91(4)	N(2)...N(5)	3.056(4)
N(2)...H(1)	2.82(4)	N(2)...H(3)	2.91(5)
O...N(1)	2.899(4)	N(5)...H(3)	2.98(5)
O...N(3)	2.888(4)	N(2)...N(3)	3.128(4)
O...H(2)	2.86(5)	N(2)...H(4)	2.71(5)
N(1)...N(3)	3.289(4)	N(2)...H(5)	2.89(4)
N(1)...H(2)	3.02(5)	N(3)...H(4)	2.99(5)
N(3)...H(2)	2.82(5)	N(3)...H(5)	2.73(4)
O...N(2)	2.950(4)	H(4)...H(5)	2.46(6)

(*c*) Hydrogen-bond data (distances in Å and angles in deg)*

D—H...A	H...A	D...A	∠DHA	∠XAH
N(3)—H(n)...N(4)	2.49(5)	3.128(5)	133(3)	83, 112, 124(1)
N(3)—H(n)...N(6)	2.51(6)	2.901(5)	110(3)	73, 107, 137(1)

*The angle N(4)...H(n)...N(6) is 108(3)°.

in an unfavorable increase in angular strain in the already strained system.

The four independent tetrahedral Ga—H distances range from 1.40 to 1.52 Å and have a mean value of 1.46 Å. There are no significant differences between the individual values. The equatorial Ga(3)—H(3) distance of 1.49(5) Å falls within the range of previously observed equatorial Ga—H bond lengths.

The distortion of the trigonal bipyramidal coordination group of Ga(3) occurs primarily as a lengthening of the axial Ga—N bond, a significant nonplanarity of the equatorial GaNNH group (which has H(3) displaced 0.37 Å from the

TABLE 8. Comparison of observed Ga—O, Ga—N, and Ga—H bond lengths

Bond	Coordination type			
		Trigonal bipyramidal		
	Tetrahedral	Equatorial	Axial	Octahedral
Ga—O Range	1.80–1.99	1.845–1.967	1.960–2.078	1.908–2.08
Mean	1.89	1.896	2.025	1.97
Number	10	8	5	20
Reference	[a,b,r]	[c,d,e]	[b,d,e]	[f,g,h,r]
Ga—N Range	1.930–2.009	1.949, 1.999	2.110–2.779	2.034–2.182
Mean	1.982	1.974	2.296	2.106
Number	27	2	7	13
Reference	[b,i–o]	[b]	[b,c,d,e]	[f,g,p,q]
Ga—H Range	1.40–1.52	1.37–1.73		
Mean	1.46	1.51		
Number	4	5		
Reference	[b]	[d,e]		

[a] $(Me_2GaOH)_4$, ref. 15.
[b] This work.
[c] $GaCl(C_{10}H_8NO)_2$, ref. 12.
[d] $[MeN(CH_2CH_2O)_2GaH]_2$, ref. 1.
[e] $[Me_2NCH_2CH_2OGaH_2]_2$ and $[Me_2NCH_2CH_2OGaMe_2]_2$, ref. 2.
[f] $[Ga_2(OH)_2Cl_2(C_{14}H_{17}N_3)_2]Cl_2.H_2O$, ref. 17.
[g] $GaH(EDTA).H_2O$, ref. 22.
[h] $Ga(acac)_3$, ref. 23.
[i] GaN, ref. 24.
[j] $(H_2GaNCH_2CH_2)_3$, ref. 25.
[k] $[D_2Ga(N_2C_3H_3)]_2$, ref. 26.
[l] Me_3NGaH_3, ref. 27.
[m] $[Me_2Ga(N_2C_3H_3)_2]_2Ni$, ref. 28.
[n] $[Me_2Ga(N_2C_3H_3)_2]_2Cu$ and $[Me_2Ga(N_2C_5H_7)_2]_2Cu$, ref. 29.
[o] $[Me_2Ga(N_2C_3H_3)_2]_2$, ref. 30.
[p] $[GaCl_2(bipy)_2]^+ [GaCl_4]^-$, ref. 31.
[q] $GaCl_3(terpy)$, ref. 32.
[r] β-Ga_2O_3, ref. 16.

mean plane in the direction of N(5)), and distortions of the valence angles at Ga(3) between the axial and the equatorial substituents. Unlike the previous five-coordinate gallium structures (1, 2, 12, 13), in which the most notable distortion of the trigonal bipyramids is the deviation of the angles between the axial substituents (which range from 150.0 to 169.1°) from linearity, the angle in the present structure, N(5)—Ga(3)—O, is 175.9(1)°. Of the angles within the equatorial group, only N(1)′—Ga(3)—N(2), 121.5(1)°, differs significantly from the "ideal" value of 120°. The angles between the axial and equatorial substituents, ideally 90°, range from 78.5(1) for N(2)—Ga(3)—N(5) to 101(2)° for O—Ga(3)—H(3).

The range of bond angles at the tetrahedrally coordinated gallium atoms, from 88.4(1)° at Ga(1) in the four-membered ring to 121(2)° for the angle N(1)—Ga(2)—H(2), represents considerable distortion from ideal tetrahedral geometry. The mean valence angles are 108.9 at Ga(1), 109.0 at Ga(2), and 109.5° at the relatively strain-free Ga(4).

The four-membered Ga_2NO ring is the first such ring to be characterized by X-ray analysis. While the related Ga_2O_2 rings contain either two five-coordinate (1, 2) or two six-coordinate gallium atoms (17), the present Ga_2NO ring contains one four-coordinate, Ga(1), and one five-coordinate gallium atom, Ga(3)′. The nonplanar ring is folded with Ga(1) and Ga(3)′ displaced by −0.0046 and −0.0043 Å from the mean plane of the ring and O′ and N(1) by 0.197 and 0.140 Å. The mean intraannular dihedral angle in the ring has a magnitude of 10.1° (individual values are given in Table 6). As a result of the severe steric constraints inherent in the fused polycyclic system, the Ga_2NO ring, with angles ranging from 85.7(1)° at Ga(3)′ to 94.2(1)° at O′, is nearly square whereas the Ga_2O_2 rings were found to have angles between 74.7 and 76.0° at Ga and between 100.0 and 105.4° at O. The nonbonded Ga...Ga contacts across the Ga_2O_2 rings are near 3.2 Å while the Ga(1)...Ga(3)′ distance across the Ga_2NO ring is considerably reduced to 2.808(1) Å.

The mean valence angle in the five-membered

Can. J. Chem. Downloaded from www.nrcresearchpress.com by 210.87.254.5 on 09/05/12
For personal use only.

Can. J. Chem. Downloaded from www.nrcresearchpress.com by 210.87.254.5 on 09/05/12
For personal use only.

GaNCCN ring is 101.2° with individual values ranging from 78.5(1) at Ga(3) to 115.3(2)° at N(2). The conformation of the ring is quite different from those observed for the related GaOCCN rings (1, 2) (on the basis of the intraannular dihedral angles) and does not correspond to a minimum energy conformation (18). This indicates a high degree of strain in the ring and is consistent with the long Ga(3)—N(5) distance. The ring conformation may be described as a distorted "envelope" with the atoms N(5), Ga(3), N(2), and C(5) forming a rough plane with C(6) displaced from this plane.

Each of the unique six-membered rings in the polycyclic system has a distorted "boat" conformation. For each ring the dihedral angles (Table 6) may be split into a group of four large magnitudes and a group of two small magnitudes. The minimum-energy boat conformation is characterized by four dihedral angles with a magnitude of 54° and two of 0° and a mean valence angle of 111.7° (19). The presence of the five-coordinate atom Ga(3) in each of the three Ga_3N_2O rings introduces a source of strain in addition to that already imposed by the fused ring system alone. As for the five-membered ring, these conformations do not correspond to any of the simple minimum-energy arrangements calculated for free cyclopentane systems (18, 19). The observed conformation must correspond to a local energy minimum but represents a system which is strained relative to the free ring. The Ga(1)—N(2)—Ga(3)—N(1)′—Ga(2)′—O′ ring, which has an equatorial–equatorial angle at Ga(3), has a mean valence angle of 113.3° while the other two Ga_3N_2O rings (Ga(1)—N(1)—Ga(2)—O—Ga(3)—N(2) and Ga(4)—N(3)—Ga(2)—O—Ga(3)—N(2)), which have equatorial–axial angles at Ga(3), consequently have smaller mean valence angles (109.5 and 108.7° respectively). Individual angles in the six-membered rings range from 97.4(1)° for N(3)—Ga(2)—O to 131.1(1)° for Ga(1)′—O—Ga(2).

The mean N(quaternary)—C and N(pyramidal)—C bond lengths of 1.477 and 1.458 Å are as expected. The N—C bonds involving the cage nitrogen atoms are somewhat longer than the others. Those involving the bridgehead atoms, N(1)—C(1) and N(2)—C(5), are both 1.480 Å, while that involving the singly bridging nitrogen atom (N(3)—C(9), 1.493(5) Å) is significantly longer than the mean value. σ-hybridization effects have been calculated (20) and appear to be primarily responsible for the slight shortening of the $C(sp^3)$—$C(sp^3)$ bonds (1.487(7)–1.528(6) Å) from the usual value of 1.537 Å. The calculated single bond distances for these C—C bonds range from 1.508–1.524 Å.

The N—H distance of 0.85(5) Å does not differ significantly from the value expected for X-ray data. The mean C—H bond length is 1.03 Å and the individual values range from 0.88–1.22(4–8) Å. The R—N—H, R—C—H, and H—C—H angles have ranges of 97–124(4), 97–122(2–5), and 93–121(3–6)° and mean values of 105, 110, and 108° respectively. The unusually long C—H distances and the extreme angles associated with the ill-defined C(11) and C(12) methyl groups (Tables 4 and 5) have not been included in the above ranges and means in view of their apparent unreliability.

The two "free" nitrogen atoms, N(4) and N(6), are involved in an intramolecular bifurcated hydrogen-bonding arrangement with H(*n*). The N...N distances (N(3)...N(4), 3.128(5) and N(3)...N(6), 2.901(5) Å) are shorter than usual (21). This shortening may be partially due to the nonlinearity of the N—H...N interactions (see Table 7*c*) but both N—H...N interactions appear to be fairly strong for such a bifurcated system. The crystal structure consists of well separated molecules. There is only one intermolecular contact less than the sum of van der Waals radii, H(3*b*)[x, y, z]...H(3*b*)[$-x$, $1-y$, $1-z$], 1.9(1) Å.

Further work is in progress in an attempt to clarify the reaction sequence leading to the above cage structure, and also to produce further examples of extensive cage structures involving Ga and N atoms, and Ga, N, and O atoms.

We thank the National Research Council of Canada for financial support and the University of British Columbia Computing Centre for assistance.

1. S. J. RETTIG, A. STORR, and J. TROTTER. Can. J. Chem. **52**, 2206 (1974).
2. S. J. RETTIG, A. STORR, and J. TROTTER. Can. J. Chem. **53**, 58 (1975).
3. A. STORR and A. D. PENLAND. J. Chem. Soc. A, 1237 (1971).
4. D. T. CROMER and J. B. MANN. Acta Cryst. A**24**, 321 (1968).
5. R. F. STEWART, E. R. DAVIDSON, and W. T. SIMPSON. J. Chem. Phys. **42**, 3175 (1965).
6. D. T. CROMER and D. LIBERMAN. J. Chem. Phys. **53**, 1891 (1970).
7. V. SCHOMAKER and K. N. TRUEBLOOD. Acta Cryst. B**24**, 63 (1968).
8. D. W. J. CRUICKSHANK. Acta Cryst. **9**, 747, 754 (1956).
9. D. W. J. CRUICKSHANK. Acta Cryst. **14**, 896 (1961).

10. W. R. BUSING and H. A. LEVY. Acta Cryst. **17**, 142 (1964).
11. C. K. JOHNSON. *In* Crystallographic computing. Munksgaard, Copenhagen. 1970. pp. 207–226.
12. M. SHIRO and Q. FERNANDO. Anal. Chem. **43**, 1222 (1971).
13. K. DYMOCK and G. J. PALENIK. Chem. Commun. 884 (1973).
14. P. B. HITCHCOCK, G. M. MCLAUGHLIN, J. D. SMITH, and K. M. THOMAS. Chem. Commun. 934 (1973).
15. G. S. SMITH and J. L. HOARD. J. Am. Chem. Soc. **81**, 3907 (1959).
16. S. GELLER. J. Chem. Phys. **33**, 676 (1960).
17. K. DYMOCK, G. J. PALENIK, and A. J. CARTY. Chem. Commun. 1218 (1972).
18. J. B. HENDRICKSON. J. Am. Chem. Soc. **83**, 4537 (1961); **85**, 4059 (1963).
19. R. BUCOURT and D. HAINAUT. Bull. Soc. Chim. Fr. 1366 (1965).
20. S. J. RETTIG. Ph.D Thesis. University of British Columbia. Vancouver, British Columbia. 1974.
21. G. C. PIMENTEL and A. L. MCCLELLAN. The hydrogen bond. Freeman, San Francisco. 1960.
22. C. H. L. KENNARD. Inorg. Chim. Acta, **1**, 347 (1967).
23. K. DYMOCK and G. J. PALENIK. Acta Cryst. B**30**, 1364 (1974).
24. R. JUZA and H. HAHN. Z. Anorg. Chem. **239**, 282 (1938).
25. W. HARRISON, A. STORR, and J. TROTTER. J. Chem. Soc. Dalton, 1554 (1972).
26. D. F. RENDLE, A. STORR, and J. TROTTER. J. Chem. Soc. Dalton, 2252 (1973).
27. D. F. SHRIVER and C. E. NORDMAN. Inorg. Chem. **2**, 1298 (1963).
28. D. F. RENDLE, A. STORR, and J. TROTTER. Chem. Commun. 406 (1974).
29. D. F. RENDLE, A. STORR, and J. TROTTER. J. Chem. Soc. Dalton. In press.
30. D. F. RENDLE, A. STORR, and J. TROTTER. Unpublished results.
31. R. RESTIVO and G. J. PALENIK. J. Chem. Soc. Dalton, 341 (1972).
32. G. BERAN, A. J. CARTY, H. A. PATEL, and G. J. PALENIK. Chem. Commun. 222 (1970).

Can. J. Chem. Downloaded from www.nrcresearchpress.com by 210.87.254.5 on 09/05/12
For personal use only.

Crystal and Molecular Structure of (±)-7,7-(2′,2′-Dimethyl)pentamethylene-1-methyl-norbornane-2-oxime

STEVEN J. RETTIG AND JAMES TROTTER

Department of Chemistry, University of British Columbia, Vancouver, British Columbia V6T 1W5

Received September 20, 1974

STEVEN J. RETTIG and JAMES TROTTER. Can. J. Chem. **53**, 765 (1975).

Crystals of (±)-7,7-(2′,2′-dimethyl)pentamethylene-1-methyl-norbornane-2-oxime are monoclinic, $a = 9.202(2)$, $b = 12.852(3)$, $c = 12.698(3)$ Å, $\beta = 110.83(2)°$, $Z = 4$, space group $P2_1/c$. The structure was solved by direct methods and was refined by full-matrix least-squares procedures to a final R of 0.048 for 1538 reflections with $I \geq 3\sigma(I)$. The crystal structure consists of pairs of molecules linked by N ... H—O hydrogen bonds (N ... O = 2.821(3) Å) to form centrosymmetric dimers. Bond distances are as follows: C—N = 1.266(3), N—O = 1.426(3), mean C(sp^3)—C(sp^3) = 1.540, and mean C(sp^3)—C(sp^2) = 1.511 Å.

STEVEN J. RETTIG et JAMES TROTTER. Can. J. Chem. **53**, 765 (1975).

Les cristaux de l'oxime de la (±)(diméthyl-2′,2′)pentaméthylène-7,7 méthyl-1 norbornanone-2 sont monocliniques $a = 9.202(2)$, $b = 12.852(3)$, $c = 12.698(3)$ Å, $\beta = 110.83(2)°$, $Z = 4$, groupe d'espace $P2_1/c$. On a résolu la structure par des méthodes directes et on l'a affinée par la méthode des moindres carrés (matrice complète) jusqu'à une valeur finale R de 0.048 pour 1538 réflections avec $I \geq 3\sigma(I)$. La structure cristalline consiste de paires de molécules liées par des ponts hydrogène N ... H—O (N ... O = 2.821(3) Å) formant des dimères centrosymétriques. Les longueurs de liaison sont les suivantes: C—N = 1.266(3), N—O = 1.426(3), valeur moyenne de C(sp^3)—C(sp^3) = 1.540, et la valeur moyenne C(sp^3)—C(sp^2) = 1.511 Å.

[Traduit par le journal]

Introduction

As part of a general approach (1, 2) to the synthesis of structurally related mono- and sesquiterpenes a simple synthetic route to camphor (**3**) based on biosynthetic ideas has been devised (3). This involves cyclization of the enol acetate (**2**) of dihydrocarvone (**1**) and the logical extension of this approach in the sesquiterpene area prompted synthesis of the enol acetate (**5**) of dihydrocryptomerion (**4**) and subjection of this to the same cyclization conditions. In this way it was hoped to achieve a simple synthesis of campherenone (**6**) which occupied a key position in the general synthetic strategy (1*b*). In the event, cyclization of the enol acetate (**5**) with boron trifluoride in wet methylene chloride provided a mixture of products from which the main components (A, B, and C) could be isolated by column chromatography (silica) and preparative g.l.c. (relative abundance of A, B, and C 5:8:1). Component A was assigned structure (**8***a*, *b*) on the basis of spectral characteristics: ν_{max}(neat) 1740 and 1410 cm^{-1}; *m/e* (relative intensity), 220 (22.5); $\tau(CCl_4)$ 9.21 (3H, s), 9.10, 9.05, 9.00, and 8.94 (6H, s). The formation of tricyclic ketones of this type was rationalized by invoking 1,5-diene cyclization of (**5**) to form an intermediate bicyclic enol acetate (**7**) which could cyclize further to yield (**8***a*, *b*). In terms of this rationalization the presence of both ketones (**8***a* and **8***b*) was expected and, although this could not be established by g.l.c., the n.m.r. supported this expectation. The separation of the suspected ketones was accomplished by conversion to the corresponding enol acetates which were separated easily by preparative g.l.c. The separated enol acetates were hydrolized to the corresponding ketones (**8***a* and **8***b*) and one of these (**8***a*) was converted to a crystalline oxime (**9**). A full X-ray crystallographic analysis of this oxime is now described, which establishes its structure (**9**) and, in addition, confirms the structural assignments indicated above. Additional evidence is required before a definitive statement can be made about the structure of components B and C in the cyclization reaction mixture.

Experimental

Full experimental details for the synthesis of compounds described in this paper have been published elsewhere (1*b*).

Recrystallization of (±)-7,7-(2′,2′-dimethyl)penta-

Can. J. Chem. Downloaded from www.nrcresearchpress.com by 210.87.254.5 on 09/05/12
For personal use only.

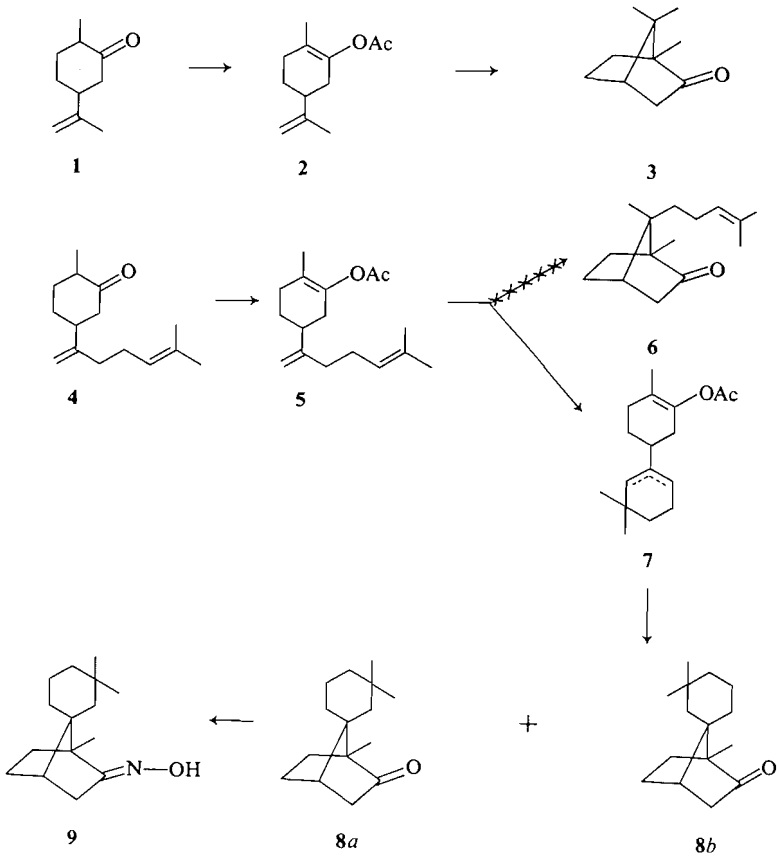

methylene-1-methyl-norbornane-2-oxime from benzene gave colorless crystals, m.p. 165–168 °C (1, 2). The crystal chosen for study was mounted with b parallel to the goniostat axis and had dimensions of *ca.* 0.5 × 0.5 × 0.7 mm. Unit-cell and space group data were obtained from film and diffractometer measurements. The unit-cell parameters were refined by a least-squares treatment of $\sin^2\theta$ values for 30 reflections measured on a diffractometer with CuK_α radiation. Crystal data are:

$C_{15}H_{25}NO$ f.w. = 235.4

Monoclinic, $a = 9.202(2)$, $b = 12.852(3)$, $c = 12.698(3)$ Å, $\beta = 110.83(2)°$, $V = 1403.6(6)$ Å^3, $Z = 4$, $\rho_c = 1.1138(5)$ g cm^{-3}, $F(000) = 520$ (20 °C, CuK_α, $\lambda = 1.5418$ Å, $\mu = 5.3$ cm^{-1}). Absent reflections: $0k0$, $k \neq 2n$ and $h0l$, $l \neq 2n$ define uniquely the space group $P2_1/c$ (C_{2h}^5, No. 14).

Intensities were measured on a Datex-automated General Electric XRD 6 diffractometer, with a scintillation counter, CuK_α (nickel filter and pulse height analyzer), and a θ–2θ scan at 2° min^{-1} over a range of (1.80 + 0.86 tan θ) degrees in 2θ, with 20 s background counts being measured at each end of the scan. Data were measured to $2\theta = 120°$ (minimum interplanar spacing 0.89 Å). The intensity of the check reflection, monitored every 40 reflections throughout the data collection, was 86% of its original intensity at the end of the data collection. Lorentz and polarization corrections and check reflection scaling were applied, and the structure amplitudes were derived. No absorption correction was made due to irregularity of the crystal surface. Of the 2061 independent reflections measured, 520 had intensities less than $3\sigma(I)$ above background where $\sigma^2(I) = S + B + (0.03S)^2$ with S = scan count and B = time averaged background count. These reflections were given zero weight in the refinement but were included in the structure factor calculations.

Structure Analysis

The structure was solved by direct methods. Sixteen sets of signs for 267 reflections with $|E| \geq 1.50$ were determined by a computer program which uses Sayre relationships in an iterative procedure (4). The starting set of reflections is given in Table 1. One set of signs was out-

TABLE 1. Basic starting set of reflections for $C_{15}H_{25}NO$

h	k	l	$\|E\|$	
0	3	10	3.87	origin determining
0	4	5	2.70	
3	7	5	3.45	
1	1	−2	2.03	
6	5	−7	3.27	
1	2	4	2.73	
4	5	−3	2.58	

Can. J. Chem. Downloaded from www.nrcresearchpress.com by 210.87.254.5 on 09/05/12
For personal use only.

Can. J. Chem. Downloaded from www.nrcresearchpress.com by 210.87.254.5 on 09/05/12
For personal use only.

standing in that it converged in 4 cycles to a set having the highest consistency index (4) (0.85) with 129 positive and 138 negative signs. An *E*-map was computed using the 267 signed values of *E* from this set. The 17 nonhydrogen atoms accounted for the 17 highest peaks on the map. Three cycles of full-matrix least-squares refinement of the positions and isotropic thermal parameters of the O, N, and C atoms gave *R* 0.160. The nonhydrogen atoms were then refined anisotropically for one cycle, reducing *R* to 0.122. A difference map at this point revealed possible locations for all 25 H atoms which were then refined isotropically for one cycle giving *R* 0.082. The entire structure was refined for one cycle resulting in *R* 0.059. At this point one of the hydrogen atoms, H(81), was clearly positioned incorrectly. A structure factor calculation omitting H(81) gave *R* 0.056. A difference map gave the correct coordinates. The entire structure was refined for two more cycles giving a final *R* of 0.048 for 1538 reflections with $I \geq 3\sigma(I)$ (3 reflections which had $|F_o - F_c| > 3\sigma(F)$ were removed from the data set in the final stages of refinement).

The least-squares refinement was based on the minimization of $\Sigma w(F_o - F_c)^2$. The scattering factors of ref. 5 were used for the nonhydrogen atoms and those of ref. 6 for the hydrogen atoms. The anisotropic thermal parameters employed in the refinement are U_{ij} in the expression

$$f = f^o\exp[-2\pi^2(U_{11}h^2a^{*2} + U_{22}k^2b^{*2} + U_{33}l^2c^{*2} + 2U_{12}hka^*b^* + 2U_{13}hla^*c^* + 2U_{23}klb^*c^*)]$$

where f^o is the tabulated scattering factor and f is that corrected for thermal motion. The weighting scheme: $w = 1$ if $|F_o| \leq 7$, $w = 7/|F_o|$ if $|F_o| > 7$ gave uniform average values of $w(F_o - F_c)^2$ over ranges of $|F_o|$ and was employed in the final stages of refinement.

On the final cycle of refinement, no parameter shift was greater than 0.33σ for the nonhydrogen atoms and 1.37σ for the hydrogen atoms; the mean parameter shift corresponded to 0.08σ. A final difference map showed maximum fluctuations of ± 0.12 e Å^{-3}. The final positional and thermal parameters appear in Tables 2 and 3. Measured and calculated structure factors have been placed in the Depository of Unpublished Data.[1]

Thermal Motion and Correction of Molecular Geometry

The ellipsoids of thermal motion for the nonhydrogen atoms are shown in Fig. 1. The thermal motion has been analyzed in terms of the rigid-body modes of translation (T), libration (L), and screw (S) motion (7) using the computer program MGTLS. The r.m.s. standard deviation in the temperature factors U_{ij} is 0.0014 Å^2 indicating that the thermal motion of the twelve ring carbon atoms, C(1)—C(12), is well described by the rigid-body thermal parameters given in Table 4 (r.m.s. $\Delta U_{ij} = 0.0022$ Å^2). The indicated modes of motion are physically reasonable; the translation tensor T is nearly isotropic while the libration tensor L is somewhat anisotropic. The location of the unique origin and the orientation of the principal axes of L indicates that the rigid-body libration of the monomer unit is constrained by the hydrogen-bonding. The origin lies near the center of gravity in *x* and *y*, but is displaced toward the hydrogen bond in *z*. The principal axes of L do not correspond to the principal moments of inertia but are oriented as follows: L_1 makes an angle of 18° with the C(7)—C(2) bond, L_2 makes an angle of 23° with the C(7)—C(12) bond, and L_3 is 19° away from the O—N bond.

The appropriate bond distances and angles have been corrected for libration (8, 9), using shape parameters q^2 of 0.08 for all atoms involved. The bonds O—N, N—C(1), C(2)—C(13), C(11)—C(14), and C(11)—C(15) have been corrected for independent motion using a riding model based on the ΔU_{ij} (10, 11). Corrected and uncorrected bond distances appear in Table 5. Bond angles (Table 6) changed by no more than 0.04°, thus corrected values will not be reported.

Results and Discussion

A general view of the molecule, with crystallographic numbering scheme, is shown in Fig. 1. Fig. 2 shows the structure viewed along *a*. Intraannular dihedral angles defining the conformations of the ring systems are given in Table 7 with e.s.d.'s calculated using the formula due to P. Huber (appendix to ref. 12). Weighted least-squares mean planes are given in Table 8. The structural parameters of (**9**) are compared with those of related compounds (13–20) and oximes (21–29) in Table 9. Important inter- and intramolecular nonbonded contacts and details of the hydrogen bonding scheme are given in Table 10.

The crystal structure consists of pairs of molecules linked by N...H—O hydrogen bonds (N...O = 2.821(3) Å) to form centrosymmetric dimers situated about the centers of symmetry at (0, 0, 0) and (0, $\frac{1}{2}$, $\frac{1}{2}$). The N...O distance is similar to those reported for other dimeric oximes: 2.84 Å in *syn-p*-chlorobenzaldoxime (23), 2.76 Å in dimethylglyoxime (25), and 2.87 Å

[1]The structure factor table is available, at a nominal charge, from the Depository of Unpublished Data, National Science Library, National Research Council of Canada, Ottawa, Canada K1A 0S2.

TABLE 2. Final positional parameters (fractional × 10^4, H × 10^3) with estimated standard deviations in parentheses

Atom	x	y	z
O	8537(2)	−522(1)	260(2)
N	9380(2)	329(1)	907(2)
C(1)	8780(2)	636(2)	1608(2)
C(2)	9424(2)	1530(2)	2396(2)
C(3)	10039(3)	1042(3)	3590(2)
C(4)	8567(3)	684(3)	3795(2)
C(5)	7257(3)	996(2)	2704(2)
C(6)	7338(3)	252(2)	1787(2)
C(7)	7852(2)	2042(2)	2374(1)
C(8)	8093(3)	2927(2)	3227(2)
C(9)	6581(3)	3467(2)	3143(2)
C(10)	5737(4)	3887(2)	1969(2)
C(11)	5390(2)	3051(2)	1065(2)
C(12)	6908(2)	2469(2)	1205(2)
C(13)	10593(3)	2203(3)	2139(3)
C(14)	4115(3)	2317(3)	1130(3)
C(15)	4788(4)	3547(3)	−105(2)
H(31)	1064(3)	157(2)	415(3)
H(32)	1069(4)	52(2)	362(2)
H(41)	846(3)	105(2)	447(2)
H(42)	865(4)	−8(3)	393(3)
H(5)	623(3)	100(2)	276(2)
H(61)	638(3)	25(2)	103(2)
H(62)	738(3)	−45(2)	195(2)
H(81)	863(3)	270(2)	402(2)
H(82)	883(4)	345(2)	308(2)
H(91)	587(3)	289(2)	332(2)
H(92)	677(4)	405(3)	372(3)
H(101)	471(3)	420(2)	197(2)
H(102)	652(3)	439(2)	181(2)
H(121)	672(2)	190(2)	63(2)
H(122)	758(2)	297(2)	99(2)
H(0)	906(4)	−60(2)	−36(3)
H(131)	1089(4)	280(3)	267(3)
H(132)	1022(3)	250(2)	142(2)
H(133)	1158(4)	178(2)	225(2)
H(141)	427(3)	198(2)	187(3)
H(142)	400(4)	170(3)	56(3)
H(143)	306(4)	269(3)	87(3)
H(151)	391(4)	404(3)	−23(3)
H(152)	457(4)	290(3)	−73(3)
H(153)	563(4)	394(3)	−18(3)

in 2-(*cis*-4-bromo-1-methylcyclohexyl)-3-(4-hydroxyimino-1-methylcyclohexyl)-*trans*-2-butene (29). The dimers are centered in the *bc* plane thus forming layers which repeat along *a* (see Fig. 2). This results in a staggering of layers which allows a compact stacking with a minimum of steric interference. All interdimer distances with the exception of H(91)...H(152), 2.23 Å, are greater than the sum of van der Waals radii (see Table 10).

The six-membered ring, C(1)—C(6), is in the boat conformation. The single atom bridge is responsible for significant deviations from the geometry expected for an unsubstituted boat. The magnitudes of the dihedral angles in the ring are considerably larger than those obtained from strain-energy minimization calculations (30). The mean bond angle in the ring, 104.9°, is significantly less than the predicted 111.7° (30). The C(2)...C(5) distance is significantly shortened from the 'ideal' 2.57 Å (30) to 2.270 Å, which is similar to corresponding distances in other norbornyl compounds (*eg.* 2.27 Å in tricyclo-[4.4.0.$0^{2,8}$]dec-3-ene-7,10-dione (13)). All atoms

Can. J. Chem. Downloaded from www.nrcresearchpress.com by 210.87.254.5 on 09/05/12
For personal use only.

TABLE 3. Final thermal parameters and their estimated standard deviations

(*a*) Anisotropic thermal parameters ($U_{ij} \times 100$ Å^2)

Atom	U_{11}	U_{22}	U_{33}	U_{12}	U_{13}	U_{23}
O	8.9(1)	7.1(1)	9.8(1)	0.3(1)	4.0(1)	−1.7(1)
N	6.5(1)	7.0(1)	7.0(1)	1.3(1)	2.5(1)	−0.1(1)
C(1)	5.5(1)	6.2(1)	6.2(1)	1.3(1)	2.1(1)	0.9(1)
C(2)	4.9(1)	8.0(1)	5.9(1)	−0.1(1)	1.8(1)	0.3(1)
C(3)	7.0(2)	11.5(2)	6.6(2)	1.8(2)	1.2(1)	1.4(2)
C(4)	9.1(2)	10.0(2)	6.7(2)	1.9(2)	3.2(1)	2.7(2)
C(5)	6.2(1)	6.3(1)	6.6(1)	0.1(1)	3.1(1)	1.0(1)
C(6)	7.0(1)	5.3(1)	8.6(2)	0.3(1)	3.4(1)	0.8(1)
C(7)	5.1(1)	6.0(1)	5.0(1)	−0.6(1)	1.9(1)	−0.3(1)
C(8)	8.2(2)	7.9(2)	6.0(1)	−1.3(1)	2.5(1)	−1.2(1)
C(9)	10.3(2)	7.9(2)	7.7(2)	0.0(2)	4.6(1)	−1.8(1)
C(10)	9.9(2)	7.2(2)	8.9(2)	1.6(1)	5.0(2)	0.1(1)
C(11)	6.3(1)	6.4(1)	6.6(1)	1.0(1)	2.8(1)	0.5(1)
C(12)	6.0(1)	5.3(1)	5.2(1)	−0.2(1)	2.5(1)	0.0(1)
C(13)	6.0(2)	10.8(2)	9.0(2)	−1.6(2)	3.0(1)	−0.6(2)
C(14)	5.7(2)	10.2(2)	11.0(2)	0.6(1)	3.1(1)	1.3(2)
C(15)	8.9(2)	9.7(2)	8.1(2)	3.4(2)	3.1(1)	2.2(2)

(*b*) Isotropic thermal parameters ($U \times 100$)

Atom	U(Å^2)	Atom	U(Å^2)	Atom	U(Å^2)
H(31)	10.2(9)	H(82)	10.8(8)	H(131)	12.7(11)
H(32)	9.3(8)	H(91)	8.8(7)	H(132)	7.9(7)
H(41)	9.8(8)	H(92)	11.6(9)	H(133)	11.0(9)
H(42)	11.8(10)	H(101)	10.7(9)	H(141)	10.4(9)
H(5)	6.2(5)	H(102)	9.8(8)	H(142)	12.5(11)
H(61)	8.8(7)	H(121)	6.1(5)	H(143)	11.3(10)
H(62)	8.1(7)	H(122)	7.2(6)	H(151)	11.2(9)
H(81)	9.6(8)	H(0)	11.5(9)	H(152)	13.6(11)
				H(153)	11.3(11)

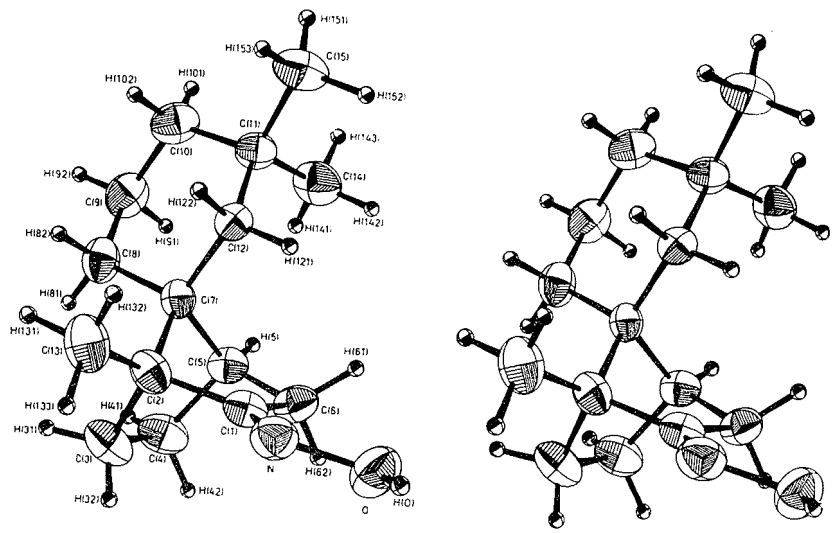

FIG. 1. A stereo view of the molecule; 25% ellipsoids are shown for oxygen, nitrogen, and carbon atoms. The atom numbering scheme is also shown.

Can. J. Chem. Downloaded from www.nrcresearchpress.com by 210.87.254.5 on 09/05/12
For personal use only.

TABLE 4. Rigid-body thermal parameters*

		Ring system carbon atoms C(1)—C(12)		
L ($\times 10$ deg^2)		202(13)	−71(12)	−39(8)
			179(20)	−16(8)
				171(10)
Principal axes of L				
	r.m.s. amplitude		Direction cosines ($\times 10^3$)	
	5.2°	779	−590	−214
	4.3	142	499	−855
	3.1	611	635	472
Principal axes of reduced T				
	r.m.s. amplitude		Direction cosines ($\times 10^3$)	
	0.23 Å	362	−927	107
	0.23	−139	−166	−976
	0.21	922	339	−189
Displacement of axes from intersecting (Å)				
Parallel to L_1			−0.08	
Parallel to L_2			0.43	
Parallel to L_3			0.38	
Effective screw translations (Å)				
Parallel to L_1			0.018	
Parallel to L_2			−0.019	
Parallel to L_3			−0.003	
Fractional coordinates of unique origin ($\times 10^4$)				
x			7314	
y			1878	
z			1524	
Fractional coordinates of center of gravity ($\times 10^4$)				
x			7664	
y			1915	
z			2405	
r.m.s. ΔU_{ij} (Å^2)			0.0022	

*Axes of reference are orthogonal angstrom axes. E.s.d.'s of components of L are given in parentheses in units of the last places shown.

in the ring undergo angular strain, the sp^2 carbon atom C(1) showing the highest strain with an angle of 108.1°. The angles at sp^3 carbon atoms range from 101.2 to 106.9°, all significantly less than the tetrahedral angle.

The bridge apex angle, C(2)—C(7)—C(5), is 92.5 and the boat to bridge angles range from 99.4 to 103.1 with a mean value of 101.6°. The two five-membered rings containing the apex atom C(7) have the envelope conformation. The dihedral angles in these rings (see Table 7) show a good relative agreement with those calculated for the low-energy conformation of cyclopentane with $\omega_1 = 0°$ (31). The mean angle in both rings is 100.9°, which is significantly less than the calculated value of 104.2° (31). It is the fact that the ring valence angles are smaller than the calculated values which accounts for the higher observed magnitudes of the dihedral angles in both five-membered rings and in the six-membered ring, C(1)—C(6), than those calculated from strain-energy minimization calculations. The steric constraints imposed by the bridging atom are responsible for these effects. Comparing the geometry of the norbornane skeleton with that observed in related compounds (see Table 9) one notes high consistency in the mean values of the various interior angles. This trend persists regardless of the nature of the compound, in particular with regard to the hybridization states at various carbon atoms. The 'ideal' mean angles in Table 9 are based on values of 109.5° at sp^3 carbons and 120° at sp^2 atoms. Introduction of sp^2 hybridized carbon atoms into the norbornyl skeleton does not significantly alter the mean interior angles but

Can. J. Chem. Downloaded from www.nrcresearchpress.com by 210.87.254.5 on 09/05/12
For personal use only.

TABLE 5. Bond lengths (Å) with estimated standard deviations in parentheses

(*a*) Nonhydrogen atoms

Bond	Distance (Å)		Bond	Distance (Å)	
	Uncorrected	Corrected		Uncorrected	Corrected
O—N	1.423(3)	1.426*	C(5)—C(6)	1.528(3)	1.533
N—C(1)	1.265(3)	1.266*	C(5)—C(7)	1.564(3)	1.573
			C(7)—C(8)	1.531(3)	1.538
C(1)—C(2)	1.501(3)	1.509	C(7)—C(12)	1.531(3)	1.538
C(1)—C(6)	1.507(3)	1.513	C(8)—C(9)	1.524(4)	1.528
C(2)—C(3)	1.549(3)	1.557	C(9)—C(10)	1.514(4)	1.521
C(2)—C(7)	1.580(3)	1.587	C(10)—C(11)	1.522(3)	1.527
C(2)—C(13)	1.503(3)	1.507*	C(11)—C(12)	1.537(3)	1.542
C(3)—C(4)	1.538(4)	1.545	C(11)—C(14)	1.530(3)	1.536*
C(4)—C(5)	1.531(3)	1.538	C(11)—C(15)	1.530(3)	1.531*

*These distances have been corrected for independent motion as well as libration (see text).

(*b*) Bonds involving hydrogen atoms

Bond	Distance (Å)	Bond	Distance (Å)
O—H(O)	1.07(3)	C(10)—H(102)	1.04(3)
C(3)—H(31)	1.00(3)	C(12)—H(121)	1.01(2)
C(3)—H(32)	0.90(3)	C(12)—H(122)	1.00(2)
C(4)—H(41)	1.01(3)	C(13)—H(131)	0.99(4)
C(4)—H(42)	1.00(3)	C(13)—H(132)	0.93(3)
C(5)—H(5)	0.98(2)	C(13)—H(133)	1.04(3)
C(6)—H(61)	1.05(3)	C(14)—H(141)	1.00(3)
C(6)—H(62)	0.93(3)	C(14)—H(142)	1.05(3)
C(8)—H(81)	0.99(3)	C(14)—H(143)	1.03(4)
C(8)—H(82)	1.02(3)	C(15)—H(151)	1.00(3)
C(9)—H(91)	1.06(3)	C(15)—H(152)	1.11(4)
C(9)—H(92)	1.01(3)	C(15)—H(153)	0.96(3)
C(10)—H(101)	1.02(3)	Mean C—H	1.01(4)*

*Root mean squared deviation from the mean in parentheses.

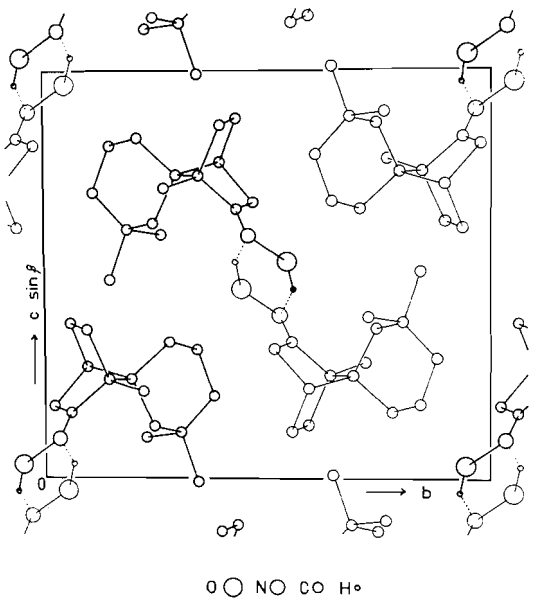

FIG. 2. The structure viewed down *a*; broken lines represent hydrogen bonds.

serves to increase angular strain in the system. Table 9 shows that, unlike the interior angles, the bond lengths in the norbornyl skeleton vary significantly between the different compounds, particularly the boat to bridge distances which range from 1.51 to 1.58 Å.

The mean bond lengths for $C(sp^3)$—$C(sp^3)$ and $C(sp^3)$—$C(sp^2)$ bonds in the C(1)—C(6) ring are 1.543 and 1.511 Å respectively, both in good agreement with the accepted means (32). The individual $C(sp^3)$—$C(sp^3)$ distances range from 1.533(3) to 1.557(3) Å. This variation is a result of steric and electronic effects in the ring. The boat to bridge distances: C(2)—C(7), 1.587(3), and C(5)—C(7), 1.573(3) Å, are significantly longer, and the C(2)—C(13) bond, 1.507(3) Å, is significantly shorter than the normal $C(sp^3)$—$C(sp^3)$ bond. These effects result, to some degree, from hybridization changes at C(2), C(5), and C(7), arising from steric distortion of the tetrahedra. The weakening of the C(2)—C(7) bond is balanced by the slight strengthening of the C(2)—C(13) bond.

Can. J. Chem. Downloaded from www.nrcresearchpress.com by 210.87.254.5 on 09/05/12
For personal use only.

Can. J. Chem. Downloaded from www.nrcresearchpress.com by 210.87.254.5 on 09/05/12
For personal use only.

TABLE 6. Bond angles (deg) with estimated standard deviations in parentheses

(*a*) Nonhydrogen atoms

Bonds	Angle (deg)	Bonds	Angle (deg)
O—N—C(1)	111.2(2)	C(2)—C(7)—C(5)	92.5(2)
N—C(1)—C(2)	122.7(2)	C(2)—C(7)—C(8)	113.3(2)
N—C(1)—C(6)	129.2(2)	C(2)—C(7)—C(12)	111.5(1)
C(6)—C(1)—C(2)	108.1(2)	C(5)—C(7)—C(8)	115.2(2)
C(1)—C(2)—C(3)	105.2(2)	C(5)—C(7)—C(12)	115.8(2)
C(1)—C(2)—C(7)	99.5(1)	C(8)—C(7)—C(12)	108.0(2)
C(1)—C(2)—C(13)	116.1(2)	C(7)—C(8)—C(9)	113.0(2)
C(3)—C(2)—C(7)	101.5(2)	C(8)—C(9)—C(10)	111.5(2)
C(3)—C(2)—C(13)	113.8(2)	C(9)—C(10)—C(11)	112.8(2)
C(7)—C(2)—C(13)	118.6(2)	C(10)—C(11)—C(12)	108.5(2)
C(2)—C(3)—C(4)	104.5(2)	C(10)—C(11)—C(14)	110.7(2)
C(3)—C(4)—C(5)	103.0(2)	C(10)—C(11)—C(15)	110.2(2)
C(4)—C(5)—C(6)	106.9(2)	C(12)—C(11)—C(14)	112.2(2)
C(4)—C(5)—C(7)	103.2(2)	C(12)—C(11)—C(15)	108.4(2)
C(6)—C(5)—C(7)	102.6(2)	C(14)—C(11)—C(15)	106.8(2)
C(1)—C(6)—C(5)	101.2(2)	C(11)—C(12)—C(7)	117.7(2)

(*b*) Angles involving hydrogen atoms

Bonds	Angle (deg)	Bonds	Angle (deg)
N—O—H(0)	102(2)	C(9)—C(10)—H(101)	107(2)
C(2)—C(3)—H(31)	110(2)	C(9)—C(10)—H(102)	105(2)
C(2)—C(3)—H(32)	110(2)	C(11)—C(10)—H(101)	109(2)
C(4)—C(3)—H(31)	112(2)	C(11)—C(10)—H(102)	106(1)
C(4)—C(3)—H(32)	113(2)	H(101)—C(10)—H(102)	118(2)
H(31)—C(3)—H(32)	107(2)	C(7)—C(12)—H(121)	110(1)
C(3)—C(4)—H(41)	111(2)	C(7)—C(12)—H(122)	108(1)
C(3)—C(4)—H(42)	108(2)	C(11)—C(12)—H(121)	111(1)
C(5)—C(4)—H(41)	111(2)	C(11)—C(12)—H(122)	106(1)
C(5)—C(4)—H(42)	114(2)	H(121)—C(12)—H(122)	104(2)
H(41)—C(4)—H(42)	110(2)	C(2)—C(13)—H(131)	110(2)
C(4)—C(5)—H(5)	114(1)	C(2)—C(13)—H(132)	114(1)
C(6)—C(5)—H(5)	112(1)	C(2)—C(13)—H(133)	110(1)
C(7)—C(5)—H(5)	118(1)	H(131)—C(13)—H(132)	105(2)
C(1)—C(6)—H(61)	111(1)	H(131)—C(13)—H(133)	108(2)
C(1)—C(6)—H(62)	112(1)	H(132)—C(13)—H(133)	111(2)
C(5)—C(6)—H(61)	117(1)	C(11)—C(14)—H(141)	117(2)
C(5)—C(6)—H(62)	117(2)	C(11)—C(14)—H(142)	109(2)
H(61)—C(6)—H(62)	99(2)	C(11)—C(14)—H(143)	111(2)
C(7)—C(8)—H(81)	113(2)	H(141)—C(14)—H(142)	106(2)
C(7)—C(8)—H(82)	107(2)	H(141)—C(14)—H(143)	108(2)
C(9)—C(8)—H(81)	109(2)	H(142)—C(14)—H(143)	106(2)
C(9)—C(8)—H(82)	110(2)	C(11)—C(15)—H(151)	115(2)
H(81)—C(8)—H(82)	105(2)	C(11)—C(15)—H(152)	107(2)
C(8)—C(9)—H(91)	107(1)	C(11)—C(15)—H(153)	107(2)
C(8)—C(9)—H(92)	111(2)	H(151)—C(15)—H(152)	115(2)
C(10)—C(9)—H(91)	108(1)	H(151)—C(15)—H(153)	107(3)
C(10)—C(9)—H(92)	110(2)	H(152)—C(15)—H(153)	105(3)
H(91)—C(9)—H(92)	109(2)		

The oxime group is slightly, but significantly, nonplanar, with O and C(1) lying below the mean plane and N, C(2), and C(6) above. The grouping about trigonal C(1) is also significantly nonplanar (see Table 8). High angular strain at C(1) is probably responsible for this non-planarity. The hydroxyl hydrogen, H(0) is rotated 9° out of the oxime mean plane, the dihedral angle C(1)[N—O]H(0) being −171(2)°. The structural features of the oxime group are similar to those in related compounds listed in Table 9. The C—N distance of 1.266(3) Å is

Can. J. Chem. Downloaded from www.nrcresearchpress.com by 210.87.254.5 on 09/05/12
For personal use only.

TABLE 7. Intraannular dihedral angles (deg)

(*a*) Cyclohexane ring

Bond	Angle	
	Obsvd.	Calcd.
C(7)—C(8)	−51.9(2)	−55.8
C(8)—C(9)	56.8(2)	55.8
C(9)—C(10)	−56.9(2)	−55.8
C(10)—C(11)	52.2(2)	55.8
C(11)—C(12)	−51.7(2)	−55.8
C(12)—C(7)	51.3(2)	55.8

(*b*) Norbornane six-membered ring

Bond	Angle	
	Obsvd.	Calcd.
C(1)—C(2)	−69.0(2)	−54.0
C(2)—C(3)	68.2(2)	54.0
C(3)—C(4)	−0.2(2)	0.0
C(4)—C(5)	−71.8(2)	−54.0
C(5)—C(6)	72.2(2)	54.0
C(6)—C(1)	−0.3(2)	0.0

(*c*) Norbornane five-membered rings

C(2), C(1), C(6), C(5), C(7)			C(2), C(3), C(4), C(5), C(7)		
	Angle			Angle	
Bond	Obsvd.	Calcd.	Bond	Obsvd.	Calcd.
C(2)—C(1)	35.6(2)	25.9	C(2)—C(3)	−34.9(2)	−25.9
C(1)—C(6)	−0.3(2)	0.0	C(3)—C(4)	−0.2(2)	0.0
C(6)—C(5)	−35.9(2)	−25.9	C(4)—C(5)	36.0(2)	25.9
C(5)—C(7)	55.8(2)	41.7	C(5)—C(7)	−55.2(2)	−41.7
C(7)—C(2)	−53.9(2)	−41.7	C(7)—C(2)	53.9(2)	41.7

TABLE 8. Weighted least-squares mean planes

(*a*) Distances (Å) of relevant atoms from the mean planes

Plane 1: the oxime group			Plane 2: C(1), C(2), C(6), N		
Atom	*d*	d/σ	Atom	*d*	d/σ
O	−0.002	1.3	N	0.004	2.4
N	0.007	3.9	C(1)	−0.013	6.5
C(1)	−0.012	6.1	C(2)	0.004	1.9
C(2)	0.002	0.8	C(6)	0.007	2.5
C(6)	0.008	3.1	O	−0.008	4.5
H(0)	0.177	5.6	H(0)	0.170	5.4

(*b*) Equations of planes $lX + mY + nZ = p$*

Plane	*l*	*m*	*n*	*p*
1	−0.3431	0.6412	−0.6864	−3.2964
2	−0.3431	0.6429	−0.6848	−3.2908

*Where *X*, *Y*, and *Z* are orthogonal angstrom coordinates derived as follows:

$$\begin{pmatrix} X \\ Y \\ Z \end{pmatrix} = \begin{pmatrix} a & 0 & c\cos\beta \\ 0 & b & 0 \\ 0 & 0 & c\sin\beta \end{pmatrix} \begin{pmatrix} x \\ y \\ z \end{pmatrix}$$

TABLE 9

(*a*) Comparison of structural parameters for norbornane derivatives (r.m.s. derivations from the mean in parentheses)

	Mean bond angles (deg)				Mean bond lengths (Å)			
	6-membered ring				6-membered ring			
	"Ideal"	Obsvd.	Boat to bridge	Apex	sp^3—sp^3	sp^3—sp^2	C=C	Boat to bridge
[a]	111.3	104.8	101.6	92.5(2)	1.543	1.511	—	1.580
[b]	113.0	105.0	100.9	94.4(2)	1.544	1.514	—	1.548
[c]	113.0	105.5	99.6	94.3(2)	1.563	1.518	1.315	1.555
[d]	109.5	104.4	101.2	97(1)	1.543	—	—	1.510
[e]	113.0	105.2	100.0	96(1)	1.567	1.515	1.34	1.510
[f]	113.0	106.0	99.5	93(1)	1.557	1.50	1.34	1.545
[g]	113.0	105.7	99.8	93(1)	1.537	1.49	1.28	1.545
[h]	113.0	105.3	101.1	92.6(8)	1.573	1.495	1.36	1.535
[i]	109.5	—	—	93(2)	1.539	—	—	1.568
[j]	116.5	—	—	92.0(8)	—	1.533	1.339	1.573
Mean	—	105.2(5)	100.5(8)	94(2)	1.552	1.510	1.329	1.547

(*b*) Comparison of structural parameters for the oxime group

	Bond lengths (Å)			Bond angles (deg)		
	C—N	N—O	O—H	Mean R—C—N	C—N—O	N—O—(H/R)
[a]	1.266(3)	1.426(3)	1.07(3)	125.9	111.0(2)	102(2)
[k]	1.27(1)	1.381(9)	0.87(9)	120.7	112.2(6)	109(5)
[l]	1.284(7)	1.395(6)	0.81(5)	132.1	113.1(4)	98(4)
[m]	1.27(4)	1.38(4)	—	122.9	112.4	—
[n]	1.284(5)	1.397(5)	1.02	118.4	111.1(2)	95
[o]	1.25(1)	1.32(2)	1.02(4)	119.8	111.4(9)	110(2)
[p]	1.288	1.415	0.77	118.9	109.7	102
[q]	1.35(4)	1.42(4)	—	119.9	113(2)	111(2)
[r]	1.276(3)	1.411(3)	—	—	111.4(7)	—
[s]	1.27(3)	1.38(3)	—	121.5	114(3)	—

[a] (±)-7,7-(2′,2′-Dimethyl)pentamethylene-1-methyl-norbornane-2-oxime, this work.
[b] Tricyclo[4.4.0.0^{2,8}]dec-3-ene-7,10-dione, ref. 13.
[c] 1,3,4,6,8,9-Hexamethyl-5-hydroxytricyclo[4.4.0.0^{5,9}]deca-3,7-dien-2-one, ref. 14.
[d] *anti*-8-Tricyclo[3.2.1.0^{2,4}]octyl *p*-bromobenzenesulfonate, ref. 15.
[e] *anti*-7-Norbornenyl *p*-bromobenzoate, ref. 16.
[f] 5-Norbornene-2,3-*endo*-dicarboxylic anhydride, ref. 17.
[g] 5-Norbornene-2,3-*exo*-dicarboxylic anhydride, ref. 18.
[h] Tricyclo[5.2.1.0^{2,6}]deca-4,8-dienyl *p*-bromobenzoate, ref. 19.
[i] Norbornane, ref. 20.
[j] Norbornadiene, ref. 20.
[k] *anti*-3′,4′-Difluoro-2-hydroxyiminopropiophenone, ref. 21.
[l] *anti*-*p*-Chlorobenzaldehyde oxime, ref. 22.
[m] *syn*-*p*-Chlorobenzaldehyde oxime, ref. 23.
[n] Glyoxime, ref. 24.
[o] Dimethyl glyoxime, ref. 25.
[p] Formamide oxime, ref. 26.
[q] *anti*-Benzil-α-monoxime *p*-bromobenzoate, ref. 27.
[r] Cyclohexane-1,4-dioxime, ref. 28.
[s] 2-(*cis*-4-Bromo-1-methylcyclohexyl)-3-(4-hydroxyimino-1-methylcyclohexyl)-*trans*-2-butene, ref. 29.

shorter than most given in Table 9 and significantly shorter than the distance of 1.287 Å predicted for a C—N double bond (33). The N—O bond, 1.426(3) Å, is somewhat longer than those reported for the other oximes. The N—O and C—N distances suggest that the N—O bond may be slightly more polar in this structure than in most of the others given in Table 9. The O—H(0) bond, 1.07(3) Å, is unusually long for X-ray data. Some of the shortening of the C(1)—N bond is probably a result of effects. The mean R—C—N angle of 126° implies that the hybrid orbitals of C(1) involved in the C—N bond have more s character than usual, resulting in a slightly shorter bond (see *e.g.* ref. 34). The C—N—O and N—O—H angles are similar to those in related compounds (see Table 9).

The cyclohexane ring, C(7)—C(12), has the

Can. J. Chem. Downloaded from www.nrcresearchpress.com by 210.87.254.5 on 09/05/12
For personal use only.

TABLE 10

(*a*) Selected intra- and intermolecular contacts

Intramolecular		Intermolecular*	
Atoms	Distance (Å)	Atoms	Distance (Å)
C(2)...C(5)	2.270(3)	O...H(0)[1]	2.60(3)
H(31)...H(41)	2.28(4)	O...H(142)[2]	2.66(3)
H(31)...H(81)	2.31(4)	O...C(14)[2]	3.364(4)
H(32)...H(42)	2.19(4)	N...N[1]	3.033(4)
H(41)...H(81)	2.22(4)	H(5)...H(101)[3]	2.53(4)
H(41)...H(5)	2.40(3)	H(91)...H(152)[4]	2.23(5)
H(5)...H(141)	2.16(4)	H(0)...H(0)[1]	2.25(6)
H(61)...H(121)	2.23(3)		
H(81)...H(92)	2.37(4)		
H(81)...H(91)	2.39(4)		
H(82)...H(131)	2.29(4)		
H(91)...H(141)	2.23(4)		
H(91)...H(101)	2.37(4)		
H(92)...H(101)	2.36(4)		
H(92)...H(102)	2.38(4)		
H(122)...H(153)	2.25(4)		
H(122)...H(132)	2.37(3)		

(*b*) Hydrogen bond data

Parameter	Value
O—H(O)...N	
H...N	1.83(3) Å
O...N	2.821(3) Å
∠DHA	152(3)°
∠C—N...H	105(1)°
	143(1)°

*Superscripts refer to atoms at positions (*1*) 2 − x, −y, −z; (*2*) 1 − x, −y, −z; (*3*) 1 − x, y − ½, ½ −z; (*4*) x, ½ −y, ½ +z.

chair conformation. The experimental dihedral angles are in good agreement with those obtained from strain-energy minimization calculations (30) for free cyclohexane (see Table 7). This distortion from the ideal chair conformation occurs primarily as a result of the 1,3-diaxial interaction between C(5) and C(14). The mean bond angle in the ring is 111.9°, slightly larger than the predicted value of 111.1° (30). The angles at fully substituted C(7) and C(11), 108.0(2) and 108.5(2)°, are near the tetrahedral angle as expected. The 1,3-diaxial interaction opens the angle at C(12) to 117.7(2)° and an interaction between the C(13) methyl group and axial hydrogen atoms H(82) and H(122) may contribute to the slight opening of the angle at C(8), 112.9(2)°, as well as to that at C(12). The angles at C(9) and C(10) are generally as expected. The bond distances in the ring range from 1.521 to 1.542 Å, with a mean value of 1.532 Å, in excellent agreement with the mean of 1.533 Å for several cyclohexanes (30). The C(11)—C(14) and C(11)—C(15) bond lengths, 1.536(3) and 1.531(3) Å, are as expected.

Bond angles and distances involving the hydrogen atoms are generally as expected. The mean C—H distance is 1.01 Å, mean C—C—H, 111°, and mean H—C—H, 108°.

We thank Dr. T. Money and Dr. D. F. MacSweeney for suggesting the problem and providing the crystals, the National Research Council of Canada for financial support, and the University of British Columbia Computing Centre for assistance.

1. (*a*) T. MONEY. Prog. Org. Chem. **8**, 29 (1973); (*b*) G. L. HODGSON, D. F. MACSWEENEY, and T. MONEY. J. Chem Soc. Perkin I, 2113 (1973).
2. G. L. HODGSON, D. F. MACSWEENEY, and T. MONEY. Chem. Commun. 766 (1971); Tetrahedron Lett. 3683 (1972).
3. J. C. FAIRLIE, G. L. HODGSON, and T. MONEY. Chem. Commun. 1196 (1969); J. Chem. Soc. Perkin I, 2109 (1973).

Can. J. Chem. Downloaded from www.nrcresearchpress.com by 210.87.254.5 on 09/05/12
For personal use only.

4. R. E. LONG. Ph.D Thesis. University of California at Los Angeles, Los Angeles, California. 1965.
5. International tables for X-ray crystallography, Vol. III. Kynoch Press, Birmingham. 1962.
6. R. F. STEWART, E. R. DAVIDSON, and W. T. SIMPSON. J. Chem. Phys. **42**, 3175 (1965).
7. V. SCHOMAKER and K. N. TRUEBLOOD. Acta Cryst. B**24**, 63 (1968).
8. D. W. J. CRUICKSHANK. Acta Cryst. **9**, 747, 754 (1956).
9. D. W. J. CRUICKSHANK. Acta Cryst. **14**, 896 (1961).
10. W. R. BUSING and H. A. LEVY. Acta Cryst. **17**, 142 (1964).
11. C. K. JOHNSON. *In* Crystallographic computing. Munksgaard, Copenhagen. 1970. pp. 207–226.
12. E. HUBER-BUSER and J. D. DUNITZ. Helv. Chim. Acta, **64**, 2027 (1961).
13. C. S. GIBBONS and J. TROTTER. J. Chem. Soc. Perkin II, 737 (1972).
14. C. A. BEAR and J. TROTTER. J. Chem. Soc. Perkin II, 330 (1974).
15. A. C. MACDONALD and J. TROTTER. Acta Cryst. **18**, 243 (1965).
16. A. C. MACDONALD and J. TROTTER. Acta Cryst. **19**, 456 (1965).
17. R. DESTRO, G. FILIPPINI, C. M. GRAMACCIOLI, and M. SIMONETTA. Tetrahedron Lett. 3223 (1969).
18. R. DESTRO, G. FILIPPINI, C. M. GRAMACCIOLI, and M. SIMONETTA. Tetrahedron Lett. 5955 (1968).
19. I. R. BELLABONO, R. DESTRO, C. M. GRAMACCIOLI, and M. SIMONETTA. J. Chem. Soc. B, 710 (1969).
20. Y. MORINO, K. KUCHITSU, and A. YOHOZECHI. Bull. Chem. Soc. Jap. **40**, 1552 (1967).
21. F. H. ALLEN, D. ROGERS, and J. TROTTER. J. Chem. Soc. B, 166 (1970).
22. K. G. JENSEN. Acta Chem. Scand. **24**, 3293 (1970).
23. B. JERSLEV. Nature, **180**, 1410 (1957).
24. M. CALLERI, G. FERRARIO, and D. VITERBO. Acta Cryst. **20**, 73 (1966).
25. W. C. HAMILTON. Acta Cryst. **14**, 95 (1961).
26. D. HALL. Acta Cryst. **18**, 955 (1965).
27. K. A. KERR, J. M. ROBERTSON, and G. A. SIM. J. Chem. Soc. B, 1305 (1967).
28. P. GROTH. Acta Chem. Scand. **18**, 128 (1968).
29. D. MOOTZ and B. BERKING. Acta Cryst. B**25**, 828 (1969).
30. R. BUCOURT and D. HAINAUT. Bull. Soc. Chim. Fr. 1366 (1965).
31. J. B. HENDRICKSON. J. Am. Chem. Soc. **83**, 4537 (1961); **85**, 4059 (1963).
32. L. E. SUTTON (*Editor*). Chem. Soc. Special Publ. No. 11, 1958, and No. 18, 1965.
33. L. PAULING. The nature of the chemical bond, 3rd ed. Cornell University Press, Ithaca, New York. 1960.
34. D. P. CRAIG and N. L. PADDOCK. *In* Nonbenzenoid aromatics. Vol. 2. Academic Press, New York. 1971. p. 322.

Can. J. Chem. Downloaded from www.nrcresearchpress.com by 210.87.254.5 on 09/05/12
For personal use only.

Crystal and Molecular Structure of 2,5-Bis(2′-hydroxyethylamino)-1,4-benzoquinone

STEVEN J. RETTIG AND JAMES TROTTER

Department of Chemistry, University of British Columbia, Vancouver, British Columbia V6T 1W5

Received October 17, 1974

STEVEN J. RETTIG and JAMES TROTTER. Can. J. Chem. **53**, 777 (1975).

Crystals of 2,5-bis(2′-hydroxyethylamino)-1,4-benzoquinone are monoclinic, a = 5.020(1), b = 19.238(3), c = 5.214(1) Å, β = 96.15(3)°, Z = 2, space group $P2_1/n$. The structure was solved by direct methods and was refined by full-matrix least-squares procedures to a final R of 0.045 for 646 reflections with $I \geq 3\sigma(I)$. The benzoquinone ring in the centrosymmetric molecule is slightly, but significantly, nonplanar. Bond distances in the compound (C—C, 1.247 (2) and 1.410 (3), C—N, 1.332 (3) and 1.457 (3), C—C, 1.384–1.514 (3), N—H, 0.89 (3), O—H, 1.07 (5), and C—H, 0.95–1.09 (3) Å) are similar to those in related compounds. The structure features an extensive network of N—H...O (N...O = 2.639 (3) and 3.033 (2) Å) and O—H...O (O...O = 2.757 (3) Å) hydrogen bonds.

STEVEN J. RETTIG et JAMES TROTTER. Can. J. Chem. **53**, 777 (1975).

Les cristaux du bishydroxy-2′méthylamino-2,5 benzoquinone-1,4 sont monocliniques, a = 5.020(1), b = 19.238(3), c = 5.214(1) Å, β = 96.15(3)°, Z = 2, groupe d'espace $P2_1/n$. On a résolu la structure par des méthodes directes et on l'a affinée par la méthode des moindres carrés (matrice complète) jusqu'à une valeur finale de R de 0.045 pour 646 réflections avec $I \geq 3\sigma(I)$. Le noyau benzoquinone dans la molécule centrosymétrique est légèrement mais toutefois pas d'une façon importante nonplanaire. Les distances de liaison dans le composé (C—C, 1.247(2) et 1.410(3), C—N, 1.332(3) et 1.457(3), C—C, 1.384–1.514(3), N—H, 0.89(3), O—H, 1.07(5) et C—H, 0.95–1.09(3) Å) sont semblables à celles trouvées dans des composés similaires. La structure comporte un réseau extensif de ponts hydrogène N—H ... O (N ... O = 2.639(3) et 3.033(2) Å) et O—H ... O(O ... O = 2.757(3) Å). [Traduit par le journal]

Introduction

An initially colorless solution of $(p\text{-}FC_6H_4)_2\text{-}\overline{BOCH_2CH_2NH_2}$ in ethanol turned deep red over a period of several months depositing a small amount of deep violet crystalline material. An X-ray crystallographic analysis of this material was undertaken in the hope that this sample would prove to be an interesting organoboron compound.

The results of the crystallographic analysis show that this material is 2,5-bis(2′-hydroxyethylamino)-1,4-benzoquinone, a compound whose structure is interesting in its own right and forms the main topic of this report. At present little is known about the reaction sequence leading to the formation of the benzoquinone. Some chemical tests are being carried out in order to solve this problem. Decomposition also occurs in other solvents (MeOH and acetone), but it is not yet known if the same product is formed. The reaction appears to be a photochemical one.

Experimental

A small quantity of 2,5-bis(2′-hydroxyethylamino)-1,4-benzoquinone was isolated as a decomposition product of *B,B*-bis(*p*-fluorophenyl)boroxazolidine, $(p\text{-}FC_6H_4)_2\text{-}\overline{BOCH_2CH_2NH_2}$, in ethanol. The dark violet crystals which were deposited from the solution were suitable for X-ray analysis after washing with cold ethanol.

The crystal chosen for study was mounted with b parallel to the goniostat axis and had dimensions of *ca.* 0.3 × 0.3 × 0.3 mm. Unit-cell and space group data were obtained from film and diffractometer measurements. The unit-cell parameters were refined by a least-squares treatment of $\sin^2\theta$ values for 20 reflections measured on a diffractometer with Cu K_α radiation. Crystal data are:

$C_{10}H_{14}N_2O_4$ f.w. = 226.2

Monoclinic, a = 5.020(1), b = 19.238(3), c = 5.214(1) Å, β = 96.15(3)°, V = 500.6(2) Å^3, ρ_m = 1.500 (flotation in aqueous KI), Z = 2, ρ_c = 1.501(1) g cm^{-3}, $F(000)$ = 240 (22 °C, Cu K_α, λ = 1.5418 Å, μ = 16.6 cm^{-1}). Absent reflections: $0k0$, $k \neq 2n$, and $h0l$, $h + l \neq 2n$ define uniquely the space group $P2_1/n$ (C_{2h}^5, No. 14).

Intensities were measured on a Datex-automated General Electric XRD 6 diffractometer, with a scintillation counter, Cu K_α (nickel filter and pulse height analyzer), and a θ–2θ scan at 2° min^{-1} over a range of

Can. J. Chem. Downloaded from www.nrcresearchpress.com by 210.87.254.40 on 09/05/12
For personal use only.

Can. J. Chem. Downloaded from www.nrcresearchpress.com by 210.87.254.40 on 09/05/12
For personal use only.

(1.80 + 0.86 tan θ) degrees in 2θ, with 20 s background counts being measured at each end of the scan. Data were measured to $2\theta = 145°$ (minimum interplanar spacing 0.81 Å). The intensity of the check reflection, measured every 40 reflections throughout the data collection, decreased slowly to a final value which was 0.90 times the original intensity. Lorentz and polarization corrections and check reflection scaling were applied, and the structure amplitudes were derived. No absorption correction was made in view of the low value of μ. Of the 1008 independent reflections measured, 357 had intensities less than $3\sigma(I)$ above background where $\sigma^2(I) = S + B + (0.05S)^2$ with S = scan count and B = time averaged background count. These reflections were given zero weight in the refinement but were included in the structure factor calculations.

Structure Analysis

The structure was solved by direct methods. Sixteen sets of signs for 139 reflections with $|E| \geq 1.50$ were determined by a computer program which uses Sayre relationships in an iterative procedure (1). The starting set of reflections is given in Table 1. One set of signs was outstanding in that it converged in one cycle to a set which had the highest consistency index (0.90) with 82 positive and 57 negative signs. The eight non-hydrogen atoms accounted for the 8 highest peaks on an E-map calculated from this set of phases. These eight atoms were refined first isotropically, then anisotropically as carbon atoms giving R 0.119. A difference map at this point revealed the positions of five of the seven hydrogen atoms, among them H(N). This information, along with bond distances and angles, and the magnitudes of the isotropic thermal parameters enabled us to identify unambiguously the nitrogen and two oxygen atoms. The remaining hydrogen atoms were located on a subsequent difference map. The entire structure (H atoms with isotropic thermal parameters) was refined for six cycles giving a final R of 0.045 for 646 reflections with $I \geq 3\sigma(I)$ (5 reflections which had $|F_o - F_c| > 3\sigma(F)$ were removed from the data set in the final stages of refinement).

The least-squares refinement was based on the minimization of $\Sigma w(F_o - F_c)^2$. The scattering factors of ref. 2 were used for the non-hydrogen atoms and those of ref. 3 for the hydrogen atoms. The anisotropic thermal parameters employed in the refinement are U_{ij} in the expression:

$$f = f^o \exp[-2\pi^2(U_{11}h^2a^{*2} + U_{22}k^2b^{*2} + U_{33}l^2c^{*2} + 2U_{12}hka^*b^* + 2U_{13}hla^*c^* + 2U_{23}klb^*c^*)]$$

where f^o is the tabulated scattering factor and f is that

TABLE 1. Basic starting set of reflections for $C_{10}H_{14}N_2O_4$

h	k	l	$\|E\|$	
2	5	2	2.23	origin determining
1	12	−3	3.27	
4	4	−3	3.72	
2	3	2	2.06	
3	15	−1	3.74	
1	1	1	1.67	
1	2	1	1.53	

TABLE 2. Final positional parameters (fractional × 10^4, H × 10^3) with estimated standard deviations in parentheses* ± $|x, y, z; 1/2 - x, 1/2 + y, 1/2 - z|$

Atom	x	y	z
O(1)	2779(4)	4540(1)	6228(3)
O(2)	7637(4)	6802(1)	5629(4)
N	3417(4)	5849(1)	7684(4)
C(1)	1433(4)	4727(1)	7978(4)
C(2)	1738(4)	5469(1)	8912(4)
C(3)	−359(5)	4291(1)	9114(4)
C(4)	3963(6)	6579(1)	8248(5)
C(5)	4978(6)	6965(1)	6020(6)
H(N)	414(6)	563(1)	643(5)
H(02)	753(9)	630(2)	475(9)
H(3)	−54(5)	382(1)	848(5)
H(4*a*)	238(7)	679(1)	870(6)
H(4*b*)	531(7)	666(2)	983(7)
H(5*a*)	376(6)	686(1)	448(6)
H(5*b*)	496(5)	751(2)	655(5)

*Coordinates are those for an asymmetric unit of a molecule centered at 0, 1/2, 1.

corrected for thermal motion. The weighting scheme: $w = 1/\sigma^2(F)$ where $\sigma^2(F)$ is derived from the previously defined $\sigma^2(I)$ gave uniform average values of $w(F_o - F_c)^2$ over ranges of $|F_o|$ and was employed in the final stages of refinement.

On the final cycle of refinement, the largest parameter shift was 0.08 σ. A final difference map showed maximum fluctuations of ±0.19 e Å^{-3}, the maxima appearing at positions expected for the oxygen lone-pair and benzoquinone ring bonding electrons. The final positional and thermal parameters appear in Tables 2 and 3 respectively. Measured and calculated structure factors have been placed in the Depository of Unpublished Data.[1]

Thermal Motion and Correction of Molecular Geometry

The ellipsoids of thermal motion for the non-hydrogen atoms are shown in Fig. 1. The thermal motion has been analyzed in terms of the rigid-body modes of translation (T), libration (L), and screw (S) motion (4) using the computer program MGTLS. The r.m.s. standard deviation in the temperature factors U_{ij} is 0.0011 Å^2 indicating that the thermal motion of the entire molecule is satisfactorily described by the rigid-body thermal parameters given in Table 4 (r.m.s. $\Delta U_{ij} = 0.0032$ Å^2).

The appropriate bond distances and angles have been corrected for libration (5, 6), using shape parameters q^2 of 0.08 for all atoms involved. The corrected and uncorrected bond lengths appear in Table 5. Bond angles, given in Table 6, changed by no more than 0.05°, thus the corrected angles are not reported.

Results and Discussion

Figure 1 shows the atom numbering scheme and Fig. 2 the packing arrangement viewed down

[1]The structure factor table is available, at a nominal charge, from the Depository of Unpublished Data, National Science Library, National Research Council of Canada, Ottawa, Canada K1A 0S2.

Can. J. Chem. Downloaded from www.nrcresearchpress.com by 210.87.254.40 on 09/05/12
For personal use only.

TABLE 3. Final thermal parameters and their estimated standard deviations

(*a*) Anisotropic thermal parameters ($U_{ij} \times 100$ Å^2)

Atom	U_{11}	U_{22}	U_{33}	U_{12}	U_{13}	U_{23}
O(1)	4.7(1)	3.8(1)	4.2(1)	−0.4(1)	3.1(1)	−0.6(1)
O(2)	5.4(1)	4.9(1)	7.8(2)	−0.9(1)	4.3(1)	−0.7(1)
N	3.9(1)	3.2(1)	3.5(1)	−0.4(1)	2.4(1)	−0.4(1)
C(1)	3.2(1)	3.2(1)	2.8(1)	0.1(1)	1.3(1)	0.1(1)
C(2)	2.9(1)	3.2(1)	2.9(1)	−0.1(1)	1.3(1)	0.2(1)
C(3)	3.7(1)	3.2(1)	3.2(1)	−0.3(1)	1.7(1)	−0.3(1)
C(4)	4.8(2)	3.1(1)	4.5(2)	−0.7(1)	2.6(1)	−0.5(1)
C(5)	4.8(2)	3.6(1)	4.6(1)	−0.4(1)	2.2(1)	0.2(1)

(*b*) Isotropic thermal parameters ($U \times 100$)

Atom	U(Å^2)	Atom	U(Å^2)
H(N)	5.5(8)	H(4*b*)	7.2(10)
H(02)	12.9(15)	H(5*a*)	5.1(8)
H(3)	4.6(7)	H(5*b*)	4.9(7)
H(4*a*)	5.9(8)		

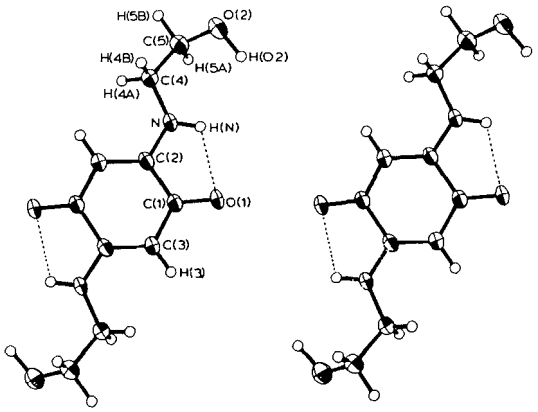

FIG. 1. Stereoscopic view of the 2,5-bis(2'-hydroxyethylamino)-1,4-benzoquinone molecule showing the atom numbering scheme and 50% probability thermal ellipsoids for the non-hydrogen atoms. Broken lines indicate hydrogen bonds.

*c**. The molecular geometry of 2,5-bis(2'-hydroxyethylamino)-1,4-benzoquinone is compared to that of related compounds in Table 7. Important inter- and intramolecular contacts and details of the hydrogen bonding arrangement are given in Table 8.

The benzoquinone ring in the centrosymmetric molecule is slightly, but significantly, nonplanar. The equation of the weighted least-squares mean plane through the six-membered ring is $-0.6787X + 0.2868Y - 0.6761Z = -0.3665$ (X, Y, and Z are orthogonal Å coordinates along a, b, and c*). Displacements of atoms from this plane are: C(1) −0.007(2), C(2) 0.007(2), C(3) 0.008(2), O(1) −0.022(2), N 0.028(3), H(3) 0.01(3), C(4) 0.069(3), and H(N) 0.05(3) Å, with symmetry related atoms displaced in the opposite direction. Nonplanarity of the benzoquinone ring has also been noted for other 2,5-diamino-1,4-benzoquinones (7–11). The intra-annular dihedral angles in the ring are alternately ±2.0°, thus the ring has adopted a slight chair conformation. The nonplanarity of the six-membered ring, the deviations of O(1) and N from the mean plane, and the small twist about the C(2)—N bond (C(3)'[C(2)—N]C(4) = 1.4(2)°) arise from steric repulsions (see Table 8(*a*)).[2]

The C(1)—O(1), C(2)—N, C(4)—N, and benzoquinone ring bond distances do not differ significantly from those in related 2,5-diamino-1,4-benzoquinones given in Table 7. The C(1)—O(1) bond, 1.247(2) Å, is significantly longer than a normal ketone double bond (*e.g.* 1.220 Å in both *p*-benzoquinone (12) and *o*-benzoquinone (13)). The C(2)—C(3)', C(1)—C(3), and N—C(2) bond lengths (1.384(3), 1.409(3), and 1.332(3) Å) are intermediate between single and double bond distances. The C(1)—C(2) bond, 1.511(3) Å, although slightly shorter than corresponding bonds in the other 2,5-diamino-1,4-benzoquinones, is significantly longer than the value of 1.485 Å expected for a

[2]Here and elsewhere in this paper primed atoms refer to those related to atoms in Table 2 by the molecular center of symmetry.

Can. J. Chem. Downloaded from www.nrcresearchpress.com by 210.87.254.40 on 09/05/12
For personal use only.

TABLE 4. Rigid-body thermal parameters of all non-hydrogen atoms*

L (× 10 deg²)	46(13)	38(9)	−24(10)
		121(10)	−23(8)
			38(9)

Principal axes of L

r.m.s. amplitude	Direction cosines (×10³)		
3.8°	−397	−876	275
2.1	−580	471	665
1.3	−712	105	−695

Principal axes of T

r.m.s. amplitude	Direction cosines (×10³)		
0.19 Å	−654	274	−705
0.18	−265	−956	−125
0.13	−709	105	698

r.m.s. ΔU_{ij} (Å²) 0.0032

*Axes of reference are orthogonal Angstrom axes. E.s.d.'s of components of L are given in parentheses in units of the last places shown.

TABLE 5. Bond lengths (Å) with estimated standard deviations in parentheses

(*a*) Bonds involving non-hydrogen atoms

	Length			Length	
Bond	Uncorrected	Corrected	Bond	Uncorrected	Corrected
O(1)—C(1)	1.245(2)	1.247	C(1)—C(2)	1.509(3)	1.511
O(2)—C(5)	1.408(3)	1.410	C(1)—C(3)	1.408(3)	1.409
N—C(2)	1.331(3)	1.332	C(2)—C(3)′	1.381(3)	1.384
N—C(4)	1.456(3)	1.457	C(4)—C(5)	1.512(3)	1.514

(*b*) Bonds involving hydrogen atoms

Bond	Length	Bond	Length
O(2)—H(02)	1.07(5)	C(4)—H(4*a*)	0.95(3)
N—H(N)	0.89(3)	C(4)—H(4*b*)	1.02(3)
C(3)—H(3)	0.96(3)	C(5)—H(5*a*)	0.98(3)
		C(5)—H(5*b*)	1.09(3)

C(sp^2)—C(sp^2) single bond. The N—C(4) bond (1.457(3) Å) is significantly longer than the expected value of 1.445 Å for an N(sp^2)—C(sp^3) single bond. The bonds O(2)—C(5), 1.410(3), and C(4)—C(5), 1.514(3) Å, are both significantly shorter than expected. This shortening is probably due to σ-hybridization effects (the angles N—C(4)—C(5) and C(4)—C(5)—O(2) are both significantly greater than the tetrahedral angle). The remaining bond distances in the molecule are normal.

The coordination groups of all trigonal atoms in the molecule (including N) are planar within experimental error. The bond angles in the central part of the molecule are again quite similar to those in related compounds (see Table 7). The small differences which do occur are probably a result of differences in the steric environments, including the intra- and intermolecular hydrogen bonding schemes. The angles N—C(4)—C(5), 113.0(2), and C(4)—C(5)—O(2), 113.9(2)°, are both significantly larger than the tetrahedral angle presumably as a result of the steric requirements imposed by the intermolecular O—H ... O hydrogen bond.

The geometry of the molecule is consistent with the resonance structures given by Kulpe (7, 8). The three most important contributors to the structure are **1**, **2**, and **3** giving the overall structure **4**.

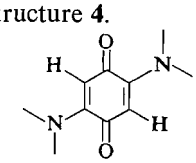

1

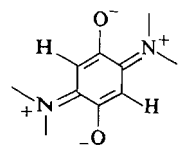

2

TABLE 6. Bond angles (deg) with estimated standard deviations in parentheses

(*a*) Non-hydrogen atoms

Bonds	Angle (deg)	Bonds	Angle (deg)
C(2)—N—C(4)	123.2(2)	N—C(2)—C(3)′	124.6(2)
O(1)—C(1)—C(2)	117.8(2)	C(1)—C(2)—C(3)′	121.1(2)
O(1)—C(1)—C(3)	123.8(2)	C(1)—C(3)—C(2)′	120.5(2)
C(2)—C(1)—C(3)	118.4(2)	N—C(4)—C(5)	113.0(2)
N—C(2)—C(1)	114.3(2)	O(2)—C(5)—C(4)	113.9(2)

(*b*) Angles involving hydrogen atoms

Bonds	Angle (deg)	Bonds	Angle (deg)
C(5)—O(2)—H(02)	105(3)	C(5)—C(4)—H(4*a*)	110(2)
C(2)—N—H(N)	115(2)	C(5)—C(4)—H(4*b*)	107(2)
C(4)—N—H(N)	122(2)	H(4*a*)—C(4)—H(4*b*)	104(3)
C(1)—C(3)—H(3)	117(2)	O—C(5)—H(5*a*)	111(2)
C(2)′—C(3)—H(3)	122(2)	O—C(5)—H(5*b*)	107(1)
N—C(4)—H(4*a*)	109(2)	C(4)—C(5)—H(5*a*)	107(2)
N—C(4)—H(4*b*)	114(2)	C(4)—C(5)—H(5*b*)	106(1)
		H(5*a*)—C(5)—H(5*b*)	113(2)

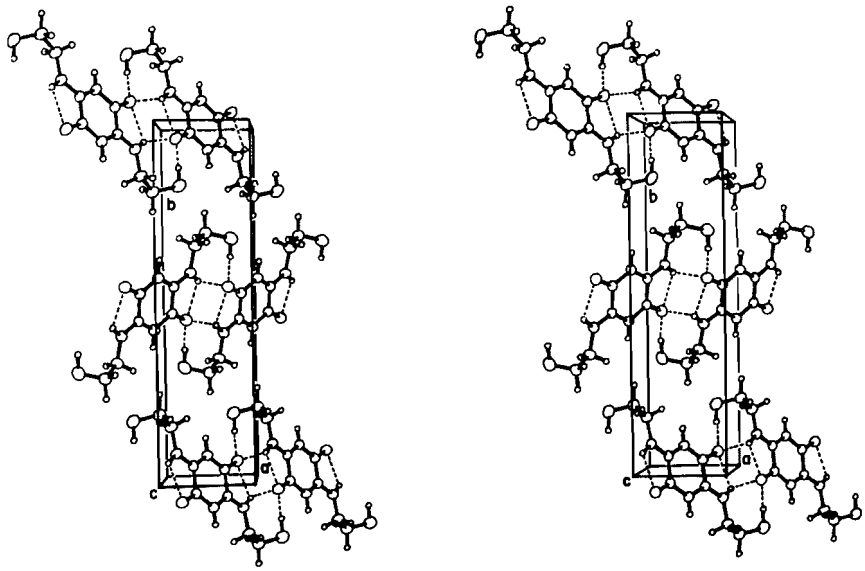

FIG. 2. The structure of 2,5-bis(2′-hydroxyethylamino)-1,4-benzoquinone viewed down *c**. Broken lines indicate hydrogen bonds.

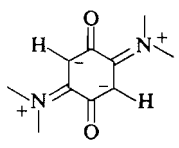

3

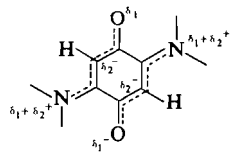

4

The crystal structure consists of molecules each linked to two others by an extensive centrosymmetric network of N—H ... O and O—H ... O hydrogen bonds to form nearly planar "ribbons" of molecules extending along [1 0 −1] (see Fig. 2). H(N) is involved in a bifurcated hydrogen bonding scheme including an intramolecular, N ... O = 2.639(3) Å, and an intermolecular N—H ... O interaction, N ... O = 3.033(2) Å. This bifurcated arrangement involving H(N) is similar to that in 3,6-dichloro-2,5-bis(methylamino)-1,4-benzoquinone (8, 9) where the corresponding N ... O distances are 2.573(7) and 2.872(7) Å. The longer N ... O

Can. J. Chem. Downloaded from www.nrcresearchpress.com by 210.87.254.40 on 09/05/12
For personal use only.

Can. J. Chem. Downloaded from www.nrcresearchpress.com by 210.87.254.40 on 09/05/12
For personal use only.

TABLE 7. Comparison of structural data for 2,5-diamino-1,4-benzoquinones

Bond	Distance (Å) This work	Reference 7*	References 8 and 9†	References 10 and 11‡
C(1)—O(1)	1.247(2)	1.237(7)	1.240(7)	1.23
C(2)—N	1.332(3)	1.341(7)	1.331(7)	1.36
C(4)—N	1.457(3)	—	1.458(7)	1.47
C(1)—C(2)	1.511(3)	1.522(7)	1.532(8)	1.52
C(2)—C(3)′	1.384(3)	1.383(7)	1.383(8)	1.36
C(3)—C(1)	1.409(3)	1.409(7)	1.413(7)	1.44

Bonds	Angle (deg) This work	Reference 7*	References 8 and 9†	References 10 and 11‡
C(3)—C(1)—O(1)	123.8(2)	124.8(6)	123.2(5)	121
C(2)—C(1)—O(1)	117.8(2)	117.4(6)	117.2(5)	120
C(1)—C(2)—N	114.3(2)	113.3(6)	110.7(5)	118
C(3)′—C(2)—N	124.6(2)	125.7(6)	130.7(5)	124
C(3)′—C(1)—C(2)	118.4(2)	117.8(6)	119.6(5)	119
C(1)—C(2)—C(3)′	121.1(2)	121.0(6)	118.6(5)	118
C(2)′—C(3)—C(1)	120.5(2)	121.2(6)	121.7(5)	123
C(2)—N—C(4)	123.2(2)	—	129.5(5)	—

*3,6-Dichloro-2,5-diamino-1,4-benzoquinone.
†3,6-Dichloro-2,5-bis(methylamino)-1,4-benzoquinone.
‡2,5-Pentamethylene-imino-1,4-benzoquinone.

TABLE 8

(*a*) Selected intra- and intermolecular contacts

Intramolecular		Intermolecular*	
Atoms	Distance (Å)	Atoms	Distance (Å)
N ... H(5*a*)	2.58(3)	O(1) ... C(1^1)′	3.205(3)
C(1) ... H(N)	2.39(3)	C(1) ... H(02^2)′	2.52(5)
C(2) ... H(4*a*)	2.57(3)	H(02) ... H(3^2)′	2.39(5)
C(3) ... H(4*a*)′	2.63(3)	H(3) ... H($5a^1$)′	2.48(4)
C(3) ... C(4)′	2.915(3)	H(4*a*) ... H($5b^3$)	2.42(4)
C(4) ... H(3)′	2.66(2)		
C(5) ... H(N)	2.62(3)		
H(02) ... H(5*a*)	2.17(5)		
H(3) ... H(4*a*)′	2.17(4)		
H(4*a*) ... H(5*b*)	2.27(4)		

(*b*) Hydrogen-bond data (distances in Å and angles in deg)*

D—H ... A	H ... A	D ... A	∠DHA	∠XAH
O(2)—H(02) ... O(1^2)	1.69(5)	2.757(3)	172(4)	117(2)
N—H(N) ... O(1^2)	2.21(3)	3.033(2)	154(3)	166.7(7)
N—H(N) ... O(1)	2.20(3)	2.639(3)	110(2)	83.1(8)

*The angle O . . . H(N) . . . O is 94(1)°. Superscripts refer to atoms at positions: (*1*), $x, y, z - 1$; (*2*), $1 + x, y, z - 1$; (*3*), $x - 1/2, 3/2 - y, 1/2 + z$.

distances in the present compound (as well as the slightly longer C(1)—O(1) bond) appear to result from the involvement of O(1) in a third hydrogen bond, O(2)—H(02) ... $O(1^2)'$ (O ...O = 2.757(3) Å). All other intermolecular contacts, the shortest of which are given in Table 8, correspond to normal van der Waals contacts.

We thank the National Research Council of Canada for financial support and the University of British Columbia Computing Centre for assistance.

1. R. E. LONG. Ph.D. Thesis, University of California at Los Angeles. Los Angeles, California. 1965.
2. D. T. CROMER and J. B. MANN. Acta Cryst. **A24**, 321 (1968).
3. R. F. STEWART, E. R. DAVIDSON, and W. T. SIMPSON. J. Chem. Phys. **42**, 3175 (1965).
4. V. SCHOMAKER and K. N. TRUEBLOOD. Acta Cryst. **B24**. 63 (1968).
5. D. W. J. CRUICKSHANK. Acta Cryst. **9**, 747 (1956); **9**, 754 (1956).
6. D. W. J. CRUICKSHANK. Acta Cryst. **14**, 896 (1961).
7. S. KULPE. Acta Cryst. **B25**, 1411 (1969).
8. S. KULPE. J. Prakt. Chem. **312**, 909 (1971).
9. S. KULPE. Z. Chem. **9**, 153 (1969).
10. S. KULPE. Tetrahedron, **26**, 2899 (1970).
11. S. KULPE. Z. Chem. **11**, 466 (1972).
12. J. TROTTER. Acta Cryst. **13**, 86 (1960).
13. A. L. MACDONALD and J. TROTTER. J. Chem. Soc. Perkin II, 476 (1973).

Can. J. Chem. Downloaded from www.nrcresearchpress.com by 210.87.254.40 on 09/05/12
For personal use only.

Can. J. Chem. Downloaded from www.nrcresearchpress.com by 210.87.254.105 on 09/05/12
For personal use only.

1-Phenyl-2,2-dialkyl Vinyl Cation

SATORU MASAMUNE, MITSURU SAKAI, AND KAZUHIKO MORIO
Department of Chemistry, University of Alberta, Edmonton, Alberta T6G 2G2

Received November 4, 1974

SATORU MASAMUNE, MITSURU SAKAI, and KAZUHIKO MORIO. Can. J. Chem. **53**, 784 (1975).

1-Phenyl-2,2-dimethyl and 1-phenyl-2,2-diethyl vinyl cations have been generated. Their n.m.r. spectral data indicate (*i*) the presence of C_{2v} symmetry in these cations, (*ii*) the positive charge being mostly localized at the vinyl α-carbon (and the aromatic ring) but not at the β-position, and (*iii*) the bisected geometry for the aromatic ring of the system.

SATORU MASAMUNE, MITSURU SAKAI et KAZUHIKO MORIO. Can. J. Chem. **53**, 784 (1975).

On a généré les cations phényl-1 diméthyl-2,2 et phényl-1 diéthyl-2,2 vinyles. Leur spectre r.m.n. indique (*i*) la présence d'une symétrie C_{2v}, (*ii*) que la charge positive est localisée principalement sur le carbon α du groupe vinyle (et sur le cycle aromatique), mais pas en position β et (*iii*) que le système de cycle aromatique a une géométrie bisectée.

[Traduit par le journal]

The successful generation and direct observation of a vinyl cation has very recently been reported by Hanack and co-workers (1). This has prompted us to disclose the results of our investigation in this area (2). Our findings are mainly in accord with theirs but offer additional information, theoretically important and experimentally advantageous: (*i*) readily available vinyl chlorides rather than the corresponding fluorides serve equally well as precursors for the generation of vinyl cations, thus the latter halides that are synthetically less accessible are not required, (*ii*) the chemical shifts of both the α- and β-carbons of the vinyl cation are unambiguously determined, (*iii*) two different cations are generated to display (to the limit of the n.m.r. time scale) the linearity of the system, a feature that requires further confirmation of this unstable and elusive system, and finally (*iv*) our quenching experiments involve direct trapping of the cations rather than the isolation of secondary products.

We have chosen (1-chloro-2,2-dimethyleth-enyl)benzene(1)[1] and (1-chloro-2,2-diethyleth-enyl)benzene (**2**) (3) as precursors and have generated the corresponding carbocations in a manner similar to that previously described (4). Methylene chloride solutions of **1** and **2** were

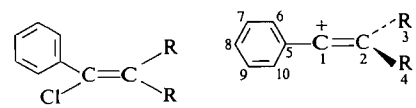

1 R = CH_3 **1′** R = CH_3
2 R = C_2H_5 **2′** R = C_2H_5

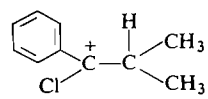

3′

NOTE: The numbering of the cation is arbitrary.

separately mixed with a 1:5 mixture of SbF_5–SO_2ClF at −130°. The resulting dark orange lower layers contained the corresponding cations **1′** and **2′** and exhibited the spectra as shown below. The p.m.r. spectra of **1′** and **2′** in Fig. 1 clearly demonstrate the equivalence of the two methyl and ethyl groups, respectively. Furthermore, the chemical shifts of the aromatic protons suggest that the π system of the aromatic ring conjugates more effectively with the empty

[1]Proton magnetic resonance spectrum of **1** ($CDCl_3$): δ 1.73 (s.3H), 2.00 (s.3H), and 7.32 (br s 5H): c.m.r. ($CDCl_3$, TMS), δ 21.8, 22.1, 125.6, 127.8, 128.1, 129.3, 130.4, and 139.6.

Can. J. Chem. Downloaded from www.nrcresearchpress.com by 210.87.254.105 on 09/05/12
For personal use only.

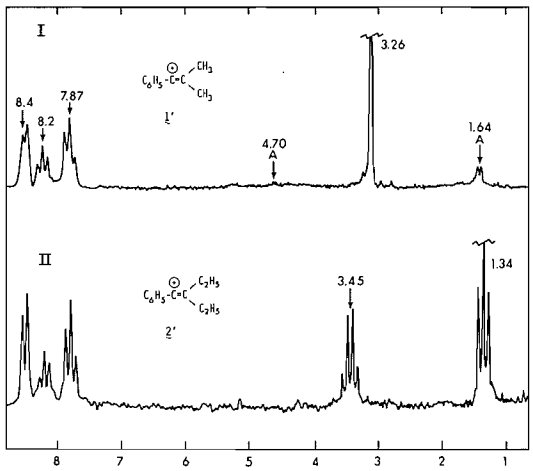

FIG. 1. Proton magnetic resonance (100 MHz) of **1′** and **2′** in SbF_5–SO_2ClF at −95°.

p-orbital of the vinyl cation rather than the double bond. This inference is in accord with the charge distribution calculated for 1-phenylvinyl cation by the MINDO/2–OPTMO program (5, 6).[2] Signals at δ 7.87, 8.2, and 8.4 are assigned to the *m*-, *p*-, and *o*-protons, respectively (5). The absorptions indicated by A have been confirmed by an independent preparation to be due to a tertiary cation **3′** contaminated in the sample.

Since off-resonance C-13 spectra did not permit unequivocal assignment of C-13 signals of **1′**, in particular, those of C(2) and C(5) of vital importance, compound **1** was labeled with C-13 either at C(1) or C(2), and also the aromatic ring was fully deuterated.[3] Figure 2 (7) shows proton-decoupled C-13 spectra of **1′** and these labeled cations. Comparison of spectra I and IV (C(1) labeled) and III (C(2) labeled) immediatedly leads to the assignment that signals A, D (overlapped with E), and G are ascribable to C(1), C(2), and C(3 and 4). Furthermore, spectrum II indicates that signal F is due to C(5) and B, C, and E are to the other aromatic carbons.[4] Another peak indicated by X appears

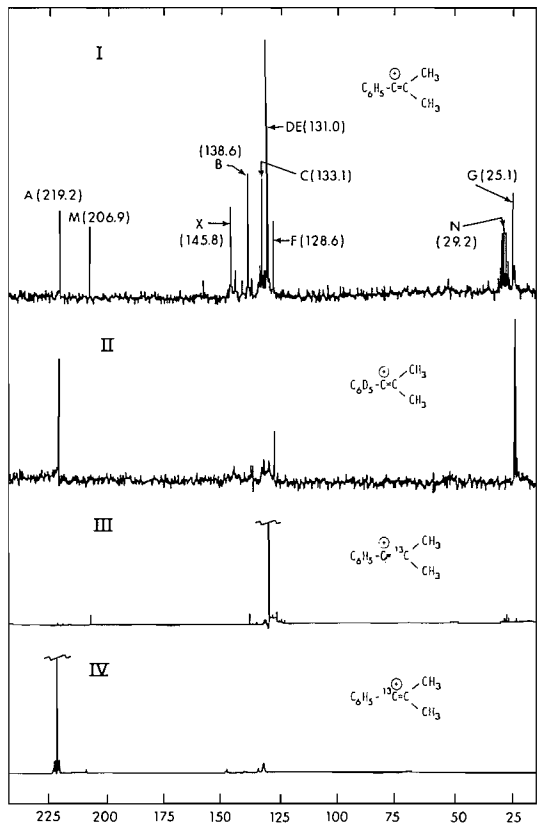

FIG. 2. Carbon-13 magnetic resonance (22.63 MHz) of **1′** and its labeled cations in SbF_5–SO_2ClF at —95°. External deuterioacetone (M and N) was used to lock the spectrometer and its signal taken as reference (N, δ 29.2).

irreproducibly in several experiments and are likely to arise from yet unidentified impurities contaminated in the superacid solution.

Thus, the equivalence of the two methyl (and ethyl) groups exhibited in both the p.m.r. and c.m.r. spectra point to the presence of C_{2v} symmetry in **1′**. The appearance of the C(2) signal in the normal olefinic region and that of the C(1) at low field clearly demonstrate that very little positive charge resides at the β-carbon of the cation even if two alkyl groups are attached to this carbon, and this aspect is being investigated further.[5] And as stated above, the chemical shifts of the aromatic protons suggest the bisected geometry for the aromatic ring of the system.

[2]The calculation also shows that this bisected geometry is *ca.* 6 kcal more stable than its geometrical isomer in which the phenyl ring and the two methyl groups are in one plane.

[3]These labeled compounds were prepared, using the corresponding C-13 benzoic acid, C-13 acetone, and deuterated toluene, respectively.

[4]The intensity of signal A, compared with those of B and C, appears to be anomously high but is not totally unexpected (8).

[5]Semi-empirical calculations (5, 9) indicate that alkyl substituents at the β-position significantly increase the positive charge density at this position.

Finally, quenching of solutions containing **1′** or **2′** with methanolic sodium methoxide at −80° provided the corresponding methoxystyrene derivatives in more that 50% yield and these experiments provide further evidence that **1′** and **2′** have indeed been generated.

The author is grateful to the National Research Council for financial support.

1. H. U. SIEHL, J. C. CARNAHAN JR., L. ECKES, and M. HANACK. Angew. Chem. **86**, 677 (1974).
2. (*a*) P. J. STANG. Prog. Phy. Org. Chem. **10**, 205 (1973); (*b*) G. MODENA and U. TONELLATO. Advan. Phys. Org. Chem. **9**, 185 (1971); (*c*) M. HANACK. Acc. Chem. Res. **3**, 209 (1970).
3. J. H. FLETCHER, O. C. DARMER, and R. B. FOX. Nomenclature of organic compounds. American Chemical Society, Washington, D.C. 1974. Chapt. 3.
4. S. MASAMUNE, M. SAKAI, A. V. KEMP-JONES, and T. NAKASHIMA. Can. J. Chem. **52**, 855 (1974).
5. K. MORIO and S. MASAMUNE. Unpublished results.
6. G. A. OLAH and C. U. PITTMAN. J. Am. Chem. Soc. **87**, 3507 (1965); G. A. OLAH, M. B. COMISARROW, and C. J. KIM. J. Am. Chem. Soc. **91**, 1458 (1969).
7. J. B. STOTHERS. Carbon-13 NMR spectroscopy. Academic Press, New York, N.Y. 1972. p. 222.
8. A. ALLERHAND, D. DODDRELL, and R. KOMOROSKI. J. Chem. Phy. **55**, 189 (1971).
9. P. J. STANG. Prog. Phy. Org. Chem. **10**, 272 (1973).

Can. J. Chem. Downloaded from www.nrcresearchpress.com by 210.87.254.105 on 09/05/12
For personal use only.

Can. J. Chem. Downloaded from www.nrcresearchpress.com by 210.87.254.6 on 09/05/12
For personal use only.

Canadian Journal of Chemistry

Published by
THE NATIONAL RESEARCH COUNCIL OF CANADA

Journal canadien de chimie

Publié par
LE CONSEIL NATIONAL DE RECHERCHES DU CANADA

Volume 53 Number 6 March 15, 1975

Volume 53 numéro 6 15 mars 1975

Nuclear Magnetic Resonance Studies of the Solution Chemistry of Metal Complexes. XIII. The Lability of the Metal–Nitrogen Bonds in the Cadmium, Zinc, and Mercury Complexes of Selected Polyaminocarboxylic Acids

DALLAS L. RABENSTEIN, GEORGE BLAKNEY, AND BRYAN J. FUHR

Department of Chemistry, University of Alberta, Edmonton, Alberta T6G 2G2

Received February 21, 1974

DALLAS L. RABENSTEIN, GEORGE BLAKNEY, and BRYAN J. FUHR. Can. J. Chem. **53**, 787 (1975).

The lability of the metal–nitrogen bonds in the Cd(II), Zn(II), and Hg(II) complexes of $(HO_2CCH_2)_2N(CH_2)_nN(CH_2CO_2H)_2$ (n = 2, 3, 4) has been investigated by proton magnetic resonance spectroscopy. The acetate methylenic protons of each of the complexes give rise to AB multiplet patterns, indicating the metal–nitrogen bonds to be inert on the n.m.r. time scale. From the temperature dependence of the multiplet patterns, the relative lability of the metal–nitrogen bonds in each series of complexes has been established. In the Cd(II) and Zn(II) complexes, the metal–nitrogen bonds become more labile as the size of the internal chelate ring increases whereas it becomes more inert in the Hg(II) complexes. Also, the mercury–proton coupling constants increase as n is increased from two to four, which is interpreted as evidence that the increased kinetic stability results from structural changes to a more linear N—Hg—N arrangement. The metal–nitrogen bonds in the Cd(II) complexes having n = 3 and 4 is more labile than in the corresponding Zn(II) complexes. The thermodynamic stability patterns of the complexes are discussed in terms of their relative kinetic stabilities.

DALLAS L. RABENSTEIN, GEORGE BLAKNEY et BRYAN J. FUHR. Can. J. Chem. **53**, 787 (1975).

On a étudié, par r.m.p., la labilité des liens métaux-azote dans des complexes du Cd(II), Zn(II) et du Hg(II) avec $(HO_2CCH_2)_2N(CH_2)_nN(CH_2CO_2H)_2$ (n = 2, 3, 4). Les protons méthyléniques de l'acétate de chaque complexe donnent lieu à des patrons de type AB sous forme de multiplets, indiquant que les liens métaux-azote sont inertes à l'échelle de temps de la r.m.n. On a pu établir, grâce à la dépendance sur la température des patrons des multiplets, la labilité relative des liens métaux-azote dans chaque série des complexes. Dans les complexes Cd(II) et Zn(II), les liens métaux-azote deviennent plus labiles à mesure que la grandeur du cycle chélate interne augmente alors qu'ils deviennent plus inertes dans les complexes du Hg(II). De plus les constantes de couplage mercure–proton augmentent lorsque n augmente de 2 à 4; on interprète ces résultats comme signifiant que la stabilité cinétique accrue résulte de changements structuraux menant à des arrangements N—Hg—N plus linéaires. Les liens métaux-azote dans les complexes avec Cd(II) dans lesquels n = 3 et 4 sont plus labiles que dans les complexes Zn(II) correspondants. On discute des patrons de stabilité thermodynamique des complexes en terme de leur stabilité cinétique relative. [Traduit par le journal]

Introduction

In their pioneering studies of the solution chemistry of ethylenediaminetetraacetic acid (EDTA) and related ligands, Schwarzenbach, Anderegg, and co-workers (1–4) found that the formation constants of metal complexes of ligands of the type

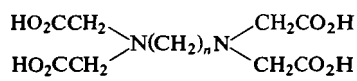

1

Can. J. Chem. Downloaded from www.nrcresearchpress.com by 210.87.254.6 on 09/05/12
For personal use only.

decrease as n is increased from two to eight, with the exception of the mercury complexes whose formation constants decrease as n is increased from two to three and then increase as n is increased from three to eight. Schwarzenbach and Anderegg proposed that larger chelate rings are favored in the Hg(II) complexes because of the tendency of Hg(II) to form linear N—Hg—N complexes. It also has been suggested that the decrease in formation constant as n is increased from two to three may indicate that some of the carboxylate groups coordinated in $Hg(EDTA)^{2-}$ are free in the Hg(II) complexes of the higher homologs (5).

Since the formation constant is determined by the ratio of the complex formation and dissociation rate constants, it seems likely that the changes in the formation constant may result from changes in the kinetic stability of the complex as the size of the internal chelate ring increases. If so, this should be reflected in the relative lability of the metal–nitrogen bonds of the different complexes, which can be determined from the complexity of the proton magnetic resonance (p.m.r.) spectra for their acetate methylenic protons (6, 7). To determine if the different stability trends do result from different changes in the kinetic stability as the size of the internal chelate ring increases, we have determined by p.m.r. the relative lability of the individual metal–nitrogen bonds in the Cd(II), Zn(II), and Hg(II) complexes of several homologs in the series represented by **1**. We have also studied the Zn(II) and Hg(II) complexes of the model ligand *N*-methyliminodiacetic acid (MIDA).

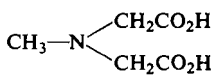

2

Experimental

1,4-Butylenediaminetetraacetic acid (1,4-BDTA) was synthesized by a method analogous to the synthesis of 1,3-propylenediaminetetraacetic acid (8). Cadmium nitrate (Fisher Certified Reagent), zinc nitrate, and mercuric nitrate (Baker Analyzed Reagents) and MIDA (K and K laboratories) were used as received.

pH measurements and 60 and 100 MHz p.m.r. measurements were made as described previously (7). 220 MHz p.m.r. measurements were made on a Varian HR-220 high resolution spectrometer at Sheridan Park, Ontario. Nuclear magnetic resonance measurements were made on samples in the pH range 6 to 8 to minimize contributions from reactions involving hydrogen or hydroxide ion (7).

Results and Discussion

Cadmium and Zinc Complexes

The 60 MHz p.m.r. spectrum of the acetate methylenic protons of $Zn(1,4\text{-}BDTA)^{2-}$ in H_2O is shown at several temperatures in Fig. 1. At 48 °C, the spectrum is a symmetrical AB pattern, the parameters for which are given in Table 1. The AB pattern indicates that, at this temperature, the zinc–nitrogen bonds are non-labile on the p.m.r. time scale (6, 7). At temperatures greater than 48 °C, the lability of the zinc–nitrogen bonds increases as evidenced by the partial collapse of the AB pattern; interchange of the protons between environments, and thus collapse of the AB pattern, can occur only by inversion of the nitrogen atom, which is possible only when the nitrogen is not metal coordinated. At temperatures less than 48 °C, the individual lines broaden at different rates, resulting in unsymmetrical AB patterns. Each half of the multiplet pattern is broadened further at 100 and 220 MHz, indicating that the broadening results from a second kinetic process, possibly a relatively slow exchange of the acetate dentates between the axial and equatorial sites. Such a process would yield an unsymmetrical

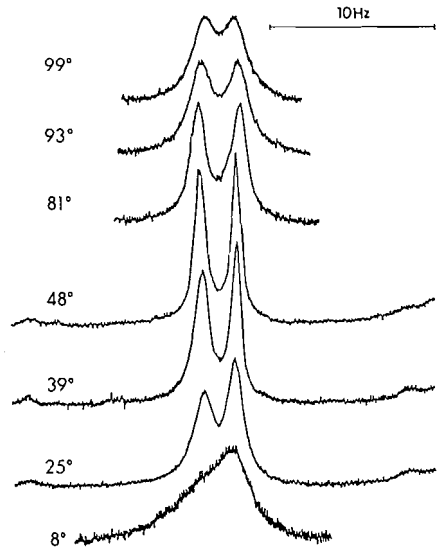

FIG. 1. Representative 60 MHz proton n.m.r. spectra of the acetate methylenic protons of $Zn(1,4\text{-}BDTA)^{2-}$ in H_2O. The pH of the solution was 8.4 at 25 °C.

TABLE 1. Nuclear magnetic resonance spectral parameters

Complex	$\lvert J_{AB}\rvert$ (Hz)	$\lvert J_{AX}\rvert$ (Hz)	$\lvert J_{BX}\rvert$ (Hz)	$\Delta\delta_{AB}$ (p.p.m.)	Other
$Zn(1,3\text{-PDTA})^{2-}$	16.3			0.220	
$Zn(1,4\text{-BDTA})^{2-}$	16.3			0.204	
$Cd(EDTA)^{2-}$ [a]	16.7	12.2	13.2	0.180	11.2 Hz[b]
$Cd(1,3\text{-PDTA})^{2-}$	16.3	11.8	15.0	0.193	
$Cd(1,4\text{-BDTA})^{2-}$	16.2	17.3	17.7	0.141	
$Hg(EDTA)^{2-}$	16.2	76	80	0.146	64.8 Hz[c]
$Hg(1,3\text{-PDTA})^{2-}$	15.7	109	115	0.105	
$Hg(1,4\text{-BDTA})^{2-}$	15.8	110	119	0.111	
$Hg(MIDA)_2^{2-}$	15.7			0.144	82.4 Hz[d]

[a]Reference 17.
[b]Cadmium – ethylenic proton coupling constant.
[c]Mercury – ethylenic proton coupling constant.
[d]Mercury – methyl proton coupling constant.

pattern if J_{AB}, ν_A, and ν_B are different for the axial and equatorial acetate groups, as in the nonlabile cobalt(III) and rhodium(III) complexes of EDTA (6, 9–11), and if $\nu_{A(axial)} - \nu_{A(equatorial)}$ is different from $\nu_{B(axial)} - \nu_{B(equatorial)}$.

The average lifetime of the nonequivalent acetate methylenic protons of $Zn(1,4\text{-BDTA})^{2-}$ before interchange is given as a function of temperature in Table 2. The AB interchange rates were obtained by matching experimental p.m.r. spectra with theoretical spectra (7) which were calculated as a function of average lifetime before AB interchange using the density matrix formalism (12).

The average lifetimes of the nonequivalent acetate methylenic protons of the Zn(II) complex of 1,3-propylenediaminetetraacetic acid, $Zn(1,3\text{-PDTA})^{2-}$, have been reported as a function of temperature previously (7). The acetate methylenic protons of $Zn(EDTA)^{2-}$ also give an AB pattern at 220 MHz, although the spectral parameters have not been reported (13).

TABLE 2. Average lifetimes of the acetate methylenic protons of $Zn(1,4\text{-BDTA})^{2-}$ and $Cd(1,4\text{-BDTA})^{2-}$ before AB interchange

	τ (s)	
T (°C)	$Zn(1,4\text{-BDTA})^{2-}$ [a]	$Cd(1,4\text{-BDTA})^{2-}$ [b]
5		0.10
23		0.050
38		0.012
51		0.0055
56	0.5	
62	0.30	
73	0.20	
80	0.095	
87	0.063	
93	0.047	
100	0.035	

[a]pH = 7.78 at 25°. Determined by lineshape analysis of 60 MHz spectra; uncertainty is 5 to 10%.
[b]pH = 7.6 at 25°. Determined by lineshape analysis of 220 MHz spectra; uncertainty is ± 10% due to slight asymmetry of the multiplet pattern.

The p.m.r. spectrum for the acetate methylenic protons of $Cd(1,4\text{-BDTA})^{2-}$ is composed of the AB part of an ABX pattern superimposed on an AB pattern. The AB part of an ABX pattern is due to the complexes of the ^{111}Cd and ^{113}Cd isotopes, which have a natural abundance of 25% and a nuclear spin of 1/2, while the AB pattern is due to 1,4-BDTA complexes of the other cadmium isotopes. The spectral parameters obtained from the 220 MHz spectrum of $Cd(1,4\text{-BDTA})^{2-}$ are given in Table 1. At 70 °C, the multiplet pattern is A_2X, indicating that the ligand is not completely dissociating from the Cd(II) in the process which results in AB interchange.[1] Approximate values for the average lifetime of the nonequivalent acetate methylenic protons of $Cd(1,4\text{-BDTA})^{2-}$ before interchange are given as a function of temperature in Table 2.

The rates of AB interchange in the Cd(II) and Zn(II) complexes of ligands of the type represented by **1** are governed by their rates of partial dissociation to yield **4** (7).

[1]AB interchange can occur when the complex has partially dissociated to form **4** (7). However, the cadmium–proton coupling will collapse only if the complex completely dissociates (14); partial dissociation of the complex to **4** followed by reformation of the metal–nitrogen bond results in no change in the spin states of the coupled nuclei.

Can. J. Chem. Downloaded from www.nrcresearchpress.com by 210.87.254.6 on 09/05/12
For personal use only.

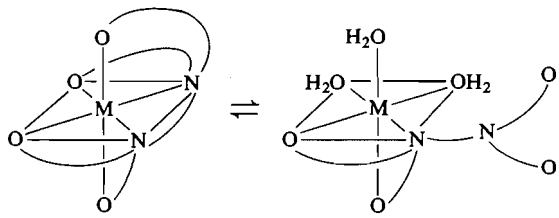

3 4

The metal–oxygen bonding in these complexes is labile at the temperatures at which the lifetimes were determined as indicated by a single AB pattern for the acetate methylenic protons. Thus, the rate determining step at these temperatures is dissociation of the metal–nitrogen bond.[2] The results in Table 2 indicate the metal–nitrogen bonding in the Cd(II) complex of 1,4-BDTA to be more labile than in the corresponding Zn(II) complex. Similar relative labilities were found for the Cd(II) and Zn(II) complexes of 1,3-PDTA (7). A comparison of the results in Table 2 with those for 1,3-PDTA (7) reveals that, for a given metal ion, the metal–nitrogen bonding in the 1,4-BDTA complexes is slightly more labile, in support of the idea that it is easier for a larger chelate ring to open (15 and references therein). Further support is derived from the AB pattern for the acetate methylenic protons of $Cd(EDTA)^{2-}$ which shows no evidence of line broadening due to AB interchange up to 100 °C (7).

Comparing the results in Table 2 with those for $Cd(1,3\text{-}PDTA)^{2-}$ and $Zn(1,3\text{-}PDTA)^{2-}$ (7), it is seen that the difference in the lability of $Cd(1,3\text{-}PDTA)^{2-}$ and $Cd(1,4\text{-}BDTA)^{2-}$ is larger than that of the corresponding Zn(II) complexes. The difference in the thermodynamic stability of the Cd(II) complexes is also larger (3), suggesting that the larger decrease in thermodynamic stability of the Cd(II) series is due, at least in part, to the decreased kinetic stability.

Opening the chelate ring involves a twisting of the aliphatic chain linking the two nitrogen atoms. To estimate an upper limit for the rate at which an iminodiacetate segment of these ligands would be expected to dissociate, the rate constant for dissociation of one MIDA ligand from $Zn(MIDA)_2^{2-}$ was determined.

$$[1]\quad Zn(MIDA)_2^{2-} \underset{k_f}{\overset{k_d}{\rightleftarrows}} Zn(MIDA) + MIDA^{2-}$$

From n.m.r. line-broadening measurements of the type described previously (16), $k_d = 40 \pm 5\ s^{-1}$ and $k_f = (1.2 \pm 0.2) \times 10^8\ M^{-1}\,s^{-1}$ at 25 °C. Taking the inverse of the lifetimes before AB interchange to be half the first order rate constants for partial dissociation to form **4** (7), the partial dissociation rate constant for $Zn(1,3\text{-}PDTA)^{2-}$ is $0.69\ s^{-1}$ at 25 °C. The difference between k_d and this value might provide an estimate of the energy barrier associated with the necessary twisting of the aliphatic chain in the formation of **4** from $Zn(1,3\text{-}PDTA)^{2-}$.

Mercury Complexes

The 220 MHz p.m.r. spectrum of $Hg(EDTA)^{2-}$ is shown as a function of temperature in Fig. 2. At 23 °C, the acetate methylenic protons give rise to a multiplet composed of the AB part of an ABX pattern superimposed on an AB pattern. The AB part of an ABX pattern is due to the EDTA complex of ^{199}Hg, which has a nuclear spin of 1/2 and a natural abundance of 16.9%, while the AB pattern is due to the EDTA complexes of the other isotopes of mercury. The ethylenic protons give rise to the A_4 part of an A_4X pattern. The spectral parameters are summarized in Table 1.

The mercury–nitrogen bonding in $Hg(EDTA)^{2-}$ is more labile than in $Cd(EDTA)^{2-}$ as evidenced by the collapse of the multiplet pattern for the acetate methylenic protons of $Hg(EDTA)^{2-}$ at higher temperatures. Indeed, collapse of the mercury–proton coupling at 70 °C indicates complete dissociation of the complex at this temperature.

The acetate methylenic protons of $Hg(1,3\text{-}PDTA)^{2-}$, $Hg(1,4\text{-}BDTA)^{2-}$, and $Hg(MIDA)_2^{2-}$ give rise to similar multiplet patterns whose spectral parameters are given in Table 1. The lines in the multiplet pattern for $Hg(1,3\text{-}PDTA)^{2-}$, however, are only very slightly broadened at 70 °C, including the satellite lines due to mercury–proton coupling, while there is no detectable broadening in the pattern for $Hg(1,4\text{-}BDTA)^{2-}$. These results indicate that, in contrast to the Cd(II) and Zn(II) complexes, the order of lability of the mercury–nitrogen bonds is $Hg(EDTA)^{2-} > Hg(1,3\text{-}PDTA)^{2-} >$

[2]Dissociation of complexes of multidentate ligands proceeds via the stepwise dissociation of the individual metal–ligand bonds. The rate of AB interchange will depend on the fraction of the complex in the different partially coordinated forms. The fraction of the complex in the various partially coordinated forms presumably is temperature dependent, which would give rise to non-linear Arrhenius plots of the type obtained with the data in Table 2 (7).

Can. J. Chem. Downloaded from www.nrcresearchpress.com by 210.87.254.6 on 09/05/12
For personal use only.

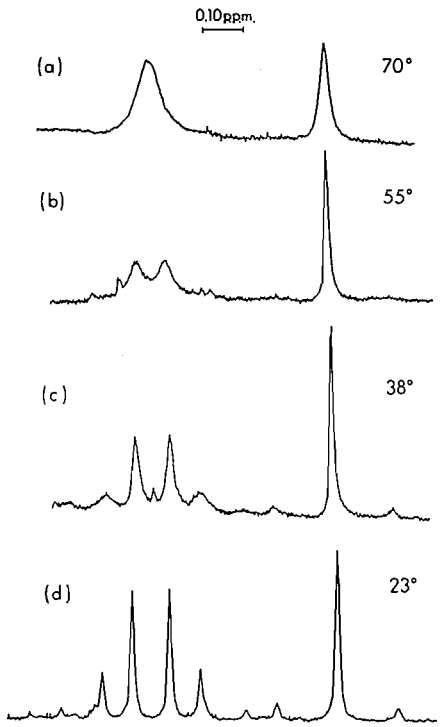

FIG. 2. Representative 220 MHz proton n.m.r. spectra of $Hg(EDTA)^{2-}$ in H_2O. The p*H* of the solution was 6.8 at 25 °C.

$Hg(1,4\text{-}BDTA)^{2-}$. Also, the coupling constants J_{AX} and J_{BX} for $Hg(1,3\text{-}PDTA)^{2-}$ and $Hg(1,4\text{-}BDTA)^{2-}$ are similar and somewhat larger than those for $Hg(EDTA)^{2-}$, suggesting that the structures of $Hg(1,3\text{-}PDTA)^{2-}$ and $Hg(1,4\text{-}BDTA)^{2-}$ are similar but different from that of $Hg(EDTA)^{2-}$. Specifically, the larger coupling in $Hg(1,3\text{-}PDTA)^{2-}$ and $Hg(1,4\text{-}BDTA)^{2-}$ indicates increased mercury s character in the mercury–nitrogen bonds which supports a more linear N—Hg—N arrangement as the size of the internal chelate ring increases (1). Two structures having the linear N—Hg—N arrangement are represented by **5** and **6**.

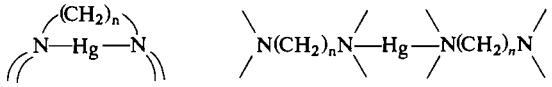

5 **6**

It is not possible to construct **5** from space filling molecular models, suggesting that coordination of Hg(II) to iminodiacetate segments of two ligands may be important in the mercury complexes of the higher homologs. An AB pattern for the acetate methylenic protons of $Hg(MIDA)_2^{2-}$, a model complex for **6**, indicates that the binding of an iminodiacetate segment by Hg(II) is sufficiently nonlabile to give the multiplet patterns observed for $Hg(1,3\text{-}PDTA)^{2-}$ and $Hg(1,4\text{-}BDTA)^{2-}$.

Summary

The decrease in the formation constants of the Cd(II) and Zn(II) complexes of **1** as the size of the internal chelate ring is increased from five membered to seven membered is accompanied by an increase in the lability of the metal–nitrogen bonds, suggesting that, in part at least, the smaller formation constants for the Cd(II) and Zn(II) complexes of the higher homologs of **1** are due to the decreased kinetic stability of these complexes. In contrast, the kinetic stability of the Hg(II) complexes of **1** increases as *n* is increased from two to three to four. Nuclear magnetic resonance coupling constant data suggests that this is accompanied by structural changes to more linear N—Hg—N bonding in the complexes of the higher homologs.

This research was supported in part by the National Research Council of Canada.

1. G. SCHWARZENBACH and G. ANDEREGG. Z. Anorg. Allgem. Chem. **282**, 286 (1955).
2. G. SCHWARZENBACH, H. SENN, and G. ANDEREGG. Helv. Chim. Acta, **40**, 1886 (1957).
3. G. ANDEREGG. Helv. Chim. Acta, **47**, 1801 (1964).
4. F. L'EPLATTENIER and G. ANDEREGG. Helv. Chim. Acta, **47**, 1792 (1964).
5. F. L. GARVAN. *In* Chelating agents and metal chelates. *Edited by* F. P. Dwyer and D. P. Mellor. Academic Press, New York, N.Y. 1964. p. 301.
6. R. J. DAY and C. N. REILLEY. Anal. Chem. **36**, 1073 (1964).
7. D. L. RABENSTEIN and B. J. FUHR. Inorg. Chem. **11**, 2430 (1972).
8. J. A. WEYH and R. E. HAMM. Inorg. Chem. **7**, 2431 (1968).
9. G. L. BLACKMER and J. L. SUDMEIER. Inorg. Chem. **10**, 2019 (1971).
10. J. L. SUDMEIER, A. J. SENZEL, and G. L. BLACKMER. Inorg. Chem. **10**, 90 (1971).
11. B. B. SMITH and D. T. SAWYER. Inorg. Chem. **7**, 2020 (1968).
12. R. M. LYNDEN-BELL. Progr. Nucl. Magn. Reson. Spectrosc. **2**, 163 (1967).
13. G. H. REED and R. J. KULA. Inorg. Chem. **10**, 2050 (1971).
14. D. L. RABENSTEIN. J. Am. Chem. Soc. **93**, 2869 (1971).
15. R. G. WILKINS. Acc. Chem. Res. **3**, 408 (1970).
16. D. L. RABENSTEIN and R. J. KULA. J. Am. Chem. Soc. **91**, 2492 (1969).
17. G. H. REED. Ph.D. Dissertation, University of Wisconsin, Madison, Wisconsin. 1968.

Can. J. Chem. Downloaded from www.nrcresearchpress.com by 210.87.254.6 on 09/05/12
For personal use only.

The Equivalent Conductivity of Aqueous Solutions of Salts of Carboxymethylcellulose: A Test of Manning's Limiting Law

JAN C. T. KWAK AND ALLAN J. JOHNSTON
Department of Chemistry, Dalhousie University, Halifax, Nova Scotia B3H 4J3
Received November 7, 1974

JAN C. T. KWAK and ALLAN J. JOHNSTON, Can. J. Chem. **53**, 792 (1975).

Measurements of the equivalent conductivity of aqueous solutions of lithium, sodium, potassium, and cesium salts of carboxymethylcellulose (CMC) at 25 °C are reported. The degree of substitution of the CMC used was 0.86, concentrations of the four salts were varied from 5×10^{-4} to 5×10^{-2} equiv l^{-1}. Results show a decrease of Λ with increasing concentration in each case. In the lower concentration range (up to 10^{-2} *N*) this decrease is in close agreement with a limiting law for conductivity recently developed by Manning. Above 10^{-2} *N* the decrease in Λ is less than the decrease predicted by the limiting law. The counterion dependence of Λ is accurately predicted by the theory, and a qualitative agreement is obtained when the theory is used to compare conductance data of polyelectrolytes with different charge densities.

JAN C. T. KWAK et ALLAN J. JOHNSTON. Can. J. Chem. **53**, 792 (1975).

On rapporte des mesures de la conductivité équivalente de solutions aqueuses de sels de lithium, de sodium, de potassium et de césium de carboxyméthylcellulose (CMC) à 25 °C. Le degré de substitution du CMC était de 0.86 et les concentrations des quatre sels variaient de 5×10^{-4} à 5×10^{-2} équiv par litre^{-1}. Dans chaque cas les résultats montrent qu'un abaissement de Λ se produit à mesure que la concentration augmente. Dans la zone de basse concentration (jusqu'à $10^{-2}N$), cet abaissement est en très bon accord avec une loi limite sur la conductivité récemment proposé par Manning. Au dessus de 10^{-2} *N*, l'abaissement de Λ est moindre que cellui prédit par cette loi. La relation de Λ avec l'ion antagoniste est bien prédite par la théorie et une relation qualitative est obtenue quand la théorie est utilisée pour comparer les données de conductivité de polyélectrolytes avec différentes densités de charge. [Traduit par le journal]

Introduction

The concentration dependence of the equivalent conductivity of polyelectrolyte solutions has been reported for polyacrylates and polymethacrylates (1, 2), polyvinylsulfonates (3), salts of carrageenan and of arabic acid (4, 5), sodium polystyrene sulfonate (6, 7), and for salts of quarternized polyvinylimidazole (8). In most cases Λ of polyelectrolyte salts decreases upon increasing the concentration, but some authors report Λ to be virtually independent of concentration (6), and in other cases a minimum in Λ is observed (4, 5, 7). The concentration dependence of Λ has normally been expressed by plotting $\Lambda - \Lambda^0$ as a function of $c^{1/2}$ and extrapolating to $c = 0$ to obtain Λ^0 of the polyelectrolyte, but in many cases this procedure led to ambiguities in the determination of Λ^0. Counterion condensation theory has shown that for polyelectrolytes with a charge density higher than a certain critical value some counterions are "condensed" on the polyion even at infinite dilution (9). Manning synthesized this counterion condensation effect and the electrostatic interactions of polyions and small ions to arrive at limiting laws for activity coefficients and osmotic coefficients (10–12). Manning's model assumes a rod-like polyion and point counterions, without interactions between different polyions or different segments of the same polyion. Application of this model to the conductance process in electrolyte solutions led to the following equation (11–13)

$$\Lambda = f(\lambda_c^0 + \lambda_p) \quad [1]$$

where f is related to the charge density parameter ξ (9, 10, 12) by

$$f = 0.87\,|z|^{-1}\,\xi^{-1} \quad [2]$$

z is the valency for the counterion, $\xi = e|\beta|/DkT$, $|\beta|$ is the charge in a unit-length of the polyelectrolyte cylinder, D the dielectric constant, k Bolzmann's constant, and T the temperature.

The appearance of λ_c^0 in eq. 1 expresses the fact that in this limiting law interactions between the uncondensed counterions are neglected. However, Debye–Hückel type interactions between the polyelectrolyte cylinder and the uncondensed counterions are taken into account,

Can. J. Chem. Downloaded from www.nrcresearchpress.com by 210.87.254.5 on 09/05/12
For personal use only.

Can. J. Chem. Downloaded from www.nrcresearchpress.com by 210.87.254.5 on 09/05/12
For personal use only.

which shows the inadequacy of treating f as the fraction of "free" ions. The conductance equation in the form of eq. 1 still contains the mobility of the polyion at finite concentration. In a recent paper, Manning (14) derived an expression for λ_p as a function of c, ξ, z, and λ_c^0. This expression allows us to calculate the complete concentration dependence of the equivalent conductivity of salt-free polyelectrolyte solutions, assuming the model on which the limiting laws are based is correct. Kwak and Hayes (15), and Scymczak, Holyk, and Ander (16) compared Manning's conductance equation to accurate data for a number of salts of polystyrenesulfonic acid. It was found that although the limiting law correctly predicted the counterion dependence when comparing polyelectrolyte salts with univalent counterions, the detailed concentration dependence in the low concentration range (below 0.01 N) was different for the two polymer samples studied. Above 0.01 N an increase in Λ was observed, whereas eq. 1 predicts a monotonous decrease in Λ with increasing concentration. These deviations from the limiting law were at least partially attributed to coiling of the polymer (15), causing the model on which the limiting law depends to break down.

It is the purpose of this investigation to compare data for the equivalent conductivity of salts of carboxymethylcellulose (CMC), a substituted polysugar with a less flexible polymer chain, to the limiting law values. The charge density of the CMC is much less than the charge density of the polystyrenesulfonates used in refs. 15 and 16, allowing for a check of the charge density dependence predicted by the limiting law. Although a report of the concentration dependence of Λ for salts of CMC has appeared (17), the values for Λ seem too high, in some cases well above 500 cm^2 ohm^{-1} $equiv^{-1}$! Rinaudo and Milas (18–20) report the equivalent conductivities of a number of salts of a high charge density CMC at one concentration (0.005 N) only. Conductance studies of salts of a few naturally occurring polysugars have been published (4, 5).

Experimental

Carboxymethylcellulose (Na-salt, Koch-Light Laboratories, Colnbrook, U.K.) was purified by repeated cation and anion exchange (Dowex 50W-X8 cation exchange resin and Dowex ANGA 542 anion exchange resin) and finally left in the H^+ form. The concentration of this stock solution was determined by titrating a weighed sample with NaOH. Weighed aliquots of HCMC were converted to the desired ionic form by adding the required amount of LiOH, NaOH, KOH, or CsOH, and finally adding the water needed to give a predetermined total weight of stock solution of each salt. This procedure is different from the one used for polystyrenesulfonates (15) and ensures that the concentrations of the different salt solutions are known relative to each other with a precision of $\pm 0.1\%$, even if the error in the actual concentration may be $\pm 1\%$. The pH of each stock solution was between 7 and 7.5. The equivalent weight of the CMC was determined by drying a weighed sample of known concentration under vacuum at 40 °C. The equivalent weight of HCMC was found to be 258 ± 2, of CsCMC 389 ± 3, corresponding to degrees of substitution of 0.85 and 0.86, respectively. In all calculations the value 0.86 will be used for the degree of substitution. Dilutions are made by weight using double distilled water ($\kappa = (1.0–1.1) \times 10^{-6}$ ohm^{-1} cm^{-1} at 25 °C). Densities of the more concentrated solutions were determined with a simple pycknometer (estimated accuracy ± 0.02%), and concentrations calculated from the known number of equiv/kg. Corrections were made for the conductance of the distilled water; for the lowest concentrations used this correction was less than 4%. No correction for hydrolysis was applied since the pH of each solution did not exceed 7.5. The conductance bridge, built around a Leeds and Northrup No. 1553 Campbell–Shackleton ratio box, and the constant temperature bath were the same as used in a previous investigation (15). Conductivity cells with cell constants 0.1527 ± 0.0001 cm^{-1} and 1.4492 ± 0.0004 cm^{-1} were used. Electrodes were lightly platinized, the reported conductivities were measured at 2000 cycles. The frequency dependence of the conductivity was determined for a few solutions. The measured conductivity increased less than 0.2% between 1 000 and 10 000 cycles.

Results and Discussion

The equivalent conductivities of Li, Na, K, and Cs carboxymethylcellulose (degree of substitution 0.86) at 25.0 °C as a function of the square root of the concentration are shown in Table 1. The results show the expected decrease in Λ over the complete concentration range studied (0.0006–0.05 N), and in this respect are markedly different from the polystyrenesulfonate salts. In Fig. 1 the experimental values for Λ (solid lines) are compared to the limiting law values for each salt, using eq. 1 (broken lines), with Manning's expression for λ_p (14). In calculating the theoretical curves, Robinson and Stokes' values for the limiting counterion mobility, λ_c^0, were used (21). Using a segment length of 5.15×10^{-8} cm (22), the charge density parameter ξ is calculated to be 1.20 (corresponding to 86% substitution per unit length of 5.15×10^{-8} cm) and $f = 0.73$. The theoretical value of λ_p, and thus of Λ, is depen-

TABLE 1. Equivalent conductivities, Λ (cm² ohm⁻¹ equiv⁻¹) of salts of carboxymethylcellulose (CMC) at 25 °C

LiCMC		NaCMC		KCMC		CsCMC	
$c \times 10^3$* (equiv. l⁻¹)	Λ	$c \times 10^3$* (equiv. l⁻¹)	Λ	$c \times 10^3$* (equiv. l⁻¹)	Λ	$c \times 10^3$* (equiv. l⁻¹)	Λ
0.498	69.7	0.498	78.5			0.498	101.4
0.598	68.5	0.599	77.2	0.598	98.0	0.598	100.1
0.797	67.4			0.798	97.2	0.798	98.4
0.997	66.1	0.997	75.2	0.997	94.0	0.997	98.2
1.296	64.4	1.296	73.2	1.296	93.0	1.296	95.5
1.994	61.7	1.994	71.2	1.994	89.9	1.995	92.8
3.989	58.9	3.989	67.3	3.988	85.8	3.992	88.8
5.989	56.6	5.986	65.7	5.987	84.6	5.991	87.1
7.980	55.4	7.983	64.4	7.983	82.7	7.991	86.0
9.980	54.5	9.869	63.4	9.990	81.6	9.995	84.9
19.98	51.4	20.00	60.3	20.00	78.8	20.04	81.9
50.14	46.5	50.08	55.9	49.90	74.4	50.49	77.3

*Relative values of concentrations of solutions of the same salt are accurate to better than ±0.1%. Relative values of concentrations of solutions of different salts are accurate to ±1.0%. Accuracy of concentration determination of HCMC stock solution is ±1%.

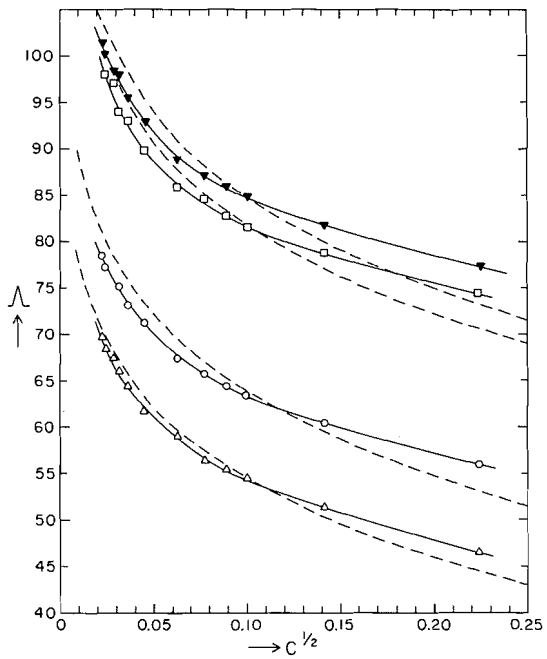

FIG. 1. Equivalent conductivity, Λ (cm² ohm⁻¹ equiv⁻¹), of LiCMC (△), NaCMC (○), KCMC (□), and CsCMC (▼) *vs.* $c^{1/2}$ (equiv.$^{1/2}$ l$^{-1/2}$). Broken lines: eq. 1 for each salt.

dent on a, the radius of the polyelectrolyte cylinder. Obviously the assignment of a cylindrical radius to any polymer chain can only be a rough approximation at best, but fortunately λ_p is not strongly dependent on a, and the change in the concentration dependence of λ_p upon varying a between realistic values is small. A cylindrical radius of 7×10^{-8} cm was used in all cases. Typically, a variation of 2×10^{-8} cm in a causes a variation of about 5% in Λ, higher values of a leading to lower values of λ_p and Λ.

It can be seen that eq. 1, using Manning's expression for λ_p, gives an excellent representation of our data for different CMC salts. Qualitatively, the curves are in good agreement at all concentrations, and below 0.005 N the concentration dependence of calculated and experimental values are in quantitative agreement. It should be stressed that this agreement in both numerical value and slopes is obtained without the use of adjustable parameters. a is not an adjustable parameter, although a reasonable choice must be made for its actual value. The predicted variation of Λ upon changing the counterion is so close that if we choose a value of a to make the theoretical and experimental values for Λ of, *e.g.* NaCMC at a given concentration, coincide (*e.g.* $a = 8.5 \times 10^{-8}$ cm would do this at $c^{1/2} = 0.04$), eq. 1 would predict Λ of the three other salts within 1%. A similar good agreement for the counterion dependence was found in the case of polystyrenesulfonates.

In order to compare both the concentration dependence and the counterion dependence of experimental values for Λ to the limiting law, Manning (14) rearranged eq. 1 to give

$$[3] \qquad \bar{\Lambda} = -\log c + \text{constant}$$

where $\bar{\Lambda}$ is a function of ξ, Λ, λ_c^0, and c. An

Can. J. Chem. Downloaded from www.nrcresearchpress.com by 210.87.254.5 on 09/05/12
For personal use only.

TABLE 2. Comparison of calculated (eq. 1) and experimental values for the equivalent conductivities of a number of polyelectrolyte salts

Polyelectrolyte	ξ	c (equiv. l^{-1})	$a \times 10^8$ (cm)	Λ_{calc}	Λ_{exp}	Reference
Na-carboxymethylcellulose	3.46	0.005	7	25.5	33.6	20
Na-polystyrenesulfonate	2.84	0.005	8	31.8	36.3	15
Na-polyacrylate (68% neutralized)	1.90	0.0044	5	47.7	42.0	2
Na-alginate	1.43	0.0058	7	57.1	48	23
Na-carboxymethylcellulose	1.20	0.005	7	68.3	66.8	This work

added advantage of this expression is that the cylindrical radius a of the polymer does not appear in $\bar{\Lambda}$. Equation 3 predicts that the $\bar{\Lambda}$'s calculated from the experimental values of Λ of different salts with the same valency counterion, when plotted against log c, should fall on a single straight line with unity slope. Although such a plot gives no information which is not already contained in Fig. 1, it does provide us with a convenient and indeed rather sensitive check of the limiting laws. Figure 2 shows this plot for the four CMC salts studied; the solid line indicates the theoretical slope only, the value of the constant in eq. 3 was not calculated. Again, we see that below 0.005 N the theoretical slope is closely obeyed. At higher concentrations the decrease in conductance is less than what is predicted by the limiting law, but the overlapping of points for the different salts shows again how closely the limiting law predicts the counterion dependence of Λ at all concentrations. In almost all cases the observed scatter in $\bar{\Lambda}$ for the four salts at the same concentration is within the limits of error of the experimental values. Deviations from the limiting slope in the case of polystyrenesulfonates (8) were attributed to coiling of this flexible vinylic polymer chain (15). The present results for the conductivity of a polyelectrolyte with a much more inflexible polymer backbone seem to support this contention. Deviations from the limiting law found at higher CMC concentrations may be due to a number of causes, including interactions between the uncondensed counterions, limited coiling of the polyion accompanied by a decrease in the degree of counterion condensation, and failing of the limiting law model of a freely draining cylinder.

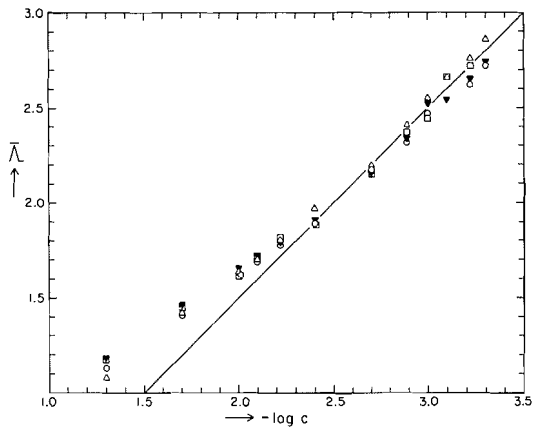

FIG. 2. $\bar{\Lambda}$ (eq. 3) *vs.* $-\log c$ for LiCMC (△), NaCMC (○), KCMC (□), and CsCMC (▼). Solid line: theoretical slope.

Equation 1 predicts the conductivity of any polyelectrolyte of finite concentration, with the charge density parameter, limiting counterion mobility, cylindrical radius, and concentration as the only variables. We have seen that this equation correctly describes both magnitude and concentration dependence of the four salts studied in this paper. The most important factor remaining is the dependence of Λ on the charge density parameter, ξ. In Table 2 we have listed calculated (eq. 1) and reported values of Λ for a number of polyelectrolytes selected to cover a range of ξ values. In discussing this table, it should be kept in mind that due to experimental conditions the uncertainty in the magnitude of Λ_{exp} in some cases may be as high as ± 2 units. Λ_{calc} is very sensitive to ξ, and therefore errors in the determination of the degree of substitution affect Λ_{calc} strongly. Also, the theory is meant to give a description of the concentration dependence of Λ rather than an *ab initio* prediction of its magnitude at a certain concentration. The qualitative agreement between Λ_{exp} and Λ_{calc} shown in Table 2 can largely be attributed to the calculation of the f parameter in eq. 1, and therefore is a qualitative confirma-

Can. J. Chem. Downloaded from www.nrcresearchpress.com by 210.87.254.5 on 09/05/12
For personal use only.

tion of the calculated influence of counterion condensation on Λ. This justifies Manning's assumption of zero mobility for the condensed ions, and contradicts earlier theories in this respect (24).

This work was supported by the National Research Council of Canada.

1. A. Oth and P. Doty. J. Phys. Chem. **56**, 43 (1952).
2. H. Eisenberg. J. Polym. Sci. **30**, 47 (1958).
3. H. Eisenberg and G. Mohan Ram. J. Phys. Chem. **63**, 671 (1959).
4. D. R. Briggs. J. Phys. Chem. **38**, 867 (1934).
5. R. E. Nelson and P. Ander. J. Phys. Chem. **75**, 1691 (1971).
6. D. O. Jordan, T. Kurucsev, and M. L. Martin. Trans. Faraday Soc. **65**, 606 (1969).
7. D. Dolar, J. Span, and S. Isaković. Biophys. Chem. **1**, 312 (1974).
8. H. P. Gregor and D. H. Gold. J. Phys. Chem. **61**, 1347 (1957).
9. F. Oosawa. Polyelectrolytes. Marcel Dekker, New York. 1971.
10. G. S. Manning. J. Chem. Phys. **51**, 924 (1969).
11. G. S. Manning. J. Chem. Phys. **51**, 934 (1969).
12. G. S. Manning. Ann. Rev. Phys. Chem. **23**, 117 (1972).
13. G. S. Manning. Biopolymers, **9**, 1543 (1970).
14. G. S. Manning. J. Phys. Chem. In press.
15. J. C. T. Kwak and R. C. Hayes. J. Phys. Chem. In press.
16. J. Scymczak, P. Holyk, and P. Ander. J. Phys. Chem. In press.
17. S. Basu and P. C. Das Gupta. J. Colloid. Sci., **7**, 53 (1952).
18. M. Rinaudo and M. Milas. C. R. Acad. Sci. C, **269**, 1190 (1969).
19. M. Rinaudo and M. Milas. C. R. Acad. Sci. C, **271**, 1170 (1970).
20. M. Rinaudo and M. Milas. J. Chim. Phys. Physicochim. Biol. **66**, 1489 (1969).
21. R. A. Robinson and R. H. Stokes. Electrolyte solutions. Butterworths, London. 1959.
22. K. Ward, Jr. and P. A. Seib. *In* The carbohydrates, chemistry and biochemistry. Vol. IIA. *Edited by* W. Pigman and D. Horton. Academic Press, New York. 1970. p. 420.
23. P. Buchner, R. E. Cooper, and A. Wasserman. J. Chem. Soc. London, 3974 (1961).
24. A. Katchalsky, Z. Alexandrowicz, and O. Kedem. *In* Chemical physics of ionic solutions. *Edited by* B. E. Conway and R. G. Barradas. Wiley, New York. 1966. p. 295.

Can. J. Chem. Downloaded from www.nrcresearchpress.com by 210.87.254.5 on 09/05/12
For personal use only.

Homogeneous Hydrogenation of Unsaturated Carboxylic Acids using Chlororhodate(I) Complexes and Rhodium(I) Diethylsulfide Complexes[1]

BRIAN R. JAMES AND FLORA T. T. NG[2]

Department of Chemistry, The University of British Columbia, Vancouver, British Columbia V6T 1W5

Received November 8, 1974

BRIAN R. JAMES and FLORA T. T. NG. Can. J. Chem. **53**, 797 (1975).

N,N-Dimethylacetamide solutions of the cyclooctene complex $[Rh(C_8H_{14})_2Cl]_2$, in the presence of excess chloride or diethylsulfide, are effective for the homogeneous hydrogenation of unsaturated carboxylic acids at *ca.* 80 °C and 1 atm H_2. Kinetic studies on the hydrogenation of maleic acid are consistent with a rate determining step involving oxidative addition of H_2 to square planar rhodium(I) olefin species. Rate constants and activation parameters agree with those determined previously from similar studies using corresponding rhodium(III) complexes and give confirmation that rhodium(I) catalysts are involved in the rhodium(III) systems. Discussion of the systems is limited by the somewhat uncertain nature of the catalysts; however, chlororhodate(I) species are involved in the chloride solutions, and bis(diethylsulfide) complexes appear likely in the sulfide systems.

BRIAN R. JAMES et FLORA T. T. NG. Can. J. Chem. **53**, 797 (1975).

Des solutions du complexe du cyclooctène, $[Rh(C_8H_{14})_2Cl]_2$, dans la *N,N*-diméthylacétamide, en présence d'excès d'ions chlorure ou de diéthylsulfure, sont efficaces pour l'hydrogénation homogène d'acides carboxyliques non-saturés à *ca.* 80 °C et 1 atm H_2. Les études cinétiques de l'hydrogénation de l'acide maléique sont en accord avec un mécanisme impliquant une étape déterminante de la réaction faisant appel à une addition oxydative de H_2 sur des espèces plan-carré de rhodium(I)-oléfines. Les constantes de vitesse et les paramètres d'activation sont en accord avec ceux déterminés auparavant lors d'études semblables utilisant les complexes correspondants du rhodium(III) et ces valeurs confirment que les catalyseurs au rhodium(I) sont impliqués dans les systèmes au rhodium(III). La discussion de ces systèmes est toutefois limitée due au fait que la nature de ces catalyseurs est un peu incertaine; toutefois des espèces de chlororhodate(I) doivent être impliquées dans les solutions contenant des ions chlorures et des complexes bis(diéthylsulfure) semblent probables dans le système au sulfure.

[Traduit par le journal]

Introduction

Earlier studies from this laboratory (1, 2) have reported on the homogeneous hydrogenation of olefinic substrates (especially unsaturated carboxylic acids) using *N,N*-dimethylacetamide (DMA) solutions of rhodium(III) chloride, and rhodium(III) sulfide complexes such as $RhCl_3(SR_2)_3$ (R = Et, CH_2Ph). Kinetic data in each case were interpreted in terms of a basic mechanism outlined in reactions 1–3.

$$[1] \qquad Rh^{III} + H_2 \xrightarrow{k_1} Rh^{I} + 2H^+$$

$$[2] \qquad Rh^{I} + \text{olefin} \xrightarrow{\text{fast}} Rh^{I}(\text{olefin})$$

$$[3] \qquad Rh^{I}(\text{olefin}) + H_2 \xrightarrow{k_2} [H_2Rh^{III}(\text{olefin})] \rightarrow Rh^{I} + \text{saturated product}$$

The systems were thought to involve initial hydrogen reduction to rhodium(I), which is stabilized by complexation to the olefin; subsequent reaction of the d^8 metal complex through oxidative addition of hydrogen leads to saturated product with regeneration of the rhodium(I) catalyst. Reactions 2 and 3 constitute a so-called and well-established "unsaturate route" for homogeneous catalytic systems involving square planar d^8 metal centers (ref. 3, p. 400).

Confirmation that rhodium(I) species are involved in the rhodium(III) systems has now been obtained by using rhodium(I) complexes directly (formed *in situ*), and comparing the kinetic data obtained with those for the rhodium(III) complexes. This paper reports on these studies; some of the work has been reported briefly elsewhere

[1]Taken from the Ph.D. thesis in Chemistry of F.T.T. Ng, University of British Columbia, Vancouver, British Columbia, 1970.

[2]Present address: Department of Chemistry, University of Guelph, Guelph, Ontario N1G 2W1.

Can. J. Chem. Downloaded from www.nrcresearchpress.com by 210.87.254.42 on 09/05/12
For personal use only.

Can. J. Chem. Downloaded from www.nrcresearchpress.com by 210.87.254.42 on 09/05/12
For personal use only.

(ref. 3, p. 275, ref. 4). Our failure to synthesize any rhodium(I)–R_2S complexes (R = alkyl or aryl) has limited our knowledge of the exact nature of the catalysts, but certain conclusions are drawn. In view of the well known poisoning of heterogeneous catalysts by sulfur compounds, the sulfur ligand systems are considered particularly interesting.

Experimental

Rhodium(III) trichloride was obtained as the trihydrate from Johnson Matthey Limited. The rhodium(I) cyclooctene dimer $[Rh(C_8H_{14})Cl]_2$, and the ethylene dimer $[Rh(C_2H_4)_2Cl]_2$, were prepared according to literature methods (5, 6).

Other materials used and the procedure used for following H_2 uptake at constant pressure have been described previously (1, 2).

Attempts to synthesize pure rhodium(I) complexes with R_2S type ligands (R = alkyl, phenyl, or benzyl) were unsuccessful, and such complexes do not appear to have been reported; procedures similar to those well-documented for synthesis of rhodium(I)–Group V ligand complexes were tried in various solvents (*e.g.* either from other labile Rh^I complexes, or from reaction of $RhCl_3 \cdot 3H_2O$ with the sulfide ligand in the absence or presence of added reducing agents). The rhodium(I) complexes were thus formed *in situ* by adding the appropriate ligand to DMA solutions of the labile dimeric rhodium(I) olefin complexes; the cyclooctene complex was especially useful since the ethylene complex decomposed slowly in the solid state (6). Addition of excess chloride or Et_2S to $[Rh(C_8H_{14})_2Cl]_2$ in DMA (Et_2S:Rh = 2) was shown by v.p.c. to liberate 2 mol of cyclooctene per mol of Rh. Such solutions were found effective for hydrogenation of maleic acid (MA) at 60–90 °C and 1 atm H_2.

Results

Spectral Studies

The $[Rh(C_8H_{14})_2Cl]_2$ dimer, **1**, is practically insoluble in DMA under vacuum or N_2 but it dissolves readily in the presence of excess chloride or Et_2S. For purposes of comparison with the previously studied rhodium(III) chloride system (1), a large excess of chloride (0.45 *M* LiCl) was used to form the *in situ* chlororhodate(I) species. An air-free solution of **1** ($\sim 10^{-3}$ *M*) in 0.45 *M* LiCl–DMA is red, and the visible spectrum is a continuum showing increasing intensity with decreasing wavelength ($\varepsilon = 230$ at 450 nm);[3] on adding a tenfold excess of MA, the spectrum slowly changed at room temperature, and a shoulder developed at 450 nm ($\varepsilon = 250$). Such spectral changes, accelerated at higher temperatures, are attributed to formation of a Rh^I(MA) complex; the complexing is "complete" at MA concentrations of 10^{-2} *M*, showing that the equilibrium constant for a reaction such as reaction 2 is $> 10^3\ M^{-1}$ at the hydrogenation conditions.

The DMA–LiCl solution of **1** in oxygen at 20 °C becomes brown due to formation of a 1:1 molecular oxygen complex (4) (Rh^IO_2;ν(0–0)895 cm^{-1}), and oxidation to higher valent rhodium species is slow. If H_2 is passed through the oxygenated solution at 80 °C for *ca.* 100 s, a red solution is obtained (longer reaction times produce some metal). The i.r. of this red solution shows a strong absorption at 1980 cm^{-1} and the disappearance of the 893 cm^{-1} band. No net gas uptake was observed, and reaction 4 is thought to occur

$$[4] \qquad Rh^IO_2 + H_2 \rightarrow Rh^{III}H_2 + O_2$$

The hydride solution was stable at 20 °C in air for several hours as evidenced from the i.r. spectra; we have been unable, however, to detect any proton signal by n.m.r. from 0–40τ. The same red hydride solution, which also showed a distinct shoulder at $\sim$475 nm (ε = 190) in the visible spectrum, could also be obtained on subjecting DMA–LiCl solutions of **1** to H_2 for a short time at 20 °C. In the presence of excess MA, however, the hydride solution was converted to the Rh^I(MA) solution; this change could be followed by visible spectroscopy at 20 °C and an isosbestic point was observed at 475 nm.

Finally, solutions of the Rh^IO_2 species under vacuum reacted with MA to again form the Rh^I(MA) species with liberation of O_2. Displacement by olefins of O_2 from d^8 molecular oxygen complexes has been noted by others (7).

During the conditions of catalytic hydrogenation (see below), the only species observed spectroscopically in solution was the Rh^I(MA) species, and this is consistent with the above findings. The Rh^I(MA) solutions reacted at 80 °C with O_2 to give finally orange solutions containing Rh^{III} chlorides with visible absorption maxima (1) at 440 nm (ε = 420) and 545 nm (ε = 125). The oxygen uptake corresponded to 0.5 mol O_2 per Rh, consistent with an oxidation of Rh^I to Rh^{III}.

Catalytic Hydrogenation

Stock solutions of **1** in 0.45 *M* LiCl–DMA

[3]Extinction coefficients as well as concentrations are expressed throughout in terms of total rhodium as monomer.

Can. J. Chem. Downloaded from www.nrcresearchpress.com by 210.87.254.42 on 09/05/12
For personal use only.

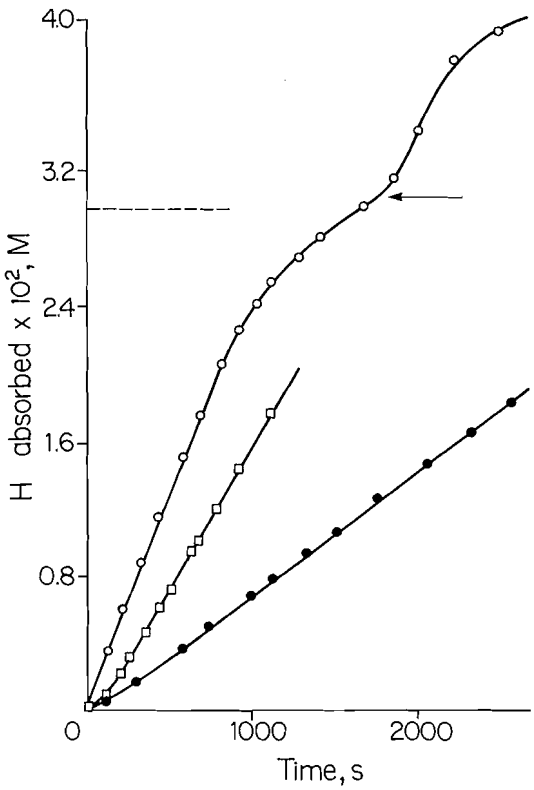

FIG. 1. Rate plots for catalytic hydrogenation of 0.03 *M* maleic acid in DMA at 80 °C, 725 mm Hg H_2 (2.32×10^{-3} *M*); ○, 5.0×10^{-3} *M* chlororhodate(I); ●, 1.8×10^{-3} *M* chlororhodate(I); □, 2.5×10^{-3} *M* rhodium(I) – diethyl sulfide; the dotted line shows the 1:1 stoichiometry for H_2:MA; the arrow marks the point of metal precipitation.

made up in air, were found to be efficient for the hydrogenation of MA at $\leq$ 1 atm H_2 around 80 °C. Typical H_2 uptake plots shown in Fig. 1 are essentially linear throughout, although the rate decreases in the regions where the ratio of H_2:MA approaches 1:1 and metal forms; a faster uptake followed metal production, and the stoichiometry for this faster reaction corresponds closely to that required for reduction of the cyclooctene. A short "autocatalytic" region was sometimes apparent at the start of the hydrogenations. In the absence of MA, metal was produced rapidly. The chlororhodate(I) solution did not hydrogenate cyclooctene homogeneously.

The kinetics for the chlororhodate(I) catalyzed hydrogenation of MA were obtained by measuring the long linear region of the uptake plots, and data are summarized in Table 1. The hydrogenation rate is seen to be first order in [Rh] and in $[H_2]$, and is independent of [MA] over the ranges of concentration used. The rate law is simply $k_2[\mathrm{Rh}][H_2]$, and the bimolecular rate constants (average = 2.1 M^{-1} s^{-1} at 80 °C) are also listed in Table 1. Data over the temperature range 70–80 °C give a good Arrhenius plot with activation parameters $\Delta H_2^{\ddagger} = 75.2 \pm 2.1$ kJ mol^{-1} and $\Delta S_2^{\ddagger} = -28.4 \pm 5.8$ J K^{-1} mol^{-1}.

The diethylsulfide catalyst was prepared *in situ* by adding Et_2S to **1** in DMA (Et_2S:Rh = 2; air was not excluded). The resulting orange-red solution was used to hydrogenate maleic, fumaric, and cinnamic acids following the same procedure used for the chlororhodate(I) solutions. Similar visible spectral changes were observed on adding MA to the catalyst solution although the initial Rh^I–Et_2S solution (ε = 460 at 450 nm) was more intensely colored than the chloride solution. The qualitative behavior of the H_2 uptake plots for MA hydrogenation (Fig. 1) was identical to that of the chloride solutions, and the kinetic dependences were found to be the same (Table 2). The average k_2 value at 80 °C is 2.85 M^{-1} s^{-1}, and the activation parameters are $\Delta H_2^{\ddagger} = 64.8 \pm 2.1$ kJ mol^{-1}, $\Delta S_2^{\ddagger} = -55.1 \pm 1.7$ J K^{-1} mol^{-1}. There was a small deuterium isotope effect ($k_2^H/k_2^D = 1.2$). Addition of (*a*), up to 0.05 *M* of the strong acid *p*-toluenesulfonic and (*b*), 0.05 *M* cyclooctene, or (*c*), a further mole of Et_2S, had little effect on the hydrogenation rate. Addition of LiCl significantly inhibited the catalysis; a constant k_2 value of 0.56 M^{-1} s^{-1} was obtained at 80 °C over a chloride concentration range of 0.01–0.125 *M*. In the absence of MA substrate, the Rh^I–Et_2S solutions were rapidly reduced by H_2 to the metal. The solutions were inactive for homogeneous hydrogenation of cyclooctene.

When a Rh^I–Et_2S solution was kept under N_2 at 80 °C for ~1 h, metal was formed, possibly through disproportionation (2). The molar conductances of stock catalyst solutions (0.2–5.0) $\times$ 10^{-3} *M* were about 1 ohm^{-1} cm^2 mol^{-1}; for 1:1 electrolytes in DMA, the values were 45–60 ohm^{-1} cm^2 mol^{-1}.

There was again evidence for formation of a molecular oxygen complex with the Rh^I–Et_2S system (8), but again under the hydrogenation conditions as for the chloride system, only a Rh^I–MA complex appeared to be present. It is of interest that the simple kinetics noted for the sulfide system were not observed for a series of

Can. J. Chem. Downloaded from www.nrcresearchpress.com by 210.87.254.42 on 09/05/12
For personal use only.

TABLE 1. Kinetic data for chlororhodate(I) catalyzed hydrogenation of maleic acid in 0.45 *M* LiCl–DMA at 80 °C unless noted otherwise

[Rh] $\times 10^3$ (M)	[MA] (M)	[H_2] $\times 10^3$ (M)	Linear rate $\times 10^5$ ($M\,s^{-1}$)	k_2 ($M^{-1}\,s^{-1}$)
1.0	0.03	2.32	0.48	2.06
1.8	0.03	2.32	0.76	1.84
2.5	0.03	2.32	1.16	2.07
4.0	0.03	2.32	1.90	2.04
5.0	0.03	2.32	2.48	2.14
2.5	0.03	0.70	0.33	1.86
2.5	0.03	1.18	0.58	1.96
2.5	0.03	1.48	0.73	1.96
2.5	0.03	2.04	1.06	2.08
2.5	0.03	2.51	1.31	2.08
2.5	0.06	2.32	1.00	1.72
2.5	0.015	2.32	1.20	2.07
2.5	0.03	2.36	0.56	0.95[a]
2.5	0.03	2.34	0.88	1.50[b]
2.5	0.03	2.30	1.80	3.13[c]

[a]70 °C.
[b]75 °C.
[c]85 °C.

TABLE 2. Kinetic data for the Rh^I–Et_2S catalyzed hydrogenation of maleic acid in DMA at 80 °C unless noted otherwise

[Rh] $\times 10^3$ (M)	[MA] (M)	[H_2] $\times 10^3$ (M)	Linear rate $\times 10^5$ ($M\,s^{-1}$)	k_2 ($M^{-1}\,s^{-1}$)
1.0	0.03	2.32	0.62	2.68
2.5	0.03	2.32	1.76	3.04
4.0	0.03	2.32	2.64	2.84
5.0	0.03	2.32	3.34	2.88
5.0	0.06	2.32	3.00	2.58
5.0	0.03	0.47	0.64	2.72
5.0	0.03	0.62	0.87	2.81
5.0	0.03	1.22	1.90	3.16
5.0	0.03	2.54	3.49	2.74
5.0	0.03	2.32	0.82	0.71[a]
5.0	0.03	2.32	0.68	0.58[b]
5.0	0.03	2.32	0.64	0.55[c]
5.0	0.03	2.32	0.66	0.57[d]
5.0	0.03	2.32	4.80	4.05[e]
5.0	0.03	2.32	4.32	3.79[f]
5.0	0.03	2.32	3.24	2.79[g]
5.0	0.03	2.32	3.21	2.76[h]
5.0	0.03	2.32	2.70	2.33[i]
5.0	0.03	2.36	1.80	1.53[j]
5.0	0.03	2.34	2.40	2.05[k]
5.0	0.03	2.30	4.32	3.76[l]

[a]0.45 *M* LiCl.
[b]0.125 *M* LiCl.
[c]0.03 *M* LiCl.
[d]0.015 *M* and 0.01 *M* LiCl.
[e]0.05 *M* *p*-toluenesulfonic acid.
[f]0.01 *M* *p*-toluenesulfonic acid.
[g]0.05 *M* cyclooctene.
[h]0.005 *M* Et_2S.
[i]D_2 in place of H_2.
[j]70 °C.
[k]74.5 °C.
[l]84 °C.

Can. J. Chem. Downloaded from www.nrcresearchpress.com by 210.87.254.42 on 09/05/12
For personal use only.

experiments in which the catalyst solutions were made up in the complete absence of oxygen. Under such conditions the rate plots for H_2 consumption analyzed for a first order dependence (*i.e.* on substrate), and the measured pseudo first order rate constants were approximately second order in [Rh] and between first and zero order in $[H_2]$.

Discussion

The k_2 values, activation parameters, and the isotope effects, are given in Table 3 with data for the Rh^{III} systems that we have studied previously. The activation parameters obtained for the Rh^{I}–Cl system are almost identical to those reported for the hydrogenation step in the $RhCl_3 \cdot 3H_2O$ catalyzed system in DMA–LiCl media, and offer convincing evidence for the same reactive Rh^{I} intermediates and the same rate determining step in both systems. The faster hydrogenation rates in the Rh^{I}–Et_2S system compared to the $RhCl_3(Et_2S)_3$ system is reflected in a lower $\Delta H_2^{\neq}$ value. However, different rhodium(I) species appear to be involved in these two systems since the ratio of Rh:Cl is different. On adding excess chloride (Cl:Rh $\geq$ 2) to the Rh^{I}–Et_2S system, which initially has one Cl per Rh, a lower limiting k_2 value of 0.56 M^{-1} s^{-1} is obtained and this is more comparable to the value of 0.33 M^{-1} s^{-1} for the $RhCl_3(Et_2S)_3$ system with three Cl per Rh. Studies on the $RhCl_3(Et_2S)_3$ system (2) showed that addition of chloride, or a strong acid, had no effect on the catalytic hydrogenation, again consistent with the present data.

The easy displacement of C_8H_{14} from $[Rh(C_8H_{14})_2Cl]_2$ has provided a general method for preparing other Rh^{I} complexes (5). The observed first order dependences on Rh give no evidence for a dimer $\rightleftharpoons$ monomer equilibrium, and indicate either that dimeric species are active or else the dimer dissociates completely to active monomer under the experimental conditions. There are a few examples of dimeric hydrogenation catalysts (ref. 3, p. 405, ref. 9), but monomeric catalysts seem highly likely in these DMA solutions with Et_2S or Cl^- cleaving the chloride bridges. Complexes such as $[Rh(CO)_2Cl]_2$ are readily cleaved by ligands, including the Cl^- ion (10), and the fact that the cyclooctene dimer is only slightly soluble in DMA but readily dissolves on addition of Cl^- or Et_2S supports monomer formation. The cyclooctene dissociates completely from the initial complex in solution, and hence Cl^-, Et_2S, or DMA will occupy the vacant coordination sites. Added cyclooctene did not interfere with the catalytic activity of such solutions. Wilkinson and coworkers (11) found that a benzene solution containing PPh_3 and $[Rh(C_8H_{14})_2Cl]_2$ (PPh_3:Rh = 3:1) gave the same kinetic results for olefin hydrogenation as using $RhCl(PPh_3)_3$ crystals in benzene.

As discussed for the previous studies using the rhodium(III) complexes (1, 2), the hydrogenations are thought to occur via the unsaturate route exemplified in reactions 2 and 3, rather than a hydride route which involves formation of a dihydride followed by reaction with olefin (ref. 3, p. 400). Indirect evidence for this is that in the absence of olefinic substrates the rhodium(I) complexes are rapidly reduced by H_2 to the metal: the sulfur ligands, for example, are weaker π-acceptors than triphenylphosphine and no stable hydrides are formed. An alternate scheme leading to the same overall kinetics is outlined in reactions 5 to 7.

$$[5] \qquad Rh^{I} + \text{olefin} \overset{K_1}{\rightleftharpoons} Rh^{I}(\text{olefin})$$

$$[6] \qquad Rh^{I} + H_2 \overset{K_2}{\rightleftharpoons} H_2Rh^{III}$$

$$[7] \qquad H_2Rh^{III} + \text{olefin} \overset{k}{\rightarrow} Rh^{I} + \text{products}$$

If K_1 is large, K_2 is small, and the Rh^{I}(olefin) complex is unreactive toward H_2, the rate law becomes $kK_2[H_2][Rh_{Total}]/K_1$. The factors governing metal precipitation, however, have not been studied, and whether the above scheme with undetectable but kinetically significant concentrations of Rh^{I} (or H_2Rh^{III}) would lead to metal production is not known with certainty. The hydride route has generally been favored for catalysis by the $RhCl(PPh_3)_3$ system which reduces *cis*-olefins faster than *trans*-olefins (maleate > fumarate), and this has been rationalized in terms of hindered approach of the substrate in a reaction such as [7] (12). The diethylsulfide system, however, reduces fumaric acid more effectively than maleic acid, and this is more readily interpreted in terms of reaction 3 involving a thermodynamically less stable Rh^{I}-

TABLE 3. Kinetic data for the hydrogenation of maleic acid using rhodium complexes in DMA

Initial complex	$k_2^{80°}$ (M^{-1} s^{-1})	$\Delta H_2^{\neq}$ (kJ mol^{-1})	$\Delta S_2^{\neq}$ JK^{-1} mol^{-1}	k_2^H/k_2^D
$RhCl_3 \cdot 3H_2O$ + LiCl[a]	1.5	76.9	−25.5	1.1
Rh^I + LiCl[b]	2.1	75.2	−28.4	—
mer-$RhCl_3(Et_2S)_3$[c]	0.33	89.4	−4.2	1.05
Rh^I + Et_2S[d]	2.85	64.8	−55.1	1.2
Rh^I + 2Et_2S + LiCl[e]	0.56	—	—	—

[a]Cl^-:Rh ≥ 100; data mostly at 1.2 *M* LiCl. Reference 1.
[b]Cl^-:Rh ≥ 100; data at 0.45 *M* LiCl; this work.
[c]Reference 2.
[d]Et_2S:Rh = 2 or 3; this work.
[e]Cl:Rh = 2 to 25; this work.

(fumaric acid) complex (8). The data in Table 3 are thus thought to refer to oxidative addition of H_2 to a square planar Rh^I–maleic acid complex.

The non-inhibition of rate on addition of one mole Et_2S to the Rh^I–Et_2S system is significant because this shows that a maximum of two sulfide ligands are coordinated per Rh. The previous work (2) had shown firstly that one Et_2S dissociated from $RhCl_3(Et_2S)_3$ prior to reduction of the complex to Rh^I, and secondly that addition of further excess sulfide had no effect on the subsequent catalytic hydrogenation. It is interesting to speculate on the nature of the various catalytic species. A likely species for reaction 3 in the Rh^I–Et_2S system is the neutral complex $RhCl(Et_2S)_2(MA)$, although we have been unable to isolate any pure Rh^I complexes from any of the catalytic systems; a maximum of one Cl per Rh can be involved, and the conductance measurements indicate no loss of chloride, at least in the absence of substrate. Several groups (13, 14) have shown that halide and not a diene ligand in complexes such as $[Rh(C_8H_{12})Cl]_2$ can be replaced in polar solvents by phosphine (L) to give solvated cationic species such as $[Rh(C_8H_{12})L_2]^+$; such species act as hydrogenation catalysts via initial dihydride formation (13). The diene ligand is presumably more strongly attached than the cyclooctene. The activation parameters for the Rh^I–Et_2S system are very similar to those reported for oxidative addition of H_2 to a number of neutral Vaska-type complexes $[IrCl(CO)L_2]$ in a range of solvents (ref. 3, p. 288), the negative activation entropy reflecting mainly the loss of translational entropy of the H_2 molecule upon coordination (15). The Rh^I–Et_2S system with added chloride could involve a less reactive $RhCl_2(Et_2S)(MA)^-$ complex, which could be the species formed *in situ* in the $RhCl_3(Et_2S)_3$ system, with addition of further chloride having little effect on reactivity as observed (2). The higher activation energy for this system is more comparable with those measured for the Rh^I–chloride systems, and these must involve anionic catalysts. These could be either $RhCl_3(MA)^{2-}$ or $RhCl_2(DMA)(MA)^-$ species. If the former, the data in Table 3 suggest decreasing reactivity toward H_2 in the trend $RhCl(Et_2S)_2(MA)$ > $RhCl_3(MA)^{2-}$ > $RhCl_2(Et_2S)(MA)^-$, which appears unlikely. The latter dichloro species thus appears more likely, and the resulting activity trend is then $RhCl(Et_2S)_2(MA)$ > $RhCl_2(DMA)(MA)^-$ > $RhCl_2(Et_2S)(MA)^-$. Oxidative addition reactions are known to be promoted by the presence of stronger σ-donors (15, 16), but in view of the limited knowledge of sulfide complexes (17) and the somewhat qualitative speculation concerning the nature of the catalytic species present, definite conclusions cannot be drawn. However, recent work from this laboratory (18) indicates that DMA is a more effective donor than chloride in some ruthenium(II) complexes (as regards reactivity toward H_2), and since chloride is a stronger donor than Et_2S (17) the relative reactivity order for the uni-negative anions seems reasonable.

The complex $RhCl_3(Et_3S)_3$ is inactive for hydrogenation in benzene solution because the initial hydrogen reduction process to Rh^I does not occur in the non-polar media (2). Wilkinson *et al.* (11) found that addition of Et_2S to $[Rh(C_8H_{14})_2Cl]_2$ in benzene (Et_2S:Rh = 2) gave inactive solutions for hydrogenation of cyclohexene, and during attempted hydrogenations the initially yellow solutions darkened during the exposure time. The results indicate that the stability and lability of the Rh^I(olefin)

Can. J. Chem. Downloaded from www.nrcresearchpress.com by 210.87.254.42 on 09/05/12
For personal use only.

Can. J. Chem. Downloaded from www.nrcresearchpress.com by 210.87.254.42 on 09/05/12
For personal use only.

complex are of paramount importance for activity of the system. Maleic acid is a better π-acceptor than cyclohexene and readily complexes with Rh^I, and the present work shows that maleic acid is hydrogenated homogeneously in preference to cyclooctene which fails to stabilize the Rh^I in DMA. Cyclooctene is similar to cyclohexene in its electronic properties and both are unlikely to stabilize Rh^I against reduction to the metal. Such reduction is almost certainly responsible for the darkening of the reaction solution noted in Wilkinson's paper. A corresponding diphenylsulfide system was said to exhibit some activity, before decomposition of the catalyst again occurred (11). If the Rh^I(olefin) complex is too stable, however, hydrogenation may not occur; this situation occurs in the case of attempted hydrogenation of tetracyanoethylene using Rh chlorides in DMA (1) and of tetrafluoroethylene using $RhCl(PPh_3)_3$ in benzene (12). An intimately related factor with these strong π-acid ligand systems is the increased electronic promotional energy necessary for the oxidative H_2 addition (12). The solvent also plays a critical role, since a maleic acid-stabilized chlororhodate(I) complex in aqueous 3 *M* HCl solution does not undergo reaction with H_2 according to reaction 3 (19). Factors for the promotion of this reaction in DMA are thought to be increased H_2 solubility, the donor power, and a possible lower dielectric constant for the non-aqueous media (1).

The short "autocatalytic" region sometimes observed at the start of the catalytic hydrogenations is attributed to some O_2 evolution from the oxygen complex (reaction 4) present in the stock catalyst solutions. The sulfide system, like the chloride system, does catalyze the oxidation of the amide solvent via an oxygen complex (4, 8), although the spectroscopic studies described for the chloride system were not carried out for the sulfide system. No autocatalytic region was observed in the hydrogenations when the catalyst solutions were made up in the absence of air, and this is consistent with O_2 having an initial deactivating effect by occupying a coordination site required for hydride or olefin. Hydrogenations catalyzed by square planar d^8 metal tertiary phosphine complexes may be markedly enhanced by the presence of traces of O_2 due to oxidation of the phosphine to non-coordinated phosphine oxide and the concomitant production of a vacant coordination site (20). Such an effect is not involved in the present Rh^I systems, as demonstrated by the good reproducibility of kinetic data, and the good agreement with data obtained from the Rh^{III} systems from which air was excluded entirely. The complex kinetic data obtained for the Rh^I–Et_2S system using the air-free catalyst solutions were therefore surprising, and are difficult to explain. The approximate second order dependence on Rh suggests that some monomer ⇌ dimer equilibrium might be involved; oxygen and a time factor could be important in promoting formation of monomeric species in the stock solutions. Some complex kinetics were observed in the $RhCl_3 \cdot 3H_2O$ catalyzed hydrogenation of MA in DMA in the absence of LiCl and these were interpreted in terms of dimeric Rh^I(MA) species.

The stoichiometric oxidation of the Rh^I(MA) complexes by O_2 at 80 °C to Rh^{III} suggests that such species will not be effective for catalytic oxygenation of olefinic substrates (21).

We thank the National Research Council of Canada and the University of British Columbia for financial support, Johnson Matthey Ltd., for loan of the rhodium, and a referee for helpful comments.

1. B. R. James and G. L. Rempel. Discuss. Faraday Soc. **46**, 48 (1968).
2. B. R. James and F. T. T. Ng. J. Chem. Soc. Dalton, 355 (1972); 1321 (1972).
3. B. R. James. Homogeneous hydrogenation. Wiley, New York. 1973.
4. B. R. James and F. T. T. Ng. Chem. Commun. 908 (1970).
5. L. Porri and A. Lionetti. J. Organomet. Chem. **6**, 422 (1966); A. van der Ent and A. L. Onderdelinden. Inorg. Syn. **XIV**, 92 (1973).
6. R. Cramer. Inorg. Chem. **1**, 722 (1962); J. Am. Chem. Soc. **88**, 2272 (1966).
7. J. P. Collman, M. Kubota, and J. Hosking. J. Am. Chem. Soc. **89**, 4809 (1967).
8. F. T. T. Ng. Ph.D. Thesis, University of British Columbia, Vancouver, British Columbia. 1970.
9. C. A. Tolman, P. Z. Meakin, D. L. Lindner, and J. P. Jesson. J. Am. Chem. Soc. **96**, 2762 (1974); B. C. Y. Hui, W. K. Teo, and G. L. Rempel. Inorg. Chem. **12**, 757 (1973).
10. L. Vallarino. Inorg. Chem. **4**, 161 (1965); D. N. Lawson and G. Wilkinson. J. Chem. Soc. 1900 (1965).
11. S. Montelatici, A. van der Ent, J. A. Osborn, and G. Wilkinson. J. Chem. Soc. A, 1054 (1968).
12. J. A. Osborn, F. H. Jardine, J. F. Young, and G. Wilkinson. J. Chem. Soc. A, 1711 (1966); F. H. Jardine, J. A. Osborn, and G. Wilkinson. J. Chem. Soc. A, 1574 (1967).
13. R. R. Schrock and J. A. Osborne. J. Am. Chem. Soc. **93**, 3089 (1971). and references therein.

14. L. M. HAINES. Inorg. Chem. **10**, 1693 (1971).
15. L. VASKA and M. F. WERNEKE. Trans. N.Y. Acad. Sci. **31**, 70 (1971).
16. M. A. BENNETT and D. L. MILNER. J. Am. Chem. Soc. **91**, 6983 (1971).
17. J. CHATT, G. J. LEIGH, and A. P. STORACE. J. Chem. Soc. A, 1380 (1971); S. E. LIVINGSTONE. Quart. Rev. **19**, 386 (1965).
18. B. R. JAMES and L. D. MARKHAM. To be published; L. D. Markham. Ph.D. Thesis, University of British Columbia, Vancouver, British Columbia. 1973.
19. B. R. JAMES and G. L. REMPEL. Can. J. Chem. **44**, 233 (1966).
20. H. VAN BEKKUM, F. VAN RANTWIJK, and T. VAN DE PUTTE. Tetrahedron Lett. 1 (1969).
21. C. W. DUDLEY, G. READ, and P. J. C. WALKER. J. Chem. Soc. Dalton, 1926 (1974).

Can. J. Chem. Downloaded from www.nrcresearchpress.com by 210.87.254.42 on 09/05/12
For personal use only.

Photocyclization Reactions of Aryl Polyenes. IX.[1] The Photocyclization of Stilbenecarboxaldehydes and 1-Formylphenyl-4-phenyl-1,3-butadienes

CARL MANNING AND CLIFFORD C. LEZNOFF
Department of Chemistry, York University, Downsview, Ontario M3J 1P3

Received September 10, 1974

CARL MANNING and CLIFFORD C. LEZNOFF. Can. J. Chem. **53**, 805 (1975).

The photocyclization–oxidation reaction of 4-stilbenecarboxaldehyde gave 3-phenanthrenecarboxaldehyde. Similarly, irradiation of 3-stilbenecarboxaldehyde gave a mixture of 2- and 4-phenanthrenecarboxaldehyde. Irradiation of 1-(*p*-formylphenyl)-4-phenyl-1,3-butadiene gave a mixture of 1-(*p*-formylphenyl)naphthalene and 8-phenyl-2-naphthaldehyde. Photocyclization of 1-(*m*-formylphenyl)-4-phenyl-1,3-butadiene yielded 1-(*m*-formylphenyl)naphthalene, 5-phenyl-2-naphthaldehyde, and 8-phenyl-1-naphthaldehyde. The surprising nature of the photocyclization–oxidation reactions of stilbenes and 1,4-diphenyl-1,3-butadienes containing formyl substituents is discussed.

CARL MANNING et CLIFFORD C. LEZNOFF. Can. J. Chem. **53**, 805 (1975).

La photocyclisation oxydative du stilbènecarboxaldéhyde-4 donne le phénanthrènecarboxaldéhyde-3. De la même manière, l'irradiation du stilbènecarboxaldéhyde-3 donne un mélange de phénanthrènecarboxaldéhyde-2 et -4. L'irradiation du (*p*-formylphényl)-1 phényl-4 butadiène-1,3 donne un mélange de (*p*-formylphényl)-1 naphtalène et de phényl-8 naphtaldéhyde-2. La photocyclisation du (*m*-formylphényl)-1 phényl-4 butadiène-1,3 conduit au (*m*-formylphényl)-1 naphtalène, aux côtés du phényl-5 naphtaldéhyde-2 et du phényl-8 naphtaldéhyde-1. On discute de la nature surprenante des produits de photocyclisation oxydative des stilbènes et des diphényl-1,4 butadiènes-1,3 portant des substituants formyle. [Traduit par le journal]

Although the photocyclization-oxidation reaction of substituted stilbenes to substituted phenanthrenes is a well-known useful preparative procedure (1, 2), the reaction fails for *p*-acetylstilbene (3), nitrostilbenes (3), and the closely related 1-nitrophenyl-4-phenyl-1,3-butadienes (4). These latter failures have been rationalized in terms of the n–π* transitions of the carbonyl and nitro groups which interfere with the normal π–π* transitions responsible for the successful photocyclization reactions in other substituted stilbenes.

The related photocyclization–oxidation reactions of 1-substituted-phenyl-4-phenyl-1,3-butadienes to substituted 1-phenylnaphthalenes, where the substituents are methoxy, methyl, fluoro, chloro, and cyano, have also been reported (5) but in light of the previous failure of *p*-acetylstilbene to photocyclize, the photocyclization of the closely related stilbenecarboxaldehydes and 1-formylphenyl-4-phenyl-1,3-butadienes were not previously attempted. One isolated example of the surprisingly successful photocyclization–oxidation of 4,4′-stilbenedicarboxaldehyde has recently been reported from our laboratory (6) and has now been extended to cover a number of formylstilbenes and 1-formylphenyl-4-phenyl-1,3-butadienes.

Irradiation of 2.5×10^{-4} *M* solutions of 4-stilbenecarboxaldehyde (**1**), synthesized by our solid-phase method (7, 8), in dry benzene containing 5×10^{-4} *M* iodine gave, after 4 days, the known 3-phenanthrenecarboxaldehyde (**2**) (9) in 40% yield as shown in Scheme 1. Similarly,

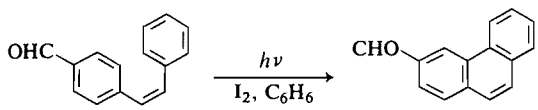

1 **2**

SCHEME 1

irradiation of 3-stilbenecarboxaldehyde (**3**) (7) gave a mixture of 2-phenanthrenecarboxaldehyde (**4**) and 4-phenanthrenecarboxaldehyde (**5**) in 25% yields as shown in Scheme 2.

Fractional crystallization of the product mixture resulted in the isolation and separation of pure **4** and **5**, the former of which was compared with the known **4** prepared as previously des-

[1]For part VIII see ref. 6.

Can. J. Chem. Downloaded from www.nrcresearchpress.com by 210.87.254.40 on 09/05/12
For personal use only.

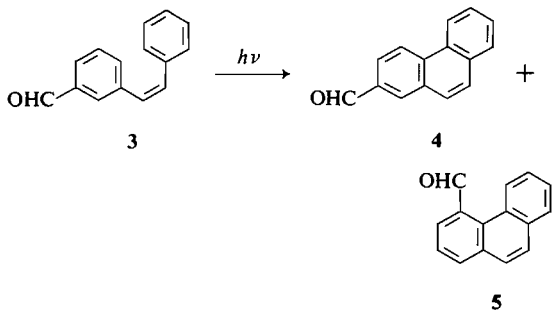

3 4 5

SCHEME 2

cribed (9) and the latter synthesized as described in the Experimental section. The ratio of **4** to **5** was approximately 10:1 based on the pure isolated compounds. Photocyclization of simple *m*-substituted stilbenes normally gives 2- and 4-substituted phenanthrenes in a 1:1 ratio (10), although photocyclization of *m*-hydroxystilbene yielded a 3:1 ratio of 2- to 4-hydroxyphenanthrenes (11).

In the photocyclization reactions of 1-substituted phenyl-4-phenyl-1,3-butadienes, there are two possible modes of cyclization, *i.e.* to the substituted or unsubstituted phenyl group. Although previous work (5) had established that the nature of the substituent had only minor influence (except for the fluoro substituent) on the direction of photocyclization, the reported failure of the photocyclization of the stilbene with an acetyl group led us to believe that the formyl group would either inhibit photocyclization or cause a dramatic influence on the direction of photocyclization.

Irradiation of 2×10^{-4} *M* solutions of 1-(*p*-formylphenyl)-4-phenyl-1,3-butadiene (**6**), prepared by our solid-phase method (7), in dry benzene containing 5×10^{-4} *M* iodine gave after 4 days a mixture of 1-(*p*-formylphenyl) naphthalene (**7**) and 8-phenyl-2-naphthaldehyde (**8**) in 35% yield as shown in Scheme 3.

Both **7** and **8** were synthesized by known procedures (9) from the appropriate methyl substituted aromatic compound. The n.m.r. spectrum of the synthesized **7** exhibited an absorption typical of an aldehydic proton at 10.00 p.p.m., whereas the aldehydic proton of synthesized **8** absorbed at 10.08 p.p.m. The n.m.r. spectrum of the mixture of **7** and **8** obtained by photocyclization of **6** exhibited appropriate absorption at 10.00 and 10.08 p.p.m., respectively, in an integrated ratio of 4:1, which strongly

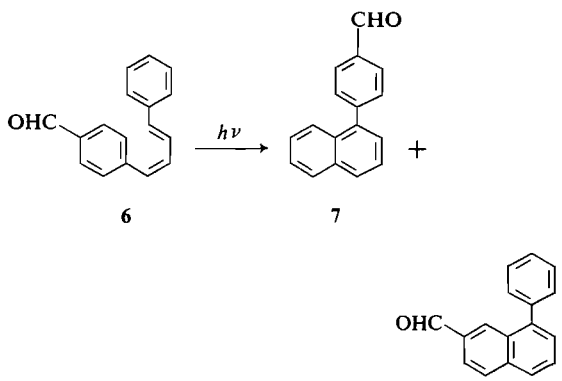

6 7 8

SCHEME 3

suggests that photocyclization occurs preferentially to the unsubstituted phenyl group of **6**.

Similarly, irradiation of 1-(*m*-formylphenyl)-4-phenyl-1,3-butadiene (**9**) (7) gave a mixture of 1-(*m*-formylphenyl)naphthalene (**10**), 5-phenyl-2-naphthaldehyde (**11**), and 8-phenyl-1-naphthaldehyde (**12**) in 40% yield as shown in Scheme 4.

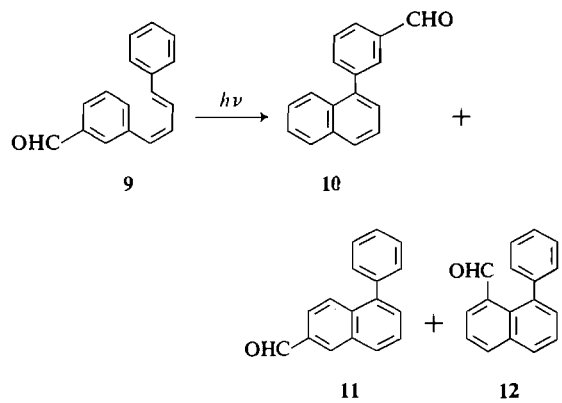

9 10 11 12

SCHEME 4

The 220 MHz n.m.r. spectrum of the mixture of **10**, **11**, and **12** showed absorptions for aldehydic protons at 10.22, 10.42, and 10.02 p.p.m. The assignment of the absorption at 10.02 p.p.m. to the aldehydic proton of **12** is assured as only this aldehydic proton is shielded by the phenyl group at the 8 position of the naphthalene nucleus. In addition, it is expected that **12** would be formed in lowest yield as formation of **12** involves photocyclization to a hindered *ortho* position (5). An absolute assignment of the aldehydic absorptions at 10.22 and 10.42 p.p.m.

Can. J. Chem. Downloaded from www.nrcresearchpress.com by 210.87.254.40 on 09/05/12
For personal use only.

TABLE 1. Spectral characteristics of the aromatic aldehydes obtained as photoproducts

Compound	Nuclear magnetic resonance spectra* δ (p.p.m.)	Ultraviolet spectra λ_{max} (nm) (ε)	Infrared spectra γ(cm^{-1})	Mass spectra† *m/e* M^+, other peaks
5	—	—	2730(w), 1702(s)	206(100), 177(70)
7	10.00	291(8300)	2730(w), 1705(s)	232(68), 203(90), 74(100)‡
8	10.08	289(3480)	2725(w), 1700(s)	232(68), 203(90), 74(100)‡
10 + 11 + 12	10.22, 10.42, 10.02	290	2720(w), 1700(s)	232(14), 203(18), 74(100)

*These values refer to the aldehydic protons.
†Figures in brackets represent percentage of base peak.
‡This mass spectrum was a mixture of 7 and 8.

TABLE 2. Synthetic aromatic aldehydes

Compound	Yield (%)	Molecular formula	Analysis (%) Found C	Found H	Calculated C	Calculated H
5	3*	$C_{15}H_{10}O$	87.10	4.78	87.35	4.89
7	15	$C_{17}H_{12}O$	87.84	5.07	87.92	5.17
8	3	$C_{17}H_{12}O$	87.72	5.02	87.92	5.17

*The yield from photolysis of 3 was 2.5%.

must remain unresolved but together indicate the presence of **10** and **11**.[2]

The mass spectra of the photoproducts of **1** and **3**, *i.e.* **2** and **4** plus **5** respectively, all exhibited molecular ions at M^+ 206 and the expected fragmentation ions $M^+ - CHO$ at 177. The mass spectra of the mixtures of **7** plus **8** and **10** plus **11** plus **12** obtained from photocyclization of **6** and **9** respectively all exhibited parent ions at M^+ 232 and fragmentation ions $M^+ - CHO$ at 203, all consistent with the assigned structures.

Although the successful photocyclization–oxidation reactions of **1** and **3** to **2** and **4** plus **5**, respectively, are surprising, considering the fact that *p*-acetylstilbene did not photocyclize, several reports in the literature *do* suggest that aromatic aldehydes and ketones can react differently under photochemical conditions. The triplet state energies of acetophenone and benzaldehyde differ by ~2 kcal/mol (12, 13), the latter being lower. The lifetimes of the triplet states of benzaldehydes are shorter than the corresponding acetophenones (14).

Since it is highly likely that photocyclization occurs by way of an excited singlet state (15) and that the lifetimes of these states are comparable for the formyl and acetyl derivatives, the relative inefficiency of the acetyl derivatives to undergo photocyclization can be accounted for in terms of their long-lived triplet states. Thus the population of molecules in the triplet state is lower for the formyl derivatives than the acetyl derivatives. If all other effects are equal (intersystem crossing in aryl carbonyls occurs with unit efficiency), the relative population in the first excited singlet state of the formyl derivatives would be greater than acetyl derivatives.

Experimental

All m.p.'s were determined on a Kofler hot stage and are uncorrected. The i.r. spectra were recorded on a Unicam SP1000 spectrometer either as neat liquids or in a Nujol mull. The u.v. spectra were measured using a Unicam SP1800 spectrometer and cyclohexane as solvent. The n.m.r. spectra were measured on a Varian A60 spectrometer using tetramethyl silane as interval standard (δ = 0) and deuteriochloroform as solvent. The 220 MHz spectrum was recorded by the Ontario Research Foundation using a HR-220 Varian spectrometer. Mass spectra were measured on a Hitachi-Perkin-Elmer RMU-6 spectrometer. Both thin- and thick-layer chromatography were performed using silica gel as adsorbent and benzene as the eluant. All photochemical reactions were carried out in a Rayonet photochemical reactor using RPR-3500 Å lamps. Microanalyses were performed by Dr. C. Daesslé of Montreal.

[2]Several attempts were made to synthesize **10** and **11** unambiguously from 1-(*m*-tolyl)naphthalene and 6-methyl-1-phenylnaphthalene in the same way as **7** and **8** were prepared, but with no success. Other methods were also unsuccessful.

Can. J. Chem. Downloaded from www.nrcresearchpress.com by 210.87.254.40 on 09/05/12
For personal use only.

Irradiation of the Stilbenes and Butadienes

The irradiations of **1**, **3**, **6**, and **9** were carried out in a manner previously described (5). The mixtures of photoproducts were obtained as a single band on preparative thick-layer chromatography and the spectral data, given in Table 1, of these mixtures were obtained and compared with some of the products prepared by classical means.

4-Phenanthrenecarboxaldehyde (**5**), m.p. 88–91°, was separated from **4** by fractional crystallization from ether at 5° for 3 days. Synthetic **5**, m.p. 88–91°, did not show a depressed m.p. on admixture with **5** prepared by photolysis.

Synthesis of 4-Phenanthrenecarboxaldehyde (5), 1-(p-Formylphenyl)naphthalene (7), and 8-Phenyl-2-naphthaldehyde (8)

Compounds **5**, **7**, and **8** were synthesized from 4-methylphenanthrene (16), 1-(*p*-tolyl)naphthalene (17), and 7-methyl-1-phenylnaphthalene (18) by the known procedure of Cymerman–Craig *et al.* (9) and their spectral and analytical data are given in Tables 1 and 2, respectively.

The authors gratefully acknowledge the help of the Atkinson Charitable Foundation for a grant in aid of this research, the Ontario Research Foundation for running the 220 MHz n.m.r. spectrum, and Dr. E. Lee-Ruff and a referee for helpful suggestions.

1. C. S. Wood and F. B. Mallory. J. Org. Chem. **29**, 3373 (1964).
2. E. V. Blackburn and C. J. Timmons. Q. Rev. **23**, 482 (1964).
3. F. B. Mallory, C. S. Wood, and J. T. Gordon. J. Am. Chem. Soc. **86**, 3094 (1964).
4. C. C. Leznoff and R. J. Hayward. Can. J. Chem. **49**, 3596 (1971).
5. C. C. Leznoff and R. J. Hayward. Can. J. Chem. **48**, 1842 (1970).
6. J. Y. Wong, C. Manning, and C. C. Leznoff. Ang. Chem. Int. Ed. **13**, 666 (1974).
7. C. C. Leznoff and J. Y. Wong. Can. J. Chem. **51**, 3756 (1973).
8. C. C. Leznoff. Chem. Soc. Rev. **3**, 65 (1974).
9. J. Cymerman-Craig, J. W. Loder, and B. Moore. Aust. J. Chem. 222 (1956).
10. F. B. Mallory and C. W. Mallory. J. Am. Chem. Soc. **94**, 6041 (1972).
11. H. Güsten and L. Klasinc. Tetrahedron, **24**, 5499 (1968).
12. W. G. Herkstroeter, A. A. Lamola, and G. A. Hammond. J. Am. Chem. Soc. **86**, 4537 (1964).
13. D. R. Kearns and W. A. Case. J. Am. Chem. Soc. **88**, 5087 (1966).
14. E. C. Lin, Y. H. Li, and R. Li. J. Chem. Phys. **53**, 2443 (1970).
15. K. A. Muszkat and E. Fischer. J. Chem. Soc. (*B*) 662 (1967).
16. R. D. Haworth. J. Chem. Soc. 1125 (1932).
17. F. Bergmann and A. Weizmann. J. Org. Chem. **9**, 352 (1944).
18. J.-M. Bonnier and J. Rinaudo. Bull. Chem. Soc. Fr. 148 (1970).

Can. J. Chem. Downloaded from www.nrcresearchpress.com by 210.87.254.40 on 09/05/12
For personal use only.

Fluorinated Alkoxides. Part VIII. Mixed Ligand Complexes of Perfluoropinacol with Ni^{2+}, Pd^{2+}, Pt^{2+} and Cu^{2+}. Solvation Equilibria between 4- and 5-coordinate Ni^{2+}

W. Stafford Cripps and Christopher J. Willis

Department of Chemistry, University of Western Ontario, London, Ontario N6A 3K7

Received October 24, 1974

W. Stafford Cripps and Christopher J. Willis. Can. J. Chem. **53**, 809 (1975).

Perfluoropinacol, $(CF_3)_2C(OH)C(OH)(CF_3)_2$, ionizes by loss of two protons, and the resulting dinegative ion (PFP^{2-}) chelates to Ni^{2+}, Pd^{2+}, Pt^{2+}, and Cu^{2+}. A variety of stable neutral complexes may be isolated if the tetracoordination of the metal ion is completed with two monodentate or one bidentate nitrogen- or phosphorus-containing ligands; square-planar structures are invariably found. The structures of these complexes are contrasted with those of analogous halides, and it is concluded that electronic effects are predominant in determining them, although steric influences may sometimes be important. The ligand field strength of the perfluoropinacolato ion is approximately equal to that of the thiocyanate ion.

The nickel complexes $Ni(PFP)_2^{2-}$ and $(PFP)Ni(RNHCH_2CH_2NHR)$ react with donor solvents (water, methanol, pyridine, etc.) to give equilibria between four- and five-coordinate solvated species; six-coordinate species are not observed. This unusual behavior is attributed to the steric hindrance imposed by the bulk of the PFP^{2-} ligand.

W. Stafford Cripps et Christopher J. Willis. Can. J. Chem. **53**, 809 (1975).

Le perfluoropinacol, $(CF_3)_2C(OH)C(OH)(CF_3)_2$, s'ionise par perte de deux protons et l'ion dinégatif qui en résulte (PFP^{2-}) se chélate au Ni^{2+}, au Pd^{2+}, au Pt^{2+} et au Cu^{2+}. On peut isoler une variété de complexes neutres stables si la tétracoordination de l'ion métallique est complétée par deux ligands monodentates ou un ligand bidentate contenant de l'azote ou du phosphore; on trouve invariablement des structures plan-carré. Les structures de ces complexes sont en opposition avec celles des halogénures analogues et on en conclut que les effets électroniques sont prédominants dans leur détermination quoique des influences stériques peuvent quelquefois être importantes. La force du champ de ligand des ions perfluoropinacolato est approximativement égale à celle de l'ion thiocyanate.

Les complexes de nickel $Ni(PFP)_2^{2-}$ et $(PFP)Ni(RNHCH_2CH_2NHR)$ réagissent avec des solvants donneurs (eau, méthanol, pyridine etc.) pour conduire à des équilibres entre des espèces solvatées et tétra ou pentacoordonnées; on n'observe aucune espèce hexacoordonnée. On attribue cette attitude anormale à des facteurs stériques imposés par la grosseur du ligand PFP^{2-}.

[Traduit par le journal]

We have previously demonstrated the value of perfluoropinacol, $HOC(CF_3)_2C(CF_3)_2OH$ (H_2PFP),[1] as a ligand to first-row transition metals (*1*). Because of the acidity of the two protons, resulting from the fluorination of the molecule, perfluoropinacol coordinates to transition metal ions as the chelating dianion, $[OC(CF_3)_2C(CF_3)_2O]^{2-}$ (PFP^{2-}), and stable complexes of Al^{3+}, VO^{2+}, CrO^{3+}, Mn^{3+}, Fe^{3+}, Co^{2+}, Ni^{2+}, Cu^{2+}, and Zn^{2+} have been prepared by reaction in solution and isolated. An analogous chelate is the oxalate ion, and the complexes $[Fe(C_2O_4)_3]^{3-}$ and $[Fe(PFP)_3]^{3-}$ appear to be similar. However, the coordination of oxalate is complicated by the possible bidentate mode of attachment of each carboxylate group, so the PFP dianion offers a useful example of an unambiguously bidentate, dinegative ligand. The resemblance between a fluorinated ligand and a halide ion has been noted elsewhere (*2*) and we find many similarities between the complexes formed by PFP^{2-} and those formed by a pair of chloride ions. This approach, in fact, is probably more useful than the formalism of comparing PFP^{2-} derivatives with alkoxides, since the fluorination of the alcohol confers on H_2PFP properties quite different from those of an unfluorinated alcohol. Our aim has therefore been to prepare a number of metal complexes of PFP^{2-} and compare their properties with analogous halide derivatives.

Those complexes which we have previously reported have been anionic species containing two or three PFP^{2-} ions. In the present work, we describe some neutral mixed ligand complexes in which one PFP^{2-} chelate and one or more

[1]Throughout this paper, we abbreviate the name of this compound to H_2PFP and its dianion to PFP^{2-}.

Can. J. Chem. Downloaded from www.nrcresearchpress.com by 210.87.254.6 on 09/05/12
For personal use only.

Can. J. Chem. Downloaded from www.nrcresearchpress.com by 210.87.254.6 on 09/05/12
For personal use only.

neutral ligands are attached to a dipositive metal ion. Many of these are compounds of nickel, where the extensive known chemistry of analogous halide derivatives has shown the possibility of various geometries of coordination for this element. We have also studied some PFP^{2-} complexes of copper(II), palladium(II), and platinum(II).

Previous work on nickel(II) has demonstrated the existence of complexes with octahedral, square planar, and tetrahedral geometries. The last description has been generally applied to a class of nonplanar, four-coordinate, paramagnetic species, even when the structure departs from strictly tetrahedral symmetry; we shall follow that practice. The tetrahalo-ions $[NiX_4]^{2-}$ (X = Cl, Br, I) are tetrahedral, whereas the phosphine–halo complexes $(R_3P)_2NiX_2$ are generally *trans*-square planar for trialkylphosphines and tetrahedral for triarylphosphines. With mixed alkyl–aryl phosphines, *e.g.* $C_2H_5P(C_6H_5)_2$, either or both geometries may be found, depending on the halide used and the conditions of reaction. Bidentate phosphines give *cis*-square planar structures.

The different geometries of coordination found in these compounds may be rationalized on either steric or electronic grounds, noting that the ligands of higher ligand field strength favor the square planar configuration in a d^8 system, and most workers have concluded that the latter effect is dominant. Although the bulkier phosphine ligands produce the tetrahedral configurations, the structures suggest that the greater degree of steric interaction is between the two halide ions. In $[(C_6H_5)_3P]_2NiCl_2$, for example, the P—Ni—P angle is 117°, while the Cl—Ni—Cl angle is 123° (3); the corresponding angles in $[(C_6H_5)_3P]_2NiBr_2$ are 110 and 126° (4). PFP^{2-} is a bulky ligand overall, but it should take up less space in the immediate coordination sphere of nickel than does a pair of halide ions. The O—Ni—O angle in the chelate ring of the square planar complex $[Ni(PFP)_2]^{2-}$ has been found to be 91° (5), so one might expect, on steric grounds, that a square planar configuration would be more likely for a phosphine–PFP nickel complex than for a phosphine–halo complex, even though a *cis*-configuration is imposed on the phosphines in the former.

We have therefore prepared a series of phosphine–PFP complexes of nickel and examined their properties. Compounds isolated were $[(C_2H_5)_3P]_2Ni(PFP)$, $[(CH_3)_2P(C_6H_5)]_2Ni(PFP)$, $[CH_3P(C_6H_5)_2]_2Ni(PFP)$, $[(C_6H_5)_3P]_2Ni(PFP)$, and (diphos)Ni(PFP) (diphos = 1,2-bis(diphenylphosphino)ethane). All five of these complexes are yellow-orange and diamagnetic, from which we conclude that they all have a *cis*-square planar configuration. A comparison of their electronic spectra in the solid state and in solution (Table 1) shows essentially no difference between the two, indicating that there is no appreciable interaction between molecules in the solid state; the bulky nature of the ligands would, of course, be expected to preclude polymerization.

The availability of structurally similar complexes of halide ions and PFP^{2-} enables us to compare the ligand field strengths of these anions. For the square planar complexes $[(C_2H_5)_3P]_2NiX_2$, the first transition is found at

TABLE 1. Visible spectra

Compound	Absorption maxima (cm^{-1})(ε)*
$K_2Ni(PFP)_2$	18200; 15600 (sh) (d.r.)
$[P(C_2H_5)_3]_2Ni(PFP)$	21800 (d.r.)
	21800 (254) (m)
	21800 (230) (b)
$[C_6H_5P(CH_3)_2]_2Ni(PFP)$	22000 (d.r.)
	21800 (263) (m)
	22000 (302) (b)
$[(C_6H_5)_2PCH_3]_2Ni(PFP)$	21600 (d.r.)
	21500 (270) (m)
	21600 (316) (b)
$[(C_6H_5)_3P]_2Ni(PFP)$	21000 (d.r.)
	21000 (274) (b)
[diphos]Ni(PFP)	22400 (d.r.)
	22500 (298) (m)
	22700 (314) (b)
[TMED]Ni(PFP)	20400 (d.r.)
	20000 (75) (m)
[TEED]Ni(PFP)	19400 (d.r.)
	19400 (70) (m)
[bipy]Ni(PFP)	24000 (d.r.)
	25600 (1640) (m)
[dibenzen]Ni(PFP)	20000 (54) (d)
[diethen]Ni(PFP)	19900 (46) (d)
[DETA]Ni(PFP)	11900; 12800; 15700; 21500; 26300 (d.r.)
	6900 (15); 11900 (12); 12800 (10); 15700 (20); 21200 (sh); 26200 (65) (m)
[TMED]Cu(PFP)	16700 (d.r.)
	17900 (68) (m)
	18200 (63) (d)
[TEED]Cu(PFP)	16400 (d.r.)
	18000 (56) (m)
	18000 (59) (d)

*sh = shoulder, d.r. = diffuse reflectance. Solvents: m = methanol, b = benzene, d = dichloromethane.

Can. J. Chem. Downloaded from www.nrcresearchpress.com by 210.87.254.6 on 09/05/12
For personal use only.

the following wavelengths: I^- at 610 nm, Br^- at 542 nm, Cl^- at 490 nm, SCN^- at 450–525 nm, and $PFP^{2-}/2$ at 460 nm.

We therefore place PFP^{2-} approximately equal to SCN^- in the spectrochemical series, with a greater ligand field strength than the halide ions, and observations on other PFP^{2-} derivatives are consistent with this assessment (6). The square planar geometry of the PFP^{2-} derivatives of nickel(II) is therefore entirely consistent with the greater ligand field strength, as compared with halide ions, so we cannot distinguish between steric and electronic effects in this series.

In an attempt to elucidate this point further, we have prepared nickel(II) complexes with PFP^{2-} and nitrogen donors. Unidentate bases such as pyridine or triethylamine were found to be unsuitable for the preparation of neutral complexes of the type $(R_3N)_2Ni(PFP)$, giving instead ionic salts $[R_3NH^+]_2[Ni(PFP)_2{}^{2-}]$. However, the use of tetra-*N*-alkyl substituted diamines such as tetramethylethylenediamine (TMED) or tetraethylethylenediamine (TEED) gave the desired complexes (TMED)Ni(PFP) and (TEED)Ni(PFP). As with the phosphine complexes, these were diamagnetic, and we therefore assume them to be *cis*-square planar, both in the solid and in solution.

In comparing these with the corresponding dihalide complexes, the position is more complicated than was the case for the phosphine complexes, since octahedral geometry occurs. $(TMED)NiCl_2$ contains octahedrally coordinated nickel in the solid state, presumably through bridging halide ions, and an octahedral–tetrahedral equilibrium exists in solution (7). The dibromide and di-iodide are exclusively tetrahedral, while the thiocyanate complex $(TMED)Ni(NCS)_2$ is insoluble and octahedral with bridging-NCS groups. It would seem likely that the occurrence of tetrahedral geometry in monomeric $(TMED)NiCl_2$ is the result of electronic, rather than steric, factors, since the metal readily increases its coordination to six by association of the complex, and the change to square planar coordination when PFP^{2-} replaces two Cl^- is consistent with the greater ligand field strength of the former. This view is confirmed by the persistence of square planar geometry in PFP^{2-} complexes when TMED is replaced by TEED or the even bulkier ligand $[C_6H_5CH_2(CH_3)NCH_2—]_2$.

The ligand 2,2′-bipyridyl (bipy) forms a series of complexes with nickel halides, with the nickel ion being uniformly six-coordinate. The compound $(bipy)_2NiCl_2$ is a monomeric nonelectrolyte (8), while $(bipy)NiCl_2$ is polymeric and octahedral through halide bridging (9); the corresponding bromides are similar (10). By contrast, we find the complex (bipy)Ni(PFP) to be monomeric and diamagnetic, and hence presumably square planar. It does not take up additional ligand to give $(bipy)_2Ni(PFP)$, nor does it form an octahedral dihydrate, as does $(bipy)NiCl_2$ (11). These results would be expected from the overall bulk of the PFP^{2-} ligand, which would tend to disfavor six-coordinate species. As for the configuration at the nickel atom in the four-coordinate complex, studies on many systems containing aromatic nitrogen donors and halide ions have shown a very fine balance between tetrahedral and square planar structures (12). Although the occurrence of the latter in (bipy)Ni(PFP) is entirely consistent with the greater ligand field strength of PFP^{2-}, the dominant effects here are probably the steric requirements of the chelating bipyridyl and PFP^{2-} rings.

Our general conclusion from a study of the nickel complexes formed by PFP^{2-} is that electronic effects make the more important contribution to determining whether 4-coordinate species adopt a tetrahedral or square-planar conformation. However, the bulk of the PFP^{2-} ligand effectively prevents the formation of a one-atom bridge between two metal ions (as commonly happens with halide ions), so the ready formation of complexes of six-coordinate nickel is prevented.

Solvation Effects and Five-coordinate Nickel

In the solid state, the nickel complexes of PFP^{2-} discussed above were invariably four-coordinate and square planar, but in several cases a change in the coordination number of the nickel through interaction with the solvent occurred in solution. For example, $K_2Ni(PFP)_2$, a purple solid, gave a yellow solution in water but purple solutions in dry methanol or ether; the latter became yellow on the addition of water. The visible spectra (Fig. 1) showed that the latter color was associated with the development of a strong absorption peak near 400 nm. By contrast, the red complex (TMED)Ni(PFP) showed no color change in a variety of solvents, suggest-

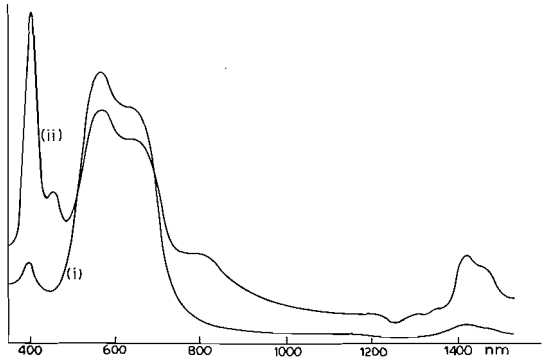

FIG. 1. Visible absorption spectrum of $K_2Ni(PFP)_2$ in (*i*) anhydrous ether, (*ii*) ether containing 1% water.

ing that the bulky tetra-*N*-alkylated ligand was preventing solvation.

Since the neutral diamine–PFP^{2-} complexes of nickel have favorable solubilities and are considerably more stable in solution than $Ni(PFP)_2^{2-}$ (which is decomposed by basic solvents), we prepared complexes using some *N*,*N*′-disubstituted diamines, in the hope that they would be less hindered and suitable for a study of solvation effects. The diamines *N*,*N*′-diethylethylenediamine (diethen) and *N*,*N*′-dibenzylethylenediamine (dibenzen) proved satisfactory, giving the complexes (diethen)Ni(PFP) and (dibenzen)Ni(PFP) as red diamagnetic solids giving red solutions in dichloromethane whose visible spectra showed a single absorption peak near 500 nm, very similar to those of the compounds (TMED)Ni(PFP) and (TEED)Ni(PFP). However, in the presence of coordinating solvents such as water, pyridine, or dimethylformamide (DMF), the solutions became green in color and the spectra changed, with the appearance of a peak at 370–390 nm. Spectra recorded in a range of solvent mixtures (Figs. 2 and 3) showed two isosbestic points, indicating that only two species were present. Pronounced thermochroic behavior was also shown, *e.g.*, the DMF solution of (dibenzen)Ni(PFP), reddish-brown at 25°, became bright green on cooling, while a methanolic solution, containing sufficient water to produce a green color at 25°, reverted to red on heating. A purple solution of $K_2Ni(PFP)_2$ in anhydrous methanol became yellow on cooling to −80°.

Although the majority of square planar nickel(II) complexes become six-coordinate if they undergo solvation, the appearance of these

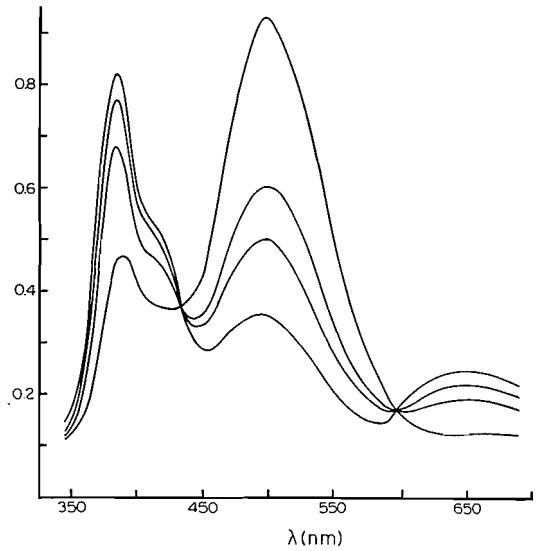

FIG. 2. Visible absorption spectra of (dibenzen)Ni(PFP) in water/methanol mixtures.

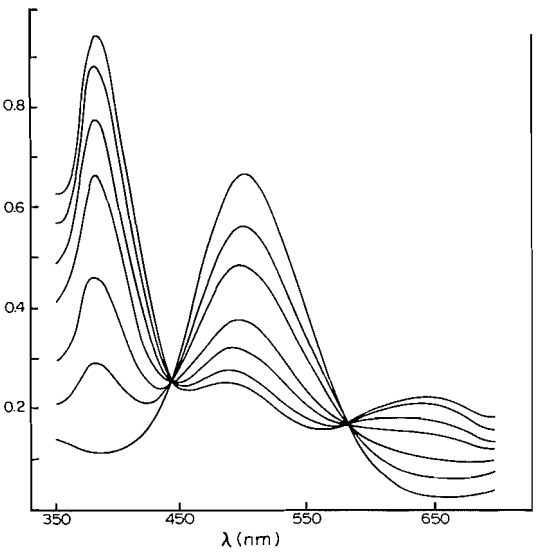

FIG. 3. Visible absorption spectra of (dibenzen)Ni(PFP) in pyridine/dichloromethane mixtures.

spectra suggested that, in this case, we were observing five-coordination. In support of this, we estimated the ratio of solvated to unsolvated species in mixed solvent from optical densities, and found this to be directly proportional to the concentration of donor solvent, as would be expected from an equilibrium of the type

$$\text{(dibenzen)Ni(PFP)} + \text{L} \rightleftharpoons \text{(dibenzen)NiL(PFP)}$$

Can. J. Chem. Downloaded from www.nrcresearchpress.com by 210.87.254.6 on 09/05/12
For personal use only.

Can. J. Chem. Downloaded from www.nrcresearchpress.com by 210.87.254.6 on 09/05/12
For personal use only.

The formation of the solvated complex is, in each case, favored by a decrease in temperature. As additional support for our suggestion that these solutions contain five-coordinate nickel, we prepared a neutral complex of Ni^{2+} with PFP^{2-} and the tridentate ligand diethylenetriamine, $NH_2CH_2CH_2NHCH_2CH_2NH_2$ (DETA). The product, (DETA)Ni(PFP), was a stable green solid, differing from the complexes prepared previously by being paramagnetic (μ_{eff} = 3.14 B.M.). It was a nonelectrolyte in methanol solution, eliminating the possibility that it could be the ionic compound $[Ni(DETA)_2]^{2+}[Ni(PFP)_2]^{2-}$, and its visible spectrum was very similar to those of our postulated five-coordinate solvates, and also to those of such well-characterized five-coordinate species as $ClNiN[CH_2CH_2N(CH_3)_2]_3 \cdot Cl$ (13). We therefore conclude that (DETA)Ni(PFP) is a monomeric species containing five-coordinate, highspin, nickel(II), whereas the analogous halide complexes (DETA)NiX_2 (X = Cl^-, Br^-), are dimeric through halide bridging and contain octahedral nickel (14).

The visible spectrum of (diethen)Ni(PFP) in dichloromethane solution containing benzylamine was very similar to that of (DETA)Ni(PFP), apart from a residual peak at 500 nm due to remaining four-coordinate species, supporting our suggestion that they are structurally alike.

The behavior of (diethen)Ni(PFP) and (dibenzen)Ni(PFP) in solution shows that they form five-coordinate 1:1 adducts with a wide variety of ligands. Ready addition occurs with good donors (water, pyridine, primary amines), which interact strongly even in low concentration, while poorer donors (methanol, ether, DMF) only give adducts in high concentrations or at low temperatures. Bulkier ligands (tertiary amines or phosphines) show no sign of interaction. Within the limitations imposed by its stability, the behavior of $Ni(PFP)_2{}^{2-}$ is similar. The restriction of solvation to a single molecule of ligand is clearly due to the bulk of the PFP^{2-} ion. Examination of molecular models shows that a distortion of the planar arrangement, which would be expected to accompany the attachment of one solvent molecule, produces a conformation of the PFP^{2-} ligand in which the CF_3 groups offer considerable hindrance to the sixth coordination site. However, it is surprising that there is insufficient room even for a second molecule of water, and this appears to be the first reported example of an equilibrium between square-planar and five-coordinate geometry for nickel associated with the addition of one water molecule.

In previous work, an equilibrium involving five coordination has been seen in the addition of pyridine to the square-planar bis(diethyldithiophosphato)nickel (15), but that system was also in equilibrium with the octahedral complex formed by the addition of a second pyridine molecule. In our studies so far, we have not seen any evidence for a six-coordinate species. It is hoped that additional information on these novel equilibria will be obtained from quantitative studies now in progress.

Copper Complexes

In the synthesis of neutral PFP^{2-} complexes of copper(II), we found *N*-alkyl substituted ethylenediamines to be the most useful co-ligands, and the complexes (TMED)Cu(PFP) and (TEED)Cu(PFP) were prepared. On the basis of their visible absorption spectra (Table 1), we suggest a square-planar configuration for these compounds. Both showed a single, broad, absorption near 550 nm with $\varepsilon \approx 60$. The spectrum did not alter when the solvent was changed from dichloromethane to methanol, showing that the latter was not coordinating to the metal.

The analogous halogen complexes (TMED)$CuCl_2$ and (TMED)$CuBr_2$ have similar absorption spectra with peaks at 700 nm (ε = 144) and 752 nm (265), respectively ($C_2H_4Cl_2$ solution) (16), which the authors consider to be consistent with an essentially planar structure, and the shift to higher energy in the position of the absorption with PFP^{2-} complexes is consistent with the greater ligand field strength of this ligand in a similar structure. However, this evidence is not strong enough to preclude some distortion from a planar configuration in the PFP^{2-} derivatives.

Palladium and Platinum Complexes

The PFP^{2-} ligand is obviously a "hard" base, in view of its structure and its ready coordination to such hard acids as Fe^{3+}, Al^{3+}, VO^{2+}, and CrO^{3+}. It would therefore be expected to show a lesser tendency to complex with the softer acids Pd^{2+} and Pt^{2+}, and our experiments have confirmed this. We were unable to prepare the anionic complexes $[Pd(PFP)_2]^{2-}$ or $[Pt(PFP)_2]^{2-}$ under conditions where Ni^{2+} readily reacted. However, the mixed ligand phosphine complexes

Can. J. Chem. Downloaded from www.nrcresearchpress.com by 210.87.254.6 on 09/05/12
For personal use only.

TABLE 2. Analytical data

Compound	Formula	Carbon		Hydrogen		Fluorine		Other	
		Calcd.	Found	Calcd.	Found	Calcd.	Found	Calcd.	Found
$K_2[Ni(PFP)_2]$	$C_{12}F_{24}O_4K_2Ni$	18.0	17.6	—	0.2	56.9	56.7	Ni: 7.3	7.3
Ni(en)(PFP)	$C_8H_8F_{12}N_2O_2Ni$	21.3	21.2	1.8	2.3	50.6	50.2	Ni: 13.0	12.8
								N: 6.2	6.4
Ni(TMED)(PFP)	$C_{12}H_{16}F_{12}N_2O_2Ni$	28.9	28.7	2.9	3.2			Ni: 11.5	11.6
								N: 6.2	5.5
Ni(TEED)(PFP)	$C_{16}H_{24}F_{12}N_2O_2Ni$	34.1	34.8	4.3	4.7	40.5	41.6	Ni: 10.4	10.4
								N: 5.0	5.0
Ni(bipy)(PFP)	$C_{16}H_8F_{12}N_2O_2Ni$	35.1	35.0	1.5	1.7	41.7	41.8	Ni: 10.7	10.8
Ni(DETA)(PFP)	$C_{10}H_{13}F_{12}N_2O_2Ni$	24.3	24.2	2.6	3.0	46.1	46.3	Ni: 11.9	12.1
$Ni[(C_2H_5)_3P]_2(PFP)$	$C_{18}H_{30}F_{12}O_2P_2Ni$	34.1	34.5	4.9	4.8	39.5	36.4	Ni: 9.6	9.4
								P: 9.7	9.9
$Ni[(CH_3)_2(C_6H_5)P]_2(PFP)$	$C_{22}H_{22}F_{12}O_2P_2Ni$	39.6	39.5	3.3	3.4	34.2	34.4		
$Ni[CH_3(C_6H_5)_2P]_2(PFP)$	$C_{32}H_{26}F_{12}O_2P_2Ni$	48.6	48.4	3.3	3.5				
$Ni[(C_6H_5)_3P]_2(PFP)$	$C_{42}H_{30}F_{12}O_2P_2Ni$	55.1	55.0	3.3	3.4	24.9	25.2		
Ni(diphos)(PFP)	$C_{32}H_{24}F_{12}O_2P_2Ni$	48.7	47.9	3.0	3.6	28.9	30.7		
$Pd[(CH_3)_2(C_6H_5)P]_2(PFP)$	$C_{22}H_{22}F_{12}O_2P_2Pd$	37.0	36.7	3.1	2.9	31.9	31.9		
$Pt[(CH_3)_2(C_6H_5)P]_2(PFP)$	$C_{22}H_{22}F_{12}O_2P_2Pt$	32.9	32.4	2.8	3.0	28.4	28.6		
$Cs_2[Cu(PFP)_2]$	$C_{12}F_{24}O_4Cs_2Cu$	14.5	14.5	—	0.6	45.9	45.6		
Cu(TMED)(PFP)	$C_{12}H_{16}F_{12}N_2O_2Cu$	28.2	28.0	3.1	3.3	44.6	44.5	Cu: 12.4	12.3
Cu(TEED)(PFP)	$C_{16}H_{24}F_{12}N_2O_2Cu$	33.9	33.9	4.2	4.3	40.2	40.4	Cu: 11.2	11.3

Can. J. Chem. Downloaded from www.nrcresearchpress.com by 210.87.254.6 on 09/05/12
For personal use only.

$[(CH_3)_2PC_6H_5]_2M(PFP)$ (M = Pt, Pd) were readily prepared from H_2PFP and the phosphino-dichlorides.

A number of analogous complexes of Pd^{2+} and Pt^{2+} have been reported, in fact the fluorinated derivatives of these metals are more numerous than their hydrocarbon analogs, where alkoxides are uncommon (17). Reaction of zerovalent metal complexes L_4M with hexafluoroacetone gives the 3-membered ring complexes $L_2\overline{MOC(CF_3)_2}$, which undergo further reaction in some cases (depending on the nature of L and M) with a second molecule of ketone to give $L_2\overline{MOC(CF_3)_2OC(CF_3)_2}$ (18, 19). The palladium(II) complex $[(C_2H_5)_3P]_2Pd(PFP)$ has been prepared by the reaction of $[(C_2H_5)_3P]_2Pd(CH_3)_2$ with H_2PFP (19), while platinum forms the unusual complex $[(C_6H_5)_3P]_2\overline{PtOC(CF_3)_2O}$, a derivative of hexafluoropropane-2,2-diol containing a four-membered chelate ring (20).

Our preparation of a stable PFP^{2-} complex of platinum demonstrates that this system is capable of existence. The fact that it is not formed in the reaction of low-valency metal complexes with hexafluoroacetone, whereas the reduction of the ketone with alkali metals (21), triethyl phosphite (22), or 2-propanol (23) leads readily to the formation of the C—C bond, has been rationalized by Stone (18) in terms of "head-to-tail" dimerization of two molecules of ketone coordinated to the same transition metal atom.

Experimental

General

Volatile compounds were handled in a conventional vacuum system. Infrared spectra were recorded on a Beckman IR-10 instrument; u.v.–visible spectra on Beckman DK or Cary 14 instruments. Microanalyses (Table 2) were performed by Alfred Bernhardt Laboratories, West Germany.

Perfluoropinacol

Caution: attention should be given to the toxic nature of this compound (23).

The most suitable method of preparation for large quantities of perfluoropinacol was found to be that based on triethylphosphite as a reducing agent (22). In a typical reaction, triethylphosphite (125 g, 0.75 mol) was cooled to 0 °C and gaseous hexafluoroacetone passed in with constant stirring, until the weight gain indicated uptake of the stoichiometric amount (1.50 mol), over a period of about 2 h.

To the resulting phosphorane was slowly added concentrated sulfuric acid (90 ml), followed by water (90 ml), stirring throughout. The solution was heated under reflux for 2 h to complete hydrolysis, then a further 50 ml of sulfuric acid added. The cooled mixture was repeatedly extracted with dichloromethane, the extract dried ($MgSO_4$), and fractionally distilled to yield crude perfluoropinacol, b.p. 110–130 °C. The product was redistilled from concentrated sulfuric acid to give anhydrous perfluoropinacol (215 g, 0.64 mol, 85% yield, b.p. 129–130 °C, m.p. 28–29 °C).

Nickel Complexes

The same general route was employed for the majority of the mixed-ligand Ni–PFP complexes. In a typical experiment, triethylphosphine (2.0 g, 17 mmol) was added slowly under nitrogen to a water–methanol solution of nickel nitrate hexahydrate (2.6 g, 8.9 mmol) and perfluoropinacol (2.8 g, 8.4 mmol). A solution of potassium hydroxide in methanol was then added dropwise with stirring to p*H* 8, and the resulting orange precipitate recrystallized from methanol/water to give bis(triethylphosphine)perfluoropinacolatonickel(II), m.p. 181°.

The same method gave:

$[(CH_3)_2P(C_6H_5)]_2Ni(PFP)$, orange, m.p. 132–133°, from methanol/water.

$[CH_3P(C_6H_5)_2]_2Ni(PFP)$, orange, m.p. 172–173°, from ethanol.

$[(C_6H_5)_2PCH_2—]_2Ni(PFP)$, golden, m.p. 228°, from methanol/water.

$[(C_6H_5)_3P]_2Ni(PFP)$. This preparation was carried out in *t*-butyl alcohol and the orange product recrystallized from chloroform/pentane, m.p. 208°.

$[(C_2H_5O)_3P]_2Ni(PFP)$. This complex could not be prepared directly, but was made by the reaction of excess triethyl phosphite with $K_2Ni(PFP)_2$ in aqueous ethanol, followed by reduction in volume and recrystallization of the precipitated product from dichloromethane/pentane.

(TMED)Ni(PFP), red, m.p. 232°, from methanol.

(TEED)Ni(PFP), magenta, m.p. 239–240° (decomp) from methanol.

(bipy)Ni(PFP), orange–brown, m.p. 280° (decomp) from ethanol/water.

The above nine complexes were diamagnetic and each showed a single peak in its ^{19}F n.m.r. spectrum in the range 70.6–71.3 p.p.m. from $CFCl_3$.

(DETA)Ni(PFP), green, m.p. 242–245° (decomp) from methanol. This complex was paramagnetic with μ_{eff} = 3.14 B.M. at 25°. It was a nonelectrolyte in methanol solution.

Palladium and Platinum Complexes

Dichlorobis(dimethylphenylphosphino)palladium(II) (0.30 g, 0.66 mmol) and H_2PFP (0.22 g, 0.66 mmol) were dissolved in methanol, and methanolic potassium hydroxide added to p*H* 8. The solution was evaporated to dryness and extracted with dichloromethane. Concentration of the extract gave $[(CH_3)_2P(C_6H_5)]_2Pd(PFP)$, off-white, m.p. 157° (decomp).

The platinum analog was similarly prepared; white, m.p. 174–175°.

Copper Complexes

TMED (1.20 g, 10.4 mmol) was slowly added to a solution of copper sulfate pentahydrate (2.0 g, 8.0 mmol) and H_2PFP (2.7 g, 8.1 mmol) in methanol/water, followed by methanolic potassium hydroxide to p*H* 8. The resulting purple precipitate was recrystallized from

acetone/water to give (TMED)Cu(PFP), m.p. 191–192° (decomp), μ_{eff} = 1.87 B.M./25°.

TEED similarly gave (TEED)Cu(PFP), purple, m.p. 195–197° (decomp), μ_{eff} = 1.87 B.M./25°.

Financial support of this work was provided by the National Research Council of Canada. We thank Dr. D. M. Barnhart for communication of his results in advance of publication.

1. M. Allan and C. J. Willis. J. Am. Chem. Soc. **90**, 5343 (1968); C. J. Willis. Chem. Commun. 944 (1972); 117 (1974).
2. R. Nyholm. Q. Rev. **24**, 1 (1970).
3. G. Garton, D. E. Henn, H. M. Powell, and L. M. Venanzi. J. Chem. Soc. 3625 (1963).
4. J. A. J. Jarvis, R. H. B. Mais, and P. G. Owston. J. Chem. Soc. A, 1473 (1968).
5. D. M. Barnhart and E. C. Lingafelter. Unpublished results.
6. C. J. Willis. Unpublished results.
7. L. Sacconi and I. Bertini. Inorg. Nucl. Chem. Lett. **2**, 29 (1966).
8. C. M. Harris and E. D. McKenzie. J. Inorg. Nucl. Chem. **19**, 372 (1961).
9. R. H. Lee, E. Griswold, and J. Kleinberg. Inorg. Chem. **3**, 1278 (1964).
10. R. J. H. Clark and C. S. Williams. Spectrochim. Acta. **23A**, 1055 (1967).
11. K. Akabori, H. Matsuo, and Y. Yamamoto. J. Inorg. Nucl. Chem. **33**, 2593 (1971).
12. E. Uhlig. Coord. Chem. Rev. **10**, 227 (1973).
13. M. Ciampolini and N. Nardi. Inorg. Chem. **5**, 41 (1966).
14. N. F. Curtis and H. K. J. Powell. J. Chem. Soc. A, 3069 (1968).
15. R. L. Carlin, J. S. Dubnoff, and W. T. Huntress. Proc. Chem. Soc. 228 (1964).
16. I. Bertini and F. Mani. Inorg. Chem. **6**, 2032 (1967).
17. F. R. Hartley. The chemistry of platinum and palladium. Wiley, New York. 1973. p. 172.
18. F. G. A. Stone. Pure Appl. Chem. **30**, 551 (1972).
19. H. D. Empsall, M. Green, and F. G. A. Stone. J. Chem. Soc. Dalton, 96 (1972).
20. P. J. Hayward and C. J. Nyman. J. Am. Chem. Soc. **93**, 617 (1971).
21. M. Allan, A. F. Janzen, and C. J. Willis. Can. J. Chem. **46**, 3671 (1968).
22. N. P. Gambaryan, Yu. A. Cheburkov, and I. L. Knunyants. Izv. Akad. Nauk. SSSR, Ser. Khim. 1526 (1964).
23. W. J. Middleton and R. V. Lindsey. J. Am. Chem. Soc. **86**, 4948 (1964).

Can. J. Chem. Downloaded from www.nrcresearchpress.com by 210.87.254.6 on 09/05/12
For personal use only.

Fluorinated Alkoxides. Part IX. The Resolution of Perfluoro(2,3-diphenylbutane-2,3-diol) and its use in preparing Optically Active Complexes of Ni^{2+} and Cu^{2+} [1]

W. Stafford Cripps and Christopher J. Willis

Department of Chemistry, University of Western Ontario, London, Ontario N6A 3K7

Received October 24, 1974

W. Stafford Cripps and Christopher J. Willis. Can. J. Chem. **53**, 817 (1975).

Perfluoro(2,3-diphenylbutane-2,3-diol), $CF_3(C_6F_5)C(OH)C(OH)(C_6F_5)CF_3$, prepared by the reductive dimerization of $C_6F_5COCF_3$, has been separated into *meso*- and DL-isomers and the latter resolved via its cinchonidine salt into optical enantiomers. The doubly ionized diol, $PDBD^{2-}$, acts as a dinegative, chelating, ligand, and neutral complexes of the form $(PDBD)ML_2$ may be isolated, where L is a neutral nitrogen- or phosphorus-containing ligand and $M = Ni^{2+}$ or Cu^{2+}. Use of the resolved diol enables optically active metal complexes to be prepared, and from their o.r.d./c.d. spectra we assign an absolute configuration to the diol. The partially fluorinated diols $CF_3(C_6H_5)C(OH)C(OH)(C_6H_5)CF_3$ and $CH_3(C_6F_5)C(OH)C(OH)(C_6F_5)CH_3$ have also been prepared from the appropriate ketones. The former, which appears to be exclusively the *meso*-isomer, has more limited chelating ability than the fully fluorinated analog, while the latter shows no ligand properties; these differences are ascribed to the reduced acidity resulting from the lower degree of fluorination.

Nuclear magnetic resonance studies suggest hindered rotation of the C_6F_5 groups through steric interaction with CF_3 groups in perfluoro(2,3-diphenylbutane-2,3-diol); an alternate explanation involving hydrogen bonding from the hydroxylic proton to aromatic fluorine atoms is considered less likely.

W. Stafford Cripps et Christopher J. Willis. Can. J. Chem. **53**, 817 (1975).

On a préparé les perfluoro (diphényl-2,3 butanediol-2,3), $CF_3(C_6F_5)C(OH)C(OH)(C_6F_5)CF_3$, par dimérisation réductrice de $C_6F_5COCF_3$; on a séparé les isomères *meso* et DL et ce dernier a été résolu en antipodes optiques par l'intermédiaire de son sel de cinchonidine. Le diol doublement ionisé, $PDBD^{2-}$ agit comme ligand dinégatif chélatant et on peut isoler des complexes neutres de la forme $(PDBD)ML_2$ dans lesquels L est un ligand neutre contenant de l'azote ou du phosphore et $M = Ni^{2+}$ ou Cu^{2+}. Si l'on utilise du diol résolu en antipodes optiques, on peut préparer des complexes métalliques optiquement actifs et en se basant sur les spectres o.r.d./c.d. on peut attribuer une configuration absolue au diol. On a aussi préparé, à partir des cétones appropriées, les diols partiellement fluorés $CF_3(C_6H_5)C(OH)C(OH)(C_6H_5)CF_3$ et $CH_3(C_6F_5)C(OH)C(OH)(C_6F_5)CH_3$. Le premier, qui semble être exclusivement l'isomère *méso*, a des propriétés chélatantes plus limitées que son analogue complètement fluoré alors que le dernier ne présente aucune propriété comme ligand; on attribue ces différences à une acidité réduite résultant du degré plus bas de fluoration.

Des études par résonance magnétique nucléaire suggèrent une rotation empêchée des groupes C_6F_5 due à des interactions stériques du groupe CF_3 dans le perfluoro diphényl-2,3 butanediol-2,3; on considère comme moins probable l'explication impliquant des liens hydrogène entre les protons hydroxyliques et les atomes de fluor du noyau aromatique.

[Traduit par le journal]

We have previously (1) reported the preparation of perfluoro(2,3-diphenylbutane-2,3-diol) (**1**) by the reductive dimerization of octafluoroacetophenone, and noted that the product appeared to contain more than one isomer. We now confirm this by the separation of the *meso*-isomer (**1***a*) and the DL-isomer (**1***b*), followed by

$$2\ C_6F_5COCF_3 \xrightarrow[h\nu]{2\text{-PrOH}}$$

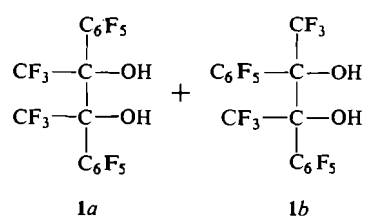

1*a* **1***b*

[1]Presented in part at the 7th International Symposium on Fluorine Chemistry, Santa Cruz, California, July, 1973.

Can. J. Chem. Downloaded from www.nrcresearchpress.com by 210.87.254.6 on 09/05/12
For personal use only.

Can. J. Chem. Downloaded from www.nrcresearchpress.com by 210.87.254.6 on 09/05/12
For personal use only.

the resolution of the latter into optical enantiomers. The initial product of dimerization was separated by fractional crystallization into approximately equal amounts of two compounds; one melting at 119–120° and the other at 129–130°. Both had elementary compositions and molecular weights corresponding to the formula $C_{16}H_2F_{16}O_2$. Their infrared spectra, while not identical, were very similar, both showing strong absorption near 3630 cm^{-1} characteristic of free O—H stretching modes.

We therefore concluded that these two compounds were the *meso*- and DL-forms of the diol. In order to decide which fraction was which isomer, we studied their interaction with a variety of optically active organic bases. The usual method of separating optical enantiomers of diols is to make an ester, *e.g.*, the phthallate, to provide an acidic function from which salts may be prepared. In the present work, this was not necessary, because the fluorination of the molecule increases the acidity of the hydroxyl group to the point where a salt may be made directly, even though the aromatic diol (pK_a = 8.85 (1)) is a considerably weaker acid than perfluoropinacol (pK_a = 5.95 (2)).

Of various bases tried, L-strychnine gave a crystalline derivative with the lower m.p. diol isomer, but fractional crystallization, followed by regeneration of the diol on acidification, gave no indication of the separation of enantiomers. This suggests that this is the *meso*-isomer (**1***a*). With the higher m.p. isomer, strychnine gave no solid derivative, but L-cinchonidine readily formed crystals which were shown by analysis to be a 1:1 adduct. This dissociated in methanol to give a conducting solution and the infrared spectrum of the solid showed no O—H absorption peaks. We therefore formulate it as an ionic salt, although the possibility of solid-state interactions through hydrogen-bonding cannot be eliminated.

The cinchonidine salt was fractionally crystallized to constant optical rotation, and acidification of the less soluble fraction yielded resolved (+)-diol, m.p. 89–90°, $[\alpha]_{589}^{20} = 96.6°$. This separation shows unambiguously that the higher m.p. fraction from the dimerization product is the DL-isomer (**1***b*), and the fact that it has a m.p. 40° higher than that of the resolved enantiomer characterizes it as a racemic compound, rather than a mixture.

The pK_a values, measured in aqueous ethanol, are 8.7 for the *meso*-isomer and 9.1 for the DL-isomer. This difference, although slight, is surprising, since the acidic nature of fluorinated diols of this type was originally ascribed to intramolecular hydrogen-bonding in the anion (2):

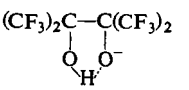

Although the need for an explanation of this "enhanced" acidity of perfluoropinacol was removed by the subsequent revision of the accepted value of the pK_a of perfluoro(*t*-butanol) (3), there has been no reason to doubt the existence of intramolecular hydrogen-bonding, on which basis one would expect a greater acidity for **1***b*, the DL-isomer, since the steric interaction between the bulky pentafluorophenyl groups required to bring the two oxygen atoms into a *syn*-conformation would appear to be less than that in the *meso*-isomer, **1***a*. The greater acidity found in the latter would suggest that hydrogen-bonding, if present, is intermolecular to solvent molecules, rather than intramolecular.

Metal Complexes

The overall objective of this work is to study the formation of complexes between highly fluorinated molecules and metal ions, as we have previously done for perfluoropinacol (4, 5). We have therefore studied the reaction of **1** with Ni^{2+} and Cu^{2+}, but we find that the fluorinated aromatic diol does not form complexes as readily as does H_2PFP. Thus, we were unable to isolate anionic complexes of either **1***a* or **1***b* of the type $[M(PDBD)_2]^{2-}$ [where $PDBD^{2-}$ = dianion of perfluoro(2,3-diphenylbutane-2,3-diol)] under conditions where perfluoropinacol readily forms $[M(PFP)_2]^{2-}$ (4), and this can be ascribed in part to the reduced acidity of the aromatic diol. Using resolved (+)-diol in solutions containing Ni^{2+} in various concentration ratios, we varied the p*H* while monitoring the optical rotary dispersion (o.r.d.) of the solutions, but in no case was any evidence seen of interaction between the ligand and the metal ion, up to the point where decomposition of the ligand began.

However, the use of a neutral co-ligand enabled us to isolate a number of stable complexes of $PDBD^{2-}$ with Ni^{2+} and Cu^{2+}, similar to those formed by perfluoropinacol (6). Nickel complexes isolated were $[(C_2H_5)_3P]_2Ni(PDBD)$, $[(CH_3)_2PC_6H_5]_2Ni(PDBD)$, (TMED)Ni(PDBD) (TMED = tetramethylethylenediamine), and

TABLE 1. Visible, optical rotary dispersion, and circular dichroism spectra (in methanol)

Compound	Visible		Optical rotary dispersion		Circular dichroism	
	λ_{max}	ε	λ_{max}	[α]	λ_{max}	Δε
(TMED)Ni[(+)-PDBD]	510	82	438	−598	474	+1.07
			504	+144	527	−0.42
			554	−407	576	+0.82
			618	+121		
(TMED)Ni[(−)-PDBD]*	510	82	439	+546	474	−0.91
			504	−134	527	+0.28
			554	+382	576	−0.72
			618	−114		
$[(C_2H_5)_3P]_2$Ni[(+)-PDBD]	470	205	387	−1200	421	+2.31
			453	+550	478	−1.00
			505	−340	531	+0.14
$[(CH_3)_2PC_6H_5]_2$Ni[(+)-PDBD]	460	286	380	−1110	412	+2.52
			446	+598	472	−0.98
			502	−272	520	+0.22
(TMED)Cu[(+)-PDBD]	561	77	544	−202	503	−0.22
			616	+51	577	+0.24
					654	−0.12

*Comparison with the data for the (+)-diol complex indicates about 93% optical purity.

(TEED)Ni(PDBD) (TEED = tetraethylethylenediamine). These four complexes were diamagnetic and had visible absorption spectra similar to those of the analogous PFP^{2-} derivatives (6); they were therefore assumed to have a square-planar coordination of ligands around nickel. Bulkier phosphine ligands, such as triphenylphosphine, did not yield stable complexes. Copper (II) gave the complex (TMED)Cu(PDBD).

Several competitive reactions were examined in which more than one potential ligand was present in solution with the metal ion. Clearcut selective chelation occurred, and the order of complexing ability was found to be PFP^{2-} > DL-$PDBD^{2-}$ > *meso*-$PDBD^{2-}$. The preferential coordination of PFP^{2-} was expected, in view of the known properties of this compound, while the superiority of the DL-isomer of the aromatic diol, although contrary to the slight difference in acidity between the two isomers, is entirely consistent with steric requirements. Consideration of Newman projections along the C—C axes of the aromatic diols shows the relative steric interactions in the coordinated ligands:

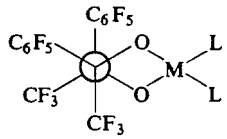

2a

coordinated *meso*-diol

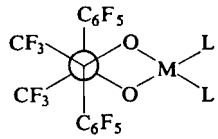

2b

coordinated DL-diol

Whereas the coordination of the *meso*-diol (**2a**) requires an axial-equatorial conformation of the C_6F_5 groups, the DL-diol may adopt a conformation in which they are *trans*-diaxial (**2b**), with reduced steric interaction.

Dissymmetric Complexes

The availability of resolved enantiomers of the aromatic diol enabled us to prepare optically active complexes of Ni^{2+} and Cu^{2+}. It is apparent from structure **2b** that the preferred conformation of the C_6F_5 groups will impose chirality on the chelate ring, and it is accepted (7) that chirality of this type is dominant over the vicinal effect of asymmetric centers in determining the optical rotatory power of a metal complex. Using the (+)-diol, dissymmetric complexes of the two metals were prepared, and essential features of the o.r.d. and c.d. (circular dichroism) spectra are shown in Table 1, while representative spectra are illustrated in Figs. 1 and 2.

These complexes represent an unusual example of a series of stable, isolable, compounds in which a chelate ring derived from a 2,3-diol contains two adjacent asymmetric carbon atoms. Although many other examples of interactions between metal ions and optically active diols are known, they mainly occur in solution without yielding solid products of established stoichiometry. It was of interest, therefore, to establish

Can. J. Chem. Downloaded from www.nrcresearchpress.com by 210.87.254.6 on 09/05/12
For personal use only.

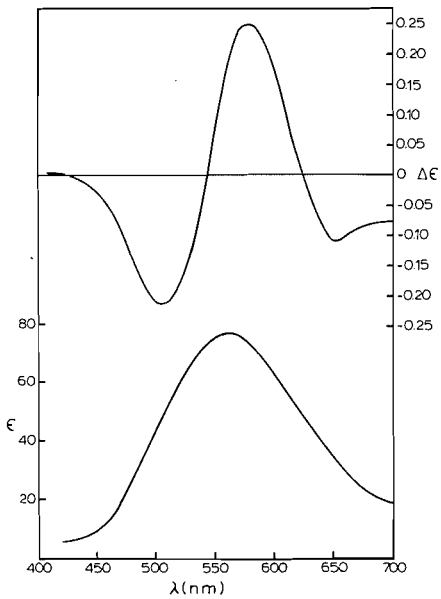

FIG. 1. Circular dichroism and visible spectra (methanol solution) of (TMED)Cu[(+)-PDBD].

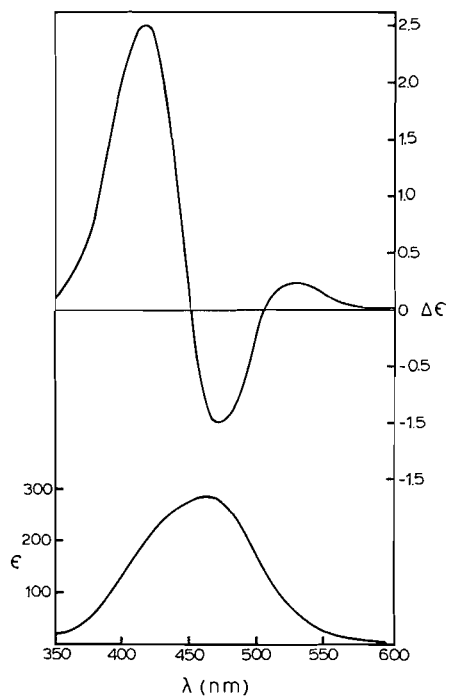

FIG. 2. Circular dichroism and visible spectra (methanol solution) of $[(CH_3)_2PC_6H_5]_2Ni[(+)\text{-PDBD}]$.

the absolute configuration of the chelate ring (and hence of the ligand itself) in the present complexes, and we have attempted to do this by a comparison of the o.r.d. spectra of the complexes with those of analogous systems of known absolute configuration.

It is convenient to refer to the conformations of the chelate rings as δ and λ

Reeves (8) investigated the configuration of a number of optically active ligands by their interaction with Cu^{2+} in ammoniacal solution ("cupra A"), where a 1:1 complex is formed, but not isolable. Using a conformationally rigid diol of known structure, subsequent workers (9) found that these solutions show a weak c.d. band at 580–600 nm and a more intense band of opposite sign near 280 nm, and established that a positive value of the former peak is associated with the δ-conformation of the chelate ring. The c.d. spectrum of our (+)-diol in cupra A shows a positive peak at 610 nm and a more intense negative peak below 300 nm, the reverse being shown by the (−)-diol. We therefore assign the δ-conformation to the coordinated (+)-isomer of $PDBD^{2-}$, *i.e.*

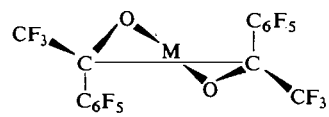

3

Additional evidence comes from studies on the conformations of a number of optically active Schiff base complexes of Ni^{2+} and Cu^{2+}. Downing and Urbach (10) found that a δ conformation in the ring of a copper complex led to a c.d. spectrum with a negative peak at 630–700 nm, a positive peak at 550–590 nm, and a further negative peak at 475–500 nm. The c.d. spectrum of (TMED)Cu[(+)-PDBD] (Table 1) is entirely consistent with this pattern, conforming our assignment of the δ-conformation to its chelated diol ring.

With the similar complexes of Ni^{2+}, several workers (11, 12) have drawn attention to the difficulty of assigning absolute configurations, so we do not feel justified in using data from the

Can. J. Chem. Downloaded from www.nrcresearchpress.com by 210.87.254.6 on 09/05/12
For personal use only.

Can. J. Chem. Downloaded from www.nrcresearchpress.com by 210.87.254.6 on 09/05/12
For personal use only.

c.d. spectra of the Ni^{2+} complexes of $PDBD^{2-}$ to support our arguments.

The extension from the assignment of a ring conformation to the assignment of an absolute configuration of each diol isomer depends on our assumption that the steric interaction between two vicinal C_6F_5 groups is greater than that between two CF_3 groups, so that the (+)-diol has the configuration illustrated in **3**. Since the difference in size between the two substituent groups is quite considerable, we consider that this assumption may be accepted with some confidence.

Partially Fluorinated Diols

In an attempt to extend the range of diols of the type RR'C(OH)C(OH)RR' which might form stable complexes with metal ions, we prepared the partially fluorinated compounds where $R = C_6F_5$, $R' = CH_3$ (**4**), and $R = C_6H_5$, $R' = CF_3$ (**5**) by reductive dimerization of the ketones $C_6F_5COCH_3$ and $C_6H_5COCF_3$ respectively.

Compound **5** had been prepared previously by Mosher and Heindel (13) who reported only one isomer, without identifying it as the *meso*- or DL-form. We also found evidence for only one isomer, which we attempted to separate into optical enantiomers as we had the fully fluorinated diol. Although strychnine gave a solid adduct with **5**, fractional crystallization showed no sign of resolution, from which we assumed it was the *meso*-form. Consistent with this, the singlet observed in the ^{19}F n.m.r. spectrum was not split when the compound was dissolved in an optically active solvent. After this work was completed, an alternate preparation of diol **5** was published (14) quoting a crystal structure on a derivative in which it was shown to have the *meso*-configuration.

Diol **5** was much less acidic than its fully fluorinated analog, having a pK_a of about 11.4. Nevertheless, it did form stable metal complexes such as $(TMED)\overline{NiOC(CF_3)(C_6H_5)C(CF_3)(C_6H_5)O}$. In competitive reactions, the fully fluorinated *meso*-diol (**1***a*) coordinated in preference to **5**, indicating that the effect of the greater acidity of the former predominated over the smaller degree of steric hindrance between the unfluorinated phenyl rings in the latter. However, diol **5** did form a complex with Ni^{2+} in the absence of any co-ligand when a solution of the diol and Ni^{2+} was made highly alkaline ($[OH^-] > 5\ M$). The resulting clear blue solution had a visible spectrum very similar to that of $Ni(PFP)_2^{2-}$ in noncoordinating solvent (6), and presumably contained a square-planar anionic complex of Ni^{2+} with diol **5**, although no solid compound could be isolated. The formation of a nickel complex under these conditions with diol **5**, but not with the other diols included in this study, may be attributed to the ligand's stability under highly basic conditions, where the diols containing pentafluorophenyl groups decomposed.

Diol **4** was produced in poor yield by the photolytic dimerization of $C_6F_5COCH_3$. As would be expected, it was less acidic than any of the other diols included in this study. It did not give an end-point on titration, nor could any evidence be found for the existence of isolable metal complexes. In the absence of salt formation with organic bases, no attempt was made to identify **4** as a *meso*- or DL-isomer.

The order of coordinating ability of the fluorinated diols covered in this study is therefore $[(CF_3)_2C(OH)—]_2 >$ DL-$[(C_6F_5)(CF_3)C(OH)—]_2 >$ *meso*-$[(C_6F_5)(CF_3)C(OH)—]_2 >$ *meso*-$[(C_6H_5)(CF_3)C(OH)—]_2 > [(C_6F_5)(CH_3)C(OH)—]_2$. With the exception of the slight difference between isomers **1***a* and **1***b*, this is the order of decreasing acidity of the diols.

^{19}F Nuclear Magnetic Resonance Spectra

We have previously (1) reported the ^{19}F n.m.r. spectra of a variety of fluorinated aromatic alcohols. The compound $C_6F_5C(CF_3)_2OH$ (**6**), for example, shows one peak associated with the CF_3 group and three others, with intensities in a 2:2:1 ratio, corresponding to the *ortho*-, *meta*-, and *para*-fluorine atoms of the aromatic ring (Table 2). By contrast, the spectra of the fully fluorinated aromatic diols studied in the present work contained the expected peak from the CF_3 groups and five equal-intensity peaks from the fluorine atoms of the aromatic rings, indicating that all five aromatic fluorine atoms were nonequivalent.

The following numbering scheme will be used to discuss these spectra; this diagram is not intended to show the conformation of the molecule.

The peak corresponding to each fluorine atom was split by fluorine–fluorine coupling and the

Can. J. Chem. Downloaded from www.nrcresearchpress.com by 210.87.254.6 on 09/05/12
For personal use only.

TABLE 2. ^{19}F nuclear magnetic resonance chemical shifts*

		meso-diol (**1***a*)	DL-diol (**1***b*)	$[(CH_3)_2PC_6H_5]_2Ni[(+)\text{-PDBD}]$	$[C_6F_5C(CH_3)(OH)—]_2$	$C_6F_5C(CF_3)_2OH$ (**6**)
CF_3	F^1,F^7	71.6	73.3	67.4	—	76.2
ortho-F	F^2	129.3	129.9	132.6	138.0	135.3
	F^6	140.5	143.2	133.4		
para-F	F^4	149.6	148.7	157.4	154.7	149.5
meta-F	F^5	160.3	159.3	164.2	162.3	160.6
	F^3	160.6	160.2	166.9		

*In p.p.m. from $CFCl_3$.

TABLE 3. Analytical data

Compound	Formula	Carbon		Hydrogen		Fluorine	
		Calcd.	Found	Calcd.	Found	Calcd.	Found
meso-diol (**1***a*)	$C_{16}H_2F_{16}O_2$	36.3	36.4	0.4	0.3	57.3	57.6
DL-diol (**1***b*)	$C_{16}H_2F_{16}O_2$	36.3	36.0	0.4	0.3	57.3	57.1
DL-diol, cinchonidine salt	$C_{35}H_{24}F_{16}N_2O_3$	51.0	51.8	2.9	2.9	36.9	37.8
(TMED)Ni[(+)-PDBD]	$C_{22}H_{16}F_{16}N_2NiO_2$	41.2	41.2	3.2	3.3	40.0	40.1
(TEED)Ni[(+)-PDBD]	$C_{26}H_{24}F_{16}N_2NiO_2$	40.9	40.7	3.7	3.8	36.9	36.7
$[(C_2H_5)_3P]_2Ni[(+)\text{-PDBD}]$	$C_{28}H_{30}F_{16}NiO_2P_2$	37.6	37.4	2.3	2.5	43.2	43.5
$[(CH_3)_2PC_6H_5]_2Ni[(+)\text{-PDBD}]$	$C_{32}H_{22}F_{16}NiO_2P_2$	44.5	44.9	2.6	2.8	35.2	34.2
(TMED)Cu[(+)-PDBD]	$C_{22}H_{16}CuF_{16}N_2O_2$	37.2	36.7	2.3	2.2	42.8	42.7
$[CH_3C(C_6F_5)OH—]_2$	$C_{16}H_8F_{10}O_2$	45.5	45.5	1.9	2.2	45.0	44.9
$(TMED)Ni[CF_3(C_6H_5)CO—]_2$	$C_{22}H_{26}F_6N_2NiO_2$	50.5	50.4	5.0	4.9	21.8	22.0

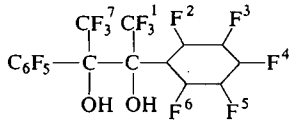

various peaks were identified by examination of the coupling pattern and use of standard decoupling techniques. The following ranges of coupling constants were found: $J(F^2–F^3) = J(F^3–F^4) = J(F^4–F^5) = J(F^5–F^6) = 21–23$ Hz; $J(F^2–F^4) = J(F^2–F^5) = J(F^3–F^6) = J(F^4–F^6) = 6–7$ Hz; $J(F^3–F^5) = 1$ Hz; $J(F^2–F^6)$ not resolved.

Coupling was also observed from the *ortho*-fluorine atoms to one of the CF_3 groups (F^1 or F^7), whose absorption peaks consisted of a complex multiplet. Irradiation of F^2 caused this to collapse to a broad singlet, while irradiation of F^6 produced a doublet ($J = 24$ Hz), indicating preferential coupling to each CF_3 group from one of the *ortho*-fluorine atoms.

The nonequivalence of the aromatic fluorine atoms indicates restricted rotation of the phenyl ring. Previous workers (15) have suggested the possibility of hydrogen-bonding from the hydroxyl group of an alcohol to an adjacent fluorine atom, but we may eliminate that in this case because the same pattern is observed in the coordinated ligand, where no hydroxyl group is present. We suggest, therefore, that the restricted rotation results from steric interaction between the *ortho*-fluorine atoms of the ring and those of one of the CF_3 groups (assuming that the diol adopts a conformation with the two phenyl rings too far apart to interact). Examination of molecular models shows that the greater degree of steric interaction is between the C_6F_5 group and the CF_3 in the vicinal position to it, rather than the *gem*-CF_3 group, and this is consistent with our observation that no such interaction is observed in **6** or in similar monohydric fluorinated alcohols. The coupling from F^2 to the CF_3 group may therefore be through-space coupling to F^7, rather than to F^1.

Additional evidence favoring our suggestion that steric interaction between C_6F_5 and CF_3 groups is dominant comes from the ^{19}F n.m.r. spectrum of the partially fluorinated diol $[C_6F_5C(CH_3)(OH)—]_2$. This shows a typical 2:2:1 set of peaks for *ortho*-, *meta*-, and *para*-fluorine atoms, indicating that the presence of the smaller CH_3 group allows free rotation of the phenyl ring.

Infrared Spectra

The infrared (i.r.) spectra of the diols **1***a* and **1***b* were very similar. The O—H stretching frequency appeared as a sharp absorption peak at 3640 cm^{-1} (**1***a*) and 3627 cm^{-1} (**1***b*) (mulls), showing the absence of hydrogen-bonding. A similar peak at 3630 ± 5 cm^{-1} has been noted previously (16) in a series of unfluorinated 1,2-diols.

Peaks associated with ring skeletal modes were seen at 1651 and 1534 cm^{-1} (**1***a*) and 1654 and 1535 cm^{-1} (**1***b*), and strong C—F stretching absorptions were present in the region 1100–1300 cm^{-1} in both compounds. The major difference in the i.r. spectra between the two isomers occurred near 1000 cm^{-1}. Whereas the *meso*-diol, **1***a*, had two sharp peaks at 995 and 945 cm^{-1}, the DL-diol had a broad, poorly resolved pair of peaks at 1010 and 990 cm^{-1}. The overall complexity of the spectra precluded any definite assignment of these peaks, but their presence provided a useful guide to the purity of the isomers.

The absence of any peaks corresponding to intramolecularly hydrogen-bonded O—H is in accord with previous work (17), which demonstrated that the fluorination of this type of molecule, while having little effect on the frequency of the O—H absorption, reduced the tendency towards hydrogen bonding.

Metal complexes of the diol isomers showed very similar i.r. spectra (the O—H peaks being, of course, absent) with the same difference in the appearance of the spectrum around 1000 cm^{-1} between complexes of **1***a* and **1***b*.

Experimental

General

Infrared spectra were recorded on a Beckman IR-10 instrument; u.v.–visible spectra on Beckman DK or Cary 14 instruments; o.r.d./c.d. spectra on a Durrum–Jasco ORD-UV-5 spectropolarimeter. Microanalyses (Table 3) were performed by Alfred Bernhardt Laboratories, West Germany.

Perfluoro(2,3-diphenylbutane-2,3-diol) (*1*).

The synthesis of the diol, as a mixture of isomers, has been described previously (1). The crude product was separated by fractional crystallization from light petroleum (b.p. 30–60°) into approximately equal amounts of two fractions; the less soluble *meso*-diol (**1***a*), m.p. 119–120°, and the more soluble DL-diol (**1***b*), m.p. 130–131°. Molecular weights (osmometric in benzene) were 535 and 543 respectively (calcd., 530).

Can. J. Chem. Downloaded from www.nrcresearchpress.com by 210.87.254.6 on 09/05/12
For personal use only.

Can. J. Chem. Downloaded from www.nrcresearchpress.com by 210.87.254.6 on 09/05/12
For personal use only.

Resolution of the DL-*diol*

Diol **1***b* (16 g, 30 mmol) and L-cinchonidine (9.0 g, 30 mmol) in a mixture of chloroform (150 ml) and hexane (20 ml) deposited a crystalline solid over a period of 3 days at 25°. Analysis showed this to be a 1:1 adduct. It had an equivalent conductance of 40 ohm^{-1} cm^2 in methanol and a molecular weight of 405 (calcd. for complete dissociation: 412) extrapolated to infinite dilution in methanol. The diol was regenerated by acidification with aqueous hydrochloric acid and extraction with dichloromethane; it had $[\alpha]_{589}^{20} = +62°$. The process was repeated to constant rotation to yield resolved (+)-diol, $[\alpha]_{589}^{20} = +96.6°$, m.p. 89–90°. Residues from the recrystallization gave an oil which yielded diol of specific rotation −42°, indicating about 45% concentration of the (−)-diol. This was used for the preparation of the metal complexes, described below, whose recrystallization provided a further degree of purification to give substantially pure (−)-diol derivatives.

Preparation of Nickel Complexes of $PDBD^{2-}$

(+)-Diol (0.30 g, 0.57 mmol) and nickel nitrate hexahydrate (0.17 g, 0.57 mmol) were dissolved in ethanol (15 ml) and TMED (0.15 g, 1.3 mmol) added slowly. Ethanolic potassium hydroxide was added dropwise to p*H* 8 and the resulting red solution filtered and evaporated to dryness. Recrystallization from ethanol gave (TMED)Ni[(+)-PDBD], red, m.p. 148° (decomp). The same procedure gave (TEED)Ni[(+)-PDBD], red.

The same procedure was used with partially resolved (−)-diol and the complex recrystallized from dichloromethane/hexane to constant rotation, yielding essentially pure (TMED)Ni[(−)-PDBD].

For both the DL-diol and the *meso*-diol, the following procedure was used. Equimolar amounts of diol and nickel nitrate were dissolved in aqueous methanol and a slight excess of TMED added. The solution was brought to p*H* 8 with methanolic potassium hydroxide and the resulting red precipitate removed by filtration, extracted with dichloromethane, and recrystallized from dichloromethane/hexane. Products were red, with m.p. 138–139° (DL-diol) and 130–131° (*meso*-diol).

The complex $[(C_2H_5)_3P]_2Ni[(+)\text{-PDBD}]$ was prepared by the slow addition of triethylphosphine (0.095 g, 0.80 mmol) under nitrogen atmosphere to a solution of (+)-diol (0.20 g, 0.38 mmol) and nickel nitrate hexahydrate (0.11 g, 0.38 mmol) in methanol, followed by the addition of methanolic potassium hydroxide to p*H* 8.5. The orange solution was evaporated to dryness and the residue extracted with dichloromethane and recrystallized from dichloromethane/hexane to yield $[(C_2H_5)_3P]_2Ni$-[(+)-PDBD], orange, m.p. 137–138°. The similar derivative of the *meso*-diol was prepared in the same way; orange, m.p. 124–125°.

The dimethylphenylphosphine complex was prepared by dissolving (+)-diol (0.30 g, 0.57 mmol) and nickel nitrate hexahydrate (0.17 g, 0.57 mmol) in ethanol under nitrogen, and slowly adding dimethylphenylphosphine (0.20 g, 1.5 mmol) followed by ethanolic potassium hydroxide to p*H* 8. The resulting solution was filtered and evaporated to dryness and the product recrystallized from 95% ethanol to give $[(CH_3)_2PC_6H_5]_2Ni[(+)$-PDBD], orange, m.p. 143°. The similar derivative of the *meso*-diol was prepared by the same route and recrystallized from dichloromethane/hexane; orange, m.p. 116°.

Preparation of (TMED)Cu[(+)-PDBD]

Copper sulfate pentahydrate (0.15 g, 0.60 mmol) and (+)-diol (0.30 g, 0.57 mmol) were dissolved in aqueous ethanol and TMED (0.20 g, 1.7 mmol) added, followed by aqueous potassium hydroxide to p*H* 8. The desired compound precipitated on concentrating the solution; it was recrystallized from ethanol to give (TMED)Cu[(+)-PDBD], purple, m.p. 88–90° (decomp).

2,3-Bis(pentafluorophenyl)butane-2,3-diol

Methyl pentafluorophenyl ketone was prepared by the Grignard reaction of acetyl chloride with pentafluorophenyl magnesium bromide (18). A solution of the ketone (5.1 g) in 2-propanol (25 ml) in a quartz tube was degassed and irradiated with ultraviolet light for 7 days. Removal of volatile material left a solid product which was recrystallized from dichloromethane/hexane to give 2,3-bis(pentafluorophenyl)butane-2,3-diol (2.1 g), m.p. 173–174°. The ^{19}F n.m.r. spectrum ($CHCl_3$ solution) showed three multiple peaks in a 2:1:2 ratio at 138.0, 154.7, and 162.3 p.p.m. from $CFCl_3$. Attempts to form nickel complexes of this diol, using methods successful with other diols, showed no evidence of interaction.

1,1,1,4,4,4-Hexafluoro-2,3-diphenylbutane-2,3-diol

Trifluoroacetophenone was prepared by the Grignard reaction of trifluoroacetic acid with phenylmagnesium bromide (19). The ketone (10 g) was dissolved in 2-propanol (22 ml) acidified with hydrochloric acid (0.2 ml) in a quartz tube, the mixture outgassed and irradiated with ultraviolet light for 8 days. Removal of solvent left a solid residue which was recrystallized from benzene/hexane to give 1,1,1,4,4,4-hexafluoro-2,3-diphenylbutane-2,3-diol (7.0 g), m.p. 154–155° (lit. m.p. (13), 155–156°). Fractional crystallization from a variety of solvents gave no evidence of the presence of more than one isomer. The ^{19}F n.m.r. spectrum showed a single peak both in chloroform (at 70.2 p.p.m. from TMS) and in (+)-α-phenethylamine (at 67.8 p.p.m.). Titration in a 1:1 ethanol/water solution gave a pK_a of about 11.4.

When equimolar quantities of this diol and L-strychnine were dissolved in a chloroform/hexane mixture, a crystalline precipitate formed. Its infrared spectrum showed the presence of both diol and strychnine, but no O—H stretching band. Fractional crystallization, followed by regeneration of the free diol by acidification and ether extraction, showed no evidence for the separation of an optically active form of the diol.

The complex (TMED)Ni$[CF_3(C_6H_5)CO—]_2$ was prepared similarly to (TMED)Ni[(+)-PDBD] and recrystallized from ethanol to give a red complex, m.p. 196–200° (decomp.).

Financial support of this work was provided by the National Research Council of Canada. We thank Dr. R. A. Haines for many helpful discussions.

1. I. S. CHANG, A. J. TOMLINSON, and C. J. WILLIS. Can. J. Chem. **50**, 512 (1972).
2. W. J. MIDDLETON and R. V. LINDSEY. J. Am. Chem. Soc. **86**, 4948 (1964).

3. I. L. KNUNYANTS and B. L. DYATKIN. Izv. Akad. Nauk. SSSR, Ser. Khim. 923 (1964).
4. M. ALLAN and C. J. WILLIS. J. Am. Chem. Soc. **90**, 5343 (1968).
5. C. J. WILLIS. J. Chem. Soc. Chem. Commun. 944 (1972).
6. W. S. CRIPPS and C. J. WILLIS. Can. J. Chem. This issue.
7. C. J. HAWKINS. *In* Absolute configuration of metal complexes. Wiley, New York. 1971. p. 200.
8. R. E. REEVES. Adv. Carbohydr. Chem. **6**, 107 (1953).
9. S. T. K. BUKHARDI, R. D. GUTHRIE, A. I. SCOTT, and A. D. WRIXON. Chem. Commun. 1580 (1968).
10. R. S. DOWNING and F. L. URBACH. J. Am. Chem. Soc. **91**, 5977 (1969).
11. R. S. DOWNING and F. L. URBACH. J. Am. Chem. Soc. **92**, 5861 (1970).
12. B. BOSNICH. J. Am. Chem. Soc. **90**, 627 (1968).
13. W. A. MOSHER and N. D. HEINDEL. J. Am. Chem. Soc. **85**, 1548 (1963).
14. D. BRYCE-SMITH, G. B. COX, and A. GILBERT. Chem. Comm. 914 (1971).
15. R. N. HASZELDINE. J. Chem. Soc. 1757 (1953).
16. L. P. KUHN. J. Am. Chem. Soc. **74**, 2492 (1952).
17. A. L. HENNE and W. C. FRANCIS. J. Am. Chem. Soc. **75**, 991 (1953).
18. A. K. BARBOUR, M. W. BUXTON, P. L. COE, R. STEPHENS, and J. C. TATLOW. J. Chem. Soc. 808 (1961).
19. A. SYKES, J. C. TATLOW, and C. R. THOMAS. Chem. Ind. Lond. **74**, 630 (1955).

Can. J. Chem. Downloaded from www.nrcresearchpress.com by 210.87.254.6 on 09/05/12
For personal use only.

Photolysis of Aqueous Solutions of 9,10-Anthraquinone-2-sulfonate. Part II. Dependence of Rates of Hydroxylation on Reaction Conditions

ARTHUR D. BROADBENT, HUGH B. MATHESON, AND RICHARD P. NEWTON

Department of Chemistry, Mount Allison University, Sackville, New Brunswick E0A 3C0

Received August 22, 1974

ARTHUR D. BROADBENT, HUGH B. MATHESON, and RICHARD P. NEWTON. Can. J. Chem. **53**, 826 (1975).

The rates of formation of hydroxy-9,10-anthraquinone-2-sulfonates, produced by irradiation of neutral and alkaline aqueous solutions of 9,10-anthraquinone-2-sulfonate (A) at 365 nm, have been measured for solutions with initial [A] ranging from 5×10^{-5} to 8×10^{-2} mol dm^{-3}, saturated with either O_2, air, or N_2. The rate of monohydroxylation was independent of the saturating gas and, for neutral solutions absorbing all the incident light, increased with increasing initial [A] reaching a constant maximum quantum yield of 0.08 above 2×10^{-2} mol dm^{-3}. In 0.1 mol dm^{-3} aqueous NaOH solution, the rate was about three times larger but had not attained a limiting value at the maximum [A] imposed by its solubility. Dihydroxy-9,10-anthraquinone sulfonates are proposed to arise from reaction of O_2 with an intermediate, rather than by further hydroxylation of monohydroxy products. The rate of dihydroxylation decreased on increasing [A] above 5×10^{-4} mol dm^{-3}, becoming essentially zero at high concentrations.

ARTHUR D. BROADBENT, HUGH B. MATHESON et RICHARD P. NEWTON. Can. J. Chem. **53**, 826 (1975).

On a mesuré à 365 nm, pour des solutions ayant des concentrations initiales de [A] allant de 5×10^{-5} à 8×10^{-2} mol dm^{-3}, saturées soit en O_2, en air ou en N_2, les vitesses de formation des hydroxyanthraquinone-9,10 sulfonates-2 produits par irradiation de solutions aqueuses, neutres ou alcalines d'anthraquinone-9,10 sulfonate-2 (A). Le taux de monohydroxylation est indépendant du gaz produisant la saturation et dans des solutions neutres absorbant toute la lumière incidente, la vitesse augmente avec l'augmentation de la vitesse initiale de [A] approchant un rendement quantique maximum constant de 0.08 au dessus de 2×10^{-2} mol dm^{-3}. Dans des solutions aqueuses de NaOH à 0.1 mol dm^{-3}, la vitesse est environ trois fois plus grande mais elle n'avait pas atteint une valeur limite à la concentration maximum de [A] imposée par sa solubilité. On propose que les dihydroxyanthraquinone-9,10 sulfonates se forment par réaction de O_2 avec un intermédiaire plutôt que par une hydroxylation ultérieure des produits monohydroxylés. Le taux de dihydroxylation diminue lorsque la concentration de [A] augmente au dessus de 5×10^{-4} mol dm^{-3} et cette vitesse devient pratiquement zéro à haute concentration.

[Traduit par le journal]

Introduction

When 9,10-anthraquinone-2-sulfonate (A) is irradiated in aqueous solution with near-ultraviolet light (λ = 300–425 nm), 1- and 2-hydroxy- (AOH) and dihydroxy-9,10-anthraquinone sulfonates ($A(OH)_2$) result, the actual product yields depending upon the photolysis conditions (1). There is evidence (2–6) that this photochemical reaction causes reduction of A and oxidation of H_2O or HO^- to $HO^\cdot$, which, in the absence of scavengers, reacts with A to produce hydroxy derivatives.

Two groups have recently established that the rate of formation of AOH (V_{AOH}) increases with increasing initial [A], even when all the incident light is absorbed. Phillips *et al.* (7) proposed the following reactions to account for this:

[1] $$A + h\nu \rightarrow A^*$$

[2] $$A^* \rightarrow A$$

[3] $$A^* + A \rightarrow A^{\cdot -} + A^{\cdot +}$$

[4] $$A^{\cdot +} + HO^- \rightarrow A + HO^\cdot$$

[5] $$A + HO^\cdot \rightarrow AOH^\cdot$$

[6] $$AOH^\cdot + O_2 \rightarrow \rightarrow AOH + HO_2^\cdot$$

A* represents the appropriate electronically excited state of A, $A^{\cdot -}$, and $A^{\cdot +}$ radical ions resulting from partial reduction and oxidation of A, respectively, and $AOH^\cdot$ the adduct from A and $HO^\cdot$.

Clark and Stonehill (8) modified and expanded this reaction scheme concluding that, if reaction 3 occurs, the initial product would be a radical ion-pair, $A^{\cdot -} \ldots A^{\cdot +}$, which either reverts to A or oxidizes H_2O or HO^-.

[7] $$A^* + A \rightarrow A^{\cdot -} \ldots A^{\cdot +}$$

[8] $$A^{\cdot -} \ldots A^{\cdot +} \rightarrow 2A$$

[9] $$A^{\cdot -} \ldots A^{\cdot +} + H_2O \rightarrow A^{\cdot -} + A + HO^\cdot + H^+$$

Can. J. Chem. Downloaded from www.nrcresearchpress.com by 210.87.254.42 on 09/05/12
For personal use only.

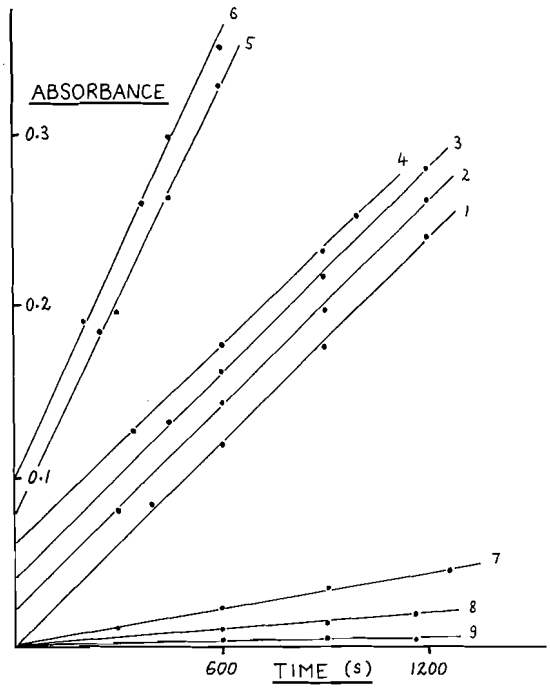

FIG. 1. Absorbance of AOH and $A(OH)_2$ as a function of time under various conditions.

Plot No.	Solvent	Salt	Gas	10^3 [A] (mol dm^{-3})	Product	λ_{max} (nm)
1	H_2O	Na^+	O_2	20	AOH	494
2	H_2O	Na^+	N_2	20	AOH	494
3	H_2O	NH_4^+	N_2	40	AOH	494
4	H_2O	NH_4^+	O_2	40	AOH	494
5	NaOH	Na^+	O_2	5	AOH	472
6	NaOH	NH_4^+	N_2	5	AOH	472
7	H_2O	Na^+	O_2	0.5	$A(OH)_2$	610
8	H_2O	Na^+	Air	0.5	$A(OH)_2$	610
9	H_2O	Na^+	N_2	0.5	$A(OH)_2$	610

Plots 1–6 successively displaced 0.02 absorbance units along the ordinate for clarity.

They also pointed out that their results were consistent with a primary process involving direct interaction of A* with H_2O or HO^-. However, the nature of AOH^-, the product of reaction 10, was not clearly identified, although several possible structures were discussed.

[10] $$A^* + H_2O \rightarrow AOH^- + H^+$$

[11] $$AOH^- \rightarrow A + HO^-$$

[12] $$AOH^- + A \rightarrow AOH^{\cdot} + A^{\cdot -}$$

In this paper, more detailed results on the effect of the initial [A] and $[O_2]$ on V_{AOH} and $V_{A(OH)_2}$ are reported. These results show that certain published observations and conclusions are erroneous.

Results

The time-independent V_{AOH} were measured over a wide range of [A] in H_2O and 0.10 mol dm^{-3} aqueous NaOH solutions of the Na^+ and the more soluble NH_4^+ salt, saturated with either O_2, air or N_2 (Figs. 1 and 2). Substitution of the Na^+ by the NH_4^+ salt had no effect on V_{AOH}, addition of excess NH_4NO_3 having no influence on V_{AOH} for the Na^+ salt in H_2O.

The maximum value for the quantum yield of AOH in H_2O solutions with [A] above 2×10^{-2} mol dm^{-3} was estimated to be $\Phi(AOH) = 0.08$, based upon the ε values in Table 1 and a value of 2.25 for the ratio of 1-$HOAQSO_3Na$ to 2-$HOAQSO_3Na$ photolysis products. Clark and Stonehill (8) have reported a maximum $\Phi(AOH)$

Can. J. Chem. Downloaded from www.nrcresearchpress.com by 210.87.254.42 on 09/05/12
For personal use only.

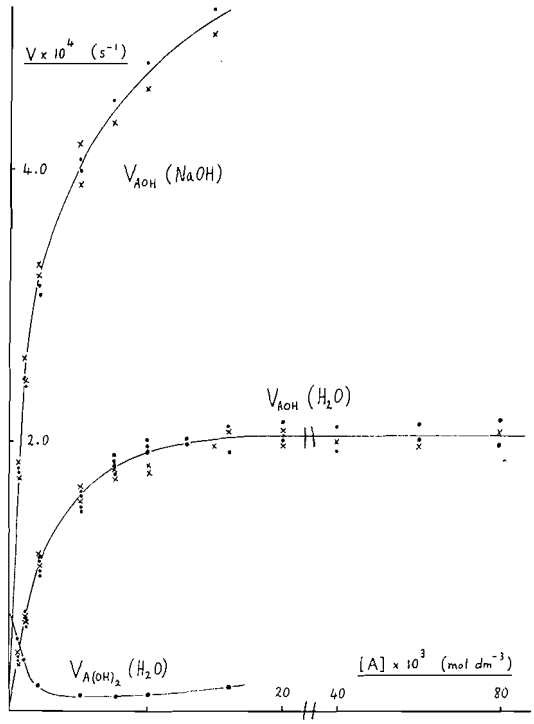

FIG. 2. Dependence of V_{AOH} and $V_{A(OH)_2}$ on [A] for solutions of the Na^+ and NH_4^+ salts saturated with O_2 or air (·) or N_2 (×).

= 0.067 in H_2O solution, based upon a value of 1.50 for the ratio of 1-$HOAQSO_3Na$ to 2-$HOAQSO_3Na$ photolysis products. Both the Φ(AOH) and the product ratio were based on low ε values (see Table 1). For solutions of A in 0.10 mol dm^{-3} aqueous NaOH only 2-$HOAQSO_3Na$ are formed and Φ(AOH) was 0.09 and 0.20 at [A] of 1.0×10^{-3} and 1.5×10^{-2} mol dm^{-3}, respectively. A limiting rate was not observed since the solubility of the Na^+ salt precludes [A] above 1.5×10^{-2} mol dm^{-3}. The higher Φ(AOH) = 0.26 in NaOH solution already published (8) was again based on erroneous ε values.

Previous studies (1) showed that photolysis of A in H_2O produces AOH and $A(OH)_2$, the latter exhibiting strong absorption at 610 nm in alkaline solution and being the major products at low [A] and high [O_2]. This absorbance at 610 nm was found to be directly proportional to the irradiation time (Fig. 1). For H_2O solutions, the derived $V_{A(OH)_2}$ decreased on increasing the [A] from 5×10^{-4} to 2×10^{-3} mol dm^{-3}, being negligible at higher [A], where the observed absorption at 610 nm is caused mainly by the

TABLE 1. Molar absorptivities (ε) for 0.1 mol dm^{-3} aqueous NaOH solutions of various hydroxy-9,10-anthraquinones (HOAQ) and for the products of photolysis of A

Compound	λ (nm)	$\varepsilon \times 10^{-3}$ (mol^{-1} dm^3 cm^{-1})*
1-HOAQ	485	4.2
2-HOAQ	465	4.9
1-$HOAQ-4-SO_3Na$	505	7.0
		7.1 (9)
1-$HOAQ-6-SO_3Na$	493	5.9
		5.7 (8)
2-$HOAQ-6-SO_3Na$	472	4.6
		3.6 (8)
2-$HOAQ-7-SO_3Na$	472	5.5
		5.4 (9)
		3.6 (8)
1-$HOAQSO_3Na$ from photolysis of A	493	6.0
2-$HOAQSO_3Na$ from photolysis of A	472	5.0

*Reference numbers in parentheses.

large excess of AOH produced. Oxygen is a necessary reaction partner for formation of $A(OH)_2$, since $V_{A(OH)_2}$ decreased on decreasing the [O_2] in solution becoming essentially zero in N_2-saturated solution (Fig. 1).

Discussion

Although Phillips *et al.* (7) claimed that a transient absorption observed on flash photolysis of A was caused by $A^{\cdot+}$, subsequent studies (10, 11) have revealed that the lifetime of A* (triplet state) is unaffected by large variations in [A]. Mechanisms including reactions 3 or 7 need not be considered.

Reactions 10–12 (8) could explain the present results. However, photolysis of A in O_2-free aqueous solution containing benzene gives not only phenol but also a larger yield of biphenyl for solutions of $pH < 7$ (12), while in alkaline solutions an enhanced yield of phenol is observed in agreement with Russian studies (4). These products can be readily detected at [A] as low as 1×10^{-4} mol dm^{-3}. These observations can only be in accord with reactions 10–12 if $AOH^{\cdot}$ or AOH^{-} is an efficient $HO^{\cdot}$ donor. The formation of biphenyl on photolysis of acidic solutions compares with the detection of this product after radiolysis of water containing benzene only when the solution was subsequently acidified (13), and is further evidence for the presence or availability of $HO^{\cdot}$ in photolyzed solutions of A.

Clark and Stonehill's reaction schemes were

Can. J. Chem. Downloaded from www.nrcresearchpress.com by 210.87.254.42 on 09/05/12
For personal use only.

Can. J. Chem. Downloaded from www.nrcresearchpress.com by 210.87.254.42 on 09/05/12
For personal use only.

introduced to explain the enhanced V_{AOH} in alkaline solution. Either of their schemes requires that the ratio of V_{AOH} in NaOH solution to V_{AOH} in H_2O should be independent of [A]. Both their data, and those reported here, show that this ratio decreases with increasing [A], indicating that reactions 10–12 are inadequate, since there is no evidence that any change in reaction mechanism occurs on increasing [A].

The same authors have also reported (14) that in anaerobic solution V_{AOH} is considerably lower than in the presence of O_2, although no actual data are given. This was rationalized in terms of reaction 6 and 13.

[13] $$AOH^{\cdot} + AOH^{\cdot} \rightarrow AOH + A + H_2O$$

In this study, V_{AOH} was independent of $[O_2]$ at all [A], and, in anaerobic solution, was certainly not half the value in aerobic solution, as required by reactions 6 and 13. In addition, these results indicate that $A(OH)_2$ are primary products of photolysis, requiring the involvement of O_2 in their formation, and that they do not arise by further hydroxylation of AOH.

The data reported here would also be consistent with a primary photochemical electron transfer reaction proposed by Russian workers (4–6, 15–17) for photolysis of aqueous solutions of anthraquinone sulfonates and also for other anthraquinone derivatives (18–20). However, some form of reverse reaction, such as reaction 15, must be considered to account for the effect of [A] on V_{AOH} and the low Φ(AOH).

[14] $$A^* + H_2O \rightarrow A^{\cdot -} + H_2O^{\cdot +} \; (A^{\cdot -} \ldots H_2O^{\cdot +})$$

[15] $$A^{\cdot -} + H_2O^{\cdot +} \; (A^{\cdot -} \ldots H_2O^{\cdot +}) \rightarrow A + H_2O$$

The enhanced V_{AOH} in alkaline solution would result partly from reduction of A* by HO^- rather than H_2O, and the maximum V_{AOH} would only be achieved at high [A] when the maximum available $HO^{\cdot}$ was captured by A.

The experimental results published to date are limited by the low selectivity of the spectrophotometric analysis, which will not clearly distinguish between the 1- and 2-hydroxy- and dihydroxyanthraquinone products, whose yields vary significantly on changing [A], $[O_2]$, and $[HO^-]$. Broadbent and Newton's product distribution data (1) and the rate data given here suggest that the product yields could be related to competitive reactions of some intermediate species such as $AOH^{\cdot}$ with A, O_2, or HO^-, in addition to any bimolecular reaction of $AOH^{\cdot}$ (reaction 13) (20).

Successful evaluation of the mechanism of the formation of AOH and $A(OH)_2$ will require more details of the precise nature of the involvement of $HO^{\cdot}$ in this reaction and clear distinction of the effect of the reaction conditions on both the primary photochemical process and on the secondary reactions leading to products.

Experimental

Sodium 9,10-anthraquinone-2-sulfonate monohydrate was purified as described previously (1). The anhydrous NH_4^+ salt was prepared by treating the barium salt with H_2SO_4, filtering off the $BaSO_4$ and neutralizing the free acid with NH_3.

Solutions of A were irradiated in a 5 cm optical cell while O_2, air, or N_2 was continuously bubbled through the solution using very narrow plastic tubing sealed into the end of the cell furthest from the stabilized Hanovia 679A 450W Hg lamp. The tubing did not interfere with the light beam and bubbling gave efficient mixing and saturation of the solution with the gas. The gas outlet was attached to a H_2O trap to ensure no air could enter the cell from outside. An almost parallel beam of light was passed through an Ealing-TFP interference filter to give radiation at 365 ± 5 nm, which then entered the solution cell.

For 0.10 mol dm^{-3} aqueous NaOH solutions, the absorbance of products at 472 nm could be measured directly as a function of time. Solutions in doubly distilled H_2O were irradiated for a given time, made strongly alkaline with one drop of concentrated NaOH solution and the absorbance of the products at 494 nm was measured. Formation of $A(OH)_2$ was detected by measurement of absorbance at 610 nm in alkaline solution. In all cases, the measured absorbance was directly proportional to the irradiation time showing that neither AOH, $A(OH)_2$, nor anthraquinone reduction products were effective internal light filters. V_{AOH} and $V_{A(OH)_2}$ were calculated in terms of the rate of increase of absorbance at the particular wavelength. Variations in V_{AOH} at fixed [A] were caused mainly by daily variations in incident light intensity. Because $A(OH)_2$ absorb light at 470–500 nm, the V_{AOH} values are more reliable at high [A] and low $[O_2]$. Similarly, slight absorption by AOH at 610 nm interferes with determination of $V_{A(OH)_2}$ at high [A].

Quantum yields were determined using potassium ferrioxalate solution as actinometer (21).

Molar absorptivities were calculated from the linear absorbance – concentration plots, for solutions of anthraquinones whose concentrations were established by potentiometric titration of the corresponding anthrahydroquinones with $K_3Fe(CN)_6$ solution. Spectra were recorded on freshly prepared alkaline solutions.

The ratio of 1-$HOAQSO_3Na$ to 2-$HOAQSO_3Na$ photolysis products and their respective ε values were determined by chromatographic separation of these products (1) and quantitative analysis of the resulting products by potentiometric titration.

The authors gratefully acknowledge the award of an operating grant and a Research Scholarship (H.B.M.) from the National Research Council of Canada.

1. A. D. BROADBENT and R. P. NEWTON. Can. J. Chem. **50**, 381 (1972).
2. B. MOONEY and H. I. STONEHILL. Chem. Ind. 1309 (1961).
3. A. D. BROADBENT. Chem. Commun. 382 (1967).
4. S. I. SHOLINA, G. V. FOMIN, and L. A. BLYUMENFEL'D. Zh. Fiz. Khim. **43**, 800 (1969).
5. A. K. CHIBISOV, V. A. KUZ'MIN, and A. P. VINOGRADOV. Dokl. Akad. Nauk SSSR, **187**, 142 (1969).
6. L. A. BLYUMENFEL'D, A. V. KARYAKIN, V. A. KUZ'MIN, G. V. FOMIN, A. K. CHIBISOV, and S. I. SHOLINA. Izv. Akad. Nauk SSSR, Ser. Khim. 2615 (1969).
7. G. O. PHILLIPS, N. W. WORTHINGTON, J. F. MCKELLAR, and R. R. SHARPE. J. Chem. Soc. A, 767 (1969).
8. K. P. CLARK and H. I. STONEHILL. J. Chem. Soc. Faraday Trans. I, **68**, 577 (1972).
9. A. D. BROADBENT. Dr. sc. techn. Dissertation, Eidgenössische Technische Hochschule, Zürich, 1963.
10. B. E. HULME, E. J. LAND, and G. O. PHILLIPS. J. Chem. Soc. Faraday Trans. I, **68**, 2003 (1972).
11. V. A. KUZ'MIN, A. K. CHIBISOV, and A. V. KARYAKIN. Int. J. Chem. Kinet. **4**, 639 (1972).
12. A. D. BROADBENT, D. HIGGINS, and H. B. MATHESON. To be published.
13. A. MANTAKA, D. G. MARKETOS, and G. STEIN. J. Phys. Chem. **75**, 3886 (1971).
14. K. P. CLARK and H. I. STONEHILL. J. Chem. Soc. Faraday Trans. I, **68**, 1676 (1972).
15. G. V. FOMIN, L. M. GURDZHIYAN, and L. A. BLYUMENFEL'D. Dokl. Akad. Nauk SSSR, **191**, 151 (1970).
16. V. A. KUZ'MIN, A. V. KARYAKIN, and A. K. CHIBISOV. Khim. Vysok. Energ. **6**, 502 (1972).
17. V. A. KUZ'MIN and A. K. CHIBISOV. J. Chem. Soc. Chem. Commun. 1559 (1971).
18. A. K. DAVIES, J. F. MCKELLAR, and G. O. PHILLIPS. Proc. Roy. Soc. London, Ser. A, **323**, 69 (1971).
19. A. K. DAVIES, R. FORD, G. A. GEE, J. F. MCKELLAR, and G. O. PHILLIPS. J. Chem. Soc. Chem. Commun. 873 (1972).
20. B. E. HULME, E. J. LAND, and G. O. PHILLIPS. J. Chem. Soc. Faraday Trans. 1. **68**, 1992 (1972).
21. J. G. CALVERT and J. N. PITTS. Photochemistry. J. Wiley and Sons, Inc., New York, 1968. p. 783.

Can. J. Chem. Downloaded from www.nrcresearchpress.com by 210.87.254.42 on 09/05/12
For personal use only.

The Structure of $(NO)_2[Ho(NO_3)_5]$, A 10-Coordinate Species

GERALD E. TOOGOOD AND CHUNG CHIEH

Department of Chemistry, University of Waterloo, Waterloo, Ontario N2L 3G1

Received August 2, 1974

GERALD E. TOOGOOD and CHUNG CHIEH. Can. J. Chem. **53**, 831 (1975).

Nitrosonium pentanitratoholmate(III), $(NO)_2Ho(NO_3)_5$, was prepared from holmium metal and dinitrogen tetroxide in anhydrous ethyl acetate. Its crystals are monoclinic with $a = 8.094$, $b = 11.979$, $c = 14.170$ Å and $\beta = 104.7°$, $Z = 4$, space group $P2_1/c$. The structure was solved by the heavy-atom method and refined by full matrix least-squares methods to an R value of 0.085 for 1514 observed reflections measured on the G.E. XRD-6 diffractometer. The structure consists of one $Ho(NO_3)_5^{2-}$ and two NO^+ ions. The holmium is 10-coordinated by five essentially symmetric bidentate nitrate groups which arrange themselves in a trigonal bipyramidal fashion around the metal with a mean Ho—O distance of 2.45 Å. The two NO^+ ions per metal occupy slightly different environments and give rise to two i.r. bands at 2250 and 2285 cm^{-1}, attributable to the (N, O^+) stretching vibration. The mean N—O distance within these ions is 1.00 Å.

GERALD E. TOOGOOD et CHUNG CHIEH. Can. J. Chem. **53**, 831 (1975).

Le pentanitratoholmate(III) de nitrosonium, $(NO)_2Ho(NO_3)_5$ a été préparé à partir de l'holmium métallique et du tétroxyde d'azote dans l'acétate d'éthyle anhydre. Les cristaux sont monocliniques avec $a = 8.094$, $b = 11.979$, $c = 14.170$ Å et $\beta = 104.7°$, $Z = 4$, groupe d'espace $P2_1/c$. On a résolu la structure par la méthode des atomes lourds et cette structure a été affinée par la méthode des moindres carrés (matrice complète) jusqu'à une valeur R de 0.085 pour 1514 réflexions observées à l'aide d'un diffractomètre G.E. XRD-6. La structure consiste d'un ion $Ho(NO_3)_5^{2-}$ et de deux ions NO^+. L'holmium est décacoordonnée par cinq groupes nitrates bidentates essentiellement symétriques qui s'arrangent d'une façon bipyramide trigonalle autour de l'atome d'holium avec une distance moyenne Ho–O de 2.45 Å. Les deux ions NO^+ occupent des environnements un peu différent et donnent lieu à deux bandes en infrarouge à 2250 et 2285 cm^{-1} attribuables à la vibration (N, O^+). La distance moyenne N—O dans ces ions est de 1.00 Å. [Traduit par le journal]

Introduction

Metal nitrates bound to one or more molecules of dinitrogen tetroxide have been prepared by various workers during the past twenty years (1–3). The nature of these compounds has been inferred from data obtained by spectroscopic and other physical methods but no definitive structural information was presented until the results of an X-ray diffraction study on $Fe(NO_3)_3 \cdot 1.5N_2O_4$ were reported by Addison and coworkers in 1973 (4). The authors of that report had realized previous to their X-ray work that this compound was unusual compared to other metal nitrate dinitrogen tetroxide adducts, particularly so far as its i.r. and Raman spectra were concerned. Their X-ray data revealed the presence of the previously unreported $N_4O_6^{2+}$ species. A more recent communication (5) which appeared during the course of our work has given preliminary data on $Cu(NO_3)_2N_2O_4$ showing that no molecular N_2O_4 exists in the structure and that bidentate nitrate groups bridge pairs of copper atoms.

In the course of our work with lanthanide metals we have prepared compounds of general formula $M(NO_3)_3 \cdot xN_2O_4$, where M = lanthanide, for all the lanthanides (except promethium). The value of x is 2 for the second half of the series but varies between 1 and 2 for the lighter elements. We formulated the compounds where $x = 2$ as $[NO]_2[M(NO_3)_5]$ (3) and this was supported by the presence of bands attributable to the N,O^+ stretching vibration in the 2280 cm^{-1} region of their i.r. spectra. In fact, two such bands were observed, separated by some 30 cm^{-1}, for each of the compounds from gadolinium to lutetium. This suggested the presence of two different environments for the NO^+ groups. To confirm this suggestion we have determined the crystal structure of $[NO]_2[Ho(NO_3)_5]$, nitrosonium pentanitratoholmate(III), using X-ray diffraction.

Experimental

Preparation of $Ho(NO_3)_3 \cdot 2N_2O_4$

The method employed was analogous to that first reported by Addison *et al.* for the copper nitrate adduct

Can. J. Chem. Downloaded from www.nrcresearchpress.com by 210.87.254.42 on 09/05/12
For personal use only.

Can. J. Chem. Downloaded from www.nrcresearchpress.com by 210.87.254.42 on 09/05/12
For personal use only.

except that extra care was taken to produce crystals of the compound suitable for X-ray work (6). Thus holmium metal was reacted with an approximately 1:1 by volume mixture of dinitrogen tetroxide and anhydrous ethyl acetate in a test tube guarded by phosphorus pentoxide against atmospheric moisture. The vigorous reaction was complete after 2 h at which stage some black residue, whose nature is unknown to us except that it is very inert, was filtered off. Addition of an appropriate excess of dinitrogen tetroxide to the filtrate will readily precipitate the desired product but not usually in a form suitable for single crystal X-ray diffraction. Since the adduct cannot be recrystallized, a "trial and error" method was employed in the step where the excess dinitrogen tetroxide was added to the initial filtrate. By varying the amount of ethyl acetate present at this stage, and controlling the rate of addition of dinitrogen tetroxide, suitable crystals were eventually obtained.

Analysis

The adduct was analyzed for holmium by thermal decomposition of the adduct to Ho_2O_3 which was collected and weighed by standard methods.

Anal. Calcd. for $Ho(NO_3)_3 \cdot 2N_2O_4$: Ho, 30.8. Found: 30.9.

X-Ray Diffraction

The crystals of $(NO)_2Ho(NO_3)_5$ are pale yellow prisms. A crystal of approximately cubic shape with edge of 0.2 mm was sealed in a capillary of 0.3 mm diameter. The crystal appeared to be stable during the course of data collection. The cell constants were established from various film data and refined by least-squares method based on 2θ values measured on the G.E. XRD-6 automatic diffractometer. The crystal data are summarized:

HoN_7O_{17} f.w. = 534.9

Monoclinic, $a = 8.094(5)$, $b = 11.979(6)$, $c = 14.170(7)$ Å, $\beta = 104.7(5)°$, $Z = 4$, $\rho_c = 2.673$, $V = 1328.9$ Å^3, F(000) = 1008, space group $P2_1/c$. $\mu_{Mo-K\alpha} = 63.0$ cm^{-1} ($\lambda_{Mo-K\alpha} = 0.7107$ Å).

The intensities of 3019 reflections ($2\theta \leq 40°$) were measured using Zr-filtered Mo–Kα radiation. Among them were four standard reflections which were measured after each 100 reflections. The intensities of the standard reflections were used as corrections (< 7%) for fluctuation over the course of data collections. The θ–2θ scan method was used and the scan range in 2θ was $\pm(0.9 + 0.3 \tan \theta)°$, with backgrounds measured at the beginning and end of each scan. The crystal was mounted with a^* along the φ axis of the goniostat. No absorption correction was made. Equivalent reflections were averaged to give 2615 independent reflections, of which 1514 had intensity I greater than the backgrounds by $3\sigma_I$ and were considered to be observed. Lorentz and polarization factors were applied to derive the structure amplitudes.

The structure was solved by heavy atom methods and refined using full-matrix least-squares methods. The revised version of least-squares program written by Doedens and Ibers was used. The atomic scattering factors for holmium are taken from Thomas–Fermi–Dirac statistical model and those of nitrogen and oxygen are from the self-consistent variational wave functions (7). Anomalous scattering corrections were made for holmium. The function minimized is $\Sigma w^2(F_o - F_c)^2$ where $w = (33.5 - 0.225F + 0.015F^2)^{-1}$, which was derived from consideration of given uniform error in each range of observed structure amplitudes. The unobserved reflections were given zero weight in the final analysis. Only the holmium atom was allowed to have anisotropic thermal parameters. The difference Fourier map showed two peaks of 3 e/Å^3 within 1 Å around the Ho atom. Other peaks are of the order of 1 e/Å^3. The final agreement index is 0.085 whereas the weighted R is 0.111. The final atomic parameters are given in Table 1.[1]

TABLE 1. Atomic coordinates (fractional × 10^4) and thermal parameters $\pm(x, y, z, x, 1/2 - y, 1/2 + z)$

Atom	x*	y	z	B(Å^2)
Ho	2511	0537	7674	†
N1	1083	1970	8893	4.0(5)
O11	1621	0962	9158	3.8(5)
O12	1167	2255	8006	4.7(4)
O13	0461	2578	9389	5.2(4)
N2	5994	0929	8799	3.6(5)
O21	7489	1026	9234	5.4(4)
O22	5495	−0019	8347	5.6(6)
O23	4881	1606	8710	4.7(4)
N3	3724	1538	6107	4.0(5)
O31	3069	2080	6682	4.8(4)
O32	3823	0500	6281	5.1(5)
O33	4116	1941	5436	5.4(5)
N4	−0937	0147	6514	3.5(5)
O41	0165	0671	6165	4.6(4)
O42	−2379	−0074	6068	5.5(5)
O43	−0414	−0133	7423	4.2(4)
N5	2593	−1773	7789	1.1(5)
O51	2483	−1241	8592	4.4(4)
O52	2698	−1315	7107	4.4(4)
O53	2738	−2846	7943	5.0(4)
N01	1848	1163	1582	9.1(10)
O01	0838	1091	0939	6.2(5)
N02	6236	1484	4491	6.8(10)
O02	7269	1768	4859	5.9(6)

*Mean estimated standard deviations with respect to the last figure are 2, 1, 1 for Ho and 26, 18, 14 for atoms in the NO_3^- groups and 42, 27, 22 for the two NO^+ groups.

†Anisotropic temperature factor for Ho = $\exp\{-2\pi^2 \times 10^{-4}(461a^{*2}h^2 + 310b^{*2}k^2 + 321c^{*2}l^2 + 20a^*b^*hk + 144a^*c^*hl + 56b^*c^*kl)\}$ with an average e.s.d. of 6×10^{-4} for the U_{ij}'s.

Results and Discussion

The structure consists of one $[Ho(NO_3)_5]^{2-}$ and two NO^+ ions; there is no molecular N_2O_4 present.

The $[Ho(NO_3)_5]^{2-}$ Group

All the nitrate ions are coordinated to the holmium and at least four can be considered as symmetrically bounded to the metal (for a

[1]Photocopies of the table of structure factors may be obtained at a nominal charge, upon request, from the Depository of Unpublished Data, CISTI, National Research Council of Canada, Ottawa, Canada K1A 0S2.

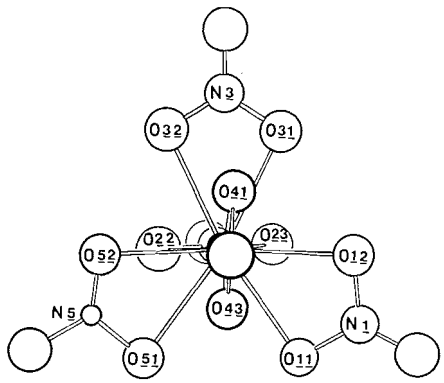

FIG. 1. The trigonal bipyramidal $Ho(NO_3)_5^{2-}$ complex looking down the axial direction.

discussion of "symmetrical" *vs.* "asymmetrical" and a general review of nitrate coordination see ref. 8). It is possible that the nitrate with its nitrogen labelled as N5 may be asymmetrically bound but it is difficult to see why this should be so. The bond distances and angles for this particular nitrate followed the same pattern throughout the refinement despite the use of different weighting schemes.

The coordination about holmium is most readily visualized in terms of the positions of the nitrogen of the five nitrate groups, that is, by considering each nitrate group as a unit)(9). These nitrogens occupy the apices of an essentially regular trigonal bipyramid which has holmium at its center as shown in Fig. 1. The planes of the two nitrate groups in the axial direction are almost perpendicular to each other, and the equatorial nitrate ions are not in the propeller fashion. An unweighted least-squares plane through Ho, N1, N3 and N5 gave the equation $0.7754X + 0.0682Y + 0.6278Z = 6.031$ referring to a, b, and c^* coordinates in Å, and the deviation of the atoms from this plane are:

Atom	Deviation	Atom	Deviation
Ho	0.05	Ce	0
N1	−0.02	N(1)	0
O11	0.39	O(2′)	0.34
O12	−0.45	O(2)	−0.34
N3	−0.02	N(2)	0
O31	−0.05	O(3)	−0.25
O32	0.06	O(4)	0.24
N5	−0.02	N(2′)	0
O51	0.42	O(3′)	0.25
O52	−0.31	O(4′)	−0.24

As a comparison the deviation of the corresponding atoms from a plane $-0.3027X - 0.9531Z = 5.44$ is also given above for the $Ce(NO_3)_5^{2-}$ ion in $(Et_3P)_2Ce(NO_3)_5$ (10). The pentanitratocerate(III) ion is situated at a special site which has C_2 symmetry and therefore the four atoms Ce, N(1), N(2), N(2′) are coplanar. A detailed examination of the two ions reveals that the arrangements of the nitrate ions are the same. The geometry of decacoordination has been discussed previously (9, 11) and it has been pointed out (9) that the highest point-symmetry achievable for these species is C_2. It is generally understood that molecules which possess certain symmetry might not be situated at crystallographic site with point symmetry corresponding to that of the molecule (12). If there were a C_2 axis for the pentanitratoholmate ion, it should be in the direction of Ho → N1. The fact that O31 and O32 are almost in the equatorial plane and O51 and O52 deviate from the plane by 0.4 and −0.3 Å indicates that the C_2 axis does not exist. The departure from C_2 symmetry may arise from the packing in the crystal and a free ion may still retain a C_2 symmetry.

The bond distances and angles with their estimated standard deviations calculated according to ref. 13 are given in Table 2. There is a slight variation in Ho—O distance but an average value of 2.45 Å compared with 2.57 (2) Å for Ce—O found in $Ce(NO_3)_5^{2-}$ (10) agrees with the contraction trend in the lanthanide series. Since no data concerning similar compounds of other elements in the series are available it is difficult to make a quantitative comparison here. The constraints imposed by the short bite of the nitrate ligand can be seen from the values found for O—Ho—O angles. In general, these can be divided into two groups, one in the range of 51–54° if both oxygen atoms are from the same nitrate and the other 68–81° if the oxygen atoms are from neighboring nitrates.

The NO^+ Groups

It is difficult to distinguish oxygen from nitrogen for the NO^+ group and the assignments of oxygen and nitrogen are based on the size of isotropic temperature factors in the initial state of structure analysis.

The bond lengths of 1.06 and 0.93 Å found for the NO^+ groups are not significantly different

Can. J. Chem. Downloaded from www.nrcresearchpress.com by 210.87.254.42 on 09/05/12
For personal use only.

Can. J. Chem. Downloaded from www.nrcresearchpress.com by 210.87.254.42 on 09/05/12
For personal use only.

TABLE 2. Bond distance and angles

(*a*) Coordination around Ho (σ = 0.02 Å and 0.6°)*

Bond	Distance (Å)	Bond	Distance (Å)
Ho—O11	2.44	Ho—O32	2.47
—O12	2.43	—O41	2.48
—O22	2.45	—O43	2.44
—O23	2.46	—O51	2.50
—O31	2.43	—O52	2.38

Bonds	Angle (deg)	Bonds	Angle (deg)
Both O from the same nitrate			
O11—Ho—O12	54.0	O41—Ho—O43	52.6
O22—Ho—O23	50.7	O51—Ho—O52	52.4
O31—Ho—O32	51.0		
Oxygens from different nitrates			
O11—Ho—O23	74.5	O32—Ho—O22	74.0
O11—Ho—O43	74.3	O51—Ho—O22	72.8
O12—Ho—O23	76.3	O51—Ho—O43	70.0
O12—Ho—O41	80.2	O52—Ho—O22	74.8
O12—Ho—O43	80.9	O11—Ho—O51	71.7
O31—Ho—O23	73.6	O12—Ho—O31	68.1
O31—Ho—O41	70.5	O32—Ho—O52	68.6
O32—Ho—O41	72.7		

*Mean bond distance = 2.45 Å.

(*b*) The nitrate groups (σ = 0.03 Å and 1°)

Bond	Distance* (Å)	Bond	Distance* (Å)
N1—O11	1.31	N4—O41	1.29
—O12	1.32	—O42	1.21†
—O13	1.21†	—O43	1.29
N2—O21	1.22†	N5—O51	1.33
—O22	1.32	—O52	1.13
—O23	1.19	—O53	1.30†
N3—O31	1.25		
—O32	1.27		
—O33	1.18†		

Bonds	Angle (deg)	Bonds	Angle (deg)
O11—N2—O12	115‡	O41—N4—O42	125
O11—N1—O13	123	O41—N4—O43	115‡
O12—N1—O13	122	O42—N4—O43	120
O21—N2—O22	118	O51—N5—O52	122‡
O21—N2—O23	128	O51—N5—O53	111
O22—N2—O23	114‡	O52—N5—O53	127
O31—N3—O32	113‡		
O31—N3—O33	124		
O32—N3—O33	123		

*Mean bond distance = 1.25 Å.
†N—O bonds not coordinated to Ho.
‡Angles of the type Ho(O, O)N.

TABLE 2. (*Concluded*)

(*c*) The NO^+ groups (σ = 0.05 Å)

Bond	Distance (Å)
N01—O01	1.06
N02—O02	0.93

(*d*) Interatomic distances from NO^+ groups to neighboring nitrate ions (σ = 0.05 Å)

Bond	Coordinates of the latter atom	Distance (Å)
N01—O12	$(x, \frac{1}{2} - y, -\frac{1}{2} + z)$	2.92
N01—O21	$(1 - x, \bar{y}, 1 - z)$	2.97
N01—O22	$(1 - x, \bar{y}, 1 - z)$	2.31
N01—O43	$(\bar{x}, \bar{y}, 1 - z)$	2.39
O01—O11	$(x, y, -1 + z)$	2.76
O01—O13	$(x, y, -1 + z)$	2.78
O01—O21	$(1 - x, \bar{y}, 1 - z)$	2.91
O01—O31	$(x, \frac{1}{2} - y, -\frac{1}{2} + z)$	2.86
O01—O43	$(\bar{x}, \bar{y}, 1 - z)$	2.69
O01—O51	$(\bar{x}, \bar{y}, 1 + z)$	2.93
N02—O23	$(x, \frac{1}{2} - y, -\frac{1}{2} + z)$	2.65
N02—O32	$(1 - x, \bar{y}, 1 - z)$	2.61
N02—O33	(x, y, z)	2.49
N02—O42	$(1 + x, y, z)$	2.90
N02—O52	$(1 - x, \bar{y}, 1 - z)$	2.63
O02—O13	$(1 + x, \frac{1}{2} - y, -\frac{1}{2} + z)$	2.93
O02—O21	$(x, \frac{1}{2} - y, -\frac{1}{2} + z)$	2.81
O02—O23	$(x, \frac{1}{2} - y, -\frac{1}{2} + z)$	2.93
O02—O33	(x, y, z)	2.88
O02—O41	$(1 + x, y, z)$	2.91
O02—O42	$(1 + x, y, z)$	2.76
O02—O52	$(1 - x, \bar{y}, 1 - z)$	2.84

and they agree with values found in literature (14). A recent report (15) showed that a compound $K_2Er(NO_3)_5$, prepared in a molten salt medium, is monoclinic with $a = 7.93$, $b = 11.92$, $c = 14.26$ Å, and $\beta = 102.8°$. These data are similar to those of $(NO)_2Ho(NO_3)_5$ and therefore indicate that the two compounds are isomorphous. A study currently being carried out (16) shows that $(NO)_2SnCl_6$ is isomorphous with K_2SnCl_6, K_2PtCl_6 etc with the NO^+ being situated at a site set corresponding to point symmetry of $\bar{4}3m$. This can be achieved through disorder of NO^+ group due to the approximate spherical shape of NO^+ ion. The disorder is also reflected in the high temperature factor for N01, O01, N02 and O02 of Table 1. The similarity between NO^+ and K^+ ions is evident. The two i.r. bands observed due to NO^+ presumably arise from the two different NO^+ environments. Both oxygen atoms in the two NO^+ ions have 6 to 7 neighboring oxygen

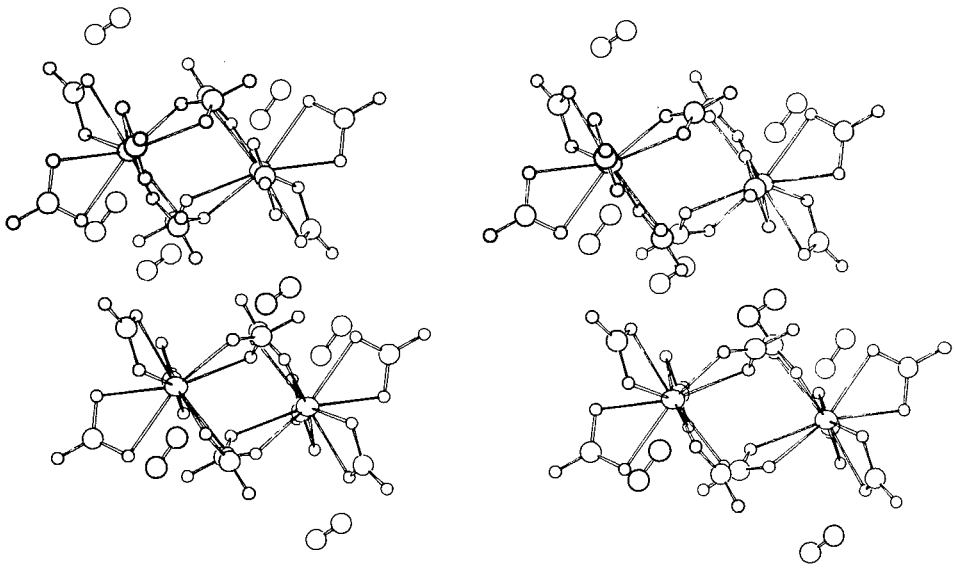

FIG. 2. A stereo-pair of the packing diagram.

at approximately the same distance but N01 has two very short contacts with other oxygen whereas N02 has four moderately close contacts with neighboring oxygen atoms. It is interesting to note that most atoms with which N01 or N02 have close contact are those involved in chelation to the metal. A stereo pair of the packing diagram is shown in Fig. 2, from which, the interionic relations are clear. In the present work, and presumably in all normal dinitrogen tetroxide – metal nitrate adducts, there is no nitrate group which is comparable to that found in the $N_4O_6^{2+}$ species in $Fe(NO_3)_3 \cdot 1.5N_2O_4$. However, in the holmium compound most of the distances between the NO^+ groups and their nearest neighboring oxygens are of comparable magnitude to those within the $N_4O_6^{2+}$ (between 2.4 and 2.7 Å) and hence it might be expected that the N,O^+ stretching vibrations would be similarly lowered. In fact the *two* i.r. bands in the spectrum of the holmium compound (2250 and 2285 cm^{-1}) are lower than, for example, in $Fe(NO_3)_3N_2O_4$ (2298 cm^{-1}), but not to the extent shown in $N_4O_6^{2+}$ (2235 cm^{-1}). It appears that the $O \ldots NO^+$ separations are not a very sensitive measure of the magnitude of the interactions between NO^+ and surrounding groups.

We are grateful to the National Research Council of Canada for financial support of this work. We thank Mr. Craig McDonald for assistance in the early stages of this work.

1. C. C. ADDISON and N. LOGAN. *In* Advances in inorganic and radio-chemistry, Vol. 6. *Edited by* H. Emeleus and A. Sharpe. 1964. p. 71, and references therein.
2. A. WALKER and J. R. FERRARO. J. Chem. Phys. **43**, 2689 (1965).
3. A. P. PENALOSA. M.Sc. Thesis, University of Waterloo, Waterloo, Ontario. 1966.
4. C. C. ADDISON, L. J. BLACKWELL, B. HARRISON, D. H. JONES, N. LOGAN, E. K. NUNN, and S. C. WALLWORK. Chem. Commun. 347 (1973).
5. L. J. BLACKWELL, T. J. KING, and A. MORRIS. Chem. Commun. 644 (1973).
6. C. C. ADDISON and B. J. HATHAWAY. J. Chem. Soc. 3099 (1958).
7. International tables for X-ray crystallography. Vol. III. Kynoch Press Birmingham. 1962. p. 201.
8. C. C. ADDISON, N. LOGAN, S. C. WALLWORK, and C. D. GARNER. Quart. Rev. **25**, 289 (1971).
9. J. G. BERGMAN and F. A. COTTON. Inorg. Chem. **5**, 1208 (1966).
10. A. R. AL-KARAGHOULI and J. S. WOOD. Chem. Commun. 135 (1970), J. Chem. Soc. Dalton, 2318 (1973).
11. E. L. MUETTERTIES and C. M. WRIGHT. Quart. Rev. **21**, 109 (1967).
12. A. I. KITAIGORODSKII. Organic chemical crystallography, Consultants Bureau, N.Y. 1961.
13. G. H. STOUT and L. H. JENSEN. X-Ray structure determination – a practical guide. Macmillan Co. 1968.
14. Tables of interatomic distances and configuration in molecules and ions; Chemical Soc. special publ. No. 11, 1958.
15. W. T. CARNALL, S. SIEGEL, J. R. FERRARO, B. TANI, and E. GEBERT. Inorg. Chem. 560 (1973).
16. D. W. A. SHARP and J. THOLEY. J. Chem. Soc. A, 3557 (1963); P. C. Chieh. To be published.

Can. J. Chem. Downloaded from www.nrcresearchpress.com by 210.87.254.42 on 09/05/12
For personal use only.

Carbon-13 Nuclear Magnetic Resonance Spectra of Isothiazole, 1,2-Dithiole, and 1,3-Dithiole Derivatives

N. PLAVAC AND I. W. J. STILL[1]

Department of Chemistry, University of Toronto, Toronto, Ontario M5S 1A1

AND

M. S. CHAUHAN AND D. M. MCKINNON

Department of Chemistry, University of Manitoba, Winnipeg, Manitoba R3T 2N2

Received October 1, 1974

N. PLAVAC, I. W. J. STILL, M. S. CHAUHAN, and D. M. MCKINNON. Can. J. Chem. **53**, 836 (1975).

Carbon-13 chemical shift data have been obtained for a number of isothiazole, benzo[*c*]-isothiazole, 1,2-dithiole, and 1,3-dithiole derivatives. A number of these compounds are thiones and the chemical shifts of the C=S carbons are discussed in the light of recent attempts to predict such chemical shifts from those of the analogous carbonyl compounds. Comparisons of substituent chemical shift (s.c.s.) effects in these heterocyclic compounds with those in simpler aromatic or conjugated systems have been made and additivity correlations tested in a number of cases.

N. PLAVAC, I. W. J. STILL, M. S. CHAUHAN et D. M. MCKINNON. Can. J. Chem. **53**, 836 (1975).

On a obtenu des données concernant les déplacements chimiques du ^{13}C d'un certain nombre de dérivés d'isothiazoles, de benzo[*c*]isothiazoles, de dithiole-1,2 et de dithiole-1,3. Un certain nombre de ces composés sont des thiones et on discute des déplacements chimiques des carbones C=S à la lumière des essais récents qui ont été faits pour prédire les déplacements chimiques de tels carbones par comparaison avec ceux de composés carbonylés analogues. On a fait une comparaison des effets de déplacements chimiques dus aux substituants (s.c.s.) dans ces composés hétérocycliques avec d'autres dans des systèmes conjugués et aromatiques plus simples et on a vérifié, dans un certain nombre de cas, des corrélations d'additivité.

[Traduit par le journal]

Introduction

A growing volume of data on carbon-13 chemical shift parameters for organic sulfur compounds in general (1–3) and sulfur-containing heterocycles in particular (4–7) has appeared in recent publications. We wish to report our own observations on five series of heterocyclic compounds, three of which may be broadly categorized as isothiazole derivatives, the others comprising 1,2-dithiole and 1,3-dithiole derivatives, respectively. Many of these compounds contain the thione functional group and, in view of a recent claim (5) to have established a linear relationship between the chemical shifts of carbonyl and thiocarbonyl carbons in compounds of the type R(C=X)R′ and R—N=C=X, we were thus particularly interested in testing the predictive value of the correlation below discovered by Kalinowski and Kessler (5) in the wider context of the heterocyclic systems already referred to.

$$\delta_{C=S} = 1.45\delta_{C=O} - 46.5 \text{ p.p.m.}$$

We were also interested in applying some of the substituent chemical shift (s.c.s.) effects in alkenes and aromatic hydrocarbons, available from recent comprehensive reviews of the carbon-13 n.m.r. literature (8, 9) to the potentially more complex systems involved in our study and we will present our findings in this regard also.

Experimental

Natural abundance proton decoupled carbon-13 n.m.r. spectra were obtained on a Varian XL-100-15 spectrometer operating at 25.16 MHz in the pulsed Fourier transform mode. The temperature of the probe was 32 ± 3°. Spectral widths of 6000 Hz, acquisition times of 0.666 s, and pulse widths of 10 μs (90° pulse = 55 μs) were routinely used. In some cases, pulse delays of 1–5 s were used to intensify quaternary carbons, and in other cases, paramagnetic chromium trisacetylacetonate[2] was used for the same purpose. The spectra were transformed

[1]To whom correspondence should be addressed.

[2]$[Cr(AcAc)_3] \approx 17$ mg/2.5 ml of solution.

Can. J. Chem. Downloaded from www.nrcresearchpress.com by 210.87.254.105 on 09/05/12
For personal use only.

Can. J. Chem. Downloaded from www.nrcresearchpress.com by 210.87.254.105 on 09/05/12
For personal use only.

using a Varian 16K-620i computer giving 4096 real points with an accuracy of ±0.1 p.p.m. Off-resonance proton decoupled spectra were obtained where deemed necessary. The deuterium of the solvent (chloroform-*d* or acetone-d_6) was used as lock and primary reference in all cases, and all chemical shifts are measured from TMS (5%) added as internal reference.

The sources of compounds used in this study, or the relevant literature references, are cited in the appropriate Table (1, 3, 4, 5, or 7). Procedures which have not been published previously appear below.

Preparation of Benzo[c]isothiazole

The procedure of Davis and White (14) gave a product contaminated with chlorinated product. It was therefore modified in that toluene was used as a solvent and the product was purified by recrystallization of its picrate.

Preparation of 4-Phenyl-1,2-dithiol-3-one

4-Phenyl-1,2-dithiole-3-thione (2.10 g, 10 mmol) (20) was added to a saturated solution of mercuric acetate in acetic acid (10 ml) and chloroform (40 ml) added. The mixture was stirred 16 h then diluted with water. Work-up afforded pale yellow needles which were recrystallized from petroleum ether (b.p. 60–80°), m.p. 81° (lit (24) m.p. 81°) (78%).

Preparation of 4,5-Diphenyl-1,2-dithiol-3-one

4,5-Diphenyl-1,2-dithiole-3-thione (2.86 g, 10 mmol) (23) was oxidized as above. Recrystallization from ethanol gave pale yellow needles, m.p. 116°, (lit. (24) m.p. 116°) (81%).

Preparation of Methyl 2-Thio-1,3-dithiole-4-carboxylate

2-Thio-1,3-dithiole-2-carboxylic acid (1.78 g, 10 mmol) (18) was added to a stirred solution of diazomethane (0.504 g, 12 mmol) in anhydrous ether (250 ml). The acid dissolved with effervescence. After 20 min the solution was filtered and evaporated to yield a yellow crystalline solid which was recrystallized from hexane as yellow flakes, m.p. 109° (98%); n.m.r. δ ($CDCl_3$) 4.12 (3H, s), 8.04 (1H, s) p.p.m.

Anal. Calcd. for $C_5H_4S_3O_2$: C, 31.41; H, 2.95; S, 50.00. Found: C, 31.46; H, 2.92; S, 50.15.

Results and Discussion

In Table 1 are gathered the chemical shift data for a series of simple isothiazole derivatives. In the case of the monomethyl derivatives these data are in good agreement with results obtained recently by Wasylishen and Becker.[3] Our data for 3-chloro-4-cyano-5-phenylisothiazole are also in good agreement with these authors' results for 4-cyanoisothiazole. In the parent compound, the C-4 carbon appears at 123.6 p.p.m., in accord with its α relationship to the polar C=N functionality. This carbon may also experience some shielding through electron release from the sulfur atom, although the examples of thiophene (in contrast to furan) (9) and our own earlier findings (3) indicate that this effect will be small. The chemical shift difference (Δδ) between C-4 and C-5 in isothiazole (24.4 p.p.m.) is, as expected, somewhat smaller than Δδ for the α- and β-carbon atoms in the presumably more polar cyclopentenone (31.3 p.p.m.) (9).

The α-, β-, and γ-shift effects for the monomethyl- and monophenylisothiazoles are collected in Table 2. It can be seen immediately from this table that these effects, especially the α- and β-effects, are quite variable and are clearly influenced by the location of the substituent and its ability to participate in conjugation with the unsaturated imine structural unit. Unfortunately, only one disubstituted compound, 4,5-diphenylisothiazole, was available and the use of the 4- and 5-phenyl s.c.s. effects gives calculated chemical shift values in only moderately good agreement with those observed. However, such departures from additivity have been noted previously even with simple *ortho*-disubstituted aromatic compounds (30, 31) and in the present case this is not at all surprising, considering the steric bulk of the phenyl substituents.

Data for a series of simple CH_3- and NO_2-substituted benzo[*c*]isothiazoles are collected in Table 3. Chemical shift data for the parent oxygen-containing analog, benzo[*c*]isoxazole, are also included for comparison. With the exception of the C-4 chemical shift in isothiazole itself, which is moved downfield (deshielded) by 11.1 p.p.m. (C-4a in the benzo-fused analog), the chemical shifts for the hetero-ring carbons are not affected very greatly by the extra fused ring. Substitution in the benzene ring does have an effect, however, on the C-3 carbon in benzo[*c*]isothiazole. For example, a methyl substituent at C-4 produces an upfield shift (γ-shielding effect) at C-3 of 1.8 p.p.m., whereas the introduction of a nitro group at C-5 or C-7 produces downfield shifts of 6.4 and 4.2 p.p.m., respectively. This latter effect can be rationalized in terms of the participation of structures such as the ones shown below.

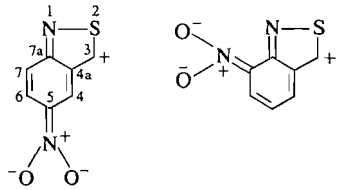

[3]R. E. Wasylishen and E. D. Becker. Personal communication.

Can. J. Chem. Downloaded from www.nrcresearchpress.com by 210.87.254.105 on 09/05/12
For personal use only.

TABLE 1. Carbon-13 chemical shifts* of isothiazoles

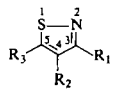

			Chemical shift								
						C_6H_5					
R_1	R_2	R_3	C-3	C-4	C-5	C-1	*Ortho*	*Meta*	*Para*	Other	Source (Reference)
H	H	H	157.0	123.4	147.8	—	—	—	—	—	†
CH_3	H	H	166.7	123.9	148.1	—	—	—	—	18.5(CH_3)	†
H	CH_3	H	158.8	134.2	143.6	—	—	—	—	11.9(CH_3)	†
H	H	CH_3	157.6	123.3	163.0	—	—	—	—	12.6(CH_3)	†
H	H	C_6H_5	158.1	119.9	167.3	130.7	126.7	129.2	129.5	—	(10)
H	C_6H_5	H	156.0	139.9	142.6	132.6	126.9	129.1	128.0	—	(11)
H	C_6H_5	C_6H_5	159.1	132.8	161.5	129.2 – 127.1 (unresolved)				—	(12)
Cl	CN	C_6H_5	151.4	105.1	176.4	127.5	129.9	127.3	132.4	112.1(CN)	(13)

*All shifts in p.p.m. relative to TMS; chloroform-*d* as solvent.
†Aldrich Chemical Co., Inc.

Can. J. Chem. Downloaded from www.nrcresearchpress.com by 210.87.254.105 on 09/05/12
For personal use only.

TABLE 2. Substituent chemical shift (s.c.s.) effects* of CH_3 and C_6H_5 in isothiazoles

Derivative	α-effect	β-effect	γ-effect
3-Methyl	+9.7	+0.5	+0.3
4-Methyl	+10.8	+1.8(C-3) −4.2(C-5)	—
5-Methyl	+15.2	−0.1	+0.6
4-Phenyl	+16.5	−1.0(C-3) −5.2(C-5)	—
5-Phenyl	+19.5	−3.4	+1.1

*In p.p.m.; positive values indicate shifts to lower field.

When both a methyl group at C-4 and a nitro group at C-5 are present, the effects are additive at C-3 (+6.4 − 1.8 = +4.6, in agreement with the observed value).

The chemical shifts of the remaining heterocyclic ring carbons (C-4a, C-7a) show a much less clear-cut influence of substitution patterns in the benzenoid ring and indeed are markedly influenced (upfield shifts of the order of 8-10 p.p.m.) only if a nitro group is located on a neighboring carbon.

As far as the benzenoid carbons (C-4, C-5, C-6, C-7) are concerned we have used the simple additivity principle to calculate predicted chemical shifts (which appear in parentheses in Table 3), using recent literature values for the C-1, *ortho*, *meta*, and *para* s.c.s. effects of methyl (9) and nitro groups (31) in aromatic systems. Considering that the total range of shifts observed for the four carbon atoms involved is at least 25 p.p.m., and that we are ignoring any variable effects produced by the heterocyclic ring, the agreement between prediction and observation is quite good. For the two monomethyl derivatives, for example, the mean deviation is 0.6 p.p.m., whereas for the two mononitro derivatives the mean deviation is less good (1.3 p.p.m.). Extension of this approach to two benzo[*c*]isothiazoles substituted by both nitro and methyl groups, as expected, gives poorer agreement, with a mean deviation of 2.3 p.p.m., although no single value deviated by more than 4.5 p.p.m.

The final series of isothiazole derivatives studied were the isothiazolinethiones, for which chemical shift data are collected in Table 4. Since, with one exception, these compounds differ only in the nature of the substituent present on the nitrogen atom, the main interest in this table centers on the chemical shift of the thiocarbonyl carbon. In the 3-isothiazoline-5-thiones (**I**) the mean value for C=S is 193.4 p.p.m., compared with 187.0 p.p.m. in the 4-isothiazoline-3-thiones (**II**), where the thione group is attached to the more electronegative nitrogen atom. These values should be contrasted with an average value for C=S of 202.9 p.p.m. which we found earlier (3) for some α,β-unsaturated thio ketones. On the other hand, Radeglia and Scheithauer (2) found the chemical shift of C=S in dithio esters of the type RCH_2CSSEt to be around 225 p.p.m. and Kalinowski and Kessler (5) reported chemical shifts for C=S in thioamides in the range 179.6–207.2 p.p.m., so that it appears that it is likely that the range of chemical shifts observed for C=S will be at least as great as that for the more familiar C=O group. We will discuss this aspect further in connection with the data obtained for the 1,2- and 1,3-dithiole derivatives (Tables 5 and 7).

The introduction of the second phenyl substituent at C-4 in 4,5-diphenyl-4-isothiazoline-3-thione produces a β-effect (C-5) of −3.7 p.p.m. and a relatively small α-effect (C-4) of +9.1 p.p.m. The corresponding shifts observed for the introduction of a C-4 phenyl group in the somewhat analogous 5-phenyl-1,2-dithiole-3-thione system (Table 5) were −2.5(β) and +9.7(α) p.p.m., respectively. The β-effect of the extra phenyl substituent on the chemical shift of C-3 (C=S) in the isothiazolinethione is quite small (+0.6 p.p.m.). Data for two other derivatives in the 3-isothiazoline-5-thione series, the *N*-methyl and *N*-phenyl analogs, do not appear in Table 4 because they were too insoluble in the solvents chloroform-*d* and acetone-d_6 used throughout this study.

In Table 5 we have collected chemical shift data for a number of phenyl-substituted 1,2-dithiole-3-thiones and 1,2-dithiol-3-ones. Although a full range of comparisons is not available because we were unable to obtain the unsubstituted dithiolone to complete the series, some comparisons are possible. For example, the much greater difference in chemical shift (Δδ) between C_α and C_β of an unsaturated enone than the corresponding unsaturated thione, discussed in our earlier paper (3), is once again evident if one compares analogous compounds. For 4-phenyl-1,2-dithiole-3-thione the Δδ value is 4.9 whereas in 4-phenyl-1,2-dithiol-3-one the corresponding value is 18.3 and in the 5-phenyl substituted analogs the Δδ values are 36.8 and 52.5 p.p.m., respectively.

Can. J. Chem. Downloaded from www.nrcresearchpress.com by 210.87.254.105 on 09/05/12
For personal use only.

TABLE 3. Carbon-13 chemical shift*† data for benzo[*c*]isothiazoles

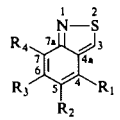

R_1	R_2	R_3	R_4	Chemical shift C-3	C-4a	C-4	C-5	C-6	C-7	C-7a	Other	Source (Reference)
H	H	H	H	144.5	134.5	122.1	124.2	128.6	121.6	161.5	—	‡
Benzo[*c*]isoxazole				155.3	118.4	124.4	120.0	131.1	114.7	156.1	—	§
CH_3	H	H	H	142.7	135.7	131.3 (131.0)	122.9 (124.9)	128.8 (128.5)	119.0 (118.7)	161.7	19.4(CH_3)	(14)
H	H	H	CH_3	144.4	134.6	119.7 (119.2)	124.4 (124.1)	127.2 (127.9)	130.9 (130.5)	161.8	17.7(CH_3)	(14)
H	NO_2	H	H	150.9	133.0	120.0 (116.8)	145.1 (143.8)	122.8 or 122.2 (123.3)	122.2 or 122.8 (122.4)	161.9	—	(15)
H	H	H	NO_2	148.7	137.6	129.6 (128.1)	127.2 (125.0)	122.8 (123.3)	140.6 (141.2)	151.7	—	(15)
NO_2	H	H	CH_3	147.4	126.7	139.4 (139.0)	124.3 (119.8)	125.6 (129.3)	140.9 (136.5)	161.9	18.4(CH_3)	(15)
CH_3	NO_2	H	H	149.1	135.9	129.7 (125.7)	144.9 (144.5)	124.2 (123.2)	120.2 (119.7)	160.9	17.4(CH_3)	(15)

*All shifts in p.p.m. relative to TMS; chloroform-*d* as solvent.
†Values in parentheses are calculated from the substituent effects (9, 31) in simple aromatic systems.
‡See Experimental.
§Aldrich Chemical Co., Inc.

Can. J. Chem. Downloaded from www.nrcresearchpress.com by 210.87.254.105 on 09/05/12
For personal use only.

TABLE 4. Carbon-13 chemical shifts* in 3-isothiazoline-5-thiones(**I**) and 4-isothiazoline-3-thiones(**II**)

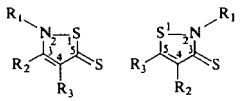

I **II**

Series	R_1	R_2	R_3	Chemical shift								Source (Reference)
							C_6H_5					
				C-3	C-4	C-5	C-1	*Ortho*	*Meta*	*Para*	Other	
I	$(CH_3)_2CH$	H	C_6H_5	149.4	131.7	192.7	132.9	127.7	128.2	127.5	56.3(*CH*) 23.5(CH_3)	(16)
I	C_6H_{11}	H	C_6H_5	149.0	131.8	192.7	132.9	127.7	128.3	127.5	63.0(*CH*) 34.2(C-2′) 25.0(C-3′) 24.7(C-4′)	(16)
I	$C_6H_5CH_2$	H	C_6H_5	150.7	131.5	194.8	133.6 133.5	(129.3–127.8)†			56.2(CH_2)	(16)
II	CH_3	H	C_6H_5	186.7	125.3	155.4	128.9	126.3	129.7	131.4	36.1(CH_3)	(17)
II	CH_3	C_6H_5	C_6H_5	187.3	134.4	151.7		(131.4 – 127.3)†			36.1(CH_3)	(18)

*All shifts in p.p.m. relative to TMS; chloroform-*d* as solvent.
†Phenyl carbons incompletely resolved.

Can. J. Chem. Downloaded from www.nrcresearchpress.com by 210.87.254.105 on 09/05/12
For personal use only.

TABLE 5. Carbon-13 chemical shifts* in 1,2-dithiole-3-thiones and 1,2-dithiol-3-ones

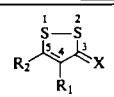

X	R_1	R_2	C-3	C-4	C-5	C_6H_5 C-1	*Ortho*	*Meta*	*Para*	Other	Source (Reference)
S	H	H	216.7	140.2	155.1	—	—	—	—	—	(19)
S	C_6H_5	H	213.8	149.2	154.1	133.2	(128.4–128.9)†			—	(20)
S	H	C_6H_5	215.6	136.0	172.8	131.7	126.9	129.6	132.2	—	(21)
S	H	p(MeO)C_6H_4	214.8	134.4	173.0	124.0	128.5	114.9	162.9	55.6(OCH_3)	(22)
S	C_6H_5	C_6H_5	214.9	145.7	170.3	134.1 133.2	(128.9, 128.5)†		130.9 130.7	—	(23)
O	C_6H_5	H	193.3	131.8	150.1	133.9	127.5	(128.7)†	(128.7)†	—	‡
O	H	C_6H_5	193.9	117.7	170.2	132.4	126.4	129.4	131.8	—	(21)
O	C_6H_5	C_6H_5	193.4§	131.6§	166.8§	134.8§ 133.8§	(131.5, 131.2, 129.8, 129.3, 129.0, 128.8)†§			—	‡

*All shifts in p.p.m. relative to TMS; chloroform-d as solvent unless otherwise indicated.
†Phenyl carbons incompletely resolved.
‡See Experimental.
§Acetone-d_6 as solvent.

TABLE 6. Substituent chemical shift (s.c.s.) effects* of C_6H_5 in 1,2-dithiole-3-thiones†

Derivative	α-effect	β-effect	γ-effect
4-Phenyl	+9.0	−1.0(C-5) −2.9(C=S)	—
5-Phenyl	+17.7	−4.2	−1.1
5-*p*-Methoxyphenyl	+17.9	−5.8	−1.9

*In p.p.m.; positive values indicate shifts to lower field.
†Unfortunately, we have been unable to obtain the parent carbonyl compound to observe the s.c.s. effects of C_6H_5 in this series.

Substituent chemical shift (s.c.s.) effects for phenyl substitution in the thione series are collected in Table 6. The α-effect produced by 5-phenyl substitution (and in the very closely similar 5-*p*-methoxyphenyl analog) is approximately twice that produced by 4-phenyl substitution, presumably due to the greater contribution of phenyl in the former case to the charged resonance contributor shown below.

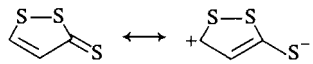

A similar doubling for the α-effects of methyl substitution at C_β *vs.* C_α in conjugated enones has already been reported by us (3). When the s.c.s. effects of phenyl were used to predict chemical shifts for C-3, C-4, and C-5 in 4,5-diphenyl-1,2-dithiole-3-thione, the agreement with the observed values was remarkably good, considering the steric bulk of the substituents and problems with the '*ortho*' effect already discussed for the isothiazole series.

For all compounds referred to in Table 5, the effects produced by the phenyl substitution on the chemical shifts of the C=S and C=O carbon atoms were rather small. The mean chemical shift observed for the C=O series of compounds is 193.5 p.p.m. and when this value is used in the empirical correlation of Kalinowski and Kessler (5) the predicted value obtained for the C=S chemical shift in this series is 234.1 p.p.m., in poor agreement with the mean value actually observed (Table 5) of 215.2 p.p.m. Similarly, as will be seen by the data in Table 7, the predicted value (using Kalinowski and Kessler's equation) of the C=S chemical shift of 1,3-dithiole-2-thione is 235.0 p.p.m., and the observed value is again approximately 20 p.p.m. to higher field at 213.3 p.p.m. We are presently unable to advance a reason for the poor correlation in this series, unlike the thioketone, thioamide, and isothiocyanate series reported by Kalinowski and Kessler. It may be worth noting that the observed chemical shift difference (C=O *vs.* C=S) for our two sets of carbonyl and thiocarbonyl compounds is approximately 20 p.p.m. in each case.

Chemical shift data on the final group of heterocyclic compounds are collected in Table 7. This group includes 1,3-dithiole-2-thione and the analogous carbonyl compound, as well as two mono- and two (symmetrically) disubstituted derivatives of the thiocarbonyl compound. It is interesting to note that the chemical shift of the C=S carbon remains essentially unaltered by being flanked by two bivalent sulfur atoms, rather than a sulfur atom and a carbon atom, as in the 1,2-dithiole analog (213.3 *vs.* 216.7 p.p.m.). If one compares a simple carboxylic acid ester with a dialkyl carbonate, for example, the Δδ for the respective carbonyl carbon atoms is approximately 15 p.p.m. (9), whereas for the case of amides and ureas (9), Δδ is slightly greater than 10 p.p.m. Thus it can be seen that the electronic effects on carbon-13 chemical shifts of oxygen, nitrogen, and sulfur run in the order O > N ≫ S. Comparing the parent thiocarbonyl compound with 1,3-dithiol-2-one, a pronounced upfield shift of the signal due to the ethylenic carbons can also be observed in the latter (118.5 *vs.* 129.4 p.p.m.).

In the mono-substituted derivatives of 1,3-dithiole-2-thione, introduction of a phenyl group produces an α-effect of +17.0 and a rather pronounced upfield shift at the β-carbon of −7.4 p.p.m. As in simple ethylene derivatives (9), introduction of a methoxycarbonyl group exerts a downfield shift on both the α- (+6.6) and the β- (+11.0) carbons, and the effect is more pronounced at the β-carbon.

In the disubstituted 1,3-dithiole derivatives, the ethylenic carbons (C-4 and C-5) are once more shifted downfield (+9.6 p.p.m.) in the dicarboxylic ester, although this is a much more pronounced shift than in dimethyl maleate (9) (+5.4 p.p.m.). It is noteworthy too that the chemical shift of the carboxylic ester carbons at 158.5 p.p.m. is at significantly higher field than that observed in diethyl maleate (9) (164.8 p.p.m.). In the 4,5-dicyano compound, the upfield shift (−6.5 p.p.m.) experienced by the ethylenic carbon atoms is again greater than that observed in maleonitrile (9) (−2.4 p.p.m.). The chemical shift observed for the CN group at

Can. J. Chem. Downloaded from www.nrcresearchpress.com by 210.87.254.105 on 09/05/12
For personal use only.

TABLE 7. Carbon-13 chemical shifts* in 1,3-dithiole-2-thiones and 1,3-dithiol-2-one

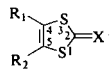

X	R_1	R_2	Chemical shift C-2	C-4	C-5	Other	Source (Reference)
S	H	H	213.3	129.4	129.4	—	(25)
O	H	H	194.1	118.5	118.5	—	(26)
S	C_6H_5	H	212.4	146.4	122.0	131.0(C-1′), 129.8(C-4′), 129.4(C-3′), 126.5(C-2′)	(27)
S	CO_2Me	H	213.7†	136.0†	140.4†	158.7†(C=O), 53.6†(OCH_3)	‡
S	CO_2Me	CO_2Me	209.2†	139.0†	139.0†	158.5†(C=O), 54.3†(OCH_3)	(28)
S	CN	CN	200.4†	122.9†	122.9†	107.1†(C≡N)	(29)

*All shifts in p.p.m. relative to TMS; chloroform-*d* as solvent unless otherwise indicated.
†Acetone-d_6 as solvent.
‡See Experimental.

107.1 p.p.m. is outside the usual range (112–126 p.p.m.) quoted (9) for the nitrile group: this may result from some contribution of charged resonance contributors as shown below.

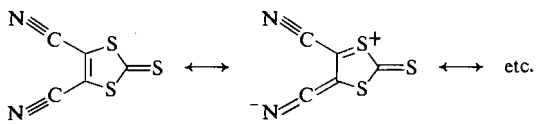

Our studies of chemical shift data and s.c.s. effects in organosulfur compounds and heterocyclic systems are continuing.

We wish to gratefully acknowledge the financial support provided by Erindale College, University of Toronto. We also thank Professor W. F. Reynolds for valuable discussions and Dr. Roderick Wasylishen for providing us with a prepublication copy of his manuscript.

1. S. PIGNATARO, L. LUNAZZI, C. BOICELLI, R. DI MARINO, A. RICCI, A. MANGINI, and R. DANIELLI. Tetrahedron Lett. 5341 (1972).
2. R. RADEGLIA and S. SCHEITHAUER. Z. Chem. **14**, 20 (1974).
3. M. S. CHAUHAN and I. W. J. STILL. Int. J. Sulfur Chem. In press.
4. R. A. ARCHER, R. D. G. COOPER, P. V. DEMARCO, and L. F. JOHNSON. Chem. Commun. 1291 (1970).
5. H-O. KALINOWSKI and H. KESSLER. Angew. Chem. Int. Ed. **13**, 90 (1974).
6. G. W. BUCHANAN, J. B. STOTHERS, and G. WOOD. Can. J. Chem. **51**, 3746 (1973); W. A. SZAREK, D. M. VYAS, A-M. SEPULCHRE, S. D. GERO, and G. LUKACS. Can. J. Chem. **52**, 2041 (1974).
7. R. D. LAPPER and A. J. POOLE. Tetrahedron Lett. 2783 (1974).
8. J. B. STOTHERS. Carbon-13 n.m.r. spectroscopy. Academic Press, New York. 1972.
9. G. C. LEVY and G. L. NELSON. Carbon-13 nuclear magnetic resonance for organic chemists. John Wiley and Sons, Inc., New York. 1972.
10. R. A. OLOFSON, J. M. LANDESBERG, R. O. BERRY, D. LEAVER, W. A. H. ROBERTSON, and D. M. MCKINNON. Tetrahedron, **22**, 2119 (1966).
11. D. LEAVER, D. M. MCKINNON, and W. A. H. ROBERTSON. J. Chem. Soc. 32 (1965).
12. G. E. BACHERS, D. M. MCKINNON, and J. M. BUCHSCHRIBER. Can. J. Chem. **50**, 2568 (1972).
13. S. NAKAGAWA, J. OKAMURA, F. SAKAI, H. HOSHI, and T. NAITO. Tetrahedron Lett. 3719 (1970).
14. M. DAVIS and A. W. WHITE. J. Org. Chem. **34**, 2985 (1969).
15. M. DAVIS and A. W. WHITE. J. Chem. Soc. C, 2189 (1969).
16. M. S. CHAUHAN, M. E. HASSAN, and D. M. MCKINNON. Can. J. Chem. **52**, 1738 (1974).
17. G. LE COUSTUMER and Y. MOLLIER. C.R. (*C*) **270**, 433 (1970).
18. D. M. MCKINNON and M. E. HASSAN. Can. J. Chem. **51**, 3081 (1973).
19. R. MAYER and J. KUBASCH. Angew. Chem. **73**, 220 (1961).
20. E. K. FIELDS. J. Am. Chem. Soc. **77**, 4255 (1955).
21. E. KLINGSBERG and A. SCHREIBER. J. Am. Chem. Soc. **83**, 2934 (1961).
22. B. BOLLCHER and A. LUTTRINGHAUS. Ann. Chem. **557**, 89 (1947).
23. M. G. VORONKOV, A. S. BROUN, and G. B. KARPENKO. J. Gen. Chem. USSR Engl. Transl. **19**, 395 (1949).
24. F. BOBERG and J. KNOOP. Ann. Chem. **708**, 148 (1967).
25. E. KLINGSBERG. J. Am. Chem. Soc. **86**, 5290 (1964).
26. F. CHALLENGER, E. A. MASON, E. C. HOLDSWORTH, and R. EMMOTT. J. Chem. Soc. 292 (1953).
27. D. LEAVER, W. A. H. ROBERTSON, and D. M. MCKINNON. J. Chem. Soc. 5104 (1962).
28. D. B. J. EASTON and D. LEAVER. Chem. Commun. 585 (1965).
29. E. KLINGSBERG. J. Am. Chem. Soc. **86**, 5290 (1964).
30. K. N. SCOTT. J. Am. Chem. Soc. **94**, 8564 (1972).
31. G. W. BUCHANAN, G. MONTAUDO, and P. FINOCCHIARO. Can. J. Chem. **52**, 767 (1974).

Can. J. Chem. Downloaded from www.nrcresearchpress.com by 210.87.254.105 on 09/05/12
For personal use only.

The Mechanism of the Microbial Hydroxylation of Steroids. Part 1. The C-21 Hydroxylation of Progesterone by *Aspergillus niger* ATCC 9142

HERBERT L. HOLLAND AND BARBARA J. AURET

Department of Chemistry, The Queen's University of Belfast, Belfast, Northern Ireland BT9 5AG

Received October 8, 1974

HERBERT L. HOLLAND and BARBARA J. AURET. Can. J. Chem. **53**, 845 (1975).

The mechanism of the C-21 hydroxylation of progesterone (**1***a*) by *Aspergillus niger* ATCC 9142 to give 11-deoxycorticosterone (**1***b*) has been studied by the use of progesterone derivatives and of C-21 deuterium labelled progesterones. The requirement of the C-21 hydroxylase system for a C-20 carbonyl group is demonstrated and the possiblity of the involvement of this group, in the C-20,21 enol form, in the C-21 hydroxylation reaction has been discussed. However, on the basis of the observed deuterium isotope effect ($K_H/K_D = 1.25$), a mechanism for the microbial C-21 hydroxylation reaction is proposed in which the rate-determining step is the direct insertion of oxygen into a C-21 carbon–hydrogen bond and not one involving enolization of the C-20 carbonyl.

In addition, C-11α and C-15β hydroxylation of both 20α- and 20β-hydroxypregn-4-ene-3-one (**2***a* and **2***b*) by *A. niger* has been observed.

HERBERT L. HOLLAND et BARBARA J. AURET. Can. J. Chem. **53**, 845 (1975).

On a étudié le mécanisme de l'hydroxylation (en position C-21) de la progestérone (**1***a*) par l'*Aspergillus niger* ATCC 9142 conduisant à la déoxy-11 corticostérone (**1***b*); cette étude a été effectuée à l'aide de dérivés de la progestérone et de progestérone marquée au deutérium en position C-21. On a démontré la nécessité d'un groupe carbonyle en C-20 pour rendre efficace le système d'hydroxylase en C-21; on discute aussi de la possibilité de l'implication du groupement carbonyle en position 20 sous forme d'énol C-20,21 lors de la réaction d'hydroxylation en C-21. Toutefois, sur la base de l'observation d'un effet isotopique ($K_H/K_D = 1.25$), on propose un mécanisme pour la réaction d'hydroxylation microbiologique en C-21 dans lequel l'étape déterminante est l'insertion directe de l'oxygène dans le lien carbone–hydrogène en C-21 et on suggère que cette réaction n'implique pas une énolisation du groupement carbonyle en position C-20.

De plus l'*Aspergillus niger* provoque l'hydroxylation en C-11α et en C-15β des hydroxy-20α et -20β pregène-4 one-3 (**2***a* et **2***b*). [Traduit par le journal]

In spite of the wide application of microbial steroid hydroxylation in both industry and research (1) and a thorough investigation of related biochemical processes (2), comparatively little is known about the chemistry of this reaction.

The proposal that microbial hydroxylation at saturated carbon proceeds by direct electrophilic insertion of oxygen into a C—H bond followed from the discovery of a relationship between microbial hydroxylation of steroids at C_n and microbial epoxidation of steroids unsaturated at C_n, demonstrating the electrophilic nature of microbial hydroxylation (3, 4) and the observation that microbial hydroxylation at saturated carbon proceeds with retention of configuration (5–7).

The question of enzymic substrate activation has received little consideration. For hydroxylation at saturated carbon, chemical analogy suggests that activation is unnecessary: oxidation of steroids at saturated carbon has been achieved under electrophilic conditions (8, 9). However, the problem of enzymic substrate activation during hydroxylation adjacent or vinylogous to carbonyl functions is potentially more complex. The substrates most commonly used (1) for microbial hydroxylations have been Δ^4-3-ketosteroids and it has been proposed (1) that, during their hydroxylation at C-2, -6, -17, or -21, activation occurs by enolization and that hydroxylation occurs by electrophilic attack of oxygen at the enol. This is shown for hydroxylation at C-21 of a C-20 ketosteroid in Scheme 1.

Precedent for such a mechanism is provided by

Can. J. Chem. Downloaded from www.nrcresearchpress.com by 210.87.254.42 on 09/05/12
For personal use only.

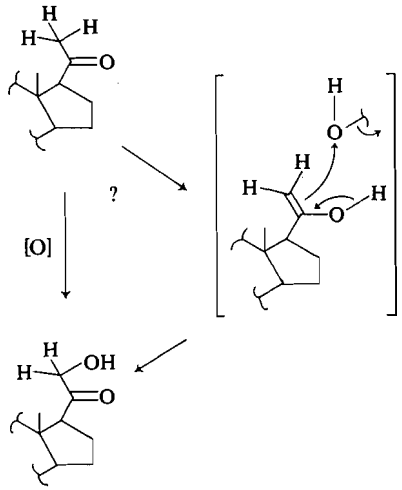

SCHEME 1. Alternative pathways for the C-21 hydroxylation of a C-20 ketosteroid.

the facile oxidation by electrophilic oxygen of steroidal enols to α-hydroperoxy or α-hydroxy ketones (10–14) and by enzymic enolization of ketosteroids (15). Further evidence, albeit circumstantial, is provided by the frequent occurrence of hydroxylations of Δ^4-3,20-diketosteroids at the axial 2β, 6β, 10β (in 19-norsteroids), and 17α positions, whereas microbial hydroxylations at 2α, 6α, 10α, and 17β are unknown (1): analogously, electrophilic attack on the corresponding enols gives exclusively axial substitution of the electrophile (11–13, 16).

To investigate activation by enzymic enolization, the C-21 hydroxylation of progesterone (pregn-4-ene-3,20-dione) (**1***a*) by *Aspergillus niger* ATCC 9142 to give 11-deoxycorticosterone (21-hydroxypregn-4-ene-3,20-dione) (**1***b*) has been examined. The absence of complicating factors such as rigid stereochemistry at C-21 and non-enzymic enolization of the C-20 carbonyl to C-21 (which does not occur under conditions of thermodynamic control (17, 18)) makes this system suitable for the present study.

Previous work (19) established that progesterone, 6β-, 11α-, 11β-, and 14α-hydroxyprogesterone, 11-ketoprogesterone, and 19-norprogesterone were hydroxylated at C-21 by *A. niger* but did not report the effect of variation of functionality at C-20: accordingly, 20α- and 20β-hydroxypregn-4-ene-3-one (**2***a* and **2***b*, respectively) were incubated with *A. niger*. In neither case was C-21 hydroxylation observed but C-15β hydroxylated (**2***c* and **2***e*) and C-11α,15β dihydroxylated (**2***d* and **2***f*) products were formed in minor amount. Their structures follow from the p.m.r. data presented in Table 1 and the Experimental section. Thus C-15β hydroxylation is characterized by a downfield shift of the signal of the C-18 methyl group, with respect to the unsubstituted (at C-15) steroid of *ca.* δ 0.3 p.p.m., and hydroxylation at C-11α produces a similar perturbation of the signal of the C-19 methyl group (20). The p.m.r. spectra of **2***c*–**2***f* accord with this and show signals due to methine protons geminal to hydroxyl of the expected multiplicity for, and in the region characteristic of, the proposed structures (20). The location of hydroxyl in **2***c*–**2***f* was confirmed by oxidation to the corresponding known ketones.

Removal of oxygen from C-20 led to a loss of hydroxylase activity in *A. niger*. Incubation of pregn-4-ene-3-one (**3***a*), the 20-methylene derivative **3***b*, and the 20-thiosteroid **3***c* produced no conversion products. The failure of *A. niger* to metabolize **3***c* is of interest in view of the facile thione–enethiol interconversion (21) and the metabolism of sulfur compounds by other strains of *A. niger* (22).

A C-20 carbonyl group is therefore essential for C-21 hydroxylation and activation of C-21 by enolization of this group has been investigated by the use of progesterone labelled with deuterium at C-21. The results are summarized in Table 2.

Progesterone fully substituted with deuterium at the enolizable carbons (**4***a*) gave, upon incubation with *A. niger*, 11-deoxycorticosterone (**5***a*) with loss of only one deuterium atom per molecule. This follows from mass spectral data (Table 2) and from the p.m.r. spectrum of **5***a*, which showed no absorption at δ 4.18 (*cf.* the spectrum of **1***a*, Table 1), and demonstrates that, if enolization is occurring during hydroxylation, it cannot be reversible with exchange of protium with the medium. It also establishes that no loss of label occurs from C-2, -4, -6, or -17 during hydroxylation. In this and subsequent incubations of labelled progesterones, starting material was recovered which showed no loss or scrambling of label.

Progesterone with one deuterium atom at C-21 (**4***b*) was prepared by hydrogenolysis of 21-iodoprogesterone with zinc and monodeuterioacetic acid, and the location of label confirmed by spectral analysis. Thus the p.m.r.

Can. J. Chem. Downloaded from www.nrcresearchpress.com by 210.87.254.42 on 09/05/12
For personal use only.

TABLE 1. Proton magnetic resonance data in deuteriochloroform solution* of progesterone, 20α-hydroxypregn-4-ene-3-one, 20β-hydroxypregn-4-ene-3-one, and the products of their metabolism by *A. niger*

Compound	δ value					
	C-11	C-15	C-18	C-19	C-20	C-21
Progesterone (**1***a*)	—	—	0.67	1.18	—	2.11
11-Deoxycorticosterone (**1***b*)	—	—	0.70	1.20	—	4.18
11-Deoxycorticosterone (**1***b*), C_6D_6 solution	—	—	0.48	0.70	—	3.95
20α-Hydroxypregn-4-ene-3-one (**2***a*)	—	—	0.72	1.20	3.70	1.26
20β-Hydroxypregn-4-ene-3-one (**2***b*)	—	—	0.78	1.18	3.70	1.14
15β,20α-Dihydroxypregn-4-ene-3-one (**2***c*)	—	4.30	1.03	1.19	3.80	1.11
11α,15β,20α-Trihydroxypregn-4-ene-3-one (**2***d*)	4.00	4.30	1.00	1.35	3.80	1.25
15β,20β-Dihydroxypregn-4-ene-3-one (**2***e*)	—	4.28	1.10	1.24	3.90	1.17
11α,15β,20β-Trihydroxypregn-4-ene-3-one (**2***f*)	4.00	4.30	1.10	1.35	3.90	1.18

*Unless otherwise stated.

TABLE 2. Conversion of *d*-progesterones **4***a*–**4***c* to 11-deoxycorticosterone by *A. niger*

Substrate	Label (%)	Product	Label (%)
2,2,4,6,6,17,21,21-d_9-Progesterone (**4***a*)	d_9, 78*	2,2,4,6,6,17,21,21-d_8-11-DOC (**5***a*)	d_8, 77.2
	d_8, 19		d_7, 18.8
	d_7, 3		d_6, 4
21-*d*-Progesterone (**4***b*)	d_1, 77.5	21-*d*-11-DOC	d_1, 58
	d_0, 22.5	(**1***b* + **5***b* + **5***c*)	d_0, 42
2,2,4,6,6,17,21,21-d_8-Progesterone (**4***c*)	d_8, 40	2,2,4,6,6,17,21,21-d_8-11-DOC	d_8, 16
	d_7, 40		d_7, 40
	d_6, 13.6	(**5***a* + **5***d* + **5***e*)	d_6, 29
	d_5, 6.4		d_5, 9
			d_4, 6

*Deuterium content values are accurate to ±0.5%.

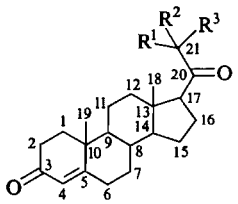

1

a $R^1 = R^2 = R^3 = H$
b $R^1 = R^2 = H; R^3 = OH$

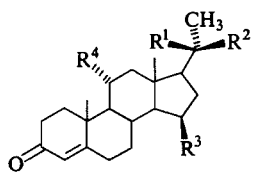

2

a $R^1 = R^3 = R^4 = H; R^2 = OH$
b $R^1 = OH; R^2 = R^3 = R^4 = H$
c $R^1 = R^4 = H; R^2 = R^3 = OH$
d $R^1 = H; R^2 = R^3 = R^4 = OH$
e $R^1 = R^3 = OH; R^2 = R^4 = H$
f $R^1 = R^3 = R^4 = OH; R^2 = H$

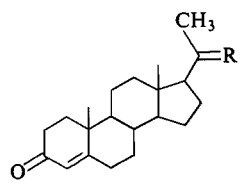

3

a $R = H_2$
b $R = CH_2$
c R = S

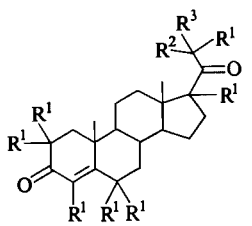

4

a $R^1 = R^2 = R^3 = D$
b $R^1 = R^2 = H; R^3 = D$
c $R^1 = R^2 = D; R^3 = H$

Can. J. Chem. Downloaded from www.nrcresearchpress.com by 210.87.254.42 on 09/05/12
For personal use only.

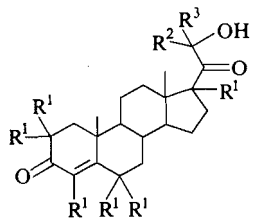

5

a $R^1 = R^2 = R^3 = D$
b $R^1 = R^2 = H; R^3 = D$
c $R^1 = R^3 = H; R^2 = D$
d $R^1 = R^2 = D; R^3 = H$
e $R^1 = R^3 = D; R^2 = H$

signal of the C-21 methyl at δ 2.11 corresponded to approximately two protons, while mass spectral analysis of **4***b* confirmed the presence of deuterium at C-21 (see Experimental).

Incubation of **4***b* with *A. niger* gave 11-deoxycorticosterone which consisted of unlabelled material **1***b* and the diastereomeric monodeuterioalcohols **5***b* and **5***c*. Mass spectral analysis showed all the label to be present at C-21: intense ions were observed at *m/e* 299 (M − CHDOH) and 271 (M − C_2HDO_2H) corresponding to the loss of C-21 and C-20 + C-21 and their substituents, respectively, whereas the ^{13}C corrected intensities of the corresponding ions at *m/e* 300 and 272, expected if label were located in the steroid nucleus, were zero. Analysis of the p.m.r. spectrum (C_6D_6 solution) of the mixture of **1***b*, **5***b*, and **5***c* showed **5***b* and **5***c* to be present in equimolar amounts. Two absorptions of equal area at δ 3.86 and 3.98, attributable to the C-21 hydrogens of **5***b* and **5***c*, were complicated by the presence of an AB quartet (J = 19 Hz) centered at δ 3.95 and assigned to the C-21 hydrogens of **1***b* but nevertheless their assignment to **5***b* and **5***c* is unambiguous. No attempt was made to assign these signals individually to **5***b* or **5***c*.

The formation of **5***b* and **5***c* in equimolar amounts shows that the two hydrogens originally present at C-21 may be lost with equal facility: by implication, the replacement of hydrogen by hydroxyl is nonstereospecific. The deuterium content of the product (**1***b* + **5***b* + **5***c*) thus enables the deuterium isotope effect of the C-21 hydroxylation to be calculated as $K_H/K_D = 1.3 \pm 0.1$.[1]

This was confirmed following synthesis of 2,2,4,6,6,17,21,21-d_8-progesterone (**4***c*) (Scheme 2) and incubation with *A. niger*. The synthesis involved loss of some deuterium during acid catalyzed hydrolysis of the intermediate 2,2,4,6,6,17,21,21-d_8-pregn-4-ene-3,20-dione 21-(2′-tetrahydropyranyl) ether but spectral analysis of **4***c* clearly indicated that deuterium content at C-21 was 2.0 atoms per molecule and that loss had taken place from C-2, -4, or -6. Thus the mass spectrum of **4***c* showed ions at *m/e* 126–129 from the fragment C-1-6 + C-19, a fragment appearing from unlabelled material **1***a* at *m/e* 124 (23) and observed in the mass spectrum of 2,2,4,6,6,17,21,21,21-d_9-progesterone (**4***a*) at *m/e* 129. The p.m.r. spectrum of **4***c* showed absorption in the region δ 2.0–2.6, essentially absent from the spectrum of **4***a* and attributable to protons adjacent or vinylogous to carbonyl; the signal of the C-21 methyl of **4***c* appeared as a singlet corresponding to approximately one proton at δ 2.11.

The 11-deoxycorticosterone formed from **4***c* consisted of the diastereomers **5***d* and **5***e*, analogous to **5***b* and **5***c*, in equimolar amount, together with **5***a* which contained a maximum

---

[1]If % d_1-progesterone is x and % d_0-progesterone is $(100 - x)$ then, in the absence of an isotope effect,

$(100 - x)d_0$-progesterone → $(100 - x)d_0$-11-DOC

and

xd_1-progesterone → $1/3xd_0$-11-DOC + $2/3xd_1$-11-DOC

In the presence of an isotope effect y, where $y = K_H/K_D$, then

$(100 - x)d_0$-progesterone → $(100 - x)d_0$-11-DOC

and

xd_1-progesterone → $(1/3)(x/y)d_0$-11-DOC + $(x - (1/3)(x/y))d_1$-11-DOC

Thus,

[1] final % d_1-11-DOC = $(x - (1/3)(x/y)) = z$

and

[2] final % d_0-11-DOC = $(100 - x) + (1/3)(x/y)$ = $(100 - z)$

Found

$x = 75.5 \pm 0.5$

$z = 58.0 \pm 0.5$

Therefore, from [1] or [2]

$y = 1.3 \pm 0.1$

Can. J. Chem. Downloaded from www.nrcresearchpress.com by 210.87.254.42 on 09/05/12
For personal use only.

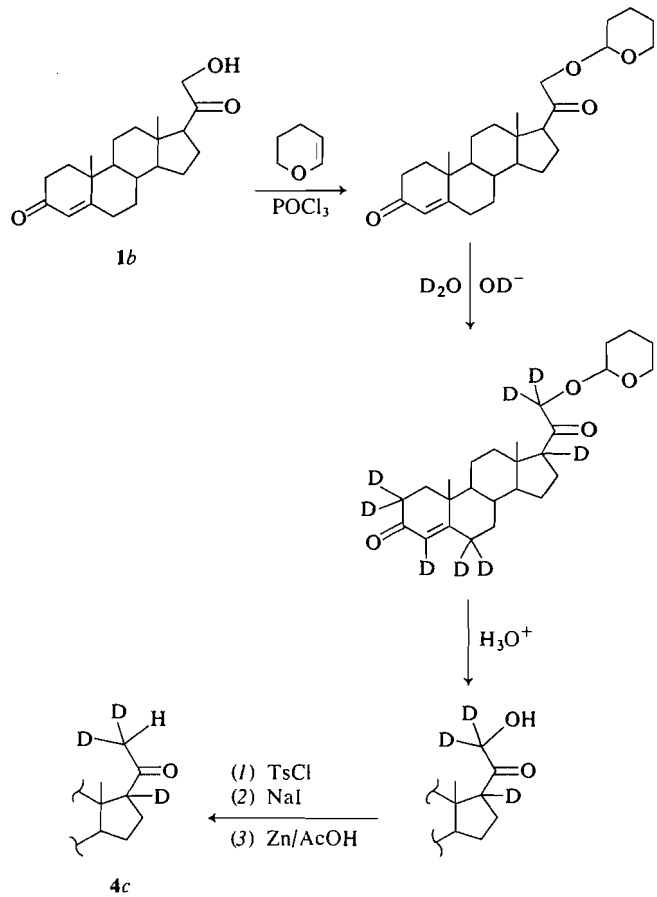

SCHEME 2. Synthesis of 2,2,4,6,6,17,21,21-d_8-progesterone (**4***c*).

of eight deuterium atoms per molecule. Proton magnetic resonance analysis was facilitated by the absence of material unlabelled at C-21 and confirmed the results of the incubation of **4***b*. Calculation of the deuterium isotope effect for the conversion of **4***c* to 11-deoxycorticosterone gave $K_H/K_D = 1.2 \pm 0.1$, in close agreement with the value obtained from the incubation of **4***b*.

The magnitude of this effect eliminates a mechanism of C-21 hydroxylation in which enolization of the C-20 carbonyl, with a rate determining loss of hydrogen from C-21, is the slow step. Primary deuterium isotope effects of between 5 and 10 for base (24–26) and acid (27) catalyzed enolizations of ketones, where the loss of α hydrogen is rate determining, have been reported. However, the effect is consistent with a mechanism of C-21 hydroxylation involving rate determining electrophilic insertion into a C—H or C—D bond. The observed value is similar to those of analogous chemical reactions such as the autoxidation of cholesterol at C-7α ($K_H/K_D = 1.8$) (28) and the insertion of a carbene into a C—H or C—D bond ($K_H/K_D = 1.8$) (29). The latter process has been the subject of calculations (30) which indicate a transition state with little C—H bond lengthening, consistent with an isotope effect of small magnitude (31). By analogy, the isotope effect of the C-21 hydroxylation may be the result of rate limiting electrophilic insertion of oxygen into a C—H or C—D bond, with little lengthening of that bond in the transition state.

This interpretation is supported by the isotope effects of enzymic hydroxylations of steroids

Can. J. Chem. Downloaded from www.nrcresearchpress.com by 210.87.254.42 on 09/05/12
For personal use only.

Can. J. Chem. Downloaded from www.nrcresearchpress.com by 210.87.254.42 on 09/05/12
For personal use only.

at nonenolizable positions. Hydroxylations at C-7β of estr-4-ene-3,17-dione (32), C-7α of cholesterol (28), C-6β of taurochenodeoxycholic acid (28), and C-11α of progesterone (6) all involve isotope effects close to unity.

This result does not, however, eliminate the C-20,21 enol from involvement in C-21 hydroxylation. Enolization may occur in which loss of hydrogen from C-21 is not rate limiting: Hine and co-workers (33, 34) have observed catalysis of the dedeuteration of α-deuteriocarbonyl compounds in which loss of deuterium is only partly rate controlling. Similar catalysis, in which the rate determining step may involve the carbonyl center (34), may occur in enzymic enolization of the C-20 carbonyl. In this event, the deuterium content of the product would depend on the relative rates of loss of protium or deuterium from C-21 and would therefore be subject to a primary isotope effect whose magnitude in this situation is unknown.[2] Exchange of deuterium at C-21 with protium from the medium does not occur during hydroxylation: the observed isotope effect is not therefore the result of an equilibration of protium and deuterium during reversible enolization.

The complexity of interpretation of the kinetic isotope effects of enzymic hydroxylations has been discussed fully (28, 32) and the isotope effect of the C-21 hydroxylation of progesterone is not open to unambiguous interpretation. It appears, however, that the effect is the result of a mechanism in which any of the C-21 C—H bonds may undergo direct insertion of oxygen, leading to the formation of 11-deoxycorticosterone directly. The microbial conversion of steroidal C-methyl groups into hydroxymethyl is well known (1) and is performed on androst-4-ene-3,17-dione by *A. niger* ATCC 9142 (35).

The C-21 hydroxylation of progesterone by *A. niger* ATCC 9142 is therefore a reaction directly analogous in mechanism to hydroxylation at saturated carbon not adjacent or vinylogous to carbonyl and not one in which the substrate is activated to electrophilic attack by enolization. The latter remains an attractive hypothesis however for axial hydroxylation at the enolizable positions of Δ^4-3-ketosteroids and will receive further consideration.

[2]J. Hine, private communication.

Experimental

Apparatus, Materials, and Methods

Melting points were determined on a Kofler heating stage and are uncorrected. Infrared spectra were recorded with a Perkin-Elmer 137, p.m.r. spectra with a Varian HA 100, using deuteriochloroform as solvent (unless otherwise stated) and TMS as internal standard, and mass spectra were obtained with an AEI MS902. Deuterium content was estimated by repeated scanning of the relevant ions and application of the appropriate corrections for ^{13}C. Accurate mass measurements were made by reference to the perfluorokerosene spectrum. Optical rotation data were obtained in chloroform solution with a Perkin-Elmer 141 polarimeter.

Column chromatography was performed on silica gel (Whatman's SG 31) and thin-layer chromatography on Merck silica $PF_{254+366}$.

Aspergillus niger ATCC 9142 was obtained from the American Type Culture Collection, Washington, D.C. and was maintained on 2% malt agar slopes.

Preparation of Substrates

Pregn-5-ene-3,20-dione Bis(ethylene acetal)

This was prepared by the method described (36) from progesterone (7.5 g). Recrystallization from acetone gave the title compound (6.8 g, 71%), m.p. 179–181° (lit. (36) m.p. 177–180°).

Pregn-5-ene-3,20-dione 3-(Ethylene Acetal)

This was prepared from pregn-5-ene-3,20-dione bis(ethylene acetal) (6 g) by the method described (37). Recrystallization from acetone gave the desired compound (3.8 g, 84%), m.p. 175–176° (lit. (37) m.p. 178–180°).

20α-Hydroxypregn-5-ene-3-one Ethylene Acetal

Sodium (9.3 g) was added portionwise to a refluxing solution of pregn-5-ene-3,20-dione 3-(ethylene acetal) (3.5 g) in 2-propanol (300 ml). When addition was complete refluxing was continued for 15 min. The solution was then poured onto ice-water (300 ml) and the precipitated solid collected by filtration, washed with water, and dried *in vacuo*. Recrystallization from ether gave the product (2.5 g, 71%), m.p. 177–179°, $[\alpha]_D^{21}$ −41.9° (*c*, 1.0) (lit. (38) m.p. 178–180°, $[\alpha]_D$ −43°).

20α-Hydroxypregn-4-ene-3-one (2a)

Sulfuric acid (8% v/v; 15 ml) was added to a solution of 20α-hydroxypregn-5-ene-3-one ethylene acetal (2.5 g) in methanol (50 ml). The solution was refluxed for 15 min, neutralized with 5% sodium bicarbonate, poured onto ice-water, and the precipitate collected by filtration and washed with water. Two crystallizations from ethyl acetate gave **2a** (1.9 *g*, 85%), m.p. 160–163°; $[\alpha]_D^{20}$ +95.4° (*c*, 1.0) (lit. (39) m.p. 161–162°, $[\alpha]_D^{22}$ +98.6°); p.m.r.: included signals at δ 0.72 (3H, s, C-18 methyl), 1.20 (3H, s, C-19 methyl), 1.26 (3H, d, J = 6 Hz, C-21 methyl), 3.70 (1H, quintet, J = 6,6,6,6 Hz, C-20 H), 5.75 (1H, d, J = 1 Hz, C-4 H).

20β-Hydroxypregn-4-ene-3-one (2b)

This was prepared from progesterone (5 g) by the method described (40). Recrystallization from aqueous methanol gave the product (3.1 g, 64% overall), m.p. 172–174°, $[\alpha]_D^{25}$ +85.2° (*c*, 1.0) (lit. (40) m.p. 174–175°, $[\alpha]_D^{20}$ +86°); p.m.r.: included signals at δ 0.78 (3H, s, C-18 methyl), 1.14 (3H, d, J = 6 Hz, C-21 methyl),

Can. J. Chem. Downloaded from www.nrcresearchpress.com by 210.87.254.42 on 09/05/12
For personal use only.

1.18 (3H, s, C-19 methyl), 3.70 (1H, m, C-20 H), 5.75 (1H, d, J = 1 Hz, C-4 H).

Pregn-4-ene-3-one (3a)

This was prepared from 3β-hydroxypregn-5-ene-20-one (3 g) by the route described (41). Recrystallization from methanol gave the product (1.4 g, 47% overall), m.p. 102–105°, $[\alpha]_D^{20}$ +124° (*c*, 0.9) (lit. (41) m.p. 102–104°, $[\alpha]_D$ +121°).

20-Methylpregna-4,20(21)-diene-3-one (3b)

This was prepared from 3β-hydroxypregn-5-ene-20-one (5 g) by the route described (42). The crude product (1.96 g) was purified by chromatography and crystallization from aqueous methanol to give the title compound (1.7 g, 34% overall), m.p. 153–156°, $[\alpha]_D^{18}$ +110° (*c*, 0.96) (lit. (42) m.p. 152–154°, $[\alpha]_D^{27}$ +112° (*c*, 1.35)).

20-Thiopregn-4-ene-3-one (3c)

This was prepared from 3β-hydroxypregn-5-ene-20-one (6 g) by the route described (43). Chromatography of the crude product on alumina gave the title compound (0.8 g, 11% overall), m.p. 112–115°.

2,2,4,6,6,17,21,21,21-d_9-Progesterone (4a)

Sodium (1 g) was added to a solution of progesterone (1 g) in dry dioxan (50 ml) and deuterium oxide (12 ml) added to this solution. The solution was refluxed for 7 days, cooled, neutralized to pH 8 with acetic acid, poured onto ice-water (150 ml), and rapidly extracted with ether. The ether extract was washed with water, dried, and evaporated to give a residue which, on crystallization from ether – light petroleum, gave the desired compound (0.64 g, 63%), m.p. 120–122°, $[\alpha]_D^{25}$ +165° (*c* 1.02, EtOH); p.m.r.: included signals at δ 0.67 (3H, s, C-18 methyl), 1.18 (3H, s, C-19 methyl), 2.0–2.6 (*ca.* 0.2H, m, protons adjacent or vinylogous to carbonyl); m.s.: *m/e* 323(100), 322(30), 321(5), 279(50), 278(10), 129(70), 128(21); analysis of ions at *m/e* 320–323 gave the following molecular isotopic composition: d_9, 78%; d_8, 19%; d_7, 3%; d_6, 0%.

21-d-Progesterone (4b)

Zinc dust (1.2 g) was added to a solution of 21-iodopregn-4-ene-3,20-dione (1.2 g) (44) in monodeuterioacetic acid (10 ml) and the mixture stirred for 10 min at room temperature. The solution was then filtered, water (100 ml) added to the filtrate, and this solution extracted with ether. The ethereal extract was washed with 2 M sodium bicarbonate, dried, and evaporated. The residue was chromatographed to give, after recrystallization from ether – light petroleum, the product (0.4 g, 46%), m.p. 120–122°; p.m.r.: included signals at δ 0.67 (3H, s, C-18 methyl), 1.18 (3H, s, C-19 methyl), 2.11 (*ca.* 2H, s, C-21 CH_2D), 5.76 (1H, broad s, C-4 H); m.s.: *m/e* 315(100), 314(30), 273(60), 272(20), 271(7), 125(30), 124(180); analysis of ions at *m/e* 314, 315 gave the following molecular isotopic composition: d_1, 77.5%; d_0, 22.5%.

Pregn-4-ene-3,20-dione 21-(2′-Tetrahydropyranyl) Ether

Phosphorous oxychloride (1 g) was added to a solution of 11-deoxycorticosterone (2.5 g) and 2,3-dihydropyran (0.64 g) in dichloromethane (50 ml) and the resulting solution stirred at 35° for 15 min. Ether (300 ml) was then added and the solution washed with 2 M sodium bicarbonate and water, dried, and evaporated to give a residue which, on crystallization from pentane, afforded the product (1.87 g, 62%), m.p. 110–113°, $[\alpha]_D^{18}$ +186° (*c*, 1.07) (lit. (45) m.p. 111–112°, $[\alpha]_D^{25}$ +183°).

2,2,4,6,6,17,21,21-d_8-Pregn-4-ene-3,20-dione 21-(2′-Tetrahydropyranyl) Ether

Sodium (1 g) was added to a solution of pregn-4-ene-3,20-dione 21-(2′-tetrahydropyranyl) ether (1.5 g) in dry dioxan (100 ml). Deuterium oxide (20 ml) was then added and the resulting solution treated as described in the preparation of 2,2,4,6,6,17,21,21,21-d_9-progesterone (**4a**). The title compound (1.36 g), after recrystallization from hexane, melted at 110–113°, $[\alpha]_D^{18}$ +181° (*c*, 0.94); m.s.: analysis of ions at *m/e* 414-422 gave the following molecular isotopic composition: d_8, 74%; d_7, 18%; d_6, 7%; d_5, 1%.

2,2,4,6,6,17,21,21-d_8-11-Deoxycorticosterone

Hydrochloric acid (37%, 5 drops) was added to a solution of 2,2,4,6,6,17,21,21-d_8-pregn-4-ene-3,20-dione 21-(2′-tetrahydropyranyl) ether (1.36 g) in hexane (100 ml) and methanol (100 ml). The mixture was stirred at room temperature for 2 h and evaporated to give a residue which was dissolved in ether, washed with 2 M sodium bicarbonate, dried, and evaporated. Recrystallization from aqueous methanol gave the product (1.0 g, 86%), m.p. 139–142°, $[\alpha]_D^{20}$ +181° (*c*, 1.0); m.s.: analysis of ions at *m/e* 330–338 gave the following molecular isotopic composition: d_8, 41%; d_7, 39%; d_6, 14%; d_5, 6%.

2,2,4,6,6,17,21,21-d_8-21-Iodopregn-4-ene-3,20-dione

This was prepared from 2,2,4,6,6,17,21,21-d_8-11-deoxycorticosterone (1 g) by the method described (44). The crude product (1.2 g) was used directly.

2,2,4,6,6,17,21,21-d_8-Progesterone (4c)

This was prepared from 2,2,4,6,6,17,21,21-d_8-21-iodopregn-4-ene-3,20-dione (1.2 g) by the procedure described for the preparation of 21-*d*-progesterone, using acetic acid in place of monodeuterioacetic acid. The product, after purification by chromatography and crystallization from aqueous methanol (0.48 g, 57%), melted at 120–121°; p.m.r.: included signals at δ 0.66 (3H, s, C-18 methyl), 1.18 (3H, s, C-19 methyl), 2.11 (*ca.* 1H, s, C-21 CHD_2), 2.0–2.6 (*ca.* 0.6H, m, protons adjacent or vinylogous to carbonyl); m.s.: *m/e* 322(80), 321(70), 320(25), 280(0.1), 279(2), 278(11), 277(37), 276(25), 275(11), 129(17), 128(60), 127(43), 126(37); analysis of ions at *m/e* 314–322 gave the following molecular isotopic composition: d_8, 40%; d_7, 40%; d_6, 13.6%; d_5, 6.4%.

Incubations with A. niger ATCC 9142

Incubations were performed in a 5-l fermentation vessel, mechanically stirred and aerated with air sterilized by passage through a Whatman Gamma 10 filter. Growth medium (2.5 l, containing Czapek Dox nutrient 33.4 g/l) was autoclaved in the fermentation vessel at 15 p.s.i. for 20 min, and then allowed to cool. A spore suspension obtained by shaking an agar slope of *A. niger* with sterile glass beads in water was then transferred to the vessel with a sterile syringe; this process was repeated so that two slopes were used to inoculate 2.5 l of medium. After 2 days growth at 28°, a solution of the substrate (1 g) in ethanol (50 ml) was added to the flask and growth allowed to continue for a further 4 days. The mycelium and medium were then separated by centrifugation, and both extracted with dichloro-

Can. J. Chem. Downloaded from www.nrcresearchpress.com by 210.87.254.42 on 09/05/12
For personal use only.

methane. The extract was dried over sodium sulfate and evaporated. Incubations with smaller quantities of substrate were performed with proportionately smaller fermentation volumes.

Progesterone (1a)

One gram gave a crude extract (0.434 g) which was subjected to preparative t.l.c. (ether) and gave: progesterone (0.16 g from ether – light petroleum), R_f 0.87, identified by m.p. and spectral comparison with an authentic sample. And *11-deoxycorticosterone* (0.21 g from aqueous methanol), R_f 0.6, identified by m.p. and spectral comparison with an authentic sample; p.m.r.: included signals at δ 0.70 (3H, s, C-18 methyl), 1.20 (3H, s, C-19 methyl), 4.18 (2H, broad s, C-21 H), 5.73 (1H, broad s, C-4 H); p.m.r. (C_6D_6) included signals at δ 0.48 (3H, s, C-18 methyl), 0.70 (3H, s, C-19 methyl), 3.95 (2H, ABq, J = 19 Hz, C-21 H), 5.81 (1H, broad s, C-4 H).

20α-Hydroxypregn-4-ene-3-one (2a)

One gram gave a crude extract (0.537 g) which was subjected to preparative t.l.c. (ethyl acetate) and gave: 20α-hydroxypregn-4-ene-3-one (**2a**) (0.3 g from aqueous methanol), R_f 0.6, identified by m.p. and spectral comparison with an authentic sample. And *15β,20α-dihydroxypregn-4-ene-3-one (2c)* (0.028 g from ethyl acetate – light petroleum), R_f 0.43 (ethyl acetate), 0.16 (ether), 0.40 (chloroform–methanol–water 188:12:1), m.p. 210–212°, M^+ 332.2358 ($C_{21}H_{32}O_3$ requires M^+ 332.2351), $[\alpha]_D^{18}$ +60° (*c*, 0.4); i.r.: ν_{max} (KBr) 3470, 1670, 1620 cm^{-1}; p.m.r.: included signals at δ 1.03 (3H, s, C-18 methyl), 1.11 (3H, d, J = 6 Hz, C-21 methyl), 1.19 (3H, s, C-19 methyl), 3.80 (1H, quintet, J = 6,6,6,6 Hz, C-20 H), 4.30 (1H, t, J = 7,7 Hz, C-15 H), 5.75 (1H, d, J = 1 Hz, C-4 H).

Oxidation of **2c** was performed as follows: a solution of **2c** (0.015 g) in acetone (5 ml) was stirred at 25° during the addition of standard chromic acid reagent (46) until the reagent was present in excess. Water (15 ml) was then added and the mixture extracted with ether. The extract was washed with 2 M sodium bicarbonate, dried, and evaporated to give a residue (0.014 g) which on crystallization from aqueous methanol gave pregn-4-ene-3,15,20-trione (0.011 g), m.p. 154–156°, $[\alpha]_D^{24}$ +198° (lit. (47) m.p. 155–157°, $[\alpha]_D^{23}$ +200°). And *11α,15β,20α-trihydroxypregn-4-ene-3-one (2d)* (0.016 g from ethyl acetate – light petroleum), R_f 0.23 (ethyl acetate), 0.1 (ether), 0.25 (chloroform–methanol–water 188:12:1); M^+ 348.2298 ($C_{21}H_{32}O_4$ requires M^+ 348.2300); m.p. 230–232°, $[\alpha]_D^{18}$ +55° (*c*, 1.3); i.r.: ν_{max} (KBr) 3470, 1670, 1620 cm^{-1}; p.m.r.: included signals at δ 1.00 (3H, s, C-18 methyl), 1.25 (3H, d, J = 6 Hz, C-21 methyl), 1.35 (3H, s, C-19 methyl), 3.80 (1H, quintet, J = 6,6,6,6 Hz, C-20 H), 4.00 (1H, sextet, J = 10,10,6 Hz, C-11 H), 4.30 (1H, t, J = 7,7 Hz, C-15 H), 5.75 (1H, d, J = 1 Hz, C-4 H).

Oxidation by the method described above gave pregn-4-ene-3,11,15,20-tetraone (0.008 g), m.p. 214–216°, $[\alpha]_D^{20}$ +309° (*c*, 0.5) (lit. (48) m.p. 218–221°, $[\alpha]_D^{23}$ +325°).

20β-Hydroxypregn-4-ene-3-one (2b)

One gram gave a crude extract (0.4 g) which was subjected to preparative t.l.c. (ethyl acetate) and gave 20β-hydroxypregn-4-ene-3-one (0.246 g from aqueous methanol), identified by m.p. and spectral comparison with an authentic sample. And *15β,20β-dihydroxypregn-4-ene-3-one (2e)* (0.04 g from diisopropyl ether–hexane), R_f 0.35 (ethyl acetate), 0.32 (ether), 0.49 (chloroform–methanol–water 188:12:1); M^+ 332.2356 ($C_{21}H_{32}O_3$ requires M^+ 332.2351), m.p. 188–190°, $[\alpha]_D^{24}$ +44° (*c*, 0.8); i.r.: ν_{max} (KBr) 3470, 1670, 1620 cm^{-1}; p.m.r.: included signals at δ 1.10 (3H, s, C-18 methyl), 1.17 (3H, d, J = 6 Hz, C-21 methyl), 1.24 (3H, s, C-19 methyl), 3.90 (1H, m, C-20 H), 4.28 (1H, t, J = 7,7 Hz, C-15 H), 5.76 (1H, d, J = 1 Hz, C-4 H).

Oxidation by the method described above gave pregn-4-ene-3,15,20-trione, m.p. 153–156°, $[\alpha]_D^{23}$ +196° (*c*, 1.0). And *11α,15β,20β-trihydroxypregn-4-ene-3-one (2f)* (0.027 g from ether), R_f 0.22 (ethyl acetate), 0.15 (ether), 0.3 (chloroform–methanol–water 188:12:1); M^+ 348.2303 ($C_{21}H_{32}O_4$ requires M^+ 348.2300), m.p. 248–252° (dec.), $[\alpha]_D^{23}$ −24° (*c*, 1.0); i.r.: ν_{max} (KBr) 3470, 1670, 1620 cm^{-1}; p.m.r.: included signals at δ 1.10 (3H, s, C-18 methyl), 1.18 (3H, d, J = 6 Hz, C-21 methyl), 1.35 (3H, s, C-19 methyl), 3.90 (1H, m, C-20 H), 4.00 (1H, sextet, J = 10,10,5 Hz, C-11 H), 4.30 (1H, t, J = 7,7 Hz, C-15 H), 5.75 (1H, d, J = 1 Hz, C-4 H).

Oxidation by the method described above gave pregn-4-ene-3,11,15,20-tetraone, m.p. 216–219°, $[\alpha]_D^{20}$ +317° (*c*, 0.4).

Pregn-4-ene-3-one (3a)

One gram gave a crude extract (0.621 g). Analysis by t.l.c. indicated the presence of starting material (R_f 0.66, ether) only. Chromatography gave **3a** (0.508 g from methanol), identified by m.p. and spectral comparison with an authentic sample.

20-Methylpregna-4,20(21)-diene-3-one (3b)

A 0.2 g sample gave a crude extract (0.137 g), t.l.c. analysis of which indicated the presence of starting material (R_f 0.6, ether) only. Preparative t.l.c. gave **3b** (0.12 g from aqueous methanol), identified by m.p. and spectral comparison with an authentic sample.

20-Thiopregn-4-ene-3-one (3c)

A 0.24 g sample gave a crude extract (0.157 g). The only steroid detectable by t.l.c. analysis was **3c** (R_f 0.23, ether), which was recovered by chromatography on alumina.

2,2,4,6,6,17,21,21,21-d_9-Progesterone (4a)

One gram gave a crude extract (0.46 g) which was subjected to preparative t.l.c. (ether) and gave 2,2,4,6,6,-17,21,21,21-d_9-progesterone (0.11 g from ether – light petroleum), R_f 0.76, identified by m.p. and spectral comparison with an authentic sample; m.s.: analysis of ions at *m/e* 320–323 gave the following molecular isotopic composition: d_9, 77%; d_8, 20%; d_7, 3%; the mass spectrum was identical with that of authentic **4a**. And *2,2,4,6,6,17,21,21-d_8-11-deoxycorticosterone (5a)* (0.124 g from aqueous ethanol), R_f 0.4, identified by m.p. and spectral comparison with unlabelled material **1b**; p.m.r.: included signals at δ 0.70 (3H, s, C-18 methyl), 1.20 (3H, s, C-19 methyl) but no absorption in the region 4.18 (C-21 CH_2OH); m.s.: *m/e* 338(20), 337(5), 336(1), 335(0.05), 305(100) (M − CD_2OH), 277(50) (M − $C_2D_2O_2H$); analysis of ions at *m/e* 335–338

Can. J. Chem. Downloaded from www.nrcresearchpress.com by 210.87.254.42 on 09/05/12
For personal use only.

gave the following molecular isotopic composition: d_8, 77.2%; d_7, 18.8%; d_6, 4%.

21-d-Progesterone (4b)

A 0.35 g sample gave a crude extract which was subjected to preparative t.l.c. (ether) and gave 21-*d*-progesterone (0.062 g from ether – light petroleum), R_f 0.8, identified by m.p. and spectral comparison with an authentic sample; p.m.r.: included signals at δ 0.67 (3H, s, C-18 methyl), 1.18 (3H, s, C-19 methyl), 2.11 (*ca.* 2H, s, C-21 CH_2D), 5.76 (1H, broad s, C-4 H); m.s.: analysis of ions at *m/e* 314, 315 gave the molecular isotopic composition as d_1, 78%; d_0, 22%. The mass spectrum was identical with that of **4***b*. And *21-d-11-deoxycorticosterone (**1***b* + **5***b* + **5***c*)* (0.074 g from aqueous methanol), R_f 0.4, identified by m.p. and spectral comparison with an authentic sample of unlabelled material; p.m.r. (C_6D_6): included signals at δ 0.48 (3H, s, C-18 methyl), 0.70 (3H, s, C-19 methyl), 3.86 (*ca.* 0.3H, broad s, C-21 C*H*DOH), 3.95 (*ca.* 0.5H, ABq, J = 19 Hz, C-21 CH_2OH), 3.98 (*ca.* 0.3H, broad s, C-21 CD*H*OH), 5.82 (1H, broad s, C-4 H); m.s.: *m/e* 331(15), 330(9), 300(26), 299(100) (M − CHDOH), 272(12), 271(50), 270(1.1) (M − $C_2DO_2H_2$); analysis of ions at *m/e* 330,331 gave the following molecular isotopic composition: d_1, 58%; d_0, 42%.

2,2,4,6,6,17,21,21-d_8-Progesterone (4c)

One gram gave a crude extract (0.594 g) which afforded, after preparative t.l.c. (ether), 2,2,4,6,6,17,21,21-d_8-progesterone (0.214 g from aqueous methanol), R_f 0.8, identified by m.p. and spectral comparison with an authentic sample. And *2,2,4,6,6,17,21,21-d_8-11-deoxycorticosterone (**5***a* + **5***d* + **5***e*)* (0.092 g from aqueous methanol), R_f 0.4, identified by m.p. and spectral comparison with an authentic sample of unlabelled material; p.m.r. (C_6D_6): included signals at δ 0.48 (3H, s, C-18 methyl), 0.70 (3H, s, C-19 methyl), 3.86 (*ca.* 0.25H, broad s, C-21 CD*H*OH), 3.95 (*ca.* 0.25H, broad s, C-21 C*H*DOH); m.s.: *m/e* 338(10), 337(15), 336(10), 335(3), 334(2), 333(0.1), 305(100) (M − CD_2OH), 277(45), 276(40) (M − $C_2D_2O_2H$); analysis of ions at *m/e* 333–338 gave the following molecular isotopic composition: d_8, 16%; d_7, 40%; d_6, 29%; d_5, 9%; d_4, 6%.

The award of a demonstratorship (to H.L.H.) from the Queen's University of Belfast is gratefully acknowledged, as is the able technical assistance of Miss H. Reid with microbiological work.

Thanks are also due to Dr. D. B. MacLean of McMaster University, Hamilton, Ontario, for reading the manuscript, and to Dr. J. Hine of the Ohio State University, Columbus, Ohio, for helpful correspondence.

1. W. Charney and H. L. Herzog. Microbial transformations of steroids: a handbook. Academic Press, New York. 1967.
2. V. Ullrich. Angew. Chem. Int. Ed. **11**, 701 (1972).
3. B. M. Bloom and G. M. Shull. J. Am. Chem. Soc. **77**, 5767 (1955).
4. F. N. Chang and C. J. Sih. Biochemistry, **3**, 1551 (1964).
5. M. Hayano, M. Gut, R. I. Dorfmann, O. K. Sebek, and D. H. Peterson. J. Am. Chem. Soc. **80**, 2336 (1958).
6. E. J. Corey, G. A. Gregoriou, and D. H. Peterson. J. Am. Chem. Soc. **80**, 2338 (1958).
7. R. Bentley. Molecular asymmetry in biology. Vol. 2. Academic Press, New York. 1970.
8. E. J. Corey and G. A. Gregoriou. J. Am. Chem. Soc. **81**, 3127 (1959).
9. A. Rotman and Y. Mazur. J. Am. Chem. Soc. **94**, 6228 (1972).
10. E. J. Bailey, J. Elks, and D. H. R. Barton. Proc. Chem. Soc. 214 (1960).
11. J. Romo, G. Rosenkranz, C. Djerassi, and F. Sondheimer. J. Org. Chem. **19**, 1509 (1954).
12. B. A. Koechlin, D. L. Garmaise, T. H. Kritchevsky, and T. F. Gallagher. J. Am. Chem. Soc. **71**, 3262 (1949).
13. V. Sanda and J. Fajkos. Coll. Czech. Chem. Commun. **26**, 2734 (1961).
14. D. N. Kirk and J. M. Wiles. Chem. Commun. 518 (1970); 1015 (1970).
15. S. K. Malhotra and H. J. Ringold. J. Am. Chem. Soc. **87**, 3228 (1965).
16. L. H. Knox, E. Velarde, S. Berger, D. Cuadriello, P. W. Landis, and A. D. Cross. J. Am. Chem. Soc. **85**, 1851 (1963); R. A. Moss, R. W. Kleinman, and K. L. Williamson. Chem. Commun. 927 (1970).
17. T. H. Kritchevsky and T. F. Gallagher. J. Am. Chem. Soc. **73**, 184 (1951).
18. C. Djerassi. Steroid reactions: an outline for organic chemists. Holden, Day Inc., San Francisco. 1963. p. 567.
19. A. Zaffaroni, C. Casas Campillo, F. Cordoba, and G. Rosenkranz. Experientia, **11**, 219 (1955).
20. J. E. Bridgeman, P. C. Cherry, A. S. Clegg, J. M. Evans, Sir Ewart R. H. Jones, A. Kasal, V. Kumar, G. D. Meakins, Y. Morisawa, E. E. Richards, and P. D. Woodgate. J. Chem. Soc. C, 250 (1970).
21. Z. Reyes and R. M. Silverstein. J. Am. Chem. Soc. **80**, 6367 (1958); **80**, 6373 (1958).
22. B. J. Auret, D. R. Boyd, H. B. Henbest, and S. Ross. J. Chem. Soc. C, 2371 (1968).
23. H. Budzikiewicz, C. Djerassi, and D. H. Williams. Structure elucidation of natural products by mass spectrometry. Vol. 2. Holden, Day, Inc., San Francisco. 1964. p. 88.
24. R. P. Bell and P. T. McTigue. J. Chem. Soc. 2983 (1960).
25. R. P. Bell and B. G. Cox. J. Chem. Soc. B, 194 (1970).
26. J. P. Calmon, M. Calmon, and V. Gold. J. Chem. Soc. B, 659 (1969).
27. J. Hine, J. C. Kaufman, and M. S. Cholod. J. Am. Chem. Soc. **94**, 4590 (1972).
28. I. Björkhem. Eur. J. Biochem. **18**, 299 (1971).
29. V. Franzen and R. Edens. Ann. Chem. **729**, 33 (1969).
30. R. C. Dobson, D. M. Hayes, and R. Hoffmann. J. Am. Chem. Soc. **93**, 6188 (1971).
31. F. H. Westheimer. Chem. Rev. **61**, 265 (1961); J. Bigeleisen. Pure Appl. Chem. **8**, 217 (1964).
32. I. Kim, C. E. Hay, and H. J. Brodie. J. Biol. Chem. **248**, 2134 (1973).
33. J. Hine, E. F. Glod, R. E. Notari, F. E. Rodgers,

and F. C. SCHMALSTEIG. J. Am. Chem Soc. **95**, 2537 (1973).
34. J. HINE, M. S. CHOLOD, and R. A. KING. J. Am. Chem. Soc. **96**, 835 (1974).
35. B. J. AURET and H. L. HOLLAND. Chem. Commun. 1157 (1971).
36. W. S. ALLEN, S. BERNSTEIN, and R. LITTELL. J. Am. Chem. Soc. **76**, 6116 (1954).
37. A. F. HIRSH and G. I. FUJIMOTO. J. Org. Chem. **35**, 495 (1970).
38. G. CAINELLI, B. KAMBER, J. KELLER, M. L. MIHAILOVIC, D. ARIGONI, and O. JEGER. Helv. Chim. Acta, **44**, 518 (1961).
39. R. B. TURNER and D. M. VOITLE. J. Am. Chem. Soc. **73**, 2283 (1951).
40. F. SONDHEIMER, C. AMENDOLLA, and G. ROSENKRANZ. J. Am. Chem. Soc. **75**, 5930 (1953).
41. C. W. SHOPPEE, R. E. LACK, and B. C. NEWMAN. J. Chem. Soc. 3388 (1964).
42. J. P. DUSZA and W. BERGMANN. J. Org. Chem. **25**, 79 (1960).
43. R. M. DODSON and P. B. SOLLMAN. U.S. Patent No. 2,873,539. June, 1958.
44. T. REICHSTEIN and H. G. FUCHS. Helv. Chim. Acta, **23**, 684 (1940).
45. A. C. OTT, M. F. MURRAY, and R. L. PEDERSON. J. Am. Chem. Soc. **74**, 1239 (1952).
46. C. DJERASSI, R. R. ENGLE, and A. BOWERS. J. Org. Chem. **21**, 1547 (1956).
47. C. DJERASSI, L. B. HIGH, J. FRIED, and E. SABO. J. Am. Chem. Soc. **77**, 3673 (1955).
48. R. D. MUIR and R. M. DODSON. U.S. Patent No. 2,823,170. February, 1958.

Can. J. Chem. Downloaded from www.nrcresearchpress.com by 210.87.254.42 on 09/05/12
For personal use only.

Reactions du phenyl-1 dimethyl-3,4 phosphole avec divers chlorures d'acides aromatiques

FRANÇOIS MATHEY, DANIEL THAVARD ET BERNARD BARTET
Institut National de Recherche Chimique Appliquée 91710 Vert-le-Petit, France

Reçu le 9 juillet 1974

FRANÇOIS MATHEY, DANIEL THAVARD et BERNARD BARTET. Can. J. Chem. **53**, 855 (1975).

Le phényl-1 diméthyl-3,4 phosphole réagit en présence d'eau avec les chlorures de benzoyles substitués et les chlorures de 2- ou 3-thienyles pour fournir des hydroxy-2 dihydro-1,2 phosphorines. La réaction est particulièrement sensible aux effets stériques. Elle échoue avec les chlorures d'acides aliphatiques. Les résultats observés ne s'expliquent pas totalement par une compétition entre la réaction d'extension de cycle et l'hydrolyse des chlorures d'acides. Une explication complémentaire est proposée. Les hydroxy-2 dihydro-1,2 phosphorines se transforment à leur tour en oxa-1 phospha-2 cycloheptadiènes-4,6 en présence de traces de NaH. Cette nouvelle extension de cycle semble moins sensible aux effets stériques mais plus aux effets électroniques. Elle échoue avec les dérivés du thiophène. Les données r.m.n. de l'ensemble des produits préparés sont présentées et discutées. On note en particulier d'importants couplages P–C–OH dans les hydroxydihydrophosphorines.

FRANÇOIS MATHEY, DANIEL THAVARD, and BERNARD BARTET. Can. J. Chem. **53**, 855 (1975).

1-Phenyl-3,4-dimethylphosphole with water and substituted benzoyl chlorides or 2- and 3-thienyl chlorides is expanded into 2-hydroxy-1,2-dihydrophosphorines. This reaction is particularly affected by steric effects. It fails with aliphatic acid chlorides. These results are not fully explained by a competition between the expansion reaction and the hydrolysis of the chlorides. A complementary explanation is proposed. The 2-hydroxy-1,2-dihydrophosphorines are in turn expanded into 1-oxa-2-phosphacyclohepta-4,6 dienes with catalytic amounts of NaH. This other expansion reaction seems to be only weakly affected by steric but more strongly by electronic effects. It fails with thienyl derivatives. Nuclear magnetic resonance data are given and discussed for all the new products. Large P–C–OH couplings in hydroxydihydrophosphorines are noteworthy.

Dans un précédent travail (1) nous avons décrit la réaction de divers phospholes avec le chlorure de benzoyle en présence d'eau. Cette réaction conduit généralement à un oxyde de (phényl-2 hydroxy-2) dihydro-1,2 phosphorine. Ayant noté qu'à l'intérieur de la série des phényl-1 phospholes diversement substitués sur les carbones du cycle, les rendements de cette réaction décroissaient rapidement avec la nucléophilie du phosphore, nous avons admis que le premier stade de l'extension de cycle comprenait une attaque électrophile de l'ion acyle sur ce même phosphore. Dans l'hydroxy acyl phosphorane qui est le stade intermédiaire de l'hydrolyse du chlorure d'acyl phospholium ainsi obtenu, le noyau phosphole se trouve certainement en position apicale-équatoriale à cause de l'angle ∠CPC intracyclique qui reste voisin de 90° (2) quel que soit le degré de coordinance du phosphore par suite de la contrainte cyclique. Dans ces conditions, d'après les théories couramment admises sur l'hydrolyse des sels de phosphonium, c'est la liaison P—C apicale du cycle qui se rompt préférentiellement à la liaison P–acyle équatoriale. Il y a ensuite recyclisation par attaque de l'anion ainsi formé sur le carbonyle. Le schéma ci-dessous résume le mécanisme que nous proposons.

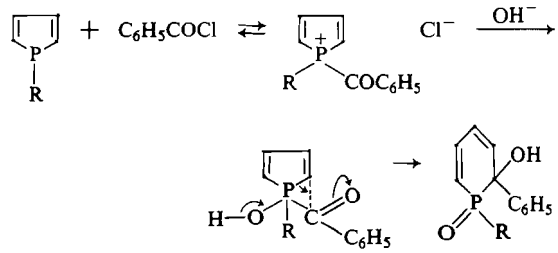

Si cette façon de voir est la bonne, on remarque que ce n'est pas l'"aromaticité" controversée des phospholes mais seulement leur contrainte cyclique qui est en jeu dans cette réaction. Ce fait vient d'être tout récemment confirmé par Smith et Smith (3) qui ont montré que l'on pouvait généraliser ce type d'extension de cycle aux phosphétanes (∠CPC ≃ 82° (4))

Can. J. Chem. Downloaded from www.nrcresearchpress.com by 210.87.254.5 on 09/05/12
For personal use only.

TABLEAU 1. Synthèse et propriétés des hydroxy-2 dihydro-1,2 phosphorines

Composé	R	Point de fusion* (°C)	Rendement (%)	Infrarouge†		
				OH	C=C	P=O
1	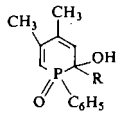	216 (toluène)	87	3164	1636, 1600, 1588	1149
2		202 (toluène)	38	3160	1630, 1587	1151
3		201 (toluène)	66	3160	1630, 1600, 1585	1145
4	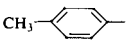	215 (toluène)	54	3160	1631, 1587	1148
5	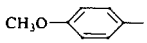	195 (toluène)	80	3145	1635, 1601, 1580	1150
6	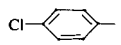	223 déc. (toluène)	75	3130	1633, 1590	1152
7	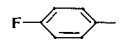	235 (alcool–eau)	61	3150	1639, 1599, 1588	1148
8	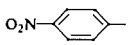	215 déc. (CH_3COOEt)	62	3115	1632, 1600, 1595	1151
9		227 (toluène)	16	3122	1632, 1587	1148
10		230 (toluène)	32	3165	1636, 1587	1156, 1144
	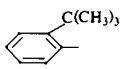		0			
			0			
			0			

*Mesurés au microscope.
†Produits en pastilles dans KBr; données en cm^{-1}.

mais que, dès que l'on passait aux phospholènes ($\angle$CPC $\simeq$ 94° (5)) et aux phospholanes ($\angle$CPC $\simeq$ 96° (4)), la réaction prenait un cours différent et conduisait à l'oxyde de la phosphine utilisée et a l'aldéhyde benzoïque. Dans ces deux derniers cas, en effet, la contrainte cyclique n'est plus suffisante pour empêcher le groupement acyle très apicophile (6) de chasser le cycle de sa position apicale-équatoriale.

Cette réaction représentant le premier exemple général d'extension de cycle des phospholes (pour divers essais d'extension de cycle des

Can. J. Chem. Downloaded from www.nrcresearchpress.com by 210.87.254.5 on 09/05/12
For personal use only.

TABLEAU 2. Résultats d'études d'hydrolyse de RCOCl

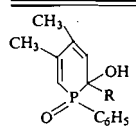

R	$10^4\ k_{H_2O}$ (s)*	Rendement en hydroxydihydrophosphorine (%)
CH_3	10.9	0
$C_6H_5CH_2$	3.60	0
4-$O_2NC_6H_4$	2.33	62
$(CH_3)_3C$	0.74	0
2-$CH_3C_6H_4$	0.0644	38
C_6H_5	0.0417	87
4-$CH_3OC_6H_4$	0.0146	80

*Données tirées de réf. 10.

phospholes dans des cas particuliers voir réfs. 7–9) et étant, de plus, le premier cas connu d'insertion du motif d'un chlorure d'acide dans la liaison P—C d'une phosphine, nous avons voulu vérifier si d'autres chlorures d'acides pouvaient remplacer le chlorure de benzoyle dans cette transformation.

Les résultats de nos essais avec les chlorures d'acides aromatiques et le phényl-1 diméthyl-3,4 phosphole sont reproduits dans le tableau 1. Tous nos essais avec les chlorures d'acides aliphatiques (CH_3COCl, $(CH_3)_3CCOCl$, $C_6H_5CH_2$-COCl, ClCO COCl, C_2H_5OCO COCl) se sont par contre soldés par des échecs. Ce fait appelle un premier commentaire.

Comme la r.m.n. du proton d'un mélange de phényl-1 diméthyl-3,4 phosphole, de chlorure de benzoyle et de triéthylamine dans le deutériochloroforme ne permet pas de mettre en évidence le sel d'acyl phospholium, on peut admettre que l'équilibre de formation de ce sel est très fortement déplacé vers la gauche. Lorsqu'on ajoute de l'eau à un tel mélange, pour pouvoir observer la formation de l'hydroxy dihydrophosphorine, il faut donc que la vitesse de transformation du sel de phospholium en phosphorine soit beaucoup plus élevée que la vitesse d'hydrolyse du chlorure d'acide. Or, d'une manière générale, les chlorures d'acides aliphatiques s'hydrolysent beaucoup plus rapidement que les chlorures d'acides aromatiques. *A priori*, on a donc là une première raison pouvant expliquer les comportements différents des chlorures d'acides aliphatiques et aromatiques. Cette raison est cependant insuffisante pour rationaliser l'ensemble de nos résultats comme le montre le tableau 2. On remarquera en particulier le cas du chlorure de *p*-nitrobenzoyle.

Une déchlorhydratation du chlorure d'acide aliphatique par la base conduisant à un cétene étant exclue dans le cas du chlorure de l'acide pivalique, la solubilisation du produit final lors du remplacement d'un chlorure aromatique par un chlorure d'acide aliphatique ne pouvant expliquer une suppression totale de la réaction d'extension de cycle (des phosphorines solubles dans le milieu réactionnel ont été obtenues à partir des P alkyl phospholes(1)), il est donc nécessaire de postuler un mécanisme réactionnel faisant explicitement intervenir le noyau aromatique. Nous proposons une stabilisation du sel d'acyl phospholium intermédiaire par délocalisation de la charge positive sur le noyau aromatique du radical acyle. Dans le cadre de

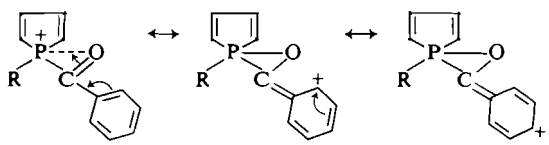

I II III

cette hypothèse il est à remarquer que les formes limites **II** et **III** sont des phosphoranes dans lesquels la tension du noyau phosphole est supprimée en position apicale-équatoriale, ce qui est très favorable.

D'autre part, on constate que le transfert électronique du noyau aromatique vers le phosphore s'effectue au détriment des positions 2, 4 et 6. Un substituant en *para* sur le noyau aromatique n'affectant que très peu les densités électroniques sur ces positions, on rationalise

Can. J. Chem. Downloaded from www.nrcresearchpress.com by 210.87.254.5 on 09/05/12
For personal use only.

Can. J. Chem. Downloaded from www.nrcresearchpress.com by 210.87.254.5 on 09/05/12
For personal use only.

TABLEAU 3. Synthèse et propriétés des oxa-1 phospha-2 cycloheptadiènes-4,6

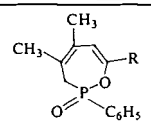

Composé	R	Point de fusion(°C)*	Rendement (%)	Infrarouge†		
				C=C	P=O	(P)—O—C‡
11	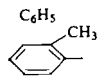	125 (méthylcyclohexane)	65	1639, 1606, 1590	1237	1066, 1045
12	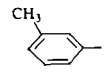	115 (hexane)	53	1645, 1630, 1590	1230	1056, 1032
13		126 (hexane)	47	1640, 1610, 1595	1238	1063, 1049
14	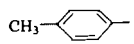	156 (hexane)	47	1640, 1610, 1588	1235	1062, 1045
15	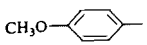	130 (hexane)	32§	1639, 1605, 1586	1233	1059, 1042‖
16	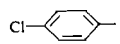	125 (hexane)	10§	1637, 1613, 1590	1250, 1234	1067, 1045
17	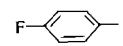	135 (hexane)	60	1642, 1613, 1602, 1592	1230	1057, 1040
18	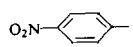	Décomposition spontanée rapide	25	1636, 1610, 1593	1250, 1238	1066, 1045
			0			
			0			

*Mesurés au microscope.
†Produits en pastilles dans KBr; données en cm^{-1}.
‡L'attribution n'est pas toujours certaine; elle a été effectuée en comparant les spectres de l'ensemble des produits de la série.
§Conditions synthétiques plus énergiques (voir partie expérimentale).
‖Le spectre comprend également une puissante bande à 1029 cm^{-1} correspondant sans doute au groupement $—OCH_3$.

Can. J. Chem. Downloaded from www.nrcresearchpress.com by 210.87.254.5 on 09/05/12
For personal use only.

ainsi le résultat *a priori* surprenant suivant lequel le rendement de la réaction d'extension de cycle ne dépend que très légèrement de la nature du substituant greffé en position 4 (comparaison de **5** et **8** par exemple). Un substituant donneur en *méta* sur le noyau augmentant au contraire les densités électroniques sur les positions 2, 4 et 6, on comprend aussi pourquoi **3** se forme avec un meilleur rendement que **4**.

Dans le thiophene on sait que seules les liaisons C_2—C_3 et C_4—C_5 ont une multiplicité nettement supérieure à 1 (voir les données structurales (11)). L'influence d'un substituant en position 2 se fait donc sentir principalement sur la position 3 et inversement. D'autre part, on sait également que les doubles liaisons sont polarisées en direction du soufre

(le sens du moment dipolaire montre bien que le soufre joue un rôle globalement électroattracteur vis-à-vis du cycle (12)). Dans ces conditions la stabilisation du sel de 3-thienyl phospholium aux dépens de la position 2 riche en électrons est plus complète que celle du sel de 2-thienyl phospholium aux dépens de la position 3 pauvre en électrons. Il est donc logique d'observer pour **10** un rendement supérieur à celui de **9**.

Enfin l'azote en position 3 dans le chlorure de l'acide nicotinique appauvrissant fortement les positions 2, 4 et 6 par suite de sa forte électronégativité déstabilise sensiblement le sel de phospholium intermédiaire, ce qui permet d'expliquer l'échec de l'extension de cycle dans ce dernier cas. Nous voyons donc que le schéma de stabilisation proposé permet en gros de rendre compte correctement des résultats observés.

La lecture du tableau 1 appelle un second commentaire. Il apparaît immédiatement que les facteurs stériques jouent un rôle prépondérant (avec R = C_6H_5, rendement 87%):

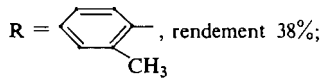

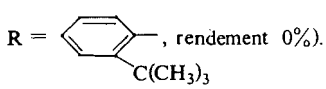

Cet effet stérique est caractéristique des réactions nucléophiles du P^{III} et constitue un argument indirect supplémentaire en faveur du mécanisme proposé.

Dans notre précédent travail (1) nous avions également montré que les hydroxy-2 dihydro-1,2 phosphorines se réarrangeaient en présence de quantités catalytiques de NaH pour donner des oxa-1 phospha-2 cycloheptadiènes-4,6.

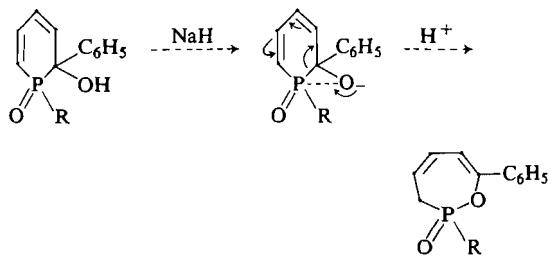

Disposant d'une gamme importante de phosphorines, nous avons voulu vérifier si leur extension en cycle heptagonal était une réaction générale. Sauf avec les dérivés thiophéniques **9** et **10**, nous avons réussi cette transformation. Le tableau 3 résume les résultats obtenus.

Nous ne ferons que deux commentaires sur cette réaction. Tout d'abord elle ne semble pas être sensible à la présence d'un substituant en *ortho* sur le noyau benzénique en position 2 (cas de la transformation **2** → **12**). Ensuite nous avons constaté que la présence d'un méthoxy ou d'un chlore en *para* sur le noyau aromatique en position 2 stabilisait la phosphorine et rendait nécessaire l'emploi de conditions plus dures pour effectuer sa conversion en cycle heptagonal (cas de **5** notamment). Nous avons alors, mais sans succès, tenté de piéger l'anion dérivé de **5** en l'alkylant par ICH_3.

Données de résonance magnétique nucléaire du proton des cycles à six et sept chainons

Ces données sont rassemblées dans les tableaux 4 et 5. La lecture du tableau 4 fait apparaître deux caractéristiques des hydroxydihydrophosphorines. (*a*) Dans de nombreux cas apparaît un important couplage P–C–O–H très sensible à la nature du solvant employé : environ 15 Hz dans le DMSO et compris entre 0 et 10 Hz dans le chloroforme. L'apparition de ces couplages traduit vraisemblablement l'existence d'un ralentissement des échanges entre OH dû à l'encombrement stérique régnant dans cette partie de la molécule. Rappelons à ce propos que fort peu de couplages P–C–O–H sont décrits dans la littérature (voir réf. 13). (*b*) Lorsque le groupement R comprend un noyau benzénique celui-ci apparaît comme un singulet élargi, sauf s'il comporte un substituant très électrodonneur

Can. J. Chem. Downloaded from www.nrcresearchpress.com by 210.87.254.5 on 09/05/12
For personal use only.

TABLEAU 4. Résonance magnétique nucleaire du proton des hydroxydihydrophosphorines

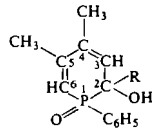

Composé	R	Solvant	$CH_3C(5)$* δ	$CH_3C(5)$* J_{H-P}	$CH_3C(4)$ δ	HC(3) δ	HC(3) J_{H-P}	HC(6) δ	HC(6) J_{H-P}	OH δ	OH J_{H-P}	PC_6H_5 δ(centre)	R—C(2)
1	C_6H_5	$CDCl_3$	2.02	~1.5	2.17	6.24	14	6.13	15.5	2.41	10.6	7.48	Ph:δ 7.31 (singulet)
2	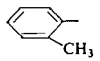	DMSO	2.01	1.5	2.14	6.18	13.9	6.08	16.7	5.77†	16.3†	7.43	Me:δ 2.43 Ph:δ 7.10 (singulet)
3	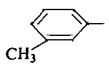	DMSO	2.0	1.5	2.11	6.09	14	5.92	16	5.85	14.8	7.44	Me:δ 2.27 Ph:δ 7.07 (singulet)
4	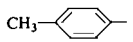	DMSO	2.01	1.5	2.12	6.11	14.2	5.94	17	5.87	15	7.48	Me:δ 2.30 Ph:δ 7.13 (singulet)
5	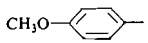	$CDCl_3$	2.02	1.5	2.17	6.19	13.5	6.05	15	2.51 (singulet fin)		7.56	OMe: δ 3.81 Ph *méta*: δ 6.91 $J_{H_oH_m}$ 8.7
6	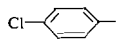	DMSO	1.99	1.5	2.12	6.13	13.3	5.92	16	Non visible‡		7.44	Ph:δ 7.28 (singulet)
7	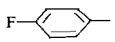	DMSO	1.98	—	2.11	6.08	13.3	5.91	15.5	Non visible‡		7.42	Ph:δ 7.05 et 7.19 (élargi)
8	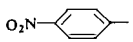	DMSO	2.04	—	2.17	6.20	16	6.0	15.1	6.36	14	7.49	Ph:*ortho*:δ 7.55 $J_{H_oH_m}$ 8.7 *méta* :δ 8.22
9		DMSO	1.97	1.4	2.10	6.08	12.6	5.96	15.3	Non visible‡		7.54	C_4H_3S:H_β:δ 6.96–7.03
10		DMSO	1.97	1.5	2.11	6.09	13.3	5.95	16	Non visible‡		7.53	C_4H_3S:H_β:δ 7.01 $J_{H_\beta H_\alpha}$ 4.9

*$CH_3C(5)$ est également couplé avec HC(6) (J_{HH} = 1.2–1.4 Hz) ce qui permet de distinguer HC(3) et HC(6).
†Dans $CDCl_3$:OH:δ 3.07, J_{HP} = 7.3 Hz.
‡Sans doute confondu avec le OH de l'eau contenue dans le DMSO.

Can. J. Chem. Downloaded from www.nrcresearchpress.com by 210.87.254.5 on 09/05/12
For personal use only.

TABLEAU 5. Résonance magnétique nucleaire du proton des oxa-1 phospha-2 cycloheptadiènes-4,6*

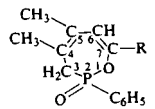

Composé	R	$CH_3C(4)$ δ	$CH_3C(4)$ J_{H-P}	$CH_3C(5)$ δ	$CH_3C(5)$ J_{H-P}	CH_2P δ	HC(6) δ	R−C(2)
11	C_6H_5	1.57	2.4	1.88	5.3	2.73–3.37	6.30	
12	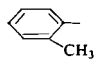	1.52	~2	1.81	4.9	2.75–3.38	5.74	CH_3:δ 2.48
13	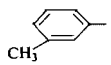	1.53	~2	1.85	5.3	2.70–3.33	6.23	CH_3:δ 2.33
14	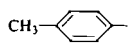	1.51	Peu visible	1.83	4.9	2.69–3.31	6.19	CH_3:δ 2.30 Ph:*méta* δ 7.11, *ortho* δ 7.64; $J_{H_oH_m}$ 8.7
15	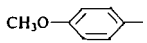	1.59	Peu visible	1.90	5	2.77–3.41	6.22	OCH_3:δ 3.85 Ph:*méta* δ 6.96, *ortho* δ 7.79; $J_{H_oH_m}$ 8.7
16	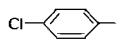	1.59	1.7	1.90	5	2.75–3.38	6.30	Ph:*méta* δ 7.37, *ortho* δ 7.74; $J_{H_oH_m}$ 8.7
17	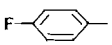	1.57	Peu visible	1.87	4.7	2.73–3.35	6.20	Ph:*méta* δ 7.06; J_{HF} 8.4; *ortho* δ 7.73; J_{HF} 5.3; $J_{H_oH_m}$ 8.9
18	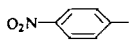	1.61	~1	1.92	5.1	2.76–3.37	6.49	Ph:*méta* δ 8.17, *ortho* δ 7.89; $J_{H_oH_m}$ 8.6

*Produits en solution dans $CDCl_3$; TMS interne.

Can. J. Chem. Downloaded from www.nrcresearchpress.com by 210.87.254.5 on 09/05/12
For personal use only.

TABLEAU 6. Résultats analytiques

Produits	Formule brute	Théorie (%)		Trouvé (cycles à six chainons)		Trouvé (cycles à sept chainons)	
		C	H	C	H	C	H
1, 11	$C_{19}H_{19}PO_2$	73.54	6.17 (P 9.98)	73.71	6.27 (P 10.17)*	73.06	5.96
2, 12	$C_{20}H_{21}PO_2$	74.06	6.52	73.34	6.63	74.12	6.48
3, 13	$C_{20}H_{21}PO_2$	74.06	6.52	73.96	6.45	73.96	6.42
4, 14	$C_{20}H_{21}PO_2$	74.06	6.52	74.07	6.34	74.08	6.62
5, 15	$C_{20}H_{21}PO_3$	70.57	6.22	70.34	6.18	70.73	6.41
6, 16	$C_{19}H_{18}PO_2Cl$	66.18	5.26 (Cl 10.28)	66.22	5.30 (Cl 9.72)	66.09	5.16
7, 17	$C_{19}H_{18}PO_2F$	69.50	5.52	69.87	5.53	69.62	5.26
8, 18	$C_{19}H_{18}PO_4N$	64.22	5.11 (N 3.94)	63.51	5.19 (N 4.20)	62.94	4.91 (N 3.89)
9	$C_{17}H_{17}PO_2S$	64.54	5.42	64.35	5.38		
10	$C_{17}H_{17}PO_2S$	64.54	5.42	64.47	5.92		

*Sur le spectre de masse, présence de l'ion moléculaire de *m/e* 310.

Can. J. Chem. Downloaded from www.nrcresearchpress.com by 210.87.254.5 on 09/05/12
For personal use only.

ou très électroattracteur qui provoque une différenciation des protons aromatiques. Ceci traduit sans doute la libre rotation du noyau benzénique autour de la liaison C(2)—R. Dans le cas de **2** cette libre rotation signifie qu'il n'y a pas d'intéraction entre le CH_3 en *ortho* et le OH ce qui est en accord avec les données i.r. qui ne montrent aucune anomalie dans la position de la bande OH. Cette absence d'intéraction explique pourquoi la réaction d'extension de cycle faisant passer de **2** à **12** se réalise aussi facilement qu'en l'absence de substituant en *ortho* comme nous l'avons noté précédemment.

A l'opposé le noyau benzénique du groupement R des cycles heptagonaux se présente toujours sous la forme d'un multiplet complexe très élargi et en moyenne plus déblindé que dans les cycles à six chaînons correspondants. Ce fait permet de soupçonner l'existence, d'ailleurs logique, d'une conjugaison entre le noyau aromatique et le système diènique du cycle bloquant la rotation du radical R autour de sa liaison avec C(7). Ce phénomène a été vérifié sur **19** homologue azoté de **11** par détermination de structure aux rayons X (14).

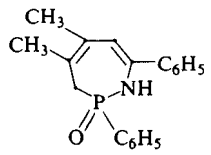

19

D'autre part, l'attribution des signaux CH_3-C(4) et $CH_3C(5)$ a été effectuée en admettant que leurs déplacements chimiques sont principalement affectés par la polarisation du système diènique induite par les doublets libres de l'oxygène ou de l'azote.

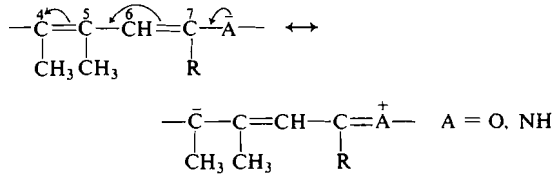

La présence d'une telle conjugaison a été mise en évidence indirectement par l'étude des propriétés chimiques de ces hétérocycles (pour A = NH on peut notamment substituer HC(6) par le brome (15)) et par l'étude de la structure de **19** (14) (la liaison N—C(7) est beaucoup plus courte qu'une liaison N—C normale). Dans ces conditions, nous attribuons le signal le plus blindé à $CH_3C(4)$. Cette conclusion est l'inverse de celle que l'on tirerait de l'étude des seuls couplages CH_3---P.

Pour finir, nous noterons le blindage anormal du proton HC(6) de **12** qui correspond d'ailleurs à une anomalie dans le spectre i.r. En effet, tous les cycles heptagonaux présentent trois bandes de doubles liaisons à environ 1640, 1610 et 1590 cm^{-1}. Pour **12** la deuxième bande, sans doute attribuable à la double liaison C(6)=C(7), est deplacée à 1630 cm^{-1}. Dans **12** existe donc vraisemblablement une intéraction entre cette double liaison et le méthyle en *ortho* sur R.

Partie expérimentale

Les spectres r.m.n. ont été réalisés par Mme R. Mankowski-Favelier sur des appareils Perkin-Elmer R12 à 60 MHz et Jeol PS 100 FT à 100 MHz. Pour la préparation du phényl-1 diméthyl-3,4 phosphole, voir réf. 16.

Synthèse des oxydes de phényl-1 hydroxy-2 diméthyl-4,5 dihydro-1,2 phosphorines

Dans un réacteur sous argon on place 3.8 g de phényl-1 diméthyl-3,4 phosphole (0.02 mol), 10 cm^3 de triéthylamine et 150 cm^3 d'éther sec. En agitant, on verse alors à température ambiante 0.04 mol de chlorure d'acide RCOCl. La triéthylamine neutralise les traces d'acide chlorhydrique toujours présentes dans le chlorure. Une fois la neutralisation terminée, on ajoute 200 cm^3 d'eau. On laisse réagir pendant 2 h. On filtre le précipité formé, on le lave à l'eau et à l'éther, puis on le sèche soigneusement. La phosphorine ainsi obtenue est simplement recristallisée. Pour les données analytiques, voir tableau 6.

Synthèse des oxydes de phényl-2 diméthyl-4,5 oxa-1 phospha-2 cycloheptadiénes-4,6 (cas général)

Dans un réacteur sous argon on place 0.01 mol d'hydroxydihydrophosphorine, 50 cm^3 de diméthylformamide anhydre et une pincée de NaH à 80% dans l'huile. On laisse agiter 4 h à température ambiante. On obtient ainsi une solution homogène légèrement colorée en jaune. On hydrolyse par 5 cm^3 d'eau, neutralise par HCl 2 *N* puis évapore à sec. On reprend le résidu par un mélange eau, chloroforme. La couche chloroformique est décantée, séchée et évaporée. Le produit ainsi obtenu est chromatographié sur colonne de silice 70–230 mesch Merck: éluant acétate d'éthyle. Le produit recherché élue avant la phosphorine (R_f 0.6). Pour les données analytiques, voir tableau 6.

*Cas particulier de **15** et **16***

Le mélange habituel est chauffé à 120 °C pendant 4 h. Le traitement est ensuite identique.

Les auteurs remercient vivement Mme. R. Mankowski-Favelier pour la réalisation des spectres r.m.n.

1. F. MATHEY. Tetrahedron, **29**, 707 (1973).
2. P. COGGON et A. T. MC. PHAIL. J. Chem. Soc. Dalton, 1888 (1973).
3. D. G. SMITH et D. J. H. SMITH. Communication orale.

Fifth International conference of organic phosphorus chemistry, Gdansk. Septembre 16–21, 1974.
4. D. E. C. CORBRIDGE. The structural chemistry of phosphorus. Elsevier, Amsterdam. 1974. p. 396.
5. A. T. MC. PHAIL, R. C. KOMSON, J. F. ENGEL et L. D. QUIN. J. Chem. Soc. Dalton, 874 (1972).
6. S. TRIPPETT. Conférence pleinière. Fifth International conference of organic phosphorus chemistry, Gdansk. Septembre 16–21, 1974.
7. I. G. M. CAMPBELL, R. C. COOKSON, M. B. HOCKING et A. N. HUGHES. J. Chem. Soc. C, 2184 (1965).
8. A. N. HUGHES et CHIT SRIVANAVIT. Can. J. Chem. **49**, 879 (1971).
9. D. W. ALLEN et I. T. MILLAR. J. Chem. Soc. C, 252 (1969).
10. I. UGI et F. BECK. Ber. **94**, 1839 (1961).
11. B. BACK, D. CHRISTENSEN, L. HANSEN-NYGAARD et J. RASTRUP-ANDERSEN. J. Mol. Spectrosc. **7**, 58 (1961).
12. T. J. BARTON, R. W. ROTH et J. G. VERKADE. J. Am. Chem. Soc. **94**, 8854 (1972).
13. C. F. GRIFFIN et S. K. KUNDU. J. Org. Chem. **34**, 1532 (1969).
14. J. P. LAMPIN, F. MATHEY et W. S. SHELDRICK. Acta Cryst. **30B**, 1626 (1974).
15. J. P. LAMPIN et F. MATHEY. Tetrahedron, **28**, 5367 (1972).
16. F. MATHEY et R. MANKOWSKI-FAVELIER, Bull. Soc. Chim. Fr. 4433 (1970).

Can. J. Chem. Downloaded from www.nrcresearchpress.com by 210.87.254.5 on 09/05/12
For personal use only.

Identification of Phenyl Vinyl Ketone and Related Compounds as 2,4-Dinitrophenylhydrazones and Pyrazolines

C. F. H. ALLEN

Chemistry Department, Rochester Institute of Technology, Rochester, New York 14623

Received September 23, 1974

C. F. H. ALLEN. Can. J. Chem. **53**, 865 (1975).

The closely interrelated, titled compounds, which have similar physical properties and which form mixtures difficult to separate, are best characterized by instrumental methods.

All α,β-unsaturated aldehydes and methyl ketones gave open-chain dinitrophenylhydrazones directly, whereas the arylated ketones form pyrazolines, as is well known.

C. F. H. ALLEN. Can. J. Chem. **53**, 865 (1975).

La façon la plus simple de caractérisé les composés mentionnés dans le titre qui sont intimement reliés entre eux, qui ont des propriétés physiques similaires et qui forment des mélanges difficiles à séparer fait appel à des méthodes instrumentales.

Tous les aldéhydes et toutes les méthyles cétones non-saturés en position α,β donnent directement des dinitrophénylhydrazones en chaîne ouverte alors que les cétones portant un groupe aryle forment, comme il est bien connu, des pyrazolines. [Traduit par le journal]

Can. J. Chem. Downloaded from www.nrcresearchpress.com by 210.87.254.40 on 09/05/12
For personal use only.

During our earlier work (1) it was found that phenyl vinyl ketone (PVK, **1**) could be isolated in quantity by chloroform extraction of an alcoholic solution of 3-chloro- or 3-dimethylaminopropiophenone containing potassium acetate (1,2), thus avoiding the many tedious, recorded methods (3–13). The usual, characteristic solid derivative, now employed for identification of isolated PVK, is 1,3-diphenyl-2-pyrazoline **9** (2, 3, 15, 16, 20).

Because PVK is such a reactive substance, mixtures, difficult to separate, are formed in alcoholic and acidic solutions of 2,4-dinitrophenylhydrazine by all usual procedures. Furthermore, the solubilities, colors, and melting points of closely related compounds, including dinitrophenylhydrazine itself, are very similar, so they are not readily separated and identified; an example is the derivative of dinitrophenylhydrazone of 3-dimethylaminopropiophenone (**4**), probably the preferable source of PVK in solution, and 1-(2,4-dinitrophenyl)-3-phenylpyrazoline (**5**).

Anticipating that 3-chloropropiophenone-DNPH (**6**) could be dehydrohalogenated to PVK-DNPH (**2**), an alcoholic solution was treated with the reagent (14). The mixture formed consisted of a small amount of the desired derivative **6**, considerable 3-ethoxypropiophenone-DNPH (**3**), and, as the main product, the bis-DNPH of 2′,2′-di-(2-benzoylethyl)-2,4-dinitrophenyl-1-hydrazine (**7**); a propoxy derivative of the latter has been previously described (18).

When **6** was dissolved in warm pyridine it at once lost hydrogen chloride, with consequent formation of the known pyrazoline **5** (19). The formation of **3** suggests that there has been a partial dehydrohalogenation of 3-chloropropiophenone to give **1**, which preferentially adds alcohol (3).

Experimental

Preparation of Compounds

3-Dimethylaminopropiophenone-DNPH (4)

A mixture of the free base from 2.2 g of the hydrochloride (17) and 25 ml of alcohol was added to a hot, previously prepared dinitrophenylhydrazinium chloride solution (14). There was no visible change but small orange-yellow crystals began to separate in 3–4 min. After 1 h in the refrigerator, 1 g of the derivative was collected on a filter; successive crops made the yield practically quantitative. The same derivative (**4**) is directly obtainable from the hydrochloride. It is also formed on employing DMF as a solvent and evaporating all the latter in a current of air on the steam bath. The substance is very slightly soluble in alcohol, ethyl acetate, and chloroform, moderately soluble in hot acetic acid (unsuitable for recrystallization), but very soluble in hot pyridine, hot DMF, Diglyme, and DMSO.

When the usual procedure for preparing dinitrophenylhydrazones was employed with **1** the product was **3**. An attempted use of trifluoroacetic acid gave 2′-trifluoroacetyl-2,4-dinitrophenylhydrazine (**8**) almost instantly; off-white needles, m.p. 163–164°.

Because DNPH is moderately soluble in cold DMF, this solvent was examined. The deep red solution of 0.2 g of the hydrazine in 1.4 ml of DMF was unchanged after addition of 1 g of PVK but the color was at once lightened on adding 3 drops of concentrated hydrochloric acid. After removal of all the solvent in a current of air, on the steam bath, a gummy mixture remained; less than

Can. J. Chem. Downloaded from www.nrcresearchpress.com by 210.87.254.40 on 09/05/12
For personal use only.

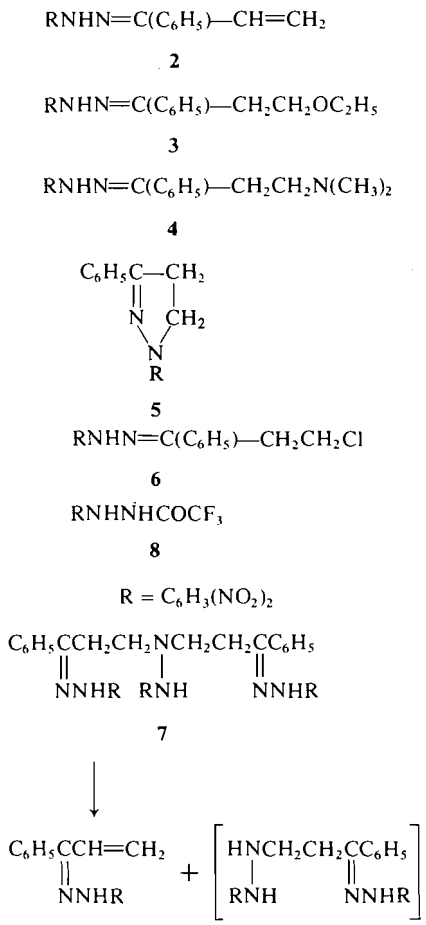

1 mg of fine red material was isolated from two runs by triturating with ethyl acetate or formate, chloroform, or ether. It melted at 188–189° (lit. (9) m.p. 195–196°). It seems obvious that PVK-DNPH (**2**) is not a suitable reference compound.

3-Chloropropiophenone (6)

To a hot suspension of 0.8 g of dinitrophenylhydrazine in 25 ml of boiling alcohol, 4 ml of concentrated hydrochloric acid was added, followed by 0.8 g of the 3-chloro ketone in 15 ml of hot alcohol; shortly, a crystalline mixture began to separate. After 4 h it was collected on a filter. Separation of the mixture was tedious. The chloro derivative **6** was always formed in a very low yield. As it was more soluble in alcohol it could be separated from **3**; the latter crystallized well from ethyl acetate or propyl alcohol. Although it was difficult to remove traces of these low-melting components, the main product was always the bishydrazone **7**. The latter is sparingly soluble in the usual solvents but dissolves easily in warm pyridine, 1-methylpyrrolidone, Diglyme, and DMF. It is best purified by dissolving in a little hot pyridine and adding an equal volume of water. The pure product melts at 243–244°, with preliminary shrinking at about 225–226°.

Occasionally the crude chloro derivative (m.p. 139–140°), which contains considerable ethoxy-DNPH (**3**), separated in a few hours. Purification was then accomplished by suspending in hot alcohol and adding sufficient ethyl acetate to give a clear solution. After several recrystallizations the analytical sample had m.p. 131°. Small amounts were purified by chromatography (45 g of Al_2O_3 in 42 ml of hexane, using a 50 ml burette). A benzene suspension was added at the top and eluted with this solvent, collecting the deep orange-red effluent. The separation was discontinued when the color became yellow (due to **3**). The reddish product that separated on evaporation of the solvent was suitable for conversion to the dinitropyrazoline **5**. The crude, chlorinated hydrazone **6** dissolved readily in warm pyridine; upon the addition of water the known (19) pyrazoline **5** separated in shiny, yellow flakes, suggestive of 'gold dust.' This pyrazoline was also identified in the colored mixtures that resulted from the interaction of **1** and dinitrophenylhydrazinium chloride in methyl and ethyl alcohols; only the pyrazoline and unchanged DNPH could be isolated from the red tar that was formed in Diglyme (24).

1,3-Diphenylpyrazoline (9)

This compound (m.p. 151–152°) is obtainable reproducibly by mixing 3 drops each of isolated **1** and phenylhydrazine in 5 ml of alcohol, and adding a trace of acetic acid (3). More recently this pyrazoline has been obtained from the Mannich salt (16) and from 3-chloropropiophenone; the literature (15) gives no details but it "is easier to get than phenyl vinyl ketone." This pyrazoline and its benzene solution show a striking brilliant blue fluorescence in u.v. light; invisible spots that may get on the skin, not removable by washing, are readily detected in this way.

Physical Properties

The remainder of this section is concerned with the characterization of PVK and closely related compounds by instrumental methods. Although none of the latter is universally applicable, mass spectroscopy appears to be the most useful. In all but one instance **7** it gave the molecular ion and characteristic fragmentation pattern. These spectra were determined by the use of a Hitachi RMS-4.

Mass Spectroscopy

2,4-Dinitrophenylhydrazine has a molecular ion at *m/e* 198 (74% M) and fragment ions at *m/e* 180 (8.5), 122 (28), 92 (16), 79 (100), 76 (44), 75 (44), and 51 (89).

Phenyl vinyl ketone-DNPH (2) has a molecular ion at *m/e* 312 (70% M) and fragment ions at *m/e* 265 (41), 264 (13), 218 (15), 189 (14), 115 (74), 105 (100), and 77 (100).

3-Ethoxypropiophenone-DNPH (3) has a molecular ion at *m/e* 358 (84% M) and fragment ions at *m/e* 329 (6.3), 312 (27), 311 (16), 295 (16), 265 (46), 119 (65), 104 (41), 103 (100), 59 (70), and 29 (75). The fragmentation pattern is very similar to that of **5**.

3-Chloropropiophenone-DNPH (6) has a molecular ion at *m/e* 348 (13% M) and fragment ions at *m/e* 312 (50), 295 (5), 265 (40), 219 (24), 218 (33), 117 (25), 116 (25), 115 (65), 104 (37), 103 (30), and 77 (100). The fragmentation pattern is very similar to that of **5**.

3-Dimethylaminopropiophenone-DNPH (4) has a molecular ion at *m/e* 357 (12% M) and fragment ions at *m/e* 355 (2), 312 (0.8), 310 (0.1), 265 (2), 115 (4), 103 (22),

TABLE 1. Analyses

Compound No.	Empirical Formula	Molecular weight	Calculated (%) C	H	N	Found (%) C	H	N
4	$C_{17}H_{20}N_5O_4Cl$	393	51.9	5.1	17.8	51.5	4.9	17.5
						51.4	4.9	17.7
3	$C_{17}H_{18}N_4O_5$	358	57.1	5.0	15.6	57.1	4.8	15.2
6	$C_{15}H_{13}ClN_4O_4$*	348	51.7	3.8	16.0	51.7	3.9	16.0
5	$C_{15}H_{12}N_4O_4$	312	57.7	3.8	17.6	57.6	3.9	17.3
7	$C_{36}H_{30}N_{12}O_{12}$	822	52.6	3.6	20.0	52.4	3.6	20.2
8	$C_8H_5F_3N_4O_5$	294	32.7	1.7		32.4	1.8	

*Calculated: Cl, 10.1. Found: 9.8.

77 (14), and 58 (100), the last attributed to $—CH_2N(CH_3)_2$.

3-Methoxypropiophenone-DNPH (26) has a molecular ion at *m/e* 344 and fragment ions comparable to the ethoxy homolog, as well as the significant one at 45 (100%) attributed to $—CH_2OCH_3$.

1,3-Diphenyl-2-pyrazoline (9) has a molecular ion at *m/e* 222 (100% M) and fragment ions at *m/e* 221 (27), 117 (8), with small amounts at 115, 111, 104, 103, 91, 75.

1-(2,4-Dinitrophenyl)-3-phenyl-2-pyrazoline (5) has a molecular ion at *m/e* 312 (100% M) and fragment ions at *m/e* 295 (23), 265 (91) plus smaller amounts at 220 (20), 219 (23), 218 (6), 165 (19), 117 (22), 116 (6), 103 (50), and 77 (36).

The pyrazoline from chalcone (25) has a molecular ion at *m/e* 388 (70% M), 386 (15), 371 (30), 356 (10), 353 (31), 340 (100), 294 (46), and small values down to 103 (13), and 77 (32).

The bishydrazone 7 decomposed in the mass spectrometer, leaving a brownish residue; because the peak intensity ratios changed during the analysis, thermal decomposition is suggested. Scale divisions (in parentheses) were measured. Found: *m/e* 329 (7), 328 (9), 325 (10), *312* (70), 298 (19), 279 (41), *265* (65), 264 (22), ***218*** (70), *217* (30), *183* (55), *115* (63), *105* (80), 104 (90), ***103*** (210), *77* (190). The values in italics are those characteristic of **2**. The value at 312 has the same *m/e* as **2** (70% M) and the isomeric dinitropyrazoline **5** (100% M); the latter also has values (bold face italic) *not found* in the above, at 295, 220, 219, 165, 117, 116, hence both **2** and **5** may be present. Although the peaks fit better for the PVK-DNPH, its presence is not unequivocally certain. However, on inspection of the structures involved it is seen that a cleavage of 7 to give this DNPH **2** is essentially a reverse Michael addition (21–23), consistent with and analogous to the formation of phenyl vinyl ketone from 3-dimethylaminopropiophenone (7). Its presence is a reasonable conclusion.

$$C_6H_5COCH_2CH_2N(CH_3)_2 \rightarrow C_6H_5COCH{=}CH_2 + HN(CH_3)_2$$

Nuclear Magnetic Resonance

These spectra were measured on a Varian A spectrometer. The chemical shifts are reported in ppm downfield from tetramethylsilane. The solvents were $CDCl_3$ and DMSO-d_6.

Compound 3: δ 1.15 (t, J = 7 Hz, 3H, O—C—CH_3), 3.20 (t, J = 5.5 Hz, 2H, N = C—CH_2), 3.85 (t, J = 5.5 Hz, N = C—C—CH_2—O—), 7.4 (m, 3H, ArH), 7.9 (m, 2H, ArH), 8.03 (d, $J_{AB} \simeq 9$ Hz, 1H, A of ABX of 2,4-DNP), 8.31 (dd, $J_{AB} \simeq 9$ Hz, $J_{BX} \simeq 2.5$ Hz, 1H, B of ABX), 9.13 (d, $J_{BX} \simeq 2.5$ Hz, 1H, X of ABX), 11.9 (broad s, 1H NH).

Compound 4: δ 2.85 (s, 6H, NMe_2), 3.3 (broad m, area uncertain since H_2O peak superimposed, =C—CH_2CH_2—N—), 7.5 (m, 3H, *m, p*-Hs of phenyl), 8.0 (m, 2H, *o*-Hs of phenyl), 8.05 (d, J_{AM} = 9 Hz, 1H, A of AMX of 2,4-DNP), 8.37 (dd, J_{AM} = 9 Hz, J_{MX} = 3 Hz, 1H, M of AMX), 8.83 (d, J_{MX} = 3 Hz, 1H, X of AMX), and 11.3 (broad s, 1H, NH).

Compound 6: ABX for dinitrophenyl at 9.12 (J = 2.5 Hz), 8.34 (J = 9 Hz, 2.5 Hz), the remaining H of this pattern is obscured by the other aromatic absorption: C_6H_5 at 7.76 (m, 2H) and 7.43 (m, 4H); AA′BB′ pattern at 3.42 (t, 2H) and 3.83 (t, 2H, NH at 11.7).

Compound 2: δ 5.86 (dd, J_{AM} = 2 Hz, J_{MX} = 17 Hz, 1H, =CH_2), 6.18 (dd, J_{AM} = 2 Hz, J_{AX} = 11 Hz, 1H, =CH_2), 6.75 (dd, J_{MX} = 1 Hz, J_{AX} = 11 Hz, 1H, =CH), 7.5 (m, 3H, *m*- and *p*-H of C_6H_5), 7.8 (m, 2H, *o*-H of C_6H_5), 8.14 (d, J_{AM} = 9 Hz, 1H, A of AMX of 2,4-DNP), 8.38 (dd, J_{AM} = 9 Hz, J_{MX} = 3 Hz, 1H, M of AMX of 2,4-DNP), 9.18 (d, J_{MX} = 3 Hz, 1H, X of AMX of 2,4-DNP), 13.0 (broad s, 1H, NH).

Compound 9: this showed a typical symmetrical AA′BB′ pattern, the two halves being centered at ~3.2 and 3.8 p.p.m. for the N—$CH_ACH_{A'}$—$CH_BCH_{B'}$—C= N moiety. The aromatic H appeared in a complex multiplet from 6.7–7.8 p.p.m.

Compound 5: ABX for DNP at 7.09 (J = 9 Hz), 8.27 (J = 9 Hz, 2.5 Hz), 8.45 (J = 2.5 Hz), phenyl at 7.44 (m, 3H), 7.67 (m, 2H), AA′BB′ at 3.43 (t, 2H) and 4.07 (t, 2H).

Ultraviolet Spectroscope

Ultraviolet absorption appears to be of less use for the identification of closely related 2,4-dinitrophenylhydrazones because, as will be noticed on inspection of the earlier literature (9), the wavelengths and extinctions of many of the derivatives are very close. This may be attributed to the fact that the major part of the molecule is the aromatic chromophore, $—C_6H_3(NO_2)_2$. In the data for the following compounds the first figure is wavelength and the second is log ε_{max}: 7, 368, 5.62; **3**, 380, 2.51; **6**, 372, 1.30; **4**, 368, 2.26; **2**, 383, 2.78 (9); **9**, 354, 1.87; **5**, 4.2, 4.52 (19); 2,4-dinitrophenylhydraz*ine*, 348, 4.12 (20), and 352, 4.17 (18).

Can. J. Chem. Downloaded from www.nrcresearchpress.com by 210.87.254.40 on 09/05/12
For personal use only.

Infrared Spectroscope

Examination of the i.r. absorption of the representative 2,4-dinitrophenylhydrazones of α,β-carbonyl compounds, $CH_2C{=}CHCHO$, $CH_2C{=}CHCOCH_3$, $C_6H_{13}CH{=}CHCOCH_3$, and $C_6H_5CH{=}CHCOCH_3$ revealed the presence of the typical NH band at 3.0–3.1 μ in each instance. The dinitrophenylhydrazone of chalcone (25) is now shown to be the lower melting isomer, m.p. 178°.

We are pleased to have had the invaluable assistance of Miss T. J. Davis for the i.r., D. Maier for the m.s., T. H. Regan for the n.m.r., D. Bush and D. Wall for the u.v. spectra, and D. Ketchum for the microanalyses, all of the Eastman Kodak Company Research Laboratory.

1. C. F. H. ALLEN, A. C. BELL, ALAN BELL, and J. A. VANALLAN. J. Am. Chem. Soc. **62**, 656 (1940).
2. C. S. MARVEL and D. J. CASEY. J. Org. Chem. **24**, 957 (1959).
3. E. P. KOHLER. Am. Chem. J. **42**, 375 (1909).
4. C. A. VAN MARLE and B. TOLLENS. Ber. **36**, 1352 (1903).
5. B. TOLLENS and H. SCHAFER. Ber. **39**, 2181 (1906).
6. F. STRAUS and A. BERKOW. Ann. **401**, 121 (1913).
7. C. MANNICH and G. HEILNER. Ber. **55B**, 356 (1922).
8. W. G. YOUNG and J. D. ROBERTS. J. Am. Chem. Soc. **68**, 649 (especially p. 650) (1946).
9. F. RAMIREZ and A. F. KIRBY. J. Am. Chem. Soc. **75**, 6028 (1953).
10. F. F. BLICKE and J. H. BURCKHALTER. J. Am. Chem. Soc. **64**, 451, (1942).
11. C. MANNICH and D. LAMMERING. Ber. **57B**, 1108 (1924); Proced. Org. React. **1**, 329.
12. J. F. NORRIS and H. B. COUCH. J. Am. Chem. Soc. **42**, 2330 (1920).
13. T. MATSUMOTO and K. HATA. J. Am. Chem. Soc. **79**, 5506 (1957).
14. C. F. H. ALLEN. J. Am. Chem. Soc. **52**, 2955 (1930).
15. K. VON AUWERS. Ber. **65**, 831 (1932).
16. A. JACOB and J. MADINAVEITIA. J. Chem. Soc. 1929 (especially p. 1931) (1937).
17. C. S. MAXWELL. Org. Synth. **23**, 30 (1943); Coll. Vol. III, 305 (1955).
18. R. F. CURTIS, C. H. HASSELL, and J. WEATHERSTON. J. Chem. Soc. 3831(1962).
19. W. L. CHAMBERS and M. L. WILLARD. J. Am. Chem. Soc. **82**, 3373 (1960).
20. J. D. ROBERTS and C. GREEN. J. Am. Chem. Soc. **68**, 214 (1946).
21. C. F. H. ALLEN and G. P. HAPP. Can. J. Chem. **42**, 641, 650, 655 (1964).
22. C. F. H. ALLEN, J. O. FOURNIER, and W. J. HUMPHLETT. Can. J. Chem. **42**, 2616 (1964).
23. C. F. H. ALLEN and W. J. HUMPHLETT. Can. J. Chem. **44**, 2315 (1966).
24. H. J. SHINE. J. Org. Chem. **24**, 252 (1959).
25. C. F. H. ALLEN and J. H. RICHMOND. J. Org. Chem. **2**, 222 (1937).
26. F. STRAUS and A. BERKOW. Ann. **401**, 121 (especially p. 144) (1913).

Can. J. Chem. Downloaded from www.nrcresearchpress.com by 210.87.254.40 on 09/05/12
For personal use only.

Neutral Solvolysis of Acyl Carbon and the Temperature Dependence of the Kinetic Solvent Isotope Effect

B. ROSSALL[1] AND R. E. ROBERTSON

Department of Chemistry, The University of Calgary, Calgary, Alberta T2N 1N4

Received September 17, 1974

B. ROSSALL and R. E. ROBERTSON. Can. J. Chem. **53**, 869 (1975).

The temperature dependence of the rate of hydrolysis of benzoic, phthalic, and succinic anhydrides have been determined in H_2O and D_2O under "neutral" conditions. Corresponding data have been obtained for methyl trifluoroacetate. While both series supposedly react by the same $B_{Ac}2$ mechanism, remarkable differences are made obvious by this investigation. Possible sources of such differences are proposed.

B. ROSSALL et R. E. ROBERTSON. Can. J. Chem. **53**, 869 (1975).

On a déterminé, dans H_2O et D_2O, dans des conditions neutres, l'influence de la température sur la vitesse d'hydrolyse des anhydrides benzoique, phtalique et succinique. On a obtenu les données correspondantes pour le trifluoroacétate de méthyle. Alors que l'on suppose que les deux séries réagissent par le même mécanisme $B_{Ac}2$, des différences importantes découlent de la présente étude. On propose diverses sources possibles pour de telles différences.

[Traduit par le journal]

Introduction

The unexpected changes in the kinetic solvent isotope effects (k.s.i.e.) with temperature found for the hydrolysis of acetic and propionic anhydrides (1) were without precedent (2–4) and did not appear to resemble the results published by Winter and Scott (5) for the methyl, ethyl, and isopropyl trifluoroacetates which, like the anhydrides and other haloacetates, are considered to react by a $B_{Ac}2$ mechanism (6). No satisfactory cause for such variation in k.s.i.e. with temperature was apparent for acetic and propionic anhydrides; hence in the hope of discovering some structural influence, the rates of hydrolysis for three other anhydrides with quite different structural features were determined in H_2O and D_2O. Rate measurements were made over a sufficient range of temperatures to permit a determination of the shape of the k.s.i.e. *vs.* T curve and to examine the temperature coefficient of $\Delta H^{\neq}$. Since Winter and Scott (5) had determined the k.s.i.e. for alkyl trifluoroacetate at three temperatures only, and had determined $\Delta C_p^{\neq}$ for ethyl trifluoroacetate, we undertook a more complete study of temperature effects on the rate of hydrolysis of methyl trifluoroacetate in both H_2O and D_2O.

[1]NRCC Postdoctoral Fellow, 1968–1970. Present address: Unilever Research, Port Sunlight Laboratory, Port Sunlight, Merseyside, U.K.

Experimental

Commercial samples of benzoic anhydride, succinic anhydride and phthalic anhydride were purified by recrystallization to constant melting point (Table 1).

Methyl trifluoroacetate was prepared by reaction of silver trifluoroacetate with methyl iodide in freshly distilled benzonitrile (8). The ester was isolated by distillation and purified by redistillation b.p. 40–41°, literature b.p. 43°.

Water and D_2O were purified by methods reported previously (1). In all D_2O experiments the %D exceeded 99.7% D.

First order rate constants for the reaction of each substrate in H_2O and D_2O were determined over the widest conveniently attainable temperature range by the conductance method used in the previous study (1) and treatment of the temperature dependence of these rates and derivation of pseudo-thermodynamic parameters followed previous formalism.

Results and Discussion

Rate determination for the solvolysis of organic substrates which produce weak electrolytes and the interpretation of the conductance–time data for these reactions present special problems which we solved previously (1). The observed pseudo first order rate constants were determined using the Guggenheim method (9) modified for weak electrolytes. The procedure may be summarized as follows: resistance readings were collected in pairs at a constant time interval, Δt apart. In addition the acid ionization constant, K_a, limiting equivalent ionic conductance, Λ_0, were required for application of the following

Can. J. Chem. Downloaded from www.nrcresearchpress.com by 210.87.254.6 on 09/05/12
For personal use only.

Can. J. Chem. Downloaded from www.nrcresearchpress.com by 210.87.254.6 on 09/05/12
For personal use only.

TABLE 1. Melting points and recrystallization solvents for acid anhydrides

Anhydride	Recrystallization solvent	Melting point (°C) This work	Literature (7)
Benzoic	Aqueous ethanol	42.6	42
Succinic	Chloroform	118.7	120
Phthalic	Benzene	131.7	132

TABLE 2. Empirical constants for the rate–temperature relation (2) for the solvolysis of acyl carbon in H_2O

Substrate	A_2	$-A_2$	$-A_3$	$n_{T_1}{}^{T_2}$
Benzoic anhydride	8.25593	2524.3274	1.2872	$24_{16}{}^{50}$
Succinic anhydride	33.88575	4054.6759	9.2282	$30_1{}^{27}$
Phthalic anhydride	185.94917	10654.3206	61.5189	$26_1{}^{16}$
Methyl trifluoroacetate	126.02044	7466.7501	41.6549	$29_1{}^{18}$

TABLE 3. Empirical constants for the rate–temperature relation (2) for the solvolysis of acyl carbon in D_2O

Substrate	A_1	$-A_2$	$-A_3$	$n_{T_1}{}^{T_2}$
Benzoic anhydride	88.85618	6367.8447	28.8520	$22_{25}{}^{60}$
Succinic anhydride	2.29799	2642.6448	−1.4460	$23_5{}^{30}$
Phthalic anhydride	45.57871	4674.4670	13.0220	$17_4{}^{20}$
Methyl trifluoroacetate	122.53008	7415.0428	40.5306	$20_4{}^{28}$

equation. In (1) where C_0 = stoichiometric concentration of anhydride at time $t = 0$; C_t = concentration of acid at time t; $C_{t+\Delta}$ = concentration of acid at time $t + \Delta$; Δ = constant time interval, approximately $2t_{1/2}$, k^0 = observed first order rate constant, C_K = cell constant.

$$[1]\quad \log\left\{\frac{1}{R_{t+\Delta}}-\frac{1}{R_t}\right\} + \log\left[1+\frac{10^3 C_K}{\Lambda_0 K_a}\left(\frac{1}{R_{t+\Delta}}+\frac{1}{R_t}\right)\right] = \log\left[\frac{C_0\Lambda_0}{2\times 10^3 C_K}(1-e^{-k\Delta})\right]-\frac{k^0 t}{2.3026}$$

Least-squares fit to eq. 1 provided k^0, the observed rate constant, and its standard deviation. For derivation of eq. 1, see ref. 1.

K_a values used were for benzoic acid in H_2O (10), benzoic acid in D_2O (11), succinic acid in H_2O (12), succinic acid in D_2O (13), phthalic acid in H_2O (14), trifluoroacetic acid in H_2O (15). K_a for phthalic acid and trifluoroacetic acid in D_2O were not available, therefore values were estimated using Rule and LaMer's law (16) and the data of Bates *et al.* (13). In order to test the reliability of the assumptions, tests of variation in observed k^0 values with changes in K_a values were made. If K_a was estimated to within $\pm 10\%$, then the error introduced into k^0 was less than 0.1%. For the cyclic anhydrides which produced dicarboxylic acids the effective ionic concentration was estimated by using the K_a (1) values, hereto, tests indicated this approximation produced no significant error in k^0.

Calculated standard deviations in k^0 were usually $<\pm 0.25\%$ and the agreement between the four experimental values for each temperature were within $\pm 0.5\%$.

The observed rate constants were fitted to the following empirical equation ($k^0 = k_{\text{observed}}$):

$$[2]\quad \log k^0 = A_1 + A_2/T + A_3 \log T + A_4 T + \ldots$$

Using only a three parameter fit to eq. 2 the empirical constants A_1, A_2, and A_3, see Table 2 for H_2O and Table 3 for D_2O were calculated

Can. J. Chem. Downloaded from www.nrcresearchpress.com by 210.87.254.6 on 09/05/12
For personal use only.

TABLE 4. Kinetic solvent isotope effect as a function of temperature

Substrate	k.s.i.e. at												
	0 °C	5 °C	10 °C	15 °C	20 °C	25 °C	30 °C	35 °C	40 °C	45 °C	50 °C	55 °C	60 °C
Acetic anhydride*	2.837	2.892	2.927	2.941	2.937	2.916	2.878	—	—	—	—	—	—
Propionic anhydride*	3.188	3.024	2.903	2.818	2.764	2.737	2.736	2.757	2.801	2.866	2.954	—	—
Benzoic anhydride	—	—	3.658	3.445	3.279	3.151	3.053	2.985	2.941	2.917	2.917	2.934	2.970
Succinic anhydride	2.579	2.633	2.676	2.709	2.733	2.748	2.754	2.753	2.744	—	—	—	—
Phthalic anhydride	2.257	2.314	2.335	2.319	2.272	2.197	—	—	—	—	—	—	—
Methyl trifluoroacetate	3.645	3.600	3.555	3.511	3.468	3.426	—	—	—	—	—	—	—

*Data included from (1).

TABLE 5. Pseudothermodynamic parameters of activation for solvolysis of acyl carbon in H_2O at 25 °C

Substrate	$10^3 k^0$ (s^{-1})	$\Delta H^{\ddagger}$ (cal mol^{-1})	$-\Delta S^{\ddagger}$ (cal deg^{-1} mol^{-1})	$-\Delta C_p^{\ddagger}$ (cal deg^{-1} mol^{-1})
Benzoic anhydride	0.4021	10 195 ± 37	39.88 ± 0.12	5 ± 3
Succinic anhydride	2.829	12 493 ± 41	28.30 ± 0.14	20 ± 4
Phthalic anhydride	10.47	11 668 ± 274	28.46 ± 0.94	124 ± 16
Methyl trifluoroacetate	8.025	8 893 ± 141	38.30 ± 0.49	85 ± 8
Ethyl trifluoroacetate*	3.29	11 530	35	67
Acetic anhydride†	2.6	9 600	38	74
Propionic anhydride†	1.5	9 510	40	31

*Reference 5.
†Reference 1.

TABLE 6. Pseudothermodynamic parameters of activation for solvolysis of acyl carbon in D_2O at 25 °C

Substrate	$10^3 k^0$ (s^{-1})	$\Delta H^{\ddagger}$ (cal mol^{-1})	$-\Delta S^{\ddagger}$ (cal deg^{-1} mol^{-1})	$-\Delta C_p^{\ddagger}$ (cal deg^{-1} mol^{-1})
Benzoic anhydride	0.1276	11 451 ± 90	37.95 ± 0.30	59 ± 5
Succinic anhydride	1.030	12 356 ± 59	30.76 ± 0.20	−1 ± 7
Phthalic anhydride	4.767	13 081 ± 91	25.29 ± 0.31	28 ± 7
Methyl trifluoroacetate	2.343	9 323 ± 51	39.30 ± 0.17	83 ± 5

for each reaction and could be used to recalculate smoothed curve values of k^0 at 5° intervals throughout the experimental temperature range. While a fourth term in T might seem to be desirable formally, the accuracy of the rate data did not justify such an extension. The kinetic solvent isotope effect, k.s.i.e. = $k_{H_2O}{}^0/k_{D_2O}{}^0$, was determined as a function of temperature, see Table 4.

An error estimate in k.s.i.e. values is provided by assuming that the error in each individual observed k^0 values was ±0.25%, then the same error was appropriate for the smoothed curve k^0 values. Consequently an error estimate on k.s.i.e. values would be ±0.5% or less.

A formal interpretation of the temperature effect on k^0 in terms of transition state assumptions permits the calculation of pseudo-thermodynamic quantities from the empirical constants A_1, A_2, and A_3 (17). The enthalpy, $\Delta H^{\ddagger}$, entropy, $\Delta S^{\ddagger}$, and heat capacity of activation, $\Delta C_p{}^{\ddagger}$, for each reaction is given in Table 5 for H_2O and in Table 6 for D_2O.

Discussion

Where comparisons are possible, our values of k.s.i.e. and of $\Delta H^{\ddagger}$ and $\Delta S^{\ddagger}$ for the hydrolysis of anhydrides agree with those published previously and lie in the range expected for a $B_{Ac}2$ mechanism (18–22). However, because we have examined the temperature dependence of the rate in both H_2O and D_2O, it is evident that these k.s.i.e. values, like those for acetic and propionic anhydrides (1), do not decrease smoothly with increasing temperature (see Fig. 1) as had been found in the hydrolysis of halides (2), sulfonyl chlorides (23), nitrates (24), and alkyl trifluoroacetates (5); the last presumably reacting by a $B_{Ac}2$ mechanism.

This departure from linearity was not uniform; the plot of log (k.s.i.e.) *vs.* $10^3/T$ for benzoic and acetic anhydrides passing through minima, while that for succinic and phthalic, like that for propionic anhydride, passed through flat maxima. Winter and Scott (5) had determined k.s.i.e. for methyl, ethyl, and isopropyl trifluoroacetate at three temperatures and had found an apparent linear decrease with temperature. We have determined the rate of hydrolysis for methyl trifluoroacetate over a wider range of temperatures in both H_2O and D_2O and found no evidence of departure from linearity of the above plot. The slope (0.88) being about the same as that found by the previous investigators.

Further empirical evidence of differences in the detailed mechanism of hydrolysis of the anhydrides and of the alkyl trifluoroacetates becomes apparent if we compare the nominal values of the temperature coefficient of the enthalpy of activation ($\Delta C_p{}^{\ddagger}$) for the two series

Can. J. Chem. Downloaded from www.nrcresearchpress.com by 210.87.254.6 on 09/05/12
For personal use only.

TABLE 7. Kinetic solvent isotope effects as pseudothermodynamic differences* for solvolysis of acyl carbon at 25 °C

Substrate	$\delta_I\Delta H^{\ddagger}$ (cal mol^{-1})	$\delta_I\Delta S^{\ddagger}$ (cal deg^{-1} mol^{-1})	$\delta_I\Delta C_p^{\ddagger}$ (cal deg^{-1} mol^{-1})
Acetic anhydride	362 ± 64	−0.91 ± 0.22	42 ± 6
Propionic anhydride	179 ± 113	−1.40 ± 0.38	−63 ± 12
Benzoic anhydride	1256 ± 127	1.93 ± 0.42	−54 ± 8
Succinic anhydride	−137 ± 100	−2.46 ± 0.34	21 ± 11
Phthalic anhydride	1413 ± 365	3.17 ± 1.25	96 ± 23
Methyl trifluoroacetate	430 ± 192	−1.00 ± 0.66	2 ± 13

*By definition $S_I\Delta X^{\ddagger} = \Delta X^{\ddagger}_{D_2O} - \Delta X^{\ddagger}_{H_2O}$.

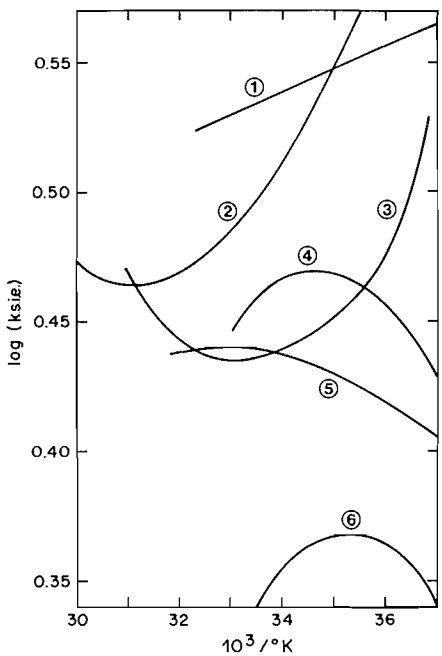

FIG. 1. The effect of temperature on the kinetic solvent isotope effect: (*1*) methyl trifluoroacetate, (*2*) benzoic anhydride, (*3*) acetic anhydride, (*4*) propionic anhydride, (*5*) succinic anhydride, (*6*) phthalic anhydride.

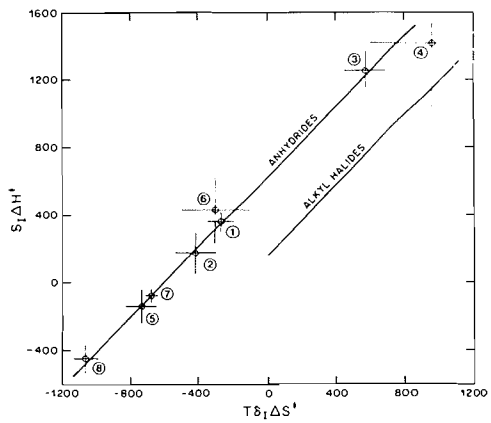

FIG. 2. A comparison of $\delta_I\Delta H^{\ddagger}$ *vs.* $T\Delta S^{\ddagger}$ values for a series of anhydrides and methyl trifluoroacetate: (*1*) acetic anhydride, 25 °C; (*2*) propionic anhydride, 25 °C; (*3*) benzoic anhydride, 25 °C; (*4*) phthalic anhydride, 25 °C; (*5*) succinic anhydride, 25 °C; (*6*) methyl trifluoroacetate, 25 °C; (*7*) acetic anhydride, 15 °C; (*8*) propionic anhydride, 35 °C.

in light and heavy water. The values of $\delta_I\Delta C_p^{\ddagger}$ (Table 7) found for the anhydrides are seen to be large and variable while the corresponding term for the methyl trifluoroacetate is less than the combined experimental error. The latter condition is normal for the hydrolysis of alkyl halides (2) and is found also for the ionization of acetic acid $\Delta C_p^0 = -36.6$ cal deg^{-1} mol^{-1} in H_2O and -38.6 cal deg^{-1} mol^{-1} in D_2O (25). The difference for the autoprotolysis of water is somewhat larger, $\Delta C_p^0 = -47$ cal deg^{-1} mol^{-1} in H_2O and -55 cal deg^{-1} mol^{-1} in D_2O (26). These relatively small differences bear but accidental resemblance to those recorded in Table 7.

We could discern no relationship between the variation in $\delta_I\Delta H$, $\delta_I\Delta S^{\ddagger}$, or $\delta_I\Delta C_p^{\ddagger}$ and the pK_a of the derived acids. However, it was found that if $\delta_I\Delta H^{\ddagger}$ was plotted against $T\delta_I\Delta S^{\ddagger}$, (see Fig. 2), the values for benzoic and phthalic anhydride (the aromatic anhydrides) are separated from values for the saturated members along the usual linear plot and this in spite of the fact that k.s.i.e. for the benzoic anhydride is the highest and the k.s.i.e. for the phthalic anhydride is among the lower values. In the $\delta_I\Delta H^{\ddagger}$ *vs.* $T\delta_I\Delta S^{\ddagger}$ plot, the point for succinic anhydride, also cyclic, is found with the saturated anhydrides. The differences noted probably relate in some way to the effect of conjugation between the phenyl and carboxyl group and such factors as

Can. J. Chem. Downloaded from www.nrcresearchpress.com by 210.87.254.6 on 09/05/12
For personal use only.

Can. J. Chem. Downloaded from www.nrcresearchpress.com by 210.87.254.6 on 09/05/12
For personal use only.

the approach of the nucleophilic water and solvation of the charged transition state but the exact relationship is not clear.[2]

One other observation, as yet unexplained, is that whereas k.s.i.e. decreases from 2.9 to 2.6 on passing from pure water to 40 vol% dioxane for acetic anhydride, and an even larger decrease occurs for methyl trifluoroacetate, benzoic anhydride shows a slight increase (20). While the decrease can be rationalized in terms of a decrease in water structure obviously the same argument will not apply for an increase. Since we are comparing results from various laboratories some allowance must be made for error, but the presence of a remarkable difference can hardly be doubted.

The changes in k.s.i.e. with T and in $\delta_I \Delta C_p^{\ddagger}$ may be related. If the $\Delta C_p^{\ddagger}$ is more negative in D_2O than in H_2O which might well be expected from a simple interpretation of the effect of temperature on the water structures, then k.s.i.e. would be expected to decrease as temperature increases. This in fact is found even though $\delta_I \Delta C_p^{\ddagger} \rightarrow 0$ under normal conditions *e.g.*, the case of the trifluoroacetates, Fig. 1. However, the decrease in k.s.i.e. with temperature for benzoic anhydride is far steeper than a $\delta_I \Delta H^{\ddagger}$ argument would require and points to an unusual influence. Moreover it should be noted that the extrema which characterize the log (k.s.i.e.) *vs.* $10^3/T$ plots for the anhydrides (Fig. 1) would not arise simply from the temperature effects on solvent structure. Some temperature dependent mechanistic change must occur which is dependent on the structure of the anhydride, the properties of D_2O and H_2O, and the wide range of mechanistic differences presently included under the definition of general acid base catalysis.

The relationship between structure and mechanism for general base catalyzed reactions has been investigated and discussed previously (21, 27–30) but not in terms of the distinction made evident in this paper. Here, a study of the temperature dependence of the k.s.i.e. and $\Delta H^{\ddagger}$ reveals characteristic differences attributable to differences in mechanism even though both series insofar as conventional tests go, hydrolyze by the same $B_{Ac}2$ mechanism (if we regard the mechanism for *t*-butyl trifluoroacetate and similar compounds as exceptional (5)).

One possible hypothesis would be the intrusion of various degrees of nucleophilic attack by OH^- or indeed the direct attack of H_2O in competition with general base catalyzed mechanism. Such a hypothesis is inconsistent with the fact that the reaction is p*H*-independent over the experimental range of temperature. Nor would a hypothesis based on the incursion of some degree of nucleophilic interaction appear to be satisfactory (31). Of course, competing reactions with different values of $\Delta H^{\ddagger}$ will give rise to changes in $\Delta C_p^{\ddagger}$ which may seem unusual (32, 33, 39). Winter and Scott (5) have shown that a change in mechanism from $B_{Ac}2$ to S_N1 probably does occur in the case of the alkyl trifluoroacetates, but this change is signalled by a dramatic change in the k.s.i.e. and in $\Delta H^{\ddagger}$ and $\Delta S^{\ddagger}$. Such changes are not at all evident as between the anhydrides and the trifluoroacetates under investigation here. Rather we are faced by a more subtle temperature dependent distinction.

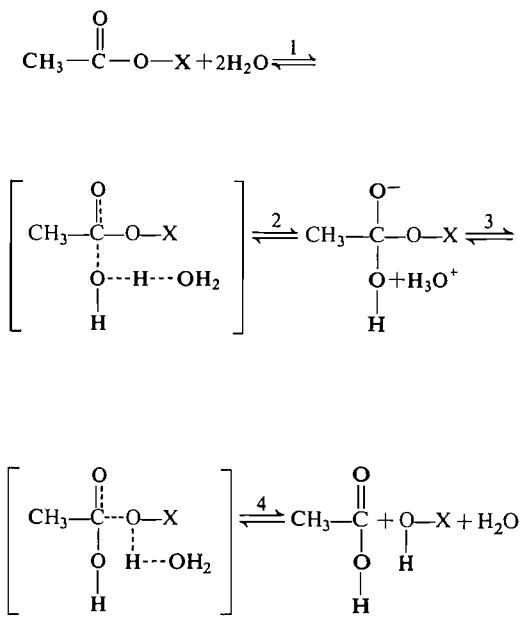

SCHEME 1. Generalized $B_{Ac}2$ mechanism for neutral hydrolysis (27).

[2]One referee drew attention to the possibility of differences arising from initial state differences as a possible contributing factor here. Such a possibility is difficult to disprove or to prove but we do not consider it a strong possibility. The major contribution to $\Delta C_p^{\ddagger}$ appears to arise in the vicinity of the anion and further appears to arise from solvation changes localized near the seat of reaction. For example, $\Delta C_p^{\ddagger}$ for the hydrolysis of both methanesulfonyl chloride and benzenesulfonyl chloride are the same (-55 cal deg^{-1} mol^{-1}).

Can. J. Chem. Downloaded from www.nrcresearchpress.com by 210.87.254.6 on 09/05/12
For personal use only.

If we accept Scheme 1 (27) as approximating the $B_{Ac}2$ mechanism then it might seem remarkable that complex temperature dependency was not observed in all cases and in fact the hydrolysis of the trifluoroacetates actually represent some kind of limiting case. We know that the latter (34–36) as well as the benzoic anhydride give evidence of ^{18}O exchange to a much greater degree than acetic anhydride, for example. However, if the rate of return k_{-1} and product formation, k_2, are fast compared to the rate at which the two oxygens become equivalent by proton transfer, significant ^{18}O exchange may not be observed. Support for such a possibility may be seen in the fact that the k.s.i.e. and the large negative values of $\Delta S^{\ddagger}$ are very similar for both series while significant differences in ^{18}O are observed. Bunton, Fuller, Perry and Shiner (21) proposed a pre-equilibrium involving a charged intermediate, as shown above, followed by partitioning between a pathway leading to a dihydroxy intermediate, admitting ^{18}O exchange, expulsion of the leaving group, and return to starting reactants. In attempting to account for the k.s.i.e. found for the spontaneous hydrolysis of acetic anhydride Bunton and Shiner (37, 38) show that differences in hydrogen bonding to such an intermediate so far exceed hydrogen bonding in bulk water as to account for observed k.s.i.e. values. It is an interesting fact that the same arguments applied to the prediction of the k.s.i.e. for methyl trifluoroacetate gave a value of 2.7, far closer to that obtained by Winter and Scott (5) and to our value for methyl trifluoroacetate, than the value which they used for comparison (21). While we regard their calculation as an oversimplification, we agree with the rather obvious principle on which it is formulated *i.e.*, that where electronic displacements develop centers of high local acidity or basicity, there will be an increase in the strength of the hydrogen bonds between these centers and the solvent water molecules.

These results point to questions which deserve further study. There is the remarkable difference in the temperature dependence of the k.s.i.e. found for the trifluoroacetates and for the anhydrides, both of which are considered to react by a $B_{Ac}2$ mechanism but which, on the basis of this evidence must differ in some significant manner. There is the difference in the temperature dependence of the same ratio among the various anhydrides as well as the existence of remarkable differences in the *apparent* $\Delta C_p^{\ddagger}$ values. There is the unprecedented difference in the *apparent* $\Delta C_p^{\ddagger}$ value for the various anhydrides in D_2O and H_2O, a fact which points to complexities in the mechanism of neutral solvolysis of the anhydrides not present in the hydrolysis of the alkyl trifluoroacetates.

The differences in $\Delta C_p^{\ddagger}$ values in H_2O and D_2O for the anhydride and trifluoroacetate series are not inconsistent with the important similarities which have led to both series being classed as reacting by general base catalysis (29). Whether this reaction is to be regarded as a single dominating concerted process (39, 40) or several stages involving pre-equilibria has been argued by several authors (27–29). We find no good reason to reject the formation of an intermediate of variable lifetime. That the trifluoroacetates are a better leaving group than the weak acid anions is accepted and this difference provides both for the difference in temperature dependency and in ^{18}O-exchange.

Scott and Robertson (41), in studying the effect of an intermediate on derived temperature coefficients for the hydrolysis of *t*-butyl chloride showed for the general mechanism

[4] $$\mathrm{A} \underset{k_2}{\overset{k_1}{\rightleftharpoons}} \mathrm{B} \underset{k_4}{\overset{k_3}{\rightleftharpoons}} \mathrm{C}, \quad \mathrm{B} \xrightarrow{2n} \mathrm{P}, \quad \mathrm{C} \xrightarrow{3n} \mathrm{P}$$

where

[5] $$k_{\text{obs}}^{\text{I}} = \frac{k_1}{1 + \dfrac{k_2}{k_3}} = \frac{k_1}{1 + \alpha}$$

that for the region I where $\alpha < 0.01$

[6] $$\Delta C_p^{\ddagger}{}_{\text{calc}} = \Delta C_{p_1}{}^{\ddagger}$$

and for region III where $\alpha > 100$

[7] $$\Delta C_p^{\ddagger}{}_{\text{calc}} = \Delta C_{p_1}{}^{\ddagger} - \Delta C_{p_2}{}^{\ddagger} + \Delta C_{p_3}{}^{\ddagger}$$

For the intermediate region II where $0.01 < \alpha < 100$ a much more complicated expression results *viz*

[8] $$\Delta C^{\ddagger}{}_{\text{calc}} = \Delta C_{p_1}{}^{\ddagger} + \frac{\alpha}{\alpha + 1}(\Delta C_{p_{2n}}{}^{\ddagger} - \Delta C_{p_2}{}^{\ddagger}) - \frac{\alpha}{(1 + \alpha)^2}\frac{(\Delta H_{2n}{}^{\ddagger} - \Delta H_2{}^{\ddagger})^2}{RT^2}$$

Can. J. Chem. Downloaded from www.nrcresearchpress.com by 210.87.254.6 on 09/05/12
For personal use only.

The spurious heat capacity term on the r.h.s. will always be positive, hence will act to reduce $\Delta C_p^{\ddagger}{}_{calc}$ and $\Delta C_{p_3}{}^{\ddagger} - \Delta C_{p_2}{}^{\ddagger}$ will probably be positive. Further complications arise since α will be temperature dependent.

In principle such a scheme could provide the basis for understanding the differences in $\Delta C_p^{\ddagger}$ characteristics between the alkyl trifluoroacetates and the anhydrides, and the differences within these series. Queen (42) has used pre-equilibria and partitioning to account for the more extreme changes in $\Delta H^{\ddagger}$ with temperature found for the hydrolysis alkyl chloroformates some of which, like the above, display general characteristics of the $B_{Ac}2$ mechanism.

The above scheme provides for complex changes in $\Delta C_p^{\ddagger}$ depending on the solvent, and on the electronic nature of the reactants. As we have shown already, these can lead to differences in k.s.i.e. with changing temperature where $\delta_I C_p^{\ddagger}$ is large. In this connection there is a related factor which deserves comment. In an investigation of the hydrolysis of substituted benzenesulfonyl chlorides (43) it was found that the $\Delta C_p^{\ddagger}$ for the *p*-methoxy member was less negative than expected by comparison with other members of the series. This was attributed to a temperature dependent interaction of the water with the methoxy group, an effect which increased with increasing temperature as the equilibrium in cooperative water structure moved toward a greater number of unbonded water molecules (44). In support of this working hypothesis we noted that $\Delta C_p^{\ddagger}$ for the hydrolysis of 2-chloro-2-methoxymethylpropane was 18 cal mol^{-1} deg^{-1} more positive than the corresponding value for *t*-butyl chloride. The ΔC_p^{0} for the ionization of 4-methoxybenzoic acid was more negative than the value for other benzoic acids (45), the change in sign in the latter case being consistent with this hypothesis and the electronic requirements as applied to the benzoic acid system. Recently Koshy (20) found values of $\Delta C_p^{\ddagger}$ for the hydrolysis of 3-methoxybenzyl nitrate in accord with this hypothesis. This same temperature dependent solvation effect must surely be present in the general base catalyzed hydrolysis involving displacement from esters, anhydrides and acid chlorides where hydrogen bonding is important. In the trifluoroacetate system $\Delta C_p^{\ddagger}$ becomes less negative by 16 cal mol^{-1} deg^{-1} on changing from Me → Et and at isopropyl (for which no $\Delta C_p^{\ddagger}$ is available) the $\Delta H^{\ddagger}$ and $\Delta S^{\ddagger}$ values resemble those for $B_{Ac}2$ displacement, while at *t*-butyl, the reaction is S_N1 (5). These changes clearly follow changes in electron density on the ether oxygen with increasing solvation and decreased positive charge on the carbonyl carbon. A similar trend is apparent in the chloroformate series studied by Queen (42). Phenyl and methyl chloroformates appear to have an intermediate in which α lies outside the midrange while ethyl and propyl show large changes in $\Delta C_p^{\ddagger}$ with temperature. For isopropyl chloroformate mixed mechanism is suspected while for *t*-Bu—O—C(=O)—Cl the reaction is claimed to be S_N1. These changes in the alkyl group have a direct effect on the hydrogen bonding of the ether-oxygen and these effects are reflected in changes in $\Delta C_p^{\ddagger}$, $\Delta H^{\ddagger}$, and in mechanism. The changes noted above were in the leaving group and the consequences in terms of mechanism were marked. Similar changes adjacent to the carbonyl carbon can change the mechanism from $B_{Ac}2$ to S_N2 or S_N1 (4, 42). These too represent extremes.

The results reported here for the anhydrides do not show such wide variation in $\Delta H^{\ddagger}$, $\Delta S^{\ddagger}$ or in k.s.i.e. as reported by Scott and Winter and by Queen but rather, differences best explained in terms of changing solvation with temperature combined with related changes in partitioning. If the structure of acetic anhydride in solution is similar to that in the gas phase (46) the ether oxygen is exposed to potential hydrogen bonding before, and in the activated state. Models suggest similar comments apply to other anhydrides. The influence of potential hydrogen bonding on the leaving group is thus a factor which may vary with the degree of bond breaking at the transition state, and as between H_2O and D_2O.

Summarizing the above qualitative arguments, we attribute the unusual temperature dependence of the k.s.i.e. to temperature dependent solvation effects and to the related effect on partitioning both of which are made evident by surprising differences in the temperature coefficients of $\Delta H^{\ddagger}$ in H_2O and D_2O. The difference in the basicity of the leaving group probably contributes to an important degree to the rate of formation of the intermediate and breakup of same. Our results reveal an unexpected problem. We trust they may contribute to its solution.

1. R. E. ROBERTSON, B. ROSSALL, and W. A. REDMOND. Can. J. Chem. **49**, 3665 (1971).
2. R. E. ROBERTSON. Prog. Phys. Org. Chem. **4**, 213 (1967).
3. L. TREINDL, R. E. ROBERTSON, and S. E. SUGAMORI, Can. J. Chem. **47**, 3397 (1969).
4. P. M. LAUGHTON and R. E. ROBERTSON. Solute–solvent interactions. *Edited by* J. F. Coetzee and C. D. Ritchie. Marcel Dekker, New York. 1969. Chapt. 7.
5. J. G. WINTER and J. M. W. SCOTT. Can. J. Chem. **46**, 2887 (1968).
6. W. P. JENCKS. Prog. Phys. Org. Chem. **2**, 63 (1964).
7. I. HEILBRON. Dictionary of organic compounds. 4th ed. Eyre and Spottiswoode, London. 1965.
8. A. J. VOGEL. Practical organic chemistry. Longman, London. 1967. p. 381.
9. E. A. GUGGENHEIM. Phil. Mag. **2**, 538 (1926).
10. R. A. ROBINSON and R. H. STOKES. Electrolyte solutions, 2nd ed. Butterworth, London. 1959. p. 518.
11. E. L. WEHRY and L. B. ROGERS. J. Am. Chem. Soc. **88**, 351 (1966).
12. G. D. PINCHING and R. G. BATES. J. Res. Nat. Bur. Standard, **45**, 322 (1950).
13. R. A. ROBINSON, M. PAABO, R. G. BATES. J. Res. Nat. Bur. Standard, **73A**, 299 (1969).
14. H. J. HAMER, G. D. PINCHING, and S. F. ACREE. J. Res. Nat. Bur. Standard, **35**, 539 (1945).
15. A. L. HENNE and C. J. FOX. J. Am. Chem. Soc. **73**, 2323 (1951).
16. C. K. RULE and V. K. LAMER. J. Am. Chem. Soc. **60**, 1974 (1938).
17. E. C. W. CLARKE and D. N. GLEW. Trans. Faraday Soc. **62**, 539 (1966).
18. M. L. BENDER. Chem. Rev. **60**, 53 (1960).
19. W. P. JENCKS and J. CARRIOLO. J. Am. Chem. Soc. **83**, 1743 (1961).
20. A. R. BUTLER and V. GOLD. J. Chem. Soc. 2305 (1961).
21. C. A. BUNTON, N. A. FULLER, S. Y. PERRY, and V. J. SHINER, JR. J. Chem. Soc. 2918 (1963).
22. J. KOSKIKALLIO, D. PAULI, and E. WHALLEY. Can. J. Chem. **37**, 1360 (1959).
23. R. E. ROBERTSON, B. ROSSALL, S. E. SUGAMORI, and L. TREINDL. Can. J. Chem. **47**, 4199 (1969).
24. K. M. KOSHY and R. E. ROBERTSON. Can. J. Chem. **52**, 2485 (1974).
25. R. GARY, R. G. BATES, and R. A. ROBINSON. J. Phys. Chem. **69**, 2750 (1965).
26. A. K. COVINGTON, R. A. ROBINSON, and R. G. BATES. J. Phys. Chem. **70**, 3820 (1966).
27. A. KIVINEN. Suomen Kemistilehti, B**38**, 159 (1965).
28. S. L. JOHNSON. Advan. Phys. Org. Chem. **5**, 237 (1967).
29. W. P. JENCKS and M. GILCHRIST. J. Am. Chem. Soc. **90**, 2622 (1968).
30. T. C. BRUICE and U. K. PANDIT. J. Am. Chem. Soc. **82**, 5858 (1960).
31. J. F. KIRSCH and W. P. JENCKS, J. Am. Chem. Soc., **86**, 837 (1964).
32. J. R. HULETT. Quart Rev. London, **18**, 227 (1964).
33. G. KOHNSTAM. Advan. Phys. Org. Chem. **5**, 121 (1967).
34. C. A. BUNTON, T. A. LEWIS, and D. R. LLEWELLYN. Chem. Ind. **11**, 54 (1954).
35. C. A. BUNTON and T. HADWICK. J. Chem. Soc. 3248 (1958).
36. H. LUDENHEIM and M. L. BENDER. J. Am. Chem. Soc. **82**, 1895 (1960).
37. C. A. BUNTON and V. J. SHINER, JR. J. Am. Chem. Soc. **83**, 42 (1961).
38. C. A. BUNTON and V. J. SHINER, JR. J. Am. Chem. Soc. **83**, 3207 (1961).
39. J. KOSKIKALLIO. Acta. Chem. Scand. **13**, 665 (1959).
40. J. HIPIN and D. P. N. SATCHELL. J. Chem. Soc. 1057 (1965).
41. J. M. W. SCOTT and R. E. ROBERTSON. Can. J. Chem. **50**, 167 (1972).
42. A. QUEEN. Can. J. Chem. **45**, 1619 (1967).
43. R. E. ROBERTSON and B. ROSSALL. Can. J. Chem. **49**, 1441 (1971).
44. G. NEMETHY and H. A. SCHERAGA. J. Chem. Phys. **36**, 3382 (1962).
45. J. W. LARSEN and L. G. HEPLER. *In* Solute–solvent interactions, *Edited by* J. F. Coetzee and C. D. Ritchie. Marcel Dekker. New York. 1969. Chapt 1.
46. H. J. V. LEDDER, F. C. MIJILHOFF, J. C. LEYTE, and C. ROMERS. J. Mol. Struct. **7**, 421 (1971).

Can. J. Chem. Downloaded from www.nrcresearchpress.com by 210.87.254.6 on 09/05/12
For personal use only.

The Copper–Selenium System at Temperatures to 850 K and Pressures to 50 kbar

RITCHIE MACLAREN MURRAY[1] AND ROBERT DONALD HEYDING

Department of Chemistry, Queen's University, Kingston, Ontario K7L 3N6

Received October 15, 1974

Can. J. Chem. Downloaded from www.nrcresearchpress.com by 210.87.254.42 on 09/05/12
For personal use only.

RITCHIE MACLAREN MURRAY and ROBERT DONALD HEYDING. Can. J. Chem. **53**, 878 (1975).

Phase relationships in the copper/selenium system in the composition range 30–70 atomic % selenium have been studied at temperatures from 298 to 850 K and at pressures to 50 kbar. A revised atmospheric pressure phase diagram is given, as well as an outline of the phase diagram at 20 kbar.

αCu_2Se is monoclinic at 298 K with $a = 14.087$, $b = 20.481$, $c = 4.145$ Å, $\beta = 90° 23'$. The $\alpha \rightarrow \beta$ (f.c.c.) transformation is complex, and occurs over a 30 K interval centered on 396 K. The overall enthalpy change is 6.4 ± 2 kJ mol^{-1}. The maximum in the DTA signal for this transition decreases slowly with increasing pressure at <1 K kbar^{-1}. The signal disappears above 42 kbar, presumably due to the formation of a high pressure modification.

Variable composition in $Cu_{2-x}Se$ (*berzelianite*) extends from $Cu_{2.00}Se$ to $Cu_{1.75}Se$ in the range 402–523 K. $Cu_{1.80}Se$, with $a = 5.765$ Å at 298 K, is stable throughout the temperature and pressure ranges investigated.

Cu_3Se_2 (*umangite*) is stable at 298 K to at least 35 kbar. Dimensions of the tetragonal cell at 298 are $a = 6.385$, $c = 4.217$ Å. At atmospheric pressure it disproportionates to $Cu_{2-x}Se$ and βCuSe at 386 K with an enthalpy change of 10.0 ± 5 kJ mol^{-1}. The reverse reaction is very slow. Above *ca.* 5 kbar it disproportionates to $Cu_{2-x}Se$ and $CuSe_2$II at a temperature less than 413 K. The reverse reaction is fast.

αCuSe (*klockmannite*) is hexagonal with $a = 3.934$, $c = 17.217$ Å at 298 K. It transforms to βCuSe at 323 K under atmospheric pressure with an enthalpy change of 0.84 ± 5 kJ mol^{-1}. This modification is C end-centered orthorhombic with $a = 3.948$, $b = 6.958$, $c = 17.239$ Å at 324 K. With increasing temperature the orthorhombic a/b ratio increases rapidly until, at 393 K, the transition to γCuSe is complete. This modification is hexagonal with $a = 3.984$, $c = 17.288$ Å at 430 K. CuSe is unstable above 5 kbar at 298 K, decomposing to form Cu_3Se_2 and $CuSe_2$II.

Marcasite-type $CuSe_2$, with $a = 5.0046$, $b = 6.182_2$, $c = 3.739_7$ Å at 298 K, disproportionates to CuSe and Se at 605 K under atmospheric pressure with an enthalpy change of 9.6 ± 4 kJ mol^{-1}. It transforms at less than 5 kbar at 298 K to the cubic pyrite modification $CuSe_2$II, with $a = 6.116$ Å. $CuSe_2$II melts congruently at 818 K and 20 kbar. The melting point increases with increasing pressure at *ca.* 3 K kbar^{-1}.

RITCHIE MACLAREN MURRAY et ROBERT DONALD HEYDING. Can. J. Chem. **53**, 878 (1975).

On a étudié les relations de phase dans le système cuivre/sélénium à des compositions allant de 30–70 atomes % de sélénium; ces études ont été effectuées entre 298 et 850 K et à des pressions de 50 kbar. On donne un diagramme de phase à pression atmosphérique modifié de même qu'une ébauche d'un diagramme de phase à 20 kbar.

αCu_2Se est monoclinique à 298 K avec $a = 14.087$, $b = 20.481$, $c = 4.145$ Å, $\beta = 90° 23'$. La transformation $\alpha \rightarrow \beta$ (f.c.c.) est complexe et se produit sur un intervalle de 30 K centré autour de 396 K. Le changement global d'enthalpie est de 6.4 ± 2 kJ mol^{-1}. Le maximum dans le signal en DTA pour cette transition diminue lentement à mesure que la pression augmente à un taux moins de 1 K kbar^{-1}. Le signal disparait au-dessus de 42 kbar, probablement dû à la formation d'une modification à haute pression.

Des compositions variables en $Cu_{2-x}Se$ (*berzelianite*) existent entre $Cu_{2.00}Se$ jusqu'à $Cu_{1.75}Se$ entre les températures de 402–523 K. Le $Cu_{1.80}Se$ avec $a = 5.765$ Å à 298 K, est stable sur tout l'intervalle des températures et des pression étudiées.

Cu_3Se_2 (*umangite*) est stable à 298 K jusqu'à au moins 35 kbar. Les dimensions de la cellule tétragonale à 298 K sont $a = 6.385$, $c = 4.217$ Å. A pression atmosphérique, il se disproportionne pour donner du $Cu_{2-x}Se$ et du βCuSe à 386 K avec un changement d'enthalpie de 10.0 ± 5 kJ mol^{-1}. La réaction inverse est très lente. Au-dessus d'environ 5 kbar il se disproportionne en $Cu_{2-x}Se$ et en $CuSe_2$II à une température plus basse que 413 K. La réaction inverse est rapide.

L'αCuSe (*klockmannite*) est hexagonal avec $a = 3.934$, $c = 17.217$ Å à 298 K. Il se transforme en βCuSe à 323 K à pression atmosphérique avec un changement d'enthalpie de $0.84 \pm$

[1]Present address: Atlantic Industrial Research Institute, c/o Nova Scotia Technical College, Halifax, Nova Scotia.

5 kJ mol^{-1}. Cette modification est orthorhombique centre sur la face C avec $a = 3.948$, $b = 6.958$, $c = 17.239$ Å à 324 K. A mesure que la température augmente le rapport a/b du système orthorhombique augmente rapidement jusqu'à 393 K; à cette température la transformation en γCuSe est complète. Cette modification est hexagonale avec $a = 3.984$, $c = 17.288$ Å à 430 K. CuSe est instable au-dessus de 5 kbar à 298 K se décomposant en Cu_3Se_2 et $CuSe_2$II.

Du $CuSe_2$ du type marcasite avec $a = 5.0046$, $b = 6.182_2$, $c = 3.739_7$ Å à 298 K, se disproportionne en CuSe et Se à 605 K à pression atmosphérique avec un changement d'enthalpie de 9.6 ± 4 kJ mol^{-1}. Il se transforme à moins de 5 kbar à 298 K pour conduire à la modification cubique de pyrite $CuSe_2$II avec $a = 6.116$ Å. Le $CuSe_2$II fond d'une façon congruente à 818 K et 20 kbar. Le point de fusion augmente avec une augmentation de pression à *ca.* 3 K kbar^{-1}.

[Traduit par le journal]

Introduction

An exhaustive review of the literature on the copper/selenium system was published recently (1). At least five compounds are formed: Cu_2Se, $Cu_{2-x}Se$, Cu_3Se_2, CuSe, and $CuSe_2$. Some of these, in one polymorphic form or another, exist as minerals. *Berzelianite*, *umangite*, and *klockmannite* correspond to $Cu_{2-x}Se$, Cu_3Se_2, and αCuSe, respectively. The mineral *krutaite* has the pyrite structure of $CuSe_2$II, but contains considerable quantities of cobalt and nickel. The mineral *athabaskaite* (Cu_5Se_4) has not been prepared synthetically.

There have been a number of reports on the properties of these compounds, particularly on the transport properties of the copper-rich phases. Often these reports do not include adequate identification of the compounds examined, and the structures must be inferred from the description of the procedures followed in their preparation.

This paper is a report on a reexamination of the copper/selenium system in the composition range 30–70 atomic % selenium, at temperatures from 298 to 850 K, and at pseudo-hydrostatic pressures to 50 kbar. A revised equilibrium phase diagram at atmospheric pressure is presented, as well as the outlines of the phase diagram at 20 kbar.

Experimental

Samples of various compositions were prepared by direct reaction of 69 grade copper and selenium (Asarco) in evacuated, sealed Pyrex or Vycor tubes in the usual way. Phases were identified by X-ray powder diffraction patterns using Philips 11.46 cm Debye–Scherrer cameras. In some instances diffraction patterns for accurate determination of unit cell dimensions were obtained in an Enraf–Nonius Guinier – de Wolff focusing camera using As_2O_3 as an internal standard.

"Kinetic" X-ray diffraction patterns above room temperature were obtained in an Enraf–Nonius Guinier – Lenne focusing camera. This camera was calibrated with respect to temperature by observing the transformations in KNO_3 (401 K) and $KClO_4$ (573 K) and the melting points of In (430 K), Sn (505 K) and Zn (573 K). In general sample heating rates were set at 5–10 K h^{-1} and film transport rates at 10 mm h^{-1} or less, using an exit slit of 1 mm and Kodak Type SB film. Specimens were prepared by painting an alcohol slurry of the selenide with high purity amorphous boron (as a binder) and silicon powder (as an internal standard) onto the platinum mesh sample holder. Above 470 K copper selenides containing more than 33 atomic % Se decomposed in the camera with the formation of $Cu_{2-x}Se$. Attempts to restrict the sublimation of selenium in such instances (for example, by sandwiching the selenide between thin graphite plates) were not successful.

A DuPont Instruments Model 990 Thermal Analyzer and DSC module were used for differential thermal analyses (DTA) in the temperature range between 223 and 673 K. The specimens were sealed in coated aluminum pans. The DSC module was calibrated with respect to temperature via the melting points of high purity Hg, In, Sn, Cd, and Bi. The same instrument was used to estimate the latent heats associated with phase transformations. For this purpose the enthalpy equivalent of the area of the DTA signal at a fixed heating rate was determined by observing the fusion of In (3.26 ± 4), Sn (7.07 ± 8), Cd (6.11 ± 8) and Zn (6.65 ± 40 kJ mol^{-1}).

The behavior of compounds in the system under high pressure was studied using devices constructed for that purpose. Exploratory "quench-and-look" experiments were conducted at room temperature between opposed anvils of supported tungsten carbide. Provision was made for rotation of one anvil with respect to the other to increase transformation rates. Samples were examined at nominal pressures to 60 kbar. In view of the large pressure gradients which are established in such uniaxial devices, no attempt was made at pressure calibration.

Differential thermal analyses were conducted at quasi-hydrostatic pressures to 50 kbar and temperatures to 850 K in a two-stage piston-cylinder apparatus.[2]

This device was used with a compound press, a 200 ton hydraulic ram serving to end load the cylinders, and a 100 ton ram to load the pistons. Details on the DTA cell

[2]Detailed drawings of the components of this device (the first and second stage pistons, the first and second stage compound cylinders, back-up plate and clamping plate) are available, at a nominal charge, from the Depository of Unpublished Data, National Research Council of Canada, Ottawa, Canada, K1A 0S2. Details on the design, construction, calibration and assembly of the high pressure DTA apparatus may be obtained from the authors.

Can. J. Chem. Downloaded from www.nrcresearchpress.com by 210.87.254.42 on 09/05/12
For personal use only.

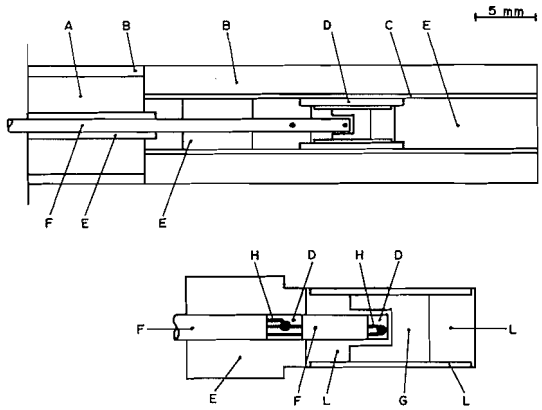

FIG. 1. High Pressure DTA Cell. The bottom drawing shows the sample capsule and thermocouple arrangement in detail. *A*, tool steel; *B*, AlSiMag; *C*, Graphite heater; *D*, boron nitride; *E*, pyrophyllite; *F*, three-hole Mullite thermocouple insulator; *G*, sample cavity; *H*, chromel/alumel thermocouples; *L*, stainless steel sample capsule.

used in the first stage cylinder (working volume 4.3 cm × 1.0 cm D) are shown in Fig. 1. The experimental procedure involved temperature sweeps at constant pressure. With the cell maintained at a temperature slightly below the transition under investigation, the pressure in the system was increased by finite intervals. At each interval, a small programmed increase and decrease in heater current carried the sample temperature through the transition in each direction. This procedure was followed through a cycle of increasing and decreasing pressure intervals. The signal from the differential thermocouple was amplified by a Keithley Model 148 Nanovoltmeter and displayed on a two pen chart recorder along with the sample thermocouple EMF. No corrections were made for the effect of pressure on thermocouple EMF.

Since the actual pressure in such a device is less than the load would indicate with increasing load (in-stroke) and greater than the load would indicate with decreasing load (out-stroke) due to internal friction, hysteresis in the transition temperature/load plots was observed. Here, in keeping with common practice, the "double value of friction" has been measured, and the equilibrium boundary in the *P–T* plane has been assumed to lie at the center of the hysteresis loop. The uncertainty invoked by this assumption is certainly greater than the probable error in apportioning the total load between the first and second stage pistons, but may well be less than the uncertainty inherent in the use of solids as pressure transmitting media. Nevertheless we estimate that the pressures observed are within 3 kbar of the true values.

The piston-cylinder apparatus was also employed in "quench-and-look" experiments using a less complicated cell than that depicted in Fig. 1. Both types of cell cooled from 773 K to room temperature in less than 5 s. In addition to powder diffraction analysis, several of these samples were sectioned, polished, and examined in an ARL electron microprobe and by optical microscopy.

Some samples were studied in a Materials Research Corporation Model XKB100 opposed diamond anvil X-ray diffraction camera at room temperature and nominal pressures to 50 kbar.

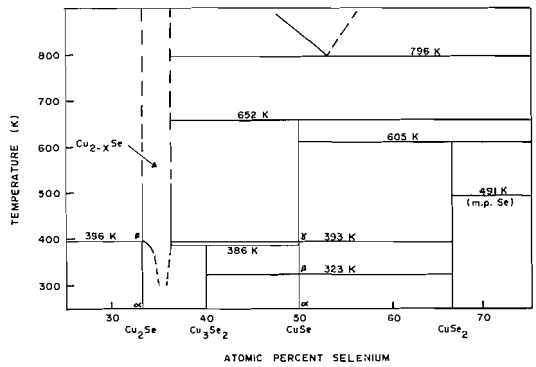

FIG. 2. Equilibrium phase diagram of the copper–selenium system at 1 bar.

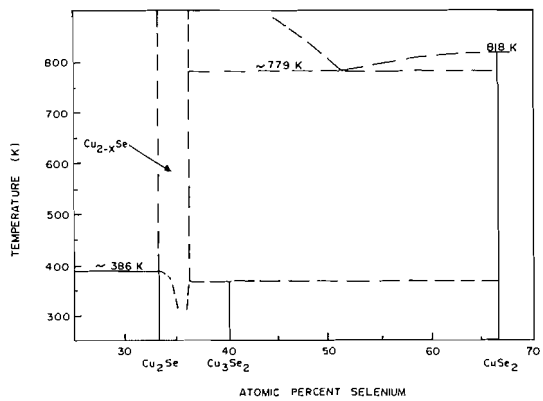

FIG. 3. Equilibrium phase diagram of the copper–selenium system at 20 kbar.

Results and Discussion

The atmospheric pressure phase diagram representing the result of this study is shown in Fig. 2. The general outlines of the phase diagram at 20 kbar are indicated in Fig. 3. In the following discussion, phase and structural relationships at each compound composition will be described in turn with reference to these figures.

Cu_2Se

Specimens of αCu_2Se (*i.e.*, the room temperature modification of Cu_2Se) at the copper rich limit of the field were prepared (*a*) by annealing samples of nominal composition *Cu_2Se* with high purity copper wire in evacuated sealed Vycor tubes at 673 K for some weeks; (*b*) by the sublimation of selenium from *Cu_2Se* at 913 K *in vacuo* (during which process long whiskers of copper are formed); and (*c*) by depositing thin films of selenium on copper foil at *ca.* 330 K and annealing at temperatures to 773 K.

Can. J. Chem. Downloaded from www.nrcresearchpress.com by 210.87.254.42 on 09/05/12
For personal use only.

Can. J. Chem. Downloaded from www.nrcresearchpress.com by 210.87.254.42 on 09/05/12
For personal use only.

Samples prepared by methods (*a*) and (*b*) gave identical well-resolved focusing camera patterns. Diffraction patterns of the product layers obtained by method (*c*), observed by X-ray transmission through the copper foil substrate in the focusing camera, were diffuse but clearly identical to those obtained in (*a*) and (*b*).

This pattern is significantly different from that given by Stevels and Jellinek (2) and much more complex than that described by Morimoto and Uchimizu (3). It can be indexed with reference to a monoclinic unit cell[3] with $a = 14.087$ Å, $b = 20.481$ Å, $c = 4.145$ Å, $\beta = 90° 23'$. This cell can be regarded as a simple monoclinic distortion of the orthorhombic unit cell ($a = 4.118$ Å, $b = 14.06$ Å, $c = 20.381$ Å) given by Stevels and Jellinek for powder specimens, and perhaps is not incompatible with the results of their single crystal studies.

Diffraction patterns of αCu_2Se at the selenium rich boundary were obtained by allowing *Cu_2Se* to undergo partial oxidation in air at 373 K.[4] These patterns were diffuse but of sufficient quality to establish that the interplanar spacings are larger than those of the same phase prepared in the presence of copper. The X-ray data are in close agreement with those observed by Stevels and Jellinek and by Heyding (4) for αCu_2Se in αCu_2Se–$Cu_{2-x}Se$ mixtures, and may be indicative of a narrow region of variable composition.

The transformations occurring in *Cu_2Se* in the temperature range 350–415 K are complex. Guinier–Lenne diffraction patterns indicate shifts in some interplanar spacings between 350 and 396 K which cannot be attributed to simple thermal expansion. There is an abrupt transition to the cubic $Cu_{2-x}Se$ ($x = 0$) phase at 396 ± 3 K. Above this temperature there are no obvious anomalies in the variation in interplanar spacings or relative intensities with increasing temperature. On the other hand, the long, asymmetric DTA signal begins at *ca.* 373 K, peaks at 409 ± 1 K, and returns to the baseline at *ca.* 415 K on heating cycles. On cooling the signal begins at 409 K and peaks at 407 K. Neither the form of the signal nor the temperature at the maximum are altered significantly by ten-fold changes in the heating rate. When the heating cycle is arrested for an annealing period within the interval below 409 K, the maximum in the signal develops in the usual way when the cycle is resumed; hence the phenomenon is not time dependent. Thus the abrupt crystallographic transformation occurs some 13 K below the maximum in a protracted DTA signal.

Comparison of these results with published data is complicated by uncertainty with respect to the composition of the various samples for which the data are given. Specimens slightly richer in selenium than *Cu_2Se* can be expected to exhibit anomalies over a protracted temperature range due to the change in composition of the $Cu_{2-x}Se$ component of the two phase mixture with increasing temperature. For example, in the data reported by Ogorelec and Celustka (5, 6) it is not clear what proportion of the anomaly in the conductivity of $Cu_{1.981}Se$ between 353 and 413 K is due to the transformation in αCu_2Se. Nevertheless our DTA results confirm the general observation that anomalies occur over a wide temperature interval. According to Routie *et al.* (7, 8) anomalies in the conductivity and thermoelectric EMF of *Cu_2Se* in the presence of copper begin at *ca.* 373 K and exhibit a maximum or discontinuity at 406 K. Similar behavior in the conductivity was observed by Okamoto (9) at slightly lower temperatures in specimens of uncertain composition. Kubaschewski and Nölting (10) have shown that the heat capacity of $Cu_{1.9975}Se$ (assumed) begins to increase abnormally at *ca.* 323 K, is very large in the interval 395–403 K, and is essentially constant above 403 K.

In his extensive study of the copper-rich selenides, Stevels (11) remarks that the temperature of 353 K observed for the $\alpha \rightarrow$ f.c.c. Cu_2Se transformation is somewhat low in comparison with DTA data giving temperatures between *ca.* 363 K ($Cu_{1.95}Se$) and 383 K ($Cu_{2.08}Se$). This latter sample apparently contained excess copper (2), and should therefore correspond to our specimens of αCu_2Se. Regardless of the rather large difference in crystallographic transition temperatures observed by Stevels and ourselves (353 K *vs.* 396 K), the occurrence of a polymor-

[3]Diffraction patterns of αCu_2Se. βCuSe, γCuSe and $CuSe_2$II have been submitted to the Joint Committee on Powder Diffraction Standards. Copies may be obtained from the authors, or, at nominal charge, from the Depository of Unpublished Data, CISTI, National Research Council of Canada, Ottawa, Canada K1A 0S2. Diffraction patterns of the other compounds are in substantial agreement with those already included in the JCPDS File.

[4]Powders of *Cu_2Se* oxidize slowly in air at room temperature with the formation of Cu_2O and $Cu_{1.8}Se$. The $Cu_{2-x}Se$ phase is much less susceptible to oxidation under the same conditions.

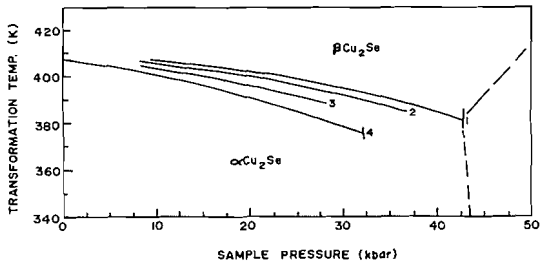

FIG. 4. Pressure dependence of the $\alpha \rightarrow \beta$ (f.c.c.) transformation temperature in Cu_2Se. Curve *1*: $Cu_{2.04}Se$, prepared by sublimation of Se from Cu_2Se. Curves *2*, *3*: Two samples of Cu_2Se prepared by direction reaction between the elements. Curve *4*: Data of Clark and Rapoport (12).

phic transition within a broad thermal effect is confirmed.

It may be significant that Stevels and Jellinek observed αCu_2Se at room temperature only in the presence of the cubic phase. The persistence of the cubic phase led to the suggestion that the f.c.c. $\rightarrow \alpha$ transformation is very slow; we did not find it to be so.

The overall enthalpy change according to our DTA data is 6.4 kJ mol^{-1}, and according to Kubaschewski and Nölting's calorimetric study (11) is 6.83 kJ mol^{-1}.

The temperature of the transformation decreases with increasing pressure as shown in Fig. 4. Here the transformation temperature has been taken as the average of the temperatures corresponding to the peak and the end of the differential signal. The T/P curves are therefore displaced to higher temperatures relative to the boundary reported by Clark and Rapoport (12) (curve 4, Fig. 4) who apparently observed well-defined peak onset temperatures and used those values. The onset of the DTA signal was not well defined in our experiments. In any case, the absolute transformation temperature *per se* is a difficult quantity to specify even at atmospheric pressure, and we would expect dT/dP to be essentially independent of the way in which T is defined.

The slope of the phase boundary observed for $Cu_{2.04}Se$ is significantly less in the 10–20 kbar range than for Cu_2Se (-0.4 K $kbar^{-1}$ *vs.* -0.8 K $kbar^{-1}$). This may be another indication of a narrow range of variable composition although, in that case, a slope of -0.8 K $kbar^{-1}$ would not have been expected from Clark and Rapoport's data since their samples were encapsulated in copper.

Assuming the enthalpy change is pressure independent, the Clausius–Clapeyron equation predicts a volume decrease during the transformation of *ca.* 0.06 cm^3 mol^{-1} ($dT/dP \simeq -0.4$ K $kbar^{-1}$; $T \simeq 400$ K; $\Delta H \simeq 6$ kJ mol^{-1}). The molar volume of αCu_2Se at 298 K, assuming the monoclinic cell proposed earlier and a cell content of 24 formula units, is 0.8% *less* than the molar volume of f.c.c. Cu_2Se at 394 K (a = 5.858 Å). A molar volume decrease could not occur during a direct transformation from the monoclinic to the cubic modification without an unrealistically high rate of thermal expansion in the monoclinic form. This is further evidence of the complexity of the transformations which occur in this phase between 343 and 409 K.

The DTA signal corresponding to the $\alpha \rightarrow \beta Cu_2Se$ transformation disappeared in Clark and Rapoport's experiments at 30 kbar. They attribute the disappearance to the formation of a high pressure Cu_2Se modification. The $\alpha \rightarrow \beta$ transformation was still evident in our experiments with Cu_2Se at 37 kbar, the highest pressure attained. However in a $Cu_{2.04}Se$ sample, the signal disappeared at about 42 kbar (curve 1, Fig. 4). This phenomenon was reversible, the signal being regained on decompression and lost again as the pressure was increased.

The boundary between the αCu_2Se and high pressure fields is assumed to be essentially vertical as shown in Fig. 4, since there was no indication of any transformation in differential thermal analyses at constant pressures close to 42 kbar. Specimens quenched from *ca.* 380 K at pressures above 42 kbar contained only αCu_2Se. Whether the high pressure field is a single phase field (Cu_2SeII) or a two phase field (*e.g.*, Cu + $CuSe_2II$) is not resolved, although of the two possibilities the former would seem to be the more likely.

Cubic βCu_2Se appears to be stable above the $\alpha \rightarrow \beta$ transformation temperature to at least 838 K. At 15 kbar no DTA signals were observed in this temperature range, and Cu_2Se samples were recovered unaltered.

$Cu_{2-x}Se$ (Berzelianite)

The compound $Cu_{2-x}Se$ occupies a field of variable composition in the phase diagram. With composition $Cu_{1.80}Se$, the cubic unit cell dimension is 5.765 Å at 298 K.[3] The space group is $F\bar{4}3m$, with Se in the face-centered sites and Cu

Can. J. Chem. Downloaded from www.nrcresearchpress.com by 210.87.254.42 on 09/05/12
For personal use only.

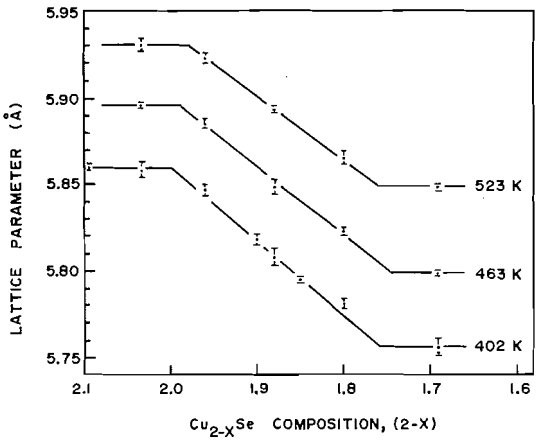

FIG. 5. The variation in the cubic lattice parameter of $Cu_{2-x}Se$ as a function of composition and of temperature. For clarity, the data at 463 and 523 K have been displaced along the ordinate by 0.03 and 0.06 Å respectively. The error bars indicate the standard deviations in *a*. The lines represent the least squares fit to the data.

distributed in non-random fashion on the octahedral, tetrahedral, and pseudo-trigonal sites in the Se sublattice (2, 13).

Compositions at the boundaries of this field at atmospheric pressure in the temperature range 402–523 K were estimated by determining the variation in unit cell dimension with nominal sample composition as indicated in Fig. 5. The field does not extend beyond Cu_2Se, and may, in fact, shift to slightly higher Se concentrations with increasing temperature. This is consistent with observations made by others (*e.g.*, Lorenz and Wagner (14), Celustka and Ogorelec (15)). The selenium-rich boundary is essentially vertical in the range 402–523 K. Much the same result was obtained by Bernardini *et al.* (16). Observations on nonequilibrated samples of composition Cu_3Se_2 suggest that the boundary may have slight positive slope from 273 to 385 K. The rather large shift to higher selenium concentrations suggested earlier (4) is not correct.

Evidence was sought for the transformation in $Cu_{1.8}Se$ at 338 K suggested by Stevels and Jellinek to account for an anomaly which they observed in the magnetic susceptibility at that temperature (2). Relative intensities of reflections in Guinier–Lenne diffraction patterns at 333, 376, and 465 K were measured and found to be identical within experimental error. Nor could this transformation be detected by DTA of $Cu_{1.8}Se$ at highest sensitivity.

Samples of nominal composition $Cu_{1.9}Se$ were examined in the high pressure DTA device. No transformations were observed. A sample of $Cu_{1.8}Se$ was annealed for 19 h at 348 K and 32 kbar, quenched, and examined by X-ray diffraction, optical microscopy, and electron probe analysis. It was unaltered. There is also evidence from experiments on other copper selenides indicating that the stability range of $Cu_{2-x}Se$ extends to the highest pressures and temperatures employed in this study.

This conclusion is in disagreement with the studies of Hinze and Neuhaus (17) which indicate that the high pressure pyrite modification of $CuSe_2$ ($CuSe_2$II) is the only copper selenide stable above 44 kbar at room temperature. These authors observed a series of pressure induced reactions in an opposed anvil device in which concentric rings of copper, $Cu_{2-x}Se$, Cu_3Se_2, $CuSe_2$, and $CuSe_2$II were formed. Copper appeared at the edge and $CuSe_2$II at the center of the anvil faces. From a knowledge of the pressure gradient in their device they ascribed a pressure stability range to each phase according to its position in the gradient.

We have observed reactions in uniaxial pressure devices very similar to those described by Hinze and Neuhaus. When samples of composition $Cu_{1.9}Se$ and $Cu_{1.8}Se$ were compressed with periodic rotation in opposed anvils at 298 K and nominal pressures of 10 kbar, mixtures of αCu_2Se, $Cu_{2-x}Se$, and Cu_3Se_2 were recovered after 1 h. Similar reactions in $Cu_{1.8}Se$ were observed in the MRC high pressure camera after several days at a nominal pressure of 27 kbar. At higher pressures, reflections due to $CuSe_2$II were observed. The mixture, containing $Cu_{1.8}Se$, αCu_2Se, Cu_3Se_2, and $CuSe_2$II, was retained on decompression. Copper was not observed as a product in these experiments.

These multiple disproportionations were not observed when other copper selenides were examined under uniaxial pressure loads. The phenomenon may be due to the abnormally high rate of diffusion of copper in $Cu_{2-x}Se$ (18, 19). In the large pressure gradients established in the specimen by the opposed anvils, mass transfer may occur not only by extrusion of the sample pellet, but also by diffusion of copper towards the edges of the anvil faces. Thus a concentration gradient may develop with copper-rich phases at the outer edge of the product lens and selenium rich phases in the center.

Can. J. Chem. Downloaded from www.nrcresearchpress.com by 210.87.254.42 on 09/05/12
For personal use only.

Can. J. Chem. Downloaded from www.nrcresearchpress.com by 210.87.254.42 on 09/05/12
For personal use only.

Cu_3Se_2 (Umangite)

The compound Cu_3Se_2 is tetragonal, space group $P\bar{4}2_1m$ (20). The unit cell dimensions obtained in this study[3] ($a = 6.385$ Å, $c = 4.271$ Å) are in good agreement with those reported earlier (4). The disproportionation to $Cu_{2-x}Se$ and CuSe is relatively slow. In DTA experiments at atmospheric pressure it occurs at 398 and 404 K for heating rates of 5 and 10 K min^{-1} respectively. In the Guinier–Lenne camera it was observed at 385 K with a heating rate of 8 K hr^{-1}. The unit cell dimension of the $Cu_{2-x}Se$ phase formed during the reaction corresponds to the selenium-rich limit of this phase as indicated in Fig. 5. The diffraction pattern of the other product of the disproportionation was ill-defined because at this temperature CuSe is involved in its own complicated $\beta \rightarrow \gamma$ transformation.

The enthalpy change associated with the disproportionation is 10.0 ± 5 kJ mol^{-1}.

The reaction of $Cu_{2-x}Se$ with CuSe to form Cu_3Se_2 below 385 K is extremely slow. Samples of *Cu_3Se_2* cooled from temperatures above 385 K contain only traces of *umangite*, and the reaction is not complete after several years at room temperature. The transformation is enhanced by pressure and shear, and may be brought essentially to completion by grinding for extended period with a mortar and pestle. Samples of *Cu_3Se_2* and of *CuSe* quenched from >673 K showed surprisingly large quantities of Cu_3Se_2, indicating that the reaction of $Cu_{2-x}Se$ with Se is more rapid than the reaction with CuSe. It was found that when mechanical mixtures of $Cu_{2-x}Se$ and $CuSe_2$II in stoichiometric proportions were ground lightly with mortar and pestle, conversion to Cu_3Se_2 was complete in less than 1 min.

It is this very rapid reaction between $CuSe_2$II and $Cu_{2-x}Se$ under shear stress which is responsible for the formation of Cu_3Se_2 in *Cu_3Se_2* mixtures in high pressure devices. The compound is formed in 1 h at room temperature between opposed anvils at 25 kbar, and at 10 kbar if the anvils are rotated.

Cu_3Se_2 is stable at room temperature to at least 35 kbar. At this pressure formation of Cu_3Se_2 from $Cu_{2-x}Se$–CuSe mixtures in the piston–cylinder synthesis cell was complete in *ca.* 12 h. The diffraction pattern of Cu_3Se_2 at 27 kbar in the high pressure camera contained no extraneous reflections.

Cu_3Se_2 was prepared *in situ* in the high pressure DTA cell. At 20 kbar no signals were observed between 273 and 865 K which might correspond to a disproportionation. However, the sample recovered contained $Cu_{2-x}Se$ and $CuSe_2$II, as well as Cu_3Se_2, indicating that some disproportionation had occurred. Apparently the disproportionation is too slow to be detected by DTA. Attempts were therefore made to determine the temperature stability limits at one pressure by a series of quench-and-look experiments.

In each experiment a sample of *Cu_3Se_2* was initially annealed at atmospheric pressure and 423 K for 1 h. Each sample could therefore be assumed to contain no Cu_3Se_2 prior to pressure increase. The pressure was raised to 18 kbar, and the temperature adjusted to the desired annealing temperature. After 1 h, the temperature and pressure were quenched simultaneously. The products contained $Cu_{2-x}Se$, Cu_3Se_2, and $CuSe_2$II in roughly the same proportions in each case. The quantity of Cu_3Se_2 recovered was no greater than that which would be formed by the reaction of $Cu_{2-x}Se$ and $CuSe_2$II either on quenching in the compacted sample or during preparation (grinding) of a specimen for powder diffraction.

These experiments indicate that the disproportionation of Cu_3Se_2 to $Cu_{2-x}Se$ and $CuSe_2$II at 18 kbar occurs at some temperature below 413 K (the lowest anneal temperature examined) and is relatively slow. Further evidence for this conclusion was obtained in quench-and-look experiments on αCuSe annealed at 18 kbar and 422 K. The product contained $Cu_{2-x}Se$ (as well as Cu_3Se_2 and $CuSe_2$II) which would not have formed were Cu_3Se_2 stable under those conditions.

CuSe

The low temperature atmospheric pressure modification of this compound, αCuSe, corresponds to the mineral *klockmannite*. Although there is some controversy in the literature as to the correct space group and structure of the mineral (21–23), the diffraction reflections can be indexed[3] with reference to a hexagonal cell with $a = 3.934$ Å and $c = 17.217$ Å in good agreement with Berry's analysis of *klockmannite* (21) and with other data on synthetic αCuSe (2, 4). The superlattice reflections observed by some authors (2, 22, 24) were not observed in samples

Can. J. Chem. Downloaded from www.nrcresearchpress.com by 210.87.254.42 on 09/05/12
For personal use only.

prepared for this study, although extra reflections have now appeared in αCuSe samples prepared in this laboratory seven years ago, indicating a slow ordering process.

αCuSe transforms abruptly to βCuSe at 324 K with an enthalpy change of 0.84 ± 5 kJ mol^{-1}. The β modification is C end-centered orthorhombic[3] with $a = 3.948$ Å, $b = 6.958$ Å, $c = 17.239$ Å at 324 K, in good agreement with the literature (2, 4).

As the temperature of the specimen is increased in the Guinier–Lenne camera, pairs of βCuSe reflections gradually coalesce (at 370 K, $a = 3.960$ Å, $b = 6.911$ Å, $c = 17.2$ Å) until, at 393 K, the transformation to γCuSe is complete. This remarkable transformation was first observed by Stevels and Jellinek (2). It cannot be detected by DTA. Both transformations are rapidly reversible.

The diffraction pattern of the γ modification can be indexed[3] with reference to a hexagonal cell, with $a = 3.984$ Å, $c = 17.288$ Å at 430 K. Although the Miller indices of the planes giving rise to diffraction are the same in αCuSe and γCuSe, and the relative intensities are remarkably similar, the rather large differences in interplanar spacings indicate that they are not isostructural.

Modifications in the αCuSe diffraction pattern are obtained when αCuSe is ground for 10 min in a mortar and pestle or compressed for short periods between opposed anvils at nominal pressures of less than 3 kbar. In this pattern the (107) reflection is unusually intense and a new reflection appears at $d = 1.64$ Å. This may indicate either a transformation or a disproportionation in CuSe at very low pressures. At slightly higher pressures (5 kbar) in the opposed anvil device with rotation, mixtures of this modification, Cu_3Se_2, and $CuSe_2$II are obtained.

At room temperature the disproportionation of αCuSe to Cu_3Se_2 and $CuSe_2$II occurred in the piston–cylinder apparatus at pressures below 10 kbar. The disproportionation is slow, and the pressure at which it occurs cannot be defined more accurately. This reaction occurs with a decrease in volume of 6.5%, assuming crystallographic densities and equal compressibilities in reactant and products.

The peritectic decomposition of CuSe was observed in the high pressure DTA cell at pressures close to atmospheric, and the decomposition temperature remained fairly constant (*ca.* 650 K) up to pressures of 5–6 kbar. At higher pressures no differential signal could be detected in the range 623–703 K. Samples quenched from this region contained $Cu_{2-x}Se$, $CuSe_2$II, and Cu_3Se_2, the latter formed by the $Cu_{2-x}Se$–$CuSe_2$II reaction on quenching.

At *ca.* 6 kbar DTA of *CuSe* exhibited a large reversible signal at 740 K. The pressure dependence of this transformation is shown in Fig. 6. Polished sections of a sample quenched from 787 K and 20 kbar were examined by optical microscopy and by electron probe. Considerable variation in composition was evident along the capsule axis. $Cu_{2-x}Se$ and $CuSe_2$II were identified, as well as Cu_3Se_2 and CuSe which formed during the quench. The identification of dendrites of $Cu_{2-x}Se$ indicates the growth of this phase from the melt, and suggests a $Cu_{2-x}Se$/$CuSe_2$II eutectic lying on the composition axis on the selenium rich side of *CuSe* as indicated in Fig. 3.

$CuSe_2$

The room temperature unit cell dimensions of orthorhombic, marcasite-type $CuSe_2$ obtained in this study[3] ($a = 5.004_6$ Å, $b = 6.182_2$ Å, $c = 3.739_7$ Å) are in good agreement with values reported in the literature (2, 4). The peritectic decomposition to $Cu_{2-x}Se$ and Se occurs at 605 K at atmospheric pressure, with a change in enthalpy of 9.6 ± 4 kJ mol^{-1}. The recombination reaction is slow.[5]

At room temperature the cubic pyrite modification, $CuSe_2$II, is formed at very low pressures (<5 kbar) although the rate of transformation is slow. "Pure" $CuSe_2$II can be prepared by

[5]An unusual feature of the disproportionation was observed during thermal analysis. As specimens were repeatedly cycled through the temperature range 548–623 K at 10 K min^{-1}, the DTA signal split into two endothermic peaks, one centered at 599 K, and the second at 609 K. On annealing for 1 h at 573 K, the original signal at 605 K was regained. When the DTA cycle was arrested at the maximum of the first peak (599 K) for 1 h, the second peak was not observed. In every case the DTA signals on cooling were identical. Samples quenched from 593 K after the double signal had been built up were mixtures of αCuSe, $CuSe_2$ and (presumably) amorphous Se, *i.e.* contained the same phases as specimens quenched from above or below the initial transition temperature. This behavior was observed in all samples known to contain $CuSe_2$. In all probability this phenomenon is a kinetic effect associated with the slow recombination of CuSe and Se, and as such should not be represented in the equilibrium phase diagram.

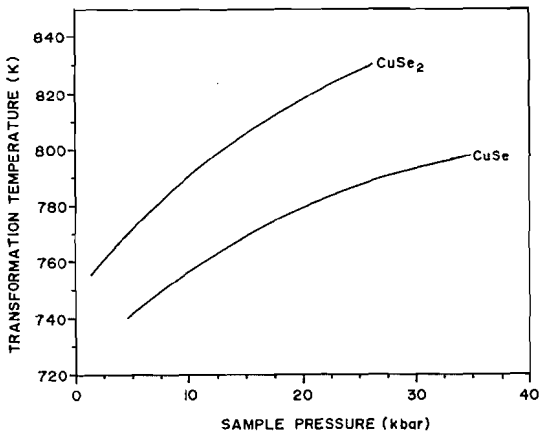

FIG. 6. The pressure dependence of the onset temperature of high pressure DTA signals in *CuSe* ($Cu_{2-x}Se$–$CuSe_2$II eutectic?) and in $CuSe_2$II (congruent melting point).

annealing $CuSe_2$ for 2 h at 12 kbar and 693 K. The unit cell dimension of the product prepared this way[3] ($a = 6.116$ Å) is in good agreement with the value reported by Bither *et al.* (25). Some $CuSe_2$II samples prepared under different conditions had a smaller unit cell with $a = 6.110$ Å. It is interesting that Bither originally reported a value of 6.123 Å (26). This range of values may be indicative of some variable composition in the pyrite structure.

Assuming crystallographic densities, the marcasite → pyrite transformation involves a 1.1% decrease in volume at atmospheric pressure.

The pyrite modification is remarkably stable at atmospheric pressure. It is stable for indefinite period at room temperature and is still present after annealing for 3 days at 483 K. In one experiment in which a mixture of the marcasite and pyrite modifications was annealed at atmospheric pressure for several hours at 623 K, decomposition of the $CuSe_2$ was observed but $CuSe_2$II was recovered unaltered.

The peritectic decomposition of $CuSe_2$ which occurs at 605 K at atmospheric pressure was observed in high pressure DTA experiments but only below 5 kbar. Above that pressure no thermal signals were observed to 723 K. Samples quenched from 5 kbar and 615 K were pure $CuSe_2$II. However, at pressures greater than 5 kbar a broad endothermic signal was observed at *ca.* 770 K. The pressure dependence of this signal is shown in Fig. 6. In some instances, liquid was extruded from the high pressure capsule during the transformation. This liquid penetrated cracks in the boron nitride sleeve, short circuiting the thermocouples and the heater. The material recovered from the sleeve was $CuSe_2$. Study of polished sections of capsules recovered intact following quenching from above the transformation temperature indicated that $CuSe_2$II is reformed completely during the quench. Electron probe analysis showed no variation in composition across the sections, and optical microscopy showed very large twinned grains with no obvious fine structure. This evidence leads to the conclusion that $CuSe_2$II melts congruently as indicated in Fig. 3.

We are indebted to Messrs. T. F. Blake, F. W. Everding, and F. F. Sziladi for assistance in the construction of our high pressure devices; to Mr. B. C. Forbes for technical assistance; and to Messrs. R. Armstrong, H. R. Holland, and D. E. Kempson for their assistance in the preparation and examination of polished sections. One of us (R.M.M.) gratefully acknowledges the award of an Alcan Postgraduate Fellowship, 1970–1973. This study was supported by operating grants from the National Research Council of Canada.

1. R. M. MURRAY. The copper–selenium system. Ph.D. Thesis, Queen's University, Kingston, Ontario. 1974.
2. A. L. N. STEVELS and F. JELLINEK. Rec. Trav. Chim. **90**, 273 (1971).
3. N. MORIMOTO and M. UCHIMIZU. *In* X-Ray powder data file. *Edited by* L. G. Berry. 19th Set, Card 19-401. Special Technical Publication 480G, A.S.T.M., Philadelphia. 1969.
4. R. D. HEYDING. Can. J. Chem. **44**, 1233 (1966).
5. Z. OGORELEC and B. CELUSTKA. J. Phys. Chem. Solids, **27**, 615 (1966).
6. Z. OGORELEC and B. CELUSTKA. J. Phys. Chem. Solids, **30**, 149 (1969).
7. R. ROUTIE, M. SUDRES, and J. MAHENC. J. Electroanal. Chem. **25**, 489 (1970).
8. R. ROUTIE, M. SUDRES, and J. MAHENC. J. Chem. Phys. **67**, 1013 (1970).
9. K. OKAMOTO. J. Appl. Phys. Jap. **10**, 508 (1971).
10. P. KUBASCHEWSKI and J. NÖLTING. Ber. Bunsenges. Phys. Chem. **77** (2), 70 (1973).
11. A. L. N. STEVELS. Philips Res. Rep. Suppl. No. 9, 124 (1969).
12. J. B. CLARK and E. RAPOPORT. J. Phys. Chem. Solids, **31**, 247 (1970).
13. W. BORCHERT. Z. Krist. **106**, 5 (1945).
14. G. LORENZ and C. WAGNER. J. Chem. Phys. **26**, 1607 (1957).
15. B. CELUSTKA and Z. OGORELEC. Croat. Chem. Acta, **41**, 73 (1969).
16. G. P. BERNARDINI, F. CORSINI, and R. TROSTI. Period. Mineral. **41**, 565 (1972).

Can. J. Chem. Downloaded from www.nrcresearchpress.com by 210.87.254.42 on 09/05/12
For personal use only.

17. E. HINZE and A. NEUHAUS. Naturwissenschaften, **56**, 136 (1969).
18. W. JOST. Diffusion in solids, liquids and gases. Academic Press, New York. 1960.
19. H. REINHOLD and H. MOHRING. Z. Phys. Chem. B**38**, 221 (1938).
20. N. MORIMOTO and K. KOTO. Science, **152**, 345 (1966).
21. L. G. BERRY. Amer. Mineral. **39**, 504 (1954).
22. C. A. TAYLOR and F. A. UNDERWOOD. Acta Crystallogr. **13**, 361 (1960).
23. F. LIPPMANN. Neues Jahrb. Mineral. Monatsh. 99 (1962).
24. J. A. ELLIOTT, J. A. BICKNELL, and R. G. COLLINGE. Acta Crystallogr. B**25**, 2420 (1969).
25. T. A. BITHER, R. J. BOUCHARD, W. H. CLOUD, P. C. DONOHUE, and W. J. SIEMONS. Inorg. Chem. **7**, 2208 (1968).
26. T. A. BITHER, C. T. PREWITT, J. L. GILLSON, P. E. BIERSTEDT, R. B. FLIPPEN, and H. S. YOUNG. Solid State Commun. **4**, 533 (1966).

Can. J. Chem. Downloaded from www.nrcresearchpress.com by 210.87.254.42 on 09/05/12
For personal use only.

Spectrophotometric Studies on Sb(III) in Hydrochloric Acid Solutions

JOHN MILNE

Department of Chemistry, University of Ottawa, Ottawa, Canada K1N 6N5

Received September 17, 1974

JOHN MILNE. Can. J. Chem. **53**, 888 (1975).

Ultraviolet spectroscopy confirms the findings of solubility studies that Sb(III) in 3–12 *M* hydrochloric acid solutions is present as an equilibrium mixture of $SbCl_4^-$ and $SbCl_6^{3-}$ ions. In the presence of H_2SO_4 a further equilibrium with the $SbCl_3(HSO_4)^-$ ion is found. The spectrum of the $SbCl_6^{3-}$ ion in solution is unlike the diffuse reflectance spectrum of this anion in $Co(NH_3)_6SbCl_6$ but is similar to that in K_3SbCl_6. The Raman spectrum of 2 *M* $SbCl_3$ in 2.8 *M* hydrochloric acid is shown to be due to the $SbCl_4^-$ ion and the spectrum is assigned under C_{2v} symmetry. The Raman spectrum of the $SbCl_6^{3-}$ ion in solution is discussed.

JOHN MILNE. Can. J. Chem. **53**, 888 (1975).

Des études par spectroscopie ultraviolette confirment les résultats obtenus par l'intermédiaire d'études de solubilité et indiquant que Sb(III) dans des solutions d'acide chlorhydrique de 3 à 12 *M* est présent sous forme d'un mélange à l'équilibre d'ions $SbCl_4^-$ et $SbCl_6^{3-}$. En présence de H_2SO_4, on trouve un autre équilibre avec l'ion $SbCl_3(HSO_4)^-$. Le spectre de l'ion $SbCl_6^{3-}$ en solution n'est pas semblable au spectre de réflexion de cet anion dans $Co(NH_3)_6SbCl_6$; il est plutôt semblable à celui de K_3SbCl_6. On montre que le spectre Raman d'une solution de 2 *M* de $SbCl_3$ dans de l'acide chlorhydrique à 2.8 *M* est dû à l'ion $SbCl_4^-$ et le spectre est attribué à une symétrie C_{2v}. On discute du spectre Raman de l'ion $SbCl_6^{3-}$ en solution.

[Traduit par le journal]

Introduction

The nature of the chloroantimonate(III) species in aqueous solution has been studied by polarographic and solubility methods (1, 2), and by Raman spectroscopy (3, 4). These studies have indicated that the $SbCl_6^{3-}$ ion is present in equilibrium with $SbCl_4^-$. The u.v. spectrum of a solution of Sb(III) in concentrated hydrochloric acid has been shown to be constant over the range of HCl concentration 6 to 12 *F* (5) and this spectrum has been attributed to the $SbCl_6^{3-}$ ion (6). There are however, reasons to question an interpretation in terms of the $SbCl_6^{3-}$ ion. The absence, in the electronic spectrum of hydrochloric acid solutions of Sb(III), Sb(V) mixtures, of an Sb(III)–Sb(V) interaction band, which is observed in solid Cs_2SbCl_6, would seem to indicate that octahedral $SbCl_6^{3-}$ is not present (7) in solution. Furthermore, the symmetric stretching mode, ν_1, of the $SbCl_6^{3-}$ ion has been shown to occur at 269 cm^{-1} (8, 9) and this is inconsistent with the assignment of the strong polarized band at 329 cm^{-1} to the breathing mode of the $SbCl_6^{3-}$ ion (3, 4). On going from solid to solution state the change in ν_1 for octahedral hexachlorometallates is not of this order of magnitude and the frequency is higher in the solid than in solution (10, 11). The discrepancies between the solution and solid vibrational spectra for SbX_6^{3-} ions have been noted before (12) and attributed to departure from O_h symmetry in these species in solution. Because of the exceptional nature of the Sb(III) – hydrochloric acid system it was considered important to apply several physical methods to confirm the presence of $SbCl_6^{3-}$ in solution.

Experimental

Antimony trichloride (Fisher) was purified by sublimation. All chloroantimonates were prepared by literature methods; SbOCl (13); $pyHSbCl_4$ (14); $Co(NH_3)_6SbCl_6$ (15); $[(CH_3)_4N]_3Sb_2Cl_9$ (2), and their purity checked by analysis.

Solution electronic spectra were done at ambient temperature (30 ± 1 °C) on a Beckman DK-2 spectrophotometer. Variable path lengths were achieved by use of quartz spacers. Diffuse reflectance spectra were measured on a Beckman DU spectrophotometer with reflectance attachment; MgO was used as reference and diluent. Raman spectra were recorded using a Jarrell-Ash 300 with 4880 Å Ar^+ laser excitation. The samples were contained in 1 mm o.d. glass tubes. Solubility studies on $Co(NH_3)_6SbCl_6$ were carried out following procedures of Haight and Ellis (2). Solubility was determined by spectrophotometric analysis for $Co(NH_3)_6^{3+}$. The λ_{max} at 475 nm for solutions of $Co(NH_3)_6Cl_3$, used for standardization, obeyed Beer's Law closely up to 2×10^{-3} *M* both in distilled water and 4 *M* HCl.

Results and Discussion

Spectrophotometry

The spectrum of Sb(III) in 12 *M* HCl consists

Can. J. Chem. Downloaded from www.nrcresearchpress.com by 210.87.254.40 on 09/05/12
For personal use only.

Can. J. Chem. Downloaded from www.nrcresearchpress.com by 210.87.254.40 on 09/05/12
For personal use only.

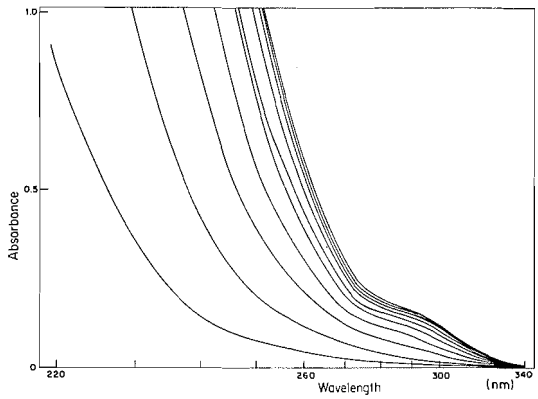

FIG. 1. Ultraviolet spectra of 10^{-3} M Sb(III) in 6.15 to 0.615 M HCl.

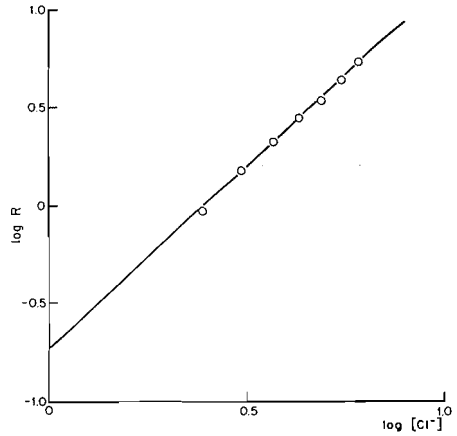

FIG. 2. Plot for the evaluation of n and K. (R = $[SbCl_{m+n}^{3-m-n}]/[SbCl_m^{3-m}]$).

of two maxima at 228 and 285 nm. Their intensities and positions at constant Sb(III) concentration remain unchanged over the HCl concentration range ~6.5 to 12 M as noted by Bonner and Goishi (5). Furthermore in 12 M HCl the spectrum obeys Beer's Law up to 0.02 M Sb(III). From these measurements the extinction coefficients at the maxima are found to be ε_{228} = 24 700 M^{-1} and ε_{285} = 2050 M^{-1}. In what follows the species giving these peaks is identified as A. As the HCl concentration is lowered from 6.5 M the peaks at 228 and 285 nm decrease and are replaced by an absorption which has a maximum below 200 nm. These changes are shown for the 285 nm peak of a 0.001 M Sb(III) solution in Fig. 1. The new species has no absorption at 285 nm and the concentration of A may be determined from the absorbance at 285 nm. Over the HCl range 6.15 to 3.07 M a single isosbestic point is observed at 224 nm indicating that two Sb(III) species are in equilibrium (A and B). Below 3.07 M HCl the short wavelength absorption shifts further below 200 nm indicating that at least one other species becomes involved. In the range where only two Sb(III) species are in equilibrium, the concentration of B may be calculated from stoichiometry

$$[B] = C_{Sb(III)} - [A]$$

where $C_{Sb(III)}$ represents total Sb(III) concentration. The equilibrium of interest is

$$SbCl_m^{(3-m)} + nCl^- \rightleftarrows SbCl_{m+n}^{3-m-n}$$

which is governed by the equilibrium constant

$$K = \frac{[SbCl_{m+n}^{3-m-n}]}{[SbCl_m^{3-m}][Cl^-]^n} \frac{f_{SbCl_{m+n}^{3-m-n}}}{f_{SbCl_m^{3-m}} f_{Cl^-}^n}$$

Ignoring the activity coefficient factor for the moment, a plot of log $[Cl^-]$ against log $\{[SbCl_{m+n}^{3-m-n}]/[SbCl_m^{3-m}]\}$ (=log R) should yield a straight line of slope n and intercept log K. Such a plot is given in Fig. 2 and from this n, is found to be 1.9 and K, 0.18 M^{-2}.

Such a plot can only be possible if there is a fortuitous cancelling of activity coefficients. Empirical equations describing the change in ionic activity coefficients, $f_\pm$, with ionic strength at moderate concentrations show an exponential dependence on ion charge (16, p. 231). One expression, introduced by Davies (17), is well known

$$\log f_\pm = -\frac{A|Z_1 Z_2|\sqrt{I}}{1+\sqrt{I}} + 0.1|Z_1 Z_2|I$$

where I represents ionic strength and A is a constant. Factoring out the ion charge part, we have

$$f_\pm = 10^{-|ZZ_2|F(I)}$$

where $F(I)$ represents the function of I. The activity coefficient of a multivalent ion, Y^{Z-}, can therefore be related to a reasonable approximation to that of a univalent ion, X^-, by the expression

$$f_{Y^{z-}} = f_{X^-}^{\,z}$$

Using this relation, it may be seen that the activity coefficient factor in the equilibrium expression with n = 2 would cancel for equilibria with m = 3 and 4, that is for

$$2Cl^- + SbCl_3 \rightleftarrows SbCl_5^{2-}$$

and

$$2Cl^- + SbCl_4^- \rightleftarrows SbCl_6^{3-}$$

Can. J. Chem. Downloaded from www.nrcresearchpress.com by 210.87.254.40 on 09/05/12
For personal use only.

it may be assumed to a reasonable approximation that f_{SbCl_3} is unity. Cancellation of the activity coefficient factor arises with no other equilibrium with a $2Cl^-$ change and, for the cases where $m \neq 3$ or 4, introduction of the appropriate factor calculated from the molal activity coefficients for HCl (18) and known density data (19) leads to large curvature in the plot. Similarly equilibria involving other than a $2Cl^-$ change lead to curves and nonintegral slopes.

These spectrophotometric results cannot indicate whether A is $SbCl_5^{2-}$ or $SbCl_6^{3-}$ but studies on the solubility of chloroantimonate(III) compounds permit this distinction.

Solubility Studies

Haight and Ellis used the solubility of $[(CH_3)_4N]_3Sb_2Cl_9$ in H_2SO_4–HCl solutions to show that $SbCl_3$, $SbCl_4^-$, and $SbCl_6^{3-}$ are in equilibria in these solutions. The question arises as to whether Sb(III) may form sufficiently stable complexes with HSO_4^- or SO_4^{2-} to affect the solubility. Mixtures of $HClO_4$–HCl could not be used to check this possibility due to the low solubility of $(CH_3)_4NClO_4$. $Co(NH_3)_6SbCl_6$ is easily prepared and has a low solubility (15) which makes it an ideal compound for solubility studies (2). On the basis of the work of Haight and Ellis the following equilibria are expected

$$[1] \quad Co(NH_3)_6SbCl_6 \rightleftarrows Co(NH_3)_6^{3+} + SbCl_6^{3-}$$

$$[2] \quad SbCl_6^{3-} \rightleftarrows SbCl_4^- + 2Cl^-$$

$$[3] \quad SbCl_4^- \rightleftarrows SbCl_3 + Cl^-$$

According to these equilibria, as chloride concentration decreases the solubility should increase. Table 1 shows that the solubility in 4 *M* HCl–$HClO_4$ mixtures falls off sharply below 3 *M* HCl. Furthermore the insoluble material is flocculent below and crystalline above 3 *M* HCl.

TABLE 1. Solubility of $Co(NH_3)_6$ $SbCl_6$ in solutions of constant total acid molarity (4 *M*)

M_{HA}	10^3S (*M*)*
4 *M* HCl	0.12
3.6 *M* HCl–0.4 *M* $HClO_4$	0.10
2.8 *M* HCl–1.2 *M* $HClO_4$	0.08
2.4 *M* HCl–1.6 *M* $HClO_4$	0.03
4 *M* $HClO_4$	0.003
4 *M* H_2SO_4	0.57

*M = mol/l.

This suggests that the equilibria given by Haight and Ellis ([2] and [3]) may not describe precisely the solubilities in this system. It should, however, be pointed out that the increasing solubility with increasing chloride concentration may be a result of ion pair formation

$$Co(NH_3)_6^{3+} + Cl^- \rightleftharpoons Co(NH_3)_6Cl^+$$

in which case the equilibria 2–3 may still be valid, but their effect would be masked.[1] Such ion pairing has been shown to be not insignificant (20). Table 1 also gives the solubility of $Co(NH_3)_6SbCl_6$ in 4 *M* H_2SO_4 which is 1000-fold greater than in 4 *M* HCl. Moreover, $SbCl_3$ yields a flocculent precipitate on contact with 4 *M* $HClO_4$ but dissolves in 4 *M* H_2SO_4. These observations show that Sb(III) is complexed in solutions containing sulfuric acid and this should be considered in interpreting the $[(CH_3)_4N]_3Sb_2Cl_9$ solubility work in HCl–H_2SO_4 mixtures. The extrapolation used by Haight and Ellis at high chloride concentrations ($0.8\ M < [Cl^-] < 4.0\ M$) should be little affected by sulfate complexing and thus the solubility curve would be accounted for in this region by the equilibria

$$[(CH_3)_4N]_3Sb_2Cl_9 \overset{K_s}{\rightleftharpoons} 3(CH_3)_4N^+ + 2SbCl_4^- + Cl^-$$

$$SbCl_4^- + 2Cl^- \overset{K_5K_6}{\rightleftharpoons} SbCl_6^{3-}$$

In the region of high $[HSO_4^-]$ the solubility may be determined by

$$SbCl_4^- + HSO_4^- \overset{K_4'}{\rightleftharpoons} SbCl_3(HSO_4)^- + Cl^-$$

Solubility, $[Cl^-]$ and $[HSO_4^-]$ are related by the expression

$$S^{5/2}[Cl^-]^{1/2} = \frac{K_2^{1/2}}{10.4}\left\{1 + K_5K_6[Cl^-]^2 + \frac{[HSO_4^-]}{[Cl^-]}K_4'\right\}$$

where S represents the solubility of the salt. This expression is identical to that of Haight and Ellis at high $[Cl^-]$ values yielding $K_S = 1.8 \times 10^{-5}$ and $K_5K_6 = 0.17$. At the low $[Cl^-]$ end of the solubility curve, correction of $[Cl^-]$ and $[HSO_4^-]$ for the various equilibria involved could not be made due to the complexity of the system. However a plot of $S^{5/2}[Cl^-]^{1/2}$ *vs.* $[HSO_4^-]/[Cl^-]$ using uncorrected $[Cl^-]$ and $[HSO_4^-]$ values should lead to the same inter-

[1]We thank one of the referees for pointing this out.

TABLE 2. Peak maxima of the electronic spectra (cm^{-1})

Sample	Dilution (v/v in MgO)	Anion maxima $10^3\bar{\nu}$		Cation maxima $10^3\bar{\nu}$
0.001 *M* $SbCl_3$ in 12.3 *M* HCl	—	34.5	43.9	—
SbOCl	—	37.7		—
$SbCl_3$	—	34.5		—
pyHCl	1:1	—		38.6
$pyHSbCl_4$	1:1	31.3		38.6
$[(CH_3)_4N]_3Sb_2Cl_9$	—	29.9	33.9	
K_3SbCl_6		30.8, 37.0, 45.0		
$Co(NH_3)_6Cl_3$	1:5	—		21.2, 29.8*
$Co(NH_3)_6SbCl_6$	1:4	27.8	37.9	20.8. 29.6

*This peak consisted of two parts indicating metallic reflectance in the spectrum of the pure compound. Upon dilution with MgO (1:5 compound/MgO) the two peaks coalesced to this maximum.

cept as the first plot and give an estimate of K_4' from the slope. The value for K_4' found was 0.017. The equilibrium constants were now used in a computer program which calculated S at the stoichiometric concentrations. From the value of S and the equilibrium constants, improved $[HSO_4^-]$ and $[Cl^-]$ values were calculated and S redetermined. This procedure was repeated until S showed no significant change. Several sets of equilibrium constants were tested. The optimum fit to solubility data of Haight and Ellis was given by $K_S = 1.85 \times 10^{-5}$, $K_5K_6 = 0.16$, $K_4' = 0.016$. As in the original solubility work, HSO_4^- dissociation was considered negligible.

The agreement between the K, calculated from the spectrophotometric measurements and K_5K_6 is remarkably good, considering the assumptions made in the determination of K and confirms that the equilibrium involved in these solutions is between $SbCl_4^-$ and $SbCl_6^{3-}$. Furthermore the electronic spectrum at high $[Cl^-]$ is due to $SbCl_6^{3-}$. Attempts to fit an equilibrium between $SbCl_3$ and $SbCl_5^{2-}$ to the solubility data, using several possible equilibria with HSO_4^- lead to nonlinear extrapolations and the best computer fit to the solubility curve was given with $K_4K_5 = 3.3$, very different from the spectrophotometric value.

Reflectance Spectroscopy

An attempt was made to identify the Sb(III) complex present in concentrated HCl by analogy with the electronic spectral bands observed in the diffuse reflectance spectra of solids known to contain specific chloroantimonate(III) ions. The data are given in Table 2. No satisfactory correlation can be found between the solution spectrum and the spectra of any of the chloroantimonate species although the parallel between the K_3SbCl_6 spectrum with the 30 800 and 37 000 cm^{-1} peaks both contributing to the solution peak at 34 500 cm^{-1}, is closest. Normally there is little shift in the band maxima of an ion upon transfer from solid to solution. The behavior of the $Co(NH_3)_6^{3+}$ ion in this work is an example of this with solid maxima at 21 200 and 29 800 cm^{-1} and solution maxima at 21 000 and 29 500 cm^{-1} (21, p. 293). On this basis it would appear there is some difference between the $SbCl_6^{3-}$ ion in solution compared to the octahedral ion in $Co(NH_3)_6SbCl_6$ (22).

In the series of chloroantimonates studied, as the number of near-neighbor chloro-ligands increases, the strongest band which is the lowest energy band in $Sb_2Cl_9^{3-}$ and $SbCl_6^{3-}$ compounds, shifts to lower energy. The u.v. absorption of $d^{10}s^2$ species has been assigned to $s \rightarrow p$ transitions (6) and it has been noted that the $s - p$ energy difference decreases as the electronegativity of the ligands bonded to such a species decreases (21 p. 186). Since in a chloro-complex or compound "Sb^{3+}" would be more electronegative than chloride ion increasing the number of Cl^- ligands would increase the electronic charge on the antimony, which would produce the same effect as decreasing ligand electronegativity. If the bonding in these chloro-antimony(III) species is principally ionic, the decrease in s–p separation with increasing number of Cl^- ligands is probably a reflection of increasing ratio of electronic to nuclear charge.

Raman Spectroscopy

A solution of 0.5 *M* Sb(III) in concentrated HCl (12.3 *M*) gives the Raman spectrum shown in Fig. 3. As the concentration of Sb(III) is de-

Can. J. Chem. Downloaded from www.nrcresearchpress.com by 210.87.254.40 on 09/05/12
For personal use only.

Can. J. Chem. Downloaded from www.nrcresearchpress.com by 210.87.254.40 on 09/05/12
For personal use only.

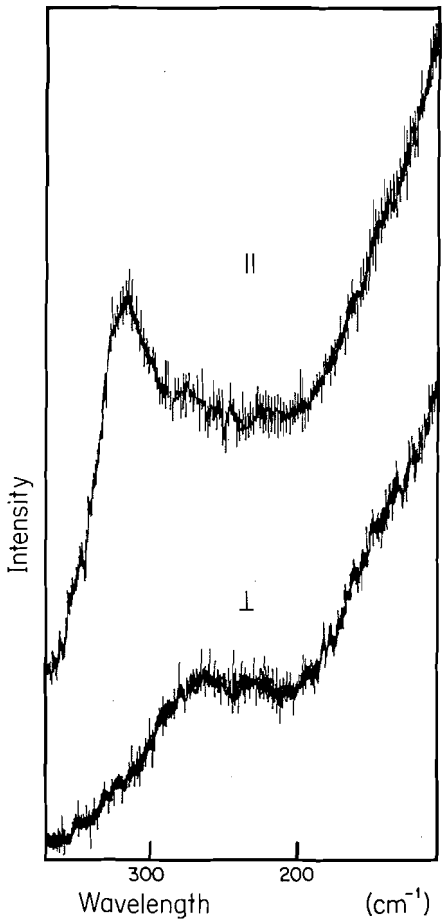

FIG. 3. Raman spectrum of $SbCl_6^{3-}$ ([Sb(III)] = 0.5 *M*).

creased the spectral profile shows virtually no change down to the limit of useful measurement at 0.02 *M* and the most intense peak remains at $325 \pm 2\ cm^{-1}$. Certainly there is no increase in relative intensity in the region of ν_1 for the octahedral $SbCl_6^{3-}$ ion in $Co(NH_3)_6SbCl_6$ at 266 cm^{-1} (8, 9, 15) as the concentration is decreased. Moreover the u.v. spectrum of the 0.02 *M* Sb(III) solution in 12.3 *M* HCl shows the typical $SbCl_6^{3-}$ spectrum. From the absorbance at 285 nm, $[SbCl_6^{3-}]$ is found to be 0.018 *M*, while using $K = 0.16$, $[SbCl_6^{3-}]$ is calculated to be 0.019 *M*. Therefore the Raman shift at 325 cm^{-1} definitely belongs to the $SbCl_6^{3-}$ ion and, as indicated above, there must be a considerable change in the nature of the $SbCl_6^{3-}$ in going from $Co(NH_3)_6SbCl_6$ to solution. In previous work

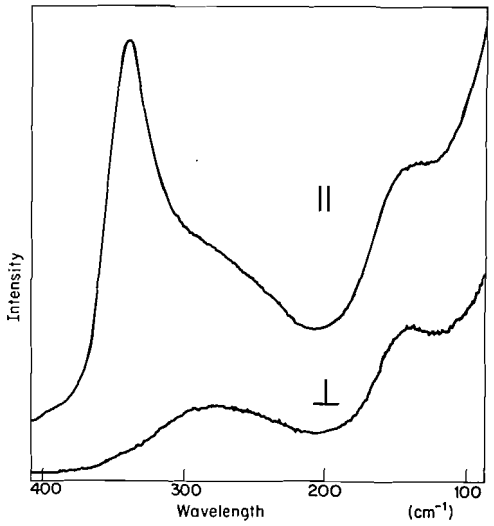

FIG. 4. Raman spectrum of $SbCl_4^-$ ([Sb(III)] = 2.0 *M*).

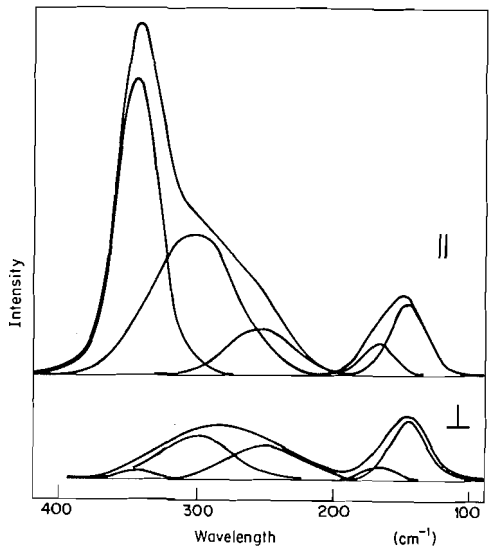

FIG. 5. Curve resolution of the Raman spectrum of $SbCl_4^-$.

TABLE 3. Assignment of the Raman spectrum of the $SbCl_4^-$ ion

Mode	Wave number	Approximate description of mode
ν_1 (A_1)	337 (10) p	ν_{sym} (eq. $SbCl_2$)
ν_2 (A_1)	300 (5) p	ν_{sym} (ax. $SbCl_2$)
ν_3 (A_1)	170 (1) p	δ_{sym} (eq. $SbCl_2$)
ν_6 (B_1)	252 (2)	ν_{asym} (eq. $SbCl_2$)
ν_7 (B_1)	146 (2)	δ_{asym} (eq. $SbCl_2$)

Can. J. Chem. Downloaded from www.nrcresearchpress.com by 210.87.254.40 on 09/05/12
For personal use only.

(4, 12) these differences have not been clearly demonstrated since the relative contribution of $SbCl_4^-$ and $SbCl_6^{3-}$ to the Raman spectrum is concentration dependent. Calculation shows that at moderate $SbCl_3$ concentrations (2 *M*) only $\frac{2}{3}$ of the Sb(III) is present as $SbCl_6^{3-}$ and the Raman spectrum consists of shifts due to $SbCl_6^{3-}$ and $SbCl_4^-$. Calculation shows that for the solution used for Fig. 3, $[SbCl_6^{3-}] = 0.47$ *M*. This spectrum has been attributed to an octahedral ion (3, 4) but the breadth of the spectral bands, the high intensity ratio of ν_2 to ν_1 for O_h symmetry species and the relative weakness of the deformation modes, suggest that $SbCl_6^{3-}$ is not octahedral in solution. It is possible that the $SbCl_6^{3-}$ ion is like XeF_6 in the vapor phase (23) consisting of an equilibrium mixture of several stereo-chemical forms. An attempt was made to apply curve resolution to the spectrum but many solutions seemed possible and the results were not considered to be meaningful.

The spectrum of 2 *M* $SbCl_3$ in 2.8 *M* HCl is given in Fig. 4. This spectrum differs from that of $SbCl_6^{3-}$ in that the relative intensity of the deformation modes is greater and the broad band centered at 288 cm^{-1}, as well as that at 332 cm^{-1}, is polarized. Calculation shows $[SbCl_4^-] =$ 1.9 *M* and the spectrum shows a close parallel to that reported by Ahlijah and Goldstein for the C_{2v} $SbCl_4^-$ ion (24). Contrary to the findings of Petrov *et al.* (4), three polarized bands are observed. The curve resolved spectra are given in Fig. 5 and the assignment in Table 3. The observation of two polarized bands in the SbCl stretching region supports C_{2v} symmetry for this ion and rules out a tetrahedral ion (4). The assignment differs from that in ref. 24 in that ν_{sym} (eq. $SbCl_2$) rather than ν_{sym} (ax. $SbCl_2$) is assigned to the highest frequency polarized band. This parallels the assignment for the SbF_4^- ion and molecular TeF_4 (25) and agrees with the X-ray work which shows that the $SbCl_{eq}$ bond is stronger than $SbCl_{ax}$ ($SbCl_{eq}$, 2.38 Å; $SbCl_{ax}$, 2.64 Å) (14).

The author is grateful to Dr. A. R. Davis of Environment Canada for the use of his Raman equipment and the National Research Council of Canada for financial assistance.

1. G. P. HAIGHT. J. Am. Chem. Soc. **83**, 85 (1961).
2. G. P. HAIGHT and B. Y. ELLIS. Inorg. Chem. **4**, 249 (1965).
3. E. MARTINEAU and J. B. MILNE. J. Chem. Soc. A, 2971 (1970).
4. K. I. PETROV, V. E. PLYUSHCHEV, V. V. FOMICHEV, and G. V. ZIMINA. Russ. J. Inorg. Chem. **16**, 696 (1971).
5. N. A. BONNER and W. GOISHI. J. Am. Chem. Soc. **83**, 85 (1961).
6. R. A. WALTON, R. W. MATTHEWS, and C. K. JORGENSEN. Inorg. Chim. Acta, **1**, 355 (1967).
7. P. DAY. Inorg. Chem. **2**, 452 (1963).
8. I. R. BEATTIE, F. C. STOKES, and L. E. ALEXANDER. J. Chem. Soc. Dalton, 465 (1973).
9. J. B. MILNE. Unpublished results.
10. I. R. BEATTIE, T. GILSON, K. LIVINGSTON, and (in part) V. FAWCETT and G. A. OZIN, J. Chem. Soc. A, 712 (1967).
11. P. J. HENDRA. Spectrochim. Acta, **23A**, 2871 (1967).
12. C. J. ADAMS and A. J. DOWNS. Chem. Commun. 1699 (1970).
13. G. BRAUER. Handbook of preparative inorganic chemistry. Academic Press, New York. 1963. p. 611.
14. S. K. PORTER and R. A. JACOBSON. Chem. Commun. 1244 (1967).
15. T. BARROWCLIFFE, I. R. BEATTIE, P. DAY, and K. LIVINGSTON. J. Chem. Soc. A, 1810 (1967).
16. R. A. ROBINSON and R. H. STOKES. Electrolyte solutions. Butterworths, Toronto. 1965.
17. C. W. DAVIES. J. Chem. Soc. 2093 (1938).
18. M. RANDALL and L. E. YOUNG. J. Am. Chem. Soc. **50**, 989 (1928).
19. Handbook of chemistry and physics. The Chemical Rubber Co., Cleveland, Ohio. 1969.
20. S. KATAYAMA. Rika Gaku Kenkyusho Hokoku, **42**, 243 (1966); Chem. Abs. **67**, 47749z (1967).
21. C. K. JORGENSEN. Absorption spectra and chemical bonding in complexes. Pergamon, Oxford. 1962.
22. D. R. SCHROEDER and R. A. JACOBSON. Inorg. Chem. **12**, 210 (1973).
23. H. H. CLAASSEN, G. L. GOODMAN, and H. KIM. J. Chem. Phys. **56**, 5042 (1972).
24. G. Y. AHLIJAH and M. GOLDSTEIN. J. Chem. Soc. A, 326 (1970).
25. C. J. ADAMS and A. J. DOWNS. Spectrochim. Acta, **28A**, 1841 (1972).

Azole Chemistry. IX.[1] A New Synthesis of Fused Pyrimidines: Tetrahydropyrimido[1,2-*a*]benzimidazoles

HOWARD ALPER[2] AND LAWRENCE PEPPER[3]

Department of Chemistry, State University of New York at Binghamton, Binghamton, New York 13901

Received July 25, 1974

HOWARD ALPER and LAWRENCE PEPPER. Can. J. Chem. **53**, 894 (1975).

2-Aminobenzimidazole and 2-amino-5,6-dimethylbenzimidazole react with various epoxy bromides in hot 2-butanone to give, after basification, 3-hydroxy-1,2,3,4-tetrahydropyrimido-[1,2*a*]benzimidazoles. The spectral properties of these heterocycles are discussed.

HOWARD ALPER et LAWRENCE PEPPER. Can. J. Chem. **53**, 894 (1975).

L'amino-2 benzimidazole et l'amino-2 diméthyl-5,6 benzimidazole réagissent avec divers bromures d'époxydes dans la butanone chaude pour conduire après basification aux hydroxy-3 tétrahydro-1,2,3,4 pyrimido-[1,2*a*] benzimidazoles. On discute des propriétés spectrales de ces hétérocycles. [Traduit par le journal]

The reaction of epoxy bromides with mercaptoazoles such as 2-mercaptoimidazole (1) and 5-mercapto-1-phenyl-1,2,3,4-tetrazole (2) represents a convenient synthetic approach to fused 1,3-thiazines (*e.g.*, **1** → **2**). A question arises as

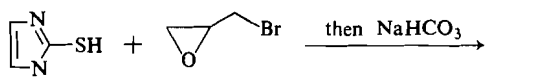

1

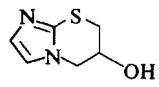

2

to whether amino azoles could also undergo this type of cyclization process and afford six-membered ring heterocycles containing two nitrogen atoms. Should such a transformation occur, it would provide a new and simple entry into fused, potentially pharmacologically active, pyrimidines. We now wish to report the synthesis of some tetrahydropyrimido[1,2-*a*]benzimidazoles, formed by treatment of 2-aminobenzimidazole and 2-amino-5,6-dimethylbenzimidazole with various epoxy bromides.

Results and Discussion

When an equimolar mixture of 2-aminobenzimidazole (**3**, $R_1 = R_2 = H$) or 2-amino-5,6-dimethylbenzimidazole (**3**, $R_1 = R_2 = CH_3$) and an epoxy halide (**4**) were refluxed in 2-butanone for 1–4 days, the hydrobromide salt of **5** was formed, either as an oil or as a solid. The salt was converted into its free base upon treatment with sodium bicarbonate. The reaction times, yields, and analytical data of the 3-hydroxy-1,2,3,4-tetrahydropyrimido[1,2-*a*]benzimidazoles (**5**) are listed in Table 1.

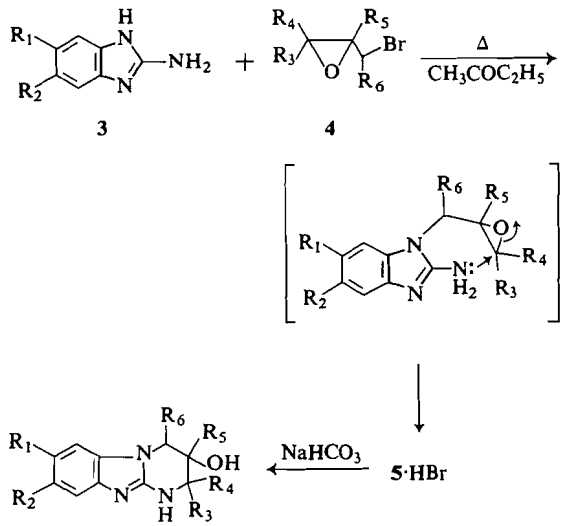

3 **4**

5·HBr

5

The initial step in the reaction process involves alkylation at a ring nitrogen to give the substituted 2,3-epoxypropane intermediate. Ogura and co-workers (3) have presented evidence for

[1]For Part VIII. see ref. 10.

[2]Present address: Department of Chemistry, University of Ottawa, Ottawa, Canada K1N 6N5.

[3]Taken in part from the B.A. (Honors) Thesis of L. Pepper, State University of New York at Binghamton, May, 1974.

Can. J. Chem. Downloaded from www.nrcresearchpress.com by 210.87.254.5 on 09/05/12
For personal use only.

Can. J. Chem. Downloaded from www.nrcresearchpress.com by 210.87.254.5 on 09/05/12
For personal use only.

TABLE 1. Products obtained from reaction of epoxy bromides (**4**) with **3**

	3	**4**				Reaction time,	Yield	Melting		Analytical data % calcd. (found)		
5	R_1, R_2	R_3	R_4	R_5	R_6	days	(%)	point (°C)	formula	C	H	N
a	H	H	H	H	H	1	17	205(dec.)	$C_{10}H_{11}N_3O$	63.48 (63.29)	5.82 (5.88)	22.22 (21.68)
b	H	H	H	CH_3	H	2	23	230–232	$C_{11}H_{13}N_3O$	65.03 (64.77)	6.40 (6.64)	20.69 (20.21)
c	H	H	H	H	CH_3	3	7	230(dec.)	$C_{11}H_{13}N_3O$	65.03 (64.77)	6.40 (6.51)	20.69 (21.19)
d	H	CH_3	CH_3	H	H	4	24	240–242	$C_{12}H_{15}N_3O$	66.36 (66.51)	6.91 (6.47)	—
e	CH_3	H	H	H	H	4	31	175(dec.)	$C_{12}H_{15}N_3O$	66.36 (66.68)	6.91 (6.73)	—
f	CH_3	H	H	H	CH_3	2	10	260(dec.)	$C_{13}H_{17}N_3O$	67.53 (67.08)	7.35 (7.32)	—

TABLE 2. Infrared and u.v. spectral data for **5**

5	Infrared (KBr disc) ν (cm^{-1}) OH	CO	N=C—N	δNH	Ultraviolet (ethanol) max (log ε) nm
a	2500–3380	1095 or 1110	1568(br)	1620	228(3.72), 253(3.69), 291(3.72)
b	2550–3350	1159	1578	1627	—
c	2600–3350	1080	1580	1628	—
d	2600–3400	1098	1577	1632	—
e	2600–3400	1095 or 1115	1570	1620	233(3.69), 250(3.62), 299(3.67)
f	2600–3300	1078	1565	1628	231(3.61), 256(3.51), 302(3.57)

the occurrence of condensation at a ring nitrogen, rather than at the amino group nitrogen, of **3**, $R_1 = R_2 = H$, in the synthesis of the related imidazo[1,2-*a*]benzimidazole system. Annelation of the pyrimidine ring to the benzimidazole then occurs by ring opening of the intermediate epoxide.

The structures of the 3-hydroxy-1,2,3,4-tetrahydropyrimido-[1,2-*a*]benzimidazoles were assigned on the basis of analytical data and spectral results. Solid state i.r. spectra (Table 2) of **5** showed sharp, characteristic carbon–oxygen stretching vibrations between 1078 and 1159 cm^{-1} (1, 2). Broad bands were observed in the region of 3400–2500 cm^{-1} and were assigned to the hydrogen–bonded stretch of the hydroxyl and amino functions (carbon–hydrogen stretching absorptions overlap in the 3050–2825 cm^{-1} region). An intense absorption appeared at 1580–1565 cm^{-1} which is due to ν(N=C—N) of the benzimidazole portion of the molecule (4).

The heterocycles (**5**) were insufficiently soluble in solvents commonly used for n.m.r. purposes. The u.v. spectra for several of the tetrahydropyrimido[1,2-*a*]benzimidazoles were recorded (Table 2) and show three absorption maxima at 228–233, 250–256, and 291–302 nm. The latter maximum is probably due, at least in part, to an $n \rightarrow \pi^*$ transition.

Electron impact mass spectra of two of the heterocycles provided important information regarding their structures. The isomeric compounds **5***b* and **5***c* each gave a parent molecular ion peak at *m/e* 203. A major fragmentation pathway of **5***b* was elimination of acetaldehyde to give an ion of *m/e* 159, possibly of structure **6**. The fused 1,3-thiazine **8**, also loses acetaldehyde

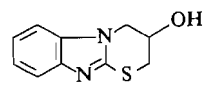

8

on fragmentation of the molecular ion (5). The tertiary alcohol **5***c* loses acetone on electron impact to afford a fragment of proposed structure **7** (*m/e* 145).

An oily by-product was formed in most of these reactions, easily separated from **5** by solubility differences. Nuclear magnetic resonance spectra of the oils lack signals due to aromatic protons. The oil is probably a polymer of the epoxy bromide.

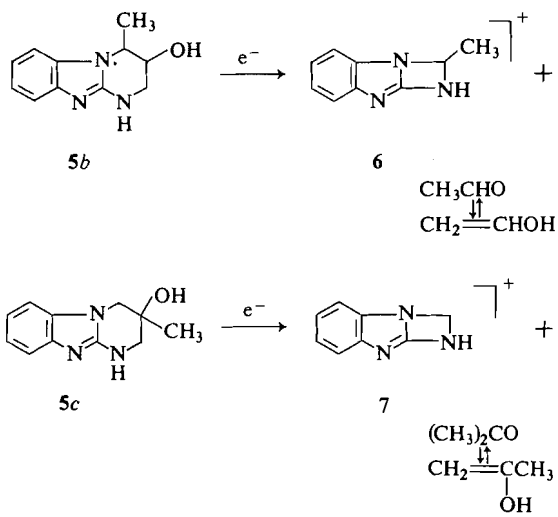

Experimental

General

Melting points were determined on a Fisher–Johns apparatus and are uncorrected. Elemental analyses were determined by Hoffmann-LaRoche Microanalytical Laboratory and by Pascher Mikroanalytisches Laboratorium, Bonn, Germany. Infrared spectra were obtained on a Perkin-Elmer 457 spectrometer and u.v. spectra were recorded on a Perkin-Elmer 202 spectrometer. Mass spectra were determined using a Varian MS902 spectrometer.

Can. J. Chem. Downloaded from www.nrcresearchpress.com by 210.87.254.5 on 09/05/12
For personal use only.

Epoxy Bromides

Epibromohydrin was commercially available. 1-Bromo-2,3-epoxy-3-methylbutane was prepared by dehydrohalogenation of 1,2-dibromo-3-methyl-3-butanol (6). Dehydrohalogenation of 2,3-dibromobutan-1-ol yielded *threo*-3-bromo-1,2-epoxybutane (7). Halogenation of 2-methyl-2-propen-1-ol gave 1,2-dibromo-2-methyl-3-propanol (8), which was then dehydrohalogenated to yield 1-bromo-2,3-epoxy-2-methylpropane (9).

General Procedure for the Reaction of 2-Aminobenzimidazole or 2-Amino-5,6-dimethylbenzimidazole with Epoxy Bromides

Equimolar amounts of the heterocycle and epoxy halide (15.6 mmol) were refluxed with stirring in 2-butanone (125–225 ml) for 1–4 days, until either the color of the solution changed or a precipitate was formed, signifying that a reaction had occurred. The reaction mixture was allowed to cool to room temperature and work-up was then effected as follows for the individual cases:

(*a*) R_1—R_6=H: the hydrobromide salt of **5***a* precipitated out of solution. If was filtered and dried. Conversion to the free base was accomplished by dissolving the salt in hot water (~300 ml), adding a small amount (5 ml) of *N*,*N*-dimethylacetamide, and basifying the solution with 5% aqueous sodium bicarbonate (to a p*H* of 8). The solution was then continuously extracted with methylene chloride. Pentane was added to the residue obtained by flash evaporation of the methylene chloride extract in order to induce precipitation of pure **5***a*.

(*b*) R_1—R_4=R_6=H, R_5=CH_3: the reaction mixture was filtered and the filtrate was concentrated to a dark oil. The oil was dissolved in ethanol and basified as described in *a*. Continuous extraction with methylene chloride, followed by solvent evaporation, gave a semi-solid from which **5***b* was isolated by addition of ether and subsequent filtration. The heterocycle was washed well with acetone.

(*c*) R_1—R_5=H, R_6=CH_3: isolation of 5*c*·HBr and basification was effected as in *b*. A small quantity of an unidentified precipitate was filtered and the filtrate was extracted continuously with methylene chloride. Flash evaporation of the organic extract gave a yellow oil which, upon standing, deposited the fused azole. The heterocycle was filtered and washed with acetone. Evaporation of the filtrate gave an oil, possibly of polymeric composition (n.m.r. $(CD_3)_2CO$: δ 2.02s, 2.87s, 3.03s).

(*d*) R_1=R_2=R_5=R_6=H, R_3=R_4=CH_3: the work-up used was that of *b* up to the point of flash evaporation of the methylene chloride extract. The oil was dissolved in the minimum amount of tetrahydrofuran. Pentane was added and the reaction mixture was then allowed to stand overnight at room temperature. Decantation of the solution gave an orange oil from which **5***d* slowly crystallized on standing.

(*e*) R_1=R_2=CH_3, R_3—R_6=H: the reaction was worked up as described for **5***b*.

(*f*) R_1=R_2=R_6=CH_3, R_3=R_4=R_5=H: the reaction was worked up as described for **5***c*.

We are grateful to the National Institutes of Health for support of this research.

1. H. ALPER and E. C. H. KEUNG. J. Org. Chem. **37**, 1464 (1972).
2. H. ALPER and R. W. STOUT. J. Heterocycl. Chem. **10**, 569 (1973).
3. H. OGURA, H. TAKAYANAGI, Y. YAMAZAKI, S. YONEZAWA, H. TAKAGI, S. KOBAYASKI, T. KAMIOKA, and K. KAMOSHITA. J. Med. Chem. **15**, 923 (1972).
4. P. BASSIGNANA, C. COGROSSI, M. GANDINO, and P. MERLI. Spectrochim. Acta, **21**, 605 (1965).
5. H. ALPER and E. C. H. KEUNG. Unpublished results.
6. S. WINSTEIN and L. GOODMAN. J. Am. Chem. Soc. **76**, 4373 (1954).
7. C. F. HISKEY, H. L. SLATES, and N. L. WENDLER. J. Org. Chem. **21**, 429 (1956).
8. M. L. WOLFROM, G. H. MCFADDEN, and A. CHANEY. J. Org. Chem. **25**, 1079 (1960).
9. E. P. ADAMS, F. P. DOYLE, D. L. HATT, D. O. HOLLAND, W. H. HUNTER, K. R. MANSFORD, J. H. NAYLER, and A. QUEEN. J. Chem. Soc. 2649 (1960).
10. H. ALPER and B. H. LIPSHUTZ. J. Org. Chem. **38**, 3742 (1973).

Can. J. Chem. Downloaded from www.nrcresearchpress.com by 210.87.254.5 on 09/05/12
For personal use only.

Carbonyl Addition Reactions: Factors Affecting the Hydrate–Hemiacetal and Hemiacetal–Acetal Equilibrium Constants

J. PETER GUTHRIE

Department of Chemistry, University of Western Ontario, London, Ontario N6A 3K7

Received August 19, 1974

Can. J. Chem. Downloaded from www.nrcresearchpress.com by 210.87.254.42 on 09/05/12
For personal use only.

J. PETER GUTHRIE. Can. J. Chem. **53**, 898 (1975).

Equilibrium constants for hydrate-hemiacetal interconversion in aqueous solution at 25° have been measured for four fluorinated carbonyl compounds: compound, alcohol, K_4 (M^{-1}): CF_3CHO, C_2H_5OH, 2.3; CF_3COCH_3, CH_3OH, 1.0; CF_3COPh, CH_3OH, 3.5; CF_3COCF_3, CH_3OH, 0.14. These values, combined with values from the literature, permit an examination of substituent effects upon the equilibrium constant for

$$-\overset{|}{\underset{|}{C}}-OH + ROH \rightleftarrows -\overset{|}{\underset{|}{C}}-OR + H_2O$$

The free energy change for this process, corrected for symmetry and steric effects, follows the equation

$$\Delta G_4'' = -0.54 + 0.63\ \Sigma\sigma^*$$

Thus electronic effects upon this equilibrium are generally small and in fact are often smaller than steric effects.

This analysis permits and justifies the calculation of free energies of formation of $-\overset{|}{\underset{|}{C}}-OH$ compounds from the (more generally measurable) free energies of formation of the analogous $-\overset{|}{\underset{|}{C}}-OR$ compounds.

J. PETER GUTHRIE. Can. J. Chem. **53**, 898 (1975).

On a mesuré, en solution aqueuse, à 25°, les constantes d'équilibre pour l'interconversion hydrate–hémiacétal de quatre composés carbonylés fluorés: le composé, l'alcool, K_4 (M^{-1}): CF_3CHO, C_2H_5OH, 2.3; CF_3COCH_3, CH_3OH, 1.0; CF_3COPh, CH_3OH, 3.5; CF_3COCF_3, CH_3OH, 0.14. Ces valeurs peuvent être combinées avec d'autres extraites de la littérature afin de permettre une évaluation de l'effet des substituants sur la constante d'équilibre

$$-\overset{|}{\underset{|}{C}}-OH + ROH \rightleftarrows -\overset{|}{\underset{|}{C}}-OR + H_2O$$

Le changement d'énergie libre au cours de cette réaction, corrigé pour la symétrie et les effets stériques, suit l'équation

$$\Delta G_4'' = -0.54 + 0.63\ \Sigma\sigma^*$$

On peut donc en déduire que les effets électroniques sur cet équilibre sont généralement petits et que de fait ils sont souvent plus petits que ceux des effets stériques.

Cette analyse permet et justifie le calcul d'énergies libres de formation de composés $-\overset{|}{\underset{|}{C}}-OH$, effectué à partir d'énergies libres de formation (généralement plus facilement mesurable) des composés $-\overset{|}{\underset{|}{C}}-OR$ qui leur sont analogues. [Traduit par le journal]

Can. J. Chem. Downloaded from www.nrcresearchpress.com by 210.87.254.42 on 09/05/12
For personal use only.

Introduction

The three related equilibria 1–3 involved in hydrate (1–6), hemiacetal (1–7), and acetal (6–12) formation from carbonyl compounds have been

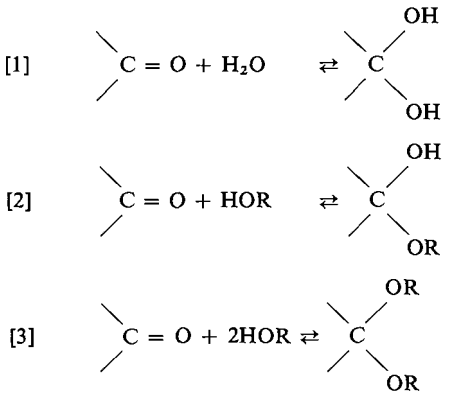

investigated in numerous laboratories. It has been found quite commonly that for a related series of compounds equilibrium constants for any one of these reactions can be correlated using the appropriate σ parameters (2, 3, 6, 12). Sander and Jencks (13) have shown that the equilibrium constants for hemiacetal and hydrate formation are often in constant proportion, depending only on the relative tendencies to add to carbonyl groups of the alcohol and water molecules. This tendency is expressed in terms of their γ parameters.

Recently it was shown (14) that a further generalization was possible in terms of the (sometimes hypothetical) reaction

since equilibrium constants for this reaction were close to unity and almost constant for a wide series of compounds and appeared to depend only upon the number of substituents on the central carbon.

This near constancy of the equilibrium constant for reaction 4 has great potential utility as a means for evaluating free energies of formation of the unobservable hydroxyl-bearing intermediates in acyl transfer reactions from the readily obtained free energies of formation of the stable methoxy or ethoxy analogs (14, 15). Accordingly it seemed essential to test the validity of this relationship for as wide a range of compounds as possible.

In the present paper are collected all available equilibrium constants from the literature, as well as some additional values determined in this laboratory. In agreement with the original generalization (14), the equilibrium constants for process 4 are close to unity for all but the most extreme cases. Inclusion of data for hemiacetals and hydrates of fluorinated aldehydes and ketones reveals that there is a small electronic effect on the equilibrium constant for reaction 4.

Results and Discussion

Equilibrium Constants for Addition to Fluorinated Aldehydes and Ketones

Fluorinated aldehydes and ketones have several advantages for the study of carbonyl addition reactions: (*a*) the trifluoromethyl group is one of the most powerful electron withdrawing groups, yet is relatively unreactive, so that electronic effects can be studied without interference; (*b*) the fluorine n.m.r. will have only signals from the trifluoromethyl group, without the massive interfering signals from solvent and other reagents which often plague the use of proton n.m.r.; (*c*) ^{19}F chemical shifts are very sensitive to substituents so that signals from hydrate and hemiacetal are well separated.

Trifluoroacetaldehyde, trifluoroacetone, trifluoroacetophenone, and hexafluoroacetone were studied in aqueous solution with varying amounts of methanol or ethanol. For all but trifluoroacetone, the free carbonyl compound is present only at unobservably low concentrations but the equilibrium between hydrate and hemiacetal is readily observed. No signals attributable to acetal were ever seen; estimation of the rate of acetal formation from the known linear free energy relation for rates of hydrolysis (16) suggests that acetal formation from these compounds would be *extremely* slow. The data are recorded in the Experimental; the final results are included in Tables 1 and 2.

Equilibrium Constants for Reaction 4

In Table 1 are collected the available data on equilibria for addition of water and methanol or ethanol to carbonyl compounds. There are numerous additional cases where only hydration or acetal equilibrium constants are available but these were not included, since equilibrium constants for reaction 4 could not be calculated without recourse to linear free energy relations to estimate the missing values. In the cases of

Can. J. Chem. Downloaded from www.nrcresearchpress.com by 210.87.254.42 on 09/05/12
For personal use only.

TABLE 1. Equilibrium constants for addition to carbonyl compounds[a]

Carbonyl compound	Hydration K[b]	Alcohol	Hemiacetal K[c]	Acetal K[d]
Formaldehyde				
CH_3O	2280[e]	MeOH	1310[f,g]	183[h]
		EtOH	860[f,i]	140[h]
Aliphatic aldehydes				
CH_3CHO	1.06[j]	MeOH	0.741[e,g]	0.0299[k,l]
		EtOH	0.496[e,i]	0.0125[k,l]
CH_3CH_2CHO	0.85[e]	MeOH	0.638[e,g]	—
		EtOH	0.417[e,i]	0.00892[k,l]
$CH_3CH_2CH_2CHO$	0.65[e]	MeOH	0.482[e,g]	0.0397[k,l]
		EtOH	0.322[e,i]	0.0108
$(CH_3)_2CHCHO$	0.615[e]	MeOH	0.360[e,g]	—
		EtOH	0.222[e,i]	0.00169[k,l]
$(CH_3)_3CCHO$	0.235[e]	MeOH	0.128[e,g]	—
		EtOH	0.102[e,i]	0.00082[k,m]
CF_3CHO	2.9×10^{4}[n]	EtOH	1.2×10^{3}[o]	—
Aromatic aldehydes				
Pyridine-4-carboxaldehyde	1.28[p]	MeOH	0.50[p]	—
		EtOH	0.27[p]	—
Aliphatic ketones				
CH_3COCH_3	1.4×10^{-3}[q]	MeOH	2.2×10^{-4}[q,g]	7.2×10^{-6}[r]
$ClCH_2COCH_3$	0.11[e]	MeOH	0.027[e,g]	—
		EtOH	0.024[e,i]	—
$ClCH_2COCH_2Cl$	10[e]	MeOH	0.58[e,g]	—
		EtOH	0.53[e,i]	—
$Cl_2CHCOCH_3$	2.9[e]	MeOH	0.081[e,g]	—
		EtOH	0.044[e,i]	—
CF_3COCH_3	35[s]	MeOH	0.88[t,s]	—
$CF_3COCH_2COCH_3$	77.2[t]	MeOH	0.63[t]	—
CF_3COCF_3	1.2×10^{6}[u]	MeOH	3.0×10^{3}[o]	—
Aralkyl ketones				
$C_6H_5COCF_3$	78[v]	MeOH	270[o]	

[a]In aqueous solution at 25°, unless otherwise noted.
[b]Dimensionless: K = [hydrate]/[carbonyl].
[c]M^{-1}.
[d]M^{-2}; standard state for water is the pure liquid.
[e]Reference 1.
[f]Reference 7.
[g]In methanol.
[h]Calculated from the free energies of formation of starting materials and products: see Appendix.
[i]In ethanol.
[j]Reference 29.
[k]Calculated from apparent equilibrium constants, by correcting for hemiacetal formation.
[l]Reference 8.
[m]Reference 11.
[n]Assumed to be the same as for CCl_3CHO (footnote *e*) see text.
[o]This work; based on the assumed value for the hydration constant and the observed equilibrium constant for hydrate + alcohol ⇌ hemiacetal.
[p]Reference 13.
[q]Reference 30.
[r]Reference 12.
[s]This work.
[t]Reference 31.
[u]Calculated from the log K–σ^* relation of ref. 2.
[v]Reference 3.

trifluoroacetaldehyde and hexafluoroacetone the equilibrium constants for hydration are unknown and could not be measured by the n.m.r. method employed in the present work; for purposes of comparison values were estimated using the linear free energy relation of Greenzaid *et al.* (2). In the case of trifluoroacetaldehyde, this is equivalent to assuming that the equilibrium constant is the same as for trichloroacetaldehyde. In any case, since the hydrate–hemiacetal equilibrium constant is directly measurable for these compounds, subsequent calculations in this paper are independent of the values of the equilibrium constants for hydration.

TABLE 2. Relative alkyl basicities: carbonyl hydrates and hemiacetals[a]

Carbonyl compound	$K_{hemiacetal}$[b] / $K_{hydrate}$	ΔG_4^{0}[c]	$\Delta G_4'$[d]	$\Delta G_4''$[e]	K_{acetal}[f] / $K_{hemiacetal}$	ΔG_4[c]	$\Delta G_4'$[d]	$\Delta G_4''$[e]
Methanol								
CH_2O	0.575	0.33	0.33	0.33		1.16	0.34	0.34
CH_3CHO	0.706	0.21	0.21	0.06	0.0404	1.90	1.08	0.31
CH_3CH_2CHO	0.717	0.20	0.20	0.05				
$CH_3CH_2CH_2CHO$	0.742	0.18	0.18	0.03	0.0824	1.48	0.66	−0.11
$(CH_3)_2CHCHO$	0.585	0.31	0.31	0.06				
$(CH_3)_3CCHO$	0.545	0.36	0.36					
4-NC_5H_4CHO[g]	0.39	0.56	0.56	0.56				
CH_3COCH_3	0.157	1.10	1.10	0.18	0.0327	2.06	1.24	0.32
$ClCH_2COCH_3$	0.25	0.82	0.82	−0.25				
$ClCH_2COCH_2Cl$	0.058	1.69	1.69	0.52				
$Cl_2CHCOCH_3$	0.028	2.12	2.12	1.05				
CF_3COCH_3	0.025	2.19	2.19	1.27				
$CF_3COCH_2COCH_3$[h]	0.0082	2.86	2.86	1.66				
CF_3COCF_3	0.0025	3.55	3.55	2.35				
$C_6H_5COCF_3$	0.063	1.64	1.64	1.49				
Ethanol								
CH_2O	0.377	0.58	0.58	0.58	0.16	1.08	0.24	0.24
CH_3CHO	0.472	0.44	0.44	0.29	0.0252	2.18	1.36	0.44
CH_3CH_2CHO	0.498	0.41	0.41	0.26	0.0214	2.28	1.46	0.54
$CH_3CH_2CH_2CHO$	0.495	0.42	0.42	0.27	0.0335	2.02	1.20	0.28
$(CH_3)_2CHCHO$	0.361	0.60	0.60	0.45	0.0137	2.54	1.72	0.80
$(CH_3)_3CCHO$	0.434	0.50	0.50	0.50	0.0080	2.87	1.97	−0.01
CF_3CHO	0.041	1.90	1.90	1.75				
4-NC_5H_4CHO[g]	0.21	0.93	0.93	0.93				
$ClCH_2COCH_3$	0.22	0.90	0.90	−0.17				
$ClCH_2COCH_2Cl$	0.053	1.75	1.75	0.68				
$Cl_2CHCOCH_3$	0.015	2.50	2.50	1.43				

[a]Equilibrium constants for the reaction $-\overset{|}{\underset{|}{C}}-OH + HOR \rightleftarrows -\overset{|}{\underset{|}{C}}-OR + H_2O$ at 25°. The standard state for reactants other than water is an ideal 1 *M* solution with an infinitely dilute reference state. The standard state for water is the pure liquid. The equilibrium constants have dimensions M^{-1}.
[b]Ratio of equilibrium constants for hemiacetal formation and hydrate formation from Table 1.
[c]Standard free energy change for the reaction indicated.
[d]Free energy change, corrected for symmetry.
[e]Free energy change, corrected for both symmetry and steric effects.
[f]Ratio of equilibrium constants for acetal formation and hemiacetal formation from Table 1.
[g]Pyridine-4-carboxaldehyde.
[h]For reaction at the carbonyl adjacent to the trifluoromethyl group.

In several cases free energies of formation for acetals and the corresponding carbonyl compounds can be calculated from values in the literature. These permit calculation of equilibrium constants for acetal formation. This was done (see Appendix) for the dimethyl and diethylacetals of formaldehyde, for which no direct measurements appear to have been reported.

In Table 2 are found the equilibrium constants for two cases of reaction 4, *i.e.* carbonyl hydrate to hemiacetal and hemiacetal to acetal. In order to make comparisons on a per hydroxyl basis, these equilibrium constants must be corrected for symmetry effects (17): the net result is that the numerical magnitude of the hemiacetal to acetal equilibrium constant is four times larger after this correction is made. Then the equilibria must be corrected for steric interactions introduced as the alkoxy group replaces a hydroxy. This was done following an approach used quite successfully in an additivity scheme for heats of formation of acetals (18); the least crowded conformation was drawn and the number of unfavorable interactions counted. The difference in these interactions is used to correct the free energy change for reaction 4.

The interactions which were considered were: the fifth-neighbour H–H interaction of the gauche butane type; the analogous fifth neighbour hydrogen – lone pair interaction, for which the values recommended by Pihlaja (18) were used, 0.77 and 0.15 kcal mol^{-1}, respectively; and the fifth neighbour H–F interaction, for which

Can. J. Chem. Downloaded from www.nrcresearchpress.com by 210.87.254.42 on 09/05/12
For personal use only.

Can. J. Chem. Downloaded from www.nrcresearchpress.com by 210.87.254.42 on 09/05/12
For personal use only.

half the axial–equatorial free energy difference for trifluoromethylcyclohexane (19) was used, *i.e.* 1.05 kcal mol^{-1}. It was assumed that the free energy change resulting from steric crowding is essentially all determined by the enthalpy change, so that enthalpies and free energies for these steric interactions are equal.[1] For the interaction between H and phenyl which would be encountered in methyl or ethyl hemiacetals or acetals of aralkyl and diaryl ketones or arylaldehydes no literature values could be found. Examination of space filling models showed that the interaction is likely to be very small. For lack of a better value this H–Ph interaction is assumed to be zero.

After these two corrections have been made to the observed free energy changes for reaction 4, the values obtained are symbolized $\Delta G_4''$ and are found in Table 2.

In order to determine whether compounds with one oxygen atom behave analogously to compounds with two oxygens, the standard free energy changes for the hypothetical reactions leading to the formation of methyl and ethyl ethers were calculated for those cases where sufficient free energy of formation data were available. The ΔG_4^0 and $\Delta G_4''$ values so obtained are found in Table 3. These values are necessarily less precise than those obtained from equilibrium studies. The $\Delta G_4''$ are corrected for symmetry and steric effects in a manner analogous to that employed for Table 2.

Figure 1 shows the dependence of ΔG_4^0, $\Delta G_4'$, and $\Delta G_4''$ upon $\sum\sigma^*$; although there is clearly a trend to the ΔG_4^0 plot, there is a great deal of scatter; the scatter is appreciably lessened by correcting for symmetry to give $\Delta G_4'$; the final values of $\Delta G_4''$, corrected for both symmetry and steric effects, show a regular linear dependence upon $\sum\sigma^*$, the sum of the σ^* values for the three substituents on the hydroxyl or alkoxyl bearing carbon. The values are fitted by the line[2]

$$[5]\quad \Delta G_4'' = (-0.66 \pm 0.12) + (0.48 \pm 0.04)\sum\sigma^*$$

determined by the method of least squares which is equivalent to

$$[6]\quad \log K_4'' = +0.48 - 0.34\sum\sigma^*$$

The only points which deviate seriously are those obtained using thermochemical calculations rather than directly evaluated equilibrium constants, and even these deviate by less than their probable errors.

The values of $\Delta G_4''$ clearly are influenced by electron withdrawal by the substituents on the central carbon, so that the initial generalization (14), that $\Delta G_4''$ was constant, is not correct. However the variation is clearly very small and only becomes appreciable for powerfully elec-

TABLE 3. Relative alkyl basicities: alcohols[a]

Alcohol	ΔG_4[b]	$\Delta G_4'$	$\Delta G_4''$
Methanol			
CH_3OH	+0.07	−0.75	−0.75
CH_3CH_2OH	+0.34	−0.07	−0.07
$(CH_3)_2CHOH$	+0.80	+0.39	+0.39
$(CH_3)_3COH$	−0.02	−0.43	−1.35
Ethanol			
CH_3CH_2OH	+0.60	−0.22	−0.22

[a]In aqueous solution at 25°: the standard state for solutes is an ideal 1 *M* solution with an infinitely dilute reference state: the standard state for water is the pure liquid. Units are kcal mol^{-1}.
[b]Calculated from values in ref. 14, with ΔG_f^0(g) for diethyl ether from ref. 24 and ΔG_t calculated from data in ref. 17*a*.

[1]This is not strictly true but entropic effects are likely to be small. Symmetry effects are explicitly taken care of in this paper leaving as the major contributions entropy of mixing effects and restrictions in the rotational freedom of a methyl (*or* trifluoromethyl) group due to steric interference (cogwheeling), (19*b*). The entropy of mixing effect results from the shift in relative population of the three conformers arising from rotation about a C—OCH_3 bond as the spread in energy levels increases with increased crowding. Estimates of this effect suggest that it amounts at most to about 0.2 kcal mol^{-1} in free energy. Entropy effects due to "cogwheeling" are difficult to estimate: where they have been invoked they amount to about 0.2 kcal mol^{-1} in free energy (19*b*). If such entropic effects were mainly responsible for the residual scatter observed in Fig. 1*c*, one would expect systematic deviations for, say, aldehyde hemiacetals relative to ketone hemiacetals, since the aldehyde hemiacetals would be less subject to steric restriction of rotation. However both sets of data show what appears to be random scatter about the least squares line. Therefore the assumption that entropy effects may be neglected appears to be valid.

[2]The correlation coefficients for these graphs are: Fig. 1*a*, 0.624; Fig. 1*b*, 0.803; Fig. 1*c*, 0.869. For Fig. 1*c*, the standard deviation of the points about the line is 0.31. The most serious deviations in Fig. 1*c* are for compounds where steric effects are expected to be large (the chloroacetones, isobutyraldehyde, and pivaldehyde). If all of the equilibria involving these compounds are deleted from the set of data, eq. 5 becomes

$$\Delta G_4'' = -0.70 + 0.49\ \Sigma\sigma^*$$

with a correlation coefficient of 0.96.

Can. J. Chem. Downloaded from www.nrcresearchpress.com by 210.87.254.42 on 09/05/12
For personal use only.

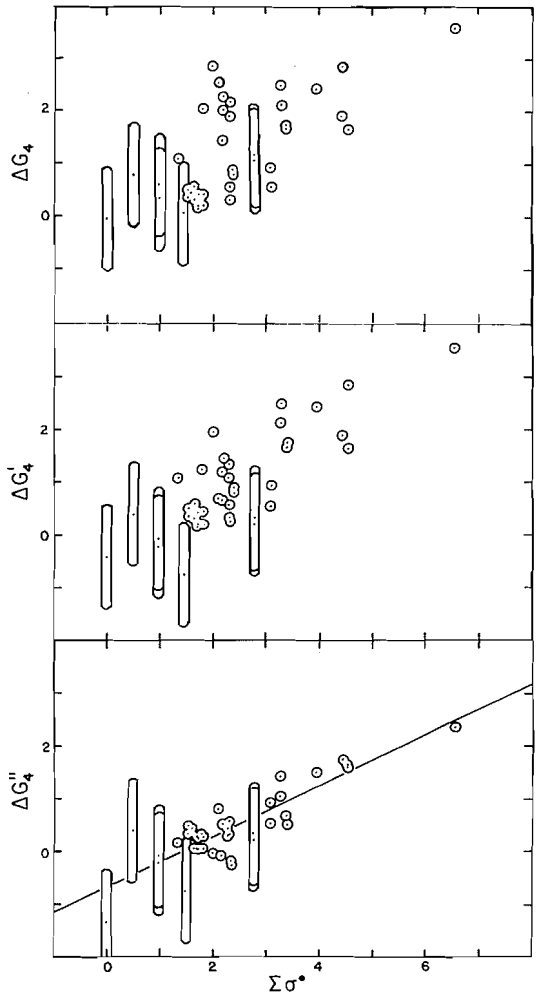

FIG. 1. Graphs of ΔG_4 (*a*), $\Delta G_4'$ (*b*), and $\Delta G_4''$ (*c*) *vs.* $\Sigma\sigma^*$, for the reaction $\gtrless$C—OH + HOR = $\gtrless$C—OR + H_2O. The elongated symbols are points based upon free energy of formation data. The line drawn in *c* was determined by weighted least squares.

tron withdrawing substituents. To keep the variation in perspective it should be noted that K_4'' varies by 300-fold, whereas $K_{\text{hydration}}$ varies by 10^9-fold. It should also be noted that the steric corrections can be as large as a factor of 28 in K_4''.

Sander and Jencks (13) have proposed the linear free energy relation

$$[7] \qquad \log K_{\text{add}} = A + \Delta\gamma$$

for addition of nucleophiles to carbonyl compounds. In this equation, A and Δ are constants for a given carbonyl compound and γ is a measure of the tendency of a nucleophile to add to carbonyl groups. γ is defined as the logarithm of the ratio of the equilibrium constants for the addition to pyridine-4-carboxaldehyde of the nucleophile and of methylamine. For the cases reported to date Δ is close to unity, although the observed dependence of $\Delta G_4''$ upon $\Sigma\sigma^*$ implies that this is a consequence of the limited set of carbonyl compounds which have been examined.

If eq. 7 is valid for all carbonyl compounds, then for the hydrate – methyl hemiacetal case of reaction 4, it would be predicted that

$$\log K = \Delta(\gamma_{CH_3OH} - \gamma_{H_2O})$$

Substituting the measured values for γ and making suitable corrections for the difference in standard state for water, this predicts that $\Delta G_4'' = +0.52\Delta$. Since $\Delta G_4''$ is dependent upon $\Sigma\sigma^*$ this implies that Δ is also dependent upon $\Sigma\sigma^*$. Since this dependence is small and since the cases examined to date have been for systems with $\Sigma\sigma^*$ in the range of 1.5–2.5, it is not surprising that Δ has appeared to be invarient. For compounds with $\Sigma\sigma^*$ in this range, examination of Fig. 1. shows that $\Delta G_4''$ is indeed close to +0.5. We are investigating other carbonyl addition reactions of aldehydes and ketones with electron withdrawing substituents to test the implications discussed above and will report on these studies later.

In view of the near constancy of the equilibrium constants for reaction 4 and of the readily analyzable nature of such variations as do occur, it seems reasonable to conclude that hydrate and hemiacetal formation constants which are not readily measurable can be obtained from the free energies of formation of the corresponding acetals. There are many cases where direct measurement of these equilibrium constants is well nigh impossible because of the extremely low magnitude of the constant or the excessive tendency of the free carbonyl compound to undergo competing side reactions. Free energies of formation for carbonyl compounds and their acetals can be calculated with adequate precision if the enthalpies of formation are available. Enthalpies of formation can in principle be measured for any compound which can be prepared in a pure state. Furthermore, methods for the estimation of enthalpies of formation either by additivity schemes (18, 20) or by semiempirical molecular orbital calculations (21) are avail-

Can. J. Chem. Downloaded from www.nrcresearchpress.com by 210.87.254.42 on 09/05/12
For personal use only.

able and provide values of quite useful precision within their range of application, which is steadily expanding. Measurement (or estimation (22)) of solubilities and vapor pressures permits calculation of free energies of formation in aqueous solution. Finally the use of eq. 5 permits calculation of the equilibrium constants for reaction 4.

The procedure for calculating a standard free energy change for a particular case of reaction 4 is (*a*) from eq. 5 and the σ* values for all groups other than the reacting hydroxyl, calculate $\Delta G_4''$; (*b*) calculate the change in strain energy, considering the least hindered conformations of product and reactant; (*c*) calculate the symmetry correction after Benson; (*d*) combine these three values to give ΔG_4^0.

The analysis of structural effects on $\Delta G_4''$, presented above and in particular the small dependence upon electronic factors and the fact that compounds with one or two oxygen atoms fit the same correlation line, appears to justify the approach which has been proposed (14, 15) in this laboratory to evaluate the free energies of formation of tetrahedral intermediates in acyl transfer reactions. This approach involved the assumption that the behavior observed for molecules with one or two oxygen atoms on the central carbon could be extrapolated to molecules with three oxygen atoms (or two oxygens and a nitrogen). The values estimated when this approach was first devised (14, 15) require recalculation using the more detailed analysis presented in this paper. In Table 4 are presented values so calculated. The deviations from the initial estimates are most severe for the ortho acids and their monoesters (14), since here the difference between $\sum\sigma^*$ for the tetrahedral species and the reference compounds used is greatest; these deviations average around 1.5 kcal mol^{-1}. For the amide hydrates and hemiacetals, (15), the deviations are smaller (*ca.* 0.7 kcal mol^{-1}), since $\sum\sigma^*$ for these compounds is smaller.

TABLE 4. Revised values for free energies of formation of tetrahedral intermediates[a]

Compound	ΔG_f^0(aq) Original	ΔG_f^0(aq) Revised[c]
H—C(OH)$_3$	−136.5[b]	−139.4
H—C(OH)$_2$(OCH$_3$)	−121.4[b]	−122.8
CH$_3$—C(OH)$_3$	−142.0[b]	−141.3
CH$_3$—C(OH)$_2$(OCH$_3$)	−126.0[b]	−124.8
H—C(OH)$_2$(N(CH$_3$)$_2$)	−65.0[d]	−65.8
H—C(OH)(OCH$_3$)(N(CH$_3$)$_2$)	−49.6[d]	−50.3
CH$_3$—C(OH)$_2$(N(CH$_3$)$_2$)	−66.6[d]	−67.3
CH$_3$—C(OH)(OCH$_3$)-(N(CH$_3$)$_2$)	−50.6[d]	−51.1

[a]In aqueous solution at 25° standard state for solutions was an ideal 1 *M* solution with an infinitely dilute reference state; standard state for water was the pure liquid.
[b]Reference 14.
[c]Recalculated from the data in refs. 14 and 15 using values of ΔG_4 calculated as described in the text.
[d]Reference 15.

Experimental

Hydration and Hemiacetal Formation from Fluorinated Aldehydes and Ketones

Trifluoroacetaldehyde ethyl hemiacetal, trifluoroacetone, trifluoroacetophenone, and hexafluoroacetone were reagent grade chemicals used without further purification. No extraneous signals were observed in the ^{19}F n.m.r. Weighed samples of the liquids were dissolved in water (or methanol for trifluoroacetophenone); hexafluoroacetone was bubbled into a weighed sample of water until a suitable increase in weight had occurred. From these stock solutions, samples with varying concentrations of alcohol were prepared.

The ^{19}F n.m.r. results and the equilibrium constants derived from them are recorded in Table 5. The values of K_4 appeared to vary with solvent composition, although this variation was relatively small. Graphs of K_4 *vs.* [Alcohol] were extrapolated to [Alcohol] = 0 to give values of K_4 in water as solvent.

Appendix

Equilibrium constants for acetal formation from formaldehyde and methanol or ethanol have not been reported but can readily be calculated from thermodynamic data in the literature. For methylal ΔG_f^0(g) = −54.03 kcal mol^{-1} can be calculated from the heat of formation (23) and the standard entropy (24). The free energy of transfer to aqueous solution can be calculated from the activity coefficient at infinite dilution (25) as ΔG_t = −1.04 kcal mol^{-1}. Then ΔG_f^0(aq) = −55.07 kcal mol^{-1}. For free (unhydrated) formaldehyde, ΔG_f^0(aq) = −24.91 kcal mol^{-1} can be calculated from the heat of formation (26) (gas phase), the standard entropy (24) (gas phase), the vapor pressure over aqueous solutions (27), and the equilibrium constant for covalent hydration (Table 1). For methanol ΔG_f^0(aq) = −56.69 kcal mol^{-1} (14). From these values, ΔG^0 for acetal formation is −3.09 kcal mol^{-1} and hence $K = 183\ M^{-2}$. For ethylal ΔH_f^0(g) = −99.13 kcal mol^{-1} (24). The standard entropy (gas phase) can be estimated after Stull (24) as S^0(g) = 99.75 e.u., so that ΔG_f^0(g) = −56.10 kcal mol^{-1}. The free energy of transfer to aqueous solution can be

TABLE 5. Determination of equilibrium constants by ^{19}F n.m.r.

Concentrations (M)			Relative peak intensities					
Carbonyl compound	Alcohol	Water	Carbonyl compound	Hydrate	Hemiacetal	$K_{hydration}$ [a]	$K_{hemiacetal}$ [b]	K_4 [c]
				Trifluoroacetaldehyde				
0.67	0.67	49.4	—	28.3	1	—	—	2.60±0.14
0.67	1.70	45.6	—	9.36	1	—	—	2.86±0.09
0.67	2.76	42.1	—	4.54	1	—	—	3.35±0.18
0.67	4.95	34.7	—	2.05	1	—	—	3.41±0.18
0.67	9.37	21.5	—	0.63	1	—	—	3.62±0.11
	0							2.3 [d]
				Trifluoroacetone				
0.43	0	55.5	1	41	—	0.74	—	—
0.38	0.51	54.2	1	37	—	0.68	—	—
0.38	0.975	53.6	1	29	0.56	0.54	0.58	1.27±0.13
0.34	3.37	48.4	1	22	2.1	0.46	0.62	1.36±0.15
0.31	5.88	43.5	1	21	2.7	0.48	0.46	0.92±0.15
0.25	9.36	36.1	1	31	8.4	0.86	0.90	1.05±0.17
	0							1.4 [d]
				Trifluoroacetophenone				
0.47	10.7	27.7	—	1	1.18	—	—	3.03±0.20
0.47	16.7	13.9	—	1	3.3	—	—	2.76±0.35
	0							3.5 [d]
				Hexafluoroacetone				
0.55	0	55.5	—	1	—	—	—	—
0.55	3.14	46.6	—	108.8	1	—	—	0.136±0.036
0.55	6.33	39.9	—	58.2	1	—	—	0.108±0.017
0.55	16.98	17.7	—	14.6	1	—	—	0.071±0.003
	0							0.14 [d]

[a] Equilibrium constant for hydrate formation: dimensionless.
[b] Equilibrium constant for hemiacetal formation: dimensions are M^{-1}.
[c] Equilibrium constant for formation of hemiacetal from hydrate: dimensions are M^{-1}; error limits are standard deviations based on the observed standard deviations in peak areas measured by electronic integration.
[d] Extrapolated to pure water as solvent.

calculated from the vapor pressure of the pure liquid (28) and the solubility in water (28) as $\Delta G_t = -1.36$ kcal mol^{-1}. Thus ΔG_f^0(aq) = -57.76 kcal mol^{-1}. For ethanol, G_f^0(aq) = -43.31 kcal mol^{-1} (14). From these values, G^0 for acetal formation is -2.92 kcal mol^{-1} and hence $K = 140\ M^{-2}$.

Values of σ* were taken from the compilation in ref. 32 for all substituents except CH_3COCH_2—, for which σ* was estimated as 0.36 times σ* for CH_3CO— (32) and 4-pyridyl, for which σ* was estimated as follows. From pK_a values for the acids X—C_6H_4--CH_2COOH (33) and the defining equations given by Charton (34), σ* values for X—C_6H_4-- could be calculated. These were plotted *vs.* Hammet σ values for X, using values from the compilation in ref. 32, and gave a good line. Then from the σ suggested for the *para* heteroatom in 4-pyridyl (32), a value for σ* of 1.26 for 4-pyridyl could be estimated.

I thank the National Research Council of Canada for financial support of this work.

1. P. LE HÉNAFF. Bull. Soc. Chim. Fr. 4687 (1968).
2. P. GREENZAID, Z. LUZ, and D. SAMUEL. J. Am. Chem. Soc. **89**, 749 (1967).
3. R. STEWART and J. D. VAN DYKE. Can. J. Chem. **48**, 3961 (1970).
4. P. LE HÉNAFF. C.R. **265**C, 175 (1967).
5. D. L. HOOPER. J. Chem. Soc. B, 169 (1967).
6. H. MALTZ. Chem. Commun. 843 (1968); H. MALTZ. Ph.D. Thesis, Yale University, New Haven, Conn. 1967.
7. P. LE HÉNAFF. C.R. **262**C, 1667 (1966).
8. H. ADKINS and E. W. ADAMS. J. Am. Chem. Soc. **47**, 1368 (1925).
9. W. H. HARTUNG and H. ADKINS. J. Am. Chem. Soc. **49**, 2517 (1927).
10. N. MINNÉ and H. ADKINS. J. Am. Chem. Soc. **55**, 299 (1933).
11. R. E. DUNBAR and H. ADKINS. J. Am. Chem. Soc. **56**, 442 (1934).
12. J. M. BELL, D. G. KUBLER, P. SARTWELL, and R. G. ZEPP. J. Org. Chem. **30**, 4284 (1965).

Can. J. Chem. Downloaded from www.nrcresearchpress.com by 210.87.254.42 on 09/05/12
For personal use only.

13. E. G. SANDER and W. P. JENCKS. J. Am. Chem. Soc. **90**, 6154 (1968).
14. J. P. GUTHRIE. J. Am. Chem. Soc. **95**, 6999 (1973).
15. J. P. GUTHRIE. J. Am. Chem. Soc. **96**, 3608 (1974).
16. M. M. KREEVOY and R. W. TAFT, JR. J. Am. Chem. Soc. **77**, 5590 (1955).
17. J. HINE and R. D. WEIMAR, JR. J. Am. Chem. Soc. **87**, 3387 (1965). S. W. BENSON, J. Am. Chem. Soc. **80**, 5151 (1958).
18. K. PIHLAJA and J. KANKARE. Acta Chem. Scand. **23**, 1745 (1969). K. PIHLAJA. Acta. Chem. Scand. **25**, 451 (1971).
19. (*a*) J. A. HIRSCH. Top. Stereochem. **1**, 199 (1967). (*b*) E. L. ELIEL. Stereochemistry of carbon compounds. McGraw-Hill, New York, N.Y. 1962.
20. S. W. BENSON. Thermochemical kinetics. Wiley, New York, N.Y. 1968.
21. N. C. BAIRD, M. J. S. DEWAR, and R. SUSTMAN. J. Chem. Phys. **50**, 1275 (1969). N. BODOR, M. J. S. DEWAR, A. HARGET, and E. HASELBACK. J. Am. Chem. Soc. **92**, 3854 (1970) and related papers in this series.
22. C. HANSCH, J. E. QUINLAN, and G. L. LAWRENCE. J. Org. Chem. **33**, 347 (1968). N. C. DENO and H. E. BERKHEIMER. J. Chem. Eng. Data, **5**, 1 (1960).
23. G. PILCHER and R. A. FLETCHER. Trans. Faraday Soc. **65**, 2326 (1969).
24. D. R. STULL, E. F. WESTRUM, JR., and G. C. SINKE. The chemical thermodynamics of organic compounds. Wiley, New York, N.Y. 1967.
25. D. L. SHAFFER and T. E. DANBERT. Anal. Chem. **41**, 1585 (1969).
26. R. A. FLETCHER and G. PILCHER. Trans. Faraday Soc. **66**, 794 (1970).
27. E. W. BLAIR and W. LEDBURY. J. Chem. Soc. 26 (1925); 2834 (1925).
28. Handbook of Chemistry and Physics. 37th ed. Chemical Rubber Publishing Co., Cleveland, Ohio. 1956.
29. J. L. KURZ. J. Am. Chem. Soc. **89**, 3524 (1967).
30. J. HINE and R. W. REDDING. J. Org. Chem. **35**, 2769 (1970).
31. Y. KODAMA, K. SATO, and K. ARAKAWA. Nippon Kagaku Zasshi, **87**, 1092 (1966); Chem. Abstr. **66**, 89031 (1967).
32. G. B. BARLIN and D. D. PERRIN. Quart. Rev. Chem. Soc. **20**, 75 (1966).
33. J. F. J. DIPPY and F. R. WILLIAMS. J. Chem. Soc. 161 (1934); 1888 (1934).
34. M. CHARTON. J. Org. Chem. **29**, 1222 (1964).

Can. J. Chem. Downloaded from www.nrcresearchpress.com by 210.87.254.42 on 09/05/12
For personal use only.

The Thermal Decomposition of Alkoxycarbonyl Thiocyanates and Isothiocyanates[1,2]

DENNIS LIOTTA AND ROBERT ENGEL

Department of Chemistry, Queens College of the City, University of New York, Flushing, New York 11367

Received July 30, 1974

DENNIS LIOTTA and ROBERT ENGEL. Can. J. Chem. **53**, 907 (1975).

Alkoxycarbonyl thiocyanates and isothiocyanates have been decomposed thermally under reduced pressure at temperatures of 240–375°. Primary systems yield primarily alkyl thiocyanates, whereas secondary and tertiary systems yield alkyl isothiocyanates. The viability of using this reaction in a conversion of primary alcohols to primary alkyl thiols and secondary and tertiary alcohols to tertiary alkyl amines is discussed.

DENNIS LIOTTA et ROBERT ENGEL. Can. J. Chem. **53**, 907 (1975).

Des thiocyanates et des isothiocyanates d'alkoxycarbonyle ont été décomposés thermiquement, sous pression réduite, à des températures allant de 240–375°. Les dérivés primaires conduisent principalement aux thiocyanates d'alkyle alors que les dérivés secondaires et tertiaires conduisent aux isothiocyanates d'alkyle. On discute de l'utilité de cette réaction pour transformer les alcools primaires en thiols primaires et les alcools secondaires et tertiaires en amines tertiaires.

[Traduit par le journal]

We have previously reported from this laboratory (1) the thermal decomposition of dialkyl phosphoroisothiocyanatidates **1** to yield the corresponding alkyl thiocyanates **2**. A logical

$$(RO)_2\overset{\overset{O}{\|}}{P}\text{—NCS} \xrightarrow{\Delta} \text{RSCN}$$

1 **2**

extension of this phosphorus containing system, which is of particular synthetic value for organic chemistry, is the thermal decomposition of the more readily available alkoxycarbonyl thiocyanates, **3**. We have now investigated the thermal decomposition of **3** and of alkoxycarbonyl isothiocyanates, **4**, over glass wool at

$$\text{ROC}\overset{\overset{O}{\|}}{\text{S}}\text{CN} \qquad \text{ROC}\overset{\overset{O}{\|}}{\text{N}}\text{CS}$$

3 **4**

temperatures of 240–375° under pressures of *ca.* 5 Torr.

Materials **3** and **4** can be considered to be compounds of the general type ROC(O)X. Others of this type have been decomposed thermally both in the liquid and vapor phases yielding RX and carbon dioxide. Investigations in which X = Cl (2, 3), SR(4), OAc(5), OC(O)R(6), and $NHS(O)_2Cl$(7) have been reported.

Although the pyrolysis conditions varied substantially in the several reports, all the previous studies resulted in proposals that the decompositions occur via ion pair intermediates. The various side reactions (predominantly elimination and Wagner–Meerwein rearrangements) which were observed in these studies were rationalized in terms of the degree of dissociation of the ion pair, as well as the basicity of X. For example, when alkyl chloroformates (X = Cl) were decomposed in the vapor phase at reduced pressure, the reaction proceeded with complete retention of configuration (3). Furthermore, no alkyl shifts were observed and the amount of olefin which was produced was small. These data have been interpreted in terms of an intimate ion pair intermediate. However, when the decomposition was accompanied via gas chromatography, substantial amounts of elimination and rearrangement products were obtained (8), presumably because of a greater degree of dissociation in the transition state.

When X = —S—C≡N (or —N=C=S), the decarboxylation reaction can, in principle, yield both an alkyl thiocyanate, R—SCN (**2**), and an alkyl isothiocyanate, R—NCS (**5**). If the decarboxylation reaction exhibits some selectivity for

[1]Taken in part from the Ph.D. Dissertation of D. Liotta, The City University of New York, 1974.

[2]Presented in part at the American Chemical Society 5th Northeast Regional Meeting, October 16, 1973, paper No. 154.

Can. J. Chem. Downloaded from www.nrcresearchpress.com by 210.87.254.6 on 09/05/12
For personal use only.

Can. J. Chem. Downloaded from www.nrcresearchpress.com by 210.87.254.6 on 09/05/12
For personal use only.

one of the isomers, this may then provide a convenient route for the conversion of an alcohol into either a thiol or an amine as these latter are readily obtainable from the alkyl thiocyanate and alkyl isothiocyanate, respectively; such overall conversions are not generally convenient by other routes for several types of reaction systems because of rearrangement and elimination processes competing effectively (7, 9).

Results and Discussion

All the reported syntheses of alkoxycarbonyl thiocyanates and isothiocynates involve reaction of a thiocyanate salt (*e.g.* Pb^{2+}, NH_4^+, K^+) with an alkyl chloroformate. The latter are obtainable (usually in high yield) by treatment of an alcohol with phosgene (10). We prefer a modified version of the method reported by Takamizawa *et al.* (11) which involves the slow addition of an alkyl chloroformate to a heterogeneous mixture of anhydrous potassium thiocyanate in dry tetrahydrofuran under a nitrogen blanket. One obtains from this reaction a mixture of the alkoxycarbonyl thiocyanate and isothiocyanate in 45–80% yield. If one uses equimolar amounts of potassium thiocyanate and alkyl chloroformate, one obtains approximately equal amounts of both isomers; if a large excess of potassium thiocyanate is used, the alkoxycarbonyl isothiocyanate is obtained almost exclusively. Moreover, this work has shown that potassium thiocyanate catalyzes the isomerization of alkoxycarbonyl thiocyanates, **3**, to the alkoxycarbonyl isothiocyanates, **4**. Both isomers undergo thermal decarboxylation to yield a mixture of alkyl thiocyanate and alkyl isothiocyanate.

The effect of pressure on the decompositions of both **3** and **4** is found to be quite significant. For example, if these decompositions are studied via gas chromatography using a 20 ft × 3/8 in. SE-30 column at 350° only very small amounts (0.5–3.0%) of the expected alkyl thiocyanate and isothiocyanate are obtained. The major product is polymer although small amounts of the dialkyl carbonates are also isolated. Since these dialkyl carbonates must be the product of at least a bimolecular process, observation of these products in "low pressure" pyrolyses over glass wool constitutes an indication that either the pressure is too high or the rate of addition to the hot surface is too rapid.

When the decompositions are performed at reduced pressures significantly high yields of alkyl thiocyanates and isothiocyanates are obtained. An optimum yield of product may be obtained under conditions described below.

The method found to effect these decompositions most efficiently is to allow the vaporized compound, **3** or **4**, to pass through a 100 cm column packed with glass wool at a pressure of 5 Torr. The pressure drop across the glass wool causes the material to flow through the column with a contact time of 3–4 min; the pyrolysate is collected in a cold trap at −78°.

The results of the pyrolyses of five alkoxycarbonyl isothiocyanates and four alkoxycarbonyl thiocyanates are given in Table 1. The temperature at which the pyrolysis is listed as being performed is that temperature at which the maximum yield of either alkyl thiocyanate or alkyl isothiocyanate was obtained. For example, when **3***b* was pyrolyzed under reaction conditions identical to those in Table 1 at 325°, a 50% yield of **2***b* was obtained. The remainder was unreacted **3***b* and trace amounts of **5***b*. When **3***b* was pyrolyzed at 375°, **2***b* was produced in 25% yield and **5***b* in 50% yield. This change in product ratio is interesting and is discussed below. When **3***b* was pyrolyzed at 350° a 90% yield of **2***b* was obtained.

From the pyrolysis temperatures given in Table 1 it is apparent that as more alkyl substituents are added to the carbinolic carbon a decrease in the temperature at which alkyl thiocyanates or alkyl isothiocyanates are produced most effectively occurs. Furthermore, the fact that in all cases isomers **3** and **4** decompose to give essentially the same product ratios (at the same temperature) suggests a common intermediate. This also is consistent with other ROC(O)X systems.

From the results in Table 1 it is also seen that **3***a*, **3***b*, **4***a*, and **4***b* yield predominantly *S*-substituted products, **3***c*, **3***e*, and **4***c* predominantly *N*-substituted products, and **3***d* and **4***d* a mixture of *N*- and *S*-substituted products.

Several sets of experiments have been performed which allow an explanation of this phenomenon in terms of an initial formation of *S*-substituted product followed, in some cases, by isomerization. The first set of experiments involved the pyrolyses of the compounds **3** and **4** at a temperature *below* those giving optimum product yield. For example, when **3***c* was pyrolyzed at 230° under typical experimental conditions a 5% conversion to **2***c* could be

TABLE 1. Pyrolysis results

Reactant	Temperature at 5 Torr (°C)	Thiocyanate* (%)	Isothiocyanate* (%)
3*a* $CH_3OC(O)NCS$	360	**2***a* CH_3SCN (81)	**5***a* CH_3NCS (4)
4*a* $CH_3OC(O)SCN$	360	**2***a* CH_3SCN (78)	**5***a* CH_3NCS (3)
3*b* $C_2H_5OC(O)NCS$	350	**2***b* C_2H_5SCN (90)	**5***b* C_2H_5NCS (5)
4*b* $C_2H_5OC(O)SCN$	350	**2***b* C_2H_5SCN (90)	**5***b* C_2H_5NCS (2)
3*c* $(CH_3)_2CHOC(O)NCS$	300	**2***c* $(CH_3)_2CHSCN$ (6)	**5***c* $(CH_3)_2CHNCS$ (84)
4*c* $(CH_3)_2CHOC(O)SCN$	300	**2***c* $(CH_3)_2CHSCN$ (3)	**5***c* $(CH_3)_2CHNCS$ (84)
3*d* $(CH_3)_2CHCH_2OC(O)NCS$	335	**2***d* $(CH_3)_2CHCH_2SCN$ (32)	**5***d* $(CH_3)_2CHCH_2NCS$ (60)
4*d* $(CH_3)_2CHCH_2OC(O)SCN$	335	**2***d* $(CH_3)_2CHCH_2SCN$ (30)	**5***d* $(CH_3)_2CHCH_2NCS$ (63)
3*e* 1-AdOC(O)NCS†	275	**2***e* AdSCN‡(0)	**5***e* AdNCS (88)

*These isolated yields are given as percentage of the theoretical yield. No rearrangement of the alkyl groups was observed.
†Ad = adamantyl.
‡No adamantyl thiocyanate was isolated.

detected in the n.m.r. spectrum of the pyrolysate; no **5***c* was observed. At 270° the pyrolysate was composed of **2***c*, 16%; **5***c*, 30%; and **3***c*, 54%. Thus it appears that **2***c* is formed initially but isomerizes readily to **5***c*.

Secondly, the product compounds themselves, *i.e.* **2**, were subjected to the same pyrolysis conditions as their precursors, **3** and **4**, with the exception of **2***e*, for which the compound is not available. In all cases, conversion to **5** occurred readily, along with some decomposition. For example, when **2***b* was subjected to the optimum pyrolysis conditions, as shown in Table 1 for **3***b* and **4***b*, a 19% conversion to **5***b* was found with the remainder being accounted for by decomposition to olefin (not isolated) and HSCN (isolated as the trimer); this rearrangement and attendant decomposition has been reported by Fava *et al.* (12). At lower temperatures (300°) a 57% conversion to **5***b* was observed with the remainder accounted for as decomposition. A mole balance of >97% was obtained for these investigations. With the secondary system, **2***c*, an even more complete conversion to **5***c* was observed.

These data serve as evidence for a mechanism partially proposed above, in which **3** and **4** decompose initially to yield **2** and carbon dioxide. This decomposition presumably occurs via a common intermediate. Negative evidence is available which argues against a preequilibrium of **3** and **4**; using pyrolysis temperatures below those listed in Table 1, where only partial conversion to products occurred and starting material could be reisolated, no conversion of **3** to **4** or **4** to **3** could ever be observed. Moreover, the formation of **5** is a secondary process, arising from rearrangement of **2**. The *amount* of **5** formed would appear to be a function of *rate* rather than *equilibrium position* as indicated by the above data.

While primary alkyl thiocyanates may be prepared more conveniently by other routes, this method does appear to be potentially important for the syntheses of secondary and tertiary alkyl isothiocyanates, not only because of the high overall yield, but also because of the lack of rearrangement and elimination products (7, 9, 13).

Furthermore, since alkyl isothiocyanates can be hydrolyzed to the corresponding amine (14) or reduced (catalytically or with lithium aluminum hydride) to the corresponding methyl amines in high yield (15), this process provides a general method for the conversion of a secondary or tertiary alcohol to the corresponding amine (or methyl amine) in 25–55% overall yield, based on normal yields in these reactions.

Experimental

Elemental analyses were performed by Schwarzkopf Microanalytical Laboratory, Woodside, New York. Nuclear magnetic resonance spectra were measured on a Varian A-60A spectrometer in CCl_4 solution using tetramethylsilane as an internal reference. Mass spectra were measured on a Varian MAT CH-7 spectrometer at 70 eV. Infrared spectra were measured on a Perkin-Elmer 237-B spectrophotometer. Phosgene (12.5% in benzene) was purchased from Matheson, Coleman, and Bell, Inc., and used without further purification. Tetrahydrofuran was dried over sodium ribbon and distilled before use. The potassium thiocyanate was dried either by fusing it and allowing it to cool in a desiccator or by allowing it to stir for 4 h over 2,2-dimethoxypropane followed by filtration and thorough washing with dry tetrahydrofuran.

General Synthesis of Alkyl Chloroformates

A typical procedure for the preparation of alkyl chloroformates is given for ethyl chloroformate. Ethanol,

Can. J. Chem. Downloaded from www.nrcresearchpress.com by 210.87.254.6 on 09/05/12
For personal use only.

Can. J. Chem. Downloaded from www.nrcresearchpress.com by 210.87.254.6 on 09/05/12
For personal use only.

TABLE 2. Yields, analyses, and properties of alkoxycarbonyl thiocyanates and isothiocyanates

Compound*	% Yield†	% Calculated C	% Calculated H	% Found C	% Found H	Melting or boiling point (°C) (Torr)	Infrared μ	Nuclear magnetic resonance δ	Mass spectra
3*a*	20	30.77	2.56	30.80	2.66	29–33 (3.0)	5.08, 5.70	3.73(s)	117
4*a*	25	30.77	2.56	30.83	2.74	42–45 (3.5)	4.59,‡ 5.60	4.18(s)	117
3*b*	26					26–27 (1.7)	5.10, 5.72	4.15(q, 2), 1.23(t, 3)	131
4*b*	35					40–42 (2.0)	4.62,‡ 5.60	3.70(q, 2), 1.21(t, 3)	131
3*c*	28	41.38	4.83	41.63	5.11	40–42 (0.8)	5.50, 5.72	4.94(m, 1), 1.37(d, 6)	145
4*c*	38	41.38	4.83	41.54	5.02	53–54 (0.6)	4.60,‡ 5.61	5.20(m, 1), 1.38(d, 6)	145
3*d*	26	45.28	5.66	46.38	6.31	35–38 (0.3)	5.07, 5.72	4.50(d, 2), 2.30(m, 1), 1.20(d,6)	115§
4*d*	46	45.28	5.66	46.51	6.38	49–54 (0.3)	4.60,‡ 5.61	4.27(d, 2), 2.27(m, 1)1.20(d, 6)	115§
3*e*	80	60.72	6.33	60.78	5.96	121–122	5.05, 5.75	1.57(s, 9), 2.11(s, 6)	237

*Compounds 3*d* and 4*d* gave analyses which were approximately 1.1 and 0.6% from the calculated % C and H, respectively. Although these compounds distill as clear, colorless liquids, they begin to yellow within 15 min after distillation, even in a nitrogen atmosphere in the dark. While the n.m.r. spectra of these compounds, taken immediately after distillation, indicate no detectable impurities, spectra of material which has been allowed to stand for 30 min shows a small but definite broadening in the peak widths. These results indicate that a small amount of decomposition occurs even under relatively innocuous conditions, and thus tends to make good analytical data unobtainable unless combustion analyses are performed immediately after distillation.

†Since isomers 3 and 4 yield the same products upon pyrolysis, mixtures of the two can be used for synthetic purposes. This is most convenient as separation of 3 and 4 is no longer necessary. Thus, the % yield of usable material is actually the sum of the yields of 3 and 4.

‡These absorptions are weak. All other i.r. spectra listed are strong.

§115 represents ($M^+ - 44$). No M^+ is observed. Apparently the molecular ion undergoes facile decarboxylation.

TABLE 3. Properties of alkyl thiocyanates and isothiocyanates

Compound	Boiling (melting) point (°C)	Infrared* (μ) (—SCN or —NCS)	Nuclear magnetic resonance (δ)
2*a*	133–134	4.61(sh)	2.61(s)
5*a*	117–119 (35)	4.73(b)	3.57(s)
2*b*	146–148	4.62(sh)	2.98(q, 2), 1.50(t, 3)
5*b*	131–132	4.79(b)	3.64(q, 2), 1.15(t, 3)
2*c*	152–154	4.65(sh)	3.48(m, l), 1.49(d, 2)
5*c*	137–138	4.82(b)	3.95(m, l), 1.31(d, 2)
2*d*	175–176	4.62(sh)	2.92(d, 2), 1.95(m, l), 0.97(d, 2)
5*d*	161–163	4.78(b)	3.33(d, 2), 1.71(m, l), 1.08(d, 2)
5*e*	(167–168)	4.70, 4.78, 4.86(b)	2.10(s, 9), 1.68(s, 6)

*sh = sharp; b = broad.

5.75 g (0.135 mol), was added dropwise to a stirred solution of phosgene in benzene (0.25 mol), cooled in an ice bath. The solution was stirred for 3 h after which the benzene and excess phosgene were removed by distillation at reduced pressure. From this was obtained 14.0 g of crude ethyl chloroformate (91%). All chloroformates were used without further purification. Adamantyl chloroformate was prepared by the method of Haas *et al.* (16).

General Synthesis of Alkoxycarbonyl Thiocyanates and Isothiocyanates

A typical procedure for the synthesis of alkoxycarbonyl thiocyanates and isothiocyanates is given below. Ethyl chloroformate, 14.0 g (0.122 mol), in 50 ml of dry tetrahydrofuran was added slowly to a suspension of 11.8 g of anhydrous potassium thiocyanate in 500 ml of dry tetrahydrofuran under a nitrogen atmosphere with vigorous stirring. The solution was allowed to stir for 6 h. The undissolved salt was removed by suction filtration and the solvent removed by distillation at reduced pressure. The resulting red oil was distilled at reduced pressure via a Vigreux column. From this was obtained 4.16 g (20%) of ethoxycarbonyl isothiocyanate, **3***b*, and 5.6 g (35%) of ethoxycarbonyl thiocyanate, **4***b*. Both of these compounds are clear, colorless liquids which yellow upon standing.

When 14 g of ethyl chloroformate (0.122 mol) was allowed to react with 36 g of anhydrous potassium thiocyanate in a procedure identical to that given above (*vide supra*), 10.40 g (65%) of ethoxycarbonyl isothiocyanate, **3***b*, was obtained.

Crude adamantyloxycarbonyl isothiocyanate, **3***e*, prepared in a similar fashion, was purified by dissolving it in a minimum amount of dichloromethane and reprecipitating it with a large volume of pentane.

Yields and pertinent physical and spectral data for all the alkoxycarbonyl thiocyanates and isothiocyanates studied are given in Table 2.

Pyrolysis Procedure

A Pyrex tube 100 cm × 2 cm was packed in the heated 85 cm portion with 65 g of Pyrex glass wool and placed in the tube oven. The pyrolysis temperature is measured by means of a thermocouple at the center of the oven. Although the pressure was maintained at 5 Torr in all cases, measured at the outlet of the collection trap, no significant differences were noted with small variations in the pressure (±2 Torr). The material to be pyrolyzed was dripped into the heated tube (250°, independently heated by a winding of Nichrome wire) at the entrance to the oven. In general, it was found that approximately 10 g of material could be pyrolyzed in a period of 1 h. Faster rates of addition usually resulted in the formation of small amounts (*ca.* 5%) of products resulting from bimolecular reactions. The contact time was estimated at 4–5 min by visual observation of condensate in the product trap after beginning of reactant addition.

Pyrolysis Results

The product mixtures were analyzed by gas–liquid chromatography (g.l.c.) using a 5 ft × 1/4 in. column of Apiezon L on Chromsorb W at temperatures of 100–150° (flow rate of He = 200 ml/min) or more conveniently with n.m.r. by measurement of the relative signal intensities of the protons adjacent to the —SCN or —NCS groups (17). The products were purified by distillation, with the exception of **5***e* which was recrystallized from a 1:1 mixture of benzene – petroleum ether. The identities of the materials were determined by comparison of their physical and spectral properties with those of authentic materials which were synthesized independently (18).

Independent Synthesis of Alkyl Thiocyanates and Isothiocyanates

Alkyl thiocyanates and isothiocyanates were prepared from the corresponding alcohols via their tosylates. The tosylates were prepared by the general method given by Fieser and Fieser (19). The tosylate was dissolved in acetone and added dropwise to a solution of excess potassium thiocyanate dissolved in acetone. The reaction was allowed to stir for 2–6 h after which it was filtered. The acetone was removed by distillation at reduced pressure and the remaining liquid (which sometimes needed further filtration) was distilled at atmospheric pressure at the appropriate temperatures given in Table 3. While the relative amounts of alkyl thiocyanate and isothiocyanate which were produced varied, significant quantities of both isomers could always be obtained.

The only compound not independently synthesized was **5***e* which is commercially available from the Aldrich Chemical Company, Inc.

Can. J. Chem. Downloaded from www.nrcresearchpress.com by 210.87.254.6 on 09/05/12
For personal use only.

1. R. ENGEL. Can. J. Chem. **47**, 1258 (1969).
2. K. L. OLIVER and W. G. YOUNG. J. Am. Chem. Soc. **81**, 5811 (1959).
3. E. S. LEWIS and W. C. HERNDON. J. Am. Chem. Soc. **83**, 1955 (1961); **83**, 1959 (1961); **83**, 1961 (1961).
4. J. L. KICE, R. A. BARTSCH, M. A. DANKLEFF, and S. L. SCHWARTZ. J. Am. Chem. Soc. **87**, 1734 (1965); J. L. KICE, R. L. SCRIVEN, E. KOUBEK, and M. BARNES. J. Am. Chem. Soc. **92**, 5608 (1970).
5. R. C. L. CHOW and D. S. TARBELL. J. Org. Chem. **32**, 2188 (1967).
6. L. M. MCDONOUGH. Chem. Ind. (London), 1501 (1965).
7. J. B. HENDRICKSON and I. JOFFEE. J. Am. Chem. Soc. **95**, 4083 (1973).
8. P. W. CLINCH and H. R. HUDSON. Chem. Commun. 925 (1968).
9. L. I. KRIMEN and D. J. COTA. *In* Organic reactions. Vol. 17. *Edited by* R. Adams. John Wiley & Sons, Inc., New York. 1969. p. 213ff.
10. S. PETERSEN. *In* Methoden der organishen chemie. Vol. 8. *Edited by* E. Miller. Georg Themie Verlag, Stuttgart, 1952. pp. 101–105.
11. A. TAKAMIZAWA, K. HIRAI, and K. MATSUI. Bull. Chem. Soc. Jap. **36**, 1214 (1963).
12. N. BARROCTA, A. MACCOLL, M. CAVAZZA, L. CONGRU, and A. FAVA. J. Chem. Soc. (B) 1264 (1971); 1267 (1971).
13. J. J. RITTER and J. KALISH. J. Am. Chem. Soc. **70**, 4048 (1948).
14. SCHMIDT *et al.* Ann. **568**, 192 (1950).
15. R. SCHROTER. *In* Methoden der organishen chemie. Vol. 11. *Edited by* E. Miller. Georg Themie Verlag, Stuttgart, 1957. pp. 600–601.
16. W. L. HAAS, E. V. KRUMKALUS, and K. GERZON. J. Am. Chem. Soc. **88**, 1988 (1966).
17. A. MATHIAS. Tetrahedron, **21**, 1073 (1965).
18. E. E. REED. Organic chemistry of bivalent sulfur. Vol. 6. Chemical Publishing Co., Inc., New York. 1966. pp. 11–226.
19. L. FIESER and M. FIESER. Reagents for organic synthesis. Vol. 1, John Wiley & Sons, Inc., New York. 1967. pp. 1180–1181.

Can. J. Chem. Downloaded from www.nrcresearchpress.com by 210.87.254.6 on 09/05/12
For personal use only.

Uses of Sydnones for Heterocyclic Syntheses

B. V. BADAMI AND G. S. PURANIK

Department of Chemistry, Karnatak University, Dharwar-580003, India

Received August 19, 1974

B. V. BADAMI and G. S. PURANIK. Can. J. Chem. **53**, 913 (1975).

N-(4-Bromo-3-chlorophenyl)sydnone is prepared and subjected to chlorination and bromination. 1,3-Dipolar addition of these sydnones with dimethyl acetylenedicarboxylate produces the substituted pyrazoles which could serve as intermediates.

B. V. BADAMI et G. S. PURANIK. Can. J. Chem. **53**, 913 (1975).

On prépare la *N*-(bromo-4 chloro-3 phényl) sydnone et on la soumet à des réactions de chloruration et de bromuration. Les réactions d'addition dipolaire-1,3 de ces sydnones avec l'acétylènedicarboxylate de méthyle conduisent à des pyrazoles substituées qui peuvent servir d'intermédiaire. [Traduit par le journal]

Can. J. Chem. Downloaded from www.nrcresearchpress.com by 210.87.254.42 on 09/05/12
For personal use only.

Sydnones unsubstituted at the 4-position undergo electrophilic substitution reactions (1). However, in view of the difficulties experienced in the synthesis of 4-halosydnones (2) an attempt was made to introduce a halogen atom at the *N*-arylglycine ethyl ester stage in the synthesis of sydnones and it resulted in the halogen entering the phenyl group rather than the side chain; this was proved by the elemental analysis and spectral data (Fig. 1) of the compound. *N*-(*m*-Chlorophenyl)glycine ethyl ester was taken as the starting material in the first instance, since there is a report that the chloro substituent in any position of the sydnone molecule enhances its biological activity (3). 3-Phenylsydnones undergo 1,3-dipolar addition with dimethyl acetylenedicarboxylate to produce the 3,4-disubstituted pyrazoles. 5-Halopyrazoles could easily be prepared by reaction of 4-halosydnones with dimethyl acetylenedicarboxylate. It is known that 1-phenylpyrazoles do not undergo halogenation in the 5-position easily (4, 5). The electrophilic attack may be initiated at the 4-position of the pyrazole ring or at the *para* position of the phenyl ring. This has been clearly interpreted by Lynch and co-workers (6) (Fig. 2).

The required *N*-(*m*-chlorophenyl)glycine ethyl ester was prepared from *m*-chloroaniline and

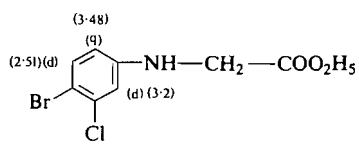

FIG. 1. Coupling constants for *N*-(4-bromo-3-chlorophenyl)glycine ethyl ester.

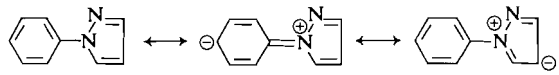

FIG. 2. Electrophilic attack on 1-phenylpyrazoles.

ethyl chloroacetate. The glycine ethyl ester was brominated in chloroform to yield *N*-(4-bromo-3-chlorophenyl)glycine ethyl ester. This was further hydrolyzed with 10% alkali and the resulting glycine subjected to nitrosation in alcoholic medium. The nitrosoglycine was heated with acetic anhydride to yield the sydnone. The sydnone was brominated in acetic acid medium to yield the 4-bromosydnone. Chlorination was effected with *N*-chlorosuccinimide to give 4-chlorosydnone. The sydnone and the 4-substituted sydnones were treated with dimethyl acetylenedicarboxylate in xylene to produce pyrazoles.

The i.r. spectrum of the sydnone carbonyl group is at 1750–1780 cm^{-1} (7). A band at *ca.* 3100 cm^{-1} is due to the sydnone C—H (7), whereas this is absent in the 4-halosydnones (8). The spectrum of pyrazoles shows absorptions at 1750 and 1740 cm^{-1} (CO_2CH_3).

Experimental

N-(m-Chlorophenyl)glycine Ethyl Ester

A mixture of ethyl chloroacetate (62.0 g), *m*-chloroaniline (64.0 g), ethanol (50 ml), and sodium acetate (60.0 g) was refluxed at 125° for 5 h in an oil bath. Water (200 ml) was then added and the precipitated ester collected and washed; recrystallized from ethanol, m.p. 105°; yield, 80.0 g.

Anal. Calcd. for $C_{10}H_{12}NO_2Cl$: C, 56.20; H, 5.62. Found: C, 55.80; H, 5.32.

Can. J. Chem. Downloaded from www.nrcresearchpress.com by 210.87.254.42 on 09/05/12
For personal use only.

N-(4-Bromo-3-chlorophenyl)glycine Ethyl Ester

N-(*m*-Chlorophenyl)glycine ethyl ester (40.0 g) was suspended in a mixture of chloroform (400 ml) and ether (200 ml), containing sodium bicarbonate (40.0 g). Bromine (5.4 ml) was added dropwise and the solution was stirred for 2 h at room temperature. The solution was filtered and the filtrate evaporated under reduced pressure. The resulting solid crystallized from petroleum ether, m.p. 85°; yield, 48.0 g.

Anal. Calcd. for $C_{10}H_{11}BrClNO_2$: C, 41.10; H, 3.76. Found: C, 40.8; H, 3.40.

Infrared (KBr) 1750 cm^{-1} (C=O); 3340 cm^{-1} (NH); n.m.r. ($CDCl_3$): 8.68 (3H, t, J_{CH_2,CH_3} = 7.5 Hz, CH_3 of $COOCH_2CH_3$), 6.08 (2H, d, $J_{CH_2,NH}$ = 6.0 Hz, CH_2 flanked between NH and ($COOCH_2CH_3$), 5.67 (2H, q, $J_{CH_2CH_3}$ = 7.5 Hz, CH_2 of ($COOCH_2CH_3$), 3.48 (1H, q, J_{ortho} = 8.0 Hz and J_{meta} = 2.5 Hz), 3.2 (1H, d, J_{meta} = 2.5 Hz), 2.51 (1H, d, J_{ortho} = 8.0 Hz).

N-(4-Bromo-3-chlorophenyl)glycine

N-(4-Bromo-3-chlorophenyl)glycine ethyl ester (40.0 g) was hydrolyzed with sodium hydroxide solution (10%, 95 ml) and ethanol (10 ml). The solution was refluxed for 1 h, then cooled and acidified. The glycine was filtered and crystallized from ethanol, m.p. 150°; yield, 30.0 g.

Anal. Calcd. for $C_8H_7BrClNO_2$: C, 36.29; H, 2.64. Found: C, 35.90; H, 3.14.

N-(4-Bromo-3-chlorophenyl)-N-nitrosoglycine

N-(4-Bromo-3-chlorophenyl)glycine (25.0 g) was suspended in a mixture of alcohol (100 ml) and water (250 ml). Sodium nitrite (8.0 g) in water (25 ml) was added at 0–5° with stirring. After 2 h of stirring the solution was acidified and the *N*-nitroso acid collected and crystallized from benzene, m.p. 125°; yield, 20.0 g.

Anal. Calcd. for $C_8H_6BrClN_2O_3$: C, 32.71; H, 2.04. Found: C, 32.34; H, 2.12.

N-(4-Bromo-3-chlorophenyl)sydnone

The above *N*-nitroso acid (20.0 g) was heated with acetic anhydride (100 ml) on a water bath for 2 h. Then it was poured into water and the solid filtered and crystallized from benzene – petroleum ether, m.p. 138°; yield, 12.5 g.

Anal. Calcd. for $C_8H_4BrClN_2O_2$: C, 34.85; H, 1.45. Found: C, 34.40; H, 1.3.

4-Bromo-N-(4-bromo-3-chlorophenyl)sydnone

N-(4-Bromo-3-chlorophenyl)sydnone (5.0 g) was dissolved in acetic acid (50 ml) containing sodium acetate (15.0 g) and cooled in ice. Bromine (1.1 ml) in acetic acid (5 ml) was added dropwise and the solution stirred for 2 h. Then it was diluted with water and the precipitated bromosydnone was crystallized from ethanol, m.p. 146°; yield, 4.0 g.

Anal. Calcd. for $C_8H_3Br_2ClN_2O_2$: C, 27.08; H, 0.84. Found: C, 26.69; H, 0.65.

4-Chloro-N-(4-bromo-3-chlorophenyl)sydnone

A solution of *N*-(4-bromo-3-chlorophenyl)sydnone (2.5 g) and *N*-chlorosuccinimide (1.6 g) in wet methanol (100 ml) was stirred for 5 min at room temperature. Evaporation of methanol furnished a slurry which was poured into water and extracted with chloroform. Evaporation of the chloroform extracts gave a residue which was crystallized from ethanol, m.p. 132°; yield, 1.8 g.

Anal. Calcd. for $C_8H_3BrCl_2N_2O_2$: C, 30.96; H, 0.96. Found: C, 31.20; H, 0.74.

Dimethyl 1-(4-Bromo-3-chloro)phenylpyrazole-3,4-dicarboxylate

N-(4-Bromo-3-chlorophenyl)sydnone (1.0 g) was dissolved in xylene (50.0 ml) and dimethyl acetylenedicarboxylate (1.0 ml) was added. The solution was refluxed until the evolution of carbon dioxide ceased. The solvent was removed under reduced pressure and the residue crystallized from petroleum ether, m.p. 142°; yield 1.2 g.

Anal. Calcd. for $C_{13}H_{10}BrClN_2O_4$: C, 41.77; H, 2.67. Found: C, 41.90; H, 3.40.

Dimethyl 1-(4-Bromo-3-chloro)phenyl-5-bromopyrazole-3,4-dicarboxylate

4-Bromo-*N*-(4-bromo-3-chlorophenyl)sydnone (1.0 g) was dissolved in dry xylene (50.0 ml) and dimethyl acetylenedicarboxylate (1.0 ml) added. On working up as in the earlier case, the compound obtained was crystallized from petroleum ether, m.p. 116°; yield, 0.9 g.

Anal. Calcd. for $C_{13}H_9Br_2ClN_2O_4$: C, 34.47; H, 1.98. Found: C, 34.07; H, 1.68.

Dimethyl 1-(4-Bromo-3-chloro)phenyl-5-chloropyrazole-3,4-dicarboxylate

4-Chloro-*N*-(4-bromo-3-chlorophenyl)sydnone (1.0 g) was dissolved in dry xylene (50.0 ml) and dimethyl acetylenedicarboxylate (1.0 ml) added. On working up as in the earlier case, the compound crystallized from petroleum ether, m.p. 104°; yield, 0.8 g.

Anal. Calcd. for $C_{13}H_9BrCl_2N_2O_4$: C, 38.23; H, 2.20. Found: C, 37.68; H, 1.88.

Our thanks are due to Mr. V. A. Desai for microanalysis, Dr. R. H. Balundgi for i.r. and Dr. C. S. Angadiyavar for n.m.r., and Prof. E. S. Jayadevappa for interest and encouragement. One of us (B.V.B.) thanks the University Grants Commission for financial support.

1. J. P. SNYDER (*Editor*). Non-benzenoid aromatics. Academic Press. 1969. p. 147.
2. C. V. GRECO, M. PESCE, and J. M. FRANCO. J. Heterocycl. Chem. **3**, 391 (1966).
3. L. B. KIER and E. B. ROCHE. J. Pharm. Sci. **56**, 149 (1967).
4. E. G. BRAIN and I. L. FINAR. J. Chem. Soc. 2435 (1958).
5. A. MICHAELIS. Ann. **385**, 1 (1911).
6. M. A. KHAN, B. M. LYNCH, and YUK-YUNG HUNG. Can. J. Chem. **41**, 1540 (1963).
7. F. H. C. STEWART. Chem. Rev. **64**, 129 (1964).
8. G. S. PURANIK and H. SUSCHITZKY. J. Chem. Soc. C, 1006 (1967).

Erratum: Theoretical Studies of some Nonbenzenoid Hydrocarbons. II

ARCHANA DASGUPTA AND NADNA K. DASGUPTA
Department of Chemistry, The University of Alberta, Edmonton, Alberta T6G 2E1
Received November 12, 1974
(Ref.: Can. J. Chem. **52**, 155 (1974))

The forename of the second author should read Nanda.

Can. J. Chem. Downloaded from www.nrcresearchpress.com by 210.87.254.40 on 09/05/12
For personal use only.

Adsorption of Polar Organic Molecules at Oil/Water and Air/Water Interfaces

ROBERT AVEYARD AND JOHN CHAPMAN
Department of Chemistry, The University, Hull HU6 7RX, England
Received October 17, 1974

ROBERT AVEYARD and JOHN CHAPMAN. Can. J. Chem. **53**, 916 (1975).

A study has been made of the adsorption of several esters of dicarboxylic acids both at the alkane/water and the air/water interface. The adsorption of *n*-butanol and *n*-heptanol at the air/water surface has also been investigated. The surface pressure (π) – surface area (A) isotherms are compared for the various films, and standard free energies of adsorption have been determined.

Attempts have been made to fit the π, A isotherms using surface equations of state based on the models of both a two-dimensional gas and a two-dimensional solution. The solution model has proved reasonably successful for fairly dilute films at the air/water surface. At higher coverages, an equation derived by Smith for liquid expanded monolayers gives a moderately good description of films of heptanol on water. A simple application of the solution model to adsorbed monolayers at the liquid/liquid interface met with little success. It is found however that two-dimensional gas equations describe such systems surprisingly well for fairly low surface concentrations.

As part of the study, the activity coefficients of methyl dodecanoate, and the diethyl esters of pentan-1,5-dicarboxylic acid and decan-1,10-dicarboxylic acid, all in dilute solution in *n*-octane at 30 °C, have been determined.

ROBERT AVEYARD et JOHN CHAPMAN. Can. J. Chem. **53**, 916 (1975).

On a fait une étude de l'adsorption de plusieurs esters d'acides dicarboxyliques aux interfaces d'alkane–eau et d'air–eau. On a aussi examiné l'adsorption du *n*-butanol et du *n*-heptanol à la surface air–eau. On compare les isothermes de pression de surface (π) et aire de surface (A) de divers films et on a déterminé les énergies libres standard d'adsorption.

On a fait des essais pour faire une corrélation des isothermes π et A utilisant des équations d'état de surface basées sur des modèles soit d'un gaz bi-dimensionnel ou d'un solution bi-dimensionnelle. Le modèle de solution s'avère raisonnablement correcte pour des films assez dilués à la surface air–eau. A des taux de recouvrement plus élevés, une équation dérivée par Smith pour des couches monomoléculaires liquides étendues donne une bonne description des films heptanol sur l'eau. Une application simple du modèle en solution à des couches monomoléculaires adsorbées à l'interface liquide–liquide n'a pas obtenu beaucoup de succès. On a trouvé toutefois que les équations d'un gaz bi-dimensionnel décrivent de tels systèmes d'une façon très correcte à des concentrations superficielles de surface relativement basses.

Dans le cadre de cette étude, on a mesuré, en solution diluée dans l'octane à 30 °C, les coefficients d'activité du dodécanoate de méthyle et des esters diéthyliques des acides pentandicarboxylique-1,5 et décanedicarboxylique-1,10. [Traduit par le journal]

Introduction

A rigorous theoretical treatment of the behavior of adsorbed films of simple amphipathic molecules at liquid surfaces has not yet been achieved. Some relatively simple and useful approaches have however been made, leading to equations of state for surface films which can be readily tested. Nevertheless, possibly as a result of the lack of sufficiently extensive and precise data, only a few thorough investigations into the applicability of these equations have been reported.

We have previously described studies of adsorbed films of 1-alkanols at alkane/water interfaces (1–3). It was shown that the Volmer equation of state, based on the model of a two-dimensional gas, and an equation based on the model of an ideal two-dimensional solution both fitted the experimental surface pressure (π), surface area (A) data reasonably well. However, there is no reliable independent check on the values of the constants of these equations (which are related to the effective sizes of molecules at the surface) required to give a fit of the data. This problem arises since it is not obvious what configurations the alkyl chains of the adsorbate, and the alkane molecules assume at the interface.

In the present paper we report studies of films

Can. J. Chem. Downloaded from www.nrcresearchpress.com by 210.87.254.6 on 09/05/12
For personal use only.

Can. J. Chem. Downloaded from www.nrcresearchpress.com by 210.87.254.6 on 09/05/12
For personal use only.

of some esters of dicarboxylic acids at the air/water and alkane/water interface, and of films of two *n*-alkanols at the air/water interface. In all these cases it is probable that the alkyl chains of the adsorbate molecules assume configurations which are essentially parallel to the interface, at least at low coverages. Thus, rough estimates of the effective areas can be made and compared with the values of the constants appearing in the various equations of state. We consider equations based both on the two-dimensional gas and two-dimensional solution models, and compare the levels of agreement the models give with the data obtained for the various systems.

Where necessary, activity coefficients of the solutes in dilute solution in alkane have been determined.

Experimental

Measurement of Surface and Interfacial Tensions

The drop-volume technique was used as described elsewhere (4). A stainless steel tip of circular cross section, radius 2.708 ± 0.002 mm, was used in conjunction with an "Agla" micrometer syringe of capacity 0.5 cm^3. The apparatus was immersed in a water thermostat, maintaining the temperature constant to within ±0.01 °C. All necessary densities were determined to within $\pm 2 \times 10^{-4}$ g cm^{-3} using a 25 cm^3 density bottle. Surface tensions were reproducible to ±0.1 mN m^{-1} and interfacial tensions to ±0.05 mN m^{-1}. The drop-volume method is not absolute but any small errors which might arise because of this are not likely to significantly affect values of π or A since these are obtained from differences in tensions (see later).

Determination of Activity Coefficients

Mole fraction activity coefficients f of the diethyl esters of pentan-1,5-dicarboxylic acid and decan-1,10-dicarboxylic acid, and of methyl dodecanoate in dilute solution in *n*-octane at 30 °C were determined using a Hitachi–Perkin Elmer Model 115 vapor pressure osmometer. The procedures involved have been described previously (3). It is difficult to assign precise errors to f. These largely arise from the graphical procedures used in the evaluation and are probably less than ±0.01.

Materials

n-Octane was supplied by Newton-Maine (England) and had a purity of ⩾ 99.5%. It was percolated through chromatographic alumina before use. Water was twice distilled using an all Pyrex glass still. The interfacial tension of the octane against the water at 30 °C was 50.80 ± 0.04 mN m^{-1} in excellent agreement with a previously recorded value (2) of 50.83 mN m^{-1}, indicating the probable absence of surface active impurities in either the water or the octane.

The following solutes were *puriss* samples obtained from Fluka: 1-heptanol (99.5%), methyl dodecanoate (99.4%), diethyl esters of methandicarboxylic acid (99.7%), pentan-1,5-dicarboxylic acid (99.4%), and dodecan-1,10-dicarboxylic acid (99.8%). The purities given in parentheses are estimates made by the use of g.l.c. in this laboratory. The 1-butanol sample (99.6%) was Hopkin and Williams (England) "Analar" grade, and the diethyl ester of butan-1,4-dicarboxylic acid used (99.7%) was a *puriss* sample from Koch-Light (England). All the esters were passed over alumina before being analyzed for purity and used.

Results

Activity Coefficients

The mole fraction activity coefficients, f, of methyl dodecanoate, and the diethyl esters of pentan-1,5- and dodecan-1,10-dicarboxylic acids (subsequently referred to as C_5 and C_{10} diesters respectively) at various mole fractions, x, in octane at 30 °C are given in Table 1. For a given value of x the monoester has a higher value of f (*i.e.* is more nearly ideal) than either of the diesters. Of the latter, the C_5 diester has the lower value of f for a given x. On the simple idea that the non-idealities arise primarily from the mixing of the polar groups with alkane, the results are, qualitatively, what would be expected.

Surface and Interfacial Tensions

The films at the alkane/water interface were formed by adsorption from the alkane phase, and in these cases x (and the mole fraction activity a) refer to concentrations in the alkane. For films

TABLE 1. Mole fraction activity coefficients, f, of solutes in solution in octane at 30 °C

$10^4 x$	f	$10^4 x$	f	$10^4 x$	f
(*a*) *Methyl dodecanoate*					
0.000	1.000	212.4	0.95_9	415.9	0.87_9
79.31	1.00_0	234.2	0.95_1	436.9	0.87_2
101.8	0.99_8	280.4	0.93_6	457.7	0.86_4
112.9	0.99_4	309.9	0.92_3	478.4	0.85_5
135.2	0.98_6	331.2	0.91_5	499.1	0.84_9
168.4	0.97_5	352.6	0.90_7	509.4	0.84_7
190.4	0.96_6	384.3	0.89_2		
(*b*) *Diethyl ester of pentan-1,5-dicarboxylic acid*					
0.000	1.000	124.1	0.95_5	245.1	0.84_3
28.46	1.00_0	146.3	0.93_2	255.9	0.83_4
45.47	0.99_8	157.4	0.92_0	277.6	0.81_7
68.05	0.99_6	179.4	0.90_0	288.4	0.80_9
90.53	0.98_6	201.4	0.88_2	309.9	0.79_3
112.9	0.96_5	223.3	0.86_2	320.6	0.78_5
(*c*) *Diethyl ester of decan-1,10-dicarboxylic acid*					
0.000	1.000	112.9	0.97_3	223.3	0.88_9
11.41	1.00_0	124.1	0.96_8	234.2	0.88_0
34.10	0.99_9	157.4	0.94_5	255.9	0.86_2
56.80	0.99_4	190.4	0.91_8	266.8	0.85_2
68.05	0.99_1	201.4	0.90_9	277.6	0.84_3
90.53	0.98_3	212.4	0.89_9		

TABLE 2. Coefficients in eq. 1 for adsorption at octane/water interface

$10^6 c_1$	$10^4 c_2$	$10^2 c_3$	$10 c_4$	Region of fit	Data points
(a) Methyl dodecanoate at 30 °C					
10.21074	−12.29171	4.47456	−4.39524	$a = 0$ to 7.1×10^{-3}	14
−12.53913	20.44650	−11.22770	20.70618	$a = 4.2$ to 30×10^{-3}	21
9.73213	−9.53085	2.21283	0.63165	$a = 2.4$ to 4.3×10^{-2}	13
(b) Diethyl ester of butan-1,4-dicarboxylic acid at 20 °C					
−1.28562	1.96280	−1.00132	1.70698	$x = 0$ to 1.8×10^{-3}	13
−3.35454	4.55127	−2.08106	3.20882	$x = 1.4$ to 5×10^{-3}	11
(c) Diethyl ester of pentan-1,5-dicarboxylic acid at 30 °C					
−1.87140	2.84115	−1.44104	2.44177	$a = 0$ to 2.2×10^{-3}	14
−3.24778	4.66644	−2.24296	3.60978	$a = 1.8$ to 15.2×10^{-3}	13
−4.42926	5.45160	−2.37959	3.62920	$a = 1.3$ to 2.5×10^{-2}	11
(d) Diethyl ester of decan-1,10-dicarboxylic acid at 30 °C					
0.74014	−0.92152	0.36181	−0.43020	$a = 0$ to 1.6×10^{-4}	7
−2.67052	4.11135	−2.11292	3.62471	$a = 1.5$ to 7.5×10^{-4}	6
−6.09513	8.92078	−4.36332	7.13311	$a = 7.4$ to 75×10^{-4}	10
−7.47751	10.87969	−5.26589	8.49388	$a = 5.7$ to 23.1×10^{-3}	14

at the air/water interface, x refers to the mole fraction of solute in the aqueous phase. In the octane + water systems all the solutes, except the diethyl ester of butan-1,4-dicarboxylic acid (C_4 diester), distribute overwhelmingly in favor of the alkane phase. For the C_4 diester, the mole fraction distribution ratio was found to be 57 ± 17 in favor of octane. Prior to adsorption experiments therefore, a large mass of the octane phase was allowed to attain distribution equilibrium with a small mass of water. Using the distribution ratio, the equilibrium concentration of C_4 diester in octane could be calculated to within 1%.

The data have been fitted with the aid of a computer, by the least squares method using a simplex procedure (5), to cubic equations of the form

$$[1] \qquad a(\text{or } x) = c_1\gamma^3 + c_2\gamma^2 + c_3\gamma + c_4$$

where γ is the surface or interfacial tension and c's are constants. For adsorption of heptanol from water and the C_4 diester from octane x was used rather than a since only very dilute solutions were employed. In the case of butanol adsorption, activity coefficients relating to 0 °C (6) were used to obtain activities. The errors incurred in using these coefficients rather than those for 20 °C are unlikely to be serious. Values of the constants in [1] for the various systems are given in Tables 2 and 3. The coefficients lead to fits of the data which are well within the reproducibility of γ (*i.e.* to within 0.05 mN m^{-1}) in all cases. The fitting was made in overlapping regions of concentration since a single fit of a whole set of data was generally slightly less satisfactory.

Various workers have studied the adsorption of alcohols at the air/water interface but usually the results have not been presented in numerical form, so that comparisons with the present data are not possible. However, Clint *et al.* (7) give the slope of the linear π–x plot for butanol adsorption at the air/water interface at 20 °C in the region $0 < \pi < 5$ mN m^{-1}. Our results are in excellent agreement (see footnote 3, Table 4). This is particularly reassuring since Clint *et al.* used the pendant-drop technique, which is absolute, to measure γ.

Calculation of Areas per Molecule at the Surface

For systems such as those studied here, where strongly surface active solutes are being adsorbed from dilute solution, it is appropriate to use the simple form of the Gibbs adsorption equation

$$[2] \qquad A = -(kT/fx)(\partial fx/\partial\gamma)$$

to obtain the area, A, per molecule at the surface (1). In eq. 2 k is the Boltzmann constant and T the absolute temperature; fx ($= a$) is the mole fraction activity of the solute in the phase from which adsorption is being studied. Substitution in eq. 2 for fx using eq. 1 yields

$$[3] \qquad A = -kT(3c_1\gamma^2 + 2c_2\gamma + c_3)/a$$

Can. J. Chem. Downloaded from www.nrcresearchpress.com by 210.87.254.6 on 09/05/12
For personal use only.

TABLE 3. Coefficients in eq. 1 for adsorption at air/water interface at 20 °C

$10^8 c_1$	$10^6 c_2$	$10^4 c_3$	$10^3 c_4$	Region of fit	Data points
(a) Butanol					
—	—	−0.80280	5.82993	$a = 0$ to 4×10^{-4}	6
−19.35945	40.08826	−28.40187	69.01458	$a = 4$ to 12×10^{-4}	11
(b) Heptanol					
−3.27779	6.66321	−4.52951	10.30715	$x = 0$ to 1.3×10^{-5}	11
0.080730	−0.078589	−0.018731	0.24770	$x = 1.2$ to 4.0×10^{-5}	13
(c) Diethyl ester of methan – dicarboxylic acid					
−10.90558	24.07734	−17.84163	44.35573	$x = 0$ to 1.8×10^{-4}	13
6.33128	−10.34398	5.04671	−6.32169	$x = 1.2$ to 3.6×10^{-4}	7
(d) Diethyl ester of butan-1,4-dicarboxylic acid					
−1.66907	3.68038	−2.71462	6.69657	$x = 0$ to 3×10^{-5}	11
−1.56742	3.45965	−2.55531	6.31424	$x = 0.5$ to 10×10^{-5}	14

Values of A (calculated by computer) were obtained only for experimentally used concentrations.

Discussion

Some General Observations

It has been noted elsewhere (2) that the π, A isotherms for films of different chain length 1-alkanols at oil/water interfaces (where the oil is a *n*-alkane) are virtually indistinguishable, suggesting that the alkanols have the same effective molecular areas at the surface. The isotherm for methyl dodecanoate is shifted to higher A values (for a given π) with respect to the alkanol curve (Fig. 1*a*), indicating a higher effective molecular area, due presumably to the larger head group. It is interesting however that for insoluble monolayers at air/water surfaces, the close-packed areas of *n*-alkanols and of esters of 1-alkanoic acids are very similar (8).

The isotherm for the C_{10} diester is shifted to considerably higher areas with respect to the curves for the monofunctional adsorbates (Fig. 1*a*). It is likely that the diester assumes orientations which are predominantly parallel to the surface, at least for higher values of A, which would result in the observed effect. Some of the quantitative aspects of the π, A curves are discussed later.

As shown in Fig. 1*b*, the π, A curves for 1-butanol and 1-heptanol adsorbed at the air/water interface differ substantially. They are both displaced to lower areas with respect to the (common) curve for 1-alkanols adsorbed at the oil/water interface. For a given value of A the difference in π for the film at the oil/water and

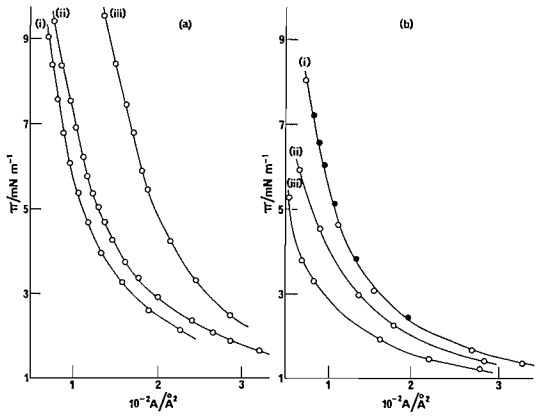

FIG. 1. π–A curves for (*a*):(*i*) dodecanol, (*ii*) methyl dodecanoate, and (*iii*) C_{10} diester (see text) at octane/water interface at 30 °C; and (*b*):(*i*) butanol, (●) and octanol (○) at dodecane/water interface, (*ii*) butanol at air/water interface, and (*iii*) heptanol at air/water interface all at 20 °C. (Results for dodecanol and octanol taken from refs. 1 and 2. Results for butanol at dodecane/water surface (20).

air/water interface is termed the "cohesive" pressure (9) since it is believed that there are interactions between adsorbate molecules at the air/water surface which are absent at the oil/water interface. However, the term "cohesive" may be misleading since different effective adsorbate areas (resulting from different orientations) for molecules at the two interface types would also contribute to a difference in π.

Standard Free Energies of Adsorption

We have determined standard free energies of adsorption, $\Delta_a\mu^0$, using the present data, and the values are consistent with the intuitive ideas con-

Can. J. Chem. Downloaded from www.nrcresearchpress.com by 210.87.254.6 on 09/05/12
For personal use only.

TABLE 4. Standard free energies of adsorption, $\Delta_a\mu^0$

Interface	Solute	T (°C)	$-\Delta_a\mu^0$ (kJ mol^{-1})
n-Octane/water	1-Dodecanol	30	23.5±0.2*
	Methyl dodecanoate	30	16.4±0.1†
	C_4 diester	20	25.7±0.2
	C_5 diester	30	26.0±0.2
	C_{10} diester	30	25.6±0.5†
Air/water	1-Butanol	20	23.0±0.1‡
	1-Heptanol	20	30.4±0.2
	C_1 diester	20	27.5±0.2
	C_4 diester	20	33.7±0.2

*From ref. 2.
†Obtained by direct determination of $(\pi/a)_0$ in linear π, a region.
‡In excellent agreement with the value of 23.0 kJ mol^{-1} obtained by Clint *et al.* (7).

cerning the orientation of the various adsorbates at the surface. $\Delta_a\mu^0$ is given by the expression

$$[4] \qquad \Delta_a\mu^0 = -RT \ln (\pi/a)_0$$

The standard states are $a = 1$ for the solution and $\pi = 1$ mN m^{-1} for the surface (1, 7). The quantity $(\pi/a)_0$ is the initial slope (at $a = 0$) of the π, a curve and can be determined directly if an initial linear section exists, or by use of the constants given in Tables 2 and 3 since

$$[5] \quad (\pi/a)_0 = -(d\gamma/da)_{a=0} = -1/(3c_1\gamma_0^2 + 2c_2\gamma_0 + c_3)$$

where γ_0 is the tension of the interface for zero adsorption. Values of the free energies are given in Table 4.

We first note that $\Delta_a\mu^0$ for the adsorption of 1-dodecanol from octane to the octane/water interface is considerably more negative than the corresponding value for methyl dodecanoate. This is probably due to the —OH group having a greater tendency than the —COOMe group to enter into H-bonding with water at the interface.

As anticipated, the C_{10} diester adsorbs much more strongly from octane to the octane/water interface than does methyl dodecanoate. It is interesting that $\Delta_a\mu^0$ for the C_5 diester and the C_{10} diester are, within the errors, equal. It seems reasonable to suppose that for these latter solutes there will be some contact between the chain methylene groups and water at the interface. If this assumption is correct the free energy of interaction of a —CH_2— group with *interfacial* water is similar to the corresponding interaction with alkane. The suggestion was made elsewhere (2) (from a consideration of free energies of adsorption of gaseous alkanes to the air/water surface, and the surface tensions and free energies of vaporisation of alkanes) that this might be the case.

The average value of $\Delta_a\mu^0$ for the adsorption of the methylene group from dilute aqueous solution to the air/water interface, calculated from the difference in $\Delta_a\mu^0$ for the two alkanols, is -2.5 kJ mol^{-1}, in agreement with previously reported values (9). This is consistent with the alkyl chains having a flat orientation in dilute films. The free energy of adsorption of *n*-alkanes (pentane to octane) from vapor to the water/vapor interface is a linear function of the chain length (10), the —CH_2— increment being -1.76 kJ mol^{-1} at 15 °C. The linear dependence implies an essentially parallel orientation of the alkanes at the surface. Further, the free energy of hydration (*i.e.* transfer from dilute vapor to dilute aqueous solution) of the methylene group is 0.67 kJ mol^{-1} at 25 °C (11). Combination of these free energy changes, neglecting the temperature difference, gives a value of -2.43 kJ mol^{-1} for $\Delta_a\mu^0$ of the methylene group in chains parallel to the water surface. This is very close to the experimentally observed value of -2.5 kJ mol^{-1}.

The lower average value of $\Delta_a\mu^0$ (-2.1 kJ mol^{-1}) observed for the —CH_2— groups in the diesters may result from a modification of the hydration of these groups caused by the two terminal polar groups. Corkill *et al.* have discussed the way in which the hydration of nonpolar groups can be altered by the proximity of polar moieties (12).

Surface Equations of State

(a) Films at the Air/Water Interface

There are two basic approaches to the treatment of adsorbed monolayers at liquid surfaces.

Can. J. Chem. Downloaded from www.nrcresearchpress.com by 210.87.254.6 on 09/05/12
For personal use only.

Can. J. Chem. Downloaded from www.nrcresearchpress.com by 210.87.254.6 on 09/05/12
For personal use only.

One is to suppose that solvent does not affect the film behavior so that the adsorbate molecules can be considered to behave as a two-dimensional gas. Alternatively, explicit account can be taken of the presence of solvent and the monolayer likened to a two-dimensional solution. The solution model is, in principle at least, the more attractive since it is more obviously in accord with reality (13*a*).

Saraga and Prigogine (14) have developed a statistical thermodynamic treatment for monolayers consisting of chain molecules (*r*-mers), disposed parallel to the surface, mixed with solvent molecules (monomers). The equation of state resulting from the model has remained almost untested for relatively simple systems such as those studied here. If the surface area of a monomer molecule is denoted σ_1, and that of an *r*-mer σ_2, the equation of state is written

$$[6]\quad \pi = -\frac{kT}{\sigma_1}\left\{\ln\left(1-\frac{\sigma_2}{A}\right)+\frac{\sigma_2-\sigma_1}{A}+\frac{\beta l}{kT}\left(\frac{\sigma_2}{A}\right)^2\right\}$$

β is an average heat of mixing per segment, and l is the fraction of nearest neighbor sites a site has within the same layer, the solution being considered to be made up of lattice planes parallel to the surface. In this work, we have followed Saraga and Prigogine and set $l = 0.5$, the value for close-packing.

Water (monomer) molecules are denoted a, the polar groups in the adsorbate (*i.e.* —OH or —COO—), b, and CH_2 and CH_3 groups (considered to be equivalent for present purposes), c. Then, β is given as (14)

$$[7]\quad \beta = \frac{n}{r}W_{ab}+\left(\frac{r-n}{r}\right)W_{ac}-\frac{n(r-n)}{r^2}W_{bc}$$

where n is the number of polar groups per *r*-mer and r is the total number of groups in the *r*-mer. The W's are heats of mixing of the various pairs of groups in the system.

Saraga and Prigogine applied eq. 6 to π, A data for insoluble films of esters of long chain carboxylic acids on water, and from the fitting of the data obtained the following values for the W

$$W_{ab} = 6.73 \times 10^{-20}\ \text{J segment}^{-1} \quad (\text{b} = \text{—COO—})$$

$$W_{ac} = 8.00 \times 10^{-21}\ \text{J segment}^{-1}$$

$$W_{bc} = 9.88 \times 10^{-20}\ \text{J segment}^{-1}$$

An independent value of $W_{ac} = 8.40 \times 10^{-21}$ J segment^{-1} was obtained from solubility data for esters in water.

Before applying eq. 6 to our own data we tested its validity for dilute monolayers of *n*-octane on water, since this system is an example of the simplest possible situation. We used the original data of Jones and Ottewill (10) and obtained values of A as described earlier. Equation 6 was rearranged to give

$$[8]\quad \frac{\pi\sigma_1}{kT}+\ln\left(\frac{A-\sigma_2}{A}\right)+\left(\frac{\sigma_2-\sigma_1}{A}\right) \doteq -\frac{\beta l}{kT}\left(\frac{\sigma_2}{A}\right)^2$$

If eq. 6 is to represent the data, a plot of the left hand side of eq. 8 against A^{-2} should be linear and pass through the origin; $\beta l/kT$ is obtained from the slope. In all our calculations we have used the value of σ_1 (6.5 Å^2) calculated by Saraga and Prigogine from the geometry of alkyl chains. The value of σ_2 ($= r\sigma_1$) for octane is thus 52 Å^2, in accord with the value obtained by the use of molecular models (Table 5). It is also noted that the molar volume of water is very similar to that of the CH_2 group. The plot of the data according to eq. 8 is shown in Fig. 2. The curve is rectilinear, passes through the origin and gives a value for $\beta l/kT = 0.84$. This corresponds to $W_{ac} = 6.7 \times 10^{-21}$ J segment^{-1}, in reasonable agreement with the value of 8.0×10^{-21} J segment^{-1} quoted by Saraga and Prigogine. Thus, eq. 6 represents the behavior of octane monolayers up to a surface coverage, θ, of about 0.3 ($A \sim 180$ Å^2) with reasonable values of the molecular parameters. For long chain esters ($C_{13}H_{27}CO_2Et$, $C_{14}H_{29}CO_2Et$, and $MeCO_2(CH_2)_{14}CO_2Me$) Saraga and Prigogine were able to obtain agreement between experiment and theory for areas per molecule down to about 400–500 Å^2, which corresponds to $\theta \sim 0.25$.

We consider now the shorter chain solutes used in the present study. Values of solute areas obtained by the use of Courtauld molecular models are compared with $\sigma_2 = r \times 6.5$ Å^2 in Table 5. The values are very similar, the largest difference (~20%) being for the C_1 diester; otherwise the values are within 5 or 6% of one another. In Fig. 3, the experimental π, A curves are compared with those given by eq. 6, using the $\beta l/kT$ given in Table 5. For the diesters, $\beta l/kT$ values are similar to those calculated from the W

TABLE 5. Molecular parameters for solutes at the air/water interface

Solute	r	$6.5r$(Å^2)	σ_2 (geometrical)	$\beta l/kT$	$\beta l/kT$(P–S)*
Octane	8	52.0	52	0.84	1.01
Butanol	5	32.5	31	0.59	—
Heptanol	8	52.0	49	0.71	—
C_1 diester†	7	45.5	54	0.46	0.59
C_4 diester‡	10	65.0	68	0.53	0.50

*Calculated using eq. 7 and values of W given in ref. 14.
†Diethyl ester of methan-dicarboxylic acid.
‡Diethyl ester of butan-1,4-dicarboxylic acid.

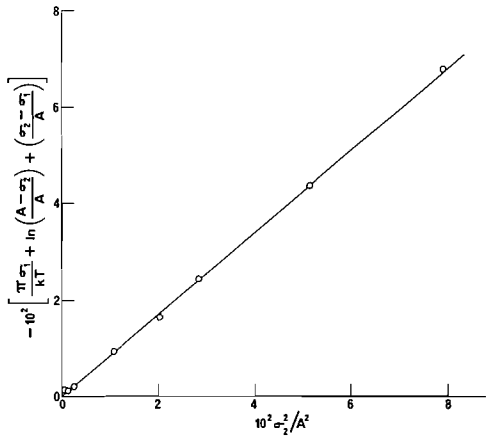

FIG. 2. Plot according to eq. 8 for *n*-octane at the air/water surface at 15 °C.

values of Saraga and Prigogine. Agreement between the experiment and theory is quite satisfactory in all cases for surface coverages, θ, less than about 0.3. It is interesting to note that the data for butanol can be equally well represented by the ideal two-dimensional gas equation $\pi A = kT$ up to values of $\pi \sim 5$ mN m^{-1}.

One of the factors contributing to the breakdown of eq. 6 at lower areas is probably the reorientation of the solute molecules. It is likely that the alkanols in particular will tend progressively to a predominantly vertical orientation as the surface concentration of solute increases. Smith (15) has presented a theoretical equation of state for liquid expanded monolayers of fatty acids on water; this state frequently exists for areas per molecule between about 30 and 60 Å^2. The equation, which contains no adjustable parameters, was found to be reasonably successful for many saturated long chain monocarboxylic acids. We have therefore sought to apply the equation to the more concentrated adsorbed films of alcohols at the air/water surface.

The equation may be written

$$[9]\quad \left(\pi + \frac{m\varepsilon A_0}{2A^2}\right)\left[A\left(1-\frac{A_0}{2A}\right)^2\right] = kT$$

It is supposed that the solute molecule acts as a stack of disks (CH_2 groups) anchored to the water by the head group. The Lennard–Jones energy parameter ε, for the interaction of disks, is taken as that for methane (2.05×10^{-21} J) (16); m is the number of carbon atoms in the molecule.

The quantity A_0 is the solute co-area, and the term $A(1 - A_0/2A)^2$ replaces $(A - A_0)$ which appears in the familiar Volmer and two-dimensional van der Waals gas equations. It was obtained by the use of the two-dimensional analogue of the scaled particle theory for fluids, which is more appropriate than the imperfect gas theory for concentrated films. Smith suggests a value of 36 Å^2 for A_0. However, we have used 26 Å^2 for the following reasons. The co-area is twice the area defined by the distance, d, of closest approach, *i.e.* $A_0 = \pi d^2/2$ (13*b*). Recently,

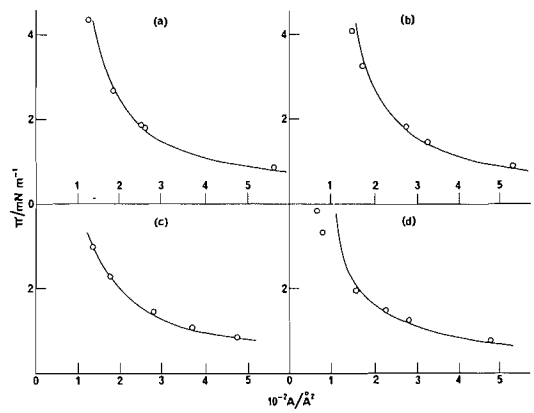

FIG. 3. π–A curves for (*a*) C_1 diester, (*b*) C_4 diester, (*c*) butanol, (*d*) heptanol all at air/water interface at 20 °C. ○ are experimental points; full curves generated by eq. 6.

Can. J. Chem. Downloaded from www.nrcresearchpress.com by 210.87.254.6 on 09/05/12
For personal use only.

Can. J. Chem. Downloaded from www.nrcresearchpress.com by 210.87.254.6 on 09/05/12
For personal use only.

Vochten and Petre (17) have reported saturation values of $A = 27$ Å^2 for adsorbed films of a series 1-alkanols at the air/water interface. If we suppose that at saturation the alkanols have a circular cross section and are hexagonally close-packed, the cross sectional area of all the alkanols studied (butanol to decanol) is 24.5 Å^2. From this, the "equilibrium" diameter, d_0, of the disks can be calculated. Using the approximate relationship $d_0 = 1.37\ d$ suggested by de Boer (18), a value of 26 Å^2 is then obtained for A_0.

It can be seen in Fig. 4 that the agreement between experiment and theory for heptanol is quite good using $A_0 = 26$ Å^2. For a given value of A in the region of 30 to 50 Å^2, the experimental and theoretical values of π do not differ by more than about 10%. However the theoretical line displays greater curvature than does the experimental π, A curve. If A_0 is set equal to 36 Å^2 the agreement is less satisfactory. We have also tested the data for butanol but in this case we do not have results extending to such low areas as for heptanol. Also, the shorter chain compound will presumably show less tendency to cohere. Again, $A_0 = 26$ Å^2 gives better absolute agreement between experiment and theory than does $A_0 = 36$ Å^2.

We have not investigated the application of eq. 9 to our data for the diesters since sufficiently high surface concentrations were not attained. In any event it would be difficult to select a suitable value of ε for the polar groups.

Finally in this section, we note that in some instances film behavior at air/water interfaces can be represented by a virial equation of state. In such cases however care has to be exercised in assigning physical significance to the coefficients. Consider the π, A data for octane for example. These results can be adequately represented, for $\theta < 0.2$, by

$$[10] \qquad \pi = kT\left(\frac{1}{A} + \frac{B^*}{A^2}\right)$$

with a value of -115 Å^2 for the second virial coefficient B^* (Fig. 5*b*). On the other hand, eq. 6 can be transformed to the virial type equation

$$[11] \quad \pi = kT\left[\frac{1}{A} + \left\{\frac{1}{2}\frac{\sigma_2^2}{\sigma_1}\left(1 - \frac{2\beta l}{kT}\right)\right\}\frac{1}{A^2} + \left\{\frac{1}{3}\frac{\sigma_2^3}{\sigma_1}\right\}\frac{1}{A^3} + \left\{\frac{1}{4}\frac{\sigma_2^4}{\sigma_1}\right\}\frac{1}{A^4} + \ldots\ldots\right]$$

Insertion of the appropriate values for $\beta l/kT$, σ_1 and σ_2 (see earlier) gives $B^* = -141$ Å^2, C^* (third virial coefficient, $\sigma_2^3/3\sigma_1$) $= 7.21 \times 10^3$ Å^4, and D^* (fourth virial coefficient, $\sigma_2^4/4\sigma_1$) $= 2.81 \times 10^5$ Å^6. The π, A curves obtained from eq. 11 by inclusion successively of B^*, C^*, and D^* terms are shown in Fig. 5*a*. Thus, although the data can be adequately fitted for $\theta < 0.2$ using only the second virial coefficient of -115 Å^2, if the solution model for the surface is accepted, the term involving the third and, at lower areas, the fourth virial coefficient should be included.

(b) Films at the Oil/Water Interface

Films of polar organic materials adsorbed at the liquid/liquid interface often behave as if they

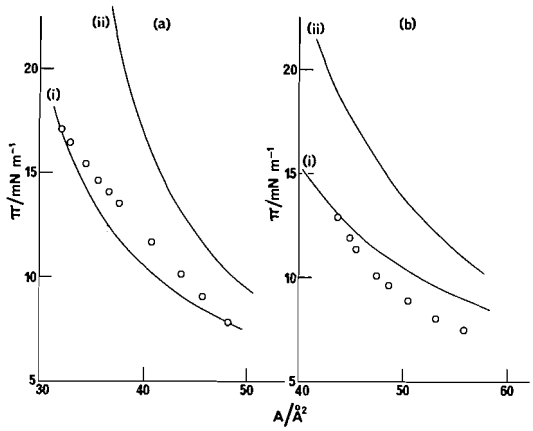

FIG. 4. π–A curves for (*a*) heptanol, (*b*) butanol at air/water interface at 20 °C. ○ are experimental points; full curves generated by eq. 9 with $A_0 = 26$ Å^2 (curves *i*) and 36 Å^2 (curves *ii*).

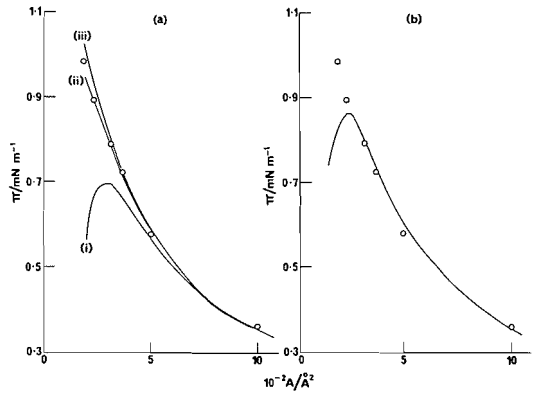

FIG. 5. π–A curves for octane at air/water surface at 15 °C. (*a*) Full lines represent curves obtained including (*i*) term in B^*, (*ii*) terms in B^* and C^*, and (*iii*) terms in B^*, C^*, and D^* in eq. 11. (*b*) Full line generated by eq. 10 with $B^* = -115$ Å^2.

Can. J. Chem. Downloaded from www.nrcresearchpress.com by 210.87.254.6 on 09/05/12
For personal use only.

were two-dimensional gases and the Volmer equation

$$[12] \qquad \pi(A - A_0) = kT$$

can be used to describe their behavior. Such films are normally considered to exhibit simpler behavior than corresponding films at the air/water interface since, if the gas model is employed to describe the data for the latter, allowances must be made for changes in lateral interactions between solute molecules as the surface concentration varies. In spite of the apparent success of the gas model, attempts have been made to fit data for films at the liquid/liquid interface using the solution model for the surface. Thus for example, the equation of state

$$[13] \qquad \pi = -\frac{kT}{\sigma_1} \ln\left(\frac{A - \sigma_2}{A - \sigma_2 + \sigma_1}\right)$$

for a two-dimensional ideal solution has been tested for alkanols at the alkane/water interface (2). The difficulty in treating such films however is that part of the adsorbate resides in the interfacial water, and part in the oil. The simplifying assumption was made in ref. 2, as elsewhere (19), that the whole of the adsorbed solute resides in the oil phase. Although data for the alkanols could be fitted by the use of eq. 13, unique values for σ_1 and σ_2 could not be obtained. The present data for methyl dodecanoate can be fitted in a similar manner. For example if σ_1 is set at 52 Å^2 corresponding to a flat orientation of octane at the interface, a reasonable fit of the data is obtained for $\sigma_2 = 73$ Å^2. However, it is not known with any certainty that the octane is parallel to the interface. Further, we find that the shape of the π, A curves for the diesters cannot be adequately represented by eq. 13. We conclude therefore that the use of eq. 13, even when a good fit of data can be obtained, does not lead to useful information about the physical reality in the system, although it can be very useful simply as a fitting equation. Similar remarks can be made about the use of eq. 6 with $\beta = 0$.

The Volmer equation describes the behavior of 1-alkanol films at oil/water interfaces very well, with $A_0 = 25$ Å^2 (2). It was previously suggested by one of us that the similarity between this value of A_0 and the close-packed areas of alkanols in insoluble monolayers might be fortuitous. However, the saturation adsorption of a series of 1-alkanols at the air/water surface reported subsequently by Vochten and Petre (see earlier discussion), provides further indication that this value of A_0 does mean that monofunctional alkyl chain compounds are oriented essentially normal to the alkane/water interface. It is very likely however that the diesters we have used in this study will be disposed parallel to the surface in films which are not very concentrated. In this case, if the Volmer model is adequate, much larger values of A_0 should be obtained. Indeed values of the order of, but greater than, the "static" geometrical areas would be expected. We find that for the C_4, C_5, and C_{10} diesters the Volmer equation fits the data for $A > 180$ Å^2 with A_0 values of, respectively, 90, 102, and 114 Å^2 (Fig. 6). The areas calculated from molecular models are respectively 68, 74, and 104 Å^2. For areas above about 300 Å^2 (not shown) the experimental π for the C_{10} diester fall about 0.2 mN m^{-1} above the Volmer curve.

For $A < 180$ Å^2, corresponding to a surface coverage of about 0.6, the experimental curves fall below those given by eq. 12 and, as can be seen in Fig. 6, approach one another. The curve for the C_4 diester (not included, for the sake of clarity, in Fig. 6) is indistinguishable from that for the C_5 diester for areas below about 120 Å^2. Taken together these observations are consistent

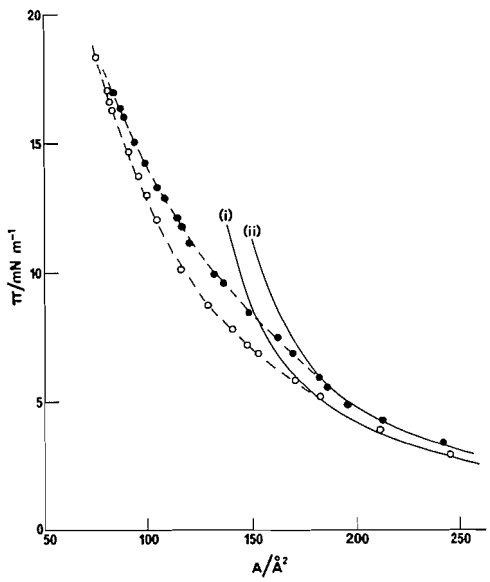

FIG. 6. π–A curves for C_5 diester (○) and C_{10} diester (●) at octane/water interface at 30 °C. Full lines generated by eq. 12 with (*i*) $A_0 = 102$ Å^2, (*ii*) $A_0 = 114$ Å^2.

with the diesters being parallel at the interface for coverages of less than 0.6, and tending towards a vertical orientation at higher coverages. The effective areas for all three diesters in a stretched vertical alignment would of course be the same.

It is perhaps surprising that an equation based on a two-dimensional gas model should be apparently more successful than one derived from a solution model, and we do not have a ready explanation for this observation. The apparent failure of the latter may be associated with the simplifying assumption that the solute resides totally in the oil at the interface. There are two circumstances, however, in which eq. 13 takes on the form of the Volmer equation. Expansion of the logarithmic term in the former gives

$$[14] \quad \pi = kT[1/(A - \sigma_2) - \sigma_1/2(A - \sigma_2)^2 + \sigma_1{}^2/3(A - \sigma_2)^3 + \ldots]$$

Equation 12 is obtained (with $A_0 = \sigma_2$) for $\sigma_1 = 0$. Alternatively, if $\sigma_1 = \sigma_2 = \sigma$, eq. 13 may be expressed

$$[15] \quad \pi = 2kT[1/(2A - \sigma) + \sigma^2/3(2A - \sigma)^3 + \ldots]$$

The second and higher terms in square brackets in eq. 15 will normally be very much smaller than the first so that to a good approximation

$$[16] \quad \pi(A - \sigma/2) = kT$$

Since in general $\sigma_1 \neq \sigma_2$, the films investigated here are behaving as if the solvent were absent ($\sigma_1 = 0$), *i.e.* as two-dimensional gases.

One of us (J.C.) is indebted to the Science Research Council for the provision of a maintenance grant.

1. R. AVEYARD and B. J. BRISCOE. Trans. Faraday Soc. **66**, 2911 (1970).
2. R. AVEYARD and B. J. BRISCOE. J. Chem. Soc. Faraday I. **68**, 478 (1972).
3. R. AVEYARD, B. J. BRISCOE, and J. CHAPMAN. J. Colloid and Interface Sci. **44**, 282 (1973).
4. R. AVEYARD and D. A. HAYDON. Trans. Faraday Soc. **61**, 2255 (1965).
5. J. A. NELDER and R. MEAD. Computer J. **7**, 308 (1965).
6. W. D. HARKINS and R. W. WAMPLER. J. Am. Chem. Soc. **53**, 850 (1931).
7. J. H. CLINT, J. M. CORKILL, J. F. GOODMAN, and J. R. TATE. J. Colloid Interface Sci. **28**, 522 (1968).
8. N. K. ADAM. Physics and chemistry of surfaces. Dover, New York. 1968. p. 50.
9. J. T. DAVIES and E. K. RIDEAL. Interfacial phenomena. 2nd. ed. Academic Press, London. 1963. p. 230.
10. D. C. JONES and R. H. OTTEWILL. J. Chem. Soc. 4076 (1955).
11. J. A. V. BUTLER and W. S. REID. J. Chem. Soc. 1171 (1936).
12. J. M. CORKILL, J. F. GOODMAN, and J. R. TATE. Trans. Faraday Soc. **65**, 1742 (1969).
13. R. AVEYARD and D. A. HAYDON. Introduction to the principles of surface chemistry. Cambridge University Press. 1973. (*a*) p. 84. (*b*) p. 23.
14. L. SARAGA and I. PRIGOGINE. Mém. Serv. Chim. de l'Etat, **38**, 109 (1953).
15. T. SMITH. J. Colloid Interface Sci. **23**, 27 (1967).
16. R. C. REID and T. K. SHERWOOD. The properties of gases and liquids. 2nd ed. McGraw-Hill, New York. 1966. p. 632.
17. R. VOCHTEN and G. PETRE. J. Colloid Interface Sci. **42**, 320 (1973).
18. J. H. DE BOER. The dynamical character of adsorption. Oxford University Press, Oxford, England. 1953. p. 173.
19. F. M. FOWKES. J. Phys. Chem. **66**, 1863 (1962).
20. R. W. MITCHELL. Unpublished results.

Can. J. Chem. Downloaded from www.nrcresearchpress.com by 210.87.254.6 on 09/05/12
For personal use only.

The Kinetics and Mechanisms of Exchange in the Binary System Manganese(II) – Adenosine 5′-Triphosphate[1]

G. P. P. KUNTZ,[2] YIU-FAI LAM, AND GEORGE KOTOWYCZ
Department of Chemistry, University of Alberta, Edmonton, Alberta T6G 2G2

Received September 23, 1974

G. P. P. KUNTZ, YIU-FAI LAM, and GEORGE KOTOWYCZ. Can. J. Chem. **53**, 926 (1975).

^{31}P n.m.r. studies on the Mn(II) – adenosine 5′-triphosphate system indicate that two n.m.r. exchange mechanisms are present in solution; namely, the Eigen–Tamm mechanism and the direct ligand exchange mechanism. Their respective contributions to the observed n.m.r. linewidths and hence to the n.m.r. exchange rate depend upon the concentration of the ligand ATP. Equations are developed to prove what n.m.r. "sees" for the Eigen–Tamm mechanism and these equations are applied to this study.

G. P. P. KUNTZ, YIU-FAI LAM et GEORGE KOTOWYCZ. Can. J. Chem. **53**, 926 (1975).

Des études r.m.n. de ^{31}P sur le système Mn(II) – adénosine 5′-triphosphate indiquent que deux mécanismes d'échange en r.m.n. sont présents dans la solution, à savoir, le mécanisme Eigen–Tamm et le mécanisme d'échange direct du ligand. Leurs contributions respectives à la largeur observée pour les bandes en r.m.n., ainsi qu'au taux d'échange en r.m.n., dépendent de la concentration du ligand ATP. On a développé des équations pour démontrer ce que la r.m.n. "voit" pour le mécanisme Eigen–Tamm et on a appliqué ces équations à l'étude actuelle. [Traduit par le journal]

Introduction

The application of nuclear magnetic resonance (n.m.r.) in the area of biochemistry is constantly increasing as n.m.r. determines not only whether two substances interact but also, in many cases, the sites of interaction. Excellent reviews in this area have been written by Roberts and Jardetzky (1), Rowe *et al.* (2), Mildvan and Cohn (3), Mildvan (4), Cohn (5), and Kotowycz and Lemieux (6).

Researchers are also applying n.m.r. exchange rate studies to two or more interacting substances, *e.g.* a metal ion, substrate, and enzyme system. In these experiments the n.m.r. exchange rate is compared with the catalytic turnover number. Mildvan and co-workers have utilized the n.m.r. exchange rate to obtain kinetic information (7–9). The n.m.r. exchange mechanism must be known before the n.m.r. exchange rate can be compared with the catalytic turnover number. This paper explicitly points out how a substrate concentration dependence study of the n.m.r. exchange rate permits one to assign the n.m.r. exchange mechanism either as Eigen–Tamm (dissociation–association), M + L = ML, or direct ligand exchange, ML + L* = ML* + L.

The present study of the Mn–ATP system demonstrates that two exchange mechanisms are present and that their respective contributions to the observed n.m.r. linewidth depends upon the concentration of ATP.

Theoretical Introduction

In the study of metal ion–ligand interactions, Eigen and Tamm (10) showed that at least four species must be considered; namely, the solvated metal ion M(aq), the solvated ligand L(aq), and outer sphere metal ion – ligand complex M(aq)L and an inner sphere metal ion – ligand complex ML. Their mechanism may be written as

$$[1] \qquad \mathrm{M(aq) + L(aq)} \underset{k_{-os}}{\overset{k_{os}}{\rightleftharpoons}} \mathrm{M(aq)L} \underset{k_{-o}}{\overset{k_{o}}{\rightleftharpoons}} \mathrm{ML}$$

where k_{os}, k_{-os}, k_o, and k_{-o} are the forward and reverse rate constants of the outer and inner sphere complexes respectively. Eigen and Tamm (10), Stengle and Langford (11), Hewkin and Prince (12), Wilkins (13), Hunt (14) and many researchers cited in these papers have demonstrated that the first step is essentially diffusion controlled and the second step, the ligand penetration step, is the rate determining step for the

[1]This is paper No. 6 in a series of nuclear magnetic resonance studies of nucleoside – and nucleotide – metal ion interactions. For paper No. 5, see ref. 17.

[2]Postdoctoral Research Associate 1973–1975.

Can. J. Chem. Downloaded from www.nrcresearchpress.com by 210.87.254.5 on 09/05/12
For personal use only.

process. A relaxation technique such as temperature jump measures the over all rate (15)

$$[2] \qquad M(aq) + L(aq) \underset{k_{-1}}{\overset{k_1}{\rightleftharpoons}} ML$$

where

$$k_1 = \frac{k_{os}}{k_{-os}} k_o = K_{os} k_o$$

$$k_{-1} = k_{-o}$$

and k_1 and k_{-1} are the forward and reverse rate constants, respectively. The K_{os} term is the outer sphere stability constant (10, 15). The overall stability constant is

$$K = k_1/k_{-1} = [ML]/[M][L]$$

To the best of the authors' knowledge, no one has proven what n.m.r. "sees" for the Eigen–Tamm mechanism. Labelling the three different species of L present in solution namely, L(aq), M(aq)L, and ML as a, b, and c, respectively, the three-site exchange theory previously presented (16, 17) may be applied to the present system. In the Appendix it is shown that the transverse relaxation rate due to the presence of the paramagnetic metal ion, T_{2p}^{-1}, is given by

$$[3] \qquad T_{2p}^{-1} = K_{os} k_o [M]$$

for the Eigen–Tamm mechanism when the rate of exchange from site a to b is rapid and the rate of exchange from site b to site c is in the chemical controlled region (16). Hence n.m.r. measurements also measure the process given in eq. 2. This has previously been assumed by Mildvan and co-workers (7–9).

If a ligand, L, is observed as it exchanges from one magnetic environment to another, then the lifetime of L, τ_L, is (18, 19)

$$[4] \qquad \tau_L^{-1} = k_L = \frac{\text{rate of decrease of L}}{\text{concentration of L}}$$

Hence n.m.r. experiments measure the pseudo-first order rate constant k_L. Equation 4 has been extensively applied to the interpretation of kinetics and mechanisms of exchange in inorganic chemistry (20, 21) and in studies of proton exchange kinetics (22, 23) to list but a few references.

The lifetime, τ_L, of L in state L(aq) for the exchange mechanism (eq. 2) is

$$[5] \qquad \tau_L^{-1} = k_1[M] = k_{-1} \frac{[ML]}{[L]}$$

and the lifetime, τ_M, of L in the complex ML is

$$[6] \qquad \tau_M^{-1} = k_{-1}$$

The lifetime τ_M is in general a quantity that cannot be directly measured as the bound signal is usually too broad or too weak in intensity to be observed. Therefore τ_M is calculated from the observable τ_L using

$$[7] \qquad \tau_M = \tau_L \frac{[ML]}{[L]}$$

Hence for the mechanism given by eq. 2, eq. 7 becomes

$$[8] \qquad \frac{\tau_M}{\tau_L} = \frac{k_1[M]}{k_{-1}}$$

[M], [ML], and [L] are the equilibrium concentrations of the free metal ion, the complex, and free ligand, respectively.

In addition to the above Eigen–Tamm mechanism, another common exchange mechanism may also be present. This mechanism is the direct ligand exchange and is written as[3]

$$[9] \qquad ML + L^* \underset{k_2}{\overset{k_2}{\rightleftharpoons}} ML^* + L$$

Then

$$[10] \qquad \tau_L^{-1} = k_2[ML]$$

and

$$[11] \qquad \tau_M^{-1} = k_2[L]$$

Finally, when both exchange mechanisms are simultaneously considered, then

$$[12] \qquad \tau_L^{-1} = k_1[M] + k_2[ML] = k_{-1} \frac{[ML]}{[L]} + k_2[ML]$$

$$[13] \qquad \tau_M^{-1} = k_{-1} + k_2[L]$$

The lifetime, τ_M, of L in the complex as well as τ_L, is no longer simple to interpret. Equation 13 is identical in form to eq. 4 in the paper by Pearson and Lanier (24). Pearson and Lanier (24) also point out that a plot of τ_M^{-1} *vs.* [L] must eventually flatten out in the high ligand concentration range. Therefore not detecting a ligand concentration dependence on τ_M^{-1} does not

[3]The ligand L* is the same as L. The * indicates that this ligand has just come off or on the metal ion. Reaction 9 is the overall exchange process. Intermediate steps which may also be present are too rapid to measure using n.m.r.

Can. J. Chem. Downloaded from www.nrcresearchpress.com by 210.87.254.5 on 09/05/12
For personal use only.

Can. J. Chem. Downloaded from www.nrcresearchpress.com by 210.87.254.5 on 09/05/12
For personal use only.

guarantee that the direct ligand exchange mechanism is absent if only a narrow ligand concentration range is studied. To show that the direct ligand exchange mechanism (mechanism 9) is absent, one must prove that $T_{2B}^{-1} \ll \tau_M^{-1}$ (24) where T_{2B}^{-1} is the transverse relaxation rate of the bound state. T_{2B}^{-1} can be estimated from the Solomon–Bloembergen equation (25)

$$[14] \quad T_{2B}^{-1} = \frac{2S(S+1)}{3}\frac{A^2}{\hbar^2}\tau_e + \frac{2}{5}\frac{S(S+1)}{r^6}\gamma_I^2\beta^2 g^2\tau_c$$

where the symbols have the usual meaning.

Experimental Procedure

Natural abundance ^{31}P n.m.r. spectra were obtained in the Fourier transform mode with proton noise decoupling on a Bruker HFX 90 NMR spectrometer (36.43 MHz) interfaced with a Nicolet computer. The deuterium resonance of the solvent D_2O was used as the lock signal. All measurements were carried out under controlled temperatures using the Bruker temperature control unit. Samples were in the probe for at least 15 min before the measurements were begun.

Transverse relaxation times were measured from the linewidths at half-height from the Fourier transformed spectra and calculated using

$$T_{2p}^{-1} = \pi[\Delta\nu_{1/2,obsd} - \Delta\nu_{1/2,o}] = \pi\Delta\nu_{1/2,p},$$

where $\Delta\nu_{1/2,obsd}$ is the observed linewidth at half-height of the ligand resonance for the metal ion solution, $\Delta\nu_{1/2,o}$ is the linewidth at half-height for the same resonance without metal ions and $\Delta\nu_{1/2,p}$ is the effective paramagnetic linewidth. Corrections were made for the $J(^{31}P—^{31}P)$ splitting of 19.5 Hz. Depending on the required resolution, the free induction decay signals were stored in either 8K or 4K data points corresponding to a frequency range of 3000 Hz. The transformed spectrum then yields 4K or 2K data points respectively.

ATP (disodium salt) of highest grade was obtained from Sigma Chemical Co. Samples were purified by passing an ATP solution through a Dowex 50 exchange resin. ATP solutions were then prepared in D_2O and adjusted to a pD of 8.2 (26) with sodium hydroxide. Stock solutions of Mn(II) were prepared from Fisher certified reagent $MnCl_2 \cdot 4H_2O$ crystals. The Mn(II) ion concentrations were calibrated against a Fisher certified atomic absorption Mn(II) standard solution by measuring the ^{31}P n.m.r. signals of 5′-AMP using both the stock and standard solutions. The ionic strength was maintained at one using tetramethylammonium chloride, TMA·Cl (Eastman Kodak Co.).

The ATP concentrations were determined by uv spectrometry ($\varepsilon_{max} = 1.54 \times 10^4$ at 260 mμ at pH 8). The metal solutions were added with calibrated H. E. Pedersen micropipets. After the addition of the metal ions, the solution pD was rechecked and was constant at 8.2 ± 0.1 in all cases.

Results and Discussion

Metal ion – ATP interactions have now been extensively studied (17, 27–39). However, the kinetics and exchange mechanisms have been difficult to study due to the high concentrations of ATP that are required. With the advent of pulse Fourier transform n.m.r. techniques, the ATP concentration range available for these studies has increased by a factor of ten. The inconsistencies in the interpretation of the previous metal ion – ATP kinetic study by n.m.r. (39) have been pointed out in previous papers (17, 35, 40, 41).

A plot of $\Delta\nu_{1/2,p}$ $(1/\pi T_{2p})$ as a function of the reciprocal of the absolute temperature for the ^{31}P resonance of ATP is shown in Fig. 1. The data for ATP concentrations of 0.1 and 0.01 M are shown in Fig. 1 whereas the results for 0.05 and 0.03 M solutions are tabulated in Table 3. Since T_{2p}^{-1} is in the chemical controlled region (16, 28, 33) it then equals the n.m.r. exchange rate τ_L^{-1}. It has previously been shown (17) that in the Mn(II) – ATP system, ATP exists in at

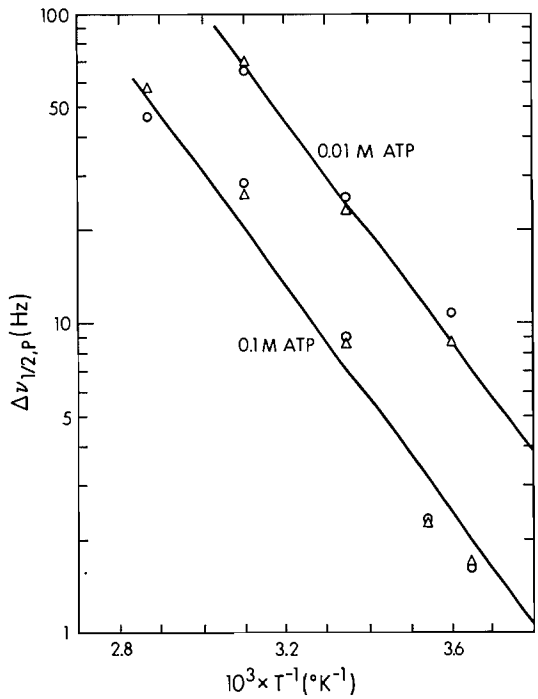

FIG. 1. Plot of $\Delta\nu_{1/2,p}$ *vs* T^{-1} ($°K^{-1}$). The γ phosphorus signal is labelled △ and the α phosphorus signal is labelled ○. The Mn(II) concentration is 1.0×10^{-5} M for all solutions. The ionic strength was maintained at one using tetramethylammonium chloride.

TABLE 1. Concentration of species in the Mn–ATP system[a]

K (M)	$[ATP]_{total}$[b]	$[Mn]_{total}$	[Mn–ATP]	[Mn]
1×10^4	0.1	1.0×10^{-5}	9.99×10^{-6}	1×10^{-8}
	0.05	1.0×10^{-5}	9.98×10^{-6}	2×10^{-8}
	0.03	1.0×10^{-5}	9.97×10^{-6}	3×10^{-8}
	0.01	1.0×10^{-5}	9.9×10^{-6}	10×10^{-8}
5×10^4	0.1	1.0×10^{-5}	9.998×10^{-6}	0.2×10^{-8}
	0.05	1.0×10^{-5}	9.996×10^{-6}	0.4×10^{-8}
	0.03	1.0×10^{-5}	9.993×10^{-6}	0.7×10^{-8}
	0.01	1.0×10^{-5}	9.98×10^{-6}	2×10^{-8}

[a]Evaluated at 27 °C, concentration is expressed in molarity units.
[b]$[ATP]_{total} \cong [ATP]$.

least three states in solution, namely free ATP (species a), metal ion – phosphate bound ATP (species b), and phosphate-metal ion-ring bound ATP (species c). In the chemical-controlled region, even if $T_{2b} = T_{2c}$ as may be true for the ^{31}P nuclei, n.m.r. sees only the a $\rightleftharpoons$ b exchange. Hence τ_L^{-1} (τ_{ab}^{-1}) is measured experimentally and τ_M^{-1} (τ_{ba}^{-1}) is calculated using eq. 7 written in the form $\tau_M^{-1} = [a]\tau_L^{-1}/[b]$. However, if the concentration of species b is not very well known, then τ_M is also not well known.

Since the stability constant for the Mn(II) – ATP complex for a solution with an ionic strength of one is not precisely known, in our calculations the present authors used $[b] \cong [Mn(II)]$ rather than $[b] = 0.8\ [Mn(II)]$ (17).

The analysis of the ATP concentration dependence on T_{2p}^{-1} is shown in Table 1. Since the ligand-to-metal ion ratio is very large, the free ATP concentration is essentially equal to the total ATP concentration in solution. The stability constant K for the Mn–ATP complex is very large and values have been reported ranging between 1×10^4 and 1.5×10^5 l mol^{-1} for an ionic strength of 0.1 (42, 43 and references therein). For the present discussion, values of the stability constant ranging from 1×10^4 to 5×10^4 l mol^{-1} have been chosen (ionic strength 1.0). The concentration of the Mn–ATP complex is very close to a constant and independent of the value of K or the ATP concentration (Table 1).

If only the exchange mechanism (mechanism 9) was present, the exchange rate would be independent of the ATP concentration over the ATP concentration range studied (eqs. 10 and 12). However, if the only mechanism present was the Eigen–Tamm mechanism (mechanism 2), then the exchange rate for 0.01 M ATP should be ten times that for 0.1 M ATP (eq. 5) as the concentration of Mn–ATP is constant (Table 1). Experimentally, from Fig. 1 it is seen that the exchange rate for 0.01 M ATP is about 3.3 times that at 0.1 M ATP.

Hence both exchange mechanisms must be simultaneously considered and the exchange rate is now governed by eq. 12. Therefore the forward rate constant, k_1, can easily be calculated based on the quantities in Table 1. The forward rate constant then ranges between $6 \times 10^8\ M^{-1}\ s^{-1}$ and $3 \times 10^9\ M^{-1}\ s^{-1}$ at 27 °C (Table 2). On the basis of temperature jump studies, Hammes and Levison (44) calculated k_1 to be $2 \times 10^9\ M^{-1}\ s^{-1}$ for the Mn–ATP system (ionic strength 0.1).

The exchange constant, k_2, for the direct ligand exchange mechanism is $1.8 \times 10^6\ M^{-1}\ s^{-1}$ (Table 2). Using these values of k_1 and k_2, the observed τ_L^{-1} for 0.05 M ATP and 0.03 M ATP are compared with the calculated values using eq. 12 (Table 3). The calculated exchange rates are compatible with the observed exchange rates. For 0.1 M ATP, the Eigen–Tamm mechanism contributes approximately 15% to the observed linewidth. The small concentration range that is feasible for this study (0.1 to 0.01 M) influenced us to analyze the data in this manner rather than by plotting $\Delta\nu_{1/2,p}$ *vs.* $[L]^{-1}$, the preferred approach. Hence our analysis of the data indicates that two n.m.r. exchange mechanisms

TABLE 2. Calculated rate constants[a]

K (M)	k_1 ($M^{-1}\ s^{-1}$)	k_2 ($M^{-1}\ s^{-1}$)
1×10^4	$(6\pm1)\times10^8$	$(1.8\pm0.3)\times10^6$
5×10^5	$(3\pm0.5)\times10^9$	$(1.8\pm0.3)\times10^6$

[a]Evaluated at 27 °C.

Can. J. Chem. Downloaded from www.nrcresearchpress.com by 210.87.254.5 on 09/05/12
For personal use only.

TABLE 3. Comparing calculated and observed exchange rates[a]

[ATP] (*M*)	$\tau_L^{-1}(s^{-1})$ Calculated	Observed
0.05	30±5	30±3
0.03	36±5	34±3

[a]Experimental conditions are listed in Fig. 1.

are required to explain the ATP concentration dependence in the binary system, Mn–ATP. The kinetic parameters thus obtained favorably compare with those obtained from other kinetic techniques as mentioned in the review article by Frey and Stuehr (40).

Summary

It has been shown that for the Eigen–Tamm exchange mechanism

$$M(aq) + L(aq) \overset{K_{os}}{\rightleftharpoons} MWL \overset{k_o}{\underset{k_{-o}}{\rightleftharpoons}} ML$$

nuclear magnetic resonance "sees" the exchange rate

$$\tau_L^{-1} = K_{os}k_o[M] = k_1[M]$$

We have also explicitly demonstrated the circumstances when a concentration dependence study is required to assign the exchange mechanisms. This understanding was then applied to the binary system Mn–ATP and it was thus seen that two exchange mechanisms are required to fit the n.m.r. lifetimes.

We wish to thank Dr. D. L. Rabenstein for valuable discussions and the National Research Council of Canada for financial support.

Appendix

The Eigen–Tamm exchange mechanism for a metal ion, M, and ligand, L, complex may be written as

$$[A1] \quad M(aq) + L(aq) \overset{k_{os}}{\underset{k_{-os}}{\rightleftharpoons}} M(aq)L \overset{k_o}{\underset{k_{-o}}{\rightleftharpoons}} ML$$

where k_{os}, k_{-os}, k_o, k_{-o} are the forward and reverse rate constants of the outer and inner sphere complexes respectively. The first step is diffusion controlled and the second step, the ligand penetration step, is the forward rate determining step. For n.m.r. exchange, mechanism A1 is rewritten as

$$[A2] \quad M(aq) + L(aq) \overset{k_{ab}}{\underset{k_{ba}}{\rightleftharpoons}} M(aq)L \overset{k_{bc}}{\underset{k_{cb}}{\rightleftharpoons}} ML$$

where $k_{ij} = \tau_{ij}^{-1}$ is the n.m.r. exchange rate of the ligand, L, going from site i to site j. From eq. 4, the above rate constants and n.m.r. exchange rates are related by the following

$$[A3] \quad \begin{aligned} k_{ab} &= k_{os}[M] \\ k_{ba} &= k_{-os} \\ k_{bc} &= k_o \\ k_{cb} &= k_{-o} \\ K_{os} &= \frac{k_{os}}{k_{-os}} \end{aligned}$$

The ligand sites are defined as free ligand, L(aq), outer sphere ligand, M(aq)L, and inner sphere ligand, ML, and are referred to as species a, b, and c respectively. The three site exchange theory that has previously been developed (16, 17) can now be applied to this system.

The change in the transverse relaxation caused by the paramagnetic metal ion in the consecutive three site exchange mechanism is

$$[A4] \quad \frac{1}{T_{2p}} = k_{ab} + k_x$$

where

$$k_x = \frac{-k_b(k_c^2 + \Delta\omega_c^2)k_{ab}k_{ba} + k_c k_{bc}k_{cb}k_{ab}k_{ba}}{[(k_b^2 + \Delta\omega_b^2)(k_c^2 + \Delta\omega_c^2) + 2(\Delta\omega_b\Delta\omega_c - k_b k_c)k_{bc}k_{cb} + k_{cb}^2 k_{bc}^2]}$$

$$k_b = T_{2b}^{-1} + k_{ba} + k_{bc}$$

$$k_c = T_{2c}^{-1} + k_{cb}$$

T_{2j} is the usual transverse relaxation time in the j environment and $\Delta\omega_j$ is the difference between the resonance frequency for site j and the actual frequency.

The outer sphere complex is usually in the fast exchange region while the inner sphere complex may be in either the fast or slow (chemical controlled) region in the n.m.r. time domain (45). In the present paper it is assumed that the inner sphere complex is in the chemical controlled region, a common occurrence for ^{31}P n.m.r. (28).

Can. J. Chem. Downloaded from www.nrcresearchpress.com by 210.87.254.5 on 09/05/12
For personal use only.

Can. J. Chem. Downloaded from www.nrcresearchpress.com by 210.87.254.5 on 09/05/12
For personal use only.

The rate of exchange of species b to species a is in the fast exchange limit. Assuming $K_{os} = 100$ for this ionic strength, then $k_{ba} = k_{-os} = k_{os}/K_{os}$ which is less than two orders of magnitude that is required for diffusion control. Hence

[A5] $$k_{ba} \gg T_{2b}^{-1}; \Delta\omega_b$$

The rate of exchange of species c to species b is in the chemical controlled region

[A6] $$\Delta\omega_c; T_{2c}^{-1} \gg k_{cb}$$

For a large stability constant (of the order of $10^4\ M^{-1}$)

[A7] $$k_{ba} \gg k_{bc} \gg k_{cb}$$

as k_{ba} is of the order of $10^9\ s^{-1}$, k_{bc} is of the order of $10^6\ s^{-1}$ or less for the first row transition metals and k_{cb} is of the order of $10^4\ s^{-1}$ (44).

In the case of manganese, the bound linewidth is always much greater than the shift so the shift terms are negligible. Hence

[A8] $$T_{2c}^{-1} \gg \Delta\omega_c$$

The inner sphere complex has a much greater linewidth than the outer sphere complex so that

[A9] $$T_{2c}^{-1} \gg T_{2b}^{-1} \gg \Delta\omega_b$$

Applying limits A5 to A9 to eq. A4, it is found that

[A10] $$\frac{1}{T_{2p}} = \frac{k_{ab}}{k_{ba}}(k_{bc} + T_{2b}^{-1})$$

Applying eq. A3, eq. A10 becomes

[A11] $$\frac{1}{T_{2p}} = K_{os}[M](k_o + T_{2b}^{-1})$$

The outer sphere bound transverse linewidth, T_{2b}^{-1}, is dipolar in nature. The distance between the metal ion and ligand is approximately 5.5 Å. T_{2b}^{-1} can be calculated from the Solomon equation (46).

[A12] $$T_{2b}^{-1} = \frac{2}{5}\frac{S(S+1)\gamma_I^2\beta^2 g^2}{R^6}\tau_c$$

T_{2b}^{-1} is of the order of 10^2 to $10^3\ s^{-1}$, much smaller than k_o ($10^6\ s^{-1}$ for Mn(II)). Equation A11 becomes

[A13] $$\frac{1}{T_{2p}} = K_{os}k_o[M]$$

When the bound shift is much greater than the bound linewidth as is true for Ni(II) and Co(II), the linewidth terms are negligible

[A14] $$\Delta\omega_c \gg T_{2c}^{-1}$$

The inner sphere complex has a greater shift than the outer sphere complex

[A15] $$\Delta\omega_c \gg \Delta\omega_b \gg T_{2b}^{-1}$$

Applying the limiting cases A5, A6, A7, A14 and A15 to eq. A4, T_{2p}^{-1} becomes

[A16] $$\frac{1}{T_{2p}} = \frac{k_{ab}}{k_{ba}}\frac{k_{bc}\Delta\omega_c^2}{(k_{cb}^2 + \Delta\omega_c^2)}$$

In the slow exchange limit (16)

[A17] $$\Delta\omega_c^2 \gg k_{cb}^2$$

and eq. A16 becomes

[A18] $$\frac{1}{T_{2p}} = \frac{k_{ab}}{k_{ba}}k_{bc} = K_{os}k_o[M]$$

which is equivalent to A13.

Therefore n.m.r. for both cases "sees" the Eigen–Tamm mechanism as a single step mechanism

[A19] $$M(aq) + L(aq) \underset{k_{-1}}{\overset{k_1}{\rightleftharpoons}} ML$$

where

$$k_1 = K_{os}k_o$$

and

$$k_{-1} = k_{-o}$$

1. G. C. K. Roberts and O. Jardetzky. Advan. Protein Chem. **24**, 447 (1970).
2. J. J. M. Rowe, J. Hinton, and K. L. Rowe. Chem. Rev. **70**, 1 (1970).
3. A. S. Mildvan and M. Cohn. Advan. Enzymology, **33**, 1 (1970).
4. A. S. Mildvan. The enzymes. Vol. 2. *Edited by* P. D. Boyer. 3rd ed. Academic Press, New York. 1970. p. 445.
5. M. Cohn. Quart. Rev. Biophys. **3**, 1 (1970).
6. G. Kotowycz and R. U. Lemieux. Chem. Rev. **73**, 669 (1973).
7. A. S. Mildvan, J. S. Leigh, and M. Cohn. Biochemistry, **6**, 1805 (1967).
8. A. S. Mildvan and M. C. Scrutton. Biochemistry, **6**, 2978 (1967).
9. T. Nowak, A. S. Mildvan, and G. L. Kenyon. Biochemistry, **12**, 1690 (1973).
10. M. Eigen and K. Tamm. Z. Elektrochem. **66**, 107 (1962).
11. T. R. Stengle and C. H. Langford. Coord. Chem. Rev. **2**, 349 (1967).
12. D. J. Hewkin and R. H. Prince. Coord. Chem. Rev. **5**, 45 (1970).
13. R. G. Wilkins. Accounts Chem. Res. **3**, 408 (1970).
14. J. P. Hunt. Coord. Chem. Rev. **7**, 1 (1971).
15. G. G. Hammes and J. I. Steinfeld. J. Am. Chem. Soc. **84**, 4639 (1962).
16. T. J. Swift and R. E. Connick. J. Chem. Phys. **37**, 307 (1962).

17. Y. F. LAM, G. P. P. KUNTZ, and G. KOTOWYCZ. J. Am. Chem. Soc. **96**, 1834 (1974).
18. H. S. GUTOWSKY, D. W. MCCALL, and C. P. SLICHTER. J. Chem. Phys. **21**, 279 (1953).
19. H. S. GUTOWSKY and C. H. HOLM. J. Chem. Phys. **25**, 1228 (1956).
20. H. W. DODGEN, A. D. JORDAN, and R. B. JORDAN. J. Phys. Chem. **77**, 2149 (1973).
21. B. J. FUHR and D. L. RABENSTEIN. Inorg. Chem. **12**, 1868 (1973).
22. E. GRUNWALD, A. LOEWENSTEIN, and S. MEIBOOM. J. Chem. Phys. **27**, 630 (1957).
23. E. GRUNWALD, A. LOEWENSTEIN, and S. MEIBOOM. J. Chem. Phys. **27**, 641 (1957).
24. R. G. PEARSON and R. D. LANIER. J. Am. Chem. Soc. **86**, 765 (1964).
25. I. SOLOMON and N. BLOEMBERGEN. J. Chem. Phys. **25**, 261 (1956).
26. P. K. GLASOE and F. A. LONG. J. Phys. Chem. **64**, 188 (1960).
27. M. COHN and T. R. HUGHES, JR. J. Biol. Chem. **237**, 176 (1962).
28. H. STERNLICHT, R. G. SHULMAN, and E. W. ANDERSON. J. Chem. Phys. **43**, 3123 (1965).
29. H. STERNLICHT, R. G. SHULMAN, and E. W. ANDERSON. J. Chem. Phys. **43**, 3133 (1965).
30. T. A. GLASSMAN, C. COOPER, L. W. HARRISON, and T. J. SWIFT. Biochemistry, **10**, 843 (1971).
31. G. P. P. KUNTZ, T. A. GLASSMAN, C. COOPER, and T. J. SWIFT. Biochemistry, **11**, 538 (1972).
32. C. M. FREY, J. L. BANYASZ, and J. E. STUEHR. J. Am. Chem. Soc. **94**, 9198 (1972).
33. F. F. BROWN, I. D. CAMPBELL, R. HENSON, C. W. J. HIRST, and R. E. RICHARDS. Eur. J. Biochem. **38**, 54 (1973).
34. T. A. GLASSMAN, C. COOPER, G. P. P. KUNTZ, and T. J. SWIFT. F.E.B.S. Lett. **39**, 73 (1974).
35. V. WEE, I. FELDMAN, P. ROSE, and S. GROSS. J. Amer. Chem. Soc. **96**, 103 (1974).
36. I. FELDMAN and V. WEE. Biochemistry, **13**, 1836 (1974).
37. D. H. BUISSON and H. SIGEL. Biochim. Biophys. Acta, **343**, 45 (1974).
38. C. F. NAUMANN, B. PRIJS, and H. SIGEL. Eur. J. Biochem. **41**, 209 (1974).
39. H. STERNLICHT, D. E. JONES, and K. KUSTIN. J. Am. Chem. Soc. **90**, 7110 (1968).
40. C. M. FREY and J. E. STUEHR. *In* Metal ions in biological systems. Vol. I. *Edited by* H. Sigel. Marcel Dekker, New York, N.Y. 1974. p. 51.
41. M. S. ZETTER, H. W. DODGEN, and J. P. HUNT. Biochemistry, **12**, 778 (1973).
42. R. PHILLIPS. Chem. Rev. **66**, 501 (1966).
43. R. M. IZATT, J. J. CHRISTENSEN, and J. R. RYTTING. Chem. Rev. **71**, 439 (1971).
44. G. G. HAMMES and S. A. LEVISON. Biochemistry, **3**, 1504 (1964).
45. T. J. SWIFT. *In* NMR of paramagnetic molecules. *Edited by* G. N. La Mar, W. DeW. Horrocks, Jr. and R. H. Holm. Academic Press, New York. 1973. p. 53.
46. I. SOLOMON. Phys. Rev. **99**, 559 (1955).

Can. J. Chem. Downloaded from www.nrcresearchpress.com by 210.87.254.5 on 09/05/12
For personal use only.

Energetics of the Ionization and Fragmentation of Phosphorus Trifluoride by Electron Impact

DAVID F. TORGERSON

Cyclotron Institute and Department of Chemistry, Texas A. & M. University, College Station, Texas 77843

AND

JOHN B. WESTMORE[1]

Department of Chemistry, University of Manitoba, Winnipeg, Manitoba R3T 2N2

Received September 5, 1974

DAVID F. TORGERSON and JOHN B. WESTMORE. Can. J. Chem. 53, 933 (1975).

Relative intensities and appearance potentials of several positive ions in the mass spectrum of PF_3 are reported as well as an ionization efficiency curve for F^-, the only negative ion of significant intensity. Probable ion fragmentation pathways are proposed, together with heats of formation of some positive ions, and ionization potentials for PF_3, PF_2·, and PF. The results are compared with available data for other Group V halides.

DAVID F. TORGERSON et JOHN B. WESTMORE. Can. J. Chem. 53, 933 (1975).

On rapporte les intensités relatives et les potentiels d'apparition de plusieurs ions positifs dans le spectre de masse de PF_3 de même que les courbes d'efficacité d'ionisation pour F^-, seul ion négatif d'intensité notable. On propose des chemins probables pour la fragmentation des ions, de même que les chaleurs de formation de quelques ions positifs et les potentiels d'ionisation de PF_3, PF_2. et PF. On compare ces résultats avec les données disponibles pour d'autres halogénures du groupe V. [Traduit par le journal]

There has been considerable interest in the ionization of the monomeric halides and hydrides of the main Group V elements, both from an experimental and a theoretical point of view. Photoelectron spectroscopy has been used to study PF_3 (1–5), other Group V halides (5–9), hydrides (3, 8–11) and PF_3-containing complexes of Ni and Pt (2, 12) and Cr, Fe, and Rh (13). Electron impact appearance potentials have been measured for NF_3 (14), PH_3 (15–20), PCl_3 (21–23), PBr_3 (24), PI_3 (25), $AsCl_3$ (7, 23, 26), $SbCl_3$ (23), AsH_3 (15, 26, 27), SbH_3, BiH_3 (15), and Ni and Co complexes containing PF_3 (28, 29). Photoionization studies have been reported for NF_3 (30) and PF_3, PCl_3, PH_3, AsH_3, and SbH_3 (31). Absorption spectra have been obtained for the hydrides and halides (32) and ionization and dissociation energies of hydrides and fluorides have been discussed (33). Molecular orbital calculations have been made for PH_3, PF_3, and $P(CH_3)_3$ (34) and for PF_3 and PF_2CN (35). In view of this extensive activity it is surprising that no electron impact studies have been published for PF_3. Consequently, we wish to report our results for this simple and important molecule.

[1]To whom correspondence should be addressed.

Results and Discussion

The positive ion mass spectrum of PF_3 at an electron energy of 70 V is shown in Table 1. Apart from background peaks due to air and water there were also small peaks of variable intensity observed at *m/e* 20, 35, 36, 37, 38, 81, 85, and 104 which could be assigned to HF^+, 20; Cl^+, 35, 37; HCl^+, 36, 38; SiF_3^+, 85; and SiF_4^+, 104. The source of HF and SiF_4 was thought to be from the reaction of PF_3 with background water, and the glass reservoir and inlet line respectively, while HCl was formed by the action of moisture on the SbF_3, PCl_3 mixture used to prepare PF_3. The peak at *m/e* 81 was tentatively assigned to P_2F^+ formed from P_2F_2 or P_2FCl as possible by-products of PF_3 preparation. For normal recording conditions no metastable peaks were observed, but at high sensitivity a metastable peak could just be detected at *m/e* 36.2, corresponding to the reaction $PF_2^+ \rightarrow PF^+ + F$ (36.23 calculated). The negative ion mass spectrum showed only F^-.

The appearance potential (a.p.) of PF_3^+ was determined from the experimental data by three procedures, namely, the "extrapolated voltage difference" (e.v.d.) method (36), the "semilogarithmic plot" (s.l.p.) method (37), and the

Can. J. Chem. Downloaded from www.nrcresearchpress.com by 210.87.254.42 on 09/05/12
For personal use only.

TABLE 1. Relative intensities and appearance potentials of positive ions in the mass spectrum of PF_3

m/e	Ion	Relative intensity (70 eV)	Appearance potential (eV)	Method
88	PF_3^+	71	11.81±0.06*	e.v.d.
			11.63±0.02*	s.l.p.
			11.64±0.09*	e.d.d.
69	PF_2^+	100	15.5 ±0.2	s.l.p.
50	PF^+	9.4	20.5 ±0.2	e.v.d.
44	PF_3^{2+}	3.9	†	
34.5	PF_2^{2+}	3.1	~40	s.l.p.
31	P^+	4.3	32.3 ±0.5	e.v.d.
25	PF^{2+}	6.9	~40	s.l.p.
19	F^+	3.6	~36	s.l.p.
15.5	P^{2+}	0.86	‡	

*Mean value = 11.65 ± 0.07 eV.
†Background CO_2 prevents determination.
‡Intensity too low for determination.

"energy distribution difference" (e.d.d.) method (38, 39), using krypton to calibrate the energy scale. Appearance potentials of fragment ions were determined by the s.l.p. method if the curves for fragment ion and Kr^+ were parallel, or nearly parallel, in the threshold region. When this was not true then the e.v.d. method was used. The results are given in Table 1 and represent the mean of several determinations.

PF_3^+

Values for the a.p. of this ion, determined by three procedures, are listed in Table 1. To some extent the values depend upon the method used for determination, the e.v.d. method giving a value slightly higher than the other methods while the s.l.p. method gave the most reproducible results. The mean value of 11.65 ± 0.07 eV is the statistically weighted average incorporating the overall standard deviation.

The i.p. of PF_3 has also been determined by photoelectron spectroscopy. The adiabatic i.p. has been reported as 11.66 eV (4) and the vertical i.p. as 12.28 eV (1), 12.3 eV (2, 3), 12.29 eV (4), and 12.27 eV (5). It is apparent that the i.p. determined by electron impact (especially as obtained by the s.l.p. and e.d.d. methods) is very close to the adiabatic value and that an earlier value of 9.71 eV obtained by photoionization (31) is incorrect.

Ionization by electron impact is a vertical ionization process and the probability of ionization to the ground vibrational state of the molecular ion will depend upon the relative shapes and positions of the potential energy surfaces of the neutral molecule and ground electronic state of the molecular ion. When the relative probability of producing the molecular ion in its lowest energy state is small the measured a.p. *may* be greater than the adiabatic i.p. of the molecule and will often be a function of the sensitivity of the ion detecting equipment. On the other hand, the measured a.p. will be smaller than the vertical i.p. (corresponding to the most probable ionizing transition) of the molecule, because of the still finite probabilities of ionization to lower vibrational states of the molecular ion. Generally, ionization potentials determined by electron impact are considered as upper limits to adiabatic ionization potentials.

Photoelectron spectroscopy shows that, for PF_3, the vertical i.p. lies some 0.6 eV above the adiabatic i.p. In spite of this, the sensitivity of the ion detecting system of the mass spectrometer is evidently high enough to detect formation of PF_3^+ in its ground state. To calculate ΔH_{f298}^0 for PF_3^+ the mean of −221.95 (40) and −219.6 kcal/mol (41) was used for ΔH_{f298}^0 (PF_3, gas).

PF_2^+

There are two plausible reactions which could lead to production of this ion

[1] $$PF_3 + e \rightarrow PF_2^+ + F + 2e$$

[2] $$PF_3 + e \rightarrow PF_2^+ + F^- + e$$

In order to distinguish between them the initial assumption was made that, at threshold, the excess energies associated with the reactions

Can. J. Chem. Downloaded from www.nrcresearchpress.com by 210.87.254.42 on 09/05/12
For personal use only.

TABLE 2. Probable ion formation reactions and heats of formation of positive ions in the mass spectrum of PF_3

Ion	Reaction	ΔH_{f298}^0(kcal/mol)
PF_3^+	$PF_3 + e \rightarrow PF_3^+ + 2e$	48 ± 3
PF_2^+	$PF_3 + e \rightarrow PF_2^+ + F + 2e$	$\leqslant 117 \pm 6$
PF^+	$PF_3 + e \rightarrow PF^+ + F_2 + 2e$	$\leqslant 252 \pm 6$*

*Based on reaction 4. See text for possible uncertainties.

were small. By taking $D(PF_2—F) = 131 \pm 10$ kcal/mol (42), and the electron affinity of F as 3.45 eV (43, 44) values obtained for the i.p. of $PF_2\cdot$ were 9.8 ± 0.6 and 13.25 ± 0.6 eV for reactions 1 and 2 respectively. The i.p. of $PF_2\cdot$ is expected to be substantially lower than that of PF_3 because of the stabilization of positive charge in the even-electron PF_2^+ by delocalization over the three atoms as indicated by the canonical forms

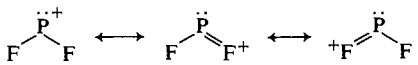

The anticipated lowering is about 1–2 eV by comparison with other AX_3 and $AX_2\cdot$ species having similar valence shell electron configurations (see, for example, Table 3). A similar, but larger, lowering is observed between CF_4 (i.p. = 14.9 eV) and $CF_3\cdot$ (i.p. = 10.1 eV) (41) where the positive charge on CF_3^+ can be delocalized over four atoms rather than three as in AX_2^+. Thus, for reaction 2 to apply, an excess energy of at least 2.5 eV would be involved. In spite of the high bond energy in PF_3 this is considered unlikely because (*a*) in the threshold region the ionization efficiency curve for PF_2^+ was so similar to that of Kr^+ that the s.l.p. method could be used to determine the a.p. of PF_2^+, and (*b*) according to Stevenson's rule (45), as the i.p. of $PF_2\cdot$ is substantially less than that of F then the products of reaction 2 should be formed without excess energy. Consequently, reaction 1 is indicated. The value obtained for the i.p. of $PF_2\cdot$ is an upper limit, though according to Stevenson's rule, excess energy for this reaction should be small at threshold. Probably, the largest uncertainty in the value comes from $D(PF_2—F)$ which depends upon an estimated value, rather than an experimental value, for $\Delta H_f(PF_2\cdot)$. The calculated value for $\Delta H_{f298}^0(PF_2^+)$ in Table 1 is based on reaction 1, using $\Delta H_{f298}^0(F) = 19.0$ kcal/mol (41), and the value quoted earlier for PF_3.

PF^+

There are three plausible reactions which could lead to production of this ion

[3] $PF_3 + e \rightarrow PF^+ + 2F + 2e$

[4] $PF_3 + e \rightarrow PF^+ + F_2 + 2e$

[5] $PF_3 + e \rightarrow PF^+ + F + F^- + e$

Calculations for these reactions are based on $\Delta H_{f298}^0(PF) = 11 \pm 10$ kcal/mol, a value estimated from D(N—H) and the mean bond energies in NH_3 and PH_3 (ref. 42, p. 132). By assuming negligible excess energies at threshold the upper limits for the i.p. of PF are calculated to be 9.8 ± 0.6, 11.4 ± 0.6, and 13.2 ± 0.6 eV for reactions 3, 4, and 5 respectively. When compared with the i.p. of PF_3 the latter value is much too high (compare values in Table 3). Considerable excess energy is required for reaction 5 to apply, but the possibility is not definitely excluded. Because of the uncertainty in the i.p. values a choice between reactions 3 and 4 is more difficult though reaction 4 is to be preferred. The i.p. of PF should exceed that of $PF_2\cdot$ because there is less opportunity for positive charge delocalization in PF^+ compared to PF_2^+. Furthermore, the i.p. of PF should be greater than that of PCl (see below, and Table 3). For comparison, using tabulated data (41), the i.p. of the isoelectronic SO molecule is calculated to be 10.65 ± 0.35 eV. The calculated value of $\Delta H_{f298}^0(PF^+)$ in Table 2 is thus based on reaction 4.

P^+ and F^+

These ions are formed in reactions of considerable excess energy since the threshold energies for the highest energy reactions leading to their formation, namely

[6] $PF_3 + e \rightarrow P^+ + 3F + 2e$

[7] $PF_3 + e \rightarrow F^+ + P + 2F + 2e$

lead to a calculated a.p. for P^+ of 25.8 eV

Can. J. Chem. Downloaded from www.nrcresearchpress.com by 210.87.254.42 on 09/05/12
For personal use only.

Can. J. Chem. Downloaded from www.nrcresearchpress.com by 210.87.254.42 on 09/05/12
For personal use only.

TABLE 3. Ionization potentials (eV) of Group V halide molecules and radicals.

Molecule	Ionization potential	Radical	Ionization potential	Molecule	Ionization potential	Method*	Reference
NF_3	13.00±0.2	NF_2·	11.73±0.09	NF	(12.07)†	p.i.	30
	13.2		12.1		12.9	Analysis of literature	33
	12.97 (adiabatic)					p.e.	9
PF_3	11.65±0.07	PF_2·	⩽9.8±0.6	PF	⩽11.4±0.6‡	e.i.	This work
	11.66 (adiabatic)					p.e.	4
PCl_3	10.75±0.2	PCl_2·	8.8±0.4	PCl	9.9±0.4	e.i.	21
	10.6 ±0.2		8.3±0.7		9.6±0.7	e.i.	22
	9.91?					p.i.	31
PBr_3	10.0 ±0.2	PBr_2·	8.7±0.6	PBr	10.2±0.6	e.i.	24
		PI_2·	9.8±0.4			e.i.	25
$AsCl_3$	10.57±0.3					e.i.	7
	10.55					p.e.	7

*e.i., electron impact mass spectrometry; p.i., photoionization; p.e., photoelectron spectroscopy.
†Estimated to be same as O_2.
‡Based on reaction 4. See text for possible uncertainties.

Can. J. Chem. Downloaded from www.nrcresearchpress.com by 210.87.254.42 on 09/05/12
For personal use only.

compared with the experimental value of 32.3 eV, and to an a.p. for F^+ of 32.7 eV compared with the experimental value of 36 eV. (For these ions the ionization efficiency curves had low energy tails which were attributed to ionization of a background impurity amounting to ~5% at *m/e* 31 and ~1% at *m/e* 19. The threshold energies were much too low to arise from fragmentation of PF_3.)

Remaining Positive Ions

Since the reactions leading to formation of these ions cannot be definitely established, no further discussion is given.

F^-

The ionization efficiency curve for F^- is shown in Fig. 1. The energy scale was calibrated by comparison with curves for the formation of O^- from CO and O_2 (46). The dissociative electron capture reaction

$$[8] \qquad PF_3 + e \rightarrow PF_2 + F^-$$

is calculated to occur at 2.25 ± 0.4 eV which is below the low energy range of our instrument. Figure 1 may show the high energy tail of the capture peak. The remainder of the ionization efficiency curve shows much structure and processes corresponding to reactions such as [2] or [5] could not be identified. The onset occurring at ~6 eV is at much too low an energy to correspond to [2].

Comparisons with other Group V Halides

It is instructive to consider the i.p. of the Group V halide molecules and radicals given in Table 3. Most values are from electron impact work. Only a few of the photoelectron spectroscopic studies cite adiabatic i.p. In some cases values have been recalculated from the original data using thermochemical information from refs. 41 and 42. Some electron impact results for PCl_3, $AsCl_3$, and $SbCl_3$ (23, 26) are not included because of their low accuracy.

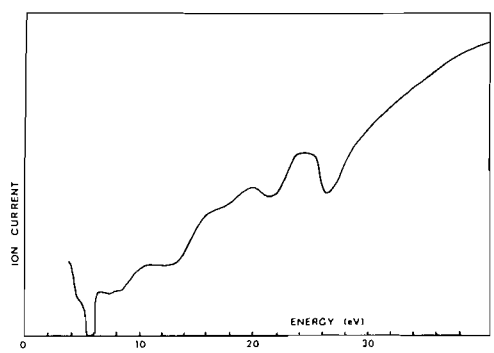

FIG. 1. Ionization efficiency curve for F^- from PF_3.

For each Group V halide in Table 3 the main fragmentation occurs according to

$$[1a] \qquad AX_3 + e \rightarrow AX_2^+ + X + 2e$$

Although Halmann and Klein (22) proposed a dissociative capture process for the formation of PCl_2^+ from PCl_3 their value of 11.8 ± 0.4 eV is clearly much too high for the i.p. of $PCl_2\cdot$. Their proposal was based on an interpretation of an ionization efficiency curve at least as complex as that of Fig. 1 and is extremely questionable. It appears that the energetically more favorable reactions analogous to [2] have very low ionization cross sections.

With the exception of PF_3 the formation of the AX^+ ion for all the other compounds in Table 3 is based on the reaction

$$[3a] \qquad AX_3 + e \rightarrow AX^+ + 2X + 2e$$

The reason for the difference is not obvious though the fragmentation may be sensitive to differences in potential energy surfaces for molecules and ion products. Other differences in behavior from PF_3 can be noted. For example, the formation of P^+ from PCl_3 occurs with little excess energy at threshold (21).

It is noteworthy that the i.p. of PCl is close to that of the isoelectronic S_2 molecule (9.9 ± 0.5 eV) (41).

It is apparent from the incomplete nature of Table 3 that further studies on the Group V halides are much needed.

Experimental

PF_3 was prepared in a vacuum rack by condensing PCl_3 onto SbF_3 using a liquid nitrogen trap. The first gases evolved on warming the sample were passed through several CO_2–acetone or CO_2–isopropanol traps to remove PCl_3, then stored in glass bulbs before use.

Mass spectra and appearance potentials were determined using a Hitachi Perkin–Elmer RMU-6D single focussing mass spectrometer, using an external potentiometer for potential measurements. For a.p. determinations ion current readings for a particular ion were taken at 0.100 V intervals upward from the ionization threshold and also at an electron energy of 50 V before and after these readings. Appearance potentials were determined relative to krypton (i.p. = 14.00 eV) and argon (i.p. = 15.76 eV) as standards.

Addendum

A referee has suggested the possibility that CF_4 might be present from the reaction of PF_3 with high vacuum grease or other organic

residues. Since CF_4 would give ions of the same nominal m/e values as PF_3 then a relatively small amount could affect the shape of some of the ionization efficiency curves. We cannot exclude this possibility but literature values (41) for a.p. of ions from CF_4, obtained by the s.l.p. method, are: CF_4^+, 14.9 ± 0.2 eV (derived value, since this ion is absent from the spectrum); CF_3^+, 16.0 ± 0.2 eV; CF_2^+, 20.3 ± 0.5 eV; CF^+, 22.6 ± 0.5 eV. Low amounts of an interfering ion are only likely to have a serious effect on the ionization efficiency curve of a more abundant ion if it has a lower a.p. than the more abundant ion. Thus CF_4^+ (which has a negligible intensity in any case) and CF_3^+ are unlikely to significantly influence the quoted a.p. for PF_3^+ and PF_2^+ respectively, while the a.p. of CF^+ is so far different from that of P^+ that a contribution to the ionization efficiency curve would be obvious. Only in the case of PF^+ could interference from CF_2^+ be troublesome.

We thank the National Research Council of Canada for financial support of this work.

1. A. W. Potts, H. J. Lempka, D. G. Streets, and W. C. Price. Phil. Trans. R. Soc. A**268**, 59 (1970).
2. J. C. Green, D. I. King, and J. H. D. Eland. Chem. Commun. 1121 (1970).
3. J. P. Maier and D. W. Turner. J. Chem. Soc. Faraday II, **68**, 711 (1972).
4. P. J. Bassett, D. R. Lloyd, I. H. Hillier, and V. R. Saunders. Chem. Phys. Lett. **6**, 253 (1970).
5. P. J. Bassett and D. R. Lloyd. J. Chem. Soc. Dalton, 248 (1972).
6. D. Betteridge, M. Thompson, A. D. Baker, and N. R. Kemp. Anal. Chem. **44**, 2005 (1972).
7. R. A. W. Johnstone and F. A. Mellon. J. Chem. Soc. Faraday II, **68**, 1209 (1972).
8. S. Cradock and D. W. H. Rankin. J. Chem. Soc. Faraday II, **68**, 940 (1972).
9. A. B. Cornford, D. C. Frost, C. A. McDowell, J. L. Ragle, and A. I. Stenhouse. Advances in mass spectrometry. Vol. 5. The Institute of Petroleum, London. 1971. p. 105.
10. G. R. Branton, D. C. Frost, C. A. McDowell, and I. A. Stenhouse. Chem. Phys. Lett. **5**, 1 (1970).
11. A. W. Potts, and W. C. Price. Proc. R. Soc. A**326**, 181 (1971).
12. I. H. Hillier, V. R. Saunders, M. J. Ware, P. J. Bassett, D. R. Lloyd, and N. Lynaugh. Chem. Commun. 1316 (1970).
13. J. F. Nixon. J. Chem. Soc. Dalton, 2226 (1973).
14. R. M. Reese and V. H. Dibeler. J. Chem. Phys. **24**, 1175 (1956).
15. F. E. Saalfeld and H. J. Svec. Inorg. Chem. **2**, 46 (1963).
16. N. V. Larin, G. G. Devyatykh, and I. L. Agafonov. Russ. J. Inorg. Chem. **9**, 110 (1964).
17. H. Neuert and H. Clasen. Z. Naturforsch. 7a, 410 (1952).
18. T. P. Fehlner and R. B. Callen. Advances in chemistry series. Vol. 72. American Chemical Society, Washington. 1968. p. 181.
19. Y. Wada and R. W. Kiser. Inorg. Chem. **3**, 174 (1964).
20. J. Fischler and M. Halmann. J. Chem. Soc. 31 (1964).
21. A. A. Sandoval, H. C. Moser, and R. W. Kiser. J. Phys. Chem. **67**, 124 (1963).
22. M. Halmann and Y. Klein. J. Chem. Soc. 4324 (1964).
23. P. Kusch, A. Hustrulid, and J. T. Tate. Phys. Rev. **52**, 840 (1937).
24. R. W. Kiser, J. G. Dillard, and D. L. Dugger. Advances in chemistry series. Vol 72. American Chemical Society, Washington. 1968. p. 153.
25. A. Finch, A. Hameed, P. J. Gardner, and N. Paul. Chem. Commun. 391 (1969).
26. W. R. Cullen and D. C. Frost. Can. J. Chem. **40**, 390 (1960).
27. F. E. Saalfeld and M. V. McDowell. Inorg. Chem. **6**, 96 (1967).
28. R. W. Kiser, M. A. Krassoi, and R. J. Clark. J. Am. Chem. Soc. **89**, 3653 (1967).
29. F. E. Saalfeld, M. V. McDowell, A. G. MacDiarmid, and R. E. Highsmith. Int. J. Mass Spectrom. Ion Phys. **9**, 197 (1972).
30. V. H. Dibeler and J. A. Walker. Inorg. Chem. **8**, 1729 (1969).
31. W. C. Price and T. R. Passmore. Discuss. Faraday Soc. **35**, 232 (1963).
32. C. M. Humphries, A. D. Walsh, and P. A. Warsop. Discuss. Faraday. Soc. **35**, 148 (1963).
33. W. C. Price, T. R. Passmore, and D. M. Roessler. Discuss. Faraday Soc. **35**, 201 (1963).
34. I. H. Hillier and V. R. Saunders. Chem. Commun. 316 (1970).
35. W. R. Hall and H. F. Hameka. Inorg. Chem. **12**, 1878 (1973).
36. J. W. Warren. Nature, **165**, 810 (1950).
37. F. P. Lossing, A. W. Tickner, and W. A. Bryce. J. Chem. Phys. **19**, 1254 (1951).
38. R. E. Winters, W. L. Courchene, and J. H. Collins. Chem. Eng. News, 44 (1966).
39. R. E. Winters, J. H. Collins, and W. L. Courchene. J. Chem. Phys. **45**, 1931 (1966).
40. R. L. Potter and V. N. DiStephano. J. Phys. Chem. **65**, 849 (1961).
41. J. L. Franklin, J. G. Dillard, H. M. Rosenstock, J. T. Herron, K. Draxl, and F. H. Field. Ionization potentials, appearance potentials, and heats of formation of gaseous positive ions: NSRDS-NBS 26. U.S. Govt. Printing Office, Washington, 1969.
42. V. I. Vedeneev, L. V. Gurvich, V. N. Kondrat'yev, V. A. Medvedev, and Ye. L. Frankevich. Bond energies, ionization potentials and electron affinities. Edward Arnold, London. 1966. p. 83.
43. D. Cubiciotti. J. Chem. Phys. **34**, 2189 (1961).
44. R. S. Berry and C. W. Reimann. J. Chem. Phys. **38**, 1540 (1963).
45. D. P. Stevenson. Discuss. Faraday Soc. **10**, 35 (1951).
46. F. H. Field and J. L. Franklin. Electron impact phenomena. Revised Ed. Academic Press, New York, 1970.

Can. J. Chem. Downloaded from www.nrcresearchpress.com by 210.87.254.42 on 09/05/12
For personal use only.

Synthesis and Characterization of Some Dibasic Tridentate Schiff Base Ligands[1]

ELMER C. ALYEA AND ABDUL MALEK

Department of Chemistry, University of Guelph, Guelph, Ontario N1G 2W1

Received August 21, 1974

ELMER C. ALYEA and ABDUL MALEK. Can. J. Chem. **53**, 939 (1975).

The synthesis and characterisation of several dibasic tridentate Schiff base ligands (H_2SB) are described. Structural formulas for the isolated ligands are suggested on the basis of infrared, nuclear magnetic resonance, and mass spectral data.

ELMER C. ALYEA et ABDUL MALEK. Can. J. Chem. **53**, 939 (1975).

On décrit la synthèse et la caractérisation de plusieurs ligands (H_2SB) dibasiques tridentates et dérivés de bases de Schiff. On propose des formules structurales pour les ligands isolés en se basant sur les données infrarouges, r.m.n. et de masse. [Traduit par le journal]

Can. J. Chem. Downloaded from www.nrcresearchpress.com by 210.87.254.6 on 09/05/12
For personal use only.

Introduction

In continuing our studies of titanium(IV) compounds having uncommon coordination numbers for titanium (1, 2) we are presently engaged in investigations involving various Schiff base ligands, particularly dibasic tridentate ONO and ONS ligands. During the characterization of complexes of the types $Ti(SB)_2$ and $(RO)_2Ti(SB)$ it became necessary, in establishing physicochemical criteria for the coordinating behavior of the ligands, to isolate and characterize by spectral methods the free Schiff base ligands under study.[2]

In this paper we report the synthesis and characterization of several potentially tridentate ONO and ONS donor Schiff base ligands (H_2SB). Structural formulas for the following ligands, depicted in their Schiff base forms, are given in Fig. 1: salicylaldehyde-2-hydroxyanil (H_2SAP), salicylaldehyde-2-hydroxyethylimine (H_2SAE), salicylaldehyde-3-hydroxypropylimine (H_2SPA), acetylacetone-2-hydroxyanil (H_2AAP), and acetylacetone-2-mercaptoanil (H_2ASP). The characterization of salicylaldehyde-2-mercaptoanil (H_2SSP) was reported earlier (3).

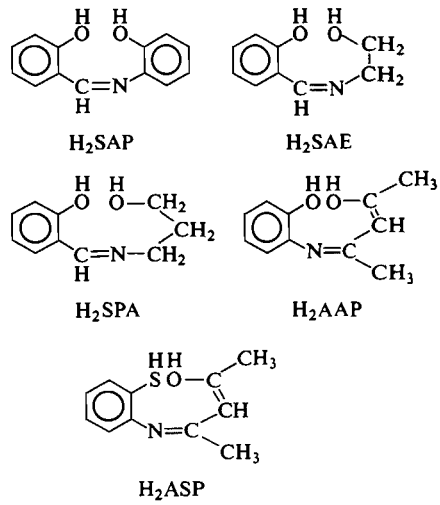

FIG. 1. Formulation of H_2SAP, H_2SAE, H_2SPA, H_2AAP, and H_2ASP.

Experimental

Chemicals

Salicylaldehyde was obtained from Fisher Scientific Company or J. T. Baker Chemical Company. The latter company also supplied acetylacetone, 3-amino-1-propanol, and 2-amino-1-ethanol. Eastman Organic Chemicals was the source of *o*-aminophenol, which was recrystallized from ethanol before use. *o*-Aminothiophenol was purchased from Matheson, Coleman and Bell. Solvents were purified and dried following standard procedures.

Physical Measurements

Elemental analyses were performed in this department by S. McKinnon and by M-H-W Laboratories, Garden City, Michigan. Infrared spectra were obtained in the region 4000–200 cm^{-1} using a Beckman IR-12 spectrophotometer. Mass spectra were recorded with a Varian Mat-7 mass spectrometer at an ionizing energy of 70 eV by L. MacDonald. Proton n.m.r. spectra were obtained with a Varian A-60A spectrometer at ambient temperatures with TMS as the internal standard.

[1]Presented in part at the 166th ACS National Meeting, Chicago, Illinois, August 26–31, 1973.

[2]For part I of a series concerning these complexes, see ref. 3.

TABLE 1. Some Properties and Analytical Data for the Ligands

Compound	Color	Melting point (°C)	Highest* *m/e* peak	Analyses (%) Found C	Found H	Found N	Calculated C	Calculated H	Calculated N
H_2SAP	Orange	195	213	73.0	5.2	6.5	73.2	5.2	6.6
H_2ASP	Colorless	86–87	207	64.0	6.6	6.7	63.8	6.3	6.8
H_2AAP	Yellowish-white	196	191	69.9	6.9	7.3	69.2	6.8	7.3
H_2SAE	Amber oil	138/1 mm†	165	64.9	6.6	8.6	65.5	6.7	8.5
H_2SPA	Amber oil	123–124/10^{-3} mm†	179	66.9	7.3	7.6	67.0	7.3	7.8

*Corresponds to parent peak.
†Distillation conditions.

TABLE 2. Characteristic infrared bands of the Schiff base ligands*

Compound	3600–2500 cm^{-1} Halocarbon	3600–2500 cm^{-1} Dimethylsulfoxide	1700–1500 cm^{-1} Halocarbon	1700–1500 cm^{-1} Dimethylsulfoxide
H_2SAP	3050w, 2925w 2620w, 2580w	3530s, 3200s, b 2880s, b	1638s, 1620m 1600m, 1542sh 1532s, 1510w	1630vs, 1605s 1585sh, 1504w
H_2SAE	3370s, b, 2940s 2890s	3350vs, b, 2750vs, b	1638vs, 1616s 1585m, 1532m 1500s	1655sh, 1610vs, b 1510vs, 1502vs
H_2SPA	3400s, b, 2940s 2870s	3430vs, b, 2900m, b	1635vs, 1615sh 1582m, 1530m 1498s	1650vs, b, 1605sh 1520s
H_2AAP	3140–2980s, b 2880sh, 2740m 2630m	3510m, 3430m 3190vs, b, 2850s, b 2740s, b, 2620m	1613vs, 1560vs 1515m, sh	1625vs, 1605vs 1578vs, 1520s 1503sh
H_2ASP	3340s	3500vs, b, 3270vs, b	1715vs, 1588vs	1725vs, 1675sh 1592vs, 1485vs

*s = strong, m = medium, b = broad, v = very, sh = shoulder, w = weak.

Preparation of the Ligands

Previous preparative methods for H_2SAP (4), H_2SAE (5), H_2SPA (6), and H_2AAP (7) are only briefly described in the literature. Nevertheless, synthetic details are not described here since their preparation follows standard methods (8) and is similar to that described below. Acetylacetone-2-mercaptoanil (H_2ASP) was prepared by the following procedure: acetylacetone (5.0 g, 50 mmol) was dissolved in 100 ml ethanol and cooled in an ice bath. *o*-Aminothiophenol (6.25 g, 50 mmol) dissolved in 50 ml ethanol and also precooled was added to the acetylacetone solution. After stirring briefly the solution was allowed to stand at room temperature overnight. The large prismatic crystals which separated were collected by filtration, washed with chilled ethanol, and dried under vacuum over P_4O_{10}.[3]

[3]Cooling is essential to avoid formation of an orange oxidation product. Our preliminary findings indicate that the oxidized species is not the simple benzothiazole, as found for H_2SSP (3).

Some of the physical properties and the analyses of the free ligands are summarized in Table 1.

Results and Discussion

Structures of the Ligands

Even though earlier workers had isolated some of the Schiff base ligands used in this study (as compared to *in situ* preparation prior to adding a metal salt), the literature is sparse with respect to spectral characterization of their structures. We have previously demonstrated that the condensation product of salicylaldehyde and *o*-aminothiophenol exists in the benzothiazoline (cyclic) form in the free ligand but readily transforms to the chelating Schiff base form in reactions with titanium alkoxides (3). Accordingly, in order to employ changes in the infrared frequencies and n.m.r. chemical shifts as criteria

Can. J. Chem. Downloaded from www.nrcresearchpress.com by 210.87.254.6 on 09/05/12
For personal use only.

TABLE 3. Nuclear magnetic resonance data for the Schiff base ligands*

Compound	—N=CH—	—OH and/or —NH	Other resonance peaks†
H_2SAP	8.95	13.75, 9.64	—
H_2SAE	8.57 (8.19)	*ca.* 7.1	3.68
H_2SPA	8.59 (8.25)	*ca.* 7.1	3.50, 1.78
H_2AAP	—	12.22, 9.90 (12.08, 8.10)	5.24(1), 1.97(6)
H_2ASP	—	6.43 (4.97)	3.20(2), 2.14(3) 1.63(3)

*In DMSO-d_6 or $CDCl_3$ (in parenthesis) with TMS as internal standard; values are in p.p.m. (δ).
†Broad multiplets centered at *ca.* 7.1 δ due to phenyl protons are omitted.

of tridentate behavior in a series of titanium(IV) complexes, it was necessary to obtain the characteristic spectral data for the ligands. This information for the free ligands is recorded in Tables 2 and 3. Broad multiplets assignable to phenyl protons were also observed in the range 6.4–7.5 δ for all of the Schiff base ligands.

The infrared spectrum of H_2SAP in dimethylsulfoxide shows several bands in the hydroxyl stretching frequency region (Table 2) and their weakening and shift to lower energy in the solid state (halocarbon mull) is compatible with even more extensive intramolecular H-bonding in the solid state. On the basis of observing frequencies at 3546 and 2730 cm^{-1} for a 0.01 *M* CCl_4 solution of H_2SAP, Baker and Shuligan (4) assigned the higher frequency to the hydroxyl of the salicylaldehyde residue (H-bonded to the azomethine nitrogen) and the lower frequency to the hydroxyl of the amine residue (H-bonded to the π-electron system of the —CH=N— bond). Our observation (Table 3) of resonance peaks at 13.75 δ and 9.64 δ which disappear with the addition of D_2O substantiates the infrared assignment of the presence of two intramolecularly-bonded hydroxyl- groups. The single proton giving a singlet at 8.95 δ in the n.m.r. spectrum of the dimethylsulfoxide-d_6 solution of H_2SAP does not exchange with D_2O and hence may be assigned to the azomethine proton (9). In monomeric $(CH_3)_2Sn(SAP)$, where distinct spin–spin coupling is observed between the tin nuclei and the azomethine proton via the N → Sn coordinate bond, the azomethine proton chemical shift has recently been reported to occur at 9.03 δ in dimethylsulfoxide-d_6 (10). Some of the strong infrared bands near 1600 cm^{-1} are doubtless associated with C=N stretching frequencies but any assignment (11) to uncoupled ν(C=N) is unwise in view of the recent exhaustive isotopic labelling study that indicates extensive vibrational coupling in Schiff bases derived from salicylaldehyde (9). The significant frequency shift of several bands in the 1700–1500 cm^{-1} region upon complexation of H_2SAP does indeed suggest vibrational coupling of the C=N and C=C stretching frequencies.

The mass spectrum of H_2SAP shows a base peak at *m/e* 213 corresponding to the parent molecular ion, $C_{13}H_{11}O_2N^+$. The high intensity is in accord with the stabilization of the molecule by strong intramolecular hydrogen-bonding. Similarly the high resistance of the ligand to hydrolysis reflects the stabilization of the azomethine bond by means of the hydrogen-bonded ring system. It is well established that chelate ring formation with metal ions allows stabilization of Schiff base —C=N— bonds (8). Additionally, it is worth noting that a very strong peak at *m/e* 120 can be assigned to the fragment

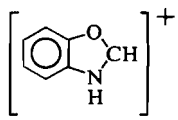

The formation of such stable heterocyclic species is characteristic of the mass spectra of *ortho*-substituted aromatic Schiff bases (12).

Schiff bases obtained from salicylaldehyde are expected to exist predominantly as the phenol-imine tautomer (8, 9). The spectral evidence obtained in this study and by previous workers (4, 11, 13) confirms that H_2SAP also can be

Can. J. Chem. Downloaded from www.nrcresearchpress.com by 210.87.254.6 on 09/05/12
For personal use only.

formulated in the Schiff base form (Fig. 1) in which intramolecular hydrogen-bonding occurs.

Salicylaldehyde condenses with 2-amino-1-ethanol and 3-amino-1-propanol to form amber oils (represented as H_2SAE and H_2SPA in this paper) which can be purified by distillation under reduced pressure. The infrared spectrum of each Schiff base is similar to that discussed above for H_2SAP, indicating their structure involves a —N=CH— linkage that is strongly hydrogen-bonded to the hydroxyl hydrogen atoms. It is reasonable to assume that the very intense bands at 1638 and 1635 cm^{-1} for H_2SAE and H_2SPA respectively have a strong ν(C=N) component because they shift to higher frequencies in dimethylsulfoxide, a solvent that is expected to weaken the intramolecular hydrogen bonds and thereby strengthen the —C=N— bond.

The single proton resonance in the n.m.r. spectra of H_2SAE and H_2SPA which occurs near 8.2 δ in $CDCl_3$ and 8.6 in DMSO-d_6 is assigned to the azomethine proton. The downfield shift in the more polar solvent is expected (10) and is of the same order of magnitude as the change in resonance position upon complexation to form titanium(IV) complexes. By integration of the phenyl resonance peaks before and after exchange with deuterium it was determined that the hydroxyl proton resonance signals are masked by the phenyl proton resonance peaks. This upfield shift of the hydroxyl proton chemical shifts for H_2SAE and H_2SPA as compared to H_2SAP can be attributed to the greater shielding of the hydroxyl protons by the more basic nitrogen atoms of the two compounds derived from aliphatic amines. In the mass spectra of H_2SAE and H_2SPA stepwise fragmentation of the aliphatic side-chain is quite evident and the parent ion is no longer the base peak as it was for H_2SAP. A metastable peak at *m/e* 85 for H_2SAE suggests the possibility that the two most intense peaks in the mass spectrum (*m/e* 106 and 133) may be related by the loss of HCN from the higher mass fragment. The spectral evidence thus supports formulation of both H_2SAE and H_2SPA in the (hydrogen-bonded) Schiff base forms shown in Fig. 1.

Although the structure of the mono-condensation product of acetylacetone with *o*-aminophenol is depicted in the Schiff base or enol-imine form in Fig. 1, H_2AAP might also be formulated in the keto-imine (**2***a*) or keto-amine (**2***b*) forms

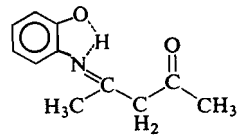

2*a*

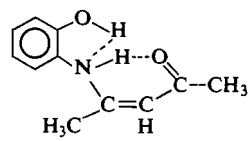

2*b*

shown above. Previous physico-chemical studies on related compounds (14, 15) gave no evidence for the keto-imine form, and in the case of condensation products of alkyl amines with acetylacetone the keto-amine form was predominant to the extent of >95 mol% in nonpolar solvents (15*a*). Our spectral evidence supports this formulation for H_2AAP, at least in $CDCl_3$ solution.

The n.m.r. spectrum of H_2AAP in $CDCl_3$ shows signals at 1.85 δ and 2.10 δ due to inequivalent methyl groups and a one-proton peak at 5.25 δ for the =CH— proton (Table 3). The broad signals at 8.10 δ and 12.08 δ are assigned to the N—H and O—H protons respectively because they disappear upon deuteration. In the halocarbon infrared spectrum (Table 2) the strong broad bands at *ca.* 3000 cm^{-1} may be assigned to the hydrogen-bonded N—H and O—H stretching frequencies expected for **2***b*. The absence of a free carbonyl stretching frequency and a methylene resonance peak in the n.m.r. spectrum clearly eliminates form **2***a* from consideration.

Significant changes occur in both the infrared and the n.m.r. spectrum of H_2AAP when DMSO-d_6 rather than $CDCl_3$ is the solvent. The strong bands attributable to ν(OH) and/or ν(NH) near 3500 and 3200 cm^{-1} might be interpreted as supporting either the keto-amine form **2***b* or the enol-imine form shown in Fig. 1. The more polar solvent might destroy any intramolecular hydrogen-bonding in particular, resulting in the observed increase in frequency. In DMSO-d_6, the methyl n.m.r. signal occurs as a singlet and the peak at 8.10 δ in $CDCl_3$ is now found at 9.90 δ; these changes may be followed by the addition of DMSO-d_6 dropwise to a $CDCl_3$ solution. Since one difference between form **2***b* and that shown in Fig. 1 for H_2AAP is a small displacement in the equilibrium position of the acidic proton, it is feasible that the signal at 9.90 δ in DMSO-d_6 is due to the hydroxyl proton (of the acetylacetone residue) of the enol-imine form. Support for this idea comes

Can. J. Chem. Downloaded from www.nrcresearchpress.com by 210.87.254.6 on 09/05/12
For personal use only.

Can. J. Chem. Downloaded from www.nrcresearchpress.com by 210.87.254.6 on 09/05/12
For personal use only.

from the development of a yellow color as the proportion of the more polar solvent is increased (the yellow color is typical of the —N=C— chromophore in Schiff bases (8)) and the possibility, supported by molecular models, that conjugation in the enol-imine form would allow the methyl groups to become magnetically equivalent. Earlier workers had suggested the enol-imine form was of major importance in the condensation products of acetylacetone with substituted anilines by measuring their acid dissociation constants (15*b*). Nevertheless, it should be pointed out that methyl groups are known to become equivalent in some solutions even when the keto-amine form is predominant (15*a*) and also that the keto-amine form is found in the crystal structure of $[Cu(AAP)]_2$ (16). Molecular models do not allow us to favor one form over the other for H_2AAP but we interpret the above evidence as indicating a tautomeric equilibrium in DMSO-d_6 that shifts virtually completely to the keto-amine form in $CDCl_3$ solution and in the solid state (both are colorless).

The mass spectrum of H_2AAP provides no useful information in discriminating between the possible tautomeric forms. However, it is interesting that in addition to the parent ion peak at *m/e* 191 (77%), the mass spectrum shows the base peak at *m/e* 134. By analogy with the *m/e* peak observed for H_2SAP, this peak may be assigned to the fragment

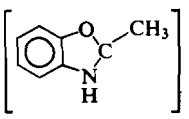

Although a dimeric nickel(II) chelate of H_2ASP has been reported (17) the isolation and characterization of the free ligand has not been discussed. Earlier work by one of us (13) and its extension in the present study indicates that the product obtained on the condensation of acetylacetone with *o*-aminothiophenol is not the Schiff base form shown in Fig. 1. Our results, summarized in Tables 2 and 3 and discussed below, indicate that H_2ASP is similar to salicylaldehyde-2-mercaptoanil (3) in having a heterocyclic benzothiazoline form, shown below. The sharpness of the bands in the solid state infrared spectrum attributable to ν(N—H) and ν(C=O) indicate that any intramolecular hydrogen-bonding must be quite weak.

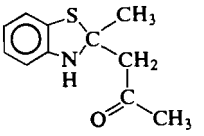

The splitting of the ν(N—H) band in DMSO solution may arise from the competition of the solvent for the hydrogen-bond (14). The n.m.r. spectrum in $CDCl_3$ showed the N—H proton peak at 4.97 δ, identified by its ready exchange with D_2O. The methylene protons give rise to signals at 2.76, 3.05, 3.13, and 3.35 δ in $CDCl_3$ solution. The inequivalence of the methylene protons is due to their proximity to the asymmetric carbon atom of the heterocyclic ring. The observed coupling constant of 17.4 Hz is as expected for this type of AB system (18). In DMSO-d_6, however, the methylene peak becomes a singlet (two-proton) at 3.20 δ. Equivalence of the methylene protons may arise as a consequence of free rotation about the asymmetric carbon to methylene carbon bond by removal of the intramolecular hydrogen bond.

The mass spectrum of H_2ASP, which shows the parent peak at *m/e* 207, also shows a very strong peak at *m/e* 150 corresponding to the fragment

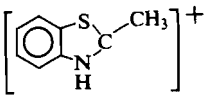

This peak is analogous to that found for H_2SSP at *m/e* 136 (3) and thus supports our formulation of H_2ASP as the benzothiazoline structure. Infrared and n.m.r. spectral evidence for tridentate ONO and ONS ligation of these dibasic tridentate Schiff base ligands in diamagnetic $Ti(SB)_2$ and $(RO)_2Ti(SB)$ complexes will be presented in a future paper.

This work was made possible by an operating grant from the National Research Council of Canada.

1. E. C. ALYEA and P. H. MERRELL. Inorg. Nucl. Chem. Lett. **9**, 69 (1973).
2. E. C. ALYEA, B. S. RAMASWAMY, A. N. BHAT, and R. C. FAY. Inorg. Nucl. Chem. Lett. **9**, 399 (1973).
3. E. C. ALYEA, A. MALEK, and P. H. MERRELL. J. Coord. Chem. **4**, 55 (1974).
4. A. W. BAKER and A. T. SHULGIN. J. Am. Chem. Soc. **81**, 1523 (1959).
5. L. H. GOODSON and H. CHRISTOPHER. J. Am. Chem. Soc. **71**, 1117 (1949).

6. J. A. BERTRAND, J. A. KELLEY, and J. L. BREECE. Inorg. Chim. Acta, **4**, 247 (1970).
7. (*a*) Y. MUTO. Bull. Chem. Soc. Jap. **33**, 1242 (1960); (*b*) W. SNIDER. J. Prakt. Chem. [2] **83**, 241 (1911).
8. R. H. HOLM, G. W. EVERETT, JR., and A. CHAKRAVORTY. Prog. Inorg. Chem. **7**, 83 (1966) and references cited therein.
9. G. C. PERCY and D. A. THORNTON. J. Inorg. Nucl. Chem. **34**, 3357, 3369 (1972).
10. K. KAWAKAMI and T. TANAKA. J. Organometal. Chem. **49**, 409 (1973).
11. N. S. BIRADAR, V. B. MAHALE, and V. H. KULKARNI. Inorg. Chim. Acta, **7**, 267 (1973).
12. D. J. ELIAS and R. J. GILLES. Aust. J. Chem. **19**, 251 (1966).
13. A. MALEK. Ph.D. Thesis, McGill University, Montreal, Quebec. 1972.
14. P. TEYSSIE and J. J. CHARETTE. Spectrochim. Acta, **19**, 1407 (1963).
15. (*a*) G. O. DUDEK and R. H. HOLM. J. Am. Chem. Soc. **84**, 2691 (1962); (*b*) D. F. MARTIN, G. A. JANUSONIS, and B. B. MARTIN. J. Am. Chem. Soc. **83**, 73 (1961).
16. G. A. BARCLAY and B. F. HOSKINS. J. Chem. Soc. 1979 (1965).
17. G. R. BRUBAKER, J. C. LATTA, and D. C. AQUINO. Inorg. Chem. **9**, 2608 (1970).
18. A. K. BOSE. Interpretive spectroscopy. *Edited by* S. K. Freeman. Reinhold Publishing Co., New York. 1965. p. 223.

Can. J. Chem. Downloaded from www.nrcresearchpress.com by 210.87.254.6 on 09/05/12
For personal use only.

An Extension of the Hückel 4N + 2 Rule to Polycyclic Non-alternant Conjugated Hydrocarbons

JERZY KRUSZEWSKI AND TADEUSZ MAREK KRYGOWSKI[1]

Institute of Chemistry, University of Gdansk, 80 216 Gdansk, Sobieskiego 18, Poland,

and

Department of Chemistry, University of Warsaw, 02 093 Warsaw, Pasteura 1, Poland

Received September 13, 1974

JERZY KRUSZEWSKI and TADEUSZ MAREK KRYGOWSKI. Can. J. Chem. **53**, 945 (1975).

A general rule of aromatic stability of non-alternant polycyclic conjugated hydrocarbons has been detailed and using aromatic stability indices, corroborated. The π-electron system is said to be relatively more stable if the difference between number of $4N + 3$-type rings minus number of $4N + 1$-type rings is 0 or divisible by 4. If not, the system is assumed to be relatively unstable. The presence of benzene rings does not affect the rule. A further extension for intramolecular H-bonded systems is also suggested. The rule suggested permits prediction of substituent effects on stability as well as the ionic form being most stable if the rule is not fulfilled.

JERZY KRUSZEWSKI et TADEUSZ MAREK KRYGOWSKI. Can. J. Chem. **53**, 945 (1975).

On a développé une règle générale permettant d'évaluer la stabilité aromatique des hydrocarbures polycycliques conjugués mais non alternants; cette règle a été corroborée en faisant appel aux indices de stabilité aromatique. On dit généralement que le système d'électrons π est relativement plus stable si la différence entre le nombre des cycles du type $4N + 3$ moins le nombre des cycles du type $4N + 1$ est 0 ou divisible par 4. Si tel n'est pas le cas, on fait l'hypothèse que le système est relativement instable. La présence de noyaux benzéniques n'affecte pas cette règle. On suggère aussi une autre extention pour les systèmes contenant des ponts hydrogène intramoléculaires. La règle suggérée permet aussi de prédire l'effet des substituants sur la stabilité de même que la forme ionique est la plus stable si la règle n'est pas suivie.

[Traduit par le journal]

The Hückel $4N + 2$ rule (1) is one of the best known and most useful rules for predicting the aromatic stability of monocyclic π-electron systems (2). An extension of this rule to polycyclic conjugated hydrocarbons has not been successfully developed. Some indirect applications, taking into account only peripheral π-bonds of these systems, led to rather good results (3), but most often in the case of alternant systems.

Recently a number of authors have reviewed the problem of aromatic stability (see *e.g.* refs. 4–8, 11–24, 35) and have suggested various quantitative measures of "aromaticity". The most advantageous seem to be those coming from quantum chemical calculations like the Hess–Schaad REPE (13) (Resonance Energy per Pi Electron) or other (7, 10, 11, 14) estimates of resonance energy. However, these calculations cannot always be carried out especially by those concerned with the practical aspects of organic chemistry such as synthesis; moreover, the quantum mechanical calculations are not always sufficiently reliable. It is clear that a simple rule as a qualitative guide to aromatic stability is needed in the area of non-alternant polycyclic conjugated hydrocarbon chemistry.

The main purpose of this paper is to present an attempt to extend the Hückel $4N + 2$ rule to polycyclic non-alternant conjugated hydrocarbons and to test it by using various indices of aromatic stability.

Indices of Aromatic Stability

The aromatic state of the molecule is most frequently associated with the following features (4, 5): (*i*) an increase of stability of the cyclic system in comparison with the polyene analogue (6, 7); (*ii*) an averaging of CC-bond lengths (8); (*iii*) an ability to sustain π-electron molecular ring current, when an external magnetic field is applied (4), and as the oldest criterion; (*iv*) a

[1]Visiting Professor at the Department of Chemistry, University of Guelph, Guelph, Ontario, N1G 2W1.

Can. J. Chem. Downloaded from www.nrcresearchpress.com by 210.87.254.40 on 09/05/12
For personal use only.

TABLE 1. Normalized expressions for some indices of aromatic stability

Representative property	Method of estimation	Form of normalized index of aromatic stability A^{N*}
1. Empirical resonance energy E_R	Heats of atomization	$A^{N}_{pb,pe} = 0.167E_R(emp)_{pb,pe}$
2. Theoretical resonance energy E_R (ref. 7)	SCF–SPO (ref. 7)	$A^{N}_{pb,pe} = 4.552E_R(D\text{-}G)_{pb,pe}$
3. Theoretical resonance energy REPE (ref. 12)	HMO (ref. 13)	$A^{N}_{pb,pe} = 15.3848REPE$
4. Theoretical resonance energy SECC (ref. 9)	SCF–PPP (ref. 10)	$A^{N}_{pb} = 2.9265SECC$

*pe and pb stand for quantities calculated per one π-electron and per one π-electron bond of the π-electron system under consideration. This type of normalization permits comparison of the aromatic stability of various molecules when only one method is applied. Normalization in the scale (0, 1) for ethylene (Kekule structure of benzene) and benzene permit, to some extent, comparison of the various methods of estimation of aromatic stability indices.

tendency to react to form substitution products instead of addition, as is characteristic for the polyene analogues (9).

These quantitative rules permit classification of π-electron systems into aromatic, nonaromatic, and antiaromatic (5). According to Breslow (6) and Dewar (7) an aromatic system is a cyclic π-electron system which is more stable than its polyene analogue, whereas that which is less stable is said to be antiaromatic. Unfortunately, application of the above rules *i–iv* to a quantitative description is not too useful unless numerical measures of aromatic stability are introduced (7–17). On the other hand, the disadvantage of the varied approaches to this problem is that the studies of aromatic stability are not comparable to one another as a result of their different definitions. To rectify the situation a general definition of aromatic stability has been suggested (18) by which the stability index A is taken to be a linear function of some carefully chosen, representative property P (eq. 1)

$$A = a + bf(P) \qquad [1]$$

This index A is normalized so that $A = 1.0$ for the benzene molecule and $A = 0.0$ for its Kekule structure (with alternant double and single bonds) or for ethylene; a and b in eq. 1 are normalization factors, which are summarized for some popular indices in Table 1. The following rules have been suggested (16) as criteria of suitability in the selection of the more predictive aromatic stability indices: (*a*) a good aromatic stability index should be greatest for benzene and should decrease monotonically in the series of linear polyacenes, with increase in number of rings, and (*b*) a good index of aromatic stability should monotonically decrease for $(4N + 2)$-annulenes and monotonically increase for $(4N)$-annulenes, when the number of π-electrons increases.

Some indices of aromatic stability are discussed now in order to clarify further considerations. The most helpful index based on point (*i*) is the REPE as introduced by Hess and Schaad (13). Accordingly, the HMO-calculated resonance energy E_R divided by the number of π-electrons is used as a quantitative measure of aromatic stability. Hess and Schaad applied this quantity successfully to many molecules both carbo- and heterocyclic π-electron systems (13, 19–24). The main idea of their treatment of resonance energy is firstly to take into account non-zero contributions to the π-electron energy of the reference state with localized bonds coming from single C—C bonds in π-electron systems, and secondly to consider E_{CC}^{π} as a function of structural environment of this CC-bond. Owing to these improvements, the classical Hückel definition of resonance energy within the HMO approximation becomes as good as those calculated on the basis of more sophisticated quantum chemical methods (19). In Table 1, the expressions used to convert various resonance energy values, defined for various methods of calculation and estimation, into the normalized form described by eq. 1 are presented. Almost any of these indices fulfill at least one of the criteria of suitability (except SECC, which does not) but it seems to be most advantageous to use $REPE^N$-values, as these quantities are available for about 500 carbo- and heterocyclic π-electron systems. Moreover, $REPE^N$ is found analytically (16) to fulfill criterion (*b*) whereas criterion (*a*) is proved empirically for the first six members of the polyacene series (16).

Can. J. Chem. Downloaded from www.nrcresearchpress.com by 210.87.254.40 on 09/05/12
For personal use only.

Can. J. Chem. Downloaded from www.nrcresearchpress.com by 210.87.254.40 on 09/05/12
For personal use only.

Among the other aromatic stability indices resulting from the rules *i–iv*, that based on the criterion of bond length averaging is also quite helpful. The classical expression for this type of index comes from Julg and Francois (8) where

$$[2] \qquad A_j = 1 - \frac{225}{n}\sum_{r=1}^{n}\left(1 - \frac{d_r}{d}\right)^2$$

n is the number of peripheral CC-bonds, d_r is the length of a given CC-bond and d is an averaged value of CC-bond lengths calculated for all peripheral bonds. The disadvantage of this definition is, however, that only peripheral and only CC-bonds are taken into consideration and that the reference bond length to measure the degree of bond averaging is the average value of the bond length. As is known from the paper of Lo and Whitehead (10), for the polyacene series this quantity increases with increase in molecular size. A considerable improvement in predicting aromatic stability was achieved when the optimal value of the bond length d_{opt} was used as reference instead of the average bond length. These quantities can be easily calculated by use of the simple harmonic oscillator model (15–18).

$$[3] \qquad d_{opt} = \frac{s + wd}{1 + w}$$

where s and d in eq. 3 are bond lengths for "pure" single and double bonds, respectively (for CC, the bond lengths in ethane and ethylene have been chosen), whereas w is the force constant ratio for stretching modes of "pure" single and double bonds. Using experimental data for s, d, and w one obtains for a CC-bond the optimal length (15)

$$[4a] \qquad d_{opt}(CC) = 1.397 \text{ Å}$$

(*i.e.* just as in benzene), whereas for other bonds the magnitudes obtained are as follows (17)

$$[4b] \qquad d_{opt}(CN) = 1.338 \text{ Å}$$

$$[4c] \qquad d_{opt}(NN) = 1.308 \text{ Å}$$

$$[4d] \qquad d_{opt}(CO) = 1.300 \text{ Å}$$

Now, having a list of optimal bond lengths for the most popular bonds in π-electron systems, one can write a general expression for the index of aromatic stability called HOMAS (Harmonic Oscillator Model of Aromatic Stability),

$$[5] \quad \text{HOMAS} = 1 - \frac{98.89}{n}\left\{\sum_{r=1}^{n_{cc}}(d_{opt}^{cc} - d_r)^2 + \sum_{r=1}^{n_{cx}}(d_{opt}^{cx} - d_r)^2 + \sum_{r=1}^{n_{cy}}(d_{opt}^{cy} - d_r)^2 + \sum_{r=1}^{n_{xy}}(d_{opt}^{xy} - d_r)^2\right\}$$

where n_{cc}, n_{cx}, n_{cy}, n_{xy} are the numbers of CC, CX, CY, and XY bonds in the given π-electron system under consideration, and obviously $n_{cc} + n_{cx} + n_{cy} + n_{xy} = n =$ number of all π-electron bonds in the system. The HOMAS index fulfills both criteria of suitability on the basis of the experimental data taken from ref. 10, and by use of Dewar's (25) bond length calculated using the SCF method (26).

It should be mentioned, that detailed analysis (27) of various indices of aromaticity led to the statement that the most reliable index of aromatic stability to discuss molecular stability is REPE^N whereas HOMAS is most reliable when considering the local aromaticity of molecules. Thus, these two indices are used in the next section to present more clearly how the suggested rule-of-thumb operates in predicting the relative "aromaticity" of the systems under consideration. On applying the indices of aromatic stability one can find in a more qualitative form how this rule works and also find that non-alternant conjugated hydrocarbons form a wide spectrum ranging from aromatic to nonaromatic to antiaromatic. However, the rule suggested operates similarly to the original Hückel $4N + 2$ rule, *i.e.* it classifies π-systems into two classes: more stable, called frequently aromatic, and less stable identified also as nonaromatic and/or antiaromatic (5).

An Extension of the Hückel 4N + 2 Rule

The original Hückel $4N + 2$ rule states that a planar, monocyclic π-electron system containing $4N + 2$ π-electrons is more stable than the appropriate polyene analogue. These systems are often called aromatic (5) whereas those containing $4N$ π-electrons are less stable and are called antiaromatic. For annulenes this rule is completely equivalent to Craig's rules (28).

In polycyclic conjugated hydrocarbon molecules one can differentiate four types of rings: those containing $4N$, $4N + 1$, $4N + 2$, and $4N + 3$ centers giving π-electrons to the system. In general non-alternant systems chiefly contain

Can. J. Chem. Downloaded from www.nrcresearchpress.com by 210.87.254.40 on 09/05/12
For personal use only.

two types of odd rings: $4N + 1$, a five-membered ring; and $4N + 3$, a seven-membered ring. The number of rings of type $4N + 1$ is denoted by F and of type $4N + 3$ by S, respectively. Then, the proposed extension to the $4N + 2$ rule has the following form. Having defined a number R as follows

$$[6] \qquad R = S - F$$

then, if $R = 0$ or is divisible by 4, the non-alternant system is assumed to be relatively stable (aromatic), whereas if $R \neq 0$ and is not divisible by 4, it is assumed to be relatively less stable (non- or anti-aromatic). The presence of rings of $4N + 2$-type (*e.g.* benzene) does not influence the stability of the system. The presence of rings containing $4N$ π-centers does not influence stability of the system if these rings do not contain carbon atoms forming C—H bonds.

To clarify this last point let us consider two examples of alternant hydrocarbons. The biphenylene molecule **1** is stable and usually classified as aromatic and the $4N$ ring ($N = 1$) is supposed to be empty according to the terminology of Clar (38). On the other hand in bicyclo[6,2,0]decapentaene (**2**), the 8-member ring ($4N$ with $N = 2$) is not empty and does

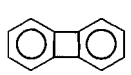

1

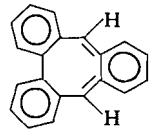

2

contain C—H bonds. Owing to its properties (35) this compound is not stable and can be classified as nonaromatic or perhaps even antiaromatic. In other words, the rule suggested may be used only for cases with empty $4N$ rings; otherwise these rings cause considerable decrease of stability.

Additionally, the above presented extension of the Hückel-type rule cannot be applied to π-systems containing non-bonding orbitals.

The above mentioned rule can also be used to predict the most stable charged (ionic) form of a given non-alternant system. If $R = 1$ or -1 the system is more stable as a cation or anion, respectively. If $R = 2$ or -2 the di-cation or di-anion is the relatively most stable form respectively. To illustrate this idea let us consider the stability of cyclopentadiene radical **3** and its anion **4**.

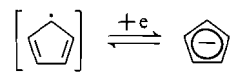

3 **4**

From rule (6) one has $R = 0 - 1 = -1$ for the radical, and hence, the system should be unstable whereas its anion is assumed to be relatively stable; this is in agreement with experience (35) as well as with the Hückel $4N + 2$ rule. A more complex situation arises when a two-cyclic system such as pentalene (**5**) is considered. This molecule is known to be stable as the dianion (30) (**6**) or in a complex

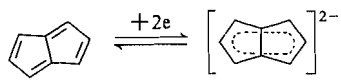

5 **6**

with Ni (31) in which it is also negatively charged. For pentalene (**5**) one has $R = 0 - 2 = -2$ and according to the rule proposed, the system is predicted to be unstable whereas its di-anion is supposed to be relatively stable. This agrees with experiment (35) and also with the low $REPE^N$ value for **5** (−0.275). Comparison of $REPE^N$ for **5** and **6** cannot be made, but for both of these species HOMAS-values have been calculated[2] as equal to 0.745 for **5** and 0.966 for **6**. Again the stability of the dianion relative to the parent molecule is evident.

In the case when both neutral and ionic systems are taken into account the more general formula for R may be used[3]

$$[6a] \qquad R = S - F - \text{net charge}$$

In order to present rule [6] for uncharged polycyclic non-alternant systems let us consider the aromatic stability of s-**7** and as-**8** indacenes. In both cases $S = 0$, and $F = 2$ (rings Nos. 1, 3), hence $R = 0 + (-2) = -2$; thus, both these systems are said to be unstable. This

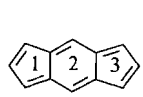

7

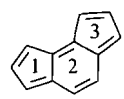

8

[2]Calculation of HOMAS values have been performed using bond lengths for **5** and **6** from Nakajima's SCF calculations (32).

[3]The authors are greatly indebted to the referee for this suggestion.

finding is in good agreement with predictions coming from the indices of aromatic stability; $REPE^N = 0.260$ and 0.362, respectively for **7** and **8**.

Another illustration of the rule is the azulene-[8, 8*a*, 1, 2-*de*]-heptalene molecule (**9**)

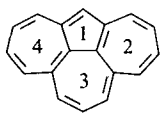

$F = 1$ (ring No. 1)
$S = 3$ (rings Nos. 2, 3, 4)

9

For this system $R = 3 - 1 = 2 \neq 0$ and thus, is not divisible by 4. This π-electron system is therefore assumed to be relatively unstable. This result is in excellent agreement with the $REPE^N$-prediction (0.138), as well as with magnetic and u.v.–spectral properties of this compound (29).

The rule presented above can be explained in a very qualitative fashion. When $R = 0$, it follows that $F = S$ and hence that each electron attracting ring of type $4N + 1$ may interact with the appropriate electron repelling ring of the $4N + 3$ type giving as a result a more convenient electron distribution in both rings. If $F \neq S$ such a pairing is not possible and the system cannot reach a more convenient charge distribution and thus, becomes less stable. This very simplified picture should be considered by use of more accurate quantum chemical calculations. To illustrate how rule [6] works values of R together with the appropriate $REPE^N$ values are given in Table 2 for representative compounds.

It is easily seen that compounds **9** and **10** do not fulfill the rule and that $REPE^N$ values are considerably lower than those for the remaining compounds **11** to **14**.

From rule [6] and its application described above one can also deduce that π-electron systems for which $R > 0$ or $R < 0$ should be stabilized by appropriate substituents: in the first case by electron-attracting substituents whereas in the second case by electron-withdrawing ones. To clarify this point let us consider penthalene **5** for which $R = -2$ and which is very unstable. Synthesis of 9-methyl-pentalene

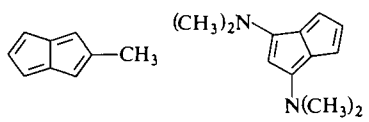

15 **16**

(33) as well as 1,3-bis-[dimethylamino]-pentalene **14** (34) support these considerations, as both Me- and $N(Me)_2$-substituents are electron donating, and hence stabilize the π-electron system of pentalene.

TABLE 2. *R*- and $REPE^N$-values for some synthetized periconcleuse non-alternant conjugated hydrocarbons*

Molecule	*R*	$REPE^N$
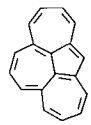 **9**	2	0.138
10	−2	0.275
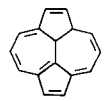 **11**	0	0.336
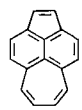 **12**	0	0.535
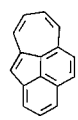 **13**	0	0.489
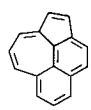 **14**	0	0.505

*Calculated from data given in ref. 19.

Can. J. Chem. Downloaded from www.nrcresearchpress.com by 210.87.254.40 on 09/05/12
For personal use only.

Can. J. Chem. Downloaded from www.nrcresearchpress.com by 210.87.254.40 on 09/05/12
For personal use only.

TABLE 3. R-, REPE^N- and HOMAS-values for some fulvalene-type molecules

Molecule	R	REPE^N*	HOMAS†
Triafulvalene 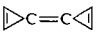	+2	−1.529	0.465
Calicene 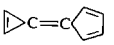	0	0.658	0.755
Fulvalene 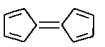	−2	−0.505	0.731
Sesquifulvalene 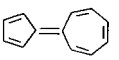	6	0.336	0.852
Heptafulvalene 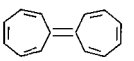	+2	−0.214	0.782

*Calculated from the data taken from refs. 13, 19–24.
†Calculated according to eq. 5 using SCF–PPP bond lengths taken from ref. 32.

Other support of the rule proposed in this paper comes from the fulvalene-type compounds. Some data for these systems are collected in Table 3. In these cases rule [6] is still more clear as interactions between the various kinds of rings are "conducted" by only one double bond. Both calicene and sesquifulvalene are assumed to be much more stable than triafulvalene, fulvalene, and heptafulvalene on the basis of the values of R and also according to the relative values of REPE^N and HOMAS. The charge distribution in these compounds is in agreement with results from experimental measurements of dipole moments (39) as well as with those from theoretical calculations (39).

The extension of the Hückel $4N + 2$ rule presented above can also be successfully applied to the problems of stability of H-bond systems. As pointed out recently (36) stability of these systems is greater if the appropriate iso-π-electronic analogue is aromatic, and less if this analogue is antiaromatic. This analogy with hydrocarbons is as follows: aromatic and antiaromatic hydrocarbons can be easily transferred into iso-π- electronic quazi-aromatic and quaziantiaromatic systems,[4] if the fragment [C···C···C] is replaced by the iso-π-electronic = A···H—D group, where A is the proton acceptor and D—H the proton donor part of the molecule. Most frequently A is the oxygen atom in a carbonyl group or the nitrogen atom in an imine group whereas DH is usually an OH- or NH_2-group.

As an example let us consider azulene (**17**) and pentalene (**5**).

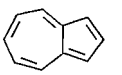

17
Azulene, $R = 1 - 1 = 0$
aromatic

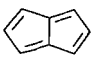

5
Pentalene $R = 0 - 2 = -2$
antiaromatic

The respective quazi-aromatic and quazi-antiaromatic systems are as follows: tropolene (**18**) and (**19**).

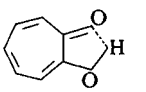

18
Stable H-bond
stable molecule

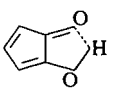

19
Still not known

These examples illustrate rather clearly the advantage of extension of the rule presented to H-bond containing systems. The rule of increase in the stability if the iso-π-electronic analogue of H-bond system is aromatic and decrease if antiaromatic, has been proved (36) within the simple Dewar-PMO model (37).

Conclusions

It seems to be reasonable to conclude that the extension of the Hückel $4N + 2$ rule presented above gives a rather good prediction of aromatic stability. Also it seems to be advantageous to use normalized indices of aromatic stability to test this rule, as agreement between predictions of the rule and values of the aromatic stability indices is more distinct and more easily interpreted.

One of the authors (T.M.K.) would like to express his gratitude to Professors A. K. Colter and W. R. Fawcett for making possible his stay as visiting professor in 1974–1975 at the University of Guelph where this paper was written.

1. E. HÜCKEL. Z. Phys. **70**, 204 (1931).
2. A. STREITWIESER JR. Molecular orbital theory. J. Wiley, New York. 1961.

[4]For a discussion see the article of D. Lloyd in ref. 5.

3. H. H. STAAB. Einfürung in der theoretische organische Chemie. Verlag—Chemie. 1963.
4. J. A. ELVIDGE and L. M. JACKMAN. J. Chem. Soc. 859 (1961); F. SONDHEIMER. Pure Appl. Chem. **7**, 363 (1964).
5. E. D. BERGMANN and B. PULLMAN (*Editors*) Proc. Int. Symp. The Israel Ac. Sci. and Hum. Jerusalem. 1971.
6. R. BRESLOW and E. MOHASCI. J. Am. Chem. Soc. **85**, 431 (1963).
7. M. J. S. DEWAR and G. J. GLEICHER. J. Am. Chem. Soc. **87**, 685 (1965).
8. A. JULG and PH. FRANCOIS. Theor. Chim. Acta, **7**, 249 (1967).
9. J. KRUSZEWSKI and T. M. KRYGOWSKI. Tetrahedron Lett. 319 (1970).
10. D. H. LO and M. A. WHITEHEAD. Can. J. Chem. **46**, 2027 (1968); **46**, 2041 (1968).
11. H. P. FIGEYS. Tetrahedron, **26**, 5225 (1970).
12. T. M. KRYGOWSKI. Tetrahedron Lett. 1311 (1970).
13. B. A. HESS and L. J. SCHAAD. J. Am. Chem. Soc. **93**, 307 (1971).
14. M. MILUN, Z. SOBOTKA, and N. TRINAJSTIĆ. J. Org. Chem. **37**, 139 (1972).
15. J. KRUSZEWSKI and T. M. KRYGOWSKI. Tetrahedron Lett. 3839 (1972).
16. T. M. KRYGOWSKI and J. KRUSZEWSKI. Bull. Ac. Pol. Sci. Ser. Sci. Chim. **20**, 993 (1972).
17. T. M. KRYGOWSKI and J. KRUSZEWSKI. Bull. Ac. Pol. Sci. Ser. Sci. Chim. **21**, 409 (1973).
18. J. KRUSZEWSKI and T. M. KRYGOWSKI. Bull. Ac. Pol. Sci. Ser. Sci. Chim. **20**, 907 (1972).
19. B. A. HESS and L. J. SCHAAD. J. Org. Chem. **36**, 3418 (1971).
20. L. J. SCHAAD and B. A. HESS. J. Am. Chem. Soc. **94**, 3068 (1972).
21. B. A. HESS and L. J. SCHAAD. J. Am. Chem. Soc. **93**, 2413 (1971).
22. B. A. HESS, L. J. SCHAAD, and C. W. HOLYOKE. Tetrahedron, **28**, 5299 (1972).
23. B. A. HESS, L. J. SCHAAD, and C. W. HOLYOKE. Tetrahedron, **28**, 3657 (1972).
24. B. A. HESS and L. J. SCHAAD. Tetrahedron Lett. 17 (1971).
25. M. J. S. DEWAR. Private communication.
26. M. J. S. DEWAR and C. DELLANO. J. Am. Chem. Soc. **91**, 789 (1969).
27. J. KRUSZEWSKI and T. M. KRYGOWSKI. Soc. Sci. Lodz, Acta Chim. **18**, 165 (1973).
28. T. M. KRYGOWSKI and J. KRUSZEWSKI. Bull. Ac. Pol. Sci. Ser. Sci. Chim. **27**, 509 (1973).
29. K. HAFNER. Pure Appl. Chem. **28**, 153 (1972).
30. T. J. KATZ and M. ROSENBURGER. J. Am. Chem. Soc. **84**, 865 (1962).
31. T. J. KATZ and N. ACTON. J. Am. Chem. Soc. **94**, 3281 (1972).
32. T. NAKAJIMA. Pure Appl. Chem. **28**, 219 (1972).
33. K. HAFNER, R. DONGAES, E. GOEDEDRE, and R. KAISER. Angew. Chem. Int. Ed. **12**, 337 (1973).
34. K. HAFNER, K. F. BAUGERT, and V. ORFANOS. Angew. Chem. Int. Ed. **6**, 451 (1967).
35. P. GARRATT and P. VOLHARDT. Aromatizität, G. Theime Verlag Stuttgart. 1973; P. GARRATT, Aromaticity, McGraw-Hill, London. 1971.
36. J. KRUSZEWSKI and T. M. KRYGOWSKI. In press.
37. M. J. S. DEWAR. The molecular orbital theory of organic chemistry. McGraw-Hill, New York. 1969.
38. E. CLAR. Polycyclic hydrocarbons. Academic Press, London. 1964; E. Clar. The aromatic sextet, J. Wiley, New York. 1972.
39. K. FUKUI, A. IMAMURA, T. YONEZAWA, and C. NAGATA. Bull. Chem. Soc. Jap. **33**, 1591 (1960).

Can. J. Chem. Downloaded from www.nrcresearchpress.com by 210.87.254.40 on 09/05/12
For personal use only.

The Role of Hemicellulose in the Delignification of Wood[1]

A. J. KERR AND D. A. I. GORING

Pulp and Paper Research Institute of Canada and Department of Chemistry, McGill University, Montreal, Quebec H9R 3J9

Received November 4, 1974

A. J. KERR and D. A. I. GORING. Can. J. Chem. **53**, 952 (1975).

Hemicellulose was selectively removed from white birch by treatment with cold alkali. Untreated and alkali-treated samples were pulped to various stages of delignification by the acid chlorite process. The acid chlorite reagent was shown to be selective for lignin removal from both samples during the first 60% of delignification.

In alkali-treated white birch, the median pore width increased considerably as acid chlorite delignification proceeded. In contrast, in untreated white birch, this parameter remained relatively constant during the first 60% of delignification.

Alkali-treated white birch delignified at a much faster rate than untreated white birch. In addition, there was a topochemical preference for removal of lignin from the secondary wall of the fibers in the hemicellulose-deficient wood. Apparently, prior removal of hemicellulose caused larger pores to be produced in the fiber walls during pulping, thereby facilitating a more rapid removal of lignin.

A. J. KERR et D. A. I. GORING, Can. J. Chem. **53**, 952 (1975).

On a enlevé d'une façon sélective l'hémicellulose du bouleau blanc par le traitement avec de l'alcali à froid. On a transformé, divers échantillons de bois non traité et traité par les alcalis, en pâte à papier jusqu'à divers stages de délignification, utilisant le processus au chlorite en milieu acide. On a démontré que durant les premiers 60% de la délignification, ce réactif enlève sélectivement la lignine provenant des deux types d'échantillons.

Dans le cas du bouleau blanc traité par les alkalis, la largeur médiane des pores augmente considérablement à mesure que la délignification au chlorite se poursuit. Par opposition, lorsque le bouleau blanc n'est pas traité, ce paramètre demeure pratiquement constant durant les premiers 60% de la délignification.

Le bouleau blanc traité par les alcalis se délignifie à une vitesse beaucoup plus grande que le bouleau blanc non traité. De plus il y a une préférence topochimique pour l'enlèvement de la lignine provenant des cellules secondaires de la fibre dans le bois déficient en hémicellulose. Apparemment l'élimination préalable de l'hémicellulose amène la production de pores plus grandes dans la fibre au cours du processus de transformation en pâte facilitant ainsi l'élimination plus rapide de la lignine. [Traduit par le journal]

Introduction

Hemicelluloses are dissolved from wood along with lignin in the early stages of kraft and acid sulfite pulping but are retained during acid chlorite pulping (1). In all three pulping processes, the sizes of lignin macromolecules removed from the wood cells correspond closely to the sizes of the cell pores at various stages of delignification (2). In kraft and acid sulfite pulping, the pore sizes (3) and the sizes of the extracted lignin macromolecules (4, 5) increase during the pulping, whereas in acid chlorite pulping both remain almost constant throughout (2).

Thus, hemicellulose removal plays an important role in chemical pulping. When hemicelluloses are retained in the wood during pulping, the cell pores and the extracted lignin macromolecules remain small and delignification is characteristically slow. However, when hemicelluloses are removed in the early stages of pulping, the pores and lignin macromolecules increase in size and delignification is much more rapid.

To test whether the increase in pore size and the faster rate of delignification is really caused by hemicellulose removal, it would be instructive to compare a highly selective delignification of whole wood with an identical treatment of wood from which hemicelluloses have been removed. The hemicelluloses should be removed by a method that does not change the chemical properties of the lignin.

It is difficult to remove significant amounts of hemicelluloses from softwoods without chemical modification or simultaneous removal of lignin

[1]This paper is dedicated to Professor C. A. Winkler of McGill University on the occasion of his sixty-fifth birthday by one of his colleagues (D.A.I.G.).

Can. J. Chem. Downloaded from www.nrcresearchpress.com by 210.87.254.105 on 09/05/12
For personal use only.

Can. J. Chem. Downloaded from www.nrcresearchpress.com by 210.87.254.105 on 09/05/12
For personal use only.

(6). Hardwood hemicelluloses are more soluble, however, and it has been shown that large amounts can be removed from white birch by a cold alkali treatment (7). Accordingly, hemicelluloses were removed from white birch with alkali and the size of the pores in the cell wall and the rates of acid chlorite delignification of untreated and alkali-treated white birch were compared.

Dissolution of hemicellulose from wood also seems to affect the topochemistry of the delignification reaction. During kraft pulping of black spruce (8), there is an initial preferential removal of lignin from the tracheid secondary wall, followed at about 50% delignification by a rapid dissolution of lignin from the compound middle lamella. In contrast, during acid chlorite pulping of black spruce, lignin dissolution occurs at the same relative rate from the secondary wall and compound middle lamella regions of the tracheids (9). The topochemical preference for early lignin removal from the secondary wall, was found to be greatest in kraft pulping and decreased in the order

$$\underset{\text{kraft}}{\text{acid}} > \underset{\text{sulfite}}{\text{neutral}} > \underset{\text{sulfite}}{\text{acid}} > \text{chlorite}$$

In seeking an explanation for the above trend, Wood *et al.* (9) noted that the order of topochemical preference is the same as the order of the extent of hemicellulose dissolution from the wood in the early stages of pulping. Hemicellulose removal is rapid initially and occurs to decreasing degrees in kraft, acid sulfite, and neutral sulfite pulping (10, 11), whereas in acid chlorite pulping there is no hemicellulose removal until more than 60% of the lignin has been dissolved (1). This parallel behaviour led Wood *et al.* (9) to propose that the topochemical effect is associated with the removal of hemicelluloses from the wood.

The present investigation provided a good opportunity to test the hypothesis of Wood *et al.* (9). If the hypothesis is correct, the alkali-treated hemicellulose-deficient wood should show a topochemical effect whereas the untreated wood should not. Accordingly, the removal of lignin from the cell walls and middle lamellae by acid chlorite delignification of both the untreated and alkali-treated birch wood was analyzed by the techniques of ultraviolet microscopy recently developed in this laboratory (12).

Experimental

A sample of 20–40 mesh sawdust was prepared from the trunk of a 46 year old birch tree. Hemicelluloses were extracted by treatment with 3% NaOH for 24 h at 30 °C to produce a sample at 78% yield with 48.4% of hemicelluloses removed.

The acid chlorite pulping was carried out according to the procedure of Wise *et al.* (13) as adopted by Timell (14) and Ahlgren and Goring (1). The chemical charge was 0.3 g of sodium chlorite and 0.1 ml of acetic acid per gram of dry wood and the reaction temperature was 70 °C. A fresh charge of chemicals was added at hourly intervals without withdrawal of any liquor. The initial liquor-to-wood ratio was 13:1.

Tappi standard methods were employed for the determination of "Klason" lignin in the wood (15) and in the acid chlorite pulps (16). The acid-soluble lignin contents were calculated from the u.v. absorbances at 205 nm of the Klason hydrolysates, using an absorptivity of 113.4 $l\,g^{-1}\,cm^{-1}$. This figure was determined by Schöning and Johansson (17) on isolated samples of white birch acid-soluble lignin. Its application to acid chlorite pulps is justified as, for both spruce and beech, Campbell and McDonald (18) found little difference between the absorptivities of acid-soluble lignins prepared from wood and acid chlorite pulp. The total lignin content of each wood and pulp sample was obtained by adding the Klason and acid-soluble lignin contents.

The Tappi standard method was employed for the determination of α-cellulose (19). The hemicellulose content was calculated by difference, yield minus lignin and α-cellulose.

Cumulative volume distributions of pore size in water-swollen pulp samples were measured by the solute exclusion technique of Stone and Scallan (3, 20, 21). The technique measures the accessibility of the samples to a number of dissolved sugars and dextrans ranging in hydrodynamic diameter from 8 Å (glucose) to 560 Å (a dextran with a molecular weight of about two million). Further details of the method are given elsewhere (22).

For specimen preparation in u.v. microscopy, matchstick-size chips about 1 mm^2 × 5 mm were cut from the 44th annual ring of the tree and were alkali extracted and delignified together with the sawdust. At each stage of delignification, chips were solvent exchanged from the water-swollen state to absolute ethanol and then to propylene oxide prior to embedding in Epon 812. Ultrathin transverse sections (0.5–3.0 μm) were cut from the embedded samples with a diamond knife mounted on a Porter-Blum ultramicrotome and were photographed in a Leitz u.v. microscope. The microscopic methods used were essentially those of Scott *et al.* (12), although a lower wavelength of 240 nm was employed. Changes in the absorptivity of *in situ* lignin produced by the acid chlorite reagent were found to be smallest at this wavelength (22).

Results

Hemicellulose Removal

The results of the alkali treatment are summarized in Fig. 1. The data show that the alkali extracts mainly the hemicelluloses, although

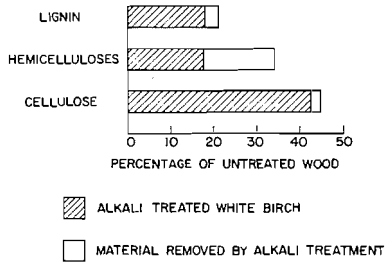

FIG. 1. Diagram illustrating the results of the cold alkali treatment of white birch.

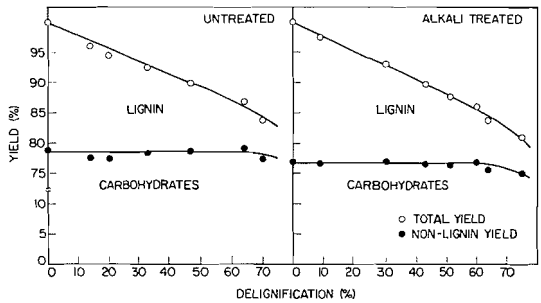

FIG. 2. Lignin and carbohydrate contents of untreated (left) and alkali-treated (right) white birch at various stages during acid chlorite delignification.

small amounts of lignin and cellulose are also removed from the wood.

To check if the lignin has been modified chemically during the alkali treatment, u.v. spectra were measured on fiber and vessel walls of untreated and alkali-treated white birch. For both morphological regions, the spectra of the untreated and alkali-treated wood were identical which indicated that the cold alkali caused no major chemical modification of the lignin.

Acid Chlorite Pulping

Yields, lignin contents, and percentage delignification are given in Table 1 and the selectivity of the delignification is illustrated in Fig. 2. The results show that only lignin is removed from both untreated and alkali-treated white birch during the first 60% of delignification. Ahlgren and Goring (1) previously observed similar behavior with black spruce. The present results, therefore, indicate that the acid chlorite reagent is selective for lignin removal not only from softwoods but also from hardwoods.

Pore Size

The cumulative pore size distribution curves for untreated and alkali-treated white birch at various stages of acid chlorite delignification are shown in Figs. 3 and 4, respectively. In all samples studied, the pore sizes were found to be distributed log normally to a good approximation (22). A similar distribution of pore sizes in various wood and pulp samples was reported previously by Ahlgren (23). The median pore

TABLE 1. Chemical compositions of the acid chlorite pulps

Pulping time (min)	Yield (%)	Klason lignin (%)	Acid-soluble lignin (%)	Total lignin (%)	Total lignin (% of original wood)	Delignification (%)
			Untreated white birch			
0	100	17.7	3.5	21.2	21.2	0
20	96.0	10.4	8.7	19.1	18.3	14
44	94.5	8.6	9.4	18.0	17.0	20
76	92.5	6.4	8.9	15.3	14.2	33
119	89.9	3.9	8.6	12.5	11.2	47
167	86.8	2.5	6.3	8.8	7.6	64
260	83.8	2.0	5.6	7.6	6.4	70
			Alkali-treated white birch (78% yield)*			
0	100	20.1	2.8	22.9	22.9	0
3.5	97.5	16.3	5.2	21.5	20.9	9
11	93.1	11.9	5.4	17.3	16.1	30
23	89.7	9.5	5.1	14.6	13.1	43
37	87.7	7.7	5.2	12.9	11.3	51
52	86.0	6.1	4.6	10.7	9.2	60
71	83.7	5.3	4.5	9.8	8.2	64
93	80.9	3.5	3.7	7.2	5.8	75

*Yield for uncooked alkali-treated wood is taken as 100%.

Can. J. Chem. Downloaded from www.nrcresearchpress.com by 210.87.254.105 on 09/05/12
For personal use only.

Can. J. Chem. Downloaded from www.nrcresearchpress.com by 210.87.254.105 on 09/05/12
For personal use only.

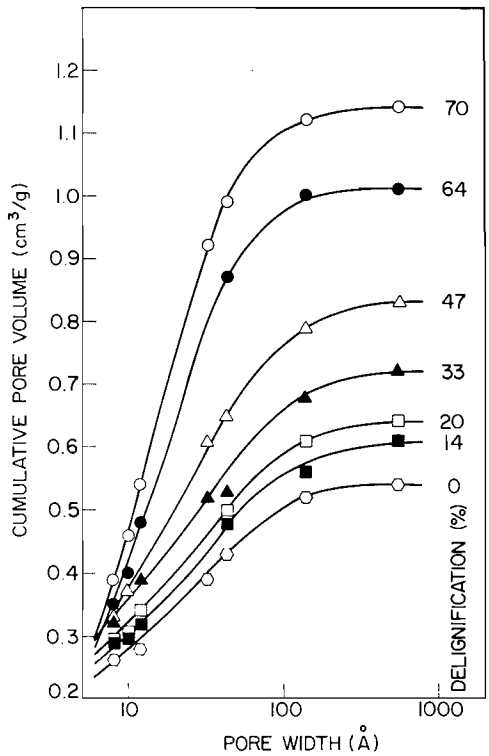

FIG. 3. Cumulative pore volume *vs.* pore width for untreated white birch at various stages of acid chlorite delignification.

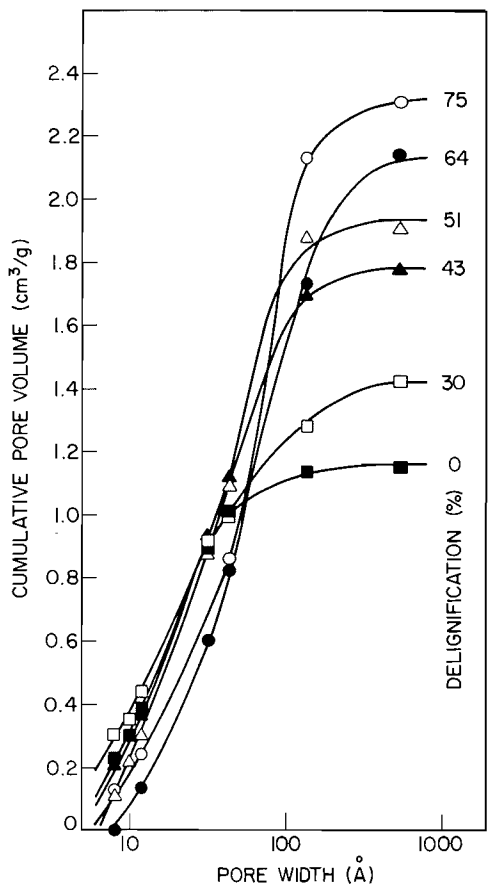

FIG. 4. Cumulative pore volume *vs.* pore width for alkali-treated white birch at various stages of acid chlorite delignification.

width, which is the pore width at one half the cell wall pore volume (or fiber saturation point) was conveniently determined for each sample from a straight line plot of the data on a log–probability diagram (22).

Median pore width is plotted against percentage delignification for both untreated and alkali-treated white birch in Fig. 5. The median pore width of alkali-treated white birch is 16.9 Å which is significantly higher than the value of 9.2 Å found for untreated white birch, indicating that hemicellulose removal causes the cell pores to increase in size.

The median pore width of untreated white birch remains fairly constant during the first 60% of acid chlorite delignification but increases slightly thereafter. A similar trend occurs in the median pore width of black spruce during acid chlorite delignification (2). In contrast to this, the median pore width of alkali-treated white birch increases throughout acid chlorite delignification (see Fig. 5). A rapid increase of the median pore width with the extent of lignin removal also occurs in kraft and acid sulfite pulping of black spruce (2, 3).

Rates of Pulping

Percentage delignification is plotted against pulping time in Fig. 6 for the acid chlorite pulps prepared from both untreated and alkali-treated white birch. It is clear that the rate of delignification of alkali-treated white birch is considerably greater than that of untreated white birch. Thus, the prior removal of hemicelluloses causes a marked increase in the rate of delignification.

This result is consistent with the findings of Procter (24) who compared the rate of delignification for western hemlock pretreated with H_2S with that for untreated wood. The H_2S pretreatment protected the hemicelluloses from dissolution during the kraft process and at the

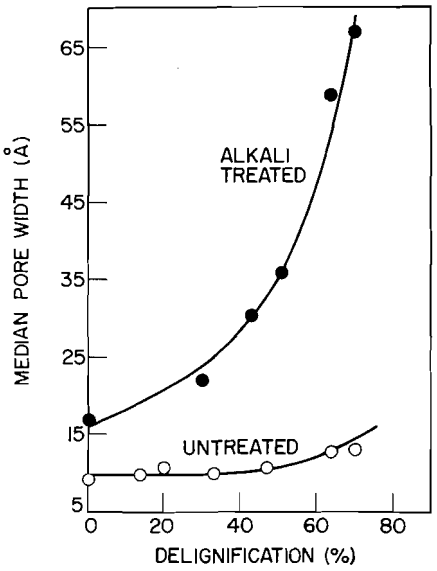

FIG. 5. Median pore width of untreated and alkali-treated white birch at various stages of acid chlorite delignification.

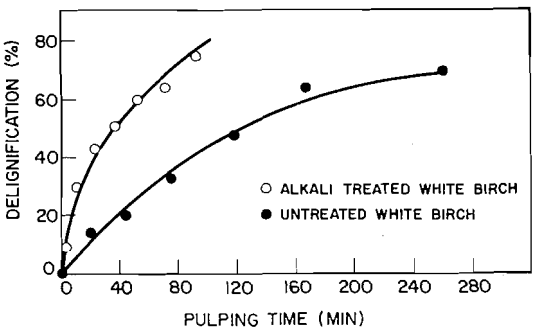

FIG. 6. Percentage delignification *vs.* pulping time for the acid chlorite pulps.

same time caused a reduction in the rate of delignification.

Topochemical Effects

The progress of acid chlorite delignification of untreated and alkali-treated white birch is illustrated for the fibers in the u.v. micrographs displayed in Fig. 7 and for the vessels in Fig. 8. As in previous studies of kraft, sulfite, and acid chlorite pulping (8, 9), no significant gradient of lignin concentration across the secondary walls of the cells can be detected at any stage of delignification.

The u.v. absorbances for the cell walls and middle lamellae of the fibers and vessels at

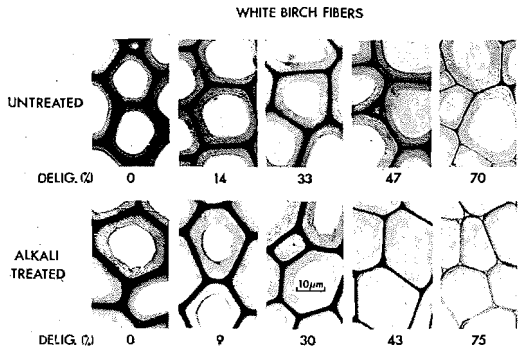

FIG. 7. Photomicrographs at 240 nm showing the progressive acid chlorite delignification of fibers in untreated and alkali-treated white birch. The photomicrographs are all of 1.0 μ sections.

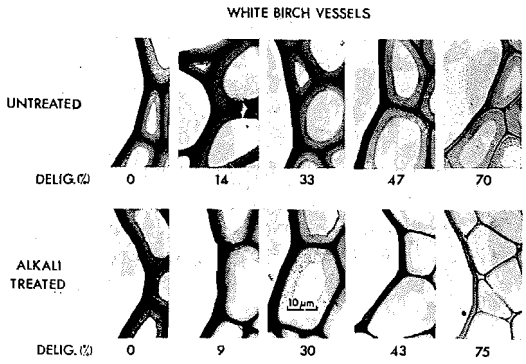

FIG. 8. Photomicrographs at 240 nm showing delignification of the vessels. The photomicrographs are all of 1.0 μ sections.

various stages of delignification are given in Table 2. The absorbances were measured at a wavelength of 240 nm and were corrected for changes in the dimensions of the morphological regions and the absorbtivity of the lignin which were produced by the chlorite treatment. Details of the correction procedures are given elsewhere (22).

The percentage of lignin removed from any morphological region of a sample at a particular stage of delignification, R_i, is given by

$$[1] \qquad R_i = 100\ A_i/A_0$$

in which A_i is the absorbance at any particular degree of delignification and A_0 is the absorbance in the original sample. The percentage of lignin removed from the secondary wall and compound middle lamella regions of the fibers and vessels

Can. J. Chem. Downloaded from www.nrcresearchpress.com by 210.87.254.105 on 09/05/12
For personal use only.

TABLE 2. Corrected 240 nm u.v. absorbances

Delignification (%)	Fiber wall	Corrected u.v. absorbances (A_1) Fiber ML	Vessel wall	Vessel-fiber ML	Fiber cell corner ML
		Untreated white birch			
0	0.33	1.23	0.90	1.39	2.02
14	0.28	1.04	0.80	1.33	1.73
20	0.25	0.97	0.75	1.14	1.14
33	0.18	0.77	0.65	1.03	0.92
47	0.16	0.60	0.57	0.76	0.62
64	0.14	0.53	0.43	0.62	0.58
70	0.13	0.33	0.34	0.51	0.31
		Alkali-treated white birch			
0	0.30	1.38	0.94	1.25	2.20
9	0.20	1.36	0.81	1.01	2.08
30	0.16	1.23	0.70	1.04	1.77
43	0.06	0.80	0.55	0.71	1.07
51	0.06	0.75	0.47	0.74	1.02
64	0.05	0.64	0.40	0.65	0.55
75	0.04	0.37	—	—	—

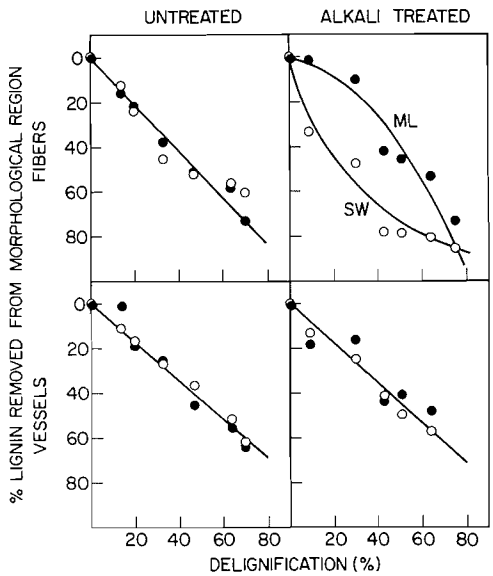

FIG. 9. Topochemistry of acid chlorite delignification of fibers and vessels of untreated and alkali-treated white birch: percentage of lignin removed from the middle lamella (ML, filled circles) and the secondary wall (SW, empty circles) *vs.* percentage of lignin removed from the whole sample (*i.e.* % delignification).

of untreated and alkali-treated white birch were calculated from the corrected u.v. absorbances using eq. 1 and are plotted against the percentage of lignin removed from the whole wood (*i.e.* percentage delignification) in Fig. 9.

No topochemical effect is apparent in either the fibers or vessels of untreated white birch. A marked topochemical effect occurs in the fibers of alkali-treated, hemicellulose-deficient white birch but not in the vessels. The results therefore indicate that hemicellulose removal produces a topochemical effect in the chlorite pulping of birch fibers.

Discussion

The results confirm that the removal of hemicellulose from birch wood (*i*) increases the average pore size in the cell wall during all stages of acid chlorite delignification; (*ii*) increases the overall rate of delignification; and (*iii*) increases the rate of delignification of the fiber wall with respect to that of the middle lamella.

What physicochemical mechanisms of delignification are indicated by the above trends?

Lignin in wood appears to be a polymeric material made up of rather short chains of phenyl propane units cross linked in a variety of ways to give a network structure. Between one third and one quarter of the lignin is found in the middle lamella region in a fairly pure form. Most of the remainder is in the secondary wall associated with the cellulose and hemicellulose moieties (25, 26).

When wood is pulped two things must happen. Firstly, the lignin network must be broken down to give macromolecules which are soluble in the

Can. J. Chem. Downloaded from www.nrcresearchpress.com by 210.87.254.105 on 09/05/12
For personal use only.

Can. J. Chem. Downloaded from www.nrcresearchpress.com by 210.87.254.105 on 09/05/12
For personal use only.

pulping solvent. Secondly, the soluble lignin must diffuse out of the secondary wall into the lumen cavity. If the pores in the cell wall are small, then the lignin network must be broken down into small fragments to allow diffusion through the wall to the lumen. This will require sustained chemical action on the lignin and will tend to result in a slow rate of delignification. If the pore size is large, the chemical breakdown of the lignin network need not be excessive because large lignin macromolecules will be capable of diffusing through the wall to the lumen.

It should be noted that, regardless of diffusion constraints, there will be a limit to the size of lignin macromolecules which will be soluble in the pulping solvent. However, both kraft and acid sulfite pulping of isolated lignins were found to produce soluble lignins with molecular weights in excess of 10^6 (27, 28) which is considerably greater than the molecular weights of soluble lignins obtained by the usual methods of delignifying wood (4, 5). Thus the constraint to lignin removal from wood does not seem to be the solubility of the isolated lignin macromolecules but rather the porous structure of the cell wall.

What the present results confirm is that the hemicellulose governs the pore size in the cell wall and thus the rate of delignification. Removal of hemicellulose increases the pore size and therefore also increases the rate of delignification. Retention of hemicellulose imposes a constraint on the diffusion of soluble lignin molecules out of the wall and therefore slows up the delignification process.

The explanation of the enhancement of the topochemical effect by the removal of hemicellulose is not as straightforward. An obvious suggestion is that the S1 layer in the secondary wall acts as a diffusion barrier to the escape of lignin dissolved from the middle lamella. However a recent study of the kraft pulping of pressure refined spruce wood showed that even when the middle lamella lignin was exposed directly to the kraft pulping liquor, it dissolved more slowly than the secondary wall lignin (29). Thus it seems that the rate of dissolution of the lignin in the middle lamella is an intrinsic property of this morphological region and is not affected by the presence of the S1 layer.

Just as the dissolution of lignin from the cell wall is governed by the porous structure of the cell wall, the dissolution of the lignin in the middle lamella will be governed by the porous structure of the middle lamella. The true middle lamella is almost pure lignin and hence will contain less hemicellulose than the cell wall. Thus hemicellulose removal is likely to have a greater effect on the pore size of the cell wall than on the pore size of the middle lamella. This may be the cause of the enhancement of the topochemical effect produced by hemicellulose removal. It is also possible that the chemical structure (*e.g.* degree of cross linking) of middle lamella lignin differs from that of cell wall lignin and that such structural differences contribute to the topochemical effect.

It is interesting to observe in Fig. 9 that the vessels showed no topochemical effect even after removal of hemicellulose. The cold alkali extraction used in the present investigation would be expected to remove only the xylan (30). Perhaps the vessels are rich in glucomannan which is not extracted by cold alkali and the presence of which would be expected to reduce the topochemical preference for lignin removal from the cell walls.

Finally it should be noted that only one type of delignification (acid chlorite) and one type of wood (white birch) have been covered by the present investigation. However, previous results for the kraft, acid sulfite, neutral sulfite (8), and acid chlorite (2, 9) pulping of spruce wood and for the kraft and neutral sulfite pulping of birch wood (31) are all consistent with the results described herein. Therefore it seems likely that the trends noted and the principles elucidated in the present paper are of general applicability to the delignification of wood.

1. P. A. AHLGREN and D. A. I. GORING. Can. J. Chem. **49**, 1272 (1971).
2. P. A. AHLGREN, W. Q. YEAN, and D. A. I. GORING. Tappi, **54**, 737 (1971).
3. J. E. STONE and A. M. SCALLAN. Pulp Paper Mag. Can. **69**, T288 (1968).
4. W. Q. YEAN and D. A. I. GORING. Svensk Papperstidn. **71**, 739 (1968).
5. J. G. MCNAUGHTON, W. Q. YEAN, and D. A. I. GORING. Tappi, **50**, 548 (1967).
6. E. BOOKER and C. SCHUERCH. Tappi, **41**, 650 (1958).
7. R. NELSON and C. SCHUERCH. J. Polymer Sci. **22**, 435 (1956).
8. A. R. PROCTER, W. Q. YEAN, and D. A. I. GORING. Pulp Paper Mag. Can. **68**, T445 (1967).
9. J. R. WOOD, P. A. AHLGREN, and D. A. I. GORING. Svensk Papperstidn. **71**, 15 (1972).

10. J. H. KALISCH and W. BEAZLEY. Pulp Paper Mag. Can. **61**, T452 (1960).
11. I. CROON. Pulp Paper Mag. Can. **66**, T71 (1965).
12. J. A. N. SCOTT, A. R. PROCTER, B. J. FERGUS, and D. A. I. GORING. Wood Sci. Technol. **3**, 73 (1969).
13. L. E. WISE, M. MURPHY, and A. A. D'ADDIECO. Paper Trade J. **122**, 35 (1946).
14. T. E. TIMELL. Tappi, **44**, 88 (1961).
15. Tappi Standard. T13m – 54.
16. Tappi Standard. T223m – 58.
17. A. G. SCHÖNING and G. JOHANSSON. Svensk Papperstidn. **68**, 607 (1965).
18. W. G. CAMPBELL and I. R. C. MCDONALD. J. Chem. Soc. 3180 (1952).
19. Tappi Standard, T203m – 58.
20. L. G. AGGEBRANDT and O. SAMUELSON. J. Appl. Polymer Sci. **8**, 2801 (1964).
21. J. E. STONE and A. M. SCALLAN. Cellulose Chem. Technol. **2**, 343 (1968).
22. A. J. KERR. Ph.D. Thesis, McGill University, Montreal. 1970.
23. P. A. AHLGREN. Ph.D. Thesis, McGill University, Montreal. 1970.
24. A. R. PROCTER. Tappi, **55**, 424 (1972).
25. B. J. FERGUS, A. R. PROCTER, J. A. N. SCOTT, and D. A. I. GORING. Wood Sci. Technol. **3**, 117 (1969).
26. B. J. FERGUS and D. A. I. GORING. Holzforschung, **24**, 118 (1970).
27. P. R. GUPTA and D. A. I. GORING. Can. J. Chem. **38**, 270 (1960).
28. A. REZANOWICH and D. A. I. GORING. J. Colloid Sci. **15**, 452 (1960).
29. A. J. KERR and D. A. I. GORING. In preparation.
30. T. E. TIMELL. Svensk Papperstidn. **63**, 472 (1963).
31. B. J. FERGUS and D. A. I. GORING. Pulp Paper Mag. Can. **70**, T314 (1969).

Can. J. Chem. Downloaded from www.nrcresearchpress.com by 210.87.254.105 on 09/05/12
For personal use only.

Studies Related to Antitumor Antibiotics. Part III.[1] Syntheses of 1,2,3,4,5,6-Hexahydro-2,3-benzazocin-5-ones as Possible Intermediates in the Biosynthesis of Mitomycins

J. WILLIAM LOWN AND TSUNEO ITOH[2]

Department of Chemistry, University of Alberta, Edmonton, Alberta T6G 2E1

Received August 29, 1974

J. WILLIAM LOWN and TSUNEO ITOH. Can. J. Chem. **53**, 960 (1975).

The synthesis of 8-methoxy-9-methyl-*N*-*p*-toluenesulfonyl-1,2,3,4,5,6-hexahydro-2,3-benzazocin-5-one (**23**) and its conversion via transannular interaction to the 2,3-dihydro-1*H*-pyrrolo-[1,2-*a*]indole ABC parent ring system of the antitumor antibiotic mitomycin C is described. The possible implication of this result in the biosynthesis of the mitosanes and the connection with the structurally and pharmacologically related pyrrolizidine alkaloids is discussed.

J. WILLIAM LOWN et TSUNEO ITOH. Can J. Chem. **53**, 960 (1975).

On décrit la synthèse de la méthoxy-8 méthyl-9 *N*-*p*-toluènesulfonylhexahydro-1,2,3,4,5,6 benzazocin-2,3 one-5 (**23**) et sa conversion, par l'intermédiaire d'une interaction transannulaire, en dihydro-2,3 1*H*-pyrrolo[1,2-*a*]indole qui comporte le système cyclique ABC du composé antitumoral et antibiotique mitomycin C. On discute de l'implication possible de ces résultats dans la biosynthèse des mitosanes et la relation avec les alkaloides pyrrolizidine qui leur sont reliés tant au point de vue de la structure que de la pharmacologie.

[Traduit par le journal]

The mitosane class of potent antitumor antibiotics (**1**), which contains several unique structural features including an aziridine group, has attracted considerable attention from synthetic chemists and pharmacologists (1, 2).

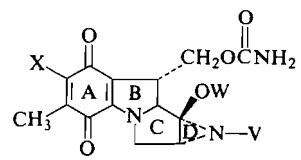

1

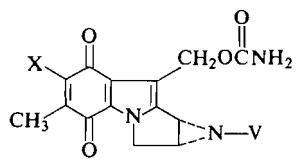

2

In part I of this series we explored some of the characteristics of the chiral aziridine moiety as they relate to the key alkylation role in the cytotoxic action of mitomycin C by irreversible cross linking of the complementary strands of DNA (3). Part II dealt with the spectroscopic evidence from c.m.r. and p.m.r. on the conjugative stabilization and conformation of the antibiotic (4). In the present paper we describe the synthesis of some 1,2,3,4,5,6-hexahydro-2,3-benzazocin-5-ones which pertain to a possible biosynthetic pathway to mitomycin C.

In early work on the biosynthesis the structural similarity of the mitosanes to indole-related compounds suggested a biosynthetic relationship of the antibiotic to tryptophan. However, several compounds structurally or biosynthetically related to the indole nucleus of mitomycin C failed to induce any increase in antibiotic yield (5, 6*a*). Neither labelled tyrosine nor tryptophan contributes label to mitomycin. Recent work by Hornemann and co-workers (6) employing radioactive labelling with ^{14}C and ^{15}N has established the involvement of D-glucose in the construction of ring A and of D-glucosamine in the formation of rings C and D (6). L-Methionine is implicated in the methylation of sites 7 and 9a (6*a*, 7) whereas citrulline is an intermediate in the insertion of the carbamoyl side chain of mitomycin (6*c*).

The introduction of the 9a bridgehead oxygen function in **1** poses considerable problems both biosynthetically and in attempted total synthesis.

[1]For part II see ref. 4.

[2]National Cancer Institute of Canada Postdoctoral Fellow 1972–1973; present address: School of Pharmaceutical Sciences, Kitasato University, Tokyo.

Can. J. Chem. Downloaded from www.nrcresearchpress.com by 210.87.254.6 on 09/05/12
For personal use only.

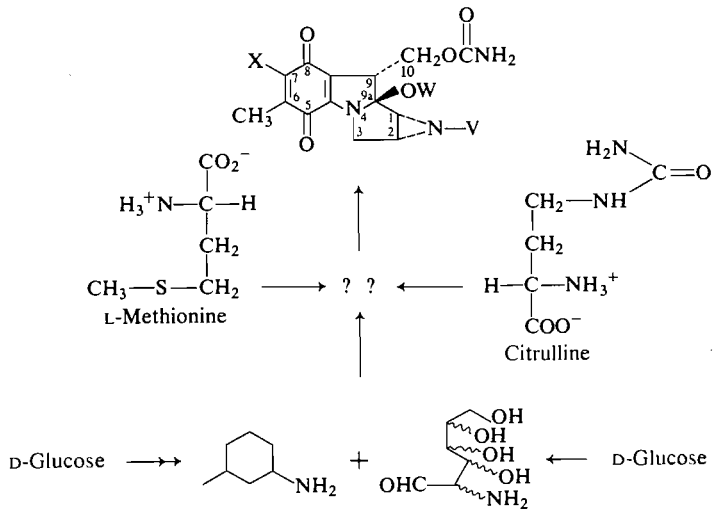

SCHEME 1

Previous synthetic explorations directed toward mitomycin have avoided the problem of introducing the 9a oxygen function and concentrated on the simpler aziridinomitosene structure, **2** (1*e*). The removal of the 9a group following enzymatic reduction of the mitosanes has been suggested as the primary mode of activation of mitomycin (2), *i.e.*

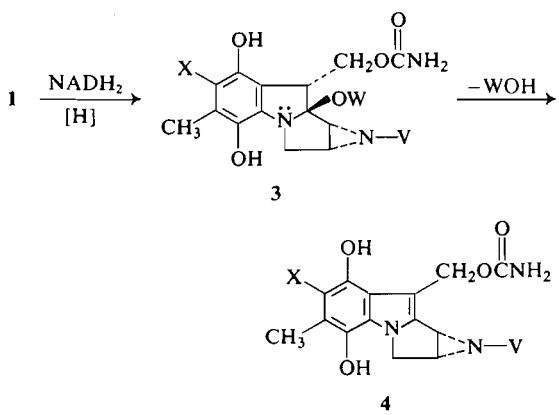

The reduced form of the aziridinomitosene (**4**) is then considered "activated", *i.e.*, capable of rapid bifunctional alkylation and hence covalent cross linking of DNA (2).

A possible clue to the origin of the 9a moiety and the biosynthetic formation of rings B and C in the mitosanes is provided by the pyrrolizidine alkaloids which they resemble in structure and function (Scheme 2) (2, 8–10). The comparison is even more striking between the pyrrole analogs of the alkaloids, *e.g.*, dehydrolasiocarpine and the activated form of mitomycin (8*b*). Compounds **6** and **4** are both bifunctional alkylating agents with similarly located linkage points. There is evidence that lasiocarpine brings about inhibition of DNA-dependent RNA-polymerase in rat liver suggesting covalent cross linking analogous to that of mitomycin C (11). Some pyrrolizidine alkaloids have mutagenic and tumor-inhibitory properties or cause chromosome breakage, and these conform to structure **6** (8*b*). The alkylating ability is for example associated with the possibility of alkyl–oxygen cleavage of the allylic ester grouping, analogous to the alkylating ability enhanced by indolic-conjugation found in **4**.

The relevant portion of the biosynthesis of the pyrrolizidine alkaloids (which proceeds from the amino acid ornithine) may be represented schematically (see Scheme 3) (12–16). An analogy for the transannular interaction envisaged in mitomycin biosynthesis is provided by the metabolic conversion of otosenine by rat liver microsomes to a pyrrole derivative considered to be dehydroretronecine (17).

Comparison of Schemes 1 and 3 suggests the intermediate formation of a hexahydrobenzazocinone followed by an analogous transannular interaction as the origin of the 9a oxygen function (see Scheme 4). Transannular interactions in cyclic aminoketones of eight or more atoms

Can. J. Chem. Downloaded from www.nrcresearchpress.com by 210.87.254.6 on 09/05/12
For personal use only.

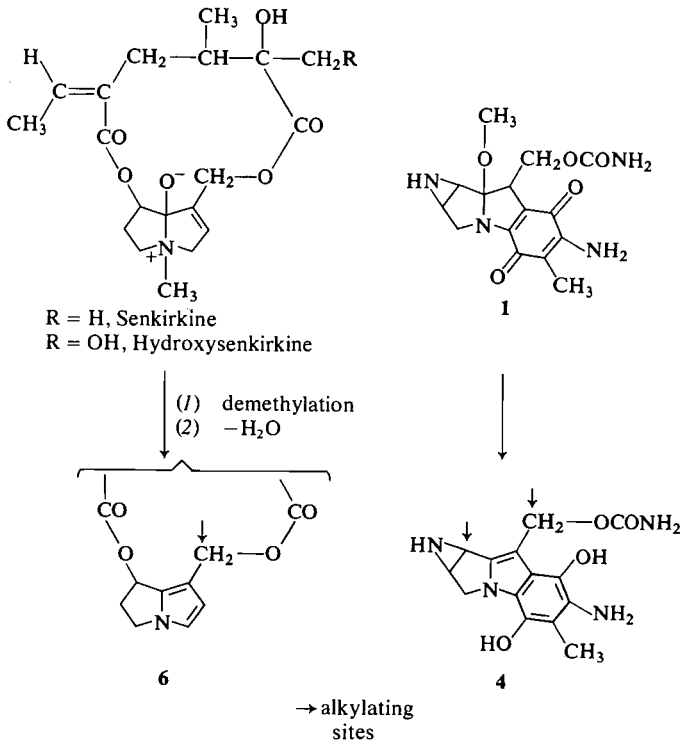

SCHEME 2

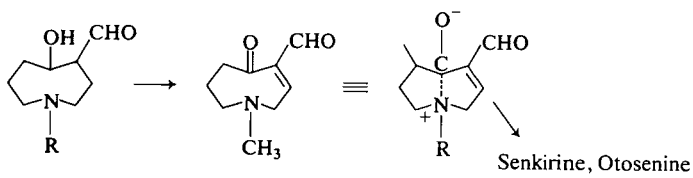

SCHEME 3

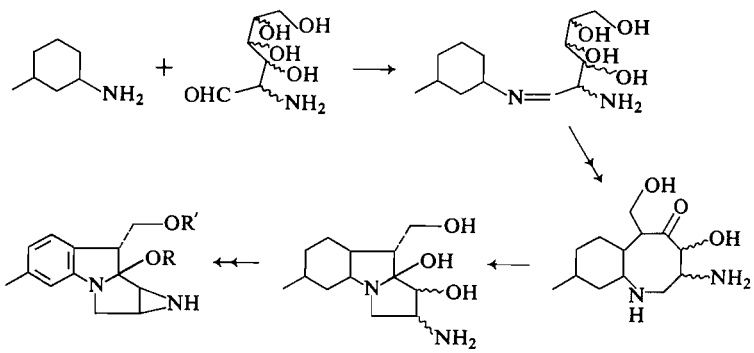

SCHEME 4

Can. J. Chem. Downloaded from www.nrcresearchpress.com by 210.87.254.6 on 09/05/12
For personal use only.

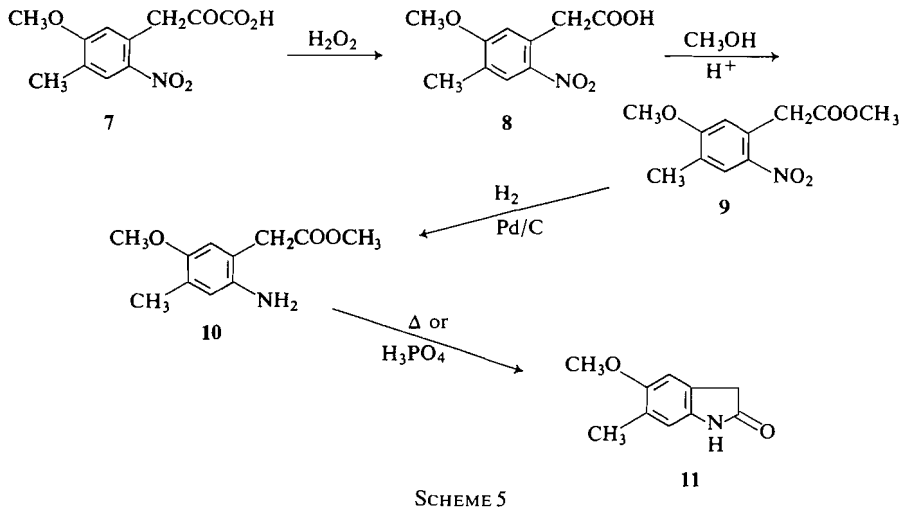

SCHEME 5

have been established by Leonard and coworkers (18*a–c*) and Johnson *et al.* (18*d*).

We considered that a comparable demonstration of the formation of rings A, B, and C from a suitably substituted hexahydrobenzazocinone would be valuable in pointing to its possible intermediacy in the biosynthesis. The interaction envisaged is different in type from that demonstrated by Leonard in that an aromatic amine is involved. However, successful ring closure of a benzazocinone might clarify the sequence of events in Scheme 4., *i.e.*, aromatization prior to transannular interaction or vice versa.

In our initial approach 5-methoxy-4-methyl-2-nitrophenylpyruvic acid (**7**) (19) was oxidatively decarbonylated to 5-methoxy-4-methyl-2-nitrophenylacetic acid (**8**) in 80% yield. Esterification of the latter followed by catalytic hydrogenation of the nitro group over palladium at atmospheric pressure afforded methyl 5-methoxy-4-methyl-2-amino-phenyl acetate (**10**) in 92.5% yield (Scheme 5).

The amino ester **10** was extremely labile and consequently, unless precautions were taken to cool the mixture during the catalytic hydrogenation, spontaneous ring closure to the indolinone **11** took place readily. This reaction

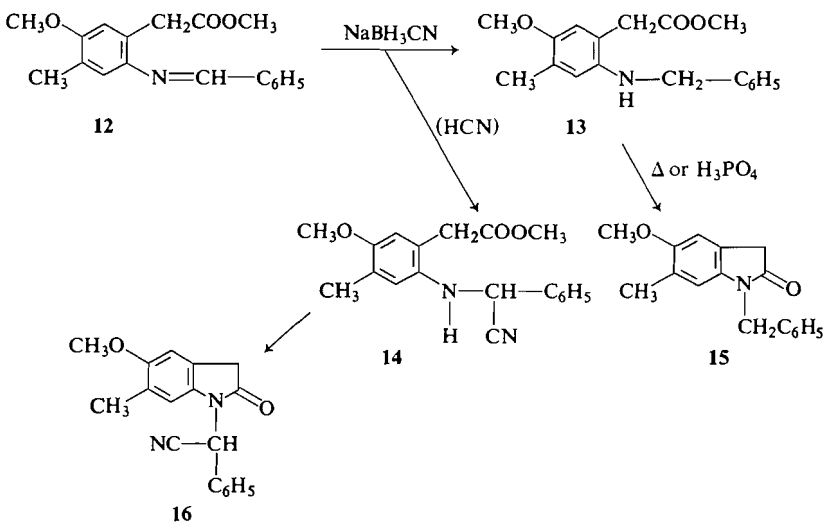

SCHEME 6

Can. J. Chem. Downloaded from www.nrcresearchpress.com by 210.87.254.6 on 09/05/12
For personal use only.

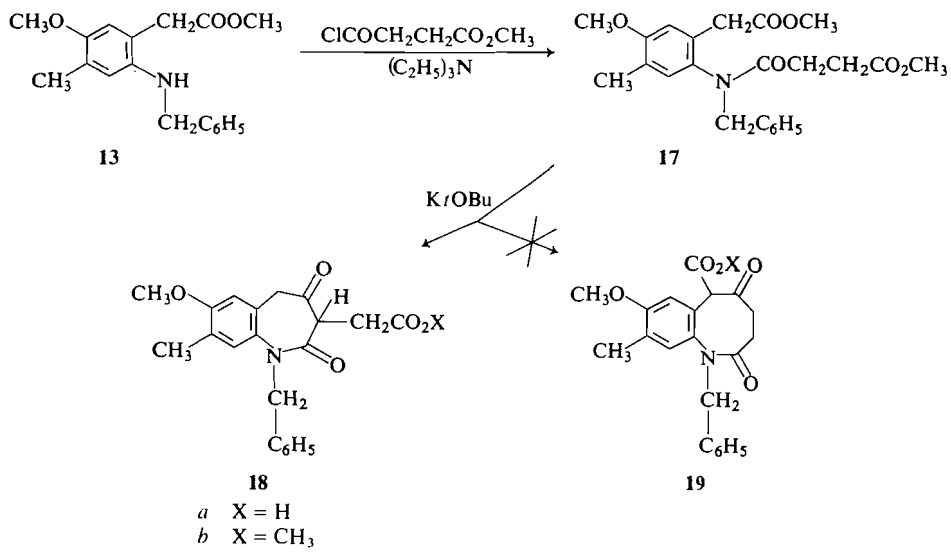

SCHEME 7

could also be accomplished quantitatively by brief warming of **10** with polyphosphoric acid. In view of its reactivity compound **10** was immediately converted into the anil **12**. Subsequent selective reduction of the imine function in the presence of the ester proved difficult; however the final method selected using sodium cyanoborohydride afforded the desired *N*-benzyl ester **13**. Careful chromatographic separation showed **13** to be accompanied by the two oxindoles **15** and **16**. The latter presumably arises from a Strecker-type addition (20) of the elements of hydrogen cyanide to **12** to form **14** which is unisolated but which would undergo rapid condensation to form **16**. Again these conclusions receive confirmation by the independent cyclization of **13** to **15** by warming with polyphosphoric acid (see Scheme 6).

Compound **13** was acylated in 72.5% yield with 3-carbomethoxypropionyl chloride to give methyl 5-methoxy-5-methyl-2-[*N*-benzyl(3′-carbomethoxypropionamido)]phenyl acetate (**17**).

Base catalyzed cyclizations to form medium sized rings are well known to give variable yields (21). In this case treatment of **17** with potassium *tert*-butoxide gave the tetrahydrobenzazepin-2,4-dione-3-acetic acid derivative **18***a* in 63% yield by a Stobbe reaction, instead of the desired hexahydrobenzazocin-2,4-dione **19** (see Scheme 7).

Evidence in support of structure **18***a* rests on the molecular composition and on the n.m.r. spectrum which shows an ABC pattern to be expected for $COCH{\cdot}CH_2CO_2H$ and not an A_2B_2 pattern which is seen in **17** and which would be expected for structure **19**. The i.r. spectrum shows absorption for seven-membered ketone at 1720 and normal acid at 1700 cm^{-1} and no evidence of chelation which would be expected for **19**. Compound **19** would also be expected to undergo ready decarboxylation.

Treatment of **18***a* with diazomethane in ether gave the ester **18***b*, the n.m.r. spectrum of which is similar to **18***a* and whose i.r. shows normal ketone and ester absorption at 1725 and 1715 cm^{-1}, respectively. In order to prevent the Stobbe reaction and favor Dieckmann condensation, an alternative approach was made via an intermediate which is incapable of forming a carbanion β to the nitrogen.

Formation of the *N*-*p*-toluenesulfonyl derivative from compound **10** proceeded smoothly in 72% yield. The product compound **20** has the distinct advantage over derivatives of the type **13** in that direct *N*-alkylation is possible via the *N*-sulfonyl anion of **20**. For example treatment of **20** with ethyl γ-bromobutyrate in the presence of potassium carbonate gave the *N*-alkylated product **22** (see Scheme 8). Treatment of **22**

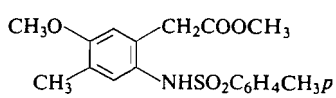

20

Can. J. Chem. Downloaded from www.nrcresearchpress.com by 210.87.254.6 on 09/05/12
For personal use only.

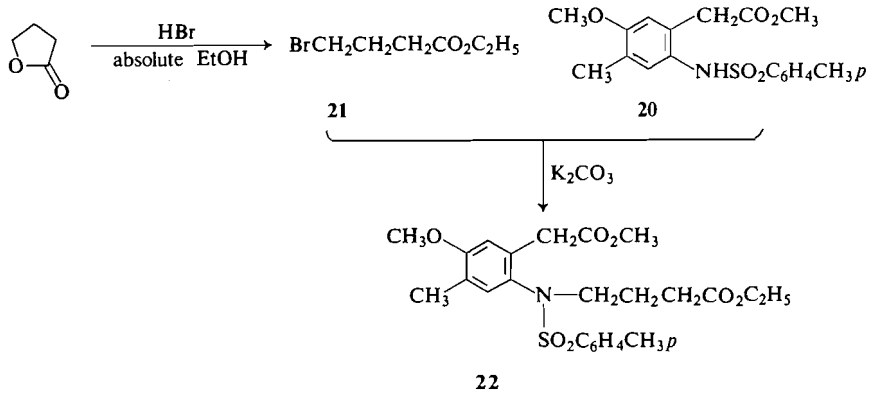

SCHEME 8

with potassium *tert*-butoxide in dry toluene afforded the desired 1,2,3,4,5,6-hexahydro-1,2-benzazocin-5-one **23** accompanied by small quantities of the analogs **24** and **25**. Compounds **24** and **25** were isolable as crystalline solids and characterized separately whereas **23** was obtained as an oil slightly contaminated with traces of **24** and **25** (Scheme 9). The spectral properties of all three compounds were consistent with their assigned structures (see Experimental).

Reductive cleavage of the N—S bond was accomplished with sodium in liquid ammonia; (this reagent has been used previously for the reductive cleavage of sulfur containing bonds (22)). The initial transannulated product **26** which was not isolated, eliminated water under these conditions to form the known compound **27** (19) in a reaction which is analogous to the conversion of **3** to **4** (Scheme 10). Compound **25** was accompanied by small amounts of **28** and **29** formed from the analogous ring closure of **24** and **25**, respectively. Compound **29** was isolated as a crystalline solid which could be characterized. The structure of **29** is given by its molecular composition and the n.m.r. spectrum which shows an ethyl ester and absence of vinylic absorptions and three groups of methylene absorptions (see Experimental).

The above experiments with model systems provide a chemical basis for the suggested intermediacy of a hexahydrobenzazacinone and its transannular interaction to form rings A, B, and C of mitomycin C during its biosynthesis. This sequence of reactions also may provide an alternative approach to the presently unsolved problem of a total synthesis of mitomycin C.

Experimental

Melting points were determined on a Fisher-Johns apparatus and are uncorrected. The i.r. spectra were recorded on a Perkin-Elmer model 421 spectrophotometer and only the principal, sharply defined peaks are reported. The n.m.r. spectra were recorded on Varian A-60 and A-100 analytical spectrometers. The spectra were measured on approximately 10–15% (w/v) solutions in $CDCl_3$, with tetramethylsilane as a standard. Line

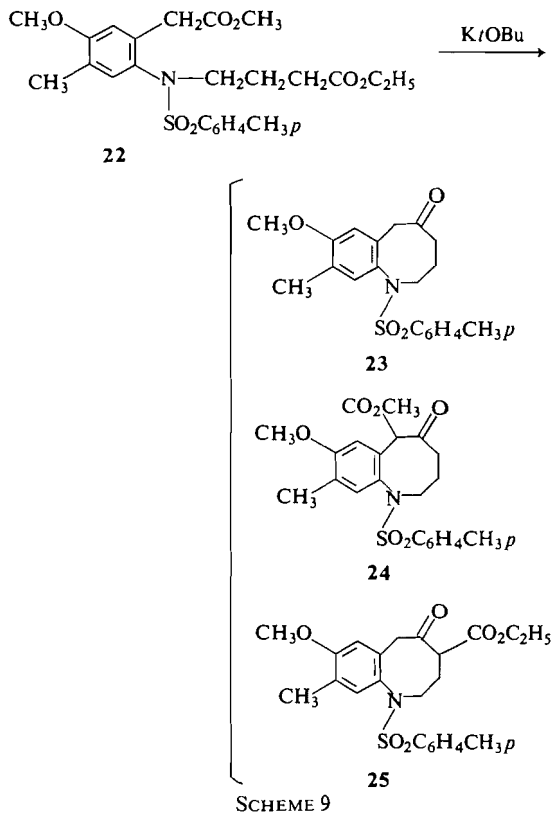

SCHEME 9

Can. J. Chem. Downloaded from www.nrcresearchpress.com by 210.87.254.6 on 09/05/12
For personal use only.

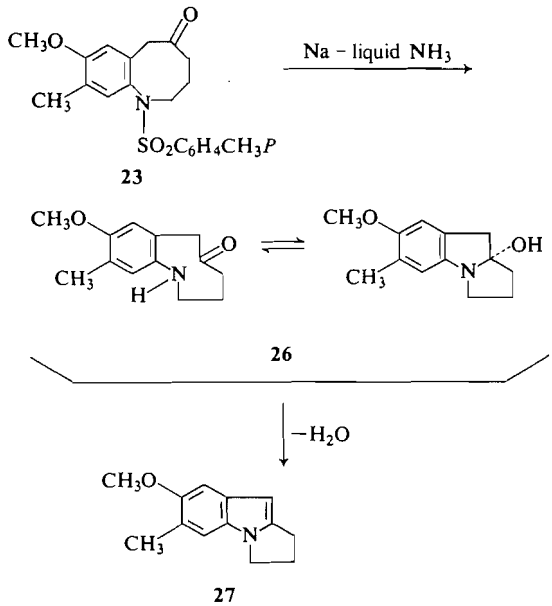

SCHEME 10

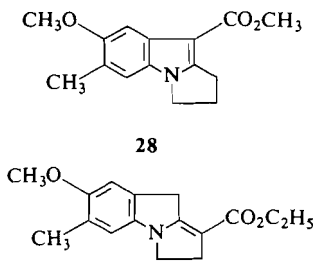

positions are reported in p.p.m. from the reference. Mass spectra were determined on an Associated Electrical Industries MS-9 double focusing high resolution mass spectrometer. The ionization energy, in general, was 70 eV. Peak measurements were made by comparison with perfluorotributylamine at a resolving power of 15000. Kieselgel DF-5 (Camag, Switzerland) and Eastman Kodak precoated sheets were used for thin layer chromatography. Microanalyses were carried out by Mrs. D. Mahlow of this department.

5-Methoxy-4-methyl-2-nitrophenylacetic Acid (8)

5-Methoxy-4-methyl-2-nitrophenylpyruvic acid 7 (25.321 g, 0.100 mol) (19) was dissolved in a solution of 40.0 g (1.0 mol) of sodium hydroxide in 130 ml of water. Ice (50 g) was added, followed by the slow addition of a solution of 27 g of 30% hydrogen peroxide in 75 ml of water with continuous stirring. The solution was set aside at room temperature for 5 h then cautiously acidified with concentrated hydrochloric acid. The resulting solid was collected and purified by recrystallization from methanol affording 18.0 g (80% yield) of compound **8**, m.p. 154°.

Anal. Calcd. for $C_{10}H_{11}O_5N$ (mol. wt. 225.0637): C, 53.33: H, 4.92; N, 6.22. Found (mass spectrum, 225.0630): C, 53.08; H, 4.80; N, 6.15.

The n.m.r. spectrum δ TMS ($CDCl_3$): 2.27 (s, 3H, CH_3), 3.97 (s, 3H, OCH_3), 4.07, (s, 2H, $—CH_2CO_2$), 6.71, 8.08 (s, 1H each, aryl). The i.r. ν_{max} ($CHCl_3$): 1710 (acid CO), 3500 cm^{-1} (acid OH).

Methyl 5-Methoxy-4-methyl-2-nitrophenylacetate (9)

A solution of 5.0 g (22 mmol) of 2-nitrophenylacetic acid **8** and 0.5 ml of concentrated sulfuric acid in 100 ml of methanol was heated under reflux for 3 h. The reaction mixture was concentrated *in vacuo* and the resulting solid collected and purified by recrystallization from methanol to give 4.0 g (76.5% yield) of compound **9** as white needles, m.p. 123–124°.

Anal. Calcd. for $C_{11}H_{13}O_5N$ (mol. wt. 239.0799): C, 55.23; H, 5.48; N, 5.86. Found (mass spectrum 239.0798): C, 55.12; H, 5.64; N, 5.78.

The n.m.r. spectrum δ TMS ($CDCl_3$): 2.26 (s, 3H, CH_3), 3.75 (s, 3H, $—CO_2CH_3$), 3.96 (s, 3H, OCH_3), 4.05 (s, 2H, $—CH_2CO_2R$), 6.75, 8.07 (s, 1H, each, aryl).

Methyl 5-Methoxy-4-methyl-2-aminophenylacetate (10)

A mixture of 7.17 g (30 mmol) of methyl 5-methoxy-4-methyl-2-nitrophenylacetate (**9**) and 1.0 g of 5% palladium-on-charcoal in 160 ml of ethyl acetate was subjected to hydrogenation at atmospheric pressure. The theoretical volume of hydrogen was absorbed in 6 h. Filtration and concentration of the solution gave a pale yellow oil which solidified on cooling. Crystallization from methanol gave 5.8 g (92.5% yield) of compound **10**, m.p. 158–160°. This material was extremely unstable and was immediately converted into the anil.

Anil of Methyl 5-Methoxy-4-methyl-2-aminophenylacetate (12)

To a solution of 4.180 g (20 mmol) of methyl 5-methoxy-4-methyl-2-aminophenylacetate **10** and 500 mg of *p*-toluenesulfonic acid in 30 ml of dry benzene was added a solution of 2.12 g (20 mmol) of benzaldehyde in 10 ml of dry benzene and the solution was stirred at ambient temperature overnight. The filtered solution was concentrated *in vacuo* to give 5.02 g (84.5% yield) of the Schiff base **12** as a yellow solid which was purified by recrystallization from methanol, m.p. 98°.

Anal. Calcd. for $C_{18}H_{19}O_3N$ (mol. wt. 297.1359): C, 72.70; H, 6.44; N, 4.71. Found (mass spectrum 297.1365): C, 72.54; H, 6.56; N, 4.68.

The n.m.r. spectrum δ TMS ($CDCl_3$): 2.22 (s, 3H, CH_3), 3.62 (s, 3H, $—CO_2CH_3$), 3.86 (s, 5H, CH_2CO_2R and OCH_3), 6.78, 6.96 (1H each, s, ring protons), 7.35–7.97 (aryl protons), 8.26 (s, 1H, $—N=CH—C_6H_5$). The i.r. spectrum ν_{max} ($CHCl_3$): 1730 cm^{-1} (C=O).

Methyl 2-Benzylamino-4-methyl-5-methoxyphenylacetate (13)

To a solution of 0.9 g of the Schiff base **12** in 5 ml of ethyl acetate was added a solution of 120 mg of sodium cyanoborohydride (23) in 3 ml of methanol, and the mixture stirred at room temperature for 6 h. The p*H*

Can. J. Chem. Downloaded from www.nrcresearchpress.com by 210.87.254.6 on 09/05/12
For personal use only.

Can. J. Chem. Downloaded from www.nrcresearchpress.com by 210.87.254.6 on 09/05/12
For personal use only.

of the solution was adjusted to 7.0 periodically by the addition of hydrochloric acid, the solution was filtered and concentrated *in vacuo*. The residual oil was treated with water and methylene chloride and the aqueous layer extracted several times with methylene chloride. Concentration of the dried extract gave 0.780 g of compound **13** as an oil.

The n.m.r. spectrum δ TMS ($CDCl_3$): 2.12 (s, 3H, CH_3), 3.54 (s, 2H, $CH_2CO_2CH_3$), 3.63 (s, 3H, CO_2CH_3), 3.73 (s, 3H, OCH_3), 4.86 (s, 2H, CH_2Ph), 6.54, 6.84, (s, 1H each, ring protons), 7.04–7.65 (m, 5H, aryl protons). The i.r. spectrum (film): 1695 (C=O), 3350 (NH) cm^{-1}.

Mol. Wt. Calcd. for $C_{18}H_{21}NO_3$: 299. Found (mass spectrum): 299.

Further elution with benzene gave 180 mg of 5-methoxy-6-methyl-*N*-1′-cyanobenzyl-2-indolinone (**16**) as a white crystalline solid, m.p. 152–153° (methanol).

Anal. Calcd. for $C_{18}H_{16}O_2N_2$ (mol. wt. 292.1212): C, 73.95; H, 5.52; N, 9.58. Found (mass spectrum 292.1213): C, 73.91; H, 5.48; N, 9.39.

The n.m.r. spectrum δ TMS ($CDCl_3$): 2.16 (s, 3H, CH_3), 3.76 (s, 2H, —CH_2); 3.89 (s, 3H, OCH_3), 6.74, (s, 1H, 4 or 7 proton), 7.06 (s, 2H, 4 or 7 proton and —N—C*H*(CN)Ph), 7.66 (s, 5H, phenyl group). Further elution with benzene gave *N*-benzyl-5-methyl-2-oxindole (**15**). The spectral and physical data on this compound were identical with those described in its synthesis below.

*5-Methoxy-6-methyl-2-indolinone (**11**)*

A mixture of 1.5 g (7.1 mmol) of the amine **10** and some polyphosphoric acid (prepared from 7.5 ml of orthophosphoric acid and 7.5 g of phosphorous pentoxide) was heated at 130–140° with stirring for 15 min. After cooling, the mixture was treated with excess of cold water and the precipitated product was collected and purified by recrystallization from methanol affording 950 mg (74.5% yield) of compound **11**, m.p. 162–164°.

Anal. Calcd. for $C_{10}H_{11}O_2N$ (mol. wt. 177.0790): C, 67.78; H, 6.26; N, 7.91. Found (mass spectrum, 177.0794): C, 67.69; H, 6.11; N, 8.02.

The n.m.r. spectrum δ TMS ($CDCl_3$): 2.23 (s, 3H, CH_3), 3.55 (s, 2H, CH_2), 3.87 (s, 3H, OCH_3), 6.87 (s, 1H), and 7.13 (s, 1H, aryl protons). The i.r. spectrum ν_{max} (film): 1655 (amide C=O), 3430 cm^{-1} (br, NH).

*N-Benzyl-5-methoxy-6-methyl-2-indolinone (**15**)*

A solution of 0.7 g (2.3 mmol) of methyl 2-benzylamino-4-methyl-5-methoxyphenyl acetate **13** in 15 ml of dry ether in a pressure bottle was warmed at 40–50° with stirring for 16 h. The solvent was removed *in vacuo* and crystallization of the residue from methanol gave 400 mg (65% yield) of *N*-benzyl-5-methoxy-5-methyl-2-indolinone (**15**), m.p. 103–104°.

Anal. Calcd. for $C_{17}H_{17}O_2N$ (mol. wt. 267.1259): C, 76.38; H, 6.41; N, 5.24. Found (mass spectrum 267.1256): C, 76.21; H, 6.51; N, 5.18.

The n.m.r. spectrum δ TMS ($CDCl_3$): 2.20 (s, 3H, CH_3), 3.67 (s, 2H, CH_2), 3.87 (s, 3H, OCH_3), 5.02 (s, 2H, NCH_2Ph), 6.78 (s, 1H), and 7.02 (s, 1H, oxindole ring protons), 7.47 (s, 5H, aryl). The i.r. spectrum ν_{max} ($CHCl_3$): 1675–1690 cm^{-1} (C=O).

*Methyl 2-[N-Benzyl-N-(3-carbomethoxypropionyl)]-amino-4-methyl-5-methoxyphenylacetate (**17**)*

To a solution of 5.3 g (17.4 mmol) of compound **13** and 1.92 g (18 mmol) of trimethylamine in 30 ml of dry benzene was added a solution of 2.61 g (17.4 mmol) of 3-carbomethoxypropionyl chloride in 10 ml of dry benzene. The mixture was stirred for 1 h then washed with water (3 × 20 ml) and the organic layer dried ($MgSO_4$). Evaporation of the solvent gave a yellow oil which was purified by chromatography on silica gel. Elution with 4.0 g (72.5% yield) of compound **17** as a yellow oil.

Anal. Calcd. for $C_{23}H_{27}O_6N$ (mol. wt. 413.1838): C, 66.81; H, 6.58; N, 3.39. Found (mass spectrum 413.1842): C, 66.61; H, 6.62; N, 3.35.

The n.m.r. spectrum δ TMS ($CDCl_3$): 2.14 (s, 3H, CH_3), 2.10–2.83 (br m, 4H, —$CH_2CH_2CO_2R$), 3.50 s, 2H, —CH_2CO_2R), 3.80 (s, 6H, CO_2CH_3), 3.96 (s, 3H, CH_3O), ABq centered at 4.52 and 5.35, J = 14 Hz (2H, —CH_2Ph), 6.79 (s, 1H), and 6.98 (s, 1H, aryl ring protons). The i.r. spectrum ν_{max} ($CDCl_3$): 1645 (amide CO), 1725 cm^{-1} (ester CO).

*1-Benzyl-7-methoxy-8-methyl-2,3,4,5-tetrahydrobenzazepin-2,4-dione-3-acetic Acid (**18a**)*

A mixture of 0.78 g (20 mmol) of potassium and 4.5 g (62 mmol) of *tert*-butyl alcohol was allowed to react in 60 ml of freshly distilled toluene in a three-necked flask purged with nitrogen. The mixture was stirred and heated below the boiling point of the alcohol–toluene azeotrope until all of the potassium had reacted. The excess of alcohol was then removed by distillation. Dry toluene was introduced to bring the total volume in the flask to 150 ml and 3.10 g (7.5 mmol) of the diester **17** in 60 ml of dry toluene was added dropwise over a period of 12 h to the reaction mixture with vigorous stirring and refluxing. After cooling, the resulting mixture was neutralized with dilute hydrochloric acid and the organic layer dried ($MgSO_4$). Removal of the solvent *in vacuo* from the filtered solution afforded 1.79 g (63% yield) of 1-benzyl-7-methoxy-8-methyl-2,3,4,5-tetrahydrobenzazepin-2,4-dione-3-acetic acid (**18a**) as an oil.

Anal. Calcd. for $C_{21}H_{21}NO_5$ (mol. wt. 367): C, 69.27; H, 6.08; N, 3.67. Found (mass spectrum 367): C, 69.53; H, 6.21; N, 3.44.

The n.m.r. spectrum δ TMS ($CDCl_3$): 2.22 (s, 3H, CH_3), 2.92–4.20 (3H, ABC COC*H*—CH_2CO_2H), 3.80 (s, 3H, CO_2CH_3), 3.90 (s, 2H, CH_2CO), ABq centered at 4.78 and 5.40, J = 14.5 Hz (CH_2Ph), 6.53 (s, 1H, ring proton), 6.9–7.5 (m, 6H, phenyl and ring protons).

The i.r. ν_{max} (KBr disc): 1645 ( ), 1700 (CO_2H), 1720 (seven-membered ring C=O) cm^{-1}.

*Methyl 1-Benzyl-7-methoxy-8-methyl-2,3,4,5-tetrahydrobenzazepin-2,4-dione-3-acetate (**18b**)*

To a solution of 1.00 g (2.7 mmol) of the tetrahydrobenzazepindioneacetic acid in 45 ml of dry ether was added by distillation, an ethereal solution of diazomethane (prepared from 1.5 g of nitrosomethylurea and 20% sodium hydroxide solution). The mixture was stirred at ambient temperature for 18 h and taken to dryness to give an oil which was purified by chromatog-

Can. J. Chem. Downloaded from www.nrcresearchpress.com by 210.87.254.6 on 09/05/12
For personal use only.

raphy on neutral alumina giving 1.02 g (97% yield) of methyl 1-benzyl-7-methoxy-8-methyl-2,3,4,5-tetrahydrobenzazepin-2,4-dione-3-acetate (**18***b*).

Anal. Calcd. for $C_{22}H_{23}NO_5$ (mol. wt. 381.1576); C, 69.27; H, 6.08; N, 6.37. Found (mass spectrum, 381.1565): C, 69.53; H, 6.21; N, 3.42.

The n.m.r. spectrum δ TMS ($CDCl_3$): 2.20 (s, 3H, CH_3), 2.85–4.25 (ABC, 3H, $COCHCH_2CO_2H$), 3.64 (3,3H, CO_2CH_3), 3.78 (s, 3H, OCH_3), 3.89 (d, 2H, $—CH_2CO$), AB quartet centered at 4.72 and 5.44, J = 14.5 Hz, $—NHCH_2Ph$, 6.52 and 7.25 (s, 1H each, ring protons), 7.20 (s, 5H, phenyl group). The i.r. ν_{max} ($CHCl_3$): 1645 ($\diagdown$N—CO$\diagup$); 1715 (CO_2CH_3) and 1725 (seven-membered ketone) cm^{-1}.

*Methyl 5-Methoxy-4-methyl-2-toluenesulfonamidophenylacetate (**20**)*

To a solution of 4.18 g (20 mmol) of the *o*-aminophenylacetate **10** in 45 ml of dry pyridine was added 3.80 g (20 mmol) of *p*-toluenesulfonyl chloride. The solution was stirred for 3 h at room temperature then the pyridine was allowed to evaporate in the fume hood. The residue was shaken with chloroform and dilute hydrochloric acid and the organic layer was dried ($MgSO_4$). Concentration of the solution afforded 5.2 g (71.5% yield) of compound **20** as white crystals, m.p. 109–110°.

Anal. Calcd. for $C_{18}H_{21}O_5NS$ (mol. wt. 363.1140): C, 59.49; H, 5.83; N, 3.86. Found (mass spectrum 363.1136): C, 59.38; H, 5.85; N, 3.71.

The n.m.r. spectrum δ TMS ($CDCl_3$): 2.10, (s, 3H, CH_3), 2.38 (s, 3H, CH_3), 3.20 (s, 2H, $—CH_2CO_2R$), 3.65 (s, 3H, CO_2CH_3), 3.77 (s, 3H, OCH_3), 6.53 (s, 1H), 7.01 (s, 1H, phenyl ring protons), AB quartet centered at 7.20 and 7.58, J = 8.0 Hz (4H, toluenesulfonyl ring protons). The i.r. spectrum ν_{max} ($CHCl_3$): 1715 (ester C=O), 3350 cm^{-1} (sulfonamide NH).

*Methyl 5-Methoxy-4-methyl-2-[N-(3-carbomethoxypropyl)]-p-toluenesulfonamidophenyl Acetate (**22**)*

A mixture of 3.63 g (10 mmol) of methyl 5-methoxy-4-methyl-2-*p*-toluenesulfonamidophenylacetate **20**, 3.66 g (20 mmol) of ethyl γ-bromobutyrate, and 4.95 g (36 mmol) of anhydrous potassium carbonate in 60 ml of dry acetone was heated under reflux with stirring for 16 h. The reaction mixture was filtered and concentrated *in vacuo* and the oil was subjected to chromatography. Removal of the solvent afforded 4.5 g (94% yield) of **22** as an oil.

Anal. Calcd. for $C_{24}H_{31}O_7N^{32}S$ (mol. wt. 477.1822): C, 60.36; H, 6.54; N, 2.93. Found (mass spectrum 477.1833): C, 60.18; H, 6.63; N, 3.15.

The n.m.r. spectrum δ TMS ($CDCl_3$): 1.29 (t, 3H, $CH_3CH_2—$), 2.03 (s, 3H, $CH_3—$), 1.61–2.52 (m, 4H, $CH_3CH_2CH_2—$), 3.31–3.56 (m, 2H, CH_2CO_2R); 3.74 (s, 3H, CO_2CH_3), 3.87 (s, 3H, $CH_3O—$), 3.90–4.45 (m, 2H, $—CH_2CH_3$), 6.30 (s, 1H), 6.87 (s, 1H, phenyl ring protons), AB quartet centered at 7.28 and 7.55, J = 8.5 Hz (4H, aryl absorption). The i.r. spectrum ν_{max} ($CHCl_3$): 1725 cm^{-1} (C=O).

*Dieckmann Condensation of Methyl 5-Methoxy-4-methyl-2-[N-(3-carbomethoxypropyl)]-p-toluenesulfonamidophenylacetate (**22**)*

A solution of 4.77 g (10 mmol) of diester **22** in 60 ml of dry toluene was added over a period of 3 h with vigorous stirring and continuous refluxing under nitrogen to a suspension of 5.75 g (0.05 mol) of potassium *tert*-butoxide in 150 ml of dry toluene. The solution was concentrated to about half the volume *in vacuo* and after cooling the filtered solution was washed with (*i*) dilute hydrochloric acid (3 × 25 ml) and (*ii*) water (2 × 15 ml) then dried ($MgSO_4$). Removal of the solvent and chromatography of the residual oil on silica gel with chloroform as eluant gave (*a*) an oil and (*b*) crystals.

Fraction *a* the oil was 8-methoxy-9-methyl-*N*-*p*-toluenesulfonyl-1,2,3,4,5,6-hexahydro-2,3-benzazocin-5-one (**23**) 0.92 g (24.6% yield).

Anal. Calcd. for $C_{20}H_{23}NO_4S$ (mol. wt. 373.1348): N, 3.14. Found (mass spectrum 373.1337): N, 3.63.

The n.m.r. spectrum δ TMS ($CDCl_3$): 0.9–2.5 (m, 6H, CH_2), 2.02 (s, 3H, CH_3), 2.43 (s, 3H, CH_3), 3.30–4.2 (m, 2H, $ArCH_2CO$), 3.82 (s, 3H, OCH_3), 6.48, 6.66 (s, 1H, each phenyl ring proton), AB quartet centered at 7.30 and 7.67, J = 8.0 Hz (4H, $—C_6H_4CH_3$). The i.r. spectrum ν_{max} ($CHCl_3$): 1705 cm^{-1} (C=O).

Fraction *b* provided sufficient material (65 mg), m.p. 110–112° for an n.m.r. spectrum confirming the presence of both **24** and **25**.

The n.m.r. spectrum δ TMS ($CDCl_3$): 1.23 (t, 3H, $CH_3CH_2—$), 1.74–2.10 (br, *ca.* 6H, methylenes), 2.12, 2.14, (s, 3H each, ring CH_3), 3.66 (s, 3H, CO_2CH_3 of **24**), 3.79, 3.81 (s, 3H each, ring OCH_3), 4.02–4.38 (q, 2H, CH_2CH_3 for **25**), 6.70 and 6.76 (s, 1H each, phenyl ring protons), AB quartets centered at 7.18 and 7.56, J = 9.0 Hz (4H each, $SO_2C_6H_4CH_3$).

The i.r. spectrum ν_{max} (KBr disc): 1733 (eight-membered ring ketone), 1715 cm^{-1} (ester C=O). Fractional recrystallization of *b* from ether afforded pure methyl 8-methoxy-9-methyl-*N*-*p*-toluenesulfonyl-1,2,3,4,5,6-hexahydro-2,3-benzazocin-5-one-2-carboxylate (**24**, 11 mg), m.p. 173°.

Anal. Calcd. for $C_{22}H_{25}O_6N^{32}S$ (mol. wt. 431.1403): C, 61.24; H, 5.84; N, 3.25. Found (mass spectrum, 431.1391): C, 61.45; H, 5.98; N, 2.89.

Recrystallization of the residue from the mother liquor gave ethyl 8-methoxy-9-methyl-*N*-*p*-toluenesulfonyl-1,2,3,4,5,6-hexahydro-1,2-benzazocin-4-carboxylate (**25**, 8 mg), m.p. 121°.

Mol. Wt. Calcd. for $C_{23}H_{27}O_6N^{32}S$: 445.1566. Found (mass spectrum): 445.1559.

*Reductive Cleavage of the N-Tosylhexahydrobenzazocinone **23** and Ring Closure to 2,3-Dihydro-7-methoxy-6-methyl-1H-pyrrolo[1,2-a]indole (**27**)*

To a stirred suspension of 873 mg (2.72 mmol) of the hexahydrobenzazocinone **23** in *ca.* 30 ml of liquid ammonia was added 230 mg (10 mgatom) of sodium and after 10 min a blue color developed. Ammonium chloride was added when the solution became colorless, then the ammonia was allowed to evaporate and methanol then water and chloroform were added. The organic layer was washed with water and dried ($MgSO_4$).

Can. J. Chem. Downloaded from www.nrcresearchpress.com by 210.87.254.6 on 09/05/12
For personal use only.

Evaporation of the solvent afforded an oil which was chromatographed on silica gel. Elution with chloroform gave 230 mg (45% yield) of 2,3-dihydro-7-methoxy-6-methyl-1*H*-pyrrolo[1,2-*a*]indole (**27**), m.p. 112–113°, as needles crystallized from *n*-hexane. The m.p. was depressed (by admixture with traces of the corresponding pyrrolo[1,2-*a*]indoles **28** and **29**) compared with literature (19) value of 116–118°. The m.p. was undepressed upon admixture with an authentic sample of **27**.

Mol. Wt. Calcd. for $C_{13}H_{15}NO$: 201.1154. Found (mass spectrum): 201.1145.

The n.m.r. spectrum δ TMS ($CDCl_3$): 2.32 (s, 3H, 6-CH_3), 2.45–2.71 (m, 2H, —$CH_2CH_2CH_2$—), 2.97 (t, 2H, —$NCH_2CH_2CH_2$—), 3.86 (s, 3H, OCH_3), 3.96 (t, 2H, —N—CH_2—CH_2CH_2—), 6.04 (s, 1H, indole H), 6.96 (s, 1H), 6.98 (s, 1H, 5 and 9 ring protons).

Fractional crystallization of the mother liquor allowed the isolation of pure **29**, m.p. 118.9°.

Mol. Wt. Calcd. for $C_{16}H_{19}NO_3$: 273.1372. Found (mass spectrum): 273.1366.

The n.m.r. spectrum δ TMS ($CDCl_3$): 1.38 (t, 3H, CH_2CH_3), 2.21 (s, 3H, CH_3), 2.57 (quintet, 2H, —CH_2—), 3.19 (t, 2H, —CH_2—), 3.89 (s, 3H, OCH_3), 3.95 (q, 2H, —CH_2), 6.94, 7.55 (s, 1H each ring protons). The n.m.r. spectrum shows in addition an absorption due to **28**, a band 3.86 (s, 3H, —CO_2CH_3). The i.r. spectrum ν_{max} ($CHCl_3$): 1683 cm^{-1} (N—C=C—C=O). The mother liquor showed the presence of compound **28**.

Mol. Wt. Calcd. for $C_{15}H_{17}NO_3$: 259.1208. Found (mass spectrum): 259.1213.

This research was supported by grants to J. W. Lown from the National Research Council of Canada and from the National Cancer Institute of Canada and by the Chemistry Department, University of Alberta. We thank Dr. A. Hogg and Mr. R. Swindlehurst for the mass and n.m.r. spectra. We wish to thank Dr. M. J. Weiss, Lederle Laboratories, Pearl River, N.Y. for supplying an authentic sample of **27** for comparison.

1. (*a*) T. Hato, Y. Sano, R. Sugawara, A. Matsumae, K. Kanamori, T. Shima, and T. Hoshi. J. Antibiot. (Tokyo) Series A, **9**, 141 (1956); (*b*) S. Wakaki, H. Marumo, T. Tomioka, G. Shimizu, E. Kato, H. Kamada, S. Kudo, and Y. Fujimoto. Antibiot. Chemother. **8**, 228 (1958); (*c*) S. Wakaki. Cancer Chemother. Rep. **13**, 79 (1961); (*d*) J. S. Webb, D. B. Cosulich, J. H. Mowat, J. B. Patrick, R. W. Broschard, W. E. Meyer, R. P. Williams, C. F. Wolf, W. Fulmor, C. Pidacks, and J. E. Lancaster. J. Am. Chem. Soc. **84**, 3185 (1962); (*e*) W. A. Remers and M. J. Weiss. J. Med. Chem. **11**, 737 (1968) and papers cited therein; (*f*) R. W. Franck and J. Auerbach. J. Org. Chem. **36**, 31 (1971); (*g*) T. Hirata, Y. Yamada, and M. Matsui. Tetrahedron Lett. 4107, (1969); (*h*) T. Takada and S. Ohki. Chem. Pharm. Bull. (Japan), **19**, 977 (1971); (*i*) T. Takada, S. Kunugi, and S. Ohki. Chem. Pharm. Bull. (Japan), **19**, 982 (1971); (*j*) T. Takada and M. Akiba. Chem. Pharm. Bull. (Japan), **20**, 1785 (1972).
2. W. Szybalski and V. N. Iyer. *In* The mitomycins and porfiromycins. Antibiotics. 1. *Edited by* D. Gottlieb and P. D. Shaw. Springer-Verlag Publishers, New York. 1967. p. 277.
3. J. W. Lown, T. Itoh, and N. Ono. Can. J. Chem. **51**, 896 (1973).
4. J. W. Lown and A. Begleiter. Can. J. Chem. **52**, 2331 (1974).
5. E. J. Kirsch. *In* Mitomycins. Antibiotics II. *Edited by* D. Gottlieb and P. D. Shaw. Springer-Verlag Publishers, New York. 1967. p. 66.
6. (*a*) U. Hornemann and J. C. Cloyd. Chem. Commun. 301 (1971); (*b*) U. Hornemann and M. J. Aikman. Chem. Commun. 88 (1973); (*c*) U. Hornemann, J. P. Kehrer, C. S. Nunez, and R. L. Ranieri. J. Am. Chem. Soc. **96**, 320 (1974).
7. E. J. Kirsch and J. Korshala. J. Bacteriol. **87**, 247 (1964).
8. (*a*) C. C. J. Culvenor, A. T. Dann, and A. T. Dick. Nature, **195**, 570 (1962); (*b*) C. C. J. Culvenor, D. T. Downing, and J. A. Edgar. Ann. N.Y. Acad. Sci. **163**, 837 (1969); (*c*) A. J. Aasen and C. C. J. Culvenor. Aust. J. Chem. **22**, 2657 (1969).
9. E. K. McLean. Pharmacol. Rev. **22**, 429 (1970).
10. V. N. Iyer and W. Szybalski. Science, **145**, 55 (1964).
11. J. Reddy, C. Harris, and D. Svoboda, Nature, **217**, 659 (1968).
12. L. B. Bull, C. C. J. Culvenor, and A. T. Dick. The pyrrolizidine alkaloids. North Holland Publishing Co., Amsterdam. 1968. F. L. Warren. *In* The alkaloids. Vol. XII. *Edited by* R. H. F. Manske. Academic Press, New York. 1970. p. 316.
13. E. Nowacki and R. U. Bjerrum. Life Sci. **5**, 157 (1962).
14. C. A. Hughes, R. Letcher, and F. L. Warren. J. Chem. Soc. 4974 (1964).
15. W. Bottomley and T. A. Geissman. Phytochemistry, **3**, 357 (1964).
16. A. McKillop. An introduction to the chemistry of the alkaloids. Butterworths. 1969. p. 134.
17. C. C. J. Culvenor, J. A. Edgar, L. W. Smith, M. V. Jago, and J. E. Peterson. Nature New Biol. **229**, 255 (1971).
18. (*a*) N. J. Leonard. Rec. Chem. Prog. **17**, 243 (1956); (*b*) N. J. Leonard, D. F. Morrow, and M. T. Rogers. J. Am. Chem. Soc. **79**, 5476 (1957); (*c*) N. J. Leonard and T. Sato. J. Org. Chem. **34**, 1066 (1969); (*d*) R. A. Johnson, M. E. Herr, H. C. Murray, and G. S. Fonken. J. Org. Chem. **33**, 3187 (1968).
19. G. R. Allen, J. F. Poletto, and M. J. Weiss. J. Org. Chem. **30**, 2897 (1965).
20. A. Strecker. Ann. **75**, 27 (1850).
21. G. R. Proctor and W. I. Ross, J. Chem. Soc. Perkin I, 885 (1972) and subsequent papers. J. P. Schaefer and J. J. Bloomfield. *In* Organic reactions. Vol. 15. *Edited by* Roger Adams. Wiley, New York. 1967. p. 1.
22. J. E. Baldwin, R. E. Hackler, and D. P. Kelly. J. Am. Chem. Soc. **90**, 4758 (1968).
23. R. F. Borch and H. D. Durst. J. Am. Chem. Soc. **91**, 3996 (1969); R. F. Borch, M. D. Bernstein, and H. D. Durst. J. Am. Chem. Soc. **93**, 2897 (1971).

Can. J. Chem. Downloaded from www.nrcresearchpress.com by 210.87.254.5 on 09/05/12
For personal use only.

Information on the Proton Affinity and Protolysis of Propane from Measurement of the Ion Cluster Equilibrium: $C_2H_5^+ + CH_4 = C_3H_9^+$

KENZO HIRAOKA AND PAUL KEBARLE

Chemistry Department, University of Alberta, Edmonton, Alberta T6G 2E1

Received December 23, 1974

KENZO HIRAOKA and PAUL KEBARLE. Can. J. Chem. **53**, 970 (1975).

The clustering equilibrium $C_2H_5^+ + CH_4 = C_3H_9^+$ [1] was measured between -60 and -110 °C in 0.5–8 Torr methane. A van't Hoff plot of K_1 leads to $\Delta H_1^0 = -6.6$ kcal/mol, $\Delta S_1^0 = -23.4$ e.u. (std. st. 1 atm), and ΔG_1^0 (300 K) $\approx +0.4$ kcal/mol. The $C_3H_9^+$ formed by [1] is probably the most stable structure of protonated propane which corresponds to a three center bond of the proton with the electrons of a C—C bond. This structure is also similar to an ethyl ion forming a three center bond with C—H in CH_4 *i.e.* the product of reaction 1. With this assumption $\Delta H_f(C_3H_9^+) = 194.5$ kcal/mol and p.a.$(C_3H_8) = 147$ kcal/mol are obtained. The pathways for the decomposition of $C_3H_9^+$ (protolysis of propane) are examined. The reaction to $C_3H_7^+ + H_2$ is shown to involve a 9 kcal/mol energy barrier compared to the decomposition to CH_4 and $C_2H_5^+$. The latter is favored at low temperature and low excitation of $C_3H_9^+$.

KENZO HIRAOKA et PAUL KEBARLE. Can. J. Chem. **53**, 970 (1975).

On a mesuré l'équilibre d'agrégation du $C_2H_5^+ + CH_4 = C_3H_9^+$ (1) à des températures allant de -60 à -110 °C et à des pressions de méthane allant de 0.5 à 8 Torr. Une courbe de van't Hoff de K_1 conduit à une valeur de $\Delta H_1^0 = -6.6$ kcal/mol, $\Delta S_1^0 = -23.4$ e.u. (std. st. 1 atm) et ΔG_1^0 (300 K) $\approx +0.4$ kcal/mol. Le $C_3H_9^+$ formé par la réaction 1 est probablement la structure la plus stable pour le propane protoné; elle correspond à un lien à trois centres impliquant le proton avec les électrons du lien C—C. Cette structure est aussi semblable à celle d'un ion éthyle formant un lien à trois centres avec le C—H dans le CH_4 *i.e.* le produit de la réaction 1. En faisant cette hypothèse on obtient $\Delta H_f(C_3H_9^+) = 194.5$ kcal/mol et p.a. de $(C_3H_8) = 147$ kcal/mol. On examine les différents chemins de décomposition du $C_3H_9^+$ (protolyse du propane). On démontre que la réaction de $C_3H_7^+ + H_2$ implique une barrière d'énergie de 9 kcal/mol si on la compare à la décomposition en CH_4 et $C_2H_5^+$. Cette dernière réaction est favorisée à basse température et pour des faibles excitations de $C_3H_9^+$.

[Traduit par le journal]

The proton affinities of alkanes apart from CH_4 have not been measured experimentally. CH_5^+ and $C_2H_7^+$ have been observed in many mass spectrometric ion molecule reaction studies. The higher compounds $C_nH_{2n+3}^+$ have been observed only rarely (1–4) and under conditions where their structure could not be deduced with certainty.

In an investigation of the ion molecule reactions in methane at pressures 0.5–8 Torr we observed the reaction equilibrium 1 in the tem-

[1] $$C_2H_5^+ + 2CH_4 = C_3H_9^+ + CH_4$$

perature range -60 to -110 °C. The next step in the clustering equilibrium could be observed at lower temperatures.

[2] $$C_3H_9^+ + 2CH_4 = C_4H_{13}^+ + CH_4$$

The measurements were obtained with a pulsed electron beam high ion source pressure mass spectrometer. The clustering reactions of the other major ion CH_5^+ and details on the experimental conditions and apparatus are given in a separate publication (5).

Van't Hoff plots for the equilibria 1 and 2 are shown in Fig. 1. The straight line obtained for [1] leads to $\Delta H_1^0 = -6.6$ kcal/mol and $\Delta S_1^0 = -23.4$ e.u. (standard state 1 atm). The error in the determinations is estimated to be about 10 to 20%. The temperature range for reaction 2 is too narrow to permit reliable determination of ΔH_2^0 and ΔS_2^0. It is evident from Fig. 1 that the second clustering interaction is much weaker. Figure 1 includes also results from an earlier measurement of equilibrium 1 by Field

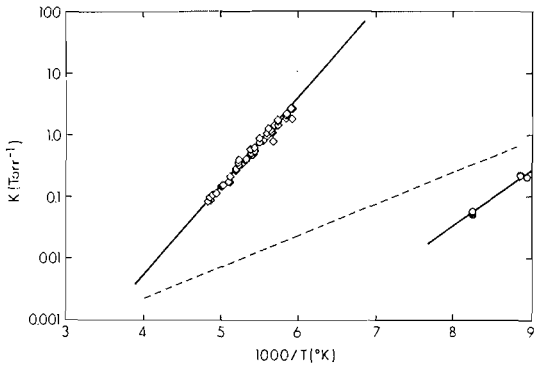

FIG. 1. Van't Hoff plots of equilibrium constant for clustering reactions: □, $C_2H_5^+ + CH_4 = C_3H_9^+$; ○, $C_3H_9^+ + CH_4 = C_4H_{13}^+$; results of Field and Beggs (6) for reaction 1 given by dashed line.

and Beggs (6). These results are in disagreement with the present work. Similar disagreements in other measurements were ascribed to inadequacies of the continuous ionization apparatus used by Field (5, 7).

Lathan *et al.* (8) have made theoretical studies of protonated ethane and found that structure **2** is some 11 kcal/mol more stable than structure **1** (Fig. 2). By analogy we assume that the lowest energy structure of protonated propane is **4**, which corresponds to a proton interacting with the σ electrons of one C—C bond. This structure is also akin to an ethyl ion, in its classical structure, interacting with the electrons of one C—H bond of methane. This suggests strongly that the $C_3H_9^+$ formed by [1] has this structure.

Using $\Delta H_f(C_2H_5^+) = 219$ kcal/mol (9) and the present $\Delta H_1 = -6.6$ kcal/mol one obtains $\Delta H_f(C_3H_9^+[1]) = 194.5$ kcal/mol and p.a.$(C_3H_8) = 146.8$ kcal/mol. This proton affinity appears of the right magnitude since

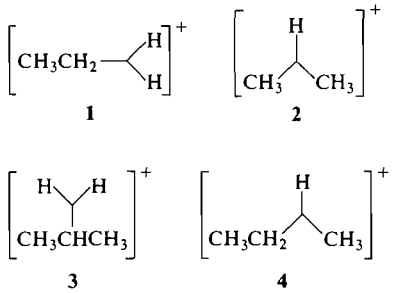

FIG. 2. Isomeric structures for protonated ethane and propane. **1** and **2** structures for ethane due to Pople and co-workers (8).

p.a.$(CH_4) = 127$ kcal/mol (10). Unfortunately the exact p.a.(C_2H_6) is not known but the limits $136 <$ p.a.$(C_2H_6) < 159$ have been set by Bohme *et al.* (11). The present p.a.$(C_3H_8) = 147$ kcal/mol predicts a difference of 20 kcal/mol between p.a.(C_3H_8) and p.a.(CH_4). Assuming that some 70% of this difference should appear between CH_4 and C_2H_6 one obtains a tentative p.a.$(C_2H_6) \approx 141$ kcal/mol.

It is interesting to note that the dissociation of $C_3H_9^+$ via [4] is more exothermic by 5 kcal ($\Delta H_f(s\text{-}C_3H_7^+) = 192$ kcal/mol (9)) than the dissociation by the reverse of reaction 1. Using the present $\Delta H_f(C_3H_9^+[1]) = 194.5$ kcal/mol one finds that [4] is exothermic by 2.5 kcal.

[4] (most stable) $C_3H_9^+ = s\text{-}C_3H_7^+ + H_2$

[-1] $= C_2H_5^+ + CH_4$

Obviously an energy barrier must exist for reaction 4. We assume that [4] must proceed via the isopropyl ion – H_2 type structure **3** shown in Fig. 2. The energy barrier between **3** and **4** may be expected to be similar but smaller than that between **1** and **2**. In agreement with this expectation it was observed (12) that at temperatures above −60 °C, $C_2H_5^+$ and CH_4 do not react according to [1] but according to [5]. An investigation (12) of the temperature dependence of [5] led to the determination of the activation energy $E_5 = 2.5$ kcal. This result predicts a difference of $E_5 + (-\Delta H_1) = 9.1$ kcal/mol between structures **3** and **4** which is close to the difference of the analogous ethane structures. This is additional evidence that the $C_3H_9^+$ formed by [1] corresponds to the stable form **4**.

[5] $C_2H_5^+ + CH_4 \rightleftarrows (C_3H_9^+) \rightarrow C_3H_7^+ + H_2$

On basis of the above energy values one can make some predictions regarding the outcome of proton transfer reactions 6 to propane.

[6] $RH^+ + C_3H_8 = R + C_3H_9^+ \xrightarrow{(3)} H_2 + C_3H_7^+(s)$; $\xrightarrow{(4)} CH_4 + C_2H_5^+$

For $146.8 <$ p.a.(R) $< 146.8 + 6.6$ stable $C_3H_9^+$ of structure **4** should be formed by the proton transfer reactions. When $146.8 + 6.6 <$ p.a.(R) $< 146.8 + 9$ dissociation of structure **4** via (*4*) is energetically possible and will probably occur. For p.a.(R) $> 146.8 + 9$ structures **3** and **4** could be formed. We expect structure **3** to dissociate via (*3*) and structure **4** largely but not exclusively via (*4*). This is in agreement with

Can. J. Chem. Downloaded from www.nrcresearchpress.com by 210.87.254.5 on 09/05/12
For personal use only.

results of Ausloos and Lias (13) who showed by means of deuterium labelling that the methane product and not the $C_2H_5^+$ contains the proton transferred to propane.

It is important to note that even the stable structure **4** of protonated propane is unstable above room temperature and dissociates by [−1]. This follows from $\Delta G_1 \approx 0.4$ kcal/mol (300 K, standard state 1 atm) obtained by extrapolation of the plot in Fig. 1.

The production of higher C_nH_{2n+3} compounds by clustering reactions like [1] is possible and some such reactions have been reported (3, 4). It will be interesting and thermochemically rewarding if many of these species turn out to be the most stable protonated alkanes.

Independently of the present work, Ausloos (14) has come to the conclusion that the $C_3H_9^+$ formed via [1] is the most stable structure.

Support of this work by the National Research Council of Canada is gratefully acknowledged.

1. R. M. Haynes and P. Kebarle. J. Chem. Phys. **45**, 3899 (1966).
2. R. P. Borkowski and P. Ausloos. J. Chem. Phys. **40**, 1120 (1969).
3. S. K. Searles, L. Wayne Sieck, and P. Ausloos. J. Chem. Phys. **53**, 849 (1970).
4. S. L. Bennett, S. G. Lias, and F. H. Field. J. Phys. Chem. **76**, 3919 (1972).
5. K. Hiraoka and P. Kebarle. To be published.
6. E. H. Field and D. P. Beggs. J. Am. Chem. Soc. **93**, 1585 (1971).
7. A. J. Cunningham, J. D. Payzant, and P. Kebarle. J. Am. Chem. Soc. **94**, 7627 (1972).
8. W. A. Lathan, W. J. Hehre, and J. A. Pople. J. Am. Chem. Soc. **93**, 808 (1971).
9. F. P. Lossing and G. P. Semeluk. Can. J. Chem. **48**, 955 (1970).
10. W. A. Chupka and J. Berkowitz. J. Chem. Phys. **54**, 4256 (1971).
11. D. K. Bohme, P. Fennelly, R. S. Hemsworth, and H. I. Schiff. J. Am. Chem. Soc. **95**, 7512 (1973).
12. K. Hiraoka and P. Kebarle. To be published.
13. P. Ausloos and S. G. Lias. J. Chem. Phys. **40**, 3599 (1964).
14. P. Ausloos. Private communication; S. G. Lias and P. Ausloos. Adv. Chem. Ser., Am. Chem. Soc. To be published.

The Photoelectron Spectrum of Methyl Tri-*t*-butylcyclobutadienecarboxylate

R. S. Brown and S. Masamune[1]

Department of Chemistry, University of Alberta, Edmonton, Alberta T6G 2G2

Received November 5, 1974

R. S. Brown and S. Masamune. Can. J. Chem. **53**, 972 (1975).

The photoelectron spectrum of the title compound has been determined and found to contain a very low ionization potential. An interpretation of the spectrum and comparison with other cyclobutadienes are presented. The effect of the substituents on the ring and hence on the ionization potential of π_2 is discussed.

R. S. Brown et S. Masamune. Can. J. Chem. **53**, 972 (1975).

On a déterminé le spectre photo-électron du composé mentionné dans le titre et on a trouvé qu'il contient un potentiel d'ionisation très bas. On présente une interprétation du spectre et une comparaison avec ceux d'autres cyclobutadiènes. On discute de l'effet des substituants sur le cycle et en conséquence sur le potentiel d'ionisation de π_2. [Traduit par le journal]

The recent report (1) of the photoelectron spectrum of a cyclobutadiene derivative (**1**) has prompted us to reveal our results concerning the vertical ionization potential of methyl tri-*t*-butylcyclobutadiene carboxylate (**2**). Both compounds are crystalline and thermally stable, but differ in important ways. Unlike **1** the substitution pattern in **2** is such that the two bonds, $C_{(1)}$—$C_{(2)}$ and $C_{(1)}$—$C_{(4)}$ can attain equivalence if the π-electrons of the system are fully delocalized (ref. 3 and references therein). Thus the geometrical distortion of the cyclobutadiene system

[1]The authors are grateful to Mr. M. Suda for his preparation of compound **3** and to the National Research Council of Canada for financial support.

Can. J. Chem. Downloaded from www.nrcresearchpress.com by 210.87.254.5 on 09/05/12
For personal use only.

results of Ausloos and Lias (13) who showed by means of deuterium labelling that the methane product and not the $C_2H_5^+$ contains the proton transferred to propane.

It is important to note that even the stable structure **4** of protonated propane is unstable above room temperature and dissociates by [−1]. This follows from $\Delta G_1 \approx 0.4$ kcal/mol (300 K, standard state 1 atm) obtained by extrapolation of the plot in Fig. 1.

The production of higher C_nH_{2n+3} compounds by clustering reactions like [1] is possible and some such reactions have been reported (3, 4). It will be interesting and thermochemically rewarding if many of these species turn out to be the most stable protonated alkanes.

Independently of the present work, Ausloos (14) has come to the conclusion that the $C_3H_9^+$ formed via [1] is the most stable structure.

Support of this work by the National Research Council of Canada is gratefully acknowledged.

1. R. M. Haynes and P. Kebarle. J. Chem. Phys. **45**, 3899 (1966).
2. R. P. Borkowski and P. Ausloos. J. Chem. Phys. **40**, 1120 (1969).
3. S. K. Searles, L. Wayne Sieck, and P. Ausloos. J. Chem. Phys. **53**, 849 (1970).
4. S. L. Bennett, S. G. Lias, and F. H. Field. J. Phys. Chem. **76**, 3919 (1972).
5. K. Hiraoka and P. Kebarle. To be published.
6. E. H. Field and D. P. Beggs. J. Am. Chem. Soc. **93**, 1585 (1971).
7. A. J. Cunningham, J. D. Payzant, and P. Kebarle. J. Am. Chem. Soc. **94**, 7627 (1972).
8. W. A. Lathan, W. J. Hehre, and J. A. Pople. J. Am. Chem. Soc. **93**, 808 (1971).
9. F. P. Lossing and G. P. Semeluk. Can. J. Chem. **48**, 955 (1970).
10. W. A. Chupka and J. Berkowitz. J. Chem. Phys. **54**, 4256 (1971).
11. D. K. Bohme, P. Fennelly, R. S. Hemsworth, and H. I. Schiff. J. Am. Chem. Soc. **95**, 7512 (1973).
12. K. Hiraoka and P. Kebarle. To be published.
13. P. Ausloos and S. G. Lias. J. Chem. Phys. **40**, 3599 (1964).
14. P. Ausloos. Private communication; S. G. Lias and P. Ausloos. Adv. Chem. Ser., Am. Chem. Soc. To be published.

Can. J. Chem. Downloaded from www.nrcresearchpress.com by 210.87.254.40 on 09/05/12
For personal use only.

The Photoelectron Spectrum of Methyl Tri-*t*-butylcyclobutadienecarboxylate

R. S. Brown and S. Masamune[1]

Department of Chemistry, University of Alberta, Edmonton, Alberta T6G 2G2

Received November 5, 1974

R. S. Brown and S. Masamune. Can. J. Chem. **53**, 972 (1975).

The photoelectron spectrum of the title compound has been determined and found to contain a very low ionization potential. An interpretation of the spectrum and comparison with other cyclobutadienes are presented. The effect of the substituents on the ring and hence on the ionization potential of π_2 is discussed.

R. S. Brown et S. Masamune. Can. J. Chem. **53**, 972 (1975).

On a déterminé le spectre photo-électron du composé mentionné dans le titre et on a trouvé qu'il contient un potentiel d'ionisation très bas. On présente une interprétation du spectre et une comparaison avec ceux d'autres cyclobutadiènes. On discute de l'effet des substituants sur le cycle et en conséquence sur le potentiel d'ionisation de π_2. [Traduit par le journal]

The recent report (1) of the photoelectron spectrum of a cyclobutadiene derivative (**1**) has prompted us to reveal our results concerning the vertical ionization potential of methyl tri-*t*-butylcyclobutadiene carboxylate (**2**). Both compounds are crystalline and thermally stable, but differ in important ways. Unlike **1** the substitution pattern in **2** is such that the two bonds, $C_{(1)}$—$C_{(2)}$ and $C_{(1)}$—$C_{(4)}$ can attain equivalence if the π-electrons of the system are fully delocalized (ref. 3 and references therein). Thus the geometrical distortion of the cyclobutadiene system

[1]The authors are grateful to Mr. M. Suda for his preparation of compound **3** and to the National Research Council of Canada for financial support.

caused by the substituents is minimized in **2**. Compound **2** was prepared by the photolysis of precursor **3** in degassed pentane at −78° accord-

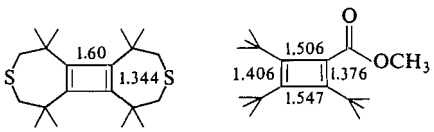

1 **2**

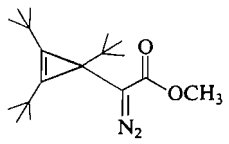

3

(Bond lengths given in Å.)

ing to published procedure (2), and upon exposure to air quickly decomposed to a mixture of oxygenated materials presumably arising from an initial dioxetane formation. The photoelectron spectra [2] of **2**, **3**, and the final oxygenated material (**4**)[3] are displayed in Fig. 1.

The assignment of the ionizations in the cyclobutadiene systems rests primarily upon the validity of sophisticated computational methods. At present there is ambiguity about several important features of cyclobutadiene itself including the ground state geometry and multiplicity (3). Notwithstanding, the first vertical ionization potential (v.i.p.) of **2** is 6.90 eV and can be most certainly assigned to the removal of an electron from π_2 of the cyclobutadiene ring.[4] At first glance this value appears to correlate well with that reported for **1** (6.89 eV) but due to the presence of the inductively withdrawing methoxycarbonyl group which lies nearly perpendicular to the plane of the ring (4), one would have expected the value for **2** to be somewhat

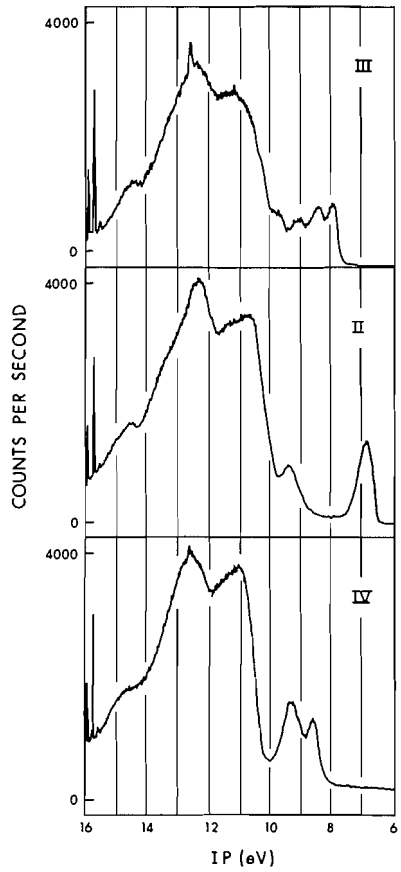

FIG. 1. Pholoelectron spectra of diazo-precursor (3), methyl tri-*t*-butylcyclobutadienecarboxylate (**2**), and the final oxygenated product (**4**).

higher than that of **1**. We feel that the constraint placed upon **1** by the two fused rings would restrict the geometry in such a way that the two double bonds will become more localized and interact less. Indeed, the single bond in **1** is found to be 1.60 Å (5), and hence the first v.i.p. assigned to π_2 in **1** should appear at somewhat higher energies than in unrestricted tetra-*t*-butylcyclobutadiene. In contrast **2** contains somewhat shorter single bonds of 1.506 and 1.547 Å (4). Apparently the presence of the methoxycarbonyl group in **2** counterbalances the effect of distortion in **1** and hence the v.i.p. are the same.

The value reported for the first v.i.p. of tri-*t*-butylcyclobutadiene of 6.83 eV (6) indicates a lower value in the absence of the methoxycarbonyl group in agreement with the above reasoning.

The ionization pertaining to the second band

[2]Spectra were determined at room temperature and 20 μ pressure using argon as an internal calibrating gas, on a MacPherson Model 36 Esca Spectrometer equipped with a He(I) excitation source. The resolution of the argon $^2P_{3/2}$–$^2P_{1/2}$ peaks was 32 meV.

[3]As yet the products of oxygenation have not been identified. The important point is that after exposure to oxygen, the cyclobutadiene ring is destroyed, and hence the low i.p. disappears.

[4]A linear combination of two molecular π orbitals (LCMO) gives a bonding orbital ($\pi_a + \pi_b$) and an antibonding orbital ($\pi_a - \pi_b$) both of which are occupied. In the text, the latter otbital is referred to as π_2.

Can. J. Chem. Downloaded from www.nrcresearchpress.com by 210.87.254.40 on 09/05/12
For personal use only.

in the p.e. spectrum of **2** (9.45 eV) cannot be assigned with absolute certainty at this time. While we cannot rigorously exclude the possibility that this band is due to some impurity,[5] careful and repeated experiments have shown no diminution of band 2 with time. If one is allowed to use CNDO/2 calculations[6] as an aid, then this band can be assigned to removal of an electron from a σ-orbital located primarily on the cyclobutadiene ring. That the ionization occurs simply from the methoxycarbonyl group can be ruled out, since the values reported for methyl acetate are 10.45 eV (n_0) and 11.16 eV (π_0) (7).

The full width at half maximum intensity (f.w.h.m.) of the first band in the p.e.s. of **2** is 0.5 eV. This in addition to the extremely broad u.v. transition from 350 to 550 nm (λ_{max} pentane 425 nm) (2) for **2** suggests a marked difference in the ground and excited state geometries, and hence a wide Franck–Condon envelope.

While in principle it may be possible to use photoelectron spectroscopy to determine ground state multiplicities (1, 8), we believe that the large f.w.h.m. in both **1** (1) and **2** preclude such a distinction. However e.s.r. and n.m.r. data provide no evidence for a triplet nature of **2** (2), and no e.s.r. signals can be detected for cyclobutadiene itself generated in a low temperature matrix (2, 4, 9).

The above i.p. for π_2 in **2** is expected to be roughly 1.5 eV lower than that for cyclobutadiene due to the presence of the substituents (the effect of substituting a *t*-butyl group for a hydrogen in ethylene is to lower the observed i.p. from 10.51 to 9.7 eV (10)). The value reported by Hedeya *et al.* (11) of 8.2 eV based upon the appearance potential of the molecular ion stands as the best present value for the first i.p. of cyclobutadiene.

[5] We can be certain that this peak is *not* due to either the starting material (**3**) or the final oxygenated product (**4**) since the p.e. spectra of these two are quite different from that of (**2**) as shown in Fig. 1.

[6] Calculations were performed on methyl trimethylcyclobutadienecarboxylate since the number of basis functions required in **2** exceeded the limits of the program. Bond lengths were maintained from the X-ray data of **2** (4) but when the *t*-butyl groups were replaced by methyl groups, the C—H bond lengths were altered accordingly.

1. G. LAUER, C. MULLER, K. W. SCHULTE, A. SCHWEIG, and A. KREBS, Angew. Chem. **86**, 597 (1974); Angew. Chem. Int. Ed. **13**, 544 (1974).
2. S. MASAMUNE, N. NAKAMURA, M. SUDA, and H. ONA. J. Am. Chem. Soc. **95**, 8481 (1973).
3. G. MAIER. Angew. Chem. Int. Ed. **13**, 424 (1974).
4. L. I. J. DELBAERE, M. N. G. JAMES, N. NAKAMURA, and S. MASAMUNE. To be published.
5. H. IRNGARTINGER and H. RODEWALD. Angew. Chem. In press.
6. A. SCHWEIG. Second IUPAC meeting on non-benzenoid aromatic compounds, Lindow, Germany. September 26, 1974.
7. D. A. SWEIGART and D. W. TURNER. J. Am. Chem. Soc. **94**, 5592 (1972).
8. R. GOMPER, F. HOLSBOER, W. SCHMIDT, and G. SEYBOLD. J. Am. Chem. Soc. **95**, 8479 (1973).
9. S. MASAMUNE, M. SUDA, H. ONA, and L. M. LEICHTER. J. Chem. Soc. Chem. Commun. 1268 (1972).
10. J. W. ROBINSON. (*Editor*). Handbook of spectroscopy, Vol. 1. CRC Press, Cleveland. 1974.
11. E. HEDEYA, R. D. MILLER, D. W. MCNEIL, D. F. D'ANGELO, and P. SCHISSEL. J. Am. Chem. Soc. **91**, 1875 (1969).

Can. J. Chem. Downloaded from www.nrcresearchpress.com by 210.87.254.40 on 09/05/12
For personal use only.

Can. J. Chem. Downloaded from www.nrcresearchpress.com by 210.87.254.42 on 09/05/12
For personal use only.

Canadian Journal of Chemistry

Published by
THE NATIONAL RESEARCH COUNCIL OF CANADA

Journal canadien de chimie

Publié par
LE CONSEIL NATIONAL DE RECHERCHES DU CANADA

Volume 53 Number 7 April 1, 1975

Volume 53 numéro 7 1 avril 1975

Dicarbonylcycloheptatrienylmolybdenum Derivatives of Silicon, Germanium, and Tin[1]

E. E. ISAACS AND W. A. G. GRAHAM

Department of Chemistry, University of Alberta, Edmonton, Alberta T6G 2E1

Received November 11, 1974

E. E. ISAACS and W. A. G. GRAHAM. Can. J. Chem. **53**, 975 (1975).

Convenient procedures are reported for the synthesis of the compounds $(\eta\text{-}C_7H_7)Mo(CO)_2MR_3$ (M = Si, R = Cl; M = Ge, R = Cl, F, Ph; M = Sn, R = Cl, Ph). The triphenyl derivatives were accessible through the anion $[(\eta\text{-}C_7H_7)Mo(CO)_2]^-$, while the MCl_3 derivatives were prepared from $(\eta\text{-}C_7H_7)Mo(CO)_2Cl$. Infrared, n.m.r., and mass spectrometric properties are reported.

E. E. ISAACS et W. A. G. GRAHAM. Can. J. Chem. **53**, 975 (1975).

On rapporte des méthodes simples pour la synthèse de composés $(\eta\text{-}C_7H_7)Mo(CO)_2MR_3$ (M = Si, R = Cl; M = Ge, R = Cl, F, Ph; M = Sn, R = Cl, Ph). On arrive aux dérivés triphénylés par l'intermédiaire de l'anion $[(\eta\text{-}C_7H_7)Mo(CO)_2]^-$ alors que l'on prépare les dérivés MCl_3 à partir de $(\eta\text{-}C_7H_7)Mo(CO)_2Cl$. On rapporte les spectres infrarouges, r.m.n. et de masse de ces composés. [Traduit par le journal]

Introduction

Although species of the type $(\eta\text{-}C_7H_7)Mo(CO)_2L$ (where L is a one-electron donor) satisfy the effective atomic number rule, few have actually been prepared. Among the known examples are $(\eta\text{-}C_7H_7)Mo(CO)_2I$ (1), $(\eta\text{-}C_7H_7)Mo(CO)_2Mn(CO)_5$ (2), $(\eta\text{-}C_7H_7)Mo(CO)_2(\sigma\text{-}C_6F_5)$ (3), and various tertiary phosphine and phosphite derivatives of the general formula $(\eta\text{-}C_7H_7)Mo(CO)(PR_3)I$ (4, 5).

We report in this paper the syntheses and properties of derivatives of the general formula $(\eta\text{-}C_7H_7)Mo(CO)_2MR_3$ (M = Si, R = Cl; M = Ge, R = Cl, F, Ph; M = Sn, R = Cl, Ph) which extend considerably the chemistry of cycloheptatrienyl systems. While this work was in progress, the preparation of several tin derivatives (6) and the crystal structures of two of them (7) were reported.

[1]Organometallic Compounds Having Metal–Metal Bonds, Part XXIV. For Part XXIII, see ref. 11.

Experimental

Melting points were determined using a Kofler hot-stage microscope. Analytical results (Table 1) were obtained by the Microanalytical Laboratory of this department. Infrared spectra of the carbonyl stretching region were measured by means of a Perkin–Elmer Model 337 spectrometer at a scanning rate of 39 cm^{-1} min^{-1}, and recorded in expanded form (1 cm of chart $\approx$ 10 cm^{-1}) on an external recorder. Spectra were calibrated with bands of gaseous CO and DBr, and are considered accurate to ± 1 cm^{-1}. Band positions quoted in Table 2 refer to the mid-point at half-height. Nuclear magnetic resonance spectra were obtained using a Varian A56-60a and results are included in Table 2. Mass spectra are given in Table 3, which lists major fragments and those common to two or more compounds.

Reactions were carried out and products recovered and purified under a nitrogen atmosphere, using Schlenk apparatus. Dichloromethane was distilled from P_4O_{10} and tetrahydrofuran from CaH_2 prior to use. In other cases, reagent grade solvents were used without purification.

Preparation of Dicarbonyl(chloro)(η-cycloheptatrienyl)-molybdenum, $(\eta\text{-}C_7H_7)Mo(CO)_2Cl$

The compound $[(\eta\text{-}C_7H_7)Mo(CO)_3][PF_6]$ (4.2 g, 10.1 mmol), prepared by the published method (8), was

TABLE 1. Analytical data, colors, melting points, and yields

Compound	% Yield	Color	Melting point (°C)	Calculated C	Calculated H	Calculated Cl	Found C	Found H	Found Cl
$C_7H_7Mo(CO)_2Cl$	82	Green	150–160 dec.	38.88	2.53	12.73	38.57	3.07	13.38
$C_7H_7Mo(CO)_2SiCl_3$	35	Red-brown	160 dec.	28.63	1.87	28.17	29.10	2.60	28.56
$C_7H_7Mo(CO)_2GeCl_3$	72	Red	166–170	25.61	1.67	25.20	25.69	1.95	25.64
$C_7H_7Mo(CO)_2GeF_3$	75	Pink	~200 dec.	29.08	1.90	—	28.94	1.73	—
$C_7H_7Mo(CO)_2SnCl_3$	68	Red-brown	182–184 dec.	23.09	1.51	22.72	23.06	1.56	22.69
$C_7H_7Mo(CO)_2GePh_3$	32	Deep red	202–205	59.29	4.05	—	59.19	4.20	—
$C_7H_7Mo(CO)_2SnPh_3$	30	Red	211–214	54.68	3.74	—	54.50	3.99	—

stirred with a large excess of sodium chloride in 100 ml of reagent acetone to which 5 ml of water had been added. The solution turned deep green immediately with vigorous gas evolution. The reaction mixture was stirred for at least 4 h to ensure complete reaction. The solvent was then removed using a water aspirator vacuum. A black residue remained which was washed with water to remove sodium hexafluorophosphate and air dried. The residue was extracted with dichloromethane, filtered, and the solvent removed using a water aspirator. Deep green crystals remained, and these were washed on a filter with ether and pentane and sucked dry affording 2.3 g (82% yield) of the product.

Preparation of Dicarbonyl(η-cycloheptatrienyl)(trichlorosilyl)molybdenum, $(\eta\text{-}C_7H_7)Mo(CO)_2SiCl_3$

To a solution containing $(\eta\text{-}C_7H_7)Mo(CO)_2Cl$ (1.2 g, 4.3 mmol) and $HSiCl_3$ (2.5 g, 18.5 mmol) in 30 ml acetonitrile at room temperature triethylamine (3.0 g, 29.7 mmol) was added dropwise. The initial green color of the solution turned red after a few minutes and stirring was continued for 1 h. The solution was filtered through Celite (degassed just prior to use) and the solvent was removed under reduced pressure. After pumping in vacuum for 24 h the residue was extracted with 20 ml dichloromethane, filtered, and *n*-heptane was added dropwise until the solution became cloudy. This was cooled at −78° affording red-brown crystals (0.5 g, 35% yield) which darkened on exposure to air and/or light.

Preparation of Dicarbonyl(η-cycloheptatrienyl)(trichlorogermyl)molybdenum, $(\eta\text{-}C_7H_7)Mo(CO)_2GeCl_3$

Trichlorogermane (1.8 g, 10.0 mmol) was added to a magnetically stirred dichloromethane solution of $(\eta\text{-}C_7H_7)Mo(CO)_2Cl$ (2.0 g, 7.2 mmol). The solution turned deep red immediately and a red precipitate formed. After stirring for 20 min the reaction mixture was filtered, the precipitate washed with ether and sucked dry. The filtrate was cooled at −20° overnight, affording more of the red crystalline product. The two batches of product were combined and recrystallized from dichloromethane (yield 2.2 g, 72%).

Preparation of Dicarbonyl(η-cycloheptatrienyl)(trifluorogermyl)molybdenum, $(\eta\text{-}C_7H_7)Mo(CO)_2GeF_3$

Solid silver tetrafluoroborate (2.3 g, 12.0 mmol) was added to a solution of $(\eta\text{-}C_7H_7)Mo(CO)_2GeCl_3$ (1.5 g, 3.6 mmol) in 25 ml acetonitrile. A white precipitate of AgCl immediately formed, with no noticeable color change. After stirring for a short period, 15 ml of ether was added and the reaction mixture was filtered and concentrated under reduced pressure. Addition of more ether precipitated an orange-red solid which was recrystallized from dichloromethane–ether to yield 1.0 g (75%) of the analytical sample.

Preparation of Dicarbonyl(η-cycloheptatrienyl)(trichlorostannyl)molybdenum, $(\eta\text{-}C_7H_7)Mo(CO)_2SnCl_3$

Anhydrous $SnCl_2$ (2.3 g, 12.0 mmol) and $(\eta\text{-}C_7H_7)Mo(CO)_2Cl$ (2.8 g, 10.0 mmol) were refluxed in dichloromethane for 12 h. The reaction mixture turned brown and a brown precipitate was formed. This was filtered, washed with dichloromethane, and sucked dry. Recrystallization from hot acetonitrile gave red-brown plate-like crystals of product (3.2 g, 68% yield).

Preparation of Dicarbonyl(η-cycloheptatrienyl)(triphenylstannyl)molybdenum, $(\eta\text{-}C_7H_7)Mo(CO)_2SnPh_3$

The reaction was conducted in a 250-ml three-necked flask with a stopcock fused to the bottom. After filling with nitrogen, the flask was charged with 10 ml of mercury and 1.0 g of sodium metal was added in small portions with stirring. After all the sodium had reacted, $(\eta\text{-}C_7H_7)Mo(CO)_2Cl$ (2.0 g, 7.2 mmol) and 100 ml of tetrahydrofuran were added. The progress of the reaction was followed by i.r. spectroscopy, specifically by the disappearance of the bands at 2023 and 1974 cm^{-1} and appearance of bands at 1926 and 1857 cm^{-1}. When the formation of the anion was complete, excess amalgam was removed through the stopcock at the bottom. Then Ph_3SnCl (2.6 g, 7.7 mmol) in 50 ml tetrahydrofuran was added and the mixture stirred overnight. The solution was filtered through Celite and the solvent removed under reduced pressure leaving a muddy brown solid. This was extracted with dichloromethane, filtered, concentrated, and chromatographed on alumina, eluting as a single red band. Recrystallization from dichloromethane – petroleum ether (60–80°) afforded 1.3 g (30% yield).

The Ph_3Ge analogue was prepared in the same manner.

Results and Discussion

Synthesis

Group IV derivatives of the $(\eta\text{-}C_7H_7)Mo(CO)_2$ moiety have been prepared in this work from $(\eta\text{-}C_7H_7)Mo(CO)_2Cl$ by three routes: insertion into the Mo—Cl bond, displacement of chloride ion by a group IV nucleophile and by reduction to the $[(\eta\text{-}C_7H_7)Mo(CO)_2]^-$ anion followed by reaction with group IV halides.

Can. J. Chem. Downloaded from www.nrcresearchpress.com by 210.87.254.42 on 09/05/12
For personal use only.

TABLE 2. Infrared carbonyl stretching frequencies n.m.r. data

Compound	Carbonyl stretching frequencies (cm^{-1})[a]		Chemical shifts C_7H_7[b]
$C_7H_7Mo(CO)_2Cl$	2023(10.0)	1975(7.7)	4.52
$C_7H_7Mo(CO)_2SiCl_3$	2011(10.0)	1963(7.7)	4.48
$C_7H_7Mo(CO)_2GeCl_3$	2027(10.0)	1985(7.9)	4.42
$C_7H_7Mo(CO)_2GeF_3$	2028(10.0)	1984(8.0)	4.00[c]
$C_7H_7Mo(CO)_2SnCl_3$	2026(10.0)	1983(7.0)	4.62[d]
$C_7H_7Mo(CO)_2GePh_3$	1980(10.0)	1923(8.3)	4.89[e,f]
$C_7H_7Mo(CO)_2SnPh_3$	1973(10.0)	1919(9.1)	4.65[e]

[a]Dichloromethane solutions; figures in parentheses are relative band heights.
[b]Chloroform-d_1 solutions relative to TMS as internal standard, except as noted.
[c]^{19}F n.m.r., singlet, −4586 Hz from $CFCl_3$.
[d]Pyridine-d_5.
[e]Phenyl region complex multiplet.
[f]$J(^{117,119}Sn—C_7H_7) = 5$ Hz.

The last of these routes is perhaps most interesting, since no previous successful synthetic use of the $[(\eta\text{-}C_7H_7)Mo(CO)_2]^-$ anion has been reported. Thus it has been reported that sodium amalgam reduction of $(\eta\text{-}C_7H_7)Mo(CO)_2I$ followed by reaction with methyl iodide afforded no $(\eta\text{-}C_7H_7)Mo(CO)_2CH_3$ (2). We observe strong infrared evidence for the formation of the anion by sodium amalgam reduction of the chloride in tetrahydrofuran, and find that the reduction product reacts with Ph_3GeCl and Ph_3SnCl forming the expected derivatives in yields of 30%.

$$(\eta\text{-}C_7H_7)Mo(CO)_2Cl \xrightarrow[THF]{Na/Hg} [(\eta\text{-}C_7H_7)Mo(CO)_2]^- \xrightarrow{Ph_3MCl\ (M = Ge, Sn)} (\eta\text{-}C_7H_7)Mo(CO)_2MPh_3$$

Surprisingly, no reaction was observed with Me_3SnCl or with Ph_3SiCl, and the reactivity of this anion merits further investigation. Recently, the synthesis of $(\eta\text{-}C_7H_7)Mo(CO)_2SnPh_3$ in 2% yield was reported by the reaction of $(\eta\text{-}C_7H_7)Mo(CO)_2Br$ with Ph_3SnLi (6); this low yield was due in part to the formation during workup of phenylchlorotin compounds.

Trichlorotin and trichlorogermanium derivatives were prepared by the insertion of $SnCl_2$ of $GeCl_2$ ($HGeCl_3$ is considered to be a source of the latter), as in the following reaction.

$$(\eta\text{-}C_7H_7)Mo(CO)_2Cl + HGeCl_3 \xrightarrow[CH_2Cl_2]{25°} (\eta\text{-}C_7H_7)Mo(CO)_2GeCl_3 + HCl$$

The trichlorogermanium compound was conveniently converted to the trifluoro derivative by means of $AgBF_4$, a reaction first applied in this area by Marks and Seyam (9). The insertion reaction of $SnCl_2$ or $SnBr_2$ with $(\eta\text{-}C_7H_7)Mo(CO)_2Br$ has been reported recently as a route to $SnCl_3$ or $SnBr_3$ derivatives respectively (6).

Trichlorosilane reacted in the following way with $(\eta\text{-}C_7H_7)Mo(CO)_2Cl$.

$$(\eta\text{-}C_7H_7)Mo(CO)_2Cl + HSiCl_3 + Et_3N \xrightarrow[CH_3CN]{25°} (\eta\text{-}C_7H_7)Mo(CO)_2SiCl_3 + Et_3NH^+Cl^-$$

Benkeser *et al.* (10) have shown that the trichlorosilyl anion, $SiCl_3^-$, is present in $HSiCl_3$–amine–CH_3CN systems, and this anion is no doubt the reactive species in the nucleophilic displacement of chloride ion.

Attempts to prepare $(\eta\text{-}C_7H_7)Mo(CO)_2Cl$ in analogy with the preparation of $(\eta\text{-}C_7H_7)Mo(CO)_2I$ (8) failed. It was discovered that only in the presence of small amounts of water does the reaction proceed to give the desired product. Thus treatment of $[(\eta\text{-}C_7H_7)Mo(CO)_3][PF_6]$ with sodium chloride or tetraethylammonium chloride in reagent acetone failed, whereas tetraphenylarsonium chloride, which contains water of hydration, reacted to give the chloride. We have included in the Experimental section a convenient preparation of $(\eta\text{-}C_7H_7)Mo(CO)_2Cl$ from sodium chloride in acetone with added water.

Physical and Spectroscopic Properties

The six derivatives prepared in this work range in color from brown to red. They are insoluble in hydrocarbon solvents and ether, and are only slightly soluble in benzene. With one exception, the compounds are very soluble in dichloromethane, acetonitrile, and acetone. The trichlorotin derivative is only sparingly soluble in

Can. J. Chem. Downloaded from www.nrcresearchpress.com by 210.87.254.42 on 09/05/12
For personal use only.

TABLE 3. Relative intensities in the mass spectra

MR_3	$SiCl_3$[a]	$GeCl_3$[b]	GeF_3[a]	$SnCl_3$[b]	$GePh_3$[a]	$SnPh_3$[b]
Source temperature[c]	100°	175°	150°	165°	210°	190°
Fragment						
$C_7H_7Mo(CO)_2MR_3^+$	2.2	1.6	8.5	—	3.5	7.8
$C_7H_7Mo(CO)MR_3^+$	1.4	0.6	—	0.1	8.5	2.7
$C_7H_7MoMR_3^+$	3.3	2.2	2.7	0.3	54.0	21.5
$C_7H_7Mo(CO)_2MR_2^+$	1.3	3.9	1.5	—	—	3.0
$C_7H_7Mo(CO)_2MR^+$	1.6	—	—	0.4	—	—
$C_7H_7MoMR_2^+$	—	—	0.3	—	6.5	20.0
$C_7H_7Mo(CO)R^+$	—	7.4	5.6	3.5	—	—
$C_7H_7MoR^+$	24.5	100.0	—	94.0	100.0	50.0
$C_5H_5MoR^+$	8.0	18.7	32.6	20.0	—	—
$Mo(CO)_2MR_3^+$	—	0.6	—	—	—	—
$Mo(CO)_2MR_2^+$	—	1.4	—	2.4	—	—
$MoMR_2^+$	—	—	100.0	—	—	—
MR_3^+	—	—	—	—	70.0	100.0
MR_2^+	—	24.8	—	15.3	16.0	37.5
MR^+	—	32.0	—	20.0	36.0	38.5
$C_7H_7^+$	100.0	72.2	33.6	100.0	26.0	2.0

[a]Measured on Associated Electrical Industries MS-2 spectrometer modified for solid samples.
[b]Using MS-12 spectrometer.
[c]Lowest source temperature necessary to produce the molecular ion, or in the case of $MR_3 = SnCl_3$, the $(P - CO)^+$ ion.

these solvents. The compounds can be handled in air for short periods but are gradually oxidized on long exposure.

All compounds were characterized by their infrared, n.m.r., and mass spectra. The infrared spectra showed the expected two bands in the carbonyl region and the ^1H n.m.r. spectra confirmed the presence of the heptahapto cycloheptatrienyl group.

The molecular formulae of the group IV compounds were confirmed by their mass spectra. Molecular ions were observed for all compounds except the trichlorotin derivative. The latter did not show a parent peak, but peaks due to loss of the two carbonyls, chlorine, dichlorotin, and tropylium from the parent were observed in low abundance.

Extraneous peaks, identified by computer fitting of the observed patterns, due to $C_{15}H_{14}O_2Cl_3Mo_2^+$ (*m/e* 525) and $C_{14}H_{14}Cl_3Mo_2^+$ (*m/e* 481) were observed in the mass spectra of both the trichlorogermanium and trichlorotin compounds but not for the trichlorosilicon derivative.[2] The pattern centered at *m/e* 481 was also observed in the mass spectrum of $C_7H_7Mo(CO)_2Cl$. It is not clear whether the extraneous peaks are due to the presence of an impurity in the starting material or are formed in the mass spectrometer, perhaps by decomposition of the solid sample during heating.

[2]These values refer to the nominal mass of the major peak in the observed isotope pattern for a particular fragment or that computed using all isotopes and their natural abundances.

We thank the National Research Council of Canada for financial support and for a postgraduate scholarship to E.E.I.

1. D. J. BERTELLI, Ph.D. Thesis, University of Washington, Seattle, Washington. 1961.
2. R. B. KING and M. B. BISNETTE. Inorg. Chem. **3**, 785 (1964).
3. M. D. RAUSCH, A. K. IGNATOWICZ, M. R. CHURCHILL, and T. A. O'BRIEN. J. Am. Chem. Soc. **90**, 3242 (1968).
4. R. B. KING and A. FRONZAGLIA. Inorg. Chem. **5**, 1837 (1966).
5. T. W. BEALL and L. W. HOUK. Inorg. Chem. **11**, 915 (1972).
6. H. E. SASSE, G. HOCH, and M. L. ZIEGLER. Z. Anorg. Allgem. Chem. **406**, 263 (1974).
7. H. E. SASSE and M. L. ZIEGLER. Z. Anorg. Allgem. Chem. **402**, 129 (1973).
8. R. B. KING. Organometallic synthesis. Vol. 1. Transition-metal compounds. Academic Press, London. 1965.
9. T. J. MARKS and A. M. SEYAM. J. Organometal. Chem. **31**, C62 (1971).
10. R. A. BENKESER, K. M. FOLEY, J. B. GRUTZNER, and W. E. SMITH. J. Am. Chem. Soc. **92**, 694 (1970).
11. E. E. ISAACS and W. A. G. GRAHAM. J. Organometal. Chem. **85**, 237 (1975)

Can. J. Chem. Downloaded from www.nrcresearchpress.com by 210.87.254.42 on 09/05/12
For personal use only.

Steric Crowding and the Reactivity of Substituted *tert*-Butyl Perbenzoates[1]

SIDDICK ICLI, KANDIL A. KANDIL, C. THANKACHAN, AND THOMAS T. TIDWELL
Department of Chemistry, University of Toronto, Scarborough College, West Hill, Ontario M1C 1A4

Received October 10, 1974

SIDDICK ICLI, KANDIL A. KANDIL, C. THANKACHAN, and THOMAS T. TIDWELL. Can. J. Chem. **53**, 979 (1975).

The relative rates of decomposition of peroxyesters in cumene at 100° and their activation parameters $\Delta H^{\ddagger}$ (kcal/mol) and $\Delta S^{\ddagger}$ (cal deg^{-1} mol^{-1}) were *tert*-butyl perbenzoate (**1**) 1.0, 34.0, 9.3; *tert*-butyl pertoluate (**7**) 1.3, 32.2, 4.8; *tert*-butyl permesitoate (**8**) 11, 31.9, 8.4; and *tert*-butyl 2,4,6-tri-*tert*-butylperbenzoate (**9**) 29, 32.9, 13.0. Each peroxyester yielded the corresponding acid as one of the products. The reactions are all interpreted as proceeding through a rate-determining scission of the O—O bond to yield a benzoyloxy radical, which then undergoes competitive decarboxylation and hydrogen abstraction from the solvent. The small rate acceleration due to a *para* substituent is interpreted as due to a polar factor and the larger rate enhancing effect of the *ortho* substituents is interpreted as due to destabilization of the ground state due to twisting of the carboxyl group out of conjugation with the ring.

SIDDICK ICLI, KANDIL A. KANDIL, C. THANKACHAN et THOMAS T. TIDWELL. Can. J. Chem. **53**, 979 (1975).

On a évalué, dans le cumène à 100°, les vitesses relatives de décomposition de peroxyesters ainsi que leurs paramètres d'activation $\Delta H^{\ddagger}$ (kcal/mol) et $\Delta S^{\ddagger}$ (cal deg^{-1} mol^{-1}); les valeurs sont pour le perbenzoate de *tert*-butyle (**1**) 1.0, 34.0, 9.3; pour le pertoluate de *tert*-butyle (**7**) 1.3, 32.2, 4.8; pour le permésitoate de *tert*-butyle (**8**) 11, 31.9, 8.4; et pour le tri-*tert*-butyl-2,4,6 perbenzoate de *tert*-butyle (**9**) 29, 32.9, 13.0. Chaque peroxyester conduit entre autre à l'acide correspondant. On interprète toutes les réactions en fonction d'une étape déterminante de la réaction qui impliquerait la scission du lien O—O conduisant au radical benzoyloxy qui subirait ensuite une décarboxylation ou enlèverait un hydrogène du solvant. On attribue la petite augmentation de vitesse due à un substituant en *para* à des facteurs polaires; par ailleurs l'augmentation importante observée lorsqu'il y a des substituants en position *ortho* implique une déstabilisation de l'état fondamental due à une rotation du groupement carboxyle hors du plan de conjugaison du cycle. [Traduit par le journal]

Introduction

Organic peresters are of widespread use as initiators of free-radical reactions. The utility of these materials justifies the intense interest in elucidating their mode of reactivity and many aspects of their chemistry are well understood (for recent reviews see ref. 1 and footnotes 3, 5, 18, and 19 of ref. 2).

Perhaps the most commonly used perester is *tert*-butyl perbenzoate (**1**), which is commercially available from several suppliers. However, several features of the chemistry of this material appear to deserve further examination.

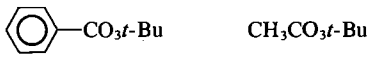

1 **2**

Firstly, *tert*-butyl perbenzoate (**1**) decomposes faster than *tert*-butyl peracetate (**2**) by a factor of about 2 but whereas **1** gives an 82.9% yield of CO_2 on thermolysis in cumene, plus residual acid (3, 4), **2** gives a 96.5% measured yield of CO_2 in cumene and no detectable residual acid (5). Both of these reactions are commonly interpreted (1) as proceeding through an initial one-bond scission to give a carboxylate–*tert*-butoxy radical pair which reacts by decarboxylation both before and after diffusion of the radical pair (eq. 1). This scheme requires that the benzoyloxy radical be formed more rapidly than acetoxy, yet the acetoxy radical undergoes decarboxylation more efficiently than benzoyloxy.

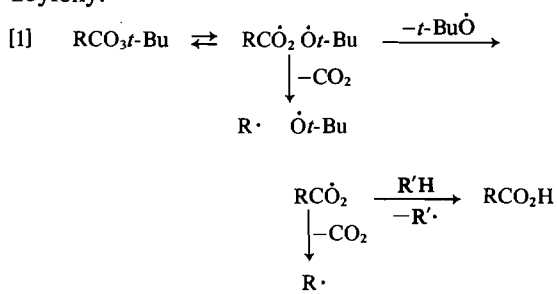

[1]The research for this paper was supported by the Defence Research Board of Canada, Grant No. 9530-129.

Can. J. Chem. Downloaded from www.nrcresearchpress.com by 210.87.254.42 on 09/05/12
For personal use only.

Can. J. Chem. Downloaded from www.nrcresearchpress.com by 210.87.254.42 on 09/05/12
For personal use only.

The cause of greater rate of reaction of the perbenzoate has occasioned much discussion, including the proposed interactions with the phenyl ring shown in **3** and **4** (6). Analogous

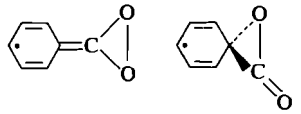

3 **4**

structures were proposed for the intermediate from naphthoyl peroxide (7). The results of CIDNP experiments with benzoyl peroxide have been interpreted in terms of the occurrence of a small amount of concerted decarboxylation on scission of the O—O bond, leading directly to phenyl radical, although this interpretation has been criticized (ref. 1*a*, p. 127).

Evidence that aliphatic acyloxy radicals decarboxylate more rapidly than aromatic ones includes the lower yields of CO_2 from the latter and the fact that the latter can be trapped by olefins to yield adducts which can be examined by electron spin resonance, whereas the former cannot (8).

The reported rate constant for decarboxylation of acetoxy is $1.6 \times 10^9\ s^{-1}$ at 60° (9), while the corresponding values reported for benzoyloxy are $1 \times 10^4\ s^{-1}$ (10*a*) at 80° and $7.4 \times 10^3\ s^{-1}$ (10*b*) at 60°.

It is of interest that benzoyl peroxide has a lesser tendency to undergo isotopic scrambling between the carbonyl and peroxidic oxygens than does acetyl peroxide (11–13). This scrambling has been proposed to occur either by sigmatropic rearrangement (11, 13*a*) or by cage recombination of radical pairs (12, 13*b*). It has been suggested (ref. 1*d*, p. 238, and ref. 12) that the opposite propensity of scrambling would have been expected for the cage recombination route for scrambling but there have been no proposals as to which substrate would be expected to scramble more rapidly by sigmatropic rearrangement.

The effect of substituents on the rate of perbenzoate thermolysis reactions has also occasioned considerable comment. The decomposition of a series of *tert*-butyl *p*-substituted perbenzoates was correlated with σ values with $\rho = -0.68$ (14). The lower reactivity of the peresters substituted with more electron-withdrawing substituents was attributed (14) to a greater ground state bond strength due to enhanced resonance contributions of the ionic structure with an electron-deficient benzoyloxy group (**5**). *Ortho* substituents in aryl peresters (6, 15, 16) and diacyl peroxides (17)

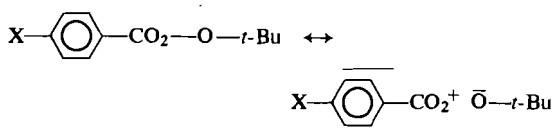

5

invariably cause enhanced reactivity, however, and these effects are as large as 10^6 for highly polarizable substituents such as iodine and sulfur. These latter effects were ascribed to direct anchimeric participation by the *ortho* substituent (6, 15) (eq. 2). The presence of

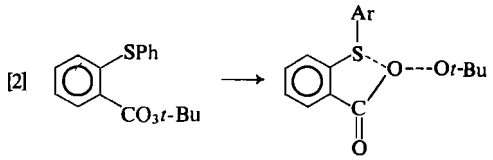

two such substituents, in the *o*,*o*′ positions, leads to no further rate increase, (16*a*) but when two percarboxy groups flank a single phenylthio group, a further rate acceleration by a factor of 81 is observed and the formation of the sulfurane **6** occurs (16*b*). This reaction was interpreted in

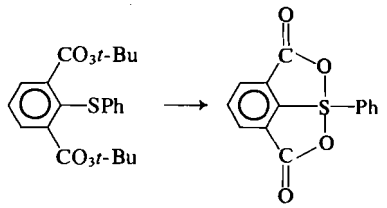

6

terms of simultaneous participation of the phenylthio group in cleavage of both perester functions (16*b*).

Alkyl groups, which are incapable of such participation, also cause modest rate enhancements in the *ortho* positions of peresters (6) and diacyl peroxides (17*a*), as does an *ortho*-phenyl group in peresters (18). Despite some proposals of a role for nonbonding steric interactions in these systems (6, 17*a*), these have been more commonly neglected or "ruled out" (ref. 1*b*, p. 497).

It appeared to us that a further investigation of steric effects in this series might result in

TABLE 1. Rates of thermal decomposition of peresters in cumene

Compound	Temperature (°C)	$k_1(s^{-1})^{a,b}$	$k_{rel}(100°)^b$	ΔH^* (kcal/mol)	ΔS^* (e.u.)
1	130.2	3.24×10^{-4}			
	115.0	5.81×10^{-5}			
	100.0[c]	9.65×10^{-6}	1.0	34.0	9.3
	99.3	9.37×10^{-6}		(33.6)[d]	(8.2)[d]
	85.0	1.320×10^{-6}			
7	115.0	6.77×10^{-5}			
	100.0[c]	1.220×10^{-5}	1.3	32.2	4.8
	99.3	1.139×10^{-5}			
	84.0	1.660×10^{-6}			
8	115.0	5.91×10^{-4}			
	100.0[c]	1.074×10^{-4}	11	31.9	8.4
	99.3	9.94×10^{-5}			
	84.0	1.464×10^{-5}			
9	115.0	1.656×10^{-3}			
	100.0[c]	2.84×10^{-4}	29	32.9	13.0
	99.3	2.67×10^{-4}			
	84.0	3.54×10^{-5}			
	70.4	5.84×10^{-6}			

[a]Average of two runs at each temperature, reproducibility ±1 to ±6%.
[b]The rate calculated for 1 at 25° is 7.41×10^{-11} s^{-1} and the calculated relative rates for 1 and 7–9 are 1.0, 2.4, 23, and 43, respectively.
[c]Calculated from data at other temperatures.
[d]In *p*-chlorotoluene, calculated from data in ref. 22.

greater understanding of the reactivity of these species. We were especially impressed with the fact that the examination of the effect of bulky *ortho* substituents on benzoate ester hydrolysis (19) and solvolyses leading to substituted benzyl cations (20) had elucidated an interrelation of steric blocking of bimolecular attack, inhibition of resonance by twisting of the ring out of conjugation with the side chain, and steric repulsion of the departing group. Accordingly, we have investigated the reactivity of a series of substituted *tert*-butyl perbenzoates.

Results

The compounds chosen for study were *tert*-butyl perbenzoate (**1**), *tert*-butyl pertoluate (**7**), *tert*-butyl permesitoate (**8**), and *tert*-butyl 2,4,6-tri-*tert*-butylperbenzoate (**9**). Compound **1** was

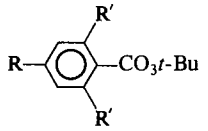

	R	R'
1	H	H
7	Me	H
8	Me	Me
9	*t*-Bu	*t*-Bu

a commercial sample, and **7**–**9** were obtained from reaction of their known acid chlorides with sodium *tert*-butylhydroperoxide.

The rates of thermal decomposition of **1** and **7**–**9** in cumene were monitored by the i.r. technique (21). Rate constants and derived activation parameters are collected in Table 1, along with suitable literature data for comparison.

The data for **1** are in quite satisfactory agreement with results obtained with *p*-chlorotoluene solvent (22*a*) and an unpublished rate constant for **1** in cumene at 105°[2] of 1.82×10^{-5} s^{-1} is in close agreement with the value for that temperature calculated from our data (1.80×10^{-5} s^{-1}). There is also reasonable agreement with rates in *n*-undecane (22*b*).

The formation of acids during the decomposition of **1** and **7**–**9** to the extent of about 10% was monitored by i.r. spectroscopy. The identity of the tri-*tert*-butylbenzoic acid from **9** was confirmed by treatment of the reaction product with diazomethane and isolation of the methyl ester, which was compared to an authentic sample.

The formation of the tri-*tert*-butylphenyl radical (**10**) from photolysis of **9** in cyclopropane

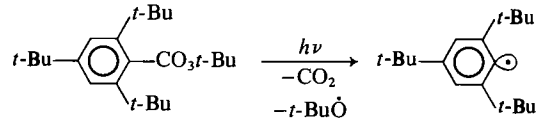

9 **10**

[2]M. J. Goldstein. Private communication.

Can. J. Chem. Downloaded from www.nrcresearchpress.com by 210.87.254.42 on 09/05/12
For personal use only.

Can. J. Chem. Downloaded from www.nrcresearchpress.com by 210.87.254.42 on 09/05/12
For personal use only.

was shown to occur by e.s.r. spectroscopy. The observed spectrum showed a main triplet with hyperfine coupling $a = 7.3$ G due to coupling with the 3,5-protons. The spectrum of 2-(3,5-di-*tert*-butylphenyl)-2,2-dimethylethyl radical could also be detected. This latter radical is derivable from **9** by an intramolecular hydrogen shift.

Radical **10** is the only phenyl radical which has been observed in solution. It was discovered recently by Barclay *et al.* (23) by bromine atom abstraction from 2,4,6-tri-*tert*-butylbromobenzene. Our e.s.r. spectra are in complete agreement with theirs and the formation of **10** from two different sources yields definitive confirmation of the structure assigned. Attempted observation of the 2,4,6-trimethylphenyl radical by photolysis of **8** was unsuccessful, however.

Discussion

The reported rates confirm the previous findings that *p*-alkyl substituents cause minimal rate enhancement of the decomposition of *tert*-butyl perbenzoates. Thus our value of 1.3 for the **7**/**1** rate ratio at 100° agrees well with the reported values of 1.1 (at 131°) and 1.4 (at 100°) (14). This enhancement is apparently due to a subtle electronic factor, in which the ground state is either destabilized by electron-donating substituents (this argument is given in ref. 14 and was mentioned in the Introduction) or the transition state is stabilized by the electron donating substituent.

The effect of the *ortho* substituents is much larger than that ascribable to the electronic factor. Further the effect is enhanced by the presence of two *ortho* substituents, as evidenced by the fact that the rate of *tert*-butyl perbenzoate decomposition is increased by a factor of 3.8 for an *ortho-tert*-butyl group at 60° (6) and 2.7 for an *ortho*-phenyl group at 110° (18) as compared to our factors of 11 for 2,4,6-trimethyl substituents and 29 for 2,4,6-tri-*tert*-butyl at 100°.

Bonding between the *ortho* substituents and the carboxy groups was invoked to explain the large rate enhancements due to *ortho*-iodo and -sulfur substituents (refs. 1*a*, p. 127, and 15). Such an effect does not seem reasonable for alkyl substituents without low-lying vacant orbitals or unshared electrons.

Direct steric compression of the alkyl groups by the carbonyl carbon and oxygens, if relieved in the transition state, would provide acceleration of these reactions. This relief of *F*-strain has been proposed as a major factor in certain ionic reactions (24, 25). However, the formation of acids in the present reactions shows that the bond between the phenyl ring and the carboxyl group is not broken in the rate-determining step of these reactions (eq. 3) so this effect cannot

$$[3] \qquad ArCO_3t\text{-}Bu \xrightarrow[r.d.]{slow} ArC\dot{O}_2 + t\text{-}Bu\dot{O}$$

be appreciable. Examination of molecular models suggests no steric interaction between the substituted aryl ring and the departing *tert*-butoxy group, so such a factor also presumably does not affect the rates.

Relief of *B*-strain has also been considered as a possible accelerating effect in free-radical reactions (26–29). However this effect depends on a rehybridization of the molecule on conversion to a free radical which reduces steric interactions. Since no rehybridization occurs on formation of the carboxy radical in the rate-determining step of these reactions this factor also can be excluded.

Apparently only conformational effects, which are significant in analogous ionic reactions (19) and on the physical properties of *ortho*-substituted benzenes (30), can explain the observed trends. The carboxyl group in the ground state for **8** and **9** would be twisted completely out of conjugation with the phenyl ring. For example, mesitoic acid has been calculated to have a twist angle of 65° (31), and similar effects have been observed in aryl ketones with *ortho* substituents (32), including *tert*-butyl groups (33). The ground state energy of these molecules will be raised by the amount of the resonance energy due to conjugation between the aryl ring and the carboxyl group. The magnitude of this interaction can be estimated from the rotational barrier of benzaldehyde of 7.9 kcal/mol (34). This value is consistent with earlier estimates of the resonance energy of this interaction as 4 kcal in benzoic acid (35*a*) and 5 kcal in benzoate esters (35*b* and *c*). Conjugation between the phenyl ring and the developing carboxy radical in the transition state will also be eliminated. However, there is reason to suspect that the magnitude of this interaction is not as large as it is in the ground state. In benzoate anions it has been proposed

Can. J. Chem. Downloaded from www.nrcresearchpress.com by 210.87.254.42 on 09/05/12
For personal use only.

that the strong delocalization of the negative charge inhibits cross-conjugation of the carboxyl group with the ring and that this difference in conjugation amounts to 0.7 kcal (ref. 35*b*, pp. 581 and 656). A similar phenomenon might well occur in the transition state leading to the radical, so that the net energy difference between the ground and transition states would be decreased by twisting the carboxyl group out of the plane.[3]

Quantitative estimates of the magnitude of this effect would depend on reliable data of the resonance energy in the benzoyloxy radical and these are not available. A simple molecular orbital treatment suggested that there was no extra resonance stabilization of the carboxyl radical relative to the carboxyl group (36*c*) but this appears unreasonable and the author pointed out that a more sophisticated treatment might give different results.

An alternative hypothesis to explain the observed rate trends is that entropy effects are responsible. In particular, the higher rate of **9** is due in part to the fact that this compound has the highest entropy of activation in this group and this favorable entropy of activation is plausible since the crowded ground state of the molecule must greatly restrict the freedom of the movement of the groups involved. On the basis of this argument the entropy of activation of **8** would be expected to be larger than was observed but this discrepancy could be due to experimental error because of the narrower range of temperatures of the rate constants of **8**.

Despite the fact that the explanation based on entropy effects accounts for the observed results, we prefer to attribute the results to ground state destabilization due to loss of resonance. Activation parameters are frequently used as a criterion of mechanism of perester reactions (21) but it has been emphasized (37) that such treatments ought to be applied with great caution due to the difficulty of obtaining reliable values. We agree with the statement of Pryor and Smith (37) that "It is probable that the rate constants, rather than the activation parameters, would be more reliable for use in classifying initiators."

The lower rate of decarboxylation of benzoyloxy radicals relative to alkyl carboxy radicals is probably due to a stronger C—C single bond between the ring and the carboxy group because of the sp^2 hybridization of the ring, as proposed by Traylor *et al.* (38).[4] This argument also suggests that rate enhancement due to formation of the α-lactone intermediate **4** does not occur, as this involves rehybridization.

Thus we believe that the major cause of the enhanced reactivity of *tert*-butyl perbenzoates with *ortho*-alkyl substituents is the increased energy of the ground states caused by the substituents forcing the carboxyl group into a conformation orthogonal to the π-system of the phenyl ring.

Experimental

Elemental analyses were performed by A. B. Gygli Microanalysis, Ltd., Toronto. Nuclear magnetic resonance spectra were measured using a Varian T-60 instrument with TMS as an internal standard. Vapour phase chromatography (v.p.c.) separations were carried out using a Varian-Aerograph 920 instrument. Kinetic measurements were carried out by i.r. (21) using Beckman IR 12 and Perkin Elmer 625 i.r. spectrophotometers and 0.06 *M* solutions of the peresters in cumene.

Cumene was purified by shaking with H_2SO_4 and then $NaHCO_3$, followed by distillation from sodium. Lucidol 90% *tert*-butylhydroperoxide was distilled using a helix packed column and aspirator pressure. The fraction boiling at 30–35° (15 Torr) was collected. Iodometric titration indicated a purity of 99%. *tert*-Butyl perbenzoate (**1**) from Aldrich or Lucidol was used as received, although one sample was purified by chromatography on Florisil using pentane–chloroform as the eluent. The kinetic behavior of the different samples was indistinguishable. *tert*-Butylbenzene was alkylated to 1,4-di-*tert*-butylbenzene (39) which was converted to tri-*tert*-butylbenzene (40) and brominated with bromine and silver nitrate (40, 41). The bromide was exchanged with *n*-butyllithium and carbonated with Dry Ice to give 2,4,6-tri-*tert*-butylbenzoic acid, (40, 41) which was converted to the acid chloride by treatment with thionyl chloride at 25° (42).

tert-Butyl 2,4,6-Tri-tert-butylperbenzoate (9)

This was prepared by the dropwise addition of the acid chloride (2.53 g, 0.0133 mol) in ether at 25° to a solution obtained from the addition of *tert*-butylhydroperoxide (6.33 g, 0.070 mol) to a pentane suspension of NaH (0.05 mol rinsed with pentane to remove oil). The mixture was stirred 24 h at 25° and was then poured into water and extracted four times with ether and the combined ether layers were washed first with water, then four times with 10% NaOH, and twice with

[3]The related 2-alkonyl radicals have been examined recently (36) and in support of our hypothesis the phenacyl radical has "little delocalization of the spin density into the aromatic ring" (36*a*).

[4]These authors also report a moderately greater tendency for decarboxylation of the *o,o'*-dimethylbenzoyloxy radical, indicating some stabilization of the benzoyloxy radical by conjugation involving the ring.

saturated NaCl solution. The solution was dried over Drierite and the solvent removed on the rotary evaporator at room temperature. Recrystallization of the solid product from pentane at 0° gave white crystals: m.p. 127–128° (with gas evolution); i.r. (cumene) 1765 cm^{-1} (C=O); n.m.r. (CCl_4) δ 1.28 (s, 9, *t*-BuO), 1.33 (s, 9, *p*-*t*-Bu), 1.40 (s, 18, *o*-*t*-Bu), and 7.35 (s, 2, Ar H).

Anal. Calcd. for $C_{23}H_{38}O_3$ (362.53): C, 76.20; H, 10.56. Found: C, 76.28; H, 10.59.

tert-Butyl Permesitoate (8)

This was prepared by a procedure analogous to that for **9** and was obtained as a colorless oil after chromatography on Florisil with pentane–chloroform: i.r. (CCl_4) 1770 cm^{-1} (C=O); n.m.r. (CCl_4) δ 1.32 (s, 9, *t*-BuO), 2.24 (s, 3, *p*-Me), 2.28 (s, 6, *o*-Me), and 6.76 (s, 2, Ar H).

Anal. Calcd. for $C_{14}H_{20}O_3$ (236.31): C, 71.16; H, 8.53. Found: C, 71.25; H, 8.55.

tert-Butyl Pertoluate (7) (14)

This was prepared by an analogous procedure.

Products of 9

A solution of **9** (0.36 g, 1 mmol) in 5 ml cumene was heated 24 h in a sealed tube at 140°. The mixture was treated with ethereal diazomethane. Volatile solvent was removed on the rotary evaporator and the residual oil separated by v.p.c. (10 ft × 0.375 in. 20% DEGS on 45–60 mesh AW Chromosorb W at 170°). One of the isolated peaks had the same retention time as methyl 2,4,6-tri-*tert*-butylbenzoate and the identity was confirmed by comparison of its n.m.r. and mass spectra with those of an authentic sample.

1. (*a*) T. Koenig. *In* Free radicals. Vol. 1. *Edited by* J. K. Kochi. John Wiley and Sons, New York, 1973. Chap. 3, p. 113; (*b*) W. H. Richardson and H. E. O'Neal. *In* Comprehensive chemical kinetics. Vol. 5. *Edited by* C. H. Bamford and C. F. H. Tipper. Elsevier, New York, 1972. Chap. 4; (*c*) L. A. Singer. *In* Organic peroxides. Vol. 1. *Edited by* D. Swern. John Wiley and Sons, New York, 1970. Chap. 5. (*d*) J. P. Lorand. *In* Inorganic reaction mechanisms. Part II. *Edited by* J. O. Edwards. John Wiley and Sons, New York. 1972. p. 207; (*e*) C. Rüchardt *et al.* Special Lectures, XIIIth International Congress of Pure and Applied Chemistry. Butterworths, London, 1971. Vol. 4. p. 223.
2. A. I. Dalton and T. T. Tidwell. J. Org. Chem. **37**, 1504 (1972).
3. L. B. Levy. Ph.D. Thesis. Harvard University, Cambridge, Mass. 1963. p. 31.
4. T. Koenig, M. Deinzer, and J. A. Hoobler. J. Am. Chem. Soc. **93**, 938 (1971).
5. J. P. Lorand. Ph.D. Thesis. Harvard University, Cambridge, Mass. 1964.
6. W. G. Bentrude and J. C. Martin. J. Am. Chem. Soc. **84**, 1561 (1962).
7. J. E. Leffler and R. G. Zepp. J. Am. Chem. Soc. **92**, 3713 (1970).
8. D. J. Edge and J. K. Kochi. J. Am. Chem. Soc. **95**, 2635 (1973).
9. W. Braun, L. Rajbenbach, and E. R. Eirich. J. Phys. Chem. **66**, 1591 (1962).
10. (*a*) D. F. De Tar. J. Am. Chem. Soc. **89**, 4058 (1967); (*b*) J. C. Bevington and J. Toole. J. Polym. Sci. **28**, 413 (1958).
11. M. J. Goldstein and H. A. Judson. J. Am. Chem. Soc. **92**, 4120 (1970).
12. J. C. Martin and J. H. Hargis. J. Am. Chem. Soc. **91**, 5399 (1969).
13. (*a*) M. J. Goldstein and W. A. Haiby. J. Am. Chem. Soc. **96**, 7358 (1974); (*b*) J. W. Taylor and J. C. Martin. J. Am. Chem. Soc. **89**, 6904 (1967).
14. A. T. Blomquist and I. A. Berstein. J. Am. Chem. Soc. **73**, 5546 (1951).
15. D. L. Tuleen, W. G. Bentrude, and J. C. Martin. J. Am. Chem. Soc. **85**, 1938 (1963).
16. (*a*) T. H. Fisher and J. C. Martin. J. Am. Chem. Soc. **88**, 3382 (1966); (*b*) J. C. Martin and M. M. Chau. J. Am. Chem. Soc. **96**, 3319 (1974).
17. (*a*) W. Cooper. J. Chem. Soc. 3106 (1951); (*b*) A. T. Blomquist and A. J. Buselli. J. Am. Chem. Soc. **73**, 3883 (1951); (*c*) J. E. Leffler, R. D. Faulkner, and C. C. Petropoulos. J. Am. Chem. Soc. **80**, 5435 (1958); (*d*) F. D. Greene, G. R. Van Norman, J. C. Cantrill, and R. D. Gillion. J. Org. Chem. **25**, 1790 (1960).
18. H. Minato, H. Matsuzaki, and K. Miwa. Bull. Chem. Soc. Jap. **41**, 249 (1968).
19. (*a*) V. R. Stimson and E. J. Watson. J. Chem. Soc. 2848, (1954); (*b*) V. R. Stimson. J. Chem. Soc. 2010 (1955); (*c*) J. G. Hawke and V. R. Stimson. J. Chem. Soc. 4676 (1956); (*d*) C. A. Bunton, A. E. Comyns, J. Graham, and J. R. Quayle. J. Chem. Soc. 3817 (1955); (*e*) S. G. Cohen and A. Schneider. J. Am. Chem. Soc. **63**, 3382 (1941); (*f*) L. R. C. Barclay, N. D. Hall, and G. A. Cooke. Can. J. Chem. **40**, 1981 (1962).
20. (*a*) L. R. C. Barclay, H. R. Sonowane, and J. C. Hudson. Can. J. Chem. **50**, 2318 (1972); (*b*) L. R. C. Barclay, J. R. Mercer, and J. C. Hudson. Can. J. Chem. **50**, 3965 (1972); (*c*) J. C. Charlton and E. D. Hughes. J. Chem. Soc. 850 (1956); (*d*) G. Baddeley and J. Chadwick. J. Chem. Soc. 368 (1951); (*e*) K. Yates and J.-J. Périé. J. Org. Chem. **39**, 1902 (1974).
21. P. D. Bartlett and R. R. Hiatt. J. Am. Chem. Soc. **80**, 1398 (1958).
22. (*a*) A. T. Blomquist and A. F. Ferris. J. Am. Chem. Soc. **73**, 3408 (1951); (*b*) V. L. Antonovskii *et al.* Zh. Fiz. Khim. **43**, 2281, 2286 (1969); Chem. Abstr. **72**, 42513m, 54559u (1970).
23. L. R. C. Barclay, D. Griller, and K. U. Ingold. J. Am. Chem. Soc. **96**, 3011 (1974).
24. J. Slutsky, R. C. Bingham, P. von R. Schleyer, W. C. Dickason, and H. C. Brown. J. Am. Chem. Soc. **96**, 1969 (1974).
25. T. T. Tidwell. J. Org. Chem. **39**, 3533 (1974).
26. G. A. Abruscato and T. T. Tidwell. J. Am. Chem. Soc. **94**, 672 (1972).
27. S. J. Cristol and H. W. Mueller. J. Am. Chem. Soc. **95**, 8489 (1973).
28. W. Duismann and Ch. Rüchardt. Chem. Ber. **106**, 1083 (1973).
29. J. W. Timberlake and M. L. Hodges. J. Am. Chem. Soc. **95**, 634 (1973); C. G. Overberger, W. F. Hale, M. B. Berenbaum, and A. B. Finestone. J. Am. Chem. Soc. **76**, 6185 (1954).

Can. J. Chem. Downloaded from www.nrcresearchpress.com by 210.87.254.42 on 09/05/12
For personal use only.

30. R. T. C. BROWNLEE, R. E. J. HUTCHINSON, A. R. KATRITZKY, T. T. TIDWELL, and R. D. TOPSOM. J. Am. Chem. Soc. **90**, 1757 (1968).
31. K. YATES and B. F. SCOTT. Can. J. Chem. **41**, 2321 (1963).
32. N. NAKAMURA and M. ŌKI. Bull. Chem. Soc. Jap. **45**, 2565 (1972).
33. D. LAUER and H. A. STAAB. Chem. Ber. **102**, 1631 (1969).
34. F. A. L. ANET and M. AHMAD. J. Am. Chem. Soc. **86**, 119 (1964).
35. (*a*) C. K. INGOLD. Structure and mechanism in organic chemistry. 2nd ed. Cornell University Press, Ithaca. 1969. p. 140; (*b*) R. W. TAFT, JR. *In* Steric effects in organic chemistry. *Edited by* M. S. Newman. John Wiley and Sons, New York. 1956. pp. 603, 672; (*c*) T. B. GRINDLEY, A. R. KATRITZKY, and R. D. TOPSOM. J. Chem. Soc. Perkin II, 289 (1974).
36. (*a*) P. H. KASAI, D. MCLEOD, JR., and H. C. MCBAY. J. Am. Chem. Soc. **96**, 6864 (1974); (*b*) T. FOSTER, D. KLAPSTEIN, and P. R. WEST. Can. J. Chem. **52**, 524 (1974); (*c*) E. HEDAYA, R. L. HINMAN, V. SCHOMAKER, S. THEODOROPULOS, and L. M. KYLE. J. Am. Chem. Soc. **89**, 4875 (1967).
37. W. A. PRYOR and K. SMITH. Int. J. Chem. Kinetics, **3**, 387 (1971).
38. T. G. TRAYLOR, A. SIEBER, H. KIEFER, and N. CLINTON. Intersci. Chem. Rep. **3** (4), 289 (1969).
39. L. F. FIESER. Organic experiments. 2nd ed. Raytheon Education Co., Lexington, Massachusetts. 1968. p. 188.
40. L. R. C. BARCLAY and E. E. BETTS. Can. J. Chem. **33**, 672, 1768 (1955).
41. L. R. BARCLAY, H. R. SONAWANE, and M. C. MACDONALD. Can. J. Chem. **50**, 281 (1972).
42. H. A. STAAB and D. LAUER. Chem. Ber. **101**, 864 (1968).

Can. J. Chem. Downloaded from www.nrcresearchpress.com by 210.87.254.42 on 09/05/12
For personal use only.

Stereospecific Spin–Spin Coupling between Hydroxyl Protons and ^{19}F Nuclei in *o*-, *m*- and *p*-Fluorophenol Derivatives. "Through-space" Interactions via the Hydrogen Bond

J. Brian Rowbotham,[1] Murray Smith, and Ted Schaefer
Department of Chemistry, University of Manitoba, Winnipeg, Manitoba R3T 2N2

J. Brian Rowbotham, Murray Smith, and Ted Schaefer. Can. J. Chem. **53**, 986 (1975).

Under conditions of slow intermolecular hydroxyl proton exchange $^6J_p^{OH,F} < 0$, $^5J_{trans}^{OH,F} > 0$, $^5J_{cis}^{OH,F} < 0$, $^4J_o^{OH,F} < 0$ in fluorophenol derivatives. $^5J_m^{OH,F}$ is remarkably insensitive to intrinsic substituent effects, yields accurate values of conformational populations of *m*-fluorophenol derivatives and can be used to demonstrate a buttressing effect on the strength of the relatively weak O—H···halogen hydrogen bond. $^4J_o^{OH,F}$ displays a stereospecific dependence opposite to that of other couplings from a side-chain proton to a ring fluorine nucleus, is apparently very sensitive to the distance between proton and fluorine nucleus and is cited as an example of a negative through-space coupling mechanism. Approximate molecular orbital calculations give some support to the last suggestion.

J. Brian Rowbotham, Murray Smith et Ted Schaefer. Can. J. Chem. **53**, 986 (1975).

Dans les dérivés du fluorophénol, dans des conditions où l'échange intermoléculaire du proton hydroxylique est lent, $^6J_p^{OH,F} < 0$, $^5J_{trans}^{OH,F} > 0$, $^5J_{cis}^{OH,F} < 0$, $^4J_o^{OH,F} < 0$. La valeur de $^5J_m^{OH,F}$ est, d'une façon remarquable, insensible aux effets intrinsèques des substituants et fournit des valeurs précises des populations conformationnelles dans les dérivés du *m*-fluorophénol; on peut aussi utiliser cette valeur pour démontrer l'influence d'un effet de répulsion sur la force de la liaison hydrogène O—H···halogène qui est relativement faible. Une dépendance stéréospécifique existe pour la valeur de $^4J_o^{OH,F}$; cette dépendance est toutefois opposée à celle des autres couplages provenant d'un proton sur une chaîne latérale avec le noyau de fluor sur le cycle. La valeur de $^4J_o^{OH,F}$ est apparemment très sensible à la distance entre le proton et le noyau de fluor et on peut la citer comme un exemple d'un mécanisme négatif de couplage à travers l'espace. Des calculs approchés d'orbitales moléculaires apportent quelques confirmations pour cette dernière suggestion. [Traduit par le journal]

Introduction

The signs and magnitudes of electron-coupled spin–spin coupling constants between nuclei in the side chain and in the benzene ring are known for toluene (1, 2) and many of its ring (3) or α-substituted derivatives (4), for benzaldehyde (5, 6), styrene (7), and aniline (8) derivatives. Their dependence on conformation has been explored in some detail, both experimentally and theoretically (7–9), and is of use in the deduction of the relative energies of conformations (4, 6) as well as in the measurement of large (10) and small (11, 12) barriers to conversion between conformers.

Accurate long-range coupling constants between hydroxyl protons and nuclei on the benzene ring until recently have been observed only for phenol derivatives (5, 13) in which the hydroxyl group is strongly hydrogen bonded to *ortho* nitro or carbonyl groups and is thereby prevented from undergoing relatively rapid intermolecular proton exchange. Under the right circumstances the preexchange lifetime of the hydroxyl protons in the halophenols is also large enough to allow the observation[2] of $^5J_m^{OH,H}$ in compounds of type *1* or *2*. The stereo-

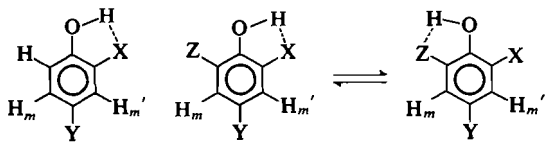

1 **2a** **2b**

specificity of this coupling then yields the relative hydrogen bond strengths between the phenolic proton and the *ortho* halogen atoms (14). The accuracy of such determinations is limited by the intrinsic substituent effects on $^5J_m^{OH,H}$. Fortunately, these perturbations on the stereo-

[1]Research associate, 1973–1974.

[2]As shown in ref. 14 the line widths of the phenolic proton resonance peaks are just as narrow as those of the ring protons.

Can. J. Chem. Downloaded from www.nrcresearchpress.com by 210.87.254.40 on 09/05/12
For personal use only.

TABLE 1. Spin–spin coupling constants in Hz* between hydroxyl protons and ring protons or fluorine nuclei in fluorophenol derivatives in dilute CCl_4 solutions

	Compound	$^{4,5,6}J_{o,m,p}^{OH,F}$	$^{5}J_{m}^{OH,H_3}$	$^{5}J_{m}^{OH,H_5}$	% *cis*†
1	2-F-6-NO_2	−0.43	0.68	0.00	0
2	2-F-4,6-diCl	−2.44	0.40	0.20	33
3	2-F-4,6-diBr	−2.58	0.38	0.20	34
4	2-F-4,6-diI	−3.49	0.25	0.28	53
5	2-F-4-Br	−4.42	0.00	0.44	100
6	2,3,5,6-tetraF	−2.49(0.59 ± 0.03)‡	—	—	50
7	3-F-6-NO_2	1.56	—	0.00	0
8	3-F-4,6-diBr	1.53	—	0.00	0
9	3-F-2,4,6-triBr	1.02(1.03)§	—	0.18(0.20)§	32 ± 3‖
10	3-F-2-NO_2	−0.35	—	0.42	100
11	4-F-2-Cl	−0.23 ± 0.03	0.00	0.45	—
12	4-F-2,6-diBr	−0.27	0.26	0.26	—

*The accuracy is estimated at 0.01 Hz for simple spectra of compounds like 2–4, 9, 12; at 0.02 Hz for others, unless otherwise indicated. See ref. 14 for the quality of the spectra.
†The *cis* conformation has the O—H bond *cis* to the C—F bond.
‡The smaller coupling is that over five bonds.
§In dilute benzene-d_6 solution.
‖Assuming $^{5}J_{trans}^{OH,H}$ as 0.57 ± 0.04 Hz.

specificity of $^{5}J_{m}^{OH,H}$ depend more on the degree of substitution than on the position of the halogen atoms, at least for **1** and **2** (14).

In this paper the signs and magnitudes of $^{4}J_{o}^{OH,F}$, of $^{5}J_{m}^{OH,F}$, and of $^{6}J_{p}^{OH,F}$ are reported for some derivatives of the corresponding fluorophenols. Their conformational dependence is investigated. The unique behavior of $^{4}J_{o}^{OH,F}$ is discussed from the viewpoint of a "through-space" (15–25) or "fragment" (26, 27) coupling mechanism. Approximate molecular orbital calculations partially corroborate the experimental conclusions.

Experimental

The derivatives of *o*, *m*, and *p*-fluorophenols were obtained commercially or by standard preparative methods (14). Samples were prepared as previously described and were degassed at concentrations of less than 5 mol%. Not all samples displayed slow intermolecular exchange of the hydroxyl proton. For example, of nine samples of 2,3,5,6-tetrafluorophenol only one yielded the couplings to the fluorine nuclei.

Proton magnetic resonance spectra were calibrated on an HA100D spectrometer at sweep widths of 1 Hz/cm and sweep rates of 0.02 Hz/s. Double resonance experiments (28, 29) yielded the signs of coupling constants. Line widths of the hydroxyl proton resonance peaks were comparable to those of the ring protons. Sample temperatures were 32 °C.

Results and Discussion

Spectral Analyses

Analyses were performed with the aid of the computer program LAME (30, 31) yielding spectral parameters for which the r.m.s. errors were generally well below 0.01 Hz. The coupling constants between ring protons themselves, and between ring protons and fluorine nuclei, were unexceptional in their magnitudes and signs (32–35) and are not tabulated here. Table 1 presents the coupling constants involving the hydroxyl protons. These are of interest in the following discussion.

The Hydroxyl Proton–fluorine Couplings, $J^{OH,F}$

Stereospecificity of $^{5}J_{m}^{OH,F}$

The energy differences between **2***a* and **2***b*, (X, Y, Z = F, Cl, Br, I) are such that comparable $^{5}J_{m}^{OH,H}$ values were measured for both *meta* protons (14). When Z = H, as in **1**, no coupling to H_{m}' was observed, indicating the predominance of the intramolecular hydrogen bonded form in the equilibrium; this is in agreement with far infrared data which gave enthalpies of formation of the intramolecular hydrogen bond, O—H···X as lying between 1.44 and 1.62 kcal/mol (36).

For compounds **6–10** in Table 1 the values of $^{5}J_{m}^{OH,F}$ are also stereospecific. Thus, in **7** and **10** the strong intramolecular O—H···ONO hydrogen bond ensures that the measured couplings are $^{5}J_{trans}^{OH,F} \equiv {}^{5}J_{t}^{OH,F} = 1.56$ Hz and $^{5}J_{cis}^{OH,F} \equiv {}^{5}J_{c}^{OH,F} = -0.35$ Hz, respectively. These two members define the solid line in Fig. 1, where $^{5}J^{OH,F}$ is plotted *vs.* % *cis* conformation of the *m*-fluorophenol derivatives. The *cis* conformation has a *cis* arrangement of O—H and C—F bonds, as illustrated in Fig. 1.

Can. J. Chem. Downloaded from www.nrcresearchpress.com by 210.87.254.40 on 09/05/12
For personal use only.

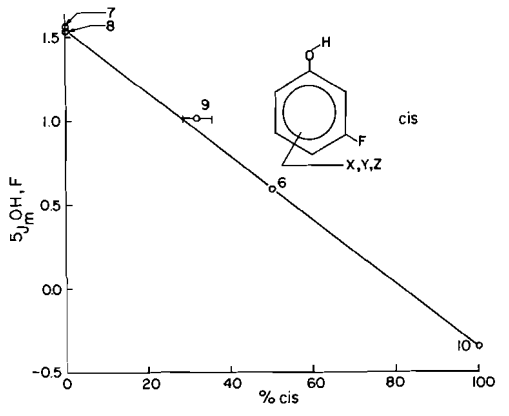

FIG. 1. The values of $^5J_m^{OH,F}$ in Hz in *m*-fluorophenol derivatives are plotted *vs.* the % *cis* conformation, in which the O—H bond lies *cis* to the C—F bond. The points are numbered in accordance with the compounds in Table 1. The point for compound **9** is plotted on the assumption that the population of the *cis* form is given by $^5J_m^{OH,H}$. See text for an elaboration of this procedure.

In compound **6** the *cis* and *trans* conformations must be equally abundant. $^5J_m^{OH,F}$ is observed to be 0.59 ± 0.03 Hz and falls on the line in Fig. 1, indicating that $^5J_m^{OH,F}$ is insensitive to intrinsic substituent effects on the electron distribution in the molecule. Furthermore, $^5J_m^{OH,F}$ is 1.53 Hz for 8, indicating 100% *trans*, and this indication is confirmed by the absence of coupling from the hydroxyl proton to the *meta* proton in the *cis* C—H bond.

In 3-fluoro-2,4,6-tribromophenol (compound **9**) $^5J_m^{OH,H}$ is 0.18 Hz. In 2,4,6-tribromophenol $^5J_c^{OH,H} + {}^5J_t^{OH,H} = 0.58$ Hz. Actually, in 10 2,4,6-trihalophenols (14) this sum varies between 0.53 and 0.61 Hz. On the assumption that $^5J_t^{OH,H}$ is 0.57 ± 0.04 Hz one has 32 ± 3% of the *cis* conformation **3***b*. This value is plotted in Fig. 1, together with the observed $^5J_m^{OH,F}$ of 1.02 Hz.

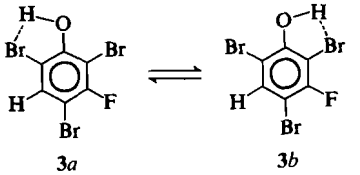

3*a* **3***b*

However, $^5J_m^{OH,F}$ may well be a better indicator of conformational populations than is $^5J_m^{OH,H}$ because it is larger in magnitude and is therefore measurable with a smaller percentage error. $^5J_m^{OH,F}$ also appears less sensitive to intrinsic substituent effects than does $^5J_m^{OH,H}$. Accordingly, using $^5J_m^{OH,F}$ and the calibration line in Fig. 1 gives 28% *cis*, *i.e.*, 28% of **3***b*.

Buttressing of the O—H···X Hydrogen Bond

Clearly, neither $^5J_m^{OH,H}$ nor $^5J_m^{OH,F}$ is compatible with equal abundances of **3***a* and **3***b*. The extra stability of **3***a* could arise for two reasons. First, the steric crowding of the three neighboring halogen atoms could cause an extra repulsion between the lone pairs of the oxygen and bromine atoms in **3***a*, forcing the O—H bond nearer the hydrogen bonded bromine atom and strengthening the interaction. Evidence for such a buttressing is adduced from i.r. spectra (37) on di-*ortho* substituted phenols. Buttressing is also consistent with the behavior of $^4J_o^{OH,F}$, to be discussed below.

Second, the dipole moment of **3***a* is larger than that of **3***b*, the dipole vectors of the O—H and C—F bonds lying more nearly parallel in the former. Classical solution theory (38) suggests the more polar isomer is favored in solvents of dielectric constant greater than unity. Experience (38) then dictates that benzene behaves[3] *as if* it had a dielectric constant of 7 to 9. Accordingly, the coupling parameters of 3-fluoro-2,4,6-tribromophenol were also measured in a dilute benzene-d_6 solution but no significant changes from the values in CCl_4 solution were found (see Table 1). More polar solvents cause intermolecular proton exchange, at least in our laboratory.

In our opinion, the likely explanation of the relative stabilities of **3***a* and **3***b*, the former being about 500 cal/mol more stable at 32 °C, involves the concept of steric crowding. The strength of the relatively weak "five-membered" O—H···X hydrogen bond in *o*-halophenols probably depends on a delicate balance between the effects of charge densities or distributions and O—H···X distances or angles and could well be altered appreciably by small changes in any of these parameters. A systematic variation of the ring substituents, combined with the advantages of $^5J_m^{OH,F}$ as an indicator of conformational populations, may lead to some interesting conclusions.

[3]That is, the relative stabilities of many conformational isomers can be predicted (38) if the dielectric constant is assumed to be larger than the observed one.

Can. J. Chem. Downloaded from www.nrcresearchpress.com by 210.87.254.40 on 09/05/12
For personal use only.

Can. J. Chem. Downloaded from www.nrcresearchpress.com by 210.87.254.40 on 09/05/12
For personal use only.

Stereospecificity of $^4J_o^{OH,F}$

Reasoning as before, one has $^4J_t^{OH,F}$ as -0.43 Hz and $^4J_c^{OH,F}$ as -4.42 Hz from the data for compounds **1** and **5** in Table 1. If these values are correct, $^4J_o^{OH,F}$ in compound **6** should be $-(4.42 + 0.43)/2 = -2.42$ Hz, comparing fairly well with the observed coupling of -2.49 Hz. The three numbers are plotted *vs.* % *cis* conformation in Fig. 2, where the end points define the solid line.

Compounds **2**, **3**, and **4** possess values of $^4J_o^{OH,F}$ which deviate considerably from the solid line in Fig. 2. A likely explanation once again calls on a small buttressing of the oxygen atom by the large *ortho* halogen atom, causing a small shift of the hydrogen atom towards fluorine. This shift need only be 0.03 Å or less in order to account for the observed deviation of $^4J_o^{OH,F}$ (see below). If the deviation of -0.07 Hz for **6** in Fig. 2 is taken as real, then the deviations are -0.07, -0.70, -0.80, and -0.95 Hz for F, Cl, Br, and I, respectively. In other words, an *ortho* fluorine substituent causes at most a very small buttressing in these phenols.

The proportions of the *cis* and *trans* forms of **2**, **3**, and **4** indicated in Fig. 2 are calculated from the $^5J_m^{OH,H}$ values in Table 1. The deviations from the line in Fig. 2 cannot arise from errors in conformational proportions. For example, for compound **4** there must occur almost 80% *cis* if the point shall fall on the line, implying $^5J_c^{H,OH} \gg {}^5J_t^{H,OH}$ and contradicting a wealth of experimental data concerning the stereospecificity of five-bond couplings to a ring nucleus in benzene derivatives. Furthermore, the internal consistency of the conclusions about the relative hydrogen bond strengths in halophenols (14) would disappear.

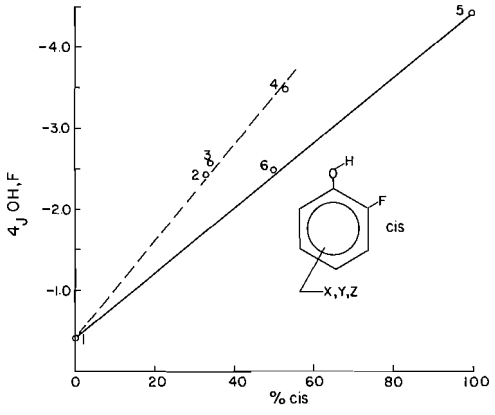

FIG. 2. A plot of $^4J_o^{OH,F}$ in Hz in some *o*-fluorophenol derivatives *vs.* the % *cis* confirmation, in which the O—H and C—F bonds are *cis* to one another. The numbering of the points conforms to that in Table 1.

The implied sensitivity of $^4J_c^{OH,F}$ to the H···F distance in the O—H···F hydrogen bond is discussed below from the viewpoint of spin–spin coupling mechanisms.

The Six-bond Coupling $^6J_p^{OH,F}$

The barrier to rotation of the hydroxyl group lies near 5 kcal/mol in a number of *o*-halophenols (39). The proportion of molecules in which the hydroxyl group lies in the plane of the ring in compounds **11** and **12** is therefore overwhelming at ambient temperatures. The measured values of -0.23 and -0.27 Hz for $^6J_p^{OH,F}$ in **11** and **12** can therefore be taken as those for a planar molecule. A similar situation holds for *p*-fluorobenzaldehyde for which $^6J_p^{F,CHO}$ is -0.44 Hz (6). If it is assumed that a coupling over six bonds in these molecules is transmitted via the π electron system of the ring (40, 41), then the hyperfine interaction constant Q_{OH}^H must be negative and small (32, 40, 41) because Q_{CF}^F is large and positive. Some e.s.r. data suggest Q_{OH}^H as -7 G (42) compared to a Q_{CF}^F of about +40 G (32, 43, 44).

$^4J_c^{OH,F}$ *as a "Through-space" Coupling*

$^4J_t^{OH,F}$ is -0.43 Hz and $^4J_c^{OH,F}$ is -4.42 Hz for the *o*-fluorophenol derivatives in Table 1. In contrast, $^4J_t^{F,CH}$ is -2.5 Hz and $^4J_c^{F,CHCl_2}$ is -0.3 Hz in derivatives of *o*-fluorobenzalchloride (4), whereas $^4J_t^{F,CHO}$ and $^4J_c^{F,CHO}$ are estimated at -1.6 and -0.2 Hz, respectively, in *o*-fluorobenzaldehyde (6). As all these couplings occur for a planar arrangement of the intervening bonds, it appears that the large negative value of $^4J_c^{OH,F}$ in *o*-fluorophenol may arise via an electron-coupled interaction which depends on the proximity of the proton and fluorine nucleus, *i.e.*, via a "through-space" or "fragment" coupling (15–27).

Such a coupling is distinct from other "direct" interactions which would involve only the O—H and C—F bonds (45) and not the other intervening bonds. Such direct interactions are important in coupling over two and three bonds.

In a hydrogen bond the proximity may be high enough so that a through-space interaction, involving overlap of the valence s orbitals on the hydrogen and fluorine atoms, may occur.

Can. J. Chem. Downloaded from www.nrcresearchpress.com by 210.87.254.40 on 09/05/12
For personal use only.

Such interactions apparently occur when the distance, r_{AB}, between the nuclei is approximately equal to or less than the sum of the van der Waals radii of atoms A and B.

Indeed, one semi-empirical theory (46) makes the coupling proportional to the square of the overlap integral between the valence s orbitals of the two relevant atoms, implying a positive coupling constant, apparently true for ^{19}F, ^{19}F through-space interactions (25). Another semi-empirical theory (27) uses a sum-over-states perturbation method in conjunction with INDO molecular orbitals, predicting large negative $^{1}H,^{19}F$ couplings at small r_{HF} values. Both theories assume a Fermi contact mechanism. The signs of through-space $^{1}H,^{19}F$ couplings are apparently unknown. On the basis of $^{4}J_c^{OH,F}$ it is now suggested that these are negative, insofar as this coupling depends at least to some extent on such a mechanism.

CNDO/2 and INDO-MO-FPT Calculations of $^{4}J_c^{OH,F}$

A standard geometry (47) was assumed for **4** but the angles ϕ and θ were varied in steps of

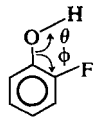

4

2°, describing a grid defined by $116° \leq \phi \leq 124°$ and $104° \leq \theta \leq 112°$. The finite perturbation was applied to the s orbital of the hydroxyl hydrogen atom in the Fock matrices (48) and yielded 50 computed values of $^{4}J_c^{OH,F}$ over the grid, partitioned between the CNDO/2 and INDO approximations. The distance between the proton and fluorine nucleus lay between 2.05 and 2.42 Å, which may be compared to 2.55 Å as the sum of the van der Waals radii of the hydrogen and fluorine atoms.

The calculated values of $^{4}J_c^{OH,F}$ ranged from +0.64 Hz at 2.42 Å to −12.9 Hz at 2.05 Å. The INDO calculations yielded a $^{4}J^{OH,F}$ of −4.5 Hz at $\phi = 120°$, $\theta = 106°$, and $r_{HF} = 2.21$ Å, while CNDO/2 gave −4.5 Hz at $\phi = 118°$, $\theta = 109°$, and $r_{HF} = 2.18$ Å.

The steep dependence of $^{4}J_c^{OH,F}$ on r_{HF} is very similar to that proposed by Myhre *et al.* (17) for coupling between side-chain protons and ring fluorine nuclei in 2,4,6-trialkylhalobenzenes, attributed to a through-space coupling mechanism. In our calculations a change of 0.03 Å in r_{HF} produces a change of 1 Hz in the vicinity of −4.5 Hz and is therefore consistent with the buttressing effect on $^{4}J_o^{OH,F}$ proposed in connection with the data in Fig. 2.

Of course, the approximate nature of the semi-empirical MO-FPT treatment does not permit the statement that the r_{HF} values which reproduce the observed J values shall also represent the lowest energy of the molecule. In fact, the calculated energy minima occur at $r_{HF} = 2.30$ Å for the CNDO/2 and at 2.35 Å for the INDO calculations, emphasizing the approximate nature of the theory.

The computations agree with our suggestion that through-space $^{1}H,^{19}F$ couplings are negative, in negation of one theory (46) but in confirmation of the sum-over-states model (27). It is true that such couplings are thought to arise from repulsive overlap of nonbonding orbitals centered on the coupled nuclei, whereas the $^{4}J^{OH,F}$ values observed here arise in a weakly (hydrogen) bonding situation. However, the sum-over-states model accommodates this situation (see p. 37 of ref. 27) and predicts a negative coupling.

Other CNDO/2 and INDO-MO-FPT Calculations

For a standard geometry (47) but with $\phi = 123.5°$ and $\theta = 108° 50'$, conforming with microwave data (49), such calculations were performed for *p*- and *m*-fluorophenol. As expected, the INDO calculations of $^{5}J_m^{OH,H}$ and $^{5}J_m^{OH,F}$ reproduced the zigzag stereospecificity of these couplings but considerably over estimated their magnitude, in line with similar results found for the corresponding fluorobenzaldehydes (6), while CNDO/2 yielded values in better agreement with the data in Table 1. Neither approximation gave a negative value for $^{5}J_c^{OH,F}$.

On the other hand, $^{6}J_p^{OH,F}$ was given as −0.15 and 0.02 Hz by INDO and CNDO/2, respectively, but became 1.63 and 0.02 Hz when the O—H group lay in a plane perpendicular to the benzene ring. The INDO results emphasize the increased probability of a σ–π interaction where the O—H group rotates out of the node of the π electron system, so that such an occurrence could be followed by observing $^{6}J_p^{OH,F}$ in an appropriate compound.

For the θ and ϕ angles as given, the *cis* form of *o*-fluorophenol yielded $^{4}J_c^{OH,F} =$

Can. J. Chem. Downloaded from www.nrcresearchpress.com by 210.87.254.40 on 09/05/12
For personal use only.

$-0.25(-0.23)$ Hz and ${}^4J_t^{OH,F} = -2.16(-0.80)$ Hz for the INDO (CNDO/2) methods, in agreement with the stereospecificity observed for the other molecules discussed above, and confirming the necessity of a close approach of H and F atoms if a large negative ${}^4J_c^{OH,F}$ value is to be observed. Hence at least part of ${}^4J_c^{OH,F}$ is probably contributed by a through-space interaction.

The observed torsion frequencies yield a twofold barrier of 2.96 kcal/mol for *p*-fluorophenol (39) whereas the calculations gave 3.17 (INDO) and 2.71 (CNDO/2) kcal/mol. Similarly, the INDO (CNDO/2) calculations predict hydrogen bond energy of 1.00 (0.97) kcal/mol but a barrier of only 3.77 (3.11) kcal/mol, as compared to a torsion barrier of 4.84 kcal/mol. Of course, an accurate calculation of barriers requires *ab inito* methods (50). The selected values quoted here perhaps indicate that the m.o. calculations in this paper have some degree of validity.

In conclusion the proportions of *cis* and *trans* isomers of halophenol derivatives can be determined fairly reliably from the stereospecific couplings over five bonds between the hydroxyl protons and ring protons or fluorine nuclei, the coupling to the latter being of relatively large magnitude and remarkably insensitive to intrinsic substituent effects. Buttressing effects on the strengths of OH···X hydrogen bonds (X = halogen) occur and are most dramatically indicated by ${}^4J_c^{OH,F}$ in *o*-fluorophenol derivatives. This coupling evidently has a large through-space component, which is very sensitive to distance between the hydroxyl proton and the fluorine nucleus. ${}^6J_p^{OH,F}$ is negative for planar *p*-fluorophenol derivatives but theory indicates substantial positive values when the hydroxyl group leaves the plane of the benzene ring.

We are grateful to the National Research Council of Canada for financial support.

1. G. KOTOWYCZ and T. SCHAEFER. Can. J. Chem. **44**, 2743 (1966).
2. M. P. WILLIAMSON, R. KOSTELNIK, and S. M. CASTELLANO. J. Chem. Phys. **49**, 2218 (1968).
3. D. J. BLEARS, S. S. DANYLUK, and T. SCHAEFER. J. Chem. Phys. **47**, 5037 (1967).
4. H. M. HUTTON, J. B. ROWBOTHAM, B. H. BARBER, and T. SCHAEFER. Can. J. Chem. **49**, 2033 (1971).
5. S. FORSÉN and R. A. HOFFMAN. J. Mol. Spectrosc. **20**, 168 (1966).
6. R. WASYLISHEN and T. SCHAEFER. Can. J. Chem. **49**, 3216 (1971).
7. M. BARFIELD, C. J. MACDONALD, I. R. PEAT, and W. F. REYNOLDS. J. Am. Chem. Soc. **93**, 4195 (1971).
8. R. WASYLISHEN, J. B. ROWBOTHAM, L. ERNST, and T. SCHAEFER. Can. J. Chem. **50**, 2575 (1972).
9. R. WASYLISHEN and T. SCHAEFER. Can. J. Chem. **50**, 1852 (1972).
10. J. PEELING, J. B. ROWBOTHAM, L. ERNST, and T. SCHAEFER. Can. J. Chem. **52**, 2414 (1974).
11. J. B. ROWBOTHAM, A. F. JANZEN, J. PEELING, and T. SCHAEFER. Can. J. Chem. **52**, 481 (1974).
12. K. CHUM, J. B. ROWBOTHAM, and T. SCHAEFER. Can. J. Chem. **52**, 3489 (1974).
13. T. SCHAEFER and G. KOTOWYCZ. Can. J. Chem. **46**, 2865 (1968).
14. J. B. ROWBOTHAM and T. SCHAEFER. Can. J. Chem. **52**, 3037 (1974).
15. D. R. DAVIS, R. P. LUTZ, and J. D. ROBERTS. J. Am. Chem. Soc. **83**, 246 (1961).
16. L. PETRAKIS and C. H. SEDERHOLM. J. Chem. Phys. **35**, 1243 (1961).
17. P. C. MYHRE, J. W. EDMONDS, and J. D. KRUGER. J. Am. Chem. Soc. **88**, 2459 (1966).
18. F. B. MALLORY, C. W. MALLORY, and M-C. FEDARKO. J. Am. Chem. Soc. **96**, 3536 (1974).
19. G. R. MILLER, A. W. YANKOWSKY, and S. O. GRIM. J. Chem. Phys. **51**, 3185 (1969).
20. R. E. RICHARDS and T. SCHAEFER. Trans. Faraday Soc. **54**, 1447 (1958).
21. J. JONAS, L. BOROWSKI, and H. S. GUTOWSKY. J. Chem. Soc. **47**, 2441 (1967).
22. E. ABUSHANAB. J. Am. Chem. Soc. **93**, 6532 (1971).
23. W. MCFARLANE. Chem. Commun. 609 (1971).
24. F. R. JEROME and K. L. SERVIS. J. Am. Chem. Soc. **93**, 1535 (1971); **94**, 5896 (1972).
25. R. D. CHAMBERS, L. H. SUTCLIFFE, and G. J. T. TIDDY. Trans. Faraday Soc. **66**, 1025 (1970).
26. K. HIRAO, H. NAKATSUJI, H. KATO, and T. YONEZAWA. J. Am. Chem. Soc. **94**, 4078 (1972).
27. K. HIRAO, H. NAKATSUJI, and H. KATO. J. Am. Chem. Soc. **95**, 31 (1973).
28. J. P. MAHER and D. F. EVANS. Proc. Chem. Soc. 208 (1961).
29. R. FREEMAN and W. A. ANDERSON. J. Chem. Phys. **37**, 2053 (1962).
30. S. M. CASTELLANO and A. A. BOTHNER-BY. J. Chem. Phys. **41**, 3863 (1961).
31. C. W. HAIGH and J. M. WILLIAMS. J. Mol. Spectrosc. **32**, 398 (1969).
32. R. WASYLISHEN and T. SCHAEFER. Can. J. Chem. **49**, 94 (1971).
33. S. CASTELLANO and R. KOSTELNIK. J. Am. Chem. Soc. **90**, 141 (1968).
34. A. D. COHEN and T. SCHAEFER. Mol. Phys. **10**, 209 (1965).
35. J. E. LOEMKER, J. M. READ, JR., and J. H. GOLDSTEIN. J. Phys. Chem. **72**, 991 (1968).
36. G. L. CARLSON, W. G. FATELEY, A. S. MANOCHA, and F. F. BENTLEY. J. Phys. Chem. **76**, 1553 (1972).
37. R. A. NYQUIST. Spectrochim. Acta, **19**, 1655 (1963).
38. R. J. ABRAHAM and E. BRETSCHNEIDER. *In* Internal rotation in molecules. *Edited by* W. J. Orville-Thomas. J. Wiley and Sons, New York. 1974.
39. W. G. FATELEY. Pure Appl. Chem. **36**, 110 (1973).
40. C. L. BELL, S. S. DANYLUK, and T. SCHAEFER. Can. J. Chem. **47**, 3529 (1969).
41. T. SCHAEFER and S. S. DANYLUK. Can. J. Chem. **47**, 4289 (1969).

42. G. P. RABOLD, K. H. BAR-ELI, E. REID, and K. WEISS. J. Chem. Phys. **42**, 2438 (1965).
43. D. R. EATON, A. D. JOSEY, W. D. PHILLIPS, and R. E. BENSON. Mol. Phys. **5**, 407 (1962).
44. W. G. ESPERSEN and R. W. KREILICK. Mol. Phys. **16**, 577 (1969).
45. M. BARFIELD and M. KARPLUS. J. Am. Chem. Soc. **91**, 1 (1969).
46. A. D. BUCKINGHAM and J. E. CORDLE. J. Chem. Soc. Faraday II, 994 (1974).
47. J. A. POPLE and M. S. GORDON. J. Am. Chem. Soc. **89**, 4253 (1967).
48. D. L. BEVERIDGE and J. A. POPLE. Approximate molecular orbital theory. McGraw Hill Book Co., New York, N.Y. 1970.
49. C. R. QUADE. J. Chem. Phys. **48**, 5490 (1969).
50. W. J. HEHRE, L. RADOM, and J. A. POPLE. J. Am. Chem. Soc. **94**, 1496 (1972).

Can. J. Chem. Downloaded from www.nrcresearchpress.com by 210.87.254.40 on 09/05/12
For personal use only.

Commentaire: Sur la sensibilité differente du vibrateur carbonyle d'acétophénones *méta* et *para* substituées aux facteurs σ_m^+ et σ_p^+

M. BERTHELOT ET C. LAURENCE

Laboratoire de Spectrochimie Moléculaire, U.E.R. de Chimie, B.P. 1044, 44037 Nantes Cédex, France

Reçu le 1 février 1974

M. BERTHELOT et C. LAURENCE. Can. J. Chem. **53**, 993 (1975).

Les conclusions de Laurence et Wojtkowiak sur la nécessité de traiter séparément les substituants *méta* et *para* dans les corrélations entre les fréquences ν_{CO} d'acétophénones *m*- et *p*-substituées et le facteur σ^+ sont confirmées. A partir d'un échantillonnage de substituants adapté au mieux au problème posé, les auteurs trouvent en effet une différence significative entre les coefficients ρ_p^+ et ρ_m^+ avec un pourcentage de confiance supérieur à 99.9%.

M. BERTHELOT and C. LAURENCE. Can. J. Chem. **53**, 993 (1975).

The conclusions of Laurence and Wojtkowiak concerning the need to treat separately *meta* and *para* substituents in correlations between the frequencies ν_{CO} for substituted acetophenones and the factors σ^+ are confirmed. From a sampling of substituents chosen to illustrate best the effect under consideration, we indeed find a significant difference between the coefficients ρ_p^+ and ρ_m^+ at a confidence level greater than 99.9%. [Journal translation]

Dans un travail récent Krueger (1) rapporte une corrélation linéaire entre la fréquence ν_{CO} de 27 acétophénones substituées sur le noyau et le facteur σ^+ (2) avec un coefficient de corrélation r de 0.988 et un écart-type s sur l'estimation de ν_{CO} par l'éq. 1 de 1.2 cm^{-1}

$$[1] \quad \nu_{CO}\,(cm^{-1}) = 11.53\sigma^+_{m\ et\ p} + 1691.5$$

Selon lui ces résultats contredisent les conclusions de Laurence et Wojtkowiak (3) sur la différence des coefficients ρ_m^+ et ρ_p^+ dans les éqs. 2 et 3 de la corrélation $\nu_{CO} = \rho^+\sigma^+ +$ constante

$$[2] \quad \nu_{CO}\,(cm^{-1}) = 14.86\sigma_m^+ + 1690.3$$
$$n = 8 \quad r = 0.969 \quad s = 1.2\ cm^{-1}$$

$$[3] \quad \nu_{CO}\,(cm^{-1}) = 10.48\sigma_p^+ + 1691.4$$
$$n = 10 \quad r = 0.983 \quad s = 1.3\ cm^{-1}$$

En effet, l'éq. 1 se rapporte à un plus grand nombre de composés et possède un coefficient de corrélation plus élevé.

A partir des coefficients ρ_p^+ et ρ_m^+ des éqs. 2 et 3 et de leurs écarts-type $s_{\rho_p^+}$ et $s_{\rho_m^+}$, si l'on teste la différence $\rho_p^+ - \rho_m^+$ en formant le rapport[1]

$$[4] \quad t = (\rho_p^+ - \rho_m^+)/s_{(\rho_p^+ - \rho_m^+)}$$

on trouve une valeur $t = 2.58$ qui correspond dans la table de distribution du t de Student (4) pour 14 degrés de liberté à une probabilité comprise entre 2 et 5% que la différence $\rho_p^+ - \rho_m^+$ soit due au hasard. Ce test ne nous paraissant pas décisif pour juger avec un grand pourcentage de confiance si $\rho_p^+ - \rho_m^+$ est significativement différent de zéro, nous avons complété l'échantillonnage de Laurence et Wojtkowiak avec 7 substituants *para* et 4 substituants *méta*. L'additivité des effets des substituants *méta* et *para* a également été étudiée sur 4 composés polysubstitués. Les fréquences ν_{CO} de 32 acétophénones sont ainsi reportées dans le tableau 1. Les résultats des corrélations correspondantes entre ces valeurs et σ^+ sont consignés dans le tableau 2.

Les valeurs ρ et s_ρ des éqs. 5 et 6 permettent de calculer une valeur $t = 4.12$ à partir de la formule 4. La table de t lue pour 25 degrés de liberté nous autorise alors à affirmer que $\rho_p^+ - \rho_m^+$ est différent de zéro avec un pourcentage de confiance supérieur à 99.9%. Les conclusions de Laurence et Wojtkowiak se trouvent ainsi confirmées sur un échantillonnage aussi nombreux que celui de Krueger. Cet échantillonnage nous paraît surtout mieux adapté au problème posé, pour les raisons suivantes:

(*a*) il ne nous paraît pas judicieux d'inclure des substituants *ortho* dans une étude voulant juger la sensibilité d'une propriété aux effets des substituants *méta* et *para*.

[1] $s_{(\rho_p^+ - \rho_m^+)}$ est l'écart-type de la différence $\rho_p^+ - \rho_m^+$. Il est égal à $\sqrt{s_{\rho_p^+}^2 + s_{\rho_m^+}^2}$.

Can. J. Chem. Downloaded from www.nrcresearchpress.com by 210.87.254.105 on 09/05/12
For personal use only.

Can. J. Chem. Downloaded from www.nrcresearchpress.com by 210.87.254.105 on 09/05/12
For personal use only.

TABLEAU 1. Fréquences carbonyle et constantes de substituant d'acétophénones *m*- et *p*-substituées

Substituant	σ_p^+	ν_{CO} (cm^{-1})	Substituant(s)	σ_m^+	ν_{CO} (cm^{-1})
4-NH_2	−1.3	1677.1	3-NH_2	−0.16	1688.3
4-OCH_3	−0.778	1683.1	3-OCH_3	+0.047	1689.6
4-OH	−0.92	1684.7	3-CH_3	−0.066	1689.7
4-SCH_3	−0.604	1685.5	3-C_6H_5	+0.109	1691.2
4-$NHCOCH_3$	−0.6	1686.4	3-I	+0.359	1694.7
4-CH_3	−0.311	1687.3	3-Br	+0.405	1695.3
4-C_2H_5	−0.295	1687.6	3-Cl	+0.399	1695.7
4-$C(CH_3)_3$	−0.256	1687.9	3-COOH	+0.322	1696.1
4-C_6H_5	−0.179	1688.6	3-CF_3	+0.520	1698.0
H	0	1691.2	3-CN	+0.562	1700.4
4-F	−0.073	1691.5	3-NO_2	+0.674	1701.2
4-Cl	+0.114	1691.6			
4-I	+0.135	1692.9		$\Sigma\sigma_{m,p}^+$	
4-Br	+0.150	1693.3	3,4,5-tri-OCH_3	−0.684	1684.9
4-CN	+0.659	1698.1	3,4-di-CH_3	−0.377	1686.8
4-CF_3	+0.612	1699.1	3,4-di-Cl	+0.513	1696.2
4-NO_2	+0.790	1700.6	3-NO_2, 4-OCH_3	−0.104	1694.3

TABLEAU 2. Corrélations entre fréquences ν_{CO} d'acétophenones *m*- et *p*-substituées et σ^+

Equation[a]	n[b]	r[c]	s[d]	s_ρ[e]
[5] $\nu = 15.50\sigma_m^+ + 1690.2$	12	0.974	1.3	1.13
[6] $\nu = 10.44\sigma_p^+ + 1691.5$	17	0.985	1.1	0.48
[7] $\nu = 10.99\sigma_{m,p}^+ + 1691.5$	28	0.975	1.3	0.49
[8] $\nu = 10.84\sigma_{m,p}^+ + 1691.6$	32	0.969	1.4	0.50

[a]Les éqs. 5 à 8 se rapportent dans l'ordre: aux composés *méta*, aux composés *para*, aux composés *méta* et *para* et enfin aux composés *méta*, *para* et polysubstitués en *méta* et *para*.
[b]Nombre de points.
[c]Coefficient de corrélation.
[d]Écart-type sur l'estimation de ν.
[e]Écart-type sur le coefficient de régression ρ.

TABLEAU 3. Comparaison des fréquences ν_{CO} expérimentales et des fréquences calculées en supposant l'additivité des effets de substituant

	Calcul de la fréquence ν_{CO}				
Substituants	ν_{CO} acétophénone	+	Incréments de substitution	= ν_{calc}	$\nu_{calc} - \nu_{expti}$
3,4,5-tri-OCH_3	1691.2		2(−1.6) − 8.1	1679.9	5
3.4-di-CH_3	1691.2		−3.9 − 0.5	1686.8	0
3.4-di-Cl	1691.2		4.5 + 0.4	1696.1	0.1
3-NO_2, 4-OCH_3	1691.2		10 − 8.1	1693.1	1.2

(*b*) de même les composés polysubstitués nous semblent à proscrire de l'échantillonnage du fait du caractère aléatoire de la loi d'additivité des effets de substituant mis en évidence dans le tableau 3 où l'on compare la fréquence ν_{CO} expérimentale des composés polysubstitués à la fréquence calculée en additionnant les incréments de substitution déterminés à partir des acétophénones monosubstituées. Ceci conduit dans l'éq. 8 à une diminution de la précision de la corrélation par rapport à l'éq. 7.

(*c*) le nombre de substituants *méta* nous semble insuffisant dans l'échantillonnage de Krueger; en tenant compte des remarques (*a*) et (*b*) il n'est que de 4 alors que notre étude porte sur 11 de ces substituants. Puisque σ_m^+ traduit l'effet de substitution avec une précision moindre que σ_p^+ (pour l'éq. 5 $r = 0.974$ et

pour l'éq. 6 $r = 0.985$), on explique ainsi en partie, le coefficient de corrélation supérieur trouvé par Krueger.

(*d*) l'étude de Krueger ne porte en réalité que sur une combinaison de 8 substituants différents (NH_2, OCH_3, CH_3, F, Cl, Br, I, NO_2) alors que notre échantillonnage contient 17 substituants très diversifiés (NH_2, $NHCOCH_3$, OCH_3, OH, SCH_3, CH_3, C_2H_5, $C(CH_3)_3$, C_6H_5, F, Cl, Br, I, COOH, CF_3, CN, NO_2). En particulier Krueger ne prend en considération qu'un seul substituant électroattracteur $\pi(NO_2)$ alors que nous étudions 4 substituants de ce type (COOH, CF_3, CN, NO_2) conformément aux recommandations de Taft *et al.* (5) sur l'importance de l'équilibre numérique à établir entre les diverses classes de substituant.

Partie expérimentale

Les composés utilisés sont des produits commerciaux purifiés par recristallisation fractionnée ou distillation sous pression réduite. Les mesures ont été effectuées en solution diluée dans du CCl_4 de qualité spectroscopique désséché sur tamis moléculaire 4 Å, à l'aide d'un appareil Beckman IR 9 étalonné avec la vapeur d'eau, purgé à 8 p.p.m. d'eau atmosphérique et dont la précision dans cette région est de 0.5 cm^{-1} et la reproductibilité de 0.1 cm^{-1}. Ces résultats, moyennes de trois mesures, sont en bon accord avec nos valeurs précédentes (3), sauf pour *p*-F, et avec les valeurs de Jones *et al.* (6) et Krueger (1).

1. P. J. KRUEGER. Can. J. Chem. **51**, 1363 (1973).
2. H. C. BROWN et Y. OKAMOTO. J. Am. Chem. Soc. **80**, 4979 (1958).
3. C. LAURENCE et B. WOJTKOWIAK. Bull. Soc. Chim. Fr. 3124 (1971).
4. F. J. ROHEF et R. R. SOKAL. Statistical tables. Freeman, San Francisco. 1969.
5. P. R. WELLS, S. EHRENSON et R. W. TAFT. *Dans* Progress in physical organic chemistry. Vol. 6. Interscience, New York. 1968. p. 147.
6. R. N. JONES, W. F. FORBES et W. A. MUELLER. Can. J. Chem. **35**, 504 (1957).

Can. J. Chem. Downloaded from www.nrcresearchpress.com by 210.87.254.105 on 09/05/12
For personal use only.

Sorption of the Inert Gases (Ar, Kr, and Xe) in Type A Zeolites

RUSSELL IAN DERRAH[1] AND DOUGLAS MORRIS RUTHVEN

Department of Chemical Engineering, University of New Brunswick, Fredericton, New Brunswick E3B 5A3

Received November 12, 1974

RUSSELL IAN DERRAH and DOUGLAS MORRIS RUTHVEN. Can. J. Chem. **53**, 996 (1975).

Theoretical potential profiles for Ar, Kr, and Xe occluded in an idealized 5A zeolite are calculated and used to evaluate the Henry's law equilibrium constants for these species. Calculations were made using the three common formulae to estimate the dispersion constants (Kirkwood–Mueller, Slater–Kirkwood, and London) and the theoretical Henry constants are compared with the values obtained directly from experimental equilibrium isotherms. For both Kr and Xe the Slater–Kirkwood formula gives the best agreement with the experimental values while, for argon, the London formula is best. At higher concentrations the isotherms for Kr can be well represented by a simple Langmuir expression with eleven sites per cavity while for Xe there appears to be a transition from localized sorption at low temperatures to a mobile adsorbed phase at higher temperatures. These conclusions are qualitatively consistent with the results of the theoretical potential calculations.

RUSSELL IAN DERRAH et DOUGLAS MORRIS RUTHVEN. Can. J. Chem. **53**, 996 (1975).

On calcule les profils potentiels théoriques de Ar, Kr et Xe occlus dans une zéolithe 5A idéalisée; on utilise les valeurs ainsi calculées pour évaluer les constantes d'équilibre de la loi d'Henry pour ces espèces. On a fait des calculs utilisant les trois formules ordinaires pour estimer les contantes de dispersion (Kirkwood–Mueller, Slater–Kirkwood et London) et l'on compare les constantes théoriques d'Henry avec les valeurs obtenues directement à partir des isothermes expérimentales d'équilibre. Pour le Kr et le Xe, la formule de Slater–Kirkwood donne la meilleure relation avec les valeurs expérimentales alors que pour l'argon, la formule de London est la meilleure. A des concentrations plus hautes, les isothermes de Kr peuvent aussi être présentés par une expression simple de Langmuir avec onze sites par cavité alors que pour Xe il semble qu'il existe une transition passant d'une sorption localisée à basse température à une phase adsorbée mobile à plus haute température. Ces conclusions sont qualitativement en accord avec les résultats des calculs potentiels théoriques. [Traduit par le journal]

The monatomic nature of the rare gas molecules makes these species ideally suited to fundamental sorption studies since the equilibrium data are amenable to a more detailed theoretical analysis than is at present feasible for more complex molecules. An added incentive for such studies has arisen from the practical requirement for a suitable adsorbent for the removal of krypton and xenon which are formed in considerable quantities during the controlled fission of uranium fuels. The sorption of argon and krypton in chabazite (1–4) and faujasite (5, 6) have been investigated in some detail. More recently the results of several experimental studies of sorption in the type A zeolites have been reported and a semi-empirical correlation of the isotherms has been given by Lee and Basmadjian (7). Kiselev and co-workers have achieved some success in the theoretical calculation of Henry's law equilibrium constants from potential theory (8–10) but, as yet, the nature of the adsorbed species remains uncertain and the similarities and differences between the isotherms for the different gases have not been examined in detail.

In the present paper experimental equilibrium isotherms for the sorption of argon, krypton, and xenon in 4A and 5A zeolites are presented and discussed in relation to the published data of other authors. In particular the present data, which were obtained at subatmospheric pressures, are compared with the recently published high pressure isotherms of Barrer, Papadopoulos, and Ramsay (11), thus allowing the validity of model isotherms to be tested over a very wide range of conditions.

Experimental

Equilibrium isotherms were measured gravimetrically using a Cahn vacuum microbalance system. Prior to the experimental measurements the sample of zeolite (Linde 4A or 5A crystals) was degassed at 400 °C, 10^{-5} Torr for several hours. The isotherms obtained under these con-

[1]Present address: C.I.L., Central Research Laboratories, McMasterville, Quebec.

Can. J. Chem. Downloaded from www.nrcresearchpress.com by 210.87.254.6 on 09/05/12
For personal use only.

Can. J. Chem. Downloaded from www.nrcresearchpress.com by 210.87.254.6 on 09/05/12
For personal use only.

ditions were perfectly reversible and reproducible and show good agreement with the isotherms of other workers who used an equally severe degassing procedure. The isotherms for xenon reported by Kitani and Takada (12) are, under comparable conditions, appreciably lower than those obtained in the present study presumably as a result of an inadequate regeneration procedure (temperatures of only 200 °C were used).

Experimental Henry's Law Constants

At sufficiently low pressures the equilibrium isotherm reduces to a simple linear expression

$$[1] \qquad c = Kp$$

where c is the sorbate concentration at equilibrium pressure p. Under the conditions of the present study (temperatures 190–398 °K, pressures 0–400 Torr) the isotherms for argon and krypton were linear over a substantial pressure range so that the Henry constants (K) could be found directly. The low temperature isotherms for xenon, however, showed significant curvature and an extrapolation procedure was needed to determine the limiting slopes. Two methods were used: the Langmuir plot and plots of log (c/p) *vs.* c, as recommended by Barrer and Davies (4). The values found in these two ways showed good agreement.

The van't Hoff plot showing the temperature dependence of the Henry constants is given in Fig. 1 which includes also the values calculated from previously reported isotherms. The values of K_0 and q_0 defined by the equation

$$[2] \qquad K = K_0 e^{q_0/RT}$$

are given in Table 1. The Henry constants for 4A and 5A zeolites are very similar. There is no significant difference between the present 4A and 5A values for krypton and argon while the 4A values calculated from the data of Harper *et al.* (15), Springer (13), Ackley and Browning (16), and Lloyd and McNees (17) are about 80% of the present values for 5A. The sorption of xenon in the 4A sieve was too slow to allow reliable equilibrium data to be obtained and even for krypton fairly high temperatures are required, thus restricting the range of concentrations over which the isotherms could be measured.

Theoretical Calculation of Henry Constants

The Henry constant may be simply expressed as a ratio of partition functions

$$[3] \qquad K = f_z \exp[(u_g - u_z)/kT]/f_g' \, kT$$

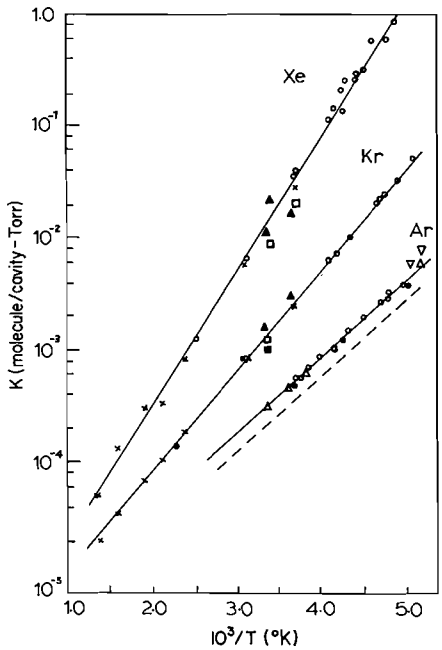

FIG. 1. Van't Hoff plot showing temperature dependence of Henry's law constants for sorption of inert gases in 4A and 5A zeolites: this work, ○, (5A); ●, (4A); △, Springer (13) (5A); ▽, Cook (14) (5A); Ackley and Browning (16), □, (5A); ■, (4A); ▲, Lloyd and McNees (17) (5A); ×, Barrer *et al.* (11); ---, data of refs. 13 and 15 for Ar-4A.

f_z is the partition function for an adsorbed molecule, f_g' is the partition function per unit volume for the gaseous molecule, $u_g - u_z$ is the difference in potential energy, and k is Boltzmann's constant. Since the rare gas molecules have no internal degrees of freedom the ratio of partition functions reduces simply to the configuration integral (Z) for a single molecule occluded within a cavity of the zeolite lattice

$$[4] \qquad K = Z/kT$$

where $Z = \int_v \exp(-u(\boldsymbol{r})/kT) \cdot d\boldsymbol{r}$ and $\boldsymbol{r}$ is the position vector.

In order to calculate the configuration integral detailed knowledge of the potential energy contours within the cavity is required. The interaction energy for an inert gas molecule, which has no permanent dipole or quadrupole moment, may be written simply as the sum of the contributions arising from dispersion (ϕ_D), repulsion (ϕ_R), and polarization (ϕ_P) energies:

$$[5] \qquad u(\boldsymbol{r}_i) = \phi_D + \phi_R + \phi_P$$

TABLE 1. Comparison of theoretical and experimental Henry constants for 5A zeolite correlated according to eq. 2

Gas	Method of calculation	Temperature range (°K)	$K_0 \times 10^6$ (molecule/cavity-Torr)	q_0 (kcal/mol)
Ar	Experimental	200–300	1.04	3.36
	Theory eq. 9	200–300	1.64	5.21
	Theory eq. 10	200–300	1.98	4.25
	Theory eq. 11	200–300	2.89	2.9
	ref. 26	80–90	—	3.0
Kr	Experimental	200–245	1.26	4.24
	Theory eq. 9	200–300	2.22	6.06
	Theory eq. 10	200–300	2.72	4.32
	Theory eq. 11	200–300	2.38	3.52
	ref. 11	273–723	—	4.66
	ref. 33	200–300	—	4.25
Xe	Experimental	200–400	1.29	5.38
	Theory eq. 9	200–350	1.21	7.78
	Theory eq. 10	200–350	1.65	5.05
	Theory eq. 11	200–350	2.15	3.62
	ref. 11	273–723	—	5.25

[6] $$\phi_D = \sum_j A_{ij}/r_{ij}^6$$

[7] $$\phi_R = \sum_j B_{ij}/r_{ij}^{12}$$

[8] $$\phi_P = -\frac{1}{2}\alpha_i \left\{\text{grad}\left(\sum_j \frac{e_j}{(r_i - r_j)}\right)\right\}^2$$

α_i is the polarizability of a sorbate molecule located at position vector r_i, r_j is the position vector of the jth ion of the zeolite lattice (charge e_j e.s.u.), and r_{ij} is the distance between probe molecule and lattice ion. The dispersion constant A_{ij} may be estimated by the Kirkwood–Mueller (18, 19), Slater–Kirkwood (20), or London (21) formulae

[9] $$(A_{ij})_{KM} = 6mc^2\alpha_i\alpha_j/(\alpha_i/\chi_i + \alpha_j/\chi_j)$$

[10] $$(A_{ij})_{SK} = 3eh\alpha_i\alpha_j/[4\pi\sqrt{m}(\sqrt{\alpha_i/n_i} + \sqrt{\alpha_j/n_j})]$$

[11] $$(A_{ij})_L = 1.5\alpha_i\alpha_j E_i E_j/(E_i + E_j)$$

m and e are respectively the mass and charge of an electron, c is the velocity of light, h is Planck's constant, χ is diamagnetic susceptibility, n is the number of electrons in the outermost shell, and E the ionization potential of species i or j. The repulsion constant B_{ij} is calculated by setting the equilibrium separation of an isolated molecule–ion pair (r_e) equal to the mean van der Waals radius (σ)

[12] $$\left\{\frac{\partial}{\partial r_{ij}}[u(r_{ij})]\right\}_{r_e} = 0$$

$$r_e = (\sigma_i + \sigma_j)/2$$

whence

[13] $$B_{ij} = \tfrac{1}{2}A_{ij}r_e^6(1 + \alpha_i e_j^2 r_e^2/3A_{ij})$$

Using eqs. 5–8, one of the eqs. 9–11, and eq. 13 the potential energy of a probe molecule at any point within the cavity may be calculated, provided that the positions of all ions in the crystal lattice are known.

In the present calculation the ionic positions given by Broussard and Shoemaker (22) were used and the small contribution arising from the Si and Al ions was neglected. An idealized A zeolite containing 4 Na^+ and 4 Ca^{2+} ions located symmetrically in the type I sites (near the centers of the 6-membered oxygen rings) was considered. Calculations were also performed assuming 8 hypothetical $NaCa^{+1.5}$ ions per cavity as suggested by Whitford (23). The resulting potential profiles agreed fairly well with those obtained using the symmetrical tetrahedral arrangement of Ca^{2+} and Na^+. A few calculations were performed using random arrangements of Ca^{2+} and Na^+. In all cases of random arrangement the polarization energy was unrealistically large as a result of the charge imbalance in the particular cavity considered.

Can. J. Chem. Downloaded from www.nrcresearchpress.com by 210.87.254.6 on 09/05/12
For personal use only.

TABLE 2. Parameters used in the estimation of dispersion constants

Gas	$\alpha \times 10^{25}$ (cm^3)	$\chi \times 10^{30}$ (cm^3/mol)	$r_0^* \times 10^8$ (cm)
Ar	16.3	31.0	1.92
Kr	24.8	47.87	2.02
Xe	40.25	72.76	2.28
$O^{-1/4}$	14.7	17.7	1.52
Ca^{2+}	4.71	22.1	0.99
Na^+	1.8	6.95	0.98

*The van der Waals radii of Ar, Kr, and Xe were calculated from force constants given by Hirschfelder *et al.* (34). The values of the ionic radii ($O^{-1/4}$, Na^+, and Ca^{2+} are those used by Barrer and Stuart (5) and Broier *et al.* (9).

TABLE 3. Dispersion and repulsion constants used in calculation of potential profiles

	Slater–Kirkwood		Kirkwood–Mueller		London	
Gas–Ion	$A \times 10^{43}$*	$B \times 10^{88}$†	$A \times 10^{43}$*	$B \times 10^{88}$†	$A \times 10^{43}$*	$B \times 10^{88}$†
Ar–$O^{-1/4}$	9.86	9.275	12.51	11.47	5.894	5.989
Ar–Ca^{2+}	4.005	19.76	7.358	20.78	1.169	18.912
Ar–Na^+	1.767	5.036	2.647	5.298	0.3933	4.6302
Kr–$O^{-1/4}$	13.40	15.30	19.14	20.95	8.485	10.465
Kr–Ca^{2+}	5.291	74.97	11.313	78.65	1.719	37.630
Kr–Na^+	2.287	9.834	4.068	10.484	0.5805	9.218
Xe–$O^{-1/4}$	18.83	34.40	30.28	51.64	12.82	25.35
Xe–Ca^{2+}	7.212	120.84	17.519	127.14	2.664	118.1
Xe–Na^+	3.053	30.24	6.317	32.19	0.9047	28.96

*In cal cm^6 mol^{-1}.
†In cal cm^{12} mol^{-1}.

Since the Si and Al atoms were neglected in the calculations, the oxygen ions were each assigned a charge of $-e/4$ after Kiselev (8). The molecular constants used in the calculations are summarized in Table 2 and the corresponding values of the dispersion and repulsion constants are given in Table 3.

The dispersion and repulsion energies at each point were obtained by direct summation of the contributions arising from interaction between a probe molecule and each ion in a $5 \times 5 \times 5$ block of cells. The electric field was calculated from the vector sum of the individual ionic contributions and the polarization energy was then obtained directly from eq. 8. A few calculations were carried out using a $10 \times 10 \times 10$ block of cells but the calculated energies showed no significant difference from those obtained for the $5 \times 5 \times 5$ block indicating that the effect of ions outside the $5 \times 5 \times 5$ block of cells could be neglected.

Potential profiles across the cavity in several directions were calculated using dispersion constants given in Table 3. The profiles which are illustrated in Figs. 2–4, were then used to calculate the configuration integral Z. The integral by which Z is defined was replaced by a double summation over radial coordinate (r) and direction, with the weighting factor $f(j)$ chosen to be proportional to the fraction of the cavity surface taken up by ions (or windows) of a particular type

$$[14] \quad Z = \sum_{j=1}^{N} f(j) \sum_{r=0}^{R} 4\pi r^2 \times \exp\left[-u(r, j)/kT\right] \cdot \Delta r$$

where

$$\sum_{j=1}^{N} f(j) = 1$$

and $R = 6.16$ Å is the maximum radius of the cavity. Further details including the values assigned to $f(j)$ are given by Derrah (24).

By an exactly similar calculation the average energy of interaction for an adsorbed molecule $\boldsymbol{u}$ was obtained from the integral

$$[15] \quad \boldsymbol{u} = \int_v \frac{u(\boldsymbol{r}_i) \cdot \exp\left(-u(\boldsymbol{r}_i)/kT\right) \cdot d\boldsymbol{r}_i}{Z}$$

Can. J. Chem. Downloaded from www.nrcresearchpress.com by 210.87.254.6 on 09/05/12
For personal use only.

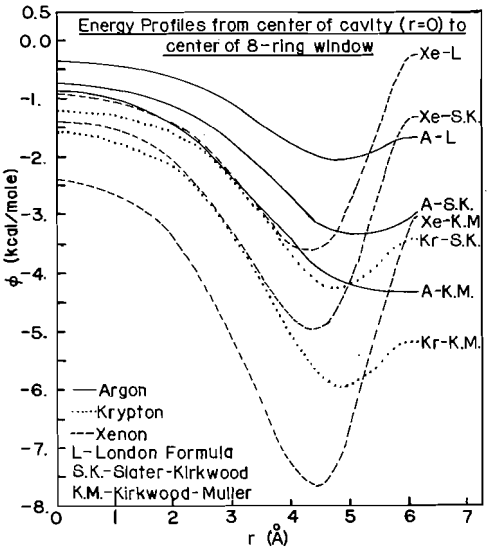

FIG. 2. Potential profiles from center of cavity to center of 8-membered oxygen window showing effect of choice of dispersion constant.

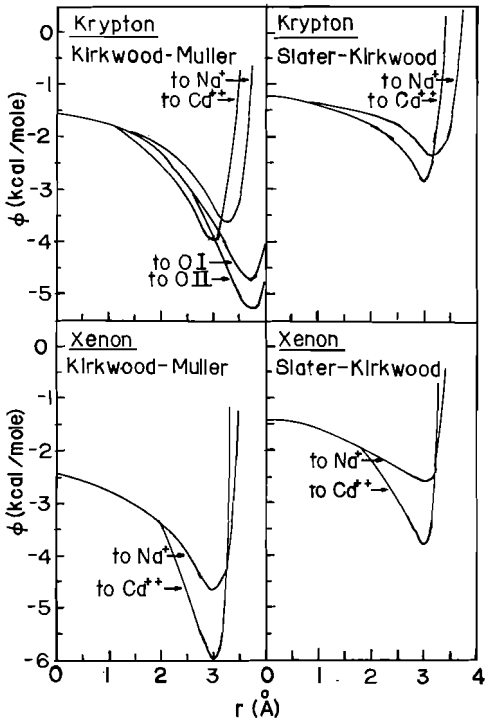

FIG. 3. Potential profiles from center of cavity to various ions showing effect of choice of dispersion constant. (The Na^+ and Ca^{2+} ions are located at the centers of the 6-membered oxygen rings. O_I denotes an oxygen shared between a 6 and 4-membered ring. O_{II} denotes an oxygen shared between an 8 and 6-membered ring.)

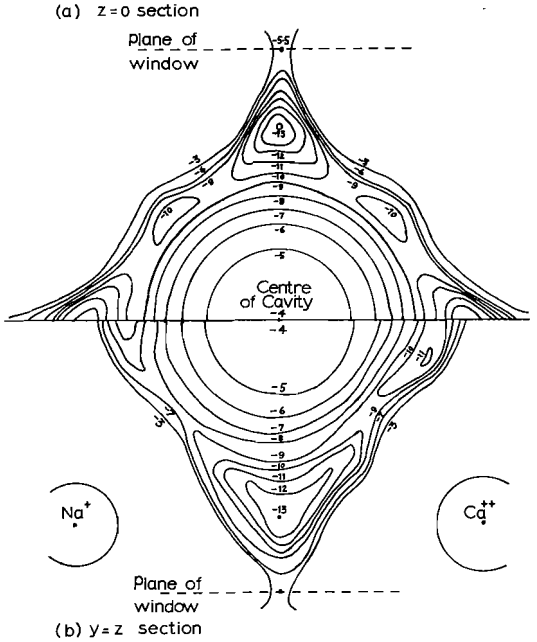

FIG. 4. Potential energy contours for a xenon atom in an idealized 5A zeolite cavity: (*a*) shows a section along a plane bisecting the unit cell through the centers of four 8-membered oxygen windows ($z = 0$ plane); (*b*) shows a section along a plane bisecting the unit cell on the diagonal ($y = z$ plane). Kirkwood–Mueller dispersion constants were used in the calculation of these contours. Potentials are given in units of 10^{-21} cal/molecule.

The theoretical values for the limiting heat of sorption q_0 were then obtained from the relation

$$[16] \qquad q_0 = -u + RT$$

It may be seen from Figs. 2 and 3 that the different methods of estimating the dispersion constants lead to significantly different potential profiles. Errors are also compounded by the addition of the terms in eq. 5 since small differences between relatively large quantities are involved. As a result of these uncertainties the potential energy profiles cannot be considered as quantitatively accurate although they give useful qualitative and semiquantitative information. It has been shown by Young and Crowell (25) that the constants in eqs. 9–11 do not exactly match the empirical potential profiles for the interaction of two inert gas molecules as obtained from crystal data although, of the three formulae, the Slater–Kirkwood expression was found to be the best approximation. This suggests that in interpreting the results of the

Can. J. Chem. Downloaded from www.nrcresearchpress.com by 210.87.254.6 on 09/05/12
For personal use only.

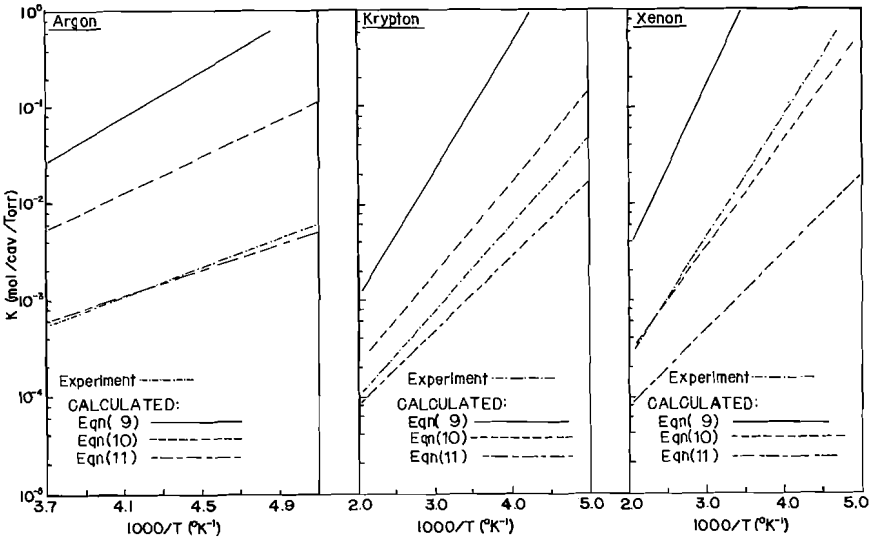

FIG. 5. Comparison of experimental Henry constants with theoretical values calculated from potential energy profiles using Kirkwood–Mueller, Slater–Kirkwood, and London dispersion constants.

present calculations one should probably consider the Slater–Kirkwood values to give the best representation of the actual energy profiles.

The Henry's law constants calculated by integration of the potential profiles are summarized in Table 1 and in Fig. 5 in which the experimental data are also shown. It may be seen that the Slater–Kirkwood expression does indeed give the best prediction of the Henry constant for both krypton and xenon and that the values for argon are correct within an order of magnitude. A somewhat better representation of the experimental data for argon is obtained from the London formula but this formula gives constants for krypton and xenon which are considerably smaller than the experimental values.

In view of the uncertainties involved in the calculation of the potential profiles, the agreement between the theoretical and experimental Henry constants may be considered satisfactory. However, it is apparent that, with the present state of knowledge, the theoretical prediction of Henry constants does not offer a viable alternative to direct experimental measurements, even for the rare gases. For more complex molecules the problems involved in the theoretical calculations are even more severe owing to the possibility of molecular rotation and the distribution of the centers of force.

Variation of Isosteric Heat with Sorbate Concentration

The concentration range covered by the argon isotherms was so low (0–1 molecule/cavity) that no significant variation in isosteric heat of sorption could be observed. The data for krypton and xenon covered a larger concentration range and in order to extend the range of temperatures over which the isosteres could be plotted, and so improve the accuracy of estimation of the isosteric heat, the present isotherms were taken in conjunction with the high pressure – high temperature isotherms of Barrer *et al.* (11).

Over the range 0–6 molecules per cavity the isosteric heat of krypton was essentially constant (~4.2 kcal/mol) while, for xenon, the isosteric heat showed a slight increase from about 5.4 to 6.0 kcal/mol. Similar near constant or slightly increasing values of isosteric heats have been observed for these gases in other zeolites (4, 6, 11) and in the case of krypton and argon in 5A zeolites the values have been confirmed by calorimetric measurements (27, 33).

Isotherm Models

Various theoretical models have been used to correlate the isotherms for sorption of inert gases in the type A zeolites. Mahajan and Walker (28), who reported isotherms for krypton in 5A

Can. J. Chem. Downloaded from www.nrcresearchpress.com by 210.87.254.6 on 09/05/12
For personal use only.

Can. J. Chem. Downloaded from www.nrcresearchpress.com by 210.87.254.6 on 09/05/12
For personal use only.

zeolite at 195, 273, and 298 °K, correlated their data in terms of the Polanyi potential theory. This theory does not really give an adequate representation of the data as different characteristic curves of W (volume sorbed) *vs.* ΔG (adsorption potential) are obtained below and above the critical temperature. Furthermore, the Polanyi theory suffers from the disadvantage that it does not reduce automatically to Henry's law in the low concentration limit. In order to obtain insight into the nature of the sorbed species a more detailed physical model is needed.

Lee and Basmadjian (7) attempted to develop a general correlation of equilibrium data for the rare gases in A type zeolites based on the theory of pore volume filling. The isotherm equation involves a relation between the effective volume of a sorbed molecule and the average free energy of adsorption. It was assumed that the average interaction energy of a mobile sorbed molecule is equal to the interaction energy (sum of the molecule–ion interactions) for a molecule in the center of the cavity. This is a poor assumption as may be seen from the potential energy profiles, illustrated in Figs. 2–4. This method of estimation gives too high a value (too near zero) for the interaction energy but the effect of this error is to some extent compensated for by calculating the polarization energy contribution from experimental data. A fairly good fit of the isotherm data is thus obtained using only a single empirical parameter.

The results of the theoretical potential calculations, which are discussed above, suggest considerable energetic heterogeneity within the zeolite cavity. One may therefore expect that single atom molecules, such as the rare gases, will be adsorbed at specific localized sites and that mobility within the cavities will be limited. It is in principle possible to distinguish between a localized and mobile adsorbed phase by analysis of the isotherms. This approach has been used in several previous studies.

Ideal localized adsorption on a set of discrete sites with no interaction between adsorbed molecules leads to the simple Langmuir expression

$$[17] \qquad bp = \theta/1-\theta)$$

where b is an equilibrium constant, $\theta = c/c_s$, and c_s is the number of sites per cavity. Weak interaction between neighboring adsorbed molecules leads to the modified expression

$$[18] \qquad bp = \{\theta/(1-\theta)\} \exp(2w\theta/RT)$$

in which allowance is made for the pair interaction energy $2w/z$ and the coordination number z is assumed to be constant for all sites. The case of ideal mobile adsorption leads to the Volmer equation

$$[19] \qquad bp = \{\theta/(1-\theta)\} \exp\{\theta/(1-\theta)\}$$

The isotherms for argon and krypton in H-chabazite (4) showed almost ideal Langmuir behavior (eq. 17) at least for $\theta < 0.65$ while the isotherms for krypton in Na-faujasite (6) were interpreted in terms of eq. 18, again suggesting localized adsorption but with some sorbate–sorbate interaction. By contrast, the isotherms for argon in both mordenite (29) and chabazite (2) have been found to obey Volmer's equation, suggesting a mobile adsorbed phase. The xenon isotherms could not however be adequately interpreted in terms of any simple model equation and this led Barrer and Davies (4) and later Barrer, Papadopoulos, and Ramsay (11) to use an empirical virial expression to correlate their data.

An alternative model isotherm has recently been developed for a system in which the sorbed molecules are confined within a particular cavity but are freely mobile within the cavity (30, 31). For such a system, simplified considerations of the reduction in free volume available to the sorbed molecules lead to the following expression for the isotherm

$$[20] \qquad c = \frac{Kp + (Kp)^2(1 - 2\beta/v)^2 + \ldots + \dfrac{(Kp)^m}{(m-1)!}(1 - m\beta/v)^m}{1 + Kp + \dfrac{1}{2!}(Kp)^2(1 - 2\beta/v)^2 + \ldots + \dfrac{(Kp)^m}{m!}(1 - m\beta/v)^m}$$

Can. J. Chem. Downloaded from www.nrcresearchpress.com by 210.87.254.6 on 09/05/12
For personal use only.

in which the small intermolecular attraction terms have been dropped. In this expression v is the cavity volume, β is the molecular volume of the sorbate molecule, and $m \leq v/\beta$ is the saturation limit, rounded to an integral number of molecules per cavity. This model has been found to provide a very satisfactory representation of the equilibrium isotherms for light hydrocarbons in type A zeolites (31) and also in H-chabazite (32). However the assumption of free molecular movement within a cavity is more likely to be correct for polyatomic molecules such as the hydrocarbons since the effect of molecular rotation will be to substantially reduce any energetic heterogeneity, thus favoring free mobility.

Argon

The range of concentration covered by the argon isotherms was insufficient to allow a reliable choice to be made between various isotherm equations. This is true also of the data of Springer (13), Cook (14), and Harper *et al.* (15) for sorption of argon in both 4A and 5A zeolites.

Krypton

The saturation capacity, as estimated from the quotient of the cavity volume of the A type zeolite and the van der Waals covolume of krypton, is about 11 molecules per cavity. The potential calculations show that there are, within the cavity, eight energetically favorable sites (type I) near the 6-membered oxygen rings and a further six favorable sites near the centers of the 8-membered oxygen windows (type II). Each type II site is in effect shared between two adjacent cavities since, although the potential minimum does not occur actually at the center of the window, it is sufficiently close to the window to prevent simultaneous occupation of the sites on either side of any particular window, while the energy barrier between the two minima on either side of a window is very small ($\sim$500 cal). (See Fig. 2.) Each window would therefore be expected to behave as a single site thus giving effectively three type II sites per cavity.

For krypton the distance between two adjacent sites (one of type I and one of type II) is about 4.09 Å which is close to the equilibrium distance between an isolated pair of krypton atoms, as estimated from the Lennard–Jones potential curve (4.04 Å). The results of the potential calculations thus suggest that with only very minor adjustments of position a cavity can accommodate eight krypton atoms in sites of type I and a further three atoms in sites of type II. Furthermore the energy difference between the type I and type II sites is not large ($\sim$1 kcal) and the distance between adjacent sites is sufficient to ensure that repulsive interactions are small. As a first approximation one may therefore expect that an idealized representation as a set of eleven equivalent noninteracting sites might be a fair approximation for this system.

Figure 6 shows the krypton equilibrium data plotted as $\ln [\theta/p(1 - \theta)]$ *vs.* θ, (c_s = 11 molecules/cavity). The data extend only up to about 50% of saturation but it is evident that, within this range, the equilibrium constant calculated according to eq. 18 is essentially constant, indicating that the ideal Langmuir model fits the data well. This was also found to be true of the data of Mahajan and Walker (28).

The adequacy of the simple Langmuir model is further illustrated in Fig. 7 in which the experimental isotherms are compared with the theoretical curves calculated according to eq. 17. Also shown are the high pressure, high temperature data of Barrer *et al.* (11) which are well represented by the theoretical curves, calculated according to eq. 17 with values of b ($=K/c_s$) estimated by extrapolation of the low temperature Henry constants according to eq. 2, with the experimental values of K_0 and q_0 given in Table 1.[2] The remarkable agreement, over such a wide range of conditions, between the experimental isotherms and the simple theoretical predictions based on an idealized Langmuir model provides strong evidence that the approximations on which the model is based are essentially correct.

Xenon

The quotient of the cavity volume and the van der Waals covolume of xenon gives a value of 9 molecules per cavity for the saturation concentration. The interpretation of the theoretical potential profiles is, however, less straightforward for xenon than for krypton. As with krypton

[2]At the higher pressures and lower temperatures the fugacity coefficient is significantly less than unity ($\sim$0.7) and Figs. 7 and 8 are therefore plotted in terms of fugacity rather than pressure.

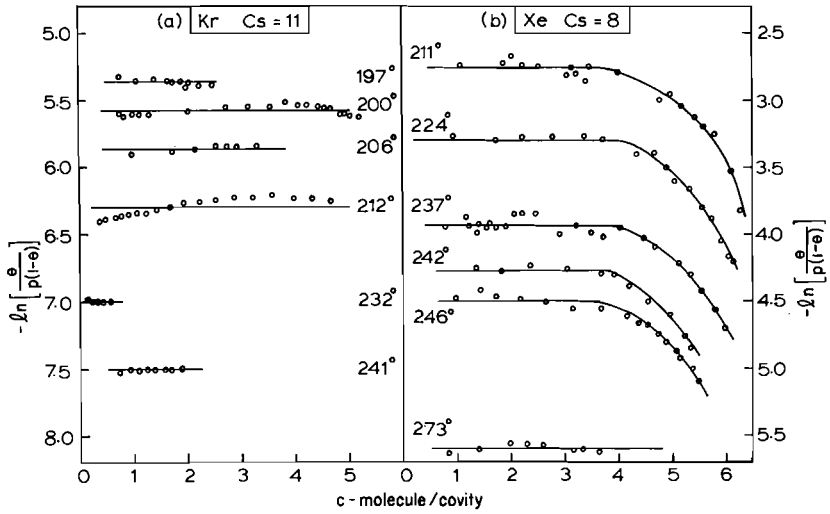

FIG. 6. Plot showing variation of equilibrium constant, calculated according to eq. 17, for Kr and Xe in 5A zeolite (temperatures in °K).

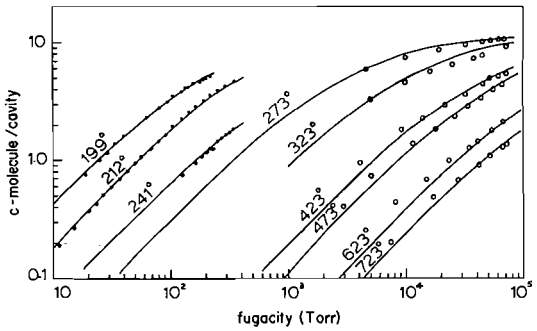

FIG. 7. Equilibrium isotherms for krypton in 5A zeolite: experimental data of Barrer *et al.* (11); ●, present experimental data; —, theoretical lines calculated according to eq. 17.

there are 8 favorable type I sites near the six-membered oxygen rings and effectively three further type II sites per cavity. The distance between adjacent sites of types I and II is, however, only 3.7 Å which is much smaller than the equilibrium separation between isolated xenon molecules (4.56 Å). It is therefore evident that the type I and type II sites cannot be simultaneously occupied.

As a first approximation we assume that the type I sites are preferentially occupied. The simplest representation of this system then becomes an idealized Langmuir model with eight equivalent noninteracting sites per cavity. Figure 6*b* shows the plot of $\ln [\theta/p(1-\theta)]$ *vs.* θ calculated from the experimental isotherms with $c_s = 8$. For $\theta < 0.5$ it is clear that the equilibrium constant calculated according to eq. 17 is indeed approximately constant so that the simplified Langmuir model is an adequate approximation. However, at higher sorbate concentrations deviations become pronounced as may be seen from Fig. 8, in which the experimental isotherms are compared with the theoretical curves calcu-

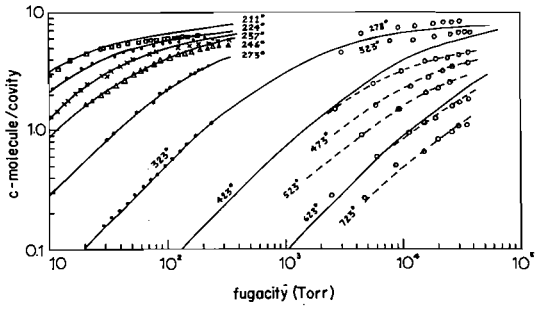

FIG. 8. Experimental isotherms for xenon in 5A zeolite. ○, experimental data of Barrer *et al.* (11); ■, ●, △, ×, present experimental data; —, theoretical lines calculated from eq. 17; ---, theoretical lines calculated from eq. 20 with β = van der Waals b = 85 Å^3 per molecule, v = 776 Å^3 per cavity, $K = 1.29 \times 10^{-6}$ exp (5380/RT) molecule/cavity Torr.

Can. J. Chem. Downloaded from www.nrcresearchpress.com by 210.87.254.6 on 09/05/12
For personal use only.

Can. J. Chem. Downloaded from www.nrcresearchpress.com by 210.87.254.6 on 09/05/12
For personal use only.

lated from eq. 17. Also shown in Fig. 8 are the high temperature, high pressure isotherms of Barrer *et al.* and it is clear that the extrapolated curves based on eq. 17 provide but a poor approximation to these isotherms.

The high temperature isotherms are however well represented by eq. 20 with the values of the Henry constant calculated by extrapolation, according to eq. 2, with the experimental values of K_0 and q_0 given in Table 1. However this equation does not fit the low temperature isotherms (or the isotherms for krypton).

The simplest interpretation of these results is that at low temperatures the molecules are adsorbed at localized sites and that there are approximately eight equivalent sites per cavity. At high temperatures and possibly also even at lower temperatures when the concentration is sufficiently high, the molecules become mobile thus occupying all the available space within the cavity. The distance between the potential minima of adjacent type I sites is 4.23 Å which is slightly smaller than the equilibrium separation between two xenon atoms (4.56 Å). The energy barriers between adjacent sites are not large ($\sim$1 kcal) and such barriers would be reduced by repulsion between neighboring adsorbed molecules. The suggestion of a transition from a predominantly localized adsorbed phase at low temperatures to a mobile adsorbed phase at high temperatures therefore seems physically reasonable but, in the absence of more direct evidence, any such conclusion is tentative. From the practical point of view the important result is that eq. 20 provides a useful method of extrapolation in the high temperature, high pressure region.

Conclusions

The Henry's law equilibrium constants and heats of sorption for the inert gases in the type A zeolites can be estimated theoretically from potential calculations and the resulting values are in satisfactory agreement with experiment. The practical limitations of this approach arise not from the difficulty of performing such calculations but rather from the present unsatisfactory state of knowledge of intermolecular forces. The use of dispersion constants calculated according to each of the three well known formulae (eq. 9–11) leads to significantly different values for the equilibrium constant. For both krypton and xenon the Slater–Kirkwood formula gives closest agreement with experiment while for argon, the London expression seems preferable.

At least up to about 50% saturation the isotherms for krypton fit a simple Langmuir model with eleven equivalent sites per cavity. The behavior of xenon is more complex and there appears to be a transition from localized adsorption to mobile adsorption at high temperatures and sorbate concentrations. Further direct evidence such as might be obtained from a calorimetric study would however be needed to substantiate such a conclusion.

1. L. A. Garden, G. L. Kington, and W. Laing. Trans. Faraday Soc. **51**, 1558 (1955).
2. L. A. Garden, G. L. Kington, and W. Laing. Proc. R. Soc. A**234**, 35 (1956).
3. G. L. Kington. Trans. Faraday Soc. **52**, 475 (1956).
4. R. M. Barrer and J. A. Davies. Proc. R. Soc. A**320**, 289 (1970).
5. R. M. Barrer and W. I. Stuart. Proc. R. Soc. A**249**, 464 (1959).
6. L. V. C. Rees and C. J. Williams. Trans. Faraday Soc. **60**, 1973 (1964).
7. A. K. K. Lee and D. Basmadjian. Can. J. Chem. Eng. **48**, 682 (1970).
8. A. V. Kiselev. Adv. Chem. **102**, 37 (1971).
9. P. Broier, A. V. Kiselev, E. A. Lesnik, and A. A. Lopatkin. Russ. J. Phys. Chem. **42**, 1350 (1966); **43**, 844 (1969).
10. P. Broier, A. A. Lopatkin, and G. P. Stepanez. Adv. Chem. **102**, 97 (1971).
11. R. M. Barrer, R. Papadopoulos, and J. D. F. Ramsay. Proc. R. Soc. A**326**, 331 (1972).
12. S. Kitani and J. Takada. J. Nucl. Sci. Technol. **2**, 7 (1965).
13. C. Springer. Ph.D. Thesis, University of Iowa, Iowa City, Iowa. 1964.
14. G. A. Cook. Argon, helium and the rare gases, Vol. I. Interscience, New York. 1961.
15. R. J. Harper, G. R. Stifel, and R. B. Anderson. Can. J. Chem. **47**, 4661 (1969).
16. R. D. Ackley and W. E. Browning. Oak Ridge National Laboratory, Oak Ridge, Tenn. Report No. Cf-61-2-32 1961.
17. M. H. Lloyd and R. A. McNees. Oak Ridge National Laboratory, Oak Ridge, Tenn. Report No. ORNL3228 1960.
18. J. G. Kirkwood. Phys. Z. **33**, 57 (1932).
19. A. Mueller. Proc. R. Soc. A**154**, 624 (1936).
20. J. C. Slater and J. G. Kirkwood. Phys. Rev. **37**, 682 (1931).
21. F. London. Z. Phys. Chem. B**11**, 222 (1930).
22. L. Broussard and D. P. Shoemaker. J. Am. Chem. Soc. **82**, 1041 (1960).
23. C. J. Whitford. Ph.D. Thesis, University of London, London, England. 1969.

24. R. I. DERRAH. Ph.D. Thesis, University of New Brunswick, Fredericton, New Brunswick. 1973.
25. D. M. YOUNG and A. D. CROWELL. Physical adsorption of gases. Butterworth, London. 1962.
26. N. DUPONT-PAVLOVSKY and J. BASTICK. C. R. Acad. Sci. Paris, **269C**, 476 (1969).
27. F. ROUQUEROL, S. PARTYKA, and J. ROUQEROL. Coll. Int. C.N.R.S. No. 201 Marseille, 1971. Proceedings Thermochimie, 547 C.N.R.S., Paris, 1972.
28. O. P. MAHAJAN and P. L. WALKER. J. Colloid Sci. **29**, 129 (1969).
29. T. TAKAISHI, A. YUSA, and F. AMAKASU. Trans. Faraday Soc. **67**, 3565 (1971).
30. D. M. RUTHVEN. Nature, Phys. Sci. **232** (29), 70 (1971).
31. D. M. RUTHVEN and K. F. LOUGHLIN. J. Chem. Soc. Faraday Trans. I, **68**, 696 (1972).
32. D. M. RUTHVEN, K. F. LOUGHLIN, and R. I. DERRAH. Adv. Chem. **121**, 330 (1973).
33. H. J. F. STROUD and N. G. PARSONAGE. Adv. Chem. **102**, 138 (1971).
34. J. O. HIRSCHFELDER, C. F. CURTISS, and R. B. BIRD. Molecular theory of gases and liquids. Wiley, New York. 1954. p. 1110.

Can. J. Chem. Downloaded from www.nrcresearchpress.com by 210.87.254.6 on 09/05/12
For personal use only.

Ion Pair Formation and Solvation Energies in Solutions of Alkali Halides in Dimethyl Sulfoxide. II. Model Calculations

MERRILL S. GOLDENBERG,[1] PEETER KRUUS, AND STEPHEN K. F. LUK[2]

Department of Chemistry, Carleton University, Ottawa, Canada K1S 5B6

Received September 10, 1974

MERRILL S. GOLDENBERG, PEETER KRUUS, and STEPHEN K. F. LUK. Can. J. Chem. **53**, 1007 (1975).

Energy calculations were carried out on models of molecular-level structures likely to be present in solutions of alkali halides in dimethyl sulfoxide (DMSO). Classical electrostatic interactions were assumed, and polarization of a DMSO molecule was assumed due to the fields of the ions only. The validity of this assumption was tested. DMSO molecules were represented by increasingly detailed models, with most calculations carried out with each molecule represented by 10 point charges and 9 polarizable bonds. A program including up to 14 such molecules and two ions was used for energy and distance calculations, and is made available. Polarization effects are as important as interactions between permanent charges for energy calculations. The configurations of minimum energy determined by classical electrostatics often do not involve overlap of the "hard-sphere radii" of neighboring species, so that the neglect of quantum mechanical repulsive forces seems justified. Energy cycles using the calculated energies for ion–solvent complexes predicted experimental cation enthalpies with some success. The form of the potential for vibration of a cation in a solvent shell was investigated and found in cases not to have an energy minimum at the shell center. Calculations including next-nearest solvating DMSO's indicate a rather loose structure. An energy profile for an anion moving from a solvent-separated ion pair position to a contact-ion pair position is presented.

MERRILL S. GOLDENBERG, PEETER KRUUS et STEPHEN K. F. LUK. Can. J. Chem. **53**, 1007 (1975).

On a effectué des calculs d'énergie sur des modèles de structures moléculaires susceptibles d'être présentes dans des solutions d'halogénures d'alkalis dans le diméthyl sulfoxyde (DMSO). On a fait l'hypothèse que des interactions électrostatiques classiques existent et que la polarisation de la molécule DMSO est due uniquement au champ des ions. On a évalué la validité de cette hypothèse. On a représenté les molécules de DMSO par des modèles de plus en plus détaillés; la plupart des calculs ont été effectués avec chaque molécule représentée par 10 charges ponctuelles et 9 liens polarisables. Pour les calculs d'énergie et de distance, on a utilisé un programme incluant jusqu'à 14 molécules de ce genre et deux ions; ce programme est disponible. Pour lés calculs d'énergie, les effets de polarisation sont aussi importants que les interactions entre les charges permanentes. Souvent les configurations d'énergie minimum déterminées par les théories électrostatiques et classiques n'impliquent pas d'interaction "rayon de sphère dure" avec les espèces environnantes et l'on peut en déduire qu'il est justifié de négliger les forces répulsives de la mécanique quantique. Les cycles d'énergie utilisant les énergies calculées pour les complexes ion–solvant ont prédit avec quelques succès les enthalpies expérimentales des cations. La forme du potentiel pour la vibration d'un cation dans une cellule de solvant a été examinée et on a trouvé dans certains cas qu'il n'y avait pas d'énergie minimum au centre de la cellule. Des calculs impliquant les molécules de DMSO plus loin que les molécules les plus près indiquent que la présence d'une structure lache. On présente un profil d'énergie pour un anion se déplaçant d'une position de paire d'ions séparés par le solvant vers une position de paire d'ions de contact. [Traduit par le journal]

Introduction

Although ultrasonic studies on ion pairing in solutions have been carried out since 1953 (1), there is still difficulty in obtaining a definitive mechanism for 2–2 electrolytes in water (2, 3). Ultrasonic absorption studies were therefore carried out on solutions of alkali halides in dimethyl sulfoxide (DMSO) (4). This provided data on systems which could possibly be described by relatively simple, yet realistic models; the ions are univalent and spherical, and the anions are essentially unsolvated (5).

These studies (4) indicated that there was an

[1]Present address: Chemistry Department, Polytechnic Institute of Brooklyn, Brooklyn, New York.

[2]Present address: Department of Chemistry, University of California, Davis, California.

Can. J. Chem. Downloaded from www.nrcresearchpress.com by 210.87.254.42 on 09/05/12
For personal use only.

Can. J. Chem. Downloaded from www.nrcresearchpress.com by 210.87.254.42 on 09/05/12
For personal use only.

excess absorption with a relaxation frequency between 3 and 8 MHz in solutions of several alkali halides in DMSO. The relaxation was assigned to the final step in the formation of a contact ion pair, with the relaxation frequency controlled by the rate of movement of a solvent molecule rather than an ion.

This paper describes attempts to investigate the energies of models of various molecular-level structures which could be present in solutions of alkali halides in DMSO. The results of such calculations, when related to experimental results (4), could eventually lead to a quite definitive picture of molecular level structures in such solutions.

The calculations involved electrostatic interaction calculations, with each DMSO molecule described by 10 point charges. Polarization of the DMSO was also included by considering each bond to have a longitudinal and transverse polarizability, so that induced dipoles are set up in the DMSO by the field set up by the ions. Some simpler models were also tested.

Such calculations have been carried out previously for aqueous systems (*e.g.* refs. 6 to 9). These have usually only involved tetrahedral and octahedral hydration for the purpose of predicting heats, entropies, and free energies of solvation. In this case, the calculations are extended to include bond polarizabilities and the presence of a second ion.

Theoretical approaches used to describe interactions in electrolyte solutions can be considered from the point of view of two limiting cases. In the one case, the solvent is considered as a continuum; in the other, a quantum mechanical interaction between ion and solvent molecules is attempted. The first approach (10–12) has the advantage of including many interactions, also those taking place at long ranges, but has the disadvantage of neglecting the detail of the ion–molecule interaction in the first solvation shells where the fields are strong. The other approach (13–17) describes such interaction in detail, but is limited to consideration of only a few molecules.

The molecular level, classical electrostatic approach used here sacrifices some of the accuracy in description of ion–molecule interaction, but with use of high-speed computers makes the inclusion of a substantial number of molecules possible. This approach would seem most suitable for this case. Interactions beyond the first solvation shells would seem to be relatively unimportant when the results are considered relative to different alkali halide salts. Direct quantum mechanical effects would seem to be of secondary importance in the case of alkali halides, and not worth pursuing at the expense of exclusion of molecules from the model.

The calculations described here include up to 2 ions and 14 solvent molecules, each molecule represented by 10 point charges and 9 polarizable bonds. The computer program used for the calculations is set up generally enough so that few changes are needed to alter it for calculations on other systems, or for inclusion of more molecules. Copies of the program are available on request from the authors (P.K.).

Results and Discussion

(I) Structure and Charge Distribution in DMSO

To calculate the structure and the charge distribution for DMSO from first principles is a monumental task. An attempt has been made at a calculation for methyl sulfoxide, but the results (18) show the dipole in a direction opposite to the experimentally determined one. Experimental data on DMSO was therefore used whenever available.

Bond distances and angles were taken from X-ray data on solid DMSO at 5 °C (19). The structure of DMSO in the liquid seems likely to resemble the solid structure rather than the gaseous structure, and structure determinations in the gas phase through electron diffraction (20) and rotational spectroscopy (21) are less precise. Table 1 gives the data used.

A semiclassical model (22, 23) of the charge distribution was used. The model consists of touching, conducting spheres centered on the atoms, with each sphere having a radius equal to the covalent bond radius of that atom. To obtain the 10 charges representing the DMSO molecule, the following data and assumptions were used. The data is summarized in Table 2.

TABLE 1. Bond distances and angles for DMSO

Bond	Distance (Å)	Bonds	Angle (deg)
S—O	1.531	O—S—C	106.7
S—C	1.798	S—C—C	97.4
C—H	1.08	S—C—H	109.5
		H—C—H	109.5

Can. J. Chem. Downloaded from www.nrcresearchpress.com by 210.87.254.42 on 09/05/12
For personal use only.

TABLE 2. Experimental and calculated parameters for DMSO

Bond (a—b)	$(\alpha_l)_{ab}$ (10^{-25} cm^3)	$(\alpha_t)_{ab}$ (10^{-25} cm^3)	r_a (Å)	r_b (Å)
C—H	7.9*	5.8*	0.772‡	0.30‡
C—S	18.8†	16.9†	0.772	1.04‡
O—S	29.0*	14.7*	0.55‡	1.04

*Reference 26.
†Reference 27.
‡Reference 24.

(*i*) Pauling's single-bond covalent radii (24) were used for all atoms except oxygen. The triple bond radius (0.55 Å as compared to 0.66 Å for the single-bond) was used for O in order to make it consistent with the S—O bond length.

(*ii*) Each bond polarizability tensor was assumed to have one longitudinal component α_l and two equal transverse components α_t (25).

(*iii*) Slater's screening rules were used to estimate the effective nuclear charge felt by the valence shell electrons in the molecule.

(*iv*) The bond moment arising from the internal field for a bond was represented as a dipole with equal and opposite point charges at the nuclei.

(*v*) The experimentally determined dipole moment (3.96 ± 0.04 D (21)) was used in the simultaneous equation solved.

(*vi*) Data for methane (26) and dimethylsulfide (27) were used to obtain bond parameters for the C—H and the C—S bonds. These parameters are very sensitive to the values of the screening constants and bond radii and the use of experimental data seems advisable.

Combining this data into equations analagous to those used by Smith and co-worker (22) gave six equations with five unknowns. Two of the equations referred to the experimental dipole moment, one to total charge neutrality, and three to net charges in the H, C, and O atoms. Four of the unknowns were the magnitudes of the charges centered on the 4 different types of atoms. The fifth was a parameter for the O—S bond.

Using only one of the dipole equations gave the following solution for the charges: C, 1.66; H, −0.202; O, −1.63; S, −0.474 ($\times 10^{-10}$ e.s.u.). These values differ somewhat from those of Jullien *et al.* (23) who used different values for the DMSO structural parameters and the dipole moment. When the values obtained are substituted into the second dipole equation, the resultant dipole component in the plane bisecting the C—S—C angle is 0.245 D. This gives a resultant dipole of 3.99 D at an angle 4° off the experimentally determined angle.

The polarizability matrices of the 9 bonds can be resolved along a common set of axes and combined to give a polarizability matrix for the whole molecule. With the axes set as shown in Fig. 1 the components α_{xx}, α_{yy}, and α_{zz} are 91.7, 87.7, and 100.3 × 10^{-25} cm^3 respectively. The averaged scalar polarizability calculated on this model is thus 93.2 × 10^{-25} cm^3. This is somewhat higher than the value of 83.72 × 10^{-25} cm^3 calculated for DMSO in ref. 28. It should be noted that only electron polarization is assumed in the model. Atomic polarization, *i.e.* distortion of the interatomic distances and bonds, is neglected. Furthermore, electrons in the various bonds are assumed independent in using bond polarizabilities. This seems to be a reasonable assumption in the case of molecules with no resonance contributions (25). Hyperpolarizability effects are also ignored (29).

Such a description of a DMSO molecule has several uncertainties. The 10 point charge description of the electronic structure in DMSO is more realistic than a multipole expression, especially for calculations where there is substantial interaction. However, a more precise description may be desirable, especially one incorporating descriptions of the electronic distributions about the O and the S atoms.

This most detailed model (A) was simplified to three different models for some calculations to test the sensitivity of the energy calculations

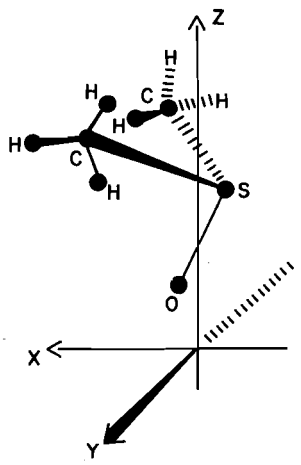

FIG. 1. Positioning of DMSO in a coordinate axis.

Can. J. Chem. Downloaded from www.nrcresearchpress.com by 210.87.254.42 on 09/05/12
For personal use only.

to the detail of the DMSO model. Model B pictured the DMSO as 4 point charges (O, S, and 2 methyls) and 3 polarizable bonds, model C as 4 point charges and a single scalar polarizability, and model D simply as a point dipole and a scalar polarizability. Most calculations were performed using model A, however, as interatomic distances could be obtained with this model.

(II) Contributions to the Interaction Energy of Ion–Solvent Structures

Regular geometric arrangements of DMSO molecules were assumed around the cation for making energy calculations. For an ion with 4 DMSO's around it, the DMSO's were set in a tetrahedron, 5 in a trigonal bipyramid, 6 in an octahedron, and 8 in a square antiprism. The permanent dipoles of the DMSO's were set pointing at the cation (Fig. 1).

Such a structure is unrealistic in that the solvent molecules would in reality not have such regular arrangements at all times. They would also be in continuous thermal motion and would be exchanging with each other. The effect of such thermal motion is difficult to evaluate and is neglected here. There has been evidence, however, that averaged over time, the cation in DMSO is in a solvent cage (30) with the oxygen atom in direct proximity to the metal and the dipole oriented towards it (31).

To construct this model in the computer, a DMSO molecule was first placed on the z-axis as shown in Fig. 1. The coordinates for the other DMSO's can then be obtained simply by rotation of the coordinates of the atoms in the first DMSO by specific amounts. Details of this procedure for the 4, 5, 6, and 8-coordinated cases considered can be found in copies of the computer programs used.

According to ref. 19, the methyl groups are eclipsed, and an activation energy of 11 kJ mol^{-1} is present for the barrier of methyl group rotation about the C—S bond (32). A calculation in which the methyl groups were rotated showed two hydrogens to be at 2.1 Å, within the van der Waals distance of 2.4 Å. It was thus assumed that the methyl groups did not rotate, and the conformation of methyl groups as depicted in ref. 19 was used throughout.

The change in the electrostatic energy due to intermolecular interaction of the permanent charges describing the molecules which took place on rotation of a DMSO molecule about its dipole was found to be negligibly small: less than 0.2% for 6 coordination of a cation with an ion–oxygen distance of 2.4 Å and less than 2% for 5 coordination of an anion with ion–oxygen distance 5.6 Å. Thus the configuration of the DMSO's about the dipole axis was left in the position in which they fell on rotation of the coordinates about the main coordinate axis.

The energy calculations were done taking account of 9 terms: (*i*) E_{AP}, the interaction energy due to permanent charges on the anion and the DMSO molecules, (*ii*) E_{AI}, that due to the permanent anion charge and induced dipoles in the DMSO's, (*iii*) E_{CP} and (*iv*) E_{CI}, the corresponding cation–molecule interaction energies, (*v*) E_{PP}, the interaction energy due to permanent charges on the DMSO, (*vi*) E_{PI}, that due to permanent charges and induced dipoles in the DMSO's, (*vii*) E_{II}, that due to induced dipoles in DMSO's, (*viii*) E_{AC}, that due to permanent charges on the anion and cation, and (*ix*) E_{ACI}, that due to induced dipoles in the ions.

In all the calculations, it was assumed that the induced dipoles were due only to the fields of the ions. This assumption is good in the case of ions, as the DMSO's around the ions were placed with sufficient symmetry so that the fields at the ion due to charge distributions in the DMSO's essentially cancel each other. The degree of validity of this assumption in the case of molecules can be illustrated by considering the three particle problem illustrated in Fig. 2, composed of an ion (I) and two molecules (II, III) modelled as polarizable dipoles pointing towards I.

Before proceeding with this, the mathematical relations for the interactions will be illustrated with the aid of Fig. 2. The relationships are set

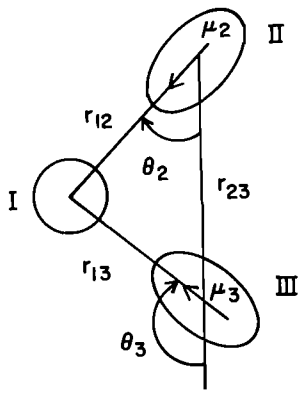

FIG. 2. Schematic illustration of 3-body interaction.

Can. J. Chem. Downloaded from www.nrcresearchpress.com by 210.87.254.42 on 09/05/12
For personal use only.

up for use of the more familiar c.g.s. e.s.u. units. The conversion of the final energy values to SI units is simple. Thus the field F at a distance r from an ion is

$$[1] \qquad F = (qr/r^3)$$

The interaction energy of an ion (I) and a permanent point-dipole μ (II) is then

$$[2] \qquad E_{q\mu} = -\mu \cdot F = -q\mu_2 \cos\theta/r_{12}^2$$

Here θ is the angle between μ and r (taken as zero in Fig. 2). The field due to a permanent dipole is

$$[3] \qquad F = \frac{-\mu}{r^3} + \frac{3r(\mu \cdot r)}{r^5} = \frac{-\mu_2}{r_{23}^2} + 3r_{23}\frac{\mu_2 \cos\theta_2}{r_{23}^4}$$

if the field at III due to II is considered. The interaction energy between two permanent point-dipoles is thus

$$[4] \qquad E_{\mu\mu} = -\mu_3 \cdot F = \frac{-\mu_2\mu_3}{r_{23}^3} \times (2\cos\theta_2 \cos\theta_3 - \sin\theta_2 \sin\theta_3)$$

A 2-dimensional model is assumed here, with μ_2 and μ_3 lying in the same plane.

The interaction energy due to polarization is given in the case of a scalar polarizability α as

$$[5] \qquad E = -\tfrac{1}{2}\alpha F^2$$

A polarizable entity in the field of an ion has energy

$$[6] \qquad E_{qi} = -q_1^2\alpha_2/(2r_{12}^4)$$

while in the field of a point-dipole it has

$$[7] \qquad E_{\mu i} = -\mu_2^2\alpha_3 (3\cos^2\theta_2 + 1)/(2r_{23}^6)$$

Finally, the energy of interaction between two induced dipoles α_2F_{12} and α_3F_{13} due to fields F_{12} and F_{13} at II and III respectively due to I is from [1] and [4]

$$[8] \qquad E_{ii} = -q^2\alpha_2\alpha_3 (2\cos\theta_2 \cos\theta_3 - \sin\theta_2 \sin\theta_3)/r_{12}^2 r_{13}^2 r_{23}^3$$

These relationships were used in the computer energy calculations and the calculations on the model in Fig. 2.

To illustrate the validity in the method of calculating energies, consider the field at II to be made up of 3 components

$$[9] \qquad F_2 = F_{12} + F_{32} + F_{32}^1$$

Here F_{12} is the field at II due to I ([1]), F_{32} the field at II due to the permanent dipole at III ([3]), and F_{32}^1 the field at II due to the dipole induced at III, $\mu_3^1 = \alpha_3F_3$. The field F_{32}^1 will be of the same form as F_{32}, with μ_3 replaced by α_3F_3. Thus $F_{32}^1 = \beta F_3$. The field F_3 can be expressed in a form analogous to [9].

By appropriate substitution, F_2 can be solved to be

$$[10] \qquad F_2 = (F_{12} + F_{32} + \beta F_{13} + \beta F_{23})/(1 - \beta^2)$$

Thus the total energy of II in this field

$$[11] \qquad E_2 = -\mu_2 \cdot F_2 - \tfrac{1}{2}\alpha_2 F_2^2$$

results in 14 terms. Of these, only 6 are considered in the calculations. These correspond to E_{CP}, E_{CI}, E_{PP}, E_{PI}, (twice), E_{II}. Note that E_{AP}, E_{AI}, E_{AC}, and E_{ACI} are nonexistent as the model in Fig. 2 has no anion. The neglected terms are all of an order β smaller than these 6. Taking the simplest model (D) with $q_1 = 4.80 \times 10^{-10}$ e.s.u., $\mu_2 = \mu_3 = 3.96 \times 10^{-18}$ e.s.u. cm, $\alpha_2 = \alpha_3 = 83.7 \times 10^{-25}$ cm^3, $\theta_2 = 45°$, and $r_{12} = r_{13} = 3.8 \times 10^{-8}$ cm, then $\beta = 0.12$. This corresponds to an oxygen–ion distance of 2.4 Å, the distance of closest approach of a DMSO to an Na^+. Thus errors of up to 15% at most can be expected through neglect of the 8 terms as the accuracy of the approximation improves as r increases. The terms E_{II} and E_{PI} contain β in the numerator, but the large values of the other factors (F_{12}, F_{13}) at small r makes them appreciably large (Fig. 5).

Ion–solvent interactions have been described in a similar way in (33), including also quadrupole, dispersion, and repulsion effects. In the actual calculations carried out here, however, it is not necessary to consider permanent dipole (or quadrupole) effects as molecules are described in greater detail by 10 point charges. Dispersion effects are assumed negligible as compared to classical electrostatic effects, and the ions and atoms in DMSO were assumed to behave as hard spheres at distances less than their crystal or covalent radii. Thus the energy is assumed to become infinitely positive if atoms in different molecules or the ion approach the sum of their radii.

For the ions, the most recently available crystal radii (34) were chosen as listed in Table 3 together with polarizabilities (35). There would be a small difference in the effective size of the

Can. J. Chem. Downloaded from www.nrcresearchpress.com by 210.87.254.42 on 09/05/12
For personal use only.

TABLE 3. Radii and polarizabilities of ions

Ion	Radius (Å)*	α (10^{-25} cm^3)†
Li^+	0.90	0
Na^+	1.21	3.0
K^+	1.51	12.3
Cs^+	1.80	31.7
F^-	1.19	7.6
Cl^-	1.65	30.4
Br^-	1.80	42.8
I^-	2.01	65.4

*Reference 34.
†Reference 35.

ion radius in the crystal and the solution (36), and the uncertainty in the measured radii are 0.05 Å. The van der Waals radius used for S was 1.85 Å and for H, 1.2 Å (22). In the solid form of DMSO, the smallest H—H distance observed was 2.51 Å, but a short H—O contact of 2.40 ± 0.3 Å was observed (19). Thus the effective radius for O in DMSO was taken to be 1.20 Å. A considerable error can arise from the uncertainty in the van der Waal's radius for oxygen, as this determines the closest distance to which the DMSO's can approach the ion. However, often electrostatic repulsion rather than "hard sphere" contact determined interatomic distances.

(III) Solvation of Alkali Metal and Halide Ions in DMSO

Solvent–ion interaction studies were initially done by setting 4, 5, or 6 DMSO around the ion as described in (*II*). For cations the DMSO dipoles were set pointing towards the ion as in Fig. 1, while for anions the orientations of the DMSO's were reversed. The DMSO molecules were initially placed far from the ion and then brought simultaneously toward the ion.

Figure 3 shows the results for cations and Fig. 4 for anions. Distances of ion–oxygen hard-sphere contact are indicated for the various ions, and DMSO–DMSO hard-sphere contact distances are also noted. It is interesting to note that the classical electrostatic calculations performed here predict in some cases a configuration of minimum energy which corresponds closely to the hard-sphere contact configuration. The source of the repulsion at low ion–DMSO distances is illustrated in Fig. 5. At $r_{C-O} < 1.9$ Å the effective induced dipole in DMSO is greater than the permanent one, and induced interactions become predominant. The magnitude and

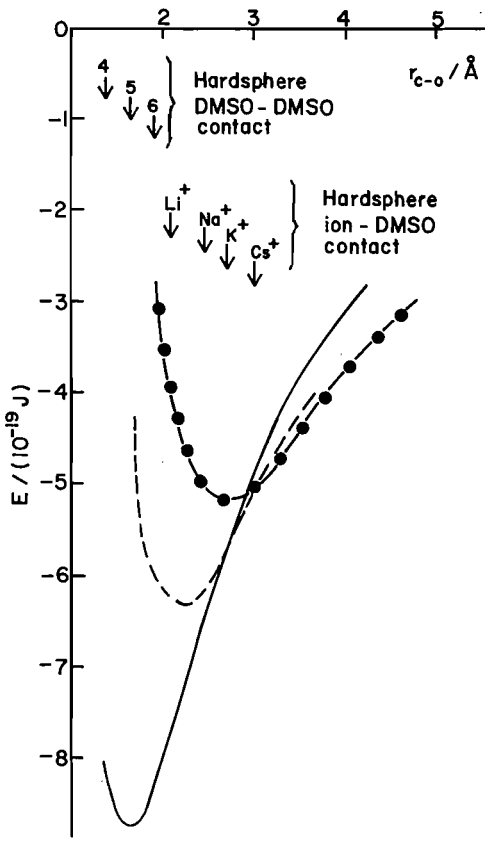

FIG. 3. Energy of cation–solvent complex with 4, 5, and 6 DMSO. —, 4; ---, 5; ●—●, 6 coordination.

positioning of the polarizability in the DMSO becomes thus of extreme importance for realistic calculations.

Figure 6 illustrates the sensitivity of the *E vs. r* curve at small *r* to the DMSO model. Model B is shown to give a smaller energy minimum at larger distances, as the polarizability is effectively closer to the cation than in Model A, thus giving larger E_{II} and E_{PI} repulsion terms. In Model C, the minimum is larger and closer in, as the polarizability is effectively further from the cation, the polarizability of the O—S bond now being located near the S atom. The simplest model (D) gives reasonable agreement with the most detailed, but the positioning of the point dipole and polarizability were adjusted to be 1.08 Å from the O atom to give agreement at large values of *r*.

A number of further calculations of cation solvation were made with solvent shells assumed to be composed of 6 DMSO's with a cation–

Can. J. Chem. Downloaded from www.nrcresearchpress.com by 210.87.254.42 on 09/05/12
For personal use only.

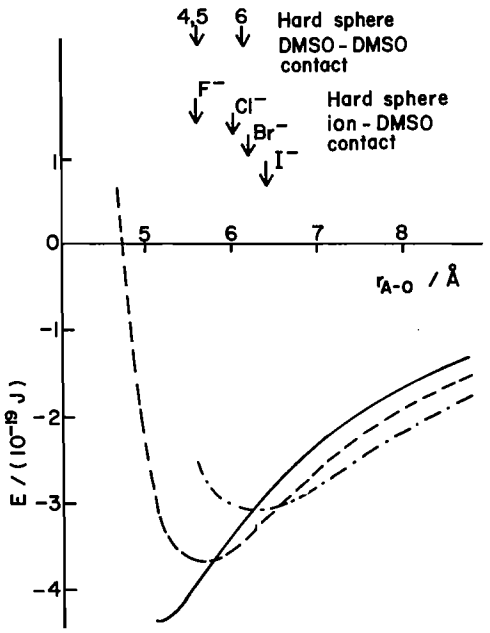

FIG. 4. Energy of anion–solvent complex with 4, 5, and 6 DMSO. —, 4; ---, 5; —·—·—, 6 coordination.

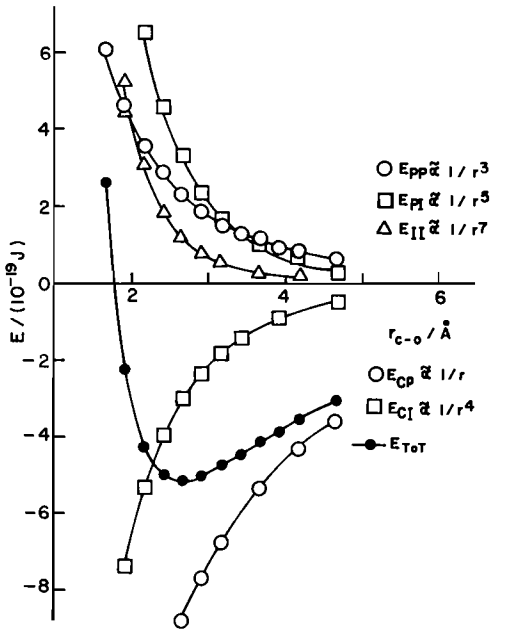

FIG. 5. Contributions to energy of cation–solvent complex (6 DMSO's, Model A).

oxygen distance of 2.4 Å. This corresponds to hard-sphere Na^+–oxygen contact.

A physical model of such a system using wax models of the DMSO molecules showed considerable free space remaining in the form of a square antiprism. The number of DMSO's was thus increased in some runs to 14, 6 nearest neighbors and 8 next-nearest neighbors. With the 6 nearest neighbors set at $r_{co} = 2.4$ Å, the 8 next-nearest neighbors were simultaneously brought towards the cation. When the dipoles of the 8 were pointing towards the cation, an energy minimum -5.8×10^{-19} J was obtained at r_{co} (for the 8) of 9.3 Å, considerably larger than the r_{co} distance of 4.2 Å where DMSO–DMSO hard-sphere contact occurs. With the directions of the dipoles of the 8 next-nearest molecules reversed, the energy again decreased when r_{co} distances were greater than the hard-sphere contact distance (9.0 Å). Thus classical electrostatics predicts a rather loose structuring of solvent about a cation. A lower-energy, less structured, and more tightly packed configuration may possibly be found by a Monte-Carlo type calculation, however.

Values of ΔH^0 for solvation of ions in DMSO (more correctly ΔU^0) can be estimated on the basis of the data in Figs. 3 and 4. Such calcula-

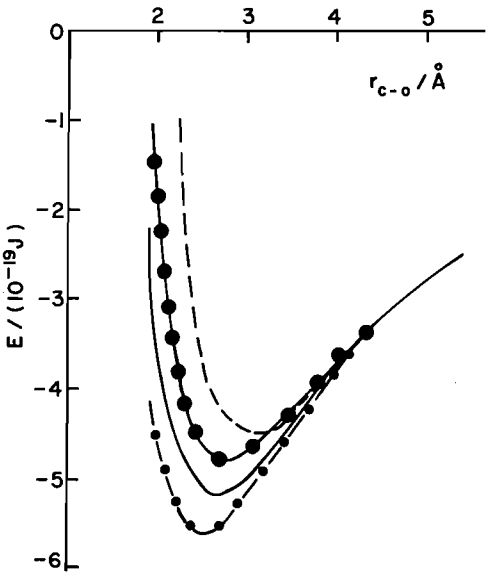

FIG. 6. Energy of cation–solvent complex (6 DMSO's) with varying detail in description of the DMSO. —, Model A (10 charges (q), 9 polarizable bonds (α) per DMSO); ---, Model B (4q, 3α); —·—·— Model C (4q, 1α, with polarizability at S atom); ●—●, Model D (μ, 1α centered 1.08 Å from O).

TABLE 4. Energy contributions to calculations of ΔH^0 of ion

Step	Ion			
	Li^+	Na^+	K^+	Cl^-
(*1*) Formation of hole in liquid	+50	+50	+50	+50
(*2*) Reorientation of DMSO about hole	+50	+50	+50	+50
(*3*) Ion-coordinating DMSO energy	−452	−391	−342	−211
(*4*) DMSO–DMSO coordination energy	−72	−56	−84	−84
(*5*) Ion-continuum interaction	−104	−101	−96	−96
(*6*) ΔH^0 solvation in DMSO (calcd)	−528	−448	−422	−291
(*7*) ΔH^0 hydration*	−531	−420	−339	—
(*8*) ΔH^0 transfer† (water → DMSO)	−28	−30	−37	—
(*9*) ΔH^0 solvation in DMSO (exptl)	−559	−450	−376	−315‡

*Reference 44.
†Reference 45.
‡From ref. 36.

tions are presented for Li^+, Na^+, K^+ and Cl^-. It will be assumed following Fig. 3 that Li^+ is 4 coordinated with an energy for the ion–solvent complex (at $r_{co} = 2.1$ Å) of -7.5×10^{-19} J; Na^+ to be 4 coordinated with an energy (at $r_{co} = 2.41$ Å) of -6.5×10^{-19} J; K^+ to be 5 coordinated with an energy (at $r_{co} = 2.7$ Å) of -5.7×10^{-19} J. From Fig. 4, Cl^- is likely to be 5 coordinated with an energy -3.5×10^{-19} J. For the cations, the coordination numbers might be larger than those listed above for cations if a higher value, *e.g.* 1.4 Å rather than 1.2 Å were used as the hard-sphere radius for O. Lower coordination numbers would be favored in liquid solutions, however, as addition of extra DMSO's into the coordination shell must lower the energy by about 50 kJ mol^{-1} (see Table 4) if the step DMSO(1) → DMSO (coordination shell) is to be exothermic.

Table 4 gives the contributions to the ΔH^0 of solvation calculated on the speculative constant energy cycle described below. The rows in Table 4 correspond to the steps:

(*1*) A hole the size of a DMSO is formed to hold the cation. This requires an energy equal to the internal latent heat of vaporization (37), $\Delta H_v - RT = 50.3$ kJ mol^{-1} at 25 °C when the figure 52.8 kJ mol^{-1} is used for the latent heat of vaporization, ΔH_v (38).

(*2*) The second step involves the simultaneous orientation of the sterically least hindered DMSO's into the appropriate coordinating positions, and nearby DMSO's into the next coordination shell. This energy is difficult, if not impossible, to calculate. An estimate was made on the basis of calculations comparing interaction energies between two DMSO's in a variety of positions in the first solvation shell. An energy of 50 kJ mol^{-1} was estimated for this step based on the difference in energy between unfavorable and favorable dipole energies, and the energy to force out interfering DMSO's (estimated as 8 kJ mol^{-1}). In an analogous problem with methanol (39), interfering molecules were not considered. The energy for the first steps was estimated as 35 ± 20 kJ mol^{-1}.

(*3*) These are simply the energies as calculated, noting that 10^{-19} J ion^{-1} equals 60.23 kJ mol^{-1}.

(*4*) The interactions between the coordinating DMSO's must be subtracted here, as they are already included in the structure in step (*2*). These terms can be computed with the general program, setting the charge on the ion equal to zero.

(*5*) Finally, the interaction between the ion and the outer coordination shells must be considered. The outer shells are considered as structureless, homogeneous, and incompressible (no electrostriction) with the macroscopic dielectric constant. The first coordination shell was considered irrotationally bound to the ion as part of a charged sphere representing the ion–DMSO complex. The radii of these spheres were determined from the furthest H-distances and were 6.8 Å for Li^+, 7.1 Å for Na^+, and 7.4 Å for K^+ and Cl^-. An expression for the ΔH was obtained from the Born equation (40), with values of the dielectric constants obtained from refs. 41–43. Use of the Born equation should be quite appropriate as the next-nearest neighbors are likely to be located at distances such that their centers are over 10 Å from the cation.

(*6*) This row gives the single ion solvation enthalpies as calculated by the above cycle.

Can. J. Chem. Downloaded from www.nrcresearchpress.com by 210.87.254.42 on 09/05/12
For personal use only.

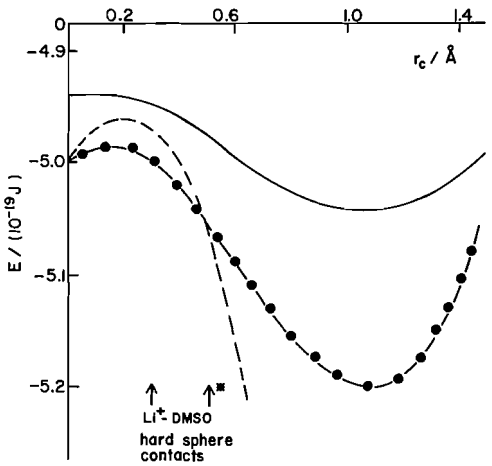

FIG. 7. Energy as a function of cation distance from the shell center with 6 coordinating DMSO: —, O atoms 3.0 Å from shell center, movement in 1,1,1 direction; ---, O atoms at 2.4 Å, movement along z axis; ●—●, O atoms at 2.4 Å, movement in 1,1,1 direction.

The values should be compared with those in row (*9*). The agreement is good, considering the crude assumptions made in (*1*), (*2*), and (*4*). It is significant that both the right order of magnitude and the correct trend are predicted.

The experimental values in row (*9*) were determined from single ion enthalpies of hydration (44) and the energy of transfer from water to DMSO (45). The difference between ΔH^0 solvation in row (*9*) between Li^+ and K^+ is 183 kJ mol^{-1} in agreement with the figure obtained from ref. 36 assuming the Li^+ value shown. The calculated ΔH^0 solvation for LiCl (−819 kJ mol^{-1}) is smaller than the experimental one (−874 kJ mol^{-1} (36)) by nearly 10%. The small changes of ΔH^0 solvation in going from Cl^- to Br^- to I^- are also predicted from the curves in Fig. 4.

For a more definitive test of the validity of the calculations on ion–solvent energies carried out, a comparison to gas phase solvation experiments such as those in ref. 46 would be desirable. No systems are yet available for which both experimental results and calculation from the general model described here exist.

(IV) Vibration of Cations in Solvent Shells

The infrared spectra of alkali metal salts in DMSO have been interpreted as due to alkali metal ions vibrating in cages under the influence of electrostatic forces (30). The frequencies for Li and Na salts are 425 and 200 cm^{-1}, irrespective of anion. It was decided to look at the energy as a function of the position of the cation in solvent shells of varying sizes. The results are shown in Fig. 7 for three types of vibrations.

In all three cases, the cation was assumed 6 coordinated. When the cation is moved along the *z* axis, then the energy is a maximum near the center and falls steeply as the cation approaches the O of the DMSO on the *z* axis. The hard-sphere contact distances with O atoms 2.4 Å from the center of the cage is shown for Li^+. The second distance (*) is for the negative side of the graph where the curve is not shown. The curves are not exactly symmetrical about r_c (distance of cation from center of cage), as the O atoms are not exactly on the coordinate axes (see Fig. 1). When the cation is taken to vibrate along the 1,1,1 direction, a minimum in the energy occurs away from the center of the cage, with a repulsion predicted from electrostatics.

The force constants for vibrations in the 1,1,1 direction are (*i*) for the O's 2.4 Å from the center, 1.3×10^{-9} N $Å^{-1}$ and (*ii*) for 3.0 Å, 6.5×10^{-10} N $Å^{-1}$. The force constants for Li^+ and Na^+ in DMSO calculated in ref. 30 are 7.7×10^{-9} N $Å^{-1}$ and 6.2×10^{-9} N $Å^{-1}$. The results are qualitatively correct, in that the force constant increases as the size of the ion cage decreases. The results calculated here are lower by nearly an order of magnitude, however. A low value would be expected, as the addition of a nonclassical exponential repulsion term would increase the curvature. As indicated in Fig. 7, vibrations in directions other than the 1,1,1 direction are also likely to have larger force constants, but to obtain a value for them it is necessary to introduce repulsion potentials smoother than the hard-sphere potential. Thus classical electrostatic considerations are not sufficient to explain the vibration phenomenon quantitatively.

The results described in this section suggest that the high-symmetry configurations used for the calculations may not necessarily be the lowest energy ones. To find lower energy, less symmetrical configurations, it would seem necessary to do Monte-Carlo type calculations. It is also likely that the solvent cages are on the average considerably larger than those predicted on the basis of O-ion hard-sphere contact in Fig. 3. Both of these effects add to the imprecision of the calculations summarized in Table 4.

Can. J. Chem. Downloaded from www.nrcresearchpress.com by 210.87.254.42 on 09/05/12
For personal use only.

TABLE 5. Energies of various configurations

System	Energy of configuration (10^{-19} J)	Energy difference (10^{-19} J)
1 Tetrahedral 4-coordinated cation, no anion	−6.5	−5.4
2 As in 1 but with anion at Na^+–Cl^- hard-sphere distance	−11.9	
3 4-coordinated cation (trigonal bipyramid less one DMSO)	−6.2	
4 As in 3 but with anion	−12.0	−5.8
5 5-coordinated cation (octahedral less one DMSO)	−5.8	
6 As in 5 but with anion	−11.0	−5.2
7 6-coordinated cation (octahedral)	−5.8	
8 As in 7 but with anion	−10.6	−5.6
9 14 DMSO's about cation 6 octahedral, 8 square antiprism	−5.8	
10 As in 9 with anion, direction of 1 DMSO reversed, ions touching	−10.5	−4.7
11 As in 9 with anion one DMSO removed from cation.	−9.3	−1.2

(V) Ion Pairs in Dimethyl Sulfoxide

Energy calculations were made on a number of configurations including both an anion and a cation. It was hoped to be able to follow the energy of configurations for the reaction: solvent-separated ion pair going to contact ion pair. The energy of the transition state could in such a case be obtained and comparison made to the kinetic data for the systems (4). This goal has not been fully reached in this study, however.

A number of calculations were made with only the first coordination shell DMSO's considered. The results are summarized in Table 5. All systems assumed a cation–oxygen distance of 2.4 Å. Results for the inclusion of 14 DMSO's are also included. All the systems assumed the cation to be Na^+ and the anion Cl^-.

The first 5 pairs of systems (*i.e.* 1 and 2, 3 and 4 etc.) each give the ΔE for a reaction. Solvated cation + free anion → solvated ion pair. Only in the case of the last set is the solvation of the anion reasonably complete. The first 4 pairs give approximately the same ΔE for this reaction -5.6×10^{-19} J configuration^{-1}, or −330 kJ mol^{-1}. In all cases E decreased monotonically as the anion approached the cation.

The value −330 kJ mol^{-1} is meaningful only for the ΔU^0 of the formation of such an ion pair in the gas phase. The ΔE is rather insensitive to the number and the configuration of the DMSO's present. If no DMSO's are present then the ΔE for the formation of the ion pair is -8.7×10^{-19} J. This assumes hard-sphere interaction occurs at an ion–ion distance 2.86 Å. The experimental value, and that calculated with an ion–ion distance of 2.51 Å and an r^{12} repulsion is -9.1×10^{-19} J (47).

When the anion in the model is somewhat solvated (system 9), then the ΔE is somewhat smaller. The ΔE for going from systems 11 to 10 is considerably smaller. The configurations for these two systems are shown in Fig. 8, with only two of the 8 next-nearest solvation molecules shown. This is a more realistic ΔU^0 for the solvent separated ion pair – contact ion pair postulated to be the cause for the excess absorption in ref. 4. The value would be even smaller if the anion in system 11 would be solvated by a third shell of DMSO's.

It is noteworthy as shown in Fig. 8 using wax models, that even with octahedral 6 coordination, there is room enough for the anion to approach nearly all the way in to the hard-sphere distance without touching the DMSO's.

Table 6 gives the energies for a number of configurations intermediate between systems 10 and 11 in Table 5. These configurations could be transition states for the contact ion pair – solvent separated ion pair reaction. In all cases the cation is in the center, the 6 nearest neighbor DMSO are at $r_{co} = 2.4$ Å and the 8 next-nearest neighbors are at $r_{co} = 9.3$ Å. Several configurations intermediate to systems 4 and 5 in Table 6 were examined, but in each case there was a hard-sphere interaction. Thus some relaxation of the DMSO's from the symmetrical positions

Can. J. Chem. Downloaded from www.nrcresearchpress.com by 210.87.254.42 on 09/05/12
For personal use only.

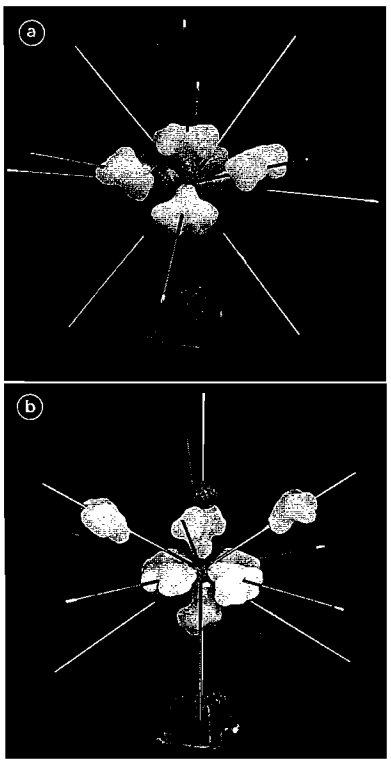

FIG. 8. Models of systems 10 and 11 of Table 5 with 6 nearest and 2 next-nearest DMSO's shown: (*a*) contact ion pair (system 10); (*b*) solvent separated ion pair (system 11).

TABLE 6. Energies of configurations intermediate to contact and solvent-separated ion pairs

	Coordinates of anion (Å)			Energy
	x	*y*	*z*	(10^{-19} J)
1.	System 10, Table 5			−10.5
2.	1.65	0.165	1.65, as (1) but one DMSO reversed	−10.3
3.	1.8	1.8	1.8	−10.2
4.	2.0	2.0	2.0	−10.2
5.	1.0	1.0	7.6	−9.07
6.	0	0	7.6	−9.29
	System 11, Table 5			

used here seems necessary for the process to proceed.

The energy difference between systems 5 and 6 suggests that an activation energy of about 0.22×10^{-19} J (13 kJ mol^{-1}) may be present in the process, but this may not be the lowest energy reaction coordinate. On the other hand, higher-energy transition states may be present which were not detected in the calculations. The energy can be lowered by about 12 kJ mol^{-1} by reversing the orientation of the next-nearest neighbor DMSO closest to the anion. This makes the activation energy for the reverse process of the order of 80 kJ mol^{-1}. The results in ref. 4 indicate a low activation energy for the process responsible for the excess ultrasonic absorption.

In order to get more meaningful results, calculations on far more configurations must be done. These should ideally be done by a Monte-Carlo type approach, allowing configurations to "relax" to their positions of lowest energy.

Conclusions

The classical electrostatic models used in the calculations presented here seem to be a good compromise between the quantum mechanical and the continuum models used for description of microscopic structures in liquids and solutions. The description of the DMSO molecule need not be as detailed as that used here for molecules farther from ions. However, specifying the coordinates of all the atoms makes it easy to extend the calculation to include repulsive forces. Thus in addition to the coulomb interactions due to the charge centered on atoms, a repulsive term of a form $C_1 \exp[-C_2(r-C_3)]$ or $C_1(C_2/r)^{C_3}$ can be added to the calculations.

For an adequate description of the solvent-separated ion pair, it seems necessary to add a third shell of solvent molecules. Most likely, about 10 molecules forming a third shell in the positive *z* half of the coordinate system seems sufficient. This would bring the number of molecules up to 24.

It would seem desirable to also include in the calculation of the electric field causing polarization the contributions from the neighboring molecules. Close to the ion, the ion field is predominant, but fields due to neighboring molecules may be significant when outer shell molecules are considered. It may however be adequate to describe the polarization through a single judiciously placed scalar polarizability rather than 9 polarizable bonds.

The most realistic configurations of the lowest energy for contact and solvent separated ion pairs as well as intermediate states can be best obtained through Monte-Carlo type calcula-

Can. J. Chem. Downloaded from www.nrcresearchpress.com by 210.87.254.42 on 09/05/12
For personal use only.

tions. The system can be allowed to find the configuration of lowest energy with one or both of the ion coordinates fixed. A promising initial configuration can be chosen on the basis of geometrical models such as shown in Fig. 8.

Incorporation of these features into the calculations are quite feasible in principle, but require more computational resources than those used for the calculations presented here. Such calculations can be set up quite generally so that other solvent systems can be studied. Because of the neglect of dispersion forces and quantum mechanical effects, the calculations are most realistic for systems involving polar molecules and/or relatively simple univalent ions.

The authors wish to thank Dr. D. R. Dickson for assistance in programming parts of the calculations, and Dr. W. J. Meath, Dr. P. M. Laughton, and Dr. J. M. Holmes for useful discussions. The project was supported financially by the National Research Council of Canada.

1. G. KURTZE and K. TAMM. Acustica, **3**, 33 (1953).
2. L. G. JACKOPIN and E. YEAGER. J. Phys. Chem. **74**, 3766 (1970).
3. A. BECHTLER, K. G. BREITSCHWERDT, and K. TAMM. J. Chem. Phys. **52**, 2975 (1970).
4. D. R. DICKSON and P. KRUUS. Can. J. Chem. **49**, 3107 (1971).
5. J. E. PRUE and P. J. SHERRINGTON. Trans. Faraday Soc. **57**, 1795 (1961).
6. F. G. GARRICK. Phil. Mag. **11**, 741 (1931).
7. J. P. BERNAL and R. H. FOWLER. J. Chem. Phys. **1**, 515 (1933).
8. A. D. BUCKINGHAM. Discuss. Faraday Soc. **24**, 151 (1947).
9. J. S. MUIRHEAD-GOULD and K. J. LAIDLER. Trans. Faraday Soc. **63**, 944 (1967).
10. K. J. LAIDLER and J. S. MUIRHEAD-GOULD. Trans. Faraday Soc. **63**, 953 (1967).
11. D. K. ROSS and S. LEVINE. Aust. J. Phys. **21**, 571 (1968).
12. P. S. RAMANATHAN and H. L. FRIEDMAN. J. Chem. Phys. **54**, 1086 (1971).
13. J. DALY and R. E. BURTON. Trans. Faraday Soc. **66**, 2408 (1970).
14. K. HAUGE and A. STOEGAARD. Acta Chem. Scand. **27**, 2683 (1973).
15. B. M. RODE. J. Chem. Soc. Faraday Trans. II, **69**, 1439 (1973).
16. A. GUPTA and C. N. R. RAO. J. Phys. Chem. **77**, 2888 (1973).
17. H. KISTENMACHER, H. POPKIE, and E. CLEMENTI. J. Chem. Phys. **59**, 5842 (1973).
18. A. RAUK, S. WOLFE, and I. G. CSIZMADIA. Can. J. Chem. **47**, 113 (1969).
19. R. THOMAS, C. B. SHOEMAKER, and K. ERIKS. Acta Cryst. **21**, 12 (1966).
20. O. BASTIANSEN and H. VIERVOLL. Acta Chem. Scand. **2**, 702 (1948).
21. H. DREIZLER and G. DENZL. Z. Naturforsch. **19A**, 512 (1964).
22. R. P. SMITH and H. EYRING. J. Am. Chem. Soc. **75**, 5183, 2012 (1953); **74**, 229 (1952); **73**, 5513, 2263 (1951).
23. J. JULLIEN, H. STAHL-LARIVIERE, and A. TRAUTMANN. Bull. Soc. Chim. Fr. 2398 (1966).
24. L. PAULING. The nature of the chemical bond, 3rd ed. Cornell University Press, Ithaca, New York. 1964.
25. J. O. HIRSCHFELDER, C. F. CURTISS, and R. B. BIRD. Molecular theory of gases and liquids. John Wiley and Sons, New York. 1964.
26. E. R. LIPPINCOTT and J. M. STUTMAN. J. Phys. Chem. **68**, 2926 (1964).
27. R. J. W. LEFEVRE. Advances in physical organic chemistry, Vol. 3. *Edited by* V. Gold. Academic Press, London. 1965. p. 50.
28. E. R. LIPPINCOTT, G. NAGARAJAN, and J. M. STUTMAN. J. Phys. Chem. **70**, 78 (1966).
29. A. D. BUCKINGHAM and B. J. ORR. Q. Rev. **21**, 195 (1967).
30. W. E. EDGELL, J. LYFORD IV, R. WRIGHT, W. RISEN, JR., and A. WATTS. J. Am. Chem. Soc. **92**, 2240 (1970).
31. B. W. MAXEY and A. I. POPOV. J. Am. Chem. Soc. **91**, 20 (1969).
32. H. MACKLE and P. A. G. O'HARE. Trans. Faraday Soc. **58**, 1912 (1962).
33. W. E. MORF and W. SIMON. Helv. Chim. Acta, **54**, 794 (1971).
34. F. G. FUMI and M. P. TOSI. J. Phys. Chem. Solids, **25**, 31, 45 (1964).
35. A. J. MICHAEL. J. Chem. Phys. **51**, 5730 (1969).
36. R. F. RODEWALD, K. MAHENDRAN, J. L. BEAR, and R. FUCHS. J. Am. Chem. Soc. **88**, 6698 (1968).
37. S. GLASSTONE. Textbook of physical chemistry, 2nd ed. D. Van Nostrand Co., Toronto. 1948.
38. T. B. DOUGLAS. J. Am. Chem. Soc. **70**, 2001 (1948).
39. D. O. ELEY and D. C. PEPPER. Trans. Faraday Soc. **37**, 581 (1941).
40. G. KORTUM. Treatise on electrochemistry. Elsevier, Amsterdam. 1965.
41. H. L. SCHLÄFER and W. SCHAFFERNICHT. Angew. Chem. **72**, 618 (1960).
42. J. DOUCET, F. CALMES-PERRAULT, and M. T. DURAND. C. Hebd. Seances, Acad. Sci. 260, 1878 (1965). *Cited in* D. MARTIN, A. WEISE, and H. J. NICLAS. Angew. Chem. Int. Ed. **6**, 318 (1967).
43. P. G. SEARS, G. R. LESTER, and L. R. DAWSON. J. Phys. Chem. **60**, 1433 (1956).
44. V. P. VASILEV, E. K. ZOLOTAREV, A. F. KUSTINSKII, K. P. MISHCHENKO, E. A. PODGORNAYA, and K. B. YATSIMIRSKII. Russ. J. Phys. Chem. **34**, 840 (1960).
45. E. M. ARNETT and D. R. MCKELVEY. J. Am. Chem. Soc. **88**, 2598 (1966).
46. J. D. PAYZANT, A. J. CUNNINGHAM, and P. KEBARLE. Can. J. Chem. **51**, 3242 (1973).
47. M. DAVIES. Some electrical and optical aspects of molecular behaviour. Pergamon, Oxford. 1965.

Can. J. Chem. Downloaded from www.nrcresearchpress.com by 210.87.254.42 on 09/05/12
For personal use only.

Reactions of Alkyl Azidoformates with Norbornylene[1]

OLIVER E. EDWARDS, JOHN W. ELDER,[2] MAURICE LESAGE, AND ROBERT W. RETALLACK[3]

Biochemistry Laboratory, National Research Council of Canada, Ottawa, Canada K1A 0R6

Received November 5, 1974

OLIVER E. EDWARDS, JOHN W. ELDER, MAURICE LESAGE, and ROBERT W. RETALLACK. Can. J. Chem. **53**, 1019 (1975).

Evidence is presented that the reactions of alkyl azidoformates with norbornylene induced by direct irradiation do not involve intermediate triazolines. The products of this, and acetophenone-photosenzitized reaction of the mixtures in cyclohexane, are described and contrasted with those from the direct photolysis of the corresponding *N*-alkoxycarbonyl triazolines. The action of aqueous dioxane at 170° converted 2,3-iminonorbornane (3-azatricylo[3.2.1.$0^{2,4}$]octane) into 3-aminonortricyclene and *syn*-7-amino-2-*exo*-hydroxynorbornane. Three preparations of derivatives of 2-*exo*-aminonorbornan-3-one are described. The trimethylsilyl ether of the enol of norbornan-2-one (2-trimethylsilyloxynorborn-2-ene) was prepared.

OLIVER E. EDWARDS, JOHN W. ELDER, MAURICE LESAGE et ROBERT W. RETALLACK. Can. J. Chem, **53**, 1019 (1975).

On présente des données indiquant que les réactions induites par irradiation directe, entre les azidoformates d'alkyles et le norbornylène, n'impliquent pas de triazolines comme intermédiaires. On donne une description des produits de ces réactions, de même que de ceux qui ont été obtenus de ces mêmes mélanges, par irradiation photosensibilisée par l'acétophénone, dans le cyclohexane. La comparaison de ces produits, montre des différences marquées par rapport à ceux qui se forment durant la photolyse directe des triazolines *N*-alkoxycarbonylées correspondantes. Sous l'action du dioxanne aqueux, à 170°, l'imino-2,3 norbornane (aza-3 tricyclo-[3.2.1.$0^{2,4}$]octane) se transforme en amino-3 nortricyclène et en *syn*-amino-7 *exo*-hydroxy-2 norbornane. On décrit trois préparations des dérivés de l'*exo*-amino-2 norbornanone-3. On a préparé l'éther triméthylsilylé de l'énol de la norbornanone-2 (triméthylsilyloxy-2 norbornène-2).

Introduction

The photolysis of azidoformates in the presence of compounds with isolated carbon double bonds (1), enol acetates (2), and of dihydropyran (3) has been shown to give aziridines. The internal photochemical addition of acyl azides to olefinic double bonds has also been described (4, 5). In the case of unreactive double bonds, comparison of the products of photochemical reaction and the reaction of the olefin with chemically generated singlet nitrenes suggested that the former also were singlet nitrene reactions (1). However, this is not necessarily true for polarized or strained olefins. These could react with electronically excited azide to give vibrationally excited triazoline. This could lose nitrogen directly or require electronic excitation by another photon before giving aziridine (eq. 1).

[1] $RCON_3^* + \text{>C=C<} \longrightarrow$

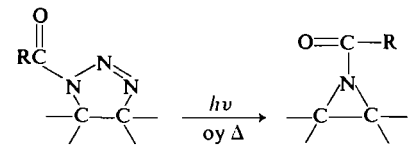

It seemed to us that comparison of photolysis of a triazoline with the photolysis of the azide–olefin mixture might throw light on this problem.

When this work was initiated (summer 1964) the acyl triazoline **1** had been described (6) as product of reaction of ethyl azidoformate with *N*-(1-cyclohexenyl)morpholine and it had been concluded that **2** was the product of reaction of benzoyl azide with norbornylene (7). Our attempts to intercept acyl triazolines in thermal reactions of ethyl azidoformate with 1-methoxycyclohexene (8) or with dihydropyran (3) were unsuccessful. However it was found that reaction of methyl and ethyl azidoformates with the reactive double bond of norbornylene was much

[1]NRCC No. 14425.

[2]Guest worker, summers of 1964 and 1972. Present address: Fairfield University, Fairfield, Connecticut.

[3]NRCC Postdoctorate fellow, 1966–1968.

Can. J. Chem. Downloaded from www.nrcresearchpress.com by 210.87.254.40 on 09/05/12
For personal use only.

Can. J. Chem. Downloaded from www.nrcresearchpress.com by 210.87.254.40 on 09/05/12
For personal use only.

more rapid than the loss of nitrogen from the adduct, which was presumed to be the triazoline **3**. The adduct rapidly lost nitrogen when heated

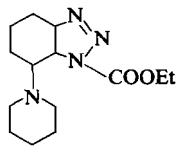

1

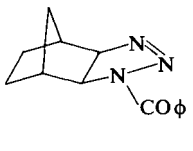

2

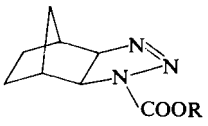

3

at 135°, when treated with acids, or when irradiated with u.v. light. The major products were the imine **4** and a tricyclic urethane A, which appeared to be a derivative of either the aziridine **5** or azetidine **6**. The n.m.r. spectrum

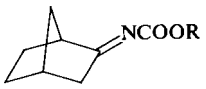

4

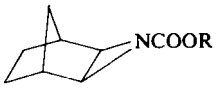

5

6

of A was more easily reconciled with structure **5** since the two protons on carbon carrying nitrogen gave a singlet at δ 2.63 ($w_{1/2}$ 2.2 Hz). However, when the alkoxycarbonyl group of A was removed by mild alkaline hydrolysis, then the resulting amine **7** heated in aqueous dioxane at 170°, the main products were nortricyclylamine (**8**) (8%), *anti*-7-amino-2-*exo*-hydroxynorbornane **28** (8%), and *syn*-7-amino-2-*exo*-hydroxynorbornane **9** (81%) (structure proof below). This suggested that "A" was actually the *N*-alkoxycarbonyl azetidine **6** and thus cast doubt on the structure of the proposed triazoline.

While this work was in progress the preparation and reaction of a number of *N*-acyl triazolines derived from norbornylene was reported (9–11) and the thermal decomposition of the apparent triazolines from azidotropones and norbornylene described (12). Evidence was also presented for triazoline formation from *t*-butyl azidoformate and birdcage hydrocarbon (13). Of more direct relevance, Scheiner reported the preparation of triazoline **3** and claimed that its photolysis gave essentially pure **5** (14). Zalkow and Oehlschlager and their co-workers (15) described the preparation, thermolysis and photolysis of **3**. Tanida *et al.* (16) showed that **3** rapidly lost nitrogen at room temperature in alcohols giving the same major product as thermolysis (presumably **5**). In all these cases the structure of **5** was deduced from n.m.r. evidence (14–16) and a band at 1190 cm^{-1} attributed to the aziridine ring (14). The only chemical evidence bearing on its structure was the ambiguous acid-catalyzed ring opening to a 2,7-disubstituted norbornane (16).

In order to decisively settle the question of structure an X-ray analysis of the *N*-*p*-bromobenzoyl derivative **10** prepared from A was carried out by Dr. Gopalakrishna (17). This determined that A actually had the aziridine structure **5** and hence that the original adduct was the triazoline **3**. Hence rearrangement took place even on ring opening of **5** in basic medium. For similar observations with the norbornylene – benzenesulfonyl azide adduct see refs. 18 and 19.

Structure Proof

The imine **4** was never obtained pure since it hydrated with great ease to **11**. This decomposed on heating or when injected onto g.l.c. columns into urethane and norbornanone. However this imine has been described as a product of thermolysis of **3** (15*b*) and its n.m.r. spectrum reported.

The amino alcohol **9** obtained by hydrolytic opening of the aziridine **7**, derived from **5**, was

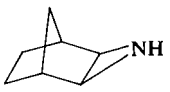

7

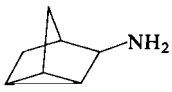

8

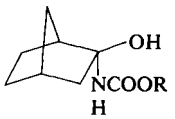

11

characterized as its *N*-benzoyl- (**12***a*) and *N*-benzyloxycarbonyl (**12***b*) derivatives (Scheme 1). The fact that it could be converted into a cyclic carbamate **13** indicated that it was either *syn*-7-amino-2-*exo*-hydroxynorbornane (**9**) or 2-*exo*-amino-3-*exo*-hydroxynorbornane (**16**). In order to establish which structure was correct we undertook independent syntheses of both.

Derivatives of 2-*exo*-amino-3-*exo*-hydroxynorbornane were prepared in three ways (Scheme 2).

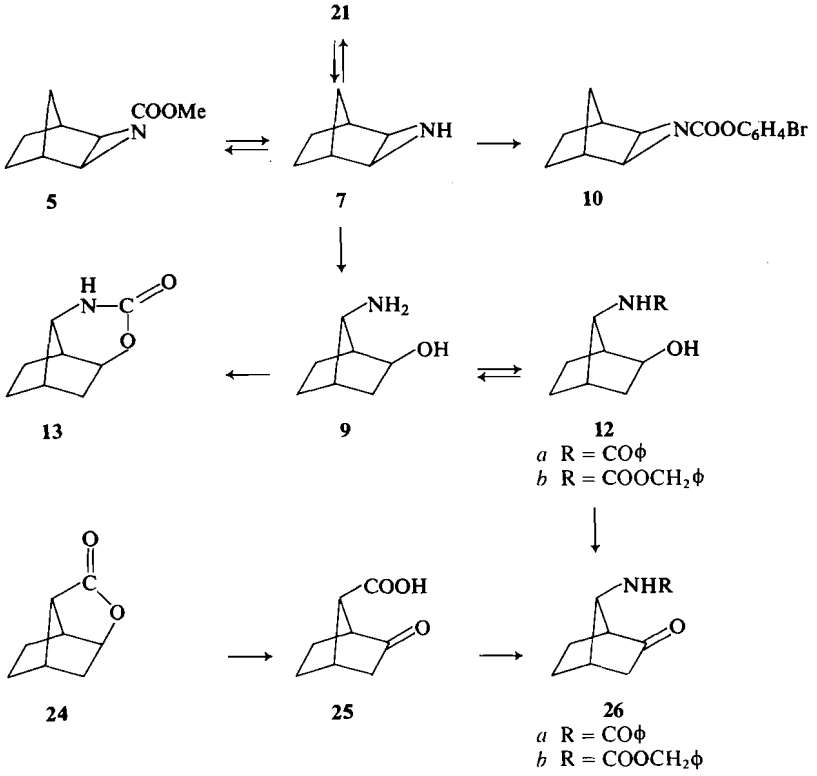

SCHEME 1

(*a*) Following Schechter *et al.* (20), a mixture of 2-*exo*-nitronorbornan-3-ols **14** was prepared by N_2O_4 addition to norbornylene. This was reduced to a mixture of the amino alcohols **15** and **16** which were converted to the *N*-benzyloxycarbonyl derivative **17** and the cyclic carbamate **18**, respectively. Oxidation of **17** gave 3-*exo*-benzyloxycarboxamidonorbornan-2-one (**20***b*).

(*b*) The enol ether of norbornanone **19** was prepared by the action of triphenylmethyl anion on the ketone in the presence of trimethylsilyl chloride. Using the method of Lessard *et al.* (21), chromous chloride catalyzed addition of *N*-chlorobenzylcarbamate to the enol ether was carried out. After mild hydrolysis of the product the *N*-benzoylcarbonyl derivative **20***b* was again obtained in low yield.

(*c*) Huisgen *et al.* (9) had claimed on the basis of n.m.r. evidence that addition of benzoyl azide to norbornylene led with loss of nitrogen to the *N*-benzoylaziridine **21**. On heating, this was reported to give the dihydrooxazoline **22**. We were unable to repeat the reported base-catalyzed hydrolysis of **22**. However acid hydrolysis gave a benzamido alcohol **23**. This could be oxidized to a benzamido ketone **20***a* which was related to the benzyloxycarbamido ketone from routes *a* and *b*. Thus the structural conclusions of Huisgen *et al.* were correct and the *exo*-nitro geometry of **14** was substantiated. Both the cyclic carbamate **18** and the derivatives **20***a* and **20***b* were distinct from the corresponding compounds obtained from **7**, hence the 2,7 disubstituted derivatives were synthesized.

The known lactone (22) of 2-*exo*-hydroxynorbornan-7-*syn*-carboxylic acid **24** was converted via the keto acid **25** into the *N*-benzoyl- (**26***a*) and *N*-benzyloxycarbonyl (**26***b*) derivatives of *syn*-7-aminonorbornan-2-one. These proved identical with the products derived from **7** hence the hydrolytic opening at 170° gives the rearranged amino alcohol **9**. The cyclic carbamate from **9** hence has structure **13**.

A significant product (8%) in the hydrolytic opening of quite pure **7** was characterized as its benzamido derivative. On oxidation this gave a benzamido ketone distinct from either **20***a* or **26***a*. The relatively sharp n.m.r. signal for the

Can. J. Chem. Downloaded from www.nrcresearchpress.com by 210.87.254.40 on 09/05/12
For personal use only.

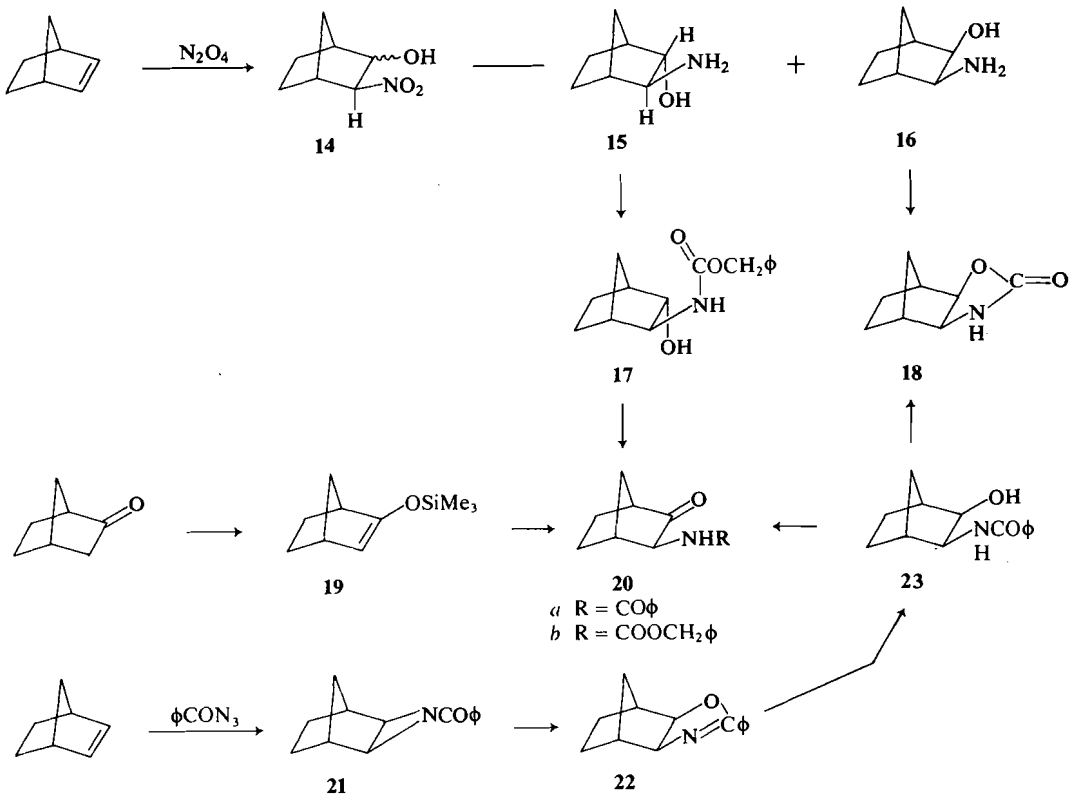

SCHEME 2

proton on the carbon carrying the benzamido group (after D_2O exchange) was consistent with a 7-benzamido function. Therefore the benzamido ketone was apparently **27** and the minor amino alcohol was most probably 7-*anti*-amino-2-*exo*-hydroxynorbornane **28**. This probably arose from small amounts of 2,3-*endo*-aziridine produced in the alcohol-catalyzed decomposition of **3**. (For its formation in thermolysis of **3** see ref. 15*b*.)

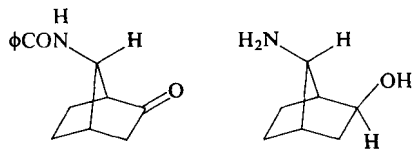

27

28

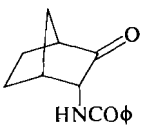

29

A very minor product (1%) encountered in the hydrolytic opening of **7** was characterized as the benzamido alcohol and ketone. It appeared that the ketone had structure **29** (2-*endo*-benzamidonorbornan-3-one) since the 2-hydrogen after exchange of the amide hydrogen using acidic deuterium oxide gave a doublet with J = 5 Hz. This was confirmed by comparison with a sample prepared from 2-*endo*-aminonorbornan-3-one (23). Hence the amino alcohol was 2-*endo*-amino-3-*exo*-hydroxynorbornane derived by hydrolytic opening without rearrangement of the 2,3-*endo*-aziridine.

Photolytic Studies

The direct irradiations were done with lamps with peak emission at 254 nm. The rate of nitrogen evolution from irradiated mixtures of ethyl azidoformate and norbornylene in cyclohexane did not change as the ratio of these changed from 1:1.7 to 1:10. However the amount of attack on solvent giving *N*-cyclohexylurethane decreased sharply with the higher

Can. J. Chem. Downloaded from www.nrcresearchpress.com by 210.87.254.40 on 09/05/12
For personal use only.

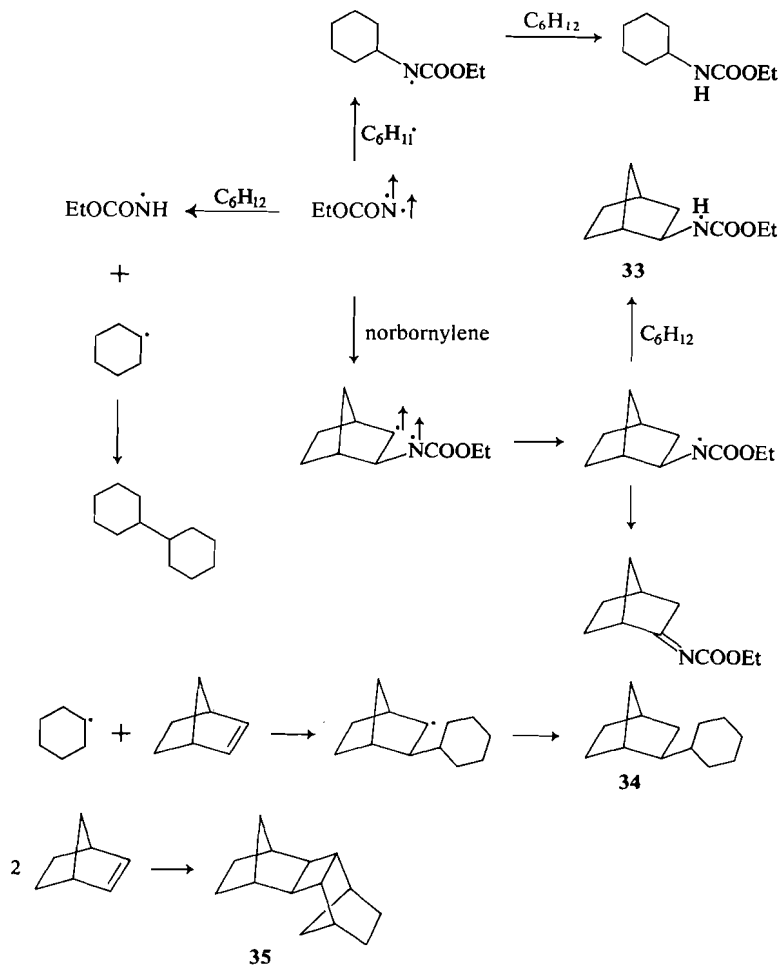

SCHEME 3

olefin concentration. Although cyclohexylurethane certainly arises by singlet nitrene insertion into CH bonds (24), this observation is not inconsistent with a competition between decomposition of excited azide and its addition to the olefin. The major product at higher olefin to azide ratios was the aziridine **5**. Most significantly, no imine **4** was produced. However when the triazolines **3** were irradiated the major products were the aziridine **5** (60–65%) and the imine **4** (20–25%).

None of the characteristic i.r. bands of the triazoline could be detected when a mixture of methyl azidoformate and norbornylene were irradiated. However under comparable conditions the triazoline photolyzed at a similar rate, hence a low steady state concentration could have escaped detection.

Acetophenone-photosensitized decomposition of ethyl azidoformate in the presence of norbornylene, with cyclohexane as solvent, gave an array of products. The ones characterized are shown in Scheme 3. Attempts to obtain photosensitized reaction of the triazoline **3** using energy transfer from acetophenone or benzophenone resulted in very slow reaction, hence where abandoned. This contrasts with the observation of Scheiner with aryl triazolines (11). The products of thermolysis and irradiation experiments are summarized in Table 1.

Discussion

The absence of products of skeletal rearrangement in the thermal or alcohol-catalyzed decomposition of the triazoline **3** means that if the zwitterion **30** is an intermediate it has a very

Can. J. Chem. Downloaded from www.nrcresearchpress.com by 210.87.254.40 on 09/05/12
For personal use only.

TABLE 1. Thermolysis and irradiation results

Compounds	Conditions	Solvent	Products
Triazoline **3** (R = CH_3)	Heat	—	**4** (19%) + **5** (70%)
	hν	Cyclohexane	**4** (20–25%) + **5** (60–65%)
Ethyl azidoformate + Norbornylene	*hν*	Cyclohexane	**5** (59%) + urethane + *N*-cyclohexylurethane (20%)
	Acetophenone photosensitized	Cyclohexane	**4** + **33** + **34** + **35** + dicyclohexyl + *N*-cyclohexylurethane

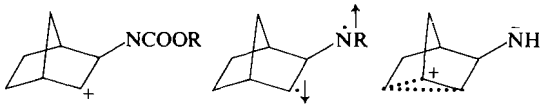

30 **31** **32**

short lifetime. However both the effect of dielectric constant on the rate (15) and the dramatic effect of protic solvents (16) on the decomposition indicate charge development in the transition state (see also ref. 12).

The formation of imine in the triazoline photodecomposition and its absence in the products from irradiation of the azide–olefin mixture excludes the intervention of the triazoline in the latter case (see eq. 1). Hence we conclude that the photoaddition of acyl azides to olefins involves singlet nitrene addition (see also ref. 4), again with a very short lifetime for any zwitterionic intermediate such as **30**.

The photosensitized reaction of azidoformates raises interesting questions. The products in the presence of norbornylene with cyclohexane as solvent clearly derive from nitrogen-centered and carbon-centered radicals. It is tempting to interpret these as arising from the triplet nitrene as illustrated in Scheme 3 (see also ref. 25). However McConaghy and Lwowski (1) have argued that 30% of the alkoxycarbonyl nitrenes produced in direct irradiation of the azidoformates are in the triplet state. If this is correct, we would expect the products shown in Scheme 3 to accompany the products derived from singlet nitrene. However in our direct irradiation studies we were unable to observe these. Thus, either their conclusion is wrong or the photosensitized reaction does not produce triplet nitrene. Indeed, McConaghy and Lwowski have suggested that either triplet excited azide or an excited acetophenone–azide complex is the initial hydrogen-abstracting species (1). If either of these species could abstract one hydrogen and lose nitrogen to give the urethanyl radical EtOCONH, all the products in Scheme 3 could be accounted for. We are unable to settle this question.

Scheiner (11*a*) has suggested that irradiation of triazolines gives C,N-diradicals with antiparallel spins (*e.g.* **31**). If this were so, one might expect to see some radical-type products. However in our direct irradiation of **3** in cyclohexane no dicyclohexyl or 2-alkoxycarboxamidonorbornane were found. Hence if such a diradical is formed it has such a short lifetime that the process is difficult to distinguish from bond reorganization synchronous with nitrogen expulsion.

The products of hydrolytic opening of the 2,3-*exo*-aziridine **7** are interesting. The aziridine was inert in dry dioxane at 170°, hence the water was playing an important role. Since no 2-*exo*-amino-3-*endo*-hydroxynorbornane was produced, the water was not assisting ionization of a C—N bond by back-side displacement. Hence it must accelerate reaction by its dielectric properties. This accords with the production of the rearranged product **9** and the nortricyclylamine. The formation of the latter has parallels in the homoenolate formation from norbornanone (26) and tricyclanone formation on deamination of 2-*exo*-aminonorbornan-3-one (27). We conclude that the aziridine **7** in aqueous dioxane at 170° opens to a zwitterion which before interception by water has the character of the delocalized ion **32**.

Experimental

Infrared spectra were taken in chloroform unless otherwise stated, and n.m.r. spectra are of deuteriochloroform solutions with tetramethylsilane as internal reference. Thin-layer chromatography was done using silica gel with G_{254} fluorescent indicator. Analytic gas liquid chromatography involved a thermal conductivity detector and an OS-138 column (20% polyphenyl ether on dimethylsilylated chromosorb W) with o.d. 0.25 in. and

Can. J. Chem. Downloaded from www.nrcresearchpress.com by 210.87.254.40 on 09/05/12
For personal use only.

Can. J. Chem. Downloaded from www.nrcresearchpress.com by 210.87.254.40 on 09/05/12
For personal use only.

length 6 ft. Preparative separations were done on a similar column 10 ft in length.

Photolyses were conducted in a Rayonet Photochemical Reactor with a cylindrical reflecting chamber and 16 lamps around the periphery.

*3-Ethoxycarbonyl-3,4,5-triazotricyclo[5.2.1.0^{2,6}]dec-4-ene (**3**, R = C_2H_5)*

A mixture of 1.23 g (12 mmol) of ethyl azidoformate and 1.95 g (21 mmol) of norbornylene in 10 ml of cyclohexane was heated in the dark at 75° for 24 h, when the azide had all reacted. The solvent and excess norbornylene were removed under reduced pressure. Since attempts at short-path distillation had resulted in some loss of nitrogen, the product was simply left under 0.1 mm pressure while agitated until the nitrogen analysis remained constant.

Anal. Calcd. for $C_{10}H_{15}N_3O_2$: N, 20.08. Found: N, 20.0.

The n.m.r. spectrum of **3** (R = C_2H_5) contained a triplet at δ 1.4, a broad 2H doublet centered at δ 2.72 (J = 9 Hz), a 1H doublet centered at δ 3.72 (J = 8.5 Hz), 2H quartet centered at 4.41 and a 1H doublet centered at 4.63 (J = 8.5 Hz). It had ν_{max} (cyclohexane) 1765 (med str), 1725 (str), 1527 (med), 1420, 1388, 1353 (str), 1150 cm^{-1} (str).

*3-Methoxycarbonyl-3,4,5-triazotricyclo[5.2.1.0^{2,6}]dec-4-ene (**3**, R = CH_3)*

Using the same molar ratios and concentration as for the ethoxy analog, reaction was much faster. The azide had completely reacted in 5 days at room temperature. After removal of unreacted solvent and norbornylene under reduced pressure the product crystallized. After recrystallization from hexane it had m.p. 35.5–37° (lit. (15*b*) m.p. 35.5°).

Anal. Calcd. for $C_9H_{13}N_3O_2$: C, 55.37; H, 6.71; N, 21.53. Found: C, 55.48; H, 6.88; N, 21.19.

Its n.m.r. spectrum contained a broad 2H doublet centered at δ 2.7 (J = 8.5 Hz), a 1H doublet centered at 3.75 (J = 8.5 Hz), a 3H singlet at 3.96, and a 1H doublet centered at 4.69 (J = 8.5 Hz).

Compound **3** (R = CH_3) had ν_{max} (cyclohexane) 1755 (str sh), 1720 (str), 1520 (med), 1380 (str), 1355 (str sh), 1147 cm^{-1} (str).

*Thermal Decomposition of **3***

When **3** (R = CH_3) was maintained at 85° for 18 h nitrogen evolution was complete. Gas–liquid chromatographic analysis on an OS-138 column showed the presence of aziridine **5** (70%), imine **4** (19%), and two minor peaks totalling 11% of peak areas.

When **3** (R = CH_3) was injected into a gas chromatograph (OS-138 column, injector block at 280°, column at 200°) the ratios of areas of peaks were: **5**, 33%, **4**, 32%, two minor products, 15%.

*Photolysis of **3** (R = CH_3)*

A solution of 375 mg of **3** (R = CH_3) in 10 ml of cyclopentane was irradiated in a Rayonet photoreactor using lamps with peak emission at 254 nm and a Vycor cell. Cooling was by water at 0° and the reaction mixture was protected from i.r. radiation by a water-filled quartz jacket. The theoretical amount of nitrogen was evolved in 3 h. Gas–liquid chromatographic analysis on an OS-138 column showed the major products to be aziridine **5** (60–65%) and imine **4** (20–25%). At least three very minor components were also evident. However no ethyl urethane, *N*-methoxycarbonyl norbornylamine or dicyclohexyl were detected.

*N-Alkoxycarbonyl 3-Azatricylo[3.2.1.1^{2,4}]octane (**5***a* *and b)*

The ethoxycarbonyl derivative (**5***a*) was an oil. Its n.m.r. gave a 1H doublet centered at δ 0.78 (J = 10 Hz), a triplet (—CH_2—CH_3) centered at 1.25, a broad 2H singlet at 2.52, a sharp 2H singlet at 2.59, and a quartet (–CH_2—CH_3) centered at 4.14.

The methoxycarbonyl derivative (**5***b*) was also an oil with ν_{max} (cyclohexane) 1710 (str), 1440 (str), 1380 (med), 1325 (med sh), 1305 (str), 1272 (str), 998 cm^{-1} (med).

*3-Azatricyclo[3.2.1.0^{2,4}]octane **7***

The *N*-alkoxycarbonyl derivative **5** could be hydrolyzed by 5 h refluxing with potassium hydroxide in methanol. The bulk of the methanol was removed under reduced pressure, the residue diluted with water and the base extracted into ether. The oily base gave n.m.r. signals at δ 0.57 (1H singlet), 0.75 (1H singlet), 1.93 (2H singlet), and a broad 2H singlet at 2.30. It was characterized and stored as its picrate, m.p. 123°.

Anal. Calcd. for $C_{13}H_{14}N_4O_7$: C, 46.16; H, 4.17; N, 16.56. Found: C, 45.98; H, 4.33; N, 16.39.

The aziridine was unchanged by heating at 172° for 16 h in dioxane under nitrogen. The base could be reconverted to **5***b* by methyl chloroformate in ether containing triethylamine at −10°. Compound **7** gave an oily *N*-benzoyl derivative **21** when treated with benzoyl chloride in ether containing trimethylamine at −10°. This gave n.m.r. signal between δ 0.7 and 1.9 (6H), a broad 2H peak at 2.58, and a sharp 2H singlet at 2.73 ($w_{1/2}$ 2.3 Hz). Benzyloxycarbonyl chloride in ether the containing triethylamine at 0° converted it to the oily *N*-benzyloxycarbonyl derivative. This gave n.m.r. signals at δ 2.45 (broad, 2H), a 2H peak at 2.59 a sharp 3H singlet at 5.15, and a 5H signal at 7.4.

Anal. Calcd. for $C_{15}H_{17}NO_2$: C, 74.05; H, 7.04; N, 5.76. Found: C, 73.90; H, 6.87; N, 6.01.

The *N-p*-bromobenzoyl derivative **10** was prepared as for the benzoyl derivative. It had m.p. 119–121° after recrystallization from methanol and gave n.m.r. signals at δ 7.83 (quartet-4H), sharp (2H) singlet at 2.80, broad (2H) singlet at 2.63, a series of broad peaks (6H) between 1.85 and 1.1, and a broad 1H doublet centered at 0.90 (J = 10 Hz).

Anal. Calcd. for $C_{14}H_{14}BrNO$: C, 57.54; H, 4.83; Br, 27.39; N, 4.98. Found: C, 57.65; H, 4.93; Br, 27.16; N, 4.98.

This derivative was used for X-ray analysis (17).

*Imine **4***

This compound was isolated by preparative g.l.c. of the reaction mixture from the decomposition of triazoline. Upon reinjection of **4** on g.l.c., it partly decomposed into norcamphor and urethane. From its i.r. spectrum it was obvious that **4** was hydrating very easily to **11** in the presence of moisture. Hence the fraction collected by g.l.c. (31 mg) was dissolved in methylene chloride (5 ml) and shaken with 0.1 *N* HCl (3 ml) for 3 h. The organic phase was separated and to it 2,4-dinitrophenylhydrazine hydrochloride (75 mg) in methanol was added. The

Can. J. Chem. Downloaded from www.nrcresearchpress.com by 210.87.254.40 on 09/05/12
For personal use only.

methylene chloride was evaporated and the methanolic solution left at room temperature to crystallize. The crystals obtained had m.p. 130–132° giving no depression on admixture with the corresponding derivative of norbornanone.

Photosensitized Decomposition of Triazoline 3

A solution of 1.03 g of the methoxycarbonyl triazoline **3** and 2 g of benzophenone in 75 ml of cyclopentane was placed in a Vycor cell. This was surrounded by a Pyrex sleeve and cooled by a cold finger with circulating ice water. The mixture was irradiated while stirred magnetically in the Rayonet apparatus using lamps with peak emission at 350 nm. In this, and a comparable experiment using the ethoxycarbonyl triazoline (2 g) and acetophenone (1.5 g) less than 30% of the theoretical amount of nitrogen was liberated in 3 days. Hence these experiments were abandoned.

Photoaddition of Ethyl Azidoformate to Norbornylene

A mixture of norbornylene (10 g, 0.106 mol) and 1.12 g (10 mmol) of ethyl azidoformate in 50 ml of cyclohexane in a Vycor apparatus with water-cooled central finger was irradiated in a Rayonet photoreactor using lamps with peak emission at 254 nm. After 4 h irradiation at approximately 20 °C the theoretical amount of nitrogen had evolved. The solvent was removed on a rotating evaporator and the residue analyzed by g.l.c. on a OS-138 column. The two main products were cyclohexyl urethane (20%) and aziridine **5** (59%). Ethyl urethane (11%) and seven other minor components were detected. However, no *N*-ethoxycarbonyl norbornylamine (**33**) or dicyclohexyl were detected.

The photolysis was repeated with the same ethyl azidoformate concentration but only 1.7 mmol of norbornylene. The rate of nitrogen evolution was unchanged but the ratio of peak areas of aziridine **5** to cyclohexyl urethane was now 1:1.

Acetophenone-photosensitized Decomposition of Ethyl Azidoformate

A mixture of 1 g (1 mmol) of ethyl azidoformate, 7.1 g (1.2 mmol) of norbornylene and 1.82 g (1.5 mmol) of acetophenone in 80 ml of cyclohexane was irradiated in a Pyrex vessel using a Rayonet photoreactor with lamps with peak emission at 350 nm. In 48 h gas evolution had stopped after 92% of the theoretical amount of nitrogen had been collected. Neither direct irradiation nor heating of the product resulted in evolution of more nitrogen. After removal of the solvent the residue was partially separated on a column of alumina (25-fold, activity II). Pentane eluted a mixture of dicyclohexyl, 2-cyclohexylnorbornane (**34**), norbornylene dimer (**35**), and acetophenone. Ether eluted a mixture of ethyl urethane, norbornanone, and acetophenone, followed by *N*-ethoxycarbonyl cyclohexylamine, then *N*-ethoxycarbonyl norbornylamine **33**. The pentane eluate was further separated by chromatography on a 25-fold ratio of alumina, activity I. The early eluates contained the hydrocarbon products almost free of acetophenone.

N-Ethoxycarbonyl-2-exo-norbornylamine 33

This was an oil with ν_{max} 3445 and 1705 cm^{-1}. Its ^1H n.m.r. spectrum had a triplet centered at δ 1.23 (CH_2CH_3), a broad 2H singlet centered at 2.22 (bridgehead hydrogens), a 6-line multiplet centered at 3.50 which collapsed to a 4-line signal on D_2O – *p*-toluenesulfonic acid exchange, a quartet centered at 4.12 (CH_2CH_3), and a broad singlet (NH) at 4.5. Its mass spectrum had peaks at *m/e* 79, 82, 90, 93, 94, 95, 102, 110, 115, 128, 154, 168, and 183 (M^+).

Anal. Calcd. for $C_{10}H_{17}NO_2$: C, 65.54; H, 9.35; N, 7.64. Found: C, 65.71; H, 9.27; N, 7.56.

It proved identical (i.r., ^1H n.m.r.) to an authentic specimen prepared from 2-*exo*-norbornylamine.

2-Cyclohexylnorbornane 34

This had ν_{max} 1453 cm^{-1} and its n.m.r. spectrum contained a broad peak (2H) centered at δ 2.18. Its mass spectrum at 10 eV had peaks at *m/e* 67, 81, 82, 95, 96, 109, 121, 122, 135, 149, and 178 (M^+).

Anal. Calcd. for $C_{13}H_{22}$: C, 87.56; H, 12.44. Found: C, 87.45; H, 12.30.

Norbornylene Dimer 35

This hydrocarbon from the photosensitized reaction had ν_{max} 1482, 1458, 1270, and 1190 cm^{-1}. Its n.m.r. spectrum contained a broad (2H) peak centered at δ 2.22, and its mass spectrum had peaks at *m/e* 79, 80, 81, 105, 159, and 188 (M^+).

Hydrolysis of 7

The aziridine 7 (2.5 g) in dioxane–water (60 ml) (1:2, v/v) was sealed under N_2 in a pressure tube and heated at 180° for 16 h. The tube was cooled, opened, the reaction mixture adjusted to p*H* 6, and evaporated to near dryness. The residue was suspended in water and made basic with potassium carbonate (12 g). The reaction was then kept at 0° while a solution of benzoyl chloride (10 g) in 15 ml of dioxane was added dropwise. After vigorous stirring for 16 h the mixture was diluted with water, the volume reduced by half to eliminate the dioxane, then the basic aqueous solution extracted with ether. The ether contained 4.6 g of viscous benzoate and dibenzoate mixture.

This mixture was separated by chromatography on activity I neutral alumina (32×). The readily eluted products (ether) were partially hydrolyzed to give a mixture of the hydroxybenzamide **12***a* and *N*-benzoyl nortricyclylamine. This mixture was separated on activity II neutral alumina (30×).

The more strongly adsorbed products from the first chromatogram proved to be a mixture of **12***a* and two minor components, which also analyzed for monobenzoates, in yields of 8 and 1%. The components could be separated by very careful rechromatography on a 40-fold ratio of alumina activity II. It was found more convenient to partially separate the components on alumina, then separate each main fraction using high pressure liquid chromatography (Waters Associates) on a Porasil A column, length 4 ft diameter 0.375 in. and elution with 2% MeOH–$CHCl_3$ (4 ml/min). In this way very pure samples of the three hydroxybenzamides were obtained.

The total yield of 7-*syn*-benzamido-3-*exo*-hydroxynorbornane was 81% and of *N*-benzoyl nortricyclylamine was 8%.

7-syn-Benzamido-2-exo-benzoyloxynorbornane

When recrystallized from benzene this had m.p. 151–152 °C and ν_{max} 3460 (med), 1720 (str), 1660 (str), 1607 (wk), 1583 (wk), and 1520 cm^{-1} (str). Its n.m.r. spectrum contained a complex set of signals (6H) between δ 1.0

Can. J. Chem. Downloaded from www.nrcresearchpress.com by 210.87.254.40 on 09/05/12
For personal use only.

and 2.3, a broad 2H singlet at 2.64, a broad 1H doublet at 4.35, a broad 1H multiplet at 5.26, and a series of peaks (10H) between 7.1 and 8.4.

Anal. Calcd. for $C_{21}H_{21}NO_3$: C, 75.20; H, 6.31; N, 4.18. Found: C, 75.25; H, 6.45; N, 3.83.

7-syn-Benzamido-2-exo-hydroxynorbornane ***12a***

This was recrystallized from acetone–hexane, m.p. 144–145°, yield, 81%. It had ν_{max} 3590 (wk), 3380 (med), 1640 (str), 1580 (med), 1530 (str), 1490 (med), 1183 (med), 1145 (wk), 1110 (wk), 970 cm^{-1} (wk). Its n.m.r. spectrum had two fairly sharp singlets at δ 0.967 and 1.10, a broad 1H singlet at 2.19, a broad 1H singlet at 2.42, a broad 2H multiplet centered at 4.12, a broad 1H (—O*H*) singlet at 4.82, a set of signals between 7.2 and 8.1 (5H), and a broad 1H (—N*H*) doublet centered at 8.45.

Anal. Calcd. for $C_{14}H_{17}NO_2$; C, 72.70; H, 7.41; N, 6.06. Found: C, 72.43; H, 7.29; N, 5.95.

7-syn-Benzamidonorbornane-2-one ***26a***

When recrystallized from methanol this melted at 200°. It had ν_{max} 3360 (med), 3420 (med), 1740 (str), 1660 (str), 1300 (wk), 1275 cm^{-1} (wk). Its n.m.r. spectrum had a series of peaks (6H) between δ 1.3 and 2.5, three broad 1H singlets at 2.74, 3.02, and 4.25, a broad (1H, —N*H*) multiplet at 6.75, and a series of peaks (5H) between 7.25 and 8.15.

Anal. Calcd. for $C_{14}H_{15}NO_2$: C, 73.34; H, 6.59; N, 6.11. Found: C, 73.07; H, 6.69; N, 6.37.

Cyclic Carbamate ***13***

A solution of 7-*syn*-amino-2-*exo*-hydroxynorbornane **9** (270 mg) in benzene (5 ml) and triethylamine (300 mg) was prepared. The solution was cooled to 0° and ethyl chloroformate (900 mg) was added slowly while stirring. The reaction was then left overnight at room temperature. The precipitate was filtered and the filtrate reduced to a syrup (392 mg). This was dissolved in ethanol and stirred vigorously with potassium carbonate (1 g) for 5 h at room temperature to hydrolyze the 2-ethoxycarbonyl function. The mixture was then diluted with water, evaporated to remove the alcohol, the aqueous solution extracted with methylene chloride, dried, and evaporated to dryness. The resulting hydroxy carbamate (340 mg) was dissolved in dioxane (15 ml), sodium hydride (300 mg) was added, and the mixture was refluxed overnight. The mixture was then evaporated to dryness and the solid residue (190 mg) carefully washed with benzene. When recrystallized from ethyl acetate – methanol the product had m.p. 165–166°; mol wt. 158 (osmometry). It had ν_{max} 3450 (wk), 3250 (wk), 3120 (wk), 1710 (str), 1363 (wk), 1133 (med), 1095 (med), 1040 (wk), 1024 (med), 1004 (wk), 985 (wk), 970 (wk) 952 cm^{-1} (wk). Its n.m.r. spectrum had a series of peaks (8H) between δ 0.8 and 3.2, a broad 1H singlet at 3.37, a broad 1H doublet (J = 5 Hz) at 4.34, and a broad (1H, –N*H*) singlet at 7.04.

Anal. Calcd. for $C_8H_{11}NO_2$: C, 62.72; H, 7.24; N, 9.14. Found: C, 62.66; H, 7.25; N, 9.14.

The cyclic carbamate could be reconverted to the original hydroxybenzamide.

7-anti-Benzamido-2-exo-hydroxynorbornane

This was sublimed at 120°/10^{-2} mm, m.p. 158–159°, yield 8%. It had ν_{max} 3500 (wk), 3410 (wk), 1675 (str), 1578 (med), 1515 (wk), 1485 (wk), 1445 (wk), 1372 cm^{-1} (med str). Its n.m.r. spectrum had a 2H singlet at δ 2.40 and a 1H singlet at 2.46 which exchanged with D_2O, a broad 1H multiplet at 3.86, a broad 1H doublet collapsing to a broad singlet on D_2O exchange and becoming a sharp singlet at 4.33 when exchanged with D_2O–H^+, and a series of peaks (5H) between 7.1 and δ 7.9.

Anal. Calcd. for $C_{14}H_{17}NO_2$: C, 72.70; H, 7.41; N, 6.06. Found: C, 72.81; H, 7.53; N, 6.10.

2-exo-Acetoxy-7-anti-benzamidonorbornane

This derivative was recrystallized from methanol–pentane, m.p. 113–115°. It had ν_{max} 3440 (wk), 1720 (str), 1655 (str), 1580 (wk), 1450 (med), 1420 (str), 1250 (str), 1070 (med), 1015 cm^{-1} (wk). Its n.m.r. had a series of peaks (6H) between δ 1.0 and 1.9, a sharp 3H singlet (O—CH_3) at 1.96, a broad 2H singlet at 2.35, a broad 1H doublet at 4.21 collapsing to a singlet on D_2O acid exchange, a broad 1H multiplet at 4.57, a broad 1H doublet (—N*H*) at 6.14, and a series of peaks (5H) between 7.1 and 7.9.

7-anti-Benzamidonorbornane-2-one ***27***

This compound was sublimed at 110°/10^{-2} mm, m.p. 150–152°. It had ν_{max} 3440 (wk), 3330 (wk), 1745 (str), 1660 (str), 1602 (wk), 1580 (wk), 1510 (str), 1485 (str), 1300 (med), 1270 (med str), 1165 (med str), 1070 cm^{-1} (med). Its n.m.r. spectrum had a broad singlet (2H) at δ 2.77, a broad doublet (1H) at 4.22, collapsing to a sharp singlet after exchange with D_2O–H^+, a broad 1H doublet (—N*H*) at 6.55, and a series of peaks (5H) between 7.1 and 7.9.

Anal. Calcd. for $C_{14}H_{15}NO_2$: C, 73.34; H, 6.59; N, 6.11. Found: C, 73.35; H, 6.74; N, 6.16.

2-endo-Benzamido-3-hydroxynorbornane

After sublimation at ~130°/10^{-2} mm this had m.p. 184–185°. It had ν_{max} 3600 (v wk), 3520 (wk sh), 3450 (med), 1650 (str), 1605 (wk), 1580 (med str), 1510 (str), 1485 (str), 1310 (wk), 1290 (med), 1012 cm^{-1} (med).

Anal. Calcd. for $C_{14}H_{17}NO_2$: C, 72.70; H, 7.41; N, 6.06. Found: C, 72.54; H, 7.37; N, 6.01.

2-endo-Benzamidonorbornane-3-one ***29***

After sublimation at 110–112°/10^{-2} mm this had m.p. 170–171°. It had ν_{max} 3420 (wk), 1750 (str), 1645 (str), 1605 (wk), 1585 (wk), 1525 (str), 1475 (str), 1340 (v wk), 1320 (v wk), 1305 (wk), 1298 (wk), 1275 (wk), 1160 (v wk), 1140 (v wk), 1080 cm^{-1} (med). Its n.m.r. spectrum had a broad 1H singlet at δ 2.72, a broad 1H singlet at 3.14, a 1H triplet centered at 4.24 which collapses to a doublet (J = 5 Hz) on exchange with D_2O–H^+, a broad 1H singlet (—N*H*) at 6.51, and a series of peaks (5H) between 7.1 and 8.0.

Anal. Calcd. for $C_{14}H_{15}NO_2$: C, 73.34; H, 6.59; N, 6.11. Found: C, 73.51; H, 6.67; N, 6.13.

Compound **29** proved identical (mixed m.p., mass spectrum, and i.r. spectrum) with a sample prepared in low yield by benzoylation of authentic 2-*endo*-amino-norbornan-3-one (21).

Nortricyclylamine Derivatives

The *O*-methyl oxime of nortricyclanone (4 g) was dissolved in dioxane (50 ml) and while cooling and stirring, $LiAlH_4$ (2 g) was added in small portions. After the addition was completed, the mixture was left at room temperature for 15 min and then refluxed for 1 h. After

Can. J. Chem. Downloaded from www.nrcresearchpress.com by 210.87.254.40 on 09/05/12
For personal use only.

that time, it was cooled, methanol was added carefully followed by a saturated Na_2SO_4 solution. The precipitate was filtered, the filtrate acidified to congo red using perchloric acid, then evaporated to dryness. The residue crystallized from MeOH, m.p. 204–206°.

Anal. Calcd. for $C_7H_{12}ClNO_4$: C, 40.02; H, 5.77; N, 6.69. Found: C, 39.74; H, 5.86; N, 6.72.

The *N*-benzoyl derivative was prepared. This crystallized from methanol – ethyl acetate, m.p. 150–151°. Its n.m.r. had a sharp 3H singlet at δ 1.25, a broad 1H singlet at 2.20, a broad (1H–C_3) doublet centered at 4.07 which collapses to a singlet upon exchange of the —NH (δ 6.32) with D_2O–acid, and aromatic protons (5H) centered at 7.75. It has ν_{max} 3445 (wk), 1655 (str), 1510 (str), 1485 cm^{-1} (str).

Anal. Calcd. for $C_{14}H_{15}NO$: C, 78.84; H, 7.09; N, 6.57. Found: C, 78.98; H, 7.06; N, 6.66.

Stability of Nortricyclylamine

The amine was treated under the same conditions as for the aziridine ring opening. The recovered base was benzoylated giving a quantitative recovery of *N*-benzoyl amine.

*2-exo-Amino-3-hydroxynorbornanes **15** and **16***

Addition of dinitrogen tetroxide in ether at −5° to norbornene following Shechter *et al.* (20), followed by overnight hydrolysis by stirring with aqueous sodium bicarbonate gave a mixture of dinitro compound and nitro alcohols. The water solution of the nitro alcohols was extracted with ether in a continuous extractor. A mixture of the nitro alcohols (6.2 g) was reduced in acetic acid by hydrogen over platinum (from 180 mg PtO_2) during 36 h. Work-up gave 5.9 g of a crystalline mixture of amino alcohols **15** and **16**.

*2-exo-Benzyloxycarboxamido-3-endo-hydroxynorbornane **17***

A mixture of the amino alcohols **15** and **16** (5.9 g) in 40 ml of 1:1 dioxane–water containing 5 g of sodium hydroxide was stirred vigorously overnight with 3 ml of benzyl chloroformate. The product was extracted into ether, then the ether washed with water, dried, and distilled. Chromatography on a 25-fold ratio of alumina (activity III) and elution with progressively increasing percentages of benzene in hexane gave benzyl alcohol, the hydroxyurethane **17** as an oil, followed by the cyclic carbamate **18**. The hydroxyurethane was distilled at a bath temperature of 105–125°/0.03 mm.

Anal. Calcd. for $C_{15}H_{19}NO_3$: C, 68.94; H, 7.33; N, 5.36. Found: C, 69.12; H, 7.49; N, 5.46.

*2-exo-Benzyloxycarboxamidonorbornan-3-one **20b***

Jones' reagent (28) (2.5 ml) was added slowly to a solution of 2-*exo*-benzyloxycarbonamido-3-*endo*-hydroxynorbornane **17** in 50 ml of acetone at 0°. After 30 min stirring at 0° the excess oxidizing agent was reduced with methanol. The bulk of the acetone was removed under reduced pressure, water added, and the product extracted into ether. The 760 mg of crystalline product was sublimed *in vacuo* then recrystallized from hexane. It was dimorphic, m.p. 104–107° (blades) and 110–112° (needles). It had ν_{max} 3430 (—NH) (med), 1758 (str), 1725 (str), 1505 (str), 1250 (str), 1060 cm^{-1} (med), and its n.m.r. spectrum had a series of signals (6H) between δ 2.10 and 1.25, a broad 2H multiplet at 2.6 (bridgehead hydrogens), a broad 1H quartet at 3.55 collapsing to a doublet (J = 2.8 Hz) after exchange with D_2O–HCl, a sharp (2H, —O—CH_2—φ) singlet at 5.08, a broad (1H, N—*H*) doublet at 5.32 collapsing to a broad singlet upon exchange with D_2O–HCl, and a sharp (5H, C_6H_5) singlet at 7.29.

Anal. Calcd. for $C_{15}H_{17}NO_3$: C, 69.48; H, 6.61; N, 5.40. Found: C, 69.47; H, 6.67; N, 5.50.

*Cyclic Carbamate **18***

2-Benzamido-3-hydroxynorbornane **23** (512 mg) and 0.5 g of potassium hydroxide were dissolved in 10 ml of methanol. The solution was refluxed under nitrogen for 16 h, cooled, acidified using hydrochloric acid, then evaporated to small volume. The residue was diluted with water and extracted with methylene chloride to remove unchanged amide. The aqueous layer was made alkaline with a large excess of potassium carbonate, then benzyloxycarbonyl chloride (1 g) added dropwise with vigorous stirring. Stirring was continued for 2 h, then the product extracted into methylene chloride, and recrystallized from *n*-hexane–$CHCl_3$ to give m.p. 136–137°. It had ν_{max} ($CHCl_3$) 3465 (med), 3260 (wk), 1745 (str), 1140 (wk), 1050 cm^{-1} (med). Its n.m.r. spectrum had a series of peaks (6H) between δ 0.9 and 2.0, a broad 1H singlet at 2.25, a broad 1H singlet at 2.46, a pair of 1H doublets (J = 7 Hz) at 3.68 (C-3) and 4.50 (C-2), and a broad (1H, N*H*) singlet at 6.88.

Anal. Calcd. for $C_8H_{11}O_2N$: C, 62.72; H, 7.24; N, 9.14. Found: C, 62.62; H, 7.19; N, 9.04.

This proved identical to the readily eluted product from the carbobenzoxylation of the mixture of **15** and **16**.

*1-Trimethylsilyloxynorbornene **19***

A solution of 2.5 g of norbornan-2-one in ether at 0° was added slowly with stirring under nitrogen to a suspension of potassium triphenylmethide in ether until the red color disappeared. Fresh salt and ketone were added until the norbornanone had been converted to enolate. Then 5.5 ml of trimethylsilyl chloride was added dropwise during 10 min at 0°. After 30 min of stirring the mixture was filtered under nitrogen pressure, the ether distilled then the product distilled in a chain of bulbs at 80°/0.3 mm, giving 4.13 g (77%) of the trimethylsilyl ether. Its n.m.r. spectrum contained a sharp 9H singlet at δ 0.11, a broad 1H singlet at 2.45, a broad 1H singlet at 2.67, and 1H doublet (J = 3.2 Hz) centered at 4.55.

Anal. Calcd. for $C_{10}H_{18}OSi$: C, 65.88; H, 9.93. Found: C, 66.03; H, 9.86.

*Conversion of **19** into **20b***

A solution of 365 mg (2 mmol) of **19** and 742 mg (4 mmol) of *N*-chlorobenzylcarbamate in 5 ml of chloroform was cooled to −78° in a carbon dioxide atmosphere. A methanol solution of 8 mmol of chromous chloride, which had been stirred with powdered calcium carbonate, was added to this under carbon dioxide during 1 h at −78°. The reaction mixture was stirred for an additional 10 min in the cold, allowed to warm to room temperature, then diluted with water. The products were extracted into methylene chloride, then separated on preparative thin-layer plates developing with 1:2 ether–hexane mixture. The 58 mg of crude **20b** after recrystallization had m.p. 108–110° and proved identical by mixture m.p. and comparison of n.m.r. spectra with the product of oxidation of **17**.

Can. J. Chem. Downloaded from www.nrcresearchpress.com by 210.87.254.40 on 09/05/12
For personal use only.

7-Benzyloxycarboxamidonorbornan-2-one 26b

Following Beckmann and Geiger (22) the lactone **24** was converted to the keto acid **25** m.p. 121–122°. This (427 mg) was converted to its sodium salt which was carefully dried, suspended in 10 ml of hexane, and converted to the acid chloride by cautious addition of 0.5 ml oxalyl chloride in hexane. The solvent and excess oxalyl chloride were removed under reduced pressure then the acid chloride distilled over a short path at 110°/10 mm. It gave a single sharp peak on g.l.c. analysis on an SE-30 column.

The acid chloride (178 mg) was dissolved in dry acetone, then added with vigorous stirring to an ice-cold solution of 1 g of sodium azide in 5 ml of water. After 2 h stirring at 0° sodium carbonate was added and the product extracted into pentane. After evaporation of the pentane below room temperature, 80 mg of acyl azide remained. This was dissolved in 2 ml of benzyl alcohol and heated at 100° for 1 h. After removal of the benzyl alcohol *in vacuo* the 7-benzyloxycarbonyl derivative **26b** had n.m.r. and i.r. spectra identical to those of the benzyloxycarboxamido ketone prepared from **9** via **12b**.

2-exo-Benzamido-3-exo-hydroxynorbornane 23

Following Huisgen *et al.* (9), the *N*-benzoyl aziridine **21** was prepared from norbornylene and benzoyl azide. This rearranged in 20 min at 240° under nitrogen into the previously described Δ^2-oxazoline **22**. Alkaline hydrolysis (KOH in refluxing methanol; see however ref. 9) failed to open this. The Δ^2-oxazoline (14.6 g) in 50 ml of 2 *N* sulfuric acid was refluxed for 4 h. The solution was diluted with 100 ml of water and extracted with methylene chloride, giving 3.7 g of starting material. The aqueous solution was basified using potassium hydroxide then extracted with chloroform. The benzamido alcohol **23** recovered from this (11 g) after recrystallization from ethyl acetate had m.p. 114–115° (lit. (9) m.p. 114.5°). It had ν_{max} 3600, 3410, and 1640 cm^{-1} and gave n.m.r. signals at δ 2.32 (broad 2H doublet) and a 2H triplet (?) centered at 3.9.

2-exo-Benzamidonorbornan-3-one 20a

An acetone solution (10 ml) of 1.3 g of the benzamido alcohol **23** was cooled to 0°. Jones' reagent (28) was added dropwise with stirring at 0° until excess oxidant persisted for 15 min. The reaction mixture was evaporated under reduced pressure, the residue taken up in water, and the solid product collected by filtration. The 1.02 g of solid, m.p. 180° was recrystallized from methanol–chloroform mixtures to give 453 mg, m.p. 209–211°. It had ν_{max} 3280, 1755, and 1635 cm^{-1}.

Anal. Calcd. for $C_{14}H_{15}NO_2$: C, 73.34; H, 6.59; N, 6.11. Found: C, 73.20; H, 6.71; N, 5.97.

2-exo-Amino-3-exo-hydroxynorbornane 16

This was prepared by hydrolysis of hydroxybenzamide **23** with sodium hydroxide in aqueous methanol at 160°. The free base had m.p. 93.5–94° after sublimation *in vacuo*.

Anal. Calcd. for $C_7H_{13}NO$: C, 66.10; H, 10.30; N, 11.01. Found: C, 65.99; H, 10.48; N, 10.89.

Its hydrochloride after recrystallization from methanol – ethyl acetate had m.p. 242°.

Anal. Calcd. for $C_7H_{14}ClNO$: C, 51.37; H, 8.56; N, 8.63. Found: C, 51.54; H, 8.49; N, 8.63.

1. J. S. McConaghy and W. Lwowski. J. Am. Chem. Soc. **89**, 2357, 4450 (1967).
2. J. F. W. Keana, S. B. Keana, and D. Beetham. J. Org. Chem. **32**, 3057 (1967).
3. I. Brown and O. E. Edwards. Can. J. Chem. **43**, 1266 (1965).
4. I. Brown, O. E. Edwards, J. M. McIntosh, and D. Vocelle. Can. J. Chem. **47**, 2751 (1969).
5. N. C. Castelluci, M. Kato, H. Zendra, and S. Masamune. Chem. Commun. 473 (1967).
6. R. Fusco, G. Bianchetti, and D. Pocar. Gazz. Chim. Ital. **91**, 849, 933 (1961).
7. R. Huisgen. Angew. Chem. **72**, 359 (1960).
8. M. Lesage. Unpublished work.
9. R. Huisgen, L. Möbius, G. Müller, H. Stangl, G. Szeimies, and J. R. Vernon. Chem. Ber. **98**, 3992 (1965).
10. R. S. McDaniel and A. C. Oehlschlager. Tetrahedron, **25**, 1381 (1969).
11. (*a*) P. Scheiner. J. Am. Chem. Soc. **90**, 988 (1968); (*b*) Tetrahedron, **24**, 2757 (1968).
12. J. D. Hobson and J. R. Malpass. J. Chem. Soc. C, 1935 (1970).
13. R. J. Steadman, A. C. Swift, and J. R. E. Hoover. Tetrahedron Lett. 2525 (1965).
14. P. Scheiner. J. Org. Chem. **30**, 7 (1965).
15. (*a*) A. C. Oehlschlager, P. Tillman, and L. H. Zalkow. Chem. Commun. 596 (1965); (*b*) A. C. Oehlschlager, R. S. McDaniel, A. Thakore, P. Tillman, and L. H. Zalkow. Can. J. Chem. **47**, 4368 (1969).
16. H. Tanida, T. Tsuji, and T. Irie. J. Org. Chem. **31**, 3941 (1966).
17. E. M. Gopalakrishna. Acta Crystallogr. **B28**, 2754 (1972).
18. J. E. Franz, C. Osuch, and M. W. Dietrich. J. Org. Chem. **29**, 2922 (1964).
19. L. H. Zalkow and A. C. Oehlschlager. J. Org. Chem. **28**, 3303 (1963). L. H. Zalkow, A. C. Oehlschlager, G. A. Cabat, and R. L. Hale. Chem. Ind. (London) 1556 (1964).
20. H. Shechter, J. J. Gardikes, T. S. Cantrell, and G. V. D. Tiers. J. Am. Chem. Soc. **89**, 3005 (1967).
21. J. Lessard, H. Driguez, and J. P. Vermes. Tetrahedron Lett. 4887 (1970).
22. S. Beckman and H. Geiger. Chem. Ber. **94**, 48 (1961).
23. K. Hohenlohe-Oehringen. Montash. Chemie, **101**, 614 (1970).
24. W. Lwowski (Editor). Nitrenes. Interscience Publishers, New York. 1970. pp. 199–206, 238–242.
25. I. Brown and O. E. Edwards. Can. J. Chem. **45**, 2599 (1967).
26. A. Nickon and J. L. Lambert. J. Am. Chem. Soc. **88**, 1905 (1966).
27. O. E. Edwards, J. W. Elder, M. Lesage, and R. W. Retallack. In preparation.
28. K. Bowden, I. M. Heilbron, E. R. H. Jones, and B. C. L. Weedon. J. Chem. Soc. 39 (1946).

A Carbon-13 Nuclear Magnetic Resonance Study of Chlorinated and Polyol Analogs of Glucose and Related Oligomers[1]

PIERRE COLSON,[2] KEITH N. SLESSOR,[3] H. J. JENNINGS, AND IAN C. P. SMITH
Division of Biological Sciences, National Research Council of Canada, Ottawa, Canada K1A 0R6
Received September 16, 1974

PIERRE COLSON, KEITH N. SLESSOR, H. J. JENNINGS, and IAN C. P. SMITH. Can. J. Chem. **53**, 1030 (1975).

Complete assignments of the carbon-13 n.m.r. spectra of the following compounds in aqueous solution are presented: 6-chloro-6-deoxy-D-glucose, 6-*O*-methyl-D-glucose, ribitol, glucitol, 4-*O*-methyl-glucitol, maltose, maltitol, 6,6′-dichloro-6,6′-dideoxymaltose, 6′-chloro-6′-deoxymaltose, isomaltose, isomaltitol, and 6′-chloro-6′-deoxyisomaltose. Some earlier assignments for maltose are reversed. Chlorination on the exocyclic carbon of the glucopyranose ring usually results in a substantial decrease in the chemical shift of the substituted carbon (−17 p.p.m.) and the next-nearest carbon (−1.2 p.p.m.); methylation leads to an increased chemical shift for the contiguous carbon (+10 p.p.m.) and only small changes for other carbons in the molecule. The response to 4-*O*-methylation in glucitol is opposite for C-3 (+0.7 p.p.m.) and C-5 (−0.8 p.p.m.) demonstrating that response of a particular carbon to substitution at a neighboring carbon depends upon the configuration of the particular carbon. Dissolution of these compounds in pyridine results in a bunching together of resonances which makes unambiguous assignments very difficult. The data for this series of compounds are useful in assigning the more complex spectra of microbial polysaccharides.

PIERRE COLSON, KEITH N. SLESSOR, H. J. JENNINGS et IAN C. P. SMITH. Can. J. Chem. **53**, 1030 (1975).

Nous présentons l'attribution complète des spectres de résonance magnétique nucléaire en carbone-13 des composés suivants étudiés en solution aqueuse: 6-chloro-6-désoxy-D-glucose, 6-*O*-methyl-D-glucose, ribitol, glucitol, maltose, maltitol, 6,6′-dichloro-6,6′-didésoxymaltose, 6′-chloro-6′-désoxymaltose, isomaltose, isomaltitol et 6′-chloro-6′-désoxyisomaltose. Certaines attributions antérieures du maltose sont inversées. La chloruration du carbone exocyclique de l'anneau glucopyranose conduit généralement à une diminution importante du déplacement chimique du carbone substitué (−17 p.p.m.) et de son voisin le plus proche (−1.2 p.p.m.); par contre, la méthylation provoque une augmentation importante du déplacement chimique du carbone substitué (+10 p.p.m.) sans influencer de façon notoire les autres carbones de la molécule. La méthylation en position 4 du glucitol est différemment ressentie par les carbones adjacents (C-3, +0.7 p.p.m.; C-5, −0.8 p.p.m.). Ceci démontre que la stéréochimie des carbones adjacents à un carbone substitué peut différencier leur comportement lors d'une substitution. La mise en solution de ces composés dans la pyridine conduit à un resserrement des résonances et l'attribution de certaines d'entre elles reste ambiguë. Les données de cette série de composés sont utiles pour attribuer les spectres plus complexes de polysaccharides microbiens.

Introduction

Simple carbohydrates have been studied extensively by ^{13}C n.m.r. (1). Numerous investigations have been devoted to glucose and related compounds (2–14) and to complex carbohydrates containing these residues (15–20). Nearly all the resonances of glucose have been resolved and assigned, particularly by the study of the influence of *O*-methylation (5–7, 10–12), *O*-acetylation (6, 10), and deuterium incorporation (2, 12, 13). Cyclic and acylic polyol spectra have also been assigned (14, 21–22). Recently, the influence of methylation on the ^{13}C chemical shifts of galactose derivatives and galactitols has been reported (23–24).

We describe here the usefulness of chlorinated and polyol derivatives of glucose and related disaccharides in the assignment process. The correlations deduced here can be used to resolve difficult assignments and related problems of other carbohydrates, such as sialic acid, which is composed of a cyclic sugar and an acyclic

[1]NRCC No. 14426.

[2]NATO Postdoctoral Fellow, 1973–1974. Permanent address: Laboratoire de Biochimie, Faculté des Sciences, Université de Liège, Sart-Tilman, B-4000-Liège (Belgium).

[3]Department of Chemistry, Simon Fraser University, Burnaby, British Columbia V5A 1S6.

Can. J. Chem. Downloaded from www.nrcresearchpress.com by 210.87.254.105 on 09/05/12
For personal use only.

Can. J. Chem. Downloaded from www.nrcresearchpress.com by 210.87.254.105 on 09/05/12
For personal use only.

polyol (20) and polymers containing glycerol side chains.

Experimental

Nuclear magnetic resonance spectra were obtained on a Varian XL-100-15 (sample tubes of outside diameter 12-mm, 32°) or a Varian CFT-20 (10-mm tubes, 30°) spectrometer with complete proton decoupling. Chemical shifts were measured relative to tetramethylsilane in a sealed concentric tube of outside diameter 5 mm and are expressed as increasingly positive with increasing frequency (decreasing field) from the resonance of Me_4Si. Differences in susceptibility correction between the 12- and 10-mm tubes were less than the experimental accuracy of 0.1 p.p.m. and were neglected. Carbohydrate samples were 100 mg/ml in neutral deuterium oxide.

Paper chromatographic analysis was carried out on Whatman No. 1 filter paper using the following solvent system: butan-1-ol, pyridine, water (6:4:3, v/v) and the mobilities of the components are given relative to that of D-glucose (R_{Glc} 1.0).

4-*O*-Methyl-D-glucose was prepared by the method of Kenner and Richards (25) and 6-*O*-methyl-D-glucose by the hydrolysis of 6-*O*-methyl-α-D-glucopyranoside (26). 4-*O*-Methyl-D-glucitol was prepared by the sodium borohydride reduction of 4-*O*-methyl-D-glucose.

Maltose and isomaltose were commercial samples used without further purification and maltitol and isomaltitol were obtained by the sodium borohydride reduction of the respective reducing disaccharides using standard procedures.

6,6′-Dichloro-6,6′-dideoxy maltose was prepared in the following way. Maltose (5 g) was treated with sulfuryl chloride and pyridine by a procedure previously described for the synthesis of fully chlorosulfated pentapyranosyl chlorides (27). In the case of maltose due to the presence of exocyclic primary hydroxyl groups specific chloro substitution of these groups occurred to yield syrupy 6′,6-dichloro-6′,6-dideoxymaltosyl chloride 2′,2,3′,3,4′-pentachlorosulfate (10.2 g, 80%). Additional 4′-chloro substitution, which normally occurs when the product of this reaction is isolated at ambient temperature (28), was avoided by the low-temperature isolation (−10 to 0°) of the product. The syrupy pentachlorosulfate (5 g) was treated with sodium iodide in aqueous acetone (29) and the resultant solution was deionized and concentrated to yield a syrup (1.5 g; 69.4%) which was shown to be homogeneous by paper chromatographic analysis (R_{Glc} 2.6) and had $[\alpha]_D$ +99.6° (*c*, 2.0 in water). Hydrolysis of the syrupy product (*N* sulfuric acid at 100° for 16 h) gave only 6-chloro-6-deoxy-D-glucose (R_{Glc} 2.5), which was characterized as its known crystalline peracetate derivative (30).

6′-Chloro-6′-deoxyisomaltose was prepared by an identical procedure to that described above. From isomaltose (0.5 g), syrupy 6′-chloro-6′-deoxyisomaltose was obtained in an overall yield of 58% (0.29 g). The product was homogeneous by paper chromatographic analysis (R_{Glc} 1.1) and hydrolysis (*N* sulfuric acid at 100° for 16 h) yielded both glucose and 6-chloro-6-deoxyglucose (paper chromatographic analysis). Recently, 6-chloro-6-deoxy-D-glucose has also been synthesized by this procedure and this preparation will be reported in detail in a subsequent communication (31).

6′-Chloro-6′-deoxymaltose was prepared according to the method of Melton and Slessor (32).

Results and Discussion

Glucose and Related Derivatives

In order to study derivatives of maltose and isomaltose chlorinated at C-6, it was first necessary to assign the resonances of the analogous monomer, 6-chloro-6-deoxy-D-glucose. In Table 1, its resonances are compared to those of glucose and 6-*O*-methyl-D-glucose. We are in agreement with the published assignments for these compounds (4, 10, 11). However, we could resolve two resonances due to C-6 in each of D-glucose and 6-chloro-6-deoxy-D-glucose and assign them to the α- and β-anomer species by taking into account the relative populations of the two anomers, as manifest in the C-1 resonances. We also distinguished between the C-2 and C-5 resonances in 6-*O*-methyl-β-D-glucose because no chemical shift effect is expected on C-2 due to methylation of C-6. Thus, the peaks at 75.9 and 75.5 p.p.m. are assigned to C-5 and C-2, respectively. The chlorination effect on the contiguous carbon occurs in the sense opposite to that of methylation and is considerably larger (*ca.* −17 and +10 p.p.m. displacements for chlorination and methylation, respectively). Qualitatively, these effects can be foreseen taking into account that the replacement of a substituent by a more polar group causes an upfield shift of the carbon bearing this substituent (33). In fact, we substitute an —OH group by an $—OCH_3$ or —Cl group and the order of polarity is —Cl > —OH > $—OCH_3$. If we refer to the ^{13}C chemical shifts observed in the alkanes (34), a −17 p.p.m. displacement is expected when a chlorine is substituted for a hydroxyl group. This comparison with alkanes is reasonable as the substitution is done on the exocyclic carbon. Chlorination at C-6 of glucose results in better resolution of the resonances due to this carbon in the two anomers (0.1 and 0.5 p.p.m. in D-glucose and 6-chloro-6-deoxy-D-glucose, respectively). The effect on the nearest neighbor carbon, a so-called β-effect, of the two substituents is nearly equivalent, −1.2 p.p.m., in the two anomers. As previously observed (4, 5), methylation usually produces negligible effects beyond the nearest neighbor carbon. However, a chemical shift change of +0.6 p.p.m. is observed on C-4 of the two anomers.

The spectra of ribitol, glucitol, and 4-*O*-

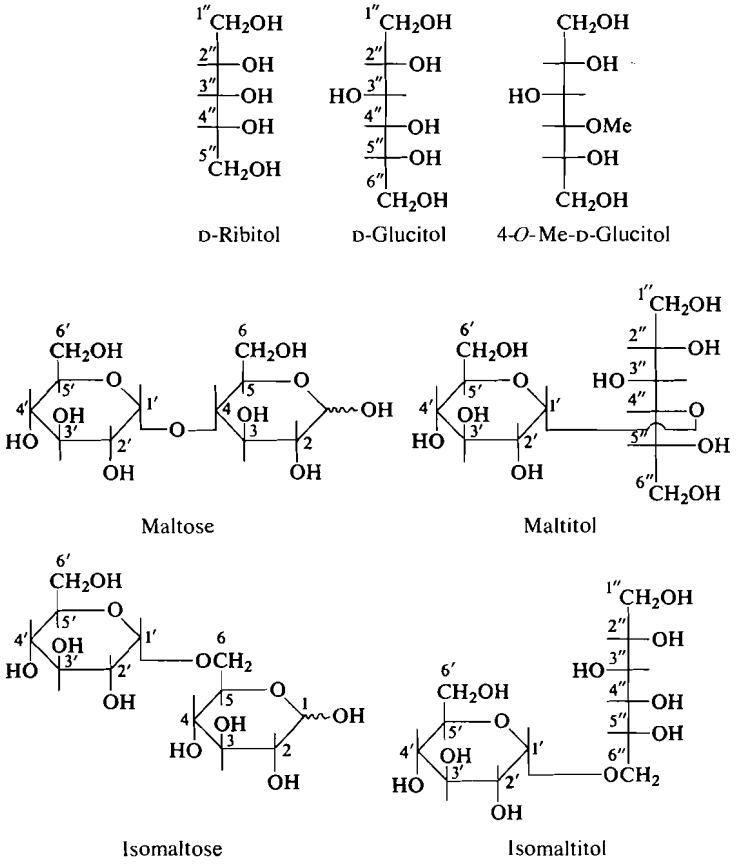

FIG. 1. Formulae of maltose, isomaltose, and some polyol derivatives related to them and to glucose.

TABLE 1. Comparison of the effects of methylation and chlorination at carbon 6 on the ^{13}C chemical shifts of glucose

	α-Anomer			β-Anomer		
	Unsubstituted	6-Cl	6-*O*-Me	Unsubstituted	6-Cl	6-*O*-Me
C-1	93.1	93.4	93.5	97.0	97.1	97.4
C-2	72.5*	72.5	72.9	75.2	75.2	75.5
C-3	73.8	73.6	74.2	77.0†	76.5	77.2
C-4	70.7	71.3	71.3	70.7	71.2	71.3
C-5	72.5*	71.4	71.3	76.8†	75.6	75.9
C-6	61.7	45.6	72.7	61.8	45.1	72.7
CH_3	—	—	60.1	—	—	60.1

*No differentiation in chemical shift observed with a resolution of 0.03 p.p.m.
†Two resonances distinguishable but no reliable method available for assigning resonances differing by so little.

methyl-D-glucitol (see Fig. 1 and Table 2) were also assigned to be used as references for polyol derivatives of disaccharides with possible extension to polysaccharides. In the following, unprimed and primed carbons will correspond to the reducing and nonreducing units of the disaccharides, respectively. Double primed carbons will represent those of polyol chains. Two resonance regions can be distinguished for secondary (70–75 p.p.m.) and primary (63–64 p.p.m.) alcohol carbon atoms. The two secondary alcohol resonances found by Voelter *et al.* (21) for ribitol could not be resolved under resolution conditions of 0.05 p.p.m. In glucitol, no un-

Can. J. Chem. Downloaded from www.nrcresearchpress.com by 210.87.254.105 on 09/05/12
For personal use only.

TABLE 2. Assignments of the ^{13}C resonances of maltose and its chlorinated and polyol derivatives

	Ribitol	Glucitol	4-*O*-Me-Glucitol	Maltose	Maltitol	6′-Chloro-6′-deoxymaltose	6,6′-Dichloro-6,6′-dideoxymaltose
C-1α				93.1		93.0	93.2
C-1β				97.1		96.9	97.0
C-1′				100.8	101.6	100.8	101.0
C-1″	63.7	64.0	63.9		64.0		
C-2α				72.5		72.4	72.4
C-2β				75.2		75.1	75.1
C-2′				73.8	73.8	73.4	72.9
C-2″	73.4*	72.4†	72.4‡		72.7		
C-3α				74.4		74.4	74.2
C-3β				77.3		77.3	77.1
C-3′				74.1	74.1	73.6	73.6
C-3″	73.4*	70.9	71.6‡		71.6		
C-4α				78.3		78.3	78.9
C-4β			61.0§	78.1		78.1	78.6
C-4′				70.5	70.6	71.2	71.2
C-4″	73.4*	72.2†	82.6		83.0		
C-5α				71.2		71.0	69.7
C-5β				75.7		75.6	74.0
C-5′				72.8	72.7	72.8	72.8
C-5″	63.7	74.1	73.3		73.6		
C-6α				62.0		62.1	46.1
C-6β				61.8		61.9	45.6
C-6′	—			61.7	61.6	45.4	45.6
C-6″		63.7	63.5		64.5		

*No resolution of these resonances observed.
†Uncertainty concerning relative assignments.
‡Differentiation based on the more important influence of 4-*O*-methylation on the resonance of C-3 than on that of C-2.
§Resonance of methyl group at C-4.

equivocal distinction between the C-2″ and C-4″ resonances can be made at present because they differ in chemical shift by so little (0.2 p.p.m.). However, regardless of the assignment, comparison of the chemical shifts of C-2″ of glucitol (72.2 or 72.4 p.p.m.) with that of ribitol (73.4 p.p.m.) demonstrates a *ca.* 1 p.p.m. influence of reversing the configuration of a neighboring carbon atom in a polyol. The peak at 63.7 p.p.m. can be attributed to C-6″ of glucitol, the conformational environment of which is more similar to those of C-1″ and C-5″ of ribitol than to that of C-1″ of glucitol (64.0 p.p.m.). Of the two possible assignments for C-3″ and C-5″ of glucitol (70.9 and 74.1 p.p.m.), that in Table 2 is chosen because it minimizes the difference in chemical shift between C-5″ of glucitol and C-2″ of ribitol which it closely resembles. In 4-*O*-methyl-D-glucitol, the methylation effect is greatest on C-4″, +10.4 p.p.m. It is of considerable interest to note that the effects of methylation at C-4″ are approximatly equal in magnitude but opposite in sign for C-3″ (+0.7 p.p.m.) and C-5″ (−0.8 p.p.m.) due to the different relative positions of the hydroxyl groups of C-3″ and C-5″ with respect to the substituent on C-4″. As no significant geminal effect, a so-called γ-effect, is foreseen, the resonance at 72.4 p.p.m. for 4-*O*-methyl-D-glucitol must be due to C-2″, whereas those at 63.9 and 63.5 p.p.m. are unambiguously attributable to C-1″ and C-6″ carbons, respectively. The resonance at 61.0 p.p.m. is assigned to the *O*-methyl group by reference to the derivatives of glucose methylated on the ring (5, 11, 19).

Glucobioses and Related Compounds

Maltose (O-α-D-Glucopyranosyl-(1 → 4)-O-α-D-glucopyranose)

Assignment of the ^{13}C n.m.r. spectrum of maltose (Fig. 2) has been previously attempted (9–11). Numerous uncertainties remain in the data of Voelter *et al.* (9) and a significant difference in chemical shift is present for all the resonances with respect to those given by other authors, due to the choice of an indirect chemical

Can. J. Chem. Downloaded from www.nrcresearchpress.com by 210.87.254.105 on 09/05/12
For personal use only.

Can. J. Chem. Downloaded from www.nrcresearchpress.com by 210.87.254.105 on 09/05/12
For personal use only.

shift reference. The assignments of C-3α and C-3β made by Dorman and Roberts (10) have to be interchanged with those of C-5α and C-5β to be consistent with the assignment of 4-*O*-methyl-D-glucose and methyl 4-*O*-methyl-α-D-glucopyranoside previously given (11, 19). As seen in Table 2, our assignment of the maltose resonances agrees very well with those of Usui *et al.* (11). In some cases, we were able to obtain better resolution for some resonances. Taking into account the relative intensities of these resonances, the peaks at 78.3 and 78.1 p.p.m. can be assigned to C-4α and C-4β, respectively, and the C-6 peaks at 62.0, 61.8, and 61.7 p.p.m. to C-6α, C-6β, and C-6′, respectively. Finally, the two peaks at 74.4 and 74.1 p.p.m. are due to C-3α and C-3′, respectively.

The maltitol assignment (Fig. 2) can be facilitated by considering that the reducing glucose unit of maltose is replaced by 4-*O*-methyl-D-glucitol. This direct comparison shows that only C-1′ differs by more than 0.5 p.p.m. with respect to the additive spectra of the constituents. This change of chemical shift by +0.8 p.p.m. demonstrates the relative effects of substitution of a glucopyranose ring by a polyol aliphatic chain or by another glucose residue. Turning to the glucitol moiety, C-4″ is displaced by +0.4 p.p.m. more on substitution with a glucosyl residue than with a methyl group. A corresponding difference of 0.3 p.p.m. exists for C-2″ and C-5″, whereas the influences of methyl and glycosyl substitution on C-3″ are equal. This underlines again the observation that the response on neighboring carbon chemical shifts to substitution depends on the orientation of their substituents relative to those of the carbon being substituted. All other resonances in the comparison correspond. Thus, the C-6′ resonance situated at 61.6 p.p.m. confirms our previous assignment of this carbon in maltose.

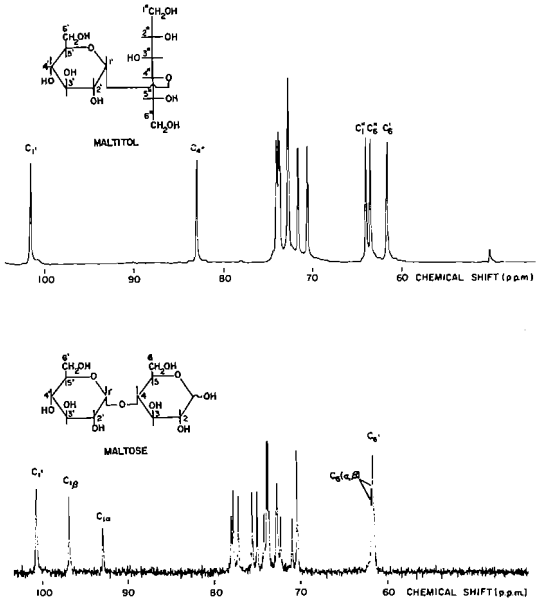

FIG. 2. ^{13}C n.m.r. spectra of maltitol and maltose, 100 mg/ml in D_2O, 32°, p*D* 7.0, spectral width 2.5 KHz, 6K data points, cycle time 1.2 s, pulse angle 45°, 21 900 and 7700 transients for maltitol and maltose, respectively.

Chlorination of C-6′ of the nonreducing unit of maltose is not expected to produce changes in the chemical shifts of reducing unit carbons, as seen in Table 2. This substitution could be expected to produce displacements of the chemical shifts of C-4′, C-5′, and C-6′, by comparison of 6-chloro-6-deoxy-α-D-glucose with α-D-glucose. However, account must be taken that the nonreducing unit is actually a glycoside. The increased shielding of C-6′ by 16.3 p.p.m. on chlorination is comparable to that observed in glucose (α, −16.1 p.p.m.; β, −16.7 p.p.m.) but a corresponding effect on C-5′ is not found. The glycosidic link at C-1′ must be responsible for this decreased sensitivity. The small displacements of C-2′ and C-3′ by −0.4 and −0.5 p.p.m., respectively, are mainly due to the chlorination effect, as well as the +0.7 p.p.m. change in chemical shift of C-4′ (Table 2).

In the dichlorinated derivative, we expect effects in the nonreducing moiety similar to those found for 6′-chloro-6′-deoxymaltose. This is generally true, including the absence of an effect of chlorination on the chemical shift of C-5′ and the decreased shielding of C-4′ (Table 2). The reducing end is comparable to glucose with the complication of a linkage at C-4. The changes in chemical shift of C-6 (α, −15.9 p.p.m.; β, −16.2 p.p.m.) are comparable to those found for 6-chloro-6-deoxy-D-glucose (Table 1). Similarly, an increased shielding is found for C-5 (α, −1.5 p.p.m.; β, −1.7 p.p.m.), in contrast to the anomalous behavior of the nonreducing end. This predicted behavior for the C-5 resonances confirms our proposed alteration of the assignments of Dorman and Roberts (10). The distinction between the C-6 resonances of the α- and β-anomers of the reducing end is enhanced relative to maltose as was found for glucose.

Can. J. Chem. Downloaded from www.nrcresearchpress.com by 210.87.254.105 on 09/05/12
For personal use only.

Isomaltose (O-α-D-Glucopyranosyl-(1 → 6)-α-D-glucopyranose)

We agree with the assignments of Usui *et al.* (11) for isomaltose itself, except that we were able to resolve more resonances, including those of C-2β and C-5β (75.3 and 75.5 p.p.m., respectively). However, the resonance region between 74.3 and 70.8 p.p.m. has to be discussed. Of the two signals at 70.8 and 71.3 p.p.m. (relative intensities 149 to 42, respectively), C-4′ must be assigned to the former, as this is the only signal of sufficient intensity to accommodate a complete carbon signal (based on an average relative intensity of 90 per carbon signal in the spectrum). The resonances of C-4α and C-4β must also be located at or in close proximity to the C-4′ signal as it has been demonstrated that C-4 of glucose derivatives exhibits little sensitivity to either anomeric change or C-6 substitution (Table 1). In addition the C-5α resonance must also be located in this region as model compounds indicate almost identical chemical shifts for C-4α, C-4β, and C-5α (Table 1). The resonance at 71.3 p.p.m. is too intense to accommodate C-5α alone which should have an approximate relative intensity of 30 based on the intensity of C-5β and the known ratio of the two anomers. Therefore two interpretations are consistent with the intensity data for the C-4α, C-4β, and C-5α signals. The signal at 71.3 p.p.m. can be assigned either to both C-4α and C-5α or to C-4β. This leaves the signal at 70.8 p.p.m. assignable to C-4β or to both C-4α and C-5α, respectively. Finally, by comparison with maltose, the C-3′ and C-3α resonances are positioned at 74.3 p.p.m. and the C-2α resonance at 73.0 p.p.m. The peaks at 73.25 and 72.7 p.p.m. are assigned to C-2′ and C-5′. As reported earlier (16, 19), the passage from the (α-1 → 4) to the (α-1 → 6) linkage has induced a change of −1.5 p.p.m. in the position of the C-1′ resonance, of −7 p.p.m. for the two C-4 resonances of the reducing moiety, and of +5 p.p.m. for the two resonances of the linked C-6 of the reducing moiety. This information is all necessary for the assignment of isomaltitol.

The assignment of isomaltitol is achieved by comparison of its spectrum with that of maltitol and by taking into account the different kind of linkage in isomaltitol (α-1 → 6). Thus, in the cyclic unit, the C-1′ and C-2′ resonances must be displaced relative to their values in maltitol. They undergo displacements of −2.1 and −0.5 p.p.m., respectively (similar to the corresponding differences between maltose and isomaltose). In the polyol chain, the substitution at C-6″ of the glucitol entity results in displacement of C-6″ and C-5″ by +6.2 and −1.0 p.p.m., respectively, whereas the other resonances are essentially unchanged from the values in glucitol. These effects are responsible for the chemical shift differences between C-3″, C-5″, and especially C-4″ in isomaltitol and maltitol, and aid in confirming the assignments between 74.2 and 70.7 p.p.m. in Table 3. Finally, the C-6″ resonance of the polyol chain is logically positioned at 69.9 p.p.m. Indeed, a carbon resonance is less shielded if linked to a methyl group or to an aliphatic chain than if linked to another ring (19). Replacement of the glucose ring by an aliphatic chain modifies the C-1′ resonance less in the (α-1 → 6) than in the (α-1 → 4) linkage (0.2 and 0.8 p.p.m., respectively). This is suggestive of the conformational influence on chemical shifts detected when comparing the relatively rigid cyclodextrins with linear (α-1 → 4) homopolymers or oligomers of glucose (19), and is due mainly to the extra degree of freedom in the linked C-6 moiety of a disaccharide relative to a linked C-4, C-3, or C-2.

In 6-′chloro-6′-deoxyisomaltose, the positions of the C-1, C-6, C-2β, C-3β, and C-5β resonances are well defined. As expected, the C-6′ resonance is the only one to undergo a drastic change in chemical shift on chlorination, −16.3 p.p.m. with respect to isomaltose. The region between 74.3 and 70.6 p.p.m. must again be discussed in greater detail. By comparison with isomaltose and isomaltitol, the C-3α and C-3′ resonances are located at 74.3 and 74.0 p.p.m., respectively, taking into account their relative intensities, whereas the C-2′ and C-2α resonances must be at 72.6 p.p.m. because they are not expected to change on chlorination of C-6′. On the other hand, the resonance at 71.9 p.p.m. can be assigned to C-5′, which undergoes an expected high-field shift. The four resonances between 71.4 and 70.6 p.p.m. (C-4α, C-4β, C-4′, C-5α) are assigned according to their relative intensities: 71.4 p.p.m. to the nonreducing end, 71.1 and 70.7 p.p.m. to the α-carbons, and 70.6 p.p.m. to a β-carbon of the reducing end. An uncertainty remains in the relative assignments of 71.1 and 70.7 p.p.m. for C-4α and C-5α.

The Influence of Dissolution in Pyridine

All compounds described above were also

TABLE 3. Assignments of the ^{13}C resonances of isomaltose and its chlorinated and polyol derivatives

	Isomaltose	Isomaltitol	6′-Chloro-6′-deoxyisomaltose
C-1α	93.4		93.4
C-1β	97.3		97.3
C-1′	99.3	99.5	99.1
C-1″		63.8	
C-2α	73.0		72.6
C-2β	75.3		75.3
C-2′	73.25	73.3*	72.6
C-2″		72.8	
C-3α	74.3		74.3
C-3β	77.2		77.2
C-3′	74.3	74.2	74.0
C-3″		70.9	
C-4α	71.3*		71.1*
C-4β	70.8*		70.6
C-4′	70.8	70.7	71.4
C-4″		72.2	
C-5α	71.3*		70.7*
C-5β	75.5		75.4
C-5′	72.7	72.8	71.9
C-5″		73.1*	
C-6α	67.1		67.0
C-6β	67.1		67.0
C-6′	61.8	61.8	45.5
C-6″		69.9	

*Uncertainty concerning relative assignments.

studied in pyridine solution. Pyridine was chosen because some chlorinated carbohydrates are only sparsely soluble in water. In pyridine the resonances cluster closely together and unambiguous assignments cannot be made without parallel studies of specifically-deuterated compounds. Therefore the data are not reported in detail but are available upon request.

One of us (P.C.) is indebted to the North Atlantic Treaty Organization for a Postdoctoral Fellowship.

1. A. S. PERLIN. *In* MTP international review of science, Organic Chemistry. Series 2. In press.
2. A. S. PERLIN and B. CASU. Tetrahedron Lett. 2921 (1969).
3. H. J. KOCH and A. S. PERLIN. Carbohyd. Res. **15**, 403 (1970).
4. A. S. PERLIN, B. CASU, and H. J. KOCH. Can. J. Chem. **48**, 2596 (1970).
5. D. E. DORMAN and J. D. ROBERTS. J. Am. Chem. Soc. **92**, 1355 (1970).
6. L. D. HALL and L. F. JOHNSON. J. Chem. Soc. Chem. Commun. 509 (1969).
7. E. BREITMAIER, G. JUNG, and W. VOELTER. Chimia, **25**, 362 (1971).
8. W. W. BINKLEY, D. HORTON, N. S. BHACCA, and J. D. WANDER. Carbohyd. Res. **23**, 301 (1972).
9. W. VOELTER, V. BILIK, and E. BREITMAIER. Collect. Czech. Chem. Commun. **38**, 2054 (1973).
10. D. E. DORMAN and J. D. ROBERTS. J. Am. Chem. Soc. **93**, 4463 (1971).
11. T. USUI, N. YAMAOKA, K. MATSUDA, K. TUZIMURA, H. SUGIYAMA, and S. SETO. J. Chem. Soc. Perkin Trans. I, 2425 (1973).
12. J. HAVERKAMP, J. P. C. M. VAN DONGEN, and J. F. G. VLIEGENTHART. Tetrahedron, **29**, 3431 (1973).
13. D. R. BUNDLE, H. J. JENNINGS, and I. C. P. SMITH. Can. J. Chem. **51**, 3812 (1973).
14. D. E. DORMAN, S. J. ANGYAL, and J. D. ROBERTS. J. Am. Chem. Soc. **92**, 1351 (1970).
15. K. TAKEO, K. HIROSE, and T. KUGE. Chem. Lett. 1233 (1973).
16. H. J. JENNINGS and I. C. P. SMITH. J. Am. Chem. Soc. **95**, 606 (1973).
17. D. R. BUNDLE, I. C. P. SMITH, and H. J. JENNINGS. J. Biol. Chem. **249**, 2275 (1974).
18. T. USUI, N. KOBAYASHI, N. YAMAOKA, K. MATSUDA, K. TUZIMURA, H. SUGIYAMA, and S. SETO. Tetrahedron Lett. 3397 (1973).
19. P. COLSON, H. J. JENNINGS, and I. C. P. SMITH. J. Am. Chem. Soc. **96**, 8081 (1974).
20. A. K. BHATTACHARJEE, H. J. JENNINGS, C. P. KENNY, A. MARTIN, and I. C. P. SMITH. J. Biol. Chem. In press.
21. W. VOELTER, E. BREITMAIER, G. JUNG, T. KELLER, and D. HISS. Angew. Chem. Int. Ed. **9**, 803 (1970).

Can. J. Chem. Downloaded from www.nrcresearchpress.com by 210.87.254.105 on 09/05/12
For personal use only.

22. J. D. ROBERTS, F. J. WEIGERT, J. I. KROSCHWITZ, and H. J. REICH. J. Am. Chem. Soc. **92**, 1338 (1970).
23. W. VOELTER, E. BREITMAIER, E. B. RATHBONE, and A. M. STEPHEN. Tetrahedron, **29**, 3845 (1973).
24. J. HAVERKAMP, J. P. C. M. VAN DONGEN, and J. F. G. VLIEGENTHART. Carbohyd. Res. **33**, 319 (1974).
25. J. KENNER and G. N. RICHARDS. J. Chem. Soc. 1810 (1955).
26. B. HELFERICH, W. KLEIN, and W. SHAFER. Ber. **59**, 79 (1926).
27. H. J. JENNINGS. Can. J. Chem. **46**, 2799 (1968).
28. H. J. JENNINGS and J. K. N. JONES. Can. J. Chem. **40**, 1408 (1962).
29. H. J. JENNINGS. Can. J. Chem. **48**, 1834 (1969).
30. B. HELFERICH and A. GNÜCHTEL. Ber. **74**, 1035 (1941).
31. H. J. JENNINGS and A. MARTIN. Unpublished results.
32. L. D. MELTON and K. N. SLESSOR. Can. J. Chem. **51**, 327 (1973).
33. D. M. GRANT and B. V. CHENEY. J. Am. Chem. Soc. **89**, 5315 (1967).
34. G. C. LEVY and G. L. NELSON. Carbon-13 nuclear magnetic resonance for organic chemists. Wiley Interscience, New York. 1972. p. 47.

Can. J. Chem. Downloaded from www.nrcresearchpress.com by 210.87.254.105 on 09/05/12
For personal use only.

Variable Temperature Nuclear Magnetic Resonance Studies of Some Five-Membered Ring Chelate Complexes

WILLIAM R. CULLEN, LAURANCE D. HALL, AND JOHN E. H. WARD[1]

Department of Chemistry, University of British Columbia, Vancouver, British Columbia V6T 1W5

Received September 16, 1974

WILLIAM R. CULLEN, LAURANCE D. HALL, and JOHN E. H. WARD. Can. J. Chem. **53**, 1038 (1975).

The temperature dependence of the n.m.r. spectra of nine ditertiary arsine chelate complexes of formula $(CH_3)_2AsC(3)(3')C(4)$ $(4')As(CH_3)_2M(CO)_3X$ has been studied (M = Mo, Cr; X = CO; M = Mn; X = halogen; (3), (3'), (4), (4') = H, F, $Si(CH_3)_3$, CN; but not all combinations). Significant variation in coupling constants, indicating a shift in the conformer populations, was found only for the $CHFCF_2$ bridged $Mn(CO)_3Cl$ complex, the CH_2CF_2 bridged $Mn(CO)_3Cl$ complex, and the CHFCHF bridged $Mo(CO)_4$ complex. In the last case the $^3J_{HH}$ coupling constants were used to estimate $\Delta H \sim 1$ kcal/mol and $\Delta S \sim 3$ e.u for the conformational equilibrium.

WILLIAM R. CULLEN, LAURANCE D. HALL et JOHN E. H. WARD. Can. J. Chem. **53**, 1038 (1975).

On a étudié, en fonction de la température les spectres r.m.n. de neuf complexes contenant une arsine ditertiaire comme chelate et possédant la formule $(CH_3)_2AsC(3)(3')C(4)$ $(4')As(CH_3)_2M(CO)_3X$ dans lesquels (M = Mo, Cr; X = CO; M = Mn; X = halogène, (3), (3'), (4), (4') = H, F, $Si(CH_3)_3$, CN; toutes les combinaisons n'ont toutefois pas été étudiées). D'une façon générale les constantes de couplage étaient semblables; toutefois on trouve des changements importants, indiquant une variation dans les populations de conformères, pour le complexe du $CHFCF_2$ ponté au $Mn(CO)_3Cl$, pour le complexe de CH_2CF_2 ponté au $Mn(CO)_3Cl$ et pour le complexe de CHFCHF ponté au $Mo(CO)_4$. Dans le dernier cas les constantes de couplage $^3J_{HH}$ ont été utilisées pour établir la valeur de $\Delta H \sim 1$ kcal/mol et $\Delta S \sim 3$ e.u pour l'équilibre conformationnel. [Traduit par le journal]

Introduction

We have completed several investigations (1–4) of the conformational preferences of five-membered chelate rings in octahedral transition metal complexes of the general type **A**, where M = Cr, Mo, W, or Mn; E = $As(CH_3)_2$ or $P(CH_3)_2$; X = Cl, Br, or I (for M = Mn)

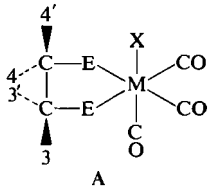

A

or CO (for M = Cr, Mo, W); and 3, 3', 4, and 4' are substituents such as: H, F, Cl, CN, and $Si(CH_3)_3$. It was shown that a "bulky" substituent such as a trimethylsilyl group prefers the "equatorial" orientation on the puckered five-membered chelate ring, whereas a fluorine substituent frequently prefers the "axial" orientation (1–4). On the other hand, certain substituents such as a chloro or cyano group do not seem to strongly favor a particular orientation. In ideal cases, the changes in the puckering of the chelate rings arising from variations in the transition metal and *cis* (axial) substituents could be roughly predicted (3, 4).

In an attempt to derive further conformational information for these systems we have carried out variable temperature n.m.r. experiments on nine selected chelate complexes. The present paper is concerned with the results of these studies.

Experimental

All the chelate complexes used in this study were prepared by methods which we have already described (1–4).

The n.m.r. spectra were obtained using an extensively modified Varian HA-100 spectrometer and were recorded in the frequency sweep mode on carefully calibrated charts, using TMS as the internal reference. Computer analyses of the n.m.r. spectra were obtained

[1]This work includes part of the material submitted by J.E.H.W. in partial fulfilment of the requirements for the Ph.D. degree in Chemistry, University of British Columbia.

Can. J. Chem. Downloaded from www.nrcresearchpress.com by 210.87.254.40 on 09/05/12
For personal use only.

TABLE 1. Chelate complexes $(CH_3)_2EC(3)(3')C(4)(4')E(CH_3)_2M(CO)_3X$ **1–9** examined by variable temperature n.m.r.[a]

Complex	3	3′	4	4′	E	M	X
1	$Si(CH_3)_3$	H	H	H	As	Cr	CO
2	CN	H	H	H	As	Cr	CO
3	H	F	H	H	As	Cr	CO
4	H	H	F	F	As	Cr	CO
5	H	H	F	F	As	Mn	Br
6	F	H	F	H	As	Mo	CO
7	F	H	F	H	As	Mn	Cl
8	H	F	F	F	As	Cr	CO
9	H	F	F	F	As	Mn	Cl

[a]The numbering also refers to A which is not intended to represent a fixed conformation.

with an IBM 360-67 computer and a modified version of the LAOCOON III program.[2]

Table 1 lists the chelate complexes **1–9** examined in this work.

Results and Discussion

The chemical shifts and coupling constants obtained by iterative computer analysis of the n.m.r. spectra of **1–9** are summarized in Tables 2 and 3, respectively. Specific details of the spectral analysis of these derivatives have been presented elsewhere (1–4).

Theory

A number of results (6–8) indicate that the energy differences between conformers of five-membered chelate rings are small. It has been shown (9) that the energy barriers to conformational inversion of these rings are also small. Thus, all conformations determined by the n.m.r. method should be subject to some degree of time averaging. Thus a single specific conformation cannot be assigned, although it may be that in some instances one section of the pseudo-rotational cycle is extensively populated (6, 7, 10, 11). Because of the experimental techniques we are using, we can discuss only those conformers which involve rotation about the carbon–carbon bond of the ethane bridge.

It is sometimes assumed for compounds undergoing dynamic intramolecular processes in solution that the n.m.r. parameters of the protons or fluorines in the individual isomers are temperature invariant (12). Usually, this assumption leads to no serious errors on the calculation of exchange rates and thermodynamic data, provided that the protons or fluorines change equally. However, it has been demonstrated (13) for rigid molecules such as the difluorethylenes that the proton chemical shifts, ^1H–^{19}F, and ^{19}F–^{19}F coupling constants may exhibit a substantial temperature dependence, while the geminal and vicinal ^1H–^1H coupling constants are essentially temperature invariant. Thus caution should be used in interpreting the data obtained from variable temperature n.m.r. studies of dynamic systems and an attempt should be made to separate the changes arising from inherent temperature dependences from those arising from alterations in the dynamic equilibrium (14).

Chelate Ring Conformational Preferences

Complexes of the Ligands $(CH_3)_2AsCH_2$-$CHXAs(CH_3)_2$ (X = $Si(CH_3)_3$, CN, F)

We have shown previously (1) that the vicinal ^1H–^1H coupling constants of the trimethylsilyl derivative **1** indicate that the bulky trimethylsilyl group adopts the equatorial orientation on the ethane bridge as in **B**, rather than the axial position as in **C** at 34°.

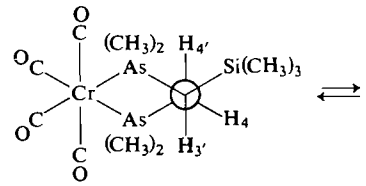

B

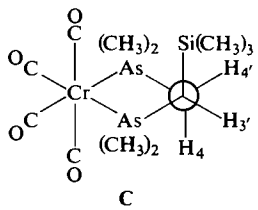

C

[2]LAOCOON III is a version of the least squares n.m.r. spectral fitting program described by Castellano and Bothner-By (5), modified by R. B. Malcolm, Chemistry Department, University of British Columbia.

Can. J. Chem. Downloaded from www.nrcresearchpress.com by 210.87.254.40 on 09/05/12
For personal use only.

Can. J. Chem. Downloaded from www.nrcresearchpress.com by 210.87.254.40 on 09/05/12
For personal use only.

TABLE 2. Chemical shifts (τ and ϕ values) for the chelate complexes **1–9**

Complex	Solvent	Temperature (°C)	3	3′	4	4′	Arsenic-methyl groups			
1	$C_6H_5NO_2$	34		9.573	7.354	8.800	8.298	8.345	8.459	8.563
2	$C_6H_5NO_2$	34		7.151	7.625	8.061	8.273	8.283	8.324	8.443
3	$C_6H_5NO_2$	34	4.203	192.44	7.374	8.529	8.390	8.436	8.486	8.581
4	C_6H_6[a]	34	9.22	9.22	105.8	105.8	9.42	9.42	9.52	9.52
5	$CDCl_3$	34	7.673	7.546	91.79	106.62	8.273	8.273	8.358	8.484
		80			[b]	[b]	[c]			
6	$(CD_3)_2CO$	−42	[b]	3.928	[b]	3.928	[c]			
		−22	[b]	3.998	[b]	3.998	[c]			
		34	212.22	4.191	212.22	4.191	8.426	8.426	8.433	8.433
		69	[b]	4.248	[b]	4.248	[c]			
		89	[b]	4.282	[b]	4.282	[c]			
7	$(CD_3)_2CO$	34	214.06[d]	3.861	219.16[d]	4.068	8.309	8.341	8.370	8.469
8	$C_6H_5NO_2$	34	5.204	220.41	120.10[d]	128.51[d]	[e]			
9	$CDCl_3$	−12	4.571	[b]	[b]	[b]	[c]			
		8	4.565	[b]	[b]	[b]	[c]			
		34	4.560	235.51	114.55[d]	121.23[d]	8.333	8.353	8.353	8.482
		89	4.530	[b]	[b]	[b]	[c]			
		145	4.531	[b]	[b]	[b]	[c]			

[a] −50° spectrum determined on a chloroform solution.
[b] ^{19}F n.m.r. spectrum not recorded.
[c] Arsenic methyl proton signals were not recorded.
[d] The stereochemical assignments of the fluorine nuclei are made arbitrarily.
[e] Data not reported due to the complexity of the arsenic methyl proton resonances.

TABLE 3. Coupling constants (Hz) for the chelate complexes **1–9**

Complex	Solvent	Temperature (°C)	$J_{33'}$	J_{34}	$J_{34'}$	$J_{3'4}$	$J_{3'4'}$	$J_{44'}$
1[a]	$C_6H_5NO_2$	34				5.2	15.9	−12.7
2[b]	$C_6H_5NO_2$	34				6.1	10.2	−13.0
3[c]	$C_6H_5NO_2$	34	49.6	3.4	3.3	15.9	49.6	−14.0
4[d]	C_6H_6	34						
5	$CDCl_3$	34	−13.2	42.0	7.0	14.9	7.2	248.4
		80	−13.1	39.4	7.4	16.2	8.1	[e]
6	$(CD_3)_2CO$	−42	51.3	−19.4	13.1	13.1	9.6	51.3
		−22	50.7	−20.2	12.4	12.4	9.2	50.7
		34	50.4	−23.0	11.6	11.6	8.4	50.4
		69	50.1	−23.7	11.5	11.5	8.1	50.1
		89	50.2	−23.9	11.5	11.5	8.0	50.2
7[f]	$(CD_3)_2CO$	34	51.7	−14.6	18.5	17.6	10.2	53.1
8[g]	$C_6H_5NO_2$	34	48.7	5.4	16.0	−22.6	−15.6	265.8
9	$CDCl_3$	−12	48.4	27.0	6.7	[b]	[b]	[b]
		8	48.5	26.7	6.9	[b]	[b]	[b]
		34	48.5	26.4	7.2	−10.9	−12.8	250.4
		89	48.8	25.8	7.3	[b]	[b]	[b]
		145	48.4	25.3	7.4	[b]	[b]	[b]

[a]The vicinal ^1H–^1H coupling constants obtained at 90° differ by < 0.2 Hz from those obtained at 34°.
[b]The vicinal ^1H–^1H coupling constants obtained at 100° differ by < 0.2 Hz from those obtained at 34°.
[c]The vicinal ^1H–^1H coupling constants obtained at 120° differ by < 0.5 Hz from those obtained at 34°.
[d]Signals arising from the CH_2 and CF_2 groups are triplets, Σ^3J_{HF} = 72 Hz. Negligible changes in the triplet spacings (^1H n.m.r. spectrum, in $CDCl_3$) were observed on cooling the sample to −50°.
[e]^{19}F n.m.r. spectrum not recorded.
[f]The vicinal ^1H–^1H coupling constant obtained at −20° differs by < 0.5 Hz from that obtained at 80°.
[g]The vicinal ^1H–^{19}F coupling constants obtained at 95° differ by < 0.5 Hz from those obtained at 34°.

We now find that the n.m.r. spectrum of **1** at 90° shows that although the chemical shifts of the three vicinal protons change from those obtained at 34° the vicinal ^1H–^1H coupling constants do not vary appreciably. This result indicates a strong preference for conformer **B** and we conclude that the ground state energy of that conformer is substantially lower than that of **C**. Calculations on the related 1,2-propanediamine chelate ring reveal that the conformer with the methyl group in the axial orientation is 0–3 kcal/mol higher in energy than the conformer with the methyl group in an equatorial orientation (6). A more recent report indicates that this difference is *ca.* 2.5 kcal/mol (8).

The cyano derivative **2** probably undergoes some degree of conformational inversion between **D** and **E** (1, 3). While the vicinal ^1H–^1H coupling constants indicate that form **D** is preferred, the relative proportions of **D** and **E** can apparently be changed by solvent variations (3). The present variable temperature n.m.r. studies reveal only small changes between the $^3J_{HH}$ values obtained at 34 and 100°. Thus, it appears that conformer **D** is highly populated at least in nitrobenzene solution.

In contrast, the vicinal ^1H–^1H and ^1H–^{19}F coupling constants of the monofluoro complex **3** unexpectedly revealed a strong preference for the fluoro substituent to adopt the axial orientation on the five-membered chelate ring (1) as in **F**.

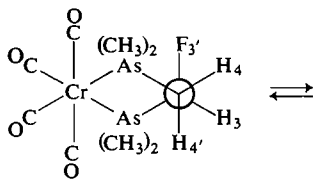

F

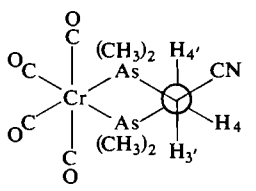

D

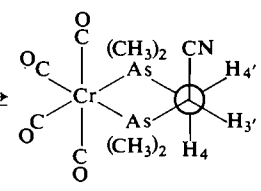

E

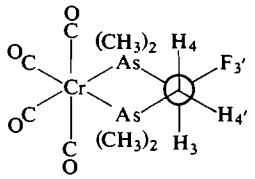

G

Can. J. Chem. Downloaded from www.nrcresearchpress.com by 210.87.254.40 on 09/05/12
For personal use only.

Can. J. Chem. Downloaded from www.nrcresearchpress.com by 210.87.254.40 on 09/05/12
For personal use only.

The ^1H n.m.r. spectrum at 120° shows that the vicinal ^1H–^{19}F coupling constants do not vary appreciably from those obtained at 34°. Thus the fluoro substituent strongly prefers the axial orientation on the five-membered chelate ring as in **F**.

Complexes of $(CH_3)_2AsCH_2CF_2As(CH_3)_2$

The appearance of the ^1H n.m.r. spectrum of the methylene region of the geminal-difluoro chromium complex **4** as a triplet suggested that inversion between two conformers is occurring rapidly on the n.m.r. time scale as in **H**. If the

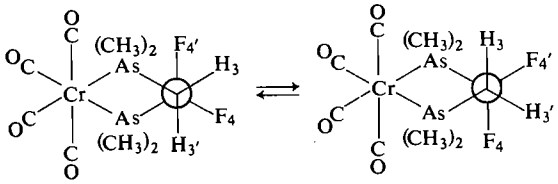

H

rate of the equilibrium reaction could be slowed down on the n.m.r. time scale, an ABXY spectrum would arise from the individually "locked" conformers. However, when the sample was cooled to −50°, only very small changes in the ^1H n.m.r. spectrum of **4** were observed and we thus conclude that the equilibrium reaction **H** is occurring quite rapidly on the n.m.r. time scale, which is not unexpected.

For the geminal-difluoro bromo manganese complex **5**, two distinct conformers **I** and **J**

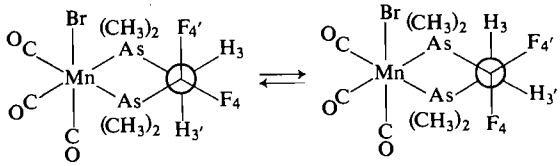

I **J**

are possible. We have previously found that the vicinal ^1H–^{19}F coupling constants of **5** are markedly solvent dependent (4) indicating that the equilibrium between **I** and **J** is being shifted by changes in the solvent. To check this conclusion, we obtained the ^1H n.m.r. spectrum of **5** at 80°. This reveals substantial changes in the $^3J_{HF}$ values. For example J_{34} decreases by *ca.* 3 Hz from 42.0 to 39.4 Hz, while $J_{3'4}$ increases by *ca.* 1 Hz, from 14.9 to 16.2 Hz. Thus, it seems that, (*i*) there is indeed an equilibrium between **I** and **J**, (*ii*) the changes in the vicinal ^1H–^{19}F coupling constants due to solvent variations are *not* due to the inherent solvent dependences of those coupling constants, and (*iii*) the equilibrium is shifted by varying the temperature or the solvent. Unfortunately, since the $^3J_{HF}$ values of the individual locked conformers **I** and **J** should be approximately the same, we cannot deduce which conformer is favored with the increase in temperature.

Complexes of $(CH_3)_2AsCHFCHFAs(CH_3)_2$

The vicinal ^1H–^1H and ^1H–^{19}F coupling constants of the vicinal-difluoro molybdenum complex **6** exhibit a marked sensitivity to temperature changes. We have already interpreted the ^3J values obtained at ambient probe temperature for this complex in terms of a dynamic equilibrium between conformers **K** and **L** (3).

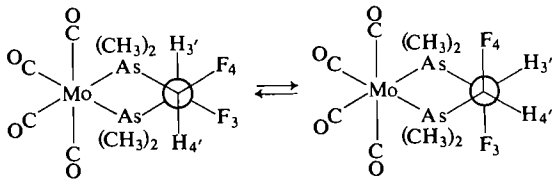

K **L**

Since the vicinal ^1H–^1H coupling constants increase with decreasing temperature, we conclude that **K** is the low energy form of **6** since that conformer contains the two protons in a mutually *trans* orientation. Because all the vicinal coupling constants obtained at 69° are equal, within the experimental error (±0.1 Hz), to these obtained at 89°, it appears that the high temperature limit has been attained at 69°. Thus at that and higher temperatures, the equilibrium consists of equal proportions of **K** and **L**.

If it is assumed that (*i*) the inherent temperature dependence of the vicinal ^1H–^1H coupling constants is negligible (13), (*ii*) conformers **K** and **L** have the same dihedral angles, and (*iii*) simple Karplus relationships (15, 16) apply to both **K** and **L**, *i.e.* they have the same Karplus coefficients, we can derive an estimate of the enthalpy difference between **K** and **L** as follows.

$$[1] \qquad {}^3J_{HH} = A\cos^2\phi \qquad 0 \le \phi \le 90°$$

$$[2] \qquad = B\cos^2\phi \qquad 90 \le \phi \le 180°$$

If ϕ is the dihedral angle and θ the in-plane projection of the "tetrahedral" angles (assumed to be 120° (15, 17)) about the ring carbon atoms as in **M**, we can derive expressions for the

TABLE 4. Thermodynamic data for the equilibrium **K** = **L**

Temperature (°K)	$^3J_{HH(obs)}$ (Hz)	K	ln K	ΔG	X
231	9.6	0.49	−0.71	326	0.67
251	9.2	0.60	−0.51	254	0.63
307	8.4	0.87	−0.14	85	0.53
342	8.1	1.0	0.0	0	0.50

vicinal ^1H–^1H coupling constants of the individual conformers **K** and **L**.

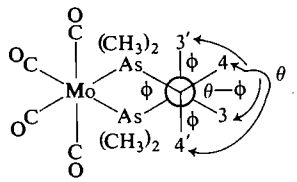

M

[3] $$^3J_{HH}(trans, \mathbf{K}) = B\cos^2(\theta + \phi)$$

[4] $$^3J_{HH}(gauche, \mathbf{L}) = A\cos^2\phi$$

Expressing the observed vicinal ^1H–^1H coupling constants, $^3J_{obs}$, as a sum of the contributions from the conformers **K** and **L**

[5] $$^3J_{obs} = X\,^3J_{HH}(trans, \mathbf{K}) + (1 - X)\,^3J_{HH}(gauche, \mathbf{L})$$

where X is the fractional population of **K**, and solving for X we find

[6] $$X = \frac{^3J_{obs} - {}^3J_{HH}(gauche, \mathbf{L})}{^3J_{HH}(trans, \mathbf{K}) - {}^3J_{HH}(gauche, \mathbf{L})}$$

The equilibrium constant K for **K** = **L** is $(1 - X)/X$, and thus

[7] $$K = \frac{^3J_{HH}(trans, \mathbf{K}) - {}^3J_{obs}}{^3J_{obs} - {}^3J_{HH}(gauche, \mathbf{L})}$$

Substituting eqs. 3 and 4 into eq. 7 yields:

[8] $$K = \frac{B\cos^2(\theta + \phi) - {}^3J_{obs}}{^3J_{obs} - A\cos^2\phi}$$

If we now assume that $A = 0.9B$ (3, 18) and $\phi = 55°$, as was revealed by X-ray determinations of a variety of related derivatives (19) and calculations based on the vicinal coupling constants of analogous complexes (3, 4), the equilibrium constant can be expressed as

[9] $$K = \frac{B\cos^2(175°) - {}^3J_{obs}}{^3J_{obs} - 0.9B\cos^2(55°)}$$

In order to obtain an estimate for B, we can solve eq. 9 for the high temperature limit (69°), where $^3J_{obs} = 8.1$ Hz and $K = 1$. This calculation yields a value of 12.6 Hz for B which is similar to those of carbocyclic systems (20, 21). Thus it seems that the electron donating properties of the two dimethylarsino groups are apparently almost equally offset by the electron withdrawing properties of the fluorine atoms.

We can now use this value of B in eq. 9 to determine the equilibrium constants K for the process **K** = **L**. These values are assembled in Table 4, together with the calculated values of ΔG and X. A plot of ΔG *vs.* T is shown in Fig. 1. Linear regression analysis of the data for this plot yields eq. 10.

[10] $$\Delta G = -2.94T + 997$$

where

$$r = 0.998$$

Thus, ΔH for the equilibrium is *ca.* 1 kcal/mol, while ΔS is *ca.* +3 e.u. The small value of ΔH is entirely consistent with our expectations that the energy barriers to conformational inversion in five-membered chelate rings are very small.

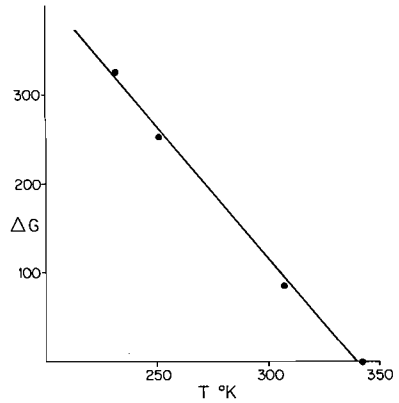

FIG. 1. Plot of ΔG *vs.* T for the variable temperature ^1H n.m.r. study of $(CH_3)_2AsCHFCHFAs(CH_3)_2$-$Mo(CO)_4$ **6**.

Can. J. Chem. Downloaded from www.nrcresearchpress.com by 210.87.254.40 on 09/05/12
For personal use only.

The slight deviation of the points from the line described by eq. 10 may arise from the failure of the Karplus coefficients for **K** and **L** to remain the same. Recent evidence (22–25) indicates that the assumption that they are the same may not be valid.

In the case of the analogous chloro manganese derivative **7** the vicinal ^1H–^1H coupling constants do not vary appreciably when the ^1H n.m.r. spectrum of the sample was taken at 80°. Thus, we conclude that the conformer with the two protons *trans* to one another, as in **N**, is highly favored relative to **O**, the conformer with a *gauche* proton–proton orientation.

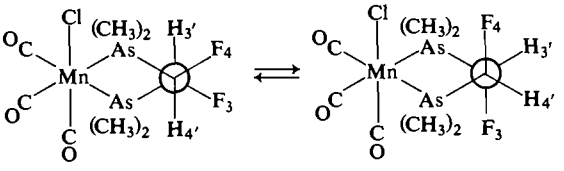

N **O**

Thus, for both **6** and **7** the low energy conformation is the form with mutually *trans* protons. Apparently the dipolar and/or steric interactions of the *cis*-chloro and single carbonyl ligand with the five-membered ring in **7** differ significantly from those interactions of the two *cis*-carbonyls with the chelate ring in **6**.

Complexes of $(CH_3)_2AsCHFCF_2As(CH_3)_2$

The ^1H and ^{19}F n.m.r. parameters obtained at 34° for the trifluoro chromium complex **8** (3) indicate a major preference for two of the fluorine atoms to have the axial orientation as in **P**. The vicinal ^1H–^{19}F coupling constants

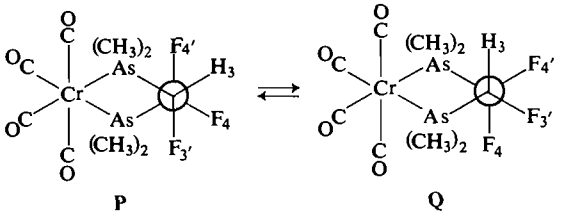

P **Q**

obtained from the ^1H n.m.r. spectrum at 95° do not appear appreciably different so the preference for **P**, which has two axial fluorine atoms, seems quite marked.

In contrast with the chromium trifluoro derivative **8** (4), the conformer of the trifluoro manganese complex **9** with the hydrogen in the axial position in **S**, has an appreciable population in equilibrium with **R** at 34°. This conclusion is based on the observations (3, 4) that one of the *gauche* ^1H–^{19}F coupling constants (*ca.* 26 Hz) in **9** is substantially higher (*ca.* 15 Hz) than that in **8**. This is probably conformationally significant since Karplus coefficients of the ethane bridge are not particularly sensitive to changes in the transition metal or its *cis*-axial ligands (3, 4). However, since the dihedral angles in the chelate rings may differ in **8** and **9** such an interpretation is not unequivocal. Our variable temperature n.m.r. studies show that the two vicinal ^1H–^{19}F coupling constants in **9** are indeed temperature sensitive: J_{34} increases from 25.3 to 27.0 Hz when the temperature is lowered from 145 to −12°, while $J_{34'}$ decreases from 7.4 to 6.7 Hz. Since the temperature dependences of these vicinal ^1H–^{19}F coupling constants are opposite, it appears that the changes observed are not due to the inherent temperature dependence of the $^3J_{HF}$ values for the individual conformers **R** and **S**. Thus, we may interpret these coupling constant changes in terms of a dynamic equilibrium between **R** and **S**. It is tempting to carry a discussion of this dynamic process further by estimating the thermodynamic parameters for this equilibrium; however, since we are unable to unambiguously assign the vicinal constants to particular nuclei, such calculations would necessarily have a restricted value. Nevertheless, since the changes observed are relatively small for a wide temperature range, we infer that the energies of conformers **R** and **S** are quite similar.

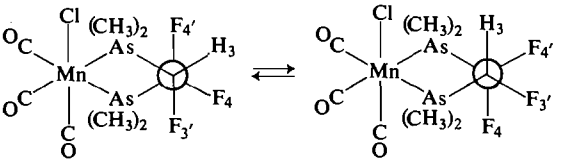

R **S**

Thus, it seems that the steric and/or dipolar interactions of the trifluoro chelate rings in **9** differ significantly from those in the chromium analog **8**. We have already noted a similar difference between the vicinal difluoro analogs **6** and **7**.

It is a pleasure to thank the National Research Council of Canada for its generous financial support of this work in the form of operating grants to L.D.H. and W.R.C., and the Alfred P. Sloan Foundation for a research fellowship to L.D.H.

Can. J. Chem. Downloaded from www.nrcresearchpress.com by 210.87.254.40 on 09/05/12
For personal use only.

1. W. R. CULLEN, L. D. HALL, and J. E. H. WARD. J. Am. Chem. Soc. **94**, 5702 (1972).
2. W. R. CULLEN, L. D. HALL, and J. E. H. WARD. Chem. Commun. 625 (1970).
3. W. R. CULLEN, L. D. HALL, and J. E. H. WARD. J. Am. Chem. Soc. **96**, 3422 (1974).
4. W. R. CULLEN, L. D. HALL, and J. E. H. WARD. J. Am. Chem. Soc. **96**, 3431 (1974).
5. S. CASTELLANO and A. A. BOTHNER-BY. J. Chem. Phys. **41**, 3863 (1964).
6. J. R. GOLLOGLY and C. J. HAWKINS. Inorg. Chem. **8**, 1168 (1969).
7. J. R. GOLLOGLY, C. J. HAWKINS, and J. K. BEATTIE. Inorg. Chem. **10**, 317 (1971).
8. L. J. DEHAYES and D. H. BUSCH. Inorg. Chem. **12**, 1505 (1973).
9. K. G. CAULTON. Inorg. Nucl. Chem. Lett. **9**, 533 (1973).
10. J. R. GOLLOGLY and C. J. HAWKINS. Inorg. Chem. **9**, 576 (1970).
11. L. D. HALL, P. R. STEINER, and C. PEDERSON. Can. J. Chem. **48**, 1155 (1970).
12. R. E. GALL, D. LANDMAN, G. P. NEUSOROFF, and J. STERNHELL. Aust. J. Chem. **25**, 109 (1972).
13. A. M. IHRIG and S. L. SMITH. J. Am. Chem. Soc. **94**, 34 (1972); A. M. IHRIG and S. L. SMITH. J. Am. Chem. Soc. **92**, 759 (1970).
14. F. R. JENSEN and B. H. BECK. J. Am. Chem. Soc. **90**, 3251 (1968); F. R. JENSEN, C. H. BUSHWELLER, and B. H. BECK. J. Am. Chem. Soc. **91**, 344 (1969); L. D. HALL and D. L. JONES. Can. J. Chem. **51**, 2914 (1973).
15. K. L. WILLIAMSON, Y.-F. L. HSU, F. H. HALL, S. WAGER, and M. S. COULTER. J. Am. Chem. Soc. **90**, 6717 (1968).
16. R. E. CRAMER. Inorg. Chem. **11**, 1019 (1972).
17. J. B. LAMBERT, J. J. POPAY, E. S. MAGYAR, and M. K. NEUBERG. J. Am. Chem. Soc. **95**, 4458 (1973).
18. K. N. SLESSOR and A. S. TRACEY. Can. J. Chem. **49**, 2874 (1971).
19. I. W. NOWELL, S. RETTIG, and J. TROTTER. J. Chem. Soc. Dalton Trans. 2381 (1972).
20. M. KARPLUS. J. Chem. Phys. **30**, 11 (1959).
21. M. KARPLUS. J. Am. Chem. Soc. **85**, 2870 (1963).
22. K. G. R. PACHLER. Tetrahedron, **27**, 187 (1971).
23. K. G. R. PACHLER. J. Chem. Soc. Perkin Trans. II, 1936 (1972).
24. R. J. ABRAHAM and G. GATTI. J. Chem. Soc. B, 961 (1969).
25. L. PHILLIPS and V. WRAY. J. Chem. Soc. Perkin Trans. II, 536 (1972).

Can. J. Chem. Downloaded from www.nrcresearchpress.com by 210.87.254.40 on 09/05/12
For personal use only.

The Crystal Structure of Dimedone

ISHWAR SINGH
Department of Chemical Technology, Mohawk College, Hamilton, Ontario L9C 1G1
AND
CRISPIN CALVO
Department of Chemistry, McMaster University, Hamilton, Ontario L8S 4M1

Received June 12, 1974

ISHWAR SINGH and CRISPIN CALVO. Can. J. Chem. **53**, 1046 (1975).

Dimedone, $C_8H_{12}O_2$, crystallizes with monoclinic symmetry, $a = 10.079(7)$, $b = 6.835(3)$, $c = 12.438(4)$ Å, $\beta = 110.24(5)°$, space group $P2_1/n$ and $Z = 4$. The structure of this compound was solved by direct methods and refined by full-matrix least-squares techniques using 1205 unique reflections to a final R of 0.047. In the solid state it exists in the enolic form and these molecules pack in the crystal in systems of infinite chains linked together by hydrogen bonds in the y direction. These results are virtually the same as recently reported by Semmingsen.

ISHWAR SINGH et CRISPIN CALVO. Can. J. Chem. **53**, 1046 (1975).

Le dimédon, $C_8H_{12}O_2$, cristallise avec une symétrie monoclinique $a = 10.079(7)$, $b = 6.835(3)$, $c = 12.438(4)$ Å, $\beta = 110.24(5)°$, groupe d'espace $P2_1/n$ et $Z = 4$. On a résolu la structure de ce composé par des méthodes directes et on l'a affinée par la méthode des moindres carrés (matrice complète) utilisant 1205 réflections uniques jusqu'à une valeur finale de R de 0.047. A l'état solide, le dimédon existe sous forme énolique et les molécules s'arrangent dans le cristal dans un système de chaines infinies liées entre elles par des ponts hydrogène dans la direction y. Ces résultats sont pratiquement les mêmes que ceux rapportés récemment par Semmingsen.

[Traduit par le journal]

Introduction

Dimedone, also known as 5,5-dimethylcyclohexane-1,3-dione, methone, or 5,5-dimethyldihydroresorcinol, can exist in the form of keto (**1**), enol (**2**), dimeric enol (**3**), and polymeric enol (**4**) structure as shown below.

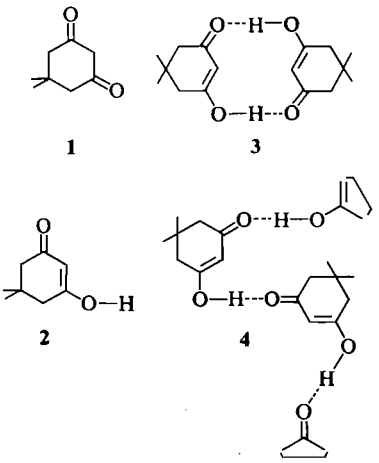

Studies in solution by infrared spectroscopy (1, 2) and C^{13} n.m.r. spectrometry (3) show the presence of both the keto and enol forms in different concentrations and under different conditions. But in the solid state dimedone can exist either in the dimeric or polymeric enol form. The dimeric enol form does not seem very probable from the geometric considerations. This study was undertaken to determine the structure in the solid state by single crystal X-ray diffraction method. While this report was in the hands of the referees a report of the structure of dimedone appeared (4). Since both results appear to be of comparable quality a detailed comparison seemed advisable.

Experimental

A crystal of dimedone having approximate dimensions $0.05 \times 0.03 \times 0.03$ cm^3 was used for all the X-ray measurements. The space group was uniquely determined as $P2_1/n$ from systematic absences (conditions limiting possible reflections: $h00$, $h = 2n$; $0k0$; $k = 2n$; $00l$, $l = 2n$; $h0l$, $h + l = 2n$). Crystal data are as follows:

$C_8H_{12}O_2$ f.w. = 140

Monoclinic, $a = 10.079(7)$, $b = 6.835(3)$, $c = 12.438(4)$ Å, $\beta = 110.24(5)°$, $V = 803.94$ Å^3 at $T = 25$ °C. $Z = 4$, $D_x = 1.15 \pm 0.05$ g/cm^3 (20 °C), $\lambda(MoK_{\bar{\alpha}}) = 0.71069$.

The dimensions of the unit cell were obtained from a least squares refinement of 13 values of 2θ measured with $MoK_{\bar{\alpha}}$ radiation using a P$\bar{1}$ Syntex automatic diffrac-

Can. J. Chem. Downloaded from www.nrcresearchpress.com by 210.87.254.6 on 09/05/12
For personal use only.

Can. J. Chem. Downloaded from www.nrcresearchpress.com by 210.87.254.6 on 09/05/12
For personal use only.

tometer. A total of 1205 unique reflections lying in the range $0 < 2\theta \leq 55°$ were measured on this diffractometer using graphite monochromatized $MoK_{\bar{\alpha}}$ radiation. Reflections were scanned in the θ–2θ mode at a rate between 2 and 24° per minute depending on the peak intensity. Backgrounds were recorded on either side of the peak and used to determine the integrated intensity together with an estimated standard deviation based upon counting statistics. Those reflections whose intensity were less than 3σ, 473 in number, were regarded as unobserved. The data were corrected for Lorentz and polarization effects but not absorption. The XRAY-71 package of programs for X-ray crystallography published by the University of Maryland as adopted for use with the CDC 6400 by H. D. Grundy were used for all computations.

The positions of 8 carbon atoms and two oxygen atoms were determined from the E map after the phases of reflections were determined by the direct method (5). These initial positions were refined with their individual isotropic temperature factors and a scale factor. This yielded a minimum R of 0.13. The atomic scattering curves were obtained from the International tables for X-ray crystallography (6). A difference electron density map at this stage revealed the positions of all the 12 hydrogen atoms of the dimedone molecule. Further refinements were carried out, using anisotropic temperature factors for the nonhydrogen atoms and isotropic temperature factors for the hydrogen atoms. Weights were given by $\omega = [0.6520 - 0.1420F_o + 0.0110F_o^2]^{-1}$. These weights were chosen so that $\omega|F_o - F_o|^2$ would locally be independent of F_o, the observed structure factor. The unobserved reflections were weighted as the observed and were also included in the refinement. The final refinement resulted in a minimum R of 0.047 and $R\omega = [\Sigma\omega|F_o - F_c|^2/\Sigma\omega|F_o|^2]^{1/2}$ equal to 0.045. The average shift/error in the final cycle of refinement and the standard deviations of an observation, $[\Sigma\omega|F_o - F_c|^2/(m - n)]^{1/2}$, were 0.097 and 0.49 respectively. A final difference Fourier map contained no more electron density variations than ± 0.34 e/Å^3. The final atomic parameters are listed in Table 1 and the observed and calculated structure factors are in Table 2.[1] A list of the bond lengths and angles with standard deviations calculated from the standard errors derived from the least-squares matrix is given in Table 3.

Description of the Structure

A view of the molecule is seen in Fig. 1. It is found that the structure of dimedone is of enol form in the solid state. In the enolic form atoms O1, C1, C2, C3, and O2 are coplanar with H6 −0.14 Å and C5 0.53 Å out of this plane. The negative deviation for H1 indicates that it is on the opposite side of the plane from C5. A plane defined by H6, O1, and C1 makes an acute angle of 7° with the plane defined by atoms O1, C1, C2, C3, and O2. This allows for increased distance between atoms H6 and H1, thereby decreasing the interaction between them. This is further supported by the fact that angle C1—C2—H1 (Table 3) is 131.4° instead of 120.00° as expected. This may arise from the repulsion between the atoms H6 and H1. Thus it seems that the presence of H6 on the side of C2, as found in this structure, rather than on the side of C6 is not really the preferred orientation but is perhaps necessary for the packing of the dimedone molecule in the solid state. The conformation of the molecule can be best described as an envelope with C5 0.62 Å out of the plane defined by O1, O2, C1, C2, C3, C4, and C6. The plane defined by C4, C5, and C6 makes an angle of 136.14° with the last plane. Deviations from this plane, (*b*) in Table 4, are positive for C1, C2, C3, and C6 and are on the same side as C5 whereas for O1, O2, and C4 they are negative.

The molecules of dimedone attains the polymeric enol structure in the solid state as evidenced by a hydrogen bond of length 1.71(4) Å between the atoms H6 of the asymmetric unit and O2 of the molecule generated by the equivalent positions $-x + \frac{1}{2}$, $y - \frac{1}{2}$, $-z + \frac{1}{2}$ and similarly O2 of the asymmetric unit is bonded through a hydrogen bond to H6 of another molecule related by the equivalent positions $-x + \frac{1}{2}$, $y + \frac{1}{2}$, $-z + \frac{1}{2}$. These chains extend in the y direction thereby allowing the dimedone molecules to pack closely. The bond angle O1—H6....O2 is 167(3)°. However, this nonlinearity is not an exception to the various hydrogen bond angles found in many other compounds (7). The other hydrogen bond lengths and angles are given in Table 5. The intermolecular H6...H1 contact distance is 2.485 Å close to corresponding intramolecular distance of 2.483 Å.

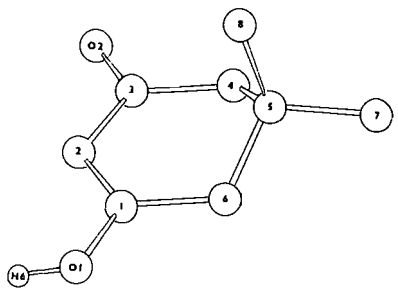

FIG. 1. Molecular structure of dimedone.

[1]Photocopies of Table 2 are available for a nominal charge from the Depository of Unpublished Data, National Science Library, National Research Council of Canada, Ottawa, Canada K1A 0S2.

TABLE 1. Atomic parameters of dimedone*

Atom	x	y	z	U_{11}	U_{22}	U_{33}	U_{12}	U_{13}	U_{23}
O(1)	0.4044(2)	−0.1504(2)	−0.3569(2)	6.9(1)	6.1(1)	6.6(1)	2.3(1)	2.6(1)	1.2(1)
†	0.4042(1)	−0.1508(2)	−0.3571(1)	5.6(1)	6.6(1)	5.7(1)	−1.3(1)	2.0(1)	1.1(1)
O(2)	0.0516(2)	0.3024(2)	−0.3597(1)	6.3(1)	5.9(1)	6.8(1)	−0.6(1)	2.5(1)	0.9(1)
†	0.0514(1)	0.3227(2)	−0.3597(1)	5.2(1)	6.0(1)	5.7(1)	−1.5(0)	2.2(1)	−0.8(1)
C(1)	0.3057(2)	−0.0172(3)	−0.4055(2)	4.9(1)	4.3(1)	5.6(1)	0.0(1)	1.5(1)	0.2(1)
†	0.3057(2)	−0.01711(2)	−0.4053(1)	4.7(1)	4.8(1)	5.0(1)	−0.0(1)	2.3(1)	−0.0(1)
C(2)	0.2352(2)	0.0833(3)	−0.3482(2)	5.0(1)	5.2(1)	4.5(1)	−0.4(1)	1.5(1)	−0.0(1)
†	0.2350(2)	0.0835(2)	−0.3484(1)	4.6(1)	5.3(1)	4.3(1)	−0.1(1)	1.7(1)	−0.0(1)
C(3)	0.1253(2)	0.2158(3)	−0.4078(2)	4.8(1)	4.0(1)	5.8(1)	0.6(1)	1.8(1)	0.9(1)
†	0.1245(2)	0.2150(2)	−0.4078(1)	4.7(1)	4.4(1)	5.1(1)	−0.1(1)	2.4(1)	−0.7(2)
C(4)	0.0898(2)	0.2430(4)	−0.5345(2)	5.5(1)	4.5(1)	5.3(1)	0.4(1)	1.1(1)	−0.3(1)
†	0.0905(2)	0.2438(2)	−0.5343(1)	5.9(1)	4.9(1)	4.8(1)	−0.5(1)	2.7(1)	−0.2(1)
C(5)	0.2133(2)	0.2080(3)	−0.5766(2)	6.2(1)	5.0(1)	4.6(1)	0.1(1)	1.7(1)	−0.2(1)
†	0.2137(2)	0.2073(2)	−0.5762(1)	5.3(1)	5.3(1)	4.1(1)	−0.1(1)	1.6(1)	−0.1(1)
C(6)	0.2770(3)	0.0088(4)	−0.5307(2)	6.1(1)	5.4(1)	5.4(1)	0.7(1)	1.9(4)	−0.6(1)
†	0.2773(2)	0.0084(2)	−0.5305(1)	5.2(1)	5.9(1)	4.8(1)	−1.1(1)	1.7(1)	−0.5(1)
C(7)	0.1603(4)	0.2048(5)	−0.7068(2)	9.6(2)	7.9(2)	5.5(2)	1.2(2)	1.8(2)	0.2(1)
†	0.1595(2)	0.2044(3)	−0.7072(1)	8.1(1)	8.3(1)	4.6(1)	−1.2(1)	1.3(1)	0.2(1)
C(8)	0.3248(3)	0.3676(5)	−0.5331(3)	8.5(2)	6.6(2)	7.7(2)	−1.9(2)	3.2(2)	0.2(1)
†	0.3247(2)	0.3680(3)	−0.5334(2)	6.7(1)	7.2(1)	7.2(1)	1.9(1)	2.5(1)	0.2(1)

Atom	x	y	z	U	Attached to
H(1)	0.2405(16)	0.0776(25)	−0.2674(18)	1.4(5)	C(2)
†	0.2552(15)	0.0648(20)	−0.2677(12)	4.8(4)	
H(2)	0.0124(24)	0.1435(34)	−0.5730(17)	2.7(5)	C(4)
†	0.0084(17)	0.1556(22)	−0.5751(13)	6.1(4)	
H(3)	0.0470(23)	0.3668(37)	−0.5560(18)	3.3(6)	C(4)
†	0.0518(16)	0.3728(24)	−0.5543(12)	5.6(4)	
H(4)	0.2122(22)	−0.0891(37)	−0.5717(17)	3.0(6)	C(6)
†	0.2100(16)	−0.0960(22)	−0.5733(12)	6.1(4)	
H(5)	0.3651(26)	−0.0138(40)	−0.5421(19)	4.9(7)	C(6)
†	0.3661(19)	−0.0129(23)	−0.5438(12)	6.4(5)	
H(6)	0.4081(32)	−0.1766(45)	−0.2848(31)	5.2(8)	O(1)
†	0.4152(21)	−0.1664(25)	−0.2865(16)	7.4(5)	
H(7)	0.2483(37)	0.1962(45)	−0.7391(26)	6.3(8)	C(7)
†	0.2341(24)	0.1803(27)	−0.7379(17)	8.8(0)	
H(8)	0.1015(32)	0.3241(55)	−0.7414(26)	7.9(10)	C(7)
†	0.1102(21)	0.3991(29)	−0.7382(15)	8.8(0)	
H(9)	0.0902(25)	0.1042(38)	−0.7324(20)	4.0(8)	C(7)
†	0.0875(19)	0.0943(28)	−0.7347(15)	8.8(0)	
H(10)	0.4093(27)	0.3428(36)	−0.5635(21)	4.8(7)	C(8)
†	0.4047(24)	0.3489(27)	−0.5576(16)	8.8(0)	
H(11)	0.3611(26)	0.3654(36)	−0.4481(27)	5.6(8)	C(8)
†	0.3609(21)	0.3789(25)	−0.4486(17)	8.8(0)	
H(12)	0.2805(26)	0.4976(53)	−0.5578(20)	4.5(7)	C(8)
†	0.2809(20)	0.4973(28)	−0.5604(15)	8.8(0)	

*U and U_{ij} have been multiplied by 100. The thermal factor is: $\exp -2\pi^2(U_{11}h^2b_1^2 + \ldots + 2U_{12}hkb_1b_2 + \ldots)$ where b_i are reciprocal vectors.
†These are the corresponding parameters from ref. 4.

Comparisons of Two Structures

The structure of dimedone reported by Semmingsen (4) is in $P2_1/c$ space group, with cell dimensions $a = 10.040(1)$, $b = 6.823(1)$, $c = 12.984(2)$ Å, $\beta = 116.20(1)°$ which on transformation to space group $P2_1/n$ does not change a and b but $c = 12.421(2)$ and $\beta = 110.20(1)°$ at 18 °C. These lattice parameters values differ from those in the present report because of the difference in temperature. We have determined the cell dimensions at different temperatures to find that the a, b, and c axes increase by 0.0012,

Can. J. Chem. Downloaded from www.nrcresearchpress.com by 210.87.254.6 on 09/05/12
For personal use only.

Can. J. Chem. Downloaded from www.nrcresearchpress.com by 210.87.254.6 on 09/05/12
For personal use only.

TABLE 3. Bond distances and angles in dimedone with standard errors in parentheses

Bond	Distance (Å)	Bonds	Angle (deg)
C3—O2	1.246(3)	O2—C3—C4	118.5(2)
C3—C4	1.500(3)	O2—C3—C2	122.5(2)
C3—C2	1.418(3)	C4—C3—C2	118.9(2)
C2—C1	1.351(3)	C3—C2—C1	120.5(2)
C2—H1	0.96(2)	H1—C2—C1	131.4(10)
		H1—C2—C3	108.3(10)
C1—O1	1.326(2)	O1—C1—C2	123.9(2)
C1—C6	1.491(3)	O1—C1—C6	113.2(2)
C6—C5	1.524(3)	C1—C6—C5	113.3(2)
C6—H4	1.00(2)	C1—C6—H4	109.0(10)
C6—H5	0.97(3)	C1—C6—H5	106.2(10)
C5—C4	1.527(4)	C6—C5—C4	107.7(2)
C5—C7	1.522(3)	C6—C5—C7	109.5(2)
C5—C8	1.526(4)	C6—C5—C8	110.5(2)
C4—H3	0.96(2)	C5—C4—C3	114.5(2)
C4—H2	1.00(2)	H3—C4—C5	113.0(16)
		H2—C4—C5	108.4(15)
		H3—C4—H2	105.3(18)
C7—H8	0.99(3)	H8—C7—C5	112.3(19)
C7—H7	0.97(4)	H7—C7—C5	111.2(15)
C7—H9	1.01(2)	H9—C7—C5	108.0(16)
C8—H10	0.96(3)	H10—C8—C5	110.2(13)
C8—H11	0.99(3)	H11—C8—C5	108.6(16)
C8—H12	0.99(3)	H12—C8—C5	109.4(15)
O1—H6	0.87(4)	C6—C1—C2	122.8(2)
		C4—C5—C7	109.5(2)
		C4—C5—C8	110.3(2)
		C7—C5—C8	109.2(2)

0.001, and 0.001 Å respectively per °C rise in temperature. This difference might be reflected in different thermal parameters between the refinements. Hamilton's (8) χ square test and Abraham and Keve's (9) half-normal probability plot can be used to compare the sets of results. This is accomplished by calculating δp_i using the following relationship

$$\delta p_i = ||p(1)_i| - |p(2)_i||/\{\sigma^2 p(1)_i + \sigma^2 p(2)_i\}^{1/2}$$

and then examining the hypothesis that δp_i are drawn from a normal population with unit variance and zero mean by testing $\delta^2 p$, which is equal to $\sum_{i-1}^{N} \delta^2 p_i$, against χ^2 with N degrees of freedom. If the calculated value of $\delta^2 p$ exceeds the tabulated value of $\chi_{N,\alpha}{}^2$, the hypothesis may be rejected with $100\alpha\%$ probability of falsely rejecting a true hypothesis. For half-normal probability plot δp_i values are plotted against the expected values, tabulated by Hamilton and Abrahams (10) for samples of size <41, and for no differences in two sets of data the plot should be a straight line of unit slope and zero intercept. Using this procedure a $\delta^2 p$ value of 49.87 for the 30 nonhydrogen positional parameters was calculated. This value falls in between the two tabulated values of $\chi^2_{30,0.05} = 43.77$ and $\chi^2_{30,0.01} = 50.89$. This does not show very significant differences between these sets of parameters. This is further shown by the half-normal probability plot for these positional parameters in Fig. 2. If it is assumed that the line passes through the origin, then a slope of 0.95 is obtained. However, the analysis of variance shows a better line determined by least squares methods with a slope of 0.72 and intercept 0.35. This slight systematic effect is perhaps due to small standard deviations obtained in Semmingsen's results, which in turn is due to 343 more reflections beyond 2θ of 55° collected by him. Similarly hydrogen positional parameters gave a value of $\delta^2 p$ of 141.4 while tabulated value for $\chi^2_{36,0.05}$ is about 51. This significant difference in the two sets can perhaps be ex-

TABLE 4. Least-squares planes and out of plane distances (11)

Atoms	Out of plane deviations (Å)
(*a*) Plane defined by O2, C3, C2, C1, O1 is $6.43x + 5.01y + 0.02z = 1.87$ with a standard deviation of 0.03 Å	
H6	−0.14
H1	0.06
C6	−0.06
C5	0.53
C4	−0.09
(*b*) Plane defined by O1, O2, C1, C2, C3, C4, and C6 is $6.47x + 5.05y - 0.392z = 2.04$	
H6	−0.18
H1	0.02
C5	0.62
O1	−0.04
O2	−0.03
C1	0.01
C2	0.04
C3	0.02
C4	−0.02
C6	0.01
(*c*) Plane defined by C1, O1, and H6 is $5.97x + 4.97y + 1.50z = 1.13$	
H4	−1.17
H1	0.29
(*d*) Plane defined by C4, C5, and C7 is $3.59x + 3.00y + 8.09z = -3.27$	
C7	−1.25
C8	1.23

TABLE 5. Hydrogen bond lengths and angles. The values in parentheses are the corresponding parameters from ref. 4

Bond	Distance (Å)	Bonds	Angle (deg)
O1---O2	2.595(2.593)	O1—H6---O2	167(177)
		C1—O1---O2	111.3(112.7)
O1—H6	0.90(0.87)	C3—O2---O1	126(129.7)
O2---H6	1.71(1.74)	C3—O2---H6	125.4(129)
		C1—O1—H6	110.7(11.1)

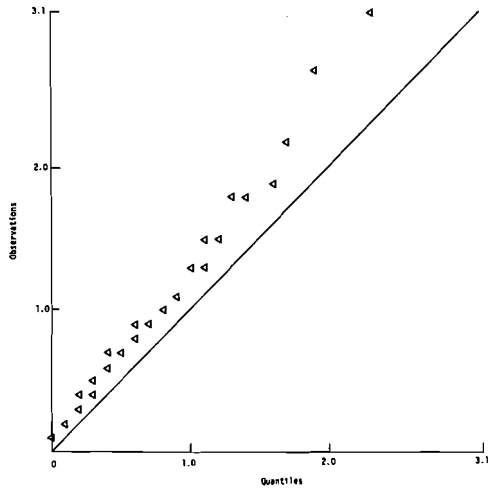

FIG. 2. δp half-normal probability plot.

plained due to different sets of scattering curves used in these two investigations and also in part due to more high angle data collected in the other investigation. As indicated in Table 1 the thermal parameters for the methyl hydrogens in dimedone were not refined by Semmingsen.

The thermal parameters U_{11}, U_{22}, and U_{33} when analyzed for any systematic differences gave 467.7 as the value of $\delta^2 p$ compared to $\chi^2_{30,0.05} = 43.77$. This significant difference probably arises from the different temperatures at which the two data sets were collected and other reasons mentioned above. It is interesting to note that in the earlier investigation of dimedone U_{12} and U_{23} gave values smaller than the present investigation.

Bond lengths and angles from two investigations are given in Table 3. A $\delta^2 p$ value of 12.62 compared to $\chi^2_{10,0105} = 18.31$ for bond lengths of nonhydrogen atoms show no differences at all. A similar analysis for bond angles of these atoms does not show any difference. The only difference of significance is the hydrogen bond angle O1—H6...O2 as noted in Table 5. However, the conformation of the molecule is exactly the same in the two investigations and the structures are of comparable accuracy.

1. R. S. RASMUSSEN, D. D. TUNCLIFF, and R. R. BRATTAINS. J. Am. Chem. Soc. **1**, 1068 (1949).
2. KOJI NAKANISHI. Infrared absorption spectroscopy – practical. Holden-Day, San Francisco, California. 1962. p. 65.
3. J. H. BILLMAN, S. A. SOJKA, and R. T. PHILIP. J. Chem. Soc. Perkins II, **14**, 2034 (1972).
4. D. SEMMINGEN. Acta Chem. Scand. **B28**, 169 (1974).
5. J. KARLE and I. L. KARLE. Acta Cryst. **21**, 849 (1966).
6. International tables for X-ray crystallography. Vol. III. Kynoch Press. Birmingham, England. 1962.
7. J. DONOHUE. Selected topics in hydrogen bonding. *In* Structural chemistry and molecular biology. W. H. Freeman and Co., San Francisco. 1968.
8. W. C. HAMILTON. Acta Cryst. **A25**, 194 (1969).
9. S. C. ABRAHAMS and E. T. KEVE. Acta Cryst. **A27**, 157 (1971).
10. W. C. HAMILTON and S. C. ABRAHAMS. Acta Cryst. **A28**, 215 (1972).
11. V. SCHOMAKER, J. WASER, R. E. MARSH, and G. BERGMAN. Acta Cryst. **12**, 600 (1959).

Can. J. Chem. Downloaded from www.nrcresearchpress.com by 210.87.254.6 on 09/05/12
For personal use only.

Studies in Solvolysis. Part VI. An Examination of the Heat Capacity of Activation for the Hydrolysis of 4-Methoxybenzyl Trifluoroacetate

JUNE GERTRUDE WINTER, JOHN PATRICK BARRON, AND JOHN MARSHALL WILLIAM SCOTT

Chemistry Department, Memorial University, St. John's, Newfoundland A1C 5S7

Received October 8, 1974

JUNE GERTRUDE WINTER, JOHN PATRICK BARRON, and JOHN MARSHALL WILLIAM SCOTT. Can. J. Chem. **53**, 1051 (1975).

The heat capacity of activation for the hydrolysis of 4-methoxybenzyl trifluoroacetate in water containing 9.05×10^{-2} mol fraction of acetone has been measured and shown to be positive. This unusual result is consistent with the notion that the ester reacts by two distinct routes: one involving acyl–oxygen fission, the other, alkyl–oxygen fission. The relative importance of the two paths for the 4-methoxy ester has been established quantitatively via a Hammett σ–ρ correlation for a series of 4-substituted-benzyl trifluoroacetates. Such an assessment allows the observed heat capacity, entropy, and enthalpy of activation to be factored into parts appropriate to each of the two reaction paths.

JUNE GERTRUDE WINTER, JOHN PATRICK BARRON et JOHN MARSHALL WILLIAM SCOTT. Can. J. Chem. **53**, 1051 (1975).

On a mesuré la capacité calorifique d'activation de l'hydrolyse du trifluoroacétate de méthoxy-4 benzyle dans l'eau contenant 9.05×10^{-2} mol d'acétone; on a trouvé que cette valeur est positive. Ce résultat inattendu est en accord avec le fait que l'ester peut réagir par deux routes distinctes: une impliquant une fission acyle–oxygène et l'autre une fission alkyle–oxygène. En faisant appel à une corrélation σ–ρ de Hammett pour une série de trifluoroacétates de benzyles substitués en position 4, on a pu établir d'une façon quantitative, pour l'ester étudié, l'importance relative des deux chemins. Une telle détermination permet d'attribuer à chacune des deux routes de la réaction les capacités calorifiques, les entropies et les enthalpies d'activation appropriées. [Traduit par le journal]

Introduction

The temperature dependence of the enthalpy of activation ($\Delta C_{p_o}^{\ddagger}$) has been measured frequently for S_N1/S_N2 solvolytic displacements (1, 2). The studies reported by Robertson's group (1) have been largely concerned with displacement reactions in pure water, whereas Kohnstam's group (2) have examined the heat capacity parameter in mixed aqueous solvents. Heat capacities of activation have also been measured for the hydrolyses of carboxylic esters and anhydrides (3–5) which usually react by an acyl–oxygen fission mechanism ($B_{Ac}2$). Both the $B_{Ac}2$ and S_N processes[1] give rise to negative heat capacities of activation. The negative sign appears to be diagnostic of reactions which include the kinetic or equilibrium production of ions from originally neutral reactants. Extensive discussions are available for such kinetic phenomena (1, 2, 6).

[1]The designations 1 and 2 have been purposefully omitted since the present paper attempts no mechanistic distinctions of this sort.

Recently we have examined the rate of hydrolysis of a series of 4-substituted-benzyl trifluoroacetates (7) and we were able to show that the 4-methoxy ester reacts by a mechanism in which alkyl–oxygen fission (S_N) and acyl–oxygen fission ($B_{Ac}2$) contribute almost equally to the observed rate.

Thus for the scheme represented by

[1] Ester $\xrightarrow{k_b}$ Product ($B_{Ac}2$ route); Ester $\xrightarrow{k_s}$ Product (S_N route)

the observed rate constant k_o is related to the $B_{Ac}2$ and S_N rate constants by

$$[2] \qquad k_o = k_b + k_s$$

where the quantity γ is defined by

$$[3] \qquad \gamma = k_s/k_b$$

The observed heat capacity of activation for a reaction proceeding according to the scheme summarized by reaction 1 is given by the readily derived expression

Can. J. Chem. Downloaded from www.nrcresearchpress.com by 210.87.254.40 on 09/05/12
For personal use only.

$$[4]\quad \Delta C_{po}^{\ddagger} = \frac{1}{1+\gamma}\Delta C_{pb}^{\ddagger} + \frac{\gamma}{1+\gamma}\Delta C_{ps}^{\ddagger} + \frac{\gamma}{(1+\gamma)^2}\frac{(\Delta H_b^{\ddagger} - \Delta H_s^{\ddagger})^2}{RT^2}$$

where $\Delta C_{pb}^{\ddagger}$ and $\Delta C_{ps}^{\ddagger}$ are respectively the heat capacities of activation for paths B and S, and $\Delta H_b^{\ddagger}$ and $\Delta H_s^{\ddagger}$ are the enthalpies of activation appropriate to the same routes. The other symbols in eq. 4 have their usual significance and the quantity γ is defined in eq. 3.

When γ is close to unity and the quantity $|\Delta H_b^{\ddagger} - \Delta H_s^{\ddagger}|$ is large (the value is *ca.* 15 kcal mol^{-1} in water, see ref. 3) the third term on the r.h.s. of eq. 4 might conceivably outweigh the normally negative values of $\Delta C_{pb}^{\ddagger}$ and $\Delta C_{ps}^{\ddagger}$ to yield a net value of $\Delta C_{po}^{\ddagger}$ which is positive.

The purpose of the present paper is to relate the above analysis of $\Delta C_{po}^{\ddagger}$ for a bifurcated mechanism to the temperature dependence of the enthalpy of activation of 4-methoxybenzyl trifluoroacetate for which the quantity γ has already been shown to approximate unity at 5.05 °C in water containing 1.2×10^{-2} mol fraction of acetone. Clearly the ubiquity of negative heat capacities of activation lends considerable interest to one which is positive in sign. Moreover, such a positive heat capacity of activation would provide further evidence for the bifurcated $S_N/B_{Ac}2$ mechanism proposed for 4-methoxybenzyl trifluoroacetate on the basis of other observations.

Experimental

The 4-substituted-benzyl trifluoroacetates were prepared and their purity established as previously described (7). Acetone was treated with potassium permanganate, dried with anhydrous potassium carbonate, and distilled (b.p. 57.5 °C). Distilled deionized water was used to prepare all solutions.

Kinetics

Rates were measured by conductance in an acetone–water mixture containing 9.05×10^{-2} mol fraction of the nonaqueous component which was added to reduce supersaturation of the substrates. Frequent density measurements were made to monitor and then maintain the composition of the solvent during preparation and use. At twelve of the eighteen temperatures for which rates are recorded for the 4-methoxy ester the density of the solvent (T = 25 °C) was 0.96284 ± 0.00004 g ml^{-1}. The remaining six density measurements averaged at 0.96249 ± 0.00023 g ml^{-1}. The variation of the rate constants arising from changes in solvent composition corresponding to the above range of densities is less than the spread of rate constants at any particular temperature. Hence errors arising from variations in the solvent composition during the course of the work are negligible. A small quantity of trifluoroacetic acid was added to the solvent to reduce the resistance of the solvent to a convenient value. Otherwise the general technique of measuring the rates was similar in most respects to that described in ref. 3. A more detailed description of the apparatus is given elsewhere (8, 9). The rate constants measured for the five esters studied are quoted in Table 1.

The temperature dependence of the rates of hydrolysis for benzyl trifluoroacetate is expressed by

$$[5]\quad \log(k/T) = -1862.7/T + 0.9781$$

in which the coefficient of $1/T$ and the constant term are least squares values. The conversion of

TABLE 1. Rates of reaction for the hydrolysis of some 4-substituted benzyl trifluoroacetates

Ester (4-X—$C_6H_4CH_2OCOCF_3$)	T (°C)	$k \times 10^4$ (s^{-1})*
—OCH_3	2.053	4.914±0.007 (4)
	3.091	5.396±0.030 (4)
	3.980	5.767±0.090 (3)
	4.019	5.902±0.025 (4)
	4.978	6.432±0.041 (8)
	5.822	6.918±0.027 (5)
	6.958	7.701±0.045 (6)
	8.138	8.575±0.022 (4)
	8.999	9.309±0.094 (4)
	9.086	9.419±0.088 (4)
	10.096	10.20 ±0.02 (4)
	11.100	11.30 ±0.02 (4)
	12.097	12.37 ±0.04 (4)
	12.846	13.23 ±0.01 (4)
	14.000	14.79 ±0.10 (6)
	14.729	15.48 ±0.13 (6)
	15.970	17.53 ±0.05 (4)
	16.887	19.26 ±0.02 (4)
—CH_3	4.97	3.849±0.013 (4)
—H†	4.97	5.295±0.003 (4)
	9.92	7.118±0.024 (4)
	14.73	9.237±0.030 (4)
—Cl	5.00	8.410±0.010 (3)
—NO_2	4.98	26.65 ±0.08 (4)

*Number of individual rate determinations in parentheses.
†At 9.9 °C, the midpoint of the temperature range $\Delta H_0^{\ddagger}$ = 8.54 kcal mol^{-1} and $\Delta S^{\ddagger}$ = −42.8 e.u. for hydrolysis of benzyl trifluoroacetate.

Can. J. Chem. Downloaded from www.nrcresearchpress.com by 210.87.254.40 on 09/05/12
For personal use only.

Can. J. Chem. Downloaded from www.nrcresearchpress.com by 210.87.254.40 on 09/05/12
For personal use only.

these numerical constants to the pseudothermodynamic quantities, $\Delta H^{\ddagger}$ and $\Delta S^{\ddagger}$, was accomplished in the usual way (3). The more extensive study of the 4-methoxy ester gave rates whose temperature dependence could be represented by[2]

$$[6] \quad \log k = 2431.4/T + 45.73537 \log T - 123.7229$$

The numerical coefficients in eq. 6 were determined using a least squares program which is based on some considerations reported by Clarke and Glew (10). The individual rates (not the meaned rates reported in Table 1) were used in the least squares computation. In the present study all but two of the 84 rates measured were accepted by the program. The two rejected rate constants deviated by more than 2.6% from the value calculated from eq. 6. The conversion of the numerical coefficients of eq. 6 to give values of $\Delta H_0^{\ddagger}$ and $\Delta S_0^{\ddagger}$ at any selected temperature and a value of $\Delta C_{p_0}^{\ddagger}$ follows usual practice (1). The value for $\Delta C_{p_0}^{\ddagger}$ was found to be 89 ± 17 cal mol^{-1} deg^{-1}. The relatively large error in the heat capacity of activation from the coefficient of log T in eq. 6 is probably a consequence of supersaturation, a problem which proved to be a significant factor in the hydrolysis of *t*-butyl trifluoroacetate (11). The various thermodynamic quantities derived from the kinetic data are reported in Table 2.

TABLE 2. Thermodynamic parameters for the hydrolysis of 4-methoxybenzyl trifluoroacetate at various temperatures*

T (°C)	$\Delta H_0^{\ddagger}$ (kcal mol^{-1})	$\Delta S_0^{\ddagger}$ (e.u.)
0.00	13.18	−25.8
9.90	14.06	−22.6
25.00	15.40	−17.9
50.00	17.63	−10.8
75.00	19.85	−4.2
100.00	22.08	2.0

*Calculated on the basis of $\Delta C_p^{\ddagger} = 89$ cal mol^{-1} deg^{-1}.

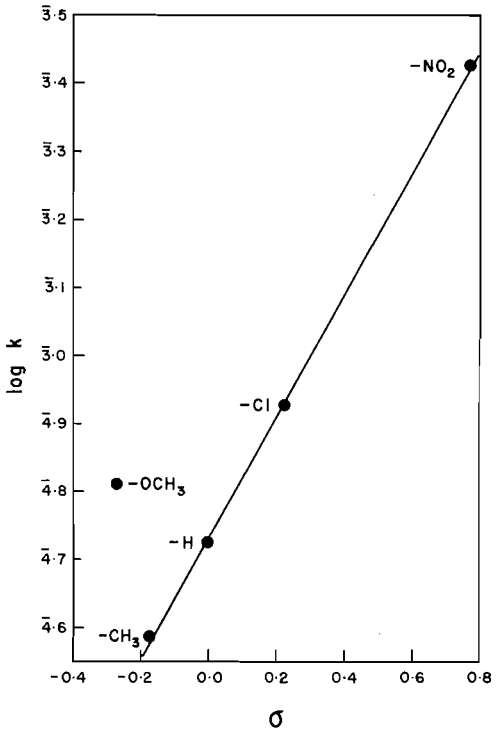

FIG. 1. Correlation of the rates of hydrolysis at 5 °C of a series of 4-substituted-benzyl trifluoroacetates with the Hammett σ parameter.

Discussion

Relative Rates, Free Energies of Activation

The general behavior of the five 4-substituted benzyl trifluoroacetates (4-X—$C_6H_4CH_2OCOCF_3$ where X = —OCH_3, —CH_3, —H, —Cl, and —NO_2) is very similar to that observed in our previous study (7) for an acetone–water mixture richer in water (1.02×10^{-2} mol fraction of acetone). The Hammett plot is also similar and the positive deviation of the 4-methoxy ester from the $B_{Ac}2$ line (see Fig. 1), as interpreted previously (see ref. 3), gives $k_s = 3.34 \times 10^{-4}$ s^{-1} and $k_b = 3.09 \times 10^{-4}$ s^{-1}, *i.e.*, the S_N and $B_{Ac}2$ routes are again of roughly equal importance in the new solvent system ($\gamma = 1.081$).

Enthalpies and Entropies of Activation

The $\Delta H_0^{\ddagger}$ and $\Delta S_0^{\ddagger}$ values for the unsubstituted ester calculated from the numerical coefficients in eq. 5 correspond to $T = 9.9$ °C

[2]Equation 6 assumes that $\Delta C_{p_0}^{\ddagger}$ is independent of temperature which is at variance with eq. 4. The $\Delta C_{p_0}^{\ddagger}$ obtained from eq. 6 is an averaged value over the range of temperatures studied. The rates measured in the present study are not considered to be sufficiently accurate to establish the temperature dependence of $\Delta C_{p_0}^{\ddagger}$ but the "large error" in $\Delta C_{p_0}^{\ddagger}$ may possibly be associated with factors implicit in eq. 4. However, the large error can be accounted for in other ways, *e.g.* the small temperature range over which the reaction rates were studied.

Can. J. Chem. Downloaded from www.nrcresearchpress.com by 210.87.254.40 on 09/05/12
For personal use only.

which is the midpoint of the experimental range over which the rates were determined. The values of $\Delta H_o^{\ddagger}$ and $\Delta S_o^{\ddagger}$ at 9.9 °C for the 4-methoxy ester both show a positive shift from the related quantities observed for the unsubstituted ester. This shift is consistent with a contribution from the S_N reaction to k_o for this ester, since the S_N reaction is characterized with a positive shift in both $\Delta H^{\ddagger}$ and $\Delta S^{\ddagger}$ (see part I (3) of the present series).

The expressions relating the observed $\Delta H_o^{\ddagger}$ and $\Delta S_o^{\ddagger}$ values for the 4-methoxy ester to parameters characterizing the separate mechanisms are

$$[7] \quad \Delta H_o^{\ddagger} = \frac{1}{1+\gamma}\Delta H_b^{\ddagger} + \frac{\gamma}{1+\gamma}\Delta H_s^{\ddagger}$$

and

$$[8] \quad \Delta S_o^{\ddagger} = \frac{1}{1+\gamma}\Delta S_b^{\ddagger} + \frac{\gamma}{1+\gamma}\Delta S_s^{\ddagger} - 2.3026R \times \{\log k_b + \gamma \log k_s - (1+\gamma)\log k_0\}$$

Using eqs. 7 and 8 in conjunction with the experimental data the enthalpies, entropies, and heat capacities characterizing the $B_{Ac}2$ and S_N reactions for 4-methoxybenzyl trifluoroacetate may be estimated.

From the value of k_b, (quoted above) the free energy of activation for the $B_{Ac}2$ mechanism, $\Delta G_b^{\ddagger}$, may be calculated as 20.71 kcal mol^{-1} (for $T = 5$ °C). Since the enthalpy of activation associated with the $B_{Ac}2$ mechanism ($\Delta H_b^{\ddagger}$) is not particularly sensitive to structure (3), the unsubstituted benzyl ester provides a model for estimating $\Delta H_b^{\ddagger}$ for the 4-methoxy ester. The value of $\Delta H_b^{\ddagger}$ for the unsubstituted ester is 8.54 kcal mol^{-1} and in the case of the 4-methoxy ester we raise this value to 9.0 kcal mol^{-1} on two counts. Firstly, the negative $\Delta C_{pb}^{\ddagger}$ anticipated for the $B_{Ac}2$ mechanism will raise $\Delta H_b^{\ddagger}$ (T changes from 9.9 → 5 °C) and secondly, the 4-methoxy ester is the least reactive ester with respect to the complete series of benzyl esters reacting by the $B_{Ac}2$ path. Combining $\Delta H_b^{\ddagger}$ and $\Delta G_b^{\ddagger}$ for the 4-methoxy ester gives $\Delta S_b^{\ddagger}$ ($T = 5$ °C) = −42.1 cal mol^{-1} deg^{-1}. For the same temperature $\Delta H_o^{\ddagger} = 13.6$ kcal mol^{-1} and $\gamma = 1.081$ which from eq. 7 gives $\Delta H_s^{\ddagger} = 17.86$ kcal mol^{-1}. From similar considerations involving eq. 8 with $\Delta S_o^{\ddagger}$ ($T = 5$ °C) = −24.1 cal mol^{-1} deg^{-1} yields $\Delta S_s^{\ddagger} = -10.1$ e.u. Combining $\Delta H_s^{\ddagger}$ and $\Delta S_s^{\ddagger}$ in the usual way yields a value of $\Delta G_s^{\ddagger}$ which is consistent with the value of k_s obtained via the Hammett plot (3.34×10^{-4} s^{-1}). The $\Delta H_s^{\ddagger}$ and $\Delta S_s^{\ddagger}$ values are in the "general region" for an S_N process in acetone–water mixtures. Moffat and Hunt (12) report $\Delta S_s^{\ddagger} = -5.8$ cal mol^{-1} deg^{-1} and $\Delta H_s^{\ddagger} = 23.0$ kcal mol^{-1} for *t*-butyl trifluoroacetate in 70% acetone–water. Since the reaction of the latter compound involves the attack at a tertiary center and the solvent systems are not identical, the S_N character of the calculated $\Delta S_s^{\ddagger}$ and $\Delta H_s^{\ddagger}$ for the 4-methoxybenzyl trifluoroacetate is adequately established by comparison.

The Heat Capacity of Activation

With $\Delta H_b^{\ddagger} = 9.00$ kcal mol^{-1} and $\Delta H_s^{\ddagger} = 17.86$ kcal mol^{-1} the final spurious heat capacity term (11) in eq. 4 can be calculated as 127.5 cal mol^{-1} deg^{-1}. This value combined with $\Delta C_{po}^{\ddagger} = 89$ then gives

$$[9] \quad 0.418\Delta C_{pb}^{\ddagger} + 0.519\Delta C_{ps}^{\ddagger} = -38.5$$

For many S_N reactions in acetone–water mixtures (2) $\Delta C_p^{\ddagger}/\Delta S^{\ddagger} = 3$ which gives $\Delta C_{ps}^{\ddagger} = -30$. Substituting this value into eq. 9 gives $\Delta C_{pb}^{\ddagger} = -55$ which is reasonable (*cf.* ref. 3) for such a process.

General Comments

The mechanistic bifurcation postulated in the case of 4-methoxybenzyl trifluoroacetate was originally devised to account for the deviation from a Hammett plot as well as an unusual value for the solvent isotope effect $k(H_2O)/k(D_2O)$ observed for this ester (7). The same hypothesis is capable of explaining the unique positive heat capacity of activation for this process. The present study further vindicates the notion that careful temperature dependence studies are of considerable mechanistic utility (1, 2) in spite of forceful statements presenting an opposite point of view (13).

The authors wish to thank the National Research Council of Canada for partly helping with the cost of this work. We also wish to express our gratitude to the technical services unit at Memorial University for their continued assistance and Dr. Peter Golding for some useful criticisms. We also thank Dr. R. E. Robertson of the University of Calgary for providing the least squares computer program.

1. R. E. ROBERTSON. *In* Progress in physical organic chemistry. Vol. 4. *Edited by* A. J. Streitwieser, Jr. and R. W. Taft. Interscience, John Wiley, London and New York. 1967. p. 213.
2. G. KOHNSTAM. *In* Advances in physical organic chemistry. Vol. 5. *Edited by* V. Gold. Academic Press, London and New York. 1967. p. 121.
3. J. G. WINTER and J. M. W. SCOTT. Can. J. Chem. **46**, 2887 (1968).
4. V. GOLD. Trans. Faraday Soc. **44**, 506 (1948).
5. R. E. ROBERTSON, B. ROSSALL, and W. A. REDMOND. Can. J. Chem. **49**, 3665 (1971).
6. G. KOHNSTAM. The transition state. Chem. Soc. Spec. Publ. No. 16. 1962. p. 176.
7. J. G. WINTER and J. M. W. SCOTT. Can. J. Chem. **50**, 1886 (1972).
8. D. J. BARNES and J. M. W. SCOTT. Can. J. Chem. **51**, 411 (1973).
9. D. J. BARNES, P. GOLDING, and J. M. W. SCOTT. Can. J. Chem. **52**, 1966 (1973).
10. E. C. W. CLARKE and D. N. GLEW. Trans. Faraday Soc. **62**, 539 (1966).
11. D. J. BARNES, M. COLE, S. LOBO, J. G. WINTER, and J. M. W. SCOTT. Can. J. Chem. **50**, 2175 (1972).
12. A. MOFFATT and H. HUNT. J. Am. Chem. Soc. **80**, 2985 (1958).
13. M. J. S. DEWAR. The molecular orbital theory of organic chemistry. McGraw Hill, London, New York. 1969. p. 283.

Can. J. Chem. Downloaded from www.nrcresearchpress.com by 210.87.254.40 on 09/05/12
For personal use only.

The Observable Thirtyfold Degenerate Camphenehydro Cation. A Stereospecific *exo*-3,2-Methyl Shift and *endo*-6,2(*exo* 6,1)-Hydride Shift

R. HASELTINE, E. HUANG, K. RANGANAYAKULU, AND T. S. SORENSEN

Department of Chemistry, University of Calgary, Calgary, Alberta T2N 1N4

Received June 25, 1974

R. HASELTINE, E. HUANG, K. RANGANAYAKULU, and T. S. SORENSEN. Can. J. Chem. **53**, 1056 (1975).

The observable camphenehydro cation **2** has been prepared and is shown to undergo two degenerate rearrangements, both well known in an indirect sense from many studies on the racemization of camphene. The results from both methods are compared and some advantages of the direct method are given; in particular it is shown that the 3,2-methyl shift is highly stereospecific. An eventual irreversible rearrangement of **2** is observed and the ion products characterized. A computer is used to systematically investigate the shortest paths from reactant to product ions.

R. HASELTINE, E. HUANG, K. RANGANAYAKULU et T. S. SORENSEN. Can. J. Chem. **53**, 1056 (1975).

On a préparé et observé le cation hydrocamphène **2**; on démontre qu'il subit deux réarrangements dégénérés qui sont chacun bien connus d'une façon indirecte à partir de plusieurs études sur la racémisation du camphène. On compare les résultats obtenus à partir des deux méthodes et on indique quelques avantages de la méthode directe; en particulier, on montre que le réarrangement du groupe méthyle de la position 3 vers la position 2 est hautement stéréospécifique. On observe un réarrangement irréversible éventuel de **2** et on caractérise les produits ioniques. On utilise un ordinateur pour étudier d'une façon systématique les chemins les plus courts entre les réactifs et les produits ioniques. [Traduit par le journal]

Introduction

The racemization of camphene, **1***a* ⇌ **1***b*, by acid catalysts is a well-known reaction dating

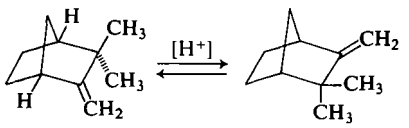

1*a* **1***b*

back over 40 years (1). Although a 3,2-methyl shift (the Nametkin rearrangement) in the intermediate camphenehydro cation **2**[1] (Scheme 1, path *A*) served to explain the racemization, it later became apparent (3) that another sequence of reactions could also explain the result (Scheme 1, path *B*), a sequence involving a Wagner–Meerwein shift in **2**, a 6,2-hydride shift[2] (6,1 if the original numbering is used), and then the reverse Wagner–Meerwein shift (abbreviated in this paper WM-6,2-WM rearrangement). In classic experiments using a ^{14}C label, Roberts and Yancey (4) and Vaughan and Perry (5) showed that both processes occur, *i.e.* there is a redundancy in the racemization mechanism. In fact, there are probably three mechanisms operative since it seems probable that a minor pathway involves tricyclene **3** as an intermediate (6, 7) (Scheme 2).

The overall nature of the 3,2-methyl shift in **2** is still controversial. Vaughan *et al.* (7), in a continuation of their earlier work, have recently suggested that, while the *exo*-3,2 shift is dominant, a measurable amount of *endo*-3,2 shift also occurs. Collins and Lietzke have, however, reanalyzed the same data (8) and conclude that the fit is equally good assuming an exclusive *exo*-3,2-methyl shift. There is, of course, a substantial body of literature (9, 10) showing preferential *exo*-3,2 shifts but *endo* shifts have been reported (11, 12).

The present study, *i.e.* the preparation of the long-lived camphenehydro cation, was undertaken in the hope that one could directly observe the ion-to-ion rearrangements shown in Scheme 1. There are certain advantages inherent in this: (*i*) It can be shown (see Results) that tricyclene most definitely cannot be an intermediate under

[1]Not until the pioneering paper of Meerwein and van Emster (2) in 1922 were carbonium ions actually postulated as intermediates in organic reactions.

[2]Cation structures in Scheme 1, for visual clarity, are not intended to distinguish between classical or nonclassical types.

Can. J. Chem. Downloaded from www.nrcresearchpress.com by 210.87.254.42 on 09/05/12
For personal use only.

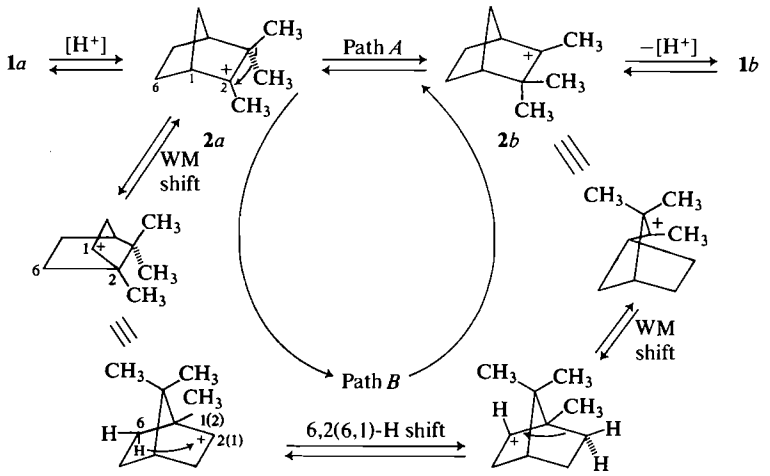

SCHEME 1

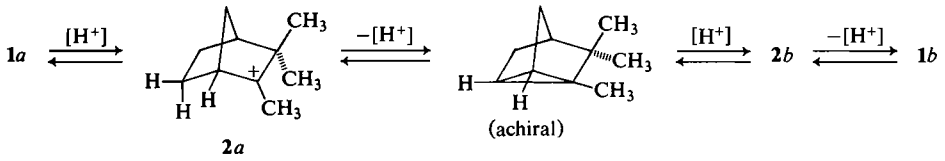

SCHEME 2

these conditions and that hopefully one needs only to consider two mechanisms. (*ii*) The n.m.r. line broadening method can be considered as a superior labelling experiment where *all* of the groups are specifically labelled. One anticipates therefore that *all* stereospecific processes may be detected.

Results

The long-lived camphenehydro cation can be prepared[3] by the addition of camphene, tricyclene, or isoborneol (but not borneol, see later) to FSO_3H or mixtures of this acid diluted with SO_2ClF at −80 to −120 °C. The ion can also be prepared in FSO_3D and in this case, there is no incorporation (other than in the initial preparation) of deuterium into the cation. No neutral intermediates are involved therefore in the degenerate rearrangements observed in this work since these would automatically incorporate deuterium in going back to the cation. The proton n.m.r. spectrum of the ion at −120 °C is shown in Fig. 1 (lower right) and the corresponding ^{13}C spectrum in Fig. 2 (bottom). Both represent 'frozen out' spectra in that all separate peaks are observable and no appreciable line broadening is apparent. The assignment of the proton peaks is based partly on the line broadening observed at higher temperatures and by comparison with chemical shifts observed for other norbornyl cations (13, 14). The assignments and measurable coupling constants are listed in Table 1. The ^{13}C chemical shift assignments (Table 1) were made from off-resonance studies, ^{13}C line-broadening studies and by comparison with ^{13}C chemical shifts observed for the 2-methyl-2-norbornyl cation.

Above −120 °C, line broadening is observed in both ^1H and ^{13}C spectra. The original spectrum is observed on recooling the sample so that the processes responsible for the line broadening are degenerate. In Fig. 1, some representative ^1H n.m.r. spectra are shown covering the temperature range −120 to −53 °C and in Fig. 2, ^{13}C spectra for −100 and −70 °C are shown. Above about −40 °C, an irreversible rearrangement becomes rapid so that line broadening cannot be studied above this temperature. This irreversible rearrangement is discussed later.

[3]Partly described in an earlier communication (13).

Can. J. Chem. Downloaded from www.nrcresearchpress.com by 210.87.254.42 on 09/05/12
For personal use only.

Can. J. Chem. Downloaded from www.nrcresearchpress.com by 210.87.254.42 on 09/05/12
For personal use only.

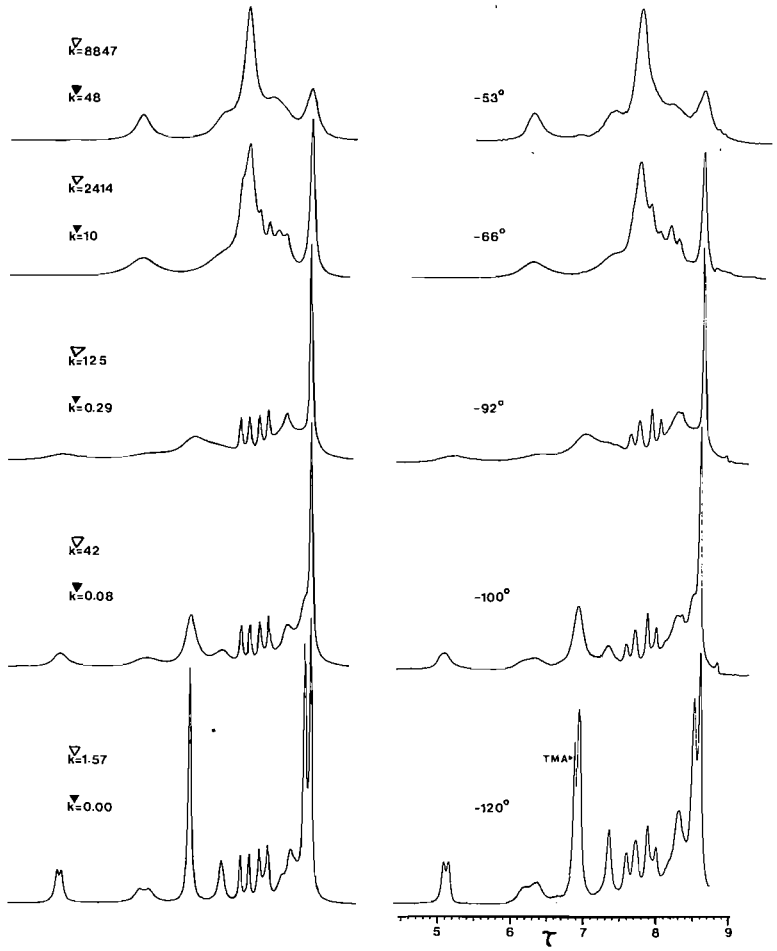

FIG. 1. Right, experimental ^{1}H n.m.r. spectra of the camphenehydro cation at various temperatures. Left, calculated ^{1}H n.m.r. spectra, $k^{\nabla} \equiv$ the *exo*-3,2-methyl shift rate in s^{-1}, $k^{\blacktriangledown} \equiv$ the WM-6,2-WM rearrangement rate in s^{-1}.

The most noticeable feature of the proton spectra obtained in the temperature range -120 to -70 °C is that all peaks broaden except for one methyl group and a four line portion (Fig. 1, temperatures -100 and -92 °C). This line-broadening pattern can be unequivocally attributed to a *stereospecific* 3,2-methyl shift. The groups becoming equivalent are shown in **I**.

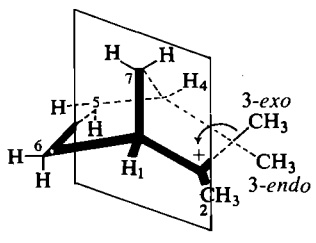

I

^{1}H spectrum		^{13}C spectrum	
$CH_3(2)$	CH_3(3-*endo*)	C_2	C_3
H_1	H_4	C_1	C_4
H_6*exo*	H_5*exo*	C_6	C_5
H_6*endo*	H_5*endo*	$CH_3(2)$	CH_3(3-*endo*)
H_7	(*syn*)	C_7	
H_7	(*anti*)	CH_3(3-*exo*)	
CH_3(3-*exo*)			

symmetry plane

Can. J. Chem. Downloaded from www.nrcresearchpress.com by 210.87.254.42 on 09/05/12
For personal use only.

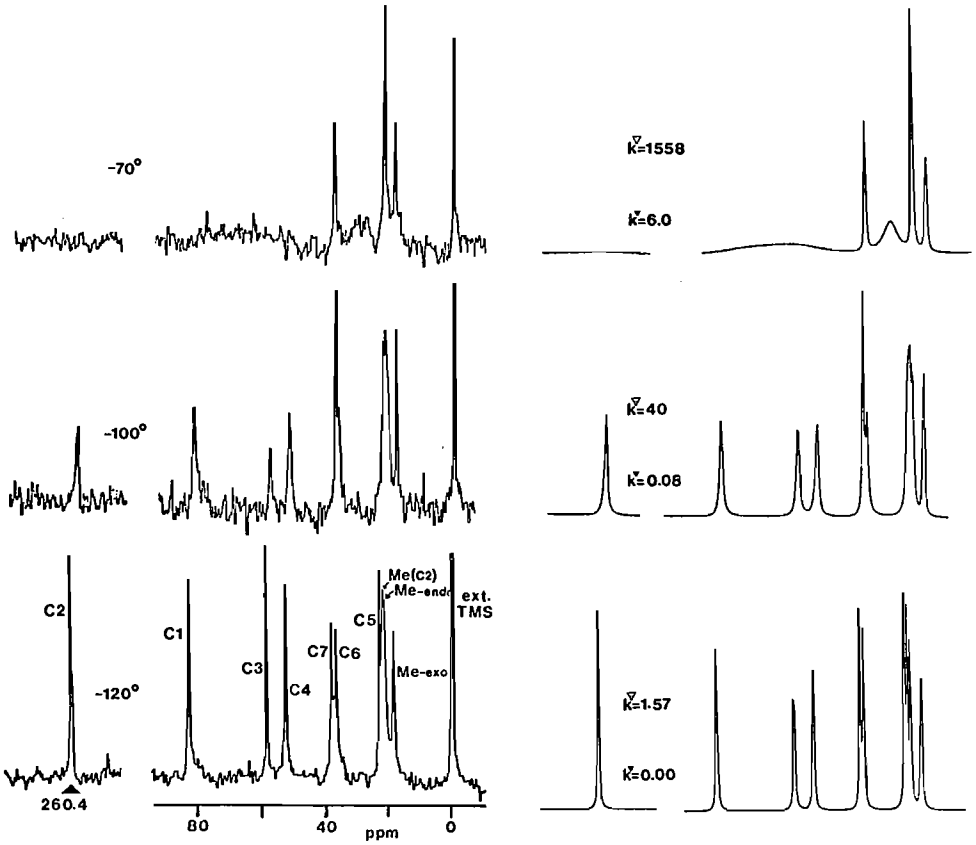

FIG. 2. Experimental and calculated ^{13}C n.m.r. spectra of the camphenehydro cation at −120, −100, and −70 °C.

TABLE 1. Magnetic resonance parameters[a] for **2**

H_1	H_4	H_5	H_6	H_7	CH_3-2	CH_3-3
5.14[b]	7.38	*exo* 8.35[c] *endo* 8.35[c]	*exo* 6.30 *endo* 8.07[c]	*syn* 7.96[d] *anti* 7.68[d]	6.96	*exo* 8.62 *endo* 8.54

C-1	C-2	C-3	C-4	C-5	C-6	C-7	Methyls
80.6	260.4	57.0	51.2	22.4	35.6	36.8	CH_3-C-2 21.3[e] *exo*-C-3 18.0 *endo*-C-3 21.3[e]

[a]In τ p.p.m. relative to internal tetramethylammonium cation = 6.90 for the ^1H spectra and in p.p.m. downfield from external TMS for the ^{13}C spectra.
[b]Doublet, J = 6.5 Hz.
[c]When averaged by the 3,2-methyl shift, the peak for the H_6 *endo* and H_5 *endo* protons is a doublet at 8.21, J = 11 Hz. Since there is a recognizeable peak at 8.3–8.4 in the frozen-out spectrum, this is assigned to H_5 *endo* and H_5 *exo*. H_6 *endo* is then assigned by interpolation.
[d]Both are AB doublets, J = 11.8 Hz. The assignment made on the assumption that H_7 *syn* will be at the higher field position.
[e]In some spectra, these peaks are resolved but no definite assignment is possible.

Although one cannot unequivocally assign the 3-*endo* and 3-*exo* methyl peaks in Fig. 1, and hence decide which migrates, the previous work on ^{14}C labelled camphene and work described in a following publication (15) makes it quite clear that this must be the 3-*exo* methyl. This fact has been assumed in **I** and will be tacitly incorporated in the subsequent discussion. The groups not undergoing exchange, therefore, are the 3-*exo*-methyl group and the C-7-*syn* and -*anti* protons, the latter giving rise to the four lines and analyzing as an AB quartet. The ^{13}C line-broadening

Can. J. Chem. Downloaded from www.nrcresearchpress.com by 210.87.254.42 on 09/05/12
For personal use only.

spectra are completely in accord with the proton assignments. All ^{13}C peaks broaden except for one methyl carbon and a CH_2 carbon (Fig. 2, -100 °C).

Starting at about -70 °C, and well before there is complete coalescence of exchanging peaks from the *exo*-3,2-methyl shift, the remaining sharp methyl peak starts to broaden (Fig. 1, -66 and -53 °C). The nature of this second, slower degenerate process is much more difficult to ascertain since most other peaks are still rather broad from the effects of the 3,2-methyl shift and because of an irreversible rearrangement, one cannot obtain spectra much above -40 °C, a temperature still below the coalescence temperature for the process. However, the two obvious choices for a second degenerate rearrangement involving the remaining methyl group are: (*i*) an *endo*-3,2-methyl shift or (*ii*) a WM-6,2-WM rearrangement (see Scheme 1).

Although both predict a broadening of the remaining methyl group, there are other crucial differences. An *endo*-3,2-methyl shift does not further average (beyond that shown in **I**) any of the other protons, while a WM-6,2-WM process will result in further broadening (assuming the peaks were not already broad). The protons becoming equivalent as a result of this process are shown in **II**.

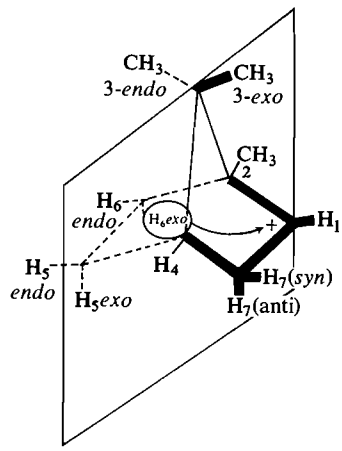

II

CH_3(3-*endo*)	CH_3(3-*exo*)
H_6*endo*	H_1
H_5*endo*	H_7*syn*
H_5*exo*	H_7*anti*
CH_3(2)	
H_4	
H_6*exo*	

symmetry plane

A *stereospecific* migration of the original C-6-*exo* proton to C-1 has been assumed (this is the 6,2-shift, if the intermediate in **II** is renumbered in the proper manner). Once again, there is solvolysis-type evidence for this stereospecificity (16, 17) but in a study of the observable 2-methyl-2-norbornyl cation (13), we have shown the process to be indeed an extremely stereospecific migration. In fact, even in the camphene hydrocation, as will be shown, there is evidence that the process, within the crude limits of the experimental measurements, must be stereospecific.

In order to differentiate between the 3,2-*endo* methyl shift and the WM-6,2-WM process, the following techniques were used.

(*i*) The double irradiation spin-saturation transfer (DISST) method of Forsén and Hoffman (18) was employed. The DISST method consists of saturating a given proton or protons while observing the position into which it is suspected they are exchanging. It is possible to analyze the results quantitatively and to measure the rate of the exchange process but in the present case, major complications arise because of the prior b , adening of peaks from the 3,2-methyl shift and we have obtained only an order of magnitude value (see later). The method is, however, equally valuable from a qualitative point of view and tells one not only that exchange is occurring but also what the mutual exchange processes are. The results of this experiment are shown in Fig. 3. The plot is an INDOR type where the variable f_2 frequency is the saturating external oscillator frequency, the observing frequency f_1 scans the averaged (from the 3,2-methyl shift) C-1–C-4 proton peak (the lowest field peak in Fig. 1, -53 °C). The other axis is the arbitrary height of this peak. This decreases when the f_2 saturating frequency begins to overlap the rather broad C-1–C-4 peak because direct saturation occurs, as expected. The dashed line in Fig. 3 represents the expected peak height behavior caused by direct saturation on the high field side of the peak, *assuming no exchange processes occurred.* That exchange between C-1–C-4 and other protons is occurring is very evident and to show the specific mutual exchanges, the graph shows the location (from Fig. 1) of the averaged C-5-*endo*–

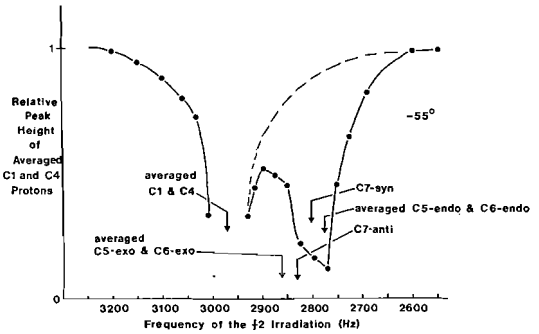

FIG. 3. Application of the n.m.r. DISST technique in detecting specific proton exchanges in the camphenehydro cation.

C-6-*endo* protons, the averaged C-5-*exo*–C-6-*exo* protons, and the separate C-7-*syn* and C-7-*anti* protons. It is apparent that the C-1–C-4 protons do exchange with the C-5-*endo*–C-6-*endo* protons and also probably with the C-7-*syn* proton since the slight asymmetry shown in Fig. 3 is quite reproducible at other temperatures and with different external oscillator power. Nothing very definite can be deduced concerning the C-7-*anti* proton since the 'resolution' of the method is poor; however, it appears very probable that the C-6-*exo*–C-5-*exo* protons are *not* exchanging within the crude limits of the experiment with the C-1–C-4 protons. It is worth emphasizing that an *endo*-3,2 shift would not have caused any of these observations and that the equivalences shown in **I** and **II** predict that the C-1–C-4 protons *should* further exchange with C-5-*endo*–C-6-*endo* and C-7-*syn* but *not* with C-7-*anti* or C-5-*exo*–C-6-*exo* (see subsequent discussion).

(*ii*) From the above discussion, it can be seen that the averaged C-1–C-4 proton peak should further broaden in the WM-6,2-WM mechanism but that no further exchanges are introduced by a 3-*endo* methyl shift process. Accurate rate constants can be calculated for both the two-methyl and three-methyl broadening processes, using the methyl peak line shapes (see next section), the latter calculated broadening pattern being identical for either of the two mechanisms being considered here. Using the derived rate constants for the three-methyl broadening, one can calculate the hypothetical behavior of the averaged C-1–C-4 proton peak and compare this with experiment (Fig. 4) (the small peak to the right is one of the growing irreversible rearrangement product peaks). The line shapes at the three

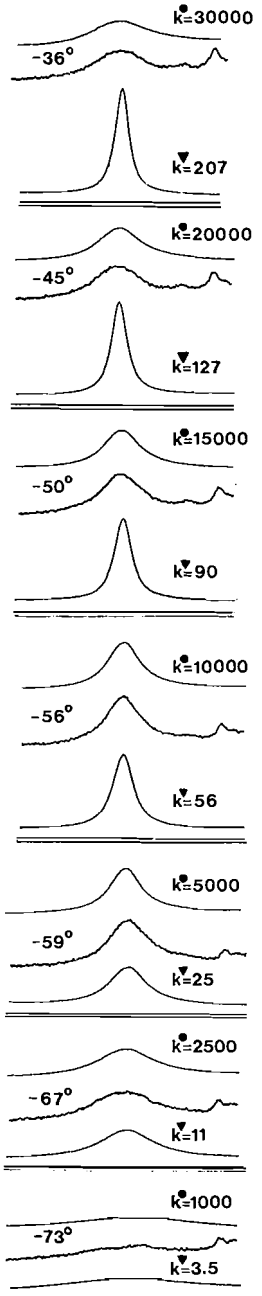

FIG. 4. Middle curve of each set: n.m.r. spectrum of the C_1–C_4 protons of the camphenehydro cation measured at various temperatures. Lower curve of each set: calculated effect on this peak due to a postulated *endo*-3,2-methyl shift in **2**, $k\triangledown$ = *exo*-3,2-methyl shift rate constant, $k\blacktriangledown$ = rate constant of the *endo*-methyl shift. Upper curve of each set: calculated effect on this peak due to a postulated WM-6,2-WM rearrangement in **2**, $k\triangledown$ as above $k\blacktriangledown$ = rate constant for the WM-6,2-WM process.

Can. J. Chem. Downloaded from www.nrcresearchpress.com by 210.87.254.42 on 09/05/12
For personal use only.

Can. J. Chem. Downloaded from www.nrcresearchpress.com by 210.87.254.42 on 09/05/12
For personal use only.

lowest temperatures are still governed by the fast *exo*-3,2-methyl shift process but starting at about −60 °C, the observed peak appears to 'mark time' before finally broadening again, starting at about −45 °C. This behavior is exactly as predicted for the WM-6,2-WM mechanism (top calculations) but totally at variance with an *endo*-3,2-methyl shift (bottom calculations).

(*iii*) The rate of the WM-6,2-WM rearrangement has been accurately measured in two related carbocations where this is the only low temperature rearrangement process. The agreement with the rate calculated from the three-methyl broadening in this work is excellent.

The above observations leave no doubt that the observed second slower degenerate rearrangement is the WM-6,2-WM rearrangement, although one must concede that a small amount of *endo*-3,2-methyl shift would be undetectable (however, see ref. 15).

Quantitative Rate Comparison of the Two Steps

One of the objects of this work concerns the comparison of rate processes observed in long-lived carbocations with those generated as intermediates under 'solvolysis-type' conditions. It is of interest therefore to calculate accurately $k_{exo\text{-}3,2\text{-methyl shift}}$ and $k_{\text{WM-6,2-WM}}$ (and hence the ratio). In addition, activation energies for both processes will be required (for temperature–rate extrapolations) since the camphene racemizations have been carried out from 100 to 180 °C, compared to the −120 to −40 °C range in the observable carbocations.

In the preliminary communication (13), the comparison of calculated and observed n.m.r. line broadening curves was done using only the methyl peaks. Matching the peaks becomes somewhat difficult however because of the distortion caused by the underlying absorptions of some of the eight other protons in the molecule. The calculations have been repeated therefore using all of these protons. The actual system consists of 17 more-or-less closely coupled protons and it is impossible to attempt an exact solution. The approximations used consist of treating the methyl groups separately, treating the C-5-*exo*, C-6-*exo*, and C-7-*anti* protons as another group and the remaining protons as a third group. Small coupling constants are mimicked by using the appropriate T_2 value while separate peaks are included for large couplings but these are all approximated as first-order couplings and a restricted number of spin states are used. In practice, most of these approximations will not seriously affect the intermediate exchange rate spectra (19) where the methyl peak matchings are made.

The rate processes for both steps are not separated enough to treat separately and the kinetic matrix used included both. In addition to changing the absolute values of $k_{exo\text{-}3,2\text{-methyl shift}}$ and $k_{\text{WM-6,2-WM}}$, it was necessary to adjust the ratio of the two in order to finally fit the observed spectra. Several of the calculated and observed spectra are shown in Fig. 1. From this comparison, the following data were obtained in the usual way: for the *exo*-3,2-methyl shift, $\Delta H^{\ddagger} = 8.4$ kcal/mol, $\sigma = 0.2$, $\Delta G^{\ddagger}_{-104\,^{\circ}\text{C}} = 8.3$ kcal/mol, $\Delta S^{\ddagger} = 0.5 \pm 1$ e.u., a typical k being 29.5 s^{-1} at −101.9 °C; for the WM-6,2-WM process, $\Delta H^{\ddagger} = 10.1$ kcal/mol, $\sigma = 0.2$, $\Delta G^{\ddagger}_{-64\,^{\circ}\text{C}} = 10.7$ kcal/mol, $\Delta S^{\ddagger} = -3 \pm 1$ e.u., a typical k being 21 s^{-1} at −59.5 °C. The calculated ^{13}C line shapes shown in Fig. 2 were made using the above activation parameters and show good agreement with the observed spectra. This provides a useful check on the validity of these.

The DISST n.m.r. method provides a further order-of-magnitude value for $k_{\text{WM-6,2-WM}}$. A value of *ca.* 10 s^{-1} at −56 °C was obtained by measuring the equilibrium C-1–C-4 peak height while irradiating the C-5-*endo*–C-6-*endo* protons and assuming a T_1 value of *ca.* 1 s.[4] The extrapolated value from the line broadening is 30.9 s^{-1} at this temperature.

A detailed discussion of both the 3,2-methyl shift and the WM-6,2-WM rearrangement is deferred at this time since it is possible to devise systems where 3,2-methyl shifts occur in the absence of the WM-6,2-WM rearrangement and vice versa (15).

Comparison with Camphene Racemization Results

The original data obtained by Roberts and Yancey have been corrected slightly by Vaughan *et al.* (20). Using a hydrated titanium dioxide catalyst at 160°, the ratio $k_{3,2\text{-shift}}/k_{\text{WM-6,2-WM}}$ was about 0.5; using aniline hydrochloride in

[4]Normally both T_1 and k can be obtained by measuring the time dependence of the peak decrease. This works at temperatures where $T_1 \sim 1/k$, a situation not realizable in this case because the C-1–C-4 proton peak is very broad from the effects of the 3,2-methyl shift (see Fig. 4), −67 °C spectrum as an example.

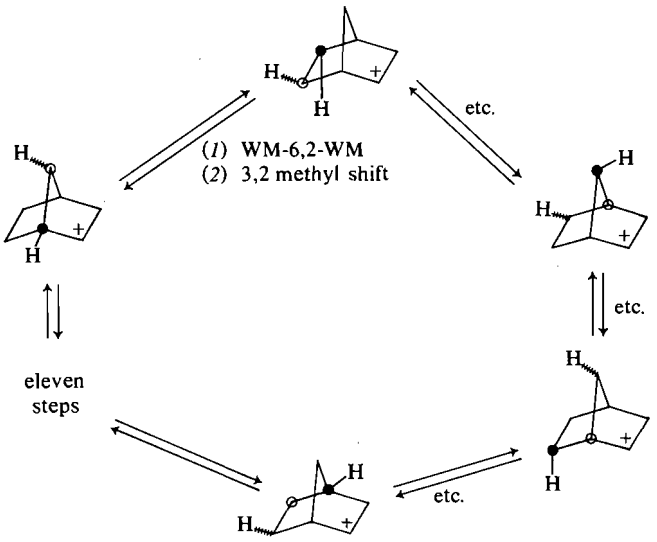

FIG. 5. Fifteenfold degenerate rearrangement cycle for the *R*-camphenehydro cation. For simplicity only two carbons and two protons are shown.

aniline at 180 °C, 0.33 and using pyruvic acid – acetonitrile at 156 °C, 4.0. In their most recent work, Vaughan and co-workers (7) have used freshly distilled pyruvic acid in acetonitrile at 137–138 °C and find the ratio 1.3. The ratios obtained in this work are 596 at −104 °C, 233 at −64 °C, 39.5 at 100 °C, 32.2 at 137 °C, and 26.7 at 180 °C. The best isothermal comparison is 1.3 for pyruvic acid – acetonitrile *vs.* 32.2 for the fluorosulfonic acid – sulfuryl chlorofluoride system (there is no evidence in fact that changes in the strong acid media affect the rates in any significant manner (13)). In extrapolating the two rates over large temperature ranges one has potentially large errors introduced. This made it necessary that we did the most careful line shape analysis possible in determining E_a. An error propagation analysis has also been carried out. At the 90% confidence level, the minimum value for this ratio in our work is 7.4 (140 as a maximum), still well above the 1.3 ratio for the acid-catalysis work. It is quite apparent that the camphene results vary significantly with the medium used so that it is not too surprising to find the above variance in the comparison to the strong acid results. We feel however that the strong acid results should serve as an 'intrinsic' ratio to which one might compare the specific changes brought about by other solvent systems.

The Thirty-fold Degeneracy of the Camphenehydro Cation

Previous labelling work on camphene has concerned only the methyl and exocyclic methylene groups but labelling the other protons (as in n.m.r. line broadening or in isotopic substitution) is equally of interest. Using alternating *exo*-3,2-methyl shifts and *endo*-6,2(*exo*-6,1)-hydride shifts one can show readily that the camphenehydro cation is 30-fold degenerate. A part of the 30-step cycle is shown in Fig. 5. The 30 structures can be divided into 15 of each enantiomer and since the two series are otherwise identical, only one needs to be considered. In completing a rearrangement cycle to give all the degenerate structures, the overall topology in this process is such that the three protons on the 'outside' of the molecule, C-6-*exo*, C-5-*exo*, and C-7-*anti* circulate, keeping their same relative order (**III**). The five protons, C-1, C-6-*endo*, C-5-*endo*, C-4, and C-7-*syn*, which lie in an equatorial belt, also circulate (**IV**), while the methyl groups occupy each of the three nonequivalent sites in turn. The five-proton group remains attached always to the same carbon so that both 'partners' are moving in the process. The three-proton group changes carbon 'partners' in a regular pattern. For each rearrangement step (within the same enantiomer group), the three-proton group

Can. J. Chem. Downloaded from www.nrcresearchpress.com by 210.87.254.42 on 09/05/12
For personal use only.

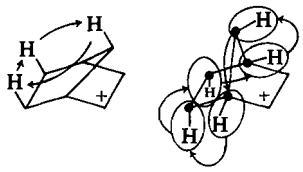

III IV

circles one position while the five protons circle two positions in the same direction (or three in reverse). This 'square dance' analogy clearly shows (V) that a double label, one in the three-proton group and one in the five-proton group, completely removes the degeneracy. The two dark lobes in V might represent for example the initial orientation of two deuterium atoms. It can be easily verified that 15 (5 × 3) steps are needed to regain the original positions.

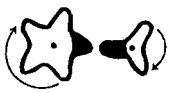

V

The Irreversible Rearrangement

The camphenehydrocation **2** rapidly rearranges at −30 °C, $k_{disappearance} = 9.8 \times 10^{-4}\ s^{-1}$. The products are a cyclohexenyl cation **4** (38%) and another 2-norbornyl cation system **5** (62%). The latter proved to be identical to a cation obtained by protonating 1,2,3-trimethyl-2-norbornene (ε-fenchene) (14) and was thus easily identified. The cyclohexenyl cation **4** was characterized from the observed n.m.r. spectrum (see structure **4**) and by comparison with the authentic specimen. This same cation is produced from a wide range of terpenes in fluorosulfonic acid, *e.g.* α-terpineol, β-pinene, sabinene, etc.

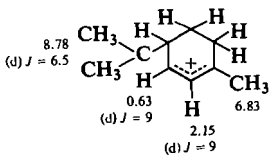

4

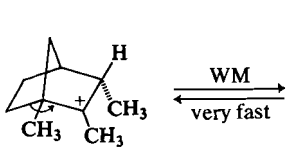

5

(+ 3-*exo* methyl and 7-*syn* methyl pair)

The cyclohexenyl cation formation is readily explained by an opening of the bicyclic ring, a reaction type first observed by Deno and Houser (21) (Scheme 3).

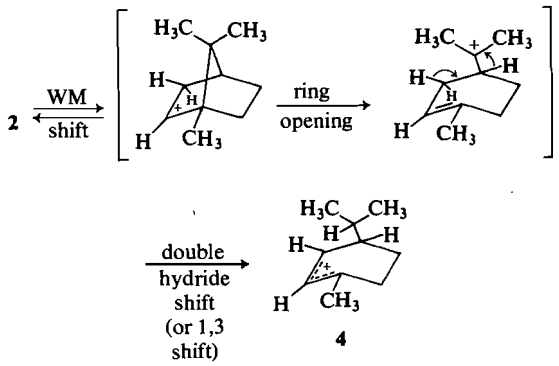

SCHEME 3

There are a great many ways by which the camphenehydro cation **2** could have formed **5**. This can be seen in the graph theory treatment of Johnson and Collins (22) as applied to trimethyl-2-norbornyl cations. For the rearrangement of **2** to **5** we have not constructed a complete graph but have simply calculated (by computer) all pathways of 10 steps or less (for four different rearrangement processes). All processes containing loops or regenerating starting material were discarded. The rearrangement processes were given the following symbols: Wagner–Meerwein 6,1–6,2 shift≡1; *exo*-3,2-shift≡2; *endo*-6,2-hydride shift≡3; double Wagner–Meerwein 7,1–7,2 shift (really two steps)≡4.

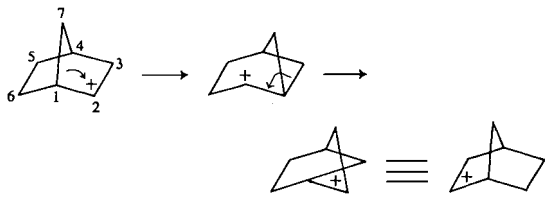

SCHEME 4

For further characterization, the *exo*-3,2-shift was broken down into 3,2-hydride shifts, 2H, and 3,2-methyl shifts, 2M. Furthermore, the substitution on C-2, *i.e.* H≡S (secondary), CH_3≡T (tertiary) was determined before and after the rearrangement, *i.e.* 2MTT refers to an *exo*-3,2-methyl shift starting with a tertiary C^+ center and ending up with another tertiary C^+ center. For rearrangement *4*, the processes 4TT-TT and

Can. J. Chem. Downloaded from www.nrcresearchpress.com by 210.87.254.42 on 09/05/12
For personal use only.

TABLE 2. Computer generated rearrangement pathways for **2** → **5**

Number of steps	
	Sequences using all four processes
7	4TT, 1TS, 2MST, 1TS, 2SS, 1ST, 2HTT
7	1TS, 4SS, 2MST, 1TS, 3SS, 1ST, 2HTT
8	4TT, 3TS, 2HSS, 1SS, 2MST,1TS, 3ST, 1TT
9	4TT, 1TS, 2MST, 4TT, 1TS, 4SS, 3SS, 1ST, 2HTT
9	1TS, 4SS, 2MST, 4TT, 1TS, 4SS, 3SS, 1ST, 2HTT
9	4TT, 1TS, 2MST, 1TS, 3SS, 4SS, 1ST, 4TT, 2HTT
9	1TS, 4SS, 2MST, 1TS, 3SS, 4SS, 1ST, 4TT, 2HTT
9	4TT, 3TS, 1SS, 2MTS, 1TS, 2HSS, 3ST, 4TT, 2HTT
10	4TT, 2HTS, 3SS, 1SS, 2MST, 1TS, 2HSS, 3SS, 2HST, 1TT
10	1TS, 4SS, 1ST, 3TS, 2HSS, 1SS, 2MST, 1TS, 3ST, 1TT
10	4TT, 3TS, 2HSS, 1SS, 2MST, 4TT, 1TS, 4SS, 3ST, 1TT
10	4TT, 1TS, 2MST, 1TS, 3SS, 1ST, 3TS, 1SS, 2HSS, 3ST
10	1TS, 4SS, 2MST, 1TS, 3SS, 1ST, 3TS, 1SS, 2HSS, 3ST
10	4TT, 1TS, 2MST 1TS, 3SS, 1ST, 3TS, 2HSS, 4SS, 3ST
10	1TS, 4SS, 2MST, 1TS, 3SS, 1ST, 3TS, 2HSS, 4SS, 3ST
	Sequences using only three processes (excluding 4)
11	1TS, 2HSS, 1SS, 2MST, 1TT, 2HTS, 1SS, 3SS, 2HSS, 3ST, 1TT
11	1TS, 2HSS, 1SS, 2MST, 3TS, 2HSS, 3ST, 1TS, 3SS, 1ST, 2HTT
12	1TS, 2HSS, 1SS, 2MST, 1TT, 3TS, 1ST, 2HTT, 3TS, 2HST, 1TS, 3ST
12	1TS, 2HSS, 1SS, 3SS, 2HSS, 1ST, 2HTS, 3SS, 2MST, 1TS, 3ST, 1TT
13	1TS, 2HSS, 1SS, 2MST, 1TT, 2HTS, 3SS, 1SS, 3SS, 1SS, 2HSS, 3ST 1TT.

4SS-SS are equivalent to 1SS and 1TT and the former were dropped. The symbol 4TT implies a secondary bicyclo[3.1.1]heptyl cation intermediate, etc.

Although rearrangement *4* is known to occur in some cases (22), there is a question concerning the activation energy for this step, *i.e.* it may be quite high. We have therefore carried out two series; in the first series, all four processes were employed. Restricting the path length to 10 steps yields 15 sequences all requiring a *4* step. In a second series, the rearrangement *4* was excluded and a path length of up to 13 steps considered. This yields five sequences, the shortest being 11 steps. In Table 2, we list the sequences for both series.

We prefer the shortest path, seven steps, involving a single *4* step. This initially converts the camphenehydro cation into the α-fenchyl cation and we have previously shown that the α-fenchyl cation gives **5** rapidly at −90 °C (14). Also, both products **4** and **5** would then arise from the initial weakening of the C-7—C-1 bond, *i.e.* it either shifts or opens up.

We are hopeful that activation energies can eventually be assigned to each of the subdivided steps, thus enabling one to predict the most probable route on a rational basis.

The Protonation of Borneol and Isoborneol in Fluorosulfonic Acid

Although not part of the investigation, an interesting sidelight to this work was the observation of an enormous difference in the rate at which protonated borneol and isoborneol were converted to the camphenehydro cation. Protonated borneol (methyl peaks at τ 8.52, 8.60, and 8.64, C—H at 4.36, broad doublet, J = 10) is

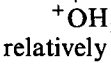

relatively stable, the heterolysis of the C—$^+OH_2$ bond does not take place readily until about −30 °C. At this temperature, only the camphenehydro cation rearrangement products **4** and **5** are formed. Protonated isoborneol, on the other hand, is very difficult to obtain. By conducting the addition at −120 °C in FSO_3H–SO_2ClF (1:4), it has been possible to obtain a spectrum which, although rather broad and featureless, is probably the 'onium' cation contaminated with some of the camphenehydro cation (methyls at τ 8.84 and 8.90, C—H, broad, at 5.08), These

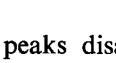

peaks disappear quite rapidly at −105 °C to yield the camphenehydro cation. Large rate differences in the solvolysis of *exo*- and *endo*-2-norbornyl derivatives are very well known (23);

Can. J. Chem. Downloaded from www.nrcresearchpress.com by 210.87.254.42 on 09/05/12
For personal use only.

however the reactions in FSO_3H are somewhat unique in that the solvent (FSO_3H) or nucleophile (FSO_3^-) assistance in the actual C—$^+OH_2$ bond breaking step is probably minimal.

Experimental

Camphene and tricyclene were a gift of the Hercules Powder Co. The ion preparation followed standard techniques previously described (24). The n.m.r. spectra were measured using a Varian Assoc. HA-100 spectrometer equipped with a variable temperature probe. Temperatures were measured by directly inserting a thermocouple into the n.m.r. tube, the reading being taken as the pen passed over the spectra region being used for the line-broadening comparison.

In the DISST technique, the audio power was varied and measurements were made on both spinning and non-spinning samples, the results being substantially the same in both cases. The external oscillator power was always allowed to load the RF circuit, the actual irradiation being accomplished by a sudden switch from a noninterfering frequency to that desired. The f_1 observing power was also kept very low to minimize any direct saturation effects.

^{13}C n.m.r. spectra were recorded on a Bruker HFX-90 Fourier transform spectrometer. Between 1K and 2K scans were collected for each temperature. The heteronuclear fluorine lock material, trifluoromethyltrichloroethene, was contained with TMS in a 5 mm capillary.

Line-broadening Calculations

In all computer calculations, the kinetic matrix used included both mutual exchange processes. The Arrhenius plot for each mutual exchange process was used to extrapolate the rates, *i.e.* the values quoted in Fig. 1 for the slower step, in the region where line-broadening effects are due to the faster process and also in the values quoted for the faster process in the temperature region where the line-broadening effects are principally due to the slower step. ^{13}C spectra were calculated using Lorenzian line shapes and using the rate constants derived from the proton comparisons.

The authors thank the National Research Council of Canada for generous financial support. We wish to thank Professor R. K. Brown for his aid in obtaining the ^{13}C n.m.r. spectra and Drs. C. Johnson and C. Collins for preprints of their work on the application of graph theory to norbornyl cation rearrangements.

1. P. Lipp and G. Stutzinger. Ber. **65**, 241 (1932).
2. H. Meerwein and K. Van Emster. Ber. **55**, 2500 (1922).
3. H. Meerwein and F. Montfort. Ann. **435**, 207 (1924).
4. J. D. Roberts and J. A. Yancey. J. Am. Chem. Soc. **75**, 3165 (1953).
5. W. R. Vaughan and R. Perry. J. Am. Chem. Soc. **75**, 3168 (1953).
6. P. Hirsjärvi, K. Heinonen, and L. Pirila. Suomen Kemistilehti B, **37**, 77 (1964).
7. C. W. David, B. W. Everling, R. J. Kilian, J. B. Stothers, and W. R. Vaughan. J. Am. Chem. Soc. **95**, 1265 (1973).
8. C. J. Collins and M. H. Lietzke. J. Am. Chem. Soc. **95**, 6842 (1973).
9. P. von R. Schleyer. J. Am. Chem. Soc. **89**, 699 (1967).
10. J. A. Berson, J. H. Hammons, A. W. McRowe, R. G. Bergman, A. Remanick, and D. Houston. J. Am. Chem. Soc. **89**, 2590 (1967).
11. A. W. Bushell and P. Wilder. Jr. J. Am. Chem. Soc. **89**, 5720 (1967).
12. P. Wilder, Jr. and W. C. Hsieh. J. Org. Chem. **36**, 2552 (1971).
13. E. Huang, K. Ranganayakulu, and T. S. Sorensen. J. Am. Chem. Soc. **94**, 1780 (1972).
14. E. Huang, K. Ranganayakulu, and T. S. Sorensen. J. Am. Chem. Soc. **94**, 1779 (1972).
15. R. P. Haseltine and T. S. Sorensen. Can. J. Chem. This issue.
16. J. A. Berson and P. W. Grubb. J. Am. Chem. Soc. **87**, 4016 (1965).
17. B. M. Benjamin and C. J. Collins. J. Am. Chem. Soc. **88**, 1556 (1966).
18. S. Forsén and R. A. Hoffman. J. Chem. Phys. **39**, 2892 (1963).
19. A. Allerhand, H. S. Gutowsky, J. Jonas, and R. A. Meinzer. J. Am. Chem. Soc. **88**, 3185 (1966).
20. W. R. Vaughan, C. T. Goetschel, M. H. Goodrow, and C. L. Warren. J. Am. Chem. Soc. **85**, 2282 (1963).
21. N. C. Deno and J. J. Houser. J. Am. Chem. Soc. **86**, 1741 (1964).
22. C. K. Johnson and C. J. Collins. J. Am. Chem. Soc. **96**, 2514 (1974); C. J. Collins, C. K. Johnson, and V. F. Raaen. J. Am. Chem. Soc. **96**, 2524 (1974).
23. G. D. Sargent. Quart. Rev. **20**, 301 (1966).
24. L. Huang, K. Ranganayakulu, and T. S. Sorensen. J. Am. Chem. Soc. **95**, 1936 (1973).

Can. J. Chem. Downloaded from www.nrcresearchpress.com by 210.87.254.42 on 09/05/12
For personal use only.

A Comparison of the Stereospecificity of Carbocation to Rearranged Carbocation Reactions under Observable Ion and Steady-state Intermediate Conditions

ROLLIN P. HASELTINE AND TED S. SORENSEN

Department of Chemistry, University of Calgary, Calgary, Alberta T2N 1N4

Received June 25, 1974

ROLLIN P. HASELTINE and TED SORENSEN. Can. J. Chem. **53**, 1067 (1975).

From observable ion studies on a series of polymethyl tertiary 2-norbornyl cations, a huge difference in the migratory aptitudes (stereospecificity) of 3-*exo* and 3-*endo* methyl groups was observed. The same trend was observed under typical acid catalysis conditions where the *same* rearrangements are involved but where the cation is in this case a fleeting intermediate. In related work, a comparison was made of the absolute rate of an *exo*-3,2-hydride and an *exo*-3,2-methyl shift and a direct measurement of the H–D isotope effect in a 3,2-hydride shift was made.

ROLLIN P. HASELTINE et TED SORENSEN. Can. J. Chem. **53**, 1067 (1975).

En se basant sur des études des ions qui peuvent être observés dans une série de cations tertiaires dérivés de polyméthyl-norbornyl-2, on a observé de grandes différences dans les aptitudes à la migration (stéréospécificité) des groupes méthyles *exo*-3 et *endo*-3. On a observé la même tendance dans des conditions de catalyse acide typique dans lesquelles les mêmes réarrangements sont observés mais où le cation n'est dans ces cas qu'un intermédiaire éphémère. Dans des travaux parallèles, on a pu faire une comparaison des vitesses absolues des transferts d'hydrures *exo*-3 vers 2 et des transferts de méthyles de *exo*-3 vers 2 et on a aussi fait une mesure directe de l'effet isotopique H–D lors du transfert d'hydrure de la position 3 vers la position 2. [Traduit par le journal]

Introduction

A study of the directly observable camphenehydro cation (1) shows that an *exo*-3,2-methyl shift in this system is preferred over a possible *endo* shift by a rate factor of at least 250 at −64 °C. However two important questions remain unanswered:

(*i*) What *is* the actual absolute rate of an *endo*-3,2-methyl shift in an observable 2-norbornyl cation? In the camphenhydro cation, a second rearrangement process which interconverts the 3-*exo* and 3-*endo* substituents (Scheme 1) makes this question impossible to answer in this case.

(*ii*) To what extent are rate comparisons derived from observable ion rearrangements applicable to solvolysis or acid-catalysis type conditions where the carbocations exist as temporal intermediates? Indications from the camphene racemization problem and the directly observable camphenehydro cation rearrangements (1) indicate some differences.

The Overall Plan

In order to allow equal statistical choice between a degenerate migration of an *exo* or *endo* methyl substituent one requires the basic three

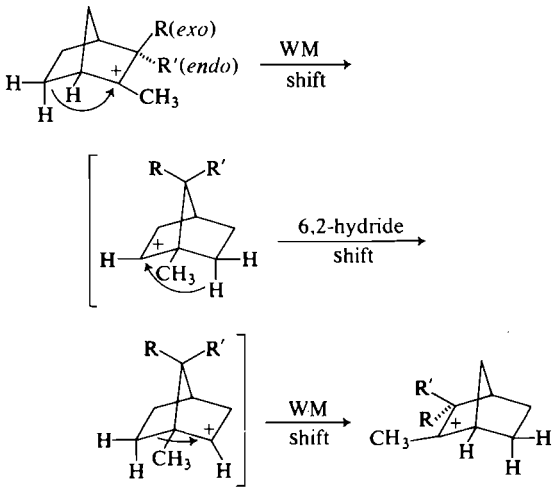

SCHEME 1

methyl groups of the camphenehydro cation **1**. In deciding first of all on systems which do not allow for interconversion of the 3-position substituents by the Scheme 1 reactions, one can consider cations with an extra methyl substituent at C-1, *i.e.* **2**. However, in order to make the rearrangement degenerate (as in the camphene-

Can. J. Chem. Downloaded from www.nrcresearchpress.com by 210.87.254.6 on 09/05/12
For personal use only.

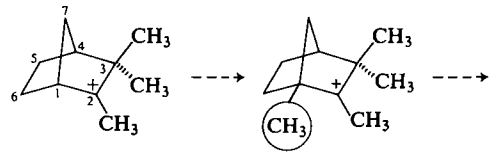

1
basic skeleton wanted

2

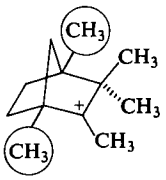

3

hydro cation) one requires a further methyl substituent at the C-4 position, giving **3**. The reason that **3** does not interconvert the 3-position methyl groups by the sequence of reactions shown in Scheme 1 can best be shown if one attempts to carry these out on **3** (Scheme 2). No symmetry plane exists in this series of reactions, *i.e.* both C-3 methyl substituents retain their separate identity. Even if **5** is kinetically accessible, as long as **5** is thermodynamically less stable than **3** it will not interfere in any way with the planned experiments.

One finds experimentally that the first Wagner–Meerwein (WM) shift process shown in Scheme 2 is extremely fast. It is so fast in fact that at all temperatures one only sees averaged n.m.r. peaks for the two cations **3** and **4**. As in another pair of this type which we have recently studied (2), the equilibrium constant **3**/**4** is not one, and so the averaged peaks are naturally more representative of the major isomer of the pair. In the structures **3***a* and **4***a*, the groups which average are given the symbols 1 and 1′, etc. It turns out,

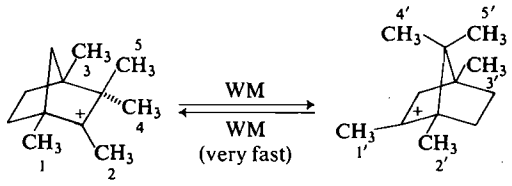

3*a* **4***a*

in this case, that one isomer, **4**, is structurally incapable of *any* low-energy degenerate rearrangements so that only **3** needs to be considered. However, for quantitative purposes, in order to compare with the camphenehydro cation results, one should know the equilibrium concentration of **3**, and there are ways to obtain this.

As it turns out, ion **3** (accompanied by **4**) is useful for studying the *exo*-3,2-methyl shift but an irreversible rearrangement which becomes very rapid by about −20 °C effectively limits the search for an *endo* shift to temperatures below this. This has led to the investigation of other systems containing the same basic five methyl groups of **3**, but with an additional methyl group in the C-7-*anti* position, structures **6** and **7**. This pair is stable (observable) up to nearly room temperature before, again, an irreversible rearrangement becomes rapid. As will be shown, besides the degenerate *exo*-3,2-methyl shift in **6**, a degenerate 3,2-hydride shift occurs in **7** and a useful direct comparison between an *exo*-3,2-hydride and *exo*-3,2-methyl shift is possible. The

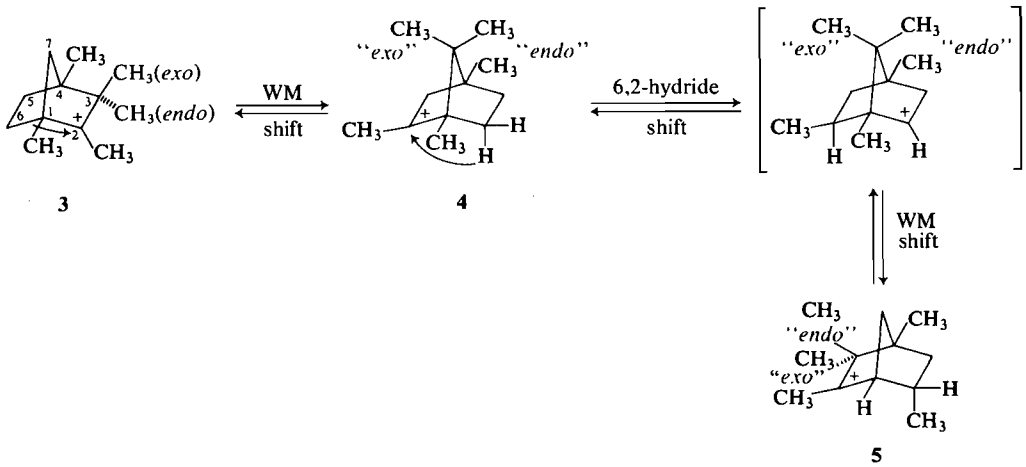

3 **4** **5**

SCHEME 2

Can. J. Chem. Downloaded from www.nrcresearchpress.com by 210.87.254.6 on 09/05/12
For personal use only.

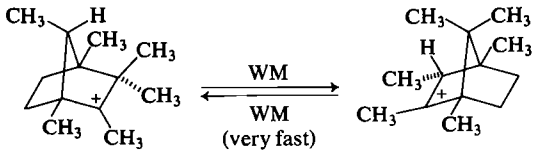

6 7

application of both degenerate rearrangements together with the WM shift leads to an overall 20-fold degenerate rearrangement process whereby five of the six methyl groups become equivalent on the n.m.r. time scale, the remaining methyl *not* becoming equivalent *unless* an *endo*-3,2-methyl shift is allowed. The extended temperature range over which **6** (and **7**) exist proves very useful in allowing one finally to obtain evidence for an *endo* shift in **6**.

Finally, a heptamethyl cation **8** was investi-

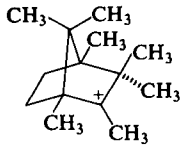

8

gated in order to test the stereospecificity and the absolute rate of the 3,2-methyl shift when a C-7-*syn* methyl substituent was present. This substituent was expected to decrease substantially the rate of an *exo*-3,2 shift but to have no effect on the *endo* shift.

It turns out that all three systems are very amenable to study involving acid-catalysis conditions, the second objective of this work. The particular acid-catalysis reaction studied was the hydrogen–deuterium substitution of the corresponding alkenes in deuterio acetic acid containing a small amount of deuterio sulfuric acid (fairly typical acid-catalysis conditions). As an illustrative example of what is being attempted, one can take the alkene **9**, a precursor of the pentamethyl cation system **3**–**4**, and show how the exchange occurs (Scheme 3). In order to exchange with solvent D, a CH_3 group must be located adjacent to a cationic center. If no rearrangement whatever occurred, only the *exo*-methylene group 2 would be exchanged. If only the WM shift were allowed, only the C-1 methyl and $=CH_2$ in **9** would eventually be exchanged. If both WM shift and an *exo*-3,2-methyl shift were allowed, three of the four methyl groups (only the one labelled 5 in structure **9** remains unexchanged) and $=CH_2$ can be exchanged (Scheme 3). If a WM shift and both *exo*- and *endo*-methyl shifts are allowed, *all* methyls in **9** will exchange (not shown in Scheme 3). There is thus a clear-cut experimental distinction to test the stereospecificity of the 3,2-methyl shift in **3**, under acid-catalysis type conditions where **3** has only a fleeting existence.

In the hexamethyl **6** and **7**, and heptamethyl **8** cation systems similar distinctions are possible.

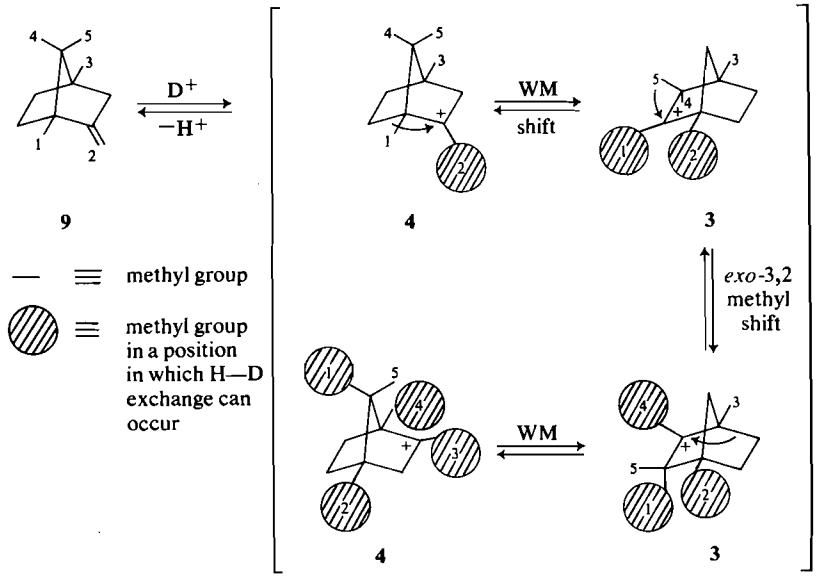

9 4 3 4 3

SCHEME 3

Can. J. Chem. Downloaded from www.nrcresearchpress.com by 210.87.254.6 on 09/05/12
For personal use only.

Can. J. Chem. Downloaded from www.nrcresearchpress.com by 210.87.254.6 on 09/05/12
For personal use only.

In the former case, allowing only an *exo*-3,2-methyl shift as well as the WM shift and 3,2-hydride shift, the precursor alkene **10** will exchange five of the six methyl groups (see structure **10**). All six will exchange if, in addition, an *endo*-3,2-methyl shift occurs.

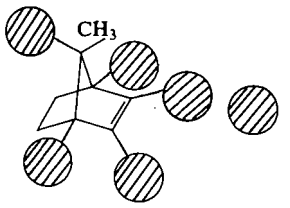

10

In the heptamethyl cation case, four of the six methyl groups in the precursor alkene **11** will exchange if only the WM shift and the *exo*-3,2-methyl shift are allowed, while all six will exchange if, in addition, an *endo*-methyl shift occurs.

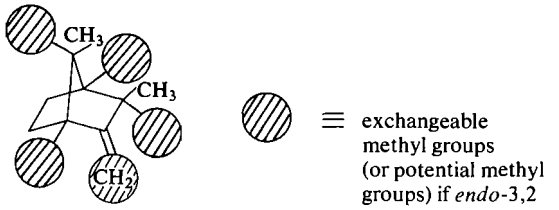

11

Since each system is somewhat different, the pentamethyl, hexamethyl, and heptamethyl cation series will be treated in order, asking in each case the following questions: (*i*) What are the relative propensities in the observable ions for *exo*- and *endo*-3,2-methyl shifts? and (*ii*) how does this ratio compare with that determined in the acid-catalyzed H–D exchange where the ions are fleeting intermediates?

Pentamethyl Cation Series 3–4

The starting material for this study was the hydrocarbon **9**. This $C_{12}H_{20}$ isomer is by far the most thermodynamically stable of the four hydrocarbons **9**, **12**, **13**, and **14** related to cations **3**–**4**. The equilibrium percentages of **9**, **12**, **13**, and **14** are 78, 14, 6.5, and 1.5%, respectively, at 25 °C in 0.5% H_2SO_4–CH_3COOH. The synthesis of these hydrocarbons will be reported separately. There is no particular advantage in using **9** to prepare the cations (other than the ready availability of the alkene) but in the H–D exchange study, where complete equilibration of the four hydrocarbons accompanies exchange, starting with **9** means that this remains the major component of the mixture.

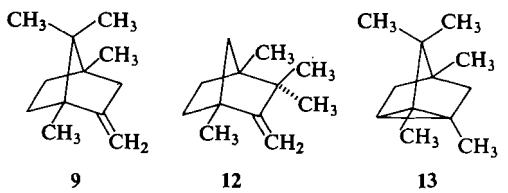

9 **12** **13**

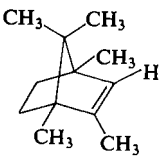

14

Addition of **9** to FSO_3H–SO_2ClF (1:4) at −120 °C gives a light yellow solution showing a very clean ^1H n.m.r. spectrum. At −120 °C, there are five separate methyl peaks in the spectrum, corresponding to the methyls numbered 1, 2, 3, 4, and 5 in the previously shown structures **3***a* and **4***a*. These averaged peaks, as well as those for the remaining protons, are reported in Table 1. The two lowest field methyl peaks are found at

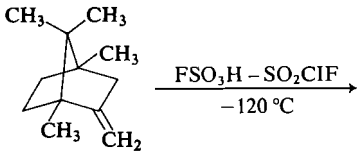

9

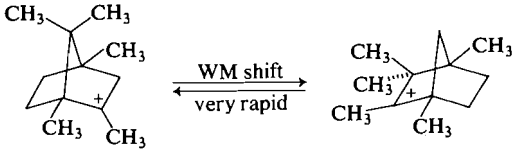

4 **3**

equilibrium mixture of these

τ 7.36 and 8.01 at −90 °C and the separation δ (65 Hz) is temperature dependent, reflecting the changing equilibrium constant, K = **3**/**4**, with temperature changes. This temperature dependence can be analyzed by a procedure pre-

TABLE 1. ^{1}H n.m.r. results

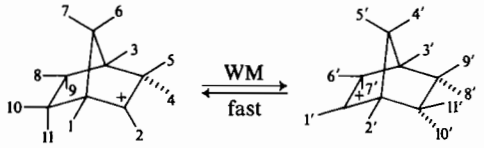

Ion	Position[a] 1–1′	2–2′	3–3′	4–4′	5–5′	6–6′	7–7′	8–8′	9–9′	10–10′	11–11′
3 (unprimed numbers) } **4** (primed numbers) }	7.36[b]	8.01[b]	8.71[c]	8.82[c]	9.00[d]	7.34b[e]	7.34b[e]	⟵ 8.2–8.6 ⟶			6.72vb
6 (unprimed numbers) } **7** (primed numbers) }	7.36	8.04	8.84[f]	8.82[g]	9.05[g]	7.17[b]	8.66[f]	7.96[h]		7.68[h]	
8		7.67	8.84		8.68	8.68			8.37[i]	7.13[i]	

[a] In τ p.p.m. from internal tetramethylammonium cation = 6.90.
[b] The assumption that **4** is more stable than **3** is based on analogy to several other systems (2, 3, 5, 12), temperature −90 °C.
[c] These assignments follow from the assigned positions for 1–1′ and 2–2′ and the positions of the coalesced peaks after exchange with 3–3′ and 4–4′.
[d] In the dominant isomer **4**, this peak is expected to be shielded more than peak 4′ because it is closer to the maximum shielding region of the cation π system.
[e] Assigned because these peaks are not line broadened by the methyl shift.
[f] Located knowing 1–1′ and 2–2′ (at −119 °C) and the averaged 1–1′, 7–7′, and 2–2′, 3–3′ at higher temperatures.
[g] Reasoning analogous to *d*.
[h] These values obtained at −30 °C and are averages, *i.e.* 8–8′ = 10–10′ *etc.* The two sets form an A_2B_2 pattern.
[i] Triplet, J = 5.5 Hz.

viously reported (2) and yields an equilibrium constant value of 0.3 at −90 °C.

As the temperature of the solution of **3**–**4** is raised above −120 °C, four of the five methyl peaks begin to broaden. This is due to a stereospecific 3,2-methyl shift in **3**, which can be categorized further as an *exo*-3,2 shift if the assignment made in Table 1 is correct, *i.e.* that the highest field peak is due to the methyl 5–5′ in structures **3***a*–**4***a* (see notes to Table 1).

The *exo*-3,2 shift results in the following averaging:

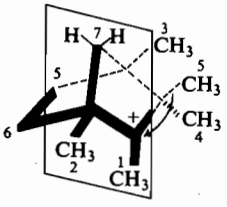

3*a*

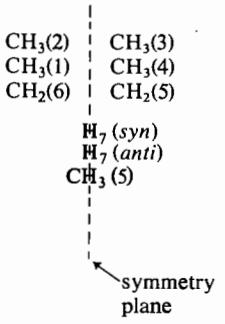

The migrating methyl 5 does not change environment (except for *R*–*S* interconversion) and remains unbroadened. The numbered peaks are already averages of **3** and **4** but the above broadening only occurs via ion **3**. The absolute rate of this shift in **3** can be related to the overall observed broadening in **3**–**4** by the relationship:

$$4 \underset{}{\overset{K}{\rightleftarrows}} 3 \xrightarrow{k_{exo\ \text{shift}}} 3'$$

The rate for the *exo*-3,2-methyl shift was obtained directly by comparing the observed spectra with spectra calculated for various values of $k_{exo\ \text{shift}}$, assuming the WM shift to be very fast and allowing K to change with temperature (an extrapolation of the observed changes at low temperature into the temperature region of line broadening). The matching spectra are not shown but are similar in principle to those of the more complex hexamethyl cation series shown in Fig. 2. A typical rate constant is 14 s^{-1} at −94 °C, $\Delta G^{\ddagger}$ = 9.4 kcal/mol. An Arrhenius plot gives $\Delta H^{\ddagger}$ = 10 ± 2 kcal/mol. The *exo*-3,2-methyl shift rate in **3** is quite similar to the value found for the camphenehydro cation, K = 14 s^{-1} *vs.* 92 s^{-1}, both at −94 °C. This indicates that the added methyl groups in **3** have only a small effect on this reaction.

Since the main point of using the **3**–**4** system is to look for an *endo*-3,2-shift, one looks for the

Can. J. Chem. Downloaded from www.nrcresearchpress.com by 210.87.254.6 on 09/05/12
For personal use only.

Can. J. Chem. Downloaded from www.nrcresearchpress.com by 210.87.254.6 on 09/05/12
For personal use only.

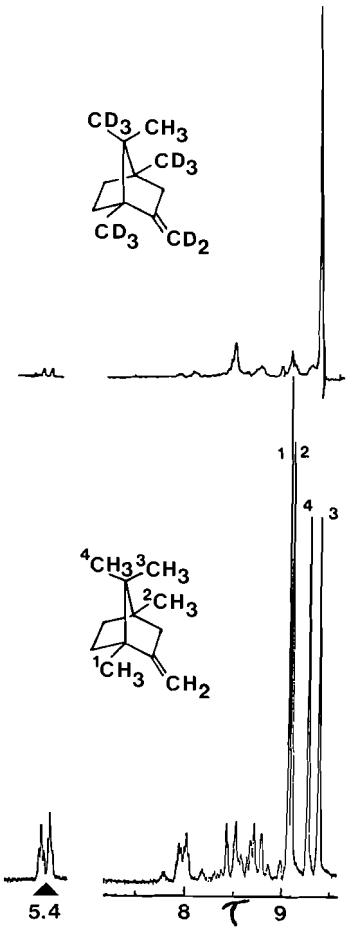

FIG. 1. Lower, n.m.r. spectrum of pure **9**. Upper, n.m.r. spectrum of pure **9** isolated after H–D exchange of $=CH_2$ and three of the four methyl groups.

remaining sharp methyl peak to broaden and eventually average with 2 and 4 (structure **3***a*). However, up to -20 °C, the highest temperature at which it was possible to still observe this peak because of a very rapid irreversible rearrangement, it still remained sharp. On analysis of this, the maximum possible rate constant for an *endo* shift must be less than 10 s^{-1} at -20 °C. Extrapolating the *exo* shift rate to -20 °C yields a minimum $k_{exo\ shift}/k_{endo\ shift}$ ratio of *ca.* 6×10^3 at -20 °C.

Turning next to the H–D exchange results, when the alkene **9** is dissolved in 0.9% D_2SO_4–CD_3COOD at 25 °C, one notices a rapid (in the n.m.r. spectrum) decrease in the size of the *exo* methylene $=CH_2$ group and the C-1 methyl peak. The C-4 and C-7-*anti* methyl peaks decrease somewhat slower. The half-life for the exchange of the protons in the latter is *ca.* 2 h at 25 °C. Within 1 day, there is virtually only one methyl peak of **9** left showing in the spectrum, the one assigned to the C-7-*syn* methyl. There are, as well, equilibrium amounts[1] of the three other hydrocarbons **12**, **13**, and **14**, each showing as well only a single methyl peak, C-3-*exo* in **12** and **13**, and C-7-*syn* in **14**. After several days in the deuterated acid, the hydrocarbons **9**, **12**, and **13** were isolated and purified. In Fig. 1, a spectrum of **9**, thus isolated, is compared to the original **9**. Comparisons of **12** and **13** are similar.

When the original solution is left at 25 °C for an extended period, it requires *ca.* 150 days for half of the remaining C-7-*syn* methyl signal in **9** to be lost. This loss may in small part be due to decomposition of **9** since there are no non-exchangeable positions to serve as a reference. However, if one assumes the total loss is due to H–D substitution brought about by an *endo*-3,2-methyl shift, the minimum rate difference for $k_{exo\ shift}/k_{endo\ shift}$ is 150 days/0.08 days $= 2 \times 10^3$.[2]

The isolation of the specifically labelled alkene **9***b* allows one to obtain the corresponding observable carbocation **3***b*–**4***b* when this is added to $DFSO_3$–SO_2ClF (1:4) at -120 °C. The n.m.r. spectrum of the resulting solution consists basically of one peak as expected, the same peak as in the all-proton ions **3**–**4** which occurred at highest field and which did not broaden (exchange). If any proof is needed, these results

[1]The relative amounts of the hydrocarbons **9**, **12**, **13**, and **14** show interesting variations with time. Very soon after dissolution of **9** in the deuterated acid the concentration of **12** increases to several times the proton equilibrium value (see previous values for these) and then slowly decreases again over a period of days to the same equilibrium value as found in the protonated case. Much more slowly, the tricyclene **13** also builds up over the proton equilibrium value and then likewise decreases. These results can be attributed to a kinetic isotope effect which favors the loss of H over D in the intermediate ions **3**–**4**.

[2]The actual relationship between the rate of loss of the proton signal and the rate of the *exo* or *endo* shift is complex. The simplest case would be one where the exchange of the C-1 methyl and $=CH_2$ positions in **9** is much faster than the 3,2-methyl shifts. This is certainly not true in the present case as far as the *exo*-3,2-shift is concerned. In this circumstance, the rate of the *exo*-3,2-methyl shift will be *faster* than that observed for the loss of protons in the C-4 and C-7-*anti* methyl groups. On two counts, therefore, the *exo* shift/*endo* shift ratio must be regarded as a minimum figure.

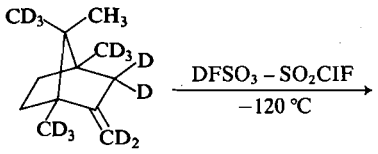

9b

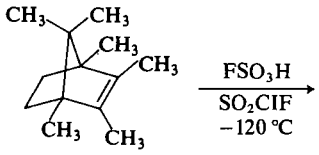

10

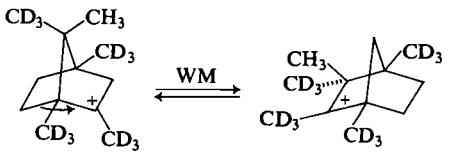

4b 3b

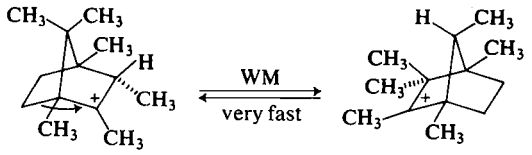

7 6

prove that the observable ion rearrangement and that occurring in the acid catalysis are the same.

However, one can now look for exchange of the CD_3 groups and the CH_3 group in the cations **3***b*–**4***b* *on a conventional kinetic basis* as opposed to the rapid rates needed to give line broadening and which we have discussed in the earlier results. Up to the temperature where the cations **3***b*–**4***b* are decomposing irreversibly at a rapid rate (and hence decreasing the size of the CH_3 signal), there is only a very slight indication of proton area 'growing' into the CD_3 peak positions. The maximum possible rate constant for the *endo*-3,2-methyl shift is *ca.* 1×10^{-3} s^{-1} at -40 °C. The minimum ratio for $k_{exo\ shift}/k_{endo\ shift}$ is now extended to *ca.* $10^4/10^{-3} = 10^7$ at -40 °C. The above results also make it obvious why no line broadening was observed for the remaining sharp methyl group in the spectrum of **3**–**4**.

Although the carbocation system **3**–**4** allows one to show a huge difference between *exo* and *endo* shifts, it has still not been possible to obtain a satisfactory measure of the actual rate of an *endo*-3,2-methyl shift. For this reason, another series was investigated.

Hexamethyl Cation Series 6–7

For reasons discussed in the Overall Plan, the five methyl groups of **3** constitute the basic requirement. In considering other systems, it was found experimentally that adding yet another methyl group to the C-7-*anti* position of **3** gave a system which was stable to much higher temperatures than was **3**. This results again in a pair of cations **6**–**7**, like **3**–**4**, averaged on the n.m.r. time scale by a very rapid WM shift. The starting material for these cations was the alkene **10**, chosen like **9**, because it is the most thermodynamically stable of the $C_{13}H_{22}$ hydrocarbons **10**, **15**, and **16** related to the ions **6**–**7**. The equilibrium concentrations of these are, 87, 8, and 4%, respectively, for **10**:**15**:**16** in 0.5% H_2SO_4–CH_3COOH at 25 °C. The synthesis and characterization of these will be reported in a separate publication.

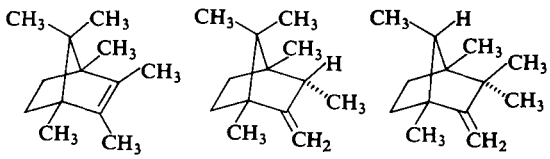

10 15 16

Addition of **10** to FSO_3H–SO_2ClF (1:4) at -120 °C results in a pale yellow carbocation solution whose n.m.r. spectrum can be satisfactorily analyzed in terms of a very rapidly equilibrating mixture of **6**–**7**. Some of the observed n.m.r. spectra are shown in Fig. 2, as a function of temperature. At the very lowest temperatures (-130 °C), six separate methyl peaks are implied (although not all resolved in the viscous solution). The chemical shifts of these and the other protons in **6**–**7** are listed in Table 1 (see notes to this table for a description of how the assignments were made). The proton at C-3 in **7** is assigned an *exo* geometry to account for the very rapid rate observed for the *exo*-3,2-hydride shift in **7**, a rate similar to that observed in a related cation (3). In addition, protonation is normally found to occur from the *exo* side in norbornyl systems (4), although the C-7-*syn* methyl substituent might possibly have been expected to have changed this. In any case, all of the results are consistent with this assigned geometry.

Can. J. Chem. Downloaded from www.nrcresearchpress.com by 210.87.254.6 on 09/05/12
For personal use only.

Can. J. Chem. Downloaded from www.nrcresearchpress.com by 210.87.254.6 on 09/05/12
For personal use only.

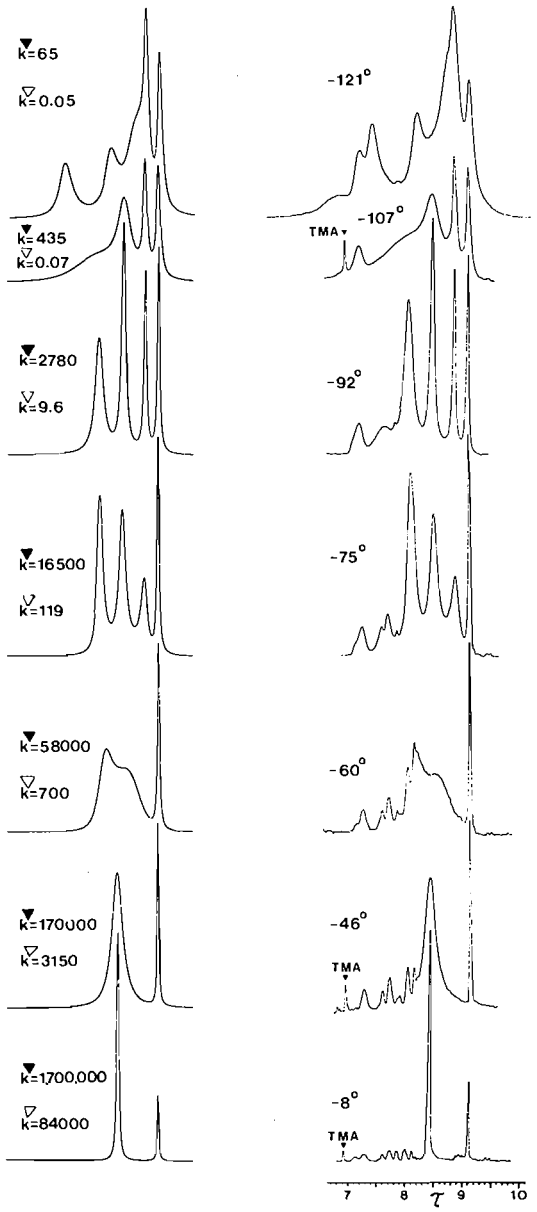

FIG. 2. Right, representative experimental ^1H spectra of the cations **6**–**7** measured at various temperatures. TMA is the reference, the tetramethylammonium cation. Left, calculated spectra for the methyl groups in **6**–**7**, $k^{\blacktriangledown}$ = rate of *exo*-3,2-hydride shift in **7** and $k^{\triangledown}$ = rate of *exo*-3,2-methyl shift in **6**.

At the temperature where six separate methyl peaks occur, one is dealing with a very similar situation to that described for the pentamethyl cation case. An analogous analysis of the temperature dependence of the separation (δ) of the two lowest field methyl peaks gives K = **6**/**7** = 0.21 at −121 °C. However, whereas in the pentamethyl ion only one line-broadening process occurs, *i.e.* that due to the *exo*-3,2-methyl shift in **3**, there are two separate line-broadening processes in **6**–**7**. As the solution is warmed above −130 °C, four (the lowest field four) of the six methyl peaks broaden and eventually coalesce so that by −92 °C (Fig. 2), one has four peaks in an area ratio 6:6:3:3. Further warming results in the two 6H peaks and the lower field of the 3H peaks broadening and eventually coalescing into a single peak so that at high temperatures (−8 °C), one has two sharp peaks of relative area 15:3 (Fig. 2).

The actual form of the broadening indicates conclusively that the lower temperature broadening is due to an *exo*-3,2-hydride shift in **7** and the higher temperature broadening to an *exo*-3,2-methyl shift in **6**. The actual equivalences are shown below:

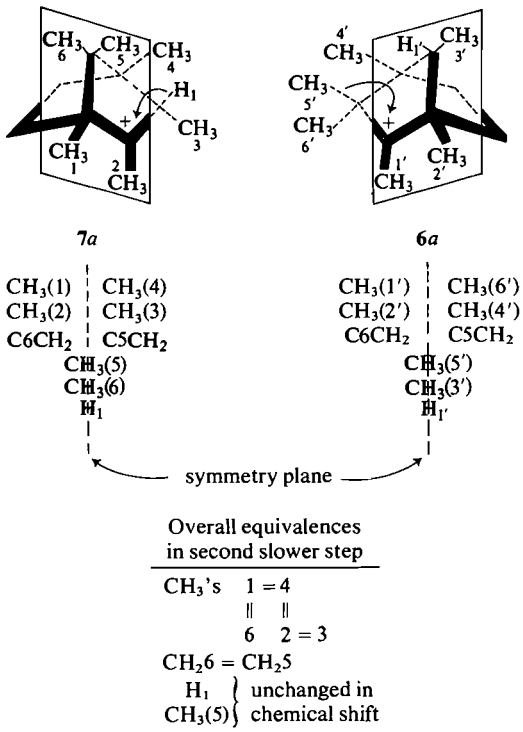

Thus, if the lowest temperature broadening had involved the *exo*-3,2-methyl shift in ***6a***, one of the two remaining unchanged methyls should have been a doublet (3–3′ in ***7a***–***6a***). From Fig. 2, −92 °C spectrum, this clearly is not the case. The

Can. J. Chem. Downloaded from www.nrcresearchpress.com by 210.87.254.6 on 09/05/12
For personal use only.

exo-3,2-hydride shift requires methyls 5 and 6 to remain unchanged and these are clearly singlets.

The calculated spectra (representative examples are shown in Fig. 2) were obtained using three different rate constants and a temperature-dependent equilibrium constant in the kinetic matrix. The rate constant for the WM process was made very large in all cases. Numerical values for $k_{3,2\text{-hydride}}$ and $k_{exo\text{-}3,2\text{-methyl}}$ can be obtained with relative ease using spectra obtained at very low temperatures (−130 to −100 °C) for the former and at the higher range (−75 to 0 °C) for the latter, avoiding in the first instance those temperatures where both rate processes contribute to line broadening (*ca.* −75 to −100 °C). Having derived rates and activation energies for the two processes, one can then check the spectra in this region for consistency, that shown in Fig. 2 at −92 °C is illustrative of the close fit of the experimental and calculated curves. A typical rate constant for the 3,2-hydride shift is 375 s^{-1} at −110 °C, $\Delta G^{\ddagger}$ = 7.4 kcal/mol. From the Arrhenius plot, $\Delta H^{\ddagger} = 7 \pm 1$ kcal/mol. For the *exo*-3,2-methyl shift, a typical rate constant is 400 s^{-1} at −67 °C, $\Delta G^{\ddagger}$ = 9.4 kcal/mol. The Arrhenius plot in this case is shown in Fig. 3 and yields $\Delta H^{\ddagger} = 9.8 \pm 1$ kcal/mol. Although the analysis needed to obtain these rate constants is admittedly complex, this should not be allowed to distract from the simple answers obtained, *i.e.* the rate for the 3,2-hydride shift in **7** and the rate for the *exo*-3,2-methyl shift in **6**. The *exo*-3,2-methyl shift rate in **6** is quite close to that observed for **3**, the extrapolated rate constant from Fig. 3 for **6** at −94 °C is 7.4 s^{-1} *vs.* 14 s^{-1} for **3**, again indicating that the additional methyl in **6** does not affect the *exo*-3,2-methyl shift rate appreciably.

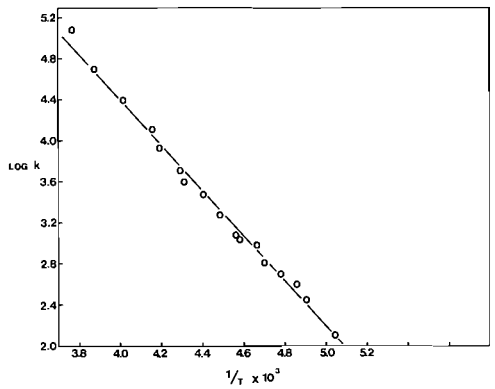

FIG. 3. Plot of log k for the *exo*-3,2-methyl shift in **6** *vs.* $1/T$.

Surprisingly, the rate of the *exo*-3,2-hydride shift in **7** is not greatly affected by the presence of the C-7-*anti* methyl substituent if one compares this with the corresponding rate in the cation **17**, $k_{exo\text{-}3,2\text{-hydride}}$ = *ca.* 270 s^{-1} at −115 °C for **17** *vs.* 125 s^{-1} for **7** at −115 °C. In the 2,3-*endo*-dimethyl-2-norbornyl cation **18**, the rate is only about 25 times as fast (5).

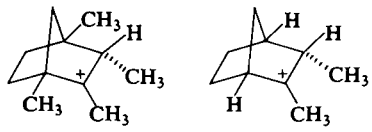

17 **18**

The sharp high-field methyl peak shown for the −8 °C spectrum in Fig. 2 can still be observed as a sharp peak at +30 °C, although an irreversible rearrangement of **6**–**7** is taking place very rapidly at this temperature. One can assign a maximum rate constant of 10 s^{-1} at +30 °C for the *endo*-3,2-methyl shift required to broaden this line (see Overall Plan). The extrapolated rate constant for the *exo*-3,2-methyl shift from Fig. 3 is 9.3×10^5 s^{-1} at 30 °C, giving the minimum ratio $k_{exo\text{-methyl shift}}/k_{endo\text{-methyl shift}} = 9.3 \times 10^4$.

The increased temperature stability of **6**–**7** relative to **3**–**4** is of interest and may be due to a statistical entropy stabilization in the former case. If one carries out a sequence 3,2-hydride shift, WM shift, *exo*-3,2 methyl shift, WM shift, 3,2-hydride shift, *etc.* on **6** and **7**, it requires 20 steps in one direction before one again reaches an identity with all of the unique methyl groups back in their original positions. This is shown in Fig. 4. There are 10 degenerate structures in **7** and 10 in **6**. The 10 structures in each correspond to a permutation of the 5 unique exchanging positions, C-1, 2, 3-*endo*, 4 and 7-*anti*, and the five unique substituents 1, 2, 3, 4, and 6 at each of these positions, the substituents maintaining an unique order with respect to one another. There are series involving both the 1*R* and 1*S* forms of the assymmetric 2-norbornyl cation (but never involving enantiomers), to give the total of 10 of each. If one follows the reaction scheme of Fig. 4 in a clockwise direction, the fixed relationship of the substituents involves a clockwise rotation in **6** and **7** to an observer facing the

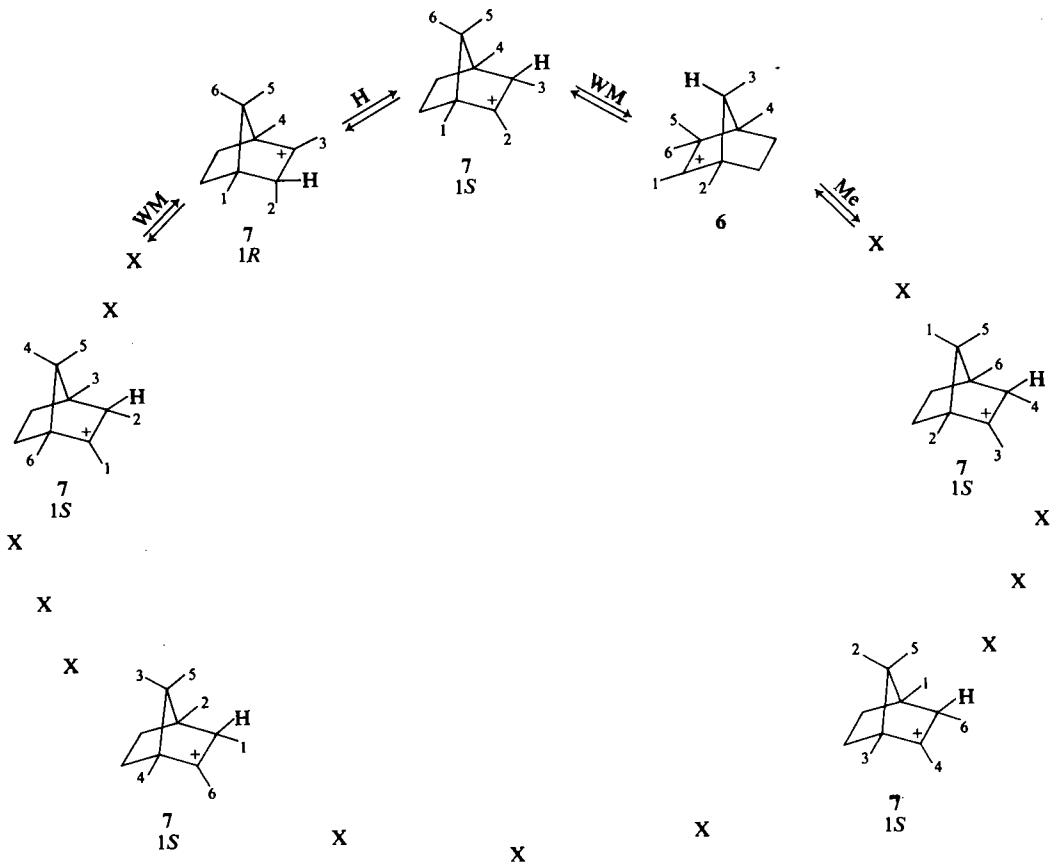

FIG. 4. Degenerate rearrangement cycle for the cations **6**, **7**. There are 10 structures for **6** and 10 for **7**. One-half in each case are 1*S* enantiomers and one-half 1*R*.

structures as written below. The C-3 proton in **7**, C-7 *syn* in **6**, resides with each of five methyl substituents 1, 2, 3, 4, and 6 in turn, and in order to get complete averaging of the coupling would require a complete sequence of steps. Experimentally the line widths in **6**–**7** are too broad (see for example the 15H peak at −8 °C in Fig. 2) to show the subtle changes expected as the coupling becomes averaged, although one can show the effects in calculations by using artificially narrow line widths.

6 and **7** series

The degeneracy present in **6**–**7** will result in a stabilization of these cations relative to other hexamethyl cations in which this degeneracy is not present by at least 1 kcal/mol. Thus, when the only doubly degenerate pentamethyl cations **3**–**4** irreversibly rearrange, they are apparently forming other more stable pentamethyl-2-norbornyl cations. When the (each) 10-fold degenerate **6**–**7** rearrange, they are directly forming a cyclopentenyl cation.

In the H–D exchange part of this work, the alkene **10** was dissolved in 0.55% D_2SO_4–CD_3COOD. The solution was then heated to 50 °C and the sequence of events shown in Fig. 5 was observed. The two largest peaks in the initial spectrum (*E*) of **10** are assigned to the C-1–C-4 and C-2–C-3 methyls, the former the higher field. The highest field of the 'single' methyl peaks is assigned to the 7-*syn* methyl, the other to the 7-*anti* methyl. Both 6H peaks decrease relatively fast, $t_{1/2}$ *ca.* 10 min for the C-2–C-3 methyls and *ca.* 40 min for the C-1–C-4 methyls. The C-7-*anti*

Can. J. Chem. Downloaded from www.nrcresearchpress.com by 210.87.254.6 on 09/05/12
For personal use only.

Can. J. Chem. Downloaded from www.nrcresearchpress.com by 210.87.254.6 on 09/05/12
For personal use only.

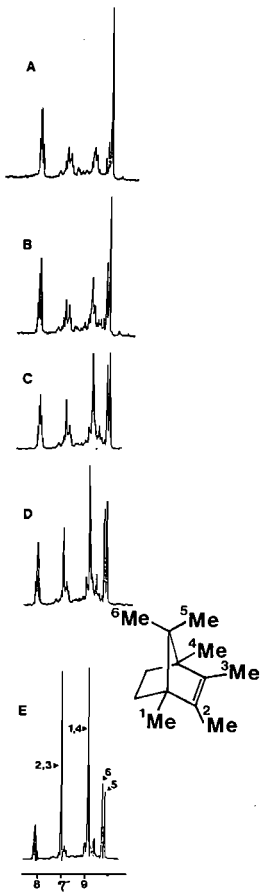

FIG. 5. The H–D exchange with time of protons in the alkene **10**, measured in 0.55% D_2SO_4–CD_3COOD at 50 °C. *E*, initial; *D*, 30 min; *C*, 45 min; *B*, 100 min; *A*, 27 h. The peak to the left is the peak height reference signal, CHD_2COOD.

methyl decreases more slowly, $t_{1/2}$ *ca.* 90 min. After 2 days, only one methyl signal remains, spectrum *A* in the Fig. 5 sequence. The two small peaks to the lower field side of the large peak in *A* are due to single CH_3 peaks in the two alkenes **16***a* and **15***a*, the proportions *ca.* 1:2.

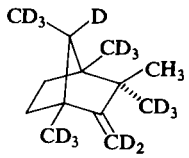

16*a*

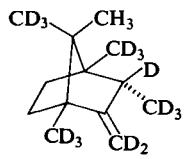

15*a*

The above solution was then kept at 25 °C for *ca.* 120 days before one-half of the remaining CH_3 peak had disappeared. The rate of this decrease is very similar to that observed in the pentamethyl alkene **9** for the related methyl group. Although the rate of H–D exchange due to the *exo*-3,2-methyl shift, *i.e.* as measured by the loss of the C-7-*anti* methyl, is slower in **10** compared to **9**, this is quite probably caused by an intrinsically slower H–D exchange rate in **10**. This occurs because the dominant deprotonation process of the cations **6–7** is loss of the C-3 proton, which does not lead of course to exchange in the methyl groups, whereas in **3–4**, the dominant loss is from a methyl group. It seems probable to us that the actual rate of the *exo*-3,2-methyl shift is similar in both the H–D exchanges in **9** and **10** so that the ratio quoted for the pentamethyl series, 2×10^3, is roughly applicable to **10**.

When a solution of **10** was kept at 50 °C for 2 days in the deuterated acid and then worked up, the pure alkene **10***a* could be isolated. Adding this to 1:1 (by weight) $DFSO_3$–SbF_5 at *ca.* −50 °C yields a solution of the carbocations **6***a*–**7***a*.

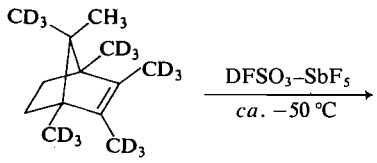

10*a*

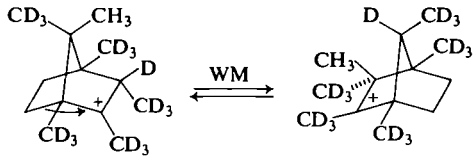

6*a* **7***a*

An n.m.r. spectrum of **6***a*–**7***a* at −30 °C is shown in Fig. 6*A*. In addition to the sharp single methyl peak of **6***a*–**7***a*, there is a small, broad peak for the residual CHD_2 protons of the five coalesced methyl peaks in **6***a*–**7***a* and some residual protons in the C-5–C-6 region which were not exchanged out in **10***a*. This spectrum can be contrasted to that shown in Fig. 2 for the all-proton analog.

When the solution of **6***a*–**7***a* was warmed to −10 °C, exchange of the remaining methyl group with the other five was finally observed. The intact CH_3 group in **6***a*–**7***a* is finding its way into the five-methyl rearrangement manifold and

Can. J. Chem. Downloaded from www.nrcresearchpress.com by 210.87.254.6 on 09/05/12
For personal use only.

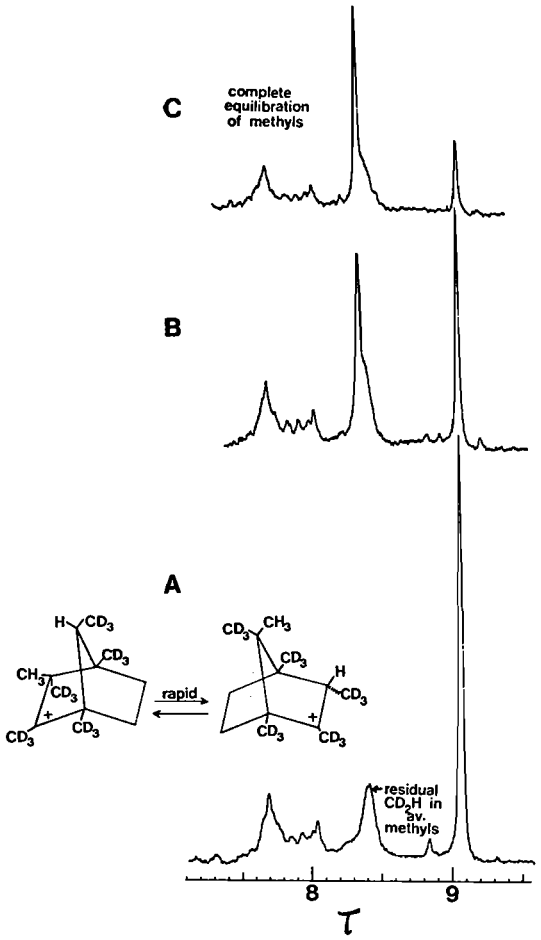

FIG. 6. The ions **6**, **7** prepared from the partially deuterated alkene **10***a*. *A*, −30°C; *B*, after 30 min at −10 °C; *C*, after complete equilibration at 0 °C.

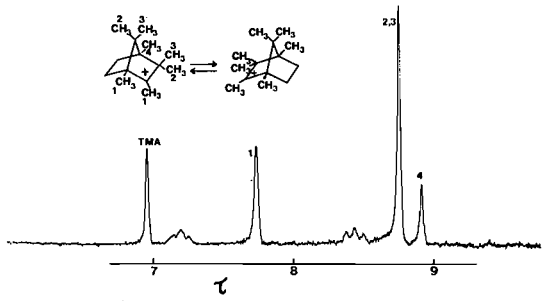

FIG. 7. Nuclear magnetic resonance spectrum at −70 °C of the carbocation **8**.

is appearing as a sharp peak[3] superimposed on the residual CD_2H protons already there. The rate constant for this process was *ca.* 4×10^{-4} s^{-1} at −10 °C. If this overall exchange is the result of an *endo*-3,2-methyl shift in cation **6***a*, then the rate constant for this shift is *ca.* 1×10^{-4} s^{-1} (taking the unfavorable equilibrium concentration of **6***a* into consideration). An actual value for $k_{exo\text{-}3,2\text{-methyl shift}}/k_{endo\text{-}3,2\text{-methyl shift}} = 7 \times 10^4/1 \times 10^{-4} = 7 \times 10^8$ at −10 °C can finally be arrived at.

Heptamethyl Cation Series **8**

Addition of the alkene **11** to FSO_3H–SO_2ClF (1:4) at −120 °C generates the carbocation **8** whose n.m.r. spectrum is shown in Fig. 7. As in

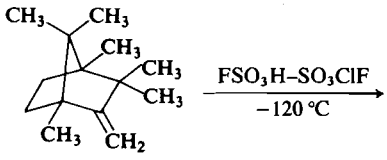

11

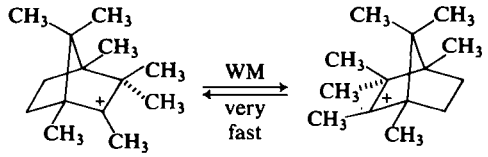

8

the other ions, the WM shift, which is degenerate in this case, is very rapid on an n.m.r. time scale. The chemical shifts for the WM averaged structure are listed in Table 1, the chemical shifts of the 3-*endo*–7-*anti* and 3-*exo*–7-*syn* methyl 'pairs' being accidentally equivalent. Up to the temperature (−50 °C) where an irreversible rearrangement becomes rapid, there is no sign of line broadening in the n.m.r. spectrum of **8**. Using the double irradiation spin-saturation transfer technique of Forsén and Hoffman (6), it was possible to observe a decrease in the size of the C-1–C-2 methyl groups on irradiation of the C-4 methyl at −50 °C. Very approximately (assuming $T_1 = 1$ s), this yields the rate constant for the exchange, $k = 1$ s^{-1}. The actual exchange

[3]The use of the much stronger acid $DFSO_3$–SbF_5 was necessary because in $DFSO_3$–SO_2ClF (1:4), there is direct exchange of solvent deuterium with carbocation protons at −10 °C, *i.e.* as soon as the CH_3 group exchanges into the five-methyl manifold it becomes exchanged out.

Can. J. Chem. Downloaded from www.nrcresearchpress.com by 210.87.254.6 on 09/05/12
For personal use only.

may be due to an *endo*- or *exo*- (or both) 3,2-methyl shift. Assuming that the rate were for an *exo*-3,2-methyl shift, the minimum factor by which the C-7-*syn* methyl slows down the *exo*-3,2-methyl shift would be $1/(2 \times 10^3)$ (from **6**–**7** data) $= 5 \times 10^{-4}$. This can be contrasted with the minimal effect of a C-7 *syn* methyl on the 3,2-hydride shift, *cf.* ions **7** and **17**. The difference is not unexpected in view of the differing steric requirements for H and CH_3 but this study puts a quantitative value on it.

In the H–D exchange studies, the hydrocarbon **11** was dissolved in 0.85% D_2SO_4–CD_3COOD and heated to 58 °C. Within 10 min at this temperature there is virtually no signal left for the C-1 methyl group or the *exo*-methylene protons of **11**. This is shown in Fig. 8*D*, the peak *1* corresponding to the residual C-1 methyl signal. After 20 h at this temperature (spectrum *C*), there is a noticeable decrease in the C-4–C-6 methyl peak relative to the others. The bath temperature was then raised to 80 °C and after 5 h at this temperature, spectrum *B* was obtained. The final spectrum *A* was obtained after a total of 9 h at 80 °C. The results obtained indicate that both *exo*- and *endo*-3,2-methyl shifts are occurring, the decrease in peaks *2* and *6* indicative of the *exo* shift and the decrease in *3* and *5* indicative of the *endo* shift. The results suggest that the *exo*-3,2-methyl shift is marginally faster.

A comparison of the *exo* and *endo* shifts in **11** with alkenes **9** and **10** is difficult because of the different temperatures involved. When exchange in **9** was carried out at 58 °C, the half-life for exchange of the C-4 and C-7-*anti* methyl groups (indicative of the *exo*-3,2-methyl shift) was *ca.* 5 min. One can estimate the half-life for the corresponding H–D exchange in **11** as perhaps 60 h

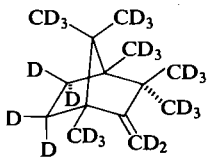

11*a*

at 58 °C, giving an approximate ratio of 1.5×10^{-3} for the decreased rate of the *exo*-3,2-methyl shift in **11**. This is of the same order of magnitude as that found in the observable ion comparisons. The rate of the *endo*-3,2-methyl shift in **11** may be somewhat faster than in **9** and **10** but there is certainly no dramatic difference.

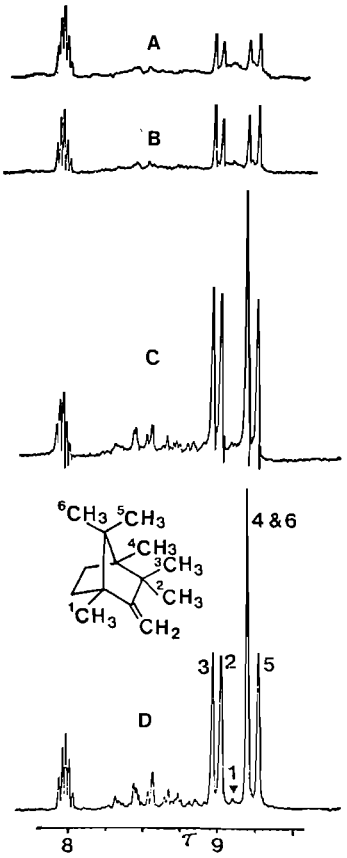

FIG. 8. The H–D exchange with time of the protons in alkene **11**, measured in 0.85% D_2SO_4–CD_3COOD. *A*, less than 10 min at 58 °C; *B*, after 20 h at 58 °C; *C*, after a further 5 h at 80 °C; *D*, after 9 h at 80 °C. The peak to the left is CHD_2COOD, which was used as a constant peak height reference.

When the deuterated acid solution of **11** is heated at 80 °C, a deep violet color develops and in order to ascertain whether the peak decrease shown in Fig. 8 is simply due to decomposition, the hydrocarbon (expected to be partly **11***a*) was reisolated. The mass spectrum of this recovered **11** (parent ions) indicated the following species and percentages: d_{11}, <1%; d_{12}, 1%; d_{13}, 2%; d_{14}, 4%; d_{15}, 6%; d_{16}, 9%; d_{17}, 12%; d_{18}, 14%; d_{19}, 15%; d_{20}, 14%; d_{21}, 11%; d_{22}, 7%; d_{23}, 3%; and d_{24} (perdeuterioalkene **11***a*), 1%. Since one is exchanging out 24 protons, there is considerable equilibrium proton content in **11**. Clearly, the results are consistent with both *exo* and *endo* shifts since a maximum d_{18} species would be produced if only one of the 3,2-methyl shifts were involved. The loss of the C-5 and C-6

Can. J. Chem. Downloaded from www.nrcresearchpress.com by 210.87.254.6 on 09/05/12
For personal use only.

methylene protons can occur via the corresponding tricyclene which appears to be a minor equilibrium constituent along with **11**.

Alternatives to an endo-3,2-Methyl Shift

The *exo*-3,2-methyl shift in the observable cations is unambiguously established because the n.m.r. line-broadening method essentially labels each unique group. Likewise, because one knows the absolute rate of this shift to be fast, it is very reasonable to interpret the H–D exchanges in the ion intermediates in terms of this. The proposed *endo*-3,2-methyl shift is so slow and the evidence is based on a much less unique labelling scheme so that alternative explanations should at least be considered.

We have been unable to formulate *any* reasonable process in the observable ions which would involve a symmetry plane developing in the 2-norbornyl cation structure and which would equate the C-3-*exo* methyl group with either the C-3-*endo* methyl or the C-2 methyl. The only processes which appear remotely possible are ones involving ring opening, rotation and reclosure, for example, as in Scheme 4. A similar

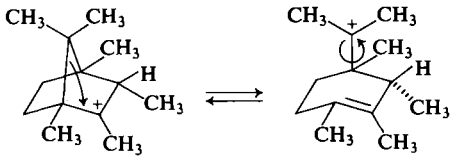

SCHEME 4

process could occur with breaking of the C-6–C-1 bond of an intermediate norbornyl cation. All things considered, the most reasonable rationalization of the CH_3 scrambling observed in Fig. 6 is to formulate the *endo* methyl shift.

In the H–D exchange work, all that is required for a methyl to exchange is that it be located next to the positive center of a carbocation intermediate. One can imagine equilibrium processes, Scheme 5, which accomplish this but do not ever equate the methyls concerned with any other (in contrast, the observable ion studies require this). The actual alkene produced from **19** would have to be thermodynamically much less stable than **10** since one can account for all of the observed g.l.c. peaks in terms of alkenes related to the ions **6**–**7** (see hexamethyl cation results). Large stability differences between these alkenes seem somewhat unlikely; however, an even stronger case for an actual *endo*-3,2-methyl shift comes from a careful analysis of the H–D substitution pattern in the alkene **11** (shown in Fig. 8 and analyzed in Scheme 6).

Experimentally, methyl 1 is very quickly exchanged. A migration of any of the four methyls 2, 3, 5, 6 allows for subsequent substitution of the 4-methyl group (which is unfortunately overlapped by 6). The actual substitution pattern for this group is consistent with this picture, *i.e.* by the time the other groups have decreased by a factor of two, the 4-methyl should have decreased by a factor of eight (the *exo* and *endo* processes occur at nearly the same rate). Hence, in Fig. 8*B*, where the decrease in peaks 2, 3, 5, and 6 is somewhat more than a factor of two, the 4-methyl has been, within experimental error, fully exchanged. This particular pattern would not likely have occurred if the exchange had taken place by some other mechanism (as in Scheme 5) and all things considered, the H–D exchange rates appear to us to reflect the *exo*- and *endo*-3,2-methyl shifts.

Direct Measurement of the H–D Kinetic Isotope Effect for a 3,2-Hydride Shift

When the alkene **10** was added to $DFSO_3$–SO_2ClF (1:4), the cations **6**–**7** which were produced had, surprisingly, a considerable C-3 proton content (Scheme 7). We have no explanation for this but in any case, when the cation solution is carefully warmed, there is preferential exchange of solvent deuterium with this position before any appreciable exchange occurs in other positions. When the line broadening due to the 3,2-D shift is analyzed, the rate is found to be about eight times slower than for the corresponding proton shift, giving $k_H/k_D = 8$ at -110 °C. This experiment is included in this paper because vicinal hydride shifts in observable cations are usually too fast to measure. The fact that the hydride shift in **6**–**7** is measurable and amenable to a rather accurate kinetic treatment made it worthwhile to show the potential for the direct measurement of isotope effects in cation rearrangements. Further studies are in progress.

Discussion

This work shows that *exo*-3,2-methyl shifts in tertiary 2-norbornyl cations are overwhelmingly preferred to *endo* shifts. Thus the recently reported (7) occurrence of an *endo*-3,2-methyl shift must be seriously questioned, as indeed Collins

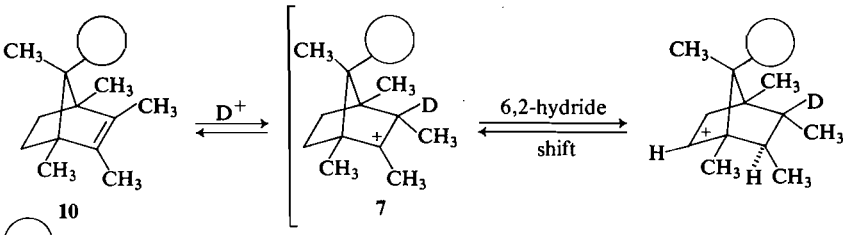

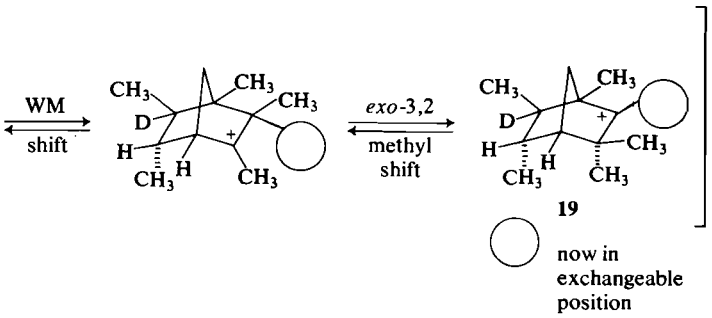

SCHEME 5

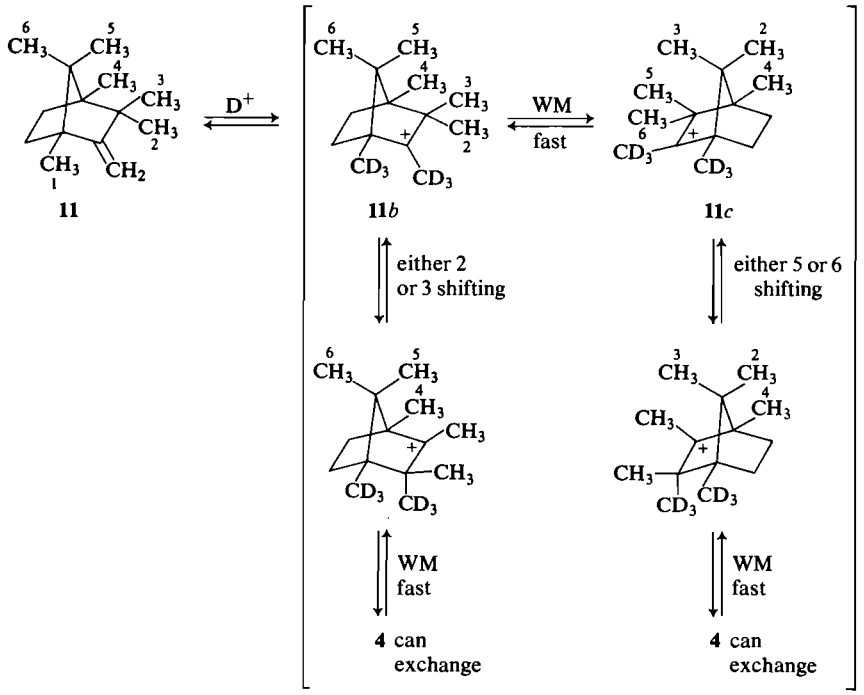

SCHEME 6

Can. J. Chem. Downloaded from www.nrcresearchpress.com by 210.87.254.6 on 09/05/12
For personal use only.

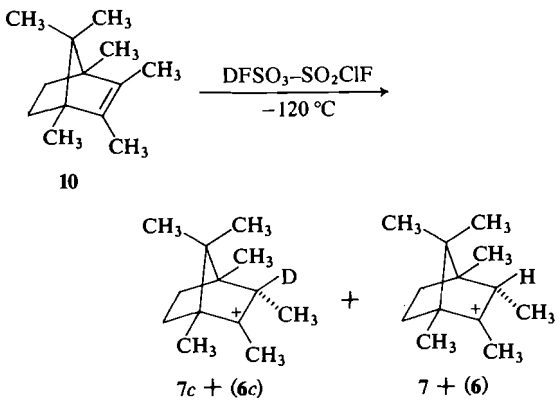

SCHEME 7

and Lietzke (8) have also done but on other grounds.

Nevertheless, the stereospecificity of the 3,2-shift is much higher in the observable ions, *cf.* for the **6**–**7** system, 7×10^8 *vs.* 2×10^3 for acid catalysis, although in part this occurs because reactions are more selective at low temperatures. Some stereospecificity for *exo*-3,2-shifts in solvolytically generated 2-norbornyl cations is a well established phenomenon (9, 10) and in the report by Vaughan and co-workers (7) concerning an *endo*-3,2-methyl shift, the *exo* shift is still reported as being dominant. The uncertainty we hope to have answered in this paper is one of quantity. This stereospecificity in 2-norbornyl cations has generally been attributed to a nonclassical structure for the ions (9, 10) or to tortional effects (9). In the present ions, the existence of the two WM-shift isomers **3**–**4** is firmly established and a nonclassical structure definitely ruled out. If one makes a normal model of the 2-norbornyl cation, the geometry looking down the C-2–C-3 bond is approximately as shown in **I**, as noted previously by Schleyer (9). There is evi-

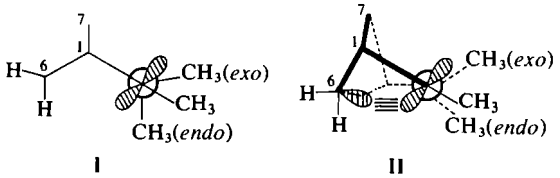

I II

dence in observable tertiary norbornyl cations for some overlap of the empty $2p_z$ orbital with a back lobe on C-6 (11) and this can be visualized as a twisting of the $2p_z$ orbital (**II**). This makes the *exo* substituent more colinear and the *endo* substituent less so and is an obvious way to rationalize the experimental facts. In more nucleophilic solvents, such as are used in acid catalysis or solvolysis work, there may be less need for internal stabilization via C-2–C-6 bonding and hence a geometry in which the stereospecificity is somewhat diminished. One might also predict that a phenyl substituent at C-2 would act in much the same way as a nucleophilic solvent, *i.e.* that it would delocalize charge from C-2 without the need for internal stabilization and that the stereospecificity would also be diminished in this case.

In determining absolute rearrangement rates for carbocations, one should in principle be able, *if* these rates are applicable to the more nucleophilic solvents, to calculate overall rates in conventional acid catalysis rearrangement reactions. Such a reaction is outlined in Scheme 8. If

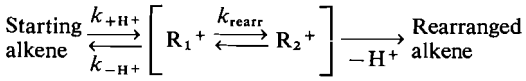

SCHEME 8

$k_{-H^+} > k_{rearr}$, then the overall rate constant is given by $k_{overall} = Kk_{rearr}$. If one could assign an accurate pK_a value to the carbocation and if the p*H* or acidity function of the solvent system were known, one could calculate $k_{overall}$. Unfortunately, k_{-H^+} seems to be competitive with k_{rearr} in the examples in this work except for the heptamethyl case or for the *endo*-3,2-methyl shifts. An ideal situation for this kind of study would in fact be a k_{rearr} rate constant somewhere between the *exo*- and *endo*-shift value, *i.e.* easily measurable as a degenerate process in observable cations and fast enough so that dilute acid solutions of well-defined p*H* and moderate temperatures could be used for the acid catalyzed rearrangement. The other possibility would be to increase k_{-H^+} in the present examples by using a more basic solvent system.

Conclusions

(*i*) From observable ion studies, there is a huge difference in the migratory aptitudes of 3-*exo* and 3-*endo* methyl groups in 2-norbornyl cations.

(*ii*) The same trend is readily apparent in acid-catalyzed rearrangements but to a lesser extent.

(*iii*) A C-7-*syn* methyl substituent has a very large effect on an *exo*-3,2-methyl shift but almost none on an *exo*-3,2-hydride shift.

Can. J. Chem. Downloaded from www.nrcresearchpress.com by 210.87.254.6 on 09/05/12
For personal use only.

(*iv*) An *exo*-3,2-hydride shift is very much faster than an *exo*-3,2-methyl shift (a factor of 1.6×10^3 at -80 °C).

Experimental

All n.m.r. measurements were made using a Varian HA-100 spectrometer equipped with a variable temperature probe. Temperatures were measured using a thermocouple inserted directly into the n.m.r. tube. For the spin-saturation transfer experiments, the precautions outlined in the preceding paper (1) were followed. The preparation of the carbocations and the quenching procedures were similar to those previously described (3).

H–D Exchange Studies

The pure alkene (2% by weight of the final solution) was added to the D_2SO_4–CD_3COOD mixture and a small sample removed for the n.m.r. study. The rates of the H–D exchanges were based on peak heights, the unchanging CHD_2 peak of the deuterated acetic acid being used as an internal standard. When the n.m.r. study had determined the time and temperature necessary for the complete exchange (specific), the same conditions were applied to the bulk solution. For the recovery of the alkenes, the acid solution was added dropwise to an ice-cold stirred solution of excess Na_2CO_3 in D_2O and the alkene extracted 3 x with ether. After drying over anhydrous K_2CO_3, the ether was removed to yield the crude alkene mixture, which could be separated by preparative g.l.c. using a 12 ft × 3/8 in. column of Carbowax 20 M at 165 °C.

Nuclear Magnetic Resonance Line-Broadening Calculations

The calculated spectra were obtained by solving the Bloch equations. The major problem in both the pentamethyl and hexamethyl series comes in the variation of the equilibrium constant with temperature. Once this relationship has been established, it is necessary to match the experimental spectra at each temperature with spectra calculated specifically for this temperature (running through a series of rate constants in order to determine the best fit). Since the calculated spectra involve only the methyl groups, the calculations need take into account only first-order coupling effects.

The authors wish to thank the National Research Council of Canada for generous financial support.

1. R. HASELTINE, E. HUANG, K. RANGANAYAKULU, and T. S. SORENSEN. Can. J. Chem. This issue.
2. T. S. SORENSEN and K. RANGANAYAKULU. Tetrahedron Lett. 2447 (1972).
3. L. HUANG, K. RANGANAYAKULU, and T. S. SORENSEN. J. Am. Chem. Soc. **95**, 1936 (1973).
4. S. J. CRISTOL, L. K. GASTON, and D. W. JOHNSTON. Tetrahedron Lett. 185 (1963); H. KWART and J. L. NYCE. J. Am. Chem. Soc. **86**, 2601 (1964).
5. A. J. JONES, E. HUANG, R. HASELTINE, and T. S. SORENSEN. J. Am. Chem. Soc. In press.
6. S. FORSÉN and R. A. HOFFMAN. J. Chem. Phys. **39**, 2892 (1963).
7. C. W. DAVID, B. W. EVERLING, R. J. KILIAN, J. B. STOTHERS, and W. R. VAUGHAN. J. Am. Chem. Soc. **95**, 1265 (1973).
8. C. J. COLLINS and M. H. LIETZKE. J. Am. Chem. Soc. **95**, 6842 (1973).
9. P. V. R. SCHLEYER. J. Am. Chem. Soc. **89**, 699 (1967) and references therein.
10. J. A. BERSON, J. H. HAMMONS, A. W. MCROWE, R. G. BERGMAN, A. REMANICK, and D. HOUSTON. J. Am. Chem. Soc. **89**, 2590 (1967).
11. G. A. OLAH, J. R. DEMEMBER, C. Y. LUI, and R. D. PORTER. J. Am. Chem. Soc. **93**, 1442 (1971).
12. E. HUANG, K. RANGANAYAKULU, and T. S. SORENSEN. J. Am. Chem. Soc. **94**, 1779 (1972).

Can. J. Chem. Downloaded from www.nrcresearchpress.com by 210.87.254.6 on 09/05/12
For personal use only.

The Activity of AgCl in AgCl–LiCl–KCl Melts

ANTHONY C. GRUNER[1] AND WILLIAM T. THOMPSON

Department of Mining and Metallurgical Engineering, McConnell Engineering Building, McGill University, Montreal, Quebec H3C 3G1

Received September 12, 1974

ANTHONY C. GRUNER and WILLIAM T. THOMPSON. Can. J. Chem. **53**, 1084 (1975).

Thermodynamic properties of silver chloride in molten silver chloride – lithium chloride – potassium chloride melts were studied using a silver chloride formation cell employing a chlorine electrode of novel design which facilitated measurements in ternary melts. The data were treated by analytical methods resulting in the generation of activity and the partial molar excess free energy at 500 °C.

The measured properties were interpreted with the aid of a model which presupposed the existence of free silver ions as well as those "bonded" to adjacent chloride ions. With three adjustable parameters it was possible to account for the thermodynamic behavior of silver chloride.

ANTHONY C. GRUNER et WILLIAM T. THOMPSON. Can. J. Chem. **53**, 1084 (1975).

On a étudié les propriétés thermodynamiques du chlorure d'argent dans des masses fondues contenant du chlorure d'argent, du chlorure de lithium et du chlorure de potassium; ces études ont été effectuées en faisant appel à une cellule à formation de chlorure d'argent munie d'une électrode à chlore redessinée pour faciliter les mesures dans des masses fondues ternaires. On a traité les données par des méthodes analytiques de façon à en déterminer la génération d'activité et les énergies libres molaires partielles à 500 °C.

On a interprété les propriétés mesurées à l'aide d'un modèle qui présuppose l'existence d'argent sous forme d'ions libres de même que d'autres "liés" à des ions chlorures adjacents. En faisant intervenir trois paramètres ajustables, il est possible d'expliquer le comportement thermodynamique du chlorure d'argent. [Traduit par le journal]

Introduction

In view of the importance of fused salt electrowinning processes to extractive metallurgy, numerous studies of molten salts and solutions thereof have been conducted by metallurgists in the past two or three decades. Of basic importance is a knowledge of the thermodynamic properties. These are useful in understanding melt structure.

Thermodynamic studies have generally been restricted to binary systems in spite of the importance of ternary solutions in many practical electrolyte systems. In recent years, however, there have been systematic investigations of silver chloride – alkali chloride ternary systems; these include the systems silver chloride – sodium chloride – potassium chloride (1) and silver chloride – sodium chloride – cesium chloride (1) and most recently, silver chloride – sodium chloride – rubidium chloride (2). The properties of these three systems are much the same because of the chemical similarity of the alkali metals from sodium to cesium. It is expected that there would be much different behavior for a ternary system of silver chloride containing lithium chloride because of the small ionic radius of lithium.

This report is concerned with the measurement and interpretation of the properties of the molten silver chloride – lithium chloride – potassium chloride system. This system is slightly more difficult to study than those cited previously because of the tendency of lithium chloride to react with atmospheric water vapor to form lithium hydroxide and hydrogen chloride. However, in other respects this system is amenable to precise study especially because of the low temperature eutectic in the lithium chloride – potassium chloride binary system. This permits useful data to be gathered on the melt without the necessity of measurements at temperatures in excess of 535 °C.

Experimental Procedure

Thermodynamic properties of molten silver chloride – lithium chloride – potassium chloride electrolytes were

[1]This work was submitted by A. C. Gruner in partial fulfilment of the requirements for the M. Eng. degree at McGill University.

Can. J. Chem. Downloaded from www.nrcresearchpress.com by 210.87.254.42 on 09/05/12
For personal use only.

Can. J. Chem. Downloaded from www.nrcresearchpress.com by 210.87.254.42 on 09/05/12
For personal use only.

determined by measuring the Gibbs free energy change for the reaction

$$Ag_{(s)} + \tfrac{1}{2}Cl_{2(g)} \rightarrow AgCl_{(l)}$$

in electrolytes of different silver chloride concentration over the approximate temperature range of 370 to 535 °C. The proven electrochemical technique which makes use of the cell

$$-Ag/AgCl\text{–}LiCl\text{–}KCl/Cl_2, C+$$

was employed exclusively in this work (3).

The cell is shown in Fig. 1; construction details of this mainly Pyrex apparatus are largely self-explanatory.

Prior to cell assembly the crucible was filled with a chloride solution. This solution was purified *in situ* by passing anhydrous hydrogen chloride vapor over the salts (4) and then filtering the melt through Pyrex wool. The solution was then purged of dissolved hydrogen chloride by bubbling argon through the melt for 2 h.

The silver electrode was a fine-silver wire 3 mm in diameter immersed about 2 cm into the melt.

The chlorine electrode basically consisted of a graphite rod in contact with the melt and a chlorine atmosphere. A detailed drawing appears in Fig. 2. The graphite rods were 6 mm in diameter and made of spectroscopic grade material. The graphite was nevertheless pretreated by baking in vacuum at 900 °C for 12 h and then in a chlorine atmosphere for 48 h. The use of the movable tapered glass joint at the bottom of the electrode assembly made it possible to achieve a cell resistance of 500 to 3000 ohm. With such a resistance chlorine diffusion to the silver electrode is effectively eliminated. It has been found that it is only when chlorine diffusion is reduced to very low values that reproducible and thermodynamically meaningful e.m.f. measurements can be made (3).

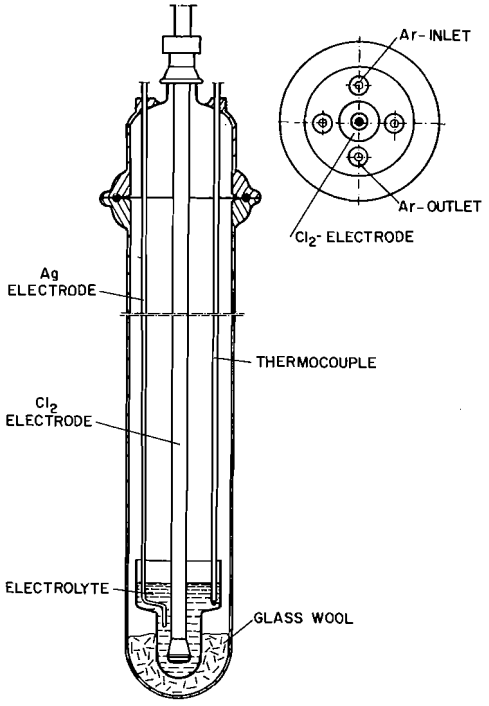

FIG. 1. Overall view of electrochemical cell.

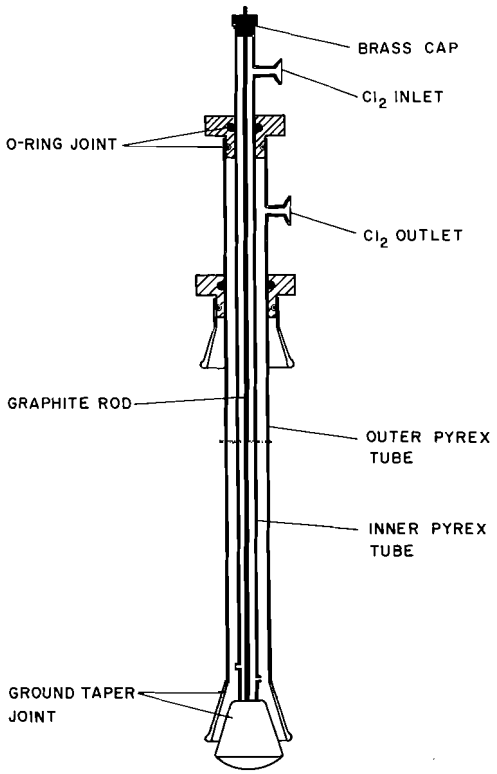

FIG. 2. Detail of chlorine electrode.

Measurements were conducted on pure silver chloride and 13 ternary solutions. Compositional changes along paths of constant lithium chloride to potassium chloride ratio were made by adding silver chloride directly to the melt. After each addition, anhydrous hydrogen chloride was bubbled through the melt followed by argon purging. The tapered glass joint at the bottom of the chlorine electrode was found to be particularly useful for such composition changes. In particular it was easy to ensure that the melt composition was uniform throughout the entire cell by simply opening the tapered joint and moving the electrode up and down a few times in the melt.

After each change in composition, it took several hours to reach a stable e.m.f. This is attributed to the time required for chlorine to saturate the electrolyte. The chlorine pressure was measured with a manometer and typically was about 10–12 Torr above atmospheric pressure.

Measurements of e.m.f. were stable to within 0.2 mV for a period of 1 h and responded immediately to changes in temperature. The values were reproducible on increasing and decreasing the temperature.

The temperature was measured with a calibrated chromel–alumel thermocouple. With it the temperature gradient within the melt was determined to be about

0.4° (C) cm^{-1}. Since the overall depth of the melt was 10 cm, the uncertainty in temperature is about $\pm 2°$ (C).

When the e.m.f. measurements of a particular composition were completed, two samples of the melt were taken for silver chloride and potassium chloride analysis. The analysis was carried out by dissolving the frozen salt mixture in ammonium hydroxide and distilled water. The silver chloride was precipitated from the solution after expelling the ammonium hydroxide (5). The precipitate was collected, dried, and weighed. The filtrate was saved and then analyzed gravimetrically for potassium chloride by using the perchlorate method (6). The lithium chloride concentration was determined by subtracting the combined weights of potassium chloride and silver chloride from the total sample weight.

During sampling partial freezing of the electrolyte may have resulted in some sample bias due to segregation. This and other systematic errors accumulate so that the mole fractions of the components were regarded as not more accurate than 1 mol%

Experimental Results

The electromotive force, E, is related to the activity of silver chloride, a_{AgCl}, the pressure of chlorine in atm, P_{Cl_2}, the absolute temperature T, and the standard formation potential E^0, by the Nernst equation.

$$[1] \quad E = \frac{RT}{2F} \ln P_{Cl_2} = E^0 - \frac{RT}{F} \ln a_{AgCl}$$

where F is the Faraday. The measured e.m.f., however, does not give E directly because of the thermoelectric effect associated with dissimilar electrodes. The silver and carbon electrodes effectively constitute a thermocouple in series with the electrochemical cell, but the small correction for this effect can be made without difficulty (7). The left hand side of eq. 1, which will be referred to as E^*, is the potential of the cell with respect to the standard chlorine electrode; that is to say, one in which the chlorine pressure is 1 standard atmosphere.

Standard Formation Potential of Silver Chloride

In order to determine the thermodynamic properties associated with AgCl in the melt, for example a_{AgCl}, the standard formation potential of pure AgCl, E^0, must be known as a function of temperature; that is, E^* must be determined for the case when the electrolyte is pure silver chloride.

Although several investigations have reported values for E^0 (3, 8–13) a redetermination was undertaken in order to test the operation of the cell. These measurements are depicted in Fig. 3.

In order to achieve a satisfactory interpolation

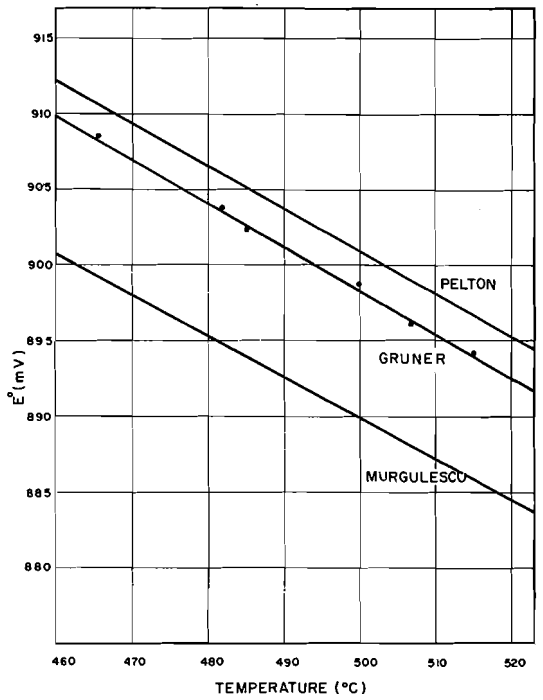

FIG. 3. Standard formation potential of silver chloride bracketed by highest and lowest reported measurements.

of the measurements, a regression analysis was performed recognizing the known difference in heat capacity between silver chloride, silver, and chlorine gas (14, 15).

$$[2] \quad (C_p)_{AgCl(l)} - (C_p)_{Ag(s)} - \tfrac{1}{2}(C_p)_{Cl_2(g)} = 4.195 - 2.07 \times 10^{-3}T - 0.02 \times 10^{5}T^{-2} \text{ cal mol}^{-1}\text{ K}^{-1}$$

It follows that

$$[3] \quad \Delta H^0 = A + 4.195T - 1.035 \times 10^{-3}T^2 + 0.02 \times 10^{5}T^{-1}$$

$$[4] \quad \Delta S^0 = B + 4.195 \ln T - 2.07 \times 10^{-3}T + 0.01 \times 10^{5}T^{-2}$$

where A and B are integration constants and ΔH^0 and ΔS^0 are the standard molar enthalpy and entropy changes for the formation of AgCl. Since

$$[5] \quad \Delta G_T^0 = -FE^0 = \Delta H^0 - T\Delta S^0$$

where ΔG^0 is the standard free energy change at temperature T, it follows that

Can. J. Chem. Downloaded from www.nrcresearchpress.com by 210.87.254.42 on 09/05/12
For personal use only.

Can. J. Chem. Downloaded from www.nrcresearchpress.com by 210.87.254.42 on 09/05/12
For personal use only.

[6] $\Sigma = -FE^0 - 4.195T + 4.195T \ln T - 0.01 \times 10^5 T^{-1} - 1.035 \times 10^3 T^2 = A - BT$

A linear regression of Σ *vs.* T gives values of $-28\,449$ cal mol^{-1} for A and -32.899 cal K^{-1} mol^{-1} for B.

The variation of E^0 with respect to temperature as determined by the regression is displayed in Fig. 3. The highest reported measurements (3) and the lowest reported measurement (11) bracket the present work and within a few mV the various determinations of E^0 concur; for all subsequent calculations discussed the following equation based upon the Σ function calculation on the present measurements was employed

[7] $E^0 = 1233.6 - 1.609T + 0.182T \ln T - 43.4T^{-1} - 4.48 \times 10^{-5} T^2$

Thus at 500 °C, $E^0 = 898.4$ mV.

Relative Partial Molar Free Energy

Thirteen different compositions in the AgCl–LiCl–KCl ternary system were studied. The compositions are depicted on the Gibbs triangle shown in Fig. 4. Points on the silver chloride – potassium chloride binary are those of Pelton and Flengas (3). Points on the silver chloride – lithium chloride binary are those of Panish *et al.* (9). The compositions studied in this investigation were limited to the central region of this system because of the Pyrex construction of the apparatus which limited the upper temperature of this investigation to 535 °C.

The e.m.f. as measured between a standard chlorine electrode and a silver electrode, E^*, is plotted *vs.* temperature in Figs. 5 and 6.

The general scatter of points is comparable with that of Panish *et al.* for the AgCl–LiCl binary system and Pelton and Flengas for the AgCl–KCl binary system shown in Figs. 7 and 8 respectively. In this respect it should be realized that the e.m.f. and temperature scales are more expanded for the present measurements owing to the limited temperature range. The lines in Figs. 5–8 represent traces of a regression analysis performed on all the data at once. Details of this analysis follows.

The difference between the electromotive force of a cell in which silver chloride is dissolved in a lithium chloride and potassium chloride melt, E^*, and that of a cell involving pure silver chloride, E^0, gives the free energy of mixing for the following process

$$(AgCl)_{(l)} + n\{(Ag,Li,K)Cl\}_{(l)} \rightarrow (n+1)\{(Ag,Li,K)Cl\}_{(l)}$$

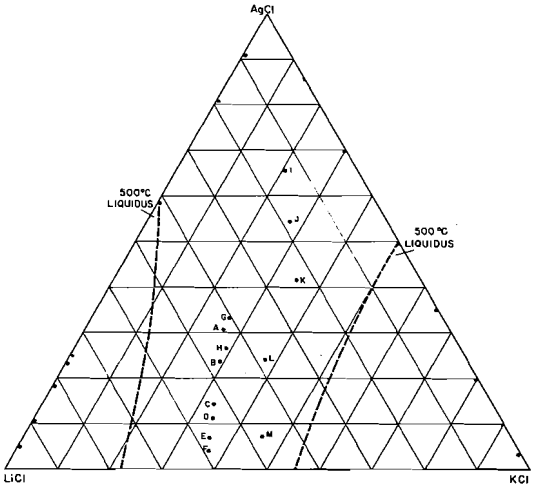

FIG. 4. Compositional points studied in the AgCl–LiCl–KCl system. Melts studied in the present investigation are given a code letter. Points on the AgCl–LiCl edge are from Panish *et al.* (9) Points on the AgCl–KCl edge are from Pelton and Flengas (3).

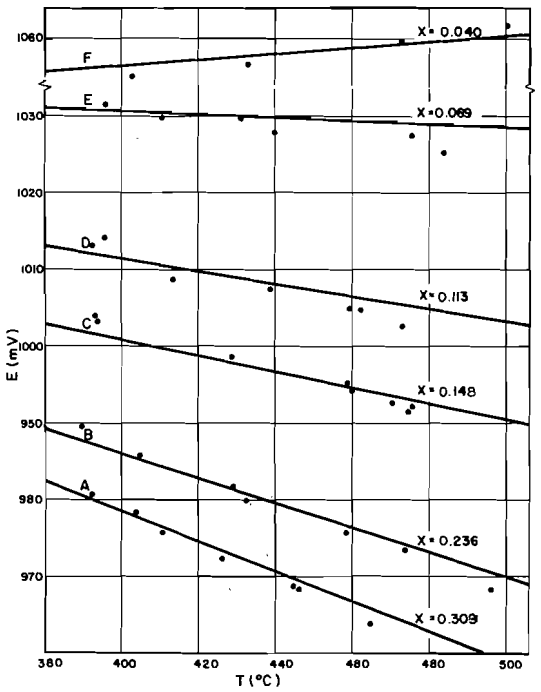

FIG. 5. Experimental measurements relative to a standard (1 atm) chlorine electrode. The mole fraction of AgCl, X, is indicated. The lines represent traces obtained by a multiple regression analysis.

Can. J. Chem. Downloaded from www.nrcresearchpress.com by 210.87.254.42 on 09/05/12
For personal use only.

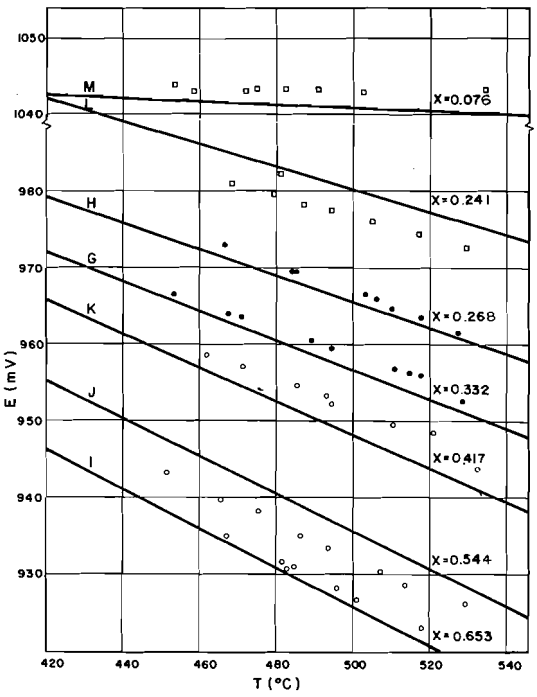

FIG. 6. Experimental measurements relative to a standard (1 atm) chlorine electrode. The mole fraction of AgCl, X, is indicated. The lines represent traces obtained by a multiple regression analysis.

where $n \gg 1$. That is to say, the relative partial molar free energy of silver chloride $\Delta\bar{G}_{AgCl}$, is

$$[8]\quad (\Delta\bar{G})_{AgCl} = \Delta\bar{H}_{AgCl} - T\Delta\bar{S}_{AgCl} = -F(E^* - E^0)$$

The relative partial molar free energy is related as indicated to the partial molar enthalpy and entropy, $\Delta\bar{H}_{AgCl}$ and $\Delta\bar{S}_{AgCl}$; these properties vary insignificantly with pressure and temperature but do vary with respect to composition. The following empirical series (16) may be employed to express these variations:

$$[9]\quad \Delta\bar{H}_{AgCl} = \sum_{j=2}\sum_{k=0} a_{jk}(\Lambda^j)(\Psi^k)$$

$$[10]\quad \Delta\bar{S}_{AgCl} = \sum_{j=2}\sum_{k=0} b_{jk}(\Lambda^j)(\Psi^k) - R \ln X_{AgCl}$$

where X_{AgCl} is the mole fraction of AgCl, $\Lambda = (1 - X_{AgCl})$, and $\Psi = X_{KCl}/(X_{LiCl} + X_{KCl})$.

The lower limits of summation guarantee Raoultian behavior of silver chloride in concentrated solutions. Combining eqs. 8–10 yields

$$[11]\quad E^* + \frac{RT}{F}\ln X_{AgCl} - E^0 = -\frac{1}{F}\sum_{j=2}\sum_{k=0}(a_{jk} - Tb_{jk})(\Lambda^j)(\Psi^k)$$

The coefficients a_{jk} and b_{jk} in the right hand side of eq. 11 were determined by a multiple linear regression analysis based upon 198 points (103 of which were determined in this investigation). An arbitrary truncation of the series is required; the following twelve coefficient series was found to express the variation E^* well.

$$\begin{aligned}[12]\quad E^* = -\frac{1}{F}\{&-3895.7\Lambda^2 + 5.8202T\Lambda^2 \\ &+ 3320.4\Lambda^2\Psi - 7.2596T\Lambda^2\Psi \\ &- 881.3\Lambda^2\Psi^2 + 0.2054T\Lambda^2\Psi^2 \\ &+ 7114.6\Lambda^3 - 6.7819T\Lambda^3 \\ &- 3246.2\Lambda^3\Psi + 4.4283T\Lambda^3\Psi \\ &- 3884.0\Lambda^3\Psi^2 + 3.5212T\Lambda^3\Psi^2\} \\ &- \frac{RT}{F}\ln(1-\Lambda) + E^0\end{aligned}$$

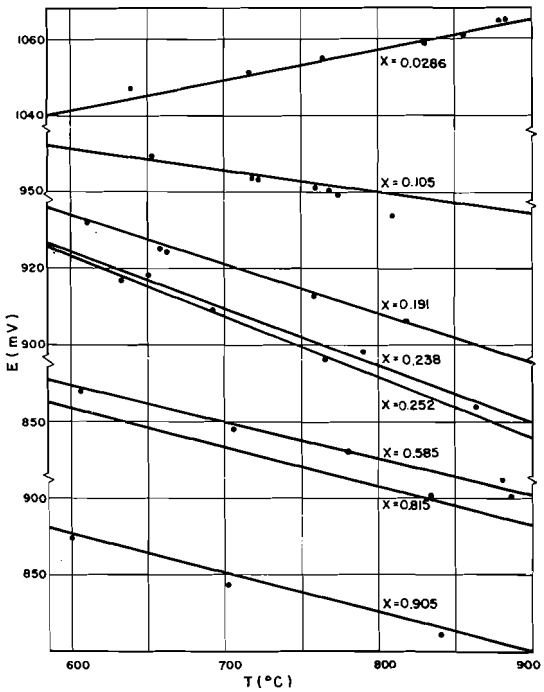

FIG. 7. Measurements of Panish *et al.* (9) for AgCl–LiCl melts relative to a standard (1 atm) chlorine electrode. The mole fraction of AgCl, X, is indicated. The lines represent traces obtained by a multiple regression analysis.

Can. J. Chem. Downloaded from www.nrcresearchpress.com by 210.87.254.42 on 09/05/12
For personal use only.

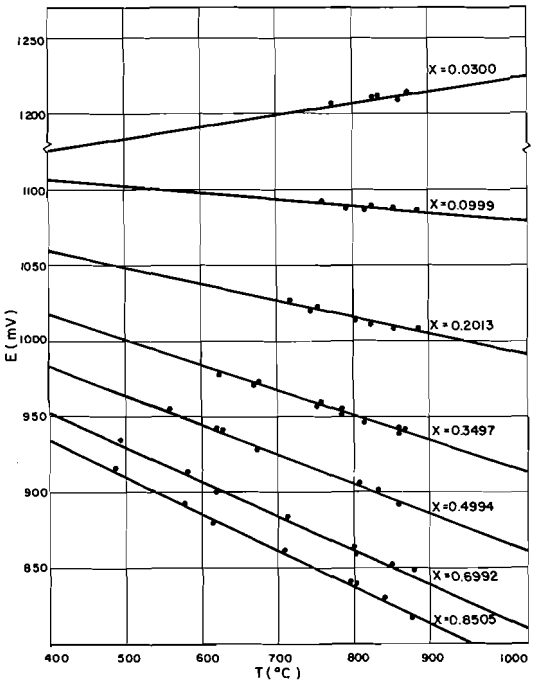

FIG. 8. Measurement of Pelton and Flengas (3) for AgCl–KCl melts relative to a standard (1 atm) chlorine electrode. The mole fraction of AgCl, X, is indicated. The lines represent traces obtained by a multiple regression analysis.

The standard deviation for the regression analysis was 2.5 mV; the mean absolute deviation was 1.8 mV. Equation 13 expresses within about 15 mV seventeen measurements made by Yang and Hudson (17) on five solutions of AgCl dissolved in LiCl–KCl eutectic ($\Psi = 0.42$).

As mentioned previously the lines which appear in Figs. 5–8 represent the behavior of eq. 12 at particular values of Λ and Ψ. The notable feature is that several of the lines are systematically above or below the experimental E^* values. This is regarded as being due mainly to an error associated with the determination of composition. For example, a variation in the AgCl mole fraction of 0.01, say, from 0.40 to 0.41, consistent with the analytical accuracy discussed previously causes a change in E^* at 500 °C of 1.6 mV. This together with temperature gradients in the cell combine to account for the slight systematic deviation most apparent in Fig. 6.

Another approach to fitting the experimental measurements would have involved the independent regression of each E^* *vs.* T line and the subsequent smoothing of the calculated relative partial molar properties. However, in view of the short temperature range covered in the present study it was felt that a single data analysis in which all measurements pertinent to this system were smoothed at once would provide a more representative empirical equation.

It may be shown that the term in braces in eq. 12 is the partial molar excess Gibbs free energy of AgCl, $\bar{G}_{AgCl}^{E}$. This property of the melt is plotted on the Gibbs triangle in Fig. 9 for a temperature of 500 °C. The lines of constant $\bar{G}_{AgCl}^{E}$ are shown extrapolated beyond the 500 °C liquidus lines.

Figure 10 illustrates the behavior of the silver chloride activity at 500 °C calculated from the excess free energy using

$$[13] \qquad a_{AgCl} = X_{AgCl} \exp\left(\frac{\bar{G}_{AgCl}^{E}}{RT}\right)$$

The form of the isotherm is similar to that empirically predicted by Moser (18).

Equation 12 in principle permits the determination of the relative partial enthalpy and entropy of AgCl. In view of the short temperature range studied and the errors associated with the measurement of E^*, these calculations would not be very reliable. Accordingly, they are not reported here.

Discussion

In recent years there has been considerable success in interpreting the thermodynamic behavior of molten salt solutions with ionic

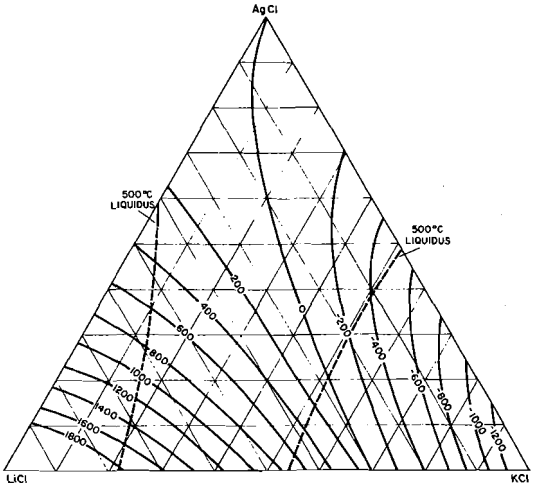

FIG. 9. Partial molar excess free energy of AgCl, $\bar{G}_{AgCl}^{E}$, at 500 °C based upon experimental measurements. The units are cal mol^{-1}.

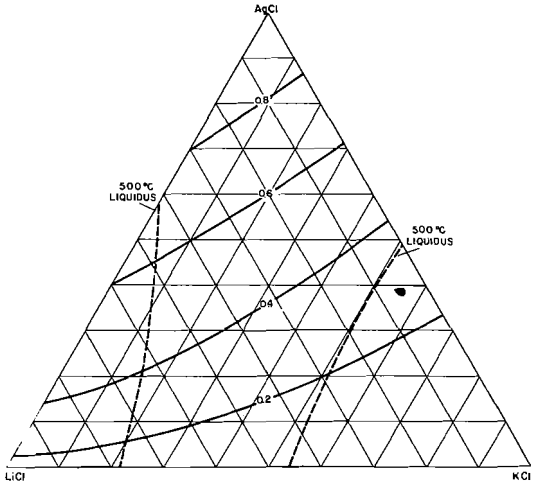

FIG. 10. Activity of AgCl (relative to liquid AgCl) at 500 °C based upon experimental measurements.

models that make reference to the existence of complex ions (19–23). It is postulated that certain cations are bound to adjacent anions; these units are treated as independent entities in the melt.

For the case of silver chloride – alkali chloride binary solutions Pelton and Flengas have proposed a dual-bonding model (3). This treatment recognizes the distinction between free silver ions and other silver ions considered to be "bonded" to adjacent anions. The model does not require postulates about the stoichiometry of this arrangement, *i.e.* it is immaterial whether the "bonded" silver exists as $AgCl_2^-$, $AgCl_3^{2-}$, etc., or silver chloride "molecules". This treatment has had success in interpreting precisely measured thermochemical properties for the silver chloride – alkali chloride binary melts from sodium chloride through to cesium chloride. This is remarkable because of the few adjustable parameters involved in the theory, one per salt.

An extension of this treatment to the ternary melts can be made as follows. Consider the isothermal formation of a mole of molten ternary solution by combining silver chloride with a lithium chloride – potassium chloride melt of fixed composition. This process may be represented as follows

$$[14]\quad X_1AgCl_{(l)} + (1 - X_1)(Li,K)Cl_{(l)} \rightarrow (Ag,Li,K)Cl_{(l)}$$

For the purpose of subsequent discussion AgCl, LiCl, and KCl will be referred to as components 1, 2, and 3 respectively.

The configurational entropy of the ternary solution is determined by the number of distinguishable ways Li^+, K^+, Ag^+, and Ag* ("bonded" silver) can be arranged over the available cationic sites. Let this multiplicity be Ω. Regarding the number of sites for a mole of solution as simply Avogadro's number, N, and α as the fraction of the total silver that exists as Ag* in the molten solution, the multiplicity is given by the following expression

$$[15]\quad \Omega = \Omega_1\Omega_2\Omega_3$$

where Ω_2 is the number of distinguishable ways of arranging X_2N lithium ions over N positions. Assuming random mixing

$$[16]\quad \Omega_2 = \frac{N!}{(N - X_2N)!(X_2N)!}$$

Ω_3 is the number of distinguishable ways of arranging X_3N potassium ions over the remaining $(N - X_2N)$ available positions.

$$[17]\quad \Omega_3 = \frac{(N - X_2N)!}{(N - X_2N - X_3N)!(X_3N)!}$$

and Ω_1 is the number of distinguishable ways of arranging the αX_1N "bonded" silver ion over the remaining $(N - X_2N - X_3N)$ available positions.

$$[18]\quad \Omega_1 = \frac{(N - X_2N - X_3N)!}{(N - X_2N - X_3N - \alpha X_1N)!(\alpha X_1N)!}$$

There is no freedom with regard to the distribution of the free silver ions or the chloride ions. Simplifying eqs. 15–18 yields for 1 mol of solution

$$[19]\quad \Omega = \frac{N!}{(X_2N)!([1 - \alpha]X_1N)!(\alpha X_1N)!(X_3N)!}$$

The total configurational entropy of the ternary solution (Ag, Li, K)Cl is determined by applying Boltzmann's equation

$$[20]\quad S_{(Ag,Li,K)Cl} = \frac{R}{N}\ln\Omega = -R[X_2 \ln X_2 + X_3 \ln X_3 + \alpha X_1 \ln \alpha X_1 + (1 - \alpha)X_1 \ln (1 - \alpha)X_1]$$

The configurational entropy for a mole of pure silver chloride is, by similar reasoning

Can. J. Chem. Downloaded from www.nrcresearchpress.com by 210.87.254.42 on 09/05/12
For personal use only.

Can. J. Chem. Downloaded from www.nrcresearchpress.com by 210.87.254.42 on 09/05/12
For personal use only.

$$[21]\quad S_{AgCl}{}^{0} = -R[\alpha^0 \ln \alpha^0 + (1-\alpha^0)\ln(1-\alpha^0)]$$

where α^0 is a fraction of silver that exists as Ag* in pure molten silver chloride. If the configurational entropy of a mole of the lithium chloride and potassium chloride melt in reaction 14 is simply given by

$$[22]\quad S_{(Li,K)Cl} = -R\left(\frac{X_2}{X_2+X_3}\ln\frac{X_2}{X_2+X_3} + \frac{X_3}{X_2+X_3}\ln\frac{X_3}{X_2+X_3}\right)$$

wherein it is assumed that the lithium and potassium ions are randomly mixed, then it is possible to evaluate the configurational entropy change for the mixing process given by reaction 14.

$$[23]\quad \Delta S = S_{(Ag,Li,K)Cl} - X_1 S^0{}_{AgCl} - (1-X_1)S_{(Li,K)Cl}$$

This will be regarded as the total entropy change for the process; that is, vibrational entropy changes will be neglected. Therefore, $\Delta S = S(\alpha, \alpha^0)$.

The enthalpy change for the reaction expressed by [14] is assumed to be mainly the result of an increase or decrease in the fraction of silver that is "bonded". A change in this fraction is expected as the character of the melt is altered by changes in the relative population of alkali cations.

Let ε_1, ε_2, ε_3 refer to the energy per mole associated with the process $Ag^+ \rightarrow Ag^*$ in pure silver chloride, "pure" lithium chloride, and "pure" potassium chloride respectively. Further, suppose that in the ternary solution, as a first approximation, the energy for this process is given by

$$[24]\quad \varepsilon = X_1\varepsilon_1 + X_2\varepsilon_2 + X_3\varepsilon_3$$

Regarding the energy liberated during the formation of the solution as being entirely due to the energy associated with a change in α, and neglecting the formal distinction between enthalpy and internal energy because the volume change on mixing is small, the enthalpy change per mole of solution for reaction 14 is given by

$$[25]\quad \Delta H = \alpha X_1(X_1\varepsilon_1 + X_2\varepsilon_2 + X_3\varepsilon_3) - \alpha^0 X_1\varepsilon_1$$

The value of α at any composition is that which results in the minimum free energy of the solution

$$[26]\quad \frac{\partial G}{\partial \alpha} = \frac{\partial H}{\partial \alpha} - T\frac{\partial S}{\partial \alpha} = 0$$

$$[27]\quad \frac{\partial H}{\partial \alpha} = X_1{}^2\varepsilon_1 + X_1X_2\varepsilon_2 + X_1X_3\varepsilon_3$$

$$[28]\quad \frac{\partial S}{\partial \alpha} = -RX_1 \ln\frac{\alpha}{1-\alpha}$$

Accordingly

$$[29]\quad X_1\varepsilon_1 + X_2\varepsilon_2 + X_3\varepsilon_3 + RT\ln\frac{\alpha}{1-\alpha} = 0$$

Rearranging

$$[30]\quad \alpha = \frac{\prod_{i=1}^{3}\left(\exp\left(\frac{-X_i\varepsilon_i}{RT}\right)\right)}{1+\prod_{i=1}^{3}\left(\exp\left(\frac{-X_i\varepsilon_i}{RT}\right)\right)}$$

by similar reasoning α^0 may be found

$$[31]\quad \alpha^0 = \frac{\exp\left(\frac{-\varepsilon_1}{RT}\right)}{1+\exp\left(\frac{-\varepsilon_1}{RT}\right)}$$

Thus ΔS, ΔH, ΔG for reaction 14 are determined entirely by the values assigned to ε_1, ε_2, ε_3. These parameters are, of course, adjustable for the purposes of fitting the experimentally observed behavior of the system. However, to be consistent with the previous work of Pelton, ε_1 and ε_3 must have the values -3500 and -5500 cal mol^{-1} respectively. Thus ε_2 was treated as the only adjustable number in fitting the experimental data reported in the previous section. That experiment however did not yield direct measurements of ΔG for reaction 14; rather, relative partial molar free energies of silver chloride were measured. These are related to the properties of reaction 14 as follows. It may be shown (16) that along a composition path of a constant Ψ that

$$[32]\quad \Delta\bar{G}_{AgCl} = -\Lambda\frac{d\Delta G_{mix}}{d\Lambda} + \Delta G_{mix}$$

where ΔG_{mix} is the integral free energy of mixing for the ternary solution. But this is equivalent to

$$[33]\quad \Delta\bar{G}_{AgCl} = -\Lambda\frac{d[\Delta G_{mix} - \Lambda(\Delta G_{mix}{}^*)]}{d\Lambda} + (\Delta G_{mix} - \Lambda\Delta G_{mix}{}^*)$$

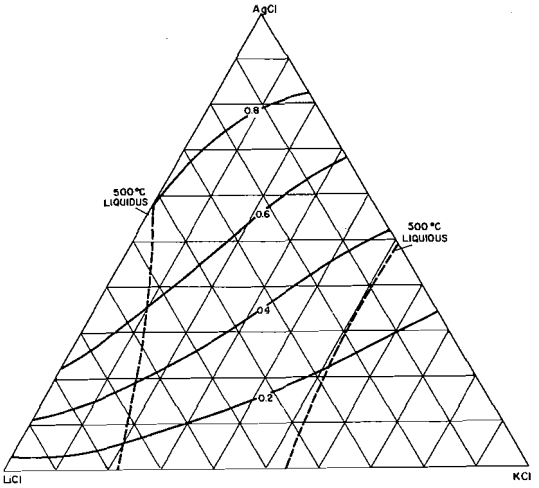

FIG. 11. Activity of AgCl (relative to liquid AgCl) at 500 °C based upon calculations using the dual-bonding model (3). Compare with Fig. 10.

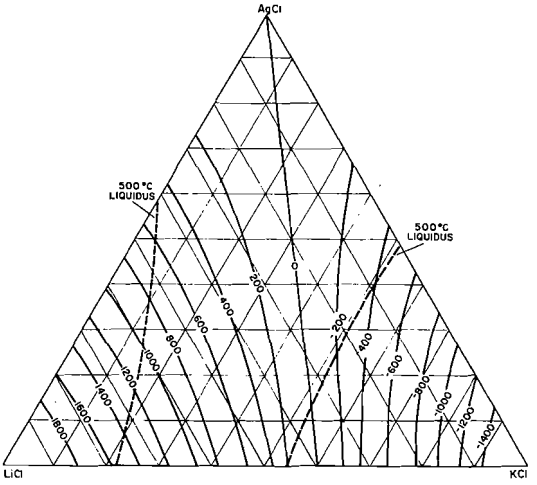

FIG. 12. Partial molar excess free energy of AgCl, $\bar{G}_{AgCl}{}^{E}$, at 500 °C based upon calculations using the dual-bonding model (3). The units are cal mol^{-1}. Compare with Fig. 9.

where the constant, $\Delta G_{mix}{}^{*}$, is the molar integral free energy of mixing of the binary lithium chloride – potassium chloride melt with the composition falling on the composition path, Ψ. The term $(\Delta G_{mix} - \Lambda\Delta G_{mix}{}^{*})$ may be recognized as the ΔG referred to previously in connection with reaction 14.

This means that by the application of eq. 33 it is possible to establish $\Delta\bar{G}_{AgCl}$ from ΔG for reaction 14.

With a value of -500 cal mol^{-1} for ε_2, $\Delta\bar{G}_{AgCl}$ was calculated and the activity at 500 °C was determined. The calculated activity isotherm appears in Fig. 11. This compares well with the measured property, Fig. 10. To further the comparison between the theoretical and measured properties, the $\bar{G}_{AgCl}{}^{E}$ isotherm was calculated using the model. This appears in Fig. 12 for a temperature of 500 °C. This may be compared with Fig. 9.

The major drawback of this treatment probably relates to eq. 22, which assumes random mixing of lithium and potassium ions. In view of the relatively large difference in ionic radius this assumption may not be entirely correct. Nevertheless, the dual-bonding model appears to be a reasonable way of interpreting the thermodynamic behavior of silver chloride – lithium chloride – potassium chloride melts.

The authors thank the National Research Council of Canada for financial support.

1. J. GUION, M. BLANDER, D. HENGSTENBERG, and K. HAGEMARK. J. Phys. Chem. **72**, 2086 (1968).
2. A. D. PELTON and S. N. FLENGAS. J. Electrochem. Soc. **118**, 1307 (1971).
3. A. D. PELTON and S. N. FLENGAS. J. Electrochem. Soc. **117**, 1130 (1970).
4. H. A. LAITINEN, W. S. FERGUSON, and R. A. OSTERYOUNG. J. Electrochem. Soc. **104**, 516 (1957).
5. I. M. KOLTHOFF and E. B. SANDELL. Textbook of quantitative inorganic analysis, 3rd ed. MacMillan, London. 1952.
6. I. M. KOLTHOFF and P. J. ELVING. Treatise on analytical chemistry. Pt. 2, Vol. 1. John Wiley and Sons, New York. 1961.
7. W. T. THOMPSON and S. N. FLENGAS. J. Electrochem. Soc. **118**, 419 (1971).
8. S. SENDEROFF and G. W. MELLORS. Rev. Sci. Instr. **29**, 151 (1968).
9. M. B. PANISH, F. F. BLANKENSHIP, W. R. GRIMES, and R. F. NEWTON. J. Phys. Chem. **62**, 1325 (1958).
10. J. LEONARDI and J. BRENET. C. R. **261**, 116 (1965).
11. I. G. MURGULESCU and S. STERNBERG. Rev. Chem. Acad. Rep. Pap. Rou. **2**, 251 (1957).
12. E. J. SALSTROM. J. Am. Chem. Soc. **56**, 1272 (1934).
13. J. HAMER. J. Electroanal. Chem. **10**, 140 (1965).
14. O. KUBASCHEWSKI, E. L. EVANS and C. B. ALCOCK. Metallurgical thermochemistry. 4th ed. Pergamon Press, London. 1967.
15. W. T. THOMPSON and S. N. FLENGAS. Can. J. Chem. **49**, 1550 (1971).
16. A. D. PELTON and S. N. FLENGAS. Can. J. Chem. **47**, 2283 (1969).
17. L. YANG and R. HUDSON. Met. Trans. **215**, 589 (1959).
18. Z. MOSER. Rev. Roum. Chem. In press.
19. E. W. DEWING. Met. Trans. **3**, 495 (1972).
20. A. D. PELTON and W. T. THOMPSON. Can. J. Chem. **48**, 10 (1970).
21. J. BRAUNSTEIN and M. BLANDER. J. Phys. Chem. **64**, 10 (1959).
22. F. R. DUKE and H. M. GARFINKEL. J. Phys. Chem. **65**, 461 (1961).
23. A. S. KUCHARSKI and S. N. FLENGAS. Can. J. Chem. **49**, 3971 (1971).

Can. J. Chem. Downloaded from www.nrcresearchpress.com by 210.87.254.42 on 09/05/12
For personal use only.

Oligoribonucleotide Synthesis. VIII.[1] Insertion of Terminal 5′-Phosphate Groupings

THOMAS NEILSON, K. V. DEUGAU, T. E. ENGLAND, AND E. S. WERSTIUK
Department of Biochemistry, McMaster University, Hamilton, Ontario L8S 4J9

Received September 6, 1974

THOMAS NEILSON, K. V. DEUGAU, T. E. ENGLAND, and E. S. WERSTIUK. Can. J. Chem. **53**, 1093 (1975).

General oligoribonucleotide synthesis using phosphotriester protection has been extended to allow insertion of terminal 5′-phosphates. Selective removal of 5′-triphenylmethoxyacetyl groups allow phosphorylation by TPS-activated mono-2,2,2-trichloroethylphosphate on protected oligomers.

THOMAS NEILSON, K. V. DEUGAU, T. E. ENGLAND et E. S. WERSTIUK. Can. J. Chem. **53**, 1093 (1975).

On a étendu la synthèse générale des oligoribonucléotides utilisant la protection par les phosphotriesters pour permettre l'introduction de phosphates-5′ terminaux. L'enlèvement sélectif de groupe triphénylméthoxyacétyl-5′ permet la phosphorylation par des monotrichloro-2,2,2 éthylphosphates activés par le TPS sur des oligomères protégés. [Traduit par le journal]

All known native transfer ribonucleic acids (tRNAs) possess a 5′-terminal phosphate. Since the stem regions of tRNA's are possible partial aminoacyl-tRNA synthetase recognition sites (2), an attractive proposition to study the elements of recognition requires short duplices of known sequence, one strand having a 5′-terminal phosphate (3). Anticodon–codon studies have shown that short oligoribonucleotide sequences bind more securely to tRNA when they possess a phosphate moiety at their 5′-terminal (4). Existing syntheses of oligonucleotides carrying a 5′-phosphate start with appropriate protection of the 5′-phosphate of mononucleotide derivatives. Various chemical functional groups have been used in this capacity (5, 6). Protected oligonucleotides are then assembled stepwise from these nucleotide units and, after deblocking, a free oligonucleotide-5′-phosphate is obtained (5).

Consequently, in our continuing efforts to synthesize discrete portions of tRNAs (1), it was necessary to develop a convenient insertion of 5′-phosphate groupings during synthesis of oligoribonucleotides using phosphotriester protection. Our method for the synthesis of oligoribonucleotide-5′-phosphates is an extension of our general method for the synthesis of oligoribonucleotides which proceeds stepwise (7) or in blocks (1, 8) from the 5′- to the 3′-terminus. The nucleoside residue, destined to become the bearer of the 5′-phosphate of the completed oligonucleotide is initially protected with a 5′-trityloxyacetyl (Trac) group which allows ready detection of the protected oligomer at all stages of its synthesis. Selective removal of the Trac group provides an unprotected oligomer with a free 5′-hydroxyl group allowing 5′-specific phosphorylation.

In this communication we describe the conversion of a trinucleoside diphosphate to 5′-trinucleotide using protected, pApUpA, as an experimental illustration. To show that phosphorylation also occurs at the 5′-position when G and C are the 5′-terminal bases in protected oligomers, data on the syntheses of pCpU and pGpG are also included. A synthetic outline is shown in Scheme 1[2] and a summary of experimental data is given in Table 1.

5′-Triphenylmethoxyacetate (**2**) of the low R_F diastereoisomer of *N*-benzoyl-2′-*O*-tetrahydropyranylnucleoside (**1**) (10) was converted to protected dinucleoside phosphate (**4**) from the high R_F diastereoisomer of *N*-benzoyl-2′-*O*-tetrahydropyranylnucleoside (**3**) (10) and mono-

[1]For part VII, see ref. 1.

[2]The abbreviations used are those suggested by IUPAC–IUB (9): Trac is triphenylmethoxyacetyl; t is 2′-*O*-tetrahydropyranyl; $\overset{*}{X}$, $\overset{*}{Y}$, and $\overset{*}{Z}$ = $\overset{b_2}{A}$, $\overset{b_2}{C}$, $\overset{b_2}{G}$, or U (*N*-benzoylnucleosides); X, Y, and Z = A, C, G, or U; p- between two characters, *e.g.* $\overset{*}{x}$tp-$\overset{*}{y}$t, indicates a 2,2,2-trichloroethyl phosphotriester internucleotide linkage.

Can. J. Chem. Downloaded from www.nrcresearchpress.com by 210.87.254.6 on 09/05/12
For personal use only.

Can. J. Chem. Downloaded from www.nrcresearchpress.com by 210.87.254.6 on 09/05/12
For personal use only.

TABLE 1. Experimental data for free and protected CpU, GpG, and ApUpA derivatives

Compound	Yield (%)	R_F in 10% CH_3OH–CH_2Cl_2	Deblocked product	Yield (%)	R_{Gp} (p.c. in solvent *A*)	R_{Gp} (t.l.c. in solvent *B*)	R_{Gp} (p.c. in solvent *C*)
4: X = A; Y = U	59	0.66	ApU	86	2.36	1.66	0.40
4: X = C; Y = U	86	0.77	CpU	82	2.40	1.54	0.45
4: X = Y = G	38	0.70	GpG	30	1.27	0.85	0.93
6: X = Z = A; Y = U	56	0.64	ApUpA	86	1.08	1.34	0.37
7: X = Z = A; Y = U	84	0.73					
10: X = C; Y = U	82	0.78					
10: X = Y = G	80	0.72					
8: X = Z = A; Y = U	59	0.62	ApUpA	93	1.08	1.34	0.37
11: X = C; Y = U	65	0.63	CpU	76	2.40	1.54	0.45
11: X = Y = G	57	0.50	GpG	20	1.27	0.85	0.93
9: X = Z = A; Y = U	70	0.20	pApUpA	66	0.16	0.12	0.80
12: X = C; Y = U	93	0.40	pCpU	64	0.51	0.91	1.15
12: X = Y = G	95	0.33	pGpG	20	0.45	0.74	0.96
10: X = A; Y = C	78	0.81	ApC	80	2.51	1.70	0.27
Gp					1.0	1.0	1.0

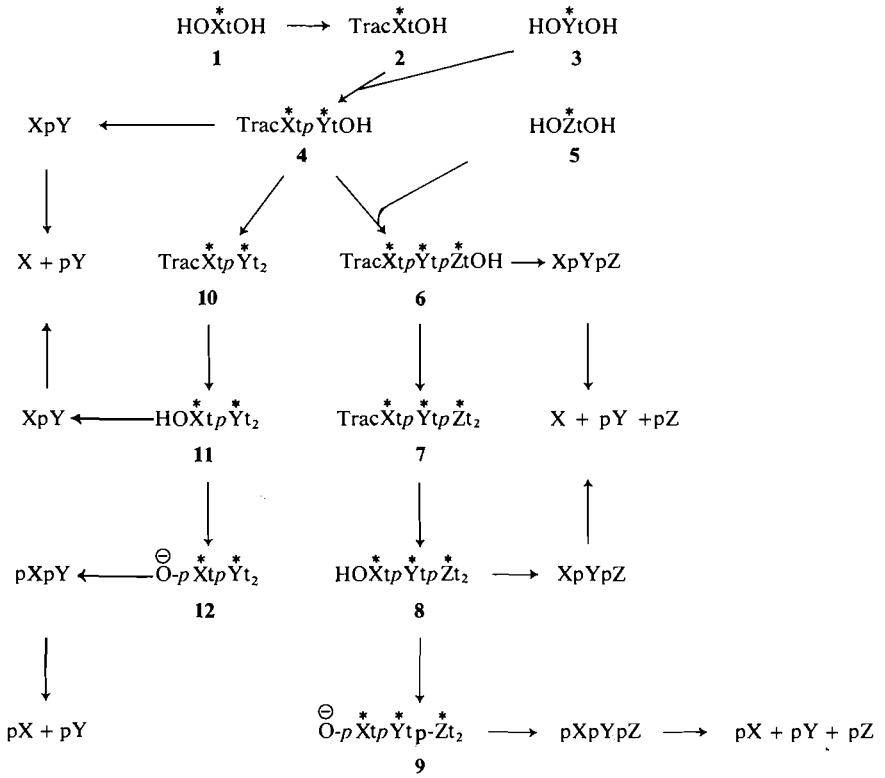

SCHEME 1

2,2,2-trichloroethylphosphate (11) using the previously described two-step coupling procedure (7). In a similar coupling, **4** and **5** were converted to a protected trinucleoside diphosphate (**6**). Each of these products was completely deblocked using the published three-step procedure (7) and the products subjected to snake venom diesterase digestion analysis.

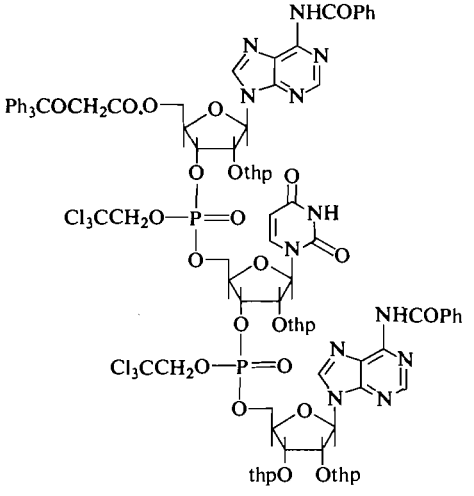

Trac XtpYtpZt2 (7: X = Z = A; Y = U)

Since specific 5′-phosphorylation is required, the 3′-hydroxyl groups of **4** and **6** must be blocked using protection which will survive the mild basic conditions used for selective removal of a 5′-trityloxyacetyl grouping. If at any time, 3′,5′-diphosphorylation was required, the 3′-hydroxyl would be left unprotected. An acid-labile blocking group seemed an appropriate choice and smooth reaction of **4** and **6** with dihydropyran in anhydrous acid medium gave the corresponding 3′-*O*-tetrahydropyranyl ethers **10** and **7**, respectively. Subsequent removal of the 5′-trityloxyacetyl from **10** and **7** to give **11** and **8**, respectively, was carried out using dilute methanolic ammonia (8).

Phosphorylation at the free 5′-hydroxyl groups of **11** and **8** using the pyridinium salt of mono-2,2,2-trichloroethylphosphate and triisopropylbenzenesulfonyl chloride (TPS) gave the pyridinium salts of **12** and **9**, respectively, which were immediately deblocked in the usual manner to give the corresponding ammonium salts of pXpY and pXpYpZ, respectively. Satisfactory

Can. J. Chem. Downloaded from www.nrcresearchpress.com by 210.87.254.6 on 09/05/12
For personal use only.

Can. J. Chem. Downloaded from www.nrcresearchpress.com by 210.87.254.6 on 09/05/12
For personal use only.

enzymic analyses were found using snake venom diesterase, with and without pretreatment with alkaline phosphatase.

Some aspects of this synthesis are worthy of note. Actual phosphorylation is accomplished after assembly of nucleotide units and, in fact, is the last step before deblocking. Thus syntheses of *any* oligoribonucleotide and its corresponding 5′-phosphate derivative are possible from the *same* starting materials and by the *same* route with only minor divergence near the end of the overall synthesis.

Methanolic ammonia cleavage behavior of various TracXt-YtOH (**4**) and their 3′-phosphate derivatives, has been discussed previously (12). The nature and sequence of the bases and the nature of the group at 3′, control the type of reaction, and its kinetics. Since the 3′-position in **10** was protected by a tetrahydropyranyl ether which should have little or no inter- or intramolecular catalytic effect, the opportunity arose to compare alkaline cleavage behavior between examples of **4** and **10**. Data in Table 2 show that substitution of the 3′-hydroxyl with a tetrahydropyranyl group causes an approximate fourfold retardation in the hydrolysis of the trityloxyacetyl group. This result is in agreement that the nature of the 3′-grouping controls the rate of cleavage.

TABLE 2. Time (h) for 50% cleavage of the Trac grouping in 0.15 *N* methanolic ammonia of various protected dinucleotides

Compound	$t_{\frac{1}{2}}$
4: X = C; Y = U	0.5
4: X = Y = G	1.0
4: X = A; Y = C	0.5
10: X = C; Y = U	2.0
10: X = Y = G	5.0
10: X = A; Y = C	2.0

Experimental

The p.m.r. spectra were recorded on a Varian T60 or Varian HA-100 spectrometer in 10–15% (w/v) DMSO-d_6–D_2O solutions and line positions are reported in p.p.m. from the reference (TMS).

Silica gel (Baker Analyzed Reagent) was used for column chromatography; and Analtech prescored silica gel plates were employed for t.l.c. The plates were usually developed in 5 or 10% methanol in methylene chloride mixtures. The t.l.c. detection was carried out using a ceric sulfate spray (1 g $H_4Ce(SO_4)_4$ in 10% aqueous sulfuric acid solution) and followed by heating the plates at 300–400 °C. Compounds containing a trityl group develop as yellow spots, while others appear as brown colorations.

Paper chromatography was performed using the descending technique on Whatman No. 1 or 3 MM paper. Analtech precoated cellulose plates (Avicel F) were used for t.l.c. of deblocked nucleotides. The solvent systems employed for p.c. on Whatman No. 1 and t.l.c. on cellulose were (*A*) ethanol – 1 *M* ammonium acetate, p*H* 7.5 (7:3, v/v) and (*B*) 1-PrOH – concentrated NH_4OH – H_2O (55:10:35, v/v), respectively. Paper electrophoresis was performed at 1400 V/66 cm using Whatman 3 MM paper and (*C*) 0.05 *M* triethylammonium bicarbonate, p*H* 8. A short wave u.v. lamp was used for detection.

It was essential that moisture be excluded form all coupling reactions. After evaporation *in vacuo* of the pyridine solution, normal pressure was restored with dry nitrogen and *not* atmospheric air. All such evaporations were carried out in the temperature range of 30–40 °C. Emulsion, frequently obtained during methylene chloride extractions of aqueous pyridine solutions, was broken by the addition of a few milliliters of saturated sodium chloride solution.

*N^6-Benzoyl-2′-O-tetrahydropyranyl-5′-O-triphenylmethoxyacetyladenosine (**2**: X = A)*

Sodium triphenylmethoxyacetate (3.64 g, 0.011 mol) (8) was evaporated *in vacuo* from anhydrous pyridine (2 × 40 ml) and finally its volume reduced to *ca.* 25 ml. The solution was sealed under nitrogen, TPS (2.00 g, 0.066 mol) added, and the reaction set aside at room temperature for 2 h. The low R_F diastereoisomer of N^6-benzoyl-2′-*O*-tetrahydropyranyladenosine (**1**: X = A) (10*b*) (2.30 g, 0.005 mol; R_F 0.48 in 10% CH_3OH–CH_2Cl_2) was evaporated *in vacuo* from anhydrous pyridine (2 × 40 ml) and finally its volume reduced to *ca.* 15 ml. This solution was then added to the trityloxyacetic acid – TPS complex (prepared above) and reaction mixture stored at room temperature for 2–3 days in the dark. A further portion of TPS (0.5 g) was added after 1 day to ensure complete esterification; t.l.c. indicated *ca.* 90% conversion into a product of R_F 0.80 in 10% CH_3OH–CH_2Cl_2. Ice (30 g) was then added to the mixture and stirring continued for a further hour. The mixture was poured into ice water (100 ml) and repeatedly extracted with methylene chloride (6 × 40 ml). The combined organic extracts were washed and evaporated to dryness *in vacuo*. The light brown glass was purified by chromatography on silica gel (80 g) in methylene chloride. Elution with methylene chloride (1000 ml) removed some impurities. Elution with 0.5% CH_3OH–CH_2Cl_2 gave some diester (R_F 0.8 in 10% CH_3OH–CH_2Cl_2). Pure N^6-benzoyl-2′-*O*-tetrahydropyranyl-5′-*O*-trityloxyacetyladenosine (2.8 g, 73%) (R_F 0.75 in 10% CH_3OH–CH_2Cl_2) was obtained on elution with 1% CH_3OH–CH_2Cl_2 (1000 ml). The p.m.r. spectrum showed signals (δ TMS) at 11.41 (1H-multiplet; N^6 amide proton), 8.66 (2H-singlet; 2- and 8-protons of A), 8.02 (2H-multiplet; *o*-benzoate protons), 7.32 (18H-multiplet; other aromatic protons), 6.20 (1 H-doublet; J = 6 Hz; 1′-anomer proton); 4.79 (1 H-singlet; thp acetal proton), 3.80 (2 H-singlet; OCH_2CO), 3.20 (2 H-multiplet; OCH_2 of thp), 1.55 p.p.m. (6 H-broad multiplet; C—CH_2 of thp).

Anal. Calcd. for $C_{43}H_{41}N_5O_8 \cdot H_2O$ (mol. wt. 773.8):

Can. J. Chem. Downloaded from www.nrcresearchpress.com by 210.87.254.6 on 09/05/12
For personal use only.

C, 66.74; H, 5.60; N, 9.05. Found: C, 66.64; H, 5.42; N, 8.81.

*N^6-Benzoyl-2′-O-tetrahydropyranyl-5′-O-triphenylmethoxyacetyladenylyl[3′-(2,2,2-trichloroethyl)-5′]2′-O-tetrahydropyranyluridine (**4**: X = A; Y = U)*

Biscyclohexylammonium mono-2,2,2-trichloroethyl phosphate (11) (1.31 g, 2.92 mmol) was dissolved in anhydrous pyridine (20 ml) with warming and converted to its pyridinium salt by repeated evaporation *in vacuo* and solution in pyridine (5 × 40 ml). TPS (1.77 g, 5.84 mmol) was then added to the pyridine salt in pyridine (10 ml). After 1 h a pyridine solution (10 ml) of N^6-benzoyl-2′-O-tetrahydropyranyl-5′-O-triphenylmethoxyacetyladenosine (**2**: X = A) (1.10 g, 1.46 mmol; R_F 0.75 in 10% CH_3OH–CH_2Cl_2) was added to the yellow solution and the reaction mixture sealed under dry nitrogen and stored at room temperature in the dark. After 2 days t.l.c. indicated complete conversion into products of R_F 0.0–0.20 in 10% CH_3OH–CH_2Cl_2. Ice (5 g) was added and the quenched reaction left for 30 min, poured into ice water (150 ml), and repeatedly extracted with methylene chloride (4 × 40 ml). The combined organic phases were washed with water (4 × 40 ml) and methylene chloride removed by evaporation *in vacuo* and replaced by anhydrous pyridine (10 ml) by repeated evaporation *in vacuo* and solution in pyridine (3 × 20 ml). TPS (443 mg, 1.46 mmol) was added to the blocked adenylate derivative and activation allowed to proceed for 30 min at room temperature. The high R_F diastereoisomer of 2′-O-tetrahydropyranyluridine (**3**: Y = U) (10*a*)(705 mg, 2.19 mmol; R_F 0.45 in CH_3OH–CH_2Cl_2) dissolved in anhydrous pyridine (10 ml) was added and the reaction mixture sealed under dry nitrogen and stored at room temperature in the dark. On the second day, a further portion of TPS (100 mg) was added to ensure complete coupling. After 3 days t.l.c. indicated complete conversion to a product of R_F 0.70 in 10% CH_3OH–CH_2Cl_2. Ice (10 g) was added to the mixture and stirring continued for a further 30 min. The reaction mixture was poured into ice water (150 ml) and repeatedly extracted with methylene chloride (6 × 50 ml). The combined organic extracts were washed with water (5 × 40 ml) and evaporated to dryness *in vacuo*, the last traces of pyridine being removed by co-distillation with toluene (3 × 20 ml). The light brown residue was dissolved in methylene chloride (50 ml) and the bulk of triisopropylbenzenesulfonic acid separated and was filtered off. The filtrate was subjected to chromatography on silica gel (50 g) in methylene chloride. Elution with 2% CH_3OH–CH_2Cl_2 gave the desired product (**4**: X = A; Y = U) (1.4 g, 75%; R_F 0.66 in 10% CH_3OH–CH_2Cl_2) on removal of solvent. The p.m.r. spectrum showed signals (δ TMS) at 12.4 (1 H-broad multiplet; N^6-proton of A), 8.65 (2 H-overlapping singlets; 2- and 8-protons of A), 8.1 (2 H-multiplet; *o*-benzoate protons), 7.4 (19 H-broad multiplet; other aromatic protons and 6-proton of U), 6.28 (1 H-doublet; J = 5 Hz; 1′-proton of A), 5.9 (1 H-doublet; J = 5 Hz; 1′-proton of U), 3.85 (2 H-singlet; OCH_2CO), 1.6 p.p.m. (12 H-broad multiplet; C—CH_2 protons of thp). Since **4** occurs as a diastereoisomeric pair (P atom is chiral center), its spectrum is not as sharp as that of **2**.

*N^6-Benzoyl-2′-O-tetrahydropyranyl-5′-O-triphenylmethoxyacetyladenylyl[3′-(2,2,2-trichloroethyl)-5′]2′-O-tetrahydropyranyluridylyl[3′-(2,2,2-trichloroethyl)-5′] N^6-benzoyl-2′-O-tetrahydropyranyladenosine (**6**: X = Z = A; Y = U)*

Similar phosphorylation (as described above for **2**; X = A) of blocked ApU (**4**; X = A; Y = U) (720 mg, 0.564 mmol; R_F 0.66 in 10% CH_3OH–CH_2Cl_2) and subsequent coupling with N^6-benzoyl-2′-O-tetrahydropyranyladenosine (**5**; Z = A) (385 mg, 0.846 mmol; R_F 0.48 in 10% CH_3OH–CH_2Cl_2) gave the desired product as a solid foam (730 mg; R_F 0.64 in 10% CH_3OH–CH_2Cl_2) in 66% yield. Complete deblocking (7) gave ApUpA in 86%; R_{Up} 0.59 (0.60 (13)) in solvent *A*. ApUpA was completely digested by snake venom diesterase to give A, pU, and pA in the ratio of 1:1:1 and by pancreatic RNase and subsequent alkaline phosphatase treatment to give ApU and A.

*N^6-Benzoyl-2′-O-tetrahydropyranyl-5′-O-triphenylmethoxyacetyladenylyl[3′-(2,2,2-trichloroethyl)--5′]2′-O-tetrahydropyranyluridylyl[3′-(2,2,2-trichloroethyl)-5′] N^6-benzoyl-2′,3′-O-ditetrahydropyranyladenosine (**7**: X = Z = A; Y = U)*

A solution of *p*-toluenesulfonic acid monohydrate (24 mg, 0.013 mmol) in dry dioxan (2 ml) containing molecular sieves (10 mg) was cooled in ice till solidified. Dihydropyran (184 mg, 0.22 mmol) was then added dropwise with stirring, followed by a dioxan solution (1 ml) of blocked ApUpA (**6**: X = Z = A; Y = U) (300 mg, 0.156 mmol; R_F 0.38 in 5% CH_3OH–CH_2Cl_2). The reaction mixture was allowed to warm up to room temperature after 30 min and stirring was continued a further 4 h. Thin-layer chromatography indicated complete conversion into a product R_F 0.50 in 5% CH_3OH–CH_2Cl_2 and the reaction mixture was neutralized with 0.15 *N* methanolic ammonia. Evaporation *in vacuo* of the solution gave a yellow oil which was purified by chromatography on silica gel (15 g) in methylene chloride. Elution with 2.5% CH_3OH–CH_2Cl_2 gave the desired product as a light brown foam (261 mg, R_F 0.50 in 5% CH_3OH–CH_2Cl_2 and 0.73 in 10% CH_3OH–CH_2Cl_2).

*N^6-Benzoyl-2′-O-tetrahydropyranyladenylyl[3′-(2,2,2-trichloroethyl)-5′]2′-O-tetrahydropyranyluridylyl-[3′-(2,2,2-trichloroethyl)-5′]N^6-benzoyl-2′,3′-O-ditetrahydropyranyladenosine (**8**: X = Z = A; Y = U)*

Blocked ApUpA (**7**: X = Z = A; Y = U) (261 mg, R_F 0.73 in 10% CH_3OH–CH_2Cl_2) was dissolved in 0.15 *N* methanolic ammonia (35 ml) and stirred for 2.5 h. Thin-layer chromatography indicated almost complete cleavage of the Trac group, R_F 0.73 (yellow) → 0.62 (black), and the reaction was quenched by evaporation *in vacuo*. The residue was subjected to chromatography on silica gel (15 g) in methylene chloride. Elution with 4% CH_3OH–CH_2Cl_2 gave the desired product (131 mg, R_F 0.62 in 10% CH_3OH–CH_2Cl_2) in 59% yield. Complete deblocking (7) gave ApUpA in 93% yield.

*N^6-Benzoyl-2′-O-tetrahydropyranyl-5′-(2,2,2-trichloroethylphosphoryl)adenylyl[3′-(2,2,2-trichloroethyl)-5′]2′-O-tetrahydropyranyluridylyl[3′-(2,2,2-trichloroethyl)-5′]N^6-benzoyl-2′,3′-O-ditetrahydropyranyladenosine (**9**: X = Z = A; Y = U)*

Biscyclohexylammonium mono-2,2,2-trichloroethyl-

phosphate (59 mg, 0.14 mmol) (11) was converted to its corresponding pyridinium salt as described earlier. TPS (85 mg, 0.28 mmol) was added to the anhydrous pyridine solution (2 ml) and activation allowed to proceed for 2 h under dry nitrogen. Blocked ApUpA (**8**: X = Z = A; Y = U) (131 mg, 0.077 mmol, R_F 0.62 in 10% CH_3OH–CH_2Cl_2) was dissolved in anhydrous pyridine (1 ml) and added to the TPS complex. The volume of the reaction mixture was reduced to 1 ml by gentle evaporation *in vacuo*. Thin-layer chromatography indicated phosphorylation was complete in 2 h, R_F 0,62 → 0.2–0.3 in 10% CH_3OH–CH_2Cl_2. Ice (0.5 g) was added and the quenched reaction left for 30 min, poured into ice water (20 ml), and repeatedly extracted with methylene chloride (6 × 5 ml). The combined organic phases were washed with water (2 × 25 ml) and evaporated to dryness *in vacuo*, the last traces of pyridine being removed by codistillation with toluene (2 × 10 ml). The residue was purified by column chromatography on silica gel (8 g) in methylene chloride. Elution with 4% CH_3OH–CH_2Cl_2 gave the desired product as a glass (98 mg, 70%; R_F 0.2 in 10% CH_3OH–CH_2Cl_2).

5′-Phosphoryladenylyl(3′-5′)uridylyl(3′-5′)adenosine (pApUpA)

Crude blocked pApUpA (**9**: X = Z = A; Y = U) (10 mg, 0.005 mmol) was dissolved in DMF (0.8 ml) and Cu/Zu couple (*ca.* 10 mg) was added and the mixture stirred overnight. Thin-layer chromatography indicated loss of all 2,2,2-trichloroethyl groups (R_F 0.2 → 0.0 in 10% CH_3OH–CH_2Cl_2). Concentrated ammonia (half diluted with methanol) (1 ml) was added and stirring continued a further day. Loss of N^6-benzoyl groups was indicated by conversion to a major species (R_F 0.7 → 0.4, cellulose plates in solvent *A*). Dowex-50 (NH_4^+ form) (*ca.* 1 g) was added and gentle stirring continued for 30 min. The resin was removed by filtration. The filtrate was reduced to *ca.* 5 ml by evaporation *in vacuo* and its p*H* adjusted to 2 with 2 *N* hydrochloric acid. Overnight stirring removed the tetrahydropyranyl groups as indicated by t.l.c. (R_F 0.4 → 0.0, cellulose plates in solvent *A*). The p*H* was adjusted to 7 with *N* ammonium hydroxide and the solution reduced to *ca.* 2 ml by evaporation *in vacuo*. pApUpA was purified by paper chromatography on Whatman 3 MM developed for 18 h in solvent *B*. The most intense band (R_F 0.2) was eluted with distilled water and the eluate stored as a frozen solution; yield 128 $o.d._{260}$ units, 66%. Alkaline phosphatase digestion gave a single product ApUpA, R_{Up} 0.59, in solvent *A*. Snake venom diesterase digestion gave pA and pU in the expected ratio of 2:1.

General Method for the Preparation of Protected Dinucleotides

Procedures similar to that described earlier for blocked ApUpA, were followed. Complete deblocking of dinucleotides **4**, **11**, and **12** gave XpY, XpY, and pXpY, respectively, in good yields (see Table 1 for details). Enzymic digestion analysis was satisfactory in all cases.

*Selective 5′-De-O-triphenylmethoxyacetylation of Protected Dinucleotides **4** and **10***

Substrates were dissolved in 0.15 *N* methanolic ammonia (12). Solutions were sealed and stored at room temperature and reaction progress monitored by t.l.c. in 10% CH_3OH–CH_2Cl_2. Half-lives of the starting materials were determined.

Financial assistance from the Medical Research Council of Canada is gratefully acknowledged.

1. T. Neilson and E. S. Werstiuk. J. Am. Chem. Soc. **96**, 2295 (1974).
2. R. W. Chambers. Prog. Nuclei Acid. Res. Mol. Biol. **11**, 489 (1971).
3. E. Ohtsuka, M. Ubasawa, S. Morioka, and M. Ikehara. J. Am. Chem. Soc. **95**, 4725 (1973).
4. M. Nirenberg and P. Leder. Science, **145**, 1399 (1964).
5. K. L. Agarwal, A. Yamazaki, P. J. Cushion, and H. G. Khorana. Angew. Chem. Int. Ed. **11**, 451 (1972).
6. K. L. Agarwal, M. Fridkin, E. Jay, and H. G. Khorana. J. Am. Chem. Soc. **95**, 2020 (1973).
7. T. Neilson and E. S. Werstiuk. Can. J. Chem. **49**, 3004 (1971).
8. E. S. Werstiuk and T. Neilson. Can. J. Chem. **50**, 1283 (1972).
9. IUPAC–IUB Commission. Biochemistry, **9**, 4022 (1970).
10. B. E. Griffin, M. Jarman, and C. B. Reese. Tetrahedron, **24**, 639 (1968). T. Neilson and E. S. Werstiuk. Can. J. Chem. **49**, 493 (1971). T. Neilson, E. V. Wastrodowski, and E. S. Werstiuk. Can. J. Chem. **51**, 1068 (1973).
11. F. Eckstein. Chem. Ber. **100**, 2228 (1967).
12. E. S. Werstiuk and T. Neilson. Can. J. Chem. **51**, 1889 (1973).
13. R. Lohrmann, D. Söll, H. Hayatsu, E. Ohtsuka, and H. G. Khorana. J. Am. Chem. Soc. **88**, 819 (1966).

Can. J. Chem. Downloaded from www.nrcresearchpress.com by 210.87.254.6 on 09/05/12
For personal use only.

Can. J. Chem. Downloaded from www.nrcresearchpress.com by 210.87.254.6 on 09/05/12
For personal use only.

On the Mechanism of Base-catalyzed Hydrogen Isotope Exchange in Cyclic Ketones

SUJIT BANERJEE AND NICK H. WERSTIUK[1]

Department of Chemistry, McMaster University, Hamilton, Ontario L8S 4M1

Received December 31, 1974

SUJIT BANERJEE and NICK H. WERSTIUK. Can. J. Chem. **53**, 1099 (1975).

The kinetics of H → D exchange in norcamphor (**1**) and of D → H exchange in norcamphor-*3,3-d*$_2$ (**6**) have been determined. The rate ratio k_{exo}/k_{endo} drops from 661 in H → D exchange to 72 for D → H exchange. These data imply the presence of a dual mechanism for *endo* exchange and emphasize the importance of isotope effects in dictating exchange selectivity.

SUJIT BANERJEE et NICK H. WERSTIUK. Can. J. Chem. **53**, 1099 (1975).

On a déterminé la cinétique de l'échange de H → D dans le norcamphre (**1**) et pour l'échange de D→ H dans le dideutéro-*3,3-d*$_2$ norcamphre (**6**). Le rapport des vitesses k_{exo}/k_{endo} tombe de 661 dans l'échange H → D à 72 pour l'échange D → H. Ces données impliquent la présence d'un mécanisme double pour l'échange *endo* et mettent en évidence l'importance des effets isotopiques dans la direction de la sélectivité de l'échange. [Traduit par le journal]

Stereoselectivity in the base-catalyzed deuteration at the 3-position of norcamphor (**1**) has been noted by several workers (1–3). Kinetic measurements have shown that in dioxane-D_2O $k_{exo}^{H\rightarrow D}/k_{endo}^{H\rightarrow D}$ is approximately 650 (2, 3).[2] As a part of our studies on the isotope exchange of bicyclic mono- and diketones (3), we have measured the dedeuteration of norcamphor-*3,3-d*$_2$ (**6**) in protic media, and have found $k_{exo}^{D\rightarrow H}/k_{endo}^{D\rightarrow H}$ to be 72.[3] In this communication we present our findings and show that the difference between H → D and D → H exchange rates provides information on the mechanism of exchange.

Rates of H → D exchange in **1** and D → H exchange in **6** were measured in 60% dioxane–H_2O (D_2O) at 30.0 °C by monitoring the decrease in substrate by mass spectrometry (2, 3). The observed rate data are listed in Table 1, and second-order rate constants derived from these are collected in Table 2. Since *exo* exchange is faster than *endo* exchange, the deuteration of **1** proceeds with predominant retention (5) to give **3** (2). If secondary isotope effects are neglected, the difference between $k_{exo}^{H\rightarrow D}$ and $k_{exo}^{D\rightarrow H}$ is then the product of the *exo* primary isotope effect and the solvent isotope effect.

For *endo* exchange, the general mechanisms outlined in Schemes 1 and 2 are expected to apply. Now, if in Scheme 1, **2**, **4**, and **5** are steady-state intermediates then

$$k_{endo}^{H\rightarrow D} = k_6 + k_1 - \frac{k_1k_2(k_4 + k_5)}{(k_2 + k_3)(k_4 + k_5) - k_3k_4}$$

Further, since

$$(k_2 + k_3)(k_4 + k_5) \gg k_3k_4$$

[1] $$k_{endo}^{H\rightarrow D} = k_6 + k_1a$$

where

$$a = \left(1 - \frac{k_2}{k_2 + k_3}\right)$$

and

[2] $$k_{endo}^{D\rightarrow H} = k_6' + k_1'a'$$

where

$$a' = \left(1 - \frac{k_2'}{k_2' + k_3'}\right)$$

If k_6 and k_6' were the major contributors to $k_{endo}^{H\rightarrow D}$ and $k_{endo}^{D\rightarrow H}$, respectively, then $k_{endo}^{H\rightarrow D}$ would exceed $k_{endo}^{D\rightarrow H}$ on account of primary and solvent isotope effects. On the other hand, although a in

[1]To whom enquiries should be addressed.

[2]$k_{exo}^{H\rightarrow D}$ and $k_{endo}^{H\rightarrow D}$ refer to the rates of protium → deuterium exchange of the *exo* and *endo* proton, respectively.

[3]A similar effect has been observed in camphor, where $k_{exo}^{H\rightarrow D}/k_{endo}^{H\rightarrow D}$ is 18 and $k_{exo}^{D\rightarrow H}/k_{endo}^{D\rightarrow H}$ is 2 (4).

TABLE 1. Variation of rates of H → D and D → H exchange in norcamphor (**1**) and norcamphor-*3,3-d*$_2$ (**6**) with base concentration*

Substrate	[NaOH(D)](M)	$k_{exo} \times 10^3$ (s^{-1})	$k_{endo} \times 10^5$ (s^{-1})
6	0.008	0.0568	
6	0.020	0.143	0.158
6	0.040	0.265	0.289
6	0.100	0.688	0.672
6	0.140		0.958
6	0.200	1.195	1.70
1	0.045	2.65	0.403†

*Single determinations unless otherwise specified.
†Average of two determinations (average deviation; 1.4%).

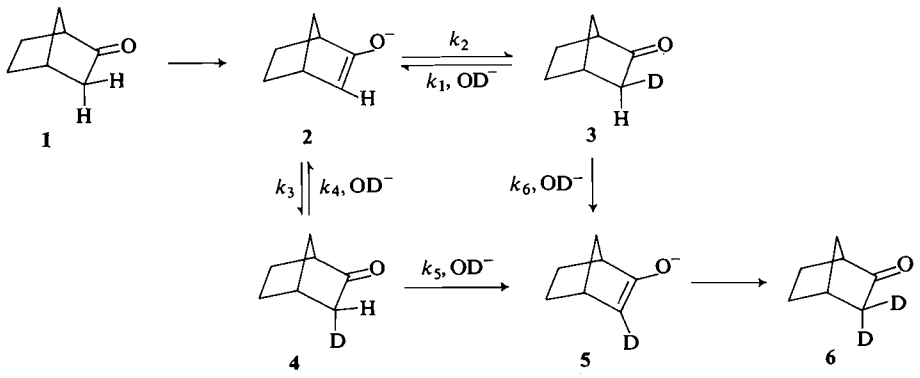

SCHEME 1. H → D exchange in norcamphor (**1**).[4]

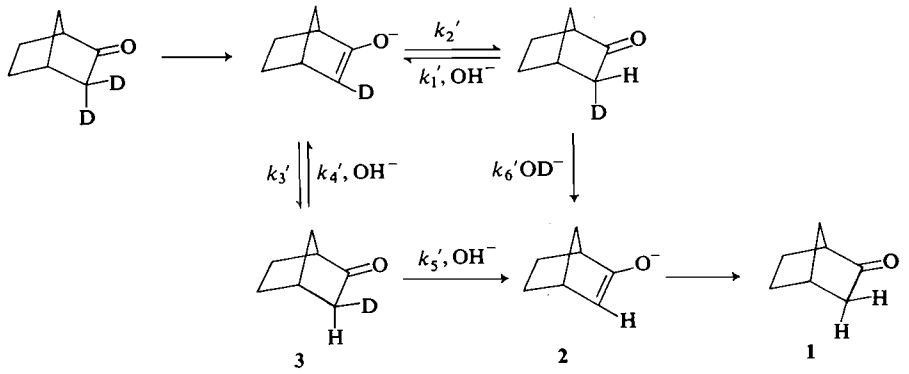

SCHEME 2. D → H exchange in norcamphor-*3,3-d*$_2$ (**6**).

[1] is small, since $k_1 \gg k_6$, $k_1 a$ is by no means negligible as compared to k_6. For $k_{endo}^{H \to D}$ (Scheme 1) a primary isotope effect operates in k_1, whereas for $k_{endo}^{D \to H}$ (Scheme 2) $k_{6'}$ is decreased relative to k_6 due to a primary isotope effect. Clearly, the influence of an isotope effect on k_1 in [1] is compensated for by a similar effect on $k_{6'}$ in [2], so that $k_{endo}^{H \to D} \approx k_{endo}^{D \to H}$.

This establishes that H → D exchange in ketones and likely sulfoxides containing two chemically different C—H bonds α to the carbonyl (sulfoxyl) groups must be described by Scheme 1 regardless of the exchange selectivity.

[4]Although the intermediates **2** and **5** are illustrated as enolates they are kinetically indistinguishable from the corresponding enols.

Can. J. Chem. Downloaded from www.nrcresearchpress.com by 210.87.254.6 on 09/05/12
For personal use only.

TABLE 2. Rate constants for H → D and D → H exchange in norcamphor (**1**) and norcamphor-*3,3-d*$_2$ (**6**)

Parameter	H → D	D → H
k_{exo} (M^{-1} s^{-1})	5.89×10^{-2}*	5.96×10^{-3}†
k_{endo} (M^{-1} s^{-1})	9.07×10^{-5}*	8.26×10^{-5}†
k_{exo}/k_{endo}	661	72

*Obtained by dividing the observed rate constant by base concentration.
†Obtained from plots of k_{obs} *vs.* [NaOH].

Since exchange of the less reactive proton must involve two pathways, the previous relative rate values determined in these systems by the exchange method (2–5) must be to some extent reexamined. We have derived more complete expressions, (which contain the isotope effects and the intrinsic selectivity), relating the various rates in water and in D_2O, and are presently continuing studies on H → D and D → H exchanges in 3-substituted norcamphors.

We thank the National Research Council of Canada for financial support.

1. A. F. THOMAS, R. A. SCHNEIDER, and J. MEINWALD. J. Am. Chem. Soc. **89**, 68 (1967).
2. G. A. ABAD, S. P. JINDAL, and T. T. TIDWELL. J. Am. Chem. Soc. **95**, 6326 (1973).
3. N. H. WERSTIUK and R. TAILLEFER. Can. J. Chem. **48**, 3966 (1970).
4. W. O. CRAIN. Ph.D. Thesis, Indiana University. 1969.
5. R. R. FRASER, F. J. SCHUBER, and Y. Y. WIGFIELD. J. Am. Chem. Soc. **94**, 8795 (1972).

Can. J. Chem. Downloaded from www.nrcresearchpress.com by 210.87.254.6 on 09/05/12
For personal use only.

Can. J. Chem. Downloaded from www.nrcresearchpress.com by 210.87.254.40 on 09/05/12
For personal use only.

Canadian Journal of Chemistry

Published by
THE NATIONAL RESEARCH COUNCIL OF CANADA

Journal canadien de chimie

Publié par
LE CONSEIL NATIONAL DE RECHERCHES DU CANADA

Volume 53 Number 8 April 15, 1975

Volume 53 numéro 8 15 avril 1975

Preparation and Thermolysis of some 1,2-Dioxetanes[1,2]

KARL R. KOPECKY, JOHN E. FILBY,[3] CEDRIC MUMFORD, PETER A. LOCKWOOD,[4] AND JAN-YIH DING

Department of Chemistry, University of Alberta, Edmonton, Alberta T6G 2E1

Received October 10, 1974

KARL R. KOPECKY, JOHN E. FILBY, CEDRIC MUMFORD, PETER A. LOCKWOOD, and JAN-YIH DING. Can. J. Chem. **53**, 1103 (1975).

Treatment of the bromohydroperoxides of 2-methyl-2-butene and ethylidenecyclohexane with cold methanolic base produces trimethyl- and 4-methyl-3,3-pentamethylene-1,2-dioxetane, **3** and **8**. Under these conditions the bromo- and iodohydroperoxides of 2,3-dimethyl-2-butene A, 1,2-dimethylcyclohexene B, and $\Delta^{9,10}$-octalin C are converted rapidly to the corresponding allylic hydroperoxides. The reaction in methylene chloride between silver ion and the bromo- and iodohydroperoxides of A and the iodohydroperoxides of B and C produces the corresponding dioxetanes in 20–30% yield: tetramethyl-1,2-dioxetane **11**, 3,4-dimethyl-3,4-butano-1,2-dioxetane **15**, and 3,4:3,4-dibutano-1,2-dioxetane **23**. About 50% of the corresponding allylic hydroperoxides also are formed as are pinacolone, ~15%, 1-acetyl-1-methylcyclopentane, ~20%, and $\Delta^{9,10}$-octalin, ~1%, from the appropriate halohydroperoxides.

All the dioxetanes are yellow, thermolyze to give only carbonyl cleavage products, and are luminescent. Reduction of **3** with bisulfite ion produced trimethyloxacyclopropane and with iodide ion 2-methyl-2,3-butanediol. Reduction of **8**, **11**, **15**, and **23** with lithium aluminum hydride at −78° gave good yields of the corresponding diols. Treatment with triphenylphosphine of **11** gave tetramethyloxacyclopropane, of **15**, a 1:3 ratio of 2-methylene-1-methylcyclohexanol and 2,3-dimethylcyclohexen-3-ol, and of **23**, 10-hydroxy-$\Delta^{1,9}$-octalin.

Activation parameters for thermolysis of the dioxetanes are (dioxetane, E_a, kcal/mol, ΔS^*, e.u.) **3**, 23.5 ± 0.5, −5 ± 2; **11**, 25.8 ± 0.5, −2 ± 2; **15**, 25.7 ± 0.7, 2 ± 2; **23**, 22.7 ± 0.9, −3 ± 3.

KARL R. KOPECKY, JOHN E. FILBY, CEDRIC MUMFORD, PETER A. LOCKWOOD et JAN-YIH DING. Can. J. Chem. **53**, 1103 (1975).

Le traitement des bromohydroperoxydes des méthyl-2 butène-2 et éthylidènecyclohexane avec une solution méthanolique de base, à froid, donne le triméthyl- et le méthyl-4 pentaméthylène-3,3 dioxétanne-1,2, **3** et **8**. Dans les mêmes conditions, les bromo- et iodohydroperoxydes du diméthyl-2,3 butène-2, A, du diméthyl-1,2 cyclohexène, B, et de la $\Delta^{9,10}$-octaline, C, conduisent rapidement aux hydroperoxydes allyliques correspondants. La réaction dans la dichlorométhane entre les ions d'argent et les bromo- et iodohydroperoxydes de A et les iodohydroperoxydes de B et C donne les dioxétannes correspondants avec des rendements de

[1]This research was supported in part by grants from the Defense Research Board, Grant Number 9530-99, and from the National Research Council of Canada.

[2]Presented in part at the 51st Annual Conference of the Chemical Institute of Canada, Vancouver, B.C., June, 1968, Abstracts p. 41, at the Symposium on Cyclic Peroxides at the Regional Meeting of the New York, New Jersey and Puerto Rico Sections of the American Chemical Society, San Juan, Puerto Rico, April 30, 1971, and at the 55th Conference of the Chemical Institute of Canada, Quebec, P.Q., June, 1972, Abstracts p. 33.

[3]Holder of a Canadian Mortgage and Housing Corporation Fellowship, 1970–1971 and a National Research Council of Canada Scholarship, 1971–1973.

[4]Holder of a National Research Council of Canada Scholarship, 1970–1973.

20–30%: tétraméthyldioxétanne-1,2, **11**, diméthyl-3,4 butano-3,4 dioxétanne-1,2, **15**, et dibutano-3,4:3,4 dioxétanne-1,2, **23**. Dans ces réactions, il se forme environ 50% des hydroperoxydes allyliques correspondants et suivant les hydroperoxydes utilisés de la pinacolone, 15% (approx), de l'acétyl-1 méthyl-1 cyclopentane, 20% (approx), et de la $\Delta^{9,10}$-octaline, 1% (approx).

Tous les dioxétannes sont des composés jaunes et luminescents, dont la thermolyse ne donne que les produits de fission carbonylique. La réduction de **3** avec le bisulphite donne le triméthyloxacyclopropane alors que les ions iodures conduisent au méthyl-2 butanediol-2,3. La réduction de **8**, **11**, **15** et **23** avec l'hydrure de lithium et aluminium à $-78°$ donne des bons rendements des diols correspondants. Le traitement de **11** avec de la triphénylphosphine transforme **11** en tétraméthyloxacyclopropane; **15** en méthylène-2 méthyl-1 cyclohexanol et en diméthyl-2,3 cyclohexèn-3-ol dans le rapport 1:3; et **23** en hydroxy-10 $\Delta^{1,9}$-octaline.

Les paramètres d'activation pour la thermolyse des dioxétannes sont (dioxétanne, E_a, kcal mol^{-1}, ΔS^* cal deg^{-1} mol^{-1}); **3**, 23.5 ± 0.5, −5 ± 2; **11**, 25.8 ± 0.5, −2 ± 2; **15**, 25.7 ± 0.7, 2 ± 2; **23**, 22.7 ± 0.9, −3 ± 3.

Introduction

In an attempt to devise a general non-photochemical reaction sequence for the conversion of alkenes to allylic hydroperoxides it was found that β-halohydroperoxides of di- and trisubstituted ethylenes gave cleavage products when treated with base (1). For example, 3-bromo-2-methyl-2-butyl hydroperoxide **1** appeared to be converted mainly to acetone and acetaldehyde. Some trimethyloxacyclopropane **2** and 3-bromo-2-methyl-2-butanol were also formed, reaction 1.

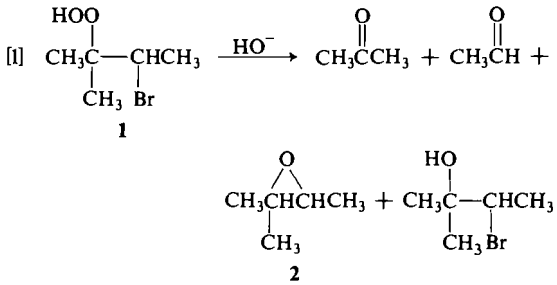

Similar behavior was exhibited by 2-bromo-1-phenylethyl hydroperoxide. Examples of such cleavage reactions had been noted already with some other suitably substituted hydroperoxides (2), where it was suggested that the cleavage products resulted from the decomposition of transient 1,2-dioxetanes.

In contrast to the reactions just described the reaction between base and β-halohydroperoxides of tetrasubstituted ethylenes apparently leads to the exclusive formation of allylic hydroperoxides (1). We thought originally that these transformations also proceeded by way of transient 1,2-dioxetanes which reacted rapidly with base to give allylic hydroperoxides more rapidly than they cleaved to give carbonyl products. A more careful study of the reactions of β-halohydroperoxides has shown that this is not so and has resulted in the isolation of the several 1,2-dioxetanes reported here. The 1,2-dioxetanes derived from 2-methyl-2-butene and from ethylidenecyclohexane are formed by treating the corresponding bromohydroperoxides with base, while the 1,2-dioxetanes of 2,3-dimethyl-2-butene, 1,2-dimethylcyclohexene, and $\Delta^{9,10}$-octalin can be prepared by treatment of the corresponding bromo- or iodohydroperoxides with silver ion. The characterization and rates of thermolysis of these 1,2-dioxetanes are described in this paper also.

Since the first reports of the preparation and thermal decomposition of trimethyl-1,2-dioxetane **3** appeared (3) a number of other members of this class of compound has been isolated from the reaction between alkenes and singlet oxygen (4) or triphenyl phosphite ozonide (5), from β-bromohydroperoxides (6), and from α-hydroperoxy acids (7).

Results

Trimethyl-1,2-dioxetane, 3

The initial indication that **3** might be stable enough to be isolated was obtained by comparing the rate of appearance of bromide ion with the rate of disappearance of peroxide content of basic methanolic solutions of the bromohydroperoxide **1** at 0°. Bromide ion was formed rapidly with a rate that appeared to be nicely first order with respect to both base and **1**. The peroxide content of the solution disappeared much more slowly. In fact, most of the peroxide content was still left when nearly all of the inorganic bromide had been released. It is clear that a rather stable bromine-free peroxidic product was formed. Evidence for the formation of a relatively

Can. J. Chem. Downloaded from www.nrcresearchpress.com by 210.87.254.40 on 09/05/12
For personal use only.

Can. J. Chem. Downloaded from www.nrcresearchpress.com by 210.87.254.40 on 09/05/12
For personal use only.

stable new compound also was obtained by n.m.r. spectroscopy. At 0° a 90:10 methanol: water solution initially 1.0 *M* in **1** and 1.1 *N* in sodium hydroxide slowly developed a yellow color. The n.m.r. spectrum of the yellow carbon tetrachloride extract, obtained after 45 min reaction, showed a new quartet centered at τ 4.80 approximately equal in area to that of the quartet at τ 5.50 due to remaining **1**. Four new signals in the methyl region of the spectrum were also present. Thus, about 50% of the starting material had been consumed. However, only about 5% acetone and acetaldehyde had been formed at this time as judged by the intensity of a singlet at τ 7.98.

The product is volatile with carbon tetrachloride and low pressure distillation of the extract at 0° gave a solution of **3** free of starting material. Carbon tetrachloride or benzene solutions of relatively pure (80 to 90%) **3** at concentrations up to 1 *M* have been made in this way in ~30% overall yield. Longer contact time with base before workup results in the formation of by-products (see below). Pure **3** was obtained as yellow crystals, m.p. 5–7°, from an isopentane extract of the reaction mixture by removing solvent at low temperature followed by low pressure distillation of the residue and crystallization of the distillate from isopentane. The i.r. spectrum showed no absorption for a hydroxyl group and very weak absorption in the carbonyl region. The n.m.r. spectrum showed signals for the methine and methyl protons with relative areas of 1.0 to 9.0. The properties of **3** found in the present work agree well with those reported (6*d*).

In solution this dioxetane may be stored at −10°) for several months with little decomposition. At higher temperatures **3** decomposes to give acetone and acetaldehyde as the only detectable products. This decomposition is accompanied by luminescence as has been reported already (3*b*, 6*d*). At 60° in aerated solutions in benzene and in carbon tetrachloride **3** has a half-life of ~25 min. It decomposes much more slowly in dilute solution than when pure or in concentrated solutions. Although we have had no explosions yet while handling **3** it certainly must be regarded as being potentially explosive in view of our experience with the tetramethyl analog (see below). This appears to have been the first example of the isolation of a 1,2-dioxetane.

Final characterization of **3** involved its reduction by iodide ion in acetic acid to 2-methyl-2,3-butanediol **4** in 50% yield. Attempted catalytic reduction of **3** over palladium on charcoal resulted in rapid cleavage of the molecule to acetone and acetaldehyde.[5] Bisulfite ion reduces **3** to the epoxide **2**, presumably by way of the intermediate **5** which would result from attack of the bisulfite ion on an oxygen atom of **3**. The reactions described so far are outlined in Scheme 1 and serve to confirm the structure **3** for the bromine-free peroxidic product of the reaction between base and **1**.

A compound with a structure such as **6** might also undergo the reactions described to give the observed products but it is not compatible with the observed molecular weight (6*d*).

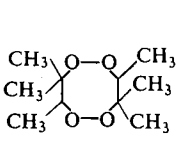

6

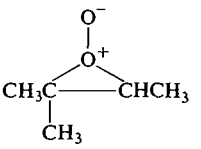

7

Another possible structure for the material in hand might be the perepoxide **7**. It might be visualized that **7** would rearrange thermally to **3** which would then very rapidly cleave to the carbonyl compounds. However, **7** probably would not be reduced to the diol **4** by iodide ion. Also, perepoxides are believed to be intermediates in the reaction between base and β-halohydroperoxides of tetrasubstituted ethylenes which produces allylic hydroperoxides exclusively and not 1,2-dioxetanes (9). Sulfoxide and amine oxide analogs of perepoxides do not rearrange to four-membered ring compounds but do undergo ring opening elimination (10). Thus, it is quite unlikely that we are dealing here with a compound of structure **7**.

When the reaction between base and **1** is allowed to proceed for too long other products in addition to **3** are formed and solutions of **3** obtained by the extraction–distillation method are quite contaminated. The other products include those of reaction 1, the diol **4**, and some unidentified materials. The routes by which these

[5]It appears that transition metals and their salts, in general, may cause rapid decomposition of 1,2-dioxetanes; inadvertent contact of solutions of **3** with cupric and ferric salts caused vigorous reaction to occur. The products were not determined. Similar behavior has been noted with tetramethyl-1,2-dioxetane (8).

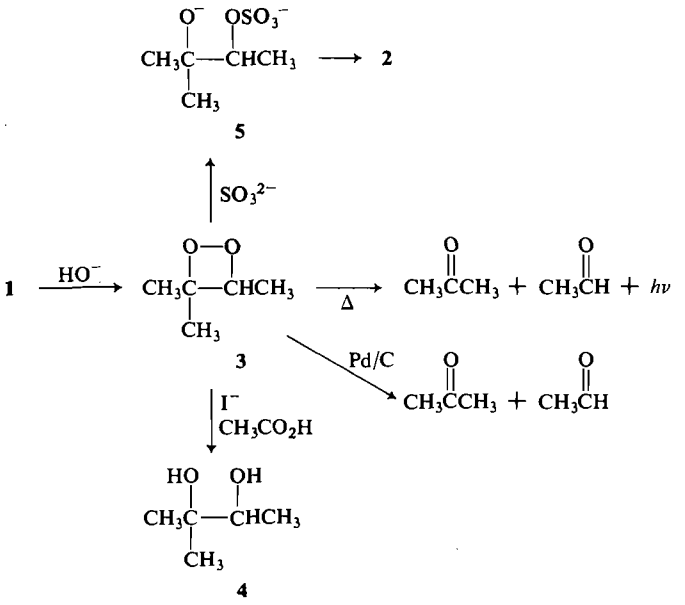

SCHEME 1

products are formed have not been identified but it has been shown that base reacts with **3** to form a variety of products among which acetaldehyde, acetone, and **4** predominate. In spite of a careful search no evidence was obtained for the formation of any allylic hydroperoxide. Control experiments showed that both possible allylic hydroperoxides (11) would have survived the reaction conditions. Diol and epoxide have been observed also during a careful study of the reaction between base and 1-chloro-2-methyl-2-propyl hydroperoxide (6*a*). The mechanisms suggested for the formation of these reduction products quite likely apply to the present system as well.

4-Methyl-3,3-pentamethylene-1,2-dioxetane **8**[6]

This compound was prepared as a result of reports of its formation on ozonolysis of ethylidenecyclohexane in pinacolone solvent (12). We have shown already that, contrary to these reports, **8** is not present among the products of ozonolysis (13) and report here the details of the reactions used for its preparation and characterization, Scheme 2.

The structure of 1-(1-bromoethyl)cyclohexyl hydroperoxide **9** follows from its n.m.r. spectrum, the methyl group protons absorb at $\tau(CCl_4)$ 8.32 which is where the analogous methyl group protons of **1** absorb (1), and by analogy with results of recent studies of bromohydrin formation from cyclohexane derivatives with exocyclic double bonds (14). These studies showed, in contrast to an earlier report (15), that the bromine atom becomes attached to the exocyclic carbon atom.

It was necessary to precipitate **9** as the 1,4-diazabicyclo[2.2.2]octane complex (16) in order to obtain pure material. We have found that this is the best method for freeing from impurities β-halohydroperoxides which are difficult to crystallize.

It appears that **8** is more sensitive to base than is **3** for the reaction between **9** and base must be interrupted quickly in comparison to the reaction between base and **1** in order to obtain pure **8** on workup. The pure dioxetane **8** is isolated by low pressure distillation at 20°. It is an unstable yellow oil, m.p. $\sim -11°$, and it is necessary to carry out all operations during its isolation and for its characterization as quickly as possible or it will be contaminated by decomposition products.

Pure **8** (97.8% active oxygen) is monomeric, mol. wt. found (cryoscopic, benzene) 155, and decomposes in benzene-d_6 at 50° with a half-life of ~15 min to acetaldehyde and cyclohexanone in 90 and 95% yield, respectively.

[6]The Chemical Abstracts will index this compound as 3-methyl-1,2-dioxaspiro[3.5]nonane.

Can. J. Chem. Downloaded from www.nrcresearchpress.com by 210.87.254.40 on 09/05/12
For personal use only.

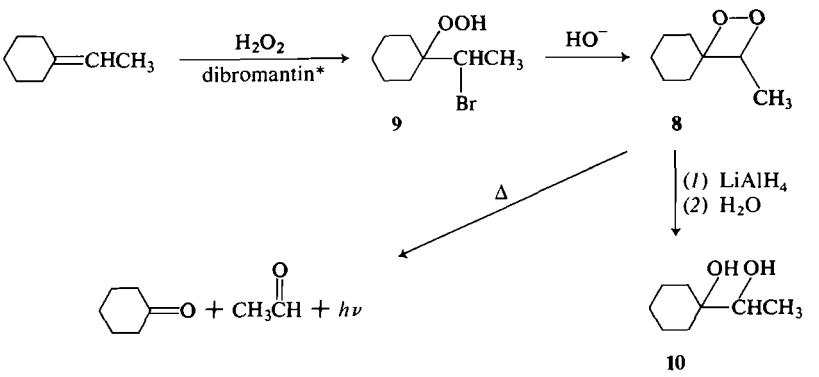

*1,3-dibromo-5,5-dimethylhydantoin

SCHEME 2

The rate of thermal decomposition of **8** appears to be about three to four times that of **3**. The decomposition is accompanied by luminescence whose intensity is greatly enhanced by the addition of 9,10-dibromoanthracene (DBA) (17). Reduction of **8** using lithium aluminum hydride at −40° gave 1-(1-hydroxyethyl)cyclohexanol **10** in 87% yield. The spectral properties of **8** are also consistent with the proposed structure.

Tetramethyl-1,2-dioxetane, 11

The reaction between base and 3-bromo-2,3-dimethyl-2-butyl hydroperoxide **12***a* produces 3-hydroperoxy-2,3-dimethyl-1-butene **13** in >98% yield (1, 9) even at −40°. After it was found that solutions of **3** emitted light when warmed to 50° an attempt was made to detect the presence of **11** by addition of a solution of **12***a* to a boiling solution of base and DBA in methanol. Luminescence could be observed clearly, suggesting that at least some **11** was formed under these conditions. However, no evidence for **11** and only trace amounts of acetone were ever detected by conventional means when the reaction between base and **12***a* was conducted under a wide variety of conditions.

When it became clear that **11** could not be isolated from **12***a* under basic conditions attempts were made to effect cyclization using silver salts. These attempts proved to be successful. In preliminary experiments only acetone and **13** appeared to be formed when **12***a* was treated with the silver salts of several strong acids. This had been observed already (2*b*). The use of silver acetate or silver benzoate does lead to the formation of reasonable amounts of **11**. A mixture of **11**, **13**, and pinacolone is formed in ratios that vary from about 1:4:1 to about 3:3:1, depending upon the solvent and temperature used, when solutions of **12***a* are shaken with suspensions of silver acetate or silver benzoate in nonpolar aprotic solvents, Scheme 3. Formation of pinacolone and **13** on treatment of **12***a* with silver tetrafluoroborate was noted recently but **11** apparently was not detected (18). Solutions of the dioxetane in solvents boiling below ~80° can be evaporated under reduced pressure at 0° to a yellow oil from which pure dioxetane may be isolated by distillation at 0.01 mm followed by crystallization of the residue from isopentane. The yellow crystals of pure **11** melt at 77–78° to a yellow liquid which emits a faint, deep blue luminescence. Optimum yields of pure dioxetane appear to be ~35%. Essentially the same distribution of products is obtained from the iodohydroperoxide **12***b* as from **12***a*.[7]

We have experienced numerous explosions with sublimed samples of **11** kept in sealed, evacuated tubes. However, samples of **11** have been kept at −20° for many months under air with little or no decomposition. Solutions up to 2 *M* in **11** do not appear to be explosive.

The proof of structure of **11** is similar to that described for **3** and **8**. It is monomeric, also mol. wt. found (cryoscopic, benzene) 112, and it was reduced to pinacol by lithium aluminum hydride in 98% yield. Acetone, 98% yield, is the

[7]The iodohydroperoxide was prepared after it was found that the iodohydroperoxide of $\Delta^{9,10}$-octalin readily formed the dioxetane on treatment with silver ion whereas the bromohydroperoxide did not, see below.

Can. J. Chem. Downloaded from www.nrcresearchpress.com by 210.87.254.40 on 09/05/12
For personal use only.

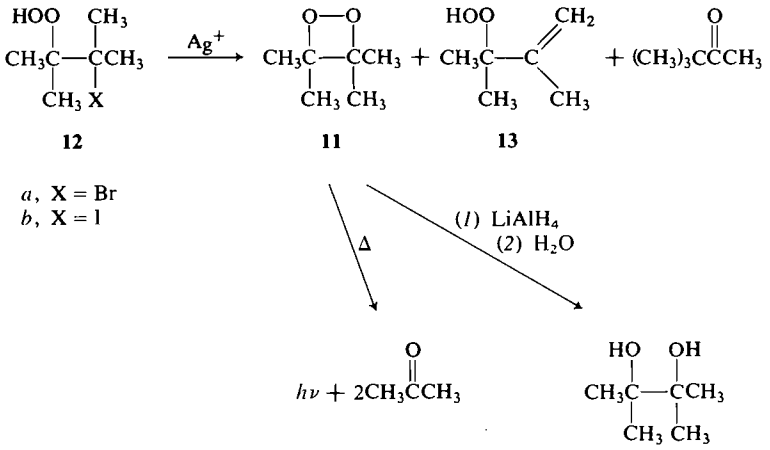

SCHEME 3

only product detectable on thermolysis of **11** in benzene or in carbon tetrachloride.

Attempts to determine the molecular weight of **11** by mass spectrometry were inconclusive. Using electron impact a very weak peak at *m/e* 116 was observed only occasionally, and its relative intensity (~0.1%) was variable from run to run when it was observed. The spectrum was very similar to that of acetone. The dioxetane appears to fragment to acetone and the acetone radical ion exclusively on electron impact. The peak seen occasionally at *m/e* 116 could result from association of an acetone molecule with the radical ion at high pressure of dioxetane. Chemical ionization using ammonium ion also resulted in cleavage of the dioxetane. Peaks due to clusters of ammonium ion with acetone molecules were observed at *m/e* 86, 134, 192, and 250. The relative intensities of the peaks varied from run to run with the peaks at higher *m/e* increasing in intensity as the probe temperature increased.

The n.m.r. spectrum of **11** consists of a sharp singlet at $\tau(CCl_4)$ 8.58. No broadening of the signal was observed even at −90° ($CFCl_3$). This may be taken as evidence against a perepoxide structure **14** in which the two pairs of vicinal methyl groups should become nonequivalent at low temperature (*4b*).[8]

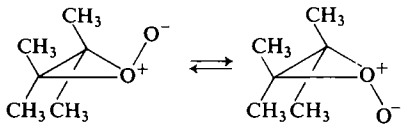

14

It was found that **11** is quite insensitive to acid and to base at 25° or below in methanol. After 48 h at 0° three methanol solutions initially 0.1 *M* in **11** of which one was neutral, one was 0.3 *N* in sodium hydroxide, and one was 0.3 *M* in trifluoroacetic acid had all lost 25 to 30% of the original dioxetane content. Acetone was the only product formed. No trace of the allylic hydroperoxide **13** could be detected in any of the reaction mixtures by n.m.r. spectroscopy. The half-life of **11** can be calculated to be ~90 h under these conditions. The rate of decomposition of **11** in methanol at 0° is then ~100 times that calculated in benzene or carbon tetrachloride (see below). At 50° in benzene the rate of decomposition of **11** is only 50% greater in the presence of 1.0 *M* trifluoroacetic acid than it is in pure benzene. Acetone was the only product detected.

Greatly enhanced rates of decomposition of **11** in methanol relative to those in benzene have been reported already (19) and shown to be due to a rapid dark reaction caused by trace amounts of impurities (8). This rapid dark reaction may mask smaller effects of acid or base on the rate of decomposition of **11** in methanol. Nevertheless, there certainly is no

[8]The barrier for the pyramidal inversion of the perepoxide of ethylene has been calculated to be 18 ± 1 kcal/mol (33).

Can. J. Chem. Downloaded from www.nrcresearchpress.com by 210.87.254.40 on 09/05/12
For personal use only.

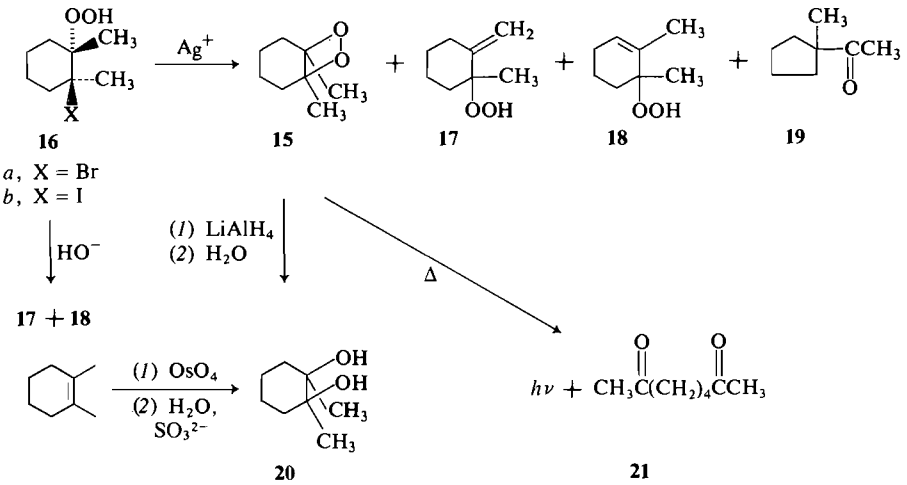

SCHEME 4

very fast acid or base catalyzed reaction of **11** in this solvent.

cis-3,4-Dimethyl-3,4-butano-1,2-dioxetane, ***15***[9]

This material was prepared, Scheme 4, in order to determine whether the route used to prepare **11** might be a general one for the synthesis of tetrasubstituted 1,2-dioxetanes. Treatment of *trans*-2-iodo-1,2-dimethylcyclohexyl hydroperoxide **16***b*[10] with a suspension of silver acetate in methylene chloride at 20° rapidly produces a mixture of four products: **15**, 1-methyl-2-methylenecyclohexyl hydroperoxide **17** (1), 2,3-dimethylcyclohexen-3-yl hydroperoxide **18** (1), and 1-acetyl-1-methylcyclopentane **19**. The ratio of **17**:**18** is about 1:4 which is quite different from the ratio, ~95:5, that is obtained on treatment of **16***a* or *b* with base. Pure **15**, 98.5% active oxygen, can be isolated in 15 to 25% yield as yellow crystals, m.p. 48–50°, by distilling it from the oily mixture of products under high vacuum at ~20° and crystallizing the distillate from pentane. This product is monomeric, mol. wt. found 142, and was reduced with lithium aluminum hydride to *cis*-1,2-dimethylcyclohexane-1,2-diol in 93% yield. Consistently higher yields of **15** were obtained from the iodohydroperoxide[7] **16***b* than from the bromohydroperoxide **16***a* which was much less reactive.

Solutions containing **15** also emit light when heated. At 100° in cyclohexane **15**, ~1 *M*, decomposed to give 2,7-octanedione **21** in 100% yield. Thermolysis of **15** in carbon tetrachloride at 100° resulted in the formation of darkened solutions whose color deepened and which slowly deposited oily droplets, presumably water, on standing at ~22°. Again the major product was **21** but some 1-acetyl-2-methylcyclopentene **22** was also formed as were smaller amounts of several other unidentified products. The amount of **22** formed was ~2% immediately after decomposition but increased slowly when the solutions were allowed to stand. It appears that **22** might be formed by an acid catalyzed cyclization of **21**. A small amount of acid could be formed as a result of some chlorine atom abstraction from solvent by the excited **21** formed from **15**. A sample of authentic **22** was prepared by heating **21** with acid (20), reaction 2.

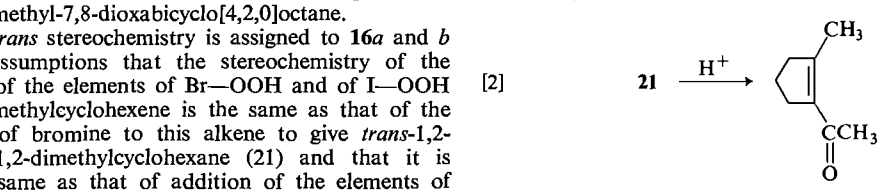

[9]Chemical Abstracts will index this compound as *cis*-1,6-dimethyl-7,8-dioxabicyclo[4,2,0]octane.

[10]The *trans* stereochemistry is assigned to **16***a* and *b* on the assumptions that the stereochemistry of the addition of the elements of Br—OOH and of I—OOH to 1,2-dimethylcyclohexene is the same as that of the addition of bromine to this alkene to give *trans*-1,2-dibromo-1,2-dimethylcyclohexane (21) and that it is also the same as that of addition of the elements of Br—OOH to $\Delta^{9,10}$-octalin, see below.

Can. J. Chem. Downloaded from www.nrcresearchpress.com by 210.87.254.40 on 09/05/12
For personal use only.

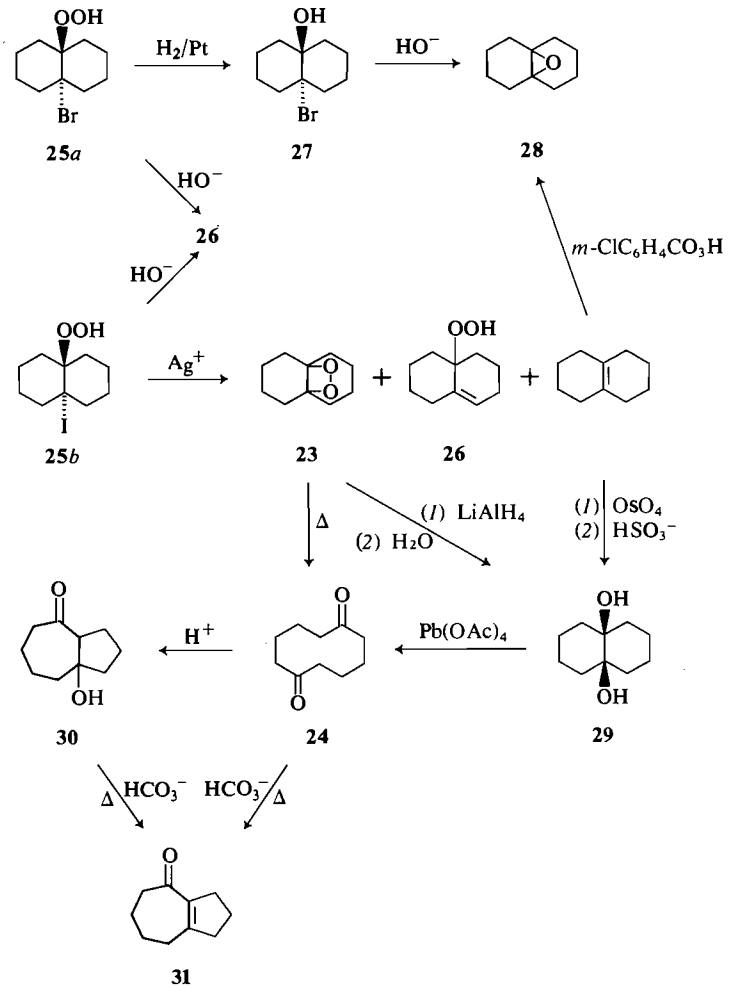

SCHEME 5

3,4:3,4-Dibutano-1,2-dioxetane, 23[11]

This material was prepared in order to assess the effect of strain in the product of thermolysis, 1,6-decanedione, **24**, on the stability and luminescence of the dioxetane. Recent calculations indicate that **24** possesses 8.2 kcal/mol of strain energy (21).

The reaction between 10-bromo-*trans*-9-decalyl hydroperoxide **25***a* and silver ion could not be used to prepare **23**. No reaction occurred at 25°. A slow reaction took place at 60° in benzene. The main product appeared to be 10-hydroperoxy-$\Delta^{1,9}$-octalin **26**. Some of the dione **24** was formed but no evidence could be found for the presence of **23** in the reaction mixture. The *trans* configuration was assigned to **25***a* because the bromohydrin **27** derived from it was converted to the epoxide **28** by base, Scheme 5. The *cis*-bromohydrin presumably would be converted to 10-hydroxy-$\Delta^{1,9}$-octalin by base (see the reaction between **23** and triphenylphosphine below).

The iodohydroperoxide **25***b* was then prepared and found to react rapidly with silver ion, Scheme 5, to produce a mixture of the dioxetane **23**, the allylic hydroperoxide **26**, and $\Delta^{9,10}$-octalin. Product yields were ~35, ~5, and ~1%, respectively. The pure dioxetane can be isolated as yellow crystals, m.p. 34–36°, by chromatography of the concentrated reaction mixture on silica gel at −50° followed by crystallization from the eluent isopentane at −78°.

[11]Chemical Abstracts will index this compound as octahydro-4a,8a-epidioxynaphthalene.

Can. J. Chem. Downloaded from www.nrcresearchpress.com by 210.87.254.40 on 09/05/12
For personal use only.

Can. J. Chem. Downloaded from www.nrcresearchpress.com by 210.87.254.40 on 09/05/12
For personal use only.

Thermolysis of **23** either in solution or neat produces a quantitative yield of pure diketone, **24**. The reaction is accompanied by emission of a faint, deep blue light which can be seen in a dark room. Reduction of **23** with lithium aluminum hydride produces 9,10-dihydroxy-*cis*-decalin **29** in 98% yield. The molecular weight of **23** was not determined, but its spectral and chemical properties are consistent with its formulation as a 1,2-dioxetane.

The reaction between **25***a* or *b* and silver ion produces no rearranged ketone product corresponding to pinacolone from **12** or to **19** from **16**. The elimination of the elements of I—OOH from **25***b* to form $\Delta^{9,10}$-octalin is a reaction which was not noticed in the other halohydroperoxide reactions although no especial effort was made to detect it.

Considerable amounts, up to 30% yields, of 9-hydroxy-4-ketodecahydroazulene **30** were isolated sometimes from initial reactions between **25***b* and silver acetate. These runs were carried out by using about equivalent amounts of reagents and, after removal of the silver salts, allowing the reaction mixtures to stand at 5° or −20° for up to 48 h. Apparently, some strong acid was generated under these reaction conditions. This catalyzed the cyclization of the diketone **24**, which was formed by decomposition of the dioxetane (subsequently discovered to be quite unstable, half-life = 16 h at 10°), to the hydroxyketone **30**. No **30** was ever found when an excess of silver acetate was used. Treatment of a solution of the diketone **24** with some trifluoroacetic acid did in fact produce **30**. The structure **30** was assigned from its spectral properties and its ready dehydration with mild base to 4-keto-$\Delta^{9,10}$-octahydroazulene **31**, which was identical with an authentic (22) sample, Scheme 5.

In common with the behavior of other halohydroperoxides from tetrasubstituted ethylenes **25***a* and *b* on treatment with base are converted to the allylic hydroperoxide **26**, exclusively.

Reduction of 1,2-Dioxetanes with Triphenylphosphine

In order to obtain some indication of the chemical reactivity of the peroxide bond in 1,2-dioxetanes some of these compounds were treated with triphenylphosphine. Triphenylphosphine reacted rapidly at 0° in carbon tetrachloride with **11**, **15**, and **23**. The yellow color of the dioxetane was discharged immediately. The nature of the reduction products depends upon the structure of the dioxetane, Scheme 6. Tetramethyloxacyclopropane **32**, 2,3-dimethyl-1-buten-3-ol **33**, and acetone were formed from the monocyclic dioxetane **11** in about 85, 10, and 5% yields, respectively. Only allylic alcohols were formed as reduction products from the bicyclic and tricyclic dioxetanes **15** and **23**. From **15** there were formed 2,3-dimethylcyclohexen-3-ol **34**, 1-methyl-2-methylenecyclohexanol **35**, and **21** in about 70, 20, and 10% yields, respectively. The only detectable products that were formed from **23** were 10-hydroxy-$\Delta^{1,9}$-octalin **36**, isolated in 31% yield, and some **24**.

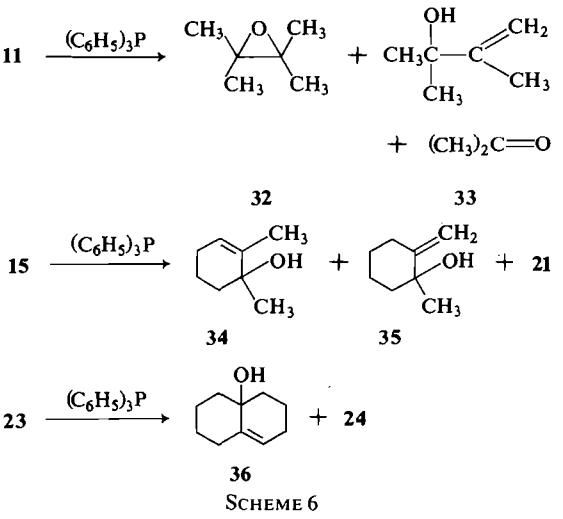

SCHEME 6

A more careful study of the reaction between **11** and triphenylphosphine has been reported already (23). The pentavalent phosphorane product of insertion into the O—O bond was isolated in nearly quantitative yield when the reaction was conducted in benzene. The phosphorane was shown to decompose rapidly to triphenylphosphine oxide and the epoxide **32** only in several solvents including carbon tetrachloride. Thus, the allylic alcohol **33**, found to be a minor product of the reaction between **11** and triphenylphosphine, probably is not formed by way of the phosphorane so that the phosphorane does not appear to be the exclusive initial product of reaction in carbon tetrachloride as it is in benzene.

The reduction products of the reaction between triphenylphosphine and the dioxetane

Can. J. Chem. Downloaded from www.nrcresearchpress.com by 210.87.254.40 on 09/05/12
For personal use only.

are consistent with the formation and subsequent decomposition of zwitterionic intermediates (24), such as **37**, formed directly or

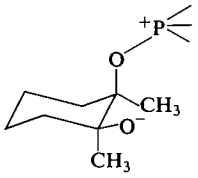

37

from pentacovalent phosphoranes. If such a zwitterion were part of an open chain system it could form an epoxide. If it were part of a cyclic system, as in **37**, in which the two oxygen functions are constrained to be *cis* the backside intramolecular displacement of triphenylphosphine oxide is impossible. Elimination occurs instead to give allylic alcohol.

It is not clear how the ketonic cleavage products are formed. The dioxetanes are stable thermally at 0°. Amines have been observed to catalyze the decomposition of *cis*-3,4-diethoxy-1,2-dioxetane to ethyl formate (25). Perhaps amines and phosphines can catalyze the cleavage of dioxetanes in similar ways.

Ultraviolet and Infrared Spectra of 1,2-Dioxetanes

All the 1,2-dioxetanes reported here are yellow as a result of a weak absorption tail which extends to ~450 nm from a low intensity maximum at ~280 nm[12], Fig. 1. The yellow color of these 1,2-dioxetanes is neither a universal nor a unique characteristic of this class of peroxide. At least some 1,2-dioxetanes are reported to be white (4*a*, 4*f*) and the endoperoxides, 2,3-dioxabicyclo[2.2.2]oct-5-ene (26) and 2,3-dioxabicyclo[2.2.2]hept-5-ene (27), are yellow. The spectrum of *cis*-3,4-diethoxy-1,2-dioxetane does not show a maximum (28) as exhibited in Fig. 1, and simple alkyl peroxides show only weak, nearly structureless absorption below 400 nm. The spectra exhibited by peroxides is thus quite dependent on their structure.

Peroxides are reported to absorb in the range 890 to 830 cm^{-1} in the i.r. (29). The dioxetanes **3**, **11**, and **15** have weak to medium intensity

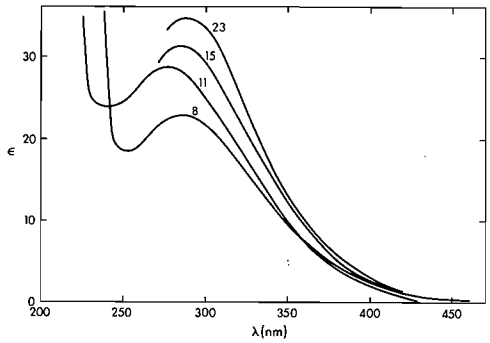

FIG. 1. Ultraviolet–visible spectra of 10^{-2} *M* dioxetanes. Solvents: **8** in heptane, **11** in carbon tetrachloride, **15** and **23** in cyclohexane.

absorptions at 886, 868, and 882 and 870 cm^{-1}, respectively.[13]

Rates of Thermolysis

The rates of thermolysis of the 1,2-dioxetanes in carbon tetrachloride or benzene were determined by a variety of methods, Table 1. Relative rates of thermolysis are included in Table 2. Rates obtained by n.m.r. analysis and by fluorescence decay measurements in the presence of DBA agree reasonably well with those obtained by iodometric analysis in those cases where comparisons were made. This is consistent with other work (6*b*, 6*c*, 28). The rate of fluorescence decay of a degassed solution of **11** containing DBA was twice that of a similar aerated solution. It was observed qualitatively that **15** and **23** also decomposed more rapidly in degassed than in aerated solutions. This phenomenon already has been studied carefully and explained (28); oxygen in aerated solutions quenches the excited state ketone or fluorescer formed on thermolysis of the dioxetane. This prevents energy from being transferred to the dioxetane which would result in its decomposition.

There appeared to be no effect of concentration on the rate of decomposition of the dioxetanes in aerated solution in the concentration range 1 to 0.01 *M*. Dioxetanes appear to be quite stable to strong acid, at least in nonpolar solvents. The rate of disappearance of **11** at 50° in benzene containing 1 *M* trifluoroacetic

[12]Solutions of dioxetane lost less than 5% of their peroxide content during the time that the spectra were recorded.

[13]NOTE ADDED IN PROOF: However the Raman spectrum of **11** has been obtained recently and shows strong absorption at 672 cm^{-1}. The i.r. bands at 868 and 882 cm^{-1} are not Raman active and thus are not O—O stretching bands.

TABLE 1. Rates of thermolysis of 1,2-dioxetanes

Dioxetane	Solvent	Concentration (M)	Temperature (°C)	Method[a]	$k \times 10^4$ (s^{-1})[b]
3	CCl_4	0.1–0.5	60.1	I	4.71±0.10
3	CCl_4	0.1	55.3	I	2.69
3	CCl_4	0.2	50.2	I	1.66
3	CCl_4	0.1–0.5	39.8	I	0.47±0.06
3	CCl_4	0.2	36.0	N	0.29
11	CCl_4	0.01–0.5	70.0	I	3.67±0.18
11	C_6H_6	0.1	70.0	I	3.77±0.05[d]
11	CCl_4	0.1–0.5	60.0	I	0.874±0.001
11	CCl_4	0.1–0.5	50.0	I	0.265±0.002
11	CCl_4	0.1	40.0	I	0.0726±0.000[d]
11	C_6H_6	0.01	52.0	F	0.50
11	C_6H_6[c]	0.01	52.0	F	0.94
11	C_6H_6[e]	0.2	50.0	I	0.41
15	C_6H_6	0.2–0.5	59.4	F	9.82±0.09
15	C_6H_6	0.2–0.3	52.0	F	4.02±0.07
15	C_6H_6	0.1	50.0	N	4.25
15	C_6H_6	0.2–1.2	37.0	F	0.612±0.011
23	C_6H_6	0.005–0.05	29.7	F	1.91±0.08
23	C_6H_6	0.03	29.7	I	1.75
23	C_6H_6	$2–5 \times 10^{-3}$	10.0	F	0.139±0.003[d]
23	C_6H_6	0.01	10.0	I	0.132

[a]I, iodometric analysis; N, n.m.r.; F, fluorescence decay with added DBA. Aerated solutions were used except as indicated.
[b]Average of three or more runs unless indicated otherwise. Errors are average error. Only one run was made when no error is given.
[c]Solution was degassed.
[d]Average of two runs.
[e]Containing 1 M trifluoroacetic acid.

TABLE 2. Relative rates and activation parameters for thermolysis of 1,2-dioxetanes

Dioxetane	Relative rate at 40°	E_a (kcal/mol) Found	E_a (kcal/mol) Calculated	$\Delta S^{\ddagger}$ (e.u.) Found (at 40°)	$\Delta S^{\ddagger}$ (e.u.) Calculated
3	6.4	23.5±0.5[a]	[b]	−5±2	−4[c]
8	~15	—	—	—	—
11	1	25.8±0.5	24.7[c]	−2±2	−5[c]
15	1.2	25.7±0.7	22.2[d]	2±2	−2[d]
23	88	22.7±0.9	22.2[d]	−3±3	−2[d]

[a]This value differs slightly from that reported (31*a*), 23.7. More kinetic runs have been made since then.
[b]E_a for thermolysis of 3 was used as a basis for the thermochemical calculations (31).
[c]Reference 31.
[d]Calculated using the method described (31).

acid was only twice that in acid-free carbon tetrachloride.

Activation parameters for the thermolysis of the dioxetanes, Table 2, were calculated from rates obtained from runs made using aerated solutions. Only rates determined by the same method at each of the different temperatures involved were used for the calculations for each compound. Under these conditions all available points of plots of log k *vs.* 1000/T fell on a straight line for each dioxetane except **11**. For this compound the point at 70° lay above the line defined by the points at 40, 50, and 60°. The rate of decomposition of **11** at 70° was reproducibly faster than expected by a factor of ~1.4 and was not affected by degassing the solution. Perhaps the concentration of oxygen in carbon tetrachloride and benzene at this temperature is too small to prevent some induced decomposition (28, 30) of **11** by the electronically excited acetone molecules which are formed by thermolysis.

Can. J. Chem. Downloaded from www.nrcresearchpress.com by 210.87.254.40 on 09/05/12
For personal use only.

Can. J. Chem. Downloaded from www.nrcresearchpress.com by 210.87.254.40 on 09/05/12
For personal use only.

The energy of activation for thermolysis of **11** is in good agreement with reported values (8, 19). The activation parameters for thermolysis of **11** and **23** agree well with those calculated on the basis of a two step biradical mechanism for the thermolysis (31). However, those for **15** do not agree with calculated values. Both **15** and **23** are calculated to have the same activation parameters for thermolysis, but **15** is clearly seen to be much more stable than **23** even on a qualitative basis in the laboratory. Indeed, **23** is the least stable tetrasubstituted 1,2-dioxetane so far prepared.[14]

Discussion

Compounds which have been assigned a 1,2-dioxetane structure have been reported numerous times (32) prior to the present work, but for most of these compounds such structures have been suggested to be improbable (ref. 31*a*, footnote 3) or are known to be incorrect on the basis of other evidence (34). It is unlikely that the stable peroxidic material isolated from autooxidation of methyl oleate (32*f*) can be a dioxetane since known disubstituted dioxetanes are too unstable thermally (6*a–c*, 31*a*) to survive the reaction conditions used.

General interest in dioxetanes was first aroused after it was proposed that these may be the critical intermediates which decompose to give the electronically excited products that emit light in some chemiluminescent and bioluminescent reactions (35). The fact that all the stable dioxetanes isolated to date are luminescent (at least in the presence of added fluorescers) lends strong support to this suggestion.[15] Since the first report of the isolation and luminescence of a stable dioxetane numerous members of this class of compound have been prepared (4–7) and many energy transfer experiments have been performed with **3** (6*d*, 37) and **11**. A review article has already been written about experiments carried out with **11** (38) and dioxetanes have been suggested as being sources of energy for some dark biological reactions (36*f*, 39). The thermochemistry and the possible mechanisms of the thermolysis of dioxetanes have been discussed elsewhere as well (28, 31, 38, 40, 41).

The isolation of stable dioxetanes also has a bearing on the mechanism of the formation of allylic hydroperoxides in the reaction between singlet oxygen and alkenes. Dioxetanes are not converted to allylic hydroperoxides either thermally or by acid or base. This shows that, in general, dioxetanes cannot be intermediates in such singlet oxygen oxidations, contrary to what has been suggested (42). It appears that in singlet oxygen reactions where both dioxetanes (or their fragmentation products) and allylic hydroperoxides are produced (4*g*, 4*j*, 42, 43) these materials are formed by parallel, not consecutive reactions.

Finally, some comments about the reported preparation of several 1,2-dioxetanes will be made. A number of alkenes are reported to have been converted to dioxetanes by the reaction with ozone in pinacolone solvent (12). Specifically, **8** reportedly was formed in high yield from ethylidenecyclohexane. However, no **8** could be detected among the products when the reaction was repeated (13, 44). Also, the reported synthesis, using this reaction, of the dioxetane of bifluorenylidene (45) could not be repeated in two laboratories (36*f*, 46). Dioxetane structures have been assigned to some products isolated, directly or after some treatment, from the reaction between singlet oxygen and phenyl substituted ethylenes (4*e*, 47). These materials appear to be exceptionally stable for dioxetanes of the structures given and the possibility remains that they are actually 1,2-dioxane derivatives formed by a 1,4-addition of singlet oxygen, reaction 3.

[3] 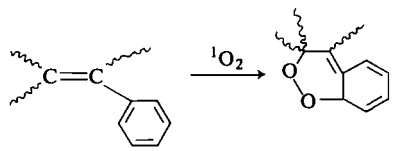

These products could rearrange to dioxetanes on heating to give cleavage products and might form products seemingly derived from dioxetanes on chemical characterization. There is ample precedent for 1,4-addition of singlet oxygen to aryl substituted ethylenes (48) and such 1,2-dioxanes have been suggested to rearrange easily to dioxetanes (47*a*, 48*a*). The endoperoxide of 1,4-dimethoxy-9,10-diphenyl-

[14]A referee has suggested that there may be compensating errors in E_a and $\Delta S^{\ddagger}$ for thermolysis of **15**, and that if $\Delta S^{\ddagger}$ were -5 e.u., E_a would become 23.2 kcal/mol.

[15]Several reviews of chemiluminescence and bioluminescence have appeared recently (36).

Can. J. Chem. Downloaded from www.nrcresearchpress.com by 210.87.254.40 on 09/05/12
For personal use only.

anthracene also rearranges readily to a dioxetane (49). A trisubstituted dioxetane structure was assigned to a product isolated from the reaction between olivetol and citral in refluxing pyridine (50). There is not enough information to decide whether the product is a dioxetane, but such a dioxetane could not have survived the reaction conditions and it is difficult to see how it could have been formed during the reported workup.

The results of some energy transfer experiments and the determination of yields of excited states formed on thermolysis of the dioxetanes **3**, **11**, **15**, and **23** will be reported later (51).

Experimental

CAUTION! All preparations and reactions of hydroperoxides and dioxetanes were carried out behind shields. Numerous small explosions and vigorous decompositions occurred throughout this research.

Melting points and boiling points are uncorrected. Ultraviolet spectra were recorded with Cary 15 and Bausch and Lomb Spectronic 600 recording spectrophotometers. Nuclear magnetic resonance spectra were recorded with Varian analytical spectrometers models HA-100, A-60, and A-56/60 (^{1}H spectra) using tetramethylsilane internal standard and with a Brucker HFX 10 spectrometer (^{13}C spectra). The latter were obtained on 0.2 to 1 *M* solutions using Fourier transform and 1000 to 4000 pulses were collected. Gas–liquid chromatography analyses were carried out on Aerograph 202 and A-90-P3 gas chromatographs. Infrared spectra were recorded on Perkin–Elmer Model 421 and Model 337 spectrophotometers. Mass spectra were obtained with A.E.I. MS-2 and MS-12 mass spectrometers. Refractive indices were measured with a Bausch and Lomb Abbe-3L refractometer.

Anhydrous magnesium sulfate was used as drying agent unless otherwise noted. Solvents were removed with a rotary evaporator unless stated otherwise. Iodometric analyses were carried out using the method of Organic synthesis (52).

Alkenes

Commercial samples of 2-methyl-2-butene, 2,3-dimethyl-2-butene, and ethylidenecyclohexane were used. The synthesis (53) of $\Delta^{9,10}$-octalin was modified to use tetralin as the starting material which doubled the amount of product formed without increasing the scale of the reaction. Use of crude material containing ~30% of the $\Delta^{1,9}$-isomer gave almost as good yields of the halohydroperoxides **25***a* and *b* as did use of the purified product. It was necessary to use isomerically pure 1,2-dimethylcyclohexene (54) and to store it under nitrogen or in evacuated ampoules in order to obtain crystalline halohydroperoxides **16***a* and *b*.

Preparation of β-Halohydroperoxides

These materials were prepared by the reaction in ether between the appropriate alkene, 98% hydrogen peroxide, and 1,3-dibromo- or 1,3-diiodo-5,5-dimethylhydantoin (Arapahoe Chemicals) using the general method described previously (1) with the following exceptions. For the preparation of the iodohydroperoxides the ether solutions, after having been extracted repeatedly with water, were shaken with cold aqueous bisulfite solution until the ether layer lost the iodine color. It was necessary to keep the temperature of the reaction mixture at −40° for at least 4 h during the preparations of **9**. Otherwise the product was contaminated by significant amounts of a material, perhaps the dibromide of ethylidenecyclohexane, which had a methyl group doublet (J = 7 Hz) absorption at τ 7.9.

Compound **12***a* has been characterized already (1, 2*c*). Compounds **1** and **16***a* were obtained previously as oils (1) but have now been prepared in pure crystalline form. All the compounds but **1** and **9** could be purified by crystallization (sometimes at −78°) of the crude product from pentane, isopentane, or hexane solvents. It was necessary to free from impurities compounds **1** and **9** by precipitating them as the 1,4-diazabicyclo[2.2.2]octane (DABCO) complexes (16), as described below for **1**, before they could be crystallized.

Properties of the β-halohydroperoxides are given in Table 3.

Preparation of 3-Bromo-2-methyl-2-butyl Hydroperoxide, 1

A 7.0 g (0.1 mol) sample of 2-methyl-2-butene was converted to the bromohydroperoxide in the usual way (1). After the repeated extraction with water the ether layer was dried and then 5.6 g (0.05 mol) of DABCO was added. The resulting solution was cooled with swirling to −78° over 20 min, during which time a precipitate was formed, and kept at −78° for 3 h. The crystals were filtered on a precooled Buchner funnel, washed twice with cold ether, and then shaken with a mixture of ether and ice water. The ether layer was shaken twice with water, dried, and concentrated to give 10.1 g of an oil. Crystallization of the oil from isopentane at −78° gave 9.0 g (50%) of **1**.

Trimethyl-1,2-dioxetane, 3

A solution of 0.4 g (0.01 mol) sodium hydroxide in 1 ml water and 3 ml methanol was added dropwise to a stirred solution of 1.9 g (0.01 mol) of pure **1** in 6 ml methanol at 0°. After 100 m the mixture was extracted with 3 × 25 ml isopentane. The combined extracts were dried and concentrated at 0° under reduced pressure. The residual yellow oil was distilled at room temperature under ~0.1 mm pressure into a cold trap. A colorless forerun was discarded. The main fraction, a yellow solid, was recrystallized twice from isopentane at −78° to give 0.1 g (10%) of yellow crystals, m.p. 5–7°, 97.2, 99.7% active oxygen; n.m.r. (CCl_4) τ 4.80 (q, J = 6.5 Hz, 1H), 8.51 (s, 3H), 8.56 (s, 3H), 8.68 (d, J = 6.5 Hz, 3H); i.r. (CCl_4): 1370, 1360, 1202, 1156, 886 cm^{-1}. This material has a very pungent odor.

Benzene or carbon tetrachloride solutions up to 1 *M* in **3** containing less than 10% of impurities can be made using crude **1**, by extracting the reaction mixture with the appropriate amounts of these solvents and, after drying, distilling the yellow extract at low temperature until the residue is pale yellow. The dioxetane, obtained in ~30% yield in this way is slightly less volatile than these solvents. Late fractions of the distillate are richer in dioxetane than are early fractions.

TABLE 3. Properties of β-halohydroperoxides

Compound	Yield (%)	Melting point (°C)	Active oxygen (%)	Nuclear magnetic resonance absorptions, $\tau(CDCl_3)$[a]
1	50[b]	−7 to −5[c]	99.2	1.4 (s, OOH), 5.56 (q, J = 7 Hz, CH), 8.32 (d, J = 7 Hz, CH_3), 8.63 and 8.72 (s, *gem.* —CH_3's)[d]
9	41[b]	44.0–45.5	99.6	2.29 (s, OOH), 5.60 (q, J = 7 Hz, CH), 8.32 (d, J = 7 Hz, CH_3), 7.9–8.8 (broad, CH_2's)
12*b*	~80	32–35 (dec.)[e]		1.48 (s, OOH), 7.95 (s, β-CH_3's), 8.50 (s, α-CH_3's)[d]
16*a*	98[f]	44–46	96.8[f]	7.8–8.7 (broad, CH_2's), 8.20 (s, 2-CH_3), 8.52 (s, 1-CH_3),[d] OOH absorption not visible
16*b*	~80	54–55 (dec.)	120–130[g]	2.41 (s, OOH), 7.8–8.5 (broad, CH_2's), 7.82 (s, 2-CH_3), 8.33 (s, 1-CH_3)
25*a*	85	114–115	99.7	2.80 (s, OOH), 8.28 and 8.50 (broad, CH_2's)
25*b*	83	~105 (dec.)	98.7	3.1 (s, OOH), 8.10 and 8.40 (broad, CH_2's)

[a]See ref. 71 for discussion of assignments of CH_3 absorptions.
[b]Yield of crystalline material. Crude material, 95% active oxygen, obtained in 90% yield is sufficiently pure for the preparation of the dioxetane.
[c]*p*-Nitrobenzoyl derivative, m.p. 86–88°. Anal. Calcd. for $C_{12}H_{14}BrNO_5$: C, 43.38; H, 4.24; Br, 24.08; N, 4.22. Found: C, 42.76, 43.16; H, 4.25, 4.36; Br, 23.92, 24.49; N, 4.35, 4.63.
[d]In CCl_4.
[e]Crystalline material free of solvent explodes within 5 min at room temperature. No attempt was made to determine the active oxygen content.
[f]For crude oily product.
[g]In spite of many attempts no satisfactory analysis was obtained on any of several samples of otherwise apparently pure (n.m.r., t.l.c.) crystalline material.

Lower yields of less pure **3** were obtained if the reaction between **1** and base was allowed to continue for much beyond 100 min. The n.m.r. spectrum of a reaction mixture after 20 h indicated the presence of about 30% acetone in addition to several other materials. Evaporation of the mixture left an oily residue which was evaporated several times with carbon tetrachloride and then taken up in their solvent. The n.m.r. spectrum of the solution was identical to that of an authentic sample of 2-methyl-2,3-butanediol **4**.

4-Methyl-3,3-pentamethylene-1,2-dioxetane, ***8***[8]

A solution of 2.3 g (0.01 mol) **9** in 6 ml cold methanol was added dropwise to a solution of 0.4 g (0.01 mol) of sodium hydroxide in 1 ml water and 3 ml methanol at 0°. The mixture was stirred for 25 min after which 10 ml water and 10 ml carbon tetrachloride were added. The yellow organic layer was shaken with 2 × 20 ml ice water, dried, and then concentrated under reduced pressure to a yellow oil. These operations were all carried out as quickly as possible at 0°. The oil was quickly distilled at 20° under 0.01 mm pressure into a cold trap. A colorless forerun was discarded. The main fraction, a yellow solid, was redistilled twice more in this way to give 180 mg (12.5%) of a yellow solid, m.p. −11°, 98.0% active oxygen, n.m.r. (CCl_4) τ 4.91 (q, J = 6.5 Hz, 1H) and 8.66 (d, J = 6.5 Hz) superimposed on broad absorption from 7.7 to 8.9 (total 13H), mol. wt. found (cryoscopic, C_6H_6): 155.

This compound appears to be considerably less stable than **3** and all operations involving it must be carried out as quickly as possible. The luminescence of **8** appeared to be considerably more intense than that of **3** in solutions of similar concentrations at similar temperatures.

Tetramethyl-1,2-dioxetane, ***11***

A solution of 4.0 g (0.02 mol) of **12***a* in 20 ml methylene chloride was added quickly to a rapidly stirred slurry of 12 g (0.07 mol) silver acetate[16] in 80 ml methylene chloride. The resulting mixture was stirred 15 min at 25° and then filtered through Celite. The pale yellow filtrate was washed with 30 ml water and with 30 ml 10% sodium carbonate, dried, and concentrated at 0° to a yellow oil. The oil was distilled at 20° under 0.01 mm pressure into a cold trap. The distillate was crystallized from isopentane at −78° to give 0.7 g (30%) yellow crystals, m.p. (sealed tube) 73–76°. This was easily sublimed to give a solid that was still yellow, m.p. (sealed tube, m.p. block preheated to 70°) 76–77° (the melt emitted a faint blue glow), 98.7% active oxygen, mol. wt. found (cryoscopic, C_6H_6): 112; ^1H n.m.r. (CCl_4) τ 8.49 (s), ^{13}C n.m.r. (acetone-d_6) 89.33 and 23.55 p.p.m. downfield from internal TMS; i.r. (CCl_4): 1380, 1370, 1202, 1168, and 868 cm^{-1}.

The residue remaining from the distillation of the crude reaction mixture was almost pure allylic hydroperoxide **13**, 1.2 g (55%), as judged from the n.m.r. spectrum. The filtrate from the crystallization of **11** was concentrated at 0° to an oil which showed strong absorption at τ 7.95 (s) and 8.9 (s), area ratio 1:3, in the n.m.r. spectrum. Pinacolone 2,4-dinitrophenylhydrazone was isolated in 15% yield from this oil.

[16]Consistently better yields of dioxetanes were obtained when silver acetate powder produced by J.T. Baker Chemical Co. was used as supplied than when other commercially available samples of silver acetate were used. Silver acetate or benzoate prepared under a variety of conditions in our laboratories were less effective, also.

Can. J. Chem. Downloaded from www.nrcresearchpress.com by 210.87.254.40 on 09/05/12
For personal use only.

Can. J. Chem. Downloaded from www.nrcresearchpress.com by 210.87.254.40 on 09/05/12
For personal use only.

Use of the iodohydroperoxide **12***b* for this preparation resulted in essentially the same product distribution as was obtained from **12***a*.

cis-3,4-Dimethyl-3,4-butano-1,2-dioxetane, ***15***[9]

A solution of 3 g (0.011 mol) **16***b* in 20 ml methylene chloride was added quickly in portions to a rapidly stirred mixture of 6 g (0.036 mol) silver acetate in 80 ml methylene chloride at 25°. At each addition the mixture turned red, then yellow. Reaction appeared to occur almost instantaneously. Five minutes after the addition was complete the mixture was filtered through Celite. The filtrate was dried and concentrated to a yellow oil, 1.3 g, which was distilled under 0.01 mm at 20°. The volatile material was crystallized from isopentane at −78°. Two recrystallizations gave 0.35 g (25%) of pale yellow crystals, m.p. 48–50°, 99.2% active oxygen, mol. wt. found (osmometric, CH_2Br_2): 134; ^1H n.m.r. ($CDCl_3$) τ 8.6 (s) superimposed on broad absorption from τ 7.9 to 8.7, ^{13}C n.m.r. (acetone-d_6) 19.61, 22.91, 34.41, and 88.34 p.p.m. downfield from internal TMS; i.r. (CS_2): 2900, 2850, 1380, 1205, 1180, 1050, 910, 882, 877 cm^{-1}. The mass spectrum (70 eV) was identical to that of 2,7-octanedione **21** (55) except that the weak $M^+ + 1$ peak in the mass spectrum of **21** was absent in that of **15**.

The mother liquor from the crystallization of **15** was concentrated to an oil which was converted to the semicarbazone derivative. This product, 0.4 g (20%), was recrystallized from aqueous methanol, m.p. 138–141°, mixed m.p. with the semicarbazone of authentic (56) 1-acetyl-1-methylcyclopentane **19** 138–141°. The authentic semicarbazone had m.p. 138–141° (lit. (57) m.p. 140.5–141°).

The residue remaining upon the distillation of **15** and **19** from the crude reaction mixture appeared to consist mainly of the allylic hydroperoxides **17** and **18** (~50% yield) in a ratio of ~1:4 as judged from the n.m.r. spectrum.

Treatment of the bromohydroperoxide **16***a* with silver acetate resulted in the formation of the same products that were formed from **16***b* but the yield of **15** was always rather low and the reaction quite slow.

3,4:3,4-Dibutano-1,2-dioxetane, ***23***[11]

A solution of 2.0 g (0.007 mol) of **25***b*, freshly recrystallized from heptane, in 20 ml methylene chloride was added quickly to a rapidly stirred suspension of 5.0 g (0.03 mol) of silver acetate in 80 ml methylene chloride at 20°. The resulting suspension was stirred for 5 min and then filtered through Celite. The filtrate was washed with cold 10% sodium bicarbonate and with ice water, then dried at 0° and concentrated at 0° to give 1.2 g yellow oil. This oil was taken up in a little pentane and the solution transferred to a jacketed chromatography column containing 12 g silica gel at −50°. All the above operations were carried out as quickly as possible. The yellow band due to the dioxetane was eluted with 0.5% ether in pentane. The fractions containing **23** (yellow) were kept at −78° until the solvent became colorless. Solvent was decanted from the yellow crystals which formed. These were taken up in a little isopentane. This solution was quickly transferred to a glass ampoule and cooled to −78° until crystallization was complete. Solvent was removed under 0.01 mm pressure at −78° leaving 0.14 g (12%) of yellow crystals which melted at 34–36° to a melt which emitted a faint deep blue glow. The melt resolidified on further heating at 3°/min at ~80° to a white solid, m.p. 98–99° (lit. (58) m.p. 99–99.5° for 1,6-cyclodecanedione). Pure **23** had 100.4% active oxygen, ^1H n.m.r. (CCl_4) τ 7.8–8.8 (broad), ^{13}C n.m.r. (acetone-d_6) 21.20, 35.12, and 87.99 p.p.m. downfield from internal TMS.

Iodometric titration of the combined dioxetane containing fractions from the chromatography indicated that the actual yield of **23** formed in each of several runs was 30 to 37%.

Further elution of the column with 0.5% ether in pentane removed the allylic hydroperoxide **26** which was formed in ~50% yield. Finally, the dione **24**, ~5% was eluted.

Concentration of the fractions which eluted before those containing **23** gave ~1% of an oil which was identified as $\Delta^{9,10}$-octalin on the basis of its n.m.r. spectrum and behavior on t.l.c.

Carbonyl Compounds from Thermal Decomposition of 1,2-Dioxetanes

Trimethyl-1,2-dioxetane, ***3***

A 0.1 *M* solution of **3** in carbon tetrachloride, containing some benzene as internal standard, was heated at 60° for 12 h in a sealed n.m.r. tube. Only signals for acetone and acetaldehyde were observed in the n.m.r. spectrum of the solution which showed that these materials were formed in 93% yield. Only product peaks due to acetone and acetaldehyde could be detected on g.l.c. analysis of the solution.

Tetramethyl-1,2-dioxetane, ***11***

A 0.1 *M* solution of **11** in carbon tetrachloride, containing some anisole as internal standard, was heated at 70° for 10 h in a sealed n.m.r. tube. The n.m.r. spectrum of the solution indicated that acetone was the only product formed in 96% yield. Only acetone could be detected on g.l.c. analysis of the solution.

4-Methyl-3,3-pentamethylene-1,2-dioxetane, ***8***

A solution of 38 mg **8** in 0.5 ml benzene-d_6, containing some benzene as internal standard, was heated at 50° for 6 h in a sealed n.m.r. tube. The only products detected were acetaldehyde in 90% yield (by n.m.r.) and cyclohexanone in 95% yield, isolated as the 2,4-dinitrophenylhydrazone after driving off the acetaldehyde by boiling the solution briefly. The half-life of **8** was ~15 min under these conditions.

Thermolysis of **8** in carbon tetrachloride at 50° gave a dark solution and some unidentified products other than acetaldehyde and cyclohexanone were detected by n.m.r. spectroscopy.

cis-3,4-Dimethyl-3,4-butano-1,2-dioxetane, ***15***

A solution of 0.1 g **15** in 10 ml pentane was allowed to stand at 25° until the yellow color had faded completely (5 d), then cooled to −10° overnight. White crystals formed, 0.1 g (100%), m.p. 43–45°, mixed m.p. with authentic (59) 2,7-octanedione **21** 43–45°.

Gas–liquid chromatography analysis of the decomposition at temperatures up to 100° of 0.1 *M* in degassed hydrocarbon solvents indicated that > 99% of the product was the dione **21**. Less than 0.03%, if any, of acetone was formed.

Can. J. Chem. Downloaded from www.nrcresearchpress.com by 210.87.254.40 on 09/05/12
For personal use only.

Thermolysis of 0.08 g **15** in 1 ml carbon tetrachloride at 100° for 15 min resulted in the formation of a dark solution. This solution darkened further when allowed to stand at −10° for 8 h and deposited droplets of a second phase. The reaction mixture was applied to a thick layer plate of silica gel which was developed with 1:10 ether:Skelly B. The major fraction was extracted from the silica gel and found to be 1-acetyl-2-methylcyclopentene **22** on the basis of its n.m.r. spectrum and semicarbazone, m.p. 221°, mixed m.p. with the semicarbazone of authentic **22** 218–220°.

Authentic **22** was prepared by the acid catalyzed cyclization (60) of 2,7-octanedione (59) and purified by column chromatography on silica gel using 1:10 ether:Skelly B as eluent, semicarbazone m.p. 218–220° (lit. (60) m.p. 221°).

3,4:3,4-Dibutano-1,2-dioxetane, 23

As was reported under the preparation of **23**, heating of **23** above its melting point produced pure 1,6-cyclodecanedione. Therefore, the yield of product is 100%.

Reduction of 1,2-Dioxetanes by Triphenylphosphine

Dioxetanes **11** and **15** were each reduced by adding 0.04 g of dioxetane in 1 ml carbon tetrachloride dropwise to 25 ml carbon tetrachloride containing 1.1 equivalents of triphenylphosphine at 0°. The yellow color of the dioxetane was discharged immediately. The relative yields of products were determined by integration of the n.m.r. spectra taken immediately after reaction. Only acetone, 5%, **33**, 10%, and **32**, 85%, could be detected as products from **11** by n.m.r. spectroscopy or by g.l.c. on an FFAP column at 30 or 66°. From **15** only **21**, 10%, **35**, 20%, and **34**, 70%, could be detected by n.m.r. spectroscopy or by t.l.c. using several solvent systems.

A solution of 0.25 g (15 mmol) of **23** in 5 ml carbon tetrachloride was slowly added to 0.430 g (16 mmol) of triphenylphosphine in 30 ml carbon tetrachloride at −10°. The resulting solution was allowed to stand for a short time. Thin-layer chromatography analysis indicated the presence of mainly **36** and a little **24** as products. Solvent was removed and the residue stirred well with 5 ml benzene. The resulting mixture was filtered and the filtrate was applied to a column of 100 g of basic alumina. Elution with 5% ether in benzene gave 0.070 g (31%) **36**, m.p. 85–87°, mixed m.p. with authentic **36** 84–87°.

Reduction of 1,2-Dioxetanes with Lithium Aluminum Hydride

The same procedure was used for reduction of all 4 dioxetanes below.

Reduction of Tetramethyl-1,2-dioxetane, 11

A solution of 0.12 g freshly sublimed **11** in 10 ml ether was added slowly to a stirred mixture of 0.2 g lithium aluminum hydride in 10 ml ether at −78°. The resulting mixture was stirred at −78° for 20 min and then allowed to warm to 20°. A solution of 10% aqueous potassium hydroxide was added slowly until a clear solution had formed. The precipitate was filtered and washed several times with ether. The combined washings and filtrate were concentrated to give 0.14 g white crystals of pinacol, m.p. 42–44°, containing 1.5 mol water of crystallization, as judged from the n.m.r. spectrum. Thus, the yield of pinacol was 100%. Recrystallization of the product from benzene gave pure pinacol, m.p. 39–41°, which had i.r. and n.m.r. spectra identical to those of authentic material.

Reduction of cis-3,4-Dimethyl-3,4-butano-1,2-dioxetane, 15

Reduction of 0.11 g of **15** and removal of the ether after workup and drying gave an oily solid which was recrystallized twice from isopentane to give 0.049 g (44%) of *cis*-1,2-dimethylcyclohexane-1,2-diol **20**, m.p. 48–50° (lit. (61) m.p. 49.5–50°), mixed m.p. with authentic **20** 46–48°. Osmium tetroxide oxidation (62) of 1,2-dimethylcyclohexene gave authentic **20**, m.p. 46–48°.

Reduction of 3,4:3,4-Dibutano-1,2-dioxetane, 23

A 20 ml fraction of the dioxetane containing eluent from the chromatographic purification of **23** was found to contain 45 mg **23** by iodometric titration. This fraction was treated with lithium aluminum hydride as described above. The crude product was repetitively evaporated with benzene and taken up in 25 ml benzene. Analysis of an aliquot of the solution for diol content using lead tetracetate (63) indicated a yield of 98%. Crystalline 9,10-dihydroxy-*cis*-decalin **29**, 15 mg (30%), m.p. 89–90°, mixed m.p. with authentic **29** 89–90°, was isolated on concentration of the remaining solution.

Oxidation of 0.55 g $\Delta^{9,10}$-octalin with osmium tetroxide (58) gave 0.60 g (88%) of the authentic *cis*-diol 29, m.p. 88–89° (lit. (58) m.p. 90°).

Reduction of 4-Methyl-3,3-pentamethylene-1,2-dioxetane, 8

Reduction of 45 mg of **8**, gave after drying and evaporation of the ether solution to a thin film, 44 mg (96%) of a colorless oil whose i.r. and n.m.r. spectra were the same (except for the OH absorptions) as those of authentic diol **10** (64). Thin-layer chromatography analysis showed no impurities.

Reduction of Trimethyl-1,2-dioxetane, 3

Sulfite Ion

Three millilitres of carbon tetrachloride containing 0.33 *M* **3** was added to a stirred solution of 0.126 g sodium sulfite in 3 ml water at 0°. The p*H* of the solution was kept between 7 and 9 by periodic addition of 10% hydrochloric acid. When all the peroxide had been consumed (KI test) the mixture was separated. The n.m.r. and i.r. spectra of the dried organic layer were identical with those of authentic (65) trimethyloxacyclopropane **2**. The aqueous layer was acidified with 10% hydrochloric acid and then treated with barium chloride solution. The precipitate was filtered, washed, and dried to give 0.162 g (70%) of barium sulfate.

Iodide Ion

A mixture of 5 ml carbon tetrachloride containing 0.1 *M* **3**, 5 ml glacial acetic acid, and 1 ml saturated aqueous potassium iodide was allowed to stand at 26° for 15 min in the dark. Sufficient 0.2 *M* aqueous sodium thiosulfate was then added to just decolorize the solution. Solid sodium carbonate was added in portions until the evolution of gas ceased. The resulting slurry was shaken for 1 h with each of 4 × 25 ml aliquots of ether. The combined ether layers were dried and concentrated to a thin film whose n.m.r. spectrum in carbon tetrachloride containing toluene as an internal standard was identical to that of authentic 2-methyl-2,3-butanediol **4**, except for the absorptions due to toluene, and indicated that the yield of **4** was 50%.

Can. J. Chem. Downloaded from www.nrcresearchpress.com by 210.87.254.40 on 09/05/12
For personal use only.

2-Methyl-2,3-butanediol, 4

Authentic **4** was prepared by shaking a mixture of 3.7 g trimethyloxacyclopropane **2** (65) and 12 ml water containing two drops of concentrated sulfuric acid at 10° until the sharp odor of **2** had faded. The homogeneous solution was neutralized with 10% aqueous sodium carbonate. Water was removed under reduced pressure and the residue was washed repeatedly with ether. The ether washings were combined, dried, and concentrated. The residual oil was distilled to give 2.35 g (53%) of **4**, b.p. 63–64° (4 mm), n_D^{28} 1.4361 (lit. (66) b.p. 75–76° (14 mm), n_D^{25} 1.4375).

Stability of Tetramethyl-1,2-dioxetane, 11, to Acid and Base

Three methanolic solutions ~0.1 *M* in **11** of which one was neutral, one was 0.3 *N* in sodium hydroxide, and one was 0.3 *M* in trifluoroacetic acid were allowed to stand at 0°. The solutions, which also contained some benzene as internal standard, were analyzed periodically by n.m.r. spectroscopy. After 48 h the neutral solution had 69%, the basic solution 75%, and the acidic solution 72% of the original amount of **11**. No product other than acetone could be detected by g.l.c. using several columns from any of the solutions at this time or after they had been allowed to stand at 22° for another 72 h when most of the dioxetane had disappeared.

7-Hydroxybicyclo[5.3.0]decan-2-one, 30

Method A

Powdered silver acetate, 9.0 g (0.054 mol), was added over a period of 30 min to a solution of 15 g (0.051 mol) of **25***b* in 100 ml methylene chloride at 0 to −10°. The mixture was stirred for 4 h at 0 to −10° and then filtered through Celite. The filtrate was washed with 3 × 50 ml 100% sodium bicarbonate solution, dried, and concentrated to give 2 g (24%) white crystals which were recrystallized twice from heptane, m.p. 96–97°, n.m.r. (CCl_4) τ 8.75 (broad, t, 1H) 7.5 (broad, 2H) and 8.6 (s, exchangeable with D_2O) superimposed on broad absorption from 7.5–8.5 (total 13H); i.r. (CCl_4): 3600 (sharp), 3480 (broad), 1700 cm^{-1}. On dilution the intensity of the 3600 cm^{-1} band increased relative to that of the 3480 cm^{-1} band.

Anal. Calcd. for $C_{10}H_{16}O$: C, 71.34; H, 9.59. Found: C, 71.09; H, 9.52.

Method B

A solution of 0.1 g of the dione **24** and 10 mg trifluoroacetic acid in 5 ml methylene chloride was allowed to stand at ~22° for 24 h and then shaken with 20 ml water. The organic layer was concentrated to an oil which was applied to a 1.5 × 9 cm column of silica gel. Elution with 1 to 5% ether in hexane removed little material. Elution with 10% ether in hexane gave 0.031 g (30%) of white crystals, m.p. 96–97.5°, mixed m.p. with product from Method A 95–97°.

Dehydration of 30 to Bicyclo[5.3.0]dec-1(7)-ene-2-one, 31

The hydroxyketone **30**, 0.2 g, was heated under reflux with 20 ml saturated sodium bicarbonate solution for 1 h. The reaction mixture was cooled and extracted with 2 × 10 ml methylene chloride. The organic layer was dried and concentrated to an oil which was purified by chromatography on silica gel. The n.m.r. spectrum of the product was identical to that of authentic (67) **31** which had n_D^{25} 1.5251 (lit. (22) n_D^{25} 1.5260). The semicarbazone had m.p. 188–190° (lit. (67) m.p. 195–200°), mixed m.p. with the semicarbazone of authentic (67) **31** 188–190°.

9-Bromo-10-hydroxy-trans-decalin, 27

Method A

A solution of 0.578 g (23 mmol) of 9-bromo-10-hydroperoxy-*trans*-decalin **25***a* in 25 ml ether was added to a solution of 0.657 g (24 mmol) of triphenylphosphine in 10 ml ether at 20–30°. The resulting solution was allowed to stand a few minutes, then cooled to −10°, and a few drops of 98% hydrogen peroxide added. The precipitate was filtered, the filtrate concentrated to an oil, and the oil adsorbed on a column of silica gel. The product was eluted with 20% ether–pentane. Repeated crystallization from isopentane gave two sharp melting fractions. One, 0.080 g, m.p. 64–66° (dec.) showed absorption due to both aromatic and aliphatic protons in the n.m.r. spectrum, no OH absorption in the i.r. spectrum, and was not further identified. The other, 0.062 g (11%), m.p. 40–41°, showed sharp absorption at 3620 cm^{-1}.

Anal. Calcd. for $C_{10}H_{17}BrO$: C, 51.52; H, 7.34; Br, 34.27. Found: C, 51.79, H, 7.27; Br, 34.23.

Method B

A mixture of 0.79 g of **25***a* and 10 mg platinum oxide in 25 ml ethanol was hydrogenated until one equivalent of hydrogen had been absorbed. The catalyst was removed, the organic layer poured into 100 ml water, and this mixture was extracted with 3 × 25 ml pentane. The combined pentane layers were washed twice with water, dried, and concentrated to a small volume. The product was crystallized at −78° and recrystallized twice from isopentane to give 0.390 g (56%) white needles, m.p. 39–41°, mixed m.p. with **27** from A 39–41°.

$\Delta^{9,10}$-Octalin Epoxide, 28

Addition of 0.78 g of **27** to 15 ml methanol containing 0.5 g potassium hydroxide produced a white precipitate almost immediately. The mixture was stirred for 1 h and poured into 20 ml water. The resulting mixture was shaken with 3 × 5 ml pentane. The combined pentane layers were shaken twice with water dried and concentrated. Distillation of the residue through a short-path still at 20 mm gave 0.34 (67%) of a colorless oil, n_D^{20} 1.4816 (lit. (68) n_D^{19} 1.4851), whose n.m.r. and i.r. spectra were identical with those of an authentic sample of **28** prepared by oxidation of $\Delta^{9,10}$-octalin with *m*-chloroperbenzoic acid and which had n_D^{20} 1.4808.

Reaction of 3-Iodo-2,3-dimethyl-2-butyl Hydroperoxide, 12b, with Base

A solution of 0.25 g freshly recrystallized **12***b* in 2 ml methanol was added to a solution of 0.05 g sodium hydroxide in 5 ml methanol. The mixture was stirred at 0° for 10 min and then diluted with water. The resulting mixture was extracted with 3 × 10 ml methylene chloride. The combined extracts were dried and concentrated to give a 0.10 g (90%) of an oil whose n.m.r. spectrum was identical to that of an authentic (1) sample of **13**.

2-Methylene-1-methylcyclohexyl Hydroperoxide, 17

Treatment of the iodohydroperoxide **16***b* with methanolic base and subsequent work-up of the reaction

mixture was carried out as described for **12***b* above. The n.m.r. spectrum of the product indicated that it consisted of **17** together with a trace of the isomeric 2,3-dimethyl-3-cyclohexenyl hydroperoxide **18**. Distillation of this material under 0.01 mm pressure at 40° gave pure (by n.m.r.) **17**, n_D^{25} 1.4840.

Anal. Calcd. for $C_8H_{14}O_2$: C, 67.57; H, 9.93. Found: C, 67.37; H, 9.95.

10-Hydroperoxy-$\Delta^{1,9}$*-octalin, 26*

Treatment of 1.25 g of the bromohydroperoxide **25***a* with methanolic base and workup of the reaction mixture as described above for **12***b* produced an oily residue. Crystallization from Skelly B gave 0.8 g (89%) white crystals, m.p. 58–59° (lit. (69) m.p. 60°).

A 95% yield of **26** was obtained when the iodohydroperoxide **25***b* was treated in this way.

10-Hydroxy-$\Delta^{1,9}$*-octalin, 36*

A 0.58 g (34 mmol) sample of the allylic hydroperoxide **26** was added to a solution of 0.1 g (21 mmol) sodium borohydride in 10 ml methanol at −10°. The solution was allowed to warm to 20°, heated on the steam bath for 5 min, and then poured into 20 ml ice water. The precipitate was filtered, washed with water, and air dried to give 0.38 g (81%) of a white solid, m.p. 83–85° (lit. (70) m.p. 87–88°).

Kinetic Studies

(A) Iodometric Method

Solutions of the dioxetanes in benzene or carbon tetrachloride in a round-bottomed flask fitted with a reflux condenser were immersed in a Colora constant temperature bath. Aliquots of the solutions were withdrawn at suitable intervals after temperature equilibrium had been reached, cooled to 0°, and titrated for peroxide content (52). Measurements on degassed solutions were made on samples in ampoules which had been degassed to 10^{-3} mm by three freeze–thaw cycles.

(B) Chemiluminescence Decay

A Turner Model 430 spectrofluorometer with the xenon lamp source turned off was used with the 60 nm emission monochromator bandwidth. Solutions of the dioxetanes containing $\sim 10^{-2}$ *M* DBA were placed in a 10 cm jacketed polarimeter type cell with one end silvered. The cell was placed in a specially made compartment with the unsilvered end centered about 2 cm from the entrance slit. Water from a constant temperature bath was circulated through the jacket and the internal temperature of the solution was measured.

(C) Nuclear Magnetic Resonance Method

A carbon tetrachloride solution of **15** in an n.m.r. tube was placed in the heated probe of the 100 MHz spectrometer. The concentration of **15** was monitored by comparing the area of the signal due to the methyl protons of **15** with total area of the signals.

The results of the kinetic runs are given in Table 1.

We wish to thank Professor W. H. Richardson for helpful comments and Dr. K. L. Loening for information about nomenclature.

1. K. R. Kopecky, J. H. van de Sande, and C. Mumford. Can. J. Chem. **45**, 25 (1968).
2. (*a*) W. H. Richardson, J. W. Peters, and W. P. Konopka. Tetrahedron Lett. 553 (1966); (*b*) M. Schulz, A. Rieche, and K. Kirschke. Chem. Ber. **100**, 370 (1967); (*c*) L. Dulog and W. Voght. Tetrahedron Lett. 5169 (1966).
3. (*a*) K. R. Kopecky and C. Mumford. 51st Ann. Conf. Chem. Inst. of Can., Vancouver, British Columbia. June, 1968. Abstr. p. 41; (*b*) K. R. Kopecky and C. Mumford. Can. J. Chem. **47**, 709 (1969).
4. (*a*) P. D. Bartlett and A. P. Schaap. J. Am. Chem. Soc. **92**, 3223 (1970); (*b*) S. Mazur and C. S. Foote. J. Am. Chem. Soc. **92**, 3225 (1970); (*c*) A. P. Schaap. Tetrahedron Lett. 1757 (1971); (*d*) G. Rio and J. Berthelot. Bull. Soc. Chim. Fr. 3555 (1971); (*e*) J. J. Bassilier and J. P. Le Roux. Bull. Soc. Chim. Fr. 4443 (1971); (*f*) J. Strating, J. H. Wieringa, H. Wynberg, and W. Adam. Tetrahedron Lett. 169 (1972); (*g*) N. M. Hasty and D. R. Kearns. J. Am. Chem. Soc. **95**, 3380 (1973); (*h*) P. D. Bartlett and M. S. Ho. J. Am. Chem. Soc. **96**, 627 (1974); (*i*) T. R. Darling and C. S. Foote. J. Am. Chem. Soc. **96**, 1625 (1974); (*j*)P. A. Burns and C. S. Foote. J. Am. Chem. Soc. **96**, 4339 (1974).
5. A. P. Schaap and P. D. Bartlett. J. Am. Chem. Soc. **92**, 6055 (1970).
6. (*a*) W. H. Richardson and V. F. Hodge. J. Am. Chem. Soc. **93**, 3996 (1971); (*b*) W. H. Richardson, M. B. Yelvington, and H. E. O'Neal. J. Am. Chem. Soc. **94**, 1619 (1972); (*c*) W. H. Richardson, F. C. Montgomery, and M. B. Yelvington. J. Am. Chem. Soc. **94**, 9277 (1972); (*d*) E. H. White, P. D. Wildes, J. Wiecko, H. Doshan, and C. C. Wei. J. Am. Chem. Soc. **95**, 7050 (1973).
7. W. Adam and J.-C. Liu. J. Am. Chem. Soc. **94**, 2894 (1972).
8. (*a*) T. Wilson, M. E. Landis, A. L. Baumstark, and P. D. Bartlett. J. Am. Chem. Soc. **95**, 4765 (1973); (*b*) P. D. Bartlett, A. L. Baumstark, and M. E. Landis. J. Am. Chem. Soc. **96**, 5557 (1974).
9. K. R. Kopecky and J. H. van de Sande. Can. J. Chem. **50**, 4034 (1972).
10. (*a*) J. E. Baldwin, G. Hofle, and S. C. Choi. J. Am. Chem. Soc. **93**, 2810 (1971); (*b*) J. E. Baldwin, A. K. Bhatnagar, S. C. Choi, and T. J. Shotridge. J. Am. Chem. Soc. **93**, 4082 (1971).
11. C. S. Foote, S. Wexler, and W. Ando. Tetrahedron Lett. 4111 (1965).
12. P. R. Story, J. A. Alford, J. R. Burgess, and W. C. Ray. J. Am. Chem. Soc. **93**, 3042 (1971); (*b*) P. R. Story, E. A. Whited, and J. A. Alford. J. Am. Chem. Soc. **94**, 2143 (1972).
13. K. R. Kopecky, P. A. Lockwood, J. E. Filby, and R. W. Reid. Can. J. Chem. **51**, 468 (1973).
14. (*a*) A. J. Sisti. J. Org. Chem. **33**, 3953 (1968); (*b*) A. J. Sisti. Tetrahedron Lett. 3305 (1970); (*c*) A. J. Sisti. J. Org. Chem. **35**, 2670 (1970).
15. J. G. Traynham and O. S. Pascual. Tetrahedron, **7**, 165 (1959).
16. A. A. Ostwald, F. Noel, and A. J. Stephenson. J. Org. Chem. **26**, 2969 (1961).
17. E. H. White, J. Wiecko, and D. F. Roswell. J. Am. Chem. Soc. **91**, 5194 (1969).

Can. J. Chem. Downloaded from www.nrcresearchpress.com by 210.87.254.40 on 09/05/12
For personal use only.

Can. J. Chem. Downloaded from www.nrcresearchpress.com by 210.87.254.40 on 09/05/12
For personal use only.

18. M. SCHULZ and K. KIRSCHKE. Z. Chem. **12**, 261 (1972).
19. (*a*) N. J. TURRO and P. LECHTKEN. J. Am. Chem. Soc. **95**, 264 (1973); (*b*) N. J. TURRO and P. LECHTKEN. Pure Appl. Chem. **33**, 363 (1973).
20. N. H. HAWORTH. J. Chem. Soc. **103**, 1249 (1913).
21. N. L. ALLINGER, M. T. TRIBBLE, and M. A. MILLER. Tetrahedron, **28**, 1173 (1972).
22. S. DEV. J. Indian Chem. Soc. **31**, 1 (1954).
23. (*a*) P. D. BARTLETT, A. L. BAUMSTARK, and M. E. LANDIS. J. Am. Chem. Soc. **95**, 6486 (1973); (*b*) P. D. BARTLETT, A. L. BAUMSTARK, M. E. LANDIS, and C. L. LERMAN. J. Am. Chem. Soc. **96**, 5267 (1974).
24. D. B. DENNY and D. H. JONES. J. Am. Chem. Soc. **91**, 5821 (1969).
25. D. C.-S. LEE and T. WILSON. *In* Chemiluminescence and bioluminescence. *Edited by* M. J. Cormier, D. M. Hercules, and J. Lee. Plenum Press, New York, N.Y. 1973. p. 625.
26. G. O. SCHENCK and W. WILLMUND. *Reported by* R. Criegee. *In* Houben-Weyl. Methoden der oganischen chemie. Vol. VIII, 4th ed. *Edited by* E. Muller. Georg Thieme Verlag. Stuttgart. 1952. p. 16.
27. G. O. SCHENCK and D. E. DUNLAP. Angew. Chem. **68**, 248 (1956).
28. T. WILSON and A. P. SCHAAP. J. Am. Chem. Soc. **93**, 4126 (1971).
29. G. J. MINKOFF. Proc. R. Soc. Lond. A**224**, 176 (1954).
30. P. LECHTKEN, A. YEKTA, and N. J. TURRO. J. Am. Chem. Soc. **95**, 3027 (1973).
31. (*a*) H. E. O'NEAL and W. H. RICHARDSON. J. Am. Chem. Soc. **92**, 6553 (1970); (*b*) H. E. O'NEAL and W. H. RICHARDSON. J. Am. Chem. Soc. **93**, 1828 (1971); (*c*) H. E. O'NEAL and W. H. RICHARDSON. J. Am. Chem. Soc. **94**, 8665 (1972).
32. (*a*) H. BLITZ. Ann. **296**, 238 (1897); (*b*) E. P. KOHLER. Am. Chem. J. **36**, 177 (1906); (*c*) E. P. KOHLER and R. B. THOMPSON. J. Am. Chem. Soc. **59**, 887 (1937); (*d*) M. BUSCH and W. DIETZ. Ber. **47**, 3277 (1914); (*e*) H. STAUDINGER. Ber. **58**, 1075 (1925); (*f*) D. SWERN, J. E. COLEMAN, H. B. KNIGHT, R. RICCUITI, C. O. WILLITS, and C. R. EDDY. J. Am. Chem. Soc. **75**, 3135 (1953); (*g*) C. E. GRIFFIN and R. E. LUTZ. J. Org. Chem. **21**, 1134 (1956).
33. K. MISLOW. Private communication.
34. (*a*) W. H. RICHARDSON and R. F. STEED. J. Org. Chem. **32**, 4182 (1967); (*b*) K. H. PAUSACKER. J. Chem. Soc. 3478 (1950); (*c*) E. F. JENNY, H. DROCSCHER, and A. MELZER. Angew. Chem. Int. Ed. Engl. **3**, 650 (1964); (*d*) B. WITKOP and J. B. PATRICK. J. Am. Chem. Soc. **73**, 2188 (1951); (*e*) B. WITKOP and J. B. PATRICK. J. Am. Chem. Soc. **73**, 2194 (1951); (*f*) B. WITKOP and J. B. PATRICK. J. Am. Chem. Soc. **74**, 3855 (1952).
35. (*a*) E. H. WHITE and M. J. C. HARDING. J. Am. Chem. Soc. **86**, 5686 (1964); (*b*) F. MCCAPRA and D. G. RICHARDSON. Tetrahedron Lett. 3167 (1964).
36. (*a*) K. D. GUNDERMANN. Angew. Chem. Int. Ed. Engl. **4**, 566 (1965); (*b*) F. MCCAPRA. Q. Rev. Chem. Soc. **20**, 485 (1966); (*c*) E. H. WHITE and D. F. ROSWELL. Acc. Chem. Res. **3**, 54 (1970); (*d*) F. MCCAPRA. Pure Appl. Chem. **24**, 611 (1970); (*e*) F. MCCAPRA. Prog. Org. Chem. **8**, 231 (1973); (*f*) E. H. WHITE, J. D. MIANO, C. J. WATKINS, and E. J. BREAUX. Angew. Chem. Int. Ed. Engl. **13**, 229 (1974); (*g*) M. M. RAUHUT. Acc. Chem. Res. **2**, 80 (1969).
37. (*a*) E. H. WHITE, J. WIECKO, and J. F. ROSWELL. J. Am. Chem. Soc. **91**, 5194 (1969); (*b*) E. H. WHITE, J. WIECKO, and C. C. WEI. J. Am. Chem. Soc. **92**, 2167 (1970); (*c*) E. H. WHITE and C. C. WEI. Biochem. Biophys. Res. Commun. **39**, 1219 (1970); (*d*) P. D. WILDES and E. H. WHITE. J. Am. Chem. Soc. **93**, 6286 (1971); (*e*) A. A. LAMOLA. Biochem. Biophys. Res. Commun. **43**, 893 (1971).
38. N. J. TURRO, P. LECHTKEN, N. E. SCHORE, G. SCHUSTER, H.-C. STEINMETZER, and A. YEKTA. Acc. Chem. Res. **7**, 97 (1974).
39. G. CILENTO. Q. Rev. Biophys. **6**, 4 (1973).
40. F. MCCAPRA. Chem. Commun. 155 (1968).
41. P. LECHTKEN and G. HOHNE. Angew. Chem. Int. Ed. Engl. **12**, 772 (1972).
42. W. FENICAL, D. R. KEARNS, and P. RADLICK. J. Am. Chem. Soc. **91**, 3396 (1969).
43. P. D. BARTLETT, G. D. MENDENHALL, and A. P. SCHAAP. Ann. N.Y. Acad. Sci. **171**, 79 (1970).
44. P. S. BAILEY, T. P. CARTER, C. M. FISCHER, and J. A. THOMPSON. Can. J. Chem. **51**, 1278 (1973).
45. N. C. YANG and R. V. CARR. Tetrahedron Lett. 5143 (1972).
46. R. CRIEGEE and A. BANCIU. Angew. Chem. **98**, 261 (1974).
47. (*a*) J.-P. LE ROUX and J.-J. BASSELIER. C.R. Acad. Sci. Paris. **271**, 461 (1970); (*b*) J. RIGAUDY, P. CAPDEVILLE, and M. MAURNY. Tetrahedron Lett. 4997 (1972).
48. (*a*) C. S. FOOTE, S. MAZUR, P. A. BURNS, and D. LERDAL. J. Am. Chem. Soc. **95**, 586 (1973); (*b*) G. RIO, D. BRICOUT, and L. LACOMBE. Tetrahedron Lett. 3583 (1972).
49. (*a*) T. WILSON. Photochem. Photobiol. **10**, 441 (1969); (*b*) J. RIGAUDY. Pure Appl. Chem. **16**, 169 (1968); (*c*) J. RIGAUDY, C. DELETANG, D. SPARFEL, and N. H. CUONG. C. R. Acad. Sci. Paris, **267**, 1714 (1968); (*d*) J. E. BALDWIN, H. H. BASSON, and H. KRAUSS, JR. Chem. Commun. 984 (1968).
50. R. K. RAZDAN and V. V. KANE. J. Am. Chem. Soc. **91**, 5190 (1969).
51. J. E. FILBY. Ph.D. Thesis. University of Alberta, Edmonton, Alberta. 1973.
52. H. B. KNIGHT and D. SWERN. *In* Organic synthesis, Coll. Vol. 4. *Edited by* N. Rabjohn. John Wiley and Sons, Inc., New York. 1963. p. 895.
53. R. A. BENKESER and E. M. KAISER. J. Org. Chem. **29**, 955 (1964).
54. G. S. HAMMOND and T. D. NEVITT. J. Am. Chem. Soc. **76**, 4121 (1954).
55. J. KOSSANYI and J. K. MOGOTO. Org. Mass Spectrom. **3**, 721 (1970).
56. H. HART and R. L. LERNER. J. Org. Chem. **32**, 2669 (1967).
57. S. NAMENTKIN and N. DELEKORSKI. Ber. **57**, 583 (1924).
58. R. CRIEGEE. Ann. **522**, 75 (1936).
59. V.-Q. YEN. Ann. Chim. Paris, **7**, 785 (1962).
60. N. H. HAWORTH. J. Chem. Soc. **103**, 1249 (1913).
61. H. MEERWEIN. Ann. **542**, 123 (1939).
62. C. A. BUNTON and M. A. CARR. J. Chem. Soc. 5834 (1963).

63. R. CRIEGEE. Ber. **64**, 260 (1931).
64. G. F. HENNION and E. J. WATSON. J. Org. Chem. **23**, 656 (1958).
65. J. READ and W. G. REID. J. Chem. Soc. 1487 (1928).
66. C. M. SUTER and H. D. ZOOK. J. Am. Chem. Soc. **66**, 738 (1944).
67. W. HÜCKEL and L. SCHNITZSPAHN. Ann. **505**, 724 (1933).
68. W. G. DAUBEN, R. C. TWIST, and R. L. MCLEAN. J. Am. Chem. Soc. **77**, 48 (1955).
69. S. MAZUR and C. S. FOOTE. J. Am. Chem. Soc. **92**, 3225 (1970).
70. G. O. SCHENCK and K.-H. SCHULTE-ELTE. Ann. **618**, 185 (1958).
71. K. R. KOPECKY and J. H. VAN DE SANDE. Can. J. Chem. **50**, 4034 (1972).

Can. J. Chem. Downloaded from www.nrcresearchpress.com by 210.87.254.40 on 09/05/12
For personal use only.

Kinetic, Electron Spin Resonance, and Product Studies of the Reaction Between 2,2-Diphenyl-1-picrylhydrazyl and 2,4,6-Tri-*t*-butylbenzenethiol

JAMES FLOOD AND KENNETH E. RUSSELL

Department of Chemistry, Queen's University, Kingston, Ontario K7L 3N6

Received October 16, 1974

JAMES FLOOD and KENNETH E. RUSSELL. Can. J. Chem. **53**, 1123 (1975).

The reaction of 2,2-diphenyl-1-picrylhydrazyl (DPPH) with 2,4,6-tri-*t*-butylbenzenethiol (TBBT) in benzene solution has been studied. The two major products, 2,2-diphenyl-1-picrylhydrazine (DPPH-H) and di-(2,4,6-tri-*t*-butylphenyl) disulfide, are those anticipated for a reaction in which DPPH abstracts hydrogen from the thiol yielding thiyl radicals which undergo coupling to produce the disulfide. About 30% of the DPPH is converted into a derivative in which a nitro group has been displaced by a 2,4,6-tri-*t*-butylphenylthiyl group. Displacement of NO_2 from DPPH by the tri-*t*-butylphenylthiyl radical is thought to constitute an important secondary reaction.

In the presence of excess thiol, the rate constant for disappearance of DPPH, determined spectrophotometrically, is $1.23 \pm 0.04\ M^{-1}\ s^{-1}$ at 25 °C, and the activation energy is 5.8 ± 0.5 kcal mol^{-1}. The rate of reaction is halved when the thiol is deuterated at the SH group, confirming that the primary step involves hydrogen transfer. Addition of DPPH-H retards the overall reaction indicating that this primary step is reversible.

An e.s.r. study of the reacting solutions shows that the concentration of thiyl radical is relatively low until most of the DPPH disappears; it also shows the slow buildup of the 2,4,6-tri-*t*-butylphenylthiyl derivative of DPPH. The e.s.r. spectrum of the latter derivative has been analyzed and shown to be consistent with nitrogen coupling constants $A_1 = 10.4 \pm 0.2$ G and $A_2 = 6.45 \pm 0.2$ G.

JAMES FLOOD et KENNETH E. RUSSELL. Can. J. Chem. **53**, 1123 (1975).

On a étudié la réaction du radical diphényl-2,2 picryl-1 hydrazyle (DPPH) avec le tri-*t*-butyl-2,4,6 benzène thiol (TBBT) en solution benzénique. Les deux produits majeurs, la diphényl-2,2 picryl-1 hydrazine (DPPH-H) et le disulfure de di(tri-*t*-butyl-2,4,6 phényl) sont ceux attendus pour une réaction dans laquelle le DPPH enlève des atomes d'hydrogène du thiol amenant la formation de radicaux thiyles qui subissent alors une réaction de couplage pour fournir le disulfure. Environ 30% du DPPH est transformé en un dérivé dans lequel le groupe nitro a été remplacé par un groupe tri-*t*-butyl-2,4,6 phénylthiyle. On croit que le remplacement du NO_2 du DPPH par un radical tri-*t*-butylphénylthiyle est une réaction secondaire importante.

En présence d'un excès de thiol la constante de vitesse pour la disparition du DPPH, tel que déterminé spectrophotométriquement, est de $1.23 \pm 0.04\ M^{-1}\ s^{-1}$ à 25 °C et l'énergie d'activation est de 5.8 ± 0.5 kcal mol^{-1}. La vitesse de la réaction est réduite de moitié quand le thiol est deutéré dans le groupe SH; ceci confirme que l'étape primaire de la réaction implique un transfert d'hydrogène. L'addition du DPPH-H retarde la réaction globale et ceci indique que l'étape primaire est réversible.

Une étude r.p.e. des solutions réagissantes montre que la concentration de radical thiyle est relativement basse jusqu'à ce que pratiquement tout le DPPH soit disparu; il montre aussi qu'il y a une accumulation lente du dérivé tri-*t*-butyl-2,4,6 phénylthiyle du DPPH. On a analysé le spectre r.p.e. de ce dernier dérivé et montré qu'il est en accord avec des constantes de couplage de l'azote $A_1 = 10.4 \pm 0.2$ G et $A_2 = 6.45 \pm 0.2$ G.

[Traduit par le journal]

Introduction

The early studies of Goldschmidt and Renn (1) demonstrated that DPPH can react with the hydrogen donor, hydroquinone, to give DPPH-H and benzoquinone. More recently it has been shown that DPPH can abstract hydrogen from aliphatic thiols (2), aromatic amines (3), and phenols (4, 5). The rate constants for the overall disappearance of DPPH vary markedly with the type of X—H bond and, in the case of phenols, with the substituents in the ring. The results have been discussed in terms of polar and steric influences on the primary hydrogen abstraction step.

DPPH-H is isolated from the various reaction mixtures in high yield. The donor molecules yield free radicals in the primary step and these may react with themselves or with a second molecule

Can. J. Chem. Downloaded from www.nrcresearchpress.com by 210.87.254.40 on 09/05/12
For personal use only.

Can. J. Chem. Downloaded from www.nrcresearchpress.com by 210.87.254.40 on 09/05/12
For personal use only.

of DPPH. Products derived from the donor are however more difficult to isolate and the importance of the various secondary reactions is not generally known. The reactions are frequently retarded by DPPH-H, suggesting that the primary hydrogen abstraction step is reversible.

One of the few reactions of DPPH to be thoroughly investigated is the reaction with 2,4,6-tri-*t*-butylphenol (6). Abstraction of the phenolic hydrogen by DPPH yields DPPH-H and the 2,4,6-tri-*t*-butylphenoxy radical; in the absence of air, the phenoxy radical does not enter into secondary reactions. Spectrophotometric and e.s.r. studies yield rate and equilibrium constants for the known primary reaction. DPPH has a relatively wide line e.s.r. spectrum and 2,4,6-tri-*t*-butylphenoxyl a narrow line spectrum and their concentrations in reaction mixtures can be readily determined. The present study of the reaction between DPPH and 2,4,6-tri-*t*-butylbenzenethiol was performed with the hope that it would lead to a corresponding understanding of the reaction between DPPH and an aromatic thiol. Comparison of the results for the hindered thiol and phenol should provide information on factors influencing reactivities of these hydrogen donors.

Experimental

Materials

2,4,6-Tri-*t*-butylbenzenethiol (TBBT) was prepared from benzene. Alkylation of benzene with *t*-butyl chloride in the presence of aluminum chloride was conducted at −40 °C (7); after two recrystallizations the 1,3,5-tri-*t*-butylbenzene was obtained in 62% yield, m.p. 71–73 °C (lit. (7) m.p. 72–73 °C, (8) m.p. 73–73.5 °C). Bromination of the tri-*t*-butylbenzene was performed according to the procedure of Betts and Barclay (9). The 2,4,6-tri-*t*-butylbromobenzene, after five recrystallizations, was obtained as white plates, yield 20%, m.p. 176–177 °C (lit. (9) m.p. 177–177.5 °C). Conversion of the 2,4,6-tri-*t*-butylbromobenzene to the corresponding thiol was effected by preparing the magnesium Grignard reagent of the bromobenzene in dry tetrahydrofuran, allowing it to react with sulfur, and reducing the product with lithium aluminum hydride (*cf.* Rundel (10)). After removal of THF by steam distillation, the TBBT was extracted from the residue by shaking with ether; the ether extracts were concentrated to give 5 ml solution and the TBBT separated by chromatography on neutral alumina. After three recrystallizations from acetone, the 2,4,6-tri-*t*-butylbenzenethiol was obtained as white needles, yield 25%, m.p. 179–181 °C (lit. (10) m.p. 180–181 °C).

DPPH (Eastman Organic Chemicals) was heated to 80 °C *in vacuo* in order to remove any complexed solvent (11). DPPH-H was used as supplied. Benzene (Fisher Scientific) was of 99 mol% grade.

Spectroscopic Studies

Benzene solutions of DPPH and TBBT were separately degassed in an apparatus similar to that used in earlier studies (6, 12). The apparatus was immersed in a thermostat for 20 min, the solutions were mixed, and the mixture transferred to an optical cell of 1 cm pathlength. The decrease in absorbance at 640 nm was observed by means of a Unicam SP600 spectrophotometer fitted with a special thermostat bath and cell holder (12). For studies with deuterated TBBT, benzene solutions of thiol were shaken with heavy water and the kinetic measurements performed using solutions saturated with heavy water. The conversion of SH to SD was estimated to be >99%. In separate studies it was shown that rates of disappearance of DPPH are the same in dry benzene as in water-saturated benzene.

Reaction mixtures for e.s.r. study were similarly prepared except that the mixed solutions were transferred to a quartz tube of 9 mm internal diameter. The e.s.r. spectra were determined by means of a Varian V4502 X-band spectrometer with 100 kHz modulation.

Reaction Products

Solutions of DPPH (2.3×10^{-3} *M*; 0.113 g) and TBBT (4.6×10^{-3} *M*; 0.160 g) in benzene were separately degassed and mixed and allowed to react for 15 h in the dark. The reaction mixture was concentrated by evaporation under reduced pressure and chromatographed on silica gel or neutral alumina, using petroleum ether and benzene as eluents.

The first pale yellow band (0.13 g) consisted of a mixture of unreacted TBBT and the corresponding disulfide as shown by n.m.r. spectra of the mixture and of authentic samples. The n.m.r. spectrum of TBBT showed bands at τ 8.65 (s, 9H; *p*-*t*-butyl), 8.36 (s, 18H; *o*-*t*-butyl), 6.40 (s, 1H; S—H), 2.57 (s, 2H; *m*-protons) and the n.m.r. spectrum of the disulfide showed bands at τ 8.71 (s, 9H; *p*-*t*-butyl), 8.66 (d, 18H; *o*-*t*-butyl), 2.78 (d, 2H; *m*-protons). The integrated absorptions of the S—H proton and of the total aromatic protons of the mixture showed that the mixture contained approximately 0.055 g TBBT and 0.080 g disulfide.

A purple band yielded 0.043 g reddish-brown material which after recrystallization and drying *in vacuo* at 60 °C gave crystals m.p. 159 °C. Identification of this material is described in the section on Results.

A brown band yielded 0.065 g brown solid; m.p. 171–173 °C (lit. (1) DPPH-H m.p. 172–173 °C), mixed m.p. with DPPH-H 171–173 °C. The mass spectra of the brown solid and DPPH-H were identical. Three other bands were observed but the yields of these were low and the materials were not identified.

Results

The major products of the reaction of DPPH with TBBT in dilute solution are DPPH-H and bis(2,4,6-tri-*t*-butylphenyl) disulfide. In addition, a reddish-brown compound (**1**) was isolated which on oxidation with lead dioxide in benzene gave a stable radical whose e.s.r. spectrum is typical of a substituted hydrazyl. Analytical data for **1** are in agreement with the values calculated

Can. J. Chem. Downloaded from www.nrcresearchpress.com by 210.87.254.40 on 09/05/12
For personal use only.

for a derivative of DPPH-H in which a nitro-group has been replaced by a 2,4,6-tri-*t*-butylphenylthio group.

Anal. Calcd. for $C_{36}H_{42}N_4O_4S$: C, 68.98; H, 6.75; N, 8.94; O, 10.21; S, 5.11. Found: C, 68.65; H, 6.65; N, 8.87; O, 10.44; S, 5.43.

The mass spectral results are shown in Fig. 1. High resolution studies yielded the following results: *m/e* 626.3 (M^+), 168.078 (Ph_2N^+), 169.086 (Ph_2NH^+), and 459.215 ($H_2NC_6H_2(NO_2)_2(SC_6H_2Bu_3^t)^+$). The cracking pattern of **1** is similar to that of DPPH-H. We thus conclude (13) that displacement of a nitro-group from DPPH by the 2,4,6-tri-*t*-butylthio radical is an important secondary process in the reaction of DPPH with TBBT. The absorption spectrum of **1** in the 250–600 nm range resembles that of 2,2-diphenyl-1-(2,6-dinitrophenyl) hydrazine rather than that of the corresponding 2,4-dinitrophenyl derivative (14) suggesting that the nitro-group has been displaced from the *para-* rather than the *ortho-* position of the picryl ring. A similar conclusion is reached on examination of the absorption spectra of solutions of the corresponding hydrazyls.

The yields of the above products from a reaction mixture initially 1.15×10^{-3} *M* in DPPH and 2.3×10^{-3} *M* in TBBT indicate that at least 60% of the DPPH is converted to DPPH-H and a further 25–30% to the thiyl derivative of DPPH. At the same time over 75% of the reacting TBBT is converted to disulfide. The stoichiometry of the reaction depends however on the concentrations of reactants. Colorimetric estimation of excess DPPH in reaction mixtures containing initially 10^{-4} *M* DPPH and 0.25×10^{-4}, 0.5×10^{-4}, 0.75×10^{-4} *M* TBBT indicated that the ratios of DPPH to TBBT reacting after 20 h at 50 °C were respectively 1.7, 1.3, and 1.1. A variation of molar ratios with concentration of reactant was

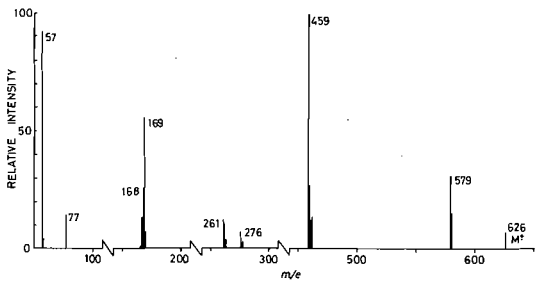

FIG. 1. Mass spectrum of hydrazine **1**.

observed in earlier studies by Brook *et al.* (15) of the reaction of DPPH with thiophenol.

The rates of disappearance of DPPH in benzene solutions were obtained for reaction mixtures containing initially 10^{-4} *M* DPPH and 5×10^{-4}, 7.5×10^{-4}, and 10×10^{-4} *M* TBBT. Plots of log [DPPH] *vs.* time are linear for the first 25% of the reaction and the apparent first order rate constants at 25 °C ($6.14 \pm 0.18 \times 10^{-4}$, $9.6 \pm 0.2 \times 10^{-4}$, and $11.8 \pm 0.5 \times 10^{-4}$ s^{-1}) indicate that the reaction is of first order with respect to TBBT. The second order rate constant at 25 °C is 1.23 ± 0.04 M^{-1} s^{-1}. Rate constants at 37.5 and 50 °C are respectively 1.57 $\pm$ 0.1 and 2.22 $\pm$ 0.1 M^{-1} s^{-1} and the overall activation energy for the disappearance of DPPH under the above reaction conditions is 5.8 ± 0.5 kcal mol^{-1}. The rate constant for the reaction of DPPH with the deuterated thiol is 0.62 ± 0.02 M^{-1} s^{-1} at 25 °C so that the apparent kinetic isotope effect is 2.0 ± 0.1. Addition of 5×10^{-4} *M* DPPH-H to a reaction mixture of 10×10^{-4} *M* DPPH and 5×10^{-4} *M* TBBT causes the rate to be halved.

Electron spin resonance spectra of a reaction mixture are shown in Fig. 2; the solution initially contained 5×10^{-4} *M* DPPH and 2×10^{-3} *M* TBBT and the spectra correspond to times of 8, 14, 21, 57, 148, and 191 min. The arrow in each spectrum marks the center of the DPPH spectrum. After 8 min the concentration of DPPH dropped to about one-half of its initial value but DPPH was the only radical observable at this stage. After 24 min the central region of the spectrum has changed significantly, suggesting that the solution contains one or more DPPH derivatives (16) in addition to DPPH itself. After 148 min the spectrum suggests the presence of a nonhydrazylic radical. The three lines of the triplet have equal intensity and the hyperfine coupling and *g* factor are 8.2 ± 0.2 G and 2.008 ± 0.001 respectively. The *g* factor is appreciably higher than those of typical nitrogen-centered free radicals such as DPPH ($g = 2.0036$) and is closer to the *g* factors of nitroxides ($g = 2.005$–2.006) (17) and of the *o*-nitrophenylsulfenylimine radical ($g = 2.0076$) (18) in which there is some unpaired spin density on sulfur. A nitrogen radical in which the nitrogen atom is adjacent to a sulfur atom would satisfy the *g* factor requirements and structures **2** and **3** are possible. The observation of Balaban *et al.* (19) that picryl-3,4-dimethoxylphenyl

Can. J. Chem. Downloaded from www.nrcresearchpress.com by 210.87.254.40 on 09/05/12
For personal use only.

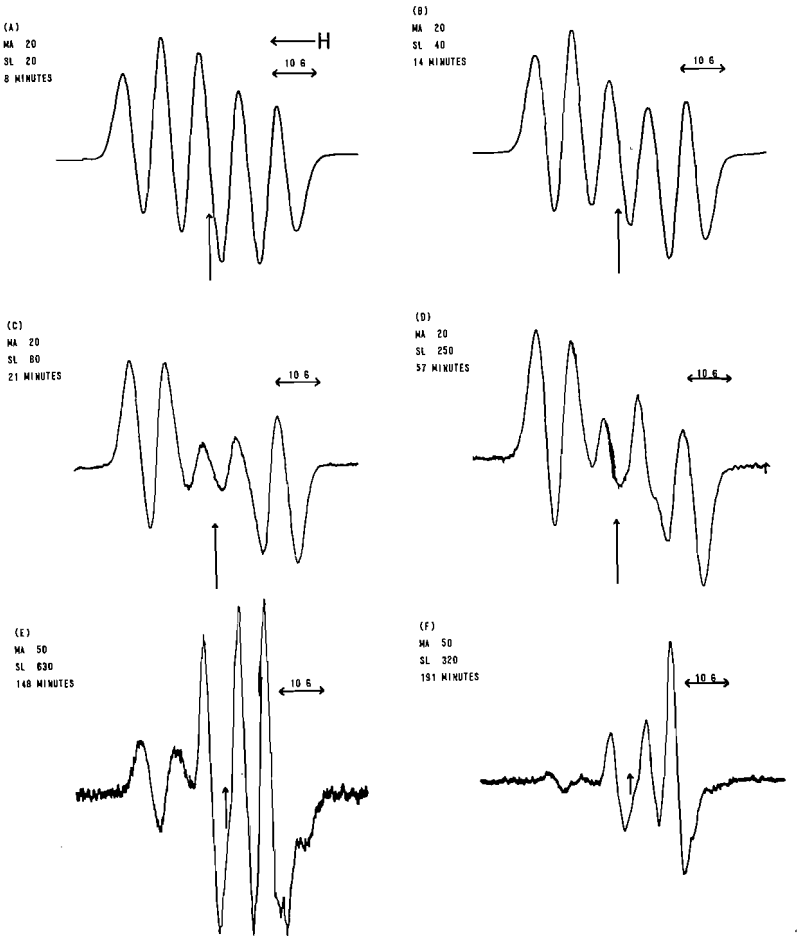

FIG. 2. Electron spin resonance spectra of a reaction mixture of DPPH and TBBT. (*A*) 8 min, (*B*) 14 min, (*C*) 21 min, (*D*) 57 min, (*E*) 148 min, (*F*) 191 min.

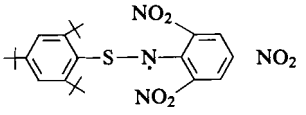

2

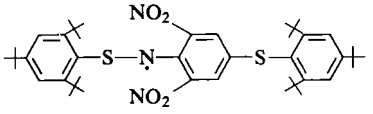

3

nitrogen gives a triplet spectrum with $a_N = 8.0$ G and $g = 2.0036$ is taken as supporting evidence for these suggested assignments.

After 191 min, the hydrazyl has almost disappeared and a singlet is superimposed on the low field line of the triplet. The g factor of the singlet is 2.010 ± 0.001 and the linewidth is close to 2 G; it appears to arise from the 2,4,6-tri-*t*-butylbenzenethiyl radical observed by Rundel (20) on u.v. photolysis or lead dioxide oxidation of TBBT in benzene or carbon tetrachloride solution. This sulfur radical is only observed at the end of the DPPH–TBBT reaction and its concentration is relatively low during the main course of the reaction, in contrast to the high concentration of 2,4,6-tri-*t*-butylphenoxyl which is observed in the corresponding reaction of DPPH with 2,4,6-tri-*t*-butylphenol (6).

Oxidation of the reddish-brown hydrazine **1** with lead dioxide in benzene solution gives a radical whose e.s.r. spectrum is shown in Fig. 3*A*. The spectrum is comparable to that of DPPH derivatives (16) and is thus attributed to the hydrazyl corresponding to the hydrazine **1**.

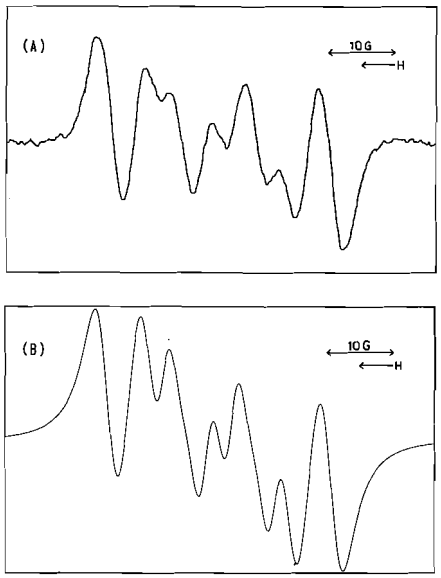

FIG. 3. (*A*) Electron spin resonance spectrum of radical obtained by lead dioxide oxidation of hydrazine **1**. (*B*) Computer simulated spectrum.

The spectrum shown was obtained in the absence of air and with a hydrazyl concentration approximately 10^{-4} *M*. Figure 3*B* shows a computer simulation of the spectrum with nitrogen coupling constants A_1 and A_2 equal to 10.4 and 6.45 G. A change in either of the coupling constants by ± 0.20 G gives simulated spectra which are discernibly different from the experimental spectrum. In spectra of various hydrazyls labelled with N^{15} at N(1) (the nitrogen atom adjacent to the picryl group), it is found that the larger coupling constant is normally associated with N(1) (16), and it is assumed that the same conclusion applies here. According to a theory developed by Walter (21), substitution of the hydrogen in the 4-position of the 2,6-dinitrophenyl group in 2,2-diphenyl-1-(2,6-dinitrophenyl-) hydrazyl by an electron donating group should lead to a decrease in the ratio A_2/A_1. The ratio is found to decrease from 0.70 (22) to 0.62 for the hydrazyl derived from **1** indicating that the 2,4,6-tri-*t*-butylphenylthio group acts as an electron donor.

Discussion

Product analysis of the reaction of DPPH with TBBT in benzene solution is most simply interpreted in terms of the following reactions:

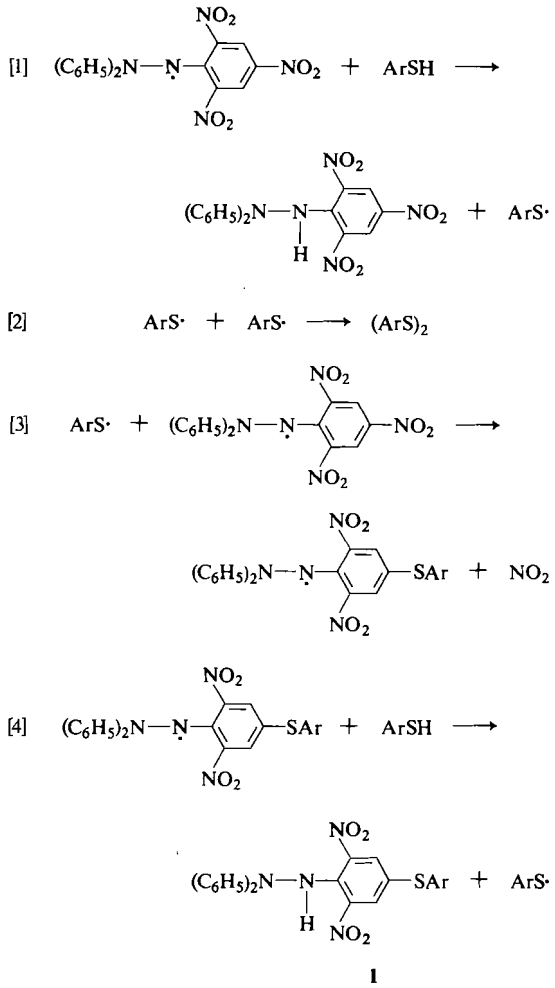

1

Reactions 1 and 2 account for the large yields of DPPH-H and the disulfide. Reactions 3 and 4 account for the formation of the hydrazine **1**. The e.s.r. spectrum of a reacting solution after 57 min is very similar to the spectrum of the hydrazyl derived from **1** and the hydrazyl is thus an intermediate as suggested in the above mechanism. Our work gives no information on the fate of the NO_2 produced in reaction 3 but studies by Weil *et al.* (16) and Kopecky and coworker (23) show that it probably attacks the *para*-position of a phenyl group of DPPH.

It has frequently been noted that hydrogen abstraction reactions involving DPPH lead both to the major product DPPH-H and to unidentified derivatives of DPPH-H (see *e.g.* (2, 3, 15)). In the reaction of DPPH with TBBT the main DPPH-H derivative is the hydrazine **1** formed almost certainly via the displacement reaction 3.

Can. J. Chem. Downloaded from www.nrcresearchpress.com by 210.87.254.40 on 09/05/12
For personal use only.

Can. J. Chem. Downloaded from www.nrcresearchpress.com by 210.87.254.40 on 09/05/12
For personal use only.

Studies of the decomposition of certain azoalkanes in the presence of DPPH (23) show that alkyl radicals can also react with DPPH at the 4-position of the picryl group. Displacement reactions of this type thus compete with dimerization of alkyl and of thiyl radicals and they may well occur to a significant extent in many other reactions of DPPH with hydrogen donors. If **2** or **3** is present in the reaction with TBBT, DPPH and its derivatives may take part to a limited extent in further displacement reactions. These assignments require additional evidence, but alternatives of the type Pic—N—Ar appear

to be much less likely since they involve rearrangement and are also susceptible to steric strain.

The observation of secondary reactions and the variation of stoichiometry with concentrations of reactants show that the rate of the hydrogen abstraction [1] cannot be identified with the rate of disappearance of DPPH. The kinetic results are based on spectrophotometric studies of the initial stages of the reaction and under these conditions the rate constants for reaction 1 may be as much as 30% lower than the quoted values for disappearance of DPPH. The reaction is subject to a deuterium isotope effect of 2.0, showing that the hydrogen abstraction reaction 1 is a rate controlling process. The retardation observed on addition of DPPH-H affords evidence that reaction 1 is reversible (5, 6). Retardation by the product DPPH-H in normal reaction mixtures is small provided that observations are limited to the initial stages of the reaction.

The observed rate constant for loss of DPPH, 1.23 M^{-1} s^{-1} at 25 °C, compares with a value of 0.14 M^{-1} s^{-1} for the corresponding reaction of DPPH with 2,4,6-tri-*t*-butylphenol. The activation energy for the reaction with TBBT, 5.8 ± 0.5 kcal/mol, is significantly lower than the activation energy for the reaction with the hindered phenol, 6.9 ± 0.2 kcal/mol (12). Thus the A factors for the two reactions are both about 2×10^4 M^{-1} s^{-1}; they could differ by a factor of 3 or so because of the uncertainties in the activation energies. The low A factor for the reaction with the phenol has been in part ascribed to steric hindrance to the hydrogen abstraction reaction (4, 5) and it had been anticipated that the A factor for the reaction with the thiol would be significantly greater than 2×10^4 M^{-1} s^{-1}. Steric hindrance is thought to be significant in the reaction of DPPH with 2-methyl-2-propanethiol (2) but further studies are required before any conclusion can be reached with regard to aromatic thiols.

We thank Professor L. R. C. Barclay for helpful discussion of the preparation of intermediates. This research was supported by a grant from the National Research Council of Canada.

1. S. Goldschmidt and K. Renn. Ber. **55**, 628 (1922).
2. K. E. Russell. J. Phys. Chem. **58**, 437 (1954).
3. J. E. Hazell and K. E. Russell. Can. J. Chem. **36**, 1729 (1958).
4. J. C. McGowan, T. Powell, and R. Raw. J. Chem. Soc. 3103 (1959).
5. J. S. Hogg, D. H. Lohmann, and K. E. Russell. Can. J. Chem. **39**, 1588 (1961).
6. P. B. Ayscough and K. E. Russell. Can. J. Chem. **43**, 3039 (1965).
7. J. M. A. Baas, H. Van Bekkum, M. A. Hoefnagel, and B. M. Wepster. Rec. Trav. Chim. **88**, 1110 (1969).
8. W. van Hartingsveldt, P. E. Verkade, and B. M. Wepster. Rec. Trav. Chim. **75**, 349 (1956).
9. E. E. Betts and L. R. C. Barclay. Can. J. Chem. **33**, 1768 (1955).
10. W. Rundel. Chem. Ber. **101**, 2956 (1968).
11. J. A. Lyons and W. F. Watson. J. Polym. Sci. **18**, 141 (1955).
12. G. J. Besserer. M.Sc. Thesis, Queen's University, Kingston, Ontario. 1967.
13. J. Flood, K. E. Russell, and J. A. Stone. J. Chem. Soc. Chem. Commun. 482 (1972).
14. A. T. Balaban, P. T. Frangopol, M. Marculescu, and J. Bally. Tetrahedron, **13**, 258 (1961).
15. A. G. Brook, R. J. Anderson, and J. Tissot van Patot. Can. J. Chem. **36**, 159 (1958).
16. M. C. Chen, K. V. Sane, R. I. Walter, and J. A. Weil. J. Phys. Chem. **65**, 713 (1961).
17. A. R. Forrester, J. M. Hay and R. H. Thomson. Organic chemistry of free radicals. Academic Press, London. 1968. Chapt. 5.
18. U. Schmidt, K. H. Kabitzke, and K. Markau. Angew. Chem. Int. Ed. Engl. **3**, 373 (1964).
19. A. T. Balaban, P. T. Frangopol, M. Frangopol, and N. Negoita. Tetrahedron, **23**, 4661 (1967).
20. W. Rundel. Chem. Ber. **102**, 1649 (1969).
21. R. I. Walter. J. Am. Chem. Soc. **88**, 1923 (1966).
22. A. T. Balaban, M. Marculescu, I. Pascaru, M. Rotaru, A. Valeriu, and M. Weiner. Z. Phys. Chem. **219**, 285 (1962).
23. K. R. Kopecky and M. Hall. Abstracts, 55th Chemical Institute of Canada Conference, Quebec. 1972. p. 46.

Effet de substituant et de solvant sur l'enthalpie de dimérisation de diméthyl-2,6 phénols. Etude par résonance magnétique nucléaire

D. BARON, M. TANGUY ET N. LUMBROSO-BADER

Université de Paris VI, Laboratoire de Chimie Physique du C.N.R.S., 2, rue Henri Dunant, 94320, Thiais, France

Reçu le 2 août 1974

D. BARON, M. TANGUY et N. LUMBROSO-BADER. Can. J. Chem. **53**, 1129 (1975).

Des valeurs précises d'enthalpie de dimérisation de phénols encombrés ont été déterminées par r.m.n.: chloro-4 diméthyl-2,6 phénol dans CCl_4 (−2.5 kcal/mol); triméthyl-2,4,6 phénol dans CCl_4 (−3.8 kcal/mol); diméthyl-2,6 phénol dans C_6H_{12} (−4.8 kcal/mol) et dans C_6H_6 (−2.3 kcal/mol).

L'étude des diméthyl-2,6 phénols parasubstitués permet, par comparaison avec des résultats antérieurs obtenus notamment sur des phénols non encombrés (1, 2), de confirmer, pour ces derniers, la prédominance des structures cycliques des dimères; les variations de ΔH_2 sont donc essentiellement dues à la répercussion de l'effet de substituant sur les propriétés acido-basiques du groupement hydroxyle (augmentation de ΔH_2 avec le pK).

De plus, les différences entre les valeurs de ΔH_2 obtenues dans CCl_4 et dans C_6H_{12} suggèrent que l'hydrogène acide n'est sans doute pas le site prépondérant de la solvatation dans CCl_4 et que la variation de ΔH_2 avec le substituant est alors certainement due à la variation de la charge électronique de l'oxygène phénolique.

D. BARON, M. TANGUY, and N. LUMBROSO-BADER. Can. J. Chem. **53**, 1129 (1975).

Some precise values for the enthalpy of dimerization of substituted phenols were determined by n.m.r.: 4-chloro-2,6-dimethylphenol in CCl_4 (−2.5 kcal/mol); 2,4,6-trimethylphenol in CCl_4 (−3.8 kcal/mol); 2,6-dimethylphenol in C_6H_{12} (−4.8 kcal/mol) and in C_6H_6 (−2.3 kcal/mol).

By comparison with earlier (1, 2) results obtained, especially on nonsterically hindered phenols, the study of the *p*-substituted 2,6-dimethylphenols confirms the predominance of cyclic structures for the dimers of the latter. The variations of ΔH_2 are thus due essentially to the influence of the substituent effect on the acid–base properties of the hydroxyl group (increase of ΔH_2 with pK).

In addition, the differences between the values of ΔH_2 obtained in CCl_4 and in C_6H_{12} suggest that the acidic hydrogen is doubtlessly not the chief site of solvation in CCl_4, and that the variation of ΔH_2 with the substituent is thus certainly due to the variation of electronic charge on the phenolic oxygen. [Journal translation]

Introduction

La structure des dimères de phénols a été très controversée (2–8). L'étude de ce problème est difficile en raison de la présence, même aux faibles concentrations, d'agrégats d'ordre supérieur (ouverts ou fermés), ce qui peut fausser très sensiblement les résultats thermodynamiques ou spectroscopiques. Il faut donc se limiter aux très grandes dilutions ou mieux aux données à dilution infinie. Profitant de la grande sensibilité aux interactions moléculaires du déplacement chimique du OH phénolique, nous avons mis au point une méthode précise de détermination des pentes à l'origine des courbes de dilution $\delta_{OH} = f(x_A{}^0)$, $x_A{}^0$ fraction molaire de phénol (1, 2). L'enthalpie de dimérisation est obtenue à partir de la variation de ces pentes avec la température.

Nos premiers travaux portaient notamment sur la détermination des enthalpies de dimérisation dans CCl_4 d'alcoyl-4 phénols non encombrés (dont le *p*-crésol, $\Delta H_2 = -6.7$ kcal/mol) ainsi que du phénol (−5.7 kcal/mol), du *p*-chlorophénol (−4.3 kcal/mol) et enfin du diméthyl-2,6 phénol (−3.2 kcal/mol). Ces résultats avaient permis de conclure à une structure ouverte des dimères, dans le cas du diméthyl-2,6 phénol, et cyclique, dans celui des alcoylphénols non encombrés. Par contre, les valeurs plus faibles obtenues avec les phénols plus acides pouvaient s'expliquer soit par une proportion importante de structures ouvertes, soit par une valeur notamment différente de la force des liaisons hydrogène due, par exemple, à une moindre basicité de l'oxygène phénolique ou à un phénomène de solvatation.

Il était donc intéressant, pour élucider ce problème, de mesurer l'effet de substituant en *para* (Cl ou Me) sur la force d'une liaison hydrogène; nous avons pour cela déterminé les enthal-

Can. J. Chem. Downloaded from www.nrcresearchpress.com by 210.87.254.6 on 09/05/12
For personal use only.

TABLEAU 1. Résultats expérimentaux* $\delta = \delta_{OH} - \delta_{CH_3} = f(x_A^0, t)$

Système	x_A^0(%)	t (°C) 10	20	30	40	50	60	70
Diméthyl-2,6 phenol/C_6H_{12}	0.20	24.0	23.1	22.3	21.6	20.9	20.4	19.9
	0.30	24.3	23.3	22.5	21.8	21.1	20.6	20.1
	0.40	24.6	23.6	22.6	21.9	21.2	20.6	20.1
	0.60	25.3	24.3	23.3	22.4	21.6	20.8	20.2
	0.80	25.8	24.6	23.5	22.6	21.8	21.1	20.4
	1.00	26.9	25.4	24.2	23.1	22.1	21.3	20.5
	1.10	27.6	26.0	24.5	23.2	22.2	21.3	20.6
	1.20	27.9	26.0	24.5	23.3	22.4	21.6	20.8
Diméthyl-2,6 phenol/C_6H_6	0.20	25.2	24.1	23.1	22.2	21.3	20.3	19.4
	0.40	25.4	24.2	23.0	22.0	21.2	20.3	19.4
	0.59	26.1	24.9	23.6	22.4	21.4	20.5	19.7
	0.90	26.3	25.0	24.0	22.8	21.9	21.0	20.2
	1.18	26.6	25.5	24.3	23.2	22.3	21.3	20.3
	1.37	26.8	25.6	24.3	23.2	22.2	21.2	20.2
	1.70	27.4	26.1	24.7	23.5	22.4	21.5	20.6
	1.86	28.0	26.3	24.9	23.7	22.7	21.6	20.5
	1.99			25.4	24.0	22.9	21.8	
	2.35	28.0	26.7	25.4	24.1	22.9	21.7	20.9
Triméthyl-2,4,6 phenol/CCl_4	0.22	19.2	18.4	17.7	16.9	16.1	15.4	14.7
	0.40	19.8	18.8	18.0	17.1	16.3	15.5	14.7
	0.55	19.9	19.0	18.0	17.1	16.3	15.6	15.0
	0.78	20.4	19.3	18.4	17.6	16.7	15.9	15.1
	0.94	21.1	20.0	18.9	17.9	17.0	16.2	15.4
	1.20	21.5	20.2	19.1	18.2	17.2	16.3	15.4
	1.40	22.2	20.8	19.5	18.3	17.3	16.5	15.7
	1.59	23.0	21.2	19.7	18.5	17.4	16.6	15.7
Chloro-4 diméthyl-2,6 phenol/CCl_4	0.21	27.7	26.8	26.0	25.2	24.4	23.7	23.1
	0.40	28.1	27.3	26.5	25.7	24.8	24.0	23.2
	0.63	28.3	27.4	26.6	25.8	25.0	24.2	23.4
	0.80	28.9	28.0	27.1	26.1	25.2	24.3	23.4
	0.99	29.3	28.2	27.3	26.4	25.5	24.6	23.9
	1.20	29.8	28.8	27.8	26.9	25.9	24.9	23.9
	1.40	30.0	28.8	27.8	26.8	25.8	24.9	24.2
	1.48	30.3	29.0	27.8	26.7	25.8	24.9	24.2
	1.60	30.8	29.4	28.2	27.1	26.1	25.2	24.4

*δ — 100 Hz (60 MHz).

pies de dimérisation dans CCl_4 de diméthyl-2,6 phénols *para* substitués que l'empêchement stérique contraint à la formation d'une seule liaison hydrogène dans le dimère. Par ailleurs, pour préciser le rôle de CCl_4, nous avons également étudié le diméthyl-2,6 phénol dans d'autres solvants "inertes" (C_6H_{12}) ou légèrement complexant (C_6H_6).

Partie expérimentale et résultats

Les phénols sont d'origine commerciale (diméthyl-2,6: Eastmann Kodak; chloro-4-diméthyl-2,6: Aldricht; triméthyl-2,4,6: K et K). Ils ont été sublimés avant utilisation. Les solvants (Eastmann Kodak Spectrograde) ont été desséchés sur tamis moléculaire Linde 4 Å. Tous les produits ont été conservés à l'abri de l'humidité.

Les déplacements chimiques ont été mesurés à 60 MHz avec un spectromètre Jeol C-60-H. Pour minimiser les effets dus à l'anistropie du milieu, seul le déplacement chimique intramoléculaire $\delta = \delta_{OH} - \delta_{CH_3}$ a été pris en considération.[1]

Le domaine de concentration permettant d'assimiler à une droite le diagramme $\delta = f(x_A^0)$, x_A^0 fraction molaire du phénol, est limité à environ $x_A^0 = 1.5\%$ dans le cas des diméthyl-2,6 phénols dans CCl_4. La concentration maximale est abaissée dans C_6H_{12} et augmentée dans le

[1]On peut rendre compte de la validité de la référence intramoléculaire $\delta_{OH} - \delta_{CH_3}$ dans le cas du diméthyl-2,6 phénol par la mesure des déplacements chimiques (en Hz) du monomère, à 30 °C, dans CCl_4 (125.1), C_6H_6 (122.8) et C_6H_{12} (121.8). Ces déplacements chimiques sont peu différent.

Can. J. Chem. Downloaded from www.nrcresearchpress.com by 210.87.254.6 on 09/05/12
For personal use only.

TABLEAU 2. Résultats analytiques: ΔH_2, $d\delta_M/dT$, δ_M et β

Système	$-\Delta H_2$	$-d\delta_M/dT$	T (°C)	δ_M*	β†
Chloro-4 diméthyl-2,6 phenol/CCl_4	2.54±0.08	0.074	10	127.2	2.09
			20	126.5	1.76
			30	125.8	1.52
			40	125.0	1.32
			50	124.3	1.15
			60	123.5	1.02
			70	122.8	0.975
Triméthyl-2,4,6 phenol/CCl_4	3.78±0.12	0.069	10	118.6	2.56
			20	117.9	2.00
			30	117.3	1.57
			40	116.6	1.27
			50	115.9	1.03
			60	115.2	0.921
			70	114.5	0.805
Diméthyl-2,6 phenol/C_6H_{12}	4.84±0.04	0.054	10	122.9	4.14
			20	122.3	3.12
			30	121.8	2.33
			40	121.3	1.79
			50	120.7	1.41
			60	120.2	1.13
			70	119.6	0.934
Diméthyl-2,6 phenol/C_6H_6	2.28±0.14	0.096	10	125.1	1.36
			20	123.9	1.25
			30	122.8	1.16
			40	121.9	1.02
			50	121.0	0.861
			60	120.2	0.760
			70	119.3	0.690

*ΔH_2 en kcal/mol.
†$\delta_M = (\delta_{OH} - \delta_{CH_3})_{x_A{}^0=0}$ en Hz (60 MHz).
‡$\beta = (d\delta/dx_A{}^0)_{x_A{}^0=0}$ en Hz/10^{-2} f.m.

benzène (*cf.* tableau 1). Huit solutions, au minimum, ont été étudiées à plusieurs températures, t, entre 5 et 75 °C environ. Des courbes $\delta_{x_A{}^0=cte} = f(t)$ on déduit les valeurs $\delta_{x_A{}^0,t}$ à sept températures: 10, 20, . . . , 70 °C.

Pour chaque température, on a la relation linéaire

$$\delta = \delta_M + \beta x_A{}^0$$

δ_M et β peuvent donc être calculés par une méthode de moindres carrés. Mais nous avons montré que généralement δ_M varie linéairement avec T (1, 2). En utilisant cette hypothèse on peut calculer δ_M et β à chaque température à partir de l'ensemble des données expérimentales d'un système.[2] Si l'hypothèse est vérifiée, la déviation standard σ, relative aux déplacements chimiques, doit être plus faible que dans le cas d'une détermination indépendante à chaque température.

Le tableau 2 rassemble les résultats obtenus. Seules les données relatives au système diméthyl-2,6 phénol – C_6H_6 ont nécessité une analyse indépendante à chaque température, une légère courbure apparaissant dans le diagramme $\delta_M = f(t)$; dans ce cas, le gradient $d\delta_M/dT$ n'est qu'une valeur moyenne. σ est toujours inférieur à 0.2 Hz (0.17 avec C_6H_6; 0.13 pour les autres systèmes).

Moyennant deux hypothèses que nous avons justifiées (1), (possibilité de négliger l'effet de milieu anisotrope et la variation, avec la température, du déplacement chimique moyen du OH dans le dimère), les pentes des diagrammes log $K_2 = f(1/T)$ et log $\beta = f(1/T)$ sont identiques. Les bonnes corrélations linéaires généralement obtenues (fig. 1) se traduisent, sauf dans le cas de C_6H_6, par une déviation standard sur ΔH_2 de l'ordre de 0.1 kcal.

[2]Pour la méthode de calcul, *cf.* réf. 1.

Can. J. Chem. Downloaded from www.nrcresearchpress.com by 210.87.254.6 on 09/05/12
For personal use only.

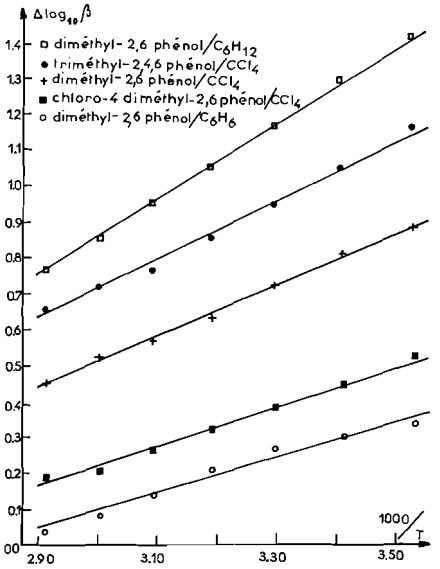

FIG. 1. Calcul de ΔH_2: corrélation $\log \beta = f(1/T)$ (les diagrammes ont été décalés en ordonnée).

Discussion

Effet de substituant en para et structure des dimères de phénols

L'introduction dans un phénol de deux groupements méthyles en *ortho* a notamment pour conséquences: (*a*) d'empêcher la formation de dimères cycliques; (*b*) d'augmenter la basicité de l'oxygène (pK_a: phénol 9.95; diméthyl-2,6 phénol 10.65; *p*-crésol 10.26; triméthyl-2,4,6 phénol 10.89); (*c*) d'augmenter par effet stérique la distance O . . . O dans le dimère ouvert, comme cela a été mis en évidence dans le cas assez voisin des complexes phénol–acétone (9).

Dans l'hypothèse d'une structure cyclique des dimères de phénols non encombrés, on ne s'attend donc pas, pour le rapport $(\Delta H_2)_{X\text{-}4}/(\Delta H_2)_{X\text{-}4(CH_3)_2\text{-}2,6}$, à une valeur rigoureusement égale à 2. On obtient en fait 1.7 à 1.8 (*cf.* tableau 3). Ceci peut s'interpréter par l'absence de différences fondamentales dans la structure des dimères du *p*-chlorophénol, du phénol et du *p*-crésol. Or nous avons montré que pour ce dernier les dimères cycliques devraient être nettement prépondérants. Il en sera donc de même pour le *p*-chlorophénol et le phénol. Par ailleurs, ces rapports, inférieurs à 2, indiquent que la force de la liaison hydrogène dans les diméthyl-2,6 phénols est plus sensible à l'augmentation de basicité de l'oxygène phénolique qu'à un allongement de la liaison hydrogène dû à un effet stérique.

De plus, on peut comparer, dans les deux séries de composés substitués en *para* (phénols non encombrés et diméthyl-2,6 phénols) l'incrément de ΔH_2 lié au changement du substituant.

Le rapport

$$(\Delta H_2)_{X\text{-}4} - (\Delta H_2)_{Y\text{-}4}/(\Delta H_2)_{X\text{-}4(CH_3)_2\text{-}2,6} - (\Delta H_2)_{Y\text{-}4(CH_3)_2\text{-}2,6}$$

est voisin de 2 pour X = Cl, Y = H et de 1.7 pour X = H, Y = CH_3.

Compte tenu de la précision obtenue sur ces rapports, on peut en conclure que les incréments liés au changement de substituant en *para* sont sensiblement deux fois plus grands dans les phénols non encombrés que dans les diméthyl-2,6 phénols. Ceci confirme encore la structure cyclique prépondérante des dimères de tous les phénols non encombrés.[3]

Effet de substituant en para et valeurs de ΔH_2

L'ensemble des résultats met en évidence, lorsque l'acidité du phénol diminue, une augmentation de la valeur absolue de l'enthalpie de dimérisation par liaison hydrogène, mesurée dans CCl_4. Avant de conclure quant à l'influence du substituant en *para* sur les valeurs de ΔH_2, il fallait examiner si cette variation pouvait provenir d'une interaction phénol–CCl_4 (11).

Pour résoudre ce problème, on a étudié le diméthyl-2,6 phénol dans d'autres solvants: C_6H_{12}, considéré comme suffisamment inerte, et C_6H_6 où une interaction est généralement admise. Par comparaison des résultats obtenus sur les deux systèmes, on peut dégager quatre critères d'interaction: (*a*) une variation non linéaire de δ_M avec la température (l'écart maximum à la linéarité est de 0.2 Hz dans le domaine étudié); (*b*) une augmentation du gradient moyen $d\delta_M/dT$; (*c*) une courbure négative dans le diagramme $\log \beta = f(1/T)$ (*cf.* fig. 1); (*d*) une diminution de $|\Delta H_2|$.

En fait, dans le cas des systèmes phénol–CCl_4

[3]Il a été proposé (10) qu'un abaissement de l'enthalpie d'autoassociation qui serait d'environ 25% par méthyle en *ortho* puisse expliquer les différences entre phénols encombrés ou non, sans faire intervenir de dimères cycliques dans le cas de phénols non encombrés. Rappelons (2) que cette hypothèse ne rend alors pas compte du fait que les ΔH_2, surtout dans le cas des alcoylphénols non encombrés, soient nettement plus grands que les ΔH des complexes phénol–acétone (4.5 à 5 kcal/mol environ) (9) bien que la basicité de l'acétone soit plus grande que celle d'un oxygène phénolique.

Can. J. Chem. Downloaded from www.nrcresearchpress.com by 210.87.254.6 on 09/05/12
For personal use only.

TABLEAU 3. Comparaison des valeurs de ΔH_2* des phénols dans CCl_4 en fonction de l'encombrement et de la substitution en *para*

Substituants		ΔH_2 pour X = Cl	H	CH_3	Différences Cl/H	H/CH_3
X-4	(A)	−4.35±0.19	−5.72±0.11	−6.67±0.21	1.37±0.30	0.95±0.32
X-4 $(CH_3)_2$-2,6	(B)	−2.54±0.08	−3.23±0.07	−3.78±0.12	0.69±0.15	0.55±0.19
Rapport (A)/(B)		1.71±0.12	1.77±0.07	1.76±0.10	2.0±0.7	1.7±0.8

*ΔH_2 en kcal/mol.

TABLEAU 4. Comparaison des valeurs des enthalpies de dimérisation par liaison hydrogène dans CCl_4 et C_6H_{12} en fonction du pK_a des phénols

Phénols	pK_a	$\Delta H_2(C_6H_{12})$	$\Delta H_2(CCl_4) - \Delta H_2(C_6H_{12})$* n
p-Chloro phénol	9.4	−5.82±0.13	0.73±0.16
p-Crésol	10.25	−9.07±0.10	1.20±0.15
Diméthyl-2,6 phénol	10.65	−4.84±0.04	1.61±0.11

*ΔH_2 en kcal/mol. Pour ΔH_2 dans CCl_4, voir tableau 3; $n = 2$ pour les phénols non encombrés; $n = 1$ pour le diméthyl-2,6 phénol.

(1, 2), on a toujours obtenu des variations linéaires de δ_M avec la température.[4] Par contre, on a effectivement observé que, pour un phénol donné, le gradient $d\delta_M/dT$ était plus élevé qu'avec C_6H_{12} mais ces variations de gradient avec le solvant ne semblent pas liées à l'acidité du phénol (2). Enfin, la très légère courbure négative qui existe dans les diagrammes log $\beta = f(1/T)$ des phénols non encombrés n'étant pas mesurable avec précision, les trois premiers critères ne permettent pas de préciser le mode d'interaction entre le phénol et CCl_4.

Par contre, on note que la différence d'enthalpie par liaison hydrogène, lorsque l'on passe de CCl_4 à C_6H_{12}, augmente avec le pK_a du phénol (*cf.* tableau 4). Ceci serait donc en faveur d'une interaction phénol–CCl_4 de type 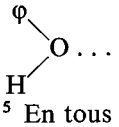 $ClCCl_3$ plutôt que φ OH . . . $ClCCl_3$.[5] En tous cas l'augmentation, avec le pK_a du phénol, de la valeur absolue de l'enthalpie de dimérisation, mesurée dans CCl_4, ne peut pas s'expliquer par l'existence d'interactions phénol–CCl_4. On peut en conclure que la variation importante des valeurs de ΔH_2 est donc essentiellement due à la répercussion, sur la force des liaisons hydrogène, des modifications de basicité de l'oxygène liées à la nature du substituant en *para*.

[4]Sauf dans le cas du *p*-chlorophénol où une variation non linéaire de δ_M avec T est observée, tant dans CCl_4(1) que dans C_6H_{12}(2).

[5]Ceci est à rapprocher des mesures de polarisation diélectrique de Gomel *et coll.* (12) qui mettent en évidence des interactions spécifiques entre solutés basiques (tels que tétrahydrofurane) et solvants chlorés.

1. D. BARON, N. LUMBROSO-BADER et M. TANGUY. J. Chim. Phys. Physicochim. Biol. **69**, 1069 (1972).
2. D. BARON, N. LUMBROSO-BADER, M. TANGUY et C. COUPRY. J. Chim. Phys. Physicochim. Biol. **69**, 1076 (1972).
3. L. J. BELLAMY et R. J. PAGE. Spectrochim. Acta, **22**, 525 (1966).
4. A. HALL et J. L. WOOD. Spectrochim. Acta, **23A**, 2657 (1967).
5. K. B. WHETSEL et J. H. LADY. Am. Chem. Soc. Div. Fuel Chem. Preprints, **11**, 210 (1967).
6. L. RACZY, E. CONSTANT et A. LEBRUN. J. Chim. Phys. Physicochim. Biol. **64**, 1180 (1967).
7. D. BARON et N. LUMBROSO-BADER. J. Chim. Phys. Physicochim. Biol. **66**, 1927 (1969).
8. J. DOS SANTOS, F. CRUEGE et P. PINEAU. J. Chim. Phys. Physicochim. Biol. **67**, 826 (1970).
9. L. LAMBERTS. J. Chim. Phys. Physicochim. Biol. **62**, 1404 (1965).
10. J. TACK. Proefschrift Doctorate, Leuven, Universiteit te Leuven, Celestijnenlaan 200F, B-3030, Heverlee. 1974.
11. A. N. FLETCHER. J. Phys. Chem. **73**, 2217 (1969).
12. B. CASTAGNA, J. M. DUMAS, M. GUERIN et M. GOMEL. J. Chim. Phys. Physicochim. Biol. **70**, 961 (1973).

Can. J. Chem. Downloaded from www.nrcresearchpress.com by 210.87.254.6 on 09/05/12
For personal use only.

Apparent Molal Volumes and Heat Capacities of some Sulfates and Carbonates in Water at 25 °C

GÉRALD PERRON AND JACQUES E. DESNOYERS[1]

Department of Chemistry, Université de Sherbrooke, Sherbrooke, Québec J1K 2R1

AND

FRANK J. MILLERO

Rosenstiel School of Marine and Atmospheric Science, University of Miami, Miami, Florida 33149

Received November 13, 1974

GÉRALD PERRON, JACQUES E. DESNOYERS, and FRANK J. MILLERO. Can. J. Chem. **53**, 1134 (1975).

The densities and volumetric specific heats of Na_2SO_4, K_2SO_4, $MgSO_4$, Na_2CO_3, $NaHCO_3$, and NaOH were measured up to an ionic strength of 1 in water at 25 °C with a flow densimeter and a flow microcalorimeter. From these data, the heat capacity for the formation of the ion pair $MgSO_4^0$ was evaluated as 84.9 J K^{-1} mol^{-1}. There is an anomalous increase in the apparent molal heat capacities of Na_2CO_3 at low concentration but the apparent molal volumes are normal. This anomaly can be suppressed with NaOH. Attempts to account quantitatively for this behavior by an hydrolysis correction were not successful.

GÉRALD PERRON, JACQUES E. DESNOYERS et FRANK J. MILLERO. Can. J. Chem. **53**, 1134 (1975).

Les masses volumiques et les chaleurs spécifiques volumiques de Na_2SO_4, K_2SO_4, $MgSO_4$, Na_2CO_3, $NaHCO_3$ et NaOH ont été mesurées dans l'eau à 25 °C au moyen d'un densimètre et d'un microcalorimètre dynamiques jusqu'à une force ionique unité. A partir de ces données le changement de capacité calorifique pour la formation de la paire d'ions $MgSO_4^0$ a été évalué à 84.9 J K^{-1} mol^{-1}. Il y a une augmentation anormale dans la capacité calorifique apparente molaire de Na_2CO_3 aux faibles concentrations mais aucune anomalie avec les volumes apparents molaires. Cette anomalie peut être supprimée par l'addition d'une faible quantité de NaOH mais les tentatives de corriger les données originales en supposant l'hydrolyse de Na_2CO_3 ont échouées.

Introduction

The thermodynamic properties of aqueous sulfate and carbonate salts are of much interest since they are normal components of sea water and other natural waters. While activity and volume data are fairly well known for most of the naturally occurring sulfates and carbonates (1), their thermochemical data are scarcer and often of doubtful accuracy. In particular, the precise heat capacities are lacking for many of these systems; these values are useful to calculate the temperature dependence of activity data (2) and to convert adiabatic compressibilities into isothermal ones (3). We therefore felt it would be useful to measure or remeasure the heat capacities of the naturally occurring carbonates and sulfates in water using a precise flow microcalorimeter (4).

The systems investigated were Na_2SO_4, K_2SO_4, $MgSO_4$, Na_2CO_3, and $NaHCO_3$. The heat capacities of NaOH were also determined to calculate the correction for the hydrolysis of Na_2CO_3. Since precise densities are required for the calculation of apparent molal heat capacities from volumetric specific heats (4), the densities of the present electrolytes were also measured with a flow densimeter (5). These volume data, when compared with literature values, can at least be used as a check of the purity of the salts and of the accuracy of the concentrations.

Experimental

The volumetric specific heats σ were measured relative to that of the solvent σ_0 with a flow microcalorimeter (4) having a precision of 0.3% (6) on $\Delta\sigma/\sigma_0$ up to the limit of the sensitivity on $\Delta\sigma$ which is 7×10^{-5} J K^{-1} cm^{-3} for a temperature rise of 1.6 K and a liquid flow rate of 0.5 cm^3 min^{-1}. The densities were determined with a flow densimeter (5) capable of evaluating differences in densities $d - d_0$ to 2 p.p.m.

All salts (Fisher Certified) were used as such after drying in a vacuum oven. The solutions were prepared by weight with deionized distilled water (Continental Deionizer). The NaOH was Fisher Certified 1 *N* stock solution. Other solutions were prepared by weight dilution with deionized water. Whenever necessary, the molarities c were calculated from the molalities m using the measured densities of the solutions. All measurements were made at 25.00 ± 0.02 °C.

[1]To whom correspondence should be addressed.

Can. J. Chem. Downloaded from www.nrcresearchpress.com by 210.87.254.42 on 09/05/12
For personal use only.

Can. J. Chem. Downloaded from www.nrcresearchpress.com by 210.87.254.42 on 09/05/12
For personal use only.

Results and Discussion

The apparent molal volumes ϕ_V and heat capacities ϕ_C were calculated in the usual manner from the densities and volumetric specific heats (6).

The differences in densities $d - d_0$ and relative differences in volumetric specific heats $(\sigma - \sigma_0)/\sigma_0$ are given elsewhere[2] along with the derived ϕ_V and ϕ_C. The density d_0 and volumetric specific heat σ_0 of pure water were taken as 0.997047 g cm^{-3} (7) and 4.1670 J K^{-1} cm^{-1} (8).

The apparent molal quantities are usually fitted to a Redlich type (9) equation in terms of c or m (6, 10).

$$[1] \quad \phi_V = \phi_V^0 + k_V\omega^{3/2}c^{1/2} + B_V'c + \ldots$$

$$[2] \quad \phi_V = \phi_V^0 + k_V\omega^{3/2}(d_0m)^{1/2} + B_Vm + \ldots$$

$$[3] \quad \phi_C = \phi_C^0 + k_C\omega^{3/2}c^{1/2} + B_C'c + \ldots$$

$$[4] \quad \phi_C = \phi_C^0 + k_C\omega^{3/2}(d_0m)^{1/2} + B_Cm + \ldots$$

where k_V and k_C are given by the limiting Debye–Hückel law as 1.868 and 28.95 in water at 25 °C for ϕ_V and ϕ_C expressed respectively in cm^3 mol^{-1} and J K^{-1} mol^{-1}. The valence factor ω is given by

$$[5] \quad \omega = 0.5 \sum_i \nu_i Z_i^2$$

There is no real advantage in expressing ϕ_V and ϕ_C in c or m. It is preferable to express them in c if we wish to back calculate d or σ. On the other hand, parameters related to m are required to calculate the pressure or temperature dependence of activity data (2). It is therefore simpler to calculate both sets of parameters. Also with multivalent electrolytes it is often preferable to express concentrations in ionic strengths. Equations 1 to 4 may be readily converted to this scale by replacing m by I_m/ω and c by I_c/ω.

Plots of $\phi_V - \omega k_V I_C^{1/2}$ and $\phi_C - \omega k_C(d_0 I_m)^{1/2}$ against I_c or I_m are shown in Figs. 1 and 2. In all cases where these functions were linear, the parameters ϕ_V^0, B_V, B_V', ϕ_C^0, B_C, B_C' were determined from a weighted least squares analysis and are summarized in Table 1.

The present volume data are in excellent agreement with those of Dunn (11), Wirth (12), Millero *et al.* (13), and Hepler *et al.* (14) with the exception of Na_2SO_4 where the present data are more positive than those of Dunn by about 0.15 cm^3 mol^{-1}. The present ϕ_V of $MgSO_4$ are also systematically 0.3 cm^3 mol^{-1} more positive than the literature values averaged by Millero

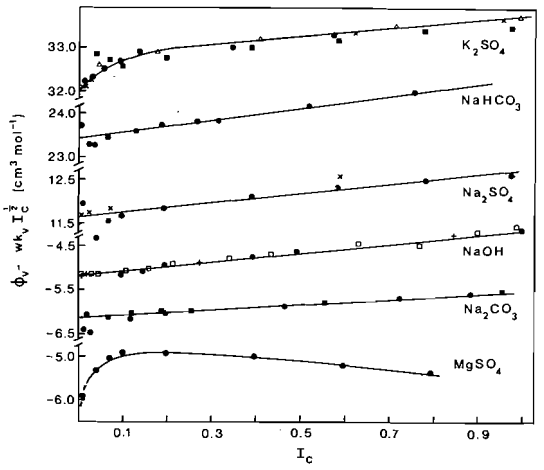

FIG. 1. Apparent molal volumes in water at 25 °C: ●, present results; ■, present results in 0.005 *m* NaOH; ×, Dunn (11); +, Hepler *et al.* (14); □, Millero *et al.* (13); △, Wirth (12).

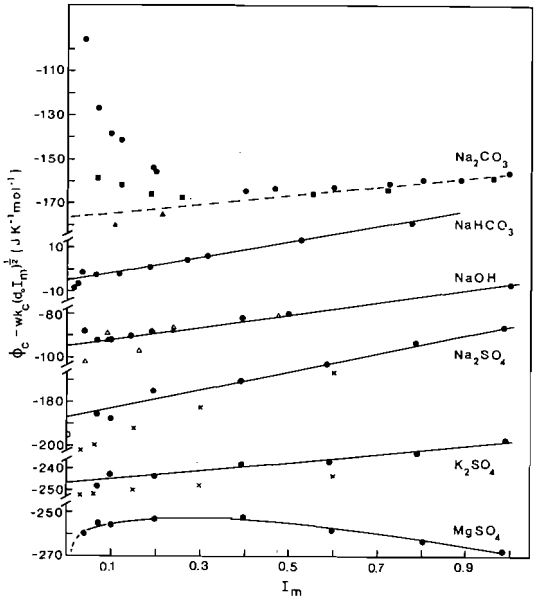

FIG. 2. Apparent molal heat capacities in water at 25 °C: ●, present results; ■, present results in 0.005 *m* NaOH; ▲, present results in 0.01 *m* NaOH; ×, Randall and Rossini (16); △, Gucker and Schminke (17); ○, Gardner *et al.* (18). In the case of K_2SO_4 ● and ■ refer to two sets of measurements in H_2O.

[2]Complete set of tabular data is available, at a nominal charge, from the Depository of Unpublished Data, CISTI, National Research Council of Canada, Ottawa, Canada K1A 0S2.

TABLE 1. Parameters of eqs. 1 to 4 for some carbonates and sulfates in water at 25 °C for ϕ_V and ϕ_C given respectively in $cm^3\ mol^{-1}$ and $J\ K^{-1}\ mol^{-1}$

Electrolyte	ϕ_V^0	B_V	B_V'	ϕ_C^0	B_C	B_C'
Na_2SO_4	11.76	2.70	2.75	−187.0	126.1	128.2
K_2SO_4	32.00			−246.9	54.7	57.4
$NaHCO_3$	23.45	1.32	1.38	−5.1	(34.0)	35.3
Na_2CO_3*	−6.13	1.77	1.79	−176.3	100.9	63.7
NaOH	−5.20	1.12	1.11	−93.2	26.5	26.4

*To extend the data up to 1 *m* an extra parameter in $c^{3/2}$ (−44.4) or $m^{3/2}$ (−11.2) is required for ϕ_C.

and co-worker (15). We have no reasons to believe that the present measurements are less reliable than the others. At any rate, the agreement is still sufficiently good that we would not expect an error much larger than 1 $J\ k^{-1}\ mol^{-1}$ in ϕ_C resulting from errors in densities and concentrations.

The agreement of the present heat capacity data with those of the literature is less satisfactory. With the exception of NaOH, where the agreement is excellent, differences of 5 to 10 $J\ K^{-1}\ mol^{-1}$ are observed with the ϕ_C of Randall and Rossini (16), Gucker and Schminke (17), and Gardner *et al.* (18). The generally good agreement between the present result and literature in the case of volumes and the proven reliability of the flow technique for heat capacity measurements (6) gives us confidence that the present data are the more accurate.

The $MgSO_4$ shows a strong departure from linearity at low concentration with both the ϕ_V and ϕ_C data. The infinite dilution ϕ_V^0 and ϕ_C^0 can be calculated from the data for $MgCl_2$ (19) and Na_2SO_4, using the additivity rule. The predicted ϕ_V^0 and ϕ_C^0 are thus $-7.46\ cm^3\ mol^{-1}$ and $-286.4\ J\ K^{-1}\ mol^{-1}$ suggesting significant association of this electrolyte in water. Since the association constant of this electrolyte is known (20), it is possible to apply to heat capacities the same treatment that was used by Millero and Masterton (15) to calculate the volume and by Leung and Millero (21) to calculate the enthalpy of an ion pair. The observed ϕ_C can be related to those of the ion pair $MgSO_4^0$ and of the free ions (Mg^{2+}, SO_4^{2-}) by the relation

$$[6]\quad \phi_C(\text{obs}) = (1-\alpha)\phi_C(MgSO_4^0) + \alpha\phi_C(Mg^{2+},SO_4^{2-})$$

where α is the fraction of free ions. The degree of association $1-\alpha$ is given by

$$[7]\quad 1-\alpha = K_a(\gamma\pm)^2 m$$

where K_a is the association constant and $\gamma\pm$ the mean activity coefficient of the electrolyte, and has been calculated by Millero and Masterton (15) for $MgSO_4$ in water at 25 °C.

The values of $\phi_C(Mg^{2+}, SO_4^{2-})$ can be calculated assuming additivity of ϕ_C at all concentrations. This is of course only an approximation since the concentration dependence of ϕ_C depends on *all* ion–ion interactions, but it becomes exact as the concentration tends to zero. From

$$[8]\quad \phi_C(Mg^{2+},SO_4^{2-}) = \phi_C(MgCl_2) + \phi_C(Na_2SO_4) - 2\phi_C(NaCl)$$

where each ϕ_C is assumed to be given by eq. 4, an approximate expression for the concentration dependence of $\phi_C(Mg^{2+},SO_4^{2-})$ can be predicted

$$[9]\quad \phi_C(Mg^{2+},SO_4^{2-}) = -286.4 + 243.2m^{1/2} - 68.2m$$

The value of $\phi_C(Mg^{2+},SO_4^{2-})$ cannot be calculated from the potassium salts since K_2SO_4 also shows signs of association.

The method developed by Leung and Millero (21) can be used to evaluate $\Delta\bar{C}_p^0(MgSO_4^0)$, the standard change in heat capacity for the formation of an ion pair. By using the relative apparent molal heat capacity, $\phi_J = \phi_C - \phi_C^0$, eq. 6 can be rearranged to

$$[10]\quad \phi_J(\text{obs}) = \alpha\phi_J(Mg^{2+},SO_4^{2-}) + (1-\alpha) \times [\phi_J(MgSO_4^0) + \phi_C^0(MgSO_4^0) - \phi_C^0(Mg^{2+},SO_4^{2-})]$$

and since

$$[11]\quad \Delta\bar{C}_p^0(MgSO_4^0) = \Delta\phi_C^0(MgSO_4^0) = \phi_C^0(MgSO_4^0) - \phi_C^0(Mg^{2+},SO_4^{2-})$$

eq. 10 becomes

$$[12]\quad \phi_J(\text{obs}) = \alpha\phi_J(Mg^{2+},SO_4^{2-}) + (1-\alpha) \times [\phi_J(MgSO_4^0) + \Delta\bar{C}_p^0(MgSO_4^0)]$$

Can. J. Chem. Downloaded from www.nrcresearchpress.com by 210.87.254.42 on 09/05/12
For personal use only.

Can. J. Chem. Downloaded from www.nrcresearchpress.com by 210.87.254.42 on 09/05/12
For personal use only.

By assuming ϕ_J for $MgSO_4^0$ is a linear function of the concentration of the ion pair $(1 - \alpha)m_T$, this equation upon rearrangement can be simplified to

$$[13] \quad [\phi_J(\text{obs}) - \alpha\phi_J(Mg^{2+},SO_4^{2-})]/(1 - \alpha) = \Delta\bar{C}_p^0(MgSO_4^0) + k(1 - \alpha)m_T$$

A plot of the left-hand side of eq. 13 against $(1 - \alpha)m$ is shown in Fig. 3. As is quite apparent from Fig. 3 ϕ_J of $MgSO_4^0$ is not linear. By using a second degree fit, a value of $\Delta\bar{C}_p^0 = 84.9$ J K^{-1} mol^{-1} is obtained for the formation of $MgSO_4^0$.

Not too much importance should be placed on the shape of $\phi_J(MgSO_4^0)$ because of the approximations made in estimating $\phi_J(Mg^{2+}, SO_4^{2-})$. The order of magnitude of the $\bar{C}_p^0(MgSO_4^0)$ (-200 J K^{-1} mol^{-1}) when compared with the heat capacity of solid $MgSO_4$ (96 J K^{-1} mol^{-1}) (22) and $\bar{C}_p^0(Mg^{2+},SO_4^{2-})$ (-286.4 J K^{-1} mol^{-1}) indicates that the ion pair still has about 80% of its hydration contribution remaining. This would suggest that these ion pairs still strongly interact with water, in agreement with volume and compressibility measurements (15, 23).

The large increase in ϕ_C of Na_2CO_3 in pure water was intriguing since no such behavior was observed with ϕ_V. The measurements were therefore repeated in 0.005 *m* NaOH instead of pure water. The ϕ_C data at low concentrations were substantially lowered while the ϕ_V data were unaffected (see Figs. 1 and 2). A few measurements in 0.01 *m* NaOH suppressed the anomally completely. This therefore suggests that the anomalously high values for ϕ_C of Na_2CO_3 were due to hydrolysis and that an estimate of the true ϕ_C^0 could be obtained by extrapolating the high concentration data (Table 1).

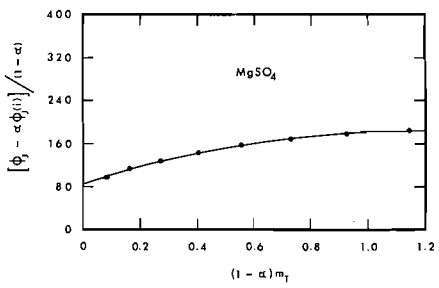

FIG. 3. Heat capacity of the formation of the ion pair $MgSO_4^0$ in water at 25 °C.

A correction can in principle be made to the data since the hydrolysis constant of Na_2CO_3 is known. If the treatment of Monk (24) is applied to ϕ_V and ϕ_C neglecting the influence of CO_2 in water, then

$$[14] \quad m\phi_C(\text{obs}) = (m - x)\phi_C(NaCO_3) + x\{\phi_C(NaOH) + \phi_C(NaHCO_3)\}$$

$$[15] \quad m\phi_V(\text{obs}) = (m - x)\phi_V(NaCO_3) + x\{\phi_V(NaOH) + \phi_V(NaHCO_3)\}$$

where x, the concentration of the carbonate that has hydrolyzed, has been estimated by Monk. Such a treatment indicates that hydrolysis should have only a small effect on ϕ_C but a large one on ϕ_V, which is the opposite of what we have observed.

The effect of CO_2 on the density and specific heat of water was investigated. The density of a saturated solution of CO_2 hardly changes from that of pure water while a significant change in specific heat is observed ($\sigma - \sigma_0 \simeq 0.0012$ J K^{-1} cm^{-3}). If σ of water saturated with CO_2 was used instead of that of pure water to calculate ϕ_C of Na_2CO_3, then most of the anomalies which we attributed to hydrolysis tended to disappear. However, deionized water was used as a reference and not water equilibrated with CO_2 in the actual experiments. This CO_2 might come from the neutralization of some of the CO_3^{2-} ions by the slight acidity of the water used (p*H* 5 to 6) (25). In a basic solution no such equilibrium would be possible which would explain the suppression of the anomaly with NaOH.

J.E.D. wishes to acknowledge Environment Canada and F.J.M. the Office of Naval Research (N00014-67-A-0201-0013) and the Oceanographic Section of the National Science Foundation (GA-17386 and GA-40532) for their support.

1. F. J. MILLERO. *In* The sea, Vol. 5. *Edited by* E. D. Goldberg. Wiley, New York. 1974.
2. J.-L. FORTIER and J. E. DESNOYERS. To be published.
3. J. E. DESNOYERS and P. R. PHILIP. Can. J. Chem. **50**, 1094 (1972).
4. P. PICKER, P.-A. LEDUC, P. R. PHILIP, and J. E. DESNOYERS. J. Chem. Thermodyn. **3**, 631 (1971).
5. P. PICKER, E. TREMBLAY, and C. JOLICOEUR. J. Solution Chem. **3**, 377 (1974).
6. J.-L. FORTIER, P.-A. LEDUC, and J. E. DESNOYERS. J. Solution Chem. **3**, 323 (1974).
7. G. S. KELL. J. Chem. Eng. Data, **12**, 66 (1967).
8. H. F. STIMSON. Am. J. Phys. **23**, 614 (1955).
9. O. REDLICH. Naturwissenchaften, **19**, 251 (1930); O. REDLICH and D. M. MEYER. Chem. Rev. **64**, 221 (1964).

10. F. J. MILLERO. Water and aqueous solutions. *Edited by* R. A. Horne. Wiley, New York. 1972. Chapt. 13.
11. L. A. DUNN. Trans. Faraday Soc. **62**, 2348 (1966).
12. H. E. WIRTH. J. Am. Chem. Soc. **59**, 2549 (1937).
13. F. J. MILLERO, E. V. HOFF, and L. KAHN. J. Solution Chem. **1**, 309 (1972).
14. L. G. HEPLER, J. M. STOKES, and R. H. STOKES. Trans. Faraday Soc. **61**, 20 (1965).
15. F. J. MILLERO and W. L. MASTERTON. J. Phys. Chem. **78**, 1287 (1974).
16. M. RANDALL and F. D. ROSSINI. J. Am. Chem. Soc. **51**, 323 (1929).
17. F. T. GUCKER and K. H. SCHMINKE. J. Am. Chem. Soc. **51**, 731 (1929).
18. N. L. GARDNER, R. E. MITCHELL, and J. W. COBBLE. J. Phys. Chem. **73**, 2029 (1969).
19. G. PERRON, J. E. DESNOYERS, and F. J. MILLERO. Can. J. Chem. **52**, 3738 (1974).
20. U. S. K. NAIR and G. N. NANCOLLAS. J. Chem. Soc. 3706 (1958).
21. W. F. LEUNG and F. J. MILLERO. J. Solution Chem. In press.
22. P. PASCAL. Nouveau traité de chimie minérale, Tome IV. Masson, Paris. p. 191. 1958.
23. F. J. MILLERO, G. K. WARD, F. K. LEPPLE, and E. V. HOFF. J. Phys. Chem. **78**, 1636 (1974).
24. C. B. MONK. J. Chem. Soc. 429 (1949).
25. W. STUMM and J'J. MORGAN. Aquatic chemistry. Wiley, New York. 1970. Chapt. 4.

Can. J. Chem. Downloaded from www.nrcresearchpress.com by 210.87.254.42 on 09/05/12
For personal use only.

The Crystal Structure of the [Pt(diethylenetriamine)Br]Br Complex

ROBERT MELANSON, JOSEPH HUBERT, AND F. D. ROCHON

Département de chimie, Université du Québec à Montréal, C.P. 8888, Montréal, Québec H3C 3P8

Received November 11, 1974

ROBERT MELANSON, JOSEPH HUBERT, and F. D. ROCHON. Can. J. Chem. **53**, 1139 (1975).

The molecular and crystal structure of the [Pt(dien)Br]Br complex (dien = diethylenetriamine) has been studied by X-ray diffraction. The compound belongs to the orthorhombic $Pca2_1$ space group and the cell parameters are: $a = 14.211$, $b = 4.940$, $c = 13.450$ Å, and $Z = 4$. The refinement of the positional and anisotropic thermal parameters, carried out by full matrix least squares calculations, converged to $R = 0.039$ and $R_w = 0.036$.

The coordination around the platinum atom is planar. The crystal consists of alternate layers of $[Pt(dien)Br]^+$ cations and Br^- ions parallel to the *ac* plane.

ROBERT MELANSON, JOSEPH HUBERT et F. D. ROCHON. Can. J. Chem. **53**, 1139 (1975).

La structure moléculaire et cristalline du complexe [Pt(dien)Br]Br (dien = diéthylènetriamine) a été étudiée par diffraction des rayons-X. Le composé cristallise dans le système orthorhombique et le groupe spatial $Pca2_1$. Ses paramètres de maille sont: $a = 14.211$, $b = 4.940$, $c = 13.450$ Å et $Z = 4$. Les coordonnées et les facteurs thermiques anisotropes ont été affinés par la méthode des moindres carrés à matrice entière jusqu'à $R = 0.039$ et $R_w = 0.036$.

La coordination autour de l'atome de platine est plane. Le cristal est formé de couches de cations $[Pt(dien)Br]^+$ et d'anions Br^- alternées, parallèles au plan *ac*.

Introduction

Kinetic studies by Basolo, Gray, and Pearson (1) on the replacement of a ligand X in complexes of the type $[Pt(diethylenetriamine)X]^+$ and $[Pt(tripyridine)X]^+$ by pyridine in aqueous solution, have shown that the $[Pt(tripy)X]^+$ complexes (tripy = tripyridine) react 1000 to 10 000 times faster than the corresponding $[Pt(dien)X]^+$ complexes (dien = diethylenetriamine). This result was somewhat surprising since $[Pt(bipy)Cl_2]$ (bipy = bipyridine) and $[Pt(en)Cl_2]$ (en = ethylenediamine) do not differ appreciably in their reactivity. The authors explained the results of their kinetic studies by the fact that the two types of complexes $[Pt(dien)X]^+$ and $[Pt(tripy)X]^+$ would have square planar structures, but the latter would be very strained. This strain would cause the complexes $[Pt(tripy)X]^+$ to be unstable and explain their high reactivity.

The crystal structures of several complexes of the types $[M(dien)X_3]$ (2, 3) and $[M(dien)_2]^{2+ \text{ or } 3+}$ (4–7) have been determined. All the complexes possess distorted octahedral geometry. The two terminal nitrogen atoms in the diethylenetriamine ligand are coordinated either *cis* or *trans* to each other. Therefore the tridentate ligand can have a planar or a bent conformation.

The crystal structure of a compound from each type of complexes [Pt(dien)X]X and [Pt(tripy)X]X was studied in our laboratory. In this paper, we report our results on the crystal structure of [Pt(dien)Br]Br.

Experimental Section

Crystal Data

$PtBr_2C_4H_{13}N_3$ f.w. = 458.08

Orthorhombic $Pca2_1$, $a = 14.211(7)$, $b = 4.940(3)$, $c = 13.450(8)$ Å, $Z = 4$, $V = 944.3(1.35)$ Å^3, $\rho_o = 3.17(5)$ g/cm^3 (flotation), $\rho_c = 3.221$ g/cm^3, λMoKα = 0.71069 Å, μMoKα = 240.57 cm^{-1}, $T = 22$ °C.

The compound [Pt(dien)Br]Br was prepared as previously described (8) and recrystallized as plates from water. The pale yellow crystals are stable to air and to X-rays. A set of precession photographs indicated that the $h0l$, $h = 2n + 1$ and $0kl$, $l = 2n + 1$ reflections are systematic absences. These extinctions are found for space groups $Pca2_1$ (no. 29) and *Pacm* (no. 57) (non-standard setting for *Pbcm*). The cell parameters were calculated by least squares refinement from the setting angles of 15 automatically centered reflections (MoKα radiation) on a Syntex P$\bar{1}$ diffractometer equipped with a graphite monochromator.

Collection and Reduction of Intensity Data

The intensity data were collected from a crystal of dimensions 0.646 × 0.093 × 0.268 mm. A total of 1647 independent reflections were measured in the region of $2\theta < 60°$ by the $2\theta/\theta$ scan technique using MoKα radiation. The data collection was done at a variable speed (24° to 1°/min) depending on the intensity of the reflection (Syntex $2\theta/\theta$ autocollection program). The

Can. J. Chem. Downloaded from www.nrcresearchpress.com by 210.87.254.105 on 09/05/12
For personal use only.

Can. J. Chem. Downloaded from www.nrcresearchpress.com by 210.87.254.105 on 09/05/12
For personal use only.

TABLE 1. Final structure parameters* and estimated standard deviations† ($\times 10^4$)

Atom	x	y	z	β_{11}	β_{22}	β_{33}	β_{12}	β_{13}	β_{23}
Pt	1801.6(4)	1968.7(11)	2500	19.5(2)	168.0(17)	29.8(3)	1.3(7)	−0.8(4)	1.2(16)
Br_1	2931(1)	4837(5)	3362(2)	35(1)	356(9)	47(1)	−33(2)	−2(1)	−20(2)
Br_2	−806(1)	3413(4)	506(2)	31.5(1)	249(7)	39(1)	−9(2)	5(1)	5(2)
N_1	2571(13)	1491(32)	1305(12)	48(9)	234(70)	29(8)	2(21)	6(7)	41(20)
N_2	811(10)	−157(32)	1817(11)	29(7)	170(53)	37(8)	9(17)	−12(6)	26(20)
N_3	875(13)	1664(36)	3733(12)	49(8)	241(70)	35(9)	−36(22)	10(7)	3(23)
C_1	1952(13)	269(52)	550(16)	34(10)	473(112)	44(12)	−45(26)	0(9)	12(30)
C_2	1310(14)	−1856(49)	1033(16)	34(9)	340(85)	56(13)	−41(28)	11(9)	0(35)
C_3	227(10)	−1583(25)	2534(22)	34(7)	119(53)	35(7)	−20(14)	−9(13)	18(44)
C_4	1(12)	335(45)	3361(17)	22(7)	371(95)	47(11)	2(21)	12(8)	9(29)

*The anisotropic thermal parameters are in the form exp $(-h^2\beta_{11} - k^2\beta_{22} - l^2\beta_{33} - 2hk\beta_{12} - 2hl\beta_{13} - 2kl\beta_{23})$.
†Standard deviations are given in parenthesis.

Can. J. Chem. Downloaded from www.nrcresearchpress.com by 210.87.254.105 on 09/05/12
For personal use only.

majority of the reflections were measured at a speed of 1°/min. A 2θ scan range of 1.2° below $K\alpha_1$ and 1.2° over $K\alpha_1$ was selected. The background time to scan time ratio was 0.40. During the data collection, two standard reflections (4,2,−1 and 2,1,−2) were measured after every 25 reflections. Their variations were less than 2% from their respective means. The 1647 independent measurements reduced to a set of 1435 independent reflections after taking out the systematically absent reflections. The 307 reflections for which the intensity was less than 2.5 $\sigma(I)$ were considered as unobserved. The standard deviation $\sigma(I)$ was calculated in the following manner:

$$\sigma^2(I) = \frac{1}{\tau}\left\{\left(T + \frac{B}{(\mathrm{BSR})^2}\right) *\mathrm{SCRT}^2 + (p*N)^2\right\}$$

where τ = transmission coefficient, T = total count, B = total background count, N = net count, BSR = background to scan time ratio, SCRT = scan rate, $p = 0.04$ long term instability constant. Finally, 1128 independent observed reflections remained. An absorption correction based on the equations of the crystal faces was then applied. The transmission factors varied from 0.0205 to 0.1321. The data were finally corrected for the Lorentz and polarization effects.

The scattering factors for platinum, bromine, carbon, and nitrogen were those of Cromer and Waber (9) and those of Stewart, Davidson, and Simpson were used for hydrogen (10). The anomalous dispersion terms of platinum ($\Delta f' = -2.05$, $\Delta f'' = 8.43$) and bromine ($\Delta f' = -0.21$, $\Delta f'' = 2.68$) (11) were included in the calculation.

Structure Determination

The $N(Z)$ test and the distribution of the normalized structure factors $|E|$ values suggested the space group $Pca2_1$ (12). The platinum atom was easily located from the three-dimensional Patterson map. The positions of all other atoms except the hydrogen atoms, were obtained by structure factor and Fourier map calculations. The refinement of the parameters was carried out by full matrix least squares calculations. In the early stages of refinement, unit weight was assigned to all observed reflections. Individual weights w according to the equation $1/w = a + bF_o + cF_o^2$ were calculated. a, b, and c were adjusted to make the distribution of $w|\Delta F|^2$ constant with respect to $|F_o|$ and $\sin\theta/\lambda$ ($a = 263$, $b = -2$, and $c = 0.005$). An isotropic secondary extinction correction (13) was also introduced. The hydrogen atoms of the methylene groups were fixed at the calculated positions, while those on the nitrogen atoms were neglected. The refinement of the scale factor, the coordinates and anisotropic temperature factors of all nonhydrogen atoms converged to $R = \Sigma(|F_o| - |F_c|)/\Sigma|F_o|$ of 0.039 and a weighted residual $R_w = [\Sigma w(|F_o| - |F_c|)^2/\Sigma w|F_o|^2]^{1/2}$ of 0.036. The standard deviation of an observation of unit weight is 1.147. The final difference Fourier map using all observed reflections did not show peaks higher than ± 1 e/Å^3.[1] The refined parameters are given in Table 1.

[1]The structure factor table is available, for a nominal charge, from the Depository of Unpublished Data, CISTI, National Research Council of Canada, Ottawa, Canada K1A 0S2.

The calculations were performed with a CDC 6400 computer. The following programs were used: NRC crystallographic programs (14), NUCLS a modified version of ORFLS, and Zalkin (FORDAP).

Results and Discussion

The structure consists of an arrangement of the complex cation $[Pt(dien)Br]^+$ and of Br^-. The atoms were labelled according to Fig. 1.

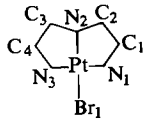

FIG. 1. Atom identification in complex cation $[Pt(dien)Br]^+$.

Structure of the Cation

A stereoscopic view of the $[Pt(dien)Br]^+$ is shown in Fig. 2. The most important bond distances and angles are listed in Table 2. Three nitrogen and one bromine atoms form the square planar coordination expected for Pt(II) complexes. The weighted best plane was calculated through the platinum, the bromine, and the three nitrogen atoms. The deviations from this plane are: Pt, 0.0000; Br_1, 0.002; N_1, −0.112; N_2, 0.120; and N_3, −0.119 Å. The angles around platinum are close to the expected 90 and 180° but there seems to be some slight deviations. The N_1—Pt—N_2 and N_2—Pt—N_3 angles (87.3, 83.4°) are smaller than the N_1—Pt—Br_1 and N_3—Pt—Br_1 angles (95.3, 94.5°). A slight strain caused by the tridentate ligand might be responsible for this deviation from the ideal square planar coordination. The Pt—Br_1 bond (2.434 Å) is of normal length (15). The Pt—N bond lengths are normal (16–19) and one Pt—N_3 bond (2.12 Å) appears significantly longer than the two other Pt—N bonds (1.98 and 1.96 Å). Values of 1.95 to 2.31 Å have been reported for Pt—N bonds.

The complex cation $[Pt(dien)Br]^+$ approxi-

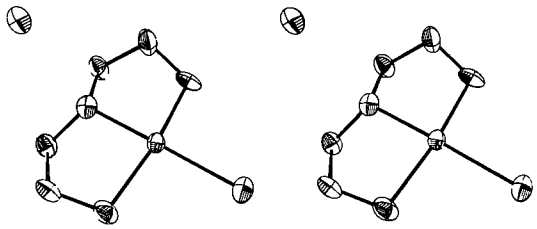

FIG. 2. Stereoscopic view of $[Pt(dien)Br]^+Br^-$.

Can. J. Chem. Downloaded from www.nrcresearchpress.com by 210.87.254.105 on 09/05/12
For personal use only.

TABLE 2. Bond distances and bond angles in the $[Pt(dien)Br]^+$ ion

Bond	Distance (Å)	Bonds	Angle (deg)
$Pt—Br_1$	2.434(2)	$Br_1—Pt—N_1$	95.3(5)
$Pt—N_1$	1.958(17)	$Br_1—Pt—N_2$	175.8(5)
$Pt—N_2$	1.982(15)	$Br_1—Pt—N_3$	94.5(5)
$Pt—N_3$	2.123(17)	$N_1—Pt—N_2$	87.3(7)
$N_1—C_1$	1.47(3)	$N_2—Pt—N_3$	83.4(7)
$N_2—C_2$	1.52(3)	$N_1—Pt—N_3$	168.2(7)
$N_2—C_3$	1.45(3)	$Pt—N_1—C_1$	106.4(13)
$N_3—C_4$	1.49(3)	$Pt—N_2—C_2$	106.4(12)
$C_1—C_2$	1.53(3)	$Pt—N_2—C_3$	110.8(12)
$C_3—C_4$	1.50(3)	$Pt—N_3—C_4$	106.6(12)
		$C_3—N_2—C_2$	117.3(15)
		$N_1—C_1—C_2$	110.0(17)
		$N_2—C_2—C_1$	101.3(16)
		$N_2—C_3—C_4$	108.0(16)
		$N_3—C_4—C_3$	110.4(17)

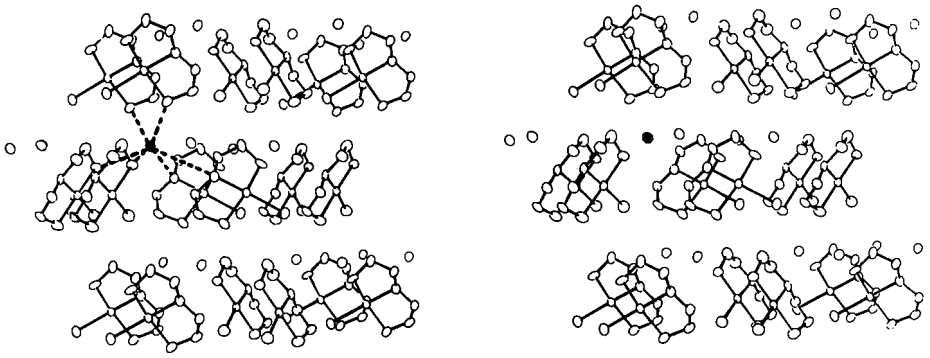

FIG. 3. Packing in the [Pt(dien)Br]Br crystal.

TABLE 3. The Br_2–N distances and related angles

Atoms	Distances (Å)	Atoms	Angle (deg)
$Br_2–N_1$*	3.514(17)	$Br_2–N_1$*–C_1*	84.2(11)
$Br_2–N_1$†	3.580(17)	$Br_2–N_1$†–C_1†	117.8(12)
$Br_2–N_2$	3.391(15)	$Br_2–N_2–C_2$	104.0(11)
$Br_2–N_3$‡	3.461(17)	$Br_2–N_2–C_3$	102.1(11)
$Br_2–N_3$§	3.407(17)	$Br_2–N_3$‡–C_4‡	83.6(11)
$Br_2–N_2$‖	4.299(17)	$Br_2–N_3$‖–C_4‖	121.7(12)

NOTE: Coordinates x, y, z except:
*$x - \frac{1}{2}, -y, z$.
†$x - \frac{1}{2}, 1 - y, z$.
‡$-x, -y, z - \frac{1}{2}$.
§$-x, 1 - y, z - \frac{1}{2}$.
‖$x, 1 + y, z$.

mates a C_s point group symmetry with a mirror plane through N_2, Pt, and Br_1 atoms.

Packing in the Crystal

Figure 3 illustrates the packing in the [Pr(dien)Br]Br crystal. The latter consists of alternate layers of $[Pt(dien)Br]^+$ cations and Br^- ions parallel to the *ac* plane.

The environment of the bromine atoms was examined to locate possible hydrogen bonding to the nitrogen atoms. Only the ionic bromide ion seems to be involved in the hydrogen bonding. Br–N distances within a range of 3.3 to 3.6 Å have been suggested for hydrogen bonding of this type (20). Five nitrogen atoms at distances smaller than 3.6 Å from the bromide

ion form a distorted pyramid. A sixth nitrogen atom N_2 located at 4.29 Å completes a trigonal antiprism geometry around Br_2 (Fig. 3). These Br_2–N contacts and the related angles are shown in Table 3. No nitrogen atoms are in the close environment (< 3.6 Å) of the bonded bromine atom (Br_1) except the two terminal atoms of the ligand (3.26 and 3.53 Å). The unfavorable angles C_1–N_1–Br_1 (152.4°) and C_4–N_3–Br_1 (151.8°) do not suggest any intramolecular hydrogen bonding of this type.

Grateful acknowledgment is made to the National Research Council of Canada for financial support and to Dr. Pi-Chang Kong for the synthesis of the analyzed compound.

1. F. Basolo, H. B. Gray, and R. G. Pearson. J. Am. Chem. Soc. **82**, 4200 (1960).
2. F. A. Cotton and R. C. Elder. Inorg. Chem. **3**, 397 (1964); F. A. Cotton and R. M. Wing. Inorg. Chem. **3**, 314 (1965); F. A. Cotton and D. C. Richardson. Inorg. Chem. **5**, 1851 (1966).
3. Yoshihiko Kushi, Kimio Watanabe, and Hisao Kuroya. Bull. Chem. Soc. Jap. **40**, 2985 (1967).
4. F. S. Stephens. J. Chem. Soc. 883, 2233, 2493 (1969).
5. M. Kobayashi, F. Marumo, and Y. Saito. Acta Cryst. B**28**, 470 (1972).
6. K. Zocchi, A. Albinati, and G. Tieghi. Cryst. Struct. Commun. **1**, 135 (1972).
7. M. Konno, F. Marumo, and Y. Saito. Acta Cryst. B**29**, 739 (1973).
8. F. G. Mann. J. Chem. Soc. 466 (1934).
9. D. T. Cromer and J. T. Waber. Acta Cryst. **18**, 104 (1965).
10. R. F. Stewart, E. R. Davidson, and W. T. Simpson. J. Chem. Phys. **42**, 3175 (1965).
11. D. T. Cromer. Acta Cryst. **18**, 17 (1965).
12. G. H. Stout and L. H. Jenson. X-Ray structure determination, Collier–Macmillan Canada Ltd., Toronto, Ontario. 1968. pp. 208, 320.
13. P. Coppens and W. C. Hamilton. Acta Cryst. A**26**, 71 (1970).
14. F. R. Ahmed, S. R. Hall, M. E. Pippy, and C. P. Huber. NRC Crystallographic Programs. NRC 2 and 2A Data Reduction Programs, NRC-3 Absorption Correction and NRC-12 Distances and Angles Calculations. World list of crystallographic computer programs. 2nd ed., Appendix. Utrecht, Oasthoek. p. 52.
15. G. B. Bokii and G. A. Kukina. J. Struct. Chem. **5**, 670 (1965).
16. W. E. Davies, W. Hewertson, R. H. B. Mais, P. G. Owston, and C. G. Patel. J. Chem. Soc. 1873 (1970).
17. C. Pedone and E. Benedetti. J. Organometal. Chem. **29**, 443 (1971).
18. G. Bombieri, E. Forsellini, and R. Graziani. J. Chem. Soc. Dalton, 525 (1972).
19. J. W. Carmichael, N. Chan, A. W. Cordes, C. K. Fair, and D. A. Johnson. Inorg. Chem. **11**, 1117 (1972).
20. W. C. Hamilton and J. A. Ibers. Hydrogen bonding in solids. New York, Benjamin. 1968. p. 15.

Can. J. Chem. Downloaded from www.nrcresearchpress.com by 210.87.254.105 on 09/05/12
For personal use only.

On the π-Donating Abilities of Sulfur and Oxygen. A Comparative Quantum Chemical Investigation of the Static and Dynamic Properties and Gas Phase Acidities of $\overset{+}{C}H_2OH$ and $\overset{+}{C}H_2SH$

FERNANDO BERNARDI
Istituto di Chimica Organica, Universita di Bologna, Italy
IMRE G. CSIZMADIA
Department of Chemistry, University of Toronto, Toronto, Ontario M5S 1A1
AND
H. BERNHARD SCHLEGEL[1] AND SAUL WOLFE
Department of Chemistry, Queen's University, Kingston, Ontario K7L 3N6
Received September 26, 1974

FERNANDO BERNARDI, IMRE G. CSIZMADIA, H. BERNHARD SCHLEGEL, and SAUL WOLFE. Can. J. Chem. **53**, 1144 (1975).

Nonempirical SCF-MO computations have been performed on CH_2O, CH_2S, and their protonated derivatives $\overset{+}{C}H_2OH$ and $\overset{+}{C}H_2SH$. The methylene group of CH_2O is strongly positive and that of CH_2S is slightly negative, because oxygen in CH_2O behaves towards carbon as a π-donor and σ-acceptor, but sulfur in CH_2S behaves as both a π- and σ-donor. The total π-overlap in CH_2O is greater than that in CH_2S.

The stable conformations of $\overset{+}{C}H_2OH$ and $\overset{+}{C}H_2SH$ correspond in each case to a structure in which all atoms lie in the same plane. In this conformation, both the C—O and C—S bond lengths are substantially shorter than those of methanol and methanethiol, indicative of conjugative interaction between the cationic center and the adjacent heteroatom. From the results of a Mulliken-type population analysis it is found that, relative to hydrogen, OH and SH behave towards an adjacent $\overset{+}{C}H_2$ group as electron-withdrawing and electron-releasing ligands, respectively. When $\overset{+}{C}H_2OH$ is considered to form from $\overset{+}{C}H_2$ and OH fragments, π-donation from O to C amounts to 0.38 electron, but σ-donation in the opposite direction amounts to 0.35 electron; the π-overlap population is 0.1496. A similar analysis of $\overset{+}{C}H_2SH$ reveals π- *and* σ-donation from S to C of 0.53 and 0.15 electron, respectively, and a π-overlap population of 0.1734, so that *sulfur forms a stronger π-bond to the adjacent cationic center.*

Geometrical isomerization of $\overset{+}{C}H_2OH$ proceeds by linear inversion at oxygen, with a barrier of 13.98 kcal/mol; but that of $\overset{+}{C}H_2SH$ proceeds by rotation about the C—S bond, with a barrier of 36.47 kcal/mol. This latter value is substantially higher than that (23 kcal/mol) computed for $\overset{+}{C}H_2OH$ with a rigid rotor model, and reflects the greater strength of the π-bond between sulfur and the adjacent cationic center.

FERNANDO BERNARDI, IMRE G. CSIZMADIA, H. BERNHARD SCHLEGEL et SAUL WOLFE. Can. J. Chem. **53**, 1144 (1975).

On a effectué des calculs non-empiriques SCF-MO sur le CH_2O, le CH_2S et leurs dérivés protonés $\overset{+}{C}H_2OH$ et $\overset{+}{C}H_2SH$. Le groupe méthylène du CH_2O est fortement positif et celui du CH_2S est faiblement négatif; ces résultats proviennent du fait que l'oxygène dans le CH_2O agit vis-à-vis le carbone comme un donneur d'électrons π et un accepteur d'électrons σ mais que le soufre du CH_2S agit comme donneur d'électrons π et d'électrons σ. Le recouvrement total d'orbitales π dans le CH_2O est plus grand que dans le CH_2S.

Les conformations stables de $\overset{+}{C}H_2OH$ et $\overset{+}{C}H_2SH$ correspondent dans chaque cas à une structure dans laquelle tous les atomes sont dans le même plan. Dans cette conformation, les longueurs de liaison C—O et C—S sont passablement plus courtes que les liaisons correspondantes du méthanol et du méthanethiol indiquant une interaction conjugative entre le centre cationique et l'hétéroatome adjacent. On trouve, à partir des résultats d'une analyse de population du type Mulliken, que par rapport à l'hydrogène, les groupes OH et SH agissent respectivement vis-à-vis un groupe $\overset{+}{C}H_2$ adjacent comme des groupes électro-affinitaires et électro-répulsifs. Lorsque l'on

[1]Holder of a National Research Council of Canada 1967 Science Scholarship.

Can. J. Chem. Downloaded from www.nrcresearchpress.com by 210.87.254.5 on 09/05/12
For personal use only.

considère que $\overset{+}{C}H_2OH$ se forme à partir de fragments $\overset{+}{C}H_2$ et OH, on calcule qu'il y a eu don d'électrons π de l'oxygène au carbone de 0.38 électrons mais un don d'électrons σ dans la direction opposée correspondant à 0.35 électrons; la population de recouvrement d'électrons π est de 0.1496. Une analyse similaire de $\overset{+}{C}H_2SH$ révèle qu'il y a des dons d'électrons π et σ du S vers le carbone qui équivalent respectivement à 0.53 et 0.15 électrons et que la population de recouvrement d'électrons π est de 0.1734 *ce qui implique que le soufre forme un lien π plus fort avec le centre cationique adjacent.*

L'isomérisation géométrique de $\overset{+}{C}H_2OH$ se produit par une inversion linéaire à l'oxygène avec une barrière de 13.98 kcal/mol; celle de $\overset{+}{C}H_2SH$ se produit toutefois par une rotation autour du lien C—S avec une barrière de 36.47 kcal/mol. Cette dernière valeur est considérablement plus élevée que celle (23 kcal/mol) calculée pour $\overset{+}{C}H_2OH$ avec un modèle de rotor rigide et implique une plus grande force du lien π entre le soufre et le centre cationique adjacent.

[Traduit par le journal]

Introduction

There is an extensive literature concerning the relative effects of oxygen and sulfur upon the properties of adjacent cationic, radical, and anionic centers (*e.g.* ref. 1). It seems that, in solution, it is easier to generate a carbanion (*e.g.* ref. 2) or radical (*e.g.* ref. 3) adjacent to sulfur than to oxygen, but the reverse is observed in the case of carbonium ions (ref. 4 and references cited therein). These various trends have usually been rationalized (2–4) in terms of appropriate conjugative interactions: $(p \rightarrow d)_\pi$ conjugation in the case of anions and radicals, with the ability of the heteroatom to enter into such conjugation being possible only for the second row atom (sulfur); p_π–p_π conjugation in the case of cations, with the magnitude of this interaction inversely proportional to the internuclear separation and, thus, favored for the system having the shorter bond length (oxygen).

It is noteworthy that, in all such rationalizations, it is the π-type interactions which are emphasized; the possible role of σ-interactions and steric effects is ignored. In addition, these rationalizations have tended to assume that the observed effects are caused by differences in the interactions between the carbon center and the adjacent heteroatom, and not by differential solvation effects. However, it now seems well established that solvation effects cannot be ignored, at least in some cases (2, 5). In the gas phase, where solvation effects are not present, the dissociation energies of CH bonds adjacent to oxygen and to sulfur are identical (6), indicating no difference in the ease of formation of a radical center adjacent to oxygen and to sulfur; and, on the basis of appearance potential measurements (6, 7), there also seems to be no significant difference in the ease of formation of *cationic* centers adjacent to oxygen and to sulfur.

It is inappropriate to conclude from such observations that one heteroatom "stabilizes" an adjacent reactive center better than or as well as the other, because in one case what is being observed is the breaking of a CH bond adjacent to *sulfur* to form a reactive center adjacent to *sulfur*; and in the other case, a CH bond adjacent to *oxygen* is broken to form a reactive site adjacent to *oxygen.*

There is no simple theoretical solution to this problem because, in addition to the point just raised, a theoretical treatment introduces two additional difficulties. Consider, for example, the heterolytic bond breaking or bond making process shown in reaction 1, in which the electron

[1] 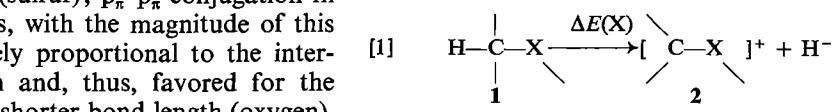

pairing scheme is formally unchanged, so that both the initial and final states have closed electron shells. The first problem is that, if we were to define stabilization energy (s.e.) in terms of the double energy difference shown in eq. 2,

$$[2] \qquad \text{s.e.} \equiv \Delta\Delta E = \Delta E(\text{S}) - \Delta E(\text{O})$$

it would be necessary to compute four different energy values. Even in the ideal situation of a reaction such as [1], only computations performed very close to the Hartree–Fock limit would allow us to hope for a minimum of two significant figure accuracy in $\Delta\Delta E$. The second problem is that, even if $\Delta\Delta E$ were considered to be reliable, it is not clear what are the relative contributions to this quantity of π-conjugative effects, σ-effects, steric effects, etc. However, what the theoretical analysis allows is a determination of the changes in bonding which take place between the heteroatom and the adjacent

Can. J. Chem. Downloaded from www.nrcresearchpress.com by 210.87.254.5 on 09/05/12
For personal use only.

Can. J. Chem. Downloaded from www.nrcresearchpress.com by 210.87.254.5 on 09/05/12
For personal use only.

carbon as a result of the chemical reaction 1 and, therefore, of the nature of the effects exerted by the heteroatoms in each case.

In previous work, we have found that a variety of the static, dynamic, and chemical properties of carbanions (8) and radicals (9) adjacent to oxygen and to sulfur are reproduced faithfully by nonempirical quantum chemical calculations, but that 3d-orbital conjugation in the case of sulfur (*i.e.*, a π-type effect) is not responsible for differences between the two systems. Rather, it is the differences in the sizes of the two heteroatoms and, therefore, differences in their electronegativities, polarizabilities, and energies of the atomic lone pair orbitals that cause these conformational and chemical differences.

The subject of the present work is a comparative quantum chemical investigation of the reaction represented by reaction 3 in which X = oxygen and sulfur. Protonated aliphatic

[3] 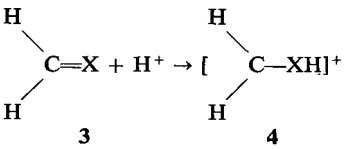

3 **4**

aldehydes, including formaldehyde (reaction 3, X = O), and protonated aliphatic ketones have been observed experimentally by Olah *et al.* (10) to display geometrical isomerism about the carbon–oxygen bond. However, the barrier to interconversion of geometrical isomers was not determined by these workers, and experimental data concerning the protonation of thioaldehydes and thioketones (reaction 3, X = S) have not yet been reported.

If the magnitude of the barrier to *rotation* about the C—X bond of **4** were to constitute a rough measure of the *π-conjugative* stabilization afforded by X, then current chemical intuition would suggest that hydroxymethylcarbonium ion should have the higher rotational barrier. Therefore, a prime objective of the present work was the computation of the energetics and mechanisms of geometrical isomerization of the cations **4** (for previous investigations of $\overset{+}{C}H_2OH$ see ref. 11), and the changes in bonding that occur in the formation of these species from **3**. In disagreement with expectation, we find $\overset{+}{C}H_2SH$ to have the higher rotational barrier, *i.e.*, that the π-conjugative effects *are greater for the second row atom* than for the first row atom. In agreement with this conclusion is the finding that the computed amount of π-charge transfer from the heteroatom to the CH_2^+ center and the π-overlap populations are greater for sulfur than for oxygen.

Method

The method employed was the single-determinant LCAO-MO-SCF procedure, in which each molecular orbital ψ_i is expressed as a linear combination of a set of contracted Gaussian type functions (eq. 4).

$$[4] \qquad \psi_i = \sum_j C_{ij}\phi_j$$

A split valence shell basis set (4-31G) has been used throughout the work (12*a*, *b*). In this basis set each inner shell is represented by a four term Gaussian expansion, and the valence shell is split into three- and one-term expansions of the inner and outer parts, respectively. The molecular orbitals were determined by solution of the Roothaan–Hartree–Fock equations using the Gaussian 70 program system (12*c*) with full optimization of the geometries of each of the four species **3** (X = O, S) and **4** (X = O, S). All computations were performed on a CDC 6600 computer at the University of Bologna.

Results and Discussion

Geometry Optimization of CH_2O and CH_2S

Table 1 lists the computed optimized geometries of formaldehyde (12*a*) and thioformaldehyde, together with the experimentally determined (13) geometries of these molecules. Formaldehyde has been investigated previously by a number of workers (11*a*, 11*c*, 14, 15), but with the exception of ref. 12*a*, the objectives were different from those of the present work, and full geometry optimization was not performed. It is evident that the optimized geometries of **3** agree well with the experimental values in both cases; this provides some confidence that the basis set employed in the work can also provide accurate geometries of the species **4**, for which experimental data are not available.

Geometry Optimization of $\overset{+}{C}H_2OH$ and $\overset{+}{C}H_2SH$

The most stable conformation in each case is the fully planar structure **5**. In each case, the energy was optimized with respect to all geometrical parameters except the C—H bond length of $\overset{+}{C}H_2OH$, kept constant at the value 1.0835 Å previously computed at the minimal basis set level (16). The optimized value of the C—H bond length for $\overset{+}{C}H_2SH$ is 1.0677 Å, and this value was kept constant in all subsequent computations

TABLE 1. The theoretically optimized and experimentally determined geometries of CH_2O and CH_2S

	CH_2O		CH_2S	
	Theoretical	Experimental	Theoretical	Experimental
r(C—X)	1.21 Å	1.21 Å	1.63 Å	1.61 Å
r(C—H)	1.08 Å	1.12 Å	1.07 Å	1.09 Å
∠HCH	116.8°	116.3°	115.6°	116.8°

TABLE 2. Optimum energies (Hartree a.u.), bond lengths (Å), and bond angles (deg) for various conformations of $\overset{+}{C}H_2OH$ and $\overset{+}{C}H_2SH$

	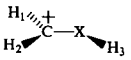		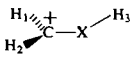		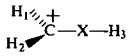	
	X = O	X = S	X = O	X = S	X = O	X = S
r(C—H)*	1.0835	1.0677				
r(C—X)	1.25	1.65	1.27	1.81	1.23	1.63
r(X—H_3)	0.96	1.36	0.96	1.37	0.96	1.35
∠H_1CH_2	122.1	117.3	122.4	117.6	122.4	120.5
∠H_2CX	122.2	119.6	—	—	—	—
∠CHX_3	124.7	100.9	124.7	96.2	180	180
E	−113.97905	−436.27448	−113.94325	−436.21639	−113.95671	−436.16782

*See text.

reported here for this species. The computed geometrical parameters of structure **5** in the two cases are summarized in Table 2. In both protonated systems

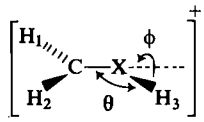

5

the C—X bonds are longer than those of the parent molecules **3** (0.04 and 0.02 Å for X = O and X = S, respectively). However, these bond lengths are substantially shorter than those of CH_3OH and CH_3SH (1.428 and 1.819 Å, respectively (17)), so that significant double bond character remains following protonation.

The H_2CX and CXH_3 bond angles (see Table 2) are of some interest, and have important consequences for the mechanisms of geometrical isomerization of the two species. Compared to CH_3OH, whose COH angle is 105.9° (17), $\overset{+}{C}H_2OH$ has a COH angle of 124.76°. In contrast, the CSH angle of $\overset{+}{C}H_2SH$ is only 4.4° larger than that of CH_3SH (17). We suggest that the origin of this large COH bond angle is the small (2.07 Å) internuclear separation that would otherwise have been present between H_2 and H_3. The movement of these nuclei away from each other leads to an opening not only of the COH angle but also of the H_2CO angle which is now greater than 120°. The H_2CS angle in $\overset{+}{C}H_2SH$ is less than 120°.

Geometrical Isomerization of $\overset{+}{C}H_2OH$ and $\overset{+}{C}H_2SH$ SCF Computations

As pointed out by others (11*a*, *b*), two mechanisms are possible for the geometrical isomerization of a species such as **4**. In the first, the transition state has the structure **6**, and the process may be termed "linear inversion" (18). In the second, the transition state has the structure **7**, and the process is one of torsion along the C—X bond.

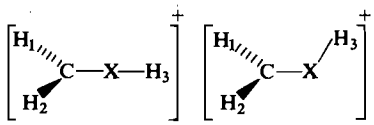

6 **7**

Linear inversion in $\overset{+}{C}H_2OH$ was studied by computation of the total energy as a function of θ = ∠COH; at θ = 124.76° (the energy minimum) and θ = 180° (the transition state) the geometry was optimized with respect to the CO

Can. J. Chem. Downloaded from www.nrcresearchpress.com by 210.87.254.5 on 09/05/12
For personal use only.

Can. J. Chem. Downloaded from www.nrcresearchpress.com by 210.87.254.5 on 09/05/12
For personal use only.

and OH bond lengths and the HCH angle. The results of these calculations are found in the first and fifth columns of Table 2, and they give a value of the barrier to linear inversion of 13.98 kcal/mol. Linear inversion in $\overset{+}{C}H_2SH$ was studied in the same way, and the results for $\theta = 100.9°$ (the energy minimum) and $\theta = 180°$ (the transition state) are collected in the second and sixth columns of Table 2. The barrier to linear inversion in this case is 66.95 kcal/mol. It will be noted that, in both cations, the optimized CX bond length in the transition state for linear inversion is slightly shorter than that of CH_2X.

The barriers to linear inversion in H_2O and H_2S are 26.4 and 37.0 kcal/mol, respectively (19). The simplest interpretation of this difference is that the bond angle of H_2O changes from 105 to 180° but that of H_2S changes from 96.4 to 180°. On this basis, the substantial decrease in the barrier to linear inversion at oxygen on going from H_2O to $\overset{+}{C}H_2OH$ is a direct consequence of the geometry relaxation in the ground state of the latter species, already discussed.

We were unable to compute an accurate value for the rotational barrier of $\overset{+}{C}H_2OH$. Optimization of the molecular geometry as a function of the dihedral angle ϕ between the HCH and COH planes led to a COH angle of 180° for $\phi = 90°$. This means that the rotation is disfavored with respect to linear inversion. An approximate value of the rotational barrier of 23 kcal/mol was obtained (*cf.* Table 2, columns one and three) by maintaining the COH angle at 124.76°, the same value as in the planar conformation. Our results parallel those of Ros (11*a*), in whose study of $\overset{+}{C}H_2OH$ rotation was found to be disfavored with respect to linear inversion with a rigid rotor model, and those of Lehn *et al.* (11*b*), who found linear inversion to be the favored process in $CH_2{=}NH$ and $CH_2{=}CH^-$.

In contrast, rotation is the favored process in $\overset{+}{C}H_2SH$. Table 2, column 4 lists the optimized geometry and energy of the transition state (7) for this process, from which the barrier is computed to be 36.47 kcal/mol. Two features of the geometry of this transition state are of interest: the C—S bond length is now 1.81 Å indicating that conjugation between carbon and sulfur has been completely destroyed; and the angle between the HCH plane and the CS bond is not zero, so that attachment of a nonconjugating SH ligand to the carbonium ion makes this center

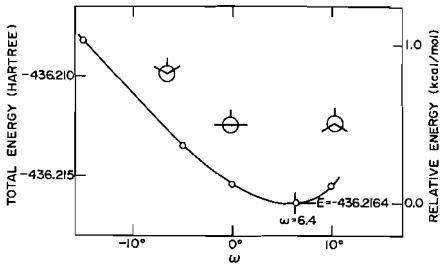

FIG. 1. The total energy of **7** (X = S) as a function of ω, the angle between the HCH plane and the C—S bond.

nonplanar. Figure 1 displays the total energy of **7** (X = S) as a function of the angle ω between the HCH plane and the CS bond, from which it is evident that, in this rotational conformation, the cation adopts the Y conformation **8**, in contrast to the corresponding anion, which adopts the W conformation **9** (8).

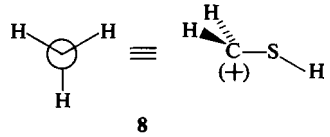

8

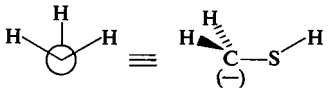

9

For the analysis of effects such as the relative stabilities of Y and W conformations, it is useful to consider the relative contributions to the total energy of nuclear and electronic effects (8, 20–22). When electronic effects dominate, the more crowded conformation (W in this case) is the more stable. On this basis, the greater stability of the W conformation in the case of the anion **9** is the result of the increased electronic interactions associated with the additional electron pair.

A Configuration Interaction Study

Closed shell restricted Hartree–Fock theory is sometimes unable to provide accurate results because of the overrestrictive nature of the wavefunction. Thus, in the computation of rotational barriers about a bond containing a significant amount of double bond character, a single determinantal approach may not be sufficient (23*a*). For example, in the computation of the rotational barrier of ethylene, unacceptably high values are obtained from a single determinantal

TABLE 3. Total energies (a.u.) computed with a single determinantal (SCF) approach and with a CI procedure for $\overset{+}{C}H_2SH$ in conformation 7 at different C—S bond lengths

Bond length (Å)	E_{SCF}	E_{CI}	CI eigenvectors
1.70	−436.21147	−436.21150	0.9999 0.86×10^{-18} -0.7476×10^{2}
1.75	−436.21499	−436.21501	0.9999 0.85×10^{-18} 0.6124×10^{-2}
1.8136	−436.21639	−436.21640	0.9999 0.81×10^{-18} -0.4755×10^{-2}

approach, but the inclusion of one additional configuration is sufficient to afford much improved results (23*b*).

Since the results just described, of rotation in $\overset{+}{C}H_2SH$, are highly significant if correct, it seemed desirable to check the role of configuration interaction. The rotational barrier was, therefore, recomputed using a limited CI procedure.[2] The configurations taken into account are the three illustrated in the following Scheme 1, where HOMO refers to the highest occupied molecular orbital, and LUMO to the lowest unoccupied molecular orbital obtained in the single determinant SCF calculation.

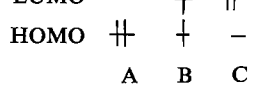

SCHEME 1

The CI energy of **7** (X = S) was computed by solving a 3 × 3 secular determinant at three C—S bond lengths: 1.6, 1.7, and 1.8136 Å, the latter corresponding to the optimized value afforded by the single determinantal approach. The results of this study are shown in Table 3. They reveal that the CI procedure does not change the energy of **7** significantly as compared to the value computed by the single determinantal approach. In addition, the eigenvectors show that the ground electronic configuration predominates. This suggests that a single configuration SCF wavefunction can be used with confidence to study rotation along a polarized bond such as C—O and C—S, even when this bond has appreciable double bond character.

[2]We thank Professor W. J. Hehre for providing us with the program.

The higher rotational barrier in $\overset{+}{C}H_2SH$ therefore seems to be real. Since as noted above, π-conjugation between carbon and sulfur is completely destroyed during rotation, we must conclude that *π-conjugation in $\overset{+}{C}H_2SH$ is greater than in $\overset{+}{C}H_2OH$*. Quantitative support for this interpretation is provided by the Mulliken-type population analysis, discussed later.

The Rotation – Linear Inversion Surfaces of $\overset{+}{C}H_2OH$ and $\overset{+}{C}H_2SH$

The dynamic properties of the two cations can be represented conveniently in the form of rotation–inversion surfaces. Equations for such surfaces were obtained by "least squares" fittings of the expression.

$$[5]\quad E = E_0 + C_1\phi^2 + C_2\phi^4 + C_3\phi^2\cos 2\theta + C_4\phi^4\cos 2\theta$$

to the SCF computed energies of a number of conformations. The inversion coordinate φ and the rotation coordinate θ are as defined previously. The energies of the conformations used in the fitting procedure are summarized in Table 4. Each of the entries in Table 4 has been fully optimized with respect to geometrical parameters other than rotation and inversion. The constants for eq. 5 are given in Table 5.

Plots of the surfaces are shown in Figs. 2 and 3. In both cations, the inversion process is energetically allowed, as indicated by paths *A* in the figures, and proceeds via the linear transition state. However, in the sulfur cation, an alternate isomerization mechanism is favored. Path *B* of Fig. 3 shows that rotation is the lower energy process. As indicated by the broken path in Fig. 2, a similar rotation in protonated formaldehyde is energetically not allowed, because any attempt to rotate H_3 about the C═O axis

Can. J. Chem. Downloaded from www.nrcresearchpress.com by 210.87.254.5 on 09/05/12
For personal use only.

TABLE 4. Data employed for the computation of the rotation – linear inversion surfaces of $\overset{+}{C}H_2OH$ and $\overset{+}{C}H_2SH$

Cation	Rotation (deg)	Inversion (deg)	Energy (a.u.)
$^+CH_2OH$	0	0	−113.956707
	0	56.46	−113.979014
	0	66.00	−113.976466
	90	32.04	−113.953336
	90	40.48	−113.950638
$^+CH_2SH$	0	0	−436.167817
	0	79.02	−436.274482
	0	82.56	−436.273962
	90	83.83	−436.216389
	90	86.83	−436.215939
	0	76.56	−436.274234

TABLE 5. Parameters of the rotation – linear inversion surfaces of CH_2OH and CH_2SH

Parameter	$\overset{+}{C}H_2OH$	$\overset{+}{C}H_2SH$
E_0	−113.956518	−436.167818
C_1	−0.021762	−0.078980
C_2	0.022422	0.020098
C_3	−0.023077	−0.032452
C_4	—	0.008962

results in a path proceeding through the linear transition state, as shown by path *B* of Fig. 2. Since the endpoints of paths *A* and *B* are identical (H_3 *anti* to H_1), these paths are indistinguishable experimentally. Hence, inversion is the only energetically allowed mechanism of geometrical isomerization in protonated formaldehyde, whereas both rotation and inversion are allowed in protonated thioformaldehyde, with rotation being the favored process.

Proton Affinities of CH_2O and CH_2S

In the quantum mechanical convention, proton affinity is defined as the difference between the energies of the protonated (MH^+) and deprotonated (M) species (eq. 6), since the energy of the proton is zero, by definition. This value is also a measure of the gas phase

$$[6] \qquad \text{p.a.(M)} = E(MH^+) - E(M)$$

basicity of the species M and the gas phase acidity of the species MH^+. The proton affinity values computed for formaldehyde and thioformaldehyde are shown in Table 6. The two values are of the same order of magnitude, with that of formaldehyde slightly greater.

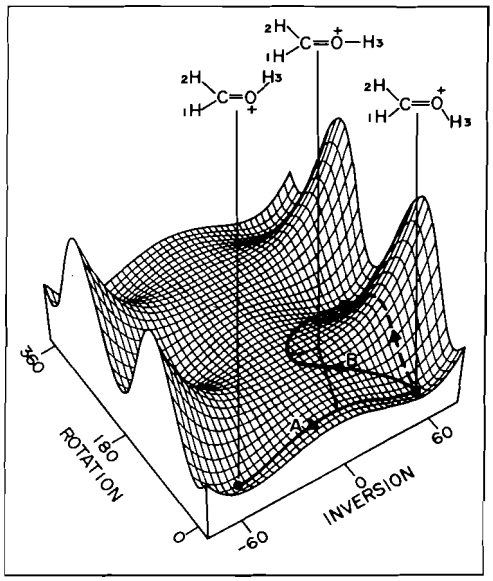

FIG. 2. The rotation – linear inversion surface of $\overset{+}{C}H_2OH$.

Mulliken Population Analyses of 3 and 4

Table 7 summarizes the net atomic charges and gross orbital populations of the valence orbitals of CH_2O and CH_2S. Table 8 lists the same data for $\overset{+}{C}H_2OH$ and $\overset{+}{C}H_2SH$.

The two parent molecules have opposite charge distributions. In formaldehyde the methylene group has a net charge of +0.51 electron, and in thioformaldehyde the net charge of this group is −0.08 electron. Alternatively, we may state that oxygen is strongly negative in formaldehyde, but sulfur is slightly positive in thioformaldehyde. Inspection of the data of

Can. J. Chem. Downloaded from www.nrcresearchpress.com by 210.87.254.5 on 09/05/12
For personal use only.

TABLE 6. Computed proton affinities (p.a.) of CH_2O and CH_2S

	Total energy (a.u.)	Proton affinity (kcal/mol)
CH_2O	−113.69252	−179.86 (−161 ± 3)*
$^+CH_2OH$	−113.97905	—
CH_2S	−435.99186	−177.4
$^+CH_2SH$	−436.27448	—

*Experimental value.

TABLE 7. Net atomic charges (q) and gross orbital populations of the valence atomic orbitals for CH_2O and CH_2S*

	CH_2O			CH_2S		
	H	C	O	H	C	S
q	+0.16	+0.17	−0.49	+0.22	−0.52	+0.08
s	0.84	1.22	1.96	0.78	1.42	1.89
p_x	—	1.10	1.90	—	1.19	1.97
p_y	—	0.73	1.27	—	0.83	1.20
p_z	—	0.79	1.36	—	1.08	0.93

*The coordinate system is 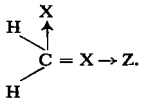 C = X → Z.

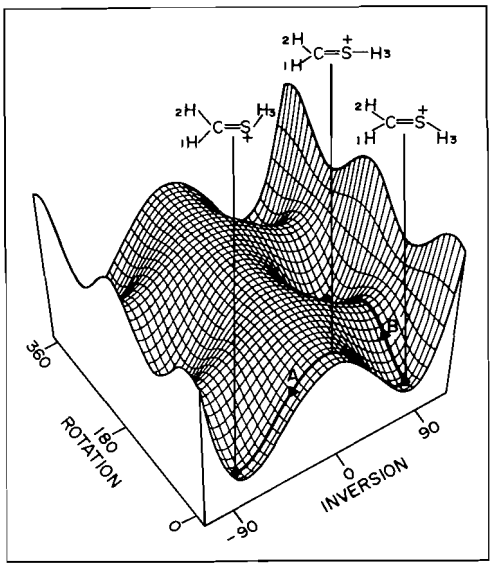

FIG. 3. The rotation – linear inversion surface of CH_2SH.

Table 7 reveals that oxygen in formaldehyde behaves as a π and a σ acceptor towards carbon, but in thioformaldehyde sulfur behaves as a π acceptor and a σ *donor*.

Both molecules belong to the C_{2v} symmetry point group. If we define two reference planes, one of which is the plane of the molecule and the other is perpendicular and bisects the HCH angle, then two types of π molecular orbitals can be distinguished, as shown below.

Structure	Orbital symmetry type	Orbital energy X = O	Orbital energy X = S
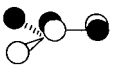	b_1	−0.4421	−0.3461
	b_2	−0.5283	−0.4062
	b_1	−0.7064	−0.6466

In terms of this representation, the total π-overlap population in formaldehyde is 0.2357 (0.2149 from b_1 and 0.0208 from b_2); and in thioformaldehyde it is 0.2257 (0.2119 from b_1 and 0.0138 from b_2), so that π-bonding between carbon and oxygen is slightly stronger than π-bonding between carbon and sulfur.

The situation is different in the protonated species. Scheme 2 displays the charge on the methylene group in $\overset{+}{C}H_3$, $\overset{+}{C}H_2OH$, and $\overset{+}{C}H_2SH$.

Can. J. Chem. Downloaded from www.nrcresearchpress.com by 210.87.254.5 on 09/05/12
For personal use only.

Can. J. Chem. Downloaded from www.nrcresearchpress.com by 210.87.254.5 on 09/05/12
For personal use only.

TABLE 8. Net atomic charges (q) and gross orbital populations of the valence atomic orbitals for $\overset{+}{C}H_2OH$ and $\overset{+}{C}H_2SH$*

	$\overset{+}{C}H_2OH$					$\overset{+}{C}H_2SH$				
	H_1	H_2	C	O	H_3	H_1	H_2	C	S	H_3
q	+0.35	+0.33	+0.31	−0.53	+0.54	+0.36	+0.35	−0.39	+0.45	+0.23
s	0.65	0.67	1.31	1.88	0.46	0.64	0.65	1.47	1.87	0.77
p_x			0.37	1.63				0.53	1.50	
p_y			1.29	1.69				1.34	1.32	
p_z			0.71	1.33				1.05	0.04	

*The coordinate system is 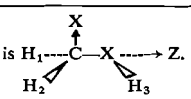

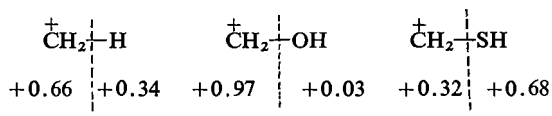

SCHEME 2

With respect to hydrogen we see that OH behaves towards $\overset{+}{C}H_2$ as an electron-withdrawing ligand by 0.31 electron, but SH behaves as an electron-releasing ligand by 0.34 electron.

Perhaps the most informative way to discuss the population analyses of these protonated species is to consider the interaction of the two fragments $\overset{+}{C}H_2$ and XH. Reference to the p_x and p_z overlap populations listed in Table 6 shows that, if $\overset{+}{C}H_2OH$ is considered to be formed by the combination of the fragments $\overset{+}{C}H_2$ and OH, π-donation from oxygen amounts to 0.38 electron. This corresponds to a charge transfer from the $2p_x$ oxygen lone pair to the vacant π orbital of $\overset{+}{C}H_2$, with the consequent formation of a relatively strong π bond between C and O. The π-overlap population is now 0.1496, less than that in $\overset{+}{C}H_2O$, so that the C—O bond in $\overset{+}{C}H_2OH$ is longer than that in CH_2O. As shown in **10**, the π-donation of 0.38 electron from O to C must be counterbalanced by a σ-donation from C to O of 0.35 in order to account for the total charge distribution δ_+.

In $\overset{+}{C}H_2SH$, a similar analysis reveals that π-donation from S to C amounts to 0.53 electron and that σ-donation from *S to C* amounts to an additional 0.15 electron. These are shown schematically in **11**. The important finding is that the π-donation from S to C (0.53 electron) is greater than that from O to C (0.38 electron).

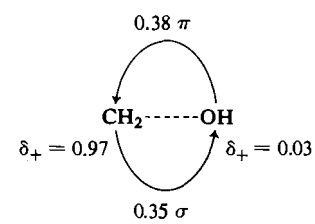

10

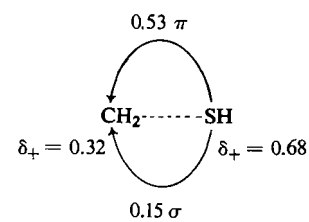

11

The π-overlap population in $\overset{+}{C}H_2SH$ is, therefore, also larger (0.1734), indicating a stronger π-bond between C and S than between C and O.

These analyses are thus in agreement with the interpretations given earlier of the rotational barriers. We must conclude that, in contrast to the current view of the nature of the interactions between first row and second row heteroatoms and an adjacent carbonium ion center, π-conjugative effects are greater for the second row atom. This result can be rationalized in terms of the interaction between the $2p_x$ heteroatom lone pair and the vacant carbon $2p_x$ orbital. The charge transfer associated with such an interaction is inversely proportional to the energy difference between the interacting orbitals so that greater stabilization is afforded by a sulfur lone pair than by an oxygen lone pair, because

the ionization potential of a second row atom is always less than that of the corresponding first row atom (*e.g.* ref. 24: H_2O, 12.61 eV; H_2S, 10.48 eV). A detailed account of this rationalization is presented elsewhere (25).

We thank NATO, the Italian CNR, and the donors of the Petroleum Research Fund, administered by the American Chemical Society, for financial support of this work.

1. C. C. PRICE and S. OAE. Sulfur bonding. Ronald Press, New York, N.Y. 1962.
2. D. J. CRAM. Fundamentals of carbanion chemistry. Academic Press, New York, N.Y. 1965.
3. Y. YANO and S. OAE. Mech. React. Org. Sulfur Compd. **4**, 167 (1969).
4. F. J. BORDWELL and P. J. BOUTON. J. Am. Chem. Soc. **78**, 854 (1956).
5. R. R. FRASER and F. J. SCHUBER. J. Am. Chem. Soc. **94**, 8795 (1972).
6. F. P. LOSSING, H. B. SCHLEGEL, and S. WOLFE. Unpublished results.
7. R. W. TAFT, R. H. MARTIN, and F. W. LAMPE. J. Am. Chem. Soc. **87**, 2490 (1965).
8. F. BERNARDI, I. G. CSIZMADIA, A. MANGINI, H. B. SCHLEGEL, M. H. WHANGBO, and S. WOLFE. J. Am. Chem. Soc. In press.
9. F. BERNARDI, I. G. CSIZMADIA, H. B. SCHLEGEL, M. TIECCO, M. H. WHANGBO, and S. WOLFE. Gazz. Chim. Ital. In press.
10. G. A. OLAH, D. H. O'BRIEN, and M. CALIN. J. Am. Chem. Soc. **89**, 3582 (1967); G. A. OLAH, M. CALIN, and D. H. O'BRIEN. J. Am. Chem. Soc. **89**, 3586 (1967).
11. (*a*) P. ROS. J. Chem. Phys. **49**, 4902 (1968); (*b*) J. M. LEHN, B. MUNSCH, and PH. MILLIE. Theor. Chim. Acta, **16**, 351 (1970); (*c*) L. M. TEL, S. WOLFE, and I. G. CSIZMADIA. Int. J. Quant. Chem. VII, 475 (1973).
12. (*a*) R. DITCHFIELD, W. J. HEHRE, and J. A. POPLE. J. Chem. Phys. **54**, 724 (1971); (*b*) W. J. HEHRE and W. A. LATHAN. J. Chem. Phys. **56**, 5255 (1972); (*c*) W. J. HEHRE, W. A. LATHAN, R. DITCHFIELD, M. D. NEWTON, and J. A. POPLE. Quantum Chemistry Program Exchange, Indiana University, Bloomington, Indiana.
13. D. R. JOHNSON, F. X. POWELL, and W. H. KIRCHOFF. J. Mol. Spectrosc. **39**, 136 (1971).
14. N. W. WINTER, T. H. DUNNING, and J. H. LETCHER. J. Chem. Phys. **49**, 1871 (1968).
15. W. MEYER and P. PULAY. Theor. Chim. Acta, **32**, 253 (1974).
16. W. A. LATHAN, L. A. CURTISS, W. J. HEHRE, J. B. LISLE, and J. A. POPLE. Prog. Phys. Org. Chem. **11**, 175 (1974).
17. Tables of interatomic distances and configuration in molecules and ions. Spec. Publ. No. 11. The Chemical Society, London. 1958; Spec. Publ. No. 18. The Chemical Society, London. 1965.
18. H. KESSLER. Tetrahedron, **30**, 1861 (1974).
19. F. B. BROWN. J. Chem. Phys. **58**, 827 (1973).
20. S. WOLFE, L. M. TEL, and I. G. CSIZMADIA. Can. J. Chem. **51**, 2423 (1973).
21. F. BERNARDI, I. G. CSIZMADIA, H. B. SCHLEGEL, J. THEODORAKOPOULOS, M. H. WHANGBO, and S. WOLFE. To be published.
22. A. LIBERLES, A. GREENBERG, and J. E. EILERS. J. Chem. Educ. **50**, 676 (1973).
23. (*a*) L. SALEM and C. ROWLAND. Angew. Chem. Int. Ed. Engl. **11**, 92 (1972); (*b*) M. H. WOOD. Chem. Phys. Lett. **24**, 239 (1974).
24. Ionization potentials, appearance potentials and heats of formation of gaseous positive ions. National Bureau of Standards, Washington, D.C., NBS 26. 1969.
25. F. BERNARDI, I. G. CSIZMADIA, and N. D. EPIOTIS. To be published.

Can. J. Chem. Downloaded from www.nrcresearchpress.com by 210.87.254.5 on 09/05/12
For personal use only.

Substituent Effects in Electron Transfer Reactions: The Preparation and Chromium(II) Reduction of 3-Formylpentane-2,4-dionatobis(ethylenediamine)cobalt(III). Preparation of the Linkage Isomer 2-Acetylbutane-1,3-dionatobis(ethylenediamine)cobalt(III)

ROBERT J. BALAHURA[1] AND N. A. LEWIS

Department of Chemistry, University of Guelph, Guelph, Ontario N1G 2W1

Received October 30, 1974

ROBERT J. BALAHURA and N. A. LEWIS. Can. J. Chem. **53**, 1154 (1975).

The preparation of the linkage isomers, 3-formylpentane-2,4-dionatobis(ethylenediamine)-cobalt(III), (**1**), and 2-acetylbutane-1,3-dionatobis(ethylenediamine)cobalt(III), (**2**), are described. The kinetics of the reaction of $Cr(OH_2)_6^{2+}$ with **1** and the parent complex, 2,4-pentanedionatobis(ethylenediamine)cobalt(III), (**3**), have been studied spectrophotometrically in acidic solution. For **1**, the reduction is described by the rate law $-$ d ln [Co(III)complex]/dt = $k[Cr^{2+}]$, and $k = 0.0863\ M^{-1}\ s^{-1}$ at 25 °C, $\mu = 1.0\ M$ ($LiClO_4$). The activation parameters for this reaction were found to be $\Delta H^{\ddagger} = 9.9 \pm 0.5$ kcal mol^{-1} and $\Delta S^{\ddagger} = -30 \pm 3$ e.u. The reaction proceeded by an inner-sphere mechanism and the product of this reaction was isolated and characterized as 2-acetylbutane-1,3-dionatotetraaquochromium(III). The linkage isomer of this complex was also prepared. The parent complex (**3**) was not reduced by $Cr(OH_2)_6^{2+}$ at an observable rate and an upper limit for the rate constant of this reaction was assigned a value of 10^{-4}–$10^{-6}\ M^{-1}\ s^{-1}$ at 25 °C. The ability of the formyl group to enhance the rate of electron transfer is discussed, and the chromium(II) reduction studies of related chelated systems are compared with the results obtained in this investigation.

ROBERT J. BALAHURA et N. A. LEWIS. Can. J. Chem. **53**, 1154 (1975).

On décrit la préparation des isomères de liaisons, formyl-3 pentanedionato-2,4 bis(éthylènediamine) cobalt(III) (**1**) et acétyl-2 butanedionato-1,3 bis(éthylènediamine) cobalt(III) (**2**). On a étudié spectrophotométriquement en solution acide la cinétique de la réaction du $Cr(OH_2)_6^{2+}$ avec **1** et avec le complexe parent pentanedionato-2,4 bis(éthylènediamine) cobalt(III) (**3**). Pour **1** la réduction est décrite par la loi de vitesse $-$ d ln [Co(III) complexe]/dt = $k[Cr^{2+}]$ et $k = 0.0863\ M^{-1}\ s^{-1}$ à 25 °C, $\mu = 1.0\ M$ ($LiClO_4$). On a trouvé que les paramètres d'activation pour cette réaction sont $\Delta H^{\ddagger} = 9.9 \pm 0.5$ kcal mol^{-1} et $\Delta S^{\ddagger} = -30 \pm 3$ e.u. La réaction se produit par un mécanisme de sphère intérieure et le produit de 'a réaction peut être isolé et caractérisé comme étant l'acétyl-2 butanedionato-1,3 tétraaquochrome(III). On a aussi préparé les isomères de liaisons de ce complexe. Le complexe parent (**3**) n'est pas réduit par $Cr(OH_2)_6^{2+}$ à une vitesse mesurable et on a attribué une limite supérieure pour la constante de vitesse de cette réaction de 10^{-4} à $10^{-6}\ M^{-1}\ s^{-1}$ à 25 °C. On discute de l'habilité du groupe formyle d'augmenter la vitesse de transfert d'électron; on compare les résultats obtenus au cours de cette étude avec ceux d'études sur la réduction par du chrome(II) de systèmes chelates apparentés. [Traduit par le journal]

Introduction

Linkage isomerism involving metal chelates is exceedingly rare (1). Generally, synthesis of separate isomers has been effected by changing reaction conditions such as solvent (2), temperature (3), counterion (4), or bulkiness of other ligands (5). In this study we wish to report on the synthesis and characterization of the linkage isomers of 3-formylpentane-2,4-dione with bis(ethylenediamine)cobalt(III), **1** and **2**.

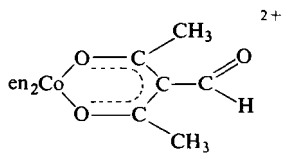

1

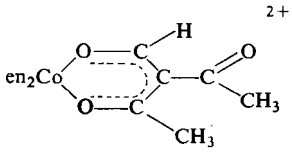

2

[1]Author to whom correspondence should be addressed.

Can. J. Chem. Downloaded from www.nrcresearchpress.com by 210.87.254.6 on 09/05/12
For personal use only.

Can. J. Chem. Downloaded from www.nrcresearchpress.com by 210.87.254.6 on 09/05/12
For personal use only.

These isomers were prepared using two different preparative procedures since both **1** and **2** were found to be stable, with respect to isomerization, upon changing reaction conditions.

Our original aim in preparing these compounds was to investigate their redox properties. There are few studies of mechanistic behavior involving chelated bridging ligands in oxidation–reduction reactions. A recent report (6) of the chromium(II) reduction of cobalt(III)-mercaptoacetate, $[Co(en)_2(OOCCH_2S)]^+$, and alkoxide, $[Co(en)_2(OOCCH_2O)]^+$ complexes has indicated that the reaction occurs via an inner-sphere process by attack of the reductant at the coordinated sulfur and alkoxide oxygen respectively. In complexes of the above type there are three potential sites for attack of the reductant and it is difficult to determine unambiguously the site of attack. The large rate difference found for reaction of the mercaptide complex with respect to the alkoxide complex has also been the source of much speculation.

A potentially simpler system involves the pseudoaromatic chelate formed with 2,4-pentanedione. It was anticipated that the complex

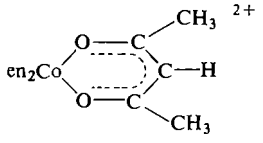

3

would react by an outer-sphere mechanism rather than one which involved attack of reductant at one of the coordinated oxygens. We hoped then to substitute the methylene hydrogen with other groups capable of acting as inner-sphere bridges towards chromium(II). The synthesis of **1** has allowed us to investigate the electron-transfer-inducing ability of the formyl group. Furthermore, reduction of **2**, where small structural changes in the chelate ring have been made, may indicate some of the factors influencing electron transfer involving chelate complexes.

It has been shown that electronic effects can be transmitted from one chelate group to another in the same complex (*7a*, *b*). Thus, a systematic variation of substituents on the chelate ring as well as a variation in the number and type of chelate groups may help to indicate the importance of electronic delocalization in electron transfer reactions. Also, it appears that the electron transfer process involves activation of the entire chelate ring and not just the bridging atom (8). This effect may be observed when comparing complexes **1** and **2**.

In inner-sphere reactions of this type, the chelates are initially bonded to chromium(III) as monodentate ligands but usually the final products involve a chelated complex. In these systems this would allow us to investigate the ring closure reactions as well as being helpful in indicating the initial position of attack of the reductant.

Experimental

Reagents

All reagent solutions were prepared in water redistilled from alkaline permanganate in an all glass apparatus. Lithium perchlorate solutions were prepared and standardized as described previously (9).

Chromium(II) perchlorate solutions were prepared by reduction of chromium(III) perchlorate using zinc–mercury amalgam. These solutions were stored and handled in an atmosphere of high-purity argon.

Kinetic Measurements

The rate of reduction of 3-formylpentane-2,4-dionatobis(ethylenediamine)cobalt(III) was followed by observing the change in absorbance of the longest wavelength maximum of the cobalt(III) complex. The kinetic runs were performed on a Beckman Acta CIII spectrophotometer with the temperature controls described previously (10). All reactions were carried out in cylindrical cells sealed with rubber serum caps in the absence of oxygen. The reactions were run under pseudo first-order conditions (reductant in a 10–50 fold excess over oxidant).

Physical Measurements

The proton magnetic resonance spectra were obtained on a Varian A60 spectrometer. The ultraviolet and visible spectra were measured on a Beckman Acta CIII spectrophotometer. The infrared spectra were recorded on a Beckman IR 12 spectrophotometer.

Preparation of Complexes[2]

$[en_2Co(ptdn)](PF_6)_2$

The compound was prepared as reported in the literature (11). It was dissolved in water and purified by ion-exchange chromatography on Rexyn 102(H) weak acid cation exchange resin (Fisher Scientific Co.) converted to the sodium ion form. Elution with 0.1 *M* NaCl separated the product from the principal impurity $[en_3Co]^{3+}$. The resin containing the desired complex was

[2]The abbreviation, acac, commonly used to denote 2,4-pentanedione (acetylacetone) was not employed in this work since a corresponding abbreviation could not be found for 1,3-butanedione. We have elected to use instead the abbreviations ptdn = 2,4-pentanedione and btdn = 1,3-butanedione based on IUPAC names.

Can. J. Chem. Downloaded from www.nrcresearchpress.com by 210.87.254.6 on 09/05/12
For personal use only.

separated physically and washed with distilled water, which was filtered off under suction. Enough distilled water was then added to the resin to make a thick slurry and concentrated HCl was added dropwise to the rapidly stirred slurry until the complex was removed from the resin, complete removal being signified by the presence of free hydrogen ions. The complex was precipitated with NH_4PF_6, filtered, washed with ether, and air-dried.

Anal. Calcd. for $[Co(C_2N_2H_8)_2(C_5O_2H_7)](PF_6)_2$: C, 19.05; H, 4.05; N, 9.86. Found: C, 19.05; H, 4.27; N, 9.84.

$[en_2Co(3\text{-formyl-ptdn})](PF_6)_2$

A mixture of dry dimethylformamide (100 ml), Davidson Molecular Sieves (15 g, 8–12 mesh, 4 Å effective pore size), and $[en_2Co(ptdn)]I_2$ (11) (5 g) recrystallized from KI was allowed to stir for 1 h to ensure dryness. Then $POCl_3$ (8 ml) was added over a 10 min interval. The reaction was slightly exothermic but there was no need to cool the reaction mixture. Stirring was continued for 2 h at room temperature.

The solution was filtered and added slowly to ether (500 ml). The mixture was stirred to extract a yellow organic material in the ethereal layer which was then decanted off. The red layer containing the desired product was gradually stirred into acetone (800 ml). A pink precipitate formed immediately and was filtered off, dissolved in water (1000 ml), and ion-exchanged as described above. The unreacted $[en_2Co(ptdn)]^{2+}$ separated from the formyl product as a red band upon elution with 0.1 *M* NaCl. The $[en_2Co(3\text{-formyl-ptdn})]^{2+}$ moved down the column as an orange band. The bands were separated physically and the complexes removed from the resin, as described in the above preparation. The formyl complex was precipitated with NH_4PF_6, washed with ether, and air-dried. Yield 1.6 g, 30.5%.

Anal. Calcd. for $[Co(N_2C_2H_8)_2(C_6H_7O_3)](PF_6)_2$: C, 20.15; N, 9.39; H, 3.86. Found: C, 19.99; N, 9.37; H, 4.01.

3-Formylpentane-2,4-dione

The free ligand, 3-formylpentane-2,4-dione was prepared following Beilstein (12) and purified by the method of Akehurst and Bartels-Keith (13). The compound was found to be unstable if stored at room temperature in a P_2O_5 dessicator under vacuum but it could be stored for several weeks at 5 °C.

$[en_2Co(2\text{-acetyl-btdn})](PF_6)_2$

The complex $[en_2Co(CO_3)]^{2+}$ (14) (2.2 g) was treated with 8 ml of 2 *M* HCl. The ligand 3-formylpentane-2,4-dione (2.1 g) was dissolved in 12 ml of 1 *M* NaOH. The ligand solution was added to the stirring metal complex solution. The reaction mixture was allowed to sit at room temperature for a week, after which time the mixture was diluted to 700 ml with distilled water and ion-exchanged as described above. Elution with 0.1 *M* NaCl separated a red and an orange band, the first being identified as $[en_2Co(ptdn)]^{2+}$ and the latter as the desired complex. Other bands of higher charge remained at the top of the column and were not identified. The orange band was eluted off the column with 0.1 *M* NaCl and was taken to dryness on a rotovap. The chloride salt obtained in this manner was converted to the PF_6^- salt using NH_4PF_6.

Anal. Calcd. for $[Co(N_2C_2H_8)_2(C_6H_7O_3)](PF_6)_2$: C, 20.15; N, 9.39; H, 3.86. Found: C, 20.12; N, 9.25; H, 4.12.

$[(OH_2)_4Cr(ptdn)]^{2+}$

A solution of 10 ml of 2,4-pentanedione and 20 ml of 0.5 *M* $[Cr(OH_2)_6]^{3+}$ in 0.2 *M* $HClO_4$ was allowed to stir in a covered flask for 48 h. A 3 ml portion of the reaction mixture was then subjected to ion-exchange on Dowex 50W-X8 cation exchange resin at 5 °C. The first band moved as a 1+ ion and was the disubstituted product, $[(OH_2)_2Cr(ptdn)_2]^+$; the second band moved as a 2+ and was the monosubstituted product $[(OH_2)_4Cr(ptdn)]^{2+}$, and the third band was unreacted $[(OH_2)_6Cr]^{3+}$. Extinction coefficients were based on the chromium concentration which was determined spectrophotometrically as chromate.

$[(OH_2)_4Cr(2\text{-acetyl-btdn})]^{2+}$

Chromatographic separation of reaction mixtures at different acidities and at a 1:1 ratio of Cr^{2+} to $[en_2Co(3\text{-formyl-ptdn})]^{2+}$ afforded this complex as the only product. Separations were obtained on Dowex 50W-X8. Elution and analysis were performed as described previously (9).

$[(OH_2)_4Cr(3\text{-formyl-ptdn})]^{2+}$

The free ligand, 3-formylpentane-2,4-dione (2 g) was added to 10 ml of 0.5 *M* $[Cr(OH_2)_6]^{3+}$ in 0.2 *M* $HClO_4$. The ligand was not immediately soluble in this solution but dissolved over a 2 h period to give a purple solution. Ion-exchange of portions of the reaction mixture was accomplished on Dowex 50W-X8 after 2 to 8 h of reaction time. Three bands were obtained, corresponding to $[(OH_2)_2Cr(3\text{-formyl-ptdn})_2]^+$, $[(OH_2)_4Cr(3\text{-formyl-ptdn})]^{2+}$, and $[(OH_2)_6Cr]^{3+}$. Increasing amounts of the disubstituted product were obtained as the reaction time was increased.

Results and Discussion

Preparation and Characterization of Complexes

The substitution of the methylene proton was accomplished by reaction of the unsubstituted complex with $POCl_3$ in dimethylformamide (DMF)

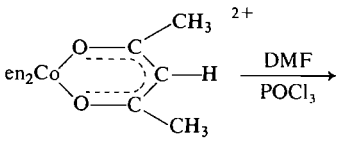

3

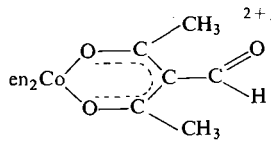

1

in a procedure similar to that of Collman *et al.* (15). The mixture of $POCl_3$ and DMF is a potent formylating agent (16), the active

Can. J. Chem. Downloaded from www.nrcresearchpress.com by 210.87.254.6 on 09/05/12
For personal use only.

species probably composed of an addition compound of $POCl_3$ and DMF (17):

$$[(CH_3)_2N{-}\overset{+}{C}H{-}Cl \leftrightarrow (CH_3)_2\overset{+}{N}{=}CH{-}Cl]\bar{O}POCl_2$$

The complex was purified by cation-exchange chromatography and eluted as the expected 2+ ion.

The linkage isomer of **1** was prepared from reaction of the free ligand, 3-formylpentane-2,4-dione with $[Co(en)_2(OH_2)_2]^{3+}$

$[Co(en)_2(H_2O)_2]^{3+}$ + 3-formyl-ptdn →

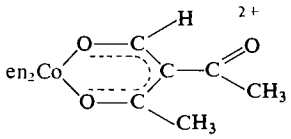

2

Purification via ion-exchange indicated that **2** is formed selectively since no trace of **1** was observed. Attempts to prepare **2** by heating **1** at elevated temperatures in a variety of solvents proved unsuccessful.

Infrared Spectra

The infrared spectra of β-diketone complexes have been well documented (18, 19). The bands that appear in the region $1515 \pm 10\ cm^{-1}$ (B band) and $1575 \pm 30\ cm^{-1}$ (A band) have been assigned to the C=O and C=C stretching modes, respectively (20). However, labelling experiments suggest that the A band corresponds to a pure C=O stretch whereas the B band is a pure C=C stretch (21, 22). Later, Mikami *et al.* showed that the two modes are coupled slightly to each other (23). The presence of these bands provides excellent proof of chelate formation. The A and B bands in the parent compound, $[Co(en)_2(ptdn)]^{2+}$, appear at 1582 and 1523 cm^{-1} (24).[3]

Previously (25), Dryden and Winston had shown that substitution of the methylene hydrogen at the 3-position results in only one band in the 1500–1600 cm^{-1} region. However, the nitro chelates prepared by Collman *et al.* (15) exhibited two bands in this region, the band at 1520 cm^{-1} being assigned to an asymmetric nitro stretching frequency. It has been found that when the group substituted for hydrogen is a double-bonded species such as acetyl, a doublet persists in the 1500–1600 cm^{-1} region. In the formyl derivative **1**, $[Co(en)_2(3\text{-formyl-ptdn})][PF_6]_2$, a spectrum as a Nujol mull also shows a doublet in this region (at 1589 and 1565 cm^{-1}). When the infrared spectrum is run as a KBr disk only one peak at 1578 cm^{-1} is observed. The free carbonyl stretching frequency of the formyl group appears at 1695 cm^{-1} in a Nujol mull and as a doublet at 1670 and 1675 cm^{-1} in a KBr disk. The carbonyl stretching frequency of the formyl group appears at 1660 cm^{-1} in the complex (3-formyl-2,4-pentanedionato)bis(2,4-pentanedionato)cobalt(III) (2). The infrared spectrum of the free ligand 3-formylpentane-2,4-dione shows a ν(C=O) at 1674 cm^{-1}.

The infrared spectrum of the linkage isomer **2** in Nujol shows intense bands at 1572 and 1587 (1610 sh) cm^{-1}. The latter band is probably due to the ν(C=O) of the coordinated aldehydo and keto oxygens of the ring. In a KBr disk only one band is observed for the coordinated keto and aldehydo ν(C=O) at 1586 cm^{-1}. The free acetyl carbonyl stretching frequency is observed at 1665 cm^{-1} in both Nujol and a KBr disk.

It is apparent that the number and type of bands obtained in the 1500 cm^{-1} region for these complexes are dependent upon the particular medium chosen in obtaining the spectrum. Thus we feel that caution should be exercised in applying Dryden's rule (25). Also, other physical studies are necessary for an unambiguous structural interpretation.

Proton Magnetic Resonance Spectra

The proton magnetic resonance spectra provide perhaps the best structural characterization of the linkage isomers. The spectra of complexes **1**, **2**, and **3** in DMSO-d_6 and D_2O are shown in Fig. 1. A tabulation of chemical shifts appears in Table 1. In D_2O the NH_2 protons on the ethylenediamine rings exchange with the solvent and are not visible. As shown in Fig. 1*a* the NH_2 protons appear as two broad peaks in the 4–6 δ region. Each peak integrates for four protons. The CH_2 protons of the ethylenediamine rings appear near or superimposed upon the solvent peak at about 2.50 δ. The shapes and positions of these peaks depend upon the solvent and nature of the

[3]Boucher and Bailar report 1565 and 1523 cm^{-1} for the iodide salt. The spectra reported in our study are for the hexafluorophosphate salts.

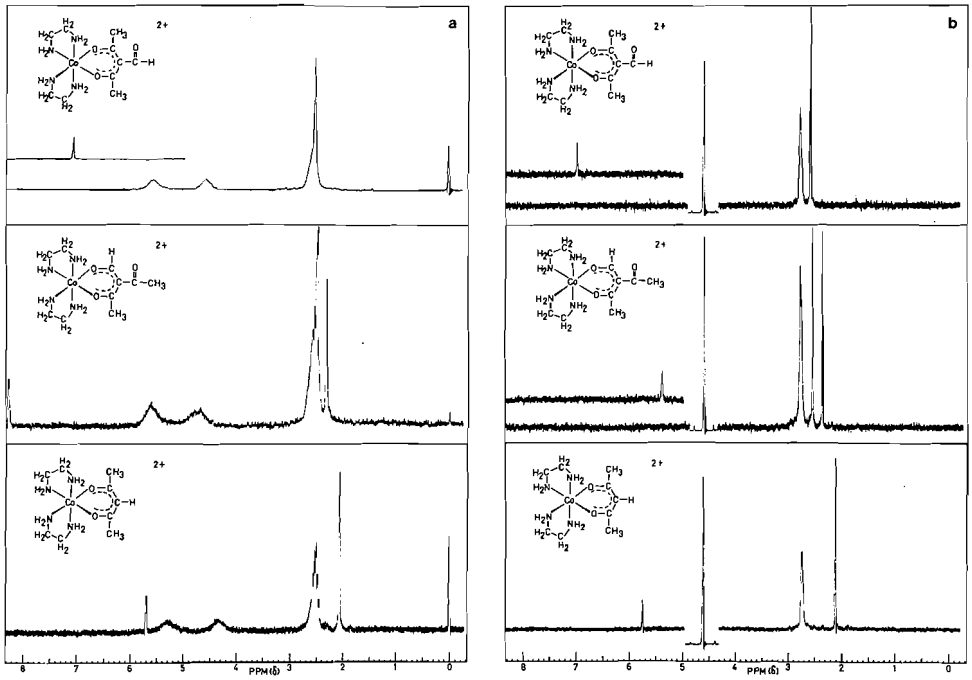

FIG. 1. (*a*) Proton magnetic resonance spectra of cobalt(III) complexes in DMSO-d_6 (offsets are 200 Hz). (*b*) Proton magnetic resonance spectra of cobalt(III) complexes in D_2O (offsets are 200 Hz).

TABLE 1. Proton magnetic resonance shifts for cobalt(III) complexes

Complex	Chemical shift (p.p.m. δ)				
	—CH_3	—CH_2—*	—C—H	—NH_2—†	Solvent‡
$en_2Co(ptdn)^{2+}$	2.08	2.52	5.70	4.35, 5.30	DMSO-d_6
	2.02	2.66	5.67		D_2O
$en_2Co(3\text{-formyl-ptdn})^{2+}$	2.45*	2.45	10.05	4.58, 5.57	DMSO-d_6
	2.48	2.70	10.01		D_2O
$en_2Co(2\text{-acetyl-btdn})^{2+}$	2.34	2.50	8.28	4.75, 5.62	DMSO-d_6
	2.50*				
	2.30	2.70	8.36		D_2O
	2.48				

*Peak occurs with solvent peak for DMSO-d_6.
†Amine protons exchange with solvent in D_2O and are not observed.
‡Chemical shifts in DMSO-d_6 are relative to TMS. Chemical shifts in D_2O are relative to HDO peak at 4.61 δ. All spectra in DMSO-d_6 originally contained a peak due to a water impurity which was shifted downfield with trifluoroacetic acid.

group in the 3-position of the 2,4-pentanedione ring.

The methylene proton in the unsubstituted complex, **3**, appears at ~5.78 δ in both DMSO-d_6 and D_2O. This is in good agreement with the position of this peak in other 2,4-pentanedione complexes (5.4–6.0 δ) (*7b*, 15). The disappearance of this peak is an excellent confirmation of substitution at the 3-position.

For complex **1** the lack of a peak in the 5–6 δ region and the appearance of a peak due to one proton at ~10 δ is expected for substitution of a formyl group in the 3-position. The fact that only a singlet is observed for the CH_3 protons of the 2,4-pentanedione ring (integration in D_2O gives 6 protons) implies that rotation about the C_3—C_{formyl} bond is fast and that there is little conjugation between the formyl group and

Can. J. Chem. Downloaded from www.nrcresearchpress.com by 210.87.254.6 on 09/05/12
For personal use only.

TABLE 2. Electronic spectra of cobalt(III) complexes*

$\lambda_{max}(\varepsilon_{max})$, nm ($M^{-1}$ cm^{-1})		
$[Co(en)_2(ptdn)][PF_6]_2$	$[Co(en)_2(3\text{-formyl-ptdn})][PF_6]_2$	$[Co(en)_2(2\text{-acetyl-btdn})][PF_6]_2$
499(146)	488(143)	489(144)
323(4430)	298(3090)	310(2410)
237(17 100)	252(27 000)	247(30 900)
217(25 600)	209(21 700)	210(21 000)

*All spectra were run in aqueous solution.

the pseudo aromatic chelate ring. This is consistent with the spectrum observed (2) for (3-formylpentane-2,4-dionato)bis(2,4-pentanedionato)cobalt(III) where only one methyl resonance was observed for the substituted chelate at 2.7 δ. In this complex the formyl proton was observed at 10.20 δ.

The proton magnetic resonance spectrum of the linkage isomer **2** is more complex than that of **1**. Again, substitution is indicated by the absence of the C_3 proton peak and the presence of a resonance due to one proton at 8.38 δ. This latter resonance is assigned to the proton on the coordinated formyl group. Two resonances are expected for the two inequivalent CH_3 groups and these are observed in D_2O at 2.30 and 2.48 δ. These results are similar to those observed (2) for the complex (2-acetylbutane-1,3-dionato)bis(2,4-pentanedionato)-cobalt(III) where the methyl groups are observed at 2.35 and 2.68 δ.

Thus the proton magnetic resonance spectra allow a clear distinction to be made between the linkage isomers.

Electronic Spectra

The positions of the absorption bands in the visible and ultraviolet regions of the spectrum for **1**, **2**, and **3** are given in Table 2. The lowest energy band in the visible region of the spectrum can be assigned to the d–d transition $^1A_{1g} \rightarrow {}^1T_{1g}$. The position of this band for the complexes reported here as well as similar complexes (24, 26) with different β-diketones does not vary appreciably. This indicates that the ligand field around the central cobalt metal remains essentially constant and is determined by the two ethylenediamine rings and the two oxygen atoms of the β-diketone. The expected $^1A_{1g} \rightarrow {}^1T_{2g}$ transition is observed as a shoulder at 376 nm in $[Co(en)_2(ptdn)]^{2+}$ but is obscured by ligand transitions in complexes **1** and **2**.

The remaining bands in the ultraviolet are due to ligand and charge-transfer transitions. In analogy to assignments made by Boucher and Bailar (24) the peaks at about 300 nm correspond to a $d\varepsilon \rightarrow \pi^*$ metal–ligand charge-transfer transition. The remaining ultraviolet bands, especially those at approximately 250 nm, can be assigned to π–π^* transitions.

It has been pointed out previously (7*b*, 27) that the methyl groups in 2,4-pentanedione complexes prevent coplanarity of acetyl and nitro groups with the chelate ring. However, halogen, sulfur, and formyl substituents can remain conjugated with the chelate ring. Thus a comparison of the ultraviolet spectra of substituted 2,4-pentanedione complexes can indicate the extent of steric inhibition of resonance of the substituents with the chelate ring. The data for complexes **1** and **2** imply that the formyl and acetyl groups are not sterically hindered from attaining coplanarity with the ring. This will be important in considering the electron transfer data.

Kinetic Studies

The kinetics of reduction of $[Co(en)_2(3\text{-formyl-ptdn})]^{2+}$ by chromium(II) follows the rate law

$$-\frac{d \ln [Co(III)complex]}{dt} = k[Cr^{2+}] = k_{obsvd}$$

A summary of the kinetic data is given in Table 3. The progress of the reaction was also followed by scanning the range from 300–700 nm with varying ratios of $[Cr^{2+}]$ and $[Co^{3+}]$ and with different hydrogen ion concentrations. A typical scan is given in Fig. 2. Good isosbestic behavior was observed in all cases with isosbestic points at 402, 430, 548, and 651 nm. The final spectrum obtained indicates that the final product of the reaction is not $Cr(OH_2)_6^{3+}$ and therefore an inner-sphere

Can. J. Chem. Downloaded from www.nrcresearchpress.com by 210.87.254.6 on 09/05/12
For personal use only.

Can. J. Chem. Downloaded from www.nrcresearchpress.com by 210.87.254.6 on 09/05/12
For personal use only.

reaction is indicated. The peak maxima obtained for the chromium(III) product were at approximately 558 and 412 nm whereas for $Cr(OH_2)_6^{3+}$ the maxima occur at 574 and 408 nm (28).

An attempt was made to study the reduction of $[Co(en)_2(ptdn)]^{2+}$ by chromium(II) but no reaction was observed under a variety of conditions. In one particular study no reaction was detected after 13 h at 55 °C for $[Cr^{2+}] = 1.87 \times 10^{-1}\ M$, $[Co^{3+}] = 7.70 \times 10^{-4}\ M$, and $[H^+] = 0.10\ M$. For comparative purposes it is probably reasonable to assume that this reaction is at least 10^4 to 10^6 times slower than the reduction of the 3-formyl derivative just described.

These results, as well as those previously described, are consistent with an inner-sphere mechanism for reduction of $[Co(en)_2(3\text{-formyl-ptdn})]^{2+}$ as outlined below

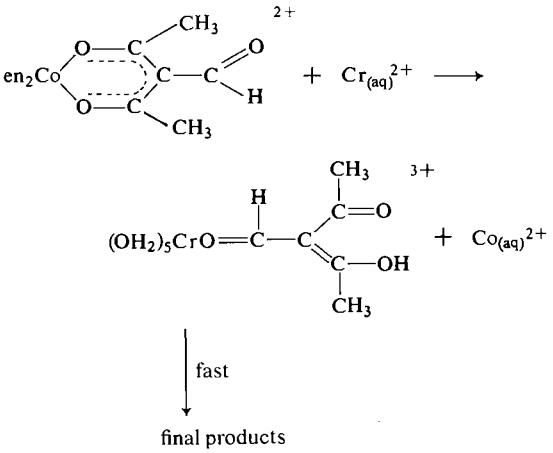

Since a monodentate complex of a substituted 2,4-pentanedione ligand was not anticipated the products of the reduction were isolated by cation exchange chromatography of reaction mixtures. Reaction mixtures with approximately 1 to 1 molar ratios of $[Cr^{2+}]$ to $[Co^{3+}]$ and varying acidity were subjected to cation exchange chromatography on Dowex 50W-X8. In all cases only one product was obtained. The average percent ligand transfer is 71% as determined by three such separations. It should be mentioned that the complex was difficult to remove from the column and based on the isosbestic behavior observed we feel that the transfer of ligand is nearly quantitative.

This product had elution characteristics of a 2+ ion. The visible–ultraviolet spectrum shows peak maxima (extinction coefficient) at 547(35.0), shoulder at 408(48.3), 309(5200), 246(13 150), and 238 nm(12 750 M^{-1} cm^{-1}). The spectrum is identical in both 1.0 M $HClO_4$ and 0.01 M $HClO_4$. Based on the extinction coefficients reported here and those of known monodentate and chelate complexes of chromium(III) (29, 30) we assign a chelate structure, **4**, to the final product obtained from the reduction. This product can be formed from the initial product of the reduction as shown below:

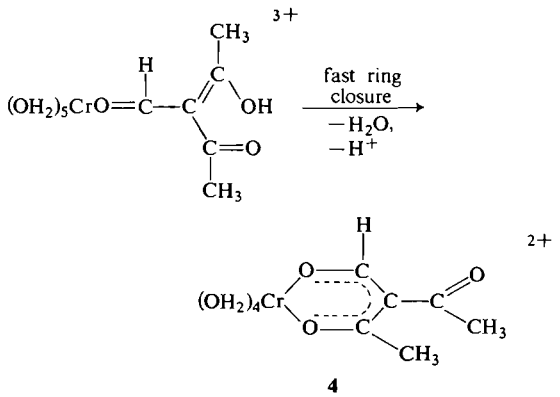

4

This reaction is expected to be extremely fast since it is known that Cr(III)–keto bonds are very labile (31, ref. 14 of (31)). In fact aquation of keto-coordinated ligands is generally characterized by half-times in the region of 20–30 ms (32, 33).[4] If ring closure were not fast, significant amounts of $Cr(OH_2)_6^{3+}$ would be expected. This would have been detected in the scan runs and isosbestic behavior would not have been observed.

Chelation between the reductant and one of the coordinated oxygens and the free formyl oxygen in the transition state could lead directly to a chelated product. Examination of molecular models, however, shows that the oxygens appear too far away in the complex to make this

[4]Unpublished observations on aquation of

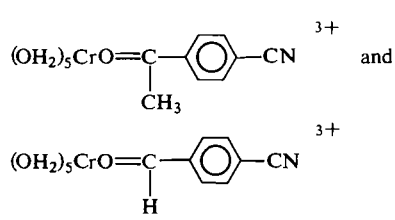

TABLE 3. Kinetic data for the reduction of 3-formylpentane-2,4-dionatobis(ethylenediamine)Co(III) by chromium(II)*

[Oxidant] ($\times 10^3$)†	[Reductant] ($\times 10^2$)†	[H$^+$]†	Temperature (°C)	k ($\times 10$) (M^{-1} s^{-1})
3.02	5.10	0.10	25.4	0.866
2.81	10.28	0.10		0.874
2.26	3.40	0.60		0.854
3.17	6.86	0.60		0.856
1.33	4.28	0.05	30.1	1.18
1.38	12.58	0.10		1.22
1.33	4.28	0.20		1.20
1.33	4.28	0.80		1.16
1.24	4.36	0.05	35.5	1.65
1.27	12.82	0.10		1.62
1.22	4.36	0.20		1.68
1.24	4.36	0.80		1.62
1.34	4.36	0.05	44.8	2.61
1.36	12.82	0.10		2.58
1.34	4.36	0.20		2.56
1.36	4.36	0.80		2.53

*For all runs ionic strength $\mu = 1.0$ ($LiClO_4$).
†Concentrations are initial values in molar units.

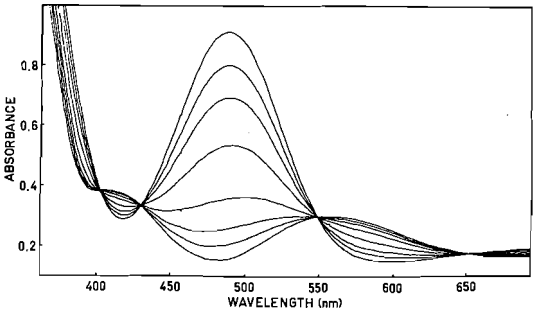

FIG. 2. Changes in the visible spectrum during reduction of (3-formyl-ptdn)bis(ethylenediamine)cobalt(III) (3.16×10^{-3} M) by Cr^{2+} (1.54×10^{-2} M); [H$^+$] = 2.86×10^{-2} M; path length = 2.0 cm; 25 °C. The spectral scans were started at 0.5, 4.0, 8.0, 16.0, 30.0, 45.0, 60.0, 130.0, and 215.0 min after mixing. The last two show no change.

mechanism attractive. In addition, reactions where chelation has been definitely shown to occur (34) are usually much faster than that observed here. If this type of mechanism were operative one might expect attack at a coordinated oxygen in the parent compound as well, resulting in an observable rate for reduction.

Synthesis of Chromium(III) Complexes

An attempt was made to prepare the chelated product obtained from electron transfer independently by reaction of the ligand, 3-formylpentane-2,4-dione with $Cr(OH_2)_6^{3+}$. Chromatography of the reaction mixture gave three complexes. Band I eluted as a 1+ ion and was formulated as $Cr(OH_2)_2$(3-formyl-ptdn)$_2^+$. Band II had elution characteristics of a 2+ band and was formulated as $Cr(OH_2)_4$(3-formyl-ptdn)$^{2+}$. Band III was identified as unreacted $Cr(OH_2)_6^{3+}$. Band II had peak maxima (extinction coefficient) in the electronic spectrum at 557(30.4), 315(4640), 244(11 600), and 231 nm (14 100 M^{-1} cm^{-1}). This product is different from that obtained from the reduction of complex **1** and is formulated as the linkage isomer of **4** as below

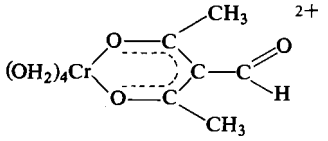

5

Substitution of the free ligand on $Cr(OH_2)_6^{3+}$ was unusually facile. Reaction mixtures containing a five-fold excess of ligand turned from blue to violet in 2 h at room temperature. The ligand was initially insoluble in water but dissolved as the reaction proceeded. If the reaction were allowed to proceed for 10 h or more, the

Can. J. Chem. Downloaded from www.nrcresearchpress.com by 210.87.254.6 on 09/05/12
For personal use only.

TABLE 4. Kinetic data for the chromium(II) reduction of $en_2Co(III)$ chelate complexes and related $(NH_3)_5Co^{3+}$ complexes[a]

Complex	$k^{25°}$ (M^{-1} s^{-1})	ΔH^{+} (kcal mol^{-1})	ΔS^{+} (e.u.)
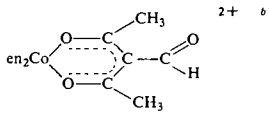 2+ [b]	0.0863	9.9±0.5	−30±3
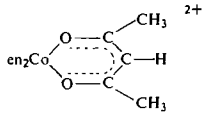 2+	10^{-4}–10^{-6}	—	—
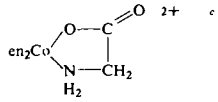 2+ [c]	2.22	8.8	−27
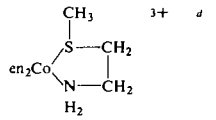 3+ [d]	0.381	5.4	−42
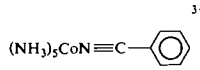 3+ [e]	0.0427	—	—
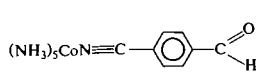 3+ [f]	8×10^{5}	—	—

[a] $\mu = 1.0\ M$ ($LiClO_4$).
[b] Reduction of the linkage isomer is not strictly first order in [Cr(II)] and [Co(III)] and no rate is reported.
[c] See ref. 37.
[d] See ref. 38.
[e] See ref. 35.
[f] See ref. 36.

spectrum of the 2+ band obtained from cation exchange chromatography was erratic and quite different from that obtained if the reaction proceeds from 2–9 h. In particular the extinction coefficient at the 315 nm peak was altered by up to 50% depending upon the particular run.

Both $[Cr(OH_2)_4(3\text{-formyl-ptdn})]^{2+}$ (from the free ligand) and $[Cr(OH_2)_4(2\text{-acetyl-btdn})]^{2+}$ (from the reduction) appear to be very stable (no decomposition occurs in 2 d at room temperature). This indicated that the free ligand decomposed to 2,4-pentanedione after 9 h in solution and the contaminant was $[Cr(OH_2)_4(ptdn)]^{2+}$. This hypothesis was strengthened by the observation that in the preparation of the cobalt complex **2** some $[Co(en)_2(ptdn)]^{2+}$ was also obtained even though **2** does not decompose to the 2,4-pentanedione complex once formed. To establish that the spectrum reported for $[Cr(OH_2)_4(3\text{-formyl-ptdn})]^{2+}$ was due only to this complex with no contamination by the 2,4-pentanedione complex, a series of product analyses were carried out over reaction times of from 2 to 8 h. Identical spectra were obtained indicating that 3-formylpentane-2,4-dione remained intact for this time period.

To verify the assignments made for **4** and **5** the complex $[Cr(OH_2)_4(ptdn)]^{2+}$ was prepared by reacting 2,4-pentanedione and $Cr(OH_2)_6^{3+}$ in acidic solution. Cation exchange chromatog-

Can. J. Chem. Downloaded from www.nrcresearchpress.com by 210.87.254.6 on 09/05/12
For personal use only.

Can. J. Chem. Downloaded from www.nrcresearchpress.com by 210.87.254.6 on 09/05/12
For personal use only.

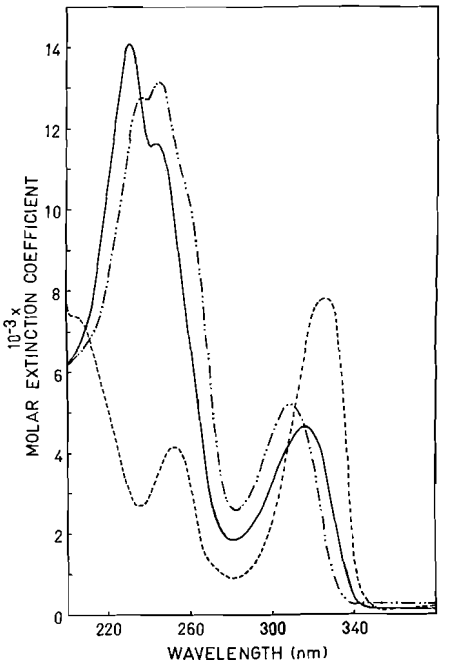

FIG. 3. Ultraviolet spectra of chromium(III) products: —, $Cr(OH_2)_4$(3-formyl-ptdn)$^{2+}$; ---, $Cr(OH_2)_4$(ptdn)$^{2+}$; ·····, $Cr(OH_2)_4$(2-acetyl-btdn)$^{2+}$.

raphy again gave three bands which eluted as 1+, 2+, and 3+ ions. The 2+ ion was formulated as $(OH_2)_4Cr(ptdn)^{2+}$ and had peak maxima (extinction coefficient) in the visible–ultraviolet at 553(27.0), 326(7880), 253(4140), and 204 nm (7380 M^{-1} cm^{-1}). This is sufficiently different from the spectra of **4** and **5** to support the previous formulations. The spectra of $[Cr(OH_2)_4$(3-formyl-ptdn)$]^{2+}$, $[Cr(OH_2)_4$(2-acetyl-btdn)$]^{2+}$, and $[Cr(OH_2)_4(ptdn)]^{2+}$ are given in Fig. 3 for comparative purposes.

Comparison of Kinetic Data With Related Systems

The kinetic parameters for reduction of $[Co(en_2)$(3-formyl-ptdn)$]^{2+}$ and related complexes by chromium(II) are collected in Table 4. Comparison of the rate of reduction of $[en_2Co(ptdn)]^{2+}$ to $[en_2Co$(3-formyl-ptdn)$]^{2+}$ and of $(NH_3)_5CoN{\equiv}C\langle\bigcirc\rangle^{3+}$ (35) to $(NH_3)_5CoN{\equiv}C\langle\bigcirc\rangle CHO^{3+}$ (36) indicates that the formyl group enhances electron transfer by a factor of approximately 10^7 M^{-1} s^{-1}. In both cases the unsubstituted complexes are probably reduced by an outer-sphere process while the substituted complexes react via inner-sphere mechanisms. For the reduction of complex **1** it appears that the chelate ring exhibits its aromatic behavior in a similar fashion to benzene in the 4-formylbenzonitrile ligand which is more reducible than the substituted chelate. Therefore, electron transfer occurs much more readily in the former complex. Also in the case of the chelate, two O—Co bonds must be stretched in the activation process prior to electron transfer whereas for the 4-formylbenzonitrile complex only stretching of the nitrogen–cobalt bond of the ligand need occur. A "remote attack" (32) mechanism has been demonstrated by product analysis in the case of the substituted chelate investigated in this work and by spectroscopic observation of the labile Cr(III) aldehyde-coordinated complex involving 4-formylbenzonitrile. In both cases the formyl group can attain planarity with the rest of the ligand and thus facilitate orbital overlap and electron transfer.

Our initial studies on reduction of the linkage isomer **2** indicate that electron transfer proceeds by a different mechanism. Changes in absorbance which occurred during electron transfer indicate that reactive intermediates are formed prior to reduction of Co(III). These changes depend upon the chromium(II) and cobalt(III) concentrations in an undetermined manner. When compared to the results obtained for reduction of **1** these differences may imply attack at the coordinated aldehyde group.[5] Studies on the reduction of **2** are in progress but are hampered by the difficulty in preparing the large quantities of complex required to ascertain the concentration dependencies of the rate and the nature of the products.

The activation parameters obtained for reduction of complex **1** are quite similar to those for reduction of $[en_2Co(O_2CCH_2NH_2)]^{2+}$ (37) where attack also occurs at the free carbonyl oxygen in an inner-sphere process. Presumably the reaction of complex **1** is slower because of the extra carbon atoms in the electron transfer path. It is known that addition of CH_2 groups in the electron transfer path causes the rate to fall sharply (38). Reduction of $[en_2Co(S(CH_3)$-

[5]It was pointed out in ref. 2 that coordinated aldehyde complexes are difficult to synthesize because the cobalt(III) oxidizes the aldehyde group. This may be a complicating factor in the electron transfer studies.

$CH_2CH_2NH_2)]^{3+}$ is an outer-sphere process and the activation parameters are different from those of the previous two complexes (8).

The authors wish to acknowledge the financial support of this research from the National Research Council of Canada.

1. J. L. BURMEISTER. Coord. Chem. Rev. **3**, 225 (1968).
2. J. P. COLLMAN and J. SUN. Inorg. Chem. **4**, 1273 (1965).
3. I. BERTINI and A. SABATINI. Inorg. Chem. **5**, 1025 (1966).
4. D. F. GUTTERMAN and H. B. GRAY. J. Am. Chem. Soc. **91**, 3105 (1969).
5. M. W. ADLARD and G. SOCRATES. J. Chem. Soc. Dalton, 797 (1972).
6. R. LANE and L. BENNETT. J. Am. Chem. Soc. **92**, 1090 (1970).
7. (*a*) J. P. COLLMAN, R. L. MARSHALL, and W. L. YOUNG (III). Chem. Ind. 1380 (1962); (*b*) J. P. COLLMAN. Angew. Chem. Int. Ed. **4**, 132 (1965).
8. M. J. GILROY. PhD Thesis, University of Florida, Gainesville, Florida. 1971. p. 70.
9. R. J. BALAHURA and R. B. JORDAN. J. Am. Chem. Soc. **92**, 1533 (1970).
10. R. J. BALAHURA and L. HUTLEY. Can. J. Chem. **51**, 3712 (1973).
11. S. Y. TYREE, JR. (*Editor*). Inorganic synthesis IX. McGraw-Hill, Toronto. 1967. p. 167.
12. BEILSTEIN, **1**, 808; **1**, 854.
13. B. D. AKEHURST and J. R. BARTELS-KEITH. J. Chem. Soc. 4798 (1957).
14. G. SCHLESSINGER. Inorganic laboratory preparations. Chemical Publishing Co., New York. 1962. p. 230.
15. J. P. COLLMAN, R. L. MARSHALL, W. L. YOUNG (III), and S. D. GOLDBY. Inorg. Chem. **1**, 704 (1962).
16. A. VILSMEIER and A. HAACK. Chem. Ber. **60**, 119 (1927).
17. T. SCHIRADO, E. GENNARI, R. MERELLO, A. DECINTI, and S. BUNEL. J. Inorg. Nucl. Chem. **33**, 3417 (1971).
18. K. NAKAMOTO. Infrared spectra of inorganic and coordination compounds. 2nd ed. Wiley–Interscience, New York., 1970. p. 247.
19. K. NAKAMOTO and P. MCCARTHY. Spectroscopy and structure of metal chelate compounds. Wiley, New York. 1968. p. 250.
20. K. NAKAMOTO and A. E. MARTELL. J. Chem. Phys. **32**, 588 (1960).
21. S. PINCHAS, B. SILVER, and I. LAULICHT. J. Chem. Phys. **46**, 1506 (1967).
22. H. MUSSO and H. JUNGE. Tetrahedron Lett. **33**, 4003 (1966).
23. M. MIKAMI, I. NAKAGAWA, and T. SHIMANOUCHI. Spectrochim. Acta, **23A**, 1037 (1967).
24. L. J. BOUCHER and J. C. BAILAR, JR. Inorg. Chem. **3**, 589 (1964).
25. R. P. DRYDEN and A. WINSTON. J. Phys. Chem. **62**, 635 (1958).
26. L. J. BOUCHER. Inorg. Chim. Acta, **6**, 29 (1972).
27. J. P. COLLMAN and E. T. KITTLEMAN. J. Am. Chem. Soc. **83**, 3529 (1961).
28. J. A. LASWICK and R. A. PLANE. J. Am. Chem. Soc. **81**, 3564 (1959).
29. D. H. HUCHITAL and H. TAUBE. J. Am. Chem. Soc. **87**, 5371 (1965).
30. R. D. BUTLER and H. TAUBE. J. Am. Chem. Soc. **87**, 5597 (1965).
31. E. S. GOULD. J. Am. Chem. Soc. **89**, 5792 (1967).
32. A. ZANELLA and H. TAUBE. J. Am. Chem. Soc., **94**, 6403 (1972).
33. R. J. BALAHURA and W. L. PURCELL. Unpublished results.
34. H. J. PRICE and H. TAUBE. Inorg. Chem. **7**, 1 (1968).
35. R. J. BALAHURA, G. B. WRIGHT, and R. B. JORDAN. J. Am. Chem. Soc. **95**, 1137 (1973).
36. R. J. BALAHURA and W. L. PURCELL. To be published.
37. F. SEDOR. PhD Thesis, University of Florida, Gainesville, Florida. 1971.
38. R. FRASER. Inorg. Chem. **3**, 1561 (1964).

Can. J. Chem. Downloaded from www.nrcresearchpress.com by 210.87.254.6 on 09/05/12
For personal use only.

Complexes of 2-Mercaptobenzothiazole with Cu(II), Ni(II), Co(II), Cd(II), Zn(II), Pb(II), Ag(I), and Tl(I)

I. P. KHULLAR AND U. AGARWALA[1]

Department of Chemistry, Indian Institute of Technology, Kanpur-208016, U.P., India

Received August 21, 1974

I. P. KHULLAR and U. AGARWALA. Can. J. Chem. **53**, 1165 (1975).

The complexes of 2-mercaptobenzothiazole with Cu(II), Ni(II), Co(II), Cd(II), Zn(II), Pb(II), Tl(I), and Ag(I) have been synthesized. Their structures have been assigned on the basis of analytical, spectral (i.r. and visible), and magnetic data.

I. P. KHULLAR et U. AGARWALA. Can. J. Chem. **53**, 1165 (1975).

On a synthétisé les complexes du mercapto-2 benzothiazole avec le Cu(II), Ni(II), Co(II), Cd(II), Zn(II), Pb(II), Tl(I) et Ag (I). On leur a attribué des structures en se basant sur les données analytiques, spectrales (i.r. et visible) et magnétiques. [Traduit par le journal]

Can. J. Chem. Downloaded from www.nrcresearchpress.com by 210.87.254.5 on 09/05/12
For personal use only.

The use of 2-mercaptobenzothiazole (**1**) as an analytical reagent (1–4) and of its complexes in industry and medicine has been known for a long time (5, 6). The structures of its complexes with a few metal ions have also been investigated using various physical techniques (7–9). In our laboratory, we have for quite some time now been interested in the complexing properties of the HNCS group (10–13). We felt it worthwhile to attempt investigating the structural aspects of the complexes of **1** with metal ions like Cu(II), Ni(II), Co(II), Cd(II), Zn(II), Pb(II), and also with Ag(I) and Tl(I).

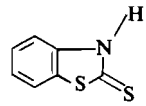

1

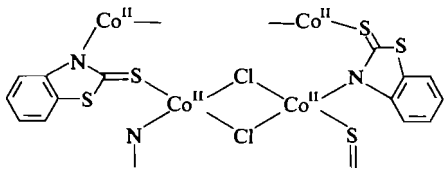

2
Structure of Co(MBT)Cl

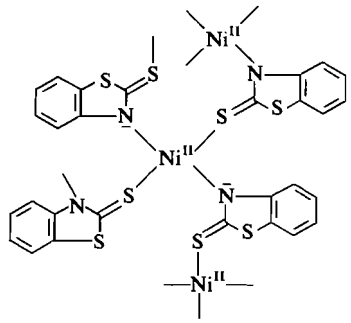

3
Structure of Ni(MBT)$_2$

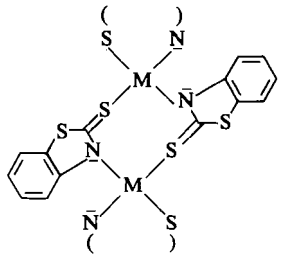

4
M = Cu(II) (Square Planar)
M = Cd(II), Zn(II), and Pb(II) (Tetrahedral)
Structure of M(MBT)$_2$

Experimental

The commercially available 2-mercaptobenzothiazole (hereafter referred to as (MBTH)) was recrystallized from hot ethanol before use.

Preparation of Complexes

(i) Bis(2-mercaptobenzothiazolato(1-))copper(II), Cu(MBT)$_2$

A solution of $CuCl_2.2H_2O$ (0.9 g, ~5 mmol) in 50 ml ethanol was added to a solution of ligand (1.7 g, ~10 mmol) in about 80 ml of ethanol. A light yellow compound was immediately precipitated which was digested on a water bath for about an hour. It was cooled, centri-

[1]To whom correspondence should be addressed.

Can. J. Chem. Downloaded from www.nrcresearchpress.com by 210.87.254.5 on 09/05/12
For personal use only.

fuged, washed repeatedly with hot ethanol and ether. The complex was dried in an air-oven at 120 °C.

Anal. Calcd. for $Cu(MBT)_2$: C, 42.5; H, 2.0; N, 7.1; S, 32.4; Cu, 16.1. Found: C, 42.4; H, 1.9; N, 7.2; S, 32.5; Cu, 16.3.

(ii) Bis(2-mercaptobenzothiazolato(1-))nickel(II), $Ni(MBT)_2$

A solution of $NiCl_2.6H_2O$ (1.2 g, ~5 mmol) in 50 ml ethanol was added to a solution of ligand (1.7 g, ~10 mmol) in about 80 ml ethanol neutralized with NH_4OH solution whereby a brown complex precipitated. After about an hour, the precipitate was centrifuged, washed repeatedly with ethanol and ether. It was dried overnight in an air-oven at 120 °C.

Anal. Calcd. for $Ni(MBT)_2$: C, 43.0; H, 2.0; N, 7.2; S, 32.8; Ni, 15.2. Found: C, 42.6; H, 2.0; N, 7.3; S, 32.9; Ni, 14.8.

(iii) Mono(2-mercaptobenzothiazolato(1-))mono chloro cobalt(II), Co(MBT)Cl

$CoCl_2$ (1.2 g, ~5 mmol), in a similar procedure as above (*ii*) gave a green colored complex.

Anal. Calcd. for Co(MBT)Cl: C, 32.3; H, 1.5; N, 5.3; S, 24.6; Co, 22.6. Found C, 32.4; H, 1.7; N, 4.9; S, 24.9; Co, 22.3.

(iv) Bis(2-mercaptobenzothiazolato(1-))cadmium(II), $Cd(MBT)_2$

$CdCl_2$ (0.8 g, ~2.5 mmol) in 50 ml water, in a similar procedure as above (*ii*) gave a cream colored complex.

Anal. Calcd. for $Cd(MBT)_2$: C, 38.4; H, 2.0; N, 5.4; S, 28.6; Cd, 24.7. Found: C, 37.8; H, 1.8; N, 6.3; S, 28.8; Cd, 25.2.

(v) Bis(2-mercaptobenzothiazolato(1-))zinc(II), $Zn(MBT)_2$

$ZnCl_2$ (0.35 g, ~2.5 mmol) in a procedure similar to (*iv*) gave a cream colored complex.

Anal. Calcd. for $Zn(MBT)_2$: C, 42.3; H, 2.0; N, 7.0; S, 32.3; Zn, 16.5. Found: C, 41.8; H, 1.8; N, 6.3; S, 32.5; Zn, 16.9.

(vi) Bis(2-mercaptobenzothiazolato(1-))lead(II), $Pb(MBT)_2$

$Pb(NO_3)_2$ (0.8 g, ~2.5 mmol) in a procedure similar to (*i*) gave a yellow colored complex.

Anal. Calcd. for $Pb(MBT)_2$: C, 32.3; H, 1.7; N, 5.4; Pb, 38.4. Found: C, 31.2; H, 1.5; N, 5.2; Pb, 37.9.

(vii) Mono(2-mercaptobenzothiazolato(1-))silver(I), Ag(MBT)

$AgNO_3$ (0.4 g, ~2.5 mmol) in a procedure similar to (*v*) gave a dark yellow colored complex.

Anal. Calcd. for Ag(MBT): C, 30.7; H, 1.4; N, 5.1; S, 23.4; Ag, 35.5. Found: C, 31.6; H, 1.6; N, 4.8; S, 24.0; Ag, 34.8.

(viii) Mono(2-mercaptobenzothiazolato(1-))thallium(I), Tl(MBT)

$TlNO_3$ (0.3 g, ~2.5 mmol) in a procedure similar to (*vii*) gave a yellow colored complex.

Anal. Calcd. for Tl(MBT): C, 22.7; H, 1.0; N, 3.8; S, 17.3; Tl, 55.1. Found: C, 22.7; H, 0.7; N, 4.6; S, 17.1; Tl, 54.0.

Analysis

The analyses of the metal ions and sulfur were carried out by the standard methods (14, 15). Carbon, hydrogen, and nitrogen analyses were performed by the Microanalytical Section of the Indian Institute of Technology, Kanpur, India.

Infrared Spectra

Infrared spectra of the ligand and of the complexes were recorded with a Perkin–Elmer Model 521 diffraction grating infrared spectrophotometer in the range of 4000–250 cm^{-1}. Samples were prepared as KBr discs. Major bands of the ligand and the complexes are given in Table 1.

Magnetic Susceptibility Measurements

The magnetic susceptibilities of these complexes were determined with the help of a Gouy balance. Mercury tetrathiocyanato cobaltate(II) was used as a magnetic susceptibility standard and the diamagnetic corrections were estimated by a method outlined by Figgis and Lewis (16).

Visible Spectra

The absorption spectra of the ligand and the complexes were recorded on a Beckman DU-2 spectrophotometer in Nujol mull between 250 and 1000 nm.

Results and Discussion

If one assumes that a particular ion adopts its normally preferred geometry in its complexes, the analytical results then suggest the ligand is behaving in a bidentate fashion. Before forming the complex, the ligand may exist either in the thione or in the thiol form. However, it is assumed here that in solution it is behaving as a tautomer rather than in any one particular form.

It is evident that in the ligand molecule, there are only two bonding sites: (*a*) the thiocarbonyl sulfur atom, and (*b*) the nitrogen atom. Since the lone pairs on the sulfur atom present in the skeleton of the ring are involved in the resonating structures of the molecule, it is therefore expected that it should have very weak coordinating ability (17). It is, therefore, assumed that it will not coordinate with the metal ions. As-

TABLE 1. Assignments of the major infrared bands of the ligand and the complexes (cm^{-1})

Ligand	Complexes§	Assignments
3110	—	$\nu_{(N-H)}$
1490	1500 ± 10 m	Thioamide band **1***
1320	1370	Thioamide band **2**†
1010	1000 ± 10 m	Thioamide band **3**‡
860	720 ± 15	Thioamide band **4**‖
—	500 ± 5 w	$\nu_{(M-N)}$
—	340 ± 20 w	$\nu_{(M-S)}$

*Due to $\nu_{(N-H)} + \nu_{(C-N)}$.
†Mainly due to $\nu_{(C-N)} + \nu_{(N-H)}$.
‡Mainly due to $\nu_{(C-N)} + \nu_{(C=S)}$.
‖Mainly due to $\nu_{(C=S)}$.
§m = medium; w = weak.

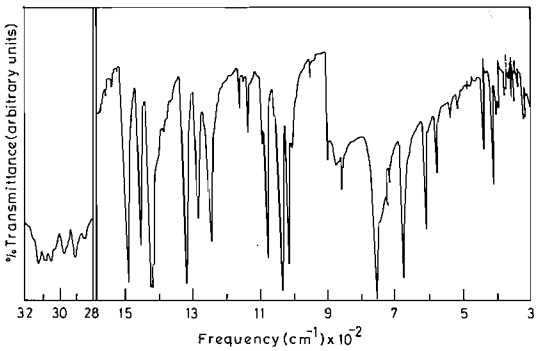

FIG. 1. Infrared spectrum of ligand 2-mercaptobenzothiazole (MBTH).

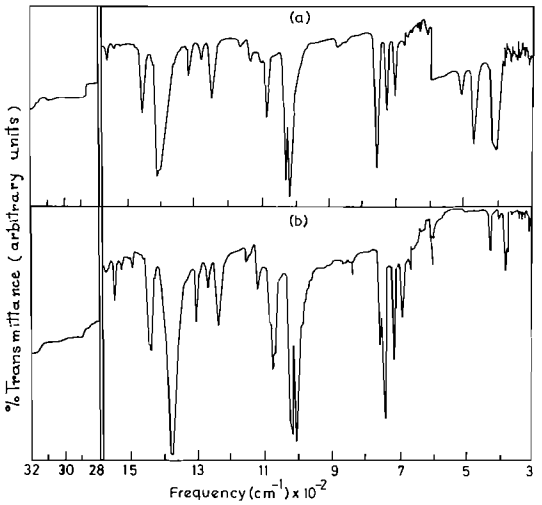

FIG. 2. Infrared spectra of (*a*) $Cu(MBT)_2$, (*b*) $Cd(MBT)_2$.

suming this there remain only two bonding sites on the ligand molecule, the ligand can therefore in some complexes behave as monodentate while in some as bidentate. In order to know the mode of bonding in the complexes, the i.r. studies of these complexes have been made.

Infrared spectra of several heterocyclic systems, in which a 5-membered ring with one or more hetero-atoms is fused to a benzene ring, have been studied and the bands around 1600, 1460, 1390, 1310, 1270, 1250, 1200, 1160, 1100, 1060, 1020, 950, 890, 850, 800, and 750 cm^{-1} have been found to be common to all the systems (18). These bands appear in the spectra of the ligand and the complexes and therefore they have been assigned to the ligand skeletal modes of vibration. Besides these bands, the bands at 3100, 1490, 1010, and 860 cm^{-1} are also present in the spectrum of the ligand. Since the ligand has one HNCS group, one should expect the bands due to N—H stretching mode, thioamide bands, **1**, **2**, **3**, **4** in the regions 3100, 1500, 1300, 1000, and 800 cm^{-1} respectively (19, 20). The bands around 3100, 1490, 1010, 860 cm^{-1} have been assigned to $\nu_{(N-H)}$, thioamide **1**, **3**, and **4** respectively. Undoubtedly the thioamide bands **1**, **3**, **4** will not be purely due to $\delta_{(N-H)}$, $\nu_{(C-N)}$, and $\nu_{(C=S)}$, but they must also be coupled with the other fundamental modes of skeletal vibrations (21). However, it is tacitly assumed that these bands arise due to contributions from $\delta_{(N-H)}$, $\nu_{(C-N)}$, and $\nu_{(C=S)}$. The major contribution from $\nu_{(C=N)}$ should be present in the band at 1318 cm^{-1}.

The direction of shifts in the positions of all the bands in the spectra of the complexes are the same. It indicates that the bonding pattern in the complexes should be similar. The major changes in the spectra of the complexes as compared to that of the ligand are as follows:

(*a*) The bands due to $\nu_{(N-H)}$ and $\delta_{(N-H)}$ are not present in the spectra of complexes. This is what one should expect if the charge balance in the complexes is to be maintained.

(*b*) The position of the band at 1320 cm^{-1} (thioamide band **2**) having major contribution from $\nu_{(C=N)}$ shifts to higher wavenumber ($\sim$1370 cm^{-1}). This shows that the bond order of C=N is increased. It indicates that metal ion is bonded to thiocarbonyl sulfur.

(*c*) The thioamide band (**4**) having major contribution from $\nu_{(C=S)}$ (22) shifts to 700 cm^{-1} region suggesting further that the metal is bonded to sulfur.

(*d*) Two new bands appear around 500 and 300 cm^{-1} in the spectra of the complexes which could be assigned to coupled vibrations having contributions from $\nu_{(M-N)}$ (23) and $\nu_{(M-S)}$ (24).

It is, therefore, concluded from the i.r. spectra (*i*) that metal ions are bonded to thiocarbonyl sulfur atom and (*ii*) that N—H group is not present. It is difficult to say from the i.r. studies if the bonding of the metal ions take place through nitrogen also. However, if in the complexes the ligand molecules take the orientation in such a way that it gives the usually preferred geometry to the metal ion, the ligand molecule should be bidentate. The only other donor atom in the ligand molecule is nitrogen. Hence it is assumed that the metal ions coordinate with the

Can. J. Chem. Downloaded from www.nrcresearchpress.com by 210.87.254.5 on 09/05/12
For personal use only.

Can. J. Chem. Downloaded from www.nrcresearchpress.com by 210.87.254.5 on 09/05/12
For personal use only.

TABLE 2. Electronic spectral bands, their assignments, crystal field parameters, and magnetic moments

Complex	Position			Assignments	Δ_1 (cm^{-1})	Δ_2 (cm^{-1})	B (cm^{-1})	C (cm^{-1})	β	Magnetic moment (B.M.)
	Band	In nm	In cm^{-1}							
$Cu(MBT)_2$	ν_1	960	10 416	—	—	—	—	—	—	Diamagnetic
	ν_2	770	12 987	$d_{xy} \rightarrow d_{z^2}$						
	ν_3	510	19 607	$d_{xy} \rightarrow d_{x^2-y^2}$						
	ν_4	410	24 390	Characteristic of copper complex having spin-pairing						
$Ni(MBT)_2$	ν_1	925	10 810	$^1A_{1g} \rightarrow {}^3A_{2g}$	20455	7290	600	3200	0.58	Diamagnetic
	ν_2	790	12 700	$^1A_{1g} \rightarrow {}^3E_g$						
	ν_3	580	17 240	$^1A_{1g} \rightarrow {}^1A_{2g}$						
	ν_4	440	22 730	$^1A_{1g} \rightarrow {}^1E_g$						
Co(MBT)Cl		740	13 513	$^4A_2(F) \rightarrow {}^4T_1(P)$	—	—	—	—	—	4.49

Can. J. Chem. Downloaded from www.nrcresearchpress.com by 210.87.254.5 on 09/05/12
For personal use only.

ligand through both the thiocarbonyl sulfur and the nitrogen atom.

Magnetic and Visible Spectral Studies

The magnetic and the spectral properties of copper, cobalt, and nickel complexes were studied to understand the spatial arrangement of the ligand molecules around the metal ions. The values of magnetic moment corrected for ligand diamagnetism, the position of the electronic absorption bands, and their most probable assignments are given in Table 2.

The magnetic moment of the green cobalt complex is 4.49 B.M. Since the orbital contribution in the tetrahedral Co(II) is much less than that of the octahedral complexes, tetrahedral cobalt(II) complexes have generally lower values of magnetic moments (4.3–4.7 B.M.) (25, 26) as compared to those of octahedral complexes (4.7–5.6 B.M.) (27, 28). The value of magnetic moment (4.49 B.M.) of the complex studied lies well within the range of tetrahedral complexes. The green color of the complex also indicates the tetrahedral geometry of the complex. The electronic spectrum of cobalt(II) complex shows a band at 740 nm. The presence of this band alone cannot distinguish between the tetrahedral and the octahedral geometry. However, the absence of any band around 450 nm suggests the tetrahedral geometry of the complex (29) and therefore, the band at 740 nm is assigned to $^4A_2(F) \rightarrow {}^4T_1(P)$ transition. Thus, on the basis of i.r., magnetic moment, color, and visible spectrum polymeric structure is tentatively proposed for the cobalt(II) complex, **2**. Because of the complete insolubility of the complex in any of the common solvents, it is assumed to be polymeric.

The nickel complex $Ni(MBT)_2$ is diamagnetic. The diamagnetism is very strong indication that the spatial arrangement of the ligand molecules around the nickel ion is square planar, since the other preferred orientations should give the value of the magnetic moment corresponding to two unpaired electrons.

The electronic spectrum of the nickel complex shows four bands at 925, 790, 580, and 440 nm. The intensities of the bands at 925 and 790 nm are relatively weak compared to those at 580 and 440 nm. For the nickel complex the symmetry has been approximated as D_{4h}. For a d^8 system, one should expect in D_{4h} symmetry six bands due to d–d transitions (three singlet → triplet, $^1A_1 \rightarrow {}^3A_2$, ^3E_g, $^3B_{1g}$ and three singlet → singlet, $^1A_{1g} \rightarrow {}^1A_{2g}$, ^1E_g, $^1B_{1g}$ transition (30). Two transition from $^1A_{1g} \rightarrow {}^3B_{1g}$ and $^1B_{1g}$ generally appear in the near u.v. region which may be masked by charge transfer bands present in this region. The other bands which appear in the spectrum of the complex have been assigned as given in Table 2. From the positions of these bands ligand field parameters Δ_1, Δ_2, B, C, and β have been evaluated. These values are also given in Table 2. As expected $\Delta_1 \gg \Delta_2$ since the donor ligand causes a marked destabilization of the b_{1g} ($d_{(x^2-y^2)}$) level while b_{2g} (d_{xy}) level remains practically nonbonding. The values of B (600) and β (0.58) indicate a substantial covalency in the bonds between the ligand donor atoms and the nickel ion. The complex is highly insoluble in all the common solvents. Thus, on the basis of i.r., magnetic moment, and electronic spectral studies square planar polymeric structure is proposed for nickel complex, **3**.

The stoichiometry of the copper complex is $Cu(MBT)_2$. Simple oxidation–reduction experiments showed that in the complex copper is present in +2 oxidation state. This is one of the few copper(II) complexes in which the spin paramagnetism is completely quenched ($\mu_{eff} = 0$) at room temperature. The diamagnetism indicates that there is strong spin–spin interaction between two cupric ions. This may take place either by the formation of a σ or δ bond by the overlap of the two d-orbitals whereby spins of the electrons are paired up or by the formation of extended molecular orbitals by the extended overlap of copper and one of the two ligand donor orbitals. However, in quite a large number of diamagnetic copper(II) complexes, partial or complete quenching is explained by the superexchange mechanism. It is very difficult to decide without complete X-ray work, whether spin–spin interaction takes place because of σ or δ bond formation or by superexchange phenomenon. On the basis of copper carboxylate complexes where quenching of paramagnetism is explained by superexchange phenomenon, the authors also prefer the quenching by superexchange mechanism. This is because of the system 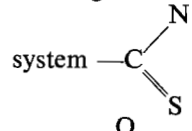 , where the bonding is similar to 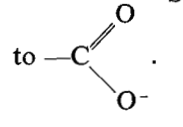 .

Can. J. Chem. Downloaded from www.nrcresearchpress.com by 210.87.254.5 on 09/05/12
For personal use only.

The spectra of diamagnetic copper carboxylate complexes show three bands in the regions 11 000, 13 500, and 26 000 cm^{-1} (31). Harris *et al.* (32) have proposed structure for the diamagnetic copper(II) complex of diazoaminobenzene in which there is metal–metal interaction and Cu^{2+} ion has square planar geometry. The electronic spectrum of this complex shows two bands at 670 and 530 nm which are assigned to $d_{xy} \rightarrow d_{z^2}$ and $d_{xy} \rightarrow d_{x^2-y^2}$ respectively. The visible spectrum of copper(II) complex shows four bands at 960, 770, 510, and 410 nm. Assuming a square planar arrangement of the ligand molecules around copper(II) ion, the bands at 770 and 510 nm are tentatively assigned to $d_{xy} \rightarrow d_{z^2}$ and $d_{xy} \rightarrow d_{x^2-y^2}$ respectively (Table 2). Tsuchida and co-workers (33, 34) indicated that all the copper complexes in which the paramagnetism is partially or completely quenched absorb around 375 nm region. In our complex, a band at 410 nm appeared which may be a similar band as detected by Tsuchida and co-workers (33, 34). This complex is completely insoluble in all the noncoordinating solvents. Thus, the insolubility in the inorganic and organic noncoordinating solvents, stoichiometry diamagnetism, visible, and i.r. spectral data indicate square-planar polymeric structure for the copper complex, **4**.

Most of the Cd(III), Zn(II), Pb(II) complexes mentioned in the literature are tetrahedral (35). The complexes are diamagnetic, therefore, the tetrahedral arrangement of the ligand molecules around Cd(II), Zn(II) and Pb(II) are assigned to these complexes (structure **4**).

Similarly Ag(I) and Tl(I) complexes are linear. These complexes are also diamagnetic. Therefore, linear structures are proposed for these complexes, **5**.

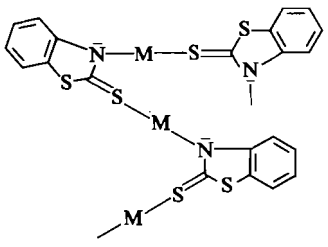

5

M = Ag(I) and Tl(I) (Linear)
Structure of M (MBT)

1. E. G. Walliczek. Talenta, **11**, 573 (1964).
2. B. C. Bera and M. M. Chakrabarthy. Microchem. J. **11**, 420 (1966).
3. A. V. Nikolaev, V. M. Shulman, L. M. Gindin, and S. V. Larionov. Izv. Sib. Otd. Akad. Nauk. SSSR, Ser. Khim. Nauk. **4**, 60 (1970).
4. I. Ubaldini. Gazz. Chim. Ital. **78**, 293 (1948).
5. (*a*) H. S. Patinkin and H. Thomas Webb. U.S. 3 524 733 (1970); (*b*) Régie Nationale des Usines, Brit. 914 787 (1963).
6. R. Davide Grassetti, J. F. Murray, Jr., M. E. Brokke, and A. D. Gutman. J. Med. Chem. **13**, 273 (1970).
7. L. N. Lomakina and E. K. Yakovskay. Zh. Anal. Khim. **24**, 1172 (1969).
8. G. Wilkinson, D. J. Gilbert, and David Rose. J. Chem. Soc. A, 2765 (1970).
9. F. Wilson and P. Merchant. J. Inorg. Nucl. Chem. **29**, 1993 (1967).
10. Umesh Agarwala, V. A. Narayan, and S. K. Dikshit. Can. J. Chem., **45**, 1057 (1967).
11. J. S. Dwivedi and U. Agarwala. J. Inorg. Nucl. Chem. **35**, 2229 (1973).
12. Lakshmi and U. Agarwala. J. Inorg. Nucl. Chem. **34**, 241 (1972).
13. I. P. Khullar and U. Agarwala. Aust. J. Chem. **27**, 1877 (1974).
14. A. I. Vogel. A text book of quantitative inorganic analysis. Longmans Green and Co. Ltd., London. 1972.
15. E. P. Treadwell and W. T. Hall. Analytical chemistry, Vol. II. John Wiley and Sons, Inc., N.Y. 1958. pp. 77, 199.
16. B. N. Figgis and J. Lewis. Modern coordination chemistry. *Edited by* J. Lewis and R. G. Wilkins. Interscience Publishers, Inc., N.Y. 1960. p. 403.
17. Robert T. Morrison and Robert N. Yoyd. Organic chemistry. 2nd ed. Prentice Hall Pvt. (Ltd.), Eastern Economy Editions, New Delhi-110001, India. 1973. p. 1076.
18. C. N. R. Rao. Chemical applications of infrared spectroscopy. Academic Press, New York. 1963.
19. C. N. R. Rao, R. Venkataraghavan, and T. R. Kasturi. Can. J. Chem. **42**, 36 (1964).
20. C. N. R. Rao and R. Venkataraghavan. Spectrochim. Acta, **18**, 541 (1962).
21. K. Nakamoto and A. E. Martell. J. Chem. Phys. **32**, 588 (1960).
22. I. Suzuki. Bull. Chem. Soc. Jap. **35**, 1286, 1449, 1456 (1962).
23. D. M. Adams and J. B. Cornell. J. Chem. Soc. A, 1299 (1968).
24. K. Nakamato. Infrared spectra of inorganic and coordination compounds. John Wiley and Sons, Inc., New York, N.Y. 1964. p. 146.
25. (*a*) R. H. Holm and F. A. Cotton. J. Chem. Phys. **31**, 788 (1959); (*b*) R. H. Holm and F. A. Cotton. J. Chem. Phys. **32**, 1168 (1960).
26. F. A. Cotton, D. M. L. Goodgame, and M. Goodgame. J. Am. Chem. Soc. **83**, 4690 (1961).
27. G. N. Tyson, Jr. and S. C. Adams. J. Am. Chem. Soc. **62**, 1226 (1940).
28. B. N. Figgis and R. N. Nyholm. J. Chem. Soc. 12 (1954).

29. A. P. B. LEVER. Inorganic electronic spectroscopy. Elsevier Publishing Co., New York. 1968. p. 322.
30. C. J. BALLHAUSEN and H. B. GRAY. Coordination chemistry, Vol. 1. *Edited by* A. E. Martell. Van Nostrand Reinhold Co., New York, 1971. p. 66.
31. A. P. B. LEVER. Inorganic electronic spectroscopy. Elsevier Publishing Co., New York. 1968. p. 360.
32. C. M. HARRIS, B. F. HOSKINS, and R. L. MARTIN. J. Chem. Soc. 3728 (1959).
33. Y. YAMADA, H. NAKAMURA, and T. TSUCHIADA. Bull. Chem. Soc. Jap. **31**, 303 (1958).
34. S. YAMADA, H. NISHIKAVA, and T. TSUCHIDA. Bull. Chem. Soc. Jap. **33**, 1278 (1960).
35. F. A. COTTON and G. WILKINSON. Advanced inorganic chemistry, a comprehensive text, 3rd ed. Interscience Publishers, Inc., N.Y. 1972.

Can. J. Chem. Downloaded from www.nrcresearchpress.com by 210.87.254.5 on 09/05/12
For personal use only.

Correlation of the Diterpenoids Sideritol and Jativatriol

CARLOS VON CARSTENN-LICHTERFELDE, FERNANDO M. PANIZO, TERESA G. DE QUESADA, BENJAMIN RODRÍGUEZ, AND SERAFIN VALVERDE

Instituto de Química Orgánica, CSIC, Juan de la Cierva 3, Madrid 6, Spain

AND

WILLIAM A. AYER AND JO-ANN H. BALL

Department of Chemistry, University of Alberta, Edmonton, Alberta T6G 2E1

Received November 21, 1974

CARLOS VON CARSTENN-LICHTERFELDE, FERNANDO M. PANIZO, TERESA G. DE QUESADA, BENJAMIN RODRÍGUEZ, SERAFIN VALVERDE, WILLIAM A. AYER, and JO-ANN H. BALL. Can. J. Chem. **53**, 1172 (1975).

The diterpenoids jativatriol (**1**) and sideritol (**2**) have been correlated by transformation of each into *ent*-17-noratis-13-en-1,16-dione (**9**). In the case of jativatriol, a simple procedure is described for transforming the *ent*-15-beyerene derivative into an *ent*-13-atisene derivative.

CARLOS VON CARSTENN-LICHTERFELDE, FERNANDO M. PANIZO, TERESA G. DE QUESADA, BENJAMIN RODRÍGUEZ, SERAFIN VALVERDE, WILLIAM A. AYER et JO-ANN H. BALL. Can. J. Chem. **53**, 1172 (1975).

On a établi une corrélation entre les diterpénoides jativatriol (**1**) et sidéritol (**2**) en les transformant chacun en *ent*-nor-17 atizène-13 dione-1,16 (**9**). Dans le cas du jativatriol, on décrit une procédure simple pour transformer le dérivé *ent*-beyérène-15 en dérivé *ent*-atizène-13.

[Traduit par le journal]

Jativatriol (**1**) (1) and sideritol (**2**) (2) are diterpenoids isolated from *Sideritis angustifolia* Lag. (family *Labiatae*). Sideritol is the first reported diterpenoid of the *ent*-atisane type which does not contain nitrogen as well as the first reported *ent*-atis-13-ene derivative. As noted previously (2) sideritol may be biogenetically related to jativatriol. Rearrangement of the latter as indicated by the arrows in **1** leads to **2**. Conceivably both compounds originate from a common intermediate arising from oxidation of the *ent*-beyer-15-ene skeleton at C-12. In this paper we describe two methods by which jativatriol has been transformed into a derivative of sideritol, confirming our previous conclusions regarding the relationship of these two compounds. In particular, this work firmly establishes the location of the secondary hydroxyl at C-1 in sideritol, a point which had previously been inferred from chemical and spectroscopic data but not directly proven.

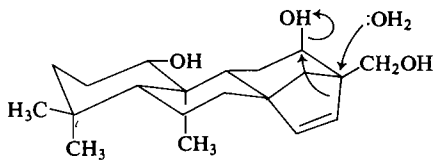

1

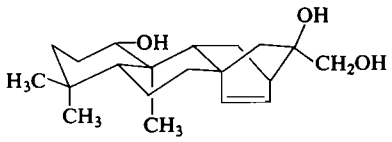

2

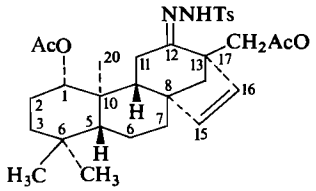

3

The transformation of an *ent*-15-beyerene derivative to an *ent*-13-atisene derivative by reductive rearrangement of a 12-tosylhydrazone has recently been reported (3). This same procedure has now been applied to the tosylhydrazone **3** derived (see Experimental) from jativatriol (**1**). The product proved to be a mixture of C-16 epimers, *ent*-1β,17-diacetoxy-16*S*-atis-13-ene (**4**) and ent-1β,17-diacetoxy-16*R*-atis-13-ene (**5**). The stereochemistry at C-16 in these epimers was established by comparing the chemical shifts of the —CH_2OAc protons in **4** and **5** with their respective dihydro deriva-

Can. J. Chem. Downloaded from www.nrcresearchpress.com by 210.87.254.105 on 09/05/12
For personal use only.

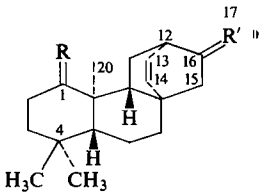

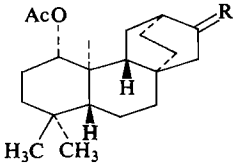

4 R = 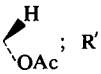 ; R′ = 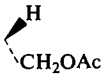

6 R =

5 R = 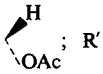 ; R′ = 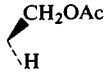

7 R =

8 R = 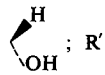 ; R′ = 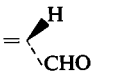

9 R = O; R′ = O

tives **6** and **7**. The large downfield shift (0.33 p.p.m.) observed for these protons as we go from **4** to **6** indicates that in **4** the acetoxymethyl is *endo* to the double bond (4) and thus has the *ent*-16*S* configuration. In agreement with this result the observed effect (upfield shift of 0.04 p.p.m.) between **5** and **7** indicates the *ent*-16*R* configuration in **5**.

A simpler method of effecting the rearrangement of jativatriol (1) to an *ent*-13-atisene derivative has also been discovered. When a solution of jativatriol in aqueous methanolic HCl is heated under reflux for several hours the aldehyde **8** (as a mixture of C-16 epimers) is obtained in 70% yield. The n.m.r. spectrum of this mixture shows aldehydic signals at δ 9.75 and 9.35 in the ratio of 1:3. Repeated recrystallization from hexane–acetone afforded the epimer displaying the δ 9.35 signal, assigned the stereochemistry shown in **8** on the basis of the upfield shift of the aldehydic signal relative to that of the minor epimer. This assignment was confirmed by reduction ($NaBH_4$) of **8** and subsequent acetylation to give compound **4**.

Oxidative decarbonylation (5) of **8** gave a compound which without further characterization was oxidized with Jones' reagent to the diketone **9**. Oxidation of sideritol (**2**) with excess Jones' reagent gave, in high yield, the same diketone (**9**), thus completing the correlation of the two series and firmly establishing the location of an oxygen function at C-1 in sideritol.

Experimental

Solutions were dried over anhydrous sodium sulfate. Melting points were determined in a Kofler apparatus and are uncorrected. The optical rotations were measured with a Perkin Elmer 141 polarimeter with 1-dm cells. Infrared spectra were recorded on a Perkin Elmer Model 257 spectrometer. Nuclear magnetic resonance spectra were measured using a Perkin Elmer Model R-12 spectrometer or a Varian XL-100 spectrometer in $CDCl_3$ solution and with tetramethylsilane as internal standard and are quoted as δ (number of protons, description of signal assignment). Elementary analyses were carried out in the Instituto de Química Orgánica, Madrid, with the aid of an automatic analyser. Silica gel Merck (60 PF_{254}) was used for preparative layer chromatography.

Preparation of ent-1β,17-Diacetoxy-15-beyeren-12-tosylhydrazone (3)

To a solution of jativatriol-1-monoacetate (1 g), obtained from jativatriol triacetate as described in ref. 1, in anhydrous pyridine (5 ml) was added acetic anhydride (5 ml). The solution was allowed to stand 30 min at 0° and then poured into water and extracted with chloroform. The chloroform layer was dried, filtered, and evaporated leaving a residue which on t.l.c. shows two components. The less polar of these corresponded to jativatriol triacetate, while the other, isolated by preparative t.l.c. (eluent benzene – ethyl acetate 1:1), is a mixture (700 mg) of 1,17- and 1,12-jativatriol diacetates (4:3 ratio according to n.m.r. data). This mixture was dissolved in acetone (20 ml) and mixed with Jones' reagent (1.5 ml). The oxidation was allowed to proceed for 2 h at room temperature. Two products were obtained and these were separated by preparative t.l.c. (eluent benzene – ethyl acetate 3:2):

ent-1β,17-Diacetoxy-15-beyeren-12-one (380 mg): m.p. 145–147° (from aqueous EtOH); $[\alpha]_D^{22}$ −238.1° (*c* 0.44, $CHCl_3$); i.r. (KBr) cm^{-1}: 3080 (olefinic CH); 2980, 2970, 2940, 2920, 2860 (CH stretching vibrations); 1735 (ester); 1710 (ketone); 1235 (C—O of ester); 761 (*cis*-1,2-disubstituted olefin); n.m.r. (δ): 5.91 (2H, AB quartet, *J* 6 Hz, olefinic H-15 and H-16), 4.47 (1H, multiplet, $w_{1/2}$ 18 Hz, axial H-1), 4.19 (2H, AB quartet, *J* 11.3 Hz, H-17), 2.02 and 2.00 (3H each, singlets, two —$OCOCH_3$), C—Me singlets at 0.94, 0.91, and 0.87.

Anal. Calcd. for $C_{24}H_{34}O_5$: C, 71.61; H, 8.51. Found: C, 71.87; H, 8.43.

ent-1β,12α-Diacetoxy-15-beyeren-17-oic acid (290 mg): m.p. 189–191° (from *n*-hexane); $[\alpha]_D^{22}$ −10.0° (*c* 1.43, $CHCl_3$); i.r. (KBr) cm^{-1}: 3400–2550, 1705 (—COOH); 3060, 762 (olefin); 1740, 1240 (—OAc); n.m.r. (δ): 8.85 (1H, broad signal, —COOH), 5.96 (2H, AB quartet, *J* 6 Hz, olefinic H-15 and H-16), 5.30 (1H, multiplet, $w_{1/2}$ 8 Hz, equatorial H-12), 4.58 (1H, multiplet, $w_{1/2}$ 18 Hz, axial H-1), 2.04 and 2.01 (3H each, singlets, two —$OCOCH_3$), three C—Me singlets accumulated at 0.87 (9H).

Anal. Calcd. for $C_{24}H_{34}O_6$: C, 68.87; H, 8.19. Found: C, 68.97; H, 8.08.

Can. J. Chem. Downloaded from www.nrcresearchpress.com by 210.87.254.105 on 09/05/12
For personal use only.

Can. J. Chem. Downloaded from www.nrcresearchpress.com by 210.87.254.105 on 09/05/12
For personal use only.

To a solution of the above ketone (300 mg) in absolute ethanol (4 ml) was added tosylhydrazide (167 mg). The solution was then heated under reflux for 10 h. A crystalline precipitate appears on cooling. Crystallization from aqueous ethanol affords pure **3** (360 mg), m.p. 164–167°; $[\alpha]_D^{22}$ −112.3° (*c* 0.52, $CHCl_3$); i.r. (KBr) cm^{-1}: 3110 (—NH—); 3060, 3030, 1600, 758, 738, 685 (aromatic and olefinic); 1720, 1240 (—OAc); 1623 (>C=N—); 1165 (—Ts); n.m.r. (δ): 7.55 (4H, A_2B_2 system, *J* 8.6 Hz, aromatic protons), 5.78 (2H, AB quartet, *J* 6 Hz, olefinic H-15 and H-16), 4.42 (1H, multiplet, $w_{1/2}$ 18 Hz, axial H-1), 4.24 (2H, AB quartet, *J* 12 Hz, H-17), 2.42 (3H, singlet, CH_3—Ph), 2.19 and 1.98 (3H each, singlets, —$OCOCH_3$ on C-17 and C-1 respectively), C—Me singlets at 0.90, 0.86, and 0.85.

Anal. Calcd. for $C_{31}H_{42}O_6N_2S$: C, 65.24; H, 7.42; N, 4.91; S, 5.60. Found: C, 65.41; H, 7.35; N, 4.82; S, 5.71.

$NaBH_4$ Reduction of 3: Compounds 4 and 5

Sodium borohydride (200 mg) was slowly added to a solution of **3** (350 mg) in a 1:1 (v/v) mixture of dioxane – absolute ethanol (10 ml). The solution was then allowed to stir at room temperature for 4 h, diluted with water, and extracted with chloroform. The residue obtained by evaporation of the solvent was then separated into two components by preparative t.l.c. (eluent benzene – ethyl acetate 85:15).

ent-1β,17-Diacetoxy-16*S*-atis-13-ene (**4**): Less polar component, crystallizes from MeOH (133 mg), m.p. 123–125°; $[\alpha]_D^{20}$ +7.3° (*c* 0.72, $CHCl_3$); i.r. (KBr) cm^{-1}: 3040, 3000, 2960, 2930, 2880, 2855, 1728, 1250, 725, 710; n.m.r. (δ): 5.98 (2H, multiplet, olefinic H-13 and H-14), 4.60 (1H, apparent doublet of doublets, axial H-1), 3.61 (2H, doublet, *J* 7.3 Hz, H-17), 2.42 (1H, multiplet, $w_{1/2}$ 12 Hz, allylic H-12), 2.01 and 1.99 (3H each, singlets, two —$OCOCH_3$), C—Me singlets at 0.88, 0.83, and 0.76.

Anal. Calcd. for $C_{24}H_{36}O_4$: C, 74.19; H, 9.34. Found: C, 74.11; H, 9.41.

ent-1β,17-Diacetoxy-16*R*-atis-13-ene (**5**), more polar component, thick oil (49 mg): $[\alpha]_D^{20}$ +30.7° (*c* 0.26, $CHCl_3$); i.r. (NaCl) cm^{-1}: 3030, 2950, 2855, 1740, 1243, 720; n.m.r. (δ): 6.09 (2H, multiplet, olefinic H-13 and H-14), 4.55 (1H, apparent doublet of doublets, axial H-1), 3.99 (2H, octet, J_{gem} 10.6 Hz, J_{vic} 6.6 Hz, H-17), 2.37 (1H, multiplet, $w_{1/2}$ 12 Hz, allylic H-12), 2.04 and 1.99 (3H each, singlets, two —$OCOCH_3$), C—Me singlets at 0.87, 0.83, and 0.78.

ent-1β,17-Diacetoxy-16S-atisane (6)

A solution of compound **4** (100 mg) in EtOH (20 ml) was hydrogenated at room temperature and atmospheric pressure over Pd/C (10%) for 16 h. Filtration and evaporation of the solvent leaves a residue (**6**; 100 mg) which crystallizes from aqueous EtOH, m.p. 99–101°; $[\alpha]_D^{20}$ −45.8° (*c* 0.58, $CHCl_3$); i.r. (KBr) cm^{-1}: 2990, 2950, 2900, 2880, 2855, 1735, 1723, 1250, 1220; n.m.r. (δ): 4.60 (1H, apparent doublet of doublets, axial H-1), 3.94 (2H, doublet, *J* 7.6 Hz, H-17), 2.02 and 1.99 (3H each, singlets, two —$OCOCH_3$), C—Me singlets at 1.11 (3H, H-20) and 0.85 (6H, two Me on C-4).

Anal. Calcd. for $C_{24}H_{38}O_4$: C, 73.80; H, 9.81. Found: C, 73.65; H, 9.80.

ent-1β,17-Diacetoxy-16R-atisane (7)

Compound **5** (40 mg) was hydrogenated in the same manner as described for **4** to give **7** (40 mg): m.p. 98–100° (aqueous EtOH): $[\alpha]_D^{20}$ +1.7° (*c* 0.46, $CHCl_3$); i.r. (KBr) cm^{-1}: 2990, 2965, 2920, 2860, 1750, 1245; n.m.r. (δ): 4.55 (1H, apparent doublet of doublets, axial H-1), 3.95 (2H, doublet, *J* 7.5 Hz, H-17), 2.03 and 2.00 (3H each, singlets, two —$OCOCH_3$), C—Me singlets at 1.11 (3H, H-20), and 0.84 (6H, two Me on C-4).

Anal. Calcd. for $C_{24}H_{38}O_4$: C, 73.80; H, 9.81. Found: C, 73.91; H, 9.68.

Rearrangement of Jativatriol (1) into ent-1β-Hydroxy-16S-atis-13-en-17-al (8)

To a solution of jativatriol (**1**, 400 mg) in absolute MeOH (10 ml), concentrated HCl was added (1.1 ml). The solution was heated under reflux for 7 h, cooled, diluted with water, and extracted with $CHCl_3$. The residue obtained by evaporation of the solvent is a complex mixture from which the main product (280 mg) can be separated by preparative t.l.c. (eluent benzene–ethyl acetate 4:1). Repeated crystallization of the major fraction from *n*-hexane affords pure **8**, m.p. 121–123°; $[\alpha]_D^{22}$ +14° (*c* 0.8, $CHCl_3$); i.r. (Nujol) cm^{-1}: 3535 (—OH); 3065, 3030, 720, 700 (olefin); 2760, 2730, 1716 (—CHO); n.m.r. (δ): 9.35 (1H, doublet, *J* 2 Hz, —*CH*O), 5.96 and 5.92 (1H each, doublet, *J* 4 Hz, H-13 and H-14 olefinic protons), 3.25 (1H, quartet, $J_{aa'}$ 9 Hz, $J_{ae'}$ 5 Hz, axial H-1), 2.86 (1H, multiplet, $w_{1/2}$ 12 Hz, allylic H-12), 2.54 (1H, multiplet, $w_{1/2}$ 20 Hz, H-16), C—Me singlets at 0.86, 0.80, and 0.66. Double resonance shows that the aldehyde proton (9.35 δ) is coupled to a complex signal at δ 2.54. Similarly the olefinic signal appears as a singlet when the allylic proton (δ 2.86) is irradiated. This last proton appears as a quartet (*J* 3.5 Hz) when the olefinic signal is irradiated.

Anal. Calcd. for $C_{20}H_{30}O_2$: C, 79.42; H, 10.00. Found: C, 79.55; H, 9.93.

The n.m.r. spectrum of the major fraction before crystallization shows aldehydic signals at 9.75 and 9.35 δ (1:3 ratio). The signal at 9.75 indicates the presence of the *ent*-16*R* isomer in this mixture. These isomers are not distinguished by t.l.c.

Preparation of 4 from 8

An ethanolic solution of compound **8** (50 mg) was reduced with $NaBH_4$ in the usual manner. The crude reduction product was acetylated (Py/Ac_2O) at room temperature to give compound **4**, identical (m.p., m.m.p., i.r., n.m.r., and $[\alpha]_D$) with that described above.

Preparation of ent-17-Noratis-13-en-1,16-dione (9) from 8

To a solution of **8** (47 mg) in DMF (15 ml) was added 1,5-diazabicyclo[4.3.0]non-5-ene (1.5 ml) and cupric acetate – 2,2′-bipyridyl complex (1:1; 9 mg). The solution was heated to 40° and dry air bubbled through the solution for 20 h. The reaction mixture was then diluted with water and extracted with ethyl ether. The residue obtained by evaporation of the ether is predominantly a single product (t.l.c.). This residue was oxidized by the Jones' method and the major component

(**9**) was separated by preparative t.l.c. Compound **9** (20 mg) crystallizes from aqueous EtOH, m.p. 137–138°; $[\alpha]_D^{22}$ +160° (*c* 0.38, $CHCl_3$); i.r. (KBr) cm^{-1}: 3050, 740 (olefin); 3000, 2960, 2860, 1720, 1710 (ketones); n.m.r. (δ): 6.15 (2H, multiplet, H-13 and H-14 olefinic protons), 3.07 (1H, multiplet, $w_{1/2}$ 9 Hz, allylic H-12), C—Me singlets at 1.07, 1.01, and 0.98; mass spectrum *m/e* (% of base peak): 286 (8, calcd. for $C_{19}H_{26}O_2$: 286.1933; found: 286.1944), 244 (36), 139 (100), 91 (35), 41 (34).

Anal. Calcd. for $C_{19}H_{26}O_2$: C, 79.68; H, 9.15. Found: C, 79.48; H. 9.03.

*Preparation of **9** from Sideritol (**2**)*

An acetone solution of compound **2** (70 mg) was oxidized with excess Jones' reagent for 12 h. A single product was obtained (61 mg) identical in all respects with compound **9** prepared from jativatriol.

1. C. VON CARSTENN-LICHTERFELDE, S. VALVERDE, and B. RODRÍGUEZ. Aust. J. Chem. **27**, 517 (1974).
2. W. A. AYER, J.-A. H. BALL, B. RODRÍGUEZ, and S. VALVERDE. Can. J. Chem. **52**, 2792 (1974).
3. K. H. PEGEL, L. P. L. PIACENZA, L. PHILLIPS, and E. S. WAIGHT. J. Chem. Soc. Chem. Commun. 552 (1973).
4. R. R. FRASER. Can. J. Chem. **40**, 78 (1962).
5. V. VAN RHEENEN. Tetrahedron Lett. 985 (1969).

Can. J. Chem. Downloaded from www.nrcresearchpress.com by 210.87.254.105 on 09/05/12
For personal use only.

Kinetics of Proton Transfer Reactions of Carbon Acids. V. Variation of Primary Deuterium Isotope Effect with Solvent Composition for the Reaction of Di-(4-nitrophenyl)methane with *t*-Butoxide in *t*-Butyl Alcohol – Toluene Mixtures

ARNOLD JARCZEWSKI AND PRZEMYSLAW PRUSZYNSKI
Institute of Chemistry, Adam Mickiewicz University, Poznan, Poland
AND
KENNETH T. LEFFEK
Department of Chemistry, Dalhousie University, Halifax, Nova Scotia B3H 4H6
Received October 24, 1974

ARNOLD JARCZEWSKI, PRZEMYSLAW PRUSZYNSKI, and KENNETH T. LEFFEK. Can. J. Chem. **53**, 1176 (1975).

The second-order rate constants, activation parameters, and primary deuterium isotope effects are reported for the proton transfer reaction from di-(4-nitrophenyl)methane to *t*-butoxide ion in a series of solvents containing varying amounts of toluene in *t*-butyl alcohol. Increasing toluene content in the solvent decreases the rate constant and increases the enthalpy of activation, while the entropy of activation becomes less negative. The isotope rate ratio k_H/k_D increases from 7.3 in 10% v/v toluene to 9.4 in 50% v/v toluene at 25 °C, corresponding to a change in $(\Delta H_D^{\ddagger} - \Delta H_H^{\ddagger})$ from 0.46 to 1.0 kcal mol^{-1} and a change in $(\Delta S_D^{\ddagger} - \Delta S_H^{\ddagger})$ from −2.4 to −1.1 cal mol^{-1} deg^{-1}. It is suggested that the negative values for $(\Delta S_D^{\ddagger} - \Delta S_H^{\ddagger})$ are due to a time lag for solvent reorganization relative to the proton transfer.

ARNOLD JARCZEWSKI, PRZEMYSLAW PRUSZYNSKI et KENNETH T. LEFFEK. Can. J. Chem. **53**, 1176 (1975).

On rapporte les constantes de vitesse du second ordre, les paramètres d'activation et les effets isotopiques primaires du deuterium pour le transfert de proton lors de la réaction du di-(nitro-4 phényl)méthane avec l'ion *t*-butylate dans une série de solvants contenant des quantités variables de toluène dans l'alcool *t*-butylique. L'augmentation du contenu en toluène dans le solvant diminue la vitesse de réaction et augmente l'enthalpie d'activation alors que l'entropie d'activation devient moins négative. A 25 °C, le rapport des vitesses k_H/k_D augmente de 7.3 lorsque l'on a 10% v/v de toluène à 9.4 lorsque l'on a 50% v/v de toluène; cette variation correspond à un changement dans le $(\Delta H_D^{\ddagger} - \Delta H_H^{\ddagger})$ de 0.46 à 1.0 kcal mol^{-1} et un changement dans $(\Delta S_D^{\ddagger} - \Delta S_H^{\ddagger})$ de −2.4 à −1.1 cal mol^{-1} deg^{-1}. On suggère que les valeurs négatives pour $(\Delta S_D^{\ddagger} - \Delta S_H^{\ddagger})$ sont principalement dues à un retard dans la réorganisation du solvant par rapport à la vitesse du transfert du proton. [Traduit par le journal]

Introduction

The reaction of di-(4-nitrophenyl)methane with alkoxide bases is the proton transfer equilibrium (1–3) shown in eq. 1. The violet color

[1] $(NO_2C_6H_4)_2CH_2 + {}^-OAlK \underset{k_2}{\rightleftharpoons} [(NO_2C_6H_4)_2CH]^- + HOAlK$

due to the anion of the substrate is stable and indicates a molar absorptivity of about 12 000 l mol^{-1} cm^{-1} in the region 510–520 nm.

The previous paper in this series (3) dealt with the primary deuterium isotope effect for the reaction with *t*-butoxide in *t*-butyl alcohol containing 10% v/v toluene. The rate ratio of 7.33 at 25 °C was found to contain an entropy of activation component, $\Delta S_D^{\ddagger} - \Delta S_H^{\ddagger}$, of −2.4 cal mol^{-1} deg^{-1}, corresponding to A_D/A_H = 0.29, which falls well outside the standard zero-point energy approximation theory of isotope effects. Almost simultaneously with this work, Caldin and Mateo (4) discovered large isotope effects for proton transfers from carbon acids to nitrogen bases when the reactions were carried out in toluene solvent.

In this paper, we have investigated the effect of increasing the toluene content of the solvent on the isotope effects in the *t*-butoxide reaction to see whether the Caldin and Mateo phenomenon extends to this type of base and also to test the

Can. J. Chem. Downloaded from www.nrcresearchpress.com by 210.87.254.42 on 09/05/12
For personal use only.

TABLE 1. Second-order rate constants for the reaction of normal and deuterated di-(4-nitrophenyl)methane with *t*-butoxide

Temperature (°C)	Solvent composition (% v/v) toluene in *t*-butyl alcohol						
	10*		20		50		80
	10^2k_{2H}†	10^2k_{2D}	10^2k_{2H}	10^2k_{2D}	10^2k_{2H}	10^2k_{2D}	10^2k_{2H}
15	—	—	49±2	5.4±0.2	27±0.5	2.6±0.05	3.0±0.1
20	123±2	16.4±0.9	58±2	6.7±0.2	35±1	3.5±0.1	4.4±0.1
25	148±3	20.2±0.4	74±3	8.2±0.3	45±1	4.8±0.2	5.8±0.5
30	182±4	25.3±1.9	94±3	11.0±0.2	57±1	6.1±0.2	8.0±0.1
35	212±3	30.3±1.0	—	—	—	—	11.3±0.1
40	266±3	37.4±0.9	—	—	—	—	14.8±0.5
45	315±4	45.0±1.0	—	—	—	—	19.2±0.4
50	—	—	—	—	—	—	27 ±2

*From ref. 3.
†k_{2H} and k_{2D} in units of l mol^{-1} s^{-1}.

TABLE 2. Activation parameters for the reaction of normal and deuterated di-(4-nitrophenyl)methane with *t*-butoxide

Parameter	Solvent composition (% v/v) toluene in *t*-butyl alcohol			
	10*	20	50	80
$\Delta H_H^{\ddagger}$ (kcal mol^{-1})	6.41±0.16	7.64±0.45	8.79±0.05	11.39±0.16
$\Delta H_D^{\ddagger}$ (kcal mol^{-1})	6.87±0.07	8.55±0.10	9.81±0.30	—
$\Delta S_H^{\ddagger}$ (cal mol^{-1}deg^{-1})	−36.2 ±0.5	−33.0 ±1.0	−30.6 ±0.2	−25.94±0.05
$\Delta S_D^{\ddagger}$ (cal mol^{-1}deg^{-1})	−38.7 ±0.3	−34.3 ±0.8	−31.7 ±1.0	—
$\Delta G_H^{\ddagger}$ (kcal mol^{-1} at 300 K)	17.3	17.5	18.0	19.2

*From ref. 3.

hypothesis proposed by Kim and Leffek (3) that the abnormal entropy contribution to the isotope effect is related to solvent composition.

Results and Discussion

Reaction Rates and Activation Parameters

Pseudo first-order rate constants for the reaction of di-(4-nitrophenyl)methane and its deuterated analog with *t*-butoxide were measured as described previously (1), using a substrate concentration of 5×10^{-5} *M* and base concentrations varying between 2.9×10^{-3} and 1.4×10^{-1} *M*. The second-order rate constants, shown in Table 1, were calculated from the slope of the plots of k_1 *vs.* *t*-butoxide concentration.

The activation parameters calculated from the second-order rate constants in Table 1 are presented in Table 2.

It may be seen that the rate constants and activation parameters in solvents containing 20, 50 and 80% v/v toluene in *t*-butyl alcohol form a series with the results in 10% v/v toluene – *t*-butyl alcohol reported earlier (3), in which the changes in these reaction characteristics are smooth. The rate constants decrease as the toluene content of the solvent is increased and are very small for solvents above 80% toluene. This result is opposite to that which we observed for the same reaction in acetonitrile – *t*-butyl alcohol mixtures (3). The second-order rate constant at 25 °C in 50% v/v acetonitrile in *t*-butyl alcohol is almost exactly 100 times faster than that in 50% toluene in *t*-butyl alcohol. However, a change from 50 to 80% acetonitrile increases the rate by a factor of 3, whereas a change from 50 to 80% toluene decreases the rate by a factor of 8. As noted previously (3), the acetonitrile results conform to the Miller–Parker solvation theory (5). The *t*-butoxide ion is a stronger proton abstractor in acetonitrile-rich solvents. If this is true for acetonitrile–alcohol mixtures, and there is a very wide range of rate measurements which support the Miller–Parker theory, it should also be true for toluene–alcohol mixtures and the rates should change in the same way.

We believe that the reason for the observed

Can. J. Chem. Downloaded from www.nrcresearchpress.com by 210.87.254.42 on 09/05/12
For personal use only.

TABLE 3. Primary deuterium isotope effects for the proton transfer reaction from di-(4-nitrophenyl)methane-d_2 to *t*-butoxide

Parameter	Solvent composition (% v/v) toluene in *t*-butyl alcohol		
	10*	20	50
k_{2H}/k_{2D} at 15 °C	—	9.07±0.50	10.08±0.08
k_{2H}/k_{2D} at 20 °C	7.50±0.43	8.66±0.39	10.12±0.35
k_{2H}/k_{2D} at 25 °C	7.33±0.21	8.94±0.50	9.38±0.44
k_{2H}/k_{2D} at 30 °C	7.19±0.56	8.54±0.31	9.34±0.35
$\Delta H_D^{\ddagger} - \Delta H_H^{\ddagger}$ (kcal mol^{-1})	0.46±0.17	0.91±0.40	1.03±0.35
$\Delta S_D^{\ddagger} - \Delta S_H^{\ddagger}$ (cal mol^{-1}deg^{-1})	−2.4 ±0.6	−1.7 ±1.0	−1.1 ±1.0
A_D/A_H	0.29±0.12	0.53±0.37	0.58±0.29

*From ref. 2.

decrease in rate with increase in toluene content arises from a second factor, the incomplete dissociation of sodium *t*-butoxide ion pairs. The fraction of sodium *t*-butoxide present as ion pairs must be much greater in toluene – *t*-butyl alcohol mixtures than in acetonitrile – *t*-butyl alcohol mixtures and the increase in the proportion of ion pairs as the toluene content is increased must override the general solvation effect.

An additional factor is that some proton transfer reactions in alcohol solution are known (6, 7) to involve solvent molecules directly in the transfer. If such a mechanism were operating, an increase in the toluene content of the solvent would make the process less favorable and result in a decrease in the rate. Our measurements do not allow a judgement as to whether this mechanism of proton transfer is present, but if it is, its importance cannot be great since the acetonitrile–alcohol mixtures show an opposite rate change. This conclusion is consistent with other work on carbon acid systems (8, 9).

Although the rate changes (*i.e.* free energy changes) for the toluene – *t*-butyl alcohol solvents are opposite to those found for the acetonitrile – *t*-butyl alcohol solvents, the enthalpy and entropy of activation changes are in the same direction. This situation is brought about by the circumstance that in both solvent systems the $\Delta H^{\ddagger}$ and $\Delta S^{\ddagger}$ changes are opposed to each other. In going from 50 to 80% toluene in *t*-butyl alcohol the increase in enthalpy outweighs the decrease in the negative entropy by 1.6 kcal mol^{-1} at 300 K, whereas for the same percentage change in the acetonitrile system, the opposite is true by 0.8 kcal mol^{-1} at 300 K.

The changes are accounted for qualitatively by our postulate previously made (3) that the energy required to break one alcohol–alkoxide hydrogen bond would be offset by the formation of a new alcohol–alcohol hydrogen bond and that it would require less energy to break out one alcohol molecule from the solvation shell if the solvent molecule immediately adjacent to it in the next solvent layer is another alcohol molecule. Hence, increase in toluene content increases the activation energy.

Isotope Effects

The isotope effects on the rate constants and activation parameters are summarized in Table 3. The two solvents studied in this work form a series with the 10% v/v toluene – *t*-butyl alcohol solvent reported earlier (2) and the isotope effects are seen to change smoothly with solvent composition, giving larger rate ratios the greater the toluene content. These rate ratios are roughly comparable to those found by Caldin and Mateo (4) for the proton transfer from 4-nitrophenylnitromethane to triethylamine and tri-*n*-butylamine in pure toluene, but very much less than the k_H/k_D of 45 which these authors reported for the same reaction with the base tetramethylguanidine.

The results of Tables 2 and 3 provide additional examples of entropy isotope effects, ($\Delta S_D^{\ddagger} - \Delta S_H^{\ddagger}$), which are negative and correspond to frequency factor ratios, A_D/A_H, of less than unity. The direction of this effect is unusual, although a few have been previously reported (10, 11). We pointed out earlier (3) that the −2.4 cal mol^{-1} deg^{-1} value in 10% toluene – *t*-butyl alcohol could not be explained on standard isotope effect theory which ignores the solvent and postulated that a solvation effect

Can. J. Chem. Downloaded from www.nrcresearchpress.com by 210.87.254.42 on 09/05/12
For personal use only.

Can. J. Chem. Downloaded from www.nrcresearchpress.com by 210.87.254.42 on 09/05/12
For personal use only.

might be involved. The entropy effects for the other two mixed solvents confirm the experimental validity of our earlier result, in that these measurements were carried out in a different laboratory with different equipment and chemical sources. They also confirm that the phenomenon is a function of solvent composition. Statistically, the results of Table 3 do not prove that the isotope effect on the entropy of activation is different in the three solvents, within a 68% confidence limit. Nevertheless, we believe this to be true, taking into account the fact that the number of measurements made is really too small for reliable statistical analysis. However, all three entropy isotope effects are negative within a 68% confidence limit or better.

In 50% v/v toluene – *t*-butyl alcohol, the isotope effects on the activation parameters fit the zero-point energy approximation for the loss of a C—H or C—D stretching vibration very well but in 10% toluene the results cannot be fitted to the theory at all. Caldin and Mateo (4) have postulated that any solvation changes accompanying proton transfer involving rotation of the solvent molecules will increase the effective mass of the proton and hence reduce the apparent effects of proton tunnelling, *i.e.* reduce k_H/k_D and A_D/A_H. However, A_D/A_H would not be expected to be reduced below a value of one by this mechanism.

The primary kinetic isotope effect gives us a probe to look at the reaction at the site of the proton transfer, in contrast to simply measuring the effect of solvent change on the activation parameters of the normal substrate molecule which include effects arising not only from the substrate molecule itself but also from a quite extensive solvent environment. From the latter type of measurements, we concluded (1) that a large part of the activation parameters seemed to arise from solvation changes in going from the initial to the transition state. Now the isotope effects show that some of this solvation change is very closely associated with the proton transfer site. While the change from C—H to C—D bond breaking cannot change the general characteristics of the solvation shell very far from this site, nevertheless $\Delta S_D^{\ddagger}$ is significantly more negative than $\Delta S_H^{\ddagger}$.

Bell suggested (12) that a time lag between the proton transfer and the reorientation of the solvent molecules could influence the size of the isotope effect. Since the proton is transferred faster than the deuteron, this effect would be larger for proton transfer and would lead to a decrease in k_H/k_D. Caldin (13) developed this idea for proton transfers involving a negative entropy of activation, which is largely controlled by the orientation of solvent molecules. In this case, the solvent molecules are held more extensively in the transition state relative to the initial state and the lag will give a positive contribution to $\Delta S^{\ddagger}$ which will be larger for $\Delta S_H^{\ddagger}$ than for $\Delta S_D^{\ddagger}$. Thus, $\Delta S_D^{\ddagger}$ will be more negative than $\Delta S_H^{\ddagger}$.

Our isotope effects fit the above postulate of Caldin in that solvent lag would be expected to be greater in the more polar solvent of 10% v/v toluene in *t*-butyl alcohol than in the 50% v/v toluene in *t*-butyl alcohol. We observe the largest negative value for $(\Delta S_D^{\ddagger} - \Delta S_H^{\ddagger})$ in the more polar solvent and this parameter becomes less negative as the polarity of the solvent is decreased by the addition of toluene. It must be noted, however, that the $\Delta S_H^{\ddagger}$ values themselves are more negative in the more polar solvent and thus do not demonstrate overtly the positive contribution to $\Delta S_H^{\ddagger}$ from solvent lag. Nevertheless, entropies of activation are complex quantities and it is quite possible that the solvent lag effect is masked in the entropy of activation by some other factor which cancels in the isotope effect, $(\Delta S_D^{\ddagger} - \Delta S_H^{\ddagger})$. This other factor may be the incomplete dissociation of sodium *t*-butoxide ion pairs.

Experimental

Materials

Di-(4-nitrophenyl)methane was prepared as described previously (1). Deuterated material was prepared from this by exchange with $NaOCH_3$–CH_3OD (3). The exchange process was carried out four times and yielded material 99% isotopically pure according to the n.m.r. spectrum.

Toluene was commercial reagent grade purified by the Walden method (14), with sodium and fractional distillation in the range 110.5 to 111.0 °C. The distillate was protected against moisture and CO_2.

Reagent grade *t*-butyl alcohol was dried over CaO, distilled from sodium metal, and then fractionally distilled at 82.4 °C. The distillate was protected from moisture and CO_2 and stored under dry O_2-free nitrogen.

Kinetic Measurements

Sodium *t*-butoxide was made by dissolving clean sodium metal in a mixture of *t*-butyl alcohol and a small amount of toluene in a flask previously flushed with nitrogen. After the sodium had dissolved, toluene was

added to bring the solvent to the required composition. The concentration of sodium *t*-butoxide was checked by titration with standard HCl using methyl orange indicator.

The proton transfer reaction was followed on a Specord UV-Vis spectrophotometer (Carl-Zeiss Jena) by scanning at a fixed wavelength in the region of 510–520 nm. The reaction cells were maintained at a constant temperature to within ± 0.1 °C. The first-order rate constants were calculated from the absorbance values by the Guggenheim method (15). The second-order rate constants were calculated from the k_1 *vs.* base concentration plots by the method of least squares using an ODRA 204 computer. Example runs have been given in an earlier publication (1).

1. A. JARCZEWSKI and K. T. LEFFEK. Can. J. Chem. **50**, 24 (1972).
2. J.-H. KIM and K. T. LEFFEK. Can. J. Chem. **51**, 2805 (1973).
3. J.-H. KIM and K. T. LEFFEK. Can. J. Chem. **52**, 592 (1974).
4. E. F. CALDIN and S. MATEO. Chem. Commun. 854 (1973).
5. A. J. PARKER. Q. Rev. **16**, 163 (1962).
6. E. GRUNWALD, C. F. JUMPER, and S. MEIBOOM. J. Am. Chem. Soc. **85**, 522 (1963).
7. E. GRUNWALD and M. COCIVERA. Disc. Faraday Soc. **39**, 105 (1965).
8. D. M. GOODALL and F. A. LONG. J. Am. Chem. Soc. **90**, 238 (1968).
9. M. M. KREEVOY and J. M. WILLIAMS. J. Am. Chem. Soc. **90**, 6809 (1968).
10. P. W. K. FLANAGAN. Diss. Abstr. **18**, 1980 (1958).
11. J. R. KEEFE and N. H. MUNDERLOH. Chem. Commun. 17 (1974).
12. R. P. BELL. Disc. Faraday Soc. **39**, 16 (1956).
13. E. F. CALDIN. *In* Reaction transition states. *Edited by* J. E. Dubois. Gordon and Breach, London. 1972. p. 247.
14. P. WALDEN. Z. Phys. Chem. **147A**, 1 (1930).
15. E. A. GUGGENHEIM. Phil. Mag. **2**, 538 (1926).

Can. J. Chem. Downloaded from www.nrcresearchpress.com by 210.87.254.42 on 09/05/12
For personal use only.

Microbiological Transformations of 17-Norkauran-16-one, *ent*-17-Norkauran-16-one, and 17-Norphyllocladan-16-one by *Aspergillus niger*[1]

ALLAN B. ANDERSON

Department of Botany and Genetics, University of Guelph, Guelph, Ontario N1G 2W1

AND

ROBERT MCCRINDLE[2] AND JAMES K. TURNBULL

Chemistry Department, University of Guelph, Guelph, Ontario N1G 2W1

Received October 28, 1974

ALLAN B. ANDERSON, ROBERT MCCRINDLE, and JAMES K. TURNBULL. Can. J. Chem. **53**, 1181 (1975).

Incubation of 17-norkauran-16-one (**3***b*) and *ent*-17-norkauran-16-one (**2***b*) with *Aspergillus niger* gives the related C-3 equatorial alcohols **3***c* and **2***c*, respectively, whereas 17-norphyllocladan-16-one (**4***b*) gives the 3β-alcohol **4***c* and the corresponding 3-ketone **4***g*. Yields of all of these products are low. Diketone **4***g* is identical with the corresponding compound derived from calliterpenone, thus confirming that calliterpenone should be formulated as **8** rather than **7**.

ALLAN B. ANDERSON, ROBERT MCCRINDLE et JAMES K. TURNBULL. Can. J. Chem. **53**, 1181 (1975).

Les incubations de la nor-17 kauranone-16 (**3***b*) et de l'*ent*-nor-17 kauranone-16 (**2***b*) avec l'*Aspergillus niger* conduisent respectivement aux alcools équatoriaux en position 3 (**3***c* et **2***c*) alors que la nor-17 phyllocladanone-16 (**4***b*) conduit à l'alcool 3β (**4***c*) et au dérivé céto-3 correspondant (**4***g*). Les rendements de tous ces produits sont bas. La dicétone **4***g* est identique avec le composé correspondant obtenu à partir de la calliterpénone; ceci confirme donc que la calliterpénone doit être représentée par la formule **8** plutôt que **7**. [Traduit par le journal]

The gibberellins (2) have attracted a large portion of diterpenoid research mainly because of their influence on the growth and development of plants. All known gibberellins are thought to have the gibbane skeleton (**1**) and to be biosynthesized in plants via *ent*-16-kaurene (**2***a*) or a derivative of this diterpene. Other tetracyclic diterpenes, such as kaurene (**3***a*) and phyllocladene (13β-kaurene; **4***a*) occur (3) naturally and we have been seeking evidence for the occurrence of gibberellin-like compounds derived from these. A study of the gibberellins in plants which produce **3***a* or **4***a* would be an obvious approach in this quest. However, since fresh tissue of such plants has not been obtainable by us[3] in sufficient quantity we have undertaken a less direct attack.

This approach was suggested by observations (6) that although *ent*-kaurene itself has little gibberellin activity, various oxygenated derivatives, all of which contain the ring D *exo*-methylene group, do exhibit significant physiological effects. We planned to submit analogous kaurene and phyllocladene derivatives for testing in bioassays that are specific for gibberellins but since such compounds were not available, synthetic routes from the parent hydrocarbons (**3***a* and **4***a*) were sought. The present paper deals with an investigation of microbial oxygenation as a means of producing the desired derivatives.

Initially, microbial hydroxylation of the more available *ent*-kaurene system was studied as a model. The norketone **2***b* was chosen as a suitable substrate for two reasons. First, carbonyl containing compounds have been successfully used (7, 8) in related steroidal work and second, the C-17 methylene group could be readily reattached by the Wittig reaction. Thus, the norketone **2***b* was incubated with submerged cultures of 13 fungal species (see Experimental) in small scale trial experiments. Transformations of the substrate were detected by t.l.c. com-

[1]For a preliminary account of part of this work see ref. 1.

[2]To whom correspondence should be addressed.

[3]Another group has failed (4) in an attempt to isolate the gibberellins from a variety of *Cryptomeria japonica* which contains (5) **4***a*.

Can. J. Chem. Downloaded from www.nrcresearchpress.com by 210.87.254.105 on 09/05/12
For personal use only.

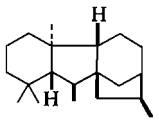

1

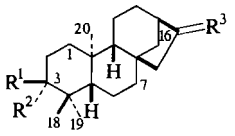

2

a $R^1 = R^2 = H; R^3 = CH_2$
b $R^1 = R^2 = H; R^3 = O$
c $R^1 = H; R^2 = OH; R^3 = O$
d $R^1 = H; R^2 = OH; R^3 = CH_2$
e $R^1 = H; R^2 = OAc; R^3 = O$
f $R^1 = H; R^2 = OAc; R^3 = CH_2$
g $R^1 + R^2 = O; R^3 = CH_2$

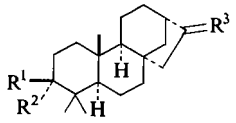

3

a $R^1 = R^2 = H; R^3 = CH_2$
b $R^1 = R^2 = H; R^3 = O$
c $R^1 = OH; R^2 = H; R^3 = O$
d $R^1 = OAc; R^2 = H; R^3 = O$
e $R^1 = OH; R^2 = H; R^3 = CH_2$
f $R^1 + R^2 = O; R^3 = O$

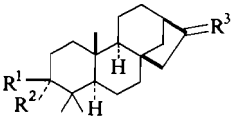

4

a $R^1 = R^2 = H; R^3 = CH_2$
b $R^1 = R^2 = H; R^3 = O$
c $R^1 = OH; R^2 = H; R^3 = O$
d $R^1 = OAc; R^2 = H; R^3 = O$
e $R^1 = OH; R^2 = H; R^3 = CH_2$
f $R^1 = OAc; R^2 = H; R^3 = CH_2$
g $R^1 + R^2 = O; R^3 = O$

parison of the culture extracts of each organism grown in the presence and absence of **2***b*. Five of these fungi, *Calonectria decora*, *Rhyzopus nigricans*, *Fusarium moniliforme*, *Coprinus lagopus*, and *Aspergillus niger*,[4] appeared to effect transformations of **2***b*. Further small scale screening incubations were then carried out with these five fungi using **3***b* and **4***b* as substrates. *Aspergillus niger* was the only organism for which there was clear t.l.c. evidence for the production of derivatives from both of these norketones. On this basis *A. niger* was selected for large scale investigation with **2***b*, **3***b*, and **4***b*.

ent-17-Norkauran-16-one

The ketone (**2***b*, ref. 10) was added in DMF to a submerged culture of *A. niger* (ATCC 26693[5]) which had been growing for 3 days in a full nutrient medium (11) under aerobic conditions. After 5 days the mycelia and aqueous medium were extracted with ethyl acetate. Column chromatography of the extract over silica gel afforded a large fraction of the substrate (**2***b*) and a minor amount of a more polar compound, m.p. 179–181°, which was recognized as a norkauranone from its n.m.r., i.r., and mass spectra. In addition, the n.m.r. spectrum indicated that this transformation product (**2***c*) had resulted from the introduction of a secondary hydroxyl group into **2***b*. The multiplicity of the resonance arising from the carbinol proton (dd, $W_{1/2} = 16$ Hz) revealed the equatorial nature of the hydroxyl group and the presence of only two vicinal protons. This eliminated all but three possible structures for the compound, namely, an *ent*-17-norkauran-16-one with an equatorial (α) hydroxyl group substituted at C-1, C-3, or C-7. A decision in favor of the second of these possibilities was readily made as follows. The hydroxy-*ent*-16-kaurene **2***d*, which was required for biological testing in any case, was prepared from the norketone **2***c* via the acetates **2***e* and **2***f* and its n.m.r. spectrum was recorded in the presence of $Eu(dpm)_3$. The induced shifts of the methyl resonances were in the normalized (12) ratio of 10.0:9.4:4.1 (3 H-19, 3 H-18, and 3 H-20, respectively) which is consistent (13) only with a 3α-hydroxy group. Further, oxidation of **2***d* afforded the corresponding ketone (**2***g*) which gave benzene-induced methyl shifts of the magnitude predicted (14) for a C-3 ketone with ring A in the expected (15) flattened chair conformation. Final confirmation of these structural assignments came from the fact that **2***c*, **2***d*, and **2***e* have identical physical and spectral characteristics with those prepared (16, 17) from diterpenoids of natural provenance.

[4]A group at the University of Western Australia are also studying (9) the metabolism of *ent*-kauranoids by fungi. We thank Professor P. R. Jefferies for discussions of unpublished results.

[5]ATCC 26693 refers to the American Type Culture Collection strain No. 26693.

Can. J. Chem. Downloaded from www.nrcresearchpress.com by 210.87.254.105 on 09/05/12
For personal use only.

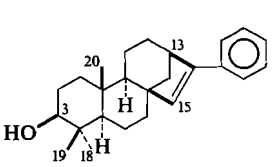

5

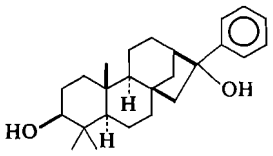

6

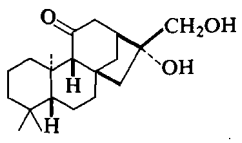

7

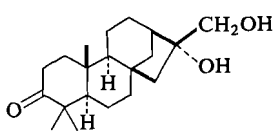

8

17-Norkauran-16-one

When the ketone **3***b* was incubated with *A. niger* (ATCC 26693) in a manner similar to that described above for its enantiomer an analogous product mixture was obtained. Much substrate was again recovered along with a small quantity of the related C-3 equatorial alcohol (**3***c*). The latter was characterized as the derived acetate **3***d* and alcohol **3***e* both of which are identical, except in sign of optical rotation, with the corresponding compounds in the *ent*-series (see above).

17-Norphyllocladan-16-one

When norphyllocladanone (**4***b*, ref. 10) was incubated as above with *A. niger*, (ATCC 26693) small amounts of two transformation products were isolated. The major, more polar, product (**4***c*), m.p. 158–160°, was readily formulated as a keto alcohol on the basis of its spectral properties and those of the corresponding acetate (**4***d*), m.p. 156–158°. The multiplicity of the carbinol proton again indicated that it is axial and only coupled to two protons and thus the hydroxyl group must be β-orientated and located at C-1, C-3, or C-7. The eventual assignment of structure **4***c* to the compound rests on the magnitude of the shifts induced by $Eu(dpm)_3$ on the methyl resonances of **5** and **4***e*. The former was produced in our initial attempt to prepare the latter. In this case solutions of phenyl lithium and methyltriphenylphosphine bromide in ether were mixed and then after 10 min at 20° the keto acetate **4***d* was added in the same solvent and the resulting mixture heated to reflux for 2 days. Work-up gave, rather than the desired acetoxy olefin (**4***f*), the unstable diol **6** which was smoothly transformed into the styrene **5** by treatment with toluene-*p*-sulfonic acid in benzene. When the Wittig reaction was repeated, but this time the phenyl lithium – methyltriphenylphosphine bromide solution was heated for 3 h before addition of **4***d*, the expected product **4***f* was formed. The $Eu(dpm)_3$ induced shifts of the methyl resonances in **5** and **4***e* are in the normalized ratios of 10.0:9.3:3.4 and 10.0:9.4:3.9, respectively, values entirely consistent for 3 H-19, 3 H-18, and 3 H-20 in the presence of a 3β-hydroxyl function.

The less polar transformation product, **4***g*, m.p. 187–189°, shows no absorption in the i.r. attributable to OH stretching but gives two strong peaks in the carbonyl region at 1712 and 1749 cm^{-1}. $Eu(dpm)_3$ shifted n.m.r. spectra of this compound suggested the structure **4***g*, a formulation which was readily confirmed by its preparation from **4***c* by oxidation with Jones' reagent.

This investigation provided us not only with **4***e* for biological testing but also with the means of resolving the controversy concerning the structure of calliterpenone. This constituent of *Callicarpa macrophylla* was originally formulated (18) as a substituted kaurane (**7**), an assignment which was subsequently challenged (19). This second group proposed, on much firmer evidence, an alternative structure **8**, based on the phyllocladane skeleton. That the latter assignment is indeed correct was shown by a direct comparison of the diketone **4***g*, prepared in this study, with the corresponding compound[6] derived (19) from calliterpenone. The two samples are identical.

Mechanism

Recently there has been considerable interest in the nature of the interaction between hydroxylating organisms and their substrates during microbial oxidation. Several groups (for leading examples see ref. 8) have pointed out that a knowledge of such interactions for a given organism might allow prediction of the position(s) of oxygenation in any substrate. The oxidations reported in this paper have several notable features relevant to such studies.

It is striking that *A. niger* inserts oxygen only equatorially at C-3 in the three norditerpenoids tested even although these include a pair of enantiomers. Previous studies (20), using other organisms, have shown that the pattern of oxi-

[6]A generous sample of this compound was supplied by Dr. Asif Zaman, Aligarh Muslim University, Aligarh, India.

Can. J. Chem. Downloaded from www.nrcresearchpress.com by 210.87.254.105 on 09/05/12
For personal use only.

Can. J. Chem. Downloaded from www.nrcresearchpress.com by 210.87.254.105 on 09/05/12
For personal use only.

dation of enantiomeric substrates is often different. It has been proposed (8) that polar functional groups such as carbonyls can interact with hydroxylating enzymes in such a way that the site of oxygenation of the substrate bears a fixed geometrical relationship to the carbonyl or other directing group. Certainly the presence of the C-16 carbonyl group in **2***b*, **3***b*, and **4***b* does facilitate hydroxylation with *A. niger*, **2***a* and **4***a* giving no detectable transformation products (see Experimental). Since in each case a reasonable amount of unreacted substrate was recovered from the *filtered* medium it seems likely that **2***a* and **4***a* were present in a physical state suitable for utilization by the organism. It is possible that substrates must contain a polar function to allow their transport through the cellular membrane to a site for hydroxylation within the cell. However, the allylic hydroxylation by *A. niger* of a wide variety of nonoxygenated olefins (21) has been reported and this presumably requires that they diffuse into the cell. Thus, it would appear that the most likely explanation for the absence of oxidation of **2***a* and **4***a* is that the enzymes responsible for remote hydroxylation can react only with substrates which contain a ketone[7] or other polar function.

If the same *A. niger* enzyme is involved in the hydroxylation of **2***b*, **3***b*, and **4***b* then the following model for the role played by the enzyme is attractive in terms of both simplicity and plausibility. First, the hydroxylase "locks on" to the oxygen function at C-16 and then interacts with the flat underside (as drawn in Scheme 1) of **2***b*, **3***b*, and **4***b*. The equatorial proton at C-3 is then singled out for attack. Possibly the enzyme "recognizes" the three axial hydrogens on the underside (Scheme 1) of ring A and allows oxidative displacement of the geminal partner of the one which is most remote from the primary binding site.

One final aspect of the oxidations of **2***b*, **3***b*, and **4***b* warrants comment, namely that only in the case of norphyllocladanone (**4***b*) was a 3-keto derivative isolated. It has been reported (22) that a strain of *A. niger* oxidizes 3β-hydroxy-5-pregnen-20-one to the 3-ketone while its enantiomer is unaffected. Other 3β-hydroxy steroids are also oxidized (23) to ketones by *A. niger*. Thus it would appear that oxidation of 3β-hydroxy decalin systems which have the same A/B ring junction configuration as that of the naturally occurring steroids is a fairly general property of some strains of this organism. Our failure to detect **3***f* from incubation of the norkauranone **3***b* might have been anticipated in view of the small amount of product **3***c* present and thus available for further transformation. Finally, it appears possible that some strains of *A. niger* may be ineffective for this oxidation of a 3β-hydroxy group to a ketone. In an experiment designed to determine if strains of *A. niger* other than ATCC 26693 can effect hydroxylation of these diterpenoid norketones, **4***b* was incubated with a strain (ATCC 10577) which is well known (7) as an efficient 11α-hydroxylator of steroids. In this case **4***c* was obtained in a yield similar to that from ATCC 26693 but notably no **4***g* could be isolated.

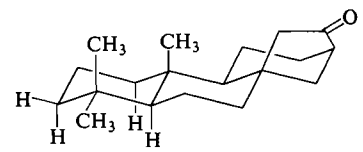

4*b*

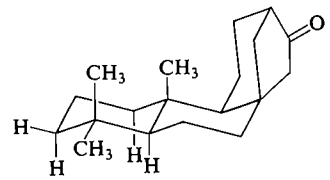

3*b*

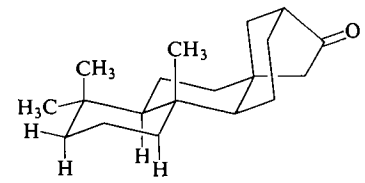

2*b*

SCHEME I

[7]Some preliminary results involving the interaction of *A. niger* with 15-deuterio derivatives of **2***b* and **2***c* may be taken to indicate the intervention of an enolate, or related, derivative at some stage in the hydroxylation process. For example, **2***b* with an *exo*-deuterium at C-15, after hydroxylation has lost an appreciable proportion of its label while recovered substrate has not. When similarly labelled, **2***c* retains almost all of its deuterium upon exposure for several days to a medium in which *A. niger* has been growing actively.

Can. J. Chem. Downloaded from www.nrcresearchpress.com by 210.87.254.105 on 09/05/12
For personal use only.

Experimental

Melting points were determined on a Kofler hot-stage apparatus and are uncorrected. For analytical and preparative t.l.c.. chromatoplates were spread with Kieselgel G. (Merck). Silica gel (Baker) used for column chromatography was 40–140 mesh. Gas–liquid chromatography was carried out with a Varian Aerograph 1200 gas chromatograph using a stainless steel column (1/8 in. × 10 ft packed with 5% SE-30) and nitrogen as carrier gas with a flow rate of 25 ml/min. Light petroleum was of b.p. 30–75°. Infrared solution spectra were recorded in carbon tetrachloride on a Beckman I.R. 12 spectrophotometer. Proton magnetic resonance spectra were run on a Varian Associates A-60A or HA 100 spectrometer, in deuteriochloroform unless otherwise stated, using tetramethylsilane as internal standard. Mass spectra were run on a Varian Associates CH7 instrument. Specific rotations were measured in chloroform unless otherwise stated using a Bellingham and Stanley polarimeter or a Bendix automatic polarimeter. *Aspergillus niger* cultures were maintained on potato dextrose agar slopes at 25°. Submerged cultures of *A. niger* for diterpenoid transformation were grown in presterilized Erlenmeyer flasks each of which was plugged with nonabsorbent cotton wool and contained a full nutrient growth medium (11) and a magnetic stirring bar. The medium was inoculated with *A. niger* under sterile conditions and the cultures were aerated by vigorous magnetic stirring.

Incubations of ent-17-Norkauran-16-one (2b) with Various Fungal Species

The ketone (**2***b*, 20mg) was incubated with 13 fungal species in essentially the fashion described below for one of them, *Aspergillus niger*, transformation being detected by comparison of the culture extract with that of a control on t.l.c. *Calonectria decora, Rhyzopus nigricans, Fusarium moniliforme, Coprinus lagopus*, in addition to *A. niger*, appeared to effect transformations, while *A. nidulans, A. ochraceous*, a *Hypomycetes* species, an *Ostracoderma* species, *Penicillium expansum*, a *Trichoderma* species, *Trichothecium roseum*, and a *Zygorhynchus* species did not.

Incubations of ent-17-Norkauran-16-one (2b) with A. niger (ATCC 26693)

An initial screening incubation was performed as follows. A 3-day-old submerged culture of *A. niger* (100 ml nutrient medium) in a 250-ml Erlenmeyer flask was inoculated with *ent*-17-norkauranone (**2***b*, 20 mg) in DMF (1 ml) and stirred vigorously for 7 days. The culture was then sonicated and the mycelium and medium were extracted with ethyl acetate (3 × 100 ml). Comparison by t.l.c. (ethyl acetate – light petroleum, 1:4) of this extract with one from a control culture inoculated with DMF (1 ml) only, showed a polar spot, in addition to that of substrate (**2***b*), not present in the control extract. Large scale incubations were carried out as follows. Vigorously stirred 3-day-old cultures of *A. niger* (2.5 l nutrient medium) in 4-l Erlenmeyer flasks were incubated with the norketone for 5 days. In a typical run, **2***b* (1.0 g) in DMF (50 ml) was added to the growing culture (5 l). After 5 days the mycelia were removed by filtration and the filtrate was then saturated with NaCl and extracted with ethyl acetate (3 × 1.5 l/2.5 l filtrate). The combined ethyl acetate extracts were evaporated to give an oil (2.8 g). The mycelia were killed by treatment with acetone, which was then allowed to evaporate at ambient temperature and pressure. The resulting tissue was ground with sand and extracted with ethyl acetate. This gave an oil (1.8 g). The two oily residues were then chromatographed separately over silica gel (100 g). The material (2.8 g) from the filtrate on elution with ether – light petroleum (1:4) gave substrate **2***b* contaminated with nonditerpenoid compounds (n.m.r. evidence). Elution with ether – light petroleum (1:1) gave an oil (0.4 g) which consisted of several compounds separable by t.l.c. (acetic acid – ethyl acetate – light petroleum, 2:5:25). One of these was not present in the corresponding fraction from a control culture. Preparative t.l.c. (same solvent, run twice) afforded this component, 3α-hydroxy-*ent*-17-norkauran-16-one (**2***c*, 45 mg). Repeated crystallization from methanol gave pure **2***c* (28 mg), m.p. 179–181° (lit. (16) 179–181°, (17) 192–193°). The material (1.8 g) from the mycelia on chromatography yielded small amounts of pure **2***c* (2 mg) and substrate (**2***b*). All fractions from both columns which contained substrate were combined and crystallized from methanol giving pure **2***b* (0.7 g). Based on substrate not recovered the yield of **2***c* was 9%.

3α-Acetoxy-ent-17-norkauran-16-one (2e)

In later incubations of **2***b* with *A. niger* it was found that **2***c* was more readily separated from column chromatography fractions (see above) as the derived acetate (**2***e*). These fractions were treated with acetic anhydride – pyridine (1:1) at 20° for 12 h and then submitted to preparative t.l.c. (chloroform). This gave the keto acetate **2***e* which on crystallization from methanol had m.p. 194–196° (lit. (17) 186°).

3α-Acetoxy-ent-16-kaurene (2f)

A solution of phenyl lithium was prepared by reacting lithium (160 mg) with bromobenzene (800 mg) in ether (20 ml). A portion (1.8 ml) of the resulting solution was added at 20° to methyltriphenylphosphine bromide (12 mg) in ether (30 ml) under nitrogen and followed 15 min later by **2***e* (45 mg) in ether (10 ml). The mixture was heated to reflux for 65 h and then worked up by treatment with water (50 ml) and extraction into ether (2 × 50 ml). Preparative t.l.c. (ethyl acetate – light petroleum, 3:17) of the product furnished 3α-acetoxy-*ent*-16-kaurene (**2***f*, 40 mg) which crystallized from light petroleum and had m.p. 151–154°; τ 5.20 (br s, 2 H-17), 5.49 (dd, 1 H-3, $w_{1/2}$ = 17 Hz), 7.96 (s, 3H, $-O_2C-CH_3$), 8.95 (s, 3 H-20), and 9.15 (s, 3 H-18 + 3 H-19); $\nu_{C=O}$ 1730 cm^{-1}.

Mol. Wt. Calcd. for $C_{22}H_{34}O_2$: 330.2559. Found (high resolution mass spectrometry): 330.2561.

3α-Hydroxy-ent-16-kaurene (2d)

The acetate (**2***f*, 53 mg) was heated with excess (200 mg) lithium aluminum hydride in refluxing dry ether for 90 min. The reaction was worked up by addition of saturated aqueous sodium sulfate. The crude product was purified by preparative t.l.c. (ethyl acetate – light petroleum, 1:4) and then crystallization from light petroleum. This gave 3α-hydroxy-*ent*-16-kaurene (**2***d*, 38 mg), m.p. 168–169° (lit. (16) 172–173°); τ 5.20 (br s, 2 H-17), 6.78 (dd, 1 H-3, $w_{1/2}$ = 17 Hz), 8.97 (s, 3 H-20), 9.02 (s, 3 H-18), and 9.22 (s, 3 H-19); τ with 0.78 molar

Can. J. Chem. Downloaded from www.nrcresearchpress.com by 210.87.254.105 on 09/05/12
For personal use only.

ratio of $Eu(dpm)_3$ to **2***d* 1.25 (s, 3 H-19), 1.73 (s, 3 H-18), 4.80 (br s, 2 H-17), and 5.75 (s, 3 H-20); ν_{OH} 3630 cm^{-1}.

ent-16-Kauren-3-one (2g)

A pyridine (2 ml) solution of alcohol **2***d* (20 mg) was added to a solution of chromium trioxide (0.5 g) in the same solvent (5 ml). After 2 h at 20°, water (80 ml) and ethyl acetate (80 ml) were added and the mixture was stirred for 4 h and then filtered. Evaporation of the ethyl acetate layer gave an oil, the major component of which was separated and purified by preparative t.l.c. (ethyl acetate – light petroleum, 1:9) and crystallization. This yielded *ent*-16-kauren-3-one (**2***g*, 8 mg), m.p. 84–85° (lit. (16) 86–87°); τ 5.20 (br s, 2 H-17), 8.75 (s, 3H, C_4—CH_3), 8.93 (s, 3 H-20), and 8.96 (s, 3H, C_4—CH_3); τ (C_6D_6) 8.80 (s, 3H, C_4—CH_3), 8.99 (s, 3H, C_4—CH_3) and 9.20 (s, 3 H-20); $\nu_{C=O}$ 1710 cm^{-1}.

17-Norkauran-16-one (3b)

(+)-Kaurene (**3***a*, 5.0 g from a *Podocarpus* species[8]) was oxidized with osmium tetroxide – sodium periodate as described previously (10) for its enantiomer. The dark product (4.7 g) was chromatographed over silica gel (200 g) and the fractions eluted with ether – light petroleum (1:8) combined and crystallized from moist methanol. The 17-norkauranone (**3***b*, 2.1 g) obtained had m.p. 116–118° [*cf.* enantiomer, **2***b*, 116–119° (10)], $[\alpha]_D$ +56° (*c*, 1.0); τ 8.91, 9.13, and 9.17 (all s, 3H, quaternary C—CH_3's); $\nu_{C=O}$ 1742 cm^{-1}.

Anal. Calcd. for $C_{19}H_{30}O$: C, 83.15; H, 11.02. Found: C, 83.11; H, 11.00.

Incubations of 17-Norkauran-16-one (3b) with A. niger (ATCC 26693)

Procedures similar to those for *ent*-17-norkauranone were used. In a typical incubation, *A. niger* cultures (4 × 2.5 l) were inoculated with **3***b* (2.0 g) in DMF (50 ml). After 5 days an oil (2.9 g) was recovered from the filtered medium by extraction with ethyl acetate. Chromatography of this oil over a silica gel column (120 g) and elution with ether – light petroleum (1:2) gave fractions containing substrate (see below). Elution with ether gave a complex mixture which contained (t.l.c.) the only component, other than **3***b*, present in the extract from the incubation but absent from that of a control culture. This compound, which had an identical mobility on t.l.c. with that of 3α-hydroxy-*ent*-17-norkauran-16-one (**2***c*) was isolated by repeated preparative t.l.c. (acetic acid – ethyl acetate – light petroleum, 2:25:25 and 2:10:25). The resulting oily 3β-hydroxy-17-norkauran-16-one (**3***c*) (4 mg) could not be induced to crystallize but had $[\alpha]_D$ +30° (lit. (9) enantiomer −45°); τ 6.78 (dd, 1 H-3, $w_{1/2}$ = 17 Hz), 8.89, 8.99, and 9.18 (all s, 3H, quaternary C—CH_3's). The compound was characterized as its acetate (see below).

An extract of the mycelia on chromatography afforded fractions containing substrate but no isolable amounts of **3***c*. All fractions containing substrate from the extracts of the medium and the mycelia were combined and crystallized from methanol. This gave pure **3***b* (1.06 g).

[8]We thank Dr. G. B. Sweet, New Zealand Forest Service, for this material.

3β-Acetoxy-17-norkauran-16-one (3d)

In later incubations of **3***b* with *A. niger*, fractions containing **3***c*, which were obtained by column chromatography over silica gel, were combined and treated with acetic anhydride – pyridine (1:1) at 20° for 14 h. Evaporation of reagents *in vacuo* and purification of the product by preparative t.l.c. (chloroform) and crystallization from light petroleum (b.p. 62–67°) gave the keto acetate **3***d*, m.p. 193–196° (*cf.* **2***e*, m.p. 194–196°), $[\alpha]_D$ +18° (*c*, 0.6); τ 5.50 (dd, 1 H-3, $w_{1/2}$ = 17 Hz), 7.98 (s, 3H, —O_2C—CH_3), 8.90 (s, 3 H-20), and 9.15 (s, 6H, C_4—CH_3's); $\nu_{C=O}$ 1735 cm^{-1}; *m/e* 332 (14%, M^+), 317 (1%), 288 (2%), 273 (26%), 272 (100%), 256 (60%), 228 (26%), and 216 (39%).

Mol. Wt. Calcd. for $C_{21}H_{32}O_3$: 332.2352. Found (high resolution mass spectrometry): 332.2350.

3β-Hydroxy-16-kaurene (3e)

A portion (2.8 ml) of a phenyl lithium solution, prepared from lithium (100 mg) and bromobenzene (800 mg) in ether (20 ml), was added to methyltriphenylphosphine bromide in ether (30 ml) under dry nitrogen. After 2 h at 20° 3β-acetoxy-17-norkauran-16-one (**3***d*, 9 mg) was added in ether (5 ml) and the mixture heated to reflux for 56 h. Decomposition with water, extraction with ether, and evaporation gave an oil (129 mg) which on t.l.c. analysis (ethyl acetate – light petroleum, 1:7) did not contain a compound of the mobility of 3α-acetoxy-*ent*-16-kaurene (**2***f*). It did contain a component of identical R_f with that of 3α-hydroxy-*ent*-16-kaurene (**2***d*). This component, 3β-hydroxy-16-kaurene (**3***e*, 5.3 mg) was recovered by repeated preparative t.l.c. (ethyl acetate – light petroleum, 1:8; chloroform) and had m.p. 168–170° (from methanol; *cf.* **2***d*, m.p. 168–169°), $[\alpha]_D$ +60° (*c*, 0.5); τ 5.20 (br s, 2 H-17), 6.78 (dd, 1 H-3, $w_{1/2}$ = 17 Hz), 8.97 (s, 3 H-20), 9.02 (s, 3 H-18), and 9.22 (s, 3 H-19); ν_{O-H} 3630 cm^{-1}; *m/e* 288 (58%, M^+), 273 (18%), 270 (22%), 255 (52%), 245 (35%), 229 (32%), 227 (53%), 159 (22%), and 91 (100%).

Mol. Wt. Calcd. for $C_{20}H_{32}O$: 288.2453. Found (high resolution mass spectrometry): 288.2454.

Incubations of 17-Norphyllocladan-16-one (4b) with A. niger (ATCC 26693)

The conditions and procedures established for both norkauranone enantiomers (**2***b* and **3***b*) were used for the incubation of **4***b* with *A. niger*. In a typical incubation, cultures (5 × 2.5 l) of *A. niger* were inoculated with the norketone (**4***b*, 2.0 g) in DMF (50 ml). The cultures were harvested after 5 days and gave an oily extract (1.25 g, total from medium and mycelia) which was chromatographed over silica gel (70 g). Elution with ether – light petroleum (1:1) gave substrate (1.36 g), while elution with pure ether gave fractions containing two compounds which were absent from the extract of a control culture. These were isolated by preparative t.l.c. (acetic acid – ethyl acetate – light petroleum, 2:5:25). The less polar transformation product, the diketone (**4***g*, 17 mg, 2.5%) on crystallization from light petroleum had m.p. 187–189°, $[\alpha]_D$ +13° (*c*, 0.8); τ 8.90, 8.95 (each s, 3H, C_4—CH_3's), and 8.99 (s, 3 H-20); τ with a 1.0 molar ratio of $Eu(dpm)_3$ to **4***g* 6.80, 7.08 (each s, 3H, C_4—CH_3's), and 7.84 (s, 3 H-20); $\nu_{C=O}$ 1749 and 1712 cm^{-1}; *m/e* 288 (100%, M^+), 273 (10%), 243 (24%), 232 (40%), 230 (23%), 202 (80%), and 201 (95%).

Can. J. Chem. Downloaded from www.nrcresearchpress.com by 210.87.254.105 on 09/05/12
For personal use only.

Mol. Wt. Calcd. for $C_{19}H_{28}O_2$:288.2089. Found (high resolution mass spectrometry):288.2086.

This sample was identical (m.p., mixture m.p., t.l.c., n.m.r., and mass spectra) with **4***g* prepared from calliterpenone (**8**) by Dr. Zaman (19). As obtained from Dr. Zaman **4***g* had m.p. 179–182°, raised to 185–188° by preparative t.l.c. (chloroform) and crystallization from light petroleum.

The more polar transformation product 3β-hydroxy-17-norphyllocladan-16-one (**4***c*, 35 mg, 5.0%), on crystallization from light petroleum had m.p. 158–160°, $[\alpha]_D$ +16° (*c*, 0.7); τ 6.75 (dd, 1 H-3, $w_{1/2}$ = 17 Hz), 7.3 (dd, 1 H-15, J_{obs}, 15α-15β = 19 Hz and 14α-15β = 3 Hz), 9.02, 9.13, and 9.24 (all s, 3H, quaternary C—CH_3's) $\nu_{C=O}$ 1750 cm^{-1}, and ν_{O-H} 3640 cm^{-1}; *m/e* 290 (100%, M^+), 275 (18%), 272 (65%), 258 (62%), 234 (29%), and 230 (24%).

Mol. Wt. Calcd. for $C_{19}H_{30}O_2$:290.2276. Found (high resolution mass spectrometry): 290.2272.

Incubation of 17-Norphyllocladan-16-one (4b) with A. niger (ATCC 10577)

Inoculation of cultures (3 × 2.5 l) of *A. niger* (ATCC 10577) with **4***b* (1.35 g) in DMF (50 ml) and then extraction of the mycelia and medium, as described above, afforded an oil (1.82 g). Chromatography of this oil over silica gel (80 g) and preparative t.l.c. of the resulting fractions gave substrate (**4***b*, 0.81 g) and the keto alcohol **4***c* (27 mg, 5%). Only a trace (< 1 mg) of material with the same R_f on t.l.c. (acetic acid – ethyl acetate – light petroleum, 2:10:25 and 2:6:15) as that of the diketone **4***g* was obtained.

Oxidation of 3β-Hydroxy-17-norphyllocladan-16-one (4c)

The keto alcohol (**4***c*, 4 mg) in acetone (5 ml) was treated with Jones' reagent (0.3 ml). After 30 min at 20° the solution was diluted with water (50 ml) and extracted with ether (2 × 50 ml) to give a compound (3 mg) which was identical by t.l.c., g.l.c. (retention time 10.3 min, 195°), i.r. and mass spectra, with the diketone (**4***g*).

3β-Acetoxy-17-norphyllocladan-16-one (4d)

Treatment of the keto alcohol (**4***c*, 35 mg) with acetic anhydride – pyridine (1:1, 5 ml) for 12 h and then evaporation of the reagents *in vacuo* gave the keto acetate (**4***d*). After preparative t.l.c. (chloroform) and crystallization from light petroleum it (28 mg) had m.p. 156–158°, $[\alpha]_D$ +27° (*c*, 1.0); τ 5.45 (dd, 1 H-3, $w_{1/2}$ = 17 Hz), 7.95 (s, 3H, —O_2C—CH_3), 9.08 (s, 3H, quaternary C—CH_3), and 9.10 (s, 6H, quaternary C—CH_3's); $\nu_{C=O}$ 1735 cm^{-1}.

Mol. Wt. Calcd. for $C_{21}H_{32}O_3$:332.2352. Found (high resolution mass spectrometry):332.2350.

3β-Acetoxy-16-phyllocladene (4f)

A portion (2 ml) of a phenyl lithium solution, prepared from lithium (160 mg) and bromobenzene (800 mg) in ether (20 ml), was added to methyltriphenylphosphine bromide (180 mg) in ether (30 ml) under dry nitrogen and the resulting yellow solution heated to reflux for 3 h. The ketoacetate (**4***d*, 28 mg) in ether (5 ml) was then added and the heating continued for 3 days. Decompositon with water (20 ml), extraction with ether (2 × 50 ml) and evaporation gave an oil (220 mg). This was subjected to preparative t.l.c. (ethyl acetate – light petroleum, 3:17) and gave the acetoxy olefin (**4***f*, 19 mg) which on crystallization from methanol had m.p. 121–123°, $[\alpha]_D$ +41° (*c*, 1.1); τ 5.29 (br s, 2 H-17), 5.52 (dd, 1 H-3, $w_{1/2}$ = 16 Hz), 8.00 (s, 3H, —O_2C—CH_3), 9.05 (s, 3H, quaternary C—CH_3), and 9.17 (s, 6H, quaternary C—CH_3's); $\nu_{C=O}$ 1735 cm^{-1}.

Mol. Wt. Calcd. for $C_{22}H_{34}O_2$:330.2559. Found (high resolution mass spectrometry):330.2560.

Preparation of Diol 6

Phenyl lithium solution (1.6 ml, from 80 mg lithium and 400 mg bromobenzene in 10 ml dry ether) was reacted with methyltriphenylphosphine bromide (120 mg) in ether (30 ml) under dry nitrogen at 20°. After 10 min the keto acetate (**4***d*, 43 mg) was added and the mixture heated to reflux for 48 h. Work-up (as above) gave an oil which on t.l.c. (ethyl acetate – light petroleum, 3:17) showed no trace of the acetoxy olefin **4***f* but only a spot of much lower R_f. The component responsible for this was isolated by preparative t.l.c. (ethyl acetate – light petroleum, 2:3 run twice). This oily diol (**6**, 20 mg) had τ 2.4–2.9 (5H, aromatic protons), 6.80 (dd, 1 H-3, $w_{1/2}$ = 15 Hz), 9.02 (s, 6H, quaternary C—CH_3's), and 9.20 (s, 3H, quaternary C—CH_3); ν_{O-H} 3633 and 3610 cm^{-1}.

Rapid decomposition of **6** to the styrene **5** was taking place and further investigations were limited to **5** (see below).

Dehydration of Diol 6

The diol (**6**, 20 mg) in benzene (20 ml) was treated with toluene-*p*-sulfonic acid (15 mg) in the presence of anhydrous calcium chloride (0.5 g) for 100 min. The drying agent and solvent were removed and the oily residue submitted to preparative t.l.c. (ethyl acetate – light petroleum, 1:4). This gave the styrene **5** (13 mg), which on crystallization from ether had m.p. 177–178°; τ 2.4–2.9 (5H, aromatic protons), 3.75 (s, 1 H-15), 6.75 (dd, 1 H-3, $w_{1/2}$ = 16 Hz), 7.1 (m, 1 H-13), 8.98, 9.20, and 9.22 (all s, 3H, quaternary C—CH_3's); τ with 1.23 molar ratio of Eu(dpm)$_3$ to **5** −0.70 (s, 3 H-19), 0.00 (s, 3 H-18), and 5.90 (s, 3 H-20); λ_{max} 264 (ε 14 600); ν_{O-H} 3650 cm^{-1}.

Mol. Wt. Calcd. for $C_{25}H_{34}O$: 350.2610. Found (high resolution mass spectrometry): 350.2612.

3β-Hydroxy-16-phyllocladene (4e)

A suspension of lithium aluminum hydride (110 mg) in ether (10 ml) was stirred under dry nitrogen at 20° for 1 h. The acetate **4***f* (20 mg) was then added in ether (6 ml) and the reaction heated to reflux for 5 h. Addition, in succession, of water (0.1 ml), aqueous sodium hydroxide (15%, 0.1 ml), and water (0.4 ml) followed by removal of the resulting precipitate and the solvent gave an oil. Preparative t.l.c. (chloroform) of this residue furnished 3β-hydroxy-16-phyllocladene (**4***e*, 18 mg) which crystallized from light petroleum and had m.p. 157–158°, $[\alpha]_D$ +3° (*c*, 0.9); τ 5.30 (br s, 2 H-17), 6.85 (dd, 1 H-3, $w_{1/2}$ = 16 Hz), 9.09 (s, 3 H-18), 9.15 (s, 3 H-20), and 9.29 (s, 3 H-19); τ with 0.4 molar ratio of Eu(dpm)$_3$ to **4***e* 4.25 (s, 3 H-19), 4.49 (s, 3 H-18), 4.95 (br s, 2 H-17), and 7.12 (s, 3 H-20); ν_{O-H} 3638 cm^{-1}.

Mol. Wt. Calcd. for $C_{20}H_{32}O$:288.2453. Found (high resolution mass spectrometry):288.2454.

Incubation of ent-Kaurene (2a) and Phyllocladene (4a) with A. niger (ATCC 26693)

Three cultures (100 ml each) of *A. niger* were grown

for 4 days and then one was inoculated with *ent*-kaurene (**2***a*, 20 mg) in DMF (1.5 ml), another with phyllocladene (**4***a*, 27 mg) in DMF (1.5 ml), and the third with DMF (1.5 ml) only. After incubation for 6 days the cultures were extracted with ethyl acetate as before (see above). The three extracts were compared by analytical t.l.c. (ethyl acetate – light petroleum, 1:9 and 1:2). No trace of products (**2***d*, **4***e*) of axial hydroxylation at C-3 in **2***a* or **4***a* was detected in the appropriate extracts, the three extracts appearing identical except for the presence of unreacted **2***a* and **4***a*. *ent*-Kaurene (**2***a*, 18 mg) and phyllocladene (**4***a*, 24 mg) were recovered by preparative t.l.c. (light petroleum).

We thank the National Research Council of Canada for an Operating Grant (to R.McC.) and a Scholarship (to J.K.T.). We are also indebted to Dr. T. Anthonsen, Trondheim, for the high resolution mass spectra and to Dr. G. L. Barron, University of Guelph for gifts of fungal cultures.

1. A. B. ANDERSON, R. MCCRINDLE, and J. K. TURNBULL. Chem. Commun. 143 (1973).
2. A. LANG. Ann. Rev. Plant Physiol. **21**, 53F (1970).
3. J. R. HANSON. The tetracyclic diterpenes. Pergamon Press, Oxford. 1968.
4. J. MACMILLAN and E. R. H. WALKER. J. Chem. Soc. Perkin Trans. I, 981 (1972).
5. R. A. APPLETON, R. MCCRINDLE, and K. H. OVERTON. Tetrahedron, **9**, 581 (1970).
6. P. W. BRIAN, J. F. GROVE, and T. P. C. MULHOLLAND. Phytochemistry, 1475 (1967).
7. W. CHARNEY and H. L. HERZOG. Microbial transformations of steroids. Academic Press, New York. 1967.
8. E. R. H. JONES. Pure Appl. Chem. **33**, 39 (1973). A. M. BELL, P. C. CHERRY, I. M. CLARK, W. A. DENNY, E. R. H. JONES, G. D. MEAKINS, and P. D. WOODGATE. J. Chem. Soc. Perkin Trans. 1. 2081 (1972).
9. J. P. BEILBY, E. L. GHISALBERTI, P. R. JEFFERIES, M. A. SEFTON, and P. N. SHEPPARD. Tetrahedron Lett. 2589 (1973).
10. R. A. APPLETON, P. A. GUNN, and R. MCCRINDLE. J. Chem. Soc. C, 1148 (1970).
11. J. C. GALBRAITH and J. E. SMITH. Brit. Mycol. Soc. Trans. **52**, 237 (1969).
12. D. G. BUCKLEY, G. H. GREEN, E. RITCHIE, and W. C. TAYLOR. Chem. Ind. 298 (1971).
13. P. V. DEMARCO, T. K. ELZEY, R. B. LEWIS, and E. WENKERT. J. Am. Chem. Soc. **92**, 2537 (1970).
14. J. D. CONNOLLY and R. MCCRINDLE. Chem. Ind. 379 (1965). D. H. WILLIAMS and N. S. BHACCA. Tetrahedron, **21**, 2021 (1965).
15. P. WITZ, H. HERRMANN, J.-M. LEHN, and G. OURISSON. Bull. Soc. Chim. Fr. 1101 (1963).
16. P. R. JEFFERIES and R. W. RETALLACK. Aust. J. Chem. **21**, 1311 (1968).
17. D. A. H. TAYLOR. J. Chem. Soc. C, 1360 (1967).
18. A. CHATTERJEE, S. K. DESMUKH, and S. CHANDRASEKHAREN. Tetrahedron, **28**, 4319 (1972).
19. S. A. AHMAD and A. ZAMAN. Tetrahedron Lett. 2179 (1973).
20. L. L. SMITH, G. GREENSPAR, R. REES, and T. FOELL. J. Am. Chem. Soc. **88**, 3120 (1966). Y. Y. LIN, M. SHIBAHARA, and L. L. SMITH. J. Org. Chem. **34**, 3530 (1969).
21. B. R. PREMA and P. K. BHATTACHARYYA. Appl. Microbiol. **10**, 529 (1962).
22. A. WETTSTEIN, F. VISCHER, and C. MEYSTRE. U.S. Patent No. 2. 844, 513 July 22, 1958; Chem. Abstr. **53**, 1629B (1968).
23. J. FRIED, R. W. THOMA, D. PERLMAN, J. E. HERZ and A. BORMAN. Recent Prog. Hormone Res. **11**, 149 (1955).

Can. J. Chem. Downloaded from www.nrcresearchpress.com by 210.87.254.105 on 09/05/12
For personal use only.

Substituted 5-Allyl-9-oxobenzomorphans. Versatile Intermediates for Investigations in the Field of Analgesics and Narcotic Antagonists. Part 1

IVO MONKOVIC

Bristol Laboratories of Canada, 100 Industrial Boulevard, Candiac, P.Q. J5R 1J1

Received October 25, 1974

IVO MONKOVIC. Can. J. Chem. **53**, 1189 (1975).

2-Tetralone has been converted to 5-allyl-2-methyl-9-oxo-benzomorphan methobromide (**4**). Thermal dequaternization of **4** afforded tertiary base **5**. Alternatively, **4** was reduced with sodium borohydride to give **7***a* or reacted with methylmagnesium iodide to give **7***b*. Dequaternization of these to tertiary bases (**8***a* and **8***b*) followed by acid-catalyzed cyclization afforded tetrahydrofurano compounds **9***a* and **9***b*, respectively. Bromocyclization of **8***b* afforded bromomethyltetrahydrofurano compound **9***c*, which was further converted to dimethylamino compound **9***d*.

IVO MONKOVIC. Can. J. Chem. **53**, 1189 (1975).

On a transformé la tétralone-2 en méthobromure d'allyl-5 méthyl-2 oxo-9 benzomorphane (**4**). La déquaternisation thermique de **4** conduit à la base tertiaire **5**. Le composé **4** peut aussi être réduit par le borohydrure de sodium pour donner **7***a* ou réagir avec de l'iodure de méthylmagnesium pour conduire à **7***b*. La déquaternisation de ces composés en bases tertiaires (**8***a* et **8***b*) suivie par une cyclisation acido-catalysée fournit respectivement les composés tétrahydrofuranno **9***a* et **9***b*. La bromocyclisation de **8***b* fournit le composé bromométhyltétrahydrofuranno **9***c* qui peut être transformé en composé diméthylamino **9***d*. [Traduit par le journal]

In recent years significant progress has been made in the field of highly potent, pure, and partial narcotic antagonists (nonabusable analgesics) by studying 14-hydroxymorphine-related compounds of general structures **I** (1) and **II** (2),

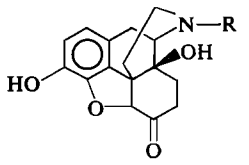

I

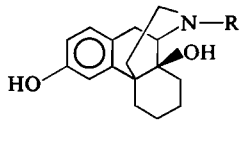

II

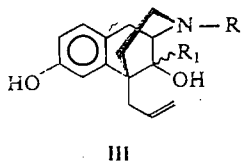

III

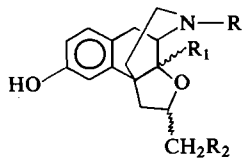

IV

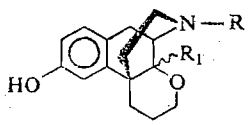

V

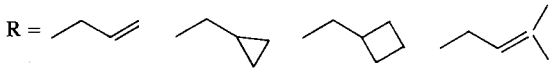

R_1 = H, alkyl; R_2 = H, Br, OH, *N*,*N*-dialkyl.

incorporating various C_3H_5 to C_5H_7 nitrogen substituents. Similar studies in the benzomorphan series have not been conducted, even though synthetic methodology to this end has been available for a number of years (3–5). The lack of interest in the 9-hydroxybenzomorphans may have been due to the finding that replacement of the 9-hydrogen by a hydroxyl group adversely affected agonist activity (Reference 6)

We wished to study the effect of varying the substituent on the nitrogen atom in the 9-hydroxybenzomorphans **III**, while incorporating at C5 a substituent suitably functionalized for the formation of an heterocyclic C-ring in the morphinan series (represented by general structures **IV** and **V**). As a pilot study in this direction, we decided to attempt a synthesis of 5-allyl-9-oxobenzomorphan **5**. At the time of inception of our work, the most promising synthetic approach to **5** appeared to be that of May and co-workers (6, 7). By analogy to their procedure, the allylation of 2-tetralone via the corresponding pyrrolidine enamine afforded allyltetralone **1**. Further alkylation of **1** by reaction with 2-chloro-*N*,*N*-dimethylethylamine and sodium *t*-pentoxide in boiling benzene afforded dialkylated tetralone **2**.

The success of our synthesis was dependent upon a successful selective bromination of ketone **2** in the presence of the double bond. This selectivity has been achieved earlier by utilization of

Can. J. Chem. Downloaded from www.nrcresearchpress.com by 210.87.254.5 on 09/05/12
For personal use only.

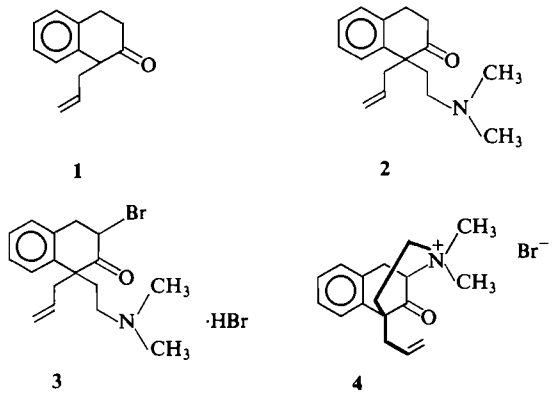

1 2 3 4

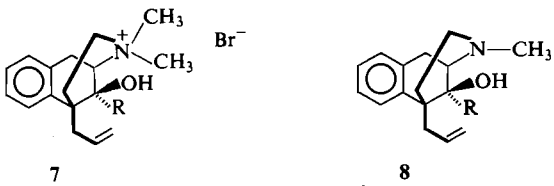

7 8

a R = H; *b* R = CH_3

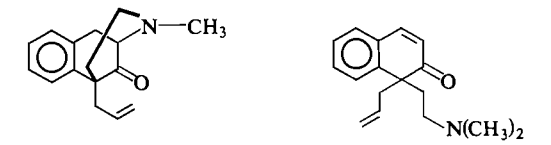

5 6

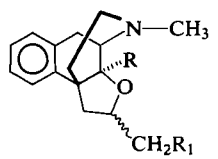

9

a R = H; R_1 = H
b R = CH_3; R_1 = H
c R = CH_3; R_1 = Br
d R = CH_3; R_1 = $N(CH_3)_2$

phenyltriethylammonium tribromide (8) and cupric bromide (9). More recently Awang and Wolfe (10) described a method utilizing pyrrolidone hydrotribromide as a brominating agent. This method was applied in the bromination of **2**, affording a reasonable yield of bromotetralone **3** (57%). The free base of **3** spontaneously cyclized to the quaternary salt **4** (3, 4). Heating a solution of **4** in 1-octanol to reflux for 15 min resulted in a mixture of benzomorphan **5** and two by-products, one of which was identified as an elimination product **6**. Alternatively, **4** was reduced with sodium borohydride in ethanol at room temperature to the 9β-hydroxybenzomorphan **7***a*, which was dequaternized as above, affording a superior yield of tertiary base **8***a* (57% overall yield from **4**), as compared to that of **5**. Similarly treatment of **4** with methylmagnesium iodide, followed by dequaternization as above without prior isolation of **7***b* resulted in tertiary base **8***b*. The stereochemical assignments of the 9-carbinols followed from the method of preparation of **7***b* (3) and from the i.r. spectra of both **8***a* and **8***b*, which exhibited broad maxima at 3400 cm^{-1} (irrespective of concentration) which are characterestic of intramolecular OH–N bonding and have been observed by Kugita and May in 5-methyl homologs (4). Acid-catalyzed cyclizations of **8***a* and *b* (boiling with concentrated hydrochloric acid) afforded the corresponding tetrahydrofuran derivatives **9***a* and **9***b*, respectively. Bromocyclization (11) of **8***b* (addition of a solution of bromine in carbon tetrachloride to a solution of **8***b* in dichloromethane) afforded bromomethyltetrahydrofurano compound **9***c* as the hydrobromide salt. Reaction of **9***c* with dimethylamine in DMF at 100° afforded the corresponding dimethylamino compound **9***d*.

Experimental

The melting points were determined on a Gallenkamp melting point apparatus and are not corrected. The i.r. spectra were recorded on a Unicam Sp-200G grating i.r. spectrometer. The n.m.r. spectra were recorded on a Varian A-60A spectrometer using deuteriochloroform as a solvent. The chemical shifts are expressed in δ values using tetramethylsilane as internal reference. Microanalyses were performed by Micro-Tech Laboratories Inc., Skokie, Ill.

3,4-Dihydro-1-allyl-2(1H)naphthalenone (1)

The 1-allyl-2-tetralone (**1**) was obtained in 78% yield by the procedure described by Murphy *et al.* (7); b.p. 79–83°/0.05 mm; i.r. (neat) 1715 cm^{-1}; n.m.r. δ 7.12 (4H, s), 4.7–6.2 (3H, m), 3.39 (1H, t, J = 6 Hz), 2.2–3.1 (6H, m).

Anal. Calcd. for $C_{13}H_{13}O$: C, 84.29; H, 7.01. Found: C 83.94; H, 7.04.

3,4-Dihydro-1-allyl-1-(2-dimethylaminoethyl)-2(1H)-naphthalenone (2)

A nitrogen atmosphere was maintained throughout this experiment. To a stirred and heated to reflux suspension of sodium hydride (17.0 g of 42.8%, washed with hexene) in benzene (300 ml) was added dropwise during 40 min t-pentyl alcohol (25.0 g), followed by a solution of allyltetralone **1** (67.0 g) in benzene (200 ml) during 30 min. The mixture was heated and stirred for another 30 min, followed by treatment with a solution of 2-chloro-*N*,*N*-dimethylethylamine (50.0 g) in benzene (80 ml) over

Can. J. Chem. Downloaded from www.nrcresearchpress.com by 210.87.254.5 on 09/05/12
For personal use only.

Can. J. Chem. Downloaded from www.nrcresearchpress.com by 210.87.254.5 on 09/05/12
For personal use only.

a period of 1 h at such a rate as not to cause excessive evolution of hydrogen. After addition was completed, the mixture was heated and stirred for 24 h. After cooling, it was extracted with 2 × 200 ml of 2 *N* hydrochloric acid and the combined extracts were warmed up to 70° to hydrolyze the *O*-alkylated product. The starting material was recovered by extraction with ether, to afford after drying, evaporation of ether, and distillation, 20.1 g of **1**. The acidic layer was basified with ammonium hydroxide and extracted with ether to afford after drying and evaporation of ether 51.8 g of **2** as an oil; i.r. (neat) 1710 cm^{-1}; n.m.r. (CCl_4) δ 7.0–7.3 (4H, m), 4.6–5.8 (3H, m), 2.8–3.2 (2H, m), 2.1–2.8 (4H, m), 1.9 (6H, s), 1.5–2.1 (2H, m). A sample for analysis was purified as the oxalate salt by recrystallization from methanol–acetone; m.p. 118–119°.

Anal. Calcd. for $C_{17}H_{23}NO{\cdot}C_2H_2O_4$: C, 65.69; H, 7.25; N, 4.03. Found: C, 65.47; H, 7.29; N, 4.06.

3-Bromo-1,4-dihydro-1-allyl-1-(2-dimethylamino)-2-(1H)naphthalenone (3)

A freshly prepared hydrogen bromide solution in ether was used to convert free base **2** (14.1 g) in ether at 0–5° to the corresponding hydrogen bromide salt. The ether was decanted and the residue, a heavy oil, was dissolved in a mixture of dichloromethane (100 ml) and THF (200 ml). This solution was stirred vigorously in the dark and to it was added dropwise during 2 h a solution of pyrrolidone hydrotribromide (27–28 g) in THF (300 ml). The mixture was allowed to stand for 3 h and then the separated solid was removed by filtration. The filtrate was concentrated *in vacuo* and the residual solid was recrystallized from 2-propanol, to afford 11.2 g of **3**, m.p. 129–131°. Another crop of 2.1 g was obtained from mother liquors for a total of 13.3 g. Recrystallization from 2-propanol afforded sample for analysis; m.p. 133–135°; i.r. (Nujol) 1735 cm^{-1}; n.m.r. δ 7.0–7.7 (4H), 3.7–5.9 (4H, m), 3.3–3.7 (2H, m), 2.4–3.2 (13H, m).

Anal. Calcd. for $C_{17}H_{22}BrNO{\cdot}HBr$: C, 48.94; H, 5.56; N, 3.36. Found: C, 49.01; H, 5.66; N, 3.21.

5-Allyl-2-methyl-9-oxo-6,7-benzomorphan Methrobromide (4)

A mixture of **3** (8.34 g), water (80 ml), ice (10 g), ether (100 ml), and concentrated ammonium hydroxide (2 ml) was shaken vigorously in a separatory funnel. The ether layer was transferred quickly to a round bottom flask and the aqueous layer was extracted with 2 × 20 ml of ether. The combined ethereal extracts were evaporated to dryness and to the residue was added dichloromethane (20 ml). After 24 h, the separated solid was removed by filtration to afford 5.23 g of **4**, m.p. 189–193°. A sample for analysis was recrystallized from methanol-2-propanol; m.p. 196–197°; i.r. (Nujol) 1735 cm^{-1}; n.m.r. (D_2O) δ 7.48 (4H, s), 5.0–6.3 (3H, m), 3.53 (3H, s), 3.37 (3H, s), 2.5–4.4 (11H, m).

Anal. Calcd. for $C_{16}H_{18}NO{\cdot}CH_3Br$: C, 60.72; H, 6.59; N, 4.17. Found: C, 60.64; H, 6.62; N, 4.23.

In another experiment **4** was obtained in 54% yield directly from **2** without prior isolation of **3**. After addition of pyrrolidone hydrotribromide to **2** was completed, the mixture was allowed to stand overnight, and then it was concentrated to a small volume and the residue was treated with ammonium hydroxide and extracted with ether as above to afford **4**.

5-Allyl-2-methyl-9-oxo-6,7-benzomorphan (5) and 1-Allyl-1-(2-dimethylaminoethyl)-2(1H)naphthalenone (6)

To hot 1-octanol (40 ml) was added quaternary salt **4** (3.36 g) and the mixture was heated to reflux under flow of nitrogen for 15 min. After cooling, to this was added ether (120 ml) and it was extracted with 1 *N* hydrochloric acid (2 × 15 ml) followed by water (5 × 20 ml). The combined extracts were extracted with petroleum ether to remove traces of octanol, basified with ammonium hydroxide, and extracted with ether to afford after drying and concentration 1.98 g of an oil, which showed three spots on t.l.c. This was chromatographed on a silica gel column with ether as eluent, to afford apart from some unidentified less polar impurity, 730 mg of **5** as a white solid, m.p. 65–67°. After treatment with ether and charcoal, the sample showed m.p. 73–75°; i.r. (Nujol) 1725 cm^{-1}; n.m.r. (CCl_4) δ 7.5 (4H, s), 4.8–6.2 (3H, m, $CH_2CH{=}CH_2$), 2.9–3.7 (3H, m, 1-H and 3-H_2), 2.75 (2H, d, J = 6 Hz, $CH_2CH{=}CH_2$), 2.37 (3H, s, N—CH_3), 1.5–2.6 (3H, m, 8-H_2 and 4α-H), 1.37 (1H, d, J = 10 Hz, 4β-H).

A hydrochloride salt crystallized slowly from acetone with ½ mol of water of crystallization; m.p. 190–192°.

Anal. Calcd. for $C_{16}H_{19}NO.HCl{\cdot}\frac{1}{2}H_2O$: C, 67.00; H, 7.38; N, 4.88 Found: C, 67.10; H, 7.31; N, 4.68.

Further elution of the column with methanol afforded 340 mg of crude **6** as an oil, which was purified as oxalate salt by recrystallization from methanol–acetone; m.p. 160–161°; i.r. (free base, neat) 1730 cm^{-1}; n.m.r. (CCl_4) δ 7.2–7.5 (4H, m), 7.25 (1H, d, J = 10 Hz, 4-H), 6.1 (1H, d, J = 10 Hz, 3-H), 4.5–5.7 (3H, m), 1.9 (6H, s), 1.6–3.1 (6H, m).

Anal. Calcd. for $C_{17}H_{22}NO{\cdot}C_2H_2O_4{\cdot}CH_3OH$: C, 63.64; H, 7.21; N, 3.71. Found: C, 63.99; H, 7.51; N, 3.70.

5-Allyl-9β-hydroxy-2-methyl-6,7-benzomorphan Methabromide (7a)

A mixture of **4** (6.73 g) and sodium borohydride (400 mg) in absolute ethanol (50 ml) was stirred for 1 h followed by careful addition of hydrogen bromide (925 mg of 48%) in water (10 ml) and the mixture was heated to 65–70° for 30 min. It was then concentrated *in vacuo* and to the residue was added dichloromethane (25 ml). The mixture was stirred and filtered to remove inorganic salts. The filtrate was evaporated to dryness and to the residue was added acetone (15 ml), causing crystallization. A white solid was removed by filtration to afford 5.54 g of **7***a*; m.p. 206–208° from methanol–acetone; i.r. ($CHCl_3$), 3495 cm^{-1}; n.m.r. ($CDCl_3$) δ 7.1–7.4 (4H, m), 4.7–6.2 (4H, m), 4.0 (3H, s), ˊ.38 (6H, s), 2.4–4.0 (8H, m), 1.4 (1H).

Anal. Calcd. for $C_{16}H_{21}NO{\cdot}CH_3Br$: C, 60.36; H 7.15; N, 4.14. Found: C, 60.73; H, 7.23; N, 4.11.

5-Allyl-9β-hydroxy-2-methyl-6,7-benzomorphan (8a)

A mixture of **7***a* (4.2 g) and 1-octanol (30 ml) was heated to reflux for 45 min. Work-up as above afforded an oil which crystallized from petroleum ether. There was obtained 2.17 g of **8***a*; m.p. 80–81°; i.r. ($CHCl_3$), 3400 cm^{-1}; n.m.r. ($CDCl_3$) δ 7.0–7.5 (4H, m), 4.8–6.2 (3H, m), 3.83 (1H, d, J = 4 Hz), 3.38 (3H, s), 1.9–3.5 (8H, m), 1.12 (1H, d, J = 7 Hz); hydrochloride salt, flakes from methanol–ether; m.p. 228–230°.

Can. J. Chem. Downloaded from www.nrcresearchpress.com by 210.87.254.5 on 09/05/12
For personal use only.

Anal. Calcd. for $C_{16}H_{21}NO{\cdot}HCl$: C, 68.68; H, 7.93; N, 5.01. Found: C, 68.77; H, 8.05; N, 4.94.

5-Allyl-9β-hydroxy-2,9α-dimethyl-6,7-benzomorphan (8b)

To a suspension of **4** (3.36 g) in dry ether (5 ml) was added 1.7 *M* solution of methylmagnesium iodide in ether (35 ml) and the mixture stirred for 45 min. The ether was then evaporated and an attempt was made to isolate quaternary salt **7***b*. However, we obtained a heavy oil, which did not crystallize. Therefore, the oil was extracted with chloroform, the extract was dried and evaporated *in vacuo* and the residual oil was pyrrolized in 1-octanol, as described above to afford 2.24 g of **8***b* as an oil; i.r. ($CHCl_3$) 3400 cm^{-1}; n.m.r. (CCl_4) δ 6.9–7.4 (3H, m), 5.8–6.5 (3H, m), 2.37 (3H, s), 1.9–3.1 (8H, m), 1.08 (3H, s), 0.9–1.1 (1H). The oil was dissolved in ether and treated with a solution of oxalic acid in acetone to afford 2.6 g of oxalate salt, m.p. 165–167°. A sample of this was recrystallized from methanol–ether, m.p. 178–180°.

Anal. Calcd. for $C_{17}H_{23}NO{\cdot}C_2H_2O_4$: C, 65.69; H, 7.25; N, 4.03. Found: C, 65.65; H, 7.26; N, 3.89.

Tetrahydrofuranobenzomorphan 9a

A solution of **8***a* (11.05 g) in concentrated hydrochloric acid (10 ml) was heated to reflux for 1 h. After cooling, it was basified with ammonium hydroxide and extracted with ether to afford, after drying and evaporation of ether, 660 mg of **8***a* as an oil. It was dissolved in dry ether and triturated with petroleum ether. The solid impurity was removed by filtration and the filtrate was treated with a solution of oxalic acid in acetone to form the oxalate salt. It crystallized from methanol–acetone with a ½ mol of methanol of crystallization, m.p. 116–118°; n.m.r. (free base, CCl_4) δ 7.0 (4H, s), 4.15–4.7 (1H, m), 3.70 (1H, d, J = 3 Hz), 2.73 (3H, s), 1.26 (3H, d, J = 6 Hz), 1.0–3.6 (9H, m).

Anal. Calcd. for $C_{16}H_{23}NO{\cdot}C_2H_2O_4{\cdot}\frac{1}{2}CH_3OH$: C, 63.59; H, 7.21; N, 4.00. Found: C, 63.27; H, 7.22; N, 4.00.

Tetrahydrofuranobenzomorphan 9b

To a concentrated hydrochloric acid (2 ml) was added oxalate salt of **8***b* (900 mg) and the mixture heated briefly to boiling. Work-up as above afforded 600 mg of **9***b* as a white solid, m.p. 79–82°; n.m.r. (CCl_4) δ 7.0 (4H, s), 4.2–4.8 (1H, m), 2.38 (3H, s), 1.4 (3H, d, J = 6 Hz), 1.0–3.4 (9H, m), 0.97 (3H, s); hydrochloride salt, m.p. 278–280° from methanol–ether.

Anal. Calcd. for $C_{17}H_{23}NO{\cdot}HCl$: C, 69.49; H, 8.23; N, 4.77. Found: C, 69.26; H, 8.24; N, 4.66.

Bromomethyltetrahydrofuranobenzomorphan 9c

To a stirred and cooled (ice bath) solution of **8***b* (2.29 g) in dichloromethane (15 ml) was added dropwise 1 *M* solution of bromine in carbon tetrachloride (8.9 ml). The solvent was then removed *in vacuo* and to the residue was added acetone (12 ml). After 2 h, the solid precipitate was removed by filtration to afford 2.6 g of **9***c*, white crystals, m.p. 228–230° from methanol–acetone; n.m.r. ($CDCl_3$) (free base) δ 7.17 (4H, s), 3.34–5.0 (1H, m), 2.37 (3H, s), 2.0–3.9 (10H, m), 1.12 (1H, d, J = 7 Hz), 1.06 (3H, s).

Anal. Calcd. for $C_{17}H_{22}NO{\cdot}HBr$: C, 48.94; H, 5.58; N, 3.36. Found: C, 49.32; H, 5.63; N. 3.23.

Dimethylaminomethyltetrahydrofuranobenzomorphan 9d

To a solution of dimethylamine in DMF (5 ml) was added the bromohydrobromide **9***c* (1.0 g) and the mixture heated in a steel bomb at 100° for 1 h and after cooling, it was partitioned between benzene and 2 *N* sodium hydroxide (50 ml). Benzene layer was washed several times with water, dried, and evaporated to dryness. The residue was dissolved in ether and extracted with 2 *N* hydrochloric acid (5 ml). The extract was concentrated *in vacuo* and the residue crystallized from methanol acetone to afford 690 mg (71%) of **9***d* as the dihydrochloride salt, with 1 mol of methanol of crystallization, m.p. 278–280°; n.m.r. (free base, CCl_4) δ 7.04 (4H, s), 4.15–4.85 (1H, m), 2.37 (3H, s), 2.23 (6H, s), 1.8–3.1 (8H, m), 1.1 (1H, m), 0.92 (3H, s).

Anal. Calcd. for $C_{19}H_{28}N_2O{\cdot}2HCl{\cdot}CH_3OH$: C, 59.25; H, 8.45; N, 6.9. Found: C, 48.84; H, 8.32; N, 6.96.

This work was supported in part by the National Research Council of Canada with a grant through its Industrial Research Assistance Programme.

1. J. W. Lewis, K. W. Bentley, and A. Cowan. Ann. Rev. Pharmacol. **4**, 241 (1971).
2. I. Monkovic, T. T. Conway, H. Wong, Y. G. Perron, I. J. Pachter, and B. Belleau. J. Am. Chem. Soc. **95**, 7910 (1973).
3. E. L. May and H. Kugita. J. Org. Chem. **26**, 188 (1961).
4. H. Kugita and E. L. May. J. Org. Chem. **26**, 1954 (1961).
5. S. Archer, N. F. Albertson, L. S. Harris, A. K. Pierson, and J. G. Bird. J. Med. Chem. **7**, 123 (1964).
6. E. L. May, H. Kugita, and J. H. Ager. J. Org. Chem. **26**, 1621 (1961).
7. J. G. Murphy, J. H. Ager, and E. L. May. J. Org. Chem. **25**, 1386 (1960).
8. A. Marquet and J. Jacques. Bull. Soc. Chim. Fr. 90 (1962).
9. E. R. Glazier. J. Org. Chem. **27**, 4397 (1962).
10. D. V. C. Awang and S. Wolfe. Can. J. Chem. **47**, 706 (1969).
11. H. Wong, J. Chapuis, and I. Monkovic. J. Org. Chem. **39**, 1042 (1974).

A Proton Magnetic Resonance Study of the Ultraviolet Photoproduct of d(TpT) in Aqueous Solution[1]

FRANK E. HRUSKA, DONALD J. WOOD,[2] KELVIN K. OGILVIE, AND JAMES L. CHARLTON

Department of Chemistry, University of Manitoba, Winnipeg, Manitoba R3T 2N2

Received August 16, 1974

FRANK E. HRUSKA, DONALD J. WOOD, KELVIN K. OGILVIE, and J. L. CHARLTON. Can. J. Chem. **53**, 1193 (1975).

The p.m.r. data of d(TpT) and its predominant u.v. photoproduct d(T[p]T) in aqueous solution are compared. The data are consistent with the presence of a *cis-syn* cyclobutane ring in d(T[p]T). Consideration of the $H_{1'}$ chemical shifts leads to the conclusion that changes in the sugar–base torsion angle of both nucleotide fragments of the parent molecule are required to bring the thymine bases into alignment for photodimerization. The coupling constants indicate that the conformation of the 5′-terminal fragment is only slightly affected by the cyclobutane ring formation. Photodimerization brings about a distortion of the sugar pucker in the 3′-terminal fragment. In this fragment both the *gauche-gauche* and *gauche-trans* conformers are significantly populated whereas the *trans-gauche* form is excluded.

FRANK E. HRUSKA, DONALD J. WOOD, KELVIN K. OGILVIE et J. L. CHARLTON. Can. J. Chem. **53**, 1193 (1975).

On compare les données de r.m.p., obtenues en solution aqueuse, pour le d(TpT) avec celles de son photoproduit u.v. d(T[p]T) prédominant. Les données sont en accord avec la présence d'un cyclobutane-*cis-syn* dans le d(T[p]T). L'examen des déplacements chimiques du $H_{1'}$ conduit à la conclusion que des changements dans l'angle de torsion sucre–base des deux fragments du nucléotide de la molécule parente sont requis pour amener les bases thymines dans une orientation appropriée pour la photodimérisation. Les constantes de couplage indiquent que la conformation du fragment 5′ terminal n'est que très peu affectée par la formation du noyau cyclobutanique. La photodimérisation amène une distorsion de la molécule de sucre plissée dans le fragment 3′ terminal. Dans ce fragment, les deux conformères *gauche-gauche* et *gauche-trans* existent d'une façon importante alors que la forme *trans-gauche* n'existe pas. [Traduit par le journal]

Introduction

Thymine photodimers possessing a cyclobutane ring are generated by u.v. irradiation of thymine (2–4).[3] In u.v. irradiated DNA the predominant photoproduct is formed from thymines adjacent on a polynucleotide strand and has been shown to possess the *cis-syn* geometry (6–12) with the *trans-syn* form as a minor product (13). Several groups have examined photodimer production in model compounds, particularly the dinucleoside monophosphates (14–17) and the abbreviated dinucleosides (18). Johns *et al.* (16) have isolated two isomeric forms of d(T[p]T), the u.v. photoproduct of d(TpT) (Fig. 1); evidence has been provided for the *cis-syn* cyclobutane geometry in the predominant product and the *trans-syn* in the minor product. Formation of the antiparallel cyclobutane ring systems (*cis-anti* and *trans-anti*) in u.v. irradiated oligo- or polynucleotides is unlikely for steric reasons.

Recently we reported a p.m.r. conformational study of d(TpT) in aqueous solution (19). For the present work we have prepared, according to the methods of Johns *et al.* (16), the predominant photoproduct of d(TpT) and obtained its 100 and 220 MHz spectra. The chemical shift and coupling constant data are shown to be consistent with the presence of a cyclobutane ring structure with the *cis-syn* geometry. Other geometries could not, however, be excluded on the basis of our p.m.r. data alone. The data reveal that thymine dimer formation at the dinucleoside monophosphate level causes distor-

[1]Presented in part at the 4th Harry Steenbock Symposium on the Structure and Conformation of Nucleic Acids and Protein – Nucleic Acid Interactions. Madison, Wisconsin, June 16–19, 1974 (1).

[2]Postdoctoral fellow.

[3]Abbreviations used: thymine: Thy; thymine photodimer: Thy[ ]Thy; (see ref. 5 for photoproduct symbolism); 2′-deoxythymidine, its 3′- and 5′-monophosphate: dT, 3′dTMP, 5′dTMP; 2′-deoxythymidylyl-(3′,5′)-2′-deoxythymidine and its u.v. photoproduct: d(TpT), d(T[p]T); their 5′- and 3′-terminal fragments: dTp-, dT[p]- and -pdT, -[p]dT.

Can. J. Chem. Downloaded from www.nrcresearchpress.com by 210.87.254.105 on 09/05/12
For personal use only.

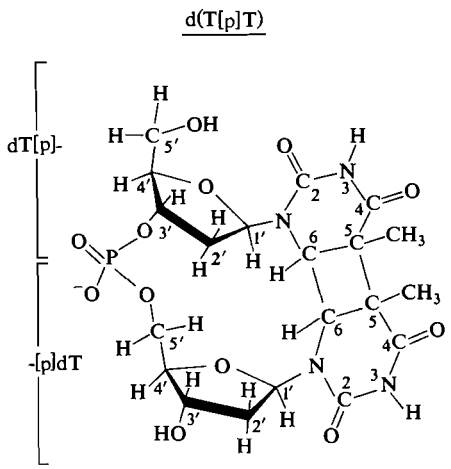

FIG. 1. The structural formula of the ultraviolet photoproduct of 2′-deoxythymidylyl-(3′,5′)-2′-deoxythymidine *i.e.* d(T[p]T). dT[p]- and -[p]dT refer to the nucleotide fragments with the free 5′- and 3′-hydroxyls, respectively.

tion of the sugar–base torsion angle of both nucleoside fragments and perturbs the conformation of the sugar–phosphate backbone. The findings are interesting in the light of evidence that local distortion of secondary structure is a consequence of dimer formation in polynucleotides (20).

Experimental

The procedure of Letsinger *et al.* (21) was used in the synthesis of d(TpT). d(TpT) (75 mg) in water (75 ml) was irradiated under nitrogen through a Pyrex (3 mm) filter with a water-cooled Hanovia 450 W medium-pressure mercury lamp. After 10 h the absorbance (267 nm) dropped to 14% of its original value. The solution was lyophilized and the residue was dissolved in water and applied to Whatmann 3 MM paper which was developed in solvent A (22). The desired photoproduct moved slightly slower than d(TpT). The product was eluted with water and rechromatographed in solvent C (22). The product was again eluted with water and lyophilized to a fine powder. The product was photoreversible to d(TpT) at 254 nm.

An aqueous (D_2O) solution of the photoproduct (0.05 *M*, p*D* = 7.0), containing 0.05 *M* TSP (sodium 3-trimethylsilylpropionate-2,2,3,3-d_4) for internal referencing, was freeze-dried three times, and dissolved in 100% D_2O. Spectra were obtained on Varian HA-100 and HR-220 MHz spectrometers. Calibration of spectra and spin-decoupling experiments were carried out by standard methods. Spectral analysis was carried out with LAME (23). Computer simulations of the spectra were used as the final test of the data. The chemical shift (δ) and coupling constant (J) data are given in Table 1.

Results and Discussion

Spectral Assignment

Figure 2 shows the experimental 220 MHz and calculated spectra of d(T[p]T) at 65 °C. Spectral assignment was carried out by comparison of these spectra with those of dT, 3′dTMP, 5′dTMP, and d(TpT) discussed previously (1, 19). Consideration of the magnetic shielding effects of phosphorylation at the 3′-position of a series of molecules, dT → 3′dTMP (1, 19), d(TpT) → d(TpTp) (24), and d(T[p]T) → d(T[p]Tp) (24), facilitated location of the $H_{2'}$, $H_{2''}$, and $H_{3'}$ bands of the -[p]dT fragment. The reasoning outlined in ref. 19 was used to distinguish the $H_{2'}$ and $H_{2''}$ of the dT[p]- fragment. In this work we argued that, in a 2′-deoxyribose which experiences no unusual distortion, *i.e.* whose conformational and bond angles fall into expected ranges (25–28), the measured values of the coupling constants $J_{2''3'}$ and $J_{3'4'}$ should be identical to within a few tenths of a Hertz. At 18 °C values of 5.7 and 3.7 Hz were obtained for the pair of $H_{2'}$–$H_{3'}$ coupling constants in dT[p]-. By the above arguments the smaller must be $J_{2''3'}$ (and the larger, $J_{2'3'}$) since it is the closer in value to $J_{3'4'}$ (3.1 Hz). The choice of $J_{2''3'}$ = 3.7 Hz and $J_{2'3'}$ = 5.7 Hz allows us to assign $H_{2'}$ to low field of $H_{2''}$ in the 2′,2″ band of dT[p]-. Interestingly, if we apply this same reasoning to the -[p]dT fragment of d(T[p]T) and choose the $H_{2'}$–$H_{3'}$ coupling constant of 3.7 Hz (rather than 8.1 Hz) for $J_{2''3'}$, we arrive at the assignment based on the shielding influence of a 3′-phosphate mentioned above. This supports the contention that our reasoning, based on the near equality of $J_{2''3'}$ and $J_{3'4'}$, is generally applicable to 2′-deoxyribosides with "normal" (25–28) conformations.

Further ambiguity exists in the assignment of the $H_{5'}$ and $H_{5''}$ spectral bands. We have assumed here the Remin and Shugar assignment (29) for ribonucleosides, although there is no justification for assuming that their assignment will hold for our series of molecules. However, wherever relevant, we point out the conformational conclusions which follow from the second choice of $H_{5'}$,$H_{5''}$ assignment.

The Eight Configurational Isomers of d(T[p]T)

Wulff and Fraenkel first listed the four isomeric types of Thy[ ]Thy (4). Actually a total of six configurationally distinct forms exist (Fig. 3) since the *trans-syn* (III) and *cis-anti* (II)

Can. J. Chem. Downloaded from www.nrcresearchpress.com by 210.87.254.105 on 09/05/12
For personal use only.

TABLE 1. Proton magnetic resonance parameters[a] for the photoproduct in aqueous solution

	dT[p]-[b]		-[p]dT[b]			dT[p]-		-[p]dT	
Parameter	18 °C	63 °C	18 °C	63 °C	Parameter	18 °C	63 °C	18 °C	63 °C
$\delta_{1'}$	5.67	5.75	6.00	6.00	$J_{2',2''}$	−13.3	−13.5	−13.5	−13.6
$\delta_{2'}$	2.63	2.64	2.33	2.28	$J_{2',3'}$	5.1	5.7	7.6	8.1
$\delta_{2''}$	2.40	2.43	2.12	2.14	$J_{2'',3'}$	3.2	3.7	3.5	3.7
$\delta_{3'}$	4.67	4.65	4.34	4.32	$J_{3',4'}$	2.6	3.1	4.2	5.2
$\delta_{4'}$	4.18	4.10	3.94	3.92	$J_{4',5'}$	3.8	4.0	1.3	1.6
$\delta_{5'}$	3.74	3.74	4.12	4.13	$J_{4',5''}$	3.8	4.0	7.1	6.8
$\delta_{5''}$	3.70	3.70	4.00	4.01	$J_{5',5''}$	−12.3	−12.3	−11.1	−12.2
δ_5	1.50	1.50	1.54	1.54	$J_{P3'}$	2.9	4.5	—	—
δ_6	4.27	4.27	4.35	4.30	$J_{P4'}$	—	—	1.6	1.4
J_{66}	5.9	6.1	5.9	6.1	$J_{P5'}$	—	—	3.9	4.7
J_{M6}	<0.3	<0.3	<0.3	<0.3	$J_{P5''}$	—	—	6.2	6.3
$J_{1',2'}$	8.5	8.1	8.6	8.3	Σ	7.6	8.0	8.4	8.4
$J_{1',2''}$	5.2	5.6	5.6	5.9	Σ'	—	—	10.1	11.0

[a]δ in p.p.m. relative to internal TSP; estimated error ±0.004 p.p.m. J and Σ in Hz; estimated error ±0.2 Hz.
[b]See Fig. 1 for symbolism.

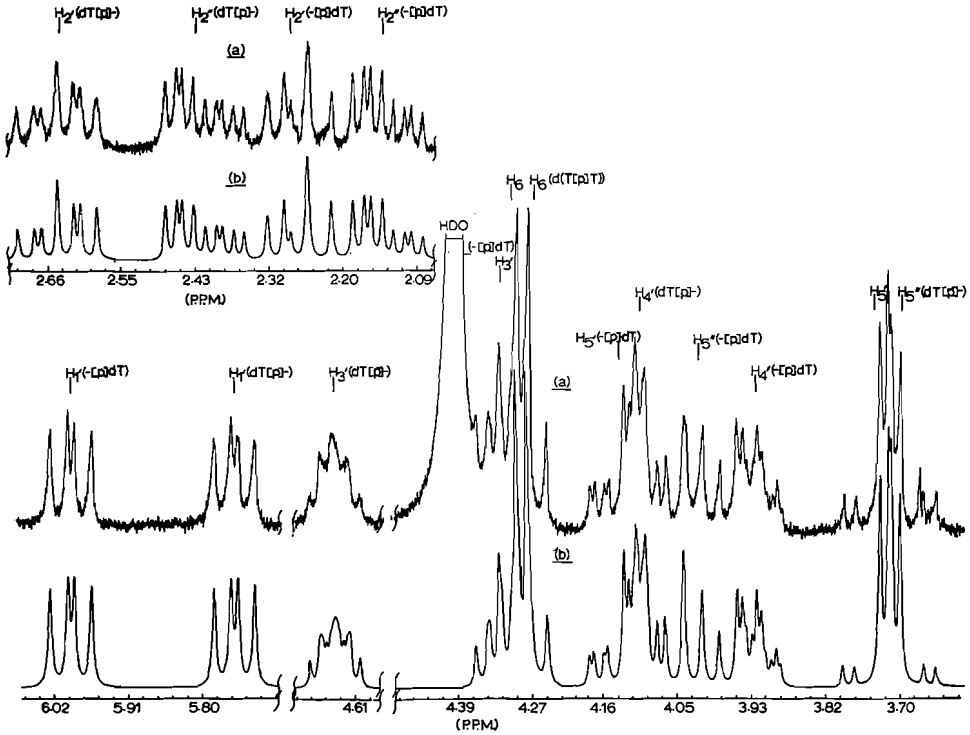

FIG. 2. (*a*) The 220 MHz spectrum of d(T[p]T) in aqueous solution: 63 °C; pD = 7.0, 0.05 M. Single scan, continuous wave, sweep width 250 Hz. Methyl hydrogen resonances not included. (*b*) Computer simulated 220 MHz spectrum.

forms exist as a pair of enantiomeric (*d,l*) forms whereas the *cis-syn* (I) and *trans-anti* (IV) forms exist as single (*meso*) diastereomers. Isomers II and III are optically active but their *d,l* labelling remains arbitrary until the optical rotatory properties of the individual enantiomers are determined. By ignoring all steric difficulties which might arise in their actual synthesis, we have been able to construct a total of *eight* configurationally distinct isomers of d(T[p]T),

Can. J. Chem. Downloaded from www.nrcresearchpress.com by 210.87.254.105 on 09/05/12
For personal use only.

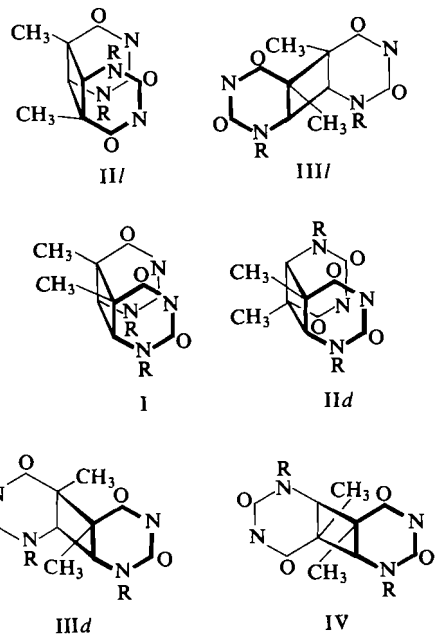

FIG. 3. The six configurational isomers of Thy[ ]Thy. I: *cis-syn*; II*d*, II*l*: *cis-anti*; III*d*, III*l*: *trans-syn*; IV: *trans-anti*. II and III each occur as an enantiomeric pair; their *d,l* labelling is arbitrary.

two for each type of cyclobutane ring. It is inconceivable that any of the four isomers with the antiparallel geometries (II and IV) will ever be synthesized and thus these will not be considered further. The generation of the four diastereomers with geometries I and III can be viewed as follows: (*i*) Configurations with geometry I (designated A_1 and A_2); A_1 will be generated from d(TpT) which has assumed a base-stacked[4] conformation with both the dTp- and -pdT fragments in the ANTI[5] conformation; A_2 is formed if both fragments are SYN. (*ii*) Configurations with geometry III (designated A_3 and A_4); A_3 will be generated from d(TpT) which has assumed a base-stacked conformation with dTp- and -pdT in their SYN and ANTI forms, respectively; A_4 will be generated if dTp- and -pdT are in their ANTI and SYN forms respectively.[6] Note that, whereas A_1 and A_2 possess the same *cyclobutane* geometry (I), A_3 and A_4 differ in that A_3 possesses one of the III*d*, III*l* pair and A_4 the other.

For steric reasons the four isomers are expected to appear in the following order of decreasing importance: $A_1 > A_3 > A_4 > A_2$. This prediction is based *solely* on the expected proportions of d(TpT) with the conformation required to generate A_1, etc. This expectation in turn is based solely on a considerable body of evidence that the ANTI conformation is favored over the SYN in pyrimidine nucleosides, with an even stronger bias for ANTI in pyrimidine-5′-nucleotides due to the repulsion of the 2-keto oxygen and the negatively charged phosphate in the SYN conformation. Interestingly, Weinblum and Johns (6) have shown that the predominant and minor photoproducts possess geometries I and III, respectively. However, since their analysis required liberation of the Thy[ ]Thy from the sugars by hydrolysis, they could not distinguish between the two possibilities for the *intact* predominant product (which we call A_1 and A_2) or for the *intact* minor product (here labelled A_3 and A_4). Our prediction points to A_1 and A_3 as the predominant and minor products observed by Weinblum and Johns.

Evidence for the Cyclobutane Ring

The following observations are consistent with the presence of a cyclobutane ring in d(T[p]T): (*a*) the 0.4 p.p.m. upfield shift of the methyl resonances of d(T[p]T) relative to those of d(TpT) compares favorably with the 0.3 p.p.m. upfield shift observed for the methyl hydrogens in the Thy to *cis-syn* Thy[ ]Thy conversion (4) and with the effect of removal of unsaturation in the propene to propane conversion (30–31); (*b*) the 3.4 p.p.m. upfield shift of the H_6 resonances of d(T[p]T) relative to d(TpT) is in good agreement with the 3.35 p.p.m. shift observed in the Thy to Thy[ ]Thy conversion (4); (*c*) the

[4]In the right-handed helical sense.

[5]ANTI and SYN refer to the conformation about the *N*-glycosyl linkages; *anti* and *syn* refer to the cyclobutane ring geometry.

[6]There is an alternate, but equivalent, way of viewing the formation of the A_1 to A_4 isomers. Viewing a d(TpT) molecule with both fragments in the ANTI conformation from the C_5 to the C_2 positions, we may label the two faces of each base as R (to the right) and L (to the left). The four isomers are generated with the following combination of faces in contact: A_1: R(dTp-), L(-pdT); A_2: L(dTp-), R(-pdT); A_3: L(dTp-), L(-pdT); A_4: R(dTp-), R(-pdT).

Can. J. Chem. Downloaded from www.nrcresearchpress.com by 210.87.254.105 on 09/05/12
For personal use only.

Can. J. Chem. Downloaded from www.nrcresearchpress.com by 210.87.254.105 on 09/05/12
For personal use only.

appearance of a large J_{66} coupling constant (5.9–6.1 Hz) in d(T[p]T) confirms the presence of covalent links between the bases.

Geometry of the Cyclobutane Ring

The work of Weinblum and Johns (6, 8) on Thy[ ]Thy fragments isolated from d(T[p]T), coupled with later studies (7, 11), provided conclusive evidence for the presence of I in the predominant d(T[p]T) product. Unfortunately, our data cannot provide an independant assignment of ring configuration for the *intact* d(T[p]T) molecule (see below). However, given the *cis-syn* assignment of Weinblum and Johns, we are able to deduce some conformational features of the cyclobutane ring.

With few exceptions crystalline cyclobutane derivatives assume a puckered conformation which confers on the ring substituents quasi-axial (*a*) and quasi-equatorial (*e*) orientations (Fig. 4).[7] The *cis-syn* form of the tetra-*N*-methyl derivative of Thy[ ]Thy, DMT[ ]DMT,[8] is puckered in the crystal state with dihedral angles of 152–153° (11).[9] Available p.m.r. evidence (9, 10) points to a puckered conformation for free *cis-syn* thymine dimers in solution. A $^3J_{66}$ value of 4.8–5.2 Hz was obtained for Thy[ ]Thy (10) and DMT[ ]DMT (9) and, on the basis of studies by Wiberg and Barth (35) and Abraham *et al.* (36), may be translated into an *apparent* dihedral angle of 138°. The 5.9–6.1 Hz values for $^3J_{66}$ suggest a somewhat flatter cyclobutane ring in d(T[p]T) with an apparent dihedral angle of 145°. One cannot, however, distinguish between the two puckered modes on the basis of $^3J_{66}$ values alone.

Nuclear magnetic resonance data for cyclobutane in the nematic phase (37) and for a variety of its derivatives in solution (38) have been interpreted in terms of a rapid interconversion between puckered forms. If one assumes that the 4.8–5.2 Hz $^3J_{66}$ values are consistent with puckered four-membered rings in Thy[ ]Thy and DMT[ ]DMT, then the chemical shift equivalence of corresponding hydrogens on the two halves of each photodimer (9, 10) may be taken as evidence for a rapid interconversion between the two equally populated puckermodes (Fig. 4), since corresponding hydrogens in either puckered form are not related by symmetry. A similar but perhaps somewhat constrained interconversion between puckered modes is also expected for d(T[p]T).

It is unfortunate that the observed $^3J_{66}$ values for d(T[p]T) cannot be used as an independent means for determining the cyclobutane ring configuration; $^3J_{66}$ values of 6.0 Hz are consistent with either puckered form of I (35, 36) or a rapid interconversion between the two modes. In one puckered form of III the 6-hydrogens are *a,a* and a $^3J_{66}$ value of about 10 Hz is expected; in the other they are *e,e* and a $^3J_{66}$ value of about 2.5 Hz is expected. Hence a rapid interconversion between essentially equally populated pucker modes with geometry III can also account for an intermediate (*ca.* 6.0 Hz) value of $^3J_{66}$. Thus little independent configurational information is provided by $^3J_{66}$ values in pyrimidine photodimers.

Several groups (9, 10, 39), in their studies of photodimerized pyrimidine *bases*, have concluded that 5–6 Hz values for J_{66} are consistent only with a vicinal relationship for the two 6-hydrogens. However, *four bond* coupling constants of this magnitude have been observed for hydrogens which constitute an *e,e* pair in other cyclobutane ring systems (35, 36). In this situation the hydrogens are separated by two zigzag (W) coupling paths which favor the appearance of large ^4J values. If one assumes that the same stereochemical rules apply to the pyrimidine photodimers, then a 5–6 Hz J_{66} value does not necessarily preclude the *cis-anti* antiparallel geometry since the two 6-hydrogens are *cis* here and, given the appropriate pucker, may constitute an *e,e* pair. Thus some caution should be exercised in deducing configurational features in the absence of conformational information about the cyclobutane ring. In this regard it is

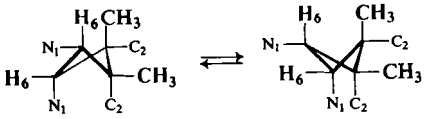

FIG. 4. Puckered forms of the cyclobutane ring.

[7]Centrosymmetrically substituted cyclobutanes may be planar (32); planar centrosymmetrically substituted (*trans-anti*) pyrimidine photodimers have been noted (33, 34).

[8]DMT: 1,3-dimethylthymine.

[9]Defined as the angle between the planes defined by three ring carbon atoms having the transannular distances in common (11).

TABLE 2. Δ(6)[a] values (p.p.m.) for a series of dinucleoside(tide)monophosphates in aqueous solution

Temperature (°C)	d(TpT)	d(TpTp)	d(T[p]T)	d(T[p]Tp)
18	0.02	0.08	0.08	0.18
65	0.05	0.10	0.03	0.14

[a]Defined as the relative shift between the 6-hydrogens of the two thymine residues.

interesting to point to the absence of an observable $^4J_{66}$ coupling constant in the "low-melting" DMT[ ]DMT isomer (10) which has been shown (40) to have the *cis-anti* geometry and to be puckered with the 6-hydrogens in *a* positions and the methyls in the less crowded *e* positions. If it assumes the same conformation (with the pair of 6-hydrogens rather than the larger methyl groups in the crowded *a,a* positions) in solution, then the absence of any observable $^3J_{66}$ coupling constant is expected.

The Molecular Configuration of d(T[p]T)

Two distinct configurational possibilities exist for d(T[p]T) molecules with the *cis-syn* cyclobutane geometry (see above). Several pieces of evidence suggest that the predominant photoproduct is generated from d(TpT) molecules with ANTI dTp- and -pdT fragments. (*a*) In Table 2 are given Δ(6) values for d(T[p]T) and d(TpT) as well as for d(TpTp) and d(T[p]Tp) from ref. 24; Δ(6) for any dimer is defined as the *relative* chemical shift for the two 6-hydrogens. Comparing the d(TpT) and d(TpTp) entries we note that 3′-phosphorylation enhances the separation of the 6-resonances by 0.05–0.06 p.p.m., whereas for the d(T[p]T) and d(T[p]Tp) entries this enhancement is 0.10–0.11 p.p.m. The enhanced influence of 3′-phosphorylation at the photodimer level seems most consistent with location of the 6-hydrogen of the -[p]dT fragment of d(T[p]T) and the -[p]dTp fragment of d(T[p]Tp) near to the 3′-position. This situation is obtained by rotation of these fragments into an extreme ANTI position (χ, the sugar–base torsion angle $\simeq -160°$) and is possible only when both fragments of the photodimer are ANTI. (*b*) An *endo*-$C_{2'}$ hydrogen should experience a deshielding of about 0.5 p.p.m. upon rotation of a pyrimidine nucleoside from its ANTI to its SYN conformation (41–43). However, in the -pdT to -[p]dT conversion $H_{2'}$ moves upfield by 0.05 p.p.m. Interestingly the $H_{2'}$ hydrogen moves upfield by 0.04 p.p.m. when U (uridine) is converted to diHU (dihydrouridine) by reduction of the C_5—C_6 double bond (44). Thus the 0.05 p.p.m. effect upon $H_{2'}$ is consistent with the disappearance of unsaturation in the C_5—C_6 bond of -[p]dT but not with ANTI to SYN conversion. (*c*) Rotation of a pyrimidine nucleoside into its SYN conformation places the 2-keto oxygen over the sugar ring and should lead to increases of 1.5–2.0 Hz in the sum $J_{4'5'} + J_{4'5''}$ and in the difference $J_{4'5'} - J_{4'5''}$ for the hydroxymethyl group (45, 46). Such changes are not observed for the dTp- to dT[p]- conversion and hence we conclude that photodimerization of d(TpT) does not require ANTI to SYN conversion of the 5′-terminal fragment. We do not think that comparison of *J* and δ values other than those discussed above is meaningful here.

The Sugar–Base Torsion Angles

In the previous section it was suggested that the nucleoside fragments in d(T[p]T) favor the ANTI conformation as in d(TpT). However, our data reveal that some reorientation about the *N*-glycosyl linkages does occur upon conversion of d(TpT) to d(T[p]T). In Fig. 5 the sugar proton chemical shifts for dT, 3′- and 5′-dTMP, d(TpT), and d(T[p]T) are shown. Since $H_{1'}$ is located near to the 2-keto oxygen of ANTI pyrimidine nucleosides, changes in χ should be reflected in δ(1′). Excepting those for d(T[p]T), all δ(1′) entries in Fig. 5 are contained in the narrow range at 6.28 ± 0.05 p.p.m. This was taken as evidence (19) that the χ value distribution for a dT fragment is not drastically affected by 3′- or 5′-phosphorylation or by incorporation into the dimer d(TpT), a contention supported by crystal data. Large upfield shifts, relative to the corresponding δ(1′) in d(TpT), are observed for δ(1′) of dT[p]- ($\simeq$0.52 p.p.m.) and -[p]dT fragments ($\simeq$0.33 p.p.m.). These effects cannot be attributed simply to the removal of the double

Can. J. Chem. Downloaded from www.nrcresearchpress.com by 210.87.254.105 on 09/05/12
For personal use only.

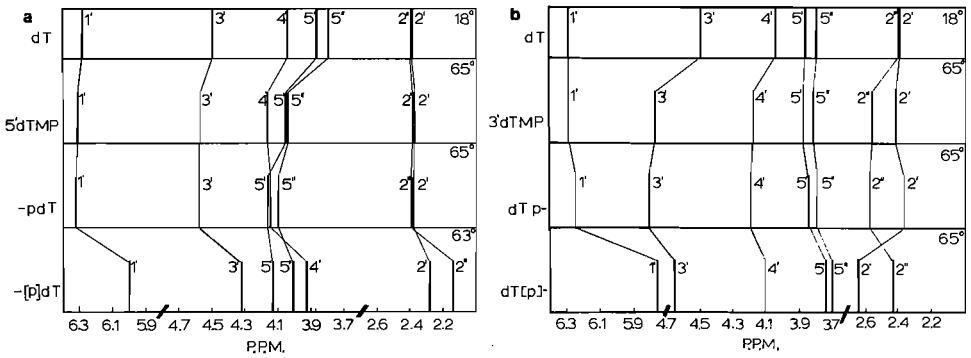

FIG. 5. (*a*) Chemical shifts of the 2′-deoxyribo hydrogens of dT, 5′dTMP, -pdT, and -[p]dT in p.p.m. relative to internal TSP. Temperature in °C indicated. (*b*) Chemical shifts of the 2′-deoxyribo hydrogens of dT, 3′dTMP, dTp-, and dT[p]- in p.p.m. relative to internal TSP. Temperature in °C indicated. Data from this work and ref. 19.

TABLE 3. 2′-Deoxyribose coupling constants for a series of molecules in aqueous solutions[a]

Coupling constant	dT	3′dTMP	dTp-	dT[p]-	5′dTMP	-pdT	-[p]dT
Trans							
$J_{1'2'}$	6.7	7.2	7.2	8.5	—	—	8.6
$J_{2''3'}$	4.6	3.7	3.8	3.2	—	—	3.5
$J_{3'4'}$	4.0	4.0	3.2	2.6	2.9	4.0	4.2
Cis							
$J_{1'2''}$	6.8	6.5	6.1	5.2	—	—	5.6
$J_{2'3'}$	6.3	6.8	6.0	5.1	—	—	7.6

[a]In Hz: dT (75 °C) from ref. 24; 3′- and 5′-dTMP (30 °C) from ref. 19; dTp- and -pdT, the fragments of d(TpT), at 18 °C from ref. 32; dT[p]- and -[p]dT, the fragments of d(T[p]T) at 18 °C.

bond character of the C_5—C_6 bond and an accompanying electron density change at $C_{1'}$; upon conversion of U to diHU (44) by reduction of the C_5—C_6 double bond, an upfield shift of only 0.04 p.p.m. is noted in $H_{1'}$. It is more likely that the 0.33 and 0.52 p.p.m. shifts can be traced to the anisotropic magnetic and electric fields associated with the C_2 carbonyls of the thymines, and the χ-dependent orientation of the carbonyls and the 1′-hydrogens. A quantitative evaluation of the χ-value distribution does not seem possible but it seems reasonable to conclude that significant readjustments in the χ angle are required of *both* nucleoside fragments in d(T[p]T).

Conformation of the Sugar Ring

The coupling constants relevant to a discussion of the 2′-deoxyribo rings of d(T[p]T) as well as of dT, 3′- and 5′-dTMP, and d(TpT) are found in Table 3. Considering first the dT[p]- data, we find that the J values are not very different from those of the corresponding monomers (dT, 3′dTMP) and the dTp- fragment of d(TpT). Thus we conclude that this unit is capable of the 2′-*endo* ↔ 3′-*endo* interconversion (26, 27, 45, 46). The data for dT[p]- are consistent with (*a*) a slight increase, relative to dTp-, in the 2′-*endo* bias[10] and (*b*) an increase of about 5° in τ_m (the amplitude of pucker (27)) estimated from the decrease in $J_{1'2''}$ and $J_{2'3'}$. The data do not reveal any significant changes in the pseudorotational parameters P for the dTp- to dT[p]- conversion. At the elevated temperature ($\simeq$65 °C) corresponding J values of dT[p]- and dTp- become more alike, indicating that the conformation of the dT[p]- approaches that of dTp- with increasing temperatures.

Larger effects of photodimerization are indicated for the sugar residue of the -[p]dT frag-

[10]Percentage (3′-*endo*) = $10\,J_{3'4'}$ serves as a useful guide for discussing the conformational weighting of the 2′-*endo* and 3′-*endo* types of pucker (27).

Can. J. Chem. Downloaded from www.nrcresearchpress.com by 210.87.254.105 on 09/05/12
For personal use only.

Can. J. Chem. Downloaded from www.nrcresearchpress.com by 210.87.254.105 on 09/05/12
For personal use only.

TABLE 4. Calculated % rotamer population for the $C_{4'}$—$C_{5'}$ and $O_{5'}$—$C_{5'}$ bonds[a]

	dTp-		dT[p]-		-pdT		-[p]dT	
	18 °C	65 °C	18 °C	63 °C	18 °C	65 °C	18 °C	63 °C
P_{gg}	54	41	54	50	65	55	46	45
P_{gt}	27	35	23	25	25	35	53	55
P_{tg}	19	24	23	25	10	10	1	0
$P_{g'g'}$					90	83	77	72
$P_{g't'}$					5	9	18	19
$P_{t'g'}$					5	8	5	9

[a] P_{gg}, P_{gt}, and P_{tg} calculated via eqs. 1–3 and expressed as percentage. $P_{g'g'}$, $P_{g't'}$, and $P_{t'g'}$ calculated via analogous equations given in ref. 19.

ment. This is made particularly clear by the magnitudes of $J_{2',3'}$ (7.6 and 8.1 Hz at 18 and 65 °C) which are the largest such values so far noted in any 2′-deoxyriboside and about 2.5 Hz larger than the corresponding values in dT[p]-. This large $J_{2',3'}$ coupling constant can be interpreted in terms of a flattening of the ring, *i.e.* a reduction in the τ_m of about 10° relative to the value in dT[p]-. The large $J_{1',2'}$ value and small $J_{2'',3'}$ and $J_{3',4'}$ values reveal a preference for the 2′-*endo* conformation though a sizeable contribution from 3′-*endo* must be present since the $J_{2'',3'}$ and $J_{3',4'}$ are comparable to, in fact slightly larger than, the corresponding values for the other molecules listed in Table 3. It is also interesting to note, in view of arguments presented earlier (19), the large differences in the $J_{2'',3'}$ and $J_{3',4'}$ values (0.7 Hz at 18 °C; 1.5 Hz at 65 °C). In all 2-deoxyribosides studied to date, including dT[p]-, this difference is never larger than 0.6 Hz and typically 0.3 Hz. This increase in the $J_{3',4'}$ value relative to $J_{2'',3'}$ could be due to a tendency for the -[p]dT fragment to favor unusually low P_N and/or unusually high P_S values (26, 27) though we cannot discount bond angle distortion in the $C_{2'}$—$C_{3'}$—$C_{4'}$ fragment as a possible interpretation.

Conformation about the $C_{4'}$—$C_{5'}$ Bond

The following relationships which assume a rapid interconversion between staggered conformations are useful for discussing trends in the conformer distribution about the $C_{4'}$—$C_{5'}$ bond (19).

$$[1] \qquad P_{gg} = (13 - \Sigma)/10$$

$$[2] \qquad P_{gt} = (\Sigma - \Delta - 3)/20$$

$$[3] \qquad P_{gg} + P_{gt} + P_{tg} = 1$$

where the P_{ij}'s are the fractional populations of the *gg*, *gt*, and *tg* conformers (Fig. 6), Σ is the observed sum, $J_{4'5'} + J_{4'5''}$, and Δ, the observed difference, $J_{4'5'} - J_{4'5''}$. The calculated values in Table 4 indicate that the dTp- to dT[p]- conversion has no large influence on the $C_{4'}$—$C_{5'}$ population distribution of the free hydroxymethyl group, with a slight bias for *gg* indicated in both instances.

Space-filling molecular models reveal that a d(T[p]T) molecule can reasonably accommodate either the *gg* or *gt* conformer of the -[p]dT fragment but close contact interactions preclude the appearance of the *tg* conformer. Interestingly, if we assume the applicability of eqs. 1–3, we find for -[p]dT significant contributions from *gg* ($\simeq$45%) and from *gt* ($\simeq$55%) but essentially no contribution from *tg* to the overall conformational blend. We must bear in mind that these estimates required us to assume a specific spectral assignment of the 5′,5″ spectral band of the -[p]dT fragment *i.e.* $H_{5'}$ to low field of $H_{5''}$. If the reverse assignment is assumed, then the calculations lead to a *gg* (45%) $\leftrightarrow$ *tg* (55%) interpretation and the exclusion of *gt*. Since the presence of *tg* cannot be easily reconciled with

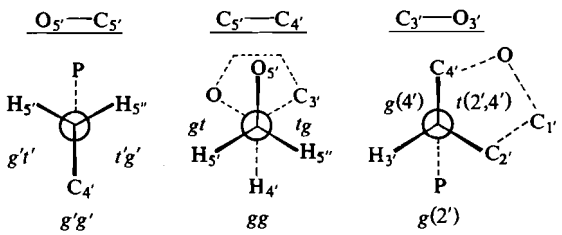

FIG. 6. Definition of the staggered conformers about the $C_{4'}$—$C_{5'}$, $O_{5'}$—$C_{5'}$, and $C_{3'}$—$O_{3'}$ bonds of a nucleotide.

Can. J. Chem. Downloaded from www.nrcresearchpress.com by 210.87.254.105 on 09/05/12
For personal use only.

model building, we feel our (Remin and Shugar (29)) assignment is the more reasonable.

Our calculations for the -[p]dT fragment are interesting since in base-stacked helical polynucleotides in the solid state the *gg* form is assumed, exclusive of *gt* and *tg* (25, 28). Thus one conformational consequence of thymine photodimerization appears to be the destabilization of the *gg* rotamer relative to *gt*. The absence of significant effects of the dTp- to dT[p]- conversion on the orientation of the free hydroxymethyl group suggests that distortion may not be transmitted to nucleoside fragments neighboring the damaged photodimer.

Conformation about the $O_{5'}$—$C_{5'}$ and $C_{3'}$—$O_{3'}$ Bonds

The magnitudes of the $^3J_{P5'}$ and $^3J_{P5''}$ coupling constants suggest that the phosphorus atom prefers a *gauche* disposition relative to both the 5′- and 5′′-hydrogens of the -[p]dT fragment (47–51), *i.e.* the *g′g′* conformer (Fig. 6) is preferred as it is in -pdT (32) and all 5′-monophosphates examined to date (25, 28, 51). Conformer populations calculated with equations (19) analogous to [1]–[3] indicate a slight decrease in the *g′g′* conformer of -[p]dT relative to -pdT (Table 4). However, no drastic reorientation about $O_{5'}$—$C_{5'}$ seems required for the -pdT to -[p]dT conversion.

In earlier work (51) correlations between Σ ($=J_{4'5'} + J_{4'5''}$) and Σ'($=J_{P5'} + J_{P5''}$) were discussed; these demonstrate that the population distribution about the $C_{4'}$—$C_{5'}$ and $O_{5'}$—$C_{5'}$ bonds of a 5′-β-nucleotide are interrelated. The interrelationship is such that when the molecule is *gg*, the *g′t′* and *t′g′* conformers are excluded and the *g′g′* state must be assumed; upon rotation out of *gg*, *g′g′* is no longer required and the molecule is allowed to populate the *g′t′* and *t′g′* forms, though *g′g′* remains the predominant form. Steric arguments for this behavior were presented (51). Our studies on d(TpT) (19) and those of Altona (52) indicate that similar correlations and interdependencies hold for the -pN fragment of dinucleoside monophosphates (NpN) as well. Interestingly the Σ,Σ' data for -[p]dT also lie near to the correlation plots in ref. 51. This supports our calculated $C_{4'}$—$C_{5'}$ and $O_{5'}$—$C_{5'}$ rotamer populations in Table 4 and the *gg* ↔ *gt* model for the -[p]dT fragment.

Correlations between Σ and Σ', and the long-range phosphorus-$H_{4'}$ coupling ($^4J_{P4'}$) have been presented (53). They demonstrate that $^4J_{P4'}$ is a simultaneous measure of the conformational distribution about the $C_{4'}$—$C_{5'}$ and $O_{5'}$—$C_{5'}$ bonds of a 5′-nucleotide and support our conclusions based on the Σ,Σ' maps. $^4J_{P4'}$ values of 1.6 Hz (18 °C) and 1.4 Hz (63°C) were revealed in the -[p]dT portion of the d(T[p]T) spectrum. These data also lie near to the $\Sigma,^4J_{P4'}$ and $\Sigma',^4J_{P4'}$ correlation plots, though the deviations seem outside of experimental error. Nevertheless we feel the agreement is adequate and in support of our conformational conclusions based on the three-bond coupling constants.

The $^3J_{P3'}$ coupling constant monitors the conformer distribution about the $C_{3'}$—$O_{3'}$ bond of the dT[p]- fragment. The values of 2.9 Hz (18 °C) and 4.5 Hz (63 °C) argue for a *gauche* orientation of $H_{3'}$ and P (47, 48) (Fig. 6). One could assume an equilibrium blend of rotamers *g*(2′) and *g*(4′). However, *g*(4′) is not compatible with the stacking of bases required for photodimerization and thus can be excluded. These values for $^3J_{P3'}$ in d(T[p]T) are the smallest noted to date. In d(TpT), values of 6.8 and 7.1 Hz were obtained at 18 and 65 °C, respectively. In certain dinucleoside monophosphates (52), $^3J_{P3'}$ values up to 9.5 Hz are noted. This suggests that in d(T[p]T) the *gauche* energy minimum in the H—$C_{3'}$—O—P fragment is nearer to the classically staggered (60°) situation. Furthermore, in contrast with the situation in other dinucleoside monophosphates, $^3J_{P3'}$ changes perceptibly (1.6 Hz) in the temperature interval 18–63 °C. Interestingly in the same interval, substantial changes (~1 Hz) are observed for $J_{3'4'}$ and Σ'. Thus some perceptible rearrangements in the vicinity of the phosphate do occur with changes in temperature. This does not seem to be the case with d(TpT) (19).

In conclusion, p.m.r. data for the predominant u.v. photoproduct of d(TpT) are discussed. The data are consistent with the presence of a puckered cyclobutane ring with the *cis-syn* geometry but do not form an independent basis for configurational analysis. Photodimerization leads to conformational changes in the ribose phosphate backbone with the larger distortions apparent in the 3′-terminal (5′-linked) nucleotide moiety.

NOTE ADDED IN PROOF: Sundaralingam (25) has suggested the symbols ω, ω′, ϕ, ϕ′, ψ, and ψ′

to denote the torsion angles about the P—$O_{5'}$, $O_{3'}$—P, $O_{5'}$—$C_{5'}$, $C_{3'}$—$O_{3'}$, $C_{5'}$—$C_{4'}$, and $C_{4'}$—$C_{3'}$ bonds of a polynucleotide backbone. Rotations were defined to be positive and can be designated as g^+ (*gauche*$^+$), t(*trans*), and g^-(*gauche*$^-$) if the angle lies in the range of staggered conformations possessing the 60, 180, and 300° (−60°) values, respectively. With this nomenclature we have noted (1) an interesting uniformity in the orientations assumed by right-handed helical polynucleotides. Thus for RNA-11 and DNA-A which are 3′-*endo* puckered we have: g^- for the P—O rotations (ω, ω'); t for the C—O rotations (ϕ, ϕ'), and g^+ for the C—C rotations (ψ, ψ'). For DNA-B which is 2′-*endo* the same scheme holds except that ψ' is t rather than g^+. Thus with this uniformity the gross conformational features of right-handed helical polynucleotides (which fall now logically into two classes differing only in pucker) are easily remembered.

The work was supported by grants from the National Research Council of Canada, the Research Corporation of New York, The North Atlantic Treaty Organization, and The Faculty of Graduate Studies of the University of Manitoba. The authors acknowledge illuminating discussions with Professor T. Schaefer and the NMR group at the University of Manitoba. We thank Dr. A. A. Grey and Ms. Valerie Robinson of the Canadian 220 MHz Centre, Sheridan Park, Ontario for obtaining the 220 MHz spectra and Dr. J. B. Rowbotham for assistance with the computer programs. Special thanks to Dr. C. Altona for allowing us to view a preprint of ref. 52.

1. F. E. Hruska, D. J. Wood, and K. K. Ogilvie. Proceedings, 4th Harry Steenbock symposium on nucleic acid structure and conformation and protein – nucleic acid interactions. Madison, Wisconsin. June 16–19, 1974. In press.
2. A. D. McLaren and D. Shugar. Photochemistry of proteins and nucleic acids. Macmillan Co., New York. 1964.
3. J. K. Setlow. *In* Current topics in radiation research. *Edited by* M. Ebert and A. Howard. North Holland Publishing Co., Amsterdam. 1965.
4. D. L. Wulff and G. Fraenkel. Biochim. Biophys. Acta, **51**, 332 (1961).
5. W. E. Cohn, N. J. Leonard, and S. Y. Wang. Photochem. Photobiol. **19**, 89 (1974).
6. D. Weinblum and H. E. Johns. Biochim. Biophys. Acta, **114**, 450 (1966).
7. G. M. Blackburn and R. J. H. Davies. J. Am. Chem. Soc. **89**, 5941 (1967).
8. D. Weinblum. Biochem. Biophys. Res. Commun. **27**, 384 (1967).
9. R. Anet. Tetrahedron Lett. 3713 (1965).
10. D. P. Hollis and S. Y. Wang. J. Org. Chem. **32**, 1620 (1967).
11. N. Camerman and A. Camerman. J. Am. Chem. Soc. **92**, 2523 (1970).
12. D. Weinblum, F. P. Ottensmeyer, and G. F. Wright. Biochim. Biophys. Acta, **155**, 24 (1968).
13. E. Ben-Hur and R. Ben-Ishai. Biochim. Biophys. Acta, **166**, 9 (1968).
14. E. Sztumpf and D. Shugar. Biochim. Biophys. Acta, **61**, 555 (1962).
15. R. A. Deering and R. B. Setlow. Biochim. Biophys. Acta, **68**, 526 (1963).
16. H. E. Johns, M. L. Pearson, J. C. LeBlanc, and C. W. Helleiner. J. Mol. Biol. **9**, 503 (1964).
17. I. H. Brown, K. B. Freeman, and H. E. Johns. J. Mol. Biol. **15**, 640 (1966).
18. M. W. Logue and N. J. Leonard. J. Am. Chem. Soc. **94**, 2842 (1972).
19. D. J. Wood, F. E. Hruska, and K. K. Ogilvie. Can. J. Chem. **52**, 3353 (1974).
20. F. N. Hayes, D. L. Williams, R. L. Ratcliffe, A. J. Varghese, and C. S. Rupert. J. Am. Chem. Soc. **93**, 4940 (1971).
21. R. L. Letsinger, K. K. Ogilvie, and P. S. Miller. J. Am. Chem. Soc. **91**, 3360 (1969).
22. K. K. Ogilvie and L. A. Slotin. Can. J. Chem. **51**, 2397 (1973).
23. C. W. Haigh and J. M. Williams. J. Mol. Spectrosc. **32**, 398 (1969).
24. D. J. Wood, K. K. Ogilvie, and F. E. Hruska. Can. J. Chem. Submitted.
25. M. Sundaralingam. Biopolymers, **7**, 821 (1969).
26. C. Altona and M. Sundaralingam. J. Am. Chem. Soc. **94**, 8205 (1972).
27. C. Altona and M. Sundaralingam. J. Am. Chem. Soc. **95**, 2333 (1973).
28. M. Sundaralingam. *In* Proceedings, international symposium on the conformation of biological molecules and polymers, symposia on quantum and biochemistry. Vol. 5. *Edited by* B. Pullman and E. D. Bergmann. Academic Press, Jerusalem. 1973. p. 417.
29. M. Remin and D. Shugar. Biochem. Biophys. Res. Commun. **48**, 636 (1972).
30. N. Sheppard and J. J. Turner. Mol. Phys. **3**, 168 (1960).
31. A. A. Bothner-By and C. Naar-Colin. J. Am. Chem. Soc. **83**, 231 (1961).
32. T. N. Margulis. J. Am. Chem. Soc. **93**, 2193 (1971).
33. J. R. Einstein, J. L. Hosszu, J. W. Longworth, R. O. Rahn, and C. H. Wei. Chem. Commun. 1063 (1967).
34. N. Camerman, S. C. Nyburg, and D. Weinblum. Tetrahedron Lett. 4127 (1967).
35. K. B. Wiberg and D. E. Barth. J. Am. Chem. Soc. **91**, 5124 (1969).
36. R. J. Abraham, M. A. Cooper, J. R. Salmon, and D. Whittaker. Org. Magn. Resonance, **4**, 489 (1972).
37. S. Meiboom and L. C. Snyder. Chem. Eng. News, **44**, 51 (1966).
38. J. B. Lambert and J. D. Roberts. J. Am. Chem. Soc. **87**, 3884 (1965).
39. G. M. Blackburn and R. J. H. Davies. Tetrahedron Lett. 4471 (1966).
40. N. Camerman, D. Weinblum, and S. C. Nyburg. J. Am. Chem. Soc. **91**, 982 (1969).
41. M. P. Schweizer, J. T. Witkowski, and R. K. Robins. J. Am. Chem. Soc. **93**, 277 (1971).

Can. J. Chem. Downloaded from www.nrcresearchpress.com by 210.87.254.105 on 09/05/12
For personal use only.

42. H. DUGAS, B. J. BLACKBURN, R. K. ROBINS, R. DESLAURIERS, and I. C. P. SMITH. J. Am. Chem. Soc. **93**, 3468 (1971).
43. F. E. HRUSKA. J. Am. Chem. Soc. **93**, 1795 (1971).
44. R. DESLAURIERS, R. D. LAPPER, and I. C. P. SMITH. Can. J. Chem. **49**, 1279 (1971).
45. F. E. HRUSKA. *In* Proceedings, international symposium on the conformation of biological molecules and polymers, symposia on quantum and biochemistry. Vol. 5. *Edited by* B. Pullman and E. D. Bergmann. Academic Press, Jerusalem. 1973. p. 345.
46. F. E. HRUSKA, A. A. SMITH, and J. G. DALTON. J. Am. Chem. Soc. **93**, 4334 (1971).
47. B. DONALDSON and L. D. HALL. Can. J. Chem. **50**, 2111 (1972).
48. L. D. HALL and R. B. MALCOLM. Can. J. Chem. **50**, 2092, 2102 (1972).
49. D. DAVIES and S. S. DANYLUK. Abstracts, second international symposium on NMR spectroscopy organized by the Chemical Society at the University of Surrey. July, 1972.
50. I. C. P. SMITH, H. H. MANTSCH, R. D. LAPPER, R. DESLAURIERS, and T. SCHLEICH. *In* Proceedings, international symposium on the conformation of biological molecules and polymers, symposia on quantum and biochemistry. Vol. 5. *Edited by* B. Pullman and E. D. Bergmann. Academic Press, Jerusalem. 1973. p. 381.
51. D. J. WOOD, R. J. MYNOTT, F. E. HRUSKA, and R. H. SARMA. FEBS Lett. **34**, 323 (1973).
52. C. ALTONA. Proceedings, 4th Harry Steenbock symposium on nucleic acid structure and conformation and protein – nucleic acid interaction. Madison, Wisconsin, June 16–19, 1974. In press.
53. R. H. SARMA, R. J. MYNOTT, D. J. WOOD, and F. E. HRUSKA. J. Am. Chem. Soc. **95**, 6457 (1973).

Can. J. Chem. Downloaded from www.nrcresearchpress.com by 210.87.254.105 on 09/05/12
For personal use only.

Oxidation of Benzylidene Acetals by Ozone

PIERRE DESLONGCHAMPS,[1] CLAUDE MOREAU,[2] DANIEL FRÉHEL, AND ROBERT CHÊNEVERT
Laboratoire de synthèse organique, Département de chimie, Université de Sherbrooke, Sherbrooke, Québec J1K 2R1
Received October 9, 1974

PIERRE DESLONGCHAMPS, CLAUDE MOREAU, DANIEL FRÉHEL, and ROBERT CHÊNEVERT. Can. J. Chem. **53**, 1204 (1975).

Oxidation of five-membered ring (1,3-dioxolan) and six-membered ring (1,3-dioxan) benzylidene acetals by ozone are reported.

PIERRE DESLONGCHAMPS, CLAUDE MOREAU, DANIEL FRÉHEL et ROBERT CHÊNEVERT. Can. J. Chem. **53**, 1204 (1975).

L'oxydation de benzylidène acétals du type dioxolanne-1,3 et dioxanne-1,3 par l'ozone est rapportée.

Can. J. Chem. Downloaded from www.nrcresearchpress.com by 210.87.254.42 on 09/05/12
For personal use only.

We have reported in a preliminary communication (1), the oxidation of aldehyde acetals to the corresponding esters and alcohols with

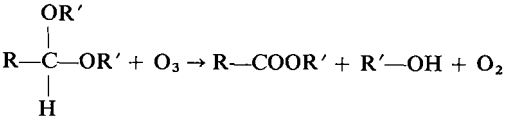

ozone. Further studies on the reactivity of the acetal function in relation to its conformation (2) led us to develop a new stereoelectronic theory for the hydrolysis of esters (3) and amides (4). We have reported in detail (5) the ozonolysis of various types of acetals such as 1,1-dialkoxyheptane, 2-alkyl-1,3-dioxolan, 2-alkyl-1,3-dioxan, 2-alkoxytetrahydropyran, and 2-alkoxytetrahydrofuran as well as α- and β-glycosides. We have also examined the oxidation of benzylidene acetals and we wish to report in detail the result of this work.

We have studied five-membered ring (1,3-dioxolan) and six-membered ring (1,3-dioxan) benzylidene acetals. 1,3-Dioxolan acetals were investigated for two reasons. First, we wanted to obtain evidence that the oxidation of acetals by ozone proceeded through the formation of a tetrahedral hemiorthoester intermediate or its equivalent (3). Secondly, we hoped to demonstrate that the oxidation of these acetals was valuable in the carbohydrate field as an attractive method for the specific esterification of an axial alcohol in conformationally rigid *cis*-1,2-cyclohexanediols. It was also of interest to examine the oxidation of a series of 4,6-*O*-benzylidene derivatives (1,3-dioxan acetals) of glycopyranosides to see if this reaction could be used for the preparation of 6-benzoate-4-hydroxy or 4-benzoate-6-hydroxy derivatives of glycopyranosides. The preparation of such partially esterified sugar derivatives can be important in carbohydrate chemistry. This route is particularly attractive because 4,6-*O*-benzylidene derivatives are normally readily available.

King and Allbutt (6) have described the stereoselective hydrolysis of dioxolenium ions and orthoesters fused to anchored six-membered rings. Mild acid hydrolysis of the dioxolenium salt **1** or the orthoester **2** afforded the axial ester – equatorial alcohol **4** with a very small amount of the isomer **5**. They further established by equilibration studies that the more stable isomer is the expected equatorial benzoate **5**, thus indicating that the formation of the isomer **4** is the result of a kinetically controlled hydrolysis of **1** and **2**. The hydrolysis of **1** and **2** proceeds through the formation of the hemiorthoester tetrahedral intermediate **3**. The intermediate **3** can assume two different conformations **6** and **7** which can give respectively the axial ester **4** and the equatorial ester **5** through an orbital assisted mechanism (3–6). However, conformer **6** is sterically favored over conformer **7** (6) and the axial ester **4** is formed selectively.

The study of the ozonolysis of 1,3-dioxolan benzylidene acetals fused to a rigid six-membered ring was therefore undertaken. If one observes the same stereoselectivity in product formation as seen in the hydrolysis of **1** and **2**, strong indirect evidence will have been obtained that the ozonolysis of acetals proceeds via the formation

[1]To whom all correspondence should be addressed.
[2]Holder of a "bourse postdoctorale France–Québec," 1973–1974.

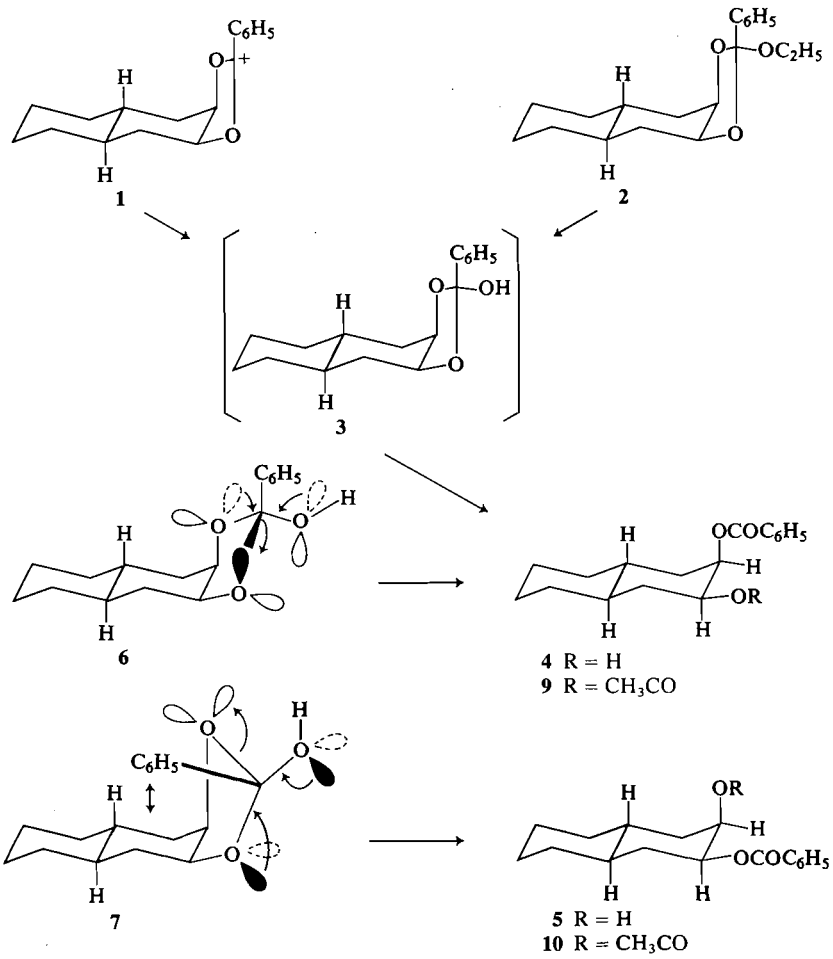

of an intermediate analogous to a hemiorthoester. Accordingly, oxidation studies on the benzylidenes derivatives **8** of 9β,10α-decalin-2β,3β-diol[3] (6) and **11** of 5α-cholestane-2β,3β-diol (7) were carried out.

Ozonolysis of **8** for 1 h at −78° in ethyl acetate gave a mixture of two isomeric hydroxy benzoates which were separated by preparative thin-layer chromatography. The major isomer (92%) was identified as the axial benzoate **4** ((6), 2β-benzoxy-3β-hydroxy-9β,10α-decalin). The minor isomer (8%) was the equatorial benzoate **5** ((6), 3β-benzoxy-2-β-hydroxy-9β,10α-decalin). The structure of the minor isomer **5** was confirmed by comparison with an authentic sample prepared by benzoylation of 9β,10α-decalin-2β,3β-diol (6).

[3]We are grateful to Professor J. F. King (University of Western Ontario) for his generous gift of this compound.

Analogous results were obtained for the ozonolysis of the cholestane benzylidene derivatives **11**. The major product (92%) was identified as the axial benzoate **12** and the minor product (8%) as the equatorial benzoate **13**. The minor isomer **13** was also compared with an authentic sample prepared by benzoylation of 5α-cholestane-2β,3β-diol (8).

The presence of minor amounts (≃8%) of the equatorial benzoate derivatives (**5** and **13**) in these reactions can be explained in two ways. Either the reaction is simply not completely stereospecific or the reaction is totally stereospecific but the axial benzoate derivatives (**4** and **12**) are converted to some extent into the more stable equatorial isomers (**5** and **13**) by equilibration during the reaction or in the work-up procedure. The second explanation was preferred because we were aware that trace amounts of acetic acid

Can. J. Chem. Downloaded from www.nrcresearchpress.com by 210.87.254.42 on 09/05/12
For personal use only.

Can. J. Chem. Downloaded from www.nrcresearchpress.com by 210.87.254.42 on 09/05/12
For personal use only.

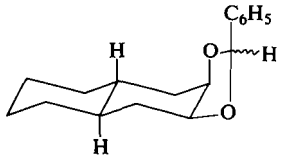

8

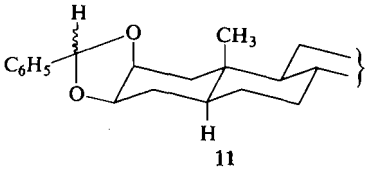

11

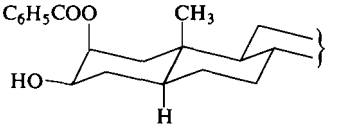

12

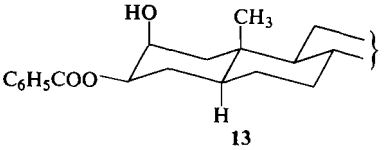

13

were produced when the ozonolysis reaction was carried out in ethyl acetate. The presence of acid could have catalyzed the isomerization. The ozonolysis of compound **8** was repeated in acetic anhydride containing sodium acetate. This solvent system is known to be useful in transforming *in situ* an alcohol function into an acetate function (5), thus eliminating the possibility of a transesterification during the work-up procedure. As expected, only one product,[4] the axial benzoate – equatorial acetate derivative **9**,[5] was isolated. Thus, the ozonolysis of benzylidene acetal **8** (or **11**) shows the same stereoselectivity as observed in the kinetic decomposition of hemiorthoester **3**. Therefore, it is logical to conclude that this oxidation reaction involves the formation of an intermediate which is either equivalent or identical to a hemiorthoester.

We have also studied the ozonolysis of the following 4,6-*O*-benzylidene derivatives of 2,3-disubstituted methyl α-D-glucopyranosides: 2,3-di-*O*-methyl **14** (m.p. 122–123° (9)), 2,3-di-*O*-acetyl **18** (10), and 2,3-di-*O*-tosyl derivative **22** (11). Ozonolysis of **14** in anhydrous carbon tetrachloride gave a mixture of the 6-*O*-benzoyl derivative **15** (60%) and the 4-*O*-benzoyl derivative **16** (40%) of methyl 2,3-di-*O*-methyl-α-D-glucopyranoside which were separated by preparative thin-layer chromatography. The 4-*O*-benzoyl derivative **16** was further converted into methyl 4-*O*-benzoyl-6-bromo-6-deoxy-2,3-di-*O*-methyl-α-D-glucopyranoside (**17**) (12); an authentic sample of **17** was prepared by oxidation of **14** with *N*-bromosuccinimide (13).

Ozonolysis of the 2,3-di-*O*-acetyl benzylidene derivative **18** in glacial acetic acid gave a mixture of the 6-*O*-benzoyl-2,3-di-*O*-acetyl- (85%) and 4-*O*-benzoyl-2,3-di-*O*-acetyl- (15%) methyl α-D-glycopyranosides (**19** and **20**) which were separated by preparative thin-layer chromatography. The identity of the 4-*O*-benzoyl derivative **20** was established by its transformation into methyl 4-*O*-benzoyl-6-bromo-6-deoxy-2,3-di-*O*-acetyl-α-D-glucopyranoside (**21**) (12). An authentic sample of **21** was prepared by oxidation of compound **18** with *N*-bromosuccinimide (13). The ozonolysis of the 2,3-di-*O*-tosyl benzylidene derivative **22** was also carried out in glacial acetic acid. Methyl 4-*O*-benzoyl-2,3-di-*O*-tosyl-α-D-glucopyranoside (**23**) was the only product isolated. This structure is proposed on the basis of its carbon-13 n.m.r. spectrum (Table 1). Compounds **15** and **16** were used as models. The C-6 of **23** must be part of a CH_2OH group since it is shielded (60.6 p.p.m.) relative to the corresponding carbon in **16** (61.1 p.p.m.). Also, C-6 in **16** is shielded relative to C-6 in **15** (63.7 p.p.m.) (14).

The other possible epimeric benzylidene derivative (m.p. 126–128°) of methyl 2,3-di-*O*-methyl-α-D-glucopyranoside is known (9). If it exists in conformation **24**, it should be inert to ozone; the lone pair orbitals of the two oxygens are not properly oriented to make **24** reactive toward ozone (1, 2, 5). However, it has been proposed that this compound can assume conformation **25** (9). If it does, it should be reactive toward ozone since **25** has proper orbital orientation. The benzylidene epimer (m.p. 126–

[4]Since only product **9** was obtained, one must also conclude that a suspension of sodium acetate in acetic anhydride does not catalyze a possible transesterification to any appreciable extent.

[5]The structure of compound **9** was firmly established by comparison with an authentic sample prepared by acetylation of the axial benzoate derivative **4**. The synthesis of the other possible isomer **10**, the equatorial benzoate – axial acetate derivative, was achieved by acetylation of the equatorial benzoate derivative **5**. This last experiment was carried out to be completely certain that no transesterification reaction occurred prior to the acetylation of the axial benzoate derivative **4**.

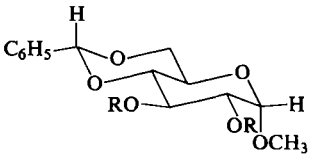

14 R = CH_3
18 R = CH_3CO
22 R = $CH_3C_6H_4SO_2$

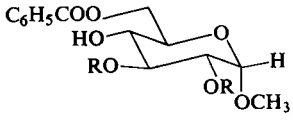

15 R = CH_3
19 R = CH_3CO

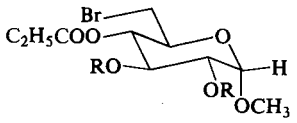

17 R = CH_3
21 R = CH_3CO

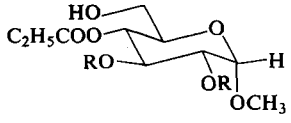

16 R = CH_3
20 R = CH_3CO
23 R = $CH_3C_6H_4SO_2$

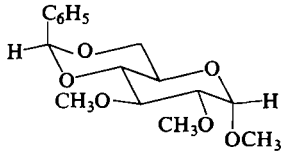

24

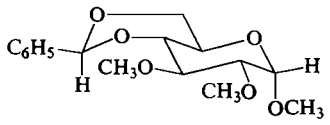

25

128°) was found to be reactive toward ozone yielding a mixture of the 6-*O*-benzoyl derivative **15** (40%) and the 4-*O*-benzoyl derivative **16** (60%) of methyl 2,3-di-*O*-methyl-α-D-glucopyranoside. This ozonolysis reaction was carried out with carbon tetrachloride which has been filtered through neutral alumina. The possibility that the epimer (m.p. 126–128°) was first isomerized by traces of acid to the epimer **14** (m.p. 122–123°) prior to the reaction with ozone seems unlikely.

It is known that methyl β-glycopyranoside can be oxidized by ozone (5) but this reaction is slow even at room temperature. Benzylidene acetals are much more reactive; the oxidation is normally completed within 2 h at −78°. Consequently, we think that the oxidation of the benzylidene acetals of alkyl-4,6-*O*-benzylidene-β-glycosides can be carried out without oxidation of the anomeric center. Thus, this new method for the synthesis of partially esterified sugars can be also used with alkyl-β-glycopyranosides.

The oxidation of an ethylidene derivative (**26**) (15) was also attempted. This reaction was carried out in acetic anhydride – sodium acetate, so that the poly-*O*-acetylated product was isolated directly. Methyl 4,6-*O*-ethylidene-2,3-di-*O*-acetyl-α-D-glucopyranoside (**26**) gave methyl 2,3,4,5-tetra-*O*-acetyl-α-D-glucopyranoside (**27**) (16) in excellent yield.

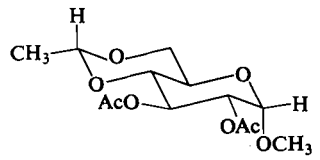

26

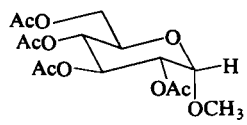

27

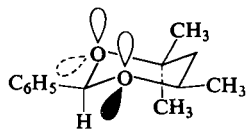

28

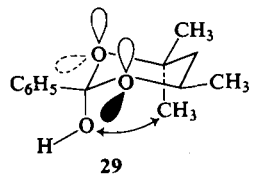

29

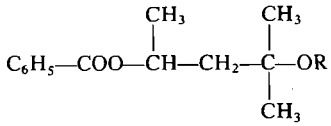

30 R = H
31 R = CH_3CO

Can. J. Chem. Downloaded from www.nrcresearchpress.com by 210.87.254.42 on 09/05/12
For personal use only.

TABLE 1. Carbon-13 n.m.r. spectra (p.p.m.)*

	C-1	C-2	C-3	C-4	C-5	C-6	C=O
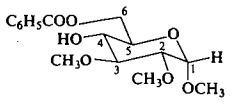 15	97.4	81.6	82.6	69.1	70.1	63.7	166.8
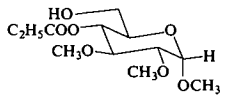 16	97.7	81.4	80.6	71.3	69.7	61.1	166.5
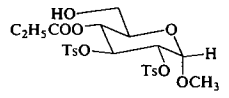 23	97.4	76.7	75.8	69.8	68.9	60.6	166.1

*We are grateful to Professor J. K. Saunders for the analysis of the spectra.

We have also studied the ozonolysis of 2-phenyl-4,4,6-trimethyl-1,3-dioxan (**28**). In this reaction, the intermediate **29** should be formed. The orientation of the orbitals of the ring oxygen atoms favors the opening of **29** in both directions equally. However, there is a strong 1,3-diaxial interaction between the OH group and the axial methyl group. The cleavage of **29** to give the secondary ester **30** eliminates this steric interaction whereas the cleavage of **29** to give the corresponding tertiary ester does not. Consequently, we think that this steric compression factor is strong enough to induce a specific cleavage of **29**. The exclusive formation of the secondary ester **30** is thus predicted. This result was confirmed experimentally and it constitutes another piece of evidence for the formation of a hemiorthoester intermediate in the ozonolysis of acetals.[6]

Experimental

The i.r. spectra were taken on a Perkin-Elmer 257 spectrophotometer. Proton n.m.r. spectra (δ value) were recorded on a Varian A-60 spectrometer in solvent indicated. Carbon-13 n.m.r. spectra were taken on a Bruker HX-90 spectrometer equipped with a Nicolet 1083 comp uter. All chemical shifts are recorded relative to internal TMS as standard. The ozonolysis reactions were carried out with a Welsbach Ozonator, model T-816. Organic solutions were dried over anhydrous magnesium sulfate and silica gel was use in all the chromatography. Microanalyses were performed by Dr. C. Daesslé, Organic Microanalyses, and by Mr. J. Tamas, Laboratoire de Microanalyse, Université de Sherbrooke.

[6]For a theoretical study related to this subject, see ref. 17.

Benzylidene Derivative of 9β,10α-Decalin-2β,3β-diol (8)

9β,10α-Decalin-2β,3β-diol ((6) 450 mg, 2.6 mmol) was dissolved in benzaldehyde (30 ml) and mixed with zinc chloride (4 g). The reaction mixture was kept for 18 h at room temperature under nitrogen. Water (50 ml) was then added and the mixture was extracted with ether. After evaporation of the dried ethereal phase, the resulting product was purified by preparative thin-layer chromatography with silica gel. The analytical sample was prepared by sublimation; m.p. 86–80°; n.m.r.: δ($CDCl_3$) 7.40 (5H, multiplet, aromatic hydrogens), 6.13 and 5.86 (1H, two singlets (ratio: 2:1), acetal hydrogen of the isomeric benzylidenes), and 4.16 (2H, multiplet, two >CHOC<).

Anal. Calcd. for $C_{17}H_{22}O_2$: C, 79.03; H, 8.58. Found: C, 79.12; H, 8.81.

Ozonolysis of 2β,3β-O-Benzylidene-9β,10α-decalin (8)

(*a*) Compound **8** (258 mg, 1 mmol) was ozonized in ethyl acetate (100 ml) at −78° (rate of ozone: 1 mmol/min) during 1 h. Residual ozone was removed by flushing the system with nitrogen. The solvent was removed *in vacuo*. The residual material contained the isomers **4** and **5** which were separated by preparative thin-layer chromatography.

2β-Benzoxy-3β-hydroxy-9β,10α-decalin (**4**) (252 mg, 92%); m.p. 105–106° (lit. (6) m.p. 106–107°); i.r.: ($CHCl_3$) 3580, 3460, and 1720 cm^{-1}; n.m.r.: δ($CDCl_3$) 8.1–7.5 (5H, two multiplets, aromatic hydrogens), 5.45 (1H, multiplet, ArCOOCH), and 3.80 (1H, multiplet, C*H*OH).

3β-Benzoxy-2β-hydroxy-9β,10α-decalin (**5**) (17 mg, 6%), m.p. 102° (lit. (6) m.p. 102–103°). An authentic sample of **5** was prepared by benzoylation of 9β,10α-decalin-2β,3β-diol by following the procedure described by King and Allbutt (6).

Can. J. Chem. Downloaded from www.nrcresearchpress.com by 210.87.254.42 on 09/05/12
For personal use only.

Can. J. Chem. Downloaded from www.nrcresearchpress.com by 210.87.254.42 on 09/05/12
For personal use only.

(*b*) Compound **8** (150 mg, 0.5 mmol) was ozonized (rate of ozone: 1 mmol/min) in acetic anhydride (100 ml) containing sodium acetate (2 g) at room temperature during 1 h. Pyridine was then added to the reaction mixture which was kept at room temperature for 24 h. Solvent was removed *in vacuo*. The resulting material was purified by preparative thin-layer chromatography and was found to be identical with an authentic sample of 3β-acetoxy-2β-benzoxy-9β,10α-decalin (**9**). The isomer **10** could not be detected by thin-layer chromatography.

*3β-Acetoxy-2β-benzoxy-9β,10α-decalin (**9**)*

2β-Benzoxy-3β-hydroxy-9β,10α-decalin (**4**, 80 mg, 0.3 mmol) was dissolved in a mixture of pyridine (10 ml) and acetic anhydride (10 ml). This mixture was kept at room temperature for 15 h. The solvent was removed *in vacuo* and the product was purified by preparative thin-layer chromatography. The analytical sample was prepared by distillation (86 mg, 94%); i.r.: ν_{max} ($CHCl_3$) 1720 cm^{-1}; n.m.r.: δ ($CDCl_3$) 8.1–7.5 (5H, two multiplets, aromatic hydrogens), 5.6 (1H, narrow multiplet, ArCOOCH), 4.98 (1H, broad multiplet, CHOAc), and 1.93 (3H, singlet, CH_3COO).

Anal. Calcd. for $C_{19}H_{24}O_4$: C, 72.13; H, 7.65. Found: C, 72.29; H, 7.29.

*2β-Acetoxy-3β-benzoxy-9β,10α-decalin (**10**)*

3β-Benzoxy-2α-hydroxy-9β,10α-decalin (**5**) was acetylated by the experimental procedure described above. Compound **10** was purified by distillation (92% yield); i.r.: ν_{max} ($CHCl_3$) 1720 cm^{-1}; n.m.r.: δ ($CDCl_3$) 8.0–7.45 (5H, two multiplets, aromatic hydrogens), 5.47 (1H, narrow multiplet, ArCOOCH), 5.10 (1H, broad multiplet, CHOAc), and 2.11 (3H, singlet, CH_3COO).

Anal. Calcd. for $C_{19}H_{24}O_4$: C, 72.13; H, 7.65. Found: C, 72.14; H, 7.71.

*2β,3β-O-Benzylidene-5α-cholestane (**11**)*

Cholestane-2β,3β-diol ((7), 200 mg, 0.5 mmol) was dissolved in benzaldehyde (30 ml) and mixed with zinc chloride (2 g). The reaction mixture was kept for 18 h at room temperature under nitrogen. Ether (500 ml) was added and the organic phase was washed with water. The dried organic phase was evaporated and the residual material was purified by preparative thin-layer chromatography to yield a mixture of the epimeric benzylidenes (**11**) which was recrystallized from acetone; m.p. 126–131°; n.m.r.: δ ($CDCl_3$) 6.12 and 5.76 (1H, two singlets (ratio 1:1), acetal hydrogen of the isomeric benzylidenes), and 4.22 (2H, multiplet, two >CHOC<).

*Ozonolysis of 2β,3β-O-Benzylidene-5α-cholestane (**11**)*

Compound **11** (135 mg, 0.27 mmol) was ozonized in ethyl acetate (50 ml) at −78° (rate of ozone: 1 mmol/min) during 1 h. The solvent was removed *in vacuo*. The residual material contained the isomers **12** and **13** which were separated by preparative thin-layer chromatography.

2β-Benzoxy-3β-hydroxy-5α-cholestane **12** (128 mg, 92%) was recrystallized from acetone; m.p. 141°; i.r.: ν_{max} ($CHCl_3$) 3580, 3460, and 1720 cm^{-1}; n.m.r.: δ ($CDCl_3$) 8.1–7.46 (5H, two multiplets, aromatic hydrogens), 5.42 (1H, narrow multiplet, ArCOOCH), and 3.75 (1H, broad multiplet, C*H*OH).

Anal. Calcd. for $C_{34}H_{52}O_3 \cdot H_2O$: C, 77.51; H, 10.32. Found: C, 77.92; H, 9.89.

3β-Benzoxy-2β-hydroxy-5α-cholestane (**13**) (9 mg, 8%) was recrystallized from acetone, m.p. 213–215°, and was found identical to an authentic sample.

*3β-Benzoxy-2β-hydroxy-5α-cholestane (**13**)*

5α-Cholestane-2β,3β-diol ((7), 115 mg, 0.28 mmol) was dissolved in dichloromethane (25 ml). Pyridine (4.5 ml) and benzoyl chloride (45 mg, 0.3 mmol) was added and the mixture was left at room temperature for 24 h. Ether was added and the organic phase was washed with an aqueous solution of sodium bicarbonate. The dried ethereal solution was evaporated and the residual material was purified by preparative thin-layer chromatography to give the benzoate derivative **13** (104 mg, 90%) which was crystallized from acetone; m.p. 213–215°; i.r.: ν_{max} ($CHCl_3$) 3580, 3460, and 1720 cm^{-1}; n.m.r.: δ ($CDCl_3$) 8.0–7.5 (5H, two multiplets, aromatic hydrogens), 5.08 (1H, broad multiplet, ArCOOCH), and 4.24 (1H, narrow multiplet, C*H*OH).

Anal. Calcd. for $C_{34}H_{52}O_2 \cdot H_2O$: C, 77.51; H, 10.32. Found: C, 77.52; H, 9.99.

Ozonolysis of Methyl 4,6-O-Benzylidene-2,3-di-O-methyl-α-D-glucopyranosides (9)

*(a) Isomer **14** (m.p. 122–123°)*

Methyl 4,6-*O*-benzylidene-2,3-di-*O*-methyl-α-D-glucopyranoside (m.p. 122–123°) (1.556 g, 5.02 mmol) was ozonized (rate of ozone: 0.5 mmol/min) in carbon tetrachloride (filtered through neutral alumina) at room temperature. The reaction was stopped after 30 min and the solvent was evaporated *in vacuo*. The residual material contained the isomers **15** and **16** which were separated by column chromatography with silica gel.

Methyl 6-*O*-benzoyl-2,3-di-*O*-methyl-α-D-glucopyranoside (**15**, 635 mg); m.p. 95–97°; $[\alpha]_{578}^{CHCl_3}$ +42°; n.m.r.: δ ($CDCl_3$) 8.1–7.5 (5H, two multiplets, aromatic hydrogens), 5.23 (1H, doublet, J = 8 Hz, ArCOOCH), 4.96 (1H, doublet, J = 3 Hz, anomeric hydrogen), 3.55 (3H, singlet, OCH_3), 3.53 (3H, singlet, OCH_3), and 3.48 (3H, singlet, OCH_3).

Methyl 4-*O*-benzoyl-2,3-di-*O*-methyl-α-D-glucopyranoside (**16**, 774 mg); m.p. 68–70°; $[\alpha]_{578}^{CHCl_3}$ +107°; n.m.r.: δ ($CDCl_3$) 8.1–7.5 (5H, two multiplets, aromatic hydrogens), 4.87 (1H, doublet, J = 3 Hz, anomeric hydrogen), 4.60 (2H, doublet, J = 3 Hz, CH_2O), 3.66 (3H, singlet, OCH_3), 3.48 (3H, singlet, OCH_3), and 3.43 (3H, singlet, OCH_3).

Anal. Calcd. for $C_{16}H_{22}O_7$: C, 58.88; H, 6.80. Found: C, 59.11; H, 6.92.

*(b) Isomer **24** (**25**) (m.p. 126–128°)*

Methyl 4,6-*O*-benzylidene-2,3-di-*O*-methyl-α-D-glucopyranoside (m.p. 126–128°) was ozonized under the same experimental conditions described for the ozonolysis of isomer **14** (m.p. 122–123°). The isomeric hydroxybenzoates **15** and **16** were isolated in 40 and 60%, respectively.

*Methyl 4-O-Benzoyl-6-bromo-6-deoxy-2,3-di-O-methyl-α-D-glucopyranoside (**17**)*

(*a*) Methyl 4-*O*-benzoyl-2,3-di-*O*-methyl-α-D-glucopyranoside (**16**, 90 mg, 0.3 mmol) and triphenyl phosphine (160 mg, 0.6 mmol) were dissolved in anhydrous dimethylformamide (5 ml). *N*-Bromosuccinimide (110 mg, 0.6 mmol) was then slowly added and the mixture was heated at 60° for 2 h (12). After cooling, water (5 ml) was added and the mixture was extracted with ether. The dried

Can. J. Chem. Downloaded from www.nrcresearchpress.com by 210.87.254.42 on 09/05/12
For personal use only.

ethereal phase was then evaporated. The residue was purified by preparative thin-layer chromatography to yield pure methyl 4-*O*-benzoyl-6-bromo-6-deoxy-2,3-di-*O*-methyl-α-D-glucopyranoside (**17**, 90 mg, 84%); oil; $[\alpha]_{578}^{CHCl_3}$ +68°; n.m.r.: δ ($CDCl_3$) 8.1–7.5 (5H, two multiplets, aromatic hydrogens), 5.13 (1H, doublet, J = 8 Hz, ArCOOCH), 4.92 (1H, doublet, J = 3 Hz, anomeric hydrogen), 3.53 (3H, singlet, OCH_3), 3.50 (3H, singlet, OCH_3), and 3.46 (3H, singlet, OCH_3).

(*b*) Methyl 4,6-*O*-benzylidene-2,3-di-*O*-methyl-α-D-glucopyranoside (**14**, 320 mg, 1.03 mmol) was dissolved in anhydrous carbon tetrachloride and heated at reflux for 1 h in presence of *N*-bromosuccinimide (280 mg, 1.60 mmol) and barium carbonate (800 mg, 4 mmol) (13). The solution was filtered through Celite and evaporated to dryness. Compound **17** was purified by preparative thin-layer chromatography (247 mg); oil; $[\alpha]_{578}^{CHCl_3}$ +71°. This product was found identical with compound **17** prepared by the procedure described above.

*Ozonolysis of Methyl 4,6-O-Benzylidene-2,3-di-O-acetyl-α-D-glucopyranoside (**18**) (10)*

Compound **18** (165 mg, 0.45 mmol) was ozonized (rate of ozone: 0.3 mmol/min) in glacial acetic acid at room temperature. The reaction was stopped after 1.5 h and the solvent was removed *in vacuo*. The residual material contained the isomers **20** (15%) and **19** (85%) which were separated by preparative thin-layer chromatography. Pure isomer **19** was isolated but isomer **20** was contaminated with a small quantity of the other isomer (**19**).

Methyl 6-*O*-benzoyl-2,3-di-*O*-acetyl-α-D-glucopyranoside (**19**); oil; $[\alpha]_{578}^{CHCl_3}$ +110°; n.m.r.: δ ($CDCl_3$) 8.0–7.4 (5H, two multiplets, aromatic hydrogens), 4.90 (2H, singlet, $ArCOOCH_2$), 3.40 (3H, singlet, OCH_3), and 2.06 (6H, singlet, two CH_3COO).

Anal. Calcd. for $C_{18}H_{22}O_9$: C, 56.53; H, 5.80. Found: C, 56.47; H, 5.97.

Methyl 4-*O*-benzoyl-2,3-di-*O*-acetyl-α-D-glucopyranoside (**20**), oil; n.m.r.: δ ($CDCl_3$) 8.0–7.4 (5H, two multiplets, aromatic hydrogens), 3.43 (3H, singlet, OCH_3), 2.7 (3H, singlet, CH_3COO), and 1.90 (3H, singlet, CH_3COO).

*Methyl 4-O-Benzoyl-6-bromo-6-deoxy-2,3-di-O-acetyl-α-D-glucopyranoside (**21**)*

(*a*) Methyl 4-*O*-benzoyl-2,3-di-*O*-acetyl-α-D-glucopyranoside (**20**, 165 mg, 0.43 mmol) and triphenyl phosphine (230 mg, 0.87 mmol) were dissolved in anhydrous dimethyl formamide (5 ml). *N*-Bromosuccinimide (160 mg, 0.87 mmol) was then added and the mixture was heated at 60° for 2 h (12). After cooling, water (10 ml) was added and the mixture was extracted with ether. The dried ethereal phase was then evaporated. The residue was purified by preparative thin-layer chromatography to yield pure methyl 4-*O*-benzoyl-6-bromo-6-deoxy-2,3-di-*O*-acetyl-α-D-glucopyranoside (**21**, 110 mg); oil; $[\alpha]_{578}^{CHCl_3}$ +61°; n.m.r.: δ ($CDCl_3$) 7.9–7.4 (5H, two multiplets, aromatic hydrogens), 5.0 (2H, singlet, CH_2Br), 3.48 (3H, singlet, OCH_3), 8.05 (3H, singlet, CH_3COO), and 1.86 (3H, singlet, CH_3COO).

(*b*) Methyl 4,6-*O*-benzylidene-2,3-di-*O*-acetyl-α-D-glucopyranoside (**18**, 360 mg, 1.0 mmol) was dissolved in anhydrous carbon tetrachloride and heated at reflux for 1 h in presence of *N*-bromosuccinimide (250 mg, 1.5 mmol) and barium carbonate (800 mg) (13). The solution was filtered through Celite and evaporated to dryness. Compound **21** was purified by preparative thin-layer chromatography (195 mg); oil; $[\alpha]_{578}^{CHCl_3}$ +61°. This product was found identical with compound **21** prepared by the procedure described above.

*Ozonolysis of Methyl 4,6-O-Benzylidene-2,3-di-O-tosyl-α-D-glucopyranoside (**22**) (11)*

Compound **22** (80 mg, 0.136 mmol) was ozonized (rate of ozone: 0.33 mmol/min) in glacial acetic acid at room temperature. The reaction was stopped after 1.5 h and the solvent was removed *in vacuo*. The residue was purified by preparative thin-layer chromatography to give methyl 4-*O*-benzoyl-2,3-di-*O*-tosyl-α-D-glucopyranoside (**23**, 60 mg, 75%); m.p. 85–88°; $[\alpha]_{578}^{CHCl_3}$ −26°; n.m.r.: δ ($CDCl_3$) 8.0–7.0 (13H, multiplets, aromatic hydrogens), 3.36 (3H, singlet, OCH_3), 2.41 (3H, singlet, $ArCH_3$), and 2.25 (3H, singlet, $ArCH_3$).

Anal. Calcd. for $C_{28}H_{30}O_{11}S_2$: C, 55.60; H, 4.99. Found: C, 55.60; H, 5.14.

*Ozonolysis of Methyl 2,3-Di-O-acetyl-4,6-O-ethylidene-α-D-glucopyranoside (**26**) (15)*

Compound **26** (940 mg, 3.09 mmol) was ozonized (rate of ozone: 0.3 mmol/min) in acetic anhydride (100 ml) containing sodium acetate (4 g) at room temperature during 2 h. The reaction mixture was then heated at 100° for 1.5 h. The solvent was removed in *vacuo* then ether was added. The ethereal phase was washed with an aqueous solution of sodium carbonate and brine. The dried organic phase was evaporated *in vacuo* and the residue was purified by column chromatography to yield methyl 2,3,4,6-tetra-*O*-acetyl-α-D-glucopyranoside (**27**, 1.109 g, 98%); m.p. 99–100°; $[\alpha]_{578}^{CHCl_3}$ +129° (lit. (8) m.p. 101–103°; $[\alpha]_{D}^{CHCl_3}$ +130°). This compound was found to be identical to an authentic sample.

*2-Phenyl-4,4,6-trimethyl-1,3-dioxan (**28**)*

Benzaldehyde (10.6 g, 0.10 mol) and 2-methylpentane-2,4-diol (18) (11.8 g, 0.10 mol) were dissolved in dry benzene (150 ml) containing a small quantity of *p*-toluenesulfonic acid. The benzene solution was heated during 3 h and the water was removed with the aid of a Dean-Stark trap. After cooling at room temperature, the reaction mixture was washed with aqueous sodium carbonate and water. The dried organic solution was evaporated and distillation of the crude product gave pure 2-phenyl-4,4,6-trimethyl-1,3-dioxan (19.3 g, 94%); b.p. 73°/150 mm; n.m.r.: δ ($CDCl_3$) 7.50 (5H, multiplet, C_6H_5), 5.81 (1H, singlet, acetal hydrogen), 4.15 (1H, multiplet, —C*H*(CH_3)—O), and 1.41 (11H, multiplet, —CH_2— and CH_3).

Anal. Calcd. for $C_{13}H_{18}O_2$: C, 75.69; H, 8.80. Found: C, 75.81; H, 8.91.

*Ozonolysis of 2-Phenyl-4,4,5-trimethyl-1,3-dioxan (**28**)*

(*a*) 2-Phenyl-4,4,6-trimethyl-1,3-dioxan (2.06 g, 0.01 mol) was dissolved in freshly distilled ethyl acetate and cooled at −78°. Ozone (1 mmol/min) was passed through the solution and the end of the reaction was indicated by the appearance of the characteristic blue color of ozone. The excess ozone was swept with a stream of nitrogen and the reaction mixture was allowed to warm up at room temperature. The solvent was evaporated *in vacuo* yielding crude 3-hydroxy-1,3-dimethylbutane benzoate (**30**, 2.18 g, 98%); i.r.: ν_{max} ($CHCl_3$) 3450 and 1710 cm^{-1}; n.m.r.:

δ ($CDCl_3$) 8.15 and 7.60 (5H, two multiplets, C_6H_5), 5.50 (1H, multiplet, $CHOCOC_6H_5$), 2.46 (1H, singlet, OH), 2.1–1.5 (2H, multiplet, CH_2), 1.38 (3H, doublet, $J = 7$ Hz, CH_3), 1.25 (6H, singlet, *gem*-dimethyl).

Acetylation of the crude product with acetic anhydride (100 ml) and sodium acetate (4 g) (reflux for 3 h) gave 4-acetoxy-4-methyl-2-pentyl benzoate (**31**) which was purified by distillation (2.22 g, 84%).

(*b*) 2-Phenyl-4,4,6-trimethyl-1,3-dioxan (2.06 g, 0.01 mol) was dissolved in freshly distilled acetic anhydride (100 ml) and sodium acetate (4 g). Ozone (1 mmol/min) was passed through the solution cooled at −78°. The end of the reaction was indicated by the appearance of the blue color of ozone. The excess ozone was swept away with a stream of nitrogen. The reaction mixture was allowed to be warmed up at room temperature and was refluxed for 3 h. The solvent was removed *in vacuo* and crude product was dissolved in ether (200 ml). The organic phase was washed with aqueous sodium carbonate (5%) and water. The organic phase was dried over magnesium sulfate, filtered, and evaporated to dryness yielding crude 3-acetoxy-1,3-dimethyl butane benzoate (**31**). Distillation *in vacuo* gave the analytical sample (2.13 g, 81%); b.p. 115°/3 mm; i.r.: ν_{max} ($CHCl_3$) 1725 cm^{-1}; n.m.r.: δ ($CDCl_3$) 8.10–7.50 (5H, two multiplets, C_6H_5), 5.46 (1H, multiplet, $CHOCOC_6H_5$), 2.25 (2H, multiplet, CH_2), 1.83 (3H, singlet, CH_3COO), 1.50 (6H, singlet, *gem*-dimethyl), and 1.37 (3H, doublet, $J = 7$ Hz, CH_3).

Anal. Calcd. for $C_{15}H_{20}O_4$: C, 68.16; H, 7.63. Found: C, 67.89; H, 7.59.

Support for this work by the National Research Council of Canada, by the Alfred P. Sloan Foundation, and by the "Ministère de l'Education" Québec is gratefully acknowledged.

1. P. DESLONGCHAMPS and C. MOREAU. Can. J. Chem. **49**, 2465 (1971).
2. P. DESLONGCHAMPS, C. MOREAU, D. FRÉHEL, and P. ATLANI. Can. J. Chem. **50**, 3402 (1972).
3. P. DESLONGCHAMPS, P. ATLANI, D. FRÉHEL, and A. MALAVAL. Can. J. Chem. **50**, 3405 (1972).
4. P. DESLONGCHAMPS, C. LEBREUX, and R. TAILLEFER. Can. J. Chem. **51**, 1665 (1973).
5. P. DESLONGCHAMPS, P. ATLANI, D. FRÉHEL, A. MALAVAL, and C. MOREAU. Can. J. Chem. In press.
6. J. F. KING and A. D. ALLBUTT. Can. J. Chem. **48**, 1754 (1970); Tetrahedron Lett. 49 (1967).
7. H. B. HENBEST, M. SMITH, and A. THOMAS. J. Chem. Soc. 3293 (1958).
8. H. B. HENBEST and M. SMITH. J. Chem. Soc. 926 (1957).
9. N. BAGGETT, J. M. DUXBURY, A. B. FOSTER, and J. M. WEBBER. Carbohyd. Res. **1**, 22 (1965); N. BAGGETT, MD. MOSIHUZZAMAN, and J. M. WEBBER. Carbohyd. Res. **11**, 263 (1969).
10. R. W. JEANLOZ and D. A. JEANLOZ. J. Am. Chem. Soc. **79**, 2579 (1957).
11. D. S. MATHERS and G. J. ROBERTSON. J. Chem. Soc. 696 (1933).
12. M. M. PONPIPOM and S. HANESSIAN. Carbohyd. Res. **18**, 342 (1971).
13. S. HANESSIAN. Carbohyd. Res. **2**, 86 (1966).
14. J. B. STOTHERS. Carbon-13 NMR spectroscopy. Academic Press, New York, N.Y. 1972.
15. J. HONEYMAN and J. W. W. MORGAN. J. Chem. Soc. 3660 (1955).
16. C. S. HUDSON and J. K. DALE. J. Am. Chem. Soc. **37**, 1264 (1915).
17. J. M. LEHN, G. WIPFF, and H.-B. BÜRGI. Helv. Chim. Acta, **57**, 493 (1974).
18. T. E. DUBOIS. Ann. Chim. 406 (1951).

Can. J. Chem. Downloaded from www.nrcresearchpress.com by 210.87.254.42 on 09/05/12
For personal use only.

Further Studies on the Assignment of Signals in ^{13}C Magnetic Resonance Spectra of Aldoses and Derived Methyl Glycosides[1]

PHILIP A. J. GORIN AND MYTOSK MAZUREK

Prairie Regional Laboratory, National Research Council of Canada, Saskatoon, Saskatchewan S7N 0W9

Received October 9, 1974

PHILIP A. J. GORIN and MYTOSK MAZUREK. Can. J. Chem. **53**, 1212 (1975).

The ^{13}C signals of most of the more common sugars and their methyl glycosides have been assigned, based on the α-carbon and β-carbon effects that occur on deuterium substitution. For pyranoses having the same hydroxyl configuration, replacement of the CH_2OH substituent at C-5 with CH_3, CO_2H, CO_2Me, or H is accompanied by displacement of the C-4, C-5, and when applicable C-6 signals. The magnitudes of the displacements in the glucopyranose and mannopyranose series are almost identical and were of aid in assigning signals in the ^{13}C spectrum of methyl (methyl α-D-mannopyranuronosid)uronate. The displacements, however, differ from corresponding ones observed in the galactopyranose series. Some assignments are made for the ^{13}C signals of structurally related methyl aldofuranosides.

PHILIP A. J. GORIN et MYTOSK MAZUREK. Can. J. Chem. **53**, 1212 (1975).

On a attribué les signaux en r.m.n. du ^{13}C de la plupart des sucres usuels ainsi que de leurs glycosides de méthyle; ces attributions ont été faites en se basant sur les effets que produisent les carbones α et β des substitutions par du deutérium. Pour des pyrannoses ayant la même configuration des groupes hydroxyles, le remplacement d'un substituant CH_2OH en C-5 par CH_3, CO_2H, CO_2Me ou H s'accompagne par un déplacement des signaux en C-4, C-5 et lorsque c'est possible en C-6. L'amplitude de ces déplacements dans les séries glucopyrannoses et mannopyrannoses sont presque identiques et a été fort utile pour attribuer les signaux dans le spectre r.m.n. du ^{13}C du (α-D-mannopyrannuronoside de méthyle)uronate de méthyle. Les déplacements diffèrent toutefois des déplacements correspondants observés en série galactopyrannose. On a fait quelques attributions pour des signaux de ^{13}C dans des aldofurannosides de méthyle qui leur sont reliés d'une façon structurale. [Traduit par le journal]

In a previous study (1), the carbon-13 magnetic resonance (^{13}c.m.r.) spectra of deuterated derivatives of αβ-D-glucose, αβ-D-mannose, and αβ-D-galactose were interpreted and discussed. With the aid of two suitable deuterated derivatives of each aldose it was possible to make an unambiguous assignment of each signal, since the signals of the ^{13}C nucleus attached to the deuteron (α-carbon) disappeared and those of the adjacent β-carbons were displaced upfield by 0.02–0.10 p.p.m. (1). Since some of the assignments carried out elsewhere have proved to be incorrect, the studies in this laboratory have been extended to most of the frequently encountered monosaccharides and certain derived methyl glycosides. The preparation of the deuterated sugars was rendered easier, in most instances, by synthetic routes previously devised for the undeuterated counterparts.

As in the above study, which was relatively brief, two deuterated derivatives of each sugar were selected and their ^{13}c.m.r. spectra rationalized by observing the expected α-carbon (2) and the β-carbon deuterium isotope effects (1) (Table 1). Although, for the most part, the signal of the α-carbon disappears, in the case of *5-*^2H derivatives of pentoses, or the *6-*^2H derivatives of 6-deoxyhexoses and methyl 6-deoxyhexopyranosides, the α-^{13}C signals appear as triplets at 0.4 p.p.m. upfield (3). The β-carbon effect appeared as an upfield shift of 0.04–0.09 p.p.m. on monodeuteration, 0.07–0.12 p.p.m. on dideuteration, and 0.17 p.p.m. for the C-3 signal of β-D-arabinopyranose-*4,5-*$^2H_3$. The signals of α- and β-anomers of reducing sugars were distinguished by following the mutarotation process by ^{13}c.m.r. spectroscopy, and those of isomeric methyl glycosides, which were components of mixtures, were obtained by reference to appropriate standards.

The assignments made by these approaches are summarized in Tables 2–6. The results obtained on the methyl glycosides can be used in interpreting the ^{13}c.m.r. spectra of polysaccharides and other sugar-containing polymers (4). Also, the following discussion will show that

[1]NRCC No. 14432.

Can. J. Chem. Downloaded from www.nrcresearchpress.com by 210.87.254.5 on 09/05/12
For personal use only.

TABLE 1. Upfield displacement of ^{13}C–C–^{2}H and ^{13}C–^{2}H signals of sugars* compared with those of corresponding ^{13}C–C–^{1}H and ^{13}C–^{1}H resonances, respectively, in p.p.m.

Sugar	Upfield displacement in p.p.m.†
αβ-D-Xylose-*3*-^{2}H	—
αβ-D-Xylose-*5*-^{2}H	C_α-4(0.07), C_β-4(0.07), C_α-5(0.42; *J* 20 Hz), C_β-5(0.37; *J* 23 Hz)
αβ-D-Arabinose-*5*-$^{2}H_2$	C_α-4(0.10), C_β-4(0.12)
αβ-D-Arabinose-*4,5*-$^{2}H_3$	C_α-3(0.10), C_β-3(0.17)
6-Deoxy-αβ-L-galactose-*4*-^{2}H	C_α-3(0.08), C_β-3(0.06), C_α-5(0.06) C_β-5(0.06)
6-Deoxy-αβ-D-galactose-*6*-^{2}H	C_α-5(0.04), C_β-5(0.04), C_α-6(0.50; *J* 20 Hz), C_β-6(0.50, *J* 20 Hz)
6-Deoxy-αβ-D-glucose-*6*-^{2}H	C_α-5(0.05), C_β-5(0.06)
6-Deoxy-αβ-D-glucose-*4*-^{2}H	C_α-3(0.08), C_β-3(0.07), C_α-5(0.06), C_β-5(0.06)
αβ-L-Rhamnose-*4*-^{2}H	C_α-3(0.06), C_β-3(0.05), C_α-5(0.05), C_β-5(0.06)
αβ-L-Rhamnose-*6*-^{2}H	C_α-5(0.09), C_β-5(0.08), $C_{\alpha\beta}$-6(0.41, *J* 18 Hz)
Methyl αβ-D-xylopyranoside-*3*-^{2}H	—
Methyl αβ-D-xylopyranoside-*5*-^{2}H	C_α-4(0.06), C_β-4(0.06)
Methyl αβ-D-arabinopyranoside-*5*-^{2}H	—
Methyl αβ-D-arabinopyranoside-*4,5*-$^{2}H_3$	C_α-3(0.08), C_β-3(0.09)
Methyl αβ-D-galactopyranoside-*4*-^{2}H	C_α-3(0.08), C_β-3(0.08), C_α-5(0.06), C_β-5(0.06)
Methyl αβ-D-galactopyranoside-*6*-$^{2}H_2$	C_α-5(0.12), C_β-5(0.11)
Methyl αβ-D-ribofuranoside-*3*-^{2}H	—
Methyl αβ-D-ribofuranoside-*5*-^{2}H	C_α-4(0.04), C_β-4(0.04)
Methyl αβ-D-arabinofuranoside-*5*-^{2}H	—
Methyl αβ-D-arabinofuranoside-*4,5*-$^{2}H_3$	C_α-3(0.04), C_β-3(0 04)
Methyl αβ-D-galactofuranoside-*4*-^{2}H	C_α-3(0.04), C_β-3(0.05), C_α-5(0.08), C_β-5(0.06)
Methyl αβ-D-galactofuranoside-*6*-$^{2}H_2$	C_α-5(0.12), C_β-5(0 12)
Methyl 6-deoxy-αβ-D-galactopyranoside-*4*-^{2}H	C_α-3(0.08), C_β-3(0 07), C_α-5(0 06), C_β-5(0.05)
Methyl 6-deoxy-αβ-D-galactopyranoside-*6*-^{2}H	C_α-5(0.04), C_β-5(0 05)
Methyl 6-deoxy-αβ-D-glucopyranoside-*6*-^{2}H	C_α-5(0.04), C_β-5(0.04)
Methyl 6-deoxy-αβ-D-glucopyranoside-*4*-^{2}H	C_α-3(0.05), C_β-3(0.06), C_α-5(0 06), C_β-5(0.05)
Methyl α-L-rhamnopyranoside-*4*-^{2}H	C_α-3(0.08), C_β-5(0.06)
Methyl α-L-rhamnopyranoside-*6*-^{2}H	C_α-5(0.05), $C_{\alpha\beta}$-6(0.32; *J* 0 68)
Methyl αβ-D-glucopyranosiduronic acid-*2*-^{2}H	C_α-3(0.04), C_β-3(0.05)
Methyl αβ-D-glucopyranosiduronic acid-*5*-^{2}H	C_α-4(0.07), C_β-4(0.07)
Methyl (methyl αβ-D-glucopyranosid)uronate-*2*-^{2}H	C_α-3(0 06), C_β-3(0.06)
Methyl (methyl αβ-D-glucopyranosid)uronate-*5*-^{2}H	C_α-4(0.06), C_β-4(0.06)

*α and β subscripts refer to C-1 configuration of sugar.
†Unless otherwise stated, the signals of carbons attached to deuterium disappear.

signal displacements observed on changing certain substituents in structurally related sugars are consistent, so that they may be of aid in interpreting the spectra of other sugars.

The chemical shifts of signals of ^{13}C nuclei of methyl α-D-glucopyranoside may be compared with those of respective nuclei in methyl α-D-aldopyranosides having a Cl conformation and the same configuration at C-2, C-3, C-4, and C-5 (Table 2). On going from methyl α-D-glucopyranoside to methyl 6-deoxy-α-D-glucopyranoside, methyl α-D-glucopyranosiduronic acid, methyl (methyl α-D-glucopyranosid)uronate, and methyl α-D-xylopyranoside, marked differences of shift were not observed for the respective C-1, C-2, C-3, and OCH_3-1 signals. Replacement of CH_2OH at C-5 with CH_3 causes C-4 and C-5 signals to be displaced at +6 p.p.m. (downfield) and −4 p.p.m., respectively.[2] These figures are +1.9 p.p.m. and −0.8 p.p.m., respectively, when comparisons are made with the spectra of

[2]Shifts are measured relative to external Me_4Si, which is always upfield from observed signals.

Can. J. Chem. Downloaded from www.nrcresearchpress.com by 210.87.254.5 on 09/05/12
For personal use only.

Can. J. Chem. Downloaded from www.nrcresearchpress.com by 210.87.254.5 on 09/05/12
For personal use only.

TABLE 2. Assignment of signals in ^{13}C spectra of configurationally related sugars. The figures of the chemical shifts are in p.p.m., as are those in parentheses, which represent the difference of the shift from that of the corresponding carbon in α-D-glucose and methyl α-D-glucopyranoside

α-D-Glucose						Methyl α-D-glucopyranoside							
C-1	C-2	C-3	C-4	C-5	C-6	C-1	C-2	C-3	C-4	C-5	C-6	OCH_3-1	OCH_3
α-D-Glucose (1)						*Methyl α-D-glucopyranoside*							
92.7	72.14	73.4	70.4	72.10	61.3	100.3	72.5	74.2	70.6	72.7	61.7	56.2	
α-D-Xylose						*Methyl α-D-xylopyranoside*							
93.3 (+0.6)	72.5 (+0.4)	73.9 (+0.5)	70.4 (0)	62.1 (−10.0)		100.6 (+0.3)	72.3 (−0.2)	74.3 (+0.1)	70.4 (−0.2)	62.0 (−10.7)		56.0 (−0.2)	
6-Deoxy-α-D-glucose						*Methyl 6-deoxy-α-D-glucopyranoside*							
93.1 (+0.4)	72.9 (+0.8)	73.6 (+0.2)	76.4 (+6.0)	68.6 (−3.5)	18.0 (−43.3)	100.3 (0)	72.6 (+0.1)	73.9 (−0.3)	76.2 (+5.6)	68.7 (−4.0)	17.6 (−44.1)	56.2 (0)	
						Methyl α-D-glucopyranosiduronic acid							
						100.7 (+0.4)	71.9 (−0.6)	73.8 (−0.4)	72.5 (+1.9)	71.9 (−0.8)	?	56.7 (+0.5)	
						Methyl (methyl α-D-glucopyranosid)uronate							
						100.8 (+0.5)	71.94 (−0.6)	73.7 (−0.5)	72.4 (+1.8)	71.87 (−0.8)	?	56.8 (+0.6)	54.2

Can. J. Chem. Downloaded from www.nrcresearchpress.com by 210.87.254.5 on 09/05/12
For personal use only.

TABLE 3. Assignment of signals in ^{13}C spectra of configurationally related sugars. The figures of the chemical shifts are in p.p.m., as are those in parentheses, which represent the difference of the shift from that of the corresponding carbon in β-D-glucose and methyl β-D-glucopyranoside

β-D-Glucose						Methyl β-D-glucopyranoside							
C-1	C-2	C-3	C-4	C-5	C-6	C-1	C-2	C-3	C-4	C-5	C-6	OCH_3-1	OCH_3
β-D-Glucose (1)						*Methyl β-D-glucopyranoside*							
96.5	74.8	76.4	70.3	76.6	61.5	104.3	74.2	76.9	70.8	76.9	61.9	58.3	
β-D-Xylose						*Methyl β-D-xylopyranoside*							
97.6 (+1.1)	75.1 (+0.3)	76.9 (+0.5)	70.3 (0)	66.3 (−10.3)		105.1 (+0.8)	74.0 (−0.2)	76.9 (0)	70.4 (−0.4)	66.3 (−10.6)		58.3 (0)	
6-Deoxy-β-D-glucose						*Methyl 6-deoxy-β-D-glucopyranoside*							
96.8 (+0.3)	75.6 (+0.8)	76.6 (+0.2)	76.1 (+5.8)	73.0 (−3.6)	18.0 (−43.5)	104.3 (0)	74.5 (+0.3)	76.7 (−0.2)	76.2 (+5.4)	73.0 (−3.9)	17.8 (−44.1)	58.3 (0)	
						Methyl β-D-glucopyranosiduronic acid							
						104.3 (0)	73.8 (−0.4)	76.5 (−0.4)	72.3 (+1.5)	75.6 (−1.3)	?	58.5 (+0.2)	
						Methyl (methyl β-D-glucopyranosid)uronate							
						104.6 (+0.3)	73.7 (−0.5)	76.3 (−0.6)	72.4 (+1.6)	75.7 (−1.2)	?	58.7 (+0.4)	56.5

Can. J. Chem. Downloaded from www.nrcresearchpress.com by 210.87.254.5 on 09/05/12
For personal use only.

TABLE 4. Assignment of signals in ^{13}C spectra of configurationally related sugars. The figures of the chemical shifts are in p.p.m., as are those in parentheses, which represent the difference of the shift from that of the corresponding carbon in α- and β-D-mannose and methyl α-D-mannopyranoside

α- and β-D-Mannose						Methyl α-D-mannopyranoside							
C-1	C-2	C-3	C-4	C-5	C-6	C-1	C-2	C-3	C-4	C-5	C-6	OCH_3-1	OCH_3
α-D-*Mannose (1)*						*Methyl α-D-mannopyranoside*							
95.0	71.7	71.3	68.0	73.4	62.1	101.9	71.2	71.8	68.0	73.7	62.1	55.9	
α-L-*Rhamnose*						*Methyl α-L-rhamnopyranoside*							
95.0 (0)	71.9 (+0.2)	71.1 (−0.2)	73.3 (+5.3)	69.4 (−4.0)	18.0 (−44.1)	101.9 (0)	71.0 (−0.2)	71.3 (−0.5)	73.1 (+5.1)	69.4 (−4.3)	17.7 (−44.4)	55.8 (−0.1)	
β-D-*Mannose (1)*						*Methyl (methyl α-D-mannopyranosid)uronate**							
94.6	72.3	74.1	67.8	77.2	62.1	102.3 (+0.4)	70.4 (−0.8)	71.1 (−0.7)	69.2 (+1.2)	72.9 (−0.8)	?	56.5 (+0.6)	54.1
β-L-*Rhamnose*													
94.6 (0)	72.4 (+0.1)	73.8 (−0.3)	72.9 (+5.1)	73.1 (−4.1)	18.0 (−44.1)								

*Suggested assignments.

Can. J. Chem. Downloaded from www.nrcresearchpress.com by 210.87.254.5 on 09/05/12
For personal use only.

TABLE 5. Assignment of signals in ^{13}C spectra of configurationally related sugars. The figures of the chemical shifts are in p.p.m., as are those in parentheses, which represent the difference of the shift from that of the corresponding carbon in α- and β-D-galactose and methyl α- and methyl β-D-galactopyranoside

α- and β-D-Galactose						Methyl α- and methyl β-D-galactopyranoside						
C-1	C-2	C-3	C-4	C-5	C-6	C-1	C-2	C-3	C-4	C-5	C-6	OCH_3-1
α-D-*Galactose (1)*						*Methyl* α-D-*galactopyranoside*						
93.6	69.8	70.56	70.63	71.7	62.5	100.5	69.4	70.6	70.4	71.8	62.3	56.3
β-L-*(or* D-*)-Arabinose*						*Methyl* β-L-*(or* D-*)-arabinopyranoside*						
93.7	69.6	69.8	69.8	63.6		101.0	69.4	69.92	69.96	63.8		56.3
(+0.1)	(−0.2)	(−0.8)	(−0.8)	(−8.1)		(+0.5)	(0)	(−0.7)	(−0.4)	(−8.0)		(0)
6-Deoxy-α-D-*galactose*						*Methyl 6-deoxy*-α-D-*galactopyranoside*						
93.3	69.2	70.4	73.0	67.4	16.7	100.5	69.0	70.6	72.9	67.5	16.5	56.3
(−0.3)	(−0.6)	(−0.2)	(+2.4)	(−4.3)	(−45.8)	(0)	(−0.4)	(0)	(+2.5)	(−4.3)	(−45.8)	(0)
β-D-*Galactose (1)*						*Methyl* β-D-*galactopyranoside*						
97.7	73.3	74.2	70.1	76.3	62.3	104.9	71.8	73.9	69.8	76.2	62.1	58.3
α-L-*(or* D-*)-Arabinose*						*Methyl* α-L-*(or* D-*)-arabinopyranoside*						
97.8	73.0	73.5	69.6	67.5		105.1	71.8	73.4	69.4	67.3		58.1
(+0.1)	(−0.3)	(−0.7)	(−0.5)	(−8.8)		(+0.2)	(0)	(−0.5)	(−0.4)	(−8.9)		(−0.2)
6-Deoxy-β-D-*galactose*						*Methyl 6-deoxy*-β-D-*galactopyranoside*						
97.3	72.8	74.0	72.5	71.9	16.7	104.8	71.5	74.1	72.4	71.9	16.5	58.3
(−0.4)	(−0.5)	(−0.2)	(+2.4)	(−4.4)	(−45.6)	(−0.1)	(−0.3)	(+0.2)	(+2.6)	(−4.3)	(−45.6)	(0)

Can. J. Chem. Downloaded from www.nrcresearchpress.com by 210.87.254.5 on 09/05/12
For personal use only.

TABLE 6. Assignments of signals in ^{13}c.m.r. spectra of various methyl aldofuranosides. Chemical shifts and the figures in parentheses, which represent the difference of the shift of a given signal from that of the corresponding methyl galactofuranoside are in p.p.m.

Methyl α-D-galactofuranoside							Methyl β-D-galactofuranoside						
C-1	C-2	C-3	C-4	C-5	C-6	OCH_3-1	C-1	C-2	C-3	C-4	C-6	C-6	OCH_3-1
		Methyl α-D-galactofuranoside							*Methyl β-D-galactofuranoside*				
103.1	77.4	75.5	82.3	73.7	63.4	56.1	109.2	81.9	77.8	84.0	72.0	63.9	56.1
		Methyl β-D-arabinofuranoside							*Methyl α-D-arabinofuranoside*				
103.2 (+0.1)	77.5 (+0.1)	75.7 (+0.2)	83.1 (+0.8)	64.2 (−9.5)		56.3 (+0.2)	109.3 (+0.1)	81.9 (0)	77.5 (−0.3)	84.9 (+0.9)	62.4 (−9.6)		56.1 (0)
		Methyl β-D-ribofuranoside							*Methyl α-D-ribofuranoside*				
109.0	75.3	71.9	83.9	63.9		56.3	104.2	72.1	70.8	85.5	62.2		56.5

Can. J. Chem. Downloaded from www.nrcresearchpress.com by 210.87.254.5 on 09/05/12
For personal use only.

CO_2H or CO_2CH_3 derivatives. When the spectra of methyl α-D-glucopyranoside and methyl α-D-xylopyranoside, and α-D-glucose and α-D-xylose are compared, respectively, only the shifts of C-5 signals are markedly different (−11 and −10 p.p.m., respectively).

The displacements of the C-4 and C-5 signals recorded for the methyl β-D-aldopyranosides are similar to those recorded above in the α-series, as are those which are obtained when the spectra of the β-anomers of glucose, 6-deoxyglucose, and xylose are compared (Table 3).

A similar approach can be used for comparison of the chemical shifts of the C-4 and C-5 signals of α- and β-D-mannose with those of α- and β-L-rhamnose on one hand and for those of methyl α-D-mannopyranoside and methyl α-L-rhamnopyranoside on the other (Table 4). Again the C-4 and C-5 signal displacements are +.5 p.p.m. and −4 p.p.m., respectively, without appreciable effects on those of C-1, C-2, and C-3. Since the result of replacing a CH_2OH group with a CH_3 group is the same in the glucopyranose and mannopyranose series, little difference would be expected between these two series when a CH_2OH group is replaced with a CO_2CH_3 group. Such a relationship allows a tentative assignment of signals in the ^{13}c.m.r. spectrum of methyl (methyl α-D-mannopyranosid)-uronate, whose deuterated derivatives would be difficult to prepare. Using the CH_2OH to CO_2Me displacements in the glucopyranose series, which are: C-2 (−0.6), C-3 (−0.5), C-4 (+1.8), and C-5 (−0.8), the nearest fit obtained by comparison of signal displacements of methyl α-D-mannopyranoside and the methyl ester are C-2 (−0.8), C-3 (−0.7), C-4 (+1.2), and C-5 (−0.8) (see Table 4).

Comparisons can be made between the shifts of ^{13}C signals of various sugars conformationally and configurationally related to galactose (Table 5). These are between: (*i*) α-D-galactose and 6-deoxy-α-D-galactose, (*ii*) the corresponding β-derivatives, (*iii*) methyl α-D-galactopyranoside and methyl 6-deoxy-α-D-galactopyranoside, and (*iv*) the corresponding β-derivatives. In each comparison the C-5 and C-4 signals are displaced by ~ −4 p.p.m. and ~ +2.5 p.p.m., respectively. The downfield displacement is less than ~ +6 p.p.m. observed in the glucopyranose series, which contains sugars with equatorial rather than axial OH-4 groups. However, on going from (*i*) α-D-galactose to β-L-arabinose, (*ii*) β-D-galactose to α-L-arabinose, (*iii*) methyl α-D-galactopyranoside to methyl β-L-arabinopyranoside, and (*iv*) methyl β-D-galactopyranoside to methyl α-L-arabinopyranoside, the C-5 signals are displaced by −9 to −10 p.p.m. This is of the same order as is observed when the signals of glucose and xylose, or their corresponding methyl pyranosides are compared.

The signals of ^{13}C spectra of some of the pyranose sugars described above and in a previous study (1) have been assigned previously by other methods. The results obtained by Perlin *et al.* (6), who correlated chemical shifts of ^{13}C nuclei with electron densities based on molecular orbital data, agree in most cases. Assignments of ^{13}C signals of αβ-D-glucose, αβ-D-mannose, β-D-galactose, β-D-allose, αβ-D-xylose, α-arabinose, methyl β-D-galactopyranoside, methyl β-D-glucopyranoside, and methyl αβ-D-xylopyranoside were in agreement. In the cases of α-D-galactose, methyl α-D-glucopyranoside, methyl α-D-galactopyranoside, and methyl α-D-mannopyranoside, some were different. Differences were also observed for the C-2, C-3, and C-4 signals of β-arabinose but since they were resolved by only 0.2 p.p.m. and less, the discrepancy may be due to the use of H_2O as solvent in their study and D_2O in ours. The latter solvent was preferred since it appeared to suppress microbial activity and was suitable for ^{1}H–^{13}C decoupling studies.

Less agreement was attained when the present data were compared with the results of Dorman and Roberts (7), who used a system of empirical constants based on steric or proximity effects to estimate chemical shift differences. Agreement was obtained when the assignments of ^{13}C signals of β-D-glucose, αβ-D-mannose, β-D-galactose, α-D-allose, β-D-xylose, αβ-L-rhamnose, β-fucose, and methyl β-D-glucopyranoside were compared. Their assignments of signals of α-D-glucose, α-D-galactose, αβ-arabinose, β-D-allose, α-D-xylose, α-fucose, and methyl α-D-glucopyranoside differed. The disagreement that exists in the cases of α- and β-arabinose can be explained partly by the differing interpretations of the ^{13}c.m.r. spectrum. Dorman and Roberts (7) reported a signal for each anomer that could not be observed by Perlin *et al.* (6) or in the present study. Their discrepancy is likely due to the slowness of recording the spectra, relative to the speed of mutarotation.

TABLE 7. Differences between the ^{13}C chemical shifts of the anomers of D-glucose, and the respective ones of D-mannose and D-galactose, in p.p.m.

C-1	C-2	C-3	C-4	C-5	C-6
		α-D-*Galactose*			
+0.9	−2.3	−2.8	+0.2	−0.4	+1.2
		α-D-*Mannose*			
+2.3	−0.4	−2.1	−2.4	+1.3	+0.8
		β-D-*Galactose*			
+1.2	−1.5	−2.2	−0.2	−0.3	+0.8
		β-D-*Mannose*			
−1.9	−2.5	−2.3	−2.5	+0.6	+0.6

The signal displacements occurring on changing the nature of the substituent at C-5 are confined to C-4, C-5 (and C-6 in some cases). Thus, these effects are over much shorter range than those observed on going from an equatorial to an axial hydroxyl group, for example, β-D-glucose to β-D-galactose or β-D-glucose to β-D-mannose. As far as these longer range effects are concerned, it is evident that on going from β-D-glucose to β-D-mannose, with an axial OH-2 group, and to β-D-galactose with an axial OH-4 group, there is little correlation between signal displacements of carbons in the corresponding positions relative to the axial OH group (Table 7). It, therefore, does not seem profitable to pursue such an approach in predicting ^{13}C chemical shifts of other sugars containing axial OH groups.

A certain number of methyl furanosides were examined and their ^{13}C c.m.r. spectra rationalized. Not surprisingly, the C-1, C-2, C-3, C-4, and OCH_3 signals of methyl β-D-galactofuranoside correspond in their shifts to those of methyl β-L-arabinofuranoside and those of the corresponding β-hexoside to those of the α-pentoside (Table 6). Evidently the CH_2OH and CHOH—CH_2OH substituents are similar in their shielding or deshielding effects and do not give rise to differences of conformation or populations of given conformations.

A few of the deuterated compounds compiled in Table 1 were prepared by routes that have not been described previously. For example, methyl α-L-rhamnopyranoside was treated with phosgene in pyridine to give the 2,3-cyclic carbonate, which was then oxidized with phosphorus pentaoxide in dimethyl sulfoxide to the 2,3-cyclic carbonate of methyl 6-deoxy-α-L-lyxohexopyranosid-4-ulose. Treatment with sodium borohydride provided a mixture containing methyl α-L-rhamnopyranoside which was identified by its ^{13}C c.m.r. spectrum and a larger proportion of another isomer, which although it was not isolated, is probably methyl 6-deoxy-α-L-talopyranoside. The action of sodium borodeuteride on the ketone provided a mixture of the *4-*^2H derivatives of the methyl 6-deoxy-α-L-hexopyranosides, which was used for assigning the ^{13}C signals of methyl α-L-rhamnopyranoside. The mixture of aldoses prepared on hydrolysis contained αβ-L-rhamnose-*4-*^2H, which aided the assignment of ^{13}C signals of αβ-L-rhamnose.

D-Ribose-*5-*^2H was prepared from 1,2-*O*-isopropylidene-α-D-allofuranose by successive periodate oxidation, sodium borodeuteride reduction and hydrolysis. D-Ribose-*3-*^2H was obtained from 1,2-*O*-isopropylidene-α-D-allofuranose-*3-*^2H in a similar fashion, except that sodium borohydride was used as reducing agent.

Experimental

Carbon-13 magnetic resonance spectra were obtained using a Varian XL-100-15 spectrometer with Fourier transform from D_2O solutions (0.85 ml) of compound (20–100 mg) contained in a coaxial glass cylinder fitting snugly within a 12 mm diameter × 8 in. tube maintained at 33°. Larger amounts of solute were dissolved in D_2O (2 ml) contained in the 12 mm × 8 in. tube similar to that described above, except that it was fitted with a Teflon vortex plug. To obtain a complete ^{13}C c.m.r. spectrum the spectral width was 5000 Hz, the acquisition time 0.4 s, and the pulse width 50 μs. In several experiments it was necessary to improve the resolution and the spectral width was narrowed to 500 Hz, with the acquisition time 4 s and the pulse width 117 μs. Under these conditions the extent of the β-carbon deuterium isotope effect could

Can. J. Chem. Downloaded from www.nrcresearchpress.com by 210.87.254.5 on 09/05/12
For personal use only.

Can. J. Chem. Downloaded from www.nrcresearchpress.com by 210.87.254.5 on 09/05/12
For personal use only.

be measured by examination of a mixture of deuterated and undeuterated material. Frequently signals were superimposed when a 5000 Hz scan was used and those could be resolved by preparation of two or three spectra with a 500 Hz sweep width and suitable offsets. Signals of CH_2 groups were recognized as triplets in partially decoupled spectra. The chemical shifts are expressed as δ_C in p.p.m., relative to external Me_4Si, whose shift relative to D_2O (lock signal) was obtained in a separate experiment.

Some of the undeuterated chemicals used were obtained commercially and they are listed below with suppliers: α-D-xylose (Fisher Scientific Co., Fair Lawn, N.J.), β-L-arabinose (Nutritional Biochemicals Corp., Cleveland, Ohio), α-L-rhamnose (Aldrich Chemical Co., Milwaukee, Wisc.), α-L-fucose, and α- and β-anomers of methyl D-glucopyranoside and methyl D-galactopyranoside, methyl α- and methyl β-D-xylopyranoside (Sigma Chemical Co., St. Louis, Mo.), α-D-glucose-*2*-^2H (Raylo Chemicals Ltd., Edmonton, Alta.), methyl β-L-arabinopyranoside (K & K Labs Inc., Plainview, N.Y.).

Other compounds were prepared according to procedures described in the appended references. These were: methyl α-L-rhamnopyranoside (8), α- and β-anomers of methyl 6-deoxy-L-galactopyranoside (9), methyl α-D-arabinofuranoside (10), methyl β-L-arabinofuranoside (11), methyl α-L-arabinopyranoside (12), methyl β-D-galactofuranoside and its minor α-anomer which are produced simultaneously (13), α- and β-anomers of methyl D-glucopyranosiduronic acid (14), methyl (methyl α-D-mannopyranosid)uronate (15), and methyl 6-deoxy-α-D-glucopyranoside (16).

The above glucopyranosiduronic acid derivatives were converted to their methyl esters by treatment for 3 h with cold 1% methanolic HCl.

Preparation of Deuterated Sugars

αβ-D-*Xylopyranose-5-*^2H, αβ-D-*Xylopyranose-3-*^2H, *and Derived Methyl* αβ-D-*Xylopyranosides*

α-D-Xylose-*5-*^2H was prepared from 1,2-*O*-isopropylidene-α-D-glucofuranose by successive oxidation with sodium periodate, reduction with sodium borodeuteride, and hydrolysis, as outlined by Isbell *et al.* (17) for the preparation of α-D-xylose-*5-*^3H.

α-D-Xylose-*3-*^2H was similarly prepared from 1,2-*O*-isopropylidene-α-D-glucofuranose-*3-*^2H, obtained from partial acid hydrolysis of 1,2:5,6-di-*O*-isopropylidene-α-D-glucofuranose-*3-*^2H (18).

Mutarotation of each of the deuterated xyloses in D_2O gave αβ-D-xylopyranose.

Each of the αβ-mixtures was treated with refluxing 3% methanolic hydrogen chloride to give methyl αβ-D-xylopyranoside.

4-^2H *and 6-*$^2H_2$ *Derivatives of Methyl* αβ-D-*galactofuranoside and Methyl* αβ-D-*Galactopyranoside*

The *4-*^2H and *6-*^2H derivatives of α-D-galactose (1) were dissolved in 0.5% methanolic hydrogen chloride which was left for 15 h at room temperature (19). The product consisted mainly of methyl αβ-D-galactofuranoside according to the ^{13}c.m.r. spectrum. The signals of methyl αβ-D-galactofuranoside were assigned once the signals of methyl αβ-D-galactopyranoside were accounted for.

The above furanosidic mixtures were converted to deuterated methyl αβ-D-galactopyranosides by refluxing in 3% methanolic hydrogen chloride for 3 h.

5-$^2H_2$ *and 4,5-*$^2H_3$ *Derivatives of* αβ-D-*Arabinopyranose, and Corresponding Deuterated Methyl* αβ-D-*Arabinopyranosides and Methyl* αβ-D-*Arabinofuranosides*

β-D-Arabinopyranose-*5-*$^2H_2$ was prepared from α-D-glucose-*6-*$^2H_2$ (1) by the method used by Isbell *et al.* (20) for the preparation of β-D-arabinopyranose-*5-*^{14}C from α-D-glucose-*6-*^{14}C.

α-D-Glucose-*5,6-*$^2H_3$ was prepared by acid hydrolysis of 1,2-*O*-isopropylidene-α-D-glucofuranose-*5,6-*$^2H_3$ (18) and converted to β-D-arabinopyranose-*4,5-*$^2H_3$ by the same procedure.

Mutarotation of each of the arabinoses in D_2O gave the αβ-pyranosidic mixtures.

Treatment of the anomeric mixture with refluxing 3% methanolic hydrogen chloride for 3 h gave a mixture of methyl αβ-D-arabinopyranoside and methyl αβ-D-arabinofuranoside. In a parallel experiment using undeuterated derivatives, the glycosidic mixture gave a ^{13}c.m.r. spectrum with 23 of the possible 24 signals. Even when a spectral width of 500 Hz was used the signal at δ_C 75.7 from methyl α- and methyl β-D-arabinofuranoside could not be resolved.

*6-Deoxy-*αβ-D-*galactose-6-*^2H, *6-Deoxy-*αβ-L-*galactose-4-*^2H, *Derived Methyl 6-Deoxy-*αβ-L-*galactopyranosides, 6-Deoxy-*αβ-L-*glucose-4-*^2H, *and Methyl 6-Deoxy-*αβ-L-*glucopyranoside-4-*^2H

Using a method analogous to that of Schmid and Karrer (21), who reduced 1,2:3,4-di-*O*-isopropylidene-6-*p*-tolylsulfonyl-α-D-galactopyranose with lithium aluminum hydride to give 1,2:3,4-di-*O*-isopropylidene-α-D-fucopyranose, the *6-*^2H derivative was obtained by using lithium aluminum deuteride.

Heyns *et al.* (22), using Pt/H_2 as reagent, reduced methyl 6-deoxy-α-L-xylohexopyranosid-4-ulose to give methyl 6-deoxy-α-L-galactopyranoside exclusively. Using Pt/D_2 we obtained the *4-*^2H derivative, and when sodium borodeuteride in water was used as a reagent, some methyl 6-deoxy-α-L-glucopyranoside-*4-*^2H was formed also, as shown by the ^{13}c.m.r. spectrum.

Hydrolysis of each deuterated glycoside or glycosides with 0.5 *M* H_2SO_4 at 100° for 6 h gave the appropriate reducing sugars. Each deuterated glycoside was equilibrated with refluxing 3% methanolic hydrogen chloride for 3 h to give the αβ-glycosidic mixture.

αβ-D-*Rhamnose-6-*^2H, αβ-L-*Rhamnose-4-*^2H, *Methyl* α-D-*Rhamnopyranoside-6-*^2H, *and Methyl* α-L-*Rhamnopyranoside-4-*^2H

Haskins *et al.* (23) hydrogenated methyl 2,3,4-tri-*O*-benzoyl-6-deoxy-6-iodo-α-D-mannopyranoside to give methyl 2,3,4-tri-*O*-benzoyl-α-D-rhamnopyranoside using Raney nickel in the presence of diethylamine. They proceeded to prepare methyl α-D-rhamnopyranoside and α-D-rhamnopyranose. The compounds were prepared as *6-*^2H derivatives by substituting deuterium for hydrogen in the reduction step.

To methyl α-L-rhamnopyranoside (6.6 g) in pyridine (30 ml), phosgene (1.2 molar-equiv.) in toluene (20 ml) was added with stirring. After 3 h, the solution was evaporated to a sirup, which was partitioned between chloroform and water. The chloroform layer was washed with water

Can. J. Chem. Downloaded from www.nrcresearchpress.com by 210.87.254.5 on 09/05/12
For personal use only.

and evaporated to a sirup which crystallized. Two recrystallizations from ethanol gave the cyclic 2,3-carbonate of methyl α-L-rhamnopyranoside (1.6 g) with m.p. 158–161° and $[\alpha]_D^{25}$ −40° (*c* 0.8, H_2O).

Anal. Calcd. for $C_8H_{12}O_6$: C, 47.06; H, 5.92. Found: C, 47.02; H, 6.01.

The carbonate (0.50 g) was oxidized in dimethyl sulfoxide (4 ml) – phosphorus pentaoxide (0.20 g) and after 3 days excess chloroform was added and the mixture washed three times with ice-cold water. Evaporation gave a sirup (0.36 g) which crystallized and two recrystallizations from diethyl ether – pentane gave the cyclic 2,3-carbonate of methyl 6-deoxy-α-L-lyxo-hexopyranosid-4-ulose (0.17 g) with m.p. 93° and $[\alpha]_D^{25}$ −120° (*c* 0.6, EtOH).

Anal. Calcd. for $C_8H_{10}O_6$: C, 47.53; H, 4.99. Found: C, 47.25; H, 4.94.

The ketone (0.15 g) in water (5 ml) was treated with sodium borohydride (50 mg) for 3 h and the reaction mixture worked up as outlined above to give a mixture of isomeric methyl 6-deoxy-α-L-hexopyranosides.

Anal. Calcd. for $C_7H_{14}O_5$: C, 47.18; H, 7.92. Found: C, 47.15; H, 8.16.

A mixture of *4-²H* derivatives was prepared using sodium borodeuteride in place of the sodium borohydride. ^{13}C spectroscopy showed that the major product was methyl 6-deoxy-α-L-talopyranose-*4-²H* but the much smaller signals of methyl α-L-rhamnopyranose-*4-²H*, which were recognized by comparison with authentic undeuterated material, were sufficient for the necessary spectral determinations to be made. Hydrolysis with 0.5 *M* H_2SO_4 at 100° for 3 h gave a mixture of 6-deoxy-αβ-L-talose-*4-²H* and αβ-L-rhamnose-*4-²H*, whose ^{13}C n.m.r. spectrum was recorded and compared with that of αβ-L-rhamnose.

2-²H and 5-²H Derivatives of Methyl αβ-D-Glucopyranosiduronic Acid and their Methyl Esters

α-D-Glucose-*2-²H* was treated with refluxing 3% methanolic hydrogen chloride for 6 h to give a mixture which was resolved partially by crystallization from EtOH to give methyl α-D-glucopyranoside-*2-²H* and a mother liquor consisting of a mixture of α- and β-glycoside.

Following the use of the α-anomer to distinguish between the C-2 and C-5 signals of its ^{13}C n.m.r. spectrum, it and its αβ counterpart were oxidized separately with platinum (14) to give methyl α-D-glucopyranosiduronic acid-*2-²H* and its αβ-anomer, respectively.

1,2-*O*-Isopropylidene-α-D-glucofuranose-5,6-$^2H_3$ (18) was similarly treated with MeOH–HCl to give methyl α-D-glucopyranoside-*5,6-²H₃* and sirupy methyl αβ-glucopyranoside-*5,6-²H₃*, which were then converted to methyl α-D-glucopyranosiduronic acid-*5-²H* and the mixed isomeric mixture, respectively.

Each of the four deuterated uronic acid fractions was treated at room temperature in 1% methanolic hydrogen chloride to give the methyl ester.

3-²H and 5-²H Derivatives of Methyl αβ-D-Ribofuranoside

To 1,2-*O*-isopropylidene-α-D-allofuranose (24; 0.50 g) in water (20 ml), sodium metaperiodate (0.75 g) was added and after 18 h the solution was deionized with Amberlite IR120 (H^+ form) and Dowex 1 (HCO_3^- form). The filtrate was evaporated to about 10 ml, sodium borohydride added and after 1 h the solution was acidified with acetic acid and decationized with Amberlite IR120 (H^+ form). The suspension was filtered off and the filtrate evaporated to a sirup to which methanol was added and evaporation carried out, the process being repeated five times. The product (0.35 g) was dissolved in water, the p*H* was adjusted to 2 with H_2SO_4, and the solution kept at 100° for 1 h. The hydrolyzate was neutralized ($BaCO_3$), filtered, and evaporated to a sirup which crystallized from EtOH–EtOAc. A further crystallization gave D-ribose with m.p. and mixture m.p. 84°.

Anal. Calcd. for $C_5H_{10}O_5$: C, 40.00; H, 6.71. Found: C, 40.10; H, 6.80.

A parallel experiment was carried out using sodium borodeuteride instead of sodium borohydride in order to prepare D-ribose-*5-²H*.

1,2:3,4-Di-*O*-isopropylidene-α-D-allofuranose-*3-²H* (18) was converted by the method of Collins (24) to give 1,2-*O*-isopropylidine-α-D-allofuranose-*3-²H* which was converted to D-ribose-*3-²H* by the method outlined above.

A mixture of α- and β-anomers of deuterated methyl D-ribofuranosides was obtained by treating the riboses with 0.5% methanolic hydrogen chloride for 10 h (19). The ^{13}C n.m.r. signals of the β-isomer were characterized by comparison with those of an authentic specimen (25).

6-Deoxy-αβ-D-glucose-6-²H and Methyl 6-Deoxy-αβ-D-glucopyranoside-6-²H

Methyl 6-deoxy-α-D-glucopyranoside-*6-²H* was prepared by lithium aluminum deuteride reduction of methyl 6-*O*-*p*-tolylsulfonyl-α-D-glucopyranoside by using the procedure of Timell *et al.* (16) who used lithium aluminum hydride as reagent.

The αβ-glycosidic mixture was prepared from methyl 6-deoxy-α-D-glucopyranoside by treatment with refluxing 3% methanolic hydrogen chloride for 3 h and 6-deoxy-αβ-D-glucose was prepared from the α-glycoside by using 0.5 *M* H_2SO_4 at 100° for 18 h.

1. P. A. J. Gorin. Can. J. Chem. **52**, 458 (1974).
2. H. Spiesecke and W. G. Schneider. J. Chem. Phys. **35**, 731 (1961).
3. F. J. Weigert and J. D. Roberts. J. Am. Chem. Soc. **89**, 2967 (1967).
4. P. A. J. Gorin and M. Mazurek. Carbohyd. Res. **39**, 3 (1975).
5. G. E. Maciel, P. D. Ellis and D. C. Hofer. J. Phys. Chem. **71**, 2160 (1967).
6. A. S. Perlin, B. Casu and H. J. Koch. Can. J. Chem. **48**, 2596 (1970).
7. D. E. Dorman and J. E. Roberts. J. Am. Chem. Soc. **92**, 1355 (1970).
8. E. Fischer. Ber. **28**, 1158 (1895).
9. J. G. Gardiner and E. Percival. J. Chem. Soc. 1414 (1958).
10. R. K. Ness and H. G. Fletcher. J. Am. Chem. Soc. **80**, 2007 (1958).
11. P. A. J. Gorin. Can. J. Chem. **40**, 275 (1962).
12. H. G. Fletcher and C. S. Hudson. J. Am. Chem. Soc. **72**, 4173 (1950).
13. E. Pacsu. Methods Carbohyd. Chem. **2**, 354 (1963).

14. S. A. BARKER, E. J. BOURNE and M. STACEY. Chem. Ind. (London) 970 (1951).
15. H. W. H. SCHMIDT. Tetrahedron Lett. 236 (1967).
16. T. E. TIMELL, W. ENTERMAN, F. SPENCER and E. J. SOLTES. Can. J. Chem. **43**, 2296 (1965).
17. H. S. ISBELL, H. L. FRUSH and J. D. MAYER. J. Res. Natl. Bur. Standards. **64A**, 359 (1960).
18. H. J. KOCH and A. S. PERLIN. Carbohyd. Res. **15**, 403 (1970).
19. P. A. LEVENE, A. L. RAYMOND and R. T. DILLON. J. Biol. Chem. **95**, 699 (1932).
20. H. S. ISBELL, N. B. HOLT and H. L. FRUSH. J. Res. Natl. Bur. Standards **57**, 95 (1956).
21. H. SCHMID and P. KARRER. Helv. Chim. Acta. **32**, 1371 (1949).
22. K. HEYNS, A. L. BARON and H. PAULSEN. Chem. Ber. **97**, 921 (1964).
23. W. T. HASKINS, R. M. HANN and C. S. HUDSON. J. Am. Chem. Soc. **68**, 628 (1946).
24. P. M. COLLINS. Tetrahedron **21**, 1809 (1965).
25. I. AUGESTAD and E. BERNER. Acta. Chem. Scand. **10**, 911 (1956).

Can. J. Chem. Downloaded from www.nrcresearchpress.com by 210.87.254.5 on 09/05/12
For personal use only.

Structure électronique de dérivés sulfures. XI.[1] Thiétanne et dérivés

CLAUDE GUIMON, DANIEL LIOTARD ET GENEVIÈVE PFISTER-GUILLOUZO
Laboratoire de Chimie Structurale – I.U.R.S. – Avenue Philippon – 64016 PAU – France

Reçu le 4 juillet 1974

CLAUDE GUIMON, DANIEL LIOTARD et GENEVIÈVE PFISTER-GUILLOUZO. Can. J. Chem. **53**, 1224 (1975).

Les structures conformationnelles du thiétanne, du thiétanne sulfoxyde et de leurs dérivés mono chlorés en position 3 ont été déterminées théoriquement à l'aide d'un procédé de minimisation de l'énergie par rapport aux facteurs géométriques sur la base de la méthode semi-empirique CNDO/2 étendue à la troisième période.

Les résultats sont en bon accord avec les données expérimentales connues. Les stabilités respectives des différents conformères sont expliquées grâce aux résultats énergétiques partiels obtenus par une partition bicentrique de l'énergie potentielle totale des molécules.

CLAUDE GUIMON, DANIEL LIOTARD, and GENEVIÈVE PFISTER-GUILLOUZO. Can. J. Chem. **53**, 1224 (1975).

The conformations of thietane, thietane sulfoxide, and their 3-chloro derivatives were obtained theoretically by minimization of the energy with respect to geometric parameters using the semi-empirical CNDO/2 method extended to the third period. The results agree well with known experimental data. The respective stabilities of the different conformers are explained by partial energy results obtained by a bicentric partition of the total potential energy of the molecules. [Journal translation]

Durant les dernières années de nombreuses approches théoriques ont été réalisées par différentes méthodes semi-empiriques (Hückel, PPP, EHT, CNDO/2) sur des molécules cycliques comportant un ou plusieurs atomes de soufre. Toutefois, les principaux travaux ont porté sur l'étude de la structure électronique d'hétérocycles conjugués à cinq ou six chaînons en relation avec leur réactivité et leurs propriétés physico-chimiques. A notre connaissance, seuls quelques travaux dispersés ont été effectués sur les cycles saturés présentant un ou plusieurs atomes de soufre. Dans le cadre d'une étude générale sur les problèmes des interactions intramoléculaires consécutives à l'introduction d'un ou de plusieurs atomes de soufre dans un cycle à quatre, cinq ou six chaînons et qui sont à l'origine de la conformation et de la réactivité même de ces composés, nous avons examiné les molécules de thiétanne, de thiétanne sulfoxyde, de chloro-3 thiétanne et de chloro-3 thiétanne sulfoxyde.

Expérimentalement pour ces composés, des études par dipolemétrie et notamment par résonance magnétique nucléaire avaient antérieurement permis de déterminer les conformations privilégiées.

Les calculs ont été effectués à l'aide de la méthode CNDO/2. La paramétrisation adoptée a été présentée antérieurement et appliquée à des sulfures, sulfoxydes et sulfones acycliques (1). Nous rappellerons seulement que les orbitales d ne sont différenciées des orbitales s et p que par le paramètre β^0 intervenant dans l'élément non diagonal de la matrice autocohérente $|\mathbf{F}|$.

On sait que cette méthode sous estime les barrières de rotation et qu'au contraire elle surestime celles d'inversion. Toutefois, ce défaut de la méthode CNDO/2 n'a que peu d'incidence sur les résultats de ce travail à cause des différences énergétiques considérables entre la barrière de torsion du cycle et celle d'inversion du soufre.

Les structures géométriques des différentes molécules et des intermédiaires envisagés lors des processus conformationnels ont été déterminées théoriquement par un procédé de minimisation énergétique (2, 3) utilisant la méthode de plus grande pente (4–7) et mis au point par l'un d'entre nous (D.L.).

Thiétanne

D'après les premiers travaux effectués (8), ce composé semblait présenter une structure plane et appartenir au groupe de symétrie C_{2v}. Ultérieurement plusieurs auteurs ont pu montrer par diverses techniques expérimentales que cette molécule n'était pas plane (symétrie C_S). La bar-

[1]Partie X, à paraître.

Can. J. Chem. Downloaded from www.nrcresearchpress.com by 210.87.254.40 on 09/05/12
For personal use only.

TABLEAU 1. Structures expérimentale (12, 16) et calculées du thiétanne et du chloro-3 thiétanne

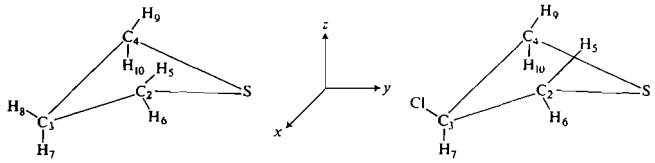

	Chloro-3 thiétanne	Thiétanne		
	Géométrie théorique optimisée	Géométrie expérimentale	Géométrie théorique optimisée	Géométrie théorique de la forme plane
Liaisons (Å)				
S–C_2	1.846	1.833	1.842	1.846
C_2—C_3	1.463	1.54	1.463	1.468
C_2—H_5	1.122	1.09	1.121	1.119
C_2—H_6	1.119	1.09	1.123	1.119
C_3—H_7	1.121	1.09	1.122	1.121
C_3—Cl	1.760			
C_3—H_8		1.09	1.124	1.121
Angles (deg)				
θ*	159.1	148.	150.1	180.
C_2SC_4	66.9	79.	69.	68.7
$C_2C_3C_4$	88.1	98.4	91.	90.3
H_5C_2S	108.9		110.8	109.5
H_6C_2S	108.8		111.1	109.5
H_7C_3X†	129.0		124.9	127.3
ClC_3X†	125.8			
H_8C_3X†			130.4	127.3

NOTE: La numérotation des atomes ainsi que le système d'axe sont identiques pour tous les calculs et tous les composés dérivés du thiétanne.
*θ est l'angle dièdre défini par les plans C_2SC_4 et $C_2C_3C_4$.
†X représente l'axe bissecteur de l'angle $C_2C_3C_4$.

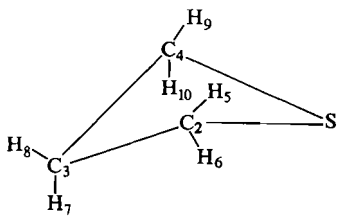

rière d'inversion déterminée par micro-ondes (9, 10) et infrarouge lointain (11) est relativement faible (de l'ordre de 274 cm^{-1}) mais plus élevée cependant que celle du triméthylène oxyde qui n'est que de 35 cm^{-1} (12–14). Ces travaux se sont d'ailleurs trouvés confirmés par ceux de Durig et Lord (15).

Compte tenu de ces données expérimentales, nous avons déterminé la forme énergétiquement favorisée pour ce composé par une optimisation complète des divers facteurs géométriques (14 degrés de liberté). La topologie obtenue est reportée dans le tableau 1. On peut noter l'excellent accord entre la structure théorique et celle observée expérimentalement par micro-ondes. En particulier, l'angle dièdre θ entre les plans C_2SC_4 et $C_2C_3C_4$ est calculé à 150.1° pour 148° expérimentalement. Les écarts observés au niveau de la liaison C—C et des angles C_2SC_4 et $C_2C_3C_4$ sont inhérents à la paramétrisation de la méthode CNDO/2 et notamment à l'évaluation des répulsions entre atomes qui sont sous estimées à courte distance.

L'optimisation d'une structure plane (huit degrés de liberté) nous a permis d'évaluer la barrière d'inversion du cycle à 0.317 kcal/mol (111 cm^{-1}). L'ensemble des données énergétiques est rassemblé dans le tableau 2. Nous avons utilisé

Can. J. Chem. Downloaded from www.nrcresearchpress.com by 210.87.254.40 on 09/05/12
For personal use only.

TABLEAU 2. Différences énergétiques entre les formes plane et non plane du thiétanne (en kcal/mol)

Liaisons	ΔE_l	ΔE_l^T	ΔE_{int}^T	ΔE_{int}^H	ΔE_{at}^T	ΔE_{el}	ΔE_{rep}	ΔE_T
C_2—S	4.099							
C_2—C_3	5.689							
C_2—H_5	0.536							
C_2—H_6	−1.403	12.855	−9.025	0.841	−3.513	125.370	−125.053	0.317
C_3—H_7	−1.906							(111 cm^{-1})
C_3—H_8	−3.081							

NOTE: ΔE_l représente la différence des énergies de liaisons entre les deux formes telles qu'elles ont été définies par Pople (voir texte). Il en est de même pour ΔE_{int} et ΔE_{at}; $\Delta E_l^T = \sum_{liaisons} \Delta E_{liaisons}$; $\Delta E_{int}^T = \sum_{interactions} \Delta E_{interactions}$; $\Delta E_{int}^H = \sum_{interactions}^{hydrogènes} \Delta E_{interaction\ entre\ hydrogènes}$ $\Delta E_{at}^T = \sum_{atomes} \Delta E_{at}$; ΔE_{el} et ΔE_{rep} sont respectivement les différences entre les énergies électroniques et de répulsions des coeurs des deux formes du thiétanne; ΔE_T est l'écart entre l'énergie totale de la forme plane et celle de la forme non plane. Elle représente donc la barrière d'inversion.

la partition bicentrique de l'énergie totale proposée initialement par Pople et Segal (17) et reprise par Gordon (18)

$$E_T = \sum_{A}^{atomes} E_A + \sum_{B>A}^{liaisons} E_{A-B} + \sum_{B>A}^{interactions} E_{A-B}$$

Cette partition est commode car elle rationalise certains concepts chimiques comme les énergies de liaison ou les interactions entre atomes non liés. De plus, ainsi que l'ont remarqué Fischer et Kollmar (19), elle présente l'avantage de répondre à trois critères: la transférabilité, la monotonie et l'importance relativement faible des termes associés aux atomes non liés.

Globalement, si l'énergie totale de répulsion pour la forme plane est bien plus faible que celle de la forme non plane, cet écart est largement compensé par la stabilisation de l'énergie électronique. Rappelons que l'énergie totale est égale à la somme de ces deux énergies qui sont de signes opposés:

$$\Delta E_T = E_{el}(\text{plan}) + E_{rep}(\text{plan}) - |E_{el}(\text{non plan}) + E_{rep}(\text{non plan})| = \Delta E_{el} + \Delta E_{rep}$$

L'analyse des termes E_A et E_{A-B} montre que la stabilité de la forme non plane est due, en partie et comme on pouvait s'y attendre, à une répulsion entre les groupements méthylène plus faible en position "pseudo-staggered" qu'en position "eclipsed," mais surtout à la stabilisation énergétique des liaisons du cycle C—S et C—C et dans une moindre mesure à celle des deux liaisons C_2—H_5 et C_4—H_9.

La matrice densité au premier ordre (tableau 3) montre la faible participation des orbitales de polarisation du soufre au niveau des charges électroniques, ce qui avait été remarqué dans des études antérieures (1) pour des atomes de soufre liés à des atomes de carbone ou d'hydrogène. L'introduction de ces orbitales de polarisation permet néanmoins de traduire correctement le moment dipolaire puisque l'écart entre la valeur théorique et la valeur expérimentale est de l'ordre de 0.1 D.

Chloro-3 thiétanne

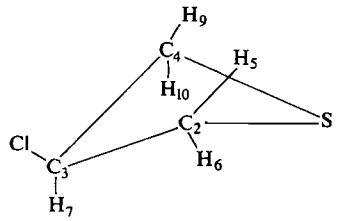

La plupart des travaux effectués sur la molécule de thiétanne substituée en 3 ont été réalisés à l'aide de la résonance magnétique nucléaire du proton (22, 23).

Wucherpfennig (22) détermine les déplacements chimiques et les constantes de couplage du thiétanne disubstitué en 3 d'une part par deux groupements méthyle et d'autre part par un groupement méthyle et un groupement hydroxyle. Il conclut dans ce dernier cas que le groupement hydroxyle se trouve en position pseudo-équatoriale. Cette même conformation est proposée pour le chloro-3 thiétanne par Keller *et al.* (23) qui ont analysé la totalité du spectre r.m.n. à l'aide des programmes NMREN et NMRIT. Cette même conformation a également été mise en évidence à partir des données de la dipolemétrie (24).

Ainsi que nous l'avions fait pour le thiétanne nous avons optimisé la structure géométrique du chloro-3 thiétanne, et dans un deuxième temps

Can. J. Chem. Downloaded from www.nrcresearchpress.com by 210.87.254.40 on 09/05/12
For personal use only.

TABLEAU 3. Répartition électronique et moment dipolaire du thiétanne

Orbitales	Soufre	C_2	C_3	H_5	H_6	H_7	H_8
$s + p_\sigma$	3.994	2.951	3.008	0.993	1.012	1.000	1.016
p_π	1.978	0.982	0.966				
d_σ	0.126						
d_π	0.037						
Charges totales	6.135	3.933	3.974	0.993	1.012	1.000	1.016
μ_{calc} (D)	1.69						
μ_{exp} (D)	1.78*	1.85†					

*Moment dipolaire déterminé en solution benzénique (20).
†Moment dipolaire déterminé en phase vapeur (21).

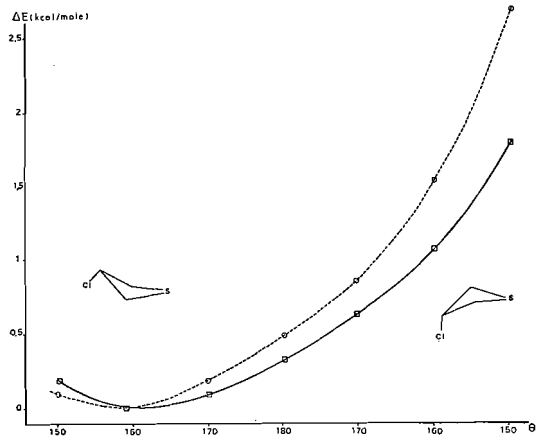

FIG. 1. Energie potentielle totale du chloro-3-thiétanne lors de l'inversion du cycle, à l'état gazeux (trait plein) et solvaté (pointillés).[2]

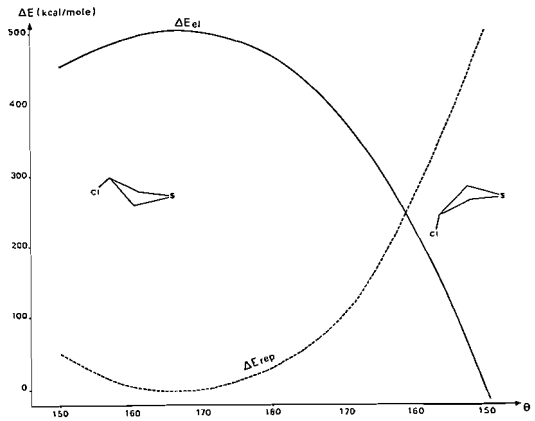

FIG. 2. Energies électronique ΔE_{el} et de répulsion ΔE_{rep} du chloro-3-thiétanne lors de l'inversion du cycle.[2]

les structures de cette molécule en fixant certaines valeurs à l'angle dièdre θ défini par les plans C_2SC_4 et $C_2C_3C_4$. La figure 1 donne les variations de l'énergie potentielle totale du chloro-3 thiétanne en fonction de cet angle θ à l'état gazeux et en solution.

L'énergie de solvatation est calculée selon la formulation proposée par Jano (25) d'après le modèle de Born (26)

$$E_{solv} = -\left(1 - \frac{1}{D_S}\right)\left|\frac{1}{2}\sum_A Q_A{}^2\gamma_{AA} + \sum_{A\neq B}\sum Q_A Q_B \gamma_{AB}\right|$$

Cette relation fait intervenir, outre la constante diélectrique du solvant D_S,[3] la répartition des charges électroniques (Q_A étant la charge nette de l'atome A) et la structure géométrique de la molécule (par les intégrales coulombiennes mono et bi-électroniques γ_{AA} et γ_{AB}).

Comme le suggéraient les données expérimentales, nous observons un seul puit de potentiel pour un angle θ égal à 159.1°, le chlore se plaçant en position pseudo-équatoriale (tableau 1). On peut noter que contrairement aux autres paramètres géométriques qui sont similaires, l'angle dièdre du cycle est nettement plus ouvert que pour le thiétanne non substitué (pour lequel il était à 150.1°). Cette valeur paraît logique si l'on considère l'interaction du chlore avec notamment les carbones des groupements méthylène voisins nettement plus élevée que celle produite par un atome d'hydrogène. Le fait qu'on ne puisse observer de composé à structure pseudo-axiale semble lié à de fortes répulsions entre

[2]L'origine des énergies est prise au point le plus bas des courbes.

[3]Dans tous nos calculs nous avons pris le cas limite: $1 - 1/D_S = 1$ c'est-à-dire $D_S = \infty$.

Can. J. Chem. Downloaded from www.nrcresearchpress.com by 210.87.254.40 on 09/05/12
For personal use only.

Can. J. Chem. Downloaded from www.nrcresearchpress.com by 210.87.254.40 on 09/05/12
For personal use only.

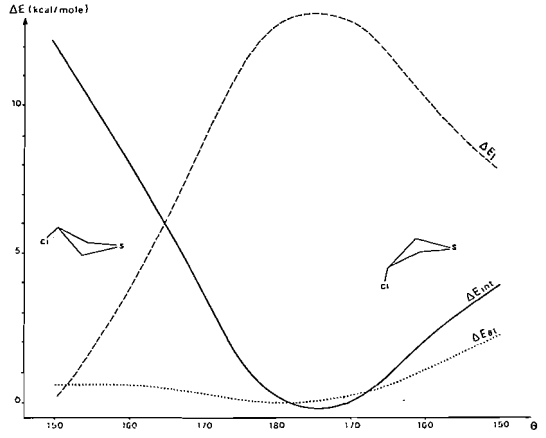

FIG. 3. Energies globales atomique ΔE_{at}, de liaisons ΔE_l et d'interactions entre atomes non liés chimiquement ΔE_{int} lors de l'inversion du cycle du chloro-3-thiétanne.[2]

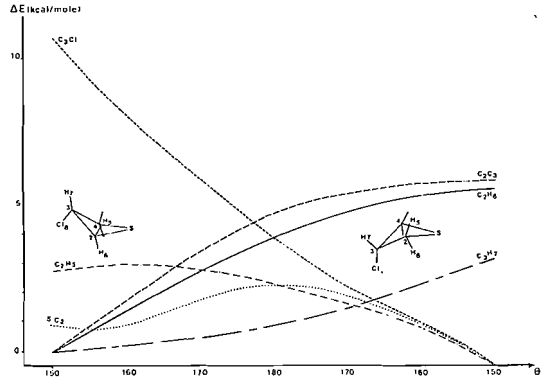

FIG. 4. Energies des liaisons du chloro-3-thiétanne lors de l'inversion du cycle.[2]

atomes (fig. 2) bien qu'on remarque la tendance de l'énergie électronique à stabiliser cette forme.

Les données énergétiques correspondant à la partition bicentrique de l'énergie totale définie précédemment sont reportées dans fig. 3. La courbe représentant les variations globales des énergies de liaison ΔE_l a un maximum pour $\theta \sim 175°$ (forme p-axiale). Les variations de l'énergie associée aux interactions entre atomes non liés chimiquement ΔE_{int} et celles de l'énergie associée aux atomes eux-mêmes ΔE_{at} possèdent un minimum également aux alentours de 175° (forme p-axiale).

Ainsi les énergies de liaisons semblent être à l'origine de la stabilisation d'un conformère par rapport à l'autre. En effet, si l'on examine fig. 4, on note que les liaisons C_2—C_3, C_2—H_6 et

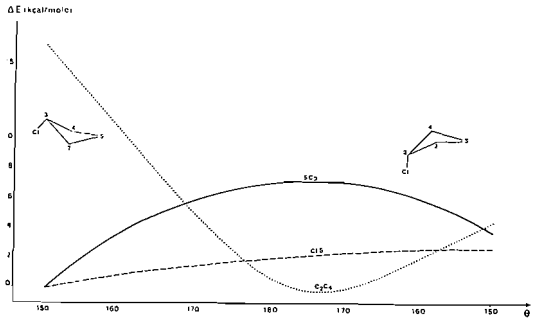

FIG. 5. Energies des principales interactions entre atomes non liés chimiquement du chloro-3-thiétanne lors de l'inversion du cycle.[2]

C_3—H_7 sont énergétiquement beaucoup plus liantes dans le dérivé p-équatorial que dans le présumé conformère p-axial alors que les liaisons C_3—Cl et C_2—H_5 sont dans une moindre mesure plus liantes pour la forme p-axiale.

Au contraire comme on peut le voir sur fig. 5, si les interactions entre les atomes de carbone C_3 et de soufre ainsi que celles entre le soufre et le chlore sont attractives dans le dérivé équatorial, ceci est fortement compensé par une diminution notable de l'interaction attractive pour ce composé entre les carbones C_2 et C_4.

La matrice densité au premier ordre (tableau 4) pour la forme privilégiée montre les mêmes caractéristiques générales que pour le thiétanne, c'est-à-dire une légère charge nette négative sur l'atome de soufre et au contraire une charge nette positive pour les autres atomes à l'exception des hydrogènes H_5. Les densités électroniques des orbitales de polarisation sont faibles: 0.147 *e* pour le soufre et 0.064 *e* pour le chlore. Le moment dipolaire calculé à 0.91 D traduit correctement la valeur expérimentale de 1.01 D (24).

Thiétanne sulfoxyde

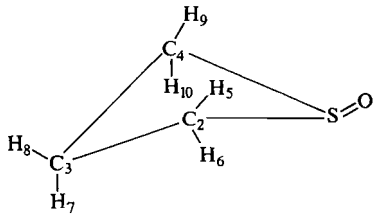

A l'encontre du thiétanne, le thiétanne sulfoxyde n'a été étudié expérimentalement qu'au travers de ses dérivés substitués. La plupart des travaux effectués ont porté sur des cycles mono-

TABLEAU 4. Répartition électronique et moment dipolaire du chloro-3-thiétanne

	S*	C_2	C_3	Cl*	H_5	H_6	H_7
Charges totales	6.146	3.929	3.896	7.176	1.000	0.971	0.983
μ_{calc} (D)	0.91						
μ_{exp} (D)	1.01 (24)						

*La charge électronique localisée sur les orbitales d du soufre est de 0.147 *e* alors que celle localisée sur les orbitales d du chlore est de 0.064 *e*.

substitués en position 3 ou disubstitués en 2,4. Il était donc intéressant de rechercher la conformation théorique du dérivé non substitué et les causes principales de sa stabilité avant d'étudier le composé substitué lui-même.

La préférence de l'atome d'oxygène pour la position axiale est bien connue dans le cas des cycles à six chaînons (27–29). Cette préférence, confirmée théoriquement par la méthode Westheimer (30), est remise en question pour les cycles de plus faibles dimensions et en particulier pour le thiétanne sulfoxyde. Wucherpfennig (22) a étudié en résonance magnétique nucléaire du proton les thiétanne, thiétanne sulfoxyde et sulfone disubstitués en position 3 par deux groupements méthyles. Des déplacements chimiques et des constantes de couplage obtenus, il déduit, à l'encontre des cycles à six chaînons, la plus grande stabilité du conformère ayant l'oxygène en position pseudo-équatoriale. On peut donc raisonnablement supposer qu'il en est de même pour le dérivé non substitué.

Comme pour son homologue non oxydé, nous avons effectué une optimisation géométrique des deux conformères possibles. De plus, nous avons calculé d'une part la barrière d'inversion du cycle ΔH_C et d'autre part la barrière d'inversion du soufre ΔH_S.

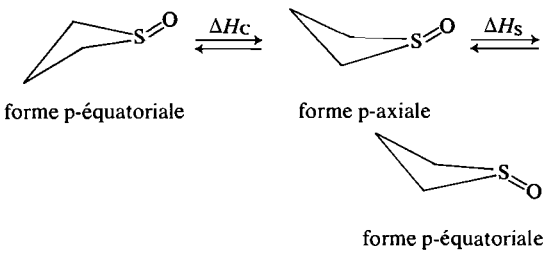

Dans le tableau 5 sont reportées les structures minimisées des deux conformères p-équatorial et p-axial. Ces structures sont très proches l'une de l'autre puisque sur les longueurs de liaison, l'écart se situe sur la troisième décimale (l'unité étant l'Angström) et que le plus grand écart sur les angles du cycle est de 1° (pour l'angle $C_2C_3C_4$). L'angle dièdre est légèrement plus ouvert dans le cas du conformère p-axial (163.2° contre 158.7°), ce qui semble logique de part l'interaction plus importante dans ce cas entre l'oxygène et les atomes C_3 et H_8. En comparant ces résultats avec les données expérimentales obtenues pour le carboxy-3 thiétanne sulfoxyde (31), il est à noter que si la longueur de la liaison C—S est proche de celle observée expérimentalement, il n'en est pas de même pour les liaisons C—C et surtout S—O. Comme nous l'avions signalé, ces différences par rapport aux valeurs expérimentales sont liées à la méthode, mais seule une optimisation de tous les paramètres géométriques rend fiable les comparaisons énergétiques entre deux conformères. Remarquons d'ailleurs que des études antérieures (18) avaient mis en évidence une meilleure traduction des barrières expérimentales par optimisation des géométries bien que celles-ci soient notablement différentes des valeurs réelles.

Pour évaluer les deux barrières d'inversion ΔH_C et ΔH_S, nous avons choisi des modèles intermédiaires entre les deux formes stables p-équatoriale et p-axiale et nous avons optimisé leur géométrie en gardant constant l'angle dièdre du cycle pour ΔH_C et l'angle XSO pour ΔH_S. Ce mode de calcul ne donne pas en réalité le "vrai chemin" conduisant d'une forme à l'autre, c'est-à-dire la vallée de l'hypersurface énergétique menant du puit de potentiel représentant le conformère p-équatorial à celui associé au conformère p-axial. Il donne un chemin légèrement différent mais qui passe par le même "col." La barrière d'inversion calculée sera donc exacte puisqu'elle est égale à la différence "d'altitude" entre le point le plus bas de l'hypersurface (puit de potentiel le plus profond) et le "col" unique situé entre les deux points.

Can. J. Chem. Downloaded from www.nrcresearchpress.com by 210.87.254.40 on 09/05/12
For personal use only.

TABLEAU 5. Structures optimisées du thiétanne sulfoxyde (formes pseudo-équatoriale et pseudo-axiale) et des quatre conformères du chloro-3 thiétanne sulfoxyde

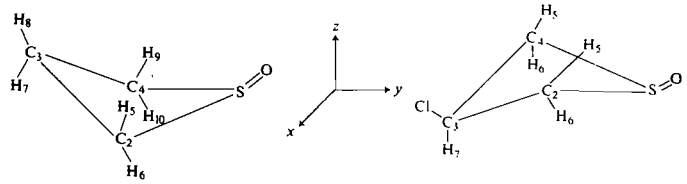

	Thiétanne sulfoxyde		Chloro-3 thiétanne sulfoxyde			
	Forme p-équatoriale	Forme p-axiale	I	II	III	IV
Liaisons (Å)						
S—O	1.663	1.663	1.662	1.658	1.661	1.660
S–C_2	1.843	1.843	1.854	1.841	1.851	1.846
C_2—C_3	1.465	1.468	1.464	1.460	1.463	1.465
C_2—H_5	1.120	1.121	1.123	1.120	1.124	1.116
C_2—H_6	1.211	1.119	1.117	1.123	1.117	1.121
C_3—H_7	1.123	1.123	1.119	1.122	1.120	1.122
C_3—H_8	1.119	1.120				
C_3—Cl			1.758	1.754	1.759	1.755
Angles (deg)						
θ*	158.7	163.2	157.2	159.2	157.9	160.3
C_2SC_4	67.8	67.4	65.6	65.7	66.4	67.4
$C_2C_3C_4$	89.2	88.2	86.6	86.4	87.6	88.8
OSY†	115.7	115.1	119.7	119.6	118.9	120.2
H_5C_2S	109.2	109.6	108.2	109.0	108.4	109.2
H_6C_2S	110.2	109.2	107.7	108.8	108.4	109.0
H_7C_3X‡	125.8	127.8	128.7	129.1	128.8	129.6
H_8C_3X‡	128.7	126.0				
ClC_3X‡			125.0	125.7	125.3	126.3

*θ est l'angle dièdre défini par l'intersection des plans C_2SC_4 et $C_2C_3C_4$.
†Y est l'axe bissecteur de l'angle C_2SC_4.
‡X est l'axe bissecteur de l'angle $C_2C_3C_4$.

Ainsi que le montre fig. 6, les deux conformères ont des énergies potentielles très voisines, la forme équatoriale étant très légèrement plus stable à l'état gazeux. L'énergie de solvatation montre une stabilisation de la forme p-équatoriale en solution. Il est d'ailleurs plus logique de comparer aux données expérimentales les résultats calculés compte tenu de cette énergie de solvatation, les diverses études par dipole métrie ou par r.m.n. ayant été effectuées sur le thiétanne sulfoxyde en solution. Les barrières d'inversion du cycle calculées pour la molécule isolée et solvatée sont néanmoins très proches puisque respectivement égales à 0.36 et 0.39 kcal/mol, différence peu significative. Cette valeur est d'ailleurs du même ordre que celle obtenue pour la molécule de thiétanne (0.32 kcal/mol).

La barrière d'inversion du soufre (fig. 7) par contre est beaucoup plus importante puisque calculée à 47 kcal/mol pour la molécule isolée, elle est de 58 kcal/mol pour le composé solvaté. Le passage d'un conformère à l'autre ne peut donc se faire que par l'inversion du cycle. Comme pour le thiétanne et son homologue substitué, la barrière d'inversion du cycle provient d'une déstabilisation électronique: la courbe ΔE_{el} représentant les différences d'énergie électronique entre les formes intermédiaires lors de l'inversion du cycle présente un maximum pour un angle dièdre θ avoisinant 170° (côté forme p-équatoriale) alors que la grandeur ΔE_{rep} représentant les écarts d'énergie de répulsion entre les coeurs en fonction de l'angle θ, croit lorsque θ diminue et a son minimum pour un angle θ proche de 170° également. Rappelons que ΔE_T (fig. 6) est la somme des termes ΔE_{el} et ΔE_{rep}. Nous n'avons pas rapporté les courbes ΔE_{el} et ΔE_{rep} correspondant à ce composé car elles sont exactement similaires

Can. J. Chem. Downloaded from www.nrcresearchpress.com by 210.87.254.40 on 09/05/12
For personal use only.

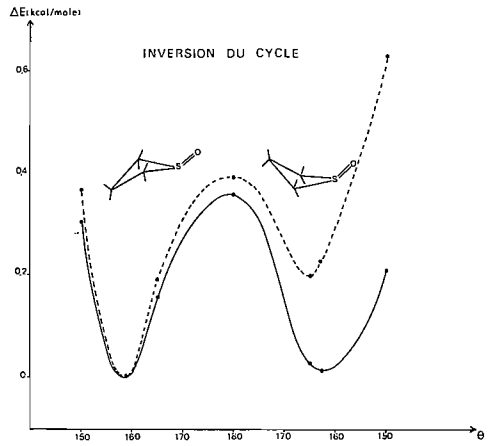

FIG. 6. Energie potentielle totale du thiétanne sulfoxyde lors de l'inversion du cycle à l'état gazeux (trait plein) et à l'état solvaté (pointillés).[2]

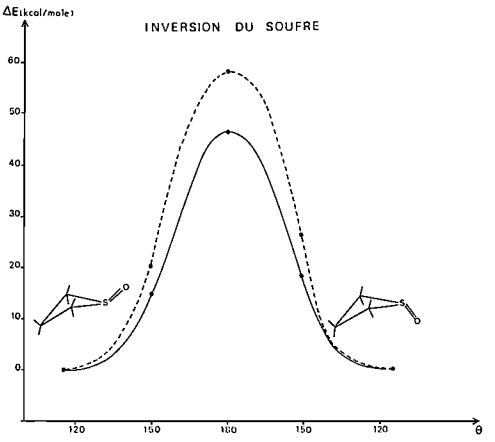

FIG. 7. Energie potentielle totale du thiétanne sulfoxyde lors de l'inversion du groupement sulfoxyde, à l'état gazeux (trait plein) et solvaté (pointillés).[2]

à celles du chloro-3 thiétanne (fig. 2). Il en est de même des variations globales des énergies associées aux atomes, des énergies associées aux liaisons chimiques et de celles associées aux interactions entre atomes non liés chimiquement (fig. 3). On remarque ici aussi que l'allure de la courbe représentant les variations $\Delta E_{\text{liaisons}}$ en fonction de θ est la même que celle représentant ΔE_{el} alors que les courbes ΔE_{at} et $\Delta E_{\text{interactions}}$ sont de même type que ΔE_{rep}, l'ordre de grandeur des variations étant cependant très différent (allant du facteur 1 à 20).

La barrière d'inversion paraît donc liée à l'affaiblissement de certaines liaisons. C'est le cas en particulier pour les liaisons S—O, S—C_2 et C_2—C_3, c'est-à-dire les liaisons formant le cycle (fig. 8), les variations énergétiques des liaisons C_2—H_5 et C_2—H_6 étant en partie compensées par celles en sens contraire de C_3—H_7 et C_3—H_8.

Par contre la destabilisation de la molécule lors de la fermeture de l'angle dièdre θ suit ΔE_{at} et surtout $\Delta E_{\text{interactions}}$.

ΔE_{at} est pratiquement défini par les variations d'énergie de l'atome de soufre (fig. 9), l'ordre de grandeur des autres énergies atomiques étant bien plus faible et celles-ci se compensant les unes les autres.

Enfin $\Delta E_{\text{interactions}}$ est dirigé surtout par l'interaction entre les atomes C_2 et C_4, l'interaction entre les atomes S et C_3 allant en sens

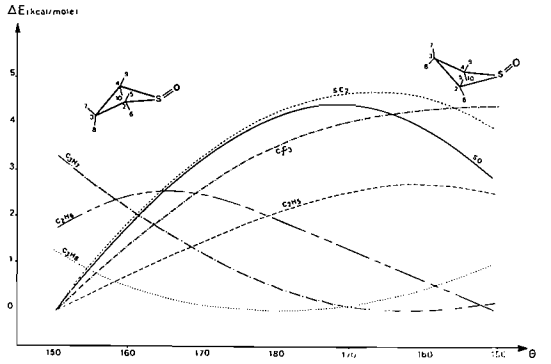

FIG. 8. Energies des liaisons du thiétanne sulfoxyde lors de l'inversion du cycle.[2]

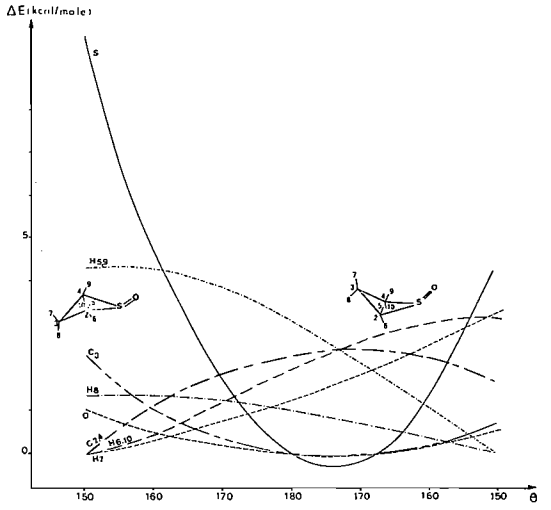

FIG. 9. Energies des atomes du thiétanne sulfoxyde lors de l'inversion du cycle.[2]

Can. J. Chem. Downloaded from www.nrcresearchpress.com by 210.87.254.40 on 09/05/12
For personal use only.

TABLEAU 6. Répartition électronique et moment dipolaire du thiétanne sulfoxyde

	Forme p-équatoriale	Forme cycle plan	Forme p-axiale	Forme S—O dans le plan C_2SC_4
S $\begin{cases} s + p \\ d \end{cases}$	$\begin{matrix} 5.411 \\ 0.455 \end{matrix}\Big\}$ 5.866	$\begin{matrix} 5.431 \\ 0.448 \end{matrix}\Big\}$ 5.879	$\begin{matrix} 5.426 \\ 0.452 \end{matrix}\Big\}$ 5.878	$\begin{matrix} 5.490 \\ 0.452 \end{matrix}\Big\}$ 5.942
O	6.316	6.315	6.313	6.233
C_2	3.955	3.949	3.949	3.951
C_3	3.983	3.989	3.987	3.988
H_5	0.964	0.972	0.982	0.978
H_6	1.000	0.990	0.984	0.991
H_7	1.001	0.995	0.989	1.004
H_8	0.997	1.000	1.003	0.992
μ_T*(D)	4.37	4.51	4.59	4.51

*Le moment dipolaire expérimental du diméthyl-3,3′-thiétanne sulfoxyde est égal à 4.03 D (22).

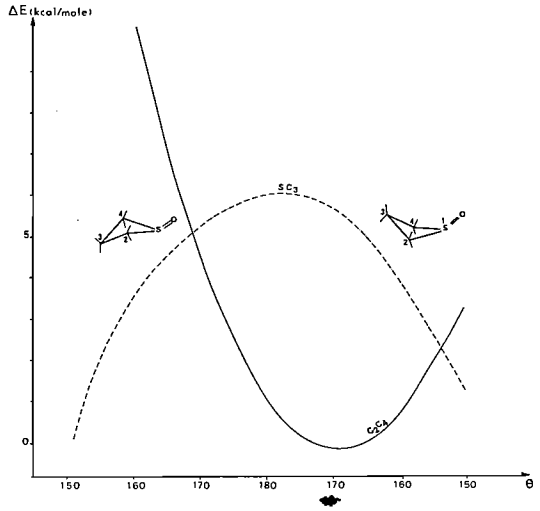

FIG. 10. Energies des principales interactions entre atomes non liés chimiquement du thiétanne sulfoxyde lors de l'inversion du cycle.[2]

contraire, c'est-à-dire vers une déstabilisation de la forme plane (fig. 10). Les interactions entre les autres atomes et en particulier entre les hydrogènes subissent des variations plus faibles. Il en est de même des interactions liantes entre l'atome d'oxygène et les atomes d'hydrogène. L'interaction O–H_5 est plus liante (0.497 kcal/mol) dans le cas du conformère p-équatorial que dans celui du conformère p-axial mais le résultat est inversé pour l'interaction O–H_6 (plus stable de 0.528 kcal/mol dans la forme p-axiale). Enfin les variations des interactions O–H_7 et O–H_8 sont beaucoup plus faibles et assez peu significatives.

En résumé, la déstabilisation du thiétanne sulfoxyde que l'on remarque lors d'une trop grande fermeture de l'angle dièdre θ s'explique par la déstabilisation de l'atome de soufre et par l'augmentation de la répulsion entre les atomes C_2 et C_4. La barrière d'inversion s'explique par l'affaiblissement de l'énergie de la liaison S—O et des énergies de liaison du cycle lorsque celui-ci tend vers une structure plane.

La matrice densité au premier ordre des deux conformères stables et de la forme intermédiaire où le cycle est plan (tableau 6) montre tout d'abord une population notable sur les orbitales d du soufre (0.45 *e*). Cette population s'affaiblit légèrement pour la forme plane du cycle alors qu'au contraire les orbitales 3s et 3p sont un peu plus chargées (notamment les orbitales de type σ). Il faut remarquer cependant que les variations de charge observées pour ces trois formes sont faibles au niveau des atomes lourds et plus sensibles pour les hydrogènes. On note en effet une nette évolution de la charge nette positive des hydrogènes en α et β du groupement sulfoxyde selon l'orientation de ce groupement. Pour le conformère p-équatorial, seul l'hydrogène H_5 a une forte charge nette positive alors que dans le conformère p-axial les deux hydrogènes en α et β en vis à vis de l'oxygène sont fortement positifs. Le moment dipolaire calculé est plus satisfaisant dans le cas de la forme p-équatoriale (4.37 D) pour une valeur expérimentale du diméthyl-3,3′ thiétanne sulfoxyde aux environs de 4 D que dans celui de la forme p-axiale (4.59 D), ce qui est cohérent avec la plus grande stabilité supposée de cette première forme en solution. Enfin pour la forme intermédiaire lors de l'inversion du soufre, on peut noter un net affaiblissement de la polarité de la liaison S—O, due pour la plus grande partie à une densité électronique plus faible sur l'orbitale p_y (p_σ) de l'oxygène. Ceci entraine

Can. J. Chem. Downloaded from www.nrcresearchpress.com by 210.87.254.40 on 09/05/12
For personal use only.

TABLEAU 7. Energies totales et partielles des quatre conformères du chloro-3-thiétanne sulfoxyde

	I	II	III	IV
Energie totale (ua)*	−70.38271	−70.38123	−70.38238	−70.37741
Energie totale + energie de solvatation (ua)	−70.42241	−70.42028	−70.42191	−70.41417
Energie électronique (ua)	−195.15741	−195.39252	−194.98874	−196.63764
Energie de répulsion (ua)	124.77470	125.01129	124.60636	126.26023

*1 ua = 627.272 kcal/mol.

d'ailleurs un affaiblissement notable de l'énergie de cette liaison qui est à l'origine de la forte barrière observée.

Chloro-3 thiétanne sulfoxyde

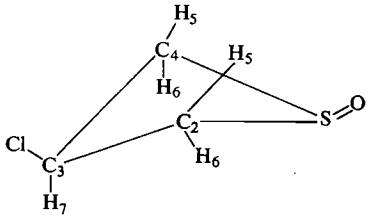

Le chloro-3 thiétanne sulfoxyde peut présenter quatre conformations différentes. Le passage des unes aux autres se fait par l'inversion du cycle (**I** à **II** et **III** à **IV**), ou inversion du soufre (**I** à **III** et **II** à **IV**).

Dans le cas du thiétanne sulfoxyde non substitué nous avions évalué théoriquement la barrière d'inversion du cycle à 0.4 kcal et celle du soufre supérieure à 50 kcal. En supposant que la substitution d'un atome d'hydrogène par un chlore ne modifie pas ou que faiblement l'ordre de grandeur de ces barrières d'inversion, on devrait donc observer dans des conditions normales de température deux formes en équilibre, une *trans* (**I** ou **II**), l'autre *cis* (**III** ou **IV**).

Les études expérimentales effectuées en résonance magnétique nucléaire du proton sur divers dérivés du thiétanne sulfoxyde en position 3 (32–34) confirment cet équilibre. Mais alors que Allenmark (31) met en évidence par rayons X une forme *trans* pour le carboxy-3 thiétanne sulfoxyde et que Arbuzov *et al.* (24) par dipolemétrie conclut à la prédominance de cette même forme pour le chloro-3 thiétanne sulfoxyde, Johnson et Siegl (32, 33), par l'analyse des spectres r.m.n., et après une séparation par chromatographie, mettent en évidence une stabilité supérieure de la forme *cis* pour les dérivés substitués en 3 par un groupement *p*-chlorophényl.

Comme précédemment, nous avons effectué une optimisation complète des structures géométriques des quatre conformères possibles de façon à comparer leur énergie respective. Les résultats de ces calculs sont reportés dans le tableau 3. Il est à noter que l'angle dièdre θ du cycle est voisin de celui calculé pour la chloro-3 thiétanne et qu'il varie relativement peu entre les quatre formes puisqu'il est de 157.2° pour le conformère *trans* avec le chlore en position équatoriale et de 160.3° pour le conformère *cis* diaxial. Cette valeur de 157.2° se rapproche de celle déduite par Arbuzov par dipolemétrie qui

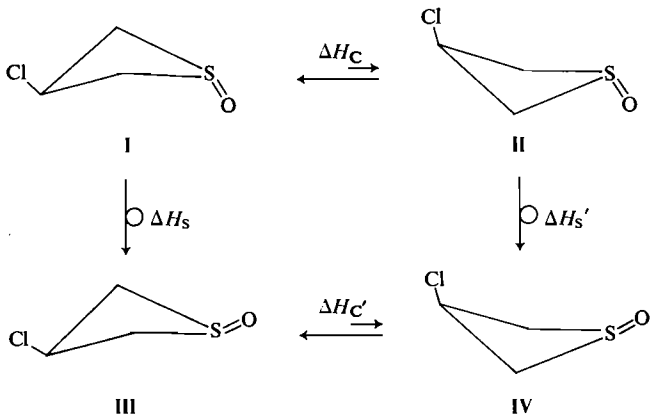

Can. J. Chem. Downloaded from www.nrcresearchpress.com by 210.87.254.40 on 09/05/12
For personal use only.

TABLEAU 8. Interactions globales et interactions principales entre les atomes de la molécule du chloro-3-thiétanne sulfoxyde dans ses quatre formes possibles (en kcal/mol)

	Energie totale d'interactions	C_2–C_4	S–C_3	S–Cl	O–C_3	O–Cl
I	−107.008	−125.399	−8.205	−4.737	−2.956	3.109
II	−106.109	−126.949	−6.305	−2.487	−2.972	2.833
III	−95.823	−115.416	−8.226	−4.760	−3.013	3.171
IV	−84.224	−102.976	−7.626	−2.594	−3.074	3.463

l'estime à 155.5°. L'introduction d'une liaison polaire sur le cycle thiétanne (S=O ou C—Cl) entraine donc un aplatissement du cycle puisque le thiétanne avait un angle dièdre voisin de 150° alors que les thiétanne sulfoxyde, le chloro-3 thiétanne et le chloro-3 thiétanne sulfoxyde ont un angle dièdre approchant 160°. Par rapport au dérivé non substitué, la différence la plus sensible se situe au niveau de l'angle OSY puisque l'écart avoisine 4°. L'atome d'oxygène se trouve donc un peu plus éloigné du cycle que dans le thiétanne sulfoxyde, ce qui réduit en particulier les interactions entre cet atome et les atomes de carbone C_3 et de chlore.

Les résultats énergétiques globaux (tableau 7) sont en excellent accord avec les données expérimentales. En effet, dans le cas des deux conformères *trans*, la forme la plus stable est celle ayant l'atome d'oxygène en position axiale et l'atome de chlore en position équatoriale. La différence d'énergie entre les deux formes *trans* est de 0.931 kcal/mol en phase gazeuse et de 1.339 kcal/mol à l'état solvaté. Une minimisation énergétique d'une forme intermédiaire (cycle plan) lors de l'inversion du cycle permet d'évaluer la barrière d'inversion entre les deux conformères *trans* à environ 2 kcal/mol, c'est-à-dire une valeur nettement plus élevée que celle du thiétanne (0.32 kcal/mol) et du thiétanne sulfoxyde (0.36 kcal). L'écart énergétique entre les deux formes *cis* est nettement plus élevé, la forme diaxiale étant de loin la moins stable (3.116 kcal/mol en phase vapeur et 4.856 kcal/mol en solution). Par contre, les deux formes énergétiquement les plus stables ont des énergies potentielles voisines, la plus stable étant la forme *trans* (de 0.208 kcal/mol à l'état gazeux et 0.316 kcal/mol à l'état solvaté) ce qui est en accord avec les conclusions d'Arbuzov *et al.* (24) et d'Allenmark (31).

Si l'on examine le tableau 7 on remarque que globalement la stabilité des formes où le chlore est en position équatoriale a son origine dans l'affaiblissement des énergies de répulsions. C'est également ce que nous avions observé pour le chloro-thiétanne et le thiétanne sulfoxyde, le détail des calculs ayant toutefois montré que les répulsions entre atomes liés jouaient un rôle prédominant (les énergies totales des liaisons étant essentiellement à l'origine de la préférence équatoriale tant du chlore que du groupement sulfoxyde).

Par contre lors de la présence de deux groupements polaires (entre **I** et **III**) les interactions entre atomes non liés jouent un rôle prédominant. Ainsi comme on peut le voir par exemple dans le tableau 8, les facteurs qui favorisent la position équatoriale du chlore entre les composés **I** et **II** sont essentiellement les interactions entre atomes non liés. En effet, si les liaisons de la forme **II** sont plus liantes de 10.246 kcal/mol les énergies atomiques sont plus stables de 10.278 kcal/mol pour la forme **I** (tableau 9) (les variations d'énergie atomique provenant en majeure partie des atomes de soufre (6.649 kcal/mol) et de chlore (3.701 kcal/mol)).

Les interactions attractives entre les atomes de chlore et de soufre ainsi que celles entre les atomes de soufre et de carbone C_3 sont bien plus importantes que celles observées pour le chloro-3 thiétanne. Comme pour ce composé, elles favorisent le conformère p-équatorial, mais de

TABLEAU 9. Différences entre les énergies atomiques globales et les énergies des atomes de soufre, d'oxygène et de chlore des conformères (I–IV) du chloro-3-thiétanne sulfoxyde (en kcal/mol)

	Energie atomique globale relative	S	O	Cl
I	0	0	0	0
II	10.278	6.649	2.321	3.701
III	3.491	4.705	0.376	0.502
IV	10.520	10.915	1.443	4.767

Can. J. Chem. Downloaded from www.nrcresearchpress.com by 210.87.254.40 on 09/05/12
For personal use only.

TABLEAU 10. Répartition électronique et moment dipolaire des quatre formes possibles du chloro-3-thiétanne sulfoxyde

Atomes	I	II	III	IV
S {s + p	5.431	5.413	5.417	5.404
S { d	0.449	0.456	0.453	0.462
O	6.303	6.306	6.304	6.295
C_2	3.953	3.956	3.959	3.967
C_3	3.897	3.898	3.895	5.890
Cl {s + p	7.099	7.080	7.095	7.074
Cl { d	0.064	0.065	0.064	0.064
H_5	0.978	0.989	0.992	0.974
H_6	0.962	0.958	0.945	0.968
H_7	0.972	0.983	0.980	0.994
μ_T	2.39	3.24	3.53	5.20
μ_{exp}		1.73 (4)		

plus compensent largement l'interaction entre les atomes de carbone C_2 et C_4 nettement plus stabilisante pour la forme **II**.

Il faut noter que les interactions O–Cl sont sensiblement voisines.

De la même façon ces interactions stabilisantes $S–C_3$ et S–Cl existent pour le conformère **III** comparativement au conformère **IV** et dans ce cas s'ajoutent à l'interaction $C_2–C_4$ plus importante dans la forme **III**. Remarquons que l'on observe également entre les deux composés une interaction répulsive entre le chlore et l'oxygène du même ordre, ce qui laisse présumer à côté des effets électrostatiques une interaction entre paires libres stabilisante (35).

Si cette analyse met en évidence clairement l'origine de la préférence équatoriale du chlore dans des interactions $S–C_3$ et S–Cl par contre l'orientation privilégiée du groupement sulfoxyde dans une direction axiale semble surtout liée à une interaction stabilisante notable entre les atomes de carbone C_2 et C_4.

Les populations atomiques des quatre conformères du chloro-3 thiétanne sulfoxyde sont reportées dans le tableau 10. Comme pour le thiétanne sulfoxyde, l'atome de soufre est chargé positivement (à l'inverse du chloro-3 thiétanne) et montre un transfert de charge sur les orbitales de polarisation d assez élevé (0.45 *e*). Au contraire, l'atome de chlore possède des orbitales d très peu chargées (0.06 *e*). Il semble donc qu'au niveau de la répartition électronique, on retrouve d'une part du côté du groupement sulfoxyde exactement les mêmes caractéristiques que pour le thiétanne sulfoxyde et d'autre part du côté du chlore celles du chloro-thiétanne. Ce fait traduit d'ailleurs les faibles interactions existant entre l'atome d'oxygène et l'atome de chlore.

De même que nos résultats énergétiques, les valeurs calculées des moments dipolaires vont dans le sens d'une prédominance du conformère *trans* (chlore en position équatoriale) comme l'avait d'ailleurs proposé Arbuzov.

Les conclusions tirées de cette approche théorique sont dans l'ensemble en bon accord avec les données expérimentales connues concernant les préférences conformationnelles des molécules étudiées. Il apparaît donc que malgré ses déficiences le CNDO/2 peut permettre d'aborder de façon raisonnable l'étude conformationnelle des cycles à cinq ou six chaînons comportant des atomes de soufre pour lesquels un traitement *ab initio* est difficilement envisageable. De telles observations avaient déjà été faites par différents auteurs (18, 19, 36); il n'en reste pas moins intéressant de comparer pour le cycle thiétanne ces données semi-empiriques à celles découlant d'un calcul *ab initio* que nous prévoyons d'effectuer.

Les auteurs remercient la Société Nationale des Pétroles d'Aquitaine pour le soutien financier accordé à l'un d'entre eux (C.G.).

1. C. GUIMON, D. GONBEAU et G. PFISTER-GUILLOUZO. J. Mol. Struct. **16**, 271 (1973).
2. A. DARGELOS, D. LIOTARD et M. CHAILLET. Tetrahedron, **28**, 5595 (1972).
3. D. LIOTARD, A. DARGELOS et M. CHAILLET. Theor. Chim. Acta, **31**, 325 (1973).
4. J. B. ROSEN. J. Soc. Ind. Appl. Math. **8**, 181 (1960).
5. J. B. ROSEN. J. Soc. Ind. Appl. Math. **9**, 514 (1961).
6. H. A. SPANG. Siam. Rev. **4**, 343 (1962).
7. H. E. ZELLNIK, N. D. SONDK et R. S. DAVIS. Chem. Eng. Prog. **58**, 35 (1962).

Can. J. Chem. Downloaded from www.nrcresearchpress.com by 210.87.254.40 on 09/05/12
For personal use only.

8. D. W. SCOTT, H. L. FINKE, W. N. HUBBARD, J. P. MCCULLOUGH, C. KATZ, M. E. GROSS, J. F. MESSERLY, R. E. PENNINGTON et G. WADDINGTON. J. Am. Chem. Soc. **75**, 2795 (1953).
9. D. O. HARRIS, H. W. HARRINGTON, A. C. LUNTZ et W. D. GWINN. J. Chem. Phys. **44**, 3467 (1966).
10. H. W. HARRINGTON. J. Chem. Phys. **44**, 3481 (1966).
11. T. R. BORGERS et H. L. STRAUSS. J. Chem. Phys. **45**, 947 (1966).
12. S. I. CHAN, J. ZINN, J. FERNANDEZ et D. W. GWINN. J. Chem. Phys. **33**, 1643 (1960).
13. S. I. CHAN, J. ZINN, et W. D. GWINN. J. Chem. Phys. **34**, 1319 (1961).
14. S. I. CHAN, T. R. BORGERS, J. W. RUSSELL, H. L. STRAUSS et W. D. GWINN. J. Chem. Phys. **44**, 1103 (1966).
15. J. R. DURIG et R. C. LORD. J. Chem. Phys. **45**, 61 (1966).
16. R. M. DODSON, E. H. JANCIS et G. KLOSE. J. Org. Chem. **35**, 2520 (1970).
17. J. A. POPLE et G. D. SEGAL. J. Chem. Phys. **44**, 3289 (1966).
18. M. S. GORDON. J. Am. Chem. Soc. **91**, 3122 (1969).
19. H. FISCHER et H. KOLLMAR. Theor. Chim. Acta, **16**, 163 (1970).
20. C. W. N. CUMPER et A. I. VOGEL. J. Chem. Soc. 3521 (1959).
21. M. S. WHITE et E. L. BEESON. J. Chem. Phys. **43**, 1839 (1965).
22. W. WUCHERPFENNIG. Tetrahedron Lett. **10**, 765 (1970).
23. W. D. KELLER, T. R. LUSEBRINK et C. H. SEDERHOLM. J. Chem. Phys. **44**, 782 (1966).
24. B. A. ARBUZOV, O. N. NURETDINOVA et A. N. VERESCHAGIN. Dokl. Akad. Nauk SSSR, **172**, 591 (1966).
25. I. JANO. C. R. **261**, 103 (1965).
26. M. BORN. Z. Phys. **1**, 45 (1920).
27. C. R. JOHNSON et D. MCCANTS, JR. J. Am. Chem. Soc. **86**, 2935 (1964).
28. J. C. MARTIN et J. J. VEBEL. J. Am. Chem. Soc. **86**, 2936 (1964).
29. J. B. LAMBERT et R. G. KESKE. J. Org. Chem. **31**, 3429 (1966).
30. N. L. ALLINGER, J. A. HIRSCH, M. A. MILLER et I. J. TYMINSKI. J. Am. Chem. Soc. **91**, 337 (1969).
31. S. ALLENMARK. Ark. Kem. **26**, 73 (1966).
32. C. R. JOHNSON et W. O. SIEGL. Tetrahedron Lett. **23**, 1879 (1969).
33. C. R. JOHNSON et W. O. SIEGL. J. Am. Chem. Soc. **91**, 2796 (1969).
34. W. O. SIEGEL et C. R. JOHNSON. Tetrahedron, **27**, 341 (1971).
35. N. D. EPIOTIS. J. Am. Chem. Soc. **95**, 3087 (1973).
36. J. B. MOFFAT et K. F. TANG. Theor. Chim. Acta, **32**, 171 (1973).

Can. J. Chem. Downloaded from www.nrcresearchpress.com by 210.87.254.40 on 09/05/12
For personal use only.

The Temperature Dependence of the Ratio k_d/k_c for Ethyl Radicals

D. G. HOOPER, M. SIMON, AND M. H. BACK
University of Ottawa, Ottawa, Canada K1N 6N5

Received October 18, 1974

D. G. HOOPER, M. SIMON, and M. H. BACK. Can. J. Chem. **53**, 1237 (1975).

The ratio of the rate constants for disproportionation and combination for ethyl radicals, k_d/k_c

$$2C_2H_5 \xrightarrow{k_d} C_2H_4 + C_2H_6$$

$$2C_2H_5 \xrightarrow{k_c} C_4H_{10}$$

has been measured over the temperature range 298–173 K in the gas phase. Ethyl radicals were produced by direct photolysis of ethylene followed by addition of hydrogen atoms to ethylene. At low temperatures the only important reactions of the radicals were combination and disproportionation. The ratio k_d/k_c was obtained from measurements of the rates of formation of ethane, butane, and butene. No change in the ratio k_d/k_c was observed over the temperature range studied, leading to the conclusion that $E_d - E_c = 0$, within the experimental error. The significance of this result is discussed in relation to other measurements in both gas and liquid phase and to the nature of the transition state for this reaction.

D. G. HOOPER, M. SIMON et M. H. BACK. Can. J. Chem. **53**, 1237 (1975).

On a mesuré les rapports des constantes de vitesse de dismutation et de combinaison des radicaux éthyles, k_d/k_c

$$2C_2H_5 \xrightarrow{k_d} C_2H_4 + C_2H_6$$

$$2C_2H_5 \xrightarrow{k_c} C_4H_{10}$$

en phase gaseuse à des températures allant de 298–173 K. On a produit les radicaux éthyles par photolyse directe de l'éthylène suivie par l'addition d'atomes d'hydrogène à l'ethylène. A basse température, les seules réactions importantes des radicaux sont les réactions de combinaison et de dismutation. On a obtenu le rapport k_d/k_c à partir des mesures des vitesses de formation de l'éthane, du butane et du butène. On n'a observé aucun changement dans le rapport k_d/k_c dans les limites des températures étudiées; ceci nous amène à conclure que $E_d - E_c = 0$ à l'intérieur des erreurs expérimentales. On discute de la signification de ce résultat en relation avec d'autres mesures en phase gaseuse et en phase liquide et en rapport avec la nature de l'état de transition pour cette réaction. [Traduit par le journal]

Introduction

When two radicals react together two reactions may occur, *viz.* combination, which involves the formation of one bond and one product molecule, and disproportionation, which involves the transfer of a hydrogen atom from one radical to the other forming two product molecules. The ratio of disproportionation to combination in a particular encounter is a characteristic of the radicals involved. Values of k_d/k_c, the rate constant ratio for disproportionation and combination, range from essentially zero for methyl radicals (insofar as this ratio may be observed in this system) to 3.1 for two *t*-butyl radicals (1). The factors determining this ratio have been much discussed but no comprehensive interpretation has yet evolved (2). The most promising empirical relation appears to be the linear dependence of log k_d/k_c on $S_d^0 - S_c^0$, the entropy difference between the products of disproportionation and of combination (3, 4). Even this correlation was shown, however, to require the introduction of a factor, β, to provide agreement with the thermodynamic interpretation of reaction rates (5). Furthermore, as more values of k_d/k_c have become available, it has become evident that the scatter of the data is too large to conclude that all radicals have a common set of linear constants in this relation (6).

Can. J. Chem. Downloaded from www.nrcresearchpress.com by 210.87.254.6 on 09/05/12
For personal use only.

Can. J. Chem. Downloaded from www.nrcresearchpress.com by 210.87.254.6 on 09/05/12
For personal use only.

If log k_d/k_c is proportional to $S_d^0 - S_c^0$, the difference in activation energy between k_d and k_c, $E_d - E_c$, must be zero or constant (7). Early studies showed that for small radicals the difference was probably zero, but because of the scatter of the data, the small temperature range covered, and the difficulty in distinguishing a temperature-dependence of k_d/k_c from concurrent changes in the mechanism of the reaction, particularly at higher temperatures, some uncertainty remains. The reaction of two ethyl radicals is the system most thoroughly studied. Measurements of k_d/k_c from the photolysis of propionaldehyde showed no change over the range 323–588 K (8). On the other hand Reid and LeRoy found that k_d/k_c increased with temperature in a higher temperature region (9). A study of the photolysis of azoethane both in the gas phase over the range 317–208 K, and in a variety of solvents over the range 358–82 K, showed that k_d/k_c increased with decreasing temperature and that $E_c - E_d$ was approximately 300 cal/mol (10). The authors, however, preferred to attribute the temperature-dependence to a factor T^n, where $n = -0.7$. In a study of the radiolysis of liquid methane in the presence of ethylene over the range 179–92 K Gillis (11) found that k_d/k_c for ethyl radicals increased with decreasing temperature giving $E_c - E_d$ of 290 cal/mol, although the actual values for k_d/k_c were higher than those obtained by Dixon *et al.* (10). In an extension of the experiments with azoethane, Stefani (12) found a heterogeneous contribution to k_d/k_c and concluded that in the gas phase the change in k_d/k_c with temperature was almost within experimental error.

These uncertainties reflect the difficulties in the measurement of a small temperature coefficient of a rate constant ratio in a radical system and the problem of comparing results from studies in the gas phase with those from the liquid phase. In the measurement of such a small temperature coefficient some advantage may be gained by making measurements at low temperatures. To accomplish this with a gas phase reaction we have studied the photolysis of ethylene at 185 nm over the temperature range 298–153 K. Several studies of this reaction (13–16) have shown that at least one primary process involves the formation of a hydrogen atom which rapidly adds to ethylene to form an ethyl radical. Subsequent reactions of the ethyl radical, which at low temperatures are mainly radical–radical reactions, may be studied.

Experimental

Research grade ethylene was obtained from Matheson Co., Whitby, Ont. The ethane impurity of 0.02 mol% was removed by gas chromatography. The cylindrical quartz reaction vessel shown in Fig. 1 was 5 cm in diameter and 114 cc in volume. The window of the vessel formed part of a Dewar flask which was designed so that cooling liquid could cover the vessel completely. To remove mercury vapor, ethylene was admitted to the vessel through two spiral traps maintained at −78 °C. The vessel was isolated by a Hoke bellows-seal stainless steel valve. A low-pressure mercury lamp was constructed of 12 mm o.d. tubing coiled to form a flat spiral. The lamp current was varied between 1 and 6 mA by addition of resistors to the circuit. The lamp was placed about 5 mm from the outside window of the Dewar flask and the lamp and flask were enclosed in a box, through which nitrogen gas was circulated to prevent absorption of light by oxygen.

In the first series of experiments the noncondensable products were separated from the condensable products and collected in a gas burette. They were subsequently analyzed on a 4 m Porapak Q column maintained at 30 °C, using a thermal conductivity detector. The total condensable products were analyzed on a 4 m Porasil A column maintained at 30 °C. In the second series of experiments, for which a flame ionization detector was used, the unreacted ethylene and products were condensed into a small detachable bulb. On warming to room temperature, air was added to bring the total pressure to atmospheric, the mixture was stirred magnetically, and samples were withdrawn with a syringe for analyses. In this analysis system only greaseless Teflon stopcocks and greaseless joints were used. This method had the advantage of giving better separation and permitting duplicate analyses for each experiment but was exact only for ratios of products, not absolute amounts. For calibration, known mixtures of the products were condensed into the bulb and the same procedure followed. A 6 m column of phenylisocyanate on Porasil gave ratios of C_2H_6/C_4H_{10}, C_4H_8/C_4H_{10}, and C_4H_6/C_4H_{10} and a 4 m column of *n*-octane on Porasil (Durapak) gave ratios of

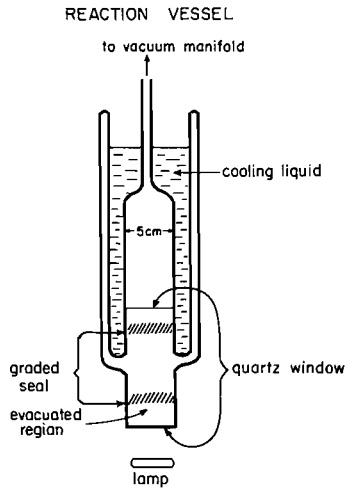

FIG. 1. Diagram of reaction vessel.

Can. J. Chem. Downloaded from www.nrcresearchpress.com by 210.87.254.6 on 09/05/12
For personal use only.

C_4H_8/C_4H_{10}, C_4H_6/C_4H_{10}, C_6H_{14}/C_4H_{10}, and C_6H_{12}/C_4H_{10}. Ratios from duplicate analyses usually agreed within 15%, while analyses on the two columns agreed within 20%, except for hexane, which because of the small amount sometimes had more error.

The photolysis was studied at 298, 195, 173, and 153 K over the range of pressures 16–125 Torr. The cooling liquid at 173 K was ethanol and at 153 K was pentane.

Results and Discussion

The photolysis of ethylene at 185 nm has been shown to involve three primary processes and it has been suggested that at least three excited states of ethylene contribute to these reactions (13). Deactivation without decomposition is also important at 185 nm.

[1] $C_2H_4 + h\nu \rightarrow C_2H_2 + H_2$

[2] $\rightarrow C_2H_2 + 2H$

[3] $\rightarrow C_2H_3 + H$

The hydrogen atoms rapidly add to ethylene and the main reacting species are the vinyl and ethyl radicals. At room temperature radical–radical reactions should predominate.

[4] $H + C_2H_4 \rightarrow C_2H_5$

[5] $C_2H_5 + C_2H_5 \rightarrow C_2H_6 + C_2H_4$

[6] $\rightarrow C_4H_{10}$

[7] $C_2H_3 + C_2H_5 \rightarrow C_2H_4 + C_2H_4$

[8] $\rightarrow C_2H_2 + C_2H_6$

[9] $\rightarrow C_4H_8$

[10] $C_2H_3 + C_2H_3 \rightarrow C_2H_4 + C_2H_2$

[11] $\rightarrow C_4H_6$

The ratio k_5/k_6 should be obtained from the ratio $[C_2H_6]/[C_4H_{10}]$ with a correction for the ethane produced in reaction 8.

The products detected and analyzed were hydrogen, acetylene, butane, ethane, butene-1, 1,3-butadiene, *n*-hexane, and hexene-1. Hydrogen and acetylene were formed directly in the primary processes 1 and 2 while the other products were formed by secondary reactions of the radicals produced in reaction 3. The ratios of the rates of formation of products relative to butane at 298 K are summarized in Table 1, and at 195, 173, and 153 K in Table 2. Typical yield–time plots are given in Fig. 2. The ratio of ethane/butane was constant over the time range studied under all conditions. Methane was not detected except in a few experiments at higher light intensity where small quantities of C_5 products were also observed. Propylene was not detected but propane was not separated from the large quantities of ethylene. The products were identified by comparison of retention time on at least two columns and by addition of small amounts of a particular product into the reaction mixture.

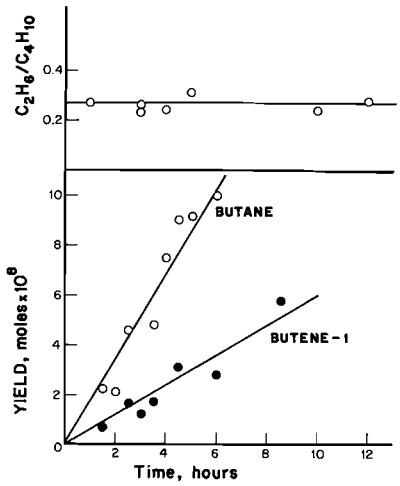

FIG. 2. Variation of the yield of butane and butene with time and of the ratio ethane/butane with time.

In the present experiments the absorbed light intensity at 27 Torr was about 4×10^{14} quanta $l^{-1}\ s^{-1}$, estimated using the value of $\Phi_{H_2} = 0.44$ measured by Glasgow and Potzinger (17). This intensity was much lower than used in previous studies; in particular in the study by Potzinger *et al.* the absorbed intensity was 1.7×10^{17} quanta $l^{-1}\ s^{-1}$ (13). The lower light intensity caused two differences between the mechanism outlined here and that proposed in the latter study. First, reaction 12 is not important in the

[12] $H + C_2H_5 \rightarrow C_2H_6$

present experiments. This is demonstrated by the constancy of the ratio $[C_2H_6]/[C_4H_{10}]$ with a change in light absorbed by a factor of six, illustrated in Figs. 3 and 4. In a second set of experiments in which the absorbed intensity was changed by a factor of four the ratio $[C_2H_6]/[C_4H_{10}]$ was also unchanged. These results are included in Table 1. An increase in absorbed intensity should favor reaction 12 over reaction 4 and hence increase the ratio $[C_2H_6]/[C_4H_{10}]$. If the ratio remains unchanged reaction 12 cannot be important.

Secondly, the formation of *n*-hexane suggests that addition of the ethyl radical to ethylene occurred followed by radical–radical reactions

TABLE 1. Rate of product formation relative to butane at 298 K*

C_2H_4 (Torr)	Relative I_{abs}	$\frac{C_2H_6}{C_4H_{10}}$	$\frac{C_4H_8}{C_4H_{10}}$	$\frac{C_4H_6}{C_4H_{10}}$	$\frac{C_6H_{14}}{C_4H_{10}}$
16	1.5	0.215	0.12		0.17
	6	0.21			
	6	0.22			
	1	0.20			
	1	0.20			
	3	0.34			
	3	0.22			
18	1.5	0.26	0.11	0.09	0.14
	6	0.29	0.17	0.13	0.07
	6	0.28	0.24	0.19	0.07
27	6	0.29	0.24	0.19	0.065
	6	0.30	0.25		0.06
	1.5	0.21	0.15	0.09	0.28
	1.5	0.26	0.15	0.10	0.15
	6	0.22			
	6	0.21			
	6	0.23			
	3	0.26			
	1	0.26			
	1	0.20			
	1	0.23			
	1	0.19			
	1	0.17			
	1.5	0.245	0.13		
	1	0.202	0.143	0.093	0.39
	1	0.22	0.14	0.097	0.43
	1	0.24	0.15	0.11	0.52
	6	0.25	0.10	0.09	0.06
	6	0.25	0.15	0.13	0.08
	6	0.275	0.18	0.14	0.085
	6	0.285	0.24	0.21	0.10
37	1	0.28			
	1	0.24			
	3	0.25			
	6	0.16			
	6	0.20			
	6	0.21			
50	1.5	0.28	0.17	0.13	0.23
	1.5	0.27	0.20	0.11	0.27
	1.5	0.285	0.21	0.12	0.34
	1.5	0.27	0.28		0.34
	1.5	0.23	0.15		
	1.5	0.25	0.13		
	6	0.295	0.20		0.075
	6	0.24	0.20	0.12	0.12
	1	0.17	0.15	0.09	0.47
	1	0.20	0.17	0.11	0.55
	1	0.22	0.16	0.11	0.75
76	1.5	0.28	0.20	0.10	
	1.5	0.30	0.36	0.30	0.38
	1.5	0.31	0.23	0.16	0.42
	1.5	0.22	0.14	0.11	
	6	0.29	0.22	0.18	0.18
	6		0.21	0.17	0.19
	6	0.30	0.23		0.17
100	1.5	0.30	0.27	0.24	
	1.5	0.32	0.24	0.15	
	6	0.28	0.21	0.17	0.19
	6	0.28	0.21		0.34
	1	0.25	0.17	0.09	0.52
	1	0.21	0.18	0.10	1.0
126	1.5	0.33	0.28	0.16	0.59

*Where the ratio is not reported, the yield was not measured.

TABLE 2. Rate of product formation relative to butane

C_2H_4 (Torr)	Relative I_{abs}	$\frac{C_2H_6}{C_4H_{10}}$	$\frac{C_4H_8}{C_4H_{10}}$	$\frac{C_4H_6}{C_4H_{10}}$	$\frac{C_2H_2*}{C_4H_{10}}$
Temperature = 195 K					
10	1.5	0.23	0.23	0.03	0.84
16	1.5	0.26	0.20	0.04	1.02
16	6	0.26			
16	6	0.20			
16	6	0.27			
16	6	0.25			
16	3	0.17			
16	1	0.26			
16	1	0.21			
	1	0.21			
27	1.5	0.29	0.19	0.05	1.04
27	6	0.27			
27	6	0.23			
27	6	0.26			
27	6	0.24			
27	6	0.31			
27	6	0.23			
27	6	0.28			
27	3	0.25			
27	3	0.16			
27	1	0.23			
27	1.5		0.30	0.06	0.86
37	6	0.33			
37	6	0.25			
37	6	0.34			
37	6	0.35			
37	3	0.31			
37	3	0.35			
37	1	0.32			
37	1	0.25			
50	1.5	0.295	0.20	0.08	1.12
50	1.5	0.28	0.22	0.07	0.99
50	1	0.24	0.30	0.08	0.80
76	1.5	0.31	0.20	0.10	
76	1	0.26	0.28	0.07	0.82
100	1.5	0.28	0.20	0.08	1.00
100	1.5	0.27	0.19	0.07	0.86
100	1	0.29	0.26	0.08	0.87

Can. J. Chem. Downloaded from www.nrcresearchpress.com by 210.87.254.6 on 09/05/12
For personal use only.

Can. J. Chem. Downloaded from www.nrcresearchpress.com by 210.87.254.6 on 09/05/12
For personal use only.

TABLE 2. (*Concluded*)

C_2H_4 (Torr)	Relative I_{abs}	$\frac{C_2H_6}{C_4H_{10}}$	$\frac{C_4H_8}{C_4H_{10}}$	$\frac{C_4H_6}{C_4H_{10}}$	$\frac{C_2H_2*}{C_4H_{10}}$
Temperature = 173 K					
16	1.5	0.335	0.35	0.017	0.97
16	6	0.27			
16	6	0.35			
16	3	0.28			
16	1	0.15			
16	1.5	0.275	0.40	0.13	0.86
27	1.5	0.405	0.40	0.025	0.96
27	6	0.35			
27	6	0.33			
27	3	0.44			
37	6	0.35			
50	1.5	0.355	0.30	0.05	1.1
76	1.5	0.295	0.31	0.06	0.72
100	1.5	0.41	0.33	0.05	
128	1.5	0.46	0.44	0.04	0.94
Temperature = 153 K					
18	1	0.49	0.51	0 016	1.1
	1	0.455	0.45	0.014	1.0
	1	0.40	0 425	0.012	1.0
27	1	0.465	0.515	0.03	1.1
	1	0.44	0.44		0.90
50	1	0.54	0.48	0.15	0.76
76	1	0.48	0.50		0.94
	1	0.595	0.55	0 054	1.05
100	1	0.56	0.59	0.03	1.0

*The relative yield of acetylene was not reported at room temperature because a small amount of decomposition occurred concurrently by mercury photosensitization at 254 nm. This was negligible at the lower temperatures.

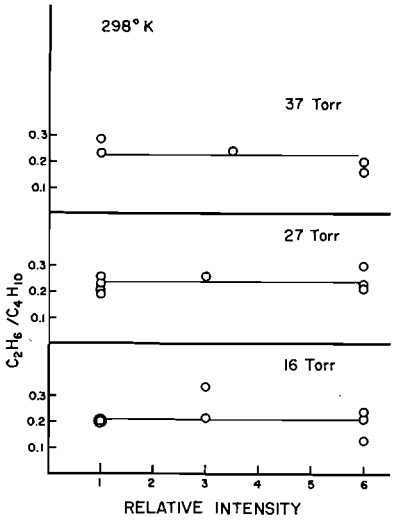

FIG. 3. Variation of the ratio ethane/butane with absorbed light intensity.

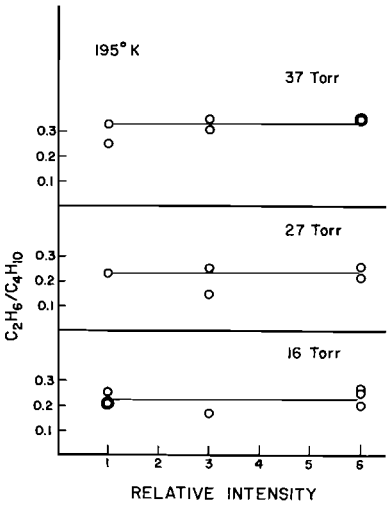

FIG. 4. Variation of the ratio ethane/butane with absorbed light intensity.

of the *n*-butyl radical. Since the ethyl radical is the most abundant radical in the system other radical–radical reactions should be unimportant. Only at very low light intensity would the addition of ethyl radicals to ethylene compete with radical–radical reactions. Hexane was, understandably, not observed in previous studies (13, 16).

[13] $C_2H_5 + C_2H_4 \rightarrow C_4H_9$

[14] $C_4H_9 + C_2H_5 \rightarrow C_4H_8 + C_2H_6$

[15] $\rightarrow C_4H_{10} + C_2H_4$

[16] $\rightarrow n\text{-}C_6H_{14}$

The rates of formation of butane and hexane are given as follows:

$$\text{Rate butane} = k_6[C_2H_5]^2$$

$$\text{Rate hexane} = \frac{k_{16}}{k_{14} + k_{15} + k_{16}} k_{13}[C_2H_5][C_2H_4]$$

Since $[C_2H_5]$ is proportional to $I_a^{1/2}$

[17] $$\frac{\text{Rate hexane}}{\text{Rate butane}} = \frac{k'[C_2H_4]}{I_a^{1/2}}$$

where k' is a composite rate constant. The ratio of hexane/butane as a function of pressure and intensity is shown in Fig. 5. The ratio was roughly linear with ethylene pressure and decreased by a factor of approximately two when

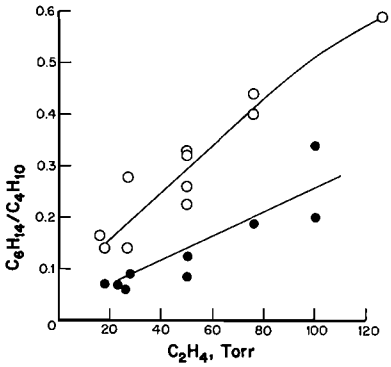

FIG. 5. Variation of the ratio hexane/butane as a function of ethylene pressure: ○, relative intensity = 1.5; ●, relative intensity = 6.

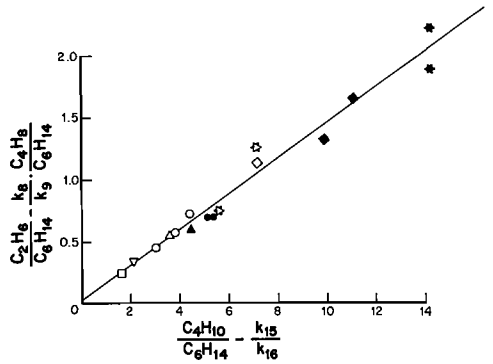

FIG. 6. Plot of eq. 18. Ethylene pressure: ✡, 16 Torr; ◇, 27 Torr; ○, 50 Torr; ▽, 76 Torr; △, 100 Torr; □, 126 Torr. Open symbols denote relative intensity of 1.5; closed symbols relative intensity 6.

the absorbed intensity increased by a factor of four.

Hexene-1 is believed to be formed by a separate primary process not involving hydrogen atoms or ethyl radicals. The kinetics of its formation are discussed in the following paper (18) and will not be further considered here.

Assuming that reactions 5, 6, 8, 9, 14, 15, and 16 account for the formation of ethane, butane, butene, and hexane, the following relation may be derived:

$$[18]\quad \frac{[C_2H_6]}{[C_6H_{14}]} - \frac{k_8[C_4H_8]}{k_9[C_6H_{14}]} = \frac{k_5}{k_6}\left[\frac{[C_4H_{10}]}{[C_6H_{14}]} - \frac{k_{15}}{k_{16}}\right] + \frac{k_{14}}{k_{16}}\left[1 - \frac{k_8}{k_9}\right]$$

where the quantity in brackets refers to the rate of formation of the product. Using measured values for k_{15}/k_{16} and k_{14}/k_{16} (1), the left-hand side of eq. 18 was plotted against

$$\left[\frac{[C_4H_{10}]}{[C_6H_{14}]} - \frac{k_{15}}{k_{16}}\right]$$

A value of k_8/k_9 was chosen so that the slope equalled the accepted value of k_5/k_6 at room temperature. As shown in Fig. 6, a value of $k_8/k_9 = 0.7$ gave a slope of 0.145. The uncertainty in k_8/k_9 was less than ± 0.2. This rather high value of k_8/k_9 means that relatively large amounts of ethane were formed in reaction 8 even though the concentration of vinyl radicals was considerably smaller than the concentration of ethyl radicals. It may be pointed out that high values of k_d/k_c for the reaction of two vinyl radicals have been reported (19, 20).

In their study of the photolysis of ethylene, Hara and Tanaka (16) reported values for the ratios C_2H_6/C_4H_{10} and C_4H_8/C_4H_{10} in excellent agreement with those obtained in the present work. Since hexane was not a product under their experimental conditions they used eq. 19 (see below) to obtain k_5/k_6. By assuming a value of 0.48 for k_8/k_9 they obtained $k_5/k_6 = 0.21$. If the value of k_8/k_9 is taken as 0.7 then from their results $k_5/k_6 = 0.17$, a value in much better agreement with previous measurements.

At 195 K and below hexane was not formed. At these temperatures the addition reaction is considerably slower and the radical–radical reactions can compete successfully. Assuming reactions 5, 6, 8, and 9 now account for the production of ethane, butane, and butene, the following equation may be derived.

$$[19]\quad \frac{[C_2H_6]}{[C_4H_{10}]} = \frac{k_5}{k_6} + \frac{k_8[C_4H_8]}{k_9[C_4H_{10}]}$$

A plot of the ratios $[C_2H_6]/[C_4H_{10}]$ against $[C_4H_8]/[C_4H_{10}]$ obtained over the pressure range 10–128 Torr at 195, 173, and 153 K is shown in Fig. 7. The line represents the values of k_5/k_6 and k_8/k_9 measured at room temperature. It is evident that the ratios measured at lower temperatures are consistent with the values of k_5/k_6 and k_8/k_9 measured at room temperature. Nevertheless for each set of ratios obtained at one temperature a line of lower slope and larger intercept could be drawn. It must be assumed however that both ratios k_5/k_6 and k_8/k_9 would change with temperature in the same direction. Clearly the ratios obtained at

Can. J. Chem. Downloaded from www.nrcresearchpress.com by 210.87.254.6 on 09/05/12
For personal use only.

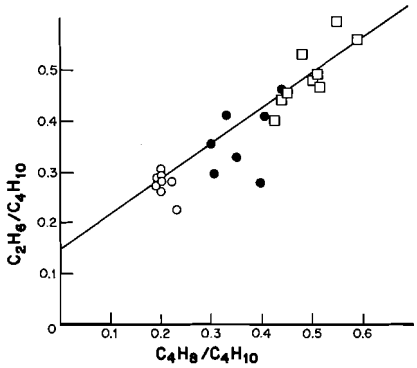

FIG. 7. Plot of eq. 19. ○, 195 K; ●, 173 K; □, 153 K. The line is drawn with intercept = 0.145 and slope = 0.7.

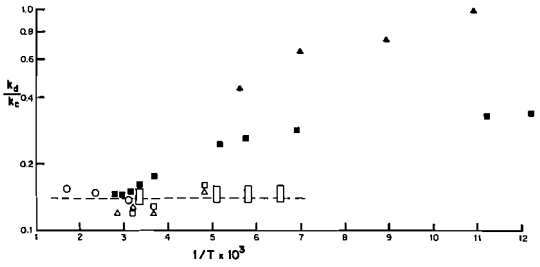

FIG. 8. Values for k_d/k_c as a function of $1/T$. ○, ref. 8; ■ and □, ref. 10; △, ref. 12; ▲, ref. 11; ▯, present work. Open symbols denote results obtained in the gas phase; filled symbols denote results obtained in the liquid phase.

the lower temperatures do not indicate an increase in both the slope and intercept of eq. 19, nor do they indicate a decrease in both these quantities. Our conclusion is that neither ratio, k_5/k_6 nor k_8/k_9, shows any change with temperature within experimental error. Over the temperature range covered by these experiments the present results indicate an upper limit to the activation energy difference for these reactions of about 30 cal/mol.

The ratio C_4H_8/C_4H_{10}, which is proportional to C_2H_3/C_2H_5, increased as the temperature decreased and increased slightly with increasing pressure. The radicals formed in reaction 3 will have some excess energy and a certain fraction may dissociate to acetylene. The exact relation between reactions 2 and 3 has not been clearly established in the photolysis of ethylene. It is not evident, however, why this ratio should depend on temperature. This question is discussed in more detail in the following paper.

In Fig. 8 values of k_d/k_c for ethyl radicals are shown in an Arrhenius plot. The constancy of k_d/k_c with changing temperature observed in the present study is in agreement with the measurements of k_d/k_c by Kerr and Trotman-Dickenson (8) over the temperature range 323–488 K. The results of Dixon *et al.* (10) from the photolysis of azoethane in the gas phase from 298–208 K appear to be in disagreement, since these authors observed an increase in k_d/k_c with decreasing temperature. In a later study of the same system, by Stefani (12), the contribution of a heterogeneous reaction to disproportionation threw some doubt on this interpretation and Stefani concluded that the change in k_d/k_c with temperature was barely significant. The results of many other measurements of k_d/k_c in the temperature range 298–373 K scatter between the values 0.12 and 0.15 (1). None of these results show any tendency for k_d/k_c to decrease above room temperature, as would be expected if the temperature coefficient measured by Dixon *et al.* persisted at higher temperatures. It must be concluded that in the gas phase k_d/k_c for ethyl radicals is independent of temperature within the experimental limits of accuracy.

The measurements by Dixon *et al.* (10) and by Gillis (11) of k_d/k_c for ethyl radicals in the liquid phase do show an increase in the ratio with decreasing temperature. Similar behavior has been observed with other radicals (2). This difference between gas and liquid phases is not easily explained. At room temperature the value of k_d/k_c is virtually the same in the gas phase and in nonpolar liquids. There is therefore no specific solvation effect on the reaction between ethyl radicals and it does not appear that the solvent in any way aids the formation of the disproportionation product. On the other hand the increase in k_d/k_c may be the result of a decrease in k_c, which may occur as rotations in the transition state become increasingly hindered in the liquid phase at low temperature and the reacting pair of radicals may more readily approach and follow the surface leading to disproportionation. An increase in internal pressure of the solvent should show a similar effect and this was observed and discussed by Dixon *et al.* (10). The difference in the volume of activation for disproportionation and combination, measured by Backman *et al.* (21) was also consistent with this interpretation.

The nature of the transition state for dispro-

Can. J. Chem. Downloaded from www.nrcresearchpress.com by 210.87.254.6 on 09/05/12
For personal use only.

portionation and combination reactions has been much discussed. The original question concerning the "common" or "separate" transition states was really an attempt to distinguish different types of collisions between the radicals, where one type of collision led to combination and another type to disproportionation. Because of the very loose nature of the collision complex, however, different orientations of the approaching radicals cannot be distinguished (22). Nevertheless within the phase space of the complex two surfaces can be distinguished but because the fraction of the radicals proceeding to disproportionation and combination in the ethyl radical complex appears invariant with temperature, our conclusion is that these two transition states are isoenergetic. Entropy or configurational factors alone must distinguish the two paths even though these factors cannot be described completely by $S_d^0 - S_c^0$, the difference in entropy between the products of disproportionation and combination.

The authors thank the National Research Council of Canada for generous financial support of this research.

1. A. F. TROTMAN-DICKENSON and G. S. MILNE. Tables of bimolecular gas reactions. NSRDS-NBS 9, 1967.
2. M. J. GIBIAN and R. C. CORLEY. Chem. Rev. **73**, 441 (1973).
3. J. N. BRADLEY. J. Chem. Phys. **35**, 748 (1961).
4. R. A. HOLROYD and G. W. KLEIN. J. Phys. Chem. **67**, 2273 (1963).
5. K. J. LAIDLER. Int. J. Chem. Kinet. **3**, 377 (1971).
6. H. H. GEORGAKAKOS, B. S. RABINOVITCH, and C. W. LARSON. Int. J. Chem. Kinet. **3**, 535 (1971).
7. R. S. KONAR. Int. J. Chem. Kinet. **2**, 419 (1970).
8. J. A. KERR and A. F. TROTMAN-DICKENSON. J. Chem. Soc. 1611 (1960).
9. L. E. REID and D. J. LEROY. Can. J. Chem. **46**, 3275 (1968).
10. P. S. DIXON, A. P. STEFANI, and M. SZWARC. J. Am. Chem. Soc. **85**, 2551 (1963).
11. H. A. GILLIS. Can. J. Chem. **49**, 2861 (1971).
12. A. P. STEFANI. J. Am. Chem. Soc. **90**, 1694 (1968).
13. P. POTZINGER, L. C. GLASGOW, and G. VON BUNAU. Z. Naturforsch. **27**, 628 (1972).
14. H. OKABE and J. R. MCNESBY. J. Chem. Phys. **36**, 601 (1962).
15. R. A. BACK and D. W. L. GRIFFITHS. J. Chem. Phys. **46**, 4839 (1967).
16. H. HARA and I. TANAKA. Bull. Chem. Soc. Jap. **46**, 3012 (1973).
17. L. C. GLASGOW and P. POTZINGER. J. Phys. Chem. **76**, 138 (1972).
18. M. SIMON and M. H. BACK. Can. J. Chem. This issue.
19. N. A. WEIR. J. Chem. Soc. 6870 (1965).
20. K. O. MCFADDEN and C. L. CURRIE. J. Chem. Phys. **58**, 1213 (1973).
21. C.-M. BACKMAN, S. CLAESSON, and M. SZWARC. Trans. Faraday Soc. **66**, 3061 (1970).
22. O. K. RICE. J. Phys. Chem. **65**, 1588 (1961).

Can. J. Chem. Downloaded from www.nrcresearchpress.com by 210.87.254.6 on 09/05/12
For personal use only.

The Mechanism of Formation of Hexene-1 in the Photolysis of Ethylene at 185 nm

M. SIMON AND M. H. BACK

Chemistry Department, University of Ottawa, Ottawa, Canada K1N 6N5

Received October 18, 1974

M. SIMON and M. H. BACK. Can. J. Chem. **53**, 1245 (1975).

In the photolysis of ethylene at 185 nm the rate of formation of hexene-1 has been measured. The ratio of the rates of formation of hexene-1 to butane varied from 0.6 to 1.4 at 298 K and fell to about 0.25 at 153 K. It is suggested that hexene-1 is formed by successive additions to ethylene to give hexamethylene which isomerizes to hexene-1.

$$C_2H_4^* + C_2H_4 \rightarrow (CH_2)_4$$
$$(CH_2)_4 + C_2H_4 \rightarrow (CH_2)_6$$
$$(CH_2)_6 \rightarrow C_6H_{12}\text{-}1$$

This interpretation is consistent with the effect of pressure of ethylene and absorbed light intensity on its rate of formation.

M. SIMON et M. H. BACK. Can. J. Chem. **53**, 1245 (1975).

On a mesuré le taux de formation de l'hexène-1 lors de la photolyse de l'éthylène à 185 nm. Les rapports des vitesses de formation de l'hexène-1 par rapport au butane varient de 0.6 à 1.4 à 298 K et tombent à environ 0.25 à 153 K. On suggère que l'hexène-1 se forme par une série d'additions successives à l'éthylène pour donner l'hexaméthylène qui s'isomérise en hexène-1. Les réactions sont

$$C_2H_4^* + C_2H_4 \rightarrow (CH_2)_4$$
$$(CH_2)_4 + C_2H_4 \rightarrow (CH_2)_6$$
$$(CH_2)_6 \rightarrow C_6H_{12}\text{-}1$$

Cette interprétation est en accord avec l'effet sur la vitesse de formation de l'hexène-1, de la pression de l'éthylène et de l'intensité de la lumière absorbée. [Traduit par le journal]

Introduction

In the photolysis of ethylene at 185 nm three primary dissociation processes have been observed (1–5).

[1] $$C_2H_4 + h\nu \rightarrow C_2H_2 + H_2$$

[2] $$\rightarrow C_2H_2 + 2H$$

[3] $$\rightarrow C_2H_3 + H$$

It has been suggested (1) that more than one excited state of ethylene is involved, but the photophysical processes that precede dissociation have not been fully clarified. Previous studies have shown that at room temperature the hydrogen atoms are removed by addition to ethylene and that the products may be accounted for by the subsequent radical–radical reactions of the ethyl and vinyl radicals.

Products of molecular weight higher than C_4 were observed to arise only by secondary reactions of accumulated products. In the present study of the photolysis of ethylene at 185 nm, however, as reported in the preceding paper (6), *n*-hexane and hexene-1 were shown not to be formed in this manner. It was suggested that *n*-hexane was formed by the addition of the ethyl radical to ethylene followed by combination of the resulting *n*-butyl radical with the ethyl radical. By analogy hexene-1 could be formed by combination of the vinyl and *n*-butyl radicals or of the ethyl and butenyl radicals. The kinetics of the formation of hexene-1, however, were not in accord with this mechanism and we have been led to suggest an independent set of reactions involving a consecutive addition of diradicals to ethylene. A somewhat similar mechanism was suggested to account for the formation of the minor product hexene-1 in the mercury-photosensitized decomposition of ethylene (7). The present paper describes the kinetics of the formation of hexene-1 in the direct photolysis of ethylene at 185 nm and discusses the evidence for a diradical mechanism.

Experimental

The apparatus, procedure, and analysis were described in the preceding paper (6). Hexene-1 was identified by coincidence of retention time with pure samples on two

Can. J. Chem. Downloaded from www.nrcresearchpress.com by 210.87.254.105 on 09/05/12
For personal use only.

columns, 4 m × ¼ in. *n*-octane on Porasil C (Durapak) at 40 °C and 3 m × ¼ in. tricresylphosphate on Chromosorb P at 30 °C. Also, small amounts of pure samples were added to the reaction mixture to test for coincidence with the reaction products. 1,5-Hexadiene, *trans*-hexene-2, *trans*-hexene-3, cyclohexane, and methylcyclopentane were well separated from hexene-1 and were shown to be absent from the reaction products.

Results and Discussion

The only two products of any importance of molecular weight higher than C_4 were *n*-hexane and hexene-1. At the highest absorbed light intensity and at long reaction times small amounts of C_5 products and other C_6 products were observed. The ratios of rates of formation of products, listed in Table 1, were obtained under conditions where these minor products were not significant. In Fig. 1 the ratio of hexene-1/butane is shown to be independent of time, and since the rate of formation of butane was previously shown to be independent of time (6) it may be concluded that hexene-1 is not formed by secondary photolysis of a product.

TABLE 1. C_6H_{12}/C_4H_{10}

C_2H_4 (Torr)	Temperature (K) 298	195	173	153
10	0.74*	0.21	0.074	
16	0.69			
18	0.56	0.41	0.30	0.30
	0.66*			
	0.71*			
	0.97*			
23	0.80*			
27	0.87*	0.35	0.30	0.20
	1.0	0.31		
	0.71			
	0.91*			
	0.97*			
	0.85			
	0.92			
	0.88			
50	0.93	0.44	0.32	0.24
	1.18	0.75		
	0.95	0.48		
	0.81*			
	0.81*			
	0.94			
	0.94			
	0.98			
76	1.20	0.53	0.44	0.26
	1.15			
	1.26			
	0.87*			
	0.90*			
	0.96*			
100	0.78*	0.55	0.33	
	0.90*	0.55		
	0.80	0.57		
	1.05			
126	1.46		0.34	

*I_{abs} was increased by a factor of four.

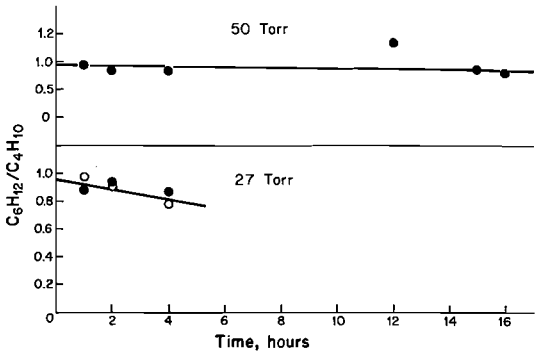

FIG. 1. The ratio of the rates for hexene-1 to butane as a function of time: ○, high intensity; ●, low intensity.

Two arguments may be advanced to show that radical combination reactions are not the main source of hexene. First, the yield of hexene is too large to arise solely from vinyl or butenyl radical reactions. From the relative yields of butane ($C_2H_5 + C_2H_5$), butene ($C_2H_3 + C_2H_5$), and hexane ($C_2H_5 + C_4H_9$) it may be shown that even at the highest pressure of 126 Torr, less than 20% of the hexene-1 produced could have been formed by radical combination reactions, ($C_4H_9 + C_2H_3$ or $C_4H_7 + C_2H_5$) and at lower pressures the fraction was much smaller. Secondly, if hexene were formed by combination of radicals then hexadiene would also be expected as a product from the corresponding combination of vinyl and butenyl radicals, and should be formed in amounts roughly comparable to those of hexane. No trace of hexadiene was observed under any conditions, although such amounts could have been measured easily.

We propose therefore that hexene is formed by a process independent of the formation of hydrogen atoms, which involves instead the successive addition of a diradical to ethylene to form hexamethylene and finally hexene-1.

I_{abs} $\quad C_2H_4 + h\nu \rightarrow C_2H_4(S)$

[1] $\quad C_2H_4(S) \rightarrow C_2H_2 + H_2$

[2] $\quad C_2H_4(S) \rightarrow C_2H_2 + 2H$

[3] $\quad C_2H_4(S) \rightarrow C_2H_3 + H$

[4] $\quad C_2H_4(S) \rightarrow C_2H_4(T)$

Can. J. Chem. Downloaded from www.nrcresearchpress.com by 210.87.254.105 on 09/05/12
For personal use only.

Can. J. Chem. Downloaded from www.nrcresearchpress.com by 210.87.254.105 on 09/05/12
For personal use only.

[5] $C_2H_4(T) \rightarrow C_2H_3 + H$

[6] $C_2H_4(T) + C_2H_4 \rightarrow 2C_2H_4$

[7] $C_2H_4(T) + C_2H_4 \rightarrow (CH_2)_4$

[8] $(CH_2)_4 + C_2H_4 \rightarrow (CH_2)_6$

[9] $(CH_2)_6 \rightarrow C_6H_{12}$-1

$C_2H_4(S)$ refers to the first excited singlet state of ethylene and $C_2H_4(T)$ to the corresponding triplet state, although this identification is tentative.

If all the hydrogen atoms are converted to ethyl radicals, which in turn disappear by combination,[1] disproportionation, and addition reactions, then the sum $2\alpha R_{C_4H_{10}} + 2\beta R_{C_6H_{14}} + \gamma R_{C_4H_8}$ represents the rate of formation of hydrogen atoms, where α, β, and γ are the corrections for the loss of radicals to disproportionation products. The ratio of this sum to the rate of formation of hexene is shown in Fig. 2 as a function of pressure at each temperature. The data for the rates of formation of products other than hexene-1 were taken from ref. 6. It is clear that the ratio becomes independent of pressure above about 50 Torr, and it must be concluded that above this pressure the excited molecule of ethylene formed in reaction 4 does not undergo any competing first-order reactions, such as reaction 5. Furthermore, the tetramethylene diradical formed in reaction 7 must react quantitatively to yield hexene-1.

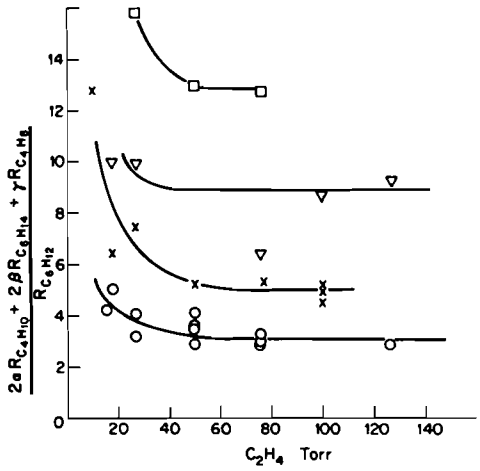

FIG. 2. The ratio $(2\alpha R_{C_4H_{10}} + 2\beta R_{C_6H_{14}} + \gamma R_{C_4H_8})/R_{C_6H_{12}}$ as a function of pressure. ○, 298 K; ×, 195 K; ▽, 173 K; □, 153 K.

[1] $C_2H_5 + C_4H_7$ is neglected.

The results of Potzinger *et al.* (1) provide some confirmation for this assumption. In the mechanism suggested by these authors one of the excited states, designated $C_2H_4^*$, reacts by competing first-order and second-order processes. Using the terminology of these authors

[f] $C_2H_4^* \rightarrow C_2H_2 + 2H$

[g] $C_2H_4 + C_2H_4^* \rightarrow$ deactivation

Reaction g was observed as a deactivation process because hexene was not analyzed by Potzinger *et al.* Higher hydrocarbon products were observed in some experiments but this aspect of the investigation was not pursued. The ratio k_g/k_f was given as 4050 l mol^{-1} at room temperature and at 50 Torr the ratio $k_f/k_g(C_2H_4)$ is approximately 0.1. If the reaction g actually led to formation of hexene then the ratio $k_f/k_g(C_2H_4)$ may be equated to our ratio $k_5/[k_7(C_2H_4)]$ and the ratio of rate constants measured by Potzinger *et al.* is in accord with the pressure-independence observed for the ratio

$$\frac{2\alpha R_{C_4H_{10}} + 2\beta R_{C_6H_{14}} + \gamma R_{C_4H_8}}{R_{C_6H_{12}}}$$

above 50 Torr. The excited molecule designated as $C_2H_4^*$ was not suggested by Potzinger *et al.* to be the triplet state. In our mechanism the triplet state is merely considered to be the most likely state to react in this manner.

It might be questioned why the tetramethylene radical should react entirely by further addition whereas the hexamethylene radical isomerizes to hexene-1. The rates of isomerization of tetramethylene and hexamethylene may be comparable to the isomerization rates of the corresponding alkyl radicals. Isomerization of *n*-butyl radical to *s*-butyl radical, in which a 1,3 hydrogen shift must occur, is much slower than isomerization of 1-hexyl to 2-hexyl, which occurs by a 1,5 hydrogen shift (8–12). By analogy, isomerization of tetramethylene to butene-1 should be slow while isomerization of hexamethylene to hexene-1 should be rapid. If the rate constant for the latter reaction is comparable to that measured for the isomerization of 1-hexyl to 2-hexyl ($\log k\ (s^{-1}) = 9.4 - 11200/2.3RT$) (12), isomerization should be many times faster than addition under the present conditions. It appears reasonable then that the addition reaction of tetramethylene radical could be faster than its

Can. J. Chem. Downloaded from www.nrcresearchpress.com by 210.87.254.105 on 09/05/12
For personal use only.

isomerization while the reverse could apply to the hexamethylene radical.

In contrast to the behavior of hexene-1, the ratio hexane/butane was found to be linearly dependent on the ethylene pressure (Fig. 5 of ref. 6), as expected from the mechanism involving radical combination reactions. This result also leads to the conclusion that hexene-1 and hexane are formed by entirely different processes.

The effect of absorbed light intensity further supports this conclusion. The ratio

$$\frac{2\alpha R_{C_4H_{10}} + 2\beta R_{C_6H_{14}} + \gamma R_{C_4H_8}}{R_{C_6H_{12}}}$$

was independent of absorbed light intensity when this was changed by a factor of four (Fig. 3). In contrast, the ratio

$$\frac{R_{C_6H_{14}}}{R_{C_4H_{10}}}$$

was inversely proportional to the square root of the absorbed light intensity (Fig. 5 of ref. 6) as expected from the mechanism involving addition of the ethyl radical to ethylene.

Effect of Temperature

The addition of radicals to ethylene is a process which requires an activation energy of several kcal/mol. In previous studies of the photolysis of ethylene at 185 nm this process was not found to be significant. In the present study the absorbed light intensity was sufficiently low that addition of ethyl radicals to ethylene was able to compete with radical–radical reactions at room temperature. At temperatures of 195 K and lower, however, no addition was observed, as indicated by the disappearance of the product *n*-hexane. The product hexene-1, on the other hand, was observed even at the lowest temperature of 153 K, although the yield was reduced. This further substantiates the view that the two products, hexane and hexene, are formed by quite different mechanisms.

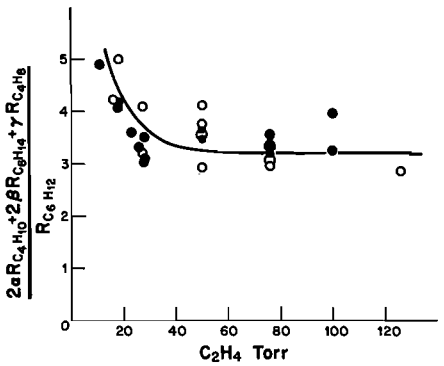

FIG. 3. The ratio $(2\alpha R_{C_4H_{10}} + 2\beta R_{C_6H_{14}} + \gamma R_{C_4H_8})/R_{C_6H_{12}}$ for absorbed intensities different by a factor of four. ●, high intensity; ○, low intensity.

In the pressure-independent region the ratio

$$\frac{2\alpha R_{C_4H_{10}} + 2\beta R_{C_6H_{14}} + \gamma R_{C_4H_8}}{R_{C_6H_{12}}}$$

may be expressed as follows

$$[10] \quad \frac{2\alpha R_{C_4H_{10}} + 2\beta R_{C_6H_{14}} + \gamma R_{C_4H_8}}{R_{C_6H_{12}}} = \frac{2k_2 + k_3}{k_4} \cdot \frac{(k_6 + k_7)}{k_7}$$

and the following equations may be derived.

$$[11] \quad \frac{\gamma R_{C_4H_8} + 2\delta R_{C_4H_6}}{R_{C_6H_{12}}} = \frac{k_3}{k_4} \cdot \frac{(k_6 + k_7)}{k_7}$$

$$[12] \quad \frac{\gamma R_{C_4H_8} + 2\delta R_{C_4H_6}}{2\alpha R_{C_4H_{10}} + 2\beta R_{C_6H_{14}} + \gamma R_{C_4H_8}} = \frac{k_3}{2k_2 + k_3}$$

The ratios in eqs. 11 and 12 were also independent of pressure above about 50 Torr. The values of these three ratios in the plateau region at each temperature are given in Table 2, and the Arrhenius plots are shown in Fig. 4. Because the yield of hexene is relatively large it may be concluded that $(k_6 + k_7)/k_7 \cong 1$ and most of the ethylene formed in reaction 4 produces hexene. The activation energy obtained from the Arrhenius plot of eq. 11 indicates therefore that $E_4 - E_3 \cong 2$ kcal/mol. The final column in Table 2 shows that the ratio $k_3/(2k_2 + k_3)$ is small compared to one and therefore may be approximated to $k_3/2k_2$ only at the highest temperature. A lower limit for $E_2 - E_3$ of about 1.5 kcal/mol may be estimated from the Arrhenius plot of eq. 12 in the region of 298 K. If E_3 is zero these estimates represent the activation energies for reactions 4 and 2 respectively.

A temperature dependence of a primary photodissociation process is unusual. The most probable cause is absorption of some of the incident radiation by vibrationally-excited ethylene, which can lead to an increased vibrational

TABLE 2. Values of the ratios of rates in the pressure-independent region

T(K)	$\frac{2\alpha R_{C_4H_{10}} + 2\beta R_{C_6H_{14}} + \gamma R_{C_4H_8}^*}{R_{C_6H_{12}}}$	$\frac{\gamma R_{C_4H_8} + 2\delta R_{C_4H_6}^*}{R_{C_6H_{12}}}$	$\frac{\gamma R_{C_4H_8} + 2\delta C_4H_6^*}{2\alpha R_{C_4H_{10}} + 2\beta R_{C_6H_{14}} + \gamma R_{C_4H_8}}$
298	3.1	0.204	0.066
195	5.0	1.36	0.28
173	8.9	2.11	0.24
153	12.8	4.42	0.35

*The correction factors, α, β, γ, δ are equal to the ratio $(k_d + k_c)/k_c$ for the particular radical–radical reaction. α and β are both well established and equal to 1.15. The value for γ was taken as 1.7, which is the value measured in ref. 6. A range of values has been reported for δ and since the most recent measurement indicates a high value, δ was taken equal to γ, 1.7. It should be emphasized that the variation of the ratios in Table 2 with pressure, absorbed intensity, and temperature is quite insensitive to the values chosen for γ and δ and the conclusions concerning the mechanism are not changed by using other values. Only the actual value of the ratio is affected and these values should therefore be accepted with caution.

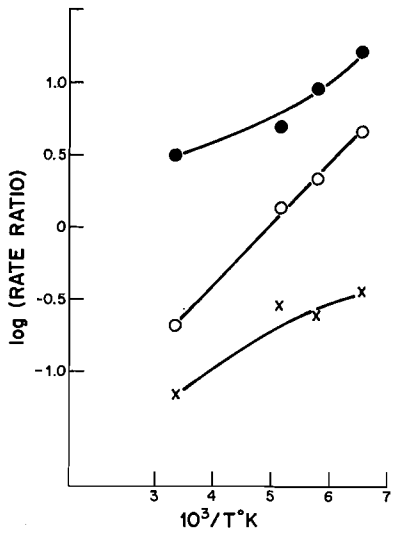

FIG. 4. Arrhenius plots of eqs. 10, 11, and 12: ●, $(2\alpha R_{C_4H_{10}} + 2\beta R_{C_6H_{14}} + \gamma R_{C_4H_8})/R_{C_6H_{12}}$; ○, $(\gamma R_{C_4H_8} + 2\delta R_{C_4H_6}/R_{C_6H_{12}}$; ×, $(\gamma R_{C_4H_8} + 2\delta R_{C_4H_6})/(2\alpha R_{C_4H_{10}} + 2\beta R_{C_6H_{14}} + \gamma R_{C_4H_8})$.

excitation of the upper state. Such "hot band" absorption is usually not appreciable at room temperature and below, but in the long-wavelength tail of a transition involving a large change in geometry, as is the case with ethylene, it can become important.[2] The reason is that a change in geometry may give a more favorable Franck–Condon factor, thus greatly favoring absorption from the vibrationally-excited level. "Hot band" absorption has in fact been observed in ethylene over the temperature range −78 to 100 °C (13). The estimated activation energy for reaction 2 of about 1.5–2.0 kcal/mol corresponds roughly to the energy of the quantum for the torsional vibration of ethylene. The ratio of reaction 2 to 3 could be particularly sensitive to small increments of energy in the upper state since the energy of the absorbed quantum (154 kcal/mol) is not far from the estimated threshold for reaction 3 (145 kcal/mol). Finally it should be noted that a temperature dependence of less than 2 kcal/mol is easily detected only in the low temperature range of the present experiments and would not be apparent in studies in the vicinity of room temperature.

Effect of Oxygen

Some experiments were done with small additions of oxygen to test for a difference in reactivity of the excited molecule producing hydrogen atoms and that giving hexene-1. The effect of oxygen on the products from the hydrogen atoms and on the hexene-1 was almost identical. The rate of formation of ethane, butane, and hexene relative to the rate in the absence of oxygen is shown as a function of oxygen pressure in Fig. 5. The pressure of oxygen required to reduce the yield of hexene by one-half was 2.7×10^{-2} Torr, while the corresponding pressure for ethane was 3.9×10^{-2} Torr. This difference is probably not significant and it may be concluded that oxygen reacts rapidly with the initially-formed singlet state and much slower with other intermediates.

Comparison of Liquid and Gas Phase Photolyses

In a recent study of the photolysis of ethylene at 185 nm in the liquid phase (15) the addition reaction of an excited ethylene molecule with another molecule of ethylene was also observed,

[2]In the A ← X transition of ammonia, a similar case, the 0,0 and 1,1 absorption bands are almost equally intense at room temperature, despite an unfavorable Boltzmann factor of about 10^{-2} for the latter (14).

Can. J. Chem. Downloaded from www.nrcresearchpress.com by 210.87.254.105 on 09/05/12
For personal use only.

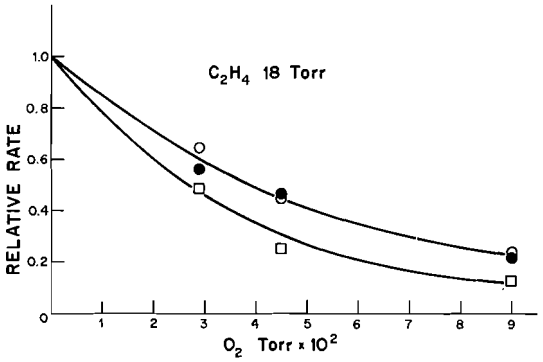

FIG. 5. Rates in the presence of oxygen relative to the rate in the absence of oxygen. ○, C_2H_6; ●, C_4H_{10}; □, C_6H_{12}.

but in this case the products were entirely C_4 molecules, the major portion being butene-1 with smaller amounts of cyclobutane and methylcyclopropane. It was suggested that butene-1 was formed by reaction of the ethylidene radical with ethylene, by either of two possible paths, the ethylidene radical being a possible configuration of the excited state. In the present study the addition reaction was suggested to proceed through a diradical, forming tetramethylene and subsequently hexamethylene. There was no evidence for formation of C_4 products by the addition reaction and the yield of butene-1 was very much smaller than observed in the liquid phase. It seems likely that the lifetime of the ethylidene radical is too short to allow bimolecular reactions to occur in the gas phase and these may be observed only in the liquid phase. Previous attempts to observe reactions of ethylidene in the gas phase have shown that its lifetime is very short and rearrangement to ethylene is very rapid (16).

In the present study the yield of hexene relative to the yield of butene plus butadiene decreased with decreasing temperature (Fig. 4) and by an extrapolation it may be estimated that the hexene formed by the diradical mechanism at −160 °C, where the experiments on liquid ethylene were done, would be only about 10% of the observed yield of hexene in the liquid phase. The diradical addition mechanism would therefore not be important at −160 °C. At this temperature the excited molecules probably undergo a rapid bimolecular reaction before reaction 4 may occur. It may be concluded that two quite distinct photoexcited molecules of ethylene are involved in the addition reaction in the liquid and in the gas phase.

The authors thank the National Research Council of Canada for financial support of this research. The authors also thank Dr. R. A. Back for helpful discussions and suggestions concerning the manuscript.

1. P. POTZINGER, L. C. GLASGOW, and G. VON BÜNAU. Z. Naturforsch. **27a**, 628 (1972).
2. H. OKABE and J. R. MCNESBY. J. Chem. Phys. **36**, 601 (1962).
3. R. A. BACK and D. W. L. GRIFFITHS. J. Chem. Phys. **46**, 4839 (1967).
4. P. BORRELL, A. CERVENKA, and J. W. TURNER. J. Chem. Soc. B. 2293 (1971).
5. H. HARA and I. TANAKA. Bull. Chem. Soc. Jap. **46**, 3012 (1973).
6. D. HOOPER, M. SIMON, and M. H. BACK. Can. J. Chem. This issue.
7. J. R. MAJER, B. MILE, and J. C. ROBB. Trans. Faraday Soc. **57**, 1342 (1961).
8. A. KOSSIAKOFF and F. O. RICE. J. Am. Chem. Soc. **65**, 590 (1943).
9. V. B. SEFTON and D. J. LEROY. Can. J. Chem. **34**, 41 (1956).
10. C. P. QUINN. Trans. Faraday Soc. **59**, 2543 (1963).
11. J. H. PURNELL. Symposium on Gas Kinetics, Szeged, Hungary. July, 1969.
12. K. W. WATKINS. J. Phys. Chem. **77**, 2938 (1973).
13. R. MCDIARMID and E. CHARNEY. J. Chem. Phys. **47**, 1517 (1967).
14. A. E. DOUGLAS. Discuss. Faraday Soc. **35**, 158 (1963).
15. SHUN-ICHI HIROKAMI and R. J. CVETANOVIĆ. J. Phys. Chem. **78**, 1254 (1974).
16. H. M. FREY and I. D. R. STEVENS. J. Chem. Soc. 1700 (1965).

Can. J. Chem. Downloaded from www.nrcresearchpress.com by 210.87.254.105 on 09/05/12
For personal use only.

Can. J. Chem. Downloaded from www.nrcresearchpress.com by 210.87.254.40 on 09/05/12
For personal use only.

Canadian Journal of Chemistry

Published by
THE NATIONAL RESEARCH COUNCIL OF CANADA

Journal canadien de chimie

Publié par
LE CONSEIL NATIONAL DE RECHERCHES DU CANADA

Volume 53 Number 9 May 1, 1975

Volume 53 numéro 9 1 mai 1975

Factor Analysis as a Complement to Band Resolution Techniques. III. Self Association in Trichloroacetic Acid

J. T. BULMER[1] AND H. F. SHURVELL[2]

Department of Chemistry, Queen's University, Kingston, Ontario K7L 3N6

Received November 22, 1974

J. T. BULMER and H. F. SHURVELL. Can. J. Chem. **53**, 1251 (1975).

Digitized infrared spectra of nine solutions of trichloroacetic acid in CCl_4 have been studied in the carbonyl stretching region. At all concentrations only two bands are visually apparent. However, factor analysis indicates the presence of four absorbing components. The contour resolution technique gives a monomer band at 1786 cm^{-1}, a dimer band at 1749 cm^{-1}, and a third band close to the dimer frequency at approximately 1735 cm^{-1}. Examination of the changes in Cauchy–Gauss shape ratio of the monomer band with increasing concentration indicates the presence of an unresolved component. The band at 1735 cm^{-1} and the unresolved band near the monomer peak at 1786 cm^{-1} are assigned to absorption of carbonyl groups in linear polymers of trichloroacetic acid. The monomer–dimer equilibrium constant was calculated from the molar absorption coefficients and absorbances of monomer and dimer bands. The average value over the concentration range 0.305 $\times$ 10^{-3} to 0.1603 *M* was 287 l/mol at 33.9 $\pm$ 0.5 °C.

J. T. BULMER et H. F. SHURVELL. Can. J. Chem. **53**, 1251 (1975).

On a étudié, pour la région de vibration du carboxyle, les spectres infrarouges chiffrés de neuf solutions d'acide trichloroacétique dans CCl_4. A toutes les concentrations, il n'y a que deux bandes qui sont apparentes d'une façon visuelle. Toutefois une analyse factorielle indique la présence de quatre composants qui absorbent. La technique de la résolution des contours donne une bande monomère à 1786 cm^{-1}, une bande dimère à 1749 cm^{-1} et une troisième bande près de la fréquence de la bande dimère à environ 1735 cm^{-1}. Un examen des changements dans les rapports des formes Cauchy–Gauss de la bande monomère, lorsque l'on augmente la concentration, indique la présence d'un composant qui n'est pas résolu. On a attribué la bande à 1735 cm^{-1} et la bande non résolue près du pic monomère à 1786 cm^{-1} à l'absorption des groupements carbonyles dans le polymère linéaire de l'acide trichloroacétique. On a calculé les constantes d'équilibre monomère–dimère à partir des coefficients molaires d'absorption et des absorbances des bandes des monomères et dimères. La valeur moyenne sur l'intervalle des concentrations 0.305 $\times$ 10^{-3} à 0.1603 *M* est de 287 l/mol à 33.9 $\pm$ 0.5 °C.

[Traduit par le journal]

Introduction

Infrared band contour resolution together with factor analysis provide a useful approach to the study of equilibria in solution. We have previously reported results of studies of self association of acetic acid (1) and complex formation between chloroform and di-*n*-butyl ether (2) in CCl_4 solutions. Our method is based on well established mathematical techniques. The band contour resolution method using digitized infrared spectra is due to Jones and co-workers (3), while factor analysis has been

[1]Present address: Department of Chemistry, University of Waterloo, Waterloo, Ontario.

[2]Author to whom correspondence should be addressed.

Can. J. Chem. Downloaded from www.nrcresearchpress.com by 210.87.254.40 on 09/05/12
For personal use only.

applied to spectrophotometric data by a number of authors (4–6). The combination of these two techniques can reveal information not easily obtained by other methods.

Our procedure determines the number of absorbing components in a complex band. If these components can be assigned to the same group vibration in various species in equilibrium, then information on the stoichiometry of the system is available. The method also leads to molar absorption coefficients of the group vibration in hydrogen bonded or complexed molecules, from which equilibrium constants can be calculated. The use of digitized spectra enables an entire band shape to be analyzed rather than using only the positions and heights of the major spectral features.

The present application is to solutions of trichloroacetic acid in CCl_4. Infrared spectra of the carbonyl stretching region show only two bands, while factor analysis indicates that four absorbing components are present. Contour resolution requires two bands at low acid concentrations with a third component at higher concentrations. A careful examination of the shape ratios of the component bands for a Cauchy–Gauss product function, reveals the increasing importance of a Gaussian component associated with the monomer band as the concentration increases.

Experimental

Fisher reagent grade trichloroacetic acid was dried in a drying pistol using P_2O_5. The sample was warmed with refluxing dimethyl ether (b.p. 34.5 °C) and a vacuum of about 0.1 Torr was used. Crystals deposited on the cooler part of the drying pistol. These were collected and stored in a dessicator. Trichloroacetic acid melts at 56.3 °C and has deliquescent crystals. Preliminary results showed that the spectrum of CCl_3COOH is quite sensitive to the presence of water. For this reason all solutions were prepared in a dry box.

Fisher spectroanalyzed carbon tetrachloride was dried over molecular sieves. Dryness was checked by monitoring water bands at 3709 and 3618 cm^{-1}. Ten solutions were prepared in the concentration range 3.05×10^{-4} to 0.1603 *M*.

Spectra were recorded using R.I.I.C. variable pathlength cells on a Perkin–Elmer model 180 spectrometer. The instrument was flushed with dry air and wavenumber calibration was checked using the known frequencies of standard compounds. A cell containing solvent was placed in the reference beam and the absorptions of sample and reference beams were balanced at 1850 cm^{-1}. Pathlengths were determined by the fringe method which only applies to short pathlengths over a small range. However, the high precision with which the R.I.I.C. cells are manufactured ensures accuracy of pathlength over the range used in this work. Details of concentrations and pathlengths of the nine solutions subjected to analysis are given in Table 1.

TABLE 1. Concentrations and pathlengths used for CCl_3COOH solutions in CCl_4

Solution	Concentration (mol/l)	Pathlength (cm)
1	0.00061	0.5019
2	0.00122	0.4827
3	0.00244	0.3101
4	0.00488	0.1327
5	0.00977	0.07037
6	0.02004	0.02242
7	0.04008	0.01043
8	0.08015	0.00564
9	0.16030	0.002281

The spectra were digitized at 0.5 cm^{-1} intervals using the manual technique described previously (7). Digitization was carried out at 301 points over the range from 1850 to 1700 cm^{-1}. Triplicate spectra were compared numerically by a small computer program to check for errors in the manual digitization. The spectra were then averaged before further processing.

Computational Techniques

Band Resolution

The computer programs for band contour resolution were supplied by R. N. Jones and are described fully in ref. 3. The Lorenzian (Cauchy) band shape usually assumed for i.r. bands (8–10) can be written:

$$[1] \qquad A_c(\nu) = X_1[1 + X_3^2(\nu - X_2)^2]^{-1}$$

where $A(\nu)$ = absorbance at wavenumber ν, X_1 = peak height, X_2 = peak position, and X_3 = band width parameter.

Perturbations due to solute–solvent interactions, or absorption by other species such as isomers, isotopic molecules, or in the present case polymeric species add Gaussian character to the i.r. band (11). The Gaussian function can be written

$$[2] \qquad A_g(\nu) = X_1 \exp[-X_4^2(\nu - X_2)^2]$$

where X_1, X_2 are as above and X_4 = Gauss band width parameter.

Equations 1 and 2 can be combined to give a product function

$$[3] \quad A_p(\nu) = X_1\left[\frac{\exp[-X_4^2(\nu - X_2)^2]}{1 + X_3^2(\nu - X_2)^2}\right]$$

The Cauchy–Gauss shape ratio is defined as

Can. J. Chem. Downloaded from www.nrcresearchpress.com by 210.87.254.40 on 09/05/12
For personal use only.

[4] $$R_{c/g} = \frac{X_3}{X_3 + X_4}$$

Functions 1 and 3 have been used to fit the observed contours of the carbonyl stretching band of CCl_3COOH in CCl_4 solutions. The fitting procedure involves sequentially increasing the number of absorbing components (NC) until a satisfactory fit is obtained between observed and calculated contours. Infrared absorption is normally recorded as transmittance (T) and this is converted to absorbance by the programs. A good fit is achieved when the function ϕ given by

[5] $$\phi = \sum_i f_i^2$$

where

$$f_i = \left[\frac{T}{T_0}\right]_{\nu(\text{obs})} - \left[\frac{T}{T_0}\right]_{\nu(\text{calcd})}$$

approaches the value of S^2NP, where NP is the number of points in the digitized spectrum and S is the standard deviation in the experimental transmittance measurements. Fluctuation in the wavenumber of the maximum difference between the observed and calculated spectrum (WFM) indicates that the correct number of components (NC) is being used. An invariant WFM indicates the necessity of an additional component at that frequency. In view of the importance of NC and the dependence of the method on an assumed band shape, an independent method for the determination of the number of absorbing components is needed and factor analysis provides this.

Factor Analysis

The mathematical technique known as factor analysis or principal component analysis applies to constitutive properties such as absorbance. The Beer–Lambert law for a single absorbing component at wavenumber ν can be written

[6] $$A(\nu) = \varepsilon(\nu)C$$

where $A(\nu)$ is the absorbance normalized to unit pathlength, $\varepsilon(\nu)$ is the molar absorption coefficient at wavenumber ν, and C is the concentration in mol/l.

For NC absorbing components in NS solutions of different concentrations the Beer–Lambert law for NW wavenumbers over an entire absorption band can be written

[7] $$\mathbf{A} = \mathbf{EC}$$

where $\mathbf{A}$ is the NW × NS normalized absorbance matrix, $\mathbf{E}$ is the NW × NC molar absorption coefficient matrix, and $\mathbf{C}$ is the NC × NS concentration matrix. Also, NW is the number of digitized points in the spectrum, NS is the number of solutions, and NC the number of absorbing components.

The method of factor analysis involves finding the rank of the absorbance matrix. The rank of $\mathbf{A}$ may be interpreted as being equal to the number of absorbing components NC. To find the rank of $\mathbf{A}$, previous workers (4, 5, 12) have formed the matrix $\mathbf{P} = \mathbf{AA}^T$ where $\mathbf{A}^T$ is the transpose of $\mathbf{A}$. This matrix $\mathbf{P}$ is a square matrix of dimension NW × NW and has the same rank as $\mathbf{A}$. The rank of $\mathbf{P}$ however, is the number of nonzero eigenvalues of $\mathbf{P}$. Thus the number of absorbing components also corresponds to the number of nonzero eigenvalues of $\mathbf{P}$. Fortunately, the nonzero eigenvalues of $\mathbf{A}^T\mathbf{A}$ (dimension NS × NS) are identical to those of $\mathbf{AA}^T$ (dimension NW × NW). Since NW is usually several hundred, while NS is about 10, it is obviously easier to handle $\mathbf{A}^T\mathbf{A}$.

In practice, experimental errors and computational procedures, in addition to absorbing components, lead to nonzero eigenvalues of $\mathbf{A}^T\mathbf{A}$. However, statistical tests (1, 4, 5) can be applied to determine which eigenvalues are really nonzero, (*i.e.*, can be attributed to absorbing components). Details of these tests formulated in the present notation have been given in ref. 1. They are: (*i*) A residual standard deviation (r.s.d.) method (5), where the residual standard deviations in the eigenvalues are compared with an estimated average standard deviation (s.d.); (*ii*) The estimation of the square root of the variance of each eigenvalue (4), where eigenvalues larger than the square root of their variances are taken to be nonzero; (*iii*) The χ^2 criterion (4), where the *smallest* number of eigenvalues (m) leading to a value of χ^2 near the expectation value, given by (NW-m)(NS-m) (13), is taken to be NC; (*iv*) An examination of the misfit between the observed absorbance matrix and an absorbance matrix regenerated using only the first m eigenvectors of $\mathbf{A}^T\mathbf{A}$ (4). Here NC is taken to be the *smallest* number of eigenvectors which give a regenerated absorbance matrix with most elements within 3 standard deviations of the corresponding observed points.

Can. J. Chem. Downloaded from www.nrcresearchpress.com by 210.87.254.40 on 09/05/12
For personal use only.

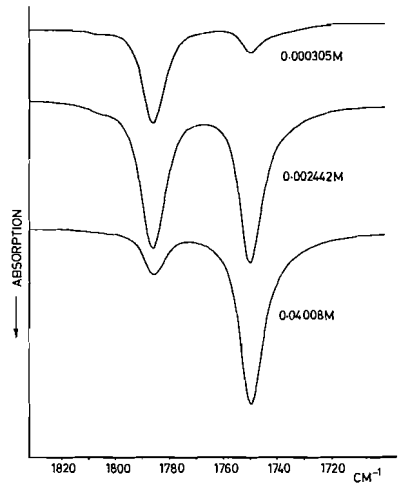

FIG. 1. Infrared spectra of the carbonyl stretching region of three solutions of trichloroacetic acid in carbon tetrachloride.

TABLE 2. Factor analysis of nine solutions of CCl_3COOH using the residual standard deviation and square root of eigenvalue variance criteria

	Eigenvalue	Residual standard deviation*	Square root of estimated variance†
1	28.607133	0.029915	0.007054
2	2.343600	0.005197	0.005697
3	0.049244	0.002955	0.005998
4	0.019383	0.001230	0.005018
5	0.002055	0.000863	0.004368
6	0.001038	0.000598	0.004340
7	0.000422	0.000446	0.005406
8	0.000298	0.000294	0.010273
9	0.000227	0.0	0.003606

*The estimated experimental standard deviation in A is in the range 0.0005 to 0.0015 (for ΔT between 0.1 and 0.3%).
†For $\Delta T = 0.2\%$.

Results and Discussion

The spectra of the carbonyl stretching region of three solutions of CCl_3COOH in CCl_4 are shown in Fig. 1. The peak at 1786 cm^{-1} decreases while the peak at 1750 cm^{-1} increases as the concentration increases. At no concentration was there any visual evidence of additional bands, although the 1750 cm^{-1} band does show some asymmetry on the low wavenumber side.

Factor Analysis

Factor analysis of nine spectra of the carbonyl region of CCl_3COOH in CCl_4 solution in the concentration range 0.61×10^{-3} to 0.16 M indicate the presence of four absorbing components.

Inspection of the residual standard deviations in Table 2 indicates that the r.s.d. of the 4th, 5th, and 6th eigenvalues lie in the range of the experimental s.d. However, there is a decrease of an order of magnitude between fourth and fifth eigenvalues, so that four absorbing components are indicated.

Table 2 also compares the eigenvalues of $\mathbf{A}^T\mathbf{A}$ with the square root of the estimated variance for a transmittance error 0.2%. It is seen that only the first four eigenvalues are larger than the square roots of their estimated variances.

The results of the regeneration of the absorbance matrix using from one up to nine eigenvectors of $\mathbf{A}^T\mathbf{A}$ are given in Table 3. Using up to 3 eigenvectors leaves many points with misfits greater than 3 standard deviations. The χ^2 values are also very large. If four eigenvectors are used 2654 out of 2700 data points agree within three estimated transmittance errors. Also $\chi_4^2 = 3107$ is comparable with the expectation value of

TABLE 3. Factor analysis of nine solutions of CCl_3COOH in CCl_4. Comparison of observed and regenerated absorbances

Number of eigenvectors	Distribution of misfit compared to estimated absorbance error*											
	0–1	1–2	2–3	3–4	4–5	5–6	6–7	7–8	8–9	9–10	10+	χ^2
1	616	222	131	145	241	175	87	83	103	94	812	1538700.0
2	975	476	228	229	271	168	65	39	42	75	141	56066.6
3	1168	616	318	260	209	72	27	13	15	7	4	17165.3
4	2015	529	110	30	14	9	2	0	0	0	0	3107.0
5	2343	304	53	6	2	1	0	0	0	0	0	1530.6
6	2488	211	10	0	0	0	0	0	0	0	0	775.1
7	2650	58	1	0	0	0	0	0	0	0	0	368.9
8	2677	32	0	0	0	0	0	0	0	0	0	218.7
9	2709	0	0	0	0	0	0	0	0	0	0	0.0

*Experimental transmittance error = 0.20%T.

Can. J. Chem. Downloaded from www.nrcresearchpress.com by 210.87.254.40 on 09/05/12
For personal use only.

1485. The results using five eigenvectors also yield results consistent with a transmittance error of 0.2% and χ_5^2 is closer to the expectation value. However, NC is taken as the *smallest* number of eigenvectors which satisfactorily reproduce the absorbance matrix.

Band Contour Resolution

Visual examination of the spectra at all concentrations between 0.61×10^{-3} and $0.16\ M$ reveals only two bands due to monomer and dimer. However, factor analysis indicates four absorbing components and previous experience with acetic acid leads us to expect two additional absorptions arising from terminal and hydrogen-bonded C=O groups in linear chain structures. The spectra of CCl_3COOH in CCl_4 solution resemble those of acetic acid in the more dilute solutions, where only two bands were apparent.

Two band fits using both Cauchy and Cauchy–Gauss product functions indicated the presence of a third absorption near 1735 cm^{-1} in addition to the monomer at 1780 cm^{-1} and dimer at 1750 cm^{-1}. Details of the results of a three band fit of the spectrum of 0.00488 M CCl_3COOH in CCl_4 using Cauchy functions are given in Table 4. This confirms the necessity for three bands, but does not directly indicate a fourth. However, examination of the Cauchy–Gauss ratio defined in eq. 4 clearly shows the increasing importance of a Gaussian component in the monomer band as the concentration increases. At the same time the dimer band retains a strongly Lorentzian character. Values of the Cauchy–Gauss ratio are listed in Table 5. This is clear evidence for the location of the fourth component predicted by factor analysis and is most likely due to the terminal carbonyl groups of linear chain structures. The 1735 cm^{-1} band is then assigned to hydrogen bonded C=O groups in the linear polymers.

TABLE 4. Resolution of the carbonyl stretching absorption region of 0.00488 M CCl_3COOH in CCl_4 solution using three Cauchy functions

Peak	Position (cm^{-1})	Height (absorbance units)
Monomer	1786.1±0.04	0.539±0.006
Dimer	1749.9±0.03	0.939±0.009
Polymer	1734.3±1.0	0.107±0.004

TABLE 5. Cauchy–Gauss ratios from a two band product function fit of nine spectra of CCl_3COOH in CCl_4 solution

Solution concentration ($\times 10^3\ M$)	Dimer $\left[\frac{X_3}{X_3+X_4}\right]_{1749}$	Monomer $\left[\frac{X_3}{X_3+X_4}\right]_{1786}$
0.610	0.994	0.927
1.22	0.991	0.830
2.44	0.990	0.788
4.88	0.995	0.714
9.77	0.986	0.711
20.04	0.994	0.683
40.08	0.999	0.611
80.15	0.993	0.584
160.3	0.993	0.507

Calculation of Molar Absorption Coefficients and Equilibrium Constants

The calculation of the monomer–dimer equilibrium constant is based on the method of Chiang and Hammaker (14). We have taken the activity coefficients of monomer and dimer to be unity. A linear least squares method is used to obtain the molar absorption coefficients of monomer and dimer from the equation

$$[8] \qquad \frac{A_2}{C_T l} = \varepsilon_2 - \frac{\varepsilon_2}{\varepsilon_1}\left(\frac{A_1}{C_T l}\right)$$

This equation is based on the assumption that only monomer and dimer are present in significant quantities in dilute solutions. The absorbances A_1 and A_2 were obtained from the resolved monomer and dimer bands for the five most dilute solutions, using a two band Cauchy–Gauss product function. The molar absorption coefficients ε_1 and ε_2 were found to be 785 and 1154 l mol^{-1} cm^{-1} for monomer and dimer respectively. An increase in the molar absorption coefficient of the C=O stretching band on hydrogen bonding is usually found and the corresponding values for ε_1 and ε_2 for acetic acid solutions in CCl_4 are 754 and 992 l mol^{-1} cm^{-1} (1).

The equilibrium constant is evaluated using the equation:

$$[9] \qquad K = \frac{1}{2C_1}\frac{A_2}{A_1}\frac{\varepsilon_1}{\varepsilon_2}$$

where

$$[10] \qquad C_1 = C_T\left(\frac{A_1\varepsilon_2}{A_2\varepsilon_1}\right)\Big/\left(1 + \frac{A_1\varepsilon_2}{A_2\varepsilon_1}\right)$$

Can. J. Chem. Downloaded from www.nrcresearchpress.com by 210.87.254.40 on 09/05/12
For personal use only.

TABLE 6. Dimerization equilibrium constants of trichloroacetic acid in CCl_4 solution as a function of concentration

Concentration (mol/l × 10^3)	Equilibrium constant (l/mol)
0.305	246
0.610	270
1.22	300
2.44	301
4.88	309
9.77	263
20.0	307
40.1	286
80.2	317
160.3	273

Values of K were obtained using $\varepsilon_1/\varepsilon_2$ from the slope of the line of eq. 8. The results are given in Table 6 for all nine solutions studied. The constant value for the apparent dimerization constant is misleading, since it suggests that only monomer and dimer are present at all concentrations. However the results of factor analysis, band resolution, and the trend in the shape of the monomer band suggest the formation of additional species such as linear polymer chains. A change in equilibrium constant with concentration was observed for acetic acid (1). The apparent absence of this effect here is most likely due to overlap of the bands and our inability to resolve the polymer components.

Conclusions

Factor analysis together with detailed band contour resolution studies indicate the presence of four absorbing components in the carbonyl stretching region of solutions of trichloroacetic acid in CCl_4. Monomeric CCl_3COOH absorbs at 1786 cm^{-1}, while the cyclic dimer absorbs at 1750 cm^{-1}. Linear chain structures, which appear to be less important in CCl_3COOH than in acetic acid in the same solvent, give rise to absorptions due to terminal and hydrogen-bonded carbonyl groups at 1786 and 1735 cm^{-1} respectively.

The apparent equilibrium constant for the monomer–dimer equilibrium does not decrease with increasing concentration in the way observed for acetic acid solutions. This is likely due to our inability to resolve the overlapping monomer/polymer and dimer/polymer bands. The average value for the dimerization equilibrium constant was found to be 287 l mol^{-1} at 33.9 °C. This is compared with previously reported values in Table 7.

It would appear that factor analysis and some detailed features of band contour resolution such as trends in the shape ratio can lead to additional information from spectra. The presence of species other than monomer and dimer in solutions of trichloroacetic in CCl_4 is not detectable from simple band contour analysis alone, nor from the calculated values of the monomer–dimer equilibrium constant at various concentrations.

1. J. T. BULMER and H. F. SHURVELL. J. Phys. Chem. **77**, 256 (1973).
2. J. T. BULMER and H. F. SHURVELL. J. Phys. Chem. **77**, 2085 (1973).
3. R. N. JONES *et al.* National Research Council of Canada Bulletin Nos. 11 and 12, 1968; No. 13, 1969.
4. Z. Z. HUGUS, JR. and A. A. EL-AWADY. J. Phys. Chem. **75**, 2954 (1971).
5. J. J. KANKARE. Anal. Chem. **42**, 1322 (1970).
6. J. S. COLEMAN, L. P. VARGA, and S. H. MASTIN. Inorg. Chem. **9**, 1015 (1970).
7. T. BULMER and H. F. SHURVELL. Can. Spectrosc. **16**, 94 (1971).

TABLE 7. Reported values for the dimerization constant of CCl_3COOH in CCl_4 solution

Temperature (°C)	Concentration (mol/l)	K (l mol^{-1})	Reference
25	0.07	530	Harris and Hobbs (15)
25	0.0016	270	Melnick *et al.* (16)
25	0.001	410	Kagarise (17)
33.9±0.5	0.000305–0.1603	287±25	This work

8. R. N. JONES, K. S. SESHADRI, N. B. W. JONATHAN, and J. W. HOPKINS. Can. J. Chem. **41**, 750 (1963); Spectrochim. Acta, **19**, 1013 (1963).
9. S. ABRAMOWITZ and R. P. BAUMANN. J. Chem. Phys. **39**, 2757 (1963).
10. J. T. SHIMOZAWA and M. K. WILSON. Spectrochim. Acta, **22**, 1591 (1966).
11. J. G. DAVID and H. E. HALLAM. J. Mol. Struct. **5**, 31 (1970).
12. G. WERNIMONT. Anal. Chem. **39**, 554 (1967).
13. Z. Z. HUGUS, JR. Private communication.
14. T. C. CHIANG and R. M. HAMMAKER. J. Phys. Chem. **69**, 2715 (1965).
15. J. T. HARRIS and M. E. HOBBS. J. Am. Chem. Soc. **76**, 1419 (1954).
16. H. E. AFFSPRONG, S. D. CHRISTIAN, and A. M. MELNICK. Spectrochim. Acta, **20**, 285 (1964).
17. R. E. KAGARISE. Infrared absorption studies of some halogenated acetic acids. Naval Research Laboratory Report No. 4955. Washington, 25, D.C. 1957.

Can. J. Chem. Downloaded from www.nrcresearchpress.com by 210.87.254.40 on 09/05/12
For personal use only.

Thermodynamic Properties of Binary Liquid Acid–Base Mixtures

HORACIO N. SÓLIMO, ROQUE RIGGIO, FRANCO DAVOLIO, AND MIGUEL KATZ

Cátedra de Físico-Química, Facultad de Ciencias Exactas y Tecnología, Universidad Nacional de Tucumán, Tucumán, Argentina

Received October 15, 1974

HORACIO N. SÓLIMO, ROQUE RIGGIO, FRANCO DAVOLIO, and MIGUEL KATZ. Can. J. Chem. **53**, 1258 (1975).

Viscosities, densities, refractive indices, and enthalpies at 25 °C were determined for the systems: propionic acid + aniline (PA + A), propionic acid + *N*,*N*-dimethylaniline (PA + DMA), and propionic acid + pyridine (PA + P). From the experimental results the excess volume, excess viscosity, excess molar free energy of activation, and excess enthalpy were calculated. The deviations from ideality for the excess thermodynamic functions are more important for the systems PA + A and PA + P than for PA + DMA. There is evidence for complex formation between propionic acid and aniline in the following molar relation: 2 $CH_3CH_2COOH \cdot C_6H_5NH_2$.

HORACIO N. SÓLIMO, ROQUE RIGGIO, FRANCO DAVOLIO et MIGUEL KATZ. Can. J. Chem. **53**, 1258 (1975).

On a déterminé, à 25 °C, les viscosités, les densités, les indices de réfraction et les enthalpies des systèmes acide propionique + aniline (AP + A), acide propionique + *N*,*N*-diméthylaniline (AP + DMA) et acide propionique + pyridine (AP + P). On a calculé, à partir de ces résultats expérimentaux le volume d'excès, la viscosité d'excès et l'énergie libre d'activation molaire d'excès et l'enthalpie d'excès. Les déviations de la courbe idéale pour les fonctions thermodynamiques en excès sont plus importantes pour les systèmes AP + A et AP + P que pour le système AP + DMA. Il semble évident qu'il y a formation de complexes entre l'acide propionique et l'aniline dans la relation molaire suivante: 2 molécules acide propionique pour une molécule d'aniline. [Traduit par le journal]

Introduction

Viscosities, densities, refractive indices, and enthalpies of some nonelectrolytes acid–base binary liquid mixtures have been studied to obtain information about the type and degree of interaction between molecules of the components. This is a continuation of our studies about thermodynamic properties (1–3).

The following systems: propionic acid + aniline (PA + A), propionic acid + *N*,*N*-dimethylaniline (PA + DMA), and propionic acid + pyridine (PA + P) were chosen because these four substances have polar characteristics and two of them (A and PA) show hydrogen bonding.

Solutions of nonelectrolytes were classified by Barker and Smith (4) as (*i*) "nonpolar" solutions, (*ii*) "polar" solutions, and (*iii*) "associated" solutions. The first system PA + A could be classified as (*iii*) and the other two systems PA + DMA and PA + P as (*ii*) and (*iii*).

In the present paper, densities, refractive indices, viscosities, and enthalpies of the three systems at different molar fractions were measured at 25 °C. From the experimental results the following thermodynamic functions have been calculated: V^E (excess molar volume), η^E (excess viscosity), G^{*E} (excess molar free energy of activation of flow), and H^E (excess molar enthalpy).

Experimental

Density

Densities were determined with a Robertson specific gravity bottle (5). All weighings were made with an accuracy of ± 0.00005 g cm^{-3}. A thermostatically controlled bath, constant to ± 0.01 °C, was used.

Refractive Index

The refractive indices for the sodium D line of the pure components and mixtures were measured with a Jena dipping refractometer with an accuracy of ± 0.00002.

Viscosity

Viscosities of pure liquids and mixtures have been determined with an accuracy of ± 0.005 cP with a Cannon–Fenske viscosimeter calibrated with doubly distilled water, benzene, and sucrose solutions (6). Kinetic energy corrections were applied to viscosity data. All these experimental methods have been described previously (1).

Calorimetric Measurements

The adiabatic jacketed calorimeter described by Loiseleur (7) was used to determine the change of enthalpy when propionic acid was mixed with aniline, *N*,*N*-dimethylaniline, and pyridine. The following

Can. J. Chem. Downloaded from www.nrcresearchpress.com by 210.87.254.5 on 09/05/12
For personal use only.

modification was made: Teflon was used instead of nylon in several parts of the calorimeter and a cellophane membrane was used between the two compartments. All measurements were made at 25 ± 1 °C, with an accuracy of ±1%.

Material and Solutions

Propionic acid, Hopkin & Williams, was dried over anhydrous sodium sulfate and fractionally distilled. The fraction distilling at 139–141 °C was collected and refractionated over potassium permanganate. The middle fraction distilling at 140.7 °C at 760 mm was collected. The purification of the other substances was described previously (1, 3).

Mixtures were prepared by mixing weighed amounts of the pure liquids. Caution was taken to prevent evaporation.

Results

In general, values of the densities, viscosities, and refractive indices were in reasonable agreement with data from the literature (8–12).

The excess thermodynamic functions (13) were calculated with the following equations:

$$[1] \qquad \eta^E = \eta - (x_1\eta_1 + x_2\eta_2)$$

$$[2] \qquad V^E = V - (x_1V_1 + x_2V_2)$$

$$[3] \qquad G^{*E} = RT[\ln \eta V - (x_1 \ln \eta_1 V_1 + x_2 \ln \eta_2 V_2)]$$

where η, η_1, and η_2 = viscosity of the mixture and of the pure components; V, V_1, and V_2 = molar volume of the mixture and of the pure components; R = gas constant, and T = absolute temperature. The molar volume V of the mixture is defined by

$$[4] \qquad V = \frac{x_1M_1 + x_2M_2}{\rho}$$

where M_1 and M_2 are the molecular weights of the components and ρ the density of the mixture.

The experimental molar fractions, densities, viscosities, refractive indices, and molar enthalpies for the three systems are listed in Tables 1, 2, and 3.

TABLE 1. Experimental values of density ρ (g cm^{-3}), viscosity η (cP), refractive index n_D, and excess molar enthalpy H^E (J mol^{-1}) for the systems PA + A at 25 °C

x_1*	ρ	η	n_D	x_1*	H^E
0.0000	1.01745	3.773	1.58392	0.0000	0
0.0996	1.01947	4.218	1.56835	0.1827	−1055
0.2015	1.02096	4.652	1.55249	0.3846	−1978
0.2966	1.02458	5.177	1.53723	0.5768	−2848
0.3880	1.02777	5.870	1.52275	0.6528	−3058
0.4955	1.03159	6.898	1.50485	0.7292	−2875
0.5962	1.03418	7.775	1.48834	0.8036	−2409
0.7160	1.03298	7.294	1.46295	0.9081	−1050
0.7994	1.02663	5.282	1.44317	1.0000	0
0.8950	1.01113	2.477	1.41618		
1.0000	0.98792	1.014	1.38476		

*x_1 = molar fraction of propionic acid.

TABLE 2. Experimental values of density ρ (g cm^{-3}), viscosity η (cP), refractive index n_D, and excess molar enthalpy H^E (J mol^{-1}) for the system PA + DMA at 25 °C

x_1*	ρ	η	n_D	x_1*	H^E
0.0000	0.95232	1.288	1.55661	0.0000	0
0.1014	0.95515	1.364	1.54488	0.1901	−490
0.2025	0.95863	1.416	1.53277	0.3194	−504
0.3050	0.96250	1.478	1.51951	0.3996	−526
0.3966	0.96652	1.527	1.50695	0.5032	−560
0.5057	0.97165	1.583	1.49068	0.5820	−528
0.6027	0.97662	1.651	1.47476	0.6154	−522
0.6922	0.98160	1.690	1.45707	0.7046	−530
0.8012	0.98720	1.657	1.43616	0.7876	−595
0.8905	0.98992	1.467	1.41571	0.7969	−603
1.0000	0.98792	1.014	1.38476	1.0000	0

*x_1 = molar fraction of propionic acid.

Can. J. Chem. Downloaded from www.nrcresearchpress.com by 210.87.254.5 on 09/05/12
For personal use only.

TABLE 3. Experimental values of density ρ (g cm^{-3}), viscosity η (cP), refractive index n_D, and excess molar enthalpy H^E (J mol^{-1}) for the system PA + P at 25 °C

x_1*	ρ	η	n_D	x_1*	H^E
0.0000	0.97710	0.886	1.50713	0.0000	0
0.0999	0.98276	1.000	1.49755	0.1939	−2094
0.1959	0.98709	1.135	1.48830	0.3759	−3931
0.2826	0.99266	1.311	1.47967	0.5195	−4420
0.3927	0.99874	1.587	1.46902	0.5776	−4368
0.5016	1.00473	1.943	1.45893	0.6971	−3783
0.6401	1.01116	2.388	1.44382	0.8012	−2723
0.7118	1.01260	2.480	1.43526	1.0000	0
0.7972	1.01156	2.353	1.42378		
0.8994	1.00355	1.755	1.40594		
1.0000	0.98792	1.014	1.38476		

*x_1 = molar fraction of propionic acid.

Each set of results was fitted with a Redlich–Kister form of the type

$$[5] \quad X^E = x_1(1 - x_1) \sum_{j=1}^{n} a_j(1 - 2x_1)^{j-1}$$

where X^E represents the excess property under consideration. The method of least-squares was used to determine the values of the coefficients a_j. In each case the optimum number of coefficients was ascertained from an examination of the variation of the standard error of estimate with n,

$$[6] \quad \sigma_x = [\sum(X_{obs}{}^E - X_{cal}{}^E)^2/(n_{obs} - n)]^{1/2}$$

The values adopted for the coefficients a_j (calculated with a IBM 1620 computer) and the standard error of the estimate σ associated with the use of eq. [5] are summarized in Table 4.

Figures 1, 2, 3, and 4 show the experimental values obtained for the excess property under consideration. The continuous curves for η^E, V^E, and H^E in Figs. 1, 2, and 3 were calculated from eq. [5] using these values for the coefficients.

Discussion

Figure 1 shows positive excess viscosities with well marked maxima. This behavior is an evidence for complex formation (14). The energy necessary to break the hydrogen bonding of the type O—H· · ·O in the propionic acid (9.34 kcal mol^{-1}) (15) is greater than the energy to break the hydrogen bonding N—H· · ·N in the aniline (3–5 kcal mol^{-1}) (16). When they are mixed, a shift of the maximum excess viscosity towards the mole fraction of the component with the most energetic hydrogen bonding is observed. In this case the maximum at $x_1 = 0.66$ is in agreement with what has been said above.

For the other two systems the excess viscosity

TABLE 4. Values of the coefficients for eq. [5] determined by the method of least squares*

System	Function	a_0	a_1	a_2	a_3	a_4	σ
PA + A	H^E	−10050	9493	−8347	−7931	14520	29
	V^E	−9.117	9.835	−1.716	−4.046	—	0.05
	η^E	18.563	−25.636	3.767	36.815	−27.490	0.09
PA + DMA	H^E	−2204	−149	152	2132	−9853	6
	V^E	−2.421	3.542	−2.325	—	—	0.03
	η^E	1.770	−1.964	1.643	−0.187	—	0.01
PA + P	H^E	−17720	2534	6552	1297	—	27
	V^E	−7.012	6.657	−3.274	−0.756	—	0.03
	η^E	4.267	−7.249	1.096	4.310	—	0.05

*Units: H^E, J mol^{-1}; V^E, cm^3 mol^{-1}; η^E, cP.

Can. J. Chem. Downloaded from www.nrcresearchpress.com by 210.87.254.5 on 09/05/12
For personal use only.

Can. J. Chem. Downloaded from www.nrcresearchpress.com by 210.87.254.5 on 09/05/12
For personal use only.

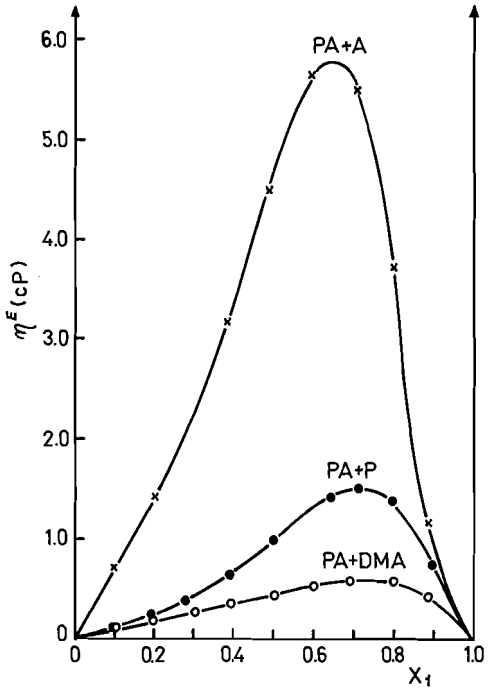

FIG. 1. η^E *vs.* x_1.

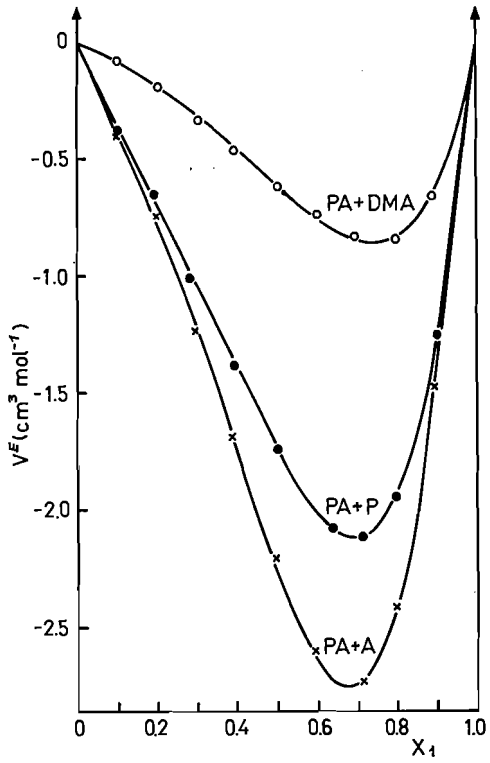

FIG. 2. V^E *vs.* x_1.

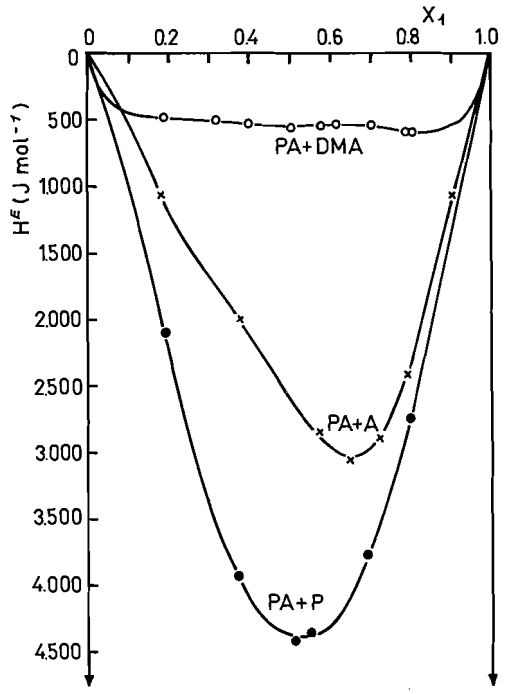

FIG. 3. H^E *vs.* x_1.

becomes less positive and for the PA + P system is meaningful, probably due to the weak bonding N···H of pyridine and the absence of hydrogen bonding in *N*,*N*-dimethylaniline (17).

Fialkov (18) concludes that for systems whose excess viscosity shows well marked maxima, the composition of the compound formed can be fixed, at least to a first examination.

From the analysis of Figs. 1 and 3 we may conclude that for the system PA + A where both components are associated in the pure state, there is evidence for a complex formation in the following molar relation $2CH_3CH_2COOH{\cdot}C_6H_5NH_2$.

For the other two systems we cannot find a molar relation because the maxima do not coincide.

The negative values of V^E in Fig. 2 for the three systems are explained by Prigogine (19) in terms of the different size of the molecules or the dipole–dipole interaction between them. This last effect is more strongly observed in the PA + A system.

Figure 3 shows that H^E for all systems are negative over the whole concentration range. The excess enthalpies of PA + P are greater

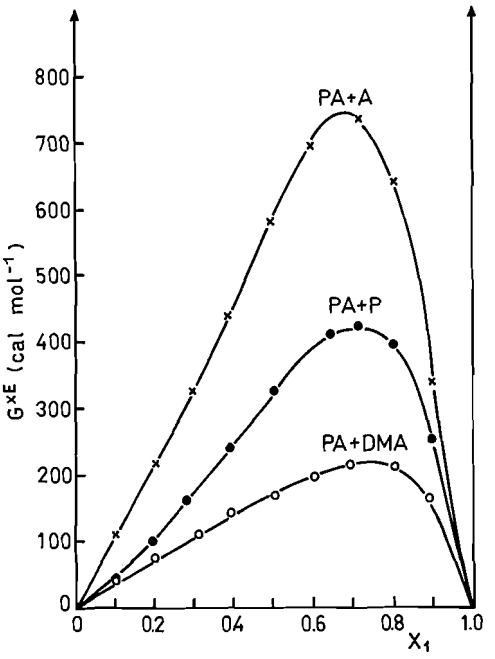

FIG. 4. G^{*E} *vs.* x_1.

than PA + A. The lower negative value for this last system can be explained by the fact that the exothermic effect in complex formation is compensated by the endothermic effect in the rupture of hydrogen bonding in each substance. In the system PA + P there is only an endothermic effect for the propionic acid.

From the analysis of Fig. 4 we may conclude that for the system PA + A more positive G^{*E} values are obtained. This result is in agreement with the expected variation of the ΔH^* and $T\Delta S^*$ functions for nonideal mixtures of the type previously described (20).

The linear variation of the molar refraction for the three systems, calculated from the refractive indices given in Tables 1, 2, and 3 by Lorenz–Lorentz formula, in terms of composition is in agreement with the conclusion of Loiseleur (21) for a large number of ideal and non-ideal systems. Neither the polar characteristics of the substances studied nor the existence of hydrogen bonding in the propionic acid and aniline seem to have any important effect on the linear dependence of this property on concentration.

This work was supported by a SECYT research grant. We are indebted to Miss Silvia Alonso for experimental assistance and to Mr. Eduardo Epstein for help in computation programs.

1. M. KATZ, P. W. LOBO, A. SANCHO MIÑANO, and H. SÓLIMO. Can. J. Chem. **49**, 2605 (1971).
2. M. KATZ, P. W. LOBO, and H. SÓLIMO. Anales Asoc. Quím. Argentina, **61**, 83 (1973).
3. H. SÓLIMO, R. RIGGIO, P. W. LOBO, and M. KATZ. Anales Asoc. Quím. Argentina, In press.
4. J. A. BARKER and F. SMITH. J. Chem. Phys. **22**, 375 (1954).
5. G. R. ROBERTSON. Ind. Eng. Chem. Anal. Ed. **11**, 464 (1939).
6. International Critical Tables. Vol. V. 1st ed. McGraw Hill Book Co., Inc. New York and London. 1929. p. 23.
7. H. LOISELEUR, J. MERLIN, and R. A. PÂRIS. J. Chim. Phys. **62**, 1380 (1965).
8. A. WEISSBERGER, E. S. PROSKAUER, J. A. RIDDIK, and E. E. TOOPS. Organic solvents. Vol. VII. 2nd ed. Interscience Publ., New York. 1955. pp. 146, 235.
9. J. TIMMERMANS. Physico-chemical constants of binary systems in concentrated solutions. Interscience Publ. New York. 1959. p. 153.
10. W. KOGLIN. Kurzes Handbuch der Chemie. Vandenhoeck & Ruprecht. Göttingen. 1953. L–Z, p. 1449 and A–Bix, p. 156.
11. International critical tables. McGraw Hill Book Co., Inc. New York and London. 1st ed. 1929. Vol. V. p. 36; Vol. VII, p. 218.
12. N. A. LANGE. Handbook of chemistry. 9th ed. McGraw Hill. Handbook Publishers. Inc. Sandusky. Ohio. 1956.
13. P. K. KATTI and M. M. CHAUDHRI. J. Chem. Eng. Data, **9**, 442 (1964).
14. R. J. FORT and W. R. MOORE. Trans. Faraday Soc. **62**, 1112 (1966).
15. E. FREEMAN. J. Chem. Phys. **21**, 1784 (1953).
16. G. C. PIMENTEL and A. L. MCCLELLAN. The hydrogen bond. W. H. Freeman & Co. San Francisco and London. 1960. p. 213.
17. V. T. DESPHANDE and K. G. PATHKI. Trans. Faraday Soc. **58**, 2134 (1962).
18. YU. YA. FIALKOV. Russ. J. Phys. Chem. **37**, 1051 (1963).
19. I. PRIGOGINE. The molecular theory of solutions. North Holland Publishing. Co., Amsterdam. 1957.
20. G. M. BARROW. Química-Física. Vol. II. Reverté ed. 1968. p. 655.
21. H. LOISELEUR. Thèse de Doctorat-ès Sciences. Lyon. 1965. p. 80.

Can. J. Chem. Downloaded from www.nrcresearchpress.com by 210.87.254.5 on 09/05/12
For personal use only.

Electron Mobilities and Ranges in Liquid Ethers: Ion-like and Conduction Band Mobilities[1,2]

JEAN-POL DODELET AND GORDON R. FREEMAN

Chemistry Department, University of Alberta, Edmonton, Alberta T6G 2E1

Received October 21, 1974

JEAN-POL DODELET and GORDON R. FREEMAN. Can. J. Chem. **53**, 1263 (1975).

The free ion yields in X irradiated ethers are larger than those in alkanes because the dielectric constants of the former liquids are greater than those of the latter. The relative increase of the free ion yield with temperature is smaller in ethers than in alkanes because the dielectric constants decrease more rapidly with increasing temperature in the former. The density normalized penetration range (thermalization length) $b_{GP}d$ of the secondary electrons in dimethyl ether (DME) is 3.5×10^{-7} g/cm^2. As the length of the *n*-alkyl groups on the ether is increased $b_{GP}d$ increases towards the value obtained for long chain *n*-alkanes, 4.5×10^{-7} g/cm^2. Electron mobilities u_e showed two types of behavior: (*i*) at low temperatures u_e approaches a value of about $2u_-$, where u_- is the mobility of the anions formed in the irradiated liquid; (*ii*) at higher temperatures the ratio u_e/u_- increases with temperature, and equals 21 in di-*n*-butyl ether (DBE) at 375 K. The activation energy of electron migration at low temperatures (ion-like mechanism) is similar to that of ion migration, 2–3 kcal/mol, while at high temperatures it increases to ~6 kcal/mol. The larger activation energy is attributed to thermal excitation of electrons from the solvated state into a conduction band, and is equal to one-half of the optical excitation energy of the solvated electrons. Electrons in water, alcohols, and ammonia at 300 K migrate by the ion-like mechanism. Electrons in alkanes migrate almost exclusively by the conduction band mechanism. A plot of the Arrhenius temperature coefficient of electron mobility against mobility in different liquids at a given temperature displays a maximum which is temperature dependent.

JEAN-POL DODELET et GORDON R. FREEMAN. Can. J. Chem. **53**, 1263 (1975).

Les éthers irradiés aux rayons X ont un rendement en ions libres plus grand que les alcanes; ceci est dû à leur constante diélectrique plus élevée. De plus, la diminution sensible de cette constante diélectrique avec l'élévation de température est responsable de la faible augmentation du rendement en ions libres comparativement aux alcanes. Le parcours moyen des électrons secondaires (jusqu'à thermalisation), normalisé pour la densité, $b_{GP}d$, est de 3.5×10^{-7} g/cm^2 pour l'éther diméthylique; il augmente avec l'alongement de la chaîne alkyle tendant vers la valeur 4.5×10^{-7} g/cm^2 obtenue pour le pentane normal. Deux types de mobilité électronique, u_e, ont été observés dans les éthers: (*i*) à basse température, u_e tend vers une mobilité dont la valeur est approximativement deux fois la mobilité anionique, u_-; (*ii*) lorsque l'on augmente la température, le rapport u_e/u_- augmente pour atteindre à 375 K la valeur 21 pour l'éther di-*n*-butylique (DBE). L'énergie d'activation, 2–3 kcal/mol, de la migration électronique à basse température est semblable à celle de la migration ionique tandis qu'à plus haute température elle augmente jusqu'à 6 kcal/mol environ. Cette dernière énergie d'activation est attribuée à l'excitation thermique des électrons depuis l'état solvaté jusqu'à la bande de conduction et vaut la moitié de l'énergie d'excitation optique. Le mécanisme de migration des électrons à 300 K dans l'eau, les alcools et l'ammoniac liquide, est de type ionique. Dans les alcanes les électrons migrent presque exclusivement par un mecanisme de bande de conduction. Le coefficient de température d'Arrhenius pour la mobilité électronique est porté en graphique en fonction de la mobilité électronique dans plusieurs liquides. Un coefficient maximum apparait à une température donnée et varie en fonction de la température.

Introduction

This article reports a continuation of the study of electron transport in dielectric liquids.

Mobilities of thermal electrons in liquid hydrocarbons range over five orders of magnitude, from 510 cm^2 V^{-1} s^{-1} in methane at 118 K to 0.003 cm^2 V^{-1} s^{-1} in ethylene at 170 K (1). The mobility depends greatly upon molecular structure (1–4 and references therein), tending to increase with increasing sphericity of the molecules. A surprising result was that the mobilities ap-

[1]This paper is dedicated to Professor C. A. Winkler of McGill University on the occasion of his sixty-fifth birthday by one of his former students (G.R.F.).

[2]Assisted financially by the National Research Council of Canada.

Can. J. Chem. Downloaded from www.nrcresearchpress.com by 210.87.254.42 on 09/05/12
For personal use only.

peared to be independent of the magnitudes of small dipole moments, $\mu \leqslant 0.5$ D, possessed by some of the molecules (5). In highly polar liquids such as water (6), alcohols (7, 8), and ammonia (9), electron mobilities are uniformly small, 10^{-3}–10^{-2} cm^2 V^{-1} s^{-1}. The purpose of the present work was to measure electron mobilities in liquids of intermediate polarity. Ethers were a suitable choice because they have moderately high gas phase dipole moments (10) and moderately low liquid phase dielectric constants (11).

The penetration ranges of secondary (~ 10 eV) electrons in ethers were studied for similar reasons. There is an empirical correlation between the mobilities of thermal electrons and the penetration ranges of secondary electrons in liquids (4, 5).

Experimental

Materials

Dimethyl ether (DME) was obtained from Matheson at a purity of 99.87%. Diethyl ether (DEE), dipropyl ether (DPE), dibutyl ether (DBE), tetrahydrofuran (THF), tetrahydropyran (THP), *p*-dioxan (PD), and *m*-dioxan (MD) were obtained from Aldrich Chemical at the highest available purity ($\geqslant$97%).

All the ethers except DME were stirred for several hours under vacuum with lithium aluminum hydride, then distilled onto sodium–potassium alloy and stirred overnight. MD reacted with the alloy, forming a white precipitate over a period of minutes. THF reacted similarly but over a period of many months, hence with a rate $\approx 10^{-5}$–10^{-6} that of MD.

DME has a low boiling point, 250 K, and was used directly from the cylinder.

Techniques

The methods of temperature control, dosimetry, charge clearing, and electron transient conductance measurements were described earlier (4, 12). However, DME, DEE, THF, and THP possessed large intrinsic specific conductivities, $>10^{-12}$ mho cm^{-1} at 300 K, that increased rapidly with temperature. For these compounds the conventional charge clearing measurements could not be made. Instead, the electron and ion conduction transient after a radiation pulse was treated as an a.c. signal, amplified, fed into a Fabritek model 1062 signal averager, and averaged over 512 pulses. Integration under the averaged transient signal gave the collected charge that resulted from an average radiation pulse. This method allowed radiolysis charge clearing measurements to be made in spite of intrinsic conductances up to 3×10^{-11} mho cm^{-1}.

The ion conductance transient obtained in the above manner displayed two portions with decay rates due to ions with different mobilities. At fields >10 kV/cm each decay portion was nearly linear with time (Fig. 1), which permitted the ionic mobilities u to be calculated from eq. 1.

$$[1] \qquad u = l^2/Vt_d$$

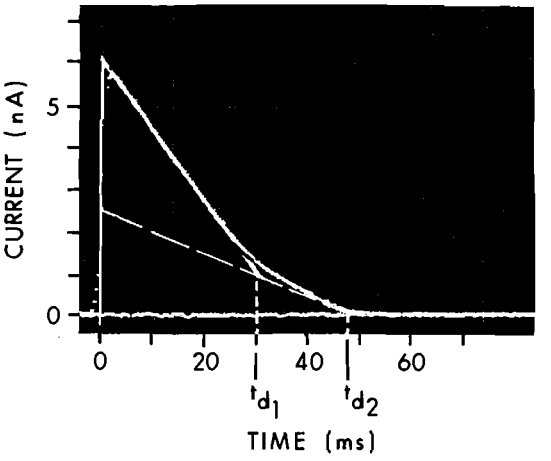

FIG. 1. Oscilloscope trace of ionic drift in di-*n*-propyl ether at 293 K. $l = 0.302$ cm and $V = 4.0$ kV. The triangles were drawn to have equal areas, corresponding to equal amounts of positive and negative charge. The lack of a sharp angle between the fast and slow decay portions is probably due to the presence of two or more slow ions with slightly different mobilities.

where l is the distance between the electrodes, V is the applied voltage, and t_d is the time required for the ion to drift the distance l.

The conductance cell (12) was coated on the outside surface with Aqua Dag (GC. Electronics TV Tube Coat) to minimize electrostatic effects caused by the flowing thermostating gas. Small ghost signals due to these electrostatic effects in uncoated cells were equivalent to an electron mobility $u_e \approx 0.001$ cm^2 V^{-1} s^{-1}, so they interfered with the electron conductance transient when u_e was <0.01 cm^2 V^{-1} s^{-1}. The ghost signals had a half life of 2 μs, so they did not interfere with the ion conductance transients, which had half lives $\sim 10^{-2}$ s.

Physical Properties of the Liquids

The densities d were obtained from the literature (13, 14). The dielectric constants ε were measured as functions of temperature with the aid of an Electro Scientific Industries model 273 capacitance bridge and a General Radio Co. model 1422-CD precision capacitor. The method of measurement and extensive data will be reported elsewhere (15). Values are listed in Table 1. They agree with data in ref. 11 within 1%, in the few cases where comparison is possible.

The intrinsic conductances of the ethers were not accurately recorded, but at 293 K they increase in the following order: PD (10^{-15} Ω^{-1} cm^{-1}) < DBE < DPE ≪ DEE (10^{-11} Ω^{-1} cm^{-1}) < DME ≈ THP < THF < MD ($\sim 10^{-10}$ Ω^{-1} cm^{-1}). The intrinsic conductance of MD was so great that the noise in it was as large as the radiation induced signal. MD also underwent radiation or electrolysis induced polymerization in the cell. The experiment with MD was abandoned.

Can. J. Chem. Downloaded from www.nrcresearchpress.com by 210.87.254.42 on 09/05/12
For personal use only.

TABLE 1. G_{fi}^0 and most probable electron range b_{GP} in liquid ethers

Liquid	T (K)	d* (g/cm³)	ε†	μ (D)‡	G_{fi}^0	b_{GP}§ (Å)	$b_{GP}d$ (10^{-8} g/cm²)	$(b_{GP}d)_{av}$ (10^{-8} g/cm²)
DME	165	0.814	10.7	1.30	0.64	42	34	35
	195	0.778	9.0		0.73	45	35	
	226	0.742	7.4		0.74	47	35	
DEE	195	0.818	8.0	1.15	0.53	41	34	35
	223	0.790	6.45		0.50	43	34	
	252	0.760	5.40		0.49	45	34	
	293	0.714	4.39		0.54	51	36	
	328	0.673	3.70		0.57	55	37	
DPE	169	0.857	5.64	1.21	0.23	46	39	39
	202	0.828	4.76		0.25	47	39	
	254	0.782	3.90		0.30	49	38	
	293	0.745	3.43		0.34	52	39	
	342	0.696	2.91		0.38	55	39	
	376	0.660	2.60		0.44	61	40	
DBE	187	0.845	4.50	1.17	0.21	49	41	42
	220	0.825	3.99		0.23	49	41	
	255	0.798	3.52		0.26	51	41	
	293	0.770	3.14		0.30	53	41	
	332	0.736	2.83		0.36	57	42	
	373	0.700	2.55		0.42	61	43	
	406	0.666	2.35		0.48	65	43	
	436	0.633	2.20		0.54	68	43	
THF	205	0.983	11.6	1.63	0.72	33	32	32
THP	231	0.935	7.28	1.6	0.45	34	32	33
	254	0.910‖	6.60		0.48	36	33	
	293	0.880‖	5.60		0.51	38	33	
PD	293	1.03	2.20	0.0	0.08	44	45	44
	335	0.982	2.15		0.12	45	44	
	374	0.939	2.08		0.16	47	44	

*References 13 and 14.
†Measured in the present work.
‡Reference 10.
§Based on the assumed value $G_{tot} = 4.3$.
‖The variation of density of THP with temperature is assumed to be the same as that of THF.

Results

Free Ion Yields and Electron Ranges

The free ion yields increased with increasing applied electric field strength. Figure 2 shows the field effect for all the ethers that could be measured at 293 K. The curves drawn through the experimental data were calculated on the basis of a single ion pair per spur model (16–19). The probability $\phi(y, E)$ that a thermalized electron–ion pair of initial intrapair separation distance y will escape geminate neutralization in the presence of an applied electric field of strength E is given by eq. 2 (12).

$$[2] \qquad \phi(y, E) = e^{-r/y}\left\{1 + e^{-\beta y}\sum_{n=1}^{\infty}\frac{(\beta y)^n}{(n+1)!}\sum_{j=0}^{n-1}(n-j)\frac{(r/y)^{j+1}}{(j+1)!}\right\}$$

where $r = \xi^2/\varepsilon kT$, $\xi = 4.80 \times 10^{-10}$ e.s.u., ε is the dielectric constant of the fluid, k is Boltzmann's constant, T is the absolute temperature, and $\beta = (\xi E/300kT)$. The free ion yield G_{fi}^E in the presence of an applied field E is given by [3] (12).

$$[3] \qquad G_{fi}^E = G_{tot}\int_0^{\infty}\phi(y,E)F(y)\,dy$$

Can. J. Chem. Downloaded from www.nrcresearchpress.com by 210.87.254.42 on 09/05/12
For personal use only.

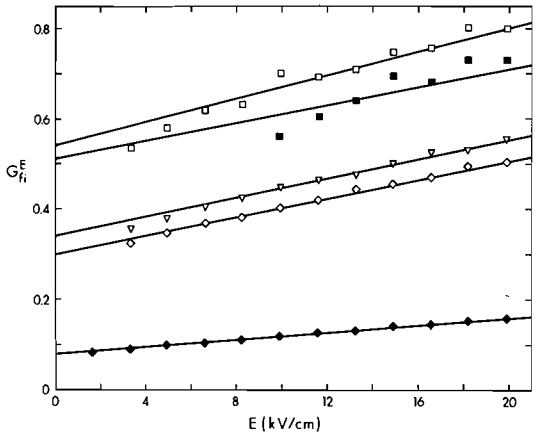

FIG. 2. Free ion yield $G_{fi}{}^E$ at field strength E in ethers at 293 K. □, diethyl ether (DEE); ■, tetrahydropyran (THP); ▽, di-*n*-propyl ether (DPE); ◇, di-*n*-butyl ether (DBE); ◆, *p*-dioxan (PD).

where G_{tot} is the total number of ion–electron pairs generated per 100 eV of energy absorbed by the fluid and $F(y)dy$ is the fraction of pairs with initial separation distances between y and $y + dy$. The distribution function used was YGP, which has a Gaussian body and a power function tail that extends the function to larger y values than would the Gaussian alone (12). The normalized equation for YGP is

$$[4]\quad \begin{cases} F(y) = 0.96\ \mathrm{YG} & y < 2.4b_{GP} \\ F(y) = 0.96\ (\mathrm{YG} + 0.5b_{GP}{}^2/y^3) & y > 2.4b_{GP} \end{cases}$$

with

$$\mathrm{YG} = (4y^2/\pi^{1/2}b_{GP}{}^3)\exp(-y^2/b_{GP}{}^2)$$

where 0.96 is a normalization factor and b_{GP} is the dispersion parameter of the Gaussian and is also the most probable value of the secondary electron range y.

Curves were fit to experimental data by selecting the value of b_{GP} that gave the minimum mean difference between the calculated and experimental free ion yields over the experimental range of field strengths used. The values of b_{GP} obtained for each ether at various temperatures are listed in Table 1. The free ion yields $G_{fi}{}^0$ extrapolated to zero applied field strength were calculated from b_{GP} and are included in Table 1.

The electron ranges in a given liquid are inversely proportional to the liquid density, so the density normalized ranges $b_{GP}d$ are also given in Table 1.

The relative variation of the free ion yield with temperature in ethers is smaller and slightly more complex than in hydrocarbons (4, 12, 20, 21). The difference is due to the relatively greater decrease of ε with increasing T in ethers than in hydrocarbons. The dielectric constant in eq. 2, and hence [3], appears only as a product with T, in r. In hydrocarbons the product εT increases with increasing T, whereas in ethers with relatively high dielectric constants, such as DME and DEE, εT decreases with increasing T. The result is that the relative variation of free ion yield with temperature is smaller in ethers than in hydrocarbons. The $G_{fi}{}^E$ *vs.* E curve for DEE at 195 K crosses the 293 and 328 K curves (Fig. 3); there is a minimum in $G_{fi}{}^E$ at about 250 K.

Ion Mobilities

The measured values of ion mobilities and their activation energies are listed in Table 2. The method does not allow one to distinguish between positively and negatively charged ions, so it is not known for certain that the faster moving ions were anions. Mobilities of cations and anions have been extensively studied in hydrocarbons (for a review see ref. 22). For these liquids the anion mobility was always greater than that of the cations. We assumed the same to be true in ethers. In diethyl ether vapor anion mobilities have been observed to be greater than those of the cations (22). However, the reverse was reported for liquid PD (23), so

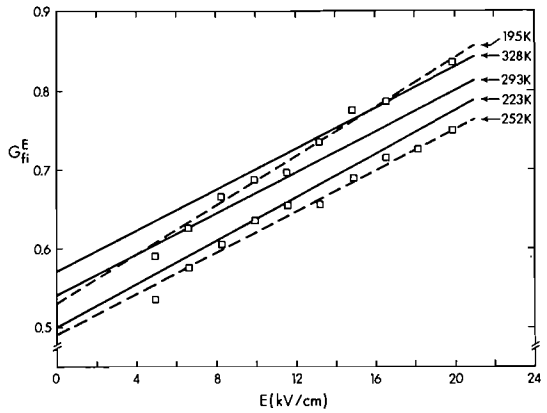

FIG. 3. Free ion yield plotted against field strength in diethyl ether at the temperatures indicated. The curves were calculated using the values of b_{GP} listed in Table 1. Experimental points are only displayed for 195 and 252 K, for clarity; the calculated curves for these two temperatures are dashed for the same reason.

Can. J. Chem. Downloaded from www.nrcresearchpress.com by 210.87.254.42 on 09/05/12
For personal use only.

TABLE 2. Positive and negative ion mobilities u_+ and u_-, liquid viscosities η, and their Arrhenius temperature coefficients $E_\pm$ and E_η in ethers

Liquid	T (K)	u_+ (10^{-4} cm^2 V^{-1} s^{-1})	u_- (10^{-4} cm^2 V^{-1} s^{-1})	$E_\pm$ (kcal/mol)	η^{-1}* (cP^{-1})	E_η (kcal/mol)
DME	165	3.0	4.6	1.4	1.3	1.2
	195	5.2	7.9		2.2	
	226	8.3	12.4		3.33	
	255	12	19		4.7	
DEE	168	0.8	1.2	1.9	0.56	1.7
	195	1.7	2.6		1.09	
	223	3.3	4.9		1.88	
	253	5.9	8.9		3.07	
	293	10	15		4.34	
	328	13	20		6.25	
DPE	215	0.9	1.4	2.4	0.72	1.9
	293	4.3	6.9		2.43	
	377	10.7	16.9		5.55	
DBE	219	0.5	1.1	2.7	0.4	2.3
	293	2.9	4.8		1.49	
	373	6.9	14		3.57	
	436	13	24		5.55	
THF	205	1.2	1.7	—	0.60	1.5
THP	231	0.8	1.2	2.8	—	—
	254	1.2	1.8		—	
	293	2.8	4.2		—	
PD	293	2.2	3.7	2.8	0.82	2.2
	336	3.9	6.7		1.33	
	374	5.9	10.1		1.72	

*Reference 13. The values are listed as η^{-1} for direct comparison with the mobilities.

our assignments remain uncertain. The ratio $(u_{fast}/u_{slow}) = 1.7 \pm 0.3$ in all the ethers.

The sum of the separately determined u_+ and u_- values was checked by calculating $(u_+ + u_-)$ from the height of the ion conductance transient, in the manner used for measuring electron mobilities (5). The two methods agreed within 10%.

Electron Mobilities

Electron conductance transients were measured on a microsecond time scale, compared to the millisecond scale used for the ion transients. The shorter time scale used for electrons was due partly to their higher mobilities and partly to their removal by reaction with trace impurities in the ethers. Addition of 10^{-3}–10^{-2} M nitrous oxide to an ether eliminated the electron signal by reacting with the electrons in a time shorter than the response time of the equipment, which was 100 ns.

The electron conductance transient method of determining mobilities (4) yields the sum of the electron and positive ion mobilities $(u_e + u_+)$. The value of u_e was obtained by subtracting u_+ from the sum. The appropriate value of u_+ was obtained by interpolation or extrapolation of data in the previous section.

The electron mobilities are listed in Table 3.

Difficulty was experienced with THF and THP. The mobility measurement involves taking the ratio of the peak magnitude of the electron conductance transient (amps) to the integrated charge collected (coulombs) after a radiation pulse. However in THF and THP the electron conductance transients were small at low temperatures and the radiolytic-charge integration was poor at high temperatures (due to large intrinsic conductances). The mobilities were estimated by measuring the conductance magnitudes at high temperatures and calculating the free ion yields (proportional to the integrated charge collected) at those temperatures by assuming $b_{GP}d$ to be constant. The amount of error introduced by this technique would be $<10\%$ because $b_{GP}d$ was observed to be nearly independent of temperature in the other ethers (Table 1) and in hydrocarbons (1, 2, 12).

Arrhenius plots of the electron and anion

Can. J. Chem. Downloaded from www.nrcresearchpress.com by 210.87.254.42 on 09/05/12
For personal use only.

Can. J. Chem. Downloaded from www.nrcresearchpress.com by 210.87.254.42 on 09/05/12
For personal use only.

TABLE 3. Mobilities of electrons in ethers

Liquid	T (K)	u_e (10^{-3} cm^2 V^{-1} s^{-1})
DEE	166	0.23
	196	0.64
	218	1.1
	240	1.8
	266	2.8
	294	5.1
	317	7.3
	337	12
DPE	293	3.7
	323	9.4
	340	14
	357	22
	378	40
DBE	238	0.44
	263	1.1
	294	3.4
	324	8.8
	351	18
	375	29
THF	293	3
THP	293	3.1
	323	6.2
	349	12
	374	19
PD	293	0.8
	352	3.7
	370	4.0

mobilities are given in Fig. 4. At low temperatures electron mobilities in some ethers are lower than ion mobilities in others, but at high temperatures the group of electron curves rises above the group of ion curves.

Discussion

Electron Ranges

The density normalized penetration ranges $b_{GP}d$ of the secondary electrons in ethers are smaller than those in the corresponding alkanes (12), compared by exchanging an —O— for a —CH_2—. However, the ether values approach those of the long chain *n*-alkanes (4.5×10^{-7} g/cm^2) as the length of the alkyl groups in the ether is increased. The chain length effect appears to be one of dilution.

The normalized ranges in ethers are larger than those in *trans*- but smaller than those in *cis*-olefins (12), compared by exchanging an —O— for a —CH=CH—.

By considering PD to be a dimer of DME, and

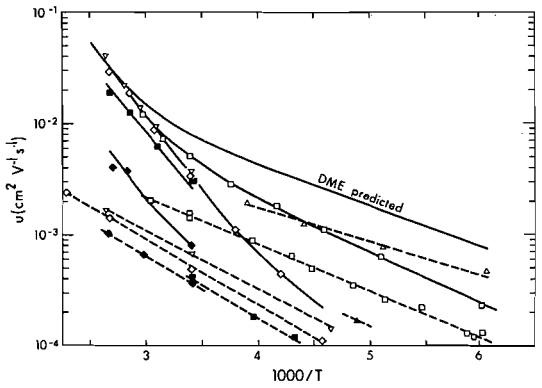

FIG. 4. Electron (—) and anion (---) mobilities in ethers. Open points, di-*n*-alkyl ethers: △, DME; □, DEE; ▽, DPE; ◇, DBE. Full points, cyclic ethers: ◆, PD; ■, THP; ▲, THF. The electron mobility curves were calculated from eqs. 12 and 13, using the parameter values in Table 5.

THF to be a closed ring form of DEE, one may detect small reductions in $b_{GP}d$ that correlate with large increases in molecular dipole moment (Table 4). It had been noted earlier (5) that small changes in molecular dipole moment had negligible effect on the ranges and mobilities of electrons in liquid hydrocarbons. The controlling factors are evidently short range interactions, but their nature is not yet clear. Transfer of electron kinetic energy to molecular vibrations and rotations through transient negative ion formation would be a tempting suggestion if it could accommodate the large difference in behavior of *cis*- and *trans*-butene-2. Of course, different mechanisms may dominate in different systems.

TABLE 4. Correlation between normalized range $b_{GP}d$ and dipole moment μ in related ethers

Liquid		μ (D)*	$b_{GP}d$ (10^{-8} g/cm^2)
PD		0.0	44
DME		1.30	35
DEE		1.15	35
THF		1.63	32

*Gas phase values from ref. 10.

Can. J. Chem. Downloaded from www.nrcresearchpress.com by 210.87.254.42 on 09/05/12
For personal use only.

Ion Mobilities

In all of the di-*n*-alkyl ethers from DME to DBE the anion and cation mobilities are related to the liquid viscosity by approximately the same relations

$$[5] \qquad u_- = (2.6 \pm 0.5)10^{-4}\eta^{-1.2}$$

$$[6] \qquad u_+ = (1.5 \pm 0.3)10^{-4}\eta^{-1.2}$$

where u_+ and u_- are in $cm^2\ V^{-1}\ s^{-1}$ and η in cP. The anion mobilities fall in the lowest hatched region of Fig. 5.

The mobility–viscosity relationships are dependent on the type of structure of the solvent molecules. For example, the ions in the cyclic ethers PD and THF have higher mobilities than those in the *n*-alkyl ethers at the same viscosity. They are higher by a factor of about two. However, the viscosity exponent in relations analogous to [5] and [6] was in the range -1.1 to -1.3 in all of the ethers studied. This simply means that the ratio of activation energies of ion mobility and viscous flow has the value $E_\pm/E_\eta = 1.2 \pm 0.1$ in these liquids.

Stokes' law predicts $u \propto \eta^{-1.0}$. Although ion migration is strongly influenced by the solvent viscosity (the ease of solvent molecular translation), the relative difficulty of rotation of the solvent molecules must also be a factor in determining the rate of ion migration in a liquid. Most types of ions do not drag a complete solvation shell with them when they diffuse, but energy requirements would result in the solvation shell of an ion being moderately highly polarized even in the transition state of a diffusion step. Thus solvent molecular rotation should be important in ion diffusion. Rotational motions in polar liquids are usually studied as dielectric relaxation times. Unfortunately, the dielectric relaxation times τ are not known as a function of temperature for any of the present ethers except DEE (24), so an extended correlation with ion mobility cannot be made. However, the activation energy of dielectric relaxation in DEE is $E_\tau = 2.0$ kcal/mol, so $u_- \propto \tau^{-0.95}$ in this liquid.

Electron Mobilities in Ethers

At low temperatures u_e in a particular ether approaches a value of about $2u_-$ in that ether. This behavior is most clearly visible in the DEE results (Fig. 4), but is also observed in those from DBE and PD. At higher temperatures the ratio u_e/u_- increases with temperature, having the value 21 in DBE at 375 K (Fig. 4). Thus the

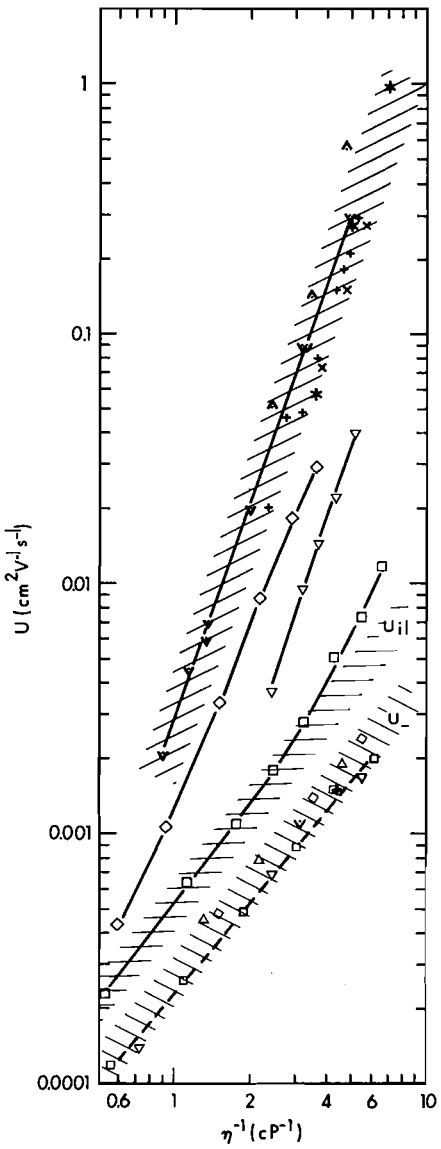

FIG. 5. Electron and anion mobilities in di-*n*-alkyl ethers and *n*-alkanes, plotted against the inverse of the liquid viscosity. The top hatched region refers to electrons in *n*-alkanes, with an inner line drawn through the hexane points for reference. The lowest hatched region refers to anions in the ethers and alkanes, with an inner line drawn through the DEE points for reference. The center hatched region is the expected range of ion-like mobilities for electrons in these liquids. The central lines represent electron mobilities in *n*-alkyl ethers. Solvent: △, DME; □, DEE; ▽, DPE; ◇, DBE; *, ethane; ∧, propane; ×, *n*-butane; +, *n*-pentane; ∨, *n*-hexane. The electron mobilities in hydrocarbons were taken from refs. 1–3 and 45; the ion mobilities in pentane and hexane are from ref. 46. The viscosities were obtained from ref. 13, by extrapolation where necessary.

Can. J. Chem. Downloaded from www.nrcresearchpress.com by 210.87.254.42 on 09/05/12
For personal use only.

activation energy of electron migration in ethers at low temperatures is approximately equal to that of ion migration, 2–3 kcal/mol, while at high temperatures the activation energy of electron migration increases to ~6 kcal/mol, more than double the value for ions. The change of activation energy signifies a change in the mechanism of migration.

The mechanism of electron migration in low temperature ethers apparently resembles that of ion migration. This implies that the diffusive jump distances are short and that solvent rearrangement is involved. Ion mobilities in the present liquids display Arrhenius type temperature dependence (Fig. 4). Thus at low temperatures u_e may be represented by [7].

$$[7] \qquad u_e(\text{low } T) = u_{il}^0 \exp(-E_{il}/RT)$$

where u_{il}^0 and E_{il} are respectively the pre-exponential factor and activation energy for ion-like migration.

Electron migration at high temperatures can be described in terms of thermal excitation from the solvated state into a conduction band. By analogy with the conductance of an n-type semiconductor (25, 26), the average mobility at high temperature is the product of the mobility u_{cb} in the conduction band and the fraction of the electrons that are in the band.

$$[8] \qquad u_e(\text{high } T) = u_{cb} \exp(-E_{cb}/RT)$$

where E_{cb} is the thermal energy barrier between the solvated electron and the conduction band.

The value of u_{cb} is usually considered to have a negative power dependence on temperature (25, 26). For the sake of discussion it will be assumed that u_{cb} in liquid ethers has the $T^{-3/2}$ dependence characteristic of electron scattering by phonons (26).

$$[9] \qquad u_{cb} = u_{cb}^0 T^{-3/2}$$

Solvated electrons do not all reside in traps of the same depth, so eq. 8 must be integrated over the distribution of E_{cb} values. This distribution is not yet known, but some information can be obtained about it by fitting calculated mobilities to the observed mobility *vs.* temperature results. It is particularly interesting to estimate E_{cb} relative to the optical excitation energies that are displayed in the optical absorption spectrum (27, 28). The thermal energies may be lower than the optical energies for a number of reasons (25, 26).

Equation 8 may be written

$$[10] \qquad u_e(\text{high } T) = u_{cb}\chi$$

where

$$[11] \qquad \chi = \frac{\int_0^\infty \exp(-E/RT)N(E)\,dE}{\int_0^\infty N(E)\,dE}$$

and $N(E)dE$ is the relative number of solvated electrons with E_{cb} values between E and $E + dE$.

The mobility at any temperature is

$$[12] \qquad u_e = (1 - \chi)u_{il}^0 \exp(-E_{il}/RT) + \chi u_{cb}$$

The calculations with [12] were systematized through the mobilities in DEE, which were measured over the greatest temperature range (Fig. 4). The mobilities at low temperatures show that $u_{il}^0 = 0.13\ \text{cm}^2\ \text{V}^{-1}\ \text{s}^{-1}$ and $E_{il} = 2.1$ kcal/mol (0.09 eV/electron) in this liquid. The mobilities at high temperatures give information about $N(E)$ and u_{cb}^0. In preliminary calculations $N(E)$ was approximated by the optical absorption spectrum reported by Jou and Dorfman (27) for electrons in DEE at room temperature (~297 K). The spectrum has an absorption maximum at the energy $E_{am} = 0.54$ eV. It has an approximately Gaussian shape on the low energy side with a dispersion parameter $\sigma = 0.18$ eV, and an approximately Lorentzian (Cauchy) shape on the high energy side with a dispersion parameter $L = 0.30$ eV. The temperature coefficient of the absorption maximum is $dE_{am}/dT \approx -0.0017$ eV/deg, while σ and L are nearly independent of temperature (28). With these parameter values the calculated temperature coefficient of the mobilities was too large, which means that the optical absorption energies are larger than E_{cb}.

In the next series of calculations the activation energy E was reduced by arbitrarily dividing it by $n > 1$, so the Boltzmann exponent in [11] became $(-E/nRT)$. It was demonstrated that this was also equivalent to leaving the Boltzmann exponent as $(-E/RT)$ and reducing the E values in $N(E)$ by dividing E_{am}, σ, and L each by n. Values of n ranging from 1.1 to 5.0 were tried, and $n = 2.0^{+0.5}_{-0.3}$ gave the best agreement with experiment. The best value of u_{cb}^0 was 23 000 $\text{cm}^2\ \text{deg}^{3/2}\ \text{V}^{-1}\ \text{s}^{-1}$, corresponding to $u_{cb} = 4.6\ \text{cm}^2\ \text{V}^{-1}\ \text{s}^{-1}$ at 294 K. Thus the thermal activation energy for electron mobility in high temperature ethers is equal to one-half of the optical excitation energy.

The value $n = 2$ might be a coincidence, but

Can. J. Chem. Downloaded from www.nrcresearchpress.com by 210.87.254.42 on 09/05/12
For personal use only.

several mechanisms of thermally activated electron migration in semiconductors lead to an exponential factor $\exp(-E/2RT)$ (26). It is not clear which, if any, of the specific mechanisms might apply to electrons in ethers, but it is tempting to speculate that the great breadth of the optical absorption spectra of solvated electrons is due to a large variation in trap depths, and that most of the observed spectrum in an ether is due to bound–continuum transitions. The possible subdivision of the optical spectra of solvated electrons into bound–bound and bound–continuum transitions has received attention recently (29–32).

The shape of $N(E)$ for thermal excitation might be expected to be different from that of the optical absorption spectrum, but a random set of trap depths could give a Gaussian shape to the low energy side of both. One might also expect the high energy side of both to be more extended than a Gaussian. However, to simplify the calculations for the series of ethers, $N(E)$ was taken to be entirely Gaussian. To facilitate comparison with optical absorption energies the factor $n = 2$ was left in the Boltzmann exponent, although it might actually belong in $N(E)$ as $(E_{am}/2)$ and $(\sigma/2)$. Hence, χ was taken as [13].

$$[13]\quad \chi = \frac{\int_0^\infty \exp\left\{-\frac{E}{2RT} - \left(\frac{E-E_{am}}{\sigma}\right)^2\right\} dE}{\int_0^\infty \exp\left\{-\left(\frac{E-E_{am}}{\sigma}\right)^2\right\} dE}$$

The optical values of E_{am} and σ again gave agreement with the experimental mobilities in DEE, but the required value of u_{cb}^0 was reduced to 13 000 $cm^2\ deg^{3/2}\ V^{-1}\ s^{-1}$. The only effect of decreasing the high energy side of $N(E)$ from a Lorentzian with $L = 0.30$ eV to a Gaussian with $\sigma = 0.18$ eV was to reduce the estimated value of u_{cb}^0 by a factor of 1.8. The high energy side of $N(E)$ contributes negligibly to the *number* of electrons in the conduction band, so reducing the hypothetical population on the high energy side merely increases the apparent *fraction* of electrons on the low energy side and correspondingly decreases the estimated value of u_{cb} (see eqs. 10 and 11). The values of u_{cb} obtained by using [13] are lower limits.

The calculated mobilities are shown in Fig. 4.

The entire set of calculations was repeated with the DBE mobilities and similar conclusions were reached. In both DEE and DBE it appears that $u_{il}^0 \approx 0.13\ cm^2\ V^{-1}\ s^{-1}$ and $E_{il} \approx 1.1\ E_\pm$. The parameters are listed in Table 5 and the calculated curve is shown in Fig. 4.

TABLE 5. Parameters for the calculation of u_e by eq. 12*

Liquid	E_{il} (eV)	u_{cb}^0 ($cm^2\ deg^{3/2}\ V^{-1}\ s^{-1}$)	E_{am}(293 K) (eV)
DME	0.07†	13 000†	0.56†
DEE	0.09	13 000	0.54‡
DPE	0.10	14 000	0.52†
DBE	0.124	12 000	0.50
THF	0.105	13 000	0.59‡
THP	0.12	13 000†	0.53
PD	0.14	13 000†	0.74

*Equation 13 was used for χ. The values $u_{il}^0 = 0.13\ cm^2\ V^{-1}s^{-1}$, $(dE_{am}/dT) = -0.0017$ eV/deg, and $\sigma = 0.33E_{am}$ (293 K) independent of temperature, were assumed for all ethers.
†Assumed.
‡Reference 27.

The calculations using [12] and [13] were then extended to all the ethers. The estimated parameter values are listed in Table 5 and the calculated curves are displayed in Fig. 4. In all cases $u_{il}^0 = 0.13\ cm^2\ V^{-1}\ s^{-1}$ and $E_{il} = (1.1 \pm 0.1)E_\pm$ were consistent with the data. The conduction band mobilities appear to be similar in all the ethers. The value $u_{cb}^0 = 13\,000\ cm^2\ deg^{3/2}\ V^{-1}\ s^{-1}$ corresponds to $u_{cb} = 2.6\ cm^2\ V^{-1}\ s^{-1}$ at 294 K. Not much weight should be given to the absolute value assigned here to u_{cb}^0 because it is highly sensitive to the assumed shape of $N(E)$ and to the temperature coefficient of E_{am}. For example, decreasing (dE_{am}/dT) to -0.0010 eV/deg would increase u_{cb} to 152 $cm^2\ V^{-1}\ s^{-1}$ at 294 K.

The only unusual result in the series is the high value of E_{am} in PD. If the apparent correlation between $N(E)$ and the optical absorption spectrum is real, solvated electrons in PD at 294 K should have an absorption maximum at $E_{am} = 0.74$ eV ($\lambda_{max} = 1.7\ \mu$). This might seem surprising in view of the relatively low dielectric constant of the liquid (Table 1), but is consistent with the observation that E_{am} is greater in polyethers than in monoethers (27). Measurement of the optical spectrum in PD will provide a test of the correlation with $N(E)$.

Experimental difficulties prevented the measurement of u_e in DME, but parameter values were estimated by comparison with those for the other alkyl ethers. The predicted mobilities in DME are shown in Fig. 4.

E_{il} is greater than E_η in all the ethers. In DEE, the only ether for which the activation energy of dielectric relaxation is known (24), $E_{il} = 1.1\ E_\tau$.

Can. J. Chem. Downloaded from www.nrcresearchpress.com by 210.87.254.42 on 09/05/12
For personal use only.

This is consistent with the suggestion that solvent molecular rotation makes a major contribution to the ion-like migration mechanism of electrons. Rotational and translational motions of the nonspherical solvent molecules are not independent of each other. The ion-like mechanism of electron migration appears to be governed by migration of the potential well through rotational–translational motions of the dipoles that constitute the well and the medium immediately surrounding it.

The ion-like migration in liquid ethers behaves like the hopping mechanism discussed for amorphous semiconductors (26, 33). A relatively short hopping distance is envisaged in both cases. Whether or not a completely new site is involved in each hop in the liquid depends on whether the hopping distance is greater or less than a molecular diameter.

Electron Mobilities in Other Liquids

Equation 10 was used to estimate the contribution of conduction bands to electron migration in water, alcohols, and ammonia at $\sim$296 K. Values of σ were obtained from known spectra (34–38), and $u_{cb}{}^0$ was taken as $\lesssim 10^5$ cm^2 deg$^{3/2}$ V^{-1} s^{-1}. The contribution of conduction bands in all these liquids was estimated to be negligible at room temperature and below. Electron migration is therefore ion-like, with $u_e/u_- = 2 \pm 1$ in water (6, 39) and alcohols (7, 40). Consistent with this conclusion, the activation energies of viscous flow (13), dielectric relaxation (24), and electron mobility (7, 39) are similar to each other in water or in a given alcohol (41). However, $u_e/u_{Cl^-} = 5$ in ammonia at 240 K (9, 42), so electron migration in this liquid might involve other processes than the simple rotational–translational motions of the solvent molecules. Molecular inversion might make a contribution to electron trap migration. Ammonia molecules invert through a planar ground state with an activation energy of 5.8 kcal/mol (43). It would be informative to measure the temperature dependences of electron migration, viscous flow, and dielectric relaxation in ammonia in the vicinity of 240 K.[3]

[3]NOTE ADDED IN PROOF: The activation energy of electron mobility of dilute solutions of sodium in liquid ammonia near 240 K is $E_u \approx 2.2 \pm 0.5$ kcal/mol, estimated from the data of Kraus (48) and Kraus and Lucasse (49). The activation energy of viscous flow of ammonia near 240 K is $E_\eta = 1.4$ kcal/mol, calculated from data in ref. 50. We now need to know E_τ and a more accurate value of E_u.

By contrast, electron migration in saturated hydrocarbons occurs almost exclusively by the conduction band mechanism. The optical absorption spectra of electrons in saturated hydrocarbons lie at lower energies than those of electrons in ethers (44), and u_e is expected to increase approximately exponentially with decreasing E_{am}. Unfortunately there is not sufficient information about the optical spectra in liquid alkanes to allow quantitative calculations to be done.

To demonstrate that electrons do not migrate to an appreciable extent by the ion-like mechanism in alkanes, the mobilities in five *n*-alkanes (1–3, 45 (*n*-pentane values)) were plotted against the inverse of the liquid viscosity (Fig. 5). The *n*-alkanes were chosen because electron mobilities are lower in these than in branched or cycloalkanes at the same viscosity. Thus the contribution of the ion-like mechanism to electron migration in the *n*-alkanes is greater than that in the other alkanes. The electron mobilities fall in the uppermost hatched region of Fig. 5, while the anion mobilities (46) fall in the lowest hatched region with the anions in *n*-alkyl ethers. The center hatched region represents the expected range of ion-like mobilities for electrons in these liquids, with $u_{il} \approx (2\text{–}3)u_-$. The electron mobilities in alkanes lie well above the ion-like region. Mobilities in ethers are intermediate. Furthermore, the steep slopes of the alkane plots indicate that the activation energy of electron mobility in *n*-alkanes (4 $\pm$ 1 kcal/mol (1–3)) is about 3-fold that of viscous flow. If the correlation between $N(E)$ and the optical spectrum is real, the activation energy is consistent with an optical absorption band centering at $\sim$0.4 eV ($\lambda_{max} \approx 3$ μ) for electrons in *n*-hexane at 300 K.

Furthermore, the mobility $u_e = 10$ cm^2 V^{-1} s^{-1} at 296 K in neohexane, with an activation energy of 1.4 kcal/mol (2), is consistent with an optical absorption band centering at $\sim$0.1 eV ($\lambda_{max} \approx 12$ μ) in that liquid.

The high mobility and low activation energy in neopentane (47) are consistent with electrons being scattered by potential wells of depth $\sim kT$ ($\lambda_{max} \approx 40$ μ) in that liquid.

The values of u_{cb} are not necessarily the same from one type of liquid to another.

Temperature Dependence of Electron Mobility in Liquids

The Arrhenius temperature coefficient E_a of electron mobility passes through a maximum as

Can. J. Chem. Downloaded from www.nrcresearchpress.com by 210.87.254.42 on 09/05/12
For personal use only.

one passes from low to high mobilities. The location and magnitude of the maximum depend on the particular values of u_{i1}^0, E_{i1}, and u_{cb}. To illustrate the effect eq. 14 was taken as an approximation of [12].

$$[14] \quad u_e = 0.1 \exp(-2000/RT) + 100 \exp(-E_{cb}/RT)$$

where u_{i1}^0 and u_{cb} are 0.1 and 100 $cm^2\ V^{-1}\ s^{-1}$, respectively, $E_{i1} = 2000$ cal/mol, and a single "effective" value of E_{cb} was used for a given liquid. Values of u_e were calculated from [14] for a series of values of E_{cb}, at $T = 280$, 300, and 320 K. The values at 280 and 320 K were used to calculate an Arrhenius temperature coefficient E_a from [15].

$$[15] \quad u_e = A_a e^{-E_a/RT}$$

E_a was then plotted against the calculated value of u_e for 300 K (Fig. 6).

With the above choice of parameters E_a has a maximum of 4.6 kcal/mol at $u_e = 0.02\ cm^2\ V^{-1}\ s^{-1}$, with $E_{cb} \approx 5.5$ kcal/mol. For $u_e \geqslant 0.1\ cm^2\ V^{-1}\ s^{-1}$, $E_a = E_{cb}$; values of E_{cb} are marked at several places along the curve in Fig. 6. For $u_e < 0.02\ cm^2\ V^{-1}\ s^{-1}$ E_a decreases with decreasing mobility, reaching $E_a = E_{i1}$ when $E_{cb} = \infty$. However, the parameter values used in this illustration place E_a within experimental error of E_{i1} when $E_{cb} > 8$ kcal/mol (>0.3 eV/electron).

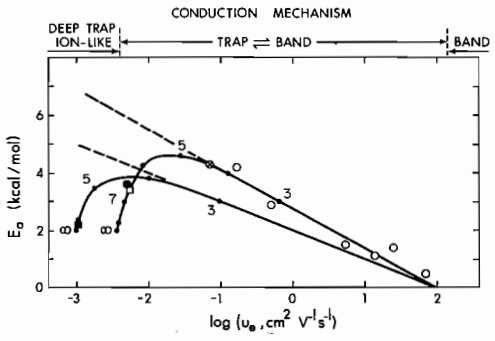

FIG. 6. Variation of the Arrhenius temperature coefficient E_a with electron mobility. The solid curves were calculated from eqs. 14 and 15: upper curve, $T = 300$ K; lower curve, $T = 215$ K. The small dots on the curves represent the points calculated using $E_{cb} = 3$, 4, 5, 6, 7, 8, and ∞ kcal/mol; alternate points are labelled with the value of E_{cb}. The experimental points at 300 K represent: ○, saturated hydrocarbons from refs. 3, 4, and 45; ⊗, n-C_6H_{14} from ref. 47; □, DEE. At 215 K: ●, estimated for n-C_6H_{14} from data in ref. 47: ■, DEE. The dashed lines are extrapolations of $u_e = 100 \exp(-E_{cb}/RT)$.

Experimental values of u_e and E_a at 300 K in a number of hydrocarbons (3, 4, 45, 47) and in DEE (in which u_{i1} agrees approximately with that of eq. 14) are included in Fig. 6. The results are consistent with the model. The scatter of the points about the line represent mainly variations in u_{cb} and experimental error.

The calculations with [14] and [15] were repeated for $T = 200$, 215, and 230 K. The curve for 215 K lies below and to the left of the 300 K curve in Fig. 6. The behavior is consistent with the experimental data available for 215 K.

We are grateful to the staff of the Radiation Research Center for help with the electronics.

1. M. G. ROBINSON and G. R. FREEMAN. Can. J. Chem. **52**, 440 (1974).
2. W. F. SCHMIDT and A. O. ALLEN. J. Chem. Phys. **52**, 4788 (1970).
3. R. M. MINDAY, L. D. SCHMIDT, and H. T. DAVIS. J. Chem. Phys. **54**, 3112 (1971).
4. J.-P. DODELET and G. R. FREEMAN. Can. J. Chem. **50**, 2667 (1972).
5. J.-P. DODELET, K. SHINSAKA, and G. R. FREEMAN. J. Chem. Phys. **59**, 1293 (1973).
6. K. SCHMIDT and M. ANBAR. J. Phys. Chem. **73**, 2846 (1969).
7. P. FOWLES. Trans. Faraday Soc. **67**, 428 (1971).
8. A. V. RUDNEV, A. V. VANNIKOV, and N. A. BAKH. High Energy Chem. Engl. Transl. **6**, 416 (1972).
9. D. S. BURNS. Adv. Chem. Ser. **50**, 82 (1965).
10. R. D. NELSON, JR., D. R. LIDE, JR., and A. A. MARYOTT. Selected values of electric dipole moments in the gas phase. NSRDS-NBS 10, Washington, D.C. 1967.
11. A. A. MARYOTT and E. R. SMITH. Tables of dielectric constants of pure liquids. NBS Circular 514, Washington, D.C. 1951.
12. J.-P. DODELET, K. SHINSAKA, U. KORTSCH, and G. R. FREEMAN. J. Chem. Phys. **59**, 2376 (1973).
13. R. W. GALLANT. Physical properties of hydrocarbons, Vols. 1 and 2. Gulf Publishing Co., Houston, Texas. 1968 and 1970.
14. R. R. DREISBACH. Physical properties of chemical compounds. Adv. Chem. Ser. **15** (1955); **22** (1959).
15. J.-P. DODELET, K. SHINSAKA, and G. R. FREEMAN. To be published.
16. L. ONSAGER. Phys. Rev. **54**, 554 (1938).
17. G. R. FREEMAN. J. Chem. Phys. **39**, 1580 (1963).
18. J. TERLECKI and J. FIUTAK. Int. J. Radiat. Phys. Chem. **4**, 469 (1972).
19. G. R. FREEMAN and J.-P. DODELET. Int. J. Radiat. Phys. Chem. **5**, 371 (1973).
20. W. F. SCHMIDT and A. O. ALLEN. J. Phys. Chem. **72**, 3730 (1968).
21. M. G. ROBINSON, P. G. FUOCHI, and G. R. FREEMAN. Can. J. Chem. **49**, 3657 (1971).
22. I. ADAMCZEWSKI. Brit. J. Appl. Phys. **16**, 759 (1965); Acta Phys. Polon. **30**, 707 (1966).
23. A. HUMMEL, A. O. ALLEN, and F. H. WATSON, JR. J. Chem. Phys. **44**, 3431 (1966).

24. F. BUCKLEY and A. A. MARYOTT. Tables of dielectric dispersion data for pure liquids and dilute solutions. NBS Circular 589, Washington, D.C. 1958.
25. C. KITTEL. Introduction to solid state physics, 4th ed. Wiley, New York. 1971. Chapt. 11.
26. N. F. MOTT and E. A. DAVIS. Electronic processes in non-crystalline materials. Clarendon Press, Oxford. 1971. Chapters. 2–4, and 7.
27. F. Y. JOU and L. M. DORFMAN. J. Chem. Phys. **58**, 4715 (1973).
28. F. Y. JOU AND G. R. FREEMAN. To be published.
29. R. LUGO and P. DELAHAY. J. Chem. Phys. **57**, 2122 (1972).
30. T. KAJIWARA, K. FUNABASHI, and C. NALEWAY. Phys. Rev. A**6**, 808 (1972).
31. N. R. KESTNER and J. JORTNER. J. Phys. Chem. **77**, 1040 (1973).
32. K. FUEKI, D.-F. FENG, and L. KEVAN. J. Chem. Phys. **59**, 6201 (1973).
33. W. E. SPEAR. Adv. Phys. **23**, 523 (1974).
34. B. D. MICHAEL, E. J. HART, and K. H. SCHMIDT. J. Phys. Chem. **75**, 2798 (1971).
35. M. C. SAUER, JR., S. ARAI, and L. M. DORFMAN. J. Chem. Phys. **42**, 708 (1965).
36. S. ARAI and M. C. SAUER, JR. J. Chem. Phys. **44**, 2297 (1966).
37. U. SCHINDEWOLF, R. VOGELSGESANG, and K. BODDEKER. Angew. Chem. **79**, 1064 (1967).
38. FARHATAZIZ, L. M. PERKEY, and R. R. HENTZ. J. Chem. Phys. **60**, 4383 (1974).
39. G. C. BARKER, P. FOWLES, D. C. SAMMON, and B. STRINGER. Trans. Faraday Soc. **66**, 1498 (1970).
40. R. A. VERMEER and G. R. FREEMAN. Can. J. Chem. **52**, 1181 (1974).
41. K. N. JHA and G. R. FREEMAN. J. Chem. Phys. **51**, 2846 (1969).
42. C. A. KRAUS and W. C. BRAY. J. Am. Chem. Soc. **35**, 1315 (1913).
43. J. D. SWALEN and J. A. IBERS. J. Chem. Phys. **36**, 1914 (1962).
44. A. EKSTROM and J. E. WILLARD. J. Phys. Chem. **72**, 4599 (1968).
45. J.-P. DODELET and G. R. FREEMAN. To be published.
46. P. H. TEWARI and G. R. FREEMAN. J. Chem. Phys. **49**, 4394 (1968).
47. R. M. MINDAY, L. D. SCHMIDT, and H. T. DAVIS. J. Phys. Chem. **76**, 442 (1972).
48. C. A. KRAUS. J. Am. Chem. Soc. **43**, 749 (1921).
49. C. A. KRAUS and W. W. LUCASSE. J. Am. Chem. Soc. **44**, 1941 (1922).
50. R. C. WEAST. (*Editor*). The handbook of chemistry and physics, 50th ed. Chemical Rubber Co., Cleveland, Ohio. 1969.

Can. J. Chem. Downloaded from www.nrcresearchpress.com by 210.87.254.42 on 09/05/12
For personal use only.

Bond Scission in Sulfur Compounds. Part X.[1] The Hydrazinolysis of Methyl *p*-Nitrophenyl Sulfate

ERWIN BUNCEL AND CLAUDIO CHUAQUI

Department of Chemistry, Queen's University, Kingston, Ontario K7L 3N6

Received October 15, 1974

ERWIN BUNCEL and CLAUDIO CHUAQUI. Can. J. Chem. **53**, 1275 (1975).

Reaction of methyl *p*-nitrophenyl sulfate with the hydrazine – hydrazine hydrochloride system in methanol gives rise to different types of behavior depending on the state of ionization of the reagent. For the $H_2NNH_2/H_2NNH_3^+$ combination the observed reaction is conversion of methyl *p*-nitrophenyl sulfate to *p*-nitrophenyl sulfate ion (alkyl–oxygen scission). For the $H_2NNH_3^+/{}^+H_3NNH_3^+$ combination, or with ${}^+H_3NNH_3^+$ alone, one observes the consecutive processes methyl *p*-nitrophenyl sulfate → *p*-nitrophenyl sulfate ion → *p*-nitrophenol (alkyl–oxygen followed by sulfur–oxygen scission). For the alkyl–oxygen scission process, *i.e.* nucleophilic displacement on the alkyl carbon, the observed pseudo first-order rate constant is given by the contributions of several nucleophilic species; $k_{obs} = k_{sol} + k_{Cl^-}[Cl^-] + k_{H_2NNH_3^+}[H_2NNH_3^+] + k_{H_2NNH_2}[H_2NNH_2]$. A method for the dissection of k_{obs} into the constituent terms is given. The sulfur–oxygen scission process is an acid catalyzed reaction and the measured kinetic data have been utilized for the derivation of the pK_a of ${}^+H_3NNH_3^+$ in methanol. Rate data for the conversion of sodium *p*-nitrophenyl sulfate to *p*-nitrophenol in methanol containing HCl have also been determined in this connection.

ERWIN BUNCEL et CLAUDIO CHUAQUI. Can. J. Chem. **53**, 1275 (1975).

La réaction du *p*-nitrophényl sulfate de méthyle avec le système hydrazine – chlorhydrate d'hydrazine dans le méthanol donne lieu à différents types de réaction dépendant de l'état d'ionisation du réactif. Pour la combinaison $H_2NNH_2/H_2NNH_3^+$, la réaction observée est la transformation du *p*-nitrophényl sulfate de méthyle en ion *p*-nitrophényl sulfate (scission alkyle–oxygène). Pour la combinaison $H_2NNH_3^+/{}^+H_3NNH_3^+$ ou avec ${}^+H_3NNH_3^+$ seul, on observe des réactions consécutives allant du *p*-nitrophényl sulfate de méthyle → l'ion *p*-nitrophényl sulfate → *p*-nitrophénol (scission alkyle–oxygène suivie par une scission soufre–oxygène). Pour le processus de scission alkyle–oxygène, *i.e.* le déplacement nucléophile sur le carbone de la chaîne alkyle, la constante de vitesse du pseudo premier ordre qui est observée est obtenue à partir des contributions de plusieurs espèces nucléophiles; $k_{obs} = k_{sol} + k_{Cl^-}[Cl^-] + k_{H_2NNH_3^+}[H_2NNH_3^+] + k_{H_2NNH_2}[H_2NNH_2]$. On donne une méthode pour la dissection du k_{obs} en ses termes constituants. Le processus de scission soufre–oxygène est une réaction acido catalysée et on a pu utiliser les valeurs cinétiques mesurées pour déterminer les valeurs de pK_a du ${}^+H_3NNH_3^+$ dans le méthanol. A cet effet on a aussi déterminé la vitesse de transformation (dans du méthanol contenant du HCl) du *p*-nitrophényl sulfate de sodium en *p*-nitrophénol.

[Traduit par le journal]

Methyl *p*-nitrophenyl sulfate is the first member of the family of mixed alkyl aryl sulfates to be subjected to intensive investigation. This particular substrate offers several possible electrophilic centers in its reactions with nucleophiles: the alkyl carbon, the sulfonyl sulfur, and the aryl carbon. So far we have reported on the neutral and alkaline methanolysis reactions (2) as well as the reaction with some anionic nucleophiles (1). We have now investigated the reaction with the hydrazine – hydrazine hydrochloride system and present here the results of the study, concentrating on the nature of the bond scission processes occurring as well as the reactivity of the various species in this system. Some related compounds which have been examined from a similar point of view are the monoalkyl and aryl sulfates (3–7), the sulfites (8, 9), and the halo sulfates (10–12).

Reactions with the $H_2NNH_2/H_2NNH_3^+$ System

Reactions performed in media containing the H_2NNH_2 and $H_2NNH_3^+$ species have been observed to follow the spectral behavior characteristic of the conversion of methyl *p*-nitrophenyl sulfate to *p*-nitrophenyl sulfate ion. Thus there is a decrease in the absorption maximum at 260 nm due to the reactant, an increase at 283 nm due to product, and a sharp isobestic point occurs at 272 nm. Figure 1 illustrates the spec-

[1]For part IX, see ref. 1.

Can. J. Chem. Downloaded from www.nrcresearchpress.com by 210.87.254.6 on 09/05/12
For personal use only.

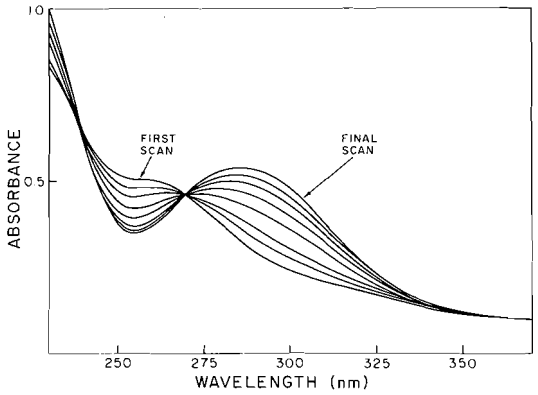

FIG. 1. Spectral scans in typical kinetic run for the conversion of methyl *p*-nitrophenyl sulfate (5.00×10^{-5} *M*) to *p*-nitrophenyl sulfate ion in the reaction with the H_2NNH_2 (7.48×10^{-5} *M*) – $H_2NNH_3^+$ (238.4×10^{-5} *M*) system in methanol at 25°.

tral changes obtained during a typical kinetic run. Plots of log $(A_\infty - A_t)$ *vs.* *t* for data at 283 nm are linear and the slope yields the pseudo first-order rate constant, k_{obs}. The reaction occurring is a nucleophilic displacement on the alkyl carbon center:

[1] $O_2N-C_6H_4-O-\underset{\underset{O}{\|}}{\overset{\overset{O}{\|}}{S}}-O-CH_3 + :Nu \longrightarrow$

$O_2N-C_6H_4-O-\underset{\underset{O}{\|}}{\overset{\overset{O}{\|}}{S}}-O^- + {}^+Nu-CH_3$

The neutral hydrazine species, H_2NNH_2, and the monoprotonated hydrazinium ion, $H_2NNH_3^+$, are both expected to be active nucleophiles towards methyl *p*-nitrophenyl sulfate. In addition, chloride ion, present as the counter ion to $H_2NNH_3^+$, is known to be reactive (1), while methanol should also partake in a neutral solvolytic reaction (2). Thus the overall pseudo first-order rate constant will be the sum of the contributions due to the various constituents, *i.e.*,

$$[2]\quad k_{obs} = k_{sol} + k_{Cl^-}[Cl^-] + k_{H_2NNH_3^+}[H_2NNH_3^+] + k_{H_2NNH_2}[H_2NNH_2]$$

The procedure used for dissection of k_{obs} into the contributing terms is given below.

In Table 1 are given the k_{obs} data obtained for various values of $[H_2NNH_2]$ and $[H_2NNH_3^+]$, while keeping the sum of the concentrations of these species constant (246×10^{-5} *M*). The k_{obs} values when plotted against $[H_2NNH_2]$ yield a linear graph as shown in Fig. 2 (line *1*) with slope 0.394 M^{-1} s^{-1} and intercept on *y* axis 6.34×10^{-4} s^{-1}. One can readily take care of the contribution due to chloride ion since $[Cl^-]$ is known and is in fact constant throughout the series of runs. (This follows from the manner of preparation of the reaction solutions in these runs, namely that a constant quantity of the dihydrochloride salt, $H_2NNH_2 \cdot 2HCl$, was used and variable quantities of CH_3ONa were added in order to generate the H_2NNH_2 and $H_2NNH_3^+$ species, see also Experimental.) Since $k_{Cl^-} = 0.011$ M^{-1} s^{-1} (1) and $[Cl^-] = 4.92 \times 10^{-3}$ *M*, one obtains $k_{Cl^-}[Cl^-] = 0.54 \times 10^{-4}$ s^{-1}, which can then be subtracted from the k_{obs} values throughout the series of runs. The derived values of $k_{obs} - k_{Cl^-}[Cl^-]$ are given in Table 1. The line obtained in plotting $k_{obs} - k_{Cl^-}[Cl^-]$ *vs.* $[H_2NNH_2]$ is of course parallel to the k_{obs} *vs.* $[H_2NNH_2]$ line, *i.e.*, slope 0.394 M^{-1} s^{-1}, intercept on the *y* axis 5.81×10^{-4} s^{-1} (Fig. 2, line *2*). Now this intercept is simply the sum of the terms $k_{sol} + k_{H_2NNH_3^+}[H_2NNH_3^+]$ and since k_{sol} is known (5.28×10^{-4} s^{-1}) from independent measurements in MeOH/$HClO_4$ solutions (1), one obtains $k_{H_2NNH_3^+}[H_2NNH_3^+]$ as equal to $(5.81 - 5.28) \times 10^{-4}$ s^{-1} or 0.53×10^{-4} s^{-1}. Hence the catalytic coefficient $k_{H_2NNH_3^+}$ is given by $k_{H_2NNH_3^+} = 0.53$

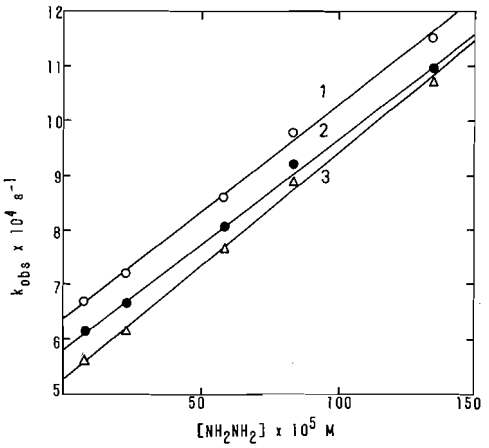

FIG. 2. Plot of rates *vs.* $[H_2NNH_2]$ for reaction of methyl *p*-nitrophenyl sulfate with the H_2NNH_2 – $H_2NNH_3^+$ system in methanol at 25°. Line *1*, k_{obs}; line *2*. $k_{obs} - k_{Cl^-}[Cl^-]$; line *3*. $k_{obs} - k_{Cl^-}[Cl^-] - k_{H_2NNH_3^+}[H_2NNH_3^+]$.

Can. J. Chem. Downloaded from www.nrcresearchpress.com by 210.87.254.6 on 09/05/12
For personal use only.

TABLE 1. Kinetic data for the reaction of methyl *p*-nitrophenyl sulfate with the $H_2NNH_2/H_2NNH_3^+$ system in methanol at 25°

$[H_2NNH_2]$ $\times 10^5$ *M*	$[H_2NNH_3^+]$ $\times 10^5$ *M*	k_{obs} $\times 10^4$ s^{-1}	$k_{obs} - k_{Cl^-}[Cl^-]$ $\times 10^4$ s^{-1}	$k_{H_2NNH_3^+}[H_2NNH_3^+]$ $\times 10^4$ s^{-1}	$k_{obs} - k_{Cl^-}[Cl^-] - k_{H_2NNH_3^+}[H_2NNH_3^+]$ $\times 10^4$ s^{-1}	k_{calcd} $\times 10^4$ s^{-1}
7.48	238.4	6.68	6.15	0.52	5.51	6.65
22.82	223.1	7.17	6.64	0.49	6.04	7.25
58.16	187.8	8.60	8.07	0.41	7.56	8.63
83.50	162.4	9.79	9.26	0.36	8.82	9.62
134.17	111.7	11.52	10.99	0.25	10.69	11.59

$\times 10^{-4}/2.46 \times 10^{-3}$ M^{-1} $s^{-1} = 0.022$ M^{-1} s^{-1}, since $[H_2NNH_3^+] = 2.46 \times 10^{-3}$ *M* when $[H_2NNH_2] = 0$ (see Experimental).

The catalytic coefficient due to the neutral hydrazine species can now be obtained readily. For each value of $[H_2NNH_3^+]$ in Table 1 one can calculate the term $k_{H_2NNH_3^+}[H_2NNH_3^+]$ and on subtraction from $k_{obs} - k_{Cl^-}[Cl^-]$ one obtains the data in the last but one column in Table 1. These data when plotted against $[H_2NNH_2]$ yield line *3* of Fig. 2. The slope of this line is now $k_{H_2NNH_2} = 0.412$ M^{-1} s^{-1}.

A check on the above method of calculating rate coefficients may be obtained by reversing the procedure and calculating the sum of the contributions due to the various nucleophilic species in eq. 2, using the values for the catalytic coefficients derived above. The results of this procedure are given in the last column of Table 1 under k_{calcd}. The agreement with the experimental values of k_{obs} is seen to be satisfactory. In addition, it can readily be shown that the difference in the slopes of lines *2* and *3* in Fig. 2 should be simply the catalytic coefficient due to $H_2NNH_3^+$. By this method, $k_{H_2NNH_3^+} = 0.024$ M^{-1} s^{-1}, which compares favorably with the value obtained by the previously outlined procedure.

Reactions with the $H_2NNH_3^+/{}^+H_3NNH_3^+$ System

Reactions performed in media containing the $H_2NNH_3^+$ and $^+H_3NNH_3^+$ species in combination, or the $^+H_3NNH_3^+$ species alone, showed spectral characteristics which were quite different in nature from those in the $H_2NNH_2/H_2NNH_3^+$ system considered above. The spectral changes observed during the course of a kinetic run are illustrated in Fig. 3 and are typical of an A → B → C process (13). In the early stages, before a significant amount of C has formed, the isosbestic point of 272 nm is somewhat poorly defined. Similarly, in the later stages of the run, when the concentration of A is insignificant, a second diffuse isosbestic point at 292 nm is indicative of the B → C process. When all three species are present in significant concentration then isosbestic behavior is lost altogether.

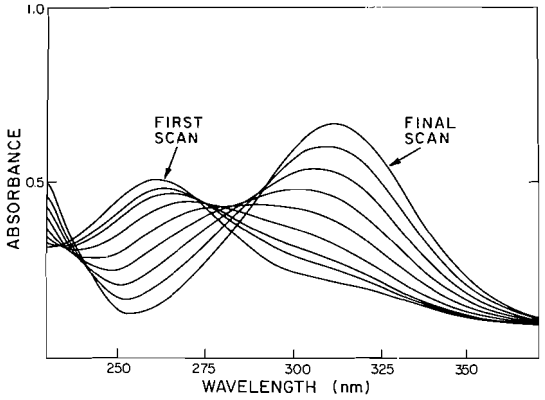

FIG. 3. Spectral scans illustrating the consecutive processes in reaction of methyl *p*-nitrophenyl sulfate (5.00×10^{-5} *M*) with the $H_2NNH_3^+$ (12.9×10^{-5} *M*) − $^+H_3NNH_3^+$ (11.7×10^{-5} *M*) system in methanol at 25°.

For these kinetic runs one can calculate the rate constants, k^A_{obs} and k^B_{obs} respectively, for the A → B and B → C steps by the method described previously (2). One obtains k^A_{obs} by plotting log $(A_\infty - A_t)$ *vs.* *t* for data at 292 nm, which corresponds to the isosbestic wavelength for the B → C conversion. Similarly, one obtains k^B_{obs} by plotting log $(A_t - A_\infty)$ *vs.* *t* at 272 nm, corresponding to the isosbestic wavelength for the A → B conversion (see also footnote 21 in ref. 2). The second plot is linear only in the latter stages of the reaction, when there is no longer a significant concentration of A remaining. The k_{obs} data are given in Table 2. Discussion of these results is deferred so as to allow

Can. J. Chem. Downloaded from www.nrcresearchpress.com by 210.87.254.6 on 09/05/12
For personal use only.

TABLE 2. Kinetic data for the reaction of methyl *p*-nitrophenyl sulfate with the $H_2NNH_3^+/^+H_3NNH_3^+$ system in methanol at 25°

$[^+H_3NNH_3^+]_0$ $\times 10^5$ *M*	$[H_2NNH_3^+]_0$ $\times 10^5$ *M*	$[^+H_3NNH_3^+]_{eq}$ $\times 10^5$ *M*	$[H_2NNH_3^+]_{eq}$ $\times 10^5$ *M*	$[Cl^-]$ $\times 10^5$ *M*	k^A_{obs} $\times 10^4$ s^{-1}	k^B_{obs} $\times 10^4$ s^{-1}	k^A_{calcd} $\times 10^4_A$ s^{-1}
24.59	—	11.72	12.87	49.18	5.42	2.88	5.40
49.18	—	30.11	19.07	98.36	5.51	4.61	5.47
98.36	—	67.48	30.88	196.72	5.69	—	5.60
245.90	—	193.60	52.30	491.80	6.02	—	5.97
491.80	—	415.21	76.59	983.60	6.58	—	6.52
365.11	126.69	360.79	131.01	983.60	6.70	—	6.69
238.42	253.38	236.77	255.03	983.60	6.82	—	6.90

prior consideration of the nature of the chemical processes and pertaining matters.

The A → B stage is the nucleophile induced conversion of methyl *p*-nitrophenyl sulfate to *p*-nitrophenyl sulfate ion (*cf.* eq. 1). The B → C stage, namely the conversion of *p*-nitrophenyl sulfate to *p*-nitrophenol, is an acid-catalyzed process (5, 14) as given by eqs. 3 and 4. The SO_3

[3] 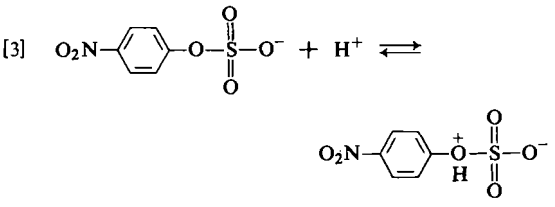

[4] 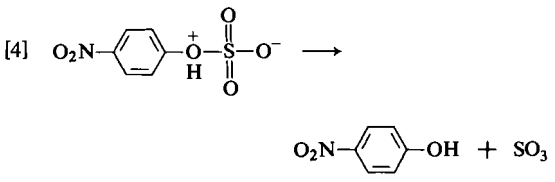

formed in eq. 4 will be converted to methyl hydrogen sulfate and, as this should be a strong acid, in the overall reaction of *p*-nitrophenyl sulfate to *p*-nitrophenol no acid is consumed. The A → B → C reaction sequence was also observed in the methanolysis of methyl *p*-nitrophenyl sulfate (2).

As has been noted, the B → C stage is an acid-catalyzed process according to eqs. 3 and 4. In eq. 3, the hydrogen ion (solvated) is derived in part from the neutral solvolytic reaction (eq. 1, Nu = CH_3OH) which generates 1 mol of acid. The second source of hydrogen ion in the present system derives from ionization of $^+H_3NNH_3^+$. Since the magnitude of k^B_{obs} reflects the $[H^+]$ present in the system, one should be able to apply these data towards an indirect determination of the pK_a of $^+H_3NNH_3^+$. There are no literature data for this pK_a pertaining to methanol, though the pK_a in water is known (−0.67) (15). The method used is described below, as it may have more general application.

As a first requirement, the rate of the acid catalyzed conversion of *p*-nitrophenyl sulfate (sodium salt) to *p*-nitrophenol was measured in media of known acidity. Rate data were obtained over a range of [HCl] in methanol and the results are given in Table 3. A plot of k_{obs} *vs.* [HCl] is linear and the slope yields the second-order rate coefficient $k_{HCl} = 1.72\ M^{-1}\ s^{-1}$. If one takes into account the incomplete dissociation of HCl in methanol, via the pK_a value of 1.23 (16), then the corrected value k_{H^+} is given by $1.86\ M^{-1}\ s^{-1}$.

One can now proceed to evaluate the pK_a of $^+H_3NNH_3^+$ in methanol. In the reaction of methyl *p*-nitrophenyl sulfate with $^+H_3NNH_3^+$, using initial reagent concentrations of 24.59×10^{-5} and 49.18×10^{-5} *M* ($[^+H_3NNH_3^+]_0$ in Table 2), one obtains for the B → C process k^B_{obs} values of 2.88×10^{-4} and 4.61×10^{-4} s^{-1}, respectively. Corresponding to these rates one calculates $[H^+]_{total}$ values of 15.52×10^{-5} and 24.85×10^{-5} *M*, respectively, using $k_{H^+} = 1.86\ M^{-1}\ s^{-1}$ as obtained independently (data on HCl-catalyzed reaction of *p*-nitrophenyl sul-

TABLE 3. Kinetic data for conversion of sodium *p*-nitrophenyl sulfate to *p*-nitrophenol in methanolic HCl at 25°

[HCl] $\times 10^5$ *M*	k_{obs} $\times 10^4$ s^{-1}
22.9	4.32
50.1	10.05
75.0	13.4
95.4	17.4
241.2	41.9

Can. J. Chem. Downloaded from www.nrcresearchpress.com by 210.87.254.6 on 09/05/12
For personal use only.

Can. J. Chem. Downloaded from www.nrcresearchpress.com by 210.87.254.6 on 09/05/12
For personal use only.

fate). To calculate the pK_a one must consider the hydrogen ion concentration derived from *p*-nitrophenyl hydrogen sulfate formed in the A → B stage.[2] Assuming complete dissociation of $O_2NC_6H_4OSO_3H$, the calculated pK_a values for $^+H_3NNH_3^+$ in the case of the above two sets of data are 3.94 and 3.77, respectively. Or, assuming that $O_2NC_6H_4OSO_3H$ has pK_a 2 in methanol, which is not unreasonable, the derived pK_a's for $^+H_3NNH_3^+$ are now 3.93 and 3.77. Moderate changes in the assumed pK_a for *p*-nitrophenyl hydrogen sulfate lead only to minor variation in the calculated pK_a of $^+H_3NNH_3^+$. Therefore, a reasonable estimate for the pK_a of $^+H_3NNH_3^+$ in methanol is 3.85. This pK_a is defined by eqs. 5 and 6:

$$[5] \qquad {}^+H_3N{-}NH_3^+ \rightleftarrows H_2NNH_3^+ + H^+$$

$$[6] \quad K_a = [H_2NNH_3^+][H^+]/[{}^+H_3NNH_3^+]$$

Though in principle the kinetic method for derivation of pK_a should have general application, in the present system there are two complicating factors. In the first place there is a limitation on observation of the B → C rate, which must not exceed the A → B rate in order to be measurable (*cf.* ref. 17). Secondly the degree of dissociation of *p*-nitrophenyl hydrogen sulfate provides slight uncertainty, which would not be present in the general case (*e.g.* acid-catalyzed ester hydrolysis). It should, however, be readily feasible to devise a suitable system such that the rate of a simple acid-catalyzed reaction would be determined in the presence of the catalyzing acid whose pK_a in the given medium is required.

The catalytic coefficients $k_{H_2NNH_3^+}$ and k_{sol} in the conversion of methyl *p*-nitrophenyl sulfate to *p*-nitrophenyl sulfate ion (eq. 2) can be independently evaluated using the derived value of the pK_a of $^+H_3NNH_3^+$. Thus the equilibrium concentration of the $H_2NNH_3^+$ species, $[H_2NNH_3^+]_{eq}$, will be given by the sum of the initial concentration, $[H_2NNH_3^+]_0$, and the contribution due to the ionization of $^+H_3NNH_3^+$. The latter term is calculated by means of eq. 6. The various data are presented in Table 2. Following the procedure used in Fig. 2, one then plots k^A_{obs} *vs.* $[H_2NNH_3^+]_{eq}$, which gave a linear graph, slope 0.058 M^{-1} s^{-1}, and intercept on the *y* axis 5.63×10^{-4} s^{-1}. Subtraction of the $k_{Cl^-}[Cl^-]$ term gave a second line, the slope yielding $k_{H_2NNH_3^+} = 0.025$ M^{-1} s^{-1}. The intercept on this graph is the neutral solvolytic rate constant, $k_{sol} = (5.32 \pm 0.06) \times 10^{-4}$ s^{-1}. These values substantiate the method for calculation of rate data as given in the previous section.

In conclusion, it has been shown in this study that the nucleophiles $H_2NNH_3^+$ and H_2NNH_2 react with methyl *p*-nitrophenyl sulfate by displacement at the aliphatic carbon with *p*-nitrophenyl sulfate ion as the leaving group. This is analogous to the alkaline methanolysis (2) and the reaction with some common anions (1).

The reactivity ratio, $k_{H_2NNH_2}/k_{H_2NNH_3^+}$, is about 20 in methanol at 25°. A preliminary Bronsted β can be derived for these nucleophiles using the estimated pK_a values 9.2 and 3.9 in methanol for the conjugate acids of these species. Thus $\beta = \Delta pK_a/\Delta \log k_{Nu} = 0.24$. The small value of β is in accord with the good leaving group present and suggests also that "α effects" (18–20) are not significant in this system.

Experimental

Methyl *p*-nitrophenyl sulfate was prepared according to the procedure described previously (21). Hydrazine hydrochloride (BDH reagent grade) was recrystallized before use. Sodium methoxide solutions were prepared by dissolving freshly cut sodium metal in dry methanol. A Bausch and Lomb SP505 spectrophotometer equipped with a thermostatted cell block was used for the spectral measurements.

The procedure used for the kinetic runs recorded in Table 1 may be illustrated for the case of the first run shown in the table. A 0.50 ml aliquot of a 1.50×10^{-2} *M* stock solution of $H_2NNH_2 \cdot 2HCl$ was placed in a 10 mm cuvette. After adding 1.00 ml of 7.73×10^{-3} *M* solution of CH_3ONa/CH_3OH, the volume was made up to 3.00 ml with methanol. The run was started by adding with a syringe 0.050 ml of a stock solution of methyl *p*-nitrophenyl sulfate in ether yielding a solution 5.00×10^{-5} *M* in substrate. The volume of the $H_2NNH_2 \cdot 2HCl$ solution added was kept constant throughout the series of runs, while the volume of CH_3ONa/CH_3OH was varied, with methanol making up the balance in each case for a total of 3.00 ml. Therefore the chloride ion concentration throughout the series was constant at 491.8×10^{-5} *M*. The constancy of the added $H_2NNH_2 \cdot 2HCl$ in this series of runs facilitates the evaluation of catalytic rate constants according to Fig. 2.

For the data presented in Table 2, the experimental design is different from the above in several respects. First, the added $H_2NNH_2 \cdot 2HCl$ is not kept constant but in fact varies throughout the series. Secondly, in the case of the first five runs no CH_3ONa/CH_3OH is added to the

[2]The correction applied is for the acid generated due to the reaction of methanol with the substrate. The competing reaction of $H_2NNH_3^+$, which also generates acid (as well as giving rise to the species $CH_3NHNH_3^+$), has been found to be negligible.

reaction solution. However, for the last two runs the CH_3ONa/CH_3OH solution is added, in an amount equivalent to $[H_2NNH_3^+]_0$.

The procedure used to derive the data of Table 3 for the conversion of *p*-nitrophenyl sulfate ion to *p*-nitrophenol was as follows. A stock solution of the sodium *p*-nitrophenyl sulfate (1.24×10^{-4} *M*) was prepared by reaction of methyl *p*-nitrophenyl sulfate with excess of sodium methoxide in methanol (2). Aliquots of this solution were added to excess of methanolic HCl in the 1 cm cuvette and made up to a total volume of 3 ml with methanol, yielding a final concentration of substrate 4.12×10^{-5} *M* and HCl concentrations as given in Table 3. This procedure circumvents the possibility that commercial *p*-nitrophenyl sulfate could be partially decomposed, as well as providing a mimic of the reaction system used in derivation of the pK_a (*i.e.* $^+H_3NNH_3^+$ + methyl *p*-nitrophenyl sulfate → *p*-nitrophenyl sulfate → *p*-nitrophenol).

We gratefully acknowledge financial support of this research by the National Research Council of Canada.

1. E. BUNCEL, C. CHUAQUI, P. FORSYTHE, S. MAHONEY, A. RAOULT, and J. WILTSHIRE. J. Chem. Soc. Perkin II. In press.
2. E. BUNCEL, A. RAOULT, and J. WILTSHIRE. J. Am. Chem. Soc. **95**, 799 (1973).
3. E. T. KAISER, M. PANAR, and F. H. WESTHEIMER. J. Am. Chem. Soc. **85**, 602 (1963).
4. B. D. BATTS. J. Chem. Soc. B, 547, (1966); 551 (1966).
5. J. L. KICE and J. M. ANDERSON. J. Am. Chem. Soc. **88**, 5242 (1966).
6. S. J. BENKOVIC and P. BENKOVIC. J. Am. Chem. Soc. **88**, 5504 (1966).
7. E. J. FENDLER and J. H. FENDLER. Chem. Commun. 1261 (1967).
8. P. A. BRISTOW, J. G. TILLETT, and D. E. WIGGINS. J. Chem. Soc. B, 1360 (1968).
9. C. A. BUNTON and G. SCHWERIN. J. Org. Chem. **31**, 842 (1966).
10. E. BUNCEL. Chem. Rev. **70**, 323 (1970).
11. E. BUNCEL. Mech. React. Sulfur Compd. **5**, 71 (1970).
12. E. BUNCEL and A. RAOULT. J. Chem. Soc. Perkin II, 691 (1972).
13. E. BUNCEL, A. RAOULT, and J. WILTSHIRE. J. Chem. Educ. **51**, 814 (1974).
14. E. BUNCEL and W. M. J. STRACHAN. Can. J. Chem. **47**, 911 (1969).
15. J. J. CHRISTENSEN, R. M. IZATT, D. P. WRATHALL, and L. D. HANSEN. J. Chem. Soc. A, 1212 (1969).
16. D. W. CLARE, D. COOK, E. C. F. KO, Y. C. MAC, and A. J. PARKER. J. Am. Chem. Soc. **88**, 1911 (1966).
17. A. A. FROST and R. G. PEARSON. Kinetics and mechanism. 2nd ed. Wiley, New York. 1961. pp. 166–171.
18. R. G. PEARSON. *In* Advances in linear free energy relationships. *Edited by* N. B. Chapman and J. Shorter. Plenum Press, London. 1972.
19. J. E. DIXON and T. C. BRUICE. J. Am. Chem. Soc. **94**, 2052 (1972).
20. J. L. KICE and E. LEGAN. J. Am. Chem. Soc. **95**, 3912 (1973).
21. E. BUNCEL and A. RAOULT. Can. J. Chem. **50**, 1907 (1972).

Can. J. Chem. Downloaded from www.nrcresearchpress.com by 210.87.254.6 on 09/05/12
For personal use only.

A Synthetic Approach to Cadinane- and Amorphane-type Sesquiterpenoids via Annelation of Cyclohexanone Derivatives with (*E*)-2-Methyl-3-hepten-5-one. A Simple Synthesis of (±)-Cadinene Dihydrochloride

EDWARD PIERS AND WYNONA M. PHILLIPS-JOHNSON

Department of Chemistry, University of British Columbia, 2075 Wesbrook Place, Vancouver, Canada V6T 1W5

Received November 18, 1974

EDWARD PIERS and WYNONA M. PHILLIPS-JOHNSON. Can. J. Chem. **53**, 1281 (1975).

The annelation of the pyrrolidine enamine of cyclohexanone with (*E*)-2-methyl-3-hepten-5-one (**7**) afforded a 7:3 mixture of the octalones **12** and **13**. Lithium–ammonia reduction of the former afforded the *trans*-fused decalone **14**, whereas, in contrast, a similar reduction of **13** gave exclusively the *cis*-fused decalone **16**. Annelation of the pyrrolidine enamine of 4-hydroxycyclohexanone with the unsaturated ketone **7** yielded a 7:3 mixture of the octalones **22** and **23**. The former was converted via a short, efficient synthetic sequence into (±)-cadinene dihydrochloride (**30**).

EDWARD PIERS et WYNONA M. PHILLIPS-JOHNSON. Can. J. Chem. **53**, 1281 (1975).

L'énamine dérivant de la pyrrolidine et de la cyclohexanone soumise à une réaction d'annelation avec la méthyl-2 heptène-3 one-5 (*E*) (**7**) conduit à un mélange 7:3 des octalones **12** et **13**. La réduction par le lithium dans l'ammoniac de **12** conduit à la décalone *trans* **14** alors qu'une réduction similaire de **13** conduit uniquement à la décalone *cis* (**16**). L'énamine dérivée de la pyrrolidine et de l'hydroxy-4 cyclohexanone soumise à une réaction d'annelation avec la cétone non-saturée **7** conduit à un mélange 7:3 des octalones **22** et **23**. Une séquence synthétique courte et efficace permet de transformer **22** en dichlorhydrate de (±)-cadinène (**30**).

The fairly large number of sesquiterpenoids which possess the basic carbon skeleton as shown in **1**[1] have by convention been divided into four classes or subgroups, differing only in the relative stereochemistry at C_1, C_6, and C_7 (1, 2). Thus, the cadinane-type (**2**) and bulgarane-type (**3**) sesquiterpenoids possess *trans*-fused six-membered rings and differ only in the relative stereochemical orientation of the isopropyl or related side chain. On the other hand, in the muurolanes (**4**) and the amorphanes (**5**), the decalin systems are *cis*-fused. Again, these two types differ only in the relative stereochemistry at C_7.

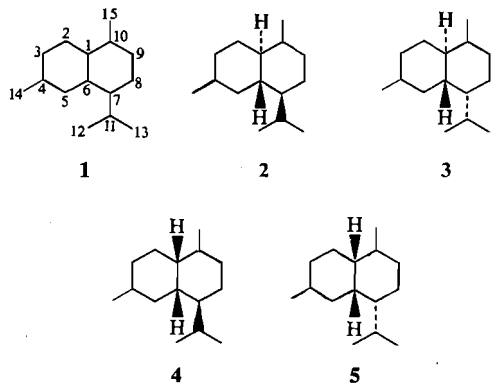

1 **2** **3** **4** **5**

The four sesquiterpenoid classes mentioned above are constituted mainly of olefinic hydrocarbons and alcohols. Structurally speaking, many of the individual members of these classes are very closely related and often differ from one another only in the position of an olefinic double bond and/or in a diastereomeric sense. Because of this, it has often been difficult to separate mixtures of these types of compounds into individual components, and the structural and stereochemical elucidation of the cadinane and related sesquiterpenoids was, in the past, often carried out with impure materials. Consequently, the chemical literature dealing with this area contains many conflicting and erroneous reports. A classic and, perhaps, extreme example of this involves the naturally occurring olefinic alcohol δ-cadinol. Since its isolation in 1922, no fewer than seven different proposals have been put forward regarding the structure and sterochemistry of this compound, the latest (3) being that δ-cadinol is actually a muurolane derivative.

[1]The numbering system shown in structure **1** is that normally used for the cadinane and related sesquiterpenoids.

Can. J. Chem. Downloaded from www.nrcresearchpress.com by 210.87.254.42 on 09/05/12
For personal use only.

Can. J. Chem. Downloaded from www.nrcresearchpress.com by 210.87.254.42 on 09/05/12
For personal use only.

Up to the present time, relatively little work has been reported concerning the synthesis of the cadinane and related sesquiterpenoids.[2] We report in this paper a simple synthetic approach which, with appropriate development and modification, should allow for the efficient synthetic entry into both the cadinane- and amorphane-type sesquiterpenoids.

Of the number of synthetic approaches which we considered and investigated in varying detail (5), the one involving annelation of a substituted cyclohexanone derivative (**6**) with (*E*)-2-methyl-3-hepten-5-one (**7**) appeared, in principle, to be the simplest and most direct (see Scheme 1).

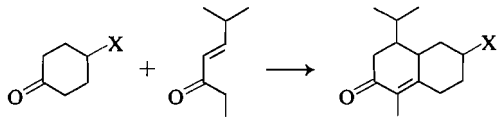

6 **7** **8**

SCHEME 1

Success of this general reaction would introduce, in one step, 14 of the 15 carbon atoms necessary for the synthesis of the cadinane and/or related sesquiterpenoids. An appropriate functional group (X) at C_6 in the annelation product **8** would then presumably allow for the introduction of the final required carbon atom.

The required α,β-unsaturated ketone **7** was prepared as follows (see Scheme 2). Treatment of isobutyraldehyde with the anion of trimethylphosphonoacetate (6) in dimethyl sulfoxide afforded, in 65% yield, the *trans*-olefinic ester **9**. Hydrolysis of the latter with potassium carbonate in aqueous methanol gave the corresponding carboxylic acid **10**. When compound **10** was allowed to react with freshly prepared ethyllithium under carefully controlled conditions (−78°, 2 h), the desired α,β-unsaturated ketone **7** was formed in excellent yield. It should be noted that the success of the latter reaction depended, to a large extent, upon a judicious choice of reaction temperature, reaction time, and reactant concentration. That is, use of reaction temperatures greater than −40°, or use of longer reaction times, resulted in the formation of considerable amounts of alcohol-containing products. On the other hand, milder reaction conditions (more dilute solutions, shorter reaction times, low temperatures) resulted in the recovery of fairly copious amounts of starting material. However, to eliminate the formation of alcohol-containing product, it was necessary to tolerate the recovery of some starting material. The latter could then be recycled and, eventually, the desired unsaturated ketone **7** was obtained in 92% yield.

Attempted annelation of cyclohexanone, 2-carbomethoxycyclohexanone, and 2-hydroxymethylenecyclohexanone with the heptenone **7**, using a variety of bases and reaction conditions, proved unsuccessful. However, when the pyrrolidine enamine of cyclohexanone (**11**) was allowed to react with **7** under carefully chosen conditions, the corresponding annelated material was formed in 83% yield (see Scheme 2). Analysis of this material by gas–liquid chromatography (g.l.c.) indicated that it consisted of a mixture of the two epimeric compounds **12** and **13**, in a ratio of approximately 7:3, respectively. Treatment of this mixture with sodium methoxide in refluxing methanol afforded a mixture of the same two components, now in a ratio of 3:1. The two compounds could be separated readily by preparative g.l.c. and spectral and analytical data clearly showed that the two materials were indeed epimers.

On the basis of conformational analysis, one would expect the octalone **12**, containing an equatorially oriented isopropyl group (*cf.* **12***a*), to be more stable than octalone **13**, possessing an axially oriented isopropyl group (*cf.* **13***a*). Hence, the major and minor products obtained from the annelation reaction were assigned structures **12** and **13**, respectively.

In order to obtain additional information regarding the stereochemistry of octalones **12** and **13**, each was subjected to reduction with lithium in liquid ammonia. Reduction of the major annelation product **12** afforded, in 78% yield, the corresponding *trans*-fused decalone **14**. Application of internuclear double resonance (INDOR) techniques (7–9)[3] to a detailed study of the proton magnetic resonance (p.m.r.) spectrum of **14** fully supported the assigned structure and stereochemistry. Specifically, the INDOR studies revealed the following first-order coupling constants: H_{3a}–H_{3e} 12.6 ± 0.4 Hz, H_{3a}–H_4 12.6 ± 0.4 Hz, H_{3e}–H_4

[2]For an excellent and comprehensive review of sesquiterpenoid synthesis, see ref. 4.

[3]We are very grateful to Professor L. D. Hall and Dr. C. W. M. Grant for carrying out the INDOR studies. Details of these experiments will be published elsewhere.

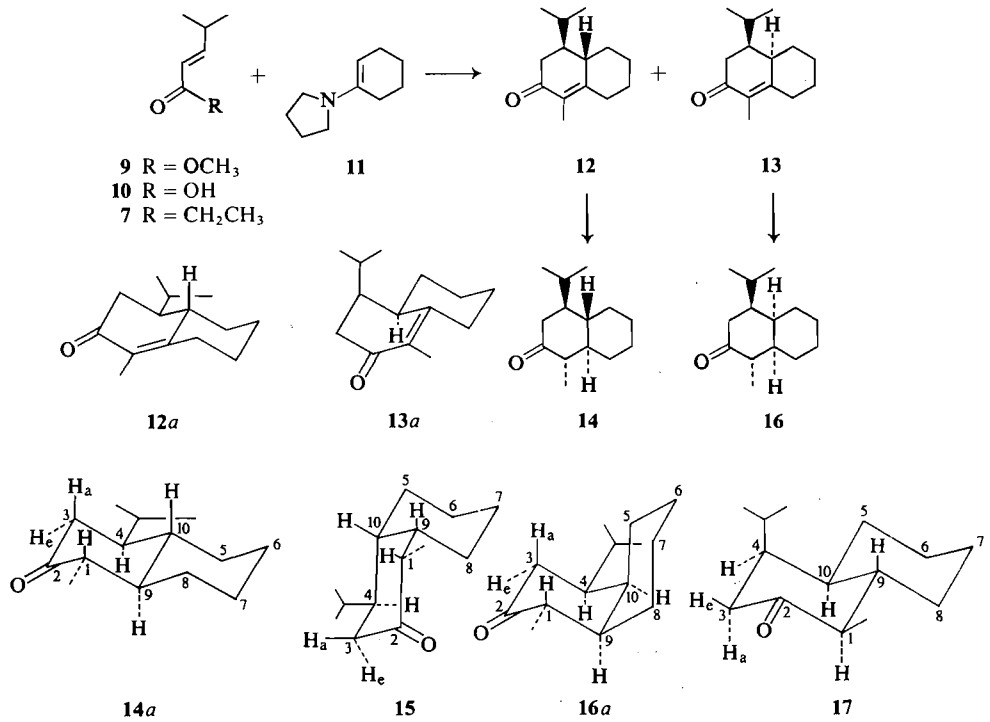

SCHEME 2

3.9 ± 0.4 Hz. It can readily be seen that these first-order coupling constants for compound **14** are fully consistent with the assigned stereochemistry (*cf.* **14***a*). Furthermore, the p.m.r. studies also revealed that the H_1 transitions for compound **14** were spread over at least 32 Hz, indicating that the H_1–H_9 coupling (*cf.* **14***a*) was an axial–axial coupling. If the H_1–H_9 coupling had been axial–equatorial, the H_1 transitions would have been spread over only 22–25 Hz, at most. These facts clearly showed that the lithium–ammonia reduction of the major annelation product (**12**) had not produced a *cis*-fused decalone, which would have had the conformation shown in **15**. The latter structure, although consistent with the observed coupling pattern for the C_3 and C_4 protons, was clearly inconsistent with the observed line width for the H_1 resonance.

Lithium–ammonia reduction of the minor annelation product **13** afforded steroselectively, in 75% yield, the corresponding *cis*-fused decalone **16**. The stereochemistry of the latter was confirmed in two ways. First of all, hydrogenation of the olefinic double bond of **13** would be expected to take place from the side opposite the axially oriented isopropyl group (*cf.* **13***a*) (steric approach control) and also produce the *cis*-fused decalone **16**. Indeed, hydrogenation of **13** over palladium-on-charcoal, followed by equilibration (sodium methoxide in methanol) of the initially formed product, afforded only decalone **16**, identical in all respects with the product obtained from the lithium–ammonia reduction. Secondly, INDOR (7–9)[3] studies on compound **16** again fully supported the assigned stereochemistry. Thus the observed first-order coupling constants (H_{3a}–H_{3e} 13.0 ± 0.4 Hz, H_{3a}–H_4 13.0 ± 0.4 Hz, H_{3e}–H_4 3.9 ± 0.4 Hz) were clearly consistent with structure **16** (*cf.* **16***a*) but were inconsistent with a corresponding decalone possessing a *trans* ring fusion (*cf.* **17**). Furthermore, the p.m.r. studies again showed that the H_1 transitions for compound **16** were spread over at least 33 Hz. As in the case of compound **14**, this fact clearly indicated that the H_1–H_9 coupling (*cf.* **16***a*) was an axial–axial coupling.

It is well known that the alkali metal – ammonia reduction of simply substituted $\Delta^{1(9)}$-2-octalones generally affords, in each case, a high proportion of the corresponding *trans*-fused 2-decalone (10–12). Therefore, the steroselective formation of the *cis*-fused decalone **16** from the

Can. J. Chem. Downloaded from www.nrcresearchpress.com by 210.87.254.42 on 09/05/12
For personal use only.

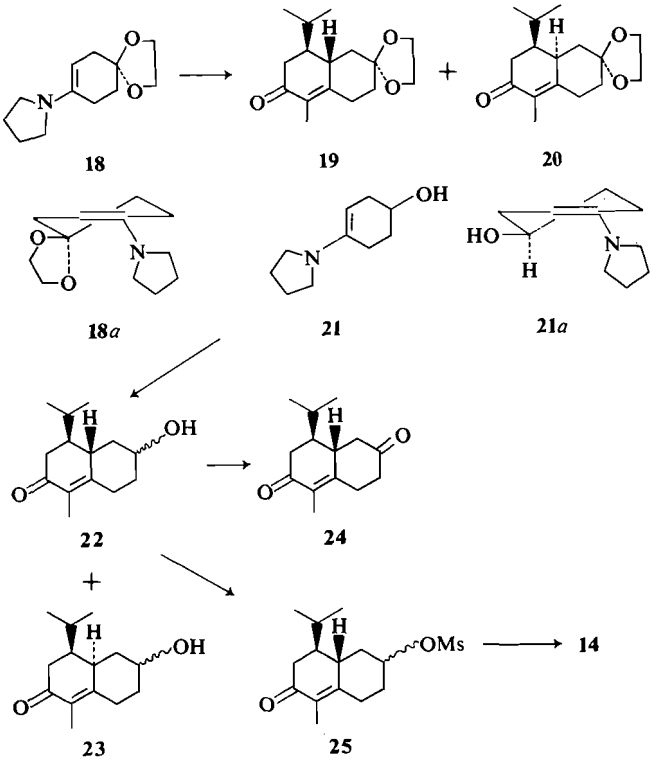

SCHEME 3

lithium–ammonia reduction of octalone **13** was initially surprising and clearly seemed to suggest that the presence of an axially-oriented substituent at the C_4 position of $\Delta^{1(9)}$-2-octalones can exert a profound effect on the stereochemical outcome of the reduction. A more detailed study and discussion of this observation can be found in the accompanying paper (13).

Having successfully realized the annelation of cyclohexanone with the α,β-unsaturated ketone **7**, we next turned our attention to the annelation of a cyclohexanone derivative containing a substituent suitable for the (later) introduction of the last one-carbon unit necessary for the synthesis of cadinane-type (or related) sesquiterpenoids. To this end, the pyrrolidine enamine of 4,4-ethylenedioxycyclohexanone (**18**) (14) was allowed to react with **7** under conditions similar to those used in the above mentioned condensation (see Scheme 3). However, the annelated product, a 4:1 mixture of octalones **19** and **20**, respectively, was obtained in only very poor yield (<10%). Attempts to improve the yield of this reaction by varying the reaction conditions were not successful. It was felt that the ketal functionality, with one of the oxygen atoms necessarily axially oriented (*cf.* **18***a*) could be sterically interfering with the approach of the vinyl ketone **7** to the β-carbon atom of the enamine **18** (anti-parallel attack (15)), thus accounting for the low yield of product. Therefore, it was decided to investigate the use of the pyrrolidine enamine of 4-hydroxycyclohexanone (**21**), which could, presumably, react from a conformation possessing an equatorially oriented hydroxyl group (*cf.* **21***a*). Condensation of **21** with the unsaturated ketone **7** was attempted under a variety of conditions and a 40% yield of a mixture of annelated products was finally realized. The crude product was equilibrated (sodium methoxide in methanol) and then subjected to analysis by g.l.c. and spectral methods. The latter revealed that this material consisted of a mixture of hydroxy octalones **22** and **23** in a ratio of approximately 7:3, respectively. The two compounds were readily separated by preparative g.l.c.

It should be noted that both **22** and **23** actually consisted of a mixture of two epimeric

Can. J. Chem. Downloaded from www.nrcresearchpress.com by 210.87.254.42 on 09/05/12
For personal use only.

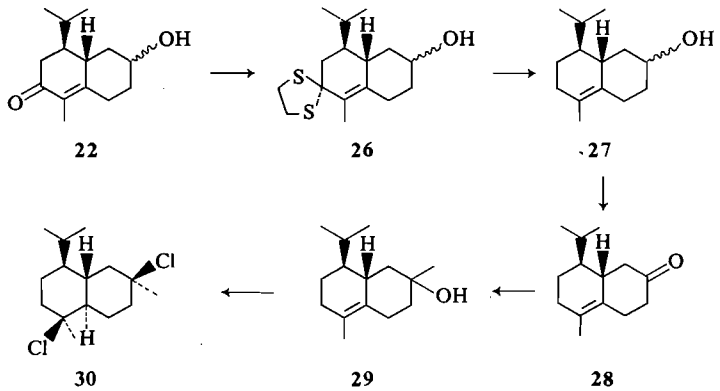

SCHEME 4

alcohols. Thus, a careful integration of the p.m.r. spectrum of the major condensation product **22**[4] indicated that the two alcohols possessing axial and equatorial hydroxyl groups were present in a ratio of approximately 3:2, respectively. That compound **22** was indeed a mixture of two epimeric alcohols was shown by chromium trioxide – pyridine oxidation (16) of this material, which produced, in 94% yield, the crystalline dione **24**. The latter, by means of g.l.c. and spectral analysis, was shown to be homogeneous.

Similarly, a careful analysis of the p.m.r. spectrum of the minor condensation product **23**[4] indicated that the epimeric alcohols were present in a ratio of approximately 1:1.

To obtain additional information regarding the relative stereochemistry (at C_4 and C_{10}) of the major and minor condensation products **22** and **23**, it was decided to correlate the former keto alcohol with the previously obtained, and structurally simpler, decalone **14**. Since assignment of the stereochemistry of the latter appeared to be on a firm basis, this correlation would provide corroborative support for the proposed stereochemistry of **22** and, by inference, of **23** as well.

Treatment of the hydroxy octalone **22** with methanesulfonyl chloride in pyridine afforded, in 85% yield, the corresponding keto mesylate **25**. Reaction of the latter with lithium in liquid ammonia containing some ethanol reduced not only the α,β-unsaturated ketone system (11, 12) but also effected hydrogenolysis of the mesylate functionality (17). Oxidation of the resulting crude product with Jones' reagent (18) produced the saturated, *trans*-fused decalone **14**, identical in every respect with a sample of the compound obtained as described previously.

In order to demonstrate the potential use of octalone **22** as an intermediate for the synthesis of cadinane-type sesquiterpenoids, and to fully confirm the stereochemical assignments outlined above, it was decided to convert **22** into racemic cadinene dihydrochloride (**30**) (19–22), the stereochemistry of which has been established unambiguously. To this end, octalone **22** was treated with ethanedithiol in the presence of boron trifluoride etherate to afford the dithioketal **26** (see Scheme 4). Desulfurization of the latter with Raney nickel in refluxing ethanol afforded, in 77% yield, the olefinic alcohol **27**. Oxidation of **27** with chromium trioxide in pyridine (16) gave, in 89% yield, the keto olefin **28**, which in turn was converted, by reaction with methyllithium in ether, into the tertiary alcohol **29** (91% yield). Treatment of the latter compound with anhydrous hydrogen chloride in anhydrous ether at 0° afforded, in 80% yield, racemic cadinene dihydrochloride (**30**). The latter was identical in every respect with an authentic sample of (±)-cadinene dihydrochloride.[5]

The enamine annelation approach to the synthesis of cadinane-type and/or related sesquiterpenoids, as outlined above, is attractive in terms of simplicity and efficiency. However, the general scheme does possess disadvantages. One of these is the production, in the annelation reaction itself, of diastereomeric products (**22**

[4]For the sake of simplicity, this material will subsequently be referred to as one compound.

[5]We are very grateful to Dr. M. D. Sutherland for a generous sample of (±)-cadinene dihydrochloride.

Can. J. Chem. Downloaded from www.nrcresearchpress.com by 210.87.254.42 on 09/05/12
For personal use only.

Can. J. Chem. Downloaded from www.nrcresearchpress.com by 210.87.254.42 on 09/05/12
For personal use only.

and **23**) which must then be separated at an early stage of the overall synthetic sequence. This complication is, however, at least partially offset by the results obtained from the lithium–ammonia reduction of the initially formed annelation products. That is, on the basis of the work reported in this paper, it is obvious that the lithium–ammonia reduction of a mixture of octalones **22** and **23** would produce a mixture of the corresponding *trans*- and *cis*-fused 2-decalones **31** and **32**, respectively. Separation at this stage of the synthetic sequence would then provide one with two distinct synthetic precursors, one (**31**) potentially convertible into cadinane-type sesquiterpenoids and the other (**32**) potentially convertible into amorphane-type sesquiterpenoids.

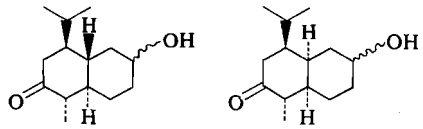

31 **32**

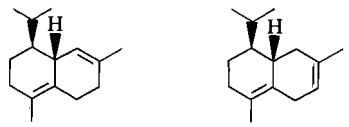

33 **34**

Another problem which must as yet be overcome involves the regioselective introduction of olefinic double bonds into various positions of an appropriate synthetic intermediate. For example, conversion of the keto olefin **28** into the natural products δ-cadinene (**33**) and ω-cadinene (**34**) would require the introduction of a methyl group at the carbonyl carbon (of **28**) and the controlled, regioselective introduction of carbon–carbon double bonds into two distinct positions. We are currently investigating methods for carrying out these transformations in a controlled fashion.

Experimental

General[6]

Melting points, which were determined on a Fisher-Johns melting point apparatus, and boiling points are uncorrected. The u.v. spectra were, unless otherwise noted, measured in methanol solution on a Unicam, model SP 800, spectrophotometer. Routine i.r. spectra were recorded on a Perkin-Elmer model 710 spectrophotometer, while comparison spectra were recorded on Perkin-Elmer models 421 or 457 spectrophotometers. The p.m.r. spectra were, unless otherwise noted, taken in deuteriochloroform solution on Varian Associates spectrometers, A-60, T-60 and/or HA-100 or XL-100. Signal positions are given in the Tiers τ scale, with tetramethylsilane as an internal standard. The multiplicity, integrated peak areas, and proton assignments are indicated in parentheses. High resolution mass spectrometric measurements were carried out on an AEI type MS-9 mass spectrometer. Gas–liquid chromatographic analyses were carried out on Varian Aerograph g.l.c. units, models 700 and/or 90-P. The following columns were employed: column A, 10 ft × ¼ in., 8% FFAP on 60–80 mesh Chromosorb G; column B, 10 ft × ¼ in., 20% Carbowax 20M on 60–80 mesh Chromosorb W; column C, 10 ft × ⅜ in., 30% Carbowax 20M on Chromosorb W. The specific column used, along with the column temperature and carrier gas (helium) flow-rate (in ml/min) are indicated in parentheses. Microanalyses were performed by Mr. P. Borda, Microanalytical Laboratory, University of British Columbia, Vancouver.

*Methyl (E)-4-Methyl-2-pentenoate (**9**)*

Sodium hydride (4.3 g of a 56% dispersion in mineral oil) was added to 50 ml of dry dimethyl sulfoxide and the resulting suspension was slowly heated under a nitrogen atmosphere to 75° and maintained at that temperature until all frothing had ceased (~45 min). The solution was cooled to room temperature and a solution of 18.2 g of trimethylphosphonoacetate in 30 ml of dimethyl sulfoxide was added. The solution was allowed to stir for 10 min and then a solution of 5.76 g of isobutyraldehyde in 30 ml of dimethyl sulfoxide was added dropwise. After the addition was complete, the reaction mixture was allowed to stir for an additional hour. Water was added and the resulting mixture was extracted thoroughly with petroleum ether (b.p. 30–60°). The combined extracts were successively washed with water and brine, and then dried over anhydrous magnesium sulfate. Removal of the solvent, followed by distillation of the residue under reduced pressure afforded 6.5 g (65%) of methyl (*E*)-4-methyl-2-pentenoate, b.p. 65°/10 mm (lit. (23) b.p. 74–75°/46 mm); n_D^{25} 1.4309 (lit. (23) n_D^{25} 1.4305); i.r. (film) λ_{max} 5.8, 6.05 μ; p.m.r. τ 8.95 (d, 6H, $-CH(CH_3)_2$, J = 7 Hz), 7.50 (m, 1H, $-CH(CH_3)_2$), 6.30 (s, 3H, OCH_3), 4.25 (d of d, 1H, H-2, $J_{2,3}$ = 16 Hz, $J_{2,4}$ = 1 Hz), 3.05 (d of d, 1H, H-3, $J_{2,3}$ = 16 Hz, $J_{3,4}$ = 7 Hz).

*(E)-4-Methyl-2-pentenoic Acid (**10**)*

To a stirred solution of 34 g of potassium carbonate in 200 ml of methanol–water was added 23 g of methyl (*E*)-4-methyl-2-pentenoate. The reaction mixture was stirred at reflux for 3 h. Most of the methanol was removed under reduced pressure and the residue was diluted with water. The resulting aqueous solution was washed with ether (washings discarded), acidified with dilute hydrochloric acid, and thoroughly extracted with ether. The combined ether extracts were successively washed with water and brine, and dried over magnesium sulfate. Removal of the solvent and distillation of the residue under reduced pressure afforded 17.2 g (82%) of

[6]This general section is applicable to the succeeding, accompanying paper (13), as well as to the present paper.

Can. J. Chem. Downloaded from www.nrcresearchpress.com by 210.87.254.42 on 09/05/12
For personal use only.

(*E*)-4-methyl-2-pentenoic acid, b.p. 75°/0.6 mm; n_D^{27} 1.4454; u.v. λ_{max} 217 nm (ε 3630); i.r. (film) λ_{max} 3.1–4.0 (broad), 5.9, 6.1 μ; p.m.r. τ 8.95 (d, 6H, —CH(CH_3)$_2$, J = 6.5 Hz), 7.25–7.8 (m, 1H, —CH(CH$_3$)$_2$), 4.2 (d of d, 1H, H-2, $J_{2,3}$ = 15.5 Hz, $J_{2,4}$ = 1.5 Hz), 2.9 (d of d, 1H, H-3, $J_{2,3}$ = 15.5 Hz, $J_{3,4}$ = 6.5 Hz), −2.15 (s, 1H, —CO_2H).

Anal. Calcd. for $C_6H_{10}O_2$: C, 63.14; H, 8.83. Found: C, 62.85; H, 8.76.

(E)-2-Methyl-3-hepten-5-one (7)

Finely cut lithium wire (25.8 g) was added to 600 ml of anhydrous ether under nitrogen. To the resulting stirred mixture was added dropwise a solution of 120 ml of ethyl bromide (previously distilled from calcium hydride) in 300 ml of anhydrous ether. During the addition the reaction mixture was kept at −10° by application of an external Dry Ice–acetone cooling bath. After the addition was complete the solution was warmed to 0°, kept at this temperature for 1 h, filtered under nitrogen, and used immediately.

A solution of 32 g of (*E*)-4-methyl-2-pentenoic acid in 540 ml of anhydrous ether was cooled to −78° (Dry Ice – acetone) and 600 ml of the previously prepared ethyllithium solution was added dropwise. After the addition was complete, the white slurry was allowed to stir at −78° for an additional hour. The cooling bath was removed and stirring was continued until a clear solution resulted. The latter was poured into rapidly stirred, ice-cold 1 *N* hydrochloric acid. The resulting mixture was thoroughly extracted with ether. The combined ether extracts were washed successively with dilute ammonium hydroxide, water, and brine and then dried over magnesium sulfate. The solvent was removed by careful distillation through a Vigreaux column at atmospheric pressure. Fractional distillation of the residue under reduced pressure yielded 17 g (92%, based on unrecovered starting material) of (*E*)-2-methyl-3-hepten-5-one (**7**), b.p. 54°/10 mm; u.v. λ_{max} 221 nm (a quantitative u.v. spectrum was not obtained, since the material contained a small amount of the corresponding β,γ-unsaturated ketone); i.r. (film) λ_{max} 5.98, 6.14 μ; p.m.r. τ 8.90 (d, 6H, —CH(CH_3)$_2$, J = 7 Hz), 8.95 (t, 3H, —CH_2CH_3, J = 7 Hz), 7.45 (q, 2H, —CH_2—CH_3, J = 7 Hz), 3.98 (d of d, 1H, H-4, $J_{4,5}$ = 16 Hz, $J_{4,6}$ = 1.5 Hz), 3.20 (d of d, 1H, H-5, $J_{4,5}$ = 16 Hz, $J_{5,6}$ = 6 Hz).

Anal. Calcd. for $C_8H_{14}O$: C, 76.19; H, 11.11. Found: C, 76.10; H, 11.12.

Preparation of Octalones 12 and 13

A mixture of 6 g (0.02 mol) of the pyrrolidine enamine of cyclohexanone (**11**) and 2.6 g (0.02 mol) of (*E*)-2-methyl-3-hepten-5-one (**7**) was stirred under nitrogen at 60° for 40 h. Anhydrous dioxan (12 ml) was added and the reaction mixture was refluxed overnight. To the resulting solution was added 1 ml of glacial acetic acid, 2 ml of water, and 0.5 g of anhydrous sodium acetate and refluxing was continued for 4 h. The cooled reaction mixture was diluted with water and the resulting mixture was extracted thoroughly with ether. The combined ether extracts were washed successively with water, dilute hydrochloric acid, water, and brine and then dried over anhydrous magnesium sulfate. Removal of the solvent, followed by distillation of the residual material under reduced pressure afforded 3.5 g (83%) of a pale yellow oil, b.p. 100°/0.2 mm. This material was shown by g.l.c. to consist of a 7:3 mixture of octalones **12** and **13**, respectively. Separation of the two components was accomplished by preparative g.l.c. (column A, 200°, 86). The major octalone **12** exhibited u.v. λ_{max} 249 nm (ε 13 600); i.r. (film) λ_{max} 6.0, 6.15 μ; p.m.r. τ 9.21, 9.11 (d, d, 6H, —CH(CH_3)$_2$, J = 7 Hz), 8.26 (s, 3H, vinyl CH_3).

Mol. Wt. Calcd. for $C_{14}H_{22}O$: 206.167. Found (high resolution mass spectrometry): 206.166.

The minor octalone **13** exhibited u.v. λ_{max} 249 nm (ε 13 400); i.r. (film) λ_{max} 6.0, 6.1 μ; p.m.r. τ 9.11 (d, 6H, —CH(CH_3)$_2$, J = 6 Hz), 8.26 (s, 3H, vinyl CH_3).

Mol. Wt. Calcd. for $C_{14}H_{22}O$: 206.167. Found (high resolution mass spectrometry): 206.166.

Lithium–Ammonia Reduction of Octalone 12

To 150 ml of liquid ammonia (distilled from sodium metal) was added 200 mg of finely cut lithium wire. After the lithium had dissolved, a solution of the octalone **12** (450 mg) in 25 ml of anhydrous ether was added dropwise over a period of 30 min. The reaction mixture was allowed to stir for an additional 1.5 h and then ammonium chloride was added to discharge the blue color. The ammonia was allowed to evaporate under a slow stream of nitrogen and the residual material was diluted with water. The resulting mixture was extracted thoroughly with ether. The combined ether extracts were washed successively with water, dilute hydrochloric acid, water, and brine and then dried over anhydrous magnesium sulfate. Removal of the ether, followed by distillation of the residual material under reduced pressure gave 350 mg (78%) of the *trans*-fused decalone **14**, b.p. 125°/0.6 mm. Analysis of the product by g.l.c. (column B, 215°, 110) revealed the presence of only one component. An analytical sample of **14** exhibited i.r. (film) λ_{max} 3.42, 3.51, 5.85 μ; p.m.r. τ 9.23, 9.13 (d, d, 6H, —CH(CH_3)$_2$, J = 7 Hz), 8.99 (d, 3H, secondary CH_3, J = 6.5 Hz).

Anal. Calcd. for $C_{14}H_{24}O$: C, 80.71; H, 11.61. Found: C, 80.48; H, 11.31.

Lithium–Ammonia Reduction of Octalone 13

The lithium–ammonia reduction of the octalone **13** was carried out via a procedure identical with that described above. From 150 mg of **13** there was obtained 115 mg (75%) of the *cis*-fused decalone **16**. Analysis of the product by g.l.c. (column B, 215°, 110) showed the presence of only one component. An analytical sample exhibited i.r. (film) λ_{max} 3.45, 5.85 μ; p.m.r. τ 9.13, 9.09 (d, d, 6H, —CH(CH_3)$_2$, J = 6 Hz), 9.02 (d, 3H, secondary CH_3, J = 6.5 Hz).

Mol. Wt. Calcd. for $C_{14}H_{24}O$: 208.183. Found (high resolution mass spectrometry): 208.182.

Hydrogenation of Octalone 13

A solution of 100 mg of the octalone **13** in 10 ml of freshly distilled ethyl acetate was hydrogenated at atmospheric pressure and room temperature over 10 mg of 10% palladium-on-charcoal. Distillation of the crude product under reduced pressure afforded 96 mg (92%) of a colorless oil, b.p. 125°/0.6 mm. This material was subjected to epimerization with sodium methoxide in refluxing methanol. The resulting product was shown

Can. J. Chem. Downloaded from www.nrcresearchpress.com by 210.87.254.42 on 09/05/12
For personal use only.

to contain 98% of one component by g.l.c. analysis (column B, 180°, 100). An analytical sample of this material exhibited i.r. and p.m.r. spectra identical with those of the *cis*-fused decalone **16**, obtained as described above.

*Preparation of Octalones **19** and **20***

A solution of 1 g of the pyrrolidine enamine of 4,4-ethylenedioxycyclohexanone (**18**) (24) and 500 mg of (*E*)-2-methyl-3-hepten-5-one (7) in 4 ml of dry dioxan was refluxed for 48 h. A solution of 0.2 g of sodium acetate in 1.1 ml of acetic acid – water (1:2) was added and refluxing was continued for 1.5 h. The cooled reaction mixture was then diluted with water and thoroughly extracted with ether. The combined ether extracts were successively washed with water, aqueous sodium carbonate, water, and brine and then dried over anhydrous magnesium sulfate. Removal of the solvent, followed by distillation of the residue under reduced pressure gave 121 mg (8%) of a viscous oil, b.p. 150°/0.1 mm. Gas–liquid chromatographic analysis (column A, 180°, 85) revealed that this material consisted of a mixture of two compounds, in a ratio of 4:1. Analytical samples were collected by preparative g.l.c. The major compound, octalone **19**, exhibited u.v. λ_{max} 243 nm (ε 13 000); i.r. (film) λ_{max} 6.05 μ; p.m.r. τ 9.18, 9.08 (d, d, 6H, —CH(CH_3)$_2$, J = 6.5 Hz), 8.23 (s, 3H, vinyl CH_3), 6.06 (s, 4H, —OCH_2CH_2O—).

Mol. Wt. Calcd. for $C_{16}H_{24}O_3$: 264.172. Found (high resolution mass spectrometry): 264.172.

The minor isomer, octalone **20**, exhibited u.v. λ_{max} 243 nm (ε 18 900); i.r. (film) λ_{max} 6.01, 6.15 μ; p.m.r. τ 9.08, 9.06 (d, d, 6H, —CH(CH_3)$_2$, J = 6.0 Hz), 8.23 (s, 3H, vinyl CH_3), 6.06 (s, 4H, —OCH_2CH_2O—).

Mol. Wt. Calcd. for $C_{16}H_{24}O_3$: 264.172. Found (high resolution mass spectrometry): 264.172.

*Preparation of Hydroxy Octalones **22** and **23***

A solution of 18 g of 4-hydroxycyclohexanone (25) and 20.7 ml of pyrrolidine in 234 ml of benzene was refluxed under a Dean–Stark water separator until no further separation of water occurred. The benzene and excess pyrrolidine were removed under reduced pressure (0.1 mm) to yield a crude, crystalline enamine, i.r. (Nujol) λ_{max} 3.0, 6.1 μ. To this material was added 13.5 g of (*E*)-2-methyl-3-hepten-5-one (7) and the resulting mixture was stirred at 50° for 17 h. At this time, the i.r. spectrum of an aliquot showed the absence of absorptions due to the vinyl ketone. Hence, an additional 5 g of the vinyl ketone 7 was added and stirring was continued for an additional 19 h. Dry dioxan was then added and the resulting solution was refluxed for 16 h. A solution of 5 g of sodium acetate in acetic acid – water (30 ml, 1:2) was added and refluxing was continued for 4 h. The cooled reaction mixture was diluted with water and thoroughly extracted with ether. The combined ether extracts were washed successively with water, dilute hydrochloric acid, water, and brine and dried over anhydrous magnesium sulfate. Removal of the solvent, followed by distillation of the residue under reduced pressure gave 14 g (40%) of a colorless oil, b.p. 200°/0.1 mm. This material was shown by g.l.c. analysis (column C, 215°, 170) to be a mixture of two components in a ratio of approximately 3:2. Subjection of this mixture to epimerizing conditions (150 ml of 2 *M* sodium methoxide in methanol, reflux 12 h) changed this ratio to 7:3, respectively. The two components were separated by preparative g.l.c. (column C, 230°, 110). The major octalone (**22**) exhibited u.v. λ_{max} 248 nm (ε 10 900); i.r. ($CHCl_3$) λ_{max} 2.75, 2.9, 6.05 μ; p.m.r. τ 9.16, 9.07 (d, d, 6H, —CH(CH_3)$_2$, J = 6.5 Hz), 8.23 (s, 3H, vinyl CH_3), 6.15, 5.82 (unresolved multiplets, 1H, —C*H*OH).

Mol. Wt. Calcd. for $C_{14}H_{22}O_2$: 222.162. Found (high resolution mass spectrometry): 222.162.

The minor octalone (**23**) exhibited u.v. λ_{max} 247 nm (ε 9300); i.r. ($CHCl_3$) λ_{max} 2.75, 2.9, 6.05, 6.15 μ; p.m.r. τ 9.07, 9.04 (d, d, 6H, —CH(CH_3)$_2$, J = 6 Hz), 8.26 (s, 3H, vinyl CH_3), 6.10, 5.78 (unresolved multiplets, 1H, —C*H*OH).

Mol. Wt. Calcd. for $C_{14}H_{22}O_2$: 222.162. Found (high resolution mass spectrometry): 222.162.

*Preparation of Dione **24***

A solution of 60 mg of chromium trioxide in 1.5 ml of dichloromethane containing 0.09 ml of pyridine was allowed to stir at room temperature for 15 min. To this solution was added a solution of 30 mg of octalone **22** in 0.5 ml of dichloromethane. The resulting reaction mixture was allowed to stir at room temperature for 25 min and was then diluted with 8 ml of ether. The ether layer was washed with water and brine and dried over anhydrous magnesium sulfate. Removal of the ether afforded 28 mg (94%) of the dione **24**, m.p. 108–110°. This material showed one peak on g.l.c. analysis (column A, 180°, 86) and exhibited u.v. λ_{max} 247 nm (ε 13 000); i.r. ($CHCl_3$) λ_{max} 5.85, 6.05, 6.15 μ; p.m.r. τ 9.20, 9.07 (d, d, 6H, —CH(CH_3)$_2$, J = 6.5 Hz), 8.12 (s, 3H, vinyl CH_3).

Anal. Calcd. for $C_{14}H_{20}O_2$: C, 76.33; H, 9.15. Found: C, 76.28; H, 9.18.

*Conversion of Hydroxy Octalone **22** into Decalone **14***

To a solution of 225 mg of octalone **22** in 6 ml of dry pyridine at 0° was added 0.15 ml of methanesulfonyl chloride. The reaction mixture was allowed to stir at room temperature for 3.5 h. Ice was added, the mixture was allowed to stir for an additional 10 min, and then was thoroughly extracted with ether. The combined ether extracts were washed with water, dilute sulfuric acid, dilute aqueous sodium bicarbonate, and brine and dried over anhydrous magnesium sulfate. Removal of the solvent afforded 280 mg (85%) of the crude oily methanesulfonate derivative **25**, i.r. (film) λ_{max} 6.0, 7.45, 8.55 μ.

A solution of this material in 1.8 ml of absolute ethanol was added dropwise to a solution of 1.35 g of lithium in 50 ml of liquid ammonia (distilled from sodium metal) at −78°. The mixture was stirred at −78° for 1 h and then at −33° for 1.5 h. Additional ethanol was added until the blue color disappeared. The liquid ammonia was allowed to evaporate, water was added to the residue, and the resulting mixture was thoroughly extracted with ether. The combined ether extracts were washed with water and brine and dried over anhydrous magnesium sulfate. Removal of the solvent gave 160 mg of a mixture of alcohols. This material was dissolved in 12 ml of acetone (distilled from potassium permanganate) and to the resulting solution was added standard chromic acid solution (18) until the orange color persisted. The

Can. J. Chem. Downloaded from www.nrcresearchpress.com by 210.87.254.42 on 09/05/12
For personal use only.

orange color was discharged by addition of isopropyl alcohol and the solvent was removed under reduced pressure. The residue was diluted with water and the mixture was thoroughly extracted with ether. The combined ether extracts were washed with water and brine and dried over anhydrous magnesium sulfate. Removal of the solvent, followed by distillation of the residue under reduced pressure afforded 136 mg (85%) of the decalone **14**, b.p. 125°/0.6 mm. This material showed one peak on g.l.c. analysis (column B, 215°, 110) and exhibited spectra (i.r., p.m.r.) identical with those of an authentic sample of the *trans*-fused decalone **14**.

Preparation of the Dithioketal 26

To a cold (0°), stirred mixture of 3.6 g of octalone **22** and 3.0 ml of ethanedithiol was added 1.4 ml of boron trifluoride etherate. The solution was allowed to warm to room temperature and then stirred for an additional 1 h. After dilution with water, the reaction mixture was thoroughly extracted with chloroform. The combined chloroform extracts were washed with water and brine and dried over anhydrous magnesium sulfate. Removal of the solvent gave 5.2 g of crude material. A benzene solution of the latter was filtered through a short column of Woelm activity I neutral alumina (20 g). The alumina column was eluted with additional benzene. Concentration of the filtrate gave a crystalline solid which, upon recrystallization from ether afforded 3.2 g (66%) of the dithioketal **26**, m.p. 105–110°; i.r. (Nujol) λ_{max} 3.0, 6.1 μ; p.m.r. τ 9.21, 9.02 (d, d, 6H, $-CH(CH_3)_2$, J = 7 Hz), 8.07 (s, 3H, vinyl CH_3), 6.67 (m, 4H, $-SCH_2CH_2S-$), 6.54, 5.86 (unresolved multiplets, 1H, $-CH(OH)-$).

Mol. Wt. Calcd. for $C_{16}H_{26}OS_2$: 298.142. Found: (high resolution mass spectrometry): 298.144.

Preparation of Alcohol 27

To a solution of 700 mg of the dithioketal **26** in 100 ml of absolute ethanol was added 10 g of commercial Raney nickel. The mixture was refluxed for 5 h, cooled, and filtered through a bed of Celite. The filtrate was concentrated and the residual oil was distilled under reduced pressure to afford 350 mg (77%) of the alcohol **27**, b.p. 120°/0.25 mm; i.r. (film) λ_{max} 3.0, 6.0 μ; p.m.r. τ 9.23, 9.09 (d, d, 6H, $-CH(CH_3)_2$, J = 6.5 Hz), 8.40 (s, 3H, vinyl CH_3), 6.36, 5.85 (unresolved multiplets, 1H, $-CH(OH)$).

Mol. Wt. Calcd. for $C_{14}H_{24}O$: 208.183. Found (high resolution mass spectrometry): 208.183.

Preparation of Octalone 28

To an ice-cold solution of 720 mg of chromium trioxide in 18 ml of anhydrous pyridine was added a solution of 350 mg of alcohol **27** in 9 ml of anhydrous pyridine. The solution was allowed to stir at room temperature for 40 h. The reaction mixture was poured into stirred anhydrous ether. Celite was added and the mixture was filtered. The filtrate was thoroughly washed with water and brine and dried over anhydrous magnesium sulfate. Removal of the solvent, followed by distillation of the oily residue under reduced pressure yielded 307 mg (89%) of a colorless oil, b.p. 130°/0.35 mm. This product was shown to be homogeneous by g.l.c. (column B, 180°, 85). An analytical sample exhibited i.r. (film) λ_{max} 5.85 μ; p.m.r. τ 9.21, 9.05 (d, d, 6H, $-CH(CH_3)_2$, J = 6.5 Hz), 8.36 (s, 3H, vinyl CH_3).

Mol. Wt. Calcd. for $C_{14}H_{22}O$: 206.167. Found (high resolution mass spectrometry): 206.168.

Preparation of Alcohol 29

A solution of 230 mg (1.06 mmol) of octalone **28** in 30 ml of anhydrous ether was cooled to 0°. To this solution was added, dropwise, 2 ml of 2.16 *M* methyllithium (4.32 mmol) in ether. After the addition was complete the solution was allowed to stir for 2 h at room temperature and was then poured into a mixture of ice and water. The ether layer was separated and washed with water and brine and dried over anhydrous magnesium sulfate. The solvent was removed and the residual oil was distilled under reduced pressure to afford 224 mg (91%) of a viscous oil, b.p. 130°/0.25 mm. This oil was shown by g.l.c. analysis (column C, 200°, 110) to contain one major component along with trace amounts of unidentified material. The major component, obtained by preparative g.l.c., was a white crystalline substance, m.p. 79–80°; i.r. (Nujol) λ_{max} 3.0, 6.1 μ; p.m.r. τ 9.21, 9.07 (d, d, 6H, $-CH(CH_3)_2$, J = 6.5 Hz), 8.81 (s, 3H, tertiary CH_3), 8.37 (s, 3H, vinyl CH_3).

Mol. Wt. Calcd. for $C_{15}H_{26}O$: 222.198. Found (high resolution mass spectrometry): 222.198.

Preparation of (±)-Cadinene Dihydrochloride (30)

A solution of 100 mg of the crystalline alcohol **29** in 10 ml of anhydrous ether was cooled to 0°. Dry hydrogen chloride gas was bubbled into the solution. At the end of 15 min, the gas flow was stopped and the solution was stirred for an additional hour. The ether was removed under reduced pressure to afford 100 mg (80%) of crystalline (±)-cadinene dihydrochloride (**30**). An analytical sample was obtained by recrystallization from *n*-hexane–methanol to afford white crystals, m.p. 104.5–106°. This sample showed no depression of melting point on admixture with an authentic sample of (±)-cadinene dihydrochloride and its i.r. spectrum was superimposable with that of the authentic sample; i.r. (Nujol), λ_{max} 3.45, 6.95, 8.75, 11.75 μ.

Anal. Calcd. for $C_{15}H_{26}Cl_2$: C, 65.01; H, 9.39. Found: C, 64.75; H, 9.52.

Financial support from the National Research Council of Canada and a National Research Council of Canada Studentship (to W.M.P.) are gratefully acknowledged.

1. J. S. Roberts. *In* Specialist periodical reports. Terpenoids and steroids. Vol. 1. The Chemical Society, London. 1971. pp. 62–64.
2. Y. Ohta, K. Ohara, and Y. Hirose. Tetrahedron Lett. 4181 (1968).
3. Y. Ohta and Y. Hirose. Bull. Chem. Soc. Japan, **46**, 1535 (1973).
4. C. H. Heathcock. *In* The total synthesis of natural products. Vol. 2. *Edited by* J. ApSimon. John Wiley and Sons, New York. 1973.
5. Wynona M. Phillips. Ph.D. Thesis. University of British Columbia, Vancouver, British Columbia. 1971.
6. L. Horner, H. Hoffmann, H. G. Wippel, and G.

KLAHRE. Chem. Ber. **92**, 2499 (1959); W. S. WADSWORTH and W. D. EMMONS. J. Am. Chem. Soc. **83**, 1733 (1961); J. BOUTAGY and R. THOMAS. Chem. Rev. **74**, 87 (1974).
7. E. B. BAKER. J. Chem. Phys. **37**, 911 (1962).
8. V. J. KOWALEWSKI. *In* Progress in n.m.r. spectroscopy. Vol. 5. *Edited by* J. W. Emsley, J. Feeney, and L. H. Sutcliffe. Pergamon Press, London. 1969.
9. R. BURTON, L. D. HALL, and P. R. STEINER. Can. J. Chem. **49**, 588 (1971).
10. R. HOWE and F. J. MCQUILLIN. J. Chem. Soc. 2670 (1956).
11. G. STORK and S. D. DARLING. J. Am. Chem. Soc. **86**, 1761 (1964).
12. M. J. T. ROBINSON. Tetrahedron, **21**, 2475 (1965).
13. E. PIERS, W. M. PHILLIPS-JOHNSON, and C. BERGER. Can. J. Chem. This issue.
14. G. STORK, A. BRIZZOLARA, H. LANDESMAN, J. SZMUSZKOVICZ, and R. TERRELL. J. Am. Chem. Soc. **85**, 207 (1963).
15. L. VELLUZ, J. VALLS, and G. NOMINÉ. Angew. Chem. Int. Ed. **4**, 181 (1965).
16. G. I. POOS, G. E. ARTH, R. E. BEYLER, and L. H. SARETT. J. Am. Chem. Soc. **75**, 422 (1953).
17. J. A. MARSHALL and H. ROEBKE. J. Org. Chem. **34**, 4190 (1969).
18. K. BOWDEN, I. M. HEILBRON, E. R. H. JONES, and B. C. L. WEEDON. J. Chem. Soc. 39 (1946).
19. V. SÝKORA, V. HEROUT, and F. ŠORM. Coll. Czech. Chem. Commun. **23**, 2181 (1958).
20. N. V. MANI. Z. Krist. **118**, 103 (1963).
21. M. D. SOFFER and G. E. GÜNAY. Tetrahedron Lett. 1355 (1965).
22. M. V. R. KOTESWARA RAO, G. S. KRISHNA RAO, and S. DEV. Tetrahedron, **22**, 1977 (1966).
23. J. B. ROGAN. J. Org. Chem. **27**, 3910 (1962).
24. M. HASLANGER and R. G. LAWTON. Synth. Commun. **4**, 155 (1974).
25. P. RADLICK and H. T. CRAWFORD. J. Org. Chem. **37**, 1669 (1972).

Can. J. Chem. Downloaded from www.nrcresearchpress.com by 210.87.254.42 on 09/05/12
For personal use only.

Synthesis and Novel Stereochemical Results in the Lithium–Ammonia Reduction of Some 4-Alkyl-$\Delta^{1(9)}$-2-octalones

EDWARD PIERS, WYNONA M. PHILLIPS-JOHNSON, and CHRISTIAN BERGER

Department of Chemistry, University of British Columbia, 2075 Wesbrook Place, Vancouver, British Columbia V6T 1W5

Received November 18, 1974

EDWARD PIERS, WYNONA M. PHILLIPS-JOHNSON, and CHRISTIAN BERGER. Can. J. Chem. **53**, 1291 (1975).

The 4-alkyl-$\Delta^{1(9)}$-2-octalones **7–11**, inclusive, prepared by conjugate addition of appropriate organocuprate reagents to the cross-conjugated dienones **13** and **14**, were subjected to lithium–ammonia reduction. Interestingly, these reductions produced, in each case, a considerably higher proportion (13–35%) of the corresponding *cis*-fused 2-decalone (**27–31**, inclusive) as compared with that normally formed in the alkali metal – ammonia reduction of $\Delta^{1(9)}$-2-octalones. The results are qualitatively explained in terms of the proposals originally set forth by Robinson.

EDWARD PIERS, WYNONA M. PHILLIPS-JOHNSON et CHRISTIAN BERGER. Can. J. Chem. **53**, 1291 (1975).

On a soumis à une réduction par le lithium dans l'ammoniac les alkyl-4 $\Delta^{1(9)}$ octalones-2 (**7** à **11**) préparées par l'addition 1–4 des réactifs organocuprates appropriés sur les diénones **13** et **14** conjuguées d'une façon croisée. Il est intéressant de noter que ces réductions produisent dans chaque cas une quantité proportionnellement plus élevée (13–35%) de la décalone-2 *cis* correspondante (**27–31** inclusivement) par opposition avec ce qui est normalement obtenu lors de la réduction par les métaux alcalins dans l'ammoniac des $\Delta^{1(9)}$ octalones-2. Les résultats sont expliqués sur une base qualitative en termes des propositions qui ont été originalement mises de l'avant par Robinson. [Traduit par le journal]

The alkali metal – ammonia reduction of α,β-unsaturated ketones is a very useful and frequently employed reaction in organic synthesis. Not only is the reaction normally efficient in terms of product yield but it also produces as the initially formed product an enolate anion, which can then be used in a variety of ways. Furthermore, in those cases where new chiral centers are formed (particularly at the β-carbon), the reaction often proceeds with high stereoselectivity. More explicitly, the latter characteristic is of noteworthy importance in the synthesis of natural products (particularly steroids and terpenoids), in which the transformation illustrated in general terms by **1** → **2** is often a requirement. Indeed, it is well known that the alkali metal – ammonia reduction of $\Delta^{1(9)}$-2-octalone systems of type **1** generally proceeds in a highly stereoselective manner, yielding a large predominance of the corresponding *trans*-fused 2-decalone system **2** (1–3).

The mechanistic details of alkali metal – ammonia reduction of α,β-unsaturated carbonyl compounds have been the subject of many reports in the chemical literature. Of particular note in this regard are the recent papers by House *et al.* (4, 5) and by Kemp and co-workers (6, 7). Furthermore, the reasons underlying the high stereoselectivity of reduction of $\Delta^{1(9)}$-2-octalones and related compounds have been the subject of a number of studies (2, 3, 8) and discussions (9–11*a*). However, there does not as yet appear to be complete agreement as to what the reasons for this high stereoselectivity actually are and a number of different proposals have been put forward. The main source of controversy has been, and appears still to be, related to the question of whether the geometry of the transition state for protonation at the β-carbon is pyramidal (2, 5, 9) or trigonal (3).

In the accompanying paper (12) we reported the preparation and lithium–ammonia reduction of the two epimeric octalones **3** and **4**. It was found that although reduction of **3** proceeded in the "normal" manner and produced only the *trans*-fused 2-decalone **5**, a similar reduction of **4** afforded stereoselectively the *cis*-fused 2-decalone **6**. This novel and initially surprising result led us to initiate an investigation into the stereochemistry of lithium–ammonia reduction of a series of analogous $\Delta^{1(9)}$-2-octalones containing an angular methyl group at C_{10} and various axially oriented alkyl groups at C_4. In particular, we report in this paper the preparation and

Can. J. Chem. Downloaded from www.nrcresearchpress.com by 210.87.254.42 on 09/05/12
For personal use only.

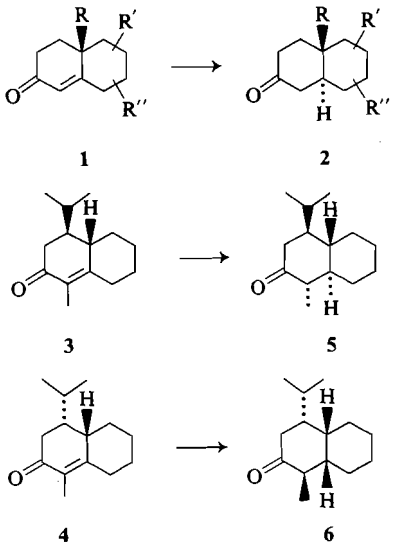

lithium–ammonia reduction of the substituted $\Delta^{1(9)}$-2-octalones **7–11**, inclusive.[1]

Preparation of the 4α-Alkyl-4aβ-methyl-4,4a,5,6,7,8-hexahydro-2(3H)-napthalenones 7–11 (see Scheme 1)

The $\Delta^{1(9)}$-2-octalones chosen for the present study were prepared by conjugate addition of appropriate cuprate reagents (14) to the cross-conjugated dienones **13** (15) and **14** (16). It is now well established that conjugate addition of Grignard reagents (copper catalyzed) or of lithium dialkylcuprate reagents to dienones such as **13** and **14** takes place both regioselectively and stereoselectively to produce the corresponding octalones with an axially oriented alkyl group at C_4 (14, 17–19). In other words, the incoming alkyl group attacks the less hindered β-carbon of the dienone system from the side opposite the already present angular methyl group. Molecular models clearly show that if approach of the reagent were to occur in a stereoelectronically allowed fashion from the other side of the molecule, the incoming alkyl group would, in the transition state, be nearly eclipsed with the angular methyl group. The resulting steric and torsional strain should be a dominant factor and, presumably, ensures that the alternate transition state (α attack at C_4) is favored.

Conjugate addition, under appropriate conditions, of lithium dimethyl-, divinyl-, and diisopropylcuprate to the cross-conjugated dienone **13** afforded, in good yields, the octalones **7**, **12**, and **9**, respectively. In each case, the reaction was highly stereoselective and the spectral properties of the product fully corroborated the assigned structure. The vinyl derivative **12** was found to be quite unstable and was therefore immediately converted, by hydrogenation in the presence of tris(triphenylphosphine)chlororhodium (20), into the corresponding ethyl derivative **8**. In a similar fashion, addition of lithium dimethyl- and diisopropylcuprate to the dienone **14** afforded the octalones **10** and **11**, respectively.

It should be noted that considerable experimentation was done to find optimum conditions for the above-mentioned conjugate additions. Therefore, it is appropriate to make a few general comments regarding these reactions. At the time this work was underway, House and co-workers (21, 22) had already reported a detailed study of the use of lithium dimethylcuprate in conjugate addition to α,β-unsaturated ketones and we therefore experienced no problems in connection with the use of this reagent. However, no analogous information was available for lithium divinyl- or diisopropylcuprate. Initially, therefore, a procedure analogous to that used by House *et al.* (21) for the preparation and use of the dimethyl reagent was also employed for the divinyl and diisopropyl reagents. However, it was found that this procedure gave rise to only a poor yield of conjugate addition product with the divinylcuprate and only recovered starting material or polymeric material in the latter case. In an attempt to enhance the reactivity of the lithium diisopropylcuprate reagent with respect to conjugate addition, the use of various additives was investigated. Indeed, it was found that fair to moderate yields of conjugate addition product could be realized if anhydrous lithium bromide was present in the reaction mixture. However, since these reactions were still rather inefficient as compared with the reactions involving the use of lithium dimethylcuprate, an alternative method of preparing the cuprate reagents was investigated. In this approach, the ether soluble cuprous iodide – tri-*n*-butylphosphine complex (23) was employed instead of cuprous iodide. The solutions of lithium divinyl- and diisopropylcuprates prepared in this manner were homogeneous in contrast to the colloidal appearance of those previously prepared. Fur-

[1]For a preliminary report regarding this work, see ref. 13.

Can. J. Chem. Downloaded from www.nrcresearchpress.com by 210.87.254.42 on 09/05/12
For personal use only.

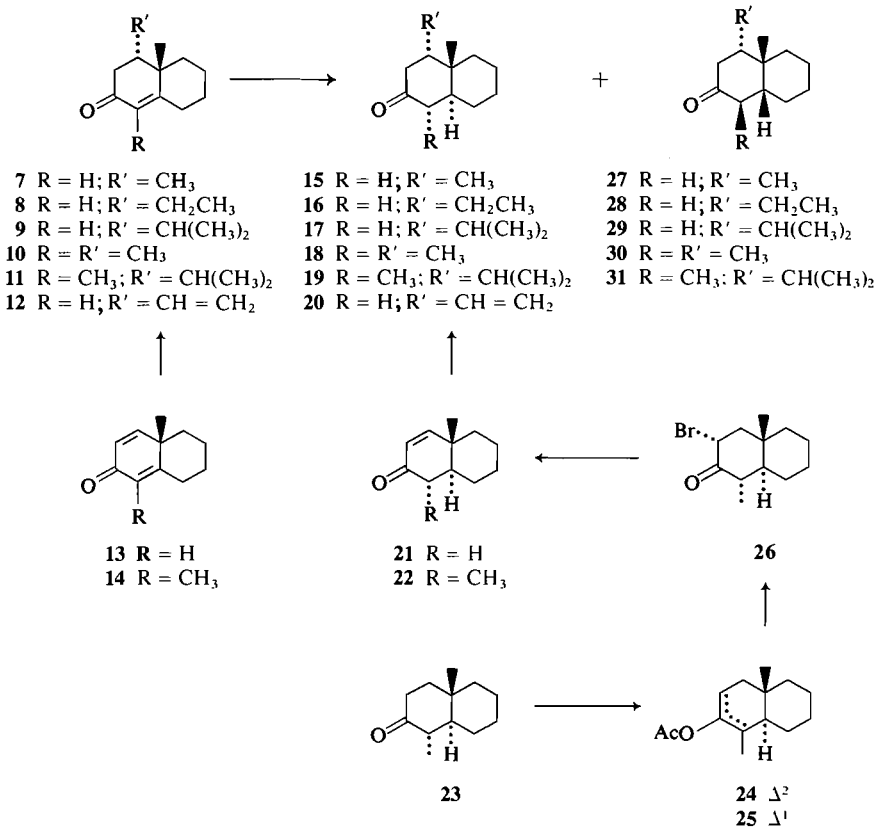

SCHEME 1

thermore, the yields of conjugate addition products were markedly improved, although, in the case of the diisopropyl reagent, the use of anhydrous lithium bromide as an additive again appeared to be advantageous.

In further attempts to improve the yields of conjugate addition products, the effect of other reaction parameters (reaction time, temperature, reactant concentration, and quenching procedure) was investigated. Firstly, it was generally found that product yields obtained upon varying the reaction time from 4 to 36 h appeared to be invariant, although use of reaction times shorter than 4 h generally resulted in the recovery of some starting material. Secondly, repetition of various reactions at different temperatures clearly revealed that the best yields were obtained at low temperatures and most of the conjugate additions were therefore carried out at −78°. Thirdly, attempted additions using a variety of reactant concentrations indicated that optimum yields were obtained when the reaction solutions were between 0.01 and 0.005 *M* in the organocuprate reagents. Finally, it was found advantageous to quench the reactions by dropwise addition of the reaction mixtures to a rapidly stirred solution of aqueous acid (see ref. 24).

It should be noted that recently, subsequent to the time at which the above-described work was carried out, there have appeared a number of reports concerning the use of lithium divinylcuprate (25–29) and related reagents (30–40) in conjugate addition to a variety of α,β-unsaturated ketones.

Preparation of the Lithium–Ammonia Reduction Products (see Scheme 1)

Having realized the efficient and stereoselective synthesis of each of the octalones required for the projected lithium–ammonia reduction studies, it was necessary to unambiguously prepare the products which could be expected from these reductions. Explicitly, this involved the preparation of the *trans*-fused 2-decalones **15–19**, and the *cis*-fused 2-decalones **27–31**. The former

Can. J. Chem. Downloaded from www.nrcresearchpress.com by 210.87.254.42 on 09/05/12
For personal use only.

Can. J. Chem. Downloaded from www.nrcresearchpress.com by 210.87.254.42 on 09/05/12
For personal use only.

compounds (**15–19**) were prepared by the conjugate addition of appropriate organocuprate reagents to the requisite α,β-unsaturated ketone. Thus, when the octalone **21** (41) was allowed to react with each of lithium dimethyl-, divinyl-, and diisopropylcuprate under conditions essentially identical with those outlined previously, the corresponding *trans*-fused 2-decalones (**15**, **20**, and **17**, respectively) were formed in good to excellent yields.[2] Hydrogenation of the vinyl derivative **20** in the presence of palladium-on-charcoal afforded, in 98% yield, the saturated decalone **16**. In a similar fashion, conjugate addition of lithium dimethyl- and diisopropylcuprate to the octalone **22**[3] gave, in excellent yields, the other two required *trans*-fused decalones **18** and **19**, respectively.

The required *cis*-fused decalones (**27–31**) were prepared by hydrogenation of the corresponding $\Delta^{1(9)}$-2-octalones **7–11**. It is well known that, under appropriate conditions, hydrogenation of Δ^4-3-keto steroids and related materials affords mainly the corresponding *cis*-fused decalone-type system. Furthermore, in the case of each of the octalones **7–11**, the presence of an axially oriented alkyl group at C_4 would tend to sterically hinder hydrogenation from the α side. In the event, hydrogenation of compounds **7–11** in 0.3 *N* ethanolic potassium hydroxide over palladium-on-charcoal afforded, in each case, a high yield (≥95%) of product which consisted nearly entirely (≥94%) of the corresponding *cis*-fused 2-decalone (**27–31**). In each case, the minor (≤6%) hydrogenation product exhibited g.l.c. retention times identical with those of the corresponding *trans*-fused 2-decalones (**15–19**).

Lithium–Ammonia Reduction of Octalones 7–11

The lithium–ammonia reduction of each of the octalones **7–11** was carried out under standardized conditions. Thus, a solution of the appropriate substrate in ether was added over a period of 30 min to a solution of lithium in anhydrous ammonia, the reaction mixture was stirred for an additional 2 h, and was then quenched by addition of ammonium chloride. Each reduction was repeated at least twice. The crude product mixtures were distilled and then subjected to analysis by g.l.c. The reduction products, the *trans*- and *cis*-fused 2-decalones, were, in each case, isolated by preparative g.l.c. and were shown to be identical with the corresponding authentic materials prepared as described above.

The composition of the reduction products was determined by integration (disc integrator) of the g.l.c. trace obtained by analysis of the product mixtures. It was found that the molar response factor was, within experimental error, the same for each pair of *cis*- and *trans*-fused 2-decalones. This factor was determined, in each case, by preparing a mixture of authentic *cis*- and *trans*-fused decalones in a ratio very similar to that observed in the lithium–ammonia reduction product. The mixture of known composition was then analyzed by g.l.c. and the ratio of the two components obtained by integration of the g.l.c. trace was found to be within experimental error, the same as the known ratio. This was not unexpected, since it is known that molecules of similar structure and molecular complexity generally have identical molar response factors (43).

The results (yields and product compositions) obtained from several reductions of each individual octalone were averaged and the resultant figures are recorded in Table 1.[4]

As can be seen from an examination of the results summarized in Table 1, small amounts (2–14%) of starting material were recovered from the lithium–ammonia reduction of octalones **7–11**. This was not surprising, since it is well known (3, 4) that alkali metal – ammonia reduction of α,β-unsaturated ketones in the absence of proton donors which are more acidic than ammonia generally leads to the recovery of some starting material. Presumably, this is largely due to the fact that some of the unreduced enone reacts with amide ion (produced when the β-carbon of the substrate is protonated by ammonia) to form either the corresponding enolate anion or the product of conjugate addi-

[2]For a discussion regarding the stereochemistry of this type of reaction, see ref. 41. The decalone **17** had been prepared previously (41) via a somewhat different, although related, method.

[3]This compound was prepared as follows. Conversion of the decalone **23** (42) into a mixture of the enol acetates **24** and **25** (85:15, respectively), followed by bromination of this mixture with bromine in acetic acid, afforded the bromoketone **26**. Dehydrobromination of the latter with anhydrous lithium bromide in hot hexamethylphosphoramide afforded octalone **22**.

[4]The results obtained from three or more reductions of each octalone (**7–11**) were found to be reproducible to within ±2%.

TABLE 1. Stereochemistry of lithium–ammonia reduction of 4-alkyl-$\Delta^{1(9)}$-2-octalones

Experiment No.	Octalone	Yield (%)*	Ratio of *trans*:*cis* decalone	Recovered starting material
1	**3**†	91	>99: 1	—
2	**4**†	80	<1:99	—
3	**7**	93	87:13	2
4	**8**	94	75:25	13
5	**9**	98	69:31	14
6	**10**	90	82:18	8
7	**11**	98	65:35	7

*Yield of distilled product, including any recovered starting material.
†See ref. 12.

tion (11*b*), both of which would be inert to reduction. This can be avoided by employing an alcohol as a proton source. However, in the presence of an alcohol, the product of reduction is generally the 2-decalol, which must subsequently be oxidized back to the decalone. In the present work, recovery of small amounts of starting material presented no problem to the analysis of product mixtures. That is, in each case, g.l.c. conditions were found in which the starting material (octalone) and the two corresponding products (*cis*- and *trans*-fused decalones) exhibited distinct retention times. Furthermore, the yields of the reduction products were higher when the additional oxidation step could be omitted. Therefore, all of the reductions were carried out in the absence of an alcohol.

From a stereochemical point of view, a number of interesting conclusions can be drawn from the results tabulated in Table 1. Firstly, the results showed that the lithium–ammonia reduction of $\Delta^{1(9)}$-2-octalones possessing an axially oriented alkyl substituent at C_4 afforded, in each case, a much greater proportion of the corresponding *cis*-fused 2-decalone than that normally found in this type of reduction. For example, whereas the parent $\Delta^{1(9)}$-2-octalone was known to afford nearly exclusively *trans*-2-decalone (3, 5), the isopropyloctalone **4** yielded only the corresponding *cis*-fused 2-decalone **6** (Expt. No. 2). Similarly, although less strikingly, the octalones **7–11** afforded upon lithium–ammonia reduction significant amounts (13–35%) of the corresponding *cis*-fused decalones **27–31**, respectively (Expt. Nos. 3–7). In contrast, a similar reduction of the parent 10-methyl-$\Delta^{1(9)}$-2-octalone was known to yield nearly exclusively *trans*-10-methyl-2-decalone (3, 5).

Secondly, the results summarized in Table 1 indicated that the presence (or absence) of an angular methyl group (at C_{10}) in these compounds had a very significant effect on the stereochemical outcome of reduction. Thus, although the C_{10}-unsubstituted octalone **4** afforded only the *cis*-fused product **6** (Expt. No. 2), the 4α-isopropyloctalones **9** and **11**, containing a 10β-methyl group, yielded significantly lower amounts (31 and 35%) of the *cis*-fused decalones (Expt. Nos. 5 and 7). Thirdly, in the case of octalones **7–11**, the results showed that the relative amount of *cis*-fused decalone in the product increased with increasing size of the axially oriented C_4-alkyl group (Expt. Nos. 3–5 and 6, 7). Finally, the results indicated that the presence or absence of a methyl group at C_1 had little or no effect on the stereochemical outcome of the reduction (Expt. Nos. 3, 5–7).

Discussion

It is important to note that, with regards to the lithium–ammonia reduction of octalones **7–11**, the results (Table 1) showed that the energy difference between the transition states leading from the starting material to the Δ^1-enolates (or enols) of the *trans* and *cis*-fused 2-decalones (**32** and **33**) was quite small. Furthermore, the conformational analysis of substituted Δ^1-octalines of the type **32** and **33** has not as yet been put on a quantitative basis and it is thus very difficult to accurately assess the magnitude of the various nonbonded interactions involved in the different conformations of possible intermediates and/or transition states. Therefore, it is difficult to offer, in *quantitative* terms, an explanation for the stereochemical results summarized in Table 1. However, we feel that the

Can. J. Chem. Downloaded from www.nrcresearchpress.com by 210.87.254.42 on 09/05/12
For personal use only.

Can. J. Chem. Downloaded from www.nrcresearchpress.com by 210.87.254.42 on 09/05/12
For personal use only.

results can be *qualitatively* explained in terms of the proposals originally set forth by Robinson (3).

Briefly, Robinson's conclusions can be summarized as follows. (*a*) The β-carbon of the intermediate anion is planar in shape and the transition state for protonation at the β-carbon should resemble this shape (reactant-like transition state).[5] It was recognized, however, that the planarity is not necessarily perfectly retained in the transition state. (*b*) The intermediate anion can adopt three different conformations (**34**, **35**, **36**),[6] each of which could theoretically lead to protonation transition states to afford **32** and/or **33**. However, considering angle and torsional strain, Robinson concluded that **36** would generally involve too high an energy (large angle strain, lack of planarity of the conjugated system) to be a likely conformation. Of the two remaining conformations, Robinson proposed that **34** would normally be favored and would lead largely to a transition state (resembling **34** in geometry) forming *trans*-fused enolate (or enol) **32**, whereas **35** would normally be more strained (less stable) and would lead mainly to a transition state (resembling **35** in geometry) forming *cis*-fused enolate (or enol) **33**. Therefore, it would be expected that for "normal" $\Delta^{1(9)}$-2-octalones (R′ = H), the transition state arising from **34** (leading to **32**) would be favored over the transition state arising from **35** (leading to **33**), thus accounting for the observed predominance of the *trans*-fused decalone in the product.

Considering now the stereochemical results obtained from the lithium–ammonia reduction of octalones **4** and **7–11**, inclusive, it is reasonable to propose that the stability gained by changing the conformation of the reduction intermediate from **34** (axial C_4-alkyl group) to **35** (equatorial-like C_4-alkyl group) would at least partially off-set the angle and torsional strain inherent in conformation **35**. If the protonation transition state is reactant like, this would result in a lowering of the energy of the transition state resembling **35** relative to that resembling **34**. Robinson's theory would thus correctly predict a higher proportion of *cis*-fused decalone product in the present examples, relative to that "normally" found.

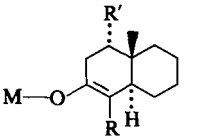

32 M = Li or H

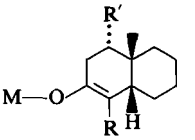

33 = Li or H

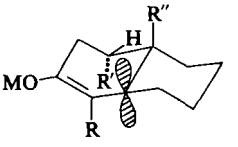

34

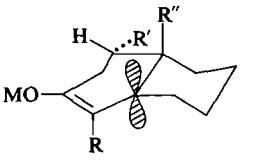

35

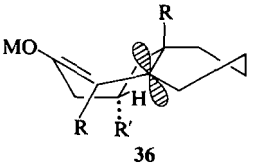

36

The effect of a C_{10} angular methyl group can also be understood in terms of Robinson's theory. In octalones **7–11**, the relative stabilization arising from changing the conformation of the intermediate from **34** to **35** would be somewhat off-set by the increased skew nonbonded interaction between the C_4-alkyl group (R′ in **35**) and the C_{10}-methyl group (R″ = CH_3 in **35**). Hence, in these octalones, the amount of *cis*-fused decalone formed on lithium–ammonia reduction would be expected to be less than in the case of octalone **4**. In the latter, as the conformation of the intermediate changes from **34** (R = R″ = H, R′ = isoPr) to **35**, there is no developing nonbonded interaction between the C_4-isopropyl group and the C_{10}-proton (R″ = H in **35**). Thus, although the magnitude of the effect of changing the C_{10}-substituent from a proton (in **4**) to a methyl group (in **9** and **11**) was not expected *a priori*, the results can be accounted for on a qualitative basis.

Finally, the effect of changing the size of the C_4-alkyl group must be mentioned. As the bulk of the C_4-alkyl group increases, it seems prob-

[5]The reasoning which led to this conclusion will not be reproduced here. However, Robinson has convincingly argued that the transition state for protonation at the β-carbon is not tetrahedral in shape (product-like transition state), since there is no correlation between product ratios and relative product stabilities.

[6]The representations used here differ slightly in detail from those in Robinson's paper. In our representations, we have taken into account the recent mechanistic work of House and co-workers (4, 5).

Can. J. Chem. Downloaded from www.nrcresearchpress.com by 210.87.254.42 on 09/05/12
For personal use only.

able that the stabilization arising from changing the alkyl group from the axial orientation (**34**) to the equatorial-like orientation (**35**) would also increase somewhat. This would make the transition state resembling **35** increasingly more favored and could thus account for the observed fact that as the C_4-alkyl group increases in size, the amount of *cis*-fused decalone obtained also increases.

Experimental[7]

4α,4aβ-Dimethyl-4,4a,5,6,7,8-hexahydro-2(3H)-naphthalenone (7)

To a stirred, ice-cold slurry of 6.84 g of cuprous iodide in 150 ml of anhydrous ether was added 34.3 ml of 2.1 *M* methyllithium in ether. To the resulting clear solution was added dropwise, over a period of 1 h, 1 g (6.2 mmol) of the cross-conjugated dienone **13**. The resulting thick yellow reaction mixture was thoroughly extracted with ether. The combined ether extracts were successively washed with water, dilute ammonium hydroxide, water, and brine and then dried over anhydrous magnesium sulfate. Removal of the solvent followed by distillation of the residue under reduced pressure gave a clear oil, b.p. 124° at 0.3 mm, which was subjected to chromatography on 40 g of silica gel. The fractions eluted with 15% ether – petroleum ether (b.p. 30–60°) contained 900 mg (82%) of the octalone **7** (19, 44), a clear colorless oil which showed a single peak on analysis by g.l.c. (column A, 190°, 86). This material exhibited u.v. λ_{max} 239 nm (ε 14 000); i.r. (film) λ_{max} 6.0, 6.15 μ; p.m.r. τ 9.02 (d, 3H, secondary CH_3, J = 7 Hz), 8.74 (s, 3H, tertiary CH_3), 4.30 (s, 1H, vinyl H).

1,4α,4aβ-Trimethyl-4,4a,5,6,7,8-hexahydro-2(3H)-naphthalenone (10)

The reaction of dienone **14** with lithium dimethylcuprate was carried out by a procedure identical with that described above for the preparation of **7**. From 1 g of dienone **14** there was obtained 1 g (92%) of the trimethyloctalone **10**, b.p. 125°/0.3 mm, which was shown to be homogeneous by g.l.c. (column A, 200°, 86); u.v. λ_{max} 249 nm (ε 13 800); i.r. (film) λ_{max} 6.0, 6.2 μ; p.m.r. τ 9.04 (d, 3H, secondary CH_3, J = 6.5 Hz), 8.74 (s, 3H, tertiary CH_3), 8.25 (d, 3H, vinyl CH_3, J = 1 Hz).

This compound was further characterized as a red 2,4-dinitrophenylhydrazone, recrystallized from ethanol, m.p. 174–175°.

Anal. Calcd. for $C_{19}H_{24}N_4O_4$: C, 61.28; H, 6.50; N, 15.04. Found: C, 60.98; H, 6.42; N, 15.11.

4aβ-Methyl-4α-vinyl-4,4a,5,6,7,8-hexahydro-2(3H)-naphthalenone (12)

A solution of 15 g of tri-*n*-butylphosphine copper(I) iodide (23) in 150 ml of anhydrous ether was cooled to −78° by an external Dry Ice – acetone bath. Addition of 22.8 ml of 3.2 *M* vinyllithium in tetrahydrofuran gave a pale green solution, to which was added, over a period of 1 h, a solution of 1 g of the dienone **13** in 50 ml of dry ether. The resulting thick yellow reaction mixture was allowed to stir at −78° for 4 h. The mixture was allowed to warm to room temperature and was then poured into 250 ml of rapidly stirring 10% hydrochloric acid. The aqueous mixture was thoroughly extracted with ether. The combined ether extracts were washed successively with water, dilute ammonium hydroxide, water, and brine and then dried over anhydrous magnesium sulfate. After removal of the solvent, the desired product was roughly separated from the high boiling material by collecting all material with a boiling point less than 130° at 0.2 mm. The resulting distillate was subjected to chromatography on 100 g of silica gel. The fractions eluted with 10% ether – petroleum ether (b.p. 30–60°) afforded 870 mg (73%) of the desired octalone **12**. The latter showed only one peak by g.l.c. analysis (column A, 195°, 100), and exhibited i.r. (film) λ_{max} 6.0, 6.2, 10.9 μ; p.m.r. τ 8.72 (s, 3H, tertiary methyl), 3.89–5.13 (m, 3H, $-CH=CH_2$), 4.25 (s, 1H, vinyl H). Due to its instability, octalone **12** was not characterized further but was immediately subjected to hydrogenation.

4α-Ethyl-4aβ-methyl-4,4a,5,6,7,8-hexahydro-2(3H)-naphthalenone (8)

The hydrogenation of the octalone **12** (708 mg) was carried out in benzene (50 ml) solution at room temperature and atmospheric pressure using tris(triphenylphosphine)chlororhodium (120 mg) as catalyst. After uptake of hydrogen had essentially ceased, the reaction mixture was filtered through a column of Woelm activity III neutral alumina (20 g). The column was eluted with an additional 100 ml of benzene. Removal of the solvent, followed by distillation of the crude product under reduced pressure afforded 650 mg of a clear colorless oil. Analysis of this material by g.l.c. (column A, 180°, 100) showed that it consisted of a mixture of the decalone **28** (~10%) and the desired octalone **8** (~90%). The mixture was separated by chromotography on 50 g of silica gel. The fractions eluted with 8% ether – petroleum ether (b.p. 30–60°) contained 57 mg of the *cis*-fused decalone **28**, while the fractions eluted with 15% ether – petroleum ether (b.p. 30–60°) contained 413 mg (58%) of the desired octalone **8**; u.v. λ_{max} 239 nm (ε 11 000); i.r. (film) λ_{max} 6.0, 6.2 μ; p.m.r. τ 9.07 (t, 3H, $-CH_2-CH_3$, J = 4 Hz), 8.73 (s, 3H, tertiary CH_3), 4.21 (broad s, 1H, vinyl H).

This compound was further characterized as a red 2,4-dinitrophenylhydrazone derivative, recrystallized from ethanol, m.p. 118–120°.

Anal. Calcd. for $C_{19}H_{24}N_4O_4$: C, 61.28; H, 6.50; N, 15.04. Found: C, 61.07; H, 6.42; N, 15.05.

4α-Isopropyl-4aβ-methyl-4,4a,5,6,7,8-hexahydro-2(3H)-naphthalenone (9)

A solution of 15 g (38 mmol) of tri-*n*-butylphosphine copper(I) iodide and 0.5 g of anhydrous lithium bromide in 150 ml of anhydrous ether was cooled to −78° with an external Dry Ice – acetone bath. A solution of isopropyllithium in pentane (39 ml, 1.86 *M*, 73 mmol) was added, forming first a dark red and then a pale aqua solution. To this solution was added, over a period of 45 min, a solution of 1 g (6.1 mmol) of the dienone **13** in 50 ml of anhydrous ether. The dark red reaction mixture was allowed to stir at −78° for an additional 5 h and was then allowed to warm to room temperature. The reaction mixture was transferred under nitrogen to a dropping funnel and then added slowly to a rapidly stirring solution of

[7]For general information, see preceding paper (ref. 12).

Can. J. Chem. Downloaded from www.nrcresearchpress.com by 210.87.254.42 on 09/05/12
For personal use only.

10% hydrochloric acid. The resulting mixture was extracted thoroughly with ether. The combined ether extracts were washed successively with water, dilute ammonium hydroxide, water, and brine and then dried over anhydrous magnesium sulfate. Removal of the solvent and distillation of the residue under reduced pressure afforded an oil which was further purified by chromatography on 25 g of silica gel. The fractions eluted with 20% ether – petroleum ether (b.p. 30–60°) gave 395 mg (95%) of the desired octalone **9**. This material showed one component by g.l.c. (column A, 180°, 86) and exhibited u.v. λ_{max} 240 nm (ε 9400); i.r. (film) λ_{max} 6.0, 6.15 μ; p.m.r. τ 9.20, 9.05 (d, d, 6H, —CH(CH_3)$_2$, J = 6.5 Hz), 8.74 (s, 3H, tertiary CH_3), 4.22 (broad s, 1H, vinyl H).

This compound was further characterized as its 2,4-dinitrophenylhydrazone derivative, recrystallized from ethanol, m.p. 153–155°.

Anal. Calcd. for $C_{20}H_{26}N_4O_4$: C, 62.16; H, 6.78; N, 14.50. Found: C, 62.01; H, 6.80; N, 14.40.

*4α-Isopropyl-1,4aβ-dimethyl-4,4a,5,6,7,8-hexahydro-2(3H)-naphthalenone (**11**)*

The reaction of lithium diisopropylcuprate with the cross-conjugated dienone **14** was carried out via a procedure identical with that described above for the preparation of octalone **9**.

From 2 g of the dienone **14** there was obtained, after chromatography of the crude product on 140 g of silica gel, 2.38 g (95%) of the desired octalone **11**. This material showed one component by g.l.c. (column A, 190°, 86) and exhibited u.v. λ_{max} 294 nm (ε 14 000); i.r. (film) λ_{max} 6.0, 6.2 μ; p.m.r. τ 9.23, 9.04 (d, d, 6H, —CH(CH_3)$_2$, J = 7 Hz), 8.73 (s, 3H, tertiary CH_3), 8.22 (s, 3H, vinyl CH_3).

This compound was further characterized as a red 2,4-dinitrophenylhydrazone derivative, recrystallized from ethanol, m.p. 134–135°.

Anal. Calcd. for $C_{21}H_{28}N_4O_4$: C, 62.98; H, 7.05; N, 13.99. Found: C, 63.13; H, 6.90; N, 13.76.

*3α-Bromo-1α,4aβ-dimethyl-trans-3,4,4a,5,6,7,8,8a-octahydro-2(1H)-naphthalenone (**26**)*

To a solution of 7.9 g (44 mmol) of the dimethyldecalone **23** (42) in 50 ml of isopropenyl acetate was added 0.1 ml of 98% sulfuric acid. The solution was refluxed under an atmosphere of nitrogen for 2.5 h. Most of the isopropenyl acetate was removed under reduced pressure and the residue was diluted with ether. The ether solution was washed successively with water, 5% aqueous sodium bicarbonate, water, and brine and dried over anhydrous magnesium sulfate. Removal of the solvent followed by chromatography of the crude product on 150 g of Woelm activity III neutral alumina, gave 9.5 g of a mixture of enol acetates **24** and **25**, in a ratio of approximately 85:15, respectively. The mixture exhibited i.r. (film) λ_{max} 5.7, 5.95 μ.

The mixture of enol acetates (9.5 g) **24** and **25** was dissolved in 100 ml of glacial acetic acid containing 10 g of anhydrous sodium acetate. To the resulting solution was added, over a period of 1 h, a solution of 7.2 g of bromine in 50 ml of glacial acetic acid. After the addition was complete, the reaction mixture was allowed to stir for an additional 15 min. The glacial acetic acid was removed under reduced pressure, the residue was diluted with water and then thoroughly extracted with ether. The combined ether extracts were washed successively with water, aqueous sodium bicarbonate, water, and brine and dried over anhydrous magnesium sulfate. Removal of the solvent gave a crystalline material which, upon recrystallization from petroleum ether (b.p. 30–60°), afforded 9.2 g (85%) of the bromoketone **26**, m.p. 69–70°; i.r. ($CHCl_3$) λ_{max} 5.8 μ; p.m.r. τ 8.99 (d, 3H, secondary CH_3, J = 6.5 Hz), 8.84 (s, 3H, tertiary CH_3), 5.13 (d of d, 1H, —C(=O)—CH(Br)—, J = 14, 6 Hz).

Anal. Calcd. for $C_{12}H_{19}OBr$: C, 55.60; H, 7.34; Br, 30.89. Found: C, 55.59; H, 7.26; Br, 30.86.

*1α,4aβ-Dimethyl-trans-4a,5,6,7,8,8a-hexahydro-2(1H)-naphthalenone (**22**)*

A solution of 4 g (15 mmol) of the bromoketone **26** and 1.5 g of anhydrous lithium bromide in 35 ml of hexamethylphosphoramide was heated to 120° and kept at this temperature for 3 h. The solution was cooled, diluted with water, and thoroughly extracted with ether. The combined ether extracts were washed thrice with water, once with brine, and dried over anhydrous magnesium sulfate. Removal of the solvent gave an oil which was shown by g.l.c. (column A, 185°, 86) to consist mainly of the desired octalone **22**, contaminated by a small amount of 1,10-dimethyl-$\Delta^{1,9}$-2-octalone. Chromatography of this material on 100 g of silica gel gave, upon elution of the column with 3% ether – benzene, 2 g (72%) of the octalone **22**. The latter exhibited u.v. λ_{max} 229 nm (ε 9200); i.r. (film) λ_{max} 6.0, 6.15 μ; p.m.r. τ 8.93 (s, 3H, tertiary CH_3), 8.92 (d, 3H, secondary CH_3, J = 7 Hz), 4.19, 3.35 (d of d, 2H, —C(=O)—C*H*=CH— and —C(=O)—CH=C*H*—, respectively, J = 9 Hz).

This compound was further characterized as a red 2,4-dinitrophenylhydrazone derivative, recrystallized from ethanol, m.p. 198–199°.

Anal. Calcd. for $C_{18}H_{22}N_4O_4$: C, 60.32; H, 6.19; N, 15.63. Found: C, 60.51; H, 6.11; N, 15.73.

*4α,4aβ-Dimethyl-trans-3,4,4a,5,6,7,8,8a-octahydro-2(1H)-naphthalenone (**15**)*

To a stirred ice-cold slurry of 2.3 g of cuprous iodide in 67 ml of anhydrous ether under nitrogen, was added 11.4 ml of 2.1 *M* ethereal methyllithium. To the resulting clear solution was added dropwise over a period of 30 min, a solution of 328 mg (2 mmol) of the octalone **21** (41) in 40 ml of anhydrous ether. The reaction mixture was allowed to stir at 0° for an additional 1.5 h and was then poured slowly into rapidly stirring 10% aqueous hydrochloric acid. The resulting mixture was thoroughly extracted with ether. The combined ether extracts were washed with water and brine and dried over anhydrous magnesium sulfate. Removal of the solvent, followed by distillation of the residue under reduced pressure, afforded 345 mg (98%) of the desired dimethyldecalone **15**, b.p. 110°/0.2 mm (lit. (44) b.p. 133–137°/9 mm). This material showed one component by g.l.c. (column A, 190°, 100) and exhibited i.r. (film) λ_{max} 3.45, 5.85 μ; p.m.r. τ 9.08 (d, H, secondary CH_3, J = 6.5 Hz), 8.87 (s, 3H, tertiary CH_3).

*1α,4α,4aβ-Trimethyl-trans-3,4,4a,5,6,7,8,8a-octahydro-2(1H)-naphthalenone (**18**)*

This compound was prepared by the reaction of

Can. J. Chem. Downloaded from www.nrcresearchpress.com by 210.87.254.42 on 09/05/12
For personal use only.

lithium dimethylcuprate with the dimethyloctalone **22** via a procedure essentially identical with that described above for the preparation of decalone **15**. The crude product obtained from 200 mg (1.2 mmol) of the octalone **22** was subjected to chromatography on silica gel (20 g). The fractions eluted with 5% ether – petroleum ether (b.p. 30–60°) afforded 189 mg (93%) of the desired *trans*-decalone **18**. An analytical sample was obtained by preparative g.l.c. (column A, 190°, 86) and exhibited i.r. (film) λ_{max} 5.85 μ; p.m.r. τ 9.10, 9.02 (d, d, 6H, secondary methyls, J = 7 Hz), 8.77 (s, 3H, tertiary CH_3), 7.97 (d of d, 1H, H-3e, J = 2.2 and 14 Hz), 7.21 (d of d, H-3a, J = 6 and 14 Hz).

This compound was further characterized as an orange 2,4-dinitrophenylhydrazone derivative, recrystallized from ethanol, m.p. 167–168°.

Anal. Calcd. for $C_{19}H_{26}N_4O_4$: C, 60.95; H, 7.00; N, 14.96. Found: C, 60.66; H, 6.87; N, 15.06.

*4aβ-Methyl-4α-vinyl-trans-3,4,4a,5,6,7,8,8a-octahydro-2(1H)-naphthalenone (**20**)*

A solution of tri-*n*-butylphosphine copper(I) iodide (4 g) in anhydrous ether (50 ml) was cooled, under nitrogen, to −78° by means of an external Dry Ice – acetone cooling bath. A solution of 3.1 *M* vinyllithium in tetrahydrofuran (6.4 ml) was added dropwise until the initially formed red solution became colorless. To this solution was added dropwise, over a period of 30 min, a solution of the octalone **21** (328 mg, 2 mmol) in 50 ml of anhydrous ether. The brown reaction mixture was allowed to stir for an additional 5 h at −78° and then allowed to warm slowly to room temperature. The reaction mixture was transferred under nitrogen to an addition funnel and was added dropwise to 100 ml of rapidly stirring 10% hydrochloric acid. The mixture was extracted thoroughly with ether. The combined ethereal extracts were washed successively with dilute ammonium hydroxide, water, and brine and dried over anhydrous magnesium sulfate. Removal of the solvent gave a viscous yellow oil which was subjected to chromatography on 50 g of silica gel. The fractions eluted with 15% ether – petroleum ether (b.p. 30–60°) contained 280 mg (73%) of the desired decalone **20**. This material was distilled (b.p. 130° at 0.15 mm) to afford an oil which showed only one component by g.l.c. (column A, 190°, 100) and exhibited i.r. (film) λ_{max} 5.85, 6.1, 10.9 μ; p.m.r. τ 8.88 (s, 3H, tertiary CH_3), 4.0–5.2 (m, 3H, —CH=CH_2).

This compound was further characterized as a dark red 2,4-dinitrophenylhydrazone derivative, m.p. 186° (from ethanol).

Anal. Calcd. for $C_{19}H_{24}N_4O_4$: C, 61.28; H, 6.50; N, 15.04. Found: C, 60.98; H, 6.41; N, 14.94.

*4α-Ethyl-4aβ-methyl-trans-3,4,4a,5,6,7,8,8a-octahydro-2(1H)-naphthalenone (**16**)*

The hydrogenation of the vinyl-substituted decalone **20** was done at atmospheric pressure and room temperature using 10% palladium-on-charcoal as catalyst and absolute ethanol as solvent. From 675 mg of decalone **20** there was obtained 670 mg (98%) of the ethyl-substituted decalone **16**. The product showed one component by g.l.c. (column A, 180° 86) and exhibited i.r. (film) λ_{max} 5.85 μ; p.m.r. τ 8.88 (s, 3H, tertiary CH_3).

This compound was further characterized as a pale orange 2,4-dinitrophenylhydrazone, m.p. 192–193° (from ethanol).

Anal. Calcd. for $C_{19}H_{26}N_4O_4$: C, 60.95; H, 7.00; N, 14.96. Found: 60.74; H, 6.89; N, 14.92.

*4α-Isopropyl-4aβ-methyl-trans-3,4,4a,5,6,7,8,8a-octahydro-2 (1H)-naphthalenone (**17**)*

To a solution of 4 g of tri-*n*-butylphosphine copper(I) iodide in 60 ml of anhydrous ether at −78° under nitrogen was added 11 ml of 1.86 *M* isopropyllithium in *n*-pentane. To the resulting aqua solution was added dropwise, over a period of 30 min, a solution of 328 mg (2 mmol) of the octalone **21** in 10 ml of anhydrous ether. After the addition was complete, the dark red reaction mixture was allowed to stir for an additional 3h at −78°, was transferred under nitrogen to an addition funnel, and then added dropwise to 50 ml of rapidly stirring 10% hydrochloric acid. The resulting mixture was thoroughly extracted with ether. The combined ether extracts were washed successively with water, dilute ammonium hydroxide, water, and brine and dried over anhydrous magnesium sulfate. Removal of the solvent gave a viscous oil which was distilled under reduced pressure (0.1 mm). All material with b.p. of less than 150° was collected. The distillate was further purified by chromatography over 35 g of silica gel. The fractions eluted with 20% ether – petroleum ether (b.p. 30–60°) contained 297 mg (72%) of the *trans*-fused decalone **17**, which crystallized on standing. Recrystallization of this material from *n*-hexane gave an analytical sample, m.p. 49–50° (lit. m.p. (41) 49–50°); i.r. ($CHCl_3$) λ_{max} 5.87 μ; p.m.r. τ 9.08, 9.17 (d, d, 6H, —CH(CH_3)$_2$, J = 6.8 Hz), 8.89 (s, 3H, tertiary CH_3).

*4α-Isopropyl-1α,4aβ-dimethyl-trans-3,4,4a,5,6,7,8,8a-octahydro-2(1H)-naphthalenone (**19**)*

This compound was prepared by the reaction of lithium diisopropylcuprate with the dimethyloctalone **22** via a procedure essentially identical with that described above for the preparation of decalone **17**. The crude product obtained from 356 mg (2.1 mmol) of octalone **22** was distilled (b.p. 120°/0.3 mm) and the distillate was further purified by chromatography on 20 g of silica gel. Elution with benzene afforded 262 mg (82%) of the desired decalone **19**, which showed one component by g.l.c. analysis (column A, 198°, 86) and exhibited i.r. (film) λ_{max} 5.85 μ; p.m.r. τ 9.21, 9.09 (d, d, 6H, —CH(CH_3)$_2$, J = 6.5 Hz), 9.00 (d, 3H, secondary CH_3, J = 6 Hz), 8.87 (s, 3H, tertiary CH_3); p.m.r. (benzene) τ 7.74 (d of d, 1H, H-3a, J = 15.5, 7.6 Hz), 7.56 (d of d, 1H, H-3e, J = 15.5, 2.4 Hz).

The product was further characterized as a yellow 2,4-dinitrophenylhydrazone derivative, recrystallized from ethanol, m.p. 145–146°.

Anal. Calcd. for $C_{21}H_{30}N_4O_4$: C, 62.67; H, 7.51; N, 13.92. Found: C, 62.55; H, 7.50; N, 13.73.

*4α,4aβ-Dimethyl-cis-3,4,4a,5,6,7,8,8a-octahydro-2(1H)-naphthalenone (**27**)*

A suspension of 20 mg of 10% palladium-on-charcoal in 15 ml of 0.3 *N* ethanolic sodium hydroxide solution was stirred for 1 h under an atmosphere of hydrogen at room temperature. A solution of 122 mg (0.68 mmol) of octalone **7** in 10 ml of ethanol was added by means of a syringe. After the calculated amount of hydrogen had been taken up, the mixture was filtered and the filtrate was concentrated under reduced pressure. The residue was diluted with water and the resulting mixture was

Can. J. Chem. Downloaded from www.nrcresearchpress.com by 210.87.254.42 on 09/05/12
For personal use only.

thoroughly extracted with ether. The combined ether extracts were washed successively with 5% hydrochloric acid, 5% aqueous sodium bicarbonate, water, and brine and dried over anhydrous magnesium sulfate. Removal of the solvent, followed by distillation of the residue under reduced pressure, gave 119 mg (97%) of the *cis*-fused decalone **27**, b.p. 110°/0.2 mm. This material was shown to be homogeneous by g.l.c. (column A, 190°, 86) and exhibited i.r. (film) λ_{max} 5.85 μ; p.m.r. τ 9.10 (d, 3H, secondary CH_3, J = 7 Hz), 8.95 (s, 3H, tertiary CH_3).

This compound was further characterized as a yellow 2,4-dinitrophenylhydrazone derivative, m.p. 161–162° (from ethanol).

Anal. Calcd. for $C_{18}H_{24}N_4O_4$: C, 59.99; H, 6.71; N, 15.55. Found: C, 59.99; H, 6.80; N, 15.46.

1β,4α,4aβ-Trimethyl-cis-3,4,4a,5,6,7,8,8a-octahydro-2(1H)-naphthalenone (30)

This compound was obtained by hydrogenation of octalone **10** under conditions identical with those used for the preparation of **27**. From 130 mg of **10** there was obtained 125 mg (95%) of a colorless oil, b.p. 115°/0.2 mm, which showed one component by g.l.c. (column A, 180°, 86). Compound **30** exhibited i.r. (film) λ_{max} 5.85 μ; p.m.r. τ 9.08, 9.01 (d, d, 6H, secondary methyls, J = 6.5 Hz), 8.92 (s, 3H, tertiary CH_3), 7.85 (d of d, 1H, H-3e, J = 13, 3.6 Hz), 7.64 (d of d, 1H, H-3a, J = 13, 14.4 Hz), 7.35 (overlapped d of q, 1H, H-1a, J = 13, 6 Hz).

The decalone **30** was further characterized as its 2,4-dinitrophenylhydrazone derivative, m.p. 213–214° (from ethanol).

Anal. Calcd. for $C_{19}H_{26}N_4O_4$: C, 60.95; H, 7.00; N, 14.96. Found: C, 60.85; H, 7.08; N, 14.93.

4α-Ethyl-4aβ-methyl-cis-3,4,4a,5,6,7,8,8a-octahydro-2(1H)-naphthalenone (28)

The hydrogenation of octalone **8** was carried out under conditions identical with those employed for the synthesis of decalone **27**. From 100 mg of octalone **8** there was obtained 96 mg (95%) of a clear colorless oil which was shown by g.l.c. analysis (column A, 180°, 86) to be greater than 95% pure. An analytical sample of the decalone **28** was collected by preparative g.l.c. and exhibited i.r. (film) λ_{max} 5.85 μ; p.m.r. τ 8.90 (s, 1H, tertiary CH_3).

This compound was further characterized as a yellow 2,4-dinitrophenylhydrazone derivative, m.p. 174° (from ethanol).

Anal. Calcd. for $C_{19}H_{26}N_4O_4$: C, 60.95; H, 7.00; N, 14.96. Found: C, 60.81; H, 6.85; N, 14.88.

4α-Isopropyl-4aβ-methyl-cis-3,4,4a,5,6,7,8,8a-octahydro-2(1H)-naphthalenone (29)

Octalone **9** was subjected to hydrogenation under conditions identical with those described previously for the preparation of decalone **27**. From 100 mg of octalone **9** there was obtained 96 mg (96%) of an oil which was shown by g.l.c. analysis (column A, 190°, 86) to consist of two components in a ratio of 95:5. The minor component exhibited a retention time identical with that of the *trans*-fused decalone **17**. An analytical sample of the major component, *cis*-fused decalone **29**, was collected by preparative g.l.c. and exhibited i.r. (film) λ_{max} 5.85 μ; p.m.r. τ 9.19, 9.10 (d, d, 6H, $-CH(CH_3)_2$, J = 6.5 Hz), 8.88 (s, 3H, tertiary CH_3).

This compound was further characterized as an orange 2,4,-dinitrophenylhydrazone derivative, recrystallized from ethanol; m.p. 180–181°.

Anal. Calcd. for $C_{20}H_{28}N_4O_4$: C, 61.84; H, 7.27; N, 14.42. Found: C, 61.86; H, 7.35; N, 14.30.

4α-Isopropyl-1β,4aβ-dimethyl-cis-3,4,4a,5,6,7,8,8a-octahydro-2(1H)-naphthalenone (31)

This compound was prepared by hydrogenation of octalone **11** via a procedure identical with that described for the preparation of decalone **27**. From 100 mg of octalone **11** there was obtained 96 mg (95%) of an oil which exhibited one component by g.l.c. (column A, 180°, 86) and produced the following spectral data: i.r. (film) λ_{max} 5.85 μ; p.m.r. τ 9.19, 9.11 (d, d, 6H, $-CH(CH_3)_2$, J = 6.5 Hz), 9.01 (d, 3H, secondary CH_3, J = 6 Hz), 8.89 (s, 3H, tertiary CH_3), 7.86 (m, 1H, H-3e, J = 14, 3.6 Hz), 7.63 (m, 1H, H-3a, J = 14, 14.3 Hz), 8.30 (m, 1H, H-1a, J = 13, 6 Hz).

This *cis*-fused decalone **31** was further characterized as its 2,4-dinitrophenylhydrazone derivative, m.p. 188–189° (from ethanol).

Anal. Calcd. for $C_{21}H_{30}N_4O_4$: C, 62.67; H, 7.51; N, 13.92. Found: C, 62.46; H, 7.28; N, 14.01.

Lithium–Ammonia Reduction of 4α-Alkyl-4aβ-methyl-4,4a,5,6,7,8-hexahydro-2(3H)-naphthalenones (7, 8, 9) and of 4α-Alkyl-1,4aβ-dimethyl-4,4a,5,6,7,8-hexahydro-2(3H)-naphthalenones (10, 11). General Procedure

To 60 ml of liquid ammonia (freshly distilled from sodium metal) was added 55 mg of finely cut lithium wire. After all the lithium had dissolved, a solution of 0.56 mmol of the appropriate octalone in 10 ml of anhydrous ether was added dropwise over a period of 30 min. The reaction mixture was allowed to stir for an additional 2 h and the blue color was then discharged by careful addition of ammonium chloride. The liquid ammonia was allowed to evaporate and the residue was diluted with water and neutralized by addition of hydrochloric acid. The resulting mixture was thoroughly extracted with ether. The combined ether extracts were washed with water and brine and dried over anhydrous magnesium sulfate. Removal of the solvent, followed by distillation of the residual material under reduced pressure afforded an oil which was subjected to analysis by g.l.c. (column A, 160–190°, 86). In each case, g.l.c. conditions were found in which the starting material (octalone), the corresponding *cis*-fused decalone, and the corresponding *trans*-fused decalone exhibited distinct retention times. The percent composition of each product was determined by integration (disc integrator). The products from each reduction were identified by isolation (preparative g.l.c.) and comparison (i.r., p.m.r.) with authentic samples prepared as described previously.

In each case, samples of *cis*-fused and *trans*-fused decalones were carefully weighed and then combined to afford authentic mixtures of known composition approximating that observed in the appropriate lithium–ammonia reduction. Analysis of these authentic mixtures by g.l.c. showed that the observed ratio was, within experimental error, identical with the known ratio; that is, in each case, the g.l.c. molar response factors of the *cis*- and *trans*-fused decalones were, within experimental error, identical.

Each lithium–ammonia reduction was carried out at

Can. J. Chem. Downloaded from www.nrcresearchpress.com by 210.87.254.42 on 09/05/12
For personal use only.

least in triplicate. The results recorded in Table 1 represent average values.

Financial support from the National Research Council of Canada and a National Research Council of Canada Studentship (to W.M.P) are gratefully acknowledged.

1. R. Howe and F. J. McQuillin. J. Chem. Soc. 2670 (1956).
2. G. Stork and S. D. Darling. J. Am. Chem. Soc. **86**, 1761 (1964).
3. M. J. T. Robinson. Tetrahedron, **21**, 2475 (1965).
4. K. W. Bowers, R. W. Giese, J. Grimshaw, H. O. House, N. H. Kolodny, K. Kronberger, and D. K. Roe. J. Am. Chem. Soc. **92**, 2783 (1970).
5. H. O. House, R. W. Giese, K. Kronberger, J. P. Kaplan, and J. F. Simeone. J. Am. Chem. Soc. **92**, 2800 (1970).
6. I. H. Elson, T. J. Kemp, D. Greatorex, and H. D. B. Jenkins. J. Chem. Soc. Faraday II, **69**, 665 (1973).
7. I. H. Elson, T. J. Kemp, D. Greatorex, and H. D. B. Jenkins. J. Chem. Soc. Faraday II, **69**, 1402 (1973).
8. S. K. Malhotra, D. F. Moakley, and F. Johnson. Tetrahedron Lett. 1089 (1967).
9. H. E. Zimmerman. *In* Molecular rearrangements. Pt. 1. *Edited by* P. de Mayo. John Wiley and Sons, Inc., New York. 1963. pp. 352–358.
10. F. Johnson. Chem. Rev. **68**, 375 (1968).
11. H. L. Dryden, Jr. *In* Organic reactions in steroid chemistry. Vol. 1. *Edited by* J. Fried and J. A. Edwards. Van Nostrand Reinhold Company, New York. 1972. (*a*) pp. 34–35; (*b*) pp. 40–42.
12. E. Piers and W. M. Phillips-Johnson. Can. J. Chem. This issue.
13. E. Piers, W. M. Phillips-Johnson, and C. Berger. Tetrahedron Lett. 2915 (1972).
14. G. Posner. Org. React. **19**, 1 (1972).
15. R. B. Woodward and T. Singh. J. Am. Chem. Soc. **72**, 494 (1950); D. Caine, P. F. Brake, J. F. DeBardelen, Jr., and J. B. Dawson. J. Org. Chem. **38**, 967 (1973).
16. P. J. Kropp. J. Org. Chem. **29**, 3110 (1964).
17. M. Pesaro, G. Bozzato and P. Schudel. Chem. Commun. 1152 (1968).
18. J. A. Marshall and T. M. Warne, Jr. J. Org. Chem. **36**, 178 (1971).
19. J. A. Marshall and R. A. Ruden. J. Org. Chem. **37**, 659 (1972).
20. J. A. Osborn, E. F. Jardine, J. F. Young, and G. Wilkinson. J. Chem. Soc. A, 1711 (1966).
21. H. O. House and W. F. Fischer, Jr. J. Org. Chem. **33**, 949 (1968).
22. H. O. House, W. L. Respess and G. M. Whitesides. J. Org. Chem. **31**, 3128 (1966).
23. G. B. Kauffman and L. A. Teter. Inorg. Syn. **7**, 9 (1963).
24. E. Piers and R. J. Keziere. Can. J. Chem. **47**, 137 (1969).
25. J. Hooz and R. B. Layton. Can. J. Chem. **48**, 1626 (1970).
26. E. J. Corey and R. L. Carney. J. Am. Chem. Soc. **93**, 7318 (1971).
27. E. J. Corey, C. U. Kim, R. H. K. Chen, and M. Takeda. J. Am. Chem. Soc. **94**, 4395 (1972).
28. R. L. Cargill, D. F. Bushey, and P. D. Ellis. J. Org. Chem. **39**, 573 (1974).
29. F. E. Ziegler and P. A. Wender. Tetrahedron Lett. 449 (1974).
30. C. P. Casey and R. A. Boggs. Tetrahedron Lett. 2455 (1971).
31. C. J. Sih, R. G. Salomon, P. Price, G. Peruzzotti, and R. Sood. J. Chem. Soc. Chem. Commun. 240 (1972).
32. C. J. Sih, P. Price, R. Sood, R. G. Salomon, G. Peruzzotti, and M. Casey. J. Am. Chem. Soc. **94**, 3643 (1972).
33. C. J. Sih, R. G. Salomon, P. Price, R. Sood, and G. Peruzzotti. Tetrahedron Lett. 2435 (1972).
34. R. Pappo and P. W. Collins. Tetrahedron Lett. 2627 (1972).
35. F. S. Alvarez, D. Wren, and A. Prince. J. Am. Chem. Soc. **94**, 7823 (1972).
36. A. F. Kluge, K. G. Untch, and J. H. Fried. J. Am. Chem Soc. **94**, 9256 (1972).
37. C. V. Grudzinskas and M. J. Weiss. Tetrahedron Lett. 141 (1973).
38. C. J. Sih, J. B. Heather, G. P. Peruzzotti, P. Price, R. Sood, and L-F. H. Lee. J. Am. Chem. Soc. **95**, 1676 (1973).
39. J. B. Heather, R. Sood, P. Price, G. P. Peruzzotti, S. S. Lee, L-F. H. Lee, and C. J. Sih. Tetrahedron Lett. 2313 (1973).
40. E. J. Corey and J. Mann. J. Am. Chem. Soc. **95**, 6832 (1973).
41. E. Piers, W. de Waal, and R. W. Britton. Can. J. Chem. **47**, 4299 (1969).
42. M. Yanagita and R. Futaki. J. Org. Chem. **21**, 949 (1956).
43. G. G. S. Dutton, K. B. Gibney, G. D. Jensen, and P. E. Reid. J. Chromatog. **36**, 152 (1968).
44. R. M. Coates and J. E. Shaw. J. Am. Chem. Soc. **92**, 5657 (1970).

Nucleic Acid Related Compounds. 16. Direct Fluorination of Uracil Nucleotides Using Trifluoromethyl Hypofluorite[1]

MORRIS J. ROBINS, G. RAMANI,[2] AND MALCOLM MACCOSS[3]

Department of Chemistry, The University of Alberta, Edmonton, Alberta T6G 2G2

Received June 3, 1974[4]

MORRIS J. ROBINS, G. RAMANI, and MALCOLM MACCOSS. Can. J. Chem. **53**, 1302 (1975).

Treatment of commercially available uracil nucleotides and dinucleoside phosphates in methanolic solutions with trifluoromethyl hypofluorite in trichlorofluoromethane (Freon 11) gave adducts which were converted into the corresponding 5-fluorouracil nucleotides in basic solution. This procedure circumvents certain problems involved in phosphorylation of the rather inaccessible and expensive 5-fluorouracil nucleosides.

Salts of both 5-fluorouridine-5′-monophosphate (5′-FUMP) and 5-fluorouridine-3′,5′-cyclic monophosphate (cFUMP) were crystallized and fully characterized. The procedure is not readily applicable to dinucleoside phosphates.

MORRIS J. ROBINS, G. RAMANI et MALCOLM MACCOSS. Can. J. Chem. **53**, 1302 (1975).

La réaction de l'hypofluorite de trifluorométhyle en solution dans de la fluorure de trichlorométhyle (Freon 11) avec des solutions méthanoliques de nucléotides et de diphosphates de nucléosides obtenus de sources commerciales donne des adduits qui sont transformés, en solution basique, en nucléotides fluorés en position 5 correspondants. Ce procédé évite certains problèmes rencontrés lors de la formation de phosphates des nucléosides, difficilement accessibles et coûteux, du fluoro-5-uracil.

Les sels des monophosphates-5′ de la fluoro-5-uridine (5′-FUMP) et du monophosphate cyclique-3′,5′ de la fluoro-5 uridine ont été cristallisés et entièrement caractérisés. Ce procédé n'est pas applicable directement aux phosphates de dinucléosides.

Previous extensive studies (1) on 5-fluoropyrimidines and their higher metabolic derivatives had uniformly involved "*de novo*" construction of the fluorinated bases from small aliphatic precursors such as the highly toxic ethyl fluoroacetate (1, 2). Chemical or enzymatic coupling of these base derivatives with a suitably functionalized sugar produced the nucleoside (see for example, 3–7 and references therein). Phosphorylation and/or coupling (with another nucleoside or nucleotide) then gave nucleotide derivatives (see for example, 8–15). Nucleotides of 5-fluorouracil have been evaluated for cytotoxicity (1, 9, 15, 16), as substrates for RNA polymerase (12), as nearest neighbor of associated DNA (17), as substrates for polynucleotide phosphorylase and in investigation of biophysical effects in the resulting homo or copolymers (13, 14), and for ribosome binding and stimulation of amino acid incorporation (14, 18).

Conventional synthetic routes to the final nucleotide products involve specific blocking, phosphorylation and/or coupling, chromatographic separation of the desired nucleotide from unreacted starting materials and polycondensation products, and then deblocking. Often these sequences have been effected in less than satisfactory overall yields. Preliminary communications from our laboratory (19, 20) have described the direct introduction of fluorine at the 5 position of uracil, cytosine, and their nucleosides in high yields using trifluoromethyl hypofluorite in organic solvents.

We now wish to report the synthesis of 5-fluorouracil nucleotides from the commercially available uracil compounds by direct fluorination. Trifluoromethyl hypofluorite in trichlorofluoromethane (CAUTION[5]) was added to

[1]For the previous paper in this series see ref. 24.

[2]Postdoctoral Fellow 1971–1973.

[3]Postdoctoral Fellow 1972–Present.

[4]Revision received December 27, 1974.

[5]CAUTION: Trifluoromethyl hypofluorite (CF_3OF) is a toxic, strong oxidizing agent. We have experienced no problems in the addition of CF_3OF in CCl_3F at $-78°$ to cold (usually $-78°$) solutions of substrates in methanol, chloroform, or aqueous mixtures. However, we have been informed of violent explosions occurring upon direct introduction of gaseous CF_3OF into methanol. Direct addition of CF_3OF to alcohols or other easily oxidizable substrates (especially at room temperature) should not be attempted.

Can. J. Chem. Downloaded from www.nrcresearchpress.com by 210.87.254.6 on 09/05/12
For personal use only.

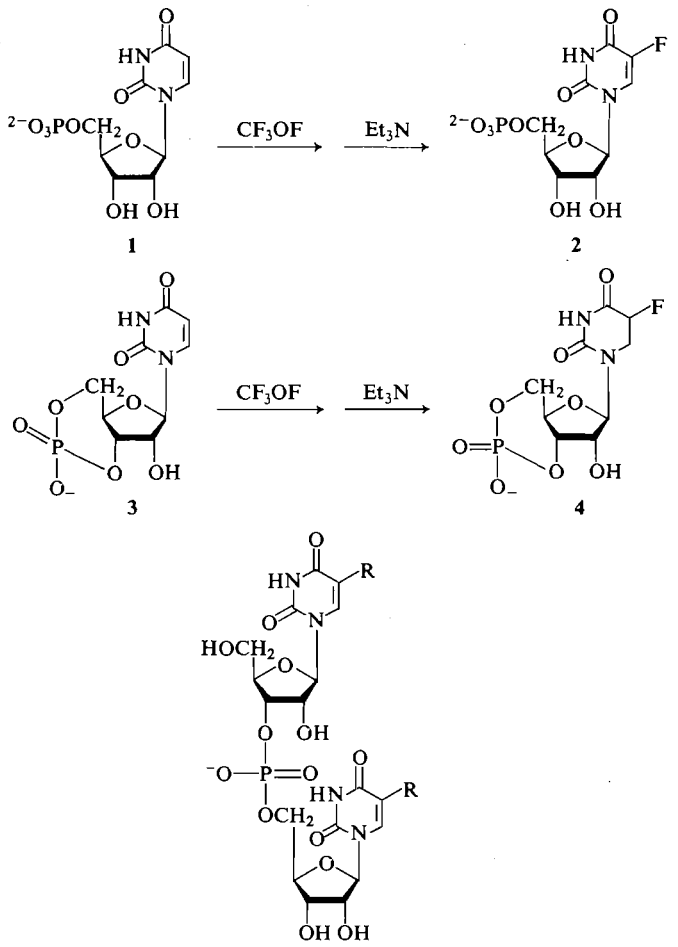

SCHEME 1

cold solutions of the nucleotide tetra-*n*-butylammonium salts in methanol or other salts in aqueous methanol (see Experimental). Reactions proceeded rapidly with loss of u.v. absorption of the uracil chromophore at 260 nm, presumably to give the 5,6-dihydrouracil adduct with fluorine at C_5 and alkoxyl or hydroxyl at C_6. Excess reagent and solvents were evaporated and the adduct residues were treated with aqueous amine solutions to generate the 5-fluorouracil products.

Reactions of the mononucleotides proceeded in good yields as estimated spectroscopically and chromatographically. Both 5-fluorouridine-5′-monophosphate (**2**) and 5-fluorouridine-3′,5′-cyclic monophosphate (**4**) (see Scheme 1) were obtained as analytically pure crystalline salts. Samples of these compounds were hydrolyzed enzymatically to give 5-fluorouridine which was rigorously identified by chromatographic; u.v., ^1H and ^{19}F n.m.r., and mass spectral; and mixture m.p. comparisons with an authentic sample (19).

Although reaction of 5′-UMP (**1**) with trifluoromethyl hypofluorite proceeded readily, quantitative generation of **2** was not observed and varying amounts (~20%) of a non-u.v. absorbing nucleotide product remained after basic treatment. Stronger base or acid treatment of this material did not generate **2** and its

Can. J. Chem. Downloaded from www.nrcresearchpress.com by 210.87.254.6 on 09/05/12
For personal use only.

Can. J. Chem. Downloaded from www.nrcresearchpress.com by 210.87.254.6 on 09/05/12
For personal use only.

structure is unknown.[6] Also, the presence of tightly associated fluoride was observed with initially precipitated samples of **2** (disodium salt). Analytical values for fluorine were essentially twice the theoretical amount. The ^1H n.m.r. spectrum of this material was in agreement with the structure of **2** and integrated intensities as well as splitting patterns precluded difluorination of the uracil ring. The corresponding ^{19}F n.m.r. spectrum contained a peak with the appropriate splitting for the C_5—F substituent plus broad absorption in the range expected for fluoride anion. A ^{31}P n.m.r. spectrum contained no evidence of P—F bonding. Reprecipitation from aqueous alcoholic solutions failed to reduce the analytical value for fluorine content. Adsorption of the sample on a carbon column, washing the column with 0.1 *N* aqueous sodium chloride solution and then distilled water, elution of the nucleotide with ammonia in ethanol–water, and conversion to the crystalline disodium salt gave **2** with analytical values in agreement with theory.

An analytically pure powder can be obtained readily by applying the reaction product directly to a Dowex 1-X2(HCO_2^-) column, elution of product with formic acid (9), and conversion to the dilithium salt of **2**. Thus, caution should be exercised in assuring that compounds are free from presumably tightly associated fluoride (see ref. 21 for a case of tightly associated mercury ions in nucleoside synthesis).

The dinucleoside phosphates uridylyl-3′ → 5′-uridine (UpU) (**5***a*), uridylyl-3′ → 5′-adenosine (UpA), and adenylyl-3′ → 5′-uridine (ApU) were subjected to this two step procedure. Preliminary studies have indicated that the adenine ring is unreactive toward CF_3OF under these mild conditions. Enzymatic hydrolysis of the product from UpU (**5***a*) using crude snake venom plus bacterial alkaline phosphatase gave 5-fluorouridine as the only u.v. absorbing component (t.l.c. and spectral comparisons). Similarly, UpA and ApU reaction products were found to give adenosine and 5-fluorouridine upon enzymatic hydrolysis. However, more careful examination of the UpU reaction mixture using electrophoresis and anion exchange chromatography on DEAE cellulose columns indicated that free 5-fluorouridine and 5-fluorouridinemonophosphate(s) were present as well as u.v. absorbing products which were not hydrolyzed to 5-fluorouridine by pancreatic ribonuclease. The desired 5-fluorouridylyl-3′ → 5′-5-fluorouridine (FUpFU) was present in less than 20% yield from starting UpU. The ApU and UpA reactions appeared to be equally complex and were not investigated further.

This study extends the convenient direct fluorination of pyrimidine bases using trifluoromethyl hypofluorite (19, 20, 22) to mononucleotides. The feasibility of employing this general method with dinucleotides was briefly investigated and found to be severely limited.

Details of the uracil adduct structure and experimental procedures for various uracil and cytosine nucleosides will be reported shortly.

Experimental

Ultraviolet spectra were determined on Cary 14 or 15 spectrophotometers by dissolving the sample in a few drops of water and then diluting accurately to 100 cc with methanol. Nuclear magnetic resonance spectra were determined in D_2O with TMS as external ^1H reference on Varian A-60, HA-100, and Brüker 90 spectrometers. Evaporations were accomplished using a Büchler rotating evaporator under reduced pressure (aspirator or vacuum pump) at 40° or lower. Mass spectra were determined by the Mass Spectroscopy Laboratory in this Department on an AEI MS-2 spectrometer using a direct probe at 70 eV and 200°.

Alkaline phosphatase (EC 3.1.3.1) (*E. coli* Type III), phosphodiesterase (EC 3.1.4.1) crude venom from *Crotalus adamanteus* (Type VI), ribonuclease (2.7.7.16) (Type I-A), uridine-5′-monophosphate (5′-UMP), uridylyl-3′ → 5′-adenosine (UpA), uridylyl-3′ → 5′-uridine (UpU), and adenylyl-3′ → 5′-uridine (ApU) were purchased from Sigma Chemical Company, St. Louis, Missouri. Trifluoromethyl hypofluorite was purchased from PCR, Inc., Gainsville, Florida. Uridine-3′,5′-cyclic monophosphate (cUMP) was a gift from Dr. R. A. Long, ICN Nucleic Acid Research Institute, Irvine, California.

Descending chromatography was effected using Whatman No. 1 paper and the following solvent systems: *A*, EtOH – 1 *M* NH_4OAc at p*H* 7.2 (7.5:3.0); *B*, 0.0005 *M* sodium borate – isopropyl alcohol (1:2); *C*, EtOH – 1 *M* NH_4OAc at p*H* 7.5 (7:3). Nucleosides obtained by enzymatic dephosphorylation were resolved by t.l.c. on Eastman silica gel sheet No. 13181 using the upper phase of EtOAc–*n*-PrOH–H_2O (4:1:2). Electrophoresis was performed on a Savant flat-plate apparatus (HV-3000A) using Whatman No. 1 paper.

5-Fluorouridine-5′-monophosphate (5′-FUMP) (2)

To a vigorously stirred solution of 0.39 g (0.001 mol) of uridine-5′-monophosphate disodium salt (**1**) (containing 6% H_2O) in 80 ml of H_2O–MeOH (14:66) at −78° was added a solution of 1.4 g (0.013 mol) of CF_3OF

[6]See ref. 23 for discussion concerning the failure of 6-hydroxy-5-fluoro-5,6-dihydrouracil adducts to be converted to 5-fluorouracils in alkaline solution.

Can. J. Chem. Downloaded from www.nrcresearchpress.com by 210.87.254.6 on 09/05/12
For personal use only.

in 10 ml of CCl_3F at −78°. The u.v. absorption of the solution at 262 nm rapidly decreased to a minimum value in ~5 min. After ~10 min further stirring, nitrogen was bubbled through the solution for 25 min to remove excess reagent while the temperature was allowed to rise to room temperature. The solution was then evaporated to dryness and the resulting white solid foam was dissolved in 5 ml of MeOH. A 10 ml portion of Et_3N–MeOH–H_2O (10:45:45) was added and the solution was stirred at room temperature overnight. Evaporation of this solution *in vacuo* gave a white solid foam which was estimated by u.v. spectroscopy to contain ~70% yield of **2**. This material was dissolved in ~5 ml of H_2O and applied to a column (2 × 20 cm) of Dowex 1-X2 (HCO_2^-) resin packed in H_2O. The column was washed with 1250 ml of H_2O and elution was begun with a linear gradient consisting of 2000 ml of H_2O in the mixing chamber and 2000 ml of 1 *N* HCO_2H in the reservoir followed by 1 *N* HCO_2H to completion. The eluate was monitored spectrophotometrically at 254 nm. Product was eluted after 3450 ml of gradient had passed through and the following 1225 ml was pooled and evaporated to dryness. This material was estimated by u.v. spectroscopy to be ~68% yield of **2**. A 60 ml portion of a solution of this solid in 120 ml of H_2O was neutralized to p*H* 7.05 (p*H* meter) with ~1.5 ml of 0.5 *N* LiOH. This solution was concentrated to ~10 ml *in vacuo* and 10 ml of MeOH was added. Acetone (70 ml) was added and the resulting mixture was allowed to stand at −10° for 4 h. The precipitate (0.1 g, 57%) was filtered, washed with acetone and then ether, and dried at 78°/0.1 mm for 3 days over KOH and P_2O_5. R_F 0.39 (*B*).

Anal. Calcd. for $C_9H_{10}FN_2O_9PLi_2$: F, 5.37. Found: F, 5.16.

Comparable results (68.5% of **2** by t.l.c. and u.v. analysis) were obtained by treating a 0.0005 mol sample of the bis(tetra-*n*-butylammonium) salt of **1** (prepared by passing an aqueous solution of disodium **1** through a column of J. T. Baker ANGC-244 (n-Bu_4N^+)) in 45 ml of methanol with 0.6 g of CF_3OF in 5 ml of CCl_3F as described above followed by similar chromophore regeneration.

A sample of **1** was fluorinated in an analogous manner, purified on a carbon column, converted into the disodium salt using a column of J. T. Baker ANGC-244 (Na^+) resin, and crystallized from acetone–water to give needles of 5-fluorouridine-5′-monophosphate disodium salt dihydrate; R_F 0.16 (*A*), 0.39 (*B*); u.v. max 270 nm (ε 9000) min 235 nm (ε 2300); n.m.r. (^1H, D_2O, TMS external) δ 8.28 (d, J_{6-5F} = 6.4 Hz, 1, H_6), (^{19}F, EtOH–H_2O, CCl_3F external) δ 164.1 (d of d, J_{5F-6} = 6.4 Hz, $J_{5F-1'}$ = 1.5 Hz, 1, F_5).

Anal. Calcd. for $C_9H_{10}FN_2O_9PNa_2.2H_2O$: C, 25.61; H, 3.34; F, 4.50; N, 6.64. Found: C, 25.80; H, 2.99; F, 4.56; N, 6.48.

This product was treated with alkaline phosphatase at p*H* 8.5 and 37° to give 5-fluorouridine as the only product as judged by t.l.c. co-chromatography with an authentic sample (19), u.v. spectra, mixture m.p., and superimposable mass spectra (M^+ *m/e* 262).

5-Fluorouridine-3′,5′-cyclic Monophosphate (cFUMP) (4)

To a vigorously stirred solution of 0.25 g (0.00072 mol) of uridine-3′,5′-cyclic monophosphate sodium salt monohydrate (**3**) in 100 ml of H_2O–MeOH (12:88) at −78° was added a solution of 0.30 g (0.003 mol) of CF_3OF in 15 ml of CCl_3F. The u.v. absorption at 261 nm rapidly vanished and excess reagent was removed by bubbling nitrogen through the solution. Solvents were removed by evaporation and the residue was stirred with 15 ml of Et_3N–MeOH–H_2O (10:45:45) for 10 h. This u.v. absorbing solution was evaporated to dryness and the resulting product **4** was dissolved in 1 ml of H_2O and 9 ml of MeOH was added followed by ~1 ml of J. T. Baker ANGC-244 (H^+) resin. The mixture was stirred until strongly acidic (p*H* < 1.5), filtered, and the resin washed with MeOH. To the combined filtrate was added 1 *N* $NaOH_{(aq)}$ dropwise until complete precipitation of the white solid salt occurred. This material was filtered and subjected to two further reprecipitation cycles to give 0.21 g (76%) of crystalline 5-fluorouridine-3′,5′-cyclic phosphate sodium salt dihydrate; R_F 0.63 (*A*), 0.50 (*B*); u.v. max 269 nm (ε 8500), min 235 nm (ε 2100); n.m.r. (^1H, D_2O, TMS external) δ 7.90 (d, J_{6-5F} = 6.4 Hz, 1, H_6), (^{19}F, D_2O, CCl_3F external) δ 164.2 (d of d, J_{5F-6} = 6.4 Hz, $J_{5F-1'}$ = 1.5 Hz, 1, F_5).

Anal. Calcd. for $C_9H_9FN_2O_8PNa{\cdot}2H_2O$: C, 28.29; H, 3.43; F, 4.97; N, 7.33. Found: C, 27.95; H, 3.10; F, 4.99; N, 7.70.

Treatment of this product with excess crude snake venom diesterase plus alkaline phosphatase at p*H* 8.5 and 37° for an extended period of time gave 5-fluorouridine only, which was identified by comparison with an authentic sample (19) as described in the above preparation of **2**.

5-Fluorouridylyl-3′ → 5′-5-Fluorouridine (FUpFU) (5b)

An aqueous solution of UpU (**5a**) was passed through a J. T. Baker ANGC-244 (n-Bu_4N^+) column and the pooled eluate was evaporated to dryness and co-evaporated three times *in vacuo* using 25 ml portions of MeOH. The residue (222 o.d. units) was dissolved in 10 ml of MeOH, cooled to −78°, and treated with 0.27 g of CF_3OF in 2.5 ml of CCl_3F at −78° with vigorous stirring. After 20 min, the solution was evaporated to dryness The residue (u.v. transparent at 260 nm) was dissolved in 15 ml of 15% aqueous ammonia and stirred for 16 h at room temperature. The solution was neutralized with J. T. Baker ANGC-244 (pyridinium$^+$) resin, filtered, and the resin washed well with H_2O. The filtrate was evaporated to dryness, the residue dissolved in a minimum volume of H_2O, and the solution passed through a column (2.2 × 8 cm) of Rexyn 101 (NH_4^+) resin. The pooled aqueous eluate was evaporated to dryness and the residue (103 o.d. units) was dissolved in H_2O. This solution was applied to a column (0.6 × 12.5 cm) of Whatman DE-52 DEAE cellulose (HCO_3^-) packed in H_2O. Elution (16 ml fractions) was begun with H_2O with constant monitoring at 254 nm. Fractions 3–6 contained 10 o.d. units of 5-fluorouridine. At fraction number 18, a linear gradient (1000 ml of H_2O in the mixing chamber and 1000 ml of 0.2 *N* triethylammonium bicarbonate in the reservoir) was begun. Fractions 24–29 contained 5-fluorouridine, 30–34 contained a small quantity of unknown material, 42–54 contained 29.6 o.d. units of two unknown components (paper chromatography, R_F 0.22 and 0.30 (*C*)), 84–94

contained 21.3 o.d. units of FUpFU (*5b*), R_F 0.27 (*C*) as indicated by the following enzymatic hydrolysis.

Compound	Paper chromatography (*C*) R_F	Electrophoretic mobility* Distance (cm)
5′-UMP (**1**)	0.10	17.2
5′-FUMP (**2**)	0.083	20.0
2′(3′)-FUMP	0.13	
cUMP (**3**)	0.42	12.9
cFUMP (**4**)	0.39	18.0
UpU (*5a*)	0.33	11.1
FUpFU (*5b*)	0.27	15.7
Uridine†	0.62	
5-Fluorouridine†	0.61	

*Whatman No. 1 paper; 0.05 *M* glycine p*H* 9.05 (NaOH); 2 kV (37 V/cm), 10–15 mA; 45 min.
†Uridine and 5-fluorouridine are resolved conveniently using the t.l.c. system indicated.

Combined fractions 84–94 were evaporated to dryness and dissolved in 1 ml of H_2O. Ribonuclease (0.5 mg) was added and the solution was allowed to stand at room temperature for 24 h. Paper chromatographic analysis of the concentrated solution showed spots at R_F 0.13 and 0.61 (*C*) corresponding to 5-fluorouridine-2′(3′)-monophosphate and 5-fluorouridine, respectively. These spots were eluted with 0.1 *N* HCl and analyzed by u.v. Three separate enzymatic determinations gave 2′(3′)-FUMP/5-fluorouridine = 0.85/1; 1.15/1; 1.2/1.

Generous support from the National Cancer Institute of Canada, The National Research Council of Canada (A5890), and The University of Alberta is gratefully acknowledged. We also wish to thank Dr. R. A. Long, ICN Pharmaceuticals, for a gift of uridine-3′,5′-cyclic monophosphate.

1. C. HEIDELBERGER. Prog. Nucleic Acid Res. Mol. Biol. **4**, 1 (1965).
2. R. DUSCHINSKY, E. PLEVEN, and C. HEIDELBERGER. J. Am. Chem. Soc. **79**, 4559 (1957).
3. M. HOFFER, R. DUSCHINSKY, J. J. FOX, and N. YUNG. J. Am. Chem. Soc. **81**, 4112 (1959).
4. N. C. YUNG, J. H. BURCHENAL, R. FECHER, R. DUSCHINSKY, and J. J. FOX. J. Am. Chem. Soc. **83**, 4060 (1961).
5. M. PRYSTAŠ and F. ŠORM. Coll. Czech. Chem. Commun. **29**, 2956 (1964).
6. M. PRYSTAŠ and F. ŠORM. Coll. Czech. Chem. Commun. **30**, 1900 (1965).
7. F. KELLER, J. E. BUNKER, and A. R. TYRRILL. J. Med. Chem. **10**, 979 (1967).
8. O. SKÖLD. Biochim. Biophys. Acta, **29**, 651 (1958).
9. J. L. DAHL, J. L. WAY, and R. E. PARKS, JR. J. Biol. Chem. **234**, 2998 (1959).
10. W. G. FARKAS, L. C. IACONO, and R. DUSCHINSKY. IVth Internatl. Cong. of Biochem. Vienna, 1958. Abstr. p. 6.
11. D. C. REMY, A. V. SUNTHANKAR, and C. HEIDELBERGER. J. Org. Chem. **27**, 2491 (1962).
12. F. M. KAHAN and J. HURWITZ. J. Biol. Chem. **237**, 3778 (1962).
13. W. SZER and D. SHUGAR. Acta Biochim. Pol. **10**, 219 (1963).
14. M. GRUNBERG-MANAGO and A. M. MICHELSON. Biochim. Biophys. Acta, **87**, 593 (1964).
15. A. BLOCH, M. H. FLEYSHER, R. THEDFORD, R. J. MAUE, and R. H. HALL. J. Med. Chem. **9**, 886 (1966).
16. C. HEIDELBERGER, J. BOOHAR, and G. D. BIRNIE. Biochim. Biophys. Acta, **91**, 636 (1964).
17. S. SLAPIKOFF and P. BERG. Biochemistry, **6**, 3654 (1967).
18. A. J. WAHBA, R. S. GARDNER, C. BASILIO, R. S. MILLER, J. F. SPEYER, and P. LENGYEL. Proc. Natl. Acad. Sci. U.S. **49**, 116 (1963).
19. M. J. ROBINS and S. R. NAIK. J. Am. Chem. Soc. **93**, 5277 (1971).
20. M. J. ROBINS and S. R. NAIK. J. Chem. Soc. Chem. Commun. 18 (1972).
21. G. L. TONG, W. W. LEE, and L. GOODMAN. J. Org. Chem. **32**, 1984 (1967).
22. D. H. R. BARTON, R. H. HESSE, H. T. TOH, and M. M. PECHET. J. Org. Chem. **37**, 329 (1972).
23. R. DUSCHINSKY, T. GABRIEL, W. TAUTZ, A. NUSSBAUM, M. HOFFER, E. GRUNBERG, J. H. BURCHENAL, and J. J. FOX. J. Med. Chem. **10**, 47 (1967).
24. M. J. ROBINS, A. S. K. LEE, and F. A. NORRIS. Carbohyd. Res. In press.

Can. J. Chem. Downloaded from www.nrcresearchpress.com by 210.87.254.6 on 09/05/12
For personal use only.

β-Carbon Shielding Effects in Carbon-13 Nuclear Magnetic Resonance Spectroscopy

H. BEIERBECK AND J. K. SAUNDERS

Département de Chimie, Université de Sherbrooke, Sherbrooke, Québec J1K 2R1

Received August 29, 1974

H. BEIERBECK and J. K. SAUNDERS. Can. J. Chem. **53**, 1307 (1975).

Carbon-13 chemical shifts in saturated hydrocarbons of staggered conformation may be derived from the corresponding resonances in ethane, propane, isobutane, and neopentane in the following way: every H—*C*—C(α)—C(β) *gauche* interaction between an α-hydrogen and a β-carbon deshields a carbon nucleus by *ca.* 4.7 p.p.m. Every exocyclic carbon–carbon *gauche* configuration H—C(α)—*C*—C(α)—C(β)—H has a deshielding effect of *ca.* 1.7 p.p.m., as the result of nonbonded hydrogen–hydrogen γ-interactions. Every nonbonded interaction between an α-hydrogen and a hydrogen on a γ-carbon makes a shielding contribution of *ca.* −4.5 p.p.m.

H. BEIERBECK et J. K. SAUNDERS. Can. J. Chem. **53**, 1307 (1975).

Nous démontrons qu'il est possible de prévoir les déplacements chimiques des carbones des hydrocarbures saturés en se basant sur les déplacements chimiques dans l'éthane, le *n*-propane, le butane tertiaire et le néopentane et en considérant le nombre des interactions *gauches* et interactions non liées de la façon suivante: chaque interaction *gauche* H—*C*—C(α)—C(β) cause un déblindage de 4.7 p.p.m. sur le carbone β. Chaque interaction *gauche* H—C(α)—*C*—C(α)—C(β)—H induit un déblindage de 1.7 p.p.m. sur le carbone β pourvu que ces derniers noyaux aient une configuration telle qu'il y ait une interaction non liée entre les hydrogènes sur les carbones S et γ. Chaque interaction non liée entre un proton α et un proton sur un carbone γ induit un blindage de −4.5 p.p.m. sur le carbone γ.

Introduction

There have been a number of attempts to correlate carbon-13 chemical shifts in saturated hydrocarbons with molecular structural features (1–6). The additivity parameters reported recently by Grant and co-workers (5, 6) appeared to be the best to date, since they were based on conformationally well defined model systems. However, the physical significance of the term β, which these authors interpreted as an inductive shielding contribution (5), seemed questionable since it was difficult to reconcile with the observation that β-substituent effects on carbon-13 chemical shifts are virtually independent of the nature of the substituent (1, 7–14).

In order to resolve this contradiction we have reexamined β-carbon shielding effects in carbon-13 n.m.r. spectroscopy and found that the prediction of carbon-13 chemical shifts with the β-substituent parameters V_g and β of refs. 5 and 6 is numerically equivalent to an interpretation of β-carbon shielding solely in terms of *gauche* interactions.

Results and Discussion

The experimental data used in this study were carbon-13 chemical shifts in saturated hydrocarbons of staggered conformation or parts of molecules which met this criterion. The data in Table 1 are a selection of chemical shifts in rigid decalin derivatives, taken from ref. 5 and those in Table 2 are resonances of carbons in portions of natural product type compounds which consist of cyclohexane rings in the chair form.

In order to extract the β-carbon substituent effects from the data in Tables 1 and 2, the α- and steric shifts were eliminated as follows. Since α-carbon shieldings are nonadditive it is best to use the resonances in ethane, propane, isobutane, and neopentane (1, 2) as references for primary, secondary, tertiary, and quaternary carbons respectively. CH_3CH_3 = 5.9 p.p.m., $CH_2(CH_3)_2$ = 16.1 p.p.m., $CH(CH_3)_3$ = 25.2 p.p.m., $C(CH_3)_4$ = 27.9 p.p.m. Groups which are three or more bonds from the carbon in question make significant shielding contributions only if there are appreciable nonbonded interactions with the hydrogens on that carbon (1,

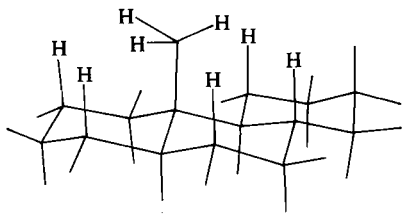

Can. J. Chem. Downloaded from www.nrcresearchpress.com by 210.87.254.105 on 09/05/12
For personal use only.

Can. J. Chem. Downloaded from www.nrcresearchpress.com by 210.87.254.105 on 09/05/12
For personal use only.

TABLE 1. Carbon-13 chemical shifts for some decalin derivatives (taken from ref. 5)*†

Carbon	Derivative	δ Experimental	δ Calculated	Δδ	δ(β)	n_β	n_{HC}	$n_{CC'}$	$n_{CC''}$	n_γ
1	*cis-syn*-1-Methyldecalin	37.2	38.1	0.9	12.0	3	2	2	2	0
2	*cis-syn*-1-Methyldecalin	29.5	30.5	1.0	17.9	3	4	0	2	1
3	*cis-syn*-1-Methyldecalin	27.4	25.6	−1.8	11.3	2	2	0	2	0
4	*cis-syn*-1-Methyldecalin	25.8	26.0	0.2	18.7	3	4	0	2	2
5	*cis-syn*-1-Methyldecalin	33.6	32.0	−1.6	17.5	3	3	1	2	0
6	*cis-syn*-1-Methyldecalin	21.9	21.1	−0.8	10.3	2	2	0	2	1
7	*cis-syn*-1-Methyldecalin	27.4	25.6	−1.8	11.3	2	2	0	2	0
8	*cis-syn*-1-Methyldecalin	20.0	21.5	1.5	17.4	3	4	0	2	3
9	*cis-syn*-1-Methyldecalin	43.0	44.6	1.6	17.8	5	3	3	4	0
10	*cis-syn*-1-Methyldecalin	38.7	38.1	−0.6	13.5	4	2	2	4	0
Me-1	*cis-syn*-1-Methyldecalin	19.8	20.3	0.5	18.4	2	4	0	0	1
1	*trans*-Decalin	34.7	35.0	0.3	18.6	3	4	0	2	0
2	*trans*-Decalin	27.2	25.6	−1.6	11.1	2	2	0	2	0
9	*trans*-Decalin	44.2	44.1	−0.1	19.0	4	4	0	4	0
1	*trans*-9-Methyldecalin	42.4	41.5	−0.9	26.3	4	5	1	2	0
2	*trans*-9-Methyldecalin	22.2	21.1	−1.1	10.6	2	2	0	2	1
3	*trans*-9-Methyldecalin	27.4	25.6	−1.8	11.3	2	2	0	2	0
4	*trans*-9-Methyldecalin	29.4	30.5	1.1	17.8	3	4	0	2	1
9	*trans*-9-Methyldecalin	34.8	34.9	0.1	6.9	4	0	4	4	0
10	*trans*-9-Methyldecalin	46.2	47.6	1.4	21.0	5	4	2	4	0
Me-9	*trans*-9-Methyldecalin	15.8	16.3	0.5	27.9	3	6	0	0	4
1	*trans-anti*-1-Methyldecalin	38.4	41.1	2.7	13.2	3	3	1	2	0
2	*trans-anti*-1-Methyldecalin	37.1	35.0	−2.1	21.0	3	4	0	2	0
8	*trans-anti*-1-Methyldecalin	31.0	30.5	−0.5	19.4	3	4	0	2	1
9	*trans-anti*-1-Methyldecalin	50.6	50.6	0.0	25.4	5	5	1	4	0

Can. J. Chem. Downloaded from www.nrcresearchpress.com by 210.87.254.105 on 09/05/12
For personal use only.

TABLE 1. (*Concluded*)

Carbon	Derivative	δ Experimental	δ Calculated	Δδ	δ(β)	n_β	n_{HC}	$n_{CC'}$	$n_{CC''}$	n_γ
Me-1	*trans-anti*-1-Methyldecalin	19.7	20.3	0.6	18.3	2	4	0	0	1
1	*trans-anti*-1-*syn*-2-Dimethyldecalin	44.3	47.6	3.3	19.1	4	4	2	2	0
2	*trans-anti*-1-*syn*-2-Dimethyldecalin	39.3	41.1	1.8	14.1	3	3	1	2	0
3	*trans-anti*-1-*syn*-2-Dimethyldecalin	35.8	35.0	−0.8	19.7	3	4	0	2	0
8	*trans-anti*-1-*syn*-2-Dimethyldecalin	31.0	30.5	−0.5	19.4	3	4	0	2	1
9	*trans-anti*-1-*syn*-2-Dimethyldecalin	49.4	50.6	1.2	24.2	5	5	1	4	0
Me-1	*trans-anti*-1-*syn*-2-Dimethyldecalin	16.1	15.8	−0.3	19.2	2	4	0	0	2
Me-2	*trans-anti*-1-*syn*-2-Dimethyldecalin	20.9	20.3	−0.6	19.5	2	4	0	0	1
1	*trans-syn*-2-*syn*-3-Dimethyldecalin	44.2	44.5	0.3	28.1	4	6	0	2	0
2	*trans-syn*-2-*syn*-3-Dimethyldecalin	39.8	41.1	1.3	14.6	3	3	1	2	0
Me-2	*trans-syn*-2-*syn*-3-Dimethyldecalin	20.3	20.3	0.0	18.9	2	4	0	0	1
1	*trans-anti*-1-*syn*-8-Dimethyldecalin	34.0	36.6	2.6	13.3	3	3	1	2	1
2	*trans-anti*-1-*syn*-8-Dimethyldecalin	35.6	35.0	−0.6	19.5	3	4	0	2	0
3	*trans-anti*-1-*syn*-8-Dimethyldecalin	28.5	25.6	−2.9	12.4	2	2	0	2	0
4	*trans-anti*-1-*syn*-8-Dimethyldecalin	35.5	35.0	−0.5	19.4	3	4	0	2	0
5	*trans-anti*-1-*syn*-8-Dimethyldecalin	35.4	35.0	−0.4	19.3	3	4	0	2	0
6	*trans-anti*-1-*syn*-8-Dimethyldecalin	21.0	21.1	0.1	9.4	2	2	0	2	1
7	*trans-anti*-1-*syn*-8-Dimethyldecalin	34.6	32.0	−2.6	18.5	3	3	1	2	0
8	*trans-anti*-1-*syn*-8-Dimethyldecalin	26.6	28.9	2.3	5.9	3	1	2	3	1
9	*trans-anti*-1-*syn*-8-Dimethyldecalin	52.4	54.1	1.7	27.2	6	5	3	4	0
10	*trans-anti*-1-*syn*-8-Dimethyldecalin	36.8	39.6	2.8	16.1	4	4	0	4	1
Me-1	*trans-anti*-1-*syn*-8-Dimethyldecalin	19.2	20.3	1.1	17.8	2	4	0	0	1
Me-8	*trans-anti*-1-*syn*-8-Dimethyldecalin	12.5	11.3	−1.2	20.1	2	4	0	0	3

*δ(exptl), observed carbon-13 chemical shift; δ(calcd), predicted carbon-13 chemical shift; Δδ, δ(calcd) − δ(exptl); δ(β), extracted β-carbon shift contribution (see text); n_β, etc, number of β-carbons, hydrogen–carbon, exocyclic and endocyclic carbon–carbon *gauche* interactions, and nonbonded γ-interactions.

†Numbering system:

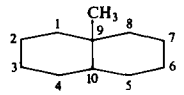

TABLE 2. Carbon-13 chemical shifts for portions of natural product type compounds, which consist of cyclohexane rings in the chair form*†‡

Carbon	Compound	δ(exptl)	δ(calcd)	Δδ	δ(β)	n_β	n_{HC}	$n_{CC'}$	$n_{CC''}$	n_γ
1	17β-Hydroxyandrostane	38.8	37.0	−1.8	27.2	4	5	1	2	1
2	17β-Hydroxyandrostane	22.2	21.1	−1.1	10.6	2	2	0	2	1
3	17β-Hydroxyandrostane	26.8	25.6	−1.2	10.7	2	2	0	2	0
4	17β-Hydroxyandrostane	29.1	30.5	1.4	17.5	3	4	0	2	1
5	17β-Hydroxyandrostane	47.2	47.6	0.4	22.0	5	4	2	4	0
6	17β-Hydroxyandrostane	29.1	30.5	1.4	17.5	3	4	0	2	1
7	17β-Hydroxyandrostane	31.8	30.5	−1.3	20.2	3	4	0	2	1
8	17β-Hydroxyandrostane	35.7	41.6	5.9	19.5	5	5	1	4	2
9	17β-Hydroxyandrostane	55.1	54.1	−1.0	29.9	6	5	3	4	0
10	17β-Hydroxyandrostane	36.4	38.3	1.9	8.5	5	0	6	4	0
11	17β-Hydroxyandrostane	21.6	21.5	−0.1	19.0	3	4	0	2	3
12	17β-Hydroxyandrostane	38.7	41.5	2.8	22.6	4	5	1	2	0
19	17β-Hydroxyandrostane	12.4	11.8	−0.6	29.0	3	6	0	0	5
6	Friedelin	41.3	37.0	−4.3	29.7	4	5	1	2	1
7	Friedelin	18.3	17.0	−1.3	20.2	3	4	0	2	4
8	Friedelin	53.1	53.0	−0.1	32.4	7	5	5	4	1
9	Friedelin	37.5	36.6	−0.9	9.6	5	0	5	5	0
10	Friedelin	59.5	57.5	−2.0	34.3	7	5	5	4	0
11	Friedelin	35.7	32.5	−3.2	28.6	4	5	1	2	2
12	Friedelin	30.5	28.0	−2.5	27.9	4	5	1	2	3
1	Germanicol	38.9	37.0	−1.9	27.3	4	5	1	2	1
5	Germanicol	55.5	57.5	2.0	30.3	7	5	5	4	0
6	Germanicol	18.2	17.0	−1.2	20.1	3	4	0	2	4
7	Germanicol	34.6	32.5	−2.1	27.5	4	5	1	2	2
8	Germanicol	40.7	40.1	−0.6	12.8	6	0	7	5	0
9	Germanicol	51.2	53.0	1.8	30.5	7	5	5	4	1
10	Germanicol	37.3	34.9	−2.4	9.4	5	0	4	6	0
11	Germanicol	21.1	21.5	0.4	18.5	3	4	0	2	3
14	Germanicol	43.3	40.1	−3.2	15.4	6	0	7	5	0
15	Germanicol	27.4	28.0	0.6	24.8	4	5	1	2	3

*See footnote * of Table 1.
†The carbon-13 chemical shifts for the steroid were taken from ref. 16, those for the terpenes are unpublished results.
‡Numbering in the terpenes:

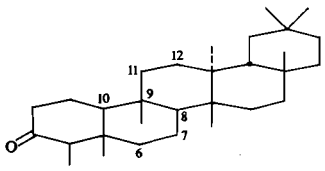

Friedelin

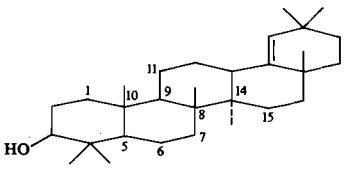

Germanicol

15). Nonbonded γ-interactions, which are the only steric interactions that need to be considered here, were assumed to make a shielding contribution of −4.5 p.p.m. Little seems to be gained by introducing a new parameter for the second and subsequent γ-interactions, as proposed by Grant and co-workers (5, 6), since the variation of steric shifts with conformational changes is not clearly understood at present.

The derivation of the β-carbon shielding contribution to the chemical shift of C(1) in 17β-hydroxyandrostane may serve as numerical example. C(1) is a secondary carbon and the α-shift is therefore eliminated by subtracting 16.1 p.p.m., the chemical shift of the secondary carbon in propane. There is one nonbonded interaction with a hydrogen on C(11) and a shift increment of −4.5 p.p.m. is subtracted to eliminate this γ-contribution. The β-carbon shielding effect on C(1) in 17β-hydroxyandrostane is therefore

$$\delta(\beta) = 38.8 - 16.1 - (-4.5) = 27.2 \text{ p.p.m.}$$

The β-carbon shielding contributions are included in Tables 1 and 2.

The configuration of the structural unit con-

Can. J. Chem. Downloaded from www.nrcresearchpress.com by 210.87.254.105 on 09/05/12
For personal use only.

TABLE 3. β-Carbon shielding parameters, in p.p.m.

	Derived from*				Derived from	
	$\{n_{HC}, n_{CC}\}$	$\{n_{HC}, n_{\beta}\}$	$\{n_{CC}, n_{\beta}\}$		$\{n_{HC}, n_{CC'}, n_{CC''}\}$	$\{n_{HC}, n_{CC'}\}$
HC	4.43	3.52	—	HC	4.72	4.73
CC	0.91	—	−3.52†	CC′	1.71	1.74
β	—	1.82	8.87†	CC″	0.04	—
RMS (P)	1.51	1.51	1.51	RMS (P)	0.70	0.69
RMS (S)	1.64	1.64	1.64	RMS (S)	1.64	1.64
RMS (T)	2.73	2.73	2.73	RMS (T)	2.16	2.14
RMS (Q)	2.01	2.01	2.01	RMS (Q)	1.86	1.89
RMS (total)	2.02	2.02	2.02	RMS (total)	1.74	1.74

*Show the interdependence defined by eqs. 2*a–c*:

$$[2a]: \delta(\beta) = n_{HC}(4.43) + n_{CC}(0.91)$$
$$[2b]: \delta(\beta) = n_{HC}(4.43 - 0.91) + n_{\beta}(2 \times 0.91) = n_{HC}(3.52) + n_{\beta}(1.82)$$
$$[2c]: \delta(\beta) = n_{CC}(0.91 - 4.43) + n_{\beta}(2 \times 4.43) = n_{CC}(-3.52) + n_{\beta}(8.87)$$

†These agree well with −3.50/8.49 (ref. 5) and −3.38/8.81 p.p.m. (ref. 6).

sisting of a carbon and its α- and β-substituents, in saturated hydrocarbons of staggered conformation, may be described by the number of H—*C*—C(α)—C(β) hydrogen–carbon and C(α)—*C*—C(α)—C(β) carbon–carbon *gauche* interactions, n_{HC} and n_{CC}. Since every β-carbon gives rise to two *gauche* interactions the sum of n_{HC} and n_{CC} is always twice the number of β-carbons, n_{β}.

$$[1] \qquad n_{HC} + n_{CC} = 2n_{\beta}$$

This means that there are three equivalent descriptions of the configuration, namely the parameter sets $\{n_{HC}, n_{CC}\}$, $\{n_{HC}, n_{\beta}\}$, and $\{n_{CC}, n_{\beta}\}$. Since β-carbon substituent effects have been found (5, 6) to correlate with $\{n_{CC}, n_{\beta}\}$, they must also correlate with $\{n_{HC}, n_{CC}\}$ and $\{n_{HC}, n_{\beta}\}$. For instance, the prediction of β-carbon shifts δ(β) in terms of $\{n_{HC}, n_{CC}\}$, with corresponding parameters HC and CC,

$$[2a] \qquad \delta(\beta) = n_{HC}HC + n_{CC}CC$$

may be converted to expressions for δ(β) in terms of $\{n_{HC}, n_{\beta}\}$ or $\{n_{CC}, n_{\beta}\}$, simply by substituting the rearranged eq. 1 into expression 2*a*.

$$[2b] \qquad \delta(\beta) = n_{HC}HC + (2n_{\beta} - n_{HC})CC = n_{HC}(HC - CC) + n_{\beta}(2CC)$$

$$[2c] \qquad \delta(\beta) = (2n_{\beta} - n_{CC})HC + n_{CC}CC = n_{CC}(CC - HC) + n_{\beta}(2HC)$$

The coefficients (CC − HC) and (2HC) of n_{CC} and n_{β} in eq. 2*c* correspond to V_g and β of refs. 5 and 6 (Table 3). The results of regression analyses between the β-carbon shifts of Tables 1 and 2 and the three sets of variables $\{n_{HC}, n_{CC}\}$, $\{n_{HC}, n_{\beta}\}$, and $\{n_{CC}, n_{\beta}\}$ clearly show the numerical equivalence of the three predictive schemes [2*a*]–[2*c*]. The root mean squares deviations are identical and the three sets of additivity parameters are interrelated according to eqs. 2*a*–2*c* (Table 3).

The important result of this demonstration is the conclusion that it is not possible to elucidate the mechanism of β-carbon shielding solely on the basis of correlation studies between observed β-carbon shift increments and structural parameters. However, the observation that β-substituent effects on carbon-13 chemical shifts are rather insensitive to the nature of the substituent (1, 7–14) favors version [2*a*], which corresponds to an interpretation of β-substituent shifts without explicitly invoking inductive effects. For this reason, and because of their interesting implications for conformational studies, the derivation of β-carbon shielding contributions in terms of *gauche* parameters has been chosen here, but with the following modification.

In Tables 1 and 2 the carbon–carbon *gauche* interactions are divided into exocyclic (CC′) and endocyclic (CC″) interactions. A regression analysis with the variable set $\{n_{HC}, n_{CC'}, n_{CC''}\}$ showed that only the parameter $n_{CC'}$ was significant (Table 3). The principal difference between the exocyclic and endocyclic carbon–carbon *gauche* configuration is the steric hydro-

Can. J. Chem. Downloaded from www.nrcresearchpress.com by 210.87.254.105 on 09/05/12
For personal use only.

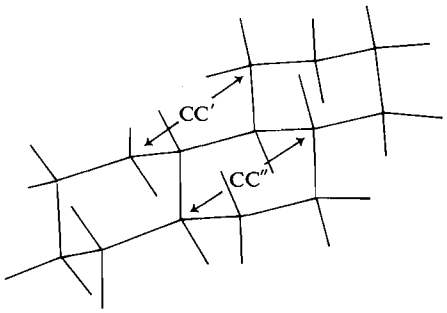

gen–hydrogen interaction H—C(α)—*C*—C(α)—C(β)—H in the exocyclic case. It is therefore possible that the shift increment $n_{CC'}CC'$ is not due to *gauche* interactions between the carbons, but to nonbonded γ-interactions between the hydrogens on these carbons. In other words, it seems that nonbonded γ-interactions shift the signal of the first carbon upfield and that of the second carbon downfield. This then leads to the

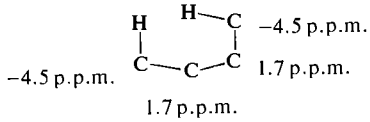

following tentative interpretation of β-carbon shielding effects. *Gauche* interactions H—*C*—C(α)—C(β) between an α-hydrogen and a β-carbon make the major contribution to the β-carbon shift. A second contribution comes from H—C(α)—*C*—C(α)—C(β)—H γ-interactions between hydrogens on an α-carbon and a β-carbon. This shielding term is linked to exocyclic carbon–carbon *gauche* interactions, which are the geometric requirement for steric γ-interactions. The carbon–carbon *gauche* interactions themselves do not seem to affect carbon-13 chemical shifts significantly.

Thus, carbon-13 chemical shifts in saturated hydrocarbons of staggered conformation may be derived from the corresponding resonances in ethane, propane, isobutane, and neopentane in the following way. Every H—*C*—C(α)—C(β) *gauche* interaction between an α-hydrogen and a β-carbon deshields a carbon nucleus by *ca.* 4.7 p.p.m. Every exocyclic carbon–carbon *gauche* configuration H—C(α)—*C*—C(α)—C(β)—H has a deshielding effect of *ca.* 1.7 p.p.m., as the result of nonbonded hydrogen–hydrogen γ-interactions. Every nonbonded interaction between an α-hydrogen and a hydrogen on a γ-carbon makes a shielding contribution of *ca.* −4.5 p.p.m.

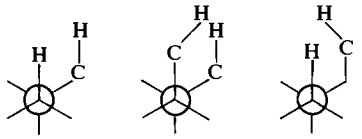

4.7 p.p.m. 1.7 p.p.m. −4.5 p.p.m.

The prediction of the chemical shifts of C(1) in androstane may serve as numerical example. Since C(1) is a secondary carbon, the reference shift is the resonance of the secondary carbon in propane (corresponding to the fragment C(2)—C(1)—C(10)). There are a total of five hydrogen–carbon, one exocyclic and two endocyclic carbon–carbon *gauche* interactions about the two bonds C(1)—C(2) and C(1)—C(10). The two endocyclic CC″ interactions do not contribute to the chemical shift.

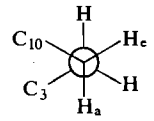

C_1—C_2

HC
H(a)—C(1)—C(2)—C(3)
CC″
C(10)—C(1)—C(2)—C(3)

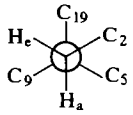

C_1—C_{10}

HC
H(a)—C(1)—C(10)—C(5)
H(a)—C(1)—C(10)—C(9)
H(e)—C(1)—C(10)—C(9)
H(e)—C(1)—C(10)—C(19)
CC′
C(2)—C(1)—C(10)—C(19)
CC″
C(2)—C(1)—C(10)—C(5)

In addition there is one nonbonded γ-interaction with a hydrogen on C(11). Therefore, the chemical shift of C(1) is predicted to be $\delta_{C(1)} = 16.10 + 5 \times 4.73 + 1.74 - 4.50 = 37.0$ p.p.m. The number of *gauche* and nonbonded interactions and the predicted carbon-13 chemical shifts are included in Tables 1 and 2.

Conclusions

Additivity parameters for predicting carbon-13 chemical shifts in saturated hydrocarbons have been proposed, which do not require the explicit assumption of inductive shielding contributions to β-substituent effects. In this interpretation of shielding the hydrogens play a major role, modifying chemical shifts through hydrogen–carbon *gauche* interactions and nonbonded hydrogen–hydrogen γ-interactions. Studies of shielding by functional groups and in conformations, where

Can. J. Chem. Downloaded from www.nrcresearchpress.com by 210.87.254.105 on 09/05/12
For personal use only.

dihedral angles differ from 60°, are expected to add further insight into the factors determining carbon-13 chemical shifts.

1. J. B. STOTHERS. Carbon-13 NMR spectroscopy. Academic Press, New York. 1972.
2. D. M. GRANT and E. G. PAUL. J. Am. Chem. Soc. **86**, 2984 (1964).
3. L. P. LINDEMAN and J. Q. ADAMS. Anal. Chem. **43**, 1245 (1971).
4. J. MASON. J. Chem. Soc. A, 1038 (1971).
5. D. K. DALLING, D. M. GRANT, and E. G. PAUL. J. Am. Chem. Soc. **95**, 3718 (1973).
6. D. K. DALLING and D. M. GRANT. J. Am. Chem. Soc. **96**, 1827 (1974).
7. J. B. GRUTZNER, M. JAUTELAT, J. B. DENCE, R. A. SMITH, and J. D. ROBERTS. J. Am. Chem. Soc. **92**, 7107 (1970).
8. E. LIPPMAA, T. PEHK, J. PAASIVIRTA, N. BELIKOVA, and A. PLATÉ. Org. Magn. Reson. **2**, 581 (1970).
9. T. PEHK, E. LIPPMAA, V. V. SEVOSTJANOVA, M. M. KRAYUSCHKIN, and A. I. TARASOVA. Org. Magn. Reson. **3**, 783 (1971).
10. G. E. MACIEL, L. SIMERAL, R. L. ELLIOTT, B. KAUFMAN, and K. CRIBLEY. J. Phys. Chem. **76**, 1466 (1972).
11. L. SIMERAL and G. E. MACIEL. J. Phys. Chem. **77**, 1590 (1973).
12. N. S. BHACCA, D. D. GIANNINI, W. S. JANKOWSKI, and M. E. WOLFF. J. Am. Chem. Soc. **95**, 8421 (1973).
13. D. D. GIANNINI, P. A. KOLLMAN, N. S. BHACCA, and M. E. WOLFF. J. Am. Chem. Soc. **96**, 5462 (1974).
14. S. H. GROVER and J. B. STOTHERS. Can. J. Chem. **52**, 870 (1974).
15. D. M. GRANT and B. V. CHENEY. J. Am. Chem. Soc. **89**, 5315 (1967).
16. J. W. APSIMON, H. BEIERBECK, and J. K. SAUNDERS. Can. J. Chem. **51**, 3874 (1973).

Can. J. Chem. Downloaded from www.nrcresearchpress.com by 210.87.254.105 on 09/05/12
For personal use only.

The Chemical Ionization Mass Spectra of Fluorotoluenes

ALEX. G. HARRISON AND PING-HUANG LIN[1]

Department of Chemistry, University of Toronto, Toronto, Ontario M5S 1A1

Received November 28, 1974

ALEX G. HARRISON and PING-HUANG LIN. Can. J. Chem. **53**, 1314 (1975).

The methane and hydrogen chemical ionization mass spectra of benzyl fluoride, the isomeric fluorotoluenes, and fluorobenzene have been determined. Reaction mechanisms have been elucidated by using CD_4 and D_2 as reagent gases. Both the CH_4 and H_2 spectra of benzyl fluoride show $C_7H_7^+$ as the major ion. In the CH_4 spectra of the fluorotoluenes MH^+ is the only abundant ion resulting from protonation while in the H_2 chemical ionization spectra considerable loss of HF and H_2 occurs from MH^+. There is no evidence for ring expansion to form tropylium type ions. The novel reactions

$$CH_5^+ + FC_6H_4R \rightarrow CH_3C_6H_4R.H^+ + HF$$

$$H_3^+ + FC_6H_4R \rightarrow C_6H_5R.H^+ + HF$$

are important reaction modes for $R = CH_3$ or H and indicate that a long-lived collision complex is formed between CH_5^+ or H_3^+ and the aromatic neutral.

ALEX G. HARRISON et PING-HUANG LIN. Can. J. Chem. **53**, 1314 (1975).

On a déterminé les spectres de masse, par ionisation chimique avec le méthane et l'hydrogène, de fluorures de benzyle. des fluorotoluènes isomères et du fluorobenzène. On a élucidé les mécanismes de réaction en faisant appel à CD_4 et D_2 comme gaz réactifs. Les spectres avec CH_4 et H_2 du fluorure de benzyle montrent la présence de $C_7H_7^+$ comme ion majeur. Dans le spectre des fluorotoluènes ionisés chimiquement par CH_4, MH^+ est le seul ion abondant résultant de la protonation; dans le spectre avec ionisation chimique par H_2, on trouve qu'il y a une perte considérable de HF et de H_2 à partir de MH^+. On ne trouve aucun support pour la présence d'une extention de cycle pour former des ions de type tropylium. Les réactions nouvelles

$$CH_5^+ + FC_6H_4R \rightarrow CH_3C_6H_4R.H^+ + HF$$

$$H_3^+ + FC_6H_4R \rightarrow C_6H_5R.H^+ + HF$$

sont des modes importants de réaction dans les cas où $R = CH_3$ ou H et indiquent qu'un complexe de collision ayant une longue vie se forme entre CH_5^+ ou H_3^+ et la molécule aromatique neutre.

[Traduit par le journal]

It is well established that, in the dissociative electron impact ionization of toluene, and many toluene derivatives, extensive isotopic scrambling occurs (1–3). The early interpretation (2, 3) of ring expansion to form symmetrical tropylium-type ions appears basically correct, although there is now evidence, for some systems, from collisional activation (4) and ion–molecule reaction studies (5) that isomeric ions in addition to tropylium ions (possibly interconverting) are present.

The possible importance of such ring expansion processes in chemical ionization has not been investigated in any detail. Field (6) has shown that, in the methane chemical ionization of toluene, the low abundance $C_7H_7^+$ ($[M—H]^+$) ion originates almost entirely by hydrogen abstraction from the methyl group. This ion probably is formed by a direct hydride abstraction by CH_5^+ and/or $C_2H_5^+$ and in such a direct process one would not anticipate ring expansion. Field's results indicated that protonated toluene, the major ion produced by methane chemical ionization, did not undergo significant fragmentation. In the absence of such fragmentation it is impossible to use isotopic labelling to assess the importance of ring expansion.

As part of a program to assess the role of ring expansion in chemical ionization processes we have determined the chemical ionization mass spectra of benzyl fluoride and the isomeric fluorotoluenes. The significance of the fluorine substituent will be discussed below. The electron

[1]Present address: Department of Chemical Engineering, Massachusetts Institute of Technology, Cambridge, Mass.

Can. J. Chem. Downloaded from www.nrcresearchpress.com by 210.87.254.5 on 09/05/12
For personal use only.

Can. J. Chem. Downloaded from www.nrcresearchpress.com by 210.87.254.5 on 09/05/12
For personal use only.

impact mass spectra of benzyl fluoride and the fluorotoluenes are practically identical, the major ions being the molecular ion (*m/e* 110) and the $[M—H]^+$ fragment ion. The appearance potentials for the $FC_7H_6^+$ fragment ions from *m*-fluorotoluene and *p*-fluorotoluene are identical (7) and this has been taken (7) as evidence that ring expansion to a fluorotropylium ion has occurred. In addition, Safe *et al.* (8) recently have measured the ratios of metastable ion intensities for the fragmentation processes

$$[1] \qquad FC_7H_6^+ \rightarrow C_7H_5^+ + HF$$

$$[2] \qquad \rightarrow C_5H_4F^+ + C_2H_2$$

and have observed differences in this ratio of less than 30% for $FC_7H_6^+$ ions generated from the four isomers. Such small differences probably originate from variations in the internal energy distributions of the fragmenting ions (9) rather than from structural differences; these results therefore provide additional support for the earlier suggestion (7) that the same ring-expanded fragment ion is formed by dissociative ionization.

Thus, there is substantial evidence that ring expansion does occur in the electron impact ionization of fluorine-substituted toluenes and it is of interest to consider the possible effect of ring expansion on the chemical ionization of these compounds. In the absence of ring expansion, protonated benzyl fluoride would be expected to show an abundant ion resulting from loss of HF since the product benzyl ion is quite stable. By contrast, in the absence of ring expansion, the loss of HF from the protonated fluorotoluenes will be energetically unfavorable since unstable tolyl ions would be formed; rather the loss of H_2 to form the more stable fluorobenzyl cations should be favored. On the other hand, if ring expansion occurs in the protonated molecules, one would anticipate facile loss of HF for all isomers since a stable tropylium cation can be formed in each case.

We have, therefore, carried out a detailed study of the chemical ionization of benzyl fluoride and the fluorotoluenes using both CH_4 and H_2 as reagent gases. To provide additional information concerning reaction mechanisms we also have used CD_4 and D_2 reagent gases. For comparison purposes the chemical ionization mass spectra of fluorobenzene with the four reagent gases have been determined.

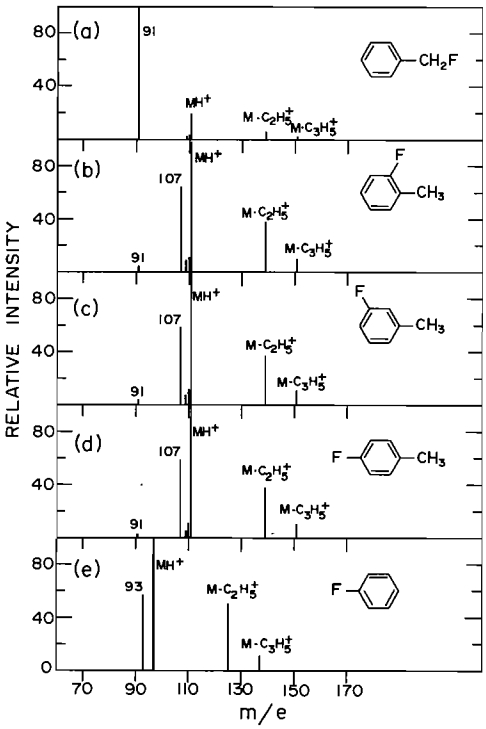

FIG. 1. CH_4 chemical ionization mass spectra of fluorine substituted toluenes and of fluorobenzene.

Methane Chemical Ionization Spectra

The methane chemical ionization mass spectra of benzyl fluoride, the isomeric fluorotoluenes, and fluorobenzene are shown in Fig. 1. For benzyl fluoride, an important peak (19% of base peak) is observed corresponding to the protonated molecule, MH^+, while the base peak is $C_7H_7^+$ at *m/e* 91. The reaction sequence presumably is

$$[3] \qquad \left.\begin{matrix} CH_5^+ \\ C_2H_5^+ \end{matrix}\right\} + C_7H_7F \rightarrow C_7H_7F.H^+ \rightarrow C_7H_7^+ + HF$$

With CD_4 as reagent gas the fragment ion peak did not shift to *m/e* 92 (*cf.* H_2 and D_2 results below) indicating that the added proton is always lost with the HF neutral.[2] In addition, low abundance ions are observed at *m/e* 139 and 151 corresponding to the collision-stabilized clustering of the $C_2H_5^+$ and $C_3H_5^+$ reactant ions with the neutral benzyl fluoride. In contrast

[2]Alternatively one cannot rule out the possibility that the reaction is a direct F^- abstraction reaction.

Can. J. Chem. Downloaded from www.nrcresearchpress.com by 210.87.254.5 on 09/05/12
For personal use only.

to the electron impact spectrum, the $[M—H]^+$ intensity is very low (<2% of base peak).

The spectra of the three fluorotoluenes all show MH^+ as the base peak with only minor formation of $C_7H_7^+$ (2–4% of base peak). The *m/e* 139 and 151 cluster ions are considerably more abundant. In addition the $[M—H]^+$ ions are more abundant than in the benzyl fluoride case but still only 4–8% of the MH^+ intensity. It is probable that, as in the toluene case (6), these ions are formed by hydride abstraction.

The spectra of the three fluorotoluenes are essentially identical and clearly distinguishable from that of benzyl fluoride. As discussed in the previous section the facile loss of HF from protonated benzyl fluoride and the practically negligible loss of HF from the protonated fluorotoluenes provides strong evidence that ring expansion has not occurred in the MH^+ species prior to fragmentation. It is surprising that the loss of H_2 from the protonated fluorotoluenes and from toluene (6) is of only minor importance. The overall reaction

$$[4]\quad CH_5^+ + C_6H_5CH_3 \rightarrow C_6H_5CH_2^+ + H_2 + CH_4$$

is 38 kcal mol^{-1} exothermic[3] and the reaction with the fluorotoluenes would be expected to be similarly exothermic. The low abundance of the $[M—H]^+$ ion suggests either that only a fraction of the exothermicity of the initial proton transfer is retained in the MH^+ ion or that there is an energy barrier additional to the endothermicity for fragmentation of MH^+.

A large ion current is observed at *m/e* 107 in the methane chemical ionization spectra of the fluorotoluenes which shifts to *m/e* 111 when CD_4 is used as reagent gas, indicating incorporation of four deuterium atoms in the product ion. Similarly, in the spectrum of fluorobenzene (Fig. 1*e*) a large ion current is observed at *m/e* 93, shifting to *m/e* 97 with CD_4 as reagent gas. In the fluorobenzene system, Munson and Ridge (13) have shown, using ion cyclotron resonance techniques, that *m/e* 93 is formed by a direct reaction between CH_5^+ and C_6H_5F. The reaction can be written as

$$[5]\quad CH_5^+ + FC_6H_4R \rightarrow CH_3C_6H_4R.H^+ + HF \qquad (R = H \text{ or } CH_3)$$

where it is suggested, although certainly not proven, that the product ion corresponds to the appropriate protonated methyl-substituted benzene. (Rearrangement to tropylium type structures cannot be excluded.) Harrison *et al.* (14) have reported $\Delta H_f(C_7H_9^+) = 224$ kcal mol^{-1} and suggested that the ion may have the protonated toluene structure. Using this heat of formation we calculate that reaction 5 is 35 kcal mol^{-1} exothermic for reaction with fluorobenzene.

The occurrence of reaction 5 is of considerable interest because it indicates that the collision of CH_5^+ with these aromatic molecules does not occur with a simple, direct proton transfer but rather that a collision complex is formed which has a lifetime sufficient for relatively complex bond rearrangements to occur.

Hydrogen Chemical Ionization Mass Spectra

The CH_4 chemical ionization of the fluorotoluenes produces very little fragmentation. To induce further fragmentation we have used H_2 as reagent gas since protonation by H_3^+ is much more exothermic[4] and one might therefore anticipate formation of more highly excited MH^+ ions.

The H_2 and D_2 chemical ionization mass spectra of benzyl fluoride, the fluorotoluenes, and fluorobenzene are displayed graphically in Fig. 2. For benzyl fluoride the MH^+ intensity is extremely small (<2% of base peak), the overwhelming proportion of the ionization being observed as *m/e* 91 ($C_7H_7^+$). In the D_2 spectrum approximately 40% of the ion current moves to *m/e* 92 ($C_7H_6D^+$) indicating that the reaction does not proceed entirely by protonation at the fluorine followed by immediate HF loss (or by direct F^- abstraction) but rather that there is addition of D^+ to the molecule with one of the hydrogens originally bonded to carbon subsequently being eliminated as HF to a significant extent. It should be noted that randomization of all the H/D in $C_7H_7F.D^+$ would lead to 88% HF loss compared to the 40% observed, so that there remains a distinct preference for loss of the added proton (or for F^- abstraction). The results are in contrast to the CD_4 chemical ionization results where no shift to *m/e* 92 was

[3]Calculated using $\Delta H_f(CH_5^+) = 221$ kcal mol^{-1} (10) and $\Delta H_f(C_6H_5CH_2^+) = 213$ kcal mol^{-1} (11). Throughout this paper all thermochemical data not given are taken from ref. 12.

[4]$\Delta H_f(H_3^+) = 264$ kcal mol^{-1} (15) corresponding to p.a.(H_2) = 100 kcal mol^{-1}. $\Delta H_f(CH_5^+) = 221$ kcal mol^{-1} (10) corresponding to p.a.(CH_4) = 127 kcal mol^{-1}.

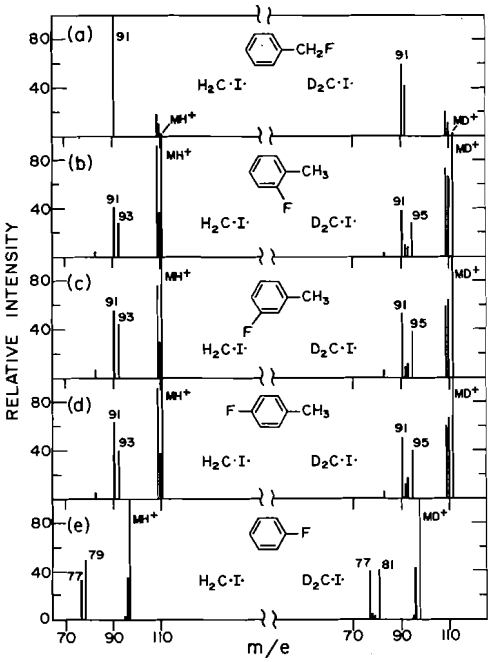

FIG. 2. H_2 and D_2 chemical ionization mass spectra of fluorine substituted toluenes and of fluorobenzene.

observed, indicating no H/D interchange in $C_7H_7F.D^+$ at lower internal energies.

The H_2 chemical ionization mass spectra of the fluorotoluenes are very similar to each other but are distinctly different from the spectrum of benzyl fluoride. As for the CH_4 spectra, the base peak is MH^+, however, much more extensive fragmentation is observed with the $[M—H]^+$ peak being 80–90% of the base peak and the $C_7H_7^+$ peak (*m/e* 91) being 50–65% of the base peak. In addition a significant ion current is observed at *m/e* 110 corresponding to the molecular ion formed by the exothermic charge transfer reaction[5]

[6] $H_3^+ + C_7H_7F \rightarrow C_7H_7F^+ + H_2 + H\cdot$

For each of the fluorotoluenes significant ion currents are observed at *m/e* 93 shifting to *m/e* 95 in the D_2 chemical ionization spectra. Similarly the H_2 chemical ionization of fluorobenzene (Fig. 2*e*) shows a product at *m/e* 79 shifting to *m/e* 81 when D_2 is used as reagent gas. The reaction occurring presumably is the fluorine-displacement reaction 7, analogous to reaction 5 with CH_5^+ as reactant

[7] $H_3^+ + FC_6H_4R \rightarrow HC_6H_4R.H^+ + HF$ (R = H or CH_3)

Assuming the *m/e* 93 product (R = CH_3) is protonated toluene (ΔH_f = 224 kcal mol^{-1}) the overall reaction is ~71 kcal mol^{-1} exothermic. The occurrence of reaction 7 shows that even with H_3^+ as reactant a long-lived complex is formed on collision with the aromatic neutral in a significant fraction of the collisions.

The observation of significant ion currents at *m/e* 91 in the chemical ionization spectra of the fluorotoluenes does not necessarily imply that ring expansion has occurred in the MH^+ ion prior to fragmentation. If this were the case one would anticipate spectra much more similar to that obtained for benzyl fluoride. In addition, any ring expansion process should involve mixing of the H/D in the MD^+ ion, yet the spectra obtained using D_2 as reagent gas show practically no incorporation of D in the fragment ion. (The low intensity peaks at *m/e* 92 and 93 in the D_2 spectra probably arise by loss of H_2 and HD from the *m/e* 95 product.) The H_2 chemical ionization spectrum of fluorobenzene shows an abundant peak at *m/e* 77 ($C_6H_5^+$) corresponding to HF loss from MH^+ and this peak also does not shift when D_2 is used as reagent gas. These results suggest either a direct F^- abstraction reaction or protonation at the fluorine followed by direct loss of HF without hydrogen interchange. The observation of the fluorine-loss peak in the fluorobenzene case provides additional evidence that the *m/e* 91 observed for the fluorotoluenes does not require ring-expansion as an explanation. Although the heat of formation of the phenyl cation is not definitely established a value ≤280 kcal mol^{-1} seems most appropriate (16). Thus the reaction

[8] $H_3^+ + C_6H_5F \rightarrow C_6H_5^+ + HF + H_2$

is calculated to be ≥22 kcal mol^{-1} exothermic and the analogous reaction with the fluorotoluenes to produce tolyl ions should also be exothermic. On the other hand the similar reaction with CH_5^+ as reactant is endothermic.

The $[M—H]^+$ peaks in the H_2 chemical ionization of the fluorotoluenes all are approximately the same intensity relative to the MH^+ base peak. The slightly lower intensity for the *meta* isomer is what would be predicted on the

[5]The recombination energy of H_3^+ is ~9.1 eV (*i.e.* the exothermicity of the reaction $H_3^+ + e \rightarrow H_2 + H$) while the ionization potentials of the fluorotoluenes are in the range 8.8–8.9 eV (12).

Can. J. Chem. Downloaded from www.nrcresearchpress.com by 210.87.254.5 on 09/05/12
For personal use only.

basis of the stability of the respective substituted benzyl ions (7, 17), however, the differences are too small to permit a reliable distinction between the isomers. If the rates of the fragmentation reaction

$$[9] \qquad MH^+ \rightarrow [M—H]^+ + H_2$$

for the various fluorotoluene isomers were controlled by the relative activation energies one would anticipate much greater differences in the $[M—H]^+/MH^+$ ratio since the *p*-fluorobenzyl cation is ~ 10 kcal mol^{-1} more stable than the *m*-fluorobenzyl cation (7, 17). However, the initial protonation reaction by H_3^+ is strongly exothermic and it is more likely that the relative rates are controlled more by the frequency factors than the activation energies at the high internal energies; consequently only slight differences in the extent of fragmentation would be expected.

In the D_2 chemical ionization spectra a significant fraction of the $[M—H]^+$ intensity moves from *m/e* 109 to *m/e* 110 (where it overlaps with $M.^+$), indicating incorporation of one deuterium in the fragment ion. This shows that at least part of the $[M—H]^+$ ion does arise by protonation followed by H_2 elimination, rather than by direct H^- abstraction. In addition it is obvious that considerable H/D interchange occurs prior to fragmentation. These results are in contrast to the results obtained by Field (6) for formation of $[M—H]^+$ in the methane chemical ionization of toluene where only a specific (hydride) abstraction of a methyl hydrogen occurred. In a related study of the reaction of H_3^+ (and D_3^+) with labelled toluenes we have found that both ring and methyl hydrogens are lost in forming the $[M—H]^+$ ion and that considerable hydrogen interchange occurs in MH^+ prior to fragmentation. These results will be reported in detail in a forthcoming publication.

Experimental

The chemical ionization mass spectra were determined using a Dupont 21-490 mass spectrometer equipped with a high-pressure chemical ionization source. The source temperature was ~ 180 °C while the samples were introduced from a heated inlet at ~ 150 °C. The reagent gas pressure cannot be measured accurately with this instrument; however, approximate measurements using a calibrated thermocouple gauge inserted in place of the solid probe indicated reagent gas pressures in the range 0.3 to 0.5 mm. Under these conditions electron impact ionization of the sample was negligible. The spectra presented in the figures are the average of several determinations under the same conditions. Spectra using the nondeuterated and deuterated reagents were obtained under the same operating conditions.

The fluorobenzene, benzyl fluoride, and the fluorotoluenes were commercially available samples and showed no impurities in their mass spectra. Reagent grade CH_4 and H_2 were obtained from Matheson and Company and were used without further purification, as was the CD_4 which was obtained from Merck, Sharp, and Dohme. The D_2 (Matheson and Co.) was passed through a heated palladium thimble prior to use to remove a low-level impurity of mass 28 (probably N_2).

The authors are indebted to the National Research Council of Canada for continued financial support and to Drs. B. Munson and D. Ridge for communication of results prior to publication.

1. J. T. Bursey, M. M. Bursey, and D. G. I. Kingston. Chem. Rev. **73**, 191 (1973).
2. H. M. Grubb and S. Meyerson. *In* Mass spectrometry of organic ions. *Edited by* F. W. McLafferty. Academic Press, New York. 1963. Chapt. 10.
3. F. Meyer and A. G. Harrison. J. Am. Chem. Soc. **86**, 4757 (1964).
4. J. Winkler and F. W. McLafferty. J. Am. Chem. Soc. **95**, 7533 (1973); J. Am. Chem. Soc. **96**, 5182 (1974).
5. J. Shen, R. C. Dunbar, and G. A. Olah. J. Am. Chem. Soc. **96**, 6227 (1974).
6. F. H. Field. J. Am. Chem. Soc. **89**, 5328 (1967).
7. J. M. S. Tait, T. W. Shannon, and A. G. Harrison. J. Am. Chem. Soc. **84**, 4 (1962).
8. S. Safe, W. D. Jamieson, and D. J. Embree. Can. J. Chem. **52**, 867 (1974).
9. (*a*) A. N. H. Yeo and D. H. Williams. J. Am. Chem. Soc. **93**, 395 (1971); (*b*) C. W. Tsang and A. G. Harrison. Org. Mass Spectrom. **7**, 1377 (1973).
10. W. A. Chupka and J. A. Berkowitz. J. Chem. Phys. **54**, 4256 (1971).
11. F. P. Lossing. Can. J. Chem. **49**, 357 (1971).
12. Ionization potentials, appearance potentials, and heats of formation of gaseous positive ions. NSRDS-NBS 26, Washington, D.C. 1969.
13. B. Munson and D. Ridge. Private communication.
14. A. G. Harrison, P. Haynes, S. McLean, and F. Meyer. J. Am. Chem. Soc. **87**, 5099 (1965).
15. M. E. Schwartz and L. J. Schaad. J. Chem. Phys. **47**, 5325 (1970).
16. A. G. Harrison. *In* Topics in organic mass spectrometry. *Edited by* A. L. Burlingame. Wiley–Interscience, New York. 1970. Chapt. 3.
17. A. G. Harrison, P. Kebarle, and F. P. Lossing. J. Am. Chem. Soc. **83**, 777 (1961).

Can. J. Chem. Downloaded from www.nrcresearchpress.com by 210.87.254.5 on 09/05/12
For personal use only.

Isotope Effect Studies on Elimination Reactions. X.[1] The Nature of the Transition State for the $E_{CO}2$ Reaction of *Para*-substituted Benzyl Nitrates with Base in 90% by Volume Ethanol–Water

PETER JAMES SMITH[2] AND CAROL AUDREY POLLOCK

Department of Chemistry, Bishop's University, Lennoxville, Quebec J0I 1Z0

AND

ARTHUR NEWCOMBE BOURNS

Department of Chemistry, McMaster University, Hamilton, Ontario L8S 4L8

Received October 28, 1974

PETER JAMES SMITH, CAROL AUDREY POLLOCK, and ARTHUR NEWCOMBE BOURNS. Can. J. Chem. **53**, 1319 (1975).

Kinetic isotope effects have been determined for the $E_{CO}2$ reaction of *para*-substituted benzyl nitrates with ethoxide in 90 vol.% ethanol–water at 20°. The nitrogen isotope effect, $(k^{14}/k^{15} - 1)100$ decreased with increasing electron-withdrawing ability of the *para*-substituent; *i.e.* 2.26, 1.95, 1.60, and 0.84 for *p*-CH_3, *p*-H, *p*-CF_3, and *p*-NO_2, respectively. Furthermore, the primary hydrogen–deuterium isotope effects increased also for electron-withdrawing substituents; *i.e.* k^H/k^D = 5.78, 6.06, 6.40, 6.67, and 7.05 for *p*-CH_3, *p*-H, *p*-Br, *p*-CF_3, and *p*-NO_2, respectively. The results are discussed in terms of a recent theoretical treatment dealing with the effect of substituents on the nature of the transition state for a concerted E2 process. The conclusion is reached that any structural change which causes one bond (carbon–hydrogen) to be weakened more at the transition state will have a corresponding effect on the other bond (oxygen–nitrogen).

PETER JAMES SMITH, CAROL AUDREY POLLOCK et ARTHUR NEWCOMBE BOURNS. Can. J. Chem. **53**, 1319 (1975).

On a déterminé les effets isotopiques cinétiques pour la réaction $E_{CO}2$ de nitrates de benzyles substitués en position *para* avec de l'éthylate dans des solutions contenant 90 vol.% éthanol–eau à 20°. L'effet isotopique de l'azote, $(k^{14}/k^{15} - 1)100$ diminue avec l'augmentation du pouvoir électro-affinitaire du substituant *para* à savoir des valeurs de 2.26, 1.95, 1.60 et 0.84 respectivement pour *p*-CH_3, *p*-H, *p*-CF_3 et *p*-NO_2. De plus les effets isotopiques primaires du deuterium par rapport à l'hydrogène augmentent aussi avec les pouvoirs électro-affinitaires des substituants à savoir k^H/k^D = 5.78, 6.06, 6.40, 6.67 et 7.05 respectivement pour *p*-CH_3, *p*-H, *p*-Br, *p*-CF_3 et *p*-NO_2. On discute des résultats en termes d'un traitement théorique récent qui examine l'effet des substituants sur la nature de l'état de transition pour des processus E2 concertés. On arrive à la conclusion que tout changement de structure qui provoque un plus grand affaiblissement d'un lien (carbone–hydrogène) dans l'état de transition aura un effet correspondant sur l'autre lien (oxygène–azote). [Traduit par le journal]

Introduction

An organic nitrate ester, $RCHONO_2$ (R′), can react with base B to produce a carbonyl compound and nitrite ion in a bimolecular carbonyl elimination ($E_{CO}2$), eq. 1. A competing process

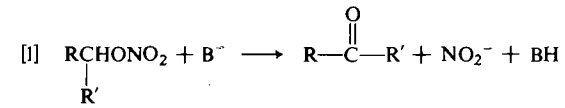

[1] $RCHONO_2 + B^- \longrightarrow R{-}C(=O){-}R' + NO_2^- + BH$

is nucleophilic displacement, eq. 2.

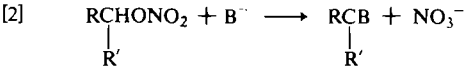

[2] $RCHONO_2 + B^- \longrightarrow RCB + NO_3^-$

The reaction of benzyl nitrate, $PhCH_2ONO_2$, with ethoxide in ethanol has been shown (2), using the deuterium exchange test and kinetic isotope effect measurements, to be a concerted one-step process with rupture of both the carbon–hydrogen and oxygen–nitrogen bonds at the transition state.

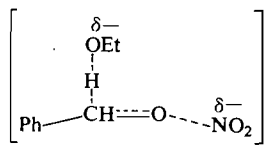

[1]For part IX see ref. 1.

[2]Author to whom correspondence should be addressed. Present address: Department of Chemistry and Chemical Engineering, University of Saskatchewan, Saskatoon, Saskatchewan S7N 0W0.

Can. J. Chem. Downloaded from www.nrcresearchpress.com by 210.87.254.40 on 09/05/12
For personal use only.

Can. J. Chem. Downloaded from www.nrcresearchpress.com by 210.87.254.40 on 09/05/12
For personal use only.

Subsequently, Pollock and Smith (3) investigated, using kinetic isotope effect measurements, the role of base and solvent in determining transition state geometry for the $E_{CO}2$ reaction of benzyl nitrate. They found that the primary hydrogen–deuterium isotope effect increased with increasing strength of the abstracting base, $k^H/k^D = 5.94$ and 6.41 at 30° for reaction with $EtO^-/EtOH$ and $t\text{-}BuO^-/t\text{-}BuOH$, respectively. The nitrogen isotope effect, $(k^{14}/k^{15} - 1)100$, decreased with increasing strength of the abstracting base; 2.07, 1.82, and 1.54% for reaction with HO^-/40 vol.% EtOH–H_2O, $EtO^-/EtOH$ and $t\text{-}BuO^-/t\text{-}BuOH$, respectively. The conclusion was reached that an increase in the strength of the abstracting base leads to a more reactant-like transition state with decreased rupture of both the carbon–hydrogen and oxygen–nitrogen bonds.

The effect of solvent on the nature of the transition state for the $E_{CO}2$ process was examined by determining rates and nitrogen isotope effects for reaction in various ethanol–water and ethanol – dimethyl sulfoxide mixtures. The nitrogen effect was found to remain essentially constant in solvent mixtures ranging from 65 vol.% EtOH–H_2O on the one hand to 80 vol.% EtOH–DMSO on the other hand where the rate constants differed by a factor of 100-fold. It was concluded that solvent plays only a minor role in determining transition state structure for the concerted elimination reaction of a neutral substrate with base.

An earlier study (1) on the E2 reaction of 2-arylethyltrimethylammonium ions with ethoxide in ethanol showed that electron-withdrawing substituents had the effect of producing a more reactant-like transition state, decreased C—H and $C—N^+$ bond rupture. Accordingly, in the present investigation, both primary hydrogen–deuterium and nitrogen isotope effects have been measured for the reaction of a series of *para*-substituted benzyl nitrates with base in 90 vol.% ethanol–water to examine whether substituents have a similar effect on transition state geometry for the reaction of a neutral substrate, benzyl nitrate with base.

In addition, it was of interest to determine whether Westheimer's curve (plot of k^H/k^D *vs.* the degree of proton transfer to base at the transition state) could be realized for the reaction of the *para*-substituted benzyl nitrates with base by varying the *para*-substituent. The primary hydrogen-deuterium effect of 5.94 (3) observed for the $E_{CO}2$ reaction of the unsubstituted compound is approaching the theoretical maximum[3] of 7 and this suggests that there might be some curvature in the plot of $\log k^H/k^D$ *vs.* $\log k$. The results of the present investigation will be discussed in the light of the theoretical treatment of Thornton (4) on the effect of substituents on the transition state geometry of an E2 reaction.

Results

Hydrogen–Deuterium Isotope Effects

The overall rate constants ($k_{E_{CO}2} + k_{S_N2}$) for reaction of a series of *para*-substituted benzyl nitrates and their α-dideuterated analogs with ethoxide in 90 vol.% ethanol–water are shown in Table 1.

When most of the compounds were reacted with ethoxide in 90 vol.% ethanol–water the carbonyl elimination reaction producing nitrite ion was in competition with an S_N2 process giving nitrate ion; *i.e.* percentage $E_{CO}2 < 100$, Table 1. It is possible, however, using methods described previously (2) to determine the deuterium isotope effect associated with the elimination process. The total rate was followed by acid–base titration and the rate constant for the carbonyl elimination reaction, $k_{E_{CO}2}$, was evaluated from the relative yields of nitrite and nitrate ions determined by the selective reduction of these ions to ammonia. In all cases, the ratio of nitrite to nitrate remained constant during the course of a kinetic run. The primary hydrogen–deuterium effects calculated from the rate data are also given in Table 1.

Hammett plots of $\log k/k_0$ *vs.* σ were obtained for the undeuterated and deuterated series. The slope, ρ, for the former is $+3.89 \pm 0.17$ while the slope of the plot for the α-dideuterated series is $+3.81 \pm 0.16$.

Nitrogen Isotope Effect Results

The results of the nitrogen isotope effect study on the $E_{CO}2$ reaction of *para*-substituted benzyl nitrates with sodium ethoxide in 90 vol.% EtOH–H_2O are shown in Table 2.

The nitrogen isotope effect for the carbonyl elimination reaction of each *para*-substituted benzyl nitrate was obtained by comparing the $^{14}N/^{15}N$ ratio of each substrate of natural

[3]This is assuming that only a stretching vibration is lost at the transition state.

TABLE 1. Rate constants and β-hydrogen–deuterium isotope effects in the $E_{CO}2$ reaction of $X\text{-}C_6H_4CY_2ONO_2$ ions with base[a] in 90 vol.% $EtOH\text{–}H_2O$

X	Y	Temperature ±0.03°	$10^5\ k_{total}$[b]	$\%E_{CO}2$	$10^5\ k_{E_{CO}2}$[b]	k^H/k^D $E_{CO}2$
CH_3	H	20	4.24	51	2.16	5.78±0.23[c]
	D		2.49	15	0.374	
H	H	20	8.80	86	7.57	6.06±0.24
	D		2.60	48	1.25	
Br	H	20	78.0	96	74.9	6.40±0.26
	D		13.4	87	11.7	
CF_3	H	20	1240	100	1240	6.67±0.27
	D		207	90	186	
NO_2	H	0	32300	100	32300	8.12±0.20
	D		3980	100	3980	

[a]The base solution was prepared by diluting sodium ethoxide in ethanol with water so that the final solution was 90 vol.% $EtOH\text{–}H_2O$.
[b]Rate constants are in $l\ mol^{-1}\ s^{-1}$.
[c]Estimated maximum uncertainty based on the reproducibility of nitrite ion yields and rate constant values.

TABLE 2. Nitrogen isotope effects for the $E_{CO}2$ reaction of *para*-substituted benzyl nitrates with base[a] in 90 vol.% $EtOH\text{–}H_2O$

Para-substituent	Temperature (deg)	Extent of reaction[b]	k^{14}/k^{15}[c]
CH_3	20	12.0	1.0227
		12.1	1.0214
		17.1	1.0239
		26.0	1.0214
		33.2	1.0234
			Mean 1.0226±0.0012
H	20	13.6	1.0185
		15.4	1.0204
		26.1	1.0193
		31.1	1.0199
		35.6	1.0195
			Mean 1.0195±0.0007
CF_3	20	12.8	1.0154
		14.6	1.0155
		23.0	1.0165
		25.8	1.0168
		28.4	1.0165
		32.3	1.0156
		36.3	1.0159
			Mean 1.0160±0.0005
NO_2	0	23.4	1.0093
		23.4	1.0095
		25.2	1.0097
		39.3	1.0091
		44.7	1.0082
		56.9	1.0095
			Mean 1.0092±0.0005

[a]The base solution was prepared from sodium ethoxide in ethanol by diluting with water so that the final solution was 90 vol.% $EtOH\text{–}H_2O$.
[b]Determined from the yield of ammonia obtained from reduction of nitrite and nitrate.
[c]The limits shown are the standard deviation.

Can. J. Chem. Downloaded from www.nrcresearchpress.com by 210.87.254.40 on 09/05/12
For personal use only.

TABLE 3. Rates and isotope effects found in the $E_{CO}2$ reaction of *para*-substituted benzyl nitrates with sodium ethoxide in 90 vol.% ethanol–water at 20°

Para-substituent	$10^5 k_{E_{CO}2}$[a]	k^{14}/k^{15}[b]	k^H/k^{Dc}
CH_3	2.16	1.0226±0.0012	5.78±0.23
H	7.57	1.0195±0.0007	6.06±0.24
Br	74.9	—	6.40±0.26
CF_3	1240	1.0160±0.0005	6.67±0.27
NO_2	32 300[d]	1.0084±0.0005[e]	7.05±0.20[e]

[a]Rate constants are in l mol^{-1} s^{-1}.
[b]The limits shown are the standard deviation.
[c]Estimated maximum uncertainty based on the reproducibility of nitrite ion yields and rate constant values.
[d]At 0°.
[e]Calculated from values determined at 0° using the equation

$$\log (k^H/k^D)_{T_1} = \log (k^H/k^D)_{T_2} \cdot \frac{T_2}{T_1}.$$

This expression was derived using the assumption that the preexponential terms cancel out; *i.e.*, $A_H = A_D$ and $A_{14} = A_{15}$. The agreement between calculated and experimental results, obtained for other systems, is reasonably good if one considers the standard deviations of the experimental isotope effects.

isotopic abundance with that of nitrite ion formed in the desired reaction of the ester carried to some known extent of completion. Selective reduction of the nitrite ion to ammonia accomplished the separation of the nitrogen of this ion from that of the nitrate ion formed in the simultaneous S_N2 displacement reaction (2). The ammonia was then converted into nitrogen gas which was first purified and then analyzed mass spectrometrically. The isotopic abundance for the reactant was obtained by analysis of the nitrogen gas similarly formed from nitrite plus nitrate produced in a reaction which had been allowed to proceed to completion.

Discussion

The present investigation on the $E_{CO}2$ reaction of the *para*-substituted benzyl nitrates was carried out at 20° with ethoxide in 90 vol.% ethanol–water. It was determined that at this temperature the rate and nitrogen isotope effect measurements could be conveniently performed for all the substrates except for the *p*-NO_2 compound, which was studied at 0°. A more aqueous solvent would lead to a decrease in the $E_{CO}2$ reaction with the solvolysis reaction becoming increasingly important making accurate determinations of both the deuterium and nitrogen isotope effects more difficult.

The kinetically significant abstracting base in solution when ethoxide in ethanol is diluted with water to give a final solution of 90 vol.% ethanol–water is probably ethoxide ion even though it has been shown (7) that the % base present as hydroxide at 25° in 90 vol.% ethanol–water is approximately 35. This view is supported by a nitrogen isotope effect study (3) on the reaction of benzyl nitrate with base in various ethanol–water mixtures where it was found that the isotope effect remained essentially constant for solvent compositions ranging from 100% EtOH to 65 vol.% EtOH–H_2O indicating that the abstracting base remains constant in this solvent composition range. It was found (3) that the nitrogen effect increased for 50 and 40 vol.% EtOH–H_2O mixtures which suggests a weaker abstracting base (4), hydroxide ion, in accordance with our earlier conclusions (1, 3).

The rate constants as well as the primary deuterium and nitrogen isotope effect results for the $E_{CO}2$ reaction of the various substituted benzyl nitrates at 20° are summarized in Table 3. The rate constants, excluding that for the *p*-NO_2 which was determined at 0°, were used to calculate the Hammett ρ value of +3.89. To our knowledge, this value is the second largest that has been determined for an E2 reaction. Only the reaction of *p*-X-phenylethyl methyl sulfoxides with *t*-BuO^-/*t*-BuOH gave a higher value, +4.4, and for this reaction it was concluded (5) that the transition state had substantial carbanion character. It is reasonable to conclude, therefore, that for the $E_{CO}2$ reaction, as well, there is considerable build-up of negative charge at the transition state.

Indeed, the Hammett ρ value of +3.89 together with a large nitrogen effect of 1.95% for reaction of the unsubstituted substrate, suggest a transition state which is carbanionic

Can. J. Chem. Downloaded from www.nrcresearchpress.com by 210.87.254.40 on 09/05/12
For personal use only.

Can. J. Chem. Downloaded from www.nrcresearchpress.com by 210.87.254.40 on 09/05/12
For personal use only.

with the proton *more than* one-half transferred to base. The only way that a large positive ρ can result in a reaction in which oxygen–nitrogen bond rupture is well advanced would be for the transfer of the proton to be well advanced as well. This conclusion receives support from the fact that the reaction of 2-phenylethyltrimethylammonium ion with ethoxide (7) has smaller values for ρ and the nitrogen effect. For this process, Steffa and Thornton (6) have established that the proton is more than one-half transferred to base at the transition state by determining the secondary effects, k^{OD^-}/k^{OH^-}.

The results of the nitrogen isotope effect study on the $E_{CO}2$ reaction of the *para*-substituted benzyl nitrates, Table 3, show a relationship between the magnitude of the effect and the electron-withdrawing or -donating ability of the *para*-substituent. It is observed that the isotope effect decreases as the *para*-substituent becomes more electron-withdrawing, *i.e.* $(k^{14}/k^{15} - 1)100$ is 2.26 and 0.84 for the *p*-CH_3 and *p*-NO_2 compounds, respectively. In fact, an approximate linear relationship is found from a plot of log $k_{E_{CO}2}$ *vs.* log $(k^{14}/k^{15} - 100)$, Fig. 1, with the smallest nitrogen effect observed for the fastest reaction where the *para*-substituent is the most strongly electron withdrawing.

It is noteworthy that the nitrogen isotope effect obtained for the reaction of the *p*-CH_3 substrate, $(k^{14}/k^{15} - 1)100 = 2.26$, is the largest value obtained for a reaction in solution. In fact, it is approximately 60% of the maximum value of 3.8% calculated on the assumption of complete oxygen–nitrogen bond rupture in the transition state (2).

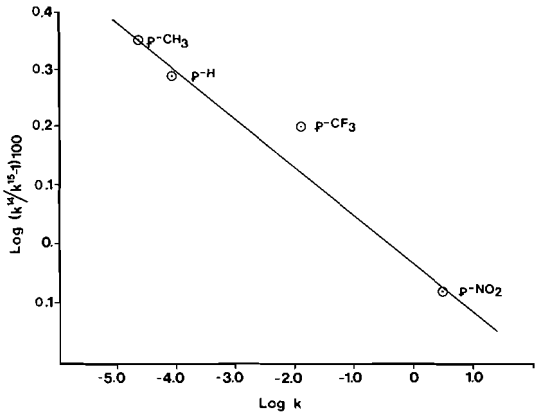

FIG. 1. Plot of log $(k^{14}/k^{15} - 1)100$ *vs.* log $k_{E_{CO}2}$ for the reaction of *para*-substituted benzyl nitrates in 90 vol.% ethanol–water at 20°.

Since the magnitude of the nitrogen effect is considered to depend on the extent to which the composite force constant of the oxygen–nitrogen bond is decreased in going to the transition state, the effect will increase regularly in a reaction series with the extent of bond weakening at the transition state. Consequently, the experimental findings indicate that the extent of O—N bond rupture is decreased in an approximate linear fashion at the transition state as the *para*-substituent becomes more electron withdrawing. Indeed, the sensitivity to substituents and the linear relationship of the nitrogen isotope effect for the elimination process with the free energy of activation makes this isotope effect potentially very useful as a monitor of changes in transition state structure. This is particularly important since it has been noted (8, 9) that the primary hydrogen–deuterium isotope effect is, in some cases, a poor indicator with respect to the degree of carbon–hydrogen bond weakening in the transition state.

A trend in the magnitude of the primary hydrogen–deuterium isotope effects with *para*-substituent is also noted, Table 3. This isotope effect increases with increased electron-withdrawing ability of the *para*-substituent, *i.e.* 5.78 and 7.05 for *p*-CH_3 and *p*-NO_2, respectively. In fact, there appears to be a relationship between the effect of substituents on the reaction rate and their effect on the magnitude of the hydrogen–deuterium isotope effect. This is seen from a plot of log k^H/k^D *vs.* log $k_{E_{CO}2}$, Fig. 2.

An interpretation of the magnitude of the primary hydrogen–deuterium effects, Table 3, in terms of the extent of C—H bond rupture requires a prior knowledge of the nature of the transition state with respect to the degree of proton transfer to base; *i.e.*, whether the proton is more than or less than one-half transferred. As was noted earlier, it is reasonable to conclude that both the large Hammett ρ and nitrogen effect are indicative of a transition state which has considerable carbon–hydrogen bond weakening. The hydrogen–deuterium results, therefore, can be interpreted in the light of Westheimer's treatment (10) with the reasonable assumption that the proton is more than one-half transferred to base at the transition state. Consequently, one can conclude that the reaction of the *p*-NO_2 compound, with the

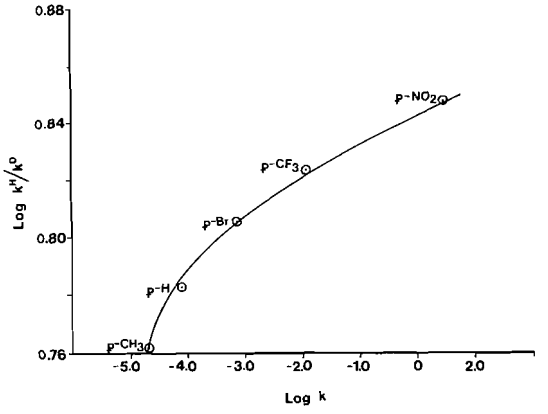

FIG. 2. Plot of log k^H/k^D *vs.* log k_{Eco2} for the reaction of *para*-substituted benzyl nitrates in 90 vol.% ethanol–water at 20°.

largest hydrogen–deuterium isotope effect, has associated with it less C—H bond rupture at the transition state than, for example, the reaction of the *p*-CH_3 compound. It should be noted that the plot of log k_{Eco2} *vs.* log k^H/k^D is similar to Westheimer's curve (plot of k^H/k^D *vs.* the degree of proton transfer to base at the transition state) where it is seen that the magnitude of k^H/k^D appears to be leveling off at a value of approximately 7 for the strong electron-withdrawing substituents, $k^H/k^D = 7.05$ for the *p*-NO_2 compound.

The conclusion that the extent of both C—H and O—N bond rupture at the transition state decreases as the *para*-substituent is made more electron withdrawing is in accord with Hammond's postulate (11) which predicts that the more facile a reaction in a reaction series the more reactant-like its transition state. Also, Thornton's theory (4), dealing with the effects of structural changes in the reactant on the nature of the transition state is consistent with the experimental results. According to this theory the geometrical change for an elimination reaction will be determined largely by the substituent effect on the parallel motion along the reaction coordinate where the relative lengths of the arrows below

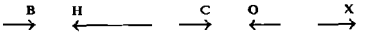

represent the relative extent to which each atom has moved when the reacting system has reached the transition state. Thornton predicts, from this reaction-coordinate representation of the transition state, that electron-withdrawing (donating) substituents at carbon should have the same effect on the C—H and O—X bond lengths at the transition state. Thornton showed that the more difficult it is for two atoms to move apart, the greater will be the extent to which they need to separate before arriving at the state of maximum energy which separates reactants and products. He then goes on to point out that an increase in electron withdrawal at carbon should make it easier to remove the proton and therefore, should result in a decrease in the extent of proton transfer to base. This, in turn, will result in shortening of the O—X bond at the transition state since the reaction coordinate motion which results in the separation of H from C also involves a separation of X from O.

It follows from the conclusion that a decrease in C—H bond rupture is accompanied by a decrease in O—N bond rupture that the carbanion character of a transition state is dependent on the *relative* change of each of these bond lengths for a transition state where there is coupling of the motion of the bonds as illustrated by Thornton's representation of the E2 transition state. Thornton (4) considered this situation and suggested that, by making H move more relative to O, and C move more relative to X, the transition state will assume an increasing carbanionic character, that is, will become more Elcb-like, the further its position along the reaction coordinate.

The plot of log k^H/k^D *vs.* log k_{Eco2}, Fig. 2, appears to resemble one-half of Westheimer's curve. It is seen that the magnitude of the hydrogen–deuterium effect becomes less sensitive to changes in the *para*-substituent as the substituent is made more strongly electron withdrawing; *i.e.* for *p*-CF_3 and *p*-NO_2. As a consequence, for the region where k^H/k^D is near the maximum, the magnitude of the isotope effect will not be a good measure of the degree of carbon–hydrogen bond rupture. For this region, nitrogen isotope effects might provide a better measure of changes in transition state geometry.

Experimental

Materials

Nitrate Esters

All the nitrate esters and their α-dideuterated analogs were prepared from the reaction of their respective benzyl halides with silver nitrate in acetonitrile using

Can. J. Chem. Downloaded from www.nrcresearchpress.com by 210.87.254.40 on 09/05/12
For personal use only.

Can. J. Chem. Downloaded from www.nrcresearchpress.com by 210.87.254.40 on 09/05/12
For personal use only.

the procedure described by Buncel and Bourns (2). All of the α-d_2 compounds were shown by n.m.r. to be at least 99% deuterated.

Benzyl nitrate. Benzyl chloride was treated with silver nitrate to give benzyl nitrate (60% yield), b.p. 62.0–62.5°/1 mm (lit. b.p. (2) 45°/0.5 mm).

p-Methylbenzyl nitrate. *p*-Methylbenzyl bromide was treated with silver nitrate to give *p*-methylbenzyl nitrate (42% yield); b.p. 72.0–73.5°/1 mm (lit. (12) 78°/0.6 mm).

p-Bromobenzyl nitrate. *p*-Bromobenzyl nitrate was prepared from the reaction of silver nitrate with *p*-bromobenzyl bromide (74% yield); b.p. 102–103°/1 mm (lit. (12) m.p. 17°).

p-Trifluoromethylbenzyl nitrate. *p*-Trifluoromethylbenzyl bromide was treated with silver nitrate to give *p*-trifluoromethylbenzyl nitrate (57% yield); b.p. 83.5–84.0°/2.5 mm; (lit. (13) 56°/0.3 mm).

p-Nitrobenzyl nitrate. *p*-Nitrobenzyl nitrate was prepared from *p*-nitrobenzyl chloride and silver nitrate (50% yield); m.p. 67.0–68.0° (lit. (12) 68.2°).

Absolute Ethyl Alcohol

This solvent was dried by the method of Lund and Bjerrum (14) and stored under anhydrous conditions.

Sodium Ethoxide

Sodium ethoxide was prepared by the action of sodium with anhydrous ethanol under strictly anhydrous conditions in a nitrogen atmosphere. The base solution was prepared by diluting the ethoxide solution with water to give the desired solvent by percentage volume to volume. The water used in the dilutions was CO_2 free.

Kinetic Measurements

The rate constants for the overall reactions as well as the rate constants for elimination were determined as described by Buncel and Bourns (2).

Nitrogen Isotope Effects

Complete Reaction and Collection of Ammonia

A sample of benzyl nitrate was added to a sodium ethoxide solution and the reaction was allowed to proceed to completion. A 5 ml aliquot of the reaction mixture was extracted with ether and the aqueous layer was added to a Kjeldahl distillation where the nitrite and nitrate were reduced by the procedure described by Buncel (2) and the ammonia was distilled into the same flask containing excess sulfuric acid. The acid was back-titrated with standard alkali, using bromocresol green as indicator, followed by the immediate addition of 3 ml of 0.01 N H_2SO_4 to prevent loss of ammonia. The titration gave the total number of moles of product formed which was usually greater than 99% of the number of moles of reactant.

Partial Reaction

The concentration of benzyl nitrate was such that when the reaction had proceeded to the desired extent of reaction, the nitrite produced would yield a volume of nitrogen of approximately 3 ml at standard conditions. The substrate was weighed into a reaction flask which was placed in a constant temperature bath and allowed to equilibrate. Similarly, the base solution of desired concentration was placed in the constant temperature bath. After approximately 30 min, the reactants were mixed and the reaction was allowed to proceed for a predetermined time, as calculated from the kinetic data. The reaction flask was then removed from the bath and its contents emptied into a separatory funnel containing ice, water, and diethyl ether. The aqueous layer was extracted four times with ether. The combined ether extracts were then washed four times with water and these washings were added to the aqueous layer which was then concentrated to a small volume, 25 ml, on a rotary evaporator.

The concentrated solution was then added to a Kjeldahl distillation flask and the nitrite ion converted into ammonia which was distilled into excess standard sulfuric acid and back-titrated as described for the preparation of the complete samples. The resulting ammonium sulfate solution was concentrated to 3 ml in preparation for its conversion to ammonia.

In all of the partial reactions where the nitrite ion was reduced to ammonia in preparation for its conversion to nitrogen gas and mass spectrometric analysis, the amount of nitrite ion was determined by the procedure described above, so that the ratio $[NO_2^-]/([NO_2^-] + [NO_3^-])$ could be used in the evaluation of nitrogen isotope effect for the $E_{CO}2$ process. The ammonium sulfate solutions were converted to nitrogen by the procedure described by Buncel and Bourns (2).

For the reaction of the *p*-nitrobenzyl nitrate at 0°, the usual method of quenching was unsatisfactory due to the fast rate of reaction. In this case, the desired extent of reaction was achieved by adding the appropriate amount of base, corresponding to the extent of reaction required, and allowing the reaction to proceed for 30 half-lives. In these cases, the concentration of the reactants was sufficiently low so that no more than 1% reaction occurred during the mixing of the reacting solutions.

The kinetic isotope effect was calculated by using the expression suggested by Baliga and Bourns (15),

$$\frac{k^{14}}{k^{15}} = \frac{\ln 1 - \dfrac{f'(1-p)}{1-f'p}}{\ln 1 - \dfrac{rf'(1-p)}{1-f'p}}$$

where f' is the mol fraction of the ester which has undergone reaction, p is the fraction of the total reaction which is substitution and r is $(^{14}N/^{15}N)_{reactant}/(^{14}N/^{15}N)_{NO_2^-}$. This is a modification of an expression derived by Stevens and Attree (16), and takes into account the fact that the reactant is being consumed by reactions other than those where the isotope effect is being measured.

This work was supported by the National Research Council of Canada.

1. P. J. Smith and A. N. Bourns. Can. J. Chem. **52**, 749 (1974).
2. E. Buncel and A. N. Bourns. Can. J. Chem. **38**, 2457 (1960).
3. C. A. Pollock and P. J. Smith. Can. J. Chem. **49**, 3856 (1971).
4. E. R. Thornton. J. Am. Chem. Soc. **89**, 2915 (1967).

5. R. BAKER and M. J. SPILLETT. J. Chem. Soc. B, 481 (1969).
6. L. STEFFA and E. R. THORNTON. J. Am. Chem. Soc. **89**, 4469 (1969).
7. B. D. ENGLAND and R. E. BURNS. Tetrahedron Lett. **24**, 1 (1960).
8. P. J. SMITH and L. M. NOBLE. Can. J. Chem. **53**, 263 (1975).
9. F. G. BORDWELL and WILLIAM J. BOYLE, JR. J. Am. Chem. Soc. **93**, 512 (1971).
10. F. H. WESTHEIMER. Chem. Rev. **61**, 265 (1961).
11. G. S. HAMMOND. J. Am. Chem. Soc. **77**, 334 (1955).
12. J. W. BAKER and J. G. HEGGS. J. Chem. Soc. 616 (1955).
13. K. M. KOSHY and R. E. ROBERTSON. Can. J. Chem. **52**, 2485 (1974).
14. H. LUND and J. BJERRUM. Ber. **64B**, 210 (1931).
15. B. T. BALIGA and A. N. BOURNS. Can. J. Chem. **44**, 363 (1966).
16. W. H. STEVENS and R. W. ATTREE. Can. J. Res. B, **27**, 807 (1949).

Can. J. Chem. Downloaded from www.nrcresearchpress.com by 210.87.254.40 on 09/05/12
For personal use only.

Synthesis and Fungicidal Activity of *N,S*-Substituted α-Thio-β-aminocrotonanilides

JAMES BENJAMIN PIERCE, ROBERT JAMES FANNING, AND ROBERT ALLAN DAVIS

Uniroyal Ltd. Research Laboratories, Guelph, Ontario and Uniroyal Chemical, Division of Uniroyal Inc., Naugatuck, Connecticut

Received November 5, 1974

JAMES BENJAMIN PIERCE, ROBERT JAMES FANNING, and ROBERT ALLAN DAVIS. Can. J. Chem. **53**, 1327 (1975).

A number of *N,S*-substituted α-thio-β-aminocrotonanilides have been synthesized. Their fungicidal activity on a number of organisms has been studied and in general it has been found that it is inferior to that of the 1,4-oxathiins to which these compounds bear some structural similarities.

JAMES BENJAMIN PIERCE, ROBERT JAMES FANNING et ROBERT ALLAN DAVIS. Can. J. Chem. **53**, 1327 (1975).

On a synthétisé un certain nombre d'α-thio β-aminocrotonanilides substitués sur l'azote et le soufre. On a étudié leur activité fungicide sur un certain nombre d'organismes et on a trouvé qu'en général ces composés sont moins actifs que les oxathiinnes-1,4 avec lesquels ils sont reliés par leur structure. [Traduit par le journal]

The discovery that certain 1,4-oxathiins and more particularly 5,6-dihydro-2-methyl-1,4-oxathiin-3-carboxanilide (Vitavax®) possess systemic fungicidal activity (1) has led us to study this and other closely related systems with the expectation that they too might exhibit biological activity (2). Among the compounds that we have synthesized and tested are the *N,S*-substituted α-thio-β-aminocrotonanilides (**I**). These compounds are derivatives of acetoacetanilide α-thioethers (**II**), a group which includes the intermediate compounds often used to produce the systemic 1,4-oxathiins (1).

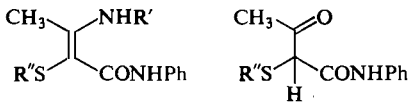

I **II**

After this work had begun a report by Mattsson and Bertilsson (3) appeared which described the synthesis and fungicidal properties of some compounds of type **I** and in particular 2-(2-hydroxyethylthio)-3-pentylamino crotonanilide which can be made by treating Vitavax with pentylamine. We wish to record here our syntheses of compounds of type **I** and our findings about their biological activities.

We have synthesized the compounds **I** by one of two routes as shown in Scheme 1. The choice of route depended largely upon the nature of the amine as it was found that in some cases the intermediate **II** underwent undesired side reactions. Thus treatment of α-(4-chlorophenylthio)acetoacetanilide (**II**, R″ = 4-chlorophenyl) with aqueous methylamine gave the deacetylated product α-(4-chlorophenylthio)acetanilide (eq. 1). The desired product **I** (R″ = *p*-chlorophenyl; R′ = CH_3) could be prepared, however, using **III** (R′ = CH_3) (4) and *p*-chlorothiophenol. Deacetylations such as that shown in equation (1) have previously been shown to occur when α-cyano (5), α,α-dichloro (6), and other α-sulfur substituted (2) acetoacetanilides are treated with base.

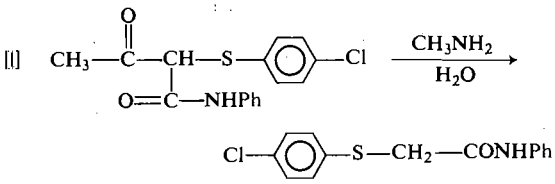

While deacetylation reactions such as the above are not too surprising, in one case of attempting to convert **II** to **I** we did discover a rather unique reaction. Thus treatment of **II** (R″ = 2-benzothiazolyl) with 40% aqueous methylamine led not to the expected **I** (R′ = CH_3; R″ = 2-benzothiazoyl) but to 2-anilinobenzothiazole in high yield (eq. 2). The product was identified by comparison of its melting point and i.r. spectrum with those of authentic ma-

Can. J. Chem. Downloaded from www.nrcresearchpress.com by 210.87.254.5 on 09/05/12
For personal use only.

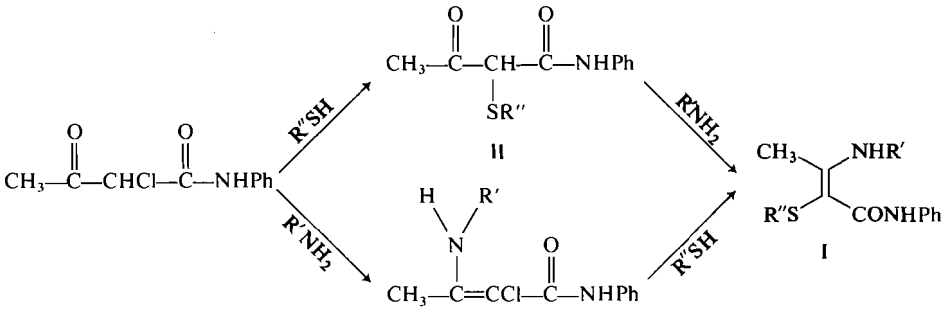

SCHEME 1

[2] 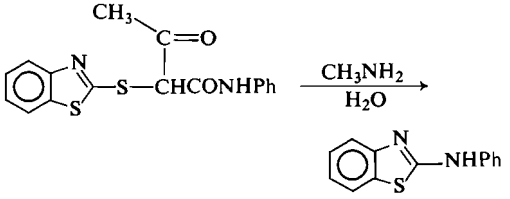

terial made by the method of Hofmann (7). At present we have no evidence concerning the mechanism of this reaction but it is hoped to study it further in the near future.

In this connection it should be mentioned that whereas the reaction of mercaptans with α-chloroacetoacetanilide in general gives excellent yields of the compounds **II**, reaction with hydrogen sulfide results predominantly in production of acetoacetanilide and sulfur (eq. 3).

[3] 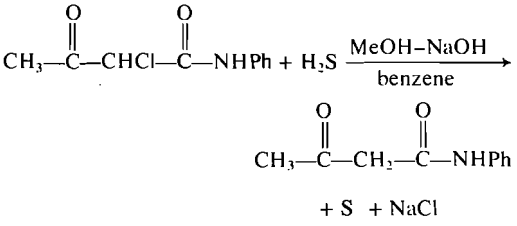

Thus repetition of the experiment of Mattsson and Bertilsson (3) in which 2-mercaptoacetoacetanilide (**II**, R″ = H) is claimed, in our hands, gave only a 78% yield of acetoacetanilide. The product, m.p. 78–84 °C, gave an i.r. spectrum identical in every way to that of authentic material. The above reaction may well proceed via the expected 2-mercaptoacetoacetanilide which then eliminates sulfur by further reaction with sodium hydrogen sulfide or sodium hydroxide (eq. 4).

In Tables 1 and 2 we have listed the compounds **I** that have been prepared for this study. Table 1 gives those prepared via intermediates

[4] 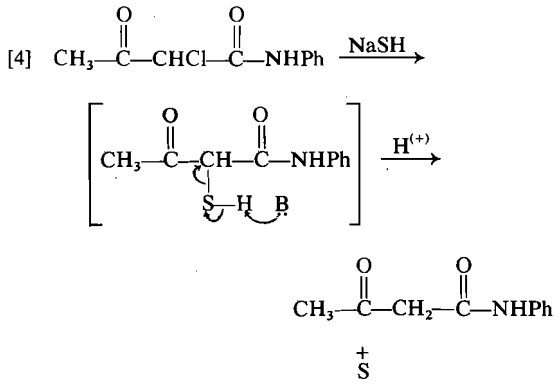

II (Scheme 1) and Table 2 those prepared via intermediates **III** (Scheme 1). The melting points, analyses, and yields obtained in going from **II** or **III** to **I** are also recorded.

We have found the fungicidal activity of these compounds to be much inferior to that of oxathiins such as Vitavax. The activity of the compounds α-(2-hydroxyethylthio)-β-aminocrotonanilide (**I**, R′ = H; R″ = HO—CH_2—CH_2—), α-(2-hydroxyethylthio)-β-methylaminocrotonanilide (**I**, R′ = Me; R″ = HO—CH_2—CH_2—), and α-(2-hydroxyethylthio)-β-anilinocrotonanilide (**I**, R′ = Ph; R″ = HO—CH_2—CH_2—) were of particular interest to us because of their close relationship to Vitavax and the intermediate used to produce Vitavax (1). However, in *in vitro* tests these compounds did not control *Alternaria solani*, *Fusarium oxysporum*, *Pythium* Spp., or *Rhizoctonia solani* at 500 p.p.m. This is in contrast to Vitavax which gives excellent control of most basidiomycetes such as *Rhizoctonia solani* and is also active on the other fungal species (8). In addition *in vivo* greenhouse tests on tomato early blight and powdery mildew on beans at 500 p.p.m. also showed these com-

Can. J. Chem. Downloaded from www.nrcresearchpress.com by 210.87.254.5 on 09/05/12
For personal use only.

TABLE 1. Compounds 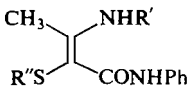 via intermediate **II** Scheme 1

R′	R″	Melting point (°C)	Yield (%)	Analysis: Calculated C	Calculated H	Calculated N	Found C	Found H	Found N
Ph	$HO—CH_2—CH_2—$	92–95	75	65.84	6.14	8.53	65.67	6.43	8.61
Ph	Ph	97–98.5	90	73.30	5.59	7.77	73.08	5.68	7.63
Ph	$Ph—CH_2—$	68–70	64	73.78	5.92	7.48	73.41	6.03	7.56
Ph		131–133	70	67.00	4.82	7.10	66.73	4.82	7.17
Ph		152–155	61	66.18	4.59	10.07	66.37	4.66	9.86
Ph	$Et_2N—C(=S)—$	108–109.5	77	63.14	6.31	10.52	62.81	6.38	10.77
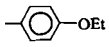	$HO—CH_2—CH_2—$	113.5–115	90	64.50	6.50	7.52	64.83	6.72	7.35
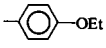	$Et_2N—C(=S)—$	119–120	78	62.29	6.59	9.48	62.02	6.72	8.86
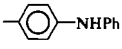	$HO—CH_2—CH_2—$	118–120	57	68.72	6.01	10.02	67.69	6.93	9.87
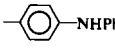	Ph	119–121	99	74.48	5.58	9.31	74.63	5.67	9.29
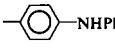	$Ph—CH_2—$	96–97.5	82	74.82	5.85	9.03	75.16	5.69	8.05
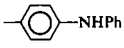	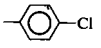	148.5–149.5	82	69.19	4.98	8.65	69.31	4.95	8.58
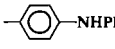		166–168.5	81	68.49	4.76	11.02	68.40	4.38	10.98
	$Et_2N—C(=S)—$	142.5–144	82	66.10	6.16	11.42	66.41	6.21	11.57

pounds to have little activity compared to the activity of Vitavax under these conditions.

Some of the compounds listed in Tables 1 and 2 did show some *in vitro* fungicidal activity. These activities are recorded in Table 3. The activities recorded for these crotonanilides all fell rapidly as the dosage of the chemical was lowered. Thus on the basis of our tests we have concluded that the fungicidal activity of these compounds is much inferior to that of oxathiins.

Experimental

The experiments described below were chosen as typical of the preparation of *N,S*-substituted α-thio-β-amino-crotonanilides (**I**) via intermediates **II** and **III**. Spectral data are given for the compounds described in these typical preparations; spectral data for the other compounds shown in Tables 1 and 2 were in full accord with their proposed structures.

Preparation via Intermediate II

α-(2-Hydroxyethylthio)-β-(4-ethoxyanilino)crotonanilide

A mixture consisting of 2-(2-hydroxyethylthio)aceto-

Can. J. Chem. Downloaded from www.nrcresearchpress.com by 210.87.254.5 on 09/05/12
For personal use only.

TABLE 2. Compounds 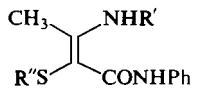 via intermediate **III** Scheme 1

R′	R″	Melting point (°C)	Yield (%)	Analysis: Calculated C	Calculated H	Calculated N	Found C	Found H	Found N
H	$HO—CH_2—CH_2—$	98–100	86	57.13	6.39	11.11	57.00	6.02	10.73
H	Ph	141–143	76	67.59	5.67	9.85	67.57	5.62	10.03
H	$EtO_2C—CH_2—CH_2—$	89–91	94	57.13	6.17	9.52	57.42	6.29	9.29
H		117–118.5	53	60.27	4.74	8.79	60.49	4.76	8.69
H		180–183	83	59.82	4.43	12.31	59.46	4.70	12.08
H	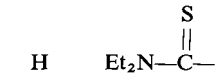	124–126	87	55.72	6.55	13.00	56.85	6.52	13.35
H	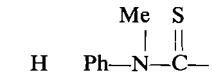	177–181	70	60.49	5.36	11.76	60.72	5.52	11.38
Me	$HO—CH_2—CH_2—$	74–77	75	58.63	6.81	10.52	59.24	6.96	10.43
Me	Ph	146–147.5	77	68.44	6.08	9.39	68.26	6.12	9.18
Me	$EtO_2C—CH_2—CH_2—$	72–75	65	58.43	6.54	9.09	58.51	6.58	9.10
Me		123.5–125.5	71	61.34	5.15	8.42	65.46	5.35	8.79
Me		150–153	78	60.84	4.82	11.83	60.91	4.85	11.61
Me		141–143	80	56.96	6.87	12.46	56.83	7.03	12.45
Me	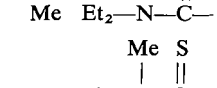	138–140	73	61.44	5.70	11.32	61.23	5.91	11.42

acetanilide (12.7 g, 0.05 mol) (2), 4-ethoxyaniline (6.9 g, 0.05 mol), 4-toluenesulfonic acid (0.1 g), and benzene (100 ml) was brought to reflux and the water formed was removed azeotropically. After 2.5 h the reaction mixture was filtered to remove a small amount of 4-ethoxyanilinium-4-toluenesulfonate salt and the benzene was then removed from the filtrate. The crude oil crystallized upon standing and was recrystallized from isopropanol to give 16.8 g or 90% of product, m.p. 113.5–115 °C; n.m.r. (DMSO-d_6): 1.30 (3H, t, J = 6 Hz), 2.33 (3H, S), 2.65 (2H, t, J = 5 Hz), 3.30–3.80 (2H, m), 3.95 (2H, q, J = 6 Hz), 5.11 (1H, t, J = 5 Hz exchange), 6.70–7.80 (5H, m), 9.78 (1H, S, exchange); i.r. (KBr): 3350, 3260, 1600, 1560, 1500, 1430, 1210 cm^{-1}.

α-(2-Benzothiazolyl)acetoacetanilide

A mixture of 2-mercaptobenzothiazole (34.4 g, 0.21 mol), 2-chloroacetoacetanilide (43.2 g, 0.21 mol), benzene (150 ml), sodium bicarbonate (17.6 g, 0.21 mol), and water (100 ml) was brought to reflux for 4 h. The phases of the hot mixture were separated and the product crystallized from the benzene phase upon cooling. Thus were obtained 51.9 g or 74% of the title compound, m.p. 123–124.5 °C.

α-(2-Benzothiazolyl)-β-(4-phenylaminoanilino)-crotonanilide

A mixture of α-(2-benzothiazolyl)acetoacetanilide (prepared as above) (17.1 g, 0.05 mol), 4-(phenylamino)-aniline (9.2 g, 0.05 mol), 4-toluenesulfonic acid (0.1 g), and benzene (125 ml) was refluxed and the water was removed azeotropically. After 2.5 h the benzene was removed and the dark residue was crystallized from ethanol giving 20.5 g or 81% of product, m.p. 166–168.5 °C; n.m.r. ($CDCl_3$): 2.32 (3H, S), 5.88 (1H, S, exchange), 6.85–7.90 (18H, m), 8.70 (1H, S, exchange), 12.77 (1H,

Can. J. Chem. Downloaded from www.nrcresearchpress.com by 210.87.254.5 on 09/05/12
For personal use only.

TABLE 3. Fungicidal activities* of some of the crotonanilides **I**

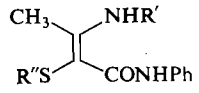

Compound **I**		Fungicidal activity (% inhibition of growth) at 500 p.p.m. on			
R′	R″	*Alternaria*	*Fusarium*	*Pythium*	*Rhizoctonia*
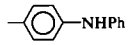	HO—CH_2—CH_2—	0	0	40	0
Ph	$(Et)_2N$—C(=S)—	25	35	0	65
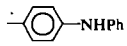	Ph	5	0	15	0
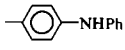	$(Et)_2N$—C(=S)—	10	5	10	25
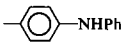	Ph—CH_2—	0	55	0	90
H		100	35	0	40
Me	EtO_2C—CH_2—CH_2—	35	20	35	0
H	Et_2N—C(=S)—	25	55	0	45
Me	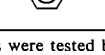	50	0	25	25

*The compounds were tested by incorporating an acetone solution of the chemical on filter paper antibiotic testing discs, placing a fungus plug in contact with the disc on a surface of an agar plate and measuring the inhibition of radial growth from the treated disc.

S, exchange); i.r. (KBr): 1555, 1600, 1435, 1425, 1300, 1210 cm^{-1}).

Preparation via Intermediate III

α-(2-Hydroxyethylthio)-β-(methylamino)crotonanilide

A solution of 2-mercaptoethanol (3.7 g, 0.045 mol), triethylamine (6.3 ml, 0.045 mol), and benzene (50 ml) was added to a solution of α-chloro-β-(methylamino)-crotonanilide (10 g, 0.045 mol) (4) in benzene (100 ml). After refluxing for 15 min a precipitate of triethylamine hydrochloride began to separate. The mixture was refluxed for 2.5 h, cooled, and extracted with water. The benzene was removed from the organic layer and the residue crystallized from isopropanol giving 9.0 g or 75% of the product, m.p. 74–77 °C; n.m.r. ($CDCl_3$): 2.30 (3H, S), 2.49 (2H, t, J = 6 Hz), 2.83 (3H, d, J = 6 Hz), 3.58 (2H, t, J = 6 Hz), 3.40 (1H, bs), 6.9–7.6 (5H, m), 9.30 (1H, S, exchange), 10.55 (1H, q, J = 6 Hz, exchange); i.r. (CCl_4): 3325, 1615, 1580, 1510, 1435, 1310, 1200 cm^{-1}.

α-(N,N-Diethyldithiocarbamoyl)-β-aminocrotonanilide

A mixture containing α-chloro-β-aminocrotonanilide (15 g, 0.071 mol), (4) the sodium salt of *N,N*-diethyldithiocarbamate trihydrate (16.1 g, 0.071 mol), and dimethylsulfoxide (50 ml) was warmed on a steam bath for 0.5 h and then poured into 500 ml of water. The precipitate was separated by filtration and recrystallized from ethanol to give 20.1 g or 87% of product, m.p. 124–126 °C; n.m.r. ($CDCl_3$): 1.28 (6H, m), 2.03 (3H, S), 3.85 (4H, m), 7.30 (5H, m), 8.08 (1H, S); i.r. ($CHCl_3$): 3490, 3375, 2975, 1625, 1580, 1500, 1430, 1310, 1270 cm^{-1}.

Reaction of α-(2-Benzothiazolyl)acetoacetanilide with Methylamine

A solution of α-(2-benzothiazolyl)acetoacetanilide (2.0 g, 0.0059 mol) in 30 ml of 40% aqueous methylamine was allowed to sit at room temperature for 4 days. Long white needles of 2-anilinobenzothiazole were gradually formed. These were filtered off, washed with a little fresh methylamine solution and air dried. Thus were obtained 1.2 g or 90.8% of 2-anilinobenzothiazole, m.p. 157–159 °C, identical in every way with an authentic sample made by the method of Hofmann (7).

Reaction of α-(4-Chlorophenylthio)acetoacetanilide with Methylamine

A sample of α-(4-chlorophenylthio)acetoacetanilide (10 g, 0.031 mol) was dissolved in 150 ml of 40% aqueous methylamine. The solution was allowed to stand at room temperature for 2.5 h and then filtered to remove the

Can. J. Chem. Downloaded from www.nrcresearchpress.com by 210.87.254.5 on 09/05/12
For personal use only.

product. A second crop was also obtained from the filtrate. The product was recrystallized from ethanol yielding 4.7 g or 51.5% of α-(4-chlorophenylthio)acetanilide, m.p. 108–110 °C. The identity of the product was proved by comparison with an authentic sample made by the reaction of α-chloroacetanilide with 4-chlorothiophenol.

Attempted Preparation of α-Mercaptoacetoacetanilide

The method of German Offen. 2,133,450 (3) was followed. Thus a solution of sodium hydroxide (8 g) in water (100 ml) was saturated with hydrogen sulfide and to this solution was added dropwise a solution of α-chloroacetoacetanilide (42.3 g) in methanol (150 ml) and benzene (150 ml). When the addition was complete (about 1 h) the mixture was stirred an additional 15 min and then filtered to remove 4.0 g or 62.5% of sulfur, m.p. 120 °C, burning with a blue flame smelling strongly of sulfur dioxide. The filtrate consisted of two phases. These were separated and the lower phase was extracted with 2 × 100 ml of ether and these ether phases combined with the upper phase. These organic phases were dried with anhydrous sodium sulfate and the solvents were then removed. The residue was recrystallized from toluene to give 28.5 g or 77.5% of acetoacetanilide, m.p. 78–84 °C. The identity of the product was confirmed as being acetoacetanilide rather than 2-mercaptoacetoacetanilide by comparison of its i.r. spectrum with that of authentic material.

Grateful acknowledgement is made to the National Research Council of Canada for financial assistance for part of this work.

1. B. Von Schmeling and M. Kulka. Science, **152**, 659 (1966); B. Von Schmeling, M. Kulka, D. S. Thiara, and W. A. Harrison. U.S. Patents 3,249,499 (May, 1966), 3,393,202 (July, 1968), 3,399,214 (August, 1968), and 3,402,241 (September, 1968); Can. Patents 787,893 (June, 1968), 791,151 (July, 1968), 842,243 (May, 1970), and 825,665 (October, 1969).
2. M. A. Corbeil, M. Curcumelli-Rodostamo, R. J. Fanning, B. A. Graham, M. Kulka, and J. B. Pierce. Can. J. Chem. **51**, 2650 (1973).
3. O. V. Mattsson and B. E. Bertilsson. German Offen. 2,133,450 (1972).
4. C. Bülow and E. King. Ann. **439**, 211 (1924).
5. R. J. Grout, B. M. Hynam, and M. W. Partridge. J. Chem. Soc. C, 1590 (1969).
6. A. J. Hodgkinson and B. Staskun. J. Org. Chem. **34**, 1709 (1969).
7. A. W. Hofmann. Ber. **20**, 1796 (1887).
8. L. V. Edgington, G. S. Walton, and P. M. Miller. Science **153**, 307 (1966).

Can. J. Chem. Downloaded from www.nrcresearchpress.com by 210.87.254.5 on 09/05/12
For personal use only.

A New Method of Preparing Hydrazonyl Halides

PEDER WOLKOFF

Department of General and Organic Chemistry, H. C. Ørsted Institute, University of Copenhagen, Universitetsparken 5, DK-2100 Copenhagen Ø, Denmark

Received September 9, 1974

PEDER WOLKOFF. Can. J. Chem. **53**, 1333 (1975).

The triphenylphosphine – carbon tetrahalide (Br, Cl) system transforms *N'*-benzoyl-*N*-arylhydrazines (**1**), *N,N*-dimethyl-, and *N*-methyl-*N*-phenyl-*N'*-benzoylhydrazines (**3**) into the corresponding hydrazonyl halides **2** and **4**.

Tribromomethyltriphenylphosphonium bromide (**7**), formed by reacting triphenylphosphine with carbon tetrabromide, is capable of transforming *N'*-benzoyl-*N*-phenylhydrazine (**1***a*) into the corresponding hydrazonyl bromide (**2***b*) in the presence of triphenylphosphine.

PEDER WOLKOFF. Can. J. Chem. **53**, 1333 (1975).

Le couple triphénylphosphine – tétrahalogénure de carbone (Br, Cl) transforme les *N'*-benzoyl *N*-arylhydrazines (**1**) ainsi que les *N,N*-diméthyl- et *N*-phényl *N'*-benzoylhydrazines (**3**) en halogénures (**2** et **4**) d'hydrazonyle correspondants.

Le bromure de tribromométhyltriphénylphosphonium (**7**) obtenu par réaction de la triphénylphosphine avec le tétrabromure de carbone peut transformer, en présence de triphénylphosphine, la *N'*-benzoyl *N*-phénylhydrazine (**1***a*) en bromure d'hydrazonyle correspondant (**2***b*).

[Traduit par le journal]

The two most important methods for the preparation of aromatic hydrazonyl halides (α-halogenobenzaldehyde arylhydrazones, **2**) are the action of phosphorus pentachloride on *N'*-benzoyl-*N*-arylhydrazines (**1**) and the halogenation of benzaldehyde arylhydrazones. The applicability of these methods is limited; the first can only be applied to hydrazonyl chlorides and the latter is generally accompanied by halogenation in the *N*-aryl part of the hydrazone (*cf.* ref. 1).

The recent work by Appel *et al.* (2) in transforming secondary amides (RCONHR') into the corresponding imidoyl halides (RCXNR') by use of the triphenylphosphine – carbon tetrahalide system (Ph_3P–CX_4) has prompted us to examine the applicability of this method also to the hydrazonyl system.

Applying the Ph_3P–CX_4 system to **1** affords **2** (see eq. 1) in 40–65% yield.

[1] $\underset{\mathbf{1}}{PhCONHNHAr} \xrightarrow{Ph_3P\text{–}CX_4} \underset{\mathbf{2}}{PhCX{=}NNHAr}$

a Ar = Ph; X = Cl
b Ar = Ph; X = Br
c Ar = 2-$NO_2C_6H_4$; X = Cl
d Ar = 3-$NO_2C_6H_4$; X = Cl
e Ar = 4-$NO_2C_6H_4$; X = Cl

Typically, CCl_4 (1 equiv.) was added to a stirred suspension of **1***a* (1 equiv.) and Ph_3P (1.25 equiv.) in dry CH_3CN. After 6 h the precipitate was filtered off and recrystallized to give **2***a* in 58% yield. The previously unknown α-bromobenzaldehyde phenylhydrazone (**2***b*, 33%) was prepared in a similar manner; the yield of **2** was increased slightly when the reaction time was extended to 20 h. The method is not limited to aromatic hydrazonyl halides but may also be applied to the preparation of aliphatic hydrazonyl halides of type **4** (see eq. 2).

[2] $\underset{\mathbf{3}}{PhCONHN(CH_3)R} \xrightarrow{Ph_3P\text{–}CX_4} \underset{\mathbf{4}}{PhCX{=}NN(CH_3)R}$

a R = Ph; X = Cl
b R = CH_3; X = Cl
c R = CH_3; X = Br

Thus reacting the Ph_3P–CBr_4 system with *N,N*-dimethyl-*N'*-benzoylhydrazine (**3***b*) affords after 2 h α-bromobenzaldehyde dimethylhydrazone (**4***c*; 39%), which has previously been prepared (but not isolated) by *in situ* bromination of the corresponding hydrazone ($PhCHNN(CH_3)_2$) (3). A mass spectrum taken of the reaction mixture confirmed the presence of bromoform and triphenylphosphine oxide.

The active reagents, transforming **1** and **3** into **2** and **4**, respectively, may be the charge–transfer complex (**5**), and the dihalogeno triphenylphosphorane (**6**), as shown by Appel *et al.* (2) in the transformation of amides into imidoyl halides.

Can. J. Chem. Downloaded from www.nrcresearchpress.com by 210.87.254.42 on 09/05/12
For personal use only.

Can. J. Chem. Downloaded from www.nrcresearchpress.com by 210.87.254.42 on 09/05/12
For personal use only.

$$\overset{+\delta}{Ph_3P} \ldots X \ldots \overset{-\delta}{CX_3} \qquad Ph_3PX_2$$
5 **6**

The sparingly soluble tribromomethyltriphenylphosphonium bromide (**7**) precipitated out instantly (88%) in dry CH_3CN by mixing CBr_4 (1 equiv.) with Ph_3P (1 equiv.) in the absence of **1** or **3** (see eq. 3); with 2 equiv. of Ph_3P the yield

[3] $$CBr_4 + Ph_3P \rightarrow (Ph_3PCBr_3)Br$$
7

of **7** was reduced to 69%. This shows that under these experimental conditions only a certain part of the Ph_3P–CBr_4 system is converted to **6** (X = Br) and dibromomethylene triphenylphosphorane (**8**) (4). Compound **7** itself was capable of transforming **1***a* into the corresponding hydrazonyl bromide **2***b* (42% after recrystallization) only in the presence of Ph_3P (see eq. 4).

[4] $$\underset{\textbf{1}a}{PhCONHNHPh} \xrightarrow{(Ph_3PCBr_3)Br + Ph_3P} \underset{\textbf{2}b}{PhCBr{=}NNHPh}$$

The formation of **2***b* may then be explained in terms of the action of **6** (X = Br) on **1***a*, where **6** (X = Br) is formed according to reaction 5, which has been proposed by Appel *et al.* (2) in accordance with the observations by Ramirez *et al.* (4) and Rabinowitz and Marcus (5) on the reaction of Ph_3P with CBr_4 and CCl_4, respectively; (see ref. 6 for a general review).

[5] $$\underset{\textbf{7}}{(Ph_3PCBr_3)Br} + Ph_3P \rightarrow \underset{\textbf{6}}{Ph_3PBr_2} + \underset{\textbf{8}}{Ph_3P{=}CBr_2}$$

This is further substantiated by the observation that dibromomethyltriphenylphosphonium bromide (**9**) is formed in 52% yield (after recrystallization), by refluxing compound **7** (1 equiv.) with Ph_3P (1 equiv.) in wet CH_3CN (see eq. 6).

[6] $$\underset{\textbf{7}}{(Ph_3PCBr_3)Br} + Ph_3P \xrightarrow[CH_3CN,\ H_2O]{} \underset{\textbf{9}}{(Ph_3PCHBr_2)Br}$$

The formation of **9** may be explained as an addition of HBr to the ylide **8** (**8** + HBr → **9**), where **8** is formed according to reaction 5. Similarly the reduction of bromomethyltriphenylphosphonium bromide to methyltriphenylphosphonium bromide by the action of Ph_3P has been reported (7).

Experimental

All melting points were taken on a Reichert melting point microscope. The aromatic hydrazonyl halides were normally recrystallized from acetonitrile.

α-Halogenobenzaldehyde Arylhydrazones

Carbon tetrachloride (1.95 ml, 20.0 mmol) was added to a stirred suspension of compound **1***a* (4.24 g, 20.0 mmol) and Ph_3P (6.55 g, 25.0 mmol) in CH_3CN (40 ml, dried by passage through an alumina column and introduced directly from the columm into the reaction flask). After 6 h the solution was cooled, crystallization was initiated by scratching, and the product filtered off. Recrystallization gave compound **2***a* in 58% yield, m.p. 128–131° (lit. (8) 129.5–130.5°). Extension of the reaction time to 20 h increased the yield of **2***a* to 64%.

Compound **1***c* (reaction time 20 h) gave **2***c* (59%), m.p. 162–164°.

Anal. Calcd. for $C_{13}H_9ClN_3O_2$: C, 56.69; H, 3.66; N, 15.24. Found: C, 56.85; H, 3.97; N, 15.48.

Compound **1***d* (reaction time 20 h) gave **2***d* (60%), m.p. 162–165°.

Anal. Found: C, 56.40; H, 3.86; N, 15.45.

Compound **1***e* (reaction time 20 h) gave **2***e* (55%), m.p. 189–192° (acetonitrile–acetone, 1:1) (lit. (9) 189–191°).

Carbon tetrabromide (6.03 g, 20.0 mmol), compound **1***a* (20.0 mmol), and Ph_3P (25.0 mmol) were mixed. After 6 h the clear solution was evaporated to dryness and extracted four times with ether, the ether was removed *in vacuo* and the residue recrystallized from ethanol to give compound **2***b* (33%), m.p. 109–111°. Extension of the reaction time to 20 h increased the yield of **2***b* to 40%.

Anal. Calcd. for $C_{13}H_{11}BrN_2$: C, 56.22; H, 4.03; N, 10.24. Found: C, 56.74; H, 4.03; N, 10.18.

α-Halogenobenzaldehyde N-Methyl-N-phenyl- and N,N-Dimethylhydrazones

Carbon tetrachloride (1.95 ml, 20.0 mmol) was added to a stirred suspension of compound **3***a* (4.52 g, 20.0 mmol) and Ph_3P (6.55 g, 25.0 mmol) in CH_3CN, (40 ml; dried as described above) with the exclusion of moisture. After 2 h, the solution was evaporated. The solid material was extracted four times with ether and the ether was removed *in vacuo*; this was followed by distillation to give **4***a* (77%), b.p. 138–143°/0.05 mm; δ 3.39 (CH_3, in $CDCl_3$) (lit. (10) δ 3.40).

Carbon tetrachloride (20.0 mmol), compound **3***b* (11) (3.28 g, 20.0 mmol), and Ph_3P (25.0 mmol) (reaction time 2 h) gave compound **4***b* (58%), b.p. 58–60°/0.05 mm; δ 2.84 (CH_3) ($CDCl_3$).

Anal. Calcd. for $C_9H_{11}ClN_2$: C, 59.18; H, 6.07; N, 15.34. Found: C, 58.78; H, 6.18, N, 15.34.

Carbon tetrabromide (20.0 mmol), compound **3***b* (20.0 mmol), and Ph_3P (25.0 mmol) (reaction time 2 h) gave compound **4***c* (39%), b.p. 82–85°/0.5 mm; δ 2.80 (CH_3) ($CDCl_3$). A mass spectrum of the reaction mixture showed both the presence of bromoform (*m/e* 254/256) and triphenylphosphine oxide (*m/e* 278).

Anal. Calcd. for $C_9H_{11}BrN_2$: C, 47.59; H, 4.88; N, 12.34. Found: C, 48.02; H, 5.23; N, 12.38.

The Reaction of Triphenylphosphine with Carbon Tetrabromide

Carbon tetrabromide (6.03 g, 20.0 mmol) was added to a stirred suspension of Ph_3P (5.25 g, 20.0 mmol) in

CH_3CN (25 ml; dried as described above). After 15 min the solution was filtered and washed carefully with ether to give compound **7** (88% yield), m.p. 230–232° (lit. (4) 246–247°).

Anal. Calcd. for $C_{19}H_{15}Br_4P$: C, 38.42; H, 2.55. Found: C, 38.57; H, 3.00.

Compound **7** crystallized from ethanol as a solvate, m.p. 242–244°.

Anal. Calcd. for $C_{19}H_{15}Br_4P \cdot C_2H_5OH$: C, 39.41; H, 3.31; Br, 49.95. Found: C, 39.20; H, 2.90; Br, 51.27.

Recrystallization of the solvated form from nitromethane gave m.p. 236–238°.

Anal. Found: C, 38.28; H, 2.95.

Carbon tetrabromide (20.0 mmol) was added to a stirred suspension of Ph_3P (10.50 g, 40.0 mmol) in CH_3CN (25 ml; dried as described above). This gave after 15 min **7** (69%), m.p. 228–230°.

Anal. Found: C, 38.91; H, 2.95.

The Reaction of N'-Benzoyl-N-phenylhydrazine with Tribromomethyltriphenylphosphonium Bromide

Compound **1***a* (2.12 g, 10.0 mmol), crude **7** (5.94 g, 10.0 mmol), and Ph_3P (2.62 g, 10.0 mmol) were stirred together under dry conditions at room temperature for 3 days in CH_3CN (20 ml; dried as described above). The mixture was evaporated to dryness, the residue extracted four times with ether, and the ether removed *in vacuo*; this was followed by recrystallization from ethanol to give compound **2***b* (42%), m.p. 108–110°; i.r. identical to that of **2***b* prepared above.

Compound **2***b* was not isolated nor detected (t.l.c.) by repeating the foregoing experiment in the absence of Ph_3P.

The Reaction of Tribromomethyltriphenylphosphonium Bromide with Triphenylphosphine

Crude **7** (2.97 g, 5.0 mmol) and Ph_3P (1.31 g, 5.0 mmol) were refluxed together for 30 min in CH_3CN (10 ml). The red solution was allowed to cool to room temperature and then filtered. The solid obtained (2.32 g) was recrystallized to give compound **9** (52%). Compound **9** crystallized from acetonitrile as a solvate, m.p. 144–147°.

Anal. Calcd. for $C_{19}H_{16}Br_3P \cdot CH_3CN$: C, 45.35; H, 3.44; N, 2.52; Br (ionic), 14.37. Found: C, 45.18; H, 3.76; N, 2.96; Br (ionic), 14.37.

Heating compound **9** at 170° overnight gave m.p. 235–238° (lit. (12) 235°).

Anal. Calcd. for $C_{19}H_{16}Br_3P$: C, 44.30; H, 3.13. Found: C, 44.30; H, 3.19.

The author is most grateful to Drs. O. Dahl and S. Hammerum for their interest and helpful comments during this work. The author also wants to thank the Danish National Research Council for financial support.

1. H. Ulrich. The chemistry of imidoyl halides. Plenum Press, New York. 1968.
2. R. Appel, K. Warming, and K.-D. Ziehn. Chem. Ber. **106**, 3450 (1973).
3. W. Walter and K. J. Reubke. Tetrahedron Lett. 5973 (1968).
4. F. Ramirez, N. B. Desai, and N. McKelvie. J. Am. Chem. Soc. **84**, 1745 (1962).
5. R. Rabinowitz and R. Marcus. J. Am. Chem. Soc. **84**, 1312 (1962).
6. H. Teichmann. Z. Chem. **14**, 216 (1974).
7. D. W. Grisley, Jr., J. C. Alm, and C. N. Matthews. Tetrahedron, **21**, 5 (1965).
8. R. Huisgen, M. Seidel, G. Wallbillich, and H. Knupfer. Tetrahedron, **17**, 3 (1962).
9. R. Huisgen, R. Grashey, H. Knupfer, R. Kunz, and M. Seidel. Chem. Ber. **97**, 1085 (1964).
10. S. Conde, C. Corral, and R. Madronero. Tetrahedron, **30**, 195 (1974).
11. E. Sedor, R. E. Freis, and H. J. Richards. Org. Prep. Proc. **2**, 275 (1970).
12. F. Ramirez and N. McKelvie. J. Am. Chem. Soc. **79**, 5829 (1957).

Can. J. Chem. Downloaded from www.nrcresearchpress.com by 210.87.254.42 on 09/05/12
For personal use only.

The Preparation and Properties of Some 2,1-Benzisoxazole and 2,1-Benzisothiazole Derivatives

MOHINDER S. CHAUHAN AND DAVID M. MCKINNON

Department of Chemistry, University of Manitoba, Winnipeg, Manitoba R3T 2N2

Received November 12, 1974

MOHINDER S. CHAUHAN and DAVID M. MCKINNON. Can. J. Chem. **53**, 1336 (1975).

A number of 2,1-benzisoxazole and 2,1-benzisothiazole compounds containing alkoxy or amino substituents in the 3-position and carboxy substituents in the 7-position, and potentially capable of valency tautomerism have been synthesized by reduction or oxidation, respectively, of suitable 2-nitro- or 2-aminoisophthalic acid derivatives. Thionation of 2-aminoisophthalic esters gave benzothiazaphosphorine derivatives. A temperature dependent n.m.r. study of the benzisoxazole and benzisothiazole derivatives indicates that in only one case, for methyl 3-methoxy-2,1-benzisothiazole-7-thionocarboxylate is there evidence for tautomerism at 200°.

MOHINDER S. CHAUHAN et DAVID M. MCKINNON. Can. J. Chem. **53**, 1336 (1975).

On a synthétisé un certain nombre de dérivés du benzisoxazole-2,1 et du benzisothiazole-2,1 contenant des substituants alkoxy et amino en position 3 et des substituants carboxy en position 7; ces composés qui sont susceptibles de présenter de la tautomérie de valence, ont été respectivement obtenus par réduction ou oxydation des dérivés appropriés des acides nitro-2 ou amino-2 isophtaliques. La thionation des esters de l'acide amino-2 isophtalique donne les dérivés benzothiaphosphorines. On a examiné les spectres r.m.n. des dérivés du benzisoxazole et du benzisothiazole à différentes températures; on n'a trouvé qu'un seul cas, celui du méthoxy-3 benzisothiazole-2,1 thiono-7 carboxylate de méthyle où de la tautomérie de valence existe à 200°. [Traduit par le journal]

2,1-Benzisoxazole (anthranil) derivatives, particularly certain 7-substituted compounds, are of interest in studies on valency tautomerism (1). The ease with which the process occurs, however, appears to depend in some measure on the solvent used (1, 2). To obtain more information on these compounds we have therefore attempted the synthesis of some other 2,1-benzisoxazoles and studied their properties. It was also of interest to compare the properties of such 7-acyl-2,1-benzisoxazoles (**1**) with the corresponding 7-thioacyl-2,1-benzisothiazoles (**2**) to determine the relative effects, if any, of the sulfur and oxygen atoms in the valency tautomerism of the compounds, since the compounds **2**, more so than **1**, parallel the structure of a benzo-1,2-dithiolium derivative (3) which demonstrates magnetic equivalence of substituents on the 3- and thioacyl positions. These comparisons were frustrated in an earlier study (1) by the lability of an aliphatic thione substituent. In this work therefore, studies were directed towards the synthesis of esters and amides possessing the required potential symmetry. The sulfur analogs of these would be expected to be sufficiently stable to provide an adequate comparison.

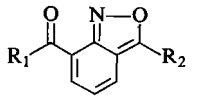

1

a $R_1 = OH; R_2 = OMe$
b $R_1 = R_2 = OMe$
c $R_1 = R_2 = Me$
d $R_1 = OH; R_2 = NMe_2$
e $R_1 = R_2 = NMe_2$
f $R_1 = OMe; R_2 = NMe_2$
g $R_1 = NMe_2; R_2 = \overset{+}{O}Me$
h $R_1 = O^-; R_2 = \overset{+}{N}HMe_2$

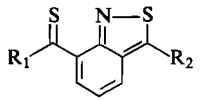

2

a $R_1 = R_2 = OMe$
b $R_1 = R_2 = NMe_2$

Syntheses were based on two methods, the reduction of *o*-nitrocarbonyl compounds or the oxidation of *o*-amino compounds. While both methods have been used for the conversion of suitable aldehydes and ketones to 2,1-benzisoxazoles (4) and are also applicable to the conversion of suitable thiocarbonyl compounds to 2,1-benzisothiazoles (5), they have not been used for the conversions of *o*-nitro- or *o*-aminoesters or thionoesters to 3-alkoxy-2,1-benzisoxazoles or 2,1-benzisothiazoles. Indeed such compounds appear to be unknown. 3-Amino-2,1-benzisoxazoles are available (6, 7) by reduction of suitable *o*-nitrobenzoic acid derivatives.

Can. J. Chem. Downloaded from www.nrcresearchpress.com by 210.87.254.105 on 09/05/12
For personal use only.

Can. J. Chem. Downloaded from www.nrcresearchpress.com by 210.87.254.105 on 09/05/12
For personal use only.

Methyl 2-nitroisophthalate (**3***a*) was reduced by stannous chloride in hydrochloric acid to methyl 2-aminoisophthalate (**3***b*). Treatment of this with hydrogen peroxide in acetic acid regenerated **3***a* but with Caro's acid 3-methoxy-2,1-benzisoxazole-7-carboxylic acid (**1***a*) was produced. Hydrolysis of an ester group had obviously accompanied the oxidative cyclization. We were unsuccessful in intercepting the required 2,1-benzisoxazole ester and other reductive methods were unsuccessful. The acid **1***a* treated with diazomethane afforded the desired ester **1***b* which has a structure of the required potential symmetry. The azide **3***c*, prepared from the amine **3***b*, failed to give **1***b* on either thermolysis or photolysis, although a similar reaction succeeded for 2,6-diacetylazidobenzene **3***d*, giving **1***c*.

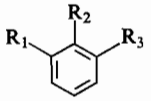

3

a $R_1 = R_3 = CO_2Me$; $R = NO_2$
b $R_1 = R_3 = CO_2Me$; $R_2 = NH_2$
c $R_1 = R_3 = CO_2Me$; $R_2 = N_3$
d $R_1 = R_3 = COMe$; $R_2 = N_3$
e $R_1 = R_3 = CONMe_2$; $R_2 = NO_2$
f $R_1 = R_3 = CONMe_2$; $R_2 = NH_2$
g $R_1 = R_3 = CSNMe_2$; $R_2 = NO_2$
h $R_1 = R_3 = CSNMe_2$; $R_2 = NH_2$
i $R_1 = R_3 = COSMe$; $R_2 = NO_2$
j $R_1 = R_3 = COSMe$; $R_2 = NH_2$
k $R_1 = R_3 = CS_2Me$; $R_2 = NO_2$

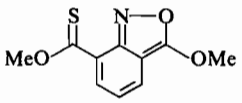

4

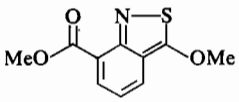

5

Thionation of **1***b* by phosphorus pentasulfide in toluene gave the 2,1-benzisothiazole **2***a* accompanied by the partially thionated compound **4** and the isomeric methyl 3-methoxy-2,1-benzisothiazole-7-carboxylate (**5**). The latter appears to be derived from **2***a* by hydrolysis of the thionoester function on the silica gel chromatogram used in separation but **2***a* appears to be otherwise stable. The ring sulfur in **2***a* is probably derived from the thionoester group in the initially thionated product **4** by valency tautomerism, similarly to a previously described example (1).

We also treated *N,N,N′,N′*-tetramethyl-2-nitroisophthalamide (**3***e*) with stannous chloride in hydrochloric acid. Two products were obtained, 3-dimethylamino-2,1-benzisoxazole-7-carboxylic acid (**1***d*) and the amine **3***f*. No 2,1-benzisoxazole **1***e* could be intercepted and other reductive methods failed to yield the desired product. The acid **1***d* was also converted by diazomethane into methyl 3-dimethylamino-2,1-benzisoxazole-7-carboxylate (**1***f*) but various attempts to form **1***e* from this by suitable chemical conversions were unsuccessful. The compound **1***f* is, however, suitable for study since it is potentially capable of valency tautomerism.

N,N,N′,N′-Tetramethyl-2-nitroisophthalamide (**3***e*) was smoothly thionated to the bisthioamide **3***g* which was reduced with stannous chloride to form a mixture of the desired *N,N*-dimethyl-3-dimethylamino-2,1-benzisothiazole-7-thiocarboxamide (**2***b*) and the amine **3***h* which were separated by fractional crystallization. The amine, as with many such structures (8), could be reoxidized to the benzisothiazole by peracetic acid.

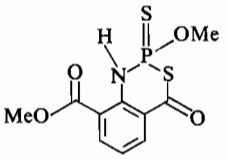

6

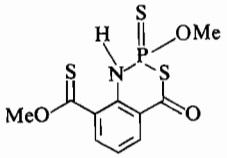

7

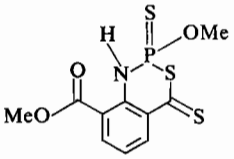

8

Methyl 2-nitroisothiolphthalate (**3***i*), prepared by treatment of 2-nitroisophthaloyl chloride with methanethiol, gave on stannous chloride reduction only methyl 2-aminoisothiolphthalate (**3***j*). No 2,1-benzisoxazole could be intercepted. The ester **3***j* could not be reoxidized to the desired 2,1-benzisoxazole by any method tried. The nitro compound **3***i* was slowly thionated by phosphorus pentasulfide in toluene to yield methyl 2-nitrotetrathioisophthalate **3***k* but this only gave what appears to be a hydrolysis product on attempted reduction. The failure to

Can. J. Chem. Downloaded from www.nrcresearchpress.com by 210.87.254.105 on 09/05/12
For personal use only.

effect suitable reduction of **3***k* in contrast to **3***i* or **3***a* is disappointing but it is probable that the nitro group is sterically hindered by the bulky sulfur functions. It is interesting that in contrast to the other compounds, which exhibit a low field displacement of aromatic protons *ortho* to the carbonyl or thiocarbonyl groups because of the electron withdrawing and anisotropic effects, the aromatic protons in **3***k* appear as a singlet.

The direct thionation of methyl 2-aminoisophthalate **3***b* with phosphorus pentasulfide gave two products, both of which contained phosphorus. The analysis, mass spectral data, and n.m.r. of one of these were in accord with the benzothiazaphosphorinethione structure **6**. This structure is analogous to some obtained by Legrand and Losac'h (9) by thionation of *N*-substituted anthranilic esters. The other compound, which was dark green, had one oxygen atom replaced by sulfur. Since a peak at 1700 cm^{-1} in **7**, due to the ester carbonyl frequency, was absent, we tentatively assign to this compound the thionoester structure **7** rather than the isomeric phosphorinedithione structure **8**.

Nuclear magnetic resonance spectra were performed in dimethyl sulfoxide. Earlier work (2) had indicated that this was a satisfactory solvent. Over the temperature range studied (40–200°) the methyl groups in **1***b* were nonequivalent, although some approach of τ values and line broadening was evident. The corresponding 2,1-benzisothiazole **2***a* exhibited coalescence at 200°. For the thioamide **2***b*, at 40° three methyl signals were observed due to the equivalent amine methyls and the nonequivalent thioamidic methyls. At 200° the latter had become equivalent but were still different from the former, two singlets being observed. These results are consistent with values for rotational barriers in thioamides (10). The net result of the alkoxy- or dimethylamino groups on the system appears to be to reduce the ease of tautomerism. The small enhancement by sulfur that is evident by comparison of the compounds **1***b* and **2***a* is expected (11) in view of the generally lower free energy of activation of reactions at sulfur atoms.

While methyl 3-dimethylamino-2,1-benzisoxazole-7-carboxylate (**1***f*) is potentially capable of tautomerism to *N*,*N*-dimethyl-3-methoxy-2,1-benzisoxazole-7-carboxamide (**1***g*), no evidence for this was obtained under the conditions studied. At 40° the amine methyl groups were nonequivalent but coalescence of their signals occurred on warming to 120°. At 200° only two signals, due to the amine and ester methyls, were apparent. It is interesting in that whereas the amine methyls in **1***f* were nonequivalent at room temperature, those in the 2,1-benzisothiazole **2***b* demonstrated equivalence in any solvent tried. The differences may be due to the greater electronegativity of the oxygen atom over sulfur in the heterocyclic ring affecting the amount of double bond character in the exocyclic carbon to nitrogen band. It is also likely that there is a significant effect of the carbonyl or thiocarbonyl group in the 7-position.

The amino methyl groups in the acid **1***d*, in contrast to the ester **1***f*, are equivalent due to its existence as the zwitterionic structure **1***h* akin to normal amino acids. The i.r. spectrum indicated a band at 2350 cm^{-1}, typical of protonated amines. When the compound was treated with sodium bicarbonate solution, to suppress protonation, the n.m.r. indicated nonequivalence of the methyl groups.

Experimental

The i.r. spectra were performed on a Perkin-Elmer model 337 spectrophotometer in liquid paraffin mulls. The n.m.r. spectra were obtained on a Varian model 56/60A spectrometer and, unless otherwise stated, in deuteriochloroform at 40°, using tetramethylsilane as an internal standard. Chromatography was performed using Camag silica gel, type D.S.F.5., supplied by Terochem Laboratories. Development of plates was carried out using benzene, with increasing proportions of chloroform, unless otherwise stated. Melting points were obtained on a precalibrated Thermopan apparatus.

Preparation of Methyl 2-Nitroisophthalate (3a)

A mixture of 2-nitroisophthaloyl chloride (9.92 g, 40 mmol) (1) and methanol (150 ml) was refluxed for 30 h. Excess methanol was removed by evaporation and the residue crystallized from a benzene – petroleum ether, 1:1 mixture, as colorless plates m.p. 133–134° (98%).

Anal. Calcd. for $C_{10}H_9NO_6$: C, 50.21; H, 3.76; N, 5.85. Found: C, 50.38; H, 3.86; N, 5.93.

The i.r. spectrum, 1735 cm^{-1} (C=O str). The n.m.r. spectrum, 6.49 (6H singlet, the methyl protons) 2.85–2.09 τ (3 H bands the aromatic protons). The mass spectrum, M^+ Calcd.: 239. Found: 239.

Preparation of 2,6-Diacetylazidobenzene (3d)

2,6-Diacetylaniline (1.77 g, 10 mmol) in 20% hydrochloric acid (20 ml) was diazotized at 0° with sodium nitrite (0.69 g). The mixture was filtered and added to sodium azide (1.5 g) in water (10 ml) and allowed to stand 16 h. The crystalline precipitate was collected,

Can. J. Chem. Downloaded from www.nrcresearchpress.com by 210.87.254.105 on 09/05/12
For personal use only.

washed, and recrystallized from petroleum ether. Colorless needles m.p. 48° were obtained (76%).

Anal. Calcd. for $C_{10}H_9N_3O_2$: C, 59.15; H, 4.44; N, 20.69. Found: C, 59.01; H, 4.52; N, 20.70.

The i.r. spectrum, 2151 cm^{-1} (N_3). The n.m.r. spectrum, 7.35 τ (6H singlet, the methyl protons), 2.13–2.84 τ (3H bands, the aromatic protons). The mass spectrum M^+ Calcd.: 203. Found: 203 (M^+), 175 ($M^+ - N_2$).

Preparation of 7-Acetyl-3-methyl-2,1-benzisoxazole (1c)

2,6-Diacetylazidobenzene (0.51 g, 2.5 mmol) in *o*-dichlorobenzene (5 ml) was refluxed 20 min. The solution slowly acquired a purple color. Evaporation and chromatography indicated a number of products but the yellow and orange bands on work-up gave a crude crystalline product which was recrystallized from petroleum ether – benzene, 1:1 mixture, as colorless needles m.p 103°, identical (mixture m.p. and i.r.) with an authentic sample (1).

Reduction of Methyl 2-Nitroisophthalate to form Methyl 2-Aminoisophthalate (3b)

Methyl 2-nitroisophthalate (2.86 g, 12 mmol) was slowly added over 10 min to a stirred solution of stannous chloride dihydrate (12 g) in concentrated hydrochloric acid (36 ml) at 25° under a nitrogen atmosphere. The mixture was stirred 1.5 h then diluted with water (100 ml). The precipitate was filtered and recrystallized from a mixture of benzene – petroleum ether, 1:1, to give the desired amine as colorless needles m.p. 102–103°. The yield was virtually quantitative.

Anal. Calcd. for $C_{10}H_{11}NO_4$: C, 57.45; H, 5.26; N, 6.70. Found: C, 57.57; H, 5.41; N, 6.82.

The i.r. spectrum 1705 cm^{-1} (C=O str). The n.m.r. spectrum, 6.17 (6H singlet, the methyl protons), 3.45 and 1.92 τ (1H triplet and 3H doublet, the aromatic protons), and 1.89 τ (2H band, the amine protons, exchanged in D_2O). The mass spectrum M^+ Calcd.: 209. Found: 209.

Oxidation of Methyl 2-Aminoisophthalate

(a) With Caro's Acid

A mixture of the amine (313 mg, 15 mmol) and Caro's acid (prepared by stirring a mixture of potassium persulfate (10 g), concentrated sulfuric acid (7 ml), and ice (50 g)) was stirred at 30° for 5 h. The mixture was diluted with water, filtered, and the residue extracted with hexane (4 × 20 ml). The combined extracts on evaporation gave starting material. The residue was crystallized from a mixture of chloroform and petroleum ether to give 3-methoxy-2,1-benzisoxazole-7-carboxylic acid (43%) as colorless needles, m.p. 160–161°. Further small amounts of products were obtained by extraction of the aqueous filtrate with methylene chloride.

Anal. Calcd. for $C_9H_7NO_4$: C, 55.95; H, 3.63; N, 7.26. Found: C, 55.79; H, 3.63; N, 7.37.

The i.r. spectrum, 1751 cm^{-1} (C=O str). The n.m.r. spectrum 6.01 (3H singlet, the methyl protons), 2.95–1.75 τ (3H bands, the aromatic protons). The mass spectrum M^+ Calcd.: 193. Found: 193.

(b) With Hydrogen Peroxide

A mixture of the amine (170 mg, 8 mmol), glacial acetic acid (5 ml), and 50% aqueous hydrogen peroxide, 1.0 ml) was left at 30° for 70 h. Work-up afforded methyl 2-nitroisophthalate (63%).

Preparation of Methyl 3-Methoxy-2,1-benzisoxazole-7-carboxylate (1b)

To a solution of diazomethane (40 mg) in ether (30 ml) was added a solution of 3-methoxy-2,1-benzisoxazole-7-carboxylic acid (58 mg, 3 mmol) in ether (20 ml). Immediate evolution of gas was evident. After ½ h, the mixture was evaporated to yield the ester, which was recrystallized from hexane as colorless needles, m.p. 134–135° (96%). The compound exhibited a strong blue fluorescence in u.v. light.

Anal. Calcd. for $C_{10}H_9NO_4$: C, 57.95; H, 4.45; N, 6.77. Found: C, 57.89; H, 4.40; N, 6.78.

The i.r. spectrum, 1764 cm^{-1} (C=O str). The n.m.r. spectrum, 6.45 (3H singlet, the ester methyl), 6.02 (3H singlet, the methoxyl protons) 2.80–1.54 τ (3H bands, the aromatic protons). The mass spectrum M^+ Calcd.: 207. Found: 207.

Preparation of Methyl 2-Azidoisophthalate (3c)

To a stirred suspension of methyl 2-aminoisophthalate (1.67 g, 8 mmol) in 50% hydrochloric acid (10 ml) was added dropwise at 0° a solution of potassium nitrite (0.7 g) in water (10 ml). The solution was stirred a further 10 min and filtered. To the stirred filtrate was added a solution of sodium azide (2.0 g) in water (15 ml). A colorless precipitate was produced. The mixture was stirred a further 2 h then the precipitate collected and recrystallized from a benzene – petroleum ether, 1:1 mixture, as colorless plates m.p. 67° (88%).

Anal. Calcd. for $C_{10}H_9N_3O_4$: C, 51.10; H, 3.83; N, 17.85. Found: C, 51.13; H, 3.96; N, 17.81.

The i.r. spectrum, 1737 (C=O str) and 2163 cm^{-1} (N_3). The n.m.r. spectrum, 6.04 (6H singlet, the methyl protons), 2.84–1.92 τ (3H bands, the aromatic protons). The mass spectrum M^+ Calcd.: 235. Found: 235.

Attempted Conversion of Methyl 2-Azidoisophthalate to Methyl 3-Methoxy-2,1-benzisoxazole-7-carboxylate

Pyrolysis of the azide (156 mg, 0.65 mmol) in boiling *o*-dichlorobenzene or photolysis of the azide (235 mg, 1 mmol) dissolved in dry benzene (350 ml) under nitrogen with a medium pressure mercury lamp in a quartz reactor for 1 h yielded traces of methyl 2-aminoisophthalate and much polymeric material.

Thionation of Methyl 3-Methoxy-2,1-benzisoxazole-7-carboxylate

The ester (250 mg, 1.2 mmol) and phosphorus pentasulfide (420 mg) in dry toluene (20 ml) were refluxed 5 h. The solvent was removed under reduced pressure and the residue treated with 5% aqueous sodium bicarbonate solution. The mixture was extracted with ether (4 × 100 ml) and the extract washed, dried, and evaporated gave a crude product which was separated by chromatography using a 1% methanol solution in chloroform as an eluent to give methyl 3-methoxy-2,1-benzisothiazole-7-thionocarboxylate as yellow plates, m.p. 128–129°, from petroleum ether (7%).

Anal. Calcd. for $C_{10}H_9NO_2S_2$: C, 50.21; H, 3.77; N, 5.86; S, 26.75. Found: C, 50.35; H, 3.89; N, 5.93; S, 26.60.

The mass spectrum M^+ Calcd.: 239. Found: 239.

Methyl 3-methoxy-2,1-benzisoxazole-7-thionocarboxylate, yellow prisms, m.p. 123–124°, from petroleum ether (4%), was also separated by chromatography.

Anal. Calcd. for $C_{10}H_9NO_2S$: C, 53.81; H, 4.03; N.

Can. J. Chem. Downloaded from www.nrcresearchpress.com by 210.87.254.105 on 09/05/12
For personal use only.

6.27; S, 14.35. Found: C, 53.71; H, 4.18; N, 6.10; S, 14.49.

The n.m.r. spectrum, 4.22 and 4.00 (two 3H singlets, the methyl protons), 2.72–1.52 τ (3H bands, the aromatic protons). The mass spectrum M^+ Calcd.: 223. Found: 223.

A small quantity of pale yellow material tentatively methyl 3-methoxy-2,1-benzisothiazole-7-carboxylate (0.5%) was also isolated. The mass spectrum M^+ Calcd.: 223. Found: 223. The i.r. spectrum, 1765 cm^{-1} (C=O str).

Preparation of N,N,N′,N′-Tetramethyl-2-nitroisophthalamide (3e)

2-Nitroisophthaloyl chloride (24.8 g, 0.1 mol) was dissolved in dry benzene (200 ml) and 40% aqueous dimethylamine solution (20 ml) was added slowly. The mixture was stirred for 3 h at 50°. The benzene layer separated, washed with saturated sodium chloride solution, dried, and evaporated gave a pale yellow product which was recrystallized from a benzene – petroleum ether, 1:1 mixture, as colorless plates, m.p. 151–152° (83%). The product was stable but turned red on prolonged exposure to light.

Anal. Calcd. for $C_{12}H_{15}N_3O_4$: C, 54.34; H, 5.65; N, 15.82. Found: C, 54.33; H, 5.70; N, 15.68.

The i.r. spectrum, 1640 cm^{-1} (C=O str). The n.m.r. spectrum 7.08 and 6.92 (two 6H singlets, the methyl protons), 2.72–2.14 τ (3H bands, the aromatic protons). The mass spectrum M^+ Calcd.: 265. Found: 265.

Reduction of N,N,N′,N′-Tetramethyl-2-nitroisophthalamide

The nitro compound (2.99 g, 12.5 mmol) was added to a stirred solution of stannous chloride (12.0 g) in concentrated hydrochloric acid (36 ml) under nitrogen. The solution was stirred 1½ h at 0°, saturated sodium chloride solution (150 ml) added, and the mixture extracted with chloroform (3 × 150 ml). Work-up of the combined chloroform extracts yielded a crystalline residue which was recrystallized from benzene to give 3-dimethylamino-2,1-benzisoxazole-7-carboxylic acid as colorless needles, m.p. 164–165° (70%).

Anal. Calcd. for $C_{10}H_{10}N_2O_3$: C, 58.25; H, 4.85; N, 13.59. Found: C, 58.32; H, 4.95; N, 13.74.

The i.r. spectrum, 1602 (tentatively asym. CO_2^- str) and 2350 cm^{-1} (N^+—H str). The n.m.r. spectrum in $CDCl_3$ 6.86 (6H singlet, the methyl protons), 2.94–2.22 (3H bands, the aromatic protons), −1.10 τ (broad 1H band, exchanged in D_2O (the acidic proton)). In D_2O saturated with $NaHCO_3$ the methyl protons were evident as two peaks at 6.94 and 7.08 τ.

Neutralization of the aqueous layer from above with sodium bicarbonate and chloroform extraction gave on evaporation a crystalline product which was recrystallized from benzene – petroleum ether, 1:1 mixture, to give *N,N,N′N′*-tetramethyl-2-aminoisophthalamide as colorless needles, m.p. 177–178° (15%).

Anal. Calcd. for $C_{12}H_{17}N_3O_2$: C, 61.27; H, 7.23; N, 17.87. Found: C, 61.19; H, 7.48; N, 17.69.

The i.r. spectrum, 1661 cm^{-1} (C=O str). The n.m.r. spectrum, 6.95 (12H singlet, the methyl protons), 3.25–2.65 τ (3H bands, the aromatic protons).

Preparation of Methyl 3-Dimethylamino-2,1-benzisoxazole-7-carboxylate (1f)

3-Dimethylamino-2,1-benzisoxazole-7-carboxylic acid (248 mg, 1.2 mmol) in dry ether (300 ml) was added to the calculated amount of diazomethane in dry ether (50 ml). The solution was left at room temperature for 5 h then the ether was removed by evaporation. The residue was crystallized from a benzene – petroleum ether, 1:1 mixture, as colorless needles m.p. 105–106° (98%).

Anal. Calcd. for $C_{11}H_{12}N_2O_3$: C, 60.00; H, 5.45; N, 12.73. Found: C, 60.04; H, 5.43; N, 12.72.

The i.r. spectrum, 1761 cm^{-1} (C=O str). The n.m.r. spectrum 7.06 and 6.84 (two 3H singlets, the amine methyls), 6.73 (3H singlet, the ester methyl), 2.72–1.98 τ (3H bands, the aromatic protons). The mass spectrum M^+ Calcd.: 220. Found: 220.

Preparation of N,N,N′,N′-Tetramethyl-2-nitroisothiophthalamide

A mixture of *N,N,N′N′*-tetramethylisophthalamide (7.0 g, 2.66 mmol) and phosphorus pentasulfide (10.0 g) in toluene (50 ml) was refluxed for 3 h. The solvent was evaporated and the residue treated with 5% sodium bicarbonate solution and extracted with chloroform (3 × 100 ml). The combined extracts were washed with water and evaporated. The residue was crystallized from benzene to give the product as yellow plates m.p. 204–205° (88%).

Anal. Calcd. for $C_{12}H_{15}N_3O_2S_2$: C, 48.48; H, 5.05; N, 16.14; S, 21.55. Found: C, 48.64; H, 5.05; N, 14.11; S, 21.66.

The n.m.r. spectrum 6.73 and 6.43 (two 6H singlets, the methyl protons), 2.96–2.41 τ (3H bands, the aromatic protons). The mass spectrum M^+ Calcd.: 297. Found: 297.

Reduction of N,N,N′,N′-Tetramethyl-2-nitroisothiophthalamide

To a solution of stannous chloride (2.5 g) in concentrated hydrochloric acid (15 ml) was added the thioamide (1.435 g, 5 mmol) and the mixture stirred under nitrogen 3 h. The mixture was filtered and the residue washed with water then dissolved in benzene. The benzene solution was washed with 50% aqueous sodium hydroxide solution, washed with water, dried, and evaporated to give a crude product which was separated by chromatography using 1% methanol in chloroform as an eluant to give starting material and a mixture of *N,N,N′,N′*-tetramethyl-2-aminoisothiophthalamide (80%) and *N,N*-dimethyl-3-dimethylamino-2,1-benzisothiazole-7-thiocarboxamide (16%). These were separated by fractional crystallization from benzene, in which the isothiazole is more soluble, to give products m.p. 207–208 and 202°, respectively.

For the amine, Anal. Calcd. for $C_{12}H_{17}N_3S_2$: C, 53.93; H, 6.37; N, 15.71; S, 24.00. Found: C, 53.63; H, 6.28; N, 15.53; S, 24.02.

The n.m.r. spectrum 6.84 and 6.46 (two 6H singlets, the methyl protons), 5.90 (broad band, exchangeable in D_2O, the amine protons), 2.11–1.54 τ (3H bands, the aromatic protons). The mass spectrum, M^+ Calcd.: 267. Found: 267. Rigorous drying was necessary for proper analysis.

For the 2,1-benzisothiazole, Anal. Calcd. for $C_{12}H_{15}N_3S_2$: C, 54.2; H, 5.65; N, 15.85; S, 24.12. Found: C, 54.44; H, 5.65; N, 15.72; S, 24.12.

The n.m.r. spectrum, 6.84 and 6.27 (two 3H singlets, the amidic methyls), 6.66 (6H singlet, the amino protons),

Can. J. Chem. Downloaded from www.nrcresearchpress.com by 210.87.254.105 on 09/05/12
For personal use only.

2.19–2.04 τ (3H bands, the aromatic protons). The mass spectrum M^+ Calcd.: 265. Found: 265.

Oxidation of N,N,N′,N′-Tetramethyl-2-aminoisothiophthalamide with Hydrogen Peroxide in Acetic Acid

The thioamide (80 mg, 0.3 mmol) in acetic acid (5 ml) was treated with 30% hydrogen peroxide (0.03 ml) and the solution heated at 50° for 1 h. The solution was diluted with water, extracted with chloroform, and the chloroform layer washed with saturated sodium bicarbonate solution. Evaporation yielded a yellow oil which on examination by chromatography, using repeated development with chloroform, yielded three yellow bands. The second of these on elution gave *N,N*-dimethyl-3-dimethylamino-2,1-benzisothiazole-7-thiocarboxamide, identical (mixture m.p. and mass spectrum) to a sample prepared above (10%).

Preparation of Methyl 2-Nitroisothiolphthalate (3i)

A mixture of 2-nitroisophthaloyl chloride (12.4 g, 50 mmol), dry benzene (150 ml), and methanethiol (19.2 g) was treated with triethylamine (30 g), and the mixture stirred 3 h. The mixture was warmed to 60° to remove excess methanethiol, then poured into water. The benzene layer was extracted with dilute sodium hydroxide and dilute hydrochloric acid, dried, and evaporated under reduced pressure to give the crude ester, which was recrystallized from a mixture of benzene and petroleum ether as colorless plates m.p. 130–131°.

Anal. Calcd. for $C_{10}H_9NO_4S_2$: C, 44.28; H, 3.32; N, 5.16; S, 23.61. Found: C, 44.44, H, 3.35, N, 5.21; S, 23.79.

The i.r. spectrum, 1635 cm^{-1} (C=O str). The n.m.r. spectrum, 7.52 (6H singlet, the methyl protons), 2.46–1.82 τ (3H bands, the aromatic protons). The mass spectrum M^+ Calcd.: 271. Found: 271.

Reduction of Methyl 2-Nitroisothiolphthalate with Stannous Chloride

A mixture of methyl 2-nitroisothiolphthalate (4.06 g, 1.5 mmol), stannous chloride dihydrate (36 g), and concentrated hydrochloric acid (100 ml) was heated at 60° for 16 h under nitrogen. Water (300 ml) was added to the reaction mixture and the precipitate filtered. The residue was extracted with boiling petroleum ether which on concentration and cooling gave methyl 2-aminoisothiolphthalate. The product was recrystallized from petroleum ether as lemon yellow plates, m.p. 93–94°, (63%).

Anal. Calcd. for $C_{10}H_{11}NO_2S_2$: C, 49.79; H, 4.56; N, 5.81; S, 26.55. Found: C, 49.69; H, 4.63; N, 5.79; S, 26.74.

The i.r. spectrum, 3300 and 3405 (NH_2 str), 1655 cm^{-1} (C=O str). The n.m.r. spectrum, 7.63 (6H singlet, methyl protons), 3.56 and 1.80 (1H triplet, 2H doublet, the aromatic protons), and 1.80 τ (2H band, the amine protons). The mass spectrum M^+ Calcd.: 241. Found: 241.

Thionation of Methyl 2-Nitroisothiolphthalate to form 3k

A mixture of methyl 2-nitroisothiolphthalate (4.06 g, 15 mmol), phosphorus pentasulfide (12.0 g), and toluene (2.50 ml) was refluxed 3 days. The mixture was filtered, washed with sodium bicarbonate solution, and evaporated to yield a brown residue. Crystallization from a benzene, petroleum ether mixture gave the tetrathioester as orange plates, m.p. 138–139°, (71%).

Anal. Calcd. for $C_{10}H_9NO_2S_4$: C, 39.60; H, 2.97; N, 4.62; S, 42.24. Found: C, 39.67; H, 3.08; N, 4.69; S, 42.48.

The n.m.r. spectrum, 7.26 (6H singlet, the methyl protons) and 2.48 τ (3H singlet, the aromatic protons). This absorption remained a singlet when the compound was dissolved in hexadeuteriobenzene. The mass spectrum M^+ Calcd.: 303. Found: 303.

Attempted Reduction of Methyl 2-Nitroisotetrathiophthalate with Stannous Chloride

A mixture of the tetrathioester (1.0 g), stannous chloride (9.0 g), and concentrated hydrochloric acid (27 ml) was heated at 60–70° for 4 h. Work-up afforded mainly starting material and traces of hydrolyzed products.

Reaction of Methyl 2-Aminoisophthalate with Phosphorus Pentasulfide

A mixture of the ester (418 mg, 2 mmol), phosphorus pentasulfide (600 mg, 1.35 mmol), and toluene (25 ml) was refluxed for 8 h. The mixture was filtered and the residue washed with benzene and the benzene washings united with the toluene. The solvent was removed *in vacuo* and the residue treated with sodium bicarbonate solution. An ether extract was dried and evaporated to yield green material which was separated by chromatography in benzene to give **7** as dark green prisms m.p. 99–100° (58%) and **6** as greenish yellow prisms m.p. 150–152° (11%).

For **7**, Anal. Calcd. for $C_{10}H_{10}NO_3PS_3$: C, 37.61; H, 3.13; N, 4.39; P, 9.71; S, 30.09. Found: C, 37.79; H, 3.25; N, 4.50; P, 9.93; S, 30.06.

The i.r. spectrum, 1675 cm^{-1} (C=O str). The n.m.r. spectrum, 6.33 (3H doublet, $J = 16$ Hz, the methoxy protons, split by phosphorus) and 5.98 τ (3H singlet, the ester methyl). The mass spectrum M^+ Calcd.: 319. Found: 319.

For **6**, Anal. Calcd. for $C_{10}H_{10}NO_4PS_2$: C, 39.60; H, 3.30; N, 4.02; P, 10.23; S, 21.12. Found: C, 39.68; H, 3.22; N, 4.68; P, 10.03, S, 21.11.

The i.r. spectrum, 1695, 1660 cm^{-1} (C=O str). The n.m.r. spectrum, 6.33 (3H doublet, $J = 16$ Hz, the methoxy protons, split by phosphorus), 6.08 τ (3H singlet, the ester methyl). The mass spectrum M^+ Calcd.: 303. Found: 303.

Nuclear Magnetic Resonance Spectral Data

These were obtained on samples dissolved in hexadeuteriodimethyl sulfoxide in degassed sealed tubes and over the temperature range 40–200°.

Methyl 3-methoxy-2,1-benzisoxazole-7-carboxylate. At 40° two singlets at 6.70 and 6.21 τ were evident. At 200°, two singlets, separated by 0.52 τ were still observed, although some line broadening was evident.

Methyl 3-methoxy-2,1-benzisothiazole-7-thionocarboxylate. At 40° two singlets were observed at 6.54 and 6.20 τ. At 200° these had coalesced into a broad singlet at 6.30 τ.

Methyl 3-dimethylamino-2,1-benzisoxazole-7-carboxylate. At 40° this exhibited three methyl absorptions. Two at 7.28 and 7.10 τ were assigned to the amine methyl and one at 6.89 τ to the ester methyl. At 120° the former became equivalent but even at 200° there was no evidence for the valency isomerism.

N,N-Dimethyl-3-dimethylamino-2,1-benzisothiazole-7-thiocarboxamide. At 40°, this exhibited three methyl signals, at 7.07 and 6.54 τ, the amidic methyls, and at 6.72 τ, the equivalent amino methyls. At 180° the peaks were still discrete. At 200° the amidic methyl peaks had collapsed to a singlet but were still nonequivalent to the amine methyl. An attempt to study the temperature dependent rotational equivalence of the amine methyls in chloroform or acetone was unsuccessful as the compound was too insoluble in these solvents below −20°.

We wish to thank the National Research Council of Canada for financial support of this research. We also wish to thank Mr. M. Arneson and Mr. R. Simanavicius for preparation of spectra.

1. D. M. McKINNON and J. Y. WONG. Can. J. Chem. **49**, 2018 (1971).
2. K. P. PARRY and C. W. REES. Chem. Commun. 833 (1971).
3. E. I. G. BROWN, D. LEAVER, and T. J. RAWLINGS. Chem. Commun. 83 (1969).
4. K. H. WUNSCH and A. J. BOULTON. Adv. Heterocycl. Chem. **8**, 277 (1967).
5. M. DAVIS. Adv. Heterocycl. Chem. **14**, 43 (1972).
6. M. JUBAULT and D. PELTIER. Bull. Soc. Chim. Fr. 2365 (1972).
7. H. MUSSO and H. SCHROEDER. Ber. **98**, 1562 (1965).
8. R. F. MEYER, B. L. CUMMINGS, P. BASS, and H. O. J. COLLIER. J. Med. Chem. **8**, 515 (1965).
9. L. LEGRAND and N. LOSAC'H. Bull. Soc. Chim. Fr. 1173 (1969).
10. R. F. HOBSON, L. W. REEVES, and F. N. SHAW. J. Phys. Chem. **77**, 1228 (1973).
11. E. C. KOOYMAN. *In* Organosulfur chemistry *Edited by* M. J. Janssen. Interscience Publishers, New York. 1967.

Can. J. Chem. Downloaded from www.nrcresearchpress.com by 210.87.254.105 on 09/05/12
For personal use only.

The Electronic Structure and Localized Molecular Orbitals in S_4N_4 by the CNDO/BW Theory

M. S. GOPINATHAN AND M. A. WHITEHEAD[1]

Theoretical Chemistry Department, 1 South Parks Road, Oxford, England

Received September 24, 1974

M. S. GOPINATHAN and M. A. WHITEHEAD. Can. J. Chem. **53**, 1343 (1975).

The energies calculated for tetranitrogen tetrasulfide, S_4N_4, by the CNDO/BW theory favor a structure with coplanar nitrogen atoms and not a structure with coplanar sulfur atoms. Both structures have been proposed from experimental studies. Localized molecular orbitals are calculated for S_4N_4 and used to choose the appropriate Lewis structure for the molecule. The hybridization at the nitrogen and sulfur atoms is discussed. There is electron delocalization in the molecule, the S—N bond is a bent bond involving pure p-orbitals on the sulfur and nitrogen atoms and there is a pure p-bent bond between the sulfur atoms on the same side of the coplanar nitrogen atoms. There is no N—N bond in S_4N_4.

M. S. GOPINATHAN et M. A. WHITEHEAD. Can. J. Chem. **53**, 1343 (1975).

Les énergies calculées pour le tétrasulfure de tétrazote, S_4N_4, par la théorie CNDO/BW favorisent une structure avec des atomes d'azote coplanaires et non pas une structure avec des atomes de soufre coplanaires. Les deux structures avaient été proposées à partir d'études expérimentales. Les orbitales moléculaires localisées peuvent être calculées pour S_4N_4 et utilisées pour choisir la structure de Lewis appropriée pour la molécule. On discute de l'hybridisation aux atomes d'azote et aux atomes de soufre. Il y a une délocalisation des électrons dans la molécule; le lien S—N est un lien courbé impliquant des orbitales p pures sur les atomes de soufre et les atomes d'azote et il y a un lien p courbé entre les atomes de soufre sur le même côté des atomes d'azote coplanaires. Il n'y a pas de lien N—N dans le S_4N_4.

[Traduit par le journal]

Introduction

The molecular structure and chemical bonding in tetranitrogen tetrasulfide, S_4N_4, are unresolved (1, 2). X-Ray and electron diffraction studies (3) and vibrational (4) and electronic (5) spectral studies lead to two proposed molecular structures, **1** and **2**, (Figs. 1 and 2). In structure **1** the four nitrogen atoms are coplanar with two sulfur atoms above and two below the plane, while structure **2** has coplanar sulfur atoms with the nitrogen atoms above and below the plane. Both structures have D_{2d} molecular symmetry. An extended Hückel theory study (6) of the energies of the two structures predicted structure **1** to be more stable. The same structures are here studied using SCFMO wavefunctions of the CNDO/BW theory (7).

There is also the problem of the electronic structure of S_4N_4. Many Lewis structures (Fig. 3, **A** to **G**) have been proposed for S_4N_4, which differ in the type of bonds present, the charge on the atoms, the number of lone-pair electrons on each atom, and the presence or absence of S—S

[1]Permanent address: Chemistry Department, McGill University, Montreal, Quebec.

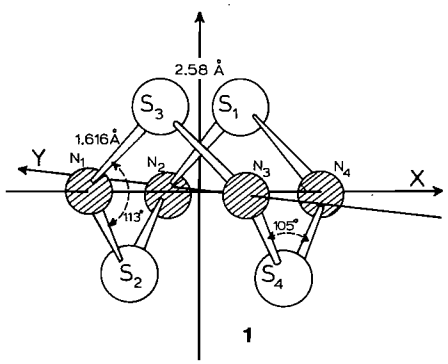

FIG. 1. The coplanar nitrogen atom structure of S_4N_4.

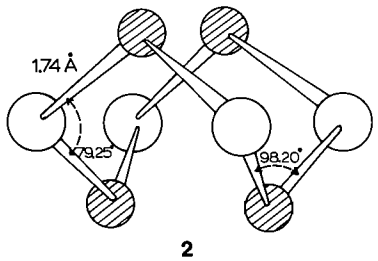

FIG. 2. The coplanar sulfur atom structure of S_4N_4.

Can. J. Chem. Downloaded from www.nrcresearchpress.com by 210.87.254.40 on 09/05/12
For personal use only.

Can. J. Chem. Downloaded from www.nrcresearchpress.com by 210.87.254.40 on 09/05/12
For personal use only.

and N—N bonds. Experimental and theoretical studies have not provided a unique atomic orbital description. From vibrational spectra, Lippincott and Tobin (4) proposed structure **2** with N—N bonds but no S—S bonds. The electronic spectrum was explained (5) using a weak S—S bond, structure **1**. A free electron treatment (8) suggested the presence of both N—N and S—S bonds, while Lindqvist (9) proposed formula **B**. From an empirical correlation between S—S bond length and s-character of the sulfur hybrid orbitals in other molecules, it was argued that a single bond involving pure po orbitals exists in S_4N_4 (9). Extended Hückel calculations (6) gave a negative bond order between the nitrogen atoms and indicated a weak S—S bond of the pσ type. The dispute over the existence of an S—S bond arises from the fact that the observed S—S distance in S_4N_4 is 2.58 Å which is longer than the normal single bond length, of 2.08 Å, and shorter than the sum of the van der Waals radii, 3.70 Å (7). A pure pσ bond between sulfur atoms does not fit (3) with the "double bond character" of the N—S bond inferred from the bond length of 1.616 Å, which is shorter than a "pure single (sp^3)" bond length of 1.764 Å. However this N—S double bond character is not consistent with the observed angles of 113° at nitrogen and 105° at sulfur. Any bonding scheme for the molecule also has to explain the electron delocalization in the S—N ring, indicated by the electronic spectrum (5), and the ^{14}N n.m.r. chemical shifts (10) and explain the unstable nature of the compound.

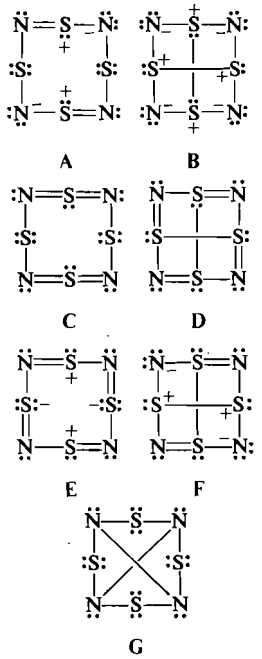

FIG. 3. Possible Lewis structures for S_4N_4.

The conventional form of molecular orbital wavefunctions cannot answer the above questions since the wavefunctions are delocalized over the entire molecular frame, and do not correspond to chemical bonds, lone pairs, etc. However, a single determinantal wavefunction, such as the CNDO/BW wavefunction, is invariant to orthogonal transformation of the occupied molecular orbitals out of which it is formed. Therefore the delocalized molecular orbitals can be transformed into Localized Molecular Orbitals (LMO's) which correspond to chemical bonds and lone pairs. Several criteria have been used to determine the transformation matrix (11) but the most successful and theoretically attractive method is that of Lennard-Jones (12), extensively applied by Ruedenberg and co-workers (13). This method uses the theory that the two electrons forming a localized bond have maximum self-repulsion. This is an intrinsic criterion (14) and does not involve any preconceived model for the electron density distribution. The method successfully describes the electronic structure of a wide variety of molecules including electron deficient molecules (15, 27), and has been applied to the CNDO/BW wavefunctions for S_4N_4 to obtain a quantitative description of the nature of the bonding.

Method of Calculation

The CNDO/BW theory is specifically parameterized to yield the correct equilibrium molecular geometry (7). The parameter set III of Boyd and Whitehead (7) has been used, together with the experimental molecular geometry: structure **1**: N—S 1.616 Å, ∠SNS 113°, ∠NSN 105° (ref. 3); structure **2**: N—S 1.74 Å, ∠SNS 98.2°, ∠NSN 79.25° (ref. 4). Only 2s and 2p functions were used in the basis set; the possibility of d-orbitals on sulfur is discussed later. The localization procedure followed that of CNDO type wavefunctions given by Gopinathan and Narasimhan (16).

Results and Discussion

Geometrical Structure

The total molecular energy calculated by the

TABLE 1. Truncated Localized Molecular Orbitals, TLMO, in S_4N_4. The numbering of the atoms and the coordinate axes refer to structure **1**

Type of LMO	N_s*	N_{p_x}	N_{p_y}	N_{p_z}	S_s†	S_{p_x}	S_{p_y}	S_{p_z}
N_1 lone pair (I)	−0.95299	0.28548	0.00513	0.00756				
S_3 lone pair					0.89418	0.14669	0.15409	−0.38646
N_1—S_3 bond	0.12185	0.39316	−0.31899	0.343203				
					0.23949	−0.29937	0.44656	−0.48681
N_1 lone pair (II)	0.00890	−0.00544	0.65906	0.646042				
				(S_2)	−0.00148	−0.05309	0.18677	0.10042
				(S_3)	−0.00535	0.064929	0.18992	0.10374
S_3—S_1 bond				(S_1)	−0.03571	0.43401	0.49203	−0.13945
				(S_3)	−0.11140	−0.48274	−0.46936	−0.12651

*N_s coefficient of atomic orbtal a on nitrogen.
†S_b coefficient of atomic orbital b on sulfur. The delocalization is given by $d = (1 - \sum_i c_{iTLMO}^2) \times 100\%$. Thus the delocalization of the N_1 lone pair is $(1 - \sum_{s,p_x,p_y,p_z} c_{N_1TLMO}^2)$, and the amount of delocalization other than to the adjacent S_2 and S_3 is given by $(1 - \sum_{\text{nitrogen orbitals}} c_i^2 - \sum_{\text{sulfur orbitals}} c_i^2)$.

CNDO/BW method is −64.72827 a.u. for structure **1** and −64.39302 a.u. for structure **2**. The average calculated S—N bond energy is 70 kcal mol^{-1} for structure **1** and 50 kcal mol^{-1} for structure **2**. Thus the coplanar nitrogen structure is more stable than the coplanar sulfur structure by 0.33525 a.u. (~200 kcal mol^{-1}). Qualitatively similar results were obtained from extended Hückel calculations (6). The latest three-dimensional X-ray diffraction study (3) also supports structure **1**. These results show structure **1** to be the correct one; structure **2** is not considered further.

Electronic Structure

There are 44 valence electrons in S_4N_4 in 22 occupied molecular orbitals. The localized CNDO/BW molecular orbitals for S_4N_4 are highly localized. The degree of delocalization of LMO can be obtained as follows.

While a given LMO approximates a given bond or lone pair in a molecule, it contains coefficients of atomic orbitals on atoms which are not those forming a localized bond or lone pair. If all the coefficients of atomic orbitals, other than those chemically considered to be involved in the bond or lone pair, are neglected, a *Truncated Localized Molecular Orbital*, TLMO (Ψ_{TLMO}) is obtained. This TLMO is not renormalized. The original LMO is normalized, and the difference

$$1 - \int \Psi_{TLMO}^2 \, d\tau$$

measures the delocalization of the original LMO. If the LMO is completely localized it equals the TLMO and the above difference is zero. Within the CNDO/BW theory, where differential overlap is neglected, this difference becomes

$$d = \left(1 - \sum_i c_{iTLMO}^2\right) \times 100$$

as a percentage of delocalization, and d goes to 0% when the LMO represents a completely localized lone pair or bond, and hence is identical to the TLMO.

The LMO's in S_4N_4 belong to five types, Table 1 and Fig. 4.

(1) Nitrogen Lone Pair (I)

This is a nitrogen 2s orbital, with 99.1% s-character. Thus there is no hybridization at the nitrogen atoms in S_4N_4. The delocalization index, d, is 1.02%; this lone pair is highly localized.

(2) Sulfur Lone Pair

This is predominantly a sulfur 2s orbital, with 80.45% s-character. The d value is 0.85%; the lone pair is highly localized.

(3) N—S Bond

The d value is 2.76%; the bond is highly localized. It is a single bond between almost pure p-orbitals on nitrogen and sulfur. The s-characters of the nitrogen and sulfur orbitals are 3.82 and 9.83% respectively. These orbitals are not directed along the N—S internuclear axis. The p-vector corresponding to the nitrogen orbital (having the x, y, z components given in Table 1) makes an angle of 6.03° with the NS axis at 21.17° to the NSS plane and the corresponding

Can. J. Chem. Downloaded from www.nrcresearchpress.com by 210.87.254.40 on 09/05/12
For personal use only.

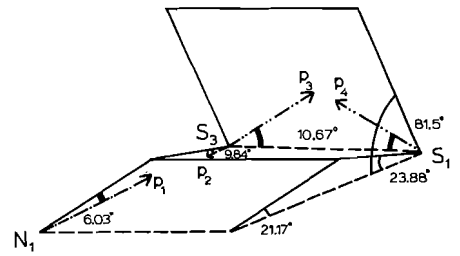

FIG. 4. Atomic orbital representation (schematic) of N—S and S—S bonds in S_4N_4 obtained from LMO's. Only one N—S bond (N_1S_3) and one S—S bond (S_1—S_3) are shown. The angles represent the deviation of the atomic hybrids from the internuclear axes and from the NSS plane. Note that the overlap occurs inside the nuclear frame, as in ref. 27 for the center bond of 1,2-$C_2B_4H_6$. Angle between p_1 and N_1—S_3 axis = 6.03°; p_1 and N_1—S_3—S_1 plane = 21.17°; p_2 and N_1—S_3 axis = 9.84°; p_2 and N_1—S_3—S_1 plane = 23.880°; p_3 and S_3—S_1 axis = p_4 and S_3—S_1 axis = 10.67°; p_3 and N_1—S_3—S_1 plane = p_4 and N_1—S_3—S_1 plane = 81.5°; where p_1 = p-orbital vector on N_1 involved in the N_1—S_3 bond, p_2 = p-orbital vector on S_3 involved in the N_1—S_3 bond, p_3 = p-orbital vector on S_3 involved in the S_3—S_1 bond, and p_4 = p-orbital vector on S_1 involved in the S_3—S_1 bond.

sulfur orbital makes an angle of 9.84° with the NS axis at 23.88° to the NSS plane (Fig. 4). Thus, maximum overlap occurs off the internuclear axis; the N—S bond is bent (17).

(4) S—S Bond

The delocalization index is 6.7% and is over the whole molecule. The orbitals in this LMO are almost pure p-orbitals on sulfur, with 2.0% s-character; the bond is between two sulfur atoms on the same side of the nitrogen plane. The S—S bond is bent, the sulfur p-orbital vectors in this LMO make angles of 10.67° with the S—S axis at 81.5° to the NSS plane.

(5) Nitrogen Lone Pair (II)

The *d* value is 14.82%. The delocalization is mainly (9.89%) to the p-orbitals of the two sulfur atoms to which the nitrogen is bonded. The remaining 5% is to all other atoms. This is a pure p-orbital lone pair on nitrogen, but more delocalized than the nitrogen s-lone pair (I) described above.

These are the only LMO's in S_4N_4. No LMO corresponds to an N—N bond; there is no N—N bond in the molecule, agreeing with the reduction products of S_4N_4 never containing N—N bonds. The LMO's show the molecule to be adequately described by the Lewis structure **B**, suggested by Lindqvist (9).

The atomic charges at nitrogen and sulfur from the present calculations are −0.329 and +0.329 respectively, again supporting structure **B** which has been shown to be consistent with the electronic spectrum of S_4N_4 (5) which requires a polar structure.

The N—S and S—S bonds are bent bonds between almost pure p-orbitals; they are weaker than normal straight bonds involving sp^n hybrids, which explains the classical "strain" in S_4N_4 and its unstable nature (4). Thus S_4N_4 is analogous to P_4 (17) where bent bonding occurs between essentially p-orbitals. The difficulty in reconciling the observed N—S and S—S bond lengths with the valence angles at nitrogen and sulfur disappears; bond lengths are not simply a function of double bond character or bond order. Thus while the N—S bond length in H_3—N—SO_3 is 1.764 ± 0.020 Å, and is assumed to be a single sp^3 bond (3), the observed N—S distance in S_4N_4 is 1.616 ± 0.010 Å. But this does not imply double bond character in the N—S bond in S_4N_4 (bond order greater than 1) nor sp^2 hybrids. The nature of a chemical bond between two atoms is determined by, (*1*) the s and p character of the bonding atomic hybrids, (*2*) the bent or straight overlap of these hybrids, and (*3*) the delocalization of these hybrids to other atoms. The S—S bond in S_4N_4 illustrates these points. The LMO shows pure p-orbitals in the bond, a considerably bent bond, and a delocalization of 6.7% to other atoms in the molecule, causing a considerable weakening of the bond even though it is a two electron single bond. This result agrees with Lindqvist's (9) prediction of a pure p-orbital bond from the correlation of observed S—S distances in S_8, $S_2O_6^{2-}$, $S_2O_4^{3-}$, and S_4N_4 with the s-character of the sulfur hybrid.

There is no satisfactory definition of bond index to measure the strength of a bond in SCFMO theory (18, 19). However, the bond order index of Wiberg (20, 21) may be used as a measure of bond strength. The index is the sum of the squares of the first-order density matrix elements between orbitals on two atoms. The Wiberg index for the N—S and S—S bonds in S_4N_4, has been calculated using the LMO's in Table 1. For the N—S bond the value is 0.907; there is an additional contribution to the N—S bond order from the delocalized N lone pair (II) of 0.16. Thus the total bond order for the N—S bond is 1.067; that for the S—S bond is 0.869. The N—S bond has little double bond character, and the S—S bond is weaker than a normal single S—S bond.

Can. J. Chem. Downloaded from www.nrcresearchpress.com by 210.87.254.40 on 09/05/12
For personal use only.

Can. J. Chem. Downloaded from www.nrcresearchpress.com by 210.87.254.40 on 09/05/12
For personal use only.

The diamagnetic ring current in S_4N_4 (10) suggests electron delocalization around the SN ring. From the LMO's the diamagnetic ring current is obviously due to the p-orbital lone pair electrons on nitrogen delocalizing into the p-orbitals on the sulfur atoms to which it is directly bonded. A recent CNDO/2 calculation of the Wiberg bond order for the S—N bonds in $N_4S_4F_4$ and S_4N_4 by Cassoux *et al.* (22) gave the values 1.3 and 1.87 for the two types of bonds in $N_4S_4F_4$ and 1.49 for the bond in S_4N_4. These authors interpreted the bond order in S_4N_4 intermediate between the values for $N_4S_4F_4$, as evidence for electron delocalization in N_4S_4. This is not true; their result is a consequence of using uniform S—N bond lengths in S_4N_4 intermediate between the two S—N bond lengths in $N_4S_4F_4$.

The present LMO picture of the molecule obtained using only s and p functions on sulfur shows electron delocalization in the molecule, and hence it is not necessary to use d-orbitals on sulfur to explain the ring current (10, 15). Turner and Mortimer's extended Hückel theory calculations (6), specifically included d-orbitals on sulfur and showed that d-orbitals do not play any role in the molecular description of S_4N_4. Similarly X_α calculations on SO_4^{2-} and SF_6 (23) have shown that there is no sulfur 3d orbital contribution to the electronic structure of these molecules. Similar conclusions have been reached by Koutecky and Musher (24) from CNDO/2 calculations on sulfur compounds of different valence states.

Conclusion

S_4N_4 has a molecular structure with coplanar nitrogen atoms. The electronic formula for the molecule is the polar Lewis structure **B**. There is no s–p hybridization at nitrogen or sulfur. The N—S and S—S bonds are bent single bonds involving pure p-orbitals. There is no N—N bond. Electron delocalization occurs by delocalization of the p-electrons in a nitrogen lone pair to the p-orbitals on the sulfur atoms to which the nitrogen is bonded. The field gradient direction at the nitrogen atom, and the relation to recent n.q.r. field gradient measurements (25) will be considered in a paper on the n.q.r. field gradients of various SN ring systems (26).

The authors deeply appreciate the warm hospitality and the keen interest in their welfare and scientific work, extended by the late Professor C. A. Coulson, FRS. M.S.G. gratefully acknowledges the award of a Commonwealth Bursary of the Royal Society, London, that made possible his visit to Oxford. M. A. W. acknowledges the award of a National Research Council of Canada Travelling Fellowship 1971–1974.

1. M. B. Goehring. Q. Rev. **10**, 437 (1959); Prog. Inorg. Nucl. Chem. **1**, 207 (1959); Angew. Chem. **73**, 589 (1961).
2. C. S. Lu and J. Donohue. J. Am. Chem. Soc. **66**, 818 (1944).
3. B. D. Sharma and J. Donohue. Acta Cryst. **16**, 891 (1963).
4. E. R. Lippincott and M. C. Tobin. J. Chem. Phys. **21**, 1559 (1953).
5. P. S. Brateman. J. Chem. Soc. 2297 (1965).
6. A. C. Turner and F. S. Mortimer. Inorg. Chem. **5**, 906 (1966).
7. R. J. Boyd and M. A. Whitehead. J. Chem. Soc. Dalton, 73, 78, 81 (1972).
8. D. Chapman and T. C. Waddington. Trans. Faraday Soc. **58**, 1679 (1962).
9. I. Lindqvist. J. Inorg. Nucl. Chem. **6**, 159 (1958).
10. J. B. Mason. J. Chem. Soc. A, 1567 (1969).
11. H. Weinstein, R. Pauncz, and M. Cohen. *In* Advances in atomic and molecular physics, Vol. 7. Academic Press, New York. 1971. p. 40.
12. J. E. Lennard-Jones. Proc. R. Soc. Lond. A**198**, 1, 14 (1949).
13. W. England, L. S. Salmon, and K. Ruedenberg. Top. Curr. Chem. **23**, 31 (1971).
14. K. Ruedenberg. *In* Modern quantum chemistry, Part 1. Academic Press, New York. 1965. p. 85.
15. E. Switkes, W. N. Lipscomb, and M. D. Newton. J. Am. Chem. Soc. **92**, 3847 (1970).
16. M. S. Gopinathan and P. T. Narasimhan. Mol. Phys. **22**, 473 (1971).
17. C. A. Coulson. Valence, 2nd ed. Oxford University Press, London. 1961.
18. R. J. Boyd. Can. J. Chem. **51**, 1151 (1973).
19. J. W. McIver, Jr., P. Coppens, and D. Nowaic. Chem. Phys. Lett. **11**, 82 (1971).
20. K. B. Wiberg. Tetrahedron, **24**, 1083 (1968).
21. C. Trindle and O. Sinanoglu. J. Am. Chem. Soc. **91**, 853 (1969).
22. P. Cassoux, J. F. Labarre, O. Glemsek, W. Kock. J. Mol. Struct. **13**, 405 (1972).
23. K. H. Johnson. *In* Advances in quantum theory, Vol. 7. *Edited by* P. O. Lowdin. Academic Press, New York. 1973. p. 143.
24. V. B. Koutecky and J. I. Musher. Theor. Chim. Acta, Berl. **33**, 227 (1974).
25. D. Benlian, M. Gourdji, and L. Guibe. J. Chem. Phys. **59**, 5382 (1974).
26. M. S. Gopinathan and M. A. Whitehead. To be published.
27. D. A. Kleier, T. A. Halgren, J. H. Hall, and W. N. Lipscomb. J. Chem. Phys. **61**, 3905 (1974).

The Origin of the Methyl Radical in the Photolysis of Propane at 123.6 nm

JANUSZ GAWŁOWSKI,[1] JAN A. HERMAN, AND PIERRE GAGNON

Groupe de Dynamique Moléculaire, Département de Chimie, Université Laval, Québec, Québec G1K 7P4

Received November 8, 1974

JANUSZ GAWŁOWSKI, JAN A. HERMAN, and PIERRE GAGNON. Can. J. Chem. **53**, 1348 (1975).

The isotopic composition of methane formed in photolysis at 123.6 nm of propane-*1,1,1-d*$_3$ under high pressure and in the presence of NO or H_2S was investigated. The results indicate that the main source of methyl radicals are the dissociation of propane and propyl radicals

$$C_3H_8 \xrightarrow{h\nu} CH_3^{\cdot} + C_2H_5^{\cdot}$$

$$C_3H_8 \xrightarrow{h\nu} H^{\cdot} + C_3H_7^{*} \rightarrow H^{\cdot} + CH_3^{\cdot} + C_2H_4$$

JANUSZ GAWŁOWSKI, JAN A. HERMAN et PIERRE GAGNON. Can. J. Chem. **53**, 1348 (1975).

On a étudié la composition isotopique du méthane formé lors de la photolyse à 123.6 nm et à presssion élevée du trideutéro-*1,1,1* propane et en présence du NO et H_2S. Les résultats indiquent que les radicaux méthyls viennent principalement de la dissociation du propane et du radical propyl

$$C_3H_8 \xrightarrow{h\nu} CH_3^{\cdot} + C_3H_5^{\cdot}$$

$$C_3H_8 \xrightarrow{h\nu} H^{\cdot} + C_3H_7^{*} \rightarrow H^{\cdot} + CH_3^{\cdot} + C_2H_4$$

Introduction

The photolysis of propane in the vacuum ultraviolet region was extensively investigated in the last decade (1–6). However, agreement relative to the primary and secondary decomposition processes of propane has not yet been achieved. The authors of refs. 1–4 and 6 consider the following five primary processes:

$$[1] \quad C_3H_8 \xrightarrow{h\nu} C_3H_6 + H_2$$

$$[2] \quad \rightarrow C_2H_4 + CH_4$$

$$[3] \quad \rightarrow C_2H_6 + CH_2^{\cdot}$$

$$[4] \quad \rightarrow C_3H_7^{\cdot} + H^{\cdot}$$

$$[5] \quad \rightarrow C_2H_5^{\cdot} + CH_3^{\cdot}$$

The fragments produced from processes 1–5 are usually highly excited and can dissociate further:

$$[6] \quad C_3H_7^{*} \rightarrow C_3H_6 + H^{\cdot}$$

$$[7] \quad \rightarrow C_2H_4 + CH_3^{\cdot}$$

$$[8] \quad C_2H_5^{*} \rightarrow C_2H_4 + H^{\cdot}$$

$$[9] \quad C_2H_4^{*} \rightarrow C_2H_2 + H_2$$

Vorachek and Koob (5) have proposed another mechanism for the photolysis of propane at 123.6 nm: (*a*) they postulate only three primary processes 1–3, (*b*) the methyl radical originates in dissociation of excited methane

$$[10] \quad CH_4^{*} \rightarrow CH_3^{\cdot} + H^{\cdot}$$

(*c*) the hydrogen atoms are formed only by dissociation of excited fragments, mainly in processes 10 and 11

$$[11] \quad H_2^{*} \rightarrow H^{\cdot} + H^{\cdot}$$

The purpose of this work is to examine which of the two proposed mechanisms, [5] and [7] or [10], are the origin of the methyl radicals produced in the photolysis of propane at 123.6 nm.

Experimental

Carefully degassed partially deuterated propane, $CD_3CH_2CH_3$, from Merck, Sharp and Dohme was used in the experiments. Its isotopic purity was better than 98%. Hydrogen sulfide and nitric oxide (Matheson Co.) were used after purification by standard methods. The mixtures of gases were irradiated with a krypton resonance lamp equipped with a CaF_2 window allowing only the transmission of the 123.6 nm wavelength photons. The construction of the lamp is already described in the literature (7). After irradiation the gases were frozen at liquid nitrogen temperature (−195 °C) and the volatile residual gases were introduced directly into a Varian

[1]Permanent address: Laboratory of Radiochemistry and Radiation Chemistry, Warsaw University, Warsaw, Poland.

Can. J. Chem. Downloaded from www.nrcresearchpress.com by 210.87.254.5 on 09/05/12
For personal use only.

TABLE 1. Isotopic composition of methane produced in photolysis of propane-1,1,1-d_3 at 123.6 nm*

Pressure (Torr)	Scavenger	CD_4	CD_3H	CD_2H_2	CDH_3	CH_4
16.6	—	1.9	42.5	3.1	3.0	49.5
16.8†	—	4.2	47.2	3.1	5.5	40.0
270	NO (13.5 Torr)	—	45.5	3.0	2.0	49.5
270	H_2S (30 Torr)	—	41.5	7.1	2.6	48.8
380	NO (20 Torr)	—	45.2	2.3	3.0	49.5
380	H_2S (41 Torr)	—	40.0	7.5	3.6	49.0

*Precision of results ± 1% absolute.
†Reference 1.

Atlas CH 7 mass spectrometer. The analyses of isotopic methanes were done at mass resolution $m/\Delta m \approx 2000$ to differentiate between m/e of interest from those originating from water, nitrogen, and oxygen.

Results and Discussion

The isotopic composition of methane formed during photolysis of pure propane-*1,1,1*-d_3 at 16.6 Torr and at 270 and 380 Torr in the presence of suitable scavengers is presented in Table 1. The first two entries in Table 1 represent results of two different experiments done under identical conditions, the first one (at 16.6 Torr) by us, the second (at 16.8 Torr) by Okabe and McNesby (1). Both sets of results show CD_3H and CH_4 to be the main products (about 90% of the total methane), but we find the CD_3H/CH_4 ratio to be practically the inverse of the ratio found by the workers of ref. 1. The reasons for this discrepancy are not clear yet. Isotopic composition differences for experiments at 270 and 380 Torr and for each scavenger are within experimental errors.

These results allow us to calculate approximately the isotopic composition of methyl radicals. In the presence of NO, methane is formed only in molecular processes, mainly in reaction 2. On the other hand, H_2S reacts very efficiently with free radicals, and therefore in its presence methane will be formed not only in molecular processes, but also from $CH_3^\cdot$ (3) and $CH_2^\cdot$ (8) radicals

$$[12] \qquad CH_3^\cdot + H_2S \rightarrow CH_4 + HS^\cdot$$

$$[13] \qquad CH_2^\cdot + 2H_2S \rightarrow CH_4 + 2HS^\cdot$$

On the assumption that (*1*) the quantum yields of molecular methane, methyl, and methylene radicals are identical for photolysis of C_3H_8 and $CD_3CH_2CH_3$ and (*2*) that methylene radical is generated with equal efficiency from both carbon ends in propane-*1,1,1*-d_3 (this is an oversimplification, because the isotope effect is not taken into account), one can estimate from the present results and from Vorachek and Koob's data (5) at 380 Torr ($\Phi_{CH_4} = 0.152$, $\Phi_{CH_3} = 0.339$, and $\Phi_{CH_2} = 0.035$)[2] the isotopic composition of methyl radicals. The calculation gives the following isotopic composition for the methyl radical: $CD_3^\cdot$, 42%; $CD_2H^\cdot$, 5%; $CDH_2^\cdot$, 4%; and $CH_3^\cdot$, 49%. The fact that more than 90% of the scavengeable methane is formed from $CH_3^\cdot$ and $CD_3^\cdot$ radicals shows clearly that processes 5 and 7 are the main sources of the methyl radical. If the assumptions of Vorachek and Koob were true, then the methyl radical should be composed mainly of CD_2H and CDH_2. Ausloos *et al.* have shown in the photolysis of $CD_3CH_2CD_3$ + NO system at 123.6 nm that the yields of CD_3H and C_2D_3H are practically equal, but the yield of $C_2D_2H_2$ is about 10-fold greater than that of CD_4 (6). Therefore, the dissociating methane in reaction 10 could only arise from the end carbon atoms in propane, and in our experiments this should correspond to CD_3H and CDH_3, which means that

$$[14a] \qquad CD_3H^* \rightarrow CD_3^\cdot + H^\cdot$$

$$[14b] \qquad \rightarrow CD_2H^\cdot + D^\cdot$$

[2]We assume that only methylene radicals in the triplet state react with H_2S. This is inferred from the results of Ausloos *et al.* relative to the yield of butanes in the propane photolysis (3). They found that this yield was practically the same in the presence of 12.9% H_2S or 5% NO. Since the precursor of butanes in the C_3H_8 + NO system is the singlet methylene radical on account of its low reactivity towards NO, we conclude that similar yield of butanes obtained by Ausloos *et al.* in the C_3H_8 + H_2S system indicate that $^1CH_2$ is no more reactive towards H_2S than it is towards NO. From Vorachek and Koob's data at 380 Torr of C_3H_8 + 5% O_2 we get: $\Phi^3_{CH_2} = \Phi_{C_2H_6} - \Phi_{\Sigma C_4H_{10}} = 0.035$.

Can. J. Chem. Downloaded from www.nrcresearchpress.com by 210.87.254.5 on 09/05/12
For personal use only.

[15*a*] $CDH_3^* \rightarrow CDH_2^{\cdot} + H^{\cdot}$

[15*b*] $\rightarrow CH_3^{\cdot} + D^{\cdot}$

In partially deuterated hydrocarbons the isotope effect favors the C—H bond dissociation compared to that of the C—D bond (9), we would then expect the following values for the ratio of the yields of the methyl radicals generated in reactions 14*a* and *b* and 15*a* and *b*: $CD_2H/CD_3 < 3$ and $CDH_2/CH_3 > 3$. The corresponding experimental values for these ratios from our results are $CD_2H/CD_3 \approx 0.12$ and $CDH_2/CH_3 \approx 0.08$. The comparison of expected with experimental CD_2H/CH_3 ratios shows clearly that the breakdown of methane in reaction 10 cannot be the main source of methyl radicals in the photolysis of propane. The calculated contribution of partially deuterated radicals $CD_2H^{\cdot}$ (5%) and $CDH_2^{\cdot}$ (4%) (Table 1) can result from accumulated experimental error and assumptions relative to the isotopic calculations; it can also originate from isotopic impurities in the reactant gas. Although one cannot eliminate reaction 10 from the mechanism its contribution to the methyl radical formation cannot exceed 10%.

This work was made possible through the financial assistance of the National Research Council of Canada.

1. H. Okabe and J. R. McNesby. J. Chem. Phys. **37**, 1340 (1962).
2. P. Ausloos, S. C. Lias, and J. B. Sandoval. Discuss. Faraday Soc. **36**, 66 (1963).
3. P. Ausloos and S. C. Lias. J. Chem. Phys. **44**, 521 (1966).
4. K. Oki, H. Akimoto, Y. Ogata, and I. Tanaka. J. Chem. Phys. **55**, 3822 (1971).
5. J. H. Vorachek and R. D. Koob. Can. J. Chem. **51**, 344 (1973).
6. P. Ausloos, R. E. Rebbert, and S. C. Lias. J. Photochem. **2**, 287 (1973/1974).
7. J. R. Gorden, Jr., R. E. Rebbert, and P. Ausloos. NBS Tech. Note 496, Natl. Bur. Stand. U.S., 1969.
8. A. A. Scala and P. Ausloos. J. Chem. Phys. **49**, 2282 (1968).
9. B. S. Rabinovitch and D. W. Setser. Adv. Photochem. **3**, 1 (1964).

Can. J. Chem. Downloaded from www.nrcresearchpress.com by 210.87.254.5 on 09/05/12
For personal use only.

^{13}C Nuclear Magnetic Resonance Studies. Part 48. ^{13}C Spectra of a Variety of Bicyclic Ketones[1]

S. H. GROVER, D. H. MARR,[2] J. B. STOTHERS, AND C. T. TAN
Department of Chemistry, University of Western Ontario, London N6A 5B7

Received November 1, 1974

S. H. GROVER, D. H. MARR, J. B. STOTHERS, and C. T. TAN. Can. J. Chem. **53**, 1351 (1975).

The ^{13}C n.m.r. spectra of a series of 37 bicyclic ketones have been recorded to examine the variations in ^{13}C shieldings with structure and with methyl substitution. Several examples of six skeletal types were included: bicyclo[4.4.0]decanones, bicyclo[4.1.0]heptanones, bicyclo-[3.1.0]hexanones, bicyclo[3.2.2]nonanones, bicyclo[3.2.1]- and -[3.3.0]octanones as well as bicyclo[2.1.1]hexan-2-one, nopinone (6,6-dimethylbicyclo[3.1.1]heptan-2-one), and two methyl derivatives of the latter. The observed trends associated with methyl substitution follow well-defined patterns and offer further support for the application of ^{13}C shieldings as aids for stereochemical assignments especially through the well known γ effects. The variation in the shieldings of the carbonyl carbons in these systems suggested that bond eclipsing interactions have an important influence on this parameter. With this notion, the heretofore puzzling variations observed for the cycloalkanones are readily interpretable in terms of their favored conformations.

S. H. GROVER, D. H. MARR, J. B. STOTHERS et C. T. TAN. Can. J. Chem. **53**, 1351 (1975).

On a déterminé les spectres r.m.n. du ^{13}C d'une série de 37 cétones bicycliques pour examiner les variations du blindage du ^{13}C en fonction de la structure et de la substitution par des groupements méthyles. Plusieurs exemples de six types de squelettes sont inclus: bicyclo-[4.4.0]déconones, bicyclo[4.1.0]heptanones, bicyclo[3.1.0]hexanones, bicyclo[3.2.2]nonanones, bicyclo[3.2.1] et [3.3.0]octanones de même que bicyclo[2.1.1]hexanone-2, nopinone (diméthyl-6,6 bicyclo[3.1.1]heptanone-2) de même que deux dérivés méthylés de cette dernière. Les tendances observées, associées avec la substitution du méthyle, suivent des patrons bien définis et offrent un support supplémentaire pour l'application des blindages du ^{13}C comme aide pour l'attribution stéréochimique spécialement grâce aux effets γ bien connus. La variation dans les blindages du groupe carbonyle dans ces systèmes suggère que des interactions provenant des éclipsages des liens ont une influence importante sur ce paramètre. Avec cette notion, les variations un peu surprenante observées jusqu'à maintenant dans les cycloalcanones sont facilement interprétables en termes des conformations les plus favorisées.

[Traduit par le journal]

Introduction

One of the most important and interesting features of ^{13}C nuclear shieldings is their remarkable sensitivity to stereochemical environment. Although this has been recognized for several years (1), a satisfactory theoretical interpretation has yet to be presented. Nevertheless, stereochemical assignments for a wide variety of systems have been obtained empirically (2) through the knowledge that the relative orientation of vicinal carbons, or of a carbon vicinal to a heteroatom, has a pronounced effect on the observed shieldings, attributed to 1,4-nonbonded interactions. The general trends and relative magnitudes of these shifts, termed γ effects, have been determined through systematic studies of series of model compounds, primarily, in cyclic systems. Much of the attention has been focussed on mono- and polycyclic six-membered ring systems because of their well-defined geometries although several bicyclic systems with other ring sizes are also attractive models. Of the latter, however, only the bicyclo[2.2.1]heptanes (ref. 3 and references therein) and bicyclo[2.2.2]octanes (4) have been examined in some detail. In these studies, a common approach has been to examine the effects of methyl substitution on the shieldings of the skeletal carbons as a function of methyl orientation since the latter is well defined. In this way, the influence of molecular geometry on the ^{13}C shieldings can be determined with minimum alteration of the bonding contributions.

Another aspect of stereochemical effects in ^{13}C spectra concerns the variation of carbonyl carbon shieldings with ring size. While the trend was

[1]Part 47, ref. 30.

[2]Present address: Stauffer Chemical, Dobbs Ferry, N.Y.

Can. J. Chem. Downloaded from www.nrcresearchpress.com by 210.87.254.42 on 09/05/12
For personal use only.

Can. J. Chem. Downloaded from www.nrcresearchpress.com by 210.87.254.42 on 09/05/12
For personal use only.

illustrated several years ago (5), no satisfactory explanation has been put forward although a conformational origin may be suspected. The relative rigidity of bicyclic skeletons, however, provides a means whereby potential conformational contributions can be controlled and tested.

For these reasons, a series of 37 bicyclic ketones, embracing 8 skeletal types, **1–8**, was selected for ^{13}C n.m.r. examination. We wish to report the ^{13}C shieldings for this series for comparison of the methyl substituent effects with other well-defined systems. The carbonyl shieldings for this series have led to an interpretation of the variation of carbonyl shieldings in the cycloalkanones (C_4–C_{17}) in terms of their preferred conformations. Both features have potential application for stereochemical elucidations.

Experimental

Materials

Apart from bicyclo[3.2.1]octan-2-one, *trans*-decal-1- and -2-one which were commercially available, the ketones were prepared by published procedures. These include bicyclo[3.1.0]hexan-3-one by CrO_3 oxidation of bicyclo[3.1.0]hexan-3-ol (6), 6,6-dimethylbicyclo[3.1.1]-heptan-2-one (nopinone) by ozonolysis of β-pinene (7), *cis*-bicyclo[3.3.0]octan-2-one (8), bicyclo[3.2.1]octan-3-one (9) and -6-one (10). Several samples were available from earlier work in this laboratory: the bicyclo[3.1.0]hexan-2-ones (11), the bicyclo[4.1.0]heptan-2-ones (11), and the 10-methyldecalones (12). Professors R. R. Fraser and J. L. Charlton kindly provided samples of bicyclo[3.2.2]nonan-6-one and bicyclo[2.1.1]hexan-2-one, respectively. 3,3-Dimethylbicyclo[3.3.0]octan-2-one was isolated as the rearrangement product obtained by homoenolization of 3,3-dimethylbicyclo[3.2.1]octan-2-one (13). Ring expansion of norcamphor with diazoethane furnished *endo*-2-methylbicyclo[3.2.1]octan-3-one (14) which upon equilibration with trifluoroacetic acid gave a mixture of the *exo* and *endo* isomers (37:63). This ring expansion reaction also gave *exo*-3-methylbicyclo[3.2.1]octan-2-one but, contrary to the original report, attempted epimerization with sodium methoxide failed to produce detectable amounts of the *endo*-3-methyl isomer. To confirm enolate formation under these conditions, an experiment with MeO^-/MeOD was carried out giving only the *endo*-3-deuterio-*exo*-3-methyl isomer in high yield. Norcamphor also served as the starting material for 2,2-dimethylbicyclo[3.2.1]octan-3-one which was generated from the 2-methyl-2-chloromethyl derivatives (15) by reduction with *t*-BuO^-/*t*-BuOH followed by CrO_3 oxidation to furnish the desired ketone identical to that reported by another route (16). The remaining examples were obtained by methylation using the sodamide – methyl iodide procedure (17). The mono- and dimethyl derivatives were, in most cases, readily separated by g.c. on SE-30 columns. The preparations and physical constants of the new compounds obtained in this work are described below.

3,3,6,6-Tetramethylbicyclo[3.1.1]heptan-2-one

Methylation of nopinone using sodamide and methyl iodide (17) afforded a mixture (550 mg) of three ketones. Gas chromatographic analysis and separation on SE-30 columns showed the mixture to contain nopinone (52%), *cis*-nopinone, the *exo*-3-methyl derivative (34%), and the desired 3,3-dimethylnopinone (14%). A sample of *cis*-nopinone, *exo*-3,6,6-trimethylbicyclo[3.1.1]heptan-2-one, exhibited the same i.r. and n.m.r. spectra as those reported (18).

Mol. wt. Calcd. for $C_{10}H_{16}O$: 152.1200. Found (*m/e*): 152.1199.

A sample of 3,3,6,6-tetramethylbicyclo[3.1.1]heptan-2-one had the following properties: $\nu_{max}(CCl_4)$ 1700 cm^{-1}; ^1H n.m.r. 0.84 (s, 3H), 1.24 (s, 3H), 1.31 (s, 3H), 1.33 p.p.m. (s, 3H).

Mol. wt. Calcd. for $C_{11}H_{18}O$: 166.1357. Found (*m/e*): 166.1359.

2,4-Dinitrophenylhydrazone, m.p. 117.5–118.5°.

7,7-Dimethylbicyclo[3.2.2]nonan-6-one

Methylation of bicyclo[3.2.2]nonan-6-one using $NaNH_2$–CH_3I (17) gave a mixture containing unreacted starting material (20%), the monomethyl ketones (43%), and 7,7-dimethylbicyclo[3.2.2]nonan-6-one (37%). The latter was isolated by preparative g.c. on a SE-30 column and found to have the following properties: $\nu_{max}(CCl_4)$ 1711 cm^{-1}; ^1H n.m.r. 1.14 p.p.m. (s, 6H); m.p. 89–90°.

Anal. Calcd. for $C_{11}H_{18}O$: C, 79.46; H, 10.91. Found: C, 79.56; H, 10.78.

The 7-methylbicyclo[3.2.2]nonan-6-ones, however, could not be separated but the mixture gave methyl signals in its ^1H spectrum at 1.16 (d, $J \sim 7.5$ Hz) and 1.13 p.p.m. (d, $J \sim 6.5$ Hz) assigned to the *exo* and *endo* isomers on the basis of the ^{13}C spectrum (see Discussion) which indicated that the two ketones were present in a 2:3 (*exo/endo*) ratio.

Anal. Calcd. for $C_{10}H_{16}O$: C, 78.89; H, 10.59. Found: C, 78.85; H, 10.64.

endo-7-Methylbicyclo[3.2.1]octan-6-one

The usual methylation procedure employed for this series gave only 4% of the *endo*-7-methyl derivative of bicyclo[3.2.1]octan-6-one. The major monomethyl derivative was found to be identical to that described by Kubota *et al.* (19) and subsequently shown to be the 7-*exo*-methyl isomer. A sample of the latter (400 mg) was dissolved in 10 ml of 3% sodium methoxide in methanol and the solution refluxed for 7 h in a nitrogen atmosphere. After dilution with 15 ml of ice water, the ketone product was isolated by pentane extraction. Gas chromatographic analysis on 20% Carbowax 4000 showed that the mixture (400 mg) contained 45% of the *exo*-7-methyl isomer and 55% of the desired *endo*-7-methylbicyclo[3.2.1]octan-6-one. Separation by preparative g.c. gave a sample of the latter having the following properties: $\nu_{max}(CCl_4)$ 1710 cm^{-1}; ^1H n.m.r., 1.10 p.p.m. (d, 3H, $J \sim 7$ Hz); 2,4-dinitrophenylhydrazone, m.p. 203.5–204.5°.

Anal. Calcd. for $C_{15}H_{18}N_4O_4$: C, 56.59; H, 5.70; N, 17.60. Found: C, 56.63; H, 5.88; N, 17.42.

As an aid for some of the assignments, several of the ketones were refluxed with 5% MeO^-/MeOD to exchange the α-protons. Specific examples are noted in the Results section. In each case, the ketone was recovered in high yield.

Spectra

Proton spectra were recorded with either Varian T-60 or HA-100 spectrometers while ^{13}C spectra were ob-

Can. J. Chem. Downloaded from www.nrcresearchpress.com by 210.87.254.42 on 09/05/12
For personal use only.

tained using a Varian XL-100-15 system operating in the Fourier transform mode, as described previously (3). The data were determined for $CDCl_3$ solutions (5–15% w/v) containing a few drops of TMS as an internal standard in 5 mm sample tubes. Peak positions were measured relative to TMS to within ±1 Hz; thus the shieldings have precisions greater than 0.1 p.p.m.

Results

The shielding data for this series of ketones are collected in Table 1. In each case, both noise and off-resonance decoupled spectra were obtained to distinguish between carbon types, the first step for the assignments. The carbonyl carbons were readily assigned from their characteristic low-field positions (1) and in the parent systems, the

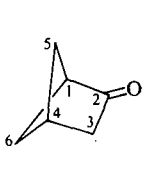

1

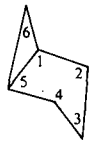

2

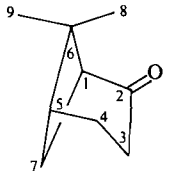

3

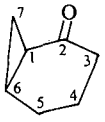

4

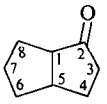

5

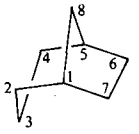

6

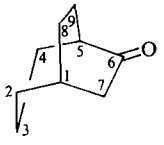

7

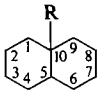

8

nonequivalent bridgehead carbons could be distinguished readily since that closer to the carbonyl is consistently less shielded. For the symmetrical compounds, the relative intensities led to straightforward assignments. From these features, the assignments for 2-oxo-**1**, 3-oxo-**2** and -**6** were completed.

The 2-oxo-**2** derivatives each have three methylene carbons which were distinguished in the monomethyl derivatives by deuterium exchange of the α-methylene protons. In the spectra of the dideuterated derivatives, one methylene signal essentially disappeared, one was shifted to higher field by ~0.2 p.p.m., by the geminal isotope effect, while the third was unaffected, establishing these as the C-3, C-4, and C-6 signals, respectively (3). From the methyl shieldings for the monomethyl derivatives, it followed that the more shielded methyl signal for the 1,5-dimethyl derivative was due to the 1-methyl carbon. In a similar manner, the assignments for the **4** derivatives were completed, again, utilizing the results for the 3,3-dideuteriomonomethyl isomers to identify the different methylene signals.

To aid the assignment for nopinone (**3**) and its derivatives, the ^{13}C spectra of apopinane (**9***a*), *cis*-pinane (**9***b*), and the nopinols (**9***c* and *d*) were also recorded; these data appear in Table 2. For **9***a*, the C-1, -2, -4, -5, and -6 assignments were straightforward and it remained to distinguish the C-3 from the C-7 signal and the *gem*-dimethyl resonances. The consistent appearance of a methylene signal near 26 p.p.m. in all spectra of the [3.1.1] series led to its assignment as C-7 since C-2 substitution could be expected to have little effect at this position. Since C-8 is essentially axial with respect to the six-membered ring and C-9 is equatorial, it was expected that C-8 would be the more shielded of the *gem*-dimethyl carbons. This was supported by an examination of the relative shifts in **3** upon addition of $Eu(fod)_3$, since the higher field methyl signal exhibited a greater downfield shift. With two methyl signals near 23 p.p.m. for **9***b* the assignments of C-8 and

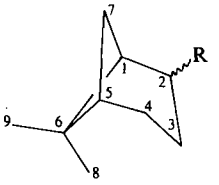

9

a R = H
b R = α-Me
c R = α-OH
d R = β-OH

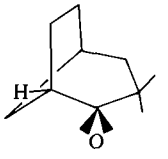

10

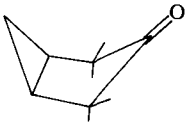

11

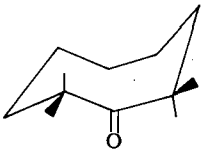

12

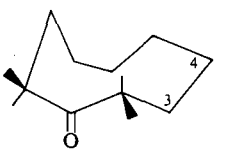

13

Can. J. Chem. Downloaded from www.nrcresearchpress.com by 210.87.254.42 on 09/05/12
For personal use only.

TABLE 1. ^{13}C shieldings of several bicyclic ketones[a]

Skeleton	Substituent	C-1	C-2	C-3	C-4	C-5	C-6	C-7	C-8	C-9	C-10	Me[b]
[2.1.1] (1)	2-Oxo	56.0	214.0	40.8	35.8	40.9	40.9					
[3.1.0] (2)	3-Oxo	12.2	40.9	217.9	40.9	12.2	13.3					
	2-Oxo	27.4	215.1	31.4	22.6	21.6	13.5					
	2-Oxo-1-Me	32.6	215.8	32.0	21.7	28.7	20.5					13.9
	2-Oxo-5-Me	35.0	214.5	33.6	29.1	30.0	20.9					21.2
	2-Oxo-1,5-Me_2	37.2	215.9	32.5	28.8	33.4	26.8					10.5 (C-1) 18.5 (C-5)
[3.1.1] (3)	2-Oxo-6,6-Me_2	57.9	214.3	32.7	21.4	40.4	41.0	25.2				22.1 (*syn*) 25.8 (*anti*)
	2-Oxo-3,6,6-Me_3	57.1	216.1	37.1	30.9	41.1	41.2	25.4				14.1; 21.9; 26.3
	2-Oxo-3,3,6,6-Me_4	58.5	219.9	43.0	37.6	42.1	40.9	25.9				22.7; 26.4; 27.6; 33.8
[4.1.0] (4)	2-Oxo	25.7	208.7	36.6	17.9	21.3	17.4	10.2				
	2-Oxo-1-Me	29.8	210.2	36.4	19.3	21.8	26.3	18.1				19.8
	2-Oxo-6-Me	34.3	208.7	35.8	18.1	28.1	23.9	17.5				24.8
	2-Oxo-1,6-Me_2	35.4	209.9	36.0	18.3	29.4	28.5	24.1				14.3 (C-1) 21.2 (C-6)
[3.3.0] (5)	2-Oxo	52.0	223.0	37.9	(26.4)	41.0	33.5	(26.2)	29.8			
	2-Oxo-3,3-Me_2	50.3	224.6	47.6	43.5	36.3	33.6	25.0	29.4			23.1 (*endo*) 25.3 (*exo*)
	2-Oxo-1,3,3-Me_3	56.4	225.1	46.9	42.4	45.5	31.8	24.4	37.4			24.9 (1-Me) 24.4 (*endo*) 25.8 (*exo*)

Can. J. Chem. Downloaded from www.nrcresearchpress.com by 210.87.254.42 on 09/05/12
For personal use only.

TABLE 1—*Continued*

Skeleton	Substituent	C-1	C-2	C-3	C-4	C-5	C-6	C-7	C-8	C-9	C-10	Me[b]
[3.2.1]	2-Oxo	51.2	214.0	34.7	32.1	34.1	(28.1)	(28.0)	38.3			
(**6**)	2-Oxo-3-Me	51.1	214.7	38.3	42.5	34.8	28.4	27.9	39.4			14.5
	2-Oxo-3,3-Me_2	50.9	218.2	42.1	46.0	35.1	28.7	28.1	35.7			30.6 31.2
	3-Oxo	35.3	50.3	211.9	50.3	35.3	29.3	29.3	37.8			
	3-Oxo-2-*exo*-Me	41.6	53.1	218.1	47.7	35.3	28.5	30.1	32.1			17.6
	3-Oxo-2-*endo*-Me	42.7	51.4	213.0	49.8	36.6	29.2	24.3	39.8			12.8
	3-Oxo-2,2-Me_2	47.7	49.7	216.3	47.1	35.9	28.4	25.4	34.1			22.9 (*endo*) 26.4 (*exo*)
	6-Oxo	32.2	(30.5)	18.9	(30.7)	46.2	221.4	43.5	37.2			
	6-Oxo-7-*exo*-Me	39.4	31.4	19.3	30.5	(46.7)	224.2	(46.9)	34.4			15.6
	6-Oxo-7-*endo*-Me	36.8	26.1	19.1	30.8	45.7	223.4	48.4	36.4			8.5
	6-Oxo-7,7-Me_2	43.1	28.1	19.2	31.2	45.8	225.4	48.1	34.4			25.2 (*exo*) 17.9 (*endo*)
[3.2.2]	6-Oxo	28.5	34.1	21.6	31.9	46.9	216.2	44.3	24.4	23.2		
(**7**)	6-Oxo-7-*exo*-Me	35.2	35.4	21.4	30.9	46.9	218.9	47.5	20.1	22.9		17.4
	6-Oxo-7-*endo*-Me	34.1	29.1	21.1	31.1	46.5	218.0	46.5	25.9	22.9		12.7
	6-Oxo-7,7-Me_2	39.6	31.4	21.0	31.4	47.0	220.1	46.4	23.3	22.7		23.2 (*endo*) 26.9 (*exo*)
[4.4.0]	1-Oxo	211.9	41.6	(25.4)	33.0	44.9	34.3	(25.1)	(25.8)	26.5	54.9	
(**8**)	1-Oxo-10-Me	215.6	37.4	26.2	(27.7)	46.1	(28.0)	26.2	21.4	32.5	48.3	15.7
	2-Oxo	48.5	210.5	41.4	(32.7)	41.6	34.2	26.1	25.6	(33.6)	43.3	
	2-Oxo-10-Me	56.8	211.2	41.3	28.0	43.7	29.4	26.6	21.1	41.6	37.6	16.5
	3-Oxo-10-Me	40.3	38.1	210.6	44.8	44.6	29.0	26.0	21.6	41.0	33.1	14.9
	4-Oxo-10-Me	40.8	20.5	40.8	210.9	57.6	22.6	25.6	21.2	41.3	39.6	16.9

[a]In p.p.m. from internal TMS in $CDCl_3$ solutions. Assignments for similar values in parentheses may be reversed.
[b]*Syn* with respect to the carbonyl group; *endo* with respect to the larger ring.

TABLE 2. ^{13}C shieldings[a] of some bicyclic nydrocarbons and alcohols

Compound	C-1	C-2	C-3	C-4	C-5	C-6	C-7	C-8	C-9	C-10
9*a*	41.1	25.4	22.4	25.4	41.1	39.1	26.7	20.5	26.8	
9*b*	48.1	36.0	33.9	23.9	41.4	38.7	26.6	(22.9)	28.3	(23.2)
α-Nopinol (**9***c*)	47.9	73.1	28.3	24.8	41.0	37.4	25.5	22.4	27.3	
β-Nopinol (**9***d*)	48.0	69.4	23.3	22.7	40.5	39.4	25.7	20.0	26.7	
6	35.2	32.8	19.1	32.8	35.2	28.9	28.9	39.7		
7	29.0	35.7	22.2	35.7	29.0	25.9	25.9	25.9	25.9	
trans-Decalin[b]	34.3	26.9	26.9	34.3	43.7	34.3	26.9	26.9	34.3	43.7
10-Methyl-*trans*-decalin[c]	42.1	22.1	27.2	29.3	45.8	29.3	27.2	22.1	42.1	33.9

[a]In p.p.m. from internal TMS. Measured for 5–15% (w/v) solutions in $CDCl_3$.
[b]From ref. 12.
[c]From ref. 20; the methyl shielding is 15.7 p.p.m.

C-10 are uncertain and for 3,3,6,6-tetramethyl-**3** the methyl assignments may not be correct; the present assignments are discussed more fully later.

As noted earlier, 3,3-dimethyl-*cis*-bicyclo-[3.3.0]octan-2-one was obtained by homoenolization of 3,3-dimethylbicyclo[3.2.1]octan-2-one. Deuterium exchange under homoenolization conditions, coupled with ^2H n.m.r. examination, permitted unequivocal identification of C-6, -7, and -8 (13) in the ^{13}C spectrum and completed the assignments, from which those for **5** and its trimethyl derivative followed readily.

In the [3.2.1] series, the parent hydrocarbon was also examined (Table 2). For the 2-oxo compounds, the spectra of the 3,3-dideuterio, 3-deuterio-3-methyl, and 1,7,7,9,10-pentadeuterio-3,3-dimethyl derivatives were also determined; the latter isomer was obtained from homoenolization experiments (13). With these data the assignments for the 2-oxo derivatives were readily completed. For the 3-oxo derivatives, the well-separated methine signals permitted straightforward assignments while the C-6 and C-7 methylene resonances were identified on the basis of an expected shielding influence of an *endo*-2-methyl at C-7 but for the *exo*-2-methyl isomer these methylene signals were not so readily assigned. By analogy with *exo*-3-methylnorcamphor (3), however, one may predict that the *exo*-2-methyl group would tend to deshield C-7 slightly and, on this basis, the C-6 and C-7 signals were taken to be those at 28.5 and 30.1 p.p.m., respectively. A comparison of the data for the 6-oxo series with that for the parent hydrocarbon led to the assignments given in Table 1 for these four derivatives. A sample of 7,7-dimethylbicyclo[3.2.1]octan-6-one containing deuterium at C-3, -4, -5, and -9 was available from homoenolization studies (20) to confirm its assignments and provide supporting evidence for those for the other 6-oxo derivatives.

For the bicyclo[3.2.2]nonan-6-ones, the spectra of the 7,7-dideuterio, 7-deuterio-7-*exo*-methyl, and 7-deuterio-7-*endo*-methyl derivatives as well as the parent hydrocarbon (Table 2) were also recorded. This permitted a ready distinction between the methine signals for the monomethyl cases. Since one signal was essentially eliminated, one was shifted upfield by 0.1 p.p.m. while the third methine signal was unaffected in the spectra of the deuterated compounds, these arose from C-7, C-1, and C-5, respectively. In addition, one of the methylene signals in each was significantly broadened, identifying the vicinal methylene carbon *anti* to the deuterium (21). Of the remaining methylene peaks, the highest field signal, ~21 p.p.m., was assigned to C-3 in the four ketones because of its similarity with C-3 in the hydrocarbon and the fact that it should be little affected by 7-substitution. All four ketones exhibited methylene absorption near 31 p.p.m. which was assigned to C-4 since this carbon should be little affected by 7-substitution. Supporting this assignment, the spectrum for 7,7-dideuteriobicyclo-[3.3.2]octan-6-one showed broadening due to vicinal C–D coupling for the 24.4 and 34.1 p.p.m. resonances. Thus it also followed that C-9 gave rise to the signal near 23 p.p.m. in the four ketones.

For the *trans*-decalones, the methylene assignments were made by comparison with the results for *trans*-decalin and 10-methyl-*trans*-decalin (Table 2) in a manner analogous to that described for the decalols (12) and some more highly substituted decalones (22). In the 2- and 3-oxo derivatives, the carbonyl group has little effect on the C-6, -7, -8, and -9 shieldings while the α-meth-

Can. J. Chem. Downloaded from www.nrcresearchpress.com by 210.87.254.42 on 09/05/12
For personal use only.

TABLE 3. Methyl substituent effects[a] in some bicyclic ketones and cyclohexanone

		Substituent effects					
			β		γ		
Skeleton	Substitution	α	C=O	$CH(CH_2)$	*gauche*	*anti*	CH[b]
[2.2.1][c]	2-Oxo-3-*exo*-Me	3.1	2.6	6.2	−3.2	0.9	−0.3
[3.2.1]	6-Oxo-7-*exo*-Me	3.4	2.8	7.2	−2.8	0.9	+0.5
[3.2.2]	6-Oxo-7-*exo*-Me	3.2	2.7	6.7	−4.3	1.3	0.0
[2.2.2][d]	2-Oxo-3-Me	2.6	3.4	6.0	−4.6	1.3	0.0
[2.2.1][c]	2-Oxo-3-*endo*-Me	3.1	2.4	5.1	−6.2	−0.4	0.5
[3.2.1]	6-Oxo-7-*endo*-Me	4.9	2.0	4.6	−4.4	−0.8	−0.5
[3.2.2]	6-Oxo-7-*endo*-Me	2.2	1.8	5.6	−5.0	1.5	−0.4
[3.2.1]	2-Oxo-3-*exo*-Me	3.6	0.7	10.4		−0.1(C-1)	
						0.7(C-5)	
	3-Oxo-2-*endo*-Me	1.1	1.1	7.4	−5.0(C-7)	−0.5(C-4)	
						2.0(C-8)	
$C_6H_{10}O$[e]	2-Me(equatorial)	3.4	1.0	9.1		0.2(C-4)	
						−0.1(C-6)	
$C_6H_{10}O$[e]	2-Me(axial)	3.6	3.6	6.0	−5.9(C-4)		
					−6.2(C-6)		
[3.2.1]	3-Oxo-2-*exo*-Me	2.8	6.2	6.3	−2.6(C-4)	0.8(C-7)	
					−5.7(C-8)		
[4.4.0]	1-Oxo-10-Me	−6.6	3.7	1.2(C-5)	−4.2(C-2)		
				6.0(C-9)	−5.3(C-4)		
					−6.3(C-6)		
					−4.4(C-8)		
	2-Oxo-10-Me	−5.7		8.3(C-1)	0.7(C=O)		
				2.1(C-5)	−4.7(C-4)		
				8.0(C-9)	−4.8(C-6)		
					−4.5(C-8)		
	3-Oxo-10-Me	−8.5		7.6(C-1)	−3.3(C-2)		
				1.3(C-5)	−3.7(C-4)		
				6.8(C-9)	−4.6(C-6)		
					−4.5(C-8)		
	4-Oxo-10-Me	−5.3		7.8(C-1)	−4.9(C-2)		
				2.7(C-5)	−1.0(C=O)		
				7.0(C-9)	−3.9(C-6)		
					−3.9(C-8)		

[a]In p.p.m. Positive values denote deshielding effects.
[b]Bridgehead carbon: C-1 in [2.2.1] and [2.2.2] ketones; C-5 in [3.2.1] and [3.2.2] series.
[c]Reference 3.
[d]Reference 4*b*.
[e]Cyclohexanone, data from ref. 23.

ylene carbons were readily identified by their characteristic shifts to lower field. In the 1- and 4-oxo derivatives, the *gauche* vicinal methylene carbon (C-9 and C-6, respectively) was characterized by its upfield shift caused by the γ effect of the carbonyl oxygen while the remaining methylene carbons in the unsubstituted ring are essentially unaffected (22), as are the β- and γ-methylene carbons in the substituted ring. Thus, the assignments for these decalones were readily completed.

Discussion

In one of the first systematic studies of substituent effects in alicyclic systems, Dalling and Grant (23) showed the remarkable reproducibility and stereochemical dependence of the effects of methyl groups on the shieldings of cyclohexane ring carbons. Similar results were subsequently obtained for the norbornane system by Roberts and co-workers (24) and in this laboratory (3) for the bicyclo[2.2.2]octanones (4*b*) and for several cyclohexanones and cyclopentanones (25). In each case, the carbons γ to the site of substitution are significantly shielded if *gauche* to the methyl group and tend to be deshielded slightly, if *anti*. To examine the trends for α-methyl substitution in the present ring systems, some pertinent data are given in Table 3, which contains the shifts observed for the skeletal

Can. J. Chem. Downloaded from www.nrcresearchpress.com by 210.87.254.42 on 09/05/12
For personal use only.

Can. J. Chem. Downloaded from www.nrcresearchpress.com by 210.87.254.42 on 09/05/12
For personal use only.

carbons in the monomethyl derivatives from their positions for the parent ketones. The first seven entries have the carbonyl in a two-carbon bridge with the α-methyl *gauche*, or approximately so, to either a one- or two-carbon bridge. It is apparent that the latter arrangement produces the larger upfield shift, as might be expected because of the smaller dihedral angle between the two γ centers; the relative shieldings of the methyl carbons exhibit the same trend. For each *exo*/*endo* pair, the β effects are somewhat diminished in the isomer having the greater negative γ shift. The last three entries in the first column of Table 3 have an equatorial α-methyl nearly eclipsed with the carbonyl group, with only one having a *gauche* γ interaction, which presumably accounts for the attenuated β effect at the adjacent bridgehead carbon. It has been generally found that the shielding of all carbons in the γ *gauche* fragment are upfield from those in the corresponding arrangement lacking the *gauche* interaction (1, 2). The remaining six entries in Table 3 are closely related, each having the methyl group in an axial orientation on a six-membered ring. The variety of γ *gauche* effects are consistently upfield for sp^3 carbons while the carbonyl carbon is much less affected. It is interesting that with three or four γ *gauche* interactions the methyl group no longer deshields the carbon to which it is bonded; also the β effects at the methine carbons are very much less than those at the methylenes. From Table 1, it is apparent that methyl substitution at the ring junctions in the [3.1.0] and [4.1.0] systems does not produce distinctive upfield shifts for the γ-carbons. This is consistent with the relatively large dihedral angles, ~120°, relating these centers. The γ shielding interactions between the nearly eclipsed vicinal methyls in the dimethyl derivatives, however, are clearly evident from the methyl carbon shieldings.

To examine the effect of the carbonyl group on the shieldings of the neighboring carbons, the relevant data are listed in Table 4, obtained by comparison of the results for the unsubstituted ketones with those for the parent hydrocarbons. The earlier data for norcamphor (3) and bicyclo[2.2.2]octanone (4*b*)[3] are included. In general, the α-methylene carbons are more strongly deshielded in the bicyclic systems than in cyclopentanone or cyclohexanone. It is also interesting that the carbonyl group tends to shield the γ-carbons in all cases. There seems to be no ready explanation for either of these trends. The upfield shifts exhibited by the β-methylene carbons, however, are consistent with γ interactions involving the carbonyl oxygen and, as expected, the effects are larger with smaller dihedral angles such that a trend is discernible. The maximum upfield shifts are found for the three decalones having the carbonyl group at either C-1 or C-4, in which cases the carbonyl oxygen must be nearly eclipsed with C-9 or C-6, respectively. The smallest shifts occur in the systems for which the carbonyl oxygen and β-methylene carbon are separated by relatively large dihedral angles, ~120°. Presumably the interaction producing these upfield shifts involves the hydrogen bonded to the affected carbon. For the β-bridgehead carbons, the bridgehead hydrogen and carbonyl oxygen are much too far apart to interact and there is no apparent trend in these data. It may be noted that in two cases the quaternary β-carbons are markedly deshielded by the carbonyl groups but this is probably a result of the elimination of a *gauche* γ interaction of the angular methyl bonded to the quaternary carbon by placement of the carbonyl at C-2 or C-4 in the decalone skeleton.

The variation of the carbonyl carbon shieldings in this series of bicyclic ketones seems particularly interesting. The values span a range of 14 p.p.m., δ_C 208.7–223.0 for the parent ketones, and there appears to be a trend which may account for the well-known but unexplained, variation of carbonyl shieldings in the monocyclic series (5). The remarkable sensitivity of this shielding to ring size has only been attributed to conformational factors in the most general terms. Although most of these bicyclic ketones can be regarded as either substituted cyclohexanones or cyclopentanones, the observed carbonyl shieldings seem to depend primarily on features other than ring size. For the simple five- and six-membered rings the carbonyl shieldings differ by 8 p.p.m. (5, 25), 220.5 and 212.0 p.p.m., respectively, in $CDCl_3$ but in **1** and **3** this absorption is near 214 p.p.m., even though their carbonyl groups are in different sized rings. As a possible explanation, it can be suggested that the number of α-bond eclipsing interactions present in each case is the more important feature. Cyclohexanone has two bond eclipsing interactions, whereas **1** and **3** have one, and cyclopentanone can be viewed as lacking such inter-

[3]The methylene shielding for bicyclo[2.2.2]octane is incorrect in the earlier paper and should read 26.1 p.p.m.

TABLE 4. Carbonyl substituent effects[a]

Skeleton	Substituent	α-C		β-C		γ-C
		CH	CH_2	CH	CH_2	
[2.2.2][b]	2-Oxo	18.3	18.5	3.9	−2.7(C-6, 7)	−1.3(C-5, 8)
[3.2.2]	6-Oxo	17.9	18.4	−0.5	−3.8(C-4)	−1.6(C-2)
					−2.7(C-9)	−0.6(C-3)
						−1.5(C-8)
[2.2.1][c]	2-Oxo	13.4	15.5	−1.0	−5.4(C-6)	−2.5(C-5)
					−0.7(C-7)	
[3.2.1]	6-Oxo	11.0	14.6	−3.0	−2.1(C-4)	−2.3(C-2)
					−2.5(C-8)	−0.2(C-3)
	2-Oxo	16.0	15.6		−0.7(C-4)	−1.1(C-5)
					−0.9(C-7)	−0.8(C-6)
					−1.4(C-8)	
	3-Oxo		17.5	0.1		0.4(C-6, 7)
						−1.9(C-8)
[4.4.0]	1-Oxo	11.2	14.7	1.2	−1.5(C-3)	−1.3(C-4)
					−7.8(C-9)	0.0(C-6)
						−1.1(C-8)
	1-Oxo-10-Me	14.4	15.3	+0.3	−1.0(C-3)	−1.6(C-4)
					−9.6(C-9)	−1.3(C-6)
						−0.7(C-8)
	2-Oxo		14.2(C-1)	−0.4	−1.6	−2.1(C-5)
			14.5(C-3)			−0.7(C-9)
	2-Oxo-10-Me		14.7(C-1)	3.7[d]	−1.3	−2.1(C-5)
			14.1(C-3)			−0.5(C-9)
	3-Oxo-10-Me		16.0(C-2)	−1.2	−1.8	−0.3(C-6)
			15.5(C-4)			−0.8(C-10)
	4-Oxo-10-Me	11.8	13.6	5.7[d]	−1.6(C-2)	−1.3(C-1)
					−6.7(C-6)	−1.6(C-7)
						−0.8(C-9)
Cyclopentanone[e]			11.6		−3.3	
Cyclohexanone[e]			14.2		−0.6	−2.7

[a]In p.p.m. Positive values denote deshielding effects.
[b]Reference 4*b*.
[c]Reference 3.
[d]Quaternary carbons.
[e]Reference 23.

actions, since its favored conformation is the half-chair (26). Inspection of molecular models indicates that α-bond eclipsing interactions should be minimal in **5** and 6-oxo-**6** and their carbonyl shieldings of 223.0 and 221.4 p.p.m., respectively, are comparable to the cyclopentanone value. The carbonyl shieldings for 3-oxo-**6** and five of the six decalones (210.5–211.9 p.p.m.) are essentially the same as that of cyclohexanone and each of these has comparable bond eclipsing. In *trans*-10-methyl-1-decalone, the somewhat lower carbonyl shielding of 215.6 p.p.m. may result from a greater degree of flattening in the ring containing the carbonyl group which would tend to reduce the *syn* axial interaction of the angular methyl at C-2. Ring flattening increases the dihedral angle between the α C—H bond and the carbonyl π-bond, thereby reducing the eclipsing interaction. The fact that the γ effect of the angular methyl group at C-2 (Table 3) is significantly less than that at C-4 and C-6 is consistent with this interpretation. The carbonyl shieldings of **7**, bicyclo[2.2.2]octanone (4*b*), and norcamphor (3) are 216.2, 216.7, and 217.4 p.p.m., respectively, which on the basis of the present proposal suggest that the carbonyl group has a single bond eclipsing interaction somewhat smaller than that in the more rigid **1** skeleton. Again, molecular models indicate that this is a reasonable interpretation. On similar grounds, the carbonyl absorption of 214.0 p.p.m. for 2-oxo-**6** can be interpreted in terms of **10** as the favored conformation having the 3-carbon bridge nearly planar.

For the ketones containing a three-membered ring, an earlier study (11) of the carbonyl shieldings led to the conclusion that cyclopropylcarbonyl conjugation could be a contributing

Can. J. Chem. Downloaded from www.nrcresearchpress.com by 210.87.254.42 on 09/05/12
For personal use only.

TABLE 5. ^{13}C shieldings of some cycloalkanones[a]

Ring	C=O	α-CH_2								ω-CH_2
4	209.1	47.7								9.7
5	220.5	38.3	23.3							
6	212.0	42.0	27.1							25.1
7	215.2	43.9	30.5	24.4						
8	218.1	42.0	27.3	25.7						24.8
9	218.1	43.6	27.0	25.1	24.4					
10	214.7	42.1	25.0	24.9	23.5					25.2
11	214.3	42.0	26.1	25.0	24.5	22.6				
12	212.7	40.4	24.8	24.7	24.3	22.6				22.5
13	212.7	42.0	26.6	25.9	25.8	24.6	23.3			
14	211.9	40.9	26.1	25.9	25.4	25.3	23.0			24.5
15	212.6	42.2	27.7	26.8_8	26.8_5	26.6	26.4	23.5		
16	212.2	42.1	27.7	27.3	27.1	26.6_2	26.5_7	23.5		26.6
17	212.1	42.4	28.3	27.9	27.7	27.3_4	27.2_6	27.0	23.8	

[a]1 *M* solutions in $CDCl_3$.

factor. This still seems reasonable for bicyclo-[4.1.0]heptan-2-one since its carbonyl signal at 208.7 p.p.m. is at appreciably higher field than that for cyclohexanone. For bicyclo[3.1.0]hexan-2-one, however, the observed shielding of 215.1 p.p.m. is also consistent with the presence of one bond eclipsing interaction, which on the basis of the foregoing, would tend to increase the carbonyl shielding from that found for cyclopentanone, as is observed. In bicyclo[3.1.0]hexan-3-one, the absorption at 217.9 p.p.m. is not so greatly different from cyclopentanone but could conceivably represent the shielding for the envelope conformation **11** since the three-membered ring probably precludes the half-chair conformer and in **11** bond opposition strain between the C-3 (C-4) and C-2 (C-5) hydrogens is minimized. The alternative envelope conformer maximizes this contribution.

Since the variations in the carbonyl shieldings in these bicyclic systems are explicable in terms of the number of bond eclipsing interactions it seems reasonable to reexamine the trends found several years ago for the monocyclic ketones (5). The data for 1 *M* solutions in $CDCl_3$ are listed in Table 5 from which it is apparent that the carbonyl carbons in 8- and 9-membered rings are appreciably deshielded relative to cyclohexanone, whereas the 7-, 10-, and 11-membered ring examples are somewhat less shielded than cyclohexanone. For the larger rings the carbonyl shieldings are essentially the same as cyclohexanone. These trends are identical to those originally reported (5) but in $CDCl_3$ the carbonyl carbons are deshielded by *ca.* 3 p.p.m., relative to the values for CS_2 solutions, presumably because of hydrogen bonding in $CDCl_3$. On the basis of bond eclipsing contributions to the carbonyl shieldings, the observed values for cyclooctanone and cyclononanone indicate that these favor conformations with one eclipsing interaction such as **12** and **13**, respectively. These are boat-chair (BC) conformations with **13** somewhat distorted to relieve bond opposition strain at C-3 and C-4. Anet and his co-workers have established that **12** is the favored conformation for cyclooctanone (27) and have shown that cyclononanone very likely exists in a single conformation of the same symmetry (28). For cyclodecanone, two of the possible boat-chair-boat (BCB) conformations are **14** and **15**. If **15** were

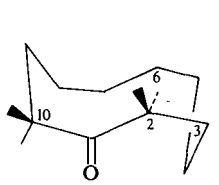

14 (BCB-3)

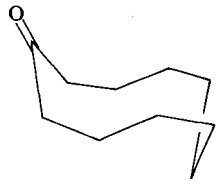

15 (BCB-1)

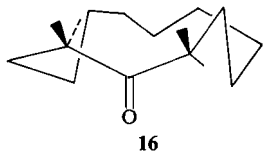

16

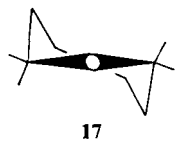

17

favored, one could anticipate a carbonyl shielding essentially the same as that for cyclohexanone whereas in **14** transannular interactions tend to maximize the separation between closely approaching hydrogens (*e.g.* on C-2 and C-6 in **14**) thereby reducing the bond eclipsing interactions of the carbonyl group (*i.e.* with the C_2—C_3 bond

Can. J. Chem. Downloaded from www.nrcresearchpress.com by 210.87.254.42 on 09/05/12
For personal use only.

Can. J. Chem. Downloaded from www.nrcresearchpress.com by 210.87.254.42 on 09/05/12
For personal use only.

and one of the α-hydrogens at C-10) and decreasing the carbonyl shielding. The observed shielding of 214.7 p.p.m. is significantly less than the cyclohexanone value of 212.0 p.p.m. The remaining BCB-2 conformation for cyclodecanone has the carbonyl group in an environment very similar to that for cyclohexanone, always eclipsed with two hydrogens on the α- and α′-carbons. Thus the carbonyl shielding results favor **14** as the preferred conformation. Anet *et al.* (28) have recently presented evidence that cyclodecanone strongly favors **14** (BCB-3) over the BCB-2 conformer and their results clearly eliminate **15** as a major contributor. Since the carbonyl shielding of cycloundecanone (214.3 p.p.m.) is very close to that for cyclodecanone, a similar preferred conformation is indicated and it has been shown that the 11-membered ring ketone probably exists as a single conformer in solution (28). The conformation of the crystalline state has recently been established (29). Anet *et al.* have also shown that cyclododecanone very probably has the same ring skeleton as cyclododecane, a "square" D_4 form, as represented by **16** with the carbonyl group at a noncorner position (28). This conformation has two bond eclipsing interactions for the carbonyl group and the observed shielding of 212.7 p.p.m. fits very well with the present interpretation. Finally it may be noted that the bond eclipsing for the carbonyl group in a twist-chair seven-membered ring (**17**) would appear to be less than that for cyclohexanone, as judged by inspection of molecular models, and the observed shielding of 215.2 p.p.m. seems very reasonable.

Although the notion that bond eclipsing interactions are important factors governing carbonyl carbon shieldings is speculative, the favored conformations indicated by the observed shieldings for the cycloalkanones are in excellent agreement with those deduced on the basis of much more rigorous information. This suggests that carbonyl shielding data may be helpful for conformation assignments in a variety of systems.

We are grateful to the National Research Council of Canada for financial support of this work. We wish to thank Inara Grikis for technical assistance and Dr. A. L. Johnson for the preparation of bicyclo[3.3.0]octan-2-one.

1. G. C. Levy and G. L. Nelson. ^{13}C nuclear magnetic resonance for organic chemists. Wiley-Interscience, New York. 1972; J. B. Stothers. Carbon-13 NMR spectroscopy. Academic Press, New York. 1972.
2. N. K. Wilson and J. B. Stothers. *In* Topics in stereochemistry. Vol. 8. *Edited by* E. L. Eliel and N. L. Allinger. Wiley-Interscience, New York. 1973.
3. J. B. Stothers, C. T. Tan, and K. C. Teo. Can. J. Chem. **51**, 2893 (1973).
4. (*a*) G. E. Maciel and H. C. Dorn. J. Am. Chem. Soc. **93**, 1268 (1971); (*b*) K. R. Stephens, J. B. Stothers, and C. T. Tan. *In* Mass spectrometry and NMR spectroscopy in pesticide chemistry. *Edited by* R. Haque and F. J. Biros. Plenum Press, New York. 1974. pp. 179–196.
5. J. B. Stothers and P. C. Lauterbur. Can. J. Chem. **42**, 1563 (1964).
6. S. Winstein and J. Sonnenberg. J. Am. Chem. Soc. **83**, 3235 (1961).
7. R. Criegee and P. Gunther. Chem. Ber. **96**, 1564 (1963).
8. A. C. Cope, H. H. Lee, and H. E. Petree. J. Am. Chem. Soc. **80**, 2849 (1958); A. C. Cope, M. Brown, and H. E. Petree. J. Am. Chem. Soc. **80**, 2852 (1958).
9. W. R. Moore, W. R. Moser, and J. E. Laprade. J. Org. Chem. **28**, 2200 (1963).
10. K. B. Wiberg and B. A. Hess. J. Org. Chem. **31**, 2250 (1965).
11. D. H. Marr and J. B. Stothers. Can. J. Chem. **45**, 525 (1967).
12. S. H. Grover and J. B. Stothers. Can. J. Chem. **52**, 870 (1974).
13. A. L. Johnson, N. O. Petersen, M. B. Rampersad, and J. B. Stothers. Can. J. Chem. **52**, 4143 (1974).
14. M. A. McKinney and P. P. Patel. J. Org. Chem. **38**, 4064 (1973).
15. C. R. Johnson and R. W. Herr. J. Org. Chem. **38**, 3153 (1973).
16. J. Wolinsky. J. Org. Chem. **26**, 704 (1961).
17. E. J. Corey, R. Hartmann, and R. A. Vatakencherry. J. Am. Chem. Soc. **84**, 2611 (1962).
18. Y. Bessiere-Chretien and M. B. Meklati. C.R. C, **269**, 1315 (1969).
19. I. Kubota, T. Matsuura, T. Tsutsui, S. Uyeo, H. Irie, A. Numato, T. Fujita, and T. Suzaku. Tetrahedron, **25**, 1659 (1966).
20. D. M. Hudyma, J. B. Stothers, and C. T. Tan. Org. Magn. Res. In press.
21. J. B. Stothers, C. T. Tan, A. Nickon, F. Huang, R. Sridhar, and R. Weglein. J. Am. Chem. Soc. **94**, 8581 (1972).
22. G. I. Birnbaum, A. Stoessl, S. H. Grover, and J. B. Stothers. Can. J. Chem. **52**, 993 (1974).
23. D. K. Dalling and D. M. Grant. J. Am. Chem. Soc. **89**, 6612 (1967); **94**, 5318 (1972).
24. J. B. Grutzner, M. Jautelet, J. B. Dence, R. A. Smith, and J. D. Roberts. J. Am. Chem. Soc. **92**, 7107 (1970).
25. J. B. Stothers and C. T. Tan. Can. J. Chem. **52**, 308 (1974).
26. E. L. Eliel, N. L. Allinger, S. J. Angyal, and G. A. Morrison. Conformational analysis. Interscience, New York. 1965. p. 202.
27. F. A. L. Anet and M. St. Jacques. J. Am. Chem. Soc. **88**, 2585 (1966); **88**, 2586 (1966); F. A. L. Anet, M. St. Jacques, and P. M. Heinrichs. Intra-Sci. Chem. Rep. **4**, 251 (1970).
28. F. A. L. Anet, A. K. Cheng, and J. Krane, J. Am. Chem. Soc. **95**, 7877 (1973).
29. P. Groth. Acta Chem. Scand. A**28**, 294 (1974).
30. S. H. Grover and J. B. Stothers. Can. J. Chem. **53**, 589 (1975).

Studies on the Synthesis of Novel Carbohydrates with Sulfur in the Ring. Part III. The Synthesis of Derivatives of 2,6-Dithio-hex-4-en-2-ulopyranosidononitriles

DOLATRAI M. VYAS AND GEORGE W. HAY[1]

Department of Chemistry, Queen's University, Kingston, Ontario K7L 3N6

Received September 23, 1974

DOLATRAI M. VYAS and GEORGE W. HAY. Can. J. Chem. **53**, 1362 (1975).

The *cis*-hydroxylation of 3,6-dihydro-3-methoxy-2-methylthio-2*H*-thiopyran-2-carbonitrile and of 3-*exo*-cyano-3-methylthio-2-thiabicyclo[2.2.1]hept-5-ene by treatment with OsO_4–pyridine afforded sulfur analogs of two new types of carbohydrates. The Diels–Alder reaction of *trans,trans*-1,4-diacetoxy-1,3-butadiene with methyl cyanodithioformate gave a one-step synthesis of methyl 3,6-di-*O*-acetyl-4,5-dideoxy-2,6-dithio-α-DL-*threo*-hex-4-en-2-ulopyranosidononitrile.

DOLATRAI M. VYAS et GEORGE W. HAY. Can. J. Chem. **53**, 1362 (1975).

L'hydroxylation *cis*, par traitement avec OsO_4 dans la pyridine, du dihydro-3,6 méthoxy-3 méthylthio-2 2*H*-thiopyrancarbonitrile-2 et de l'*exo* cyano-3 méthylthio-3 thia-2 bicyclo[2.2.1]-heptène-5 conduit aux analogues sulfurés de deux nouveaux types de carbohydrates. La réaction de Diels–Alder entre le diacétoxy-1,4 butadiène-1,3 *trans,trans* et le cyanodithioformate de méthyle fournit une synthèse en une étape du di-*O*-acétyl-3,6 didésoxy-4,5 dithio-2,6 α-DL-*thréo*-hexène-4 ulopyrannosidononitrile-2. [Traduit par le journal]

Introduction

Previous reports (1, 2) from this laboratory have described the synthesis of 3,6-dihydro-3-methoxy-2-methylthio-2*H*-thiopyran-2-carbonitrile (**1**) (2*a*) and 3-*exo*-cyano-3-methylthio-2-thiabicyclo[2.2.1]hept-5-ene (**2**)[2] (2*b*, *c*) by facile Diels–Alder reactions between methylcyanodithioformate (MCDF) and 1-methoxy-1,3-butadiene and cyclopentadiene, respectively. These compounds are useful precursors for the synthesis of more highly substituted novel carbohydrates with sulfur in the ring. Of particular interest is compound **2** which affords access to a series of bicyclic sugars distinct from those previously synthesized (3–5).

The sulfur atoms are the most nucleophilic centers in compounds **1** and **2**, and they react preferentially with most of the electrophilic reagents commonly used to add to carbon–carbon double bonds. Thus, in studies of a series of 3,6-dihydro-2*H*-thiopyrans reported previously (1, 2), attempts to achieve *trans*-hydroxylations by epoxidation with a variety of peracids or *cis*-hydroxylation with such normally effective reagents as neutral $KMnO_4$ or OsO_4–H_2O_2–*t*-BuOH led only to the oxidation of the sulfur atoms and the concomitant stabilization of the cyclic double bond[3] towards further addition. However, the *cis*-hydroxylation of carbon–carbon double bond can be achieved by OsO_4–pyridine, a system which is unreactive towards sulfur (8). Furthermore, Brown and his co-workers (9) have demonstrated the sensitivity of osmic acid to steric control during the hydroxylation of 2-methoxy-5,6-dihydro-2*H*-pyran and *cis*-2,5-dimethoxy-5,6-dihydro-2*H*-pyran; similar results have been reported by Banasek and Zamojski (10).

This paper describes the products of the osmic acid hydroxylation of **1** and **2**, and the synthesis of methyl 3,6-di-*O*-acetyl-4,5-dideoxy-2,6-dithio-α-DL-*threo*-hex-4-en-2-ulopyranosidononitrile (**3**). The conformations and structures assigned to these unusual carbohydrates were based primarily on the p.m.r. spectroscopic data.

[1]To whom inquiries should be addressed. This research was sponsored by Operating Grant A1921 from the National Research Council of Canada.

[2]Heterocyclic nomenclature has been employed arbitrarily. Alternative names (6) are: methyl 4,5-dideoxy-3-*O*-methyl-2,6-dithio-β-DL-*glycero*-hex-4-en-2-ulopyranosidononitrile (**1**) (1); methyl 3,4,5-trideoxy-3,6-*C*-methylene-2,6-dithio-α-DL-*threo*-hex-4-en-2-ulopyranosidononitrile (**2**). The structural formula of only one stereoisomer is given in the text.

[3]The rationalization of the unreactivity of this double bond in the oxidized products in terms of inductive, field, and/or conformational effects will be reported in a succeeding paper (*cf.* ref. 7).

Can. J. Chem. Downloaded from www.nrcresearchpress.com by 210.87.254.105 on 09/05/12
For personal use only.

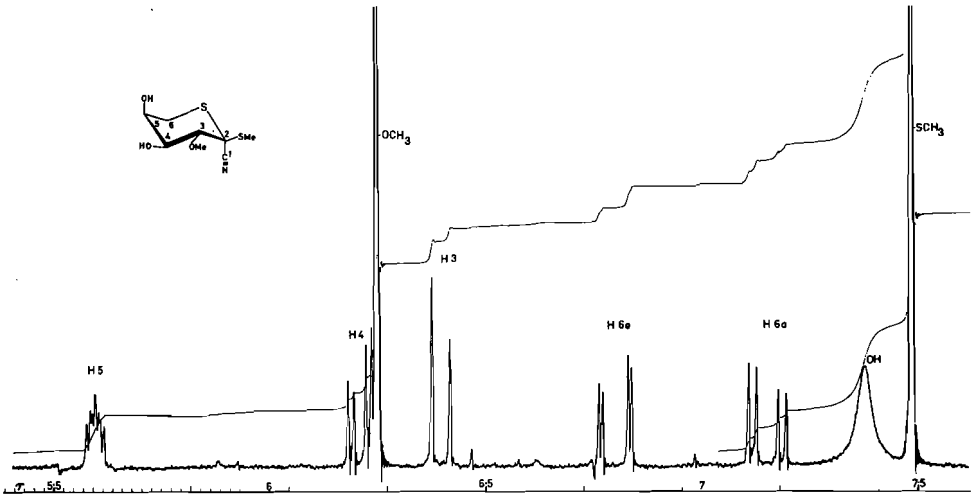

FIG. 1. The 220 MHz p.m.r. spectrum of compound **4** in chloroform-*d*.

Results and Discussion

Osmic acid reacted with **1** to give 80% yield of product, the analysis of which by t.l.c. revealed the presence of only two compounds, one in trace amounts. The major product (**4**) was obtained in a pure crystalline form in 70% overall yield by recrystallization from acetone – petroleum ether. The infrared spectrum of **4** revealed no oxidation of the sulfur but exhibited a strong absorption (3333 cm^{-1}) due to OH.

The structure and conformation of **4** were deduced from the 220 MHz p.m.r. spectrum (Fig. 1); on this evidence compound **4** was designated as methyl 3-*O*-methyl-2,6-dithio-α-DL-*arabino*-2-hexulopyranosidononitrile.

The one-proton doublet at τ 6.40 was assigned to the H-3 proton, J = 9.2 Hz, a value typical of coupling between vicinal diaxial protons. The C-6 methylene protons formed the MX portion of an AMX system centered at τ 6.98. The MX moiety had $J_{6a,5e}$ = 4 Hz, and $J_{6e,5e}$ = 2 Hz. The A portion of the system was the one-proton multiplet centered at τ 5.60 and was assigned to H-5. The one-proton quartet centered at τ 6.21 was attributed to H-4 with $J_{3a,4a}$ = 9.2 Hz, and $J_{4a,5e}$ = 3 Hz. These p.m.r. data are consistent with an attack by OsO_4 on the olefinic bond in **1** from the side opposite to the quasi-equatorial methoxyl group. The p.m.r. coupling constants also indicate that **4** occurs exclusively in the $^5C_2$(L) conformer in chloroform-*d* solution. This preference may reflect the stabilization resulting from the fewer 1,3-nonbonded interactions in the $^5C_2$(L) as compared to the $^2C_5$(L) conformer. Moreover, the recently reported destabilizing "hockey stick" effect (11), arising from orbital repulsion

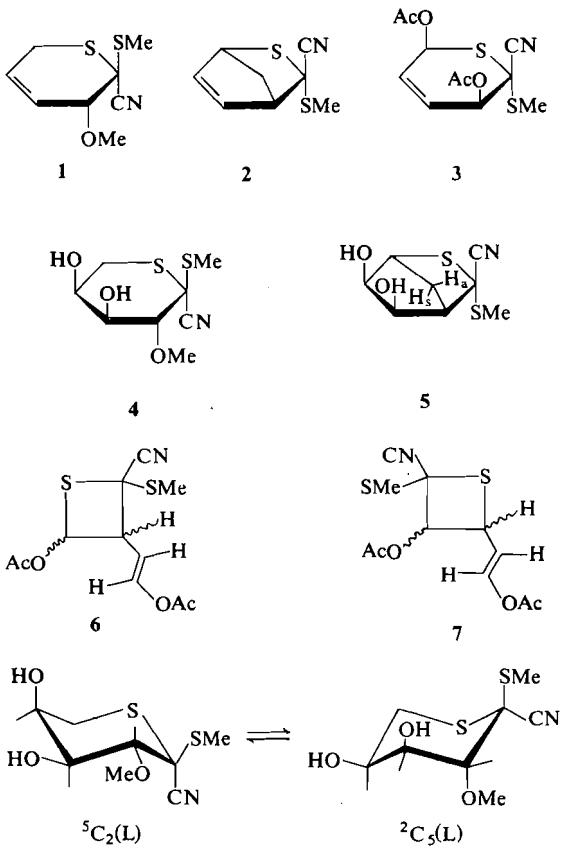

Can. J. Chem. Downloaded from www.nrcresearchpress.com by 210.87.254.105 on 09/05/12
For personal use only.

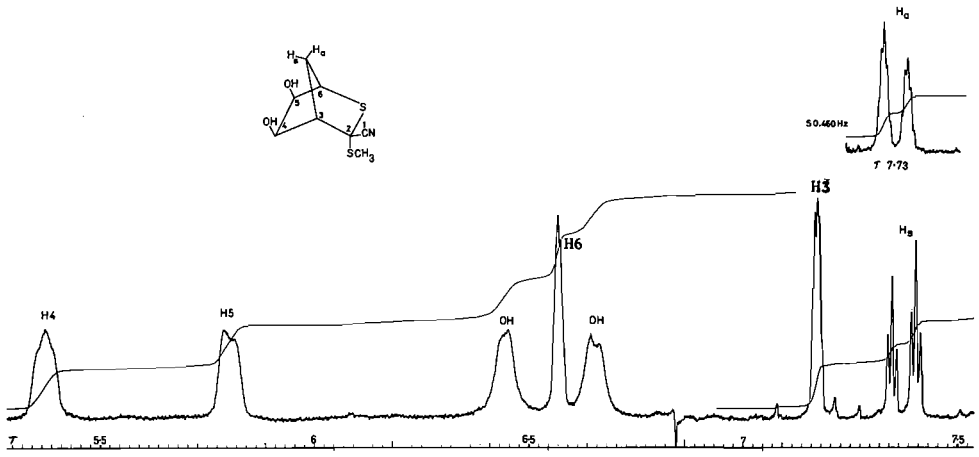

FIG. 2. The 220 MHz p.m.r. spectrum of compound **5** in chloroform-*d*.

between a sulfur atom in the ring and a β axial heteroatom-containing substituent (*e.g.*, OMe) present in the $^2C_5$ conformation of **4**, would add to the instability of that conformer. In the case of compound **1** it was revealed that of the two anomeric substituents the cyano group had the dominant "anomeric effect" (12) and showed a greater tendency to be axially disposed. This phenomenon in compound **4** may account further for the preponderance of the $^5C_2$ over the $^2C_5$ conformer.

The OsO_4–pyridine hydroxylation of **2** afforded one pure crystalline product (**5**). The elemental analysis and the i.r. spectral data for **5** were consistent with the proposed structure.

Steric considerations for this reaction strongly favor the osmic acid attack on the olefin from the less hindered *exo* side, since the hydroxylation proceeds via the osmate ester of the glycol (13). On this assumption compound **5** was tentatively designated as methyl 3-deoxy-3,6-*C*-methylene-2,6-dithio-α-DL-*talo*-hex-2-ulo-pyranosidononitrile. A similar rationale has been offered by Daniels and Fischer (14) to explain the OsO_4-catalyzed hydroxylation of the furan – maleic anhydride Diels–Alder adduct.

Analysis of the 220 MHz spectrum of **5** (Fig. 2) corroborated the stereoselectivity of the osmic acid attack on **2**. The methylene bridge hydrogens exhibited a complex AB system centered at τ 7.56. The coupling pattern revealed that the A portion centered at τ 7.38, resulted from the geminal coupling of 12 Hz and equal vicinal couplings of 2 Hz with two other protons. The B portion, centered at τ 7.73, showed the geminal coupling of 12 Hz and also coupling with more than two protons, thus accounting for the unresolved multiplet character of the signal. This could be rationalized in terms of a "W"-type long range coupling (15) between the *anti*-proton of the methylene bridge and H-5 and H-4 which, in this case, must be *endo*. Such long range couplings have been observed in several bicyclic systems (7, 16). On this basis the A and B portions of the signal were assigned to the *syn* and *anti* protons of the methylene bridge, respectively. This analysis of the AB system further corroborated the postulated control of the approach of osmic acid to compound **2**. Other signal assignments are documented in Table 1. These were made through proton decoupling experiments on the assumption that the H-6 proton in **5** should resonate at lower field than the H-3 proton. This assumption has been verified experimentally in the 2-thiabicyclo[2.2.1]heptane system (17), where the bridgehead proton on the carbon α to sulfur resonates at lower field than the other bridgehead proton. On account of the highly coupled nature of the spectrum of **5** proton decoupling experiments did not result in any drastic simplification of signals but only slight sharpening of the peaks was observed. Signals due to the hydroxyl protons were readily identified since they showed considerably different chemical shifts at different sample concentrations.

The reaction of *trans,trans*-1,4-diacetoxy-1,3-butadiene with MCDF in refluxing benzene afforded one crystalline product (**3**) which was

Can. J. Chem. Downloaded from www.nrcresearchpress.com by 210.87.254.105 on 09/05/12
For personal use only.

TABLE 1. Proton magnetic resonance data for compounds **3**, **4**, and **5***

Compound	Chemical shifts (τ values) H-3	H-4	H-5	H-6	Other signals	Coupling constants (Hz)
4†	6.40(d)	6.21(q)	5.60(m)	6.98	7.49(s), SCH_3 6.25(s), OCH_3	$J_{3,4} = 9.2$; $J_{4,5} = 3$; $J_{6,6} = 15$; $J_{6,5} = 4$; $J_{6,5} = 2$
5†	7.18(m)	5.80(m)	5.38(m)	6.57(m)	7.50(s), SCH_3 6.66, 6.45(bp), OH 7.73, H_{anti} 7.38, H_{syn}	$J_{H_a,H_s} = 12$ $J_{H_s,H_3} = J_{H_sH_6} = 2$ $J_{H_a,H_3} \sim J_{H_aH_6} \simeq 2$ $J_{H_a,H_4} \sim J_{H_aH_5} \leq 0.25$ Hz
3‡	4.30(m)	3.92(m)	3.92(m)	4.05(m)	7.58(s), SCH_3 7.80(s), OAc 7.87(s), OAc	

*In chloroform-*d* with internal TMS standard.
†220 MHz p.m.r. data.
‡60 MHz p.m.r. data.

characterized from its p.m.r. (Fig. 3; Table 1) and mass spectra. The possibility of compound **3** being a 1,2-cycloaddition adduct (**6** or **7**) was ruled out on the basis of its 60 MHz p.m.r. chemical shift data. The two one-proton resonances at τ 4.05 and 4.30 are consistent only with the allylic hydrogen signals in **3**, as the allylic protons in **6** and **7** would resonate at approximately τ 5.5 (18) and 7.0 (19), respectively. This structural assignment was substantiated by the mass spectral data of **3** which revealed a fragmentation pattern which is consistent only with the normal Diels–Alder adduct **3**. The *m/e* peaks at 170, 128, and 86 can be attributed to [1,4-diacetoxy-1,3-butadiene $(C_8H_{10}O_4)]^{+\cdot}$, $[C_8H_{10}O_4–CH_2CO]^{+\cdot}$, and $[C_8H_{10}O_4–2CH_2CO]^{+\cdot}$, respectively. 1,4-Diacetoxy-1,3-butadiene arises from the retro Diels–Alder fragmentation of **3**. Such a fragmentation for compounds **6** and **7** was considered to be less likely. However, further convincing evidence for structure **3** is provided by *m/e* peaks at 239, 180, and 138 which could only be attributed to the following fragmentation pattern resulting from the six-membered ring adduct **3**.

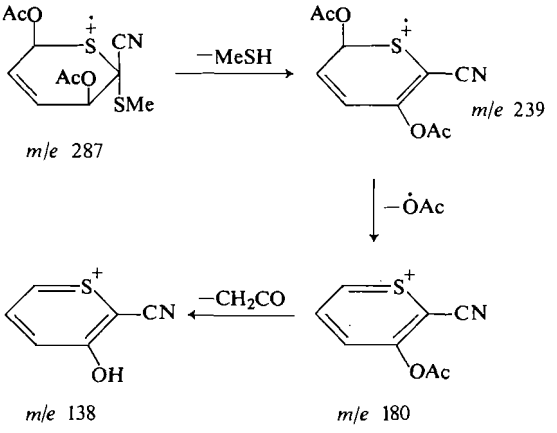

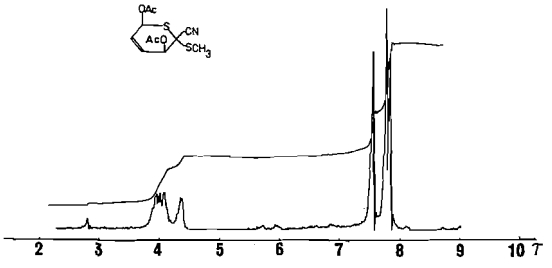

FIG. 3. The 60 MHz p.m.r. spectrum of compound **3** in chloroform-*d*.

Because Diels–Alder reactions are stereospecific (20), leading exclusively to *cis* adducts when the diene has *trans,trans* geometry, the relative stereochemistry at C-3 and C-6 in **3** was assigned as *cis*. The configuration at the anomeric center was assumed to be α on the basis that the *endo* rule with respect to the cyano function was obeyed; open-chain dienes are known to obey the *endo* rule at low temperatures (20). Moreover theoretical studies by Hoffmann and Woodward (21) have shown that, for dienophiles having a conjugated π system, the *endo* addition to the diene is energetically more favorable.

Experimental

General Procedures

Melting points were determined with a Fisher-Johns

Can. J. Chem. Downloaded from www.nrcresearchpress.com by 210.87.254.105 on 09/05/12
For personal use only.

Can. J. Chem. Downloaded from www.nrcresearchpress.com by 210.87.254.105 on 09/05/12
For personal use only.

melting point block and are uncorrected. Evaporations were conducted at 40° under reduced pressure (25 mm Hg) in a rotary evaporator. Infrared spectra were recorded on a Perkin-Elmer Model 180 spectrometer. Proton magnetic resonance spectra were obtained using a Varian T60 or a Varian HR 200 spectrometer with tetramethylsilane (TMS) (τ 10.00) as internal standard. Mass spectra were determined with a JOEL-JMS 01SC double focussing spectrometer at 75 eV and 100 nA. Thin-layer chromatography (t.l.c.) was performed on Eastman silica gel 'Chromagram' sheets and components were detected by using an iodine chamber.

Reaction of 3,6-Dihydro-3-methoxy-2-methylthio-2H-thiopyran-2-carbonitrile (1) with Osmic Acid

Osmium tetroxide (1g) in 4 ml dry pyridine was added to a solution of compound (**1**) (0.66 g) in 6 ml dry pyridine. The reaction mixture was stirred at room temperature for 21 h whereupon 1.8 g of sodium bisulfite (20 ml pyridine + 30 ml H_2O) was added and stirred for an additional 4 h. This was followed by extraction with CH_2Cl_2 (6 × 25 ml) and dried over $MgSO_4$. Evaporation of the solvent afforded a thick syrup (0.62 g), which showed two spots on t.l.c. (1:9 EtOAc–CH_2Cl_2); the component with greater R_f was only present in trace quantities. On crystallization from acetone and petroleum ether (b.p. 60–80°) 0.5 g of pure crystalline material (**4**) was obtained, which gave one spot on t.l.c., m.p. 132°; ν_{max} (KBr disc) 3333 (OH) and 2222 cm^{-1} (C≡N); τ ($CDCl_3$), see Table 1.

Anal. Calcd. for $C_8H_{13}NO_3S_2$: C, 40.83; H, 5.57. Found: C, 40.79; H, 5.68.

Osmic Acid Cis Hydroxylation of Compound 2

To 0.71 g of adduct **2** in 6 ml dry pyridine was added 1.0 g of OsO_4 in 5 ml of dry pyridine. The reaction mixture was stirred at room temperature for 18 h, followed by a work-up similar to that of the preceding case resulted in a white solid which upon recrystallization (methylene chloride – petroleum ether, b.p. 110–125°), afforded 0.6 g **5** as colorless crystals, m.p. 105–106°; ν_{max}(KBr disc) 3448 (OH) and 2222 cm^{-1} (C≡N); τ ($CDCl_3$), see Table 1.

Anal. Calcd. for $C_8H_{11}NO_2S_2$: C, 44.22; H, 5.10. Found: C, 44.36; H, 5.43.

trans,trans-1,4-Diacetoxy-1,3-butadiene

This compound was prepared in 56% yield from 25 g of cyclooctatetraene by the published procedure of Hill and Carlson (22), m.p. 100–102° (lit. (22) m.p. 103–104°).

Reaction of MCDF with trans,trans-1,4-Diacetoxy-1,3-butadiene

Diene (0.49 g) was refluxed for 24 h with MCDF (prepared from 1.8 g *N,N,N,N*-tetraethylammonium cyanodithioformate) in 20 ml benzene. The solution was concentrated to approximately 5 ml, which upon standing afforded analytically pure crystals (0.23 g), m.p. 68–70°; ν_{max}(KBr disc) 2222 (C≡N), 1748 (C=O), and 1667 cm^{-1} (C=C); τ ($CDCl_3$), see Table 1; *m/e* 287($M^{+\cdot}$)(7), 239(5), 180(5), 170(88), 138(25), 128(90), 86(73), and 43 a.m.u. (100).

Anal. Calcd. for $C_{11}H_{13}NS_2O_4$: C, 45.99; H, 4.56; S, 22.30. Found: C, 45.73; H, 4.68; S, 22.26.

The n.m.r. of the mother liquor was identical to that of the crystalline material; no other cycloaddition product was detected.

1. D. M. Vyas and G. W. Hay. J. Chem. Soc. Perkin I. 180 (1975).
2. (*a*) D. M. Vyas and G. W. Hay. Chem. Commun. 1411 (1971); (*b*) D. M. Vyas and G. W. Hay. Can. J. Chem. **49**, 3755 (1971); (*c*) D. M. Vyas and G. W. Hay. Am. Chem. Soc. 162nd National Meeting, Washington, D. C. 1971. Abstr. CARB. 036.
3. J. S. Brimacombe, M. E. Evans, E. J. Forbes, A. B. Foster, and J. M. Webber. Carbohydr. Res. **4**, 239 (1967).
4. B. Fraser-Reid and B. J. Carthy. Can. J. Chem. **50**, 2928 (1972).
5. W. Meyer Zu Reckendorf and U. Kamprath-Scholtz. Chem. Ber. **105**, 673 (1972).
6. J. K. N. Jones and W. A. Szarek. *In* The total synthesis of natural products. *Edited by* J. ApSimon. Wiley-Interscience, New York. 1973. p. 27.
7. C. R. Johnson, J. E. Keiser, and J. C. Sharp. J. Org. Chem. **34**, 860 (1969).
8. C. Djerassi and R. R. Engle. J. Am. Chem. Soc. **75**, 3838 (1953).
9. R. M. Srivastava and R. K. Brown. Can. J. Chem. **49**, 1339 (1971); T. P. Murray, U. P. Singh, and R. K. Brown. Can. J. Chem. **49**, 2132 (1971).
10. A. Banasek and A. Zamojski. Carbohydr. Res. **25**, 453 (1972).
11. N. S. Zefirov, V. S. Blagoveshchensky, I. V. Kazimirchik, and N. S. Surova. Tetrahedron, **27**, 3111 (1971).
12. R. U. Lemieux. *In* Molecular rearrangements. *Edited by* P. de Mayo. Wiley-Interscience, New York. 1963. p. 713.
13. R. Criegee. Ann. **522**, 75 (1936); N. A. Milas and S. Sussman. J. Am. Chem. Soc. **58**, 1302 (1936).
14. R. Daniels and L. Fischer. J. Org. Chem. **28**, 320 (1963).
15. L. M. Jackman and S. Sternhall. *In* Applications of nuclear magnetic resonance spectroscopy in organic chemistry. 2nd ed. Pergamon Press, Oxford. 1969. p. 334.
16. J. C. Muller, J. P. Fleury, and U. Schiedeggar. Org. Magn. Res. **2**, 77 (1970).
17. R. R. Fraser, J. Durst, M. R. McClory, R. Viau, and Y. Y. Wigfield. Int. J. Sulphur Chem. **3**, 133 (1971).
18. K. Yamada, M. Yoshioka, and N. Sugiyama. J. Org. Chem. **33**, 1240 (1968).
19. A. Ohno, Y. Ohnishi, and G. Tsuchihashi. Tetrahedron **25**, 871 (1969).
20. J. Sauer. Angew. Chem. Int. Ed. **6**, 16 (1967).
21. R. Hoffmann and R. B. Woodward. J. Am. Chem. Soc. **87**, 4388 (1965).
22. R. K. Hill and R. M. Carlson. J. Org. Chem. **30**, 2414 (1965).

Secondary Deuterium Isotope Effects on Carbonyl Ylide Intermediates

VESNA VUKOV AND ROBERT J. CRAWFORD
Department of Chemistry, University of Alberta, Edmonton, Alberta T6G 2G2

Received September 11, 1974

VESNA VUKOV and ROBERT J. CRAWFORD. Can. J. Chem. **53**, 1367 (1975).

The formation of vinyldihydrofuran (**6**) and dihydrooxepine (**5**) is sensitive to deuterium substitution at the terminal methylene of 2,3-divinyloxirane. Intra- and intermolecular isotope effects have been examined and suggest that **5** is produced on a competitive basis with **6** from a common intermediate.

VESNA VUKOV et ROBERT J. CRAWFORD. Can. J. Chem. **53**, 1367 (1975).

La formation du vinyldihydrofurane (**6**) et de la dihydrooxépine (**5**) est sensible à l'introduction de deutérium dans le méthylène terminal du vinyl-2,3-oxirane. On a déterminé les effets isotopiques intra- et intermoléculaires et ceux-ci suggèrent que **5** est produit en competition avec **6** à partir d'un intermédiaire commun.

Introduction

Scheme 1 has been suggested (1, 2) to explain the racemization of (+)-2,3-divinyloxirane (**1**) along with its isomerization to 3-vinyl-2,3-dihydrofuran (**6**) and 4,5-dihydrooxepine (**5**). A sigmatropic ($\sigma^2a + \pi^2s$) process for the production of **6** was ruled out on the basis of the negligible rotation of **6** produced from (+)-**1**. The planar carbonyl ylide **2** was thus adopted as a common intermediate. Chuche and coworkers (2) have demonstrated that the thermal isomerization of **7** gives rise to only **8** and **9**.

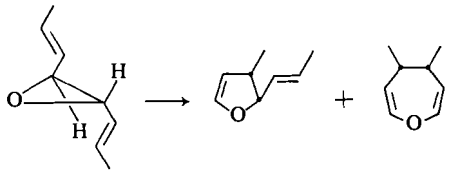

7 **8** **9**

Orbital symmetry considerations (3) suggest that **8** was produced by a five-center (6π) disrotatory ring closure of a carbonyl ylide analogous to **3**. It was suggested that a three-center (4π electron) conrotatory ring closure generated the *cis*-oxirane (**10**) which undergoes a rapid boat-like Cope rearrangement to **9**. The independently synthesized oxirane **10** produced only **9** upon thermolysis at 70° (2).

The carbonyl ylide **3** can be produced in more than one way in that it may be the result of a nonallowed disrotatory ring opening of **1**, the racemization being favored by 5.2 kcal mol^{-1} over the rearrangement process (1). It may also be produced by an isomerization of the carbonyl

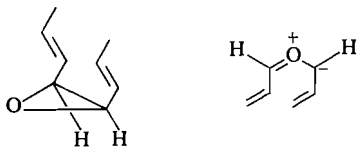

10 **11**

ylide **2** into the carbonyl ylide **3** by rotation about the carbon–oxygen bond of the ylide as shown in Scheme 1. The possibility of a conrotatory ring opening directly from the *trans*-oxirane (**1**) to a carbonyl ylide such as **11** for the production of **5** and **6** (or **8** and **9** from **7**) has been ruled out on both kinetic (4) and stereochemical grounds (2).

Dolbier and Alonso (5) have examined thermal reactions wherein the product determining step has demonstrated a secondary deuterium kinetic isotope effect of greater than unity ($k_H/k_D > 1.0$) in processes in which a new bond is being formed to the isotopically substituted center. Generally such bond forming processes result in inverse isotope effects ($k_H/k_D < 1.0$). They have suggested that "such isotope effects are derived from the rotation of a methylene group of a conjugated system to a nonconjugated, orthogonal conformation in the transition state." They suggested that the dramatic lowering of the torsional force constant of the methylene twisting motion is primarily responsible for the observed isotope effects (5, 6) in reactions involving "the product forming destruction of resonance stabilized biradicals." The carbonyl ylides are examples of resonance stabilized biradicals (7) and it is the

Can. J. Chem. Downloaded from www.nrcresearchpress.com by 210.87.254.42 on 09/05/12
For personal use only.

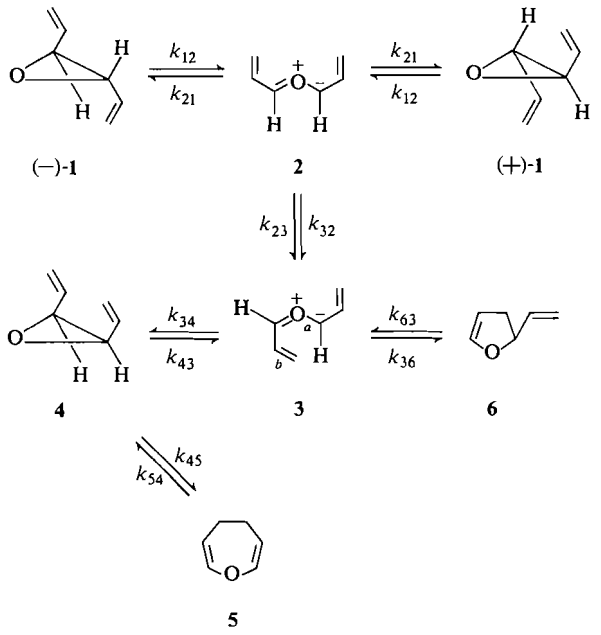

SCHEME 1

purpose of this paper to determine the magnitude of the isotope effects of the reactions in Scheme 1, and to compare these with those observed by Dolbier (5) for the purpose of examining the generality of their suggestion. Generally the isotope effects are rationalized in terms of the changes in force fields caused by the creation of new isotopically sensitive normal modes (6, 8). Seltzer (9) has demonstrated that for addition reactions where an olefinic methylene is transformed to a tetrahedral carbon that an inverse isotope effect ($k_H/k_D < 1.0$) is observed whereas in the reverse of this the normal isotope effect is encountered (10). The generalization that the transformation of an sp^2 methylene to an sp^3 methylene resulted in inverse isotope effects whereas an $sp^3 \rightarrow sp^2$ transformation gave the normal isotope effect has been widely used in the interpretation of secondary deuterium isotope effects; although not rigorously accurate, it provides a useful guide since it does correspond to the introduction of, or elimination of, new normal modes.

Results and Discussion

The secondary deuterium kinetic isotope effect upon the initial step, k_{12}, of Scheme 1 is most readily obtained by comparing k_α (where $k_\alpha = 2k_{12}$) the rate of racemization of (−)-**1** with that of k_α'[1] the rate of racemization of (−)-**1**-d_4. This material was synthesized as outlined in Scheme 2. The racemization rates were

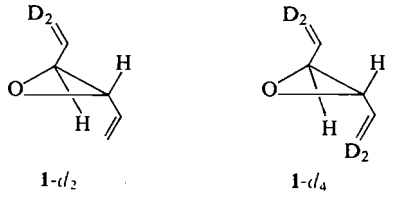

measured, in the gas phase, at 150.04 ± 0.02° with samples of (−)-**1** and (−)-**1**-d_4 being heated concurrently. For **1**, k_α is (5.18 ± 0.07) × 10^{-5} s^{-1} and for **1**-d_4, k_α' is (4.78 ± 0.04) × 10^{-5} s^{-1}. Thus k_H/k_D for the first step (**1** → **2**) is 1.08 ± 0.02, or in terms of the free energy change per deuterium, $\delta\Delta G^{\ddagger}/n$, is 16 ± 4 cal mol^{-1}, much smaller in magnitude and of opposite sign, than the 80–120 cal mol^{-1} frequently observed when a new bond is being formed at the isotopically substituted center.

Since **4** gives only **5** (12) and both **5** and **6** are stable under the reaction conditions then we know that k_{54}, k_{43}, and k_{63} are small relative

[1]In this paper all of the rate constants primed refer to reactions with the tetradeuterated substrate whereas the unprimed rate constants (k_x) refer to the nondeuterated system.

Can. J. Chem. Downloaded from www.nrcresearchpress.com by 210.87.254.42 on 09/05/12
For personal use only.

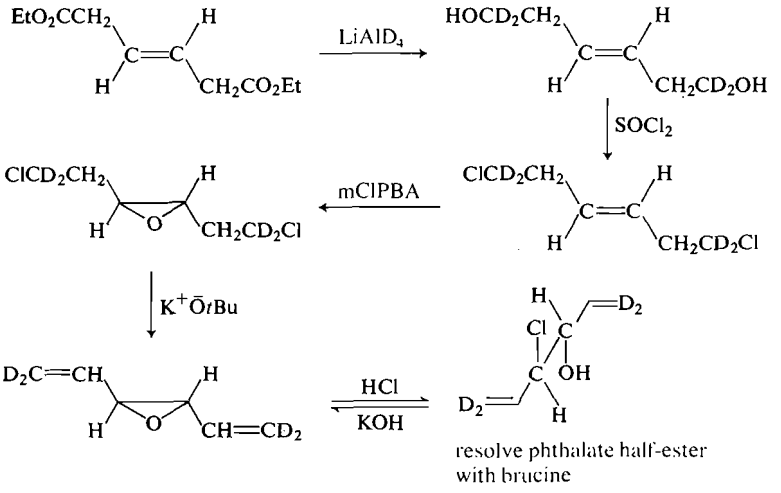

SCHEME 2

TABLE 1. Steady-state rate expression for Scheme 1 and measured rate constants at 192.45°

Reaction	k	$10^5 k$ (s^{-1})
1 → **5**	$\frac{2k_{12}k_{23}k_{34}}{(2k_{21}+k_{23})(k_{32}+k_{34}+k_{36}) - k_{32}k_{23}}$	7.32±0.02
1-d_4 → **5**-d_4	$\frac{2k_{12}'k_{23}'k_{34}'}{(2k_{21}' + k_{26}')(k_{32}'+k_{34}'+k_{36}') - k_{32}'k_{23}'}$	6.31±0.05
1 →**6**	$\frac{2k_{12}k_{23}k_{36}}{(2k_{21}+k_{23})(k_{32}+k_{34}+k_{36}) - k_{32}k_{23}}$	2.99±0.02
1-d_4 → **6**-d_4	$\frac{2k_{12}'k_{23}'k_{36}'}{(2k_{21}'+k_{23}')(k_{32}'+k_{34}'+k_{36}') - k_{32}'k_{23}'}$	2.69±0.02

to other competing processes and they can be omitted from steady state calculations. Using the steady-state approximation for the intermediates **2**, **3**, and **4** the rate expressions, for Scheme 1, are given in Table 1. The rate constants for the production of **5**-d_4 and **6**-d_4 from **1**-d_4 are listed in Table 1 with those measured concurrently for **1** going to **5** and **6** at 192.43 ± 0.02°. The product ratio **6**/**5** was assessed by analytical gas chromatography (g.c.) to be 2.45 ± 0.04. The yield of oxepine was slightly increased on deuteration to produce the ratio **6**-d_4/**5**-d_4 of 2.36 ± 0.03.

The intramolecular isotope effect upon the production of **6** was measured by n.m.r. analysis of the vinyldihydrofuran produced on the isomerization of a sample of **1**-d_2 at 192.43 ± 0.02°.

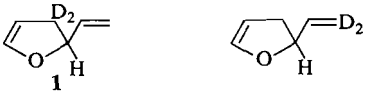

6-d_2-A **6**-d_2-B

The **6**-d_2 produced proved to be a 52:48 mixture of A:B giving an intramolecular isotope effect of 0.92 ± 0.02. Such an intramolecular isotope effect is rationalized readily in the conventional sense that the creation of new bending modes at the isotopically substituted center brings about a greater decrease in the transition states zero-point energy on going to **6**-d_2-A than for that proceeding to **6**-d_2-B. The change in free energy per deuterium ($\delta\Delta G^{\ddagger}/n$) of −38 ± 10 cal mol^{-1} is somewhat smaller than is normally expected but may be a reflection of the transition state being similar in character to the inter-

Can. J. Chem. Downloaded from www.nrcresearchpress.com by 210.87.254.42 on 09/05/12
For personal use only.

Can. J. Chem. Downloaded from www.nrcresearchpress.com by 210.87.254.42 on 09/05/12
For personal use only.

mediate and that as a consequence bond formation has not progressed very significantly. There should be little, or no, difference between this intramolecular isotope effect and the corresponding intermolecular isotope effect measured by comparing the rate of formation of **6** *vs.* **6**-d_4 (13); however, as a post-transition state intermediate this cannot be obtained directly from the kinetic data. Using the product proportions obtained from the infinity tubes on the steady-state rate constants it can be shown that:

$$\frac{d[\mathbf{6}]}{d[\mathbf{5}]} = \frac{k_{36}}{k_{34}} = 2.45 \pm 0.04$$

and

$$\frac{d[\mathbf{6}\text{-}d_4]}{d[\mathbf{5}\text{-}d_4]} = \frac{k_{36}'}{k_{34}'} = 2.36 \pm 0.03$$

Dividing the former by the latter we obtain:

$$\frac{k_{36}}{k_{34}}\frac{k_{34}'}{k_{36}'} = 1.04 \pm 0.03$$

Using the intramolecular value for the reaction **3** → **6** of 0.92 we obtain a value for k_{34}/k_{34}' of 0.89 ± 0.05. Such an inverse isotope effect suggests that the isotopically substituted methylenes are undergoing, in the course of the reaction, a large increase in the force field caused by the creation of new isotopically sensitive normal modes (6, 8). This does not seem reasonable in terms of the process **3** → **4**, an alternative more compatible with the isotope effect is that **5** is being formed directly from **3**. Rotation about the carbon–oxygen bond *a* in **3** produces **5**. This motion is symmetry allowed if it occurs in a conrotatory fashion with respect to rotation about the double bond *b* of **3**. This is consistent with the stereochemical observation of Pommelet *et al.* (2) that **7** produces **9** upon heating, and that no *trans*-4,5-dimethyl-4,5-dihydrooxepine is observed.

Arnold and Karnischky (14) have demonstrated that the disrotatory ring opening of a 5-oxabicyclo[2.1.0]pentane can occur at 120°, thus demonstrating that this motion may be more available than expected from orbital symmetry considerations. Recent theoretical considerations by Berson and Salem (15) suggest that such "forbidden" processes may in fact be concerted and stabilized by subjacent orbital effects. With these factors in mind we propose as an alternative Scheme 3 which is equally capable of rationalizing all of the stereochemical and kinetic data for the 2,3-divinyloxiranes. Table 2 lists the isotope effects observed here in terms of Scheme 3.

We conclude from this work that the secondary deuterium isotope effects observed for the system under investigation are readily rationalized in the conventional sense (11) where the introduction of new bonds to the isotopically labelled position results in an inverse isotope effect, and that transformations such as 1 → 2 and 1 → 3 which do not involve changes in bonding to the isotopically labelled center result in small normal isotope effects. Our data also indicate that a major portion of the dihydrooxepine formed from *trans*-1,2-divinyloxirane does so in a step that is directly competitive with the formation of vinyldihydrofuran rather than arising exclusively from *cis*-2,3-divinyloxirane. Whereas we had anticipated that the transformation of **3** → **5** would give a normal isotope effect, by analogy with the observations of Dolbier and Alonso (5), the inverse isotope effect was observed. This may be reconciled if the transformation **3** → **5** requires little or no twisting of the terminal methylene, a factor which Dolbier suggests is important to his cases where the normal isotope effect is observed in reactions where new force bending constants are created. As indicated earlier the free energy change for **3** → **5**, $\delta\Delta G^{\neq} = -38 \pm 4$ cal mol^{-1}, is small and its attenuated nature may in fact be due to some contribution from the methylene twisting. It should be noted that the carbonyl ylide intermediates are expected to be more stable, on the basis of successful trapping experiments and spectroscopic observations (7, 14), than the putative diradical intermediate of the 1,1-divinylcyclopropane to vinylcyclopentene rearrangement (5).

TABLE 2. Secondary deuterium isotope effects for rates as labelled in Scheme 3

Reaction	n*	k_H/k_D	$\delta\Delta G^{\neq}/n$ (cal mol^{-1})
(−)-**1** → (±)-**1**	4	1.08±0.02	16±4
1 → **3**	4	1.15±0.02	32±4
3 → **5**	2†	0.92±0.02	−38±4
3 → **6**	4	0.88±0.04	−30±10

*Where n is the number of deuteriums involved.
†This value is taken from the intramolecular rate comparing **6**-d_2-A and **6**-d_2-B.

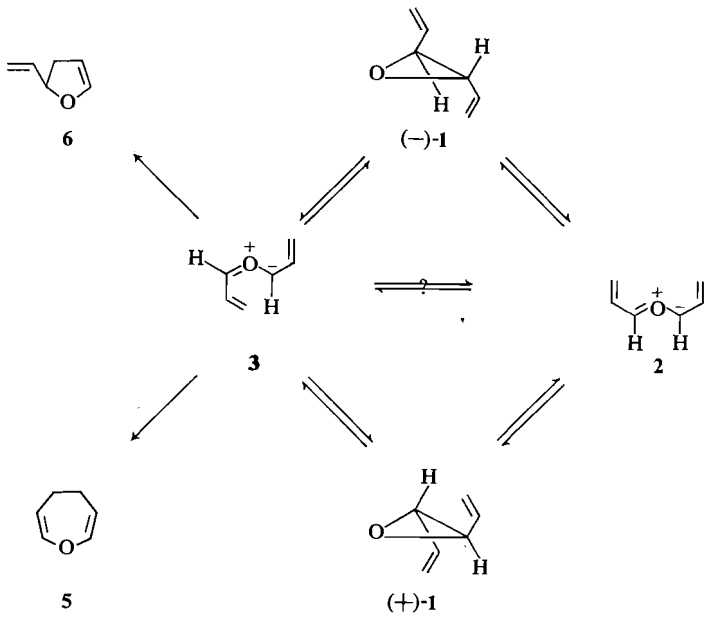

SCHEME 3

Experimental

The n.m.r. spectra were recorded on Varian A-60 and A-100 analytical spectrometers. The analytical g.c. was carried out using a Perkin-Elmer 900 GE equipped with capillary columns and a Hewlett-Packard 3370A Electronic Integrator. Mass spectra were determined on an AEI MS-9 double focussing high resolution spectrometer.

Preparation of trans-3-Hexene-1,6-diol-1,1,6,6-d_4

Diethyl *trans*-3-hexenedioate (29 g, 145 mmol) was dissolved in dry ether and added dropwise to a solution of lithium aluminum deuteride (7 g, 166 mmol) in ether (300 ml) which was maintained at 0°. The reaction was then allowed to warm to room temperature and stirred overnight. The excess reducing agent was destroyed by the careful addition of wet ether followed by a saturated solution of sodiumpotassium tartarate (200 ml). The organic layer was separated and the aqueous portion was subjected to continuous ether extraction, 12 h. The combined ether solutions were dried and the solvent removed. The diol was then subjected to silica gel chromatography 10.2 g (67%).

The n.m.r. spectrum, δ TMS ($CDCl_3$) 5.5 (multiplet, 2H), 3.6 (singlet, 2H), and 3.3 (broad doublet, 4H).

Preparation of trans-1,6-Dichloro-3-hexene-1,1,6,6-d_4

trans-3-Hexene-1,6-diol-*1,1,6,6-d_4* (9.77 g, 81 mmol) was added dropwise to freshly distilled, stirred thionylchloride (24 g, 203 mmol) maintained at 0°. Stirring was continued for an additional 2 h followed by the addition of a few drops of pyridine. The mixture was then warmed to 60° for 3 h. Water was added and the mixture extracted with chloroform. The organic layer was washed once with 2 *N* hydrochloric acid, then with saturated sodium carbonate. After drying over molecular sieves (4 Å) the solvent was removed and the residue distilled 9.3 g (74%) at 64°/5 Torr, (lit. (16) value of nondeuterated material 80°/13 Torr).

Preparation of trans-1,6-Dichloro-3,4-epoxyhexane-1,1,6,6-d_4

The freshly distilled dichloride (9 g, 57 mmol) was dissolved in methylene chloride (100 ml) and added dropwise to a solution of *m*-chloroperbenzoic acid (14.6 g, 84 mmol) in methylene chloride (200 ml). The solution was stirred and maintained at room temperature overnight. The *m*-chlorobenzoic acid was removed by filtration and the solvent removed on a rotary evaporator. Ether was then added to the residue and the solution was washed with a 10% solution of sodium sulfite until a negative KI – starch paper test was achieved. After washing with saturated sodium carbonate the ether solution was dried over molecular sieves (4 Å). Upon removal of the ether the residue was vacuum distilled at 65°/4 Torr, to give 8.8 g (89%).

The n.m.r. spectrum, δ TMS ($CDCl_3$), 3.0 (doublet, 4H), 1.05 (triplet, 2H).

*Preparation of 2,3-Divinyloxirane-d_4 (**1**-d_4)*

Potassium *t*-butoxide (11.2 g, 110 mmol) was added to a solution of *trans*-1,6-dichloro-3,4-epoxy-hexane-*1,1,6,6-d_4* (8.8 g, 50 mmol) in absolute ether (100 ml) and the mixture was stirred overnight at room temperature. Moisture was rigorously excluded. The mixture was then filtered and the solid washed with fresh ether. The combined filtrates were washed with water and dried over anhydrous sodium sulfate. The ether solution was used directly for the next step. An aliquot of this solution was subjected to preparative g.c. (β,β′-oxydipropionitrile on Chromosorb at 60°) and an n.m.r. spectrum taken and was found consistent with the spectrum of the nondeuterated material (1).

*Resolution of **1**-d_4*

The oxirane **1**-d_4 was converted to *threo*-4-chloro-1,5-

Can. J. Chem. Downloaded from www.nrcresearchpress.com by 210.87.254.42 on 09/05/12
For personal use only.

Can. J. Chem. Downloaded from www.nrcresearchpress.com by 210.87.254.42 on 09/05/12
For personal use only.

hexadiene-3-ol-*1,1,6,6-d*$_4$ and converted to the phthalate half-ester followed by resolution of the brucine salt. The conversion to **1**-*d*$_4$ was achieved in the same manner as described for the nondeuterated material (1).

The n.m.r. spectrum of the isolated (−)-**1**-*d*$_4$ displayed less than 1% absorption in the region assigned to the terminal methylene. The integration ratio of the low field vinyl protons at δ 5.6 to the oxirane ring protons at δ 3.25 was 1.01:1.00.

Preparation of Monoethyl trans-3-Hexenedioate

A solution of diethyl *trans*-3-hexenedioate (10 g, 50 mmol), *trans*-3-hexenedioic acid (17.4 g, 120 mmol), and 95% ethanol (10.3 ml) in butyl ether (6.2 ml) with concentrated hydrochloric acid (3 ml) was refluxed for 2 h. The volatile components were then removed on a rotary evaporator and the residue fractionated. The first fraction, b.p. 115°/4 Torr, consisted mainly of the diester; second fraction, b.p. 130°/4 Torr, is the half-ester. Further purification was achieved by extracting an ethereal solution of the second fraction with a 5% sodium bicarbonate solution followed by acidification and ether extraction. After drying and removal of ether the half-ester was distilled, b.p. 118°/0.3 Torr, 9 g (46%).

The n.m.r. spectrum, δ TMS ($CDCl_3$) 10.45 (singlet, 1H), 5.8 (multiplet, 2H), 4.2 (quartet, 2H), 3.15 (broad multiplet, 4H), 1.25 (triplet, 3H).

Preparation of trans-6-Hydroxy-3-hexenoic Acid

Sodium (6.6 g, 0.23 g-at.) was added in small portions to a solution of monoethyl *trans*-3-hexenedioate (15 g, 87 mmol) in liquid ammonia (450 ml) containing absolute ethanol (14.4 ml) (17). After completion of addition a small amount of ethanol was added to remove the blue color. The solution was stirred overnight and the ammonia allowed to evaporate. Upon addition of water and acidification, the solution was continuously extracted using ether. The ether layer was dried and concentrated to give 5.3 g (45%) of crude hydroxy acid. The compound was difficult to purify and thus was used directly for the next step.

Preparation of trans-3-Hexene-1,6-diol-1,1-d$_2$

The crude hydroxy acid (5.3 g, 41 mmol) from the above experiment was dissolved in ether (75 ml) and added to a slurry of lithium aluminum deuteride (1.88 g, 45 mmol) in ether (75 ml). The reaction mixture was kept under nitrogen and stirred for 2 h. Excess reducing agent was destroyed by the addition of wet ether and the diol was worked up as described above for the tetradeuterated diol.

The n.m.r. spectrum, δ TMS ($CDCl_3$) 5.5 (multiplet, 2H), 4.6 (triplet, 2H), 3.7 (singlet, 2H), 2.25 (multiplet, 4H).

Preparation of trans-3,4-Epoxy-1,5-hexadiene-1,1-d$_2$ *(1-d*$_2$*)*

The conversion of the diol of the previous preparation to the dichloride was accomplished in the same manner as that described earlier for the tetradeuterio compound. Epoxidation was carried out as described above followed by dehydrohalogenation using potassium *t*-butoxide. The pure **1**-*d*$_2$ was isolated by preparative g.c.

A 100 MHz n.m.r. spectrum δ TMS ($CDCl_3$) 6.8–5.2 (multiplet), 3.2 (doublet). Careful integration gave intensities of 2.02:1.00.

Conversion of 1-d$_2$ *to 6-d*$_2$*-A and 6-d*$_2$*-B*

Pure epoxide, **1**-*d*$_2$, was placed in break-seals such that the pressure at 192° was 600 Torr. These degassed samples were then heated to 192° for 22 h. The cooled samples were then reattached to the vacuum line and the product transferred to a sample vial. Ether was added and the mixture was separated by preparative g.c. (20% Carbowax 1500 at 40°). The vinyldihydrofuran-*d*$_2$ was placed in an n.m.r. sample tube, $CDCl_3$ and TMS added, and the sample degassed before analysis.

Careful integration of the low and high field signals gave a ratio (R) of 5.28 ± 0.11. The mol fraction n of **6**-*d*$_2$-A present is given by the equation $n = (R - 2)/(1 + R)$ and thus 0.522 ± 0.008.

Kinetic Measurements

The kinetic measurements were carried out as described previously except that in each case samples of the nondeuterated oxirane **1** were measured concurrently.

The authors wish to acknowledge the financial support of the National Research Council of Canada and fruitful correspondence with Prof. Wm. R. Dolbier, Jr.

1. R. J. Crawford, V. Vukov, and H. Tokunaga. Can. J. Chem. **51**, 3718 (1973).
2. J. C. Pommelet, N. Manisse, and J. Chuche. Tetrahedron, **28**, 3929 (1972).
3. R. B. Woodward and R. Hoffmann. Angew. Chem. Int. Ed. Engl. **8**, 781 (1969).
4. J. C. Paladini and R. J. Crawford. Can. J. Chem. **52**, 2098 (1974).
5. W. R. Dolbier, Jr. and J. H. Alonso. J. Am. Chem. Soc. **95**, 4421 (1973); S. H. Dai and W. R. Dolbier. J. Am. Chem. Soc. **94**, 3946 (1972).
6. I. Safarik and O. P. Strausz. J. Phys. Chem. **76**, 3613 (1972).
7. A. Robert, J. J. Pomeret, and A. Foucaud. C. R. Acad. Sci. Paris, **270C**, 1739 (1970). A. Dahmen, H. Hamberger, R. Huisgen, and V. Markowski. Chem. Commun. 1192 (1971). H. Hamberger and R. Huisgen. Chem. Commun. 1190 (1971). H. J. H. MacDonald and R. J. Crawford. Can. J. Chem. **50**, 428 (1972). J. C. Paladini and J. Chuche. Tetrahedron Lett. **46**, 4383 (1971).
8. M. J. Stern and M. Wolfsberg. Pure Appl. Chem. **8**, 325 (1964).
9. S. Seltzer. J. Am. Chem. Soc. **83**, 1861 (1961).
10. S. Seltzer. J. Am. Chem. Soc. **83**, 2625 (1961).
11. E. A. Halevi. Progr. Phys. Org. Chem. **1**, 109 (1963).
12. E. L. Stogryn, M. H. Gianni, and A. J. Passannante. J. Org. Chem. **29**, 1275 (1964).
13. K. B. Wiberg. Physical organic chemistry. John Wiley and Sons. Inc., New York. 1963. p. 351.
14. D. R. Arnold and L. A. Karnischky. J. Am. Chem. Soc. **92**, 1404 (1970).
15. J. A. Berson and L. Salem. J. Am. Chem. Soc. **94**, 8917 (1972).
16. G. Wittig and F. Wingler. Ber. **97**, 2146 (1964).
17. L. A. Paquette and N. A. Nelson. J. Org. Chem. **27**, 2272 (1962).

The Extraction of Mercury and Methylmercury by Diphenylthiocarbazone-treated Polyurethane Foams

ARTHUR CHOW AND DANIEL BUKSAK
Department of Chemistry, University of Manitoba, Winnipeg, Manitoba R3T 2N2
Received November 15, 1974

ARTHUR CHOW and DANIEL BUKSAK. Can. J. Chem. **53**, 1373 (1975).

Dithizone-treated polyurethane foams which are easily prepared in the laboratory, are shown to efficiently extract mercury(II) and methylmercury(II) chloride from aqueous solution over a wide p*H* range for mercury concentrations below 10 p.p.m. The mercury is firmly held but can be recovered for analysis by eluting with acetone if desired. The extraction of both forms of mercury from domestic water, river water, raw sewage, and secondary-treated sewage is shown to be acceptable.

ARTHUR CHOW et DANIEL BUKSAK. Can. J. Chem. **53**, 1373 (1975).

Des mousses de polyuréthane, traitées par le dithizone, peuvent être facilement préparées au laboratoire et on montre qu'elles peuvent extraire d'une façon efficace le mercure(II) et le chlorure de méthylmercure(II) de solutions aqueuses à des p*H* très variés et pour des concentrations de mercure en bas de 10 p.p.m. Le mercure est fortement retenu mais si on le désire il peut être récupéré pour analyse par élution avec de l'acétone. On montre qu'il y a une extraction acceptable des deux formes de mercure provenant d'eaux domestiques, d'eaux de rivière, d'eaux d'égout brutes et d'eaux d'égout traitées d'une façon secondaire.
[Traduit par le journal]

The extraction of inorganic pollutants from aqueous solutions has been accomplished with a variety of techniques for many elements. Methods such as ion exchange (1), coprecipitation (2), freeze concentration (2), gas chromatography (3), and others have been applied to specific problems but often have limited applicability because of nonselectivity or because of a necessary, extensive pretreatment.

Mercury has been recovered from brine solutions by extraction with high molecular weight amines (4) although this was not specific for only mercury. Some agricultural products and by-products have been shown (5) to adsorb nonquantitatively some mercury(II) chloride and methylmercury(II) chloride. In a previous paper (6) SH-treated polyurethane foam was used to extract mercury(II) and methylmercury(II) chloride from solution but this technique was not fully acceptable because of the low capacity and the complex preparation of the foam.

Diphenyldithiocarbazone (dithizone) has been used as a complexing agent for mercury with the complex being extracted into carbon tetrachloride (7, 8) and other solvents (9). Solvent extraction methods have a distinct disadvantage because of the limited sample volume that can be conveniently handled. Because of this and other difficulties, several attempts have been made to immobilize the dithizone on some form of matrix. Pierce and Peck (10) used dithizone on silica gel for a column chromatographic separation of mercury. Ueno and co-workers (11, 12) prepared hydrophobic gel particles containing dithizone by two methods and showed that a column of these could extract about 1 to 2 mg per 10 ml of material. Mercury was recovered and the column regenerated by using a sulfuric acid – potassium bromide solution. Braun and Faraq have used polyurethane foam which had been treated with zinc diethyldithiocarbamate or zinc dithizonate in a plastizer such as tributylphosphate to extract mercury (13) and other metals (14). These foams were shown to be efficient for collecting mercury(II) from solutions ranging in concentration from 0.72 to 72 p.p.b. Mercury could be removed from the column by using sodium thiosulfate solution. The effect of other metals in the solution on the extraction of mercury was not indicated. The application to methylmercury(II) or to real samples was not discussed.

Polyurethane foam has been used previously as an extraction medium for cigarette filters (15), oil spills (16, 17), phenol adsorption (18), polychlorinated biphenyls (19), and for mercury (6) and other metals.

It was felt that because of the wide concern

Can. J. Chem. Downloaded from www.nrcresearchpress.com by 210.87.254.6 on 09/05/12
For personal use only.

Can. J. Chem. Downloaded from www.nrcresearchpress.com by 210.87.254.6 on 09/05/12
For personal use only.

about mercury in the environment (20), a simple extraction method which would permit the removal of trace amounts of mercury(II) and methylmercury(II) chloride from aqueous samples would be useful. This would be especially useful if it permitted the extraction to be carried out in the field and the analysis to be done in the laboratory. Polyurethane foam constitutes an easily-available material which is quite inert to most solvents and is easily manipulated. Dithizone is a good complexing agent for mercury although it is not completely specific (9), and can function over a wide range of acidities. For these reasons, a detailed study of the direct use of dithizone with flexible polyurethane foam was undertaken.

Experimental

Apparatus and Reagents

A Baird Atomic Model 530 γ spectrometer with a Model 810C well-type NaI (Tl) detector was used to measure the radioactivity of the samples. A Coleman Model 38A p*H* meter was used to determine the acidity of the samples. All chemicals used were reagent grade and all water used was double distilled and deionized unless otherwise indicated. Methylmercury-203(II) chloride and mercury-203(II) chloride were obtained from ICN Research Products, Montreal and NEN Canada, Dorval, respectively. The flexible polyurethane foams were obtained as cylindrical plugs, 2.2 × 4.0 cm (DisPo brand, Canlab, Winnipeg) which fit snugly into glass columns 20 cm in length which were equipped with a Teflon stopcock.

Procedure

The polyurethane foams were soaked in a solution of 0.1 mg/ml dithizone in acetone for 1 h, drained, and then left to dry overnight in a vacuum dessicator. Two dithizone-treated foams were placed in each glass column with enough water to completely immerse them. Any air in the foams was removed by compressing them several times with a glass plunger. The column was now ready for use. Prior to the addition of a sample, the water was drained from the column, the foams compressed several times, and any residual water removed by blowing air through the foams.

Samples were prepared by taking an appropriate aliquot of the required radioactive mercury tracer, adding the desired amount of a solution of the inactive mercury compound, and diluting it to 100 ml at the appropriate acidity. The radioactivity of each individual sample in a beaker was counted five times on the γ spectrometer for 50 s, and the average taken. The sample was then transferred to a column containing two foams and the empty beaker counted again to permit the most accurate estimate of the actual radioactivity used. Normal samples had an activity of about 1000 ± 4 c.p.s. which corresponded to roughly a 0.002 p.p.b. mercury solution; the background was about 20 ± 1.5 c.p.s. The air was removed from the foams by compressing them several times and the sample then permitted to flow through the column by compressing the foams and then blowing air through them. The radioactivity of the recovered sample was compared with that of the original added sample to determine the percentage of mercury extracted by the foams. Since the radio activity *not* extracted was used for calculation and this was often quite small, the precision of the measurement of the extraction was about ±0.3%. Where multiple samples were used, the average has been reported and an average deviation was obtained of about ±0.5% of the percentage extraction. Although a much simpler format could be used in practice, the above procedure allowed a more precise evaluation in the laboratory.

Results

The effect of various acidities was evaluated for extraction by dithizone-treated foams for both mercury(II) and methylmercury(II) chloride using 100 ml samples containing tracer only at flow rates of 1 and 3 ml per min. The results are recorded in Table 1. Both mercury compounds were extracted from the aqueous phase at the slower flow rate with 94% or greater efficiency between p*H* 1 to 10. The faster flow rate gave more variable results and was less quantitative. Other experiments have shown a change in the extraction from 89% at 5 ml per min to 98.5% at 0.5 ml per min at p*H* 5.5 for similar solutions. Mercury(II) chloride was efficiently extracted at about p*H* 5 to 10 while methylmercury(II) chloride was best extracted at p*H* 1.2.

The amount of mercury used in these experiments was extremely small with respect to the amount of dithizone held by the foam and so

TABLE 1. Effect of p*H* and flow rate on extraction of mercury

Compound	p*H*	Extraction (%) Flow rate, 1 ml/min	Flow rate, 3 ml/min
$HgCl_2$ (0.002 p.p.b.)	0	98.6	—
	1.3	95.1	89.2
	3.8	96.0	94.7
	5.0	96.5	—
	7.0	—	86.0
	9.6	96.6	90.0
	11.3	79.3	58.9
CH_3HgCl (0.002 p.p.b.)	0	23	—
	1.2	100.0	99.0
	3.8	97.2	73.7
	6.5	98.3	—
	7.2	—	69.6
	9.5	98.7	74.1
	11.3	97.6	86.7

Can. J. Chem. Downloaded from www.nrcresearchpress.com by 210.87.254.6 on 09/05/12
For personal use only.

the reaction should strongly favor complex formation if the reaction is possible. Some dithizone was washed from the foams during the passage of the samples but no attempt was made to correlate the amount with the acidity of the solution.

The working range for mercury compounds was evaluated using a series of solutions varying in mercury concentration from 400 and 10 p.p.m. to the lower limit of the diluted tracer alone without nonradioactive carrier. This lower limit was calculated to be roughly 2×10^{-10} g per 100 ml sample on the basis of the measured radioactivity. It can be seen from the results shown in Table 2 that almost quantitative recovery of both mercury compounds was obtained up to a concentration of 5 or 10 p.p.m. *i.e.* a total amount of 0.5 or 1.0 mg. From the values for mercury(II) chloride, it can be seen that the total capacity of the dithizone-treated foams was much greater but that at high concentrations quantitative extraction would not occur. The more significant data indicate that even the most minute amounts of both mercury compounds were quantitatively removed from aqueous solution by the dithizone-treated foams. Additional experiments have shown that the treated foams were able to concentrate 96 and 99% of mercury(II) and methylmercury(II) chloride even when the samples were diluted by a factor of 10 to 1000 ml of 0.0002 p.p.b. solutions at p*H* 5.5 and 1.3 respectively.

TABLE 2. Effect of concentration on extraction of mercury

Compound	Concentration of sample	Extracted by foam (%)	p*H* of sample
$HgCl_2$	0.002 p.p.b.	98.4	5.5
$HgCl_2$	4 p.p.b.	98.5	5.5
$HgCl_2$	40 p.p.b.	99.1	5.5
$HgCl_2$	400 p.p.b.	97.2	5.5
$HgCl_2$	4 p.p.m.	99.7	5 5
$HgCl_2$	40 p.p.m.	62.3	5.5
$HgCl_2$	400 p.p.m.	33.4	5.5
CH_3HgCl	10 p.p.b.	99.7	1.3
CH_3HgCl	100 p.p.b.	99.7	1.3
CH_3HgCl	500 p.p.b.	99.9	1.3
CH_3HgCl	1 p.p.m.	100.0	1.3
CH_3HgCl	5 p.p.m.	93.0	1.3
CH_3HgCl	10 p.p.m.	98.9	1.3
CH_3HgCl	5 p.p.m.	93.5	5.5
CH_3HgCl	10 p.p.m.	94.3	5.5
CH_3HgCl	0.2 p.p.b.	98.2	1.3
CH_3HgCl	0.002 p.p.b.	99.2	1.3
CH_3HgCl	0.2 p.p.b.	99.3	5.5
CH_3HgCl	0.002 p.p.b.	99.4	5.5

After the extraction of mercury(II) and methylmercury(II) chloride by dithizone-treated foams, the complex was shown to be firmly held by attempting elution with water. In all cases 100 ml of water removed none of the mercury activity and a few experiments showed that 400 ml of water removed less than 0.1% with no dithizone color being seen in the eluant. Hydrochloric acid at 1 and 3 *M* removed less than 5% of the mercury but up to 50% of the methylmercury chloride. Attempts to recover the mercury using 0.1 *M* sodium thiosulfate solution with a 1 ml per min flow rate were unsuccessful with only 55% of the radioactivity being extracted. Mercury could however, be quantitatively removed from the foams by simply extracting with 100 ml of acetone. This procedure removes both the dithizone and the mercury simultaneously. The determination of the recovered mercury was made by counting the radioactive tracer for these experiments so that the same analytical method could be used for all the concentrations studied and so that the most minute amounts could be determined. In practice, the recovered mercury would be determined by the established techniques of X-ray fluorescence, spectrophotometry, atomic absorption or flameless atomic absorption spectroscopy, etc. as was required for the particular amount anticipated.

The recovery of the complexed mercury with 100 ml of acetone resulted in an increase in the concentration of the metal by a factor of ten for the 1 l samples. For the other samples, no attempt was made to increase the mercury concentration although much smaller volumes of acetone would provide a significant recovery of the complexed mercury. The results indicate that much larger concentration factors could be obtained for large volumes of dilute solutions since these foams have a significant mercury capacity and there was no significant loss of complex during the passage of water.

For comparison with the foregoing data, foams which had not been treated with dithizone were examined for the extraction of the mercury compounds under similar conditions. It was found that the plain foams would extract more than 60% of the mercury(II) chloride tracer but that 40% of this extracted mercury was washed off with the passage of 100 ml of water. Similarly,

45% of methylmercury(II) chloride was extracted and 40% of this was washed off with the first 100 ml of water to pass through the foam. An additional 100 ml removed 13% more of the extracted radioactivity. Thus it can be seen that the addition of dithizone to the foams greatly increased the ability of the foam both to extract and retain mercury.

The ability of dithizone-treated foams to extract mercury from a variety of matrices was considered very important to possible applications. Initial studies showed that a concurrent 10 or 100 p.p.m. concentration of copper, magnesium, calcium, aluminum, iron, or zinc did not appreciably influence the quantitative extraction of 0.002 p.p.b. solutions of mercury(II) or methylmercury(II) chloride where at least 96% mercury extraction was achieved. These metals were chosen because they are the most concentrated ones which occur in both the local water and sewage where they are present at 0.1 to 35 p.p.m. levels.

Natural samples contain a wide variety of components and because of this, several aliquots were taken of tap water, river water, raw sewage, and secondary-treated sewage. These sewage samples had been analyzed previously in this laboratory and were known to contain calcium, magnesium, aluminum, iron, zinc, chromium, lead, copper, manganese, nickel, silver, lithium, and bismuth, of which only the first four were above the 1 p.p.m. level.

Only minor amounts of copper, silver, zinc, and lead were present which might possibly interfere with the complexation of mercury. These metals should not affect the extraction of mercury other than to slightly lower the capacity of the foams for mercury, unless saturation was approached. These samples were spiked with the radioactive mercury tracers to provide a means to evaluate the efficiency of the extraction from these complex matrices. The results of this study which are shown in Table 3, indicated that in comparison to the extraction from distilled water, the extraction of mercury(II) chloride is somewhat less effective with about 80 to 90% being extracted at about p*H* 1. At the natural p*H* of the samples taken, it was found that approximately 10% less mercury was removed. For methylmercury(II) chloride, however, almost quantitative recovery was achieved from all the samples at both the natural and the adjusted acidities. No attempt was made to increase the extraction efficiency by using masking agents for the wide variety of diverse ions known to be present since in practice, the exact matrix would probably be only vaguely known and any addition might be unwieldy for the separational system. Thus it can be seen that both mercury compounds can be extracted from complex matrices with good efficiency using the dithizone-treated foams, without extensive treatment of the samples.

TABLE 3. Extraction of mercury from various matrices

Compound	Matrix	p*H*	Extraction (%)
$HgCl_2$	Double-distilled H_2O	5.5	97.1
	Double-distilled H_2O	3.8	96.0
	Tap H_2O	6.5	88.5
	Tap H_2O	7.2	70.4
	Tap H_2O	1.3	98.3
	River H_2O*	8.1	78.7
	River H_2O	1.3	84.3
	Raw sewage	6.9	63.7
	Raw sewage	1.2	77.8
	Treated sewage	7.4	71.1
	Treated sewage	0.9	83.5
CH_3HgCl	Double-distilled H_2O	5.5	97.8
	Double-distilled H_2O	3.4	99.5
	Double-distilled H_2O	1.2	100.0
	Tap H_2O	6.5	89.9
	Tap H_2O	7.2	96.9
	Tap H_2O	1.3	97.1
	River H_2O*	8.1	94.2
	River H_2O	1.3	99.2
	Raw sewage	6.9	95.2
	Raw sewage	1.2	98.8
	Treated sewage	7.4	96.4
	Treated sewage	1.2	99.7

*Water taken from shoreline of Red River inside Winnipeg, Manitoba, Canada.

Conclusions

The preparation of polyurethane foam containing dithizone may be easily carried out in the laboratory. These dithizone-treated foams efficiently absorb mercury(II) and methylmercury(II) chloride over a wide p*H* range at various flow rates. Both of the mercury compounds are quantitatively extracted from the most dilute solutions up to 10 p.p.m. and are retained strongly enough by the foam to permit the passage of excess water without significant loss. The mercury can be totally recovered from the foams by simple extraction with acetone.

The dithizone-treated foams provide a simple means of extracting methylmercury(II) and mercury(II) chloride from both simple and

Can. J. Chem. Downloaded from www.nrcresearchpress.com by 210.87.254.6 on 09/05/12
For personal use only.

complex aqueous systems. The technique permits the use of a wide variety of conditions and has been demonstrated to function well even for complex, real samples.

The use of dithizone-treated foams thus offers a new and efficient method for the extraction and concentration of both methylmercury(II) and mercury(II) chloride which may prove useful especially for trace amounts both in the laboratory and in the field. The application of similar techniques for other metals is presently being investigated.

The authors thank the National Research Council of Canada and the Research Board, University of Manitoba for their financial assistance.

1. W. RIEMAN. Ion exchange in analytical chemistry. Pergamon Press, New York. 1970.
2. E. W. BERG. Physical and chemical methods of separation. McGraw-Hill, New York. 1963.
3. R. W. MASHIER and R. E. SIEVERS. Gas chromatography of metal chelates. Pergamon Press, New York. 1965.
4. F. L. MOORE. Environ. Sci. Tech. **6**, 525 (1972).
5. M. FRIEDMAN and A. C. WAISS. Environ. Sci. Tech. **6**, 457 (1972).
6. M. A. J. MAZURSKI, A. CHOW, and H. D. GESSER. Anal. Chim. Acta, **65**, 99 (1973).
7. H. IRVING, S. J. H. COOKE, S. C. WOODGER, and R. J. P. WILLIAMS. J. Chem. Soc. Lond. 1847 (1949).
8. H. IRVING, G. ANDREWS, and E. J. RISDON. J. Chem. Soc. Lond. 541 (1949).
9. A. K. DE, S. M. KHOPKAR, and R. A. CHALMERS. Solvent extraction of metals. Van Nostrand Reinhold Co., London. 1970.
10. T. B. PIERCE and P. F. PECK. Anal. Chim. Acta, **26**, 557 (1962).
11. Y. SEKIZUKA, T. KOJIMA, T. YANO, and K. UENO. Talanta, **20**, 979 (1973).
12. K. UENO, T. YANO, and T. KOJIMA. Anal. Lett. **5**(7), 439 (1972).
13. T. BRAUN and A. B. FARAG. Anal. Chim. Acta, **71**, 133 (1974).
14. T. BRAUN and A. B. FARAG. Anal. Chim. Acta, **69**, 85 (1974).
15. R. L. STRICKMAN. U.S. Pat. 3 618 618 (November, 1971); Chem. Abstr. **76**, 97 051 (1972).
16. R. G. WILL and J. F. GRUTSCH. U.S. Pat. 3 617 552 (November, 1971); Chem. Abstr. **76**, 27 828 (1972).
17. E. C. A. CADRON and L. JOURQUIN. Belg. Pat. 764 805 (August, 1971); Chem. Abstr. **76**, 158 071 (1972).
18. R. C. SCHLICHT and F. C. MCCOY. U.S. Pat 3 617 531 (February, 1972); Chem. Abstr. **76**, 155 054 (1972).
19. H. D. GESSER, A. CHOW, F. C. DAVIS, J. F. UTHE, and J. REINKE. Anal. Lett. **4**, 883 (1971).
20. E. A. JENNE. At. Absorpt. Newsl. **13**, 106 (1974).

Can. J. Chem. Downloaded from www.nrcresearchpress.com by 210.87.254.6 on 09/05/12
For personal use only.

The Vibrational Spectra and Structure of Dimethyl Carbonate and its Conformational Behavior[1]

J. E. KATON AND M. D. COHEN

Department of Chemistry, Miami University, Oxford, Ohio 45056

Received October 28, 1974

J. E. KATON and M. D. COHEN. Can. J. Chem. **53**, 1378 (1975).

The infrared spectra of dimethyl carbonate in the liquid and solid phases and the Raman spectrum of the liquid phase are reported. The evidence suggests that dimethyl carbonate exists as an equilibrium mixture of at least two conformers in the liquid state. An experimental value for the enthalpy difference of the two conformers of 2.6 ± 0.5 kcal/mol is obtained from the temperature dependency of the infrared spectrum.

Dimethyl carbonate crystallizes as an oriented polycrystalline film and polarized infrared spectra of the solid have been obtained. These have been utilized, along with the liquid phase data to obtain an improved vibrational assignment. There appears to be a solid–solid phase change in dimethyl carbonate in the vicinity of 140 K, but the details of this change are not known.

J. E. KATON et M. D. COHEN. Can. J. Chem. **53**, 1378 (1975).

On rapporte le spectre infrarouge du carbonate de diméthyle dans les phases liquide et solide et le spectre Raman de la phase liquide. Les données suggèrent que le carbonate de diméthyle existe sous forme d'un mélange à l'équilibre d'au moins deux conformères dans l'état liquide. On obtient une valeur expérimentale pour la différence d'enthalpie entre les deux conformères de 2.6 ± 0.5 kcal/mol à partir de la dépendance sur la température des spectres infrarouges.

Le carbonate de diméthyle cristallise sous forme de film polycristallin orienté et on a pu obtenir les spectres infrarouges polarisés du solide. On a utilisé ceux-ci de même que les données en phase liquide pour obtenir des attributions vibrationnelles améliorées. Il semble qu'il y a un changement de phase solide–solide dans le carbonate de diméthyle à proximité de 140 K, mais on ne connait pas les détails de ce changement. [Traduit par le journal]

Introduction

Ever since the concept of hindered internal rotation about single bonds was established, it has been expected that esters of simple carboxylic acids might exist in a conformational equilibrium in their fluid states. Such an equilibrium is expected, on theoretical grounds, to involve the two planar conformations shown below.

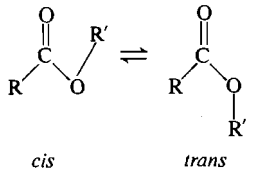

cis *trans*

The nomenclature used here is probably the most common, although many other investigators use the reverse notation of *cis* and *trans*.

Very many investigators have sought experimental evidence for the existence of such an equilibrium, but conclusive results have been very difficult to obtain. Jones and Owen (1) have recently written a very comprehensive review of this previous work. The conclusion which must be drawn from this previous work is that there has not appeared in the literature any report of the experimental confirmation of the existence of *trans* conformers of esters except "when ring-formation dominates the molecular structure (lactones) and possibly when the alkyl group R′ becomes too large to be accommodated in the space allowed by the *cis* structure" (1). The latter case has been discussed in more detail by Oki and Nakanishi (2, 3) and George *et al.* (4). Both of these groups have observed the presence of a conformational equilibrium in *t*-butyl formate (but not in *t*-butyl acetate). Their results indicate that the *cis* structure is the more stable, but whereas Oki and Nakanishi reported the enthalpy difference between conformers to be 2.2 ± 0.7 kcal/mol by n.m.r. methods, George *et al.* found the value to be 150 ± 20 cal/mol by infrared methods. In addition, Oki and Nakanishi (3) have reported that methyl *t*-butyl carbonate exists as a conformational

[1]Supported in part by the U.S. Air Force under contract F33615-73-C-5013.

Can. J. Chem. Downloaded from www.nrcresearchpress.com by 210.87.254.42 on 09/05/12
For personal use only.

Can. J. Chem. Downloaded from www.nrcresearchpress.com by 210.87.254.42 on 09/05/12
For personal use only.

equilibrium in which the most stable conformer is the one in which the methyl group has the *cis* conformation while the *t*-butyl group possesses the *trans* conformation. Their data are not very conclusive, however.

It would appear that the ideal simple compound for investigation of such a conformational equilibrium is dimethyl carbonate. In the case of dimethyl carbonate the only possible conformers are those which differ by internal rotation about the C—O bonds. In addition, there is a statistical weight factor of two in dimethyl carbonate which is not possessed by other simple esters such as methyl formate or methyl acetate. This leads to higher populations of the *cis–trans* conformer, thereby making it easier to detect experimentally (the nomenclature used here arises from the possibility of two ester groups orienting in either the *cis* or *trans* conformation). As Jones and Owen (1) point out, the barrier to rotation in dimethyl carbonate should be lower than that in other esters due to greater electron delocalization. This has no direct bearing on the equilibrium, but does have implications with regard to the experimental approach.

The temperature dependence of the dipole moment of dimethyl carbonate has been reported by Mizushima and Kubo (5) and the results interpreted in terms of one conformer only, the *cis–cis*. Collingwood *et al.* (6) have studied the vibrational spectra of the compound and report that they found no evidence for the existence of a second conformer. They conclude that the structure is the *cis–cis* conformer on the basis of the contours of the vapor phase infrared spectrum and the small number of polarized Raman bands in the liquid phase. The latter is evidence for a C_{2v} structure and the *trans–trans* form is too sterically hindered to be considered seriously.

We have previously given a preliminary report (7, 8) of the results of a thorough study of the vibrational spectra of dimethyl carbonate and the evidence that it exists in a conformational equilibrium mixture in the liquid phase. We report the details and complete results herewith.

Experimental

Dimethyl carbonate was purchased from Aldrich Chemical Company, Incorporated, and fractionally distilled. The constant boiling fraction (90 °C/760 mm Hg) was used for spectral studies. Although the infrared spectrum of the redistilled material was identical to the original, it was found that the solid–solid phase change discussed later could only be readily observed with the redistilled material.

Infrared spectra in the 4000–250 cm^{-1} region were recorded on a Perkin–Elmer Model 180 infrared spectrophotometer and those in the 300–50 cm^{-1} region on a Digilab, Inc., Model FTS-14, Fourier Transform spectrometer. Raman spectra were recorded on a Cary Model 81 Raman spectrometer using an argon ion laser source.

Low temperature infrared spectra were obtained utilizing a conventionally designed low temperature infrared cell mounted in an evacuable chamber fitted with windows for the passage of the infrared beam. The cell was cooled by a stream of nitrogen gas which had been previously cooled by passing through a copper coil immersed in liquid nitrogen and whose flow rate could be controlled by a needle valve. The temperature was monitored by a thermocouple in contact with one of the cell windows. Nominal temperatures as low as 120 K could be reached by controlling the flow of nitrogen gas.

Polarized infrared spectra were obtained utilizing the standard Model 180 polarizer accessory consisting of a gold wire grid mounted on a silver bromide substrate. Oriented polycrystals were obtained by simply cooling the sample below the freezing point, usually fairly rapidly (about 10°/min). No annealing was necessary.

The liquid phase infrared and Raman spectra of dimethyl carbonate are reproduced in Figs. 1 and 2. Typical polarized infrared spectra of crystalline dimethyl carbonate at nominal temperatures of 253 K have been previously published (8) and those at 120 K are reproduced in Figs. 3 and 4. The observed infrared and Raman bands of the liquid and high temperature solid phase are given in Table 1. The frequency accuracy is expected to be ± 4 cm^{-1} in the Raman spectrum and ± 2 cm^{-1} in the infrared spectra, at the worst.

Results

Conformational Behavior

If one studies the liquid phase Raman spectrum of dimethyl carbonate carefully, one is led to the conclusion that it is a rather unusual spectrum for a single compound in a single conformation. Overtones and combination bands are nearly always absent in the Raman spectrum unless they are intensified by Fermi resonance. As a result, one usually sees a few less Raman lines than the number of fundamental modes of vibration predicted for the molecule in question. This is generally true due to the fact that a few fundamental modes are usually weak or so closely spaced that they are unresolvable. Whatever the structure of dimethyl carbonate, it should have 30 fundamental modes of vibration active in the Raman spectrum. Although there are 28 distinct Raman bands, it is clear that not all of the fundamental modes are being resolved. In the CH stretching region there are six ob-

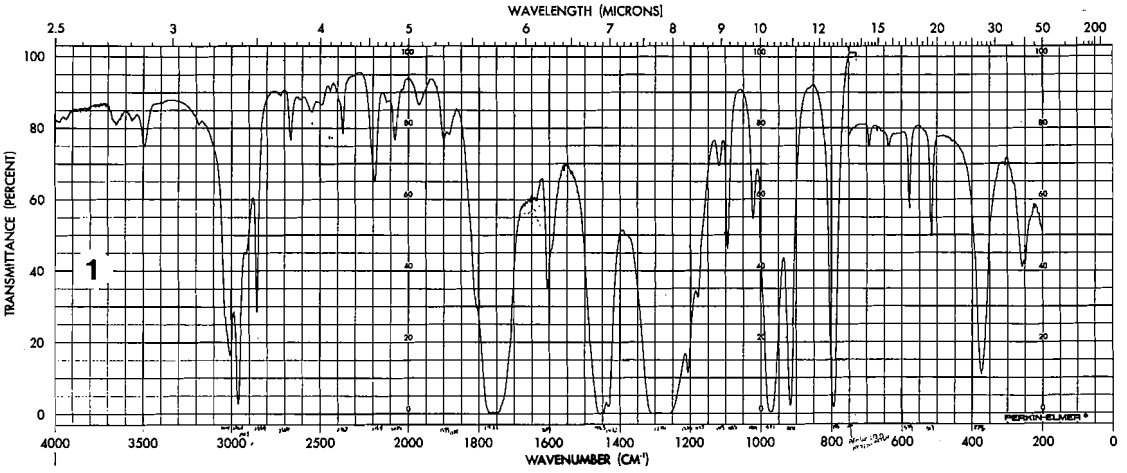

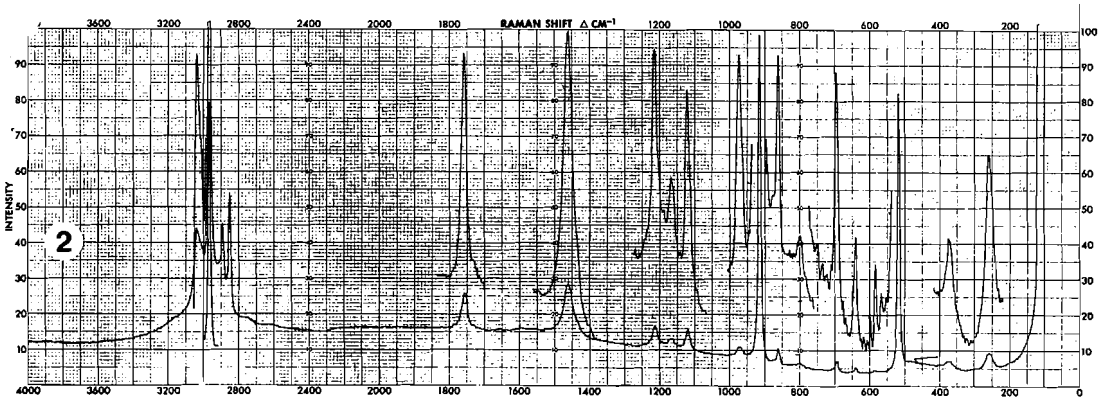

FIG. 1. The infrared spectrum of dimethyl carbonate (liquid, nominal path length 0.05 mm).
FIG. 2. The Raman spectrum of liquid dimethyl carbonate.

served bands, but three are obviously too low in frequency for fundamental modes of methyl esters. Two can be readily assigned as overtones of two CH_3 bending modes in Fermi resonance with the fundamentals. These are very typical features in the spectra of many compounds containing methyl groups. The third is a weak shoulder which can be assigned as a combination band. We are therefore failing to resolve three fundamentals in this region. A similar behavior occurs in the 1400–1500 cm^{-1} region where one expects six CH_3 bending modes. Only two Raman bands can be observed here, however, and they are not well-resolved. It is then clear that the Raman spectrum has more bands than are expected for a single compound in a single conformation. This immediately leads one to suspect a conformational equilibrium. Comparison with the liquid phase infrared spectrum indicates that nearly all of the Raman bands have infrared counterparts (although this is formally not expected for a C_{2v} molecule, it is quite reasonable in view of the nature of the A_2 modes and is discussed later). Several of the observed bands disappear, however, when the sample is cooled and the infrared spectrum of the crystal recorded. This is still further evidence for the existence of a conformational equilibrium in the liquid phase. All of these bands that disappear on cooling are quite weak in *either* the infrared or Raman spectrum, however, and this is probably the reason that Collingwood *et al.* failed to recognize the existence of a second conformer. This behavior is illustrated by the bands at 1095, 863, 640, and 583 cm^{-1}. The first and last are very weak in the Raman but relatively

Can. J. Chem. Downloaded from www.nrcresearchpress.com by 210.87.254.42 on 09/05/12
For personal use only.

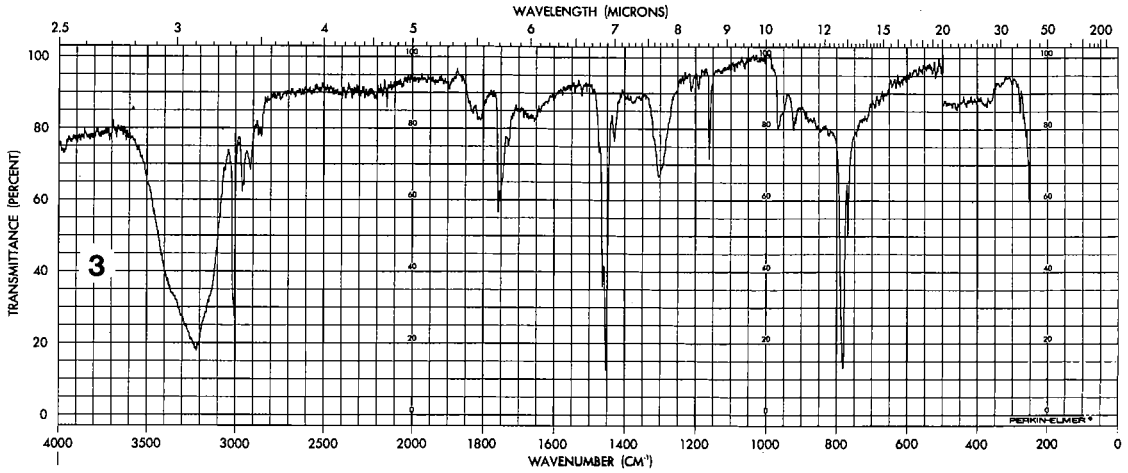

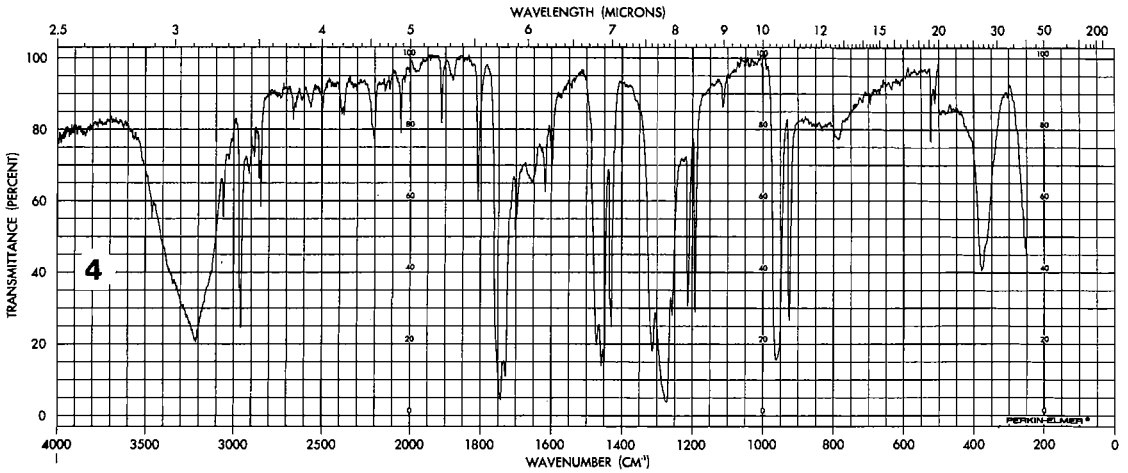

FIG. 3. The polarized infrared spectrum of dimethyl carbonate at 120 K (reference polarizer setting at 0°). The broad band centered at about 3200 cm^{-1} is due to a small amount of ice on the windows.

FIG. 4. The polarized infrared spectrum of dimethyl carbonate at 120 K (reference polarizer setting at 90°). The broad band centered at about 3200 cm^{-1} is due to a small amount of ice on the windows.

strong in the infrared while the second and third show the reverse behavior. A fifth band at 2189 cm^{-1} in the infrared spectrum of the liquid disappears on crystallization. This band can be readily assigned as the overtone of the 1095 cm^{-1} band, of course. There are other minor features in the spectra that behave similarly.

As a final test of a conformational equilibrium, the temperature dependence of the relative infrared absorbances of two bands, one of which disappears in the crystal spectrum, were measured. Since relatively long path lengths were required for these measurements, the 1095 cm^{-1} band overlapped the 1120 cm^{-1} band rather strongly. Therefore the 580/518 cm^{-1} pair were chosen for the measurements since they were relatively well isolated. Their weakness leads to relatively large absorbance errors, however. The relative absorbances of the 580/518 cm^{-1} bands as a function of temperature over the range 13–47 °C were measured. The graph of the logarithm of these ratios versus the reciprocal of the absolute temperature has a good deal of scatter due to inherent lack of accuracy, but it generally shows the trend expected for bands due to different conformers (8). The line was obtained by least squares analysis and treatment of the data in the standard way (9) yields

Can. J. Chem. Downloaded from www.nrcresearchpress.com by 210.87.254.42 on 09/05/12
For personal use only.

TABLE 1. The observed vibrational bands of dimethyl carbonate (in cm^{-1})[a]

Raman (liquid)	Infrared (liquid)	Polarized infrared[b] θ	Polarized infrared[b] θ + 90°	Assignment
	3978 vw			$\nu_{22} + \nu_{11} = 3980$
	3938 vw			$\nu_8 + \nu_1 = 3944$
	3661 w			$\nu_3 + \nu_6 + \nu_{23} = 3661$
	3565 vw			$\nu_3 + \nu_4 + \nu_{24} = 3568$
	3505 mw			$2\nu_3 = 3520$
			3478 vw	$\nu_9 + \nu_{17} = 3479$
	3193 vw			$\nu_3 + \nu_4 = 3196$
3036 mP	3028 sh		3038 sh	ν_1, ν_{16}
		3016* m		ν_{25}
3016 sh	3007 ms	3009* m	3005 w	ν_{11}
		2973 w		$\nu_6 + \nu_3 = 2969$
			2964* m	ν_2
2964 vsP	2961 s	2961 w	2960* m	ν_{17}
2915 sh	2914 vw	2908 vvw	2908 vw	$\nu_4 + \nu_{18} = 2916$
2891 sP				$2\nu_5$ F.R. ν_2
2850 sP	2857 m	2861 vw	2855 w	$2\nu_4$ F.R. ν_2
	2665 mw		2662 vw	$\nu_5 + \nu_6 = 2667$
	2614 vw		2624 vw	$\nu_5 + \nu_{27} = 2621$
				$\nu_4 + \nu_{13} = 2617$
	2549 w		2550 vvw	$2\nu_{20} = 2558$
	2491 vw			$\nu_{20} + \nu_6 = 2488$
	2441 vw			$\nu_5 + \nu_{22} = 2431$
	2398 sh			$\nu_7 + \nu_{20} = 2399$
	2369 mw	2362 w	2365 w	$\nu_6 + \nu_{27} = 2372$
		2335 w	2340 w	$\nu_6 + \nu_7 = 2329$
			2223 sh	$\nu_4 + \nu_{28} = 2233$
			2205 w	$\nu_8 + \nu_{20} = 2195$
	2189 m			Conformer ($2 \times 1095 = 2190$)
	2121 vw			$\nu_4 + \nu_{29} = 2122$
	2077 mw			$\nu_8 + \nu_{27} = 2079$
	2037 vw	2037 vvw	2037 vw	$\nu_8 + \nu_7 = 2036$
	1971 w		1970 vvw	$\nu_5 + \nu_9 = 1976$
	1904 mw		1906 w	$\nu_6 + \nu_{23} = 1901$
	1885 mw	1895 vw		$\nu_8 + \nu_{22} = 1889$
	1847 sh	1835 w	1843 vvw	$2\nu_{28} + \nu_{10} = 1851$
	1810 sh	1812 w	1808 w	$\nu_4 + \nu_{24} = 1808$
		1780 m	1781 m	
		1769 m	1766 sh	ν_3 (crystal components)
1758 mP	1760 vs	1755 sh	1751 s	
		1731 vw	1729 mw	
	1706 sh	1705 vw	1705 w	$\nu_{10} + \nu_{26} = 1710$
		1653 vvw	1653 w	$\nu_{22} + \nu_{23} = 1659$
	1637 vw		1635 w	$\nu_7 + \nu_9 = 1638$
	1606 m	1604 vw	1609 w	$\nu_8 + \nu_{23} = 1608$
1595 vvw	1596 sh			Conformer?
		1558 vw	1558 w	$\nu_{13} + \nu_{24} = 1564$
		1540 vvw	1540 w	$\nu_{10} + \nu_{20} = 1549$
	1508 sh	1504 vvw	1506 vw	$\nu_7 + \nu_{24} = 1492$
				F.R. ν_5, ν_{19}
1461 mP	1458 vs	1460* sh	1460* m	ν_5, ν_{19}
1453 sh			1452.7* ms	ν_{12}
		1451.0* m		ν_{26}
	1436 m	1429 w	1434* m	ν_{18}
			1430* m	ν_4
1270 vvw	1279 vs	1294 ms	1294 vw	ν_{20}
			1268 mw	$\nu_7 + \nu_{30} = 1256$?
1215 mP	1209 w	1208 vw	1208 m	ν_6, ν_{21}

Can. J. Chem. Downloaded from www.nrcresearchpress.com by 210.87.254.42 on 09/05/12
For personal use only.

TABLE 1. (*Concluded*)

Raman (liquid)	Infrared (liquid)	Polarized infrared[b] θ	Polarized infrared[b] θ + 90°	Assignment
1190 vvw		1190 vvw	1190 mw	ν_{13}
	1181 w			Conformer?
1165 m		1158 w	1158 vw	ν_{27}
1122 mP	1120 w	1117 vvw	1117 w	ν_7
1094 vw	1095 m			Conformer
	1021 mw			Conformer
		989 vvw	982 vw	$\nu_{28} + \nu_{29} = 984$
974 w	973 s	969 mw	969 ms	ν_{22}
916 sP	916 s	920 w	920 m	ν_8
863 wP	862 vvw			Conformer
799 vw	797 s	786 ms	786 w	ν_{28}
695 w	692 w		690 vvw	ν_{23}
640 w	637 w			Conformer
599 vvw				Conformer
583 vw	580 m			Conformer
518 sP	518 m	519 vvw	519 w	ν_9
372 w	372 ms	375 w	373 m	ν_{24}
260 mP	257 m	257 m	252 m	ν_{10}
200 vvw	198 vw			ν_{14}, ν_{29}
	136 m			ν_{15}, ν_{30}

[a] v = very, w = weak, m = medium, s = strong, sh = shoulder, F.R. = Fermi Resonance, P = polarized.
[b] High temperature solid phase except where designated *, low temperature solid phase.

a value of ΔH of 2.6 ± 0.5 kcal/mol. These results, taken together, suggest that the liquid phase of dimethyl carbonate exists as a conformational equilibrium of at least two conformers.

Vibrational Assignment

Collingwood *et al.* (C.L.W.) have published an assignment based on vapor phase infrared contours and Raman polarization data. The assignment assumes, however, that only the *cis–cis*, C_{2v}, structure is present. Their lack of infrared spectra of the crystal has therefore led to certain misassignments. In addition, we find ourselves in disagreement with C.L.W. in regard to the experimental observation of a number of weak bands. Finally, we have assigned two of the A_2 modes from our low temperature solid phase infrared spectrum under the assumption that the site symmetry of dimethyl carbonate in this phase is lower than C_{2v}. This assumption is discussed further in the next section. The assignments of the fundamental modes are compared in Table 2.

In the CH stretching region our assignment of the liquid phase spectrum is essentially identical with that of C.L.W. There are three accidental degeneracies (ν_1 with ν_{16}, ν_2 with ν_{17}, and ν_{11} with ν_{25}). In the 120 K spectrum, however, the latter two degeneracies are split.

The first assignment disagreement between C.L.W. and ourselves occurs in the CH_3 bending region. This is a very difficult region because six fundamental modes occur here and there is a great deal of accidental degeneracy. Although our liquid infrared data agrees with that of C.L.W., our Raman data does not. C.L.W. observe Raman bands at 1456 and 1414 cm^{-1}. We have searched for the 1414 cm^{-1} band, but are unable to find it. We do observe a shoulder at 1453 cm^{-1}, however, on a major band at 1461 cm^{-1}. Since our infrared spectrum has bands at 1458 and 1436 cm^{-1}, it seems clear that the 1453 cm^{-1} shoulder must be the A_2 CH_3 antisymmetric bending mode, ν_{12}. Since symmetric methyl bending modes are almost invariably lower in frequency than the corresponding antisymmetric modes, we prefer to assign 1436 cm^{-1} as ν_4 and ν_{18} and the 1458 cm^{-1} band as ν_5, ν_{19}, and ν_{26}. At 120 K, the degeneracy between ν_4 and ν_{18} is split, but that between ν_5 and ν_{19} is not. In addition, we observe two bands at 1452.7 and 1451.0 cm^{-1} of opposite polarization in the oriented crystal at

Can. J. Chem. Downloaded from www.nrcresearchpress.com by 210.87.254.42 on 09/05/12
For personal use only.

TABLE 2. Assignment of fundamental modes of vibration of dimethyl carbonate

C_{2v} symmetry species	Frequency number	Approximate mode	Frequency		Collingwood *et al.* (6)[c]
			Liquid[a]	Solid[b]	
A_1	ν_1	νCH_3 (asym)	3028	3038	3032
	ν_2	νCH_3 (sym)	2961	2964[e]	2964[d]
	ν_3	$\nu C{=}O$	1760	1751	1774
	ν_4	δCH_3 (sym)	1436	1430[e]	1458
	ν_5	δCH_3 (asym)	1458	1460[e]	1414[d]
	ν_6	δCH_3 (rock)	1209	1208	1195[d]
	ν_7	νOCO (sym)	1120	1117	1116[d]
	ν_8	$\nu CH_3{-}O$	916	920	922
	ν_9	δOCO	518	519	857[d]
	ν_{10}	δCOC	257	255	518
A_2	ν_{11}	νCH_3 (asym)	3007	3009[e]	3004
	ν_{12}	δCH_3 (asym)	1453[d]	1452.7[e]	1432
	ν_{13}	δCH_3 (rock)	1190[d]	1190	1234[d]
	ν_{14}	CH_3O torsion	198	—	—
	ν_{15}	CH_3 torsion	136	—	—
B_1	ν_{16}	νCH_3 (asym)	3028	3038	3032
	ν_{17}	νCH_3 (sym)	2961	2960[e]	2965
	ν_{18}	δCH_3 (sym)	1436	1434[e]	1458
	ν_{19}	δCH_3 (asym)	1458	1460[e]	1414[d]
	ν_{20}	νOCO (asym)	1279	1294	1299
	ν_{21}	δCH_3 (rock)	1209	1208	1160[d]
	ν_{22}	$\nu CH_3{-}O$	973	969	989
	ν_{23}	δOCO_2 (rock)	692	690	634
	ν_{24}	δCOC	372	374	579[d]
B_2	ν_{25}	νCH_3 (asym)	3007	3016[e]	3004
	ν_{26}	δCH_3 (asym)	1458	1451.0[e]	1432
	ν_{27}	δCH_3 (rock)	1165[d]	1158	1210[d]
	ν_{28}	δOCO_2 (rock)	797	786	801
	ν_{29}	CH_3O torsion	198	—	—
	ν_{30}	CH_3 torsion	136	—	—

[a]Infrared value unless otherwise indicated.
[b]High temperature solid phase infrared value unless otherwise indicated.
[c]Vapor phase infrared value unless otherwise indicated.
[d]Raman liquid value.
[e]Low temperature solid phase value.

120 K. These bands, which can only be resolved by utilizing the polarizer, are assigned to ν_{12} and ν_{26}.

The CH_3 rocking modes are all assigned in the 1150–1250 cm^{-1} region, but our data are quite different from that reported by C.L.W. They observed no infrared vapor bands in this region, but did observe liquid phase bands at 1162, 1176, and 1210 cm^{-1}. They assigned the four methyl rocking modes from their Raman spectra with the four bands and their relative intensities being 1160 (2), 1195 (4), 1210 (1), and 1234 (1). The 1195 cm^{-1} band was reported to be polarized. We do not observe the 1234 cm band, the 1215 cm^{-1} band is the strongest Raman band in this region and we find it to be polarized, the 1190 cm^{-1} band is very weak, and the 1165 cm^{-1} is the second strongest in the region. A liquid phase infrared band is found corresponding to the 1215 band, but not to the 1165 and 1190 cm^{-1} bands. The crystal infrared spectrum has bands at 1190 and 1158 cm^{-1}, however. This assignment requires that two of the methyl rocks remain accidentally degenerate and ν_6 and ν_{21} have been chosen as corresponding to the strongest Raman and infrared band observed. The choice for ν_{13} and ν_{27} is then arbitrary and we have chosen the highest frequency as ν_{13}.

The four skeletal stretching modes involving the ether-like bonds present no difficulty and we agree with C.L.W. as to their assignment.

The only fundamentals remaining to be assigned are the skeletal bending modes. These are expected below 900 cm^{-1}, where the remaining nonassigned bands are found. Because

Can. J. Chem. Downloaded from www.nrcresearchpress.com by 210.87.254.42 on 09/05/12
For personal use only.

Can. J. Chem. Downloaded from www.nrcresearchpress.com by 210.87.254.42 on 09/05/12
For personal use only.

of a lack of crystal spectra, C.L.W. assigned as fundamentals bands at 857, 634, and 579 cm^{-1}. These correspond to a second conformer, however, as we have previously discussed. They then assigned five Raman bands between 500–198 cm^{-1} as difference bands, the lowest of the ground states being 792 cm^{-1}. This must certainly be incorrect since at room temperature such a high level could not be significantly populated.

The two OCO_2 rocking modes are expected to be the highest in frequency of the skeletal bending modes and C.L.W. have assigned ν_{28} by infrared vapor phase contours. We therefore agree in our assignment of ν_{28}, but assign ν_{23}, the in-plane rocking mode to the next highest frequency found in the solid, 692 cm^{-1}.

There are three more nontorsional skeletal bending modes and three major bands remaining in both the infrared and Raman spectra. Two of these Raman bands are polarized and therefore correspond to the two remaining A_1 modes, ν_9 and ν_{10}. The higher frequency one is chosen as δOCO and the lower as δCOC since the former could be expected at a higher frequency. The remaining depolarized Raman band is then assigned as the B_1, δCOC bending mode.

In a number of studies of compounds containing methoxy groups (10–12), it has been reported that methoxy torsions occur in the range 170–215 cm^{-1} and the corresponding methyl torsions at 130–150 cm^{-1}. We therefore assign the two methoxy torsions, ν_{14} and ν_{29}, as being accidentally degenerate at 198 cm^{-1} and the two methyl torsions as being accidentally degenerate at 136 cm^{-1}.

Crystal Spectra

We have earlier reported (7, 8) that dimethyl carbonate can be crystallized between alkali halide windows as a highly oriented film. We have earlier reported that this phenomenon is rather general with other compounds (13). It is therefore feasible to study the polarized infrared spectra of dimethyl carbonate at low temperatures. Unfortunately, the crystal structure of dimethyl carbonate has not been reported and the results of a polarized infrared spectral study are therefore not unambiguously interpretable. Nevertheless, some information can be drawn from such low temperature studies.

If the sample used is one that has been purified, there appears to be a solid–solid phase change at a nominal temperature of about 140 K. The orientation of the crystals is not destroyed by this phase change since strong polarization effects are noted in the spectra of both phases. Comparison of the spectra in Figs. 3 and 4 with those published earlier (8) leads to the conclusion that the low temperature phase spectra are much more complicated than those of the higher temperature phase, with a great deal of band splitting and sharpening. The change in the spectra is a sudden one, however, and therefore indicates an actual change in crystal or molecular structure. The high temperature solid phase spectra have no significant temperature dependency, but the low temperature solid phase spectra do. In general, the splittings observed in the spectra of the low temperature phase increase as the temperature is lowered. This behavior is typical of crystal splittings in organic crystals, due probably to lattice contraction effects.

The three A_2 modes which are above the low frequency transmission limit of the windows are all methyl modes which might be expected to be accidentally degenerate with other methyl modes of the same type but of different symmetry. This appears to be true with ν_{11}, but ν_{12} and ν_{13} do appear to be resolved in the Raman spectrum of the liquid. In the high temperature solid phase infrared spectrum ν_{12} and ν_{13} also appear, but ν_{11} does not. If the assignment is correct, this indicates that the site symmetry of the high temperature crystal is less than C_{2v}. In the low temperature solid phase infrared spectra a new band appears which can be assigned to ν_{11}. It must be noted, however, that this assignment is quite arbitrary. The band may simply be due to crystal splitting, *i.e.* the same molecular mode split by intermolecular interactions. Nevertheless, ν_{11}, ν_{12}, and ν_{13} must occur very near their present assignment frequencies.

Conclusions

The spectral data for dimethyl carbonate are all consistent with the existence of a conformational equilibrium in the liquid state. In view of previous structural studies, the major conformer must be the *cis–cis*, C_{2v} structure. The second structure would be expected, on theoretical grounds, to be the *cis–trans* C_s structure. There is no experimental evidence confirming this structure as a second conformer, however.

The ΔH value obtained experimentally is quite high, but is in the range predicted for ester conformations (1). It corresponds to a relative concentration of the second conformer of about 1% at ambient temperatures in the absence of a statistical weight factor. If the second conformer is the *cis–trans* structure it would possess a statistical weight factor of two, doubling its relative concentration. If the second conformer is one in which one methyl group is not coplanar with the remainder of the molecule, however, the statistical weight factor would be four.

The recording of the solid state infrared spectra of dimethyl carbonate has, in addition to providing evidence for the conformational equilibrium, allowed improvements in the assignment of the fundamental modes of vibration. Collingwood *et al.* have assigned second conformer bands as fundamentals of the *cis–cis* conformer and these assignments have been corrected.

Dimethyl carbonate crystallizes as an oriented polycrystalline film and polarized infrared spectra may be obtained. In the absence of a known crystal structure, these cannot be fully interpreted. Nevertheless, they indicate that the site symmetry is lower than C_{2v}. It appears that dimethyl carbonate undergoes a solid–solid phase transition in the neighborhood of 140 K, but the exact nature of this transition is not known.

We wish to express our appreciation to Dr. G. L. Carlson of Carnegie–Mellon University and Mr. R. J. Jakobsen of Battelle–Columbus for making their Cary 81 Laser Raman spectrometer and Digilab FTS-14 Infrared Fourier Transform Spectrometer available to us.

1. G. I. L. Jones and N. L. Owen. J. Mol. Struct. **18**, 1 (1973).
2. N. Oki and H. Nakanishi. Bull. Chem. Soc. Jap. **43**, 2558 (1970).
3. N. Oki and H. Nakanishi. Bull. Chem. Soc. Jap. **44**, 3419 (1971).
4. W. O. George, D. V. Hassid, and W. F. Maddams. J. Chem. Soc. Perkin II, 952 (1973).
5. S. Mizushima and M. Kubo. Bull. Chem. Soc. Jap. **14**, 15 (1938).
6. B. Collingwood, H. Lee, and J. K. Wilmshurst. Aust. J. Chem. **19**, 1637 (1966).
7. J. E. Katon and M. D. Cohen. Paper 362, Pittsburgh Conference on Analytical Chemistry and Applied Spectroscopy, Cleveland, Ohio, 1974.
8. J. E. Katon and M. D. Cohen. Can. J. Chem. **52**, 1994 (1974).
9. S. Mizushima. Structure of molecules and internal rotation. Academic Press, New York. 1954.
10. G. Williams and N. L. Owen. Trans. Faraday Soc. **67**, 950 (1971).
11. T. Miyazawa. Bull. Chem. Soc. Jap. **34**, 691 (1961).
12. G. Williams, N. L. Owen, and J. Sheridan. Trans. Faraday Soc. **67**, 922 (1971).
13. J. E. Katon, D. Sinha, M. G. Griffin, and D. A. Condit. Can. J. Chem. **50**, 3255 (1972).

Can. J. Chem. Downloaded from www.nrcresearchpress.com by 210.87.254.42 on 09/05/12
For personal use only.

Vibrational Spectra of $N_2H_5HC_2O_4$ and $N_2D_5DC_2O_4$

R. SAVOIE AND M. GUAY

Département de Chimie, Université Laval, Québec, Québec G1K 7P4

Received November 15, 1974

R. SAVOIE and M. GUAY. Can. J. Chem. **53**, 1387 (1975).

Infrared and Raman spectra of $N_2H_5HC_2O_4$ and $N_2D_5DC_2O_4$ have been recorded at various temperatures between 77 and 300 K. The results at 300 K are consistent with the known crystal structures of these solids. A phase transition has been detected at ~240 K in $N_2D_5DC_2O_4$ and although there are similarities between the two stable solid phases of this compound, the low-temperature form appears to be centrosymmetric and to have a larger unit cell than the high-temperature modification.

R. SAVOIE et M. GUAY. Can. J. Chem. **53**, 1387 (1975).

Les spectres de vibration du composé $N_2H_5HC_2O_4$ et ceux de son analogue deutérié ont été obtenus à diverses températures entre 77 et 300 K. Les résultats à 300 K s'interprètent bien d'après les structures cristallines connues de ces espèces. On a par ailleurs mis en évidence une transition cristalline à ~240 K dans $N_2D_5DC_2O_4$. Même si les deux phases solides de ce dernier composé sont assez semblables, les spectres suggèrent pour la modification stable aux plus basses températures une structure centrosymétrique et une maille élémentaire augmentée par rapport à celle de la phase stable à température ambiante.

Introduction

Proton magnetic resonance investigations of hydrazinium hydrogen oxalate ($N_2H_5HC_2O_4 \equiv$ HyHOx) have shown this crystal to consist of $N_2H_5^+$ and $HC_2O_4^-$ ions (1). This has been confirmed by an X-ray diffraction structure determination (2) followed by a neutron diffraction study (3). The crystal was found to belong to the $P2_1/m$ (C_{2h}^2) space group of the monoclinic system, with two formula units per unit cell. In this structure, the $N_2H_5^+$ ions are required by symmetry to have a perfectly staggered configuration since they are located in mirror planes (at $y = \frac{1}{4}, \frac{3}{4}$), where they are linked together into zigzag chains by in-plane $NH^+\cdots N$ hydrogen bonds. Other hydrogen atoms are involved in bifurcated and trifurcated bonds with the cross-linking oxalate ions which form planar chains through very short (0.245 nm) and symmetrical or statistically disordered hydrogen bonds. The oxalate chains run parallel to each other in the $y = 0, \frac{1}{2}$ planes.

Two independent vibrational studies of HyHOx have already been reported. Selvarajan (4) has published the room-temperature infrared spectrum of the solid in a KBr matrix and the Raman spectrum of the powder, the latter of poor quality due, in part, to the weakness of the exciting source (He–Ne laser). Lindgren *et al.* (5), from a comparative infrared study of HyHOx and its deuterated analog (DyDOx) at liquid-nitrogen temperature, concluded that the $O\cdots H\cdots O$ bonds become asymmetrical when hydrogen is substituted by deuterium in this compound. This prompted an X-ray diffraction study of both crystalline HyHOx and DyDOx, by Thomas (6), who confirmed the noncentrosymmetric structure of the latter (space group: $P2_1(C_2^2)$, $Z = 2$). Still not definitely established, however, is the exact location of the H or D atoms linking the oxalate ions in these solids.

The present study was initiated for the purpose of complementing the diffraction studies and to gather information on the crystal structures of HyHOx and DyDOx at low temperature, as the occurrence of a crystalline phase change had already been indicated in HyHOx by low-temperature X-ray photographs (3).

Experimental

The HyHOx used in this study was prepared as described by Turrentine (7), by mixing warm solutions of hydrazine and oxalic acid (reagent grade, Fisher Scientific Co.). The deuterated product was prepared in a similar manner, from N_2D_4 (97% atom D) in heavy water (99.7% atom D) from Merck, Sharp, and Dohme, and $D_2C_2O_4$ obtained by reacting D_2SO_4 with CaC_2O_4. From the relative intensities of infrared bands attributable to mixed isotopic species, it is estimated that the degree of deuteration of the final product was ~95%.

The Raman spectra of polycrystalline samples were obtained from powders placed in a Dewar-type cryostat with flat windows at the end and cooled by a flow of cold nitrogen gas. In the infrared, Nujol and Fluorolube mulls were used. They were held between CsI (for the mid-infrared)

Can. J. Chem. Downloaded from www.nrcresearchpress.com by 210.87.254.105 on 09/05/12
For personal use only.

Can. J. Chem. Downloaded from www.nrcresearchpress.com by 210.87.254.105 on 09/05/12
For personal use only.

or crystalline quartz (for the far-infrared) windows in a conventional liquid nitrogen cryostat.

The single crystals of HyHOx for the Raman polarization study were grown by slow evaporation of saturated aqueous solutions. The location of the crystallographic axes in the crystals studied (1.5 × 1 × 5 mm) was found by X-ray diffraction. Raman spectra were recorded with the laser beam entering the crystal along the crystallographic *b* axis, the latter being perpendicular to a pair of parallel crystal faces. However, since the crystal shape was such that the axis of observation (*a* or *c* crystal axis) was not perpendicular to a crystal face, extinction of the Raman bands was never complete when expected. The polarization effects were nevertheless sufficiently pronounced to characterize unambiguously different vibrational species.

A Spex (Model 1400) and a Jarrell–Ash (Model 25-100) spectrometer with a CRL (Model 52A) argon laser were used for the Raman experiments. The infrared spectra were obtained with a Perkin–Elmer (Model 621) spectrophotometer (200–4000 cm^{-1} region) and a RIIC (Model FS-720) interferometer coupled to a FTC-100 Fourier transform computer for the 20–400 cm^{-1} region. The slit widths of the spectrometers were generally adjusted so as to get a resolution of 2 cm^{-1} or better and the frequencies reported later are probably accurate within ±2 cm^{-1} in the case of sharp peaks.

Results and Discussion

The low-frequency (20–600 cm^{-1}) infrared and Raman spectra of HyHOx and DyDOx at low and room temperatures are reproduced in Figs. 1 and 2. Complements of the Raman spectra are shown in Fig. 3. The corresponding infrared spectra (600–3500 cm^{-1}) are not reproduced, being essentially similar to those already reported (4, 5). To facilitate the discussion, the spectra of crystalline HyHOx will be analyzed first, using the closely resembling room-temperature spectra of the deuterated compound. The low-temperature spectra of DyDOx will be discussed separately since they differ appreciably from those at room temperature.

HyHOx

The vibrational correlation diagrams for the $N_2H_5^+$, $C_2O_4^{2-}$, and H^+ ions in crystalline HyHOx are given in Table 1, for the centrosymmetric $P2_1/m$ (C_{2h}^2) structure deduced from the diffraction studies.

The correlation diagram for the $H_2N—NH_3^+$ ion indicates that the fundamental vibrations of this species, whether they are symmetric (*A'*) or not (*A''*) with respect to the symmetry plane at the site, should give in each case one Raman and one infrared-active component ($A_g + B_u$ or $B_g + A_u$) in the crystal. This is effectively the case for the two fundamental stretching vibrations of the NH_2 group responsible for the 3292/3293 and 3357/3364 cm^{-1} infrared/Raman pairs of bands (in the room-temperature spectra), the latter pair belonging to the asymmetric stretch since the vibration at 3364 cm^{-1} has B_g symmetry (Fig. 3*A*).

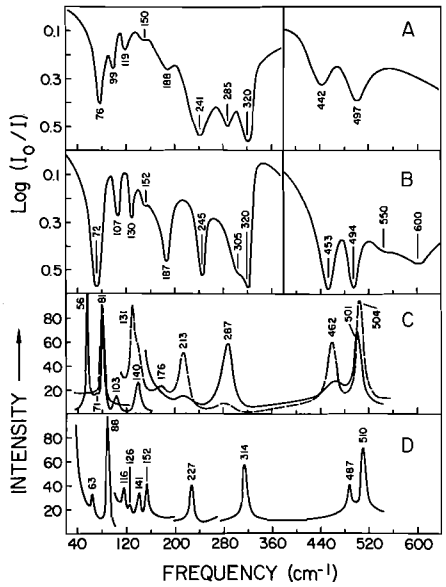

FIG. 1. Infrared spectra of polycrystalline $N_2H_5HC_2O_4$ at (*A*) 300 K and (*B*) 77 K. Polarized Raman spectrum of a single crystal at (*C*) 300 K (—A_g and ···B_g species). Raman spectrum of the powder at (*D*) 77 K.

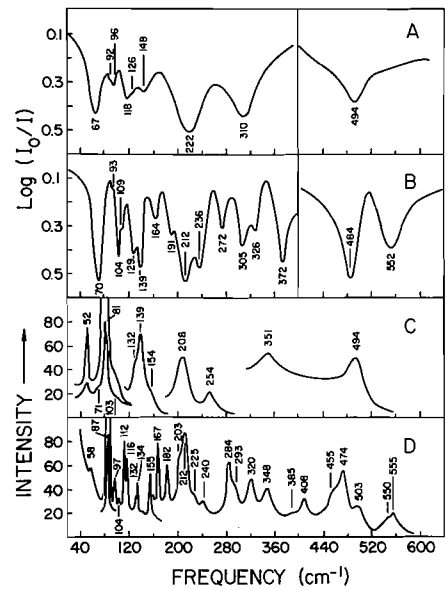

FIG. 2. Infrared spectra of polycrystalline $N_2D_5DC_2O_4$ at (*A*) 300 K and (*B*) 77 K. Corresponding Raman spectra at (*C*) 300 K and (*D*) 77 K.

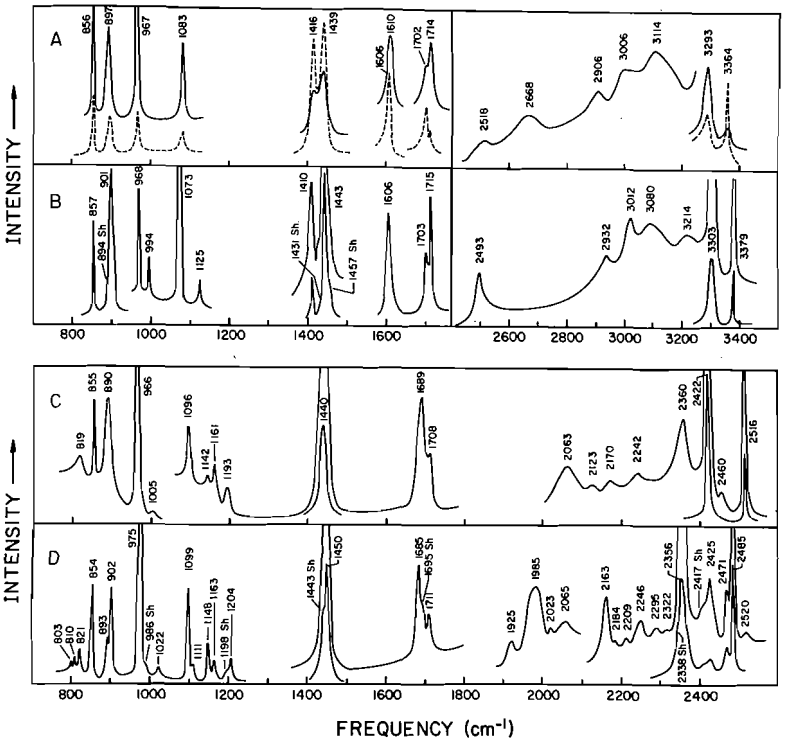

FIG. 3. Polarized Raman spectrum of a single crystal of $N_2H_5HC_2O_4$ at (*A*) 300 K (—A_g and $\cdots B_g$ species). Raman spectrum of the powder at (*B*) 77 K. Raman spectra of polycrystalline $N_2D_5DC_2O_4$ samples at (*C*) 300 K and (*D*) 77 K.

TABLE 1. Vibrational correlation diagrams for the $N_2H_5^+$, H^+, and $C_2O_4^{2-}$ ions in crystalline hydrazinium hydrogen oxalate

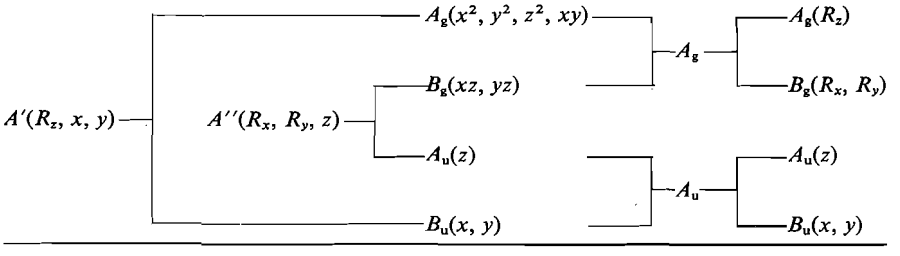

Similarly, the N—N stretching mode is characterized by the 968(infrared)/967(Raman) pair, the Raman-active mode having A_g symmetry as it arises from a symmetric (*A'*) vibration in the free ion.

Bands due to the vibrations of the hydrazinium ions are readily identified from the spectra of the deuterated compound and those of the hydrazinium halides (8). They do not reflect the crystal structure very well because some of them are very weak or nearly degenerate. For instance, only three Raman bands at 1416, 1606, and 1610 cm^{-1}, with infrared counterparts at 1412 and 1609 cm^{-1}, can be attributed to the four H—N—H

Can. J. Chem. Downloaded from www.nrcresearchpress.com by 210.87.254.105 on 09/05/12
For personal use only.

Can. J. Chem. Downloaded from www.nrcresearchpress.com by 210.87.254.105 on 09/05/12
For personal use only.

bending modes. The Raman spectrum of DyDOx, however, shows four peaks in the 1096–1193 cm^{-1} region. Similarly, the four N—N—H bending vibrations (wagging and rocking modes) are characterized by two infrared peaks only (at 1084 and 1120 cm^{-1}). As for the torsion about the N—N axis, expected to occur in the 500–650 cm^{-1} region as in $(N_2H_5)_2SO_4$ (4) and the hydrazinium halides, it has not been detected.

The fundamental vibrations of the $C_2O_4^{2-}$ ions in crystalline hydrazinium hydrogen oxalate are either symmetrical with respect to the center of inversion located midway between the two carbon atoms (A_g species), in which case they are predicted (see Table 1) to give a doublet in the Raman spectrum of the crystal ($A_g + B_g$), or asymmetrical with respect to it (A_u species), in which case they should be characterized by an infrared-active doublet ($A_u + B_u$). This pattern is readily recognized in the spectra, although the predicted factor-group splitting of the infrared-active vibrations is not apparent. For example, two of the four CO stretching modes are infrared-active only (1343 and 1727 cm^{-1}), whereas the remaining two occur as doublets in the Raman spectrum, at 1439 ($A_g + B_g$) and 1702(B_g)/1714(A_g). Similarly, the C—C stretching vibration is Raman-active only, the A_g and B_g vibrational components in the crystal having identical frequencies at room temperature (either 856 or 897 cm^{-1}, one of the two peaks being presumably due to a combination mode), as shown in the polarized Raman spectrum (Fig. 3*A*).

The other vibrations of the oxalate ions are nearly frequency coincident with the corresponding modes in $NaHC_2O_4$ and in $NaHC_2O_4 \cdot H_2O$ (9), in which the $HC_2O_4^-$ network is quite similar to that in HyHOx. The infrared bands at 241 and 320 cm^{-1} are thus assigned to the normally infrared-active rocking and wagging (symmetric C—C—O_2 bending) modes, whereas that at 497 cm^{-1} belongs to the asymmetric O—C—O bending mode. The corresponding symmetric vibration is responsible for the 501(A_g)/504(B_g) cm^{-1} Raman doublet. However, the two Raman-active rocking and wagging modes were not detected. Finally, the weak infrared band at 150 cm^{-1} is tentatively assigned to the torsional mode.

Although the number of optically active lattice modes (at $k = 0$) in crystalline HyHOx is expected from Table 1 to be rather large, the low-frequency region of the spectra can be reasonably well interpreted, using polarization data and frequency shifts upon deuteration. The librational modes of the $N_2H_5^+$ ions, in particular, are easily identified. Oscillations about the N—N axis, involving mainly the hydrogen atoms, are characterized by the 442/462 cm^{-1} infrared (A_u)/Raman (B_g) pair of bands, which are strongly temperature dependent and are shifted by a factor of 1.32 upon deuteration (462 → 351 cm^{-1}). Other librational motions of the hydrazinium ions take place in planes of symmetry of the crystal (285(B_u)/287(A_g) cm^{-1}), or perpendicular to them (188(A_u)/213(B_g) cm^{-1}).

The librational modes of the oxalate ions should be Raman-active only and occur as a series of doublets (A_g/B_g species) with mean frequency in the ratio 1:1.3:1.6 (assuming the frequency to be inversely proportional to the square root of the moment of inertia). Observed Raman bands at 81 cm^{-1} ($A_g + B_g$), 103 cm^{-1} (A_g), and 131/140 cm^{-1} (B_g/A_g) fit this pattern very well, except that the B_g counterpart of the 103 cm^{-1} mode has not been detected. Also expected in this region are three bands due to translational modes ($2A_g + B_g$) of the hydrazinium ions, which are probably strongly coupled to the librational motions of the oxalate ions. The two A_g modes involve layers of hydrazinium ions oscillating between layers of oxalate ions and are expected to have relatively low frequencies. The strong Raman band at 56 cm^{-1} likely accounts for at least one of these two vibrations. The B_g mode in which the hydrazinium ions move against the $HC_2O_4^-$ layers, in the general direction of the NH···O bonds, is expected to have a higher frequency. The remaining peak at 176 cm^{-1} in the Raman spectrum is tentatively assigned to this vibration. The other translational modes in HyHOx should be infrared active only ($6A_u + 6B_u$). Some of these involve mainly the H^+ ions and are responsible for the very broad absorption feature with maximum near 650 cm^{-1} in the infrared spectrum (5). Others involve mostly the heavier ions since they must account for the very low-frequency infrared-active modes at 76, 99, and 119 cm^{-1}.

The vibrational spectra of crystalline HyHOx, which can be well interpreted on the basis of the centrosymmetric crystal structure deduced from the diffraction studies, show no sudden change as the temperature is lowered to 77 K. This, however, does not necessarily mean that the phase transition detected below about 173 K by

Can. J. Chem. Downloaded from www.nrcresearchpress.com by 210.87.254.105 on 09/05/12
For personal use only.

X-ray diffraction (3) is not real. The suggested doubling of the *c* unit cell dimension at low temperature can occur with only minor modifications of the actual crystal structure and result in essentially similar vibrational spectra. In any case, it seems that the O···H···O bonds remain the same as the temperature is lowered, since the characteristic broad absorption band in the 300–1500 cm^{-1}, as well as the narrow transmission peak (10) near 720 cm^{-1}, are still present in the infrared spectrum at 77 K.

DyDOx

The neutron diffraction study of Thomas (6) has shown that the crystal structure of N_2D_5-DC_2O_4 at room temperature is best described by the noncentrosymmetric space group $P2_1$ (C_2^2). In this structure, the various ions are all located on general positions of the unit cell, so that all vibrational components in the solid, instead of being either Raman or infrared-active only, should be active in both types of spectra. This prediction is generally not verified in this case, most likely because the crystal structure departs only slightly from that of HyHOx. The weak infrared activity of the C—C stretching mode (at 853 or 888 cm^{-1}) in DyDOx nevertheless confirms the lowering of symmetry of the oxalate ions upon deuteration.

In the course of the present study, it was early realized that the vibrational spectra of DyDOx at liquid-nitrogen temperature could not be interpreted on the same basis as those at room temperature. The low and high-frequency regions in particular differed markedly at these two temperatures (see Figs. 2 and 3). A careful temperature dependence study indicated that the changes observed in the spectra upon cooling the samples occurred over an extended temperature range, approximately from 240 to 200 K, whereas the reverse transformation took place from 240 to 275 K upon warming. The marked spectral changes in DyDOx near 240 K indicate the occurrence of a genuine phase transition in this solid.

The average vibrational frequencies of the oxalate ions in DyDOx are almost identical in the two solid phases, which suggests that the structural parameters of these ions in the DOx···DOx··· chains remain essentially unchanged in the low-temperature phase (phase II). However, it should be noted that splitting of infrared bands due to the Ox ions occur at the transition (for example, $222 \rightarrow 212 + 236\ cm^{-1}$, $310 \rightarrow 305 + 326\ cm^{-1}$...). Such splittings were predicted above for HyHOx and DyDOx in phase I (high-temperature phase), but were not observed in the infrared spectra of these solids. This apparent lack of vibrational coupling can be explained by the fact that two Ox ions in any primitive cell are separated by Hy^+ or Dy^+ ions. If this interpretation is correct, observed splittings in DyDOx phase II could result from adjacent Ox ions being orientationally different. For example, alternate DOx ions in a chain could have their C_2O_4 planes oriented in different directions. This would of course imply a doubling of the unit cell, which would be consistent with the increased number of bands in the spectra (particularly in the Raman spectrum) of phase II.

The spectra of the $N_2D_5^+$ ions also reflect the phase transition, as shown by the 2400 cm^{-1} region of the Raman spectra (Fig. 3), where the characteristic doublet of the NH_2 group at 2422/2516 cm^{-1} in phase I is replaced by that at 2356/2485 cm^{-1} in phase II. The corresponding frequencies in the room-temperature infrared spectrum of HyHOx are 3292/3357 cm^{-1}. The frequency of the NH stretching vibration of $NHDND_3^+$ species isolated in DyDOx, 3320 cm^{-1}, is very nearly the average of the latter two. The presence of a singlet in this region indicates that the H atoms in the NHD—ND_3^+ and NDH—ND_3^+ species are equivalent. This is consistent with the X-ray diffraction findings that the two D atoms of the ND_2 groups of the ND_2—ND_3^+ ions are nearly equivalent in phase I. In the low temperature modification, the doublet at 3320/3328 cm^{-1} is indicative of a more pronounced departure from planar symmetry of the Dy^+ ions. The possibility of disorder in the relative orientations of the oxalate chains in DyDOx, as suggested by Thomas (6), should therefore be considered, especially since the phase transition in the solid could result from an ordering of the system. The fact that the bands attributable to the oxalate ions in the room-temperature vibrational spectra of DyDOx are somewhat broader than the corresponding ones in HyHOx could be due to orientational disorder of the Ox chains in the deuterated compound. It seems extremely unlikely, however, that the changes in the spectra at ~240 K are caused solely by an ordering of the Ox chains, although it is possible that more important structural changes are triggered by such a process. Whatever the situation in phase I, the sharpness of the bands in the low-tempera-

ture vibrational spectra is indicative of an ordered crystal. Furthermore, the obvious tendency for the infrared and Raman bands to have different frequencies suggests a centrosymmetric structure for phase II, which would require that adjacent chains (or chains in alternate layers) be oriented in opposite directions in the low-temperature form.

The authors gratefully acknowledge financial support of this work by the National Research Council of Canada. We are also indebted to Professor A. Cabana (Université de Sherbrooke) for temporary use of his Raman spectrometer, and to Professor A. Beauchamp (Université de Montréal) and Dr. R. Dubey for their help in locating the crystallographic axes in monocrystals of hydrazinium hydrogen oxalate.

1. L. PRATT and R. E. RICHARDS. Trans. Faraday Soc. **49**, 744 (1953), C. M. DEELEY, P. LEWIS, and R. E. RICHARDS. Trans. Faraday Soc. **50**, 556 (1954); J. TEGENFELDT and I. OLOVSSON. Acta Chem. Scand. **25**, 101 (1971).
2. N. A. K. AHMED, R. LIMINGA, and I. OLOVSSON. Acta Chem. Scand. **22**, 88 (1968).
3. A. NILSSON, R. LIMINGA, and I. OLOVSSON. Acta Chem. Scand. **22**, 719 (1968).
4. A. SELVARAJAN. Indian J. Pure Appl. Phys. **8**, 342 (1970).
5. J. LINDGREN, J. DE VILLEPIN, and A. NOVAK. Chem. Phys. Lett. **3**, 84 (1969).
6. J. O. THOMAS. Acta Cryst. B**29**, 1767 (1973).
7. J. W. TURRENTINE. J. Am. Chem. Soc. **32**, 577 (1910).
8. P. GLAVIČ and D. HADŽI. Spectrochim. Acta, **28**A, 1963 (1972); V. SCHETTINO and R. E. SALOMON. Spectrochim. Acta, **30**A, 1445 (1974).
9. J. DE VILLEPIN and A. NOVAK. Spectrochim. Acta, **27**A, 1259 (1971).
10. J. C. EVANS. Spectrochim. Acta, **18**, 507 (1962).

Can. J. Chem. Downloaded from www.nrcresearchpress.com by 210.87.254.105 on 09/05/12
For personal use only.

Can. J. Chem. Downloaded from www.nrcresearchpress.com by 210.87.254.42 on 09/05/12
For personal use only.

Canadian Journal of Chemistry

Published by
THE NATIONAL RESEARCH COUNCIL OF CANADA

Journal canadien de chimie

Publié par
LE CONSEIL NATIONAL DE RECHERCHES DU CANADA

Volume 53 Number 10 May 15, 1975 Volume 53 numéro 10 15 mai 1975

Crystal and Molecular Structure of *B*-Phenyl-*diptych*boroxazolidine, $C_6H_5BN(CH_2CH_2O)_2$

STEVEN J. RETTIG AND JAMES TROTTER

Department of Chemistry, University of British Columbia, Vancouver, British Columbia V6T 1W5

Received November 8, 1974

STEVEN J. RETTIG and JAMES TROTTER. Can. J. Chem. **53**, 1393 (1975).

Crystals of *B*-phenyl-*diptych*boroxazolidine are monoclinic, $a = 8.4977(4)$, $b = 9.0617(5)$, $c = 7.0105(3)$ Å, $\beta = 111.627(3)°$, $Z = 2$, space group $P2_1$. The structure was solved by direct methods and was refined by full-matrix least squares procedures to a final R of 0.040 for 967 reflections with $I \geq 3\sigma(I)$. The bond lengths involving nonhydrogen atoms have been corrected for thermal motion. Bond lengths are: B—O, 1.460(3) and 1.474(3), B—N, 1.666(3), B—C, 1.613(3), C—O, 1.411(3) and 1.419(3), C—N, 1.485(3) and 1.486(3), $C(sp^3)$—$C(sp^3)$, 1.514(4) and 1.524(4), C—C(ar), 1.384–1.400(4–6), mean C—H, 0.98(4), and N—H, 0.87(5) Å. The crystal structure consists of discrete molecules of *B*-phenyl-*diptych*boroxazolidine each linked to two others by N—H. . .O hydrogen bonds (O. . .N = 2.914(3) Å) to form continuous spirals along *b*.

STEVEN J. RETTIG et JAMES TROTTER. Can. J. Chem. **53**, 1393 (1975).

Les cristaux de la *B*-phényl-*diptych*boroxazolidine sont monocliniques $a = 8.4977(4)$, $b = 9.0617(5)$, $c = 7.0105(3)$ Å, $\beta = 111.627(3)°$, $Z = 2$, groupe d'espace $P2_1$. La structure a été résolue par la méthode directe et affinée par les méthodes des moindres carrés (matrice complète) avec une valeur finale de R de 0.040 pour 967 réflections avec $I \geq 3\sigma(I)$. Les longueurs des liaisons impliquant des atomes autres que l'hydrogène sont corrigées pour les mouvements thermiques. Les longueurs des liaisons sont B—O, 1.460(3) et 1.474(3), B—N, 1.666(3), B—C, 1.613(3), C—O, 1.411(3) et 1.419(3), C—N, 1.485(3) et 1.486(3), $C(sp^3)$—$C(sp^3)$, 1.514(4) et 1.524(4), C—C(ar) 1.384–1.400(4–6) valeur moyenne C—H, 0.98(4) et N—H 0.87(5) Å. La structure cristalline consiste de molécules individuelles de *B*-phényl-*diptych*-boroxazolidine chacune liée à deux autres par des liens N—H. . .O (O. . .N = 2.914(3) Å) formant des spirales continues le long de l'axe *b*. [Traduit par le journal]

Introduction

The cyclic structures of *triptych*boroxazolidine, **1**, (triethanolamine borate (1)) and two ethanolamine diarylborinates (*B*,*B*-diphenylboroxazolidine, **2***a*, (2) and *B*,*B*-bis(*p*-fluorophenyl)-boroxazolidine, **2***b*, (3)) featuring intramolecular N → B coordination, as first proposed by Brown and Fletcher (4), have recently been established by X-ray crystallography. This report describes the structure of the diethanolamine ester of phenylboronic acid, *B*-phenyl-*diptych*boroxazolidine (**3**). The N → B interaction in each of these three types of boron esters was supported by a good deal of chemical evidence (5). With this report, conclusive proof of the existence of the N → B interaction has been presented for each type of boroxazolidine.

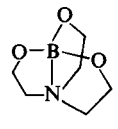

1

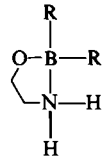

2

a, R = C_6H_5
b, R = *p*-FC_6H_4

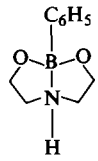

3

Experimental

B-Phenyl-*diptych*oboroxazolidine was prepared as previously described (6, 7). Recrystallization from ethanol–acetone gave colorless needles, elongated along *b*. The crystal chosen for study was mounted with *b* parallel to the goniostat axis and had dimensions of *ca.* 0.3 × 0.7 × 0.3 mm. Unit-cell and space group data were obtained from film and diffractometer measurements. The unit-cell parameters were refined by a least squares treatment of $\sin^2\theta$ values for 24 reflections measured on a diffractometer with CuK_α radiation. Crystal data are:

$C_{10}H_{14}BNO_2$ f.w. = 191.0

Monoclinic, $a = 8.4977(4)$, $b = 9.0617(5)$, $c = 7.0105(3)$ Å, $\beta = 111.627(3)°$, $V = 501.83(4)$ Å^3, $\rho_m = 1.266$ (flotation in aqueous KI), $Z = 2$, $\rho_c = 1.2642(1)$ g cm^{-3}, $F(000) = 204$ (23 °C; CuK_α, $\lambda = 1.5418$ Å, $\mu = 7.0$ cm^{-1}). Absent reflections: $0k0$, $k \neq 2n$, space group $P2_1$ (C_2^2, No. 4).

Intensities were measured on a Datex-automated General Electric XRD 6 diffractometer, with a scintillation counter, CuK_α (nickel filter and pulse height analyzer), and a θ–2θ scan at 2° min^{-1} over a range of $(1.80 + 0.86 \tan\theta)°$ in 2θ, with 10 s background counts being measured at each end of the scan. Data were measured to $2\theta = 145°$ (minimum interplanar spacing 0.81 Å). The r.m.s. deviation of the intensity of the check reflection, measured every 40 reflections throughout the data collection, from its mean value was 0.9%. The final intensity was 1.012 times the initial value. Lorentz and polarization corrections and check reflection scaling were applied, and the structure amplitudes were derived. No absorption correction was made in view of the low value of μ. Of the 1062 independent reflections measured, 84 had intensities less than $3\sigma(I)$ above background where $\sigma^2(I) = S + B + (0.06S)^2$ with S = scan count and B = time-averaged background count. These reflections were given zero weight in the refinement but were included in the structure factor calculations.

Structure Analysis

The systematic absences allow space groups $P2_1$ or $P2_1/m$. The noncentrosymmetric space group $P2_1$ was indicated by the E statistics. The structure was solved by direct methods, 189 reflections with normalized structure factor $|E| \geq 1.35$ being used in the symbolic addition procedure for noncentrosymmetric crystals (8). The phases of the 5 0 −5, 8 0 −1, and 8 1 −2 reflections were fixed to define the origin. During a manual expansion carried out among those 56 reflections with $|E| \geq 1.85$, symbol phases were assigned to the 2 9 −2, 4 7 −2, 3 9 −2, and 7 0 −8 reflections and the phase of 6 0 2 was strongly indicated to be 500 mc. These eight planes comprise the basic set of reflections given in Table 1.

TABLE 1. Basic starting set of reflections for $C_{10}H_{14}BNO_2$

h	*k*	*l*	|*E*|	Phase (mc)
5	0	−5	2.73	0 } origin determining
8	0	−1	2.62	0 } origin determining
8	1	−2	2.10	0 } origin determining
6	0	2	2.06	500 fixed
2	9	−2	2.62	*e*
4	7	−2	2.72	*a*
3	9	−2	2.40	*b*
7	0	−8	2.76	*c*

The phase of the 2 9 −2 reflection was indicated to be ±250 mc. The enantiomorph was set by allowing this symbol phase (*e*) to have only one starting value of +250 mc, thus constraining the phase of this reflection to lie between 0 and 500 mc. The basic set of reflections was split into eight starting sets by allowing symbols *a*, *b*, and *c* two starting values each. These eight starting sets were used as input to a computer program which determines phases using the tangent formula (9–10). The values of overall *t*, overall α, Q, and Rk on the final cycle for each set of phases are given in Table 2.

An *E*-map calculated from set 6, which had the lowest value of Rk and greatest number of phases determined, clearly gave the structure, the 14 highest peaks accounting for the 14 nonhydrogen atoms. Two cycles of full-matrix least squares refinement of the positional and isotropic thermal parameters of the nonhydrogen atoms gave R 0.17. The y coordinate of O(1) was fixed to define the origin. Four cycles of anisotropic refinement reduced R to 0.075 and a difference map revealed the positions of the hydrogen atoms. The entire structure (H atoms with isotropic thermal parameters) was refined for six cycles giving a final R of 0.040 for 967 reflections with $I \geq 3\sigma(I)$ (11 reflections which had $|F_o - F_c| > 3\sigma(F)$ were removed from the data set in the final stages of refinement).

The least squares refinement was based on the minimization of $\Sigma w[|F_o| - |F_c/(1 + qI)|]^2$ where q is the extinction parameter and I the uncorrected intensity. The final value of q was 9.00×10^{-7} e^{-2}. The scattering factors of ref. 11 were used for the nonhydrogen atoms and those of ref. 12 for the hydrogen atoms. Anomalous scattering factors from ref. 13 were used for the nonhydrogen atoms. The anisotropic thermal parameters employed in the refinement are U_{ij} in the expression

$$f = f^0 \exp[-2\pi^2(U_{11}h^2a^{*2} + U_{22}k^2b^{*2} + U_{33}l^2c^{*2} + 2U_{12}hka^*b^* + 2U_{13}hla^*c^* + 2U_{23}klb^*c^*)]$$

where f^0 is the tabulated scattering factor and f is that corrected for thermal motion. The weighting scheme, $w = 1/\sigma^2(F)$ where $\sigma^2(F)$ is derived from the previously defined $\sigma^2(I)$ gave uniform average values of $w(|F_o| - |F_c|)^2$ over ranges of $|F_o|$ and was employed in the final stages of refinement.

The absolute configuration of the molecule (for the particular crystal used) has been determined through the anomalous scattering of the nonhydrogen atoms. Enantiomorph A is represented by the coordinates in

Can. J. Chem. Downloaded from www.nrcresearchpress.com by 210.87.254.42 on 09/05/12
For personal use only.

TABLE 2. Results for the eight starting sets in the phase determination procedure

Set	a (mc)	b (mc)	c (mc)	t	α	Q	Rk	N
1	250	250	0	0.72	126	0.27	0.27	180
2	250	250	500	0.75	127	0.25	0.27	184
3	250	−250	0	0.85	150	0.14	0.24	184
4	250	−250	500	0.85	148	0.15	0.24	184
5	−250	250	0	0.68	113	0.31	0.29	177
6	−250	250	500	0.77	141	0.22	0.18	187
7	−250	−250	0	0.79	141	0.20	0.22	182
8	−250	−250	500	0.80	143	0.19	0.23	184

TABLE 3. Results of Hamilton's test

Parameter compared	Enantiomorph A	Enantiomorph B	B/A	Significance level*
Conventional $R \times 100$ (3σ data)	4.069	4.077	1.0020	>90
Conventional $R \times 100$ (all F)	4.363	4.372	1.0019	>90
Weighted† $R \times 100$ (3σ data)	5.327	5.343	1.0029	>95
Weighted $R \times 100$ (all F)	5.492	5.507	1.0027	>95

*This is the % probability that enantiomorph A is the correct absolute configuration.
†Weighted $R = \Sigma w(|F_o| - |F_c|)^2 / \Sigma w|F_o|^2$.

Table 4 referred to a right-handed axial system and enantiomorph B, the mirror image of A, was generated by changing the y coordinates of A to $1 - y$. Both enantiomorphs were refined and Hamilton's test (14) applied to the resulting R factor ratios. The results of this test, compiled in Table 3, strongly indicate that enantiomorph A is the correct one (the R values in Table 3 are not from the final cycle of refinement).

On the final cycle of refinement the largest parameter shift was 0.09σ. The mean error in an observation of unit weight was 1.44. A final difference map showed maximum fluctuations of ± 0.2 e Å^{-3}. The final positional and thermal parameters appear in Tables 4 and 5 respectively. Measured and calculated structure factors have been placed in the Depository of Unpublished Data.[1]

Thermal Motion and Correction of Molecular Geometry

The ellipsoids of thermal motion for the nonhydrogen atoms are shown in Fig. 1. The thermal motion has been analyzed in terms of the rigid-body modes of translation (T), libration (L), and screw (S) motion (15) using the computer program MGTLS. The r.m.s. standard deviation in the temperature factors U_{ij} is 0.0013 Å^2 indicating that the molecule as a whole (r.m.s. $\Delta U_{ij} = 0.0044$ Å^2) is not a good

[1]The structure factor table is available, at a nominal charge, from the Depository of Unpublished Data, CISTI, National Research Council of Canada, Ottawa, Canada K1A 0S2.

TABLE 4. Final positional parameters (fractional × 10^4, H × 10^3) with estimated standard deviations in parentheses

Atom	x	y	z
O(1)	5275(2)	2782	1596(3)
O(2)	6544(3)	2652(3)	−1003(3)
N	4556(2)	4598(3)	−1118(3)
B	6136(3)	3586(4)	441(4)
C(1)	3718(4)	3470(4)	1366(4)
C(2)	3024(3)	4076(4)	−787(4)
C(3)	5295(4)	2745(4)	−2983(4)
C(4)	4570(4)	4296(4)	−3188(4)
C(5)	7735(3)	4555(3)	1833(4)
C(6)	7975(3)	4972(4)	3826(4)
C(7)	9323(4)	5868(4)	4985(5)
C(8)	10462(4)	6359(4)	4161(7)
C(9)	10264(4)	5957(5)	2193(7)
C(10)	8919(3)	5064(4)	1049(5)
H(N)	473(5)	553(6)	−82(6)
H(1*a*)	295(5)	279(6)	165(6)
H(1*b*)	387(6)	427(6)	230(7)
H(2*a*)	223(5)	479(6)	−98(6)
H(2*b*)	254(5)	328(5)	−184(6)
H(3*a*)	433(4)	200(4)	−317(5)
H(3*b*)	574(5)	262(5)	−411(6)
H(4*a*)	542(4)	500(5)	−340(5)
H(4*b*)	350(5)	451(5)	−417(6)
H(6)	718(5)	468(5)	450(6)
H(7)	945(6)	610(7)	647(8)
H(8)	1146(6)	689(6)	505(7)
H(9)	1096(6)	631(6)	155(7)
H(10)	873(4)	485(5)	−35(6)

Can. J. Chem. Downloaded from www.nrcresearchpress.com by 210.87.254.42 on 09/05/12
For personal use only.

Can. J. Chem. Downloaded from www.nrcresearchpress.com by 210.87.254.42 on 09/05/12
For personal use only.

TABLE 5. Final thermal parameters and their estimated standard deviations

(*a*) Anisotropic thermal parameters ($U_{ij} \times 100$ Å^2)

Atom	U_{11}	U_{22}	U_{33}	U_{12}	U_{13}	U_{23}
O(1)	4.3(1)	3.4(1)	6.7(1)	−0.2(1)	1.6(1)	1.3(1)
O(2)	5.6(1)	4.2(1)	6.2(1)	1.4(1)	1.2(1)	−1.4(1)
N	3.7(1)	2.5(1)	4.5(1)	0.0(1)	1.1(1)	−0.2(1)
B	3.7(1)	2.7(1)	4.9(1)	0.2(1)	1.1(1)	0.1(1)
C(1)	5.0(1)	5.4(2)	5.5(1)	−0.3(1)	2.6(1)	−0.4(1)
C(2)	3.5(1)	5.1(2)	5.5(1)	−0.0(1)	1.4(1)	−0.4(1)
C(3)	5.7(1)	4.1(1)	5.6(1)	0.1(1)	2.5(1)	−1.1(1)
C(4)	5.8(2)	4.7(2)	4.7(1)	0.4(1)	1.9(1)	0.3(1)
C(5)	3.3(1)	3.0(1)	4.9(1)	0.4(1)	1.0(1)	0.2(1)
C(6)	4.6(1)	3.8(1)	5.0(1)	0.4(1)	1.1(1)	0.4(1)
C(7)	5.4(1)	5.3(2)	5.8(2)	0.7(1)	−0.3(1)	−1.0(1)
C(8)	4.3(1)	4.5(2)	9.4(3)	−0.5(1)	−0.2(1)	−1.2(2)
C(9)	3.8(1)	6.0(2)	10.4(3)	−0.7(1)	2.5(2)	0.4(2)
C(10)	4.5(1)	5.3(2)	6.7(2)	−0.5(1)	2.3(1)	−0.3(1)

(*b*) Isotropic thermal parameters ($U \times 100$)

Atom	U (Å^2)	Atom	U (Å^2)
H(N)	7.7(12)	H(4*a*)	6.1(9)
H(1*a*)	7.4(11)	H(4*b*)	6.1(9)
H(1*b*)	8.0(12)	H(6)	6.3(9)
H(2*a*)	7.1(11)	H(7)	9.6(15)
H(2*b*)	7.1(11)	H(8)	9.1(13)
H(3*a*)	5.5(9)	H(9)	8.6(13)
H(3*b*)	7.3(10)	H(10)	6.5(10)

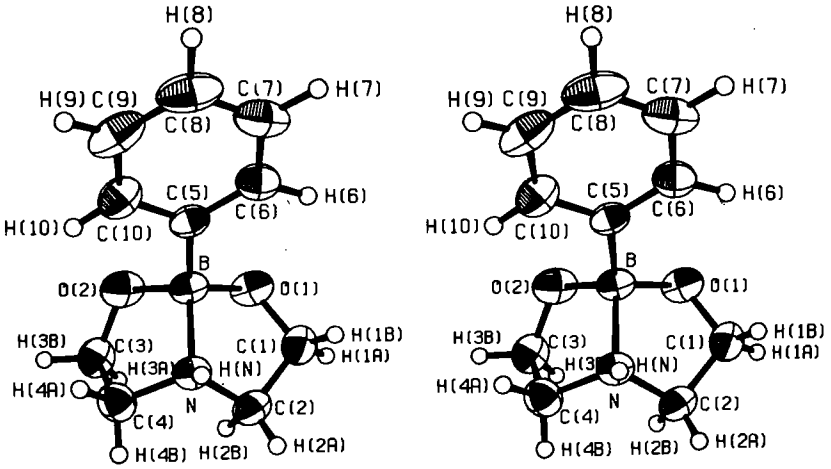

FIG. 1. Stereoscopic view of the *B*-phenyl-*diptych*boroxazolidine molecule showing the atom numbering scheme and 50% probability thermal ellipsoids for the nonhydrogen atoms.

rigid body. Examination of the individual ΔU_{ij} revealed considerable independent motion of the oxygen atoms. Two different 7-atom groups: C(5)–C(10) and B (r.m.s. $\Delta U_{ij} = 0.0019$ Å^2); and C(1)–C(5), N, and B (r.m.s. $\Delta U_{ij} = 0.0024$ Å^2) were adequately described by the rigid body thermal parameters given in Table 6.

The appropriate bond distances and angles have been corrected for libration (16, 17), using shape parameters q^2 of 0.08 for all atoms involved. Both corrected and uncorrected bond

TABLE 6. Rigid-body thermal parameters*

	C(5)–C(10), B			C(1)–C(5), B, N		
L (deg²)	24(5)	3(3) 24(4)	13(2) 2(3) 12(4)	15(4)	1(2) 11(2)	3(2) 4(2) 13(5)
Principal axes of **L**	r.m.s. amplitude			Direction cosines (×10³)		
	5.8°	795	344	499	4.3°	646	419	638
	4.7	308	−939	155	3.5	757	−456	−467
	1.9	522	30	−852	2.9	96	786	−611
Principal axes of reduced **T**	r.m.s. amplitude			Direction cosines (×10³)		
	0.22 Å	−418	205	885	0.21 Å	−358	−2	933
	0.19	900	227	372	0.19	891	299	342
	0.14	−124	952	−279	0.15	−279	955	−104
Displacement of axes from intersecting (Å)								
Parallel to L_1	1.51			0.22				
Parallel to L_2	−0.58			−0.64				
Parallel to L_3	−0.43			0.07				
Effective screw translations (Å)								
Parallel to L_1	−0.004			−0.011				
Parallel to L_2	0.018			−0.007				
Parallel to L_3	−0.031			0.026				
Fractional coordinates of unique origin (×10⁴)								
x	6559			5848				
y	4614			4321				
z	1501			159				
Fractional coordinates of center of gravity (×10⁴)								
x	8725			4978				
y	5217			3924				
z	2673			−661				
r.m.s. ΔU_{ij}	0.0019			0.0024 Å²				

*Axes of reference are orthogonal angstrom axes. Estimated standard deviations of components of **L** are given in parentheses in units of the last places shown.

lengths appear in Table 7. The changes in the bond angles were insignificant, thus only the uncorrected values are given in Table 8.

Results and Discussion

Figure 1 shows a general view of the molecule and the crystallographic numbering scheme. Figure 2 shows the packing arrangement viewed down c^*. Intraannular dihedral angles defining the conformations of the fused five-membered rings are listed in Table 9 and the weighted least squares mean plane in Table 10. Nonbonded inter- and intramolecular distances and details of the hydrogen bonding scheme appear in Table 11.

The crystal structure consists of discrete molecules of *B*-phenyl-*diptych*oroxazolidine, each linked to two others by N—H. . .O hydrogen bonds (N. . .O = 2.914(3) Å) to form continuous spirals about a 2_1 axis along *b*. The O. . .N distance is between the values of 2.874(2) and 2.941(3) Å for similar hydrogen bonds in **2***a* and **2***b* respectively. Aside from the hydrogen bond, there is only one intermolecular distance which is significantly shorter than the sum of van der Waals radii, C(6). . .H(3*a*), 2.60(4) Å. All other intermolecular contacts, the shortest of which are listed in Table 11, correspond to normal van der Waals interactions.

The conformations of the two five-membered rings are significantly different as shown in Table 9. This is due in part to intermolecular steric forces of which the O(1). . .H(N)—N hydrogen bond and the C(6). . .H(3*a*) contact

Can. J. Chem. Downloaded from www.nrcresearchpress.com by 210.87.254.42 on 09/05/12
For personal use only.

TABLE 7. Bond lengths (Å) with estimated standard deviations in parentheses

(*a*) Nonhydrogen atoms

Bond	Distance		Bond	Distance	
	Uncorrected	Corrected		Uncorrected	Corrected
B—O(1)*	1.469(3)	1.474	C(1)—C(2)	1.508(4)	1.514
B—O(2)*	1.457(3)	1.460	C(3)—C(4)	1.520(4)	1.524
B—N	1.661(3)	1.666	C(5)—C(6)	1.388(4)	1.400
B—C(5)	1.610(3)	1.613	C(6)—C(7)	1.395(4)	1.398
C(1)—O(1)*	1.417(3)	1.419	C(7)—C(8)	1.371(5)	1.379
C(3)—O(2)*	1.405(3)	1.411	C(8)—C(9)	1.377(6)	1.384
C(2)—N	1.482(3)	1.485	C(9)—C(10)	1.389(5)	1.393
C(4)—N	1.481(3)	1.486	C(10)—C(5)	1.391(4)	1.398

(*b*) Bonds involving hydrogen atoms

Bond	Distance	Bond	Distance
N—H(N)	0.87(5)	C(4)—H(4*a*)	1.02(4)
C(1)—H(1*a*)	0.97(5)	C(4)—H(4*b*)	0.94(4)
C(1)—H(1*b*)	0.96(5)	C(6)—H(6)	0.99(4)
C(2)—H(2*a*)	0.91(5)	C(7)—H(7)	1.03(5)
C(2)—H(2*b*)	1.01(4)	C(8)—H(8)	0.98(5)
C(3)—H(3*a*)	1.03(4)	C(9)—H(9)	0.92(5)
C(3)—H(3*b*)	1.00(4)	C(10)—H(10)	0.96(4)

*These bonds have been corrected for independent motion as well as libration.

are most important. The observed dihedral angles in the rings are in good agreement with those obtained for free cyclopentanes from energy minimization calculations (18) for $\omega_1 = 20.0°$ (B—O(1)—C(1)—C(2)—N) and $\omega_1 = -35.0°$ (B—O(2)—C(3)—C(4)—N), also shown in Table 9. The observed magnitudes of the dihedral angles are larger than the calculated values since the mean valence angles in the rings, 105.3° for the O(1) ring and 105.4° for the O(2) ring, are slightly greater than the calculated value of 104.2° (18). Bond angles in the five-membered rings range from 101.0(2)° for O(1)—B—N to 111.4(2)° for B—O(2)—C(3).

The C—N, C—O, and C—C distances in the fused five-membered rings do not differ significantly from corresponding bonds in the other boroxazolidines **1**, **2***a*, and **2***b* (1–3). As in **2***a* and **2***b*, the C—C distances (C(1)—C(2), 1.514(4), and C(3)—C(4), 1.524(4) Å) are significantly shorter than the value of 1.537 Å expected for a $C(sp^3)$—$C(sp^3)$ single bond while the C—N distances (C(2)—N, 1.485(3), and C(4)—N, 1.486(3) Å) correspond to normal $C(sp^3)$—$N(sp^3)$ single bonds. The two B—O bonds, B—O(1), 1.474(3), and B—O(2), 1.460(3) Å, are significantly different. This difference appears to be due to the fact that O(1) is involved in the N—H. . .O hydrogen bond while O(2) is not. The B—O(1) distance compares well with the B—O distances of 1.484(3) Å in **2***a* and 1.471(4) in **2***b* which both involve hydrogen-bonded O atoms. The B—O distances in this compound, as well as in **2***a* and **2***b*, are somewhat longer than in **1**, where all three B—O distances were found to be 1.43(1) Å. The B—N bond, 1.666(3) Å, is similar to the values of 1.647(9) for **1**, 1.653(3) for **2***a*, and 1.652(4) Å for **2***b*.

The phenyl ring is planar within experimental error (see Table 10). None of the phenyl hydrogen atoms is significantly displaced from the mean plane but the B atom is displaced by a small, but significant 0.07 Å (23σ) from the phenyl ring mean plane. Small, but significant, displacements of the B atom from phenyl mean planes were also noted in the structures of **2***a* and **2***b*. This deviation represents a folding of the phenyl group away from the B—N bond and, as can be seen in Fig. 2, probably results from intermolecular steric effects. The phenyl ring is oriented such that it is slightly twisted about the B—C(5) bond with respect to the two O atoms, the dihedral angles are: O(1)[B—

Can. J. Chem. Downloaded from www.nrcresearchpress.com by 210.87.254.42 on 09/05/12
For personal use only.

TABLE 8. Bond angles (deg) with estimated standard deviations in parentheses

(*a*) Nonhydrogen atoms

Bonds	Angle (deg)	Bonds	Angle (deg)
B—O(1)—C(1)	110.7(2)	O(1)—C(1)—C(2)	106.2(2)
B—O(2)—C(3)	111.4(2)	N—C(2)—C(1)	103.4(2)
B—N—C(2)	105.3(2)	O(2)—C(3)—C(4)	106.3(2)
B—N—C(4)	104.3(2)	N—C(4)—C(3)	103.2(2)
C(2)—N—C(4)	114.8(2)	B—C(5)—C(6)	122.5(2)
O(1)—B—O(2)	112.9(2)	B—C(5)—C(10)	120.9(2)
O(1)—B—N	101.0(2)	C(10)—C(5)—C(6)	116.6(2)
O(1)—B—C(5)	114.6(2)	C(5)—C(6)—C(7)	122.0(3)
O(2)—B—N	101.8(2)	C(6)—C(7)—C(8)	120.0(3)
O(2)—B—C(5)	112.0(2)	C(7)—C(8)—C(9)	119.5(3)
N—B—C(5)	113.2(2)	C(8)—C(9)—C(10)	120.3(3)
		C(9)—C(10)—C(5)	121.8(3)

(*b*) Angles involving hydrogen atoms

Bonds	Angle (deg)	Bonds	Angle (deg)
B—N—H(N)	111(3)	H(3*a*)—C(3)—H(3*b*)	109(3)
C(2)—N—H(N)	111(3)	N—C(4)—H(4*a*)	107(2)
C(4)—N—H(N)	110(3)	N—C(4)—H(4*b*)	109(2)
O(1)—C(1)—H(1*a*)	112(3)	C(3)—C(4)—H(4*a*)	108(2)
O(1)—C(1)—H(1*b*)	112(3)	C(3)—C(4)—H(4*b*)	120(3)
C(2)—C(1)—H(1*a*)	113(2)	H(4*a*)—C(4)—H(4*b*)	108(3)
C(2)—C(1)—H(1*b*)	108(3)	C(5)—C(6)—H(6)	122(2)
H(1*a*)—C(1)—H(1*b*)	106(4)	C(7)—C(6)—H(6)	116(2)
N—C(2)—H(2*a*)	113(3)	C(6)—C(7)—H(7)	118(3)
N—C(2)—H(2*b*)	105(2)	C(8)—C(7)—H(7)	122(3)
C(1)—C(2)—H(2*a*)	114(2)	C(7)—C(8)—H(8)	118(3)
C(1)—C(2)—H(2*b*)	112(2)	C(9)—C(8)—H(8)	122(3)
H(2*a*)—C(2)—H(2*b*)	108(3)	C(8)—C(9)—H(9)	122(3)
O(2)—C(3)—H(3*a*)	112(2)	C(10)—C(9)—H(9)	117(3)
O(2)—C(3)—H(3*b*)	114(2)	C(9)—C(10)—H(10)	120(2)
C(4)—C(3)—H(3*a*)	109(2)	C(5)—C(10)—H(10)	118(2)
C(4)—C(3)—H(3*b*)	107(3)		

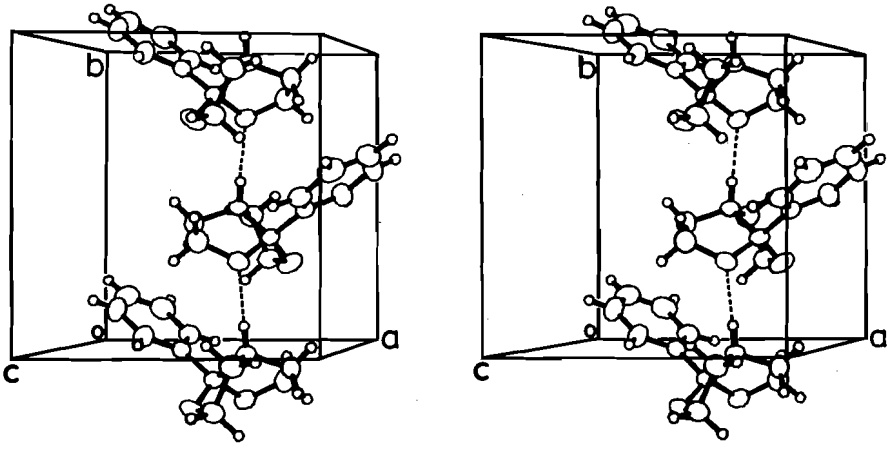

FIG. 2. The structure of *B*-phenyl-*diptych*boroxazolidine viewed down *c**. Broken lines indicate hydrogen bonds.

Can. J. Chem. Downloaded from www.nrcresearchpress.com by 210.87.254.42 on 09/05/12
For personal use only.

TABLE 9. Intraannular dihedral angles (deg)

Bond	Angle		Bond	Angle	
	Observed	Calculated		Observed	Calculated
B—O(1)	16.7(2)	20.0	B—O(2)	11.9(2)	14.9
O(1)—C(1)	−34.5(3)	−39.2	O(2)—C(3)	−30.9(3)	−36.5
C(1)—C(2)	37.3(3)	43.4	C(3)—C(4)	37.1(3)	44.0
C(2)—N	−25.8(2)	−31.2	C(4)—N	−28.4(2)	−35.0
N—B	6.9(2)	7.0	N—B	11.6(2)	12.5

TABLE 10. Distances of relevant atoms from the weighted least squares mean plane* C(5)–C(10) phenyl ring ($\chi^2 = 4.22$)

Atom	d	d/σ
C(5)	0.003	1.1
C(6)	−0.003	0.8
C(7)	0.000	0.1
C(8)	0.003	0.7
C(9)	0.000	0.1
C(10)	−0.004	1.0
B	0.071	23.0
H(6)	0.023	0.6
H(7)	−0.045	0.8
H(8)	−0.093	1.7
H(9)	0.058	1.1
H(10)	0.065	1.5

*The equation of the mean plane is $-0.4639X + 0.8131Y - 0.3517Z = 0.1039$ where X, Y, and Z are orthogonal Å coordinates along a, b, and c^*.

TABLE 11

(*a*) Selected intra- and intermolecular contacts

Intramolecular		Intermolecular*	
Atoms	Distance (Å)	Atoms	Distance (Å)
O(1)...C(6)	3.001(3)	O(1)...C(4)[1]	3.337(4)
O(2)...C(10)	2.963(4)	O(2)...H(9)[2]	2.59(5)
C(2)...H(4*b*)	2.59(3)	C(6)...H(3*a*)[3]	2.60(4)
C(2)...C(3)	3.121(4)	H(3*a*)...H(6)[1]	2.46(5)
C(4)...H(2*b*)	2.43(4)	H(4*a*)...H(6)[4]	2.47(5)
H(N)...H(4*a*)	2.15(5)		
H(N)...H(2*a*)	2.19(6)		
H(2*b*)...H(4*b*)	2.36(5)		

(*b*) Hydrogen-bond data (distances in Å and angles in deg)

D—H...A	H...A	D...A	∠DHA	∠XAH
N—H(N)...O(1)[3]	2.11(5)	2.914(3)	154(3)	107(1), 119(1)

*Superscripts refer to atoms at positions: [1] $1 - x, y - \frac{1}{2}, -z$; [2] $-x, y - \frac{1}{2}, -z$; [3] $1 - x, \frac{1}{2} + y, -z$; [4] $x, y, z - 1$.

Can. J. Chem. Downloaded from www.nrcresearchpress.com by 210.87.254.42 on 09/05/12
For personal use only.

C(5)]C(6), 18.9°, and O(2)[B—C(5)]C(10), −33.2(3)°.

The C—C bond lengths in the phenyl ring range from 1.379–1.400 Å with a mean value of 1.392 Å. The difference between the extreme values is significant. The bond distances in the ring decrease as they are removed from the boron substituent, an effect noted also for the phenyl rings of compounds **2***a* and **2***b* where it is slightly more pronounced. The mean values for the three groups are 1.399, 1.396, and 1.382 Å corresponding to values of 1.403, 1.394, and 1.380 for **2***a* and 1.403, 1.391, and 1.378 Å for **2***b*. The B—C bond length of 1.613(3) Å is similar to the mean values of 1.616 and 1.621 Å for **2***a* and **2***b* but shorter than the values of 1.631–1.648(8) Å in the tetraphenylborate anion (19).

The angles in the phenyl ring range from 116.6(2) to 122.0(3)°, showing some significant deviations from 120°. The angle at C(5), carrying the boron substituent, is 116.6(2)° and the other angles (mean values are given for equivalent pairs) are 121.9, 120.2, and 119.5° for atoms *ortho*, *meta*, and *para* to C(5). A similar variation is noted for the unsubstituted phenyl groups of **2***a* where the corresponding angles have mean values of 115.9, 122.3, 120.0, and 119.7°. The small angle at C(5) indicates that the B substituent is electron releasing (20), which would result in a small residual negative charge on the aromatic π system.

The mean C—H, mean C(ar)—H, and N—H bond lengths of 0.98(4), 0.98(4), and 0.87(5) Å are as expected for X-ray data. The bond angles involving the hydrogen atoms (Table 8) are generally as expected. There is one angle, C(3)—C(4)—H(4*b*), 120(3)°, which is significantly different from the expected value. This probably results from intramolecular steric interactions, the nonbonded contacts C(2). . .H-(4*b*), H(N). . .H(4*b*), and H(2*b*). . .H(4*b*) are all less than the sum of van der Waals radii.

We would like to thank Dr. A. Storr for preparing the sample, the National Research Council of Canada for financial support, and the University of British Columbia Computing Centre for assistance.

1. Z. Taira and K. Osaki. Inorg. Nucl. Chem. Lett. **7**, 509 (1971).
2. S. J. Rettig and J. Trotter. Can. J. Chem. **51**, 1288 (1973).
3. S. J. Rettig and J. Trotter. Acta Cryst. B**30**, 2139 (1974).
4. H. C. Brown and E. A. Fletcher. J. Am. Chem. Soc. **73**, 2808 (1951).
5. H. K. Zimmermann. Adv. Chem. Ser. No. **42**, 23 (1964).
6. R. L. Letsinger and N. Remes. J. Am. Chem. Soc. **77**, 2489 (1955).
7. O. C. Musgrave and T. O. Park. Chem. Ind. London. 1552 (1955).
8. J. Karle and I. L. Karle. Acta Cryst. **21**, 849 (1966).
9. J. Karle and H. Hauptman. Acta Cryst. **9**, 635 (1956).
10. M. G. B. Drew. Private communication; M. G. B. Drew, D. H. Templeton, and A. Zalkin. Acta Cryst. B**25**, 261 (1969).
11. D. T. Cromer and J. B. Mann. Acta Cryst. A**24**, 321 (1968).
12. R. F. Stewart, E. R. Davidson, and W. T. Simpson. J. Chem. Phys. **42**, 3175 (1965).
13. D. T. Cromer and D. Liberman. J. Chem. Phys. **53**, 1891 (1970).
14. W. C. Hamilton. Acta Cryst. **18**, 502 (1965).
15. V. Schomaker and K. N. Trueblood. Acta Cryst. B**24**, 63 (1969).
16. D. W. J. Cruickshank. Acta Cryst. **9**, 747, 754 (1956).
17. D. W. J. Cruickshank. Acta Cryst. **14**, 896 (1961).
18. J. B. Hendrickson. J. Am. Chem. Soc. **83**, 4537 (1961); **85**, 4059 (1963).
19. R. J. Sime, R. P. Dodge, A. Zalkin, and D. H. Templeton. Inorg. Chem. **10**, 537 (1971).
20. O. L. Carter, A. T. McPhail, and G. A. Sim. J. Chem. Soc. A, 822 (1966).

Can. J. Chem. Downloaded from www.nrcresearchpress.com by 210.87.254.42 on 09/05/12
For personal use only.

Homogeneous Catalysis of Hydrogen Isotope Exchange between D_2 and Ethanol by Dichlorotris(triphenylphosphine) Ruthenium(II)[1]

GRAEME STRATHDEE AND RUSSELL GIVEN

Research Chemistry Branch, Atomic Energy of Canada Limited, Whiteshell Nuclear Research Establishment, Pinawa, Manitoba R0E 1L0

Received November 22, 1974

GRAEME STRATHDEE and RUSSELL GIVEN. Can. J. Chem. **53**, 1442 (1975).

Rates of D_2–ethanol exchange catalyzed by solutions of dichlorotris(triphenylphosphine) ruthenium(II) in 1:1 benzene–ethanol are reported as a function of the concentrations of ruthenium, deuterium, triphenylphosphine, and HCl. The rates were extremely fast, and approached 10^{-3} mol D_2 l^{-1} s^{-1} at 333 K with 1.3 mmol/l Ru. Over the temperature range 263 to 303 K, the apparent activation energy was 85 kJ/mol. The kinetics have been interpreted in terms of a mechanism in which activation of D_2 by $RuCl_2L_3$ is rate-controlling. A comparison is made between the characteristics of this homogeneous catalyst and those of the related $RhClL_3$.

GRAEME STRATHDEE et RUSSELL GIVEN. Can. J. Chem. **53**, 1442 (1975).

On rapporte les vitesses de l'échange D_2–éthanol catalysé par des solutions de dichlorotris-(triphénylphosphine) ruthenium(II) dans des solutions 1:1 benzène–éthanol; ces vitesses ont été déterminées en fonction des concentrations de ruthenium, de deuterium, de triphénylphosphine et de HCl. Les vitesses sont extrêmement rapides et s'approchent de 10^{-3} mol D_2 l^{-1} s^{-1} à 333 K avec 1.3 mmol/l Ru. Entre les températures de 263 et 303 K, l'énergie d'activation apparente est de 85 kJ/mol. On a interprété la cinétique en terme d'un mécanisme dans lequel l'activation du D_2 par $RuCl_2L_3$ est déterminante pour la vitesse de la réaction. On fait une comparaison entre les caractéristiques de ce catalyseur homogène et celles du composé similaire $RhClL_3$. [Traduit par le journal]

Introduction

Dichlorotris(triphenylphosphine)ruthenium-(II) is a highly effective homogeneous catalyst for the hydrogenation of olefins and acetylenes in ethanol–benzene solution (1). Catalytic activity has been attributed to the formation of the monohydride, $RuHClL_3$ (L = triphenylphosphine)

[1] $$RuCl_2L_3 + H_2 \rightleftarrows RuHClL_3 + HCl$$

followed by olefin insertion into the Ru—H bond (2, 3). James has reviewed this topic in detail (4).

Because the component reactions of equilibrium 1 are fast (2), $RuCl_2L_3$ was of interest to us as a catalyst for D_2 – protic solvent exchange, with potential applicability in processes for the enrichment of deuterium. Since each cleavage of D_2 by $RuCl_2L_3$ would lead to exchange, this complex was potentially more effective than, say, $RhClL_3$ in benzene–ethanol where the slow deuterium transfer to the solvent was preceded by oxidative addition of D_2 to $RhClL_3$ (5).

In this work, we have studied the kinetics of D_2–ethanol exchange catalyzed by $RuCl_2L_3$ in 1:1 benzene–ethanol solution. A mechanism is proposed in which $RuCl_2L_3$ is the active catalyst species. A comparison has been made with the function of the closely related rhodium catalyst $RhClL_3$.

Experimental

The $RuCl_2L_3$ was purchased from Strem Chemicals and used as received.

Anal. Calcd. for $C_{54}H_{45}P_3RuCl_2$: C, 67.6; H, 4.7; P, 9.7; Ru, 10.5; Cl, 7.4. Found: C, 67.6; H, 4.7; P, 9.7; Ru, 9.1; Cl, 8.3.

Benzene and ethanol were each percolated through beds of activated Linde 4A molecular sieves to remove water. Each was distilled in a stream of flowing nitrogen, flushed with N_2 for at least 0.5 h, and stored in an N_2-purged glove box (typically 20 p.p.m. O_2). The N_2-saturated solvents were transferred by syringe to the reaction flask.

The deuterium gas (Matheson) was purified as previously described (6). Other reagents were used as received. The absence of triphenylphosphine oxide in the triphenylphosphine (Alpha Inorganics) was confirmed by infrared and n.m.r. spectrometric analyses.

Hydrogen isotope exchange reactions were conducted in a 93 ml glass gas–liquid contactor with efficient mag-

[1]AECL No. 5061.

Can. J. Chem. Downloaded from www.nrcresearchpress.com by 210.87.254.42 on 09/05/12
For personal use only.

Can. J. Chem. Downloaded from www.nrcresearchpress.com by 210.87.254.42 on 09/05/12
For personal use only.

netic stirring as previously outlined (5). Initial D_2 exchange rates were calculated with the relation

$$[2] \qquad -d[D_2]/dt = \ln [(n_0 - n_e)/(n_t - n_e)]A/t$$

where n_0, n_t, and n_e were the mol% D_2 in the gas phase at $t = 0$ and $t = t$ s, and at equilibrium, and A was the gas:liquid mole ratio given by A = initial D_2 (mol) ÷ solution volume (l). Plots of log D_2 against t were linear over several half-lives.

Since the D_2 exchange reaction rates were relatively rapid, about 10^{-4} mol l^{-1} s^{-1}, it was necessary to demonstrate that rate measurements were not D_2-mass-transfer-limited. In our 93 ml capacity reaction cell, the D_2 exchange rates were independent of stirring speed above about 1000 r.p.m. for D_2 = 2.73 mmol/l, Ru = 1.3 mmol/l in 20 ml solution. The catalyst solution was generally stirred at 3000 r.p.m. to generate the gas–liquid dispersion.

The effect of additives on the D_2 exchange rate was determined after injection of gaseous reagents by syringe, or by dissolution of the solids and addition as solutions in the ethanol. In some experiments, the reference D_2 exchange rate was followed for two half-lives before the additive was introduced.

Hydrogen solubility in 1:1 benzene–ethanol was measured with a precision of ±2% at 273, 298, and 323 K by a modified gas stripping technique (7). Within this temperature range, the solubility of H_2 (at 101 kPa) is given by

$$[3] \quad [H_2] = 2.42 \times 10^{-3} \exp\left[\frac{2.22}{R}\left(\frac{1}{T} - \frac{1}{273}\right)\right]$$

where R = gas constant (kJ/mol), T = temperature, K.

The dependence of [HCl] on $[H_2]$ and [Ru] was determined with the cell shown in Fig. 1. The glass–AgCl/Ag electrode couple was used to detect and measure the concentration of HCl by use of the calibration curve

$$[4] \qquad [HCl] = \exp 0.0428 \text{ [e.m.f. (mV)} - 604.5]$$

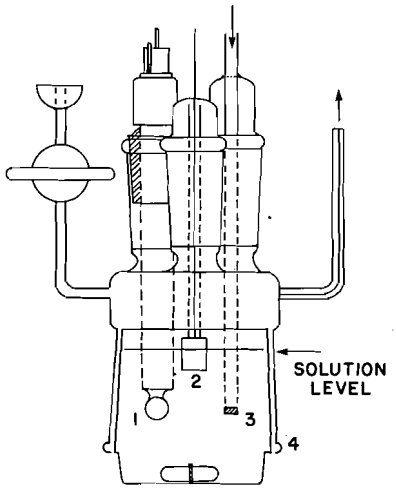

FIG. 1. Apparatus for measurement of HCl released as a function of H_2 pressure: 1, glass electrode; 2, AgCl/Ag electrode; 3, porous glass sparger; 4, T/S 60/50.

obtained by separate experiments with HCl solutions in 1:1 benzene–ethanol. Hydrogen, or an H_2–N_2 mixture, was presaturated with solvent vapor and was slowly bubbled through the cell until no further increase in cell e.m.f. was noted. Purging the vessel with N_2 reversed the reaction, and [HCl] became negligible. Other experiments showed that dissolved HCl was not stripped from solution by the gas stream.

Results

A set of data from a typical experiment are shown in Fig. 2. The overall isotope exchange reactions

$$[5] \qquad D_2 + C_2H_5OH \rightarrow HD + C_2H_5OD$$

$$[6] \qquad HD + C_2H_5OH \rightarrow H_2 + C_2H_5OD$$

commenced with the injection of the ethanol. No significant induction period occurred with solutions of $RuCl_2L_3$ alone. However, if excess triphenylphosphine, L, was initially added to the system, or if the temperature was below about 293 K, a slow increase to a limiting reaction rate was observed. In these cases, the final slopes of plots of log D_2 *vs.* t were used to calculate initial rates.

First-order decay plots for D_2 and HD were usually linear over several half-lives. From the data in Fig. 2, the apparent isotope effect $2k_{HD}/k_{D_2}$ = 1.13 was calculated, both from the maximum mol% HD and directly from the ob-

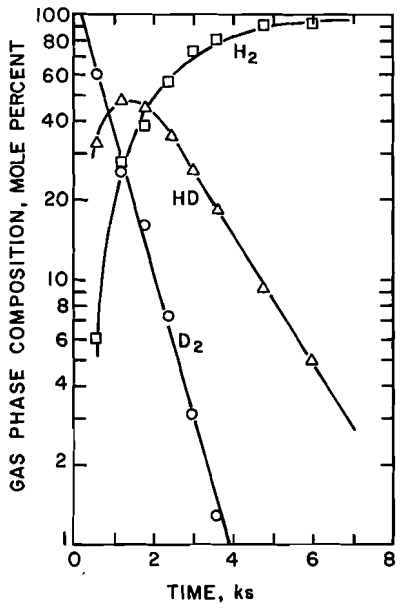

FIG. 2. Data for a typical exchange reaction. [Ru], 1.3 mmol/l; $[D_2]_0$, 2.7 mmol/l; T, 298 K.

served rates of disappearance of HD and D_2 (5). Experimental half-lives were typically 600 s in our reaction cell, but were as short as 60 s at the highest Ru concentrations. In runs with low partial pressures of D_2, care was taken to add sufficient N_2 to avoid admission of O_2 to the cell.

The Effect of D_2 and Ru Concentration on Initial Exchange Rates

Figure 3 shows the effect of D_2 concentrations between 0.4 to 2.90 mmol/l (D_2 partial pressures from 13 to 93 kPa) and ruthenium concentrations from 0.52 to 5.2 mmol/l on initial D_2 exchange rates in 1:1 (by volume) benzene–ethanol.

The form of these data is similar to that obtained for olefin hydrogenation reactions catalyzed by $RuCl_2L_3$ (3). The maximum rate for each $[Ru]_0$ may be calculated from the intercepts of plots of (Rate of D_2 exchange)$^{-1}$ *vs.* $[D_2]_0{}^{-1}$. The slopes and intercepts for the best straight lines through the data plotted in this way are listed in Table 1.

The experimental half-life for the D_2 exchange reaction was short (less than 100 s) at high [Ru]. Because D_2 uptake by $RuCl_2L_3$ occurred during a significant portion of this interval, we consider our measurements of these fast exchange rates to be somewhat low. This conclusion is supported by the fact that lines through plots of (D_2 exchange rate)$^{-1}$ *vs.* $[Ru]_0{}^{-1}$ were found to intercept the ordinate at positive values instead of at the origin.

TABLE 1. Parameters for best straight lines through $[Ru]_0$/Rate *vs.* $1/[D_2]$ data

$[Ru]_0$ (mmol/l)	Slope ($\times 10^3$) (mol s l^{-1})	Intercept (s)
1.3	7.77	5.09
2.5	7.35	5.18
4.0	12.2	3.71
5.6	16.9	2.09

Errors on experimental rates were estimated to be $\pm 5\%$, except at the highest [Ru] when the errors may have been $\pm 15\%$. There was no exchange of D_2 in blank experiments in which $RuCl_2L_3$ was omitted. Also, neither $RuCl_3 \cdot xH_2O$, nor 1% Al_2O_3-supported Ru metal, catalyzed D_2 exchange under our conditions. Therefore, there was no residual reaction rate due to the presence of these potential trace contaminants.

Temperature Dependence

The effect of temperature on the rate of D_2 exchange was determined between 263 and 333 K. These data are plotted in Fig. 4 as 1/rate *vs.* $1/T$. Pronounced curvature is evident below 3.3×10^{-3} K^{-1} (above 30°C). Since the temperature-dependence of the solubility of H_2 in 1:1

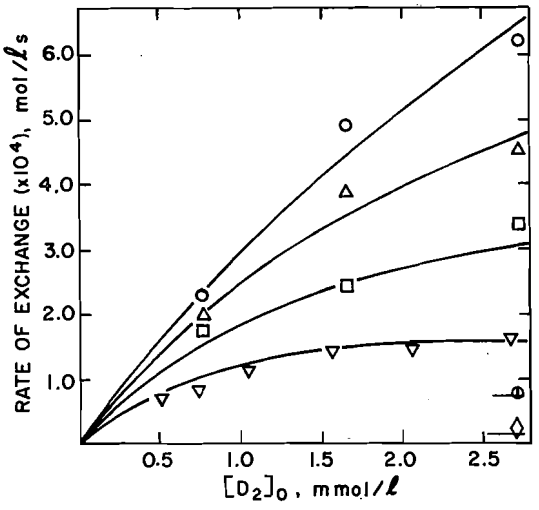

FIG. 3. The dependence of D_2 exchange rate on $[D_2]_0$ at concentrations of ruthenium, mmol/l, at 298 K: ○, 5.6; △, 4.0; □, 2.5; ▽, 1.3; ⊙, 0.8; ◇, 0.25.

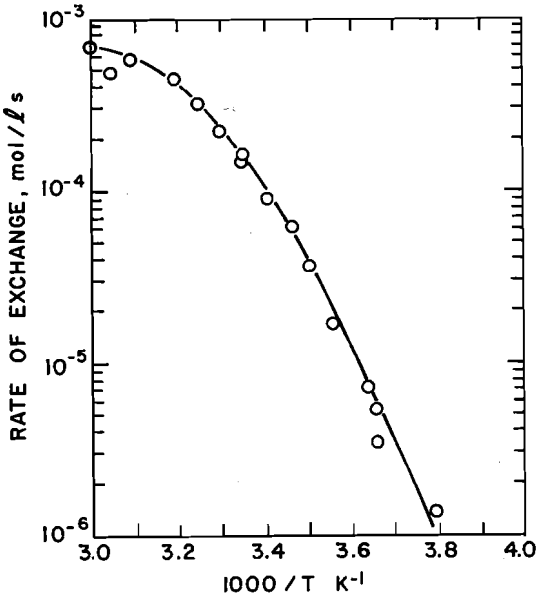

FIG. 4. The effect of temperature on the rate of D_2–C_2H_5OH exchange catalyzed by $RuCl_2L_3$.

Can. J. Chem. Downloaded from www.nrcresearchpress.com by 210.87.254.42 on 09/05/12
For personal use only.

Can. J. Chem. Downloaded from www.nrcresearchpress.com by 210.87.254.42 on 09/05/12
For personal use only.

benzene–ethanol was slight between 273 and 323 K, Fig. 4 reflects the variation in the equilibrium distribution of catalytically active Ru species, and the influence of the D_2-mass-transport on the exchange rate.

From the slope of the best straight line through the data in Fig. 4 between 263 and 303 K, an apparent activation energy, E_a, for the D_2 exchange reaction was calculated to be 85 kJ mol^{-1}.

At lower reaction temperatures, longer times were required to approach the maximum limiting values reported in Fig. 4. For example at 273 K ($[D_2]_0$ = 2.52 mmol/l, [Ru] = 1.3 mmol/l), no change in the gas phase composition was observed during the first 1.8 ks of contact. This effect arose because the active catalyst species required more time to equilibrate at these temperatures, and was probably an indication that the initial rate of D_2 activation was slow. In this case, the catalyst solution required about 1 ks to change from the brown color characteristic of $RuCl_2L_3$ in benzene to the red-violet of $RuHClL_3$ in H_2-saturated benzene–ethanol. At 303 K, the color change occurred within a few seconds.

Effects of Additives

These experiments were conducted under the standard conditions: temperature, 298 K; $[D_2]_0$ = 2.74 mmol/l; [Ru] = 1.3 mmol/l.

Triphenylphosphine

Addition of L increased the final rate of D_2 exchange as shown in Fig. 5. However, L initially inhibited the reaction. For example with a 10:1 excess of L:Ru, the exchange rate accelerated for about 2 ks before the maximum rate was established. This phenomenon is illustrated in Fig. 6.

If this behavior is related to the L ligand dissociation equilibrium reported by James and Markham (8)

[7] $$RuCl_2L_3 \rightleftarrows RuCl_2L_2 + L$$

and if the rate constant for the activation of D_2 for exchange is greater for $RuCl_2L_3$ than for $RuCl_2L_2$, then addition of L would be expected to increase the final rate as shown in Fig. 5. The initial inhibition of D_2 exchange by excess L cannot be explained in a similar way, since one would predict from reaction 7 that excess L would always enhance the rate of D_2 exchange. This topic is discussed further in the section on reaction mechanism.

Anhydrous HCl and Chloride Ion

The rate of exchange was enhanced by addition of anhydrous HCl. This effect was slightly greater than with L. The data are also included in Fig. 5.

If the rate determining step in the overall D_2 exchange reaction was the cleavage of D_2 by

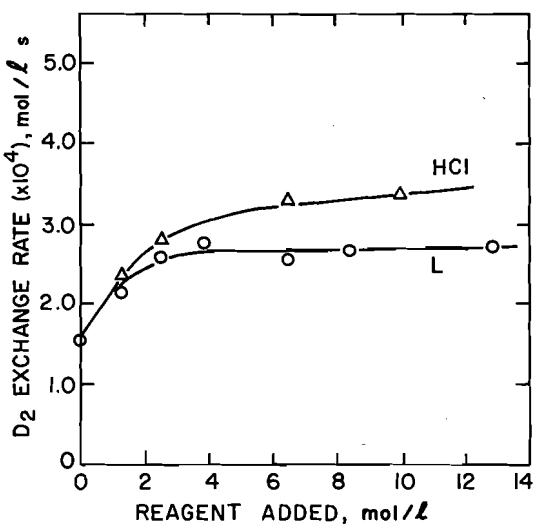

FIG. 5. The effect of excess L and HCl on the rate of D_2 exchange.

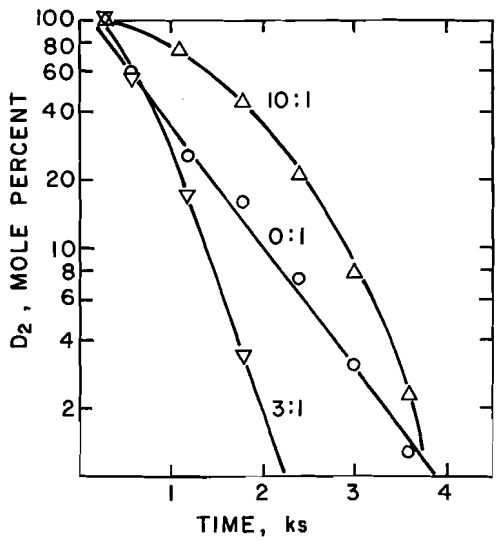

FIG. 6. The characteristic initial inhibition of D_2 exchange by excess L, as a function of the L:Ru ratio.

Can. J. Chem. Downloaded from www.nrcresearchpress.com by 210.87.254.42 on 09/05/12
For personal use only.

$RuCl_2L_3$ (3)

[8] $RuCl_2L_3 + D_2 \rightleftarrows RuDClL_3 + DCl$

then the exchange rate would have been expected to increase as equilibrium 8 was shifted to the left by excess HCl. Chloride ion, added as LiCl, had no effect on the rate of exchange, but this may have been due to a low activity of Cl^- because of ion-pair dimer formation (9) to yield Li_2Cl_2 in 1:1 benzene–ethanol. If Cl^- was added as $(CH_3)_4NCl$, a slight increase in the D_2 exchange rate was observed in agreement with the results for HCl.

If Cl^- dissociation occurred from Ru-containing species in solution, the effect of added Cl^- would be less than expected. A 10:1 excess of LiBr had no effect on the D_2 exchange rate, although the catalyst solution was maroon rather than the normal red-violet. Some halide exchange likely occurred with the active catalyst. The extent of Cl^- dissociation from either $RuCl_2L_3$ or $RuHClL_3$ has not been found to be great (8, 10).

When a 75:1 excess of HCl was added to the Ru catalyst, the solution turned bright yellow. Both the absorption maxima at 360 and 520 nm, characteristic of $RuCl_2L_3$ solutions containing $RuHClL_3$, were absent under these conditions although D_2 exchange remained fast. This indicated that the distribution of catalytically active species differs in strongly acidic media. The monohydride, $RuHClL_3$ is known to be unstable in the presence of excess HCl (11).

Bases

Ammonia, methylamines, and LiOH all inhibited the D_2-exchange reaction. A 4-fold excess of each base (:Ru) reduced the rate by two orders of magnitude under the usual conditions. Undoubtedly, neutralization of the DCl produced by reaction 8 drove the equilibrium to the right thereby lowering the concentration of catalytically active $RuCl_2L_3$. This result was expected, since the monohydride has been synthesized in nonbasic aprotic solvents by a related procedure (3).

Oxygen

If added O_2 exceeded 10 O_2:1Ru the D_2 exchange reaction ceased. Less O_2 reduced the rate for a short period (300 s) after which it returned to the original value. The capability of these solutions to recover from the effect of admission of small amounts of O_2 is highly desirable from the practical point of view, and is undoubtedly related to the activity of $RuCl_2L_3$ for the $2H_2 + O_2$ recombination reaction reported by Vaska and Tadros (12). Oxidation of L either to triphenylphosphine oxide (13), or to Ru-containing species, presumably occurs at higher O_2 concentrations at which the rate of activation of O_2 by the complexes must exceed the rate of H_2 cleavage. Retention of catalytic activity by $RuCl_2L_3$ in the presence of O_2 is not novel, since Lyons has observed isomerization of olefins under such conditions (14).

Carbon Monoxide

The Ru catalyst was immediately and irreversibly poisoned for D_2 exchange by CO. A stable Ru–carbonyl complex was likely formed. Stephenson and co-worker have discussed these reactions (15).

The Hydrogen-uptake Equilibrium

The electrochemical cell:

[9] Glass | HCl (1:1 C_6H_6–C_2H_5OH) | AgCl, Ag

was employed to measure HCl released upon cleavage of H_2 by the overall reaction 1. Because the slope of the calibration curve (cell e.m.f. *vs.* log [HCl]) was low (*cf.* eq. 4) small errors in the measurement of e.m.f. resulted in large errors in the interpolated values of [HCl]. For example, at 1 mmol/l the error was estimated to be 5%/mV. Our data are shown in Fig. 7 for [HCl] as a function of [Ru] and equilibrium [H_2]. Even at 100 kPa partial pressure of H_2, the conversion of $RuCl_2L_3$ to $RuHClL_3$ was only partially complete.

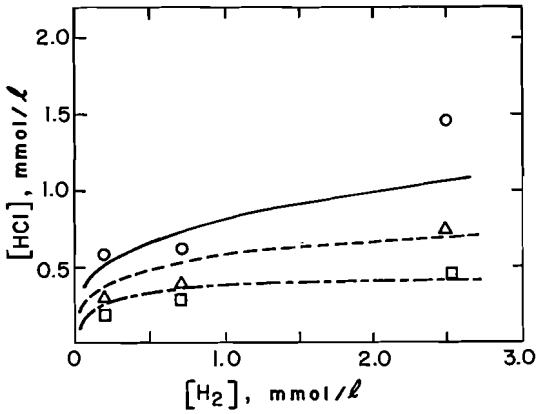

FIG. 7. The dependence of the equilibrium concentration of HCl on the concentrations of H_2 and total Ru. [Ru], mmol/l: □, 0.49; △, 0.98; ○, 2.0.

Can. J. Chem. Downloaded from www.nrcresearchpress.com by 210.87.254.42 on 09/05/12
For personal use only.

Discussion

Species in Solution

Many previous studies of the catalytic activity of solutions of $RuCl_2L_3$ have been directed towards understanding the mechanisms of hydrogenation of unsaturated organics, particularly terminal olefins and acetylenes. The hydrogen activation step itself, reaction 1, has not been studied in detail. Since James and Markham have reported that $RuCl_2L_3$ was extensively dissociated in both benzene and dimethylformamide solutions, it was of interest to determine if this complex or the species $RuCl_2L_2$ formed by reaction 7 dominated the rate law.

The major species present in hydrogenated solutions of $RuCl_2L_3$ are known to be $RuCl_2L_3$, $RuCl_2L_2$, $RuHClL_3$, and $RuHClL_2$ (3, 4, 10, 16). The deuterium exchange rates discussed above were generally measured under conditions at which the concentrations of these species had reached equilibrium. These rates could therefore be used as a direct measure of the concentration of species which activated D_2 or HD and promoted D-transfer to the protic solvent. A deuteron (as DCl) is released in the cleavage of the D_2 molecule by $RuCl_2L_3$ (*cf.* reaction 8), and the rate of D^+ transfer to the ethanol hydroxyl pool is effectively instantaneous (17) and irreversible

[10] $\quad DCl + C_2H_5OH \rightarrow C_2H_5OD + HCl$

Thus each D_2-activation event resulted in detectable exchange. Only $RuCl_2L_3$ and $RuCl_2L_2$ may cleave D_2 and promote D-transfer to the protic solvent. In a separate study (11) we have discussed the kinetics and mechanism of H_2–D_2 exchange catalyzed by $RuHClL_3$. The monohydride does not promote D_2–C_2H_5OH exchange at a significant rate. For example, at $[RuHClL_3] = 1.1$ mmol/l, $[D_2] = 2.7$ mmol/l, and 298 K the exchange rate was only 4 μmol D_2 l^{-1} s^{-1}, about a factor of 35 lower than with $RuCl_2L_3$.

Reaction Mechanism

The reaction scheme summarized in Table 2 may be used to explain the kinetics of the exchange reaction at low degrees of D_2 conversion. Equilibria involving HD and H_2 have been omitted. If it is assumed that the rate law has the following form (note that the labelling system of Table 2 has been used)

TABLE 2. Mechanism of D_2–ethanol exchange catalyzed by $RuCl_2L_3$ (L = triphenylphosphine)

[7]	$RuCl_2L_3$	$\overset{K_7}{\rightleftarrows}$	$RuCl_2L_2 + L$
[8]	$RuCl_2L_3 + D_2$	$\overset{k_8}{\rightarrow}$	$RuDClL_3 + DCl$
[11]	$RuCl_2L_2 + D_2$	$\overset{k_{11}}{\rightarrow}$	$RuDClL_2 + DCl$
[10]	$DCl + C_2H_5OH$	$\overset{k_{10}}{\rightarrow}$ fast	$HCl + C_2H_5OD$
[−8]	$RuDClL_3 + HCl$	$\overset{k_{-8}}{\rightarrow}$	$RuCl_2L_3 + HD$
[−11]	$RuDClL_2 + HCl$	$\overset{k_{-11}}{\rightarrow}$	$RuCl_2L_2 + HD$
[12]	$RuDClL_3$	$\overset{K_{12}}{\rightleftarrows}$	$RuDClL_2 + L$

$$[13] \quad -d[D_2]/dt = (k_8[RuCl_2L_3] + k_{11}[RuCl_2L_2])[D_2]$$

Then from the mass balance expression for total ruthenium

$$[14] \quad [Ru]_0 = [RuCl_2L_3] + [RuCl_2L_2] + [RuDClL_3] + [RuDClL_2]$$

the following may be derived

$$[15] \quad -d[D_2]/dt = \frac{(k_8 + k_{11}K_7/[L])[Ru]_0[D_2]}{1 + \frac{K_7}{[L]} + \frac{K_8[D_2]_0}{[HCl]} + \frac{K_8K_{12}[D_2]_0}{[L][HCl]}}$$

Addition of excess $[L]:[Ru]_0$ has been shown to increase the exchange rate, therefore $k_8 > k_{11}K_7/[L]$. If the rate law 15 is then dominated by the term

$$[16] \quad -d[D_2]/dt = k_8[RuCl_2L_3][D_2]$$

expression 13 becomes approximately

$$[17] \quad -d[D_2]/dt = \frac{k_8[Ru]_0[D_2]}{1 + \frac{K_7}{[L]} + \frac{K_8[D_2]_0}{[HCl]} + \frac{K_8K_{12}[D_2]_0}{[L][HCl]}}$$

Qualitatively, eq. 17 predicts that the D_2 exchange rate will increase with both added L and HCl, as observed.

Values for the rate constant k_8 and equilibrium constant K_7 may be calculated in the following way. By use of the data in Fig. 7, the sum

Can. J. Chem. Downloaded from www.nrcresearchpress.com by 210.87.254.42 on 09/05/12
For personal use only.

$[RuCl_2L_3] + [RuCl_2L_2]$ is given by $[Ru]_0 - [HCl]$ at a fixed $[H_2]$ (or $[D_2]$). Since the slopes of plots of $[Ru]_0$/Rate *vs.* $1/[D_2]$ (*cf.* Table 1) yield values for $(1 + K_7/[L])/k_8$, two equations in K_7 and k_8, for example at $[Ru]_0 = 1.3$ and 2.5 mmol/l, may be solved simultaneously to yield $K_7 = 1.3 \times 10^{-4}$ mol/l and $k_8 = 210$ l mol^{-1} s^{-1}.

The intercepts of those plots at $1/[D_2] = 0$ correspond to $(K_8/[HCl] + K_8K_{12}/[L][HCl])/k_8$. By assuming that dissociation of L from $RuHClL_3$ is slight, *i.e.* $K_{12} \doteq 0$, then $[Ru]_0$/Rate $= K_8/k_8[HCl]$. At that limiting condition of high $[D_2]$, $[HCl] \doteq [Ru]_0$, therefore Rate $= k_8[Ru]_0^2/K_8$. A plot of the limiting rates at $1/[D_2] = 0$ against $[Ru]_0^2$ gives a straight line of slope $k_8/K_8 = 80$ l mol^{-1} s^{-1}. Constant K_8 is therefore calculated to be 2.6.

The low value of K_7 suggests that the dissociation of L from $RuCl_2L_3$ in 1:1 benzene–ethanol is not as extensive as in benzene alone or in DMF (8). However, it explains the relative insensitivity of the overall exchange reaction rate to the addition of excess L. Our evaluation of the magnitude of K_8 was determined primarily by the form of the data reported in Fig. 7, and is the first reported in the literature.

The rate constant k_8 is large, but is consistent with the efficiency with which $RuCl_2L_3$ activates molecular hydrogen (or D_2) in this solvent system. If the species $RuCl_2L_2$ is active at all, k_{11} is probably less than 10% of k_8, *i.e.* 21 l mol^{-1} s^{-1}, however, we have been unable to demonstrate this conclusively.

We have no satisfactory explanation for the initial inhibition of D_2 exchange by excess L. It was pointed out in the section Effects of Additives that experiments with excess L would always be expected to yield higher D_2 exchange rates than if no excess L was added. The slow initial exchange can be accounted for if equilibrium 18 is significant under our conditions,

[18] $$RuCl_2L_3 + L \rightleftarrows RuCl_2L_4$$

providing that the component reaction rates are slow with respect to the rate of deuterium uptake by $RuCl_2L_3$. We do not favor this possibility, since Caulton has shown by ^{31}P n.m.r. experiments that dissociation of L from $RuCl_2L_4$ to yield $RuCl_2L_3$ is essentially complete in $CHCl_3$ at 303 K (16).

Comparison of $RuCl_2L_3$ with $RhClL_3$

This study has provided evidence that $RuCl_2L_3$ cleaves molecular hydrogen at a specific rate which is greater than that for the dissociated species $RuCl_2L_2$. The thorough investigations of solutions of the isoelectronic rhodium catalyst $RhClL_3$ by Halpern and Wong (18) and by Tolman *et al.* (19) have shown that the specific rate of activation of H_2 by $RhClL_2$ was at least 10^4 greater than by $RhClL_3$. In the ruthenium system, it may be essential to have Ru(II) stabilized by three L to provide the metal with sufficient electron density to promote D—D cleavage. The complex $RuCl_2L_3$ would possess 16 metal valence shell electrons, whereas $RuCl_2L_2$ would contain only 14. Although $RhClL_3$ and $RhClL_2$ are isoelectronic with $RuCl_2L_3$ and $RuCl_2L_2$ respectively, the detailed mechanisms of D_2-cleavage are dissimilar. In the rhodium case, oxidative addition of D_2 to the Rh atom is favored presumably because Rh(I) to Rh(III) conversion is more facile in $RhClL_2$ compared to $RhClL_3$. In the ruthenium system, no overall Ru-oxidation state change is required, (*cf.* reaction 8) although the formation of $RuHClL_3$ via a seven-coordinate Ru(IV) intermediate $RuH_2Cl_2L_3$ as proposed by Harrod *et al.* (20) has not been disproven. Apparently, reduction in the coordination number of the Ru metal ion is not accompanied by enhanced reactivity towards molecular hydrogen. It follows that access of H_2 is not impeded by the stereochemical requirements of the ligands in $RuCl_2L_3$.

Applicability of $RuCl_2L_3$ to Deuterium Enrichment

This catalyst is among the most active which we have studied for the exchange of deuterium between hydrogen gas and protic solvents. It has the desirable characteristic that the rapid hydrogen activation reaction is also rate-controlling for the exchange. In contrast, when the activation of D_2 is slow, or is not rate-determining, such as with complexes of the type $RhXL_3$ or $IrX(CO)L_2$ (X = halogen, L = alkyl or arylphosphine), then optimum deuterium exchange rates cannot be realized.

Although the D_2 conversion rates with $RuCl_2L_3$ were rapid in terms of the capability of typical stirred-tank experimental reactors, an improvement in rate of approximately two orders of magnitude would be required to make

the catalyst attractive for D enrichment purposes. Since the solubility limit of this complex is low, and since the D_2 conversion rates fall off with increasing gas pressure, $RuCl_2L_3$ is unsatisfactory for this application.

The authors wish to thank their colleagues for helpful discussions, particularly M. Tomlinson and Dr. N. H. Sagert, and D. Bell and his assistants of the Analytical Science Branch for the deuterium analyses.

1. D. Evans, J. A. Osborn, F. H. Jardine, and G. Wilkinson. Nature, **208**, 1203 (1965).
2. P. S. Hallman, D. Evans, J. A. Osborn, and G. Wilkinson. Chem. Commun. **7**, 305 (1967).
3. P. S. Hallman, B. R. McGarvey, and G. Wilkinson. J. Chem. Soc. A, 2143 (1963).
4. B. R. James. Homogeneous hydrogenation. Wiley–Interscience, Toronto. 1972. p. 83.
5. G. G. Strathdee and R. M. Given. Can. J. Chem. **52**, 2216 (1974).
6. G. G. Strathdee and M. J. Quinn. Can. J. Chem. **50**, 4289 (1972).
7. G. G. Strathdee and R. M. Given. J. Catal. **30**, 30 (1973).
8. B. R. James and L. D. Markham. Inorg. Chem. **13**, 97 (1974).
9. P. M. Henry and O. Marks. Inorg. Chem. **10**, 373 (1971).
10. B. R. James and L. D. Markham. J. Catal. **27**, 442 (1972).
11. G. G. Strathdee and R. M. Given. Can. J. Chem. **53**, 106 (1975).
12. L. Vaska and M. E. Tadros. J. Am. Chem. Soc. **93**, 7099 (1971).
13. B. W. Graham, K. R. Laing, C. J. O'Conner, and W. R. Roper. J. Chem. Soc. D, 1237 (1972).
14. J. E. Lyons. Chem. Commun. 562 (1971).
15. T. A. Stephenson and G. Wilkinson. J. Chem. Soc. **28**, 945 (1966).
16. K. G. Caulton. J. Am. Chem. Soc. **96**, 3005 (1974).
17. E. Grunwald, C. F. Jumper, and S. Meiboom. J. Am. Chem. Soc. **84**, 4664 (1962).
18. J. Halpern and C. S. Wong. J. Chem. Soc. Chem. Commun. 629 (1973).
19. C. A. Tolman, P. Z. Meakin, D. L. Lindner, and J. P. Jesson. J. Am. Chem. Soc. **96**, 2762 (1974).
20. J. F. Harrod, D. F. R. Gilson, and R. Charles. Can. J. Chem. **47**, 1431 (1969).

Can. J. Chem. Downloaded from www.nrcresearchpress.com by 210.87.254.42 on 09/05/12
For personal use only.

Thermodynamics of Mixed Electrolyte Solutions

JAMES SANGSTER AND FABIO LENZI

Département du Génie Chimique, Ecole Polytechnique, Université de Montréal, Montréal, Québec H3C 3A7

Received August 16, 1974

JAMES SANGSTER and FABIO LENZI. Can. J. Chem. **53**, 1410 (1975).

A general thermodynamic expression has been derived for the deviation Δ from Zdanovskii's rule. Conditions have been deduced under which Δ vanishes, and examples given. For nonzero values of Δ it has been shown by means of an example that Δ may be evaluated in some cases by the introduction of empirical assumptions, such as Harned's rule. The use of Zdanovskii's rule in facilitating the integration of the McKay–Perring equation has been discussed briefly.

JAMES SANGSTER et FABIO LENZI. Can. J. Chem. **53**, 1410 (1975).

Une expression générale thermodynamique a été dérivée pour la déviation Δ de la règle de Zdanovskii. Des conditions ont été déduites, avec exemples à l'appui, sous lesquelles Δ devient zéro. Pour les valeurs de Δ différentes de zéro, il a été démontré, au moyen d'un exemple, que le Δ peut être évalué dans certains cas en introduisant des suppositions empiriques, telles que la règle de Harned. L'utilité de la règle de Zdanovskii pour faciliter l'intégration de l'équation de McKay–Perring a été brièvement examinée.

Introduction

Zdanovskii (1) in 1936 proposed a simple empirical rule relating the concentrations of aqueous salt solutions under isopiestic conditions (that is, at the same water activity, a_w). Suppose that a ternary solution of electrolytes 1 and 2 at molalities m_1 and m_2 is in isopiestic equilibrium with two binary solutions at molalities m_{10} and m_{20}. The rule states that

$$[1] \qquad 1/m = y_1/m_{10} + y_2/m_{20}$$

where $m = m_1 + m_2$, $y_1 = m_1/m$, and $y_2 = m_2/m$. An alternative form of the rule may be obtained by multiplying eq. 1 by m

$$[2] \qquad 1 = m_1/m_{10} + m_2/m_{20}$$

Equation 1 is an approximation to actual behavior, and Kirgintsev and Luk'yanov (2) measured deviations from Zdanovskii's rule for a large number of electrolyte pairs. They proposed the equation

$$[3] \qquad 1/m = y_1/m_{10} + y_2/m_{20} + by_1y_2$$

where b is an empirical parameter.

Zdanovskii's rule, eq. 1 or 2, has proved to be a useful relation for estimating the water activity of multicomponent aqueous solutions up to high concentration (3), and of supersaturated single-solute solutions (4). It has also been used to simplify the integration of the McKay–Perring equation for obtaining activity coefficients in mixed electrolyte solutions (2, 5).

Until recently, no theoretical justification of this empirical rule had been attempted. In this paper we shall derive a general thermodynamic expression for the deviation from Zdanovskii's rule, and examine a number of particular cases in which it vanishes or may be calculated with the help of empirical assumptions.

General Treatment

The general condition for isopiestic equilibrium among binary and ternary aqueous electrolyte solutions is

$$[4] \qquad \nu_1 m_{10}\phi_{10} = \nu_2 m_{20}\phi_{20} = \bar{\nu} m \phi_{12}$$

where ν_1 and ν_2 are the numbers of ions per molecule of electrolytes 1 and 2 respectively, $\bar{\nu} = \nu_1 y_1 + \nu_2 y_2$, ϕ_{10} and ϕ_{20} are the osmotic coefficients of the binary solutions, and ϕ_{12} the osmotic coefficient of the ternary solution.

After a few steps, eq. 4 can be rewritten as

$$[5] \qquad 1 = m_1/m_{10} + m_2/m_{20} + \Delta$$

where Δ is the Zdanovskii deviation term, given by

$$[6] \qquad \Delta = (\bar{\nu}\phi_{12} - \nu_1 y_1 \phi_{10} - \nu_2 y_2 \phi_{20})/\bar{\nu}\phi_{12}$$

Equation 6 is an explicit expression for Δ in terms of osmotic coefficients; for the analysis of special cases later in this paper, we need Δ in terms of activity coefficients. We use the following relation (ref. 6, eq. 34-33) for ϕ_{12}

Can. J. Chem. Downloaded from www.nrcresearchpress.com by 210.87.254.42 on 09/05/12
For personal use only.

Can. J. Chem. Downloaded from www.nrcresearchpress.com by 210.87.254.42 on 09/05/12
For personal use only.

$$[7]\quad \phi_{12} = 1 + \frac{\nu_1 y_1}{\bar{\nu} m}\int_0^m m\mathrm{d}(\ln\gamma_1) + \frac{\nu_2 y_2}{\bar{\nu} m}\int_0^m m\mathrm{d}(\ln\gamma_2)$$

and the following relation (ref. 6, eq. 23-22) for ϕ_{i0}

$$[8]\quad \phi_{i0} = 1 + \frac{1}{m_{i0}}\int_0^{m_{i0}} m_{i0}\mathrm{d}(\ln\gamma_{i0})$$

where $i = 1, 2$. In these equations γ_1 and γ_2 are activity coefficients of component electrolytes in the mixed solution, and γ_{10} and γ_{20} are activity coefficients in the isopiestic single-salt solutions.

Cases in which $\Delta = 0$

(*i*) At infinite dilution all osmotic coefficients approach unity, and it can be seen from eq. 6 that in this case Δ vanishes. Mikhailov (7) attempted to show this by assuming the Debye–Hückel limiting law expressions for the osmotic coefficients of mixed and single electrolyte solutions. He derived the equation

$$[9]\quad 1/m = y_1/m_{10} + y_2/m_{20} + Q/(-\ln a_w)^{\frac{1}{2}}$$

for solutions under isopiestic equilibrium. In this equation Q is a function of the Debye–Hückel limiting law slope, conversion factors, y, ionic charges, and valence types of the electrolytes in the mixed solution. The function Q is independent of concentration, identically zero for symmetrical mixtures, and positive and finite for unsymmetrical mixtures. Mikhailov concluded that at low concentrations Zdanovskii's rule (eq. 1) and its improved version (eq. 3) contradict the Debye–Hückel theory in the case of unsymmetrical mixtures.

This is an error in interpretation, for actually there is no contradiction. We need only throw eq. 9 into the alternative form of eq. 2. We make the substitution $-\ln a_w = 1000\bar{\nu} m\phi_{12}/M_w$, where M_w is the molar mass of water. Multiplying the resulting equation by m, we obtain

$$[10]\quad 1 = m_1/m_{10} + m_2/m_{20} + Q' m^{1/2}$$

where Q' combines terms which are independent of concentration. Thus as $m \to 0$, Δ vanishes, and eq. 2 represents the zero concentration limiting behavior of all electrolyte mixtures.

(*ii*) Although at finite concentrations osmotic coefficients may be different from unity, we found (*3a*) that there are some mixtures, symmetrical or not, which conform exactly to Zdanovskii's rule. An example is the system $NaCl–BaCl_2–H_2O$, for which representative data are given in Table 1; $\Delta = 0$ for this system within experimental uncertainty.[1] Thus for systems such as this one, we have the simple relation (from eq. 6)

$$[11]\quad \bar{\nu}\phi_{12} = \nu_1 y_1 \phi_{10} + \nu_2 y_2 \phi_{20}$$

i.e., ϕ_{12} is a linear function of composition under isopiestic conditions.

Cases in which $\Delta \neq 0$

When neither of the previous conditions (*i*) or (*ii*) holds, the integrals in eqs. 7 and 8 must be evaluated in order to obtain an expression for Δ. These require expressions for activity coefficients in mixed and single electrolyte solutions. For simplicity we will examine the case of two 1:1 electrolytes and use data for the system NaCl(1)–KCl(2)–H_2O at 25 °C as an example.

For γ_1 and γ_2 we use the Harned-type relations (ref. 6, eq. 34-27)

$$[12]\quad \log\gamma_1 = \log\gamma_{1(0)} - \alpha_{12} m_2$$

$$[13]\quad \log\gamma_2 = \log\gamma_{2(0)} - \alpha_{21} m_1$$

which are assumed to be valid for systems at constant total molality m. In these equations α_{12} and α_{21} are independent of composition at a given m, but may otherwise vary with m; $\gamma_{1(0)}$ and $\gamma_{2(0)}$ are activity coefficients of the electrolytes in their own solutions at molality m. For $\gamma_{1(0)}$ and $\gamma_{2(0)}$ we use the Guggenheim-type expressions (ref. 6, eq. 22-20)

$$[14]\quad \log\gamma_{1(0)} = -A_\gamma m^{1/2}/(1 + m^{1/2}) + B_1 m$$

$$[15]\quad \log\gamma_{2(0)} = -A_\gamma m^{1/2}/(1 + m^{1/2}) + B_2 m$$

where A_γ is the Debye–Hückel limiting slope and B_1 and B_2 are empirical parameters. If now we substitute eqs. 12–15 in eq. 7, the final result is (ref. 6, eq. 23-39)

$$[16]\quad \phi_{12} = 1 - 2.303\{A_\gamma m^{1/2}\,\sigma(m^{1/2})/3 - [\bar{B} - y_1 y_2(\alpha_{12} + \alpha_{21})]m/2\}$$

where $\bar{B} = y_1 B_1 + y_2 B_2$ and $\sigma(m^{1/2})$ is a simple function of molality (ref. 6, eq. 23-40). The expressions for ϕ_{10} and ϕ_{20} are obtained from eq. 8 and those analogous to eqs. 14 and 15. The result is

[1] If the error in the molalities measured at isopiestic equilibrium is ± 0.0005, this will cause an uncertainty of a few units in the fourth decimal place of Δ.

TABLE 1. The Zdanovskii deviation quantity Δ for the system NaCl(1)–$BaCl_2$(2)–H_2O at 25 °C

a_w	m	y_1	m_{10}	m_{20}	Δ*
0.9678	0.9026	0.8179	0.9728	0.6832	0.0005
0.9678	0.8288	0.5924	0.9728	0.6832	0.0008
0.9678	0.7609	0.3430	0.9728	0.6832	0
0.9453	1.5562	0.9087	1.6226	1.0983	−0.0009
0.9453	1.4140	0.6919	1.6226	1.0983	0.0004
0.9453	1.2673	0.4150	1.6226	1.0983	0.0008
0.9083	2.3044	0.7491	2.6185	1.6998	0.0006
0.9083	2.0521	0.4909	2.6185	1.6998	0.0006
0.9083	1.8017	0.1616	2.6185	1.6998	0.0001

*As defined by eq. 5 (experimental data from ref. 8).

TABLE 2. Comparison of experimental and calculated values of Δ for the system NaCl(1)–KCl(2)–H_2O at 25 °C. $y_1 = 0.472$, $y_2 = 0.528$

			−Δ	
m	m_{10}	m_{20}	Experimental*	Calculated
2.1025	2.0098	2.1618	0.0073	0.0070
2.3640	2.2480	2.4368	0.0083	0.0078
2.6872	2.5452	2.7791	0.0087	0.0086
3.1210	2.9372	3.2455	0.0093	0.0101
3.7173	3.4699	3.8918	0.0111	0.0106
4.3226	3.9968	4.5514	0.0119	0.0113

*From eq. 5 and experimental data of ref. 11.

[17] $$\phi_{i0} = 1 - 2.303[A_\gamma m_{i0}^{1/2} \sigma(m_{i0}^{1/2})/3 - B_1 m_{i0}/2]$$

where $i = 1, 2$. We may now compare calculated and experimental values of Δ for the system NaCl–KCl–H_2O. This is shown in Table 2, where Δ has been calculated from eqs. 6, 16, and 17; the α's were those of Robinson (9) and the B's were taken from a standard reference (ref. 6, pp. 644–645). The experimental and predicted values of Δ agree within experimental uncertainty.[1]

Evaluation of the McKay–Perring Integral

The essential step in the McKay–Perring method (10) of calculating activity coefficients is the evaluation of an integral of a function $f(y)$ expressing the variation of the total molality m with composition under isopiestic conditions. In particular cases, $f(y)$ assumes simple analytical forms; these cases are based on deviations from Zdanovskii's rule, though not always explicitly.

In the simplest case $\Delta = 0$ and therefore the integral is zero also (2). When $\Delta \neq 0$, Kirgintsev and Luk'yanov (2) and Allakhverdov and Stepin (5) use a $f(y)$ defined in the manner of eq. 3; their equations differ only in the form of the deviation term by_1y_2. Robinson (9) uses the "isopiestic ratio" $R \equiv m_{10}/m$, which in some cases can be represented by $R = 1 - cy_2 - dy_2^2$, where c and d are empirical constants. The integrand then becomes d/m_{10}; this quantity is identical with the b of Kirgintsev and Luk'yanov (7). Thus Zdanovskii's rule, and deviations from it, constitute the basis of these evaluations of the McKay–Perring integral.

We wish to thank a referee for much helpful advice in the preparation of the final form of this paper.

Can. J. Chem. Downloaded from www.nrcresearchpress.com by 210.87.254.42 on 09/05/12
For personal use only.

1. A. B. ZDANOVSKII. Trudy Solyanoi Lab. Nauk SSSR, Vol. 6. 1936.
2. A. N. KIRGINTSEV and A. V. LUK'YANOV. Russ. J. Phys. Chem. **40**, 953 (1966).
3. (*a*) H. CHEN, J. SANGSTER, T. T. TENG, and F. LENZI. Can. J. Chem. Eng. **51**, 234 (1973); (*b*) J. SANGSTER and F. LENZI. Can. J. Chem. Eng. **52**, 392 (1974).
4. J. SANGSTER. T. T. TENG, and F. LENZI. Can. J. Chem. **51**, 2626 (1973).
5. G. R. ALLAKHVERDOV and B. D. STEPIN. Russ. J. Phys. Chem. **47**, 217 (1973).
6. G. N. LEWIS and M. RANDALL. Thermodynamics, 2nd ed. *Revised by* K. S. Pitzer and L. Brewer, McGraw–Hill, New York. 1961.
7. V. A. MIKHAILOV. Russ. J. Phys. Chem. **42**, 1414 (1968).
8. R. A. ROBINSON and V. E. BOWER. J. Res. Natl. Bur. Stand. **69**A, 19 (1965).
9. R. A. ROBINSON. J. Phys. Chem. **65**, 662 (1961).
10. H. A. C. MCKAY and J. K. PERRING. Trans. Faraday Soc. **49**, 163 (1953).
11. A. N. KIRGINTSEV and A. V. LUK'YANOV. Russ. J. Phys. Chem. **37**, 1501 (1963).

Can. J. Chem. Downloaded from www.nrcresearchpress.com by 210.87.254.42 on 09/05/12
For personal use only.

Raman Spectral Studies of Cadmium–Nitrite Interactions in Aqueous Solutions and Crystals[1]

DONALD E. IRISH AND RODERICK V. THORPE[2]

Department of Chemistry, University of Waterloo, Waterloo, Ontario N2L 3G1

Received November 14, 1974

DONALD E. IRISH and RODERICK V. THORPE. Can. J. Chem. **53**, 1414 (1975).

Raman spectra of aqueous solutions containing Cd^{2+} and NO_2^- clearly reveal the presence of solvated nitrite ion and of complexes. A band at 861 cm^{-1} is characteristic of the latter. The free nitrite concentration was measured from the intensity of the 817 cm^{-1} line and the average ligand number was evaluated for solutions with composition prescribed by the mole-ratio method. Four cumulative formation constants were deduced: $\beta_1 = 61.6$; $\beta_2 = 993$; $\beta_3 = 2390$; $\beta_4 = 1899$. Evidence that nitrite chelates Cd^{2+} through the two oxygen atoms is presented. The diagnostic spectral evidence consists of a high intensity, high frequency deformation mode and low intensity N—O stretching Raman bands with frequencies almost identical to those of the solvated nitrite ion. Data are also presented for solid $Cd(NO_2)_2$ and $K_{x-2}Cd(NO_2)_x$ ($x = 3, 4, 5$).

DONALD E. IRISH et RODERICK V. THORPE. Can. J. Chem. **53**, 1414 (1975).

Les spectres Raman de solutions aqueuses contenant du Cd^{2+} et du NO_2^- montrent clairement la présence d'ions nitrites solvatés de même que la présence de complexes. Une bande à 861 cm^{-1} est caractéristique de ces derniers. On a mesuré la concentration en nitrite libre à partir de l'intensité de la bande à 817 cm^{-1} et on a évalué le nombre moyen de ligands pour des solutions ayant une composition prescrite par la méthode des rapports molaires. On a déduit quatre constantes de formation cumulative: $\beta_1 = 61.6$; $\beta_2 = 993$; $\beta_3 = 2390$; $\beta_4 = 1899$. On présente des résultats indiquant que le nitrite se chélate au Cd^{2+} par l'intermédiaire des deux atomes d'oxygène. Cette conclusion, basée sur les spectres, est obtenue en se basant sur un mode de déformation de haute intensité et de haute fréquence et sur des bandes d'élongation N—O en spectroscopie Raman qui sont de basse intensité et qui ont des fréquences pratiquement identiques à celles des ions nitrites solvatés. On présente aussi des données pour le $Cd(NO_2)_2$ et le $K_{x-2}Cd(NO_2)_x$ ($x = 3, 4, 5$) à l'état solide.

[Traduit par le journal]

Raman spectra of aqueous solutions of alkali metal nitrites only exhibit lines characteristic of the solvated nitrite ion; no lines characteristic of the nitrite ion bonded to a cation are observed despite the very high solubilities of these salts (1). In contrast, divalent cations such as Ni^{2+}, Mg^{2+}, Ca^{2+}, and Zn^{2+} form complexes with nitrite ion and Raman lines attributable to both the bound and free forms of the anion are observed (2, 3). From measurement of the relative integrated intensities of the lines in the deformation region it was possible to evaluate stepwise stability constants for the species $ZnNO_2^+$ and $Zn(NO_2)_2$; values of 1.4 and 0.9 mol^{-1} l at 25° were obtained for K_1 and K_2 (3). That work has now been extended to a study of the species formed between Cd^{2+} and NO_2^- in water. In addition to a determination of the stability constants for four mononuclear complexes, structures of the species are proposed consistent with the parameters of the vibrational lines. Spectra of related solids are also reported.

Experimental

In preliminary experiments eleven solutions were prepared in accordance with the Job method of continuous variations (4, 5). A stock solution of $Cd(ClO_4)_2$ was prepared by reacting weighed amounts of CdO (J. T. Baker Analyzed Reagent grade, 99.2%) with the stoichiometric amount of $HClO_4$. The p*H* was adjusted to between 6 and 6.8 with 1 *M* NaOH and weighed quantities of $NaNO_2$ (Baker and Adamson, A.C.S. Reagent Grade) were added. The sum of the concentrations $[Cd^{2+}] + [NO_2^-]$ was kept constant at 1.43 mol l^{-1} and the Job variable ($f = [NO_2^-]/1.43$) varied from 0.26 to 1.0.

Stability constants were evaluated from data obtained from four series of solutions prepared as above but with compositions in accord with the mole-ratio method (5).

[1]Presented in part at the 57th Canadian Chemical Conference of the Chemical Institute of Canada, Regina, Saskatchewan, June 2–5, 1974.

[2]Present address: Customs and Excise Branch, Laboratory and Scientific Services Division, Revenue Canada, 490 Sussex Drive, Ottawa K1A 0L5.

Can. J. Chem. Downloaded from www.nrcresearchpress.com by 210.87.254.5 on 09/05/12
For personal use only.

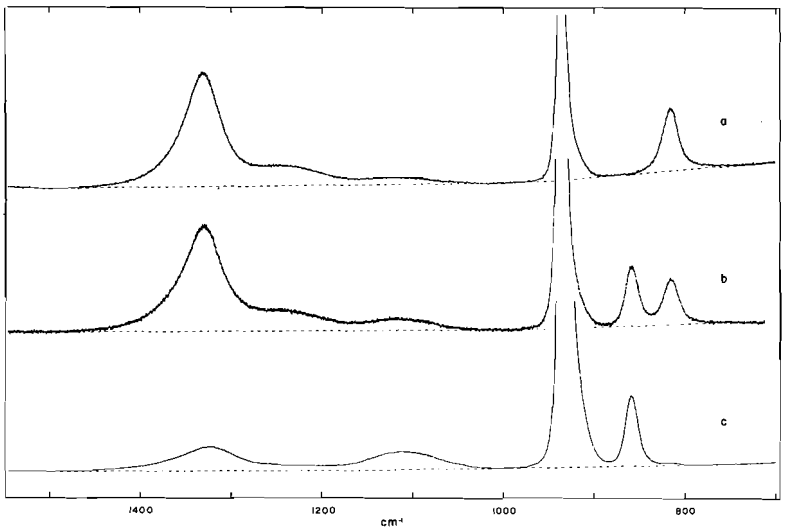

FIG. 1. Comparison of Raman spectra of $NaNO_2$ and Cd^{2+}–NO_2^- solutions from 700 to 1500 cm^{-1}: (*a*) 1.475 *M* $NaNO_2$; (*b*) 0.400 *M* Cd^{2+}, 3.62 *M* NO_2^-; (*c*) 0.896 *M* Cd^{2+}, 1.852 *M* NO_2^-.

These solutions were analyzed for NO_2^- by permanganate titration (6). Concentrations of Cd^{2+} and ClO_4^- were obtained from the weights of materials used. All solutions were filtered through a Millipore 0.100 μ filter prior to spectral measurements.

Raman spectra, excited by the 514.5 nm line of a Coherent Radiation Model 52G argon ion laser, were recorded on a Cary 81 spectrophotometer, modified as described previously (7). Samples were at the ambient temperature of the sample compartment (approximately 25 °C). All band intensities, measured as areas, were ratios relative to the intensity of the 935 cm^{-1} line of ClO_4^-. The use of this internal standard compensated for possible refractive index or color effects. Raman spectra of $Cd(ClO_4)_2$ and $NaClO_4$ solutions were used to establish the baseline. Band contours were resolved into components by a modification of the computer procedure, CURVER, described elsewhere (8). Initially the spectra, recorded repeatedly and at slow scan, were digitized using a model 21, Ruscom Logics Limited digitizer which transferred the *x* and *y* coordinates of points on a band contour to a magnetic tape via a Digi-Data Corporation tape drive unit. These data, in proper format, were used in conjunction with a PDP-11 model 20 computer and a modified CURVER program. An empirical line shape (7) which most closely fitted the symmetrically-shaped nitrite bands was employed. The line intensity of particular importance for evaluation of equilibrium constants, *viz.* the 817 cm^{-1} line, overlaps with other lines to only a small extent and thus accurate intensity measurements could be made.

Anhydrous $Cd(NO_2)_2$ was prepared from barium nitrite and cadmium sulfate as suggested by Rây (9). The purest compound prepared was analyzed for NO_2^- and showed 44.59% (predicted, 45.01%). The analysis and spectra of the solid were recorded after careful dehydration in a vacuum oven at 70 °C for several hours. The salt partially decomposed when placed in water or ethanol. Salts of the general formula $K_{x-2}Cd(NO_2)_x$, where *x* is 3, 4, or 5, were prepared by partial dehydration of solutions containing the requisite amount of KNO_2 and $Cd(NO_2)_2$ and were dried *in vacuo* at 70°. When *x* was 5, nitrite analysis gave 50.72% (predicted, 50.03%). This solid did not noticeably decompose when placed in water. Raman spectra of the powders were obtained as previously described (10). A few spectra were obtained with a Jarrell-Ash Model 100 double monochromator equipped for photon counting with an S.S.R. 1105 data converter. Infrared spectra were obtained on a Beckman IR-9 spectrophotometer fitted with a Wilks model-9 multiple internal reflectance attachment and a 60° KRS-5 prism (10, 11).

Results and Discussion

Spectral Features

The nitrite ion (C_{2v} symmetry) generates three coincident infrared and Raman lines. For 5.8 mol l^{-1} aqueous $NaNO_2$ solutions these are: $\nu_1(A_1)$, 1331 cm^{-1}, symmetric stretch; $\nu_2(A_1)$, 817 cm^{-1}, deformation; $\nu_3(B_1)$, 1242 cm^{-1}, antisymmetric stretch. They are illustrated in Fig. 1*a*. Two lines of ClO_4^-, the internal standard, are also seen in that figure at 935 and 1116 cm^{-1}. On addition of Cd^{2+} a new polarized line appears at 861 cm^{-1} (Fig. 1*b*) and grows in intensity at the expense of the 817 cm^{-1} line as the $[Cd^{2+}]/[NO_2^-]$ ratio increases (Fig. 1*c*). Less distinctive changes occur in the 1200–1400 cm^{-1} region; lines characteristic of the new species occur almost at the same positions as those of solvated NO_2^- and differ largely in molar intensity (Fig.

Can. J. Chem. Downloaded from www.nrcresearchpress.com by 210.87.254.5 on 09/05/12
For personal use only.

Can. J. Chem. Downloaded from www.nrcresearchpress.com by 210.87.254.5 on 09/05/12
For personal use only.

1*c*). This region will be discussed in more detail below.

The intensity measurements from the Job experiment (peak-height intensities; half-width was found to be constant to ± 1 cm^{-1}) are illustrated in Fig. 2. The unsymmetrical appearance of the plot and the maximum at approximately $f = 0.72$ suggest the presence of complexes of higher order than 1 : 1. The maximum is not very sharp and thus the complexes are not expected to have extremely high formation constants. For $f < 0.8$ the intensity of the 817 cm^{-1} line is very small and its molar intensity is also much less than that of the 861 cm^{-1} line. On this line-height scale (relative to 1 mol l^{-1} ClO_4^-) the ratio of molar intensities is about 0.7, estimated at $f = 0.72$.

Stability Constants from Mole-ratio Experiments

The mole-ratio method was applied to determine the identity of complexes formed by cadmium and nitrite in aqueous solution and to evaluate their formation constants. Solutions were prepared with metal concentrations, in four different series, of 1.00, 0.90, 0.40, and 0.30 mol l^{-1} respectively. The Raman spectrum of each solution was recorded in the 730 to 1000 cm^{-1} region and for selected solutions, also in the 1000 to 1520 cm^{-1} region. Because of overlap between the 817 and 861 cm^{-1} nitrite deformation bands, all spectra were digitized and curve resolved as described above. During the curve resolving, an extra component band had to be invoked, *ca.* 845 cm^{-1}, to fit the band contour of the 730 to 907 cm^{-1} region (Fig. 3).

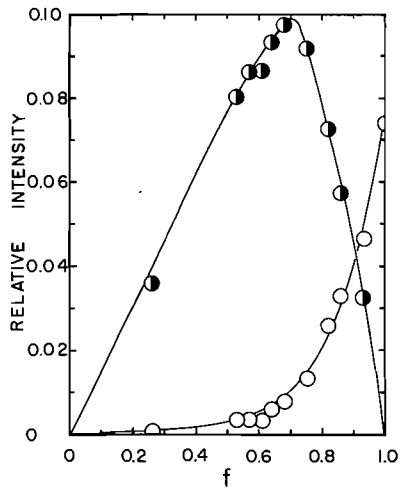

FIG. 2. Job method of continuous variations plot of relative intensity against f: ◑, relative intensity of 861 cm^{-1} bound nitrite band; ○, relative intensity of 817 cm^{-1} free nitrite band.

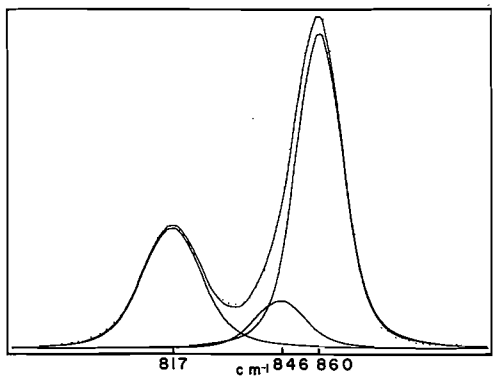

FIG. 3. Curve resolving of the nitrite deformation spectral region of a Cd–NO_2 aqueous solution ($\bar{n} = 3.48$).

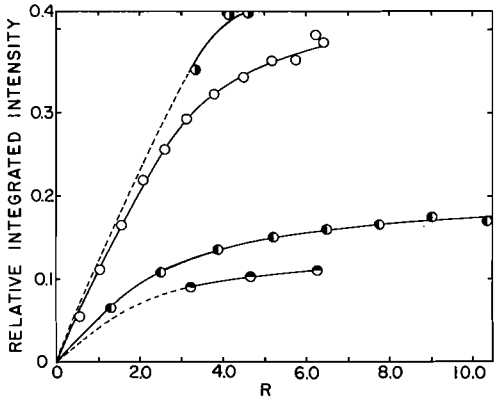

FIG. 4. Relative integrated intensity of the 861 cm^{-1} band against nitrite-to-cadmium mole ratio: ◑, 1.00 *M* Cd^{2+}; ○, 0.90 *M* Cd^{2+}; ◐, 0.40 *M* Cd^{2+}; ◓, 0.30 *M* Cd^{2+}.

Figure 4 is a plot of the relative intensity of the combined 861 and 845 cm^{-1} bands against R, the ratio of the concentrations of the total nitrite-to-cadmium for the four series. The steep slopes (increasing as cadmium concentration increases from one series to the next) and gradual levelling off at relatively low ligand-to-metal ratios (10 or less), again manifest the fairly high stability of the cadmium nitrite complexes formed. The difficulty of determining the molar intensities of the components of the band contour of bound nitrite led to the decision to determine stability constants from measurements of the 817 cm^{-1}, free nitrite band intensity. The molar intensity of this line was obtained from measurements on $NaNO_2$

Can. J. Chem. Downloaded from www.nrcresearchpress.com by 210.87.254.5 on 09/05/12
For personal use only.

solutions. A plot of relative integrated intensity of the free nitrite 817 cm^{-1} band against nitrite concentration is linear (Fig. 5). A least squares calculation was performed and gave a molar intensity, J_F, of 0.068 l mol^{-1}.

Using the measured J_F value for the free nitrite 817 cm^{-1} band, the free nitrite concentrations in the solutions were found from the curve resolved intensities by the simple relation

$$[1] \qquad C_F = I_F/J_F$$

Therefore, $\bar{n}$, the average ligand number of the complexes, was found using the total nitrite and metal concentrations

$$[2] \qquad \bar{n} = (C_T - C_F)/C_M$$

$\bar{n}$ was found to have a maximum value of 3.59 in the concentration ranges studied; thus, substantial concentrations of complexes of higher order than 1:4 were not anticipated. Only mononuclear complexes are indicated because the data from four different molar ratio experiments lie on the same curve of $\bar{n}$, as derived from eq. 2, plotted against observed free nitrite concentration (Fig. 6).

The GAUSS-Z least squares method (12) was employed in an IBM 360-75 computer program (13) to calculate β, the cumulative formation constants. Using initial guesses of β (with literature values as a guide), the program calculates new $\bar{n}$ by the equation

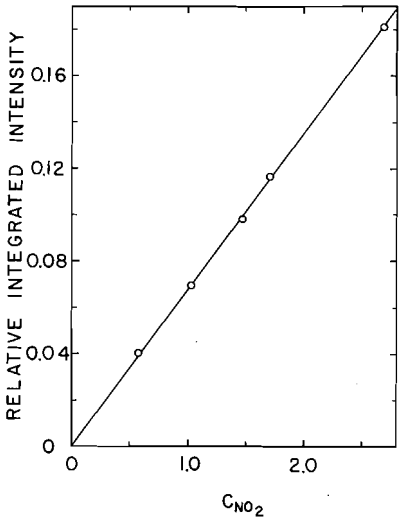

FIG. 5. Relative integrated intensity of the 817 cm^{-1} band against total nitrite concentration for standard $NaNO_2$ solutions.

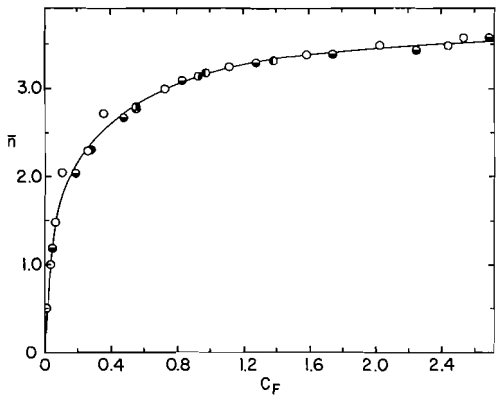

FIG. 6. $\bar{n}$ against free nitrite concentration for mole-ratio experiments: ◐, 1.00 *M* Cd^{2+}; ○, 0.90 *M* Cd^{2+}; ◒, 0.40 *M* Cd^{2+}; ◑, 0.30 *M* Cd^{2+}.

$$[3] \qquad \bar{n} = \frac{\beta_1 C_F + 2\beta_2 C_F^2 + ...}{1 + \beta_1 C_F + \beta_2 C_F^2 + ...}$$

The $\bar{n}$ are then refined in an iterative procedure to minimize the sum of the square of the difference between $\bar{n}_{calcd}$ (calculated by eq. 3) and $\bar{n}$ (initially calculated by eq. 2). The final value of the residual $R = \sum |\bar{n} - \bar{n}_{calcd}| / \sum \bar{n}$ was 1.65%. The results are presented in Table 1. Except for the first six points, for which the intensity of the free nitrite 817 cm^{-1} band is low, all solutions have values of ΔC_F less than 5% of the C_F values observed experimentally.

The logarithms of the cumulative stability constants, β_1, β_2, β_3, and β_4 are 1.79, 3.00, 3.38, and 3.28 respectively when concentrations are expressed in mol l^{-1}; the standard deviations in the logarithms are 0.053, 0.032, 0.024, and 0.011 respectively, and the unweighted sum of the squares of the deviations is 0.0948. The stepwise constants K_1 to K_4 are 61.6, 16.1, 2.41, and 0.79. Following the usual conventions (14) the log β values are compared with those obtained by other methods in Table 2. Curves of the degree of formation of each species, $\alpha = C_i/C_M$, are illustrated in Fig. 7. Extrapolations were made to lower concentrations using the computed β_1 because as log C_F becomes smaller than −2.6 only one complex species concentration is significant, *viz.* $[CdNO_2^+]$.

The Raman spectrum of one solution was examined from 710 to 1000 cm^{-1} at 31 and 61.5 °C and at 28.5 and 71 °C. The small changes in the relative intensities of the 817 and 861 cm^{-1} bands indicated a slight decrease in the concen-

TABLE 1. Free nitrite concentration and $\bar{n}$

$[Cd^{2+}]$ (mol/l)	$[ClO_4^-]$ (mol/l)	$[NO_2^-]$ (mol/l)	C_F (mol/l)	$\bar{n}$	$\bar{n}_{calcd}$	$(C_F)_{calcd}$* (mol/l)	ΔC_F† (mol/l)
0.897	1.783	0.47	0.010	0.51	0.479	0.041	0.031
0.896	1.872	0.93	0.037	1.00	1.125	−0.078	−0.115
0.896	1.848	1.40	0.066	1.48	1.477	0.077	0.011
0.896	1.860	1.85	0.115	1.94	1.810	0.229	0.114
0.896	1.851	2.33	0.265	2.31	2.319	0.253	−0.012
0.896	1.814	2.80	0.368	2.71	—	—	—
0.896	1.800	3.41	0.728	2.99	2.958	0.760	0.032
0.896	1.804	4.02	1.118	3.24	3.208	1.146	0.028
0.896	1.797	4.63	1.588	3.39	3.387	1.596	0.008
0.896	1.807	5.16	2.029	3.49	3.494	2.029	0.000
0.896	1.804	5.57	2.460	3.48	3.568	2.373	−0.087
0.897	1.828	5.75	2.544	3.57	3.580	2.539	−0.005
0.398	0.803	0.52	0.052	1.18	1.325	−0.008	−0.060
0.399	0.809	1.00	0.191	2.03	2.117	0.155	−0.036
0.400	0.816	1.55	0.485	2.66	2.702	0.469	−0.016
0.400	0.817	2.07	0.837	3.08	3.042	0.853	0.016
0.400	0.818	2.59	1.279	3.28	3.280	1.278	−0.001
0.400	0.831	3.10	1.744	3.39	3.429	1.728	−0.016
0.400	0.815	3.62	2.250	3.43	3.535	2.206	−0.044
0.400	0.815	4.14	2.700	3.58	3.601	2.700	0.000
0.299	0.606	0.97	0.279	2.30	2.351	0.267	−0.012
0.298	0.598	1.38	0.556	2.78	2.789	0.549	−0.007
0.299	0.617	1.87	0.934	3.13	3.107	0.941	0.007
0.995	2.012	3.31	0.557	2.77	2.791	0.534	−0.023
0.993	2.002	4.12	0.976	3.17	3.132	1.010	0.034
0.996	2.009	4.60	1.303	3.31	3.289	1.324	0.021

*$(C_F)_{calcd} = C_T - (C_B)_{calcd}$.
†$\Delta C_F = (C_F)_{calcd} - (C_F)$.

TABLE 2. Stability constants for Cd^{2+}–NO_2^- complexes*

Method	Temperature	Medium	log β_1	log β_2	log β_3	log β_4	Reference
Ram	~25	var	1.79	3.00	3.38	3.28	This work
MHg	25	3 ($NaClO_4$)	1.80	3.01	3.81	3.11	15
cal	25	3 ($NaClO_4$)	1.76	3.08	3.70		16
pol	30	1 (KNO_3)	1.7	1.85	3.1		17
pol	25	2.5 ($NaClO_4$)	1.8	2.3	3.2		18
pol	25	2 ($NaClO_4$)	1.78	2.85	3.53	2.70	19
sp	~25	var	1.74				20
sp	25	1 ($NaClO_4$)	1.7				21
spJ	25	→0	2.4				21

*Ram = Raman spectra; MHg = e.m.f. with amalgam electrode; cal = calorimetry; pol = polarography; sp = spectrophotometry; spJ = spectrophotometry by Job's method; var = ionic medium varied; → 0 = constants extrapolated to zero ionic strength.

tration of bound nitrite with 30 and 40° temperature increases. These results imply that the net complex formation for the concentrations of species examined is slightly unstable with respect to temperature increases.

Comparing the different results in Table 2 there seems to be general agreement that log β_1 is about 1.8. Ultraviolet spectrophotometry to date has not made possible evaluation of the number of complexes or their formation constants (20, 21). Garnier (22) has pointed out, however, that the spectrophotometric results are not inconsistent with the presence of four complexes. The absorption (*ca.* 31 000 cm^{-1}) is a colligative property of bound nitrite ion, independent of the number of nitrite ions bound to the metal ion. The polarographic study of Jain and Gaur (17) failed to make allowance for the competitive complexing between cadmium and nitrate ions (23). The results of Swinarski and Grodzicki (19) are more in

Can. J. Chem. Downloaded from www.nrcresearchpress.com by 210.87.254.5 on 09/05/12
For personal use only.

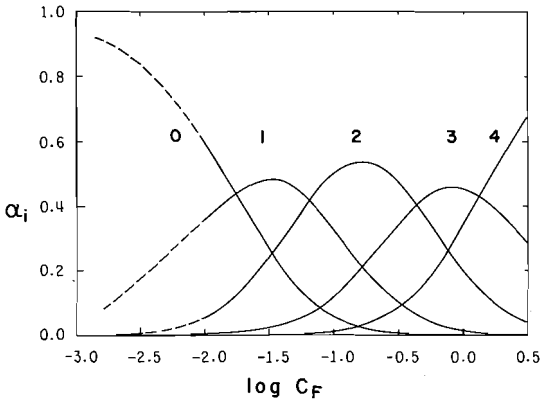

FIG. 7. Formation curves: α against log free nitrite concentration.

accord with the present work. The best agreement, however, is with the e.m.f. study of Leden (15). Gerding (16) also favored Leden's constants; he used them as starting values and adjusted them to give the best fit to his calorimetric data. He evaluated only three constants but noted that his data indicated a fourth complex. Possibly its detection has been sporadic because solution compositions have not spanned a sufficiently wide composition range.

Assignments and Structure

As noted previously, the symmetric stretching mode is observed *ca.* 1331 cm^{-1} and the antisymmetric stretching mode occurs *ca.* 1242 cm^{-1} for free nitrite. Upon addition of cadmium to a solution of sodium nitrite, no additional bands are evident in the 1000 to 1520 cm^{-1} Raman spectral region (*cf.* ref. 1). However, a noticeable decrease occurs in the molar intensity of the nitrite stretching bands. This can be noted by referring to Fig. 1. To convert the three spectra in the figure to the same scale as spectrum *a*, it is necessary to multiply the intensity of spectrum *b* by approximately two and that of spectrum *c* by approximately 2.5. Even with this conversion it is evident that the Raman molar intensities of the stretching modes of bound nitrite are less than half those of free nitrite.

The half-width of the 1331 cm^{-1} band increases from about 43 cm^{-1} for 5.8 mol l^{-1} $NaNO_2$ to about 66 cm^{-1} when the ratio of bound-to-free nitrite is 6.5. The results suggest that a bound nitrite stretching mode is nearly coincident ($\pm$10 cm^{-1}) with the 1330 cm^{-1} free nitrite stretching mode. Because of low intensity and overlap with the ν_3 line of perchlorate no significant trend was observable in the 1240 cm^{-1} region.

The digitized data facilitated another comparison of the band contours of free and bound nitrite. Point by point intensities were converted to a scale relative to 1 mol l^{-1} perchlorate and are plotted in Fig. 8 for a cadmium nitrite solution and sodium nitrite solution having equivalent concentrations of free nitrite. Although significant errors in the plot may exist, especially near the low intensity contour of the *ca.* 1116 cm^{-1} perchlorate band, a difference intensity contour, with maxima *ca.* 1337, 1249, and 1115 cm^{-1}, is evident. The occurrence of the largest intensity at about 1337 cm^{-1} further supports the contention that at least one bound nitrite stretching mode occurs within 10 cm^{-1} of the symmetric stretching mode of free nitrite. The difference intensity maximum *ca.* 1115 cm^{-1} is probably not real since large errors are inherent in measuring the difference between two low intensity contours. This postulate is substantiated by the fact that no intensity was observed at *ca.* 1115 cm^{-1} in the spectra of cadmium nitrite solutions not containing perchlorate. The difference intensity *ca.* 1249 cm^{-1} is apparently genuine since intensity is observed in this region for cadmium nitrite solutions containing a very low concentration of free nitrite.

None of the common types of coordination of

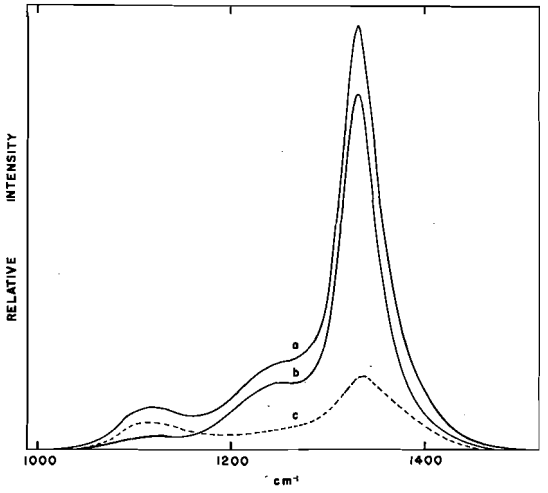

FIG. 8. Intensity due to bound nitrite in the Raman nitrite stretching region: (*a*) 4.14 *M* total NO_2^-, 2.70 *M* free NO_2^-, 1.44 *M* bound NO_2^-; (*b*) 2.69 *M* $NaNO_2$ (all free); (*c*) difference intensity, (*a*) − (*b*).

Can. J. Chem. Downloaded from www.nrcresearchpress.com by 210.87.254.5 on 09/05/12
For personal use only.

Can. J. Chem. Downloaded from www.nrcresearchpress.com by 210.87.254.5 on 09/05/12
For personal use only.

nitrite ligand to a cation would produce the observed spectral results. Observed N-bonded complexes have the bound antisymmetric stretch raised to approximately 1345 to 1497 cm^{-1}, whereas in O-bonded and bridged complexes, this band occurs at even higher frequencies (22, 24–28). The symmetric stretching frequency may rise or remain unshifted in N-bonded complexes but upon O-bonded coordination this band generally shifts to much lower frequency. Garnier (22) reports infrared and Raman spectra of a saturated aqueous solution of $K_2Cd(NO_2)_4$ which are similar to some of the spectra observed here. His infrared spectra show that the antisymmetric stretch of bound nitrite occurs *ca.* 1230 cm^{-1} or essentially unchanged from that of free nitrite. His postulate to explain the observed spectra is that the complexes contain bidentate-coordinated O-bonded linkages. Intuitively, this explanation is reasonable, since a molecular orbital approach would predict a lowering of the bond order with this coordination, lowering the nitrite stretching frequency, but the ring rigidity tends to increase the force constant for stretching, so that the frequency lowering effect is partly cancelled. It is possible then that little shifting of the N—O stretching frequencies will occur on the basis of his proposal. The decreased electron density in the N—O bonds would contribute to a decreased polarizability and an increased bond dipole; thus low Raman intensity and high infrared intensity can be rationalized. Raman resonance is not an acceptable explanation because the absorbance is negligible at the wavelength of the exciting line. Depolarization studies of cadmium nitrite solutions did not reveal any new information because of the high depolarization ratio of the symmetric stretch and considerable band overlap in this region.

The relatively high frequency, 861 cm^{-1}, of the deformation mode also supports bidentate O-bonding. Structures containing either N-bonded or O-bonded ligands have been reported and the deformations are lower than about 850 cm^{-1} (24–29). On the other hand bridging or chelation gives a higher frequency, >860 cm^{-1} (28, 30). The ring rigidity in the proposed bidentate structure would also force the deformation mode to higher frequency. The curve resolved spectra (Fig. 3) suggested two bands in this region at 846 and 861 cm^{-1}. These positions are reminiscent of those observed on dehydration of $LiNO_2 \cdot H_2O$ (842 and 872 cm^{-1}) (31). Their existence for the $Cd(NO_2)_x^{2-x}$ species may imply that whereas the nitrite ions for the most part chelate the Cd^{2+} giving rise to the 861 cm^{-1} line, a smaller fraction are oriented in monodentate fashion, possibly in the higher complex, giving the 846 cm^{-1} line.

The oxygen–cation bonds probably have high ionic character (22); a broad, weak polarized line at 240 cm^{-1} is assigned to the symmetric stretch and depolarized lines at 324 and 446 cm^{-1} are assigned to rocking and wagging modes respectively (24). The bonding of possibly eight-coordinated cadmium(II) can be understood in terms of three-center bonds discussed by Bullock and Tuck (32) for $[Hg(NO_2)_4]^{2-}$ (*vide post*).

Spectra of Related Solids

The Raman and infrared lines from the deformation and stretching modes of NO_2^- in several solids are presented in Table 3. The positions of the weak, broad bands above 1200 cm^{-1} are estimated to ± 5 cm^{-1}. The spectrum of $Cd(NO_2)_2$ is particularly interesting. The 874 cm^{-1} deformation is high in frequency and intensity. The stretching modes are weak in comparison and also when compared to the lines of $NaNO_2$; and yet they are not markedly shifted from the positions observed for alkali metal nitrites (30). These observations and those to follow suggest that also in the solid state nitrite ion chelates Cd^{2+}. The structure is represented by

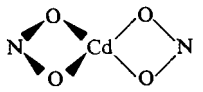

D_{2d} symmetry would account for coincidence of Raman and i.r. spectral lines. Raman lines at 347 and 382 cm^{-1} are believed to arise from cadmium–oxygen stretching motions. Lines observed at 48, 62, 71, 85, 94, 120–135, and 190 cm^{-1} are mostly lattice modes.

The solid $K_2Cd(NO_2)_4$ has been examined previously (22, 29, 33). Goodgame and Hitchman (33) have demonstrated that $K_2Cd(NO_2)_4$ and $K_2Hg(NO_2)_4$ are isomorphous. They argued that NO_2^- chelates the group 2B metal ions in both of these compounds and a structure similar to the coordination polyhedron inferred from X-ray and neutron scattering data for $K_3[Hg(NO_2)_4]NO_3$ results (34, 35). The infrared spectral data of Bullock and Tuck (32), Garnier (22), and Good-

Can. J. Chem. Downloaded from www.nrcresearchpress.com by 210.87.254.5 on 09/05/12
For personal use only.

TABLE 3. Vibrational frequencies (cm^{-1}) for powdered $Cd(NO_2)_2$ and $K_{x-2}Cd(NO_2)_x$*

$Cd(NO_2)_2$		$K_3Cd(NO_2)_5$		$KCd(NO_2)_3$	$K_2Cd(NO_2)_4$		
						Infrared	
Raman	Infrared	Raman	Infrared	Raman	Raman	Reference 33	Reference 22
		828 (m)	828 (m)	828 (m)	828 (vw)		
		850 (vs, sp)	850 (s)	850 (vs, sp)	850 (vs, sp)	851 (m, sp)	851
							855 (sh)
		860 (m, sh)		860 (m, sh)	865 (m)	858 (w, sp)	860
874 (s, sp)	874 (s)						
		1048 (w)					
		1065 (w)		1069 (w)	1069 (w)		
1257 (w, br)	1246 (m, br)	1230 (w, br)	1223 (sh, br)	1223 (sh, br)			
1280 (w)	1280 (s, br)	1271 (w, br)	1273 (s, br)	1276 (w, br)	1272 (m, br)	1266 (vs, br)	1260 (vs, br)
1305 (mw)	1302 (vw)?	1301 (w)		1301 (w)	1301 (m)		
		1326 (s)		1326 (s)	1326 (w, sh)		
1342 (m)	1346 (w)	1345 (m)	1344 (w)	1345 (m)	1345 (s)		
		1358 (sh)		1358 (sh)	1358 (sh)		

*Abbreviations: s, strong; m, medium; w, weak; sp, sharp; br, broad; sh, shoulder; v, very.

Can. J. Chem. Downloaded from www.nrcresearchpress.com by 210.87.254.5 on 09/05/12
For personal use only.

game and Hitchman (33) confirmed that $K_3[Hg(NO_2)_4]NO_3$ and $K_2Hg(NO_2)_4$ contain the same $[Hg(NO_2)_4]^{2-}$ unit. Consequently the evidence is quite strong for bidentate O-bonded coordination (although not for equal Cd—O distances) for the complexes studied in this work. The higher frequency of the deformation band of $Cd(NO_2)_2$, compared with $K_2Cd(NO_2)_4$, is attributable to a more symmetrical arrangement with stronger Cd—O bonds. Greater overlap between sp^3 hybrid orbitals of Cd^{2+} and nonbonding sp^2 hybrid orbitals of each oxygen would result in stronger bonds for the four-coordinated species than the eight-coordinated species (*cf.* ref. 32).

The crystals formed from compositions $x = 3$ and $x = 5$ are probably double salts containing KNO_2 and $K_2Cd(NO_2)_4$. The lines at 828, 1230, and the markedly higher intensity at 1326 cm^{-1} suggest uncoordinated nitrite. The weak 1048 cm^{-1} line is attributable to NO_3^- resulting from slight decomposition.

In conclusion we infer that Cd^{2+} is chelated by nitrite ion in the solids and in aqueous solution. The mode of attachment is particularly favorable for the first two complexes in solution; monodentate O-bonding occurs to some extent in the third or fourth complex. The diagnostic spectral features of the chelation are low-intensity Raman bands in the N—O stretching region with frequencies almost identical to those of the solvated nitrite ion and a high intensity, high frequency deformation mode. The infrared intensities will be intense in the stretching region because of the increased bond polarity. These conclusions lead us to believe that Zn^{2+} in aqueous solution is also chelated by nitrite ion. The deformation occurs at 867 cm^{-1} and the observations in the stretching region (3) appear to meet the conditions specified above. $Zn(NO_2)_2$ is the highest complex in aqueous solution; it should also have D_{2d} symmetry as described above for the unit in solid $Cd(NO_2)_2$. The bonding would involve overlap of sp^3 hybrid orbitals of Zn^{2+} and sp^2 nonbonding orbitals of the oxygen atoms. But the smaller size of the Zn^{2+} ion precludes higher coordination of this type. Although higher complexes do not form in solution, $Cs_2Zn(NO_2)_4$ can form in the crystalline state. Then the nitrite ions are forced to coordinate in monodentate arrangement and the deformation drops to 847 cm^{-1} while ν(N—O) occurs at 1167 cm^{-1} and ν(N=O) at about 1380 cm^{-1} (22, 33).

The support of the National Research Council of Canada is gratefully acknowledged. We also wish to thank Mr. F. Grossman and other members of the Computer Center of the university for their assistance, Professor R. Stuart Tobias for providing the GAUSS-Z program, M. H. Brooker for helpful discussion, and P. J. M. Gleeson for performing checks on the computations.

1. D. E. Irish and M. H. Brooker. Trans. Faraday Soc. **67**, 1916 (1971).
2. M. H. Brooker. Ph.D. Thesis. University of Waterloo, Waterloo, Ontario. 1969.
3. M. H. Brooker and D. E. Irish. Trans. Faraday Soc. **67**, 1923 (1971).
4. P. Job. Ann. Chim. **9**, 113 (1928); **6**, 97 (1936).
5. M. T. Beck. Chemistry of complex equilibria. Van Nostrand Reinhold, London. 1970. p. 86 ff.
6. A. Vogel. Quantitative inorganic analysis. 2nd Ed. Longmans Green, Toronto. 1951. p. 285.
7. J. D. Riddell, D. J. Lockwood, and D. E. Irish. Can. J. Chem. **50**, 2951 (1972).
8. A. R. Davis, D. E. Irish, R. B. Roden, and A. J. Weerheim. Appl. Spectrosc. **26**, 384 (1972).
9. P. C. Rây. J. Chem. Soc. **111**, 159 (1917).
10. T. G. Chang and D. E. Irish. Can. J. Chem. **51**, 118 (1973).
11. M. H. Brooker and D. E. Irish. Spectrochim. Acta, **28A**, 701 (1972).
12. R. S. Tobias and M. Yasuda. Inorg. Chem. **2**, 1307 (1963).
13. T. G. Chang. Ph.D. Thesis. University of Waterloo, Waterloo, Ontario. 1972.
14. L. G. Sillén and A. E. Martell. Stability constants of metal-ion complexes. Special Publication No. 17. The Chemical Society, London. 1964.
15. I. Leden. Dissertation, University of Lund, Lund, Sweden. 1943. p. 88.
16. P. Gerding. Acta Chem. Scand. **20**, 2771 (1966).
17. D. S. Jain and J. N. Gaur. Bull. Acad. Polon. Sci. Ser. Sci. Chim. **13**, 615 (1965).
18. V. F. Toropova and F. M. Batyrshina. Izv. Vyssh. Uchebn. Zaved. Khim. Khim. Tekhnol. **4**, 11 (1961); Chem. Abstr. **55**, 17180h (1961).
19. A. Swinarski and A. Grodzicki. Rocz. Chem. **39**, 1155 (1965).
20. H. J. Maria, A. Wahlborg, and S. P. McGlynn. J. Chem. Phys. **49**, 4925 (1968).
21. E. G. Vassian and W. H. Eberhardt. J. Phys. Chem. **62**, 84 (1958).
22. A. Garnier. J. Chim. Phys. **67**, 1440 (1970).
23. A. R. Davis and R. A. Plane. Inorg. Chem. **7**, 2565 (1968).
24. J. R. Durig and D. W. Wertz. Appl. Spectrosc. **22**, 627 (1968).
25. M. J. Cleare and W. P. Griffith. J. Chem. Soc. A, 1144 (1967).
26. D. M. Adams. Metal–ligand and related vibrations. Arnold, London. 1967. pp. 296–299.
27. J. Chatt, L. A. Duncanson, B. M. Gatehouse, J. Lewis, R. S. Nyholm, M. L. Tobe, P. F. Todd, and L. M. Venanzi. J. Chem. Soc. 4073 (1959).

28. D. M. L. GOODGAME and M. A. HITCHMAN. Inorg. Chem. **3**, 1389 (1964); **4**, 721 (1965); **6**, 813 (1967).
29. M. LE POSTOLLEC, J. P. MATHIEU, and H. POULET. J. Chim. Phys. **60**, 1319 (1963).
30. B. J. HATHAWAY and R. C. SLADE. J. Chem. Soc. A, 1485 (1966).
31. M. H. BROOKER and D. E. IRISH. Can. J. Chem. **49**, 1289 (1971).
32. J. J. BULLOCK and D. G. TUCK. J. Chem. Soc. 1877 (1965).
33. D. M. L. GOODGAME and M. A. HITCHMAN. J. Chem. Soc. A, 612 (1967).
34. D. HALL and R. V. HOLLAND. Inorg. Chim. Acta, **3**, 235 (1969).
35. L. F. POWER, K. E. TURNER, and F. H. MOORE. Inorg. Nucl. Chem. Lett. **8**, 809 (1972).

Can. J. Chem. Downloaded from www.nrcresearchpress.com by 210.87.254.5 on 09/05/12
For personal use only.

Carbon-13 Chemical Shifts of Furanosides and Cyclopentanols. Configurational and Conformational Influences[1]

R. GEORGE S. RITCHIE, NATSUKO CYR, BRIAN KORSCH, HANS J. KOCH, AND ARTHUR S. PERLIN

Department of Chemistry, McGill University, Montreal, Quebec H3C 3G1

Received November 1, 1974

R. GEORGE S. RITCHIE, NATSUKO CYR, BRIAN KORSCH, HANS J. KOCH, and ARTHUR S. PERLIN. Can. J. Chem. **53**, 1424 (1975).

Assignments for the ^{13}C chemical shifts of methyl aldopento- and hexofuranosides and of cyclopentane polyols are reported, and these chemical shifts are evaluated with respect to all combinations of configurational arrangements of the ring substituents. A *cis* configuration of vicinal substituents is generally associated with a substantial increase in shielding, as compared with the *trans* analog. Among the furanosides, however, changes in configuration involving O-3 and C-5 are accompanied by a complex shielding pattern: *e.g.*, effects on C-3 are minor, C-4 is more shielded in *cis* than in *trans* isomers, and C-4 and C-5 of hexosides are more shielded than those of pentosides. Variations in shielding attributable to *cis* or *trans* arrangements of substituents in a 1,3-relationship are encountered in only a few instances; however, it is noteworthy that C-4 is *less* shielded when O-1 and O-3 are *cis* than when *trans*. These diverse effects are considered also in relation to steric interactions and to conformational influences on ^{13}C chemical shifts in the five-membered ring series.

R. GEORGE S. RITCHIE, NATSUKO CYR, BRIAN KORSCH, HANS J. KOCH et ARTHUR S. PERLIN. Can. J. Chem. **53**, 1424 (1975).

On rapporte les attributions de déplacements chimiques du ^{13}C pour les aldopento- et hexofurannosides de méthyle et pour une série de cyclopentanepolyols; on évalue ces déplacements chimiques par rapport à toutes les combinaisons d'arrangements configurationnels des substituants du noyau. Par opposition aux analogues *trans*, on associe généralement une augmentation substantielle du blindage avec une configuration *cis* des substituants vicinaux. Toutefois parmi les furannosides, les changements de configuration impliquant O-3 et C-5 sont accompagnés par un patron de blindage complexe, *e.g.* les effets sur C-3 sont mineurs, C-4 est plus blindé dans les isomères *cis* que dans les isomères *trans* et C-4 et C-5 des hexosides sont plus blindés que ceux des pentosides. On ne rencontre que quelques cas où des variations dans le blindage sont attribuables aux arrangements *cis* et *trans* des substituants en position 1,3; toutefois il est à noter que C-4 est moins blindé quand O-1 et O-3 sont *cis* que lorsqu'ils sont *trans*. On considère aussi ces divers effets en relation avec les interactions stériques et les influences conformationnelles sur les déplacements chimiques du ^{13}C dans une série de cycles à cinq membres. [Traduit par le journal]

Introduction

Earlier studies (1–6) have dealt with configurational and conformational effects on ^{13}C n.m.r. chemical shifts in the pyranose series of carbohydrates and selected substituted cyclohexanols. The recognition of such steric effects in the spectra of these compounds proved to be relatively straightforward because of the unique geometry of the six-membered ring: namely, the existence of two chair conformations, in which the substituents are either axial or equatorial. By contrast, the furanose and cyclopentane rings are more flexible structures, conformers of which may differ relatively little in energy and hence readily interconvert as envelope and twist forms; *i.e.*, those conformations in which one and two atoms, respectively, are out of the plane of the ring. Therefore, a representative conformer may be difficult to define for a given substituted five-membered ring. The value of ^{1}H–^{1}H coupling in this context has, of course, long been recognized (7). However, ^{13}C n.m.r. data, by providing complementary stereochemical information, should enhance the reliability of conformational analysis in this area.

As described in a preliminary report (8), configurational differences between isomeric furanoses are readily recognizable by variations

[1]This paper is dedicated to Professor C. A. Winkler of McGill University on the occasion of his sixty-fifth birthday by one of his colleagues (A.S.P.).

Can. J. Chem. Downloaded from www.nrcresearchpress.com by 210.87.254.42 on 09/05/12
For personal use only.

TABLE 1. ^{13}C chemical shifts[a] of some disubstituted cyclopentanols, and substituent effects (in parentheses) on C-1 of cyclopentanols

Compound[b]	C-1	C-2	C-3	C-4	C-5	CH_3
Cyclopentanol	75.1 (0)	36.0	24.1	[c]	[c]	—
2-CH_3,1-ol[d]	76.3 (+1.9)	40.9	35.6	23.2	32.1	15.8
2-CH_3/1-ol[d]	80.9 (+6.5)	43.3	35.0	22.6	32.9	19.4
3-CH_3,1-ol[d]	74.3 (−0.1)	45.2	34.1	33.5	36.5	22.2
3-CH_3/1-ol[d]	74.3 (−0.1)	45.4	33.0	33.8	36.3	21.8
1,2-diol	74.8 (−0.3)	[c]	31.2	20.3	[c]	—
1/2-diol	79.7 (+4.6)	[c]	32.4	21.3	[c]	—
1,3-diol	73.4 (−1.7)	44.6	[c]	34.0	[c]	—
1/3-diol	73.2 (−1.9)	44.9	[c]	33.7	[c]	—

[a]In p.p.m. from upfield, external TMS; (shielding, negative; deshielding, positive).
[b](,) and (/) designate *cis* and *trans*, respectively.
[c]For clarity, symmetric ^{13}C signals have been deleted.
[d]Reference 12.

in ^{13}C chemical shifts. A more definitive analysis of chemical shift data for these compounds and a fuller account of the shielding influences observed is contained here, together with a comparative study on cyclopentanols. Configurational inversion rarely introduces a large change in the conformation of pyranoses but might lead to a gross effect on the pseudorotational itinerary of furanoses (*e.g.*, ref. 9). Hence, the influences on shielding noted below are ascribed empirically to known changes in configuration, although it is clear that an unknown conformational factor is included and may even make a major contribution to shielding.

Results and Discussion

Cyclopentanols

Because there are close analogies between the spectral characteristics of pyranoses and cyclohexanes, it is of interest to study data on cyclopentanols in conjunction with the furanosides. As in the cyclohexane series (10, 11) steric hindrance (due to CH_3–CH_3 and CH_3–OH interactions) in cyclopentanes is associated with upfield shifts (12), at least for the substituted ^{13}C nuclei when two related isomers are compared. For example, C-1 and C-2 of *cis*-1,2-dimethylcyclopentane and -2-methylcyclopentanol are more shielded than those of their *trans* isomers (12). When there are two or more hydroxyl groups on the ring, the interactions become more complex. Studying these effects in the cyclopentane series should facilitate the unravelling of the ^{13}C chemical shifts of furanosides.

Since numerous cases of the consistent additivity of substituent effects have been found (13, 14) for various types of ^{13}C nuclei, the validity of these effects in the cyclopentanol series has been studied. Thus, some disubstituted cyclopentanes were compared with cyclopentanol to determine the influence on C-1 of a hydroxyl group or a methyl group at various positions in the ring. The data are summarized in Table 1 for all combinations of diols and, for comparison, the methylcyclopentanols reported by Christl *et al.* (12). When one compares the primary carbinol signals of the following alcohols, where steric effects are minimal, values[2] similar to those observed for the *trans* examples of Table 1 are obtained; this suggests that the *trans* arrangement *per se* makes little contribution to the chemical shift.[3]

$$\overset{*}{C}H_3CH_2OH \rightarrow HOCH_2\overset{*}{C}H_2OH \qquad +4.6 \text{ p.p.m.}$$

$$\overset{*}{C}H_3CH_2\overset{*}{C}H_2OH \rightarrow HOCH_2CH_2\overset{*}{C}H_2OH \qquad -1.9 \text{ p.p.m.}$$

The substituent effect of a methyl group is distinctly different from that of a hydroxyl: carbon-1 in *cis*-2-methylcyclopentanol is deshielded relative to that of cyclopentanol, whereas the corresponding *cis*-diol is slightly more shielded. This is difficult to reconcile only on the basis of steric effects. Similarly, for the C-3-methyl compounds, C-1 is essentially unaffected, whereas it is more strongly shielded in the related *cis*- and *trans*-1,3-diols. That the γ

[2]Using TMS as the standard for ^{13}C chemical shifts, a negative value refers to increased shielding, and a positive one to a downfield shift.

[3]As a referee has noted, these comparisons may not be entirely valid because the *gauche* conformer of ethylene glycol should be important as a result of intramolecular hydrogen bonding.

Can. J. Chem. Downloaded from www.nrcresearchpress.com by 210.87.254.42 on 09/05/12
For personal use only.

TABLE 2. Experimental chemical shifts for cyclopentane polyols and their deviations (in parentheses) from those calculated using substituent parameters for cyclopentanols

Cyclopentanols	C-1	C-2	C-3	C-4	C-5
1,2,3-Triol	72.8 (−0.3)	74.8 (+0.3)	—	29.9	—
1,3/2-Triol	76.6 (−1.4)	85.1 (+0.8)	—	29.1	—
1,2/3-Triol	72.5 (−0.4)	79.9 (+0.5)	76.8 (−1.0)	29.0	29.0
1,4/2-Triol	78.4 (−0.4)	78.2 (−0.4)	41.8[a]	70.1 (−1.4)	41.9[a]
1,2,3/4-Tetrol	70.7 (−0.5)	74.2 (+1.6)	79.3 (1.6)	76.4 (+0.5)	39.1
1,2,4/3-Tetrol	69.9 (−1.3)	76.9 (−0.8)	82.5 (+0.1)	74.0 (−2.3)	38.4
1,2/3,4-Tetrol	69.5 (−1.5)	77.1 (−0.6)	—	—	39.2
1,3/2,4-Tetrol	74.1 (−2.0)	83.0 (+0.4)	—	—	38.4
1,4/2,3-Tetrol	75.8 (−0.3)	78.6 (+0.9)	—	—	38.8
1,2,3,4/5-Pentol	76.5 (+0.5)	72.0 (+1.1)	—	—	84.1 (+3.2)

[a]May be interchanged.

effect of the hydroxyl group is greater than that of the methyl has been noted in other systems (11, 13*a*, 14). Only with the 1,2-*cis*- and 1,2-*trans*-cyclopentane diols is the expected stronger shielding of C-1 of the former than of the latter noted.

It was found that the empirical substituent effects given in Table 1 are useful for predicting the chemical shifts of each substituted carbon nucleus of polyols of cyclopentane. The reasonably good agreement obtained for some triols, tetrols, and a pentol with the experimental values is demonstrated in Table 2. A typical calculation is shown below using the values in parentheses in Table 1.

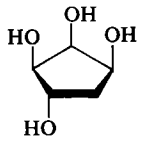

1.2.3/4-Tetrol

C-1: 75.1 + (−0.3) + (−1.7) + (−1.9) = 71.2

C-2: 75.1 + (−0.3) + (−0.3) + (−1.7) = 72.8

C-3: 75.1 + (−1.7) + (−0.3) + (+4.6) = 77.7

C-4: 75.1 + (−1.9) + (−1.9) + (+4.6) = 75.9

The deviations (shown in parentheses in Table 2) are the experimental chemical shifts minus the calculated values. In most cases, the error is small enough to confirm the assignment of each carbon signal, although it appears to increase as more and more hydroxyls are added. This suggests that the ^{13}C chemical shift depends to a small extent on interactions which are not considered here.

The change from the *trans*-1,2-diol arrangement to the *cis*, involves an increase in shielding of 4.6 p.p.m., whereas 1,3-interactions seem relatively unimportant (~0.2 p.p.m.) when comparing members of the same set. Hence, given one member of a series for which the assignments are known, such as a cyclopentanetetrol, it is to be expected that the spectrum of all other members can be estimated by using only the vicinal *cis–trans* conversions. The experimental chemical shifts of the triols and tetrols (Table 2) were then tested for the consistency of this approach. For the triols, 1,2-effects ranged from 3.8–5.2 p.p.m. (average 4.6), whereas they were slightly worse for the tetrols: 3.4–6.3 p.p.m. (average 4.8 p.p.m.). A sample conversion test is as follows:

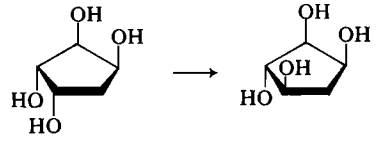

1.2/3.4-Tetrol 1.2.4/3-Tetrol

1,3-arrangements
C-1: +0.4 p.p.m.
C-2: −0.2 p.p.m.

1,2-arrangements
C-3: +5.4 p.p.m.
C-4: +4.5 p.p.m.

This illustrates further that nonvicinal effects are small. However, as will be seen in conjunction with furanosides (below), such effects may sometimes be substantial.

Can. J. Chem. Downloaded from www.nrcresearchpress.com by 210.87.254.42 on 09/05/12
For personal use only.

Can. J. Chem. Downloaded from www.nrcresearchpress.com by 210.87.254.42 on 09/05/12
For personal use only.

Effect of Ring Closure on α,ω-Butanols

Dehydration of derivatives of butane-1,4-diol gives the corresponding saturated, five-membered heterocycles. The chemical shift patterns of these compounds illustrate important features to be found in the furanoside spectra. For example, the carbons bonded to the ring oxygen are more deshielded (6–10 p.p.m.) than those in the open-chain polyols, as shown by the data in Table 3. Similar deshielding effects are observed when carbinol groups are methylated (4, 5), so that ring closure amounts to an internal *O*-alkylation. The most dramatic case is for 1,4-anhydroerythritol (**2**),[4] in which the α-carbons are at lower field than the β-carbons. The latter, being incorporated in the *cis*-2,3-diol arrangement, experience an increase in shielding, just as in the cyclopentanol series; in 1,4-anhydro-D-threitol (**4**) because of the *trans*-2,3-diol arrangement these ^{13}C nuclei follow the usual order: secondary less shielded than primary (13*a*).

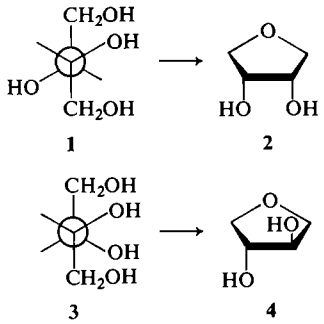

These anhydrides may be considered in relation to their parent polyols. Thus, when the secondary hydroxyl groups of erythritol (**1**), favoring an *anti* orientation, are brought into a vicinal *cis* relationship on ring closure (**2**) an upfield shift of 1.2 p.p.m. is observed for C-2 (and C-3). On the other hand, the hydroxyl groups of threitol are expected to be *gauche* (**3**) but should more closely approach an *anti* disposition on ring closure (**4**), which should contribute to the deshielding of 4.5 p.p.m. observed. Deshielding (by 5.4 p.p.m.) is also found for C-2 (and C-3) in the *cis* to *trans* configurational change in going from **2** to **4**, an effect comparable to that observed with the cyclopentanols (Table 1).

[4]Chemical shifts for this, and other 1,4-anhydro derivatives, have been reported recently by Que and Gray (15).

TABLE 3. Effects of ring closure of butane α,ω-diols: ^{13}C chemical shifts of tetrahydrofuran rings and related systems in D_2O (p.p.m. from TMS)

	C-1	C-2
Butane-1,4-diol	62.6	29.2
Tetrahydrofuran	68.6	26.2
meso-Erythritol (**1**)	63.9	73.2
1,4-Anhydroerythritol (**2**)	72.7	72.0
D-Threitol (**3**)	63.9	72.8
1,4-Anhydrothreitol (**4**)	73.8	77.4

Methyl Tetrofuranosides

In extending this study to the methyl glycofuranosides, additional effects due to the methoxyl and alkyl groups were assessed. The alternating *trans* configuration of methyl α-threoside (**9**, R = H) is considered first, as it has the least number of steric interactions. Carbon-1 now has two electronegative oxygens, both of which are "alkylated," and therefore is the least shielded of the nuclei. Carbon-2 also experiences more deshielding: a "β-effect"; *i.e.*, in a series of alkanes, where one hydrogen is replaced by an OH group, there is not only a shift downfield for the α-carbon (36–51 p.p.m.) but a smaller shift (5–10 p.p.m.) of the β-carbon (13*b*, 14). By analogy, this extra oxygen on C-1 in furanoses (relative to a 1,4-anhydrotetritol) causes C-2 to shift to lower field than C-3. As alkylation of the extra oxygen on C-1 would only promote an upfield shift for C-2 of $\sim 1.7 \pm 0.7$ p.p.m. (13*c*) the signal of the latter will always occur at lower field than C-3, even for the glycosides. When **9** (R = H) is compared with 1,4-anhydro-D-threitol (**4**), there is little change at C-3 and C-4. Since C-4 (and C-1) is more shielded than C-3 (and C-2) in compound **4**, the same order should be expected for **9** (R = H). Hence the shielding order for tetroside **9**: C-1 ≪ C-2 < C-3 < C-4 < OMe. A partial spectrum of methyl α-D-threoside is represented by Fig. 1, in comparison with the remaining tetrosides and compound **4**.

The β-anomer **10** (R = H) has a *cis* 1,2-interaction, so that C-1 and C-2 become more shielded (5.6 and 3.1 p.p.m., respectively) than in **9** (R = H). As the 1,3-interaction differences are assumed to be small, the chemical shifts of the other nuclei should not be materially changed. Experimentally, this trend is observed but the numerical differences for C-3 and C-4

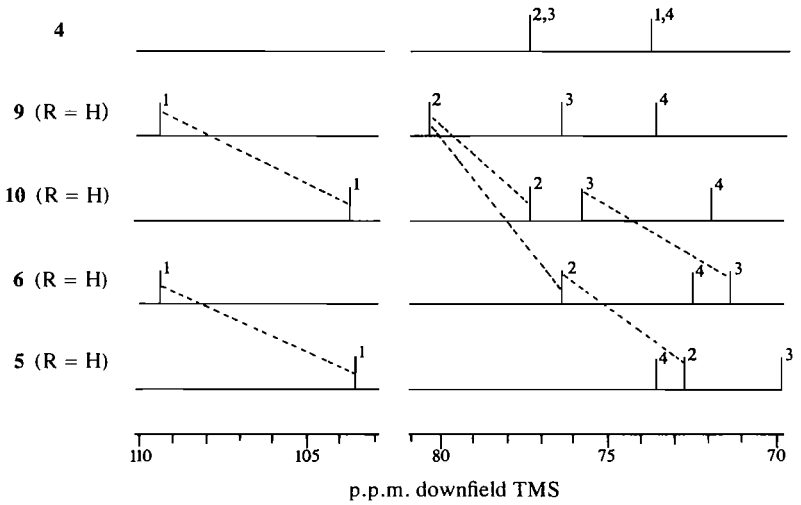

FIG. 1. Correlation of the ^{13}C chemical shifts of the ring carbons in the methyl tetrofuranosides and 1,4-anhydro-D-threitol.

are much larger than found for the cyclopentane triols, possibly due to the presence of the ring oxygen.

When comparing **6** (R = H) with **9** (R = H), the *cis* 2,3-interaction generates comparable shieldings for both C-2 and C-3. Now signal C-3 appears at higher field than C-4 in **6** (R = H) and the chemical shift for C-2 is similar to that in compound **10** (R = H). On proceeding to **5** (R = H), a compound containing all groups on the same side of the ring, C-2, flanked by two *cis* groups (OH, OMe), shifts to higher field than C-4. (The assignments of the C-4 signals were confirmed by reference to the proton-coupled spectra.) Carbon-3 in compound **5** (R = H) appears to be abnormally strongly shielded, for its position should be essentially that found in **6** (R = H), based on the cyclopentanol data. In this series, C-4 of the β-anomer is more shielded than that of the α-anomer; however, wide variations in the chemical shifts for C-4 of the higher homologs do not make this a general rule. Finally, the chemical shift of C-1 is *not* an indicator of anomeric character, as it generally is in the pyranoside series, but is a relative quantity, dependent upon the orientation of the group at C-2 (see also ref. 16).

Methyl Aldopento- and Hexofuranosides

Replacement of an α-H with a primary carbinol group, causes strong deshielding:

$\overset{*}{C}H_3OH \rightarrow HOCH_2\overset{*}{C}H_2OH$	12.6 p.p.m.
$CH_3\overset{*}{C}H_2OH \rightarrow CH_3\overset{*}{C}HOHCH_2OH$	11.6 p.p.m.
$\overset{*}{C}H_4 \rightarrow \overset{*}{C}H_3CH_2OH$	20.0 p.p.m. (13*d*)
$CH_3\overset{*}{C}H_3 \rightarrow CH_3\overset{*}{C}H_2CH_2OH$	20.2 p.p.m. (13*d*)

Hence, replacement of a 4-hydrogen in tetroside **9** by CH_2OH causes such a large downfield shift for the C-4 signal of the pentosides, that it resonates at lower field than any of the other secondary (and primary) ^{13}C nuclei. Thus, the shielding order for the alternating *trans* compound, pentoside **9**, is C-1 ≪ C-4 < C-2 < C-3 < C-5 < OMe.

Chain extension to the hexosides (R = $CHOHCH_2OH$) does little to change the chemical shifts of the ring carbons but C-5 becomes deshielded. Since C-2, in open-chain compound **1** (Table 3), is more shielded than that in the all *trans*-cyclopentane 1,3/2,4-tetrol (Table 2), it is to be expected that C-5 of a hexoside, which is a part of a side chain, will be more shielded than C-3. Thus, the shielding order for methyl β-D-galactofuranoside (**9**) must be C-1 ≪ C-4 < C-2 < C-3 < C-5 < C-6 < OMe.

When one correlates the chemical shifts of pentosides and hexosides, as for the tetrosides (Fig. 1), using the adjacent *trans–cis* conversions, one arrives at the assignments given in Table 4.

Can. J. Chem. Downloaded from www.nrcresearchpress.com by 210.87.254.42 on 09/05/12
For personal use only.

TABLE 4. Carbon-13 chemical shifts of methyl glycofuranosides[a]

	Glycoside	C-1	C-2	C-3	C-4	C-5	C-6	OMe	Σ/*n*
5	α-D-*erythro*	103.6	72.8	69.9	73.6	—	—	56.7	75.3
	α-D-*ribo*	103.1	71.1	69.8	84.6	61.9	—	55.5	74.3
	α-D-*allo*	103.8	72.3	69.9	85.9	72.7	63.5	56.6	75.0
6	β-D-*erythro*	109.6	76.4	71.4	72.6	—	—	56.6	77.3
	β-D-*ribo*	108.0	74.3	70.9	83.0	62.9	—	55.3	75.7
	β-D-*allo*	109.0	75.6	72.7	83.4	73.8	63.9	56.4	76.4
7	α-D-*lyxo*	109.2	77.0	72.2	81.4	61.5	—	56.9	76.9
	α-D-*manno*	109.7	77.9	72.5	80.5	70.6	64.5	57.2	76.1
8	β-D-*lyxo*	103.3	73.2	71.0	82.1	62.7	—	56.7	74.8
	β-D-*manno*	103.6	73.1	71.2[b]	80.7	71.0[b]	64.4	56.8	74.4
9	α-L-*threo*	109.4	80.5	76.4	73.7	—	—	55.5	79.1
	α-L-*arabino*	109.2	81.8	77.5	84.9	62.4	—	56.0	78.6
	β-D-*galacto*	109.9	81.3	78.4	84.7	71.7	63.6	55.6	77.9
10	β-L-*threo*	103.8	77.4	75.8	72.0	—	—	56.2	77.0
	β-L-*arabino*	103.1	77.4	75.7	82.9	62.4	—	56.3	76.3
	α-D-*galacto*	103.8	78.2	76.2	83.1	74.5	64.1	57.2	76.7
11	α-D-*xylo*	103.0	77.8	76.2	79.3	61.6	—	56.7	75.8
	α-D-*gluco*	104.0	77.7	76.6	78.8	70.7	64.2	57.0	75.6
12	β-D-*xylo*	109.7	81.0	76.0	83.6	62.2	—	56.4	78.2
	β-D-*gluco*	110.0	80.6	75.8	82.3	70.7	64.7	56.3	77.2

[a]Data for the *arabino* and/or *ribo* pentofuranosides are also given in refs. 16 and 17. Assignments for C-2 and C-3 of the β-*arabino* compound shown above are the reverse of those cited in ref. 16.
[b]Assignments may be interchanged.

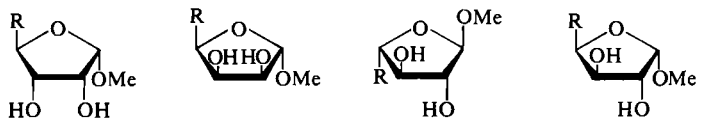

5 7 9 11

R = H (tetroside); CH_2OH (pentoside); CHOH—CH_2OH (hexoside)

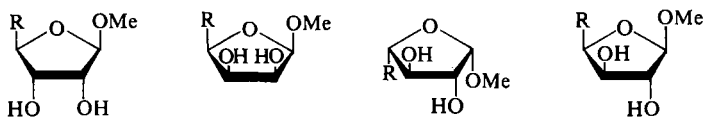

6 8 10 12

In helping to unequivocally define those assignments of signals which are close together, the anomers of methyl D-*gluco*- and D-*allo*-hexofuranoside-3*d* and -4*d* were prepared. The spectra of the deuterated compounds were essentially the same as those of the nondeuterated species, save for the facts that: the signal for the deuterated carbon was usually not observed above the background noise and nuclei β to the deuterium were barely perceptively more shielded (~0.05 p.p.m.) than those of the nondeuterated compounds. This approach has already been utilized for pyranosides (2, 6, 18).

Assignments were also greatly facilitated by analyses of the proton coupled ^{13}C spectra (see Experimental).

Analysis of Shielding Factors in Furanosides

Variations in shielding associated with configurational changes were evaluated for all combinations of the different *cis–trans* arrangements of ring substituents (OH, OCH_3, R).

Can. J. Chem. Downloaded from www.nrcresearchpress.com by 210.87.254.42 on 09/05/12
For personal use only.

TABLE 5. Calculated ^{13}C shielding terms (X) associated with *cis vs. trans* configurations of substituents in five-membered rings (p.p.m.)

Compounds	X (*cis–trans*)					
	1,2	1,3	1,4	2,3	2,4	3,4
Cyclopentane tetrols						
C-1	−4.6	−0.3	0.2	1.8	0.5	0.2
C-2	−5.3	0.5	−0.3	−3.3	0.2	0.1
1,4-Anhydropentitols						
C-2	—	—	—	−5.8	0.2	0
C-3	—	—	—	−6.2	0.3	−1.5
C-4	—	—	—	−2.0	1.9	−2.9
C-5	—	—	—	0.1	0.3	−1.4
Methyl tetrofuranosides						
C-1	−5.8	−0.2	—	0	—	—
C-2	−3.4	−0.2	—	−4.4	—	—
C-3	−1.1	−0.4	—	−5.5	—	—
C-4	−0.3	1.4	—	0.2	—	—
Methyl pentofuranosides						
C-1	−5.8	0.6	−0.2	−0.3	0.2	0.4
C-2	−4.0	−0.2	−0.1	−5.4	1.1	0.9
C-3	−1.0	−0.2	−0.5	−5.4	0.9	0.4
C-4	−0.9	2.3	0.2	0.2	0.1	−2.4
C-5	−0.2	0.1	0.8	0	0.2	−0.3
Methyl hexofuranosides						
C-1	−5.8	0.2	−0.3	−0.4	0	0.2
C-2	−3.5	−0.5	−0.5	−4.7	1.0	0.4
C-3	−1.5	−0.9	−0.2	−5.3	1.0	−0.1
C-4	−0.5	2.1	−0.2	0.6	−0.5	−3.9
C-5	0.6	−0.8	1.0	0.2	−0.1	−2.5

For this purpose it was assumed (*a*) that the chemical shift of a given ^{13}C nucleus is affected by the sum of all 1,2-, and 1,3-*trans* and -*cis* arrangements,[5] and (*b*) that the shielding influence on a carbon in a given *cis* or *trans* arrangement is a constant for the same configuration in all of the isomeric compounds. Using the chemical shift data of Table 4, shielding contributions associated with individual arrays of substituent pairs were then calculated (see Experimental), and are listed in Table 5. This table also includes data for the cyclopentane tetrols and, in addition, values calculated from ^{13}C chemical shifts reported (15) for 1,4-anhydropentitols. The following comments summarize these findings, and other information contained in Table 4, for each of the ^{13}C nuclei:

(*a*) Only the *cis*-1,2 arrangement introduces an important contribution for C-1, because the latter is uniformly about 6 p.p.m. more shielded in the *cis*, than in the *trans*, anomer.

(*b*) For C-2 both the *cis*-1,2 and -2,3 configurations are consistently associated with greater shielding than their *trans* counterparts, the *cis*-1,2 being characterized by less of an impact (by about 1.5 p.p.m.) than the *cis*-2,3.

(*c*) Stronger shielding of C-3 is also ascribable to the *cis*-2,3 as compared with the *trans*-2,3 configuration. In marked contrast, however, a *cis* arrangement of O-3 and C-5 differs relatively little from the *trans* in its apparent effect on the chemical shift of C-3. This is analogous to earlier observations (8) on *cis* and *trans* arrangements of O-3 and C-1 in ketofuranoses.

(*d*) In almost all *cis* and *trans* combinations of O-3 and C-5 a shielding influence on C-4 is attributable to the *cis* configuration of these nuclei, although the increase in shielding is more marked in the hexoside than in the pentoside or 1,4-anhydropentitol series. This

[5]That is, in a transformation such as α-anomer → β-anomer, C-1 is expected to be affected not only by the configurational change of O-1 with respect to O-2 but also by the accompanying changes in the disposition of O-1 relative to O-3 and O-5.

Can. J. Chem. Downloaded from www.nrcresearchpress.com by 210.87.254.42 on 09/05/12
For personal use only.

Can. J. Chem. Downloaded from www.nrcresearchpress.com by 210.87.254.42 on 09/05/12
For personal use only.

suggests that the greater steric perturbation expected from C-5 in the structure —C(5)-HOH—C(6)H_2OH as compared with —C(5)-H_2OH, is a possible source of the stronger shielding observed.

(*e*) Whereas C-5 of the pentosides exhibits little change in shielding due to a *cis*, as compared to a *trans*-O-3,C-5 arrangement, an increase (by ~2.5 p.p.m.) in the shielding of C-5 of the corresponding hexoside is evident. As just noted with respect to C-4, this difference also might be attributable to the expected increase in steric crowding around C-5 of the hexoside. Nevertheless, an effect similar to those on C-4 and C-5 associated with this extension of the carbon chain is not noticeably transmitted to C-3 as well.

(*f*) In general, *cis* substituents bearing a 1,3-relationship differ little from the *trans* isomers in their effect on shielding. However, a unique type of influence is indicated by the fact that C-4 of pento- or hexofuranosides is *deshielded* (by 2 p.p.m.) when there is a *cis*, in contrast to a *trans*, arrangement of O-1 and O-3. This means, for example, that in comparing each of the α,β anomeric pairs having the *gluco*, *manno*, and *allo* configurations the C-4 shielding differences for these pairs are observed to be −3.5, ~0, and +2.5 p.p.m., respectively, although no such variation should be expected if the vicinal O-3,C-5 configuration inversion is the sole factor.

(*g*) The anomeric *O*-methyl carbons and C-6 are affected to only a small degree by these diverse changes in configuration (Table 4). Perhaps consistent with such characteristics, is the likelihood that rotational isomerism about the C-1,O-1 or C-4,C-5 bond will tend to favor a disposition for OCH_3 or C-6 that is furthest removed from other nuclei of the molecule. Although, seemingly by contrast, axial anomeric OCH_3 substituents in the pyranoside series are more shielded than equatorial ones (4), this difference is not related to the relative arrangement of OCH_3 and O-2, because the same axial:equatorial difference is found for the *manno* (OCH_3 and O-2 *anti*) as for the *gluco* (*gauche*) configuration.

Conformational Influences

Although a wide array of shielding effects on the different ^{13}C nuclei is evident among the foregoing data, chemical shifts calculated by reference to Table 5 generally agree with the observed values to better than ±0.6 p.p.m. Hence the shielding associated with a given modification appears to be a consistent, characteristic quantity.[6] As noted at the outset, such a steric change is expected to include a conformational component, information about which is a prime objective of these studies.

Some measure of how conformational changes influence shielding may be gained from the estimates made earlier (8) of diamagnetic contributions to the chemical shifts. Thus, various possible forms of β-ribofuranose have been considered relative to β-ribopyranose, in the light of the fact that most ^{13}C nuclei of the latter are more shielded than those of the furanose.[7] It is found that if C-3, for example, is above the plane of the ring (envelope form E^3 (9)) less shielding of most ^{13}C nuclei of the furanose than of the pyranose molecule is indeed to be anticipated, whereas if C-3 were down (E_3), only relatively small chemical shift differences between these isomers might be expected. It may be noted also that such estimates (8) of diamagnetic contributions suggest that a *cis–trans* configurational change at C-3 and C-4, *e.g.*, β-ribofuranose to β-xylofuranose, *need not* be accompanied by a large change in shielding at C-3. This possibility is of particular interest in the light of the experimental finding (Table 5) that the shielding effect on C-3 in such circumstances is very small.

The current data, by themselves, do not provide an obvious basis for defining conformation. However, when viewed together with ^1H–^1H and ^{13}C–^1H coupling constants, these chemical shift values and shielding analyses should help to substantially reduce the number of pseudorotational forms that need be considered for a given molecule.

^{13}C Shielding and Steric Interactions

Steric compression appears in many in-

[6]The four aldopentose configurations are represented here, and four of the eight in the aldohexose series. Since the chemical shifts of configurationally related pentosides and hexosides are closely similar (aside from the increased shielding of C-4 and C-5 of the hexosides) (Table 5), it is likely that analogous results will be found for furanosides of the other aldohexoses: *i.e.*, close similarities between the *xylo* and *ido*, *arabino* and *altro*, etc., isomers.

[7]This shielding difference is general for configurationally-related five- and six-membered ring isomers (8, 19).

Can. J. Chem. Downloaded from www.nrcresearchpress.com by 210.87.254.42 on 09/05/12
For personal use only.

stances to be associated with an increase in the shielding of ^{13}C nuclei (10, 13, 14). Thus, a comparison of chemical shift differences between diastereoisomeric cyclohexane derivatives (10, 20, 21) and pyranoses (4, 5) shows that as free energy increases within the series so also, in a relatively consistent fashion, does ^{13}C shielding. A similar trend is found among the current data (Table 4); average chemical shift values (as a measure of the state of overall ^{13}C shielding within each of the molecules (4, 21)) form the following sequences.

tetrosides: **9 < 6 < 10 < 5**

pentosides: **9 < 12 < 7 < 10 < 11 ≈ 6 < 8 ≈ 5**

hexosides: **9 < 12 < 10 < 6 < 7 < 11 < 5 < 8**

That is, those furanosides that have an all-*trans* arrangement of substituents (**9**) and are expected to be most stable (22–24), also possess on the average the least shielded ^{13}C nuclei. Similarly, the introduction of *cis* substituents is accompanied by upfield shifts, and a high incidence of *cis* substituents (**5** or **8**) is associated with the most strongly shielded ^{13}C nuclei.

Hence, as with six-membered ring compounds, it appears reasonable to regard the configurational influences on ^{13}C chemical shifts described here as a reflection of destabilizing steric interactions.

Experimental

^{13}C Nuclear Magnetic Resonance Spectra

^{13}C magnetic resonance spectra of the glycosides were measured at a frequency of 22.63 MHz with a Bruker, WH-90 FT spectrometer, employing a ^{2}H-lock. Deuterium oxide was used as solvent and the signal of tetramethylsilane (in a coaxial tube) served as an external standard. ^{13}C spectra of the cyclopentanols, in water, were recorded with a Varian HA-100 CW spectrometer operating at 25.15 MHz, using the signal of ^{13}C-enriched methyl iodide in a coaxial capillary for the homonuclear field-frequency lock.

Support for some of the signal assignments in the glycofuranoside series was obtained by reference to ^{1}H-coupled spectra of these compounds. Thus, since C-2 can couple with fewer protons (across two and three bonds) than C-3 or C-4 it was expected to account for the least complex signal of the three in a coupled spectrum, and C-4 to give the most complex signal because it can interact with the largest number of protons. A distinction between the C-5 signal of a hexofuranoside and the C-2 or C-3 signal was provided by the finding (assumed to apply generally) that direct coupling ($^{1}J_{C,H}$) for the latter two nuclei is about 10 Hz larger than that for exocyclic C-5. In a number of instances, the conclusions reached on the basis of the comparisons cited above were cross-checked by reference to the coupled spectra of the specifically deuterated compounds, since this verified sources of the two- and three-bond ^{1}H couplings. Signals produced by primary carbons (C-5 of pentosides, C-6 of hexosides) were readily assigned from their triplet appearance (due to directly bonded ^{1}H-coupling).

Numerical Analysis of ^{13}C Chemical Shifts

A comparison of chemical shifts was made between a compound selected as a reference within a given series and each isomer (m) of the series. The observed difference (D_m^k) in the chemical shift of carbon k in the isomer (m = 1, 2, etc.) relative to that of the reference was expressed as the algebraic sum of the individual shielding terms (X_n^k), one for each arrangement of a substituent pair. Then, for carbon k:

$$D_m^{\,k} = \sum_{1}^{n} X_n^{\,k}\, C_{mn}$$

where C = 1 for a *trans* → *cis* interconversion, −1 for *cis* → *trans*, or 0 for no change in configuration.

As an example, the comparison of C-1 of methyl β-alloside (6) with that of the (arbitrary) reference compound, methyl α-alloside (**5**), involves conversion of a *trans* anomer (**6**) into a *cis* (**5**). Hence

$$D_m^{\,1} = 103.8(\delta_{C\text{-}1} \text{ of } \mathbf{5}) - 109.0(\delta_{C\text{-}1} \text{ of } \mathbf{6}) = -5.2$$

Therefore,

$$-5.2 = X_1(1) + X_2(1) + X_3(-1) + X_4(0) + X_5(0) + X_6(0)$$

where X_1, X_2, etc. describe shielding contributions from the six *cis–trans* arrangements of the ring substituents, (1,2) (1,3) (1,4) (2,3) (2,4) (3,4), respectively. Hence, for each carbon (k) of the pento- and hexofuranosides there are six unknowns (X_n^k) and eight compounds (Table 4) for comparison. From the resulting set of seven simultaneous equations, a least-squares fit for the solutions to the six unknowns was determined. Calculations performed with an IBM-360 computer using the double precision IMSL subroutine LLSQAR gave the results recorded in Table 5.

The maximum deviation obtained in recalculating the shift differences from these numbers was ±0.6 p.p.m.

Preparation of Glycosides

Methyl glycofuranosides were prepared by the Fischer reaction (25), *i.e.*, by reaction of the sugars with methanol in the presence of an acid catalyst. The conditions used were varied according to the individual sugar and, in general, correspond to experimental procedures described by various earlier workers, and summarized by Green (26). Mixtures of glycosides were fractionated by conventional preparative chromatographic methods. The ^{13}C n.m.r. spectra described here, as well as the p.m.r. spectra, furnished additional checks on the purity and identity of the various glycosides.

1,2:5,6-Di-O-isopropylidene-α-D-allofuranose-4-d

1,2:5,6-Di-*O*-isopropylidene-α-D-*ribo*-hexofuranos-3-ulose (27) (2.5 g) in D_2O (10 ml) and pyridine (50 ml) was heated for 5 min at 95° and then kept at ambient

temperature for 18 h. The solvents were removed *in vacuo* and the deuterium exchange procedure repeated three times.[8] This was followed by reduction with aqueous borohydride. A solution of the final product in hot petroleum ether (65–110°) was clarified with charcoal and, upon cooling, deposited crystals of the title compound; m.p. 70–73°; deuterium content estimated by n.m.r. spectroscopy, > 95%.

1,2:5,6-Di-O-isopropylidene-α-D-glucofuranose-4-d

Prepared from 1,2:5,6-di-*O*-isopropylidene-α-D-allofuranose-4-*d* (above) by inversion at C-3, as described for preparation of the 3-deuterio analog (5).

D-*Glucose-4-d and* D-*Allose-4-d*

Prepared by hydrolysis of the two foregoing di-*O*-isopropylidene derivatives, respectively, in aqueous solution in the presence of Amberlite 1R-120 (H^+) resin.

The authors gratefully acknowledge the generous support provided by the National Research Council of Canada and the Pulp and Paper Research Institute of Canada. They also express their thanks to J. Marion and R. Simoneau for valuable assistance.

1. A. S. PERLIN and B. CASU. Tetrahedron Lett. 2931 (1969).
2. L. D. HALL and L. F. JOHNSON. Chem. Commun. 509 (1969).
3. D. E. DORMAN and J. D. ROBERTS. J. Am. Chem. Soc. **92**, 1355 (1970).
4. A. S. PERLIN, B. CASU, and H. J. KOCH. Can. J. Chem. **48**, 2596 (1970).
5. H. J. KOCH and A. S. PERLIN. Carbohydr. Res. **15**, 403 (1970).
6. N. CYR, A. S. PERLIN, and M. A. WHITEHEAD. Can. J. Chem. **50**, 814 (1972).
7. R. J. ABRAHAM, L. D. HALL, L. HOUGH, and K. A. MCLAUCHLAN. Chem. Ind. (London) 213 (1962); J. Chem. Soc. 3699 (1962).
8. A. S. PERLIN, N. CYR, H. J. KOCH, and B. KORSCH. Ann. N.Y. Acad. Sci. **222**, 935 (1973).
9. J. F. STODDART. Stereochemistry of carbohydrates. Wiley-Interscience, New York. 1971. p. 97.
10. D. K. DALLING and D. M. GRANT. J. Am. Chem. Soc. **89**, 6612 (1967); **94**, 5318 (1972).
11. J. D. ROBERTS, F. J. WEIGERT, J. J. KROSCHWITZ, and H. J. REICH. J. Am. Chem. Soc. **92**, 1338 (1970).
12. M. CHRISTL, H. J. REICH, and J. D. ROBERTS. J. Am. Chem. Soc. **93**, 3463 (1971).
13. J. B. STOTHERS. Carbon-13 NMR spectroscopy in organic chemistry. Vol. 24. Academic Press, New York. 1972. (*a*) pp. 139–140; (*b*) p. 139; (*c*) p. 143; (*d*) pp. 56 and 140.
14. G. C. LEVY and G. L. NELSON. Carbon-13 nuclear magnetic resonance for organic chemists. Wiley-Interscience, New York. 1972.
15. L. QUE, JR. and G. R. GRAY. Biochem. **13**, 146 (1974).
16. T. USUI, S. TSUSHIMA, N. YAMAOKA, K. MATSUDA, K. TUZIMURA, H. SUGIYAMA, S. SETO, K. FUJILDA, and G. MIYAJIMA. Agr. Biol. Chem. (Japan), **38**, 1409 (1974).
17. E. BREITMAIER, G. JUNG, and W. VOELTER. Chimia, **26**, 136 (1972).
18. P. A. J. GORIN. Can. J. Chem. **52**, 458 (1974).
19. A. S. PERLIN, P. HERVE DU PENHOAT, and H. S. ISBELL. Adv. Chem. **117**, 39 (1973).
20. G. W. BUCHANAN, D. A. ROSS, and J. B. STOTHERS. J. Am. Chem. Soc. **88**, 4301 (1966).
21. A. S. PERLIN and H. J. KOCH. Can. J. Chem. **48**, 2639 (1970).
22. C. T. BISHOP and F. P. COOPER. Can. J. Chem. **41**, 2743 (1963).
23. R. U. LEMIEUX. *In* Molecular rearrangements. Pt. II. *Edited by* P. de Mayo. Interscience. 1964. p. 716.
24. S. J. ANGYAL. Angew. Chem. **8**, 157 (1969).
25. E. FISCHER. Ber. **26**, 2400 (1893).
26. J. W. GREEN. Advan. Carbohydr. Chem. **21**, 95 (1966).
27. W. SOWA and G. H. S. THOMAS. Can. J. Chem. **44**, 836 (1966).
28. K. N. SLESSOR and A. S. TRACEY. Can. J. Chem. **47**, 3984 (1969).
29. G. M. CREE and A. S. PERLIN. Can. J. Biochem. **46**, 765 (1968).

[8]No significant exchange is effected by treatment of this ketone for a short period (28), whereas in the preparation of the analogous D-psicose derivative the intermediate ketone undergoes rapid exchange (29).

Can. J. Chem. Downloaded from www.nrcresearchpress.com by 210.87.254.42 on 09/05/12
For personal use only.

2-Deacetylchelocardin: A Degradation Product of Chelocardin

DANIEL T. W. CHU, D. L. GARMAISE, AND E. BERNSTEIN

Department of Research, Abbott Laboratories, Limited, P.O. Box 6150, Montreal, Quebec H3C 3K6

Received August 2, 1974

DANIEL T. W. CHU, D. L. GARMAISE, and E. BERNSTEIN. Can. J. Chem. **53**, 1434 (1975).

A novel chemical transformation is described in which chelocardin **1**, under normal ketalization conditions, is converted with elimination of the 2-acetyl group, to the bisdioxolane **2**. Hydrolysis of **2** yields 2-deacetylchelocardin **4**. The properties of the tricarbonylmethane system in **1** and of the 1,3-cyclohexanedione system in **4** are found to be profoundly modified by the presence of the 4-amino and the 12*a*-hydroxyl group.

DANIEL T. W. CHU, D. L. GARMAISE et E. BERNSTEIN. Can. J. Chem. **53**, 1434 (1975).

On décrit une nouvelle transformation chimique au cours de laquelle la chélocardine **1**, sous les conditions normales d'acétalisation, est transformée, par une élimination du groupe acétyle en position 2, en bisdioxolanne **2**. L'hydrolyse de **2** conduit au déacétyl-2 chélocardine **4**. On trouve que les propriétés du système tricarbonylméthane de **1** et du système cyclohexanedione-1,3 de **4** sont affectés d'une façon profonde par la présence d'un groupe amino en position 4 et d'un groupe hydroxyle en position 12*a*. [Traduit par le journal]

Chelocardin, a potent broad spectrum antibiotic produced by *Nocardia sulphurea* (NRRL-2822), was isolated in 1956 and was first described in 1962 (1, 2). Its structure was established by Mitscher *et al.* as **1** (3).

The 2-acetyl-1,3-cyclohexanedione system in ring A suggests a parallel with the tricarbonylmethane antibacterial agents. The purpose of this work was to investigate the chemical behavior of this triketone system and to compare it with the properties of model compounds.

It has been reported that the acetyl group of 2-acetyldimedone is readily split by refluxing dilute sulfuric acid (4). Chelocardin would not withstand such conditions but it was found that a compound later shown to be 2-deacetylchelocardin (**4**) was formed, unreproducibly and in very low yield, when chelocardin was heated with hydrochloric acid in glacial acetic acid.[1] However, a novel transformation of chelocardin (**1**) into 2-deacetylchelocardin (**4**) has been developed as illustrated in Scheme 1.

Ketalization of chelocardin hydrochloride in benzene in the presence of a large excess of ethylene glycol and *p*-toluenesulfonic acid gave an 80% yield of the 1,3-bisdioxolane derivative **2** in which the 2-acetyl group has been eliminated. Its n.m.r. spectrum possesses only two singlets corresponding to the C-6 and C-9 methyl groups. The absence of another singlet signal in the region of δ 0.7–2 (corresponding to the methyl group of the ketalized 2-acetyl group) and the disappearance of the acetyl singlet (δ 2.56 in the parent compound) indicates the loss of the 2-acetyl side chain. This is further substantiated by the disappearance of the band at 1690 cm^{-1} (which represents one of the carbonyl groups in the tricarbonylmethane system) in its i.r. spectrum. All the other n.m.r. signals are consistent with the assigned structure.

Further confirmation of the structure was obtained by converting it to a carbobenzoxy derivative **3**. The i.r. spectrum of **3** showed carbamate absorption at 1720 cm^{-1}. Its n.m.r. spectrum showed the characteristic methylene protons as doublets at δ 1.87 and 2.50, with $J = -15$ Hz, and two sharp singlets for the 6- and 9-methyl groups at δ 2.33 and 2.36, respectively. All the other signals were consistent with the assigned structure.

Hydrolysis of **2** in hydrochloric acid – acetone solution gave 2-deacetylchelocardin (**4**) in 72% yield. Its n.m.r. spectrum showed two singlets at δ 2.15 and 2.35 (6- and 9-methyl groups) and a doublet at δ 5.6 for the H_4 proton indicating that there was no epimerization of the C_4 hydrogen.

This novel chemical transformation (**1** → **4**) can also be achieved by using other diols. For example, treatment of the chelocardin with 1,2-propanediol, under the same reaction conditions, gave the bisdioxolane derivative **5** which was then transformed to the corresponding carbobenzoxy derivative **6** upon treatment with

[1]Dr. W. Rosenbrook, Abbott Laboratories, North Chicago, Ill. Private communication.

Can. J. Chem. Downloaded from www.nrcresearchpress.com by 210.87.254.105 on 09/05/12
For personal use only.

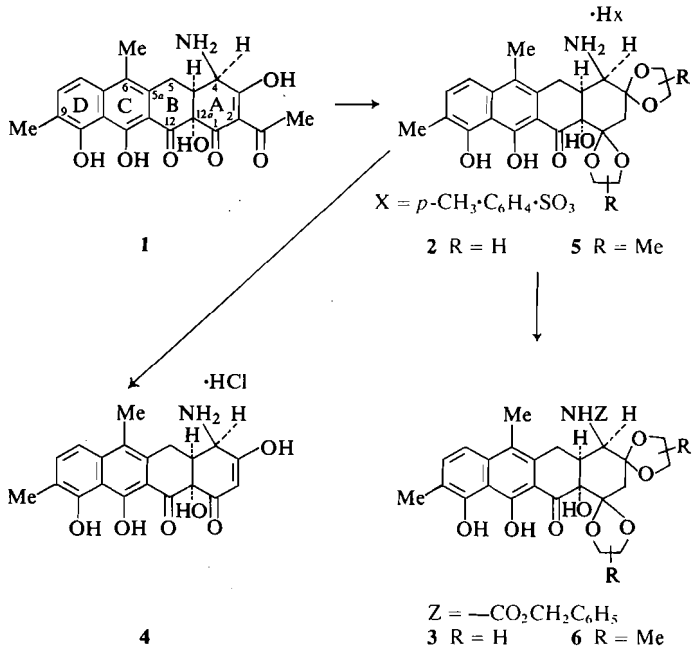

SCHEME 1

carbobenzoxy chloride. Hydrolysis of **5** gave again 2-deacetylchelocardin (**4**).

The elimination of the acetyl group could not be achieved by using ethanol in place of a 1,2-diol or by simple reflux with *p*-TSA in benzene. Additionally, *N*-carbobenzoxychelocardin (**7***a*) and *N*-acetylchelocardin (**7***b*) were recovered unchanged on treatment with ethylene glycol under the same ketalizing conditions.

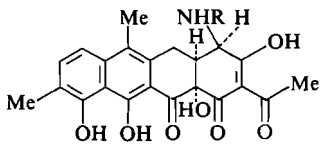

7
a R = —$CO_2CH_2C_6H_5$
b R = —Ac

It appears then that the unaltered 4-amino group and the presence of a 1,2-diol are required for the reaction to proceed. The importance of the 4-amino group was substantiated further by the observation that 2-acetyldimedone was recovered unchanged when treated with ethylene glycol and *p*-TSA in refluxing benzene.

Unfortunately, other simple triacetyl compounds with a 4-amino group, either with or without the 12*a* hydroxyl group, are not readily available and hence it is not possible to determine whether the presence of the 12*a* hydroxyl is necessary for this transformation. In the absence of further experimental evidence, it is difficult to be definite about the mechanism of this cleavage reaction. At the present moment, we favor the reaction course illustrated in Scheme 2.

The primary approach by the diol is to the exocyclic carbonyl group in the tautomeric form **1***a*. The C-3 carbonyl group serves as the electron sink, owing to the slightly positive charge created by the hydrogen bonding with the 4-amino group. There is other experimental evidence showing that the exocyclic carbonyl group is the most reactive center of the three carbonyl groups and this will be reported later. The initial Michael reaction yields the hemiacetal **8**, which cyclizes by attacking either the C-1 or C-3 to give **9** or **10**. These intermediates are stabilized by elimination of the 2-acetyl group to form **11** or **12** by a retrograde aldol reaction after protonation of C_1 or C_3 carbonyl group. Compound **11** (or **12**) upon the elimination of a molecule of acetic acid gives the intermediate **11***a* (or **12***a*) which is subsequently converted into the bisdioxolane **2**. It has been reported that 1,3-cyclohexanedione and 2-bromo-5,5-dimethylcyclohexanedione-1,3 under the same

Can. J. Chem. Downloaded from www.nrcresearchpress.com by 210.87.254.105 on 09/05/12
For personal use only.

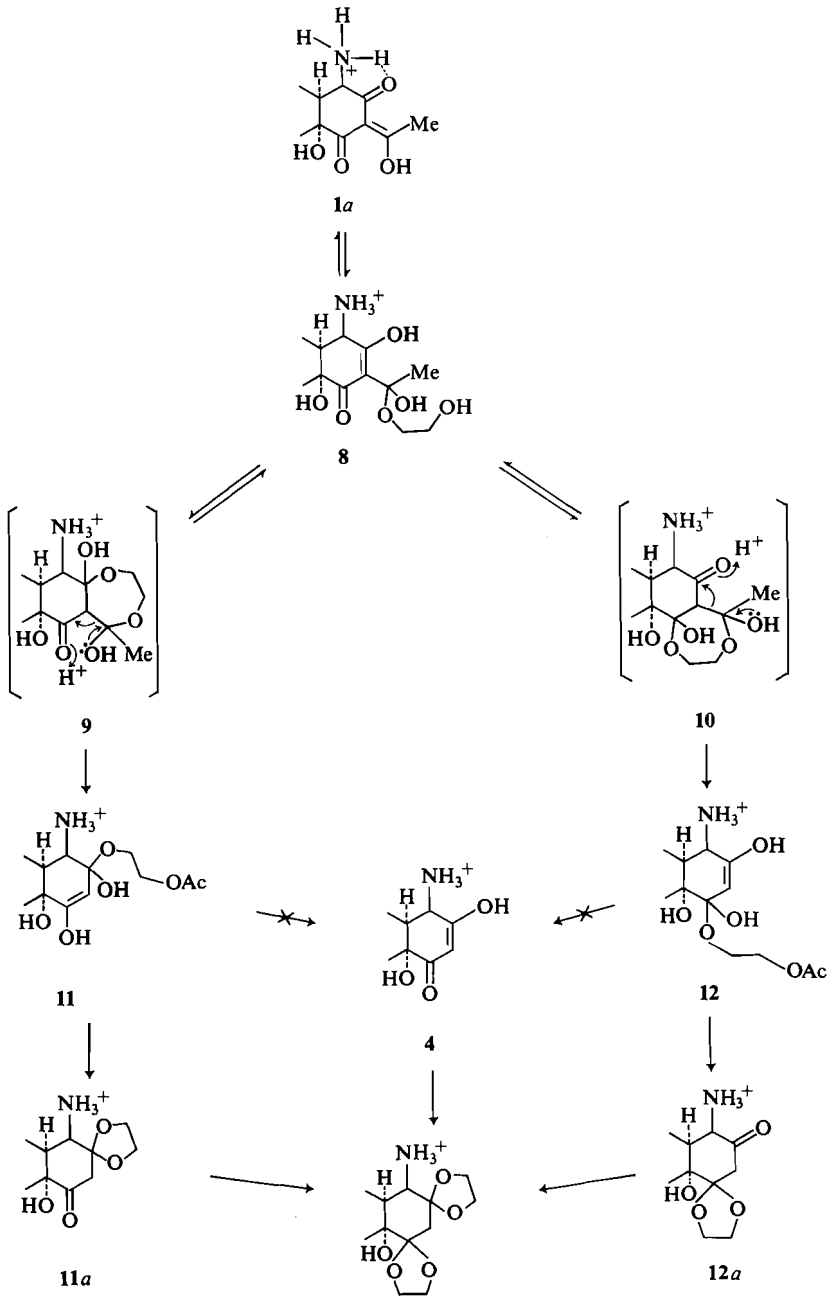

SCHEME 2

ketalization conditions gave the corresponding bisdioxolane (5, 6). We have found that **4** obtained by hydrolysis of the bisdioxolane **2** gives **2** in good yield when treated with ethylene glycol and *p*-TSA. It would be tempting to propose an alternative scheme (**11** → **4** → **2**) involving compound **4** as an intermediate which then would be converted to **2**. But during the course of the reaction, no such intermediate **4** was observed by t.l.c. Since the transformation of **4** into **2**

Can. J. Chem. Downloaded from www.nrcresearchpress.com by 210.87.254.105 on 09/05/12
For personal use only.

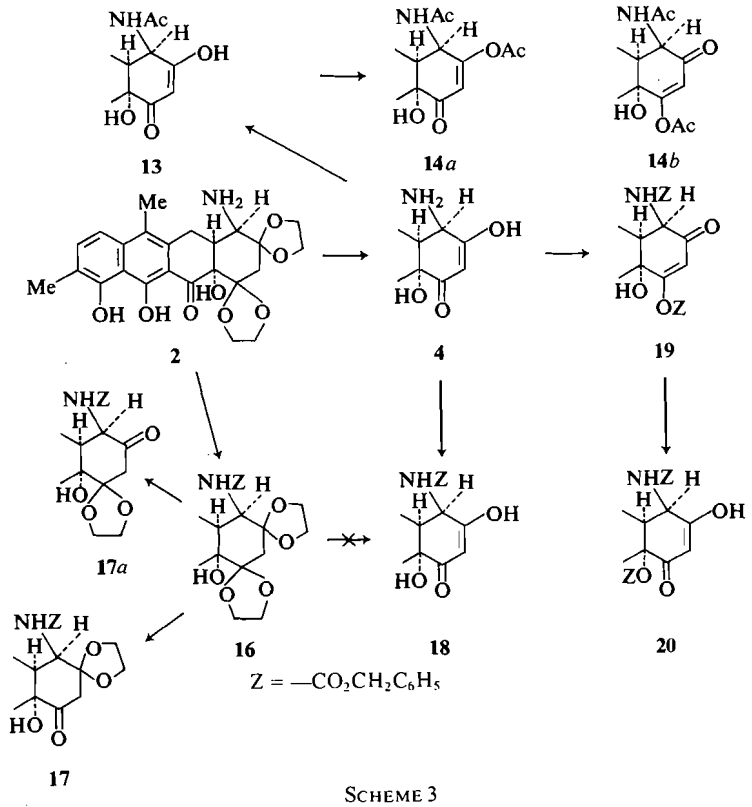

SCHEME 3

under similar conditions required more than 10 h to complete, it is unlikely that the elimination ketalization involves **4** as an intermediate.

Reactions of Deacetylchelocardin

The acylation and alkylation of deacetylchelocardin did not follow the course which might have been expected from model compounds. The unusual behavior of ring A of 2-deacetylchelocardin (**4**) is illustrated in Scheme 3.

Cautious treatment of **4** with acetic anhydride gave the *N*-monoacetyl derivative **13** which was converted on further acetylation to a mixture of *N,O*-diacetyl derivatives **14***a* (or **14***b*) and an *N,O,O*-triacetyl derivative. The diacetyl and triacetyl derivatives were readily hydrolyzed back to the *N*-monoacetyl compound **13**, indicating that there was no trace of *C*-acylation at the 2-position. The addition of sodium acetate to the reaction mixture did not affect this result and none of the *O*-acetyl groups could be rearranged to the 2-position. In contrast, cyclohexane-1,3-dione and dimedone have been converted to the 2-acetyl derivatives by heating with acetic anhydride in the presence of sodium acetate (4, 7). Cyclohexane-1,3-diones yield 2-alkyl derivatives exclusively when treated with α-haloketones (8) but when *N*-benzoyldeacetylchelocardin (**15**) was treated with chloroacetone in refluxing tetrahydrofuran or in refluxing aqueous methanol, the starting material was recovered unchanged.

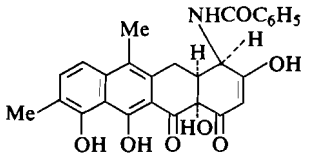

15

Although the C-2 alkylation of acyclic 1,3-diones is readily effected via the thallium salt (9) and can also be achieved, in lower yields, with cyclic 1,3-diones (10), deacetylchelocardin (**4**) yielded only *O*-alkyl derivatives.

The bisdioxolane **2** yielded an *N*-carbobenzoxy derivative **16**, which on hydrolysis yielded a monoketone-monodioxolane **17** (which may also be represented as the 3-keto-1-dioxolane

Can. J. Chem. Downloaded from www.nrcresearchpress.com by 210.87.254.105 on 09/05/12
For personal use only.

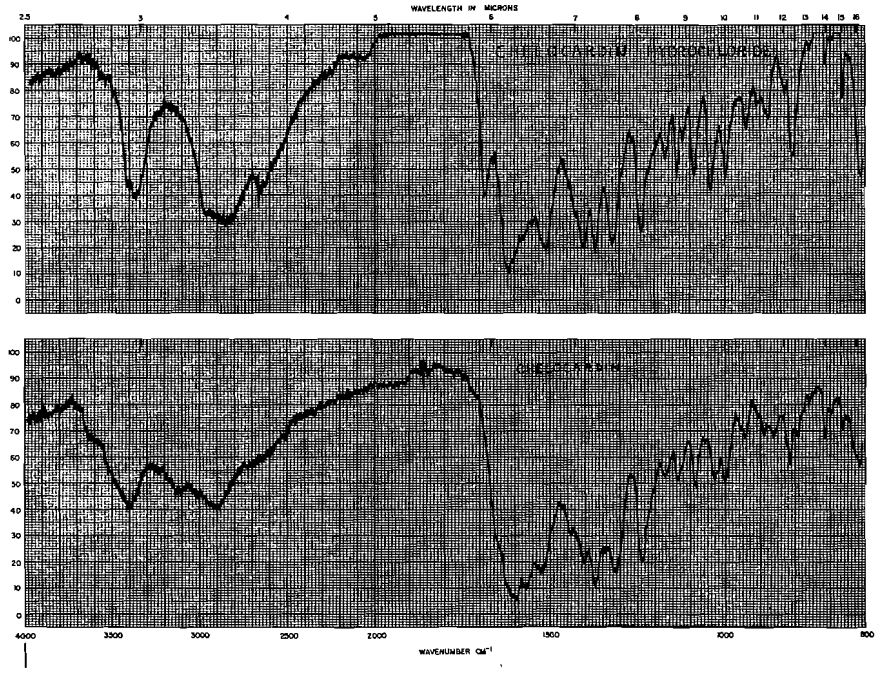

FIG. 1. Infrared spectra of chelocardin and chelocardin hydrochloride as KBr dispersion.

17*a*) and not the 2-deacetylcarbobenzoxy derivative **18**.

Deacetylchelocardin yielded a monocarbobenzoxy derivative **18** and a monobenzoyl derivative **15** when treated cautiously with 1 equiv. of the appropriate reagent. On treatment with excess carbobenzoxy chloride, a dicarbobenzoxy derivative **19** was formed. This substance, on treatment with base, did not hydrolyze to the monocarbobenzoxy derivative but instead rearranged to a stable isomeric dicarbobenzoxy compound, which is formulated as **20**.

The relative ease of this rearrangement (presumably caused by the participation of the neighboring 12*a* hydroxyl group) together with the steric hindrance due to the *N*-carbobenzoxy group at the 4-position, makes it unlikely that the carbobenzoxy group would be in the 3-position.

In summary, we have observed that the presence of the 4-amino and 12*a*-hydroxyl groups profoundly modified the behavior of the tricarbonylmethane system in chelocardin (**1**) and the 1,3-dione system in deacetylchelocardin (**4**).

Experimental Section

The i.r. spectra were recorded on Beckman model IR8 infrared spectrophotometer. The n.m.r. spectra were recorded on Varian Associates A-60 and HA-100 spectrometers in deuterated solvents; resonance positions are given on the δ scale (p.p.m.) relative to internal tetramethylsilane. The n.m.r. peaks were designated as follows: s, singlet; d, doublet; t, triplet; q, quartet; m, multiplet; b, broad. The high resolution mass spectra were determined on Associated Electrical Industries MS-902 Double Focussing mass spectrometer and were processed on an IBM 1800 computer.

The i.r. absorption spectra of chelocardin and its hydrochloride are shown in Fig. 1. Since the various derivatives reported here have the basic β-hydroxy-α,β-unsaturated carbonyl function which would have a similar absorption to the β-diketone system, very little change in the carbonyl absorption region (1580–1680 cm^{-1}) was observed. However, the changes in relative intensity of the carbonyl absorptions correlated with the structural changes. Thus, only the relevant difference in absorption bands will be mentioned in the experimental section.

2-Deacetylchelocardin-1,3-bisdioxolane (2)

p-Toluenesulfonic acid (6 g; 35 mmol) was added to a suspension of β-chelocardin hydrochloride (14.5 g; 32.4 mmol) in benzene (1500 ml) and followed by the addition of ethylene glycol (17 g; 0.27 mol). The mixture was then refluxed for 48 h with vigorous stirring and azeotropic removal of water. The benzene was decanted. *p*-Toluenesulfonic acid (0.5 g; 3.8 mmol) and ethylene glycol (3 g; 50 mmol) were then added to the benzene portion and the solution refluxed for an additional 3 h. The solution was then evaporated under reduced pressure nearly to dryness. After the addition of ethanol (25 ml), the solution was slowly poured with stirring into ether (1200 ml). The mixture was then filtered and the residue washed with ether yielding 9.5 g solid material.

Can. J. Chem. Downloaded from www.nrcresearchpress.com by 210.87.254.105 on 09/05/12
For personal use only.

Can. J. Chem. Downloaded from www.nrcresearchpress.com by 210.87.254.105 on 09/05/12
For personal use only.

The solid residue left earlier (after decantation of the benzene) was suspended in 1000 ml of benzene. After the addition of *p*-toluenesulfonic acid (1 g; 6.5 mmol) and ethylene glycol (7 g; 0.11 mmol) this mixture was refluxed for an additional 40 h with removal of water. The second reaction was worked up in a similar manner to the prior ketalization using 15 ml ethanol and 800 ml ether to give 6.5 g solid. Thin-layer chromatographic analysis of the above two solid materials showed one homogeneous spot. The combined product was 16 g (80%) which showed a loss of the 1690 cm^{-1} band in the i.r. spectrum and an n.m.r. spectrum completely consistent with the assigned structure as **2**. (The n.m.r. spectra obtained from chelocardin derivatives in which the 4-amino group is not converted to an amide are usually of poor resolution.) During the course of the reaction, t.l.c. did not show the presence of compound **4**.

Transformation of 2 into 3

Water (25 ml) was added to a solution of **2** (450 mg; 0.72 mmol) in methanol (25 ml) and the mixture was cooled to 3–5 °C. After the addition of sodium bicarbonate (0.5 g; 5.9 mmol) benzylchloroformate (1.3 g; 8 mmol) was added slowly. The ice bath was removed after 5 min and the reaction stirred for an additional 1½ h. The p*H* was adjusted to approximately 1 by the addition of dilute hydrochloric acid at ice temperature and the mixture extracted with chloroform. The organic phase was dried over sodium sulfate, filtered, and evaporated under reduced pressure almost to dryness. After the addition of a small amount of ether the solution was poured with stirring into hexane. Evaporation to a smaller volume and filtration gave a residue which after drying yielded 400 mg (96%) of carbobenzoxy deacetylchelocardin dioxolane **3**. The i.r. spectrum showed a carbamate absorption at 1720 cm^{-1}; n.m.r. ($CDCl_3$): δ 1.87 (d, 1H, C_2-*H*, $J_{ab} = -15$ Hz), 2.33 (s, 3H, C_6-CH_3), 2.36 (s, 3H, C_9-CH_3), 2.50 (d, 1H, C_2-*H*), 3.77 (m, 10H, C_5-*H*; —O—CH_2CH_2—O—), 4.29 (s, 1H, C_{12a}-O*H*), 4.71 (m, 1H, C_{4a}-*H*), 5.17 (s, 2H, —O—CH_2 C_6H_5), 5.21 (d, 1H, C_4-*H*), 7.37 (m, 7H, C_7-*H*, C_8-*H*, and C_6H_5), 10.11 (s, 1H, C_{10}-O*H*), 15.95 (s, 1H, C_{11}-O*H*); *m/e* 591.2097 (calcd.: 591.2105).

Anal. Calcd. for $C_{32}H_{33}NO_{16}$: C, 64.97; H, 5.58; N, 2.37; O, 27.07. Found: C, 64.86, H, 5.39; N, 2.41; O, 26.77.

2-Deacetylchelocardin (4)

The bisdioxolane **2** (10 g; 16 mmol) was dissolved in acetone (500 ml) and 30% hydrochloric acid (500 ml) and the solution was heated at 50 °C for 45 h. An equal volume of saturated sodium carbonate solution was added slowly (to a p*H* of 2–3) and the mixture was then shaken with chloroform. A precipitate was thrown down and this was isolated by filtration. The filtrate was separated into two layers and the chloroform fraction was decanted. The aqueous layer was reextracted with *n*-butyl alcohol. The alcohol portion was then washed with water twice, dried over magnesium sulfate, and filtered. After evaporation under reduced pressure, the crude product was dissolved in ethanol and the solution poured with stirring into ether. The resulting precipitate was collected by filtration to give a total yield of solid of 6 g. The product was further purified by filtration through Sephadex LH20 using 0.01 *M* HCl in methanol as eluent giving 4.6 g (72%) pure 2-deacetylchelocardin hydrochloride (**4**); n.m.r. ($(CD_3)_2SO$): δ 2.15 (s, 3H, C_6-CH_3), 2.35 (s, 3H, C_9-CH_3), 3.25 (m, 5H), 5.6 (d, 1H, C_4-*H*), 7.32 (d, 1H, C_7-*H*, $J_{7,8} = 8.5$ Hz), 7.58 (d, 1H, C_8-*H*), 8.81 (b, 1H, O*H*); *m/e* 369.1211 (calcd.: 369.1207).

Preparation of Substituted Bisdioxolane 5

β-Chelocardin hydrochloride (570 mg; 1.2 mmol) was suspended in benzene (70 ml). After the addition of *p*-TSA (0.12 g; 1.5 mmol) propylene glycol (340 mg; 4.4 mmol) was added. The mixture was then refluxed with azeotropic water removal for 64 h. After concentration under reduced pressure to a small volume, the residue was poured with stirring into *n*-hexane. Filtration yielded 650 mg of the title compound (**5**).

Conversion of 5 to Carbobenzoxy Derivative 6

Compound **5** (300 mg; 0.46 mmol) was dissolved in 50% aqueous methanol (30 ml) and was cooled to 5 °C. Sodium bicarbonate (100 mg; 1.2 mmol) was added, followed by the addition of benzyl chloroformate (300 mg; 0.2 mmol). After stirring for 2 h at room temperature, the reaction mixture was diluted with water and extracted with chloroform. The organic phase was dried, filtered, and evaporated under reduced pressure to a very small volume. Addition dropwise to well stirred hexane gave solid **6** which was isolated by filtration, yielding 290 mg (98%). The i.r. spectrum showed a carbamate absorption at 1720 cm^{-1}; n.m.r. ($CDCl_3$): δ 1.20 (m, 6H, —OCH_2CH(CH_3)—O), 1.97 (m, 1H, C_2-*H*), 2.34 (s, 3H, C_6-CH_3), 2.37 (s, 3H, C_9-CH_3), 2.60 (m, 1H, C_2-*H*), 3.81 (m, 8H, C_5-CH_2; —OCH_2—CH—O), 4.24 (m, 1H, C_{12a}-O*H*), 4.66 (m, 1H, C_{4a}-*H*), 5.15 (s, 2H, —O—$CH_2C_6H_5$), 5.20 (m, 1H, C_4-*H*), 7.36 (m, 7H, C_7-*H*; C_8-*H* and C_6H_5), 10.13 (s, 1H, C_{10}-O*H*), 15.96 (s, 1H, C_{11}-O*H*).

Anal. Calcd. for $C_{34}H_{37}NO_{10}$: C, 65.90; H, 5.98; N, 2.26; O, 25.85. Found: C, 66.00; H, 6.20; N, 2.21; O, 25.30.

Acetylation of 2-Deacetylchelocardin (4)

Deacetylchelocardin hydrochloride (**4**) (100 mg; 0.25 mmol) was added to a stirred solution of sodium acetate (20 mg; 0.25 mmol) in acetic anhydride (4 ml). After 10 min, the starting material was completely converted to a mixture of two products A and B. After 1 h, the reaction mixture consisted of two products B and C with the loss of A. The R_f values of A, B, and C (developed on silica gel using a solvent system of hexane – ethyl acetate – formic acid 40:60:5) were 0.30, 0.41, and 0.63, respectively. The reaction was worked up after an additional 1 h by pouring into 20 ml ice cold water and stirring for 30 min. The solvents were removed by filtration and the solid was taken up in chloroform, washed twice with water, and dried. Evaporation of the solvent under reduced pressure gave 119 mg crude mixture. Forty milligrams of this was eluted from a silica gel column giving 10 mg sample of a *N,O,O*-triacetylated product C confirmed by mass spectroscopy. The product B was isolated by gel filtration through Sephadex LH20 column using methanol as eluent. Its structure was confirmed to be *N,O*-diacetylated product **14***a* or *b* confirmed by mass spectroscopy. The presence of normal fragmentation pattern excluded the presence of a phenolic acetate group. Compound A could be prepared in high purity by following the reaction by t.l.c. and stopping the reaction

Can. J. Chem. Downloaded from www.nrcresearchpress.com by 210.87.254.105 on 09/05/12
For personal use only.

after a short time even though the starting material was still present. The i.r. and n.m.r. spectra of the pure sample were consistent with the assigned structure of the *N*-monoacetyl derivative (**13**).

*N-Benzoyldeacetylchelocardin (**15**)*

Benzoyl chloride (34.6 mg; 0.25 mmol) dissolved in tetrahydrofuran (2 ml) was added dropwise to a stirred solution of 2-deacetylchelocardin hydrochloride (**4**) (100 mg; 0.25 mmol) in 12 ml of 30% aqueous THF. The p*H* was adjusted to between 8 and 8.5 with 7% sodium hydroxide solution. When the addition was completed, the stirring was continued for ½ h at room temperature and the aqueous solution acidified to p*H* ~ 2 with 5% hydrochloric acid. After the addition of more water, the precipitate was filtered, washed with water and a small amount of ether, then dried, yielding 84 mg product. The i.r. spectrum showed a carbamate absorption at 1720 cm^{-1} (weak). The n.m.r. spectrum was consistent with the assigned structure **15**. Its mass spectrum had a *m/e* peak at 473.1470 (calcd. for $C_{27}H_{23}NO_7$ 473.1474).

*N-Carbobenzoxydeacetylchelocardin (**18**)*

To a solution of deacetylchelocardin hydrochloride (**4**) (200 mg; 0.49 mmol) in 20 ml of 30% aqueous THF (adjusted to a p*H* 8.5 with 7% sodium hydroxide) carbobenzoxy chloride (84 mg; 0.49 mmol) in tetrahydrofuran (5 ml) was added dropwise over a 30 min period. At the end of the reaction the p*H* was 7 and the starting material was converted completely into two products, one major. Water (500 ml) was then added, the p*H* adjusted to 2, and the product extracted with ether (2 × 50 ml) which was dried and evaporated under reduced pressure to dryness. Recrystallization from benzene followed by glacial acetic acid afforded a pure product m.p. 223–226 °C; *m/e* was found to be 503.1572 (calcd. for $C_{28}H_{27}NO_8$ 503.1580). The i.r. spectrum showed a carbamate absorption at 1720 cm^{-1}; n.m.r. ($CDCl_3$): δ 2.24 (s, 3H, C_6-C*H*$_3$), 2.32 (s, 3H, C_9-C*H*$_3$), 3.25 (m, 1H, C_5-*H*), 3.46 (d, 1H, C_2-*H*, $J_{ab} = -15$ Hz), 4.44 (d, 1H, C_2-*H*), 5.16 (s, 2H, —C*H*$_2$—C_6H_5), 5.39 (m, 1H, N*H*), 5.88 (m, 1H, C_4-*H*), 7.45 (m, 8H, C_7-*H*; C_8-*H*; C_6H_5; O*H*), 15.0 (bs, 1H, O*H*).

*Preparation of Monodioxolane (**17**)*

The carbobenzoxybisdioxolane **16** (110 mg; 0.2 mmol) was dissolved in a mixture of acetone (11 ml) and hydrochloric acid (5.5 ml, 30%). After heating at 50 °C for 5½ h, water (55 ml) was added and the mixture filtered. The solid was purified by dry column chromatography on silica gel using ethyl acetate as eluent yielding 85 mg (84%) monodioxolane **17** (or **17***a*). Its mass spectrum showed the *m/e* at 547.1856 (calcd. for $C_{30}H_{29}NO_9$ 547.1842); n.m.r. ($CDCl_3$): δ 2.27 (s, 3H, C_6-C*H*$_3$), 2.33 (s, 3H, C_9-C*H*$_3$), 2.75 (m, 2H, C_2-C*H*$_2$), 3.52 (m, 7H, —OC*H*$_2$C*H*$_2$—O; C_5-C*H*$_2$, N*H*), 4.50 (m, 1H, C_5-*H*), 4.68 (sb, 1H, C_{12a}-O*H*), 5.13 (s, 2H, OC*H*$_2$—C_6H_5), 5.87 (d, 1H, C_4-*H*), 7.35 (m, 7H, C_7-*H*; C_8-*H*; C_6H_5), 10.17 (s, 1H, C_{10}-O*H*), 15.75 (bs, 1H, C_{11}-O*H*).

*Preparation of Dicarbobenzoxy Derivative **19***

2-Deacetylchelocardin hydrochloride (**4**) (190 mg; 0.47 mmol) was dissolved in a mixture of methanol (10 ml) and ether (10 ml). Sodium bicarbonate (190 mg; 2.4 mmol), followed by carbobenzoxy chloride (500 ml; 3 mmol) was added and the mixture was stirred at ice temperature for ½ h. After stirring at room temperature for a further 2 h, the p*H* of the mixture was adjusted to 3 by the addition of dilute hydrochloric acid solution. The mixture was then extracted with chloroform which was subsequently filtered and evaporated to give a solid residue. A small quantity of ethanol was added to dissolve this solid, which was subsequently reprecipitated by the addition of a small amount of ether and then a large amount of hexane. Filtration gave 190 mg of pure **19** (64%). Its i.r. spectrum showed an enol carbonate absorption at 1775 cm^{-1}. Its n.m.r. spectrum contained a characteristic singlet at δ 5.15 having an intensity corresponding to four protons when compared to the two aromatic methyl signals and was assigned to the four methylene protons of the benzyl groups. Mass spectrum showed *m/e* at 637.1935 (calcd. 637.1948).

Anal. Calcd. for $C_{36}H_{31}NO_{10}$: C, 67.82; H, 4.87; N, 2.20; O, 25.12. Found: C, 67.60; H, 5.03; N, 2.34; O, 25.48.

*Base Treatment of **19***

Compound **19** (130 mg; 0.2 mmol) was added to a mixture of ethanol (10 ml) and aqueous saturated sodium carbonate solution (2 ml). After stirring for 30 min, the p*H* of the mixture was adjusted to 3 followed by extraction with chloroform, which was washed subsequently, dried, filtered, and evaporated to dryness under reduced pressure. The residue was purified by gel filtration through Sephadex LH20 using 0.01 *M* HCl in methanol as eluent; 75 mg of pure **12***a* carbonate derivative **20** was isolated. Its i.r. spectrum showed a carbonate absorption at 1755 cm^{-1} and carbamate absorption at 1720 cm^{-1}.

Anal. Calcd. for $C_{36}H_{31}NO_{10}$: C, 67.82; H, 4.87; N, 2.20; O, 25.12. Found: C, 67.68; H, 4.91; N, 2.41; O, 25.19.

*Transformation of 2-Deacetylchelocardin (**4**) into **2***

2-Deacetylchelocardin (**4**) (40.5 mg; 0.1 mmol) was dissolved in benzene (10 ml). *p*-Toluenesulfonic acid (22 mg; 0.19 mmol) was added to the solution and followed by the addition of ethylene glycol (34 mg; 0.54 mmol). The mixture was then refluxed with vigorous stirring and azeotropic removal of water. The progress of the reaction was monitored by t.l.c. and the reaction was nearly complete in about 11 h. After refluxing for 16 h, the benzene solution was then evaporated under reduced pressure nearly to dryness. After the addition of ethanol (1 ml), the solution was added slowly with stirring into ether (50 ml). The mixture was filtered and the residue was washed with ether yielding 45 mg solid material (91%) which gave i.r. and n.m.r. spectra identical to those of 2-deacetylchelocardin-1,3-bisdioxolane (**2**).

We thank R. S. Egan and M. I. Levenberg of Abbott Laboratories for the n.m.r. and mass spectra, respectively, and the staff of the microanalytical department of Abbott Laboratories for the elemental analysis.

1. T. J. Oliver, J. F. Prokop, R. R. Bower, and R. H. Otto. Antimcrob. Ag. Chemother. 583 (1962).
2. A. C. Sinclair, J. R. Schenck, G. G. Post, E. V. Cardinal, S. Burokas, and H. H. Fricke. Antimicrob. Ag. Chemother. 592 (1962).
3. L. A. Mitscher, Wm. Rosenbrook, Jr., W. W.

ANDRES, R. S. EGAN, J. SCHENCK, and J. V. JUVARKAR. Antimicrob. Ag. Chemother. 38 (1970); L. A. MITSCHER, J. V. JUVARKAR, WM. ROSENBROOK, JR., W. W. ANDRES, J. SCHENCK, and R. S. EGAN. J. Am. Chem. Soc. **92**, 6070 (1970).
4. W. DIECKMANN and R. STEIN. Ber. **37**, 3370 (1904).
5. M. W. CRONYN and J. E. GOODRICH. J. Am. Chem. Soc. **74**, 3331 (1952).
6. E. CORTES and F. WALLS. Bol. Inst. Quim. Univ. Nac. Auton. Mex. **17**, 165 (1965).
7. H. SMITH. J. Chem. Soc. 803 (1953).
8. H. STETTER and R. LAUTERBACH. Ann. **652**, 40 (1962).
9. E. C. TAYLOR and A. MCKILLOP. Acc. Chem. Res. **3**, 338 (1970).
10. J. M. MCINTOSH and P. M. BEAUMIER. J. Can. Chem. 843 (1973).

Can. J. Chem. Downloaded from www.nrcresearchpress.com by 210.87.254.105 on 09/05/12
For personal use only.

Kinetics of the Fully Inhibited Thermal Decomposition of Bistrifluoromethyl Peroxide, CF_3OOCF_3[1]

BERNARD DESCAMPS AND WENDELL FORST

Molecular Dynamics Group, Department of Chemistry, Université Laval, Québec, Québec G1K 7P4

Received December 2, 1974

BERNARD DESCAMPS and WENDELL FORST. Can. J. Chem. **53**, 1442 (1975).

The pyrolysis of CF_3OOCF_3 (BTMP) was studied in the gas phase from 5 to 100 Torr BTMP pressure and between 197 and 244 °C in a clean nickel reactor by the static method. CF_3O radicals, due to the initial split $CF_3OOCF_3 \xrightarrow{[1]} 2CF_3O$, were scavenged by SO_3F radicals produced *in situ* by the thermal decomposition of their dimer $S_2O_6F_2$. Under these conditions, CF_3OOSO_2F is the only product of BTMP pyrolysis, as shown by gas chromatographic analysis. Thus the BTMP pyrolysis becomes fully inhibited and the rate of accumulation of CF_3OOSO_2F is a measure of k_1. The rate constant k_1 turns out to be pressure-insensitive under the experimental conditions, from which it is inferred that k_1 is actually $k_{1\infty}$, the limiting high-pressure unimolecular rate constant for reaction 1. Its temperature dependence yields the result

$$k_{1\infty}\ (s^{-1}) = 10^{15.9\pm0.23} \exp\{-(46.2 \pm 0.5\ \text{kcal/mol})/RT\}$$

This result is compared with other values of the O—O bond dissociation energy in BTMP. The experimental expression for $k_{1\infty}$ is used to construct the pressure falloff of k_1 following the procedure of Forst. The calculation confirms that falloff begins only below 10 Torr.

BERNARD DESCAMPS et WENDELL FORST. Can. J. Chem. **53**, 1442 (1975).

La pyrolyse du CF_3OOCF_3 (BTMP) a été étudiée en phase gazeuse par la méthode statique à des pressions de 5 à 100 Torr de BTMP, et des températures variant entre 197 et 244 °C, dans un réacteur "propre" en nickel. Les radicaux CF_3O, provenant de la scission initiale $CF_3OOCF_3 \xrightarrow{[1]} 2CF_3O$, ont été captés par les radicaux SO_3F produits *in situ* par la décomposition thermique de leur dimère $S_2O_6F_2$. Sous ces conditions, CF_3OOSO_2F est le seul produit de la pyrolyse du BTMP, comme nous l'avons démontré par analyse chromatographique. Ainsi la pyrolyse du BTMP devient totalement inhibée et la vitesse d'accumulation du CF_3OOSO_2F est la mesure de k_1. La constante de vitesse k_1 s'avère être insensible à la pression sous nos conditions expérimentales, d'où nous concluons que k_1 est en fait $k_{1\infty}$, la constante de vitesse monomoléculaire de la réaction 1 dans la limite des hautes pressions. Sa dépendance de température donne

$$k_{1\infty}\ (s^{-1}) = 10^{15.9\pm0.23} \exp\{-(46.2 \pm 0.5\ \text{kcal/mol})/RT\}$$

On compare ce résultat à d'autres valeurs de l'énergie de la liaison O—O dans le BTMP. L'expression expérimentale pour $k_{1\infty}$ est ensuite utilisée pour la reconstitution de la courbe de la chute de k_1 avec la pression, suivant la procédure de Forst. Ce calcul confirme que k_1 ne chute qu'au dessous de 10 Torr.

Introduction

The pyrolysis of bistrifluoromethyl peroxide CF_3OOCF_3 (BTMP) is a complex reaction initiated by CF_3O radicals (1).[2] Even initial rate measurements yield an overall rate constant that actually involves, in our interpretation (1), rate constants for three different reaction steps, two of which are the initial split of BTMP into two radicals and their recombination

$$CF_3OOCF_3 \underset{[2]}{\overset{[1]}{\rightleftharpoons}} CF_3O + OCF_3$$

Thus the rate of the unimolecular dissociation of BTMP into two CF_3O radicals is not directly accessible to measurement. Because of the intrinsic interest of simple bond-fission unimolecular reactions, it seemed worthwhile to attempt to modify the course of the pyrolysis in such a way that only reaction 1 would occur, which can be accomplished by scavenging all CF_3O radicals.

[1]This paper is dedicated to Professor C. A. Winkler of McGill University on the occasion of his sixty-fifth birthday by one of his former students (W.F.).

[2]Microfiche available from Canadian Theses Division, Cataloguing Branch, National Library of Canada, 395 Wellington Street, Ottawa, Canada K1A 0N4, for $2.00. Quote Canadian Theses on Microfiche No. 18946.

Can. J. Chem. Downloaded from www.nrcresearchpress.com by 210.87.254.42 on 09/05/12
For personal use only.

Can. J. Chem. Downloaded from www.nrcresearchpress.com by 210.87.254.42 on 09/05/12
For personal use only.

Several compounds, *e.g.* SF_4, O_2, and CF_4 are known (2) to form adducts with CF_3O radicals, but these adducts generally are not stable above 200 °C, the temperature of BTMP pyrolysis. Schumacher and co-workers (3) have found that the fluorosulfate free radical SO_3F is not only an efficient scavenger for CF_3O radicals via the reaction

[3] $$SO_3F + CF_3O \rightarrow CF_3OOSO_2F$$

but the trifluoromethyl peroxyfluorosulfonate CF_3OOSO_2F (TPS) so formed is stable around 230 °C. As a result, they were able to use reaction 3 to successfully scavenge CF_3O radicals produced in the process $CF_3OF \rightarrow CF_3O + F$.

The purpose of this work is to use reaction 3 to scavenge all CF_3O radicals produced in reaction 1. Hopefully, the BTMP pyrolysis thus becomes fully inhibited, making it possible to determine k_1, the rate constant for the unimolecular fission of BTMP into two CF_3O radicals.

Experimental

Materials

Peroxydisulfuryl difluoride $S_2O_6F_2$, the source of SO_3F radicals, was prepared by the method of Shreeve and Cady (4) from Sulfan-B (Baker & Adamson) and F_2. The method produces as byproduct substantial amounts of SO_3F_2 which were removed by distillation. Purity of $S_2O_6F_2$ was checked by infrared, but this method does not reveal traces of the fluorine fluorosulfate SO_3F_2 impurity because of the similarity of their infrared spectra (5).

Other materials were as described before (1).

Apparatus

The same static system described previously (1) was employed, with the same "clean" nickel reactor. The reactor was conditioned with 5–6 Torr of BTMP for several minutes immediately prior to a run.

Analysis

Analysis was done by gas chromatography with a gas density detector. The analytical problem was a difficult one and is described elsewhere (6). While we estimate the precision of successive analyses done on the same day to be about 5%, the actual accuracy over the several months it took to complete this work was only within 10 or 15% because of temperamental behavior of the chromatographic column. Consequently experimental error in the reported *individual* rate constants is somewhat larger than it would be in a better-behaved system. However these individual errors seem to average out in a *collection* of rate constants obtained at the same temperature because an excellent Arrhenius plot is obtained (Fig. 4 and eq. 9).

Infrared analysis was used for the determination of COF_2.

It is the property of the gas density detector that weight of component x is proportional to corrected peak area $S_x = F_x S_x'$. Here (7) S_x' is the actual peak area corresponding to component x and F_x is a correction factor given by $M_x/(M_x - M_c)$, where M_x = molecular weight of component x, M_c = molecular weight of carrier gas (28.013 since nitrogen was used). Thus $F_x = 1.19728$ for BTMP, 1.17951 for TPS, and 1.16468 for $S_2O_6F_2$.

Procedure

Mixtures of BTMP and $S_2O_6F_2$, prepared in a standard gas-handling system, were introduced into the reactor by expansion from a reference volume. Because both compounds are heavy gases, they mix by diffusion only very slowly and a magnetic mixer had to be used to insure proper mixing. Inasmuch as $S_2O_6F_2$ tends to be strongly adsorbed on the walls, the mixing vessel (and also the reference volume) was heated to 100 °C. Analysis of mixtures after prolonged mixing at 100 °C or condensing in liquid air always showed that composition had remained unchanged; in particular, analysis established the absence, even in trace amounts, of compounds other than BTMP and $S_2O_6F_2$.

The total pressure in the reactor was monitored by a pressure transducer. After a predetermined reaction time, corresponding to no more than ~5% decomposition of BTMP, the contents of the reactor were condensed in a liquid nitrogen trap, and after warm-up and remixing an aliquot was analyzed by gas chromatography.

On introduction into the reactor, the equilibrium between $S_2O_6F_2$ and SO_3F radicals is established practically instantaneously (see Preliminary Results), so that the initial partial pressure of BTMP (P_0) must be calculated from the measured total pressure inside the reactor (P_t). Suppose a gas mixture containing, at room temperature, a mol of BTMP and b mol of $S_2O_6F_2$, was introduced into the reactor. At reactor temperature, x mol of $S_2O_6F_2$ dissociate to form $2x$ mol of SO_3F radicals; thus the total number of mol in the reactor is $a + b + x$. The partial pressures of the radicals and their dimer are $P_{SO_3F} = 2xP_t/(a + b + x)$, $P_{S_2O_6F_2} = (b - x)P_t/(a + b + x)$, and the equilibrium constant is $K_p = 4x^2P_t/(a + b + x)(b - x)$. Since K_p is known (eq. 6), x can be calculated. Then $P_0 = aP_t/(a + b + x)$.

$S_2O_6F_2$ condenses easily (b.p. ~ 67 °C), so that the highest pressure attainable in the reference volume before condensation took place limited the maximum pressure in the reactor to about 250 Torr.

Preliminary Results

The fluorosulfate free radicals SO_3F were generated *in situ* by the thermal homolytic cleavage of their dimer, the peroxydisulfuryl difluoride $S_2O_6F_2$, a well-known reaction (8–11)

$$S_2O_6F_2 \underset{[5]}{\overset{[4]}{\rightleftharpoons}} 2SO_3F$$

The equilibrium constant for this reaction in the gas phase was measured as a function of temperature by Dudley and Cady (8) who give

[6] $$\log_{10} K_p\,(\text{atm}) = 7.981 - 4.785 \times 10^3\, T^{-1}$$

To be useful for inhibition purposes, the equilibrium between the fluorosulfate free radical

Can. J. Chem. Downloaded from www.nrcresearchpress.com by 210.87.254.42 on 09/05/12
For personal use only.

and its dimer must be established in a time that is short compared with the time it takes for BTMP to yield measurable amounts of products at the reaction temperature (~250 °C); in addition, neither the radical nor its dimer must decompose themselves. To check this, 90 Torr of dimer $S_2O_6F_2$ was introduced into the reactor at 253.5 °C. The dissociation of the dimer increases the number of molecules, and from eq. 6 about a 50% pressure increase could be expected at 254 °C; however, after a brief initial pressure disturbance in the reactor due to the introduction of the gas and its heat-up, no pressure change was noted in the reactor, suggesting that the equilibrium between SO_3F and its dimer is established practically instantaneously. At this temperature, the half-life of the (uninhibited) BTMP pyrolysis at initial pressures of 20 Torr or higher is about 2 h, as determined from initial rates (1), so that the dimer $\rightleftharpoons 2SO_3F$ equilibrium is certainly established quickly enough. After 37 min at 253.5 °C, the contents of the reactor were trapped out and analyzed by chromatography. The initial amount of the dimer was recovered *in toto* and no other compounds were detected, indicating that no measurable degradation of the dimer or of the radical had occurred. Clearly then the dimer $\rightleftharpoons 2SO_3F$ equilibrium has all the useful properties for inhibition purposes.

If a mixture of BTMP and $S_2O_6F_2$ is introduced into the reactor, only reactions 1, 3, 4, and 5 will take place if all CF_3O radicals are scavenged. If not, other reactions of CF_3O radicals will occur (1), leading ultimately to the formation of COF_2 and CF_3OF. Of the two products, which are produced in equimolar amounts, COF_2 is very easily determined by infrared, and therefore we have used COF_2 as indicator of the degree of scavenging. The practical problem is to determine the $S_2O_6F_2$:BTMP ratio necessary to cause the disappearance of COF_2; we refer here to "cold" dimer, as measured out during the preparation of gas mixtures, and not to the actual amount of dimer present at reactor temperatures. The results are shown in Fig. 1 from which it may be deduced that about a twofold excess of (cold) $S_2O_6F_2$ over BTMP is necessary for complete disappearance of COF_2 (it can be calculated from eq. 6 that at 233 °C between 50 to 75% of the dimer is dissociated, depending on pressure). However even if the $S_2O_6F_2$:BTMP ratio is unity, only about 0.5% of BTMP ends up as COF_2, an amount that is quite clearly unimportant because the rate constant k_1 remains unchanged (Fig. 1).

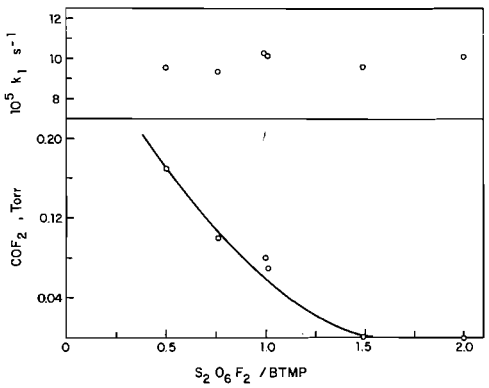

FIG. 1. Effect of varying $S_2O_6F_2$/BTMP ratio at 233.3 °C. $S_2O_6F_2$/BTMP is the ratio of pressures of the two compounds in cold mixtures. Initial pressure of BTMP in reactor constant at $P_0 \sim 17.5$ Torr. Upper portion, rate constant k_1 as a function of $S_2O_6F_2$/BTMP; lower portion, COF_2 produced in the reactor as a function of $S_2O_6F_2$/BTMP.

Results

Preliminary results show that in gas mixtures containing (at room temperature) at least equal amounts of $S_2O_6F_2$ and BTMP, the overall reaction around 250 °C is simply

[7] $CF_3OOCF_3 + S_2O_6F_2 \rightarrow 2CF_3OOSO_2F$

This can be interpreted as the result of the sequence of reactions

[1] $CF_3OOCF_3 \rightarrow 2CF_3O$ (rate-determining)

[3] $CF_3O + SO_3F \rightarrow CF_3OOSO_2F$

Reaction 3, like every reaction between two radicals, can be reasonably expected to have a large rate constant, of the order of the collision number; reaction 1, on the other hand, must be a rather slow process because it will have an appreciable activation energy. In our system, the concentration of SO_3F radicals in equilibrium with their dimer is fairly high, of the order of the concentration of BTMP itself, so that we have $k_3[SO_3F] \gg k_1$; thus reaction 1 is rate-determining. Since the equilibrium dimer $\rightleftharpoons 2SO_3F$ is established practically instantaneously, the CF_3O radicals, which are produced at a comparatively slow rate, encounter a SO_3F radical before they have a chance to encounter one of their own kind, and are effectively removed via reaction 3, the product TPS having

Can. J. Chem. Downloaded from www.nrcresearchpress.com by 210.87.254.42 on 09/05/12
For personal use only.

been shown to be stable at the temperature of the experiment. Such efficient scavenging of CF_3O radicals means that their steady-state concentration is very low, which insures that the reverse reaction 2 is suppressed, in addition to all the other reactions of CF_3O radicals mentioned in ref. 1.

Consequently the rate of formation of TPS can be taken to be a measure of the rate of reaction 1, the unimolecular fission of BTMP into two CF_3O radicals. Let the initial pressure of BTMP in the reactor at time t_0 be P_0, and let ΔP represent the amount of BTMP decomposed in the time interval Δt; then the ratio of concentrations (or pressures) of product and reactant at time $t = t_0 + \Delta t$ is r = [TPS]/[BTMP] $= 2\Delta P/(P_0 - \Delta P)$, whence $\Delta P = rP_0/(r + 2)$. The ratio r is obtained directly from gas chromatographic peaks as $r = (S_{TPS}/S_{BTMP}) \times (M_{BTMP}/M_{TPS})$, where S_x and M_x are the corrected peak area (see Experimental) and molecular weight, respectively, of component x. The first-order rate constant k_1 is then given by

$$[8] \qquad k_1 = \frac{1}{P_0 - \Delta P/2}\frac{\Delta P}{\Delta t} = \frac{2r}{\Delta t(r + 4)}$$

where $P_0 - \Delta P/2$ is the mean pressure of BTMP during the interval Δt.

Calculation of k_1 by eq. 8 assumes that ΔP rises linearly with Δt. Figure 2 shows that this is indeed the case, except that some curvature appears at very small Δt, corresponding to about 0.5% decomposition of BTMP. The reasons for this are not quite clear; analytical difficulties at such small conversions, or possibly a slight delay in the establishment of complete equilibrium between the SO_3F radicals and their dimer, may be a factor. The latter possibility seems more probable since the length of the curved portion appears to be more related to the absolute value of the time interval than to the amount of conversion. The consequence is that our practice to calculate k_1 from the amount of TPS present at ~5% decomposition may lead to a slight underestimation of k_1, although we believe it to be smaller than the fluctuation in k_1 due to experimental error (Table 1).

Figure 3 shows k_1 as a function of total pressure P_t in the reactor, at fixed initial pressure P_0 of BTMP. Clearly there is no discernible effect within experimental error; the same conclusion emerges from the complete results at five temperatures shown in Table 1. The manifest constancy of k_1 (within experimental error) at any one temperature, regardless of P_0, revealed at the same time in Table 1, shows that the reaction is in fact of the expected first order. If the reaction were some kind of second-order bimolecular process (between BTMP and $S_2O_6F_2$ or SO_3F) giving TPS directly, we would have $\Delta P/\Delta t = kP_0(P_t - P_0)$. Since P_t in our experiments is constant (Table 1), $P_t - P_0$ is proportional to the concentration of $S_2O_6F_2$ or SO_3F. Then $k_1 \sim \Delta P/P_0\Delta t = k(P_t - P_0)$, or, in other words, k_1 should *decrease* with increasing P_0, whereas for a unimolecular process k_1 can only

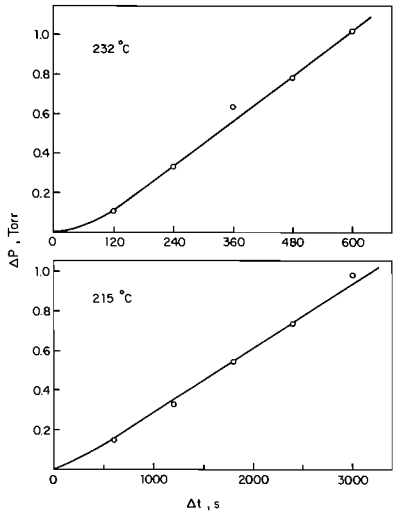

FIG. 2. Amount of BTMP decomposed (ΔP) as a function of reaction time (Δt) at two temperatures. Initial pressure of BTMP in reactor is P_0 = 17.5 Torr in both cases; thus ΔP = 1 Torr represents 5.7% decomposition. Each experimental point represents a separate experiment.

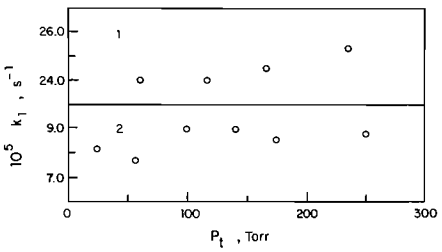

FIG. 3. Rate constant k_1 as a function of total pressure P_t in reactor: (*1*) 244.0 °C, P_0 constant at ~19 Torr; (*2*) 233.4 °C, P_0 constant at ~9 Torr. P_t is the sum of partial pressures of BTMP, SO_3F, and $S_2O_6F_2$. P_0 is the initial partial pressure of BTMP in the reactor.

Can. J. Chem. Downloaded from www.nrcresearchpress.com by 210.87.254.42 on 09/05/12
For personal use only.

TABLE 1. Rate constants for reaction 1 at five temperatures

T(°C)	a*	P_t (Torr)†	P_0 (Torr)†	r	$10^{-3}\Delta t$, (s)	$10^5 k_1$ (s^{-1})†
197.3	0.0531	196.4	9.6	0.0927	16.3	0.270
	0.101	204.4	19.2	0.1006	17.1	0.287
	0.302	205.0	58.2	0.1040	16.5	0.307
	0.399	200.5	75.6	0.09049	17.1	0.259
	0.500	206.8	98.2	0.09746	17.1	0.278
					Average =	0.280
208.6	0.0560	211.5	10.8	0.1059	5.4	0.956
	0.0996	221.1	20.1	0.1039	5.4	0.939
	0.200	219.0	40.3	0.1065	5.4	0.961
	0.299	215.7	59.7	0.09940	5.4	0.898
	0.400	211.3	78.7	0.1089	5.4	0.982
	0.500	210.7	98.5	0.1117	5.4	1.01
	0.499	207.7	96.9	0.1487	7.2	0.996
					Average =	0.963
216.4	0.0288	208.9	5.4	0.09306	3.0	1.52
	0.0527	218.1	10.3	0.1020	2.7	1.84
	0.0983	243.4	21.6	0.09444	2.4	1.92
	0.200	224.6	40.8	0.1035	2.4	2.10
	0.302	222.6	61.6	0.1126	3.0	1.83
	0.401	214.2	78.9	0.1088	2.7	1.96
	0.500	218.4	100.7	0.1068	2.1	2.48
					Average =	1.95
232.4	0.0421	137.3	4.8	0.1098	0.6	8.9
	0.0534	252.9	11.7	0.1081	0.6	8.77
	0.101	282.7	25.2	0.1041	0.6	8.46
	0.199	236.2	41.3	0.1152	0.6	9.34
	0.302	224.6	59.9	0.1074	0.6	8.72
	0.398	222.3	78.9	0.1047	0.6	8.50
	0.500	222.9	100.3	0.1145	0.6	9.28
					Average =	8.85
243.9	0.0274	191.6	4.3	0.1054	0.22	23.3
	0.100	235.1	19.8	0.1147	0.22	25.3
	0.200	227.6	38.6	0.1093	0.22	24.2
	0.300	231.5	59.6	0.1188	0.22	26.2
	0.401	227.0	79.1	0.1065	0.22	23.5
	0.499	232.7	102.3	0.1139	0.22	25.1
					Average =	24.6

*Mole fraction of BTMP in cold (BTMP + $S_2O_6F_2$) mixtures.
†Last decimal not significant.

increase or remain constant. The fact that our k_1 is constant under our experimental conditions shows that it is actually $k_{1\infty}$, the limiting high-pressure unimolecular rate constant for reaction 1.

The average rate constant at each of the five temperatures, as given in Table 1, is denoted $k_{1\infty}$ and is plotted in Fig. 4 in the form of an Arrhenius plot which yields the activation energy $E_{1\infty} = 46.2$ kcal/mol. The full least squares result is

$$[9] \quad k_{1\infty} = 10^{15.94\pm0.23} \exp\{-(46\,200 \pm 510)/RT\}\ s^{-1}$$

As a first approximation, we may take $E_{1\infty}$ to be equal to $D(CF_3O—OCF_3)$, the strength of the O—O bond in BTMP. In fact, the value $D(CF_3O—OCF_3) = 46.2$ kcal/mol appears to fit in quite well with other information, thermochemical and kinetic, available about the uninhibited pyrolysis (1) of BTMP.

Levy and Kennedy (12) first reported $D(CF_3O—OCF_3) = 40.6 \pm 5$ kcal/mol, based on measurements of the equilibrium $CF_3OOCF_3 \rightleftharpoons CF_3OF + COF_2$, and later (13) determined $D(CF_3O—OCF_3) = 46.2 \pm 0.33$ from the temperature dependence of initial rate in BTMP pyrolysis. Our value for the O—O bond strength

Can. J. Chem. Downloaded from www.nrcresearchpress.com by 210.87.254.42 on 09/05/12
For personal use only.

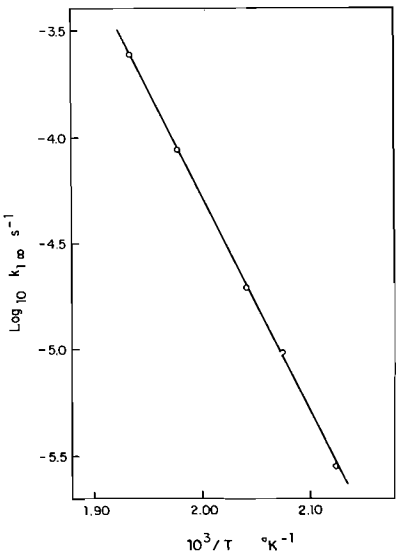

FIG. 4. Arrhenius plot for average k_1 of Table 1 (denoted as $k_{1\infty}$). The activation energy is $E_{1\infty} = 46.2 \pm 0.5$ kcal/mol.

thus agrees exactly with their second determination, an agreement that is no doubt entirely fortuitous. Not only does our interpretation of the (uninhibited) pyrolysis (1) differ fundamentally from theirs, but we also find the temperature dependence of the initial rate yields an activation energy 3.5 kcal/mol higher than theirs (49.7 kcal/mol).

Equation 9 shows that reaction 1 has a rate constant with the expected "high" pre-exponential factor (A_∞) typical of simple bond-fission unimolecular reactions (ref. 14, p. 178). For example, in the pyrolysis of hexafluoroazomethane, a very similar molecule, experiment gives (15) $A_\infty = 10^{16.2}$. If it is assumed that randomization of internal energy precedes decomposition, *i.e.* that the decomposition of BTMP is statistical, the information contained in eq. 9 can be used to reconstruct the thermal falloff curve for k_1 following the deconvolution procedure of Forst (ref. 14, chapt. 11, sect. 2). The usefulness of this procedure has been demonstrated in a number of instances (16–25). Briefly, the procedure consists of showing that if k_∞ in a thermal system is known in the form $k_\infty = A_\infty \exp(-E_\infty/RT)$, the microcanonical unimolecular rate constant of specified energy $k(E)$ can be written (neglecting centrifugal effects)

$$[10] \quad k(E) = A_\infty N(E - E_\infty)/N(E) \qquad (E \geqslant E_\infty)$$

where $N(E)$ and $N(E - E_\infty)$ are the densities of states of the reactant molecule at energies E and $E - E_\infty$, respectively. Thus only the experimental k_∞ and properties of the reactant molecule are necessary; no transition state need be postulated since no transition state properties are involved in eq. 10. The rate constant $k(E)$ of eq. 10 can then be substituted into the usual (statistical, or RRKM) rate constant integral to yield

$$[11] \quad k/k_\infty = \frac{1}{Q}\int_0^\infty \frac{N(x)e^{-x/RT}\,dx}{1 + \dfrac{A_\infty N(x)}{ZPN(x + E_\infty)}}$$

where Q = partition function, Z = collision number, and P = pressure. Numerical evaluation of the integral for several values of P then gives the falloff curve.

Figure 5 shows the result of calculations done for BTMP at the midpoint of the temperature range investigated, in the form of the usual $\log(k_1/k_{1\infty})$ *vs.* $\log P_0$ plot obtained by numerical integration of eq. 11. It can be seen that the falloff is quite slow, even for a molecule the size of BTMP, because of its low vibrational frequencies. Figure 5 thus bears out our experimental results which show that the rate constant k_1 is virtually pressure-independent above $P_0 \sim 10$ Torr. This conclusion would not be modified by some other reasonable choice of the collision diameter. In this instance, the

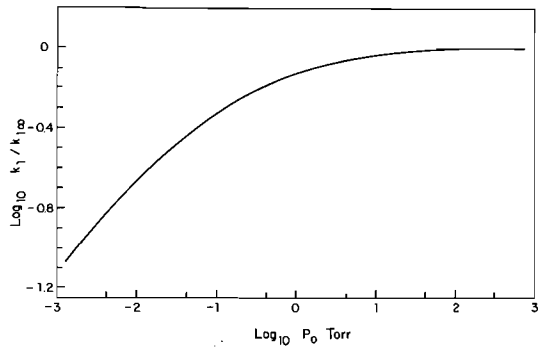

FIG. 5. Calculated fall-off curve for k_1 at 216.4 °C. Values of $k_1/k_{1\infty}$ obtained from eq. 11. Densities of states calculated by the method of steepest descents (ref. 14, append. p. 395 ff.). Vibrational frequencies of BTMP used (26) (in cm^{-1}): 64, 94, 134, 211, 228, 340, 445, 490, 558, 610, 627, 634, 673, 713, 975, 1065, 1125, 1166, 1191, 1240, 1265, 1287. All are nondegenerate, except the first (CF_3 torsion at 64 cm^{-1}) which is doubly degenerate. Collision diameter of BTMP taken to be 4.8 Å.

pressure falloff of the rate constant is located at pressures so low as to make them virtually inaccessible to measurement.

The authors are grateful to the National Research Council of Canada and the Province of Quebec Ministry of Education for financial support.

1. B. DESCAMPS and W. FORST. To be published; B. DESCAMPS. PhD Thesis, Université Laval, Québec, Québec. 1972.
2. J. R. MORTON and K. F. PRESTON. Chem. Phys. Lett. **18**, 98 (1973).
3. J. CZARNOWSKI, E. CASTELLANO, and H. J. SCHUMACHER, Z. Phys. Chem. Frankfurt am Main, **65**, 225 (1969).
4. J. M. SHREEVE and G. H. CADY. Inorg. Synth. **1**, 124 (1963).
5. F. B. DUDLEY and G. H. CADY. J. Am. Chem. Soc. **79**, 513 (1957).
6. B. DESCAMPS and W. FORST. Anal. Chem. In press.
7. A. G. NERHEIM. Anal. Chem. **35**, 1640 (1963).
8. F. B. DUDLEY and G. H. CADY. J. Am. Chem. Soc. **85**, 3375 (1963).
9. E. CASTELLANO, R. GATTI, J. E. SICRE, and H. J. SCHUMACHER. Z. Phys. Chem. N.F. **42**, 174 (1964).
10. R. A. STEWART, S. FUJIWARA, and F. AUBKE. J. Chem. Phys. **48**, 5524 (1968).
11. P. M. NUTKOWITZ and G. VINCOW. J. Am. Chem. Soc. **91**, 5956 (1969).
12. J. B. LEVY and R. C. KENNEDY. J. Am. Chem. Soc. **94**, 3302 (1972).
13. R. C. KENNEDY and J. B. LEVY. J. Phys. Chem. **76**, 3480 (1972).
14. W. FORST. Theory of unimolecular reactions. Academic Press, New York. 1973.
15. E. LEVENTHAL, C. R. SIMONDS, and C. STEEL. Can. J. Chem. **40**, 930 (1962).
16. W. FORST. J. Phys. Chem. **76**, 342 (1972).
17. W. FORST. *In* Reaction transition states. *Edited by* J. E. Dubois. Gordon and Breach, New York. 1972. p. 75.
18. H. M. FREY, R. G. HOPKINS, and I. C. VINALL. J. Chem. Soc. Faraday I, **68**, 1874 (1972).
19. H. M. FREY and I. C. VINALL. Int. J. Chem. Kinet. **5**, 523 (1973).
20. K. J. MINTZ and R. J. CVETANOVIĆ. Can. J. Chem. **51**, 3386 (1973).
21. K. J. MINTZ and D. J. LEROY. Can. J. Chem. **51**, 3534 (1973).
22. L. SZIROVICZA and R. WALSH. J. Chem. Soc. Faraday I, **70**, 33 (1974).
23. J. A. BARNARD, A. T. COCKS, and R. K. LEE. J. Chem. Soc. Faraday I, **70**, 1782 (1974).
24. M. CHRISTANSON, D. PRICE, and R. WHITEHEAD. J. Phys. Chem. **78**, 2326 (1974).
25. S. H. LIN and H. EYRING. Ann. Rev. Phys. Chem. **25**, 65 (1974).
26. J. R. DURIG and D. W. WERTZ. J. Mol. Spectrosc. **25**, 467 (1968).

Can. J. Chem. Downloaded from www.nrcresearchpress.com by 210.87.254.42 on 09/05/12
For personal use only.

Crystal Structure of and Electron Paramagnetic Resonance of Mn^{2+} in $Cd_2(NH_4)_2(SO_4)_3$

HOK NAM NG AND CRISPIN CALVO

Department of Chemistry, McMaster University, Hamilton, Ontario L8S 4M1

Received September 24, 1974

HOK NAM NG and CRISPIN CALVO. Can. J. Chem. **53**, 1449 (1975).

The room temperature structure of $Cd_2(NH_4)_2(SO_4)_3$ (CAS), isotypic with the mineral langbeinite $K_2Mg_2(SO_4)_3$ has been refined by full-matrix least squares methods. The structure is cubic with $a = 10.362(7)$ Å and space group $P2_13$. There are two inequivalent sites for the cation Cd^{2+} and e.p.r. spectra of doped Mn^{2+} show that Cd^{2+} was substituted in both sites with preferential occupancy by Mn^{2+} in a 1:3 ratio. Refinement of X-ray data on a mixed crystal of the stoichiometry $Cd_{0.84}Mn_{1.16}(NH_4)_2(SO_4)_3$ shows that site I contains 82% Mn^{2+} while site II has 38%. The zero-field splitting parameter D was calculated for Mn^{2+} in two sites using a point-charge model and confirms that Mn^{2+} substitutes into site I with greater preference. Although a monoclinic ferroelectric phase of CAS has been suggested below 90 K, no change in space group symmetry could be detected at 80 K. The proton second moment, calculated by the van Vleck's formula, and compared with the experimental values, suggests a tunneling motion of the protons among the four vertices of the ammonium tetrahedron.

HOK NAM NG et CRISPIN CALVO. Can. J. Chem. **53**, 1449 (1975).

La structure, telle qu'elle existe à la température ambiante, de $Cd_2(NH_4)_2(SO_4)_3$ (CAS), isostructural du minéral langbeinite $K_2Mg_2(SO_4)_3$, a été affinée par moindres carrés (matrice complète). La structure est cubique avec $a = 10.362(7)$ Å et appartient au groupe d'espace $P2_13$. Le cation Cd^{2+} occupe deux sites non-équivalents; le spectre r.p.e. du composé additionné de traces de Mn^{2+} montre que Cd^{2+} est substitué dans les deux sites par Mn^{2+} avec une occupation préférentielle dans le rapport de 1 : 3. L'affinement des données de rayons-X d'un cristal mixte de stoichiométrie $Cd_{0.84}Mn_{1.16}(NH_4)_2(SO_4)_3$ montre que le site I contient 82% de Mn^{2+} alors que le site II n'en contient que 38%. Le paramètre de couplage D à champ nul a été calculé pour Mn^{2+} dans chacun des sites utilisant un modèle de charge ponctuelle et confirme que Mn^{2+} se substitue dans le site I avec une préférence plus grande. Quoiqu'il a été suggéré que le CAS existe dans une phase monoclinique ferroélectrique à des températures inférieures à 90 K, on n'a pas pu détecter de changement de groupe d'espace à 80 K. Le "moment secondaire du proton", calculé par la formule de van Vleck et comparé avec les valeurs expérimentales, suggère un mouvement du à un effet tunnel des protons parmi les quatre sommets du tétraèdre de l'ammonium. [Traduit par le journal]

Introduction

A large number of double sulfates with the general formula $A_2B_2(SO_4)_3$ (where A is a monovalent metal or ammonium and B is a divalent metal) are isostructural with the mineral langbeinite $K_2Mg_2(SO_4)_3$. These crystals are cubic with the space group $P2_13$ and contain four formula units per unit cell. One of them, $Cd_2(NH_4)_2(SO_4)_3$ (CAS), has been known for a long time to undergo a phase transformation and become ferroelectric below 90 K (1, 2). Recently another member of the family, $Cd_2Tl_2(SO_4)_3$ (CTS) was reported to have a ferroelectric phase below 130 K (3). The ferroelectric phase of both crystals is believed to have the space group $P2_1$. The dielectric anomaly of CAS has aroused considerable interest in the nature of this ferroelectric phase transformation (4–6). While Dvořák (6) predicts from group theoretical considerations that the ferroelectric phase should have new unit cell vectors, $a_1' = a_1 - a_2$, $a_2' = a_1 + a_2$, and $a_3' = a_3$ with the cell volume doubled, Aizu (5) suggests that the primitive cell is tripled as a result of the condensation of triply degenerate pairs of conjugate lattice vibration modes with wave length three times the lattice constant. Since no accurate atomic parameters for CAS have been published, we have obtained more structural information on this compound by X-ray diffraction and electron paramagnetic resonance (e.p.r.). Some preliminary e.p.r. results for Mn^{2+} in CAS were reported by Tatsuzaki (7).

Experiments

Crystals of CAS were grown by slow evaporation at 85 °C of a solution containing $3CdSO_4.8H_2O$ and $(NH_4)_2SO_4$ in the proper stoichiometric ratio. A good quality single crystal was selected and ground into a

Can. J. Chem. Downloaded from www.nrcresearchpress.com by 210.87.254.105 on 09/05/12
For personal use only.

Can. J. Chem. Downloaded from www.nrcresearchpress.com by 210.87.254.105 on 09/05/12
For personal use only.

sphere of 0.30 mm diameter for X-ray intensity measurements. For e.p.r. studies about 0.2 mol% of $MnSO_4.4H_2O$ was added to the starting solution, and tetrahedrally shaped crystals with edges of about 1 mm were used. X-Ray intensity data were collected on a Syntex $P\bar{1}$ automatic diffractometer using graphite monochromatized MoKα radiation and θ–2θ scan at variable rate. Reflections whose intensities, corrected for background, were less than three times their standard deviation were considered unobserved. A total of 294 symmetry independent reflections were collected within $2\theta \leq 45°$, of which 257 were considered observed. The data were corrected for Lorentz, polarization, and absorption effects ($\mu R = 0.66$). The lattice constant was determined by a least squares fit to fifteen 2θ values measured with the automatic diffractometer. The crystal data are shown in Table 1.

A Varian V-4503 spectrometer with a 12 in. rotatable magnet was used for e.p.r. measurements. The microwave cavity was operated at 35 GHz in the cylindrical TE_{011} mode. A Varian Fieldial unit was used for regulating and measuring the magnetic field. The crystals were aligned by X-ray technique and spectra were recorded by rotating the magnetic field around crystals mounted along either the [110] or [111] axes.

Results

Refinement of the X-ray data was performed on a CDC 6400 computer with a full-matrix least squares program. The final coordinates of $K_2Mg_2(SO_4)_3$ (8) were used as initial parameters for the refinement. The scattering curves for Cd^{2+}, N, S, and O were taken from the *International Tables for X-Ray Crystallography* (9) and those for Cd and S were corrected for anomalous dispersion. A weighting function $\omega = (A + B|F_o| + C|F_o|^2)^{-1}$ was used with coefficients chosen so that $\omega(\Delta F^2)$, involving the square of the difference between the observed and calculated structure factors, would be independent of the local average of $|F_o|$. Unobserved reflections whose observed structure factors are larger than the calculated value were given zero weight, otherwise they were given a value 0.9 times the local minimum of $|F_o|$. Refinement was terminated when all the calculated shifts were less than 0.3 of the errors. The final R value is 0.016 and the weighted R value

$$R_\omega = \left[\frac{\sum\omega(|F_o| - |F_c|)^2}{\sum\omega|F_o|^2}\right]^{1/2}$$

is 0.020. The coefficients of the weighting function are 4.16, −0.0826, and 0.0008 for A, B, and C respectively. The final positional and thermal parameters are listed in Table 2. The observed and calculated structure factors (with no H atoms) are listed in Table 3.[1]

TABLE 1. CAS crystal data

Parameter	Value
Space group	$P2_13$
a (Å)	10.362(7)
V (Å^3)	1112.58
ρ_{calcd} (g/cm^3)	3.28
Z	4
μ (cm^{-1})	44.1

Proton magnetic resonance (p.m.r.) data indicate the existence of general reorientation of the ammonium ions at room temperature (10, 11). Goc *et al.* suggest a "tunneling" motion in which each proton is distributed with equal probability over the four vertices of the ammonium tetrahedron (12). For each of the two inequivalent ammonium groups in CAS, one hydrogen atom should be on a threefold axis and may be considered as the apex of the tetrahedron, while the other three hydrogen atoms are related by this threefold axis. Four possible configurations of these ammonium groups may be envisaged: (*1*) both apices pointing in the [111] direction, (*2*) both along the [$\bar{1}\bar{1}\bar{1}$] direction, (*3*) the nearest neighbors pointing towards each other, and (*4*) the nearest neighbors pointing away from each other. Model *3* results in the hydrogen atoms at the apices being 2.0 Å apart and therefore was rejected. Standard hydrogen atomic scattering factors were used (9). The other models were tested against the X-ray data by rotating each NH_4 group as a rigid tetrahedral group around the N—H bond along the threefold axis so that reasonable O...H distances could be found for hydrogen bonding. Model *1* consistently gave an R value of 0.023. One configuration of model *4* gave an R value of 0.018 and one other configuration of model *2* gave an R value of 0.017. Although models *1* and *3* may be rejected for the orientation of the ammonium groups, it is not possible to determine the positions of the hydrogen atoms based on X-ray data and the R values. The estimated standard deviations for these positions amount to 0.03 fractional coordinates for both models *2* and *4*, which corresponds to an estimated error of the order of 0.4 Å for the N—H bonds. A dynamic model for the hydrogen atoms appears to be

[1]Table 3 is available, at a nominal charge, from the Depository of Unpublished Data, CISTI, National Research Council of Canada, Ottawa, Canada K1A 0S2.

Can. J. Chem. Downloaded from www.nrcresearchpress.com by 210.87.254.105 on 09/05/12
For personal use only.

TABLE 2. Positional and thermal parameters of CAS at 25 °C (e.s.d. in parentheses)

Atom	Position type	x	y	z	U_{11}*	U_{22}	U_{33}	U_{12}	U_{13}	U_{23}
Cd(1)	4*b*	0.5806(1)	0.5806(1)	0.5806(1)	0.013(1)	0.013(1)	0.013(1)	−0.0008(8)	0.0008(8)	0.0008(8)
Cd(2)	4*b*	0.8368(1)	0.8386(1)	0.8368(1)	0.013(1)	0.013(1)	0.013(1)	−0.0012(9)	0.0012(9)	0.0012(9)
N(1)	4*b*	0.065(2)	0.065(2)	0.065(2)	0.022(8)	0.022(8)	0.022(8)	−0.0010(10)	0.0010(10)	0.0010(10)
N(2)	4*b*	0.301(2)	0.301(2)	0.301(2)	0.028(10)	0.028(10)	0.028(10)	−0.0010(10)	0.0010(10)	0.0010(10)
S	12*a*	0.6253(2)	0.4745(2)	0.2603(2)	0.0111(9)	0.010(1)	0.009(1)	0.0022(7)	−0.0004(8)	−0.0009(8)
O(1)	12*a*	0.6588(7)	0.5002(7)	0.3959(6)	0.040(3)	0.046(4)	0.022(3)	−0.001(4)	−0.001(3)	−0.015(3)
O(2)	12*a*	0.7406(7)	0.4963(7)	0.1834(7)	0.026(3)	0.047(3)	0.032(4)	0.005(3)	0.022(3)	0.008(3)
O(3)	12*a*	0.5788(6)	0.3423(6)	0.2451(6)	0.033(3)	0.014(3)	0.047(4)	−0.005(3)	−0.020(3)	0.004(3)
O(4)	12*a*	0.5257(6)	0.5622(6)	0.2152(6)	0.024(3)	0.030(4)	0.047(4)	0.010(3)	−0.012(3)	−0.001(3)

*Calculated from $\beta_{ij} = 2\pi^2 b_i b_j U_{ij}$ where $T = \exp[-(\beta_{11}h^2 + 2\beta_{12}hk + \ldots)]$ is the thermal factor appearing in the structure factor expression and b_i's are reciprocal lattice vectors.

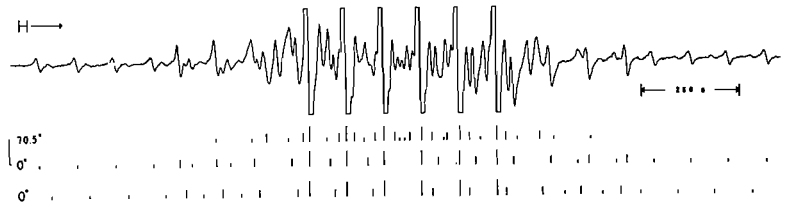

FIG. 1. Electron paramagnetic resonance spectrum of Mn^{2+} in CAS with H ∥ [111] (analysis is shown below the spectrum. Lines unaccounted for in the analysis are attributed to the 70.5° spectrum of site II.)

very likely and the final answer must await a single crystal neutron diffraction study.

Electron paramagnetic resonance spectra of CAS doped with Mn^{2+} were taken at room temperature by rotating the magnetic field around the [110] and [111] axes of the crystals. Spectral resolution was generally poor due to the large number of resonance lines. However, a few observations may be made from these complex spectra. First there exist two inequivalent sites of Mn^{2+} with the intensity ratio of their resonance lines about 1:3. Secondly, the crystalline field around both sites is axially symmetric with the symmetry axis (the z-axis) parallel to the body diagonal of the cubic unit cell, as Tatsuzaki observed (7). It may be concluded that the Mn^{2+} substitutes at both sites of the Cd^{2+}. The simplest spectral pattern (Fig. 1) was found when the magnetic field was along the [111] axis. There are four symmetry equivalent sites related by the twofold screw axes for each of the two inequivalent Mn^{2+}. The direction of the static magnetic field in this case is parallel to the z-axis of one site while it makes an angle of 70.5° with the z-axis of the other three sites. The result is that two sets of spectra are observed and each set consists of two Mn^{2+} spectra with an intensity ratio of 1:3. The two sets of spectra shown in Fig. 1 have again an intensity ratio of about 1:3, suggesting preferential occupation of the two inequivalent sites by the Mn^{2+}. Also, the 70.5° spectrum in each set should have a zero-field splitting ($3\cos^2\theta - 1$) times that for the 0° spectrum, as observed (Fig. 1).

The spectra were analyzed by using the equations for resonance fields by Bleaney and Trenam (13). The hyperfine splitting due to ^{55}Mn was found to be almost isotropic at 97 ± 5 G. The spectral parameters are given in Table 4.

It is not possible to establish from e.p.r. experiments alone which spectrum belongs to which one of the two inequivalent sites of Mn^{2+} since the site symmetries are the same, *i.e.* trigonal. The fact that greater concentration of Mn^{2+} was found in one site implies that the Mn^{2+} may also prefer the same site even at higher concentration levels. Consequently, crystals of the stoichiometry $Mn_xCd_{2-x}(NH_4)_2(SO_4)_3$ were grown by using a 1:1 ratio of Cd and Mn in the starting solution. The Mn content of the sample was analyzed colorimetrically by oxidation of Mn^{2+} to MnO_4^- with KIO_4. The value of x was found to be 1.16 ± 0.05. X-Ray data were collected on a spherical crystal (radius = 0.018 cm) and the structure was assumed to be isomorphous with CAS. The data were corrected as above and the model was refined by using a full-matrix least squares program with the site occupancy as an additional variable. The structure, with a = 10.262(8) Å, refined to a final R value of 0.051 and R_ω of 0.052. The result shows that cation site I contained 0.82 ± 11 Mn while site II contained 0.38 ± 11. The total Mn content of x = 1.2 agrees well with our chemical analysis. If we assume that the site preference of Mn^{2+} is the same at both low and high concentration the set of e.p.r. spectra with the higher intensity and larger D-splitting would correspond to Mn^{2+} in site I.

The solution to the question of site occupancy may be sought in another way. The various mechanisms giving rise to the zero-field splitting

TABLE 4. Electron paramagnetic resonance parameters of CAS (e.s.d. in parentheses)

Parameter	Site I	Site II
$g_\parallel$*	1.992(1)	1.992(1)
$\|A\|$	97(3)	97(3) G
D†	−171(5)	−162(5) G
$(a - F)$	4.3(1.0)	4.8(1.0) G

*Poor spectral resolution did not permit a determination of $g_\perp$.
†The signs of D and $(a - F)$ are relative, but the sign of D is supposed to be negative from a point-charge calculation.

Can. J. Chem. Downloaded from www.nrcresearchpress.com by 210.87.254.105 on 09/05/12
For personal use only.

Can. J. Chem. Downloaded from www.nrcresearchpress.com by 210.87.254.105 on 09/05/12
For personal use only.

of a ^6S state ion in trigonal symmetry have been discussed by Sharma, who derived expressions relating the zero-field splitting parameter D to the crystal field (14). The results were applied by Sharma to the case of Mn^{2+} in $CdCl_2$. We performed a similar calculation for Mn^{2+} in CAS by direct lattice summation to a maximum radius of 30 Å. The atomic coordinates from the structure refinement were used and the atoms were treated as point charges whose magnitude was equal to their formal charge. Using a 10 Dq value of 9000 cm^{-1} and a spin–orbit coupling constant of 300 cm^{-1} for Mn^{2+}, we obtained a value of $D = -214$ G for Mn^{2+} in site I and $D = -168$ G for site II. It is conceivable that the lattice may distort in the immediate vicinity of the site due to substitution by a cation of different size. The positions of the nearest oxygen atoms around each site were then altered in such a way that the average Mn—O distance was 2.19 Å but with O—Mn—O angles the same as in the case of Cd^{2+}. D changes by -3 G for both site I and site II. Comparison with the experimental values in Table 4 indicates that the assignment of site for the Mn^{2+} is correct.

We also attempted to verify that the space group of CAS in the ferroelectric phase below 90 K is $P2_1$, and to clarify whether the cell is doubled or tripled by taking precession photographs of the crystal at 80 K. Unfortunately neither the change in space group nor doubling or tripling of the cell constant could be detected at this temperature. Application of a static electric field up to 1.2 kV/cm along a cube axis of the crystal, in order to maintain a single-domain crystal in the ferroelectric phase, also proved to be of no avail in detecting those changes. Electron paramagnetic resonance spectra were also recorded at 77 K. A definite change of the spectral pattern was observed with the appearance of more Mn^{2+} sites than at room temperature, thus indicating a phase transition to a space group of lower symmetry. However, the spectra proved to be too complex to permit an unambiguous analysis.

Discussion

The room temperature structure of CAS projected along the [001] axis is shown in Fig. 2. The important bond lengths and bond angles are listed in Table 5. The structure is essentially the same as that of langbeinite ($K_2Mg_2(SO_4)_3$) (8). The sulfate group is slightly distorted with an

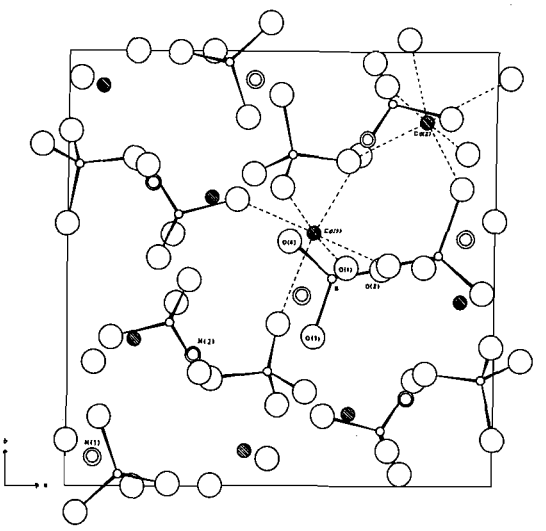

FIG. 2. Structure of CAS projected along [001].

average S—O bond length of 1.458 Å. Both Cd^{2+} ions have a distorted octahedral environment with the major distortion along the threefold axis. The shorter average cation–oxygen distance in site I is consistent with the observation that occupation of this site is preferred by Mn^{2+}, whose ionic radius is slightly smaller than that of Cd^{2+}. Each oxygen atom from a sulfate group is bonded to only one cation. The two ammonium groups have irregular environments, the first has a coordination number of 12 and the second has a coordination number of 9. The K^+ ions in langbeinite are coordinated in a similar fashion.

Goc *et al.* investigated the n.m.r. linewidths of CAS and concluded that the intramolecular contribution to the proton second moment was reduced to zero due to general reorientation of protons in the ammonium groups (12). They obtained a second moment of 0.80 G^2 for the powdered sample. The theoretical second moment for molecular reorientation of the ammonium groups by the van Vleck's formula (15), in the case of powdered CAS, is

$$S = 358.08 \sum r_{ij}^{-6}$$

where r_{ij} is the distance between centers of the groups. Using the results of our structural refinement and summing over $r_{ij} \leq 15$ Å, we obtained a value of 1.54 G^2. (Goc *et al.* reported a calculated value of 0.81 G^2 by using the atomic positions of langbeinite while we obtained a

TABLE 5. Molecular geometry of CAS* (e.s.d. in parentheses)

Atom or group	Bond	Distance (Å)	Bonds	Angle (deg)
SO_4 group	S—O(1)	1.472(7)	O(1)—S—O(2)	107.5(4)
	—O(2)	1.454(8)	—O(3)	110.5(4)
	—O(3)	1.460(7)	—O(4)	111.3(4)
	—O(4)	1.452(7)	O(2)—S—O(3)	110.9(4)
			—O(4)	108.1(4)
			O(3)—S—O(4)	108.5(4)
NH_4(I) group and environment	N(1)—O(1)11 ×3	2.97(1)		
	—O(2)4 ×3	3.22(1)		
	—O(2)6 ×3	3.37(1)		
	—O(3)4 ×3	3.36(1)		
	—O(4)4 ×3	3.22(1)		
NH_4(II) group and environment	N(2)—O(2)6 ×3	3.18(1)		
	—O(3) ×3	2.97(1)		
	—O(4)6 ×3	3.06(1)		
Cd(1) environment	Cd(1)—O(1) ×3	2.239(7)	O(1)—Cd(1)—O(1)2	97.3(3)
	—O(2)5 ×3	2.281(8)	—O(2)5	80.5(3)
			—O(2)10	88.6(3)
			—O(2)9	174.0(3)
			O(2)5—Cd(1)—O(2)9	93.9(3)
Cd(2) environment	Cd(2)—O(3)5 ×3	2.261(7)	O(3)5—Cd(2)—O(3)9	97.7(2)
	—O(4)4 ×3	2.283(6)	—O(4)4	89.4(2)
			—O(4)8	86.9(2)
			—O(4)12	170.9(2)
			O(4)4—Cd(2)—O(4)8	85.3(2)

*The number following the atom identification designates the symmetry operation in the order listed in the *International Tables of X-Ray Crystallography*; thus O(2)4 is generated from the position of O(2) in Table 2 by the symmetry operation $\frac{1}{2} + x, \frac{1}{2} - y, -z$.

value of 1.61 G^2 with these coordinates.) While the value of 1.54 G^2 is high compared with the experimental values of 0.80 G^2, Andrew and Eades (16) pointed out that for general molecular reorientation about the center of gravity, the intermolecular contribution to the second moment was further reduced and r_{ij}^{-6} should be replaced by ξG_{ij}^2 where

$$G_{ij} = \frac{1}{4r_{ij}R_1R_2} \ln\left[\frac{r_{ij}^2(R_1 - R_2)^2}{r_{ij}^2 - (R_1 + R_2)^2}\right]$$

and R_1 and R_2 are the distances of the protons from the centers of gravity of the groups and ξ was given a value of 0.63. Using these reduced interproton vectors the second moment of powdered CAS was calculated to be 1.17 G^2. Although there might be some contribution to the second moment from nuclei other than protons, this contribution is expected to be much smaller than the 0.1 G^2 found for NH_4Cl (17) since ^{16}O has zero nuclear magnetic moment. We also calculated the angular dependence of the second moment for a single crystal CAS. The results are plotted in Fig. 3. Although the shape of the

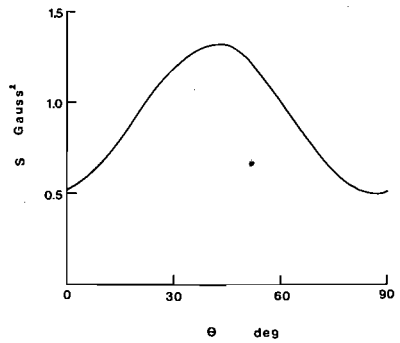

FIG. 3. Calculated angular dependence of proton second moment of CAS. ($\theta = 0°$ corresponds to H ∥ [100] and $\theta = 90°$ corresponds to H ∥ [010]).

curve and the values of the extrema (0.51 and 1.32 G^2) agree well with the experiments of Goc *et al.*, there is a difference in phase by 45°, *i.e.*, the theoretical minimum of S is to be found with the magnetic field along a cube axis and not along the [110] axis as they reported. Since the intramolecular proton contribution appears to be zero, the calculated second moment is inde-

Can. J. Chem. Downloaded from www.nrcresearchpress.com by 210.87.254.105 on 09/05/12
For personal use only.

pendent of the positions of the hydrogen atoms obtained from diffraction experiments, which must be taken as "statistical average" positions.

We conclude from these studies that CAS has the langbeinite structure at room temperature with redistribution of the hydrogen atoms among the vertices of the ammonium groups. Previous n.m.r. studies (10, 11) indicate that there is negligible change in linewidth or relaxation time of the proton resonance in going from room temperature to 77 K. This together with the observation of a similar phase transformation of $Cd_2Tl_2(SO_4)_2$ at 130 K by Brezina and Glogarová suggests that motion of the NH_4 groups in CAS is not "frozen-in" and is not responsible for the ferroelectric phase transformation, as it was found to be the case in many other ammonium salts. Some motional change of the sulfate group may be responsible for bringing about the structural change of CAS and CTS.

This research has been supported by a grant from the National Research Council of Canada.

1. F. JONA and R. PEPINSKY. Phys. Rev. **103**, 1126 (1956); F. JONA and G. SHIRANE. Ferroelectric crystals. Pergamon Press, New York. 1962.
2. H. OHSHIMA and E. NAKAMURA. J. Phys. Chem. Solids, **27**, 481 (1966).
3. B. BREZINA and GLOGAROVÁ. Phys. Status Solidi, A**11**, K39 (1972).
4. M. GLOGAROVÁ and J. FOUSEK. Phys. Status Solidi, A**15**, 579 (1973).
5. K. AIZU. J. Phys. Soc. Jap. **32**, 135 (1972).
6. V. DVOŘÁK. Phys. Status Solidi, B**52**, 93 (1972).
7. I. TATSUZAKI. J. Phys. Soc. Jap. **17**, 582 (1962).
8. V. A. ZEMANN and J. ZEMANN. Acta Cryst. **10**, 409 (1957).
9. J. S. KASPER and K. LONDSDALE. (*Editors*). International tables for X-ray crystallography, Vol. III. Kynoch Press, Birmingham. 1959.
10. G. BURNS. Phys. Rev. **123**, 64 (1961).
11. I. TODO and I. TATSUZAKI. Phys. Lett. Neth. **23**, 519 (1966).
12. R. GOC, Z. PAJAK, and A. POSPIESZALSKA. Phys. Status Solidi, B**59**, K31 (1973).
13. B. BLEANEY and R. S. TRENAM. Proc. R. Soc. **223**, 1 (1954).
14. R. R. SHARMA. Phys. Rev. B**3**, 76 (1971).
15. J. H. VAN VLECK. Phys. Rev. **74**, 1168 (1948).
16. E. R. ANDREW and R. G. EADES. Proc. R. Soc. Lond. A**216**, 398 (1953).
17. H. S. GUTOWSKI, G. E. PAKE, and R. BERSOHN. J. Chem. Phys. **22**, 643 (1954).

Can. J. Chem. Downloaded from www.nrcresearchpress.com by 210.87.254.105 on 09/05/12
For personal use only.

Photolysis of Pyridazine in the Gas Phase

JAMES R. FRASER, L. H. LOW, AND NEIL A. WEIR
Chemistry Department, Lakehead University, Thunder Bay, Ontario P7B 5E1

Received October 11, 1974

JAMES R. FRASER, L. H. LOW, and NEIL A. WEIR. Can. J. Chem. **53**, 1456 (1975).

Pyridazine was photolyzed with long wave ultraviolet radiation (3650–3663 Å) over the temperature range 100–160 °C. Nitrogen and vinylacetylene were the main products, their quantum yields at 110 °C being 0.12 ± 0.05 and 0.09 ± 0.04, respectively. Nitrogen formation is not significantly inhibited by the presence of oxygen and no isomerization of *cis*-but-2-ene was observed during photolyses. It appears that some reaction occurs from the excited singlet, S (n → π*) A, but this state is efficiently deactivated photophysically. It is suggested that vinylacetylene is formed from a C_4H_4 diradical by means of a 1,3 H-atom migration, and isotope effects observed for the photolysis of pyridazine-d_4 support C—H bond fission.

JAMES R. FRASER, L. H. LOW et NEIL A. WEIR. Can. J. Chem. **53**, 1456 (1975).

On a photolysé la pyridazine avec une radiation ultraviolette de grande longueur d'onde (3650–3663 Å), à des températures allant de 100–160 °C. L'azote et le vinyl-acétylène sont les produits principaux et leurs rendements quantiques à 110 °C sont respectivement de 0.12 ± 0.05 et 0.09 ± 0.04. La formation d'azote n'est pas inhibée d'une façon significative par la présence d'oxygène et on n'a pas observé d'isomérisation du butène-2 *cis* durant les photolyses. Il semble que quelques réactions se produisent à partir d'un état excité singulet, S (n → π*) A ; cet état est toutefois désactivé d'une façon efficace par des processus photo-physiques. On suggère que le vinyl-acétylène se forme à partir du radical C_4H_4 par l'intermédiaire d'une migration 1,3 d'un atome d'hydrogène; les effets isotopiques observés lors de la photolyse de la pyridazine-d_4 sont en accord avec une fission du lien C—H. [Traduit par le journal]

Introduction

The photochemistry of a number of 1,4-diazines has been studied in detail, and relationships between excited states and mechanisms of isomerization have been elucidated (1–4). By comparison, knowledge of the photochemistry of 1,2-diazines is very limited, although a considerable amount of data related to photophysical processes occurring in these molecules has been amassed (5–9).

Electron impact induced fragmentation of pyridazine results in the production of nitrogen and another ionic species, $C_4H_4^{2+}$, which, on the basis of metastable ion detection, was tentatively assigned the cyclobutadienyl dication structure (10).

The diazines have chemical structures similar to those of diazirines which undergo photolytic and thermolytic isomerizations or decompositions into nitrogen and a number of small hydrocarbons (11, 12). Some evidence has been obtained for the production of carbenes as intermediates and a transition state involving simultaneous rupture of two C—N bonds has been postulated (13).

1-Pyrazolines and substituted 1-pyrazolines undergo similar photochemical decompositions into nitrogen and vibrationally excited cyclopropanes which subsequently isomerize (14, 15) an intermediate excited singlet methylene produced by two simultaneous C—N bond fissions, rapidly undergoing ring closure (16).

Pyridazine is of particular interest, since it can be seen that an analogous decomposition would produce a diradical which could conceivably ring close to yield cyclobutadiene. The object of this work was to investigate the photoreactions of pyridazine.

Experimental

Photolyses were carried out in a conventional "static" system using a Pyrex reaction vessel (120 cm^3) which had been "aged" by the pyrolysis of hexamethyldisiloxane at 500 °C for 16 h. The associated vacuum system and analytical train incorporated greaseless stopcocks. The reaction vessel was housed in a coaxial furnace, the temperature of which was maintained to ±0.1 °C. Analyses were carried out by gas chromatography (Hewlett Packard Research Chromatograph) the products from the reaction vessel being divided into two fractions, one condensable and the other noncondensable at −205 °C (pumped liquid N_2), which were subsequently transferred to a temperature programmed 10 ft column containing Celite coated with 12% Carbowax and to a 6 ft molecular sieve column (5A) at 30 °C respectively. The Carbowax column effluent passed through a f.i.d., while the molecular sieve column was used along with a katharometer and helium was the carrier gas. The nature of

Can. J. Chem. Downloaded from www.nrcresearchpress.com by 210.87.254.5 on 09/05/12
For personal use only.

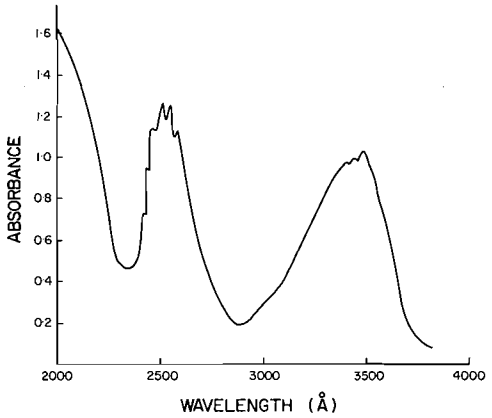

FIG. 1. Ultraviolet spectrum of pyridazine; pressure 23 Torr at 95 ± 1 °C, path length 1 cm.

the gases was confirmed by mass spectrometry, small samples of the column effluent being introduced directly into the R.MU7 mass spectrometer. Unreacted pyridazine was separated at −20 °C (salt bath) and determined, after expansion into a standard volume, by pressure measurement of 60 °C. The ultraviolet source was a medium pressure 100 W Hg arc (Hanovia).

Light from the arc passed through a standard filter to isolate the 3650–3663 Å band (17) and was focused by means of a lens into a parallel beam which traversed the reaction vessel.

Quantum yields were determined by potassium ferrioxalate actinometry (18). Solutions (0.006 *M*) were irradiated at 20 °C under the same conditions as the above reaction vessel, and were stirred by bubbling through them a stream of pure N_2. The quantum yield of Fe^{2+} formation was assumed to be 1.21 (18), and the fraction of light absorbed by a solution was determined using a phototube (R.C.A. Type 1P28) powered by a 120 V d.c. (Dry Cell) power supply. The output of the phototube was measured using a microvolt meter (Keithley Model 155).

The ultraviolet spectrum of gaseous pyridazine (pressure 23 Torr) shown in Fig. 1, was measured at 95 ± 1 °C using a Cary 14 spectrophotometer, fitted with a heated sample holder, which contained a quartz cell (Rho Scientific Anaerobic cell) with a path length of 1 cm. The cell was filled after evacuation by molecular distillation of pyridazine at 10^{-5} Torr.

Pyridazine (Aldrich) was dried over anhydrous $MgSO_4$ for 24 h and repeatedly distilled under reduced pressure in presence of nitrogen. Gas chromatographic analyses on two columns showed only one peak. Pyridazine-d_4 (Merck, Sharp and Dohme) was used without further purification.

Results

Pyridazine was photolyzed over the temperature range 100–160 °C (the vapor pressure being insufficiently high at temperatures below 100 °C). The noncondensable fraction yielded one product which was identified as nitrogen, and only one product could be separated from the condensable fraction. This product was subjected to the following analyses, the results of which are shown below.

(*a*) Infrared gas phase spectra showed the following main bands: 3300 (s), 2990 (s), 2120 (w), 1670 (w), 1450 (s), 1300 (m), 970 cm^{-1} (w).

(*b*) Mass spectrometry indicated a molecular weight of 52 which corresponds to the mass of a molecule formed by the loss of nitrogen from pyridazine. The molecular ion had the highest relative abundance and high resolution measurements indicated an *m/e* value of 52.0312 which would correspond to a C_4H_4 entity ($C_4H_4 \equiv$ 52.0313).

(*c*) Nuclear magnetic resonance analyses in deuterated chloroform showed two main bands, a sharp singlet at τ 7.2 p.p.m., and a multiplet centered at τ 4.65 p.p.m.

(*d*) The ultraviolet spectrum of a gaseous sample showed a broad band extending to 2500 Å. It was noted, however, that after standing at room temperature for a short period, the sample underwent polymerization, a yellow deposit forming on the walls of the gas cell. The u.v. spectrum of samples then showed a large bathochromic shift.

The C_4H_4 fragment could conceivably have one of three structures (cyclobutadiene omitted), *i.e.*, butatriene, vinylacetylene, or methylene cyclopropene. The above i.r. and n.m.r. data appear to favor vinylacetylene (*e.g.* the singlet at τ 7.2 p.p.m. and the peaks at 3300 and 2120 cm^{-1} suggest the presence of the —C≡CH group). The above spectral measurements were made on an authentic sample of vinylacetylene, and similar data obtained (*e.g.* a singlet at τ 7.15 p.p.m., a multiplet centered on τ 4.55 p.p.m., i.r. absorptions at 3300, 2980, and 2130 cm^{-1}). No evidence for the allene or the *exo*-double bond structures could be obtained, and it is concluded that the major products of photolysis of pyridazine are nitrogen and vinylacetylene; other products, if formed, were present in insufficient quantities for i.r. spectral estimation.

The stoichiometry of the decomposition is shown in Fig. 2 and it can be seen that while there is a good correspondence between pyridazine depletion and nitrogen formation, the vinylacetylene yield was consistently lower, possibly on account of the polymerization which occurs during the analysis. (Vinylacetylene is known to polymerize readily at room tempera-

Can. J. Chem. Downloaded from www.nrcresearchpress.com by 210.87.254.5 on 09/05/12
For personal use only.

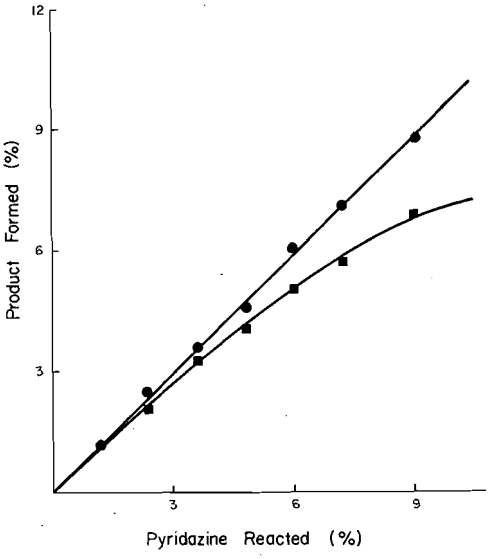

FIG. 2. Demonstration of the stoichiometry of the reaction at 110 °C, pyridazine pressure 25 Torr: ○, nitrogen produced; □, vinylacetylene produced (both as percent of initial reactant).

ture, but no polymer was observed in the reaction vessel.) Beyond about 20% decomposition Fig. 2 becomes curved, presumably due to decreasing pyridazine concentration (and hence light absorption).

Studies of the reaction were therefore restricted to the first 5% of the pyridazine decomposition. The effect of surfaces on the reaction was investigated and identical runs were carried out in an unpacked and in a packed (with Pyrex tubes) vessel, both of which had been aged as previously described and had surface–volume ratios of 1.2 and 8.3 cm^{-1} respectively. The rates of nitrogen and vinylacetylene formation for the unpacked vessel were 2.4×10^{-8} and 2.0×10^{-8} mol l^{-1} s^{-1} respectively and for the packed vessel were 2.5×10^{-8} and 1.86×10^{-8} mol l^{-1} s^{-1}, respectively. It is concluded that the reaction is homogeneous.

The extent of the purely thermal decomposition of pyridazine was investigated over the temperature range 100–160 °C and no detectable amounts of either product of the photoreaction were obtained.

The rate of nitrogen formation was found to be directly proportional to the pyridazine pressure (as would be expected for low extents of absorption) and to the light intensity (Table 1).

TABLE 1. Photolysis of pyridazine (26 Torr) at 102 °C with varying u.v. (3650–3663 Å) intensities

$R_{N_2} \times 10^8$ (mol l^{-1} s^{-1})	I (%)	R_{N_2}/I
2.66	100	0.026
2.37	81.7	0.029
1.54	64.3	0.024
1.26	46.6	0.027
0.81	33.4	0.024
0.506	22.0	0.023

Vinylacetylene formation conforms to a similar relationship, but the data are more scattered.

Quantum yields for nitrogen formation were almost invariant, with values of 0.12 ± 0.05 over the pyridazine pressure range 5–45 Torr, but those for vinylacetylene decreased with increasing pressure, *e.g.* at 5 Torr, $\Phi = 0.09 \pm 0.04$ and at 50 Torr, $\Phi = 0.06 \pm 0.02$ (measured at 110 °C).

It would appear from these results and from the light intensity data that chain decompositions are not involved.

Photolysis of pyridazine-d_4 under identical conditions at 110 °C yielded nitrogen and C_4D_4 (presumably vinylacetylene-d_4). No significant isotope effect was observed for nitrogen formation; $(R_{N_2})_H/(R_{N_2})_D = 1.04 \pm 0.01$ but for vinyl acetylene (v) the ratio $(R_v)_H/(R_v)_D$ was 1.65 ± 0.2, these measurements being made at 3% decomposition.

The photolysis was carried out in the presence of a number of added gases, and the results are shown in Fig. 3.

It can be seen that the inhibiting effects of CO_2, O_2, and *cis*-but-2-ene are comparable. The O_2 pressure had to be limited to 30 Torr to minimize explosion hazards. The effects of argon and CO_2 on vinylacetylene formation are very similar to those shown in Fig. 3, but both O_2, and to a lesser extent, *cis*-but-2-ene depress vinylacetylene yields and appear to react with small amounts of vinylacetylene and/or its precursor, a number of additional products, of which only acetylene was positively identified, being formed.

No evidence for isomerization of the *cis*-but-2-ene was obtained.

Discussion

The following scheme qualitatively accounts for the experimental data.

Can. J. Chem. Downloaded from www.nrcresearchpress.com by 210.87.254.5 on 09/05/12
For personal use only.

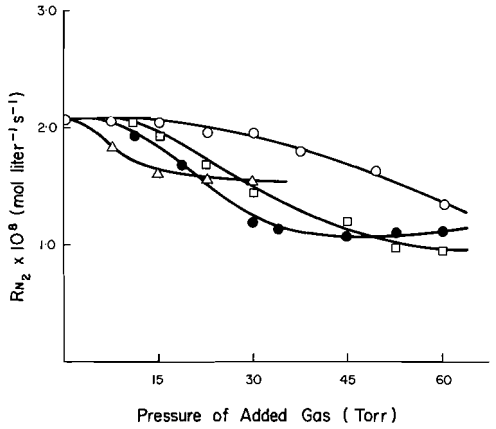

FIG. 3. Photolysis of pyridazine (22 Torr) at 105 °C in presence of added gases: ○, argon present; △, oxygen present; □, CO_2 present; ●, *cis*-but-2-ene present.

$$[1] \quad C_4H_4N_2 \xrightarrow{h\nu} [C_4H_4N_2]^* \rightarrow N_2 + [\cdot C_4H_4\cdot]^*$$

$$[\cdot C_4H_4\cdot]^* \rightarrow CH{\equiv}C{-}CH{=}CH_2$$

Absorption of light produces an excited pyridazine molecule which by analogy with previous data (13) could be a diradical with the structure

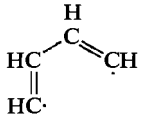

No evidence was obtained for a two-step decomposition. However the lifetime of a diazomethane type intermediate monoradical would be very short at temperatures above 100 °C. The diradical subsequently isomerizes by means of a 1,3-H atom migration to produce vinylacetylene.

Due to the presence of two filled nonbonding molecular orbitals in pyridazine, two n → π* transitions are possible; however, one of these, is symmetry forbidden. Absorption of ultraviolet radiation (λ = 3650–3663 Å) yields the vibrationally excited singlet, S* (7, 8) which is symmetry allowed [S (n → π*) A]. This species undergoes vibrational relaxation on collision with added gas molecules and this is reflected in decreased product yields (Fig. 3).

Pyridazine is anomalous in that the photophysical deactivation of the S (n → π*) A state is very facile (7). In addition to fluorescence of low intensity, rapid internal conversion to the symmetry forbidden singlet, S (n → π*) F, vibrational relaxation to the S_0 state and intersystem crossing to the triplet T (n → π*) occur. Since the energy of the triplet lies close to that of the S (n → π*) F state, further rapid intersystem crossing to this singlet occurs, the singlet subsequently returning to the ground state by internal conversion (the triplet lifetime is less than 10^{-6} s) (7) before appreciable numbers of encounters are made with oxygen and *cis*-but-2-ene molecules; a similar conclusion was reached by Srinivasan (19) regarding the photodecomposition of cycloheptanone. A plausible reaction scheme is summarized as follows.

$$[2] \quad \text{Pyridazine } (S_0) \xrightarrow{h\nu} S_1^*[S\ (n \rightarrow \pi^*)\ A]$$

$$[3] \quad S_1^* + M \rightarrow S_1 + M \text{ (M is a molecule which removes vibrational excitation on collision)}$$

$$[4] \quad S_1^* \rightarrow T_1^*$$

$$[5] \quad S_1^* \rightarrow \text{products } (N_2 + C_4H_4)$$

$$[6] \quad S_1 \rightarrow T_1 \rightarrow S\ (n \rightarrow \pi^*)\ F \rightarrow S_0$$

$$[7] \quad S_1 \rightarrow S\ (n \rightarrow \pi^*)\ F \rightarrow S_0$$

The low photochemical quantum yields are consistent with efficient partitioning of energy into photophysical processes.

The data shown in Fig. 3 could be interpreted in terms of some decomposition occurring from vibrationally excited pyridazine, the added gases removing vibrational energy by collision, and hence reducing the N_2 yield.

The excited singlet is undoubtedly formed (7), and since intersystem crossing is rapid, the excited triplet could also be present; both could yield the products.

The results obtained from reactions carried out in presence of O_2 and *cis*-but-2-ene would suggest that if triplets are indeed involved, they must be short lived excited species which decompose before significant amounts of quenching by either O_2 or *cis*-but-2-ene can take place.

From previous studies (19), it would appear that the concentrations of O_2 used in the present work would be sufficient to quench a large proportion of pyridazine triplets, and the observation that the deactivating effect of O_2 is com-

Can. J. Chem. Downloaded from www.nrcresearchpress.com by 210.87.254.5 on 09/05/12
For personal use only.

parable with that of CO_2 would suggest that no such quenching takes place.

In addition, the absence of a detectable extent of isomerization of *cis*-but-2-ene would support the above conclusions.

Because of the apparent complexity of the reactions in which O_2 and *cis*-but-2-ene are present, it was not possible to obtain unequivocal information regarding either the nature or electronic multiplicity of the C_4H_4 precursor of vinylacetylene. There is evidence that the singlet state is predominant in tetramethylene diradicals derived from the photodecomposition of saturated six-ring azo compounds (20), and the inhibiting effects of argon and CO_2 on vinylacetylene formation suggest that a vibrationally excited species is involved. Such excited diradicals frequently ring-close to form the corresponding alicyclic compounds which isomerize to form unsaturated open chain molecules (21). By analogy, the C_4H_4 diradical would yield excited cyclobutadiene and/or excited methylene cyclopropene, neither of which would be expected to have more than transitory existence, and vinylacetylene would be formed by isomerization.

An alternative mechanism involves a unimolecular isomerization of C_4H_4, the H-atom undergoing a 1,3 migration. Such reactions have been observed for vibrationally excited (40 kcal mol^{-1}) alkyl radicals (22) and probably involve cyclic transition states, there being sufficient excitation in the bending modes to ensure repeated encounters of the two ends of the radicals. A qualitatively similar mechanism of formation of vinylacetylene from excited butadiene was suggested by Lossing and co-worker (23), a H-atom on the 2 C-atom interacting with the double bond between C-atoms 3 and 4, the encounter being facilitated by the excited bending modes of the 2–3 bond.

The significant deuterium isotope effect qualitatively supports the rupturing of a C—H bond as a prerequisite for hydrogen migration. However, the effect is considerably less than would be expected for a purely thermally activated process, confirming to some extent the involvement of a vibrationally excited C_4H_4 species.

The authors gratefully acknowledge the technical assistance of Mr. D. Corbett and Mr. S. Spivac and the financial assistance of the National Research Council of Canada.

1. F. LAHMANI and N. IVANOFF. Tetrahedron Lett. 3913 (1967).
2. F. LAHMANI, N. IVANOFF, and M. MAGAT. C.R. Acad. Sci. **263**, 1005 (1966).
3. M. MAGAT, N. IVANOFF, F. LAHMANI, and M. PILENI. J. Chim. Phys. 212 (1970).
4. T. BREWER and S. H. JONES. J. Phys. Chem. **75**, 3769 (1971).
5. L. GOODMAN and R. W. HARRELL. J. Chem. Phys. **30**, 1131 (1959).
6. L. GOODMAN. J. Mol. Spectrosc. **6**, 109 (1961).
7. B. J. COHEN and L. GOODMAN. J. Chem. Phys. **46**, 713 (1967).
8. K. K. INNES, J. P. BYRRE, and I. G. ROSS. J. Mol. Spectrosc. **22**, 125 (1967).
9. K. K. INNES, W. C. TINCHER, and E. F. PEARSON. J. Mol. Spectrosc. **36**, 114 (1970).
10. M. H. BENN and T. S. SORENSEN. Chem. Commun. 574 (1967).
11. H. M. FREY. Photolysis of diazirines. *In* Organic photochemistry. IUPAC, Butterworths, London. 1965.
12. M. T. H. LIU and K. TORIYAMA. Can. J. Chem. **51**, 2393 (1973).
13. H. M. FREY and M. T. H. LIU. J. Chem. Soc. A, 1916 (1970).
14. F. H. DORER. J. Chem. Phys. **73**, 3109 (1969); **74**, 1142 (1970).
15. S. H. BAUER. J. Am. Chem. Soc. **91**, 3688 (1969).
16. E. L. ALLRED and R. L. SMITH. J. Am. Chem. Soc. **91**, 6766 (1969).
17. J. G. CALVERT and J. N. PITTS. Photochemistry. J. Wiley, New York. 1967.
18. C. G. HATCHARD and C. A. PARKER. Proc. R. Soc. Lond. A**235**, 518, (1956).
19. R. SRINIVASAN. J. Am. Chem. Soc. **81**, 5541 (1959).
20. N. C. YANG and D-H. YANG. J. Am. Chem. Soc. **80**, 2913 (1958).
21. P. CADMAN, A. F. TROTMAN-DICKENSON, and H. M. MEUNIER. J. Am. Chem. Soc. **91**, 7640 (1969).
22. E. A. HARDWIDGE, C. W. LARSON, and B. S. RABINOVITCH. J. Am. Chem. Soc. **92**, 3278 (1970).
23. J. COLLIN and F. P. LOSSING. Can. J. Chem. **35**, 778 (1957).

Can. J. Chem. Downloaded from www.nrcresearchpress.com by 210.87.254.5 on 09/05/12
For personal use only.

Etude spectroscopique de l'aniline dans les solvants

P. MÉALLIER, A. BERTHELON ET B. POUYET

Laboratoire de photochimie, laboratoire associé au département de chimie organique, Université Claude Bernard Lyon I, Villeurbanne, France

Reçu le 9 mai 1974[1]

P. MÉALLIER, A. BERTHELON et B. POUYET. Can. J. Chem. **53**, 1461 (1975).

L'influence des solvants sur la position et l'intensité des bandes d'absorption a été étudiée entre 200 et 400 nm. Nous nous sommes intéressés plus particulièrement au moment spectroscopique et au déplacement de la bande située à 280 nm.

Alors qu'avec les solvants hydroxylés, la bande d'absorption de l'amine est déplacée vers les courtes longueurs d'onde, que la valeur du moment dipolaire diminue en passant de l'état fondamental à l'état excité, nous avons le phénomène inverse avec les solvants non hydroxylés.

L'importance du transfert de charge, la structure de la molécule ainsi que le comportement des diverses solutions lors d'une photooxydation sont précisées.

P. MÉALLIER, A. BERTHELON, and B. POUYET. Can. J. Chem. **53**, 1461 (1975).

The effect of change of solvent on the positions and intensities of absorption bands of some aromatic amines between 200 and 400 nm has been examined. In particular, the behavior of the band at 280 nm has been studied.

In hydroxylic solvents, this band is displaced towards shorter wavelengths, and the dipole moment in the excited state of the molecule is smaller than in the ground state. The opposite effects are found when nonhydroxylic solvents are used.

The results show how the molecular structure is altered by charge transfer effects and can explain how different solvents affect photochemical oxidation processes.

Introduction

L'aniline et les toluidines présentent dans le domaine de longueurs d'onde compris entre 200 et 400 nm deux bandes d'absorption. Pour étudier l'oxydation photochimique de ces amines, il faut donc choisir une source qui émette soit à 230, soit à 280 nm.

Afin de faciliter les conditions expérimentales lors de l'oxydation, nous avons choisi la bande d'absorption située vers les plus grandes longueurs d'onde.

L'étude spectroscopique préliminaire se rapporte donc au comportement de cette bande d'absorption, c'est-à-dire aux variations d'intensité et aux variations de longueurs d'onde dans différents solvants.

A l'aide de ces résultats, nous nous proposons également de préciser la nature de la transition qui est tantôt définie comme une bande caractéristique du benzène (1), tantôt comme une bande nouvelle due au substituant.

Kimura *et al.* (2), par une étude théorique, laissent prévoir que l'on est en présence "d'une bande de transfert, caractéristique d'un transfert de l'électron entre les substituants et le cycle". C'est cette bande située vers 280 nm que nous nous proposons d'étudier.

Notre travail comprendra donc deux parties: (*1*) étude de l'intensité (moment spectroscopique); (*2*) étude de la position des maxima d'absorption en fonction de la nature des solvants.

Appareillage

Toutes nos expériences ont été réalisées sur un spectrophotomètre SP 800 A muni du dispositif d'expansion d'échelle SP 820. La précision des mesures est d'environ ± 1 Å, soit $\pm 10\ cm^{-1}$ dans le domaine de longueur d'onde considéré.

Etude du moment spectroscopique

Afin de définir l'influence des substituants sur un cycle benzénique, Sklar (3) et Platt (4) ont introduit la notion de "moment spectroscopique" ou "moment de migration".

Suivant la répartition des charges envisagées par Platt, nous avons attribué: le signe + au carbone portant le groupement amino; le signe − au carbone portant le groupement en position *ortho*; le signe + au carbone portant le groupement en position *méta*; le signe − au carbone portant le groupement en position *para*.

[1]Révision reçue le 10 janvier 1975.

Can. J. Chem. Downloaded from www.nrcresearchpress.com by 210.87.254.105 on 09/05/12
For personal use only.

Can. J. Chem. Downloaded from www.nrcresearchpress.com by 210.87.254.105 on 09/05/12
For personal use only.

TABLEAU 1. Valeurs des moments spectroscopiques mesurés dans différents solvants

Solvant	Aniline	*o*-Toluidine	*m*-Toluidine	*p*-Toluidine
Hexane	48.7	58.2	49.7	49
Cyclohexane	50.3	59.2	51.4	50.2
Benzène	51.3	62.2	53.7	54.7
Ether éthylique	54.3	62.5	53.7	53.2
Acétate d'éthyle	53.2	63.2	52.7	53.2
Dioxanne	63	65.2	54.7	53.7
THF	52.5	65.2	54.2	53.7
DMF	76	65.2	57.2	54.2
DMSO	57.7	67.2	57.5	56
Décaline	50.7	61	52	47.7
$CHCl_3$	44.5	56.2	47	48.2
CCl_4	60.7	75	58.2	61.2
Butanol	43	51.2	44	43
Propanol	42	54.2	43.8	45.5
Ethanol	43	51.2	44.2	45.5
Méthanol	42	48.2	42	41.2
Eau	39	44.2	39.8	40

TABLEAU 2. Moments spectroscopiques pour la bande située à 2800 Å exprimés en $(\text{cm mol/l})^{1/2}$

		m		
Molécule	ε_{max}	Calculé	Mesuré	$\Delta m = m_{mes} - m_{calc}$
Aniline	1700		48.7	
o-Toluidine	2070	34	58	+24
m-Toluidine	1740	34	49.7	+15.7
p-Toluidine	1760	47	50.2	+3.2

Les groupements CH_3 et NH_2 étant donneurs d'électrons, nous obtenons les relations suivantes: l'*o*-toluidine, moment $= k(m_a^2 + m_b^2 - m_a \cdot m_b)^{1/2}$; la *m*-toluidine, moment $= k(m_a^2 + m_b^2 - m_a \cdot m_b)^{1/2}$; la *p*-toluidine, moment $= k(m_a^2 + m_b^2 + 2m_a \cdot m_b)^{1/2}$. m_a et m_b étant les modules des moments spectroscopiques des groupements NH_2 et CH_3.

On prend $k = 1$ afin d'obtenir les résultats en $(\text{cm mol/l})^{1/2}$. Le moment spectroscopique ainsi défini permet de connaître théoriquement la variation d'intensité qu'entraîne la substitution d'un groupement à un autre. Ballester *et al.* (5) ont relié ce concept à l'expérience à l'aide d'une relation empirique:

$$\varepsilon_{max} = 40 \sum_{1}^{6} m_i - 250$$

en prenant zéro pour le moment spectroscopique du benzène et en ne considérant que les transitions pour lesquelles $\varepsilon_{max} \geqslant 350$. ε_{max} = coefficient d'absorption moléculaire à la longueur d'onde où l'absorption est maximale. m_i = moment spectroscopique de chaque substituant.

En appliquant à la relation précédente les valeurs des coefficients d'absorption moléculaire que nous avons mesurés, nous avons obtenu les résultats consignés dans les tableaux 1 et 2.

Dans le tableau 2, nous avons comparé les résultats expérimentaux aux résultats théoriques en utilisant l'hexane comme solvant et en prenant respectivement pour les moments spectroscopiques des groupements CH_3 et NH_2, les valeurs +9 et +38 (6).

Ainsi que Platt le signale dans sa publication, le calcul théorique du moment spectroscopique d'une amine aromatique diffère notablement d'une mesure expérimentale. Cette différence est due à l'interaction très forte entre noyau aromatique et substituant. L'écart maximum étant obtenu pour l'*o*-toluidine, où la déformation du cycle entraîne les modifications de symétrie les plus importantes (7).

Nous ne pouvons donc espérer aucune indication quant aux densités électroniques du cycle aromatique à partir de ces résultats.

TABLEAU 3. Caractéristiques des solvants utilisés

Solvant	n_D^{25C}	D^{25C}	$\frac{n_D^2-1}{2n_D^2+1}$	$\frac{D-1}{D+2}-\frac{n_D^2-1}{n_D^2+2}$
Hexane	1.372	1.890	0.1861	0.0001
Octane	1.395	1.948	0.1940	0.0004
Cyclohexane	1.424	2.023	0.2016	0.0018
Chloroforme	1.442	4.806	0.2104	0.2927
trans-Décaline	1.466	2.172	0.2170	0.064
Tétrachlorure de carbone	1.459	2.238	0.2159	0.168
Ether éthylique	1.351	4.335	0.1765	0.3120
Benzène	1.498	2.284	0.2275	0.0051
Dioxanne	1.417	2.209	0.2005	0.0363
Acétate d'éthyle	1.369	6.02	0.1835	0.398
Tétrahydrofurane	1.404	7.39	0.1965	0.436
DMF	1.427	37.6	0.2042	0.667
DMSO	1.478	48.9	0.2206	0.674
Butanol	1.397	17.8	0.1940	0.6066
Propanol	1.375	20.1	0.1862	0.6299
Ethanol	1.359	24.3	0.1804	0.6641
Méthanol	1.326	33.62	0.1678	0.7113
Eau	1.332	80.37	0.1701	0.7585

Cependant, si l'on considère une molécule donnée, mise en solution dans différents solvants, il sera possible de suivre l'évolution du moment spectroscopique de cette molécule en fonction des solvants choisis.

Ainsi la variation du moment spectroscopique de chaque amine au cours de l'étude a été de: 37 pour l'aniline; 30.8 pour l'*o*-toluidine; 18.4 pour la *m*-toluidine; 21.2 pour la *p*-toluidine.

Ces variations sont importantes avec les solvants non hydroxylés, faibles avec les solvants hydroxylés.

Etude du déplacement du maximum d'absorption

Pour suivre le déplacement du maximum d'absorption, nous avons utilisé l'équation de McRae et Basu (8–10). Cette relation fait intervenir les effets suivants: effet de dispersion; effet d'induction (dû au soluté); effet Starck (dû au solvant); effet d'orientation. La variation générale est égale à la somme de ces quatre effets.

$$\bar{\nu}_{\text{vapeur}} - \bar{\nu}_{\text{solution}} = \Delta\bar{\nu}_{\text{dispersion}} + \Delta\bar{\nu}_{\text{induction}} + \Delta\bar{\nu}_{\text{Starck}} + \Delta\bar{\nu}_{\text{orientation}}$$

avec pour chaque terme les relations suivantes:

$$\Delta\bar{\nu}_{\text{dispersion}} = \frac{2}{hca^3}\left(\frac{n_D^2-1}{n_D^2+2}\right)\frac{E}{\varepsilon+E} \times (|\bar{M}_{ef}|^2 + \varepsilon(\alpha_g - \alpha_e))$$

$$\Delta\bar{\nu}_{\text{induction}} = \frac{1}{hca^3}\frac{n_D^2-1}{2n_D^2+1}(\mu_e^2 - \mu_f^2)$$

$$\Delta\bar{\nu}_{\text{Starck}} = \frac{6}{hca^6}\mu_f^2(\alpha_f - \alpha_e) \times \left(\frac{D-1}{D+2} - \frac{n_D^2-1}{n_D^2+2}\right)^2$$

$$\Delta\bar{\nu}_{\text{orientation}} = \frac{2}{hca^3}\mu_f(\mu_e - \mu_f) \times \left(\frac{D-1}{D+2} - \frac{n_D^2-1}{n_D^2+2}\right)$$

où h = constante de Planck, c = vitesse de la lumière, a = rayon d'Onsager du soluté, μ_f = moment dipolaire à l'état fondamental, μ_e = moment dipolaire à l'état excité, α_f = polarisabilité du soluté à l'état fondamental, α_e = polarisabilité du soluté à l'état excité, M_{ef} = moment de transition de la bande du soluté, ε = énergie d'excitation moyenne du soluté, E = énergie d'excitation du solvant, n_D = indice de réfraction en utilisant la raie D du sodium et D = constante diélectrique.

Les caractéristiques des solvants utilisés sont consignées dans le tableau 3.

Le déplacement du maximum d'absorption, noté dans le tableau 4, est déterminé en prenant comme référence le spectre de l'amine à l'état vapeur. Le signe plus (+) étant pris lorsqu'il y a déplacement de la bande vers les grandes

Can. J. Chem. Downloaded from www.nrcresearchpress.com by 210.87.254.105 on 09/05/12
For personal use only.

TABLEAU 4. Déplacement des bandes d'absorption en cm^{-1} dans les solvants

Solvant	Aniline	*o*-Toluidine	*m*-Toluidine	*p*-Toluidine
Hexane	62	62	62	58
Octane	102	180	180	180
Cyclohexane	171	180	180	180
Chloroforme	183			
trans-Décaline	243	360	360	420
Tétrachlorure de carbone	303			176
Ether éthylique	363	489	471	579
Benzène	363	430	420	480
Dioxanne	483	669	839	635
Acétate d'éthyle	539	609	650	635
Tétrahydrofurane	660	729	714	851
DMF	1012	1082	1060	1293
DMSO	1125	1198	1173	1390
Butanol	0	360	180	180
Propanol	−151	246	120	118
Ethanol	−246	180	60	
Méthanol	−528	0	−61	−60
Eau	−749	−503	−557	−538

longueurs d'onde, le signe moins (−) lorsqu'il y a déplacement inverse.

Effets de dispersion et d'induction

Pour déterminer l'importance de ces deux effets, nous avons tracé les spectres d'absorption des anilines en utilisant des solvants apolaires. Nous avons obtenu les résultats suivants, fig. 1.

Ce déplacement, dû à la somme des deux effets, peut, en première approximation, être considéré comme constant pour l'ensemble des solvants. Ceci à condition que la variation du rapport $n_D^2 - 1/(2n_D^2 + 1)$ pour les solvants polaires, soit comprise dans l'intervalle de variation de ce même rapport pour les solvants non polaires utilisés dans la relation (11)

$$\Delta\bar{\nu} = f\left(\frac{n_D^2 - 1}{2n_D^2 + 1}\right)$$

Nous obtenons donc pour ces derniers, les déplacements suivants:

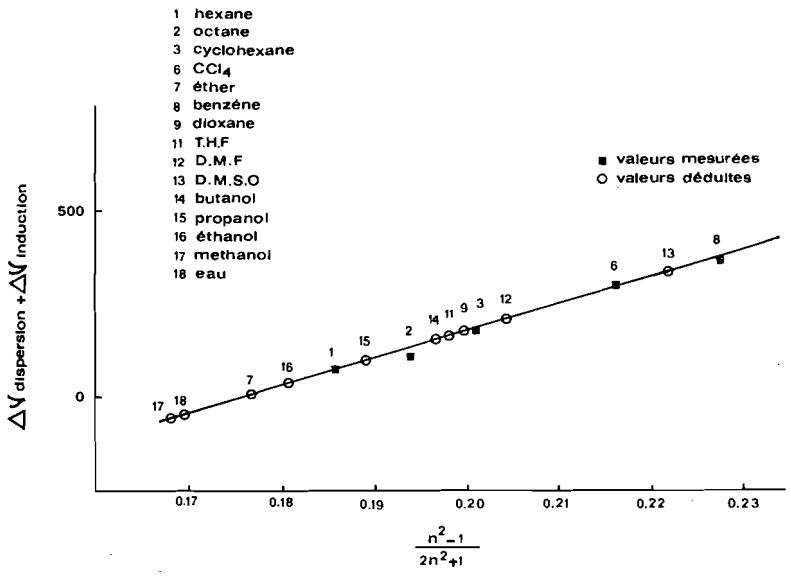

FIG. 1. Effets de dispersion et d'induction pour les solvants étudiés.

Can. J. Chem. Downloaded from www.nrcresearchpress.com by 210.87.254.105 on 09/05/12
For personal use only.

Can. J. Chem. Downloaded from www.nrcresearchpress.com by 210.87.254.105 on 09/05/12
For personal use only.

Solvant	Déplacement (cm^{-1})
Ether éthylique	10
Acétate d'éthyle	58
THF	144
DMF	195
DMSO	311
Dioxanne	180
Butanol	125
Propanol	90
Ethanol	35
Méthanol	−65
Eau	−50

Effet d'orientation

L'effet Starck, toujours très faible, peut être négligé, ce qui nous conduit à un déplacement dû aux forces d'orientation, égal à:

Solvant	Déplacement (cm^{-1})
Ether éthylique	353
Acétate d'éthyle	481
THF	516
DMF	817
DMSO	814
Dioxanne	303
Butanol	−125
Propanol	−241
Ethanol	−280
Méthanol	−463
Eau	−729

Ce qui nous donne la fig. 2, où nous remarquerons une pente positive pour les solvants non hydroxylés, une pente négative pour les solvants hydroxylés.

Discussion

Dans certains solvants, le moment dipolaire de l'aniline à l'état fondamental est connu (12–14), nous pouvons alors calculer la valeur du moment dipolaire lorsque la molécule est à l'état excité.

Nous avons effectué ce calcul pour l'aniline en solution dans le dioxanne et dans l'éther éthylique, à partir de la relation

$$\Delta\bar{\nu}_{\text{orientation}} = f\left(\frac{D-1}{D+2} - \frac{n^2-1}{n^2+2}\right)$$

La pente de la droite obtenue est

$$\text{pente} = \frac{2}{hca^3}\,\mu_f(\mu_e - \mu_f) = 1280$$

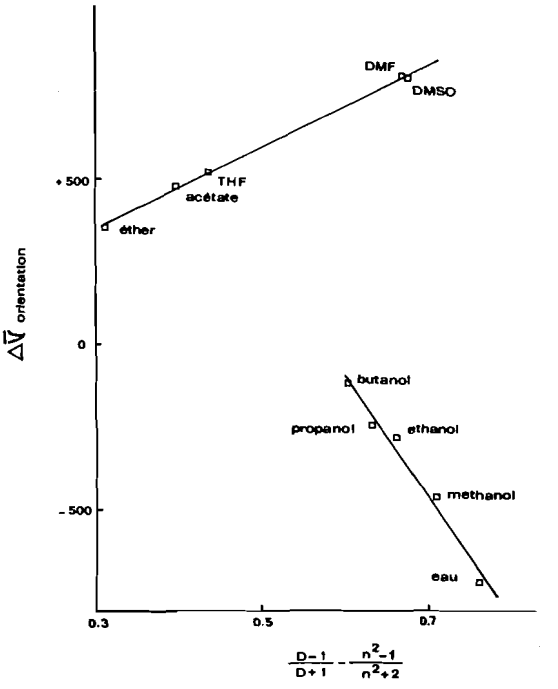

FIG. 2. Effets d'orientation pour les solvants étudiés.

avec $h = 6.62 \times 10^{-34}$; $c = 3 \times 10^8$ m/s; $a = 3.3$ Å ce qui conduit à $\mu_e = 4.4$ D (éther éthylique) et $\mu_e = 4.3$ D (dioxanne).

Ce calcul n'est pas possible pour l'aniline en solution dans l'eau ou dans les alcools. Dans ce cas, nous ne pouvons déterminer que la variation du moment dipolaire au cours de la transition.

En appliquant la relation précédente, nous avons trouvé pente de la droite = −4100 ce qui conduit à $\mu_e < \mu_f$.

Nous remarquons donc un comportement différent entre amine et solvant, selon qu'il existe ou non des groupements non hydroxylés dans ce dernier. Nous avons en effet, avec les solvants non hydroxylés: augmentation du moment spectroscopique et du moment dipolaire de l'amine à l'état excité lorsque la constante diélectrique du solvant augmente. Avec les solvants hydroxylés, nous avons le phénomène inverse. Une étude sur l'association soluté–solvant, en appliquant la méthode de calcul signalée par Gosh et Basu (15), nous a permis de mettre en évidence la formation de complexes 1:1 entre amine et solvant. A partir des valeurs obtenues pour la constante d'équilibre, nous avons calculé les variations d'enthalpies accompagnant cette complexation.

Can. J. Chem. Downloaded from www.nrcresearchpress.com by 210.87.254.105 on 09/05/12
For personal use only.

L'existence de ces liaisons soluté-solvant explique le déplacement de la bande d'absorption vers les grandes longueurs d'onde avec les solvants non hydroxylés, le déplacement vers les courtes longueurs d'onde avec les solvants hydroxylés.

En effet, si nous appelons: E_T = l'énergie de transition de l'aniline dans différents solvants; E_{S_0} = l'énergie de la molécule d'aniline dans son état fondamental; E_{S_1} = l'énergie de la molécule d'aniline dans son premier état singulet excité; X_0 = l'énergie de la molécule d'aniline associée au solvant, (état fondamental); X = l'énergie de la molécule d'aniline associée au solvant (état excité).

La connaissance de $X_0 - E_{S_0}$ nous permet de situer le niveau énergétique de l'état fondamental de l'amine associée par rapport à l'amine à l'état vapeur ou dans un solvant inerte. $X = X_0 + E_T$ = valeur énergétique du premier singulet excité de l'amine en solution. $X - E_{S_1}$: permet de situer le niveau énergétique de l'état S_1 de l'amine associée, par rapport à l'amine à l'état vapeur ou dans un solvant inerte.

L'expression $X_0 - E_{S_0}$ représente en fait l'énergie de solvatation de l'amine, valeur que nous avons précédemment calculée (16). Les valeurs de E_T pour l'aniline ont été déterminées pour la bande O—O, grâce aux courbes de fluorescence réalisées au laboratoire (17). L'énergie de transition prise comme référence correspond à une solution d'aniline dans l'hexane.

On obtient les résultats suivants:

	E_T	$X_0 - E_{S_0}$ (kcal/mol)	$X - E_{S_1}$ (kcal/mol)
Référence	94.347		
Dioxanne	91.488	0.575	−2.28
Acétate d'éthyle	91.633	2.081	−0.63
Tétrahydrofurane	91.339	1.945	−1.06
Butanol	91.773	0	−2.57
Propanol	91.928	0.20	−2.62
Éthanol	91.928	0.50	−2.82

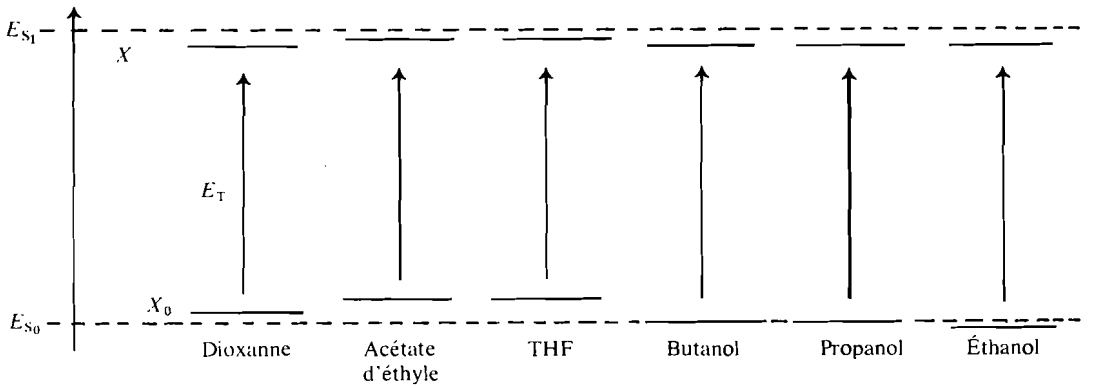

Résultats non surprenants où l'on constate que la différence entre les énergies $X - E_{S_1}$ augmente avec la polarité du solvant. Il y a une exception toutefois avec le dioxanne dont nous avons déjà signalé le comportement particulier lorsqu'on l'utilise comme solvant de l'aniline (16).

On remarquera d'une part, pour les solvants non hydroxylés: l'énergie de l'aniline à l'état fondamental est plus élevée lorsqu'il y a association que lorsque cette même molécule est libre; que l'énergie nécessaire à la transition varie dans le même sens.

Si cette dernière remarque reste valable avec les solvants hydroxylés, par contre l'état énergétique du complexe soluté-solvant se situe à un niveau inférieur.

Les liaisons conduisant à des effets opposés, nous avons pensé qu'elles devaient donner au soluté tantôt un rôle d'accepteur d'électrons, tantôt un rôle de donneur d'électrons.

Cette hypothèse nous conduit à la représentation suivante. Solvants non hydroxylés (type dioxanne)

[i] 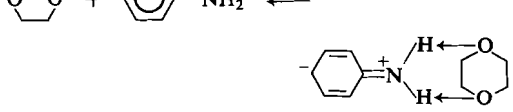

Solvants hydroxylés

[2] 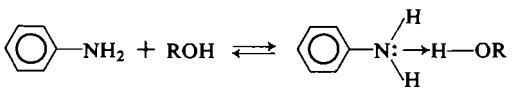

Dans le premier cas, l'association amine–solvant favorise la migration des électrons libres de l'azote sur le cycle, dans le second cas, la liaison hydrogène localise les électrons libres de l'azote et diminue la résonance.

Ce résultat est confirmé par l'étude des *NN'*-méthyl aniline et *NN'*-éthyl aniline, où les variations du moment spectroscopique (Δm) deviennent très faibles. Dans ce cas, la possibilité de liaisons hydrogènes entre les groupements portés par l'azote et les atomes d'oxygène des solvants étant pratiquement nulle, nous trouvons *N,N'*-méthyl aniline, $\Delta m = 2.1$; *N,N'*-éthyl aniline, $\Delta m = 3.1$, alors que pour l'aniline, nous avons $\Delta m = 37$.

L'existence des liaisons hydrogène, telles que nous les avons représentées, nous permet également de vérifier l'hypothèse de Kimura *et al.* (2), à savoir la possibilité d'un transfert de charge, ce transfert de charge pouvant augmenter de 22% l'intensité de la bande d'absorption.

Dans notre cas, nous aurions possibilité maximale de transfert avec les solvants non hydroxylés, possibilité minimale de transfert avec les solvants hydroxylés, le transfert pouvant être considéré comme constant lorsque l'on passe de l'état vapeur à l'amine en solution dans l'hexane solvant inerte (18).

En appelant ε_h = coefficient d'absorption molaire de l'aniline dans l'hexane et ε_e = coefficient d'absorption molaire de l'aniline dans l'eau, nous devons avoir

$$\varepsilon_h - 0.22\varepsilon_h = \varepsilon_e$$

Le calcul nous donne, $\varepsilon_e = 1326$; l'expérience, $\varepsilon_e = 1300$.

Conclusion

L'étude spectroscopique de l'aniline dans différents solvants nous a permis de mettre en évidence:

L'existence de liaisons soluté–solvant où selon la nature de celui-ci, le soluté se comportera soit en accepteur d'électrons, soit en donneur d'électrons au sein du complexe 1:1 formé.

D'expliquer les variations d'intensité de la bande d'absorption considérée, ainsi que les déplacements de sa longueur d'onde maximale d'absorption.

D'attribuer à la molécule d'aniline une configuration plane, seule compatible avec l'existence d'un transfert de charge azote-cycle.

Enfin de prévoir un rendement chimique plus élevé lors d'une oxydation photochimique dans un solvant non hydroxylé, que dans un solvant hydroxylé, si, comme on peut le supposer, le mécanisme d'oxydation fait intervenir la molécule d'amine dans son état excité.

1. L. DOUB et J. M. VANDENBELT. J. Am. Chem. Soc. **69**, 2714 (1947).
2. K. KIMURA, H. TSUBOMURA et S. NAGAKURA. Bull. Chem. Soc. Jap. **37**, 1336 (1964).
3. J. R. SKLAR. J. Chem. Phys. **10**, 135 (1942).
4. J. PLATT. J. Chem. Phys. **19**, 263 (1951).
5. M. BALLESTER, J. RIERA et L. SPIALTER. J. Am. Chem. Soc. **86**, 4276 (1964).
6. Chemical application of spectroscopy. Interscience Publishers, New York. 1968. p. 271.
7. M. BALLESTER, J. RIERA et L. SPIALTER. J. Am. Chem. Soc. **86**, 4271 (1964).
8. E. G. MCRAE. J. Phys. Chem. **61**, 562 (1957).
9. S. BASU. Adv. Quantum Chem. **1**, 145 (1964).
10. M. LAMOTTE et JOUSSOT DUBIEN. J. Chim. Phys. **66**, 161 (1969).
11. B. WOTJKOWIAK et G. LAUNAY. Bull. Soc. Chim. Fr. **9**, 3036 (1969).
12. S. NAGAKURA et H. BABA. J. Am. Chem. Soc. **74**, 5693 (1952).
13. C. CURRAN et G. K. ESTOK. J. Am. Chem. Soc. **72**, 4575 (1950).
14. A. V. FEW et J. W. SMITH. J. Chem. Soc. 753 (1949); 2663 (1949).
15. B. GOSH et S. BASU. Trans. Faraday Soc. **61**, 2097 (1965).
16. P. MÉALLIER, J. RANDEAU et B. POUYET. Spectrochim. Acta, **27A**, 2243 (1971).
17. G. PERICHET. Communication personnelle.
18. L. ABELLO et G. PANNETIER. Bull. Soc. Chim. **5**, 1645 (1966).

Can. J. Chem. Downloaded from www.nrcresearchpress.com by 210.87.254.105 on 09/05/12
For personal use only.

Substituent Effects of Phosphorus and Arsenic Containing Groups in Aromatic Substitution. IV.[1] Nitration of Aromatic Phosphine Oxides

EDMUND MALINSKI AND ANTONINA PIEKOS
Institute of Chemistry, University of Gdansk, Gdansk, Poland
AND
TOMASZ A. MODRO[2]
Department of Chemistry, University of Toronto, Toronto, Ontario M5S 1A1

Received December 23, 1974

EDMUND MALINSKI, ANTONINA PIEKOS, and TOMASZ A. MODRO. Can. J. Chem. **53**, 1468 (1975).

The nitration of some tertiary phosphine oxides $ArP(O)R_2$ in aqueous sulfuric acid has been investigated. All compounds studied react as conjugate acids. When the phosphinyl group is bonded directly to the benzene ring, high deactivation and *meta*-orientation is found, accompanied in most cases by some substitution at the *ortho* position. The substituent effects of the "quasiphosphonium" group $P(OH)R_2^+$ are compared with those of structurally related systems and are discussed in terms of p_π–d_π interactions of the oxygen and the phosphorus atom.

EDMUND MALINSKI, ANTONINA PIEKOS et TOMASZ A. MODRO. Can. J. Chem. **53**, 1468 (1975).

On a étudié la nitration de quelques oxydes de phosphines tertiaires, $ArP(O)R_2$, dans l'acide sulfurique aqueux. Tous les composés étudiés réagissent sous forme d'acides conjugués. Quand le groupe phosphinyle est lié directement au noyau benzénique, on trouve que le noyau est désactivé et l'orientation se fait principalement en *meta*; dans la plupart des cas il y a un peu de substitution en position *ortho*. On compare les effets de substituant du groupe "quasiphosphonium" $P(OH)R_2^+$ avec ceux de systèmes qui lui sont reliés d'une façon structurale et on discute de ces effets en terme d'interactions p_π–d_π de l'oxygène et de l'atome de phosphore.
[Traduit par le journal]

We have recently demonstrated (1) that the deactivating effect of the phosphorus positive pole in aromatic nitration is drastically decreased when the "classical" phosphonium substituent PMe_3^+ is replaced by the "quasiphosphonium" $P(OH)_3^+$ obtained by protonation of phosphonic acid group. This change in reactivity was attributed to back-donating interactions between oxygen atoms and phosphorus, resulting in a high degree of charge delocalization in the $P(OH)_3^+$ substituent.

In terms of the availability of the oxygen nonbonding electrons for the p_π–d_π interactions with phosphorus atom, protonated tertiary phosphine oxides of the type $Ph—P(OH)R_2^+$ occupy an intermediate position between the quaternary phosphonium ions $Ph—PR_3^+$ and the protonated aromatic phosphonic acids, $Ph—P(OH)_3^+$. Quantitative comparison of the reactivities in these structurally related series should provide further information on the detailed nature of the factors influencing substituent effects in such systems. We have therefore studied the nitration of some tertiary phosphine oxides of the type $Ph(CH_2)_nP(O)R_2$, differing in alkyl groups R and in ring – phosphorus atom distance (n = 0, 1, 2), and compared these results with previous data obtained for various aromatic systems containing phosphorus atom in a side chain.

Experimental

Solvents were purified by conventional methods. Melting and boiling points are uncorrected. Thin-layer chromatography was carried out on standard glass plates covered with Kieselgel G (E. Merck) and developed by iodine vapors. Column chromatography was performed using Kieselgel 60 (E. Merck); for all chromatographic experiments solvent system benzene – chloroform – isopropyl alcohol (2:1:1) was used. Solutions of sulfuric acid were obtained by diluting AnalaR sulfuric acid (d 1.83) with distilled water and standarized with aqueous NaOH. AnalaR nitric acid (d 1.42) was distilled from an equal volume of concentrated H_2SO_4 immediately before use.

The u.v. spectra were recorded using a Perkin–Elmer 402 or a Carl Zeiss–Jena VSU-2 spectrophotometer; n.m.r. spectra were obtained with a Tesla BS-487 (80 MHz) spectrometer with TMS or HMDSO as internal

[1]For part III of this series see ref. 3.
[2]To whom correspondence should be addressed.

TABLE 1. Tertiary phosphine oxides

Compound	Melting point (°C)	Boiling point (°C)	λ_{max} (H_2O) (nm)	ε_{max}	R_f	Reference
1	113–116 (lit. 107–109)		263	550	0.44	7
2	51–52 (lit. 55–56)	112–114/0.4 mm	263	600	0.60	2, p. 144
3	44–45 (lit. 43–44)		263	640	0.71	8
4	139–141 (lit. 141–142)		266	850	0.72	4
5	42–44 (lit. 42)	206–208/14 mm	259	180	0.60	9
6		216–218/15 mm	259	170	0.60	

standards. Infrared spectra were recorded on a Unicam SP-200 spectrophotometer.

Substrates

Phenyldimethyl- (**1**), phenyldiethyl- (**2**), and phenyldiisopropylphosphine (**3**) oxides were prepared by oxidation of the corresponding phosphines (ref. 2, p. 34), according to the reported procedure (ref. 2, p. 144). Phenyldi(chloromethyl)phosphine oxide (**4**) was synthesized according to Yagupolskii and Yufa (4) by reaction of $PhPCl_4$ with diazomethane. Benzyldiethylphosphine oxide (**5**) was prepared from diethyl phosphite by reaction with ethylmagnesium bromide followed by benzyl bromide (5); β-phenylethyldiethylphosphine oxide (**6**) was obtained by degradation of the quaternary β-phenylethyldiethylphenylphosphonium bromide, following the procedure reported by Meisenheimer *et al.* (6) for the dimethyl derivative. The purity of substrates was controlled chromatographically (single spot on the t.l.c. plate). Since all phosphine oxides studied save compound **4** are highly hygroscopic, they were dried under reduced pressure over P_2O_5 until no absorption band due to water molecules could be found in their i.r. spectra. The properties of compounds **1–6** are collected in Table 1.

Kinetics

Rate measurements were carried out as described before (1). The extent of reaction was determined from the variation in the absorbance at 260–280 nm in samples of the reaction mixture, quenched at suitable times in large volumes of water. In all cases good second-order kinetics during individual kinetic runs were observed.

Product Determination

Substrate, **1–4**, (5×10^{-3} mol) was added slowly to a 10-fold excess of nitric acid (d 1.5)[3] at 0°, then kept at room temperature for 24 h. Nitric acid was evaporated under reduced pressure at room temperature and the residue dried in vacuum over KOH. The nitration product (quantitative yield) was then examined chromatographically (t.l.c.) and spectroscopically (n.m.r., i.r., u.v.). Substrate **4** gave single-component nitration product; in case of **1–3** two products were present in the reaction mixture. Reaction products formed in nitration of compounds **1–3** were separated by column chromatography and the following pure mononitroderivatives were obtained:

From substrate **1**:

(3-nitrophenyl)dimethylphosphine oxide, 90%, m.p. 183–184° (from acetone–hexane); λ_{max} 263 nm; ε 7200; R_f 0.44.

(2-nitrophenyl)dimethylphosphine oxide, 10%, m.p. 79–81°; λ_{max} 270 nm; ε 4300; R_f 0.53.

From substrate **2**:

(3-nitrophenyl)diethylphosphine oxide, 93%, m.p. 112–113° (from acetone–hexane); λ_{max} 263 nm; ε 6900; R_f 0.60.

(2-nitrophenyl)diethylphosphine oxide, 7%, oil; λ_{max} 270 nm; ε 3700; R_f 0.66.

From substrate **3**:

(3-nitrophenyl)diisopropylphosphine oxide, 99%, m.p. 152–153° (from acetone–hexane); λ_{max} 263 nm; ε 6200; R_f 0.71.

(2-nitrophenyl)diisopropylphosphine oxide, *ca.* 1%, oil; λ_{max} 270 nm; ε 4400; R_f 0.76.

From substrate **4**:

(3-nitrophenyl)di(chloromethyl)phosphine oxide, 100%, m.p. 152–154° (lit. (4) m.p. 154–155°); λ_{max} 266 nm; ε 6900; R_f 0.72.

For the (3-nitrophenyl)dimethylphosphine oxide the following n.m.r. spectrum was obtained ($CDCl_3$): 1.76 (d, 6H), $J_{CH_3,P}$ = 14 Hz; 7.66 (triplet of doublets, 1H), $J_{H_5,H_{4,6}}$ = 7 Hz; $J_{H_5,P}$ = 3 Hz; 7.87–8.37 (m, 2H); 8.47 (doublet of triplets, 1H), $J_{H_2,P}$ = 13 Hz; $J_{H_2,H_{4,6}}$ = 2 Hz.

Nuclear magnetic resonance spectrum of the (2-nitrophenyl)dimethylphosphine oxide showed: 1.85 (d, 6H), $J_{CH_3,P}$ = 14 Hz; 7.50–7.95 (m, 2H); 8.14 (quartet of doublets, 1H), J_{H_3,H_4} = 7 Hz; $J_{H_3,P}$ = 3 Hz; J_{H_3,H_5} = 2 Hz; 8.47 (quartet of doublets, 1H), $J_{H_6,P}$ = 13 Hz; J_{H_6,H_5} = 7 Hz; J_{H_6,H_4} = 2 Hz.

Structural assignments for the nitration products of compounds **2–4** were obtained in the same manner.

[3]For isolation purposes nitric acid is a better reaction medium than sulfuric acid. We have found that this change of the medium has no effect on the product composition.

TABLE 2. Second-order rate coefficients for nitration in aqueous sulfuric acid at 25.0°

	$10^2 k_2$ (l mol^{-1} s^{-1})*					
H_2SO_4 (%)	$PhP(O)Me_2$ (1)	$PhP(O)Et_2$ (2)	$PhP(O)i\text{-}Pr_2$ (3)	$PhP(O)(CH_2Cl)_2$ (4)	$PhCH_2P(O)Et_2$ (5)	$PhCH_2CH_2P(O)Et_2$ (6)
67.4						0.780
69.1						3.03
70.4					0.146	11.4
73.1					1.29	
74.1					4.57	
75.6					9.27	
82.0	0.0152	0.0243	0.0230	0.135		
83.7	0.137	0.135	0.0694	0.659		
84.6		0.304	0.136			
84.9				1.90		
85.6	0.753	0.988	0.618			
86.6	1.85	1.48	0.943			
87.4	2.70					

*±7%.

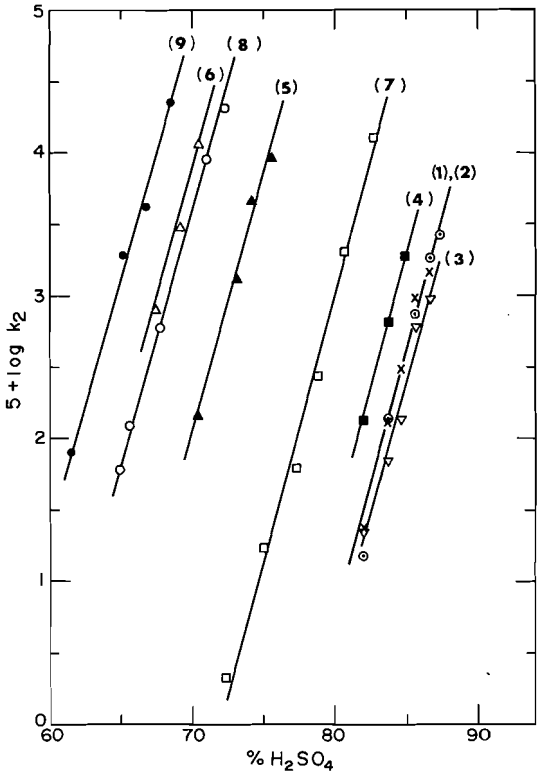

FIG. 1. Variation of rate coefficients (l mol^{-1} s^{-1}) with acidity for nitration in sulfuric acid; (**1**), PhP(O)Me_2; (**2**), PhP(O)Et_2; (**3**), PhP(O)*i*-Pr_2; (**4**), PhP(O)$(CH_2Cl)_2$; (**5**), $PhCH_2P(O)Et_2$; (**6**), $PhCH_2CH_2P(O)Et_2$; (**7**), $PhPO_3H_2$; (**8**), $PhCH_2PO_3H_2$; (**9**), $PhCH_2CH_2PO_3H_2$.

Results and Discussion

Second-order rate constants for nitration in sulfuric acid are listed in Table 2. Rate profiles are shown in Fig. 1; included are data (10) for $Ph(CH_2)_nPO_3H_3^+$ (n = 0, 1, 2) system for comparison.

All plots of log k_2 *vs.* acidity are satisfactorily linear ($r > 0.99$) and to a first approximation parallel to each other (slope values = 0.34–0.40). According to arguments presented before (1), this type of rate–acidity dependence obtained for nitration proves that for a given acidity range all substrates react entirely as protonated species. In all cases, the reactivity data reflect therefore the effect of the substituent of the "quasiphosphonium" structure, $-\overset{|}{\underset{|}{P}}(OH)^+$. The parallelism of the rate profiles allowed an evaluation of relative reactivities by standard overlap technique. The pertinent data related to the reactivity of benzene are collected in Table 3.

Table 3 shows clearly that in the protonated phosphine oxides the substituent $P(OH)R_2^+$ deactivates the ring to a much higher extent than does the protonated phosphonic group $P(OH)_3^+$, the ratio of reactivities $k_{rel(PO_3H_3^+)}/k_{rel(PEt_2OH^+)}$ for the series $Ph(CH_2)_nX$ being equal to 200, 25, and 10 for n = 0, 1, and 2, respectively. In fact, the $P(OH)Me_2^+$ group, when bonded directly to the benzene ring, shows a slightly stronger deactivating effect (by a factor of three) than the "pure" trimethylphosphonium pole. This is in agreement with results of Eaborn and co-workers (13), who found that in the protodetrimethylsilylation reaction, involving fully protonated substrates, deactivation decreases in the same order. The observed order of reactivities suggests that the back-donation of electrons due to a single oxygen atom in the protonated phosphinyl group is too weak to outweigh the −I effect of the OH group. The effect of successive methylene groups introduced between the ring and the substituent (compounds **5** and **6** in Table 3), when considered in terms of the approach discussed previously (10), shows again the close resemblance of the substituent effects of the $P(OH)R_2^+$ and PMe_3^+ groups.[4] In the extreme case of the protonated phosphonic acid group, on the other hand, three equivalent resonance structures of type **B** contribute significantly to the charge distribution and therefore decrease effectively the total electron-withdrawing properties of the substituent:

$$\underset{\mathbf{A}}{-\overset{|}{\underset{|}{P^+}}-OH} \leftrightarrow \underset{\mathbf{B}}{-\overset{|}{\underset{|}{P}}=OH^+}$$

The behavior of phenyldi(chloromethyl)phosphine oxide (**4**) is of some interest. Despite the presence of two strongly electronegative atoms, this compound is more reactive (by a factor of five) than the corresponding dimethyl derivative (**1**). This result, seemingly contradictory to the usual structural effects on the net polarity of substituents, remains however in excellent agreement with some conclusions obtained from

[4]The ratio log $(k_{rel}^{CH_2X}/k_{rel}^{X})/-\log k_{rel}^{X}$, considered as a measure of the relative contributions of the inductive and mesomeric interactions to the net polar effect of substituent X, has almost the same value for X = PMe_3^+ and X = $P(OH)Et_2^+$.

TABLE 3. Relative reactivities for nitration in aqueous sulfuric acid (25.0°)

Compound	Substrate	Relative reactivity* (Benzene = 1)
1	$Ph—P(OH)Me_2^+$	5.50×10^{-8}
2	$Ph—P(OH)Et_2^+$	5.50×10^{-8}
3	$Ph—P(OH)i\text{-}Pr_2^+$	3.48×10^{-8}
4	$Ph—P(OH)(CH_2Cl)_2^+$	27.6×10^{-8}
5	$Ph—CH_2P(OH)Et_2^+$	7.17×10^{-3}
6	$Ph—CH_2CH_2P(OH)Et_2^+$	0.32
7	$Ph—P(OH)_3^+$	1.1×10^{-5}†
8	$Ph—CH_2P(OH)_3^+$	0.18†
9	$Ph—CH_2CH_2P(OH)_3^+$	3.2†
10	$Ph—PMe_3^+$	1.6×10^{-7}‡
11	$Ph—CH_2PMe_3^+$	6.6×10^{-3}§

*Obtained by the stepwise comparison of the overlapping sections of the corresponding parallel rate profiles; *e.g.* **6** with benzene, **5** with **6**, etc.
†Taken from ref. 10.
‡Taken from ref. 11.
§In nitromethane. Taken from ref. 12.

n.m.r. spectroscopic investigations concerning the detailed nature of bonding in phosphorus-containing systems. An increase in shielding of the phosphorus atom by electron-withdrawing groups caused by an increase in p_π–d_π conjugation is generally observed (14); for example, replacement of methyl by chloromethyl at the phosphoryl function $—\overset{|}{\underset{|}{P}}=O$ results in an upfield ^{31}P chemical shift, and also the contributions to shielding of the tetravalent phosphorus atom from directly bonded groups were found to decrease in the order $Ph \geqslant CH_2Cl > CH_3$ (15). Van Wazer and Letchner demonstrated (16) that the π-bonding order for the PO bond in OPZ_3 type molecules increases from 0.35 to 0.50 when $Z = CH_3$ is changed to $Z = CH_2Cl$. These authors found also that for $Z = t$-Bu, the π-bonding is virtually nonexistent, and explained this result in terms of the large value of the Z—P—Z angle, inhibiting π-electron feedback from the oxygen. This interpretation could also be applied to explain why the phenyldiisopropylphosphine oxide (**3**) exhibits the lowest reactivity among the phosphine oxides studied in this work. The observed relative deactivating effects in substrates **1** and **4** to our knowledge represent the first example in which electronegative groups modify the p_π–d_π bonding order at phosphorus to the extent that is reflected in the increase of the reactivity of the adjacent system in an electrophilic reaction.

Preparative nitration of tertiary arylphosphine oxides has not been extensively studied; in the reported cases exclusive *meta*-substitution with respect to the phosphinyl group was observed (17). Since we found an unusually high discrimination between *ortho* and *para* positions during nitration of benzenephosphonic acid (1) (18% *ortho* and no *para* substitution), we have determined the product composition for nitration of compounds **1–4** in order to establish how far this intramolecular selectivity is general for the "quasiphosphonium" systems.

The nitration of phenyldimethylphosphine oxide (**1**) resulted in formation of two products, easily demonstrated by t.l.c. and p.m.r. of the reaction mixture. When separated by column chromatography, two mononitroderivatives of **1** (in 90% and 10% yield) were obtained. On the basis of spectroscopic characteristics, the main product was recognized as (*m*-nitrophenyl)-dimethylphosphine oxide, such a result being in full agreement with the general directing pattern of phosphonium and "quasiphosphonium" substituted benzene derivatives. The second product was identified as the corresponding *ortho*-nitrocompound. The proton resonance of the methyl groups in this isomer occurs at 0.09 p.p.m. (in $CDCl_3$) to low field of the corresponding doublet of the *meta*-isomer. In the aromatic region, the low-field C_6-hydrogen (*ortho* to phosphorus, $\delta = 8.47$) and C_3-hydrogen (*ortho* to NO_2, $\delta = 8.14$) can be easily distinguished from the C_4 and C_5-hydrogen signals and show the pattern expected for the 1,2-disubstituted structure. The same analysis showed that the minor product formed in nitration of **2** (7%), as well as of **3** (*ca.* 1%) are *ortho*-nitroderivatives; no sign of the A_2B_2 pattern expected for the *para*-nitroproduct was observed. The *ortho* structure of the isolated minor components of nitration products was also supported by their i.r. and u.v. characteristics. The i.r. spectra of the individual products showed at the region of 800–900 cm^{-1} (out-of-plane C—H deformation vibrations) absorption bands expected for the 1,3 and 1,2 substitution patterns, respectively. The intensity of the absorption in the u.v. region was considerably lower for the side-products than for the main products, which is in agreement with the previously observed decrease in intensity in the order $\varepsilon_p > \varepsilon_m > \varepsilon_o$ for all such nitro-substituted benzene derivatives containing phosphorus.

TABLE 4. Partial rate factors for nitration in aqueous sulfuric acid, 25.0°

Substituent	$f_o \times 10^7$	$f_m \times 10^7$	f_p	$\delta\Delta G_o^{\neq}/\delta\Delta G_m^{\neq}$
$P(OH)Me_2^+$	0.16	1.48	—	1.14
$P(OH)_3^{+*}$	60	270	—	1.14
$P(OH)_2H^{+*}$	10	50	—	1.13

*Taken from ref. 1.

In agreement with results reported by Yagupolskii and Yufa (4), nitration of phenyldi-(chloromethyl)phosphine oxide (**4**) gave a single product which was identified as pure *meta*-nitroderivative; no isomeric substitution products could be detected.

The decreasing proportion of the *ortho*-nitration with the increase in the size of the alkyl groups in $P(OH)R_2^+$ substituent (10%, 7%, *ca.* 1% for R = Me, Et, *i*-Pr, respectively) clearly results from the increase of the steric hindrance for the attack at *ortho* positions. More important however is that in all cases the products of *para*-substitution are formed in negligible amounts if at all. This pattern of intramolecular selectivity follows closely the orientation found in nitration of benzenephosphonic (protonated and unprotonated) and benzenephosphonous ($Ph—PO_2H_2$) acids (1). Since it seems reasonable to assume that steric requirements of the $P(OH)_3^+$, $P(OH)_2H^+$, and $P(OH)Me_2^+$ substituents are similar, the values of partial rate factors for these systems can be directly compared also with respect to the reactivity of the *ortho* positions (Table 4). Although the reactivities of the given position in these substrates differ significantly, the ratio of the substituent effects on the free energy of activation at the *ortho*- and *meta*-positions, $\delta\Delta G_o^{\neq}/\delta\Delta G_m^{\neq}$ has the same value. This can be considered as an indication of a common mechanism for intramolecular selectivity operating in all systems in which phosphorus atom, bonded to at least one oxygen, is attached to the aromatic ring.

Substituents of the −I, −M type are known to give in nitration an *o*/*p* ratio usually >2 (ref. 18, chapt. 9.1.3); however the discrimination of the *para* position in electrophilic substitution of the "quasiphosphonium" type of benzene derivatives seems to be much more pronounced.[5] The possibility must therefore be considered that with these substituents, when there is no steric hindrance, the initial specific interaction with the electrophile species occurs at the substituent, followed then by a selective transfer of the electrophile to the *ortho* position of the ring. The nature of such specific effects is not clear, as in other cases when the specific electrophile–substituent interactions are taken into account (ref. 18, chapt. 5.3.4). However, summarizing the evidence presented in this and previous papers, we feel it reasonable to consider organophosphorus groups of the structural type $—\overset{|}{\underset{|}{P(O)}}$ or $—\overset{|}{\underset{|}{P(OH)^+}}$ as a rather unusual group of substituents, which deactivate the ring in electrophilic substitution with distinctive *meta*/*ortho* orientation and rigorous discrimination of the *para*-substitution. It is worth mentioning that nitration of phenylboronic acid in strongly acidic media (19) provides an example which probably resembles most closely this pattern of substituent effects.

[5]We have recently observed a similar pattern of *meta*/*ortho* orientation with negligible *para*-substitution for positive bromination of tertiary aromatic phosphine oxides (20).

1. T. A. MODRO and A. PIEKOS. Tetrahedron, **28**, 3867 (1972).
2. K. SASSE. Methoden der organischen Chemie, Vol. XII/1. Georg Thieme Verlag, Stuttgart. 1963.
3. T. A. MODRO and A. PIEKOS. Phosphorus, **3**, 195 (1974).
4. L. M. YAGUPOLSKII and P. A. YUFA. Zh. Obshch. Khim. **28**, 2853 (1958).
5. M. J. KABACHNIK, T. A. MASTRYUKOVA, and A. E. SHIPOV. Zh. Obshch. Khim. **35**, 1574 (1965).
6. J. MEISENHEIMER, J. CASPER, M. HORING, W. LAUTER, L. LICHTENSTADT, and W. SAMUEL. Ann. Chem. **449**, 213 (1926).
7. G. WITTIG and U. SCHOLLKOPF. Chem. Ber. **87**, 1318 (1954).
8. K. D. BERLIN and M. NAGABHUSHANAM. Chem. Ind. 974 (1964).
9. V. S. TSIVUNIN, G. KH. KAMAI, and V. V. KORMACHEV. Zh. Obshch. Khim. **35**, 1819 (1965).
10. T. A. MODRO and A. PIEKOS. Tetrahedron, **29**, 2561 (1973).
11. A. GASTAMINZA, T. A. MODRO, J. H. RIDD, and J. H. P. UTLEY. J. Chem. Soc. B, 534 (1968).

12. F. L. RILEY and E. ROTHSTEIN. J. Chem. Soc. 3860 (1964).
13. R. W. BOTT, B. F. DOWDEN, and C. EABORN. J. Chem. Soc. 6306 (1965).
14. S. TRIPPETT. (*Editor*). Organophosphorus chemistry. Specialist Periodical Report, The Chemical Society, London. 1972. Vol. 3, Chapt. 11; 1973. Vol. 4, Chapt. 11.
15. J. W. EMSLEY, J. FEENEY, and L. H. SUTCLIFFE. High resolution NMR spectroscopy, Vol. 2. Pergamon Press, Oxford. 1966. p. 1052.
16. J. R. VAN WAZER and J. H. LETCHER. Topics in phosphorus chemistry, Vol. 5. Interscience, New York. 1967. p. 169.
17. H. R. HAYS and D. J. PETERSEN. Organic phosphorus compounds, Vol. 3. *Edited by* G. M. Kosolapoff and L. Maier. Wiley–Interscience, New York. 1972. p. 396.
18. J. G. HOGGETT, R. B. MOODIE, J. R. PENTON, and K. SCHOFIELD. Nitration and aromatic reactivity. Cambridge University Press, London. 1971.
19. D. R. HARVEY and R. O. C. NORMAN. J. Chem. Soc. 3822 (1962); W. SEAMON and J. R. JOHNSON. J. Am. Chem. Soc. **53**, 711 (1931).
20. E. MALINSKI, A. PIEKOS, and T. A. MODRO. Unpublished results.

Reactions of OH, CH_2OH, Br_2^-, and $(CNS)_2^-$ Free Radicals with Cysteine at p*H* 5.3

GREESH CHAND GOYAL[1] AND DAVID ANTHONY ARMSTRONG
Department of Chemistry, University of Calgary, Calgary, Alberta T2N 1N4

Received November 4, 1974

GREESH CHAND GOYAL and DAVID ANTHONY ARMSTRONG. Can. J. Chem. **53**, 1475 (1975).

The products of radiolysis of cysteine in nitrous oxide saturated solutions at p*H* 5.3 have been investigated both in the absence of other solutes and in the presence of 1 *M* methanol, 0.5 *M* KBr, and 0.2 *M* NaCNS. The results can be explained by a mechanism in which the free radicals •OH, $•CH_2OH$, $•Br_2^-$, and $•(CNS)_2^-$ all react with the cysteine (CysSH) sulfhydryl group to form CysS• as a major intermediate product. Minor yields (0.2 molecules per 100 eV) of ammonia observed in the case of attack by $•Br_2^-$ may result from attack on the NH_3^+ group or α-hydrogen by this species. Cysteine trisulfide was observed in all systems with a yield 0.12 ± 0.03 molecules per 100 eV and is probably formed from minor secondary reactions of CysS• radicals. In agreement with previous conclusions based on the analysis of products from deaerated solutions the majority of CysS• radicals form CysSSCys.

GREESH CHAND GOYAL et DAVID ANTHONY ARMSTRONG. Can. J. Chem. **53**, 1475 (1975).

On a examiné les produits de radiolyse de la cystéine dans des solutions saturées en oxyde nitreux à un p*H* de 5.3 en l'absence d'autres solutés de même qu'en présence de méthanol 1 *M*, de KBr 0.5 *M* et de NaCNS 0.2 *M*. Les résultats peuvent être expliqués par un mécanisme dans lequel les radicaux libres •OH, $•CH_2OH$, $•Br_2^-$ et $•(CNS)_2^-$ réagissent tous avec le groupe sulfhydryle de la cystéine pour former le radical CysS• comme un produit intermédiaire majeur. Les rendements mineurs (0.2 molécules par 100 eV) d'ammoniac observés dans le cas de l'attaque par $•Br_2^-$ peuvent provenir d'une attaque, par cette espèce, soit sur le groupe NH_3^+ soit sur l'hydrogène en α. Dans tous les cas, on a observé la formation de trisulfure de cystéine et le rendement est de 0.12 ± 0.03 molécules par 100 eV; ce composé se forme probablement à partir de réactions secondaires mineures des radicaux CysS. La majorité des radicaux CysS• forment CysSSCys; cette conclusion est en accord avec d'autres énoncés précédemment et qui étaient basés sur l'analyse des produits provenant de solutions desquelles l'air avait été enlevée.
[Traduit par le journal]

Introduction

Previous studies of the γ (1, 2) and pulse radiolysis (3, 4) of aqueous oxygen free solutions of cysteine ($HSCH_2CH(NH_3^+)CO_2^-$) and the related molecule cysteamine ($HSCH_2CH_2NH_3^+$) (5) have shown that the major products can be explained by the following mechanism, in which the abbreviation CysSH is used for the cysteine structure:

[1] $H_2O \rightsquigarrow •OH\ •H\ e_{aq}^-\ H^+\ H_2O_2\ H_2$

[2] $•OH + CysSH \rightarrow CysS• + H_2O$

[3] $•H + CysSH \rightarrow CysS• + H_2$

[4] $•H + CysSH \rightarrow Cys• + H_2S$

[5] $e_{aq}^- + H^+ \rightarrow •H$

[6] $e_{aq}^- + CysSH \rightarrow Cys• + SH^- \ (\xrightarrow{H^+} H_2S)$

[7] $Cys• + CysSH \rightarrow CysH + CysS•$

[8] $CysSH \rightleftharpoons CysS^- + H^+$

[9] $CysS• + CysS^- \rightleftharpoons CysS\overset{\bullet}{S}^-Cys$

[10] $CysS• + CysS• \rightarrow CysSSCys$

[11] $CysS• + CysS\overset{\bullet}{S}^-Cys \rightarrow CysS^- + CysSSCys$

[12] $H_2O_2 + 2CysSH \rightarrow CysSSCys + 2H_2O$

More recently Purdie *et al.* (6) have investigated the radiolysis of penicillamine ($HSC(CH_3)_2CH(NH_3^+)CO_2^-$ = HSPen) and have found clear evidence for the production of a significant yield of penicillamine trisulfide (PenSSSPen). Since this behavior is quite different from previous observations of cysteine radiolysis and may have implications for an understanding of differences in their abilities as protectors (6), we have reinvestigated the cysteine system to determine whether any trisulfide is in fact formed. We have also broadened the scope of our study to determine the products resulting from the reactions of $•(Br_2)^-$, $•(CNS)_2^-$, and $•CH_2OH$ with cysteine. Pulse

[1]Present address: Department of Chemistry, Brandeis University.

Can. J. Chem. Downloaded from www.nrcresearchpress.com by 210.87.254.6 on 09/05/12
For personal use only.

Can. J. Chem. Downloaded from www.nrcresearchpress.com by 210.87.254.6 on 09/05/12
For personal use only.

TABLE 1. Solute systems and radical balances at pH 5.3

Solute system	$k_{OH + Solute}$ ($M^{-1}s^{-1} \times 10^{-9}$)	Major reacting radical species	$k_{CysSH + Radical}$ ($M^{-1}s^{-1} \times 10^{-9}$)	Primary radical yields from the literature				$2\{G(CysS)_2 + G(CysSSSCys)\}$ observed experimentally
				G_H	G_{OH}	$G_{e_{aq}^-}$	Total	
N_2O	—	•OH	19.0[a]	0.60	2.90	3.05	6.6[b]	6.8
				0.60	3.15	3.15	6.9[c]	
$N_2O + CH_3OH$	0.9[d]	$•CH_2OH$	0.10[e]	0.60	2.90	3.05	6.6[b]	6.3
$N_2O + Br^-$	1.2[d]	$•Br_2^-$	~0.1[f]	0.50	3.40	3.05	7.0[g]	7.2
$N_2O + CNS^-$	11[d]	$•(CNS)_2^-$	~0.05[f]	0.50	3.40	3.05	7.0[g]	7.2

[a]Taken from ref. 4.
[b]Yields taken from ref. 13.
[c]Yields calculated from yield-reactivity curves in ref. 14 on the basis $\Sigma k_{OH+S}[S] = 1.9 \times 10^8\ s^{-1}$ and $\Sigma k_{e_{aq}^- + S}[S] = 3.5 \times 10^8\ s^{-1}$.
[d]From refs. 16 and 17.
[e]From ref. 9, assuming the same value as for cysteamine.
[f]From ref. 7.
[g]Yields taken from ref. 13 with G_H modified as in ref. 15 and G_{OH} increased by 0.5 per 100 eV on the basis of yield–reactivity curves (ref. 14) to take account of the higher solute concentrations ($\Sigma k_{OH+S}[S] = 0.8–2.2 \times 10^9\ s^{-1}$).

Can. J. Chem. Downloaded from www.nrcresearchpress.com by 210.87.254.6 on 09/05/12
For personal use only.

radiolysis experiments (7) show that the rate constants for reaction with CysSH by the former two radicals increase markedly in the pH region where —SH ionizes (pK CysSH 8.3 (8)) and above pH 8 they are assumed to react preferentially with $CysS^-$ (7), presumably to cause oxidation to CysS. Our present interest lay in determining the mechanism of reaction at pH 5.3, where the rate constants are still appreciable (see Table 1) even though CysSH is un-ionized.

In the case of the $\cdot CH_2OH$ radical two reactions are conceivable, since alcohol radicals may

[13] $CysSH + \cdot CH_2OH \rightarrow CysS\cdot + CH_3OH$

[14] $CysSH + \cdot CH_2OH \rightarrow Cys\cdot + CH_2O + H_2S$ (or $SH^- + H^+$)

behave as hydrogen atom acceptors (9) or as reducing agents (10, 11). The prior observation (9) of a pseudo first-order build up of —S$\dot{S}^-$— anions in the pulse radiolysis of N_2O-saturated solutions containing 1.13 mM cysteamine and higher concentrations of methanol was taken as evidence for the cysteamine analogs of reactions 13 and 9, the former being rate controlling. While vitiating the possibility of reaction 14 for the cysteamine system, this evidence does not completely exclude it since minor contributions of —S$\dot{S}^-$— from the sequence of reactions 14, 7, and 9 may not alter the rate of production significantly from that expected for reactions 13 and 9 alone. In the present system the yield of reaction 14 can be determined from the alanine yield.

Experimental

Potassium bromide and sodium thiocyanate from the Baker Chemical Company and L-cysteine from Mann Research Laboratories were used without further purification. The methanol was A.C.S. certified reagent grade. High purity nitrous oxide from the Matheson Co. was freed from traces of NO and other noncondensible gases by several cycles of sublimation, condensation, and pumping at −196 and −132 °C. After this it was stored in a bulb on the vacuum line. Cysteine solutions of pH 5.3 were prepared in fresh, triply distilled water containing the solutes needed for the production of the radicals being investigated. Following this 5 ml aliquots were transferred to the carefully cleaned pyrex cells and attached to the vacuum line. After thorough degassing (2) the samples were equilibrated with N_2O at 760 mm and sealed. Prior to irradiation they were stored in a refrigerator. Immediately after irradiation the analysis for amino-containing products was performed on a Technicon amino acid analyzer. Norleucine was used as an internal standard and elution buffers of pH 3.10, 3.30, and 4.50 were employed in succession for periods of 50, 60, and 50 min, respectively. A final buffer of pH 5.0 was used to elute ammonia. Standardization procedures and other details of the amino acid analyses may be found in ref. 2.

All irradiations were performed at 23 °C in a "Gamma Cell 220" purchased from Atomic Energy of Canada. The dose rate, which was determined by ferrous sulfate dosimetry assuming $G(Fe^{3+}) = 15.6$ (p. 217 of ref. 12), was 4.5×10^{16} eV ml^{-1} min^{-1}.

Results

Chromatograms of the irradiated solutions exhibited clearly resolved peaks due to residual cysteine and to alanine, cystine, cysteine trisulfide, norleucine (internal standard), and ammonia in the order given. The cysteine trisulfide was a minor product in all solutions, while ammonia was only detectable in the KBr solutions. In solutions containing methanol a small unidentified peak appeared before the residual cysteine. It corresponded to a G of about 0.1, assuming a ninhydrin sensitivity equal to that of alanine. No other peaks of any significance were observed.

Experiments with each solute system were performed at several doses in the range 1.0 to 6.0×10^{18} eV ml^{-1}. Yield–dose plots calculated

TABLE 2. G values of amino-containing products and nitrogen balance from N_2O-saturated 10^{-2} M cysteine solutions with added solutes at pH 5.3

	No added solute		1 M CH_3OH		0.5 M KBr		0.2 M NaCNS	
Product	G value	G(N)	G value	G(N)	G value	G(N)	G value	G(N)
CySSCy	3.25±0.25	6.50	3.05±0.2	6.10	3.43±0.3	6.86	3.48±0.2	6.96
CyH	0.88±0.05	0.88	0.89±0.06	0.89	0.83±0.05	0.83	0.77±0.06	0.77
CySSSCy	~0.14	0.28	~0.12	0.24	~0.15	0.30	~0.10	0.20
NH_3					0.20±0.04	0.20		
Total N		7.65		7.25		8.2		7.95
−CySH[a]	7.9±0.5		7.3±0.5		8.5±0.5		8.1±0.5	

[a]Determined from the decrease in the cysSH peak.

from the peak areas were linear, both for the products and for residual cysteine. The G values calculated from their slopes are presented in Table 2. In each case there is an excellent nitrogen balance, showing that the overall stoichiometry:

$$[15]\quad G(-\mathrm{CysSH}) = 2G(\mathrm{CysS})_2 + 2G(\mathrm{CysSSSCys}) + G(\mathrm{CysH})$$

holds. Thus one can conclude that all significant products, other than H_2S which was previously found to follow the alanine yield closely (2), have been determined.

Discussion

The amount of cystine formed from hydrogen peroxide would be negligible here since reaction 12 has a half life of ~10 h (2*b*) and our solutions were analyzed immediately after the radiolyses, which were themselves of less than 2 h duration. Hence only reactions initiated by ·H, ·OH, and e_{aq}^- or by the solute radicals formed from them need be considered. Table 1 gives the yields of primary radicals estimated for our conditions from data in the literature. From the concentration of N_2O (2.8×10^{-2} *M*) and the rate constants for reactions 6 ($9 \times 10^9\ M^{-1}\ s^{-1}$ (1, 2)) and 16 ($9 \times 10^9\ M^{-1}\ s^{-1}$, average of two values on p. 55 of ref. 12):

$$[16]\quad e_{aq}^- + N_2O + (H_2O) \rightarrow N_2 + OH + OH^-$$

we calculate that 0.78 e_{aq}^- per 100 eV would undergo reaction 6. Since $G_H = 0.6$ (ref. 12, p. 140) in the absence of solutes and $k_3/k_4 = 3.5$ (2*a*), a further yield of 0.13 alanyl radicals per 100 eV would be formed in reaction 4, giving a total yield of alanine molecules from reaction 7 of ~0.9 per 100 eV. This is in excellent agreement with the yield reported in Table 2 for solutions with only N_2O and cysteine. The alanine yield in the 1 *M* CH_3OH solutions is the same, showing that reaction 13 is in fact the only important mode of $\cdot CH_2OH$ attack on CysSH at p*H* 5.3. From Table 1 the yields of G_H in 0.5 *M* KBr and 0.2 *M* NaCNS are expected to be lower and this also appears to be reflected in the smaller alanine yields for these solutions in Table 2.

From the rate constants in column two of Table 1 and k_2 in column four it can be shown that 8, 24, and 17% of the OH radicals react directly with CysSH in the CNS^-, Br^-, and CH_3OH solutions, respectively. The remainder are converted to $\cdot(CNS)_2^-$, $\cdot Br_2^-$, and $\cdot CH_2OH$ by reactions 17–18, 19–20, and 21, respectively:

$$[17]\quad OH + CNS^- \rightarrow OH^- + \cdot CNS$$

$$[18]\quad \cdot CNS + CNS^- \rightleftharpoons \cdot(CNS)_2^-$$

$$[19]\quad \cdot OH + Br^- \rightarrow OH^- + \cdot Br$$

$$[20]\quad \cdot Br + Br^- \rightleftharpoons \cdot Br_2^-$$

$$[21]\quad \cdot OH + CH_3OH \rightarrow H_2O + \cdot CH_2OH$$

The ubiquitous occurrence of trisulfide in a yield of 0.1–0.15 molecules per 100 indicates that it is not a product of specific reactions of any one radical, for example:

$$[22]\quad \mathrm{CysSH} + OH \rightarrow \mathrm{Cys}\cdot + \mathrm{HSOH} \rightarrow S + H_2O$$

$$[23]\quad S + \mathrm{CysSSCys} \rightarrow \mathrm{CysSSSCys}$$

In fact the relative constancy of the disulfide and trisulfide yields in Table 2 is best explained if all four radical species attack CysSH to produce CysS· through reactions 2, 13, 24, and 25:

$$[24]\quad \mathrm{CysSH} + \cdot Br_2^- \rightarrow \mathrm{CysS}\cdot + 2Br^- + H^+$$

$$[25]\quad \mathrm{CysSH} + \cdot(CNS)_2^- \rightarrow \mathrm{CysS}\cdot + 2CNS^- + H^+$$

and CysSSSCys arises from secondary reactions of CysS·. One possibility is the cleavage of sulfenium radicals formed in reaction 26, *viz*:

$$[26]\quad \mathrm{CysS}\cdot + \mathrm{CysSH} \rightleftharpoons \mathrm{CysS}\overset{\cdot}{\underset{H}{S}}\mathrm{Cys}$$

$$[27]\quad \mathrm{CysS}\overset{\cdot}{\underset{H}{S}}\mathrm{Cys} \rightarrow (\mathrm{CysSSH} + \mathrm{Cys}\cdot)_{\text{solvent cage}} \rightarrow (\mathrm{CysSS}\cdot + \mathrm{CysH})_{\text{solvent cage}} \rightarrow \mathrm{CysSS}\cdot + \mathrm{CysH}$$

followed by:

$$[28]\quad \mathrm{CysSS}\cdot + \cdot\mathrm{SCys} \rightarrow \mathrm{CysSSSCys}$$

Tung and Stone (18) have proposed reaction 29

$$[29]\quad \mathrm{CysS}\overset{\cdot}{S}^-\mathrm{Cys} + H_2O \rightarrow \mathrm{CysSS}\cdot + \mathrm{CysH} + OH^-$$

above p*H* 7 and an analogous reaction has been postulated in penicillamine (6). However, further work will be required to confirm the occurrence of reaction 27 for the protonated form of the anion. The important point here is that, in accord with previous conclusions (1–5), cysteine trisulfide is a relatively minor product. Thus the significant difference between the radiation chemistry of penicillamine and cysteine in this respect is confirmed.

Can. J. Chem. Downloaded from www.nrcresearchpress.com by 210.87.254.6 on 09/05/12
For personal use only.

Can. J. Chem. Downloaded from www.nrcresearchpress.com by 210.87.254.6 on 09/05/12
For personal use only.

The relatively minor pathway responsible for the small yield of ammonia in the $\cdot Br_2^-$ system is not at present understood. However, one may note that the attack of $\cdot Cl_2^-$ on cystine produces ammonia in an even larger yield (19). Possibly the negative charge and strong oxidizing power of these radicals facilitates their attack at the NH_3^+ group (*cf.* ref. 19) or the adjacent α-hydrogen, causing hydrolysis and deamination, for example:

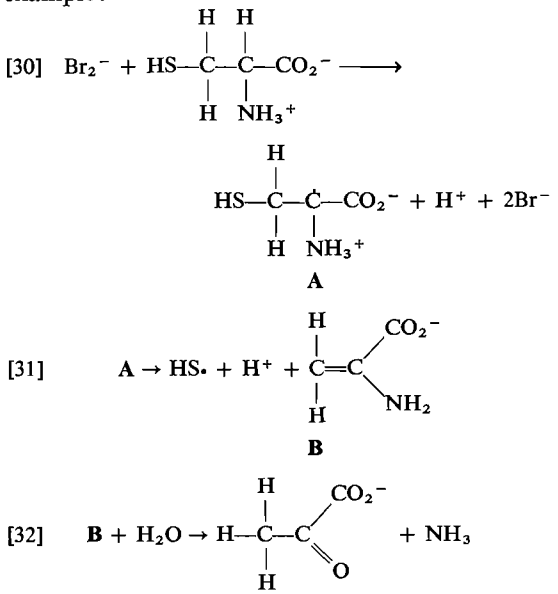

From the major reactions proposed the following radical balance equation should hold:

$$[33]\quad 2[G(\mathrm{CysS})_2 + G(\mathrm{CysSSSCys})] = G_{\mathrm{H}} + G_{\mathrm{OH}} + G_{e_{aq}^-}$$

Reference to Table 1 substantiates its validity within the experimental uncertainty of ±0.5 per 100 eV for all of the solute systems.

This work was supported by the Defence Research Board of Canada Grant No. 1675-03 and the National Research Council of Canada Grant No. A3571. The authors are grateful to Drs. M. H. Benn and F. C. Adam for their help and to Dr. J. W. Purdie for samples of cysteine trisulfide.

1. A. El. Samahy, H. L. White, and C. N. Trumbore. J. Am. Chem. Soc. **86**, 3177 (1964). A. Al-Thannon, R. M. Peterson, and C. N. Trumbore. J. Phys. Chem. **72**, 2395 (1968).
2. V. G. Wilkening, Manohar Lal, M. Arends, and D. A. Armstrong. (*a*) Can. J. Chem. **45**, 1209 (1967); (*b*) J. Phys. Chem. **72**, 185 (1968).
3. J. P. Barton and J. E. Packer. Int. J. Radiat. Phys. Chem. **2**, 159 (1970).
4. M. Z. Hoffman and E. Hayon. J. Phys. Chem. **77**, 990 (1973).
5. G. E. Adams, G. S. McNaughton, and B. D. Michael. *In* Chemistry of ionisation and excitation. *Edited by* G. R. A. Johnson and G. Scholes. Taylor and Francis, London. 1967. p. 281.
6. J. W. Purdie, H. A. Gillis, and N. V. Klassen. Can. J. Chem. **51**, 3132 (1973).
7. G. E. Adams, J. E. Aldrich, R. H. Bisby, R. B. Cundall, J. L. Redpath, and R. L. Willson. Radiat. Res. **49**, 278 (1972).
8. R. E. Benesch and R. Benesch. J. Am. Chem. Soc. **77**, 5877 (1955).
9. G. E. Adams, G. S. McNaughton, and B. D. Michael. Trans. Faraday Soc. **64**, 902 (1968).
10. G. E. Adams and R. L. Willson. Chem. Soc. Ann. Rep. 207 (1970).
11. R. L. Willson. Chem. Soc. Chem. Commun. 1425 (1970).
12. I. G. Draganić and Z. D. Draganić. The radiation chemistry of water. Academic Press, New York. 1971.
13. G. E. Adams, J. W. Boag, J. Currant, and B. D. Michael. *In* Pulse radiolysis. *Edited by* M. Ebert, J. P. Keene, A. J. Swallow, and J. H. Baxendale. Academic Press, London. 1965. p. 117.
14. Z. D. Draganić and I. G. Draganić. J. Phys. Chem. **77**, 765 (1973).
15. Z. D. Draganić and I. G. Draganić. J. Phys. Chem. **76**, 2733 (1972).
16. R. L. Willson, C. L. Greenstock, G. E. Adams, R. Wageman, and L. M. Dorfman. Int. J. Radiat. Phys. Chem. **3**, 211 (1971).
17. L. M. Dorfman and G. E. Adams. Reactivity of hydroxyl radicals in aqueous solutions. U.S. Department of Commerce, N.B.S. No. 46, Washington, D.C. 1973.
18. T-L. Tung and J. A. Stone. J. Phys. Chem. **78**, 1130 (1974).
19. D. Giles and D. W. Grant. Chem. Ind. 1437 (1970).

Facile Synthesis of Thiols and Sulfides

JEAN-ROCK BRINDLE AND JEAN-LOUIS LIARD
Département des Sciences Pures, Université du Québec, Rimouski, Québec G5L 3A1
Received November 4, 1974

JEAN-ROCK BRINDLE and JEAN-LOUIS LIARD. Can. J. Chem. **53**, 1480 (1975).

Sulfurated sodium borohydride reacts with benzylic halides to give high yields of α-toluenethiol or benzylic polysulfides depending upon the experimental conditions and the mode of hydrolysis.

Aliphatic halides and dibenzylic halides react in the same manner as benzylic halides for a given experimental condition whereas benzylic halides substituted with other groups can be totally or partially reduced depending on the stability of the substituent towards $NaBH_2S_3$.

Halogens directly attached on the aromatic ring do not react with $NaBH_2S_3$.

JEAN-ROCK BRINDLE et JEAN-LOUIS LIARD. Can. J. Chem. **53**, 1480 (1975).

La réaction de $NaBH_2S_3$ avec les halogénures benzyliques conduit à une production quantitative d'α-toluènethiol ou de polysulfures benzyliques dépendant des conditions expérimentales employées et du mode d'hydrolyse choisi.

Les halogénures aliphatiques et les halogénures dibenzyliques réagissent de la même manière que les halogénures benzyliques sous des conditions expérimentales similaires, alors que les halogénures benzyliques substitués par d'autres groupes, peuvent être réduit totalement ou partiellement dépendant de la stabilité du deuxième groupe vis-à-vis $NaBH_2S_3$.

Les halogénures directement fixés sur un noyau benzénique ne réagissent pas avec $NaBH_2S_3$.

[Traduit par le journal]

Martin and Greco (1) and Tsurugi and Nakabayaski (2) have already reported the synthesis of thiols (1) and sulfides (2) from benzylic halides in very moderate yields. This report describes a significant improvement of the existing synthetic procedures resulting from the use of sulfurated sodium borohydride (3) as a new reagent for the preparation of thiols or sulfides from halogenated compounds.

From Table 1, it can be seen that after treatment with $NaBH_2S_3$, the predominance of a given benzylic sulfurated compound depends largely upon the method of hydrolysis and the experimental conditions used. Considering benzyl chloride as a typical case, we notice that hydrolysis with sodium hydroxide favors greatly the production of sulfides in every case except when a high temperature and an excess of reducing agent are used. At constant temperature, an increase in the molar ratio of the sulfurated hydride increases the production of thiols and the same effect is observed when there is an increase in temperature at constant molar ratio. From these observations it is normal to find very high yields of thiols when an excess of reducing agent and high temperature are used, this effect being independant of the method of hydrolysis. Experimental conditions avoiding large excess of $NaBH_2S_3$ give moderate yields of thiols and sulfides when acidic hydrolysis is used but give high yields of sulfides when hydrolysis is made with a 10% sodium hydroxide solution.

Table 2 shows the reactivity of different organic iodides, chlorides, or bromides and shows that the general trend previously observed with benzyl halides is also verified with other benzylic and aliphatic halides. Methyl iodide reacts the same way as benzyl iodide under similar experimental conditions yielding mainly the corresponding thiol. For aliphatic chlorides, such as *t*-butyl chloride and 2-(chloroethyl)benzene, it appears that the same type of reactivity is obtained except when steric hindrance is important enough to inhibit reaction as seems to be the case with *t*-butyl chloride. 1-(Bromoethyl)benzene reacts in a fashion similar to benzylic bromide yielding similar proportions of the corresponding thiol and polysulfides. *p*-Dibenzylic chlorides give excellent yields of the corresponding dithiols. With substituted benzylic chlorides, such as *p*-nitrobenzyl chloride, the reaction proceeds normally under mild experimental conditions

Can. J. Chem. Downloaded from www.nrcresearchpress.com by 210.87.254.105 on 09/05/12
For personal use only.

Can. J. Chem. Downloaded from www.nrcresearchpress.com by 210.87.254.105 on 09/05/12
For personal use only.

TABLE 1. Reaction of benzylic halides with $NaBH_2S_3$

					Benzylic thiol and sulfides									
					Hydrolysis with HCl 10%					Hydrolysis with NaOH 10%				
					Thiol	Sulfides				Thiol	Sulfides			
T (°C)	Molar ratio $\frac{NaBH_2S_3}{C_6H_5CH_2X}$	Reaction time (h)	X	$C_6H_5CH_2X$ consumed (%)	—SH	Total	Mono	Di	Poly	—SH	Total	Mono	Di	Poly
20	2:1	66	F	40	7	33	7	7	19					
20	2:1	16	F	42	3	39		6	33					
20	1:1	16	Cl	92	38	54	6	28	20	5	87	9	62	16
20	1:1	16	Br	100	11	89		34	55	7	93	7	64	22
20	1:1	16	I	100	13	87	4	31	52					
20	4:1	65	F	95	22	73	2	22	49					
20	4:1	16	Cl	100	55	45	6	17	22	—	100	19	38	43
20	4:1	16	Br	100	75	25	5	12	8					
20	4:1	16	I	100	85	15	3	12						
65	1:1	16	F	40	25	15	15							
65	1:1	16	Cl	100	78	22	12	10		13	87	59	28	
65	1:1	16	Br	100	62	38	28	7	3					
65	1:1	16	I	100	58	42	34	8						
65	4:1	16	F	100	99	Traces								
65	4:1	16	Cl	100	99	Traces				87	13		13	
65	4:1	16	Br	100	69	31	3	10	18					
65	4:1	16	I	100	95	5	3	2						

Can. J. Chem. Downloaded from www.nrcresearchpress.com by 210.87.254.105 on 09/05/12
For personal use only.

TABLE 2. Reactivities of organic halides

Reagent	T (°C)	Molar ratio $\frac{NaBH_2S_3}{reagent}$	Reaction time (h)	Products Hydrolysis with HCl 10%
CH_3I	20	4:1	64	Mainly CH_3SH
	20	1:1	64	CH_3SH (70%) $CH_3S_2CH_3$ (15%) CH_3SCH_3 (15%)
$(CH_3)_3CCl$	20	4:1	16	No reaction
	65	4:1	16	Complex mixture of thiols and polysulfides
$C_6H_5CH_2CH_2Cl$	65	4:1	16	$C_6H_5CH_2CH_2SH$ (90%)
$C_6H_5CH(Br)CH_3$	65	4:1	16	$C_6H_5CH(SH)CH_3$ (30%) Polysulfides (70%)
p-$ClCH_2C_6H_4CH_2Cl$	65	8:1	16	$HSCH_2C_6H_4CH_2SH$ (80%)
p-$NO_2C_6H_4CH_2Cl$	65	8:1	16	*p*-$NH_2C_6H_4CH_2SCH_2C_6H_4NH_2$ (48%) Aminated polysulfides (52%)
	20	1:1	16	*p*-$NO_2C_6H_4CH_2SH$ (53%) Nitrated polysulfides (47%)
p-$NO_2C_6H_4CH_2Br$	20	4:1	16	*p*-$NH_2C_6H_4CH_2SCH_2C_6H_4NH_2$ (52%) Aminated polysulfides (48%)
	20	1:1	16	*p*-$NO_2C_6H_4CH_2SH$ (traces) Nitrated polysulfides (90%)
C_6H_5X(F, Cl, Br, I)	65	4:1	16	No reaction

Can. J. Chem. Downloaded from www.nrcresearchpress.com by 210.87.254.105 on 09/05/12
For personal use only.

to give nitrated thiols and polysulfides. With stronger reaction conditions, the reaction proceeds further to transform the nitro group into the amino group.

From the already known selectivity of $NaBH_2S_3$, it can be said that substituted benzylic chlorides would react normally to give the corresponding thiols and sulfides especially if the substituted group is inert to $NaBH_2S_3$, as is the case for ester, acid, ether, or olefinic groups. The same conclusion may be applied to *p*-nitrobenzyl bromide as shown by the results of Table 2.

In conclusion it is important to note that aromatic halides are inert to $NaBH_2S_3$ as shown in Table 2 whereas aliphatic and benzylic halogenated compounds give excellent yields of the corresponding sulfurated products. Actually, the main advantage of sulfurated sodium borohydride over the older reagents for the production of thiols and sulfides from halogenated compounds, is that $NaBH_2S_3$ generally leads to an almost quantitative yield of thiols or sulfides depending essentially upon the choice of the reaction conditions and the mode of hydrolysis, whereas older methods (1, 2) give more moderate yields and call for specific reagents in order to assure the production of thiols or of sulfides.

Experimental

The n.m.r. measurements were made with a Perkin-Elmer R-12A apparatus. The i.r. measurements were made with a Pye Unicam SP 200G spectrophotometer.

Typical Procedures for the Reaction of $NaBH_2S_3$ and Organic Halides

The experimental conditions for the reductions have been described in earlier works (4, 5) and the separation of the reaction products has been made by evaporation or distillation of α-toluenethiol followed by separation over column chromatography using silica gel and a mixture of hexane–CCl_4 as eluant, in order to isolate the sulfides. The identification of these sulfurated compounds has been confirmed by a comparative study of the n.m.r. chemical shifts with the authentic products as mentioned by Grant and Van Wazer (6).

Optimal Conditions for the Reaction of Benzyl Chloride

To a suspension of 0.20 mol (26.40 g) of $NaBH_2S_3$ prepared as described by Lalancette (3) in 200 ml of tetrahydrofuran, 0.05 mol (6.33 g) of benzyl chloride in 100 ml of tetrahydrofuran was added dropwise. The reaction mixture was stirred and refluxed for 16 h and was then evaporated to dryness, under reduced pressure, at room temperature. The residual solid was covered with 200 ml of ethyl ether and 10% hydrochloric acid was added until the p*H* of the reaction mixture was 1.0. The precipitated sulfur was filtered off and the filtrate washed repeatedly with ethyl ether. The organic fraction was then dried over $MgSO_4$ and the evaporation of ether gave a 99% yield of α-toluenethiol. A similar reaction using equimolar quantities of $NaBH_2S_3$ and benzyl chloride at 65° for 16 h was hydrolyzed with a 10% sodium hydroxide solution until the p*H* of the reaction mixture was 11.0. The ethereal fraction was dried over $MgSO_4$ and the evaporation of ether gave a mixture of thiol and sulfides. After evaporation of the α-toluenethiol (13%), the residual solid was analyzed by a column chromatography study using a silica gel column and a mixture of hexane–CCl_4 as eluant. The separation gave 59% of benzyl sulfide and 29% of benzyl disulfide.

The positive identification of all products was made by a comparative n.m.r. study with authentic samples.

The authors thank the National Research Council of Canada (Grant A6830) for financial assistance.

1. D. J. Martin and C. C. Greco. J. Org. Chem. **33**, 1275 (1968).
2. J. Tsurugi and T. Nakabayashi. J. Org. Chem. **24**, 807 (1959).
3. J. M. Lalancette, A. Frêche, and R. Monteux. Can. J. Chem. **46**, 2754 (1968).
4. J. M. Lalancette and J. R. Brindle. Can. J. Chem. **48**, 735 (1970).
5. J. M. Lalancette and J. R. Brindle. Can. J. Chem. **49**, 2990 (1971).
6. D. Grant and J. R. Van Wazer. J. Am. Chem. Soc. **86**, 3012 (1964).

The Rearrangement of Aryl Thiohydrazonates

ARTHUR J. ELLIOTT

Department of Chemistry, McMaster University, Hamilton, Ontario L8S 4M1

AND

PATRICK D. CALLAGHAN, MARTIN S. GIBSON, AND STEVEN T. NEMETH

Department of Chemistry, Brock University, St. Catharines, Ontario L2S 3A1[1]

ARTHUR J. ELLIOTT, PATRICK D. CALLAGHAN, MARTIN S. GIBSON, and STEVEN T. NEMETH. Can. J. Chem. **53**, 1484 (1975).

Rearrangement and cyclization of a series of *p*-nitrophenyl and heteroaryl thiohydrazonates ArSCAr′ = $NNHC_6H_3XY(2,4)$, where the displaced substituent X is Br or F and the remaining substituent Y is Br or NO_2, occurs under suitable basic conditions to the corresponding 7-substituted 2-aryl-4-*p*-nitrophenyl- and -4-heteroaryl-4*H*-1,3,4-benzothiadiazines, *e.g.* **13** → **19**. Under these or suitable acidic conditions, the 4,6-dimethyl-2-pyrimidinyl thiohydrazonate rearranges to the thiohydrazide $Ar'CSNHNArC_6H_3XY(2,4)$, apparently the first case of thiohydrazonate-thiohydrazide rearrangement; such acidic treatment produces cleavage of some other heteroaryl thiohydrazonates.

Independent syntheses of two of the 4-heteroaryl-substituted benzothiadiazines are reported.

ARTHUR J. ELLIOTT, PATRICK D. CALLAGHAN, MARTIN S. GIBSON et STEVEN T. NEMETH. Can. J. Chem. **53**, 1484 (1975).

Le réarrangement et la cyclisation d'une série de thiohydrazonates de *p*-nitrophényles et d'hétéroaryles ArSCAr′ = $NNHC_6H_3XY(2,4)$ dans lesquels le substituant déplacé X est Br ou F et l'autre substituant Y est Br ou NO_2 se produit dans des conditions basiques appropriées pour conduire aux aryl-2 *p*-nitrophényl-4 et aux hétéroaryl-4 4*H*-benzothiadiazines-1,3,4 substituées en position 7, *e.g.* **13** donne **19**. Dans ces conditions et/ou dans des conditions acides appropriées, le thiohydrazonate de diméthyl-4,6 pyrimidinyle-2 se réarrange pour fournir le thiohydrazide $Ar'CSNHNArC_6H_3XY(2,4)$ et ceci est apparamment le premier cas d'un réarrangement thiohydrazonate en thiohydrazide; un tel traitement acide produit généralement une coupure d'autres thiohydrazonates d'hétéroaryles.

On rapporte des synthèses indépendantes de deux des benzothiadiazines substitués par des hétéroaryles-4. [Traduit par le journal]

Huisgen *et al.* (1) have noted that whereas thermolysis of 2,5-diphenyltetrazole in phenol gave *N′*,*N′*-diphenylbenzohydrazide, the corresponding reaction in thiophenol gave phenyl *N*-phenyl(thiobenzohydrazonate) (**1**); the corresponding *p*-tolyl thiohydrazonate was prepared similarly. Both thiohydrazonates were stable under the conditions of formation at 160–170°. Thermal rearrangement of **1** to *N′*,*N′*-diphenyl-(thiobenzohydrazide) (**2**) under conditions where oxygen analogs (aryl hydrazonates) rearrange satisfactorily to *N′*,*N′*-diarylhydrazides was attempted later by Hegarty *et al.* (2) but without success.

$PhC(SPh)=NNHPh$ (**1**) $\qquad$ $PhCSNHNPh_2$ (**2**)

Our approach to the problem of rearrangement of aryl thiohydrazonates has involved two considerations: (*i*) the *S*-aryl ring should be made electron deficient by substitution and/or incorporation of heteroatom(s); (*ii*) rearrangement should be further facilitated by employing basic conditions to increase the nucleophilicity of the terminal nitrogen of the hydrazonyl system or, where the *S*-aryl group is basic, by employing acidic conditions to increase the electrophilicity of that group. In most cases substituents in the *N*-aryl group were chosen with a view to synthesis of 4*H*-1,3,4-benzothiadiazine derivatives as indicated below.

Initially the hydrazonyl bromide **3** was treated with *p*-nitrothiophenol in ethanol (EtOH) in presence of triethylamine (NEt_3) to give the thiohydrazonate **13**. By contrast with the corresponding reaction of **3** with thioacetate ion, there was apparently no conversion of **3** to hydrazonyl sulfide (3); also, neither *p*,*p*-dinitrodiphenyl sulfide nor *p*,*p*-dinitrodiphenyl disulfide was detected in the reaction mixture. Other

[1]Address for correspondence.

Can. J. Chem. Downloaded from www.nrcresearchpress.com by 210.87.254.40 on 09/05/12
For personal use only.

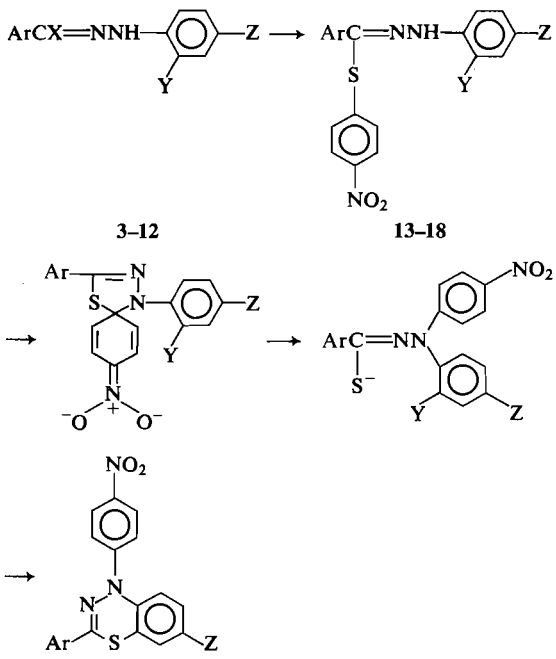

3, 13, 19	Ar = Ph; X = Z = Br; Y = F
4, 14	Ar = Ph; X = Y = Z = Br
5, 15, 20	Ar = *p*-$CH_3OC_6H_4$; X = Y = Z = Br
6, 16, 21	Ar = *p*-ClC_6H_4; X = Y = Z = Br
7, 17	Ar = Ph; X = Cl; Y = Br; Z = H
8	Ar = Ph; X = Y = Br; Z = SCN
9, 18, 22	Ar = 5-Bromo-2-thienyl; X = Y = Z = Br
10, 23	Ar = Ph; X = Y = Br; Z = NO_2
11	Ar = Ph; X = Cl; Y = Z = Br
12	Ar = Ph; X = Cl; Y = Z = H

SCHEME 1

hydrazonyl halides were similarly converted to corresponding *p*-nitrophenyl thiohydrazonates **14–18**, except in the case of **8** where competing reaction of *p*-nitrothiophenoxide ion with the thiocyanato group occurred leading to a complex mixture, possibly containing disulfides (4), from which a small yield of **17** was isolated (Scheme 1). The structures of the thiohydrazonates were confirmed by examination of mass spectra which revealed characteristic loss of the elements of *p*-nitrothiophenol from the molecular ions (5).

When the thiohydrazonate **13** was treated with EtOH–NEt_3 at reflux, the product isolated was not the isomeric *N'*,*N'*-diaryl(thiobenzohydrazide) (product of rearrangement) but the thiadiazine **19** (product of rearrangement and cyclization). Thiohydrazonates **15**, **16**, and **18** similarly gave thiadiazines **20**, **21**, and **22**, respectively, but no thiadiazine was obtained from **17**, a result consistent with earlier observations (3). The primary product from **10** and *p*-nitrothiophenol, presumably the thiohydrazonate, similarly was converted to **23**, whilst the conversion of **14** to **19**, sluggish in EtOH–NEt_3, was achieved readily by employing the perhaps unnecessarily forcing conditions of reflux with sodium hydroxide and NEt_3 in dimethylformamide (DMF).

These reactions differ from the rearrangement of aryl hydrazonates which lead to *N'*,*N'*-diarylhydrazides (2, 5) and resemble rather those reactions of hydrazonyl halides with thioacetate ion in which a hydrazonyl thioacetate, presumed as intermediate, undergoes rearrangement and cyclization by displacement of transiently activated *o*-halogen to a 4-acetyl-4*H*-1,3,4-benzothiadiazine (3). In the absence of definite evidence for involvement of an intermediate *N'*,*N'*-diaryl(thiobenzohydrazide) in thiadiazine formation, it is reasonable to assume that such an intermediate is consumed as it is formed.

A group of heteroaryl thiohydrazonates (**24–29**, **30***a*, and **31***a*) was next prepared by treatment of **4** with (*i*) the appropriate thiol in EtOH–NEt_3 or (*ii*) the sodium salt of the thiol; **30***b* and **31***b* were prepared similarly from the appropriate thiols and hydrazonyl halides **3** and **12**, respectively (Scheme 2). As in the above preparations of *p*-nitrophenyl thiohydrazonates, no hydrazonyl sulfides were detected in the reaction mixtures. Also, as with the *p*-nitrophenyl analogs, loss of the elements of the heterocyclic thiol from the molecular ions was a characteristic feature of the mass spectra of these heteroaryl thiohydrazonates.

It had been reported that **1** undergoes hydrolysis to PhCONHNHPh in concentrated hydrochloric acid – methanol (1) and that the analogous hydrazonate behaves similarly (2). Such conditions should presumably be avoided for the heteroaryl thiohydrazonates if rearrangement is desired. After experimentation, it was noted that **16** and an analogous hydrazonate (**14**; O instead of S in formula) were stable in concentrated hydrochloric acid – benzene under certain conditions and this system was adopted for the work in hand. When the pyrimidinyl thiohydrazonate **24** was so treated, the isomeric thiohydrazide **32** was obtained in 55% yield, providing the first instance in this work of a

Can. J. Chem. Downloaded from www.nrcresearchpress.com by 210.87.254.40 on 09/05/12
For personal use only.

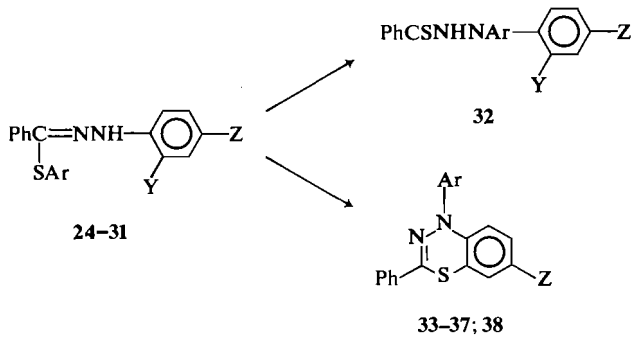

Y = Z = Br except for **30***b* (Y = F; Z = Br) and **31***b* (Y = Z = H)
24, **32** Ar = 4,6-Dimethyl-2-pyrimidinyl
25 Ar = 1-Phenyl-5-tetrazolyl
26, **33** Ar = 2-Quinoxalinyl
27, **34** Ar = 5-Nitro-2-pyridinyl
28 Ar = 2-Pyridinyl
29, **35** Ar = 4-Methyl-2-quinolinyl
30, **36** Ar = 2-Benzothiazolyl
31, **37** Ar = 2-Benzoxazolyl
38 Ar = H

SCHEME 2

thiohydrazonate → thiohydrazide rearrangement which was not complicated by subsequent reactions. However, with the tetrazolyl thiohydrazonate **25**, it was noted that acidic cleavage supervened to give the corresponding thiol and hydrazonyl chloride **11**, providing incidentally further evidence for structural assignment **25**; the presence of the hydrazide ($PhCONHNHC_6H_3Br_2$) was also indicated (t.l.c.), suggesting that some hydrolysis was occurring. Compound **25** could be reconstructed from the component thiol and **11** in EtOH–NEt_3. Acidic cleavage was also implicated in the more complex reaction of the quinoxalinyl thiohydrazonate **26** from which **11** was obtained, although none of the corresponding thiol was isolated. Compound **27** also gave a complex mixture under these conditions; no single product was isolated but there was some indication (p.m.r.) that the isomeric thiohydrazide was present. Compounds **28** and **29** were stable under these conditions.

The acid-catalyzed hydrolysis of hydrazonates has been interpreted in terms of protonation of the hydrazonate oxygen atom (2) and similar considerations can be applied to acidic cleavage and hydrolysis of thiohydrazonates, *i.e.* protonation of the thiohydrazonate sulfur atom and subsequent reaction involving chloride ion or water. However, with the present cases, alternative protonation of heteroatom(s) of the heteroaryl ring may occur, some of which would create a situation conducive to rearrangement, and the reaction course is presumably regulated by competition between these possibilities. The acid-catalyzed rearrangement **24** → **32** would thus proceed as follows:

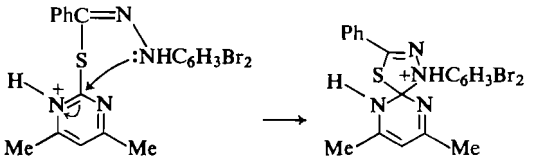

Attention was next turned to the behavior of heteroaryl thiohydrazonates under basic conditions. In view of the above results with *p*-nitrophenyl analogs, it was considered likely that thiadiazines would result if S → N heteroaryl migration occurred. When the heteroaryl thiohydrazonates were treated with EtOH–NEt_3 at reflux, the corresponding thiadiazines were obtained in the following cases: **26** → **33**, **27** → **34**, **29** → **35**, **30***a* and *b* → **36**. With **30***a* there was evidence (t.l.c.) for the involvement of an intermediate, possibly the isomeric thiohydrazide, in the conversion to **36**. Under these reaction conditions, **24** rearranged to the thiohydrazide **32** after which decomposition slowly set in, whilst **25** was decomposed extensively. Unlike **27**, no reaction was observed with **28** and no reaction was observed with **31***a* or *b*, the latter having been chosen as a case where

Can. J. Chem. Downloaded from www.nrcresearchpress.com by 210.87.254.40 on 09/05/12
For personal use only.

Can. J. Chem. Downloaded from www.nrcresearchpress.com by 210.87.254.40 on 09/05/12
For personal use only.

any rearrangement could not be followed by thiadiazine formation. When treated with sodium hydroxide and NEt_3 in DMF, however, **31***a* gave **37** but the yield was poor owing to hydrolysis of the benzoxazole ring. Finally, the structures of two of the thiadiazines (**33** and **34**) were confirmed by alternative syntheses from **38** and 2-chloroquinoxaline and 2-chloro-5-nitropyridine, respectively.

It is interesting that so few instances of simple rearrangement of aryl thiohydrazonates to thiohydrazides have been observed but it would seem likely that more examples could be found along the lines of this work. It may be that in many cases equilibrium favors the aryl thiohydrazonate (unlike similar aryl hydrazonates) rather than the thiohydrazide under the conditions which have been employed and that thiadiazine formation constitutes a process for displacement of equilibrium. Regardless, however, of whether the thiohydrazide is involved as intermediate, the S → N aryl migration taking place in formation of thiadiazines can be seen as a Smiles-type rearrangement. For migrating heterocyclic rings, such rearrangements have been studied principally in the pyridine (6) and *s*-triazine (7) series, although there are clearly many other possibilities.

Experimental

Proton magnetic resonance spectra ($CDCl_3$) were recorded on Varian A-60 and T-60 spectrometers using tetramethylsilane as internal standard; the presence of exchangeable protons was confirmed by use of D_2O. Mass spectra were recorded on Hitachi Perkin-Elmer RMU-6A and AEI-MS902 spectrometers; data are quoted as *m/e* values for the lowest isotopic species, bromine excepted (^{81}Br and ^{79}Br).

Hydrazonyl halides were prepared by published methods (3, 5, 8), as were 4,6-dimethylpyrimidine-2-thiol (9), quinoxaline-2-thiol (10) (from 2-chloroquinoxaline (11)), and 5-nitropyridine-2-thiol (12).

DMF and NEt_3 were stored over NaOH for at least 4 days before use.

Preparation of p-Nitrophenyl Thiohydrazonates

As general procedure, the hydrazonyl halide (0.01 mol) and *p*-nitrothiophenol (0.01 mol) were stirred together in EtOH (25 ml) and NEt_3 (1 ml) at room temperature for 2 h; for **3** and **4** the quantities of EtOH and NEt_3 were 40 ml and 3 ml, respectively, and reaction time was 1 h. The product was filtered off, washed, dried, and purified by crystallization.

Compound **3** gave *p-nitrophenyl N-4-bromo-2-fluorophenyl(thiobenzohydrazonate)* (**13**) (3.0 g, 67%) as orange prisms, m.p. 153–155° (from benzene–ethanol); i.r. (Nujol) 3280 cm^{-1} (NH).

Anal. Calcd. for $C_{19}H_{13}BrFN_3O_2S$: C, 51.12; H, 2.91; Br, 17.94; N, 9.42. Found: C, 51.4; H, 3.1; Br, 18.0; N, 9.1.

Compound **4** gave **14** (4.5 g, 90%) as yellow plates, m.p. 173–175° (from benzene–ethanol).

Anal. Calcd. for $C_{19}H_{13}Br_2N_3O_2S$: C, 44.97; H, 2.56; N, 8.28; S, 6.31. Found: C, 45.23; H, 2.79; N, 8.56; S, 6.16.

Compound **5** gave **15** (3.1 g, 57%) as yellow needles, m.p. 164° (from ethanol); p.m.r. δ 9.1 (s, NH), 8.0 (A), and 7.0 (B) (A_2B_2q, J = 9.0 Hz), 8.25–7.3 (m, 7H), and 3.9 (s, 3H); mass spectrum (70 eV) *m/e* 539/537/535 (M^+), 457/455 (M^+ − HBr), 384/382/380 (M^+ − $NO_2C_6H_4SH$), 304/302, 278/276, 277/275, 252/250/248 ($Br_2C_6H_3NH$), 225/223/221, 198/196, 171/169, 170/168, 155 ($NO_2C_6H_4SH$), 151, 133, 90, and 63.

Anal. Calcd. for $C_{20}H_{15}Br_2N_3O_3S$: C, 44.70; H, 2.79; Br, 29.80. Found: C, 44.52; H, 2.68; Br, 29.83.

Compound **6** gave **16** (3.4 g, 63%) as yellow needles, m.p. 158–160° (from benzene–hexane).

Anal. Calcd. for $C_{19}H_{12}Br_2ClN_3O_2S$: C, 42.11; H, 2.22; N, 7.76. Found: C, 42.27; H, 2.25; N, 7.69.

Compound **7** gave **17** (2.62 g, 62%) as yellow needles, m.p. 159° (from ethanol).

Anal. Calcd. for $C_{19}H_{14}BrN_3O_2S$: C, 53.27; H, 3.27; N, 9.81. Found: C, 53.7; H, 3.4; N, 10.0.

Compound **8** (2.09 g, 0.005 mol) reacted under the normal conditions with evolution of HCN to give an orange-yellow solid. Chromatography on Florisil and elution with hexane–ether (4:1) gave **17** which crystallized from EtOH as yellow needles (0.4 g, 18%), m.p. 159°, identical with the foregoing sample of **17**. Further elution gave yellow tarry material from which no solid product was obtained.

Compound **9** gave **18** (2.8 g, 55%) as yellow needles, m.p. 170° (from ethanol).

Anal. Calcd. for $C_{17}H_{10}Br_3N_3O_2S_2$: C, 34.46; H, 1.69; Br, 40.54; N, 7.09. Found: C, 34.68; H, 1.74; Br, 40.51; N, 6.99.

Rearrangement of p-Nitrophenyl Thiohydrazonates and Formation of Substituted 4H-1,3,4-Benzothiadiazines

Compound **13** (1.0 g), EtOH (15 ml), and NEt_3 (15 ml), were boiled under reflux for 2.75 h. *7-Bromo-4-p-nitrophenyl-2-phenyl-4H-1,3,4-benzothiadiazine* (**19**) crystallized slowly from the reaction mixture and was isolated, after cooling, as orange prisms (0.75 g, 79%), m.p. 228–229°.

Anal. Calcd. for $C_{19}H_{12}BrN_3O_2S$: C, 53.52; H, 2.82; Br, 18.78; N, 9.86. Found: C, 53.3; H, 2.9; Br, 18.8; N, 9.8.

Compound **14** (1.0 g), NaOH (0.1 g), DMF (10 ml), and NEt_3 (2.5 ml) were boiled under reflux for 2 h. When cool, the crystalline precipitate (0.77 g, 90%) m.p. 225–227°, was collected; crystallization from benzene gave **19** as orange prisms, m.p. 227–229°, identical with the previous sample of **19**.

Compound **15** (2.0 g), EtOH (20 ml), and NEt_3 (20 ml) were boiled under reflux for 2 h. The solution was concentrated *in vacuo* and the orange solid was collected, washed, and dried. Crystallization from benzene gave the *thiadiazine* (**20**) (1.2 g, 74%) as orange prisms, m.p. 217° (dec.).

Anal. Calcd. for $C_{20}H_{14}BrN_3O_3S$: C, 52.63; H, 3.07; Br, 17.54. Found: C, 52.54; H, 2.97; Br, 17.65.

Compound **16** (2.0 g), treated as for **15** above, gave

Can. J. Chem. Downloaded from www.nrcresearchpress.com by 210.87.254.40 on 09/05/12
For personal use only.

21 (0.7 g, 40%) as orange-yellow needles, m.p. 253–254° (dec.) (from benzene).

Anal. Calcd. for $C_{19}H_{11}BrClN_3O_2S$: C, 49.51; H, 2.39; N, 9.12. Found: C, 49.47; H, 2.41; N, 8.96.

Compound **17** (0.5 g), treated as for **15** above, gave a yellow gum which contained at least four components (t.l.c.), none of which was **17** or was fluorescent. Attempts to isolate solid products were unsuccessful.

Compound **18** (1.5 g), EtOH (15 ml), and NEt_3 (15 ml) were boiled under reflux for 4 h, cooled, and the product was filtered off. Compound **22** (0.8 g, 64%) crystallized from benzene–hexane as orange-brown prisms, m.p. 213°.

Anal. Calcd. for $C_{17}H_9Br_2N_3O_2S_2$: C, 39.92; H, 1.76; Br, 31.31; S, 12.52. Found: C, 39.62; H, 1.75; Br, 31.50; S, 12.65.

Compound **10** (3.10 g) was treated with *p*-nitrothiophenol in the manner described above for **5**. A sample (1.0 g) of the crude product was boiled under reflux with EtOH (10 ml) and NEt_3 (10 ml) for 4 h and the solution was then concentrated. The solid was collected, triturated with boiling acetone and benzene, and then crystallized from dioxan to give **23** as red prisms (0.37 g, 45% overall from **10**), m.p. 274° (dec.).

Anal. Calcd. for $C_{19}H_{12}N_4O_4S$: C, 58.16; H, 3.06; N, 14.29. Found: C, 58.6; H, 3.1; N, 14.0.

Preparation of Heteroaryl Thiohydrazonates

(i) The hydrazonyl halide (0.01 mol) and the thiol (0.01 mol) were stirred together in EtOH (30 ml) and NEt_3 (1 ml) at room temperature for 2 h; for preparations of **30** (*a* and *b*) and **31** (*a* and *b*), reaction times were 1 and 3 h, respectively, and the quantity of NEt_3 was increased to 3 ml. The product was filtered off (after dilution with water in the case of **27**), washed, dried, and purified by crystallization.

Compound **4** and quinoxaline-2-thiol gave the *thiohydrazonate* (**26**) (3.2 g, 63%) as yellow prisms, m.p. 142–143° (from hexane–toluene); p.m.r. δ 9.18 (s, NH), 8.52 (s, 1H) ,and 8.1–7.1 (m, 12H); mass spectrum *m/e* 516/514/512 (M^+), 435/433, 434/432, 381/379/377 ($Br_2C_6H_3NHC_8H_5N_2$), 354/352/350 ($M^+ - C_8H_5N_2SH$), 300/298, 251/249/247, 219, 170/168, 162 ($C_8H_5N_2SH$), 129, 121, 118, 103, and 91.

Anal. Calcd. for $C_{21}H_{14}Br_2N_4S$: C, 49.03; H, 2.72; Br, 31.13. Found: C, 49.01; H, 2.63; Br, 31.35.

Compound **4** and 5-nitropyridine-2-thiol gave **27** (3.4 g, 83%) as yellow plates, m.p. 144–145° (from ethanol – ethyl acetate). Analytical figures were discrepant. Proton magnetic resonance δ 9.25 (s, NH), 9.25 (d, 1H, $J = 2.5$ Hz), 8.4–7.98 (m, 3H), and 7.65–7.3 (m, 7H); mass spectrum *m/e* 510/508/506 (M^+), 477/475/473, 429/427, 428/426, 376/374/372 ($Br_2C_6H_3NC_5NH_3NO_2$), 354/352/350 ($M^+ - NO_2C_5H_3NSH$), 347, 309/307/305, 305/303, 295/293/291, 251/249/247 ($Br_2C_6H_3N$), 241, 198, 170/168, 155 ($NO_2C_5H_3NS$), 121, 103, and 76.

Compound **4** and benzothiazole-2-thiol gave **30***a* (4.8 g, 93%) as cream prisms, m.p. 128–130° (from benzene–ethanol).

Anal. Calcd. for $C_{20}H_{13}Br_2N_3S_2$: C, 46.24; H, 2.50; Br, 30.83; N, 8.09. Found: C, 46.5; H, 2.7; Br, 30.6; N, 8.0.

Compound **3** and benzothiazole-2-thiol gave **30***b* (1.4 g, 31%) as cream prisms, m.p. 100–102° (from ethanol).

Anal. Calcd. for $C_{20}H_{13}BrFN_3S_2$: C, 52.40; H, 2.84; N, 9.17; S, 13.97. Found: C, 52.1; H, 2.6; N, 8.9; S, 14.0.

Compound **4** and benzoxazole-2-thiol gave **31***a* (3.5 g, 69%) as reddish prisms, m.p. 136–138° (from benzene–hexane).

Anal. Calcd. for $C_{20}H_{13}Br_2N_3OS$: C, 47.71; H, 2.58; N, 8.35. Found: C, 48.27; H, 2.87; N, 8.20.

Compound **12** and benzoxazole-2-thiol gave **31***b* (2.5 g, 72%) as yellowish prisms, m.p. 116–117° (from benzene–hexane).

Anal. Calcd. for $C_{20}H_{15}N_3OS$: C, 69.57; H, 4.35; N, 12.17. Found: C, 59.76; H, 4.47; N, 12.03.

(ii) Sodium salts of thiols were prepared by addition of 1 equiv. of sodium to the thiol in EtOH and were then precipitated by addition of dry ether, collected, and stored *in vacuo*. The hydrazonyl halide **4** (0.01 mol) and the sodium salt of the thiol (0.01 mol) were stirred together in dry acetonitrile (30 ml) for 2 h, and the product was then filtered off, washed, dried and purified by crystallization. For preparation of **25**, EtOH (30 ml) was used as solvent and the product was collected after pouring the reaction mixture into water.

The sodium salt of 4,6-dimethylpyrimidine-2-thiol gave the *thiohydrazonate* (**24**) (3.7 g, 75%) as colorless needles, m.p. 118° (from hexane); i.r. (Nujol) 3280 cm^{-1} (NH); p.m.r. δ 9.15 (s, NH), 8.1–7.95 (m, 2H), 7.55–7.1 (m, 6H), 6.62 (s, 1H) and 2.32 (s, 6H); mass spectrum *m/e* 494/492/490 (M^+), 461/459/457, 413/411, 359/357/355 ($Br_2C_6H_3NHC_6H_7N_2$), 354/352/350 ($M^+ - C_6H_7N_2SH$), 310/308, 278/276, 251/249/247, 225, 170/168, 140 ($C_6H_7N_2SH$), 121, 103, 82, 77, and 67.

Anal. Calcd. for $C_{19}H_{16}Br_2N_4S$: C, 46.34; H, 3.25; Br, 32.52; N, 11.38. Found: C, 46.4; H, 3.4; Br, 32.6; N, 11.7.

The sodium salt of 1-phenyltetrazole-5-thiol gave **25** (4.7 g, 89%) as fawn needles, m.p. 171–172° (dec.) (from hexane–toluene); p.m.r. δ 9.05 (s, NH) and 7.9–7.25 (m, 13H).

Anal. Calcd. for $C_{20}H_{14}Br_2N_6S$: C, 45.28; H, 2.64; N, 15.85. Found: C, 45.53; H, 2.61; N, 15.75.

The sodium salt of pyridine-2-thiol gave **28** (3.5 g, 76%) as colorless needles, m.p. 131° (from hexane–toluene).

Anal. Calcd. for $C_{18}H_{13}Br_2N_3S$: C, 46.65; H, 2.81; Br, 34.56; N, 9.07. Found: C, 47.0; H, 3.1; Br, 34.8; N, 8.8.

The sodium salt of 4-methylquinoline-2-thiol gave **29** (3.8 g, 73%) as pale yellow prisms, m.p. 117–118° (from hexane–toluene).

Anal. Calcd. for $C_{23}H_{17}Br_2N_3S$: C, 52.37; H, 3.23; Br, 30.36; N, 7.97. Found: C, 52.3; H, 3.4; Br, 30.3; N, 7.9.

Behavior of Heteroaryl Thiohydrazonates under Acidic Conditions

(i) Compound **24** (1.0 g) was dissolved in warm benzene (30 ml) and concentrated HCl (10 ml) was added. The two-phase mixture was heated without agitation on a steam bath for 1 h and then cooled. The benzene layer was separated, washed with aqueous $NaHCO_3$ solution and water, and then dried and evaporated *in vacuo*. Crystallization from hexane–toluene gave the *thiobenzohydrazide* (**32**) (0.55 g, 55%) as bright yellow prisms, m.p. 142°; i.r. (Nujol) 3340 cm^{-1} (NH); p.m.r. δ 9.7 (s, NH), 8.1–7.15 (m, 8H), 6.47 (s, 1H), and 2.3 (s, 6H); mass

Can. J. Chem. Downloaded from www.nrcresearchpress.com by 210.87.254.40 on 09/05/12
For personal use only.

spectrum *m/e* 494/492/490 (M^+), 461/459/457, 413/411, 359/357/355, 310/308, 278/276, 251/249/247, 225, 197, 170/168, 121, 103, 77, and 67.

Anal. Calcd. for $C_{19}H_{16}Br_2N_4S$: C, 46.34; H, 3.25; Br, 32.52; N, 11.38. Found: C, 46.4; H, 3.2; Br, 32.5; N, 11.6.

(ii) Compound **25** (2.0 g) in benzene (50 ml) and concentrated HCl (20 ml) was treated as above. The benzene layer was washed with 2 *M* NaOH (50 ml) and the alkaline solution was acidified with concentrated HCl to precipitate a white solid which was filtered off and dried *in vacuo*. Crystallization from toluene gave 1-phenyltetrazole-5-thiol (0.4 g, 60%) as needles, m.p. 157° (dec.) (lit. (13) m.p. 147–150° (dec.)).

Anal. Calcd. for $C_7H_6N_4S$: C, 47.19; H, 3.37; N, 31.46; S, 17.98. Found: C, 47.38; H, 3.24; N, 30.98; S, 17.98.

The benzene solution was evaporated and the residue chromatographed on Florisil (toluene as eluant) to give **11** (0.6 g, 41%) as needles, m.p. 105–108° (from hexane) (lit. (3) m.p. 109–110°); p.m.r. δ 8.05 (s, NH), 7.6–7.4 (m, 2H), and 7.2–6.85 (m, 6H); mass spectrum *m/e* 390/388/386 (M^+), 354/352/350 (M^+ − HCl), 273/271, 251/249/247, 237/235/233, 225/223/221, 171/169, 170/168, 143/141, 119/117, 103, 89, 77.

Thin-layer chromatography indicated that the only other product from the reaction was almost certainly $PhCONHNHC_6H_3Br_2$.

Compound **11** (0.38 g) and 1-phenyltetrazole-5-thiol (0.18 g) isolated from the above reaction were stirred together with EtOH (5 ml) and NEt_3 (0.2 ml) for 2 h at room temperature and the mixture was then poured into water. Isolated by means of ether, compound **25** (0.05 g) crystallized from toluene as needles, m.p. and mixture m.p. 171–172° (dec.).

(iii) Compound **26** (2.0 g) in benzene (50 ml) and concentrated HCl (20 ml), treated as above, gave a mixture of at least eight components (t.l.c.); compound **11**, separated by chromatography (Florisil, hexane–toluene), crystallized from hexane as needles (0.2 g, 13%), m.p. 104–108°, identical with the previous sample.

(iv) Compound **27** (2.0 g), treated with concentrated HCl as above, gave a mixture of at least eight components, none of which could be separated in crystalline form. The product had the following spectral characteristics; i.r. (CCl_4) 3320 cm^{-1} (NH); p.m.r. δ 9.9 (s, NH), 9.02 (d, 1H, J = 2.5 Hz), 8.4–7.25 (m, *ca.* 10H), and 6.7 (d, 1H, J = 9.0 Hz).

The following compounds were unaffected by treatment with concentrated HCl – benzene under the above conditions: **28** and **29**, and **16** and an analogous hydrazonate (**14**; O instead of S).

Behavior of Heteroaryl Thiohydrazonates under Basic Conditions; Formation of Substituted 4H-1,3,4-Benzothiadiazines

(i) Compound **27** (2.0 g), EtOH (10 ml), and NEt_3 (10 ml) were boiled under reflux for 2 h, cooled, and the product was filtered off, washed, and dried. Crystallization from benzene gave *7-bromo-4-(5-nitro-2-pyridinyl)-2-phenyl-4H-1,3,4-benzothiadiazine* (**34**) (1.31 g, 79%) as yellow needles, m.p. 223°.

Anal. Calcd. for $C_{18}H_{11}BrN_4O_2S$: C, 50.59; H, 2.58; N, 13.11. Found: C, 50.8; H, 2.8; N, 12.9.

Compound **26** (2.57 g), EtOH (10 ml), and NEt_3 (10 ml) were boiled under reflux for 2 h. The solution was cooled, poured into 5% acetic acid (700 ml), and the product was filtered off, washed, and dried. Crystallization from benzene gave **33** (2.03 g, 94%) as yellow needles, m.p. 211–212°.

Anal. Calcd. for $C_{21}H_{13}BrN_4S$: C, 58.20; H, 3.00; Br, 18.48. Found: C, 58.05; H, 2.92; Br, 18.66.

Compound **29** (2.0 g), EtOH (10 ml), and NEt_3 (10 ml) were boiled under reflux for 2 h, cooled, and the product was filtered off, washed, and dried. The product was chromatographed on Florisil and the fraction containing the yellow fluorescent component (eluted with $CHCl_3$) was collected and evaporated. Crystallization from benzene gave **35** (0.2 g, 16%) as yellow needles, m.p. 204°; mass spectrum *m/e* 447/445 (M^+), 348, 315, 284, 283, 278, 263, 223, 177/175, 176/174, 159, 149, 142, 140, 130, 115, 103, 89, and 79.

Anal. Calcd. for $C_{23}H_{16}BrN_3S$: C, 61.88; H, 3.59; Br, 17.94; N, 9.42. Found: C, 61.6; 59.0; H, 4.2, 3.6; Br, 17.8, 18.0; N, 8.5.

Compound **30***a* (1.0 g), EtOH (20 ml), and NEt_3 (20 ml) were boiled under reflux for 3.5 h, cooled, and the product was collected. Crystallization from benzene gave **36** as yellow needles (0.43 g, 51%), m.p. 196–197°; compound **30***b* similarly gave **36** (80%), m.p. and mixture m.p. 196–197°.

Anal. Calcd. for $C_{20}H_{12}BrN_3S_2$: C, 54.79; H, 2.74; Br, 18.26; N, 9.59. Found: C, 54.9; H, 2.6; Br, 18.1; N, 9.7.

Compounds **28**, and **31***a* and *b* were unaffected after 2 h under the above conditions, whilst **25** was extensively decomposed. Compound **24** rearranged to **32**, reaction being virtually complete after 30 min (t.l.c.); the product (**32**) isolated after 2 h was contaminated with at least three other substances (t.l.c.) and could not be obtained pure.

(ii) Compound **31***a* (2.0 g), NaOH (0.2 g), DMF (15 ml), and NEt_3 (2.5 ml) were boiled under reflux for 3 h. The dark mixture was concentrated *in vacuo* to half bulk, chilled, and the brown solid was collected, washed with EtOH, and dried. After crystallization from cyclohexane, **37** (0.4 g, 24%) was obtained as pale green prisms, m.p. 158–161°.

Anal. Calcd. for $C_{20}H_{12}BrN_3OS$: C, 56.87; H, 2.84; N, 9.95. Found: C, 57.02; H, 2.94; N, 9.76.

Alternative Syntheses of Thiadiazines 33 and 34

Compound **38** (3) (1.02 g), 2-chloroquinoxaline (0.54 g), acetonitrile (20 ml), and NEt_3 (3 ml) were boiled under reflux for 4 h. Solvent was removed *in vacuo* and the solid was washed with water and dried. Crystallization from benzene gave **33** (0.9 g, 62%), m.p. and mixture m.p. 211–212°.

Compound **38** (1.02 g) and 2-chloro-5-nitropyridine (0.53 g) similarly gave **34** (1.1 g, 76%), m.p. and mixture m.p. 223°.

Under these conditions, **38** did not react with 2-chloro-4,6-dimethylpyrimidine or with 2-chloropyridine.

We thank the National Research Council of Canada for financial support, and Imperial Chemical Industries Ltd. for samples of pyridine-2-thiol and 4-methylquinoline-2-thiol.

1. R. HUISGEN, J. SAUER, and M. SEIDEL. Chem. Ber. **94**, 2503 (1961).
2. A. F. HEGGARTY, J. A. KEARNEY, and F. L. SCOTT. J. Chem. Soc. Perkin II, 1422 (1973).
3. I. T. BARNISH and M. S. GIBSON. J. Chem. Soc. C, 854 (1970).
4. M. M. KAYSER and M. S. GIBSON. Can. J. Chem. **51**, 3499 (1973).
5. A. J. ELLIOTT, M. S. GIBSON, M. M. KAYSER, and G. A. PAWELCHAK. Can. J. Chem. **51**, 4115 (1973).
6. Y. MAKI, M. SUZUKI, and T. MASUGI. Chem. Pharm. Bull. **16**, 559 (1968); O. R. RODIG, R. E. COLLIER, and R. K. SCHLATZER. J. Org. Chem. **29**, 2652 (1964).
7. S. TSUNODA, T. SHIOJIMA, Y. HASHIDA, S. SEKIGUCHI, and K. MATSUI. Bull. Chem. Soc. Jap. **46**, 3499 (1973).
8. I. T. BARNISH, P. D. CALLAGHAN, and M. S. GIBSON. J. Chem. Soc. Perkin I, 215 (1974).
9. R. R. HUNT, J. F. W. MCOMIE, and E. R. SAYER. J. Chem. Soc. 525 (1959).
10. F. J. WOLF, R. M. WILSON, and M. TISHLER. J. Am. Chem. Soc. **76**, 2266 (1954).
11. A. H. GOWENLOCK, G. T. NEWBOLD, and F. S. SPRING. J. Chem. Soc. 622 (1945).
12. A. R. SURREY and H. G. LINDWALL. J. Am. Chem. Soc. **62**, 1697 (1940); W. T. CALDWELL and E. C. KORNFELD. J. Am. Chem. Soc. **64**, 1695 (1942).
13. M. FREUND and H. HEMPEL. Ber. **28**, 74 (1895).

Can. J. Chem. Downloaded from www.nrcresearchpress.com by 210.87.254.40 on 09/05/12
For personal use only.

Tetrafluoro- and Octafluoro[4.2]paracyclophanes

ROBERT FILLER AND EUI W. CHOE

Department of Chemistry, Illinois Institute of Technology, Chicago, Illinois 60616

Received August 19, 1974

ROBERT FILLER and EUI W. CHOE. Can J. Chem. **53**, 1491 (1975).

Synthetic sequences for the preparation of 6,7,9,10,14,15,17,18-octafluoro[4.2]paracyclophane (**1**) and 6,7,9,10-tetrafluoro[4.2]paracyclophane (**2**) are outlined. The u.v. absorption of compound **1** is hypsochromically shifted more than 20 nm from the long wavelength band (286–291 nm) characteristic of the [2.2]paracyclophanes.

ROBERT FILLER et EUI W. CHOE. Can. J. Chem. **53**, 1491 (1975).

On décrit les séquences de la synthèse de l'octafluoro 6,7,9,10,14,15,17,18[4.2]paracyclophane (**1**) et du tétrafluoro 6,7,9,10[4.2]paracyclophane. Le spectre d'absorption ultraviolet du composé **1** est déplacé d'une façon hypsochrome par plus de 20 nm par rapport à la bande à longueur d'onde longue (286–291 nm) caractéristique des [2.2]paracyclophanes.

[Traduit par le journal]

Can. J. Chem. Downloaded from www.nrcresearchpress.com by 210.87.254.5 on 09/05/12
For personal use only.

In previous papers we described the syntheses and properties of octafluoro[2.2]paracyclophane (1) and tetrafluoro[2.2]paracyclophane (2). We report here the syntheses of 6,7,9,10,14,15,17,18-octafluoro[4.2]paracyclophane (**1**) and its tetrafluoro analog (**2**), as outlined in Schemes 1 and 2, respectively.

While compound **1** was obtained in pure form after an arduous separation from its open-chain analog, *p*-$CH_3C_6F_4(CH_2)_4C_6F_4CH_3$-*p*, **2** could not be separated cleanly from the corresponding open-chain compound, which was also formed in the final reaction to give a 50:50 mixture (by p.m.r. spectral analysis).

We have discussed previously (2) the influence of polyfluoroaryl rings on the u.v. spectra of [2.2]paracyclophanes and speculated on the possible roles of attractive and repulsive transannular interactions. In the present study we observed the effect of bridge length by comparing the spectra of the octafluoro[2.2]- and [4.2]-paracyclophanes (Fig. 1). When the value of *m* decreases from 4 to 2, a large bathochromic shift (269 nm → 291 nm) occurs, which may reflect enhanced ring distortions with increased proximity of the fluoroaromatic nuclei. This argument requires further scrutiny in light of recent studies on [6]paracyclophane (3). The spectrum of **1** more closely resembles that of its open-chain model (Fig. 1). A similar, though less pronounced, behavior has been observed in the corresponding nonfluorinated analogs (4).

Experimental

All melting points are uncorrected. Infrared spectra were measured on a Perkin-Elmer Model 257 spectrophotometer or a Beckman IR-8 i.r. spectrometer using sodium chloride cells with a path length of 0.1 mm. Ultraviolet spectra in cyclohexane were obtained on a Beckman DK-2 spectrophotometer.

Proton magnetic resonance spectra were obtained on a Varian A-60 n.m.r. spectrometer. Chemical shifts are reported in p.p.m. relative to tetramethylsilane as internal standard. Fluorine magnetic resonance spectra were obtained on a Varian DA-60-IL spectrometer operating at 56.44 MHz in the high resolution mode. Chemical shifts were measured by the sideband technique and are reported in p.p.m. upfield or downfield from hexafluorobenzene as internal standard. Unless otherwise noted, all spectra were obtained at approximately 15% concentration in carbon tetrachloride.

Elemental analyses were conducted by Micro-Tech Laboratories, Inc., Skokie, Illinois and M-H-W Laboratories, Garden City, Michigan.

1,4-Bis(pentafluorophenyl)-2-butene

To the solution of pentafluorophenylmagnesium bromide, prepared under nitrogen by treating 6.08 g (0.25 g-atom) of magnesium with 61.8 g (0.25 mol) of bromopentafluorobenzene in 125 ml of anhydrous ether at 15°, was added 26.82 g (0.125 mol) of *trans*-1,4-dibromo-2-butene in 100 ml of anhydrous ether at a moderate rate. The resulting mixture was stirred for 28 h at reflux temperature and hydrolyzed by adding crushed ice and 150 ml of Jilute hydrochloric acid. The ether layer was separated, washed with water and a saturated ammonium chloride solution, dried ($MgSO_4$), and evaporated *in vacuo* to give a brown solid. Recrystallization from 95% ethanol with 8 g of activated charcoal afforded 33 g (67.8%) of white needles; m.p. 94–94.5°; n.m.r. (CCl_4): δ 5.64 (m, 2, vinylic) and 3.42 (m, 4, methylene).

1,4-Bis(pentafluorophenyl)butane

Hydrogenation of 1,4-bis(pentafluorophenyl)-2-butene was conducted in ethyl acetate solution in a Parr apparatus using 5% palladium-on-charcoal to give 87% of the desired product, m.p. 71.5–74°.

1,4-Bis(2',3',5',6'-tetrafluorophenyl)butane

To a solution of lithium aluminum hydride (10 g, 0.264 mol) in 240 ml of 1,2-dimethoxyethane, was added slowly

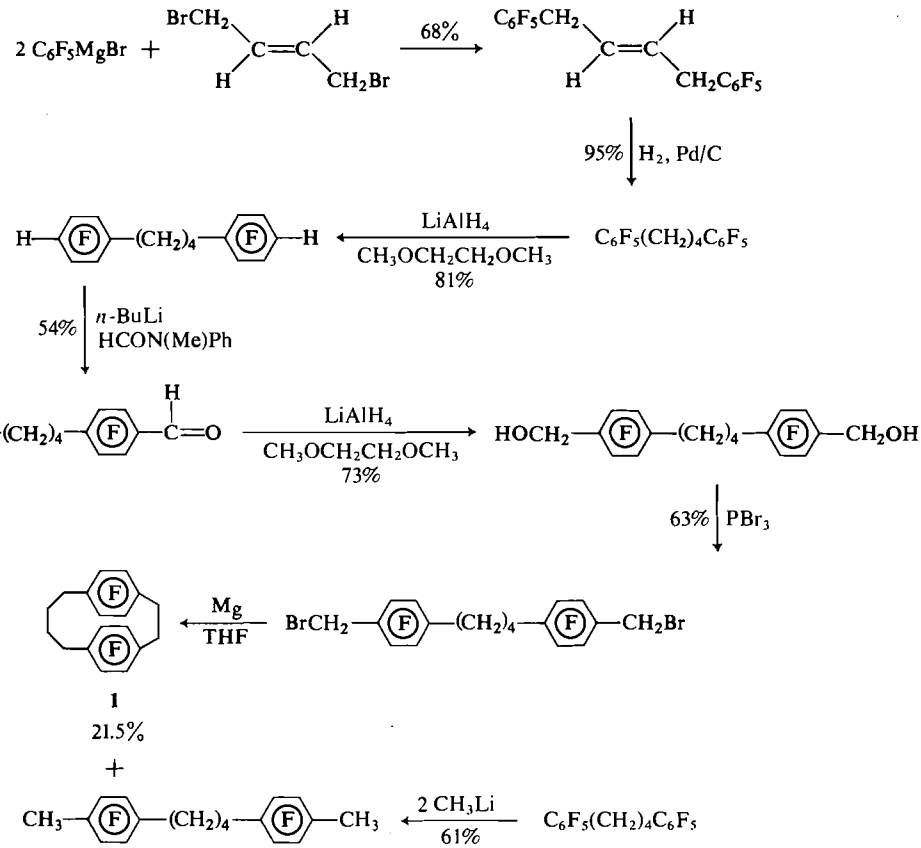

SCHEME 1

at 15°, 30 g (0.075 mol) of the bis(pentafluorophenyl)-butane. The resulting mixture was refluxed for 16 h. After decomposition of excess lithium aluminum hydride by adding a few drops of water followed by hydrolysis with dilute sulfuric acid, the mixture was poured into 2 l of water and a white solid precipitated. After decantation, the water layer was extracted with ether. The ether extract was used to dissolve the white solid, the solution was dried ($MgSO_4$), and evaporated *in vacuo* to give a white solid. Recrystallization from 95% ethanol afforded 22 g (81.3%) of product: m.p. 81.5–83°; n.m.r. δ 6.88 (triplet of triplet, 2, aromatic), 2.81 (m, 4, benzylic), and 1.71 (q, 4, J_{HH} = 3.38 Hz, methylene).

1,4-Bis(4′-formyl-2′,3′,5′,6′-tetrafluorophenyl)butane

To a solution of 0.12 mol *n*-butyllithium (75.4 ml of 15% *n*-butyllithium in hexane) cooled to −78°, was added slowly 21.2 g (0.06 mol) of the bis(tetrafluorophenyl)-butane in 400 ml of anhydrous ether. The resulting milky solution was allowed to react for 2 h. *N*-Methylformanilide (16.24 g, 0.12 mol) in 160 ml of ether was added and stirred for 3 h. After hydrolyzing with 100 ml of water and 100 ml of 6 *N* hydrochloric acid, the mixture was extracted with 1 l of ether. The ether extract was washed, dried ($MgSO_4$), and evaporated *in vacuo* to give a white solid. Trituration of this solid with 30 ml of ether and filtration gave 13.25 g (53.9%) of the bisaldehyde, m.p. 128–129°; i.r. ($CHCl_3$) 2770 (aldehyde C—H), 1705 (C=O), and 1485 cm^{-1} (polyfluoroaromatic ring); p.m.r. ($CDCl_3$) showed a triplet at δ 10.3, J_{HCCF} = 1.1 Hz (2H, —C_6F_4—CHO), a complex multiplet centered at 2.88 (4H, benzylic protons), and a quintet centered at 1.80, J_{HH} = 3.38 Hz (4H, methylene protons).

1,4-Bis(4′-hydroxymethyl-2′,3′,5′,6′-tetrafluorophenyl)-butane

To a solution of 1.52 g (0.04 mol) of lithium aluminum hydride in 250 ml of 1,2-dimethoxyethane, 20.5 g (0.05 mol) of bisaldehyde in 250 ml of 1,2-dimethoxyethane was added slowly at 15° and the mixture was stirred for 90 min. After addition of 100 ml of dilute hydrochloric acid, the mixture was poured into 3 l of water. The white solid was filtered and washed with water. Recrystallization from benzene gave 15 g (72.5%) of the diol, m.p. 172–174°; i.r. (CCl_4) 3400 and 3330 cm^{-1} (O—H).

1,4-Bis(4′-bromomethyl-2′,3′,5′,6′-tetrafluorophenyl)-butane

A mixture of 23.3 g (0.0563 mol) of bisdiol and 30.54 g (0.1126 mol, 10.71 ml) of phosphorus tribromide was heated at 140° for 5 h and then cooled and poured into 500 ml of water. The yellow solid was filtered, washed successively with water, a 5% sodium carbonate solution, then water, and dried in air. Recrystallization from carbon

Can. J. Chem. Downloaded from www.nrcresearchpress.com by 210.87.254.5 on 09/05/12
For personal use only.

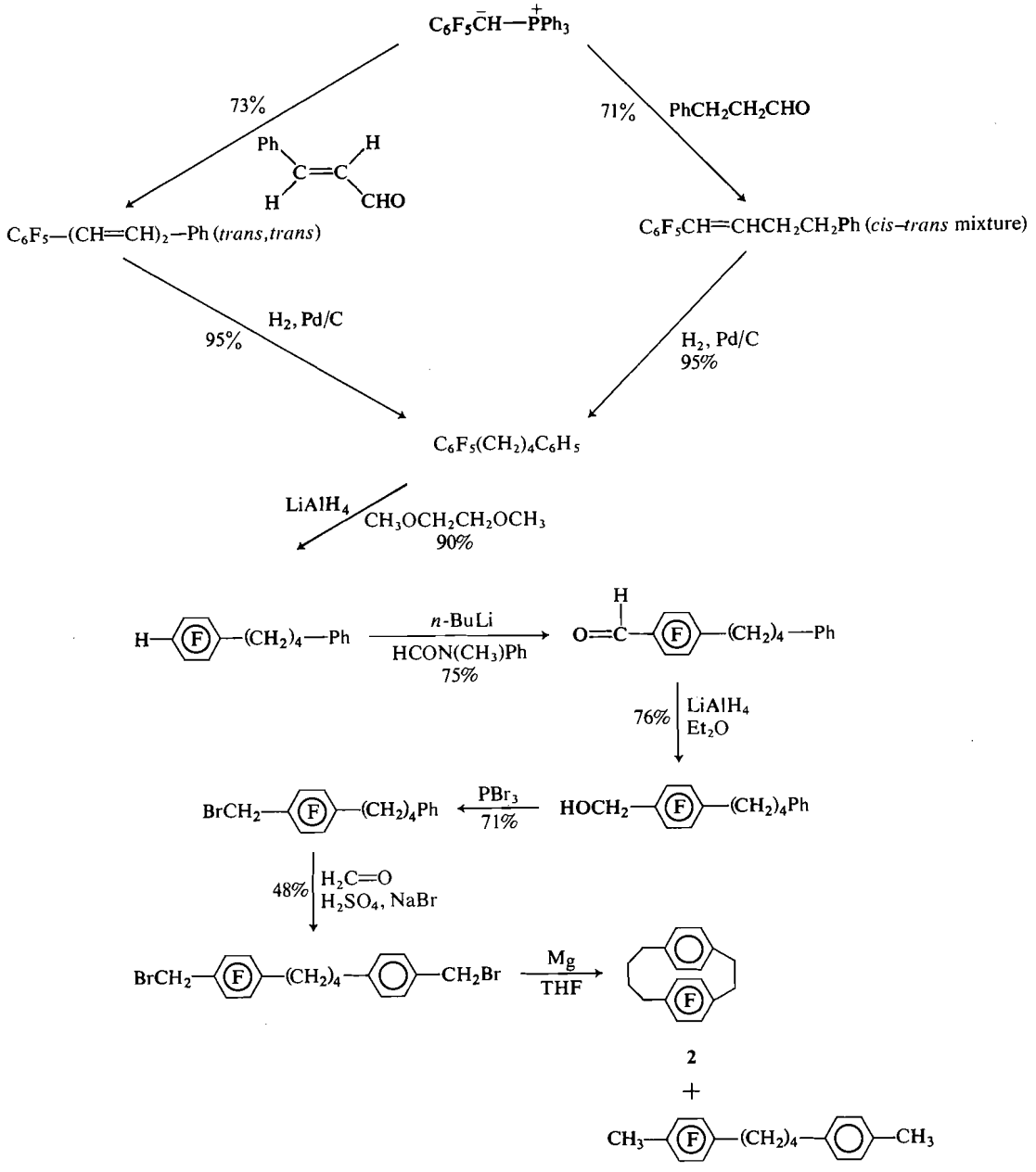

SCHEME 2

tetrachloride (400 ml) afforded 19.0 g (62.5%) of product as white needles. Sublimation at 150° (0.1 Torr) gave white crystals, m.p. 163.5–165°.

Anal. Calcd. for $C_{18}H_{12}Br_2F_8$: C, 40.03; H, 2.24. Found: C, 40.34; H, 2.26.

6,7,9,10,14,15,17,18-Octafluoro[4.2]paracyclophane (1)

To one-half of 0.3648 g (0.015 g-atom) of magnesium metal in 5 ml of tetrahydrofuran and a few crystals of iodine in a 250 ml three-necked flask, was added one-half of a tetrahydrofuran solution (105 ml) of 6.6 g (0.0122 mol) of the bisbromomethyl compound. After the mixture was stirred vigorously for 2 h, the Grignard reagent started to form. After two-thirds of the original magnesium had been consumed, the other half of magnesium and the solution of the starting material were added. After stirring for 72 h, 40 ml of tetrahydrofuran was added and the mixture stirred for an additional 60 h. The mixture was acidified with 150 ml of water and 60 ml of dilute hydrochloric acid. Filtration and air drying, followed by

Can. J. Chem. Downloaded from www.nrcresearchpress.com by 210.87.254.5 on 09/05/12
For personal use only.

Can. J. Chem. Downloaded from www.nrcresearchpress.com by 210.87.254.5 on 09/05/12
For personal use only.

sublimation (410° (0.1 Torr)) of the resulting white solid, gave 2.5 g of white sublimate. Analysis of the p.m.r. (CCl_4) spectrum of this sublimate revealed the presence of 16% of starting material, 39% of octafluoro[4.2]paracyclophane (**1**), and 43% of reduction product, 1,4-bis(4′-methyl-2′,3′,5′,6′-tetrafluorophenyl)butane. The yield of **1** was estimated to be 1 g (21.5%). The residue from the sublimation was 2.7 g of polymeric material.

Recrystallization of the sublimate from pentane gave 0.42 g of starting material. The pentane-soluble portion was chromatographed with a 90:10 mixture of pentane–benzene on 1300 g of neutral alumina using a 5 ft column, to give about 1.0 g of material. Recrystallization from 95% ethanol gave 0.42 g of the reduced product, 1,4-bis(4′-methyl-2′,3′,5′,6′-tetrafluorophenyl)butane, m.p. 141–143° (no depression when admixed with an authentic sample); n.m.r. δ 2.27 (t, 6, $^4J_{HF}$ = 2.25 Hz, methyl), 2.75 (4, m, benzylic), and 1.67 (4, m, methylene β to C_6F_5). Evaporation of the ethanol-soluble portion gave a white solid which was recrystallized from 8 ml of 95% ethanol to give 80 mg of reduced product. Evaporation of the ethanol-soluble portion and recrystallization of the residue from 0.75 ml of methylcyclohexane gave 20 mg of white crystals of pure **1**. Sublimation at 125° (0.05 Torr) gave an analytical sample, m.p. 174.5–175.5°; n.m.r. (CCl_4) δ 3.27 (m, 4, —C_6F_4—CH_2CH_2—C_6F_4—), 2.57 (m, 4,—C_6F_4—CH_2—CH_2—CH_2—CH_2—C_6F_4—), and 1.70 (m, 4, —C_6F_4—$CH_2CH_2CH_2CH_2$—C_6F_4—); u.v. λ_{max} (cyclohexane) 222 shoulder and 269 nm (log ε, 3.87 and 3.16); mass spectrum *m/e* (relative intensity) 380 (51.3) (m^+), 204 (18.9) (CH_2—C_6F_4—$CH_2CH_2^+$), 176 (100) (CH_2—C_6F_4—CH_2^+), 28 (91) ($CH_2CH_2^+$).

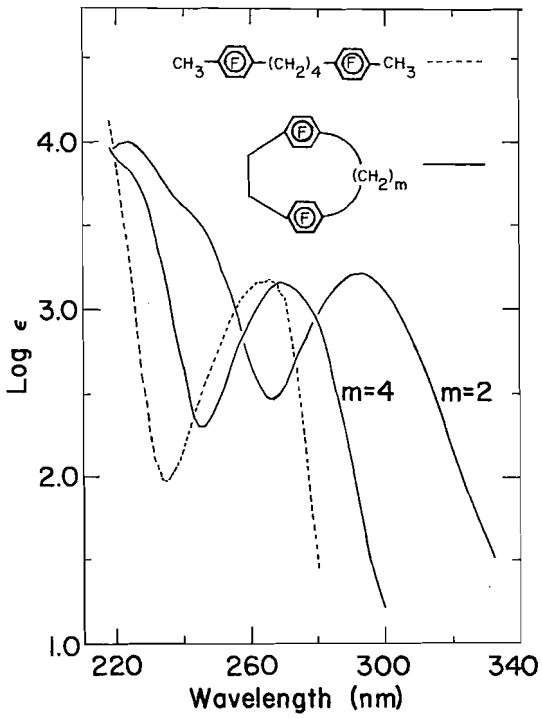

FIG. 1. Ultraviolet spectra of octafluoro[2.2]- and [4.2]paracyclophanes and open-chain model; solvent, cyclohexane.

Anal. Calcd. for $C_{18}H_{12}F_8$: C, 56.85; H, 3.18. Found: C, 56.64; H, 3.11.

1,4-Bis(4′-methyl-2′,3′,5′,6′-tetrafluorophenyl)butane

To an ethereal solution (20 ml) of 5 g (0.0128 mol) of 1,4-bis(pentafluorophenyl)butane, 15.85 ml of 5% methyllithium in ether was added sufficiently slowly to allow a gentle reflux under nitrogen. The resulting mixture turned light yellow, was stirred for 15 h, and hydrolyzed by adding ice and 6 *N* hydrochloric acid. Additional ether was required to extract the mixture. The ether layer was separated, dried ($MgSO_4$), and evaporated *in vacuo* to give a light yellow solid. Recrystallization from 95% ethanol, followed by two recrystallizations from Skelly B, with charcoal, gave 3 g (61.3%) of product, m.p. 141–145°. Sublimation at 140° (0.05 Torr) gave pure material, m.p. 141.5–143°.

Anal. Calcd. for $C_{18}H_{14}F_8$: C, 56.55; H, 3.69. Found: C, 56.60; H, 3.74.

2,3,4,5,6-Pentafluorobenzyltriphenylphosphonium Bromide

A mixture of 26.2 g (0.1 mol) of triphenylphosphine and 26.1 g (0.1 mol) of pentafluorobenzyl bromide in 180 ml of *p*-xylene was heated under reflux for 20 h. A white solid began to separate within ½ h. The white solid was collected and washed with 100 ml of *p*-xylene. Recrystallization from a 95:5 mixture of ether–methanol gave 51 g (97.5%) of the phosphonium salt: m.p. 240–241°; n.m.r. ($CDCl_3$) δ 8.15–7.60 (m, 15, aromatic) and two multiplets separated by 14 Hz, centered at 5.58 (2, C_6F_5—CH_2—P—).

Anal. Calcd. for $C_{25}H_{17}F_5BrP$: C, 57.38; H, 3.27. Found: C, 57.27; H, 3.11.

1-Pentafluorophenyl-4-phenylbutane

In a 1-l three-necked flask, equipped with a magnetic stirrer, a reflux condenser, a pressure equalizing dropping funnel connected to a nitrogen supply, and a 125 ml Erlenmeyer flask connected to the reaction flask with Gooch tubing for solid addition, was placed 0.12 mol of *n*-butyllithium (75.36 ml of 15% *n*-butyllithium in hexane, Foote Mineral Co.) in 400 ml of dry benzene. To this solution, cooled to 15° by a water bath, was added 62.76 g (0.21 mol) of 2,3,4,5,6-pentafluorobenzyltriphenylphosphonium bromide in an Erlenmeyer flask disposed in a dive position, over a period of 10 min. The resulting orange-yellow solution was stirred for 1 h at room temperature and then brought to reflux. To the hot phosphorane solution, was added slowly 0.132 mol of hydrocinnamaldehyde or *trans*-cinnamaldehyde. The red color disappeared and the resulting mixture was heated under reflux for 14 h and filtered. The filter cake was washed with additional benzene, with water, 50 ml of ether, and then dried to give 30 g (90%) of triphenylphosphine oxide.

The filtrate (benzene layer) was evaporated *in vacuo* to give a mixture of *cis* and *trans* isomers of 1-pentafluorophenyl-4-phenyl-1-butene (70.9%) (b.p. 104–108° (0.05 Torr)), or *trans,trans*-1-pentafluorophenyl-4-phenyl-1,3-butadiene (73%), respectively. The butadiene: m.p. 145–147°; i.r. ($CHCl_3$) 1515, 1494, 1000, and 965 cm^{-1}; n.m.r. ($CDCl_3$) δ 7.6–6.3 (m, ArH and vinyl). The *trans,trans* configuration was supported by the presence of λ_{max} (EtOH) 327 and a shoulder at 314 nm (5) and by the ab-

TABLE 1. Physical and analytical data for substituted 1-pentafluorophenyl-4-phenylbutanes

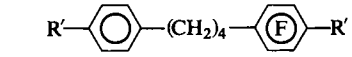

R′	R″	Recrystallization solvent	% yield	Melting or boiling point °C (Torr)	Analysis (%) Calculated C	Calculated H	Found C	Found H
H	H		90	124–125.5 (1.3)*	68.08	5.00	68.60	4.18
H	CHO	Et_2O	75.3	70.5–72	65.81	4.55	66.11	4.62
H	CH_2OH	Hexane	76.0	43.5–45	65.38	5.16	65.59	5.32
H	CH_2Br	CH_3OH	71.4	70–71	54.42	4.03	54.37	4.42
CH_2Br	CH_2Br	Skelly B – sublimation at 120° (1 Torr)	48	118.5–120	48.18	3.46	48.20	3.51

*n_D^{25} 1.5033.

sence of out-of-plane rocking of H atoms attached to a *cis* double bonded carbon (976 cm^{-1}) in its i.r. spectrum (6).

Anal. Calcd. for $C_{16}H_9F_5$: C, 64.87; H, 3.06. Found: C, 64.91; H, 3.54.

Hydrogenation of this butene or butadiene over 5% palladium-on-charcoal afforded 95% of 1-pentafluorophenyl-4-phenylbutane: b.p. 115–118° (1 Torr), m.p. 17–20°; $n_D^{26.5}$ 1.4982.

Anal. Calcd. for $C_{16}H_{13}F_5$: C, 64.00; H, 4.36. Found: 64.28; H, 4.35.

1-(4′-Bromomethyl-2′,3′,5′,6′-tetrafluorophenyl)-4-phenylbutane

This compound was prepared via the same series of reactions and procedures described earlier in the synthesis of octafluoro[4.2]paracyclophane. Pertinent data are collected in Table 1.

1-(4′-Bromomethyl-2′,3′,5′,6′-tetrafluorophenyl)-4-(4″-bromomethylphenyl)butane

This compound was prepared from its precursor above by a bromomethylation procedure described previously (7). The relevant data are found in Table 1.

6,7,9,10-Tetrafluoro[4.2]paracyclophane (2)

The mono Grignard reagent, prepared by reaction of 6.02 g (0.015 mol) of 1-(4′-bromomethyl-2′,3′,5′,6′-tetrafluorophenyl)-4-(4″-bromomethylphenyl)butane in 60 ml of tetrahydrofuran and 0.40 g (0.0165 g-atom) of magnesium turnings, was stirred for 48 h under a nitrogen atmosphere. The resulting mixture was acidified with 100 ml of water and 40 ml of dilute hydrochloric acid, filtered, and washed with water. Sublimation of the white solid at 150° (0.1 Torr) gave 0.28 g of sublimate whose p.m.r. spectrum revealed that this substance was about a 50:50 mixture of the intramolecularly cyclized product, **2** (δ's similar to those for compound **1**), and its open-chain analog, *p*-$CH_3C_6F_4CH_2CH_2CH_2CH_2C_6H_4CH_3$-*p*, (—$C_6F_4$-$CH_3$), δ 2.27 (t), $^4J_{HF}$ = 2.25 Hz. Efforts to separate the two components by column chromatography on alumina, followed by fractional crystallizations from various solvents, *e.g.*, acetone, hexane, methylcyclohexane, acetic acid, and ethanol, were unsuccessful.

1. R. FILLER and F. N. MILLER. Chem. Ind. 767 (1965).
2. R. FILLER and E. W. CHOE. J. Am. Chem. Soc. **91**, 1862 (1969).
3. V. V. KANE, A. D. WOLF, and M. JONES, JR. J. Am. Chem. Soc. **96**, 2643 (1974).
4. D. J. CRAM, N. L. ALLINGER, and H. STEINBERG. J. Am. Chem. Soc. **76**, 6132 (1954).
5. E. A. BRAUDE, J. Chem. Soc. 379 (1950).
6. K. LUNDE and L. ZECHMEISTER. Acta Chem. Scand. **8**, 1421 (1954).
7. G. KUBICZEK and L. NEUGEBAUER. Monatsh. **81**, 917 (1950); Chem. Abstr. **45**, 4211d (1951).

Can. J. Chem. Downloaded from www.nrcresearchpress.com by 210.87.254.5 on 09/05/12
For personal use only.

Reaction of 2,5-Dimethylfuran with Ethyl Propiolate: The Chemistry of Ethyl 1,4-Dimethyl-7-oxabicyclo[2.2.1]hepta-2,5-diene-2-carboxylate[1]

ARCHIBALD WILSON MCCULLOCH AND ALISTER GAVIN MCINNES

Atlantic Regional Laboratory, National Research Council of Canada, Halifax, Nova Scotia B3H 3Z1

Received December 9, 1974

ARCHIBALD WILSON MCCULLOCH and ALISTER GAVIN MCINNES. Can. J. Chem. **53**, 1496 (1975).

Thermal reaction of 2,5-dimethylfuran (**1**) and ethyl propiolate (**2**) affords the Diels–Alder adduct (**3**) and seven additional products, all of which are derived from **3**. The major products, depending on the conditions, are the *endo-exo* 2:1 diadducts (**4** and **5**) and two nortricyclenes (**8** and **10**). The last two products arise by homo Diels–Alder type dimerization of **3** (to give **10**) and subsequent Diels–Alder retrogression (to give **8**). The minor reaction products include a third nortricyclene (**9**), isomeric with **8**.

ARCHIBALD WILSON MCCULLOCH et ALISTER GAVIN MCINNES. Can. J. Chem. **53**, 1496 (1975).

La réaction thermique du diméthyl-2,5 furanne (**1**) et du propiolate d'éthyle (**2**) conduit à l'adduit de Diels–Alder (**3**) et à sept produits additionnels qui sont tous dérivés de **3**. Les produits majeurs, dépendant des conditions expérimentales, sont les diadduits *endo-exo* 2:1 (**4** et **5**) et les deux nortricyclènes (**8** et **10**). Les deux derniers produits proviennent d'une dimérisation du type homo Diels–Alder de **3** (pour donner **10**) et d'une rétrogration Diels–Alder subséquente (pour donner **8**). Les produits mineurs de la réaction incluent un troisième nortricyclène (**9**) isomère de **8**. [Traduit par le journal]

Introduction

Although Diels–Alder reactions of substituted furans with esters of acetylenedicarboxylic acid have been thoroughly investigated (1–3), the corresponding reactions utilizing propiolic acid esters have received little attention. In recent communications we have described $AlCl_3$ acceleration of the reactions of 2-methyl-, 2-phenyl-, 2,5-dimethyl-, and 2,5-diphenylfuran with the latter type of dienophile. The adducts produced in this way were shown to rearrange readily *in situ* to substituted phenolic compounds (4, 5). In the present communication we wish to describe the results of an investigation of the thermal reaction of 2,5-dimethylfuran **1** and ethyl propiolate **2**: this has revealed the high reactivity of the 2-carbethoxyoxanorbornadiene system.

Results and Discussion

The reaction of **1** and **2** at 95° proceeds slowly. In addition to the expected oxanorbornadiene adduct **3** we have isolated *seven* other products. These are the 2:1 diadducts **4** and **5**, the cyclobutene **6**, the β-carbethoxyfuran **7**, and the nortricyclene derivatives **8**, **9**, and **10**. The product composition is dependent on the initial reactant ratio, as well as reaction time and temperature (Table 1).

Adducts of type **3** are difficult to obtain. In fact **3** is the only 1:1 adduct of any furan with **2** as yet isolated. We have previously reported its formation (15%) via the $AlCl_3$-promoted reaction of **1** and **2** at −60° (5). The problem in obtaining such compounds is due to the lesser dienophilic reactivity of propiolate esters compared to esters of acetylenedicarboxylic acid and the susceptibility of the adducts to further reaction, as evidenced by their facile $AlCl_3$-catalyzed aromatization (5).

The results from Table 1, together with those derived from monitoring (p.m.r.) reactions between **1** and **2**, and from several additional independent experiments (see Experimental), showed that the formation of all seven products in the present study can be traced to the initially formed Diels–Alder adduct **3**. The reaction pathways involve (*i*) further Diels–Alder reaction of **3** with **1** (to give **4** and **5**); (*ii*) homo Diels–Alder reaction of **3** with itself (to give **10**) or with **2** (to give **8** and/or **9**?); (*iii*) Diels–Alder retrogressions of **3** (to give **7**) or of product **10** (to give **8**); and (*iv*) 2 + 2 cycloaddition of **2** to **3** (to give **6**). These transformations are summarized in Scheme 1. It is noteworthy that product **8** arises predominantly via dimerization

[1]NRCC No. 14490.

Can. J. Chem. Downloaded from www.nrcresearchpress.com by 210.87.254.40 on 09/05/12
For personal use only.

TABLE 1. Effect of reaction parameters on product composition

Reaction parameters			Yields* (%)							
Reactant ratio 1:2	Time (days)	Temperature (°C)	3	4	5	6	7	8	9	10
2:1	2	120†	—	—	20	—	1	62	—	—
1:2	7	95‡	1.7	2.6	3.4	1.6	0.4	37	0.8	15
2:1	2	95†	3.6	23	4	—	—	7	—	3
2:1	7	95†	2.3	8	4	—	0.4	23	—	12
1:1	2	95†	11	18	1.4	—	—	14	—	8

*Yields were estimated by integration of the appropriate p.m.r. signals in the various column fractions. Isolated yields (see Experimental) are somewhat lower due to normal losses during separation and purification.
†Yields based on 2.
‡Yields based on 1.

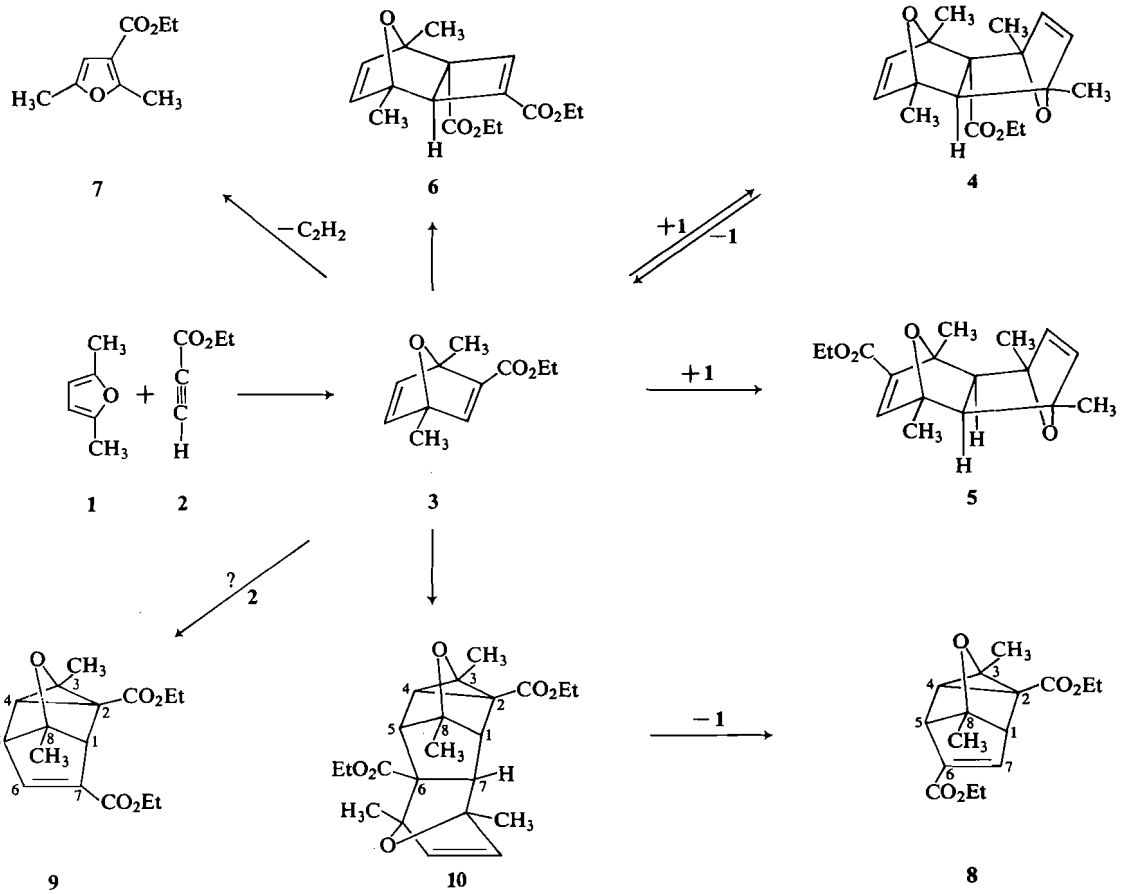

SCHEME 1

Can. J. Chem. Downloaded from www.nrcresearchpress.com by 210.87.254.40 on 09/05/12
For personal use only.

Can. J. Chem. Downloaded from www.nrcresearchpress.com by 210.87.254.40 on 09/05/12
For personal use only.

of **3** to **10** and subsequent Diels–Alder retrogression, rather than by direct reaction of **3** with **2**. Compound **10**, incidentally, is not formed at 95° by Diels–Alder addition of **1** to **8**.

Formation of diadducts **4** and **5** is not surprising since Diels–Alder additions of furans to oxanorbornadienes are well known (6–8). Thus, initial reaction of **3** with **1** affords **4**, derived by addition at the activated double bond of **3**. (Diadduct **4** is thermally unstable and when heated alone at 95° undergoes partial retrogression to **3** and **1**.) Addition of **1** to **3** under more forcing conditions (120°) occurs at the less substituted double bond of **3** to give **5**. Such behavior would be anticipated (see below) on the basis of previous work on related systems (6). An unexpected aspect of these additions, however, is their regioselectivity; we could not

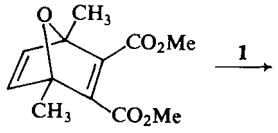

11

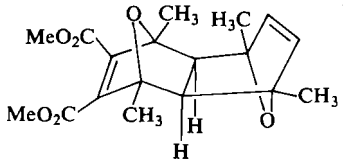

12

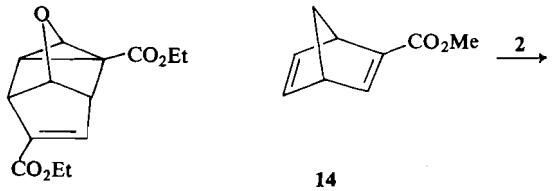

13 **14**

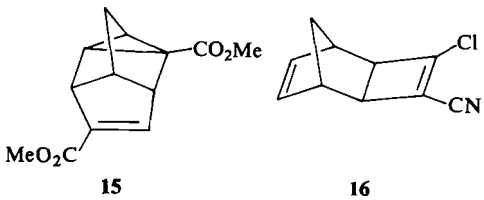

15 **16**

detect any stereoisomers of **4** or **5**. Slee and LeGoff (8) have recently reported that analogous addition of **1** to oxanorborandiene **11** at 100° gives a low yield (10%) of diadduct **12** only.

The nortricyclenes **8**, **9**, and **10** (and the structurally related derivative **13**, isolated from the thermal reaction of furan with **2** (7)), are the first such compounds to be derived from the oxanorbornadiene system, although similar compounds have been produced from norbornadienes (9–11). Although the most important route to **8** obviously involves dimerization of **3** to **10**, we cannot completely rule out the possibility of direct homo Diels–Alder addition of **2** to **3**. It may be that the minor isomer **9** is the product of such addition.[2] Direct 2,6-addition (107°/7 days) of **2** to methyl bicyclo[2.2.1]hepta-2,5-diene-2-carboxylate **14** has been reported to give a 30% yield of **15** (9). This latter product may actually arise via an intermediate analogous to **10**.

The 2 + 2 cycloadduct structure **6** has been tentatively assigned to one of our minor products on the basis of spectral evidence (see below). Its formation may be accounted for by an ionic cycloaddition mechanism similar to that proposed by Sasaki *et al.* (11) to explain their isolation of the cyclobutene **16** as a by-product (6%) from the reaction of norbornadiene with chlorocyanoacetylene.

Structures

The elucidation of the structures of the various reaction products was based primarily on their p.m.r. (Tables 2 and 3), i.r., and mass spectral properties (see Experimental). The monoadduct **3** has been isolated and characterized previously (5).

Diadducts 4 and 5

The p.m.r. spectrum (Table 2) of each of these compounds shows signals for one carbethoxyl and four methyl groups and for five other hydrogens, indicating an overall diadduct structure. In the case of **4** there are four olefinic (two AB quartets) and one methine hydrogen, indicating a diadduct formed by addition of **1** to the activated double bond of **3**. In the spectrum of **5**, on the other hand, there are signals for three olefinic (one at low field, deshielded by the carbethoxyl) and two methine (AB quartet) protons, an arrangement compatible only with a diadduct formed by addition of **1** to the less substituted double bond of **3**.

No molecular ion is observed in either mass spectrum. The base peak in each case is at *m/e*

[2]We were unable to detect any product analogous to **10** which could be postulated as a precursor of **9**.

TABLE 2. 60 MHz p.m.r. data for **4**, **5**, **6**, and **7**

Compound	Chemical shifts* (δ)				
	$-CO_2CH_2CH_3$ (q)	$-CO_2CH_2CH_3$ (t)	$-CH_3$ (s)	$=CH-$	Ring junction $-CH$
4†	4.02	1.05	1.17, 1.44, 1.47, 1.55	Superimposed AB quartets: (*i*) centered at 6.16, $\Delta\nu_{ab} = 6.5$, $J_{ab} = 5.4$ Hz (*ii*) centered at 6.17 $\Delta\nu_{ab} = 3.9$, $J_{ab} = 5.6$ Hz	3.00 (s)
5‡	4.23	1.30	1.43, 1.53, 1.57 (6H)	6.32 (2H, s), 7.02 (1H, s)	AB quartet centered at 2.55, $\Delta\nu_{ab} = 6.6$, $J_{ab} = 7.5$ Hz
6‡	4.15, 4.23	1.23, 1.30	1.47, 1.68	AB quartet centered at 6.33, $\Delta\nu_{ab} = 12.8$, $J_{ab} = 5.4$ Hz; 7.20 (1H, d, $J \sim 0.8$ Hz)	2.95(1H, d, $J \sim$ 0.8 Hz)
7‡	4.27	1.33	2.25 (b), 2.52	6.24 (bs, coupled to CH_3)	

*b = broad, s = singlet, d = doublet, t = triplet, q = quartet.
†In C_6D_6.
‡In $CDCl_3$.

96, reflecting the overwhelming tendency of these compounds to eliminate **1** by Diels–Alder retrogression.

The assignment of *endo-exo* stereochemistry to both **4** and **5** was based on their p.m.r. spectra and the fact that such additions are kinetically favored (6). The expected mode of addition of **1** to either double bond of **3** is to the oxygen-bridged face of the latter (12). Thus two product configurations are likely in each case, namely *endo-endo* **17***a* (or *b*) and *endo-exo* **4** (or **5**). The presence of signals for four nonequivalent olefinic hydrogens in the spectrum of **4** eliminates the symmetrical *endo-endo* isomer **17***a* in this case. It is impossible to assign *endo-endo* or *endo-exo* stereochemistry unequivocally to isomer **5** on the basis of its p.m.r. spectrum, which is compatible with either. However, all previous work in this (6, 7) and other (8) laboratories indicates that the kinetically favored diadducts possess *endo-exo* stereochemistry. Supporting evidence for this assignment in the case of **5** is derived from the chemical shift of the ring-junction hydrogens (quartet, $\Delta\nu_{ab} = 6.6$ Hz, centered at 2.55 δ), which is close to that (2.72 δ) of the corresponding hydrogens in **12** (8).

*Nortricyclenes **8**, **9**, and **10***

The mass and p.m.r. spectra of **8** indicate a product derived from one molecule of **1** and two of **2**. The p.m.r. spectrum (Table 3) shows signals for four single hydrogens, only one of which appears in the olefinic region. The chemical shifts of the three methine protons are in accord with those of similar hydrogens in related compounds (7, 9, 11). Two of these protons have approximately the same chemical shift, suggesting that they occupy similar environments (H-1, H-5), while the third is located at high field, consistent with it being on a cyclopropane ring. Moreover, the chemical shift of the vinylic hydrogen is consistent with deshielding by a carbethoxyl group and is very similar to that of the corresponding proton in **15** (9). In addition it is vicinally coupled to only one hydrogen. As expected, the chemical shifts of the two bridgehead methyl groups are significantly different. Verification of the structure was provided by the ^{13}C n.m.r. spectrum. We have reported full ^{13}C data for **8** (and **13**) elsewhere (7).

The spectral properties of compound **9** are, as expected, very similar to those of its isomer **8**. The main points of difference, leading to the assignment of structure **9** are in the chemical shifts and multiplicities of H-1 and H-5 (Table 3). These changes reflect the new position of the olefinic proton in **9**. The hydrogen at C-1, now subject to the deshielding effect of a second carbethoxyl group and no longer vicinal to any other hydrogen, appears as a narrow triplet at 3.49 δ (a downfield shift relative to the same

Can. J. Chem. Downloaded from www.nrcresearchpress.com by 210.87.254.40 on 09/05/12
For personal use only.

Can. J. Chem. Downloaded from www.nrcresearchpress.com by 210.87.254.40 on 09/05/12
For personal use only.

TABLE 3. 60 MHz p.m.r. data for nortricyclenes **8, 9,** and **10** (in C_6D_6)

	Chemical shifts* (δ)							
Compound	$-CO_2CH_2$ CH_3 (q)	$-CO_2CH_2$ CH_3(t)	$-CH_3$ (s)	Ring junction CH	=CH—	H-1	H-4	H-5
8	3.90, 4.02	0.90, 1.00	1.03, 1.81	—	7.16(q, H-7) $J_{1,7} = 3.6$, $J_{5,7} = 1.1$ Hz	2.90(q) $J_{1,7} = 3.6$, $J_{1,5} = 0.9$ Hz	2.27(d) $J_{4,5} = 2.0$ Hz	3.07(quintet) $J_{4,5} = 2.0$, $J_{5,7} = 1.1$, $J_{1,5} = 0.9$ Hz
9	3.98, 4.10	0.99, 1.05	1.01, 1.84	—	6.90(q, H-6) $J_{5,6} = 3.6$, $J_{1,6} = 1.0$ Hz	3.49(t) $J_{1,5} = 1.1$, $J_{1,6} = 1.0$ Hz	2.04(d) $J_{4,5} = 1.9$ Hz	2.24(m) $J_{5,6} = 3.6$, $J_{4,5} = 1.9$, $J_{1,5} = 1.1$ Hz
10	3.89, 4.07	0.97, 1.03	1.38, 1.66, 1.77, 1.90	3.02(s)	AB quartet centered at 5.96, $\Delta\nu_{ab} = 4.0$, $J_{ab} = 5.6$ Hz	2.50(s)	1.75(d) $J_{4,5} = 1.8$ Hz (partially obscured by CH_3)	2.35(d) $J_{4,5} = 1.8$ Hz

*s = singlet, d = doublet, t = triplet, q = quartet, m = multiplet.

Can. J. Chem. Downloaded from www.nrcresearchpress.com by 210.87.254.40 on 09/05/12
For personal use only.

proton in **8** of 0.59 p.p.m.). The hydrogen at C-5, on the other hand, which is now coupled vicinally to two other hydrogens but is no longer deshielded by an adjacent carbethoxyl, is observed as a broad multiplet centered at 2.24 δ (an upfield shift of 0.83 p.p.m.).

The weak molecular ion at *m/e* 388 and base peak at *m/e* 96 indicate that compound **10** is a 2:2 product from which **1** may be readily lost. Infrared absorptions at 1737 and 1718 cm^{-1} suggest two quite different types of ester group. The p.m.r. spectrum of **10** (Table 3) shows signals for two carbethoxyl and four *C*-methyl groups, an AB quartet for two olefinic hydrogens, and signals for four single methine hydrogens (at 1.75, 2.36, 2.50, and 3.02 δ). The signal at highest field was assigned to the cyclopropyl hydrogen H-4: this is coupled (J = 1.8 Hz) to the hydrogen resonating at 2.36 δ which can therefore be assigned to H-5. Since H-1 and H-5 are located in similar environments, the remaining signals may be assigned to H-1 (2.50 δ) and the ring-junction hydrogen (3.02 δ). The lack of coupling between the latter two protons necessitates that the dihedral angle between them approximates 90° and allows assignment of stereochemistry **18** or **19**. The latter configuration, however, would require approach of the diene component to the face of the dienophile opposite to the oxygen bridge. Such an approach is unlikely on steric grounds (6, 12).

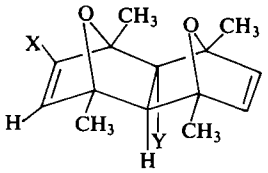

17

a X = H; Y = CO_2Et
b X = CO_2Et; Y = H

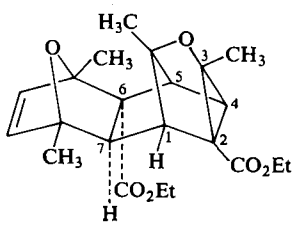

18

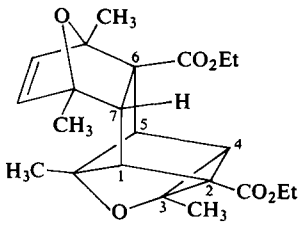

19

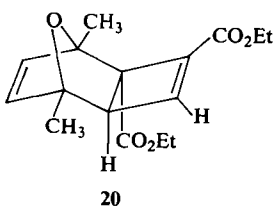

20

Compound 6

The molecular ion of this compound is at *m/e* 292 indicating a 1:2 product. The p.m.r. spectrum (Table 2) shows two nonequivalent carbethoxyl groups and two nonequivalent *C*-methyl groups, together with an AB quartet for two olefinic hydrogens and two one-proton doublets ($J \approx 0.8$ Hz), one due to a methine (2.95 δ) and the other to an olefinic (7.20 δ) hydrogen. The i.r. spectrum shows absorptions in the carbonyl region at 1727 and 1737 cm^{-1}, in accord with the presence of both conjugated and saturated ester groups. The cyclobutene ring is assigned an *exo* relationship to the bridged ring since approach in this direction is known to be least sterically hindered (12). The available evidence is equally consistent with cyclobutene structure **20**. However, the requirements of the proposed ionic cycloaddition mechanism (*cf.* 11) would favor **6**.

Compound 7

The mass spectrum indicates a molecular weight of 168 and the p.m.r. spectrum (Table 2) shows characteristic signals for one carbethoxyl and two *C*-methyl groups, and for one single hydrogen in the olefinic region. Confirmatory evidence for the furan structure is provided by the chemical shifts of the hydrogens of the two ring methyl groups and the magnitude of the coupling (~1 Hz) between the hydrogens of one of these groups (2.25 δ) and the adjacent ring hydrogen (6.24 δ).

Experimental

The p.m.r. spectra were recorded on a Varian A-60A spectrometer equipped with a V-6058A spin decoupler, using tetramethylsilane as internal standard. The i.r. spectra were obtained in CCl_4 solution on a Perkin-Elmer 521 spectrometer and the mass spectra with a

Can. J. Chem. Downloaded from www.nrcresearchpress.com by 210.87.254.40 on 09/05/12
For personal use only.

Dupont-C.E.C. 21-491 spectrometer. Unless stated otherwise the source of heat used in all reactions was a steam bath. Column chromatography was performed on Mallinckrodt silicic acid, 100 mesh, using $CHCl_3$ to elute. For preparative thin-layer chromatography (p.l.c.) Merck silica gel HF-254 (1.5 mm layers) was used, with $CHCl_3$ to elute.

Reaction of 2,5-Dimethylfuran **1** *with Ethyl Propiolate* **2**

General Procedure

The reaction of **1** and **2** was carried out under varying conditions (Table 1) using the following procedure. A mixture of **1** and **2** was heated and at the end of the desired reaction period unreacted starting materials were removed by azeotroping with EtOH. The oily residue obtained was then submitted to column chromatography. The products eluted in the following order: **7**, **8**, **3**, **9**, **6**, **10**, **5**, and **4**.

(*A*) A reaction mixture of **1** (6.98 g, 0.073 mol) and **2** (3.67 g, 0.037 mol) was maintained at reflux for 48 h (heating mantle). Obtained as products. (*i*) *compound* **7** as a pale yellow oil (0.060 g, 1%), n_D^{23} 1.4690; parent ion at *m/e* 168 (51%) ($C_9H_{12}O_3$ requires 168), base peak at *m/e* 43, strong ions at *m/e* 139 (77%) and 123 (70%); ν_{max} 1717 cm^{-1}; (*ii*) *compound* **8** as a pale yellow oil (3.34 g, 62%), n_D^{25} 1.4844; parent ion at *m/e* 292 (5%) ($C_{16}H_{20}O_5$ requires 292), base peak at *m/e* 43, strong ions at *m/e* 249 (17%), 247 (11%), 246 (12%), 221 (12%), 219 (22%), 218 (11%), 204 (10%), 176 (7%), 175 (9%), 173 (10%), 152 (13%), 147 (12%), 139 (13%), 96 (32%), and 77 (16%); ν_{max} 1715, 1721 cm^{-1}; (*iii*) an oil (2.40 g), containing *ca.* 90% *compound* **5** (*ca.* 19%). The pure compound was obtained by repeated p.l.c. as a pale yellow oil, n_D^{26} 1.4813. No parent ion was observed, base peak at *m/e* 96, strong ions at *m/e* 168 (7%), 139 (7%), and 43 (29%); ν_{max} 1713 cm^{-1}.

(*B*) From a reaction of **1** (9.6 g, 0.10 mol) and **2** (19.6 g, 0.20 mol) at 95° for 7 days were obtained: (*i*) an oil (1.14 g), mainly **8**, contaminated by a small amount of **7**; (*ii*) pure **8** (1.90 g); (*iii*) an oil (6.01 g), mainly **8** but contaminated by **3**; (*iv*) an oil (0.340 g), which on p.l.c. gave *compound* **9** as a pale yellow oil (0.076 g, 0.3%), n_D^{26} 1.4888; parent ion (very weak) at *m/e* 292 ($C_{16}H_{20}O_5$ requires 292), base peak at *m/e* 43, strong ions at *m/e* 249 (23%), 246 (27%), 221 (18%), 200 (53%), 175 (16%), 173 (23%), and 77 (23%); ν_{max} 1717 (sh), 1721 cm^{-1}; (*v*) an oil (1.128 g), which on repeated p.l.c. gave *compound* **6** (0.368 g, 1.3%) as a pale yellow oil, n_D^{26} 1.4911; parent ion at *m/e* 292 (48%) ($C_{16}H_{20}O_5$ requires 292), base peak at *m/e* 218, strong ions at *m/e* 248 (16%), 247 (25%), 219 (26%), 203 (68%), 190 (30%), 175 (48%), 173 (68%), 96 (74%), and 43 (74%); ν_{max} 1727, 1737 (sh) cm^{-1}. This fraction also afforded compounds **9** (0.061 g, 0.2%) and **10** (0.418 g, 2.2%); (*vi*) *compound* **10** (1.774 g, 9.1%) as a pale yellow oil, n_D^{25} 1.6553; parent ion (very weak) at *m/e* 388 ($C_{22}H_{28}O_6$ requires 388), base peak at *m/e* 96, strong ions at *m/e* 249 (30%), 227 (13%), 178 (33%), and 43 (88%); ν_{max} 1718, 1737 cm^{-1}; (*vii*) an oil (0.765 g), which on p.l.c. gave a mixture (0.599 g, 4.2%) of **4** and **5** in an approximate ratio of 3:5.

(*C*) From a reaction of **1** (6.98 g, 0.073 mol) and **2** (3.67 g, 0.037 mol) at 95° for 48 h were obtained: (*i*) a yellow oil (3.68 g), repeated p.l.c. of which gave (*a*) compound **8** (0.342 g, 6%), (*b*) compound **3** (0.260 g, 3.6%), identical to material obtained previously (5), and (*c*) *compound* **4** (1.634 g, 15%) as an oil which gradually crystallized, m.p. 40–43°; no parent ion was observed, ion of highest mass at *m/e* 217 (3%) ($M - CO_2Et$), base peak at *m/e* 96, strong ions at *m/e* 201 (3%), 159 (3%), 152 (4%), 149 (3%), 81 (6%), 77 (4%), and 43 (39%); ν_{max} 1711, 1738 cm^{-1}; (*ii*) an oil (2.06 g), p.l.c. of which gave (*a*) compound **10** (0.162 g, 2%) and (*b*) a mixture of **4** and **5** (1.14 g, 11%) in a ratio of 7:4.

(*D*) Two other reactions were performed, both at 95°. One used a 1:1 (2 days) and the other a 2:1 (7 days) reactant ratio. The product compositions of these and of reactions *A–C* above were estimated by integration of the appropriate p.m.r. signals in the various column fractions and are summarized in Table 1.

(*E*) A reaction of **1** (9.6 g, 0.1 mol) and **2** (19.6 g, 0.2 mol) at 95° was monitored daily by p.m.r. for 1 week. This showed that **3** and **4** were the major products initially, and that the amounts of **8** and **10** increased with time, at the expense of **3** and **4**.

Retrogression of Compound **4**

A sample of pure **4** was heated at 95°. Thermal breakdown to a mixture of **3** and **1** of 12% (1 h) and 25% (4 h) was observed (p.m.r.).

Attempted Reaction of **8** *with* **1**

Equimolar amounts of **8** and **1** were heated at 95° for 48 h. Compound **8** remained unreacted, the only change being some oxidative breakdown of **1**.

Dimerization of **3** *to Compound* **10**

(a) Attempted Reaction of **3** *with* **2**

Equimolar amounts of **3** and **2** were heated at 95°; p.m.r. showed that **2** remained unreacted while **3** was converted to **10** (**10**:**3** = 1:1 after 3 h, = 3:1 after 9 h). Small amounts of **8** were also formed. There was also evidence of considerable polymerization.

(b) Reaction of **3** *with* **1**

Equimolar amounts of **3** and **1** were heated at 95°. After 2.5 h the molar ratio of products (p.m.r.) was **3**:**4**:**10** = 7:2:4. No **5** was observed. After 7 h only a trace of **3** remained, the major products being **10** and **4** (approximate ratio 2:1).

(c) Direct Thermolysis of **3**

A 100 mg sample of **3** was heated at 95° for 21 h. Repeated p.l.c. (1% MeOH–$CHCl_3$) gave compounds **8** (10 mg) and **10** (27 mg, 27%).

Retrogression of **10**: *Formation of Compound* **8**

A pure sample of **10** was heated on an oil bath maintained at 120°. Smooth conversion to **8** (20% in 2 h, 50% in 6 h, 80% in 12 h) was observed (p.m.r.). The reaction was significantly slower at 95°.

We gratefully acknowledge the very useful contributions made to this work by R. Richard (NRCC summer student, 1972) and D. Ettinger (research assistant, 1972–1973). Our thanks go also to P. F. Seto for the i.r. spectra.

1. A. S. Onishchenko. Diene synthesis. Israel Program for Scientific Translations, Jerusalem. 1964. Chapt. VII.
2. H. Prinzbach, P. Vogel, and W. Auge. Chimia, **21**, 469 (1967).

3. A. W. McCULLOCH, B. STANOVNIK, D. G. SMITH, and A. G. McINNES. Can. J. Chem. **47**, 4319 (1969).
4. A. W. McCULLOCH and A. G. McINNES. Can. J. Chem. **49**, 3152 (1971).
5. A. W. McCULLOCH and A. G. McINNES. Can. J. Chem. **52**, 143 (1974).
6. A. W. McCULLOCH, D. G. SMITH, and A. G. McINNES. Can. J. Chem. **51**, 4125 (1973).
7. A. W. McCULLOCH, D. G. SMITH, and A. G. McINNES. Can. J. Chem. **52**, 1013 (1974).
8. J. D. SLEE and E. LEGOFF. J. Org. Chem. **35**, 3897 (1970).
9. A. J. SOLO, B. SINGH, and J. N. KAPOOR. Tetrahedron, **25**, 4579 (1969).
10. C. F. HUEBNER, E. DONOGHUE, L. DORFMAN, F. A. STUBER, N. DANIELI, and E. WENKERT. Tetrahedron Lett. 1185 (1966).
11. T. SASAKI, S. EGUCHI, M. SUGIMOTO, and F. HIBI. J. Org. Chem. **37**, 2317 (1972).
12. J. G. MARTIN and R. K. HILL. Chem. Rev. **61**, 537 (1961).

Can. J. Chem. Downloaded from www.nrcresearchpress.com by 210.87.254.40 on 09/05/12
For personal use only.

Synthesis of Substituted Hydrindanes. Part I. Products Arising from the Cyclization of Acetonyl Cyclohexanones and Acetonyl Cyclohexadiones

ANDRÉ BETH, JACQUES PELLETIER, ROBERT RUSSO, MARCEL SOUCY, AND ROBERT H. BURNELL[1]

Département de Chimie, Université Laval, Québec 10, Québec G1K 7P4

Received July 23, 1974

ANDRÉ BETH, JACQUES PELLETIER, ROBERT RUSSO, MARCEL SOUCY, and ROBERT H. BURNELL. Can. J. Chem. **53**, 1504 (1975).

The preparation and cyclizations of certain 1,4-diketones have been studied as a route to substituted hydrindan-2-one systems. Other types of products encountered are also described.

ANDRÉ BETH, JACQUES PELLETIER, ROBERT RUSSO, MARCEL SOUCY et ROBERT H. BURNELL. Can. J. Chem. **53**, 1504 (1975).

On a étudié la préparation de certaines dicétones-1,4 ainsi que leur cyclisation comme moyen d'arriver au système hydrindanone-2 substitué. On décrit aussi d'autres types de produits qui ont été rencontrés. [Traduit par le journal]

While investigating synthetic routes which could lead to both *Lycopodium* alkaloids possessing the fawcettimine skeleton and certain terpenes we have investigated the preparation of several hydrindan-2-one systems. We were particularly interested in models of type **1** in which R_3 and R_4 would represent either a nine-membered nitrogen containing ring or sidechains susceptible to cyclization to this medium-sized ring.

We decided that cyclohexa-1,3-diones offered certain advantages of reactivity and availability as starting materials and for most of the trial series we chose the readily available dimedone although some sequences have started from dihydroorcinol. Acrylonitrile condenses readily with dimedone in the presence of triethylamine (1) and we have found that by careful adjustment of the p*H* after the reaction, the pure monocyanoethyl derivative **2***a* is obtained directly in yields exceeding 70%. Alkylation of the latter with ethyl β-bromolevulinate in the presence of sodium hydride in dimethoxyethane gave only a poor yield of the triketo ester **3***a*. A similar compound, **3***b* was prepared from 2-allyldihydroorcinol **2***b*, again in low yield but the conditions necessary to cyclize these multifunctional compounds (to give **4***a* and **4***b*) were never achieved. The number of possible reactions of each compound (**3***a* and **3***b*) in reagents normally favoring cyclization, prohibited a meaningful analysis of the products.

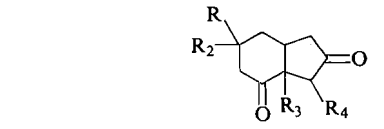

1

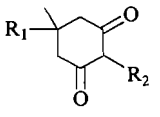

2

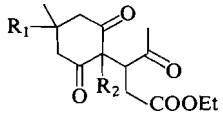

3

a $R_1 = CH_3$; $R_2 = CH_2CH_2CN$
b $R_1 = H$; $R_2 = CH_2CH{=}CH_2$
c $R_1 = CH_3$; $R_2 = CH_2CH{=}CH_2$

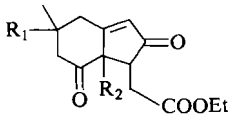

4

To further investigate the formation of the five-membered ring, simpler models were sought containing as essential elements the "quaternary" carbon atom and a side chain possessing only one carbonyl residue. Consequently cyanoethyldimedone **2***a* was alkylated in high yield with propargyl bromide to give **5***a*, forming the quaternary center and a less enolizable symmetrical 1,3-diketone. The triple bond was hydrated in virtually quantitative yield to the triketo-

[1]To whom correspondence should be addressed.

Can. J. Chem. Downloaded from www.nrcresearchpress.com by 210.87.254.6 on 09/05/12
For personal use only.

Can. J. Chem. Downloaded from www.nrcresearchpress.com by 210.87.254.6 on 09/05/12
For personal use only.

nitrile **6***a* which did not cyclize under basic conditions but afforded only the triketone **6***c* arising from a retro-Michael reaction while acidic conditions tended to open the six-membered ring (retro-Claisen) before effecting the closure, the major product being the cyclopentenone **7**. The analogous allyl-triketone **6***b*, prepared via compound **5***b* (propargylation of **2***c*) and hydration of the triple bond, was more resistant but again the only products isolated in attempted cyclizations were those resulting from expulsion of one of the side chains.

The vulnerability of the β-diketo system to cleavage suggested that internal alkylation might be more rewarding than internal condensation. To convert one of the carbonyl groups in the cyano-diketone **5***a* to a potential leaving group we reduced selectively one of the carbonyl groups and the product (**8***a*) was transformed to both the tosyl and acetyl derivatives (**8***b* and *c*, respectively). Later we found that even under forcing conditions the second carbonyl is quite resistant to sodium borohydride reduction. Since the best method we had found for hydrating the triple bond in the propargyl residue involves a methanolic solution containing a trace of trichloroacetic acid, we felt that it might be possible to isolate the diketone as the corresponding diketal providing the reaction mixture is not decomposed in water. After hydrating the triple bond in the tosyl derivative **8***b*, the volatile products were simply evaporated at or below room temperature *in vacuo* and the crystalline product shows no carbonyl absorption in the i.r. spectrum. Since mild hydrolysis of this material (or just recrystallizing from less than anhydrous solvents) affords the diketone **10***b*, the addition to the triple bond did take place. Elemental analysis of the ketal, with other spectral characterization, showed it to be the cyclic ketal **9**.

The normal procedure for hydrating the triple bonds in all three compounds **8***a*, *b*, and *c* was without consequence affording the corresponding diketones **10***a*, *b*, and *c*. Attempts to cyclize these compounds gave different results. The alcohol **10***a* suffers ring-opening by retroaldolization under all but the mildest conditions; certainly neither the cyclopentenone **11***a* which could arise by condensation nor the internal alkylation product, cyclopentanone **11***b* was isolated. The tosylate **8***b* cyclizes rapidly at room temperature in methanolic sodium methoxide but forms the (predicted?) substituted cyclopropane **12**. Varying the conditions had no apparent effect on the direction of enolization or carbanion formation and only in one reaction, in *t*-butyl alcohol containing sodium *t*-butoxide, was a different product obtained. We tentatively postulate the latter to be the substituted spiro[4.4.0.$0^{1,7}$]tricyclodecane **13** (see Experimental). The acetyl derivative **8***c* was recovered unchanged from several attempted cyclization reactions, but in one case afforded the spiro[5.4.1]-bicyclodecane system **14**.

One further type of ring closure was tried on molecules containing virtually the same functional groups. Alkylation of cyanoethyldimedone **2***a* with 2,3-dichloropropene afforded the chloro-alkene **15***a* which was reduced to the keto-alcohol **15***b* now suitably functionalized to

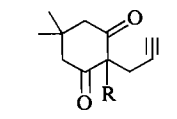

5

a R = CH_2CH_2CN
b R = $CH_2CH{=}CH_2$

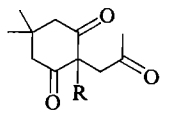

6

a R = CH_2CH_2CN
b R = $CH_2CH{=}CH_2$
c R = H

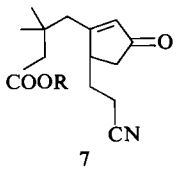

7

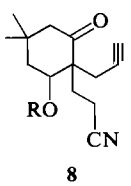

8

a R = H
b R = Ts
c R = Ac

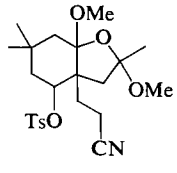

9

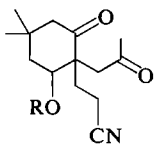

10

a R = H
b R = Ts
c R = Ac

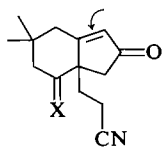

11

a X = H,OH
b X = =O, no double bond (arrow)

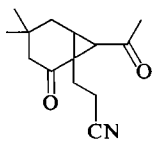

12

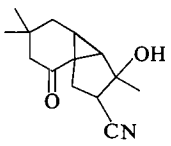

13

attempt cyclization in concentrated acids, as described by Lansbury (2). We had previously failed to prepare enol esters or ethers with the terminal double bond. It was felt that this chloro-alkene (**15***b*) should form the five-membered ring but in cold sulfuric acid the reaction was extremely complex and the nitrile appeared to be the most susceptible function. In refluxing formic acid the molecule (**15***b*) was surprisingly stable affording only the *O*-formyl derivative **15***c*. While this type of cyclization is feasible, most examples in the literature involve benzylic or allylic hydroxyl groups.

The attractiveness of the synthetic route from cyclohexa-1,3-diones lay in the fact that the formation of the quaternary center isolates the two carbonyl groups while preserving a symmetrical molecule: one carbonyl serving as the means to cyclize the five-membered ring while the other is suitably placed for the final synthetic goal or for modifying the six-membered ring. The difficulties encountered in performing the cyclization forced a reassessment of the route. By eliminating one of the two oxygen functions (the hydroxyl in **8***a* for instance) the ring closure should be relatively facile since the competing reactions (retroaldol and retro-Michael) are either impossible or considerably less probable. For certain syntheses, however, an additional problem is introduced, that of reestablishing the oxygen function at the carbon atom adjacent to the quaternary center with acceptable selectivity.

Of several methods tried, the dehydration of the keto-alcohol **8***a* was best accomplished with phosphorus oxychloride in pyridine but the quality of the reagents affects the yield of olefin **16***a* drastically. As in previous series boron trifluoride – trichloroacetic acid catalyzed hydration of the triple bond affords the diketone **16***b*. Cycloaldolization of the latter in methanolic potassium hydroxide is rapid, as is the hydrolysis of the nitrile and the acidic product from the reaction is cyclopentenone **17***a*.

Our first attempt to cyclize the diketo-olefin **16***b* was with sodium hydride in dimethoxyethane (reflecting perhaps previous difficulties) and this reaction had produced three products, the major being an acid isomeric with **17***a* and with quite similar spectral characteristics. We felt at the time that this might be the desired cyclization product and that the smaller quantity of a neutral material from this same reaction was

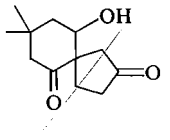

14

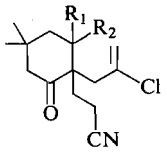

15

a $R_1, R_2 = O$
b $R_1 = H; R_2 = OH$
c $R_1 = H; R_2 = OCHO$

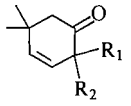

16

a $R_1 = CH_2CH_2CN; R_2 = CH_2C{\equiv}CH$
b $R_1 = CH_2CH_2CN; R_2 = CH_2COCH_3$
c $R_1 = CH_2CH{=}CH_2; R_2 = CH_2C{\equiv}CH$
d $R_1 = CH_2CH{=}CH_2, R_2 = CH_2COCH_3$

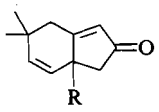

17

a $R = CH_2CH_2COOH$
b $R = CH_2CH_2COOMe$
c $R = CH_2CH_2CN$
d $R = CH_2CH{=}CH_2$

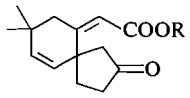

18

a R = H
b R = Me

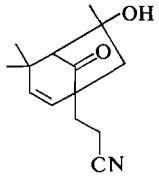

19

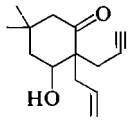

20

the nitrile **17***c*. When hydrolysis of the nitrile afforded the cyclized acid **17***a*, identical with that from the easier hydroxide cyclization, we were forced to reexamine the anomalous sodium hydride cyclization product. The u.v. spectrum of the latter (λ_{max} 221 nm, ε 6900) suggested an α,β-unsaturated acid rather than a conjugated five-membered ring ketone such as **17***a* (λ_{max} 233 nm, ε 13 000). Other spectral considerations (see Experimental) imply that the anomalous product has the structure **18***a* and its formation can be imagined as combined aldolization and Claisen-type ring closures followed by β-diketone cleavage. The third product from this cyclization was also a nitrile but contained a hydroxyl group. Spectral data, analysis, and con-

Can. J. Chem. Downloaded from www.nrcresearchpress.com by 210.87.254.6 on 09/05/12
For personal use only.

Can. J. Chem. Downloaded from www.nrcresearchpress.com by 210.87.254.6 on 09/05/12
For personal use only.

sideration of the reactions likely to occur suggest that this new material is the alternate aldolization product **19**.

The analogous series starting with allyl- (**2***c*) rather than cyanoethyldimedone (**2***a*) was also carried through to the cyclized material by the methods already discussed. Thus allyldimedone (**2***c*) is propargylated to afford the diketone **5***b* in which one carbonyl group is then selectively reduced to give the ketol **20**. While we separated the predominant solid isomer in which the hydroxyl group is equatorial both isomers separately or as a mixture are dehydrated to the olefin **16***c*. Hydration of the triple bond affords the diketone **16***d* which cyclizes to the conjugated enone **17***d*. In this compound we assume the three olefinic double bonds (terminal, cyclic, and conjugated) to be sufficiently different to allow selective modification.

Another approach to compounds of type **1** might be to introduce R_3 and R_4 by a Diels–Alder reaction should enediones such as **1***a* show sufficient reactivity as dienophiles. Not finding products of this nature in the literature, we attempted to prepare them. The fact that hydrindenone **22***a* can be readily prepared from indene (3) prompted a few experiments aimed at functionalizing the allylic methylene group but these failed due to the superior reactivity of the angular methine. To exclude this possibility we synthesized compounds with angular ester functions (**22***c* and *d*). The carbomethoxy groups could be readily eliminated after cyclization (vinylogous β-keto esters) and since synthesis from indene was no longer advantageous we prepared these keto esters from α-carboalkoxycyclohexanones. Alkylation with propargyl bromide (giving **23***a*, *b*, and *c*), hydration of the triple bond (affording **24***a*, *b*, and *c*), and cyclization of the diketo esters lead to the enones **22***c* and *d* in satisfactory yields. Varying the conditions of the ring formation also gave the decarboxylated enones **22***a* and *b*. Our Experimental was adapted from methods described by Raphael (4). The allylic functionalization proved equally unsatisfactory with the angular substituent and a variety of conditions (see Experimental) affecting allylic oxidations afforded starting material as the only tractable product.

One experiment was performed to introduce an angular substituent in compound **22***a* by conjugate addition to the enone system. Treatment

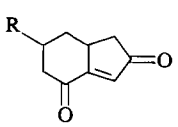

21

a $R = CH_3$
b $R = H$

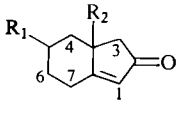

22

a $R_1 = R_2 = H$
b $R_1 = CH_3$; $R_2 = H$
c $R_1 = H$; $R_2 = COOEt$
d $R_1 = CH_3$; $R_2 = COOMe$

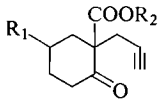

23

a $R_1 = H$; $R_2 = Et$
b $R_1 = CH_3$; $R_2 = Et$
c $R_1 = R_2 = CH_3$

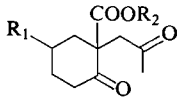

24

a $R_1 = H$; $R_2 = Et$
b $R_1 = CH_3$; $R_2 = Et$
c $R_1 = R_2 = CH_3$

of the latter with tetrakis(iodotri-*n*-butylphosphine) copper and vinyl lithium (5) affords the vinylhydrindanone **25** in modest yield. We hope to use this reaction later in another synthesis.

It had become evident that while the five-membered ring is easily grafted onto the cyclohexanone, the second ketone (perhaps as a latent substituent) would be best introduced at the outset. Arylidene or alkylidene residues, which could later be transformed into carbonyl groups by ozonolysis proved cumbersome and the yields in some steps were extremely poor. Finally the ketone was protected as the dioxalane by the following route.

α-Benzylidene or α-ethylidene cyclohexanones are converted to their spiro-ketals (**26***a* and *b*) and then cleaved by ozonolysis to give the monoketals of the corresponding α-diketones (**27***a* and *b*). Direct alkylation gives largely the dialkylated product **28***a*, the presence of which is easily revealed in the n.m.r. spectrum of the material (**28***b*) arising from the hydrogenation of the triple bonds. By first preparing the hydroxymethylene derivatives then alkylating, the monopropargylated products (**28***e* and *f*) are obtained in satisfactory yield and the hydration of the triple bond can be performed without hydrolysis of the spiro-ketal after slight modification of the conditions. Both diketones **28***g* and *h* were prepared but only the latter was cyclized to the enone **29**, which is a protected form of the desired enedione **21***a*. However, despite numerous attempts to remove the dioxolane moiety

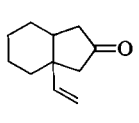

25

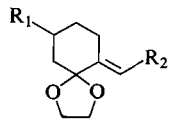

26

a $R_1 = H; R_2 = CH_3$
b $R_1 = CH_3; R_2 = Ph$

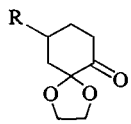

27

a R = H
b R = CH_3

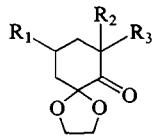

28

a $R_1 = H; R_2 = R_3 = CH_2C{\equiv}CH$
b $R_1 = H; R_2 = R_3 = CH_2CH_2CH_3$
c $R_1 = H; R_2 = R_3 = {=}CHOH$
d $R_1 = CH_3; R_2 = R_3 = {=}CHOH$
e $R_1 = R_2 = H; R_3 = CH_2C{\equiv}CH$
f $R_1 = CH_3; R_2 = H; R_3 = CH_2C{\equiv}CH$
g $R_1 = R_2 = H; R_3 = CH_2COCH_3$
h $R_1 = CH_3; R_2 = H; R_3 = CH_2COCH_3$
i $R_1 = CH_3; R_2 = H; R_3 = CH_2CH{=}CH_2$

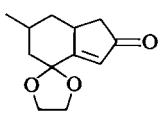

29

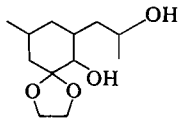

30

none was successful, in most cases hydrolysis destroyed the molecule beyond recognition. The enone spiro-ketal **29** showed great reluctance to undergo Diels–Alder cycloadditions.

As a variant to the method described above and to avoid the hydrolysis of the spiro-ketal during hydration of the triple bond (in **28***e* and *f*) we investigated a parallel route involving allylation of the activated keto-ketal **28***d*. The nature of this product (**28***i*) was confirmed by preparing a sample from the propargyl containing analog **28***f* by hydrogenation over Lindlar catalyst. The hydroxylation of the double bond using mercuric acetate followed by sodium borohydride also reduces the existing ketone moiety to give the diol **30** which is oxidized (Sarett reagent) to the diketo-ketal **28***h*. The latter on reduction with sodium borohydride also affords the diol **30**. This route however offers no advantage, either in yield or ease of manipulation.

Experimental

The normal conditions and instruments for the spectra quoted are: u.v. ethanol solutions, Beckman DK-1A; i.r. Perkin Elmer 457 and Beckman IR 12; n.m.r. Varian A60 and Bruker HX 90, internal TMS standard, coupling constants are given in parentheses; mass spectra, Varian M66. Elemental analyses were performed by Mr. R. Dulude, Chemistry Department, Université Laval and by Dr. F. Pascher, Bonn.

2-Cyanoethyl-5,5-dimethylcyclohexa-1,3-dione (2a)

Dimedone (7 g) is added to a solution of isopropanol (15 ml) and triethylamine (5 ml) in water (15 ml) under nitrogen. Freshly distilled acrylonitrile (3.5 ml) is introduced and the mixture refluxed for 3 h then cooled in ice (*ca.* 2 h) to crystallize the 2,2-bis(2-cyanoethyl)-5,5-dimethylcyclohexa-1,3-dione, m.p. 145° (1.5 g, 12%) (lit. (6) m.p. 146–147°). The filtrate is acidified (dilute hydrochloric acid) to p*H* 6, precipitating the cyanoethyldimedone **2***a* (6.7 g, 70%), m.p. 153–154°; λ_{max} 262 (16 100) and 290 (sh. 7400) nm; ν_{KBr} 2550, 2260, 1640, and 1565 cm^{-1}; δ_{CDCl_3} *gem*-dimethyl s 1.1, $-CH_2CO$ s 2.4, $-CH_2CH_2CN$ m 2.5, and OH (enol) s 8.15.

Anal. Calcd. for $C_{11}H_{15}NO_2$: C, 68.3; H, 7.8; N, 7.3. Found: C, 68.5; H, 7.9; N, 7.6.

2-Allyl-5-methylcyclohexa-1,3-dione (2b)

This was prepared following essentially the method of Rosenmund (7), m.p. 135–136°.

Anal. Calcd. for $C_{10}H_{14}O_2$: C, 72.3; H, 8.5. Found: C, 72.1; H, 8.4.

2-Allyl-5,5-dimethylcyclohexa-1,3-dione (2c)

This was prepared by the method of Rosenmund (7), m.p. 145–146° (lit. 145–146°); λ_{max} 262 (13 800) nm; ν_{KBr} 3080, 3010, 2600, 1638, and 1560 cm^{-1}; δ_{CDCl_3} *gem*-dimethyl s 1.07, $-CH_2CO-$ s 2.37, $-CH_2-CH{=}CH_2$ d(6.0) 3.12, m 5.0 and m 5.8; *m/e* 180 (M+), 165, 124, 109, 97, 96, 95, 83 (base), and 81.

Anal. Calcd. for $C_{11}H_{16}O_2$: C, 73.3; H, 8.9. Found: C, 73.4; H, 8.8.

Ethyl 3-[1-(2-Cyanoethyl)-4,4-dimethyl-2,6-dioxocyclohexyl]-4-oxopentanoate (3a)

Sodium hydride (2.35 g) washed free of mineral oil, is suspended in dimethoxyethane (100 ml) under nitrogen. The cyanoethyldimedone **2***a* (4.8 g) is added and after 2 h, ethyl β-bromolevulinate (5.58 g) is introduced dropwise and the mixture is stirred at 48° for 12 h. The reaction mixture is decomposed in water and ether extraction affords a neutral oil (2.5 g) and starting material (3.4 g) from the aqueous phase on acidification. The oil is chromatographed over Florosil. The benzene – 4% ether eluate is the ester **3***a* (0.5 g), m.p. 123–124°; ν_{KBr} 2260, 1740, 1725, 1715, 1695 cm^{-1}; δ_{CDCl_3} *gem*-dimethyl s 0.8, CH_3CH_2O t(7.2) 1.21, and q(7.2) 4.1, CH_3CO s 2.16, $CO-CH-CH_2COOR$ d of d (2.5 and 10.5) 3.70, d of d(8.5 and 10.5) 3.11 and d of d (8.5 and 2.5) 2.51; *m/e* 335 (M+), 290, 262, 248 (base), 220, 207, and 83.

Anal. Calcd. for $C_{18}H_{25}NO_5$: C, 64.5; H, 7.5; N, 4.2. Found: C, 64.3; H, 7.7; N, 4.5.

Ethyl (1-Allyl-4-methyl-2,6-diketocyclohexyl)-4-ketopentanoate (3b)

This is prepared from allyldihydroorcinol **2***b* (8.3 g) as described for **5***a*, except the mixture is heated at 65° for 20 h after standing at room temperature for 4 h. Chromatography affords the ester **3***b* (3.1 g, 20% yield),

Can. J. Chem. Downloaded from www.nrcresearchpress.com by 210.87.254.6 on 09/05/12
For personal use only.

Can. J. Chem. Downloaded from www.nrcresearchpress.com by 210.87.254.6 on 09/05/12
For personal use only.

m.p. 90–91°; ν_{KBr} 3080, 1735, 1720, 1713, 1690, and 1210 cm^{-1}; δ_{CDCl_3} CH_3CH d(6.8) 1.15, CH_3CH_2O-*t*(7.0) 1.18, and q 4.03, CH_3CO s 2.21, CO—$CHCH_2COOR$ d of d(17.5 and 3.0) 2.65, d of d(17.5 and 8.5) 3.29 and d of d(8.5 and 3.0) 4.18 and the vinyl pattern 4.9 to 6.4; *m/e* 308 (M+), 265, 235.

Anal. Calcd. for $C_{17}H_{24}O_5$: C, 66.2; H, 7.8. Found: C, 66.1; H, 7.9.

2-Propargyl-2-(2-cyanoethyl)-5,5-dimethylcyclohexa-1,3-dione (5a)

To potassium (1.02 g) dissolved in *t*-butyl alcohol (50 ml) under nitrogen, is added cyanoethyldimedone **2***a* (4.8 g) followed by propargyl bromide (4.5 ml) dropwise and the mixture is refluxed for 15 h. After cooling and pouring into ice water, the propargyl derivative **5***a* crystallizes (4.7 g, 83%), m.p. 157–158°; λ_{max} 283 (1060) nm; ν_{KBr} 3265, 2260, 2128, 1740, and 1710 cm^{-1}; $\delta_{pyridine\text{-}d_5}$ *gem*-dimethyl s 0.85 and s 0.95, —CH_2—CO s 2.76, H—C≡C—CH_2 t(2.5) 2.86 and d(2.5) 2.95; *m/e* 231 (M+), 191, 163, 147, 84, and 83.

Anal. Calcd. for $C_{14}H_{17}NO_2$: C, 72.7; H, 7.4; N, 6.1. Found: C, 72.7; H, 7.6; N, 6.1.

2-Acetonyl-2-(2-cyanoethyl)-5,5-dimethylcyclohexa-1,3-dione (6a)

To the propargyl derivative **5***a* (4 g) in methanol (150 ml) and ethoxyethanol (5 ml) is added aqueous sulfuric acid (0.3 ml of 1 *N*) and Dowex 50W-X4 resin (0.9 g) charged with mercuric ions (8). The mixture is stirred for 18 h and after neutralizing with ammonia, the resin is filtered and the solvents evaporated. The residue (**6***a*) crystallizes on contact with acetone (4.5 g, quantitative), m.p. 115–116°; ν_{KBr} 2260, 1730, 1705, 1700 cm^{-1}; $\delta_{acetone\text{-}d_6}$ *gem*-dimethyl s 1.17, CH_3COCH_2 s 2.08, and —CH_2CO s 3.08; *m/e* 249 (M+), 234, 207 (base), 206, 190, 179, 178, 167, 164, 109, and 108.

Anal. Calcd. for $C_{14}H_{19}NO_3$: C, 67.4; H, 7.7; N, 5.6. Found: C, 67.2; H, 7.6; N, 5.6.

NOTE: Owing to a certain loss of activity of the treated resin on standing, this hydration is more reproducible using the boron trifluoride – trichloroacetic acid method described later (see **10***c*).

Cyclization of the Triketonitrile 6a

(a) With Potassium t-Butoxide (retro-Michael)

Potassium (180 mg) is dissolved in *t*-butyl alcohol (10 ml) under nitrogen and after cooling 2-acetonyl-2-cyanoethyldimedone (**6***a*) (1.4 g) is added and stirring continued for 35 min. The reaction mixture is poured into ice water and acidified with hydrochloric acid (28 ml, 2 *N*). Extraction affords an oil (1.2 g) from which *2-acetonyldimedone* (**6***c*) crystallizes, m.p. 134–135° (lit. (9) 132–133°); λ_{max} 263 (14 400) and λ_{max} (NaOH) 289 (24 600) nm; ν_{KBr} 1723, 1650, and 1570 cm^{-1}; δ_{CDCl_3} *gem*-dimethyl s 1.10, CH_3COCH_2 s 2.17 and s 3.44, ring CH_2CO s 2.35, OH(enol) 9.67.

Anal. Calcd. for $C_{11}H_{16}O_3$: C, 67.3; H, 8.2. Found: C, 67.5; H, 8.2.

(b) With Ethanolic Hydrochloric Acid (retro-Claisen etc.)

To the triketone **6***a* (1.39 g) in dry ethanol (30 ml) is added concentrated hydrochloric acid (1 ml) and the mixture is refluxed for 24 h. After decomposition in ice water, the product (**7**) (1.2 g) is obtained by extraction and purified by molecular distillation (cold finger): λ_{max} 224 (6000) nm; ν_{film} 2260, 1740 (ester), 1705, and 1640 (conjugated cyclopentenone) cm^{-1}; δ_{CCl_4} *gem*-dimethyl s 1.05, CH_3CH_2O t(7.3) 1.26, and q (7.3) 4.15, CH_2COOR s 2.21, =CH—CO broad s 5.97; *m/e* 277 (M+), 247, 231, 189, 164, 163, 149, 148 (base), and 108.

2-Propargyl-2-(2-cyanoethyl)-3-hydroxy-5,5-dimethylcyclohexanone (8a)

Sodium borohydride (135 mg) is added to a solution of 2-propargyl-2-cyanoethyldimedone (**5***a*) (1.15 g) in methanol (80 ml) and the mixture stirred at room temperature for 4 h. Water (10 ml) is added and the mixture concentrated to about one-third volume before pouring into water and extracting with chloroform. The equatorial hydroxy-ketone **8***a* (1.05 g, 90%) crystallizes from methanol, m.p. 178–179°; ν_{KBr} 3420, 3280, 2260, 1705 cm^{-1}; $\delta_{pyridine\text{-}d_5}$ (90MHz) *gem*-dimethyl two s 0.91 and 1.00, —CHOH d of d(10.0 and 5.5) 4.72 and s 5.0; *m/e* 233, 216, 159, 158 (base), 135, 130, 116, and 101.

Anal. Calcd. for $C_{14}H_{19}NO_2$: C, 72.1; H, 8.2; N, 6.0. Found: C, 72.2; H, 8.3; N, 6.2.

The hydroxy-ketone gives the *O-tosyl derivative* **8***b* (88% yield) on treatment with tosyl chloride in pyridine. The product crystallizes on pouring the reaction mixture into ice water, m.p. 165° (from methanol); ν_{KBr} 3280, 2260, 1715, 1605, 1195, and 1185 cm^{-1}; δ_{CDCl_3} *gem*-dimethyl two s 0.95 and 1.10, —CH_2CO s 2.27 (broad), tosyl s 2.5 and ABq (J_{AB} = 8.5 Hz) 7.6, C*H*OTs d of d(9.0 and 7.5) 5.30; *m/e* 387 (M+, weak) 216, 215, 200, 188, 173, 159, 158, 155, 133, and 119.

Anal. Calcd. for $C_{21}H_{25}NSO_4$: C, 65.1; H, 6.5; N, 3.6. Found: C, 64.8; H, 6.4; N, 3.7.

Acetylation of hydroxy-ketone **8***a* in acetic anhydride – pyridine on a steam bath for 2 days affords the *O-acetyl derivative* **8***c* (78% after recrystallization), m.p. 129–130°; ν_{KBr} 3310, 2260, 2140, 1735, 1710, 1250, 1240 cm^{-1}; δ_{CDCl_3} *gem*-dimethyl two s 0.99 and 1.11, HC≡C—CH_2—*t*(2) 1.83 and d(2.0) 2.53, CH_3CO s 2.08, C*H*—O—Ac d of d(9.0 and 7.0) 5.63.

Anal. Calcd. for $C_{16}N_{21}NO_3$: C, 69.8; H, 7.7; N, 5.1. Found: C, 69.9; H, 7.7; N, 5.1.

2-Acetonyl-2-(2-cyanoethyl)-3-hydroxy-5,5-dimethylcyclohexanone (10a)

Hydration of the triple bond was accomplished by the Dowex resin method (see **6***a*) but yields were more reproducible using the following (in all three cases superior to 80%).

The *O*-acetyl derivative **8***c* (420 mg) is dissolved in warm methanol (35 ml) and without cooling mercuric oxide (21 mg), trichloroacetic acid (2 mg), and boron trifluoride etherate (1 ml) are added. After stirring for 2 h and pouring into dilute sulfuric acid, the methyl-ketone **10***c* (358 mg, 80%) was obtained by chloroform extraction.

The hydroxy-ketone **10***a*, m.p. 84–85°; ν_{KBr} 3420, 2260, 1710, and 1705 cm^{-1}; δ_{CDCl_3} *gem*-dimethyl two s 1.03 and 1.08, CH_3CO s 2.21, CHOH d of d(10.0 and 7.0) 4.43 and s 3.2; *m/e* 239 (M+), 208, 194 (base), 191, 164, 148, and 108.

Anal. Calcd. for $C_{14}H_{21}NO_3$: C, 66.9; H, 8.4; N, 5.6. Found: C, 67.0; H, 8.6; N, 5.6.

The tosylate **10***b*, m.p. 135–136°; ν_{KBr} 2260, 1725, 1715,

Can. J. Chem. Downloaded from www.nrcresearchpress.com by 210.87.254.6 on 09/05/12
For personal use only.

1605, 1195, 1185 cm^{-1}; δ_{CDCl_3} *gem*-dimethyl two s 0.99 and 1.05, CH_3COCH_2 s 2.05 and ABq (J_{AB} = 18.0 Hz) 2.76, CH_3-aromatic s 2.47, CH—O—Ts d of d(5.32) 5.39, aromatic H ABq (J_{AB} = 8.2 Hz) 7.36.

Anal. Calcd. for $C_{21}H_{27}NSO_5$: C, 62.2; H, 6.7; N, 3.5. Found: C, 62.1; H, 6.9; N, 3.9.

The acetate **10c**, m.p. 143–144°; ν_{KBr} 2260, 1735, 1710, 1700, 1255, 1245 cm^{-1}; δ_{CDCl_3} *gem*-dimethyl two s 1.16 and 1.23, CH_3CO two s 2.12 and 2.29, CHOAc d of d(10.0 and 8.0) 5.77.

Anal. Calcd. for $C_{16}H_{23}NO_4$: C, 65.5; H, 7.9; N, 4.8. Found: C, 65.5; H, 7.9; N, 4.8.

2,8-Dimethoxy-4-tosyloxy-9-cyanoethyl-2-methyl-perhydrobenzfuran (9)

The *O*-tosyl derivative **8b** (3.9 g) is hydrated as above but instead of pouring into dilute acid, the reaction mixture is evaporated *in vacuo* affording a white solid (3.7 g by filtration), m.p. 93–94°; ν_{KBr} 2260, 1605, 1198, and 1185 cm^{-1}; δ_{CDCl_3} *gem*-dimethyl s 1.00, $CH_3C(OCH_3)$ s 1.40, CH_3 aromatic s 2.47, 2 × CH_3O two 2 3.18 and 3.32, C*H*OTs d of d(10.0 and 7.0) 5.32, aromatic ABq (J_{AB} = 8.5 Hz) 7.70; *m/e* 451 (M+).

Anal. Calcd. for $C_{23}H_{33}O_6SN$: C, 61.2; H, 7.4; N, 3.1. Found: C, 61.3; H, 7.4; N, 3.2.

Cyclizations of Diketo-tosylate 10b

(a) 1-(2-Cyanoethyl)-4,4-dimethyl-7-acetobicyclo-[4.1.0]heptan-2-one (12)

To a methanolic solution of sodium methoxide (sodium (11.5 mg) in methanol (20 ml)), the diketo-tosylate **10b** (202 mg) is added and the mixture stirred at room temperature for 2.5 h. Chloroform extraction, after pouring the mixture into ice water, gives a clear oil (130 mg) which is chromatographed over alumina III. The benzene – 10% ether eluate is the substituted cyclopropane **12** (85 mg, 73%), m.p. 85–86°; λ_{max} 210 (8300) nm; ν_{KBr} 3060, 2260, 1703 (broad) cm^{-1}; δ_{CDCl_3} *gem*-dimethyl two s 0.90 and 1.00, CH_3CO s 2.33, *no* vinyl or aromatic protons; *m/e* 233 (M+), 218, 193, 191, 190, 176, 160, 151, 149, 148 (base). A sample is sublimed for analysis.

Anal. Calcd. for $C_{14}H_{19}NO_2$: C, 72.1; H, 8.2; N, 6.0. Found: C, 72.0; H, 8.1; N, 6.0.

This same product (**12**) is obtained by refluxing the tosylate **10b** and pyrrolidine in benzene with a Dean–Stark water separator.

(b) 9-Cyano-8-hydroxy-2-oxo-4,4,8-trimethyl-tricyclo[4.4.0.0^{1,7}]decane (13)

To a cold solution of sodium *t*-butoxide (sodium (18.6 mg) in *t*-butyl alcohol (20 ml)), is added the diketo-tosylate **10b** (325 mg) and stirring continued for 3 h at room temperature. The reaction is stopped by pouring into ice water and extracting with ether gives a viscous oil (219 mg) which crystallizes on contact with benzene to afford the spiro compound **13** (175 mg, 75%), m.p. 159–160°; ν_{KBr} 3410, 3045, 2265, 1685 cm^{-1}; δ_{CDCl_3} (90 MHz) *gem*-dimethyl two s 0.90 and 0.97, $CH_3C(OH)$ s 1.46, —CH—CN t (1.5) 2.62, no vinyl or aromatic protons; *m/e* 233 (M+) 218, 190, 177, 176, 134, 125 (base) 107, 106.

Anal. Calcd. for $C_{14}H_{19}NO_2$: C, 72.1; H, 8.2; N, 6.0. Found: C, 72.1; H, 8.1; N, 5.8.

Cyclization of Diketo-acetate 10c

Potassium (40 mg) is dissolved in *t*-butyl alcohol (30 ml) and to this solution is added the diketo-acetate **10c** (293 mg). After 12 h at 40° the reaction mixture is decomposed in ice water and the neutral products (202 mg) obtained by extraction. Chromatography over alumina III gave a *keto-nitrile* **14** (30 mg), m.p. 141–142°; ν_{KBr} 3390, 1740, and 1710 cm^{-1}; δ_{CDCl_3} *gem*-dimethyl two s 0.92 and 1.13, —CH(OH)— m 4.0 and s (broad) 3.25; *m/e* 210 (M+) 195, 182, 154, 149, 126 (base), 125, 110, and 109.

Anal. Calcd. for $C_{12}H_{18}O_3$: C, 68.5; H, 8.6. Found: C, 68.7; H, 8.7.

Other attempted cyclizations either gave back the starting material or in one case (concentrated hydrochloric acid in ethanol) hydrolyzed the product to the alcohol **10a**.

2-(2-Chloropropen-2-yl)-2-(2-cyanoethyl)-5,5-dimethylcyclohexa 1,3-dione (15a)

To a solution of cyanoethyldimedone **2a** (1.93 g) in dimethylformamide (distilled from sodium hydride) under nitrogen, is added sodium hydride – mineral oil (2 g). After warming at 60° for 17 h, 2,3-dichloropropene (5 ml) is added dropwise and heating continued for 6 h. The crude product obtained by extraction is chromatographed over alumina III affording the crystalline chloroalkene **15a** (1.34 g, 50%), m.p. 116–117° (from ether); ν_{KBr} 3120, 2260, 1730, 1700, 1645, and 900 cm^{-1}; δ_{CDCl_3} *gem*-dimethyl two s 0.84 and 1.21, $—CH_2—CCl=CH_2$ ABq (J_{AB} = 14.5 Hz) 2.74 and two s 5.32 and 5.47; *m/e* 269 and 267 (M+), 232, 231, 229, 227, 218, 201, 199.

Anal. Calcd. for $C_{14}H_{18}NO_2Cl$: C, 62.8; H, 6.8; N, 5.2. Found: C, 63.2; H, 6.7; N, 5.3.

NOTE: vacuum sublimation of **15a** gives the propargyl derivative **5a**.

2-(2-Chloropropen-2-yl)-2-(2-cyanoethyl)-3-hydroxy-5,5-dimethylcyclohexanone (15b)

The diketone **15a** (566 mg) is reduced with sodium borohydride (56 mg) in methanol (50 ml). The colorless oil obtained crystallizes on contact with ether to give the hydroxy-ketone **15b** (505 mg, 90%), m.p. 97–98°; ν_{KBr} 3440, 3010, 2260, 1690, 1645, and 900 cm^{-1}; δ_{CDCl_3} *gem*-dimethyl two s 0.95 and 1.14, $CH_2—CCl=CH_2$ ABq (J_{AB} = 14.5 Hz) 2.87 and s 5.42, —CH(OH)— m 4.35 and s 3.0.

Anal. Calcd. for $C_{14}H_{20}NO_2Cl$: C, 62.3; H, 7.5; N, 5.2. Found: C, 62.7; H, 7.6; N, 5.2.

Cyclizations attempted in concentrated sulfuric acid gave intractable products and refluxing in 97% formic acid afforded the *O-formate* **15c**, m.p. 122–123°; ν_{KBr} 2260, 1730, 1710, 1635, 1180, 1165, and 900 cm^{-1}; δ_{CDCl_3} very similar to **15b** but no OH proton, —OC*H*O s 8.14; *m/e* 299 and 297 (M+, weak) 262 (base), 211, 209, 190, 174, 134, 133, 132.

Anal. Calcd. for $C_{15}H_{20}O_3NCl$: C, 60.5; H, 6.8; N, 4.7. Found: C, 60.8; H, 6.8; N, 4.7.

2-Propargyl-2-(2-cyanoethyl)-5,5-dimethylcyclohex-3-enone (16a)

The hydroxy-ketone **8a** (2.33 g) is dissolved in pyridine (50 ml, freshly distilled from calcium hydride). After cooling to 0°, fresh phosphorous oxychloride (9 ml) is added and the solution allowed to warm to room temperature and then heated at 60° for 20 h. The reaction

Can. J. Chem. Downloaded from www.nrcresearchpress.com by 210.87.254.6 on 09/05/12
For personal use only.

mixture is poured very slowly into stirred ice water affording the crystalline unsaturated ketone **16***a* (1.46 g, 68%), m.p. 86–87°; ν_{KBr} 3260, 3030, 2260, 2120, 1715, and 780 cm^{-1}; δ_{CDCl_3} (90MHz) *gem*-dimethyl two s 1.06 and 1.10 —CH=CH— ABq (J_{AB} = 10.0 Hz) 5.7 (broadened by W coupling); *m/e* 215 (M+), 176, 173, 159, 158, 135 (base), 133, 132, 131, 119, 117, and 105.

Anal. Calcd. for $C_{14}H_{17}NO$: C, 78.1; H, 8.1; N, 6.5. Found: C, 78.1; H, 8.0; N, 6.6.

NOTE: The yield in this elimination varied greatly with the duration of the reaction (19 h, 68%; 23 h, 45%; and 44 h, 20%) and the quality of the reagents. An alternative method employing tosyl chloride in pyridine (65° for 2 days) never gave more than 52% and then only after column chromatography (alumina III).

*2-Acetonyl-2-(2-cyanoethyl)-5,5-dimethylcyclohex-3-enone (**16***b*)

The triple bond in **16***a* (1.36 g) is hydrated as given above for **10***a* affording the methyl-ketone **16***b* (1.05 g, 71%) after column chromatography. Although pure, as shown by t.l.c., this product has never crystallized; ν_{KBr} 3020, 2260, 1715, 1705, and 1365 cm^{-1}; δ_{CDCl_3} (90MHz) *gem*-dimethyl two s 1.06 and 1.14, CH_3-$COCH_2$— s 2.09 and ABq (J_{AB} = 16.5 Hz) 2.75, ring —CH_2CO— ABq (J_{AB} = 14.5 Hz) 2.46, —CH≡CH— ABq (J_{AB} = 10.0 Hz) 5.63. To characterize this product the solid intermediate cyclic acetal is isolated (like **9** but double bond and no *O*-tosyl), m.p. 71–72°; ν_{KBr} 3010, 2260, 1075 cm^{-1}.

Anal. Calcd. for $C_{16}H_{25}O_3N$: C, 68.8; H, 9.0; N, 6.0. Found: C, 69.0; H, 9.0; N, 6.0.

Hydrolysis of this derivative affords the diketone **16***b* quantitatively.

*Cyclization of **19**b*

(a) With Potassium Hydroxide

Under nitrogen, the diketone **16***b* (0.7 g) is boiled in "previously boiled" water and a solution of potassium hydroxide (1.0 g) in "boiled" water (2.7 ml) is added. Refluxing is continued for 12 h and after cooling, diluting with water, salt, and ice the solution is extracted to remove a small quantity of neutral material (23 mg). Acidification of the aqueous solution at 0° and chloroform extraction affords the cyclized acid **17***a* (530 mg, from ether – petroleum ether), m.p. 87–88°; λ_{max} 233 (13 000) nm; ν_{KBr} 3300–2500 (broad), 3010, 1725, 1670, 1620 cm^{-1}; δ_{CHCl_3} 1710, 1688, and 1625 cm^{-1}; δ_{CDCl_3} *gem*-dimethyl two s 0.93 and 1.18, —$COCH_2$— ABq (J_{AB} = 18.0 Hz) 2.27, —CH_2—C(=CH)— s (broad) 2.53 and s (broad) 5.97, —CH=CH— ABq (J_{AB} = 9.5 Hz) 5.50, COOH s (broad) 9.9; *m/e* 234 (M+), 162, 161 (base), 133, 118, 117.

Anal. Calcd. for $C_{14}H_{18}O_3$: C, 71.8; H, 7.8. Found: C, 72.1; H, 7.8.

Treating the acid **17***a* with excess ethereal diazomethane at room temperature gave the *methyl ester* **17***b*, b.p. 97–98° at 0.03 nm; similar properties to the acid: ν_{film} 3010, 1738, 1710, 1625 cm^{-1}; *m/e* 248, 175, 162, 161 (base), 159, 133, 119, 117.

*(b) With Sodium Hydride (**18***a*, **17***c*, *and **19**)*

Under nitrogen, sodium hydride (275 mg; mineral oil suspension) is introduced into dimethoxyethane (50 ml, distilled from sodium hydride). After 20 min, the diketone **16***b* (1.4 g) in dimethoxyethane (15 ml) is added drop by drop. The solution becomes red and is stirred overnight at room temperature. Dilution with ice water and extraction gives a neutral fraction (660 mg) containing several products as shown by t.l.c. (see below). Acidification and extraction of the aqueous phase affords the unsaturated acid **18***a* ([6-(4,4-dimethyl)spiro[5.4]dec-2-en-8-on]ylidene acetic acid) as a yellow solid (541 mg) which is crystallized from petroleum ether – benzene and finally sublimed, m.p. 123–124°; λ_{max} 221(6900) nm; ν_{KBr} 3500–2500 (broad), 3030, 1745, 1690, 1660, 1613, 1268, and 1250 cm^{-1}; δ_{CDCl_3} *gem*-dimethyl two s 1.0 and 1.04, —CH_2—C(=CH—COOH ABq (J_{AB} = 13.0 Hz, allylic coupling 1 Hz) 2.3 and s (broad) 5.80, —CH=CH— ABq (J_{AB} = 9.5 Hz) 5.53; *m/e* 234, 216, 163, 160 (base), 145, 133, 132, 117, and 105.

Anal. Calcd. for $C_{14}H_{18}O_3$: C, 71.8; H, 7.4. Found: C, 71.3; H, 7.7.

The *methyl ester* **18***b* is prepared quantitatively using diazomethane.

The neutral fraction from the reaction above (660 mg) is chromatographed over neutral alumina (II). Elution with benzene gave an unidentified mixture (110 mg) but benzene–ether eluted the *nitrile* **17***c* (118 mg) which could not be induced to crystallize; λ_{max} 232 (13 250) nm: ν_{film} 3020, 2260, 1710, and 1625 cm^{-1}; δ_{CDCl_3} (90MHz) *gem*-dimethyl two s 0.94 and 1.20, —CH_2—CO— ABq 2.26, —CH_2—C(=CH— s (broad) 2.53 and s (broad) 5.98, —CH=CH— ABq (J_{AB} = 10.0 Hz) 5.28. Hydrolysis (6 h in 5% aqueous sodium hydroxide) afforded the acid **17***a*, m.p. 87–88° identical with the sample above.

Further elution (ether–chloroform) gives another *nitrile* **19** m.p. 114–115°; ν_{KBr} 3440, 3030, 2260, 1710, and 785 cm^{-1}; δ_{CDCl_3} *gem*-dimethyl two s 1.02 and 1.06, $CH_3C(OH)$—CH_2— s 1.51 and ABq (J_{AB} = 14.5 Hz) 2.03, —COC*H*—C(—OH s 2.35, —CH=CH— ABq (J_{AB} = 10.0 Hz) 5.73; *m/e* 233, 191 (base), 180, 165, 137, and 109.

Anal. Calcd. for $C_{14}H_{19}O_2N$: C, 72.1; H, 8.2; N, 6.0. Found: C, 72.2; H, 8.2; N, 6.0.

*2-Allyl-2-propargyl-5,5-dimethylcyclohexa-1.3-dione (**5b**)*

Prepared from 2-allyldimedone (**2***c*) (24 g) by essentially the method described above for **5***a*. The propargyl derivative crystallizes from *n*-pentane (25.8 g, 89%), m.p. 58–59°; ν_{KBr} 3290, 3080, 2115, 1718, 1680, 1638 cm^{-1}; δ_{CDCl_3} (90MHz) *gem*-dimethyl two s 0.96 and 1.11, HC≡C—CH_2— t(2.7) 1.92 and d(2.7) 2.62, —CH_2-CH=CH_2 d(7.1) 2.65, q of t(18.0, 8.0, 7.1) 5.55 and m(18.0, 8.0) 5.05; *m/e* 218 (M+), 203, 179, 177, 175, 135, 134 (base), and 121.

Anal. Calcd. for $C_{14}H_{18}O_2$: C, 77.0; H, 8.3. Found: C, 77.1; H, 8.3.

*2-Allyl-2-propargyl-3-hydroxy-5,5-dimethylcyclohexanone (**20**)*

Sodium borohydride (2.02 g) reduction of the diketone **5***b* (16.46 g) in methanol (150 ml) affords the crude hydroxy-ketone **20** (16.4 g, 98%) which from the n.m.r. spectrum and t.l.c. is a mixture of epimeric alcohols but

Can. J. Chem. Downloaded from www.nrcresearchpress.com by 210.87.254.6 on 09/05/12
For personal use only.

the equatorial isomer, the major product (4.04 g) crystallizes in part from ether – petroleum ether and the spectral and other characteristics quoted refer to this epimer, m.p. 75–76°; ν_{KBr} 3420, 3250, 2080, 2110, 1700, and 1640 cm^{-1}; δ_{CDCl_3} (90MHz) *gem*-dimethyl two s 0.89 and 1.08, $HC{\equiv}C{-}CH_2{-}$ t(2.5) 2.08 and d(2.5) 2.54, $-CH_2{-}CH{=}CH_2$ d(7) 2.56, q of t(18.0, 9.0, 7.0) 5.45, and m(18.0, 9.0) 5.1, $-CHOH$ d of d(10.5 and 6.5) 4.32; (in the crude product the axial hydroxyl $-CHOH$ gives d of d(6.5 and 6.0) 4.16).

Anal. Calcd. for $C_{14}H_{20}O_2$: C, 76.3; H, 9.2. Found: C, 76.4; H, 9.3.

The *tosylate* was prepared in pyridine with tosyl chloride, m.p. 112–113° (from ether); ν_{KBr} 3280, 1710, 1640, 1600, 1192, and 1180 cm^{-1}.

Anal. Calcd. for $C_{21}H_{26}O_4S$: C, 67.4; H, 7.0. Found: C, 67.2; H, 7.0.

2-Propargyl-2-allyl-5,5-dimethylcyclohex-3-en-1-one (16c)

The keto-alcohol **20** (500 mg) is dissolved in pyridine (20 ml) and phosphorus oxychloride (2.07 ml) is added with vigorous stirring at room temperature. The mixture is then warmed at 57° for 46 h before cooling and pouring into ice water. After chloroform extraction (and removal of the pyridine by shaking several times with dilute hydrochloric acid, washing and drying) the unsaturated ketone **16c** (352 mg, 77%) is obtained as an oil; ν_{KBr} 3210, 3080, 3020, 1713, and 1640 cm^{-1}; δ_{CDCl_3} *gem*-dimethyl two s 1.03 and 1.09, $HC{\equiv}C$ t(2.7) 2.01, $-CH{=}CH_2$ m 5.6 and m 5.04, $-CH{=}CH-$ ABq (J_{AB} = 9.8 Hz) broadened by W coupling) 5.68.

Semicarbazone, m.p. 164–165° (dec.).

Anal. Calcd. for $C_{15}H_{21}N_3O$: C, 69.5; H, 8.2; N, 16.2. Found: C, 69.6; H, 8.2; N, 16.4.

8-Allyl-5,5-dimethylhydrinda-3,6-dien-2-one (17d) via 16d

The triple bond in **19c** is hydrated as described for **10a** affording the diketone **16d** in yields exceeding 90%; ν_{CHCl_3} 3080, 3005, 1720, 1710, 1360 cm^{-1}; δ_{CDCl_3} (90 MHz) *gem*-dimethyl two s 1.11 and 1.13, $CH_3COCH_2{-}$ s 2.07 and ABq (J_{AB} = 17.0 Hz) 2.44, $CH_2CH{=}CH_2$ d(7.1) 2.28, m 5.55 and m 5.0, ring CH_2CO ABq 2.41, $-CH{=}CH-$ ABq (J_{AB} = 10.0 Hz) 5.65; *m/e* 220 (M+), 205, 178, 177, 163, 162, 147, 138, 137 (base). This product (**16d**) was unstable and was normally cyclized immediately. The diketone **16d** (1.2 g) is refluxed for 15 h in a solution of potassium hydroxide (1.8 g) in water (36 ml) and methanol (10 ml). The clear liquid obtained (1.15 g) is purified by evaporative distillation (76–77° at 0.09 mm); λ_{max} 233 (14 200) nm; ν_{CHCl_3} 3080, 3010, 1705, 1670, and 1625 cm^{-1}; δ_{CDCl_3} (90MHz) *gem*-dimethyl 0.94 and 1.20, $-CH_2CO-$ ABq (J_{AB} = 18.0 Hz) 2.32, $-CH_2CH{=}CH_2$ d(7.0) 2.34, m 5.4 and m 5.0, $-CH_2-C(=CH-CO)$ s(broad, sharpens on irradiation at 5.90) 2.53 and s(broad) 5.90, $-CH{=}CH-$ ABq (J_{AB} = 10.0 Hz) 5.50; *m/e* 202 (M+), 162, 161 (base), 133, 118, 117, and 105.

Anal. Calcd. for $C_{14}H_{18}O$: C, 82.1; H, 9.0. Found: C, 82.4; H, 8.9.

2-Propargyl-2-carboethoxycyclohexanone (23a)

Potassium (4.12 g) is dissolved in *t*-butyl alcohol (150 ml) and to the refluxing solution under nitrogen is added 2-carboethoxycyclohexanone (17 g) and 30 min later propargyl bromide (13.1 g). After 30 min of reflux, the cooled solution is decomposed in ice water and ether extracted. Vacuum distillation gave the alkylated product **23a** (16 g, 77%), b.p. 74–77° at 0.1 mm; ν_{film} 3295 ($C{\equiv}C-H$), 2128 ($C{\equiv}C$), 1740, and 1710 (ester and ketone) cm^{-1}; δ_{CCl_4} CH_3CH_2O- t(7.2) 1.26 and q(7.2) 4.22, $H-C{\equiv}C-CH_2-$ t(2.7) 2.08 and ABq (J_{AB} = 17.3 Hz, split by $\equiv CH$, 2.7) 2.58. *Semicarbazone*, m.p. 152–153° (lit. (4) 152.7–153.5°).

Anal. Calcd. for $C_{13}H_{19}O_3N_3$: C, 58.9; H, 7.2; N, 15.8. Found: C, 59.2; H, 7.3; N, 15.5.

2-Propargyl-2-carboethoxy-4-methylcyclohexanone (23b)

Prepared from α-carboethoxy-4-methylcyclohexanone in 81% yield as described above, b.p. 72–74° at 0.1 mm; ν_{film} 3290, 2128, 1730, 1710, 1210 cm^{-1}; δ_{CCl_4} CH_3CH d(4.9) 1.05, CH_3CH_2O- t(7.2) 1.23 and q(7.2) 4.19, $H-C{\equiv}C-CH_2-$ t(2.5) 2.09 and ABq (J_{AB} = 17.3 Hz, split by $\equiv CH$, 2.5) 2.67.

2-Propargyl-2-carbomethoxy-4-methylcyclohexanone (23c)

The α-carbomethoxy-4-methylcyclohexanone (prepared using dimethylcarbonate (10)) was alkylated as described above affording the product **23c** in 86% yield after distillation, b.p. 94–98° at 0.5 mm; ν_{film} 3295, 2130, 1745, 1720, 1225 cm^{-1}; δ_{CCl_4} CH_3CH d(5.6) 1.07, $H-C{\equiv}C-CH_2-$ t(2.5) 2.04 and ABq (centered at) 2.78, CH_3O- s 3.75.

2-Acetonyl-2-carboethoxycyclohexanone (24a)

To the carboethoxypropargylcyclohexanone **23a** (16.0 g) in methanol (50 ml) is added water (1.5 ml) and concentrated sulfuric acid (0.05 ml). Dowex 50 W-X4 resin, previously treated with mercuric ions (8) (500 mg), is introduced and after warming for a few minutes the mixture is stirred overnight. The filtered solution is neutralized with ammonium hydroxide, dried over sulfate, evaporated, and filtered through a short silica gel column in benzene solution. After distillation (85–90° at 0.1 mm) the yield of methyl-ketone **24a** was 95% (16.5 g); ν_{film} 1733, 1708 cm^{-1}; δ_{CCl_4} CH_3CH_2O- t(7.2) 1.21 and q(7.2) 4.15, CH_3COCH_2- s 2.10 and s 2.79. *Bis-semicarbazone*, m.p. 220–221° (lit. 12) 214° (dec.).

Anal. Calcd. for $C_{14}H_{24}O_4N_6$: C, 49.4; H, 7.1; N, 24.7. Found: C, 49.7; H, 7.3; N, 24.5.

2-Acetonyl-2-carboethoxy-4-methylcyclohexanone (24b)

Prepared in 53% yield using Dowex resin (as above) or in 85% yield following the boron trifluoride – trichloroacetic acid procedure (see **24c** below), b.p. 92–96° at 0.1 mm, on standing the product **24b** finally crystallized, m.p. 64–66° (from pentane); ν_{KBr} 1735, 1708, 1238 cm^{-1}; δ_{CCl_4} CH_3CH d(4.8) 1.00, CH_3CH_2O- t(7.3) 1.21, and q(7.3) 4.12, CH_3COCH_2- s 2.12 and s 2.96.

Anal. Calcd. for $C_{13}H_{20}O_4$: C, 65.0; H, 8.4. Found: C, 65.1; H, 8.4.

2-Acetonyl-2-carbomethoxy-4-methylcyclohexanone (24c)

To red mercuric oxide (7.8 g), anhydrous methanol (16 ml), boron trifluoride etherate (3.1 ml), and trichloro-

Can. J. Chem. Downloaded from www.nrcresearchpress.com by 210.87.254.6 on 09/05/12
For personal use only.

acetic acid (156 mg) is added the propargyl-keto ester **23c** (114 g) in methanol (250 ml) at a rate to ensure a mild reflux. The mixture is stirred for 2.5 h before pouring into water (1 l) and acidifying with sulfuric acid. The yellow oil obtained by extraction gave the crystalline product **24c** on standing (109 g, 88%), m.p. 102–103° (from methylene chloride – petroleum ether); ν_{KBr} 1745, 1715 cm^{-1}; δ_{CDCl_3} CH_3CH d(5.0) 1.06, CH_3COCH_2— s 2.23 and s 3.05, CH_3O— s 3.87.

Anal. Calcd. for $C_{12}H_{18}O_4$: C, 63.7; H, 8.0. Found: C, 63.6; H, 8.2.

9-Carboethoxyhydrind-1(8)-en-2-one (22c)

Prepared as described for **22d** in yields up to 70%. After silica gel chromatography: ν_{film} 1740–1700 (ester and ketone), 1625 (conjugated double bond), 850 (double bond) cm^{-1}; δ_{CCl_4} CH_3CH_2O— t(7.0) 1.22 and q(7.0) 4.19, CH_2COCH ABq centered at 2.36 and s 5.93. *Semicarbazone*, m.p. 216–217° (dec.).

Anal. Calcd. for $C_{13}H_{19}O_3N_3$: C, 58.8; H, 7.2; N, 15.8. Found: C, 58.7; H, 7.4; N, 15.4.

5-Methyl-9-carbomethoxyhydrind-1(8)-en-2-one (22d)

To a solution prepared by dissolving potassium (15.6 g) in *t*-butyl alcohol (600 ml) is added at room temperature, the solid powdered diketo ester **4c** (84.6 g) in several portions during 20 min. After stirring for 45 min the mixture is poured into ice water and acidified (p*H* 4) with concentrated hydrochloric acid. Extraction gave a neutral fraction, the enone **22d** (43.9 g) and an acid (24.2 g) arising from ring fission. The enone was distilled, b.p. 98–103° at 0.05 mm; λ_{max} (EtOH) 232 (13 600) nm; ν_{film} 1740–1710 (ester and ketone), 1630 (conjugated double bond) cm^{-1}; δ_{CCl_4} CH_3CH d(7.0) 1.00 (mixture of stereoisomers), CH_3O s 3.72, =CH— s 5.91. *Semicarbazone*, m.p. 205–206° (dec.).

Anal. Calcd. for $C_{13}H_{19}N_3O_3$: C, 58.8; H, 7.2; N, 15.8. Found: C, 58.7; H, 7.3; N, 15.2.

5-Methylhydrind-1(8)-en-2-one (22b)

Cyclization of the diketo ester **23b** (4.8 g) by refluxing with 5% aqueous sodium hydroxide (50 ml) for 6 h under nitrogen affords the unsaturated ketone **22b** (2.6 g, 87%) after extraction and chromatography (silica gel); λ_{max} (EtOH) 231 (16 400) nm; ν_{film} 1709, 1623, and 838 cm^{-1}; δ_{CCl_4} CH_3CH d(7.0) 1.00, =CH— s 5.81. *Semicarbazone*, m.p. 220–221°.

Anal. Calcd. for $C_{11}H_{17}N_3O$: C, 63.7; H, 8.3; N, 20.3. Found: C, 63.5; H, 8.5; N, 19.9.

8-Vinylhydrindan-2-one (5)

To tetrakis[iodo(tri-*n*-butylphosphine)copper(I)] (15.7 g, prepared by the method of Kauffmann (11)) dissolved in tetrahydrofuran (50 ml) and cooled to −78° is added vinyl lithium (0.08 mol) in tetrahydrofuran. After 10 min the enone **22a** (2.72 g) is added in tetrahydrofuran (15 ml) and the temperature allowed to rise to 0°. Stirring is continued for 1 h and the mixture is poured into saturated ammonium chloride solution, ether extracted, and carefully chromatographed (silica gel) to afford the vinylhydrindanone **25** (1.1 g, 34%); ν_{film} 3095 (vinyl), 1740, 1633, 993, and 911 cm^{-1}; δ_{CCl_4} CH_2=CH— d of d(1.5 and 17.3) 5.05, d of d (1.5 and 11.3) 5.10, and d of d(18.5 and 10.0) 5.98. *Semicarbazone*, m.p. 214–215°.

Anal. Calcd. for $C_{12}H_{19}N_3O$: C, 65.1; H, 8.6; N, 19.0. Found: C, 65.4; H, 8.6; N, 18.5.

Cyclohexa-1,2-dione-1-ethyleneketal (27a)

α-Ethylidenecyclohexanone (85 g, lit. (12)), ethylene glycol (80 g), and *p*-toluene sulfonic acid (1.5 g) are dissolved in benzene (400 ml) and refluxed 12 h in a Dean–Stark apparatus. The spiro-ketal **26a** is isolated in the usual manner (92 g, 80%), b.p. 39–42° at 0.1 mm; ν_{film} 1670 cm^{-1}; δ_{CCl_4} CH_3CH= d(7.2) 1.61 and q of t(7.2 and 1.8) 5.65, —OCH_2CH_2O— s 3.88.

The spiro-ketal **26a** (30 g) in pyridine (68 ml) and methylene chloride (136 ml) is cooled to −78° and ozone (~5% in oxygen) is bubbled into the solution until a blue coloration persists. The solution is allowed to warm to ambient and the solvents removed in vacuum. Distillation affords the keto-ketal **27a** (16.1 g), b.p. 45–50° at 0.1 mm; ν_{film} 1735 cm^{-1}; δ_{CDCl_3} —OCH_2CH_2O— s 3.97. *2,4-Dinitrophenylhydrazone*, m.p. 169–170° (lit. (13) 171°).

Anal. Calcd. for $C_{14}H_{16}N_4O_6$: C, 50.0; H, 4.8; N 16.7. Found: C, 49.8; H, 4.9; N, 16.3.

3,3-Dipropargylcyclohexa-1,2-dione-1-ethyleneketal (28a)

To sodium hydride (1.8 g) in benzene (50 ml) is rapidly added the ketal-ketone **27a** (6.24 g) and the mixture refluxed 1 h. After cooling to room temperature, propargyl bromide (4.8 g) is added dropwise and the reaction is allowed to stand overnight. After pouring into ice water and extracting, the mixture (seen by t.l.c.) is chromatographed over alumina III affording the dipropargyl compound **28a** (2.3 g) which eventually crystallized, m.p. 87–88°; ν_{film} 3280, 3270, 2120, 1718, 1200, 1108, and 1092 cm^{-1}; δ_{CCl_4} —CH_2—C≡CH ABq (J_{AB} = 17.0 Hz, split by ≡CH, 2.7) 2.66 and —OCH_2CH_2O— s 4.0.

Anal. Calcd. for $C_{14}H_{16}O_3$: C, 72.4; H, 6.9. Found: C, 72.7; H, 6.9.

Further elution gave mixtures of dipropargyl, monopropargyl, and starting material (600 mg).

Hydrogenation of the dipropargyl derivative **28a** over 10% palladium-on-carbon gave the *3,3-di-n-propylcyclohexa-1,2-dione-1-ethyleneketal* **28b** as a liquid after chromatography: ν_{film} 1715, 1200, 1109, and 1040 cm^{-1}; δ_{CCl_4} CH_3CH_2 m 0.94 (6H) and —OCH_2CH_2O— s 3.96 (4H).

3-Hydroxymethylenecyclohexa-1,2-dione-1-ethyleneketal (28c)

Very dry sodium methoxide (from sodium (16 g) is taken up in benzene (300 ml) and methyl formate (75 ml) is added. The mixture is stirred for 30 min and the addition of more benzene (300 ml) precedes the addition of the ketal-ketone **27a** (41.6 g). After 20 h the mixture is decomposed in ice water and hydroxymethylene **28c** is extracted into iced 2% potassium hydroxide in the usual manner. The distilled product (20.3 g, 41%; b.p. 73–74° at 0.2 mm) crystallized from pentane, m.p. 40–41°; ν_{film} 1715, 1643, 1585 cm^{-1}; δ_{CCl_4} —OCH_2CH_2O— m 4.13, =CHOH s 8.84 and s 13.78 (disappears on adding D_2O).

3-Propargylcyclohexa-1,2-dione-1-ethyleneketal (28e)

The hydroxymethylene **28c** (2.6 g) is added to potas-

Can. J. Chem. Downloaded from www.nrcresearchpress.com by 210.87.254.6 on 09/05/12
For personal use only.

sium *t*-butoxide (from potassium (0.55 g) in *t*-butyl alcohol (30 ml)) and after 10 min stirring, propargyl bromide (1.67 g) is added dropwise. The mixture is refluxed 1 h and then cooled, poured into ice cold dilute hydrochloric acid, and ether extracted. The crude product (1.65 g) is chromatographed over alumina III and the fraction eluted with carbon tetrachloride is the product **28***e* (1.01 g, 37%), m.p. 63–64°; ν_{KBr} 3270, 2120, 1725, and 1185, 1085, 1040 cm^{-1}; δ_{CCl_4} —CH—C=O m 2.79 and —OCH_2CH_2O m 3.99.

Anal. Calcd. for $C_{11}H_{14}O_3$: C, 68.0; H, 7.3. Found: C, 68.1; H, 7.4.

3-Acetonylcyclohexa-1,2-dione-1-ethyleneketal (28g)

The propargyl derivative **28***e* (2.5 g) is hydrated using the Dowex resin method (see **4***a*) to give the liquid acetonyl-ketone **28***g* (1.5 g, 52%); ν_{film} 1730, 1714, 1195, 1113, and 1040 cm^{-1}; δ_{CCl_4} CH_3CO s 2.13 and —OCH_2-CH_2O— m 3.94. *Bis-semicarbazone*, m.p. 208–209° (dec.).

Anal. Calcd. for $C_{13}H_{22}N_6O_4$: C, 47.8; H, 6.8; N, 25.7. Found: C, 48.1; H, 6.9; N, 25.8.

2-Benzylidene-5-methylcyclohexanone

3-Methylcyclohexanone (13.4 g) and benzaldehyde (10.6 g) are added to a solution of sodium hydroxide (4.0 g) in water. The mixture is refluxed for 3 h and is allowed to stand at room temperature overnight. Extraction with methylene chloride which is washed, dried, and evaporated gives a viscous oil affording the benzylidene derivative (17.9 g, 89%) by distillation (b.p. 108–110° at 0.04 mm). The product crystallizes slowly, m.p. 41–42°; λ_{max} (EtOH) 290 (13 100) nm; ν_{KBr} 3060, 3040, 1685, and 1600 cm^{-1}; δ_{CDCl_3} CH_3CH d(7.2) 0.97, aromatic s (5H) 7.38 and =CH— s 7.50.

Anal. Calcd. for $C_{14}H_{16}O$: C, 84.0; H, 8.1. Found: 83.9; H, 8.1.

The residue from the distillation is taken up in methanol and on cooling affords a small quantity (0.49 g) of the *2,6-bisbenzylidene-3-methylcyclohexanone*, m.p. 118–119°; λ_{max} 316 (11 500) nm; ν_{KBr} 3100, 3020, 1668, 1610, 705, and 695 cm^{-1}; δ_{CDCl_3} CH_3CH d(7.2) 1.28, aromatic s 7.48, =CH— two s 7.70 and 7.83.

Anal. Calcd. for $C_{21}H_{20}O$: C, 87.5; H, 7.0. Found: C, 87.6; H, 7.0.

4-Methylcyclohexa-1,2-dione-2-ethyleneketal (27b)

The benzylidene (from above, 89.5 g) is converted to the spiro-ketal **26***b* (79 g, 72% as described for **26***a*, m.p. 52–53°; λ_{max} 242 (14 250) nm; ν_{KBr} 3040, 1605, 1580, 1200, 1050, and 710 cm^{-1}; δ_{CDCl_3} CH_3CH d(7.2) 0.93, —OCH_2CH_2O— M 4.08, =CH— s 6.78 and aromatic s 7.34.

The benzylidene spiro-ketal **26***b* (24.4 g) in pyridine (100 ml) and methylene chloride (200 ml) is cooled in a Dry Ice – acetone bath and ozone (5% in oxygen) bubbled through the solution until the blue coloration persists (*ca.* 3 h). The solution is allowed to warm to room temperature, washed with 2% hydrochloric acid, sodium bicarbonate, and saturated sodium chloride, and evaporated. Distillation affords the ketal-ketone **27***b* (15.9 g, 93%), b.p. 71–72° at 0.35 mm; n_D^{23} 1.4651; ν_{film} 1735, 1200, 1050 cm^{-1}; δ_{CDCl_3} CH_3CH d(7.2) 1.05 and —OCH_2-CH_2O— m 4.00. The product was characterized as the semicarbazone but the spiro-ketal is also hydrolyzed under these conditions to give: *4-Methylcyclohexa-1,2-dionebis-semicarbazone*, m.p. 251–252°.

Anal. Calcd. for $C_9H_{16}N_6O_2$: C, 45.0; H, 6.7; N, 35.0. Found: C, 44.9; h, 6.8; N, 34.3.

3-Propargyl-5-methylcyclohexa-1,2-dione-1-ethylene-ketal (28f)

The hydroxymethylene **28***d* is prepared as described above (for **28***c*) in 81% yield. The product is normally used directly for the alkylation but a redistilled portion (b.p. 72–74° at 0.15 mm) was characterized: n_D^{27} 1.5095; λ_{max} 282 (8200) nm; ν_{1720}, 1660 and 1595 cm^{-1}; δ_{CDCl_3} CH_3CH d(7.2) 1.07, —OCH_2CH_2O— m 4.13, =CH—OH s 7.31 and s 8.92.

The crude hydroxymethylene **28***d* (46.4 g) is propargylated (as described for **28***c*) affording the alkylated product **28***f* (31.4 g, 76%) by distillation b.p. 85–86° at 0.13 mm, n_D^{24} 1.4879. Cooling affords a solid which is recrystallized from hexane with difficulty, m.p. 42–43°; ν_{KBr} 3300, 2130, 1735, 1200, and 1040 cm^{-1}; δ_{CDCl_3} CH_3CH d(7.2) 1.03, —OCH_2CH_2O— s 3.98.

3-Acetonyl-5-methylcyclohexa-1,2-dione-1-ethylene-ketal (28h)

The propargyl derivative **28***f* (5.2 g) is hydrated as described above for **23***a*. The reaction mixture is poured into ice – 2% sulfuric acid and extracted immediately. The crude product is chromatographed over alumina III to give the acetonyl compound **28***h* (5.2 g, 92%), m.p. 73–74°; ν_{KBr} 1735 (ketone adjacent to ketal), 1720, 1200, 1030 cm^{-1}; δ_{CDCl_3} CH_3CH d(7.2) 1.03, CH_3CO s 2.16, —OCH_2CH_2O— m 3.97.

Anal. Calcd. for $C_{12}H_{18}O_4$: C, 63.7; H, 8.0. Found: C, 63.9; H, 8.1.

6-Methylhydrind-3(9)-en-2,4-dione-4-ethyleneketal (29)

The diketo-ketal **28***h* (8.8 g) in *t*-butyl alcohol (50 ml) is added at room temperature to the solution resulting from dissolving potassium (1.72 g) in *t*-butyl alcohol (75 ml). After stirring for 1 h the reaction mixture is poured into ice water and extracted in the usual manner affording neutral (7.7 g) and acidic products (1.1 g). Chromatography of the former affords the pure enone **29** (4.3 g, 53%), m.p. 53–55°; λ_{max} 234 (13 200) nm; ν_{KBr} 1705, 1630, 1180, 1040 cm^{-1}; δ_{CCl_4} CH_3CH d(7.2) 1.06, —OCH_2CH_2O— s 3.92 and =CH— s 5.75. *Semicarbazone*, m.p. 207–208° (dec.).

Anal. Calcd. for $C_{13}H_{19}N_3O_3$: C, 58.8; H, 7.2; N, 15.8. Found: C, 58.7; H, 7.2; N, 15.9.

Hydrolysis of the ketal was tried using hydrochloric acid in tetrahydrofuran, a trace of perchloric acid in the same solvent, magnesium sulfate in benzene–water, and exchange with acetone catalyzed by *p*-toluene sulfonic acid. The last method afforded starting material and other methods gave no tractable products. Dilute aqueous hydrochloric acid gave the diketo-ketal **28***h* in almost quantitative yield (by hydration and retroaldolization presumably).

3-Allyl-5-methylcyclohexa-1,2-dione-1-ethyleneketal (28i)

The hydroxymethylene **28***d* (9.9 g) is alkylated with allyl bromide (7.5 g) in *t*-butyl alcohol containing potassium *t*-butoxide (as described in the propargylation to give **23***a*). The alkyl-ketone **28***i* (4.9 g, 47%) is obtained

by distillation, 72–76° at 0.04 mm; n_D^{23} 1.4790; ν_{film} 3080, 1645, 895 (=CH_2) and 1735, 1200, 1040 cm^{-1}; δ_{CCl_4} CH_3CH d(7.2) 1.00, —OCH_2CH_2O— m 3.98, CH_2=CH— complex 4.9 to 6.0.

This same compound resulted by hydrogenation of the propargyl derivative **28***f* (5.63 g) in acetone (50 ml) over Lindlar catalyst (800 mg) in the presence of quinoline (100 mg). Distillation gave the allyl compound **28***i* (5.01 g, 88%).

*3(2-Hydroxy-n-propyl)5-methyl-2-hydroxycyclohexanoneethyleneketal (**30**)*

Mercuric acetate (5.35 g) in water (17 ml) is diluted with tetrahydrofuran (17 ml). The allyl ketone **28***i* (3.5 g) is added and the coloration disappears in 15 s. After 5 min stirring, a solution (17 ml) of 0.5 *M* sodium borohydride in 3 *M* aqueous sodium hydroxide is added. The mixture is saturated with sodium chloride and benzene extracted. Evaporation affords the solid diol **30** (3.92 g, 93%), m.p. 131–132° (from acetone – petroleum ether); ν_{KBr} 3340, 1170, 1045 cm^{-1}; ν_{CCl_4} CH_3CH d(7.2) 0.93, CH_3CHOH— d(7.3) 1.24 and s 3.27, —CHOH— s 3.43, O*H* (2H) s 3.12 disappears on adding D_2O), OCH_2CH_2O m 4.10.

Anal. Calcd. for $C_{12}H_{22}O_4$: C, 62.6; H, 9.6. Found: C, 62.4; H, 9.5.

Sodium borohydride reduction of the diketone **28***h* affords this same diol **30** in 98% yield.

*Oxidation of Diol **30***

The ketal-diol **30** (10.7 g) dissolved in pyridine (100 ml) is oxidized with chromium trioxide (18.8 g) in pyridine (200 ml). The mixture is allowed to stand for 24 h and the dione **28***h* (8.4 g, 79%) isolated in the normal manner (identical with **28***h* prepared earlier).

We acknowledge financial support from the National Research Council of Canada and from the Commission de la Recherche Scientifique, Gouvernement du Québec.

1. J. A. Adamcik and R. J. Flores. J. Org. Chem. **29**, 572 (1964).
2. P. T. Lansbury, E. J. Nienhouse, D. J. Scharf, and F. R. Hilfikev. J. Am. Chem. Soc. **92**, 5649 (1970).
3. J. E. Horan and R. W. Schiessler. Org. Synth. **41**, 53 (1961). R. A. Benkeser, R. K. Agnihotri, M. L. Burrous, E. M. Kaiser, J. M. Mallan, and P. W. Ryan. J. Org. Chem. **29**, 1313 (1964).
4. A. M. Islam and R. A. Raphael. J. Chem. Soc. 4086 (1952).
5. J. Hooz and R. B. Layton. Can. J. Chem. **48**, 1626 (1970).
6. I. N. Nazarov and S. I. Zav'Yalov. Zhur. Obskchei. Kim. **24**, 469 (1954); Chem. Abs. **49**, 6142 (1955).
7. K. W. Rosenmund and H. Bach. Ber. **94**, 2393 (1961).
8. M. S. Newman. J. Am. Chem. Soc. **75**, 4730 (1953).
9. H. J. Schaeffer and R. Vince. J. Org. Chem. **27**, 4502 (1962). L. Jurd and B. J. Bergot. Tetrahedron, **21**, 3699 (1965).
10. A. P. Krapcho, J. Diamanti, C. Cayen, and R. Bingham. Org. Synth. **47**, 20 (1967).
11. G. B. Kauffman and L. A. Teter. Inorg. Synth. **7**, 9 (1963).
12. G. Lardelli, V. Lamberti, W. T. Weller, and A. P. De Jonge. Rec. Trav. Chim. **86**, 481 (1967).
13. R. H. Jaeger and H. Smith. J. Chem. Soc. 160 (1955).

Can. J. Chem. Downloaded from www.nrcresearchpress.com by 210.87.254.6 on 09/05/12
For personal use only.

Structure of Nickel Orthophosphate

CRISPIN CALVO AND ROMOLO FAGGIANI

Institute for Materials Research, McMaster University, Hamilton, Ontario L8S 4M1

Received October 18, 1974

CRISPIN CALVO and ROMOLO FAGGIANI. Can. J. Chem. **53**, 1516 (1975).

$Ni_3P_2O_8$ crystallizes in the monoclinic system with space group $P2_1/c$ with $a = 5.830(2)$, $b = 4.700(2)$, $c = 10.107(4)$ Å, $\beta = 91.22(2)°$, and $Z = 2$. The structure was refined by full-matrix least squares methods to a final R value of 0.035 using 986 symmetry independent reflections. The structure is isotypic with that of sarcopside, which in turn is related to that of olivine with vacant cation sites ordered. The Ni ions are octahedrally coordinated in two types of sites with average Ni—O bond lengths of 2.081 and 2.067 Å. The mean P—O bond length is 1.547 Å although the tetrahedron shows some unusually large distortions with bond lengths ranging from 1.521 to 1.595 Å.

CRISPIN CALVO et ROMOLO FAGGIANI. Can. J. Chem. **53**, 1516 (1975).

Le $Ni_3P_2O_8$ cristallise dans le système monoclinique avec un groupe d'espace $P2_1/c$ avec $a = 5.830(2)$, $b = 4.700(2)$, $c = 10.107(4)$ Å, $\beta = 91.22(2)°$ et $Z = 2$. On a affiné la structure par la méthode des moindres carrés (matrice complète) jusqu'à une valeur finale de R de 0.035 utilisant 986 réflexions non-équivalentes. La structure est isostructurale avec celle de la sarcopside qui est à son tour reliée à celle de l'olivine avec des sites cationiques vacants ordonnés. Les ions Ni sont coordonnés d'une façon tétraédrique dans deux types de site avec des longueurs de liaison moyenne Ni—O de 2.081 et de 2.067 Å. La longueur moyenne de la liaison P—O est 1.547 Å même si le tétraèdre montre des distorsions particulièrement grandes alors que les longueurs de liaison s'étalent entre 1.521 et 1.595 Å. [Traduit par le journal]

Introduction

A large number of distinct structural types are known for compounds represented as $M_3P_2O_8$. Amongst these only the sarcopside structure (1) is based upon a close-packed array of oxygen atoms. This structure is in fact olivinelike (2) with vacant cation site ordered and results in a change from an orthorhombic to a monoclinic cell. Joubert *et al.* (3) have shown that a metastable sarcopsidelike structure can be formed by the reaction of olivinelike $Li_2M_2P_2O_8$ plus MSO_4, with M = Mg or Co at reaction temperatures of 660 and 680 °C respectively. Approximate atomic positions, obtained from a powder pattern, are available for these forms of $Mg_3P_2O_8$ and $Co_3P_2O_8$ (3). These compounds transform to the stable "γ" $Zn_3P_2O_8$ structure type (4) at 820 and 870 °C for M = Mg and Co respectively (3). The structure of this form of $Mg_3P_2O_8$ was refined from single crystal data (5) while that of $Co_3P_2O_8$ was refined from powder data (6). The cation coordination numbers in this structure are six for the site at the center of symmetry and four or five for the cation site in the general position, depending upon the specific cation.

Moore (1) has refined the structure of sarcopside, whose composition was $(Fe_{0.78}Mn_{0.21}Mg_{0.01})_3P_2O_8$, but no attempt was made to investigate the cationic partitioning. In nature sarcopside does not occur as a primary phase but is found with graftonite or triphylite (7). The stabilization of graftonite has been attributed to cations of large radii (8) although as with the γ-$Zn_3P_2O_8$ structural type the cationic coordination numbers are variable. It is possible that ions of small radii play a role in stabilizing the sarcopside structure. However, $Fe_3P_2O_8$ has been prepared isotypic with both graftonite (9–11) and sarcopside (10). One form of $Mn_3P_2O_8$ is isotypic with graftonite and the other is not sarcopsidelike (12). Moore has suggested that sarcopside might be an exsolution from triphylite, which has the olivine structure, following a reaction formally much like that proposed by Joubert *et al.* (3). *A priori* ionic radii considerations suggest that $Ni_3P_2O_8$ should behave like $Co_3P_2O_8$ and therefore the fact that the sarcopside structure is the stable form of $Ni_3P_2O_8$ is curious.

Experimental

Crystals were grown from a stoichiometric mixture of NiO_2 and P_2O_5 in a platinum crucible heated in an induction furnace. The melt was cooled slowly across the solidification temperature (1350 °C (13)). Crystals whose size were a few millimeters across were obtained.

Can. J. Chem. Downloaded from www.nrcresearchpress.com by 210.87.254.5 on 09/05/12
For personal use only.

Can. J. Chem. Downloaded from www.nrcresearchpress.com by 210.87.254.5 on 09/05/12
For personal use only.

One of these crystals, ground to a sphere with 0.15 mm as its diameter, was used to collect the X-ray data. Accurate parameters were derived by a least squares fit to the 2θ values of 15 high angle reflections measured with a Syntex PĪ diffractometer, using graphite monochromatized MoK$_\alpha$ (λ_α = 0.71069 Å) radiation. The crystal data, measured at 21 °C, are as follows:

$Ni_3P_2O_8$ f.w. = 365.88

monoclinic, a = 5.830(2), b = 4.700(2), c = 10.107(4) Å, β = 90.22(2)°, V = 276.9 Å^3, Z = 2, ρ_m = 4.38 g/cm^3, ρ_x = 4.38 g/cm^3, space group $P2_1/c$.

The intensities of 1398 reflections within a quadrant up to 2θ = 65° were measured. Reflections were scanned at a rate dependent upon the peak intensity. A total of 986 were symmetry independent and of positive measure after correcting for background. The background was the average of the values measured at either side and one degree removed, in 2θ, from the peak. Reflections whose intensity measure were greater than 3σ, with σ determined from the counting statistics, were considered observed. Absorption corrections were made.

The structure was refined using the positional coordinates of the atoms reported for sarcopside (1), with the unit cell converted to the present designation. A parameter correcting for secondary extinction was varied. Atomic scattering factors, dispersion corrected, were obtained from Cromer and Waber (14) and Cromer (15). The structure was refined by full-matrix least squares refinement, using a program[1] where weights were chosen as

$$\omega = [0.435 + 0.0093F_o + 0.00085F_o^2]^{-1}$$

At convergence, when all the calculated shifts were less than $\frac{1}{3}$ of the standard errors, R = 0.035 and $R_\omega = \{(\Sigma\omega|F_o - F_c|^2)/\Sigma\omega F_o^2\}^{1/2}$ was 0.047. The final structural parameters are in Table 1. The observed and calculated structure factors have been placed in the Depository of Unpublished Data.[2]

Description of the Structure

The structure of $Ni_3P_2O_8$ consists of hexagonally close packed layers of oxygen atoms along (100). The cations are in two types of octahedrally coordinated sites and the phosphorus atom in tetrahedral interstices (Fig. 1). The mean NiO bond length for the cation on the center of symmetry is 2.081 Å and the Ni(2)—O bond lengths average to 2.067 Å. Similarly in sarcopside (1) the average M—O bond length for the cation at the center of symmetry is the larger. Individual bond lengths and angles are in Table 2.

Both NiO_6 octohedra are distorted significantly with edges shared with the PO_4 group, O(2)—O(4) for Ni(1) and O(3)—O(4) for Ni(2),

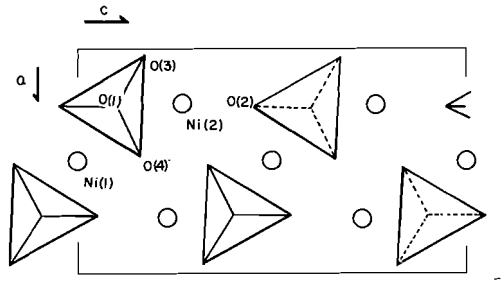

FIG. 1. The (010) projection of sarcopside. The PO_4 tetrahedra are indicated and the Ni(1) and Ni(2) sites are shown as circles.

contracted so as to subtend angles of 71.8 and 69.1° at Ni(1) and Ni(2) respectively. The Ni(1)O_6 group share O(1)—O(4) edges with two Ni(2)O_6 groups. In addition O(2) is shared between Ni(2) and the Ni(1)O_6 group generated by the glide plane. In turn the Ni(2)O_6 group shares four oxygen atoms, two of each of type O(3) and O(4), one each with four Ni(2)O_6 related to each other by $\pm a$, $\pm b$ (Fig. 2).

The average P—O bond length is 1.547 Å, a value higher than the grand mean reported by Baur (16). As in sarcopside, the overbonded O(3) shows the longest bond in the tetrahedron and P—O(1) the shortest. The edges shared with the NiO_6 are substantially contracted below the ideal tetrahedral value.

Discussion

The present structure poses a number of problems. One concerns the stability of the sarcopside structure relative to an olivinelike structure with disordered cation vacancies. Further, the stability of a sarcopside form of $Ni_3P_2O_8$ con-

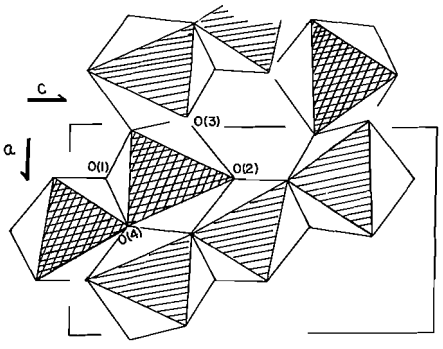

FIG. 2. The edge shared octahedral sites of sarcopside. Oxygen atoms lie at the corners of the octahedra. The ruled octahedra are filled with cations. Those octahedra with cross hatching contain cations at or near y = 0 and the remainder lie at or near $y = \frac{1}{2}$.

[1]Program was written by J. S. Stephen.

[2]Complete set of tabular data is available, at a nominal charge, from the Depository of Unpublished Data, CISTI, National Research Council of Canada, Ottawa, Canada K1A 0S2.

Can. J. Chem. Downloaded from www.nrcresearchpress.com by 210.87.254.5 on 09/05/12
For personal use only.

TABLE 1. Atomic parameters for $Ni_3P_2O_8$ with estimated standard deviations in parentheses*

Atom	x	y	z	U_{11} (Å^2)	U_{22} (Å^2)	U_{33} (Å^2)	U_{12} (Å^2)	U_{13} (Å^2)	U_{23} (Å^2)
Ni(1)	$\frac{1}{2}$	0	0	0.0082(3)	0.0048(3)	0.0065(3)	0.0007(2)	0.0007(2)	−0.0003(2)
Ni(2)	0.24174(7)	−0.01420(8)	0.27437(4)	0.0066(2)	0.0051(2)	0.0061(2)	0.0001(1)	−0.0003(1)	0.0002(1)
P	0.25138(12)	0.42209(16)	0.09485(7)	0.0068(3)	0.0039(3)	0.0055(3)	0.0002(2)	0.0000(2)	0.0003(2)
O(1)	0.2671(4)	0.7447(5)	0.1018(2)	0.0113(9)	0.0053(9)	0.0089(9)	0.0005(7)	0.0017(7)	−0.0007(7)
O(2)	0.2567(4)	0.1918(5)	0.4575(2)	0.0127(9)	0.0076(9)	0.0063(8)	−0.0009(7)	−0.0004(7)	−0.0003(7)
O(3)	0.0507(4)	0.2993(5)	0.1732(2)	0.0094(9)	0.0097(9)	0.0103(9)	0.0004(7)	0.0023(7)	0.0013(7)
O(4)	0.4666(4)	0.2650(5)	0.1619(2)	0.0076(8)	0.0069(0)	0.00971(9)	0.0001(7)	−0.0026(6)	0.0014(7)

*The U_{ij} appear in the structure factor expression as $T = \exp[-2\pi^2(h^2b_1^2U_{11} + \ldots + 2hkb_1b_2U_{12} + \ldots)]$ and the b_i's are reciprocal lattice vectors.

TABLE 2. Bond lengths and angles in $Ni_3P_2O_8$*

Bond	Distance (Å)	Bonds	Angle (deg)	Bonds	Angle (deg)
Ni(1)—O(1)	2.098(2) 2×	O(1)—Ni(1)—O(2)*a*	86.2(2)		
—O(2)*a*	2.076(2) 2×	—O(4)	96.7(2)		
—O(4)	2.069(2) 2×	O(2)*a*—Ni(1)—O(4)	71.8(2)		
Ni(2)—O(1)	2.088(2)	O(1)—Ni(2)—O(2)	172.0(1)	O(2)—Ni(2)—O(3)	96.2(2)
—O(2)	2.044(2)	—O(3)	91.2(1)	—O(3)*b*	89.7(2)
—O(3)	2.099(2)	—O(3)*b*	93.4(2)	—O(4)	99.1(2)
—O(3)*b*	1.999(2)	—O(4)	80.6(1)	—O(4)	86.8(2)
—O(4)	2.190(2)	—O(4)*b*	85.2(1)	O(3)—Ni(2)—O(3)*b*	89.4(2)
—O(4)*b*	2.083(2)	O(3)*b*—Ni(2)—O(4)	157.5(2)	—O(4)	69.1(1)
		—O(4)*b*	113.3(2)	—O(4)*b*	157.2(1)
		O(4)—Ni(2)—O(4)*b*	88.0(2)		
P—O(1)	1.521(2)	O(1)—P—O(2)*a*	112.8(1)	O(2)*a*—P—O(3)	112.5(1)
—O(2)*a*	1.536(2)	—O(3)	113.4(1)	—O(4)	101.8(1)
—O(3)	1.538(2)	—O(4)	113.3(1)	O(3)—O(4)	102.0(1)
—O(4)	1.595(2)				

*Symmetry transformations: $a = x, \frac{1}{2} - y, \frac{1}{2} + z$, $b = -x, \frac{1}{2} + y, \frac{1}{2} - z$.

TABLE 3. Unit cell data on structures isotypic with sarcopside

Compound	*a* (Å)	*b* (Å)	*c* (Å)	β (deg)
$Ni_3P_2O_8$	5.830	4.700	10.107	91.22
Sarcopside*	6.026	4.768	10.437	90.0
$(Fe, Zn)_3P_2O_8$†	6.006	4.771	10.404	91.07
$Mg_3P_2O_8$‡	5.911	4.734	10.214	91
$Co_3P_2O_8$	5.92	4.75	10.334	91.04

*Reference 1.
†Reference 17.
‡Reference 3.

trasted with the metastability of analogous forms of $Mg_3P_2O_8$ and $Co_3P_2O_8$ is unexpected. Finally it should be possible to relate the deviation of the β from 90° in sarcopside to the composition.

Olivine, A_2BO_4, is a structure based upon an hexagonal closest packing of oxygen atoms with each oxygen atom bonded to one B and three A type cations. The structure is orthorhombic with B tetrahedrally coordinated to oxygen atoms and lying on a crystallographic mirror plane. The 2(*a*) type sites, corresponding to the centers of symmetries at 0,0,0 and $0,\frac{1}{2},\frac{1}{2}$ of the sarcopside cell are filled with A type cations in the olivine structure. A disordered olivine structure for $Ni_3P_2O_8$ would lead to variations in P—O bond lengths of 0.06 Å (1.595–1.53 Å) since the cationic site vacancies would lead to oxygen atoms with 2 or 3 neighbors. Such disorder should be unlikely if an alternate structure is available. However, in $Co_3V_2O_8$ a spinel structure with disordered vacancy has been found (3) although V—O bond length variations up to 0.11 Å are expected (17).

At present those subtle contributions to the free energy which stabilize the sarcopside form of $Ni_3P_2O_8$ rather than the γ-$Zn_3P_2O_8$ form characteristic of $Co_3P_2O_8$ and $Mg_3P_2O_8$ are unknown. Accurate calculated structural energies and refinement of the metastable forms of the latter might provide some clues however.

The variation of the β angle seems to be related to the size and shape of the octahedral hole available for M(2). As seen in Fig. 2 this structure contains rows of MO_6 groups running along $(10\bar{1})$ and alternately at levels of $y = 0$ and $\frac{1}{2}$. Every 4th octahedral site in a row is unfilled. In olivine the additional cations lie adjacent to these empty sites and they share oxygen atoms with six separate rows. Thus in sarcopside this source of lateral stability is lost and adjacent rows slide relative to each other as the phosphate groups rotate. These rotations distort the octahedral site particularly through O(3) and O(4). This distortion should be largest for the smaller cation, a trend qualitatively in agreement with the results

Can. J. Chem. Downloaded from www.nrcresearchpress.com by 210.87.254.5 on 09/05/12
For personal use only.

shown in Table 3. The cationic distribution in $(Fe, Zn)_3P_2O_8$ (18) would be of interest with regards to this question.

The long P—O(4) bond is not explained by either the Baur relationship (16) between bond length and Pauling bond strength at the oxygen atoms nor by the Brown and Shannon bond strength sums (19). The former would suggest a P—O(4) bond length that is too short by 0.03 Å and the latter that one or more of the bonds to O(4) are too short. The O(3)—O(4) and O(2)—O(4) edges are shared with Ni(2) and Ni(1) respectively and the angles subtended by these edges at the phosphorus atom are near 102°. This would suggest that the O—O repulsion might be in part responsible for the weakening of this P—O(4) bond.

This research was supported with a grant from the National Research Council of Canada.

1. P. B. MOORE. Am. Miner. **57**, 24 (1972).
2. L. W. FINGERS. Am. Cryst. Assoc. Summer Meeting, Carleton University, Ottawa, Canada. 1970. p. 66.
3. J. C. JOUBERT, G. BERTHET, and E. F. BERTAUT. Z. Kristallogr. **136**, 98 (1972).
4. C. CALVO. J. Phys. Chem. Solids, **24**, 141 (1963).
5. A. G. NORD and P. KIERKEGAARD. Acta Chem. Scand. **22**, 1466 (1968).
6. A. G. NORD. Acta Chem. Scand. Ser. A, **28**, 164 (1974).
7. C. S. HURLBUT, JR. Am. Miner. **50**, 1698 (1967).
8. C. CALVO. Am. Miner. **53**, 742 (1968).
9. J. KORINTH and P. ROYEN. Z. Anorg. Allg. Chem. **313**, 121 (1961).
10. P. B. MOORE. Private communication.
11. E. KOSTINER and J. REA. Inorg. Chem. **13**, 2876 (1974).
12. J. S. STEPHENS. Ph.D. Thesis. McMaster University, Hamilton, Ontario. 1967.
13. J. F. SARVER. Trans. Brit. Ceram. Soc. **65**, 191 (1966).
14. D. T. CROMER and J. T. WABER. Acta Cryst. **18**, 104 (1965).
15. D. T. CROMER. Acta Cryst. **18**, 17 (1965).
16. W. H. BAUR. Acta Cryst. B**30**, 1195 (1974).
17. E. E. SAUERBREI, R. FAGGIANI, and C. CALVO. Acta Cryst. B**29**, 2304 (1973).
18. YU. K. KABALOV, M. A. SIMONOV, and O. V. YAKUBOVICK. Dokl. Acak. Nauk. SSSR, **210**, 830 (1973).
19. I. D. BROWN and R. D. SHANNON. Acta Cryst. A**29**, 266 (1973).

Can. J. Chem. Downloaded from www.nrcresearchpress.com by 210.87.254.5 on 09/05/12
For personal use only.

Radiolysis of Liquid Nitrous Oxide: Alcohol and Carbonyl Additives[1]

TERANCE E. M. SAMBROOK AND GORDON R. FREEMAN
Chemistry Department, University of Alberta, Edmonton, Alberta T6G 2E1
Received November 22, 1974

TERANCE E. M. SAMBROOK and GORDON R. FREEMAN. Can. J. Chem. **53**, 1521 (1975).

Methanol, ethanol, acetaldehyde, and acetone were added separately over wide concentration ranges to liquid nitrous oxide at 183 K. The oxygen and nitrogen dioxide yields were reduced from their G values of 2.7 and 5.6, respectively, to 0 by <8 mol% organic solute. The nitrogen yield decreased from 13.1 to about 11 over the same concentration region, but continued to decrease as the nitrous oxide was progressively diluted by the solute. The results are consistent with the previous mechanism II. The nitrogen yields from dilute solutions of nitrous oxide in the carbonyl compounds are smaller than those from similar solutions in the alcohols. The smaller yields are attributed to electron scavenging by the carbonyl compounds in competition with the nitrous oxide.

TERANCE E. M. SAMBROOK et GORDON R. FREEMAN. Can. J. Chem. **53**, 1521 (1975).

Du méthanol, de l'éthanol, de l'aldéhyde acétique et de l'acétone furent ajoutés tour à tour, à des concentrations très différentes à l'oxyde azoteux liquide à 183 K. Les rendements en oxygène et en bioxyde d'azote sont réduits de leur valeur initiale, de 2.7 et 5.6 respectivement, à 0 par une quantité inférieure à 8 mol% en soluté organique. Le rendement en azote décroit de 13.1 à 11 pour le même domaine de concentration et décroit encore au fur et à mesure que l'oxyde azoteux est dilué par le soluté. Les résultats sont en accord avec le mécanisme II précédent. Les rendements d'azote, pour les solutions diluées en oxyde azoteux, dans les composés carbonyles, sont inférieurs aux rendements dans les alcools. Ces rendements inférieurs sont attribués à la capture des électrons par les composés carbonyles en compétition avec l'oxyde azoteux.

Introduction

The present article is a continuation of a study of the radiolysis of liquid nitrous oxide (1, 2). The purpose is twofold: (*i*) to increase the small amount of information available about the radiolysis of inorganic liquids; (*ii*) to help elucidate the radiolysis mechanisms in organic liquids to which nitrous oxide has been added as an electron scavenger.

Experimental

The methods of sample preparation, irradiation, and analysis were the same as those reported earlier (1, 2).

Anhydrous ethanol (U.S. Industrial Chemicals Co.) and spectral grade acetone (Baker Chemical Co.) were used as supplied. Acetaldehyde obtained from Fisher Scientific Co. was vacuum distilled before use and the middle fraction retained. Methanol supplied by Baker Chemical Co. was refluxed with 1.5 g of 2,4-dinitrophenylhydrazine and 1 ml of concentrated sulfuric acid per litre of methanol, and then distilled.

The irradiation dose rate, using appropriate corrections for the electron densities, was 3×10^{17} eV/(g min) and the dose was 3×10^{18} eV/g. The irradiation temperature was 183 K, maintained with a methanol slush bath.

[1]Assisted by the National Research Council of Canada.

Results

Nitrogen Yields

Values of $G(N_2)$ are plotted against the electron fraction ε_s of organic solutes in Figs. 1 and 2. The presence of an alcohol or carbonyl compound decreases the nitrogen yield from the radiolysis of nitrous oxide. In the absence of additive $G(N_2) = 13.1$. Each yield curve contains an inflection (Figs. 1 and 2), which indicates a change of reaction mechanism.

Yields of Oxygen and Nitrogen Dioxide

The addition of <8 mol% of an alcohol or carbonyl compound reduces the yields of oxygen and nitrogen dioxide to 0 (Fig. 3). The relative rate of reduction of the latter is about double that of the former.

Products from the Organic Liquids

The yields of gaseous products from the organic liquids at 183 K are listed in Table 1. The hydrogen yields from the methanol and ethanol are somewhat lower than those reported earlier for similar temperatures and doses (3, 4). One can deduce from the earlier work that the present alcohols contained $\sim 10^{-5}$ M of an

Can. J. Chem. Downloaded from www.nrcresearchpress.com by 210.87.254.105 on 09/05/12
For personal use only.

Can. J. Chem. Downloaded from www.nrcresearchpress.com by 210.87.254.105 on 09/05/12
For personal use only.

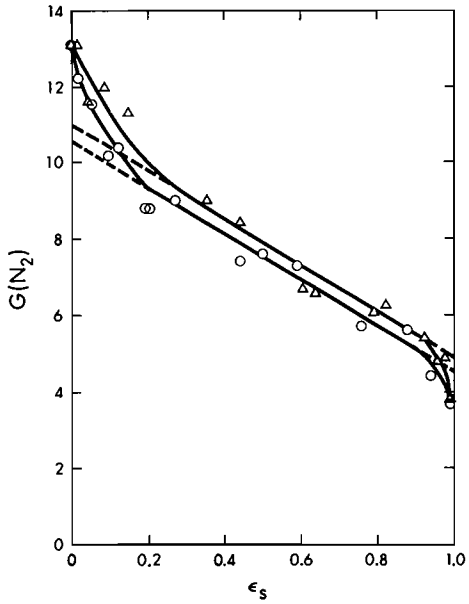

FIG. 1. $G(N_2)$ from liquid nitrous oxide, as a function of alcohol concentration. ε_s = electron fraction of solute. ○, methanol; △, ethanol.

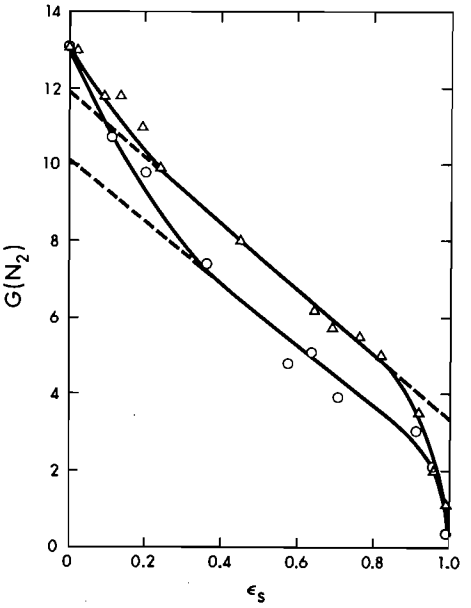

FIG. 2. $G(N_2)$ from liquid nitrous oxide as a function of carbonyl compound concentration. ε_s = electron fraction of solute. ○, acetaldehyde; △, acetone.

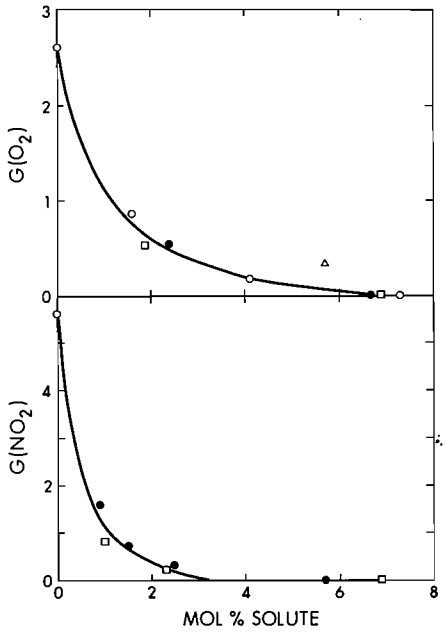

FIG. 3. Yields of oxygen and nitrogen dioxide from nitrous oxide. Solute: ●, methanol; ○, ethanol; △, acetaldehyde; □, acetone.

TABLE 1. Gaseous product yields from the organic liquids at 183 K

Liquid	$G(H_2)$	$G(CH_4)$	$G(CO)$
CH_3OH	4.0	—	—
C_2H_5OH	4.8	—	—
CH_3CHO	1.3	1.0	1.4
CH_3COCH_3	0.9	0.7	—

electron scavenging impurity. This small quantity of impurity would not affect the nitrous oxide results.

Addition of nitrous oxide to the alcohols decreased the hydrogen yields in the manner reported earlier (3, 4).

The formation of hydrogen, methane, and carbon monoxide from acetaldehyde and acetone were unaffected by the addition of nitrous oxide. This was demonstrated (5) by basing the hydrogen, etc., yields solely upon the energy initially absorbed by the carbonyl compound, *e.g.*,

$$[1] \qquad g(H_2) = G(H_2)/\varepsilon_{carb}$$

where ε_{carb} is the electron fraction of carbonyl compound in the solution. It was found that $g(H_2)$, $g(CH_4)$, and $g(CO)$ were independent of

Can. J. Chem. Downloaded from www.nrcresearchpress.com by 210.87.254.105 on 09/05/12
For personal use only.

nitrous oxide concentration up to 40 mol%, within experimental error (±0.1 units).

Discussion

Nitrogen Yields

A plot of $G(N_2)$ against ε_s has an approximately linear central portion (2). Extrapolation of this portion to the left axis gives the yield of nitrogen from the direct radiolysis of nitrous oxide that cannot be reduced by the solute. The phenomenological name given to this yield was the "plateau" value $g(N_2)^{plat}_{N_2O}$ (2). Extrapolation of the linear portion of the plot to the right axis gives $g(N_2)_s$, the yield of nitrogen obtained from the reaction of nitrous oxide with electrons generated by radiolysis of the solute (2).

Values of these quantities obtained from Figs. 1 and 2 are listed in Table 2. The solutes methanol, ethanol, and acetaldehyde gave $g(N_2)^{plat}_{N_2O} = 10.6 \pm 0.5$, the same as the value obtained with many hydrocarbons (2).

The results are compatible with the earlier mechanism II (2).

Addition of an organic solute RH apparently reduces the nitrogen yield by way of [2] (2)

[2] $$N_2O^+ + RH \rightarrow N_2O + RH^+$$

The ionization potentials of the organic solutes (6 ,7) are lower than that of nitrous oxide (Table 2), so the charge transfer [2] is exothermic. The fact that 20–30% of organic solute is required to reach the linear portions of the curves in Figs. 1 and 2 is consistent with the relative difficulty of scavenging positive charges in spurs (2). The free ion yield is expected to be small because the dielectric constant of the liquid is low (1.97 at 183 K), so [2] would have to occur mainly in the spurs.

The large value of $g(N_2)^{plat}_{N_2O} \geqslant 10$ (Table 2) indicates that the organic oxy compounds do not inhibit the decomposition of N_2O^*.

[3] $$N_2O^* \rightarrow N_2 + O$$

The same behavior was true of hydrocarbon solutes (2).

The value $g(N_2)^{plat}_{N_2O} = 11.9$ obtained with acetone was relatively high (Table 2), and similar to the value 11.6 obtained with propyne and toluene (2). These compounds cause a smaller than normal decrease in nitrogen yield, for reasons unknown.

Oxygen and Nitrogen Dioxide Yields

The variations of the O_2 and NO_2 yields with alcohol or carbonyl compound concentration (Fig. 3) are similar to those obtained with hydrocarbons (2). In particular, the concentration dependences of the yields are nearly the same as those obtained with olefins and the same mechanism (2) appears to apply.

$G(N_2)_s$

Electrons are generated by radiolysis of the solute as well as of the nitrous oxide.

[4] $$RH \rightsquigarrow RH^+ + e^-$$

These electrons can undergo [5], provided that enough nitrous oxide is present. Extrapolation

[5] $$e^- + N_2O \rightarrow N_2O^- \rightarrow N_2 + O^-$$

of the linear portion of the curves in Figs. 1 and 2 to the right axis reveals the maximum yield of nitrogen obtained through electrons generated in [4]. This yield is designated $g(N_2)_s$.

The values $g(N_2)_s = 4.5$ and 4.9 obtained for methanol and ethanol solutes, respectively (Table 2), are similar to the value 4.6 reported earlier for methanol (3) and 5 ± 1 deduced for many saturated and unsaturated hydrocarbons (2).

For the saturated compounds $g(N_2)_s$ appears to be approximately equal to the yield of [4], *i.e.* to the ionization yield in the liquid. However, there is no apparent reason why the ionization yield in acetaldehyde or acetone should be much smaller than those in the alcohols, yet the values of $g(N_2)_s$ for the carbonyl compounds are much lower than those for the alcohols (Table 2). The carbonyl compounds are themselves electron scavengers, so [6] competes with [5] and provides a smaller value of $g(N_2)_s$.

[6] $$R_2CO + e^- \rightarrow R_2CO^-$$

TABLE 2. Values of extrapolated nitrogen yields from nitrous oxide solutions at 183 K, and ionization potentials

Solute	Ionization potential* (eV)	$g(N_2)^{plat}_{N_2O}$†	$g(N_2)_s$‡
CH_3OH	10.85	10.6	4.5
C_2H_5OH	10.48	11.0	4.9
CH_3CHO	10.25	10.1	2.0
CH_3COCH_3	9.75	11.9	3.2

*Gas phase ionization potential, i.p. (N_2O) = 12.89 eV. Refs. 6 and 7.
†Estimated error is ±0.5 units.
‡Estimated error is ±0.3 units.

In the earlier work (2) butadiene-1,3 was the only efficient electron scavenger used as a solute, and it was the only hydrocarbon that gave a low value of $g(N_2)_s$, 1.9. Thus, electron scavenging by the solvent, *e.g.* [6], offers a plausible interpretation of low values of $g(N_2)_s$.

1. T. E. M. SAMBROOK AND G. R. FREEMAN. J. Phys. Chem. **78**, 28 (1974).
2. T. E. M. SAMBROOK and G. R. FREEMAN. J. Phys. Chem. **78**, 32 (1974).
3. K. N. JHA and G. R. FREEMAN. J. Chem. Phys. **48**, 5480 (1968).
4. K. N. JHA and G. R. FREEMAN. J. Chem. Phys. **51**, 2846 (1969).
5. T. E. M. SAMBROOK. Ph.D. Thesis, University of Alberta, Edmonton, Alberta. 1973.
6. R. W. KISER. Introduction to mass spectrometry and its applications. Prentice–Hall, Englewood Cliffs, N.J. 1965.
7. H. HURZELER, M. G. INGRAM, and J. D. MORRISON. J. Chem. Phys. **28**, 76 (1958).

Can. J. Chem. Downloaded from www.nrcresearchpress.com by 210.87.254.105 on 09/05/12
For personal use only.

The Question of σ Participation in the Bonding of Fluorosubstituted Arenes to Chromium Tricarbonyl. A ^{19}F Nuclear Magnetic Resonance Investigation

JOHN L. FLETCHER AND MICHAEL J. MCGLINCHEY

Department of Chemistry, McMaster University, Hamilton, Ontario L8S 4M1

Received October 16, 1974

JOHN L. FLETCHER and MICHAEL J. MCGLINCHEY. Can. J. Chem. 53, 1525 (1975).

^{19}F n.m.r. chemical shifts of free fluoroarenes have been correlated with the Swain–Lupton field and resonance parameters. Comparison of these data with the corresponding $Cr(CO)_3$ complexes shows little change in the transmission of mesomeric effects by *para*-substituents. *Meta*-substituents which interact primarily by a field effect have very little influence on the fluorine chemical shift in the complexes suggesting that the σ framework of the ring interacts with the chromium.

JOHN L. FLETCHER et MICHAEL J. MCGLINCHEY. Can. J. Chem. 53, 1525 (1975).

On a établi une corrélation entre les déplacements chimiques en r.m.n. du ^{19}F de fluoroarènes libres avec les paramètres de résonance et de champ de Swain–Lupton. La comparaison de ces données avec celles des complexes $Cr(CO)_3$ correspondants montre peu de changements dans la transmission des effets mésomériques par les substituants *para*. Les substituants *méta* qui interagissent principalement par un effet de champ ont très peu d'influence sur le déplacement chimique du fluor dans les complexes; ceci suggère que les électrons σ du cycle interagissent avec le chrome. [Traduit par le journal]

Introduction

The bonding of arenes to the chromium tricarbonyl moiety has provoked much speculation over the past few years. There is much compelling evidence from reactivity data (1–7), dipole moment measurements (8), molecular orbital calculations (9), and n.m.r. chemical shifts (10–13) to suggest that the $Cr(CO)_3$ group is strongly electron-withdrawing, perhaps comparable to a *para*-nitro group. On the other hand, the transmission of π-substituent effects in complexed arenes has been shown to be largely unchanged from that in the free arenes (14–17). This apparent dichotomy has only recently been explored by Bodner and Todd (18) who proposed a model in which there is "a net withdrawal of electron density from the σ-framework of the arene ring with little or no concomitant reduction in π-electron density". This prompts us to publish the results of our own investigation into this problem.

It has long been thought that changes in ^{19}F n.m.r. chemical shifts of *para*-substituted fluorobenzenes reflect changes in the π-electron density at the C_4 position (19), and attempts have been made to separate such chemical shift data into inductive and resonance components via empirical correlations with inductive and resonance constants derived from reactivity considerations (20). The original observations of Taft (20) have been extended to include correlations of ^{1}H (21), ^{11}B (21), and ^{13}C (18) n.m.r. shift data with the field and resonance parameters devised by Swain and Lupton (22).

We have now utilized these empirical correlations of ^{19}F n.m.r. chemical shifts of a series of substituted fluorobenzene chromium tricarbonyls with the Swain–Lupton field and resonance parameters to probe the models of ring–metal bonding in arene chromium tricarbonyls.

Experimental

^{19}F nuclear magnetic resonance spectra were recorded on a Varian DP-60 spectrometer and ^{13}C spectra on a Bruker WH-90 spectrometer; mass spectra were recorded on a C.E.C. 21-110-B spectrometer. Infrared spectra were recorded as Nujol mulls.

All complexes were prepared by heating the appropriate fluoroarene under reflux with chromium hexacarbonyl following the procedure of Strohmeier (23) and purified by repeated sublimations.

The complexes were characterized by a combination of infrared, n.m.r., and mass spectrometry together with comparisons of literature melting points where available (1, 11, 23, 24). Relevant data are presented in Tables 1 and 2.

Results and Discussion

^{19}F and ^{13}C Nuclear Magnetic Resonance Data

Swain and Lupton (22) proposed that an empirical relationship exists between ^{19}F n.m.r. chemical shifts in *meta*- or *para*-substituted fluorobenzenes and field and resonance para-

Can. J. Chem. Downloaded from www.nrcresearchpress.com by 210.87.254.105 on 09/05/12
For personal use only.

TABLE 1. Nuclear magnetic resonance and infrared data for *para*-substituted arenes and complexes

Substituent	Δ^{F*} Complex	Δ^{F*} Free	Δ^{C}† Complex	Δ^{C}† Free	$6\%\mathcal{F} + 94\%\mathcal{R}$	ν_{CO}‡ *E*	ν_{CO}‡ *A*
H	135.9	113.1	−93.50	−127.97	0.0	1930	1996
CH_3	137.8	118.8	−90.21	−125.05	−0.136	1921 1926	1980
OCH_3	142.4	124.4	−85.95	−120.22	−0.445	1911	1980
Cl	137.2	116.1	−88.74	−126.02	−0.109	1909 1938	1979
NH_2	146.2	127.1	−83.80	−117.85	−0.638	1909	1980
F	134.0	120.0	−86.97	−123.58	−0.273	1910 1930	1980
CF_3	133.5 60.5	108.3 62.5	−94.34	−131.45	+0.213	1908 1950	1979

*^{19}F chemical shifts of *para*-substituted fluorobenzenes and $Cr(CO)_3$ analogs, measured as 2% solutions in benzene relative to internal $CFCl_3$.
†^{13}C chemical shifts of C_4 in monosubstituted benzenes and $Cr(CO)_3$ analogs; all values taken from ref. 18 except for CF_3 substituent (this work) and measured relative to internal TMS.
‡Carbonyl stretching frequencies (cm^{-1}) for *para*-substituted fluoroarene complexes.

meters and follows an equation of the form

$$[1] \qquad \Delta^F = f\mathcal{F} + r\mathcal{R}$$

where $\mathcal{F}$ and $\mathcal{R}$ are respectively the field and resonance constants characteristic of particular substituents and f and r are weighting factors determined by optimizing the difference between experimental and calculated data using a standard linear regression program to maximize the linear correlation coefficient.

The originally quoted values (22) of f and r for *para*-substituted fluorobenzenes are 35% and 65% respectively, which we calculate to have a low linear correlation coefficient using the substituents H, F, Cl, CH_3, CH_3O, NH_2, and CF_3. We find a better fit (correlation coefficient, $\bar{r}$, of 98.8%) for $f = 9\%$ and $r = 91\%$. Application of the same technique to the ^{19}F n.m.r. chemical shifts of the corresponding *para*-substituted fluorobenzene chromium tricarbonyl complexes

TABLE 2. Nuclear magnetic resonance and infrared data for *meta*-substituted complexes

Substituent	Δ^{F*} complex	ν_{CO}† *E*	ν_{CO}† *A*
H	135.9	1930	1996
CH_3	135.3	1910 1924	1980
OCH_3	136.7	1910	1979
Cl	136.6	1907 1939	1978
NH_2	136.3	1901	1976
F	136.4	1909 1937	1980
CF_3	135.8 62.4	1910 1950	1980

*^{19}F chemical shifts of *meta*-substituted fluorobenzenes and $Cr(CO)_3$ analogs, measured as 2% solutions in benzene relative to internal $CFCl_3$.
†Carbonyl stretching frequencies (cm^{-1}) for *meta*-substituted fluoroarene complexes.

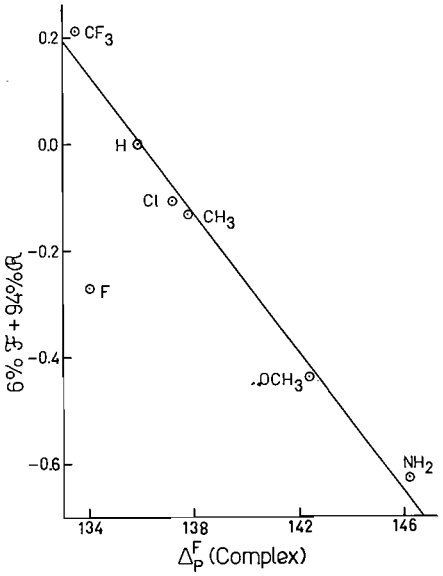

FIG. 1. Plot of ^{19}F chemical shifts of *para*-substituted fluorobenzene chromium tricarbonyls (measured in p.p.m. to high field of $CFCl_3$) against $6\%\mathcal{F} + 94\%\mathcal{R}$.

Can. J. Chem. Downloaded from www.nrcresearchpress.com by 210.87.254.105 on 09/05/12
For personal use only.

Can. J. Chem. Downloaded from www.nrcresearchpress.com by 210.87.254.105 on 09/05/12
For personal use only.

yields f and r values of 6% and 94%, $\bar{r}$ = 99.4% (see Fig. 1). This remarkable constancy of the dominance of the resonance parameter in the transmission of substituent effects is most gratifying especially as a recent ^{13}C n.m.r. study showed exactly comparable behavior (18). The correlation between the ^{19}F chemical shifts in *para*-substituted fluorobenzenes and the ^{13}C chemical shift of the C_4 carbon in the corresponding monosubstituted arenes is well established (25), and this relationship still holds in most cases when the arenes are complexed (see Fig. 2).

In contrast to the *para* isomers, *meta*-substituted fluorobenzenes show a greater than 95% dependence of the ^{19}F chemical shift on $\mathscr{F}$, the field parameter, (or as Taft (20) showed, Δ_m^F is directly proportional to σ_I). Upon complexation, however, a dramatic change occurs in that the ^{19}F chemical shifts of a wide variety of *meta*-substituted fluoroarenes (including ones of vastly differing electronic characteristics, such as CF_3 or NH_2) are almost all the same. The chemical shifts all fall within a narrow range of rather less than 2 p.p.m. (see Table 2), and show no obvious correlation with the electronic properties of the *meta*-substituent, whereas the free arenes cover a range almost five times as large as this (20).

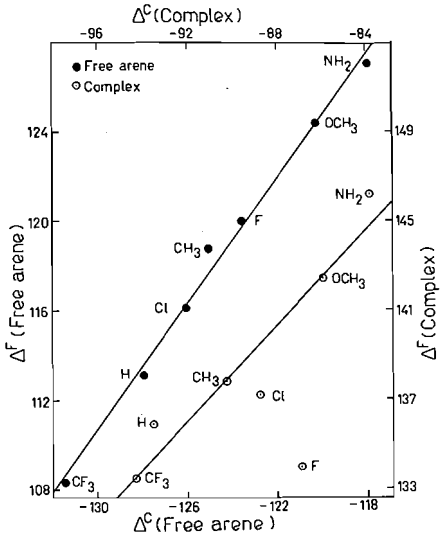

FIG. 2. Plot of ^{13}C chemical shifts of C_4 in monosubstituted benzenes and chromium tricarbonyl analogs against ^{19}F chemical shifts of *para*-substituted fluorobenzenes and tricarbonyl analogs. ^{19}F chemical shifts are in p.p.m. to high field of $CFCl_3$ and ^{13}C chemical shifts are in p.p.m. to low field of TMS.

Thus, the fluorine atom in the complex seems hardly able to distinguish any other *meta*-substituent from hydrogen, and is completely different to the *para* isomers where substituent dependence is very pronounced.

A fundamental change has clearly occurred in the arene ring upon complexation and, making the usual assumptions that mesomeric effects are transmitted predominantly via the π system while inductive effects primarily concern the σ framework, we are left with the following conclusions.

The chemical shifts of the fluorine atoms in the complexes reveal an indifference to the identity of the *meta*-substituent; thus it would seem that since this effect is transmitted almost entirely via the σ system, then the σ system itself must have been drastically modified. Indeed this would suggest participation by the σ framework of the ring in the arene–metal bond formation such as has been suggested by Drago and co-worker (26) from molecular orbital calculations. The observed upfield shift of about 20–25 p.p.m. relative to the uncomplexed arenes has been attributed to a partial sp^2–sp^3 rehybridization (27) which seems reasonable in light of the above evidence.

Since the transmission of substituent effects from the *para* position is scarcely changed upon complexation, and we have further shown this effect to be transmitted predominantly by a resonance effect, then, if this goes entirely via the π system of the ring, the π system must be essentially unperturbed by complexation. Conversely, if one could consider that the chromium atom were involved in the mechanism of transmission of the substituent effect, then it is not necessary to assume that the π-electron density remains unchanged. Furthermore, any modification of the π system would certainly affect the aromatic ring current and work to elucidate this point is currently being undertaken.

So it is clear that, upon complexation, there still remains an effective pathway by which a *para*-substituent can deliver its mesomeric effect while the net withdrawal of electron density from the σ framework seriously curtails the ability of a *meta*-substituent to bring about its inductive effect.

Infrared Data

The infrared spectra of the *meta*- and *para*-substituted fluorobenzene chromium tricarbonyl complexes reveal, as one might have anticipated

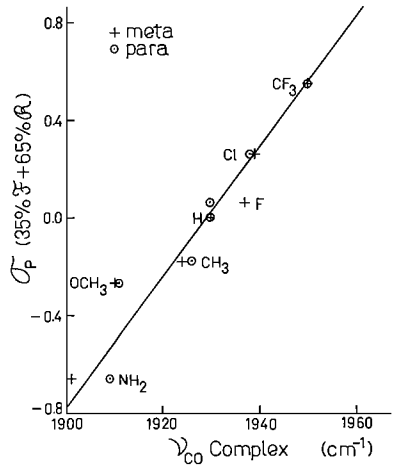

FIG. 3. Plot of carbonyl stretching frequencies (*E* mode) for *meta* and *para*-substituted fluorobenzene chromium tricarbonyls against Hammett's σ_p values (30) or 35%$\mathcal{F}$ + 65%$\mathcal{R}$ (22).

from the work of Brown *et al.* (15–17) and Reeves and co-workers (14), a good correlation between corresponding ν_{CO} stretching vibrations and a measure of the overall electron-accepting or -donating capability of a substituent whether it be *meta* or *para* to the fluorine. Thus a plot of ν_{CO} (*E* mode) against Hammett's σ_p, or against (35%$\mathcal{F}$ + 65%$\mathcal{R}$) using Swain's parameters, shows a linear correlation of 96.3% (see Fig. 3). Furthermore, as previously noted by Brown and co-worker (17), substituent effects are approximately additive, thus a plot of corresponding carbonyl stretching frequencies in the fluorinated and nonfluorinated complexes is linear with a slope very close to unity and an intercept of $\sim$10 cm^{-1}. That is, the additional fluoro substituent raises the carbonyl frequency by an approximately constant amount and is thus behaving as an acceptor of electron density in these systems.

Despite repeated syntheses of the *p*-difluorobenzene chromium tricarbonyl complex, an anomalous ^{19}F chemical shift was obtained (see Figs. 1 and 2) while its infrared and mass spectra were quite normal. The *para*-fluoro substituent would only fall on the line of Fig. 1 if one assumed an ($f\mathcal{F}$ + $r\mathcal{R}$) value of +0.13, *i.e.*, fluoro would need to be a much stronger electron-withdrawing substituent in these systems than implied by both Taft and Swain–Lupton values. As mentioned above, the carbonyl infrared data support the contention of fluorine as a relatively strong electron-withdrawing group in these instances. It is also worth noting that the ^{19}F chemical shift of the *para*-fluoro substituent in the bis(arene)chromium system was anomalously low (28).

The electronic environment in the complexed ring of arene chromium tricarbonyls appears to be considerably different from that in the corresponding bis(arene)chromium complexes. In the latter case there is a marked dependency of fluorine chemical shifts on both *meta*- and *para*-substituents (28) and this is presumably a reflection of the lack of carbonyl groups which act as an electron buffer (29). Thus, in the chromium tricarbonyl complexes an electron-donating substituent makes the ring electron rich and so electron density is siphoned off via the chromium into the π^* orbitals of the carbonyl ligands leading to a decrease in ν_{CO}; vice versa, electron-withdrawing groups produce an increase in ν_{CO}. This self-compensating mechanism is not available in symmetrically substituted bis(arene)-chromium complexes (28) and thus the arene ring itself must accommodate the relative excess or deficit of electron density; this in turn is reflected in the n.m.r. chemical shifts of nuclei such as ^{13}C or ^{19}F in the ring.

Interestingly, in the bis(arene)chromium systems, the ^{19}F n.m.r. spectra of CF_3 groups directly bonded to complexed arene rings exhibit downfield shifts of 4–6 p.p.m. relative to those of the uncomplexed arenes (28). In the $Cr(CO)_3$ analogs[1] this trend is also observed but the downfield shifts are approximately one-third the magnitude (see Tables 1 and 2).

Conclusions

^{19}F n.m.r. studies of *meta*- and *para*-substituted fluoroarene chromium tricarbonyl complexes indicate that transmission of resonance effects within the ring differs little from the free arenes but inductive effects are greatly diminished. This is rationalizable on the basis of withdrawal of σ-electron density from the ring with either little change in π-electron density of the ring or diminution of π-electron density in the ring if one invokes the concept of participation by the chromium atom in transmission of substituent effects between *para* positions.

[1] $(CF_3 \cdot C_6H_5)Cr(CO)_3$ shows ^{19}F absorption at 61.7 p.p.m. and ν_{CO} at 1908, 1940, and 1980 cm^{-1}.

Can. J. Chem. Downloaded from www.nrcresearchpress.com by 210.87.254.105 on 09/05/12
For personal use only.

We thank the National Research Council of Canada and McMaster University Science and Engineering Research Board for financial support, and Mr. J. I. A. Thompson for technical assistance. We also thank Mr. B. G. Sayer and Mr. A. R. Boate for the ^{13}C n.m.r. spectra.

1. B. NICHOLLS and M. C. WHITING. J. Chem. Soc. 551 (1959).
2. M. ASHRAF. Can. J. Chem. **50**, 118 (1972).
3. D. N. KURSANOV, V. N. SETKINA, and B. G. GRIBOV. J. Organomet. Chem. **37**, C35 (1972).
4. E. O. FISCHER, H. ESSLER, W. FROHLICH, J. P. MORTENSEN, and W. SEMMLINGER. Chem. Ber. **91**, 2763 (1958).
5. M. ASHRAF and W. R. JACKSON. J. Chem. Soc. Perkin Trans. **2**, 103 (1972).
6. J. D. HOLMES, D. A. K. JONES, and R. PETTIT. J. Organomet. Chem. **4**, 324 (1965).
7. W. S. TRAHANOVSKY and D. K. WELLS. J. Am. Chem. Soc. **91**, 5870 (1969).
8. E. O. FISCHER and S. SCHREINER. Chem. Ber. **92**, 938 (1959).
9. D. G. CARROLL and S. P. McGLYNN. Inorg. Chem. **7**, 1285 (1968).
10. W. McFARLANE and S. O. GRIM. J. Organomet. Chem. **5**, 147 (1966).
11. H. P. FRITZ and C. G. KREITER. J. Organomet. Chem. **7**, 427 (1967).
12. J. T. PRICE and T. S. SORENSON. Can. J. Chem. **46**, 515 (1968).
13. R. V. EMANUEL and E. W. RANDALL. J. Chem. Soc. A, 3002 (1969).
14. A. WU, E. R. BIEHL, and P. C. REEVES. J. Organomet. Chem. **33**, 53 (1971).
15. D. A. BROWN and H. SLOAN. J. Chem. Soc. 3849 (1962).
16. D. A. BROWN and D. G. CARROLL. J. Chem. Soc. 2822 (1965).
17. D. A. BROWN and J. R. RAJU. J. Chem. Soc. A, 1617 (1966).
18. G. M. BODNER and L. J. TODD. Inorg. Chem. **13**, 360 (1974).
19. J. W. EMSLEY and L. PHILLIPS. Prog. Nucl. Magn. Reson. Spectrosc. **7**, 47 (1971).
20. R. W. TAFT. J. Am. Chem. Soc. **79**, 1045 (1957).
21. A. R. SIEDLE and G. M. BODNER. Inorg. Chem. **11**, 3108 (1972).
22. L. G. SWAIN and E. C. LUPTON, JR. J. Am. Chem. Soc. **90**, 4328 (1968).
23. VON W. STROHMEIER. Z. Naturforsch. **17b**, 627 (1962).
24. G. JAOUEN, L. TCHISSAMBOU, and R. DABARD. C.R. Acad. Sc. Paris, Ser. C, **274**, 654 (1972).
25. E. E. MACIEL and J. J. NATTERSTAD. J. Chem. Phys. **42**, 2427 (1965).
26. S. E. ANDERSON, JR. and R. S. DRAGO. Inorg. Chem. **11**, 1564 (1972).
27. V. S. KHANDKAROVA, S. P. GUBIN, and B. A. KVASOV. J. Organomet. Chem. **23**, 509 (1970).
28. M. J. McGLINCHEY and T.-S. TAN. Can. J. Chem. **52**, 2439 (1974).
29. G. KLOPMAN and K. NOACK. Inorg. Chem. **7**, 579 (1968).
30. L. P. HAMMETT. Chem. Rev. **17**, 125 (1953).

Can. J. Chem. Downloaded from www.nrcresearchpress.com by 210.87.254.105 on 09/05/12
For personal use only.

Five-coordinate Bromobis(dialkyldithiocarbamate) Complexes of Arsenic, Antimony, and Bismuth

GEORGE E. MANOUSSAKIS, CONSTANTINOS A. TSIPIS, AND CHRISTOS C. HADJIKOSTAS
Laboratory of Inorganic Chemistry, University of Thessaloniki, Thessaloniki, Greece
Received October 8, 1974

GEORGE E. MANOUSSAKIS, CONSTANTINOS A. TSIPIS, and CHRISTOS C. HADJIKOSTAS. Can. J. Chem. **53**, 1530 (1975).

Fifteen bromobis(dialkyldithiocarbamate) complexes of arsenic, antimony, and bismuth have been prepared by reacting the corresponding tris(dialkyldithiocarbamates) with bromine. The structure of these compounds is studied by i.r., n.m.r., and electronic spectra. From the interpretation of the spectroscopic data it is deduced that each dithiocarbamate group acts as a bidentate ligand. The spectral data are discussed and compared to those of the corresponding tris(dialkyldithiocarbamate) complexes.

GEORGE E. MANOUSSAKIS, CONSTANTINOS A. TSIPIS et CHRISTOS C. HADJIKOSTAS. Can. J. Chem. **53**, 1530 (1975).

On a préparé 15 complexes bromobis(dialkyldithiocarbamate) de l'arsenic, de l'antimoine et du bismuth en faisant réagir les tris(dialkyldithiocarbamate) correspondants avec le brome. On a étudié la structure de ces composés par i.r., r.m.n. et spectroscopie électronique. A partir de l'interprétation des données spectroscopiques, on peut déduire que chaque groupe dithiocarbamate agit comme un ligand bidentate. On discute des données spectrales et on les compare avec celles des complexes tris(dialkyldithiocarbamate) correspondants.
[Traduit par le journal]

Introduction

In recent years a number of papers have been published on the reactions between dithiocarbamate complexes (both transition and non-transition elements) and halogens (1–12). The products of these reactions are usually halogenodithiocarbamate complexes, in which the central atom has an unusual oxidation number. From our point of view the paper of Willemse and Steggerda (12) on the oxidation of dithiocarbamate ligands is particularly interesting. According to these authors, halogenation of diethyldithiocarbamate complexes of iron(III), cobalt(III), antimony(III), and copper(II) gives compounds in which the dithiocarbamate ligand is oxidized to a positive ion, presumably with an S-tetrathian ring, and the metals are present as halogenated negative ions, for instance $SbCl_6^-$. After the above mentioned observations, the study of halogenation of the dialkyldithiocarbamate complexes of arsenic, antimony, and bismuth, which were prepared in this laboratory (13–14), was considered of interest.

In particular this paper deals with the preparation and study of fifteen bromobis(dialkyldithiocarbamate) complexes of arsenic, antimony, and bismuth of the general formula $BrM(R_2dtc)_2$ (where in the dithiocarbamato group, R_2dtc, R = Et, *i*-Bu, or Bz, $R_2 = (CH_2)_4$ or $(CH_2)_5$ abbreviated as Pyrr and Pip respectively, and M = As, Sb, or Bi).

As far as we know the above mentioned compounds are new compounds, except the bromobis(diethyldithiocarbamato)arsine, which has already been prepared and studied (15). The characterization and study of the prepared compounds were done by elemental analysis, molecular weight determination, and by i.r., n.m.r., and electronic spectroscopy.

Experimental

Measurements

Infrared spectra were recorded in the region 4000–650 cm^{-1} with a Perkin–Elmer 257 spectrophotometer. The complexes were studied as KBr disks and, in some cases, as chloroform solutions. No significant differences between solid-state and solution spectra were noted. Proton n.m.r. spectra were recorded on a Varian A 60A (60 MHz) instrument in $CDCl_3$ and C_6H_6 solutions using TMS as an internal standard. Electronic spectra were measured on a Zeiss PMQ II spectrophotometer with freshly prepared $CHCl_3$ solutions at about 30 °C. Molecular weights were determined using a Perkin–Elmer molecular weight apparatus Model 115 at a concentration range 3×10^{-3} to 6×10^{-4} *m* in $CHCl_3$ solution.

Preparation

The tris(dialkyldithiocarbamate) complexes of arsenic, antimony, and bismuth were prepared according to the published method (13).

Can. J. Chem. Downloaded from www.nrcresearchpress.com by 210.87.254.5 on 09/05/12
For personal use only.

Can. J. Chem. Downloaded from www.nrcresearchpress.com by 210.87.254.5 on 09/05/12
For personal use only.

The bromobis(dialkyldithiocarbamate) complexes were prepared as follows:

Bromobisdiethyl-, Bromobisdiisobutyl-, and Bromobisdibenzyldithiocarbamate Complexes of Arsenic, Antimony, and Bismuth

To a solution of the tris(dialkyldithiocarbamate) complex (5 mmol) in 100 ml CCl_4, or, for the compounds $Bi(Et_2dtc)_3$ and $As(Bz_2dtc)_3$, in a mixture of 150 ml CCl_4 and 50 ml $CHCl_3$, a solution of bromine (2.5 mmol) in 15 ml CCl_4 was added dropwise, while stirring constantly. After the addition of the bromine solution, the mixture was stirred at room temperature for 4–5 h. The mixture was then concentrated to about 30 ml and after addition of methanol the bromobis(dialkyldithiocarbamate) complexes were precipitated. Purified precipitates were obtained by dissolving them in a small amount of benzene and then precipitating with methanol or petroleum ether (b.p. 40–60 °C). The pure materials were dried under vacuum at room temperature. In the course of reprecipitating the bromobis(dibenzyldithiocarbamate) complexes by addition of methanol or petroleum ether to the benzene solution, viscous oils were obtained which were solidified on drying under vacuum. The prepared complexes are soluble in chloroform, methylene chloride, benzene, carbon tetrachloride, and acetone and insoluble in methanol, ethanol, ether, petroleum ether, and water.

Bromobipyrrolidyl-, and Bromobipiperidyldithiocarbamate Complexes of Arsenic, Antimony, and Bismuth

To a solution of the corresponding tris(dialkyldithiocarbamate) complex (5 mmol) in 100 ml $CHCl_3$ a solution of bromine (2.5 mmol) in 25 ml $CHCl_3$ was added dropwise, while stirring constantly. After the addition of the bromine solution the mixture was stirred at room temperature for 4–5 h. The mixture was then filtered and the precipitate washed with methanol and recrystallized from a mixture of dimethylformamide and methanol. The bromobis(dialkyldithiocarbamate) complexes obtained are insoluble in common organic solvents and water, but are soluble in dimethylformamide and dimethylsulfoxide, and slightly soluble in chloroform and methylene chloride.

The analytical data of the compounds studied are given in Table 1.

Results and Discussion

When the tris(dialkyldithiocarbamate) complexes of arsenic, antimony, or bismuth in carbon tetrachloride or chloroform solution are reacted with 1 equiv. of bromine, one of the three dithiocarbamate groups is displaced by a bromine atom.

Although, in some cases, bromine was used in excess (twofold of the required quantity), dibromodialkyldithiocarbamates were not isolated. This may be attributed to the easier detachment of one of the three dithiocarbamate groups, due to the stereochemically active lone pair of electrons of the central atom (13, 16, 17), while the presence of a bromine atom in the molecule of the bromoderivatives, because of its $-I$ inductive effect, strengthens the binding between the central atom and the remaining two dithiocarbamate ligands.

Conductance measurements in nitrobenzene solution indicate that the compounds studied are nonelectrolytes.

Infrared Spectra

In Table 2 are listed the relevant i.r. data for our new compounds with their assignments.

The most characteristic bands of the compounds studied are the "thioureide" bands near 1500 cm^{-1}, which indicate considerable double bond character in the C⋯N bond.

In bromobis(dialkyldithiocarbamate) complexes the stretching frequencies of the C⋯N bonds are higher than those of the corresponding tris(dialkyldithiocarbamate) complexes. This may be due to the $-I$ inductive effect of bromine atom, as well as to their different stereochemical structures. The observed shifting of the C⋯N bands to higher frequencies in the studied bromoderivatives relative to the corresponding trisdithiocarbamates follows the sequence As > Sb > Bi. Taking into consideration that the presence of the bromine atom reduces the electron density on bismuth atom more than on antimony and arsenic ones the observed sequence is abnormal. This discrepancy may be attributed to the more pronounced π-back donation in bismuth compounds than in those of antimony and arsenic. The π-back donation also seems to be more pronounced in bromoderivatives than the corresponding trisdithiocarbamates. Considering that the π-back donation is, generally, favored by the square pyramidal structure (18) and the fact that this structure was already established for the bromobis(diethyldithiocarbamato)arsine (15), we can accept the same structure for all the compounds studied.

Certain bands in the 800–1000 cm^{-1} region (Table 2) are attributed to the stretching vibration of C⋯S bonds (19, 20). The single band around 1000 cm^{-1} in the spectra of all the compounds studied (except dibenzylderivatives of arsenic and antimony) is evidence of bidentate linking of dithiocarbamato groups (21–23).

The existence of splitting in the C⋯N bands in some of the compounds studied, especially in those of arsenic, may be considered as evidence of inequivalent bonding of the dithiocarbamato groups or vibration mixings. Similar splittings have been observed by other authors (21, 23–25).

Can. J. Chem. Downloaded from www.nrcresearchpress.com by 210.87.254.5 on 09/05/12
For personal use only.

TABLE 1. Analytical data for the bromobis(dialkyldithiocarbamate) complexes of arsenic, antimony, and bismuth

Compound	Color	Yield (%)	Melting point† (°C)	C (%)		H (%)		N (%)		Br (%)		S (%)		M* (%)		Molecular weight	
				Calcd.	Exp.	Calcd.	Exp.	Calcd.	Exp.	Calcd.	Exp.	Calcd.	Exp.	Calcd.	Exp.	Calcd.	Exp.
$BrAs(Et_2dtc)_2$	White	82	132–135	26.61	26.04	4.47	4.22	6.20	6.07	17.70	17.5	28.42	27.9	16.60	16.4	451.4	454
$BrSb(Et_2dtc)_2$	Yellowish	88	131–133	24.11	23.85	4.05	3.93	5.62	5.26	16.04	15.8	25.74	26.0	24.44	24.1	498.2	502
$BrBi(Et_2dtc)_2$	Yellow	94	139–141	20.52	19.84	3.44	3.28	4.78	4.59	13.65	13.3	21.91	21.6	35.70	35.6	585.4	680
$BrAs(i\text{-}Bu_2dtc)_2$	White	70	141–143	38.36	38.06	6.44	6.38	4.97	4.85	14.18	13.8	22.76	22.3	13.29	13.5	563.6	569
$BrSb(i\text{-}Bu_2dtc)_2$	Yellowish	79	147–148	35.42	35.14	5.94	5.85	4.59	4.48	13.09	12.9	21.01	21.5	19.95	19.4	610.4	618
$BrBi(i\text{-}Bu_2dtc)_2$	Yellow	86	155–156	30.99	31.14	5.20	5.14	4.02	4.06	11.45	11.1	18.38	18.7	29.96	29.9	697.6	840
$BrAs(Bz_2dtc)_2$	Yellowish	61	92(d)	51.50	51.43	4.03	4.05	4.00	4.08	11.42	11.3	18.33	18.0	10.71	10.3	699.6	710
$BrSb(Bz_2dtc)_2$	Yellow	73	93(d)	48.27	48.42	3.78	3.87	3.75	3.69	10.70	10.4	17.18	17.5	16.31	16.0	746.4	755
$BrBi(Bz_2dtc)_2$	Yellow	84	100(d)	43.22	43.27	3.38	3.42	3.36	3.35	9.58	9.2	15.38	15.1	25.07	25.2	833.7	1362
$BrAs(Pyrrdtc)_2$	White	76	197–199	26.85	26.64	3.60	3.60	6.26	6.33	17.86	17.4	28.67	29.3	16.75	16.5	447.3	451
$BrSb(Pyrrdtc)_2$	Yellowish	84	234(d)	24.30	24.48	3.26	3.30	5.67	5.67	16.17	16.4	25.95	25.5	24.64	24.3	494.1	503
$BrBi(Pyrrdtc)_2$	Yellow	91	245(d)	20.66	20.77	2.77	2.79	4.82	4.84	13.74	13.5	22.06	22.4	35.95	36.1	581.4	594
$BrAs(Pipdtc)_2$	White	82	194–196	30.32	30.15	4.24	4.21	5.89	5.85	16.81	16.7	26.98	26.4	15.76	15.4	475.4	472
$BrSb(Pipdtc)_2$	White	90	229(d)	27.60	27.77	3.86	3.83	5.36	5.31	15.30	15.1	24.56	24.9	23.31	22.8	522.2	538
$BrBi(Pipdtc)_2$	Yellow	95	246(d)	23.65	23.68	3.31	3.30	4.60	4.58	13.11	12.8	21.04	21.6	34.29	34.3	609.4	618

*M = As, Sb, or Bi.
†d = decomposition.

TABLE 2. Relevant i.r. frequencies (cm^{-1}) of the compounds studied with their assignments (KBr disks)*

Compound	ν(C···N)	ν(C···S)	Compound	ν(C···N)	ν(C···S)
		988m			992w (br)*
$BrAs(Et_2dtc)_2$	1529vs	837m	$BrBi(Bz_2dtc)_2$	1476vs	880w
	1496vs	845m			
	1515vs(sh)	987m		1532vs	992m
$BrSb(Et_2dtc)_2$	1492vs	846m	$BrAs(Pyrrdtc)_2$	1483vs	946m
		838m			939m
					832m
					994m
$BrBi(Et_2dtc)_2$	1500vs	982w	$BrSb(Pyrrdtc)_2$	1514vs	946m
		843m		1483vs	938m
					831m
	1510vs	980w			993m
$BrAs(i\text{-}Bu_2dtc)_2$	1492vs	880w	$BrBi(Pyrrdtc)_2$	1484vs	939m
		858w			826m
	1508s(sh)	974m		1524vs	1001vs
$BrSb(i\text{-}Bu_2dtc)_2$	1496vs	880w	$BrAs(Pipdtc)_2$	1506vs	886s
		859w			
		969w			1003s
$BrBi(i\text{-}Bu_2dtc)_2$	1484vs	878w	$BrSb(Pipdtc)_2$	1507vs	887s
		1002m			999s
$BrAs(Bz_2dtc)_2$	1485vs	988m	$BrBi(Pipdtc)_2$	1486vs	884s
		878w			
		1003m			
$BrSb(Bz_2dtc)_2$	1482vs	988m			
		877w			

*vs = very strong, m = medium, br = broad, sh = shoulder, w = weak, s = strong.

TABLE 3. Proton chemical shifts, τ (p.p.m.), of bromobis(dialkyldithiocarbamate) complexes of arsenic, antimony, and bismuth in $CDCl_3$ and C_6H_6 solutions*

		$-N(CH_2CH_3)_2$		$-N\left(CH_2-CH\begin{matrix}CH_3\\CH_3\end{matrix}\right)_2$			$-N(CH_2-C_6H_5)_2$	
Compounds	Solution	$-CH_2-$	$-CH_3$	$-CH_2-$	$-CH=$	$-CH_3$	$-CH_2-$	$-C_6H_5$
Arsenic	$CDCl_3$	6.14 q	8.65 t	6.35 d	7.60 m	9.02 d	4.90 s	2.61 s
	C_6H_6	6.85 q	9.30 t	6.69 d	8.02 m	9.38 d	5.37 s	2.91 s
Antimony	$CDCl_3$	6.15 q	8.65 t	6.36 d	7.62 m	9.02 d	4.98 s	2.58 s
	C_6H_6	6.91 q	9.25 t	6.64 d	7.97 m	9.34 d	5.26 s	2.89 s
Bismuth	$CDCl_3$	6.24 q	8.67 t	6.42 d	7.63 m	9.03 d	5.16 s	2.69 s
	C_6H_6	6.76 q	9.15 t	6.58 d	7.70 m	9.25 d	5.34 s	2.89 s

*q = quartet, t = triplet, d = doublet, m = multiplet, s = singlet.

Proton Nuclear Magnetic Resonance Spectra

The signals of the proton n.m.r. spectra of the compounds studied are listed in Table 3. The absence of splitting in n.m.r. signals does not directly imply that the two dithiocarbamate ligands are bonded equivalently. This can be assigned to the isolation of the alkyl groups from the metal–sulfur bonds (26). The signals of the more distant protons are shifted less to lower fields in comparison to the signals of the corresponding tris(dithiocarbamates). This is something which can be expected, for the bromine atom in the dithiocarbamate molecules withdraws more of the electron density from the alkyl groups towards the central atom. This means that the deshielding effect is more pro-

Can. J. Chem. Downloaded from www.nrcresearchpress.com by 210.87.254.5 on 09/05/12
For personal use only.

TABLE 4. Electronic spectra of bromobis(dialkyldithiocarbamate) complexes of arsenic, antimony, and bismuth

Compound	Band I		Band II		Band III	
	ν_{max} (kK)	log ε_{mol}	ν_{max} (kK)	log ε_{mol}	ν_{max} (kK)	log ε_{mol}
$BrAs(Et_2dtc)_2$	39.3	4.53	33.2(sh)*	4.02	—	—
$BrSb(Et_2dtc)_2$	38.8	4.60	31.2(sh)	3.77	—	—
$BrBi(Et_2dtc)_2$	39.4	4.56	31.2(sh)	3.77	27.0	3.75
$BrAs(i\text{-}Bu_2dtc)_2$	38.7	4.60	33.4(sh)	4.17	—	—
$BrSb(i\text{-}Bu_2dtc)_2$	38.5	4.63	32.8(sh)	4.00	—	—
$BrBi(i\text{-}Bu_2dtc)_2$	38.1	4.62	31.2(sh)	3.84	27.2	3.54
$BrAs(Bz_2dtc)_2$	38.5	4.52	33.2(sh)	4.18	—	—
$BrSb(Bz_2dtc)_2$	38.3	4.66	31.6(sh)	3.92	—	—
$BrBi(Bz_2dtc)_2$	38.4	4.67	31.4(sh)	3.93	27.2	3.88
$BrAs(Pyrrdtc)_2$	39.5	4.61	33.2(sh)	4.10	—	—
$BrSb(Pyrrdtc)_2$	39.0	4.66	33.2(sh)	4.00	—	—
$BrBi(Pyrrdtc)_2$	40.0	4.63	30.8(sh)	3.77	27.5	3.78
$BrAs(Pipdtc)_2$	38.9	4.59	33.6(sh)	4.13	—	—
$BrSb(Pipdtc)_2$	38.5	4.65	32.6(sh)	4.01	—	—
$BrBi(Pipdtc)_2$	38.8	4.54	30.8(sh)	3.72	27.2	3.75

*sh = shoulder.

nounced for the more distant protons of the bromoderivatives.

Paradoxically the behavior of the less distant protons (methylene) is the opposite. The signals of methylene protons are shifted to a higher field region (more shielding). This discrepancy may be assigned to the different location of these protons in the shielding cone of the C⋯N bond.

The proton signals of the compounds studied are subjected to benzene induced solvent shifts (Table 3). This effect is attributed to the formation of van der Waals complexes between benzene molecules (solvent) and the bromobis(dialkyldithiocarbamates) (solute) (14). The observed values of the solvent shifts increase as the stretching frequencies of the C⋯N bonds increase.

Electronic Spectra

The electronic spectra of the arsenic and antimony compounds show two absorption bands in the ultraviolet region. In the spectra of bismuth compounds there is a third maximum near the visible region (Table 4).

The high intensity band (Band I) at 38–40 kK is assigned to an intraligand $\pi \rightarrow \pi^*$ transition (27). The position of band I is not much affected by the presence of the central atom. The sequence in the bromoderivatives studied is Bi ≥ As ≥ Sb; in the corresponding tris(dialkyldithiocarbamate) complexes it is As > Sb > Bi. This discrepancy is perhaps a further indication for the more pronounced π-back donation in the case of bismuth derivatives in agreement with i.r. data. The position of band I in bromoderivatives is shifted to higher frequencies relative to tris(dithiocarbamate) complexes. Band I depends also on the electron releasing ability of the $-NR_2$ group. The increase of the basic character of the amine group leads to blue shifts.

Band II (inflection point) is attributed to another $\pi \rightarrow \pi^*$ transition (28). This inflection is more pronounced in arsenic than in antimony compounds and it almost disappears in bismuth ones. This band is evidence of inequivalent linking of dithiocarbamate ligands (27).

Molecular Weights

The compounds studied are monomeric in $CHCl_3$ solution at the concentration range 10^{-3}–10^{-4} *m*, except the bismuth compounds which show a tendency for dimerization. This tendency decreases with increasing basicity of amine group. This may be due again to π-back donation, which has as a result the decrease of electron density on bismuth atom. Therefore weak interaction forces exist between bismuth of one molecule and a bromine atom of another molecule.

1. P. T. BEURSKENS, H. J. A. BLAAUW, J. A. CRAS, and J. J. STEGGERDA. Inorg. Chem. 7, 805 (1968).
2. P. T. BEURSKENS, J. A. CRAS, and J. J. STEGGERDA. Inorg. Chem. 7, 810 (1968).

Can. J. Chem. Downloaded from www.nrcresearchpress.com by 210.87.254.5 on 09/05/12
For personal use only.

3. P. T. BEURSKENS, J. A. CRAS, and J. G. M. VAN DER LINDEN. Inorg. Chem. **9**, 475 (1970).
4. H. C. BRINKHOFF, J. A. CRAS, J. J. STEGGERDA, and J. WILLEMSE. Recl. Trav. Chim. Pays-Bas, **88**, 633 (1969).
5. H. C. BRINKHOFF. Recl. Trav. Chim. Pays-Bas, **90**, 377 (1971).
6. F. BONATI and G. MINGHETTI. Chim. Ind. Milan, **52**, 1204 (1970).
7. R. M. GOLDIN, C. M. HARRIS, K. J. JESSOP, and W. C. TENNANT. Aust. J. Chem. **25**, 2567 (1972).
8. J. P. FACKLER, A. AVDEEF, and R. G. FISCHER. J. Am. Chem. Soc. **95**, 774 (1973).
9. H. J. A. BLAAUW, R. J. F. NIVARD, and G. J. M. VAN DER KERK. J. Organomet. Chem. **2**, 236 (1964).
10. Y. NIGO, I. MASUDA, and K. SHINRA. Chem. Commun. 476 (1970).
11. A. AVDEEF, J. P. FACKLER, and R. G. FISCHER. J. Am. Chem. Soc. **92**, 6972 (1970).
12. J. WILLEMSE and J. J. STEGGERDA. Chem. Commun. 1123 (1969).
13. G. E. MANOUSSAKIS and C. A. TSIPIS. J. Inorg. Nucl. Chem. **35**, 743 (1973).
14. G. E. MANOUSSAKIS and C. A. TSIPIS. Z. Anorg. Allg. Chem. **398**, 88 (1973).
15. R. BALLY. C.R. Acad. Sc. Paris, t. **271**, 1436 (1970).
16. G. E. MANOUSSAKIS, E. D. MIKROMASTORAS, and C. A. TSIPIS. Z. Anorg. Allg. Chem. **403**, 87 (1974).
17. S. L. LAWTON, C. J. FUHRMEISTER, R. G. HAAS, C. S. JARMAN, and F. G. LOHMEYER. Inorg. Chem. **13**, 135 (1974).
18. C. FURLANI. Coord. Chem. Rev. **3**, 141 (1968).
19. M. L. SHANKARANARAYANA and C. C. PATEL. Spectrochim. Acta, **21**, 95 (1965).
20. G. DURGAPRASAD, D. N. SATHYANARAYANA, and C. C. PATEL. Can. J. Chem. **47**, 631 (1969).
21. F. BONATI and R. UGO. J. Organomet. Chem. **10**, 257 (1967).
22. H. A. MEINEMA and J. G. NOLTES. J. Organomet. Chem. **25**, 139 (1970).
23. A. N. BHAT, R. C. FAY, D. F. LEWIS, A. F. LINDMARK, and S. H. STRAUSS. Inorg. Chem. **13**, 886 (1974).
24. C. O'CONNOR, J. D. GILBERT, and G. WILKINSON. J. Chem. Soc. 84 (1969).
25. R. N. JOWITT and P. G. H. MITCHELL. J. Chem. Soc. A, 1702 (1970).
26. J. P. BIBLER and D. G. KARRAKER. Inorg. Chem. **7**, 982 (1968).
27. H. P. KOCH. J. Chem. Soc. 401 (1949).
28. M. J. JANSSEN. Recl. Trav. Chim. Pays-Bas, **79**, 1066 (1960).

Can. J. Chem. Downloaded from www.nrcresearchpress.com by 210.87.254.5 on 09/05/12
For personal use only.

Erratum: Sur l'existence des composés P_4Se_x ($x \leqslant 3$) et $P_4Se_{3-n}S_n$ ($n = 1,2$)

YVES MONTEIL ET HENRI VINCENT
Laboratoire de Physico-Chimie Minérale I, Associé au C.N.R.S. n° 116, Service du Professeur Cueilleron, Université Claude Bernard, 43 boulevard du 11 novembre 1918, 69621 Villeurbanne, France
Reçu le 17 septembre 1974
(Ref.: Can. J. Chem. **52**, 2190 (1974))

La date de reçu doit être le 20 novembre 1973.

Erratum: The Crystal Structure of Tripotassium bis(Oxalato)-dioxovanadate(V) Trihydrate

R. E. DREW, F. W. B. EINSTEIN, AND SUSAN E. GRANSDEN
Department of Chemistry, Simon Fraser University, Burnaby 2, British Columbia V5A 1S6
Received September 17, 1974
(Ref.: Can. J. Chem. **52**, 2184 (1974))

The date of receipt, missing in the original article, is November 9, 1973.

Can. J. Chem. Downloaded from www.nrcresearchpress.com by 210.87.254.6 on 09/05/12
For personal use only.

Can. J. Chem. Downloaded from www.nrcresearchpress.com by 210.87.254.5 on 09/05/12
For personal use only.

Canadian Journal of Chemistry

Published by
THE NATIONAL RESEARCH COUNCIL OF CANADA

Journal canadien de chimie

Publié par
LE CONSEIL NATIONAL DE RECHERCHES DU CANADA

Volume 53 Number 11 June 1, 1975

Volume 53 numéro 11 1 juin 1975

Reaction of 4,4′-Bis(dimethylamino)triphenylmethyl Tetrafluoroborate with Alkoxide Ions. I. Determination of Ion-pair Dissociation Constant for Sodium Alkoxides

KENNETH T. LEFFEK AND ANDREJ SUSZKA[1]

Department of Chemistry, Dalhousie University, Halifax, Nova Scotia B3H 4H6

Received November 6, 1974

KENNETH T. LEFFEK and ANDREJ SUSZKA. Can. J. Chem. **53**, 1537 (1975).

The second-order rate constants have been determined for the reaction of 4,4′-bis(dimethylamino)triphenylmethyl tetrafluoroborate carbonium ion with sodium methoxide in methanol and sodium ethoxide in ethanol. The results have been used to evaluate the ion-pair dissociation constants for the two alkoxides. The activation parameters for the two reactions with the free alkoxide ions are also reported.

KENNETH T. LEFFEK et ANDREJ SUSZKA. Can. J. Chem. **53**, 1537 (1975).

On a déterminé les constantes de vitesse du deuxième ordre des réactions du carbocation du tétrafluoroborate de bis(diméthylamino)-4,4′ triphénylméthyle avec le méthylate de sodium dans le méthanol et avec l'éthylate de sodium dans l'éthanol. On a utilisé les résultats obtenus pour évaluer les constantes de dissociation des paires d'ions des deux alcoolates. On rapporte aussi les paramètres d'activation des deux réactions avec les ions alcoolates libres.

[Traduit par le journal]

Introduction

It has been pointed out recently (1) that despite the fact that ion association of alkali metal alkoxides must play an important part in the kinetics of their reactions in alcohol solution, few investigations have been made directly of this phenomenon by measurement of reaction rates. In the present study, the kinetics of the reaction of sodium methoxide and ethoxide, in the corresponding alcohol solvents, with 4,4′-bis(dimethylamino)triphenylmethyl tetrafluoroborate (malachite green) have been investigated and the ion-pair dissociation constants of the alkoxides have been calculated from the rate constant measurements.

The reaction of malachite green with methoxide, which is a clean formation of the methyl ether by combination of the methoxide ion with the carbonium ion was previously studied by Ritchie *et al.* (2, 3). Their experiments were made at 25 °C using tertiary amine solutions in methanol, buffered by strong organic acids, as a source of methoxide ions. Later sodium methoxide in methanol was used and the rate measurements carried out with a stopped-flow spectrophotometer. An ion-pair dissociation constant of $1.03 \times 10^{-2}\ M^{-1}$ was assumed for sodium methoxide and the second-order rate constant for malachite green was found to be $1250\ M^{-1}\ s^{-1}$ at 25 °C. The reaction of methanol itself with the carbonium ion was found to be negligible and our observations confirm this.

Results and Discussion

Two series of kinetic measurements have been made at a number of different temperatures be-

[1]Killam Postdoctoral Fellow 1972–1973.

Can. J. Chem. Downloaded from www.nrcresearchpress.com by 210.87.254.5 on 09/05/12
For personal use only.

tween 0 and 35° at various concentrations of sodium methoxide in methanol and sodium ethoxide in ethanol. The substrate concentration was 3×10^{-6} *M* and the alkoxide concentrations were always in large excess, between 3×10^{-4} and 1×10^{-2} *M*. The pseudo first-order rate constants, k_1, calculated by the Guggenheim method and plotted against the alkoxide concentration, gave straight lines over the lower range of alkoxide concentration but at higher concentrations the rate constants fell on a curve below the line as shown in Fig. 1 for the methoxide reaction. The pseudo first-order rate constants and the corresponding second-order rate constants, calculated by the method of least squares applied to the seven lower concentrations, for both the methoxide and ethoxide reactions are shown in Table 1. The second-order rate constant for methoxide ion reaction at 25 °C is about 18% lower than the value recorded by Ritchie *et al.* (3).

The curvature of the plots in Fig. 1 is no doubt due to metal alkoxide ion-pair formation in the solutions at higher concentration, as suggested by Ritchie *et al.* (3). The dissociation constant of the ion-pair is given by

$$[1] \qquad K = \frac{[Na^+][\bar{O}Alk]}{[Na^+\bar{O}Alk]}$$

If the total methoxide concentration, as free ion and ion-pair, is denoted c then

$$[2] \qquad K = \frac{[\bar{O}Alk]^2}{c - [\bar{O}Alk]}$$

and

$$[3] \qquad [\bar{O}Alk] = \tfrac{1}{2}(-K \pm \sqrt{K^2 + 4Kc})$$

The relation between k_{obs} and the second-order rate constants for a reversible equilibrium is

$$[4] \qquad k_{obs} = k_2[\bar{O}Alk] + k_{-2}$$

where k_2 and k_{-2} are the second-order rate constants for the forward and backward reactions respectively. It can be seen from Fig. 1 that k_{-2} is very small compared to $k_2[\bar{O}CH_3]$ and, therefore, it may be omitted. Combination of eqs. 3 and 4 gives

$$[5] \qquad k_{obs} = k_2\left\{\frac{-K \pm \sqrt{K^2 + 4Kc}}{2}\right\}$$

which may be transformed into

$$[6] \qquad k_{obs}\left(\frac{1}{k_2{}^2K}\right) + \frac{1}{k_2} = \frac{c}{k_{obs}}$$

Equation 6 represents a straight line relation between k_{obs} and c/k_{obs} with an intercept equal to $1/k_2$ and a slope equal to $1/k_2{}^2K$.

The slopes and intercepts were calculated by the least squares method applied to the six higher concentrations in Table 1 for the methoxide and ethoxide reactions. The intercepts yielded values of k_2 which agreed reasonably well with those of Table 1, but the k_2 values of Table 1 are more precise, so these were combined with the slopes to give the dissociation constants shown in Table 2.

The above treatment assumes that the reactivity of the ion-pair is very much less than the free alkoxide ion. There is, of course, no absolute proof for this, but there is circumstantial evidence that the nucleophilic power of anion reagents is seen only when the anion exists in solution as a free ion. In 1956, Bevan and Monk (4) showed that the differences in the second-order rate constants for the reaction of sodium, potassium, magnesium, calcium, and strontium thiosulfates with *n*-propyl bromide in

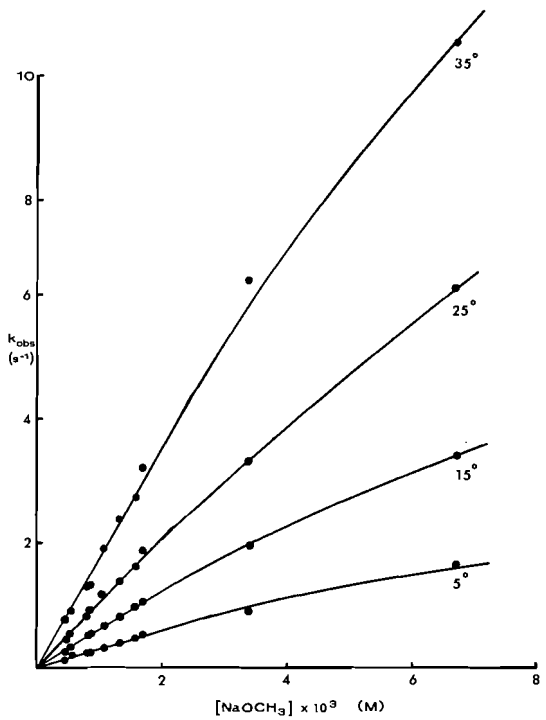

FIG. 1. Plot of pseudo first-order rate constant against sodium methoxide concentration.

TABLE 1. First and second-order rate constants for the reaction of sodium methoxide and sodium ethoxide with 4,4′-bis(dimethylamino)triphenylmethyl fluoroborate

Temperature (°C)	$10k_1$ (s^{-1}) for 10^4 [$NaOCH_3$] (M) 4.2	5.2	7.8	8.4	10.5	13.1	15.7	16.8	33.7	67.3	$10^{-1}k_2$ ($l\,mol^{-1}\,s^{-1}$)
0	1.52	1.70	2.63	2.77	3.12	3.92	4.56	5.63	7.89	14.5	30.4±0.8
5	1.44	2.18	3.03	2.71	3.96	5.12	5.92	5.47	9.53	16.9	37.7±0.9
10	2.09	2.65	3.80	4.02	5.18	6.48	7.91	7.53	13.7	29.2	49.6±0.4
15	2.86	3.39	5.16	5.66	6.67	8.43	9.81	10.77	19.7	34.4	64.2±0.7
20	3.94	4.40	6.62	7.55	9.00	11.08	12.7	15.0	27.3	47.8	84.3±1.3
25	4.80	5.45	8.36	9.42	11.06	13.8	16.5	19.0	33.5	61.4	106 ±1
30	6.05	7.20	10.94	12.5	14.5	17.8	21.3	24.6	45.3	83.1	138 ±1.5
35	7.71	9.06	13.4	13.3	19.1	23.6	27.4	31.7	62.3	105.5	176 ±3

Temperature (°C)	$10k_1$ (s^{-1}) for 10^4 [$NaOC_2H_5$] (M) 3.2	4.5	4.8	6.4	7.3	8.0	9.6	11.3	22.7	45.5	91.0	$10^{-1}k_2$ ($l\,mol^{-1}s^{-1}$)
10	3.58	3.77	5.14	6.98	6.78	8.06	9.88	9.05	15.3	30.1	54.2	101± 3
15	4.09	4.38	6.68	8.39	8.35	10.5	13.1	12.8	22.9	40.0	66.3	128± 5
20	5.60	6.31	8.60	11.6	12.1	14.6	17.7	19.6	33.9	57.2	93.8	174± 5
25	7.41	7.89	11.3	14.9	16.9	18.6	22.4	25.5	44.0	76.3	114	229± 6
30	8.72	11.0	13.9	19.2	23.5	23.3	27.8	36.0	58.8	96.9	169	293± 7
35	12.2	17.6	19.3	25.2	34.0	31.0	38.7	49.2	80.0	125	245	408±11

TABLE 2. Alkoxide ion-pair dissociation constants

Temperature (°C)	$10^2\,K$ ($Na^+\bar{O}CH_3/CH_3OH$)	$10^2\,K$ ($Na^+\bar{O}C_2H_5/C_2H_5OH$)
0	0.8	—
5	0.6	—
10	0.8	0.7
15	1.6	0.6
20	2.3	0.6
25	2.6	1.1
30	4.0	0.6
35	3.5	0.9

a mixed ethanol–water solvent could be eliminated completely if the rate constant was calculated with respect to the free thiosulfate ion. They assumed that ion-pairs in solution made no contribution to the reaction velocity and the rate constants for the free thiosulfate ion were found not only to be independent of the cation present but also independent of the ionic strengths of the solution (4).

Cram *et al.* (5) investigated the rates of racemization and exchange of 1-phenylmethoxyethane-1-*d* in dimethyl sulfoxide – potassium *tert*-butoxide. The order of the reaction in potassium *tert*-butoxide and other kinetic observations led them to conclude that potassium *tert*-butoxide in DMSO is largely in the form of ion-pairs, but that only the dissociated *tert*-butoxide ion is chemically active with the reactivity of the ion-pairs vanishingly small in comparison.

In the present investigation, the validity of the assumption that the ion-pairs are very unreactive may be judged by making a comparison between our kinetically derived dissociation constants and the literature values calculated from conductance measurements. The values of the dissociation constants in Table 2 are not of high precision and it is not possible to distinguish a clear change with temperature for the sodium ethoxide. Nevertheless, the result $K = 1 \times 10^{-2}\ M^{-1}$ at 25 °C for sodium ethoxide is of the same order of magnitude but lower than the value of $2.0 \times 10^{-2}\ M^{-1}$ from conductance measurements (6). For sodium methoxide, the only value in the literature is the assumed one from the kinetic study by Ritchie *et al.* (3) of 1.03×10^{-2}

Can. J. Chem. Downloaded from www.nrcresearchpress.com by 210.87.254.5 on 09/05/12
For personal use only.

Can. J. Chem. Downloaded from www.nrcresearchpress.com by 210.87.254.5 on 09/05/12
For personal use only.

M^{-1} which is somewhat less than our 2.6×10^{-2} M^{-1} at 25 °C. Potassium methoxide has been reported (1, 7) as 1 to 2×10^{-2} M^{-1}, calculated from conductance measurements.

The derivation of the ion-pair dissociation constants ignores salt effects due to activity coefficients. The justification of this is that Ritchie *et al.* (3) found no such salt effect in the reaction of malachite green with hydroxide ion in water up to a concentration of added salt of 10^{-2} M and also reported (3) that Taft had found a salt effect of only 10% for added salt concentrations between 0.05 and 1 M for the same reaction. For our alkoxide reactions, there is clearly no ionic strength effect on the second-order rate constants up to alkoxide concentrations of 2×10^{-3} M, as can be seen from Fig. 1. The changes in k_2 values between 2×10^{-3} M and 1×10^{-2} M fit the ion-pair theory very well within the precision of the rate measurements, thus it is assumed that activity coefficient effects must be much smaller than the ion-pairing effect.

The relative sizes of the methoxide and ethoxide ion-pair dissociation constants is reasonable, since not much difference between them would be expected, but from qualitative studies, the ethoxide, if anything, should be the smaller since the free ethoxide ion will not be as strongly stabilized by solvation as the free methoxide ion.

The second-order rate constants of Table 1 allow the evaluation of the activation parameters for the two reactions. These activation parameters are given in Table 3.

The enthalpy of activation of the ethoxide reaction is slightly larger than that for methoxide which is opposite to what would be predicted from the greater solvation stability of the methoxide ion. The importance of solvent reorganization as a major or even the dominant factor in the activation process was pointed out in 1935 by Ogg and Polanyi (8) and later by Moelwyn-Hughes and Glew (9) for nucleophilic substitution reaction. Caldin and co-worker (10, 11) and recently we (12) have made similar arguments for proton transfer from organic acids to alkoxides, and Ritchie *et al.* (3) have published such arguments for the reactions of this study. Despite this, we do not find the activation enthalpy higher for the methoxide reaction than for the ethoxide reaction as would be expected if solvent reorganization were the only factor. However, the 8 to 9 kcal mol^{-1} observed for these reactions is very similar to the 7 to 11 kcal mol^{-1} found for proton transfers (10, 12–14) and the entropies of activation bear a similar general equivalence. Therefore, the activation parameters are consistent with the presence of a major solvent reorientation factor, although this cannot be controlling the activation process entirely.

TABLE 3. Activation parameters for the reaction of 4,4′-bis(dimethylamino)triphenylmethyl fluoroborate with methoxide and ethoxide

Parameter	Methoxide	Ethoxide
$\Delta H^{\ddagger}$ (kcal mol^{-1})	7.9±0.1	9.0±0.3
$\Delta S^{\ddagger}$ (cal deg^{-1} mol^{-1})	−18.1±0.5	−12.8±0.9

Experimental

Materials

Commercial methanol was fractionally distilled, passed through a 60 × 2.5 cm column filled with Linde molecular sieve 3A, then through a 20 × 2.5 cm column filled with Dowex 50WX8, and finally distilled again. The Dowex resin was dried *in vacuo* at 90 °C for several hours before packing the column.

Anhydrous ethanol was prepared by drying commercial absolute ethanol with Mg turnings. The traces of basic material were removed by fractional distillation from anhydrous sulfanilic acid.

Sodium alkoxide solutions were prepared by dissolving clean sodium metal in alcohol in flasks protected from moisture and carbon dioxide. All solutions were prepared in a glove bag containing dry nitrogen and stored in flasks sealed with rubber serum caps. The concentrations of the alkoxides were determined by titration with standard HCl solution using methyl red as the indicator.

4,4′-Bis(dimethylamino)triphenylmethyl tetrafluoroborate was prepared by adding a slightly acidic solution of sodium tetrafluoroborate to an aqueous solution of malachite green hydrochloride. The precipitated malachite green tetrafluoroborate was recrystallized from water and dried over P_2O_5.

Kinetic Measurements

The reaction rates were measured using a stopped-flow spectrophotometer according to the standard procedure described previously (12, 15). For each set of reagent conditions, two or three trial runs were made and observed on the oscilloscope in the nonstorage mode. If these appeared satisfactory and reproducible, the oscilloscope was switched to the storage mode and between four and six runs were made in rapid succession and superimposed on the oscilloscope screen. These runs nearly always superimposed exactly giving one very slightly broadened trace. The first-order rate constant was calculated from a photograph of the composite trace. The low initial concentration of the substrate dye gave a transmittance at the beginning of a run of about 90%. The quality of the runs was about as good as it is possible to get with a stopped-flow spectrophotometer.

The authors are grateful for financial support by the National Research Council of Canada and also to the Killam Trust for a Killam Memorial Fellowship to Andrej Suszka.

1. J. R. JONES. Prog. React. Kinet. **7**, 1 (1973).
2. C. D. RITCHIE, W. R. SAGER, and E. S. LEWIS. J. Am. Chem. Soc. **84**, 2349 (1962).
3. C. D. RITCHIE, G. A. SKINNER, and V. G. BADDING. J. Am. Chem. Soc. **89**, 2063 (1967).
4. J. R. BEVAN and C. B. MONK. J. Chem. Soc. 1396 (1956).
5. D. J. CRAM, C. A. KINGSBURY, and B. RICKBORN. J. Am. Chem. Soc. **83**, 3688 (1961).
6. J. BARTHEL, G. SCHWITZGEBEL, and R. WACHTER. Z. Phys. Chem. Neue Folge, **55**, 33 (1967).
7. A. G. OGSTON. Trans. Faraday Soc. **321**, 1679 (1936).
8. R. A. OGG and M. POLANYI. Trans. Faraday Soc. **31**, 604 (1936).
9. E. A. MOELWYN-HUGHES and D. GLEW. Proc. R. Soc. A**212**, 260 (1952).
10. E. F. CALDIN. J. Chem. Soc. 3345 (1959).
11. E. F. CALDIN and G. LONG. Proc. R. Soc. A**228**, 263 (1955).
12. A. JARCZEWSKI and K. T. LEFFEK. Can. J. Chem. **50**, 24 (1972).
13. E. F. CALDIN and J. C. TRICKETT. Trans. Faraday Soc. 772 (1953).
14. E. F. CALDIN, M. KASPARIAN, and G. TOMALIN. Trans. Faraday Soc. **64**, 2802 (1968).
15. J.-H. KIM and K. T. LEFFEK. Can. J. Chem. **51**, 2805 (1973).

Can. J. Chem. Downloaded from www.nrcresearchpress.com by 210.87.254.5 on 09/05/12
For personal use only.

Electrical Conductivity and Phase Transformation Studies on Pure and Doped (Mg^{2+}, Zn^{2+}, Cu^{2+}, and Mn^{2+}) Crystals of K_2SO_4

MAHADEVA NATARAJAN AND ETALO A. SECCO

Department of Chemistry, St. Francis Xavier University, Antigonish, Nova Scotia B0H 1C0

Received July 19, 1974[1]

MAHADEVA NATARAJAN and ETALO A. SECCO. Can. J. Chem. **53**, 1542 (1975).

Electrical conductivity measurements have been made on single crystals of undoped potassium sulfate and on single crystals of K_2SO_4 doped with divalent ions, *viz.* Mg^{2+}, Zn^{2+}, Cu^{2+}, and Mn^{2+}. The presence of the divalent ion increases the cation migration energy. The lower defect formation energy is attributed to the lower symmetry of K_2SO_4 relative to the high symmetry cubic systems previously studied.

The presence of the dopants and dopant concentration, *i.e.* Cu^{2+}, show varying effects on the magnitude and nature of the conductivity discontinuity at the orthorhombic–hexagonal phase transition temperature. The phenomenon of "pretransition", 350 to 425 °C, is observed in both pure and doped crystals. Preannealing the crystal contributes to interesting behavior on all the crystals studied. The σ–T behavior of K_2SO_4 crystal doped with radioactive ^{65}Zn, however, exhibits a simpler linear dependence and the absence of "pretransition" anomaly.

MAHADEVA NATARAJAN et ETALO A. SECCO. Can. J. Chem. **53**, 1542 (1975).

On a fait des mesures de conductivité électrique sur des monocristaux de sulfate de potassium pur et sur des monocristaux de K_2SO_4 dopés avec des ions divalents comme Mg^{2+}, Zn^{2+}, Cu^{2+}, et Mn^{2+}. La présence d'ions divalents augmente l'énergie de migration du cation. On explique l'énergie plus faible de formation de défaut par la symétrie moindre de K_2SO_4 relativement aux systèmes de symétrie cubique qui ont été étudiés antérieurement.

Les impuretés, ainsi que leur concentration, *i.e.* Cu^{2+}, ont des effets variables sur l'amplitude et la nature de la discontinuité de la conductivité à la température de la transition orthorhombique–hexagonale. On observe le phénomène de "prétransition," 350 à 425 °C, dans les cristaux purs et dans les cristaux dopés. Le recuit des cristaux donne lieu à un comportement intéressant. La relation σ–T du cristal de K_2SO_4 dopé avec du ^{65}Zn radioactif est toutefois linéaire et on note dans ce cristal l'absence d'une anomalie de prétransition. [Traduit par le journal]

Introduction

Electrical conductivity measurements (1–4) on alkali halides have provided a simple and useful model for the transport mechanism in these solids involving point defects. However, such measurements have largely been restricted to crystals like KCl, KBr, CsCl, etc., which belong to a high symmetry crystal system. The existing data on defect energies in low symmetry crystals are inadequate and cannot provide a clear picture of the transport mechanism in such solids. Recently, reports on low symmetry crystals have appeared in the literature (5–8) indicating some very interesting features in the transport properties which may be linked to different conduction mechanism(s).

We have recently investigated the electrical properties in single crystals of potassium sulfate, both pure and doped with Mg^{2+}, Zn^{2+}, Cu^{2+}, and Mn^{2+}. In the case of Cu^{2+} dopant attention was also focussed on the effects of different levels of doping on the conductivity behavior of K_2SO_4. These cations show varying effects, not only on the conductivity features of the low temperature orthorhombic form but also on the magnitude of the conductivity discontinuity at the crystallographic transformation to the hexagonal form and on the conductivity of the hexagonal phase. It was also of interest to examine the recently reported (9) phenomenon of "pretransition" in K_2SO_4 monocrystals by the conductivity technique.

The source of K_2SO_4 was Fisher Certified grade (99.98%) which was further purified by crystallization. Single crystals of K_2SO_4 were prepared by slow evaporation of the aqueous solution. Seed crystals were washed and allowed to grow in saturated solution; crystals grew to $\sim$10 mm $\times$ 5 mm. The phase change in K_2SO_4 precludes growth from the melt since the crystal ruptures on cooling.

Doped K_2SO_4 crystals were similarly grown

[1]Revision received December 23, 1974.

Can. J. Chem. Downloaded from www.nrcresearchpress.com by 210.87.254.40 on 09/05/12
For personal use only.

Can. J. Chem. Downloaded from www.nrcresearchpress.com by 210.87.254.40 on 09/05/12
For personal use only.

from aqueous solutions containing 2 mol% of the respective divalent cation. Cu^{2+} doped K_2SO_4 crystals were grown from solutions containing 5.0, 3.0, 2.0, 1.0, 0.5, 0.1, and 0.05 mol% Cu^{2+}. Iodimetric titrations of the Cu^{2+} doped crystals, however, indicated ~20% of the original solution Cu^{2+} was incorporated in the K_2SO_4 crystal as shown in Table 1. The crystal Cu^{2+} shows a linear dependence on solution Cu^{2+} concentration. K_2SO_4 crystals grown in 1.0–5.0% solutions were clear and transparent while the lower concentration crystals displayed an opaque or milky appearance.

Radioactive ^{65}Zn metal (AECL Catalog No. Zn 65 S-1) was dissolved in H_2SO_4 to obtain ^{65}Zn doped K_2SO_4 crystals with specific activity ~1 count min^{-1} mg^{-1}. ^{65}Zn, $t_{1/2}$ ~ 245 d, emits γ (1.14 MeV) and β^+ (0.32 meV) radiations. The growth rate of single crystals was observed to occur in decreasing order as follows: $Cu^{2+} \approx Zn^{2+} > Mn^{2+} > Mg^{2+}$. All crystals showed a strong tendency to form contact twins and gave hexagonal bipyramids on full growth along the *c*-axis; the crystallographic axes *a* and *b* formed the basal plane.

Goniometric measurements confirmed all crystals to be orthorhombic and that the crystals grew along the *a* axis in the form of prisms terminated by the pyramidal planes.

Electrical conductivity measurements were made on crystals polished to sizes *ca.* 5 mm × 5 mm ⊥ to (100), ⊥ to (011) planes, and also ⊥ to the pyramidal planes; the experimental procedure for these measurements as described earlier (10, 11), maintained the crystal by a spring-loaded support between stainless steel leads using polished platinum discs as electrodes. The cell was heated at <25 °C per hour in a cylindrical well-type furnace. Temperature was measured by using standardized chromel–alumel thermocouples with a L & N potentiometer. The crystal conductivity was measured on a GR 1608-A bridge; the temperature was stabilized to ±1 °C prior to each measurement. The reproducibility of the conductivity values on heating–cooling cycle was excellent in the intrinsic region but was lacking in the temperature region prior to the pretransition effect.

TABLE 1. Dependence of Cu^{2+} incorporated in crystal relative to initial solution

Cu^{2+} (mol %)	
Solution	K_2SO_4
5.0	0.97
3.0	0.58
2.0	0.24
1.0	0.19
0.5	0.11
0.1	0.09

Results and Discussion

Undoped K_2SO_4 Crystals

The plot of the logarithm of electrical conductivity, σ, *vs.* the reciprocal of temperature, $1000/T$ K, for pure K_2SO_4 is presented in Fig. 1. The room temperature σ value is 2.1×10^{-8} $(\Omega\ cm)^{-1}$ ⊥ to the (100) plane and 0.79×10^{-8} $(\Omega\ cm)^{-1}$ ⊥ to the (011) plane. Earlier reports (6, 12), using single crystals of K_2SO_4, have indicated appreciable anisotropic conductivity behavior up to 350 °C, with the same temperature dependence for all three principal crystallographic directions, suggesting a common transport mechanism.

The conductivity ⊥ to (100) is higher than that ⊥ to (011) over the temperature range 200–625 °C. The low temperature conductivity follows a linear dependence corresponding to activation energies of 0.20 eV and 0.10 eV ⊥ to (100) and (011) faces, respectively. The conductivity ⊥ to (100) begins its rise at ~320 °C accompanied by an activation energy of 0.80 eV. This energy value refers to the cation migration energy in K_2SO_4; such high migration energies have re-

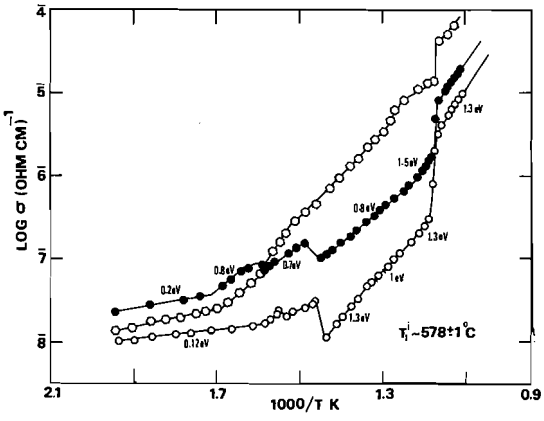

FIG. 1. Logarithm of electrical conductivity *vs.* $1000/T$ K for pure K_2SO_4 single crystal: ●, ⊥ to (100) face; ○, ⊥ to (011); ⬡, polycrystalline sample.

Can. J. Chem. Downloaded from www.nrcresearchpress.com by 210.87.254.40 on 09/05/12
For personal use only.

cently been reported for orthorhombic K_2SO_4 (6) and K_2CrO_4 (8).

The conductivity shows a sluggish increase up to ~356 °C, and an anomaly is observed at ~358 °C. Above this temperature the conductivity increases slowly with an activation energy ~0.70 eV up to ~418 °C where a sharp drop in conductivity occurred. The behavior of the sample in this region is comparable to the behavior observed for K_2CrO_4 (8) single crystals. Recently, Kolonotsova *et al.* (9) have reported a "pretransition" phenomenon in single crystals of potassium sulfate by diffuse X-ray scattering techniques. The "pretransition" is considered to be a preparatory stage that can extend over a wide temperature interval, caused by structural changes not associated with the formation of the new phase. Such changes could be described in general as an intermediate structural state between the low and high temperature modifications. According to Kolonotsova *et al.* (9) the most probable mechanism of such states is associated with cooperative atom shifts, caused by the appearance of point defects.

The anomalous conductivity behavior in the region above 375°C is also supported by the anomalous specific heat observed by Watanabe *et al.* (13), who attributed the excess specific heat to the onset of rotation of the sulfate radical. Thus, it is likely that the anomalous behavior in potassium chromate single crystals observed earlier (8) could also arise from pretransition effects and the onset of rotation by chromate radical.

Above 420 °C the (100) conductivity dependence is essentially linear with an activation energy of 0.80 eV. At 555 °C, the activation energy rises to 1.5 eV; it is not clear whether or not this represents the true intrinsic region in view of its lack of reproducibility; as evident later it varies in doped crystals. Thus, defect formation energy values are not reliable if deduced from these activation energy values. The conductivity shows a sharp discontinuity between 578 and 585 °C due to the orthorhombic–hexagonal phase transformation. Above 585 °C the conductivity with an activation energy of 1.30 eV refers to the hexagonal structure; the 1.30 eV value is in excellent agreement with that reported for Ag_2SO_4 (5).

The conductivity behavior $\perp$ to (011) face parallels the pattern observed for (100) face in the range 375–425 °C. The log $\sigma - 1/T$ dependence is essentially linear over the 425–580 °C range with a mean activation energy of 1.2 eV although we have identified segments of this temperature range with activation energies of 1.3, 1.0, and 1.30 eV. The higher activation energy of 1.2 eV, relative to 0.8 eV for (100) plane, after the "pretransition" phenomenon might incorporate the association enthalpy for the complex involving any impurity divalent ion and cation vacancies. The major transition is again evident by the abrupt rise in conductivity in the region 577–585 °C. The activation energy of 1.30 eV reappears for the hexagonal phase.

The polycrystalline σ–T data are situated between the (100) and (011) single crystal curves up to 350 °C. Above 350 °C the polycrystalline conductivity curve rises above the (100) curve and resembles the (011) single crystal slope, *viz.* 1.2 eV, with no evidence of "pretransition" phenomenon or anomalies. This crystalline behavior parallels that observed for polycrystalline potassium chromate (8). Although the activation energies below the major transition temperature are comparable in both K_2CrO_4 (8) and K_2SO_4, 1.0 and 1.2 eV, respectively, the hexagonal phase values differ appreciably from each other. This latter energy difference could arise from a more fluid-like nature of the K_2CrO_4 hexagonal phase relative to its sulfate counterpart.

Differential thermal analysis heating traces confirmed the "pretransition" effects for K_2SO_4 single crystals in the temperature range 375–425 °C and the absence of any such effect for the polycrystalline K_2SO_4 sample.

Doped (Mg^{2+}, Zn^{2+}) K_2SO_4 Crystals

Figure 2 shows the plot of logarithm of con-

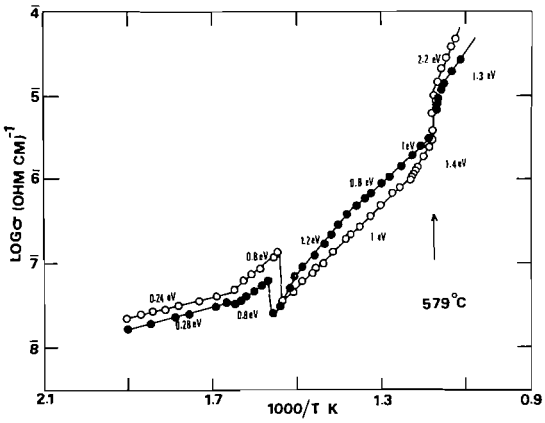

FIG. 2. Logarithm of electrical conductivity *vs.* 1000/T K for Mg^{2+} doped K_2SO_4 crystals: ○, and Zn^{2+} doped K_2SO_4 crystals; ●, measured $\perp$ to (011) face.

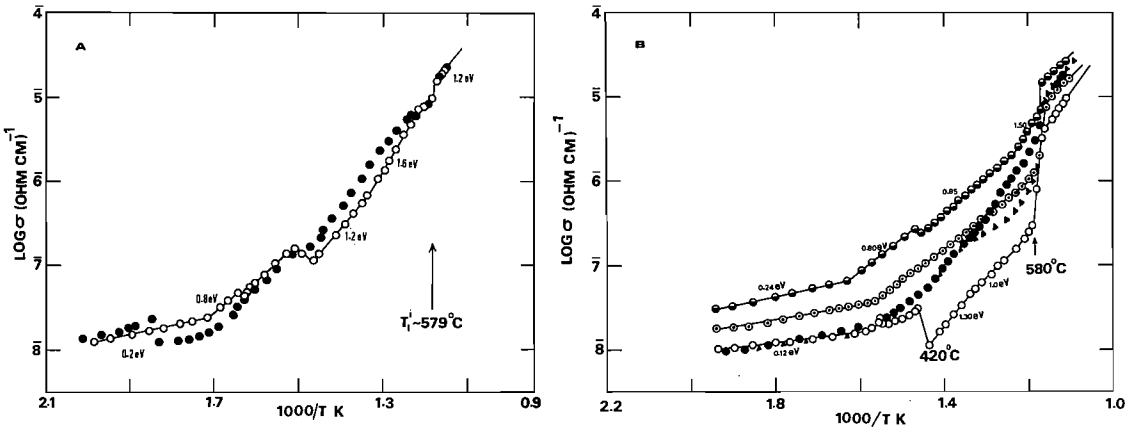

FIG. 3. (*A*) Logarithm of electrical conductivity *vs.* 1000/*T* K for Cu^{2+} doped K_2SO_4 crystals measured ⊥ to (011) face: ●, untreated crystals; ○, crystal preannealed at 330 °C for 15 min and cooled to 200 °C at ~2°/min. (*B*) Logarithm of electrical conductivity *vs.* 1000/*T* K for Cu^{2+} doped K_2SO_4 single crystals at different doping levels and pretreatment measured ⊥ to (011): ○, K_2SO_4 undoped; ▲, 0.1% Cu^{2+} grown K_2SO_4 preannealed for 30 min; ●, 0.1% Cu^{2+} grown K_2SO_4 preannealed for 60 min; ⊙, 0.5% Cu^{2+} grown K_2SO_4 preannealed for 60 min; ◒, 5% Cu^{2+} grown K_2SO_4 preannealed for 30 min.

ductivity σ *vs.* 1000/*T* K for K_2SO_4 crystals doped with Mg^{2+} (open circles) and Zn^{2+} (filled circles) measured ⊥ to (011) face. The initial slopes correspond to activation energies of 0.24 and 0.28 eV suggesting this to be due to physical defects, *e.g.* dislocations. This region is followed by an energy of 0.80 eV, in both samples, attributed to the cation migration energy. The initial higher conductivity of the Mg^{2+} doped K_2SO_4 relative to Zn^{2+} doped sample may be due to its smaller ionic radius, 0.66 Å compared to 0.74 Å, and the probability that Mg^{2+} is an interstitial impurity whereas Zn^{2+} may be present as a substitutional impurity.

The "pretransition" discontinuity appears at 370 °C for Zn^{2+} and 380 °C for Mg^{2+} doped crystals. The Mg^{2+} curve shows an activation energy of 1.0 eV after the "pretransition" effect and rising to 1.4 eV just prior to the major transition whereas the Zn^{2+} shows an activation energy of 1.2 eV and decreasing to 1.0 eV over the same temperature interval. The unusual energy trend for Zn^{2+} might incorporate the association enthalpy of divalent ion – cation vacancy complex which dissociates with increasing temperatures.

The magnitude of the jump in conductivity at the major transition, 579–585 °C, is less than that observed in the pure crystal. Above 585 °C, the conductivity of Mg^{2+} shows a higher temperature dependence than does Zn^{2+}, with activation energies of 2.2 and 1.3 eV, respectively.

Doped (Cu^{2+}) K_2SO_4 Crystals

The plot of logarithm of conductivity σ *vs.* 1000/*T* K for two crystals of K_2SO_4 containing Cu^{2+} measured ⊥ to (011) face is given in Fig. 3*A*; untreated crystal represented by filled circles and preannealed crystal, maintained at 330 °C for 15 min and cooled to 200 °C at rate of 2 °C/min, represented by open circles.

Preannealing the crystal lowers the conductivity and erases the anomaly observed at ~280 °C for the untreated crystal. The cation migration energy of 0.80 eV is reproduced here. A somewhat subdued "pretransition" effect, 350–420 °C, is followed by an activation energy of 1.20 eV. As the temperature increases the activation energy rises to 1.60 eV, reproducible to 0.10 eV for preannealed crystals, on its approach to the major transition temperature. Assuming this latter region to be the intrinsic region, the vacancy formation energy is calculated as 1.60 eV (Cu^{2+} enters the lattice substitutionally (14) giving rise to Schottky defects). Such a parallel increase in activation energy prior to the transition temperature occurred also in pure and Mg^{2+} doped K_2SO_4 crystals. The less exciting conductivity discontinuity at the transition temperature and the lower activation energy of 1.20 eV for the hexagonal phase conductivity relative to the pure crystal suggest that the Cu^{2+} doped K_2SO_4 crystal exists in highly comparable mobility configurations.

Can. J. Chem. Downloaded from www.nrcresearchpress.com by 210.87.254.40 on 09/05/12
For personal use only.

Can. J. Chem. Downloaded from www.nrcresearchpress.com by 210.87.254.40 on 09/05/12
For personal use only.

Figure 3*B* presents σ–T plots for K_2SO_4 crystals incorporating different levels of Cu^{2+} dopant and varying preanneal treatment. The σ–T curve for undoped K_2SO_4 (open circles) is included for comparison. It is evident that the conductivity of K_2SO_4 is enhanced by the level of Cu^{2+} concentration. The filled triangles represent measurements on 0.1% Cu^{2+} grown K_2SO_4 crystal preannealed for ~30 min beyond the pretransition temperature. The σ values are in excellent agreement with those of undoped K_2SO_4 up to 400 °C and the high sharp jump in σ near the phase transition ~580 °C is also evident. The filled circles refer to the same Cu^{2+} content crystal preannealed for ~60 min under identical conditions. These σ values fall on the established curve and the σ–T plot becomes linear but the discontinuity at ~580 °C is less well-defined.

The dotted circles represent 0.5% Cu^{2+} grown K_2SO_4 crystal preannealed for 60 min under identical conditions; well-defined linear slopes are observed. The half-filled circles represent a similarly preannealed 5% Cu^{2+} grown K_2SO_4 crystal. The data for 0.5% and 5% crystals were highly reproducible yielding an activation energy of 0.85 ± 0.05 eV for the cation migration and 1.4 ± 0.2 eV for the defect formation.

Doped (Mn^{2+}) K_2SO_4 Crystals

The logarithm of conductivity σ *vs.* 1000/T K for two crystals of K_2SO_4 doped with Mn^{2+} measured across the pyramidal faces is presented in Fig. 4; untreated crystal identified by filled circles and preannealed crystal, held at 425 °C for 15 min and slowly cooled to 200 °C, identified by open circles.

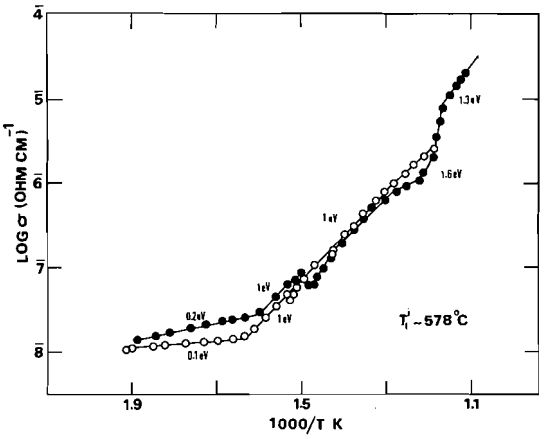

FIG. 4. Logarithm of electrical conductivity *vs.* 1000/T K for Mn^{2+} doped K_2SO_4 crystals measured across pyramidal face: ●, untreated crystal; ○, crystal preannealed at 425 °C for 15 min and slowly cooled to 200 °C.

Heat treatment lowers the initial activation energy to 0.10 eV relative to Cu^{2+} value of 0.20 eV. The cation migration energy of 1.0 eV is slightly higher than 0.80 eV recorded for the previous crystals. The "pretransition" effect is more prominent in the fresh crystal 379–406 °C, whereas the effect is barely discernible in the heated crystal. The fresh crystal shows an activation energy of 1.6 eV immediately following the "pretransition" effect and again prior to the major transition temperature while observing 1.0 eV between these two regions; the preannealed crystal, on the other hand, observes an activation energy of 1.0 eV throughout this temperature interval. The 1.6 eV region is not reproducible to 0.2 eV and therefore not reliable for defect formation energy evaluation; this latter energy value could be useful since Mn^{2+} is known to enter the K_2SO_4 lattice substitutionally (15) and expected to generate Schottky vacancies. The conductivity discontinuity at the orthorhombic–hexagonal transition lacks the sharpness observed in the undoped crystals.

Doped (Radioactive Zn^{2+}) K_2SO_4 Crystals

The σ–T data for preannealed Mn^{2+} doped K_2SO_4 crystal and Cu^{2+} doped K_2SO_4 crystal revealed (*i*) an appreciable lowering of the initial activation energy and (*ii*) the reduction in the intensity of the "pretransition" anomaly. The availability of radioactive ^{65}Zn prompted us to incorporate ^{65}Zn in the K_2SO_4 crystal to assess the effect, if any, of a constant internal energy source in the doped crystal.

The plot of the logarithm of conductivity σ *vs.* 1000/T K for two crystals of K_2SO_4 (one containing inactive Zn^{2+} and the other containing radioactive Zn^{2+}) measured ⊥ to (011) face is given in Fig. 5.

As expected the presence of the radioactive source raises the conductivity in the low temperature region with an appreciable lowering of the activation energy, 0.05 eV. The presence of ^{65}Zn also eliminates the anomaly and stabilizes the cation migration energy contribution, *i.e.* 0.85 ± 0.05 eV, prior to the major transition temperature of 579 °C. The effect of the radioactive ^{65}Zn dopant is interpreted to preclude secondary conductivity contributions arising from structural defects, ion-vacancy complex association, etc. to

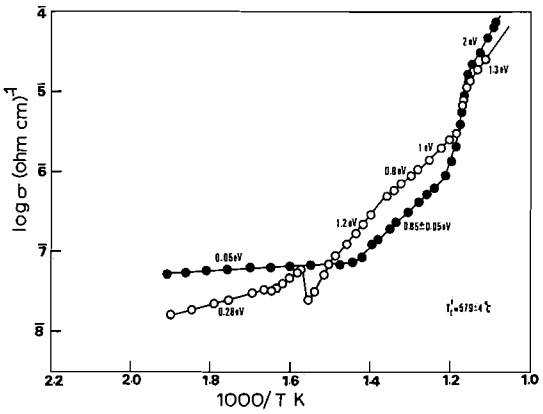

FIG. 5. Logarithm of electrical conductivity *vs.* $1000/T$ K for inactive Zn^{2+} doped K_2SO_4 crystal: ○, and radioactive Zn^{2+} doped K_2SO_4 crystal; ●, measured ⊥ to (011) face.

yield a less complex σ–T pattern of behavior; the exact interpretation must await more detailed studies.

Summary

The cation vacancy migration energy in K_2SO_4 is found to be 0.9 ± 0.1 eV. From the above conductivity measurements the defect formation energy is estimated to be 1.4 ± 0.2 eV. A decrease in lattice symmetry appears to favor Scottky defect formation and hence lower the defect formation energy; the case of CsCl supports this interpretation where defect formation energies of 1.40 eV and 2.20 eV are reported for the *Pm*3*m* (low symmetry) and *Fm*3*m* (high symmetry) phases (16, 17), respectively.

While ionic size might be the predominant factor contributing to the conductivity features of Mg^{2+} or Zn^{2+} doped K_2SO_4, the characteristic features of Mn^{2+} or Cu^{2+} doped crystals could be linked to d-electrons of the dopants, especially for a Jahn–Teller ion like Cu^{2+}. It would be worthwhile to obtain additional experimental results on crystals incorporating other transition metal ions to sort out these contributing factors.

The onset of the orthorhombic–hexagonal transformation, represented by T_t^i at $579° \pm 4$ °C as shown in the figures, is neither affected by the dopants nor by the crystallographic direction of measurement.

The phenomenon of "pretransition" is observed for all fresh crystals; the specific features of the phenomenon depend, however, on the crystallographic direction of measurement and the type of impurity ion. The persistence of this "pretransition" in preannealed crystals minimizes the confidence of any evaluation of defect formation energy or association enthalpy value. Furthermore, defect formation energies calculated from conductivity data on powder samples cannot be considered too reliable.

In conclusion, any interpretation contained above regarding defect energies should be taken only as suggestive of a trend for low symmetry crystal systems. The transport mechanism does involve defects as in the high symmetry alkali halides, but in the absence of comprehensive studies, theoretical and experimental, it is not possible at this time to describe a detailed model.

The authors are grateful to the National Research Council of Canada and the University Council for Research for financial support, and to Professor W. T. Foley for the goniometric measurements.

1. A. B. LIDIARD. Handbuch der physik. Vol. 20, Springer–Verlag, OHG Berlin. 1957. p. 246.
2. L. W. BARR and A. B. LIDIARD. Phys. Chem. **10**, 151 (1970).
3. M. HARTMANOVA. Fys. cas. **22**, 1 (1972).
4. C. NADLER and J. ROSSEL. Phys. Stat. Sol. (a) **18**, 711 (1973).
5. A. POLISHCHUK and T. M. SHURKHAL. Ukr. Khim. Zh. **38**(8), 833 (1972).
6. S. RADHAKRISHNA and K. P. PANDE. Phys. Stat. Sol. (a) **16**, 433 (1973).
7. L. N. COJOCARU, T. COSTEA, I. NEGOESCU, and G. PODEANU. Z. Phys. Chem. Neue Folge, **85**, 225 (1973).
8. M. NATARAJAN and E. A. SECCO. Can. J. Chem. **52**, 2436 (1974).
9. E. V. KOLONOTSOVA, E. E. KULAGO, N. I. BYAKOVA, and I. E. MIKHAILENKO. Sov. Phys. Dokl. **18**(5), 332 (1973).
10. P. N. MEHROTRA. Ph.D. Thesis, Indian Institute of Technology, Kanpur, India. 1968.
11. M. NATARAJAN and E. A. SECCO. Can. J. Chem. **52**, 712 (1974).
12. C. RAMASASTRY, Y. V. G. S. MURTI, and B. S. V. S. R. ACHARYULU, Modern aspects of solid state chemistry. Plenum Press, New York. 1970. p. 377.
13. T. WATANABE, K. SAKAI, and S. IWAI. Acta Cryst. A, **28**(4) Suppl. 187 (1972).
14. R. YU. ABDULSABIROV, YU. S. GREZNEV, and M. M. ZARIPOV. Sov. Phys. Solid State **12**(2), 509 (1970).
15. B. V. R. CHOWDARI and P. VENKATESWARLU. J. Chem. Phys. **48**, (1) 318 (1968).
16. (*a*) I. M. BOSWARWA. Phil. Mag. **16**, 827 (1967); (*b*) I. M. BOSWARWA and A. B. LIDIARD. Phil. Mag. **16**, 803 (1967).
17. (*a*) Z. MORLIN. Acta Phys. Acad. Sci. Hung. **21**(2), 137 (1966); (*b*) M. NATARAJAN, B. PRAKASH, and C. N. R. RAO. J. Chem. Soc. A, 2291 (1971).

Can. J. Chem. Downloaded from www.nrcresearchpress.com by 210.87.254.40 on 09/05/12
For personal use only.

Studies of β-Diketone Complexes of Rhenium. VII. The Crystal and Molecular Structure of Oxodichloropentane-2,4-dionatotriphenylphosphinerhenium(V)

C. J. L. LOCK[1] AND CHE'NG WAN

Institute for Materials Research, McMaster University, Hamilton, Ontario L8S 4M1

Received September 17, 1974

C. J. L. LOCK and CHE'NG WAN. Can. J. Chem. **53**, 1548 (1975).

The crystal structure of oxodichloropentane-2,4-dionatotriphenylphosphinerhenium(V) has been studied by single crystal X-ray methods. The crystals are triclinic with lattice parameters $a = 11.023(8)$ Å, $b = 13.523(8)$ Å, $c = 9.360(7)$ Å, $\alpha = 90.2(1)°$, $\beta = 114.1(1)°$, $\gamma = 67.7(2)°$. The space group is $P\bar{1}$ and there are two formula weights per unit cell. A total of 2891 reflections, of which 2447 were observed, were examined, and the structure was refined by full matrix least squares to an R_2 value of 0.0782. The ligands are arranged around the rhenium atom such that the nearest six atoms are at the corners of a very distorted octahedron. Most of this distortion appears to be caused by nonbonding repulsive interactions. The short oxo–phosphine distance, 2.85(1) Å, suggests the possibility of a weak bonding interaction. Observed bond distances (Re—Cl, 2.35 Å av; Re—O(oxo), 1.69(1) Å; Re—O(diketone), 1.99(1), 2.10(1) Å; Re—P, 2.431(4) Å) are close to those observed previously in similar compounds.

C. J. L. LOCK et CHE'NG WAN. Can. J. Chem. **53**, 1548 (1975).

On a étudié la structure cristalline de l'oxodichloropentanedionato-2,4 triphénylphosphine-rhénium(V) à l'aide des méthodes de rayons-X de cristal unique. Les cristaux sont tricliniques avec des dimensions de mailles $a = 11.023(8)$ Å, $b = 13.523(8)$ Å, $c = 9.360(7)$ Å, $\alpha = 90.2(1)°$, $\beta = 114.1(1)°$, $\gamma = 67.7(2)°$. Le groupe d'espace est $P\bar{1}$ et il y a deux molécules par maille. On a examiné un total de 2891 réflections desquelles 2447 ont été observées; la structure a été raffinée par la méthode des moindres carrés (matrice complète) jusqu'à une valeur R_2 de 0.0782. Les ligands sont arrangés autours de l'atome de rhénium d'une façon telle que les 6 atomes les plus près sont dans les coins d'un octaèdre très tordu. Il semble que la plus grande partie de la distortion soit causée par des interactions répulsives non-liées. La courte distance oxo–phosphine, 2.85(1) Å, suggère la possibilité d'une interaction liante faible. Les valeurs observées pour les distances de liaison (Re—Cl, 2.35 Å moyen; Re—O(oxo), 1.69(1) Å; Re—O(dicétone), 1.99(1), 2.10(1) Å; Re—P, 2.431(4) Å) sont près des valeurs observées antérieurement pour des composés similaires. [Traduit par le journal]

Introduction

The reaction of acetylacetone with oxotrichlorobis(triphenylphosphine)rhenium(V) (**1**) or oxodichloroethoxobis(triphenylphosphine)rhenium(V) (**2**) yields a number of different products depending on the reaction conditions (1). It has been shown (2, 3) that the group *trans* to the oxo group in **1** and **2** is very susceptible to attack and the expected product of the above reaction is oxodichloropentane-2,4-dionatotriphenylphosphinerhenium(V) (**3**); initial attack of **1** or **2** would involve the replacement of the group *trans* to the oxo-oxygen by one end of the chelating ligand. A small amount of a compound of stoichiometry corresponding to **3** was obtained in some reactions, but only as a minor component. The title compound can exist in four geometric isomers, however, and a further three isomers have been isolated (4). It was of interest to see whether the structure of **3** was the one expected and whether the structure would give any clue to the low yields obtained in the reactions. We now report the structure of **3**.

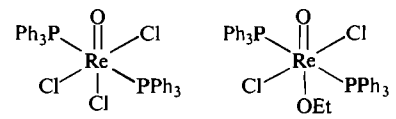

1 **2**

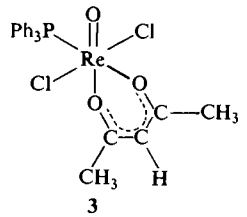

3

[1]Author to whom correspondence should be addressed.

Can. J. Chem. Downloaded from www.nrcresearchpress.com by 210.87.254.6 on 09/05/12
For personal use only.

Can. J. Chem. Downloaded from www.nrcresearchpress.com by 210.87.254.6 on 09/05/12
For personal use only.

Experiments

$ReOCl_2(acac)P(C_6H_5)_3$ was prepared from $ReOCl_2(OEt)[P(C_6H_5)_3]_2$.[2] A purple solution of $ReOCl_2(OEt)[P(C_6H_5)_3]_2$ (2 g) (5) and acetylacetone (2 ml) in benzene (50 ml) was boiled until it turned bright green (about 1 min) and then poured into light petroleum ether (b.p. 40–60°, 400 ml). The mixture was stirred vigorously and the precipitate allowed to settle. If the supernatant liquid was still appreciably green, it was decanted and set aside, green crystals of the compound separating; these were handpicked from some orange material.

Anal. Calcd. for $C_{23}H_{22}Cl_2O_3PRe$: C, 43.5; H, 3.5; P, 4.9; Cl, 11.2. Found: C, 43.1; H, 4.2; P, 5.0; Cl, 11.3.

Single crystals were obtained by crystallizing the compound from a mixture of methylene chloride and petroleum ether (80–100 °C). Crystals obtained from this solvent mixture at room temperature were usually twinned or fern-like with small crystals grouped around the main axis. If the temperature of crystallization was maintained constant at about 0 °C, nontwinned plate-like crystals were obtained suitable for X-ray diffraction purposes.

Crystallography

Two crystals were cut from a large crystal chosen because it had sharp extinctions and optical homogeneity when examined through a polarizing microscope. Crystal I, with dimensions 0.09 × 0.10 × 0.12 mm, and Crystal II, with dimensions 0.09 × 0.14 × 0.11 mm, were both mounted along their longest dimensions which were parallel to b^* and c^* respectively.

A series of Weissenberg and precession photographs showed the crystal was triclinic. Cell parameters were determined from $0kl$ and $hk0$ precession photographs which were calibrated with a diffraction pattern of TiO_2 (rutile: $a = 4.5929(5)$ and $c = 2.9591(3)$ Å (6)) and β was measured from the spindle reading. The density of a few crystals was determined in a tetrabromoethane – carbon tetrachloride mixture. The parameters were:

$C_{23}H_{22}Cl_2O_3PRe$ f.w. = 634.5

Triclinic, $a = 11.023(8)$, $b = 13.523(8)$, $c = 9.360(7)$ Å, $\alpha = 90.2(1)$, $\beta = 114.1(1)$, $\gamma = 67.7(2)°$, $V = 1158$ Å^3, $P\bar{1}$, (C_i^1, No. 2) $\rho_o = 1.76(4)$, $Z = 2$, $\rho_c = 1.82$ (22°, MoKα, $\lambda = 0.71069$ Å), $\mu = 58.6$.[3]

Photographs were taken of the layers nkl, $n = 0$–4 and hkm, $m = 0$–3 for crystal I and the first layer perpendicular to [110] for crystal II. All photographs were recorded on an integrating precession camera, using zirconium filtered MoKα radiation. The intensities of all reflections were measured with a Joyce–Loebl microdensitometer. The unobserved reflections were assigned an intensity equal to the minimum observed intensity in that region of reciprocal space. Standard errors, σ, were assigned by the method of Ibers (7) and Hughes (8) and weights, $w = 1/\sigma^2$, were used throughout the refinement. The measured intensities were corrected for Lorentz and polarization effects, but absorption corrections were not applied. The maximum error in F_o which could be introduced is 10%; the average error was much smaller.

Solution and Refinement

The Patterson functions projected on (100) and (001) gave the positions of the rhenium, chlorine, and phosphorus atoms. The magnitudes of the Re–Cl and Re–P peaks were consistent with $P\bar{1}$ symmetry and showed no splitting. All other nonhydrogen atoms were located by successive Fourier and electron difference syntheses. The phosphorus atom was distinguished from the chlorine atoms by its proximity to the carbon atoms of the phenyl groups. Refinement of the structure was by full matrix least squares treating the phenyl groups as rigid bodies (9, 10) but using individual isotropic temperature factors for each atom in the group (11). The program used was GROUPLS[4] for the CDC 6400 computer. At the beginning of the refinement, temperature factors, which had previously been isotropic for all atoms, were made anisotropic for the Re, P, Cl, and O atoms. Refinement was terminated when no parameter shifted by more than 1/20th of its estimated standard deviation at $R_1 = 0.0802$ and $R_2 = 0.0782$.[5] Of the 2891 measured reflections, 2447 were observed; 2558 reflections were given nonzero weight in the refinement. These included all observed reflections, except three which were of very doubtful accuracy because they were on the edge of the backstop shadow, and all unobserved reflections for which $F_c > F_{min}$ (114). F_{min} was the minimum observed intensity in that region of reciprocal space. For these unobserved reflections ($F_c > F_{min}$), the value of Δ, used in calculating the least squares matrix, was defined as $F_c - 0.6F_{min}$. The 2891 reflections represent about 43% of the reflections theoretically accessible with a precession angle of 30°.

The final electron difference map was essentially featureless, the only significant peaks being 2.2 e/Å^3 at 0.46, 0.81, 0.71, near the rhenium atom and between the rhenium and phosphorus atoms, and 2.1 e/Å^3 (0.29, 0.85, 0.69) between the rhenium atom and O2. The lowest valley was −1.2 e/Å^3 (0.33, 0.83, 0.02) close to O1. In all calculations, the atomic scattering factors given in the *International Tables for X-Ray Crystallography* were used for Cl, P, O, and C (12) and those of Cromer and Waber were used for Re (13). Anomalous dispersion corrections given by Cromer (14) were used for Re, Cl, and P. The calculated atom parameters are given in Table 1 and the values of F_o, F_c, and σ are given in Table 2.[6]

Results and Discussion

The principal intramolecular distances and angles for $ReOCl_2(acac)P(C_6H_5)_3$ are given in

[2]acac$^-$ is the anion of the ketoenolate form of acetylacetone, $C_5H_7O_2^-$; Et is ethyl, C_2H_5.

[3]The cell used in this work is the Niggli (30) reduced cell, as used in *Crystal Data* (31). It may be transformed into the Delaunay (32) reduced cell, $a = 13.829$, $b = 13.523$, $c = 11.174$ Å, $\alpha = 111.8$, $\beta = 98.7$, $\gamma = 132.5°$ by the transformation matrix (110/010/101).

[4]Program GROUPLS was written locally by J. S. Stephens.

[5] $R_1 = \dfrac{\Sigma||F_o| - |F_c||}{\Sigma|F_o|}$; $\quad R_2 = \left\{\dfrac{\Sigma\omega(|F_o| - |F_c|)^2}{\Sigma\omega F_o^2}\right\}^{1/2}$.

[6]Table 2 is available, at a nominal charge, from the Depository of Unpublished Data, CISTI, National Research Council of Canada, Ottawa, Canada K1A 0S2.

Can. J. Chem. Downloaded from www.nrcresearchpress.com by 210.87.254.6 on 09/05/12
For personal use only.

TABLE 1

(*a*) Atom parameters for $ReOCl_2(acac)P(C_6H_5)_3$ ($\times 10^3$)*

Atom	*x*	*y*	*z*	*U* (Å²)
Re	367.49(8)	−168.49(5)	−257.33(8)	
Cl1	259.5(6)	−292.2(4)	−267.2(7)	
Cl2	438.3(5)	−24.6(3)	−206.6(5)	
P	621.8(5)	−298.3(3)	−146.5(5)	
O1	396(1)	−179(1)	−22(1)	
O2	173(1)	−58(1)	−291(1)	
O3	371(1)	−177(1)	−436(1)	
C1	333(2)	−114(1)	45(2)	57(4)
C2	205(2)	−30(1)	−38(2)	57(5)
C3	130(2)	−6(2)	−199(2)	72(6)
C4	412(2)	−147(1)	225(2)	66(5)
C5	−18(2)	93(1)	−274(2)	62(5)
C11	914(2)	−177(2)	−259(2)	83(7)
C12	973(2)	−254(2)	−124(2)	66(5)
C13	884(2)	−292(2)	−91(2)	66(5)
C14	735(2)	−251(2)	−193(2)	41(4)
C15	676(2)	−173(3)	−328(2)	57(5)
C16	765(2)	−136(2)	−361(2)	54(4)
C21	835(2)	−369(2)	400(2)	78(6)
C22	808(2)	−449(2)	316(2)	78(6)
C23	745(2)	−430(2)	151(2)	68(5)
C24	709(2)	−329(2)	69(2)	50(4)
C25	736(2)	−248(2)	152(2)	58(4)
C26	800(2)	−269(2)	318(2)	72(5)
C31	688(2)	−621(2)	−337(2)	76(6)
C32	771(2)	−566(2)	−338(2)	111(9)
C33	753(2)	−470(2)	−277(2)	86(7)
C34	651(2)	−430(2)	−215(2)	63(5)
C35	568(2)	−486(2)	−215(2)	85(6)
C36	586(2)	−581(2)	−276(2)	99(8)

(*b*) Anisotropic temperature factors U_{ij} ($\times 10^3$)†

Atom	U_{11}	U_{22}	U_{33}	U_{12}	U_{13}	U_{23}
Re	45.4(5)	42.3(4)	50.1(5)	−16.6(3)	22.9(4)	−15.5(3)
Cl1	74(3)	68(3)	118(4)	−43(3)	56(3)	−41(3)
Cl2	67(3)	36(2)	58(2)	−24(2)	26(2)	−11(2)
P	44(2)	34(2)	42(2)	−17(2)	21(2)	−11(2)
O1	62(7)	22(5)	71(7)	−16(5)	51(7)	−13(5)
O2	62(8)	62(8)	73(8)	−13(6)	43(8)	−30(6)

*Estimated standard deviations from the least squares programs are given in brackets. The atoms C11, C12, . . . C16; C21, C22 . . . C26; etc., were refined as three groups and the estimated standard deviations are derived from the group refinement.

†The temperature factor parameters U_{ij} were obtained from $\beta_{ij} = 2\pi^2 b_i b_j U_{ij}$ where β_{ij}'s appear as a temperature effect through $\exp[-(\beta_{11}h^2 + \ldots 2\beta_{12}hk + \ldots)]$ in the structure factor expression and b_i are the reciprocal lattice vectors.

Table 3 and the molecule is illustrated in Fig. 1.[7] The ligands are arranged around the rhenium atom such that the bound atoms are at the apices of a very rough octahedron. The structure is that of the expected isomer of $ReOCl(acac)P(C_6H_5)_3$ shown as **3**.

The Re—O(oxo) bond length (1.69(1) Å) agrees well, within the errors, with values of 1.60(5) to 1.73(6) Å found in other compounds containing the oxo-group (15–17), and the Re—P distance (2.431(4) Å) is in fair agreement with previous results (18, 19). The two Re—Cl distances in $ReOCl_2(acac)P(C_6H_5)_3$ (2.339(5) and 2.376(7) Å), while close to those observed in $Re(acac)_2Cl_2$ (20) and $Re(acac)Cl_2(P(C_6H_5)_3)_2$ (19), are shorter than those found in many compounds of Re(V) (18). Ibers and co-workers have

[7]Figures 1 and 2 were prepared with the aid of the program ORTEP written by Johnson (28).

TABLE 3. Selected intramolecular distances and angles in $ReOCl_2(C_5H_7O_2)P(C_6H_5)_3$

Atom pair	Distance (Å)	Atom pair	Distance (Å)
Bonded distances			
Re—Cl1	2.376(7)	C1—C2	1.33(2)
Re—Cl2	2.339(5)	C2—C3	1.36(3)
Re—P	2.431(4)	C1—C4	1.53(3)
Re—O1	2.10(1)	C3—C5	1.54(2)
Re—O2	1.99(1)	P—C14	1.80(1)
Re—O3	1.69(1)	P—C24	1.81(1)
O1—C1	1.24(2)	P—C34	1.85(1)
O2—C3	1.24(3)		
Nonbonded distances			
Cl1–O1	2.97(1)	O1–O2	2.64(1)
Cl1–O2	2.92(1)	O2–O3	2.99(2)
Cl1–O3	3.08(2)	P–O1	3.08(2)
Cl2–O1	3.00(2)	P–O3	2.85(1)
Cl2–O2	2.92(2)	P–Cl1	3.646(6)
Cl2–O3	3.04(1)	P–Cl2	3.379(4)

Bond pair	Angle (deg)	Bond pair	Angle (deg)
Cl1—Re—Cl2	164.0(3)	Re—O1—C1	131(1)
Cl1—Re—P	98.7(2)	Re—O2—C3	132(1)
Cl1—Re—O1	82.9(4)	O1—C1—C2	122(2)
Cl1—Re—O2	83.5(5)	O2—C3—C2	125(2)
Cl1—Re—O3	97.0(5)	C1—C2—C3	125(3)
Cl2—Re—P	90.6(2)	O1—C1—C4	113(2)
Cl2—Re—O1	84.9(4)	O2—C3—C5	117(2)
Cl2—Re—O2	84.4(5)	C2—C1—C4	125(3)
Cl2—Re—O3	96.7(5)	C2—C3—C5	118(3)
P—Re—O1	85.3(3)	Re—P—C14	113.6(2)
P—Re—O2	165.5(4)	Re—P—C24	113.2(3)
P—Re—O3	85.5(3)	Re—P—C34	114.4(3)
O1—Re—O2	80.7(5)	C14—P—C24	103.8(3)
O1—Re—O3	170.6(4)	C14—P—C34	104.6(3)
O2—Re—O3	108.6(5)	C24—P—C34	106.5(3)

opined (21) that the Re—Cl distances observed in most Re(V) compounds are unduly long because of steric effects. He suggests that a "normal" distance is that observed in $ReNCl_2(P(C_6H_5)_3)_2$ (2.377(2) Å) (22) which is very close to the distances observed for our compound. If the error limits derived from the inverse matrix are realistic, it appears that the Re—Cl distances in $ReOCl_2(acac)P(C_6H_5)_3$ are significantly different. This appears to be caused by interaction with the phosphine group, since, although the Cl—O distances do not vary markedly, the P—Cl1 and P—Cl2 distances differ by 0.27 Å. The longer Cl1—P and Cl—Re distances are probably caused by the interaction between Cl1 and a phenyl group since the calculated Cl1—H(C35) distance of 2.46 Å is considerably shorter than the van der Waals radius sum of 2.93 Å and the corresponding Cl2—H(C5) distance of 2.70 Å.

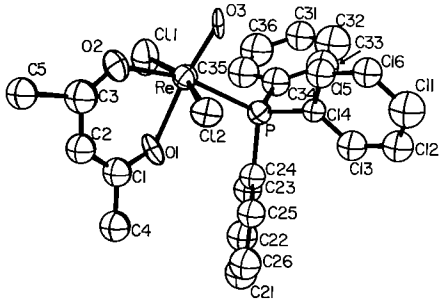

FIG. 1. The molecular structure of $ReOCl_2(C_5H_7O_2)P(C_6H_5)_3$. The numbering of the atoms is as in Table 1.

Distances within the β-ketoenolate group do not vary significantly from the average values reported by Lingafelter and Braun (23), and the

Can. J. Chem. Downloaded from www.nrcresearchpress.com by 210.87.254.6 on 09/05/12
For personal use only.

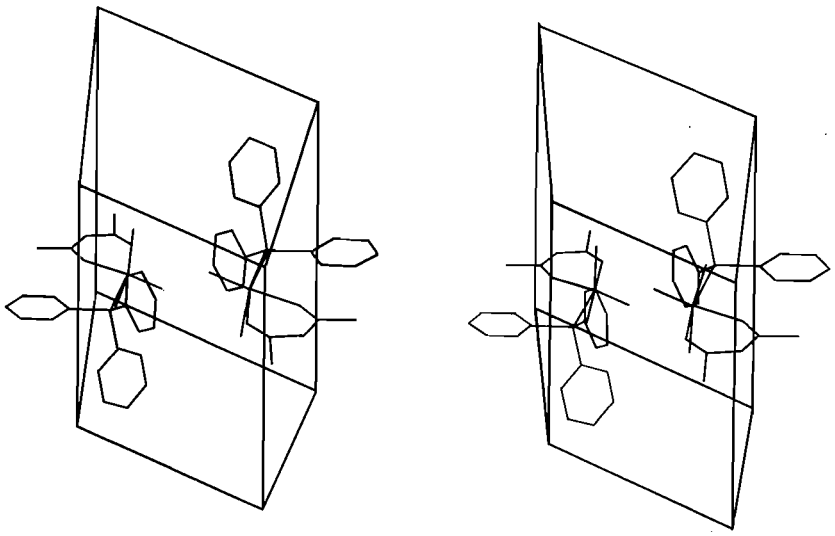

FIG. 2. Stereogram (stereoscopic pair of perspective projections) of two molecules of $ReOCl_2(acac)P(C_6H_5)_3$ in the unit cell viewed down the b^* axis. The c^* and a axes run roughly parallel to the top and side edges of the paper respectively.

dihedral angle of 16° between the ReO1O2 and O1C1C2C3O2 fragments is within the range normally observed. However, the two rhenium–oxygen (ketone) distances (2.10(1) and 1.99(1) Å) appear to be significantly different. The lower value for the oxygen *cis* to the oxo-group is in fair agreement with values we have found previously for similar compounds (19, 20), but the Re–O distance for the oxygen atom *trans* to the oxo-group is longer than any of the others. Long bonds to atoms *trans* to multiply bonded oxo and nitrido ligands have been observed before (15–17, 21, 22, 24, 25). It has been postulated that strong π-bonding in Re=O groups weakens the bonding to the *trans* ligand (3), but Bright and Ibers (18) have put forward the more reasonable explanation that the effect is caused by steric repulsion of other ligands.

Certainly, the arrangement of the O1, O2, O3, P atoms suggests fairly strong steric interactions. Even though the O3–O1 distance is about 0.2 Å longer than the normal van der Waals (v.d.W.) radii sum (2.8 Å) (29),[8] the O2–O1 distance is shorter by about 0.15 Å than the v.d.W. radii sum, as are both the P–O1 and P–O3 distances (difference 0.2 and 0.45 Å respectively). Some shortening of "nonbonded" distances between ligand atoms is not unusual and the structure is slightly distorted in such a manner to relieve repulsive interactions. O1 and O3 are about 0.05 Å out of the least squares plane through O1O2O3P on one side and O2 and P by the same distance on the other. The rhenium atom is displaced 0.03 Å out of the plane on the same side as O1. Nevertheless, the P–O3 distance is unusually short. It is nearly 0.25 Å shorter than previously observed P–O distances in similar compounds (15, 19, 20) and 0.3 Å shorter than similar P–N distances (18). Since normal forms of the repulsion interaction are assumed to be $1/r^{12}$ or $\exp(-r)$, this extra shortening would require a large amount of energy which would be obtained from an increased attractive interaction. The Re—O3 and Re—P bonds are not unusually short so that it appears that the "bonding" interaction must be directly between O3 and the phosphine group.

Such an interaction is consistent with the observed thermal breakdown of $ReOCl_2(acac)P(C_6H_5)_3$ in the mass spectrometer. Peaks corresponding to $(C_6H_5)_3PO^+$ and $Re_2(acac)_2Cl_4^+$ are observed (4) which could arise from

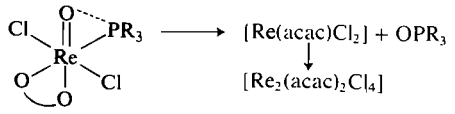

The packing of the molecules within the unit cell is shown in Fig. 2. In the ***a*** direction we can

[8]Similar distances have been observed in vanadyl β-ketoenolates (26, 27).

Can. J. Chem. Downloaded from www.nrcresearchpress.com by 210.87.254.6 on 09/05/12
For personal use only.

consider the packing as a double chain, the links being pairs of molecules related by the inversion center at $\frac{1}{2}, \frac{1}{2}, \frac{1}{2}$. Contact within this pair of molecules is such that the hydrogen atoms on the third phenyl ring of one molecule come close to O3 and Cl2 on the other molecule. Along the chain the intermolecular contact is between the first phenyl ring of one molecule and Cl1 and the β-ketoenolate ring on the next.

In the ***c*** direction each double chain contacts the next through C4 methyl groups and the third phenyl rings. In the ***b**** direction contact is between the C5 methyl groups and the first phenyl rings. All distances for the contacts mentioned above lie close to the values calculated from the sum of van der Waals radii. In addition further contact can occur between each phenyl ring and its centrosymmetrically related neighbor. Thus ring 3 lies 3.7 Å from the $\frac{1}{2}, \frac{1}{2}, \frac{1}{2}$ neighbor and ring 2 lies 3.5 Å from the $\frac{1}{2}, \frac{1}{2}, 0$ neighbor. In the case of ring 1 the related ring is obtained by inversion through $0, 0, \frac{1}{2}$, but in this case there is not substantial overlap of the rings, the shortest inter-ring C–C distance being 4.6 Å.

We thank the National Research Council of Canada for financial support of this work.

1. D. E. Grove, N. P. Johnson, C. J. L. Lock, and G. Wilkinson. J. Chem. Soc. 490 (1965).
2. J. Chatt and G. A. Rowe. J. Chem. Soc. 4019 (1962).
3. N. P. Johnson, C. J. L. Lock, and G. Wilkinson. J. Chem. Soc. 1054 (1964).
4. W. D. Courrier. Ph. D. Thesis, McMaster University, Hamilton, Ontario. 1971.
5. N. P. Johnson, C. J. L. Lock, and G. W. Wilkinson. Inorganic syntheses, Vol. 9. McGraw Hill, Inc., New York. 1967. p. 147.
6. D. T. Cromer and K. Herrington. J. Am. Chem. Soc. **77**, 4708 (1955).
7. J. A. Ibers. Acta Cryst. **9**, 652 (1956).
8. E. W. Hughes. J. Am. Chem. Soc. **63**, 1737 (1941).
9. C. Scheringer. Acta Cryst. **16**, 546 (1963).
10. S. J. LaPlaca and J. A. Ibers. Acta Cryst. **18**, 511 (1965).
11. L. F. Dahl and W. E. Oberhansli. Inorg. Chem. **4**, 629 (1965).
12. J. A. Ibers. International tables for X-ray crystallography. Vol. III. Kynoch Press, Birmingham. 1962. p. 201.
13. D. T. Cromer and J. I. Waber. Acta Cryst. **18**, 104 (1965).
14. D. T. Cromer. Acta Cryst. **18**, 17 (1965).
15. H. W. W. Ehrlich and P. G. Owston. J. Chem. Soc. 4368 (1963).
16. F. A. Cotton and S. J. Lippard. Inorg. Chem. **4**, 1621 (1965).
17. F. A. Cotton and S. J. Lippard. Inorg. Chem. **5**, 416 (1966).
18. D. Bright and J. A. Ibers. Inorg. Chem. **8**, 709 (1969).
19. I. D. Brown, C. J. L. Lock, and Che'ng Wan. Can. J. Chem. **52**, 1704 (1974).
20. (*a*) C. J. L. Lock and Che'ng Wan. Chem. Commun. 1109 (1967); (*b*) I. D. Brown, C. J. L. Lock, and Che'ng Wan. Can. J. Chem. **51**, 2073 (1973).
21. P. W. R. Corfield, R. J. Doedens, and J. A. Ibers. Inorg. Chem. **6**, 197 (1967).
22. R. J. Doedens and J. A. Ibers. Inorg. Chem. **6**, 204 (1967).
23. E. C. Lingafelter and R. L. Braun. J. Am. Chem. Soc. **88**, 2951 (1966).
24. D. Bright and J. A. Ibers. Inorg. Chem. **7**, 1099 (1968).
25. D. Bright and J. A. Ibers. Inorg. Chem. **8**, 703 (1969).
26. R. P. Dodge, D. H. Templeton, and A. Zalkin. J. Chem. Phys. **35**, 55 (1961).
27. P. K. Hon, R. L. Belford, and C. E. Pfluger. J. Chem. Phys. **43**, 1323 (1965).
28. C. K. Johnson. U.S. Atomic Energy Commission Report, ORNL-3794. Revised June, 1965.
29. L. Pauling. Nature of the chemical bond. 2nd ed. Cornell University Press, Ithaca, New York. 1945. p. 189.
30. P. Niggli. Handbüch der experimentalphysik, Vol. 7, Part 1. Akademische Verlagsgesselschaft, Leipzig. 1928.
31. J. D. H. Donnay, H. M. Ondik, and G. M. Wolten. Crystal data, 3rd ed., Vol. 2. U.S. Dept. of Commerce, N.B.S. and Joint Comm. on Powder Diffr. Standards, 1973. p. 2.
32. B. Delaunay. Z. Krist. **84**, 109 (1933).

Can. J. Chem. Downloaded from www.nrcresearchpress.com by 210.87.254.6 on 09/05/12
For personal use only.

A Convenient Preparation of *meso*-Tetra(4-sulfonatophenyl)porphyrin

CLAUDIA A. BUSBY
Department of Chemistry, Harvard University, Cambridge, Massachusetts 02138
AND
ROBERT K. DINELLO
Department of Biological Chemistry, Harvard Medical School, Boston, Massachusetts 02115
AND
DAVID DOLPHIN[1]
Department of Chemistry, The University of British Columbia, Vancouver, British Columbia V6T 1W5

Received November 25, 1974

CLAUDIA A. BUSBY, ROBERT K. DINELLO, and DAVID DOLPHIN. Can. J. Chem. **53**, 1554 (1975).

The sulfonation of *meso*-tetraphenylporphyrin, in concentrated sulfuric acid followed by neutralization and dialysis, provides an efficient and convenient route to *meso*-tetra(4-sulfonatophenyl)porphyrin.

CLAUDIA A. BUSBY, ROBERT K. DINELLO et DAVID DOLPHIN. Can. J. Chem. **53**, 1554 (1975).

La sulfonation de la *meso*-tétraphénylporphyrine, dans l'acide sulfurique concentré, suivie par une neutralisation et une dialyse fournit une méthode efficace et facile d'obtenir la *meso*-tétra(sulfonato-4 phényl) porphyrine. [Traduit par le journal]

The initial studies by Winkelman (1) on the localization of *meso*-tetra(4-sulfonatophenyl)-porphyrin in tumors have been followed by an increasing interest in this water soluble porphyrin. This interest has been stimulated by the ready availability (2) of *meso*-tetraphenylporphyrin (TPP) **1** and its conversion into *meso*-tetra(4-sulfonatophenyl)porphyrin **2** by direct sulfonation.

Two methods for this sulfonation have recently been reported. Both methods bring about the sulfonation in hot sulfuric acid and differ only in the isolation and purification of the product. The method developed by Fleischer *et al.* (3) invokes preparation of the tetra-ammonium salt which is purified by six precipitations from methanol–acetone but, in our hands, a good recovery of the product always results in its contamination with ammonium sulfate. To remove the inorganic salts one must sacrifice large amounts of the product at each stage with a resultant poor yield.

The second method reported by Srivastava and Tsutsui (4) requires dilution of the reaction mixture and addition of lime to the resulting large volume of aqueous solution in order to remove the sulfuric acid as calcium sulfate. A number of time-consuming and cumbersome filtrations and concentrations are then required to isolate the product, which is always contaminated with inorganic salts unless careful precautions are taken, which again result in a lowering of the yield.

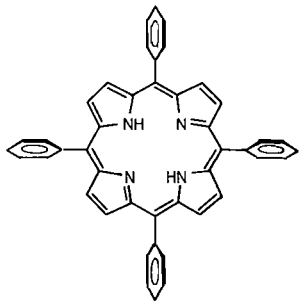

1

We wish to report here the preparation and simplified purification procedure which involves dialysis to remove inorganic contaminants and results in a 75% overall yield from TPP.

[1]Author to whom correspondence should be addressed.

Can. J. Chem. Downloaded from www.nrcresearchpress.com by 210.87.254.105 on 09/05/12
For personal use only.

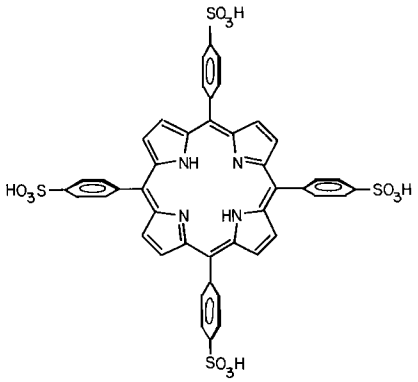

2

Experimental

Powdered TPP (2) (2 g) was suspended in concentrated sulfuric acid (50 ml) in a 250 ml round-bottomed flask equipped with a drying tube. The mixture was heated in a steam bath for 6 h and then left to stand overnight. At the beginning of the reaction the viscous mixture was occasionally swirled to dissolve the porphyrin. Water (150 ml) was then carefully added and the mixture was allowed to cool to room temperature. The green protonated porphyrin was collected by filtration and washed once with a little acetone. The porphyrin and Celite were suspended in water (150 ml) and neutralized with saturated sodium bicarbonate until the green solution turned purple. The mixture was filtered to remove Celite and unreacted TPP, and the filtrate was dialyzed four times to remove inorganic contaminants.

The dialyses were carried out using cellulose dialysis tubing with a pore diameter of 4.8 nm (Fisher), which had been previously boiled in distilled water for 15 min and then rinsed. Each dialysis was carried out for 3 h against a 40-fold excess of stirred distilled water. The solution was concentrated to 50 ml, filtered, and evaporated to dryness. Tetrasodium *meso*-tetra(4-sulfonatophenyl)porphyrin was recrystallized from methanol–ethanol and dried for 1 h at 110° to give 3 g of the dodecahydrated salt. The anhydrous product was prepared by heating *in vacuo* at 150° for 24 h.

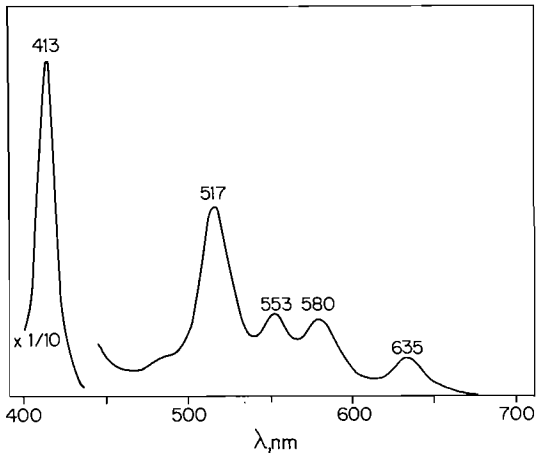

FIG. 1. The optical absorption spectrum of **2** in H_2O.

Anal. Calcd. for $C_{44}H_{26}N_4O_{12}S_4Na_4$: N, 5.48; S, 12.52. Found: N, 5.17; S, 12.29.

Nuclear magnetic resonance $\delta(D_2O)$ (DSS) A, 7.27(d); B, 8.11(d), J_{AB} = 7 Hz; C, 7.80 (s).

Visible absorption $\lambda(H_2O)$ (nm) (see Fig. 1): 414, 516, 553, 579, and 633.

C.A.B. thanks the National Institutes of Health for a predoctoral trainee fellowship, and R.K.D. thanks The National Science Foundation for a predoctoral fellowship. The support of the National Institutes of Health (Grant No. AM 14343) and the National Research Council of Canada is gratefully acknowledged.

1. J. WINKELMAN. Experientia, **23**, 949 (1967).
2. A. D. ADLER, F. R. LONGO, J. D. FINARELLI, J. GOLDMACHER, J. ASSOUV, and T. KORSAKOFF. J. Org. Chem. **32**, 476 (1967).
3. E. G. FLEISCHER, J. M. PALMER, T. S. SRIVASTAVA, and A. CHATTERJEE. J. Am. Chem. Soc. **93**, 3162 (1971).
4. T. S. SRIVASTAVA and M. TSUTSUI. J. Org. Chem. **38**, 2103 (1973).

Can. J. Chem. Downloaded from www.nrcresearchpress.com by 210.87.254.105 on 09/05/12
For personal use only.

Nuclear Magnetic Resonance Studies of Enantiomeric Internal Rotational Isomers of 1- and 3-Arylhydantoins in Achiral and Chiral Solvents

LAWRENCE D. COLEBROOK AND SIDDIK ICLI

Department of Chemistry, Sir George Williams Campus, Concordia University, Montreal, Quebec H3G 1M8

AND

FRANK H. HUND

Department of Chemistry, University of Rochester, Rochester, New York 14627

Received November 13, 1974

LAWRENCE D. COLEBROOK, SIDDIK ICLI, and FRANK H. HUND. Can. J. Chem. **53**, 1556 (1975).

^1H and ^{13}C n.m.r. spectra have been determined for a number of 1- and 3-arylhydantoins in achiral and chiral solvents. These compounds, which have enantiomeric rotational isomers, show restricted internal rotation about the aryl C—N bond at normal probe temperatures. Chemical shifts between corresponding protons on the pairs of rotamers, induced by diastereomeric solute–solvent interactions in the chiral solvent, are strongly dependent on the location of the protons in the solute molecules. In conjunction with ^1H and ^{13}C chemical shifts, these data provide information on the geometry of the solvated species. No splitting of signals resulting from the presence of diastereomeric solvates was observable in the ^{13}C spectra. Activation parameters for hindered internal rotation, determined by complete p.m.r. line shape analysis using signals of the diastereotopic methyl groups in the 5-position, show some solvent dependence.

LAWRENCE D. COLEBROOK, SIDDIK ICLI et FRANK H. HUND. Can. J. Chem. **53**, 1556 (1975).

On a déterminé les spectres r.m.n. du ^1H et du ^{13}C d'un certain nombre d'hydantoines arylées en position 1 ou 3 dans des solvants achiraux et chiraux. Ces composés, qui ont des isomères de rotation énantiomères, montrent la présence d'une rotation interne empêchée autour du lien N—C aryle aux températures normales d'études. Les solvants chiraux provoquent des interactions diastéréoisomères soluté–solvant qui induisent des déplacements chimiques, entre les protons correspondants sur les paires de rotamères, dont l'amplitude dépend fortement sur la position des protons de ces molécules solutées. Si on utilise ces données en relation avec les déplacements chimiques des ^1H et ^{13}C, on peut déduire des informations sur la géométrie des espèces solvatées. Dans les spectres ^{13}C, on n'a pas pu observé de dédoublements de signaux qui résulteraient de la présence d'espèces solvatées diastéréoisomères. Les paramètres d'activation pour la rotation empêchée interne, tels que déterminés par une analyse complète de la forme des lignes des spectres r.m.p. et faisant appel aux signaux des groupes méthyles diastéréotopes en position 5, montrent une certaine dépendance sur le solvant.

[Traduit par le journal]

Following the initial demonstration by Pirkle (1), it has become well established that chemical species which are enantiomeric in achiral media, and hence exhibit identical properties, may be distinguished by their n.m.r. spectra in suitable optically active solvents. The distinction between the spectra of the *d* and the *l* forms of the solute is possible because of a chiral solvent induced diastereomeric relationship between the two forms, resulting from the formation of short lived solute–solvent associated species (1). For the spectra of the enantiomers to be rendered nonidentical it is necessary that the solute–solvent interactions be strong enough to produce closely associated solvates and for the solvent molecules to have a high degree of magnetic anisotropy so that the chemical shift differences between corresponding nuclei in the diastereomeric solvates will be large enough to be resolved. Pirkle and Beare (2) have found 2,2,2-trifluorophenylethanol (TFPE) to be a suitable optically active solvent for this purpose in many cases. This compound is capable of forming strong intermolecular hydrogen bonds to many types of solute molecules, thus forming sufficiently stable solvates, and has sufficient magnetic anisotropy associated with the phenyl group to produce adequate chemical shift differences in a number of instances.

We now report the n.m.r. spectral behavior

Can. J. Chem. Downloaded from www.nrcresearchpress.com by 210.87.254.5 on 09/05/12
For personal use only.

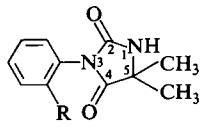

1

a R = CH_3
b R = Br

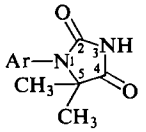

2

a Ar = 2-Methylphenyl
b Ar = 2,3-Dimethylphenyl
c Ar = 2,4-Dimethylphenyl
d Ar = 2,5-Dimethylphenyl

of some 1- and 3-arylhydantoins, which can exist in two enantiomeric forms as a result of restricted internal rotation about the aryl C—N bond (3–5), in the optically active solvent *S*-(+)-TFPE. Because of steric interaction between the *ortho* substituent on the aryl group and the substituents on the hetero ring adjacent to the point of attachment, the molecules are constrained to adopt conformations with large dihedral angles between the rings in the conformational ground states. Since the hetero rings should be approximately planar (5), and are symmetrically substituted with respect to the plane of the ring, the two rotational isomers are enantiomeric in the absence of chiral media.

The arylhydantoins studied in this project, or compounds of similar structure, had been shown previously (6) to have high barriers to internal rotation (free energies of activation within the range 17–21 kcal/mol) in conventional solvents and were expected to have sufficiently long lifetimes before interconversion of the rotational isomers at normal probe temperatures that isomeric integrity would be maintained over the time scale of the measurements.

The geminal dimethyl groups in the 5-position are diastereotopic and, in the compounds chosen for this study, are anisochronous at normal probe temperatures, giving rise to well resolved doublets with separations of 0.227–0.276 and 0.037–0.055 p.p.m. for the 1- and the 3-aryl series, respectively, in the ^1H spectrum. At elevated temperatures the 5-dimethyl doublet collapses to a singlet as the rate of rotamer interconversion increases and the environments of the methyl groups become averaged. The line shapes over an intermediate range of temperatures may be employed to measure rate constants for interconversion and hence to obtain activation parameters for the hindered rotation process (4).

Results and Discussion

Proton Magnetic Resonance Spectra

An examination of the ^1H n.m.r. spectra of the 1-aryl- and the 3-arylhydantoins in solution in the chiral solvent reveals characteristically different behavior for the two substitution patterns. This results from a very marked dependence of the extent of line doubling resulting from solute–solvent interactions on the location of the nuclei in the molecules. In the 3-arylhydantoins examined, only the *o*-methyl signal of **1***a* showed splitting. Although, in principle, the two signals resulting from the diastereotopic (in achiral media) 5-methyl groups should show further splitting in (+)-TFPE solution, no additional multiplicity or line broadening was observed. Thus, of the 3-arylhydantoins examined, only **1***a* shows evidence of line doubling in the chiral solvent.

In contrast, all of the 1-arylhydantoins examined exhibited spectral changes in the chiral solvent (Table 1). Although distinguishable doubling of the hetero ring methyl signals was not observed, the lines were broadened in all cases, indicating a small chemical shift difference between corresponding methyl groups in the diastereomeric solvates. Well resolved signals were exhibited by the nonequivalent *ortho* and *meta* aryl methyl groups of the two rotational isomers.

The magnitude of the chiral solvent induced chemical shift differences between corresponding aryl methyl groups in the rotamers is strongly dependent on the location of the methyl group, *i.e. ortho*, *meta*, or *para* to the hetero substituent. Chemical shift differences are listed in Table 2. The largest chemical shift difference between the aryl methyl groups of the diastereomeric solvates is exhibited by the *o*-methyl groups, 0.12–0.13 p.p.m. in the 1-arylhydantoin series (in the 3-arylhydantoin, **1***a*, the corresponding chemical shift difference is much smaller, 0.05 p.p.m.). A similar chemical shift difference (0.12 p.p.m.) is exhibited by the *m*-methyl groups of **2***c*, which has a 2,3-substitution pattern on the aromatic ring. In **2***d*, which has a 2,5-substitution pattern, the chemical shift difference between the *m*-methyl group signals is smaller, 0.06 p.p.m. In contrast to the other aryl methyl groups, the *p*-methyl protons of **2***c* (with a 2,4-substitution pattern) showed a single signal which did not change

Can. J. Chem. Downloaded from www.nrcresearchpress.com by 210.87.254.5 on 09/05/12
For personal use only.

Can. J. Chem. Downloaded from www.nrcresearchpress.com by 210.87.254.5 on 09/05/12
For personal use only.

TABLE 1. Proton chemical shifts* of 1-arylhydantoins

Compound	Solvent	5-Methyl	Aryl methyl		
			Ortho	*Meta*	*Para*
2*a*	DMSO-d_6	1.18,1.45	2.18	—	—
	Pyridine	1.23,1.50	2.28	—	—
	(+)-TFPE	0.95,1.19	1.93	—	—
			2.05		
2*b*	DMSO-d_6	1.17,1.42	2.05	2.27	—
	Pyridine	1.27,1.52	2.17	2.17	—
	(+)-TFPE	0.94,1.18	1.80	2.02	—
			1.93	2.14	
2*c*	DMSO-d_6	1.16,1.42	2.13	—	2.29
	Pyridine	1.29,1.54	2.24	—	2.28
	(+)-TFPE	0.95,1.18	1.91	—	2.17
			2.04		
2*d*	DMSO-d_6	1.18,1.46	2.14	2.30†	—
	Pyridine	1.25,1.52	2.26	2.26†	—
	(+)-TFPE	0.97,1.22	1.92	2.14†	—
			2.05	2.20	

*In p.p.m. from TMS.
†5-Methyl of aryl group.

TABLE 2. Chemical shift differences and coalescence temperatures for aryl methyl proton signals, and approximate free energies of activation for internal rotation of 1-aryl hydantoins in (+)-TFPE solution

Compound	Aryl methyl	Chemical shift difference (p.p.m.)*	Coalescence temperature (°C)	$\Delta G^{\ddagger}$† (kcal/mol)
2*a*	*Ortho*	0.12	81.5	18.6
2*b*	*Ortho*	0.13	117.0	20.4
	Meta	0.12	117.0	20.5
2*c*	*Ortho*	0.13	81.0	18.5
	Para	0.0		
2*d*	*Ortho*	0.13	80.5	18.5
	Meta	0.06	68.5	18.3

*Chemical shift difference at normal probe temperatures.
†Approximate free energy of activation at the coalescence temperature, calculated on the basis that coalescence results only from internal rotation within the solute molecules.

TABLE 3. Methyl group and heterocyclic ring carbon-13 chemical shifts* of 3-(*o*-tolyl)-5,5-dimethylhydantoin (**1***a*) and 1-(2,5-dimethylphenyl)-5,5-dimethylhydantoin (**2***d*)

Compound	Solvent	C-2	C-4	C-5	5-Me	Aryl methyl	
						Ortho	*Meta*
1*a*	DMSO	154.1	176.3	58.0	24.4,25.1	16.9	
	(+)-TFPE	156.3	178.1	59.6	24.1,24.8	17.2	
2*d*	Morpholine	155.6	179.1	65.7	22.3,25.1	18.1	20.6
	(+)-TFPE	155.4	179.0	66.7	21.8,24.3	17.9	20.5

*In p.p.m. from TMS.

Can. J. Chem. Downloaded from www.nrcresearchpress.com by 210.87.254.5 on 09/05/12
For personal use only.

its appearance at the lowest attainable temperature (about 0°).

On warming the samples, the magnitude of the chiral solvent induced splitting decreased until coalescence occurred at the temperature reported in Table 2. Loss of nonequivalence with increasing temperature could result from a shift towards the unassociated species in the equilibrium involving solute, solvent, and the diastereomeric solvates, from an increase in the rate of internal rotation in the solute molecules, or from a combination of these processes. The experimental evidence, based on the appearance of the spectra as a function of temperature, a comparison of coalescence temperatures, and measurements of free energies of activation, is not sufficient to establish the relative importance of these processes, but does suggest that both contribute to the temperature dependence of the spectra.

Carbon-13 Spectra

In principle, doubling of signals in the spectra of the enantiomeric mixture of rotational isomers when it is dissolved in the optically active solvent should occur in the ^{13}C as well as in the ^{1}H n.m.r. spectrum. If a major contribution to the shielding difference between ^{13}C nuclei in the two rotational isomers results from local magnetic anisotropy differences, as is the case for ^{1}H nuclei, the chemical shift difference (in p.p.m.) should be similar to that in the ^{1}H spectrum for ^{13}C nuclei in similar environments. On the basis of the observed ^{1}H chemical shift differences in the chiral solvent, the ^{13}C separation would be expected to be near the resolution limit of the instrument.

The ^{13}C spectra of **1***a* and **2***d* in the chiral solvent showed no additional splitting or definite line broadening resulting from diastereomeric solute–solvent interactions (Table 3). In addition to the small shift differences expected if anisotropy effects are important, the rather high temperature (*ca.* 55°) of the ^{13}C probe may have precluded observation of signal doubling by reducing the concentration of solute–solvent complex through a shift in the equilibrium and by reducing the lifetimes of the rotational isomers of the solute.

Although the ^{13}C spectra do not provide direct evidence for the existence of diastereomeric solute–solvent complexes, information is provided on the sites of bonding between solute and solvent molecules. A comparison of the ^{13}C spectra of **1***a* in DMSO and in the chiral solvent shows that the carbonyl carbon signals are shifted downfield about 2 p.p.m. in the hydrogen bonding chiral solvent with respect to the positions in the nonhydrogen bonding achiral solvent. Such shifts are typical of the carbon atoms of carbonyl groups subject to hydrogen bonding (7). With the exception of C-5, the chemical shifts of the remaining methyl and hetero ring carbon atoms are similar in the two solvents. The chemical shifts of **2***a* in the two hydrogen bonding solvents, morpholine and (+)-TFPE are similar, except for that of the C-5 carbon atom. Because of overlap with the aryl carbon signals from the chiral solvent, interpretation of the hydantoin aryl carbon spectrum was not attempted.

Proton Chemical Shifts

Comparison of the proton chemical shifts of the 1-arylhydantoins in achiral and chiral solvents (Table 1) provides further evidence for the existence of a strong association complex between the solute molecules and the chiral solvent and for its geometry. Use of the chiral solvent causes consistent upfield shifts for the C-5 methyl and the aromatic methyl protons, indicating that these protons lie in regions of shielding produced by the magnetic anisotropy of the solvent molecules. The greatest shielding effects in the 1-arylhydantoin series are experienced by the 5-methyl and the *o*-methyl protons, indicating that these groups are closest to the region of maximum shielding of the solvent phenyl groups. Models for the association complexes of the type which have previously been suggested by Pirkle *et al.* (8) may be based on the ^{1}H and the ^{13}C spectra of the arylhydantoins. One of the probable modes of association of a 1-arylhydantoin which is consistent with the experimental evidence and permits close association between solute and solvent molecules is depicted in Fig. 1 for one of the rotational isomers. The corresponding complex for the other isomer would have the solute aryl group rotated through approximately 180°. Complex formation results primarily from hydrogen bonding between the chiral alcohol and a carbonyl group of the hydantoin. Secondary attractive interactions between the π-electron systems of the solute and the solvent aryl groups appear to be responsible for deter-

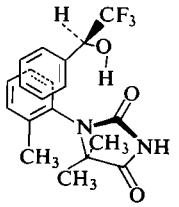

FIG. 1. Conformation of a solvate between *S*-(+)-2,2,2-trifluorophenylethanol (TFPE) and one of the rotational isomers of a 1-arylhydantoin.

mining the conformation of the complex. The greatest effects of the magnetic anisotropy of the solvent phenyl group would be exerted on those nuclei located in the immediate vicinity of the solute aryl group and the hetero substituent near the point of attachment, resulting in maximum sensitivity to differences in stereochemical environments in the two rotational isomers and in maximum overall shielding. The lack of sensitivity of a *p*-methyl substituent to the signal doubling effect of the chiral solvent is consistent with the similar environments of this group with respect to the solvated solvent molecules in the two solute isomers. The proposed model is consistent with the chemical shift evidence, which suggests that the solvent phenyl group is displaced towards the hydantoin moiety.

Barriers to Internal Rotation

Since the arylhydantoins are present in (+)-TFPE solution as strongly solvated species, it may be expected that the barriers to internal rotation about the aryl C—N bonds in the solute molecules will be influenced by the solvent. Activation parameters may be determined by complete line shape analysis of the 5-methyl signals as a function of temperature, for (+)-TFPE as well as for more traditional solvents. The only complication which is present in the spectra of (+)-TFPE solutions is the small amount of line broadening which is present at lower temperatures. Over the temperature range (84.5–110.5°, compound **2***a*) where collapse of the 5-methyl doublet occurs this broadening is small or absent because of the reduced concentration of the solvated species at high temperatures.

Complete line shape analyses of the 5-methyl group spectra were carried out, and the activation parameters calculated, for 1-(*o*-tolyl)-5,5-dimethylhydantoin (**2***a*) in pyridine, DMSO-d_6, and (+)-TFPE solutions (Table 4). Errors for the (+)-TFPE solution are somewhat higher than for the other solvents because of difficulty in estimating the correct natural linewidth for use in the line shape calculations.

TABLE 4. Activation parameters (100 °C) for 1-(2-methylphenyl)-5,5-dimethylhydantoin (**2***a*)*

Solvent	ΔH^* (kcal/mol)	ΔS^* (e.u.)	ΔG^* (kcal/mol)
Pyridine	13.1±0.7	−14±2	18.2±0.1
DMSO-d_6	15.2±0.5	−9±2	18.5±0.1
(+)-TFPE	15.4±1.1	−10±3	19.2±0.1

*Errors are 90% confidence limits.

The rotational barriers show a correlation with the expected solvating ability of the solvents. Thus, the free energy of activation is higher by 1.0 kcal/mol in (+)-TFPE than in pyridine, which is expected to solvate the solute molecules less efficiently. An intermediate position is occupied by DMSO-d_6.

Free energies of activation were also calculated at the coalescence temperatures of the 5-methyl doublets of **2***a–d* (Table 5). Because of the temperature dependence of the free energy function, these values are less useful than the data in Table 4, which are calculated at a common temperature, but they indicate higher barriers to internal rotation in (+)-TFPE, relative to the other solvents, in all cases. Free energies of activation are about 1.1 kcal/mol higher in (+)-TFPE than in pyridine solution. In most cases, coalescence temperatures are raised about 20°, from about 81° in pyridine to about 101° in (+)-TFPE. An exception is the 2,3-dimethylphenyl compound (**2***b*) which exhibits an increase of about 15° in its coalescence temperature in (+)-TFPE compared to 2-chloropyridine, possibly because a different achiral reference solvent was employed. The higher ΔG^* of **2***b* in all the solvents is attributed to buttressing between the *ortho* and the *meta* aryl methyl groups.

The feasibility of determining activation parameters for restricted internal rotation within solute molecules by employing the temperature dependence of the signals arising from corresponding protons in each association complex in a chiral solvent has recently been demonstrated (9). This method is applicable if the collapse of the signal doubling resulting from diastereomeric solute–solvent interactions

Can. J. Chem. Downloaded from www.nrcresearchpress.com by 210.87.254.5 on 09/05/12
For personal use only.

TABLE 5. Free energies of activation of 1-aryl-5,5-dimethylhydantoins at the coalescence temperatures of the 5-dimethyl signals

Compound	Solvent	Chemical shift difference (p.p.m.)	Coalescence temperature (°C)	$\Delta G^{\ddagger}$* (kcal/mol)
2*a*	Pyridine	0.272	80.5	18.1
	DMSO-d_6	0.276	87.5	18.4
	(+)-TFPE	0.238	101.0	19.2
2*b*	2-Chloropyridine	0.260	135.0	21.0
	DMSO-d_6	0.250	138.0	21.2
	(+)-TFPE	0.227	150.0	21.8
2*c*	Pyridine	0.253	81.0	18.1
	DMSO-d_6	0.267	86.0	18.4
	(+)-TFPE	0.228	102.0	19.3
2*d*	Pyridine	0.260	81.5	18.2
	DMSO-d_6	0.273	90.5	18.6
	(+)-TFPE	0.230	102.0	19.3

*Calculated from rate constants obtained by computer simulation of the line shapes in the coalescence region. Estimated errors are ±0.1 kcal/mol.

is a consequence of an increase in the rate of interconversion of the rotational isomers of the solute molecules with increasing temperature, rather than to a decrease in the concentration of the associated complexes. A similar analysis of the temperature dependence of the aryl methyl signals in the present series of compounds is probably not fully justified, since the coalescence temperatures were appreciably higher (68.5–117.0°) than those (26–30°) reported for (+)-TFPE solutions and, in consequence, the stability of the association complexes might be expected to be lower.

An indication that decreases in the stability of the association complex with increasing temperature are at least in part responsible for the disappearance of the signal doubling follows from the observation that the range of temperature dependence below the coalescence point was two to three times greater for the aryl methyl signals than for the 5-dimethyl signals, the spectra showing a decrease in chemical shift difference with increasing temperature. This temperature effect has been reported previously (9). Because of this complication, complete line analysis of the temperature dependent aryl methyl group spectra was not attempted. However, calculation of $\Delta G^{\ddagger}$ at the coalescence temperatures, using the chemical shift differences measured at normal temperatures, yielded values quite close to those obtained by analysis of the 5-dimethyl group spectra (Tables 2 and 5). Since the error involved in ignoring the temperature dependence of the chemical shift differences would have the effect of reducing the calculated values of $\Delta G^{\ddagger}$, this method provides lower limits for the free energies of activation. The reported values (Table 2) obtained by this method are all lower than those obtained from the 5,5-dimethyl group signals at coalescence (Table 5), consistent with this interpretation, but the usefulness of the comparison is limited by the different temperatures involved.

The parallel increase in the coalescence temperatures of the aryl methyl (chiral solvent induced) and the 5,5-dimethyl doublets of the internally buttressed compound, **2***b*, compared to the less hindered compounds, even though the chemical shift differences are similar (Tables 2 and 5), is further evidence that internal rotation in the solute molecules contributes to the temperature dependence of the doublets resulting from the presence of diastereomeric solvates.

Experimental

Materials

The 1-arylhydantoins were prepared from the appropriate aniline derivative and *N*-(2-bromo-2-methylpropionyl)urea (obtained by reaction between 2-bromo-2-methylpropionyl bromide and urea (10)) by the method of Mazover (11).

The 3-arylhydantoins, **1***a* and *b*, were prepared from *o*-tolyl isocyanate and *o*-bromophenyl isocyanate, respectively, and 2-methylalanine by the method of Behr and Clarke (12)

These compounds were characterized through their

Can. J. Chem. Downloaded from www.nrcresearchpress.com by 210.87.254.5 on 09/05/12
For personal use only.

p.m.r. and i.r. spectra and elemental analysis or mass spectra. Samples for ^1H and ^{13}C measurements were prepared in 2–3 *M* concentrations.

S-(+)-Trifluoromethylphenylethanol (TFPE) was obtained from Burdick and Jackson, Inc.

Magnetic Resonance Measurements

Proton magnetic resonance spectra were determined using a Varian HA-100 or a JEOL 4H-100 spectrometer equipped with standard variable temperature apparatus, and operating in the field sweep mode. For the variable temperature experiments, temperatures were determined immediately before or after each spectrum was taken by measuring the peak separation of a standard Varian ethylene glycol temperature reference sample, and they are believed to be accurate to $\pm 2°$. Adequate time was allowed for temperature equilibration to take place before spectra were measured.

Carbon-13 magnetic resonance spectra were determined at 25.12 MHz using a Varian HA-100 spectrometer equipped with an 8 mm spinning sample probe and a Varian V-3530 wide sweep accessory, and operating in the C.W. mode. Broad band proton decoupling was provided by a Varian V-3512-1 noise modulated heteronuclear spin decoupler. Spectra were accumulated (about 100 scans) in a C-1024 time averaging computer, using sweep widths of 100–200 Hz and scan times 10–25 s. The instrument was internally locked on a decoupled solvent line for the achiral solvents, and on an enriched (85%) methyl iodide sample contained in a capillary for the solutions in the chiral solvent.

The procedures used for complete line shape analysis of the temperature dependent proton spectra have been described earlier (4).

This work was supported by grants from the National Research Council of Canada.

1. W. H. Pirkle. J. Am. Chem. Soc. **88**, 1387 (1966).
2. W. H. Pirkle and S. D. Beare. J. Am. Chem. Soc. **90**, 6250 (1968); W. H. Pirkle, T. G. Burlingame, and S. D. Beare. Tetrahedron Lett. 5849 (1968).
3. W. E. Bentz, L. D. Colebrook, J. R. Fehlner, and A. Rosowsky. Chem. Commun. 974 (1970).
4. L. D. Colebrook, H. G. Giles, A. Granata, S. Icli, and J. R. Fehlner. Can. J. Chem. **51**, 3635 (1973).
5. P. H. Bird, L .D. Colebrook, A. R. Fraser, and H. G. Giles. Chem. Commun. 225 (1974).
6. J. R. Fehlner. Ph.D. Thesis, University of Rochester, Rochester, New York. 1970; S. Icli. Ph.D. Thesis, Sir George Williams University, Montreal, Quebec. 1974.
7. J. B. Stothers. Carbon-13 n.m.r. spectroscopy. Academic Press, Inc., New York. 1973. p. 495.
8. W. H. Pirkle, R. L. Muntz, and I. C. Paul. J. Am. Chem. Soc. **93**, 2817 (1971).
9. A. Mannschreck, V. Jonas, and B. Kolb. Angew. Chem. Int. Ed. Eng. **12**, 909 (1973).
10. S. R. Safir, H. Dalalian, W. Fanshawe, K. Cyr, R. Lopresti, R. Williams, S. Upham, L. Goldman, and S. Kushner, J. Am. Chem. Soc. **77**, 4840 (1955).
11. Y. G. Mazover. J. Gen. Chem. USSR, **22**, 1700 (1952).
12. L. Behr and H. T. Clarke. J. Am. Chem. Soc. **54**, 1630 (1932).

Can. J. Chem. Downloaded from www.nrcresearchpress.com by 210.87.254.5 on 09/05/12
For personal use only.

Horseradish Peroxidase. XVII. Reactions of Compounds I and II with *p*-Aminobenzoic Acid in Deuterium Oxide[1,2]

C. D. HUBBARD,[3] H. B. DUNFORD,[4] AND W. D. HEWSON

Department of Chemistry, University of Alberta, Edmonton, Alberta T6G 2E1

Received October 31, 1974

C. D. HUBBARD, H. B. DUNFORD, and W. D. HEWSON. Can. J. Chem. **53**, 1563 (1975).

The kinetics of reactions of horseradish peroxidase compounds I and II (HRP-I and HRP-II, respectively) with *p*-aminobenzoic acid have been studied in ordinary water and in deuterium oxide solution over a p*H* (p*D*) range 3–10, at 25° and at an ionic strength of 0.11. Under the conditions of the experiments the rate of reaction is first order both in substrate concentration and in enzyme concentration in both solvents. An analysis of the p*H* dependence of the second-order rate constant in H_2O confirms the presence of two acid dissociation groups on the enzyme with pK_a's of 8.6 and ~0 for HRP-II, whereas for HRP-I the data suggest a pK_a of 5.1 on the enzyme and reveal, as previously shown, the influence of the ionization of the substituted ammonium group of the substrate. In deuterium oxide the p*D* profiles are similar to those in water but significant shifts for both kinetic and acid dissociation constants are observed for both compounds.

The numerical values of the isotope effects taken together with previous results in general confirm that with labile substrates the group of pK_a 8.6 in H_2O on HRP-II is involved in general acid catalysis. *p*-Aminobenzoic acid is intermediate between labile and somewhat unreactive substrates and behaves similarly to the ferrocyanide ion in that both acid dissociation groups (pK_a's 8.6 and ~0) are influential in the catalysis of substrate oxidation by HRP-II. The kinetic isotope effect for the HRP-I reaction with *p*-aminobenzoic acid at high p*H* (p*D*) is consistent with a rate determining proton transfer but the group of pK_a 5.1 in H_2O remains unidentified.

C. D. HUBBARD, H. B. DUNFORD et W. D. HEWSON. Can. J. Chem. **53**, 1563 (1975).

On a étudié la cinétique de la réaction des composés I et II de la peroxydase du raifort (respectivement HRP-I et HRP-II) avec l'acide *p*-aminobenzoique; ces mesures ont été faites pour des solutions dans de l'eau ordinaire et de l'oxyde de deutérium à des p*H* (p*D*) allant de 3–10 à 25° et à une force ionique de 0.11. Dans les conditions des expériences, la vitesse de la réaction est du premier ordre en substrat et en concentration d'enzyme dans chacun des solvants. Une analyse de la dépendance sur le p*H* de la constante de vitesse du deuxième ordre dans l'eau confirme la présence de deux groupes de dissociation acide sur l'enzyme avec des pK_a de 8.6 et approximativement 0 pour HRP-II; pour HRP-I, les données suggèrent un pK_a de 5.1 sur l'enzyme et mettent en évidence, tel que démontré précédemment, l'influence de l'ionisation du groupe ammonium substitué du substrat. Dans l'oxyde de deutérium, les profils de p*D* sont similaires à ceux dans l'eau mais on observe pour chacun des composés des déplacements importants à la fois pour la cinétique et pour les constantes de dissociation des acides.

Les valeurs numériques des effets isotopiques, par comparaison avec les résultats antérieurs, confirment d'une façon générale qu'avec des substrats labiles le groupe de pK_a à 8.6 dans l'eau du HRP-II est impliqué dans une catalyse acide générale. La réactivité de l'acide *p*-aminobenzoique est intermédiaire entre celle d'un substrat labile et celle d'un substrat assez peu réactifs; cet acide réagit d'une façon similaire vis à vis l'ion ferrocyanure si l'on considère que les deux groupes de dissociation acide (pK_a de 8.6 et ~0) ont une influence dans la catalyse d'oxydation du substrat par HRP-II. Pour la réaction de HRP-I avec l'acide *p*-aminobenzoique, l'effet isotopique cinétique, à haut p*H* (p*D*) est en accord avec une étape déterminante indiquant un transfert de protons; le groupe de pK_a à 5.1 dans l'eau demeure non-identifié.

[Traduit par le journal]

Introduction

Horseradish peroxidase (EC 1.11.1.7 donor – H_2O_2 oxidoreductase) has been shown for a large variety of reducing substrates AH_2, to follow the general mechanism (1–3)

[1] $$HRP + H_2O_2 \rightarrow HRP\text{-}I$$

[1]This paper is dedicated to Professor C. A. Winkler of McGill University on the occasion of his sixty-fifth birthday by one of his former students (H.B.D.).

[2]For the previous three papers in this series see refs. 4, 10, and 9.

[3]On sabbatical leave from the Department of Chemistry, University of New Hampshire, Durham, New Hampshire.

[4]To whom correspondence should be addressed.

Can. J. Chem. Downloaded from www.nrcresearchpress.com by 210.87.254.40 on 09/05/12
For personal use only.

Can. J. Chem. Downloaded from www.nrcresearchpress.com by 210.87.254.40 on 09/05/12
For personal use only.

[2] $HRP\text{-}I + AH_2 \rightarrow HRP\text{-}II + AH$

[3] $HRP\text{-}II + AH_2 \rightarrow HRP + AH$

where HRP refers to the native enzyme and HRP-I and HRP-II are compounds I and II containing two and one oxidizing equivalents, respectively, in excess to that of HRP. This mechanism was found to account for the major features of oxidation of the bacterial metabolite *p*-aminobenzoic acid (PABA) at any given p*H* (4). Some complications which occurred were (*i*) slow attack on the enzyme by free radical oxidation products, which became detectable when reaction 3 was studied at high p*H* where it occurs at a slow rate; (*ii*) formation of HRP-I–PABA and HRP-II–PABA complexes at low p*H* which react with an additional PABA molecule. These oxidation reactions of an enzyme–substrate complex with an additional substrate molecule occurred at a slower rate than the direct reaction of the enzyme with substrate. Since the substrate binding appears to be non-productive then reaction involving the enzyme substrate complex is not the major reaction pathway.

Several reducing substrates have been shown to exhibit marked p*H* dependences in their reactions with HRP-I and HRP-II (4–10) and in the case of the HRP-II reactions with iodide, ferrocyanide, and *p*-cresol, p*H* dependences were determined in both H_2O and D_2O in an attempt to elucidate further the mechanisms of the reactions (11).

The present study is concerned with the comparison of the p*H* dependences of the HRP-I and HRP-II reactions with PABA in light and heavy water under reaction conditions where the complications in mechanism, outlined above, are avoided.

Experimental

Materials

Horseradish peroxidase was purchased from Boehringer Mannheim GmbH as a salt suspension. All samples used were from batch Nos. 7403424 and 7024524, and were prepared for use by extensive dialysis against triply distilled water and subsequent Millipore filtration. Enzyme purity and concentration were determined from absorbance measurements at 280 and 403 nm.

Deuterium oxide, 99.7%, was purchased from Diaprep, Milwaukee, Wisconsin and used without further purification. Triply distilled water was used throughout. *p*-Aminobenzoic acid and buffering reagents were highest quality commercial products and used without further purification.

Spectra

Routine observations of the spectra of HRP and its compounds, and some slower kinetic runs were made on a Cary 14 spectrophotometer equipped with a jacketed cell holder through which temperature controlled water was circulated.

pH Measurements

The p*H* of both water and deuterium oxide solutions was measured on an Orion 801 p*H* meter using a Fisher combination electrode, No. 13-639-90, calibrated with standard buffers. The measured p*H* of deuterium oxide solutions was corrected to a value for the %atom fraction of deuterium (94% for HRP-II reactions and 92% for HRP-I reactions) assuming to a first approximation that the change in p*H* between 100% H_2O and 0% H_2O solutions is linear (11). Results used in interpreting the kinetic and equilibrium parameters as a function of solution acidity in the heavy water solutions are based upon measured p*H* + 0.38 for HRP-II reactions and measured p*H* + 0.37 for HRP-I reactions (12).

Kinetics

All kinetic experiments except for a few in the basic region where the reaction of HRP-II with PABA is quite slow, were carried out using a Gibson-Durrum stopped-flow spectrophotometer fitted with a 2 cm path length observation cuvette. The temperature for all reactions reported is 25.0 ± 0.2° and the ionic strength 0.11. The method of data collection has been described previously (5, 7). Since the observed signal change was very small compared with the total signal, signal amplitudes at various times are utilized directly in data analysis. All traces were single kinetic processes yielding excellent first-order plots, linear for several half-lives. A minor deviation occurs at the commencement of the HRP-II reaction traces and is perhaps worthy of further investigation but it does not interfere with the treatment of data obtained at 425 nm for the compound II reactions. The conversion of HRP-I to native enzyme was monitored at 411 nm.

Typical kinetic runs were carried out as follows. The substrate solution at appropriate p*H*, buffer concentration and ionic strength was introduced into the stopped-flow drive syringe and allowed to attain thermal equilibrium, while a solution containing native enzyme was thermally equilibrated in the reservoir of the stopped-flow instrument. An appropriate small volume of stock hydrogen peroxide solution for HRP-I reactions and additionally stock potassium ferrocyanide solution for HRP-II reactions was injected into the enzyme solution to convert ~90% of the native enzyme into the desired compound. The solution was then introduced rapidly into the other stopped-flow syringe and kinetic determinations commenced. All experiments were carried out under pseudo first-order conditions. For runs below about p*H* 6, the buffer required to achieve a buffer ionic strength of 0.01 in the mixed solution was contained in the substrate syringe to prevent interference before mixing from competing reactions brought about by acidic solution.

For the deuterium oxide runs the same stock buffers of ionic strength 0.2, made up in light water, were used. The other components contributing to the protium content were the enzyme itself, and the hydrogen peroxide and potassium ferrocyanide solutions. In most runs the stock

Can. J. Chem. Downloaded from www.nrcresearchpress.com by 210.87.254.40 on 09/05/12
For personal use only.

substrate solution was also made up in deuterium oxide and suitable adjustments made to retain a constant protium content. The final ionic strength was always 0.11 as in the light water experiments.

Enzyme solutions were of initial native enzyme concentrations in the range 0.8–0.9 μM for the compound II reactions and about 1.5 μM in the reactions of compound I. Small differences are attributable to different enzyme samples. Minor kinetic differences arising from different enzyme samples were normalized by comparing kinetic data measured under identical conditions with the different batches in the most convenient region of measurement (about pH 7 for compound II and pH 7–10 for compound I). Acetic acid – acetate ion or glycine buffers were used in the region of pH of 3.0 to 5.0. It was noticed that the reproducibility of the kinetic observations for HRP-II reactions was slightly reduced in acetate buffers particularly when the solutions were on the basic side of the pK_a of acetic acid, suggesting that the acetate ion may be involved in interfering with the reactions studied. Because the effects were small and the kinetic data fitted into the pattern obtained over the whole pH region, no corrections were made.

Substrate concentrations were chosen to yield conveniently measurable kinetics. In both reaction series a second molecule of substrate is involved in the reaction at higher substrate concentrations, an effect which is more pronounced at lower pH, and therefore in the pH range below 5, substrate concentrations were kept at a low level so as to circumvent the need for substrate concentration dependence plots and correction factors to the observed kinetic constants. However, at a few pH values checks of the substrate concentration dependence were made and good agreement with previous observations was obtained (4).

Results

The rate constants, $k_{2,app}$ and $k_{3,app}$ determined by dividing the pseudo first-order constants obtained from the stopped-flow traces by substrate concentrations in light water for the reactions of HRP-I and HRP-II with PABA confirm the results obtained earlier within experimental error (4) and provide the necessary references for comparing k^D/k^H ratios. These rate constant data are available from the authors upon request. Comparisons of the light and heavy water results for the reactions of HRP-I and HRP-II with PABA are shown in Figs. 1 and 2.

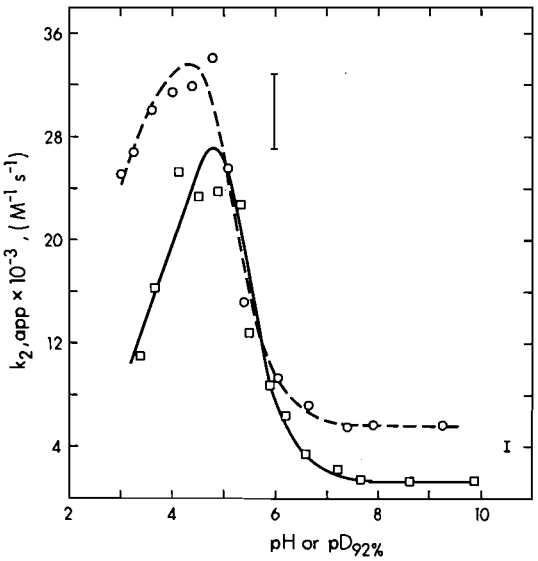

FIG. 1. Plot of the second-order rate constant, $k_{2,app}$, for the reaction of HRP-I with PABA *vs.* pH or pD in light water (dashed curve) and 92% D_2O (solid curve). $pD_{92\%} = pH_{reading} + 0.37$. The error bars show the magnitudes of $\pm 20\%$ error for two different values of k. The curves were computed by nonlinear least-squares analysis of eq. 7.

Discussion

The k^D/k^H ratios for HRP-II reactions with iodide ion, ferrocyanide ion, and *p*-cresol indicated that two reaction mechanisms were applicable (4). For the facile reactant, *p*-cresol, acid catalysis was observed which involved an acid group on HRP-II with a pK_a of 8.6. Since ionization of this group had no influence on the HRP-II spectrum, the group was assumed to be a distal group (7) and the ratio k^D/k^H of 0.45 indicated a rate-controlling proton transfer (11). For the less labile substrate, iodide ion, on the other hand, the log k *vs.* pH profile was linear with a slope of -1 over the pH range 2–9 which together with the consideration of the diffusion-controlled limit for a bimolecular reaction indicates an acid group with a pK_a of approximately 0 (5). A k^D/k^H value of 4.0 is consistent with a prior equilibrium between H_3O^+ (or D_3O^+) and the reactive acid form of HRP-II. Since this reactive form is present in vanishingly small amounts in pH ranges where the enzyme has stability, the absence of any detectable shifts in the HRP-II spectrum in moderately acidic solution does not rule out the possibility that the acid enzyme is protonated in a proximal position, either the fifth or sixth coordination position of the heme iron (11). A self-consistent explanation is that for the facile reactant *p*-cresol, catalysis by the distal group of pK_a 8.6 involves intramolecular general acid catalysis, in which the rate-controlling step is partial transfer of the proton to the proximal group in the fifth coordination position of the heme iron, believed to involve a nitrogen coordinated to iron (13) and to be the

Can. J. Chem. Downloaded from www.nrcresearchpress.com by 210.87.254.40 on 09/05/12
For personal use only.

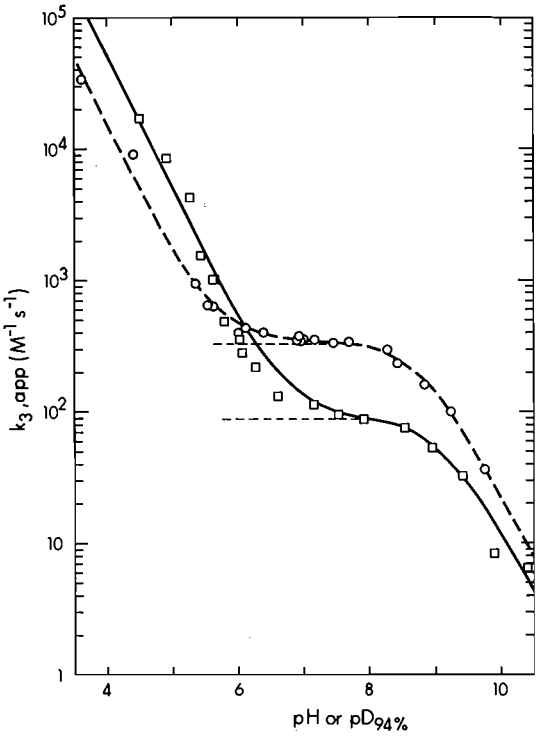

FIG. 2. Plot of log of the second-order rate constant, $k_{3,app}$ for the reaction of HRP-II with PABA *vs.* p*H* or p*D* in light water (dashed curve) and 94% D_2O (solid curve). $pD_{94\%} = pH_{reading} + 0.38$. The curves were computed by nonlinear least squares analysis of eq. 8. The horizontal portions of the curves indicate the values of k_1 (eq. 8).

imidazole ring of a histidine residue (14). Only a slight transfer of charge is required, so that the parameter which can be determined from the p*H*–rate profile is the pK_a of the distal group. For the difficult reactant, iodide ion, on the other hand, in accordance with the Hammond postulate (15, 16), total proton transfer is required and only H_3O^+ (or D_3O^+) is a strong enough acid to protonate the histidine residue, which because it is bound to Fe(IV) (17–19) has a pK_a of approximately 0. The latter catalytic mechanism is therefore specific acid catalysis (11). The ferrocyanide ion is an intermediate type of reactant in which the influence of both acid groups with pK_a's of 8.6 and 0 is felt. Intermediate k^D/k^H ratios were observed for the reaction of HRP-II with ferrocyanide ion: 2.6 ± 0.3 at high p*H* and 2.9 ± 0.6 at low p*H*. The ratio of $k^D/k^H > 1$ in basic solutions was somewhat surprising and was rationalized in terms of the relative bond distances in the transition state (11). However with the exception of the latter complication, the postulated explanation involving the two types of catalysis provided a simple and an overall self-consistent explanation of many rather diverse observations. An illustration of the two types of catalysis is given in Fig. 2 of ref. 10, which, however, should be revised in the following way. It would appear likely that if an imidazole group occupies the fifth coordination position of the heme iron, it would retain its proton. An analogy might be based upon the data of George *et al.* (20). Their data yield a value of

$$[4] \quad K = 1.5 \times 10^{-5} = \frac{[H^+][FeIm]}{[ImH^+][Fe^{III}H_2O]}$$

for the binding of imidazolium ion in the sixth coordination position of ferrimyoglobin

[5] 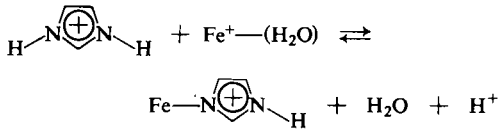

This may be comparable to the equilibrium involving imidazole in the fifth coordination position of HRP-II (pK_a ~0) although at this stage there is no evidence as to whether the Fe(IV) in the acid form of HRP-II is five-coordinate or whether H_2O replaces imidazole in the fifth coordination position.

The reactions of HRP-II with ferrocyanide and PABA display a remarkably similar p*H* dependence (8). The k^D/k^H ratios for the reaction of HRP-II with PABA displayed in Fig. 2 are of interest in that $k^D/k^H < 1$ in basic solution and > 1 in acidic solution in accord with the explanations involving a rate-limiting partial proton transfer in basic solution and a prior equilibrium involving H_3O^+ (or D_3O^+) in acidic medium.

Reaction of HRP-I

For the p*H* (or p*D*) dependence of the reaction of HRP-I with PABA, the simplest empirical equation which fits the experimental data is

$$[6] \quad k_{2,app} = \frac{A_1'(1 + [H^+]/A_2')}{(1 + [H^+]/A_3')(1 + [H^+]/A_4')}$$

Best-fit parameters for this equation and the corresponding equation for D_2O are summarized in Table 1. The parameter A_1' is clearly the rate constant at high p*H* and $k^D/k^H = 0.21$ (±13%) in accord with a rate-controlling proton (or deuteron) transfer. (The above isotope effect and all

TABLE 1. Parameters obtained from analysis of the second-order rate constant $k_{2,app}$ *vs.* p*H* or p*D* for the reduction of HRP-I by PABA (eq. 6)

Parameter	H_2O results		Results in 92% D_2O
	Previous*	Present	
A_1'	4.5×10^{3}	5.6×10^{3} (±6%)†	1.3×10^{3} (±7%)
A_2'	1.3×10^{-6}	9.1×10^{-7} (±22%)	1.3×10^{-7} (±16%)
A_3'	7.7×10^{-6}	6.1×10^{-6} (±26%)	3.2×10^{-6} (±19%)
A_4'	2.0×10^{-3}	1.7×10^{-3} (±38%)	2.8×10^{-4} (±25%)

*Reference 4.
†All quoted errors are standard deviations obtained from the nonlinear least-squares fit to the experimental data.

subsequent isotope effects are extrapolated linearly to 100% D_2O.) This represents the first kinetic isotope measurement for a reaction of HRP-I. The parameter A_4' appears to correspond to the acid dissociation constant of the substituted ammonium group of PABA determined independently to be 3.5×10^{-3} *M* (4) but in the light of other evidence on the mechanism of HRP-I reactions, the interpretation of A_2' and A_3' is less straightforward. It appears that there is an acid group in the active site of HRP-I with a pK_a value (5.1 ± 0.2) identical within experimental error to that of the carboxylic acid group on PABA (10) which complicates the interpretation. There is no evidence for the role of a very acid group in the active site of HRP-I nor for an inverse isotope effect in acid solutions, as in the HRP-II reactions. It might be tempting to speculate that the distal group of pK_a 8.6 catalytically important in HRP-II reactions and the group of pK_a 5.1, also a distal group,[5] important in HRP-I reactions, are identical and the shift in the ionization constant is a reflection of changes in the electronic and/or steric environment between compounds I and II (10). Studies of HRP-I with *N*-substituted PABA will hopefully lead to a clearer interpretation of the p*H* dependence of the reaction.

Reaction of HRP-II

The p*H* dependence of the reaction of HRP-II with PABA can be accounted for using the empirical equation

$$[7] \qquad k_{3,app} = \frac{A_1[H^+](1 + [H^+]/A_2)}{(1 + [H^+]/A_3)}$$

in which the A_n represent adjustable parameters. A comparison of the present results with those obtained earlier (4) is shown in Table 2. For reactions studied in D_2O, with the p*H* meter readings adjusted by a constant factor as described above, the best fit to the equation analogous to [7] is also given in Table 2. A kinetic interpretation (4) based on eq. 7 is

$$[8] \qquad k_{3,app} = \frac{\frac{k_1[H^+]}{K_{1E}}\left(1 + \frac{k_2[H^+]}{k_1K_{2E}}\right)}{1 + \frac{[H^+]}{K_{1E}}}$$

so that the rate constant k_1, the acid dissociation constant K_{1E}, and the ratio K_{2E}/k_2 can be computed from the best-fit data obtained in both H_2O and D_2O, with results also shown in Table 2. The constants in eq. 8 and a list of the kinetic and equilibrium isotope effects extrapolated to 100% D_2O by assuming the parameters depend linearly upon deuterium content over the small range of the extrapolation are given in Table 3. The ratio K_{1E}^{D}/K_{1E}^{H} is 0.48 (±47%) and k_1^{D}/k_1^{H} is 0.25 (±81%). The value of k_1^{D}/k_1^{H} may also be estimated from the data in Fig. 2. Although a clearly defined region in which the rate is independent of p*H* does not exist, the slopes of the plots tend to approach 0 at intermediate p*H*; p*H* independent values of k_1^{D} and k_1^{H} are obtained where the second derivatives of the plots are equal to 0. The corresponding values of k_1^{D} and k_1^{H}, indicated in Fig. 2, are in agreement with the values obtained from the best-fit parameters in Table 2. An inspection of Fig. 2 reveals a slightly less satisfactory fit of eq. 7 to the experimental data for runs in 94% D_2O particularly on the slightly acidic side of the neutral point. This does give some cause for concern but at present there is neither any evidence of differences in mechanism in the two solvents, nor any precedent for this possibility which would be implied by use of different functions to fit the two sets of data.

[5]There is little or no effect of p*H* on the HRP-I spectrum in the Soret region. J. Stillman and H. B. Dunford, unpublished results.

Can. J. Chem. Downloaded from www.nrcresearchpress.com by 210.87.254.40 on 09/05/12
For personal use only.

TABLE 2. Parameters obtained from analysis of the second-order rate constant $k_{3,app}$ *vs.* p*H* or p*D* for the reduction of HRP-II by PABA (eqs. 7 and 8 and analogs for D_2O)

Parameter	H_2O results		Results in 94% D_2O
	Previous*	Present	
A_1	1.9×10^{11}	2.3×10^{11} (±12%)†	1.2×10^{11} (±22%)
A_2	2.1×10^{-6}	2.2×10^{-6} (±11%)	1.7×10^{-7} (±23%)
$A_3 = K_{1E}$ (M)	2.1×10^{-9}	1.4×10^{-9} (±14%)	7.1×10^{-10} (±33%)
$A_1A_3 = k_1$ (M^{-1} s^{-1})	4.9×10^{2}	3.2×10^{2} (±26%)	8.5×10 (±55%)
$A_2/A_1A_3 = K_{2E}/k_2$ (M^2 s)	4.3×10^{-9}	6.9×10^{-9} (±37%)	2.0×10^{-9} (±78%)

*Reference 4.
†All quoted errors are standard deviations obtained from the nonlinear least-square fit to the experimental data.

TABLE 3. Summary of kinetic and equilibrium isotope effects for the reduction of HRP-II by PABA*

Parameter from eq. 8	Description	Isotopic ratio
k_1^D/k_1^H	Rate constant near neutral p*H*	0.25
k_2^D/k_2^H	Rate constant in acidic region	3.3
K_{1E}^D/K_{1E}^H	Group of $pK_a = 8.6$ in H_2O	0.48
pK_{2E}^D/pK_{2E}^H	Group of $pK_a \sim 0$	0.58

*Isotopic ratios corrected to 100% D_2O.

Consequently the very small deviation exhibited for the curve fit for the H_2O results is taken as assurance that the same functional equation is applicable for the results in heavy water. Some explanation may now be offered for the apparently anomalous value of k^D/k^H of 2.6 obtained in the basic region where the slopes of the plots of log k_1 *vs.* p*H* (or p*D*) are -1 in the reaction of HRP-II with ferrocyanide (11). The slopes are equal to k_1/K_{1E} so that any error in K_{1E} is reflected in the value of k_1. The value of K_{1E}^D/K_{1E}^H of 1.2 ± 0.4 for the HRP-II–ferrocyanide reaction was surprising and introduction of the result for the present study, 0.48, would reduce k_1^D/k_1^H close to unity for the HRP-II–ferrocyanide reaction, in better accord with the overall explanation of the trend in isotope effects. In this regard, it is of interest to note that both k_1^D/k_1^H and K_{1E}^D/K_{1E}^H are less than 1 for the reaction of *p*-cresol with bovine lactoperoxidase compound II.[6] There is a gross similarity in the behavior of compound II formed for both HRP and lactoperoxidase (21, 22).

The value of k_2^D/k_2^H for the HRP-II–PABA reaction may be determined in the acid region where the log $k_{3,app}$ *vs.* p*H* (or p*D*) plots have slopes of -1 (Fig. 2). The result is $k_2^D/k_2^H = 3.3$ in excellent agreement with the value of 2.9 obtained in the same p*H* region for the HRP-II–ferrocyanide reaction. It appears likely that both ferrocyanide and PABA are reacting at the diffusion-controlled limit with an acid form of HRP-II at low p*H* (4) whereas iodide does not.

The results for the reaction of the acid form of HRP-II with PABA and ferrocyanide in both light and heavy water can be correlated in an attempt to estimate $pK_{2E}^D - pK_{2E}^H$ for HRP-II. The cause of the k^D/k^H values being greater than 1 for the HRP-II reactions with ferrocyanide and PABA in acid solutions is mainly a concentration effect. Since acids in heavy water have smaller dissociation constants (23) the concentration of protonated HRP-II is larger in D_2O than in H_2O provided the p*D* is sufficiently greater than pK_{2E}^H as illustrated in Fig. 3. Therefore, the reactive acid form of HRP-II is present in higher concentration in D_2O than in H_2O in the region where the log $k_{3,app}$ *vs.* p*H* (or p*D*) plots have slopes of -1. If it were possible to study HRP-II reactions at a p*H* (or p*D*) of about -2, then the kinetic isotope effect should almost com-

[6]R. J. Maguire and H. B. Dunford, unpublished results.

Can. J. Chem. Downloaded from www.nrcresearchpress.com by 210.87.254.40 on 09/05/12
For personal use only.

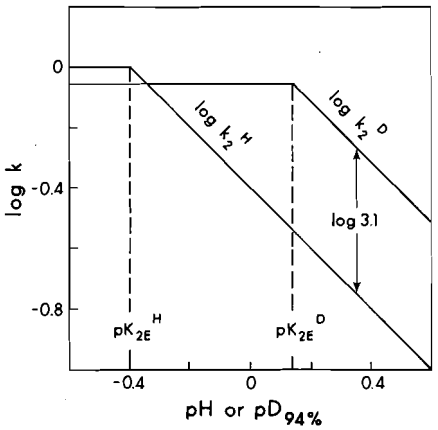

FIG. 3. Schematic representation of the pH– or pD-rate profile for a diffusion-controlled reaction if it could be studied in very acid solution. Rate constant data in the diagram, on a relative scale, are applicable to both the ferrocyanide and PABA reactions with the acid form of HRP-II. The small shift in the diffusion controlled rate when pH or pD < pK_{2E}^{H} is calculated on the basis of the viscosity ratios of light and heavy water at 25°. The mean difference in rate between the light and heavy water reactions of HRP-II with ferrocyanide and PABA where the slopes of the plots are −1 is 3.1 ± 0.2. The value of $pK_{2E}^{D} - pK_{2E}^{H}$ (extrapolated to 100% D_2O) can be estimated as 0.58 units from the plot.

pletely disappear since all of the HRP-II would be completely protonated (or deuterated) and every collision is effective for a diffusion-controlled reaction. However, one small isotope effect would remain in very acid solution and this would be attributable to the solvent isotope effect on the diffusion coefficients of reactants. Since diffusion coefficients of solutes are inversely proportional to the coefficient of viscosity, η, of solvent (25), there should be a k^D/k^H value of 0.81 as illustrated in Fig. 3 since η^D/η^H is 1.23 at 25° (24). The difference $\Delta pK = pK_{2E}^{D} - pK^{H}_{2E} = 0.58$ obtained by extrapolating the data of Fig. 3 to 100% D_2O may be compared to the prediction from an equation of Bell

$$[9] \qquad \Delta pK = 0.41 + 0.02pK^{H}$$

from which ΔpK should have a value of 0.41 (26).

Recently, a pH-dependent study of the cytochrome c peroxidase oxidation of ferrocyanide was interpreted in terms of total electrostatic charge of reactants using extended Debye–Hückel theory (27). Aside from the neglect of the charge in the active site of the enzyme (4, 28) this approach would fail to account for the kinetic and equilibrium hydrogen/deuterium isotope effects observed in the present and previous studies on HRP-II reactions (11) and to account for the pH dependences of all three classes of reactions with HRP-II, as typified by the substrates *p*-cresol, ferrocyanide ion or PABA, and iodide ion.

The authors are grateful to Dr. J. Stillman for experimental advice, to Prof. D. Dolman for helpful discussions concerning imidazole binding and to the National Research Council of Canada for financial support.

1. B. CHANCE. Arch. Biochem. Biophys. **41**, 416 (1952).
2. P. GEORGE. Nature, **169**, 612 (1952).
3. P. GEORGE. Biochem. J. **54**, 267 (1953).
4. H. B. DUNFORD and M. L. COTTON. J. Biol. Chem. In press.
5. R. ROMAN, H. B. DUNFORD, and M. EVETT. Can. J. Chem. **49**, 3059 (1971).
6. R. ROMAN and H. B. DUNFORD. Biochemistry, **11**, 2076 (1972).
7. J. E. CRITCHLOW and H. B. DUNFORD. J. Biol. Chem. **247**, 3703 (1972).
8. M. L. COTTON and H. B. DUNFORD. Can. J. Chem. **51**, 582 (1973).
9. J. E. CRITCHLOW and H. B. DUNFORD. *In* Oxidases and related redox systems. *Edited by* T. E. King, H. S. Mason, and M. Morrison. University Park Press, Baltimore. 1973. pp. 355–365.
10. H. B. DUNFORD. Physiol. Vég. **12**, 13 (1974).
11. J. E. CRITCHLOW and H. B. DUNFORD. J. Biol. Chem. **247**, 3714 (1972).
12. P. K. GLASOE and F. A. LONG. J. Phys. Chem. **64**, 188 (1960).
13. T. YONETANI and H. YAMAMOTO. *In* Oxidases and related redox systems. *Edited by* T. S. King, H. S. Mason, and M. Morrison. University Park Press, Baltimore. 1973. p. 279.
14. D. W. SMITH and R. J. P. WILLIAMS. Struct. Bonding, **7**, 1 (1970).
15. G. S. HAMMOND. J. Am. Chem. Soc. **77**, 334 (1955).
16. M. G. EVANS and M. POLYANYI. Trans. Faraday Soc. **34**, 11 (1938).
17. P. GEORGE. Nature, **169**, 612 (1952).
18. A. EHRENBERG. Svensk. Kem. Tidskr. **74**, 103 (1962).
19. R. H. FELTON, G. S. OWEN, D. DOLPHIN, and J. FASER. J. Am. Chem. Soc. **93**, 6332 (1971).
20. P. GEORGE, G. I. H. HANANIA, D. H. IRVINE, and I. ABU-ISSA. J. Chem. Soc. 5689 (1964).
21. R. J. MAGUIRE and H. B. DUNFORD. Biochemistry, **11**, 937 (1972).
22. R. J. MAGUIRE and H. B. DUNFORD. Can. J. Chem. **51**, 1721 (1973).
23. P. M. LAUGHTON and R. E. ROBERTSON. *In* Solute–solvent interactions. *Edited by* J. F. Coetzee and C. D. Ritchie. Marcel Dekker, N.Y. 1969. p. 399.
24. E. F. CALDIN. Fast reactions in solution. Wiley, N.Y. 1964. p. 11.
25. G. N. LEWIS and R. T. MACDONALD. J. Am. Chem. Soc. **55**, 4730 (1933).
26. R. P. BELL. The proton in chemistry. Cornell University Press, Ithaca, N.Y. 1959. Chapt. XI.
27. H. C. JORDI and J. E. ERMAN. Biochemistry, **13**, 3736 (1974).
28. G. G. HAMMES and R. A. ALBERTY. J. Phys. Chem. **63**, 274 (1959).

Can. J. Chem. Downloaded from www.nrcresearchpress.com by 210.87.254.40 on 09/05/12
For personal use only.

Nitration of 3,4-Dimethylacetophenone and 3,4-Dimethylbenzophenone. Formation and Rearomatization of Adducts

ALFRED FISCHER, COLIN CAMPBELL GREIG, AND ROLF RÖDERER
Department of Chemistry, University of Victoria, Victoria, British Columbia V8W 2Y2

Received November 15, 1974

ALFRED FISCHER, COLIN CAMPBELL GREIG, and ROLF RÖDERER. Can. J. Chem. **53**, 1570 (1975).

Nitration of 3,4-dimethylacetophenone in acetic anhydride gives a mixture of *cis*- and *trans*-2-acetyl-4,5-dimethyl-4-nitro-1,4-dihydrophenyl acetate as the main product, together with 3,4-dimethyl-2-, 3,4-dimethyl-5-, and 3,4-dimethyl-6-nitroacetophenone. Analogous products are obtained from 3,4-dimethylbenzophenone. Rearomatization of the adducts under mildly acidic conditions occurs via 1,4-elimination of nitrous acid to form 2-acetyl- and 2-benzoyl-4,5-dimethylphenyl acetate, respectively. In strongly acidic conditions elimination of acetic acid accompanied by 1,2- and 1,3-shifts of the nitro group occurs to form the 2- and 5-nitro derivatives of the parent ketones. The rearomatization to the nitro derivatives involves the intermediate formation of an *ipso*-cyclohexadienyl cation which may be trapped by anisole or mesitylene to form biphenyl derivatives.

ALFRED FISCHER, COLIN CAMPBELL GREIG et ROLF RÖDERER. Can. J. Chem. **53**, 1570 (1975).

La nitration de la diméthyl-3,4 acétophénone dans l'anhydride acétique donne un mélange d'acétates d'acétyl-2 diméthyl-4,5 nitro-4 dihydro-1,4 phényle *cis* et *trans*; aux côtés de ces produits principaux, il se forme aussi de la diméthyl-3,4 nitro-2, de la diméthyl-3,4 nitro-5 et de la diméthyl-3,4 nitro-6 acétophénone. On obtient des produits analogues à partir de la diméthyl-3,4 benzophénone. La réaromatisation des produits d'addition dans des conditions d'acidité faible, s'effectue par une élimination 1,4 d'acide nitreux conduisant, suivant les cas, à la formation d'acétates d'acétyl-2 et de benzoyl-2 diméthyl-4,5 phényle. Dans des conditions d'acidité forte, il y a une élimination d'acide acétique accompagnée par des réarrangements 1,2 et 1,3 du groupe nitro, pour conduire aux dérivés nitro-2 et nitro-5 de la cétone de départ. La réaromatisation des dérivés nitrés implique la formation intermédiaire d'un cation *ipso*-cyclohexadiényle qui peut être piégé par l'anisole ou le mésitylène pour conduire à des dérivés biphényles.
[Traduit par le journal]

Introduction

Ipso nitration of methylbenzenes and their derivatives in acetic anhydride gives diastereoisomeric adducts which are derivatives of 4-nitro-1,4-dihydro-*p*-tolyl acetate (1, 2). Such adducts readily undergo rearomatization reactions. Secondary acetate adducts (to which discussion is confined in this report) afford aryl acetates by elimination of nitrous acid (1*a–e*) and nitroarenes by elimination of acetic acid accompanied by migration of the nitro group. Elimination of acetyl nitrate and reversion to the original aromatic is also observed with some adducts. Thus, the *o*-xylene adduct exhibits a 1,2-shift of the nitro group to form 3-nitro-*o*-xylene (3) whereas those from 3-chloro- (1*e*) and 3- and 4-cyano-*o*-xylene (1*d*) exhibit 1,3-shifts of nitro as well as the elimination of acetyl nitrate. Formation and potential rearomatization reactions of methylbenzene adducts are depicted for toluene, the parent methylbenzene, in Scheme 1. It should be noted that not all of the rearomatization reactions have actually been observed for any one of the adducts previously studied and, in particular, the nitro rearrangement and acetyl nitrate elimination reactions have neither been looked for, nor observed, in the case of the toluene adduct itself.

The present study, which is concerned with the effect of the oxo group, is a continuation of our investigations of substituent effects on the formation and rearomatization reactions of adducts of substituted *o*-xylenes.

Results and Discussion

Nitration of 3,4-dimethylacetophenone in acetic anhydride formed a mixture of 68% diene adducts, 20% 3,4-dimethyl-6-nitroacetophenone, and small amounts of the 2-nitro and 5-nitro isomers. The diastereoisomeric acetoxynitro adducts **1***a* and *b* were isolated by chromatography. The relative yields of the products and the absence of adducts resulting from attack at the 4-(*ipso*) position are consistent with the combined directing effects of the acetyl and the two methyl

Can. J. Chem. Downloaded from www.nrcresearchpress.com by 210.87.254.6 on 09/05/12
For personal use only.

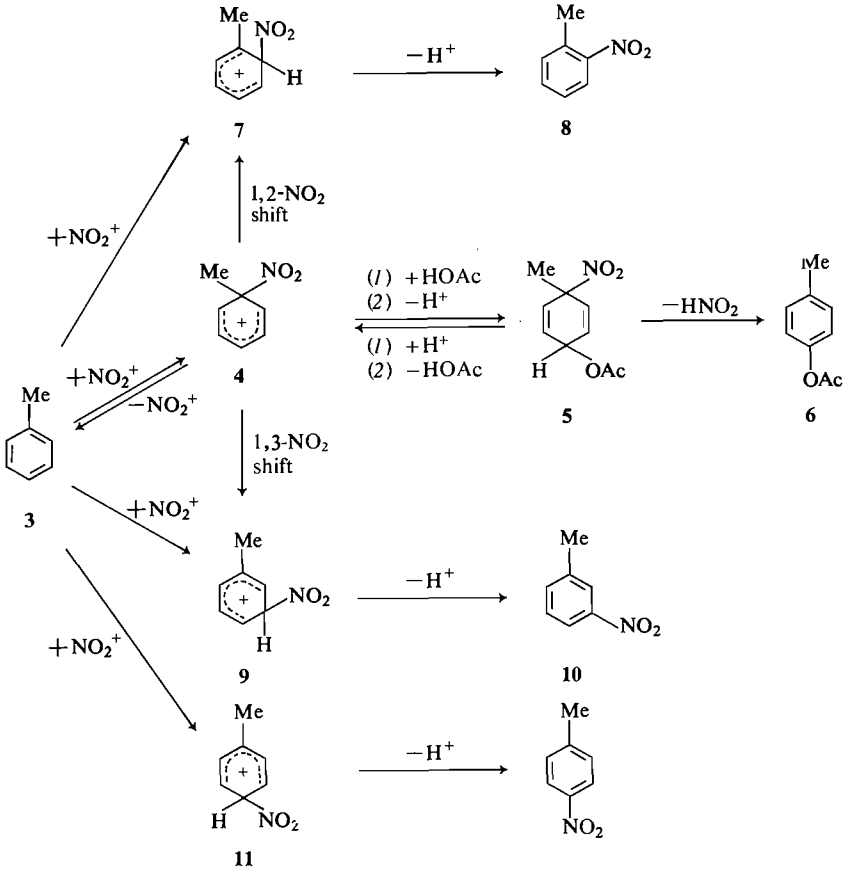

SCHEME 1. Formation and potential rearomatization reactions of methylbenzene adducts.

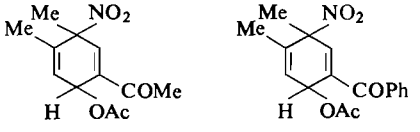

1 2

a NO_2, OAc *trans*
b NO_2, OAc *cis*

substituents. The *ortho* methyl groups should favor electrophilic attack in the positional order 3 = 4 > 6 > 5 = 2. The acetyl group, which is deactivating, would be expected to reduce the reactivity at the 4-(*para*) position to a greater extent than at the 2- and 6-(*ortho*) positions and least of all at the 3- and 5-(*meta*) positions. The observed order, 3 > 6 > 5 ~ 2 > 4, is in accord with these expectations.

Nitration of 3,4-dimethylacetophenone with mixed acid was carried out by Buu-Hoî *et al.* (4) who reported that 3,4-dimethyl-6-nitroacetophenone, m.p. 120° was obtained in 75% yield together with 3,4-dimethyl-5-nitroacetophenone. Brändström and Carlsson (5) repeated this reaction and they obtained a 2:1:1 mixture of 3,4-dimethyl-2-nitroacetophenone, m.p. 122°, 3,4-dimethyl-6-nitroacetophenone, m.p. 80°, and 3,4-dimethyl-5-nitroacetophenone. They concluded that Buu Hoî *et al.* (4) incorrectly identified the isomer of m.p. 120°. The n.m.r. spectra clearly identify each isomer (see Experimental) and our work confirms Brändström and Carlsson's observations that the isomer of m.p. 120° is the 2-nitro compound and that the isomer having m.p. 80° is 3,4-dimethyl-6-nitroacetophenone. However, the relative yields of substitution products that they found, in which the 2-nitro isomer predominates, is quite different from the

Can. J. Chem. Downloaded from www.nrcresearchpress.com by 210.87.254.6 on 09/05/12
For personal use only.

Can. J. Chem. Downloaded from www.nrcresearchpress.com by 210.87.254.6 on 09/05/12
For personal use only.

relative yields that we observed, where the 6-nitro isomer predominates. We suggest that under both sets of conditions the nitronium ion is the active electrophile and that its relative rate of attack at the nuclear positions is the same. Under the highly acidic conditions pertaining in sulfuric acid (Brändström and Carlsson's conditions) diene adducts are not stable and, if formed, will be readily converted back to the precursor cyclohexadienyl cation (5-Ac-2-Me-**4**)[1] which, by shift of the nitro group, followed by loss of a proton, will give the 2-nitro and 5-nitro substitution products of 3,4-dimethylacetophenone (*cf.* Scheme 1: **4** → **7** → **8** and **4** → **9** → **10**, see below). Thus the predominant attack by nitronium ion at the 3-(*ipso*) position will under their conditions lead to an increased yield of the 2-nitro and 5-nitro isomers. If the ratio of attack at the 2, 3, 5, and 6 positions that we observed, ~6, 68, ~6, and 20%, respectively, is assumed to be the same in sulfuric acid, and if the 68% of *ipso* attack leads to the 2-nitro and 5-nitro derivatives in the same ratio that we found for the rearrangements (3:1) then the observed yields of 2-, 5-, and 6-nitro derivatives would be 57, 23, and 20%, respectively. This is quite close to the 2:1:1 ratio found by Brändström and Carlsson. This provides a clear illustration of how *ipso* attack followed by rearrangement can complicate the interpretation of positional reactivity determined from the isomer distribution of the final substitution products (3, 6, 7).

Nitration of 3,4-dimethylbenzophenone gave the diastereoisomeric adducts **2***a* and *b*, in approximately 70% yield, the three 3,4-dimethylnitrobenzophenone isomers, and 3,5-dinitro-*o*-xylene. Because of the complexity of the spectrum of the reaction product it was not possible to measure the yields of the individual nitro substitution products. The formation of 3,5-dinitro-*o*-xylene is indicative of attack by the nitrating electrophile, assumed to be the nitronium ion, at the position *ipso* to benzoyl. The resulting 4-nitro-*o*-xylene would be expected to nitrate in the vacant *meta* position to form the 3,5-dinitro-*o*-xylene. However, study of the nitration of 4-nitro-*o*-xylene has shown that it is quite unreactive towards nitric acid in acetic anhydride under the conditions used for nitration of the dimethylbenzophenone.[2] The mode of formation of the dinitro-*o*-xylene is thus unexplained.

Rearomatization of **1** and **2** under aprotic, weakly acidic (acetic acid) and moderately acidic conditions (5% sulfuric acid in acetic acid, trifluoroacetic acid) gave the corresponding acetates, 2-acetyl-4,5-dimethylphenyl acetate and 2-benzoyl-4,5-dimethylphenyl acetate, by 1,4-elimination of nitrous acid. During the course of the slow elimination reaction of **1** in acetic acid, epimerization was evident. Under more strongly acidic conditions (50% sulfuric acid in acetic acid, 78% aqueous sulfuric acid) or in the presence of the Lewis acid boron trifluoride, a mixture of the 3,4-dimethylacetophenone (29%) and its 2-(53%) and 5-nitro (18%) derivatives, or 3,4-dimethylbenzophenone (37%) and its 2-(36%) and 5-nitro (27%) derivatives was obtained, respectively. The two distinct pathways for rearomatization reflect those observed for the *o*-xylene adduct 2-Me-**5** (3), and its derivatives 6-Cl-2-Me-**5** (1*e*), and 5-CN-2-Me-**5** (1*d*).

Clearly, the outcome of the competition between the two rearomatization pathways depends upon the acidity of the reaction medium and the results are explicable in terms of the previously proposed mechanisms (1*d*, *e*, 3). In the 1,4-elimination (E2) of nitrous acid (Scheme 1: **5** → **6**) a basic species (normally a solvent molecule) is required to abstract the proton. Under conditions of very high acidity the ability of the solvent to abstract the proton is markedly reduced and the 1,4-elimination pathway is disfavored with respect to the second rearomatization process. This involves the acid-catalyzed unimolecular loss of acetate to (re)form the *ipso*-cyclohexadienyl cation **4** which can in principle undergo (*i*) loss of the nitro group as a nitronium ion, to reform **3**; (*ii*) a 1,2-nitro shift to form **7**, which is in turn deprotonated to the 2-nitro derivative **8**; and (*iii*) a 1,3-nitro shift to form **9**, in turn deprotonated to the 3-nitro derivative **10**. The acidity at which the transition from the E2 to cation pathway occurs depends upon the substituents present in the adduct. Thus in the intermediate acidity range (5% sulfuric acid in acetic acid, or trifluoroacetic acid), where the less deactivated 6-Cl-2-Me-**5** has already exhibited the E2 to cation transition (1*e*), **1** and **2** still follow the E2 pathway. For **1** and **2** the transition is effected

[1]When reference is made to compounds as derivatives of those depicted in Scheme 1 the numbering system follows that of toluene itself *i.e.* the position to which the methyl substituent is attached is always taken as the 1-position.

[2]Unpublished work with B. Fowler.

Can. J. Chem. Downloaded from www.nrcresearchpress.com by 210.87.254.6 on 09/05/12
For personal use only.

at higher acidities. The fact that epimerimization of **1***b* occurred in the course of the elimination reaction in acetic acid indicates that (reversible) cation formation does occur at low acidities. Presumably, the lifetime of the cation under these conditions is too short to allow the nitro shift processes (**4** → **3**, **7**, **9**) to occur.

The particular rearomatization processes which occur from the cation are determined by the substituents. For 2-Me-**4** only a 1,2-nitro shift, leading eventually to 3-nitro-*o*-xylene, is observed (*cf.* **4** → **7** → **8**). The other potential reactions of the *ipso*-cyclohexadienyl cation, *viz.* a 1,3-nitro shift followed by deprotonation to the isomeric nitro aromatic (*cf.* **4** → **9** → **10**), and the loss of the nitro group as nitronium ion, leading to parent aromatic (*cf.* **4** → **3**) but not the 1,2-nitro shift, are realized in the cases of 6-Cl-2-Me-**5**, (1*e*), 3-CN-2-Me-**5**, and 5-CN-2-Me-**5** (1*d*). In adducts **1** and **2**, which give rise to the cations 5-Ac-2-Me-**4** and 5-Bz-2-Me-**4**, respectively, all three processes are observed. The relative yields of the products indicate that in the case of 5-Ac-2-Me-**4** the 1,2-shift of the nitro group (**4** → **7**) is the most favored process; loss of the nitronium ion (**4** → **3**) occurs less readily and the 1,3-shift of the nitro group (**4** → **9**) occurs to the least extent. The data for **2** suggest that 1,2-shift of the nitro group in the cation is not so favored over the other processes as it is in the case of **1**. This may be attributed to the steric effect of the benzoyl substituent (larger than acetyl) which would be expected to inhibit the 1,2-nitro shift. For both **1** and **2** it is clear that the shift of the nitro group must be intramolecular. A dissociation–renitration process would give the 6-nitro derivative which is not observed; indeed in the case of **1**, 3,4-dimethyl-6-nitroacetophenone would be expected to be the major product, since the results of the nitration of 3,4-dimethylacetophenone show that of the unsubstituted positions the 6-position is the most activated. The fact that no 3,4-dimethyl-6-nitroacetophenone is obtained from the rearomatization of **1** (nor 3,4-dimethyl-6-nitrobenzophenone from **2**) although the precursor cyclohexadienyl cation (5-Ac-2-Me-**11**) is the most stable of the non-*ipso* cations also confirms the expectation that the direct 1,4-nitro shift is unlikely and shows that a non-*ipso* cation (5-Ac-2-Me-**9**) undergoes deprotonation (to 5-Ac-2-Me-**10**) much more rapidly than it rearranges to a more stable cation (*cf.* **9** → **11**). We suspect that this last is a general conclusion since no evidence for the rearrangement of a non-*ipso* nitrocyclohexadienyl cation has ever been adduced. Furthermore, the parallel observation that the only acetyl adducts which have ever been observed have the nitro group attached to an *ipso* position and the irreversibility of nitration, show that the *only* fate of a non-*ipso* nitrocyclohexadienyl cation is deprotonation.

ipso-Cyclohexadienyl cations from tertiary acetate precursors (*e.g.* 4-Me-**4**) are trappable by nucleophiles other than acetic acid (*e.g.* methanol) to give other adducts (1*f*, *g*). The epimerization observed in the course of the rearomatization of **1***a* in acetic acid indicates that the secondary acetate adducts can undergo exchange reactions by formation of the cation and its subsequent combination with a nucleophile. The coupling reactions with aromatic substrates presumably follow this process, illustrated for the parent adduct **5** (Scheme 2). The cation substitutes in the aromatic to form as the immediate product the nitroaryl adduct **12** which readily undergoes elimination of nitrous acid to form the biphenyl derivative **13**. The biphenyl derivatives **14**, **15**, and **16** obtained by reaction of **1** with mesitylene and with anisole and by reaction of **2** with mesitylene, as well as that (**17**) previously reported from reaction of 6-Cl-2-Me-**5** with mesitylene, all have precisely the structures expected if they were formed by the pathway shown in Scheme 2. In the nitration of 1,2-dialkylbenzenes (*e.g.* *o*-xylene) and of hemimellitene with 90% nitric acid at low temperatures, coupling occurs to form polyalkylbiphenyls, which may be further nitrated (8). It is significant that such coupling takes place with substrates which when reacted with nitric acid in acetic anhydride are known to, or would be expected to, give good

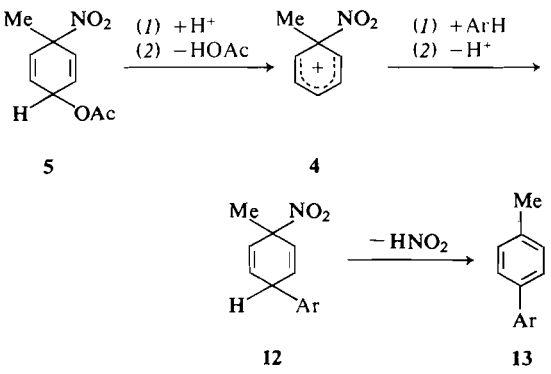

SCHEME 2

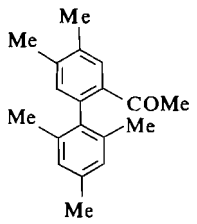

14

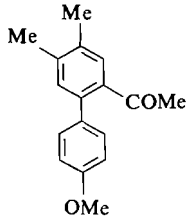

15

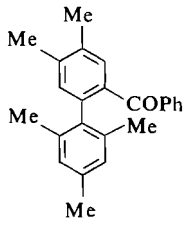

16

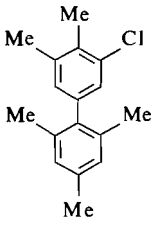

17

yields of secondary acetate adducts, and does not occur with substrates which do not form adducts (*e.g.* mesitylene) or which form only tertiary acetate adducts (*e.g. p*-xylene). It seems clear that the mechanism of this coupling reaction is just that shown in Scheme 2 except that the *ipso*-cyclohexadienyl cation **4** is generated by *ipso* attack of nitronium ion on the hydrocarbon. The susceptible hydrocarbons have a highly activated *ipso* position *para* to an unsubstituted position. Toluene itself was not observed to couple (8*a*) but since only a small amount of *ipso* attack occurs with toluene (1*c*) only a very small amount of coupling product would be expected. Cross coupling of two different arenes also occurs but only if one of the components is of the type required for successful self-coupling. Clearly the second component is merely filling the role of the aromatic which is substituted, not that which becomes the active electrophile. The high yields of biphenyl derivatives which are obtained from **1** and **2** indicate that the reaction has potential synthetic utility. The reaction is obviously related to the Scholl reaction of dehydrogenation condensation of aromatics (9) but has the important advantage over the latter that it provides a mixed biaryl product.

Reaction of **1** and **2** with sodium methoxide in methanol resulted in rearomatization by 1,4-elimination of nitrous acid accompanied by cleavage of the ester function.

Experimental

Nuclear magnetic resonance spectra at 220 MHz were determined on the Varian HR 200 spectrometer at the Ontario Research Foundation, Sheridan Park, Ontario. Microanalyses were by Dr. D. McGillivray. Nitric acid was purified by distilling the fuming acid (300 cm^3) at 100 Pa from urea (10 g) and sulfuric acid (500 cm^3). Alumina was deactivated with 3% of 10% acetic acid. Ether and pentane were dried by distillation from sodium and phosphorus pentoxide, respectively.

Nitration of 3,4-Dimethylacetophenone

A solution of freshly distilled nitric acid (10 cm^3, 0.24 mol) in acetic anhydride (40 cm^3) was added to 3,4-dimethylacetophenone (20 g, 0.14 mol) in acetic anhydride (60 cm^3) at $-40°$. The yellow reaction mixture was allowed to stand at 2° overnight after which time the n.m.r. spectrum indicated that approximately 70% of dienes had been formed. The mixture was worked up in the normal manner (10) to yield an oil consisting of (by n.m.r.) 68% dienes, 20% 3,4-dimethyl-6-nitroacetophenone, and lesser amounts of 3,4-dimethyl-2-nitroacetophenone and 3,4-dimethyl-5-nitroacetophenone. Chromatography on alumina at $-20°$ and elution with pentane and ether–pentane mixtures gave a mixture of 3,4-dimethylnitroacetophenones (1.2 g, 6 mmol) in the 50–70% ether fractions, *trans*-2-acetyl-4,5-dimethyl-4-nitro-1,4-dihydrophenyl acetate (**1***a*, 10.7 g, 42 mmol) in the second 70% ether fraction, a mixture of **1***a* and *b* (5.4 g, 21 mmol) in the first 100% ether fraction, and *cis*-2-acetyl-4,5-dimethyl-4-nitro-1,4-dihydrophenyl acetate (**1***b*, 1.0 g, 4 mmol) in the second 100% ether fraction.

Recrystallization of **1***a* from chloroform–pentane gave colorless crystals, m.p. 95.5–97°; u.v. (CH_3OH) 212.5 nm (ε 1130 $m^2\ mol^{-1}$); i.r. (Nujol) 1730 and 1245 ($OCOCH_3$), 1680 ($COCH_3$), 1545 and 1380 (NO_2), and 930 cm^{-1}; n.m.r. ($CDCl_3$) τ 3.08 (d, 1, 3-*H*) 3.83 (m, 1, 1-*H*), 4.00 (m, 1, 6-*H*), 7.62 (s, 3, $COCH_3$), 7.98 (s, 3, $OCOCH_3$), 8.09 (s, 3, 4-CH_3), 8.15 (t, 3, 3-CH_3), J_{13} = 0.90, J_{16} = 4.07, $J_{1,5-CH_3}$ = 1.26, $J_{6,5-CH_3}$ = 1.31 Hz; irradiation at 8.15 collapsed the multiplet at 3.83 to a doublet of doublets and that at 4.00 to a doublet, allowing the initial assignment of chemical shifts and coupling constants to be made to simulate the spectrum, the simulation then being refined to give the listed parameters.

Anal. Calcd. for $C_{12}H_{15}NO_5$: C, 56.91; H, 5.96; N, 5.53. Found: C, 56.61; H, 5.96; N, 5.45.

Recrystallization of **1***b* from chloroform–pentane gave colorless crystals, m.p. 120–120.5°; u.v. (CH_3OH) 213.5 nm (ε 1100 $m^2\ mol^{-1}$); i.r. (Nujol) 1730 and 1240 ($OCOCH_3$), 1680 ($COCH_3$), 1550 and 1380 (NO_2), 1020 and 940 cm^{-1}; n.m.r. ($CDCl_3$), τ 3.14 (d, 1, 3-*H*), 3.90 (m, 1, 1-*H*), 4.03 (m, 1, 6-*H*), 7.62 (s, 3, $COCH_3$) 7.95 (s, 3, $OCOCH_3$), 8.13 (t, 3, 5-CH_3). 8.17 (s, 3, 4-CH_3), J_{13} = 0.82, J_{16} = 3.83, $J_{1,5-CH_3}$ = 1.30, $J_{6,5-CH_3}$ = 1.28 Hz; irradiation at 8.08 collapsed the multiplet at 3.90 to a doublet of doublets and then at 4.30 to a doublet allowing the assignment of chemical shifts and coupling constants which were then refined as in the case of **1***a*.

Anal. Calcd. for $C_{12}H_{15}NO_5$ (M_r 253): C, 56.91; H, 5.96; N, 5.53. Found (249): C, 57.03; H, 5.93, N, 5.47.

Identical arguments to those adduced for the structure of the adduct from 3,4-dimethylbenzonitrile (**1***d*) can be made for the assignment of structure **1** to the 3,4-dimethylacetophenone adducts. The assignment is supported by the effect of the shift reagent tris-(1,1,1,2,2,3,3-heptafluoro-7,7-[$^2H_6$]dimethyl-4,6-[$^2H_3$]octanedionato)europium(III) {Eu([$^2H_9$]fod)$_3$} (Table 1). In both **1***a* and *b* the acetate methyl absorption moved downfield more rapidly

Can. J. Chem. Downloaded from www.nrcresearchpress.com by 210.87.254.6 on 09/05/12
For personal use only.

TABLE 1. Relative gradients (gradient 1-OAc = 1.00) of proton chemical shifts for diene adducts resulting from the addition of Eu([$^2H_9$]fod)$_3$

Compound	1-H	3-H	6-H	4-CH_3	5-CH_3	2-Ac	2′-H
1*a*	1.97	0.46	0.73	0.22	0.08	0.52	—
1*b*	1.94	0.40	0.73	0.08	0.09	0.51	—
2*a*	2.20	0.40	0.65	0.22	0.07	—	0.38
2*b*	2.40	0.40	0.66	0.04	0.08	—	0.42

than that of any of the other methyl groups, confirming the expectation of coordination of the reagent at the acetate function. The allylic hydrogen (1-H) peak moves downfield more rapidly than that of the adjacent vinyl hydrogen (6-H) which in turn moves more rapidly than that of the remote vinyl hydrogen (3-H), in accord with the increasing distance between the europium and the respective hydrogens. Similarly, in both **1***a* and *b*, the acetate methyl absorption moves more rapidly than that of the acetyl methyl which moves more rapidly than that of the 5-methyl, again in accord with the increasing distance between europium and the respective methyl groups. However, the 4-methyl peak in **1***a* moves more than twice as rapidly as the similar peak of **1***b* whereas the shift gradients for all other pairs of corresponding protons of **1***a* and *b* are not significantly different and on this basis the stereochemistry is assigned with 4-methyl and acetate *cis* in **1***a* and thus **1***a* as the *trans* adduct and the complementary assignment for **1***b*.

Nitro Compounds.

The residues from early column fractions containing the nitro compounds were combined and rechromatographed on alumina. 3,4-Dimethyl-6-nitro-acetophenone was eluted with 25% ether–pentane, m.p. 79–80° (lit. (5) m.p 80°); i.r. (Nujol) 1700 (C=O), 1545 and 1370 (NO_2); n.m.r. ($CDCl_3$), τ 2.15 (s, 1, 5-*H*), 2.72 (s, 1, 2-*H*), 7.50 (s, 3, $COCH_3$), 7.65 (s, 6, 3-CH_3 and 4-CH_3); mass spectrum (70 eV) *m/e* (relative intensity) 193 (32, M), 178 (100, *M* − CH_3), 151 (74), 103 (40), 91 (30), 43 (60). 3,4-Dimethyl-5-nitroacetophenone could not be obtained pure but was obtained in a mixture with the 6-nitro isomer: n.m.r. ($CDCl_3$), τ 1.85 (d, 1, *J* = 1.5 Hz, 6-*H*), 2.00 (d, 1, *J* = 1.5 Hz, 2-*H*), 7.40 (s, 3, $COCH_3$), 7.67 (s, 6, 3-CH_3 and 4-CH_3).

Anal. Calcd. for $C_{10}H_{11}NO_3$: C, 62.17; H, 5.74; N, 7.25. Found: C, 62.04; H, 5.60; H, 7.00.

3,4-Dimethyl-2-nitroacetophenone was isolated in a small amount from the 40% ether–pentane fraction on rechromatography of the nitro compounds. It was more readily obtained from the product of rearomatization of **1** using boron trifluoride (see below), m.p. 118° (lit. (5) m.p. 122°); i.r. 1700 (C=O), 1540 and 1350 cm^{-1} (NO_2); n.m.r. ($CDCl_3$) τ 2.45 (d, 1, *J* = 8 Hz, 6-*H*), 2.70 (d, 1, *J* = 8 Hz, 5-*H*), 7.48 (s, 3, $COCH_3$), 7.58 (s, 3, 3-CH_3), 7.80 (s, 3, 4-CH_3); mass spectrum (70 eV) *m/e* (relative intensity) 193 (6, M), 178 (100, *M* − CH_3), 151 (80), 103 (42), 91 (41), 43 (45), 42 (34).

Anal. Calcd. for $C_{10}H_{11}NO_3$: C, 62.17; H, 5.74; N, 7.25. Found: C, 62.00; H, 5.50; N, 7.48.

The three nitro substitution products have definitive n.m.r. spectra. 3,4-Dimethyl-2-nitroacetophenone has two *ortho* protons which give rise to a typical AB quartet with an 8 Hz coupling. Its 5-nitro isomer has *meta* protons and these give an AB quartet with a 1.5 Hz coupling. The 6-nitro isomer has *para* protons which appear as two singlets. None of the peaks overlap and this facilitates the detection of the individual isomers in mixtures.

2-Acetyl-4,5-dimethylphenol and 2-Acetyl-4,5-dimethylphenyl Acetate

Diene **1** (3 g) was added to a concentrated solution of sodium methoxide in methanol (5 cm^3). After neutralization with ammonium chloride and evaporation of excess methanol the residue was extracted with ether. Evaporation of the ether and recrystallization of the residue from petroleum ether gave 2-acetyl-4,5-dimethylphenol, m.p. 71.5–72.5° (lit. (11) m.p. 71°); i.r. (Nujol) 3300–3500 (OH), 1650 cm^{-1} ($COCH_3$); n.m.r. ($CDCl_3$) τ 2.50 (s, 1, 3-*H*), 3.20 (s, 1, 6-*H*), 7.45 (s, 1, $COCH_3$), 7.76 (s, 1, CH_3), 7.80 (s, 1, CH_3); mass spectrum (70 eV) *m/e* (relative intensity) 164 (36, M) (100, *M* − CH_3), 121 (5), 91 (12), 77 (14), 43 (15).

The phenol (278 mg) was dissolved in acetic anhydride (5 cm^3), 5 drops of sulfuric acid were added, and the mixture maintained at 35° for 30 min. The mixture was neutralized and extracted with ether. Removal of the ether gave 2-acetyl-4,5-dimethylphenyl acetate which was recrystallized from ethanol–water, m.p. 59–60°; i.r. (Nujol) 1780 ($OCOCH_3$) and 1700 cm^{-1} ($COCH_3$); n.m.r. ($CDCl_3$) τ 2.42 (s, 1, 3-*H*), 3.13 (s, 1, 6-*H*), 7.50 (s, 3, $COCH_3$), 7.69 (s, 3, CH_3), and 7.73 (s, 3, CH_3); mass spectrum (70 eV) *m/e* (relative intensity) 206 (6, M) 164 (62, *M* − CH_2CO), 149 (100), 91 (16), 43 (35).

Anal. Calcd. for $C_{12}H_{14}O_3$: C, 69.89; H, 6.84. Found: C, 69.78; H, 6.80.

*2-Acetyl-2′,4,4′,5,6′-pentamethylbiphenyl (**14**)*

Boron trifluoride etherate (1 cm^3) was diluted with ether (3 cm^3); the solution was added dropwise to a solution of diene **1** (2 g, 7.9 mmol) and mesitylene (5 cm^3) in methylene chloride (3 cm^3) and the mixture left to stand for 4 h. After work-up, chromatography on silica gel and elution with ether–pentane gave mesitylene in the 5% ether fraction, the biphenyl (1.47 g, 5.5 mmol) in the early 20% ether fractions and a mixture of 3,4-dimethyl-2- and 3,4-dimethyl-5-nitroacetophenone (300 mg, 1.6 mmol) in the later 20% ether fractions. After recrystallization from ethanol, 2-acetyl-2′,4,4′,5,6′-pentamethylbiphenyl had m.p. 74°; i.r. (Nujol) 1675 (C=O) 1610, 1275, 1220, 890, and 860 cm^{-1}; n.m.r. ($CDCl_3$) τ 2.44 (s, 1, 3-*H*), 3.11 (m, 3, 3′-*H*, 5′-*H*, and 6-*H*); 7.74 (s, 9, 4-CH_3, 4′-CH_3, and 5-CH_3) 8.10 (s, 9, 2′-CH_3, 6′-CH_3, and $COCH_3$); mass spectrum (70 eV) *m/e* (relative intensity) 266 (56, M) 251 (100, *M* − CH_3) 193 (78), 178 (43), 152 (54), 132 (47), 118 (100), 115 (49), 103 (55), 89 (67), 44 (71).

Anal. Calcd. for $C_{18}H_{22}O$: C, 85.67; H, 8.23. Found: C, 85.84; H, 8.23.

*2-Acetyl-4′-methoxy-4,5-dimethylbiphenyl (**15**)*

A solution of boron trifluoride etherate (1 cm^3) in ether

Can. J. Chem. Downloaded from www.nrcresearchpress.com by 210.87.254.6 on 09/05/12
For personal use only.

Can. J. Chem. Downloaded from www.nrcresearchpress.com by 210.87.254.6 on 09/05/12
For personal use only.

(5 cm^3) was added to a mixture of diene **1** (2 g, 7.9 mmol) and anisole (5 cm^3) at 0°. The mixture turned bright blue. After work-up and chromatography on silica gel, elution with 10% ether–pentane washed down excess anisole. Elution with 20% ether–pentane gave 2-acetyl-4′-methoxy-4,5-dimethylbiphenyl (230 mg, 0.9 mmol); n.m.r. ($CDCl_3$) τ 2.64 (s, 1, 3-*H*), 2.73 (d, 2, J = 8 Hz, 3′-*H* and 5′-*H*), 2.83 (s, 1, 6-*H*), 3.05 (d, 1, J = 8 Hz, 2′-*H* and 6′-*H*), 6.18 (s, 3, OCH_3), 7.68 (s, 6, 4-CH_3 and 5-CH_3), 8.00 (s, 3, $COCH_3$); mass spectrum (70 eV) *m/e* (relative intensity) 254.141 (19, M_r ($^{12}C_{17}{}^{1}H_{18}{}^{16}O_2$) 254.131), 149, (100), 132 (82), 104 (58), 83 (69), 77 (70), 43 (95.) Further elution with 20% ether–pentane gave 3,4-dimethyl-6-nitroacetophenone (700 mg, 3.6 mmol) and 3,4-dimethyl-2-nitroacetophenone (240 mg, 1.2 mmol).

Reaction of Diene 1 with Boron Trifluoride

Diene **1** (1.5 g, 5.0 mmol) was added to boron trifluoride etherate (1.5 cm^3). A vigorous reaction ensued. After work-up followed by chromatography on silica gel and elution with 20% ether–pentane there was obtained 3,4-dimethylacetophenone (245 mg, 1.7 mmol), 3,4-dimethyl-5-nitroacetophenone (245 mg, 1.3 mmol), and 3,4-dimethyl-2-nitroacetophenone (550 mg, 2.8 mmol). The identity of the products was confirmed by comparison of R_f values on thin-layer chromatography with those of authentic samples and by n.m.r.

Reaction of Diene 1 with 78% Sulfuric Acid

Diene **1** (500 mg) was stirred overnight with 78% (by weight) sulfuric acid. The n.m.r. of the product obtained after work-up showed 35% 3,4-dimethylacetophenone, 48% 3,4-dimethyl-2-nitroacetophenone, and 16% 3,4-dimethyl-5-nitroacetophenone. The identity of the components was confirmed by t.l.c.

Other Rearomatization Reactions of Diene 1

In each case diene **1** (100 mg) was reacted with the appropriate reagent in an n.m.r. tube and the products determined by n.m.r. and confirmed by t.l.c. Reaction with 50% sulfuric acid in acetic acid gave 23% 3,4-dimethylacetophenone, 61% of 3,4-dimethyl-2-nitro-, and 16% of 3,4-dimethyl-5-nitroacetophenone. Reaction with 5% sulfuric acid in acetic acid gave only 2-acetyl-4,5-dimethylphenyl acetate as did reaction with neat trifluoroacetic acid and reaction with neat acetic acid. Reaction with acetic acid was slow at ambient temperature ($t_{1/2} \sim 10$ days) and epimerization of the mixture in which **1*b*** predominated to a mixture in which **1*a*** was the major diastereoisomer occurred. At 120° elimination to the acetate was complete in 10 min. The rate of rearomatization was measured in 65% (by weight) trifluoroacetic acid – 35% [$^2H_4$]acetic acid mixture and at a probe temperature of 35°, by integrating over the upfield part of the diene region of the n.m.r. spectrum at measured time intervals. A plot of log(integral) against time was linear leading to a first-order rate constant of 4.0×10^{-4} s^{-1}.

Nitration of 3,4-Dimethylbenzophenone

A solution of nitric acid (8 cm^3, 0.2 mol) in acetic anhydride at −70° was added to a stirred solution of the ketone (20 g, 0.10 mol) in acetic anhydride (20 cm^3) also at −70°. The temperature of the reaction mixture was allowed to rise to 5° and held at this temperature overnight. Diene adduct **2** (9.7 g, 30 mmol) crystallized from the reaction mixture and was filtered off. The filtrate was worked up in the normal manner to yield a semicrystalline product from which more adduct **2** (4.3 g, 14 mmol) was filtered off after the addition of ether (50 cm^3). The residue (15.8 g) obtained after evaporation of the ether from the filtrate was chromatographed on deactivated alumina at −25°. Elution with ether–pentane gave 3,4-dimethylbenzophenone (0.5 g, 2 mmol) in the 20–30% ether fractions, 3,4-dimethyl-5-nitrobenzophenone (1 g, 4 mmol) in the 40–50% ether fractions, a mixture 3,4-dimethyl-2-nitro- and 3,4-dimethyl-6-nitrobenzophenone (2.5 g, 10 mmol) in the third 50% ether fraction, a mixture of 2- and 6-nitro isomers (0.7 g, 3 mmol) and diene adduct **2** (4.2 g, 13 mmol) in the 60–70% ether fractions from which the adduct **2** crystallized. In other nitration reactions 3,5-dinitro-*o*-xylene was isolated from early column fractions: n.m.r. ($CDCl_3$) τ 1.53 (d, 1, J = 2 Hz, 4-*H*), 1.75 (d, 1, J = 2 Hz, 6-*H*), 7.50 (s, 6, 1-CH_3 and 2-CH_3). Chromatography of the diene fractions at −45° gave the individual diastereoisomers **2*a*** and ***b***. *Trans* adduct **2*a*** was formed in larger amount (3:1) than *cis* adduct **2*b***. At higher temperatures adduct **2*a*** decomposed on the column and 2-benzoyl-4,5-dimethylphenyl acetate, eluted in the early column fractions, and 2-benzoyl-4,5-dimethylphenol, eluted with methanol, were formed. Adducts constituted 65–75% of the reaction product before work-up.

trans-2-Benzoyl-4,5-dimethyl-4-nitro-1,4-dihydrophenyl acetate (**2*a***) was recrystallized from chloroform–pentane, m.p. 118°; u.v. (CH_3OH) 255 nm (ε 1330 m^2 mol^{-1}); i.r. (Nujol) 1740 and 1250 ($OCOCH_3$), 1660 (C=O), 1560 (NO_2), 730 cm^{-1}; n.m.r. (220 MHz, $CDCl_3$) τ 2.22 (d, 2, J = 8 Hz, 2′-*H* and 6′-*H*), 2.38 (t, 1, J = 8 Hz, 4′-*H*), 2.51 (t, 2, J = 8 Hz, 3′-*H* and 5′-*H*), 3.46 (d, 1, 3-*H*), 3.60 (m, 1, 1-*H*), 3.90 (m, 1, 6-*H*), 8.01 (s, 3, $OCOCH_3$), 8.04 (s, 3, 4-CH_3), 8.10 (t, 3, 5-CH_3), J_{13} = 1.38, J_{16} = 3.60, $J_{1,5-CH_3}$ = 1.43, $J_{6,5-CH_3}$ = 1.43 Hz.

Anal. Calcd. for $C_{17}H_{17}NO_5$(M_r 315): C, 64.75; H, 5.43; N, 4.44. Found (307): C, 64.74; H, 5.29; N, 4.43.

cis-2-Benzoyl-4, 5-dimethyl-4-nitro-1,4-dihydrophenyl acetate (**2*b***) was recrystallized from chloroform–pentane, m.p. 128–130° (dec.); u.v. (CH_3OH) 252 nm (ε 1140 m^2 mol^{-1}); i.r. (Nujol) 1735 and 1250 ($OCOCH_3$), 1660 (C=O), 1560 (NO_2), 730 cm^{-1}; n.m.r. (220 MHz, $CDCl_3$) τ 2.11 (d, 2, J = 8 Hz, 2′-*H*, 6′-*H*), 2.37 (t, 1, J = 8 Hz, 4′-*H*), 2.50 (t, 2, J = 8 Hz, 3′-*H* and 5′-*H*), 3.54 (d, 1, 3-*H*), 3.68 (m, 1, 1-*H*), 3.93 (m, 1, 6-*H*), 7.99 (s, 3, $OCOCH_3$), 8.10 (t, 3, 5-CH_3), 8.26 (s, 3, 4-CH_3), J_{13} = 1.41, J_{16} = 3.21, $J_{1,5-CH_3}$ = 1.46, $J_{6,5-CH_3}$ = 1.43 Hz; in the 60 MHz spectrum irradiation of the methyl triplet collapsed the multiple t at 3.07 to a doublet of doublets and that at 3.95 to a doublet. The decoupled spectrum was simulated and refined to give coupling constants and chemical shifts for the hexadiene ring protons. These coupling constants together with the estimated coupling constants to the methyl group were then used to simulate the undecoupled 220 MHz spectrum and the simulation refined to give the listed coupling constants and chemical shifts.

Anal. Calcd. for $C_{17}H_{17}NO_5$ (M_r 315): C, 64.75; H, 5.43; N, 4.44. Found (306): C, 64.72; H, 5.16; N, 4.33.

The arguments for the structure of **2** are similar to those for the structure **1** and are likewise supported by the similar effects of shift reagent. The assignment of **2*a*** as the *trans* and **2*b*** as the *cis* adduct follows from the more rapid downfield shift of the 4-methyl peak in the former.

Can. J. Chem. Downloaded from www.nrcresearchpress.com by 210.87.254.6 on 09/05/12
For personal use only.

Nitro Compounds

The three nitro substitution products were obtained from the nitration mixture after chromatography and crystallization. The 2-nitro and 5-nitro isomers were also isolated from rearomatization reactions.

3,4-Dimethyl-2-nitrobenzophenone had m.p. 103–104°; i.r. (Nujol) 1680 (C=O), 1545 and 1375 cm^{-1} (NO_2); n.m.r. ($CDCl_3$) τ 2.20 (m, 2, 2′-*H* and 6′-*H*), 2.39 (m, 1, 4′-*H*), 2.53 (m, 2, 3′-*H* and 5′-*H*), 2.63 (d, 2, 6-*H*), 2.71 (d, 2, 5-*H*), 7.57 (s, 3, 3-CH_3), 7.69 (s, 3, 4-CH_3), J_{56} = 7.9, $J_{2'3'}$ = 8.1, $J_{2'4'}$ = 1.3, $J_{2'5'}$ = 0.6, $J_{2'6'}$ = 1.6, $J_{3'4'}$ = 7.5, $J_{3'5'}$ = 1.4 Hz; addition of the shift reagent to this isomer shifted the quartet of lines of the 2′-*H* and 6′-*H* down to τ 1.15 and the doublet (J = 8 Hz) of the 6-H to 1.65. Only three protons were moved substantially downfield confirming the identification as the 2-nitro isomer since there are only three protons *ortho* to the carbonyl group where the europium is expected to complex. Mass spectrum (70 eV) *m/e* (relative intensity) 255 (19, M), 238 (3, M − OH), 178 (23, M − C_6H_5), 165 (17), 162 (35), 149 (10), 132 (9), 105 (100), 77 (36).

3,4-Dimethyl-5-nitrobenzophenone had m.p. 64–69°; i.r. (Nujol) 1660 (C=O), 1540 and 1365 cm^{-1} (NO_2); n.m.r. ($CDCl_3$) 2.04 (d, 1, J = 2 Hz, 6-*H*), 2.19 (d, 1, J = 2 Hz, 2-*H*), 2.24 (q, 2, J = 2 Hz and J = 8 Hz, 2′-*H* and 6′*H*), 2.45 (m, 3, 3′-*H*, 4′-*H*, and 5′-*H*), 7.57 (s, 6, 3-CH_3 and 4-CH_3); addition of the shift reagent moved four aromatic protons to much lower field (τ 1.2). There are four protons *ortho* to the carbonyl group in the 5-nitro isomer and thus the identification of this isomer is confirmed. Mass spectrum (70 eV) *m/e* (relative intensity) 255 (80, M), 238 (80, M − OH), 105 (100), 77 (100).

Anal. Calcd. for $C_{15}H_{13}NO_3$: C, 70.58; H, 5.13; N, 5.49. Found: C, 70.31; H, 5.04; N, 5.29.

3,4-Dimethyl-6-nitrobenzophenone had m.p. 80°; i.r. (Nujol) 1680 (C=O), 1530 and 1360 cm^{-1} (NO_2); n.m.r. ($CDCl_3$) τ 2.02 (s, 1, 5-*H*), 2.26 (q, 2, J = 2 Hz and J = 8 Hz, 2′-*H* and 6′-*H*), 2.53 (m, 3, 3′-*H*, 4′-*H* and 5′-*H*), 2.79 (s, 1, 2-*H*), 7.60 (s, 3, CH_3), 7.64 (s, 3, CH_3); mass spectrum (70 eV) *m/e* (relative intensity) 255.083 (30, M_r ($^{12}C_{15}{}^{1}H_{13}{}^{14}N^{16}O_3$) 255.090), 178 (47, M − C_6H_5), 165 (23), 162 (100), 132 (25), 105 (94), 77 (50).

The structures of the three nitro substitution products are readily assigned from their n.m.r. spectra. In each case the aromatic region exhibits the complex multiplets from the protons of the benzoyl ring in addition to the peaks of the nitro-substituted ring, the patterns for which are similar to the dimethylnitroacetophenone analogs. 3,4-Dimethyl-2-nitrobenzophenone exhibits the AB quartet with an 8 Hz coupling of the two *ortho* protons of the substituted ring at higher field than the multiplets of the phenyl ring. The 5-nitro isomer exhibits for the *meta* protons of the substituted ring an AB quartet with a 2 Hz coupling of which the low field doublet (6-H) is at lower field than the phenyl ring multiplets, and the higher field doublet (2-H) overlaps the phenyl ring part of the spectrum. The 6-nitro isomer exhibits two singlets for the *para* protons of the substituted ring, one of which (5-H) lies at lower field and the other (2-H) at higher field than the phenyl ring multiplets.

2-Benzoyl-4,5-dimethylphenol and 2-Benzoyl-4,5-dimethylphenyl Acetate

Diene **2** was treated with a concentrated solution of sodium methoxide as described above for diene **1**. After work-up, 2-benzoyl-4,5-diemthylphenol was obtained, m.p. 112–113.5° (lit. (12) m.p. 111–112°); i.r. (Nujol) 1635 cm^{-1} (C=O); n.m.r. ($CDCl_3$) τ 2.44 (m, 5, C_6H_5), 2.72 (s, 1, 3-*H*), 3.15 (s, 1, 6-*H*), 7.75 (s, 3, 5-CH_3), 7.87 (s, 3, 4-CH_3); mass spectrum (70 eV) *m/e* (relative intensity) 226 (7, M), 225 (8, M − H), 149 (25, M − C_6H_5), 120 (10), 105 (30), 93 (14), 91 (50), 77 (100).

The phenol was acetylated with acetic anhydride containing sulfuric acid to give 2-benzoyl-4,5-dimethylphenyl acetate, m.p. 69–70°; i.r. (Nujol) 1720 ($OCOCH_3$), 1670 (C=O), 1285, 1210, 1180, 735, and 705 cm^{-1}; n.m.r. ($CDCl_3$) τ 2.2 (m, 2, 2′-*H* and 6′-*H*), 2.45 (m, 3, 3′-*H*, 4′-*H*, and 5′-*H*), 2.65 (s, 1, 3-*H*), 3.01 (s, 1, 6-*H*), 7.65 (s, 3, 5-CH_3), 7.71 (s, 3, 4-CH_3), 8.08 (s, 3, $OCOCH_3$); mass spectrum *m/e* 268 (M).

*2-Benzoyl-2′,4,4′,5,6′-pentamethylbiphenyl (**16**)*

A solution of diene **2** (2 g, 6.3 mmol) and mesitylene in methylene chloride was treated with boron trifluoride etherate as described for diene **1**. After work-up, chromatography on silica gel and elution with pentane and 15% ether–pentane gave mesitylene in the pentane fractions, the biphenyl (1.8 g, 5.5 mmol) in the early ether–pentane fractions followed by 3,4-dimethyl-2- and 3,4-dimethyl-5-nitrobenzophenone (90 mg, 0.4 mmol). After recrystallization from ethanol 2-benzoyl-2′,4,4′,5,6′-pentamethylbiphenyl had m.p. 98–99.5°; i.r. (Nujol) 1675 (C=O), 1265, 900 and 725 cm^{-1}; n.m.r. ($CDCl_3$) τ 2.7 (m, 5, C_6H_5), 2.72 (s, 1, 3-*H*), 3.02 (s, 1, 6-*H*), 3.26 (s, 2, 3′-*H* and 5′-*H*), 7.71 (s, 6, 4-CH_3 and 5-CH_3), 7.81 (s, 3, 4′-CH_3) 8.03 (s, 6, 2′-CH_3 and 6′-CH_3); mass spectrum (70 eV) *m/e* (relative intensity) 328 (20, M) 313 (58, M − CH_3), 251 (100, M − C_6H_5), 132 (100), 105 (60), 77 (50), 43 (78).

Anal. Calcd. for $C_{24}H_{24}O$: C, 87.76; H, 7.37. Found: C, 87.70; H, 7.23.

Reaction of Diene 2 with Trifluoroacetic Acid

Trifluoroacetic acid (2.5 cm^3) was added dropwise to a stirred solution of diene **2** (1 g) in chloroform (10 cm^3). Brown fumes of NO_2 were given off. After work-up, 2-benzoyl-4,5-dimethylphenyl acetate was obtained, identified by n.m.r. and t.l.c.

Reaction of Diene 2 with Acetic Acid

A solution of diene **2** (0.5 g) in acetic acid (5 cm^3) was heated under reflux for 30 min. Brown fumes of NO_2 were given off. After work-up, 2-benzoyl-4,5-dimethylphenyl acetate was obtained. When the reaction was carried out at ambient temperature it took 14 days to go to completion.

Thermolysis of Diene 2

A solution of diene **2** (0.5 g) in toluene (10 cm^3) was heated under reflux. Brown fumes of NO_2 were given off. The toluene was distilled off and the residue was characterized as 2-benzoyl-4,5-dimethylphenyl acetate by n.m.r. and t.l.c.

Reaction of Diene 2 with Boron Trifluoride Etherate

Diene **2** (3 g, 9.5 mmol) was added to boron trifluoride etherate (3 cm^3). A vigorous reaction ensued. After work-up and chromatography on silica gel and elution with 20% ether–pentane, 3,4-dimethylbenzophenone (640 mg, 3 mmol), 3,4-dimethyl-5-nitrobenzophenone (580 mg, 2.3 mmol), and 3,4-dimethyl-2-nitrobenzophenone (770 mg, 3.0 mmol) were obtained.

Reaction of Diene 2 with 78% Sulfuric Acid

Diene **2** (0.5 g, 1.6 mmol) was stirred with 78% sulfuric acid (2 cm^3) overnight. After work-up and chromatography on silica gel, 3,4-dimethylbenzophenone (112 mg, 0.5 mmol), 3,4-dimethyl-5-nitrobenzophenone (100 mg, 0.4 mmol), and 3,4-dimethyl-2-nitrobenzophenone (120 mg, 0.5 mmol) were obtained.

Reaction of Diene 2 with Mesitylene in Acetic Acid Containing Sulfuric Acid

A solution of sulfuric acid (1.35 cm^3) in acetic acid (2.5 cm^3) was added dropwise to a solution of diene **2** (2 g, 6.3 mmol) in mesitylene (10 cm^3). After stirring for 1.5 h the mixture was neutralized and worked-up. Chromatography on silica gel and elution with pentane removed the excess mesitylene. Elution with 20% ether–pentane gave 2-benzoyl-2′,4,4′,5,6′-pentamethylbiphenyl (810 mg, 2.5 mmol) and a mixture of 3,4-dimethyl-2-nitro- and 3,4-dimethyl-5-nitro-benzophenone (640 mg, 2.5 mmol).

1. (*a*) D. J. BLACKSTOCK, A. FISCHER, K. E. RICHARDS, J. VAUGHAN, and G. J. WRIGHT. Chem. Commun. 641 (1970); (*b*) D. J. BLACKSTOCK, J. CRETNEY, A. FISCHER, M. P. HARTSHORN, K. E. RICHARDS, J. VAUGHAN, and G. J. WRIGHT. Tetrahedron Lett. 2793 (1970); (*c*) A. FISCHER and J. N. RAMSAY. J. Chem. Soc. Perkin II, 237 (1973); (*d*) A. FISCHER and C. C. GREIG. J. Chem. Soc. Chem. Commun. 396 (1973); A. FISCHER and C. C. GREIG. Can. J. Chem. **52**, 1231 (1974); (*e*) A. FISCHER and C. C. GREIG. J. Chem. Soc. Chem. Commun. 50 (1974); (*f*) A. FISCHER and J. N. RAMSAY. J. Am. Chem. Soc. **96**, 1614 (1974); (*g*) A. FISCHER and J. N. RAMSAY. Can. J. Chem. **52**, 3960 (1974).
2. R. C. HAHN and D. L. STRACK. J. Am. Chem. Soc. **96**, 4335 (1974).
3. P. C. MYHRE. J. Am. Chem. Soc. **94**, 7921 (1972).
4. N. P. BUU HOÎ, B. ECKERT, and R. ROYER. J. Org. Chem. **17**, 1000 (1952).
5. A. BRÄNDSTRÖM and S. A. I. CARLSSON. Acta Chem. Scand. **21**, 983 (1967).
6. C. L. PERRIN and G. A. SKINNER. J. Am. Chem. Soc. **93**, 3389 (1971).
7. R. C. HAHN and M. B. GROEN. J. Am. Chem. Soc. **95**, 6128 (1973).
8. I. PUKAS and E. K. FIELDS. J. Org. Chem. (*a*) **31**, 4204 (1966); (*b*) **32**, 589 (1967).
9. A. T. BALABAN and C. D. NENITZESCU. *In* Friedel Crafts and related reactions. Vol. II. *Edited by* G. A. Olah. Interscience, New York, N.Y. 1964. Chapt. XXIII.
10. A. FISCHER, C. C. GREIG, A. L. WILKINSON, and D. R. A. LEONARD. Can. J. Chem. **50**, 2211 (1972).
11. J. VÈNE, M. KERFANTO, and D. RAPHALEN. Bull. Soc. Chim. Fr. 1813 (1963).
12. A. H. BLATT. J. Org. Chem. **20**, 598 (1955).

Can. J. Chem. Downloaded from www.nrcresearchpress.com by 210.87.254.6 on 09/05/12
For personal use only.

Juvabione and its Analogs.[1] Juvabione and $\Delta^{4'}$-Dehydrojuvabione Isolated from the Whole Wood of *Abies balsamea*, have the *R,R* Stereoconfigurations, not the *R,S*

JOHN FIEVE MANVILLE

Department of the Environment, Canadian Forestry Service, Western Forest Products Laboratory, 6620 N.W. Marine Drive, Vancouver, British Columbia V6T 1X2

Received December 4, 1974

JOHN FIEVE MANVILLE. Can. J. Chem. **53**, 1579 (1975).

The petroleum ether soluble fractions from the whole wood meal of a number of native *Abies balsamea* (L.) Mill. var. *balsamea* and var. *phanerolepis* Fern. contain varying amounts of several juvabione analogs. These include the previously reported (+)-juvabione (**1***a*), atlantones (**2**), and lasiocarpenone (**3**). This paper describes the first isolation of (+)-$\Delta^{4'}$-dehydrojuvabione (*R,R*) (**5***a*) and proves the *R,R* stereoconfiguration for (+)-juvabione (**1***a*) isolated from native *Abies balsamea*. These results require that those samples previously isolated from a Slovak fir and which have the *R,S* stereoconfigurations, be renamed (+)-epijuvabione (**6**) and (+)-$\Delta^{4'}$-dehydroepijuvabione (**7**).

JOHN FIEVE MANVILLE. Can. J. Chem. **53**, 1579 (1975).

On a extrait des sciures entières de bois d'un certain nombre d'*Abies balsamea* (L.) Mill. var. *balsamea* et var. *phanerolepis* Fern. avec de l'éther de pétrole; les fractions solubles de ces variétés de notre pays contiennent des quantités variables de plusieurs analogues de juvabione. Ceux-ci incluent les produits rapportés précédemment à savoir la (+)-juvabione (**1***a*), les atlantones (**2**) et la lasiocarpénone (**3**). Dans ce travail, on décrit la (+)-$\Delta^{4'}$-déhydrojuvabione (*R,R*) (**5***a*) qui est isolée pour la première fois et l'on prouve la stéréoconfiguration *R,R* pour la (+)-juvabione (**1***a*) isolée d'*Abies balsamea*. Ces résultats impliquent que des échantillons isolés précédemment à partir d'un sapin Slovaque et qui ont des configurations *R,S* doivent être renommées (+)-épijuvabione (**6**) et (+)-$\Delta^{4'}$-dehydroépijuvabione (**7**). [Traduit par le journal]

Introduction

A number of continuing studies at the Western Forest Products Laboratory on the extractive composition of Canadian coniferous species (1–5) have shown that, in addition to (+)-juvabione (*R,R*) (**1***a*), several other related sesquiterpenes

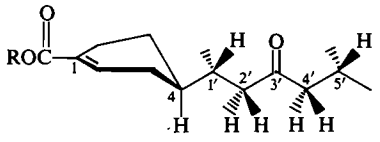

1

a R = CH_3

b R = H

occur in many of the true firs (*Abies* sp.). These previously identified compounds include the atlantones (**2**) (4) and lasiocarpenone (**3**) (3).

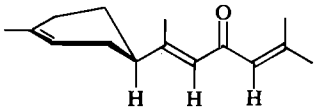

2 (*Z* + *E* isomers)

[1]Presented in part at the 167th National Meeting of the American Chemical Society, Los Angeles, California, April 1974.

Douglas fir (*Pseudotsuga menziessi* (Mirb.) Franco) also contains several juvabione analogs

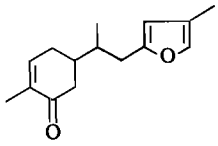

3

(1, 6), including todomatuic acid (*R,R*) (**1***b*) and *cis*-dihydrotodomatuic acid (*R*) (**4***b*).

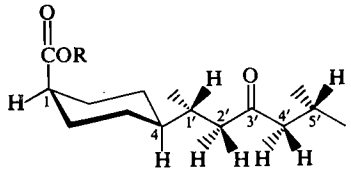

4

a R = CH_3

b R = H

The chemistry of the wood of balsam fir (*Abies balsamea* (L.) Miller) was largely ignored by extractive chemists until 1965, when Slama and Williams (7) discovered that paper towelling made from the wood of balsam fir contained an insect juvenile hormone analog (IJHA), which

Can. J. Chem. Downloaded from www.nrcresearchpress.com by 210.87.254.105 on 09/05/12
For personal use only.

Can. J. Chem. Downloaded from www.nrcresearchpress.com by 210.87.254.105 on 09/05/12
For personal use only.

they first described as "the paper factor." Subsequently Bowers *et al.* (8) in 1966, isolated the only active component from native balsam fir and named this compound (+)-juvabione (**1***a*). Its structure was shown to be identical with the methyl ester of (+)-todomatuic acid (**1***b*) which had been first isolated (9) from bisulfite-treated pulp oil of a Japanese fir (*Abies sachalinensis* Schmidt).

In 1963, Nakazaki and Isoe had assigned (10) the *R,R* stereoconfigurations to (+)-todomatuic acid (**1***b*), after comparing the molecular rotations of **1***b* and its conversion products with a related series of natural compounds of known absolute stereochemistry. Thus (+)-juvabione (**1***a*) was described as (+)-4(*R*)-[1′(*R*)-5′-dimethyl-3′-oxohexyl]-1-cyclohexene-1-carboxylic acid methyl ester.

This paper will prove the stereochemistry of (+)-juvabione (**1***a*), isolated from the whole wood of *Abies balsamea* (L.) Mill. var. *balsamea* and var. *phanerolepis* Fern., to be *R,R* and will describe the first isolation and structural identification of (+)-$\Delta^{4'}$-dehydrojuvabione (*R,R*) (**5***a*).

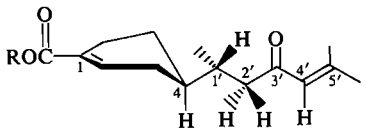

5

a R = CH_3
b R = H

The more recent literature, which "proves" a different stereochemistry for "natural (+)-juvabione" has, to this point, been purposely ignored so as to not unduly confuse the reader. A separate discussion of this *second* stereochemistry was considered necessary to establish clearly the correctness of *both* assignments.

Clarification of Assignments of Stereochemistry to (+)-Juvabione

Following the initial discovery of "the paper factor" in North American balsam fir wood, Slama returned to Czechoslovakia in 1966 and with Cerny and co-workers (11) isolated two IJHA from a Slovak fir, which was purported to be a balsam fir, growing in the arboretum at Banska Stiavnica. Their study published in 1967 revealed the presence of, not only one compound (**6**) described as being (+)-juvabione but also a

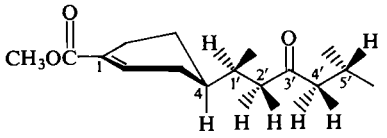

6

second, slightly more active, IJHA (**7**) which they called dehydrojuvabione.

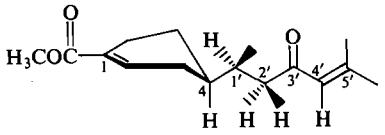

7

The next pertinent publications in this area were by Pawson *et al.* (12), in which the synthesis and absolute stereochemistry of all four diastereoisomers of juvabione were described. At this point, Pawson *et al.* (12) obtained a sample of the compound (**6**) isolated by Cerny *et al.* (11) and described by them as "natural (+)-juvabione" in order to assign the absolute stereoconfigurations to the natural product. At the same time, trivial names were given to the four diastereoisomers of juvabione.

Pawson *et al.* (12), not realizing the possibility that there could be two naturally occurring isomers of juvabione and believing that both isolations came from balsam fir trees, felt obliged to correct the original assignment of stereoconfiguration. They pointedly stated that the absolute stereochemistry of "natural (+)-juvabione" was *R,S*, not *R,R* as previously inferred by the study of Nakazaki and Isoe (10) on todomatuic acid (**1***b*). This *R,S* assignment was based on detailed optical rotatory dispersion (o.r.d.) and circular dichroism (c.d.) spectral comparisons between this natural product (**6**) and those of the four synthesized isomers of juvabione. Since an X-ray determination of structure for a key intermediate had been carried out (12*b*), there could be no question about the correctness of this assignment. Their *R,S* assignment for "natural (+)-juvabione" was widely accepted.

The stereospecific synthesis of *d,l*-juvabione as described in a recent paper (13), must in fact give (±)-epijuvabione. Also, the hydrolysis of this synthetic material gives (±)-epitodomatuic acid not (±)-todomatuic acid as was deduced by these authors who were guided by the literature.

Slama *et al.* (14) have just published a super-

Can. J. Chem. Downloaded from www.nrcresearchpress.com by 210.87.254.105 on 09/05/12
For personal use only.

lative text titled "Insect Hormones and Bioanalogues" in which they unfortunately imply the original assignment by Nakazaki and Isoe (10) is erroneous and that (+)-juvabione has the *R,S* stereoconfigurations.

Nevertheless, this *R,S* assignment has not been universally accepted (1, 6). In fact, as this study will prove, natural (+)-juvabione (**1***a*) isolated from balsam fir has the *R,R* stereoconfigurations. At first, this statement seems to contradict an assignment of stereochemistry based on an absolute X-ray determination of structure but, as will be shown, the assignment of stereochemistry to that compound isolated by Cerny and coworkers (11) is not in question. The resolution of this seemingly contradictory statement lies in the previously unrealized facts that there must be *two* naturally occurring forms of (+)-juvabione (**1***a* and **6**) and that both assignments of stereochemistry are correct. However only one isomer is (+)-juvabione (**1***a*), the other is (+)-epijuvabione (**6**).

Since Bowers *et al.* (8) did not obtain either o.r.d. or c.d. curves for their isolated (+)-juvabione and original samples were no longer available, it was necessary to repeat their isolation (present study) to determine the absolute stereochemistry of (+)-juvabione. The study of Pawson *et al.* (12) indicated that comparisons of $[\alpha]_D$ values and melting points of the derived acids were basically unreliable in differentiating between the *R,S* and *R,R* isomers of (+)-juvabione.

Re-examination of the work of Cerny *et al.* (11) has provided an explanation for the fact that a *second* isomer of (+)-juvabione was actually isolated. Recent investigations indicate that this sampled tree, from the grove labeled as "*A. balsamea* L." in the arboretum at Banska Stiavnica, is not a balsam fir. This Slovak fir is now labeled as "*A. balsamea* – dubious – dying" but it is possibly a putative cross.[2]

This should be a lesson to all who work with biological materials. It indicates the need for all chemical and other investigations to be carried out only on authentic samples obtained from typical populations sampled and/or identified by experts. Arboretum samples should be avoided.

[2]Private communications with L. Greguss, Banska Stiavnica, Czechoslovakia; O. Sziklai and J. G. Worrall, Faculty of Forestry, University of British Columbia, Vancouver, B.C.; and E. von Rudloff, National Research Council of Canada, Saskatoon, Saskatchewan.

The sample (**6**) isolated by Cerny *et al.* (11) should be known as (+)-epijuvabione, since it was *not* isolated from the wood of *Abies balsamea* (L.) Mill. and it was *not* the first isolation of "natural (+)-juvabione."

Thus, it is now apparent that Pawson *et al.* (12*a*) using this *second* isolated "natural (+)-juvabione" ((+)-epijuvabione (*R,S*) (**6**)) from a "Slovak fir" and assuming it to be identical with (+)-juvabione [*R,R*] (**1***a*) isolated (8) from a native *A. balsamea*, named the wrong isomer (+)-juvabione, resulting in the ensuing confusion in the chemical literature (1, 6, 10, 11, 13, 14).

The correct names of the four diastereoisomers of juvabione will be (+)-juvabione (*R,R*), (+)-epijuvabione (*R,S*), (−)-juvabione (*S,S*), and (−)-epijuvabione (*S,R*).

Isolation

The petroleum ether soluble fractions from the ethanol extracts of the whole wood of balsam firs were pale yellow mobile oils. They were partially separated by ion exchange chromatography on DEAE-Sephadex A-25 (15), selecting only the neutrals fraction for study. Gas–liquid chromatographic (g.l.c.) analysis revealed (see Fig. 1) the presence of up to six major components which did not correspond to any of the common fatty

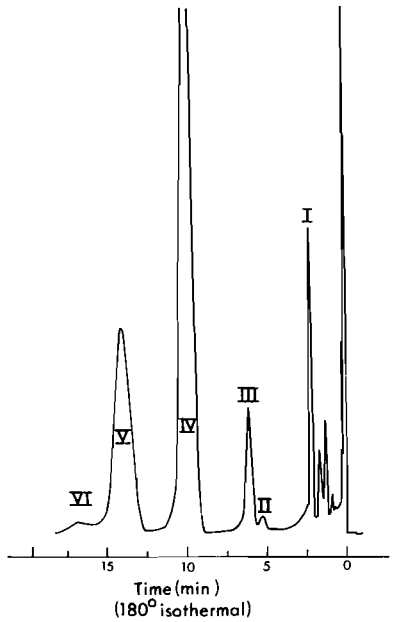

FIG. 1. Gas–liquid chromatogram of the petroleum ether solubles from the whole wood of *Abies balsamea* var. *phanerolepis* Fern.

Can. J. Chem. Downloaded from www.nrcresearchpress.com by 210.87.254.105 on 09/05/12
For personal use only.

or resin acid methyl esters. Silicic acid column chromatography effected separation of some of the major components from the extractive mixture. Compounds **2**, **8**, and **3**, corresponding to peaks I, II, and III on the g.l.c. chromatogram, were separated from the rest by eluting with petroleum ether – ether (5:1); next were eluted (petroleum ether – ether, 4:1) two compounds (**2***a* and **5***a*) that gave rise to peaks IV and VI. Finally, a more polar component (peak V) was eluted. The identification of this unknown alcohol will be the subject of a forthcoming publication.

The last eluted (g.l.c.) component (**5***a*) (peak VI) was eventually separated from **1***a* by repeated column chromatography using Woelm silica gel-I and petroleum ether – ether (4:1) as developing solvent.

This sample of **5***a*, however, contained a mixture of C_{22} and C_{24} *n*-alcohols which crystallized from an acetone solution on standing in the freezer overnight.

Results

The first three major components were identified by g.l.c. retention times (r_t) (relative to internal (+)-juvabione), nuclear magnetic resonance (n.m.r.), and mass spectrometry (m.s.) relative to authentic materials isolated from *Abies lasiocarpa* and provided by Dr. E. P. Swan of this laboratory (2–4). They were the atlantones (**2**), r_t 0.25, manool (**8**), r_t 0.53, and lasiocarpenone (**3**) r_t 0.63. The latter compound, if present, causes a bright red-purple streak on the freshly exposed wood surface[3] and a red-purple spot on silicic acid t.l.c. plates to appear, when reacted with Ehrlich's reagent (5).

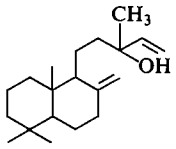

8

This study indicates a considerable degree of variation in the amounts of the various components in each wood sample (Table 1). Moreover, not all wood samples were found to contain manool (**8**) and/or, lasiocarpenone (**3**). Only one sample contained **3**; it was a balsam fir from Newfoundland (*A. balsamea* var. *phanerolepis* Fern.). The presence of **3** might serve as a means for chemotaxonomic differentiation between the varieties of *A. balsamea*. Further work on the occurrence of lasiocarpenone (**3**) is underway.

The fourth major component (peak IV) reported in this study had p.m.r., i.r., and mass spectra similar to those reported (1, 6, 8, 12) for (+)-juvabione (*R,R*) (**1***a*). The o.r.d. and c.d. curves were in accord with the published data (1, 12) for the *R,R* isomer of (+)-juvabione. The purity (g.l.c. 99.4%) of this isolated material was significantly improved over earlier isolations and had $[\alpha]_D^{25}$ +82.6°, which is much higher than earlier reported (1, 6, 12) and very close to the $[\alpha]_D^{25}$ of the saponified product **1***b* ($[\alpha]_D$ +85.6°, lit. (8) value +87°).

Compound **5***a*, corresponding to peak VI (g.l.c.), had the empirical formula $C_{16}H_{24}O_3$ as determined by high resolution mass spectrometry. The i.r. spectrum showed the compound to be an α,β-unsaturated ketone in *s-cis* conformation (1621, 1690 cm^{-1}) and an α,β-unsaturated carboxylic acid methyl ester (bands at 1441, 1654, and 1720 cm^{-1}). The p.m.r. and mass spectra were very similar to those reported (11) for (+)-dehydroepijuvabione (**7**). Whereas in general, the p.m.r. showed only slight random variations (±0.02 p.p.m.) between observed and quoted δ values (11), one of the C-5′ methyl groups resonated to higher field by 0.08 p.p.m. (δ 1.88 *vs.* 1.96) for **5***a* relative to the same group in **7**. Also the observed $[\alpha]_D^{23}$ of +57° was much lower than reported (11) for **7** ($[\alpha]_D$ +102°).

These spectroscopic similarities (i.r., m.s.) and differences (n.m.r., $[\alpha]_D$), together with the known fact that (+)-epijuvabione (**3***a*) isolated from a tree in an arboretum in Czechoslovakia was *R,S* (12), indicated that **5***a* was most likely to contain the *R,R* stereoconfigurations; whereas the Czechoslovakian sample (**7**) was undoubtedly, although never shown to be, the *R,S* isomer. Thus the "dehydrojuvabione" isolated by Cerny and co-workers (11) should be referred to as (+)-$\Delta^{4'}$-dehydroepijuvabione (**7**).

The *R* stereoconfiguration was assigned to C-4 based on the facts that the $[\alpha]_D$ was positive and the o.r.d. curve (Fig. 2) for **5***a* was similar to the o.r.d. curves of the *R,R* and *R,S* isomers of juvabione (12*a*) and clearly unlike either the *S,S*

[3]It is important to first remove the bark to eliminate any possible wood surface contamination from the bark constituents, which are known to contain varying amounts of other Ehrlich's positive compounds (indole acetic acid, its derivatives and catabolism products) and which can give rise to *false* positive indications of the occurrence of lasiocarpenone (**3**) in the heartwood.

TABLE 1. *Abies balsamea*, physical and chemical data

Tree No.	Site*	Age (years)	Diameter (cm)	Yield (% o.d. wood) EtOH	Yield (% o.d. wood) Petroleum ether	% (g.l.c.) of petroleum ether soluble neutrals **2** (r_t 0.25)	**8** (r_t 0.54)	**3** (r_t 0.63)	**1***a* (r_t 1.00)	**5***a* (r_t 1.66)
1	1	48	18.1	3.12	0.65	4.7	5.8	<1	68.6	6.5
2†	2	85	8.5	4.49	2.12	6.8	<1	6.8	56.9	4.1
3	3	83	21.8	3.18	0.66	<1	14.2	<1	10.9	66.5
4	3	76	23.3	3.71	0.81	<1	9.1	<1	23.0	62.7
5	4	47	23.8	2.61	0.68	<1	8.8	<1	82.3	6.0
6	4	58	25.8	2.83	0.48	<1	4.0	<1	47.0	37.6

*Site locations: (*1*) C.F.S. Research Forest, Petawawa, Ontario; (*2*) 10 miles outside St. John's, Newfoundland; (*3*) Fife Lake Road 4.7 miles north of main Gargantua Road and (*4*) Miron Lake Road 4.0 miles north of main Gargantua Road, both inside Lake Superior Provincial Park, Ontario.

†Bracted variety (var. *phanerolepis* Fer.), gave red-purple color with Ehrlichs' reagent.

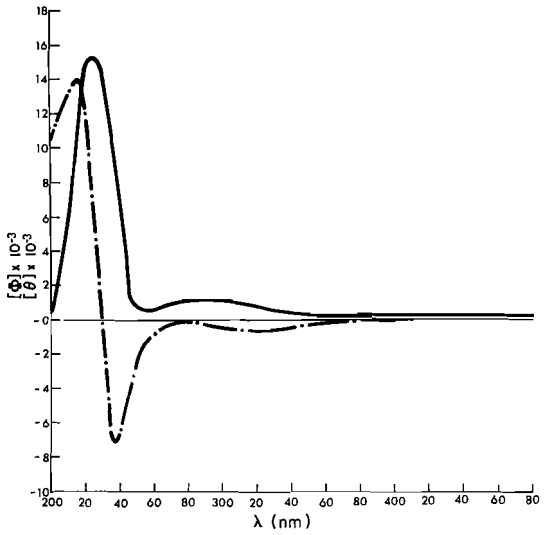

FIG. 2. The o.r.d. (———) and c.d. (—·—·) curves for $\Delta^{4'}$-dehydrojuvabione (**5***a*).

or *S,R* isomers; (Note: this center has always been shown (3, 7, 8) to be *R* for all naturally occurring samples). The remaining center (C-1′) could not be unambiguously assigned from either the o.r.d. or c.d. curves of **5***a* because of extra absorption bands present due to the conjugated double bond. However, this center was proven to be *R* by observing the o.r.d. curve of fully hydrogenated **5***a* (compounds **4***a* and **9**) (1).

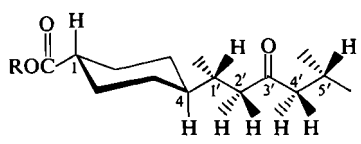

9

In keeping with the nomenclature now established for the isomers of juvabione, this new compound (**5***a*), isolated from *A. balsamea* growing in North America and described as (+)-4(*R*)-[1′(*R*)-5′-dimethyl-3′-oxohex-4′-ene]cyclohex-1-ene-1-carboxylic acid methyl ester, should be known as (+)-$\Delta^{4'}$-dehydrojuvabione.

It is interesting to speculate on the fact that Bowers and co-workers (8) were not successful in finding (+)-$\Delta^{4'}$-dehydrojuvabione (**5***a*) in the whole wood extract of a North American grown balsam fir. One possibility is that **1***a* was not an IJHA under the screening conditions, whereas the *R,S* isomer (**7**) was an IJHA (11). Thus any fraction of the extract containing **5***a* but no **1***a* would not have been investigated due to the fact that they were only looking for the active component(s) of this extract. Another possibility is that **5***a* does not occur in sufficient amounts in all balsam fir trees to have been detected as a separate component by their separation and/or screening procedures.

This latter possibility is supported by the observation of a considerable degree of tree-to-tree variation in the relative amounts of the various extractives. In particular, the amounts of dehydrojuvabione (**5***a*) (see Table 1) range from a low of 4.1% of the petroleum ether soluble neutrals to a high of 66.5%, whilst juvabione (**1***a*) goes from 56.9 to 10.9% in the same tree. Undoubtedly, some of this variation is due to site differences; however, trees 5 and 6 which are from the same site show a considerable variation in the relative amounts of **5***a* and **1***a*. It is believed that such variations reflect the individualistic biochemical differences that exist between trees and that no two trees are identical.

Can. J. Chem. Downloaded from www.nrcresearchpress.com by 210.87.254.105 on 09/05/12
For personal use only.

Can. J. Chem. Downloaded from www.nrcresearchpress.com by 210.87.254.105 on 09/05/12
For personal use only.

In summary, this study has shown the atlantones (**2**), manool (**8**), lasiocarpenone (**3**), (+)-juvabione (*R,R*) (**2***a*), (+)-$\Delta^{4'}$-dehydrojuvabione (*R,R*) (**5***a*), together with an unknown alcohol (g.l.c. peak V), to be present in the whole wood of balsam fir.

Experimental

The general methods and spectral measurements followed the format outlined previously (1). All retention times (g.l.c. r_t) are relative to internal (+)-juvabione (**1***a*). Optical rotations were recorded on a Perkin Elmer-141-Polarimeter made available by the Chemistry Department, University of British Columbia. The o.r.d. and c.d. curves for compounds **5***a* and **1***a* were kindly provided by Dr. V. Toome of the Physical Chemistry Department, Hoffman-LaRoche Inc., Nutley, N.J.

Table 1 lists chemical constituents data for each individual tree studied in this investigation, together with its site location, age, and diameter. The *A. balsamea* (L.) Mill. tree No. 2 was the only sample of the bracted variety (var. *phanerolepis* Fern.) and was kindly provided by Dr. John Hudak, Canadian Forestry Service (C.F.S.), St. Johns, Newfoundland. Tree No. 1 came from the Petawawa Forest Experiment Station, Petawawa, Ontario. Trees numbered 3–6 were provided by Dr. R. Whitney of the Great Lakes Forest Research Centre, Sault Ste. Marie, Ontario.

Trees 1, 2 and 3 were studied in detail, including the isolation of individual components. Trees 4–6 were examined by g.l.c.

Isolation

In each case, debarked whole wood was air dried and ground in a Wiley mill to pass a 5-mm screen. The wood meal was then extracted over a 12-h period in an all-glass Soxhlet apparatus with ethanol. The recovered yellow oils were taken up in methanol–water (6:4) (100 ml/g of extract) and the petroleum ether (b.p. 65–70°) solubles were extracted. These extracts were then dried (Na_2SO_4) and the petroleum ether removed under reduced pressure. Yields and other details are listed in Table 1. These oils were redissolved in ether-methanol and chromatographed on a column of DEAE-Sephadex-A25 according to an established procedure (15). Elution with the starting solvent yielded a neutrals fraction (80% yield). The column was then stripped with 4% formic acid solution and the acids fraction was set aside for study at some future date. Analysis by g.l.c. of the neutrals fraction confirmed the presence of **1***a*, **2**, **3**, **8**, and **5***a* (see Fig. 1). Compounds **1***a* and **5***a* could be easily recovered as a pair by chromatographing the petroleum ether solubles on a column of Woelm – silica gel. Then by careful rechromatographing, using petroleum ether – diethyl ether (3:1) at lower loadings, it was possible to obtain samples of **1***a* and **5***a* which were free of each other. In this liquid chromatography, 20 ml fractions were collected and monitored by g.l.c. and t.l.c.: fractions 1–32 contained traces of **2**, **3**, and **8**; 33–40 contained **1***a*; 41–49 contained a mixture of **1***a* and **5***a*, and 50–60 contained **5***a*. The fractions containing **5***a* were dissolved in acetone and placed in the freezer (−10°) for 12 h during which time the C_{22} and C_{24} *n*-alcohols (identified by g.l.c. r_t values (0.99 and 1.84), m.s., and n.m.r.) crystallized out together and were filtered from solution.

Compound 1a ((+)-Juvabione)

Compound **1***a* was a colorless oil, which by g.l.c. was better than 99% pure; it had physical and spectral parameters in accord with those published (1, 8, 11) for (+)-juvabione (*R,R*), except for $[\alpha]_D^{25}$ (*c* 1.1, $CHCl_3$) +82.6°; (*c* 1.2, MeOH) +77.9° which are greater than those reported earlier (1, 8, 11). Compound **1***a* was saponified to todomatuic acid (**1***b*), m.p. 58.5–61° and $[\alpha]_D^{25}$ (*c* 0.5, EtOH) +85.6°, lit. (8) m.p. 57–59°, $[\alpha]_D$ +87°.

Compound 5a ((+)-$\Delta^{4'}$-Dehydrojuvabione)

Compound **5***a* was a colorless oil and had t.l.c. r_t 0.36 (silicic acid, petroleum ether – ether, 3:1), g.l.c. r_t 1.66, and $[\alpha]_D^{25}$ (*c* 0.68, CH_3OH) +49.0° or +57.4° (*c* 1.08, $CHCl_3$). The o.r.d. (*c* 0.322, C_2H_5OH; 23°) $[\Phi]_{700}$ +86°, $[\Phi]_{500}$ +197°, $[\Phi]_{411}$ +262° (peak), $[\Phi]_{365}$ +195° (trough), $[\Phi]_{284}$ +1157° (peak), $[\Phi]_{250}$ +717° (trough), $[\Phi]_{226}$ +15 372°, $[\Phi]_{200}$ 0°. The c.d. (0.012197 M, C_2H_5OH; 23°) $[\theta]_{388}$ 0°, $[\theta]_{325}$ −590°, $[\theta]_{274}$ −94°, $[\theta]_{237}$ −7175°, $[\theta]_{230}$ 0°, $[\theta]_{216}$ +13 530° $[\theta]_{200}$ +10 660°. The p.m.r. (100 MHz $CDCl_3$) δ 6.94_6 (1H, multiplet, H_2), 6.06_7 (1H, septet, J = 1.2 Hz, H_4'), 3.71_5 (3H, singlet, methyl ester), 2.14_1 (3H, doublet, J = 1.2 Hz, C-5′ *cis*-methyl), 1.88_3 (3H, doublet, J = 1.2 Hz, C-5′ *trans*-methyl), 0.90_5 (3 H, doublet, J = 6.5 Hz, C-1′ methyl), 2.7–1.0 (10 H). Mass spectrum (*m/e*): 264(0.6%) (M), 232(11.5) ($M-32$), 205(1.7), 204(4.1), 177(1.1), 167(3.8), 166(18.8) 164(1.3), 151(2.9), 139(2.0), 137(1.7), 134(33.4), 131(1), 126(1.5), 125(15), 123(1.4), 121(1.1), 107(11.02), 99(14), 98(24.3), *83*(100), 79(9.8), 59(4.3), and 55(25.4). Infrared (cm^{-1}) 2915 (broad band) vs, 1715 vs, 1685 s, 1649 m, 1616 s, 1436 s, 1381 m, 1313 w, 1256 vs, 1214 m, 1086 s, 1026 m, 924 w, 804 vw, 751 vw, 726 w and 707 w.

Mol. wt. Calcd. for $C_{16}H_{24}O_3$: 264. 1724. Found (high resolution mass spectrometry): 264. 1757.

Hydrogenation of 5a

Compound **5***a* (183 mg) was dissolved in methanol (12 ml) containing palladium-on-charcoal (10% Pd, 200 mg). Hydrogenation was conducted at room temperature at 24 p.s.i. in a Parr bomb for 4 h. After removal of the catalyst by filtration, the product was recovered. Gas–liquid chromatography showed complete reaction with two products (g.l.c. r_t 0.40 and 0.55; **4***a* and **9** (3)) in a ratio of 1:2 with $[\alpha]_D^{25}$ (*c* 0.44, methanol) −6.7°. The o.r.d. curve of this mixture (*c* 0.443, methanol; 23°) $[\Phi]_{400}$ ≃0°, $[\Phi]_{350}$ −145°, $[\Phi]_{307}$ −871°, $[\Phi]_{292}$ 0°, $[\Phi]_{266}$ +1597°, molecular amplitude −24.7, was in agreement with that reported earlier (1).

The author wishes to thank Dr. V. Toome for providing the o.r.d. and c.d. curves of juvabione and $\Delta^{4'}$-dehydrojuvabione, and Drs. L. Greguss, O. Sziklai, E. von Rudloff, J. G. Worral, and Mr. S. Rowe for helpful discussions on the species identifications. Excellent technical assistance was provided by Mr. John Consiglio.

1. I. H. Rogers, J. F. Manville, and T. Sahota. Can. J. Chem. **52**, 1192 (1974).
2. H. S. Fraser and E. P. Swan. BiMon. Res. Notes, **29**(2), 13 (1973).

3. H. S. FRASER and E. P. SWAN. BiMon. Res. Notes. In press.
4. E. P. SWAN. Can. J. Chem. **45**, 1588 (1967).
5. H. S. FRASER and E. P. SWAN. BiMon. Res. Notes, **28**(5), 32 (1972).
6. T. SAKAI and Y. HIROSE. Chem. Lett. (Jap.) 491 (1973); 825 (1973).
7. K. SLAMA and C. M. WILLIAMS. Proc. Nat. Acad. Sci. U.S. **54**, 411 (1965).
8. W. S. BOWERS, H. M. FALES, M. J. THOMPSON, and E. C. UEBEL. Science, **154**, 1020 (1966).
9. R. TUTIHASI and T. HANAZAWA. J. Chem. Soc. (Jap.) **61**, 1041 (1940); Chem. Abstr. **37**, 258 (1943).
10. M. NAKAZAKI and S. ISOE. Bull. Chem. Soc. (Jap.) **36**, 1198 (1963).
11. V. CERNEY, L. DOLEJS, L. LABLER, F. SORM, and K. SLAMA. Coll. Czech. Chem. Commun. **32**, 3926 (1967).
12. (*a*) B. A. PAWSON, H. C. CHEUNG, S. GURBAXANI, and G. SAUCY. J. Am. Chem. Soc. **92**, 336 (1970); (*b*) J. F. BLOUNT, B. A. PAWSON, and G. SAUCY. Chem. Commun. 715 (1969).
13. J. FICINI, J. D'ANGELO, and J. NOIRE. J. Am. Chem. Soc. **96**, 1212 (1974).
14. K. SLAMA, M. ROMANUK, and F. SORM. *In* Insect hormones and bioanalogues. Springer–Verlag, New York. 1974. p. 170–177.
15. D. F. ZINKEL and J. W. ROWE. Anal. Chem. **36**, 1160 (1964).

Can. J. Chem. Downloaded from www.nrcresearchpress.com by 210.87.254.105 on 09/05/12
For personal use only.

Combinatorial Entropy of Mixing Molecules that Differ in Size and Shape. A Simple Approximation for Binary and Multicomponent Mixtures

MARC D. DONOHUE AND JOHN M. PRAUSNITZ

Chemical Engineering Department, University of California, Berkeley, California 94720

Received October 1, 1974

MARC D. DONOHUE and JOHN M. PRAUSNITZ. Can. J. Chem. **53**, 1586 (1975).

For liquid solutions, the combinatorial entropy of mixing is commonly calculated using either (*a*) the ideal-solution model (suitable for mixtures of simple spherical molecules) or (*b*) the Flory lattice model (suitable for mixtures of chainlike molecules). Based on the lattice theories of Huggins, Staverman, Tompa, and Lichtenthaler for molecules of arbitrary size and shape, this work proposes an *ad hoc* generalization of Flory's formula for the combinatorial entropy of mixing in binary and multicomponent solutions. The generalized Flory model yields results that are always intermediate between those obtained from (*a*) and (*b*). Parameters required for the calculations are found from molecular structure data (bond angles and distances). Illustrative calculations are given for the system carbon tetrachloride – octamethylcyclotetrasiloxane.

MARC D. DONOHUE et JOHN M. PRAUSNITZ. Can. J. Chem. **53**, 1586 (1975).

Pour des solutions liquides, on calcule généralement l'entropie combinatoire de mélange en faisant appel soit (*a*) au modèle de la solution idéale (applicable pour des mélanges de molécules sphériques simples) ou (*b*) au modèle de réseau de Flory (applicable aux mélanges de molécules sous forme de chaines). En se basant sur les théories de réseau de Huggins, Staverman, Tompa et Lichtelthaler pour des molécules de grosseur et de forme arbitraire, ce travail propose une généralisation *ad hoc* de la formulation de Flory pour les entropies combinatoires de mélange dans des solutions binaires et à plusieurs constituants. La généralisation du modèle de Flory conduit à des résultats qui sont toujours intermédiaires entre ceux obtenus à partir de (*a*) ou de (*b*). On trouve les paramètres requis pour les calculs en se basant sur des données de structures moléculaires (angle de valence et distance). On donne des calculs illustrant la méthode pour le système tétrachlorure de carbone – octaméthylcyclotétrasiloxanne.

[Traduit par le journal]

Can. J. Chem. Downloaded from www.nrcresearchpress.com by 210.87.254.40 on 09/05/12
For personal use only.

To interpret and correlate thermodynamic properties of liquid mixtures, it is customary to reduce experimental data by calculating residual properties, that is, properties in excess of those calculated from a model which serves as a reference. The values of the residual properties, in particular that of the residual entropy, depend on the reference model chosen. In this work we propose a reference model which is simple to use and which interpolates smoothly between the two common reference models.

Residual Properties

A residual property is defined as the observed change in that property upon mixing (at constant temperature and pressure) minus the calculated change in that property upon mixing (at the same temperature, pressure, and composition) where the calculation is determined by the choice of reference model. Two common reference models are the ideal solution introduced by Raoult nearly 100 years ago, and the athermal lattice due primarily to Flory (1) and to Huggins (2).

Residual Entropy

For a binary solution containing N_1 molecules of component 1 and N_2 molecules of component 2, the residual entropy is given by

$$[1] \qquad S^R = \Delta S(\text{observed}) - \Delta S^C$$

where superscript R stands for residual and superscript C stands for combinatorial; ΔS^C is determined by the choice of reference model.

Ideal solution

$$[2] \qquad \frac{\Delta S^C}{R} = -\left[N_1 \ln \frac{N_1}{N_1 + N_2} + N_2 \ln \frac{N_2}{N_1 + N_2}\right]$$

Flory lattice

$$[3] \qquad \frac{\Delta S^C}{R} = -\left[N_1 \ln \phi_1 + N_2 \ln \phi_2\right]$$

where R is the gas constant and ϕ is the site fraction

TABLE 1. Exponent in Generalized Flory Equation for combinatorial entropy of mixing

	$10^3\ p_i$ for r =								
$10^2\ q/r$	2	3	4	5	10	25	50	100	1000
100	1000	1000	1000	1000	1000	1000	1000	1000	1000
95	989	995	996	997	998	999	999	999	1000
90	953	978	985	988	992	995	996	997	999
85	888	949	964	971	982	988	990	992	996
80	783	904	933	946	967	978	982	985	991
75		839	890	912	946	964	971	976	984
70		750	831	866	918	946	956	963	976
65			752	805	883	922	938	948	965
60				725	838	893	914	928	953
55					781	857	886	904	937
50					710	813	851	875	918
45						758	808	840	895
40						690	755	796	866
35						603	690	743	832
30							607	676	790
25								590	737
20								471	668
15									572
10									428

$$\phi_1 = \frac{N_1 r_1}{N_1 r_1 + N_2 r_2}$$

$$\phi_2 = \frac{N_2 r_2}{N_1 r_1 + N_2 r_2}$$

where r_i is the number of lattice sites occupied by molecule i.

Both eqs. 2 and 3 always give positive ΔS^C. When $r_1 = r_2$, eqs. 2 and 3 are identical. However, when r_1 and r_2 are not equal, eq. 3 always gives a combinatorial entropy larger than that given by eq. 2 at the same N_1 and N_2. Much discussion of these equations has led Hildebrand (3) to the conclusion that eq. 2 gives a lower limit to the combinatorial entropy of mixing and eq. 3 gives an upper limit; the "true" combinatorial entropy lies in between.

Equations 2 and 3 can be combined into a single expression by introducing one exponent p for each component

$$[4]\quad \frac{\Delta S^C}{R} = -\left[N_1 \ln \frac{N_1 (r_1)^{p_1}}{N_1 (r_1)^{p_1} + N_2 (r_2)^{p_2}} + N_2 \ln \frac{N_2 (r_2)^{p_2}}{N_1 (r_1)^{p_1} + N_2 (r_2)^{p_2}}\right]$$

When $p_1 = p_2 = 0$, eq. 4 reduces to eq. 2 and when $p_1 = p_2 = 1$, eq. 4 reduces to eq. 3. Hildebrand's conclusion, then, suggests that the exponent p_i lies somewhere between zero and unity.

Evaluation of Exponent p_i

Modifications of eq. 3 have been presented by several authors, including Huggins (2), Staverman (4), and Tompa (5) and most recently by Lichtenthaler *et al.* (6*a*, *b*).[1] The modifications introduced by Lichtenthaler, similar to those of Tompa, provide a reasonable method for calculating ΔS^C for mixtures of molecules differing in size as well as shape. Combinatorial entropies calculated from Lichtenthaler's expression lie in between those found from eqs. 2 and 3. However, Lichtenthaler's equation is cumbersome and cannot be generalized to mixtures containing more than two components. We propose here that eq. 4 be used to calculate combinatorial entropies of mixing with exponents p_i based on Lichtenthaler's work as discussed below.

The size of a molecule i is given by the parameter r_i and the external surface area of that molecule is given by the parameter q_i. When the lattice coordination number is designated by z, the product $q_i z$ gives the number of external lattice-site contacts available to molecule i for interaction with other, nearest-neighbor molecules. The ratio $(q/r)_i$ is a measure of the molecule's shape; for a monomer $q/r = 1$. As r becomes very large,

[1] Misprint in eq. 4 of ref. 6*a* corrected in eq. 9 of ref. 6*b*.

Can. J. Chem. Downloaded from www.nrcresearchpress.com by 210.87.254.40 on 09/05/12
For personal use only.

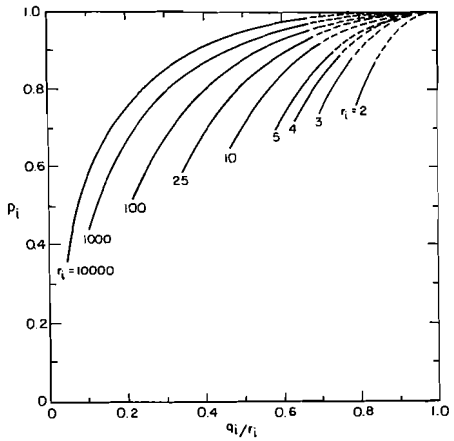

FIG. 1. Exponent in Generalized Flory Equation for combinatorial entropy of mixing.

TABLE 2. Structural parameters for molecules of some common fluids (relative to methane)

	Fluid	r	$100\,q/r$
n-Alkanes	CH_4	1.0	100
	C_2H_6	1.60	87.5
	C_3H_8	2.20	81.8
	C_4H_{10}	2.80	78.6
	C_5H_{12}	3.39	76.5
	C_6H_{14}	4.01	75.0
	C_7H_{16}	4.58	73.9
	C_8H_{18}	5.18	73.1
n-Alkenes	C_2H_4	1.40	90.5
	C_3H_6	1.99	83.4
	C_4H_8	2.59	79.5
	C_6H_{12}	3.77	75.5
	C_8H_{16}	4.96	73.4
Spherical molecule fluids	CF_4	1.60	85.6
	CCl_4	3.06	68.9
	$C(CH_3)_4$	3.38	66.7
	$Si(CH_3)_4$	3.80	64.1
	$(CH_3)_8(SiO)_4$	9.75	46.9
Cycloalkanes	C_5H_{10}	2.88	73.4
	C_6H_{12}	3.43	69.5
Aromatics	Benzene	2.83	77.8
	Toluene	3.44	74.4
	Naphthalene	4.33	71.6
	Anthracene	5.81	68.6
Other fluids	Isopentane	3.39	72.5
	Isobutane	2.80	74.2
	Isooctane	5.18	69.7
	H_2O	1.035	98.9
	Phenol	3.15	75.7
	Nitroethane	2.38	79.2
	Chloroethane	2.12	82.5

$q/r \to 2/3$ for a linear chain, and $q/r \to 0$ for a sphere (or cube). For a globular molecule the parameter q/r lies between zero and unity.

To use eq. 4, we postulate that for molecule i, p_i depends only on r_i and on $(q/r)_i$. We then calculate p_i by applying eq. 4 to the case where molecules i are mixed with monomers j ($r_j = q_j = 1$). The exponent p_i is found by obtaining the best possible agreement between ΔS^C as obtained from eq. 4 and ΔS^C as obtained from Lichtenthaler's model. (A more precise explanation of "best possible agreement" is given in the Appendix.) Results of these calculations are shown in Table 1 and in Fig. 1.

Evaluation of Parameters r and q

To obtain numerical values for r and q, we use bond angle and bond distance data as described by Bondi (7). Parameters r and q depend only on molecular size and structure; they are independent of temperature or density.

Table 2 gives parameters r and q for molecules of some common fluids. The parameters listed are relative to those for methane, *i.e.* in Table 2, $r = q = 1$ for methane.

Parameters r are found from van der Waals volumes v^* as calculated by Bondi's group-contribution method (7). For the results shown in Table 2

$$[5] \qquad r_i = v_i^*/v^*(\text{methane})$$

where $v^*(\text{methane}) = 17.1\ \text{cm}^3/\text{mol}$.

Parameters q are found by a procedure slightly different from Bondi's, as described by Lichtenthaler (6). Lichtenthaler's equation for ΔS^C is based on a simple cubic lattice with coordination number equal to 6; it follows that the surface area of a cube of volume v^* is given by $6(v^*)^{2/3}$. Following Lichtenthaler, we represent molecule i by a rectangular box with linear dimensions l_x, l_y, and l_z. The parameter q_i, as reported in Table 2, is calculated from

$$[6] \qquad q_i = \frac{2(l_x l_y + l_x l_z + l_y l_z)_i}{6(v^*)^{2/3}_{\text{methane}}}$$

Linear dimensions l_x, l_y, and l_z are found from molecular structure data.

Parameters r and q shown in Table 2 are arbitrarily normalized with respect to methane. Therefore if these parameters are used in eq. 4, the calculations are based on a monomer whose size is equal to that of methane. If we wish to use some

Can. J. Chem. Downloaded from www.nrcresearchpress.com by 210.87.254.40 on 09/05/12
For personal use only.

Can. J. Chem. Downloaded from www.nrcresearchpress.com by 210.87.254.40 on 09/05/12
For personal use only.

other molecule as the monomer, a new set of parameters r and q can be calculated by simple scaling

[7] r_i(relative to monomer j) = $\dfrac{r_i(\text{relative to methane})}{r_j(\text{relative to methane})}$

[8] q_i(relative to monomer j) = $\dfrac{q_i(\text{relative to methane})}{q_j(\text{relative to methane})}$

In obtaining ΔS^C from eq. 4, one must decide on an appropriate choice for the monomer. This choice may well differ from one mixture to another.

To obtain numerical results with eq. 4, a monomer must be chosen to obtain numerical values for r and q/r. While these parameters in turn influence the value of p (Table 1), we must emphasize that the calculations leading to Table 1 and Fig. 1 are independent of the choice of monomer (see Appendix). In finding values of the exponent p which give best agreement between eq. 4 and Lichtenthaler's equation, it was *not* necessary to use a particular molecule (such as methane) for the monomer. Therefore while Table 2 gives numerical results based on a particular choice of monomer, the results shown in Table 1 and Fig. 1 are independent of that choice; they are not linked with the structural parameters given in Table 2.

Results

We refer to eq. 4 as the Generalized Flory Model. Its main advantage follows from its simplicity; molecular parameters r and q can be calculated from molecular structure data and parameters p can then easily be estimated from Table 1 or Fig. 1.

For binary mixtures of monomers with long linear chains, or for mixtures of linear chains differing markedly in length, parameter p_i is close to unity for both components and, as expected, there is little difference between eqs. 3 and 4. However, for mixtures containing either bulky molecules or short chains, combinatorial entropies calculated from eq. 4 are appreciably smaller than those found from eq. 3. To illustrate, it is convenient first to define an excess combinatorial entropy and second, to present a numerical example shown by Figs. 2 and 3.

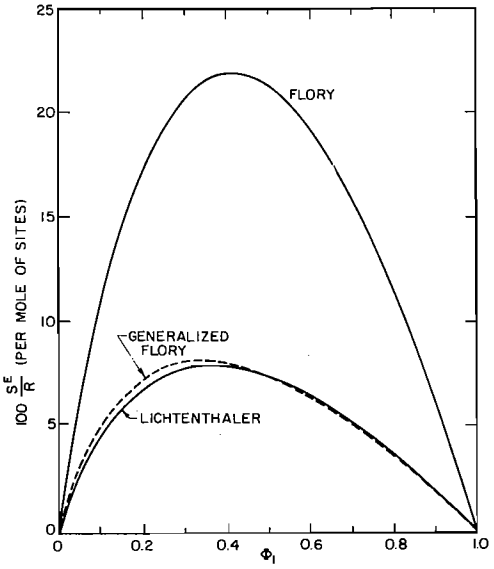

FIG. 2. Excess combinatorial entropy (per mol of sites) for binary mixture of monomers with cubes ($r = 10$, $q/r = 0.464$).

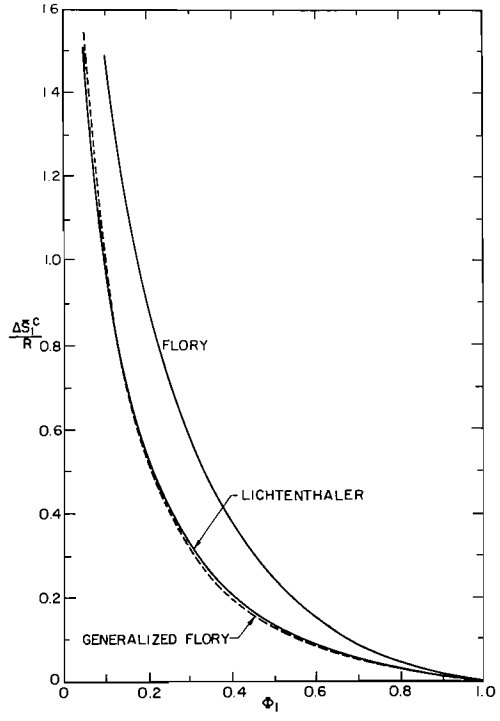

FIG. 3. Partial molar combinatorial entropy of monomers in a binary mixture with cubes ($r = 10$, $q/r = 0.464$).

Can. J. Chem. Downloaded from www.nrcresearchpress.com by 210.87.254.40 on 09/05/12
For personal use only.

The excess combinatorial entropy per mole of sites, designated by S^E, is defined by

$$[9]\quad \frac{S^E}{R} = \left[\frac{\Delta S^C}{R}\left(\begin{matrix}\text{per mole}\\ \text{of mixture}\end{matrix}\right) + \left(\frac{N_1}{N_1+N_2}\right)\ln\frac{N_1}{N_1+N_2} + \left(\frac{N_2}{N_1+N_2}\right)\ln\frac{N_2}{N_1+N_2}\right] \times \left[\frac{N_1+N_2}{r_1N_1+r_2N_2}\right]$$

Figure 2 shows the excess combinatorial entropy of mixing for a solution containing monomers ($q_1 = r_1 = 1$) and large cubes ($r_2 = 10$, $(q/r)_2 = 0.464$). Calculations were performed, first, using the Flory Model ($p_1 = p_2 = 1$) and second, using the Generalized Flory Model ($p_1 = 1$, $p_2 = 0.646$). The corresponding partial molar combinatorial entropies for the monomer are shown in Fig. 3.

Similar calculations were performed for a solution containing monomers ($q_1 = r_1 = 1$) and very large cubes ($r_2 = 100$, $(q/r) = 0.215$); the results are qualitatively similar to those shown in Figs. 2 and 3 but now the difference between eqs. 3 and 4 is even more pronounced.

Evaluation of r and q. Effect of Monomer Size

To use eq. 4, it is necessary to specify for each component values of r and q/r which are relative to those of a chosen monomer size. In general, the choice of monomer size affects the numerical value of ΔS^C; only when all p_i are the same does the monomer size cancel. The need to specify the size of a monomer is not peculiar to the Generalized Flory Model; the same need arises if one wants to use the combinatorial-entropy formulas of Huggins (2), Staverman (4), Tompa (5), or Lichtenthaler (6). Specification of monomer size must be based on physical considerations, that is, on the dimensions and flexibility of the molecules present in a particular mixture. The higher the flexibility, the smaller the monomer size.

To illustrate the effect of monomer size, we consider a binary mixture of globular molecules differing appreciably in size, carbon tetrachloride – octamethylcyclotetrasiloxane (OMCTS). In the first calculation we consider carbon tetrachloride to be the monomer; thus $r_1 = q_1 = 1$ and $r_2 = 3.19$ and $(q/r)_2 = 0.680$. In the second calculation we consider carbon tetrachloride not as a monomer but as a globular molecule and we choose methane as the monomer. In this case $r_1 = 3.06, (q/r)_1 = 0.689$; for OMCTS $r_2 = 9.77$ and $(q/r)_2 = 0.468$. Calculated excess combinatorial entropies are shown in Fig. 4.

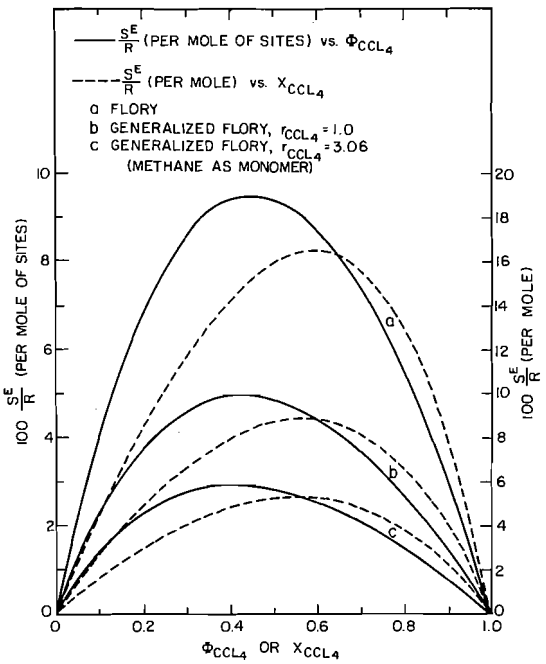

FIG. 4. Effect of monomer size on excess combinatorial entropy for mixtures of carbon tetrachloride with octamethylcyclotetrasiloxane.

Figure 4 shows that the choice of monomer size has an appreciable effect on the combinatorial entropy for this particular binary mixture; we have intentionally chosen this mixture of spherical molecules to dramatize the effect. As the shape of the larger molecule becomes less spherical and more chainlike, the effect of monomer size declines rapidly.

Experimental data of Marsh and Tomlins (8) were used to calculate residual entropies for carbon tetrachloride – OMCTS; results are shown in Fig. 5. In this case the residual entropy obtained from the data is strongly dependent on the expression used for the combinatorial entropy. The residual entropy is negative when the Flory combinatorial entropy is used but it is positive when the ideal-combinatorial entropy is used. Calculations based on the generalized Flory combinatorial entropy are in semiquantitative agreement with those obtained from hard-sphere calculations based on the Carnahan–Starling ver-

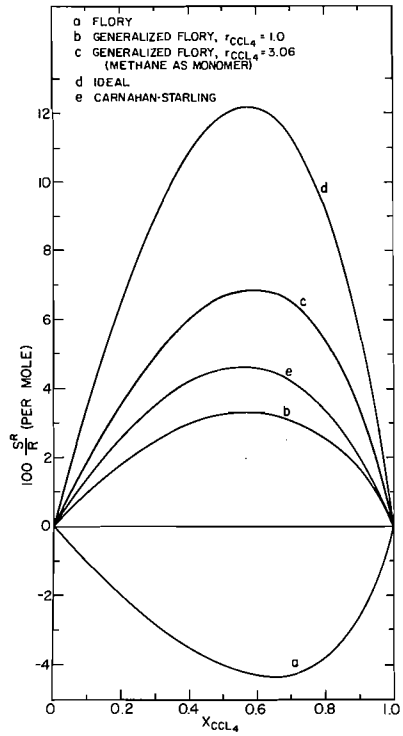

FIG. 5. Residual entropy per mol for mixtures of carbon tetrachloride and octamethylcyclotetrasiloxane at 25 °C.

sion of Percus–Yevick theory (9). In the latter calculations the hard-sphere diameters were obtained from pure-component entropy-of-vaporization data which yielded 5.25 Å for carbon tetrachloride and 8.12 Å for OMCTS. Volumetric data for the mixture were also obtained from Marsh and Tomlins (8).

The residual entropy of mixing for carbon tetrachloride – OMCTS can be calculated from an equation of state as discussed by Marsh (10). Using Marsh's calculations and observed entropies of mixing, we have used eq. 1 to find "empirical" combinatorial entropies of mixing; we then compared these "empirical" combinatorial entropies with those calculated from eq. 4. We hoped thereby to obtain information on which monomer size in eq. 4 gives the best results. However, no conclusion can be reached because, as shown by Marsh (10), the residual entropy of mixing is sensitive to the equation of state used. In other words, the uncertainty in the calculated residual entropy, caused by arbitrary choice of an equation of state, is as large as the uncertainty in eq. 4, caused by the arbitrary choice of monomer size.

Generalization to Multicomponent Mixtures

Equations 2 and 3 are readily extended to ternary (and higher) mixtures as discussed in many textbooks. By analogy (and without proof) we suggest that for a mixture of m components, the extension of eq. 4 is

Generalized Flory Model

$$[4a] \qquad \frac{\Delta S^C}{R} = -\sum_{i=1}^{m} N_i \ln \frac{N_i r_i^{p_i}}{\sum_{i=1}^{m} N_i r_i^{p_i}}$$

Conclusion

For most workers in the thermodynamics of liquid solutions, it is common practice to use *residual* functions for interpretation and correlation of experimental data. The residual functions are either expressed by empirical equations or by theoretical relations obtained from a partition function. While residual volumes and residual enthalpies of mixing are not affected, residual entropies and residual free energies are often sensitive to the choice of combinatorial entropy used for reducing the experimental data. This work presents a convenient method for calculating combinatorial entropies of mixing for mixtures of molecules differing in both size and shape.

While we cannot say with assurance what the "correct" combinatorial entropy is, the simple equation presented here (eq. 4) permits reduction of experimental data in a manner which interpolates rationally between the upper and lower limits as given by Flory's and Raoult's equations.

The authors are grateful to the American Gas Association, the Gas Processors' Association, and the National Science Foundation for financial support, to the Computer Center, University of California, Berkeley, for the use of its facilities, and to K. W. Won, D. S. Abrams, and R. N. Lichtenthaler for helpful discussions.

1. P. J. FLORY. Principles of polymer chemistry. Cornell University Press, Ithaca, N.Y. and London. 1953.
2. M. L. HUGGINS. Ann. N.Y. Acad. Sci. **43**, 1 (1942).
3. J. H. HILDEBRAND. J. Chem. Phys. **15**, 225 (1947).
4. A. J. STAVERMAN. Rec. Trav. Chim. Pays-bas, **69**, 163 (1950).
5. H. TOMPA. Trans. Faraday Soc. **48**, 363 (1952).
6. (*a*) R. N. LICHTENTHALER, D. S. ABRAMS, and J. M. PRAUSNITZ. Can. J. Chem. **51**, 3071 (1973); (*b*) R. N. LICHTENTHALER, D. D. LIU, and J. M. PRAUSNITZ. Ber. Bunsenges. **78**, 470 (1974).

Can. J. Chem. Downloaded from www.nrcresearchpress.com by 210.87.254.40 on 09/05/12
For personal use only.

7. A. BONDI. Physical properties of molecular crystals, liquids and glasses. John Wiley and Sons, Inc., New York. 1968.
8. K. N. MARSH and R. P. TOMLINS. Trans. Faraday Soc. **66**, 783 (1970).
9. G. A. MANSOORI, N. F. CARNAHAN, K. E. STARLING, and T. W. LELAND, JR. J. Chem. Phys. **54**, 1523 (1971).
10. K. N. MARSH. J. Chem. Thermodyn. **3**, 355 (1971).

Appendix

Calculation of Exponent p

Exponents p_1 and p_2 in eq. 4 were first calculated by forcing agreement between ΔS^C as found from eq. 4 and ΔS^C as found from Lichtenthaler's equation (eq. 4 in ref. 6). In this calculation component 1 was chosen as the monomer; thus $r_1 = q_1 = p_1 = 1$. To use Lichtenthaler's equation, we varied the dimensions of molecule 2 and then, from simple geometry, calculated the corresponding r_2 and q_2. For various values of r_2 and q_2, parameter p_2 was found with results shown in Table 1 and Fig. 1.

The exponent p_2 was also determined by a second calculation in which we forced agreement between $\Delta \bar{S}_1{}^C$ as found from the Generalized Flory Model and $\Delta \bar{S}_1{}^C$ as found from Lichtenthaler's equation. Again, molecule 1 is the monomer with $r_1 = q_1 = p_1 = 1$.

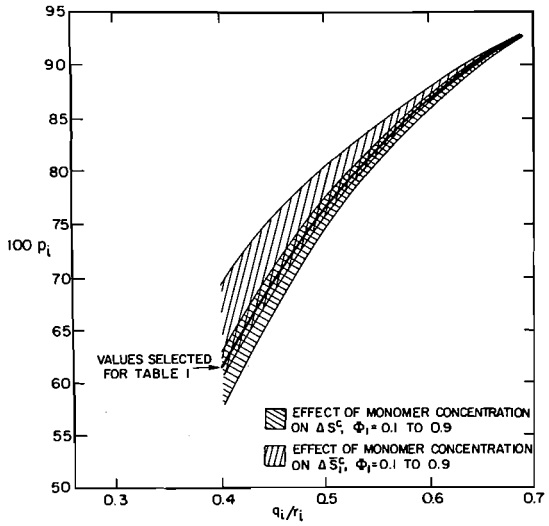

FIG. 6. Effect of monomer concentration on p_i for $r_i = 15$.

In both calculations, exponent p_2 is a weak function of segment fraction Φ, as illustrated in Fig. 6. As indicated by the dark line in Fig. 6, a representative value of p was chosen such as to give good agreement for both calculations (ΔS^C and $\Delta \bar{S}_1{}^C$). These representative values are given in Table 1 and Fig. 1.

Can. J. Chem. Downloaded from www.nrcresearchpress.com by 210.87.254.40 on 09/05/12
For personal use only.

Electron Spin Resonance Studies and Electronic Structure of *trans*-$[Ti(H_2O)_4F_2]^+$

PAVLE ILIJA PREMOVIĆ AND PAUL RONALD WEST
Department of Chemistry, University of Victoria, Victoria, British Columbia V8W 2Y2

Received July 25, 1974[1]

PAVLE ILIJA PREMOVIĆ and PAUL RONALD WEST. Can. J. Chem. **53**, 1593 (1975).

At p*H* 1.0–1.6 aqueous titanium(III) solutions containing added fluoride ion exhibit e.s.r. signals of *trans*-$[Ti(H_2O)_4F_2]^+$, $g = 1.9460 \pm 0.0005$, $a_{Ti} = 17.9 \pm 0.2$ G. The variation in the intensity of the optical and e.s.r. spectra with added fluoride ion indicate >90% conversion to the complex at [Ti]:[F] = 1:2. The *trans* geometry of the complex is established from the spectrum in D_2O, a 1:2:1 triplet with $a_F = 7.5 \pm 0.5$ G, and from the axial symmetry (D_{4h}) apparent in the frozen solution spectrum, $g_{\parallel} = 1.968$, $g_{\perp} = 1.932$.

The optical spectrum shows two bands assigned to the $^2B_{2g} \rightarrow {}^2B_{1g}$ (15 200 cm^{-1}) and $^2B_{2g} \rightarrow {}^2A_{1g}$ (23 300 cm^{-1}) transitions. Calculations based on the e.s.r. and optical spectra suggest covalent character in the in-plane π and σ bonding of the complex.

PAVLE ILIJA PREMOVIĆ et PAUL RONALD WEST. Can. J. Chem. **53**, 1593 (1975).

A des p*H* allant de 1.0 à 1.6, des solutions aqueuses de titane(III) contenant des ions fluorures ajoutés, montrent un signal r.p.e. du $[Ti(H_2O)_4F_2]^+$-*trans*, $g = 1.9460 \pm 0.0005$, $a_{Ti} = 17.9 \pm 0.2$ G. On note une variation de l'intensité des spectres optique et r.p.e. lorsqu'on ajoute des ions fluorures; cette variation indique que la conversion vers le complexe est plus grande que >90% lorsque la concentration de [Ti]:[F] = 1:2. On a établi que le complexe possède la géométrie *trans* en se basant sur le spectre dans le D_2O alors qu'on observe un triplet 1:2:1 avec $a_F = 7.5 \pm 0.5$ G et aussi sur l'existence d'une symétrie axiale (D_{4h}) observée pour le spectre de la solution congelée $g_{\parallel} = 1.968$, $g_{\perp} = 1.932$.

Le spectre optique montre deux bandes qui ont été assignées aux transitions $^2B_{2g} \rightarrow {}^2B_{1g}$ (15 200 cm^{-1}) et $^2B_{2g} \rightarrow {}^2A_{1g}$ (23 300 cm^{-1}). Des calculs basés sur les spectres r.p.e. et optique suggèrent un caractère covalent pour les liaisons π et σ dans le plan du complexe.

[Traduit par le journal]

Introduction

Through analysis of the e.s.r. spectra of titanium(III) complexes considerable information concerning the nature of the bonding can be obtained. Provided that the orbital angular momentum is quenched sufficiently by the effects of the coordinating ligands, the $3d^1$ configuration of titanium(III) gives rise to an e.s.r. signal. Analogous systems are found in the VO^{2+} ion $3d^1$ and in the case of copper(II) where a "hole" in the d shell occurs. Detailed e.s.r. studies on complexes of the latter two species have been extensively reported. However, many fewer comprehensive examinations of titanium(III) complexes have been published (1–6).

Several accounts describing the spectrum of the $[Ti(H_2O)_4F_2]^+$ ion, **1**, have appeared. Garif'yanov and Semenova (1*b*) prepared green hydrated complexes $[Ti(H_2O)_{6-n}F_n]^{(3-n)}$ which exhibited an intense slightly assymetric resonance line ($g = 1.946 \pm 0.001$; linewidth 20 G) over the concentration range from 0.01 to 0.001 *M* titanium(III). Assignment of species as the complex **1** was made without any detailed optical or other experimental study. Waters and Maki (2) briefly referred to preparation of the paramagnetic complex, **1**, in aqueous solution, in conjunction with a report on ^{47}Ti and ^{49}Ti hyperfine structure in the $Ti(OCH_3)^{2+}$ spectrum. Of particular note are the references in both of these studies to a strong axial perturbation by the coordinating ligands. Such an axial perturbation creates a well-separated orbital singlet ground state and a long spin–lattice relaxation time. The result is a relatively narrow line and a much reduced **g**-tensor anisotropy in this complex. Glebov has reported calculation of the electronic energy levels of a series of titanium(III) complexes, and speculated on the assignment of the e.s.r. absorption in the aqueous titanium(III) solution containing added F^- ion as being $[Ti(H_2O)_5F]^{2+}$ (7).

In the present study, the structure of the paramagnetic complex in such solutions is firmly established as the *trans*-$[Ti(H_2O)_4F_2]^+$ ion on

[1]Revision received January 3, 1975.

Can. J. Chem. Downloaded from www.nrcresearchpress.com by 210.87.254.6 on 09/05/12
For personal use only.

Can. J. Chem. Downloaded from www.nrcresearchpress.com by 210.87.254.6 on 09/05/12
For personal use only.

the basis of detailed e.s.r. studies in H_2O and D_2O. A simple theory of the electronic structure of the complex is developed that is consistent with its observed physical properties.

Experimental

All spectra were recorded on a Varian E-6S X band e.s.r. spectrometer operating at 100 kHz modulation. Samples were contained in standard Varian E-248 aqueous solution cells.

Sample preparation was as previously described (19). The titanium(III) solutions were prepared by dissolving the metallic sponge (Fisher) with gentle heating in approximately 1 *N* HCl or H_2SO_4. An N_2 atmosphere was employed to minimize oxidation of titanium(III) ion. Alternatively Fisher Reagent titanium(III) chloride solution (20%) was used directly without qualitative change in any results. Titanium(III) solutions in aqueous acid containing fluoride or bromide as the anion were prepared by dissolving titanium(III) carbonate in the appropriate concentrated acid (HBr or HF) and diluting to the desired concentration. Titanium(III) carbonate was prepared by the method of Semenova (1*c*). In preparing solutions of the $[Ti(H_2O)_4F_2]^+$ complex by addition of NaF or KF, p*H* adjustment was made by addition of the appropriate concentrated acid. For study in heavy water, concentrated $TiCl_3$ solution was added to D_2O (Merck) such that the sample contained 98% D_2O.

The *g* factors are quoted relative to DPPH, $g = 2.0036$, employing a Varian E 232 dual cavity assembly in which the field shift between the cavities had been carefully determined. The integrated intensity of the 1st derivative signal was used to calculate the absolute concentration of the paramagnetic species by reference to standard samples of $Cu(H_2O)_6^{2+}$, $Cr(NH_3)_6^{3+}$, $Mn(H_2O)_6^{2+}$, and $VO(H_2O)_5^{2+}$. Approximate digital calculation was used to determine the integrated intensity of the signal (8). Frozen solutions were obtained by rapidly quenching the sample in liquid nitrogen, maintaining the sample in the Varian E-246 insert Dewar.

The u.v. and visible spectra were recorded on a Cary Model 17 instrument.

Results

By adding slightly more than 2 equiv. of fluoride ion (aqueous HF, KF, or NaF) to a violet solution of the $Ti(H_2O)_6^{3+}$ ion prepared from the sulfate, chloride, or bromide (0.1 *M*) we obtained a green solution that exhibited a rather broad e.s.r. absorption signal. One can discern the presence of unresolved hyperfine structure compatible with a triplet (1:2:1) splitting, Fig. 1*a*. When prepared in D_2O by the same route, the e.s.r. signal now showed a distinct triplet splitting through interaction with two equivalent ^{19}F nuclei, thus indicating the stoichiometry titanium(III):fluoride of 1:2, Fig. 1*b*. Spectral parameters for this complex are given in Table 1. At higher gain, the satellite

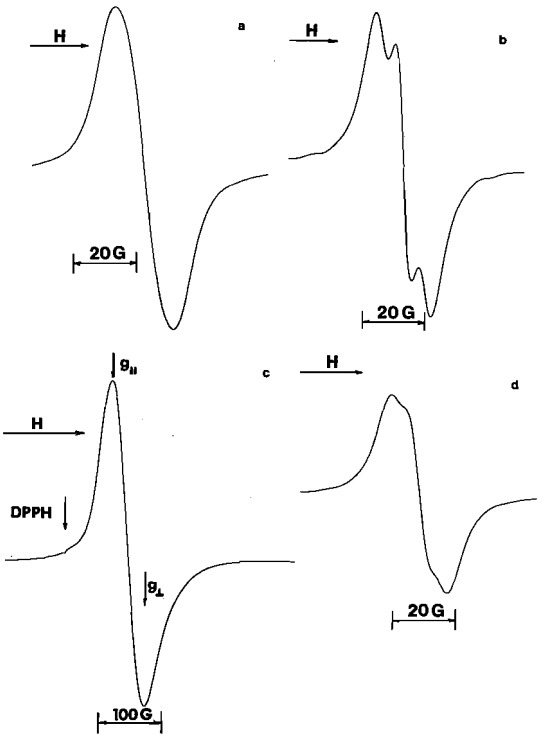

FIG. 1. Electron spin resonance spectra of TiF_2^+ ions in aqueous solution (p*H* 1.0): (*a*) $TiCl_3$ (0.02 *M*), NaF (0.06 *M*) in H_2O, 25 °C; (*b*) $TiCl_3$ (0.02 *M*), NaF (0.06 *M*) in D_2O, 25 °C; (*c*) $TiCl_3$ (0.01 *M*), NaF (0.03 *M*) in H_2O, frozen solution at 77 K; (*d*) $TiCl_3$ (0.06 *M*), NH_4F (0.06 *M*) in D_2O, 25 °C.

lines from ^{47}Ti and ^{49}Ti interaction were evident in both spectra, and revealed the same fluorine hyperfine splitting.

The p*H* dependence of the intensity of the e.s.r. absorption is shown in Fig. 2 for a 0.01 *M* solution derived from $TiCl_3$. From a constant maximum level under acidic conditions (p*H* 1.0–1.6) the signal steadily diminishes until it is no longer observed at p*H* 3.5.

TABLE 1. Electron spin resonance data for *trans*-$[Ti(H_2O)_4F_2]^+$

Parameter	Value
$g_{\parallel}$	1.968 ± 0.002
$g_{\perp}$	1.932 ± 0.002
g_0*	1.9460 ± 0.0005
a_{Ti}	17.9 ± 0.2 G
a_F†	7.5 ± 0.5 G
a_H	0.2 – 0.4

*g_0(calculated) = 1.944; by expression 13.
†Measured from $[Ti(D_2O)_4F_2]^+$.

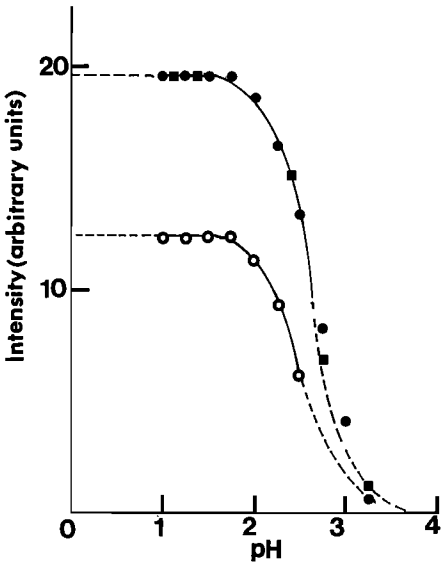

FIG. 2. p*H* dependance of proposed TiF_2^+ ion. Upper curve, e.s.r. signal intensity: ●, H_2O; ■, D_2O, relative to reading at p*H* 1.0. Lower curve, absorbance at 660 nm: ○, relative to reading at p*H* 1.0. $TiCl_3$ = 0.02 *M*, NaF = 0.06 *M*.

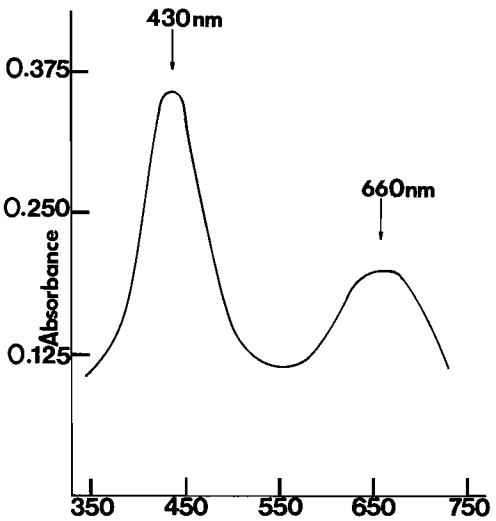

FIG. 3. Optical spectrum of TiF_2^+ in aqueous solution at p*H* 1.3; $TiCl_3$ (0.1 *M*), NaF (0.25 *M*).

In the p*H* range 1.0–2.5 the green aqueous solution derived from titanium fluoride, chloride, bromide, or sulfate exhibited the same optical spectrum in the presence of 2.5–4.0 equiv. of fluoride ion, with maxima at 430 nm ($\varepsilon \sim 3.4$) and 660 nm ($\varepsilon \sim 2$) (see Fig. 3). The decay in the intensity of these absorptions smoothly followed the decay of the e.s.r. signal to p*H* 2.5 (Fig. 2). Such behavior indicates an identity between the complex responsible for the green color and the paramagnetic species. Beyond p*H* 2.5, turbidity due to the onset of precipitation rendered optical readings unreliable. However the e.s.r. signal, though diminishing, persisted to p*H* 3.3 with sharp precipitation occurring at p*H* > 3.5. Note that in the presence of fluoride ion such samples no longer exhibited the $[Ti(H_2O)_4(OH)_2]^+$ e.s.r. signal normally observed in the p*H* region 1.0–3.5 (18). Therefore, it is likely that fluoride ion remained coordinated to titanium(III) ions undergoing hydrolysis, for example reaction 1.

[1] $[Ti(H_2O)_4F_2]^+ + OH^- \rightleftharpoons [Ti(H_2O)_3F_2(OH)]$

Qualitatively, precipitation produced a rose-white solid in contrast to the brown-black mass observed in the hydrolysis of $TiCl_3$ solution.

Variation of the e.s.r. signal intensity, Fig. 4*b*, indicated that $[Ti(H_2O)_4F_2]^+$ was one of the most stable complexes in solution. A relatively sharp breaking point was observed near a ratio of 1:2, and the depression of e.s.r. signal intensity with further increase in fluoride ion was gradual. Measurement of the integrated intensity of the maximum signal (see Experimental) indicated that 100 ± 10% of the titanium(III) was in the complex. Changes in absorbance at 430 and 660 nm, Fig. 4*a*, were compatible with the e.s.r. observations, though now loss of intense $Ti(H_2O)_6^{3+}$ bands was being monitored. At a mole ratio higher than 1:6 we observe a small shift of the 430 nm band to higher wavelength (450 nm) with 10% higher extinction coefficient. This observation is consistent with either significant population of higher complexes (1), or a second coordination shell effect of fluoride ion.

The evidence for $Ti(H_2O)F_2^+$ is in good agreement with the conclusions of other workers (1, 9, 10) and at variance with the experimental results of Glebov (7). The e.s.r. spectrum obtained from $TiCl_3$ in D_2O on addition of ammonium fluoride at a 1:1 mole ratio (Glebov's conditions for the supposed $[Ti(H_2O)_5F]^{2+}$ species in H_2O) again shows the symmetrical 1:2:1 triplet, Fig. 1*d*. Therefore the species present must actually be $[Ti(D_2O)_4F_2]^+$. Of some interest is the markedly lower resolution of the triplet splitting in the Ti^{3+}–NH_4F sys-

Can. J. Chem. Downloaded from www.nrcresearchpress.com by 210.87.254.6 on 09/05/12
For personal use only.

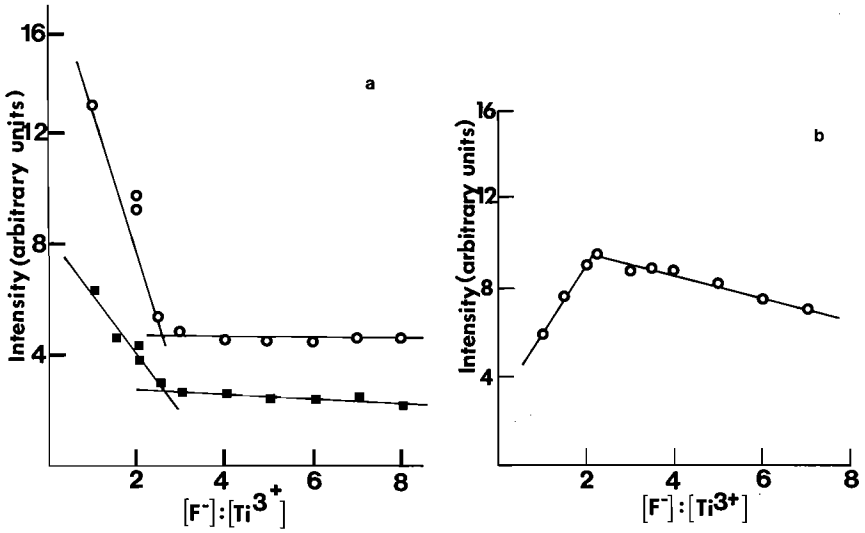

FIG. 4. Dependance of TiF_2^+ concentration on added fluoride ion. (*a*) Variation of absorbance of TiF_2^+ at: ○, 430 nm; ●, 660 nm; $TiCl_3$ (0.15 *M*) at p*H* 1.3; (*b*) Variation in e.s.r. signal intensity, $TiCl_3$ (0.01 *M*) at p*H* 1.1.

tem, relative to the higher resolution shown in Fig. 1*b* for a Ti^{3+}·NaF·D_2O sample. When titanium(III) concentration was varied from 0.01 to 0.1 *M* in the presence of NH_4F, the line broadening persisted, indicating the effect was not due to concentration dependent relaxation processes. Since spatially NH_4^+ exactly replaces an H_4O^{2+} unit in water structure (11), we tentatively ascribe the effect to association of ammonium ion with the complex in the second coordination sphere. Some delocalization of unpaired spin density to the second coordination sphere may provide additional hyperfine splitting.

The spectrum of a frozen solution of $TiCl_3$–NaF in H_2O is shown in Fig. 1*c* (Table 1). From the slight distortion of the linewidth, we conclude axial symmetry for the complex with much reduced **g**-tensor anisotropy and ^{19}F hyperfine tensor anisotropy. The values of $g_{\parallel}$ and $g_{\perp}$ (Fig. 1*c*) are assigned as the maximum limits of the anisotropy apparent in the nearly isotropic line that is observed (12). The calculated *g* factor is found to be in reasonable agreement with the isotropic *g* factor measured at room temperature.

Structure Assignment

The e.s.r. signal arises from the $[Ti(H_2O)_4F_2]^+$ complex ion, and this species is sufficiently stable to be the predominant form of titanium(III) in solution at $[Ti^{3+}]:[F^-] = 1:2$. The equivalence of the two fluorine ligands shown by the single h.f.s. constant, and the axial symmetry apparent from the frozen solution spectrum are only consistent with two axial fluoride ion ligands and four water molecules in the equatorial plane. The fluoride ion dependence of the e.s.r. spectrum (Fig. 4*b*) indicates that higher complexes of the type $[Ti(H_2O)_{6-n}F_n]^{(3-n)+}$ do not provide observable e.s.r. signals. The *trans* complex will have a well-separated orbital singlet resulting from a strong axial perturbation and leading to the requisite long spin–lattice relaxation time for the observation of the spectrum. Nonappearance of signals from the other possible ions $[Ti(H_2O)_{6-n}F_n]^{(3-n)+}$ is then direct confirmation of residency of the unpaired electron in ground states where the degeneracy is only slightly lifted by field distortions providing short spin–lattice relaxation times, and extremely broad resonance lines.

Discussion

The symmetry of the *trans*-$[Ti(H_2O)_4F_2]^+$ ion is D_{4h}. We propose that the ground electronic state is $^2B_{2g}$ (unpaired electron in b_{2g}* (d_{xy}) orbital). The e.s.r. spectrum provides direct confirmation of this assignment when the available alternative energy levels are considered.

If the electron were in an ^2E_g state (e_g*1 (d_{xz}) and e_g*2 (d_{yz}) orbitals), the degeneracy

Can. J. Chem. Downloaded from www.nrcresearchpress.com by 210.87.254.6 on 09/05/12
For personal use only.

Can. J. Chem. Downloaded from www.nrcresearchpress.com by 210.87.254.6 on 09/05/12
For personal use only.

probably only slightly split by field distortion would result in a short spin–lattice relaxation time and a broad resonance line. Note here the line width (D_2O) at 25 °C is only 5 G.

Next, for the $^2B_{1g}$ state (b_{1g}* ($d_{x^2-y^2}$) orbital) we would expect larger isotropic proton hyperfine splitting from the water ligands through σ bonding involving the b_{1g}* orbital and the a_1 (H_2O) orbitals. Also one might expect $g_\perp$ to be higher than the observed value (1.932), since the $^2B_{1g} \rightarrow {}^2E_g$ electronic transition would be relatively higher in energy compared to $^2B_{2g} \rightarrow {}^2E_g$.

In the $^2A_{1g}$ state (a_g*1 and a_g*2 orbitals; d_{z^2}, 4s) we would expect a higher isotropic h.f.s. constant for fluorine nuclei through the enhanced σ bonding. In addition the h.f.s. for titanium should be higher. In D_{4h} symmetry the d_{z^2} and 4s orbitals belong to the same irreducible representation and a direct contribution of spin density at the metal nucleus is allowed. For the $^2A_{1g}$ state, we would expect $g_\parallel$ to be very close to 2.0023 since the B_{1g} and B_{2g} states cannot mix with the ground state of A_{1g} symmetry under the perturbation of the angular momentum operator. The $g_\perp$ value would also be closer to 2.0023 since the $^2A_{1g} \rightarrow {}^2E_g$ transition will be expected to be high in energy.

Finally we consider the possibility of the unpaired electron being in any other metal orbital to be highly unlikely in view of the expected high energy of such states.

We now proceed to examine the assigned ground state $^2B_{2g}$ in more detail. Only states of B_{1g} and E_g symmetry can mix with this ground state under perturbation of the angular momentum operator. Therefore we need consider only molecular orbitals belonging to the representations b_{1g}*, b_{2g}*, and e_g*. The relevant antibonding MO's are

$$[2]\quad b_{1g}^* = \alpha_1 d_{xy} - \tfrac{1}{2}\alpha_1'[p_y^1 + p_x^2 - p_y^3 - p_x^4]$$

$$[3]\quad b_{2g}^* = \alpha_2 d_{x^2-y^2} - \tfrac{1}{2}\alpha_2'[-\sigma_x^1 + \sigma_y^2 + \sigma_x^3 - \sigma_y^4]$$

$$[4]\quad e_g^*1 = \varepsilon d_{xz} - \frac{1}{2^{1/2}}\varepsilon'[p_x^5 - p_x^6] - \frac{\varepsilon''}{2^{1/2}}[p_z^1 - p_z^3]$$

$$[5]\quad e_g^*2 = \varepsilon d_{yz} - \frac{1}{2^{1/2}}\varepsilon'[p_y^5 - p_y^6] - \frac{\varepsilon''}{2^{1/2}}[p_z^2 - p_z^4]$$

It is assumed that each of the oxygen ligand atoms has available 2s, $2p_x$, $2p_y$, and $2p_z$ orbitals and each fluorine $2p_x$, $2p_y$, and $2p_z$ for the formation of MO's with titanium 3d orbitals. The six ligands are placed on the $\pm x$, $\pm y$, and $\pm z$ axes and are labelled by superscripts starting with 1 on the $+x$ axis and proceeding counterclockwise with the 5th and 6th ligands (fluorine) placed on the $+z$ and $-z$ axes respectively. In the above states the σ^i are hybrid orbitals on oxygen given by expression 6 with a plus sign indicating the ligands on the positive x, y axes

$$[6]\qquad \sigma^i = np^i \pm (1 - n^2)^{1/2}s^i$$

and a minus sign those ligands on negative x, y axes. A value of n equal to $(\frac{2}{3})^{1/2}$ corresponds to sp^2 hybridization on the ligand atom.

The appropriate effective spin Hamiltonian for Ti^{3+} in a tetragonal field is given by expression 7

$$[7]\quad \mathcal{H} = \beta_e g_\parallel H_z S_z + \beta_e g_\perp (H_x S_x + H_y S_y) + A S_z I_z + \beta(S_x I_x + S_y I_y)$$

where

$$[8]\quad g_\parallel = 2.0023 - \frac{8\lambda\alpha_1^2\alpha_2^2}{\Delta E_{x^2-y^2}} \times \left[1 - \frac{1}{2}\frac{\alpha_1'\alpha_2'}{\alpha_1\alpha_2}T(n) - \left(\frac{\alpha_2'}{\alpha_2}\right)S - \left(\frac{\alpha_1'}{\alpha_1}\right)\Pi_1\right]$$

$$[9]\quad g_\perp = 2.0023 - \frac{2\lambda\alpha_1^2\varepsilon^2}{\Delta E_{xz}} \times \left[1 - \frac{1}{2^{1/2}}\left(\frac{\varepsilon'\alpha_1'}{\varepsilon\alpha_1}\right) - \left(\frac{\alpha_1'}{\alpha_1}\right)\Pi_1 - \frac{1}{2^{1/2}}\left(\frac{\varepsilon'}{\varepsilon}\right)\Pi_1\right]$$

The complete expression for $g_\perp$ contains an additional term within the square brackets namely

$$-\frac{1}{2^{1/2}}\left(\frac{\varepsilon''}{\varepsilon}\right)\Pi_2$$

that arises from out-of-plane π bonding with oxygen $2p_z$ orbitals. In view of the low energy of $2p_z$, the contribution of this term will be negligible and it is omitted from the final expression 9 for $g_\perp$.

$$[10]\quad A = P\left[-\alpha_1^2\left(\frac{4}{7} + K_0\right) - \frac{8\lambda\alpha_1^2\alpha_2^2}{\Delta E_{x^2-y^2}} - \frac{6\lambda\alpha_1^2\varepsilon^2}{\Delta E_{xz}}\right]$$

Can. J. Chem. Downloaded from www.nrcresearchpress.com by 210.87.254.6 on 09/05/12
For personal use only.

$$[11] \quad B = P\left[\alpha_1^2\left(\frac{2}{7} - K_0\right) - \frac{11}{7}\cdot\frac{\lambda\alpha_1^2\varepsilon^2}{\Delta E_{xz}}\right]$$

The parameter $\lambda = 154\ \text{cm}^{-1}$ is the spin–orbit coupling constant for the free ion in the appropriate valence state, K_0 is the Fermi contact term for the titanium nucleus, and $\Delta E_{x^2-y^2}(\Delta E_{(^2B_{2g} \rightarrow {}^2B_{1g})})$ and $\Delta E_{xz}(\Delta E_{(^2B_{2g} \rightarrow {}^2E_g)})$ are the transition energies to the $^2B_{1g}$ and ^2E_g states respectively. The parameter $P = -25.7 \times 10^{-4}\ \text{cm}^{-1}$ for $^{47,49}Ti^{3+}$ was obtained by extrapolation (13, 14), as defined by expression 12 where r is average orbital radius.

$$[12] \quad P = g_e g_N \beta_e \beta_N \langle r^{-3} \rangle \text{ av}$$

In eqs. 8 and 9, the integral $T(n)$ is taken over all ligand functions and S, Π_1, and Π_2 are the group overlap integrals.

$$S = 2\langle d_{xy}|p_y{}^1\rangle$$
$$\Pi_1 = 2\langle d_{x^2-y^2}|\sigma^1\rangle$$
$$\Pi_2 = 2\langle d_{xz}|p_x{}^5\rangle$$

Expressions 10 and 11 can be written as follows after substituting from expressions 8 and 9 neglecting small contributions to A and B ($\leqslant 0.05$).

$$[13] \quad A = -KP - \frac{4}{7}\alpha_1^2 \cdot P + (g_\parallel - 2.0023)P + \frac{3}{7}(g_\perp - 2.0023)P$$

$$[14] \quad B = -KP + \frac{2}{7}\alpha_1^2 P + \frac{11}{14}(g_\perp - 2.0023)P$$

where $K = \alpha_1^2 K_0$

For the isotropic solution spectra

$$[15] \quad g_0 = \tfrac{1}{3}(g_\parallel + 2g_\perp)$$

and

$$[16] \quad a = \tfrac{1}{3}(A + 2B) = -KP - (g_0 - 2.0023)P$$

The spin density at the titanium nucleus may be given in terms of

$$[17] \quad \chi = \frac{4\pi}{S}\sum_{ns}(|\Psi_{ns}(0)\uparrow|^2 - |\Psi_{ns}(0)\downarrow|^2) = -\frac{3}{2}\frac{KP}{g_e g_N \beta_e \beta_N}$$

Electrons in d orbitals cannot contribute directly to χ, but finite values of this parameter result from polarization of the inner filled s orbitals by the unpaired electrons.

The expressions for $g_\parallel$ and $g_\perp$ are deficient in that they do not contain terms for the charge-transfer (c.t.) states. These c.t. terms are of the same general form as those for the d–d states. For the present complex, one predicts that these will be of minor importance since it is clear from the optical spectrum that c.t. transitions if present occur at fairly high energy ($>50\,000\ \text{cm}^{-1}$.)

It is worth noting that in the derivation of the above expressions several other approximations have been made including omission of spin–orbit coupling of the ligand atoms and ligand–ligand overlap.

Hyperfine Interactions

Titanium

The titanium isotopes ^{47}Ti (7.32% abundance; $I = 5/2$) and ^{49}Ti (5.46%; $I = 7/2$) have equivalent gyromagnetic ratio [$\gamma(^{49}\text{Ti})/(\gamma^{47}\text{Ti}) = 1.00026 \pm 0.00002$] and give rise to a familiar pattern of two overlapping spectra of six and eight lines respectively, appearing as satellites of the main intense central line (^{46}Ti, ^{48}Ti, ^{50}Ti).

The measured value of the isotropic h.f.s. constant a_{Ti} is 17.9 ± 0.2 G (Table 1). Through eqs. 16 and 17 using $P = -25.7 \times 10^{-14}\ \text{cm}^{-1}$ we calculate as a result that $\chi = -2.3$ a.u., in agreement with other titanium complexes (2, 3, 5).

However, calculation of the χ value using unrestricted Hartree–Fock methods (15) reveals that polarization of both 2s and 3s are important, with negative contributions from the 3s orbital. In these calculations covalency has been found to be important.

Fluorine

The fluorine 2s orbitals have no interaction with the orbitals (e_g and b_{2g}) derived from the cubic $^2T_{2g}$ state since the overlap integrals are zero, for example $\langle 2s|e_g\rangle = 0$. However, charge-transfer from the 2s orbital to vacant metal orbitals derived from the E_g cubic states, 4s and 4p orbitals is possible. The latter orbitals can accept ligand electrons of either spin orientation but exchange with the $^2B_{2g}$ state will increase the transfer probability for electrons of the same spin as the titanium(III) $3d^1$ unpaired electron.

Can. J. Chem. Downloaded from www.nrcresearchpress.com by 210.87.254.6 on 09/05/12
For personal use only.

Hence negative spin density is achieved in the fluorine 2s orbital.

In the present study we obtained an isotropic h.f.s. constant a_F for $[Ti(H_2O)_4F_2]^+$ as 7.5 $\pm$ 0.5 G (Table 1).

Spin density in the fluorine 2s orbital is given by eq. 18

$$[18] \qquad \rho_s = \frac{a_F}{A_{2s}}$$

where

$$[19] \qquad A_{2s} = \frac{8}{3}\pi g_e \beta_e g_N \beta_N |\Psi(0)_{2s}|^2$$

is the hyperfine interaction of a single unpaired 2s electron in a fluoride ion. Taking the value for $A_{2s} = 1.57\ cm^{-1}$ (16) we obtain $\rho_{2s} = -0.0011$ comparable in magnitude to values obtained for other transition metal fluorides (17). Similar ρ_s values are obtained for the TiF_2^+ species in a range of alcoholic solvents (2, 18) where nearly the same isotropic a_F value is observed for two equivalent fluorine nuclei. We infer the same geometry in all the TiF_2^+ species. Moreover, the magnitude of the hyperfine splitting is consistent with the axial (*trans*) geometry assumed from the frozen solution spectrum; since equatorial (*cis*) fluorine splitting should be enhanced by greater covalent interaction with the ligand

Hydrogen (Water Ligands)

Resolution of the fluorine h.f.s. in D_2O strongly indicates the existence of proton hyperfine structure from water ligands in the H_2O solution, Fig. 1*a*. Approximate calculation based on the improved resolution indicates a h.f.s. a_H for four water ligands (8H) of *ca.* 0.2 to 0.4 G.

Since the proton interaction is observed for the complex it is evident that $\alpha_1' > 0$ and that in-plane π bonding exists. Such bonding permits some spin density at hydrogen through spin–polarization as suggested previously for *trans*-$[Ti(H_2O)_4((CH_3)_3COH)X]$ (5) and for *trans*-$[Ti(H_2O)_4(OH)_2]^+$ (19).

For the *t*-butyl alcohol complex, the estimation of Johnson *et al.* (5) gave a total spin density of $\sim$0.22 on four equatorial water molecules with $a_H = 1.8$ G in their case. On this basis in *trans*-$[Ti(H_2O)_4F_2]^+$, the total spin density on the water ligands is in the range 0.03–0.06. However, the use of the Q_{OH}^H factor in the former study (5) is open to question in view of the determination through ^{17}O labelling that $Cu(II)(H_2O)_6$ has $p = 0.22$ on oxygens while no evidence of hydrogen hyperfine splitting is seen (20).

Optical Spectrum and g-Values

The expressions 8 and 9 can be rewritten in the form

$$[20] \qquad g_{\parallel} = 2.0023 - \frac{8\lambda}{\Delta E(^2B_{2g} \rightarrow {}^2B_{1g})} \cdot K_{\parallel}$$

$$[21] \qquad g_{\perp} = 2.0023 - \frac{2\lambda}{\Delta E(^2B_{2g} \rightarrow {}^2E_g)} \cdot K_{\perp}$$

where

$$[22] \qquad K_{\parallel} = \alpha_1^2\alpha_2^2\left[1 - \frac{1}{2}\frac{\alpha_1'\alpha_2'}{\alpha_1\alpha_2}T(n) - \left(\frac{\alpha_2'}{\alpha_2}\right)S - \left(\frac{\alpha_1'}{\alpha_1}\right)\Pi_1\right]$$

$$[23] \qquad K_{\perp} = \alpha_1^2\varepsilon^2\left[1 - \frac{1}{2^{1/2}}\left(\frac{\varepsilon'\alpha_1'}{\varepsilon\alpha_1}\right) - \left(\frac{\alpha_1'}{\alpha_1}\right)\Pi_1 - \frac{1}{2^{1/2}}\left(\frac{\varepsilon'}{\varepsilon}\right)\Pi_1\right]$$

The values of $K_{\parallel}$ and $K_{\perp}$ have been regarded as the "orbital-reduction factors" (21) and these parameters are usually employed to estimate covalency. It is clear from expressions 8 and 9 that $0 \leqslant K_{\parallel}, K_{\perp} \leqslant 1$, and that both factors tend to one as the corresponding bonding tends to be ionic and vice versa.

Since only the limiting ionic value for λ(154 cm^{-1}) is available for titanium(III) covalency might better be expressed by eq. 24.

$$[24] \quad \text{Covalency factor} = \left[K\frac{\lambda(\text{covalent})}{\lambda(\text{ionic})}\right] = \frac{\Delta g \cdot \Delta E}{n\lambda(\text{ionic})}$$

where n = symmetry dependent integer, $n = 8$ for D_{4h}; $\Delta g = 2.0023 - g_{\parallel}$ ($g_{\perp}$); ΔE = energy of appropriate electronic transition.

Clearly if λ(covalent) is actually lower than λ(ionic) calculated values of the "covalency factor" will be lower than K itself.

Since the optical spectrum shows two electronic bands at $\sim$15 200 cm^{-1} (660 nm) and 23 300 cm^{-1} (430 nm) either one might correspond to the $^2B_{2g} \rightarrow {}^2B_{1g}$ transition, expression 20. We find that expression 24 gives a value of 0.45 for the low energy (15 200 cm^{-1}) possibility and 0.68 for the high energy transition. Taking into consideration the high charge density (low effective ionic radius) of the axial fluoride ligands, simple crystal field theory would pre-

dict a tetragonally *compressed* octahedron (22). Accordingly, the 15 200 cm^{-1} band is then assigned to $^2B_{2g} \rightarrow {}^2B_{1g}$ and the higher energy band to the $^2B_{2g} \rightarrow {}^2A_{1g}$ transition. Since the covalency parameter is only 0.45 we conclude that both in-plane π bonding and σ bonding are relatively covalent. It is improbable that *only* one or other is highly covalent. Observation of hydrogen hyperfine splitting from H_2O ligands is clearly consistent with significant in-plane π bonding. We should stress that the actual value of $K_{\|}$ will be somewhat higher (*ca.* 0.60) if a reduction in λ due to covalency of 30% is assumed.

By first postulating an ideal ionic case *e.g.* $\lambda = 154$ cm^{-1} and $K_{\perp} = 1$ we can calculate the upper limit of the energy of the $^2B_{2g} \rightarrow {}^2E_g$ transition as 4300 cm^{-1}, eq. 21. However we note that fluoride ion is characterized by its π donor properties (23), suggesting that the overall covalency factor could be conservatively estimated as 0.6–0.8. Then $\Delta E(^2B_{2g} \rightarrow {}^2E_g)$ falls to 2500–3200 cm^{-1}. On the other hand the relatively low energy of the $^2B_{2g} \rightarrow {}^2A_{1g}$ transition (23 300 cm^{-1}) is consistent with the expected low covalent σ bonding between the metal ion and the axial fluorines. The marked stability of the *trans*-$[Ti(H_2O)_4F_2]^+$ ion is also consistent with substantial metal–fluorine π bonding.

The authors thank the National Research Council of Canada and the University of Victoria for support through operating grants. One of us (P.P.) acknowledges support through a National Research Council of Canada Fellowship.

1. (*a*) V. I. Avvakumov, N. S. Garif'yanov, and E. I. Semenova. Sov. Phys. JETP, **12**, 847 (1961); (*b*) N. S. Garif'yanov and E. I. Semenova. Dokl. Akad. Nauk SSSR, **140**, 157 (1961); (*c*) E. I. Semenova. Dokl. Akad. Nauk SSSR, **143**, 1368 (1962).
2. E. L. Waters and A. H. Maki. Phys. Rev. **125**, 233 (1962).
3. (*a*) S. Fujiwara and M. Codell. Bull. Chem. Soc. Jap. **37**, 49 (1964); (*b*) S. Fujiwara, K. Nagashima, and M. Codell. Bull. Chem. Soc. Jap. **37**, 773 (1964); (*c*) T. Watanabe and S. Fujiwara. J. Magn. Reson. **2**, 103 (1970).
4. W. Giggenbach and C. H. Brubaker, Jr. Inorg. Chem. **8**, 1131 (1968).
5. R. Johnson, P. W. Murchison, and J. R. Bolton. J. Am. Chem. Soc. **92**, 6354 (1972).
6. I. B. Goldberg, D. H. Hern, and W. F. Goeppinger. J. Phys. Chem. **77**, 678 (1973).
7. (*a*) V. A. Glebov. Zh. Strukt. Khim. **11**, 809 (1970); (*b*) V. A. Glebov. Dokl. Akad. Nauk SSSR, **190**, 1378 (1970).
8. F. W. Cope. A method for the digital calculation of absolute free radical concentrations. N.A.D.C.-MR-6804, U.S. Naval Air Development Center, Johnsville, Penn. 1968.
9. R. J. H. Clark. The chemistry of titanium and vanadium. Elsevier Publishing Company, London. 1968. p. 153.
10. D. P. Graddon. An introduction to coordination chemistry. Pergamon Press, New York. 1961. p. 135.
11. R. N. O'Brien, W. J. Michalik, and E. Zacny-Zaklad. To be published.
12. (*a*) N. M. Atherton. Electron spin resonance, theory and applications. Halsted Press (John Wiley and Sons), New York, N.Y. 1973. p. 190; (*b*) F. K. Kneubühl. J. Chem. Phys. **33**, 1074 (1960).
13. B. R. McGarvey. J. Phys. Chem. **71**, 51 (1967).
14. A. J. Freeman and R. E. Watson. Magnetism, Vol. IIa. *Edited by* G. T. Rado and H. Suhl. Academic Press, Inc., New York, N.Y. 1965. p. 167.
15. (*a*) J. H. Wood and G. W. Pratt, Jr. Phys. Rev. **107**, 995 (1957); (*b*) V. Heine. Phys. Rev. **107**, 1002 (1957); (*c*) R. E. Watson and A. J. Freeman. Phys. Rev. **120**, 1134 (1969); (*d*) A. J. Freeman and R. E. Watson. Phys. Rev. **123**, 2027 (1961).
16. T. Moriya. Prog. Theor. Phys. Kyoto, **16**, 23 (1956).
17. T. P. P. Hall, W. Hayes, R. W. H. Stevenson, and J. Wilkens. J. Chem. Phys. **38**, 1977 (1963).
18. P. I. Premović and P. R. West. Unpublished results.
19. P. I. Premović and P. R. West. Can. J. Chem. **52**, 2919 (1974).
20. D. Getz and B. L. Silver. J. Chem. Phys. **61**, 630 (1974).
21. M. Gerloch and J. R. Miller. Prog. Inorg. Chem. **10**, 1 (1968).
22. H. L. Schläfer and G. Gliemann. Basic principles of ligand field theory. Wiley, New York, N.Y. 1969. p. 32.
23. J. E. Huheey. Inorganic chemistry. Harper and Row, New York, N.Y. 1972. p. 349.

Can. J. Chem. Downloaded from www.nrcresearchpress.com by 210.87.254.6 on 09/05/12
For personal use only.

The Hydrolysis of Cyclic Orthoesters. Stereoelectronic Control in the Cleavage of Hemiorthoester Tetrahedral Intermediates

PIERRE DESLONGCHAMPS,[1] ROBERT CHÊNEVERT, ROLAND J. TAILLEFER, CLAUDE MOREAU,[2] AND JOHN K. SAUNDERS

Laboratoire de synthèse organique, Département de chimie, Université de Sherbrooke, Sherbrooke, Québec J1K 2R1

Received November 1, 1974

PIERRE DESLONGCHAMPS, ROBERT CHÊNEVERT, ROLAND J. TAILLEFER, CLAUDE MOREAU, and JOHN K. SAUNDERS. Can. J. Chem. **53**, 1601 (1975).

The synthesis of several cyclic dialkoxy orthoesters is reported. Acid hydrolysis of these orthoesters under kinetically controlled conditions gives the corresponding hydroxy esters only. Conformationally rigid cyclic mixed orthoesters give a hydroxy ester by exclusive loss of the axial alkoxy group. A cyclic orthoester can have nine different *gauche* conformations. It is shown that they are hydrolyzed through only one *gauche* conformer. These results bring further experimental evidence that there is a stereoelectronic control in the cleavage of tetrahedral intermediates in the hydrolysis of esters.

PIERRE DESLONGCHAMPS, ROBERT CHÊNEVERT, ROLAND J. TAILLEFER, CLAUDE MOREAU et JOHN K. SAUNDERS. Can. J. Chem. **53**, 1601 (1975).

La synthèse de plusieurs dialkoxy orthoesters cycliques est rapportée. L'hydrolyse en milieu acide de ces orthoesters conduit aux hydroxy esters par contrôle cinétique. De plus, les orthoesters mixtes ayant une conformation rigide s'hydrolysent en éjectant le groupe alkoxy axial. Théoriquement, un orthoester cyclique peut prendre neuf conformations *gauches* différentes, cependant il est démontré qu'il préfère s'hydrolyser par un seul conformère. L'ensemble de ces résultats confirme qu'il y a un contrôle stéréoélectronique lors de la fragmentation d'un intermédiaire tétrahédrique durant l'hydrolyse des esters.

We have recently described a new stereoelectronic theory for the cleavage of the tetrahedral intermediate in the hydrolysis of esters (1) and amides (2). In this new theory (3), the precise conformation of the intermediate hemiorthoester or hemiorthoamide is very important. We have proposed that there is a direct relationship between the conformation of the tetrahedral intermediate and the nature of the products formed as a result of its breakdown. We have further postulated that the stereoselective decomposition of this intermediate is determined by the orientation of the lone pair orbitals on the heteroatoms; specific cleavage of a carbon–oxygen or a carbon–nitrogen bond being allowed only if the other two heteroatoms (oxygen or nitrogen) of the tetrahedral intermediate each have an orbital oriented antiperiplanar to the leaving *O*-alkyl or *N*-alkyl group.

This new theory originated from our study on the oxidation of acetals with ozone to give esters (4). We assumed that this reaction proceeds via the formation of a hemiorthoester tetrahedral intermediate or its equivalent. Product formation from this reaction was then explained by selective decomposition of this postulated intermediate according to the new stereoelectronic theory.

However, we could not use the results obtained from the oxidation of acetals to verify the new theory because it is experimentally difficult to demonstrate that a hemiorthoester intermediate is formed in the course of this reaction. Consequently, it became important to obtain direct independent experimental evidence for the selective cleavage of hemiorthoesters. These results were necessary to confirm the new stereoelectronic theory.[3]

Acid-catalyzed hydrolysis of orthoester doubtless proceeds through the formation of such a hemiorthoester intermediate as described in the following equation (6). Therefore, the preparation of several cyclic orthoesters was undertaken.

[1]To whom all correspondence should be addressed.

[2]Holder of a bourse postdoctorale France–Québec, 1973–1974.

[3]For recent experimental and theoretical studies related to this subject, see ref. 5.

Can. J. Chem. Downloaded from www.nrcresearchpress.com by 210.87.254.40 on 09/05/12
For personal use only.

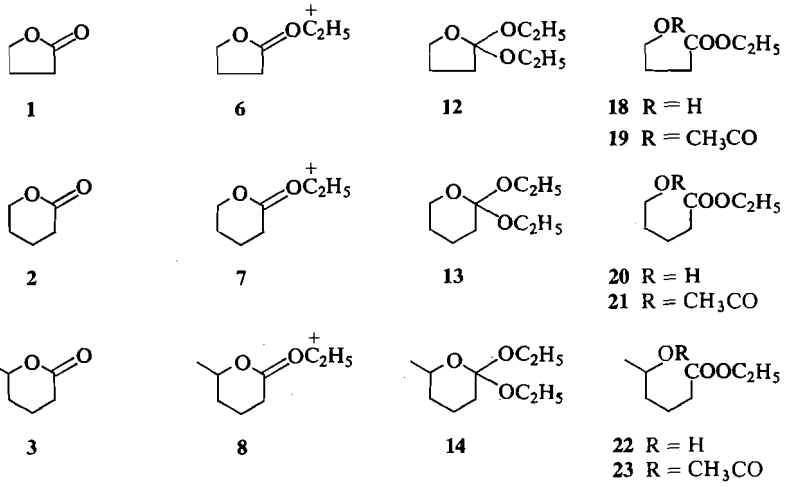

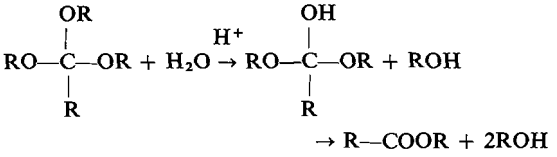

It was hoped that a study of the mild acidic hydrolysis of such orthoesters would give the experimental evidence needed to prove that the selective cleavage of hemiorthoesters does indeed take place. We wish to report in detail the result of this investigation.

Meerwein and his co-workers have described the reaction of triethyloxonium tetrafluoroborate with lactones (7); they have also reported that the resulting ethyl lactonium salts react with sodium ethoxide to yield the corresponding diethoxy cyclic orthoester. For example, γ-butyrolactone (**1**) gave the ethyl-γ-butyrolactonium salt **6** which was then converted into 1,1-diethoxytetrahydrofuran (**12**). We have utilized this two-step sequence for the preparation of the cyclic orthoesters **12–17**.[4]

The hydrolysis was carried out by stirring the orthoester in distilled water, at 0°, with a small amount of *p*-toluenesulfonic acid. The analysis of the product of the reaction was carried out after 20 min and then after 12 h. The corresponding hydroxyester or lactone are the two possible products of the reaction. For instance, the orthoester **12** can give the hydroxy ester **18** or the lactone **1**. The crude reaction mixture was treated directly with a large excess of pyridine and acetic anhydride. In this manner, the hydroxy ester was converted into the corresponding acetoxy ester (for example, **18** into **19**). The relative amount of acetoxy ester and lactone were measured by vapor phase chromatography and the results are described in Table 1.

We have verified that the hydrolysis of orthoester is a very fast reaction; when 1 drop of aqueous acid is added to a chloroform solution of an orthoester in a n.m.r. tube, proton nuclear magnetic resonance shows the instantaneous disappearance of starting material. For our study, we have allowed a period of 20 min for the hydrolysis; the reaction is highly selective, more than 94% of the acetoxy ester is produced. If the period allowed for the hydrolysis is much longer (12 h), the formation of a larger quantity of lactone is observed. This result shows that the hydroxy ester can give the lactone under the conditions of the hydrolysis but this is a relatively slow process. This means that the small percentage of lactone which appears to be present after 20 min, does not come from the lactonization of the hydroxy ester during the hydrolysis. The presence of minor amounts of lactone in these reactions can therefore be explained in two ways: (*a*) the hydrolysis of orthoesters is simply not specific; (*b*) the reaction is totally specific yielding only the hydroxy ester but this product would then be converted to a small extent into the corresponding lactone during the acetylation process. The second explanation was preferred because the acetylation of a secondary alcohol is not instant-

[4]We are grateful to Miss Madeleine Bélisle for her technical help in the preparation of these compounds.

Can. J. Chem. Downloaded from www.nrcresearchpress.com by 210.87.254.40 on 09/05/12
For personal use only.

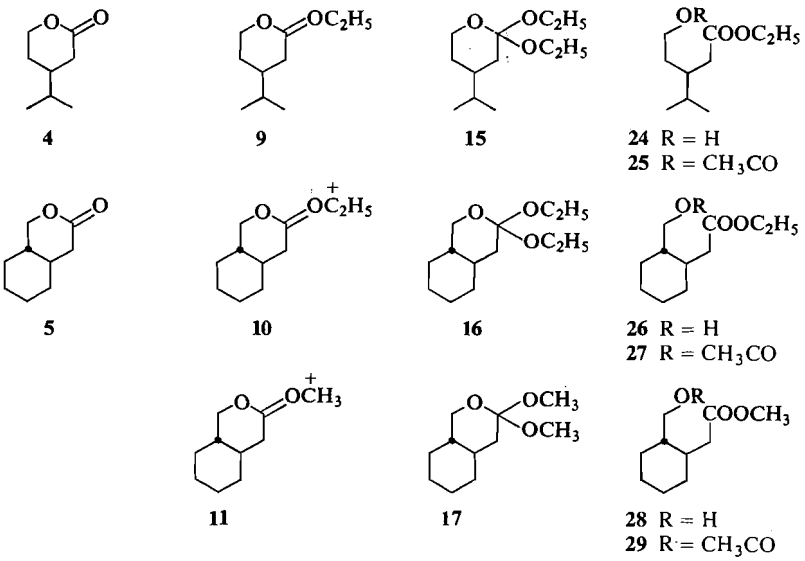

TABLE 1. Hydrolysis of orthoesters*

Orthoester	Time	Acetoxy ester (%)	Lactone (%)
12	20 min	95	5
	12 h	53	47
13	20 min	96	4
	12 h	72	28
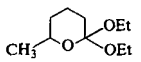 14	20 min	97	3
	12 h	54	46
15	20 min	94	6
	12 h	64	36
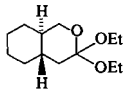 16	20 min	96	4
	12 h	trace <1	>99

*The hydrolysis product was treated with pyridine and acetic anhydride and the relative proportion of acetoxy ester and lactone was analysed by vapor phase chromatography.

Can. J. Chem. Downloaded from www.nrcresearchpress.com by 210.87.254.40 on 09/05/12
For personal use only.

Can. J. Chem. Downloaded from www.nrcresearchpress.com by 210.87.254.40 on 09/05/12
For personal use only.

TABLE 2. Carbon-13 n.m.r. spectral data for the orthoesters, lactones, and hydroxy esters

	1	2	3	4	5	6	7	8	9	10	11	12	13
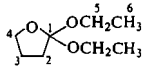 **12**	118.4	30.9	28.1	63.6	57.0	15.2							
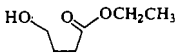 **18**	174.5	31.1	27.9	61.8	60.6	14.2							
1	178.1	27.8	22.3	68.8									
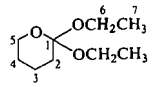 **13**	111.8	31.6	20.8	25.1	64.1	56.3	15.3						
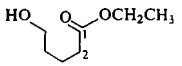 **20**	174.2	34.1	21.5	32.0	61.7	60.4	14.2						
2	171.2	29.8	19.1	22.7	69.4								
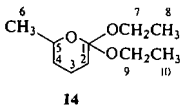 **14**	112.3	30.9	20.7	32.3	69.6	21.6	57.1	15.4	55.2	15.4			
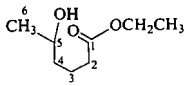 **22**	173.9	34.2	21.2	38.7	67.4	23.2	60.4	14.3					

Can. J. Chem. Downloaded from www.nrcresearchpress.com by 210.87.254.40 on 09/05/12
For personal use only.

TABLE 2. (*Concluded*)

	1	2	3	4	5	6	7	8	9	10	11	12	13
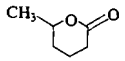 **3**	171.3	29.3	19.5	28.8	74.4								
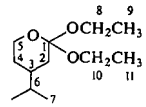 **15**	112.0	35.2	38.5	28.5	63.6	32.4	19.5	57.0	15.4	55.5	15.4		
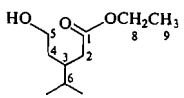 **24**	174.5	37.7	36.3	34.5	60.8	30.8	19.2	60.5	14.2				
4	171.4	34.0	37.8	26.4	68.4	32.4	19.2						
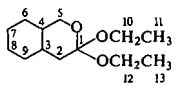 **16**	112.4	38.4	37.4	41.2	68.7	32.8	26.0	26.0	27.4	57.2	15.3	55.2	15.3
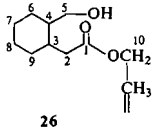 **26**	174.2	32.9	39.6	44.9	65.2	29.7	26.0	26.0	27.2	60.3	14.2		
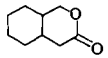 **5**	171.4	37.4	36.5	38.2	74.7	32.5	25.3	25.3	27.2				

Can. J. Chem. Downloaded from www.nrcresearchpress.com by 210.87.254.40 on 09/05/12
For personal use only.

aneous under the conditions used and pyridine could easily catalyze the lactonization reaction.

We have, therefore, looked for a more direct method of analysis. There was a good possibility that carbon-13 n.m.r. spectroscopy could be utilized to analyze mixtures of hydroxy ester and lactone. This was found to be the case since each hydroxy ester gave a different carbon-13 spectrum than the corresponding lactone as can be seen in Table 2.[5] The hydrolysis of the orthoesters was repeated. The reaction was carried out in a n.m.r. tube by addition of aqueous acid to a chloroform solution of the orthoester. The reaction mixture was analyzed by carbon-13 n.m.r. After 10 min, the hydrolysis of the orthoesters was complete. The hydroxy ester was formed exclusively; no lactone product was detected at this time (1% of lactone would have been observed). After shaking for 30 min, lactone formation was observed.

The hydrolysis of orthoesters goes through the formation of a hemiorthoester intermediate. Consequently, the preceding results constitute rigorous experimental evidence that hemiorthoesters do indeed break down in a specific manner and these results can be used to support the stereoelectronic theory.

The exclusive formation of hydroxy ester from the mild acid hydrolysis of orthoesters can be explained in the following manner. The simple six-membered cyclic orthoester **13** can be taken as a good example because it is preferable to discuss precise conformation in a six rather than in a five-membered ring. Also, we can assume that no conformational change takes place during the hydrolysis, since the experimental results are the same for both rigid and conformationally labile cyclic orthoesters.

There are nine *gauche* conformers which are theoretically possible for the cyclic orthoester **13**. They are described in Scheme 1. The next task is to define which conformers of **13** should be taken into consideration. It is logical to assume that the hydrolysis of **13** will proceed through the most energetically favored conformers which have at the same time, proper orbital orientation to permit the cleavage of a carbon–oxygen bond. A detailed examination of each conformer shows that six of them (**B**, **C**, **D**, **G**, **H**, and **I**) are readily eliminated. There is a severe 1,3-synperiplanar interaction[6] between the two ethyl groups in conformers **B** and **D**; thus the population of these conformers

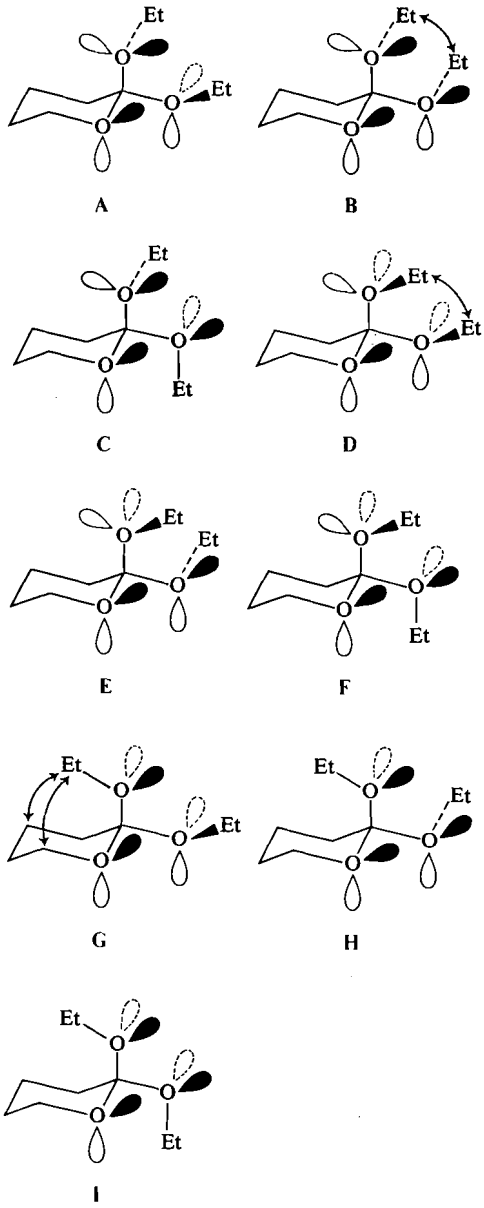

SCHEME I

[5]Proton nuclear magnetic resonance spectroscopy could not be used because of signal overlap. Also, vapor phase chromatography or any other type of chromatography could not be utilized because the hydroxy ester can be easily converted into the corresponding lactone either by heat, or by acid or base catalysis.

[6]A 1,3-synperiplanar interaction is equivalent to a 1,3-diaxial interaction in a six-membered ring.

Can. J. Chem. Downloaded from www.nrcresearchpress.com by 210.87.254.40 on 09/05/12
For personal use only.

at equilibrium will be very small. Conformers **G**, **H**, and **I** can also be ruled out by utilizing a similar argument; the ethyl group of the axial ethoxy group in each conformer is in a 1,3-synperiplanar arrangement with two methylenes (C_3 and C_5) of the ring; thus there are two severe 1,3-synperiplanar steric interactions in **G**, **H**, and **I**. The population of these conformers will also be very small at equilibrium and they can therefore be neglected.

The remaining four conformers **A**, **C**, **E**, and **F** do not have strong steric interactions. The magnitude of the anomeric effect (8), which occurs whenever two lone pair orbitals are in a 1,3-synperiplanar arrangement is approximately the same in each conformer. Two of such orbital arrangements are present in conformers **A**, **E**, and **F**. Conformer **C** has three. Thus, these four must represent the real conformers of **13**.

Conformer **C** must be eliminated as a reactive conformer simply because it does not have proper orbital orientation on two oxygen atoms to permit the cleavage of the C—O bond of the third oxygen atom. We have prepared the tricyclic orthoester **30**[7] (9) which is a perfect rigid model for conformer **C**. When compound **30**

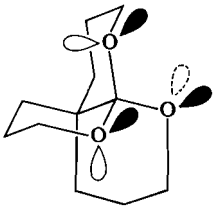

30

was submitted to the mild acidic conditions used for the hydrolysis of the preceding orthoesters, it was found to be completely stable after 24 h at room temperature. Consequently, we have obtained strong experimental support that conformer **C** is nonreactive. Indeed, it is a remarkably stable conformer and can therefore be eliminated.

The remaining conformers **A**, **E**, and **F** have each two oxygens with proper orbital orientation to cleave the C—O bond of the third oxygen atom. They will therefore be considered separately.

The cleavage of conformer **A** (Scheme 2) can

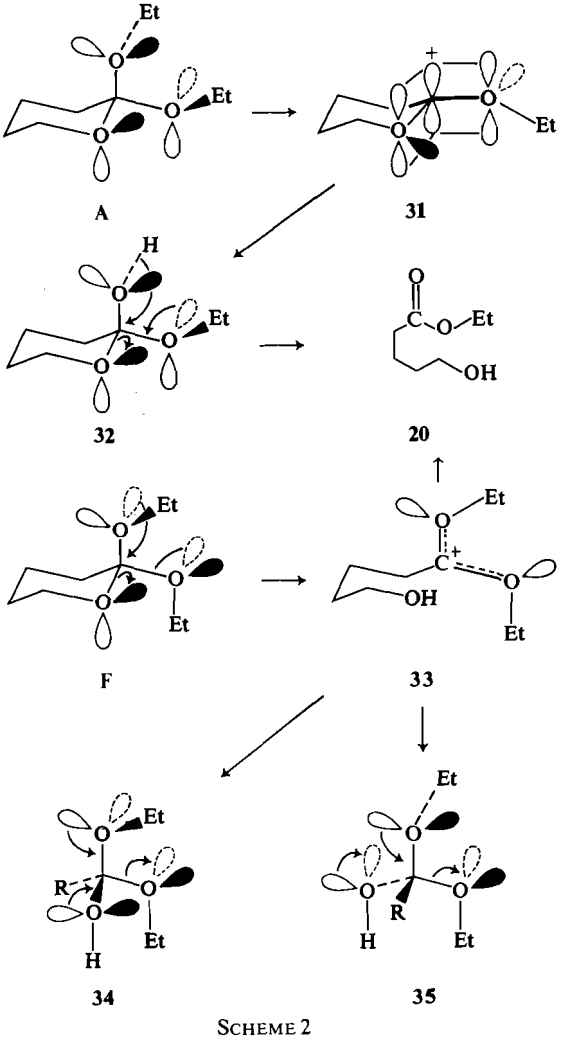

SCHEME 2

only give the dioxolenium ion **31** because of the orbital orientation (1). This ion **31** will then be attacked by water on the β face to form specifically the hemiorthoester **32** in which the ring oxygen and the OEt oxygen each have an orbital antiperiplanar to the C—OH bond which has just been formed. Attack by water on the α face of ion **31** would result in a hemiorthoester with a ring in a boat form. The hemiorthoester **32** can break down in the direction of the hydroxy ester **20** only; the OH and the OEt groups each have an orbital oriented antiperiplanar to the ring oxygen–C_2 bond. The conversion of **32** into δ-valerolactone (**2**) is a higher energy process because the ring oxygen atom does not have proper orbital orientation to assist the cleavage of the C—OEt bond.

[7]We are grateful to Messrs. Normand Beaulieu and Yvon Couture for their technical help in the preparation of this compound.

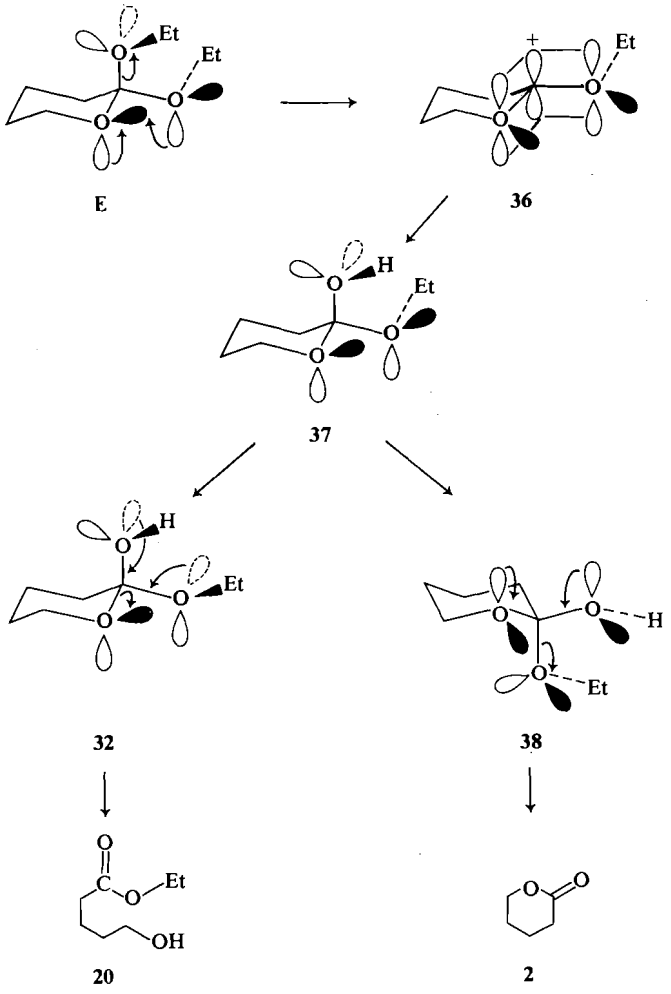

SCHEME 3

Conformer **F** (Scheme 2) should also yield the hydroxy ester **20** exclusively, since orbital orientation permits only the cleavage of the ring oxygen–carbon bond, yielding the dioxolenium ion **33**. Hydration of this ion **33** can be done in two ways giving the hemiorthoesters **34** and **35**. Nevertheless each hemiorthoester **34** and **35** can then break down to give only the hydroxy ester **20**.

Conformer **E** (Scheme 3) has proper orbital orientation to permit the cleavage of the axial ethoxy group; the ion **36** will thus be formed and hydration will then give the hemiorthoester **37**. The hemiorthoester **37** does not have proper orbital orientation to permit the cleavage of a carbon–oxygen bond. To break down, **37** will have to rotate one of its C—O bonds to obtain a reactive conformer.[8] For example, a rotation of the C—OEt bond will give **32** which will break down to give the hydroxy ester **20**. A chair inversion of **37** to **38** is also possible in a conformationally labile system; this new intermediate **38** should give δ-valerolactone (**2**). Thus, lactone formation could have been observed to some extent via conformer **E** if the orthoester is a conformationally labile system.

The preceding discussion on the manner by which conformers **A**, **E**, and **F** should break

[8]We have previously postulated (3) that a tetrahedral intermediate which does not have proper orbital orientation to break down, will prefer to undergo rotational changes to give new tetrahedral intermediates which may have orbitals properly aligned to undergo C—O bond cleavage.

Can. J. Chem. Downloaded from www.nrcresearchpress.com by 210.87.254.40 on 09/05/12
For personal use only.

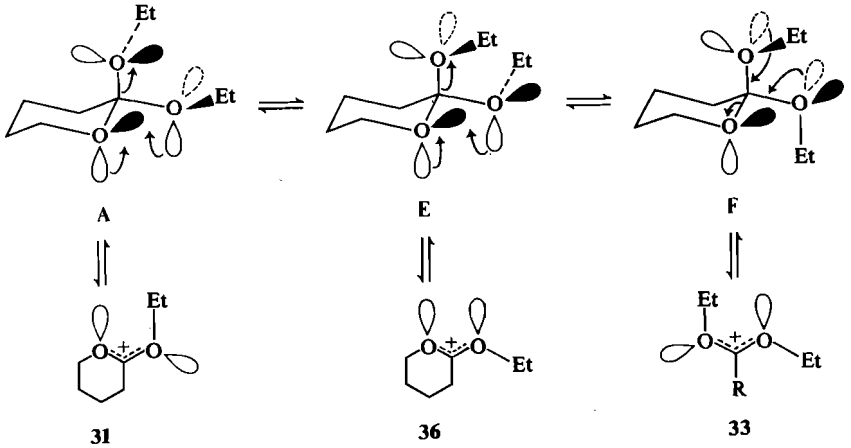

SCHEME 4

down indicates that each of them is, in principle, a reactive conformer. If the relative stability of the dioxolenium ions is taken into consideration, we believe conformer **E** can be eliminated. Conformers **A**, **E**, and **F** are going to form the dioxolenium ions **31**, **36**, and **33**, respectively (Scheme 4). The ions **31** and **33** are *trans* and the ion **36** is *cis*. It is known that *trans*-dioxolenium ions are more stable than *cis*-dioxolenium ions (10), just as *trans*-esters are more stable than *cis*-esters (11). If this difference in stability between **31**, **33**, and **36** is also operative in the transition states which are going to form these dioxolenium ions, the cleavage of conformer **E** should be a higher energy process. Conformer **E** could thus be eliminated on this basis.

It is more difficult to find arguments to differentiate between conformer **A** and conformer **F**; however, the formation of the ion **31** from **A** should be an easier operation than formation of **33** from **F**. In principle, the formation of a cyclic dioxolenium ion (**31**) should be favored over an acyclic dioxolenium ion (**33**) when the starting orthoester is cyclic. Furthermore, cleavage of conformer **A** gives two molecules, the cyclic ion **31** and ethanol whereas conformer **F** gives only one molecule, the ion **33**. This entropy factor should favor conformer **A** over conformer **F** as the reactive species. Similarly, a kinetic argument can be used to favor conformer **A**. The k value for the reformation of **F** from the cyclization of **33** must be much greater than the corresponding k value for the reformation of **A** by reaction of **31** with ethanol which is diluted in the solvent. Conformer **A** is in rapid equilibrium with conformer **F** (also with conformers **C** and **E**) by bond rotation. If the barrier to give **31** from **A** is lower by more than 2.5 kcal/mol than the barrier to give **33** from **F** (or the barrier to give **36** from **E**), the orthoester **13** will prefer to be hydrolyzed via conformer **A** only.

It is possible, in principle, to devise a simple experiment to find out if conformer **F** is reactive when compared to conformer **A**. If the stereoelectronic theory is applied, it is interesting to note that conformer **A** will give the hydroxy ester **20** by the loss of its axial ethoxy group. Conformer **F** is predicted to form **20** by ejecting its equatorial ethoxy group. Scheme 2 describes these operations; with regard to **F**, both intermediates **34** and **35** will hydrolyze by ejecting the same ethoxy group, which is the equatorial one in conformer **F**. Thus, if the preparation of rigid cyclic orthoesters having two different alkoxy groups can be realized, it should be easy to differentiate between these two pathways.

We have already developed a method for the synthesis of such conformationally rigid cyclic orthoesters. For instance, lactone **5** was converted into the salt **10** which gave the cyclic orthoester **16**. This successful synthesis of a rigid cyclic orthoester by sequential introduction of the alkoxy groups is ideal for the synthesis of mixed orthoesters, if the last step is stereospecific. If the stereoelectronic theory is valid, the addition of alkoxide ion to a rigid lactonium salt, such as that of **10**, should indeed be completely stereospecific.

When the salt **10** was treated with sodium methoxide in a mixture of methanol and isopropyl alcohol, the mixed orthoester **39** was obtained with a small quantity ($\simeq 3\%$) of the

Can. J. Chem. Downloaded from www.nrcresearchpress.com by 210.87.254.40 on 09/05/12
For personal use only.

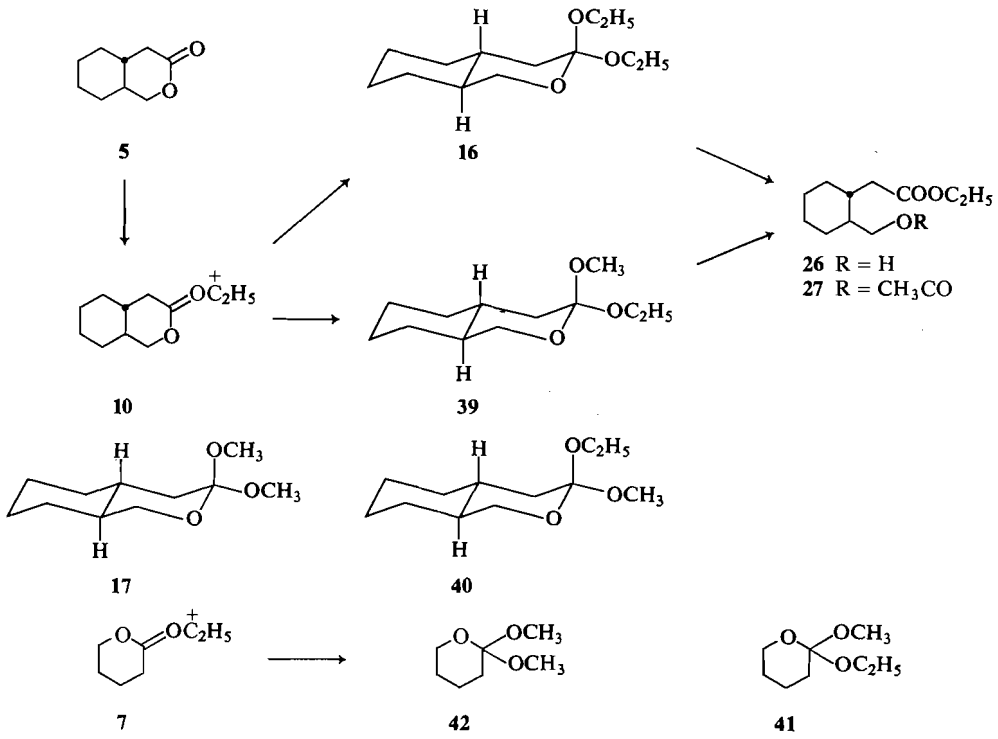

SCHEME 5

dimethoxy orthoester **17** (Scheme 5). None of the other possible mixed orthoester **40** was present. The addition of sodium methoxide to **10** is thus completely stereospecific. The stereoelectronic rule permits the formation of **40** from **10** but the attack of methoxide ion at the α face of the salt **10** would give **40** in a high energy conformation; the orthoester ring of **40** would be in a boat form. The α attack is therefore much less favored than the β attack which yields **39** directly in its more stable conformation. The small quantity of **17** must be formed by a secondary process. When the salt **10** was reacted with sodium methoxide in pure methanol, this secondary process became more important, since **17** was formed in 60% and **39** in 40% yield.[9]

[9]Under certain conditions, this unexpected reaction can become the major process! When the simple ethyl lactonium salt **7** was treated with sodium methoxide in methanol, none of the mixed orthoester **41** was isolated; the dimethoxy orthoester **42** was the only orthoester isolated. We have also shown that the diethoxy orthoester **13** is completely stable in presence of sodium methoxide in methanol. We think that this reaction occurs via the intermediate ketene acetal which can be formed by reaction of sodium methoxide with the lactonium salt. We are presently studying this new reaction.

The methyl lactonium salt **11** was prepared by reaction of lactone **5** with trimethyloxonium tetrafluoroborate (Scheme 6). An authentic sample of the dimethoxy ester **17** was prepared by reacting **11** with sodium methoxide in methanol. The methyl lactonium salt **11** was also reacted with sodium ethoxide in ethanol and a mixture of the mixed orthoester **40** (95%) and the diethoxy orthoester **16** (5%) was isolated. The lactonium salt **11** was also reacted with deuterated sodium methoxide and the mixed cyclic orthoester **43** was obtained with a small amount (10%) of the completely deuterated orthoester **44**; none of the isomeric orthoester **45** was formed.

The diethoxy orthoester **16** shows two distinct quadruplets for the methylenes of the two ethoxy groups in its n.m.r. spectrum. We have assigned the high-field quadruplet (3.55 δ) for the methylene of the axial ethoxy group and the low-field quadruplet (3.60 δ) for the methylene of the equatorial ethoxy group. Similarly, the cyclic dimethoxy orthoester **17** shows two different singlets at 3.18 and 3.28 δ which are, respectively, attributed to the axial and equatorial methoxy groups. This assignment is based on the chemical shift of α- and β-methyl glycopyranosides. It is

Can. J. Chem. Downloaded from www.nrcresearchpress.com by 210.87.254.40 on 09/05/12
For personal use only.

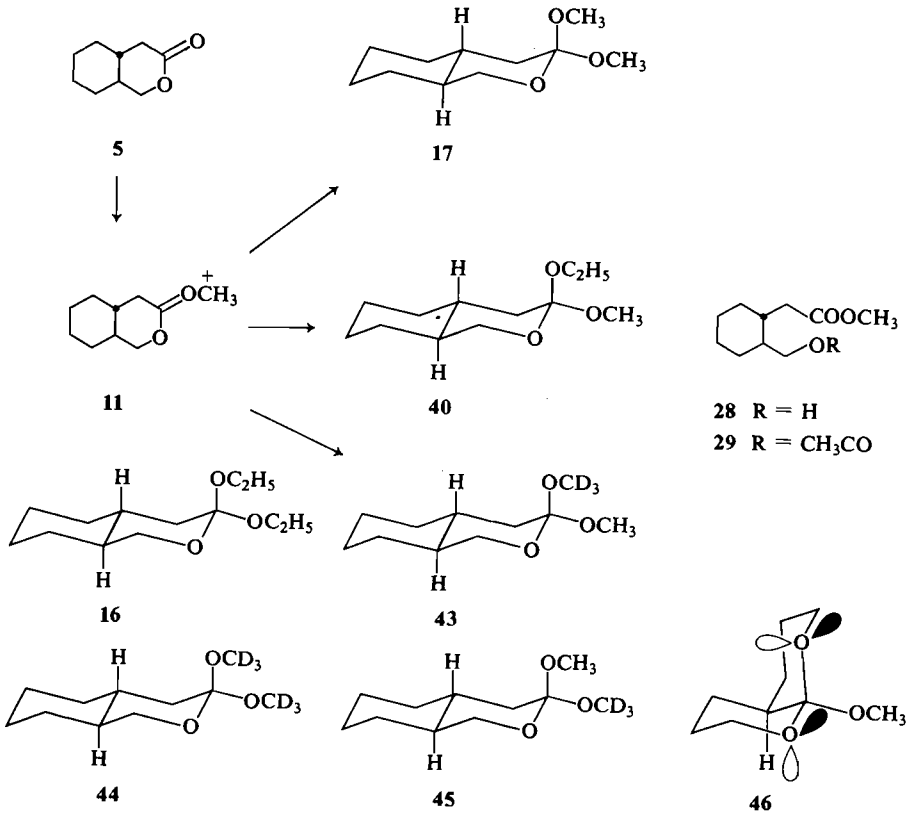

SCHEME 6

known that the axial methoxy group of α-glycoside always appears at a higher field than the equatorial methoxy group of β-glycoside (12). We have also prepared the bicyclic orthoester **46** (9) which is a good model for an orthoester having an equatorial methoxy group. The chemical shift of the methoxy group of **46** appears at 3.33 δ.

The stereochemistry of the mixed cyclic orthoesters **39**, **40**, and **43** was established by p.m.r. spectroscopy with the aid of compounds **16**, **17**, and **46** as models. The n.m.r. spectrum of the mixed orthoester **39** showed a singlet at 3.22 δ for the axial methoxy group and a quadruplet at 3.61 δ for the equatorial ethoxy group. The absence of a quadruplet at $\simeq$3.55 δ proves that **40** was not present with **39**. The mixed orthoester **40** displayed a quadruplet at 3.56 δ for the axial ethoxy group and a singlet at 3.32 δ for the equatorial methoxy group. Again, the reaction mixture of **40** did not show a singlet at $\simeq$3.22 δ which would have indicated the presence of the other mixed orthoester **39**. The mixed cyclic orthoester **43** showed a singlet at 3.32 δ for the equatorial methoxy group. No signal was observed at $\simeq$3.20 δ indicating that the other possible isomer **45**, was not formed with **43**. The relative proportions of **39**/**17**, **40**/**16**, and **43**/**44** were easily established by measuring the relative intensity of their respective molecular ions by mass spectrometry.

The orthoesters **39**, **40**, and **43** were hydrolyzed with water containing *p*-toluenesulfonic acid. The reaction mixture was then treated with pyridine and acetic anhydride and the resulting acetoxy esters were isolated. Compound **39** (containing $\simeq$3% of **17**) gave the acetoxy ethyl ester **27** containing a small quantity of **29** ($\simeq$3%). Compound **40** (containing $\simeq$5% of **16**) gave the acetoxy methyl ester **29** containing a small quantity of **27** ($\simeq$5%). The relative proportions of **27** and **29** were determined by vapor phase chromatography analysis. Finally, the hydrolysis of **43** (containing 10% of **44**) gave the acetoxy methyl ester **29**. Mass spectral analysis of **29** indicated the formation of a small amount (10%) of the deuterated acetoxy methyl ester (**29**, $CH_3 = CD_3$).

Can. J. Chem. Downloaded from www.nrcresearchpress.com by 210.87.254.40 on 09/05/12
For personal use only.

Can. J. Chem. Downloaded from www.nrcresearchpress.com by 210.87.254.40 on 09/05/12
For personal use only.

The above results show that the hydrolysis of cyclic orthoesters proceed by the loss of the axial methoxy group. Conformer **F** can be eliminated as a reactive conformer; consequently, the hydrolysis of cyclic dialkoxy orthoester takes place through the reaction of conformer **A**.

We would like to point out that the successful stereospecific synthesis of mixed cyclic orthoesters constitutes rigorous evidence for the direction of attack of the alkoxide on the cyclic dioxolenium ions. Also, the stereospecificity observed in the hydrolysis of these mixed cyclic orthoesters demonstrates that this reaction proceeds according to the same principle in the opposite direction.

The synthesis of more complex cyclic orthoesters is now in progress. The study of the hydrolysis of these substances should bring further results to support the new stereoelectronic theory.[10]

Experimental

The i.r. spectra were taken on a Perkin-Elmer 257 spectrophotometer; proton n.m.r. spectra (δ-value) were recorded on a Varian A-60 spectrometer in solvent indicated. Carbon-13 n.m.r. spectra were taken on a Bruker HX-90 spectrometer equipped with a Nicolet 1083 computer. All chemical shifts are recorded relative to internal TMS as standard. The vapor phase chromatographic analyses were done on a Varian 600-D chromatograph. Mass spectra were run in a Hitachi-Perkin Elmer RMU-6 spectrometer. Microanalyses were performed by Dr. C. Daesslé, Organic Microanalyses, Montreal.

Lactones 1, 2, 3, and 5

γ-Butyrolactone (**1**) and δ-valerolactone (**2**) are commercial products. They were distilled before use. Lactones **3** and **5** were obtained by Baeyer–Villiger oxidation (13) of commercial 5-methylcyclopentanone and *trans*-hydrindanone (14).

Lactone 4

2-Methyl-5-isopropylcyclohexen-2-one was treated by ozone in ethyl acetate at −78°; ozonides were destroyed by hydrogenation (platinum oxide) in the same solvent at 0°. The crude 3-isopropyl-4-formylbutanoic acid was reduced by sodium borohydride in basic aqueous medium at 0°. After acidification and extraction with ether, the crude lactone was treated with *p*-toluenesulfonic acid in refluxing benzene for 3 h. Distillation gave pure lactone **4**: b.p. 93–94°/0.8 mm, 84%; i.r.: ν_{max} (film) 1735, 1250, 1210, 1070 cm^{-1}; n.m.r.: δ($CDCl_3$) 0.93 (6H, doublet, J = 5.5 Hz, methyls), 1.2–2.2 (4H, multiplet, —*CH*$_2$—*CH*—*CH*(CH_3)$_2$), 2.2–3.0 (2H, multiplet, —CH_2—COO—), 4.0–4.7 (2H, multiplet, —COO—CH_2—).

Anal. Calcd. for $C_8H_{14}O_2$: C, 67.57; H, 9.92. Found: C, 67.37; H, 9.87.

O-Alkyl Lactonium Tetrafluoroborates (6–11)

General Method of Preparation

Lactone (10 mmol) and trialkyloxonium tetrafluoroborate (15) or trialkyloxonium antimony hexachloride ((16), 10 mmol) were dissolved in anhydrous dichloromethane (35 ml). The solution was magnetically stirred at room temperature during 3 h. Dry diethyl ether was added until turbid. The mixture was kept at 0° overnight. The crystals (white needles) were filtered and washed with ether–dichloromethane 5:1. The salts are extremely hygroscopic and any manipulation has to be done under controlled atmosphere.

Lactonium salt 6 (BF_4^-): m.p. 41–42° (*O*-tolunitrile) (lit. (7) m.p. 42° (same solvent)); i.r.: ν_{max} (CH_2Cl_2) 1550, 1000–1200 cm^{-1}; n.m.r.: δ(CD_2Cl_2) 1.53 (3H, triplet, J = 7.0 Hz, —CH_2—*CH*$_3$), 2.63 (2H, multiplet, methylene at C-4), 3.40 (2H, triplet, J = 7.5 Hz, methylene at C-3), 4.97 (2H, quartet, J = 7.0 Hz, —*CH*$_2$—CH_3), 5.33 (2H, triplet, J = 7.5 Hz, methylene at C-5).

Lactonium salt 7 (BF_4^-): m.p. 96–98° dec. (ether–CH_2Cl_2); i.r.: ν_{max} (CH_2Cl_2) 1550, 1000–1200 cm^{-1}; n.m.r.: δ(CD_2Cl_2) 1.48 (3H, triplet, J = 7.5 Hz, —CH_2—*CH*$_3$), 2.18 (4H, multiplet, methylenes at C-4 and C-5), 3.02 (2H, multiplet, methylene at C-3), 4.82 (2H, quartet, J = 7.5 Hz, —*CH*$_2$—CH_3), 5.16 (2H, multiplet, methylene at C-6).

Lactonium salt 8 ($SbCl_6^-$): m.p. 127–128° dec. (ether–CH_2Cl_2); i.r.: ν_{max} (CH_2Cl_2) 1500, 1000–1200 cm^{-1}; n.m.r.: δ(CD_2Cl_2), 1.43 (3H, doublet, J = 7.0 Hz, —CH—*CH*$_3$), 1.62 (3H, triplet, J = 7.5 Hz, —CH_2—*CH*$_3$), 2.10 (4H, multiplet, methylenes on C-4 and C-5), 3.03 (2H, multiplet, methylene on C-3), 4.80 (2H, quartet, —*CH*$_2$—CH_3), 5.42 (1H, multiplet, —O—*CH*—CH_3).

Lactonium salt 9 ($SbCl_6^-$): m.p. 131–132° dec. (ether–CH_2Cl_2); i.r.: ν_{max} (CH_2Cl_2) 1550, 1000–1200 cm^{-1}; n.m.r.: δ(CD_2Cl_2) 0.94 (6H, doublet, J = 5.5 Hz, —CH(CH_3)$_2$), 1.47 (3H, triplet, J = 7.0 Hz, —O—CH_2—*CH*$_3$), 2.03 (4H, multiplet, methylene on C-4, C-5 and —*CH*(CH_3)$_2$), 2.92 (2H, multiplet, methylene at C-3), 4.80 (2H, quartet, J = 7.0 Hz, —O—*CH*$_2$—CH_3), 5.17 (2H, multiplet, methylene on C-6).

Lactonium salt 10 ($SbCl_6^-$): m.p. 124–125° dec. (ether–CH_2Cl_2); i.r.: ν_{max} (CH_2Cl_2) 1550, 1000–1200 cm^{-1}; n.m.r.: δ(CD_2Cl_2) 1.50 (3H, triplet, J = 7.0 Hz, —O—CH_2—*CH*$_3$), 1.0–2.0 (10H, multiplet, ring hydrogens), 2.50–3.12 (2H, multiplet, methylene at C-3), 4.72–5.12 (2H, multiplet, methylene at C-6), 4.84 (2H, quartet, J = 7.0 Hz, —O—*CH*$_2$—CH_3).

Lactonium salt 11 ($SbCl_6^-$): m.p. 148–149° dec. (CH_2Cl_2–hexane); i.r.: ν_{max} (CH_2Cl_2) 1550, 850–1100 cm^{-1}; n.m.r.: δ(CD_2Cl_2) 1.0–2.3 (10H, multiplet, ring hydrogens), 2.9–3.4 (2H, multiplet, methylene at C-3), 4.56 (3H, singlet, —O—CH_3), 4.7–5.2 (2H, multiplet, methylene at C-6).

[10]One referee commented on the possibility that only one antiperiplanar lone pair might be sufficient to allow a specific cleavage. It is certainly possible to have a cleavage with the aid of only one lone pair. For instance, compound **30** can be hydrolyzed under more vigorous acidic conditions. However, we think that a specific cleavage with two lone pairs is a much easier process. Whenever it can occur, cleavage with the aid of one lone pair cannot compete.

Can. J. Chem. Downloaded from www.nrcresearchpress.com by 210.87.254.40 on 09/05/12
For personal use only.

*Orthoesters **12–17***

General Method of Preparation

A solution of *O*-alkyl lactonium tetrafluoroborate (10 mmol) in 35 ml of dichloromethane was prepared as described above. This solution was added dropwise and under dry nitrogen atmosphere to a solution of sodium alkoxide (30 mmol) in 35 ml of alcohol cooled to −78°. The reaction was magnetically stirred at this temperature for 1 h. The reaction mixture was then allowed to warm up to room temperature and ether was added. The organic phase was washed with an aqueous solution of sodium bicarbonate, dried over potassium carbonate, and evaporated to dryness yielding crude orthoester. Orthoesters were purified by distillation under vacuum.

*Orthoester **12**:* b.p. 72°/20 mm (lit. (7) b.p. 60–61.5°/10 mm); yield 85% (lit. (16) 83%); i.r.: ν_{max} (film) 1000–1200 cm^{-1}; n.m.r.: δ($CDCl_3$) 1.18 (6H, triplet, J = 7.0 Hz, —O—CH_2—CH_3), 1.8–2.5 (4H, multiplet, methylene at C-3 and C-4), 3.60 (4H, quartet, J = 7.0 Hz, —O—CH_2—CH_3), 4.0 (2H, multiplet, methylene at C-5); m.s.: *m/e* 160 (M^+), 102 ($M^+ - C_4H_{10}$), 87 ($M^+ - C_4H_9O$).

Anal. Calcd. for $C_8H_{16}O_3$: C, 59.98; H, 10.07. Found: C, 59.74; H, 10.09.

*Orthoester **13**:* b.p. 72–74°/20 mm (71%); i.r.: ν_{max} (film) 1000–1200 cm^{-1}; n.m.r.: δ($CDCl_3$) 1.18 (6H, triplet, J = 7.5 Hz, —O—CH_2—CH_3), 1.65 (6H, multiplet, methylenes at C-3, C-4, and C-5), 3.55 (4H, quartet, J = 7.5 Hz, —O—CH_2—CH_3), 3.70 (2H, multiplet, methylene at C-6); m.s.: *m/e* 174 (M^+), 129 ($M^+ - C_2H_5O$).

Anal. Calcd. for $C_9H_{18}O_3$: C, 62.04; H, 10.41. Found: C, 62.16; H, 10.22.

*Orthoester **14**:* b.p. 42°/0.8 mm (80%); i.r.: ν_{max} (film) 1000–1200 cm^{-1}; n.m.r.: δ($CDCl_3$) 1.18 (6H, triplet, J = 7.5 Hz, —O—CH_2—CH_3), 1.20 (3H, doublet, J = 6.5 Hz, —CH—CH_3), 1.66 (6H, multiplet, methylenes at C-3, C-4, and C-5), 3.55 and 3.61 (4H, two quartets, J = 7.5 Hz, —O—CH_2—CH_3), 3.60 (1H, multiplet, —CH—CH_3); m.s.: *m/e* 188 (M^+), 143 ($M^+ - C_2H_5$).

Anal. Calcd. for $C_{10}H_{20}O_3$: C, 63.80; H, 10.71. Found: C, 63.93; H, 10.42.

*Orthoester **15**:* b.p. 82–83°/1.7 mm (85%); i.r.: ν_{max} (film) 1000–1200 cm^{-1}; n.m.r.: δ($CDCl_3$) 0.90 (6H, doublet, J = 5.0 Hz, —CH—$(CH_3)_2$), 1.18 (6H, triplet, J = 7.0 Hz, —O—CH_2—CH_3), 1.47 (4H, multiplet, methylenes at C-3 and C-5), 2.05 (2H, multiplet, proton at C-4 and —$CH(CH_3)_2$), 3.58 (4H, two unresolved quartets, J = 7.0 Hz, —O—CH_2—CH_3), 3.80 (2H, multiplet, methylene at C-6); m.s.: *m/e* 216 (M^+), 171 ($M^+ - C_2H_5O$).

Anal. Calcd. for $C_{12}H_{24}O_3$: C, 66.63; H, 11.18. Found: C, 66.33; H, 11.12.

*Orthoester **16**:* b.p. 80–81°/0.4 mm (80%); i.r.: ν_{max} (film) 1000–1200 cm^{-1}; n.m.r.: δ($CDCl_3$) 1.18 (6H, triplet, J = 7.0 Hz, —O—CH_2—CH_3), 1.0–2.0 (12H, multiplet, ring hydrogens), 3.50 (2H, multiplet, methylene at C-6), 3.55 (2H, quartet, —O—CH_2—CH_3 axial), 3.60 (2H, quartet, —O—CH_2—CH_3 equatorial); m.s.: *m/e* 228 (M^+), 183 ($M^+ - C_2H_5O$).

Anal. Calcd. for $C_{13}H_{24}O_3$: C, 68.38; H, 10.59. Found: C, 68.55; H, 10.64.

*Orthoester **17**:* b.p. 84–86°/4.0 mm (74%); i.r.: ν_{max} (film) 1000–1200 cm^{-1}; n.m.r.: δ($CDCl_3$) 0.9–2.1 (2H, multiplet, ring hydrogens), 3.18 (3H, singlet, —O—CH_3 axial), 3.28 (3H, singlet, —O—CH_3 equatorial), 3.4–3.8 (2H, multiplet, —CH_2—O—); m.s.: *m/e* 200 (M^+), 169 ($M^+ - CH_3O$).

Anal. Calcd. for $C_{11}H_{20}O_3$: C, 65.97; H, 10.07. Found: C, 65.74; H, 10.03.

*Orthoester **39***

A solution of *O*-ethyl lactonium salt ***10*** (1.04 mmol) in 5 ml of dichloromethane was added dropwise and under dry nitrogen atmosphere to a solution of sodium methoxide (10.4 mmol) in methanol (3 ml) and isopropyl alcohol (10 ml) cooled to −78°. The reaction was magnetically stirred at this temperature for 1 h. The reaction mixture was allowed to warm up at room temperature and work-up as described in the general method furnished the crude orthoester **39**: yield 76%; i.r.: ν_{max} (film) 1000–1200 cm^{-1}; n.m.r.: δ($CDCl_3$) 0.8–2.2 (2H, multiplet, ring hydrogens), 1.22 (3H, triplet, J = 7.0 Hz, —CH_2—CH_3), 3.22 (3H, singlet, —O—CH_3 axial), 3.61 (2H, quartet, J = 7.0 Hz, —O—CH_2—CH_3, equatorial); m.s.: *m/e* 214 (M^+), 183 ($M^+ - CH_3O$), 169 ($M^+ - C_2H_5O$). A peak at *m/e* 200 indicated the presence of ≃3% of compound **17**.

*Orthoester **40***

A solution of *O*-methyl lactonium salt ***11*** (1.30 mmol) in 5 ml of dichloromethane was added dropwise and under dry nitrogen atmosphere to a solution of sodium ethoxide (13 mmol) in absolute ethanol (5 ml) and isopropanol (10 ml) cooled to −78°. The reaction was magnetically stirred at this temperature for 1 h. Work-up as described in general method gave crude orthoester **40**: yield 73%; i.r.: ν_{max} (film) 1000–1200 cm^{-1}; n.m.r.: δ($CDCl_3$) 0.8–2.2 (2H, multiplet, J = 7.0 Hz, ring hydrogens), 3.32 (3H, singlet, —O—CH_3, equatorial), 3.36 (2H, quartet, J = 7.0 Hz, —O—CH_2—CH_3, axial); m.s.: *m/e* 214 (M^+), 183 ($M^+ - CH_3O$), 169 ($M^+ - C_2H_5O$). A peak at *m/e* 228 indicated the presence of ≃5% of compound **16**.

*Orthoester **43***

A solution of *O*-methyl lactonium salt ***11*** (3.0 mmol) in 5 ml of dichloromethane was added dropwise and under dry nitrogen atmosphere to a solution of sodium methoxide (11.0 mmol) in deuterated methanol (3 ml) and isopropanol (5 ml) cooled to −78°. Usual work-up gave orthoester **45**: yield 79%; i.r.: ν_{max} (film) 1000–1200 cm^{-1}; n.m.r.: δ($CDCl_3$) 0.8–2.2 (2H, multiplet, ring hydrogens), 3.32 (3H, singlet, —O—CH_3, equatorial), 3.4–3.8 (2H, multiplet, —O—CH_2—); m.s.: *m/e* 203 (M^+), 172 ($M^+ - CH_3O$), 169 ($M^+ - CD_3O$). A peak at *m/e* 206 indicated the presence of ≃10% of compound **44**.

Orthoester Hydrolysis

General Procedure (Vapor Phase Chromatographic Analysis)

Orthoester (1 mmol) was dissolved in dichloromethane (1 ml) and poured on cold water (1 ml) containing a small amount of *p*-toluenesulfonic acid (10^{-3} *M*). A rigorous agitation was maintained at 0 °C for 20 min. Reaction mixture was dissolved in cooled pyridine (30 ml), excess acetic anhydride was added, and left overnight at room temperature. The excess acetic anhydride was destroyed by methanol with cooling. The solvents were removed

in vacuo and the crude product was analysed by v.p.c. (SE-30 10%, 5 ft × $\frac{1}{8}$ in. Chromasorb W, 100–200 mesh, 100° or specified).

Hydrolysis of Orthoester ***12***

Compound ***1:*** (5%); retention time 1.0 min.

Compound ***19:*** (95%); retention time 5.5 min; i.r.: ν_{max} (film) 1740, 1240, 1170 cm^{-1}; n.m.r.: $\delta(CDCl_3)$ 1.25 (3H, triplet, J = 7.0 Hz, —O—CH_2—CH_3), 1.50–1.85 (2H, multiplet, AcO—CH_2—CH_2—), 2.00 (3H, singlet, CH_3—COO—), 2.18–2.50 (2H, multiplet, —CH_2—COO—), 4.10 (2H, quartet, J = 7.0 Hz, —O—CH_2—CH_3).

Anal. Calcd. for $C_8H_{14}O_4$: C, 55.16; H, 8.10. Found: C, 55.16; H, 8.40.

Hydrolysis of Orthoester ***13***

Compound ***2:*** (4%); retention time 0.9 min.

Compound ***21:*** (96%); retention time 5.4 min; i.r.: ν_{max} (film) 1740, 1240, 1170 cm^{-1}; n.m.r.: $\delta(CDCl_3)$ 1.25 (3H, triplet, J = 7.0 Hz, —O—CH_2—CH_3), 1.70 (4H, multiplet, AcO—CH_2—CH_2—CH_2—), 2.03 (3H, singlet, CH_3—COO—), 2.35 (2H, multiplet, —CH_2—COO—), 4.13 (2H, multiplet, AcO—CH_2—), 4.17 (2H, quartet, J = 7.0 Hz, —O—CH_2—CH_3).

Anal. Calcd. for $C_9H_{16}O_4$: C, 57.43; H, 8.57. Found: C, 57.23; H, 8.33.

Hydrolysis of Orthoester ***14***

Compound ***3:*** (3%); retention time 2.0 min.

Compound ***23:*** (97%); retention time 7.7 min; i.r.: ν_{max} (film) 1735, 1240, 1170 cm^{-1}; n.m.r.: $\delta(CDCl_3)$ 1.18 (3H, doublet, J = 6.0 Hz, —CH—CH_3), 1.25 (3H, triplet, J = 7.0 Hz, —O—CH_2—CH_3), 1.60 (4H, multiplet, AcO—CH_2—CH_2—CH_2—), 2.05 (3H, singlet, CH_3—COO—), 2.35 (2H, multiplet, —CH_2—COO—), 4.18 (2H, quartet, J = 7.0 Hz, —O—CH_2—CH_3), 4.91 (1H, multiplet, —O—CH—).

Anal. Calcd. for $C_{10}H_{18}O_4$: C, 59.39; H, 8.97. Found: C, 59.49; H, 8.95.

Hydrolysis of Orthoester ***15***

Compound ***4:*** (6%); retention time 3.0 min.

Compound ***25:*** (94%); retention time 6.8 min; i.r.: ν_{max} (film) 1735, 1235, 1170 cm^{-1}; n.m.r.: $\delta(CDCl_3)$ 0.88 (6H, doublet, J = 6.0 Hz, *gem*-dimethyl), 1.27 (3H, triplet, J = 7.0 Hz, —O—CH_2—CH_3), 1.4–2.0 (4H, multiplet, —CH_2—CH—$CH(CH_3)_2$), 2.05 (3H, singlet, CH_3—COO—), 2.10–2.40 (2H, multiplet, —CH_2—COO—), 4.18 (4H, quartet, J = 7.0 Hz and multiplet, —O—CH_2—CH_3 and AcO—CH_2—).

Anal. Calcd. for $C_{12}H_{22}O$: C, 62.58; H, 9.63. Found: C, 62.30; H, 9.44.

Hydrolysis of Orthoester ***16***

Compound ***5:*** (4%); retention time 8.1 min (column temperature 150°).

Compound ***27:*** (96%); retention time 18.7 min; i.r.: ν_{max} (film) 1735, 1235, 1165 cm^{-1}; n.m.r.: $\delta(CDCl_3)$ 1.2–2.2 (12H, multiplet, ring hydrogens and —CH_2—COO—), 1.26 (3H, triplet, J = 7.0 Hz, —O—CH_2—CH_3), 2.06 (3H, singlet, CH_3—COO—), 4.08 (2H, multiplet, AcO—CH_2—), 4.18 (4H, quartet, J = 7.0 Hz, —O—CH_2—CH_3 and AcO—CH_2—).

Anal. Calcd. for $C_{13}H_{22}O_4$: C, 64.44; H, 9.15. Found: C, 64.21; H, 9.24.

Hydrolysis of Orthoester ***17***

Compound ***5:*** (5%); retention time 8.1 min (column temperature 150°).

Compound ***29:*** (95%); retention time 13.7 min; i.r.: ν_{max} (film) 1735, 1230, 1160 cm^{-1}; n.m.r.: $\delta(CDCl_3)$ 0.8—2.0 (10H, multiplet, ring hydrogens), 2.07 (3H, singlet, CH_3—COO—), 2.0–2.6 (2H, multiplet, —CH_2—COO—), 3.68 (3H, singlet, —O—CH_3), 4.07 (2H, multiplet, AcO—CH_2—).

Anal. Calcd. for $C_{12}H_{20}O_4$: C, 63.14; H, 8.83. Found: C, 62.99; H, 8.93.

Hydrolysis of Orthoester ***39***

Compound ***5:*** (5%); retention time 8.1 min (column temperature 150°).

Compound ***29:*** (3%); retention time 13.7 min.

Compound ***27:*** (92%); retention time 18.7 min.

Hydrolysis of Orthoester ***40***

Compound ***5:*** (4%); retention time 8.1 min (column temperature 150°).

Compound ***29:*** (91%); retention time 13.7 min.

Compound ***27:*** (5%); retention time 18.7 min.

Hydrolysis of Orthoester ***43***

Compound ***5:*** (6%); retention time 8.1 min (column temperature 150°).

Compound ***29:*** (94%); retention time 13.7 min.

Mass spectral analysis of **29** (M − 60) indicated the presence of 10% of the deuterated methyl ester.

General Procedure (C-13 Nuclear Magnetic Resonance Analysis)

Orthoester (1 mmol) was dissolved in deuterated chloroform in a n.m.r. tube. Cold water (1 ml) containing a trace of *p*-toluenesulfonic acid (10^{-3} M) was added with vigorous shaking. Spectras were immediately taken. See Table 2 for results.

Support for this work by The National Research Council of Canada and by The Ministère de l'Education, Québec, is gratefully acknowledged.

1. P. DESLONGCHAMPS, P. ATLANI, D. FRÉHEL, and A. MALAVAL. Can. J. Chem. **50**, 3405 (1972).
2. P. DESLONGCHAMPS, C. LEBREUX, and R. TAILLEFER. Can. J. Chem. **51**, 1665 (1973).
3. P. DESLONGCHAMPS. Pure Appl. Chem. In press.
4. P. DESLONGCHAMPS and C. MOREAU. Can. J. Chem. **49**, 2465 (1971); P. DESLONGCHAMPS, C. MOREAU, D. FRÉHEL, and P. ATLANI. Can. J. Chem. **50**, 3402 (1972); P. DESLONGCHAMPS, P. ATLANI, D. FRÉHEL, A. MALAVAL, and C. MOREAU. Can. J. Chem. **52**, 3651 (1974).
5. E. A. LUCKEN. J. Chem. Soc. 2954 (1959); J. F. KING and A. D. ALLBUTT. Can. J. Chem. **48**, 1754 (1970); E. L. ELIEL and F. W. NADER. J. Am. Chem. Soc. **92**, 584 (1970); H. B. BÜRGI, J. D. DUNITZ, and E. SHEFTER. J. Am. Chem. Soc. **95**, 5065 (1973); H. B. BÜRGI, J. D. DUNITZ, and E. SHEFTER. Acta Cryst. B**30**, 1517 (1974); J. M. LEHN, G. WIPFF, and H. B. BÜRGI. Helv. Chim. Acta, **57**, 493 (1974); H. B. BÜRGI, J. M. LEHN, and G. WIPFF. J. Am. Chem. Soc. **96**, 1956 (1974); H. B. BÜRGI, J. D. DUNITZ, J. M. LEHN, and G. WIPFF. Tetrahedron, **30**, 1563 (1974),

Can. J. Chem. Downloaded from www.nrcresearchpress.com by 210.87.254.40 on 09/05/12
For personal use only.

and J. M. LEHN and G. WIPFF. J. Am. Chem. Soc. **96**, 4048 (1974).
6. E. H. CORDES. *In* Progress in physical organic chemistry. Vol 4. *Edited by* A. Streitwieser and R. W. Taft. Interscience, New York, 1967. pp. 1–44; E. H. CORDES and H. G. BULL. Chem. Rev. **74**, 582 (1974).
7. H. MEERWEIN, P. BORNER, O. FUCKS, H. J. SASSE, H. SCHRODT, and J. SPILLE. Chem. Ber. **89**, 2060 (1956).
8. R. U. LEMIEUX. Pure Appl. Chem. **25**, 527 (1971); H. BOOTH and R. U. LEMIEUX. Can. J. Chem. **49**, 777 (1971); E. L. ELIEL. Angew. Chem. **84**, 779 (1972); Angew. Chem. Int. Ed. Eng. **11**, 739 (1972).
9. S. M. MCELVAIN and G. R. MCKAY. J. Am. Chem. Soc. **77**, 5601 (1955).
10. B. G. RAMSEY and R. W. TAFT. J. Am. Chem. Soc. **88**, 3058 (1966).
11. R. HUISGEN and H. OTT. Tetrahedron, **6**, 253 (1959).
12. S. A. BARKER, J. HOMER, M. C. KEITH, and L. F. THOMAS. J. Am. Chem. Soc. **80**, 6098 (1958); A. KONOWAL and A. ZAMOJSKI. Roczniki Chem. **44**, 1607 (1970).
13. J. MEINWALD and E. FRAUENGLASS. J. Am. Chem. Soc. **82**, 5235 (1960).
14. G. A. HAGGIS and L. N. OWEN. J. Chem. Soc. 389 (1953); E. ALI and L. N. OWEN. J. Chem. Soc. 2111 (1958); W. HUCKEL, and W. EGERER. Ann. Chem. 645, 162 (1961).
15. H. MEERWEIN. Org. Syn. **46**, 113, 120 (1966).
16. H. MEERWEIN, E. BATTENBERG, H. GOLD, E. PFEIL, and G. WILLFANG. J. Prakt. Chem. **154**, 83 (1939).

Can. J. Chem. Downloaded from www.nrcresearchpress.com by 210.87.254.40 on 09/05/12
For personal use only.

Photoionization Cross Sections at 11.6–11.8 eV

JO ALLAN BERAN, ANIL KUMAR DHINGRA,[1] WU-SCHYONG LIU, AND DONALD FOSTER MULLICA

Department of Chemistry, Texas A & I University, Kingsville, Texas 78363

Received August 26, 1974

JO ALLAN BERAN, ANIL KUMAR DHINGRA, WU-SCHYONG LIU, and DONALD FOSTER MULLICA. Can. J. Chem. **53**, 1616 (1975).

The relative photoionization cross sections of a homologous series of alkanes, alkenes, alkyl chlorides, aldehydes, ethers, ketones, and alcohols have been determined at 11.6–11.8 eV using an argon resonance lamp. Correlations have been made between the photoionization cross sections and the molecular polarizability, the diamagnetic susceptibility, and the electron ionization cross sections of the molecules. No general correlation was found to exist but linear correlations were observed within each molecular class of compounds. These results are in general agreement with earlier studies on the electron ionization cross sections at 70 eV.

JO ALLAN BERAN, ANIL KUMAR DHINGRA, WU-SCHYONG LIU et DONALD FOSTER MULLICA. Can. J. Chem. **53**, 1616 (1975).

On a déterminé, à 11.6–11.8 eV utilisant une lampe à résonance d'argon, les sections efficaces relatives de photoionisation de séries analogues d'alcanes, d'alcènes, de chlorures d'alkyle, d'aldéhydes, d'éthers, de cétones et d'alcools. On a fait des corrélations entre les sections efficaces de photoionisation et la polarisabilité moléculaire, la susceptibilité diamagnétique et les sections efficaces d'ionisation électronique des molécules. On n'a trouvé aucune corrélation générale; toutefois on a observé des corrélations linéaires à l'intérieur de chaque classe moléculaire de composés. Ces résultats sont en accord général avec des études antérieures sur les sections efficaces d'ionisation électronique à 70 eV.

[Traduit par le journal]

Introduction

Theoretical and experimental electron ionization cross sections for a large number of atoms and molecules have been studied quite extensively at high energies (70 eV and above) over the past several years. These data have been used quite extensively for the evaluation of radiation chemical data and for the study of ion–molecule reactions.

The energy region for ion–molecule reactions has been extended more recently (1, 2) with the availability of intense monochromatic sources of light in the low energy region (<20 eV) (3), however, data on the experimental and theoretical photoionization cross sections at these energies have been minimal. Some studies have been reported on the photoionization cross sections of nitric oxide (4) and low molecular weight hydrocarbons (5) but no extensive body of data has been collected on photoionization cross sections as in the case with electron ionization cross sections.

Several investigators have made attempts to correlate electron ionization cross sections with some ground state molecular property of the molecule under study. Otvos and Stevenson (6) suggested that molecular ionization cross sections could be determined by the addition of constituent atomic cross sections; however, errors in their calculations invalidated the results. Lampe *et al.* (7) did an extensive study of ionization cross sections and found that the additivity postulate did not hold, but that a correlation with the polarizability of the molecule did exist. Later work has shown that a correlation with diamagnetic susceptibility is also probable (8).

Recently extensive studies and a review of earlier work on ionization cross sections have been reported by Harrison *et al.* (9) and Beran and Kevan (10) at 70 eV, in which they have reported that correlations do exist between the cross sections and the molecular polarizability and the diamagnetic susceptibility within a molecular class of compounds but that a general correlation for all molecules does not exist.

We have attempted to extend these studies into the low energy region by studying the rela-

[1]Present address: Department of Chemistry, Royal Military College of Canada, Kingston, Ontario.

Can. J. Chem. Downloaded from www.nrcresearchpress.com by 210.87.254.40 on 09/05/12
For personal use only.

Can. J. Chem. Downloaded from www.nrcresearchpress.com by 210.87.254.40 on 09/05/12
For personal use only.

tive photoionization cross sections at 11.6 to 11.8 eV, utilizing an argon resonance lamp as the energy source. We have attempted correlations between the photoionization cross sections and the molecular polarizability and the diamagnetic susceptibility of a system of molecules to see if such correlations are valid as they are at higher energies (70 eV). Our results at low energy show that such correlations do exist within a molecular class of compounds as had been reported earlier at 70 eV by Beran and Kevan (10). In addition a correlation has been drawn between the photoionization cross sections and electron ionization cross sections at 70 eV.

Experimental

All compounds were obtained commercially and used without further purification, but were degassed before use. In most cases the purities were quoted to be greater than 99% although some of the ketones were quoted at less than 99% pure. All the liquid samples used in this study were doubly distilled prior to use.

An argon resonance lamp was utilized for the photoionization studies. The lamp was filled on a mercury-free vacuum line capable of achieving pressures less than 1×10^{-6} Torr. A LiF window was used on the lamp. The detailed construction technique of the lamp and the operational characteristics of an argon resonance lamp, fitted with a LiF window, have been described in an article by Gorden *et al.* (11). The lamp was powered by a 2450 MHz Raytheon microwave generator. The discharge of the lamp was kept at least 15 cm removed from the window and was operated at low intensities ($\sim 10^{12}$ quanta/s) to reduce the formation of F centers in the LiF window. Under these conditions the fluctuation of intensity of the lamp during the course of an experimental run was minimal.

The irradiation of the sample was carried out by coupling the lamp to the photoreaction cell which contained two parallel-plate stainless steel electrodes, the window of the lamp being located at the edge of the two electrodes. The electrodes were insulated from the body of the cell. The total ion current generated from the photoionization of the sample was monitored by a Keithley 602 electrometer.

Since its photoionization quantum yield is well established at the argon resonance wavelength (12), nitric oxide was used as the reference gas in this study and all the results reported here are relative to its behavior. It also has a low absorption coefficient such that ions are uniformly distributed throughout the gas and meaningful saturation current values are obtained over a wide pressure range (13). The saturation ion current generated on irradiating NO was also used to determine the absolute intensity of the light entering the cell (11). This is given by

$$[1] \qquad {}^{q}a = 6.24 \times 10^{18}(i_{NO}/\eta_{NO})$$

where ${}^{q}a$ is the absolute intensity of the absorbed light in quanta s^{-1}, i_{NO} is the saturation current of NO in amperes, and η_{NO} is the ionization quantum yield (11) for NO. By adjusting the microwave power and the distance of the discharge from the window the intensity of the lamp was kept at $\sim 10^{12}$ quanta s^{-1}.

The photoionization cross section, Q, may be determined from the total ion current, I_t, by using the following relationship

$$[2] \qquad I_t = QLdN$$

where L is the intensity of the incident radiation, d is the ionization path length, and N is the number of molecules per cm^3 in the reaction cell. For a given set of experiments the intensity L and the ionization path length, d, were kept constant. Since N is proportional to the pressure, a plot of the total current I_t *vs.* pressure should be linear with a slope proportional to the photoionization cross section of the molecule.

All current *vs.* pressure plots in this study were linear. The slopes of the plots were determined by a computer least squares fit to the experimental points. The standard deviation of the fit was within 1%. Four or more pressure plots were determined in most cases for each molecule studied, the slope of the NO plot being used as the standard. The photoionization cross section of a molecule was obtained by taking the ratio of the slopes of the molecule to that of NO. The average deviation of these slopes was in most cases no more than 5%.

Results and Discussion

Relative Phototionization Cross Sections

The relative photoionization cross sections for various series of organic compounds were determined at the argon wavelength radiation and are reported in Table 1. These values are the average of four or more determinations. All the values reported in this work are relative to the cross section of nitric oxide, which was assigned a value of one. In addition Table 1 lists the standard deviation from the mean values of the cross section. In the case of liquid samples the upper limit of each series was determined by the volatility of the compound since the samples were run at room temperature. In some cases, *e.g.* methane, the ionization potential was higher than the energy emitted by the lamp (11.6–11.8 eV) and hence, their cross sections could not be determined.

The results in Table 1 show various examples of the effect of structural isomerism on the cross section of the molecule, *e.g.* butenes, pentenes, butyl alcohols, etc. It is observed from Table 1 that the cross sections for the various isomers are almost the same and that, within experimental error, the cross sections are independent of structure within a given class of compounds. However, if one compares the cross sections

TABLE 1. Experimental photo- and electron ionization cross sections and calculated molecular polarizabilities and diamagnetic susceptibilities for several homologous series

Number	Compound	Photoionization cross section* (11.6–11.8 eV)	Standard deviation	Molecular polarizability†	Diamagnetic susceptibility‡	Electron ionization cross section§ (70 eV)
			Alkanes			
1	C_2H_6	0.07	0.01	43.42	29.1	8.51
2	C_3H_8	0.97	0.20	61.27	40.45	11.5
3	C_4H_{10}	1.56	0.23	79.12	51.8	15.3
4	C_5H_{12}	2.28	0.25	96.97	63.15	18.6
5	C_6H_{14}	2.76	0.33	114.82	74.5	22.5
			Alkenes			
6	C_2H_4	0.91	0.02	39.89	20.5	6.93
7	C_3H_6	1.83	0.03	57.74	31.85	10.2
8	iso-C_4H_8	2.85	0.06	75.59	42.8	13.3
9	1-C_4H_8	2.93	0.08	75.59	43.2	13.7
10	*cis* and *trans* 2-C_4H_8	3.10	0.22	75.59	42.0	13.85
11	1-C_5H_{10}	4.06	0.14	93.54	54.55	—
12	2-C_5H_{10}	4.00	0.10	93.54	53.35	—
13	$CH_3CH{:}C(CH_3)_2$	3.94	0.14	93.54	54.15	—
14	$CH_2{:}CHCH_2CH(CH_3)_2$	5.61	0.17	111.41	67.1	—
15	$CH_3CH{:}CHCH(CH_3)_2$	5.53	0.10	111.41	66.2	—
			Alkyl chlorides			
16	C_2H_5Cl	1.64	0.10	62.3	44.7	12.0
17	*n*-C_3H_7Cl	2.98	0.07	80.2	56.0	15.6
18	iso-C_3H_7Cl	2.81	0.06	80.2	57.25	—
19	*n*-C_4H_9Cl	4.60	0.08	98.0	67.4	19.9
			Ketones			
20	CH_3COCH_3	3.13	0.11	62.3	34.6	10.5
21	$CH_3COC_2H_5$	3.62	0.10	80.2	46.0	13.3
22	$C_3H_7COCH_3$	4.10	0.25	98.0	57.4	15.7
23	iso-$C_3H_7COCH_3$	3.93	0.26	98.0	58.25	—
24	$C_2H_5COC_2H_5$	4.44	0.22	98.0	57.4	16.3
			Aldehydes			
25	C_2H_5CHO	2.42	0.08	62.3	34.2	9.66
26	C_3H_7CHO	3.19	0.16	80.2	45.6	—
27	iso-C_3H_7CHO	3.16	0.08	80.2	46.5	12.8
			Ethers			
28	CH_3OCH_3	1.50	0.12	50.4	32.5	9.61
29	$C_2H_5OC_2H_5$	2.62	0.09	86.1	55.2	16.0
30	$C_3H_7OC_3H_7$	3.62	0.14	121.8	78.7	20.4
31	$(\text{iso-}C_3H_7)_2O$	3.76	0.14	121.8	79.7	—
32	$(n\text{-}C_4H_9)_2O$	4.98	0.06	157.6	100.6	—
33	*n*-$C_4H_9OCH_3$	3.59	0.12	104.0	66.6	18.7
34	*tert*-$C_4H_9OCH_3$	3.05	0.13	104.0	69.0	—
			Alcohols			
35	C_2H_5OH	0.50	0.03	49.9	33.8	8.92
36	*n*-C_3H_7OH	0.89	0.02	67.8	45.15	—
37	iso-C_3H_7OH	0.80	0.02	67.8	47.05	—
38	*n*-C_4H_9OH	1.47	0.09	85.7	56.5	—
39	*sec*-C_4H_9OH	1.59	0.10	85.7	58.4	—
40	iso-C_4H_9OH	1.52	0.06	85.7	57.4	—
41	*tert*-C_4H_9OH	1.69	0.05	85.7	61.9	—

*Relative to NO as 1.
†Reference 14, in units of 10^{-25} cm^3.
‡Reference 14, in units of 10^{-6} cgs e.m.u./mol.
§References 9 and 10, all values relative to argon cross section, in units of 10^{-16} cm^2.

Can. J. Chem. Downloaded from www.nrcresearchpress.com by 210.87.254.40 on 09/05/12
For personal use only.

TABLE 2. Effect of structural isomerism on cross section

Molecule	Cross section	Molecule	Cross section
C_2H_5CHO	2.39	C_2H_5OH	0.50
CH_3COCH_3	3.13	CH_3OCH_3	1.50
C_3H_7CHO	3.17*	C_4H_9OH	1.57*
$CH_3COC_2H_5$	3.62	$C_2H_5OC_2H_5$	2.62

*Average of different isomers.

of structural isomers belonging to different functional classes, as shown in Table 2, one does not observe the same values of cross sections. Similar behavior in the trend of cross sections at a higher energy (75 eV) was observed by Harrison *et al.* (9).

Table 1 also lists the molecular polarizability and the diamagnetic susceptibility values taken from the literature (14) and used for correlations in this study. In addition in Table 1, for comparison purposes, are listed the values of electron ionization cross sections at 70 eV. These values have been taken partly from the work of Beran and Kevan (10) and partly from Harrison *et al.* (9); however, for uniformity all these electron ionization cross sections are relative to the cross section of argon used by Beran and Kevan.

Correlation of Cross Sections with Molecular Parameters

The correlations of relative photoionization cross sections with molecular polarizability and diamagnetic susceptibility are shown in Figs. 1–3. The numbers in the figures refer to the numbers for the compounds in Table 1. The numerical values of the molecular polarizability and diamagnetic susceptibility used for these correlations are listed in Table 1 and are taken from the work of Beran and Kevan (14). These workers calculated the molecular polarizability using LeFevre's method of additivity of bond polarizabilities (15), and the diamagnetic susceptibility using the semi-empirical method of Haberditzl (16). In instances where the values of these two parameters were not available for certain molecules, they were calculated using LeFevre's method and Haberditzl's method, respectively. In addition to the correlations shown in Figs. 1–3, correlations can also be made with values of molecular polarizability and diamagnetic susceptibility calculated using other semi-empirical methods, *e.g.*, Lippincott–Stutman's δ-function model (17) for molecular polarizability and Baudet's method (18) for diamagnetic susceptibility. In each of these cases, however, the correlations obtained are similar to those reported in Figs. 1–3.

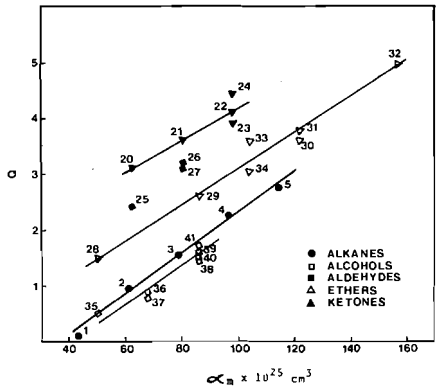

FIG. 1. Relative photoionization cross sections (Q) *vs.* molecular polarizabilities (α_m) for alkanes, alcohols, aldehydes, ethers, and ketones.

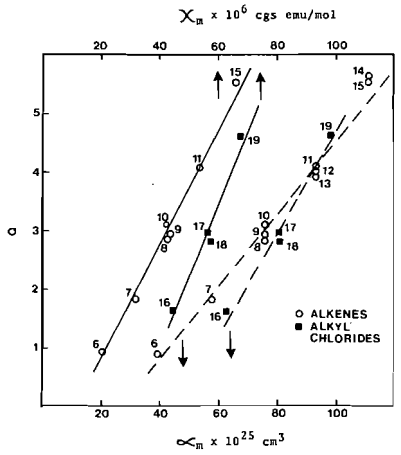

FIG. 2. Relative photoionization cross sections (Q) *vs.* molecular polarizabilities (α_m) and diamagnetic susceptibilities (χ_m) for alkenes and alkyl chlorides.

It is observed from the figures that a good linear correlation exists between the cross section and the molecular polarizability and diamagnetic susceptibility for each of the homologous series of compounds studied. These linear correlations are drawn from a least square fit. Although no linear correlation has been drawn for the aldehydes, their values are

Can. J. Chem. Downloaded from www.nrcresearchpress.com by 210.87.254.40 on 09/05/12
For personal use only.

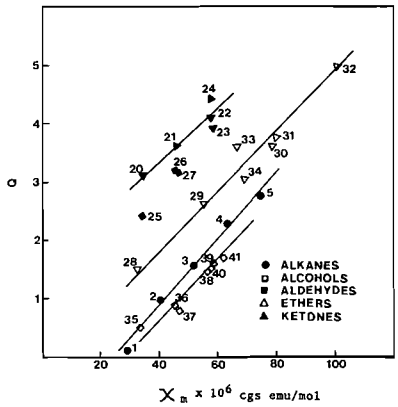

FIG. 3. Relative photoionization cross sections (Q) *vs.* diamagnetic susceptibilities (χ_m) for alkanes, alcohols, aldehydes, ethers, and ketones.

indicated on Figs. 1 and 3 to give a general idea for comparison with other series of compounds.

It is obvious from the figures that no general correlation exists for all the molecules for either the molecular polarizability or diamagnetic susceptibility; however, there is a linear correlation within a homologous series in each case. Thus a knowledge of either the molecular polarizability or the diamagnetic susceptibility of molecules should permit the estimation of cross sections for other members of the series.

In the case of molecular polarizability correlations, our conclusions are in complete accord with those at 70 eV by Harrison *et al.* (9) and Beran and Kevan (10). On studies conducted on the same series of compounds, as in this study, they observed that a correlation existed within each class of compounds but not overall. In addition a semi-empirical equation was derived by Beran and Kevan between molecular polarizability and cross section. A similar equation, which takes into account the slope and intercept of the correlations, can now be derived for low energies (11.6–11.8 eV) from our results. A look at Fig. 1 shows that the slopes of the various correlations (except for the alkenes and alkyl chlorides) are the same, within experimental error, and hence a semi-empirical equation can be written in which the slopes of all the correlations are adjusted to one slope. However, we feel that such an equation would be of limited value and that cross sections can be obtained readily by simple extrapolation.

In the case of diamagnetic susceptibility correlations, however, our conclusions are in distinct contrast to those reached at 70 eV by Beran and Kevan (10). They observed that a general correlation, as proposed earlier by Stevenson and Schissler (8) existed between the cross section and the diamagnetic susceptibility for the molecular classes: alkanes, alkenes, alkyl chlorides, ethers, ketones, and aldehydes. This general correlation, however, was not complete as the fluorine substituted compounds were found to deviate from it. From our results, as in the case of molecular polarizability correlation, we observe that a correlation exists only within each molecular class of compounds but not overall.

We observe from Fig. 3 that the slopes of the alkanes, alcohols, ethers, and ketone correlations are the same, within experimental error, hence it would again be possible for us to write a semi-empirical equation relating the cross section with the diamagnetic susceptibility.

Correlation of Photoionization Cross Sections with Electron Ionization Cross Sections

The correlation of relative photoionization cross sections at 11.6–11.8 eV with electron ionization cross sections at 70 eV is shown in Fig. 4. The values of the cross sections at 70 eV are taken from the literature and are listed for reference in Table 1. For the alcohol series, values of cross sections at 70 eV were not available.

From Fig. 4 it is observed that a good linear correlation is exhibited by molecules which are members of the same class of compounds. This shows that the photoionization cross sections can be predicted from the electron ionization cross sections or vice versa. This result seems significant in that a large body of data does exist for the electron ionization cross sections, since most of this data can be determined easily using mass spectrometric techniques. However, data on photoionization cross sections is very meager as the energy sources for such studies are relatively new. Hence such a correlation can be used for finding ionization cross sections at 11.6–11.8 eV. On the other hand we could also use this correlation to predict cross sections at 70 eV. For example, the electron ionization cross sections at 70 eV for the alcohols are not known except for ethyl alcohol. Using this cross section and assuming that the slope of the correlation is the same as for the alkanes, ketones, and ethers (this assumption would seem reasonable when one considers the fact

Can. J. Chem. Downloaded from www.nrcresearchpress.com by 210.87.254.40 on 09/05/12
For personal use only.

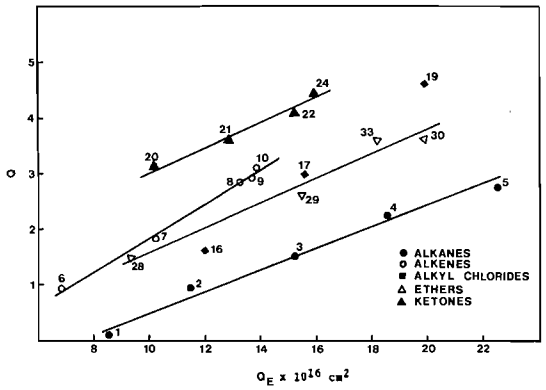

FIG. 4. Relative photoionization cross sections (Q) *vs.* electron ionization cross sections (Q_E) at 70 eV.

that the slopes for the alkanes, ketones, ethers, and alcohols are almost the same in all the other correlations studied in this work) one could draw a correlation for the alcohols in Fig. 4 and from it predict the electron ionization cross sections at 70 eV for the alcohol in question.

Conclusions

The relative photoionization cross sections of a number of molecules have been determined at 11.6–11.8 eV. Correlations have been made between the photoionization cross sections and the molecular polarizability and the diamagnetic susceptibility of the molecules to see if such correlations could be extended to the low energy region, as had been previously observed at the high energy region. From our results it is concluded that no apparent general correlation is valid but that each is valid within a given molecular class of compounds for both parameters used in the correlations. In addition a correlation is also observed with electron ionization cross sections at 70 eV. It should be mentioned here that a relation between the electron ionization cross section and the photoionization cross section was first shown by Bethe (19). The Bethe approximation has been applied successfully by Seaton (20) in determining the electron ionization cross sections from a knowledge of photoionization cross sections.

These correlations are similar to those observed at 70 eV except for the diamagnetic susceptibility case. Beran and Kevan (10) observed a general correlation when this parameter was used for the alkanes, alkenes, alkyl chlorides, ketones, ethers, and aldehydes; however, we find a correlation within each class only. This difference in observation can be attributed to the fact that photoionization and electron ionization are quite different phenomena. In photoionization only the outer electrons are ejected regardless of the photon energy while in the electron ionization process the inner shell electrons may also be ejected. Furthermore, in photoionization only one electron is ejected while in electron ionization more than one electron may be ejected leading to multiple ionization. In addition diamagnetic susceptibility is proportional to the square root of the polarizability times the square root of the number of electrons in the atom (21). Therefore, the observation at 11.6–11.8 eV that a correlation with diamagnetic susceptibility exists within each molecular class does not seem unfounded.

We wish to thank the Robert A. Welch Foundation for support of this work.

1. J. R. McNesby and H. Okabe. Adv. Photochem. **3**, 157 (1964).
2. P. Ausloos and S. G. Lias. J. Chem. Phys. **45**, 524 (1966).
3. R. Gorden, R. Doepker, and P. Ausloos. J. Chem. Phys. **44**, 3733 (1966).
4. (*a*) K. Watanabe, F. F. Marmo, and E. C. Y. Inn. Phys. Rev. **91**, 1155 (1953); (*b*) K. Watanabe. J. Chem. Phys. **22**, 1564 (1954).
5. R. I. Schoen. J. Chem. Phys. **37**, 2032 (1962).
6. J. W. Otvos and D. P. Stevenson. J. Am. Chem. Soc. **78**, 546 (1956).
7. F. W. Lampe, J. L. Franklin, and F. H. Field. J. Am. Chem. Soc. **79**, 6129 (1957).
8. D. P. Stevenson and D. P. Schissler. *In* The chemical and biological actions of radiations, Vol. V. *Edited by* M. Haissinsky. Academic Press Ltd., London. 1961. Chapt. 2.
9. A. G. Harrison, E. G. Jones, S. K. Gupta, and G. P. Nagy. Can. J. Chem. **44**, 1967 (1966).
10. J. A. Beran and L. Kevan. J. Phys. Chem. **73**, 3866 (1969).
11. R. Gorden, R. Rebbert, and P. Ausloos. U.S. Natl. Bur. Stand. Technical Note 496, 1969.
12. K. Watanabe, F. M. Matsunage, and H. Sakai. Appl. Opt. **6**, 391 (1967).
13. P. Ausloos and S. G. Lias. Radiat. Res. Rev. **1**, 75 (1968).
14. J. A. Beran and L. Kevan. J. Phys. Chem. **73**, 3860 (1969).
15. R. J. W. LeFevre. Adv. Phys. Org. Chem. **3**, 1 (1966).
16. W. Haberditzl. Angew. Chem. Int. Ed. **5**, 288 (1966).
17. E. R. Lippincott and J. M. Stutman. J. Phys. Chem. **68**, 2926 (1964).
18. J. Baudet. J. Chim. Phys. Physiol. Chim. Biol. **58**, 228 (1961).
19. H. Bethe. Ann. Phys. **5**, 325 (1930).
20. M. J. Seaton. Phys. Rev. **113**, 814 (1959).
21. J. G. Kirkwood. Phys. Z. **33**, 57 (1932).

Can. J. Chem. Downloaded from www.nrcresearchpress.com by 210.87.254.40 on 09/05/12
For personal use only.

Structural Studies of $(\pi\text{-}C_5H_5)_2MX_2$ Complexes and their Derivatives. The Structure of Bis(π-cyclopentadienyl)titanium Dichloride

ABRAHAM CLEARFIELD, DAVID KEITH WARNER,[1] CARLOS HERMAN SALDARRIAGA-MOLINA, AND RAMANATHAN ROPAL

Department of Chemistry, Ohio University, Athens, Ohio 45701

AND

IVAN BERNAL

Department of Chemistry, University of Houston, Houston, Texas 77004

Received September 27, 1974

ABRAHAM CLEARFIELD, DAVID KEITH WARNER, CARLOS HERMAN SALDARRIAGA-MOLINA, RAMANATHAN ROPAL, and IVAN BERNAL. Can. J. Chem. **53**, 1622 (1975).

The crystal and molecular structure of bis(π-cyclopentadienyl)titanium dichloride, $(C_5H_5)_2TiCl_2$, has been determined from three dimensional X-ray data. The crystals are triclinic with $a = 7.882(5)$, $b = 19.478(10)$, $c = 12.156(9)$ Å, $\alpha = 90.46(2)$, $\beta = 102.58(2)$, $\gamma = 143.49(2)°$. Intensity data (3742 reflections above background) were collected by the θ–2θ scan method using an automated counter diffractometer. The structure was refined in space group $P\bar{1}$ by block-diagonal least squares methods to a conventional R of 0.032. Since $Z = 4$, there are two symmetry independent molecules per unit cell. However, these two molecules are almost identical structurally. The coordination about the titanium atom formed by the two chlorine atoms and the centroids of the cyclopentadiene rings is that of a distorted tetrahedron. The average Ti—Cl bond distance is 2.364(3) Å and Ti—Cp—(centroid) 2.058 Å. The C—C distances vary from 1.339(11) to 1.419(9) Å. The structural results are compared to those for similar type molecules.

ABRAHAM CLEARFIELD, DAVID KEITH WARNER, CARLOS HERMAN SALDARRIAGA-MOLINA, RAMANATHAN ROPAL et IVAN BERNAL. Can. J. Chem. **53**, 1622 (1975).

On a déterminé la structure cristalline et moléculaire du dichlorure de bis (π-cyclopentadiènyl) de titane, $(C_5H_5)_2TiCl_2$, à partir de mesures rayons-X tridimensionnelles. Les cristaux sont tricliniques, $a = 7.882(5)$, $b = 19.478(10)$, $c = 12.156(9)$ Å, $\alpha = 90.46(2)$, $\beta = 102.58(2)$, $\gamma = 143.49(2)°$. Les intensités ont été mesurées par la méthode de balayage θ–2θ avec un diffractomètre automatique (3742 reflexions ont une intensité supérieure au bruit de fond). On a affiné la structure dans le groupe d'espace $P\bar{1}$ par la méthode des moindres carrés (bloc diagonal) jusqu'à un facteur d'accord R de 0.032. Puisque $Z = 4$, il y a deux molécules indépendantes par unité asymétrique. Toutefois ces deux molécules ont des structures pratiquement identiques. La coordination de l'atome de titane, formée de deux atomes de chlore et des centres des cycles cyclopentadiènes est celle d'un tétraèdre déformé. La distance moyenne du lien Ti—Cl est de 2.364(3) Å et celle de Ti—Cp (centre) est de 2.058 Å. Les distances C—C varient de 1.339(11) à 1.419(9) Å. On compare ces résultats structuraux avec ceux de molécules de type semblable. [Traduit par le journal]

Introduction

Bis(π-cyclopentadienyl)titanium(IV) dichloride, hereafter referred to as either titanocene dichloride or Cp_2TiCl_2, was prepared in 1954 by Wilkinson and Birmingham (1), who suggested from infrared studies that the molecule contains π-bonds between the Ti and the two cyclopentadienyl moieties. In 1957, Natta *et al.* (2) isolated the adduct of titanocene dichloride with diethyl aluminum as part of their studies of the mechanism of Ziegler catalysis in the polymerization of ethylene. The isolation of this compound was an important achievement since Natta and his associates were attempting then to show that the Ziegler catalysts for the polymerization of ethylene are, in general, bimetallic compounds containing organometallic bonds.

In 1966, an electron diffraction study was reported (3) in which Cp_2TiCl_2 was described as a prismatic sandwich in which the Cp rings are inclined towards each other at an angle of 58.5°. The Ti—Cl and Cl—Ti—Cl parameters were listed as 2.24 Å and 100°, respectively.

[1]Portions of this paper are based on the M.S. Thesis of D. K. Warner, presented to the Chemistry Department, Ohio University, Athens, Ohio, March, 1969.

These results are significantly different from those obtained in single crystal, X-ray (4), and neutron (5) diffraction studies of closely related substances.

In the solid state, titanocene dichloride has been studied twice by single crystal X-ray diffraction methods (6, 7). In the first report (6) no positional parameters were given. The second one (7) gives positional parameters but the results are not very accurate. For example, the C—C distances range from 1.32(4) to 1.50(4) Å. Thus, for the purposes of more accurate comparisons (4, 5, 8–10) these results are not very useful. Since, at the same time, we were aware that there are serious twinning problems with *most* crystals of titanocene dichloride, we decided to continue with our study on a non-twinned crystal we had obtained earlier (see Experimental). The results of that study are given below.

Experimental

Titanocene dichloride (Arapahoe Chemical Co.) of unknown purity was recrystallized from a 1:1 xylene–chloroform mixture. The m.p. of the resulting crystals was 287–288 °C, compared with the value of 287 ± 2 °C given by Wilkinson and Birmingham (1). Titanium was determined by fuming a sample of the crystals with perchloric acid in order to destroy the organic matter, precipitating the hydrous oxide with ammonia, and igniting to TiO_2. Chloride was determined gravimetrically as AgCl and carbon and hydrogen by standard combustion analysis.

Anal. Calcd: Ti, 19.24; Cl, 28.48; C, 48.23; H, 4.05. Found: Ti, 19.44; Cl, 28.36; C, 48.26; H, 4.01.

Crystals used for the X-ray study were obtained from hot benzene. They were small, bright red prisms which appeared, from optical examinations,[2] to have a 2-fold axis of symmetry. Crystals grown from other solvents under a variety of conditions were invariably twinned. Even with those grown from hot benzene, only a few were untwinned. Survey photographs taken with both Weissenberg and precession cameras failed to show the presence of any symmetry axes higher than 1. A set of three noncoplanar axes was chosen from photographs of an untwinned crystal and subjected to a reduced cell calculation. The reduced cell dimensions were: $a = 7.89$, $b = 11.58$, $c = 12.17$ Å, $\alpha = 108.0$, $\beta = 102.7$, and $\gamma = 89°$. These values are in substantial agreement with those reported by Tkachev and Atovmyan (7).

Accurate unit cell dimensions were obtained with a CAD-4 four-circle diffractometer (Enraf-Nonius) at 24 ± 1 °C. Subroutines SEARCH, INDEX, AND DETCELL (11) were used to collect 25 reflections at high and moderate (2θ) angles. The reflections were scanned at both ±2θ by the θ–2θ scan technique using a graphite monochromated beam of MoKα radiation ($\lambda = 0.7107$ Å) at a take-off angle of 4°. The Bragg angles were accurately determined by program DETCELL which automatically centers reflections while compensating for wavelength dispersion. Then the cell dimensions were obtained from a least squares calculation using the θ_1 values and $\lambda K\alpha_1 = 0.70926$ Å. This cell is related to the previous one by the transformation

$$\begin{pmatrix} A \\ B \\ C \end{pmatrix}_R = \begin{pmatrix} 1 & 0 & 0 \\ 2 & 1 & 0 \\ 0 & 0 & 1 \end{pmatrix} \begin{pmatrix} a \\ b \\ c \end{pmatrix}$$

where, A_R, B_R, and C_R are the reduced cell constants.

The transformed cell dimensions are given in Table 1 along with other crystallographic data of interest. The density of a crystal was determined by flotation in a solution of iodobenzene in carbon tetrachloride.

The crystal chosen for intensity data collection was almost cubic in shape and approximately 0.12 mm on an edge. The crystal to counter distance was 208 mm and the crystal to aperture distance 173 mm. Intensity data were collected by the θ–2θ scan method using a variable scan rate ranging from about 0.25°/min for the weakest reflections to about 10°/min for the strongest ones. The angular scan width was also variable and amounted to $3 \times (1.0 + 0.5 \tan\theta)°$. The right and left backgrounds were scanned for half the time required for the total peak scan. During data collection two standard reflections were recorded every time a set of 24 reflections was collected and those were used to place all the reflections on a common scale. The change in the intensities of the standards was small, random, and the maximum fluctuation about the mean was ±4%. A total of 13 508 reflections was scanned of which 3742 had intensities with $I \geq 3\sigma(I)$, where

$$\sigma(I) = (\text{Total counts} + \text{Background counts})^{1/2}$$

and were, thus, considered as observed.

The data were corrected for Lorentz and polarization effects but not for absorption or extinction. The absorption coefficient is small ($\mu R = 1.46$ cm^{-1}) (12) and the

TABLE 1. Crystal data

Parameter	Value	
Chemical formula	$(C_5H_5)_2TiCl_2$	
Molecular weight	243.00	
Crystal system	Triclinic	
Cell dimensions	Reduced cell	Working cell
	$a = 7.882(5)$ Å	7.882(5) Å
	$b = 11.590(10)$	19.478(10)
	$c = 12.156(9)$	12.156(9)
	$\alpha = 108.04(2)°$	90.46(2)
	$\beta = 102.58(2)$	102.58(2)
	$\gamma = 89.47(2)$	143.49(2)
Cell volume	$V = 1023.5$ Å^3	
Space group	$P\bar{1}$	
D(c)	1.577 g cm^{-3}	
D(m)	1.60	
Z	4 molecules/unit cell	
μ(MoKα)	11.7 cm^{-1}	
μR	1.46 cm^{-1}	

[2]A description of some of the common crystal shapes encountered in the growth of crystals of Cp_2TiCl_2 is given in ref. 19. Most of them are shapes of twins.

crystal was quite uniform in shape so that we estimate, from previous experience with absorption corrections on compounds of this type (4), that the error introduced by this omission amounts to no more than 2%.

Solution and Refinement of the Structure

The intensity data set was collected and indexed using the diffractometer working cell rather than the reduced cell dimensions. We decided at this point to find out the correctness of the solution of the structure of titanocene dichloride by Tkachev and Atovmyan (7), by using their positional parameters as a starting point in our refinement. Their positional parameters were transformed into those required for the working cell, using the transformation

$$x = X + 2Y$$

$$y = Y$$

$$z = Z$$

where x, y, and z are the fractional coordinates in our working cell and X, Y, and Z are the coordinates reported by Tkachev and Atovmyan (7). After refinement of the scale and the individual isotropic thermal parameters we obtained an $R(F)$ factor of 0.12, where

$$R(F) = \frac{\sum ||F_o| - |F_c||}{\sum |F_o|}$$

Refinement was continued by allowing for anisotropic thermal motion of all the atoms in the asymmetric unit, which lowered the $R(F)$ factor to 0.045. At this point, the positions of the hydrogen atoms were added at idealized positions which assume (*a*) that the Cp ring is a perfect pentagon and (*b*) that the hydrogen atoms lie in the same plane as the carbon atoms. The second assumption is certainly reasonable on the basis of the results obtained by neutron diffraction (5) for the closely related $(CH_2)_3(C_5H_4)_2TiCl_2$. The calculation of the positional parameters for the hydrogen atoms was carried out using program HYDROGEN (13) (C—H = 0.91 Å; C—C—H = 126°). The hydrogen atoms were assigned isotropic thermal parameters one unit (Å^2) larger than that of the carbons to which they are attached. When the values of the positional parameters of the nonhydrogen atoms shifted by less than 0.1 of their standard deviations, refinement was considered to be complete (14). The final value of $R(F)$ was 0.032 and that of the weighted residual

$$wR(F) = \left[\frac{\sum w(|F_o| - |F_c|)^2}{\sum wF_o^2}\right]^{1/2}$$

was 0.023. The function minimized was $\Sigma w(|F_o| - |F_c|)^2$, with weights, w, given by

$$w = \frac{1}{\{1 + [(F_o - P_2)/P_1]^2\}}$$

where $P_1 = 30$ and $P_2 = 90$.

A final difference Fourier map was featureless, with residual density ranging from a maximum of 0.3 e/Å^3 to a minimum of -0.3 e/Å^3. The scattering factors for the nonhydrogen atoms were taken from the compilation by Hanson *et al.* (15) in the neutral atom form. A correction for anomalous dispersion (the real term only) was included also in the refinement. The hydrogen atom scattering factors were those given by Stewart *et al.* (16).

The final set of coordinates and isotropic temperature parameters for the nonhydrogen atoms is listed in Table 2, while the positional parameters of the hydrogen atoms are given in Table 3. The anisotropic thermal parameters for the nonhydrogen atoms are listed in Table 4 and a listing of the observed and calculated structure factors is available from the Depository of Unpublished Data.[3]

At this point a comment on the solution of the structure by Tkachev and Atovmyan (7) is in order. Although we found that their positional parameters led to a smooth refinement of our data, their wide range of C—C distances may be traceable to difficulties with the quality of their data crystal (*vide supra*) similar to those we have experienced in the solution and refinement of the structure of Cp_2ZrCl_2, which is isomorphous with titanocene dichloride. We found that one of the two molecules in the asymmetric unit ($P\bar{1}$, $z = 4$) is either disordered or has high amplitudes of thermal motion in the Cp rings. Furthermore, this has independently been confirmed by Prout (17),[4] who has described similar difficulties with Cp_2ZrCl_2. As a result, we have abandoned further work

TABLE 2. Positional parameters ($\times 10^5$ for Ti and Cl atoms; $\times 10^4$ for all others) and isotropic thermal parameters for nonhydrogen atoms

Atom	x	y	z	B_{iso} (Å^2)
Ti(1)	08451(12)	23852(5)	38868(4)	2.12(3)
Ti(2)	69697(12)	26533(5)	88274(5)	2.19(3)
Cl(1)	94044(20)	08492(8)	44418(8)	4.06(6)
Cl(2)	36900(22)	36697(9)	58585(7)	4.45(6)
Cl(3)	04737(20)	41515(8)	07156(7)	4.04(6)
Cl(4)	71713(24)	15454(9)	93356(8)	4.61(6)
C(1)	5463(8)	0737(3)	2858(4)	5.24(30)
C(2)	6098(8)	1195(3)	4008(3)	4.54(28)
C(3)	7814(8)	2325(4)	4161(3)	4.59(27)
C(4)	8409(8)	2639(4)	3156(4)	4.64(28)
C(5)	6889(9)	1642(4)	2322(4)	4.92(29)
C(6)	3556(8)	2466(3)	3137(3)	4.11(25)
C(7)	5740(7)	3539(3)	4044(3)	4.48(27)
C(8)	5535(8)	4163(3)	3677(4)	5.67(33)
C(9)	3230(9)	3447(4)	2560(4)	5.17(31)
C(10)	1973(9)	2396(4)	2244(3)	4.99(27)
C(11)	2658(9)	1969(4)	7930(4)	5.34(34)
C(12)	3796(9)	2484(4)	9122(4)	6.54(38)
C(13)	3354(9)	1773(4)	9703(3)	5.88(30)
C(14)	2021(9)	0853(4)	8874(5)	6.51(32)
C(15)	1672(8)	0992(4)	7795(4)	6.53(31)
C(16)	1110(8)*	3704(4)	8247(3)	5.15(36)
C(17)	1198(9)*	4417(3)	8372(4)	6.26(31)
C(18)	8548(10)	3806(5)	7543(4)	5.27(30)
C(19)	6907(8)	2731(4)	6893(3)	5.00(30)
C(20)	8493(10)	2661(4)	7338(3)	5.53(32)

*Add unity to these coordinates in order to refer all atoms to the same molecule.

[3]Photocopies of the structure factor table are available for a nominal charge from the Depository of Unpublished Data, CISTI, National Research Council of Canada, Ottawa, Canada K1A 0S2.

[4]We thank Professor Prout for sending us his results prior to publication.

TABLE 3. Idealized positions ($\times 10^4$) and isotropic thermal parameters for hydrogens

Atom	x	y	z	B_{iso} (Å^2)
H(1)	4284	−0044	2505	6.24
H(2)	5431	0778	4583	5.54
H(3)	8503	2828	4859	5.59
H(4)	9649	3405	3053	5.64
H(5)	6835	1591	1533	5.92
H(6)	3199	1868	3133	5.11
H(7)	7124	3810	4776	5.48
H(8)	6753	4932	4118	6.67
H(9)	2616	3649	2088	6.16
H(10)	0301	1735	1529	5.99
H(11)	2584	2251	7313	6.34
H(12)	4730	3207	9486	7.54
H(13)	3894	1908	0537*	6.87
H(14)	1423	0212	9021	7.51
H(15)	0860	0484	7061	7.52
H(16)	2648*	3895	8722	6.14
H(17)	2816*	5203	8935	7.26
H(18)	7947	4080	7438	6.27
H(19)	4989	2134	6241	6.00
H(20)	7873	2001	7063	6.53

*Add unity to these coordinates in order to refer all atoms to the same molecule.

on the structure of zirconocene dichloride using our current set of data.

Description of the Structure and Discussion

In spite of the fact that the substance crystallizes with two independent molecules in the asymmetric unit, they have almost identical molecular parameters. This is readily shown by consideration of the bond lengths and angles given in Table 5. The Ti—Cl and Ti—C distances in both molecules are the same within experimental error (approximately 0.002 Å for the former and 0.009 Å for the latter). Similarly, the corresponding Cl—Ti—Cl, Cl—Ti—(ring centroid, Cp) and Cp—Ti—Cp angles are essentially identical for the two of them. In fact, the only discernible difference is the slightly shorter (average) C—C distance in molecule 2. However, this difference can readily be traced to the larger librational motion of the rings of this molecule about the metal – (ring centroid) vector. This phenomenon has been observed

TABLE 4. Anisotropic thermal parameters ($\times 10^5$ for Ti and Cl atoms; $\times 10^4$ for all others) for nonhydrogen atoms, thermal factor = $\exp[-(\beta_{11}h^2+\beta_{22}k^2+\beta_{33}l^2+\beta_{12}hk+\beta_{13}hl+\beta_{23}kl)]$

Atom	β_{11}	β_{22}	β_{33}	$2\beta_{12}$	$2\beta_{13}$	$2\beta_{23}$
Ti(1)	03055(26)	00579(5)	00425(4)	02280(21)	00901(17)	00418(7)
Ti(2)	03205(27)	00594(5)	00386(4)	02294(21)	00907(17)	00383(7)
Cl(1)	05945(54)	00751(8)	00817(8)	03535(38)	01433(35)	00681(13)
Cl(2)	07611(66)	01108(10)	00575(7)	05096(48)	−00084(34)	−00031(13)
Cl(3)	05949(55)	00810(8)	00499(6)	03477(39)	00353(30)	00144(12)
Cl(4)	10287(78)	01340(11)	00673(7)	06855(56)	02151(41)	00803(15)
C(1)	0327(20)	0097(4)	0136(5)	0292(16)	−0057(15)	−0049(7)
C(2)	0481(21)	0117(4)	0103(4)	0402(18)	0280(15)	0126(7)
C(3)	0658(25)	0141(5)	0086(3)	0555(16)	0179(20)	0058(7)
C(4)	0680(26)	0154(5)	0151(5)	0605(22)	0368(19)	0194(7)
C(5)	0765(28)	0259(7)	0055(3)	0834(27)	0153(15)	0101(7)
C(6)	0569(23)	0110(4)	0127(4)	0441(18)	0315(17)	0102(7)
C(7)	0344(19)	0111(4)	0105(4)	0326(16)	0155(14)	0081(7)
C(8)	0593(25)	0079(4)	0186(6)	0340(18)	0448(20)	0135(8)
C(9)	0912(30)	0198(6)	0169(5)	0792(25)	0638(22)	0299(9)
C(10)	0697(26)	0186(6)	0072(3)	0635(23)	0241(16)	0093(7)
C(11)	0628(26)	0199(6)	0143(5)	0647(24)	0353(20)	0214(9)
C(12)	0531(25)	0110(5)	0211(6)	0414(20)	0217(21)	0007(9)
C(13)	0726(29)	0222(7)	0083(4)	0676(18)	0322(26)	0135(9)
C(14)	0655(29)	0108(5)	0245(7)	0418(21)	0559(25)	0224(10)
C(15)	0336(21)	0119(5)	0131(5)	0257(18)	0075(17)	−0037(8)
C(16)	0598(25)	0201(6)	0102(4)	0617(23)	0312(17)	0176(8)
C(17)	0715(29)	0081(4)	0106(4)	0263(19)	0369(19)	0083(7)
C(18)	1466(43)	0243(7)	0177(6)	1119(33)	0841(28)	0351(11)
C(19)	0546(24)	0192(6)	0047(3)	0491(22)	0157(14)	0097(7)
C(20)	1207(38)	0151(5)	0110(4)	0740(27)	0555(23)	0151(8)

and discussed elsewhere (4, 5, 8–10, 17) for similar molecules.

Both molecules have the familiar, distorted-tetrahedral shape found in related molecules (4, 5, 8–10, 17, 18) in which the four ligands to the central metal ion are the centroids of the two Cp rings and the two X ligands (X = halides, S, O, etc.). The configuration of the two molecules, including the shapes of the ellipsoids of thermal motion are shown in Fig. 1, where the numbering scheme used in the tables is also given. The metal–chlorine and the metal–Cp distances are identical with those found in (1,1′-trimethylenedicyclopentadienyl) titanium dichloride, $(CH_2)_3(C_5H_4)_2TiCl_2$, which contains a $—(CH_2)_3—$ chain spanning the two Cp

TABLE 5. Bond distances (Å) and angles (°) in $(C_5H_5)_2TiCl_2$

Ti(1) environment		Ti(2) environment	
Bond	Distance	Bond	Distance
Ti(1)—Cl(1)	2.367(2)	Ti(2)—Cl(3)	2.363(1)
—Cl(2)	2.361(1)	—Cl(4)	2.365(2)
—C(1)	2.366(6)	—C(11)	2.365(9)
—C(2)	2.387(7)	—C(12)	2.357(9)
—C(3)	2.394(9)	—C(13)	2.385(8)
—C(4)	2.347(8)	—C(14)	2.372(6)
—C(5)	2.357(7)	—C(15)	2.326(6)
—C(6)	2.394(8)	—C(16)	2.371(7)
—C(7)	2.388(7)	—C(17)	2.376(5)
—C(8)	2.360(5)	—C(18)	2.332(5)
—C(9)	2.354(5)	—C(19)	2.349(5)
—C(10)	2.350(6)	—C(20)	2.374(7)
Average Ti(1)—Cl	2.364(3)	Average Ti(2)—Cl	2.364(1)
Average Ti(1)—C	2.370(9)	Average Ti(2)—C	2.369(9)
Ti(1)—Cp(1)*	2.060(—)	Ti(2)—Cp(3)	2.059(—)
—Cp(2)	2.056(—)	—Cp(4)	2.059(—)
Average Ti(1)—Cp	2.058(—)	Average Ti(2)—Cp	2.059(—)

C—C distances in the cyclopentadienyl rings

	Bond	Distance		Bond	Distance
Ring 1	C(1)—C(2)	1.399(7)	Ring 2	C(6)—C(7)	1.378(6)
	C(2)—C(3)	1.345(7)		C(7)—C(8)	1.419(9)
	C(3)—C(4)	1.372(7)		C(8)—C(9)	1.382(7)
	C(4)—C(5)	1.390(8)		C(9)—C(10)	1.372(9)
	C(5)—C(1)	1.396(6)		C(10)—C(6)	1.375(9)
Ring 3	C(11)—C(12)	1.369(7)	Ring 4	C(16)—C(17)	1.339(11)
	C(12)—C(13)	1.373(7)		C(17)—C(18)	1.364(10)
	C(13)—C(14)	1.347(9)		C(18)—C(19)	1.362(9)
	C(14)—C(15)	1.356(7)		C(19)—C(20)	1.361(11)
	C(15)—C(11)	1.346(9)		C(20)—C(16)	1.356(6)
	Ring 1, mean C—C	1.380(10)		Ring 2, mean C—C	1.385(6)
	Ring 3, mean C—C	1.358(6)		Ring 4, mean C—C	1.356(5)

Bond angles around the Ti tetrahedron

Bonds	Angle	Bonds	Angle
Cl(1)—Ti(1)—Cl(2)	94.43(6)	Cl(3)—Ti(2)—Cl(4)	94.62(6)
Cl(2)—Ti(1)—Cp(1)	106.07(5)	Cl(3)—Ti(2)—Cp(3)	106.52(6)
Cp(1)—Ti(1)—Cp(2)	130.89(5)	Cp(3)—Ti(2)—Cp(4)	131.04(6)
Cl(1)—Ti(1)—Cp(1)	106.48(6)	Cl(3)—Ti(2)—Cp(3)	106.52(5)
Cl(1)—Ti(1)—Cp(2)	106.60(6)	Cl(3)—Ti(2)—Cp(4)	106.83(5)
Cl(2)—Ti(1)—Cp(2)	106.43(6)	Cl(4)—Ti(2)—Cp(4)	105.39(5)

TABLE 5 (*Concluded*)

Bond angles on the cyclopentadienyl rings					
	Bonds	Angle		Bonds	Angle
Ring 1	C(5)—C(1)—C(2)	107.2(5)	Ring 2	C(10)—C(6)—C(7)	109.0(5)
	C(1)—C(2)—C(3)	108.2(5)		C(6)—C(7)—C(8)	106.9(5)
	C(2)—C(3)—C(4)	109.6(5)		C(7)—C(8)—C(9)	107.4(5)
	C(3)—C(4)—C(5)	107.7(5)		C(8)—C(9)—C(10)	108.6(6)
	C(4)—C(5)—C(1)	107.2(6)		C(9)—C(10)—C(6)	108.1(6)
Ring 3	C(15)—C(11)—C(12)	107.2(6)	Ring 4	C(20)—C(16)—C(17)	109.9(6)
	C(11)—C(12)—C(13)	108.1(5)		C(16)—C(17)—C(18)	107.3(6)
	C(12)—C(13)—C(14)	107.3(6)		C(17)—C(18)—C(19)	107.9(6)
	C(13)—C(14)—C(15)	108.5(6)		C(18)—C(19)—C(20)	108.2(6)
	C(14)—C(15)—C(11)	108.8(6)		C(19)—C(20)—C(16)	106.7(6)
	Average C—C—C ring 1	108.0(4)		Average C—C—C ring 2	108.0(4)
	Average C—C—C ring 3	108.0(4)		Average C—C—C ring 4	108.0(5)

*Cp = the centroid of the ring.

TABLE 6. Equation of mean plane through the cyclopentadienyl rings and displacement of atoms from these planes

Plane containing	Equation	χ^2	Atom	Displacement
C(1)...C(5)	$-0.9001x - 0.2662y - 0.344z = 3.888$	7.75	C(1)	−0.0023
			C(2)	−0.0063
			C(3)	0.0127
			C(4)	−0.0138
			C(5)	0.0098
C(6)...C(10)	$0.6706x + 0.6087y - 0.4240z = 1.750$	9.92	C(6)	0.0111
			C(7)	−0.0046
			C(8)	−0.0036
			C(9)	0.0104
			C(10)	−0.0133
C(11)...C(15)	$-0.8252x - 0.5564y - 0.0968z = 2.0468$	12.53	C(11)	0.0171
			C(12)	−0.0112
			C(13)	0.0012
			C(14)	0.0094
			C(15)	−0.0166
C(16)...C(20)	$-0.3843x + 0.6657y - 0.6396z = 4.8324$	7.90	C(16)	−0.0049
			C(17)	0.0090
			C(18)	−0.0096
			C(19)	0.0066
			C(20)	−0.0011

rings. An interesting consequence of which is the fact that, whereas in titanocene dichloride the Cp rings are staggered, in the bridged compound the Cp rings are eclipsed. This difference in ring orientation has no effect on the C—C distances or on the Ti—Cl bond lengths. It influences the molecular geometry, nonetheless, since it causes changes in the Cp—Ti—Cp, Cp—TiCl, and the Cl—Ti—Cl angles. For the two compounds the values are (130.97, 106.40, and 94.53(6)°) and (132.64, 105.95, and 93.69(5)°), respectively, for titanocene dichloride and the $-(CH_2)_3-$ bridged derivative. Thus, the smaller the Cp—Ti—Cp angle, the greater the values of the other two, which implies that this is a very compact molecular system in

TABLE 7. Intermolecular closest approach distances less than 3.2 Å

Bond	Distance (Å)
Cl(4)—H(5)	2.749
Cl(4)—H(10)	2.997
Cl(3)—H(9)	2.838

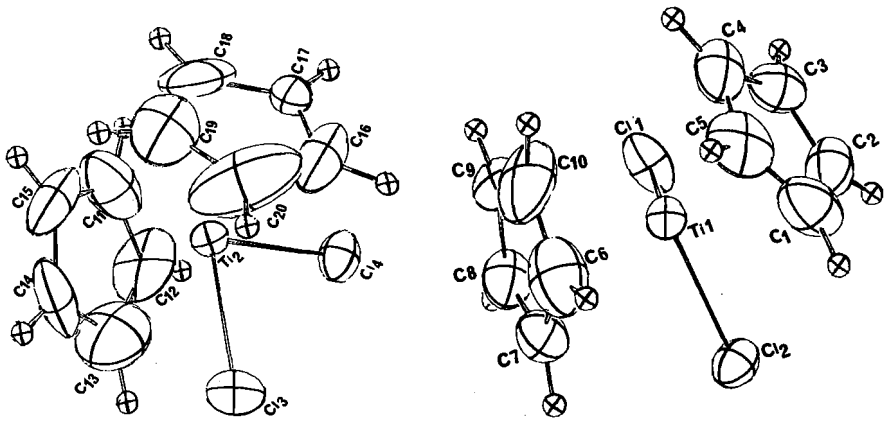

FIG. 1. The shapes of the two molecules in the asymmetric unit and the numbering system employed in labelling the atoms as they appear in the tables. Both these molecules were drawn as stereo pairs but only one view was selected; the ellipsoids of thermal motion are at 50% probability level and were drawn using Johnsons's ORTEP program.

TABLE 8. Comparison of molecular parameters for $(CH_2)_3(C_5H_4)_2MCl_2$ and $(C_5H_5)_2MCl_2$ complexes

Chemical formula	M—Cl (Å)	Cl—M—Cl (deg)	Cp—M (Å)	Cp—M—Cp (deg)	Cp—M—Cl (deg)	C—C (Å)	C—C—C(inCp) (deg)
$(CH_2)_3(C_5H_4)_2TiCl_2$	2.368(2)	93.69(5)	2.061	132.64	105.95	1.399(3)	108.0(5)
$(C_5H_5)_2TiCl_2$	2.364(2)	94.53(6)†	2.059	130.97†	106.40	1.380(10)*	108.0(5)
						1.356(6)	108.0(5)
$(CH_2)_3(C_5H_4)_2ZrCl_2$	2.441(2)	96.92(7)	2.193	129.46	106.45	1.394(10)	108.0(5)
$(CH_2)_3(C_5H_4)_2HfCl_2$	2.423(3)‡	95.87(8)	2.176‡	129.52	106.60	1.399(15)	108.0(9)

*Two molecules in the asymmetric unit ($P\bar{1}$). This is the one with lower thermal parameters for the Cp ring.
†Note the difference in these angles between the bridged and the nonbridged species. This change is probably due to the fact that the bridged compounds have eclipsed rings which are so oriented as a result of the constraints imposed on their geometry by the propylene chain. The rings in the nonbridged compounds are almost exactly staggered.
‡Note the lanthanide contraction effect. The result is the same for the metal–chlorine bond as for the metal – Cp ring distance.

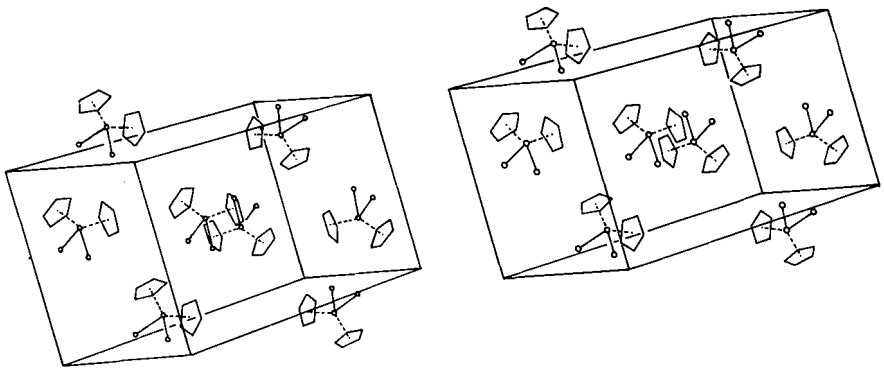

FIG. 2. This is a stereo packing diagram of the contents of the unit cell, also drawn using ORTEP.

which there is a fine balance between the Cp_2Ti and the $TiCl_2$ fragments that can readily be influenced by changes in either (*i.e.*, orientation of the rings as a result of constraints imposed by bridges, etc.).

The equations of the mean planes through the cyclopentadiene rings and the deviations of the carbon atoms from these planes are given in Table 6. In titanocene dichloride the deviations of the carbons from their mean plane are larger than those found in $(CH_2)_3(C_5H_4)_2MCl_2$, M = Ti, Zr, and Hf, as was to be expected in

view of the fact that the former exhibits larger freedom of librational motion of the Cp rings about the metal – (ring centroid) vector.

The distances of closest approach are listed in Table 7 and a packing diagram is shown in Fig. 2. Finally, a comparison of the molecular parameters (averaged values) for $(C_5H_5)_2TiCl_2$ and $(CH_2)_3(C_5H_4)_2MCl_2$ (M = Ti, Zr, and Hf) is presented in Table 8.

1. G. WILKINSON and J. M. BIRMINGHAM. J. Am. Chem. Soc. **76**, 4281 (1954).
2. G. NATTA, P. PINO, G. MAZZANTI, and U. GIANNINI. J. Am. Chem. Soc. **79**, 2975 (1957).
3. N. V. ALEKSEEV and I. A. RONOVA. Zh. Strukt. Khim. **7**, 103 (1966).
4. B. R. DAVIS and I. BERNAL. J. Organomet. Chem. **30**, 75 (1971).
5. E. F. EPSTEIN and I. BERNAL. Inorg. Chim. Acta, **7**, 211 (1973).
6. O. V. STAROVSKII and YU. T. STRUCHOV. Dokl. Akad. Nauk. SSSR, **135**, 620 (1960).
7. V. V. TKACHEV and L. O. ATOVMYAN. J. Struct. Chem. (Russ.), **13**, 263 (1972); Chem. Abstr. **77**, 25844f (1973).
8. E. F. EPSTEIN and I. BERNAL. J. Organomet. Chem. **26**, 229 (1971).
9. C. H. SALDARRIAGA-MOLINA, A. CLEARFIELD, and I. BERNAL. J. Organomet. Chem. **60**, 79 (1974).
10. C. H. SALDARRIAGA-MOLINA, A. CLEARFIELD, and I. BERNAL. Inorg. Chem. **13**, 2880 (1974).
11. Enraf-Nonium manual for CAD-4 system, Delft, Holland. 1972.
12. International tables for X-ray crystallography, Vol. 3. The Kynoch Press, Birmingham, England. 1967. p. 162.
13. A. STANISLOWSKI and B. FRENZ. Program HYDROGEN, Texas A & M University Crystallography Library, College Station, Texas.
14. F. R. AHMED, S. R. HALL, M. E. PIPPY, and C. P. HUBER. NRCC crystallographic programs for the IBM/360, National Research Council of Canada, Ottawa, Canada.
15. H. P. HANSON, F. HERMAN, J. D. LEA, and S. SKILLMAN. Acta Cryst. **17**, 1040 (1964).
16. R. F. STEWART, E. R. DAVIDSON, and W. T. SIMPSON. J. Chem. Phys. **42**, 3175 (1965).
17. K. PROUT, T. STANLEY CAMERON, R. A. FORDER, and (in part) S. R. CRITCHLEY, B. DENTON, and G. V. REES. Acta Cryst. B**30**, 2290 (1974).
18. M. A. BUSH and G. A. SIM. J. Chem. Soc. A, 2225 (1971).
19. D. K. WARNER. M. S. THESIS, Ohio University, Athens, Ohio. 1969.

Electron Spin Resonance Studies on $Ti(H_2O)_6^{3+}$ in Frozen Aqueous Solutions of Titanium(III) Chloride, Bromide, Iodide, and Sulfate

PAVLE ILIJA PREMOVIĆ AND PAUL RONALD WEST

Department of Chemistry, University of Victoria, Victoria, British Columbia V8W 2Y2

Received November 14, 1974

PAVLE ILIJA PREMOVIĆ and PAUL RONALD WEST. Can. J. Chem. **53**, 1630 (1975).

Strongly acidic aqueous solutions of titanium(III) chloride, bromide, iodide, or sulfate (0.02 *M* metal ion) provide no detectable e.s.r. signal at room temperature. In the frozen solution (77 K) an identical spectrum is observed from each sample with $g_{\parallel} = 1.994 \pm 0.001$ and $g_{\perp} = 1.896 \pm 0.001$. A maximum signal is observed at 6–8 *M* added anion, indicating not all titanium(III) species are e.s.r. active. Analysis indicates that the local symmetry of the $Ti^{3+}(3d^1)$ ions providing the signal is D_3. It is proposed that these ions are $Ti(H_2O)_6^{3+}$ species located in sites in the ice structure subject to a strong asymmetric electric field from nearby counter ions. Since the spectrum is independent of anion, the counter ions are unlikely to be in the first or second coordination shell of the Ti^{3+}.

PAVLE ILIJA PREMOVIĆ et PAUL RONALD WEST. Can. J. Chem. **53**, 1630 (1975).

Lors de l'examen par r.p.e. à température de la pièce, de solutions fortement acides de chlorure, de bromure, d'iodure et de sulfate de titane(III) (0.02 *M* en ion métallique) on n'observe aucun signal. Dans des solutions congelées (77 K) on observe un spectre identique pour chaque échantillon avec $g_{\parallel} = 1.994 \pm 0.001$ et $g_{\perp} = 1.896 \pm 0.001$. On observe un signal maximum par addition de 6–8 *M* d'anions; ceci indique que toutes les espèces de titane(III) ne sont pas actives en r.p.e. Une analyse indique que la symétrie locale des ions $Ti^{3+}(3d^1)$ fournissant le signal est D_3. On propose que ces ions sont des espèces $Ti(H_2O)_6^{3+}$ situées dans des sites de la structure de la glace qui sont sujets à des champs électriques asymétriques très forts provenant des ions antagonistes voisins. Puisque le spectre est indépendant de l'anion, il semble improbable que les ions antagonistes soient dans la première ou dans la deuxième sphère de coordination du Ti^{3+}. [Traduit par le journal]

Introduction

The ground state of a d^1 ion such as Ti^{3+} is ^2D, separated in the free ion by a rather large energy, 80 378 cm^{-1} from the first excited state ^2S (the $3d^1 \rightarrow 4s^1$ transition) (1). An ideal octahedral ligand field (O_h symmetry) splits the ^2D state into a low lying $^2T_{2g}$ state and an upper $^2E_{2g}$ state. The acidic aqueous solutions of the titanium(III) halides, $TiCl_3$, $TiBr_3$, and TiI_3, have been studied both chemically and spectroscopically, and are believed to contain only octahedrally solvated titanium ions, $Ti(H_2O)_6^{3+}$ (2–4).

The broad weak band in the optical spectrum of the $Ti(H_2O)_6^{3+}$ ion is assigned to the $^2T_{2g} \rightarrow {}^2E_{2g}$ transition (5). One interesting feature of the spectrum is the asymmetric character of the visible absorption band. This band consists of a broad maximum at 21 000 cm^{-1} with a pronounced shoulder at $\sim$17 000 cm^{-1}. The splitting is considered to arise from a nuclear configurational instability in the excited state *i.e.* from the Jahn–Teller effect (6). The ideal octahedral ion $Ti(H_2O)_6^{3+}$ cannot be stable because of the threefold degeneracy of the $^2T_{2g}$ ground state, and a tetragonal distortion is required so that a nondegenerate ground state exists *i.e.* ($^2B_{2g}$). However the theoretical background of the Jahn–Teller effect gives no direct information concerning the magnitude of the deviation from octahedral symmetry, or a choice between a static distortion and a dynamic equilibrium between limiting structures. It is however expected that the splitting of the $^2T_{2g}$ ground state will be smaller than that of the excited $^2E_{2g}$ state.

No e.s.r. signals have been detected in solutions of $Ti(H_2O)_6^{3+}$ ions at room temperature since the residual angular momentum in the $^2T_{2g}$ ground state cancels the spin angular momentum. Eventual small axial or other distortion might possibly partially "quench" the orbital angular momentum, but the expected rather short T_1 (spin–lattice relaxation time) will render the e.s.r. signal undetectable.

We now report the appearance of identical

Can. J. Chem. Downloaded from www.nrcresearchpress.com by 210.87.254.42 on 09/05/12
For personal use only.

Can. J. Chem. Downloaded from www.nrcresearchpress.com by 210.87.254.42 on 09/05/12
For personal use only.

e.s.r. signals in frozen aqueous solutions of $TiCl_3$, $TiBr_3$, and TiI_3 at 77 K which we assign to $Ti(H_2O)_6^{3+}$ ions under the influence of a strong asymmetric electric field generated indirectly by the negative counter ions present.[1] A similar signal is observed from a frozen $Ti_2(SO_4)_3$ solution.

Experimental

All spectra were recorded on a Varian E-6S X Band e.s.r. spectrometer operating at 100 kHz modulation. Samples were contained in 5 mm cylindrical quartz cells and frozen by plunging into liquid nitrogen. Spectra were recorded while the sample was cooled in a Varian E-246 insert Dewar accessory.

The commercial 20% $TiCl^3$ solution (Fisher); or 15% $Ti_2(SO_4)_3$ solution (B.D.H., [Cl] < 0.02%) were used directly. The $TiBr_3$ and TiI_3 salts were prepared by the method of Semenova from the $Ti_2(CO_3^{2-})_3$ salt (8). The concentrations of anions were varied by either addition of the reagent grade salts (NaCl, KBr, KI, and Na_2SO_4) or concentrated acids (48%HBr, 37.5% HCl, 56%HI, and 98% H_2SO_4).

The g factors are quoted relative to DPPH $g = 2.0036$, measured by means of a dual cavity assembly.

Results

Strongly acidic solutions of titanium(III) chloride ($pH \leq 1.0$) provide no detectable e.s.r. signal at room temperature. However, a rapidly frozen solution of 0.02 M $TiCl_3$ in 2 M HCl provides the spectrum shown in Fig. 1, assigned to a species with axial symmetry with $g_{\parallel} = 1.994 \pm 0.001$ and $g_{\perp} = 1.896 \pm 0.001$. The result confirms the reported observation of Glebov (7).

We now report that a frozen solution of 0.03 M $Ti_2(SO_4)_3$ in 3.75 M H_2SO_4 provided an experimentally identical spectrum under conditions where chloride ion is totally absent. Moreover both a commercial $Ti_2(SO_4)_3$ solution (B.D.H.) and a solution prepared by dissolving Ti sponge in concentrated H_2SO_4 gave the same result. To further test the sensitivity of the observed spectrum to the nature of the anion we have prepared samples of both the iodide and the bromide salts of titanium(III) (8). The method involves precipitation of titanium(III) carbonate from a $TiCl_3$ solution and thorough water-washing until no further

[1]Recently Glebov reported the e.s.r. spectrum of a frozen hydrochloric acid solution of $TiCl_3$ with pronounced g factor anisotropy ($g_{\parallel} = 1.98$ and $g_{\perp} = 1.89$). However the assignment of the structure $Ti(H_2O)_5Cl^{2+}$ made without experimental or theoretical justification overlooks the true significance of the results (7).

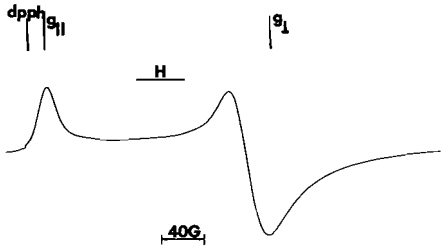

FIG. 1. Electron spin resonance spectrum of $Ti(H_2O)_6^{3+}$ in frozen aqueous solution: $Ti^{3+} = 0.02$ M, [HCl] = 6 N, 77 K.

chloride ion is detected. The $Ti_2(CO_3)_3$ is then dissolved in either aqueous HBr or HI to prepare solutions of titanous ion. Frozen solutions (77 K) prepared by this procedure [Ti] = 0.02 M, $[I^-]$ or $[Br^-] = 6$ M showed the *same spectrum* as recorded for the sulfate or chloride, Fig. 2. Even if a conservative estimate of say 10 mol% residual chloride is assigned to the solid carbonate, the ratio of $[Cl^-]$ to $[I^-]$ in the final solution would still be 10^4. It seems clear that the species providing the spectrum is independent of the anion selected, and hence does not contain anion in the first coordination shell.

A further convincing series of experiments relied upon the dependence of the signal intensity toward anion concentration. Employing 0.01 M titanium(III), a qualitatively identical spectrum was recorded at 2 M concentration of all the anions. In all cases the intensity gradually increased reaching a maximum at 4–8 M added anion. At elevated anion concentrations (> 10 M) further resonances due to additional species were apparent. Then the spectra were clearly different for Cl^-, Br^-, I^-, and SO_4^{2-}, showing a direct influence of the anion in the first coordination shell.

Of all the anions that were examined, sulfate

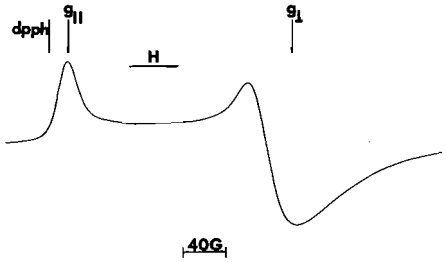

FIG. 2. Electron spin resonance spectrum of $Ti(H_2O)_6^{3+}$ in frozen aqueous solution: $Ti^{3+} = 0.02$ M, [HI] = 6.9 N, 77 K.

Can. J. Chem. Downloaded from www.nrcresearchpress.com by 210.87.254.42 on 09/05/12
For personal use only.

provided the weakest spectrum with a maximum intensity (7.5 *M* sulfate) that was only 40% of the strongest signal obtained with the halide ions. However addition of any one of NaCl, KBr, or KI to the sample caused an increase in intensity to the maximum observed with the halide ions alone, again with no change in the spectral parameters (line width or position). These experiments indicate that the studies with TiI_3 and $TiBr_3$ prepared via the carbonate route are indeed independent of chloride ion.

Our tentative assumption was that the species was $Ti(H_2O)_6^{3+}$ located in a site in the solid where a distortion of the local symmetry of the Ti^{3+} ions was created by nearby anionic species. As further tests of this hypothesis we have varied the Ti(III) concentration from 0.01 to 0.1 *M* with no appearance of resonances due to triplet Ti^{3+}---Ti^{3+} species over a wide-field sweep. Moreover we have observed that changing halide ion concentration by adding the salts (KI, KBr, or NaCl) gave the same effect as adding the corresponding concentration of the mineral acid. Therefore no specific effect of other cations (Na^+, K^+, H^+) on the e.s.r. active ions is indicated.

Discussion

The appearance of an e.s.r. signal in the frozen solutions of the titanous salts clearly indicates that a distortion of the pure octahedral O_h symmetry of the $Ti(H_2O)_6^{3+}$ species has occurred. Two lines of evidence can be used to identify the nature of the effect: (*i*) dependence of the signal on the chemical constitution of the sample, (*ii*) parameters of the observed spectrum.

There is no doubt that the signal is independent of the anion in the series Cl^-, Br^-, I^-, and SO_4^{2-}. Since dissolution of the pure metallic sponge in either concentrated reagent H_2SO_4 or in analyzed grade HCl gave samples with identical spectra, no systematic spurious impurity is suspected either. Since signal intensity increases with anion concentration, we conclude *not all* Ti^{3+} ions are located in the same environment. Clearly then we are not dealing with a (hypothetical) temperature dependent relaxation process of the $Ti(H_2O)_6^{3+}$ species that would render its spectrum observable at 77 K. Bearing in mind the uncertainty of even approximate concentration comparison in the frozen solution samples we estimate that less than 50% of the nominal Ti(III) concentration is e.s.r. active in the sample giving the most intense spectrum. In any event the fact that signal intensity *does increase* on addition of anion shows that 100% of the titanium(III) ions present do not contribute to the signal at low anion concentration.

The absence of specific effect of the anions on the spectrum leads us to suggest that while these counter ions are stabilized in water structures in the vicinity of the metal ion, they do not form a part of the first or second coordination shells. Although all four ions (Cl^-, Br^-, I^-, and SO_4^{2-}) are spherically symmetric their ionic radii and charge density are sufficiently different to project some spectral differences if neighboring (second shell) effects on the d^1 ions were primarily responsible for the distortion from octahedral symmetry. Hence, we favor the remaining alternative; that the ice structure requirements of closely situated anions and cations in turn cause a distortion of the local symmetry of the $Ti(H_2O)_6^{3+}$ unit located in that ice structure. Accordingly at low anion concentration fewer $Ti(H_2O)_6^{3+}$ would be at the required separation from a counter ion to be affected by its presence.

However the actual local symmetry of the Ti^{3+} ion in the structure is a rather complex question. In the following discussion we consider several important possibilities and compare the predicted spectrum with that actually observed.

D_{4h}

In D_{4h} symmetry, the five orbitals of a $3d^1$ configuration split into four energy states: $^2B_{2g}(d_{xy})$, doubly degenerate $^2E_{2g}(d_{xz}, d_{yz})$, $^2B_{1g}(d_{x^2-y^2})$, and $^2A_{1g}(d_{z^2})$. Consider that the Ti^{3+} ion is an octahedral ligand field of six water ligands with a small tetragonal distortion, *i.e.* D_{4h} symmetry with $^2B_{2g}$ as the ground state. The corresponding expression for $g_\parallel$ is

$$g_\parallel = 2.0023 - \frac{8\lambda}{\Delta E(^2B_{2g} \rightarrow {}^2B_{1g})} \cdot \phi_\parallel$$

where $\lambda = 154\ cm^{-1}$, ΔE refers to the electronic transition from the $^2B_{2g}$ to the $^2B_{1g}$ state, and $\phi_\parallel$ is a complex function employed to estimate covalency. The magnitude of ϕ is mainly determined by the appropriate molecular orbital coefficients. However the value of ϕ lies between 0 and 1 tending to unity as the σ and π bonding becomes more ionic, and conversely. Assuming

Can. J. Chem. Downloaded from www.nrcresearchpress.com by 210.87.254.42 on 09/05/12
For personal use only.

that we are dealing with a nearly purely ionic case *i.e.* $\phi_{\|} \rightarrow 1$ we can easily calculate (from $g_{\|}$ (exp) = 1.994 ± 0.001) that $\Delta E(^2B_{2g} \rightarrow {}^2B_{1g})$ would be as high as 154 000 cm^{-1}. Since we would expect the energy of this transition to be in the range 15 000–22 000 cm^{-1} (1–5) we must anticipate an unrealistically high covalency, *e.g.* $\phi_{\|} = 0.10$ to 0.15 to accommodate this possibility.

In an octahedral field with elongated tetragonal distortion (D_{4h} symmetry) the ground state might be expected in some cases to be $^2A_{2g}(d_{z^2})$ and corresponding expressions for the $g_{\|}$ and $g_{\perp}$ are

$$g_{\|} = 2.0023$$

$$g_{\perp} = 2.0023 - \frac{6\lambda}{\Delta E(^2A_{1g} \rightarrow {}^2E_{2g})} \cdot \phi_{\perp}$$

Now we expect $g_{\|}$ to be close to the free electron value, but $\Delta E(^2A_{1g} \rightarrow {}^2E_{2g})$ would have to be assigned an improbably *low* value ≤ 8700 cm^{-1}. Normally the transition lies between 25 000 and 45 000 cm^{-1}.

On the basis of the above discussion, we tentatively reject D_{4h} as the local point symmetry.

D_{2d}

Consideration of a $3d^1$ ion in a tetrahedral field with tetragonal distortion (D_{2d} symmetry) would involve nearly equivalent expressions and subsequent analysis would be qualitatively identical to D_{4h}.

D_{2h}

The d^1 ion in an octahedral field with a small rhombic distortion (D_{2h} symmetry) has five energy states: $^2B_{1g}$, $^2B_{2g}$, $^2B_{3g}$, and two ^2A_g states. Now the e.s.r. spectrum cannot exhibit true axial symmetry. The difference between g_x and g_y arises from the difference in energy between the $^2B_{2g}$ and $^3B_{3g}$ states.

$$g_z = g_{\|} = 2.0023 - \frac{8\lambda}{\Delta E(^2B_{1g} \rightarrow {}^2A_{1g})} \cdot \phi_z$$

$$g_x = 2.0023 - \frac{2\lambda}{\Delta E(^2B_{1g} \rightarrow {}^2B_{3g})} \cdot \phi_x$$

$$g_y = 2.0023 - \frac{2\lambda}{\Delta E(^2B_{1g} \rightarrow {}^2B_{2g})} \cdot \phi_y$$

Since our observed spectrum indicates that $g_x \simeq g_y$, then clearly the objection to D_{2h} becomes analogous to the arguments presented for D_{4h} (*vide supra*).

D_3

If the ligand field is determined primarily by the six oxygen atoms of the water ligands an approximately octahedral symmetry with a small axial trigonal distortion (D_3 symmetry) can also be considered.

In this symmetry the five orbitals are split into three energy states, one belonging to the A_1 representation and the other two to the E_1 representation. The appropriate combinations are

$$A_1 \qquad d_0$$

$$E_1 \quad \begin{cases} \sqrt{2/3}d_{-2} + \sqrt{1/3}d_1 \\ \sqrt{2/3}d_2 + \sqrt{1/3}d_{-1} \end{cases}$$

$$E_2 \quad \begin{cases} \sqrt{1/3}d_{-2} - \sqrt{2/3}d_1 \\ \sqrt{1/3}d_2 - \sqrt{2/3}d_{-1} \end{cases}$$

If pure octahedral symmetry exists, the energies of the A_1 and E_1 states are lowest and equal. A small axial distortion lifts the degeneracy and makes either A_1 or E_1 the ground state. If we are dealing with D_3 symmetry then our experimental g values are only consistent with A_1 as the ground state (if E_1 were the ground state both $g_{\|}$ and $g_{\perp}$ are predicted to be close to zero).

Consider A_1 as the ground state and assuming that we are dealing with a purely ionic case with $\Delta E(A_1 \rightarrow E_1) \gg \lambda$ we have

$$g_{\|} = 2.0023$$

$$g_{\perp} = 2.0023 - \frac{2\lambda}{\Delta E(A_1 \rightarrow E_1)} - \frac{4\lambda}{\Delta E(A_1 \rightarrow E_2)}$$

On the basis of this expression and assuming $\Delta E(A_1 \rightarrow E_2)$ is in the range 15 000–22 000 cm^{-1} (*i.e.* by analogy to $\Delta E(^2B_{2g} \rightarrow {}^2B_{1g})$ in D_{4h} symmetry) one calculates that $\Delta E(A_1 \rightarrow E_1) <$ 5600 cm^{-1}. Since the experimental value of $g_{\|}$ is rather lower than the free electron value, the assumption implicit in the above expression (*i.e.* $\Delta E(A_1 \rightarrow E_1) \gg \lambda$ for $\lambda = 154$ cm^{-1}) is not strictly valid, and $\Delta E(A_1 \rightarrow E_1)$ may be much lower than 5600 cm^{-1}.

Notwithstanding, the experimental g values are undoubtedly more consistent with D_3 local symmetry of the titanium(III) complex unit giving the spectrum than with the other possibilities that have been discussed.

On the basis of present data we are unable to make comment on the nature of the ice structure involved, for either anion or cation; or indeed whether the distortion of the field about the Ti(III) arises from the location of the ions near a phase boundary of two forms of ice structure.

The support of the National Research Council of Canada and of the University of Victoria in the form of operating grants is gratefully acknowledged. One of us (P.P) thanks the National Research Council for assistance through a National Research Council of Canada Fellowship.

1. C. E. MOORE. Atomic energy levels. U.S. Bur. Stand. Circ. No. 467, 1964.
2. (*a*) F. E. ILSE and H. HARTMANN. Z. Phys. Chem. Leipz. **197**, 239 (1951); (*b*) H. HARTMANN, H. L. SCHLÄFER, and K. H. HANSEN. Z. Anorg. Allg. Chem. **284**, 153 (1956).
3. R. L. PECSOCK, A. N. Fletcher. Inorg. Chem. **1**, 155 (1954).
4. H. J. GARDNER. Aust. J. Chem. **20**, 2357 (1967).
5. (*a*) C. K. JØRGENSEN. Absorption spectra and chemical bonding in complexes. Pergamon, Oxford. 1962; (*b*) C. J. BALHAUSEN. Ligand field theory. McGraw–Hill, New York. 1962; (*c*) R. J. H. CLARK. The chemistry of titanium and vanadium. Elsevier, Amsterdam. 1968.
6. A. D. LIEHR. Prog. Inorg. Chem. **3**, 281 (1962).
7. (*a*) V. A. GLEBOV. Zh. Strukt. Khim. **11**, 809 (1970); (*b*) V. A. GLEBOV. Dokl. Akad. Nauk SSSR, **190**, 1378 (1970).
8. E. I. SEMENOVA. Dokl. Akad. Nauk SSSR, **143**, 1368 (1962).

Can. J. Chem. Downloaded from www.nrcresearchpress.com by 210.87.254.42 on 09/05/12
For personal use only.

Substituent Effects on the Ionization Equilibria of 9-Aryl-9-fluorenols and 10-Aryl-10-hydroxyanthracen-9-ones

TREVOR W. TOONE, EDWARD LEE-RUFF, AND ALAN C. HOPKINSON
Department of Chemistry, York University, Downsview, Ontario M3J 1P3

Received October 10, 1974

TREVOR W. TOONE, EDWARD LEE-RUFF, and ALAN C. HOPKINSON. Can. J. Chem. **53**, 1635 (1975).

The title compounds were prepared and their basicities measured. In both systems the major part of the molecule is held planar, while an aryl group is free to rotate. This may interact with the positive charge but steric hindrance to the *ortho* hydrogens may be expected to oppose planarity. In these systems no evidence was found for a reduction of the normal σ^+ value due to failure to achieve planarity. A formula is presented which gives the approximate degree of resemblance (α) of the transition state to the products and, in the case of the ionization of triarylmethanols, α is found to be linear with pK_R+. It is suggested that this could resolve the apparent contradiction between the Hammett equation and the Hammond postulate.

TREVOR W. TOONE, EDWARD LEE-RUFF et ALAN C. HOPKINSON. Can. J. Chem. **53**, 1635 (1975).

On a préparé les composés mentionnés dans le titre et on a mesuré leur basicité. Dans chacun des systèmes, la plus grande partie de la molécule est maintenue à l'état planaire alors que le groupe aryle est en rotation libre. Celui-ci peut interagir avec la charge positive mais on s'attend à ce que l'empêchement stérique des hydrogènes ortho s'oppose à la planarité. Dans ces systèmes, on n'a trouvé aucune preuve amenant une réduction de la valeur normale du σ^+ qui viendrait d'un empêchement à la planarité. On présente une formule qui donne un degré approximatif de ressemblance (α) de l'état de transition avec les produits et l'on trouve dans le cas de l'ionisation des triarylméthanols qu'α varie d'une façon linéaire avec le pK_R+. On suggère que ceci pourrait résoudre la contradiction apparente entre l'équation de Hammett et le postulat de Hammond. [Traduit par le journal]

The current controversy concerning the detection of unusual substrate ratios in some electrophilic aromatic substitution reactions (see ref. 1 for summaries of opposing arguments), claimed to be the result of very early transition states, may reopen an earlier controversy which surrounded the establishment of a discrete set of Hammett-type substituent constants for use in electrophilic aromatic substitution and similar reactions. Brown and Okamoto (2) established such a set of parameters in the face of opposition (3) which claimed that such a set would be valueless because of a variable resonance effect. Deno (4) justified their use in aryl carbonium ion – aryl alcohol equilibria claiming that it is not so important how much charge is delocalized in the substituent but that the amount should remain constant throughout the reaction series. Yukawa and Tsuno (5) have attempted to correlate rates and equilibria with a linear mixture of σ and σ^+, to allow for different degrees of development of positive charge in the transition state from one reaction series to another but their method has been criticized (6) for failing to show any correlation between ρ (reaction constant) and R (the fitting parameter); also, improved 'fit' may arise simply from inclusion of an extra parameter and may have no physical significance.

On the other hand, Hammond's postulate (7) requires that the more reactive the substrate, the more the transition state should be expected to resemble the reactants. In reactions in which a partial positive charge is generated in the transition state, such as the S_N1 solvolyses used to establish σ^+ (2), the reactivity is varied by changing the substituent on the phenyl group, and this in turn must change (perhaps only slightly) the position of the transition state along the reaction coordinate and the degree of positive charge generated in the transition state. Since Stock and Brown (8) have shown that σ^+ parameters do in fact correlate a large body of data, then it is likely that the movement of the transition state along the reaction coordinate is proportional from one series to another as the substituent varies. This proportionality must be included in the reaction constant, ρ, together with the usual terms measuring the suscepti-

Can. J. Chem. Downloaded from www.nrcresearchpress.com by 210.87.254.5 on 09/05/12
For personal use only.

TABLE 1. Physical data for indicators

Compound		Melting point (°C)		Analysis (%) Calculated		Found	
No.	Aryl group	This work	Literature (ref.)	C	H	C	H
		(a) 9-Aryl-9-fluorenols					
1	4-Methoxyphenyl	85–86	87–88(20)		—		—
2	4-Methylphenyl	84–86	85.5–86.5(14)		—		—
3	Phenyl	84–85	85(21)		—		—
4	3-Methoxyphenyl	87.5–89	89–90(14)		—		—
5	3-Chlorophenyl	79–80	81–82(14)		—		—
6	3-Trifluoromethylphenyl	94.5–95.5	—	73.6	4.02	73.7	4.01
		(b) 10-Aryl-10-hydroxy-anthracen-9-ones					
7	4-Methoxyphenyl	209–210	206–207(22)	79.7	5.11	79.7	5.08
8	4-Methylphenyl	220–222	—	84.0	5.37	83.6	5.47
9	Phenyl	216–217	214(23)		—		—
10	3-Phenylphenyl	213–214	—	86.2	5.02	86.0	5.12
11	3-Trifluoromethylphenyl	208–210	—	70.2	3.84	70.0	3.73

bility of the system to electronic influences. The effect of the former will be to make ρ less negative for these reactions, since less charge is generated in the transition state in those reactions going via a more stable carbonium ion, and the $\sigma_{effective}$ for reactive compounds will lie closer to σ than σ^+, whereas for less reactive compounds $\sigma_{effective}$ will lie closer to σ^+ than to σ.

Unfortunately, studies of resonance effects in systems such as carbonium ions are frequently complicated by the twisting out-of-plane of aryl groups, as noted by Brown (8). A further complication could arise in cases such as the triaryl carbonium ion, in which it has been suggested (9) that two rings are twisted more than the third. Recently, however, this proposition has been contested (10). In the present study we examine the reduction of resonance through twisting of the aryl group in situations in which only one aryl group was free to rotate. We then compare our pK_{R+} values with the previously reported rate constants for the solvolysis of 9-phenylfluorenyl chlorides.

Experimental

Indicators

9-Aryl-9-fluorenols were prepared by the addition of an ethereal solution of 9-fluorenone to the required aryl magnesium bromide. The complex so formed was broken down by treatment with dilute acid and the crude product extracted with ether, followed by crystallization from a suitable solvent.

10-Aryl-10-hydroxyanthracen-9-ones were prepared by the dropwise addition of the required aryl magnesium bromide to a rapidly stirred suspension of anthraquinone in ether under reflux. Work-up was as for the fluorenol derivatives.

Physical data on the indicators are summarized in Table 1.

Measurements

Optical densities were measured at λ_{max} of the carbonium ion in 1 cm cells on a Unicam SP1800 spectrophotometer. Stock indicator solutions were made up in Analar methanol. Aliquots of these were transferred in a 5 µl syringe to 10 ml volumetric flasks and diluted with sulfuric acid solutions of the required strength. By weighing the flask before and after each addition it was possible to correct for small differences in indicator concentration and the changes in acid strength, by using the method of Katritzky and co-workers (11).

In the case of 10-(*m*-trifluoromethylphenyl)-10-hydroxyanthracen-9-one decomposition of the indicator occurred too rapidly for the above method to be used. Instead, solutions were made up by volume, by adding 0.05 ml of stock indicator solution to exactly 10 ml of acid solution. The resulting solution was shaken rapidly and quickly transferred to a cell, a time of about 15 s. The decrease in optical density with time was followed for a further 60–100 s and the plot extrapolated back to the time of mixing. The value so obtained was uncorrected for small differences in indicator concentration but an average correction of 0.2% was applied to the acid strength.

In all cases an acid solution of approximately the same strength as the test solution was used as reference in the spectrophotometer and care was taken to keep the temperature at 25° (±1), since the variation of pK_{R+}'s of carbinols with temperature is considerable (12).

Results and Discussion

Basicity measurements on the two series of compounds are summarized in Table 2. Both series of indicators give good linear plots of

Can. J. Chem. Downloaded from www.nrcresearchpress.com by 210.87.254.5 on 09/05/12
For personal use only.

TABLE 2. Results of basicity studies and spectral data

Compound[a]	pK_{R+}[b]	Slope of log ([R⁺]/[ROH]) *vs.* $-H_R$	λ_{max}[c]	log ε[d]
1[e]	−7.64	1.00	548	4.51
2	−9.43	0.96	518	4.48
3[e,f]	−10.82	1.00	497	4.60
4	−11.11	0.99	497	4.36
5[e]	−12.60	1.01	508	4.45
6[e]	−13.16	1.01	510[h]	4.39
7[g]	—	—	—	—
8	−9.89	0.85	550	4.07[i]
9	−10.81	0.87	530	4.21[i]
10	−11.15	0.87	486	4.10[j]
11[e]	−12.17	0.88	534	3.95

[a]Numbering as in Table 1.
[b]Calculated from $pK_{R+} = mH_R + \log([R^+]/[ROH])$, following ref. 24.
[c]9-Aryl-9-fluorenyl cations exhibit a visible spectrum consisting of two peaks, a smaller peak centered around 470 nm and a larger peak usually close to 520 nm. The visible spectrum of the 9-aryl-9-anthraquinonyl cation consists of two peaks, a smaller usually close to 480 nm and a larger close to 530 nm.
[d]In 96% sulfuric acid unless otherwise stated.
[e]The spectrum of the carbonium ion shows a small increase in intensity with increasing acid concentration. The method of Katritzky (ref. 25) was used to calculate ionization ratios.
[f]In acetic acid – water – sulfuric acid $pK_{R+} = -10.27$ and log ε = 4.57 (ref. 26).
[g]Decomposes too quickly for measurement in sulfuric acid.
[h]In the spectrum of the carbonium ion, the shorter wavelength peak at λ = 461 nm is more intense, having log ε = 4.42.
[i]In 88% sulfuric acid, as decomposition occurs rapidly in more concentrated acid.
[j]In 84% sulfuric acid, for reasons as in [i].

pK_{R+} *vs.* σ^+, as shown in Fig. 1. Neither shows curvature attributable to reduced resonance through twisting of the aryl group. Since it is likely that steric hindrance to planarity of the aryl group is greatest in the 10-aryl-10-hydroxyanthracen-9-ones, it is unfortunate that 10-(*p*-methoxyphenyl)-10-hydroxyanthracen-9-one decomposes too rapidly in sulfuric acid for measurements to be taken, as this compound is the most likely to exhibit this effect. The reaction constants for the two series are −4.28 for the fluorenols and −2.71 for the 10-hydroxyanthracen-9-ones. The lower value in the latter case is consistent with a higher degree of solvation of these cations, which may be deduced (13) from their lower slopes of log ([R⁺]/[ROH]) *vs.* $-H_R$. It is likely that the reduced ability of substituents to delocalize the positive charge is compensated by increased interaction with the solvent.

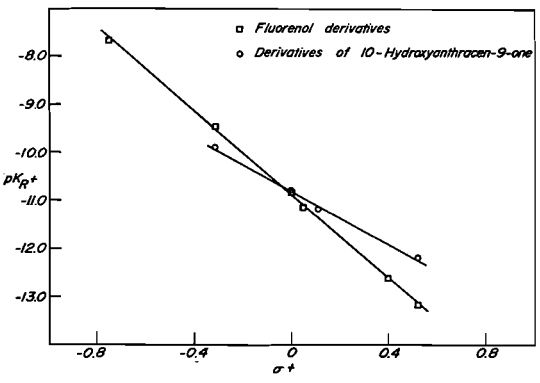

FIG. 1. Plot of pK_{R+} value against σ^+ constants.

If pK_{R+} values of 9-aryl-9-fluorenols are compared with those of similarly substituted aryldiphenyl carbinols (14) it may be seen that joining the phenyl rings in the *ortho* positions reduces the stability of the associated carbonium ion by a factor of 10^4. (The differences are 4.24 p*K* units for aryl = *p*-methoxyphenyl, 4.19 for *p*-methylphenyl, and 4.19 for phenyl.) This may be attributed to the introduction of 'antiaromaticity', since the joined system is effectively a dibenzocyclopentadienyl cation, a 12 π-electron system.

The solvolyses of 9-aryl-9-fluorenyl chlorides have been studied in 90% aqueous acetone at 25° (14) and the rates correlate well with σ^+ (correlation coefficient 0.995) with a reaction constant of −2.85. Similar correlation was found by Bolton *et al.* (15) for the solvolyses in 90:10 ethanol–acetone. Since both pK_{R+} values and

Can. J. Chem. Downloaded from www.nrcresearchpress.com by 210.87.254.5 on 09/05/12
For personal use only.

TABLE 3. Comparison of rates of solvolysis with basicity

Substrate	Solvent	Slope of log k (solvolysis) *vs.* pK_{R+} [a]	Correlation coefficient
9-Aryl-9-fluorenyl chlorides [b]	90:10 ethanol–acetone [c]	0.76	0.994
	90:10 acetone–water [d]	0.67	0.997
	90:10 acetone–water + lithium chloride [d]	0.58	0.996
Triarylmethyl chlorides [e]	60:40 acetone–ethanol [f]	0.72	
Diarylmethyl chlorides [g]	80:20 acetone–water [h]	0.71	
	Ethanol [h]	0.81	
	Ethanol [i]	0.77	
	Methanol [j]	0.83	
	2-Propanol [j]	0.73	

[a] pK_{R+} values are for carbonium ion-alcohol equilibria.
[b] pK_{R+} values from present work.
[c] Rate data from ref. 15.
[d] Rate data from ref. 14.
[e] pK_{R+} values from ref. 27.
[f] Rate data from ref. 28.
[g] pK_{R+} values from ref. 9.
[h] Rate data from ref. 29.
[i] Rate data from ref. 30.
[j] Rate data from ref. 31.

logarithms of rate constants are linear with respect to σ^+, it follows that they will be linear with respect to each other. Values of the slopes of plots of log k (from the ionization of chlorides) *vs.* pK_{R+} (from the equilibrium with the carbinol) for three different series of compounds in a variety of solvents are given in Table 3.

It is reasonable to expect pK_{R+} values of closely related compounds to vary by a constant factor in going from solvent to solvent (16); therefore the slopes of log k (solvolysis in solvent s) *vs.* pK_{R+} (in sulfuric acid) are probably very close to log k (in s) *vs.* pK_{R+} (in s). The question then arises of the reason for the less than unit slope.

Pearson and Dillon (17) examined the correlation between rates and equilibria of carbon acid ionizations and found only a rough correlation between log k (ionization) and pK_a, with a slope of approximately 0.6; this was interpreted as the degree of proton transfer from acid to base in the transition state. It is pointed out, however, that on theoretical grounds even this rough correlation is unexpected, since, in accord with Hammond's postulate (7), the weaker acids would be expected to have a greater degree of proton transfer in the transition state than the stronger acids. These data have been reexamined by Jones (18) who incorporates recent, more accurate data and shows that the plot does show the expected curvature.

Taft and co-workers (19) have measured the rates of reaction of several triaryl carbonium ions with water and show that plots of log k (reaction) *vs.* pK_{R+} were linear but only for ions containing similar substituents.

It is likely, therefore, that the slopes of about 0.7 obtained for log k (solvolysis) *vs.* pK_{R+} correspond to the degree to which the transition state resembles the carbonium ion, i.e. in the transition state a charge of about +0.7 is developed. It should be remembered, however, that the charge in the transition state probably varies with reactivity of the substrate, although this change is probably small over the range of reactivities in this investigation.

In an attempt to put Hammond's postulate on a more quantitative basis, the normal energy profile for a simple reaction may be greatly simplified to that of Fig. 2. Since $\tan\theta = \Delta G^{\ddagger}/\alpha = (\Delta G^{\ddagger} - \Delta G^0)/(1 - \alpha)$, then α, which may vary between 0 and 1 and is a rough estimate of the distance the transition state lies between reactant and product along the reaction coordinate, may be calculated using eq. 1 for those reactions for which both $\Delta G^{\ddagger}$ and ΔG^0

$$[1] \qquad \alpha = \Delta G^{\ddagger}/(2\Delta G^{\ddagger} - \Delta G^0)$$

have been measured. One such reaction is the reaction of triaryl carbonium ions with water, for which data are collected in Table 4.

With the exception of the sesquixanthyl cation, which has an unusually low activation energy, the plot of α *vs.* pK_{R+} shows excellent

Can. J. Chem. Downloaded from www.nrcresearchpress.com by 210.87.254.5 on 09/05/12
For personal use only.

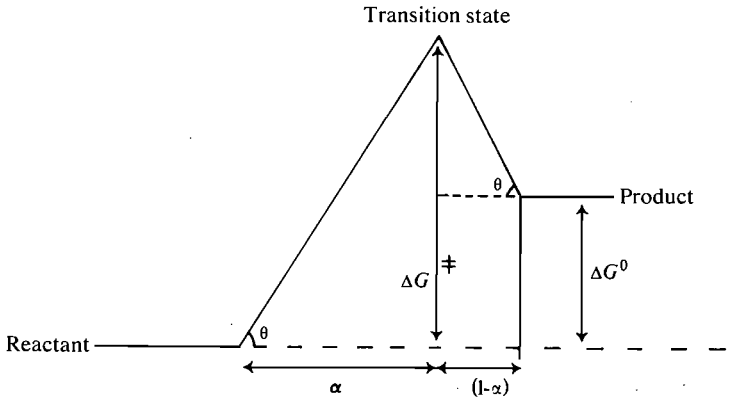

FIG. 2. Reaction profile in which the slope of the lines connecting the transition state with the reactants and with the products have the *same* magnitude but opposite sign.

TABLE 4. α for reaction of triaryl carbonium ions with water at 25°

Carbonium ion	pK_{R^+} (ref.)	$\Delta G^{\ddagger}$ (ref.)	α
Sesquixanthyl	9.05(32)	17.6(33)	0.770
$(4\text{-}N(CH_3)_2\cdot C_6H_4)_2C_6H_5\cdot C^+$	6.90(34)	22.5(19)	0.632
$(2,6\text{-DiMeO}\cdot C_6H_3)_3C^+$	5.88(33)	20.0(33)	0.625
$(4\text{-}N(CH_3)_2\cdot C_6H_4)(C_6H_5)_2C^+$	4.75(34)	20.6(19)	0.593
$(2,4\text{-DiMeO}\cdot C_6H_3)_3C^+$	3.2[a]	15.8(33)	0.580
9-(4-MeO·C_6H_4)xanthyl	1.48(33)	16.3(33)	0.533
9-Phenylxanthyl	1.02(33)	15.9(33)	0.523
$(4\text{-MeO}\cdot C_6H_4)_3C^+$	0.82(27)	16.2(19)	0.518
$(4\text{-MeO}\cdot C_6H_4)_2C_6H_5\cdot C^+$	−1.02(12)	14.9(19)	0.478
$(4\text{-MeO}\cdot C_6H_4)(C_6H_5)_2C^+$	−3.51(12)	13.5(33)	0.425

[a]Unpublished work by K. Sano and R. W. Taft, quoted from ref. 33.

linearity, with a correlation coefficient of 0.995 and slope of 0.020 (Fig. 3). $\Delta G^{\ddagger}$ does not show good linearity with ΔG^0 (correlation coefficient 0.971 excluding the sesquixanthyl cation). This is perhaps surprising in view of the success of the Hammett equation, which is frequently used to correlate free energies and activation energies of very different reactions.

Another reaction for which data on both $\Delta G^{\ddagger}$ and ΔG^0 are available is the rate of ionization of carbon acids, for which data are collected in Table 5.

In this case the treatment is a little less successful. A plot of α *vs.* pK_a has correlation coefficient 0.962. If the data on ethyl cyanoacetate, the pK_a of which is known only approximately, and 1-chloronitroethane, the pK_a of which was determined by a different method, are omitted, the correlation coefficient for the remaining three points is 1.000.

To extend the principle to incorporate our

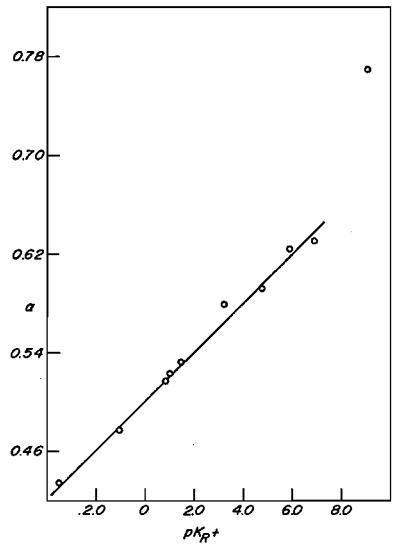

FIG. 3. Plot of the distance along the reaction coordinate, α, against pK_{R^+} for the triarylcarbonium ions.

Can. J. Chem. Downloaded from www.nrcresearchpress.com by 210.87.254.5 on 09/05/12
For personal use only.

TABLE 5. α for ionization of carbon acids

Carbon acid	pK_a [a]	$\Delta G^{\neq}$ [b]	α
Nitroacetone	5.10	17.24	0.626
1-Chloronitroethane	6.80 [c]	19.85	0.653
Ethyl nitroacetate	5.82	15.61	0.671
Ethyl cyanoacetate	~8.0	17.81	0.721
Malonitrile	11.19	15.86	0.964

[a]From ref. 17 unless otherwise stated.
[b]Calculated from data in ref. 17.
[c]Reference 35.

TABLE 6. α for reaction of 9-aryl-9-fluorenyl cations with water

Compound	Substituent	$\Delta G^{\neq}$ [a]	ΔG^0	α	pK_{R^+}
1	*p*-OMe	17.7	10.43	0.709	−7.64
2	*p*-Me	20.1	12.87	0.735	−9.43
3	H	21.5	14.76	0.761	−10.82
4	*m*-OMe	21.5	15.16	0.772	−11.11
5	*m*-Cl	23.2	17.19	0.794	−12.60

[a]Reference 15.

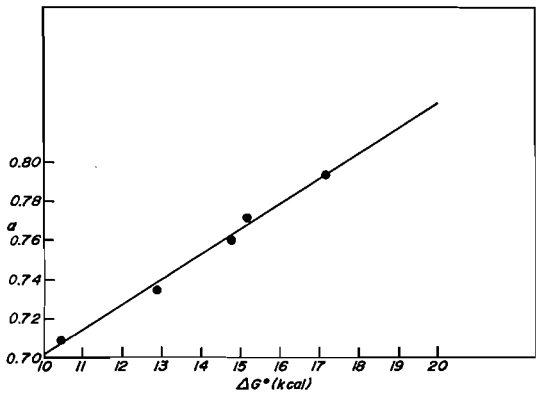

FIG. 4. Plot of α against ΔG^0 for the 9-aryl-9-fluorenyl cations.

results, we plotted α *vs.* ΔG^0 (Table 6 from the pK_{R+} values in Table 2) for the 9-arylfluorenols and obtained a linear plot (Fig. 4) with a correlation coefficient of 0.996. The $\Delta G^{\neq}$ values for the calculation of α were obtained from the kinetic data of Bolton *et al.* (15) and are referred to a different solvent system (9:1 ethanol–acetone). However, to calculate α for our solvent system, a constant difference in ΔG^0 would be involved and would not change the linearity of the plot.

While the parameter α is certainly an approximation, its linearity with pK (which must be limited as α approaches zero or unity) would seem to explain the success of the Hammett equation in the face of the apparently contradicting Hammond postulate. α also provides a simple method of converting equilibrium data into rate data, once the relationship between α and pK is established for a particular series.

The authors would like to thank the National Research Council of Canada for continued financial support.

1. G. A. OLAH. Acc. Chem. Res. **4**, 240 (1971); J. H. RIDD. Acc. Chem. Res. **4**, 248 (1971).
2. H. C. BROWN and Y. OKAMOTO. J. Am. Chem. Soc. **79**, 1913 (1957).
3. P. B. D. DE LA MARE. J. Chem. Soc. 4450 (1954); V. GOLD and D. P. N. SATCHELL. J. Chem. Soc. 2743 (1956).
4. N. C. DENO and W. L. EVANS. J. Am. Chem. Soc. **79**, 5804 (1957).
5. Y. YUKAWA and Y. TSUNO. Bull. Chem. Soc. Japan **32**, 960 (1959).
6. C. D. JOHNSON. The Hammett equation. Cambridge University Press. 1973.
7. G. S. HAMMOND. J. Am. Chem. Soc. **77**, 334 (1955).
8. L. M. STOCK and H. C. BROWN. Adv. Phys. Org. Chem. **1**, 35 (1963).
9. N. C. DENO, P. T. GROVES, and G. SAINES. J. Am. Chem. Soc. **81**, 5790 (1959).
10. I. I. SCHUSTER, A. K. COLTER, and R. J. KURLAND. J. Am. Chem. Soc. **90**, 4679 (1968).
11. C. D. JOHNSON, A. R. KATRITZKY, and S. A. SHAPIRO. J. Am. Chem. Soc. **91**, 6654 (1969).
12. M. J. COOK, N. L. DASSANAYAKA, C. D. JOHNSON, A. R. KATRITZKY, and T. W. TOONE. To be published.
13. D. G. LEE and R. CAMERON. J. Am. Chem. Soc. **93**, 4724 (1971).
14. C. EABORN, R. C. GOLESWORTHY, and M. N. LILLY. J. Chem. Soc. 3052 (1961).
15. R. BOLTON, N. B. CHAPMAN, and J. SHORTER. J. Chem. Soc. 1895 (1964).
16. E. M. ARNETT. Prog. Phys. Org. Chem. **1**, 223 (1963); M. A. PAUL and F. A. LONG. Chem. Rev. **57**, 1 (1957).
17. R. G. PEARSON and R. L. DILLON. J. Am. Chem. Soc. **75**, 2439 (1953).
18. J. R. JONES. Prog. Phys. Org. Chem. **9**, 241 (1972).
19. R. A. DIFFENBACH, K. SANO, and R. W. TAFT. J. Am. Chem. Soc. **88**, 4747 (1966).
20. M. GOMBERG and C. C. BUCHLER. J. Am. Chem. Soc. **45**, 207 (1923).
21. C. L. ARCUS and M. M. COOMBS. J. Chem. Soc. 3977 (1954).
22. F. F. BLICKE and O. J. WEINHAUFF. J. Am. Chem. Soc. **54**, 1460 (1932).
23. E. DE BARNETT and J. W. COOK. J. Chem. Soc. 2631 (1923).

Can. J. Chem. Downloaded from www.nrcresearchpress.com by 210.87.254.5 on 09/05/12
For personal use only.

24. K. YATES and R. A. MCCLELLAND. J. Am. Chem. Soc. **89**, 2686 (1967).
25. A. R. KATRITZKY. A. J. WARING, and K. YATES, Tetrahedron, **19**, 465 (1963).
26. W. N. WHITE and C. A. STOUT. J. Org. Chem. **27**, 2915 (1962).
27. N. C. DENO, J. J. JARUZELSKI, and A. SCHRIESHEIM. J. Am. Chem. Soc. **77**, 3044 (1955).
28. A. C. NIXON and G. E. K. BRANCH. J. Am. Chem. Soc. **58**, 492 (1936).
29. E. D. HUGHES, C. K. INGOLD, and N. A. TAHER. J. Chem. Soc. 949 (1940).
30. J. F. NORRIS and C. BANTA. J. Am. Chem. Soc. **50**, 1804 (1928).
31. S. ALTSCHER, R. BALTZLY, and S. W. BLACKMAN. J. Am. Chem. Soc. **74**, 3649 (1952).
32. J. C. MARTIN and R. G. SMITH. J. Am. Chem. Soc. **86**, 2252 (1964).
33. R. A. DIFFENBACH. Ph.D. Thesis, Pennsylvania State U. 1968.
34. N. C. DENO, J. J. JARUZELSKI, and A. SCHRIESHEIM. J. Org. Chem. **19**, 155 (1954).
35. J. ARMAND and P. SOUCHAY. C. R. **225**, 2112 (1962).

Can. J. Chem. Downloaded from www.nrcresearchpress.com by 210.87.254.5 on 09/05/12
For personal use only.

Etude des spectres de vibration des dérivés monosubstitués en position 5 de l'isothiazole[1]

GILBERT MILLE,[2] JEAN-CLAUDE POITE,[3] JACQUES CHOUTEAU[2] ET JACQUES METZGER[3]

Faculté des Sciences de l'Université d'Aix-Marseille III, Avenue Henri Poincaré – 13397, Marseille, Cedex 4, France

Reçu le 16 septembre 1974

GILBERT MILLE, JEAN-CLAUDE POITE, JACQUES CHOUTEAU et JACQUES METZGER. Can. J. Chem. **53**, 1642 (1975).

Les spectres i.r. sous différents états et les spectres Raman en phases condensées d'une série de dérivés de l'isothiazole monosubstitués en position 5, C_3NSH_2Y (Y = CH_3, CD_3, Cl, Br, I) ont été analysés. Une attribution des modes fondamentaux de vibration de ces molécules est proposée.

GILBERT MILLE, JEAN-CLAUDE POITE, JACQUES CHOUTEAU, and JACQUES METZGER. Can. J. Chem. **53**, 1642 (1975).

The i.r. absorption spectra in different physical states and the Raman spectra in the liquid or solid state of 5-monosubstituted isothiazole derivatives, C_3NSH_2Y (Y = CH_3, CD_3, Cl, Br, I) have been analyzed. An assignment of the fundamental modes of vibration of these molecules is given.

Introduction

Dans la continuation du programme de recherches en série hétérocyclique et, plus particulièrement, isothiazolique (1, 2) nous avons examiné les spectres i.r. sous différents états (liquide, solution, vapeur) et Raman (liquide ou solide) d'une série de dérivés de l'isothiazole C_3NSH_2Y (Y = CH_3, CD_3, Cl, Br et I) monosubstitués en position 5. Récemment, dans une courte note (2), nous avons proposé une attribution partielle des modes normaux de vibration des monométhylisothiazoles, en indiquant que dans le méthyl-5 isothiazole il paraissait exister une interaction entre une vibration de squelette et l'oscillation de valence νC—C*.[4] C'est pour préciser les mouvements susceptibles de se coupler, lors d'une substitution en position 5, que nous avons entrepris l'étude i.r. et Raman de ces molécules.

Conditions expérimentales

Préparation des composés

Les dérivés substitués en position 5 de l'isothiazole ont été obtenus par la méthode classique de lithiation de l'isothiazole par le *n*-butyllithium à −80 °C (3).

Le bromo-5 isothiazole est obtenu en faisant réagir le brome à 0 °C sur une suspension d'isothiazolyl-5 lithium. Une température trop basse favorise, par un processus d'échange, la formation de bromo-4 et de dibromo-4,5 isothiazole (4).

Nous donnons ci-dessous les résultats et les caractéristiques des composés obtenus.

Y-5 isothiazole	Rendement (%)	Point d'ébullition (mm Hg) ou de fusion (°C)	Résonance magnétique nucléaire (δ/TMS dans CCl_4) 3	4	5	Ultraviolet (solvant, éthanol) λ_{max}	ε
CH_3 ou CD_3	40	142/760	8.24	6.92	2.56	243	(8960)
Cl	34	149/760	8.37	7.35	—	243	(6700)
Br	38	56/23	8.32	7.4	—	241	(7300)
I	45	70	8.25	7.4	—	245	(9400)

Spectres infrarouges

Les spectres i.r. ont été enregistrés sur spectrographes Perkin-Elmer, modèles 125 et 225. Pour l'étude à l'état gazeux nous avons utilisé une cellule chauffante Perkin-Elmer de 5 cm d'épaisseur, à fenêtre de KBr ou CsI. A l'état dissous, les concentrations étaient voisines de 0.2 mol/l. Le tétrachlorure de carbone a été employé dans les régions de 3000 et de 1500 à 1300 cm^{-1}, le tétrachlorure d'éthylène, le sulfure de carbone et le cyclohexane ont respectivement été utilisés entre 2000 et 1400 cm^{-1}, 1350 et 450 cm^{-1}, et entre 450 et 200 cm^{-1}. Les coefficients d'extinction molaire apparents ont été mesurés aux maximum des bandes d'absorption.

[1]Ce mémoire recouvre une partie de la Thèse de Doctorat ès Sciences Physiques devant être soutenue au cours de l'année scolaire 1974–1975 par G. M.

[2]Centre technique de spectrographie infrarouge.

[3]Laboratoire de Chimie organique A.

[4]C* désigne l'atome de carbone du groupement méthyle.

Can. J. Chem. Downloaded from www.nrcresearchpress.com by 210.87.254.42 on 09/05/12
For personal use only.

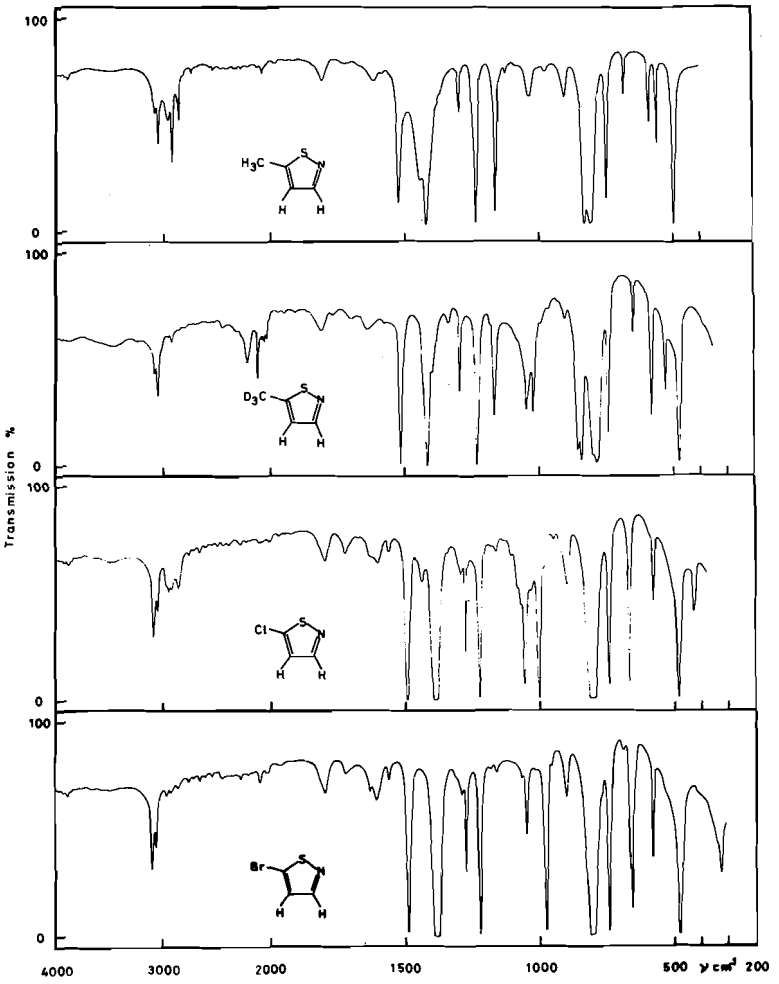

FIG. 1. Spectres des dérivés monosubstitués en position 5 de l'isothiazole.

Spectres Raman

Les échantillons à l'état liquide et solide ont été examinés dans des tubes capillaires, avec un spectrographe Raman Coderg, type PH 1 équipé d'un laser He–Ne de 100 mW émettant à 6328 Å. Les facteurs de dépolarisation ont été corrigés d'après la méthode décrite par Bribes et Gaufres (5). Les intensités ont été chiffrées de 0 à 10 par comparaison avec la raie la plus forte de chacun des spectres.

Résultats expérimentaux

Les spectres i.r. des méthyl-5, trideutériométhyl-5, chloro-5 et bromo-5 isothiazoles à l'état liquide sont reproduits dans la fig. 1. Le tableau 1 renferme sous forme de suites les fréquences i.r. et Raman des vibrations fondamentales et de quelques vibrations harmoniques ou de combinaison des hétérocycles C_3NSH_2Y. Dans le tableau 2 sont mentionnées les fréquences des vibrations propres au groupement trideutériométhyle.

Dans ces deux tableaux les fréquences infrarouges mesurées à l'état dissous sont suivies du coefficient d'extinction molaire (nombres en italiques) et lorsque les composés ont été examinés à l'état vapeur de la structure de vibration rotation (A, B ou C) des bandes. L'intensité des raies de diffusion, chiffrée de 0 à 10, et le facteur de dépolarisation succèdent aux fréquences Raman.

Analyse des spectres

Dans l'hypothèse d'une symétrie C_s (2) les 18 modes fondamentaux de l'hétérocycle C_3NSH_2X[5] actifs en i.r. et en Raman peuvent se

[5]X désigne les atomes Cl, Br, I ou C dans le cas où les substituants sont CH_3 et CD_3.

Can. J. Chem. Downloaded from www.nrcresearchpress.com by 210.87.254.42 on 09/05/12
For personal use only.

Can. J. Chem. Downloaded from www.nrcresearchpress.com by 210.87.254.42 on 09/05/12
For personal use only.

TABLEAU 1. Fréquences des vibrations fondamentales et de quelques vibrations harmoniques ou de combinaison des hétérocycles C_3NSH_2Y

	CH_3			CD_3			Cl			Br			I			Suites	Attributions
Infrarouge	3088	A	*10*	3084		*5*	3103		*43*	3100		*8*	3100	*4*			$\nu(C_4H)$
Raman	3089	3	0.30	3089	2	0.10	3107	1	0.20	3102	1	0.10	3091	1/2			
Infrarouge	3059	A	*29*	3053		*19*	3060		*62*	3058		*15*	3060	*9*			$\nu(C_3H)$
Raman				3057	1	0.10	3064	1	0.30	3063	1	0.25	3060	1/2			
Infrarouge	1800		*14*	1807		*8*	1800		*64*	1798		*6*	1803	*8*			$2\gamma(C_3H)$
Infrarouge	1606		*6*				1605		*64*	1605		*10*	1609	*9*			$2\gamma(C_4H)$
Infrarouge	1524		*40*	1520		*81*	1501		*782*	1489		*72*	1481	*52*			
Raman				1520	2	0.10	1500	1	0.20	1488	1/2	0.10			I		ω_1
Infrarouge	1421	A	*120*	1420		*146*	1399		*1480*	1392	A	*202*	1377	*276*			
Raman	1418	5	0.30	1420	3	0.45	1397	3	0.50	1386	2	0.50	1381	*2*	II		ω_2
Infrarouge	1296		*6*	1298		*12*	1282		*105*	1276		*16*	1270	*10*			
Raman	1298	6	0.20	1298	8	0.10	1283	8	0.10	1275	10	0.10	1266	*2*	III		ω_3
Infrarouge	1233	A	*102*	1232		*163*	1228		*720*	1224	A	*110*	1220	*94*			
Raman	1240	2	0.20	1234	1	0.35	1232	1/2	0.50	1226	1/2	0.40					$\delta(CH)$
Infrarouge	1164	B	*55*	1171		*26*	1009		*800*	982	A	*75*	959	*38*			
Raman	1166	3/2	0.10	1171	1/2	0.10	1011	1/2	0.55	982	1/2	0.45	961	1	IV		ω_4
Infrarouge							1165		*19*	1162		*4*	1163	*3*			$2\Gamma_1$
Infrarouge							1076		*33*	1068		*4*					$\Gamma_1 + \Gamma_2$
Infrarouge	1038	B	*6*	1023		*21*	1060		*252*	1049	B	*17*	1047	*9*			
Raman	1041	3/2	0.10	1026	1	0.60	1062	1	0.10	1053	1/2	0.10	1051	1/2			$\delta(CH)$
Infrarouge	~1000e			965		*4*	992		*33*	958		*4*					
Raman				970	1/2	0.10											$2\Gamma_2$
Infrarouge	900	C	*14*	903		*8*	901		*71*	900	C	*16*	900	*13*			$\gamma(C_3H)$
Infrarouge	832	A	*75*	846		*57*	820		*1040*	817	A	*218*	816	*233*			
Raman	835	1	0.20	845	3	0.10	821	3/2	0.10	817	2	0.10	824	1	V		ω_5
Infrarouge	805	C	*188*	785		*128*	803		*1480*	803	C	*246*	804	*282*			$\gamma(C_4H)$
Infrarouge	753	A	*43*	747		*35*	750		*256*	749	A	*87*	749	*149*			
Raman	750	7	0.30	745	8	0.15	751	2	0.30	749	2	0.35	745	2	VI		ω_6
Infrarouge	685	A	*5*	654		*8*	675		*214*	661	A	*38*	658	*76*			
Raman	684	10	0.20	654	10	0.10	671	10	0.10	662	8	0.10	656	4	VII		ω_7
Infrarouge	589	C	*12*	573		*23*	584		*62*	582	C	*20*	582	*21*	Γ		Γ_1
Raman										586	1/2	0.60					
Infrarouge	499	C	*140*	483		*95*	493		*1080*	486	C	*166*	484	*141*	Γ		Γ_2
Raman	503	1/2	0.70	485	1/2	0.60	497	1/2	0.75	488	1/2	0.45					
Infrarouge	563	A	*15*	533		*11*	435		*48*	334		*8*	281	*5*			
Raman	564	3	0.20	536	3	0.20	439	3	0.15	338	7	0.20	281	10	VIII		ω_8
Infrarouge	295		*2*	265		*3*				206		*7*					
Raman	300	3	0.40	268	1	0.60	254	2	0.50	210	4	0.50	184	5	δ(CX)		$\delta(C_5X)$
Infrarouge	240		*2*	231		*2*											
Raman	241	3	0.50	232	1	0.75	236	1	0.75				164	1	γ(CX)		$\gamma(C_5X)$

NOTE: Les notations $\nu(C_iH)$, δ(CH), δ(CX), $\gamma(C_iH)$, γ(CX), correspondent respectivement aux vibrations de valence, de déformation dans le plan et hors du plan des liaisons CH et CX. Les fréquences appartenant à des mouvements de noyau, possédant la symétrie *A'*, ont été notées ω_x ($x = 1$ à 8), celles dues aux oscillations de noyau hors du plan : Γ_1 et Γ_2; e, épaulement.

TABLEAU 2. Fréquences des vibrations fondamentales du groupement trideutériométhyle

	ν_a	ν'_s			ν_s			$r_\perp$	
Infrarouge	~2230e	2220	*9*		2122	*18*		855	*46*
Raman		2221	1/2	0.65	2121	6	0.10		
	δ_a	δ's			δ_s			$r_\parallel$	
Infrarouge	~1040*e	1047	*25*		~1068*e			~765e	
Raman		1052	2	0.20					

NOTE: Les vibrations du groupement trideutériométhyle sont désignées par: ν_a, ν'_s, ν_s (valence); δ_a, δ'_s, δ_s (déformation) et $r_\perp$, $r_\parallel$ (balancement); e, épaulement.
*Fréquence relevée à l'état liquide.

décomposer en 13 mouvements A' (2ν(CH) + 2δ(CH) + δ(CX) + ν(CX) + 7ω)* et 5 vibrations A'' (2γ(CH) + γ(CX) + 2Γ)*. Nous examinerons successivement les oscillations des liaisons CH et du squelette C_3NSX, puis celles propres aux groupements méthyle et trideutériométhyle.

Vibrations des liaisons CH

Vibrations de valence ν(CH)

Les spectres i.r. de tous les dérivés monosubstitués en position 5 de l'isothiazole présentent vers 3093 ± 10 et 3056 ± 4 cm^{-1} (Tableau 1) deux absorptions auxquelles correspondent dans le spectre Raman des raies polarisées. Ces fréquences étant respectivement proches de celles des mouvements $\nu(C_4H)$[6] et $\nu(C_3H)$[7] des hétérocycles isothiazoliques (1, 2) peuvent être attribuées à des vibrations de valence des mêmes liaisons.

Vibrations de déformation δ(CH)

Par analogie avec les attributions proposées pour ces mouvements dans l'isothiazole (1) et ses dérivés (1, 2) les deux absorptions vers 1227 ± 7 et 1041 ± 19 cm^{-1} auxquelles correspondent en Raman des raies de diffusion polarisées, peuvent être rattachées à des vibrations δ(CH) dans les composés isothiazoliques monosubstitués en position 5.

Vibrations de déformation γ(CH)

Par analogie avec le méthyl-5 isothiazole (2), les mouvements γ(CH) des isothiazoles monosubstitués en 5 peuvent être situés à 901 ± 2 et 795 ± 10 cm^{-1}. Effectivement comme dans le spectre du méthyl-5 isothiazole (2) ces bandes ont une structure de type C dans le spectre du bromo-5 isothiazole à l'état vapeur (Tableau 1) et manquent dans les spectres Raman (Tableau 1).

Vibrations du squelette C_3NSX

Vibrations de symétrie A'

En raison de la structure de vibration–rotation de type A ou B des bandes i.r. d'une part, de l'intensité et de la polarisation des raies Raman correspondantes, d'autre part, six suites de fréquences vers 1502 ± 22, 1399 ± 22, 1284 ± 14, 831 ± 15, 750 ± 3, 670 ± 16 cm^{-1} doivent être rattachées à des vibrations de symétrie A'. Les absorptions classées dans les suites I, II, III, VI et VII peuvent être reliées à des oscillations comparables aux modes ω_1, ω_2, ω_3, ω_6 et ω_7 du méthyl-5 isothiazole (2). Par contre la suite de fréquences vers 831 cm^{-1} précédemment attribuée dans le méthyl-5 isothiazole à la vibration ω_4 (2) semble devoir l'être au mouvement ω_5. En effet, tandis que pour les alkyl-5 isothiazoles les fréquences classées dans les suites I, II et V ont des positions plus élevées que les oscillations ω_1, ω_2 et ω_5 de l'isothiazole (1) ces fréquences sont, pour les halogéno-5 isothiazoles, proches des vibrations correspondantes de l'isothiazole (1). Signalons que les absorptions de la suite VII ont des fréquences toujours plus élevées ($15 < \Delta\nu < 46$ cm^{-1}) que le mode ω_7 correspondant de l'isothiazole (1). Ceci est analogue aux observations faites pour le mouvement ω_7 des dérivés substitués en position-5 du thiazole (6).

Les spectres i.r. de l'isothiazole et des deutério isothiazoles (1) montrent deux maximums d'absorption ou raies de diffusion (7) attribuables à des mouvements de symétrie A' entre 950 et 815 cm^{-1} tandis que les spectres i.r. et Raman des

[6]La notation νC_iH correspond aux vibrations de valence des liaisons C_iH. "i" (3, 4, ou 5) désignant la position de l'atome de carbone dans le cycle isothiazolique.

[7]Les symboles ν, δ, γ, ω et Γ sont définis dans la réf. 2 et dans le tableau 1.

Can. J. Chem. Downloaded from www.nrcresearchpress.com by 210.87.254.42 on 09/05/12
For personal use only.

halogéno-5 isothiazoles n'en présentent qu'un, assigné à l'oscillation ω_5. Tandis que la vibration de noyau ω_4 de l'isothiazole se manifeste par une bande infrarouge et Raman moyenne à 869 cm^{-1} aucune bande i.r. ou raie Raman de position voisine, susceptible d'appartenir à un mouvement de symétrie A' n'est observée dans les spectres des alkyl- et halogéno-5 isothiazoles. On note par contre l'existence de deux bandes i.r. et Raman classées dans les suites IV et VIII ayant des positions respectivement très voisines de deux absorptions attribuées, dans les dérivés homologues du thiazole substitués en position-5 au mode ω_5 et ν(CX) (6). On peut donc par analogie avec cette molécule envisager que les bandes des suites IV et VIII résultent du couplage du mouvement ω_4 avec la vibration ν(CX). Dans le spectre du deutério-5 isothiazole (1) où la vibration ν(CD) est située à une fréquence beaucoup plus élevée que le mode ω_4 on observe bien une bande à 922 cm^{-1} voisine de celle du mode ω_4 de l'isothiazole et une bande à 2320 cm^{-1} due à une oscillation ν(CD) pratiquement pure.

Nous avons attribué les modes δ(CX) par comparaison avec les dérivés du thiazole substitués sur le carbone 5 (6). La raie Raman correspondante est généralement polarisée.

Vibrations de symétrie A''

Deux suites de bandes vers 581 $\pm$ 8 et 491 $\pm$ 8 cm^{-1} proches des vibrations Γ_1 et Γ_2 de l'isothiazole (1) du deutério-5 isothiazole (1) et du méthyl-5 isothiazole (2) sont observées. Les enveloppes correspondantes sont de type C dans le spectre du bromo-5 à l'état vapeur (Tableau 1) et comme pour l'isothiazole (1) les raies de diffusion, lorsqu'elles apparaissent sont faibles et dépolarisées.

Par comparaison avec les dérivés homologues du thiazole (6) une raie Raman faible et dépolarisée peut être attribuée à l'oscillation γ(CX) sauf pour le bromo-5 isothiazole pour lequel elle n'a pas été observée.

Vibrations des substituants CH_3 et CD_3

Les attributions propres au groupement méthyle antérieurement proposées pour le méthyl-5 isothiazole (2) sont confirmées par l'examen de son homologue trideutériométhylé. Les vibrations du substituant CD_3 ont été assignées par analogie avec les trideutériométhylnaphtalènes (8) et sont consignées dans le tableau 2. L'ensemble de ces attributions se trouve justifié par la bonne concordance entre les valeurs des rapports isotopiques calculés à partir de nos données et celles calculées par Krimm (9) sur des bases théoriques et par Dizabo (8) sur des bases expérimentales.

Dans chaque classe de symétrie on peut remarquer aussi la bonne concordance entre le produit de Teller Redlich théorique et l'expérimental. Ces produits sont respectivement pour le trideutériométhyl-5 et le méthyl-5 isothiazole de 0.190 et 0.191 dans le cas des oscillations de symétrie A' et de 0.276 et 0.301 en ce qui concerne les modes A''.

1. J. L. Meyer, G. Davidovics, J. Chouteau, J. C. Poite et J. Roggero. Can. J. Chem. **49**, 2254 (1971).
2. G. Mille, G. Davidovics, J. C. Poite et M. Guiliano. C.R. **276B**, 31 (1973).
3. M. P. L. Caton, D. H. Jones, R. Slack et K. R. M. Wooldridge. J. Chem. Soc. 446 (1964).
4. J. C. Poite. Thèse Sciences, Marseille. 1972.
5. J. L. Bribes et R. Gaufres. J. Chim. Phys. **67**, 1168 (1970).
6. G. Davidovics. Thèse Sciences, Marseille. 1969.
7. G. Mille, S. Senez et J. Chouteau, C.R. **279B**, 211 (1974).
8. P. Dizabo. Thèse Sciences, Paris. 1965.
9. S. Krimm. Adv. Polym. Sci. **II**, 94.

Can. J. Chem. Downloaded from www.nrcresearchpress.com by 210.87.254.42 on 09/05/12
For personal use only.

The Stereochemistry of Some Organic Derivatives of Group Vb Elements. Part X.[1,2] The Crystal and Molecular Structure of Triphenylarsenic Difluoride

ANN AUGUSTINE, GEORGE FERGUSON, AND FRANK C. MARCH
Chemistry Department, University of Guelph, Guelph, Ontario N1G 2W1

Received December 4, 1974

ANN AUGUSTINE, GEORGE FERGUSON, and FRANK C. MARCH. Can. J. Chem. **53**, 1647 (1975).

The crystal structure of triphenylarsenic difluoride has been determined from three-dimensional X-ray diffractometer data. Crystals of Ph_3AsF_2 are orthorhombic, space group *Pbcn*, with four molecules of $C_{18}H_{15}AsF_2$ in a unit cell of dimensions $a = 6.270$, $b = 16.593$, $c = 14.519$ Å; molecular symmetry C_2 is required. The structure was solved by the heavy atom method and refined by full-matrix least-squares calculations to a final residual R of 0.054 for 979 intensities regarded as "observed" ($I > 3\sigma(I)$). The crystals contain well separated discrete molecules. The arsenic atom has near regular trigonal bipyramidal geometry with apical fluorine atoms (As—F 1.834(7) Å) and equatorial phenyl rings (mean As—C 1.925(5) Å). Idealized D_3 symmetry is not achieved because of unequal rotations of the phenyl rings about the As—C bonds.

ANN AUGUSTINE, GEORGE FERGUSON et FRANK C. MARCH. Can. J. Chem. **53**, 1647 (1975).

On a déterminé la structure cristalline du difluorure de triphénylarsenic à l'aide de données tri-dimensionnelles obtenues avec un diffractomètre à rayon-X. Les cristaux de Ph_3AsF_2 sont orthorhombiques, groupe d'espace *Pbcn*, avec quatre molécules de $C_{18}H_{15}AsF_2$ dans la cellule de base dont les dimensions sont $a = 6.270$, $b = 16.593$, $c = 14.519$ Å. Une symétrie moléculaire C_2 est requise. On a résolu la structure par la méthode des atomes lourds et on l'a affinée par la méthode des moindres carrés (matrice complète) jusqu'à une valeur résiduelle finale R de 0.054 pour 979 intensités considérées comme "observées" ($I > 3\sigma(I)$). Les cristaux contiennent des molécules bien séparées. L'atome d'arsenic a une géométrie pratiquement bipyramidale trigonale régulière avec des atomes de fluor aux sommets (As—F 1.834(7)Å) et des noyaux phényles en positions équatoriales (valeur moyenne de As—C 1.925(5)Å). La symétrie D_3 idéalisée n'est pas obtenue à cause de rotations inégales des noyaux phényles autour des liaisons As—C.
[Traduit par le journal]

Introduction

The series of compounds R_3MX_2 (R = alkyl or aryl; M = As, Sb, or Bi and X = halogen) are well known from spectroscopic studies (2, 3) to be generally 5-coordinate nonionic species with near regular trigonal bipyramidal geometry at the metal atom. Anomalies exist with the compounds $(CH_3)_3AsX_2$ where X = Br and I; these compounds apparently being more correctly formulated as $(CH_3)_3AsX^+,X^-$ with tetrahedral geometry at the As atom (3, 4). A number of the trigonal bipyramidal R_3MX_2 species have been subjected to crystallographic analysis *e.g.* $(CH_3)_3AsCl_2$ (4), $(CH_3)_3SbX_2$ (X = Cl, Br, I) (5), Ph_3SbCl_2 (6), and Ph_3BiCl_2 (7). No fluoride derivatives have been examined by X-ray methods and we report here the structure of Ph_3AsF_2.

[1]Research conducted as part of the Final Honours Year research project of Ann Augustine.

[2]For part IX see ref. 1.

Experimental

Crystal Data

$C_{18}H_{15}AsF_2$ f. w. = 334.2

Orthorhombic, $a = 6.270(1)$, $b = 16.593(3)$, $c = 14.519(2)$ Å, $U = 1510.5$ Å^3, $Z = 4$, molecular symmetry 2, $D_c = 1.470$, $F(000) = 696$, CuK_α($\lambda = 1.5418$ Å), $\mu = 34.7$ cm^{-1}, space group *Pbcn* (D_{2h}^{14}) from the systematic absences $hk0$, k = odd; $h0l$, $h + l$ = odd; $0kl$, l = odd.

Small lathe-shaped crystals were obtained from Dr. G. S. Harris.[3] The crystal chosen for the data collection was cut to the approximate dimensions 0.10 × 0.10 × 0.20 mm^3. The cell dimensions were obtained from a least-squares refinement of the setting angles of 12 high order reflexions measured on a Hilger and Watts Y290 diffractometer. The intensity data were collected using nickel filtered CuK_α X-radiation ($\lambda = 1.5418$ Å) by the $\theta/2\theta$ scan technique with a symmetric scan of 0.70°, consisting of 70 0.01° steps of 1 s duration. Stationary crystal-stationary counter background counts of 17.5 s duration were measured at each end of the integrated scan. Three reflexion intensities were monitored as

[3]Chemistry Department, The University, St. Andrews, Fife, Scotland.

Can. J. Chem. Downloaded from www.nrcresearchpress.com by 210.87.254.5 on 09/05/12
For personal use only.

TABLE 1. Atomic positional[a] and thermal[b,c] parameters

Atom[d]	x	y	z	U_{11}	U_{22}	U_{33}	U_{12}	U_{13}	U_{23}
As	0	24955(4)	1/4	385	491	414	0	−16	0
F	2793(5)	2475(2)	2852(3)	39	69	52	1	−7	0
C(11)	0	1332(4)	1/4	47	55	34	0	−1	0
C(12)	1779(10)	913(3)	2207(4)	71	60	62	16	10	3
C(13)	1715(13)	79(3)	2193(5)	104	52	74	21	5	−9
C(14)	0	−341(5)	1/4	113	58	58	0	13	0
C(21)	741(8)	3067(3)	1398(3)	51	40	45	−1	−1	−2
C(22)	−824(9)	3537(3)	952(3)	66	53	49	0	−9	1
C(23)	−310(12)	3949(4)	148(4)	106	65	51	−5	−3	7
C(24)	1788(14)	3858(4)	−212(4)	110	70	51	−17	11	−2
C(25)	3320(11)	3403(3)	223(4)	84	75	47	2	10	0
C(26)	2804(8)	3000(3)	1027(3)	54	54	48	−5	13	−5
H(12)	319	123	198						
H(13)	307	−26	194						
H(14)	0	−97	1/4						
H(22)	−241	358	125						
H(23)	−147	432	−21						
H(24)	220	417	−84						
H(25)	490	336	−8						
H(26)	399	264	137						

[a]Fractional coordinates $\times 10^5$ for As, $\times 10^4$ for C and F, $\times 10^3$ for H.
[b]Temperature factor = $\exp[-2\pi^2(U_{11}h^2a^{*2} + U_{22}k^2b^{*2} + \ldots + 2U_{23}klb^*c^*)]$.
[c]Values multiplied by 10^4 for As, by 10^3 for C and F. The estimated standard deviations range from 0.0006 to 0.0008 for As and from 0.002 to 0.006 for C and F.
[d]Numbering for H atoms is the same as the C atom to which they are bonded.

standards at regular intervals throughout the data collection, but did not vary significantly, indicating that both crystal and beam stability were good. Each intensity was corrected for background and the estimated standard deviation for each was given by $\sigma I = [S + 4(B_1 + B_2) + (0.05I)^2]^{1/2}$, where S, B_1, and B_2 are the scan, first background, and second background counts, respectively. A total of 1301 independent intensities were measured in the sphere $1.5° < \theta < 72°$, of which 979 were greater than three times their e.s.d.'s and were regarded as "observed." The data were corrected for Lorentz, polarization and absorption effects (8); minimum and maximum transmission coefficients were 0.62 and 0.73, respectively.

Structure Solution and Refinement

The space group *Pbcn* has three special sites of multiplicity 4, two with $\bar{1}$ symmetry, and one with 2-fold symmetry. Only the last is possible for Ph_3AsF_2 and this was confirmed by the three-dimensional Patterson function from which we deduced coordinates for the arsenic, fluorine, C(11), and C(14) atoms. One cycle of least-squares refinement of F, in which the scale factor and overall temperature factor were varied, yielded $R = \Sigma||F_o| - |F_c||/\Sigma|F_o| = 0.21$. A difference F_o synthesis was then calculated and yielded chemically sensible positions for the remaining nonhydrogen atoms. In all calculations of F_c the atomic scattering factors for As, C, and F were from ref. 9 and those for H were from ref. 10. Only the observed data were used in the refinement cycles and the function minimized was $\Sigma\omega(F_o - F_c)^2$. Absolute weights (based on $\sigma(F_o)$) were used throughout the refinement and anomalous dispersion corrections for As were included at later stages. The structure was refined by full matrix least-squares calculations, with all atoms allowed individual isotropic vibration parameters, to give $R = 0.10$. All nonhydrogen atoms were allowed anisotropic thermal motions and the refinement converged with $R = 0.056$. A final difference Fourier synthesis revealed peaks in positions corresponding to all the phenyl hydrogen atoms. The highest peak which did not correspond to a hydrogen atom was approximately 0.5 e/Å^3 and was close to the arsenic atom. Theoretical positions were calculated for the hydrogen atoms using C—H = 1.08 Å and two further cycles of refinement, with the hydrogen atoms included ($Uiso$ = 0.063 Å^2) but not refined, gave convergence with $R = 0.054$ and $R_\omega = [\Sigma\omega(F_o - F_c)^2/\Sigma\omega F_o^2]^{1/2} = 0.093$. The maximum shift in any parameter on the last cycle was 0.3 of its e.s.d.

The final atomic positional and thermal parameters are listed in Table 1. Bond lengths and angles are given in Table 2. Figure 1 is a stereoscopic view of the molecule, showing the atomic numbering scheme; the molecular packing is shown in Fig. 2. A table of measured and calculated structure factors has been placed in the Depository of Unpublished Data.[4]

Results and Discussion

As expected the molecules are nonionic 5-coordinate species, the arsenic atom having a near regular trigonal bipyramidal geometry with the fluorines in apical positions. The molecule possesses crystallographic C_2 symmetry, with

[4]A complete set of Tables is available, at a nominal charge, from The Depository of Unpublished Data, CISTI, National Research Council of Canada, Ottawa, Canada K1A 0S2.

Can. J. Chem. Downloaded from www.nrcresearchpress.com by 210.87.254.5 on 09/05/12
For personal use only.

TABLE 2. Distances (Å) and angles (°)

(*a*) Bonded atoms

Atoms	Distance (Å)	Atoms	Angle (deg)
As—F	1.834(3)[a]	F—As—C(21)′	90.4(2)
As—C(11)	1.931(7)	C(11)—As—C(21)	119.6(1)
As—C(21)	1.918(4)	C(21)—As—C(21)′	120.7(3)
C(11)—C(12)	1.381(7)	C(12)—C(11)—C(12)′	119.6(7)
C(12)—C(13)	1.383(8)	C(12)—C(11)—As	120.2(3)
C(13)—C(14)	1.356(9)	C(11)—C(12)—C(13)	118.9(6)
C(21)—C(22)	1.410(7)	C(12)—C(13)—C(14)	122.1(7)
C(22)—C(23)	1.391(8)	C(13)—C(14)—C(13)′	118.2(8)
C(23)—C(24)	1.423(11)	C(26)—C(21)—C(22)	120.5(4)
C(24)—C(25)	1.374(10)	C(26)—C(21)—As	120.2(3)
C(25)—C(26)	1.384(8)	C(22)—C(21)—As	119.2(4)
C(26)—C(21)	1.406(7)	C(21)—C(22)—C(23)	119.7(5)
C—C_{av}	1.390(7)	C(22)—C(23)—C(24)	118.0(6)
F—As—F′	177.9(2)	C(23)—C(24)—C(25)	122.4(6)
F—As—C(11)	88.9(1)	C(24)—C(25)—C(26)	119.3(6)
F—As—C(21)	90.6(2)	C(25)—C(26)—C(21)	120.0(5)

(*b*) Nonbonded contacts < 3.70 Å[b]

Atoms	Distance (Å)	Atoms	Distance (Å)
F···F^{I}	2.950(6)	C(22)···C(25)^{II}	3.683(8)
F···C(26)^{I}	3.321(6)	C(23)···C(23)^{III}	3.535(12)

[a]Distance corrected for thermal motion.
[b]The Roman numerals refer to the following equivalent positions: I $1-x, y, \frac{1}{2}-z$; II $x-\frac{1}{2}, \frac{1}{2}-y, -z$; III $-x, 1-y, -z$.

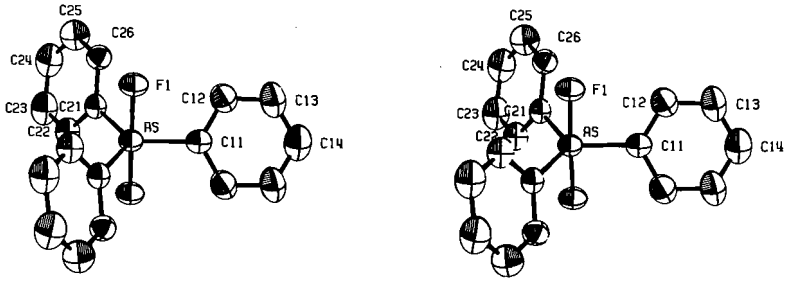

FIG. 1. Stereo view of Ph_3AsF_2. The thermal ellipsoids are drawn at the 50% level.

the As atom and two carbon atoms of one phenyl ring (C(11) and C(14)) lying on the two-fold axis; the small significant angular deviations from regular trigonal bipyramidal geometry at the As atom (∠F—As—F 177.9(2)° ∠F—As—C(11) 88.9(1)°) are doubtless caused by crystal packing effects. The molecule does not possess idealized D_3 symmetry mainly because the rotations of the phenyl groups about the As—C bonds are in opposite senses. (Table 3). The mean As—C bond distance (1.925(7) Å) is slightly longer than is generally observed for As—C(phenyl) bonds where the metal atom has tetrahedral geometry (normally in the range 1.89–1.91 Å *e.g.* ref. 11). The As—F distance, 1.834(3) Å, is slightly longer than that predicted from covalent radii data (12) and is much longer than As—F distances in hexafluorarsenate ions, *e.g.* 1.67 Å (13). There are no pentavalent As—F systems in the literature with which to compare the As—F distance found in Ph_3AsF_2.

The distances and angles in the phenyl rings vary within normal limits for structures of this kind with C—C(aromatic) = 1.390(7) Å; and ∠C—C—C 119.9(7)°. The As atom lies slightly off the planes of the two phenyl rings (Table 3),

Can. J. Chem. Downloaded from www.nrcresearchpress.com by 210.87.254.5 on 09/05/12
For personal use only.

TABLE 3. Mean plane data

(*a*) Equations[a] of planes (as in the expression $AX + BY + CZ - D = 0$)

Plane	Atoms	A	B	C	D
1	C(11)—C(14)	−0.3661	0.0027	−0.9306	−3.3747
2	C(21)—C(26)	−0.2882	−0.7958	−0.5326	−5.2628

(*b*) Distances (Å) of atoms from the planes

Plane	
1	C(11) 0.003(0); C(12) −0.012(6); C(13) 0.018(7); C(14) −0.005(0); As 0.008(0)
2	C(21) −0.002(4); C(22) 0.005(5); C(23) −0.010(6); C(24) 0.009(7); C(25) −0.003(6); C(26) 0.001(5); As 0.034(0).

(*c*) Rotation of the phenyl planes about the As—C bonds (with respect to the F—As—C plane)

Plane	
1	−37.1(3)°
2	24.2(4)°

[a] *X*, *Y*, and *Z* are angstrom coordinates parallel to unit cell axes *a*, *b*, and *c*, respectively.

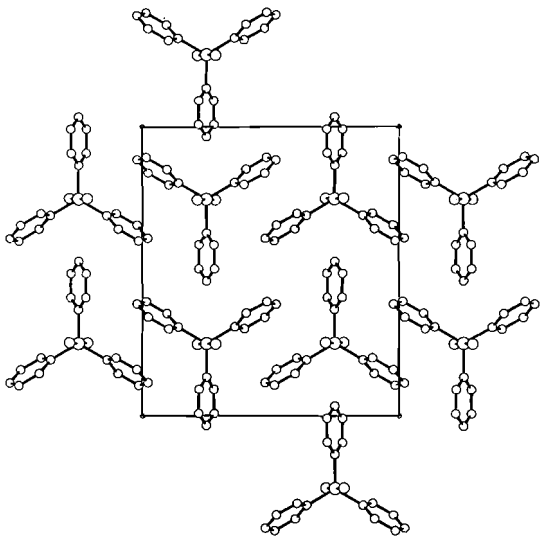

FIG. 2. The crystal structure of Ph_3AsF_2 viewed down *a*.

and the rings are rotated about their respective As—C bonds with respect to the F—As—C plane by −37.1° for plane 1 (atoms C(11)—C(14)) and 24.2° for plane 2 (atoms C(21)—C(26)).

The crystal structure is shown in Fig. 2. The shortest intermolecular contacts, listed in Table 2(*b*), correspond to normal van der Waals distances.

We are grateful to the National Research Council of Canada for financial support via operating grants (to G.F.). The many calculations were performed on the University IBM 370/155 computer system using locally modified versions of the X-Ray 72 system (14). The stereo figure was prepared with the assistance of Johnson's ORTEP (15).

1. G. FERGUSON, F. C. MARCH, and D. R. RIDLEY. Acta Cryst. In press.
2. T. B. BRILL and G. G. LONG. Inorg. Chem. **9**, 1980 (1970).
3. M. H. O'BRIEN, G. O. DOAK, and G. G. LONG. Inorg. Chim. Acta, **1**, 34 (1967).
4. M. B. HURSTHOUSE and I. A. STEER. J. Organometal. Chem. **27**, C11 (1971).
5. A. F. WELLS, Z. Kristallogr. Miner. **99**, 367 (1938).
6. T. N. POLYNOVA and M. A. PORAI-KOSHITS. Zh. Strukt. Khim. **7**, 691 (1966).
7. D. M. HAWLEY and G. FERGUSON. J. Chem. Soc. A, 2539 (1968).
8. P. COPPENS, L. LEISEROWITZ, and D. RABINOVICH. Acta Cryst. **18**, 1035, (1965).
9. International tables for X-ray crystallography. Vol. III. Kynoch Press, Birmingham. 1965.
10. R. F. STEWART, F. R. DAVIDSON, and W. T. SIMPSON. J. Chem. Phys. **42**, 3175 (1965).
11. G. FERGUSON and E. W. MACAULEY. J. Chem. Soc. A, 1, (1969).
12. L. PAULING. The nature of the chemical bond. 3rd ed. Cornell University Press, Ithaca, N.Y. 1960.
13. C. LAU, H. LYNTON, and J. PASSMORE. J. Chem. Soc. Dalton, 2535 (1973).
14. J. M. STEWART. Technical Report TR-192. University of Maryland Computer Science Centre, College Park, Maryland. 1972.
15. C. K. JOHNSON. ORTEP. Report ORNL-3794. Oak Ridge National Laboratory, Oak Ridge, Tennessee. 1965.

Can. J. Chem. Downloaded from www.nrcresearchpress.com by 210.87.254.5 on 09/05/12
For personal use only.

The Ionization of Picric Acid in Ethanol–Sulfolane and *t*-Butyl Alcohol – Sulfolane Mixtures at 30 °C

MAURIZIO CASTAGNOLO, ANGELO DE GIGLIO, ANGELO DELL'ATTI, AND GIUSEPPE PETRELLA

Institute of Physical Chemistry, University of Bari, Via Amendola, 173 70126 Bari, Italy

Received November 25, 1974

MAURIZIO CASTAGNOLO, ANGELO DE GIGLIO, ANGELO DELL'ATTI, and GIUSEPPE PETRELLA. Can. J. Chem. **53**, 1651 (1975).

Dissociation constants at 30 °C of picric acid have been determined by a spectrophotometric method in ethanol–sulfolane and *t*-butyl alcohol – sulfolane mixtures over the entire solvent composition range. Picric acid behaves as a weak acid in all mixtures. In pure sulfolane, picric acid undergoes simple dissociation for $c < 0.08\ M$ ($pK_{HPi} = 7.6$). At concentrations higher than 0.08 *M* more complex equilibria have been observed and interpreted assuming $Pi(HPi)_2^-$ as the principal picrate species in solution. Complex behavior of dependence of association constant on solvent composition was observed; in both solvent mixtures association of picric acid decreases with decrease of dielectric constant. This behavior was discussed in terms of preferential solvation of picric acid by alcohols. the more basic components of the mixtures. A reaction mechanism of four alcohol molecules with one acid molecule accounts for the behavior observed.

MAURIZIO CASTAGNOLO, ANGELO DE GIGLIO, ANGELO DELL'ATTI et GIUSEPPE PETRELLA. Can. J. Chem. **53**, 1651 (1975).

On a déterminé à 30 °C, par une méthode spectrophotométrique, dans des mélanges éthanol–sulfolanne et alcool *t*-butylique – sulfolanne à toutes les compositions du solvant, les constantes de dissociation de l'acide picrique. L'acide picrique se comporte comme un acide faible dans tous les mélanges. Dans le sulfolanne pur, l'acide picrique subit une dissociation simple à $c < 0.08\ M$ ($pK_{HPi} = 7.6$). A des concentrations plus élevées que 0.08 *M*, on a observé des équilibres complexes qui ont été interprétés en faisant l'hypothèse que $Pi(HPi)_2^-$ est l'espèce principale du picrate dans la solution. On a observé un comportement complexe de la dépendance de la constante d'association sur la composition du solvant; dans les deux mélanges de solvant, l'association de l'acide picrique diminue lorsque la constante diélectrique diminue. On discute de ce comportement en terme d'une solvatation préférentielle de l'acide picrique par les alcools qui sont les composants les plus basiques des mélanges. On peut rationaliser les résultats à l'aide d'un mécanisme de réaction impliquant quatre molécules d'alcool pour une molécule d'acide. [Traduit par le journal]

Introduction

Previous results of conductivity measurements, performed in our laboratory, on some electrolytes in water–sulfolane and methanol–sulfolane mixtures have shown association behavior in contrast to the predictions of the electrostatic theory. In water–sulfolane, alkali chlorides (1–3) and hydrochloric acid (4) are associated to ion pairs despite the high value of the dielectric constants. The association constant of lithium chloride, very high in pure sulfolane ($K_A = 14\,595$), decreases on adding methanol even though the dielectric constant of the solvent mixtures decreases (5).

These findings show that, in these solvent mixtures, the influence of specific solute–solvent interactions on ionic equilibria is very important. In order to obtain more information about these effects, acidity constants of picric acid in ethanol–sulfolane and *t*-butyl alcohol – sulfolane mixtures have been determined at 30 °C by spectrophotometric measurements.

Experimental

Reagents

Commercial sulfolane (Shell Company) was purified as described by Desbarres *et al.* (6) and then vacuum distilled three times over sodium hydroxide pellets.

Ethanol and *t*-butyl alcohol (C. Erba RP) were purified by distillation, after refluxing for many hours over anhydrous calcium oxide. The distilled fractions were kept over molecular sieves.

Picric acid (C. Erba RP) was recrystallized three times from acetone and dried *in vacuo* for 3 h at 80 °C (m.p. 121 °C).

Apparatus

Spectrophotometric measurements were made using a Zeiss PMQ II spectrophotometer equipped with

Can. J. Chem. Downloaded from www.nrcresearchpress.com by 210.87.254.6 on 09/05/12
For personal use only.

TABLE 1. Properties of solvent mixtures at 30 °C

Number	w_2	x_2	ρ (g/cc)	ε	[ROH] (mol/l)
		Ethanol–sulfolane			
1	0.00	0.0000	0.7810	23.8	16.95
2	14.89	0.0629	0.8314	25.2	15.36
3	40.25	0.2052	0.9303	28.2	12.07
4	60.93	0.3742	1.0254	31.8	8.10
5	78.18	0.5787	1.1219	36.0	5.31
6	92.66	0.8288	1.2118	40.5	1.93
7	100.00	1.0000	1.2618	43.3	0.00
		t-Butyl alcohol – sulfolane			
8	0.00	0.0000	0.7755	11.5	10.46
9	15.15	0.0992	0.8249	13.3	9.44
10	40.70	0.2974	0.9236	18.3	7.39
11	61.33	0.4945	1.0211	24.6	5.33
12	78.38	0.6910	1.1170	31.6	3.26
13	93.15	0.8935	1.2131	39.3	1.12

temperature control accessories. Stoppered Ultrasil quartz cells of 1, 0.5, and 0.1 cm path length were used. The cells were thermostated at 30.0 ± 0.1 °C during experiments.

Procedure

Solvent mixtures were made up by weight. Stock solutions for each system were prepared by weighing picric acid and solvent, and working solutions were obtained by weight dilution. Spectrophotometric measurements were made at 420 nm, the wavelength at which picrate ion and picric acid molar absorptivities have their maximum difference. Molar absorptivities of picrate ion and picric acid were determined for each system by adding to a solution of picric acid concentrated solutions of 1,3-diphenylguanidine and $HSbCl_6$ respectively, in the same solvent.

Results

The properties of the solvent mixtures ethanol–sulfolane and *t*-butyl alcohol – sulfolane are listed in Table 1, where w_2 and x_2 are sulfolane weight per cent and mole fraction, ρ and ε are densities and dielectric constants at 30 °C, [ROH] are the concentrations in mol/l of alcohol in solvent mixture. Densities and dielectric constants were obtained by interpolation from literature data for ethanol–sulfolane mixtures (7) and by interpolation from unpublished data for *t*-butyl alcohol – sulfolane mixtures.[1]

Analytical concentrations of picric acid and total concentrations of picrate ion species, spectrophotometrically determined, are listed in Table 2. Identifying numbers are the same as the first column of Table 1.

[1]A. Sacco. Unpublished results from this laboratory.

Discussion

The ionization constant for a weak acid which dissociates according to reaction

[1] $$HA \rightleftharpoons H^+ + A^-$$

is

[2] $$K_{HA} = \frac{[A^-][H^+]f_{H^+} \cdot f_{A^-}}{[HA]f_{HA}}$$

Neglecting activity coefficients (at very low ionic strength) eq. 3 is obtained

[3] $$\log [A^-] = \tfrac{1}{2} \log K_{HA} + \tfrac{1}{2} \log [HA]$$

A plot of log $[A^-]$ *vs.* log [HA] should yield a straight line with a slope of 0.5 and intercept $\frac{1}{2} \log K_{HA}$. From the intercept, then, it is possible to calculate the K_{HA} value.

Our spectrophotometrical data were interpreted on the basis of eq. 3. Experimental values of log $[Pi^-]$ and log [HPi] for systems 1–6 and 8–13 were analyzed by a least squares method. Equation 3 holds good as may be seen by standard deviation values σ and by the slope values given in Table 3. In Table 3 dissociation constants of picric acid at 30 °C obtained from eq. 3 are reported.

In pure sulfolane (system 7) it was found that in solutions more dilute than 0.08 *M* the trend of log $[Pi^-]$ *vs.* log [HPi] was like that of the other systems studied. In solutions more concentrated than 0.08 *M* experimental data gave a straight line with a greater slope than 0.5.

This behavior may be interpreted in the light of recent theoretical work by Caruso and co-

Can. J. Chem. Downloaded from www.nrcresearchpress.com by 210.87.254.6 on 09/05/12
For personal use only.

TABLE 2. Analytical and photometric data for ionization of picric acid in ethanol–sulfolane and *t*-butyl alcohol – sulfolane mixtures at 30 °C

Number	$c \times 10^4$	$[Pi^-] \times 10^4$	Number	$c \times 10^4$	$[Pi^-] \times 10^4$
1	1.15	0.814	2	1.00	0.669
	1.86	1.11		2.01	1.14
	5.17	2.30		5.74	2.28
	6.46	2.56		12.9	4.06
	11.5	4.47		26.9	5.98
	17.9	5.24		59.2	9.25
3	1.68	1.11	4	2.31	1.21
	4.20	2.12		6.94	2.43
	9.24	3.43		20.8	4.84
	18.9	5.20		57.8	8.43
	40.3	8.27		231.3	18.8
5	2.46	0.852	6	3.13	0.270
	7.10	1.57		7.83	0.427
	21.3	2.86		78.3	1.32
	63.9	5.02		363.7	2.93
	236.8	9.84		965.2	5.19
				2150	7.88
7	49.7	0.120		4410	11.7
	99.4	0.168			
	154.6	0.193	8	0.564	0.263
	276.0	0.276		1.41	0.467
	414.0	0.309		2.82	0.704
	828.0	0.543		4.66	0.960
	1381	1.23		11.8	1.57
	2201	2.50		23.6	2.24
9	0.483	0.219	10	1.07	0.437
	1.09	0.355		3.22	0.883
	3.15	0.660		7.89	1.47
	10.5	1.28		16.7	2.11
	27.3	2.02		32.8	2.92
11	5.25	1.36	12	9.41	1.07
	13.1	2.38		30.0	1.97
	39.4	4.35		85.6	3.35
	104.0	6.98		428.0	8.05
	547.0	17.5		1060	11.8
13	5.23	0.240			
	18.3	0.437			
	52.3	0.774			
	262.0	1.73			
	1160	3.79			

workers (8). As suggested, our data have been plotted in the form of $-\log [Pi^-]$ *vs.* $-\log c$ (c = analytical HPi concentration). Such a plot is shown in Fig. 1. As may be seen there are two linear portions with slopes of 0.46 when $c < 0.08\ M$ and 1.56 when $c > 0.08\ M$.

According to Caruso's treatment, the slope of 0.46 when $c < 0.08\ M$ indicates that at low concentrations simple dissociation [1] mainly occurs in solution. By extrapolation of this linear portion of the curve to $-\log c = 0$, the value of $10^{-7.6}$ may be calculated for K_{HPi}.

The slope of the curve at higher concentrations indicates that more complex equilibria than simple dissociation [1] occur in solution. Previous data (9–11) suggest that in pure sulfolane, a typical dipolar aprotic solvent, anions are stabilized by conjugation, forming AHA^-, $A(HA)_2^-$, or more complex species.

Eller and Caruso (12), by conductometric measurements of picric acid in sulfolane at 30 °C, suggest that only polymer formation can explain the magnitude of the experimental slope ($d \log \Lambda / d \log c = -0.96$). $Pi(HPi)_2^-$ was proposed by Kolthoff *et al.* (13) as the predominant picrate species present in acetonitrile at concentration greater than 0.1 M on the basis

Can. J. Chem. Downloaded from www.nrcresearchpress.com by 210.87.254.6 on 09/05/12
For personal use only.

Can. J. Chem. Downloaded from www.nrcresearchpress.com by 210.87.254.6 on 09/05/12
For personal use only.

TABLE 3. Results of analysis of photometric data by eq. 3 using a least squares method

Number	σ	Slopes	pK_{HPi}
1	0.02	0.51	3.66
2	0.02	0.53	3.62
3	0.01	0.49	3.72
4	0.01	0.52	3.72
5	0.00	0.49	4.40
6	0.02	0.52	5.54
8	0.01	0.50	4.60
9	0.01	0.49	4.82
10	0.02	0.49	4.56
11	0.01	0.51	4.22
12	0.01	0.51	4.82
13	0.01	0.51	5.90

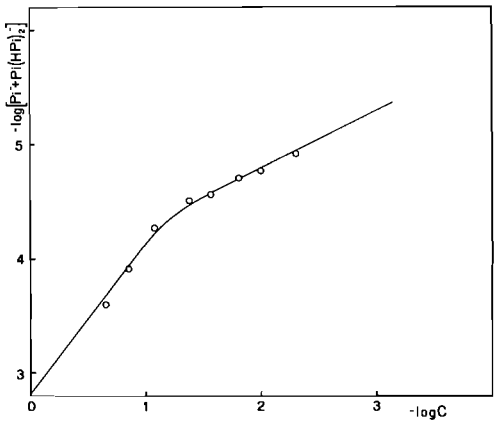

FIG. 1. Spectrophotometric data of picric acid in sulfolane. The line is the theoretical curve for equilibria 4–6 ($K_{HPi} = 10^{-7.6}$, $K_{(HPi)_2} = 10^{-1.9}$, and $K_{Pi(HPi)_2^-} = 10^4$).

of spectrophotometrical data. A graph of $-\log [Pi^-]$ *vs.* $-\log c$ shows very similar behavior, in shape and slopes (0.48 and 1.45), to our data.

Thus it is possible to suppose that in sulfolane also the mechanism of ionization of picric acid and the corresponding equilibrium constants are

[4] $$HPi \rightleftharpoons H^+ + Pi^-$$

$$K_{HPi} = \frac{[H^+][Pi^-]f^2}{[HPi]}$$

[5] $$2HPi \rightleftharpoons (HPi)_2$$

$$K_{(HPi)_2} = \frac{[(HPi)_2]}{[HPi]^2}$$

[6] $$Pi^- + (HPi)_2 \rightleftharpoons Pi(HPi)_2^-$$

$$K_{Pi(HPi)_2^-} = \frac{[Pi(HPi)_2^-]}{[Pi^-][(HPi)_2]}$$

Certainly it may be possible that the species Pi^- and $Pi(HPi)_2^-$ in these equilibria have different spectral properties; however photometric data were analyzed on the basis of identical molar absorptivities of picrate species at 420 nm. The identical assumption was made by Kolthoff *et al.* for the same anions in acetonitrile (13) and was suggested by Eller and Caruso (12).

In order to derive the values of the constants $K_{(HPi)_2}$ and $K_{Pi(HPi)_2^-}$, taking for K_{HPi} the value of $10^{-7.6}$ determined above, the procedure suggested by Caruso was used. As shown in the mathematical derivations in the microfilm edition of ref. 12, analytical picric acid concentration c is

[7] $$c = [HPi] + 2K_{(HPi)_2}[HPi]^2 + \frac{1}{f}B + \frac{1}{f}\frac{2K_{HPi}K_{(HPi)_2}K_{Pi(HPi)_2^-}[HPi]^3}{B}$$

where B is

[8] $$B = (K_{HPi}[HPi] + K_{HPi}K_{(HPi)_2} \times K_{Pi(HPi)_2^-}[HPi]^3)^{1/2}$$

and total concentration of picrate ion species is

[9] $$[Pi^-] + [Pi(HPi)_2^-] = \frac{1}{f}B$$

Neglecting activity coefficients, for an assumed set of equilibrium constants K_{HPi}, $K_{(HPi)_2}$, and $K_{Pi(HPi)_2^-}$, [HPi], and $([Pi^-] + [Pi(HPi)_2^-])$ values for different concentrations c may be respectively calculated by eqs. 7 and 9. Thus, for each set of equilibrium constants, a theoretical curve $-\log([Pi^-] + [Pi(HPi)_2^-])$ *vs.* $-\log c$ is obtained. This procedure was iterated using different values of $K_{(HPi)_2}$ and $K_{Pi(HPi)_2^-}$, in order to obtain the best agreement between theoretical and experimental data.

The theoretical curve obtained for $K_{HPi} = 10^{-7.6}$, $K_{(HPi)_2} = 10^{-1.9}$, and $K_{Pi(HPi)_2^-} = 10^4$, fits the experimental data very well, as may be seen in Fig. 1.

Let us now consider the association behavior of picric acid with solvent composition change. In Fig. 2 the curves of the logarithms of the

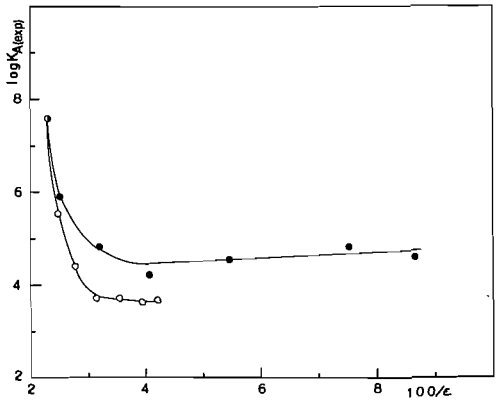

FIG. 2. Association constants of picric acid in ethanol–sulfolane (○) and *t*-butyl alcohol – sulfolane (●) mixtures.

association constants against the reciprocal of dielectric constant are shown.

If the association constant were controlled only by electrostatic forces, the Fuoss (14) equation would be valid

$$[10] \qquad \ln K_A = \ln \frac{4\pi N a^3}{3000} + \frac{e^2}{a\varepsilon kT}$$

where N is Avogadro's number, a the ion size, e the electron charge, ε the dielectric constant, k the Boltzmann constant, and T the absolute temperature. On the basis of eq. 10, the plot $\log K_A$ *vs.* $1/\varepsilon$ should be linear with positive slope.

On the contrary, for the two systems studied, the trends are not linear and association increases with increase of dielectric constant in spite of electrostatics. Clearly this behavior can only be explained by assuming that in our solvent mixtures solute–solvent interactions affect association phenomena much more than short range ion–ion interactions which depend only on the dielectric constant of the solvent.

In pure sulfolane, picric acid is weaker than in ethylic and *t*-butyl alcohols ($pK_{HPi} = 7.6$, 3.7, and 4.6 respectively). HPi reacts mainly with the alcohol which is the more basic component and sulfolane acts as an inert solvent. As suggested by Shedlowsky (15), the equilibria in solution and relevant constants should be

$$[11] \qquad HPi + n\text{ROH} \rightleftharpoons HPi\,.\,n\text{ROH}$$

$$K_1 = \frac{[HPi \cdot n\text{ROH}]}{[HPi][\text{ROH}]^n}$$

$$[12] \qquad HPi\,.\,n\text{ROH} \rightleftharpoons \text{ROH}_2^+.\text{ROH}_{(n-1)}\text{Pi}^-$$

$$K_2 = \frac{[\text{ROH}_2^+ \cdot \text{ROH}_{(n-1)}\text{Pi}^-]}{[HPi \cdot n\text{ROH}]}$$

$$[13] \qquad \text{ROH}_2^+\,.\,\text{ROH}_{(n-1)}\text{Pi}^- \rightleftharpoons \text{ROH}_2^+ + \text{ROH}_{(n-1)}\text{Pi}^-$$

$$K_3 = \frac{[\text{ROH}_2^+][\text{ROH}_{(n-1)}\text{Pi}^-]}{[\text{ROH}_2^+ \cdot \text{ROH}_{(n-1)}\text{Pi}^-]}$$

The three equations show that picric acid reacts with n molecules of alcohol, forming a complex which rearranges to an ion pair, which then dissociates. Under these conditions, eqs. 11 and 12 are controlled by specific solute–solvent interactions, while eq. 13 is controlled by electrostatics.

Then, according to eq. 10, $1/K_3 = K_A = K_0 \exp b$, where $K_0 = 4\pi N a^3/3000$ and $b = e^2/a\varepsilon kT$.

The overall constant for the equilibria 11–13 is

$$[14] \qquad K_1K_2K_3 = \frac{K_1K_2}{K_A} = \frac{[\text{ROH}_2^+][\text{ROH}_{(n-1)}\text{Pi}^-]}{[HPi][\text{ROH}]^n}$$

The experimental association constant $K_{A(exp)}$, neglecting activity coefficients, is

$$[15] \qquad K_{A(exp)} = \frac{[HPi]}{[\text{ROH}_2^+][\text{ROH}_{(n-1)}\text{Pi}^-]}$$

Evidently

$$[16] \qquad K_{A(exp)} = \frac{K_A}{[\text{ROH}]^n K_1K_2}$$

By taking logarithms, eq. 16 may be written

$$[17] \qquad \log K_{A(exp)} + n \log [\text{ROH}] = \log K_0 - \log K_1K_2 + \frac{0.434e^2}{100akT}\left(\frac{100}{\varepsilon}\right)$$

According to D'Aprano and Fuoss (16) it is possible that four alcohol molecules react with picric acid, one molecule forming ROH_2^+ species, and the other three solvating the three nitro-groups of picrate anion by hydrogen bonds. A plot of $\log K_{A(exp)} + 4 \log [\text{ROH}]$ *vs.* $100/\varepsilon$ should yield a straight line with slope $0.434e^2/100akT$ and intercept $\log K_0 - \log K_1K_2$.

Such plots for picric acid in ethanol–sulfolane and *t*-butyl alcohol – sulfolane mixtures are shown in Fig. 3. As can be seen, the graphs are reasonably linear. Higher deviation was observed in the case of pure *t*-butyl alcohol. The values of the ion size parameter a of picric acid, obtained from the slopes, are 4.7 and 2.2 Å

Can. J. Chem. Downloaded from www.nrcresearchpress.com by 210.87.254.6 on 09/05/12
For personal use only.

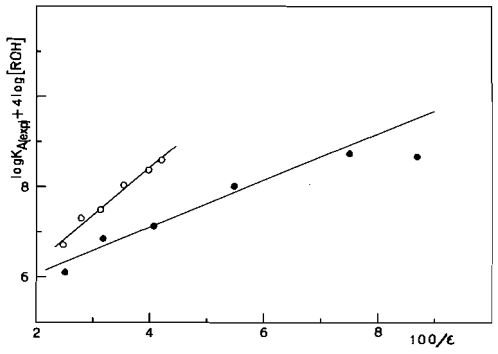

FIG. 3. Test of eq. 17 ($n = 4$) for ionization of picric acid in ethanol–sulfolane (○) and *t*-butyl alcohol – sulfolane (●) mixtures.

for *t*-butyl alcohol – sulfolane and ethanol–sulfolane mixtures respectively. Even if the last value is lower than might be expected, it is reasonable to expect lower values in ethanol than in *t*-butyl alcohol mixtures, keeping in mind the molecular size of the two alcohols studied.

From intercept values, which are 4.16 and 5.06 for ethanol–sulfolane and *t*-butyl alcohol – sulfolane mixtures respectively, it is possible to derive for the K_1K_2 products the values $10^{-5.6}$ and $10^{-5.7}$ respectively.

This result shows that, in the proposed reaction sequence [11]–[13], the interactions between hydroxyl group and picric acid are scarcely affected by different alkyl groups in the two alcohols.

1. M. CASTAGNOLO, L. JANNELLI, G. PETRELLA, and A. SACCO. Z. Naturforsch. **26**a, 755 (1971).
2. A. SACCO, G. PETRELLA, and M. CASTAGNOLO. Z. Naturforsch. **26**a, 1306 (1971).
3. G. PETRELLA, M. CASTAGNOLO, A. SACCO, and L. LASALANDRA. Z. Naturforsch. **27**a, 1345 (1972).
4. M. CASTAGNOLO and G. PETRELLA. Electrochim. Acta. **19**, 855 (1974).
5. G. PETRELLA and M. CASTAGNOLO. Z. Naturforsch. **28**a, 1149 (1973).
6. J. DESBARRES, P. PICHET, and R. L. BENOIT. Electrochim. Acta. **13**, 1899 (1968).
7. O. SCIACOVELLI. Boll. Sci. Fac. Chim. Ind. Bologna, **27**, 173 (1969).
8. N. G. SELLERS, P. M. P. ELLER, and J. A. CARUSO. J. Phys. Chem. **76**, 3618 (1972).
9. R. L. BENOIT, M. RINFRET, and R. DOMAIN. Inorg. Chem. **11**, 2603 (1972).
10. D. H. MORMAN and G. A. HARLOW. Anal. Chem. **39**, 1869 (1967).
11. J. F. COETZEE and R. J. BERTOZZI. Anal. Chem. **43**, 961 (1971).
12. P. M. P. ELLER and J. A. CARUSO. Can. J. Chem. **51**, 448 (1973).
13. I. M. KOLTHOFF, S. BRUCKENSTEIN, and M. CHANTOONI. J. Am. Chem. Soc. **83**, 3927 (1961).
14. R. M. FUOSS. J. Am. Chem. Soc. **80**, 5059 (1958).
15. T. SHEDLOVSKY. *In* Electrolytes. *Edited by* B. Pesce. Pergamon Press Inc., New York, N.Y. 1962. p. 146.
16. A. D'APRANO and R. M. FUOSS. J. Phys. Chem. **73**, 400 (1969).

Can. J. Chem. Downloaded from www.nrcresearchpress.com by 210.87.254.6 on 09/05/12
For personal use only.

Photoisomerization of Bicyclo[3.1.1]heptan-2-ones in Methanol: Chemical Transformations of 'Verbanones'[1]

ALEX G. FALLIS

Department of Chemistry, Memorial University of Newfoundland, St. John's, Newfoundland A1C 5S7

Received December 5, 1974

ALEX G. FALLIS. Can. J. Chem. **53**, 1657 (1975).

The products (predominantly unsaturated aldehydes) from photolysis in methanol of a series of 6,6-dimethylbicyclo[3.1.1]heptan-2-ones are reported. These results are rationalized on the basis of stereochemical interactions and the apparent preference for cleavage to occur adjacent to the less highly substituted α-carbon but more stable alkyl radical. It is concluded that the photochemical behavior of α-cyclobutyl ketones displays a closer parallel to the α-cyclopropyl ketones than previously recognized and that cleavage will occur preferentially on the side of the carbonyl group remote from the four-membered ring whenever possible. The synthetic steps involved in the preparation of the ketones from 'pinene' precursors are described.

ALEX G. FALLIS. Can. J. Chem. **53**, 1657 (1975).

On rapporte les produits (principalement des aldéhydes non-saturés) formés lors de la photolyse dans le méthanol d'une série de diméthyl-6,6 bicyclo[3.1.1]heptanones-2. On rationalise les résultats en se basant sur les interactions stéréochimiques et la préférence apparente pour que la coupure se produise dans la position adjacente à celle du carbone α moins substitué mais possédant le radical alkyle le plus stable. On en conclut que le comportement photochimique des α-cyclobutyl cétones montre un parallélisme plus près de celui des α-cyclopropyl cétones qu'il n'avait été reconnu auparavant; de plus, chaque fois que cette coupure sera possible, la coupure se produira préférentiellement sur le côté du groupement carbonyle éloigné du cycle à quatre membres. On décrit les étapes synthétiques impliquées dans la préparation des cétones à partir de précurseur du type 'pinène'. [Traduit par le journal]

Introduction

Interest in the photochemistry of cyclic ketones is widespread but in spite of considerable attention, some facets are still imperfectly understood. The use of simple, photoinduced cleavage reactions of cycloalkanones in organic synthesis has been less than might be anticipated due in part to difficulty in predicting product ratios accurately. In general, the major product upon photolysis of saturated cyclic ketones in solution results from preferential photoinduced cleavage adjacent to the more highly substituted α-carbon (1). At the outset of our work, only two exceptions to this generalization appeared to have been reported other than for cyclic α-cyclopropyl ketones, which are known (2) to form a special class and usually cleave on the side of the carbonyl function remote from the three-membered ring.

One such exception *cis*-verbanone (**1**) was reported (3) to give the unsaturated aldehyde **2** as the only significant product upon photolysis in methanol. The second example also involved an α-ketocyclobutane system. Irradiation of *trans*-5,5,7,7,8,8-hexamethylbicyclo[4.2.0]octan-2-one (**3**) gave rise to aldehyde **4**, a product derived from cleavage of the least substituted bond α to the carbonyl group (4).

We were intrigued by the reason for this 'abnormal' behavior particularly in the case of *cis*-verbanone since the p.m.r. data reported in support of **2** assigned the vinyl hydrogens of its semicarbazone derivative to a multiplet at δ

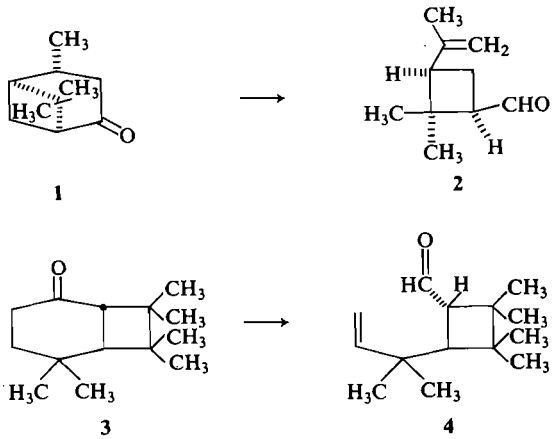

[1]Presented in part at the 55th Canadian Chemical Conference of the Chemical Institute of Canada, Quebec, Quebec, June 5–7, 1972. A preliminary report has been published (50).

Can. J. Chem. Downloaded from www.nrcresearchpress.com by 210.87.254.105 on 09/05/12
For personal use only.

TABLE 1. Proton magnetic resonance signals

Protons	δ ($CDCl_3$) (sparingly soluble)	δ (CCl_4) Matsui (3)
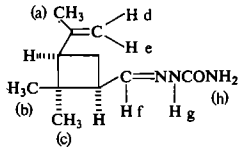		
a	1.68(3H, br s)	1.65(3H, br s)
b	0.84(3H, s)	1.27(3H, s)
c	1.24(3H, s)	0.89(3H, s)
d	4.67(1H, br s, $w_{\frac{1}{2}}$ = 5 Hz)	6.65(2H, br q)
e	4.89(1H, br s, $w_{\frac{1}{2}}$ = 6 Hz)	
f	7.14(1H, d, J = 5.7 Hz)	4.38(1H, br s)
g	*10.12(1H, br s)	
h	*5.92(2H, br s)	9.02(2H, br s)
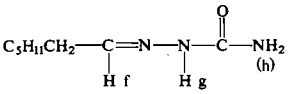		
(*n*-Heptanal semicarbazone)		
f	7.19(1H, t, J = 5.3 Hz)	
g	*10.05(1H, br s)	
h	*5.85(2H, br s)	

*Signals disappear on shaking with D_2O.

6.65 p.p.m., more nearly in accord with the range expected for cyclobutene olefinic protons. Thus, the structural assignment might have been in error and the photolytic behavior of the ketone unexceptional.

Results and Discussion

The photolysis of a methanol solution of *cis*-verbanone in a quartz tube was repeated but gave two unsaturated aldehydes in a ratio of 7:1. The important signals of the p.m.r. spectrum of the semicarbazone derivative of the major isomer are listed in Table 1 and are clearly consistent with the assigned structure **2** although they differ considerably from those reported by Matsui (3).[2] Significantly, the chemical shift and multiplicity of the vinyl hydrogen signals are as expected for geminal olefinic protons of the type found in **2** and the position of these signals is not compatible with a cyclobutene structure. In addition, the proton H_f appears as a distinct doublet (J = 5.7 Hz) whereas for the isomeric cyclobutene aldehyde (see **7**), it would appear as a triplet. The assignment of the cyclobutyl methyl signals has been reversed in accord with previous work on pinene derivatives (5) which indicates that the *trans*-methyl function lies in the deshielding zone of the unsaturated side chain. The assignment of the semicarbazone hydrogen signals was verified by D_2O exchange and comparison with model systems such as *n*-heptanal semicarbazone. (Although semicarbazones are not ideal derivatives for n.m.r. study, due to their low solubility, the signal due to the hydrogen on nitrogen (H_g) has occasionally been incorrectly assigned or missed entirely in related systems.) Additional support for the structural assignment is provided by the p.m.r. spectrum of **2** itself which displayed a doublet at δ 9.75 p.p.m. J = 1 Hz due to the aldehydic hydrogen, a broad singlet at δ 1.67 due to the vinyl methyl group and broad singlets at δ 4.71, $w_{\frac{1}{2}}$ = 4 Hz and δ 4.90, $w_{\frac{1}{2}}$ = 6 Hz for the vinyl hydrogens.

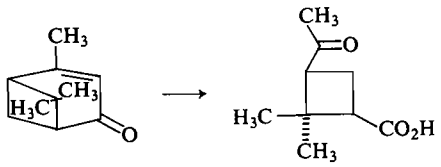

5 6

[2]We have not encountered material which corresponds to the spectral characteristics reported.

Can. J. Chem. Downloaded from www.nrcresearchpress.com by 210.87.254.105 on 09/05/12
For personal use only.

Can. J. Chem. Downloaded from www.nrcresearchpress.com by 210.87.254.105 on 09/05/12
For personal use only.

Ozonolysis of **2** followed by oxidation with Jones' reagent gave *cis*-pinononic acid (**6**) which was identical on the basis of spectral and mixture melting point comparison with an authentic sample. This sample was prepared from verbenone (**5**) by ozonolysis followed by oxidative work-up with 30% hydrogen peroxide and thus firmly established the structure of the major photolysis product as **2**.

The minor isomer is assigned the cyclobutene structure **7**. The i.r. spectrum indicates that the product is an aldehyde ν_{max} (CCl_4) 2810sh, 2710, 1730 cm^{-1}. This is supported by the p.m.r. spectrum which contained a triplet at δ 9.78, J = 2 Hz due to the aldehydic hydrogen and a multiplet at δ 6.09, representing two protons, as expected for the cyclobutene olefinic protons. The correctness of the structural assignment was further established by thermally induced ring opening to give the octadienal **8**, a situation that would not have pertained if the double bond were not in the four-membered ring. The p.m.r. spectrum of **8** displayed a doublet at δ 1.11, J = 6.5 Hz due to the saturated methyl substituent, the *gem*-dimethyl group appeared as a six-proton singlet at δ 1.73 and the aldehydic hydrogen as a triplet at δ 9.72, J = 2 Hz. The assignment of the vinyl hydrogen resonances (100 MHz) δ 6.21 (H_2, d of d, J = 10.5, 15 Hz), 5.70 (H_1, d of br s, J = 10.5 Hz), 5.40 (H_3,d of d, J = 6.5, 15 Hz) is consistent with related work on butadienes (6).

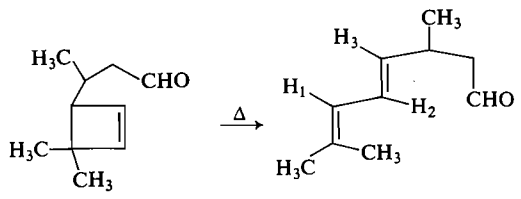

7 8

The preferential photolytic formation of **2** was previously rationalized on the basis of the efficient orbital overlap felt to be provided by the fixed geometry of this ring system and the suggestion that the β-hydrogen atom migration was probably concerted with ring cleavage to give the cyclobutane product directly (3, 7). However, in the light of evidence that diradicals are discrete intermediates for Norrish Type I reactions (8) this may be an oversimplification. More recently, in the case of related bridged-ring ketones such as camphor and bicyclo[3.2.1]-octan-2-one, the diradical intermediates formed upon photolysis have been observed directly by chemically induced dynamic nuclear spin polarization (CIDNP) (9).

Examination of molecular models (Dreiding, Prentice-Hall) suggested that steric interactions between the bridge and C_4 methyl groups may be partially responsible for the preferential formation of the cyclobutane aldehyde. If so, photolysis of suitable ketones with this interaction removed or reduced would be expected to give increased amounts of cyclobutene aldehydes resulting from bond rupture adjacent to the more highly substituted α-carbon.

A suitable model in which this interaction is absent is nopinone (**9**) which lacks the C_4 methyl substituent. Photolysis of nopinone in methanol gave rise to two major products **11** and **12** in a ratio of 4:1.[3] Thus, although **12** is a significant product and the relative amount of it has increased this aldehyde does not predominate and nonbonded interactions are not the only factor influencing the product distribution. By comparison, irradiation of *trans*-verbanone (**10**), whose behavior might be expected to parallel that of nopinone since the nonbonded interaction under consideration is also absent, gave predominately the cyclobutene aldehyde **7** in a 2:1 ratio (**7**:**2**).

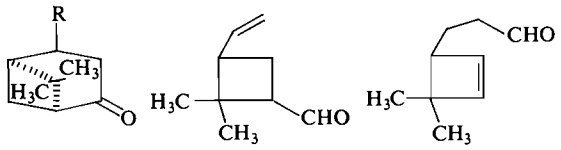

9 R = H
10 R = CH_3

11 **12**

The structures assigned to **11** and **12**, which are analogous to the products from *cis*-verbanone, are supported by spectral data. The p.m.r. spectrum of the major isomer contained a doublet J = 2 Hz at δ 9.74 for the aldehydic hydrogen while the vinyl proton appeared as a multiplet at δ 5.5–5.9, one of the terminal methylene hydrogens as a singlet at δ 5.04, and the remaining one as a doublet of multiplets J = 6 Hz at δ 4.91. In addition, a synthesis of the *cis*- and *trans*-methyl ketones derived from **11** has been

[3]While this work was in progress, we learned of parallel studies on nopinone by Professor N. J. Turro, Columbia University, whom we thank for exchange of information and subsequently another report on nopinone has appeared (7).

Can. J. Chem. Downloaded from www.nrcresearchpress.com by 210.87.254.105 on 09/05/12
For personal use only.

reported by Shaffer and co-workers (7) who have noted, as have we, that further irradiation gave rise to 4-isopropenyl-5-hexenal (**13**) a Norrish Type II product.

The spectrum of the minor isomer was consistent with structure **12**: the aldehydic hydrogen gave rise to a triplet at δ 9.78, $J = 2$ Hz, the olefinic protons appeared as a multiplet δ 6.10, and the saturated alcohol derived from **12** has been compared with an authentic sample by others (7).

The photochemical results clearly require a more detailed explanation and consideration of the relative stability of the alkyl portion of the diradicals involved is appropriate. Unfortunately, accurate figures for radical stability in solution do not appear to be available, however, values (see Table 2) based on bond dissociation energies of gaseous hydrocarbons (10) provide an approximate measure of relative stability whose order would not be expected to change appreciably in solution. Significantly, the primary radicals *n*-propyl and isobutyl are slightly more stable than the cyclobutyl radical. This implies that if other factors are equal photoinduced cleavage of α-cyclobutyl ketones adjacent to the least substituted α-carbon is slightly preferred in contrast to the earlier generalization (1). Consistent with this view, as was kindly pointed out by a referee, the hybridization of the four-membered ring is such that the adjacent single bond will have higher s-character resulting in a slightly stronger bond with a lower tendency to cleave as is observed for α-cyclopropyl ketones. Thus in the absence of other directing influences, the cyclobutene aldehyde(s) would be expected to be the minor photolysis product(s) as found for nopinone. The balance between the two competing pathways is undoubtedly delicate and steric effects will exert a strong influence.[4]

TABLE 2. Relative scale of radical stabilities (10)

Radical		$\Delta H^{\circ}_{298.2}$(kcal/mol)
tert-Butyl		91
Isopropyl Cyclohexyl	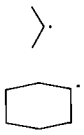	94
Cyclopentyl		95
n-Propyl Isobutyl		98
Cyclobutyl		99
Methyl	CH_3·	102
Cyclopropyl		103

In simple cyclohexanones, it has been found by Wagner (11), Agosta (12) and their respective co-workers that a β-substituent exerts a directing effect which increases the amount of product derived from cleavage on the side of the carbonyl function remote from the substituent. If this directing effect is operative in these bicyclic systems cleavage adjacent to the cyclobutane ring should be enhanced for the verbanones relative to nopinone but for *cis*-verbanone this was not the case. Thus, the product distributions can now be reconsidered in the light of the radical stability data as well as the steric interactions.

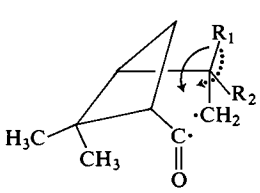

A $R_1 = R_2 = H$
B $R_1 = H; R_2 = CH_3$
C $R_1 = CH_3; R_2 = H$

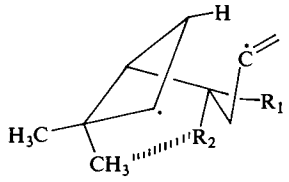

D $R_1 = R_2 = H$
E $R_1 = H; R_2 = CH_3$
F $R_1 = CH_3; R_2 = H$
G $R_1 = R_2 = CH_3$

Photolysis of nopinone results in preferential cleavage on the side of the carbonyl group remote from the four-membered ring to form **A** which gives the major product. The minor isomer arises from **D** and, although there may be a slight nonbonded methyl–hydrogen interaction, this is not sufficient to inhibit the formation of significant amounts of cyclobutene aldehyde.

Cleavage of *cis*-verbanone in the preferred sense affords **B** which requires only a slight rotation (↻) to permit hydrogen abstraction to give the major product. In addition, as the requisite rotation occurs in this diradical inter-

[4]It should be realized that the numerical difference in relative stabilities between primary and cyclobutyl radicals is of similar magnitude to the probable error in the measurement, nevertheless, the trend must be real.

Can. J. Chem. Downloaded from www.nrcresearchpress.com by 210.87.254.105 on 09/05/12
For personal use only.

mediate, any nonbonded methyl–methyl interaction is relieved. In contrast, bond fission adjacent to the cyclobutane ring gives **E** which must adopt a conformation possessing nearly a 1,3-diaxial methyl–methyl interaction (3.7 kcal/mol) (13) for hydrogen abstraction to proceed. This is probably sufficient to permit reclosure to starting material to compete efficiently and to minimize the formation of cyclobutene aldehyde **7**.

The results for *trans*-verbanone are consistent with this interpretation. Intermediate **C** requires considerable rotation (↻) to achieve a conformation suitable for hydrogen abstraction to occur and in accord with 'the principle of least motion' one should expect the predominant path to be that which requires minimum energy in changing the positions of atoms in the reactant to their corresponding positions in the product (14). This rotation introduces an unfavorable steric interaction with the bridge methyl group such that ring closure may occur in preference. In contrast, the other pathway resulting in fission adjacent to the cyclobutane ring to give **F** does not suffer this restriction (compare **E**) and allows the reaction to funnel through to cyclobutene product even though this cleavage is slightly less preferable initially.

The validity of this explanation was tested as follows. In a molecule such as **14**, the path to the cyclobutane aldehyde is blocked and unless a more deep seated rearrangement occurs **15** should be the only aldehydic product. However, formation of **15** will be unfavorable, since it must arise via intermediate **G**, which contains the unfavorable diaxial interaction discussed previously. Consistent with this, the major photolysis product is the saturated ester **16**, the first ketene derived product encountered in the series. The formation of **16**, requires an intermediate of type **H** which must approach the geometry between that found in bicyclo[3.1.1]-heptanes and the more highly strained bicyclo[2.1.1]hexanes (15); thus, in the other cases aldehydes are produced in preference. The structure of the ester is established by its i.r. carbonyl absorption at 1733 cm^{-1} and C—H stretch due to the methoxyl function at 2820 cm^{-1}. The absence of signals below the methoxy methyl resonance at δ 3.60 in the p.m.r. spectrum clearly indicates that the four-membered ring is saturated. Attempts to isolate the cyclobutene aldehyde **15** or trap it as its acetal were unsuccessful

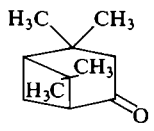

14

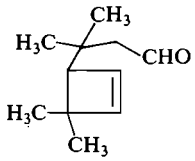

15

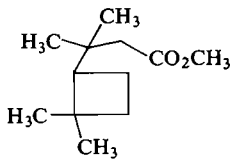

16

as it underwent a rapid Norrish Type II reaction to give cyclobutanol **18**. It appears that this γ-hydrogen abstraction is faster than the initial α-cleavage. This is consistent with the results of Lewis and co-workers (16) who found that γ-hydrogen abstraction from a secondary alkyl center is approximately 10 times more rapid than α-cleavage of *tert*-alkyl phenyl ketones. In the above case, although a primary center is involved, six equivalent hydrogens are available and the geometry is favorable. A small amount of the diene **17** may also be formed but it has not been positively identified. The ester:aldehyde ratio varied with time but an average value based on the cyclobutanol present at 65–70% conversion of starting material was 1.5:1 (**16**:**15**), compared with the value of 1:1.6 found by Coyle for cyclohexanone (17).

The i.r. spectrum of **18** contains hydroxyl bands at 3585 and 3300 (broad) cm^{-1} in addition to bands at 3020, 1625, and 860 cm^{-1} indicating the presence of a double bond. The cyclobutene nature of this double bond was established by the p.m.r. spectrum (100 MHz) which contained two separate doublets due to the olefinic protons, $J = 3$ Hz at δ 6.25 and 6.13. This is in reasonable agreement with related systems (18, 19) but in this case since the allylic couplings are apparently near zero, it is not possible to explicitly assign these signals. As anticipated for a cyclobutene system thermal ring opening on the gas chromatograph afforded a butadiene. The resonance for the proton on the carbon bearing the hydroxyl function appears as a 'quintet like' multiplet $J \sim 8.5$ Hz at δ 4.11 possessing unresolved fine structure. Both the

position and the appearance of this signal are similar to these reported for 3-isopropylcyclobutanols and amines (20). To ascertain with more certainty the environment of this hydrogen, the spectrum was recorded in the presence of a shift reagent [$Eu(fod)_3$]. This caused the signals due to the adjacent methylene hydrogens to shift downfield and improved the resolution so they appeared as a three-line multiplet (2H) $J = 8.5$ Hz and a distorted doublet of doublets $J = 2.5$, 6 Hz representing two protons. Coupling constants of cyclobutanes cover a wide

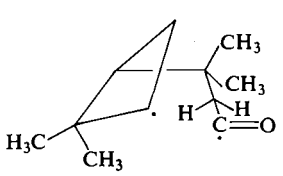

H

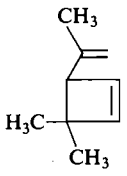

17

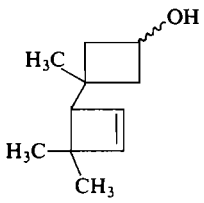

18

range due to the ability of the ring to adopt a number of conformations but generally the vicinal *cis*-coupling constant is larger than the *trans*-coupling constant (19). However, since the stereochemistry of the alcohol function is not established it is not possible to assign these signals with certainty at present. Although several reagents were examined conditions were not found by which the alcohol could be oxidized cleanly to a cyclobutanone.

Thus, it is suggested that the photolytic behavior of α-ketocyclobutane systems has more in common with α-cyclopropyl ketones than has previously been recognized. It is anticipated that upon photolysis in methanol α-ketocyclobutanes will generally display a slight preference to cleave on the side of the carbonyl group remote from the four-membered ring (*i.e.*, less substituted side) unless conformational preferences, geometric constraints, or radical stabilities dictate otherwise.[5]

Present literature examples can be rationalized on this basis in keeping with the generalization that the major photoproducts from cycloalkanones result from cleavage to form the most stable alkyl–acyl diradical whenever possible.

For example, the previous conclusion that "cleavage, next to a cyclobutane ring, is normal" (2) was primarily based on the photolysis of **19** and **21**. However, for the intermediate diradical which would result from fission remote from the four-membered ring, H_1 is geometrically inaccessible such that ring closure should compete efficiently and **20** is thus the aldehyde expected. For carvonecamphor (**21**), the ester arises from a *tert*-cyclobutyl radical in preference to a primary alkyl radical in accord with expectations. Similarly the spiro ketone **23** gives the anticipated product arising from a *tert*-cyclobutyl radical intermediate. The final example (**25**) appears initially to be an exception to the above suggestions but, in fact, gives the expected product when the geometric constraints in the system are considered since cleavage on the side of the carbonyl group remote from the ring gives an intermediate in which the abstraction of the requisite hydrogen (H_2) from the β-carbon appears difficult from models. In addition, **26** results from the favorable abstraction of a tertiary hydrogen.[6]

A referee has suggested our results can be equally well explained on the basis of a concerted mechanism. However, the original experimental evidence supporting a concerted process, based on the photolysis of 2-methylcyclohexanone, has been shown to be in error (8) and the photochemically generated diradical from 2-methylcyclohexanone has been detected by

[5]Generally, α-cleavage of cycloalkanones proceeds from a triplet excited state (21). The possibility that the product distributions for the bicycloheptanones are a consequence of different products from singlet and triplet excited states rather than resulting from the stability and conformations of the intermediate diradicals was rendered unlikely by quenching studies. Irradiation of *cis*- and *trans*-verbanone in the presence of 1,3-cyclohexadiene (1 and 5 *M*) caused a complete suppression of detectable aldehydic products.

[6]Since submission of this manuscript grandisol has been synthesized by photolysis of a substituted verbanone in methanol to give the cyclobutane aldehyde as the major product in accord with expectations (51).

Can. J. Chem. Downloaded from www.nrcresearchpress.com by 210.87.254.105 on 09/05/12
For personal use only.

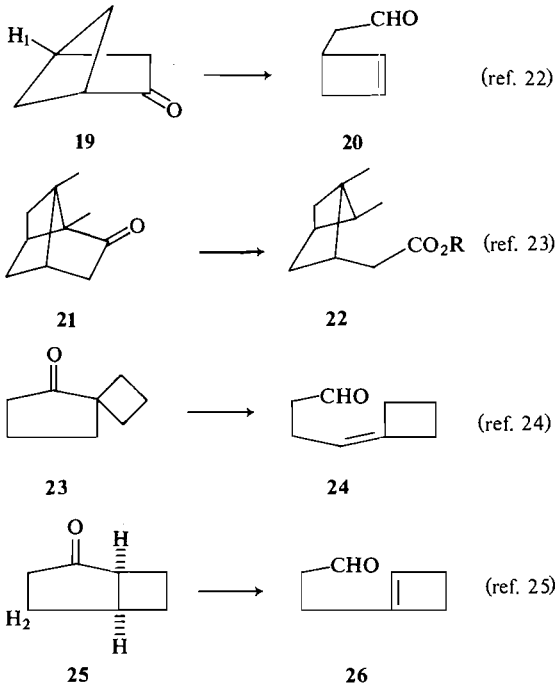

CIDNP (9). An attempt to detect diradicals upon photolysis of *cis*-verbanone in the cavity of an e.s.r. spectrometer was unsuccessful[7] but the experimental evidence for related systems (8–11, 21) favors the biradical rather than the concerted mechanism for the photolysis of cyclic ketones in solution.[8] Once formed the biradical partitions itself between disproportionation to yield alkenal(s), disproportionation to yield ketene, and recoupling to yield ground state ketone. As indicated above the relative importance of recombination (ring closure) *vs.* hydrogen abstraction is influenced by radical stability and the ease of formation of the transition states required for hydrogen transfer. Thus substituents and conformational preferences exert a significant influence on the product distribution. When two or more pathways are involved the quantum yield is not an accurate reflection of the importance of recombination unless the recoupling rates from each intermediate are equal, which is unlikely. Thus, to clearly distinguish between the competition for recombination and hydrogen abstraction, data for both cyclobutene and cyclobutane aldehyde formation are required. Unfortunately a referee's suggestion that "quantum yields might be conclusive" is overly optimistic, although they are indicative. The quantum yields (Φ_{-K}) (7, 11) for nopinone (0.32) and *cis*-verbanone (0.40) are between those of cyclohexanone (0.20) and 2-methylcyclohexanone (0.50) suggesting that in each case some ring closure competes favorably with hydrogen abstraction; for although these figures indicate that the forward disproportionation reaction is facile the efficiency does not approach unity and steric effects on the competition are undoubtedly subtle. Barltrop and Coyle (8) have estimated that 33% of the biradical formed on photolysis of 2,3-dimethylcyclohexanone reverts to ketone rather than product. Thus these data support the conformational and radical stability arguments enunciated above to rationalize the product distributions in these bicyclo[3.1.1]heptan-2-ones.

Preparation of 'Verbanones'

The ketones used in this study have been prepared previously; nevertheless, they are not readily available especially in the case of *trans*-verbanone. During and after the completion of this work, several reports appeared concerning transformations in these systems. The pertinent portion of our own work in this area is outlined below.

Verbenone (**5**) was prepared from α-pinene by allylic oxidation in improved yield when the chromium trioxide – pyridine reagent was prepared and utilized *in situ* (26, 27). Catalytic hydrogenation of verbenone (Pd/C) in methanol containing pyridine afforded *cis*-verbanone (**1**) (28) uncontaminated with the saturated alcohol (29, 30).

Previously, the standard route to *trans*-verbanone (**10**) has been via *trans*-verbenol (**32**) followed by reduction and oxidation to give a mixture of *cis*- and *trans*-verbanones 55:45 (28). Since the more stable isomer frequently predominates when α,β-unsaturated ketones are reduced with lithium in liquid ammonia verbenone (**5**) was reduced to give a mixture in which the *cis*:*trans* ratio was reversed 45:55. (Similar reduction with sodium in hexamethyl-

[7]N. J. Gogan and C. K. Chu are thanked for conducting this experiment.

[8]The possibility that this is a special case involving a concerted pathway cannot be completely excluded but no 'proven' example for a photoinduced α-cleavage has been reported.

Can. J. Chem. Downloaded from www.nrcresearchpress.com by 210.87.254.105 on 09/05/12
For personal use only.

TABLE 3. Debromination of 3-bromonopinone (**29**)

Reagent	Temperature	Time	Apoverbenone
Li_2CO_3–LiBr, DMF	150°	1.5 h	~10% plus **9** and **29**
Diazabicyclo[5.4.0]undecane	100°	15 min	~5% plus **9**
Diazabicyclo[5.4.0]undecane, DMF	150°	3 h	~6% plus **9**
tert-BuOK, *tert*-BuOH	Reflux	12 h	~3% plus **9**
$NaHCO_3$, DMSO	180°	1 h	0 plus **29**
tert-BuOK, DMSO	Reflux	12 h	~3% plus **9**
Triethylamine	Reflux	3 h	0 plus **9** and **29**
Collidine	Reflux	3 h	~2% plus **9** and **29**

NOTE: Attempted debrominations via the ketal, semicarbazone, and 2,4-dinitrophenylhydrazone derivatives were also unsuccessful.

phosphoramide gave a *cis*:*trans* ratio of 35:65.) In an attempt to improve the amount of *trans*-ketone produced the catalytic hydrogenation of *trans*-verbenol (**32**) was examined in *tert*-butyl alcohol and 50% aqueous methanol, since it is known (28) that the *cis*:*trans* ratio decreases in polar solvents but in each case the *cis*-isomer predominated. If a bulkier group is attached to the alcohol function hydrogenation of the double bond from the desired direction should be encouraged; however, hydrogenation of the acetate **33** in acetic acid gave a *cis*:*trans* ratio of 2:1 after hydrolysis and oxidation, whereas the trimethyl silyl derivative was reduced to only a slight extent at atmospheric pressure.

As separation was tedious attention was turned to a stereoselective synthesis of *trans*-verbanone (10) the essential step of which was the 1,4-conjugate addition of dimethyl copper lithium to apoverbenone (**30**). It was envisaged that the reagent would approach from the less hindered side of the molecule away from the dimethyl bridge to give the desired ketone. It is reported that apoverbenone can be prepared by dehydrobromination of 3-bromonopinone (**29**) in collidine (31). In our hands, this approach was unsuccessful and several other dehydrobromination procedures were examined as summarized in Table 3. New Zealand workers have experienced this same difficulty (32) and thus this approach to apoverbenone was abandoned. However, Grimshaw and co-workers have developed conditions for the preparation of apoverbenone in 77% yield by treating *cis*-bromonopinone[9] with lithium carbonate – lithium bromide in dimethyl sulfoxide at 150° for 60 h (33).

Selenium dioxide and dichlorodicyanobenzoquinone (DDQ) have been widely used in the steroid field to effect dehydrogenations (34). Reactions with DDQ were not encouraging and SeO_2 was investigated especially since it has been reported that verbenone can be prepared from verbanone using SeO_2 in ethanol although no yield is given (35). Several solvents were examined, dioxane, *tert*-butyl alcohol, ethanol, acetic acid, and while the reaction with nopinone (**9**) worked reasonably well on a modest scale (~1 g) yields dropped when it was scaled up. Thus, reactions were run in refluxing dioxane to approximately 70% completion to afford apoverbenone (**30**) in 40% yield. The selenium produced as a byproduct of the reaction causes ring fission and renders the reaction unsuitable for large scale preparation of apoverbenone. However, material was obtained to study the conjugate addition with dimethyl copper lithium which proceeded smoothly to give *trans*-verbanone in 80% yield uncontaminated with the *cis*-isomer. French workers have noted this also and have published a detailed study of the addition of dimethyl copper lithium and copper complexed methyl magnesium iodide to both verbenone and apoverbenone (36). These reactions thus constitute a stereoselective route to *trans*-verbanone. Jones and Webb have developed a different route to *trans*-verbanone starting with pinocamphone (*trans*-2,6,6-trimethylbicyclo[3.1.1]heptan-3-one) (37).[10]

An alternative preparation of apoverbenone involves allylic oxidation of apopinene (**28**) (31,

[9]The stereochemistry of substituted compounds in these series is frequently designated by α and β. However, different workers use different conventions (*cf.* ref. 33) and thus we prefer to designate the substituent as *cis*- or *trans*-relative to the *gem*-dimethyl bridge.

[10]These bicyclic systems may be named as pinane derivatives (IUPAC Rule A75-2); however, we favor the von Baeyer system (IUPAC Rule A31) due to its general applicability.

Can. J. Chem. Downloaded from www.nrcresearchpress.com by 210.87.254.105 on 09/05/12
For personal use only.

Can. J. Chem. Downloaded from www.nrcresearchpress.com by 210.87.254.105 on 09/05/12
For personal use only.

38). The standard route to apopinene (other than from natural sources) proceeds via catalytic decarbonylation of myrtenal but gave disappointing yields in our hands (39). An earlier report (40) outlined the preparation of apopinene by dehydration of nopinol (**31**) with potassium bisulfate and while apopinene is produced, there are additional components. Similarly, alkyl lithium treatment of nopinone tosylhydrazone gives a mixture of products (41).

Reduction of nopinone with $LiAlH_4$ gives a mixture of *cis*- and *trans*-alcohols in which the *cis*-isomer predominates (42). The use of a bulkier reagent such as 'Red-al' (sodium *bis*(2-methoxyethoxy)aluminum hydride) in refluxing benzene afforded better than 95% of the *cis*-isomer which crystallized directly upon work-up. Early attempts to form the brosylate of this alcohol resulted in a rearranged product (43) and thus a dehydration procedure must be conducted under nonacidic conditions to avoid rearrangement. Various combinations of alumina and Florisil with amines and thionyl chloride – pyridine were examined but in all cases, other products were formed in addition to the desired olefin. The procedure adopted utilized phosphorus oxychloride – pyridine at 0° and gave a 50% yield of apopinene which was oxidized to apoverbenone with chromium trioxide – pyridine in dichloromethane. The tetramethyl ketone **14** was prepared by conjugate addition of dimethyl copper lithium to verbenone.

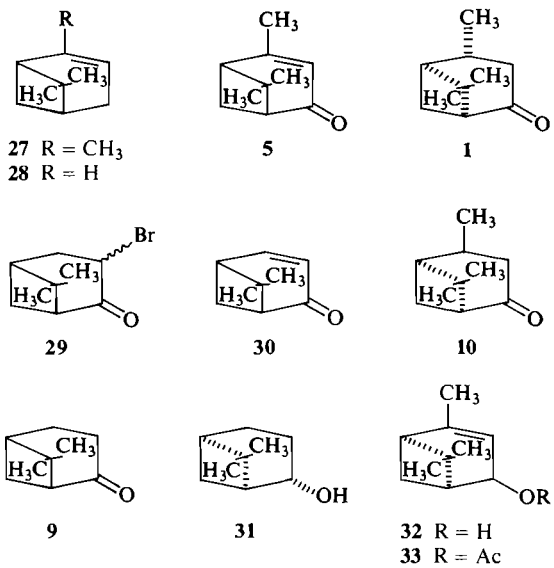

27 R = CH_3
28 R = H

5

1

29

30

10

9

31

32 R = H
33 R = Ac

Experimental

Melting points were determined in capillary tubes with a Thomas-Hoover Uni-Melt apparatus and are uncorrected. Microanalyses were performed by Alfred Bernhardt, West Germany.

Infrared spectra were recorded in carbon tetrachloride solution, unless otherwise indicated, on a Perkin-Elmer 237B grating spectrophotometer and were calibrated with the 2850 and 1601 cm^{-1} bands of polystyrene film. Ultraviolet spectra were recorded on a Perkin-Elmer 202 ultraviolet–visible spectrophotometer and were calibrated with the 279.4 nm band of a Holmium filter. Proton magnetic resonance spectra were measured using a Varian Model A-60, Varian Model EM-360, or Varian Model HA-100 spectrometer in carbon tetrachloride solutions, unless otherwise stated, containing tetramethylsilane as an internal standard. Band positions are reported in parts per million downfield from TMS (δ scale).

The g.l.c. analyses were conducted on a Varian Aerograph gas chromatograph Model 1720 with helium as carrier gas on an 8 ft × ¼ in., 13% SE-30 column supported on Chromosorb W (AW-DMCS) (70–80 mesh) or on an 8 ft × ¼ in., 20% Carbowax 20M column supported on Chromosorb W (AW-DMCS) (70–80 mesh).

Solutions in organic solvents were dried over anhydrous magnesium sulfate and stripped of solvent with a Büchi rotary evaporator connected to a water aspirator. Irradiations were conducted using a water cooled Hanovia 450 W medium pressure mercury arc source.

Verbenone (4,6,6-Trimethylbicyclo[3.1.1]hept-3-ene-2-one) (5)

Commercial (±)α-pinene (20 g, 0.147 mol, Aldrich) in dichloromethane (100 ml) was added dropwise to chromium trioxide – pyridine reagent prepared *in situ* in dichloromethane (1500 ml) from pyridine (240 g, 3 mol) and chromium trioxide (150 g, 1.5 mol, dried over P_2O_5 15 h/12 mm). The reaction was stirred mechanically for 48 h at room temperature after which time the bulk of the dichloromethane was removed by decantation and concentrated. The dark residue remaining in the reaction flask was extracted thoroughly with ether as was the residue resulting from the concentration of dichloromethane. The ether solutions were combined and washed successively with 10% aqueous $NaHCO_3$, 10% aqueous HCl until washings remained acidic, 10% aqueous $NaHCO_3$, water, and dried. Distillation of the residual oil which remained after removal of the solvent provided 12.1 g (55%) of verbenone (**5**); b.p. 108–110°/11 mm (lit. (44) b.p. 100–102°/5 mm); i.r. 1690 (C=O) cm^{-1}; p.m.r. δ 0.99 (3H, s), 1.50 (3H, s), 2.00 (3H, d, J = 1.5 Hz), 5.57 (1H, q, J = 1.5 Hz, CH=C) p.p.m.

cis-Verbanone (cis-4,6,6-Trimethylbicyclo[3.1.1.]heptan-2-one) (1)

A methanol solution (60 ml) of verbenone (**5**) (5.7 g, 0.038 mol) containing pyridine (0.6 ml, 0.006 mol) was stirred with 5% Pd/C (0.20 g) under hydrogen at atmospheric pressure until 1.05 molar-equiv. of hydrogen were absorbed. The mixture was filtered and g.l.c. analysis indicated a single product was present. The oil obtained after removal of solvent was dissolved in ether (50 ml) and the ether solution extracted with 10% aqueous HCl, water, and dried. The solution was filtered,

Can. J. Chem. Downloaded from www.nrcresearchpress.com by 210.87.254.105 on 09/05/12
For personal use only.

concentrated, and distilled to give 5 g (87%) of the *cis*-ketone **1**; b.p. 91–92°/11 mm (lit. (44) b.p. 104–105°/15 mm); i.r. 1710(C=O) cm^{-1}; u.v. (CH_3OH) 275sh nm (ε 34); p.m.r. δ 0.99 (3H, s), 1.17 (3H, d, J = 6.5 Hz) 1.33 (3H, s) p.p.m.

Lithium–Ammonia Reduction of Verbenone: cis- and trans-Verbanone

Small pieces of lithium (1 g) were added to liquid ammonia (450 ml) contained in a three-necked 1-l round bottom flask equipped with a solid carbon dioxide condenser and a pressure equalizing dropping funnel. After all the lithium had reacted verbenone (3 g, 0.020 mol) in anhydrous petroleum ether (5 ml) was added. The solution was stirred for 1 h and solid ammonium chloride was added in small portions until the blue color dispersed. After the ammonia had evaporated water (100 ml) and ether (100 ml) were added, the aqueous layer further extracted with ether, and the combined extracts dried. To facilitate the analysis, the liquid product remaining after removal of the solvent was dissolved in acetone (20 ml) and treated with Jones' reagent (45). Analysis of the resulting ketone mixture by g.l.c. indicated the ketones were formed in a *trans*:*cis* ratio of 55:45. Repeated spinning band distillation (3) (b.p. 42–44°/0.3 mm) afforded a sample of *trans*-verbanone (**10**) containing 5% of the *cis* isomer **1**.

Ketone Photolysis

cis-Verbanone (1)

cis-Verbanone (0.200 g, 1.32 mmol) in dry methanol (15 ml, distilled from magnesium) to which sodium bicarbonate (~15 mg) had been added was flushed with nitrogen, stoppered, and irradiated in a quartz tube for 1–2 h. (Longer reaction times were required when Pyrex vessels were employed.) The methanol was removed, petroleum ether (20 ml) was added, the solution filtered, and concentrated. Gas–liquid chromatographic analysis at 85% conversion of starting material indicated the two aldehyde products were present in a ratio of 7:1 (**2**:**7**); (minor components ~4%, possibly oxetanes have not been examined). The products were purified by t.l.c. on silica gel (10% ether–hexane). Alternatively samples of **2** were collected from the gas chromatograph. The major component *cis*-1-formyl-2,2-dimethyl-3-isopropenylcyclobutane (**2**) had the following spectral properties; i.r. 2800 (CHO), 2705 (CHO), 1720 (C=O), 1640 (C=C) cm^{-1}; p.m.r. δ 0.87 (3H, s, CH_3), 1.36 (3H, s, CH_3), 1.67 (3H, br s, C=C—CH_3), 4.71 (1H, br s, $w_{\frac{1}{2}}$ = 4 Hz, C=C—H), 4.90 (1H, br s, $w_{\frac{1}{2}}$ = 6 Hz, C=C—H), 9.75 (1H, d, J = 1.7 Hz, CHO) p.p.m.

Aldehyde **2** was further characterized as its semicarbazone derivative prepared according to the method of Fieser (46), crystallized from MeOH–H_2O, m.p. 176–178°.

Anal. Calcd. for $C_{11}H_{19}N_3O$: C, 63.13; H, 9.15; N, 20.08. Found: C, 63.08; H, 9.04; N, 20.25.

The minor component 3-(2′,2′-dimethylcyclobutane-3′-enyl)butanal (**7**) had the following spectral properties; i.r. 2810 sh (CHO) 2710 (CHO), 1730 (C=O), 1640 (C=C) cm^{-1}; p.m.r. δ 0.97 (3H, d, J = 6 Hz, CH_3—CH), 1.18 (6H, s, CH_3, CH_3) 6.09 (2H, m, J = 3 Hz, CH=CH), 9.78 (1H, t, J = 2 Hz, CHO) p.p.m.

Aldehyde **7** was further characterized as its semicarbazone derivative prepared according to the method of Fieser (46), crystallized from MeOH–H_2O, m.p. 116–118°.

Anal. Calcd. for $C_{11}H_{19}N_3O$: C, 63.13; H, 9.15; N, 20.08. Found: C, 62.92; H, 8.91; N, 20.42.

trans-Verbanone (10)

Irradiation was conducted as described above for *cis*-verbanone. At 75% conversion of starting material the aldehyde ratio was 1:2 (**2**:**7**).

Nopinone (9)

Nopinone (0.450 g, 3.26 mmol) in dry methanol (40 ml, distilled from magnesium) to which sodium bicarbonate (~35 mg) had been added was flushed with nitrogen, stoppered, and irradiated in a quartz tube for 2–3 h. Work-up as above gave an oil which contained the two aldehydes **11** and **12** in a 4:1 ratio, established by integration of the methyl signals in the p.m.r. spectrum. The major isomer *cis*-1-formyl-2,2-dimethyl-3-vinylcyclobutane (**11**) was purified by preparative g.l.c.; i.r. 2810sh (CHO), 2700 (CHO) 1720 (C=O), 1635 (C=C) cm^{-1}; δ 0.94 (3H, s, CH_3), 1.29 (3H, s, CH_3), 4.91 (1H, d of m, J = 6, ~2.5 Hz, C=CH), 5.04 (1H, s, C=CH), 5.5–5.9 (1H, m, CH=C), 9.74 (1H, d, J = 2 Hz, CHO) p.p.m.

A sample enriched in the minor isomer 3-(2′,2′-dimethylcyclobut-3′-enyl)propanal (**12**) was prepared by t.l.c. on silica, (petroleum ether followed by 5% ether–hexane); i.r. 2810sh (CHO), 2700 (CHO), 1720 (C=O), 1635 (C=C) cm^{-1}; p.m.r. δ 1.10 (3H, s, CH_3), 1.17 (3H, s, CH_3), 6.10 (2H, m, CH=CH), 9.78 (1H, d, J = 2 Hz, CHO) p.p.m.

In some runs a small quantity of another aldehydic component 4-isopropenyl-5-hexenal (**13**) derived from photolysis of **11** was detected and isolated by g.l.c.; i.r. 2810 (CHO), 2715, (CHO), 1725 (C=O) cm^{-1}; p.m.r. δ 1.65 (3H, br s, C=CCH_3), 4.73 (2H, br s, C=CH_2), 5.10 (2H, br s, C=CH_2) 5.4–6.1 (1H, m, CH=C), 9.72 (1H, t, J = 1.5, CHO) p.p.m.

4,4,6,6-Tetramethylbicyclo[3.1.1]heptan-2-one (14)

A sample of the tetramethylketone **14** (0.030 g, 1.81 mmol) in dry methanol (20 ml, distilled from magnesium) to which sodium bicarbonate (~18 mg) had been added was flushed with nitrogen, stoppered, and irradiated in a quartz tube for 20–25 h. The methanol was removed, petroleum ether – diethyl ether (2:1) (30 ml) was added, the solution filtered, and concentrated. Gas–liquid chromatographic analysis indicated 65% of the starting material had been consumed and two new major components were present in a ratio of 1.5:1 (**16**:**18**). (The amount of **18** present decreased as photolysis time increased.) The major component **16** was identified as methyl 3-methyl-3-(2′,2′-dimethylcyclobutyl)butanoate and was purified by t.l.c. on silica gel (5% ether–hexane) or collected from the gas chromatograph; i.r. 2820(OCH_3) 1733 (C=O) cm^{-1}; p.m.r. δ 1.00 (6H, s, CH_3, CH_3), 1.11 (3H, s, CH_3), 1.17 (3H, s, CH_3), 2.17 (2H, s, CH_2CO), 3.60 (3H, s, OCH_3) p.p.m.

The second component 3-methyl-3-(2′,2′-dimethylcyclobut-3′-enyl)cyclobutan-1-ol (**18**) was purified by t.l.c. on silica gel (5% ether–hexane); i.r. 3585 (OH), 3450–3150 (OH), 1625 (C=C) cm^{-1}; p.m.r. δ 1.03 (3H, s, CH_3), 1.13 (6H, s, CH_3, CH_3), 3.6 (1H, br s, OH), 4.12 (1H, m, J ~ 8.5 Hz, CHOH), 6.23 (2H, 2d, J = 3 Hz, CH=CH) p.p.m.

Can. J. Chem. Downloaded from www.nrcresearchpress.com by 210.87.254.105 on 09/05/12
For personal use only.

*cis-Pinononic Acid (cis-3-Acetyl-2,2-dimethylcyclobutane Carboxylic Acid (**6**)*

*From Verbenone (**5**)*

A sample of verbenone (1.5 g 0.01 mol) in dichloromethane (25 ml) was cooled to ~ −70° in a solid carbon dioxide – acetone bath and a stream of oxygen containing ~7% ozone passed through the solution until it retained a permanent blue color. A solution of 30% hydrogen peroxide (5 ml) was added to the cold solution, it was warmed to room temperature, and the mixture stirred vigorously for 12 h. Water (50 ml) was added, the aqueous solution extracted with dichloromethane, the dichloromethane extracts combined, dried, and concentrated. Carbon tetrachloride was added to the remaining solution from which the acid crystallized with scratching on cooling, 1.1 g (64%), m.p. 129–130° (lit. (47) m.p. 129°); i.r. 3200–2800 (CO_2H) 1760 sh (C=O), 1700 (C=O) cm^{-1}; p.m.r. δ 0.88 (3H, s, CH_3), 1.35 (3H, s, CH_3), 2.03 (3H, s, CH_3CO), 2.87 (1H, t, J = 8.5 Hz, CHCO), 11.58 (1H, s, CO_2H) p.p.m.

*From cis-1-Formyl-2,2-dimethyl-3-isopropenylcyclobutane (**2**)*

The aldehyde **2** (0.230 g, 1.51 mmol) was dissolved in dichloromethane (10 ml), cooled to ~ −70° in a solid carbon dioxide – acetone bath and a stream of oxygen containing ~7% ozone passed through the solution until it retained a permanent blue color. The solution was warmed to room temperature and the solvent removed under reduced pressure without external heat behind a safety shield. Acetone (10 ml) was added followed by Jones' reagent (45), dropwise as a titration, to the stirred solution until the characteristic orange color of the reagent persisted for approximately 20 min. Water (25 ml) was then added and the aqueous layer extracted with ether. The ether extracts were washed with water, dried, filtered, and the solvent removed. The semisolid residue which remained was crystallized from $CHCl_3$–CCl_4 to give fine prisms 0.18 g (70%), m.p. 129–130° (lit. (47) m.p. 129°), mixture m.p. with sample prepared above 129–130°.

*3,7-Dimethyl-4,6-octadienal (**8**)*

A sample of the cyclobutene aldehyde **7** (0.060 g, 0.39 mol) was dissolved in hexane (0.1 ml), injected in small portions into the gas chromatograph (injector temperature 210°; column temperature 140°, detector temperature 250°) and the peak corresponding to the ring opened material collected to give the butadiene **8** as an oil 0.035 g (58%); i.r. 2805 (CHO), 2705 (CHO), 1725 (C=O), 1655 (C=C) cm^{-1}; p.m.r. δ 1.11 (3H, d, J = 6.5 Hz, CH_3CH) 1.73 (6H, s, CH_3, CH_3), 9.72 (1H, t, J = 2 Hz, CHO), vinyl signals 100 MHz, 5.40 (1H, d of d, J = 6.5, 15 Hz), 5.70 (1 H, d of br s, J = 10.5 Hz), 6.21 (1H, d of d, J = 10.5, 15 Hz) p.p.m.

The butadiene aldehyde **8** was further characterized as its semicarbazone derivative m.p. 91–92° prepared according to the method of Fieser (46).

Anal. Calcd. for $C_{11}H_{19}NO_3$: C, 63.13; H, 9.15; N, 20.08. Found: C, 63.42; H, 9.03; N, 20.36.

*Nopinone (6,6-Dimethylbicyclo[3.1.1]heptan-2-one) (**9**)*

A sample of β-pinene (60g, 0.44 mol, Aldrich) was treated with ozone according to the procedure of Meinwald and Gassman (48) to give nopinone 35 g (57%), b.p. 96–97°/18 mm (lit. (48) b.p. 83–86°/12 mm); i.r. 1715 (C=O) cm^{-1}; u.v. (CH_3OH) 275 nm (ε 33); p.m.r. δ 0.85 (3H, s, CH_3), 1.35 (3H, s, CH_3) p.p.m.

*trans-Verbenyl Acetate (4,6,6-Trimethyl-2-acetoxybicyclo[3.1.1]heptan-3-one (**33**)*

trans-Verbenyl acetate was prepared by rearrangement of the product from lead tetraacetate oxidation of α-pinene according to the method of Whitham (49). The sample had b.p. 105–106°/12 mm (lit. (50) b.p. 97–98°/9 mm).

Reduction

(*a*) The acetate (1 g) in glacial acetic acid (20 ml) was stirred in a hydrogen atmosphere with 5% Pd/C, 50% water wet (0.30 g) until a molar quantity of hydrogen was utilized. The solution was filtered, concentrated, and stirred with alcoholic KOH for 1 h, water (100 ml) was added and the aqueous solution extracted with ether. The ether extracts were concentrated and oxidized with Jones' reagent to give a 2:1 mixture of *cis*:*trans* verbanone as determined by g.l.c. analysis.

(*b*) *trans*-Verbenol (0.10 g) (prepared by alkaline hydrolysis of the acetate) in *tert*-butyl alcohol (15 ml) was hydrogenated using a 5% Pd/C (0.050 g) catalyst. Filtration, removal of the *tert*-butyl alcohol and oxidation of the residual oil with Jones' reagent afforded a 3:1 mixture of *cis*:*trans* verbanone.

(*c*) Similar reduction of *trans*-verbenol using 50% aqueous methanol as the solvent gave a *cis*:*trans* ratio of 3:2.

*3-Bromonopinone (6,6-Dimethyl-3-bromobicyclo[3.1.1]heptan-2-one) (**29**)*

Bromine (~0.25 g) was added dropwise to a stirred solution of nopinone (0.20 g, 1.45 mmol) in carbon tetrachloride (15 ml) containing sodium carbonate 0.20 g) and boron trifluoride etherate (3 drops) until the color of the last drop of bromine was not dispersed by stirring for a further 5 min. Water (50 ml) was added and the solution was extracted with chloroform, the combined extracts washed with water, dried, filtered, and evaporated. The oil so obtained 0.285 g (90%) contained the two isomeric bromoketones in a ~3:1 ratio (*trans*:*cis*) by g.l.c. analysis. For the trial dehydrobrominations the mixture was used as obtained but when dissolved in hexane (7 ml) the *trans*-isomer could be isolated by fractional crystallization, m.p. 67–68° (lit. (32) m.p. 69.5–70°), i.r. 1725 (C=O) cm^{-1}; u.v. (CH_3OH) 301 nm (ε 104); p.m.r. δ 0.84 (3H, s, CH_3), 1.39 (3H, s, CH_3), 4.27 (1H, d of d, J = 3.5, 7.5 Hz, CHBr) p.p.m.

A sample of the *cis*-isomer was collected from the gas chromatograph, m.p. 109–110° (lit. (32) m.p. 109.5–110.5°); i.r. 1728 (C=O) cm^{-1}; u.v. (CH_3OH) 282 nm (ε 100); p.m.r. δ 0.87 (3H, s, CH_3), 1.39 (3H, s, CH_3), 4.68 (1H, d of d, J = 8, 10 Hz, CHBr) p.p.m.

Dehydrobrominations were carried out under standard literature conditions as indicated in Table 3.

*cis-Nopinol (cis-6,6-Dimethylbicyclo[3.1.1]heptan-2-ol) (**31**)*

Nopinone (0.675 g, 4.89 mmol) in benzene (10 ml) was added to 'Red-al' (2 ml) and the solution refluxed for 3 h. Moist benzene was added dropwise followed by

Can. J. Chem. Downloaded from www.nrcresearchpress.com by 210.87.254.105 on 09/05/12
For personal use only.

dropwise addition of water and then careful addition of 10% aqueous HCl until the complex just dissolved. This solution was extracted with ether, dried and filtered to give a solid, m.p. 90–92°, upon removal of solvent. Gas–liquid chromatographic analysis indicated a single component. Recrystallization from methanol–water afforded the alcohol 0.60 g (88%) as fine needles, m.p. 100–101° (lit. (42) m.p. 101.5–102°); i.r. 3590 (OH), 3300–3460 (OH) cm^{-1}; p.m.r. δ 1.07 (3H, s, CH_3), 1.22 (3H, s, CH_3), 4.18 (1H, m, CHOH) p.p.m.

Apoverbenone (6,6-Dimethylbicyclo[3.1.1]hept-3-en-2-one) (30)

Dehydration of Nopinone

A sample of nopinone (1.38 g 0.01 mol) in dioxane (2 ml) was added to dioxane (80 ml) and the solution refluxed under nitrogen. Selenium dioxide (1.32 g, 0.012 mol sublimed from concentrated nitric acid) was added and reflux continued for 6.5 h. The reaction mixture was cooled at room temperature, a solution of 20% ether – petroleum ether (50 ml) added, and the mixture filtered. The solvent was removed and the product purified by distillation on a spinning band column, b.p. 60–62°/4 mm (lit. (33) b.p. 48.5–49°/1.9 mm) to give apoverbenone 0.55 g (40%).

Allylic Oxidation of Apopinene

The oxidation was conducted as described above for α-pinene. Apopinene (12 g, 0.098 mol) in dichloromethane (100 ml) was added dropwise to a dichloromethane solution containing the red oxidizing agent prepared by adding chromium trioxide (100 g, 1 mol) to a cold solution of dichloromethane (800 ml) containing pyridine (160 g, 2 mol). The reaction mixture was stirred for 48 h at room temperature and worked-up as above to give apoverbenone as an oil which was purified by distillation, b.p. 60–62°/4 mm (lit. (33) b.p. 48.5–49°/1.9 mm), 6.1 g (45%); i.r. 1690 (C=O) cm^{-1}; p.m.r. δ 1.02 (3H, s, CH_3), 1.51 (3H, s, CH_3), 5.85 (1H, d, J = 9 Hz, C=CH—C=O), 7.40 (1H, d of d, J = 9, 5.5 Hz, CH=C—C=O) p.p.m.

Apopinene (6,6-Dimethylbicyclo[3.1.1]hept-2-ene) (28)

cis-Nopinol (18 g, 0.128 mol) was dissolved in dry pyridine (100 ml) and cooled to 0° in an ice bath. To this solution was added with stirring $POCl_3$ (19.5 g, 0.128 mol) and stirring continued for 30 min. Gas–liquid chromatographic analysis indicated the presence of 75% olefin plus 23% of an unidentified component. A saturated solution of sodium carbonate was slowly added to the cold solution until it was basic and the aqueous solution was extracted with ether. The combined extracts were washed with water, a 10% aqueous solution of tartaric acid, dried, filtered, and the solution concentrated. Distillation of the residue at atmospheric pressure gave apopinene, b.p. 138–140°, 7.8 g (50%) (lit. (39) b.p. 140.5°); p.m.r. δ 0.87 (3H, s, CH_3), 1.23 (3H, s, CH_3), 5.48 (1H, d of m, J = 9 Hz, CH=C), 6.08 (1H, m, C=CH) p.p.m.

trans-Verbanone (trans-4,6,6-Trimethylbicyclo[3.1.1.]heptan-2-one (10)

Cuprous iodide (6.85 g, 0.036 mol) in anhydrous ether (100 ml), contained in a flask equipped with a condenser, serum cap, magnetic stirrer, and maintained under nitrogen, was cooled to −60° by means of a solid carbon dioxide – acetone bath and a molar-equiv. of methyl lithium in hexane (Alfa) added, causing a yellow precipitate to form. The temperature was then raised to 0° and a second equiv. of the methyl lithium solution added as a titration until the yellow precipitate just dissolved. The unsaturated ketone (2.5 g, 0.018 mol) was then added, the reaction stirred at 0° for 1 h and then quenched by the addition of a saturated aqueous solution of ammonium chloride. The product was isolated by extraction with ether, the extracts dried, and the *trans*-verbanone so obtained distilled on a spinning band column, b.p. 51–52°/4 mm (lit. (44) b.p., 104–105/20 mm) 2.3 g (83%). Gas-liquid chromatographic analysis did not reveal the presence of any *cis*-verbanone; i.r. 1712 cm^{-1}; u.v. (CH_3OH) 278 sh nm (ε 41); p.m.r. δ 0.81 (3H, s), 1.05 (3H, d, J = 6.5 Hz), 1.32 (3H, s) p.p.m.

4,4,6,6-Tetramethylbicyclo[3.1.1]heptan-2-one (14)

The procedure utilized was the same as outlined for the preparation of *trans*-verbanone above. A sample of verbenone (5 g, 0.33 mol) was added to 2 molar-equiv. of preformed dimethyl copper lithium at 0° and the reaction stirred at 0° for 1 h. The reaction was quenched by the dropwise addition of a saturated aqueous solution of ammonium chloride, the ether layer separated, the aqueous solution extracted with ether, and the combined extracts dried. Distillation of the product afforded the tetramethyl ketone, b.p. 60–62°/0.5 mm (lit. (36) b.p. 52–56°/0.05), 4.2 g (82%); i.r. 1715 (C=O) cm^{-1}; u.v. (CH_3OH) 278 sh nm (ε 40); δ 0.99 (3H, s, CH_3), 1.06 (3H, s, CH_3), 1.16 (3H, s, CH_3), 1.34 (3H, s, CH_3) p.p.m.

We are grateful to Memorial University of Newfoundland and the National Research Council of Canada for financial support of this research and to Professor P. Yates for his encouragement.

1. G. Quinkert. Pure Appl. Chem. **9**, 607 (1964).
2. O. L. Chapman and D. S. Weiss. *In* Organic photochemistry. Vol. 3. *Edited by* O. L. Chapman. Marcel Dekker, New York, N.Y. 1973. p. 243.
3. T. Matsui. Tetrahedron Lett. 3761 (1967).
4. P. J. Nelson, D. Ostrem, J. D. Lassila, and O. L. Chapman. J. Org. Chem. **34**, 811 (1969).
5. L. R. Subramanian and G. S. K. Rao. Tetrahedron, **35**, 1749 (1969).
6. R. T. Hobgood and J. H. Goldstein. J. Mol. Spectrosc. **12**, 76 (1964); A. A. Bothner-By and R. K. Harris. J. Am. Chem. Soc. **87**, 3445 (1965).
7. G. W. Shaffer, A. B. Doerr, and K. L. Purzycki. J. Org. Chem. **37**, 25 (1972).
8. C. C. Badcock, M. J. Perona, G. O. Pritchard, and B. Rickborn. J. Am. Chem. Soc. **91**, 543 (1969); J. A. Barltrop and J. D. Coyle. Chem. Commun. 1081 (1969).
9. G. L. Closs and C. E. Doubleday. J. Am. Chem. Soc. **94**, 9248 (1972).
10. J. G. Calvert and J. N. Pitts, Jr. Photochemistry. John Wiley and Sons, Inc., New York, N.Y. 1966. p. 824.
11. P. J. Wagner and R. W. Spoerke. J. Am. Chem. Soc. **91**, 4437 (1969).
12. W. C. Agosta and W. H. Schrieber. J. Am. Chem. Soc. **93**, 3947 (1971).

13. N. L. ALLINGER and M. A. MILLER. J. Am. Chem. Soc. **83**, 2145 (1961).
14. F. O. RICE and E. TELLER. J. Chem. Phys. **6**, 489 (1938); J. HINE. J. Org. Chem. **31**, 1236 (1966); O. S. TEE. J. Am. Chem. Soc. **91**, 7144 (1969).
15. E. M. ENGLER, J. D. ANDOSE, and P. VON R. SCHLEYER. J. Am. Chem. Soc. **95**, 8005 (1973).
16. F. D. LEWIS and T. A. HILLIARD. J. Am. Chem. Soc. **94**, 3852 (1972); F. D. LEWIS and R. W. JOHNSON. J. Am. Chem. Soc. **94**, 8914 (1972).
17. J. D. COYLE. J. Chem. Soc. B, 1736 (1971).
18. L. A. PAQUETTE and J. H. BARRETT. J. Am. Chem. Soc. **88**, 1718 (1966).
19. I. FLEMING and D. H. WILLIAMS. Tetrahedron, **23**, 2747 (1967).
20. I. LILLIAN and R. A. DOUGHTY. J. Am. Chem. Soc. **89**, 155 (1967).
21. N. J. TURRO, J. C. DALTON, K. DAWES, G. FARRINGTON, R. HAUTALA, D. MORTON, M. NIEMCZYK, and N. SCHORE. Acc. Chem. Res. **5**, 92 (1972).
22. J. MEINWALD and R. A. CHAPMAN. J. Am. Chem. Soc. **90**, 3218 (1968).
23. J. MEINWALD, P. A. SCHNEIDER, and A. F. THOMAS. J. Am. Chem. Soc. **89**, 70 (1967).
24. N. J. TURRO and D. R. MORTON. J. Am. Chem. Soc. **93**, 2569 (1971).
25. T. S. CANTRELL and J. S. SOLOMAN. J. Am. Chem. Soc. **92**, 4656 (1970); R. L. CARGILL, T. Y. KING, and A. B. SEARS. J. Org. Chem. **36**, 1423 (1971).
26. W. G. DAUBEN, M. LORBER, and D. S. FULLERTON. J. Org. Chem. **34**, 3587 (1969).
27. R. RATCLIFFE and R. RODEHORST. J. Org. Chem. **35**, 4000 (1970).
28. A. F. REGAN. Tetrahedron, **25**, 3801 (1969).
29. I. DRISHAUS. Chem. Abstr. **50**, 3501 (1956); German Patent No. 828,244. January 17, 1952.
30. H. J. RINGOLD. J. Am. Chem. Soc. **82**, 961 (1960).
31. J. A. RETAMAR. Bull. Soc. Chim. Fr. 1227 (1966).
32. J. M. COXON, R. P. GARLAND, and M. P. HARTSHORN. Aust. J. Chem. **23**, 1069 (1970).
33. J. GRIMSHAW, J. T. GRIMSHAW, and H. R. JUNEJA. J. Chem. Soc. Perkin I, 50 (1972).
34. D. WALKER and J. D. HIEBERT. Chem. Rev. **67**, 153 (1967).
35. P. C. GUHA and P. L. N. RAO. J. Indian Inst. Sci. **22A**, 326 (1939); Chem. Abstr. **34**, 3255 (1940).
36. Y. BESSIÈRE-CHRÉTIEN and G. GRISON. Bull. Soc. Chim. Fr. 3103 (1970).
37. R. A. JONES and T. C. WEBB. J. Chem. Soc. C, 3926 (1971).
38. Y. CHRÉTIEN-BESSIÈRE and J. P. MONTHÉARD. Chem. Abstr. **62**, 9182 (1965); French Patent No. 1, 377, 525. November 6, 1964.
39. H. E. ESCHINAZI and H. PINES. J. Org. Chem. **24**, 1369 (1959).
40. G. KOMPA and T. HASSELSTROEM. Ann. Acad. Sci. Fennicae, Ser. A30, 3 (1930).
41. Y. BESSIÈRE-CHRÉTIEN and J. P. BRAS. C. R. C, **268**, 2221 (1969).
42. S. WINSTEIN and N. J. HOLNESS. J. Am. Chem. Soc. **77**, 3054 (1955).
43. P. VON R. SCHLEYER, W. E. WATTS, and C. CUPAS. J. Am. Chem. Soc. **86**, 2722 (1964).
44. S. COFFEY (*Editor*). Rodd's chemistry of carbon compounds. 2nd Ed. Vol. II, Part C. Elsevier Publishing Co., Amsterdam 1969. p. 184.
45. K. BOWDEN, I. M. HEILBRON, E. R. H. JONES, and B. C. L. WEEDON. J. Chem. Soc. 39 (1946); A. BOWERS, T. G. HALSALL, E. R. H. JONES, and A. J. LEMIN. J. Chem. Soc. 2555 (1953).
46. L. F. FIESER. Experiments in organic chemistry. 3rd Ed. D. C. Heath and Co., Boston, Mass. 1955. p. 85.
47. P. C. GUHA and K. GANAPATHI. Chem. Ber. **69**, 1185 (1936).
48. J. MEINWALD and P. G. GASSMAN. J. Am. Chem. Soc. **82**, 5445 (1960).
49. G. H. WHITHAM. J. Chem. Soc. 2232 (1961).
50. A. G. FALLIS. Tetrahedron Lett. 4573 (1972).
51. P. D. HOBBS and P. D. MAGNUS. Chem. Commun. 856 (1974).

Can. J. Chem. Downloaded from www.nrcresearchpress.com by 210.87.254.105 on 09/05/12
For personal use only.

Oxidation of Dibenzo[*a*,*e*]fluoranthene by Osmium Tetroxide

P. JACQUIGNON, O. PERIN-ROUSSEL, AND F. PERIN
Institut de Chimie des Substances Naturelles, C.N.R.S., 91190 Gif-sur-Yvette, France
AND
O. CHALVET
Centre de Mécanique Ondulatoire, 23 rue du Maroc, 75019 Paris, France
AND
J. M. LHOSTE
Fondation Curie-Institut du Radium, Section Biologie, 91405 Orsay, France
AND
A. MATHIEU
Fondation Curie-Institut du Radium, 26 rue d'Ulm, 75005 Paris, France
AND
B. SAPERAS AND P. VIALLET
Laboratoire de Chimie Physique, Faculté des Sciences, Chemin de Villeneuve, 66000 Perpignan, France
AND
F. ZAJDELA
Unité 22 I.N.S.E.R.M., Institut du Radium, Bâtiment 110, 91405 Orsay, France
Received June 10, 1974[1]

P. JACQUIGNON, O. PERIN-ROUSSEL, F. PERIN, O. CHALVET, J. M. LHOSTE, A. MATHIEU, B. SAPERAS, P. VIALLET, and F. ZAJDELA. Can. J. Chem. **53**, 1670 (1975).

Dibenzo[*a*,*e*]fluoranthene is treated by osmium tetroxide, the nature, structure, and configuration of the compound obtained (a *trans* dihydro diol) are defined taking into account the chemical, theoretical, and physicochemical arguments.

P. JACQUIGNON, O. PERIN-ROUSSEL, F. PERIN, O. CHALVET, J. M. LHOSTE, A. MATHIEU, B. SAPERAS, P. VIALLET et F. ZAJDELA. Can. J. Chem. **53**, 1670 (1975).

On traite le dibenzo[*a*,*e*]fluoranthène par le tétroxyde d'osmium; on définit la nature, la structure et la configuration du composé obtenu (un dihydro diol *trans*) en tenant compte d'arguments chimiques, théoriques et physicochimiques. [Traduit par le journal]

Recently we presented a preliminary note (1) on the properties of dibenzo[*a*,l]pyrene (**1**) and dibenzo[*a*,*e*]fluoranthene (**2**). The fact that the hydrocarbon **2** is strongly cancerogenic has been confirmed by recent experiments (2) achieved with a product whose structure has no ambiguity.

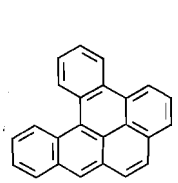

1

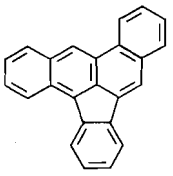

2

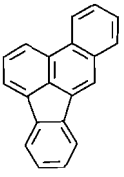

3

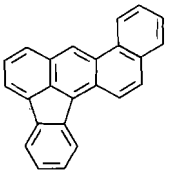

4

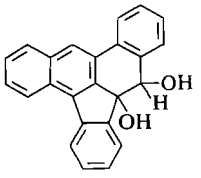

5

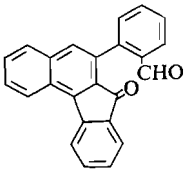

6

[1]Revision received January 15, 1975.

Can. J. Chem. Downloaded from www.nrcresearchpress.com by 210.87.254.42 on 09/05/12
For personal use only.

Can. J. Chem. Downloaded from www.nrcresearchpress.com by 210.87.254.42 on 09/05/12
For personal use only.

We must note that contrary to **1** this molecule does not seem to possess a geometric region corresponding to the definition of the "K zone" following the terminology of Pullman and Pullman (3). Consequently, it was interesting to submit it to the action of osmium tetroxide in order to determine the presence of a bond with a marked ethylenic character of the K zone type (4).

The first observation that we have made relates to the slowness of the reaction between **2** and osmic anhydride. In fact, contrary to the majority of the cases described in the literature for the series of benzo[*a*]anthracene (5) the time of contact to obtain an appreciable quantity of the complex had to be extended to 40 days. (Note: the action on the lower homolog **3** is not easier since in this case, the reaction must be continued for several months.) On the other hand, the oxidation of the isomer (**4**), or naphto[2,1-*b*]fluoranthene, which has been studied equally from the theoretical and spectroscopic points of view, occurs in a very short period of time.

These operations were carried out using the method of Criegee *et al.* (6) modified by Cook and Schoental (5). After dissociation of the complex, treatment, and chromatography, we have isolated a compound which is proved, as we expected, to be a dihydrodiol. This is confirmed by the mass spectrum, the microanalysis, and the infrared spectrum. For the position of the reactive bond, a chemical proof as well as the examination of the n.m.r. spectra allowed us to conclude that the two OH groups were situated on the carbons 5 and 5*a* and from this fact, that the diol corresponds to formula **5**. Indeed, from the chemical point of view, the oxidation by lead tetraacetate (7) breaking the 5–5*a* bond, leads to (formyl-2-phenyl)benzo[*c*]-fluorenone (**6**), the structure of which is defined without ambiguity by the resonance spectra of the protons, microanalysis, and fragmentation in mass spectrometry.

Confirmation of this structure was obtained by the complete analysis of the resonance spectrum of aromatic protons of both the diol and the parent hydrocarbon which confidently identifies all the protons of the molecules. Furthermore, the n.m.r. analysis provided information on the conformation of the diol obtained. Thus, it appears that the mechanism of reaction of osmium tetroxide with aromatic hydrocarbons parallels closely that established for reactions with aliphatic or cycloaliphatic compounds. Then, the diols formed by the action of osmium tetroxide should have a *cis* conformation (6) and only in the course of biochemical degradation could *trans* diols be formed directly from the hydrocarbons (8).

However, we have been somewhat surprised to be unable to obtain the cleavage of **5** in benzofluorenone (**6**) by sodium periodate, a specific reactive for the oxidation of *cis* glycols; and for this operation, to have to use lead tetraacetate with which the cleavage occurs very easily. Since the same phenomenon was observed for the oxidation into (formyl-2-phenyl)-1-fluorenone (**8**) of the diol **7** obtained from the lower homolog **3** of the hydrocarbon **2**, this observation suggested a *trans* conformation for these glycols.

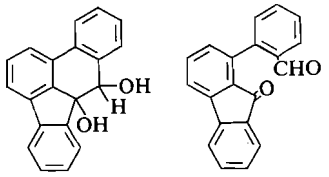

7 8

This assumption was further supported by a comparative examination of the spectra of diol **5** in the infrared taken in the solid state in KBr (bands OH, 3280 and 3370 cm^{-1}) and in solution in CS_2 (bands OH, 3550 and 3580 cm^{-1}). The shift of the characteristic bands, that we also find in the spectrum of diol **8** (KBr, 3300 cm^{-1}; CS_2, 3670 and 3550 cm^{-1}; $CHCl_3$, 3670 and 3550 cm^{-1}), does not appear consistent with the intramolecular hydrogen bond usually present in the *cis diols* (9). The variations observed suggest that the two OH groups are at a distance from each other, and thus situated on each side of the molecule midplane.

These indirect chemical and spectroscopic observations do not constitute unquestionable evidence of the *trans* type configuration. Direct evidence from the n.m.r. spectrum is not available since only one proton is directly bonded to the hydrocarbon framework and since no observable coupling between the hydroxylic protons is present.

For this reason, dihydro-5,5*a*-dibenzo[*a*,*e*]-fluoranthene (**9**) was prepared by the method of Vingiello and Youssef (10) and its n.m.r.

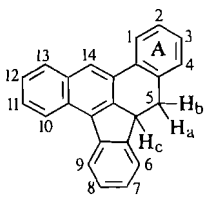

9

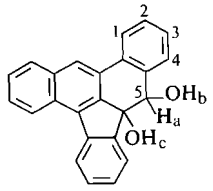

5

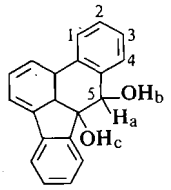

7

spectrum was analyzed and compared with that of the two diols **5** and **7**.

The spectrum of the dihydrogenated compound **9** exhibits three aliphatic protons (designated as a, b, and c in the formula) characterized by their chemical shifts and their coupling constants (δ (p.p.m.): $H_a = 4.09$, $H_b = 2.67$, $H_c = 3.56$; $J_{ab} = 14.5$ Hz, $J_{bc} = 14.3$ Hz, $J_{ac} = 6$ Hz). Thus, the high field proton H_b should be geminal and strictly *trans* with respect to the two others. Indeed, a large vicinal coupling could arise only from a strict *cis* or *trans* configuration, but the former one with a zero dihedral angle is sterically impossible in a cyclohexane type structure. Finally, the smallest coupling corresponds to a vicinal *gauche* interaction.

The assignment of H_a and H_c is easily made by double resonance experiments because in the lower field one H_a exhibits a coupling of 0.8 Hz with the neighbor aromatic H_4 proton and even a smaller long distance coupling with H_2 (*ca.* 0.5 Hz). On the other hand, the H_c resonances are very little broadened, but still exhibit an unresolved coupling with the H_6 proton. On the contrary, the high field resonances of H_b exhibit only very little, if any, coupling with H_4.

In the diol compounds **5** and **7** the remaining proton appears at 4.925 and 4.920 p.p.m. respectively. The decoupling experiments confirmed that the corresponding lines had the same structure, due to long distance coupling to H_4 (0.9 Hz) and H_2 (0.5 Hz), as H_a. Consequently, H_b and H_c have been substituted by hydroxylic groups, in agreement with the assumed *trans* configuration.

The H_a proton exhibits a downfield shift of 0.83 p.p.m. upon diol substitution. This shift could appear small when compared to downfield shifts of about 2 p.p.m. of geminal protons in cyclohexanol, but it does not correspond to the simple effect of the geminal OH group. As a matter of fact, the H_a proton has a more marked equatorial character in the dihydrogenated compound **9** than in the diol, resulting in a lowfield shift due to steric repulsion with H_4. Indeed, the $J_{H_a-H_c}$ coupling, in compound **9**, is nearly a *gauche* coupling, but the $J_{H_a-OH_b}$ coupling (11.4 Hz) certainly corresponds to a more widely opened geminal angle. Thus, the H_a proton is probably displaced a little further from the molecular plane, resulting in less steric interaction with H_4.

Considering the importance of this conclusion of a *trans* diol configuration with respect to the assumed mechanism of the diol formation and to the problems of the metabolism and cancerogenic activity of these compounds, a systematic n.m.r. investigation of the configuration of the diols obtained by osmium tetroxide and *o*-quinone reduction from related hydrocarbons possessing a true "K zone", has been undertaken. These results, which will be reported in detail elsewhere (11), indicate that the behavior of dibenzofluoranthene (**2**) with respect to osmium tetroxide is not at all an exception due to some steric or electronic reasons but is a common rule. As a matter of fact, *trans* diols, which could often be assigned by n.m.r. much more easily because of high symmetry and vicinal HH couplings, have been found for any aromatic hydrocarbon treated by osmium tetroxide, in contrast with the diols obtained by reduction of quinone which correspond to a *trans* H structure. No direct evidence for *cis* diols has been yet found, contrary to the structure assumed until now. For example, the unsymmetrical diol **10** exhibits a vicinal coupling $J_{H_a-H_d}$ of 3.9 Hz corresponding to a *gauche* configuration, which could be attributed to a *cis* configuration, but could correspond as well to two equatorial protons as revealed by the detailed analysis of the n.m.r. spectrum of the whole molecule.

But, in spite of its importance, this question was not the purpose of this work and the

Can. J. Chem. Downloaded from www.nrcresearchpress.com by 210.87.254.42 on 09/05/12
For personal use only.

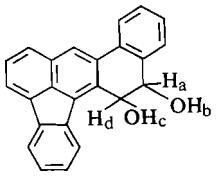

10

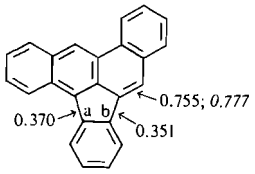

2

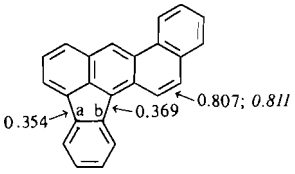

4

FIG. 1. Calculated bond orders for hydrocarbons **2** and **4**.

problem, presently under active investigation, will be reported and discussed later (11) from the point of view of the n.m.r. analysis as well as that of its chemical aspects with respect to previous assignments.

In regard to dibenzofluoranthene, chemical investigations, such as the possible diol conversion, are continuing in order to obtain a chemical proof of this structural assignment, more specific than the unsuccessful periodate oxidation. It is, however, worthwhile to mention that we were not able to obtain the corresponding epoxide until now.

In conjunction with these practical results, the prediction of the eventual reactive zone has been undertaken by the theoretical calculation of the bond indices of the hydrocarbons **2** and **4**.

We know that naphthalene (**11**), anthracene (**12**), and benzanthracene (**13**) react with osmium tetroxide uniquely on the bond possessing the strongest ethylenic character and therefore the greatest bond order, the reaction being faster the higher the bond order. Using the method of Pariser, Parr, and Pople (12) we obtain for these hydrocarbons the three values indicated in the formulas and which agree well with the experimental results.

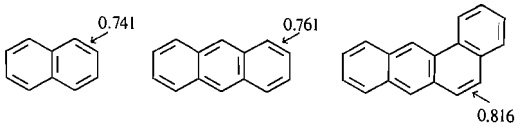

11 12 13

For the hydrocarbons **2** and **4** and assuming all the bonds of equal length ($\beta = -2.39$ eV) an analogous calculation leads to the values indicated in Fig. 1.

The indices of 0.755 for **2** and 0.807 for **4** which are the highest for each molecule could thus appear satisfactory since they situate the attack at the position where it does occur.

Nevertheless, the chosen parameters for the two molecules do not allow us to obtain a correct description of the electronic absorption spectrum, the "theoretical" spectrum being displaced too much towards the visible.

Thus it appears necessary to make the preceding calculation more precise by taking the values of β (thus the bond length) different from the rest of the molecule for the bonds a and b of Fig. 1. This value of β has been deduced by interpolation of the values (Table 1) used by Mulliken and Parr (13) for butadiene and benzene.

TABLE 1. Values for β used for butadiene and benzene (13)

Bond	Length (Å)	β (eV)	Index p
C1—C2 butadiene	1.34	−2.92	0.977
C2—C3 butadiene	1.46	−1.68	0.212
Benzenic	1.39	−2.39	0.666

This leads to a mean value $\beta_a = \beta_b = -1.90$ eV and a bond index $p_a = p_b = 0.360$. With this new parameter we then obtain the values of *0.777* and *0.811* respectively for the bond orders C5—C5*a* of **2** and C5—C6 of **4** (Fig. 1) which thus preserve the strongest character of a double bond.

Likewise this same value of mean B obtains the best correlation between the theoretical and experimental spectra of the two hydrocarbons (Table 2).

The u.v. absorption spectra of the compounds **2** (Fig. 2) and **4** (Fig. 3) show strong analogies between them and yet are clearly distinguishable from that of benzanthracene (14) and from phenyl benzanthracene (Fig. 4). The latter presents all the characteristics of the tetraphenic series: band α forbidden, bands p, β, and β' permitted. On the other hand, the relative intensities of the various bands bring the hydrocarbons **2** and **4** nearer to the fluoranthenes for which the electronic spectra presents the

Can. J. Chem. Downloaded from www.nrcresearchpress.com by 210.87.254.42 on 09/05/12
For personal use only.

Can. J. Chem. Downloaded from www.nrcresearchpress.com by 210.87.254.42 on 09/05/12
For personal use only.

TABLE 2. Comparison of theoretical and experimental spectra for compounds **2** and **4**

Band	Spectrum	
	Theoretical	Experimental
Hydrocarbon **2**		
p	382.6	390
α	384	Band masked
β	320	330
Hydrocarbon **4**		
p	372.9	380
α	348.9	Band masked
β	325.5	325

following structure: band p permitted, band α forbidden, bands β and β′ permitted.

The absorption spectra confirm a convenient choice of parameters and consequently constitute a nonnegligible proof of the validity of theoretical calculation of the bond orders of dibenzo[*a*,*e*]fluoranthene. These calculations have been confirmed by the chemical results.

Thus the low relative value of 0.777 for the reactive bond order, possibly associated with the steric requirements, could explain the slowness of the attack by osmium tetroxide. This appears more correct especially as the same calculation applied to benzofluoranthene (**3**) leads to an index of 0.767, appreciably lower, for the bond involved in the reaction. Now we have effectively established that this hydrocarbon reacts even more slowly than its superior homolog.

When the biological results concerning the hydrocarbons **2** and **4**, their benzologs, and nitrogenous analogs are published, we propose to continue our investigations and to extend them to other cancerogenic hydrocarbons apparently lacking in the K zone that present the family of more condensed homologs of fluoranthene.

Experimental

The melting points were determined either in a capillary tube on a Buchi apparatus or on a metallic block heated electrically and with an electronic temperature detection (laboratory built apparatus).

The centesimal analyses were made by the Laboratoire de Microanalyse du C.N.R.S. at Gif-sur-Yvette.

The u.v. spectra in hexane have been read on a spectrophotometer Safas 1800 modified by the laboratory, and the i.r. spectra, on a KBr disk and in solution in CS_2, on a Perkin–Elmer 225 apparatus.

The n.m.r. spectra at 100 MHz, have been recorded at high resolution in a 10 mm diameter cell on a Varian XL 100 machine at 34 °C. The concentrations of solutions in $CDCl_3$ were from 1 to 3 × 10^{-2} *M*.

The protons were identified by selective decoupling, tickling, and INDOR. Using chloroform as internal reference, the values of chemical displacement (*d*) indicated in p.p.m. have been converted to TMS taking $d(CHCl_3) = 7.26$ p.p.m.

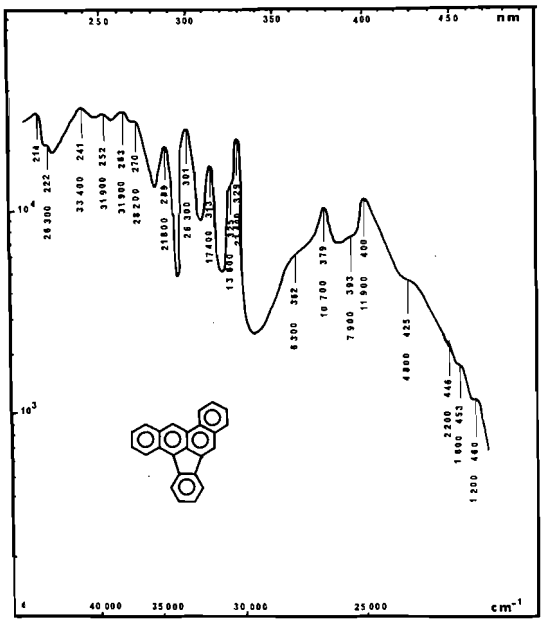

FIG. 2. Ultraviolet spectra of **2**.

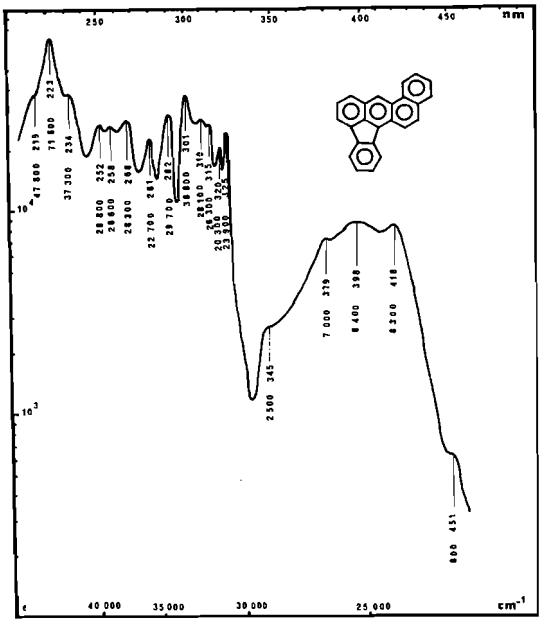

FIG. 3. Ultraviolet spectra of **4**.

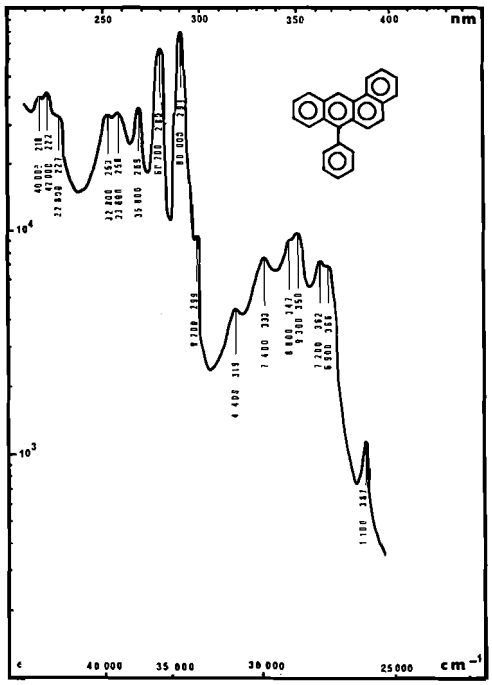

FIG. 4. Ultraviolet spectra of phenyl benzanthrene.

Oxidation by Osmium Tetroxide

The technique used for the three hydrocarbons **2**, **3**, and **4** is that designed by Cook and Schoental (5).

5,5a-Dihydroxy-5,5a-dihydrodibenzo[a,e]fluoranthene (5)

The solution of 1.2 g of dibenzofluoranthene (**2**), 1 g of osmium tetroxide, and 790 mg of pyridine in 120 ml of dry benzene is maintained at 30° for 3 to 4 weeks. Then the brown solution is decanted and the solid brown complex is dissolved in a minimum of methylene chloride. This solution is agitated and treated with an equivalent volume of an aqueous solution of potassium hydroxide (2%) and mannitol (10%). The operation is repeated several times until the aqueous phase is colorless. The organic phase is washed with water, dried with Na_2SO_4, and the solvent is evaporated under vacuum. The recrystallization in benzene of the solid obtained gives 540 mg of fine colorless needles, m.p. (inst.) 224–225° (slow decomposition from 195°); n.m.r.: δ p.p.m.: H_a = 4.925, H_b = 2.95, H_c = 2.23, H_1 = 8.21, H_2 and H_3 = 7.425 to 7.465, H_4 = 7.90, H_6, H_9, and H_{13} = 7.92 to 8.01, H_7 and H_8 = 7.425 to 7.465, H_{10} = 8.56, H_{11} and H_{12} = 7.575, H_{14} = 8.04; $J_{H_a-H_b}$ (H, OH) = 11.4 Hz; $J_{H_a-H_c} \simeq 0.5$ Hz, $J_{H_b-H_c} \simeq 0$.

Anal. Calcd. for $C_{24}H_{16}O_2$ (mol. wt. 336); C, 85.70; H, 4.80; O, 9.51. Found (336, mass spectrum): C, 84.55; H, 4.85; O, 9.21.

The treatment of the reactive benzene solution with mannitol and potassium hydroxide permits the recovery of 460 mg of the initial hydrocarbon.

A second test using double the quantity of osmium tetroxide under the same conditions yielded 730 mg of recrystallized dihydrodiol. The hydrocarbon–dihydrodiol mixture from the treatment of the mother liquors can be separated on an alumina column eluted with benzene for the hydrocarbon and then with chloroform for the diol.

5,5a-Dihydroxy-5,5a-dihydrobenzo[b]fluoranthene (7)

The above technique, with an equivalent of osmium tetroxide, starting with 500 mg of benzo[*b*]fluoranthene (**3**) and after a time of contact of 3 months, leads to the recovery of 250 mg of hydrocarbon and of 130 mg of dihydrodiol recrystallized in benzene into brilliant, colorless needles, m.p. (inst.) 242–243° (decomposition from 215°). n.m.r.: δ p.p.m.: H_a = 4.92, H_b = 2.90, H_c = 2.165; $J_{H_a-H_b}$ = 11.4 Hz, $J_{H_a-H_c}$ = 0.8 Hz, $J_{H_b-H_c} \simeq 0$. Very complex spectrum of aromatic protons, H_1 = 7.92, H_2, H_3, H_7, and $H_8 \simeq 7.42$, H_4 = 7.69, H_6 and H_9 = 7.72 and 7.84, H_{10}, H_{11}, and $H_{12} \simeq 7.52$.

Anal. Calcd. for $C_{20}H_{14}O_2$ (mol. wt. 286): C, 83.89; H, 4.93. Found: C, 83.59; H, 4.84.

5,6-Dihydroxy-5,6-dihydronaphtho[2,1-a]fluoranthene (10)

With the naphtho[2,1-*a*]fluoranthene (**4**) and an equimolar quantity of osmic anhydride, the reaction is completed after 48 h. The hydrocarbon (310 mg) gave 210 mg of fine colorless needles of diol (**10**) after recrystallization in benzene, m.p. (inst.) 194–195° (decomposition from 180°); n.m.r.: only the glycolic part of the spectrum has been analyzed; δ p.p.m.: H_a (H_5) = 5.02, H_b (OH_5) = 2.82, H_c (OH_6) = 1.98, H_d (H_6) = 5.77; $J_{H_a-H_b}$ = 10.3 Hz, $J_{H_c-H_d}$ = 7.0 Hz, $J_{H_a-H_d}$ = 3.9 Hz.

Anal. Calcd. for $C_{24}H_{16}O_2$ (mol. wt. 336): C, 85.70; H, 4.80. Found: C, 84.23; H, 4.96.

(Formyl-2-phenyl)-6-benzo[c]fluorenone (6)

All the attempts to produce oxidative cleavage of the diol **5** by metaperiodate by the described methods (15, 16) at different conditions of temperature and p*H*, have led only to the recovery of the initial product.

On the other hand, oxidation by lead tetraacetate using the technique of Boyland and Wolf (7) occurs very easily. The mixture of 350 mg of diol **5** and 1 g of lead tetraacetate in 100 ml of benzene is agitated at room temperature. After 3 h the chromatography of a sample on a thin layer of silica shows the disappearance of the initial product and the presence of a single compound (orange spot). The benzene solution is then filtered, washed successively with 1 *N* hydrochloric acid, with an aqueous solution of Na_2CO_3, then with water. After drying on Na_2SO_4 the solvent is evaporated under vacuum. The reddish residue is chromatographed on a silica column. The elution of a dark red ring by benzene, after evaporation of the solvent, gives fluorenone (**6**) the recrystallization of which in ethanol produces 290 mg of orange prismatic needles, m.p. 217–218°. Mass spectrum: molecular peak at 334, important peak at 305 by loss of —CHO; n.m.r. (The protons are numbered keeping the numbering of the diol or the hydrocarbon.): H_5(CHO) = 9.92 (coupling 0.7 Hz characteristic of the *ortho* substituted benzaldehydes), H_1, H_2, H_3, H_4 (phenyl) = 7.51 to 7.66, H_6 and H_9 = 8.075 and 8.12, H_7 and H_8 = 7.38, H_{10} = 8.61, H_{11} and H_{12} = 7.69, H_{13} = 7.895, H_{14} = 7.63.

Anal. Calcd. for $C_{24}H_{14}O_2$ (mol. wt. 334): C, 86.21; H, 4.23; O, 9.57. Found: C, 86.52; H, 4.50; O, 9.69.

Can. J. Chem. Downloaded from www.nrcresearchpress.com by 210.87.254.42 on 09/05/12
For personal use only.

(Formyl-2-phenyl)-1-fluorenone (8)

Same technique as previously cited for diol **7**. Test with periodate negative. The product recrystallizes from the benzene – petroleum ether mixture in yellow crystals, m.p. 108–109°.

Anal. Calcd. for $C_{20}H_{12}O_2$ (mol. wt. 284): C, 84.48; H, 4.26. Found: C, 83.82; H, 4.39.

5,5a-Dihydrodibenzo(a–e)fluoranthene (9)

This hydrocarbon was prepared following the method of Vingiello and Youssef (11) with a view to its study in n.m.r. δ p.p.m.: $H_a = 4.09$, $H_b = 2.67$, $H_c = 3.56$; $J_{H_a-H_b} = 14.5$ Hz, $J_{H_a-H_c} = 6$ Hz, $J_{H_b-H_c} = 14.3$ Hz. $H_1 = 8.385$, H_2 and $H_3 = 7.40$ to 7.46, $H_4 = 7.742$, H_6, H_9, and $H_{13} = 8.04$ to 8.08, $H_{10} = 8.68$, H_{11} and $H_{12} = 7.58$, $H_{14} = 8.10$.

This work was supported by the Institut National de la Santé et de la Recherche (CRL. N° 74.4.086.09 and 74.4.108.09) and by the Régie Français des Tabacs (S.E.I.T.A.).

1. O. Perin-Roussel, F. Perin, and P. Jacquignon. Tetrahedron Lett. **14**, 1227 (1974).
2. F. Zajdela et al. To be published.
3. A. Pullman and B. Pullman. Cancérisation par les substances chimiques et structure moléculaire. Masson, Paris, 1955. p. 216.
4. G. M. Badger. J. Chem. Soc. 1809 (1950).
5. J. W. Cook and R. Schoental. J. Chem. Soc. 170 (1948).
6. R. Criegee, B. Marchand, and H. Wannonius. Ann. Chem. **99**, 550 (1942).
7. E. Boyland and G. Wolf. Biochem. J. **47**, 64 (1950).
8. J. N. Daly, D. M. Jerina, and B. Witkop. Experientia, **28**, 1129 (1972).
9. L. P. Kuhn. J. Am. Chem. Soc. **74**, 2492 (1952).
10. F. A. Vingiello and A. K. Youssef. Chem. Commun. **68** (1968).
11. J. M. Lhoste, J. Mispelter, M. Croisy-Delcey, O. Perin-Roussel, F. Perin, and P. Jacquignon. To be published.
12. (*a*) R. Pariser. J. Chem. Phys. **21**, 568 (1953); (*b*) R. G. Parr. Quantum theory of molecular electronic structure. Benjamin, New York. 1964. pp. 240 and 257; (*c*) J. A. Pople. Trans. Faraday Soc. **49**, 1375 (1953).
13. R. S. Mulliken and R. G. Parr. J. Chem. Phys. **19**, 1271 (1951).
14. I. Berenblum, R. Schoental, and E. R. Holiday. Cancer Res. **3**, 689 (1943).
15. M. S. Newman and S. Blum. J. Am. Chem. Soc. **86**, 5598 (1964).
16. H. I. Hadler and A. C. Kryger. J. Org. Chem. **25**, 1896 (1960).

Can. J. Chem. Downloaded from www.nrcresearchpress.com by 210.87.254.42 on 09/05/12
For personal use only.

Etudes expérimentales et théoriques des déplacements chimiques du carbone-13 en serie isothiazolique

ROBERT FAURE, JEAN-RICHARD LLINAS ET EMILE-JEAN VINCENT

Laboratoire de Chimie Organique Physique, Université d'Aix-Marseille III, Rue Henri Poincaré, 13013 Marseille, France

ET

MICHEL RAJZMANN

Laboratoire de Chimie Industrielle, Université d'Aix-Marseille III, Rue Henri Poincaré, 13013 Marseille, France

Reçu le 14 août 1974

ROBERT FAURE, JEAN-RICHARD LLINAS, EMILE-JEAN VINCENT et MICHEL RAJZMANN. Can. J. Chem. **53**, 1677 (1975).

Dans le cadre d'une étude générale par r.m.n. d'hétérocycles pentagonaux à deux hétéroatomes, nous avons déterminé en résonance du ^{13}C les déplacements chimiques, les couplages vicinaux $^1J_{^{13}C-H}$ et les couplages à longue distance d'une série d'isothiazoles diversement substitués. A cette occasion nous avons pu comparer les effets de divers substituants à l'effet du groupe d'hétéroatomes, et montrer l'influence prépondérante de sa dissymétrie sur la grandeur des paramètres observés. De plus la comparaison avec les résultats de calculs théoriques fondés sur le modèle CNDO a montré des insuffisances qui justifient la recherche d'une représentation mieux adaptée de l'atome de soufre par introduction des orbitales d; étude qui entre dans la paramétrisation en CNDO, des éléments de la troisième ligne que nous poursuivons par ailleurs.

ROBERT FAURE, JEAN-RICHARD LLINAS, EMILE-JEAN VINCENT, and MICHEL RAJZMANN. Can. J. Chem. **53**, 1677 (1975).

During a general n.m.r. study of five-membered heterocycles with two hetero-atoms, we measured the ^{13}C chemical shifts, the vicinal couplings $^1J_{^{13}C-H}$ and the long range couplings for a series of variously substituted isothiazoles. At that time we were able to compare the effects of the various substituents to the effect of the group of hetero-atoms and to demonstrate the predominant influence of dissymmetry of the latter on the values of the observed parameters. Moreover, a comparison with theoretical results based on a CNDO model showed deficiencies which justify the search for a representation better adapted, by the introduction of d orbitals, to the sulfur atom. Studies of CNDO parametrization for third row elements are being undertaken by other means. [Journal translation]

Introduction

Dans le cadre de l'étude des hétérocycles pentagonaux à caractère aromatique, nous avons entrepris l'analyse des spectres du carbone-13 de l'isothiazole **1** et de quelques uns de ses dérivés monosubstitués. Les déplacements chimiques et les constantes de couplage $^nJ_{CH}$ des différents carbones du cycle ont pu être attribués sans ambiguité grâce à l'examen des dérivés monométhylés. L'effet des substituants sur les déplacements chimiques a fait l'objet de nombreux travaux (1–10), et dans la série isothiazolique les résultats obtenus confirment généralement ces diverses études. En ce qui concerne les couplages J_{CH} à longue distance, ces effets de substituants sont relativement faibles devant l'effet de dissymétrie dû au groupement hétéroatomique S—N. Les grandeurs observées en r.m.n. peuvent être interprétées en fonction des modèles de la chimie quantique: nous avons pour cela utilisé les résultats obtenus dans le cadre de l'approximation CNDO. Toutefois les corrélations observées ne relèvent encore que du domaine qualitatif.

1

Partie expérimentale

Les spectres du carbone-13 ont été enregistrés sur un spectromètre Varian NV-14 opérant à la fréquence de 15.087 MHz et équipé d'un système à transformée de Fourier. Les déplacements chimiques sont rapportés au signal du TMS choisi comme référence interne, et sont obtenus sur les spectres découplés par bruit, avec une erreur inférieure à 0.1 p.p.m. pour une largeur spectrale

Can. J. Chem. Downloaded from www.nrcresearchpress.com by 210.87.254.42 on 09/05/12
For personal use only.

Can. J. Chem. Downloaded from www.nrcresearchpress.com by 210.87.254.42 on 09/05/12
For personal use only.

TABLEAU 1. Déplacements chimiques du carbone-13 en série isothiazolique et de l'isoxazole

Compose	δ*			
	C_3	C_4	C_5	Substituant
Isothiazole	157.7	124.1	148.7	—
Isoxazole	150.0	104.5	158.9	—
Methyl-3 isothiazole	167.1	124.5	149.1	18.5
Methyl-4 isothiazole	159.3	134.8	144.3	11.8
Methyl-5 isothiazole	158.3	124.2	163.7	12.4
Formyl-5 isothiazole	159.6	129.4	165.3	183.0
Cyano-4 isothiazole	159.2	110.1	158.8	113.4

*δ en p.p.m. par rapport au TMS.

TABLEAU 2. Constantes de couplage $^nJ_{CH}$ (en Hz)

Compose	$^1J_{C_3H_3}$	$^1J_{C_4H_4}$	$^1J_{C_5H_5}$	$^2J_{C_3H_4}$	$^2J_{C_4H_3}$	$^2J_{C_4H_5}$	$^2J_{C_5H_4}$	$^3J_{C_3H_5}$	$^3J_{C_5H_3}$	Divers
Isothiazole	183.7	172.6	186.1	8.0	14.2	5.9	9.1	11.2	6.0	
Isoxazole	188.1 (188.0)*	184.6 (184.0)*	203.5 (203.0)*	6.2	14.2	4.4	11.3	6.2	4.3	
Methyl-3 isothiazole	—	170.4	185.5	†	—	5.2	9.0	†	—	$^1J_{C_6H_6} = 128.1$ $^3J_{C_4H_6} = 3.0$
Methyl-4 isothiazole	180.7	—	184.5	—	†	†	—	10.4	5.3	$^1J_{C_6H_6} = 128.4$ $^3J_{C_5H_6} = 5.3$ $^3J_{C_3H_6} = 4.3$ $^3J_{C_6H_{3\text{ ou }5}} = 2.1$
Methyl-5 isothiazole	181.5	170.3	—	7.9	14.0	—	†	—	†	$^1J_{C_6H_6} = 129.9$ $^3J_{C_4H_6} = 4.4$ $^3J_{C_6H_4} = 2.3$
Formyl-5 isothiazole	188.2	175.6	—	7.0	13.7	—	6.0	—	6.0	$^1J_{C_6H_6} = 187.6$ $^3J_{C_6H_4} = 3.1$ $^2J_{C_5H_6} = 32.0$
Cyano-4 isothiazole	193.4	—	194.3	—	13.8	3.9	—	9.4	4.4	$^3J_{C_6H_{3\text{ ou }5}} = 3.3$

*Référence (14).
†Couplage non résolu.

de 3500 Hz (accumulation sur 8192 points). Les constantes de couplage sont mesurées sur les spectres non découplés, avec une erreur absolue de 0.5 Hz. Pour bénéficier du gain de sensibilité provenant de l'effet nucléaire Overhauser, le système de spins a été irradié durant l'intervalle de temps compris entre deux impulsions successives, selon la technique du 'gate decoupling' (11). Les spectres ont été enregistrés à la température de 28° à partir de produits commerciaux, sans purification ultérieure, en solution à 60% en volume dans l'acétone deuteriée, excepté pour le dérivé cyané qui a été étudié en solution saturée dans le même solvant. L'analyse des spectres non découplés, en haute résolution a été effectuée au premier ordre; les spectres du proton ayant été eux-mêmes interprétés au 1er ordre (15, 16).

Résultats

Les déplacements chimiques et les constantes de couplage relatifs aux composés étudiés sont rassemblés dans les tableaux 1 et 2. L'attribution des déplacements chimiques des trois carbones de l'isothiazole dont le spectre totalement découplé se présente sous forme de trois pics d'intensité à peu près égale[1], a été réalisée sans

[1]Une étude de la relaxation spin–réseau a montré que les T1 des trois carbones de l'isothiazole sont sensiblement identiques (12).

Can. J. Chem. Downloaded from www.nrcresearchpress.com by 210.87.254.42 on 09/05/12
For personal use only.

TABLEAU 3. Effets de substitution sur les déplacements chimiques des atomes de l'isothiazole

	δ*		
Substituant	C_3	C_4	C_5
Methyl-3	9.4	0.4	0.4
Methyl-4	1.6	10.7	−4.4
Methyl-5	0.6	0.1	15.0
Formyl-5	1.9	5.3	16.6
Cyano-4	1.5	−14.0	+10.1

*δ en p.p.m. par rapport à l'isothiazole.

ambiguité par l'étude comparative des spectres des dérivés monométhylés. La perturbation apportée par un groupement méthyle se traduit par un déblindage du carbone substitué d'une quantité de l'ordre de 10 p.p.m., tout en n'influençant que très peu les déplacements chimiques des autres carbones du cycle (tableau 3). Cette attribution est confirmée par les deux observations suivantes: tout d'abord, le carbone en position α de l'atome d'azote résonne à champ plus faible que l'atome de carbone adjacent au soufre comme cela avait déjà été observé pour la molécule de thiazole (13); d'autre part, le carbone C_4 en position β des deux hétéroatomes est moins déblindé que les précédents, et le couplage $^1J_{C_4H_4}$ associé, toujours inférieur aux couplages $^1J_{C_3H_3}$ et $^1J_{C_5H_5}$ (14).

Sur les spectres non découplés on a pu déterminer les couplages à longue distance $^2J_{CH}$ et $^3J_{CH}$ pour tous les carbones à l'exception de celui qui porte le substituant, pour lequel on observe un multiplet très mal résolu. L'attribution a été réalisée par analogie avec l'ensemble des dérivés monométhylés, la valeur de ces couplages étant très peu affectée par la substitution par un groupement méthyle (1). En ce qui concerne le formyl-5 et le cyano-4 isothiazole les déplacements chimiques sont attribués par analyse des spectres non découplés, plus simples que les précédents, et par comparaison des diverses constantes de couplage.

Discussion

Dans le tableau 3 se trouvent regroupées les variations de déplacements chimiques crées par les différentes substitutions opérées sur l'isothiazole. Les groupements méthyles provoquent sur le carbone en α un déblindage d'environ 10 p.p.m., une vériation de cet ordre ayant déjà été observée sur des hétérocycles pentagonaux analogues (2, 4, 5); cette perturbation est beaucoup plus importante (+15 p.p.m.) lorsque le substituant alcoyle est situé en α du soufre, comme dans le cas du méthyl-2 thiophène (10).

Les effets des substituants saturés sur les atomes de carbone en α sont très atténués sauf pour ceux qui sont également en α du soufre; dans ce cas, on observe pour le carbone 5 du méthyl-4 isothiazole une variation de déplacement chimique égale à −4.4 p.p.m.; ce phénomène est d'ailleurs comparable à ce que l'on observe pour les carbones occupant des positions identiques dans le méthyl-4 thiazole et le méthyl-3 thiophène, pour lesquels on a respectivement pour les carbones 5 et 2 des variations égales à −5.4 (13) et −4.3 p.p.m. (10). La présence du groupement cyano provoque en position 5 du cycle isothiazolique, un important effet de déblindage (+10.1 p.p.m.) que l'on n'observe pas pour des pyridines substituées par ce même groupement. L'ordre de grandeur des couplages $^nJ_{CH}$ ($n > 1$) est relativement élevé, ainsi qu'on a déjà pu le noter pour des cycles pentagonaux comportant un ou deux hétéroatomes, et particulièrement lorsqu'on passe des molécules de pyrrole ou de thiophène au cycle isothiazolique (4, 10).

A l'inverse des hétérocycles hexagonaux, les couplages $^2J_{CH}$ sont sensiblement supérieurs aux couplages $^3J_{CH}$ et, au sein de chacune de ces deux familles, la dissymétrie du cycle isothiazolique induit des variations très importantes contrairement aux cycles pentagonaux symétriques pour lesquels ces variations sont inexistantes: $^2J_{C_4H_3} \gg {}^2J_{C_4H_5}$ et $^3J_{C_3H_5} > {}^3J_{C_5H_3}$. On retrouve d'ailleurs un tel phénomène dans le cas de l'isoxazole, molécule dans laquelle le facteur de dissymétrie est le groupement O—N.

Les substitutions opérées sur le cycle isothiazolique par des groupements méthyles ont pour effet d'abaisser les valeurs des constantes de couplage J_{CH} et dans le cas particulier de la substitution en position 4 on a pu observer comme dans le cas de la méthyl-3 pyridine (6) que les couplages vicinaux à travers un carbone substitué par un méthyle étaient multipliés par un facteur de l'ordre de 0.9 par rapport aux valeurs déterminées sur le composé non perturbé.

	$^3J_{C_3H_5}$	$^3J_{C_5H_3}$
Isothiazole	11.2	6.9
Me-4 isothiazole	10.4	5.3

Can. J. Chem. Downloaded from www.nrcresearchpress.com by 210.87.254.42 on 09/05/12
For personal use only.

TABLEAU 4. Comparaison des déplacements chimiques théoriques et expérimentaux*

Molécule	Atome	Théorie ($\delta_{C_6H_{6th}} - \delta_i$)	Experience ($\delta_i - \delta_{C_6H_{6\ exp}}$)
Isothiazole	3	4.70	29.0
	4	−15.3	−4.6
	5	0.2	20.0
Methyl-3 isothiazole	3	8.2	38.4
	4	−18.7	−4.2
	5	−5.3	20.4
	6	−89.9	−110.2
Methyl-4 isothiazole	3	3.6	30.6
	4	−11.9	6.1
	5	−5.6	15.6
	6	−93.2	−116.9
Methyl-5 isothiazole	3	0.8	29.6
	4	−20.4	−4.5
	5	3.5	35.0
	6	−93.3	−116.3
Formyl-5 isothiazole	3	−8.70	30.9
	4	−22.1	0.7
	5	−7.0	36.8
	6	−39.4	54.3
Cyano-4 isothiazole	3	−8.0	30.5
	4	−20.0	−18.6
	5	−9.9	30.1
	6	−66.2	−15.3

*$\delta_{C_6H_{6th}} = 52.9$; $\delta_{C_6H_{6\ exp}} = 128.7$ (14).

TABLEAU 5. Comparaison des constantes de couplage $^1J_{^{13}C-H}$ théoriques et expérimentales

Molécule	Atome	Théorie	Experience
Isothiazole	3	142.2	183.7
	4	129.1	172.6
	5	126.0	186.1
Methyl-3 isothiazole	3	—	—
	4	131.1	170.4
	5	123.0	185.5
	6	94.7*	128.1
Methyl-4 isothiazole	3	143.4	180.7
	4	—	—
	5	129.8	184.5
	6	94.8*	128.4
Methyl-5 isothiazole	3	140.5	181.5
	4	131.1	170.3
	5	—	—
	6	95.1*	129.9
Formyl-5 isothiazole	3	143.5	188.2
	4	131.7	175.6
	5	—	—
	6	135.3	187.6
Cyano-4 isothiazole	3	146.0	193.4
	4	—	—
	5	128.2	194.3
	6	—	—

*Valeurs moyennes.

Les substitutions, en position 4 et 5, par les groupements insaturés CN ou CHO, entrainent une augmentation des couplages $^1J_{CH}$ et une diminution sensible des couplages à longue distance.

Partie théorique

Les déplacements chimiques ont été calculés selon la méthode de Pople (17) et les constantes de couplage dans le cadre de la théorie des perturbations finies (18). Dans le cas des déplacements chimiques la fonction d'onde est déterminée dans l'approximation CNDO/S (19), dont l'un d'entre nous a montré qu'elle était le mieux adapté pour ce type de calcul (20). En ce qui concerne les constantes de couplage, faute de pouvoir utiliser, du fait de la présence de l'atome de soufre, la méthode INDO (21) nous avons mis en oeuvre la méthode CNDO/2 (22). A partir de cette fonction d'onde nous avons calculé le terme de contact de Fermi, nous limitant ainsi à l'évaluation des couplages entre atomes liés, car les couplages à longue distance font intervenir d'autres types d'interactions (23).

Les résultats sont montrés dans les tableaux 4 et 5 et la divergence évidente entre valeurs

expérimentales et valeurs théoriques est certainement due à une paramétrisation inadéquate de l'atome de soufre. La recherche d'une paramétrisation mieux adaptée doit être poursuivie par introduction des orbitales d, études que nous poursuivons par ailleurs.

1. P. C. LAUTERBUR. J. Chem. Phys. **43**, 360 (1965).
2. T. F. PAGE. T. ALGER et D. M. GRANT. J. Am. Chem. Soc. **87**, 5333 (1965).
3. H. L. RETCOFSKY et R. A. FRIEDEL. J. Phys. Chem. **71**, 3593 (1967); **72**, 2619 (1968).
4. F. J. WEIGERT et J. D. ROBERTS. J. Am. Chem. Soc. **90**, 3543 (1968).
5. R. G. REES et M. J. GREEN. J. Chem. Soc. B, 387 (1968).
6. F. J. WEIGERT, J. HUSAR et J. D. ROBERTS. J. Org. Chem. **38**, 1313 (1973).
7. R. J. PUGMIRE, D. M. GRANT, L. B. TOWNSEND, et R. K. ROBINS. J. Am. Chem. Soc. **95**, 2791 (1973).
8. G. ELLIS et R. G. JONES. J. Chem. Soc. Perkin II, 437 (1972).
9. R. G. PARKER et J. D. ROBERTS. J. Org. Chem. **35**, 996 (1970).
10. K. TAKAHASHI, T. SONE et K. FUJEDA. J. Phys. Chem. **74**, 2765 (1970).
11. W. V. PHILIPSBORN, Angew. Chem. Int. Ed. **10**, 472 (1971).
12. R. FAURE et E. J. VINCENT. Résultats non publiés.
13. R. GARNIER, R. FAURE, A. BABADJAMIAN et E. J. VINCENT. Bull. Soc. Chim. Fr. 1040 (1972); E. J. VINCENT, R. PHAN-TAN-LUU et J. METZGER. C. R. **270**, 666 (1970).
14. J. B. STOTHERS. Carbon-13 NMR spectroscopy. Academic Press, N.Y. 1972.
15. J. C. POITE. Thèse. Marseille. 1973.
16. R. E. WASYLISHEN, J. B. ROWBOTHAM et T. SCHAEFER. Can. J. Chem. **52**, 833 (1974).
17. J. A. POPLE. J. Chem. Phys. **37**, 53 (1962).
18. J. A. POPLE, J. W. MCIVER et N. S. OSLUND. J. Chem. Phys. **49**, 2960 (1968).
19. J. DEL BENE et H. H. JAFFE. J. Chem. Phys. **48**, 1807 (1968).
20. M. RAJZMANN. Thèse. Marseille. 1973.
21. J. A. POPLE, D. L. BEVERIDGE et P. A. DOBOSH. J. Chem. Phys. **47**, 2026 (1967).
22. J. A. POPLE et G. A. SEGAL. J. Chem. Phys. **43**, S136 (1965).
23. G. J. KARABATSOS et C. E. ORZECH, JR. J. Am. Chem. Soc. **86**, 3574 (1964).

Can. J. Chem. Downloaded from www.nrcresearchpress.com by 210.87.254.42 on 09/05/12
For personal use only.

Alkylation of 1-Methyl-2-piperidones[1]

PIERRE DESLONGCHAMPS, UKKEN O. CHERIYAN, AND DENNIS R. PATTERSON
Laboratoire de synthèse organique, Département de chimie, Université de Sherbrooke, Sherbrooke, Québec J1K 2R1
Received October 23, 1974

PIERRE DESLONGCHAMPS, UKKEN O. CHERIYAN, and DENNIS R. PATTERSON. Can. J. Chem. **53**, 1682 (1975).

The alkylation of 1-methyl- and 1,3-dimethyl-2-piperidone is reported in good yield.

PIERRE DESLONGCHAMPS, UKKEN O. CHERIYAN et DENNIS R. PATTERSON. Can. J. Chem. **53**, 1682 (1975).

L'alkylation de la méthyl-1 et de la diméthyl-1,3-pipéridone est rapportée avec un excellent rendement.

Can. J. Chem. Downloaded from www.nrcresearchpress.com by 210.87.254.40 on 09/05/12
For personal use only.

In the course of our investigation which led to the development of a new stereoelectronic theory for the hydrolysis of amides[1] it was necessary to prepare *N*-dialkylated imidate salts. Some of those salts can be easily produced from the appropriate 3-alkyl-1-methyl-2-piperidones. The direct alkylation of 1-methyl-2-piperidones was therefore considered.

The α-alkylation of 1-methyl-2-pyrrolidone (3) and of *N*,*N*-dialkylamides (4) has been reported but the yields were moderate.[2] This is presumably due to the base used ($NaNH_2$) to produce the enolate salt of the amide function because when *n*-butyl lithium was used to generate the dilithioamide of secondary amide, high yield of α-alkylated secondary amides was obtained (6).

We would like to report the optimum experimental conditions that we have found for the alkylation reaction of *N*-methyl six-membered lactams.[3]

We have found that 1-methyl-2-piperidone (**1**) can be converted into **2** or **3** in high yield with the proper alkyl iodide. The lithium enolate of **1** was generated with lithium dimethylamide in benzene. A slight excess of the base and alkylating agent ensured complete alkylation. There were no detectable amounts of *O*-alkylated or bis-alkylated products. 1,3-Dimethyl-2-piperidone (**2**) could be further alkylated to give the bis-α-alkylated products **4** and **5** in excellent yield. Consequently, this method provides a convenient route to α-disubstituted-*N*-alkyl lactams.

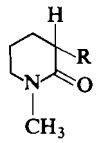

1 R = H
2 R = CH_3
3 R = C_2H_5

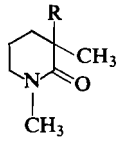

4 R = CH_3
5 R = C_2H_5

We would like to point out that α-alkylation of an amide function has a great potential in organic synthesis. Generation of the lithium enolate with appropriate base seems easy. No side reactions occur presumably because the amide function does not react with its lithium enolate during its formation. Also, *O*-alkylation of the lithium enolate does not occur in normal conditions. The amide function is a versatile and fairly chemically stable functional group which is at the oxidation level of an acid. Still, it can be easily converted to the corresponding amine, acid, ester, and aldehyde function (10).

Experimental

The i.r. spectra were taken on a Perkin-Elmer 257 spectrophotometer; proton n.m.r. spectra were recorded on a Varian A-60 spectrometer. The chemical shifts are reported in δ-values relative to tetramethylsilane as internal standard. The vapor phase chromatographic (v.p.c.) analysis was done on a Varian aerograph model 90-P. Mass spectra were taken on a Hitachi-Perkin-Elmer RMU-6 mass spectrometer. Microanalyses were carried out by Mr. J. Tamas, Laboratoire de microanalyse, Université de Sherbrooke.

[1]References 1 and 2 and unpublished work by D. R. Patterson, this laboratory, 1974.

[2]For alkylation of amides having another stabilizing group in α-position, see ref. 5.

[3]Reaction of the lithium enolate salt of 1-methyl-2-piperidone has been reported during the course of this work (7); α-alkylation of β-lactams is known (8); for an example of α-alkylation of an α-alkyl-*N*-substituted lactam, see ref. 9.

Can. J. Chem. Downloaded from www.nrcresearchpress.com by 210.87.254.40 on 09/05/12
For personal use only.

Reagents

The alkyl iodides were washed with aqueous sodium thiosulfate, dried over anhydrous calcium chloride, and distilled. *N*-Butyl lithium in hexane (2.2 *M*) supplied by Alpha Products was used in all experiments. Benzene was dried over sodium hydride and distilled. 1-Methyl-2-piperidone (Chemical Procurement Laboratories) was dried over molecular sieves (type 4A, Fisher Scientific) and distilled. Dimethylamine was used as a solution in benzene: a solution of the amine ($\simeq 1.2$ *M*) was prepared by bubbling the gas for 4 h through benzene and this solution was diluted with an equal amount of benzene and the concentration was determined by titration (11).

1,3-Dimethyl-2-piperidone (2)

A solution of dimethylamine in benzene (33 ml, 39.6 mmol) was added dropwise to a magnetically stirred cold (ice bath) solution of *n*-butyl lithium in hexane (15 ml, 33 mmol) under an atmosphere of argon. The white slushy precipitate formed was stirred (ice bath) for 0.5 h. Addition of 1-methyl-2-piperidone (**1**; 3.5 g, 31.5 mmol) to this mixture gave a pale yellow homogeneous solution. The solution was heated for 1 h at 50–60 °C under vacuum (15–20 mm) to remove excess dimethylamine. Methyl iodide (4.68 g, 33 mmol) in benzene (10 ml) was then added to the cold (ice bath) magnetically stirred reaction mixture. Stirring was continued for 2 h at room temperature. Water (10 ml) was then added and the benzene layer was separated. The aqueous phase was then extracted with dichloromethane. The combined extract was washed with a small quantity of water and dried over sodium sulfate. The solvent was removed by distillation and the resulting oil was filtered through a column of silica gel with dichloromethane to yield after removal of the solvent, a pale yellow liquid (3.75 g). Distillation gave 1,3-dimethyl-2-piperidone (**2**; 3.25 g, 83%) which was shown to be pure (> 98%) by v.p.c.; b.p. 92–94 °C/5 mm (lit. (12) b.p. 113–114 °C/18 mm); i.r.: ν_{max} ($CHCl_3$) 1625 cm^{-1}; n.m.r.: δ($CDCl_3$) 1.25 (3H, doublet, CH_3—CH), 1.52–2.2 (4H, multiplets), 2.3–2.6 (1H, multiplet), 2.98 (3H, singlet, N—CH_3), and 3.2–3.5 (2H, multiplets); m.s.: *m/e* 127 (M^+), 112 ($M^+ - CH_3$).

1-Methyl-3-ethyl-2-piperidone (3)

The lithium enolate was generated from 1-methyl-2-piperidone (**1**; 3.5 g, 31.5 mmol) in benzene by the method described above. Ethyl iodide (5.14 g, 33 mmol) in benzene (10 ml) was added dropwise. The stirring was continued for 8 h at room temperature. Work-up as described above gave 1-methyl-3-ethyl-2-piperidone (**3**; 3.7 g, 85%) which was shown to be pure (> 98%) by v.p.c.; b.p. 78–79 °C/1 mm (lit. (13) b.p. 87–90 °C/2 mm); i.r.: ν_{max} ($CHCl_3$) 1625 cm^{-1}; n.m.r.: δ($CDCl_3$) 0.96 (3H, triplet, $J = 6$ Hz, CH_2—CH_3), 1.2–2.5 (7H, multiplet), 2.98 (3H, singlet, N—CH_3), and 3.2–3.5 (2H, multiplet); m.s.: *m/e* 141 (M^+), 126 ($M^+ - CH_3$).

1,3,3-Trimethyl-2-piperidone (4)

1,3-Dimethyl-2-piperidone (**2**; 2.4 g, 18.2 mmol) was converted into its lithium enolate by lithium dimethylamide in benzene prepared from *n*-butyl lithium (9 ml, 19.8 mmol) and dimethylamine (20 ml, 24 mmol) solutions. Methyl iodide (2.85 g, 20 mmol) in benzene (10 ml) was added to the cold reaction mixture. Stirring was then continued for 15 h at room temperature. Work-up as described above gave 1,3,3-trimethyl-2-piperidone (**4**; 2.3 g, 86%) which was shown to be pure (> 98%) by v.p.c.; b.p. 72–74 °C/1 mm (lit. (12) b.p. 106–107 °C/18 mm); i.r.: ν_{max} ($CHCl_3$) 1620 cm^{-1}; n.m.r.: δ($CDCl_3$) 1.21 (6H, singlet, two CH_3), 1.7–2.0 (4H, multiplet), 3.00 (3H, singlet, N—CH_3), and 3.2–3.5 (2H, multiplet); m.s.: *m/e* 141 (M^+), 126 ($M^+ - CH_3$).

1,3-Dimethyl-3-ethyl-2-piperidone (5)

1,3-Dimethyl-2-piperidone (**2**; 2.47 g, 19.5 mmol) was converted into its lithium enolate by lithium dimethylamide in benzene prepared from *n*-butyl lithium (10 ml, 2.2 mmol) and dimethylamine (22 ml, 26.4 mmol) solutions. Ethyl iodide (3.5 g, 22 mmol) in benzene (10 ml) was added to the cold reaction mixture. Stirring was then continued for 24 h at room temperature. Work-up as described above gave 1,3-dimethyl-3-ethyl-2-piperidone (**5**; 2.38 g, 80%) which was shown to be pure (> 98%) by v.p.c.; b.p. 80–82 °C/20 mm; i.r.: ν_{max} ($CHCl_3$) 1620 cm^{-1}; n.m.r.: δ($CDCl_3$) 0.83 (3H, triplet, CH_2—CH_3), 1.18 (3H, singlet, C—CH_3), 1.4–2.0 (6H, multiplet), 2.98 (3H, singlet, N—CH_3), and 3.3–3.5 (2H, multiplet); m.s.: *m/e* 155 (M^+), 140 ($M^+ - CH_3$).

Anal. Calcd. for $C_9H_{17}NO$: C, 69.63; H, 11.04. Found: C, 69.62; H, 10.81.

Support for this work by the National Research Council of Canada, and by the Ministère de l'Education, Québec, is gratefully acknowledged.

1. P. DESLONGCHAMPS, C. LEBREUX, and R. TAILLEFER. Can. J. Chem. **51**, 1665 (1973).
2. P. DESLONGCHAMPS. Pure Appl. Chem. In press.
3. P. G. GASSMAN and B. L. FOX. J. Org. Chem. **31**, 982 (1966).
4. H. L. NEEDLES and R. E. WHITFIELD. J. Org. Chem. **31**, 989 (1966).
5. L. C. CHENEY, W. B. WHEATLEY, M. E. SPEETER, W. M. BYRD, W. E. FITZGIBBON, W. F. MINOR, and S. B. BINKLEY. J. Org. Chem. **17**, 770 (1952). P. A. J. JANSSEN and J. C. JANSSEN. J. Am. Chem. Soc. **78**, 3862 (1956). R. B. MOFFETT and B. D. ASPERGREN. J. Am. Chem. Soc. **79**, 4462 (1957). A. L. SEARLES and D. RESSLER. J. Am. Chem. Soc. **80**, 3656 (1958). O. MARTENSSON and E. NILSSON. Acta Chem. Scand. **14**, 1129 (1960); **15**, 1026 (1961). K. SHIMO, S. WAKAMATSU, and T. INOUE. J. Org. Chem. **26**, 4868 (1961).
6. R. L. GAY and C. R. HOUSER. J. Am. Chem. Soc. **89**, 1647 (1967).
7. B. M. TROST and R. A. KUNZ. J. Org. Chem. **39**, 2475 (1974).
8. T. DURST, R. VAN DEN ELZEN, and R. LEGAULT. Can. J. Chem. **52**, 3206 (1974).
9. J. L. HERRMANN, R. J. CREGGE, J. E. RICHMAN, C. L. SEMMELHACK, and R. H. SCHLESSINGER. J. Am. Chem. Soc. **96**, 3702 (1974).
10. B. C. CHALLIS and J. CHALLIS. *In* The chemistry of amides. *Edited by* S. Patai and J. Zabicky. Interscience Publishers. London, New York. 1970. pp. 731–857.
11. A. I. VOGEL. *In* Elementary practical organic chemistry. Longmans, Green and Co. Ltd. London. 1958. pp. 698–699.
12. N. J. LEONARD and F. P. HAUCK, JR. J. Am. Chem. Soc. **79**, 5279 (1957).
13. H. MOHRLE and H. WEBER. Chem. Ber. **105**, 368 (1972).

Polar Substituents in Pericyclic Reactions: Mechanistic Course of the $2\pi + 2\pi$ Photocycloaddition of Dimethyl 1,4-Dihydro-1,4-ethenonaphthalene-2,3-dicarboxylate

CHRISTOPHER OWEN BENDER AND DEE WINTON BROOKS

Department of Chemistry, University of Lethbridge, Lethbridge, Alberta T1K 3M4

Received November 7, 1974

CHRISTOPHER OWEN BENDER and DEE WINTON BROOKS. Can. J. Chem. **53**, 1684 (1975).

Deuterium labeling studies are consistent with the initial photochemical $2\pi + 2\pi$ closure of singlet excited dimethyl 1,4-dihydro-1,4-ethenonaphthalene-2,3-dicarboxylate (**4**) proceeding via bridging between the vinyl and vinyl diester moieties and not via the vinyl–benzo bridging mode favored by Grovenstein and by the Epiotis polar pericyclic theory. The possible involvement of the charge-transfer excited state of **4** in the reaction is discussed.

CHRISTOPHER OWEN BENDER et DEE WINTON BROOKS. Can. J. Chem. **53**, 1684 (1975).

Des études de marquages au deuterium sont en accord avec une fermeture photochimique initiale $2\pi + 2\pi$ de l'état excité singulet du dihydro-1,4 éthéno-1,4 naphtalènedicarboxylate de diméthyle (**4**) se produisant par l'intermédiaire d'un pont entre les portion vinyle et vinyle diester et non pas par un intermédiaire du pont vinylbenzo favorisé par Grovenstein et aussi par la théorie péricyclique polaire d'Epiotis. On discute de l'implication possible d'un état de transfert de charge de **4** dans la réaction. [Traduit par le journal]

Introduction

Recent configuration-interaction calculations by Epiotis indicate that strongly polar substituents can in some cases reverse the usual Woodward–Hoffmann formulations for concerted pericyclic processes (1). In particular, Epiotis predicts that for polar $2\pi + 2\pi$ systems, photoadditions should occur in the s + a mode. An interesting situation pertains in the case of rigid polar molecules when the s + a mode of closure is precluded by geometry, and an illustrative case discussed by Epiotis is that of hexadiene **1**, which gives no intramolecular $2\pi + 2\pi$ photoaddition product (2).[1] In an attempt to test further the theory in a rigid system, we had examined (3) the photoformation of cyclooctatetraenes from 2-cyanobenzobarrelene (**2**), it being assumed that the initial step in the reaction involves a concerted $2\pi + 2\pi$ cycloaddition to give a quadricyclic intermediate (*e.g.*, see **5** and **7**, Scheme 1).

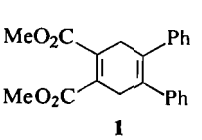

1

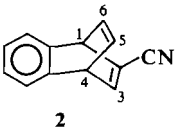

2

Of the three possible $2\pi + 2\pi$ modes of closure of **2** (between benzo–vinyl, vinyl–vinylcyano, or benzo–vinylcyano groups) the theory predicts that bonding to the polar vinylcyano bridge should be the least favored since steric prohibition prevents a concerted cyclization in the s + a mode. Nevertheless, the predicted benzo–vinyl cycloaddition, the preferred mode of closure in benzobarrelene itself (4), was not observed; only $2\pi + 2\pi$ cyclizations involving the vinylcyano bridge occurred, 65% to the vinyl and 35% to the benzo group.

A contentious point with regard to the study with **2** is that the single cyano group may not impart significant polar character to the barrelene, thus making it a poor test system.[2] To overcome this objection we have sought to examine a more potent polar species. Since the photoaddition of dimethyl maleate to cyclohexene gives the *trans*-cyclobutane **3**, a reaction cited by Epiotis as being a polar $2\pi + 2\pi$ process (1), we thought that the intramolecular photoadditions of 2,3-dicarbomethoxybenzobarrelene (**4**) would be an analogous and a pertinent polar system to investigate.

Interestingly, much of the photochemistry of **4** has been determined by Grovenstein *et al.* (5),

[1]We thank the author for a preprint of this article.

[2]Private communication with Professor N. D. Epiotis.

Can. J. Chem. Downloaded from www.nrcresearchpress.com by 210.87.254.6 on 09/05/12
For personal use only.

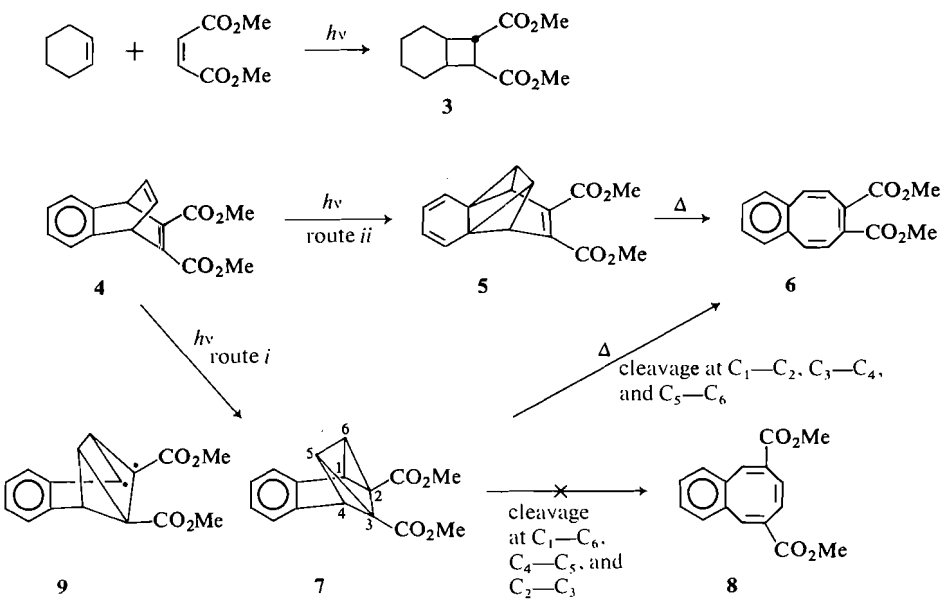

SCHEME I

who report that the direct irradiation of **4** yields 7,8-dicarbomethoxybenzocyclooctatetraene (**6**). However, the mechanism of formation of **6**, which could conceivably involve either of two initial $2\pi + 2\pi$ photoaddition pathways (route *i*, vinyl–vinyldiester bonding or route *ii*, benzo–vinyl bonding; see Scheme 1), was not elucidated, other than it being noted that route *ii* seemed to be more reasonable on the grounds that it would yield only one COT (**6**), whereas route *i* should give rise to two COT's (**6** and **8**). Route *ii* is also favored by the Epiotis polar theory.

We have now carried out deuterium labeling studies to determine the initial $2\pi + 2\pi$ bonding preference of barrelene **4**. Our results reveal that the vinyl–vinyldiester route (*i.e.*, route *i*) is solely utilized in the formation of COT **6**.

Results

To distinguish between the two possible $2\pi + 2\pi$ cycloaddition pathways which can lead to COT **6**, the mixture of deuterated barrelenes **10** and **11** was synthesized by cycloadding dimethylacetylene dicarboxylate to 2-deuterionaphthalene. It can be seen from inspection of Scheme 2 that although both routes *i* and *ii* can produce aromatically labeled COT (**17**), only route *i* can yield COT product **16** containing the label at C-6 whereas only route *ii* can yield COT product **18** containing the label at C-5.

The total deuterium content of the mixture of **10** and **11** was found to be 0.99 ± 0.08 but the relative amounts of **10** and **11** could not be ascertained directly from analysis of the n.m.r. spectrum of the mixture because of overlap of the barrelene vinyl and aromatic signals. The distribution was obtained, however, from inspection of the n.m.r. spectrum of the deuterated COT photoproducts (*vide infra*). The mixture of barrelenes **10** and **11** was irradiated directly in cyclohexane and in methanol solvent systems and runs at both low and high conversions were carried out to evaluate the possible isotope effects arising from the differing deuterium locations in the starting barrelene mixture. The resulting deuterated COT products were isolated by column chromatography and the deuterium distributions were analyzed by n.m.r. spectroscopy (see Table 1). The assignments of the protons in the undeuterated COT **6** follow from comparison of its spectrum with that of other benzo-COT's (see Table 2). The assignments were confirmed by examining the spectrum upon adding the lanthanide shift reagent tris(perfluorobutylpivaloylmethanato)europium, $Eu(fod)_3$. As shown in Fig. 1, the addition of increasing amounts of $Eu(fod)_3$ consistently moves the

Can. J. Chem. Downloaded from www.nrcresearchpress.com by 210.87.254.6 on 09/05/12
For personal use only.

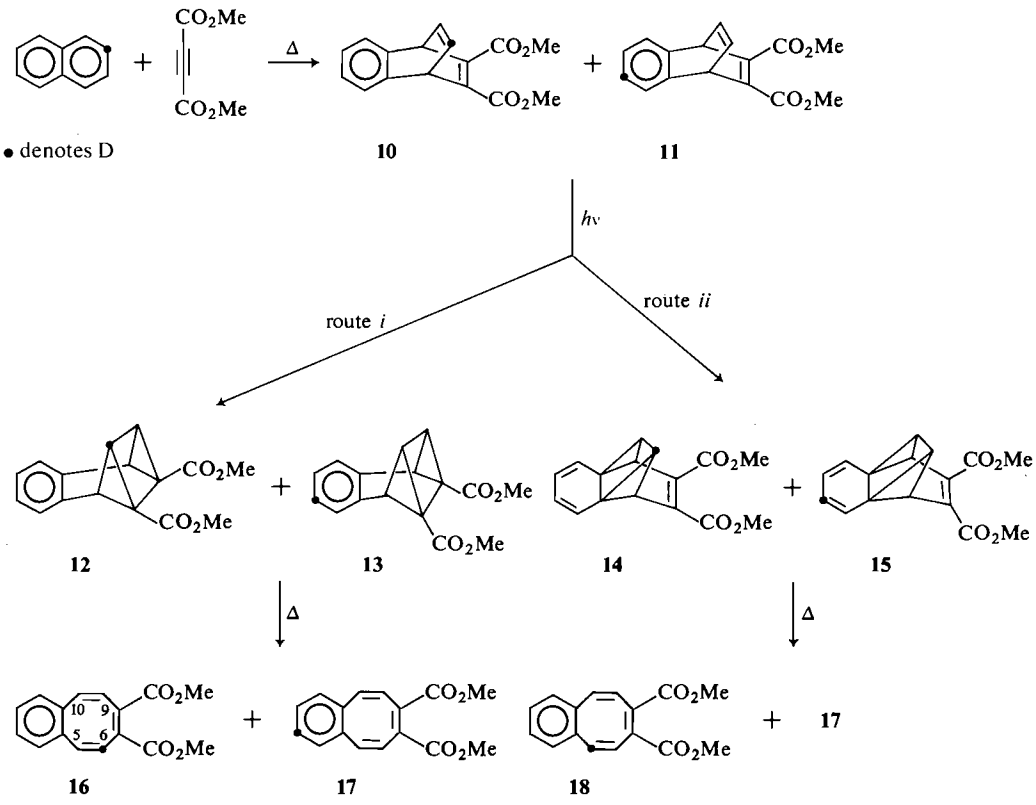

SCHEME 2

H-6(9) doublet further downfield than the H-5(10) doublet (at molar ratio 0.27 the two doublets converge to a singlet at τ 2.92), which accords with H-6(9) being closer than H-5(10) to the ester–lanthanide complexation centers.

In the case of the deuterated COT products, the n.m.r. spectra are essentially the same as that for **6**, except that there are now two types of signal for H-5. Besides the *doublet* centered at τ 3.34 (*A*B, J = 11.5 Hz) arising from coupling to H-6 (A*B*, J = 11.5 Hz) there is a *singlet* at τ 3.34 which results from the absence of coupling when C-6 is partially deuterated.

The quantum yields for the formation of COT **6** were also investigated to ascertain the relative efficiency of the reaction; in cyclohexane the appearance Φ is 0.16 ± 0.02 whereas in methanol it is 0.10 ± 0.01.

TABLE 1. Observed and theoretical hydrogen distributions in labeled cyclooctatetraene product

	Hydrogen distribution				
Item	Aromatic	H-5	H-6	OCH_3	% conversion
1 C_6H_{12}, exp[a]	3.43±0.12	1.98±0.04	1.62±0.12	6.00	22
2 C_6H_{12}, exp	3.49±0.11	2.00±0.08	1.55±0.08	6.00	81
3 CH_3OH, exp	3.43±0.13	1.98±0.11	1.57±0.05	6.00	28
4 CH_3OH, exp	3.48±0.07	1.97±0.04	1.52±0.04	6.00	82
5 route *i*, calcd[b]	3.51±0.04	2.00	1.51±0.04	6.00	
6 route *ii*, calcd[b]	3.51±0.04	1.51±0.04	2.00	6.00	

[a]Errors estimated from scatter of n.m.r. signal integrations.
[b]Corrected for 99 ± 8% deuterium incorporation, equally divided between aromatic and olefinic locations.

Can. J. Chem. Downloaded from www.nrcresearchpress.com by 210.87.254.6 on 09/05/12
For personal use only.

TABLE 2. The n.m.r. data of aromatic and vinyl protons of cyclooctatetraenes[a]

Assignment	Description and signal position, τ		
	6[b]	Benzo-COT[c]	7-CN-Benzo-COT[d]
Aromatic	2.75–3.07[e] m	2.72–3.27 m	2.72–3.05 m
H-5	3.34 d, $J_{5,6}$ = 11.5	3.53 d, $J_{5,6}$ = 10.5	3.32 d, $J_{5,6}$ = 11.5
H-6	3.87 d, $J_{5,6}$ = 11.5	4.08 d, $J_{5,6}$ = 10.5	4.11 d, $J_{5,6}$ = 11.5
H-7	—	4.19 s	—
H-8	—	4.19 s	3.46 d, $J_{8,9}$ = 4
H-9	3.87 d, $J_{5,6}$ = 11.5	4.08 d, $J_{9,10}$ = 10.5	4.03 d of d, $J_{8,9}$ = 4 $J_{9,10}$ = 11.5
H-10	3.34 d, $J_{5,6}$ = 11.5	3.53 d, $J_{9,10}$ = 10.5	3.35 d, J = 11.5

[a]CCl_4 solutions run on HA-100 MHz n.m.r. with TMS as internal standard; coupling constants are given in Hz.
[b]This work.
[c]Reference 4.
[d]Unpublished data.
[e]τ 2.85 (m, H-2 and H-3) and τ 3.02 (m, H-1 and H-4).

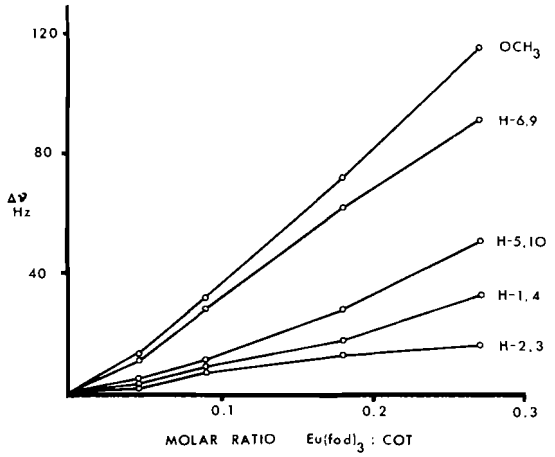

FIG. 1. Variation of chemical shift for the protons in COT **6** with increasing concentrations of the shift reagent $Eu(fod)_3$.

Discussion

It can be seen from Table 1 that irradiation of barrelene mixture **10** and **11** leads to COT product **16** containing the olefinic label uniquely at C-6 and thus the COT formation cannot proceed (within experimental error) via the benzo–vinyl bridging mechanism favored by Grovenstein and by the Epiotis polar theory. The observation that only **6** is formed from the proposed intermediate **7** can be attributed to the preferred rupture of the C_1—C_2 bond of **7**, since favorable stabilization from the carbomethoxy and benzo groups is afforded both radical centers in the ensuing species **9**. An alternative explanation is provided by the fact that in cyclopropanes electron withdrawing substituents strengthen the bond opposite, while weakening the bonds adjacent (6).

Also from Table 1, it can be seen that a comparison of the integrated area of the aromatic region with that of the well separated olefinic region of deuterated COT product provides a method of determining the relative amounts of **10** and **11** present in the original deuterated barrelene mixture. From each run, the two areas are of equal magnitude and it therefore seems reasonable to assume that the mixture is comprised of equal amounts of **10** and **11** and hence to conclude that no measurable isotope effect is observed either in the original preparation of the deuterated barrelenes, or in the subsequent photolysis of the mixture.

The reason for investigating the photolysis of barrelene mixture **10** and **11** in two solvent systems was to relate the photochemical studies of **2** and **4**, the former of which was studied in

Can. J. Chem. Downloaded from www.nrcresearchpress.com by 210.87.254.6 on 09/05/12
For personal use only.

Can. J. Chem. Downloaded from www.nrcresearchpress.com by 210.87.254.6 on 09/05/12
For personal use only.

cyclohexane and the latter in methanol. Although the large increase in solvent polarity on going from cyclohexane to methanol does decrease the efficiency of the reaction by about 40%, the overall mechanism of formation of **6** appears to be unaffected (see Table 1). Thus COT formation from both **4** and vinylcyano-2,3-naphthobarrelene (7) occurs exclusively via initial $2\pi + 2\pi$ bonding between vinyl and polar vinyl groups, whereas COT formation from **2** occurs predominately via this route (3) and it is only in the cases of the unsubstituted benzobarrelene (4) and 1,2-naphthobarrelene (8) that initial aromatic–vinyl bridging has been observed. We therefore conclude that if the cyclization step is product controlling then the Epiotis polar theory seems unable to correctly predict the preferred modes of $2\pi + 2\pi$ photoclosure in polar barrelene systems.

With regard to the nature of the excited-state species involved in the formation of COT **6**, Grovenstein has shown that the acetone sensitized irradiation of **4** yields di-π-methane rearrangement product together with some unidentified material but COT **6** appears to be absent. The singlet excited state of **4** is therefore implicated in the COT formation. Interestingly, the u.v. spectrum of **4** shows a long wavelength band at 335 nm (ε 40) in cyclohexane (334 nm inflexion (ε 60) in methanol) and this may be due to a charge-transfer transition (*cf.* the long wavelength band of benzobarrelene at 277 nm (ε 710) in cyclohexane (4)). A similar red-shifted long wavelength band for 2,3-dicyanobenzobarrelene (313 nm (ε 760) in ethanol) has been attributed by Cookson and Dance to a charge-transfer transition (9). The effect of solvent polarity on the quantum efficiency of the formation of COT **6** is also in support of the reacting singlet excited state of **4** being the charge–transfer state. If we assume that the quantum yields measured here do in fact reflect the excited state reaction rates for the formation of **6**, then a minimum interpretation of the decrease in Φ on going to more polar solvent is that the activation energy for the rearrangement of excited **4** in methanol is increased relative to that in cyclohexane because in polar solvent the stabilization afforded the charge-transfer state of **4** is greater than that afforded the less polar (and more product-like) transition state leading to **6**. If the charge-transfer state of **4** is the reacting singlet excited-state species, then since the mechanism of formation of **6** proceeds via bonding between vinyl and vinyldiester groups, it is tempting to speculate that the charge-transfer arises from an intramolecular donation of an electron from the vinyl group to the vinyldiester acceptor. Recently, Bryce-Smith *et al.* (10) have pointed out that donor–acceptor properties of olefins are of critical importance in connection with their ability to undergo 1,2-photoadditions to benzene. Perhaps also, charge-transfer contributions are of similar importance in directing the initial mode of photochemical $2\pi + 2\pi$ bridging in barrelene systems.

Experimental

The n.m.r. spectra were recorded on a Varian HA-100 spectrometer. Cyclohexane solvent was prepared for photolyses by scrubbing with 10% of its volume of 30% fuming sulfuric acid, followed by washing with 10% aqueous sodium hydroxide, drying ($MgSO_4$), and finally distilling from calcium hydride. Methanol solvent was prepared for photolyses by refluxing with basic furfural, according to the method of Morton and Mark (11), followed by fractionation on a 6 ft column packed with 8 mm Raschig rings.

*Preparation of Deuterated Barrelene Mixture **10** and **11***

A solution of 10.0 g (0.0483 mol) of 2-bromonaphthalene in 50 ml of dry THF (CaH_2) was added dropwise over a period of 0.5 h to a stirred mixture of 1.2 g (0.0515 mol) of magnesium turnings in 20 ml of THF. The reaction was maintained at reflux throughout the addition and during a further 1 h period, by which time the magnesium was consumed. The mixture was cooled in an ice bath and 20 ml of 99%-d_1 CH_3OD was added dropwise with stirring. After stirring for an additional 0.5 h, 100 ml of a 20% aqueous solution of NH_4Cl was added, the mixture was extracted with 250 ml of ether, and the extract was washed (2 × 100 ml), dried ($MgSO_4$), and concentrated *in vacuo*. The residue was taken up in cyclohexane and chromatographed on a silicic acid column (CC7, 100–200 mesh; 3 × 35 cm) with cyclohexane as eluting agent. The first major band yielded, after crystallization from hexane, 4.6 g (74%) of 2-deuterionaphthalene, m.p. 80–81.5° (lit. 80°).

A mixture of 3.0 g (23.3 mmol) of 2-deuterionaphthalene and 1 ml (8.0 mmol) of dimethyl acetylenedicarboxylate was sealed in a 250 ml pressure bottle (Fisher) and heated on an oil bath at 155–160° with stirring for 72 h. After cooling, the reaction mixture was taken up in 10 ml of benzene and chromatographed on a silicic acid column (2 × 35 cm). Elution with 1 l of cyclohexane brought off the unreacted deuterionaphthalene; elution with 5% ether in cyclohexane gave 384 mg of an oil. The oil was rechromatographed on a 2.5 × 200 cm column of silicic acid with 5% ether in cyclohexane as eluting agent; 250 ml fractions were collected. Fractions 32–34 contained 30.2 mg of an unidentified oil; 38–45 gave 308.2 mg of an oil which upon crystallization from methanol yielded 231.2 mg (11%) of colorless crystals of the deuterated mixture **10** and **11**, m.p. 74–76° (lit. (5)

Can. J. Chem. Downloaded from www.nrcresearchpress.com by 210.87.254.6 on 09/05/12
For personal use only.

77.0–77.5°); n.m.r. (CCl_4) τ 2.78–3.21 (m, aromatic and vinyl, 5.01 ± 0.08 H), 4.82–4.90 (m, bridgeheads, 1.92 ± 0.10 H), and 6.38 (s, OCH_3, 6.00 H, assumed).

*Direct Irradiations of Deuterated Barrelene Mixture **10** and **11***

Approximately 4.0 m*M* solutions of the barrelene mixture **10** and **11** in either cyclohexane or methanol solvent contained in a 250 ml water-cooled photolysis well, were irradiated with Pyrex-filtered light provided by a 450 W Hanovia medium pressure mercury arc. The solutions were purged with nitrogen prior to and during irradiations. The photolysates were concentrated *in vacuo* and the percentage conversion of starting material was determined by n.m.r. spectroscopy; see Table 1. The residues were then chromatographed on a silicic acid column (2.5 × 200 cm) with 5% ether in cyclohexane as eluting agent; 250 ml fractions were collected. In a typical run (entry 2, Table 1), 248.0 mg of mixture **10** and **11** in 250 ml of cyclohexane was irradiated for 1 h. The residue was chromatographed and the contents of fractions 32–34 were short-path distilled (85°/0.1 mm Hg) then crystallized from methanol to give 21.5 mg of COT product, m.p. 74–76° (lit (5) 77.0–77.5°); see Table 1 for deuterium distributions. Fractions 35–50 contained 189.3 mg of an oily mixture of starting material and COT product.

Quantum Yield Determinations

Quantum yields of the direct irradiation of barrelene **4** (5) were determined on a "merry-go-round" fitted with a 450 W Hanovia medium pressure mercury arc and surrounded by a water-cooled quartz immersion well. Light of wavelength 276 nm was isolated by a two compartment quartz cell fitting concentrically around the immersion well. One compartment contained a 2.0 cm path length of a solution of 533 g of nickel sulfate hexahydrate and 300 g of cobaltous sulfate heptahydrate per 1.0 l of 5% aqueous H_2SO_4. The other compartment contained a 0.2 cm path length of a solution of 1 g of bismuth trichloride per 0.5 l of 10% HCl; transmittance was 263–290 nm with a maximum at 276 nm (8%). Before irradiation, solutions of **4** (*ca.* 0.04 mmol) contained in calibrated (for differences in light transmittance) 20 × 150 mm quartz test-tube-like photolysis cells were deoxygenated by flushing with dried, pyrogallol scrubbed, commercial high-purity nitrogen. The tubes were sealed under a positive pressure of nitrogen which was maintained throughout the course of the irradiation. For each run two samples of **4** were irradiated; one sample was a solution of **4** in cyclohexane and the other was a solution of **4** in methanol. The lamp output was determined by potassium ferrioxalate actinometry (12). The photolysates were concentrated *in vacuo*, a known amount of *p*-xylene was added as internal standard, and the product composition was determined by n.m.r. analysis; the peak areas were calibrated against authentic mixtures of similar constitution. Conversions were kept below 17% and the quantum yields were determined from the average of two runs for each solvent. The Φ for the appearance of COT **6** were: $\Phi_{MeOH} = 0.10 \pm 0.01$ and $\Phi_{cyclohexane} = 0.16 \pm 0.02$.

*Effect of Lanthanide Shift Reagent on the Nuclear Magnetic Resonance Spectrum of COT **6***

The n.m.r. spectrum of COT **6** (30 mg) was recorded in CCl_4 (0.65 ml containing 1% TMS) in the presence of increasing amounts of a solution of $Eu(fod)_3$ in CCl_4 (107 mg in 2.00 ml). The shift reagent was dispensed by syringe. At molar ratio 0.27 of $Eu(fod)_3$:COT the olefinic protons coalesced to a singlet at τ 2.92 as did the aromatic protons at τ 2.69. The results are summarized in Fig. 1.

The authors thank the Spectroscopic Services Laboratory of the University of Alberta for the 100-MHz n.m.r. spectra, and gratefully acknowledge the financial support of the National Research Council of Canada, the University of Lethbridge Research Committee, and the President's Research Scholarship in Arts and Science (awarded to D. W. B., 1974). We also thank the referees for their helpful comments.

1. N. D. Epiotis. J. Am. Chem. Soc. **94**, 1941 (1972).
2. N. D. Epiotis. Angew. Chem. Int. Ed. Eng. **13**, 751 (1974).
3. C. O. Bender and S. S. Shugarman. Chem. Commun. 934 (1974).
4. H. E. Zimmerman, R. S. Givens, and R. M. Pagni, J. Am. Chem. Soc. **90**, 6096 (1968).
5. E. Grovenstein, Jr., T. C. Campbell, and T. Shibata. J. Org. Chem. **34**, 2418 (1969).
6. H. Günther. Tetrahedron Lett. 5173 (1970).
7. C. O. Bender and H. D. Burgess. Can. J. Chem. **51**, 3486 (1973).
8. H. E. Zimmerman and C. O. Bender. J. Am. Chem. Soc. **92**, 4366 (1970).
9. R. C. Cookson and J. Dance. Tetrahedron Lett. 879 (1962).
10. D. Bryce-Smith, A. Gilbert, B. Orger, and H. Tyrrell. Chem. Commun. 334 (1974).
11. A. A. Morton and J. G. Mark. Ind. Eng. Chem. Anal. Ed. **6**, 151 (1934).
12. C. G. Hatchard and C. A. Parker. Proc. R. Soc. (London), A**235**, 518 (1956).

Can. J. Chem. Downloaded from www.nrcresearchpress.com by 210.87.254.42 on 09/05/12
For personal use only.

Agelasine: A Novel Quaternary 9-Methyladenine from the Sponge *Agelas dispar*

ERNEST CULLEN AND JOHN P. DEVLIN
Pharma Research Canada Ltd., Pointe Claire, Quebec H9R 1G8

Received February 26, 1975

ERNEST CULLEN and JOHN P. DEVLIN. Can. J. Chem. **53**, 1690 (1975).

The isolation of a novel quaternary 9-methyladenine from the sponge *Agelas dispar* is described. The constitution (**1**) is assigned on the basis of degradative and spectroscopic data.

ERNEST CULLEN et JOHN P. DEVLIN. Can. J. Chem. **53**, 1690 (1975).

On décrit la méthode de séparation d'un nouveau sel quaternaire de la méthyl-9 adénine provenant de l'éponge *Agelas dispar*. On attribue la structure (**1**) en se basant sur les données spectroscopiques et les résultats obtenus par dégradation de la molécule.

[Traduit par le journal]

We have examined the pharmacological behavior of the extractives of a large number of marine organisms with the aim of uncovering novel directives for drug design. We herein report the isolation and characterization of a major constituent, agelasine (**1**), of the sponge *Agelas dispar* Duchassaing and Michelotti.

The residue on evaporation of the ethanol extract of a freeze-dried preparation of *A. dispar* was triturated with benzene. The insoluble portion on recrystallization from acetonitrile yielded **1**[1] (2% on dry weight basis) as colorless plates, m.p. 190–195° dec.; ν_{max} (KBr) 3320, 3140, 1652, 1610 cm^{-1}; and λ_{max} (CH_3OH) 271 nm (log ε 3.91). Elemental analyses indicated the empirical formula $C_{26}H_{40}N_5Cl \cdot \frac{1}{2}H_2O$. Recrystallization from 2-butanone–dimethylformamide provided the anhydrous form ($C_{26}H_{40}N_5Cl$), m.p. 197–200° dec. While a molecular ion was not observed in the mass spectrum, principle ions were found at *m/e* 421 ($C_{26}H_{38}N_5$), 308/310 ($C_{20}H_{33}Cl$), 273 ($C_{20}H_{33}$), 272 ($C_{20}H_{32}$), 191 ($C_{14}H_{23}$), and 149 ($C_6H_7N_5$). The n.m.r. spectrum ($CDCl_3$) exhibited a complex group of signals at δ 0.5–2.3 (29H); the remaining signals were as follows: δ 4.12 (s, 3H, —N—CH_3), 5.3–5.9 (m, 4H), 7.67 (broad s, 2H, —NH_2, disappeared on addition of D_2O), 8.47 (s, 1H), and 10.84 (s, 1H).

When agelasine was heated under reflux in xylene and the reaction mixture cooled a crystalline solid separated, m.p. 300–302° (from CH_3OH); ν_{max} (KBr) 3280, 3110, 1672, 1600, 1575 cm^{-1}; and λ_{max} (H_2O) 261 nm (log ε 4.03) (at p*H* 2, 7, and 11). The n.m.r. and mass spectra identified this substance as a mono-*N*-methyladenine. The i.r. and u.v. absorptions were in agreement with those reported (1, 2) for 9-methyladenine (**2**). This assignment was confirmed by a comparison with synthetic **2** prepared by the direct methylation of adenine (3).

The aforementioned mass spectral data and the thermal behavior described above suggested that agelasine was a quaternary derivative of 9-methyladenine. The quaternary iodide ($C_{26}H_{40}N_5I$), m.p. 171–173°, was readily obtained by treatment of an aqueous solution of **1** with KI. The nitrate ($C_{26}H_{40}N_6O_3$), m.p. 174–175°, was similarly formed.

The release of the 9-methyladenine moiety as the hydrochloride was rapidly effected by hydrogenation of **1** (H_2/5% Pd–C) in ethanol. A nonpolar fragment was also isolated as a colorless oil which by analysis and mass spectroscopy (M^+ 274, *m/e* 259, *m/e* 205, *m/e* 191) was assigned the molecular formula $C_{20}H_{34}$; two olefinic protons were present in the n.m.r. spectrum ($CDCl_3$) as a broad multiplet at δ 5.0–5.5. Further hydrogenation (H_2/Pt_2O/ethyl acetate – HCl) of this oil provided the tetrahydro derivative $C_{20}H_{38}$ (M^+ 278, *m/e* 263, *m/e* 193); the n.m.r. spectrum ($CDCl_3$) exhibited only a complex group of signals at δ 0.7–2.0. The nonpolar fragment can therefore be classified as a dicyclic hydrocarbon con-

[1]The i.r., n.m.r., and mass spectra of all compounds have been recorded and are in agreement with the structures assigned. Only specially relevant spectral data are reported. All crystalline compounds gave correct elemental analyses.

taining two double bonds. The fragmentation patterns observed in the mass spectra of both the nonpolar fragment and its tetrahydro derivative are similar to the patterns observed with the carbodicyclic diterpenes (4). The precise constitution of this substance is presently under investigation.

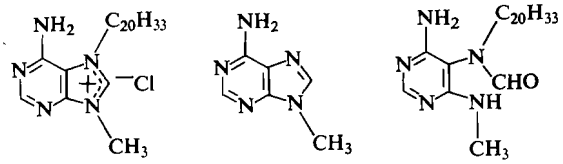

1 2 3

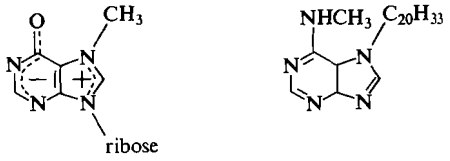

4 5

Treatment of an aqueous solution of **1** with 2 *N* Na_2CO_3 precipitated a white crystalline solid (**3**), m.p. 105–108° (from isopropyl ether); ν_{max} (KBr) 3440 (sh), 3340, 3220, 2920, 1660, and 1590 cm^{-1}; λ_{max} (C_2H_5OH): p*H* 7, 260 nm (log ε 3.77); p*H* 2, 271 nm (log ε 3.98); p*H* 11, 260 nm (log ε 3.80). The molecular formula ($C_{26}H_{41}N_5O$) was supported by analyses and the mass spectrum (M^+ 439). The n.m.r. ($CDCl_3$) spectrum exhibited signals at δ 2.9 (d, 3H, $NHCH_3$; $+D_2O$, s, 3H), 7.9 (s, 1H, C2-H or —NC*H*O), and 8.1 (s, 1H, —N—C*H*O or C2-H). The —$NHCH_3$ signal at δ 2.9 demonstrated that the nucleophilic attack occurred at C-8, with subsequent ring cleavage. The ease with which this hydrolysis occurred, encouraged us to assign N-7 as the site of quaternization with the positive charge delocalized as shown (**1**); an assignment which was supported (5) by the rapid exchange of the C8-H (δ 10.84 in $CDCl_3$; δ 10.13 in CD_3SOCD_3; δ 11.5 in C_5D_5N) of agelasine with D_2O when the n.m.r. spectrum was run in C_5D_5N. The low-field position of this proton is in agreement with that of the C-8 proton of 7-methylinosine (6) (**4**, δ 9.64 in CD_3SOCD_3) which is in a similar environment.

The constitution **1** was therefore considered for agelasine and **3** for that obtained upon treatment with 2 *N* Na_2CO_3. This assignment was supported by the ring closure of **3** with NaH in dimethylacetamide to provide **5**, $C_{26}H_{39}N_5$ (M^+ 421), as colorless plates, m.p. 163–165° (from acetonitrile); ν_{max} (KBr) 3280, 2940, 1615, 1550 cm^{-1}. The u.v. absorption (λ_{max} (C_2H_5OH): p*H* 7 and 11, 272 (log ε 4.12); p*H* 2, 282 nm (log ε 4.17)) corresponded to that anticipated for a 7-alkyladenine (7). The n.m.r. spectrum ($CDCl_3$) exhibited signals at δ 3.50 (d, 3H, —$NHCH_3$; $+D_2O$, s, 3H), 7.85 (s, 1H, C2-H), and 8.55 (s, 1H, C8-H).

To our knowledge, agelasine is the first quaternary derivative of adenine to be found in nature. Agelasine has a very broad spectrum of pharmacological activity although many of these effects can be ascribed to its saponin-like nature. These aspects will be described in a forthcoming paper.

We are grateful to Dr. K. R. Freter for his interest and encouragement, to Dr. H. J. Förster for high resolution mass spectral data, and to Dr. Finn Sander and Dr. Reiswig of the Bellairs Research Institute of McGill University at St. James, Barbados for the collection and identification of *Agelas dispar*. The technical assistance of Mr. R. Becker is gratefully acknowledged.

1. B. C. Pal and C. A. Horton. J. Chem. Soc. 400 (1964).
2. R. K. Robins and H. H. Lin. J. Am. Chem. Soc. **79**, 490 (1957).
2. T. Fujii, S. Sakurai, and T. Uematsu. Chem. Pharm. Bull. **20**, 1334 (1972).
4. C. R. Enzell and R. Ryhage. Arkiv. Kemi, **23**, 367 (1965).
5. M. Maeda, M. Saneyoshi, and Y. Kawazoe. Chem. Pharm. Bull. **19**, 1641 (1971).
6. P.O.P. Ts'o, N. S. Kondo, R. K. Robins, and A. D. Broom. J. Am. Chem. Soc. **91**, 5625 (1969).
7. N. J. Leonard, K. L. Carraway, and J. P. Helgeson. J. Heterocycl. Chem. **2**, 291 (1965).

Can. J. Chem. Downloaded from www.nrcresearchpress.com by 210.87.254.42 on 09/05/12
For personal use only.

Can. J. Chem. Downloaded from www.nrcresearchpress.com by 210.87.254.40 on 09/05/12
For personal use only.

Canadian Journal of Chemistry

Published by
THE NATIONAL RESEARCH COUNCIL OF CANADA

Journal canadien de chimie

Publié par
LE CONSEIL NATIONAL DE RECHERCHES DU CANADA

Volume 53 Number 12 June 15, 1975

Volume 53 numéro 12 15 juin 1975

Synthesis of some A-Ring Steroidal Cyclopropanols

J. F. TEMPLETON AND C. W. WIE

Faculty of Pharmacy, University of Manitoba, Winnipeg, Manitoba R3T 2N2

Received November 28, 1974

J. F. TEMPLETON and C. W. WIE. Can. J. Chem. **53**, 1693 (1975).

The preparation of two epimeric secondary cyclosteroid alcohols in the steroidal A-ring by an intramolecular 1,3-elimination of bromide with zinc–copper couple is described. Isomerization of the *endo*-cyclopropanol to the *exo*-cyclopropanol is shown to occur with either the couple or zinc acetate. Solvolysis of the cyclopropyl tosylates is discussed. Spectral data are recorded.

J. F. TEMPLETON et C. W. WIE. Can. J. Chem. **53**, 1693 (1975).

On décrit la préparation, par une élimination intramoléculaire 1,3 d'ion bromure par le couple zinc–cuivre, de deux alcools secondaires épimères d'un cyclostéroide dans le cycle A. On montre que l'isomérisation du cyclopropanol *endo* en cyclopropanol *exo* se produit avec le couple zinc–cuivre ou avec l'acétate de zinc. On discute de la solvolyse des tosylates de cyclopropyle. On rapporte les données spectrales. [Traduit par le journal]

Introduction

Few examples of steroids containing the cyclopropanol moiety have been reported. Recently several cyclopropanosteroids which contain a tertiary cyclopropanol, prepared by means of methylene addition to enolic derivatives have been prepared (1–3) and a photochemical product isolated (4). We describe here a short synthesis under mild conditions of two epimeric secondary cyclosteroid cyclopropanols prepared by an intramolecular 1,3-elimination.

Results and Discussion

Treatment of 17β-hydroxy-5α-androstan-3-one (**1**) with 2 mol of bromine in acetic acid affords the dibromoacetate (**2**) (5). Reduction of this sterically hindered ketone with sodium borohydride proceeds rapidly to give a mixture of the 3α- and 3β-hydroxy epimers (**3***a* and **4***a*). Fractional crystallization of the epimers gave a low yield of the pure dibromoalcohols. The major product from the reduction is the 3α-epimer determined by the p.m.r. spectra of the alcohols (**3***a* and **4***a*) and the acetates (**3***b* and **4***b*). The alcohols (**3***a* and **4***a*) show the presence of a triplet at 4.27 δ (J = 2.5 Hz) and 3.80 δ (J = 10.0 Hz) consistent with axial–equatorial coupling of an equatorial proton at C-3 and diaxial coupling of an axial proton at C-3, respectively (6). Similarly the p.m.r. spectra of the acetate (**3***b*) contain a triplet at 5.70 δ (J = 2.5 Hz) and the acetate (**4***b*) a triplet at 5.27 δ (J = 10.0 Hz), in agreement with the assignment of **3***a* as the 3α- and **4***a* as the 3β-derivatives.

Treatment of the 3α-dibromoalcohol (**3***a*) with a freshly prepared 2% zinc–copper couple in ethanol at room temperature showed by t.l.c. and g.l.c. analysis the formation of three major products and no starting material after ½ h. The less polar material (by t.l.c.) was largely dissolved by petroleum ether and extraction of the crude reaction mixture gave a crystalline compound from the petroleum ether soluble portion shown by p.m.r. (7*a*) and mass spectra

(*7b*) to be an isomeric mixture of 17β-acetoxy-5α-androstan-2- and 3-ene (**5**) which was not further purified. The petroleum ether mother liquor gave a further crystalline substance as a minor product. This product was identified as 2β,4β-cyclo-5α-androstane-3β,17β-diol 17-acetate (**6***a*) which gave a diacetate (**6***b*) (see below). The petroleum ether insoluble residue on fractional crystallization from ether gave as the major product 2β,4β-cyclo-5α-androstane-3α,17β-diol 17-acetate (**7***a*) which yielded a diacetate (**7***b*) identified on the basis of the following evidence. Carbon and hydrogen analysis and the presence of an ion at *m/e* 332 in the mass spectrum was

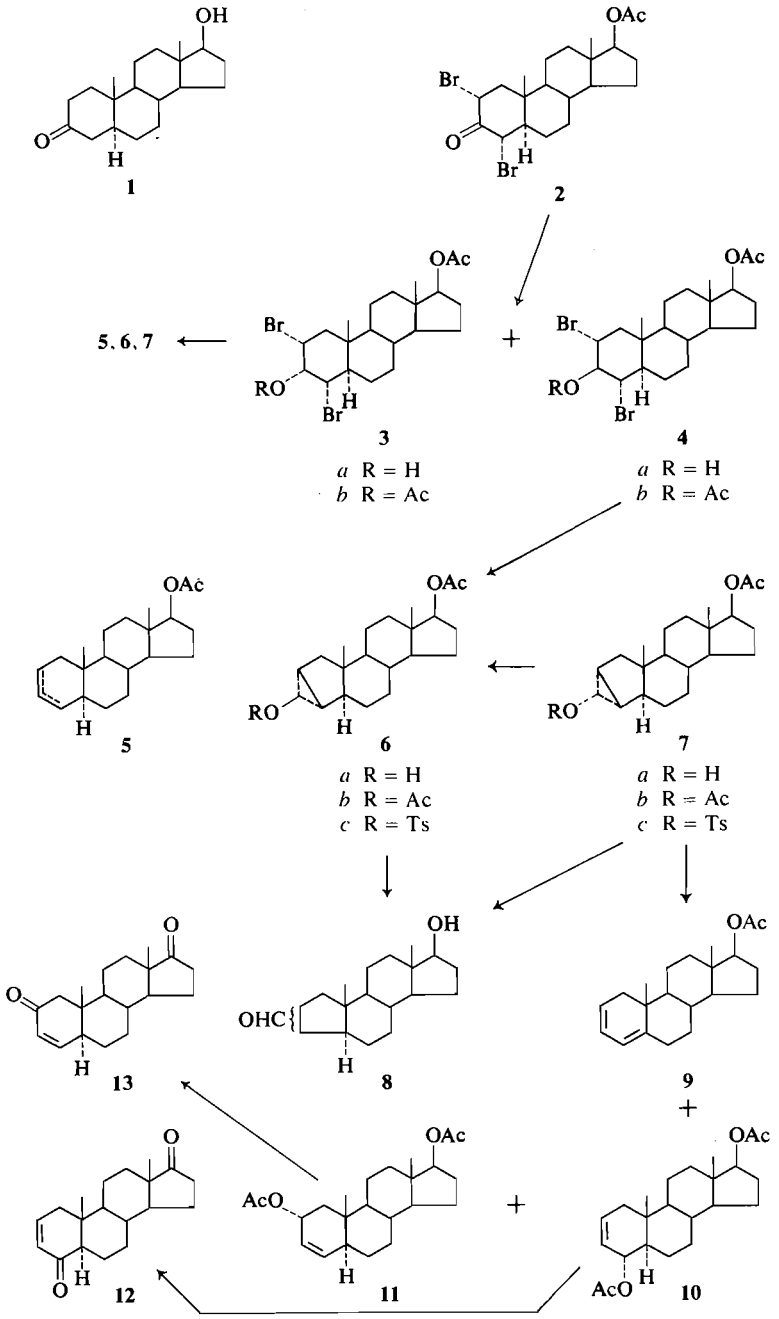

Can. J. Chem. Downloaded from www.nrcresearchpress.com by 210.87.254.40 on 09/05/12
For personal use only.

Can. J. Chem. Downloaded from www.nrcresearchpress.com by 210.87.254.40 on 09/05/12
For personal use only.

consistent with the molecular formula of **7***a*. The i.r. spectrum of **7***a* showed the presence of hydroxyl absorption and a weak absorption at 3030 and 3049 cm^{-1} consistent with cyclopropyl C—H stretching vibrations. Acetylation incorporated a second acetyl group indicating the presence of a single hydroxyl function. The p.m.r. spectrum of the diacetate (**7***b*) showed no olefinic protons, however, the presence of a triplet at 4.25 δ (J = 6.0 Hz) is consistent with a cyclopropyl acetate having an acetoxy function at C-3 with the *endo* configuration. Compound **7***a* on treatment with alcoholic potassium hydroxide was converted into a noncrystalline product which showed the presence of aldehyde carbonyl absorption (1720 cm^{-1}) and C—H stretching (2700 and 2800 cm^{-1}) which would be expected from opening of the cyclopropanol ring in **7***a* to give the A-nor derivatives (**8**) containing an aldehyde function in either the C-2 or C-3 position. The p.m.r. spectrum also contained an aldehyde proton and loss of the signals associated with the cyclopropanol ring.

Similar treatment of the 3β-dibromoalcohol (**4***a*) with a zinc–copper couple gave only one major product identical with the minor product (**6***a*) from the reaction with the 3α-dibromoalcohol (**3***a*). The chemical shift and coupling constant of the proton at C-3 of the diacetate (**6***b*) (δ 3.63, unresolved triplet) demonstrates the *exo* configuration of the cyclopropanol (8). Reaction of **6***a* with alcoholic potassium hydroxide, as with compound **7***a*, gave an uncrystalline aldehyde product having an identical i.r. and p.m.r. spectrum with the previous product (**8**) from **7***a*. The greater formation of the olefinic products (**5**) from the 3α- rather than the 3β-dibromoalcohol is consistent with the greater ease of elimination of the 3α- (axial) alcohol and the lesser stability of the *endo* alcohol.

The formation of the 3β-cyclopropanol (**6***a*) from the 3α-epimer (**7***a*) occurs under the reaction conditions with the zinc–copper couple. Also the 3α-cyclopropanol in methanol containing zinc acetate is converted slowly into the 3β-epimer. This conversion most probably involves the opening and reclosing of the cyclopropane ring. A proposed mechanism is shown in Scheme 1 showing addition of zinc acetate at either C-2 or C-4. Sterically the *endo* isomer will be the thermodynamically less stable product and ring closure then yields the more

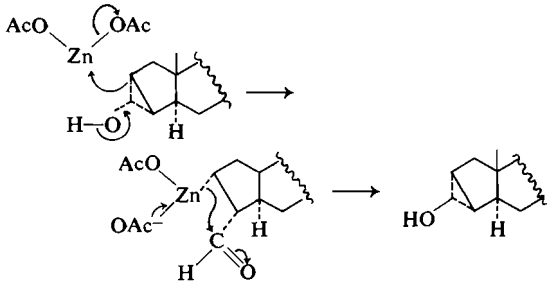

SCHEME 1

stable *exo* isomer. An analogous ring opening has been shown to occur by reaction of a cyclopropanol with mercuric acetate (9).

The *endo* and *exo* assignments of the cyclopropanols **7***a* and **6***a* are in agreement with the assignments of the configuration for the dibromoalcohols **3***a* and **4***a*, respectively.

When the dibromoacetates (**3***b* and **4***b*) were similarly treated with zinc–copper couple only a mixture of the olefinic products was detected in the reaction as determined by t.l.c.

Further evidence for the stereochemical assignment of the epimeric alcohols was provided by solvolysis of the corresponding tosylates (**6***c* and **7***c*) with sodium acetate in acetic acid. In the case of the isomers, *endo*-bicyclo[3.1.0]-hexyl 6-*p*-toluenesulfonate and *exo*-bicyclo-[3.1.0]hexyl 6-*p*-toluenesulfonate, a solvolysis rate of 25 000 and <0.01, respectively, relative to cyclopropyl *p*-toluenesulfonate was found (8). The *endo* isomer gave *cis*-2-cyclohexen-1-yl acetate as the isolated product. 2β,4β-Cyclo-5α-androstane-3β,17β-diol 17-acetate 3-tosylate (**6***c*) was recovered unchanged after refluxing for 20 h with sodium acetate in acetic acid. Similar treatment of 2β,4β-cyclo-5α-androstane-3α,17β-diol 17-acetate 3-tosylate (**7***c*) gave no starting material and a mixture of products after 15 min. The u.v. and p.m.r. spectrum of the less polar material indicated it to be principally 17β-acetoxyandrosta-2,4-diene (**9**) (10). The more polar material could be separated by chromatography into two pure substances identified as 5α-androst-2-ene-4α,17β-diol diacetate (**10**) and 5α-androst-3-ene-2α,17β-diol diacetate (**11**). Hydrolysis of these products followed by oxidation led to 5α-androst-2-ene-4,17-dione (**12**) and 5α-androst-3-ene-2,17-dione (**13**), respectively. The position of the unsaturated ketone was established by comparison of the p.m.r. spectrum with that of the known corresponding 17β-

Can. J. Chem. Downloaded from www.nrcresearchpress.com by 210.87.254.40 on 09/05/12
For personal use only.

acetates (11). The stereochemistry of the acetates was not determined directly; however, addition to the least hindered side of the intermediate cation would yield the 2α- and 4α-acetates.

Experimental

For general experimental details and apparatus see ref. 12; 220 MHz spectra were recorded by the Canadian 220 MHz NMR Centre, Ontario Research Foundation, Sheridan Park, Ontario for compounds **3***a*, **4***a*, **10**, **11**, **12**, and **13**.

Work-up Procedure

Reactions were extracted with ether (unless otherwise stated) and the combined extracts washed with water, saturated brine, dried over anhydrous sodium sulfate, filtered, and evaporated at reduced pressure to give the crude reaction product.

Thin-layer Chromatography

Silica gel coated glass plates were developed in 5% ethyl acetate in chloroform.

Gas–Liquid Chromatography

A Varian Aerograph Series 1800 chromatograph equipped with a hydrogen flame ionization detector and a Pyrex glass column packed with 2% OV-17 on Chromosorb GHP, 60–80 mesh, internal diameter 2 mm, length 180 cm was used. The detector temperature was 300°, column temperature 240°, and the carrier gas (N_2) flow rate was 40 ml/min. All compounds were injected as their trimethylsilyl derivatives at a concentration of 10 μg/μl.

Acetylation

To a 10% solution of the steroid in dry pyridine was added one-half the volume of acetic anhydride. After standing overnight at room temperature, the reaction was poured into an ice-water mixture and allowed to stand for 30 min followed by acidification with dilute hydrochloric acid and ether extraction.

Zinc–Copper Couple

A homogenous, consistently active, zinc–copper couple was prepared as follows. Finely powdered cupric acetate monohydrate (8 g, 0.04 mol) and zinc dust (130 g, 2 mol) were thoroughly mixed with a pestle and mortar. To avoid excessive frothing the mixture was added portionwise to a mechanically stirred solution of boiling glacial acetic acid (275 ml). After addition a further 200 ml of cold acetic acid was added and the slurry filtered with suction and washed several times with ether without allowing all of the ether to evaporate. The ether-moist couple was kept under ether and used as soon as possible.

2α,4α-Dibromo-17β-acetoxy-5α-androstan-3-one (2)

Prepared by the method of Jones and Ship (5). Material of m.p. 184–190° was used for reduction.

2α,4α-Dibromo-5α-androstane-3α,17β- and 3β,17β-diol 17-Acetate (3a) and (4a)

Sodium borohydride (946 mg) in ethanol (50 ml) was added to a slurry of 17β-acetoxy-2α,4α-dibromo-5α-androstan-3-one (**2**) (15 g) in ethanol (200 ml). The mixture was stirred for 5 min at room temperature, during which time dissolution occurred, and poured into ice-cold 1 *N* sulfuric acid (1 l). Extraction with dichloromethane yielded a crude product which on crystallization from chloroform gave 2α,4α-dibromo-5α-androstane-3β,17β-diol 17-acetate (4*a*) (527 mg); m.p. 248–252°, second crop (982 mg), m.p. 235–240°. Further recrystallization from dichloromethane gave **4***a*, (746 mg); m.p. 253–255°; $[\alpha]_D$ −46°; i.r. ν_{max} (KBr) 3413 (hydroxyl), 1706 (ester C=O) cm^{-1}; p.m.r. δ ($CDCl_3$) 4.59 (1, t, J = 8.0 Hz, 17α-proton), 4.10 (1, m, 2β-proton), 3.94 (1, t, J = 10.0 Hz, 4β-proton), 3.80 (1, t, J = 10.0 Hz, 3α-proton), 2.39 (1, q, J = 13.0 and 5.0 Hz, 1β-proton), 2.03 (3, s, 17-acetoxy methyl), 0.88 (3, s, 19-methyl), 0.78 (3, s, 18-methyl) p.p.m.

Anal. Calcd. for $C_{21}H_{32}O_3Br_2$: C, 51.23; H, 6.55; Br, 32.25. Found: C, 51.08; H, 6.42; Br, 33.81.

The mother liquor was evaporated and crystallized from acetone–dichloromethane to give 2α,4α-dibromo-5α-androstane-3α,17β-diol 17-acetate (3.2 g); m.p. 202–205°. Further recrystallization gave **3***a*, m.p. 206–207°; $[\alpha]_D$ −24°; i.r. ν_{max} (KBr) 3472 (hydroxyl), 1706 (ester C=O) cm^{-1}; p.m.r. δ ($CDCl_3$) 4.59 (1, t, J = 8.0 Hz, 17α-proton), 4.35 (1, m, 2β-proton), 4.27 (1, t, J = 2.5 Hz, 3β-proton), 4.20 (1, q, J = 11.0 and 2.5 Hz, 4β-proton), 2.03 (3, s, 17-acetoxy methyl), 0.89 (3, s, 19-methyl), 0.77 (3, s, 18-methyl) p.p.m.

Anal. Calcd. for $C_{21}H_{32}O_3Br_2$: C, 51.23; H, 6.55; Br, 32.25. Found: C, 51.09; H, 6.42; Br, 33.07.

Column chromatographic separation of the acetylated crude 2,4-dibromoalcohols gave a 4:1 ratio of 3α- to 3β-acetates.

2α,4α-Dibromo-5α-androstane-3α,17β-diol Diacetate (3b)

2α,4α-Dibromo-5α-androstane-3α,17β-diol 17-acetate (**3***a*) (95 mg) (m.p. 206–207°) was acetylated. The crude reaction product was recrystallized from methanol to give 2α,4α-dibromo-5α-androstane-3α,17β-diol diacetate (77 mg); m.p. 228–229°; $[\alpha]_D$ −19°; i.r. ν_{max} (CCl_4) 1761, 1742 (ester C=O) cm^{-1}; p.m.r. δ (CCl_4) 5.70 (1, t, J = 2.5 Hz, 3β-proton), 4.58 (1, t, J = 8.0 Hz, 17α-proton), 4.33 (1, m, 2β-proton), 4.16 (1, q, J = 11.0 and 2.5 Hz, 4β-proton), 2.18 (3, s) and 2.02 (3, s, 3- and 17-acetoxy methyl), 0.90 (3, s, 19-methyl), 0.76 (3, s, 18-methyl) p.p.m.; m.s. *m/e* 534 (M^+, weak).

Anal. Calcd. for $C_{23}H_{34}O_4Br_2$: C, 51.70; H, 6.41; Br, 29.91. Found: C, 51.70; H, 6.36; Br, 29.90.

2α,4α-Dibromo-5α-androstane-3β,17β-diol Diacetate (4b)

2α,4α-Dibromo-5α-androstane-3β,17β-diol 17-acetate (**4***a*) (100 mg) was acetylated. Successive recrystallization from methanol gave the 2α,4α-dibromo-5α-androstane-3β,17β-diol diacetate (73 mg); m.p. 217–218°; $[\alpha]_D$ −34°; i.r. ν_{max} (CCl_4) 1761, 1742 (ester C=O) cm^{-1}; p.m.r. δ (CCl_4) 5.27 (1, t, J = 10.0 Hz, 3α-proton), 4.60 (1, t, J = 8.0 Hz, 17α-proton), 4.28 (1, m, 2β-proton), 3.92 (1, t, J = 10.0 Hz, 4β-proton), 2.42 (1, q, J = 13.0 and 5.0 Hz, 1β-proton), 2.12 (3, s) and 2.01 (3, s, 3- and 17-acetoxy methyl), 0.88 (3, s, 19-methyl), 0.76 (3, s, 18-methyl) p.p.m.; m.s. *m/e* 534 (M^+, weak).

Anal. Calcd. for $C_{23}H_{34}O_4Br_2$: C, 51.70; H, 6.41; Br, 29.91. Found: C, 51.91; H, 6.37; Br, 29.93.

2β,4β-Cyclo-5α-androstane-3β,17β-diol-17-Acetate (6a)

To a slurry of 2α,4α-dibromo-5α-androstane-3β,17β-diol 17-acetate (**4***a*) (600 mg) in ethanol (18 ml), was

Can. J. Chem. Downloaded from www.nrcresearchpress.com by 210.87.254.40 on 09/05/12
For personal use only.

added freshly prepared 2% zinc–copper couple (9 g). The mixture was mechanically stirred for ½ h at room temperature. The reaction was filtered and the ethanol evaporated at reduced pressure with minimal heating. Cold aqueous sodium bicarbonate was added and the products extracted with ether. The crude product showed one major spot on t.l.c. and contained >98% 2β,4β-cyclo-5α-androstane-3β,17β-diol 17-acetate on g.l.c. Successive recrystallization from methanol gave the alcohol (222 mg); m.p. 130–132°; $[\alpha]_D$ +24° (dioxane); i.r. ν_{max} (KBr) 3546 (hydroxyl), 3040 (cyclopropyl C—H), 1727 (ester C=O) cm^{-1}; m.s. *m/e* 332 (M^+).

Anal. Calcd. for $C_{21}H_{32}O_3$: C, 75.85; H, 9.70. Found: C, 75.97; H, 9.75.

2β,4β-Cyclo-5α-androstane-3α,17β-diol 17-Acetate (7a)

2α,4α-Dibromo-5α-androstane-3α,17β-diol 17-acetate (**3***a*) (1 g) was treated with zinc–copper couple similarly to (**4***a*). The crude product showed three spots on t.l.c. and three peaks on g.l.c. On stirring with petroleum ether (7 ml), the insoluble material was collected (456 mg, m.p. 134–136°). Successive recrystallization from acetone ether gave 2β,4β-cyclo-5α-androstane-3α,17β-diol 17-acetate (350 mg); m.p. 143–146°; $[\alpha]_D$ +17° (dioxane); i.r. ν_{max} (KBr) 3509 (hydroxyl O—H), 3049 and 3030 (cyclopropyl C—H), 1727 (ester C=O) cm^{-1}; m.s. *m/e* 332 (M^+).

Anal. Calcd. for $C_{21}H_{32}O_3$: C, 75.85; H, 9.70. Found: C, 76.12; H, 9.63.

From the petroleum ether solution was recovered 85 mg, m.p. 105–127° of crystalline material which was stirred with petroleum ether (10 ml). The petroleum ether soluble portion was filtered through alumina, the p.m.r. spectrum (7) of the combined fractions (41 mg) corresponded to a mixture of 17β-acetoxy-5α-androst-2- and 3-ene; p.m.r. δ (CCl_4) 5.14–5.62 (2, m, olefinic protons), 4.56 (1, t, J = 8.0 Hz, 17α-proton), 1.96 (3, s, acetoxy methyl), 0.76, (6, s, 18- and 19-methyl) p.p.m. (*7a*); m.s. *m/e* 316 (M^+), 262 ($M^+ - 54$)(*7b*). The petroleum ether insoluble material (12 mg) was recrystallized from methanol to give a sample which was identical to **6***a* by mixed melting point and i.r. and m.s. spectra.

Higher overall yields of the cyclopropanols were obtained by treating the mixture of 3α- and 3β-dibromo-alcohols (**3***a* and **4***a*) directly with the zinc–copper couple. Separation of the products was carried out by extraction of the crude solid residue with petroleum ether (10% w/v). The 3α-cyclopropanol was recrystallized from the petroleum ether insoluble portion. The 3β-cyclopropanol and olefinic mixture was fractionally recrystallized from the petroleum ether soluble portion.

Similar treatment of the diacetates (**3***b* and **4***b*) gave only the olefinic mixture (**5**) by t.l.c. and i.r.

2β,4β-Cyclo-5α-androstane-3β,17β-diol Diacetate (6b)

2β,4β-Cyclo-5α-androstane-3β,17β-diol 17-acetate (**6***a*) (120 mg) was acetylated. The crude reaction product showed a single spot on t.l.c. Recrystallization of the crude product from methanol gave the 2β,4β-cyclo-5α-androstane-3β,17β-diol diacetate (100 mg); m.p. 142–143°; $[\alpha]_D$ +23°; i.r. ν_{max} (CCl_4) 3050 (cyclopropyl C—H); 1736 (ester C=O), cm^{-1}; p.m.r. δ ($CDCl_3$) 4.51 (1, t, J = 8.0 Hz, 17α-proton), 3.63 (1, unresolved t, 3α-proton), 1.94 (3, s) and 1.90 (3, s, 3- and 17-acetoxy methyl), 0.85 (3, s, 19-methyl), 0.74 (3, s, 18-methyl) p.p.m.; m.s. *m/e* M^+ (not detected), 332 ($M^+ - CH_2CO$).

Anal. Calcd. for $C_{23}H_{34}O_4$: C, 73.76; H, 9.15. Found: C, 73.93; H, 9.07.

2β,4β-Cyclo-5α-androstane-3β,17β-diol 3-Tosylate 17-Acetate (6c)

To a solution of 2β,4β-cyclo-5α-androstane-3β,17β-diol 17-acetate (**6***a*) (500 mg) in anhydrous pyridine (5 ml) was added *p*-toluenesulfonyl chloride (600 mg). The mixture was allowed to stand overnight at room temperature and the brown solution was poured into ice water. The product was extracted with ether and the ether solution was washed with cold 1 *N* sulfuric acid. The crude reaction product was dissolved in acetone and the solution was stirred with activated charcoal and filtered. Successive recrystallization from acetone at room temperature gave 2β,4β-cyclo-5α-androstane-3β,17β-diol 17-acetate 3-tosylate (**6***c*) (450 mg); m.p. 155–156°; $[\alpha]_D$ +19°; i.r. ν_{max} (CCl_4) 3030 (broad, cyclopropyl and aromatic C—H), 1730 (ester C=O), 1595 (aromatic C=C), 1188 and 1176 (tosyl S=O) cm^{-1}; p.m.r. δ ($CDCl_3$) 7.62 (4, q, AA′XX′, $J_{AX} = J_{A'X'}$ = 8.0 Hz, *p*-substituted aromatic protons), 4.61 (1, t, J = 8.0 Hz, 17α-proton), 3.56 (1, unresolved t, 3α-proton), 2.47 (3, s, aromatic methyl protons), 2.01 (3, s, acetoxy methyl), 0.75 (6, s, 18- and 19-methyl) p.p.m.

Anal. Calcd. for $C_{28}H_{38}O_5S$: C, 69.10; H, 7.87; S, 6.59. Found: C, 69.00; H, 7.86; S, 6.50.

2β,4β-Cyclo-5α-androstane-3α,17β-diol 17-Acetate (7a) with Zinc–Copper Couple

To 2β,4β-cyclo-5α-androstane-3α,17β-diol 17-acetate (*7a*) (100 mg) in ethanol (5 ml) was added freshly prepared 2% zinc–copper couple (1.5 g). Conversion of *7a* to **6***a* was monitored by t.l.c. and g.l.c. After 48 h the reaction was filtered, poured into aqueous sodium bicarbonate, and ether extracted. The crude product was acetylated followed by chromatography on alumina. A combined fraction of 58 mg corresponding to **6***b* was obtained. Recrystallization from methanol gave 26 mg of material identical to **6***b* by mixture m.p. and i.r. spectrum.

2β,4β-Cyclo-5α-androstane-3α,17β-diol 17-Acetate (7a) with Zinc Acetate

2β,4β-Cyclo-5α-androstane-3α,17β-diol 17-acetate (*7a*) (100 mg) was dissolved in a saturated solution of zinc acetate in ethanol (30 ml). The reaction was allowed to stand at room temperature for 5 days, poured into water, and the products extracted with ether. The crude product which gave two major spots on t.l.c., corresponding to **6***a* and *7a* was acetylated. The acetylation product was chromatographed on alumina, from which a combined fraction of 64 mg corresponding to **6***b* was obtained. Recrystallization from methanol gave 30 mg of material which was identical to **6***b* by mixture melting point and i.r. spectrum.

2β,4β-Cyclo-5α-androstane-3α,17β-diol Diacetate (7b)

2β,4β-Cyclo-5α-androstane-3α,17β-diol 17-acetate (115 mg) (*7a*) was acetylated. Successive recrystallization of the crude product from methanol gave the 2β,4β-cyclo-5α-androstane-3α,17β-diol diacetate (58 mg); m.p. 147–148°; $[\alpha]_D$ +14°; i.r. ν_{max} (CCl_4) 3049 (cyclopropyl C—H), 1736 (ester C=O), cm^{-1}; p.m.r. δ ($CDCl_3$) 4.60 (1, t, J = 8.0 Hz, 17α-proton), 4.25 (1, t, J = 6.0 Hz,

Can. J. Chem. Downloaded from www.nrcresearchpress.com by 210.87.254.40 on 09/05/12
For personal use only.

3β-proton), 2.12 (3, s) and 2.01 (3, s, 3- and 17-acetoxyl methyl), 0.94 (3, s, 19-methyl), 0.78 (3, s, 18-methyl) p.p.m.; m.s. *m/e* M^+ (not detected) 332, ($M^+ - CH_2CO$).

Anal. Calcd. for $C_{23}H_{34}O_4$: C, 73.76; H, 9.15. Found: C, 73.54; H, 9.17.

2β,4β-Cyclo-5α-androstane-3β,17β-diol 17-Acetate (6a) with Methanolic Potassium Hydroxide

2β,4β-Cyclo-5α-androstane-3β,17β-diol 17-acetate (100 mg) in methanolic potassium hydroxide (0.36 *M*, 5 ml) was refluxed for 1 h. No starting material was detected on t.l.c. after 30 min of reaction. The solution was poured into water and neutralized with dilute sulfuric acid. The products were extracted with ether and showed i.r. ν_{max} (CCl_4) 3620 (hydroxyl), 2800 and 2700 (aldehyde C—H), 1720 (aldehyde C=O) cm^{-1}; p.m.r. δ (CCl_4) 9.62 (aldehyde proton), 3.58 (17α-proton), 0.78 (19-methyl), 0.70 (18-methyl) p.p.m.

2β,4β-Cyclo-5α-androstane-3α,17β-diol 17-Acetate (7a) with Methanolic Potassium Hydroxide

2β,4β-Cyclo-5α-androstane-3α,17β-diol 17-acetate (100 mg) was treated with methanolic potassium hydroxide as for **6a**. Spectra (i.r. and p.m.r.) of thc crude product were identical to the above product from **6a**.

2β,4β-Cyclo-5α-androstane-3α,17β-diol 17-Acetate 3-Tosylate (7c)

2β,4β-Cyclo-5α-androstane-3α,17β-diol 17-acetate (**7a**) (1.9 g) was treated with *p*-toluenesulfonyl chloride (2.4 g) in anhydrous pyridine (20 ml) as for **6a**. The crude reaction product was recrystallized from acetone to give the tosylate (**7c**) (1.7 g); m.p. 111–112° (dec.); $[\alpha]_D$ +36°; i.r. ν_{max} (CCl_4) 3020 (broad, cyclopropyl and aromatic C—H), 1730 (ester C=O), 1595 (aromatic C=C), 1190 and 1175 (tosyl S=O), cm^{-1}; p.m.r. δ ($CDCl_3$) 7.62 (4, q, AA′XX′, $J_{AX} = J_{A'X'} = 8.0$ Hz, *p*-substituted aromatic protons); 4.63 (1, t, $J = 8.0$ Hz, 17α-proton), 4.53 (1, t, $J = 6.0$ Hz, 3β-proton), 2.45 (3, s, aromatic methyl), 2.02 (3, s, acetoxy methyl), 0.83 (3, s, 19-methyl), 0.75 (3, s, 18-methyl) p.p.m.

Anal. Calcd. for $C_{28}H_{38}O_5S$: C, 69.10; H, 7.87; S, 6.59. Found: C, 69.05; H, 7.66; S, 6.54.

Acetolysis of 2β,4β-Cyclo-5α-androstane-3β,17β-diol 17-Acetate 3-Tosylate (6c)

A solution of anhydrous sodium acetate (400 mg) and acetic anhydride (1 ml) in acetic acid (10 ml) was refluxed for 1 h. The solution was cooled to 100–105°, the tosylate (**6c**) was added (100 mg) and the resulting mixture was stirred and maintained at 100–105° in an oil bath. The reaction was followed by t.l.c. at appropriate time intervals. After 20 h the solution was poured into ice water (100 ml) and the product immediately crystallized. The crystals were filtered and washed with water, dried *in vacuo* over P_2O_5 at room temperature for 4 days. The crude product (98 mg, m.p 153.5–155.5°) was further recrystallized from acetone to give a sample (82 mg) of 155–156°; the mixture m.p. of this sample with the starting material showed no depression and gave an identical i.r. spectrum with that of the starting material.

Acetolysis of 2β,4β-Cyclo-5α-androstane-3α,17β-diol 17-Acetate 3-Tosylate (7c)

2β,4β-Cyclo-5α-androstane-3α,17β-diol 17-acetate 3-tosylate (500 mg) was treated with a solution of anhydrous sodium acetate (2.2 g) and acetic anhydride (5.5 ml) in acetic acid (55 ml) as for **6c**. No starting material was detected on t.l.c. after 15 min of reaction time. The reaction was poured into ice water and the products were extracted with ether. The crude product (394 mg) was chromatographed on alumina. Elution with 2–5% benzene – petroleum ether (60:90) gave 93 mg crystalline material; p.m.r. δ (CCl_4) 5.75–5.32 (m, olefinic protons), 4.52 (t, 17α-proton), 1.95 (s, acetoxy methyl), 0.91 (s, 19-methyl), 0.77 (s, 18-methyl) p.p.m.; which on recrystallization from methanol gave 17β-acetoxyandrosta-2,4-diene (**9**); m.p. 98–99°; u.v. λ_{max} (EtOH) 266 (log ε, 3.69), 272–273 nm (log ε, 3.65) (lit. (10) m.p. 102–104°; u.v. λ_{max} 266 (log ε, 3.78), 272–273 nm (log ε, 3.74).

Elution with 25–50% benzene – petroleum ether gave 113 mg which was recrystallized from methanol to give 5α-androst-2-ene-4α,17β-diol diacetate (**10**); m.p. 188–189°; $[\alpha]_D$ +153°; i.r. ν_{max} (CCl_4) 3030 (vinylic C—H), 1735 (ester C=O), 1728 (allylic ester C=O), 1650 (alkene C=C) cm^{-1}; p.m.r. δ ($CDCl_3$) 5.86 (1, m, olefinic proton), 5.73 (1, m, olefinic proton), 5.20 (1, m, 4β-proton), 4.57 (1, t, $J = 8.0$ Hz, 17α-proton), 2.02, 2.01 (6, 2s, acetoxy methyl), 0.95 (3, s, 19-methyl), 0.77 (3, s, 18-methyl) p.p.m.; m.s. *m/e* 374 (M^+).

Anal. Calcd. for $C_{23}H_{34}O_4$: C, 73.76; H, 9.15. Found: C, 73.86; H, 8.92.

Elution with 50–75% benzene – petroleum ether gave 67 mg which was recrystallized from methanol to give 5α-androst-3-ene-2α,17β-diol diacetate (**11**); m.p. 147–148°; $[\alpha]_D$ −47°; i.r. ν_{max} (CCl_4) 3030 (vinylic C—H), 1735 (ester C=O), 1728 (allylic ester C=O), 1650 (alkene C=C) cm^{-1}; p.m.r. δ ($CDCl_3$) 5.59 (2, m, olefinic protons), 5.27 (1, m, 2β-proton), 4.57 (1, t, $J =$ 8.0 Hz, 17α-proton), 2.02, 2.01 (6, 2s, acetoxy methyl) 0.86, (3, s, 19-methyl), 0.77 (3, s, 18-methyl) p.p.m.; m.s. *m/e* 374 (M^+).

Anal. Calcd. for $C_{23}H_{34}O_4$: C, 73.76; H, 9.15. Found: C, 73.71; H, 9.00.

5α-Androst-2-ene-4,17-dione (12) from 10

5α-Androst-2-ene-4α,17β-diol diacetate (**10**) (60 mg) was refluxed with methanolic potassium hydroxide (0.36 *M*, 1.5 ml) for 1 h. The reaction was poured into water and the product was extracted with ether. The crude product was oxidized with Jones' reagent (13) and the resulting dione recrystallized from ether (24 mg); m.p. 180–180.5° (lit. (14) m.p. 172–175°); i.r. ν_{max} (KBr) 3040 (vinylic C—H), 1730 (five-membered ring C=O), 1675 (α,β-unsaturated six-membered ring C=O) cm^{-1}; p.m.r. δ ($CDCl_3$) 6.81 (1, octet, $J = 10.0$, 6.0, and 2.5 Hz, C-2 olefinic proton), 6.01 (1, octet, $J = 10.0$, 3.0, and 1.0 Hz, C-3 olefinic proton), 0.90 (3, s, 19-methyl), 0.88 (3, s, 18-methyl) p.p.m.; m.s. *m/e* 286 (M^+).

5α-Androst-3-ene-2,17-dione (13) from 11

5α-Androst-3-ene-2α,17β-diol diacetate (**11**) (50 mg) was treated with methanolic potassium hydroxide and Jones' reagent (13) as for compound **10**. The crude product was recrystallized from ether to give the dione (21 mg); m.p. 146–147°; i.r. ν_{max} (KBr) 3030 (vinylic C—H), 1745 (five-membered ring C=O), 1667 (α, β-unsaturated six-membered ring C=O) cm^{-1}; p.m.r. δ ($CDCl_3$) 6.59 (1, q, $J = 10.0$ and 2.0 Hz, C-4 olefinic

proton), 5.99 (1, octet, J = 10.0, 3.0, and 1.0 Hz, C-3 olefinic proton), 0.92 (3, s, 19-methyl), 0.88 (3, s, 18-methyl) p.p.m.; m.s. m/e 286 (M^+).

Financial assistance from the Research Board, University of Manitoba, and the Medical Research Council of Canada is gratefully acknowledged.

1. J. F. TEMPLETON and C. W. WIE. Tetrahedron Lett. 3955 (1971).
2. W. F. JOHNS and K. W. SALAMAN. J. Org. Chem. **36**, 1952 (1971).
3. J. M. CONIA and C. GIRARD. Tetrahedron Lett. 2767 (1973).
4. P. GULL, H. WEHRLI, and O. JEGER. Helv. Chim. Acta, **54**, 2158 (1971).
5. J. B. JONES and S. SHIP. Biochim. Biophys. Acta, **258**, 800 (1972).
6. N. S. BHACCA and D. H. WILLIAMS. Applications of NMR spectroscopy in organic chemistry. Holden–Day, Inc. San Francisco. 1964. p. 51.
7. (*a*) M. L. CRAGG, C. W. DAWEY, D. N. HALL, G. D. MEAKINS, E. E. RICHARDS, and T. L. WHATELEY. J. Chem. Soc. C, 1266 (1966); (*b*) M. SPITELLER-FRIEDMAN and G. SPITELLER. Org. Mass Spectrom. **1**, 231 (1968).
8. U. SCHÖLLKOPF. Angew. Chem. Int. Ed. 7, 588 (1968).
9. A. DEBOER and C. H. DEPUY. J. Am. Chem. Soc. **92**, 4008 (1970).
10. B. BERKOZ, A. D. CROSS, M. E. ADAME, H. CARPIO, and A. BOWERS. J. Org. Chem. **28**, 1976 (1963).
11. H. TADA and Y. K. SAWA. J. Org. Chem. **33**, 3347 (1968).
12. J. F. TEMPLETON and C. W. WIE. Can. J. Chem. **49**, 3636 (1971).
13. K. BOWDEN, I. M. HEILBRON, E. R. H. JONES, and B. C. L. WEEDON. J. Chem. Soc. 39 (1946).
14. P. D. KLIMSTRA. U.S. Patent No. 3,166,578; Chem. Abstr. **62**, P9207b (1965).

Can. J. Chem. Downloaded from www.nrcresearchpress.com by 210.87.254.40 on 09/05/12
For personal use only.

Investigation on the Favorable Formation of 5α-Cholestan-3α-ol and 5-Cholesten-3α-ol by Catalytic Hydrogenation

MASAYOSHI ISHIGE AND MICHIO SHIOTA

Chemical Laboratory, Ochanomizu University, Otsuka, Bunkyo-ku, Tokyo, Japan

Received December 5, 1974

MASAYOSHI ISHIGE and MICHIO SHIOTA. Can. J. Chem. **53**, 1700 (1975).

Catalytic hydrogenation of 5α-cholestan-3-one was investigated to examine the factors influencing the selective formation of the axial 3α-ol and it has been found that the most satisfactory yield of 3α-ol is realized using Urushibara nickel A, the nickel catalyst treated by acid, in hydrocarbon solvents at lower temperatures under high pressure. Preparation of epicholestanol and epicholesterol by this method is described.

MASAYOSHI ISHIGE et MICHIO SHIOTA. Can. J. Chem. **53**, 1700 (1975).

On a examiné l'hydrogénation catalytique de la 5α-cholestanone-3 afin d'examiner les facteurs influençant la formation sélective de l'alcool axial-3α; on a trouvé que le meilleur rendement de cet alcool est obtenu en utilisant un nickel A d'Urushibara alors que le catalyseur de nickel est traité par de l'acide, que des hydrocarbures sont utilisés comme solvant à température plus basse et à plus haute pression. On décrit la préparation, par cette méthode, de l'épicholestanol et de l'épicholestérol. [Traduit par le journal]

Introduction

Previously we reported a study on the stereochemistry of the reduction of 5α-cholestan-3-one with water as a hydrogen donor in the presence of precipitated metals (1).

In continuation, we investigated the catalytic hydrogenation of 5α-cholestan-3-one with Urushibara nickel (U-Ni in abbreviation), U-Co, Raney-Ni, and platinum catalysts in hydrocarbon and alcohol solvents to examine the conditions for the selective hydrogenation of the ketone to 3α-ol.

Two types of catalytic reductions have hitherto been known for the stereoselective formation of the axial steroid 3α-alcohols, which have attracted attention with experimental and theoretical interests (2–7); these are the ordinary hydrogenation catalyzed by metallic catalysts in strong acidic media (2–4, *cf.* ref. 5) and the reduction with homogeneous iridium and rhodium complexes in aqueous isopropyl alcohol under reflux (8–12). Unfortunately, it is difficult to apply these methods to the selective hydrogenation of unstable steroidal ketones which are sensitive to acid and heat, *e.g.* 5-cholesten-3-one. The reduction of these compounds must be performed under the fairly milder reaction condition.

Among a few examples of the prepondrance of steroid 3α-alcohols attained in neutral media (13–17), an intriguing experiment has been demonstrated by Ruzicka and Goldberg (13); that is, epicholesterol (5-cholesten-3α-ol) is obtained by the nickel-catalyzed hydrogenation of 5-cholesten-3-one in cyclohexane at ambient temperature and hydrogen pressure. This hydrogenation might fulfill the requirements for the reduction of unstable ketones to 3α-alcohols. However, no examples have been shown on the application of the method to other cases and the details of the yield of the product and a part of the procedure are unavailable from the literature.[1] The solvent effect of hydrocarbons on stereochemistry in the hydrogenation of steroidal ketones has never been investigated sufficiently. We have thus undertaken a more extensive study of the catalytic hydrogenation of 5α-cholestan-3-one in neutral solvents at low temperature under high hydrogen pressure.

In this paper we will describe the results of the study on the factors which influence the selective formation of the axial 3α-ol and also a convenient route for the preparation of epicholestanol (5α-cholestan-3α-ol) and epicholesterol (5-cholesten-3α-ol).

[1]They have described that 631 mg of 5-cholesten-3-one is hydrogenated to 535 mg of crude epicholesterol (*ca.* 84%), from which the product melting sharply at 141 °C is obtained by repeating recrystallizations from EtOH. The method of replacement of water on the nickel catalyst by cyclohexane was not reported.

Can. J. Chem. Downloaded from www.nrcresearchpress.com by 210.87.254.40 on 09/05/12
For personal use only.

TABLE 1. Hydrogenation of 5α-cholestan-3-one with various catalysts in *t*-butyl alcohol and cyclohexane[a]

Catalyst	Weight (g)[b]	Weight of ketone (g)	Solvent	Amount (ml)	Reaction temperature (°C)	H_2 pressure (kg/cm²)	Composition of the products (%)[c]	
							3α-ol	3β-ol
U-Ni-A	5	0.5	*t*-BuOH	20	35	110	51	49
Raney-Ni(W5)	1.5	1.5	*t*-BuOH	30	35	100	52	48
U-Co-A	10	1.5	*t*-BuOH	50	35	100	59	41
U-Co-B	10	1.5	*t*-BuOH	50	35	100	34	66
Raney-Co	4	1.5	*t*-BuOH	50	45	115	31	69
U-Ni-A	5	1.5	Cyclohexane	30	35	100	87	13
U-Ni-B	5	1.5	Cyclohexane	30	35	100	75	25
Raney-Ni(W5)	1.5	1.5	Cyclohexane	30	35	100	77	23
U-Co-A	5	1.5	Cyclohexane	30	35	100	66	34
PtO_2	0.02	0.1	Cyclohexane	3	35	100	78	22

[a]The hydrogenation was carried out for more than 3 h in order to reduce the ketone completely.
[b]Weight of ppt-Ni, ppt-Co, and Raney-alloy except PtO_2.
[c]By gas chromatography.

Results and Discussion

Hydrogenation of 5α-Cholestan-3-one

Catalysts and Solvents

Some workers have proposed generalized rules to predict the stereochemistry of the reduction products from cyclic ketones by catalytic hydrogenation (ref. 18 footnote 23 and refs. 19 and 20) but their application seems to be restricted.

It has been shown that in the reduction of the substituted cyclohexanones catalysts and solvents have some effect on the stereochemistry of the products (cf. ref. 20 and references therein; 21). Therefore, the effects of catalysts and solvents were investigated in the reduction of 5α-cholestan-3-one in *t*-BuOH and cyclohexane. The results are tabulated in Table 1.

In *t*-BuOH, the use of U-Ni-A and Raney-Ni catalysts resulted in the formation of almost equivalent amounts of 3α-ol and 3β-ol. The reactions with U-Ni-A in other alcohols, such as *n*-propyl, isopropyl, and *n*-butyl alcohol, gave almost the same results as in the case in *t*-BuOH (47–52% of 3α-ol). Under similar conditions, U-Co-A was slightly selective for the formation of 3α-ol, whereas U-Co-B and Raney-Co were less selective.

As is shown in Table 1, it is noteworthy that a good yield of epicholestanol has been realized by using cyclohexane as a solvent, especially, the excellent result in the presence of U-Ni-A. In the case with the active catalyst possessing basic surface, such as U-Ni-B, Raney-Ni, and platinum catalysts, the proportion of 3α-ol was somewhat decreased as compared with the above case with U-Ni-A and little difference among the results with the above three catalysts was observed.

In the reduction with U-Ni-A in other hydrocarbons, including *n*-pentane, *n*-hexane, *n*-heptane, isooctane, and methylcyclohexane, epicholestanol was found to predominate in the products. The results are given in Table 2.

The results in the table show that the stereoselectivity is generally independent of the kinds of hydrocarbons. Decalin and benzene were undesirable as solvents, for they caused the strong diminution of the reduction rate and selectivity.

It should be noted that the replacement of the water on catalyst by organic solvents is a quite critical procedure for the reduction because a small quantity of the remaining water causes the decrease of the reduction rate and selectivity. Thus, the catalyst must be repeatedly rinsed with *t*-BuOH before washing with the hydrocarbons used as reaction media. A trace of *t*-BuOH, of course, remains unremoved on the catalyst surface but the residual alcohol brings about no troubles for practical usage.

The result was also fairly satisfactory in ethyl ether (78% of 3α-ol) but not so promising in dioxane (56%). As usual, the reduction was strongly retarded in dioxane.

Reaction Temperature and Hydrogen Pressure

It has been suggested that the general factors influencing the composition of two epimers resulting from cyclohexanone derivatives include

Can. J. Chem. Downloaded from www.nrcresearchpress.com by 210.87.254.40 on 09/05/12
For personal use only.

Can. J. Chem. Downloaded from www.nrcresearchpress.com by 210.87.254.40 on 09/05/12
For personal use only.

TABLE 2. Effect of solvent on selectivity in the hydrogenation of 5α-cholestan-3-one with U-Ni-A catalyst

Catalyst	Weight (g)[a]	Weight of ketone (g)	Reaction temperature (°C)	Reaction time (h)	H_2 pressure (kg/cm^2)	Solvent	Amount (ml)	Composition of the products (%)[b]	
								3α-ol	3β-ol
U-Ni-A[c]	1	0.1	35	3	100	*n*-Pentane	3	82	18
U-Ni-A	5	1.5	35	3	90	*n*-Hexane	30	80	20
U-Ni-A	5	1.5	35	3	100	*n*-Heptane	30	83	17
U-Ni-A	5	1.5	35	3	90	Isooctane	30	84	16
U-Ni-A[d]	5	1.5	35	3	100	Cyclohexane	30	87	13
U-Ni-A	5	1.5	35	3	100	Methylcyclohexane[e]	30	80	20
U-Ni-A[c]	0.7	0.1	35	4	68	Ether	3	78	22
U-Ni-A	10	1.5	45	10	130	Dioxane	50	56	44

[a]Weight of ppt-Ni.
[b]By gas chromatography.
[c]Small-scale hydrogenation.
[d]The datum is identical with the one cited in Table 1.
[e]Ketone reacted, 53%.

TABLE 3. Effects of reaction temperature and hydrogen pressure on selectivity in the hydrogenation of 5α-cholestan-3-one with U-Ni-A in cyclohexane

Catalyst	Weight (g)[a]	Weight of ketone (g)	Reaction temperature (°C)	H_2 pressure (kg/cm²)	Reaction time (h)	Composition of the products (%)[b]	
						3α-ol	3β-ol
U-Ni-A[c]	0.7	0.1	80	115	2.5	71	29
U-Ni-A[c]	0.7	0.1	35	100	2.5	86	14
U-Ni-A	0.7	0.1	68–74	Atmospheric pressure	3.5	46	54
U-Ni-A	0.7	0.1	13–16	Atmospheric pressure	7.0	72	28

[a]Weight of ppt-Ni.
[b]By gas chromatography.
[c]Small-scale hydrogenation.

acidity or basicity of media, reaction temperature, hydrogen pressure, and catalytic activity (21). In the hydrogenation of 5α-cholestan-3-one, we also observed that the selectivity of the products was variable with the changes of reaction temperature and hydrogen pressure. The results of the hydrogenation of 5α-cholestan-3-one with U-Ni-A in cyclohexane are summarized in Table 3.

From the results cited in the table and other observations, the general tendencies of these effects are represented as follows. (*i*) The proportion of 3α-ol decreases with an increase in reaction temperature. The reaction at lower temperatures (below 15 °C), even at high pressure, is very slow and gives poor results; a suitable temperature range is 30–35 °C. (*ii*) A high pressure of hydrogen is favorable for the formation of 3α-ol; generally, a pressure greater than 50 kg/cm² is recommended.

Epimerization and Tautomerization

Considerable work indicates that the reaction rate should be considered to be an important factor controlling the proportion of epimers obtained. Additional factors influencing stereochemistry in hydrogenation of cyclic ketones have been shown to be the epimerization between the alcohols produced (20, 22, 23) and intermediacy of the enol form of ketone during the reduction (24–26).

Eliel has described (27) that, as the fast hydrogenation is favorable for the formation of axial alcohol, the reaction facilitated by adding mineral acid is the most likely to yield products rich in axial alcohol, since the acid medium may promote rapid desorption of the alcohol once formed and decrease the chance for equilibration between two epimers.

In our experiments, the hydrogenation of 5α-cholestan-3-one proceeded more slowly in cyclohexane than in *t*-BuOH; for example, after the 1-h reaction, 95% of the starting ketone was found to be reduced in *t*-BuOH, whereas only 45% of the ketone reacted in cyclohexane.

From these results, it is suggested that the fast reaction does not necessarily favor the occurrence of the axial alcohol.[2]

With regard to epimerization, we confirmed that no more than 2% of cholestanol and 10% of epicholestanol could be epimerized when the conversion was effected by maintaining each epimer in cyclohexane at 35 °C for 48 h in the presence of excess amounts of U-Ni-A under a hydrogen pressure of 100 kg/cm². In *t*-BuOH, the epimerization proceeded about twice as fast as that in cyclohexane. It may be concluded from these facts that, in the present reduction, the isomerization between two steroid alcohols proceeds very slowly and consequently that the stereoselectivity in question is scarcely affected by epimerization. However, the situation would be more complex at elevated reaction temperatures. At 60 °C, conversion of epicholestanol to cholestanol, in fact, occurred more readily, with the accompanying formation of a small amount of hydrocarbons. After periods as long as 12 h, the resulting mixture was, for example, found to

[2]At lower reaction temperatures (below 15 °C), the reduction was strongly retarded and the portion of 3α-ol was decreased.

Can. J. Chem. Downloaded from www.nrcresearchpress.com by 210.87.254.40 on 09/05/12
For personal use only.

Can. J. Chem. Downloaded from www.nrcresearchpress.com by 210.87.254.40 on 09/05/12
For personal use only.

TABLE 4. Catalytic hydrogenation of 5-cholesten-3-one to epicholesterol (3α-ol) and cholesterol (3β-ol)

Catalyst	Weight (g)[a]	Substrate (g)	Solvent (ml)		H_2 pressure (kg/cm^2)	Reaction temperature (°C)	Reaction time (h)	Composition of the products (%)[b]	
								3α-ol	3β-ol
U-Ni-A	5	1.5	Cyclohexane	30	100	35	2.5	94	6
U-Ni-A	10	1.5	Dioxane	50	105	35	6	77	23
U-Co-A	10	1.5	*t*-Butyl alcohol	50	115	35	4	55	45
Raney-Ni(W5)	1.5	1.5	Cyclohexane	25	105	35	1	90	10

[a]Weight of ppt-Ni, ppt-Co, and Raney alloy.
[b]By gas chromatography.

Can. J. Chem. Downloaded from www.nrcresearchpress.com by 210.87.254.40 on 09/05/12
For personal use only.

contain 16% of cholestanol and some hydrocarbons (*ca.* 1%) by gas chromatographic analysis.

According to Anderson and MacNaughton (24), and Friedman and Turkevich (25), it is to be expected that the reduction of 5α-cholestan-3-one takes place mainly through direct addition of hydrogen across the C=O double bond when the ketone undergoes the hydrogenation at 35 °C. In some cases, the enol mechanism might, however, participate in the course of the reaction. For example, when the cobalt-catalyzed reduction of 5α-cholestan-3-one in *t*-BuOH, which gave 61% of 3α-ol, was stopped at 30–50% completion of the run, the gas chromatogram of the reaction mixture, treated with a trimethylsilyl reagent, often showed a small peak of unknown substance in the region of alcohols, together with three peaks of known compounds. It was found that the compound giving this peak was readily converted to 5α-cholestan-3-one when the sample was filtered through silica gel layer with *n*-hexane eluent. The pure steroidal ketone did not react with trimethylsilyl reagent but a sample of ketone in contact with a trace of acid reacted with the reagent to yield the trimethylsilyl ether, which gave the identical gas chromatogram peak as in the above case. From these facts, the peak is reasonably assigned to the trimethylsilyl ether resulting from the enol tautomer of the ketone. When the reduction was carried out in the presence of a trace of hydrochloric acid, the yield of 3α-ol was raised to 77% and the peak area of the enol in the gas chromatogram was observed to be increased as compared with the one in the absence of acid.

These results would suggest the possibility of participation of the enol form in the present reaction.

Steric Factor

On the basis of the fact that substituted cyclohexanones are hydrogenated preferably to give the corresponding axial alcohols in EtOH with Raney-Ni, Mitsui *et al.* (28) have stated that the favorable formation of axial alcohols will take place from the cyclohexanone derivatives in the presence of Raney-Ni catalyst. The results have been interpreted in terms of the stabilities of the adsorbed transition complexes due to the catalyst hindrance.

In the nickel-catalyzed reduction of 5α-cholestan-3-one in alcohol media, the preferential production of axial alcohol could not be observed under the conditions employed, as was described above. If the product-determining step is related to the one of formation of adsorbed species, this fact indicates that the equatorial side at C-3 of the steroid may be shielded from the attack of the metal. It is generally inferred that alcohol media strongly adsorbed on the catalyst surface may act not only as useful proton donors to facilitate the reaction but also as materials influencing the stereochemistry of the adsorption of cyclic ketones. If this is the case, the angular methyl group at C-10 and the rigid ring system of the steroidal ketone might behave as the catalyst hindrance for the β-side approach of the catalyst.

On the other hand, hydrocarbon solvents may be weakly adsorbed on the metal surface. Thus, the substrate could be allowed to interact with the metal surface freely enough to form the more stable species adsorbed on the equatorial side (28).

Preparation of Epicholestanol and Epicholesterol

It has now been found that nickel catalysts are effective for the preparation of epicholestanol when they are used in cyclohexane at 30–35 °C under the high pressure of hydrogen. Of all the catalysts used, U-Ni-A is the most suitable because the catalyst is easily obtained and the yield of the axial 3α-alcohol is excellent.

It is notable that this hydrogenation method could be applied to the reduction of 5-cholesten-3-one to epicholesterol without any isomerization or saturation of the 5,6-double bond of the ketone. No hydrogenolysis occurred during the reaction, as well. Some results are listed in Table 4.

With an analogous trend as in the case of epicholestanol, cyclohexane as a solvent played an important part in increasing the yield of epicholesterol and this solvent effect was conspicuously marked under high hydrogen pressure. The reactions at higher temperatures (*e.g.* at 80 °C) decreased the yield of the 3α-ol and caused the formation of some by-products.

Urushibara cobalt A (U-Co-A) also catalyzed the hydrogenation of 5-cholesten-3-one when used in *t*-BuOH but the catalyst was less proper for the present purpose because the formation of the 3α-ol was not so predominant.

Can. J. Chem. Downloaded from www.nrcresearchpress.com by 210.87.254.40 on 09/05/12
For personal use only.

Experimental

All melting points were measured on a hot stage and are uncorrected. Infrared spectra were recorded on KBr discs with a JASCO IR-G instrument and n.m.r. spectra were taken in chloroform-*d* and carbon tetrachloride with a JEOL C-60HL spectrometer using tetramethylsilane as an internal reference.

Catalysts

Preparation of Precipitated Nickel (1, 29)

A warmed aqueous solution of nickel chloride (4.04 g of $NiCl_2 \cdot 6H_2O$ in 10 ml of water) (*ca.* 80 °C) was added to hot zinc dust mud (10 g of zinc powder and 3 ml of water) at once with vigorous shaking. The deposit was collected and washed successively with water, ethanol, and ether and then dried on a filter paper;[3] yield, 10–11 g.

U-Ni-A Catalyst (16, 29)

A 13% aqueous solution of acetic acid (*ca.* 6 ml) was added all at once to precipitated nickel (10 g). The reaction vessel was occasionally shaken to prevent the contents from foaming over due to the violent evolution of hydrogen. When the reaction subsided, additional aqueous acetic acid was added until the solid matter settled, and then the supernatant liquid was decanted. Twice more the acid treatment was carried out using each *ca.* 30 ml of aqueous acetic acid and at an end of the acid treatment we could observe the faint green of the solution. The nickel catalyst thus obtained was washed by suspension in water and decantation until the washings were neutral to litmus. When we used hydrocarbon as a solvent in hydrogenation, the further washing processes were repeated several times with *t*-butyl alcohol and the hydrocarbon successively. The catalyst contains about 0.8 g of nickel (29).

U-Ni-B Catalyst (29, 30)

This catalyst was obtained from precipitated nickel (5 g) by using a 10% aqueous solution of sodium hydroxide (*ca.* 100 ml), instead of acetic acid solution in the case of U-Ni-A. The catalyst is dark grey and contains about 1 g of nickel and large amounts of zinc.

U-Co-A and U-Co-B Catalysts (29)

U-Co catalysts were prepared from 4.04 g of $CoCl_2 \cdot 6H_2O$ and 10 g of zinc powder by a similar procedure described in the preparation of U-Ni catalysts.

Raney-Ni Catalyst (W5)

Raney nickel catalyst (W5) was obtained from 1.5 g of Raney alloy according to the usual procedure (31). The nickel was washed successively with water (about 50 °C), *t*-butyl alcohol, and cyclohexane.

Hydrogenation of 5α-Cholestan-3-one

Hydrogenation with U-Ni-A in Cyclohexane

As a typical example, the hydrogenation with U-Ni-A in cyclohexane will be described. The freshly obtained U-Ni-A (from 5 g of precipitated nickel) and cyclohexane (30 ml) were transferred to a 100-ml autoclave equipped with a magnetic stirring device. 5α-Cholestan-3-one (1.5 g) was added and the hydrogenation was conducted at 35 °C for 3 h with stirring of 1000 cycle/min under the hydrogen pressure of 100 kg/cm². From the resultant mixture, the nickel was removed by filtration and then the filtrate was evaporated *in vacuo*. Recrystallization of the crude crystals from methanol yielded *ca.* 1.2 g of epicholestanol (80% yield); m.p. 188–189 °C (lit. (32) m.p. 186–187 °C); i.r. (KBr, cm^{-1}): 3300 (sharp, strong), 1030 and 1000; n.m.r. (CCl_4, TMS): δ 3.90 (broad equatorial H at C-3).

Small-scale Hydrogenation under High Pressure

The reduction using no more than 100 mg of 5α-cholestan-3-one was carried out in an autoclave equipped with a magnetic stirring device in the following manner. To a 5-ml Erlenmeyer flask was added 5α-cholestan-3-one (100 mg), cyclohexane (3 ml), and a given amount of catalyst (*cf.* Tables 1–4). The flask was attached to the adaptor and then settled in the autoclave as shown in Fig. 1. The hydrogenation was performed under the given condition in the usual manner. By this method, small amount of sample (1–100 mg) can be easily hydrogenated under high pressure without any special device.

Hydrogenation of 5-Cholesten-3-one

Hydrogenation with U-Ni-A in Cyclohexane

By using U-Ni-A (from 5 g of precipitated nickel), 5-cholesten-3-one (1.5 g) was hydrogenated in cyclohexane (30 ml) at 35 °C for 2.5 h with stirring of 1000 cycle/min at 100 kg/cm² pressure. After the removal of solid matter from the resultant mixture by filtration, evaporation of the filtrate *in vacuo* gave the crystals. The crystals gave 1.38 g of epicholesterol (92% yield) and 0.08 g of cholesterol (5% yield), when they were chromatographed on silica gel (150 g, 3.5 cm(ϕ) × 31 cm column) with an eluent of *n*-hexane–ether (9:1).

Epicholesterol: m.p. 139–140 °C (lit. (13) m.p. 141 °C); i.r. (KBr, cm^{-1}) 3350 (sharp, strong), 1022, 1007, 993, and 800; n.m.r. (chloroform-*d*, TMS): δ 5.45 (olefinic proton, broad doublet, J = 5.0 Hz) and 4.03 (equatorial proton at C-3, broad). The relative intensities of these peaks were approximately 1:1. By addition of a few drops of D_2O, the collapsed peak centered at δ 4.03 changed into the broad triplet peak with J = 3.0 Hz. Acetylation of the above-obtained epicholesterol af-

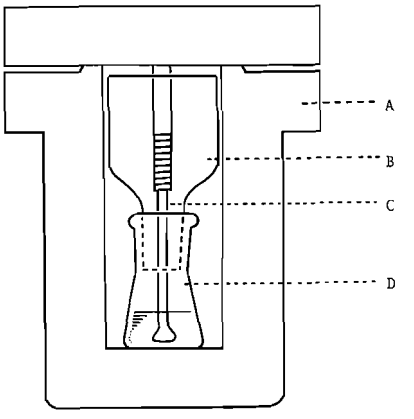

FIG. 1. Small-scale High-pressure Hydrogenator: *A*, autoclave; *B*, adaptor; *C*, stirrer (glass); *D*, Erlenmeyer flask.

[3]When the precipitated nickel thus obtained is used immediately after the preparation, we can neglect the washing processes with ethanol and ether. The dried precipitated nickel can be stored in a desiccator for a long period.

forded the acetate of m.p. 84–85 °C (lit. (13) m.p. 85 °C).[4]

Hydrogenation with U-Co-A in t-BuOH

The hydrogenation of 5-cholesten-3-one (1.5 g) catalyzed by U-Co-A was carried out in *t*-BuOH at 35 °C for 4 h at 115 kg/cm² hydrogen pressure. From the crude product, 0.75 g of epicholesterol (50% yield) and 0.74 g of cholesterol (49% yield) were isolated by column chromatography using silica gel. When cyclohexane solvent was used instead of *t*-BuOH, the reduction with U-Co-A proceeded very slowly and the proportion of 3α-ol in the products was lower than that obtained using *t*-BuOH.

Hydrogenation with Raney-Ni in Cyclohexane

By using the Raney-Ni freshly obtained as described above, 5-cholesten-3-one (1.5 g) was hydrogenated in cyclohexane (25 ml) at 35 °C for 1 h at 105 kg/cm² hydrogen pressure. The crude product was chromatographed on silica gel to give 1.22 g of epicholesterol (81% yield).

Gas–Liquid Partition Chromatographic Analyses

The analyses for data in Tables 1–4 were made by gas chromatography, after treatment of the products with *N,O*-bis(trimethylsilyl)acetamide. Gas–liquid partition chromatography analytical conditions: 3 m glass column packed with 1.5% Silicone OV-17 on silanized Shimalite W (80–100 mesh); temperature, *ca.* 250 °C; detector, HFID. All the chromatograms showed that the starting material was completely converted into the alcohols under the conditions employed.

1. M. ISHIGE, M. SHIOTA, and Y. IDENO. Can. J. Chem. **51**, 3923 (1973).
2. G. VAVON and B. JAKUBOWICZ. Bull. Soc. Chim. Fr. **53**, 581 (1933); Chem. Abstr. **27**, 5749 (1933).
3. L. RUZICKA, H. BRÜNGGER, E. EICHENBERGER, and J. MEYER. Helv. Chim. Acta, **17**, 1407 (1934).
4. J. T. EDWARD and J.-M. FERLAND. Can. J. Chem. **44**, 1311 (1966).
5. W. G. DAUBEN, E. J. BLANZ, JR., J. JIU, and R. A. MICHELI. J. Am. Chem. Soc. **78**, 3752 (1956).
6. Y. WATANABE, Y. MIZUHARA, and M. SHIOTA. Can. J. Chem. **47**, 1495 (1969).
7. J. H. BREWSTER. J. Am. Chem. Soc. **76**, 6361 (1954).
8. Y. M. Y. HADDAD, H. B. HENBEST, J. HUSBANDS, and T. R. B. MITCHELL. Proc. Chem. Soc. 361 (1964).
9. P. A. BROWNE and D. N. KIRK. J. Chem. Soc. C, 1653 (1969).
10. J. C. ORR, M. MERSEREAU, and A. SANFORD. Chem. Commun. 162 (1970).
11. H. B. HENBEST and T. R. B. MITCHELL. J. Chem. Soc. C, 785 (1970).
12. Y. M. Y. HADDAD, H. B. HENBEST, J. HUSBANDS, T. R. B. MITCHELL, and J. TROCHA-GRIMSHAW. J. Chem. Soc. Perkin Trans. I, 596 (1974).
13. L. RUZICKA and M. W. GOLDBERG. Helv. Chim. Acta, **19**, 1407 (1936).
14. M. DELÉPINE and A. HOREAU. C.R. **202**, 995 (1936); Chem. Abstr. **30**, 4812 (1936).
15. C. DJERASSI, A. J. MANSON, and M. GORMAN. J. Am. Chem. Soc. **77**, 4925 (1955).
16. M. ISHIGE and M. SHIOTA. Synthesis, 171 (1973).
17. H. B. HENBEST and A. ZURQIYAH. J. Chem. Soc. Perkin Trans. I, 604 (1974).
18. D. H. R. BARTON. J. Chem. Soc. 1027 (1953).
19. E. OTT and R. SCHROTER. Ber. **60**, 624 (1927).
20. R. J. WICKER. J. Chem. Soc. 2165 (1956).
21. A. SKITA and W. FAUST. Ber. **64**, 2878 (1931).
22. E. L. ELIEL and S. H. SCHROETER. J. Am. Chem. Soc. **87**, 5031 (1965).
23. D. CORNET and F. G. GAULT. J. Catal. **7**, 140 (1967); Chem. Abstr. **66**, 6074 (1967).
24. L. C. ANDERSON and N. W. MACNAUGHTON. J. Am. Chem. Soc. **64**, 1456 (1942).
25. L. FRIEDMAN and J. TURKEVICH. J. Am. Chem. Soc. **74**, 1669 (1952).
26. I. N. KAUDER and T. I. TAYLOR. Science, **113**, 238 (1951).
27. E. L. ELIEL. Stereochemistry of carbon compounds. McGraw-Hill, New York, San Francisco, Toronto, London. 1962. pp. 243–244.
28. S. MITSUI, H. SAITO, Y. YAMASHITA, M. KAMINAGA, and Y. SENDA. Tetrahedron, **29**, 1531 (1973).
29. K. HATA. Urushibara catalysts. University of Tokyo Press, Tokyo 1971.
30. Y. URUSHIBARA. Bull. Chem. Soc. Jap. **25**, 280 (1952).
31. H. ADKINS and H. R. BILLICA. J. Am. Chem. Soc. **70**, 695 (1948); *cf.* E. C. HORNING (*Editor*). Org. Synth. Coll. **3**, 176 (1955).
32. C. W. SHOPPEE. J. Chem. Soc. 1138 (1946).
33. T. OKAMOTO and Y. KAWAZOE. Chem. Pharm. Bull. 11, 643 (1963); N. S. BHACCA and D. H. WILLIAMS. Applications of NMR spectroscopy in organic chemistry. Holden-Day, Inc., San Francisco. 1964. p. 88.

[4]In the n.m.r. spectrum of the acetate, 6-olefinic proton (δ 5.26) was observed to resonate at the upperfield by 0.19 p.p.m. from that of epicholesterol (*cf.* ref. 33).

Can. J. Chem. Downloaded from www.nrcresearchpress.com by 210.87.254.40 on 09/05/12
For personal use only.

Acid Catalyzed Rearrangements of Conjugated Cyclopropyl and Epoxy Ketones

E. LEE-RUFF AND P. KHAZANIE
Department of Chemistry, York University, Toronto, Ontario M3J 1P3

Received October 11, 1974

E. LEE-RUFF and P. KHAZANIE. Can. J. Chem. **53**, 1708 (1975).

A series of spiro[*n*.2]alkan-2-ones and their 6 and 7 oxa derivatives were subjected to acid catalysis. In the former series, products arising from hydroxy(cyclopropyl)carbinyl cations are observed, while in the latter series epoxide oxygen protonation appears to be the dominant reaction pathway. A novel oxavinylcyclopropane rearrangement is reported.

E. LEE-RUFF et P. KHAZANIE. Can. J. Chem. **53**, 1708 (1975).

On a soumis à une catalyse acide une série de spiro[*n*.2]alkanones-2 ainsi que leurs dérivés oxa 6 et 7. Dans la première série, on a observé des produits dérivant des cations hydroxy(cyclopropyl)carbinyles alors que dans les dernières séries, il semble que la protonation de l'oxygène de l'époxyde soit le chemin réactionnel prédominant. On rapporte un nouveau réarrangement oxavinylcyclopropane. [Traduit par le journal]

Can. J. Chem. Downloaded from www.nrcresearchpress.com by 210.87.254.40 on 09/05/12
For personal use only.

The interaction of cyclopropyl and epoxide groups with an adjacent electron-deficient center continues to be a topic of extreme interest. The recent results on the acid catalyzed rearrangements of epoxy ketones reported by Williams *et al.* (1) and the interest in the protonation of cyclopropanes and epoxides (2) prompted us to report the results of the acid rearrangements of a series of spiro[*n*.2]alkanones and their 6 and 7 oxa derivatives. These systems were chosen because of their conformational semblance to the bisected forms of cyclopropylcarbinyl and epoxycarbinyl cations allowing for maximum conjugation of the three-member ring with the adjacent carbocationic center (3, 4).

Ketones **1**–**8** were prepared from the corresponding alkylidene cycloalkanones by a slightly modified three step sequence described in ref. 5. The *syn* and *anti* isomers **2**, **4** and **3**, **5**

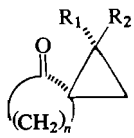

1 $R_1 = R_2 = H; n = 3$
2 $R_1 = CH_3; R_2 = H; n = 3$
3 $R_1 = H; R_2 = CH_3; n = 3$
4 $R_1 = R_2 = CH_3; n = 3$
5 $R_1 = R_2 = H; n = 4$
6 $R_1 = CH_3; R_2 = H; n = 4$
7 $R_1 = H; R_2 = CH_3; n = 4$
8 $R_1 = R_2 = CH_3; n = 4$

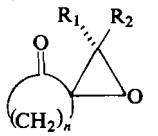

9 $R_1 = R_2 = CH_3; n = 3$
10 $R_1 = H; R_2 = CH_3; n = 4$
11 $R_1 = R_2 = CH_3; n = 4$

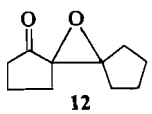

12

were obtained from the corresponding *syn*- and *anti*-2-ethylidenecycloalkanones, respectively.

The rearrangements of all cyclopropyl ketones were carried out in acidic benzene solutions at room temperature or under reflux. The results for the spiroheptanones are shown in Scheme 1. Ketone **1** appeared to be stable at room temperature in acidic benzene. Upon reflux it was slowly polymerized. However with polyphosphoric acid (PPA) a small amount (10%) of 2-ethylcyclopent-2-enone (**13**) was isolated as was also reported by Conia and Amice (6).

Ketones **2** and **3** were slightly more reactive and in refluxing H_2SO_4–C_6H_6, both gave identical mixtures of **14** and **15**. The structure of **14** was established by its synthesis from condensation of cyclopentanone and propionaldehyde. The structure of **15** was confirmed by its independent synthesis from the PPA rearrangement of **14**, a reaction which has been reported for several 2-alkylidenecyclopentanones (7). Upon prolonged reaction of **2** or **3** increasing amounts of **15** were obtained at the expense of **14**. In a separate study it was shown that **14** rearranged

Can. J. Chem. Downloaded from www.nrcresearchpress.com by 210.87.254.40 on 09/05/12
For personal use only.

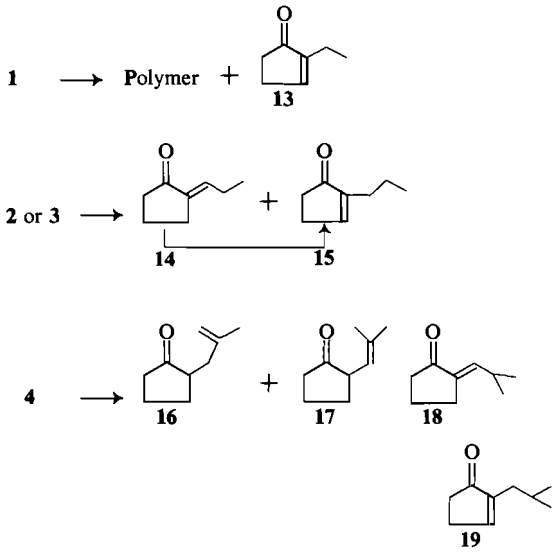

SCHEME 1. Rearrangement of spiroheptanones

to **15** under the same conditions. Reaction of the dimethyl derivative **4** gave a mixture of ketones **16** and **17**. The identity of these ketones was established on the basis of their spectral data and hydrogenation to 2-isobutylcyclopentanone which was independently synthesized. There was no evidence for the formation of ketones **18** and **19**. The relative rates for the acid catalyzed rearrangements determined by g.l.c. monitoring of starting material were found to be in the order **4** > **2** and **3** > **1**.

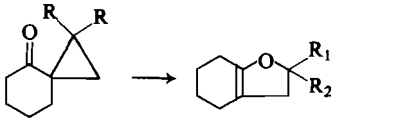

The homologous cyclohexanones appeared to be quite acid labile relative to the cyclopentanones and *at room temperature* all gave the corresponding hexahydrobenzofurans **20–22** as the only products. The structural assignments of the products were based on spectral data and independent synthesis (8). In a qualitative study, it was shown that the rearrangement rates of these ketones were in the order **8** > **7** and **6** > **5**.

The rearrangements of the epoxy ketones followed a different course from the cyclopropyl ketones. Reaction of ketones **9**, **11**, and **12** all gave the ring expanded β-diketones **23**, **24**, and **25**, respectively. The structures of diketones

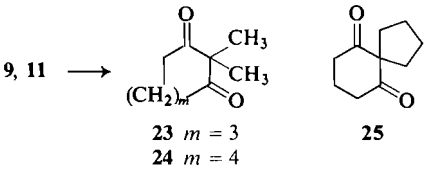

23 and **24** were unequivocally established by their independent syntheses from dimethylation of cyclohexan-1,3-dione and cycloheptan-1,3-dione (9, 10), respectively. The structure of **25** was inferred on the basis of its spectral data and comparison of this with a previously reported preparation (1, 11). The reaction of ketone **10** in acid gave a complex mixture containing no volatile material. The major product (23%) was a crystalline material which analyzed for 2 equiv. of **10** and 1 equiv. of water. The spectral data indicated the structure **26**.

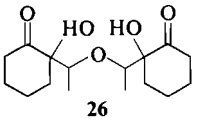

Discussion

The rearrangements of cyclopropyl ketones **1–4** to the enones **13–17** can be rationalized in terms of the mechanistic sequence shown in Scheme 2. Initial protonation of the carbonyl oxygen leads to the formation of a delocalized oxahomoallylic cation **27** and subsequent 1,2

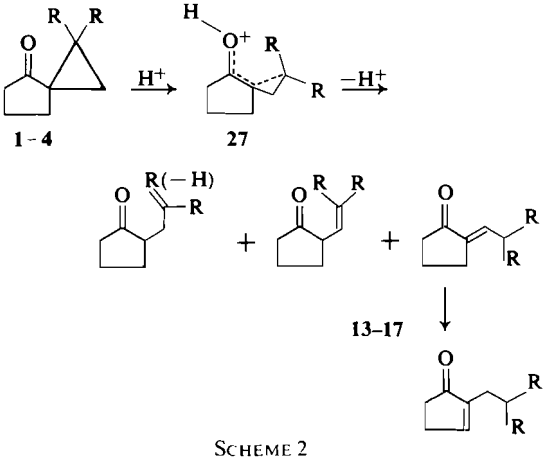

SCHEME 2

Can. J. Chem. Downloaded from www.nrcresearchpress.com by 210.87.254.40 on 09/05/12
For personal use only.

hydrogen transfer followed by loss of proton or direct proton elimination would result in the observed products. Cyclopentanones **13** and **15** are most likely secondary products since it was shown independently by Conia and us (7) that 2-alkylidenecyclopentanones rearrange under acidic conditions to the more stable 2-cyclopentenones. Although there is evidence for the delocalization of the positive charge in protonated cyclopropyl ketones from n.m.r. deshielding effects (12, 13), there have not been any reported products exhibiting this effect after quenching with base. Our present study indicates that there is significant positive charge developed at C-7 (**5–8**, C-6 in **1–4**) in the transition state of the rate determining step in these systems based upon the relative rates of rearrangement of ketones **1–4** and **5–8**. Furthermore reaction of **4** and **8** with acidic methanol led to their instantaneous conversion to ketoethers **28** and **29**, respectively.

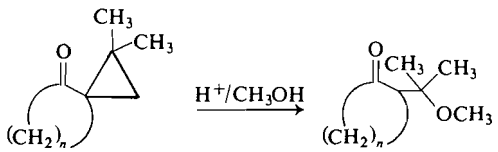

4, 8 **28** $n = 3$ **29** $n = 4$

The rearrangements of ketones **5–8** to the hexahydrobenzofurans **21–23** is formally analogous to a protonated version of the oxavinylcyclopropane rearrangement (14). Conceivably a 1-oxacyclopent-2-enyl cation **31** is formed from protonated cyclopropylketone **30** by a symmetry

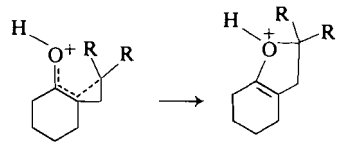

30 **31**

allowed cyclization. A similar observation was reported by Pittman and McManus (15); however in their systems there was evidence only for the formation of the tautomeric 1-oxacyclopent-1-enyl cation. That no bicyclic dihydrofurans are detected in the cyclopentanone series can be rationalized in terms of ring strain effects due to the difference in ring size.

The acidic rearrangements of the epoxy ketones follow a completely different course from the cyclopropyl ketones. All of the products can be explained in terms of an initial epoxide oxygen protonation followed by 1,2 acyl shifts. The difference in reactivities between cyclopropyl and epoxy ketones is due to the inclusion of an additional and equally competing basic oxygen in the latter. Similar observations were made by other workers (1, 16, 17) and in all cases 1,3-diketones resulting from C_β—O cleavage and acyl shift were obtained. These results are in contrast to the thermolytic study on the identical systems (18) where 1,3-diketones were obtained from initial C_α—O cleavage followed by 1,2 alkyl shift. The selectivity of these rearrangements provide a useful synthetic pathway for the preparation of 2,2-dialkylated or 2-monoalkylated (provided the alkyl group stabilizes a positive charge) two carbon ring-expanded 1,3-diketones from cyclic monoketones. That the epoxycarbinyl cation or the 1-oxabicyclobutonium ion does not play an important role in these rearrangements is evident from the absence of any oxetanyl derivatives as would be expected if these ions were quenched by base (19).

Experimental

Melting points were uncorrected. The i.r. spectra were recorded with a Unicam SP 1000 instrument. The n.m.r. spectra were measured on a Varian A-60, Ha-100, and EM-360 spectrometers. Samples were dissolved in CCl_4 and $CDCl_3$ solvents using TMS as the internal standard. Vapor phase chromatographic analyses and collections were performed on a Varian Aerograph Series 1700 instrument using the following columns: (*A*) a 5 ft 4 in. steel column (0.25 in. o.d.) packed with 3% SE-30 on Varaport 30, (*B*) a 6 in. aluminum column (0.25 in. o.d.) packed with 10% FFAP on Chromosorb P, (*C*) a 6 ft glass column (0.25 in. o.d.) packed with 6% SE-30 + 4% QF-1 on Chromosorb W AW, DMCS treated, and (*D*) a 9 ft alumina column (0.25 in. o.d.) packed with 3% OV 25 on Chromosorb W, high performance, 80–100 mesh. Microanalysis were performed by Gygli Microanalytical Labs, Toronto. All of the starting materials were prepared according to procedures described in refs. 18 and 20.

Rearrangement of Spiro[2.4]heptan-2-one (1) with Sulfuric Acid

The title compound (100 mg) was dissolved in 10 ml benzene containing 100 mg of 95% sulfuric acid. The solution was refluxed on an oil bath for 15 min. The work-up of the reaction mixture gave a polymeric material and 18 mg of the starting material.

Rearrangement of anti-6-Methylspiro[2.4]heptan-2-one (3) with Sulfuric Acid

Ketone **3** (80 mg) was dissolved in 10 ml benzene containing 80 mg of 95% sulfuric acid. The solution was refluxed for 10 min. It was then cooled in an ice bath and worked-up by standard procedures. Vapor phase chroma-

Can. J. Chem. Downloaded from www.nrcresearchpress.com by 210.87.254.40 on 09/05/12
For personal use only.

tography (column *C*) of the crude mixture showed 4% 2-propyl-2-cyclopentenone (**15**), 6% *anti*-2-propylidenecyclopentanone (**14**), 11% of an unidentified product, and 60% of the starting material. Upon refluxing for a longer period (total time: 45 min) the v.p.c. of the mixture showed only **15** and an unidentified product. Preparative t.l.c. gave 19 mg of **15**.

Compound ***14***: b.p. 63–64°/1.5 mm (lit. (21) b.p. 81–82°/11 mm); i.r. (CCl_4) 1150, 1202, 1285, 1408, 1462, 1650 (C=C), 1720 cm^{-1} (C=O); n.m.r. (CCl_4) δ 1.07 (3H, t) 1.6–2.83 (8H, m), 6.37 (1H, m).

Anal. Calcd. for $C_8H_{12}O$: C, 77.41; H, 9.67. Found: C, 77.40; H, 9.52.

Compound ***15***: b.p. 59–60°/113 mm; i.r. (CCl_4) 1060, 1105, 1715, 3040 cm^{-1}; n.m.r. (CCl_4) δ 0.92 (3H, t, J = 7 Hz), 1.12–2.70 (8H, m), 7.2 (1H, m); *m/e* 124.

Anal. Calcd. for $C_8H_{12}O$: C, 77.41; H, 9.67. Found: C, 77.30; H, 9.63.

*Rearrangement of syn-6-Methylspiro[2.4]heptan-2-one (**2**) with Sulfuric Acid*

The same procedures employed for ketone **3** was used. Reaction of 70 mg of **2** gave 17 mg of ketone **15**. Ketone **14** was detected in the mixture by v.p.c. to the extent of 6% after 10 min of reaction.

*Preparation of anti-2-Propylidenecyclopentanone (**14**)*

A mixture of cyclopentanone (16.8 g, 0.2 mol), propionaldehyde (11.6 g, 0.2 mol), and 0.5% KOH (20 ml) was stirred at 0° for 30 min and then at room temperature for 15 h. Using standard work-up conditions 11.2 g of a fraction, b.p. 70–100°/1.2 mm, was obtained. This fraction was then treated with orthophosphoric acid and benzene and worked-up in the usual manner to give 6.9 g (27%) of *anti*-2-propylidenecyclopentanone (**14**) identical in all respects with a sample obtained above.

*Preparation of 2-n-Propyl-2-cyclopentenone (**15**)*

A mixture of *anti*-2-propylidenecyclopentanone (1.0 g) and polyphosphoric acid (1:1 mixture of P_2O_5 and H_3PO_4 aged for 10 h at 100°) was heated at 100° for 30 min in a flask equipped with a condenser. Water (7 ml) was added to the cooled mixture and 50 ml of ether was added for extraction. The ether layer was washed with brine, dried over anhydrous magnesium sulfate, and ether evaporated to give 0.85 g of a crude liquid which was purified by distillation, b.p. 59–60°/1.3 mm; yield 0.51 g (51%). This was identical in all respects with a sample prepared above.

*Rearrangement of anti-2-Propylidenecyclopentanone (**14**) with Sulfuric Acid*

anti-2-Propylidenecyclopentanone (80 mg) was dissolved in 10 ml benzene containing 80 mg 95% sulfuric acid. The reflux and work-up as described in the rearrangement of **3**, gave 33 mg of 2-propyl-2-cyclopentenone (**15**) and approximately 7 mg of the starting ketone.

*Rearrangement of 6,6-Dimethylspiro[2.4]heptan-2ψone (**4**) in Sulfuric Acid*

Ketone (**4**) (75 mg) was dissolved in 6 ml Anal R benzene and the solution was cooled in an ice bath. The benzene which froze at this temperature was allowed to thaw and to this solution 125 mg of 95% sulfuric acid was added at the thawing temperature. The solution was stirred at this temperature for 1 min. It was then neutralized with sodium bicarbonate solution and worked-up in the usual way to give 56 mg of a crude mixture, which when analyzed by v.p.c. (column *C*) showed enone **16** (11 mg), **17** (10 mg), and unreacted **4** (22 mg). Compounds **16** and **17** were collected on v.p.c.

Compound ***16***: i.r. 3080, 1740, 1155, 897 cm^{-1}; n.m.r. δ 1.71 (3H, s), 2.70–1.60 (9H, m), 4.69 (2H, bs) p.p.m.

Anal. Calcd. for $C_{10}H_{14}O$: C, 78.92; H, 10.67. Found: C, 78.72; H, 10.53.

Compound ***17***: i.r. 3050–3100, 1745, 1150 cm^{-1}; n.m.r δ 1.55 (3H, s), 1.62 (3H, s), 1.6–3.0 (7H, m), 4.90 (1H, d).

Anal. Calcd. for $C_{10}H_{14}O$: C, 78.92; H, 10.67. Found: C, 78.80; H, 10.45.

*Preparation of anti-2-Isobutylidenecyclopentanone (**18**)*

A mixture of 16.8 g (0.2 mol) of cyclopentanone, 14.4 g (0.2 mol) of isobutyraldehyde, and 20 ml of 0.5% KOH was stirred at 0° for 30 min and then at room temperature for 12 h. The reaction mixture was worked-up to give 12.4 g of a fraction, b.p. 80–100°/1.2 mm which was then treated with orthophosphoric acid C_6H_6; yield of product, 7.7 g (28%); b.p. 62–63°/1.5 mm (lit. (22) b.p. 86°/11 mm); i.r. (CCl_4) 945, 1142, 1178, 1205, 1290, 1410, 1466, 1653, 1722, 2960 cm^{-1}; n.m.r. (CCl_4) δ 1.02 (6H, d), 1.62–2.8 (7H, m), 6.23 (1H, a doublet of triplets); λ_{max} (EtOH) 246 nm (ε 8004); *m/e* 124.

*Hydrogenation of anti-2-Isobutylidenecyclopentanone (**18**)*

The title ketone (58 mg) was hydrogenated at atmospheric pressure with 8 mg of platinum oxide in 6 ml of ethyl acetate. One equivalent of hydrogen was taken up whereupon the hydrogen uptake ceased. The solution was filtered and the solvent removed under reduced pressure to give 53 mg of essentially pure 2-isobutylcyclopentanone (analyzed by v.p.c., column *A*); i.r. (neat) 1183, 1392, 1410, 1432, 1480, 1492, 1756 (C=O stretch) cm^{-1}; n.m.r. (CCl_4) δ 0.77–1.1 (6H, two doublets centered at 0.83 (J = 1.5 Hz) and 0.9 (J = 1.5 Hz), 1.15–2.4 (10H, m): *m/e* 126.

*Hydrogenation of Compound **16***

A solution of 25 ml of the title compound in 6 ml ethyl acetate was hydrogenated over 5 mg of platinum oxide. Work-up and isolation gave 2-isobutylcyclopentanone in almost quantitative yield. This ketone had i.r. and n.m.r. spectra identical with those of a sample prepared by hydrogenation of *anti*-2-isobutylidenecyclopentanone.

*Hydrogenation of Compound **17***

This compound was hydrogenated just as ketone **16** and gave 2-isobutylcyclopentanone in quantitative yield. The i.r. and n.m.r. of this compound were identical with those of a sample prepared by hydrogenation of **16**.

*Rearrangement of Spiro[2.5]octan-2-one (**5**) with Sulfuric Acid*

Ketone **5** (75 mg) was dissolved in 6 ml Anal R benzene containing 130 mg of 95% sulfuric acid. The solution was stirred for 83 h at room temperature and then neutralized with 7% sodium bicarbonate solution. The mixture was taken up with an additional 25 ml benzene, the benzene layer washed neutral with saturated sodium chloride solution, dried, and evaporated to give 76 mg of a crude

Can. J. Chem. Downloaded from www.nrcresearchpress.com by 210.87.254.40 on 09/05/12
For personal use only.

product. Vapor phase chromatography (column *C*) of this sample showed **5** and 2,3,4,5,6,7-hexahydrobenzofuran (**20**) in a ratio of 1:6. The mixture was purified by preparative t.l.c. (silica gel) to give 42 mg of **20**. The i.r. and n.m.r. spectra of this compound were identical with those of the sample obtained by independent synthesis described below.

Synthesis of 2,3,4,5,6,7-Hexahydrobenzofuran (20)

Starting from the ethylene ketal of 2-cyclohexanoneacetate, the title compound was prepared by the following steps according to ref. 8.

Lithium Aluminum Hydride Reduction of the Ketal Ester

Following standard procedures for the LAH reductions of esters using 1.4 g (0.005 mol) of the above ketal ester and 300 mg (0.008 mol) of lithium aluminum hydride in 30 ml anhydrous ether, 1.1 g of ketal alcohol was obtained. This compound was purified by vacuum transfer: i.r. (CCl_4) 925, 952, 1057, 1090, 1160, 1445, 2920, 3400 cm^{-1}; n.m.r. (CCl_4) δ 1.0–2 (11H, m), 3.33–4.2 (7H, m, 3.88, s).

Hydrolysis of the Ketal Alcohol

Using the procedure described for the hydrolysis of ketal alcohol (8) from 0.8 g of ketal alcohol in 15 ml acetone and 5 ml water containing 15 mg of *p*-toluenesulfonic acid was obtained 0.6 g of hemiketal: i.r. (CCl_4) 900, 947, 1008, 1084, 1447, 2940, 3400 cm^{-1}; n.m.r. (CCl_4) δ 0.83–2.6 (11H, m), 3.3–4.05 (2H, m), 4.45 (1H, s).

Preparation of 2,3,4,5,6,7-Hexahydrobenzofuran (20)

The above hemiketal was heated to 125° and distilled at 28 mm to give the title compound in quantitative yield with the elimination of water: i.r. (CCl_4) 890, 933, 982, 1202, 1282, 1382, 1443, 1610, 2850, and 2930 cm^{-1}; n.m.r. (CCl_4) δ 4.17 (2H, t, J = 9 Hz), 2.47 (2H, t, J = 9 Hz), 1.2–2.2 (8H, m). These spectra were identical with the spectra described in the literature (8) and the product obtained in the rearrangements of **20**.

Rearrangement of anti-7-Methylspiro[2.5]octan-2-one (7) with Sulfuric Acid

Ketone 7 (75 mg) was dissolved in 8 ml Anal R benzene containing 120 mg of 95% sulfuric acid. The solution was stirred for 7 h at room temperature. It was then worked-up in ether by standard procedure to give 54 mg of 2-methyl-2,3,4,5,6,7-hexahydrobenzofuran (**21**) as the sole product. This compound displayed i.r. and n.m.r. spectra identical with those of the compound obtained by independent synthesis (8).

Rearrangement of syn-7-Methylspiro[2.5]octan-2-one (6) with Sulfuric Acid

The above procedure was used for the acid reaction of ketone **6**. Using 80 mg of **6**, 60 mg of 2-methyl-2,3,4,5,6,7-hexahydrobenzofuran (**21**) was obtained as the sole product. Its spectral data were identical with the sample prepared above.

Rearrangement of 7,7-Dimethylspiro[2.5]octan-2-one (8) with Sulfuric Acid

The same conditions described in the acid catalysis of **5** were used and from 75 mg of ketone **8**, 51 mg of 2,2-dimethyl-2,3,4,5,6,7-hexahydrobenzofuran was obtained after 8 h. The spectral data of this compound were identical with the compound obtained by independent synthesis described below.

Synthesis of 2,2-Dimethyl-2,3,4,5,6,7-hexahydrobenzofuran (22)

From ethyl 2-cyclohexanone acetate (23), the title compound was prepared as follows.

Preparation of Ethylene Ketal of 2-Cyclohexanoneacetate

A solution of ethyl 2-cyclohexanone acetate (3.68 g, 0.02 mol), ethylene glycol (1.24 g, 0.02 mol), and *p*-toluenesulfonic acid (20 mg) in 75 ml benzene was refluxed with a Dean Stark trap until no more water was collected. The reaction mixture was neutralized with sodium methoxide and worked-up with additional 75 ml benzene to give 4 g (89%) of the ketal: i.r. (neat) 927, 950, 1038, 1097, 1160, 1280, 1293, 1450, 1733; n.m.r. (CCl_4) δ 1.05–2.65 (14H, m, a triplet at 1.19, J = 7 Hz), 3.85 (4H, s), 4.5 (2H, q, J = 7 Hz), 3.85 (4H, s), 4.5 (2H, q, J = 7 Hz).

The Reaction of 2-Cyclohexanone Ethylene Ketal with Methylmagnesium Iodide

To a solution of methyl magnesium iodide (0.03 mol) in 40 ml anhydrous ether was added ketal ester (3.42 g, 0.015 mol) in 60 ml ether over a period of 30 min at room temperature. The mixture was refluxed for 1 h, decomposed with a saturated solution of ammonium chloride, and worked-up in the usual way to give 2.3 g (72%) of dimethyl carbinol: i.r. (neat) 912, 948, 1020, 1045, 1085, 1130, 1150, 1223, 1258, 1366, 1380, 1450, 1465, 3430 cm^{-1}; n.m.r. (CCl_4) δ 1–1.95 (17H, m, singlet at 1.1), 3 (1H, OH, disappeared with D_2O), 3.92 (4H, s).

Hydrolysis of the Ketal Alcohol

The ketal alcohol was dissolved in 50 ml acetone and 15 ml water containing 40 mg of *p*-toluenesulfonic acid. The solution was heated to reflux on an oil bath for 1 h. The mixture was cooled, excess acetone removed under reduced pressure and extracted with ether to give the hemiketal in equilibrium with some 2-(2′-methyl-2′-hydroxypropyl)cyclohexanone in 86% yield: i.r. (neat) 878, 948, 970, 1025, 1080, 1140, 1157, 1275, 1364, 1382, 1450, 1712 (weak), 3400 cm^{-1}; n.m.r. (CCl_4) δ 0.93–2.4 (17H, m, with a singlet at 1.33), 3.2–3.8 (1H, a broad multiplet.)

Preparation of 2,2-Dimethyl-2,3,4,5,6,7-hexahydrobenzofuran (22)

The hemiketal was heated to 130° and distilled to give 2,2-dimethylhexahydrobenzofuran with the elimination of water in quantitative yield, b.p. 80–82°/18 mm (lit. (24) b.p. 85°/15 mm); i.r. (neat) 785, 868, 907, 1086, 1143, 1193, 1220, 1235, 1270, 1298, 1369, 1380, 1450, 1711, 2840, 2930, 2970 cm^{-1}; n.m.r. (CCl_4) δ 1.28 (6H, s), 1.66 (4H, m), 1.93 (4H, m), 2.29 (2H, m).

Rearrangement of 2-Isopropylidenecyclopentanone Oxide (9)

A solution of ketone **9** (100 mg) in 10 ml benzene containing 50 mg of 95% sulfuric acid was stirred at room temperature for 15 min. The reaction was quenched with 4 ml of 10% sodium bicarbonate solution and worked-up using the usual procedure. The sole product from **9** was identified as 2,2-dimethylcyclohexane-1,3-dione (71%): i.r. (neat) 1000, 1028, 1132, 1285, 1315, 1380, 1463, 1695,

Can. J. Chem. Downloaded from www.nrcresearchpress.com by 210.87.254.40 on 09/05/12
For personal use only.

1725 cm^{-1}; n.m.r. (CCl_4) δ 1.21 (6H, s), 1.65–2.25 (2H, m), 2.43–2.83 (4H, m). This compound was synthesized independently (9). The spectra of the synthesized sample were identical with those of the sample obtained by acid catalysis of **9**.

Rearrangement of 2-Isopropylidenecyclohexanone Oxide (11)

The procedure described for the acid catalysis of **9** was followed and from 200 mg of epoxyketone 131 mg of 2,2-dimethylcyclopentane-1,3-dione was obtained as the sole product in 15 min: i.r. (CCl_4) 868, 950, 1100, 1313, 1380, 1447, 1462, 1702, 2860, and 2950 cm^{-1}; n.m.r. (CCl_4) δ 1.17 (6H, s), 1.6–2.05 (4H, m), 2.2–2.6 (4H, m). This compound was synthesized independently from dimethylation of cyclopentane-1,3-dione (9) and the spectra of the two samples were identical.

Rearrangement of 2-Cyclopentylidenecyclopentanone Oxide (12)

Following the procedure described for the acid catalysis of **9**, using 200 mg of **12** and 75 mg of 95% sulfuric acid in 20 ml benzene, 158 mg of the product **25** was obtained. The reaction was complete in 10 min: i.r. (neat) 1032, 1080, 1104, 1275, 1313, 1450, 1692, 1722, 2865, 2950 cm^{-1}; n.m.r. ($CDCl_3$) δ 2.62 (4H, t), 1.40–2.35 (10H, m). The spectral properties of this compound were identical with those described in the literature (1).

Rearrangement of 2-Ethylidenecyclohexanone Oxide (10)

Ketone **10** (150 mg) was dissolved in 15 ml benzene containing 60 mg of 95% sulfuric acid and the solution stirred at room temperature for 3 h. The mixture was extracted with an additional 30 ml benzene, and the extract washed with saturated aqueous sodium chloride solution until neutral. The benzene was removed under reduced pressure. The v.p.c. of the residual sample showed a multitude of peaks. A comparison of the i.r. and the n.m.r. spectra of the crude mixture with those of the products collected on v.p.c. indicated decomposition of the products on the column. Upon addition of 15 ml ether a white solid precipitated, m.p. 109–111° (23%). This was filtered off and recrystallized from a mixture of *n*-hexane and benzene.

The structure of this compound was identified as the condensation product **26** on the basis of its spectral properties: i.r. (KBr pellet) 790, 835, 930, 1006, 1032, 1093, 1170, 1195, 1253, 1385, 1450, 1712, 2860, 2940, 3480 cm^{-1}; n.m.r. ($CDCl_3$) δ 1.32 (6H, d, J = 6 Hz), 1.48–2.9 (16H, m), 5.3 (2H, quartet), 3.62 (2H, a broad singlet, disappeared with D_2O); *m/e* 298 (M^+), 280 ($M^+ - 18$), 262 ($M^+ - 36$).

We would like to thank the National Research Council of Canada for financial support of this work.

1. J. R. Williams, G. M. Sarkisian, J. Quigley, A. Hasiuk, and R. Vander-Vennen. J. Org. Chem. **39**, 1028 (1974).
2. C. J. Collins. Chem. Rev. **69**, 543 (1969). G. Karabatsos, N. Hsi, and S. Meyerson. J. Am. Chem. Soc. **92**, 621 (1970). R. A. Wohl. Chimia, **28**, 1 (1974).
3. F. A. Van-Catledge. J. Am. Chem. Soc. **95**, 1173 (1973).
4. W. C. Danen. J. Am. Chem. Soc. **94**, 4835 (1972).
5. W. G. Dauben and G. H. Berezin. J. Am. Chem. Soc. **85**, 468 (1963). D. H. Morr and J. B. Stothers. Can. J. Chem. **45**, 225 (1966).
6. J. M. Conia and P. Amice. C. R. Acad. Sci. Paris C, **271**, 1018 (1970).
7. J. M. Conia and P. Amice. Bull. Soc. Chim. Fr. 3327 (1968).
8. W. E. Harvey and D. S. Tarbell. J. Org. Chem. **32**, 1579 (1967).
9. S. Swaminathan, S. Ramachandran, and S. K. Sankarappa. Tetrahedron, **20**, 1119 (1964).
10. B. Eisert, F. Haupter, and K. Schank. Liebigs Ann. **665**, 55 (1963).
11. S. P. Pappas, R. M. Gresham, and M. J. Miller. J. Am. Chem. Soc. **92**, 5797 (1970).
12. C. V. Pittman, Jr. and G. A. Olah. J. Am. Chem. Soc. **87**, 2998 (1965); **87**, 5123 (1965).
13. N. C. Deno, H. G. Richey, Jr., J. S. Liu, J. D. Hodge, J. J. Houser, and M. J. Wisotsky. J. Am. Chem. Soc. **84**, 2016 (1962).
14. D. E. McGreer and J. W. McKinley. Can. J. Chem. **51**, 1487 (1973).
15. C. U. Pittman, Jr. and S. P. McManus. J. Am. Chem. Soc. **91**, 5915 (1969).
16. H. O. House and R. L. Wassan. J. Am. Chem. Soc. **78**, 4394 (1956).
17. M. Nojima, K. Hinoue, and N. Tokura. Bull. Chem. Soc. Jap. **43**, 827 (1970).
18. P. G. Khazanie and E. Lee-Ruff. Can. J. Chem. **51**, 3173 (1973).
19. H. G. Richey, Jr. and D. V. Kinsman. Tetrahedron Lett. 2505 (1969).
20. P. Khazanie. Ph.D. Thesis, York University. Toronto. 1974.
21. H. Wehrli, C. Lehman, P. Keller, J. J. Bonet, K. Schaffner, and O. Jeger. Helv. Chim. Acta, **49**, 2218 (1966).
22. L. Birkofer, S. M. Kim, and H. D. Engles. Chem. Ber. **95**, 1495 (1962).
23. A. Segre, R. Viterbo, and P. Parisi. J. Am. Chem. Soc. **79**, 3503 (1957).
24. L. H. Brannigan and P. S. Tarbell. J. Org. Chem. **35**, 639 (1970).

^{13}C Chemical Shifts of Quinolizidines. 2. ^{13}C Spectra of Some *Nuphar* Alkaloids[1]

ROBERT T. LALONDE, THOMAS N. DONVITO, AND AMY I-M. TSAI

Department of Chemistry, State University of New York, College of Environmental Science and Forestry, Syracuse, New York 13210

Received December 2, 1974

ROBERT T. LALONDE, THOMAS N. DONVITO, and AMY I-M. TSAI. Can. J. Chem. **53**, 1714 (1975).

The ^{13}C n.m.r. spectra of nine *Nuphar* alkaloids: deoxynupharidine, 7-epideoxynupharidine, nupharidine, 7-epinupharidine, nupharolutine, 7-epinupharolutine, thiobinupharidine, thionuphlutine B, and neothiobinupharidine, have been determined. Also examined were the spectra of five model compounds, 2,2,4,4-tetramethylthiolane, 3(a)-methyl-3(e)-methylthiomethylquinolizidine, 3(e)-methyl-3(a)-methylthiomethylquinolizidine, 3(e)-methylthio-3(a)-methylquinolizidine, and 3-methylfuran. This latter group of spectra were used to assist the chemical shift assignments of the *Nuphar* alkaloids. The most significant findings of this study are: (*i*) axial methyl and thiomethylene groups are shielded more than their equatorial counterparts in all cases; (*ii*) axial and equatorial hydroxyl groups substituted at C-7 of deoxynupharidine and 7-epideoxynupharidine give α-, β-, and γ-effects in ring B similar to those in carbocyclic systems but also produce small upfield shifts in ring A especially at the carbons α to nitrogen; (*iii*) the effect of a 3-furyl group located at C-4 appears to have nearly the same effect on quinolizidine ring carbons as a methyl group in the same position, the effects being shielding and deshielding at the various ring carbons; (*iv*) *N*-oxide formation results in α-, β-, γ-, and δ-shielding and deshielding effects consistent with the incorporation of an axial oxygen into a *trans*-fused system or the formation of a *cis*-fused quinolizidine *N*-oxide; and (*v*) methylene or methyl groups attached to C-2 and C-4 of a thiolane, including that in the skeleton of the C_{30} thiaspirane alkaloids, experience deshielding δ-effects.

ROBERT T. LALONDE, THOMAS N. DONVITO et AMY I-M. TSAI. Can. J. Chem. **53**, 1714 (1975).

On a déterminé les spectres r.m.n. ^{13}C de neuf alkaloides *Nuphar*: la déoxynupharidine, l'épi-7 déoxynupharidine, la nupharidine, l'épi-7 nupharidine, la nupharolutine, l'épi-7 nupharolutine, la thiobinupharidine, la thionuphlutine B et la néothiobinupharidine. On a aussi examiné les spectres de 5 composés modèles soit le tétraméthyl-2,2,4,4 thiolanne, la méthyl-3(a) méthyl-3(e) thiométhylquinolizidine, la méthyl-3(e) méthyl-3(a) thiométhylquinolizidine, la méthylthio-3(e) méthyl-3(a) quinolizidine et la méthyl-3 furanne. On a utilisé ce dernier groupe de spectres pour aider dans les attributions de déplacements chimiques des alkaloides du *Nuphar*. Les résultats les plus significatifs de cette étude sont: (*i*) que dans tous les cas les groupes méthyles axiaux et les groupes thiométhylènes sont plus blindés que leur contrepartie équatoriale; (*ii*) lorsque des groupes hydroxyles axiaux et équatoriaux sont attachés en position C-7 de la déoxynupharidine et de l'épi-7 déoxynupharidine, des effets α, β et γ sont obtenus dans le cycle B et ces derniers sont semblables à ceux observés dans des systèmes carbocycliques; ils produisent toutefois aussi de petits déplacements vers les hauts champs dans le cycle A particulièrement pour les carbones en position α de l'azote; (*iii*) il semble qu'un groupe furyl-3 situé en position C-4 a le même effet sur les carbones du cycle quinolizidine qu'un groupe méthyle dans la même position; les effets sont du blindage et du déblindage pour divers atomes de carbone du cycle; (*iv*) la formation d'un oxyde d'azote conduit à des effets de blindage et de déblindage α, β, γ et δ qui sont en accord avec l'incorporation d'un oxygène axial dans un système lié d'une façon *trans* ou à la formation d'une *N*-oxyde quinolizidine *cis*; et (*v*) les groupes méthylènes et méthyles attachés aux positions C-2 et C-4 d'un thiolanne, y compris ceux dans le squelette des alkaloides du thiaspirane en C_{30}, sont soumis à des effets de déblindage δ.

[Traduit par le journal]

Introduction

In a continuation of the study of the ^{13}C nuclear magnetic resonance spectra (c.m.r.) of quinolizidine systems (**1**), the spectra of nine *Nuphar* alkaloids have been determined. These include the six C_{15} alkaloids deoxynupharidine (DON) (**1**), 7-epideoxynupharidine (7-epiDON) (**2**), nupharidine (**3**), 7-epinupharidine (**4**), nupharolutine (**5**), and 7-epinupharolutine (**6**), and also the three C_{30} alkaloids thiobinupharidine

[1]Part 1, ref. 1.

Can. J. Chem. Downloaded from www.nrcresearchpress.com by 210.87.254.6 on 09/05/12
For personal use only.

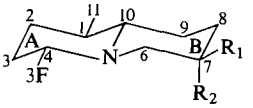

1 $R_1 = H; R_2 = \underset{12}{CH_3}$

2 $R_1 = \underset{12}{CH_3}; R_2 = H$

5 $R_1 = OH; R_2 = \underset{12}{CH_3}$

6 $R_1 = \underset{12}{CH_3}; R_2 = OH$

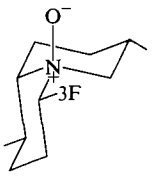

3

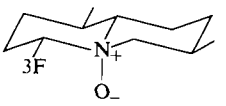

4

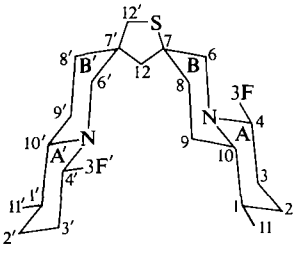

7

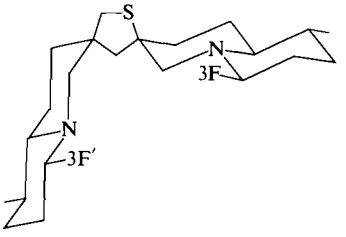

8

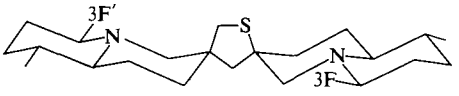

9

10

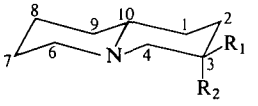

11 $R_2 = \underset{12}{CH_2}\underset{13}{SCH_3}; R_1 = \underset{11}{CH_3}$

12 $R_2 = \underset{11}{CH_3}; R_1 = \underset{12}{CH_2}\underset{13}{SCH_3}$

13 $R_2 = \underset{11}{CH_3}; R_1 = \underset{12}{SCH_3}$

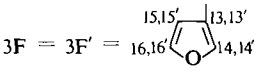

(TBN) (**7**), thionuphlutine B (TN-B) (**8**), and neothiobinupharidine (NTBN) (**9**). The c.m.r. of the five model compounds 2,2,4,4-tetramethylthiolane (**10**), 3(e)-methyl-3(a)-methylthiomethylquinolizidine (**11**)[2], 3(a)-methyl-3(e)-methylthiomethylquinolizidine (**12**), 3(e)-methylthio-3(a)-methylquinolizidine (**13**), and 3-methylfuran were also determined to assist in the chemical shift assignments of the above-mentioned *Nuphar* alkaloids. The c.m.r. of other naturally occurring and synthetic quinolizidine derivatives have been reported (3), however this is the first report of the c.m.r. of *Nuphar* alkaloids, a group of *trans*-fused quinolizidines whose conformational rigidity is enhanced principally by the C-4 located 3-furyl, the strong equatorial preference (4) of which confines the A-ring to one chair form and thereby furnishes a quinolizidine system somewhat simplified for the study of n.m.r. properties. Thus the *Nuphar* alkaloids were studied to obtain information helpful in future structure studies of not only this one class of alkaloids but other quinolizidine systems as well.

[2]The letters e and a refer to equatorial and axial and are applicable here because the quinolizidine system is *trans*-fused (2). This nomenclature is used for purposes of clarity instead of the *t* and *c* nomenclature method used previously (1, 2).

Experimental

Spectra

The spectra were obtained as follows: p.m.r. with Varian A-60A and XL-100-15 spectrometers using $CDCl_3$ solutions; i.r. with a Perkin-Elmer 137, neat; mass with a Hitachi-Perkin-Elmer RMU6E using an all-glass heated inlet system at 200° and 70 eV; c.m.r. with a Varian

Can. J. Chem. Downloaded from www.nrcresearchpress.com by 210.87.254.6 on 09/05/12
For personal use only.

Can. J. Chem. Downloaded from www.nrcresearchpress.com by 210.87.254.6 on 09/05/12
For personal use only.

TABLE 1. ^{13}C chemical shifts and splitting of the C-15 alkaloids and the sulfur-containing model compounds[a,b]

Carbon No.	Compound									
	1	**2**	**3**	**4**	**5**	**6**	**10**	**11**	**12**	**13**
1	35.72 (d)	36.50 (d)	29.78 (d)	30.45 (d)	35.11 (d)	36.86[c](d)		29.82 (t)	29.84 (t)	30.28 (t)
2	33.98 (t)	34.13[c](t)	32.31 (t)	33.36 (t)	33.78 (t)	33.52 (t)	53.52 (s)	35.17[c](t)	35.70 (t)	36.15 (t)
3	34.96 (t)	35.17 (t)	26.67 (t)	28.54 (t)	34.43 (t)	35.27 (t)	59.36 (t)	35.20[c](s)	35.70 (s)	43.06 (s)
4	60.33 (d)	61.14 (d)	74.00 (d)	72.56 (d)	59.87 (d)	59.67 (d)	45.89 (s)	66.71 (t)	66.69 (t)	66.59 (t)
5							47.34 (t)			
6	58.19 (t)	61.47 (t)	57.85 (t)	72.16 (t)	63.45 (t)	63.57 (t)	33.74 (q)	56.69 (t)	57.02 (t)	56.62 (t)
7	28.66 (d)	31.19 (d)	25.41 (d)	25.86 (d)	69.48 (s)	67.11 (s)	29.00 (q)	26.04 (t)	26.01 (t)	25.85 (t)
8	30.56 (t)	33.71[c](t)	25.50 (t)	32.49 (t)	38.55 (t)	36.94[c](t)		24.83 (t)	24.82 (t)	24.67 (t)
9	25.74 (t)	30.34 (t)	20.57 (t)	24.30 (t)	28.21 (t)	26.87 (t)		33.24 (t)	33.19 (t)	32.99 (t)
10	69.75 (d)	69.54 (d)	79.41 (d)	79.03 (d)	68.51 (d)	68.07 (d)		62.98 (d)	63.32 (d)	64.90 (d)
11	19.07 (q)	19.26 (q)	18.60 (q)	18.72[d](q)	19.30 (q)	19.15 (q)		26.64 (q)	22.51 (q)	23.45 (q)
12	17.57 (q)	20.13 (q)	18.30 (q)	18.72[d](q)	25.48 (q)	26.26 (q)		43.38 (t)	49.41 (t)	9.89 (q)
13	130.40 (s)	129.47 (s)	119.51 (s)	117.09 (s)	129.65 (s)	129.11 (s)		17.68 (q)	18.29 (t)	
14	139.64 (d)	139.92 (d)	141.91 (d)	142.51 (d)	139.68 (d)	139.70 (d)				
15	109.93 (d)	109.94 (d)	111.53 (d)	112.24 (d)	109.64 (d)	109.29 (d)				
16	143.08 (d)	143.19 (d)	143.23 (d)	143.08 (d)	143.25 (d)	143.67 (d)				

[a]In p.p.m. from TMS.
[b]s = singlet; d = doublet; t = triplet; q = quartet.
[c]Assignments may be reversed.
[d]Single peak due to two carbons.

Can. J. Chem. Downloaded from www.nrcresearchpress.com by 210.87.254.6 on 09/05/12
For personal use only.

XL-100-15 operating in the FT mode at 25.16 MHz and ambient temperature. Solutions for c.m.r. were 0.3–0.5 *M* in $CDCl_3$ containing 1% TMS (δ 0.00 p.p.m.) in 12 mm tubes. Field/frequency lock was established on the deuterium resonance of $CDCl_3$. Between 1 and 10K transients were used for fully decoupled spectra and nearly four times that number for off resonance decoupled spectra. Single frequency decoupling (s.f.d.) experiments were carried out with the decoupler in the low power mode (about 110 dB) and adjusted to the resonance frequency of the individual proton to determine the decoupled carbon signal. Chemical shifts are accurate to ±0.1 p.p.m.

Analyses

The g.l.c. were carried out on a Varian-Aerograph 200 chromatograph using a stainless steel 5 ft × 0.25 in. column containing 20% SE-30 on Chromosorb W, 60–80 mesh at 98°. Retention times (R_t) are given in minutes.

The elemental analysis was performed by Galbraith Laboratories, Knoxville, Tennessee.

Materials

Compounds **11** and **12** were prepared as previously reported (5). The preparation and isolation of the deuterium labeled and unlabeled *Nuphar* alkaloids **1–9** (6–12) and **7-6-d_1** have been previously reported. Some samples were obtained by the transformation of the more abundant *Nuphar* alkaloids. In these cases the identity of the synthetic sample was established by physical and spectral evidence. The synthesis of 3(e)-methylthio-3(a)-methylquinolizidine (**13**) has been accomplished in this laboratory and will be reported in a future publication.

2,2,4,4-Tetramethylthiolane (10)

A 100 g sample of 2,2,4,4-tetramethyltetrahydrofuran, used as obtained from Eastman Organic Chemicals, was dissolved in 75 ml of benzene and the resulting solution was heated to reflux and stirred vigorously for 16 h with 64 g of phosphorus pentasulfide in a manner similar to a previously reported procedure for preparing 2,4-dimethylthiazole (13). The liquid was decanted from the red solid, filtered, concentrated on a rotary evaporator, and refiltered. Gas–liquid chromatography of the filtrate showed three major and several minor components. Distillation gave a 45 g mixture of the three major components in a ratio of 29:52:19 by g.l.c. with retention times of 3.2, 4.8, and 5.9 respectively. Separation by spinning band distillation gave three components each having *m/e* 144 (M^+). Fraction 1 (R_t 3.2) contained a double bond by p.m.r. and i.r. but was not further characterized. The major fraction was 2,2,5,5-tetramethylthiolane: g.l.c. R_t 4.8; b.p. 41–43°/13.6 mm (lit. (14) b.p. 56°/25 mm); p.m.r. δ 1.43 (s, 12H, CH_3), 1.96 (s, 4H, CH_2) (lit. (15) 1.41, 1.91, CCl_4); c.m.r. δ 55.10 (q, CH_3), 44.89 (t, C-3) 32.69 (s, C-2); i.r. 3.39, 3.43, 6.88, 7.33, 8.82 μ; mass spectrum, *m/e* (relative intensity) 144 (M^+, 30), 129(100), 95(50), 75(36), 59(24), 55(25), 41(27).

The third fraction was **10**: g.l.c., R_t 5.9; b.p. 49–50°/13.9 mm; p.m.r. δ 1.23 (s, 6H, C-7), 1.49 (s, 6H, C-6), 1.71 (s, 2H, C-3), 2.77 (s, 2H, C-5); i.r. 3.39, 3.48, 6.90, 7.23, 7.37, 8.87, 8.96 μ; mass spectrum, *m/e* (relative intensity) 144 (M^+, 33), 129(100), 95(18), 59(28), 55(53), 41(33).

Anal. Calcd. for $C_8H_{16}S$: C, 66.60; H, 11.18. Found: C, 66.48; H, 10.98.

3-Methylfuran

The method of Gilman and Burtner (16) was employed to prepare 3-methylfuran: c.m.r. δ 9.60 (q, CH_3), 112.50 (d, C-4), 120.13 (s, C-3), 139.63 (d, C-2), 143.06 (d, C-5), s.f.d. was employed to make the assignments of the doublets.

Assignments and Results

The resonance assignments were assisted by off-resonance decoupling, single frequency decoupling (s.f.d.), and our earlier c.m.r. study of the isomeric methylquinolizidines (1). The values and assignments of the chemical shifts of the C_{15} alkaloids and the model compounds are presented in Table 1 and those of the C_{30} alkaloids in Table 2. A comparison of the shift positions of the alkaloids and the model compounds is made in Fig. 1.

The reporting of assignments and results will begin with a treatment of the C_{15} amines and *N*-oxides. Thereafter the sulfur-containing model compounds will be dealt with and finally the sulfur-containing C_{30} alkaloids will be treated.

C_{15} Amines and N-Oxides

The off-resonance proton decoupled spectra of DON (**1**), 7-epiDON (**2**), nupharidine (**3**), and 7-epinupharidine (**4**) show two quartets, five triplets, seven doublets, and one singlet which fall in three distinct regions, 15–40, 55–80, and 110–145 p.p.m. The singlet obviously results from C-13, the only quaternary carbon in these molecules. The signals of nupharolutine, **5**, and 7-epinupharolutine, **6**, fall in the same three regions and show the same splittings as those above except in both cases one doublet is replaced by a singlet. This new singlet is assigned to C-7 which, as expected and shown in Fig. 1, is greatly deshielded relative to DON and 7-epiDON as a result of equatorial or axial α-hydroxyl substitution.

In the case of DON, the quartet at 19.07 p.p.m. is assigned to C-11 and that at 17.57 p.p.m. to C-12. These DON quartet assignments are consistent with finding the two 7-epiDON equatorial methyls at 19.26 and 20.13 p.p.m. The more shielded of the two quartets exhibited by both **5** and **6** correlates with the position of C-11 in the spectra of DON and 7-epiDON, and is assigned accordingly, whereas the second quartet is deshielded in both cases because of β-hydroxyl substitution and therefore is assigned to C-12.

TABLE 2. ^{13}C chemical shifts and splittings of the C_{30} alkaloids [a,b]

Carbon No.	Compound		
	NTBN(9)	TBN (7)	TN-B (8)
1,1′	35.57[d],36.15[d] (d,d)	36.30 (d,d)[e]	35.91[d],36,07[d,f]
2,2′	33.77[c] (t)	33.82[c] (t,t)	33.74[c] (t)
3,3′	34.93,35.80[d] (t,t)	35.31[c] (t,t)[e]	35.55[d],36.42[d]
4,4′	60.24[c] (d)	59.92,60.15 (d,d)	60.09[c] (d)
6	65.26 (t)	65.97 (t)	64.13,64.33[g] (t,t)
6′	63.05 (t)	63.41 (t)	64.13,64.33[g] (t,t)
7	57.08 (s)	57.04 (s)	59.56 (s)
7′	47.33 (s)	49.20 (s)	46.74 (s)
8	40.78 (t)	39.64 (t)	39.30
8′	36.52[d] (t)	37.46 (t)	37.78
9,9′	28.16,29.45 (t,t)	28.84,29.46 (t,t)	28.42,29.11 (t,t)
10,10′	68.63,69.29 (d,d)	68.87,69.87 (d,d)	69.02,69.41 (d,d)
11,11′	19.12[c] (q)	19.20[c] (q)	19.20[c] (q)
12	54.54 (t)	45.26 (t)	50.59 (t)
12′	39.14 (t)	42.69 (t)	42.77 (t)
13,13′	129.96,130.06 (s,s)	131.10[c] (s)	128.71[c] (s)
14,14′	139.51,139.65 (d,d)	140.09,139.94 (d,d)	139.50[c] (d)
15,15′	109.65,110.33 (d,d)	109.87,109.95 (d,d)	109.26,110.04 (d,d)
16,16′	142.93,143.31 (d,d)	143.09[c] (d)	142.97,143.38 (d,d)

[a]In p.p.m. from TMS.
[b]s = singlet, d = doublet, t = triplet, q = quartet.
[c]Single peak due to two carbons.
[d]These four peaks may be interchanged; most likely assignment is given.
[e]May be (d,t).
[f]At least one of these is (d).
[g]One of these values can be assigned to C-6, the other to C-6′.

The most deshielded DON triplet is assigned to C-6 since C-6 is α to nitrogen. Of the four remaining triplets, C-2 (33.98 p.p.m.) and C-8 (30.56 p.p.m.) can be assigned by direct comparison with the corresponding carbons in 1(e)- and 3(a)-methylquinolizidine.[3] The triplet at 34.96 p.p.m. is assigned to C-3 because this is the signal closest to the 35.45 p.p.m. resonance of C-3 in 4(e)-methylquinolizidine. The chemical shift of C-9 in 1(e),7(a)-dimethylquinolizidine, estimated by the method (1) of calculating methyl decalin chemical shifts and adjusting for the presence of nitrogen, is 26.15 p.p.m. Because the 3-furyl group will have little effect on C-9, the DON triplet at 25.74 p.p.m. is assigned to this carbon.

Three of the seven DON doublets are much more deshielded than the rest and of these three the two most deshielded ones are assigned to C-14 and -16, the carbons next to oxygen in the furan ring. The correspondence of chemical shift values with those of the same two carbons in 3-methylfuran[4] is good. The most shielded furan doublet is assigned to C-15, the chemical shift of which is moved upfield by 2.6 p.p.m. relative to C-4 in 3-methylfuran. However the shielding of C-15 in DON is reasonable if the furan ring assumes a conformation in which the C-14 and -4 protons are eclipsed. C-15 is then γ-gauche to both C-3 and nitrogen. Such a conformation of the 3-furyl group is observed for deoxynupharidine hydrobromide in the crystalline state (17).

Of the remaining four DON doublets the two most deshielded ones are assigned to the carbons α to nitrogen. Thus, C-10 and -4 are assigned to 69.75 and 60.30 p.p.m., respectively, based on the shift positions of C-10 in 1(e)-methylquinolizidine and C-4 in 4(e)-methylquinolizidine (1). Further support for the assignment of these doublets will be given in the discussion of the single frequency decoupled spectrum of NTBN. The remaining two DON doublets at 35.72 and 28.66 p.p.m. are assigned

[3]Our earlier study showed that the presence of a methyl substituent on the quinolizidine system had little effect on the carbons more distant than two bonds away unless γ-gauche interactions resulted (1). This finding makes it possible to use the methylquinolizidine shift data to assist the assignments of some of the *Nuphar* alkaloid signals notwithstanding the presence of two methyl groups in the alkaloids.

[4]See the Experimental section for the chemical shift values of 3-methylfuran.

Can. J. Chem. Downloaded from www.nrcresearchpress.com by 210.87.254.6 on 09/05/12
For personal use only.

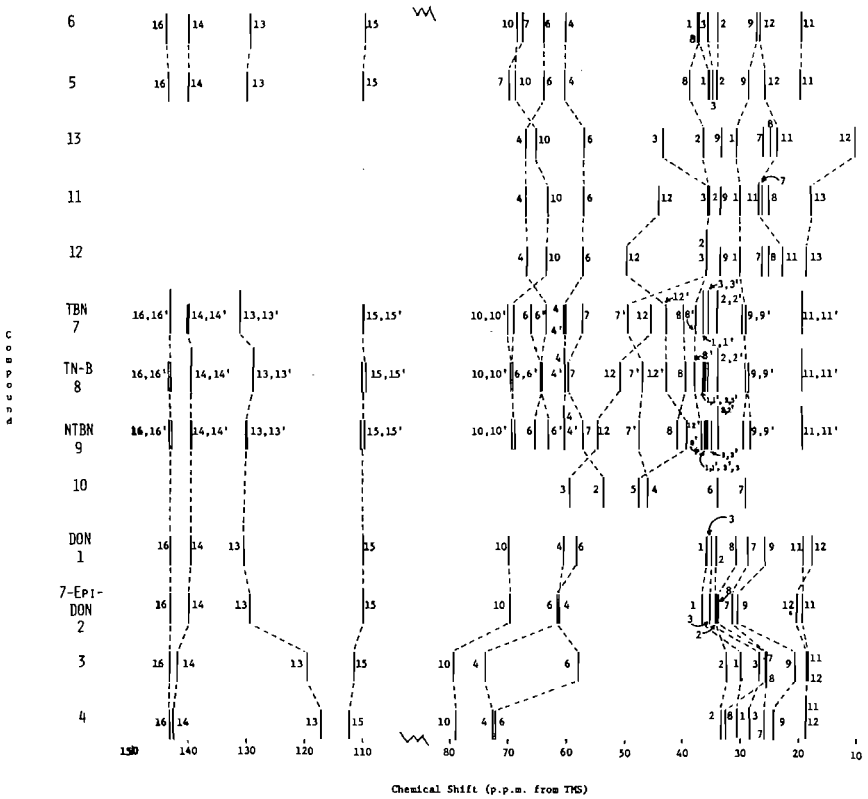

FIG. 1. Chemical shift correlation of some C_{15} and C_{30} *Nuphar* alkaloids.

to C-1 and -7, respectively, based on chemical shift agreement with the corresponding carbons in 1(e)- and 3(a)-methylquinolizidine (1).

As expected the resonances of the five ring-A carbons, including C-10, are nearly the same in the spectra of DON (**1**), 7-epiDON (**2**), nupharolutine (**5**), and 7-epinupharolutine (**6**). The assignments of the five carbons constitute consistent sets, the largest variations in which will be considered in the discussion section. However, because the C-7 methyl group is equatorial in 7-epiDON, the resonances of ring-B carbons 6, 7, 8, and 9 as well as the 7(e)-methyl (C-12) are deshielded relative to DON by amounts consistent with the observed differences between 3(e)- and 3(a)-methylquinolizidine. Of the 7-epiDON peaks at 33.71, 34.13, and 35.17 p.p.m., the first or second may be assigned to C-8 and the remaining two to C-2 and -3, the most likely assignments being shown in Table 1. As for the ring-B carbons in **5** and **6**, the assignment of C-7 has already been treated above; the assignments of the remaining carbons are made with the assistance of those for DON and 7-epiDON and known β- and γ-hydroxyl substituent effects (18). Thus replacement of the C-7 hydrogen of 7-epiDON by an axial hydroxyl results in the deshielding of C-6 and -8 by the amounts given in Table 3, amounts slightly less than half of those observed in the replacement of the C-7 hydrogen by an equatorial hydroxyl in DON. The γ-gauche effect of the axial hydroxyl in **6** shields C-9 relative to 7-epiDON. In contrast the antiperiplanar effect of the equatorial tertiary hydroxyl in **5** deshields C-9 relative to DON. This deshielding is consistent with that observed in 1-substituted adamantanes (19) but is opposite to the γ-effect caused by substituting an equatorial heteroatom at a secondary carbon (20).

Because 7-epinupharidine is *trans*-fused[5] the *N*-oxide oxygen is axial in both A- and B-rings. Therefore shielding of all the carbons γ to the

[5]R. Parthasarathy, R. T. LaLonde, and A. I-M. Tsai, unpublished results.

Can. J. Chem. Downloaded from www.nrcresearchpress.com by 210.87.254.6 on 09/05/12
For personal use only.

TABLE 3. Changes[a,b] in A- and B-ring and methyl ^{13}C chemical shifts generated by substituting a hydroxyl at C-7 in deoxynupharidine[c] and 7-epideoxynupharidine[d]

Carbon *i*	Ring location and position[e] of carbon *i*	$\Delta\delta_C{}^7$(eq)OH[f]	$\Delta\delta_C{}^7$(ax)OH[g]
1	A	−0.61	+0.36
2	A	−0.20	−0.61
3	A	−0.53	+0.10
4	A, δ	−0.46	−1.47
6	B, β	+5.26	+2.10
7	B, α	+40.82	+35.92
8	B, β	+7.99	+3.23
9	B, γ	+2.47	−3.47
10	A, B, δ	−1.24	−1.47
11	A	+0.23	−0.11
12	B, β	+7.91	+6.13

[a]In p.p.m.
[b]Positive values indicate deshielding.
[c]DON.
[d]7-epiDON.
[e]Relative to C-7 but not more than three bonds removed.
[f]$\Delta\delta_C{}^{7(e)OH} = \delta_C{}^i$ nupharolutine $- \delta_C{}^i$ DON.
[g]$\Delta\delta_C{}^{7(a)OH} = \delta_C{}^i$ 7-epinupharolutine $- \delta_C{}^i$ 7-epiDON.

new oxygen occurs. Thus C-1, -3, -7, -9, and -13 are shielded by 6.05, 6.64, 5.33, 6.04, and 12.38 p.p.m., respectively, relative to 7-epiDON. The 7-epinupharidine triplets due to C-2 and -8 and the intensity enhanced quartet due to the two equatorial methyl groups occur close to the corresponding signals exhibited by 7-epiDON and are assigned accordingly.

Three 7-epinupharidine peaks, one triplet and two doublets, are assigned to the carbons α to nitrogen. Relative to 7-epiDON, these signals are deshielded because of the β axial substituent, oxygen, and the positive charge on nitrogen. The triplet is assigned to C-6, the only methylene adjacent to nitrogen. The doublets at 72.56 and 79.03 p.p.m. are assigned to C-4 and -10, respectively, because C-4 always occurs upfield from C-10 in DON and 7-epiDON as well as in the C_{30} *Nuphar* alkaloids, discussed below.

As for the *cis*-fused nupharidine (**3**) (21), the resonances of ring-A C-1, -4, -10 (doublets), C-2 and -3 (triplets) and C-11 (quartet), occur close to the chemical shifts of the same carbons in 7-epinupharidine (**4**). The C-12 quartet also occurs very close to the corresponding methyl quartet of **4** because these methyls have the same substitution pattern and a similar stereochemical environment. The same is true for the C-7 doublet. The only triplet in the region occupied by carbons α to nitrogen is assigned to C-6. The remaining two triplets are from C-8 and -9, shifted upfield from their positions in 7-epinupharidine. C-8 undergoes a γ-gauche interaction with C-1 whereas C-9 feels a β-axial effect from C-1 instead of the β-equatorial effect experienced by the same carbon in 7-epinupharidine.

Sulfur-containing Model Compounds

The off-resonance proton decoupled spectrum of 2,2,4,4-tetramethylthiolane (**10**) shows two quartets, each due to two carbons, two triplets, and two singlets. The C-2 methyl protons are differentiated from those at C-4 by their lower chemical shift which follows from analogy with 2,2,4,4-tetramethyloxolane (22). As a result, an s.f.d. experiment allows the assignment of the 33.74 p.p.m. quartet to the C-2 methyls. This chemical shift value is close to the 32.69 p.p.m. methyl resonance of 2,2,5,5-tetramethylthiolane. The remaining quartet at 29.00 is assigned to the C-4 methyls. Similarly the C-3 and -5 hydrogens are clearly differentiated by chemical shift differences of their proton resonances. Therefore, of the two c.m.r. triplets, that at 59.36 p.p.m. is assigned to C-3 because it collapses to a singlet when the protons on C-3 are irradiated. Irradiation of the C-5 protons collapses the 47.34 p.p.m. triplet. The singlets at 53.52 and 45.84 p.p.m. are assigned to C-2 and

Can. J. Chem. Downloaded from www.nrcresearchpress.com by 210.87.254.6 on 09/05/12
For personal use only.

Can. J. Chem. Downloaded from www.nrcresearchpress.com by 210.87.254.6 on 09/05/12
For personal use only.

C-4, respectively, because the chemical shift of the former agrees with that of C-2 of 2,2,5,5-tetramethylthiolane found at 55.10 p.p.m.

The ring carbons in **10** are deshielded 28.2 to 14.7 p.p.m. relative to those reported for thiolane (23). The direction and magnitudes of these shifts are reasonable considering the methyl cyclopentane parameters of Roberts and coworkers (24).

The off-resonance proton decoupled spectrum of 3(e)-methyl-3(a)-methylthiomethylquinolizidine (**12**) shows two quartets, eight triplets, one doublet, and one singlet which is nearly coincidental with one of the triplets. The assignment of the doublet is obvious since each stereoisomer contains a single methine (C-10). The resonances of C-6, -7, -8, and -9 in **11** and **12** are assigned by assuming that they resonate close to the corresponding carbons of quinolizidine. The CH_2—S resonance of **11** is at 43.38 p.p.m. based on s.f.d. C-2 and -3 are assigned to the peaks at 35.17 and 35.20 p.p.m. on the expectation of the effects α and β substitution will have on quinolizidine. γ-Axial shielding puts the C-1 resonance at 29.82 p.p.m., upfield from C-1 of quinolizidine (33.62 p.p.m.) and near the C-1 resonance (28.50 p.p.m.) of 3(a)-methylquinolizidine. Of the two quartets, the one at lower field (26.64 p.p.m.) is assigned to the axial methyl since it has greater β substitution. The methyl attached to sulfur has no substituents closer than three bonds away and accordingly is assigned to the higher field quartet at 17.68 p.p.m.

The only significant spectral differences between **11** and **12** are those expected on the basis of the stereochemical differences; the thiomethylene is deshielded and the C-3 methyl group is shielded in the latter compound. The different chemical shift of the C-3 methyls and the nearly identical chemical shift of the methylthio methyls adds support to the assignment of all the quartets.

The off-resonance proton decoupled spectrum of **13**, relative to that of **11** and **12**, contains one less triplet due to the replacement of the methylthiomethylene by a methylthio group. Two additional features distinguish the spectrum of **13** from that of **11** and **12**. One is the low field position of C-3, caused by the directly attached sulfur. The other is the appearance of the thiomethyl group at 9.89 p.p.m., a position considerably higher than that exhibited by the same group in **11** and **12**. This observation seems to indicate a γ-gauche interaction of the C-3 axial methyl with the C-3 thiomethyl.

The C_{30} Alkaloids

The C_{30} alkaloids include two DON or 7-epiDON moieties joined at C-7 and the C-7 methyl directly and through sulfur. Appropriately, the three C_{30} alkaloids examined gave spectra very similar to the C_{15} alkaloid, DON, with the following exceptions: the C-7 doublet of DON becomes a pair of widely separated singlets displaced downfield in the spectra of the C_{30} alkaloids; the peak due to the C-7 methyl group is absent and two new methylene resonances appear; each of the other peaks in DON appears as a pair of closely spaced or coincidental peaks and each of the ring B (or B′) carbons resonate downfield from those of DON. The resonance assignments are treated below.

The furan ring and methyl carbon signals of the three alkaloids appear close to the chemical shifts of the corresponding carbons in DON and 7-epiDON. The assignments are made accordingly. Each of the alkaloids gives two triplets and three or four apparent doublets in the region characteristic of carbon α to nitrogen. However the display of three apparent doublets by TN-B and NTBN really represents two distinguishable doublets plus an additional coincidental pair of doublets as indicated by signal intensity. In the case of NTBN, the two coincidental doublets at 60.24 p.p.m. are assigned to C-4 and -4′ on the basis of s.f.d., the result of which also supports the assignment of the C-4 resonance of DON and 7-epiDON (*vide ultra*). C-10 and -10′ doublets at 68.63 and 69.29 p.p.m. are assigned by elimination. C-10, -10′, -4, and -4′ in TBN and TN-B then are assigned by chemical shift matching with NTBN. The triplets in the same region are assigned to C-6 and -6′, an assignment supported in the case of TBN by the disappearance of the 65.97 p.p.m. triplet in the spectrum of TBN-*6*-d_1. Disappearance of this signal is attributed to the reduction of nuclear Overhauser enhancement and development of unperturbed carbon–deuterium coupling (3*c*).

Each of the alkaloids gives a pair of singlets in the 47–57 p.p.m. region. The one further downfield in each case is less intense and is assigned to the quaternary carbon (C-7) adjacent

Can. J. Chem. Downloaded from www.nrcresearchpress.com by 210.87.254.6 on 09/05/12
For personal use only.

to sulfur, as in the case of **10** (*vide ultra*). The remaining higher field singlet is assigned to C-7′. These assignments are supported by observing the disappearance of the less intense singlet in the spectrum of TBN-*6*-d_1. The loss of the C-7 signal is attributed to the lengthening of the relaxation time of C-7 as hydrogen on C-6 is replaced by deuterium. A similar observation has been made for deuterium derivatives of phenanthrene (**25**). Interestingly, the deshieldings of C-7 relative to C-3 in **13**, and C-7′ relative to C-3 in **11** and **12**, are consistent with the shift observed for a quaternary ring carbon upon making it the spiro carbon in a spiro[5.4]alkane (**26**).

The only remaining nontriplet signals needing attention are the C-1 and -1′ doublets which in the case of TBN are coincident at 36.30 p.p.m., a chemical shift agreeing well with that of C-1 in DON. C-1 and -1′ are separate doublets appearing in the 35.5–36.2 p.p.m. region of the spectra of TN-B and NTBN. Their exact position cannot be located with certainty because some C-3 and -3′ signals occur within the same narrow region.

The remaining peaks are all triplets. The spectrum of each of the three alkaloids shows four triplets in a region (36–55 p.p.m.) completely devoid of peaks in the spectra of the C-15 compounds. Through s.f.d. of the thiomethylene protons of NTBN, the 39.14 p p.m. triplet is assigned to C-12′ and, by another similar decoupling, the 54.54 p.p.m. triplet is assigned to C-12. The triplets at 45.26 and 42.69 p.p.m. in the spectrum of TBN are assigned to C-12 and -12′, respectively, because C-12 is expected to become shielded and C-12′ deshielded as a result of the change in the stereochemistry of these carbons relative to the quinolizidine rings. The 50.59 p.p.m. triplet given by TN-B is assigned to C-12 since this chemical shift is between that of C-12 in the spectra of TBN and NTBN. Thus the C-12 assignments are consistent with the number of axial and equatorial interactions in which C-12 is involved. The 42.77 p.p.m. triplet given by TN-B is assigned to C-12′ since the chemical shift agrees well with that of C-12′ in TBN and both methylenes are axial in the A′B′ quinolizidines.

The second pair of triplets which appears in the 36–55 p.p.m. region is assigned to C-8 and -8′. C-8 is assigned the lower field position in each case for two reasons. First, the methyl groups substituted at the α position in model thiolane **10** appear at lower field than those attached to the β′ position. C-8 and -8′ methylenes are in the same relation to the thiolane ring as the two kinds of methyl groups are in **10**. Secondly, sulfur and C-6 and -8 are similarly juxtaposed as are sulfur and C-6′ and -8′. Since the spectrum of TBN-*6*-d_1 puts C-6 at lower field than C-6′, the analogy is extended to C-8 and -8′. The latter two are shifted downfield from the corresponding carbon (C-2) in **11**, **12**, and **13**. The deshieldings are consistent with the δ-effect on methyl carbon in 1,1,3,3-tetramethylcyclohexane (27) but more closely analogous to the δ-effect on the corresponding methylene carbons in dispiro[5.1.5.2]pentadecane (26).

The two triplets furthest upfield are assigned to C-9 and -9′ because they appear close to the chemical shift of C-1 in **11** and only 2 p.p.m. upfield from C-9 of 7-epiDON. The remaining triplets are assigned to C-2, -2′, -3, and -3′ on the basis of chemical shift correspondence with the same carbons in DON and 7-epiDON.

Discussion

The most significant observations made in this study are: the chemical shift differences of methyl and thiomethylene groups as a function of conformation; the effect of the equatorial 3-furyl group on the chemical shift of quinolizidine ring carbons; the effect of *N*-oxide formation; the effect of C-7 hydroxyl group incorporation; and the δ-effect on some quinolizidine methylene groups. The last two topics have already been discussed briefly in connection with the assignments and will not be treated further. The first four topics will be discussed below in the order just given, but before doing so, a brief comment will be made regarding the general spectral appearance related to gross symmetry characteristics of the C_{30} alkaloids.

TBN and NTBN appear to have pseudo C_2 symmetry whereas TN-B does not. Therefore, relative to TN-B, TBN, and NTBN might be expected to show greater numbers of coincidental or nearly coincidental signals arising from the near equivalence of carbons, especially those furthest removed from the pseudo twofold axis of symmetry. That such is not the case is likely due to preferred conformations of two quinolizidine moieties twisted about the spiro carbons of the thiolane ring, a factor which would enhance the intrinsic shielding difference due to nonequivalence. It is true that the shielding non-

Can. J. Chem. Downloaded from www.nrcresearchpress.com by 210.87.254.6 on 09/05/12
For personal use only.

equivalence of carbon is manifest differently by rings B and B′ on the one hand and A and A′ on the other, but in the direction opposite to what might be expected on the basis of apparent symmetry alone. Thus Fig. 1 will show that both C-6, -6′ and C-8, -8′ are more widely separated in the two C_{30} alkaloids possessing pseudo C_2 symmetry than they are in the less symmetrical structure, TN-B. Therefore it appears that the microscopic electronic effects and steric interactions are much more important than symmetry in influencing overall spectral appearance.

The axial C-7 methyl of DON appears upfield from the equatorial counterpart in 7-epiDON, a relation reversed from that of the p.m.r. where the axial methyl protons are deshielded relative to the equatorial ones (5, 7, 10, 11). However the 2.56 p.p.m. increment in the c.m.r. is somewhat greater than the 1.51 p.p.m. shift difference for the methyl groups in 3(e)- and 3(a)-methylquinolizidine (1). Indeed there appears to be no regular increment between equatorial and axial methyls in any of the 1-, 2-, and 3-methylquinolizidine pairs (1).[6] Thus the equatorial–axial shift observed for the C-7 methyl group in DON and 7-epiDON is in the right direction but the magnitude of the shift is inexplicable.

The thiomethylene and methylene carbons of **11**, **12**, and the C_{30} alkaloids follow the equatorial–axial shift relation observed for the C-7 methyl of DON and 7-epiDON as well as that reported for the exocyclic methylene of the epimeric lupinine benzoates (3*b*). The C-12 and 12′ resonances are shielded in direct relation to the number of axial interactions in which these carbons are involved. One of the major problems associated with the structure determination of the C_{30} thiaspirane alkaloids was the configuration of C-7 and -7′, the full solution of which was not obtainable from the p.m.r. studies but as illustrated here, is readily achieved from the c.m.r. examination of the C-12 and -12′ carbons.

Also noteworthy is the shielding of C-12 and -12′ in the C_{30} alkaloids relative to the corresponding carbons, C-3 and -5, respectively, in the tetramethylthiolane **10**. This result is attributed to the increased steric compression of C-12 and -12′ caused by replacing the methyl groups of **10** by the quinolizidine moieties.

One way to ascertain the effect of the 4(e)-(3-furyl) group on quinolizidine carbons is to calculate the chemical shift values for 1(e), 7(e)-, and 1(e),7(a)-dimethylquinolizidine, using Grant's hydrocarbon parameters (28) and our CH to N parameters (1), and then to compare these values, by difference, with those observed for each of the corresponding carbons in DON and 7-epiDON. The result of such a comparison is given in Table 4 which demonstrates that the effect of the 3-furyl group is to shift corresponding carbons in DON and 7-epiDON in the same direction within 1 p.p.m.[7] The extent and direction of the shift resulting from the presence of the 4(e)-(3-furyl) group is nearly the same as that observed from the substitution of an equatorial methyl group at the same position (1, 29).

The effect of changing a quinolizidine to a quinolizidine *N*-oxide, without the complications of changing the ring fusion, is seen by comparing the spectra of 7-epiDON (2) and 7-epinupharidine (4). Quinolizidine carbons β, γ, and δ to the new oxygen atom shift, on the average, +10.53, −6.02, and +0.99 p.p.m., respectively, on transforming the amine to the *trans*-fused *N*-oxide. The β- and γ-carbon shifts agree with the +10.16 β-carbon and −5.78 p.p.m. γ-carbon shifts associated with converting 1,2-, 1,3-, and 1,4-dimethylpiperidines to the corresponding *N*-oxides (3*a*). The magnitude of the shielding of the carbons γ to oxygen is nearly that expec-

[6]The methyl resonances of the two 2-methylquinolizidines differ by 4.33 p.p.m. giving an increment per γ-*gauche* interaction difference equal to −2.16. The gauche interactions include those of the nonbonding electron pair on nitrogen. The methyl resonances of the two 1-methylquinolizidines differ by 4.98 p.p.m. giving an increment per *gauche* interaction equal to −2.49 p.p.m., a value considerably in excess of the −0.76 value given by the pair of 3-methylquinolizidines. Possibly a partial answer to the problem rests in the γ-antiperiplanar effect of nitrogen on the C-3 equatorial methyl. This effect is shielding and even more so than a γ-*gauche* effect (20). Consequently, the small equatorial–axial increment might result from such antiperiplanar shielding of an equatorial methyl rather than an abnormally small γ-*gauche* shielding of an axial methyl. However this explanation fails to explain the different increments for C-1 and -3 pairs although some difference might be expected since the substitution patterns of the two antiperiplanar systems are not the same.

[7]The one anomaly at C-7 results from the failure of the method in predicting the chemical shift at C-3 of the methyl substituted quinolizidines (C-7 of DON and 7-epiDON). Thus the method gives chemical shifts for C-3 of 3(a)- and 3(e)-methylquinolizidine which are 2.51 p.p.m. upfield and 2.48 p.p.m. downfield respectively from the values observed (1).

TABLE 4. Changes in ^{13}C chemical shifts generated by substituting a 4(e)-3(furyl) group[a,b]

Carbon *i*	Position[d]	$\delta_C{}^i$, Dimethylquinolizidine[c] 1(e),7(a)-	$\delta_C{}^i$, Dimethylquinolizidine[c] 1(e),7(e)-	$\Delta\delta_C{}^{DON}$[e]	$\Delta\delta_C{}^{7\text{-epiDON}}$[f]
1	δ	37.25	37.25	−1.53	−0.75
2	γ	33.94	33.94	+0.04	+0.19
3	β	26.09	26.09	+8.87	+9.08
4	α	56.52	56.52	+3.81	+4.62
6	γ	61.85	65.57	−3.66	−4.10
7	δ	26.12	32.62	+2.54	−1.43
8	ε	30.38	33.94	+0.18	−0.23
9	δ	25.49	29.73	+0.25	+0.61
10	γ	68.81	68.81	+0.94	+0.73

[a]In p.p.m.
[b]Positive values indicate a downfield shift.
[c]Calculated chemical shift values for carbon *i* in each of the two dimethylquinolizidines; see text for method of calculation.
[d]Relative to C-4.
[e]$\Delta\delta_C{}^{DON} = \delta_C{}^i$ DON $- \delta_C{}^i$ 1(e),7(a)-dimethylquinolizidine.
[f]$\Delta\delta_C{}^{7\text{-epiDON}} = \delta_C{}^i$ 7-epiDON $- \delta_C{}^i$ 1(e),7(e)-dimethylquinolizidine.

ted from γ-axial substitution (1, 28). However the deshielding of the β-carbon is larger by about 4.7 p.p.m. than the usually observed β-axial substitution effect and is attributed in part to the positive charge on nitrogen.

The comparison of DON (**1**) with nupharidine (**3**) is somewhat more complicated, in relation to the comparison of **2** with **4**, because of the change in the ring fusion stereochemistry. Both C-7 and -8 in **3** are shielded, C-7 as a result of the *N*-oxide oxygen being axial in ring-B and C-8 by the axial C-1. Also C-1, -3, and -9 are shielded, entirely or partially, as a result of new axial interactions. The resonance of C-6 in nupharidine is maintained near its DON position as a result of the shielding C-1, -3, and -13 γ-gauche interactions offsetting the deshielding effects of the positive charge at adjacent nitrogen, a β-axial interaction with *N*-oxide oxygen and a δ-interaction with C-15. In contrast, C-4, -6, and -10 in 7-epiDON and C-4 and -10 in DON undergo, upon *N*-oxidation, large downfield shifts which are attributed to charge and β-axial effects.

N-Oxidation also results in shifts of furan ring carbons 13, 14, and 15 but not 16. C-14 and -15 are deshielded by nearly the same amount, of the order of 1.6–2.6 p.p.m. but C-13 is shielded 10.89 and 12.38 p.p.m., respectively, in the *N*-oxidation of DON and 7-epiDON. These larger upfield shifts undoubtedly are due, at least in part, to the newly developed γ-gauche interaction of C-13 with the *N*-oxide oxygen atom. The smaller deshieldings of C-14 and -15 are consistent with known δ effects in general (30) but *syn*-diaxial effects in particular (31). The nature of the δ interaction in the *N*-oxides is illustrated through the use of Newman projections and the results of the X-ray studies (21).[5] The latter show that the C-14 hydrogen and the axial hydrogen are eclipsed in both *N*-oxides. As a result there are in each of the *N*-oxides two δ interactions which are analogous to the *syn*-diaxial interaction in polycyclic cyclohexane systems. In the case of nupharidine, C-15 interacts with C-6; C-14 interacts with *N*-oxide oxygen. But in the case of 7-epinupharidine, C-15 interacts with *N*-oxide oxygen; C-14 interacts with C-6.

The outcome of the DON and 7-epiDON oxidation represents two different stereochemical possibilities open to *N*-oxidation of a quinolizidine, the one being oxidation with inversion of nitrogen, the other being retention.[8] Of all the spectral changes resulting from *N*-oxidation of the two amines, the magnitude of the C-6 shift appears to reflect in the most obvious manner the difference in the stereochemical outcome.

The authors are grateful to the National Science Foundation for an equipment grant to the Department of Chemistry, State University of New York, College of Environmental Science and Forestry toward the purchase of the XL-100-15 spectrometer and the VFT 100

[8]Inversion and retention refer here to the overall result relative to the more stable ring-fusion stereochemistry of the starting quinolizidine. In principle however, DON and 7-epiDON may undergo oxidation in the same stereochemical mode, one as the *cis*-fused amine, the other as the *trans*-fused amine.

Can. J. Chem. Downloaded from www.nrcresearchpress.com by 210.87.254.6 on 09/05/12
For personal use only.

computer used in this study. Support of this work by the National Institutes of Health, U.S. Public Health Service (Grant No. AI-10188) is gratefully acknowledged. We also acknowledge the assistance of Mr. L. McCandless in determining the spectra, Dr. C. F. Wong for alkaloid samples, and Mr. N. Muhammad in preparing 3-methylfuran.

1. R. T. LALONDE and T. N. DONVITO. Can. J. Chem. **52**, 3778 (1974).
2. T. M. MOYNEHAN, K. SCHOFFIELD, R. A. Y. JONES, and A. R. KATRITZKY. J. Chem. Soc. 2637 (1962); C. D. JOHNSON, R. A. Y. JONES, A. R. KATRITZKY, C. R. PALMER, K. SCHOFFIELD, and R. J. WELLS. J. Chem. Soc. 6797 (1965).
3. (*a*) D. W. COCHRAN. Ph.D. Dissertation. Indiana University, Bloomington, Indiana. 1971; (*b*) E. WENKERT, B. CHAUNCY, K. G. DAVE, A. R. JEFFCOAT, F. M. SCHELL, and H. P. SCHENK. J. Am. Chem. Soc. **95**, 8427 (1973); (*c*) E. WENKERT, J. S. BINDRA, C.-J. CHANG, D. W. COCHRAN, and F. M. SCHELL. Acc. Chem. Res. **7**, 46 (1974).
4. F. BOHLMANN, E. WINTERFELDT, P. STUDT, H. LAURENT, G. BOROSCHEWSKI, and K-M. KLEINE. Chem. Ber. **94**, 8522 (1972).
5. R. T. LALONDE, C. F. WONG, and H. G. HOWELL. J. Org. Chem. **36**, 3703 (1971).
6. C. F. WONG, E. AUER, and R. T. LALONDE. J. Org. Chem. **35**, 517 (1970).
7. C. F. WONG and R. T. LALONDE. Phytochemistry, **9**, 659 (1970).
8. R. T. LALONDE, E. AUER, C. F. WONG, and V. P. MURALIHAREN. J. Am. Chem. Soc. **93**, 2501 (1971).
9. R. T. LALONDE, C. F. WONG, and W. P. CULLEN. Tetrahedron Lett. 4477 (1970).
10. R. T. LALONDE, C. F. WONG, and K. C. DAS. J. Am. Chem. Soc. **95**, 6342 (1973).
11. R. T. LALONDE, C. F. WONG, and K. C. DAS. J. Am. Chem. Soc. **94**, 8522 (1972).
12. G. I. BIRNBAUM. Tetrahedron Lett. 4149 (1965); O. ACHMATOWICZ and J. T. WRÓBEL. Tetrahedron Lett. 129 (1964); O. ACHMATOWICZ, H. BANAZEK, G. SPITELLER, and J. T. WRÓBEL. Tetrahedron Lett. 927 (1964).
13. G. SCHWARTZ. *In* Organic synthesis. Vol. 3. *Edited by* E. C. Horning. John Wiley and Sons, Inc., New York. 1955. p. 332.
14. V. V. SMIRNOV, S. B. ZOTOV, and F. V. KRASNYUK-MADRI. Khim. Geterotsikl. Soedin. 173 (1968). *Cited in* Chem. Abstr. **70**, 3691 (1969).
15. E. T. STROM, W. L. ORR, B. S. SNOWDEN, JR., and D. E. WOESNER. J. Phys. Chem. **71**, 4017 (1967).
16. H. GILMAN and R. R. BURTNER. J. Am. Chem. Soc. **55**, 2903 (1933).
17. K. ODA and H. KOYAMA. J. Chem. Soc., 1450 (1970).
18. N. K. WILSON and J. B. STOTHERS. *In* Topics in stereochemistry. Vol. 8. *Edited by* E. L. Eliel and N. L. Allinger. Interscience Division, John Wiley & Sons, New York. 1974.
19. T. PEHK, E. LIPPMAA, V. V. SEVOSTJANOVA, M. M. KRAYUSCHKIN, A. I. TARASOVA. Org. Magn. Reson. **3**, 783 (1971).
20. E. L. ELIEL, W. F. BAILEY, L. D. KOPP, D. M. GRANT, R. BERTRAND, K. A. CHRISTENSEN, D. K. DALLING, M. W. DRECH, E. WENKERT, F. M. SCHELL, and D. W. COCHRAN. J. Am. Chem. Soc. **97**, 322 (1975).
21. J. OHRT, R. PARTHASARATHY, R. T. LALONDE, and C. F. WONG. J. Cryst. Mol. Struct. **3**, 3 (1973).
22. Sadtler nuclear magnetic resonance spectra. Sadtler Research Laboratories, Inc., Philadelphia. 1972. No. 13886M.
23. L. F. JOHNSON and W. C. JANKOWSKI. Carbon-13 NMR spectra. John Wiley and Sons, New York. 1972. p. 48.
24. M. CRISTL, H. J. REICH, and J. D. ROBERTS. J. Am. Chem. Soc. **93**, 3463 (1971).
25. R. S. OZUBKO, G. W. BUCHANAN, and I. C. P. SMITH. Can. J. Chem. **52**, 2493 (1974).
26. D. ZIMMERMAN, R. OTTINGER, J. REISSE, H. CRISTOL, and J. BRUGIDOU. Org. Magn. Reson. **6**, 346 (1974).
27. D. DODDRELL, C. CHARRIER, B. L. HAWKINS, M. D. CRAIN, L. HARRIS, and J. D. ROBERTS. Proc. Natl. Acad. Sci. U.S. **67**, 1588 (1970).
28. D. K. DALLING, D. M. GRANT, and E. G. PAUL. J. Am. Chem. Soc. **95**, 3718 (1973).
29. D. K. DALLING and D. M. GRANT. J. Am. Chem. Soc. **94**, 5318 (1972).
30. J. J. KROSCHWITZ, M. WINOKUR, H. J. REICH and J. D. ROBERTS. J. Am. Chem. Soc. **91**, 5927 (1969).
31. S. H. GROVER. Ph.D. Dissertation, University of Western Ontario. London. 1973.

Can. J. Chem. Downloaded from www.nrcresearchpress.com by 210.87.254.6 on 09/05/12
For personal use only.

Theoretical and Experimental Investigation of Primary Reactions in Sodium Diffusion Flames[1,2]

KENNETH J. MINTZ[3] AND DONALD J. LE ROY[4]

Lash Miller Chemical Laboratories, Department of Chemistry, University of Toronto, Toronto, Ontario M5S 1A1

Received December 18, 1974

KENNETH J. MINTZ and DONALD J. LE ROY. Can. J. Chem. **53**, 1726 (1975).

The determination of rate constants of reactions of the type Na + RX = NaX + R by the diffusion flame method is critically investigated, both theoretically and experimentally. More precise methods than those used heretofore are developed for calculating rate constants from experimental data, *viz.* evaluation of the effective nozzle radius, a generalization of the Heller criterion, an improvement in the theory of the visibility limit, and allowance for wall reaction and halide consumption. These methods were applied to previous data on the reaction Na + C_2H_5Cl as well as to new data on the reaction of sodium with CH_3Cl, CH_3Br, CH_3I, and C_2H_5Br.

KENNETH J. MINTZ et DONALD J. LE ROY. Can. J. Chem. **53**, 1726 (1975).

On a examiné d'une façon critique, sur des bases théoriques et expérimentales, la détermination, par la méthode de diffusion de flamme, des constantes de vitesse de réactions du type Na + RX = NaX + R. On a développé des méthodes plus précises que celles utilisées jusqu'à maintenant pour calculer les constantes de vitesse à partir des données expérimentales à savoir une évaluation du rayon effectif du bec, une généralisation du critère de Heller, une amélioration de la théorie de la limite de la visibilité et une allocation pour les réactions des parois et la consommation des halogénures. On a appliqué ces méthodes à des données antérieures pour la réaction de Na + C_2H_5Cl de même qu'à de nouvelles données pour la réaction du sodium avec CH_3Cl, CH_3Br, CH_3I et C_2H_5Br. [Traduit par le journal]

(I) Introduction

Reactions between alkali metal atoms and halogenated compounds have been studied extensively, both by the diffusion flame method of Polanyi (1) and by molecular beam techniques. However, relatively few comparisons have been made between rate constants determined by the two methods (2, 3). Since improvements in molecular beam technology will undoubtedly enable more precise reaction cross sections to be determined in the future it seemed desirable to reexamine the theoretical basis of the diffusion flame method so that meaningful comparisons can be made. A more immediate reason for undertaking the present investigation was that a thorough understanding of these primary reactions was a necessary prelude to the quantitative investigation of the reactions of free radicals formed in diffusion flames, which will be the subject of a forthcoming publication of the present authors (4).

In a typical diffusion flame reaction atomic sodium, at a known vapor pressure and mixed with an inert carrier gas, enters the reactor through a nozzle where it comes into contact with the other reagent. Ideally, the velocity in the nozzle is sufficiently high to avoid diffusion of the "atmospheric" reagent into the nozzle but low enough so that diffusion is the major means of mass transport of the sodium after it issues from the nozzle. The halide atmospheric reagent is normally at much higher concentration than the sodium and moves through the reactor relatively slowly so that the concentration of sodium in the reactor as it diffuses away from the nozzle will be approximately spherically symmetrical about the nozzle tip. Under these conditions

$$[1] \quad \frac{\partial^2 N}{\partial r^2} + (2/r)\frac{\partial N}{\partial r} - k_1 NA/D_N = 0$$

where N is the concentration of nozzle reagent, A is the concentration of the atmospheric reagent, D_N is the diffusion coefficient of the

[1]NRCC No. 14572.

[2]The authors are grateful to the National Research Council of Canada for financial assistance in support of this research.

[3]Present address: Explosives Research Laboratories, Canadian Industries Limited, McMasterville, Quebec.

[4]Present address: Division of Chemistry, National Research Council of Canada, Ottawa, Canada K1A 0R6.

Can. J. Chem. Downloaded from www.nrcresearchpress.com by 210.87.254.6 on 09/05/12
For personal use only.

Can. J. Chem. Downloaded from www.nrcresearchpress.com by 210.87.254.6 on 09/05/12
For personal use only.

nozzle reagent, r is the radial distance from the nozzle opening, and k_1 is the rate constant of the primary reaction to be determined.

By assuming that A is constant throughout the reaction but vanishes inside the nozzle, eq. 1 is readily solved to yield the well-known equation of Hartel and Polanyi (5)

$$[2] \qquad k_1 = \left[\frac{\ln [(N_0 r_0)/(N_R R)]}{R - r_0}\right]^2 D_N/A$$

in which N_R is the concentration of the nozzle reagent at some distance R from the nozzle and N_0 is its concentration at the origin, *i.e.* a radius r_0 close to the nozzle.

Hartel and Polanyi equated r_0 to the nozzle radius, r_n, and N_0 to the concentration of the nozzle reagent issuing from the nozzle, N_n. They also assumed that the value of N_R at the radial distance R was a fixed observable quantity. In sodium flame work N_R is taken to be the visibility limit of the sodium fluorescence observed when the system is illuminated with yellow sodium D resonance radiation (*ca.* 10^{-5} Torr).

Equation 2, with the above assumption regarding N_0, r_0, and N_R, has been used in most sodium diffusion flame work. As the result of a careful investigation, Heller (6) found empirically that for satisfactory results the linear velocity in the jet, $\bar{v}$, should be related to the diffusion coefficient, D_N, through the equation

$$[3] \qquad 5 \leqslant \bar{v}/D_N \leqslant 12 \text{ cm}^{-1}$$

Cvetanović and Le Roy (7), and later Smith (8) took into consideration the nonuniformity of the atmospheric reagent (the halide) resulting from its consumption in the primary reaction. Although the simultaneous partial differential equations involved could not be solved in closed form, approximate equations were derived and extensive numerical calculations made (9).

Reed and Rabinovitch (10, 11) pointed out that the total rate of consumption of the nozzle reagent calculated from eq. 2 on the assumption that $r_0 = r_n$ and $N_0 = N_n$ would not necessarily be equal to the rate of influx of the nozzle reagent. To get around this discrepancy they proposed that in general $N_0 \neq N_n$, but they retained the relation $r_0 = r_n$.

The same authors showed that the visibility limit of sodium resonance fluorescence corresponding to the quantity N_R in eq. 2 would not be independent of R because the light reaching the eye of the observer as one looks at the edge of the "flame" comes, not from a single point at radius R, but from all points within the reactor along the line of sight tangent to the visible flame. It follows that the apparent visibility limit will depend on the value of R. Various approximate formulae have been given to make allowance for this effect (11, 12). The subject of visibility limit has also been treated by the present authors (13).

(II) The Diffusion Flame in a Nonreactive System

In this section we examine the case in which there is no halide present in the atmospheric gas. For spherical diffusion in such a system the third term of eq. 1 vanishes, and if we let $N \to 0$ as $r \to \infty$ the solution is

$$[4] \qquad N = B/r$$

where B is to be determined by a boundary condition.

Mass conservation requires that the flow rate of nozzle reagent (*e.g.* Na) in the nozzle be equal to the rate at which it diffuses across the boundary of any sphere of radius r in the reactor at some distance from the nozzle, *viz.*

$$[5] \qquad \pi r_n^2 \bar{v} N_n = -4\pi D_N r^2 (dN/dr)_r$$

Thus, from eqs. 4 and 5

$$[6] \qquad N = \bar{v} r_n^2 N_n/(4 D_N r)$$

For spherical diffusion to obtain at a small radius r_0 this requires that

$$[7] \qquad N_0 = \bar{v} r_n^2 N_n/(4 D_N r_0)$$

Two simple options are evident:

(*1*) We can equate r_0 to r_n, *i.e.* assume that spherical diffusion occurs from the surface of a sphere of radius r_n. In this case the concentration of the nozzle reagent on the surface of that sphere is not, in general, equal to N_n but is given by the relation

$$[8] \qquad \text{e.i.c.: } N_0 = \bar{v} r_n N_n/(4 D_N)$$

This is referred to as the "effective initial concentration" or e.i.c. model, and is equivalent to that used by Reed and co-workers for the case of a reactive atmospheric reagent (10–12).

(*2*) We can equate N_0 to N_n, *i.e.* assume that spherical diffusion occurs from the surface of a sphere on which the concentration of nozzle

Can. J. Chem. Downloaded from www.nrcresearchpress.com by 210.87.254.6 on 09/05/12
For personal use only.

reagent is equal to N_n. The radius of the sphere will not, in general, be equal to r_n but will be given by the relation

[9] e.n.r.: $r_0 = \bar{v}r_n^2/(4D_N)$

This is referred to as the "effective nozzle radius" or e.n.r. model.

It should be noted that Hartel and Polanyi's assumptions that $N_0 = N_n$ *and* $r_0 = r_n$ cannot be true in general for a nonreactive atmospheric reagent, but only if $\bar{v}/D_N = 4/r_n$.

A reasonable assumption to make would be that for spherically symmetrical diffusion to take place from the surface of a sphere of radius r_0 the diffusion velocity, V, across the surface of this sphere should be equal to the maximum velocity of the nozzle reagent inside the nozzle, *i.e.* the velocity in the center of the nozzle, which is equal to $2\bar{v}$. The value of V for a radius r_0 is given by (ref. 14, p. 462)

[10] $V = -D_N[\mathrm{d} \ln N/\mathrm{d}r]_{r_0}$

Thus, on the basis of the above assumption $\bar{v}/D_N$ should be equal to $1/2r_0$. For the e.i.c. and e.n.r. models this predicts that $\bar{v}/D_N$ should be equal to $1/2r_n$ and $\sqrt{2}/r_n$, respectively. In our experiments with a nonreactive atmospheric gas and a nozzle of radius 0.095 cm we found empirically that $\bar{v}/D_N$ had to be in the range 15 to 20 cm^{-1} in order to obtain good spherical flames. This is very close to the value predicted by the e.n.r. model, which is therefore preferred for a nonreactive atmospheric gas.

(III) The Diffusion Flame in a Reactive System

If the only process leading to depletion of the nozzle reagent is its chemical reaction in the primary process then, for spherical diffusion and A constant, eqs. 1 and 2 apply and

[11] $N_r = (N_0 r_0/r) \exp[-\beta(r - r_0)]$

where $\beta = (k_1 A/D_N)^{1/2}$.

Mass conservation requires that the total rate of reaction of sodium from $r = r_0$ to $r = R$, say, plus its rate of diffusion out of a sphere of radius R, be equal to its rate of influx into the reactor. Thus from eq. 11

[12] $\pi r_n^2 \bar{v} N_n = 4\pi D_N N_0 r_0 (1 + \beta r_0)$

From eq. 12 it follows that for the e.i.c. model

[13] $r_0 = r_n$

$$N_0 = \frac{N_n \bar{v} r_n}{4D_N(1 + \beta r_n)}$$

while for the e.n.r. model

[14] $N_0 = N_n$

$$r_0 = [-1/\beta + (1/\beta^2 + \bar{v}r_n^2/D_N\beta)^{1/2}]/2$$

The method used in Part II to calculate reasonable values of $\bar{v}/D_N$ can also be applied here. For the e.i.c. model this yields

[15] $\bar{v}/D_N = 1/2r_n + \beta/2$

For the e.n.r. model

[16] $\bar{v}/D_N = \sqrt{2}/r_n + \beta/2$

The value of β is typically of the order of 2 cm^{-1}. Heller developed his criterion (eq. 3) using a nozzle of radius 0.25 cm, for which the e.i.c. and e.n.r. models predict values of $\bar{v}/D_N$ of *ca.* 3 and 6.6 cm^{-1} respectively. Thus the e.n.r. model is more in line with Heller's criterion for reactive systems. It was shown in Part II that the e.n.r. model provided an excellent criterion for spherical flames in nonreactive systems. We therefore propose that rate constants derived from diffusion flame experiments should be based on the e.n.r. model and that Heller's criterion be replaced by eq. 16.

The assumption that A is constant throughout the system and vanishes at $r = r_0$ was eliminated by Cvetanović and Le Roy (7), who used approximate methods to solve the simultaneous differential eqs. 1 and 17

[17] $$\frac{\partial^2 A}{\partial r^2} + \frac{2}{r}\frac{\partial A}{\partial r} - k_1 N A/D_A = 0$$

In the present work we have solved these equations by the boundary-value finite-difference method (15) with an optimized variable step-size, using an IBM 370/65 computer (see also Parts V and VI).

(IV) Wall Effects

Previous workers have assumed that as long as the visible flame did not touch the walls of the reactor the latter could be assumed to have an *infinite* radius insofar as the solution of eq. 1 was concerned. This assumption is easily tested. By comparing the rate of influx of nozzle reagent

Can. J. Chem. Downloaded from www.nrcresearchpress.com by 210.87.254.6 on 09/05/12
For personal use only.

with its total rate of consumption within a sphere of radius R_w equal to the radius of the reaction vessel,[5] using the "infinite reactor" eq. 11, it is easily shown that in much of the previous research on sodium diffusion flames an appreciable fraction of the sodium must have reached the walls of the reactor. It follows that the boundary condition $N \to 0$ as $r \to \infty$ was not applicable.

In setting up a "finite reactor" model some assumption has to be made about the fate of the sodium atoms reaching the wall. The assumption made here is that the concentration of sodium approaches zero at the walls as the result of adsorption on the finely divided sodium halide deposit and reaction with the organic halide reagent.

Using the e.n.r. conditions that $N_0 = N_n$, the nozzle reagent concentration distribution is given by

$$[18] \quad N_r = (N_n r_0'/r)\frac{\sinh[\beta(R_w - r)]}{\sinh[\beta(R_w - r_0')]}$$

When r_0' is calculated from eq. 18 in the same manner that r_0 was calculated in Part III we obtain the expression

$$[19] \quad \beta \coth[\beta(R_w - r_0')](r_0')^2 + r_0' = r_n^2\bar{v}/4D_N$$

However, the magnitudes of the quantities concerned are such that coth $[\beta(R_w - r_0')]$ can be equated to unity, and so r_0' is given by eq. 14.

Using the correct visibility limit (Part V), it was found that the "infinite reactor" model always overestimates the value of the rate constant k_1 when wall reaction occurs. Furthermore, the extent of wall reaction is underestimated by a considerable amount when N is calculated according to the "infinite reactor" model. It was found that the percentage of wall reaction increases with increasing flame radius and with decreasing N_n. Systematic errors in rate constants can therefore arise by simply following the recommendation (6) to use flames 1.8 cm in radius or more, or the recommendation (16) to use low values of N_n when studying fast reactions.

In the new experimental work reported later in this paper we have minimized the amount of wall reaction by using a reactor with a diameter of 17.8 cm, several times that used in previous work.

[5]The reactor is normally a cylinder of radius R_w.

(V) Visibility Limit and the Evaluation of Primary Rate Constants

We have previously discussed the visibility limit in nonreactive systems, with particular emphasis on its application to the determination of cross sections for the quenching of Na(^{2}P) atoms (13). In this section we describe its numerical evaluation, derived from a calibration experiment in a nonreactive system, and then discuss its application to the evaluation of primary rate constants in reactive systems.

For a nonreactive atmospheric gas the concentration of sodium at a point p on the line of sight perpendicular to the nozzle axis and tangent to the edge of the visible flame of radius R at a distance S from the nozzle axis is, from eq. 4, given by

$$[20] \quad N_p = B(R^2 + S^2)^{-1/2}$$

where $B = \bar{v}r_n^2N_n/4D_N$ (eq. 6).

For the purpose of the following treatment we assume that the sodium D radiation enters the reaction vessel as a parallel beam having an intensity I_F at the entrance window, which is perpendicular to the nozzle axis and at a distance R_F from the nozzle. It is evident that this beam will be attenuated as it passes through the sodium vapor between the visible flame and the entrance window and, furthermore, the attenuation will not be uniform across the axis of the reactor. The greatest attenuation will be along the nozzle axis. At a point on the axis x cm from the entrance window the sodium concentration will be given by the expression

$$[21] \quad N_x = B/(R_F - x)$$

Assuming Beer's law absorption, the rate of attenuation at the point x will be given by

$$[22] \quad -\mathrm{d}\ln I/\mathrm{d}x = \varepsilon N_x = \varepsilon B/(R_F - x)$$

where ε is the extinction coefficient. The intensity at the flame edge on the nozzle axis is then equal to $I_F(R/R_F)^{\varepsilon B}$.

From measurements made by Cvetanović (17) using the usual type of commercial sodium lamp, $\varepsilon \approx 3.6 \times 10^{10}$ cm^2 mol^{-1}. Values of B are usually of the order of 10^{-14} mol cm^{-2}. Thus the attenuation of the incident light beam due to

absorption between the entrance window and the line of sight can be neglected and the intensity along the line of sight can be considered to be uniform and equal to I, say.

The rate of light absorption, I_a, at the point p will be given by

$$[23] \quad (I_a)_p = I\varepsilon N_p = I\varepsilon B/(R^2 + S^2)^{1/2}$$

The rate of fluorescence at that point will be given by the Stern–Volmer expression

$$[24] \quad F_p = (I_a)_p/(1 + \tau k_Q(Q)) = I\varepsilon B(R^2 + S^2)^{-1/2}/(1 + \tau k_Q(Q))$$

where τ is the lifetime of the radiating state, k_Q is the rate constant for the quenching of the resonance fluorescence, and (Q) is the concentration of the quencher.

If α is the area of the aperture of the eye and D is its distance from the nozzle axis then the total amount of fluorescence originating on the line of sight that can be seen is equal to the visibility limit ν, where

$$[25] \quad \nu = [\alpha I\varepsilon B/4\pi(1 + \tau k_Q(Q))] \times \int_{-R_w}^{R_w} \frac{dS}{(R^2 + S^2)^{1/2}(D + S)^2}$$

where R_w is the radius of the reactor.[6]

The above treatment differs from that of Reed and co-workers (11, 12, 18) by the inclusion of the solid angle effect. Serious errors can be made for large values of R_w and small values of D if this effect is neglected. The effect of the quenching term was first noted, and utilized, by the present authors (13). It will not be discussed further here, except to note that it could be of some importance when applying the visibility limit (evaluated in a nonreactive system) to a reactive system where the quenching cross section of the halide is large.

In applying the visibility limit to the evaluation of primary rate constants it will be assumed that the quantities α, I, ε, and (Q) of eq. 25 remain the same as in the nonreactive system. We can then define a working value of the visibility limit

$$[26] \quad L = 4\pi\nu[1 + \tau k_Q(Q)]/\alpha I\varepsilon = B\int_{-R_w}^{R_w} \frac{dS}{(R^2 + S^2)^{1/2}(D + S)^2} = BC$$

For the present observer (K.J.M.), L was equal to $3.2_5 \times 10^{-16}$ mol cm^{-4}. If we multiply this value by D^2 (400 cm^2) the result (1.3×10^{-13} mol cm^{-2}) can be compared with the values of 4.7×10^{-14}, 6.13×10^{-14}, and 5.98×10^{-14} mol cm^{-2} obtained by Reed and co-workers (11, 18, 12). The differences could be accounted for by assuming that the eye of their observer was *ca.* 14 cm from the nozzle axis, rather than 20 cm, as in our experiments.

To apply the visibility limit in evaluating k_1 in a reactive system in which A is assumed to be constant, the e.n.r. formulation is used and wall effects are neglected, we note that the analog of eq. 26 is

$$[27] \quad L = BC = N_n r_0 \times \int_{-R_w}^{R_w} \frac{\exp\{-\beta[R^2 + S^2)^{1/2} - r_0]\}\, dS}{(R^2 + S^2)^{1/2}(D + S)^2}$$

where r_0 is given by eq. 14. The value of β, and hence k_1, is obtained by using a computer program to adjust β until the integral is equal to the known quantity $BC/N_n r_0$.

If we wish to allow for halide depletion it becomes necessary to consider eqs. 1 and 17 in the context of the visibility limit. Equation 27 is no longer an exact expression for the latter, but the value of β obtained by neglecting halide depletion can be used to give a first approximation to N_R when solving eqs. 1 and 17 simultaneously. In the latter stages of the calculation we approach self-consistency among eqs. 1 and 17 and the equation

$$[28] \quad L = BC = \int_{-R_w}^{R_w} \frac{\phi[(R^2 + S^2)^{1/2}]\, dS}{(D + S)^2}$$

where $\phi[(R^2 + S^2)^{1/2}]$ is the appropriate distribution function for sodium calculated numerically.

(VI) The Reaction Na + C_2H_5Cl

The work of Cvetanović and Le Roy (19) on the reaction Na + C_2H_5Cl remains as the most extensive investigation of the effect of temperature on the rate constant of a diffusion flame

[6]Reference 13 treats the problem in a somewhat different, but equivalent, way but unfortunately contains a number of typographical errors: in eq. 6 and subsequent equations the quantities $D + S$ and D should read $(D + S)^2$ and D^2.

Can. J. Chem. Downloaded from www.nrcresearchpress.com by 210.87.254.6 on 09/05/12
For personal use only.

Can. J. Chem. Downloaded from www.nrcresearchpress.com by 210.87.254.6 on 09/05/12
For personal use only.

reaction. Previous workers calculated "single temperature" activation energies by measuring k_1 at a single temperature and calculating E from the expression

$$[29] \quad k_1 = p\sigma^2(8\pi RT/\mu)^{1/2} \exp(-E/RT)$$

assuming p = unity and $\sigma^2 = 35$ Å^2 for all sodium flame reactions.

Cvetanović and Le Roy (19) measured k_1 over the range 533 to 653 K. Allowance was made for halide depletion (7) but they used the Hartel–Polanyi assumptions $r_0 = r_n$ and $N_0 = N_n$ and a simple visibility limit ($N_R = 7 \times 10^{-6}$ Torr). By assuming $\sigma^2 = 35$ Å^2 they found $p = 1.0 \pm 0.3$, in good agreement with the original proposal of Hartel and Polanyi (5). In the light of the improvements in the theory discussed in this paper it seemed worthwhile to reanalyze their results. The appropriate diffusion coefficients are described in Appendix 1.

The original data (19) were used to calculate k_1 to four degrees of approximation: (*a*) the infinite reactor model (eq. 2) using the Hartel–Polanyi assumptions and the simple visibility limit; (*b*) the infinite reactor model and the simple visibility limit, but with the e.n.r. assumption; (*c*) the infinite reactor model with the e.n.r. assumption and a corrected visibility limit (LD^2 was estimated to have been 6×10^{-14} mol cm^{-2} in their experiments); (*d*) the finite reactor model (eq. 19) with the e.n.r. assumption, the corrected visibility limit, and with correction for halide consumption.

The rate constants calculated according to (*b*) were between $\frac{1}{5}$ and $\frac{1}{8}$ as large as those for (*a*). However, this decrease was more than overcome when the corrected visibility limit was used; the values for (*c*) were 20 to 40% larger than for (*a*). The additional refinement of calculation (*d*) gave values very close to those of (*c*), averaging less than 2% greater.

Use of the e.i.c. rather than the e.n.r. assumption made very little difference in calculations (*b*) and (*c*). The Arrhenius parameters derived from (*d*) and based on eq. 30,

$$[30] \quad k_1 = A \exp(-E/RT)$$

where $\log A = 14.9 \pm 0.1$, $E = 10.3 \pm 0.4$ kcal mol^{-1}, as compared to 15.1 ± 0.2 and 11.2 ± 0.4, respectively, obtained by Cvetanović and Le Roy (19).[7] By assuming $\sigma^2 = 35$ Å^2 the value of p in eq. 29 derived from calculation (*d*) was 0.9 ± 0.3. Thus the main conclusions derived from the earlier work are substantiated.

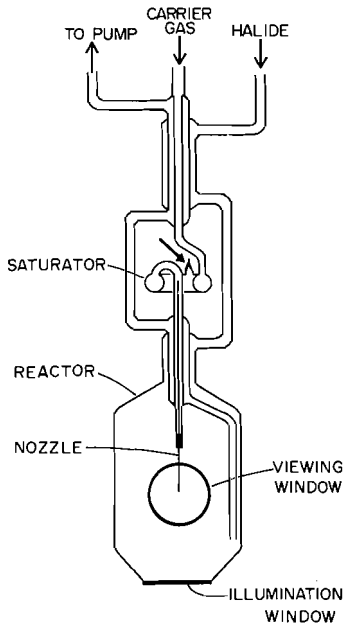

FIG. 1. Sodium diffusion flame apparatus.

It should be emphasized that large effects were produced by introducing the e.n.r. (or e.i.c.) assumption and the corrected visibility limit, and although these largely cancelled each other out in the present calculations they cannot be expected to do so in general. Furthermore, the corrections for halide depletion and wall reaction, although small in this case, can be expected to be quite important for faster reactions or different experimental conditions.

(VII) Experimental

The apparatus is shown in Fig. 1. The sodium still was glass-blown onto the apparatus at the point marked with an arrow during the preparatory stage. The sodium was carefully distilled in several stages under vacuum, after which the still was removed. The halides used were reagent grade, purified by trap-to-trap distillation under vacuum. The carrier gases used were prepurified grade N_2 and ultrahigh purity grade helium. They were passed through a quartz tube filled with copper turnings at

[7]Throughout this paper bimolecular rate constants are expressed in units of cm^3 mol^{-1} s^{-1}.

TABLE 1. Rate constants of the reactions Na + CH_3Cl and Na + C_2H_5Br

Na + CH_3Cl			Na + C_2H_5Br		
T (°C)	log k_1	Reference	T (°C)	log k_1	Reference
336	11.5 ± 0.1	This work	268	13.2 ± 0.1	This work
389	11.8 ± 0.1	This work	247	13.3 ± 0.1	This work
260	10.7	5	240	12.8	5
270	10.9	23	275	13.0	22
313	11.1	10	263	12.7	26
325	11.8	25	247	12.4	27
219	11.8	24*			

*Mean life method.

about 600 °C, a red-hot tungsten filament, and a liquid N_2 trap before passing over the molten Na in the saturator. A mass-flowmeter was used to measure the flow rate of the carrier gas.

The nozzle consisted of a 0.175 cm diameter nickel tube welded to Kovar which in turn was joined to Pyrex. This design allowed the saturated stream of Na in the carrier gas to contact only nickel once it left the saturator. The degree of saturation of sodium in the carrier gas was estimated by total product analysis together with the literature data (20, 21) on the vapor pressure of Na. Using a reactor with a glass nozzle and N_2 as the carrier gas, the degree of saturation ranged from 57% at 241 °C to 25% at 321 °C (with considerable scatter in the data). With He as the carrier, the degree of saturation was even smaller. Using the reactor with the nickel nozzle, 80% saturation of Na in N_2 could be achieved even at higher temperatures. However, for He used as the carrier, the degree of saturation was found to be a strong function of its pressure, ranging from 25% at 3 Torr to near 80% at 10 Torr or higher. This is apparently the first time that the assumption that the carrier gas is saturated with Na has actually been tested. Clearly, reaction of Na with glass decreases the apparent percent saturation, though obviously that is not the only factor involved. Since the degree of saturation depends on the design of the apparatus and is rather unreproducible, it would seem most advisable to measure in each experiment the total amount of product in order to be able to apply the formula for the rate constant with confidence.

The Na lamp was placed under the reactor so that the light entered through the bottom plane glass window. The resonance emission was observed through the window of the reactor at right angles to the incident beam. The outside of the reactor was painted black to help in seeing the emission.

Separate electrical resistance furnaces were constructed for the saturator and the reactor. Their temperatures were controlled by Wheatstone bridge circuits with platinum resistance thermometers as the sensors. Although the furnaces were controlled to 0.1 °C, the spatial variations inside the furnaces were of the order of a degree.

A F & M Model 700 dual column gas chromatograph equipped with flame ionization detectors was used for the analysis of the products. Several aliquots of the product mixture (which also contained excess halide reagent) were analyzed for each run.

(VIII) The Reaction Na + CH_3Br

Nineteen separate experiments were done on this reaction using a wide variety of conditions (with either N_2 or He as the carrier gas): temperatures from 241–389 °C, total pressure 2.8–98 Torr, flame diameter 0.68–1.68 cm, Na_n 2.1–289 × 10^{-11} mol/cm^3. Careful analysis of our data indicated that the rate constants did not drift with any experimental parameter other than temperature. Therefore we believe that the diffusion flame method properly applied does yield accurate absolute values of the rate constant, rather than merely relative values in homologous series as has been suggested. An Arrhenius plot of our rate constants yields: log A = 14.0 ± 0.4, E = 2.1 ± 1.2 kcal/mol. Our rate constants fall in between those determined by previous diffusion flame studies (log k_1 = 13.3 at 240 °C (22), 12.6 at 250 °C (16), 12.8 at 270° (23)). Frommer and Polanyi (24) using the mean life method found log k_1 = 12.2 at 200 °C and 12.8 at 240 °C, a much steeper temperature dependence than that found here. From our results, the reaction cross section, assuming p = 1.0, is 10 Å^2 for this reaction, compared to 31 Å^2 for the reaction Na + C_2H_5Cl (section VI). Hence it seems quite possible that the suggestion by Hartel and Polanyi that all reactions of this type have the same σ^2 (35 Å^2) is only a rough approximation. It should be pointed out that no attempt was made to reanalyze any of the earlier work. This also applies to previous work referred to in the subsequent sections of this paper.

(IX) The Reaction Na + CH_3Cl

The rate constants obtained here as well as in previous work are shown in Table 1. From our data, the Arrhenius parameters are: log A = 16, E = 8 kcal/mol. The other data are in

Can. J. Chem. Downloaded from www.nrcresearchpress.com by 210.87.254.6 on 09/05/12
For personal use only.

Can. J. Chem. Downloaded from www.nrcresearchpress.com by 210.87.254.6 on 09/05/12
For personal use only.

reasonable agreement with ours, except that determined by the mean life method.

(X) The Reaction Na + C_2H_5Br

The results are shown in Table 1. There appears to be a significant discrepancy between our results and those of previous workers. From our work, there does not seem to be any difference between the rate constant of this reaction and that of Na + CH_3Br in this temperature range.

(XI) The Reaction Na + CH_3I

Our one value is $\log k_1 = 14.7 \pm 0.1$ at 249 °C, compared to previous values of 14.0 at 240–270 °C (5) and 14.3 at 276 °C (26). Because of the speed of this reaction, the correction for depletion of the halide is quite appreciable; hence the discrepancy between our results and previous work (in which no correction was made) may be due to this effect. Assuming, as seems most probable, that the activation energy of this reaction is zero, then $\sigma^2 = 35$ Å^2, exactly the value assumed by Hartel and Polanyi (5).

Appendix

The effective diffusion coefficient for a species i, whose mole fraction is very small, has been approximated by (28–30)

$$[31] \qquad D_i = \left(\sum \frac{x_j}{D_{ij}}\right)^{-1}$$

where x_j are the mole fractions and D_{ij} are the binary diffusion coefficients. It can be shown on the basis of rigorous kinetic theory applied to a ternary mixture of uniform density that the maximum error in eq. 31 is less than 0.1% for $x_i < 0.001$.

The binary diffusion coefficients were calculated from eq. 32 (ref. 14, p. 539)

$$[32] \quad D_{ij} = 0.0026280 \times \frac{(T^3(M_i + M_j)/2M_iM_j)^{1/2}}{P\sigma_{ij}{}^2\Omega^{(1,1)*}T/(\varepsilon_{ij}/k)}$$

where M is the molecular weight, P is the pressure, Ω is the collision integral, values of which are tabulated (ref. 14, p. 1126). σ, ε are Lennard–Jones parameters calculated by the usual combination rules for nonpolar molecules

$$\sigma_{ij} = (\sigma_i + \sigma_j)/2$$

$$\varepsilon_{ij} = (\varepsilon_i\varepsilon_j)^{1/2}$$

For nonpolar–polar mixtures, the values of σ_{ij} and ε_{ij} were calculated by the method given by Hirschfelder *et al.* (ref. 14, p. 600).

Lennard–Jones parameters used are from Hirschfelder *et al.* (ref. 14, p. 1111) with the exception of Na which comes from Ashton and Hayhurst (31). These predict a value of 0.70 cm^2/s for D_{Na-N_2} at 527 K, in good agreement with the experimental value of 0.68 ± 0.03 cm^2/s determined by Cvetanović and Le Roy (32).

1. M. Polanyi. Atomic reactions. Williams and Norgate, London. 1932.
2. K. R. Wilson and D. Herschbach. J. Chem. Phys. **49**, 2676 (1968).
3. J. P. Toennies. Ber. Buns. Phys. Chem. **72**, 927 (1968).
4. K. J. Mintz and D. J. Le Roy. To be published.
5. H. v. Hartel and M. Polanyi. Z. Phys. Chem. B**11**, 97 (1930).
6. W. Heller. Trans. Faraday Soc. **33**, 1556 (1937).
7. R. J. Cvetanović and D. J. Le Roy. Can. J. Chem. **29**, 597 (1951).
8. F. Smith. J. Chem. Phys. **22**, 1605 (1954).
9. R. J. Cvetanović. Can. J. Chem. **34**, 54 (1956).
10. J. F. Reed and B. S. Rabinovitch. J. Phys. Chem. **59**, 261 (1955).
11. J. F. Reed and B. S. Rabinovitch. J. Phys. Chem. **61**, 598 (1957).
12. E. M. Nemeth and J. F. Reed. J. Phys. Chem. **70**, 3096 (1966).
13. K. J. Mintz and D. J. Le Roy. Chem. Phys. Lett. **10**, 280 (1971).
14. J. O. Hirschfelder, C. F. Curtiss, and R. B. Bird. Molecular theory of gases and liquids. Wiley, New York. 1954.
15. L. Fox. The numerical solution of two-point boundary problems in ordinary differential equations. Clarendon Press, Oxford. 1957.
16. J. N. Haresnape, J. M. Stevels, and E. Warhurst. Trans. Faraday Soc. **36**, 465 (1940).
17. R. J. Cvetanović. Ph.D. Thesis. University of Toronto, Toronto, Ontario. 1951.
18. E. D. Kaufman and J. F. Reed. J. Phys. Chem. **67**, 896 (1963).
19. R. J. Cvetanović and D. J. Le Roy. J. Chem. Phys. **20**, 1016 (1952).
20. M. Sittig. Sodium. Reinhold, New York. 1956. p. 452.
21. N. Nesmeyanov. Vapour pressures of the elements. Academic Press, New York. 1963. p. 443.
22. H. v. Hartel, N. Meer, and M. Polanyi. Z. Phys. Chem. B**19**, 139 (1932).
23. W. Heller and M. Polanyi. Trans. Faraday Soc. **32**, 633 (1936).
24. L. Frommer and M. Polanyi. Trans. Faraday Soc. **30**, 519 (1934).
25. J. F. Reed and B. S. Rabinovitch. J. Chem. Phys. **27**, 988 (1957).
26. A. G. Evans and H. Walker. Trans. Faraday Soc. **40**, 384 (1944).

27. F. RIDING, J. SCANALAN, and E. WARHURST. Trans. Faraday Soc. **52**, 1354 (1954).
28. J. O. HIRSCHFELDER and C. F. CURTISS. Third Int. Symp. Combust. 1949. p. 124.
29. D. F. FAIRBANKS and C. R. WILKE. Ind. Eng. Chem. **42**, 471 (1950).
30. R. E. WALKER, N. DEHAAS, and A. A. WESTENBERG. J. Chem. Phys. **32**, 1314 (1960).
31. A. F. ASHTON and A. N. HAYHURST. Trans. Faraday Soc. **66**, 833 (1970).
32. R. J. CVETANOVIĆ and D. J. LE ROY. J. Chem. Phys. **20**, 343 (1952).

Can. J. Chem. Downloaded from www.nrcresearchpress.com by 210.87.254.6 on 09/05/12
For personal use only.

A Kinetic Study of the Thermal Isomerization of $(CH_3)_2AsC{=}CAs(CH_3)_2CF_2CF_2Mn_2(CO)_8$ and Related Complexes

WILLIAM R. CULLEN AND FRANK L. HOU

Chemistry Department, University of British Columbia, Vancouver, British Columbia V6T 1W5

Received January 13, 1975

WILLIAM R. CULLEN and FRANK L. HOU. Can. J. Chem. **53**, 1735 (1975).

The kinetics of the unimolecular isomerization reaction

$$M(CO)_4M'(CO)_4As(CH_3)_2C{=}CAs(CH_3)_2CF_2CF_2 \rightarrow M(CO)_4As(CH_3)_2M'(CO)_4C{=}CCF_2CF_2$$

have been studied. The ΔH^* values in kcal mol^{-1} are 36.8 ± 2.0 (M = M′ = Mn), 46.8 ± 0.5 (M = M′ = Re), 39.2 ± 2.8 (M = Mn, M′ = Re). The mechanism of the rearrangement is discussed.

WILLIAM R. CULLEN et FRANK L. HOU. Can. J. Chem. **53**, 1735 (1975).

On a étudié la cinétique de la réaction d'isomérisation unimoléculaire suivante:

$$M(CO)_4M'(CO)_4As(CH_3)_2C{=}CAs(CH_3)_2CF_2CF_2 \rightarrow M(CO)_4As(CH_3)_2M'(CO)_4C{=}CCF_2CF_2$$

Les valeurs de ΔH^* sont de 36.8 ± 2.0 (M = M′ = Mn), 46.8 ± 0.5 (M = M′ = Re), 39.2 ± 2.8 (M = Mn, M′ = Re) kcal/mol. On discute du mécanisme de ce réarrangement.
[Traduit par le journal]

Introduction

The ligand $f_4$fars,

$$(CH_3)_2AsC{=}CAs(CH_3)_2CF_2CF_2$$

has an almost unique ability to react with metal carbonyl clusters to give stable complexes in which the ligand has displaced two terminal carbon monoxide molecules from different metal atoms (1). For example, in $f_4farsFe_3(CO)_{10}$ the ligand bridges the two equivalent iron atoms which are also bridged by two CO and an $Fe(CO)_4$ moiety (2, 3). This particular complex on warming undergoes a rearrangement with cleavage of an As–cyclobutene bond and formation of a new Fe–cyclobutene bond. The structure of the product of formula "$f_4$fars"$Fe_3(CO)_9$ is shown in Fig. 1 (3, 4). This was an early example of a ligand cleavage reaction. Recently the phenomenon has been recognized in a number of instances (5, 6).

It is important to understand the bond-making and breaking which occurs in these reactions since some are analogous to processes of catalytic importance; but most systems are not convenient for quantitative study. Fortunately the rearrangement reaction shown in Fig. 2 is quantitative. Here, the bridged derivative $f_4farsMn_2(CO)_8$, **1**, (6, 7) is converted quantitatively into its isomer "$f_4$fars"$Mn_2(CO)_8$, **2**, on heating (7, 8).

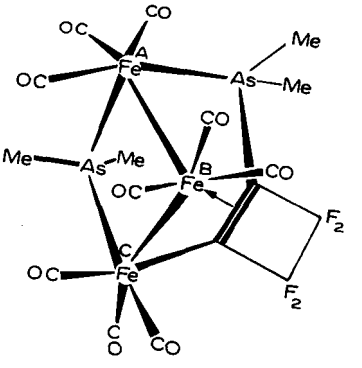

FIG. 1. The structure of "$f_4$fars"$Fe_3(CO)_9$.

The present investigation is concerned with a kinetic study of this reaction and the related ones involving $f_4farsRe_2(CO)_8$ and $f_4farsMnRe(CO)_8$.

Experimental

The complexes $f_4farsM_2(CO)_8$ (M = Mn or Re) were prepared as described previously (7).

Can. J. Chem. Downloaded from www.nrcresearchpress.com by 210.87.254.6 on 09/05/12
For personal use only.

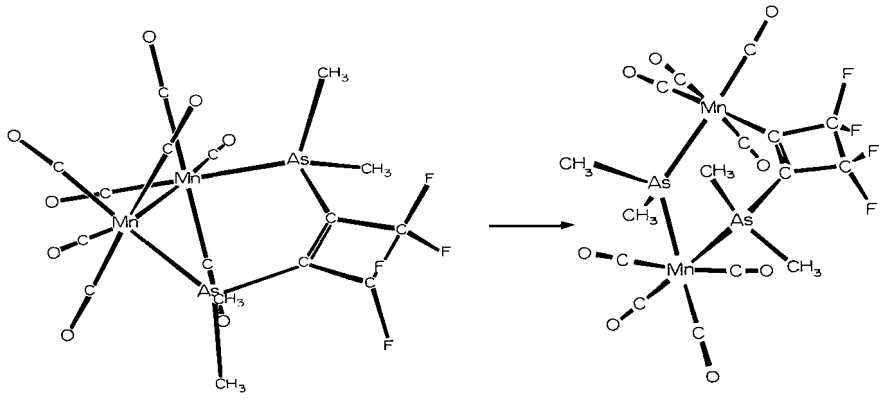

1 2

FIG. 2. The structures of $f_4farsMn_2(CO)_8$, **1**, and its isomer "f_4fars"$Mn_2(CO)_8$, **2**, which is produced on heating **1**.

Reaction of f_4fars with $MnRe(CO)_{10}$

f_4fars (1.8 g, 5.4 mmol) and $MnRe(CO)_{10}$ (1.7 g, 3.3 mmol) were refluxed in *m*-xylene for 6 h. The solvent was removed and the residue chromatographed on Florisil. The second yellow band which eluted with 95:5 petroleum ether/diethyl ether contained the product $f_4farsMnRe(CO)_8$. This was crystallized from *n*-hexane at −78° (0.25 g, 3%), ^1H n.m.r. (C_6D_6 solution): singlets at 0.72 and 0.80 p.p.m. downfield from TMS; ^{19}F n.m.r. (C_6D_6 solution): singlet at 106.2 p.p.m. upfield from $CFCl_3$; ν(CO) (C_6H_{12} solution): 2086(6), 2008(9), 1997(8), 1976(10), 1950(5), 1933(9), 1924(8), 1914(6) cm^{-1}.

Anal. Calcd. for $C_{16}H_{12}As_2F_4MnO_8Re$: C, 24.1; H, 1.5. Found: C, 24.4; H, 1.8.

Kinetic Studies

In a typical experiment 0.0206 g of $f_4farsMn_2(CO)_8$ was dissolved in 0.5402 g of C_6H_6 in an n.m.r. tube. The tube was degassed, sealed, and heated to 139°. The progress of the thermal rearrangement was followed by taking the ^1H n.m.r. spectrum every 15 min. Integration of one of the two product absorptions shown in Fig. 3*a* gave the extent of reaction. The results are shown in Table 1. The graph of log [$f_4farsMn_2(CO)_8$] at time *t* *vs.* *t* is linear indicating the conversion is first order in $f_4farsMn_2(CO)_8$. The slope gives $k = 3.00 \times 10^{-2}\ min^{-1}$.

The thermal rearrangements of $f_4farsRe_2(CO)_8$ and $f_4farsMnRe(CO)_8$ were followed in a similar manner. The former compound, in addition to undergoing the expected known rearrangement, also seemed to decompose slowly by a different route at the high temperatures used. Typical n.m.r. spectra obtained from $f_4farsMnRe(CO)_8$ are seen in Fig. 3*b*. The reaction does not go to completion as the spectrum after 95 min does not change on further heating. Furthermore there seem to be two products (see discussion). However in both cases integration of the major product peaks gave data which resulted in good first order plots. In the case of the mixed carbonyl only initial data (~2 half-lives) were used, since it is possible that the products achieve equilibrium with the starting complex which is present in about 10% of its original concentration.

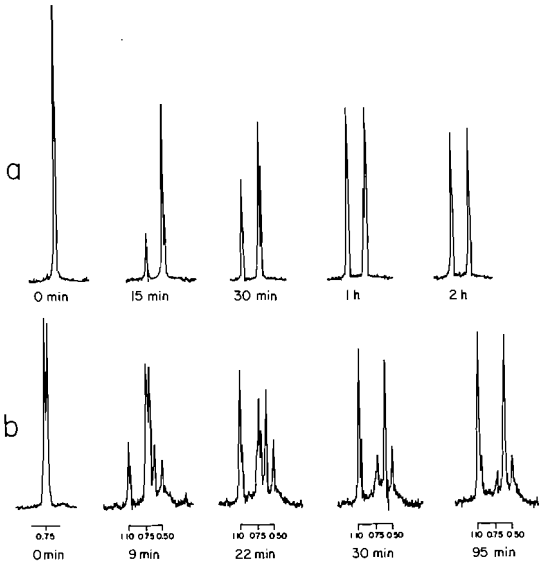

FIG. 3. Nuclear magnetic resonance spectra as a function of time obtained after heating (*a*) $f_4farsMn_2(CO)_8$, (*b*) $f_4farsMnRe(CO)_8$.

The rate constants derived in this way at various temperatures are listed in Table 2.

Results and Discussion

The new complex $f_4farsMnRe(CO)_8$ is obtained by heating f_4fars with $MnRe(CO)_{10}$. It presumably has the same bridged structure, **3**, as $f_4farsMn_2(CO)_8$ (Fig. 2, **1**). The n.m.r. spectrum of the mixed carbonyl derivative shows two arsenic methyl resonances (seen in Fig. 3*b* at zero time) and these must be due to the inequivalent ends of the ligand once com-

Can. J. Chem. Downloaded from www.nrcresearchpress.com by 210.87.254.6 on 09/05/12
For personal use only.

TABLE 1. Isomerization of $f_4farsMn_2(CO)_8$ at 139°

Time (min)	Calculated concentration of $f_4farsMn_2(CO)_8$ (arbitrary units)
0	50
15	32.5
30	24.0
45	14.0
60	10.0
75	6.0
90	4.0
105	3.0
120	0

plexed. The symmetrical manganese and rhenium analogs show only a singlet (Fig. 3*a*) so the "cyclohexene" ring (**1** in Fig. 2) is conformationally mobile.

The mass spectrum of $f_4farsMn_2(CO)_8$ and its isomer (Fig. 2, **1** and **2**) are identical indicating that the thermal isomerization under investigation takes place in the mass spectrometer. Thus the mass spectrum of $f_4farsMnRe(CO)_8$ should be that of the product isomers, **4** and **5**, since two are possible in this case.

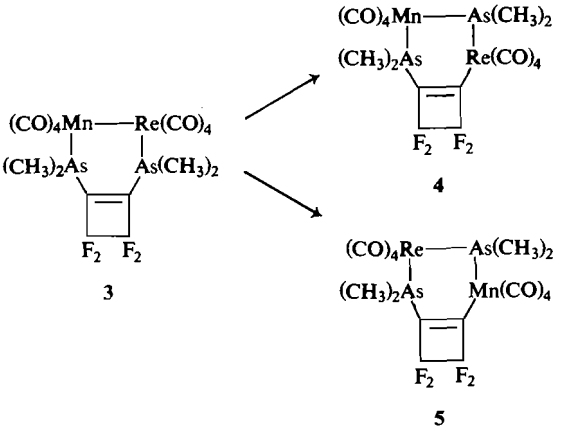

Apart from the usual parent ion followed by the loss of eight CO groups the mass spectrum shows a weak series of peaks corresponding to the sequence $\overline{C{=}CAs(CH_3)_2CF_2CF_2}.Mn(CO)_n$, n = 4–0. The corresponding sequence from a $Re(CO)_n$ moiety is absent. This indicates that only one of **5** or **4** is produced to any great extent and it seems likely that **5** would fragment in the observed manner.

In solution the rearrangement produces a major product with singlets at 1.10 and 0.60 p.p.m., which is presumably **5**, and a minor one with singlets at 1.08 and 0.50 p.p.m., presumably **4** (Fig. 3*b*).

Kinetic Results

The observed rate constants for the isomerization reaction are listed in Table 2. The activation enthalpies $\Delta H^{\ddagger}$ were derived from the Arrhenius plots. Although the temperature studies were minimal we consider that the magnitudes and trends of the parameters are significant.

The magnitude of $\Delta H^{\ddagger}$ for the manganese reaction is very similar to that reported by Poë and co-workers (9, 10) for the reaction of $Mn_2(CO)_{10}$ with oxygen (36.8 ± 0.4 kcal mol^{-1}). Substitution reactions of the type $Mn_2(CO)_9P(OC_6H_5)_3 + P(OC_6H_5)_3$ have similar activation energies (9, 10) and it seems that steric effects result in a lowering of the value for both types of reactions. It is argued that these reactions proceed via homolytic fission of the Mn—Mn bond. The analogous intermediate in the present set of reactions would be **6** in Fig. 4.

The σ–σ* transition (11) for $f_4farsMn_2(CO)_8$ occurs at 365 nm (ε = 9700) which is at longer wavelength than the parent carbonyl (343 nm) possibly indicating a weaker Mn—Mn bond. The bond length of the Mn—Mn bond in the parent carbonyl is 2.92 (3) Å whilst that of the f_4fars derivative is 2.971 (3) Å (8) again indicating a weaker interaction. The wavelength of the σ–σ* transition in the other complexes is 330 nm for $f_4farsRe_2(CO)_8$ and 340 nm for $f_4farsMnRe(CO)_8$, and thus the order of energy (and possibly of bond strength) for the three complexes is Mn_2 < MnRe < Re_2 which is that obtained for our kinetic $\Delta H^{\ddagger}$ values (Table 2). Even so homolytic cleavage as a first step cannot be regarded as being substantiated, and some contradiction comes from the observation that the free radical scavenger 3,5-di-*tert*-butyl-*O*-benzoquinone failed to affect the rate of isomerization of $f_4farsMn_2(CO)_8$.

In addition to the homolytic cleavage intermediate **6**, two other possible candidates are shown in Fig. 4. In **7**, coordinative unsaturation is achieved by forming the carbonyl bridged species. This type of intermediate has been postulated for halogen cleavage reactions (12, 13). In **8**, unsaturation is achieved by breaking the arsenic–metal bond.

Can. J. Chem. Downloaded from www.nrcresearchpress.com by 210.87.254.6 on 09/05/12
For personal use only.

TABLE 2. Kinetic and thermodynamic data for the isomerization of $f_4$farsMM′$(CO)_8$

	T (K)	k (min^{-1})	ΔH^* (kcal mol^{-1})*	ΔS^* (e.u.)
$f_4$farsMn$_2(CO)_8$	404	1.07×10^{-2}	36.8±2.0	15.0±4.7
	412	3.00×10^{-2}		
	420	5.92×10^{-2}		
$f_4$farsRe$_2(CO)_8$	466	6.93×10^{-3}	46.8±0.5	23.2±1.1
	470	1.09×10^{-2}		
	475.5	1.87×10^{-2}		
$f_4$farsMnRe$(CO)_8$	426.5	6.93×10^{-2}	39.2±2.8	20.9±2.8
	429	8.98×10^{-2}		
	435	1.68×10^{-1}		

*Errors are estimated from the Arrhenius plots.

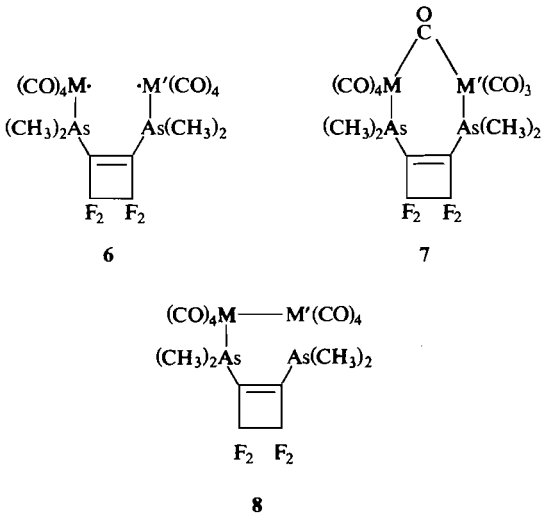

FIG. 4. Possible reaction intermediates for the thermal isomerization of $f_4$farsMM′$(CO)_8$.

In the case of all three intermediates it is possible to devise reasonable reaction paths leading to the final product. For example, oxidative addition of the As—C bond of **8** to the M′$(CO)_4$ moiety gives the correct atomic disposition.[1] Some of the rearrangements could be facilitated by temporary coordination of the double bond of the cyclobutene fragment in a manner analogous to that seen in "$f_4$fars"$Fe_3(CO)_9$ (Fig. 1).

The racemization of h^5-$C_5H_5MnP(C_6H_5)_3(NO)(COOR)$ has an activation enthalpy of 31.1 kcal mol^{-1} (15) and is believed to occur via phosphine dissociation. Thus our value of 36.8 kcal mol^{-1} could indicate arsenic dissociation to give **8**. The high activation entropy values (Table 2) could support some sort of dissociative intermediate.

[1]A similar mechanism has been suggested (14) for the reaction of $Re_2(CO)_{10}$ with $HSiCl_3$.

The authors are grateful to the National Research Council of Canada and the University of British Columbia for financial support.

1. W. R. CULLEN. Adv. Inorg. Chem. Radiochem. **15**, 323 (1972).
2. P. J. ROBERTS, B. R. PENFOLD, and J. TROTTER. Inorg. Chem. **9**, 2137 (1970).
3. W. R. CULLEN, D. A. HARBOURNE, B. V. LIENGME, and J. R. SAMS. Inorg. Chem. **9**, 702 (1970).
4. F. W. B. EINSTEIN, A. M. PILOTTI, and R. RESTIVO. Inorg. Chem. **10**, 1947 (1971).
5. M. I. BRUCE, G. SHAW, and F. G. A. STONE. J. Chem. Soc. Dalton Trans. 1667 (1973); R. T. SIMPSON, S. JACOBSON, and A. J. CARTY. J. Chem. Soc. Chem. Commun. 388 (1973); A. J. DEEMING and M. UNDERHILL. J. Chem. Soc. Dalton Trans. 2727 (1973); A. J. DEEMING, R. E. KIMBER, and M. UNDERHILL. J. Chem. Soc. Dalton Trans. 2589 (1973); A. J. CARTY, G. FERGUSON, H. N. PAIK, and R. RESTIVO. J. Organomet. Chem. **74**, C14 (1974); A. F. FOUST, M. S. FOSTER, and L. F. DAHL. J. Am. Chem. Soc. **91**, 5631 (1969).
6. L. Y. Y. CHAN and F. W. B. EINSTEIN. J. Chem. Soc. Dalton Trans. 111 (1973).
7. J. P. CROW, W. R. CULLEN, and F. L. HOU. Inorg. Chem. **11**, 2125 (1972).
8. F. W. B. EINSTEIN and A. C. MACGREGOR. J. Chem. Soc. Dalton Trans. 783 (1974).
9. J. P. FAUCETT, A. J. POË, and M. V. TWIGG. J. Chem. Soc. Chem. Commun. 267 (1973).
10. R. JACKSON and A. J. POË. Abstracts XVIth International Coordination Chemistry Conference, Dublin, 1974. Paper 3.20.
11. R. A. LEVENSON, H. B. GRAY, and G. P. CEASAR. J. Am. Chem. Soc. **92**, 3653 (1970).
12. L. I. B. HAINES, D. HOPGOOD, and A. J. POË. J. Chem. Soc. A, 429 (1968).
13. L. I. B. HAINES and A. J. POË. J. Chem. Soc. A, 2826 (1969).
14. J. K. HOYANO and W. A. G. GRAHAM. Inorg. Chem. **11**, 1265 (1972).
15. H. BRUNNER and H. D. SCHINDLER. Chem. Ber. **104**, 2467 (1971).

Can. J. Chem. Downloaded from www.nrcresearchpress.com by 210.87.254.6 on 09/05/12
For personal use only.

Configurational Entropy Change of Sodium Pyrophosphate

KIANG Y. LEUNG

School of Physics, University of Science of Malaysia, Penang, Malaysia

Received January 13, 1975

KIANG Y. LEUNG. Can. J. Chem. **53**, 1739 (1975).

Based on an analysis of the observed crystal structures of the phases of anhydrous sodium pyrophosphate, a calculation of the configurational entropy change of the system between the ordered ambient-temperature phase and the disordered hexagonal phase above 600 °C has been carried out. The result is $0.218R$ cal mol^{-1} deg^{-1} where R is the gas constant.

KIANG Y. LEUNG. Can. J. Chem. **53**, 1739 (1975).

En se basant sur une analyse des structures cristallines observés pour les diverses phases du pyrophosphate de sodium anhydre, on a effectué un calcul du changement d'entropie configurationnelle du système entre la phase ordonnée à la température de la pièce et la phase hexagonale désordonnée observée au dessus de 600 °C. Le résultat est $0.218R$ cal mol^{-1} deg^{-1}, où R est la constante des gaz. [Traduit par le journal]

Introduction

Anhydrous sodium pyrophosphate has a number of interesting order–disorder phase transformations between ambient temperature and its melting point. Leung (1) has studied in some detail the crystal structures of the phases of the system and the crystal structure of the ambient phase has been reported (2). A second paper on the crystal structure of the first phase above ambient temperature is under preparation.

Calculations of the configurational entropy of an order–disorder phase transformation have been carried out on a number of systems. Pauling (3) first calculated it for ice and Stephenson and Hooley (4) had worked on the ferroelectric crystal, potassium dihydrogen phosphate, both of which gave good agreement with the experimental values. In 1967, Okada (5) discussed the specific heat anomaly and calculated the configurational entropy change at the phase transition in copper formate tetrahydrate. Similar work was followed by Makita and Miki (6) on sodium trihydrogen selenite in 1970.

In this paper we calculate the configurational entropy change of sodium pyrophosphate based on the observed crystal structures of the phases of the system. Special attention is drawn to the idealized structure of the system discussed in (2) since all the observed phases can be described as a deviant from it. The present entropy calculation is feasible because certain structural features exist in the phase transformations which are summarized in Table 1. First, the ratio of the a and b axes is approximately $\sqrt{3}$ so that it is possible to inscribe a regular hexagon in the ab plane of the unit cell. Second, the sodium atoms and the bridging oxygen atoms of the pyrophosphate groups all lie in planes close to $z = 0$ and $z = \frac{1}{2}c_o$ and they occupy the highly symmetrical positions as shown in Fig. 1. Third, based on structural analysis, Leung and Calvo (2) inferred that the bridging oxygen atom of each pyrophosphate group is bonded to one of the three nearest coplanar sodium atoms (Fig. 1) and it is the change of orientation of this bond that gives rise to the observed phase transformations. Finally, it is found in ref. 1 that it is possible to divide the crystal into layers parallel to the ab plane at intervals $\frac{1}{2}c_o$ and that these layers can be considered as being weakly held together by sodium atoms between the terminal oxygen atoms of pyrophosphate groups in adjacent layers (*cf.* Na(3) and Na(4) of ref. 2).

All these features make it possible to state two basic postulates on the configurations that can exist within the system. From these postulates, we calculate the entropy change which could then be compared with experimental results. Unfortunately, however, at the time of writing, such results are not yet available.

Basic Postulates

Based on the structural features of the system we first divide the crystal into *basic cells*, having dimensions a_o, b_o, and $\frac{1}{2}c_o$, *i.e.* half the size of the crystal unit cell of the ambient-temperature phase. Then we propose the following postu-

TABLE 1. Phase transformations of sodium pyrophosphate*

Phase	Temperature (°C)	Space group	Cell dimensions a (Å)	b (Å)	c (Å)	β (deg)
I	20 → 405	$P2_12_12_1$	9.367(5) $\equiv a_0$	5.390(2) $\equiv b_0$	13.480(8) $\equiv c_0$	
II	405 → 515	$C2/c$	a_0	b_0	$2c_0$	93
III	515 → 520	Cc or $C2/c$	a_0	b_0	$3c_0$	90
IV	520 → 550					
V	550 → 700	$P6_3/mmc$	b_0	b_0	c_0	

*Reference 1.

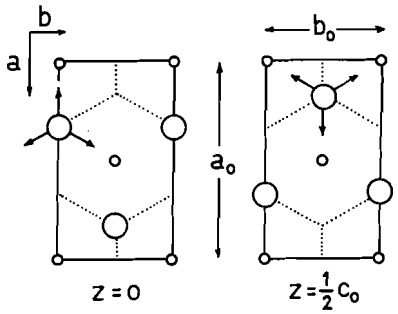

FIG. 1. Unit cell in ab plane at $z = 0$ and $z = \frac{1}{2}c_0$. Ratio $a_0:b_0$ is $\sqrt{3}$ approximately. Small circle represents sodium and large circle represents pyrophosphate group. Arrows from large circle represent the three possible bonds between sodium and bridging oxygen. P–P vector of pyrophosphate group is parallel to c axis. Note the inscribed regular hexagon in dotted lines.

lates regarding the configurations of the cells which can exist in the phases of the system:

Postulate (I). The bridging oxygen atom of each pyrophosphate group must be directed towards one of the three nearest coplanar sodium atoms.

Postulate (II). Each of the sodium atoms coplanar with the bridging oxygen atoms must have one and only one bridging oxygen atom of a pyrophosphate group directed towards it.

Fig. 2 shows that there can be only *eight* basic configurations satisfying these two postulates. We shall see below how a layer of the crystal can by constructed using these basic configurations.

One-Dimensional Checkerboards

We first consider a one-dimensional array of n basic cells along the b axis, each cell to be "filled" with an appropriate basic configuration. Following Okada (5), we call this array a one-dimensional checkerboard. Postulates *I* and *II* are to be observed in the process of filling the cells. Let $R(n)$ be the total number of arrangements of the n cells in this one-dimensional model. Then $R(n)$ can be divided into eight terms $R_i(n)$ $(i = 1, \ldots, 8)$ corresponding to each of the eight possible basic configurations in the nth cell. For example, $R_1(n)$ is the number of arrangements with configuration C_1 in the nth cell. Obviously

$$[1] \qquad R(n) = \sum_{i=1}^{8} R_i(n)$$

An array of $(n + 1)$ cells can be built by adding one cell next to the nth. However, a given configuration in the nth cell cannot take on all the eight possible basic configurations in the $(n + 1)$th cell without violating postulates *I* and *II*. For example, configuration C_1 can be followed only by configurations C_1, C_4, and C_5. In other words, for the case of $(n + 1)$ cells built by adding one cell next to the nth, we have

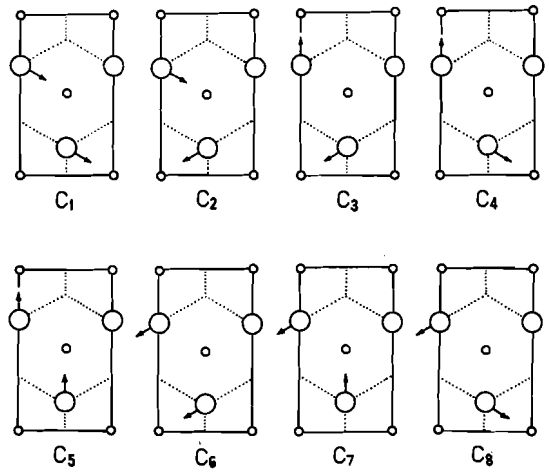

FIG. 2. Basic configurations of the system. Arrow shows orientation of bridging oxygen of a pyrophosphate group (large circle) to a coplanar sodium (small circle).

$$
\begin{aligned}
R_1(n+1) &= R_1(n) + R_2(n) + R_5(n) + R_7(n) \\
R_2(n+1) &= \quad\; R_2(n) + R_5(n) + R_7(n) \\
R_3(n+1) &= \quad\; R_2(n) + R_5(n) + R_7(n) \\
R_4(n+1) &= R_1(n) + R_2(n) + R_5(n) + R_7(n) \\
R_5(n+1) &= R_1(n) + R_2(n) + R_5(n) + R_7(n) \\
R_6(n+1) &= R_3(n) \quad\quad\; + R_6(n) \\
R_7(n+1) &= R_3(n) + R_4(n) + R_6(n) + R_8(n) \\
R_8(n+1) &= R_3(n) + R_4(n) + R_6(n) + R_8(n)
\end{aligned} \qquad [2]
$$

On addition, the l.h.s. of [2] becomes $R(n+1)$ using [1] and the r.h.s. can be simplified using [2] in terms of $R(n)$, $R(n-1)$, and $R(n-2)$. The result is the recurrence relation

$$R(n+1) = 4R(n) - 2R(n-1) + R(n-2) \qquad [3]$$

which is a linear difference equation of the third order

$$R(n+3) - 4R(n+2) + 2R(n+1) - R(n) = 0 \qquad [4]$$

where $n = 1, 2, \ldots$. To solve [4], we assume

$$R(n) = \beta^n \qquad [5]$$

which when substituted in [4] gives the cubic determinantal equation

$$\beta^3 - 4\beta^2 + 2\beta - 1 = 0 \qquad [6]$$

There are three roots to [6]: one real, A, and two complex, B_1 and B_2, which are conjugates to each other. If we write $B_1 = \rho e^{i\phi}$ where ρ = mod B_1 and ϕ = the phase angle, then $B_2 = \rho e^{-i\phi}$. A general solution of [4] can then be taken as

$$R(n) = c_1 A^n + \rho^n(c_2 \cos n\phi + c_3 \sin n\phi) \qquad [7]$$

where the constants c_1, c_2, and c_3 are to be determined from the boundary conditions

$$
\begin{aligned}
R(1) &= 8 \\
R(2) &= 28 \\
R(3) &= 98
\end{aligned} \qquad [8]
$$

which can be readily verified directly.

For later calculations, only the asymptotic value of ln $R(n)$ for very large n is needed. If $A > \rho$, [7] can be written in the form

$$R(n) = A^n\left(c_1 + \left(\frac{\rho}{A}\right)^n \times (c_2 \cos n\phi + c_3 \sin n\phi)\right) \qquad [9]$$

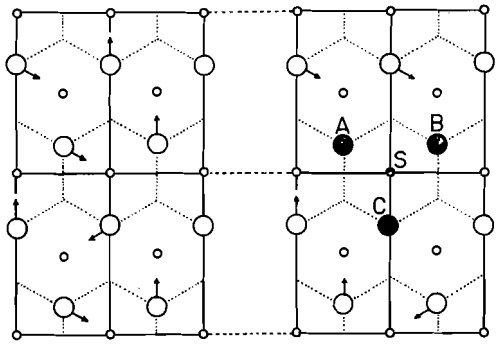

FIG. 3. The matching of two one-dimensional checkerboards to form a two-dimensional checkerboard.

giving

$$\ln R(n) = n \ln A + \ln\left(c_1 + \left(\frac{\rho}{A}\right)^n \times (c_2 \cos n\phi + c_3 \sin n\phi)\right) \qquad [10]$$

For very large n, the second term is negligible with respect to the first. We have, therefore

$$\lim_{n\to\infty} \ln R(n) = n \ln A \quad \text{if} \quad A > \rho \qquad [11]$$

Similarly

$$\lim_{n\to\infty} \ln R(n) = n \ln \rho \quad \text{if} \quad A < \rho \qquad [12]$$

Numerical calculations show that

$$A = 3.5116279 \text{ and } \rho = 0.5336429 \qquad [13]$$

so that [11] will be used in later calculations.

Two-Dimensional Checkerboards

Two-dimensional checkerboards can be obtained by putting two one-dimensional checkerboards alongside each other. It is then necessary to consider the *matching probability* of the individual cells. Referring to Fig. 3, consider a sodium atom such as S. In order to have postulates *I* and *II* satisfied, one of the following cases must hold:

(*a*) Bridging oxygen atom A *away* from S *and* bridging oxygen atom B *away* from S *and* bridging oxygen atom C *towards* S; probability $= \frac{5}{8} \times \frac{5}{8} \times \frac{3}{8}$.

(*b*) Bridging oxygen atom A *away* from S *and* bridging oxygen atom B *towards* S *and* bridging oxygen atom C *away* from S; probability $\frac{5}{8} \times \frac{3}{8} \times \frac{5}{8}$.

(*c*) Bridging oxygen atom A *towards* S *and* bridging oxygen atom B *away* from S *and*

bridging oxygen atom C *away* from A; probability = $\frac{3}{8} \times \frac{5}{8} \times \frac{5}{8}$.

Cases (*a*), (*b*), and (*c*) are mutually exclusive so that the total probability p is their sum, *i.e.* $p = 225/512$. Since there are n sites such as S for two one-dimensional checkerboards of n basic cells, the final matching probability P is given by

$$[14] \qquad P = p^n = (225/512)^n$$

Let $T(n,m)$ be the total number of possible arrangements when m one-dimensional checkerboards each of n basic cells are matched together. By definition

$$[15] \qquad T(n,1) = R(n)$$

For $m > 1$, it is obvious

$$[16] \quad T(n,m) = T(n,m-1) \cdot R(n) \cdot P = R(n)^m \cdot P^{(m-1)}$$

Taking logarithms, we have

$$[17] \quad \ln T(n,m) = m \ln R(n) + (m - 1) \ln P$$

When m and n are large, this can be simplified using [11] and [14]. Neglecting the term $n \ln p$ with respect to the others, the result becomes

$$[18] \qquad \ln T(n,m) = mn \ln (Ap)$$

This is the logarithm of the number of arrangements in a two-dimensional checkerboard, a quantity which is necessary to calculate the entropy. For sodium pyrophosphate the number of basic cells mn in a layer up the c-axis is $N/2$ where N is the number of molecules in that layer. If N refers to one mole of the crystal, and if k_B is Boltzmann's constant, it follows from [18] that the configurational entropy S of the system is given by

$$[19] \qquad k_B \ln T(n,m) = k_B \frac{N}{2} \ln (Ap) = \tfrac{1}{2} R \ln (Ap)$$

where R is the gas constant. Substituting the numerical values of A and p from [13] and [14] respectively, we have

$$[20] \qquad S = 0.218R \text{ cal mol}^{-1} \text{ deg}^{-1}$$

Actually, two-dimensional checkerboards themselves are stacked to form a three-dimensional crystal. Since interactions between adjacent layers are weak and the crystal is large enough to neglect the edge effect, no modification is necessary and [20] holds for the entire crystal.

Discussion

Equation 20 represents the configurational entropy change when the system changes from an ordered state to a disordered state when *any one* of the eight basic configurations (Fig. 2) is equally likely to occur in the system. This state of affairs corresponds to the transformations from the ordered ambient-temperature phase to the completely disordered hexagonal phase above 600 °C.

Experimentally we can measure the enthalpy ΔQ_i at each of the observed phase transition temperatures T_i of the system, and the total change of entropy is then given by

$$[21] \qquad \Delta S = \sum_i \frac{\Delta Q_i}{T_i}$$

where the summation is over the entire range of the phase transformations.

In the absence of experimental data which, at the time of writing, are in the process of being measured, it is of some interest to compare the anticipated results with some known entropy changes for orientational transformations in general. In the present calculation, we have neglected statistical Boltzmann factors in the partition function; that is, we assumed that all the eight basic configurations were energetically equivalent. Without neglecting this factor the calculated value would be smaller. Secondly, the transformations of the system between 500 and 600 °C as determined by differential thermal analysis (1), are generally such that the transition temperatures can only be estimated within about 3°. This means in measuring the enthalpy of the system, we would have to drop part of it over the temperature range. This was probably the case in copper formate tetrahydrate where Okada (5) observed a slightly higher theoretical value of the entropy, namely, 1.06 *vs.* 0.78 cal mol^{-1} deg^{-1}. In the case of sodium trihydrogen selenite (6), the agreement was very much better (1.59 *vs.* 1.53 cal mol^{-1} deg^{-1}) even though the statistical Boltzmann factors are again neglected.

It must be emphasized finally that result [20] follows directly from postulates *I* and *II* imposed on the system and it remains for measurements such as [21] to provide an experimental verification. A positive outcome will certainly lead to a better understanding of the mechanisms responsible for the phase transformations of the system of sodium pyrophosphate.

The author wishes to acknowledge with thanks many interesting discussions with Dr. Liew Yong Choy and Professor G. W. Groves, of the School of Physics, University of Science of Malaysia, Penang, Malaysia and with Professor Crispin Calvo of the Department of Chemistry, McMaster University, Hamilton, Ontario.

1. K. Y. LEUNG. Ph.D. Thesis. McMaster University, Hamilton, Ontario. 1973.
2. K. Y. LEUNG and C. CALVO. Can. J. Chem. **50**, 2519 (1972).
3. L. PAULING. J. Am. Chem. Soc. **57**, 2680 (1935).
4. C. C. STEPHENSON and J. G. HOOLEY. J. Am. Chem. Soc. **66**, 1397 (1944).
5. K. OKADA. Phys. Rev. **164**, 683 (1967).
6. Y. MAKITA and H. MIKI. J. Phys. Soc. Jap. **28**, 1221 (1970).

Mechanism of the Direct Photochemical Decomposition of Thietane and its Derivatives in the Vapor Phase, in Solution, and in Glassy Matrices

DAVID R. DICE[1] AND RONALD P. STEER[2]

Department of Chemistry and Chemical Engineering, University of Saskatchewan, Saskatoon, Saskatchewan S7N 0W0

Received January 8, 1975

DAVID R. DICE and RONALD P. STEER. Can. J. Chem. **53**, 1744 (1975).

The direct photolyses of thietane, 3-ethyl-2-propylthietane, and 3-methylthietane in the vapor phase, in solution, and in glassy matrices at low temperatures have been examined. The effects of varying the photolysis wavelength, the temperature, the pressure and the phase of the substrate, and of adding inert thermalizers on the nature and yields of the various products have been measured. The results are interpreted in terms of initial C—S cleavage to give a 1,4-biradical which may, in the gas phase, decompose or ring close before complete equilibration of the various rotamers is achieved, or which may be thermalized in condensed media and trapped in glassy matrices at low temperature.

DAVID R. DICE et RONALD P. STEER. Can. J. Chem. **53**, 1744 (1975).

On a étudié la photolyse directe du thiétanne, de l'éthyl-3 propyl-2 thiétanne et du méthyl-3 thiétanne en phase vapeur, en solution et dans des matrices vitreuses à basse température. On a mesuré les effets de la longueur d'onde de photolyse, de la température, de la pression, de la phase du substrat et de l'addition de thermaliseurs inertes sur la nature et le rendement des différents produits. On interprète les résultats en invoquant tout d'abord la rupture du lien C—S conduisant à un biradical-1,4 qui, en phase gazeuse, peut se décomposer ou reformer le cycle avant qu'un équilibre complet entre les divers rotamères ait pu s'établir, ou qui peut être thermalysé en milieux condensés et rester pris dans les matrices vitreuses à basse température.

[Traduit par le journal]

Introduction

Biradical intermediates have been postulated in numerous systems to explain the differences between the stereochemistry which is observed and that which is predicted for concerted reactions on the basis of the Woodward–Hoffmann "rules". In particular, the photodecomposition of the cyclic ketones (1) and cyclic azo compounds (2) have been extensively studied and compelling evidence for biradical intermediates has been obtained in these systems. Less complete investigations have been carried out on the cyclic ethers (3) and cyclic sulfides (4, 5).

The photochemistry of the thietane ring system in solution has been previously examined by Padwa and Gruber (4*a*) and in the gas phase by Weibe and Heicklen (4*b*). In the former work, the intermediacy of 1,4-biradicals was suggested although conclusive evidence for them was not obtained. In the latter work several intermediates of unspecified structure were introduced to explain the effects of varying the excitation wavelength on the yields of the C_2 and C_3 products. Subsequent investigations showed (5*b*) that the mechanism proposed in this study was unnecessarily complicated and could be simplified by taking into account the fact that propylene was the product of a slow secondary reaction between the reaction products and the substrate.

In previous communications we have presented evidence that 1,4-biradicals are intermediates in both the direct (5*a*) and mercury sensitized (5*b*) decomposition of 3-ethyl-2-propylthietane (EPT) in the gas phase. Triplet 1,4-biradicals from the mercury sensitized decomposition of EPT exhibit substantially longer lifetimes than the corresponding singlets produced on direct excitation and may readily be brought into thermal equilibrium with their surroundings by the addition of moderate pressures of inert thermalizing gases. The question of the nature of the biradicals produced on direct excitation has remained in doubt, however.

In this paper the results of experiments to elucidate the mechanism of the direct photolysis of thietane in the vapor phase and in solution are presented. It is shown that the primary process in the photodecomposition of thietanes

[1]Present address: Department of Chemistry, University of Western Ontario, London, Ontario.

[2]To whom correspondence should be addressed.

Can. J. Chem. Downloaded from www.nrcresearchpress.com by 210.87.254.6 on 09/05/12
For personal use only.

Can. J. Chem. Downloaded from www.nrcresearchpress.com by 210.87.254.6 on 09/05/12
For personal use only.

involves the formation of 1,4-biradical intermediates and that subsequent reactions of these species lead to the observed products. Evidence that singlet biradicals formed under different conditions exhibit different chemistries is presented.

Experimental

Apparatus

The vapor phase photolysis apparatus and light sources have been previously described (*5b*). Liquid phase photolyses were conducted in a 5 mm inside diameter quartz tube which could be connected to a vacuum system for degassing of samples and analysis of gaseous products. The light source for the liquid phase photolysis was a Hanovia 100 W medium pressure mercury lamp used in conjunction with a Vycor 7910 filter to isolate wavelengths greater than 250 nm. Photolyses of low temperature glasses were carried out using this same light source together with a 10 cm cell constructed of stainless steel and quartz which was cooled in a cryostat compatible with the Cary 14 spectrophotometer (6).

The light source used in the measurement of the direct photolysis quantum yields was an Osram 450 W high pressure xenon arc lamp. The desired region of the spectrum was isolated using a Zeiss M4Q-III quartz prism monochromator adjusted for a 10 nm bandwidth. Diethyl ketone (Koch-Light) was used as the primary actinometer, assuming that $\Phi(CO) = 1.0$ at 200 °C (7).

Materials

3-Ethyl-2-propylthietane (EPT), synthesized by the method of Searles *et al.* (8), was purified and separated into its *cis* and *trans* isomers by preparative gas chromatography using dinonylphthalate and Ucon Polar 50-HB-2000 columns. The purified starting materials were determined by g.c. analysis to be 99.9+% *trans*-EPT and 99.6% *cis*-EPT. 3-Methylthietane was prepared by the method of Bordwell and Hewett (9) and was purified by preparative g.c. Thietane (Eastman) was purified by preparative g.c. and was 99.99% pure.

Solvents for the liquid phase photolyses (cyclohexane and 3-methylpentane) were purified by repeated shaking with concentrated H_2SO_4 followed by washing with saturated aqueous $NaHCO_3$ and distilled water. The resulting materials were dried over molecular sieve and finally distilled through a spinning band column.

CO_2 and SF_6 (Matheson) were trap-to-trap vacuum distilled at temperatures at which their vapor pressures were less than 1 Torr, and were degassed at −196 °C prior to use. Traces (<1 p.p.m.) of an unidentified, innocuous impurity which could not be removed by this method remained in the SF_6. Ar (Matheson) was passed through a 10 ft by $\frac{1}{4}$ in. copper column which was packed with cleaned copper shot and which was heated to the temperature at which the characteristic color of copper oxide appeared on the outside of the tubing. No oxygen could be detected in these gases by g.c.

Analysis

Products were separated from one another and from residual reactants by low temperature trap-to-trap distillation prior to g.c. analysis, using standard high vacuum techniques. To prevent losses of ethylene when separating Ar from the other reactants and products, distillation at −210 °C (solid N_2) was necessary.

A Gow-Mac 69-500 thermal conductivity g.c. with a 10 ft by $\frac{1}{4}$ in. stainless steel column packed with Porapak Q was used to analyze the products which were noncondensable at −130 °C; condensables were analyzed using an F & M dual column flame ionization g.c. A 10 ft by $\frac{1}{8}$ in. stainless steel column packed with 10% tricresyl phosphate on Chromosorb P was used for most of the analyses. A 10 ft by $\frac{1}{8}$ in. column of 40% $AgNO_3$ in ethylene glycol on Chromosorb P preceded by a 1 ft length of tricresyl phosphate was used to separate the 3-heptene isomers. Products were identified by comparing their g.c. retention times with those of authentic samples. Identitities were confirmed by mass spectrometry. For some analyses a g.c. coupled to an AEI-MS12 mass spectrometer with a Biemann-Watson type helium separator was used.

Results

Vapor Phase Photolysis

In addition to the ethylene and propylene previously reported (*5b*), subsequent investigation has revealed that 1,2-dithiocane (DTO) is also formed in small yields when thietane (THT) is photolyzed in the vapor phase. The quantum yields of these products determined at wavelengths of 254, 290, and 313 nm, and temperature of 25 and 200 °C are shown in Table 1. Within experimental error, $\Phi(C_2H_4) + \Phi(DTO) = 1.0$ at all wavelengths for temperatures $\geq$200 °C. There is, however, a marked drop in $\Phi(DTO)$ on going from a wavelength of 313 nm to 254 nm and at 25 °C $\Phi(C_3H_6) + \Phi(DTO) < 1.0$. Within experimental error the rates of formation of both ethylene and propylene are independent of exposure time to at least 1% decomposition. However, it has been previously shown (*5b*) that propylene results from a slow reaction involving primary photoproducts and the measured $\Phi(C_3H_6)$ therefore depends on the extent of decomposition.

At 313 nm increasing the temperature from 25 to 235 °C caused an increase in the rates of formation of all products measured. These results are shown in Table 2. The results at low temperatures are somewhat less accurate than those at higher temperatures because of the tendency for polymer to collect on the cell windows and thereby reduce the intensity slightly as the run progressed. The decrease in intensity of the transmitted light over the course of a run was less than 5% at the lowest temperatures measured, however, and most of the data were collected at 200 °C where the deposition of polymer was insignificant. At temperatures

Can. J. Chem. Downloaded from www.nrcresearchpress.com by 210.87.254.6 on 09/05/12
For personal use only.

TABLE 1. Quantum yields in the direct photolysis of thietane vapor

P (THT) (Torr)	T (°C)	λ (nm)	$\Phi(C_2H_4)$†	$\Phi(C_3H_6)$	Φ(DTO)
46	25	313	0.48	—	—
40*	200	313	0.89	0.07	0.07
40	200	290	1.00	0.06	—
10	200	254	1.00	0.09	—
40*	200	254	1.01	0.12	0.01
30	200	254	0.99	—	—

*Average of three runs.
†± 0.05, maximum deviation of three runs.

TABLE 2. Effect of temperature on the direct photolysis of thietane vapor at 313 nm

	Rates (μmol min^{-1})		
T (°C)	C_2H_4* (×10^3)	C_3H_6* (×10^5)	DTO† (×10^3)
25	4.40	3	1.2
27	4.52	2	—
45	4.47	8	—
51	4.82	12	—
63	4.70	24	—
89	5.20	37	—
90	4.97	33	—
100	—	—	2.0
137	5.18	33	—
150	5.38	39	3.2
177	5.70	46	—
200	—	—	3.4
205	6.05	52	—
215	5.99	120	—
235	6.18	270	3.9
278‡	—	420	—

*P(THT) = 10.0 Torr; Pyrex filter with medium pressure lamp; $I_a = 6.92 \times 10^{-9}$ einstein min^{-1}. Total photolysis time = 300 min.
†P(THT) = 23.1 Torr; 313 nm liquid filter, high pressure lamp; $I_a = 5.17 \times 10^{-8}$ einstein min^{-1}. Total photolysis time = 30 min; assuming flame response equivalent to *n*-propyl disulfide.
‡Extensive thermal decomposition.

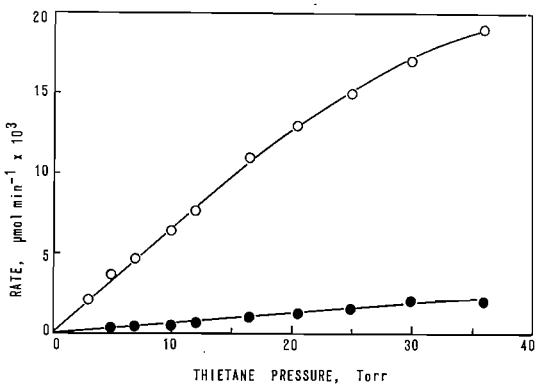

FIG. 1. Variation of $R(C_2H_4)$ and $R(C_3H_6)$ as functions of P(THT) in the direct photolysis of thietane vapor at 313 nm and 200 °C: ○, C_2H_4; ●, C_3H_6.

greater than about 235 °C, thermal decomposition of thietane took place at a significant rate.

The effect of varying the substrate pressure on the rates of formation of ethylene and propylene when thietane was photolyzed at 313 nm and 200 °C is shown in Fig. 1. The deviation from linearity of $R(C_2H_4)$ as a function of thietane pressure at higher pressures is to be expected in systems which follow the Beer–Lambert Law. The addition of up to an atmosphere of inert deactivating agents, CO_2, SF_6, or Ar, had no appreciable effect on the yields of either ethylene or propylene (*cf.* Table 3).

The major products detected in the direct photolysis of either *cis*- or *trans*-EPT at a wavelength of 254 nm and a substrate pressure of approximately 0.5 Torr were isomerized substrate, 1-butene, and *cis*- and *trans*-3-heptene. Small amounts of ethane, ethylene, propane, and propylene were also present, but were not analyzed routinely as the sum of the yields of the C_2 and C_3 products was less than 0.1% of the sum of the yields of C_4 and C_7 products.

The yields of 1-butene and of *cis*- and *trans*-3-heptene were directly proportional to substrate pressure (*cf.* Table 4), within experimental error. The addition of 760 Torr of CO_2 as an inert thermalizer, or of 10 Torr of NO as a radical scavenger, had no significant effect on the rates of formation of the measured products.

The only −130 °C noncondensable product in the photolysis of 3-methylthietane at 313 nm and 25 °C was propylene. At 60 or 205 °C traces of 2-methyl-1-propene were also present in the reaction products. There was no evidence for any ethylene formation under any of the conditions of photolysis investigated.

TABLE 3. Effect of added gases on the direct photolysis of thietane vapor at 313 nm*

Added gas	P(THT) (Torr)	P(Added gas) (Torr)	Rates (μmol min^{-1}) $C_2H_4 \times 10^3$	Rates (μmol min^{-1}) $C_3H_6 \times 10^4$
CO_2†	0.5	0	0.35	—
CO_2†	0.5	685	0.35	—
CO_2†	0.5	702	0.36	—
CO_2§	5.0	0	3.61	—
CO_2§	5.0	342	3.53	—
CO_2§	10.0	0	6.80	—
CO_2§	10.0	670	6.82	—
Ar§	5.0	0	3.60	3.7
Ar§	5.0	228	3.24	3.6
Ar§	5.0	628	3.33	—
Ar§	25.0	0	18.0	19
Ar§	25.0	650	17.1‡	20
SF_6‖	5.0	0	3.83	—
SF_6‖	5.0	620	3.45	—
SF_6‖	5.0	725	3.60	—

*λ = 313 nm (Pyrex filter and medium pressure lamp), T = 205 °C, $I_a = 4.0 \times 10^{-9}$ einstein min^{-1}.
†t = 1500 min.
‡Distillation at −210 °C.
§t = 300 min.
‖t = 150 min.

Condensed Phase Photolysis

Photolysis of thietane either as a neat liquid or in hydrocarbon solvents at room temperature is complicated both by the large numbers of products formed and by the formation of extensive amounts of a solid white material. Mass spectral analysis of this solid, which was insoluble in benzene, acetone, or carbon disulfide, indicated that this product is likely polymeric. There was no evidence of any product with a molecular weight of 138 (thioformaldehyde trimer) either in the solid itself or in benzene washings of the solid.

The major −130 °C noncondensable product in the liquid phase photolysis was ethylene. No propylene was detected. At least 20 different products condensable at −130 °C were detectable by gas chromatography, but only one of these, *n*-propyl disulfide, was present in sufficient quantities to be identified on the g.c.–m.s. combination. Traces of a product with a retention time identical to that of cyclohexene were also detected when cyclohexane solutions were photolyzed.

The relative rates of formation of ethylene and *n*-propyl disulfide are shown in Table 5. The decrease in the rates of product formation with increasing photolysis time is due to the consumption of the substrate and the increasing amount of light scattered from the cell by the solid material formed during the course of the run. However, within experimental error, the ratio of the rate of formation of ethylene to that of *n*-propyl disulfide is independent of the length of photolysis, indicating that these two products are not likely formed as a result of secondary photodecomposition.

Thietane was also photolyzed in several glassy matrices at low temperatures, and the u.v.–visible absorption spectra of the resulting mixtures were measured. Photolysis of thietane at −180 °C at a concentration of 0.02% by volume in EPA (diethylether:isopentane:ethanol, 5:5:2 by volume) or 3-methylpentane resulted in a new absorption with λ_{max} = 310 nm. Upon warming there was a slight decrease in intensity of this absorption (*cf.* Fig. 2). Near the softening point of the glass a reaction producing a white solid took place, and the λ_{max} of the photoinduced absorption shifted to shorter wavelengths. At about −50 °C, λ_{max} of this absorption was 300 nm. Recooling the mixture produced no significant spectral changes other than about a 20% increase in the absorbance due to contraction of the solvent.

Analysis of the solid product formed upon warming of the mixture was done by mass spectrometry. The low eV mass spectrum indicated that at least two products having molecular weights of 120 and 138 are present in the

Can. J. Chem. Downloaded from www.nrcresearchpress.com by 210.87.254.6 on 09/05/12
For personal use only.

Can. J. Chem. Downloaded from www.nrcresearchpress.com by 210.87.254.6 on 09/05/12
For personal use only.

TABLE 4. Rates of product formation in the direct photolysis of 3-ethyl-2-propylthietane at 313 nm* and 200 °C

Starting isomer	*P*(EPT) (Torr)	*P*(Addend) (Torr)	Rates (μmol/24 h)					
			Isomerized substrate	1-Butene	*trans*-3-Heptene	*cis*-3-Heptene	Total 3-heptene	*trans*-3-Heptene / *cis*-3-Heptene
cis	4.9	—	2.52†	1.66	0.59	1.20	1.79	0.49
cis-	8.2	—	—	2.44	0.99	1.97	2.96	0.50
cis-	4.9	10‡	—	1.70	0.62	1.15	1.77	0.54
cis-	4.9	760§	—	—	0.57	1.20	1.77	0.48
trans-	4.9	—	1.29	1.37	1.87	0.28	2.15	6.59
trans-	7.5	—	—	1.83	2.97	0.42	3.39	7.05
trans-	7.9‖	—	1.48	—	2.24	0.31	2.54	7.24

*313 nm (Pyrex filter and medium pressure lamp).
†Corrected for 0.3% *trans*-isomer in substrate.
‡NO.
§CO_2.
‖$T = 100$ °C.

TABLE 5. Rates of formation of ethylene and *n*-propyl disulfide from the photolysis of thietane in cyclohexane*

Time (h)	$R(C_2H_4)$ (μmol h^{-1})	$R(C_6H_{10}S_2)$ (μmol h^{-1})	$\frac{R(C_6H_{10}S_2)}{R(C_2H_4)}$
12.0	7.25	0.11_5	0.016
1.0	14.9	0.23_2	0.016

*λ > 250 nm (Vycor 7910 filter and medium pressure lamp), $T = 25$ °C, [THT] = 0.15 mol l^{-1}.

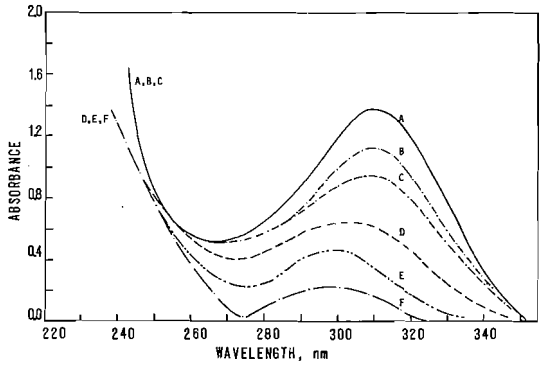

FIG. 2. Effect of temperature on the u.v. spectra of products formed in the photolysis of thietane in EPA at −180 °C: (*A*) $T = -180$ °C; (*B*) $T = -160$ °C; (*C*) $T = -140$ °C; (*D*) $T = -120$ °C; (*E*) $T = -50$ °C; (*F*) $T = +25$ °C.

solid. No such products were detected in the solid material formed in the liquid phase photolysis at room temperature.

Discussion

Vapor Phase Photolysis

Partial isomerization of the 3-heptene products and of the EPT substrate on direct photolysis of either *cis*- or *trans*-EPT is consistent with the formation of biradical intermediates in the primary photochemical step. From a consideration of molecular orbital symmetries (10) it is apparent that if a concerted photocycloreversion reaction were to occur from the excited state of thietanes, it should involve the *supra-supra* mode with 100% retention of configuration. The corresponding *antara-antara* split can likely be ruled out on steric grounds (10*b*). Therefore, the major mechanistic route in the photodecomposition of EPT and, by analogy, of thietane itself, must involve biradicals.

Cleavage of either *cis*- or *trans*-EPT at C_2—S would form 1,4-biradical **1**, while cleavage at C_4—S would result in the formation of 1,4-biradical **2**.

[1] 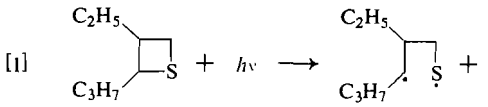

1

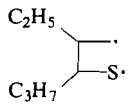

2

1 could subsequently ring close, or decompose to form 3-heptene and thioformaldehyde while **2** could ring close, or decompose to 1-butene and butanethial. Because of their thermal instability the thials would not have been detected with the analytical techniques used.

Biradical **1** is of principal interest because the isomeric composition of the 3-heptene product indicates the conformation of this biradical at the instant of its decomposition. If internal rotations about the C—C bonds of this biradical are fast compared with either its rate of decomposition or its rate of ring closure, thermal equilibrium would be achieved among the various biradical rotamers. On subsequent decomposition an equilibrium value of the ratio *R*(*trans*-3-heptene)/*R*(*cis*-3-heptene) would then be obtained. Such a thermal equilibrium distribution of the rotational conformers of the biradical is obviously not achieved in the direct photolysis of EPT as the value of *R*(*trans*-3-heptene)/*R*(*cis*-3-heptene) depends on the conformation of the starting isomer of EPT. This ratio equals 0.506 for the photolysis of *cis*-EPT and 6.88 for the photolysis of *trans*-EPT, independent of pressure. Internal rotation about the C—C bonds of biradical **1** must therefore occur at a rate which is comparable to the rate of its decomposition into 3-heptene and thioformaldehyde. Since the amount of isomerized substrate is also of the same order of magnitude as the amount of 3-heptene formed, the rate of ring

Can. J. Chem. Downloaded from www.nrcresearchpress.com by 210.87.254.6 on 09/05/12
For personal use only.

Can. J. Chem. Downloaded from www.nrcresearchpress.com by 210.87.254.6 on 09/05/12
For personal use only.

closure must be comparable to that of internal rotation.

A minimum of 57% of the products must come from the decomposition or ring closure of biradicals **1** and **2**. In such a "worst case" calculation it is first assumed that isomerized products have a 1,4-biradical precursor. Second, it is assumed that the *minimum* amount of unisomerized product resulting from the biradical can be calculated by assuming that there is an equilibrium in the *cis*- and *trans*- conformations (about bond C_3—C_4) of biradical **1**. The equilibrium constant used in this calculation was derived from a value of $\Delta G_{298}^0 = 0.33$ kcal mol^{-1} for the *trans*- and *cis*-rotamers of the triplet biradical (*trans*- lower in energy), measured in the mercury sensitized decomposition of EPT (*5d*). Since the value of *R*(*trans*-3-heptene)/*R*(*cis*-3-heptene) observed in the direct photolysis differs greatly from the equilibrium value, the actual amount of product resulting from an intermediate biradical should be substantially greater than 57%. While a molecular split cannot be ruled out unequivocally from this data, it is apparent that, if such a process occurs at all, it must be of minor importance in the direct photolytic decomposition of gaseous EPT.

The yield of 1-butene, the product resulting from initial C_4—S cleavage of EPT, is less than the total yield of the isomeric 3-heptenes, the ultimate products of initial C_2—S cleavage. This inequality is more pronounced for *trans*-EPT (*R*(3-heptene)/*R*(1-butene) = 1.71:1) than for *cis*-EPT (*R*(3-heptene)/*R*(1-butene) = 1.13:1). Two factors may contribute to this. First, a preference for C_2—S (compared to C_4—S) cleavage of EPT might be due to electronic effects because the biradical from C_2—S cleavage has one secondary radical center and should therefore be somewhat more stable than the biradical from C_4—S cleavage, which has only primary radical centers. However, even if C_2—S and C_4—S were to cleave with equal probability in EPT, steric effects in the resulting biradicals should yield the observed trend in the product ratios. From a consideration of biradical geometries it is apparent that cleavage of *cis*-EPT between C_4—S forms a biradical which is initially *cis-cis*[3] and which can rotate to a lower energy *trans-trans* biradical (see Fig. 3). There should therefore be a preponderance of the conformers of biradical **2** in the *trans-trans* conformation. However, cleavage of *trans*-EPT between C_4—S gives a *cis-trans* biradical that can only rotate to an approximately equiergic *trans-cis* conformation. A 1,4-biradical which is *trans* across C_2—C_3 cannot ring close, but can only decompose (11–13). Thus, biradical **2** from *trans*-EPT should undergo a greater amount of ring closure than biradical **2** from *cis*-EPT. Moreover, as rotation about bond C_2—C_3 appears somewhat less restricted in biradical **1** than in biradical **2**, there should be a higher proportion of biradical **1** in the *trans*-(C_2—C_3) conformation than there will be for biradical **2**. This should make decomposition more favorable from biradical **1** than from biradical **2**, and

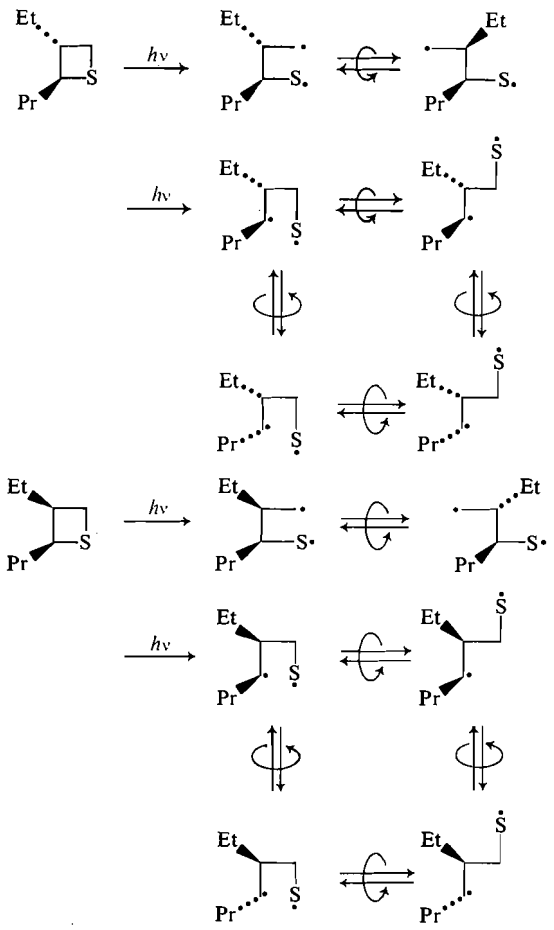

FIG. 3. Rotational conformations of biradicals **1** and **2**: Et = C_2H_5; Pr = C_3H_7; ↻ rotation about a biradical C—C bond.

[3]The conformation of the biradical is labelled first with respect to its conformation about the C_2—C_3 bond, and second, with respect to the conformation of the substituents.

Can. J. Chem. Downloaded from www.nrcresearchpress.com by 210.87.254.6 on 09/05/12
For personal use only.

even more favored when the substrate is *cis*-EPT.

Evidence that the direct photolysis of thietane vapor must also produce a biradical intermediate is (*a*) that DTO is formed, (*b*) that $\Phi(C_2H_4)$ is less than unity under certain conditions, (*c*) that $\Phi(C_2H_4)$ is temperature dependent, and (*d*) that the direct photolysis of thietane vapor with added cyclopentadiene results in the formation of a product which has its origin in the addition of a 1,4-biradical to cyclopentadiene (5*c*). These observations are inconsistent with molecular scission. Because substitution of the ring by alkyl groups does not substantially alter the nature of the primary process in the photolysis of the cyclobutananones (1*a*, *b*, *d*) and other compounds yielding biradical intermediates, it might also be expected that the photolyses of thietane and EPT in their lowest lying singlet states both involve biradical intermediates. The lack of ethylene formation in the photolysis of 3-methylthietane indicates that it is unlikely that any cross ring reactions are taking place. Therefore, the sole primary process in the direct photolysis of thietane vapor is likely cleavage of either C—S bond to form a 1,4-biradical, reaction 2.

[2] 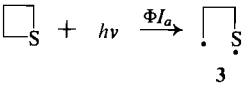

3

The lifetime of biradical **3** is probably at least as short as that of biradical **1** since the former has considerably fewer vibrational modes with which to dissipate any "excess" vibrational energy. It is apparent, therefore, that DTO must be formed by the attack of **3** on thietane, rather than by the combination of two biradicals. Even if the biradical combination reaction were diffusion controlled and had zero activation energy, the steady state concentration of biradicals would be so low that, under the conditions of these experiments, the rate of biradical combination would be about 10^{15} times slower than the observed rate of DTO formation. Thus, reaction of biradical **3** with the substrate to form a secondary intermediate biradical, **4**, which subsequently ring closes to form DTO (5*c*) is indicated. The reactions are:

[3] 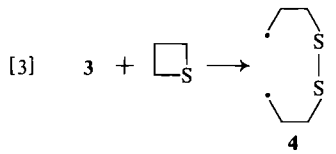

4

[4] **4** ⟶ DTO

Electrophilic attack by the thiyl portion of the biradical is predicted to occur predominately at the sulfur atom of thietane (16). This prediction is borne out by experiment as no products of the addition of **3** to thietane other than the cyclic disulfide were detected.

The question of the nature of biradicals **1**, **2**, and **3** at the instant of their formation and at the time of their subsequent reactions now must be considered. The biradical formed by breaking a C—S bond in the ground electronic state of thietane (*i.e.* by thermal decomposition) must be in its lowest lying singlet state initially and must lie on the same potential hypersurface as ground state thietane. Electronic excitation requires a transition between two different potential surfaces, however. Therefore, if photoexcitation of thietane results in C—S cleavage without intervening radiationless transitions, the initially formed biradical must lie on an excited singlet state potential surface. If, however, the excited state of thietane is not wholly unbound with respect to C—S separation then the biradical could be formed in a highly vibrationally excited ground state via predissociation (15). While it is not possible to determine unequivocally from the present data which of these processes is occurring in thietane, because no hint of any structure is apparent in the long wavelength band of the gas phase u.v. absorption spectrum (14), we assume that the upper state is unbound and that predissociation is not occurring. In any event, the lack of effect of thermalizing gases on the absolute or relative yields of the olefin products from either thietane or EPT indicates that hot triplet biradicals which are readily deactivated at moderate pressures (5*c*) are not involved in the direct photolysis mechanism. Intersystem crossing in either the excited thietane or the initially formed biradicals is therefore ruled out.

In this biradical mechanism both ethylene and thioformaldehyde would be formed by the unimolecular decomposition of biradical **3**, reaction 5.

[5] $\mathbf{3} \rightarrow C_2H_4 + CH_2S$

From thermochemical (17, 18) and spectroscopic data (19*a*, *b*, *c*), theoretical calculations (19*d*), and on the basis of the above arguments it is evident that thioformaldehyde could be formed in a low lying singlet excited state via

Can. J. Chem. Downloaded from www.nrcresearchpress.com by 210.87.254.6 on 09/05/12
For personal use only.

the dissociation of an electronically excited singlet biradical. There is at present insufficient evidence to draw any conclusions about the electronic state of the initial products of biradical decomposition, however.

If reaction 2 is the only primary process in the photolysis of thietane, it is apparent that biradical **3** must undergo reactions other than [3] and [5], as only at high temperatures does $\Phi(C_2H_4) + \Phi(DTO)$ approach 1.0 for photolysis at 313 nm. No other products were detected which could result from reaction of biradical **3**, other than the polymer which deposited on the cell walls. It therefore appears that a reasonable additional reaction of a ground state biradical **3** is ring closure, reaction 6, forming a vibrationally hot ground state thietane molecule.

[6] 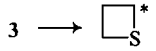

Such a hot molecule is expected to undergo the following further reactions:

[7] 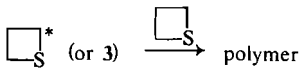

[8] 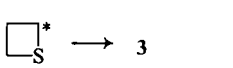

[9] 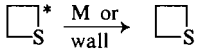

The corresponding overall ring closure process does occur to a significant extent on direct photolysis of EPT because substantial amounts of isomerized substrate are detected in that system. Thietane itself should exhibit similar behavior.

The biradical formed in reaction 8 need not necessarily be on the same potential hypersurface as the biradical formed in reacion 2, and might therefore undergo different reactions. The relative importance of reactions 6 to 9 is difficult to assess because the amount of polymer formed could not be measured. Qualitatively, less polymer is formed at higher temperatures, in agreement with the proposed mechanism. However, the lack of effect of up to an atmosphere of deactivating gases on the yield of ethylene in the thietane photolysis, or on the yields of any measured products in direct EPT photolysis, indicates either that the hot ring-closed molecule is efficiently quenched even at low pressures, or more likely, that any hot ring-closed products do not decompose or react further to give products which would be detected using the analytical techniques employed.

We believe that this latter alternative is correct. Thermal decomposition of thietane at temperatures of 250 °C in the dark photolysis cell yielded considerable amounts of an involatile, polymeric, yellow oil together with small amounts of hydrogen sulfide, ethylene, ethane, propylene, and propane. Ethylene was not a major product under the conditions employed. The polymer formed in the vapor phase photolysis may therefore be formed via the reaction of hot ground state thietane in a process analogous to thermolysis. The formation of small amounts of ethane, ethylene, propane, and propylene in the photolysis of EPT is also consistent with the fragmentation of a hot precursor.

The fraction of biradicals forming ring-closed products is greater in the EPT photolysis than in the photolysis of thietane itself. Not less than 43% of the observed products results from the ring closure of the biradical in the photolysis of *cis*-EPT at 200 °C and 313 nm for example. (Since this excludes the contribution of ring closure forming unisomerized substrate, the actual amount of ring closure will in fact, be greater than 43%.) However, by comparison, at 200 °C ring closure accounts for less than 4% of the products in the photolysis of thietane at 313 nm. ($\Phi(C_2H_4) + \Phi(DTO) = 0.96$.) Thus ring closure is less efficient in the unsubstituted thietane, consistent with its smaller number of vibrational modes.

The observed decrease in $\Phi(C_2H_4)$ as the wavelength of photolysis is decreased may be explained on a similar basis. As the energy input to the biradical is increased its rate of unimolecular decomposition must also increase. Consequently, the lifetime of the biradical will decrease, as will the probability of its collision with a thietane molecule to form DTO via reactions 3 and 4.

If one assumes that reaction 3 is the rate determining step in the formation of DTO, a plot of $\ln \{\Phi(C_2H_4)/\Phi(DTO)\}$ as a function of $1/T$ should be linear with an intercept of $\ln (A_5/A_3[THT])$ and slope of $(E_{a_3} - E_{a_5})/R$ (where A's are the Arrhenius preexponential factors, E_a's are the activation energies, and R is the gas constant). This plot is shown in Fig. 4, and is linear within experimental error. The

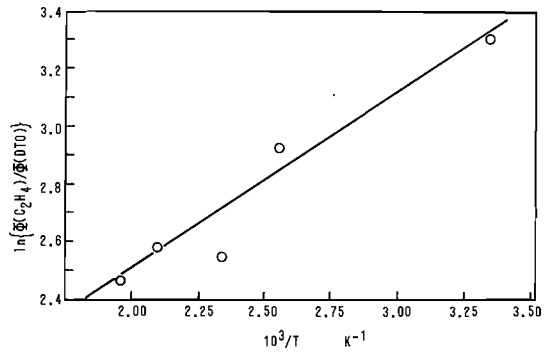

FIG. 4. Plot to determine the activation energy difference of reactions 3 and 6.

calculated activation energy difference, $E_{a_3} - E_{a_5} = 0.32 \pm 0.04$ kcal mol^{-1}.

Also, the lack of effect of adding high pressures of inert gases tends to indicate that reaction 8 is of limited importance in producing analyzable products. If one assumes that feedback via reaction 8 to produce ethylene does not occur to any significant extent, then

$$R(C_2H_4) = \frac{k_5\Phi I_a}{k_5 + k_6 + k_3[THT]}$$

At low pressures $I_a \simeq I_0\{\varepsilon l\}[THT]$ and therefore

$$R(C_2H_4) = \frac{k_5\Phi I_0\varepsilon l[THT]}{k_5 + k_6 + k_3[THT]}$$

and

$$1/R(C_2H_4) = \frac{k_3}{k_5\Phi I_0\varepsilon l} + \frac{k_5 + k_6}{k_5\Phi I_0\varepsilon l[THT]}$$

A plot of $1/R(C_2H_4)$ *vs.* 1/[THT] should therefore give a straight line with the ratio of slope/intercept $= (k_5 + k_6)/k_3$ at low thietane pressures. This plot is shown in Fig. 5. The value of $(k_5 + k_6)/k_3 = 6.3 \pm 1.1 \times 10^{-3}$ mol/l.

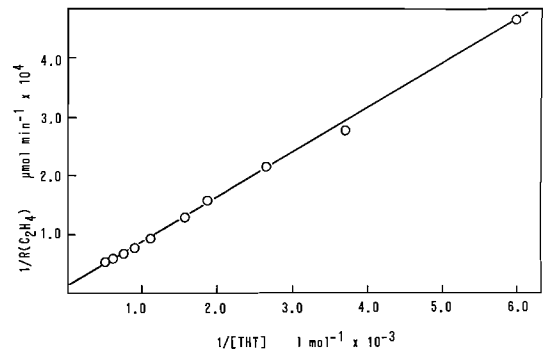

FIG. 5. Plot to determine the value of $(k_5 + k_6)/k_3$.

Condensed Phase Photolysis

There are three mechanisms which could lead to the formation of *n*-propyl disulfide in the photolysis of thietane in liquid solution. The first of these, the combination of two biradicals followed by H-abstraction, can be eliminated because the steady state concentration of biradicals must be small and it is very unlikely that the 1,4-biradical would have a lifetime sufficiently long to migrate from the solvent cage and encounter another biradical. A second mechanism might involve attack of the vibrationally relaxed (21) biradical on thietane in a reaction analogous to that postulated to lead to DTO in the gas phase. Subsequent H-abstraction from the solvent by biradical **4** could then yield the observed product. This reaction also seems unlikely as no DTO was detected in the liquid phase photolysis and it is difficult to see why H-abstraction should be so much more highly favored than ring closure in solution. The most probable mechanism involves H-abstraction by the alkyl portion of the biradical **3** to form a monoradical, *n*-propanethiyl, reaction 10.

[10] $\quad 3 + RH \rightarrow CH_3CH_2CH_2S\cdot + R\cdot$

Similar H-abstraction reactions have been observed in other systems involving biradicals in solution (22). Subsequently the combination of two *n*-propanethiyl radicals lead to the formation of *n*-propyl disulfide via reaction 11.

[11] $\quad 2CH_3CH_2CH_2S\cdot \rightarrow C_3H_7SSC_3H_7$

The fact that no 1,6-hexanedithiol is formed is consistent with this third mechanism because the rate of H-abstraction from solvent by the thiyl portion of the biradical will not be competitive with reaction 10 as shown by the following calculation. If it is assumed that the 1,4-biradical behaves essentially as if it were two independent monoradicals (a good assumption (20)), then very satisfactory estimates of the activation energies of H-abstractions by each end of the biradical can be calculated using the approach of Zavitsas (23). Using a C—S stretching frequency of 725 cm^{-1}, a C—S bond distance of 1.82 Å, and a C—S bond dissociation energy of 74.5 kcal mol^{-1} (23), the calculated E_a for H-abstraction from cyclohexane by a thermal thiyl radical is 16 kcal mol^{-1}. If a value of $E_a = 10$ kcal mol^{-1} is used for H-abstraction from cyclohexane by *n*-propyl radicals

Can. J. Chem. Downloaded from www.nrcresearchpress.com by 210.87.254.6 on 09/05/12
For personal use only.

Can. J. Chem. Downloaded from www.nrcresearchpress.com by 210.87.254.6 on 09/05/12
For personal use only.

(24) and similar Arrhenius preexponential factors are assumed for the two reactions, H-abstraction by the alkyl end of the 1,4-biradical should be of the order of 10^4 times faster than H-abstraction by the thiyl end at 298 °K.

Concentration changes due to thermal expansion of the solvent accounts for the slight decrease in the intensity of the absorption band centered near 310 nm on warming from −180 to −140 °C after photolysis of thietane in glassy matrices. It is quite clear, however, that at the softening point of the glass (∼ −140 °C) a chemical reaction takes place producing a second absorber having $\lambda_{max} \simeq 300$ nm and a white solid. While it is impossible to draw definite conclusions about the nature of the species responsible for these absorption bands, the following is nonetheless apparent. First it is unlikely that the absorption at 310 nm is due to trapped thioformaldehyde, as monomeric CH_2S should have a considerably different electronic absorption spectrum (19). The only other unstable species which could have the observed spectrum is trapped biradical **3**. Second, because the disappearance of the unstable absorber occurs concomitantly with the appearance of both a new stable absorber having $\lambda_{max} = 300$ nm and two new products of molecular weight 120 and 138, reactions converting trapped biradical **3** to other stable products must be occurring at the softening point of the glass. The solid of molecular weight 138 is likely a mixture of symmetrical and unsymmetrical trimers of thioformaldehyde, while the product of molecular weight 120 is almost certainly *o*-dithiane. This latter species has an absorption at $\lambda_{max} = 300$ nm ($\varepsilon = 290\ M^{-1}\ cm^{-1}$) (25) and may be produced by the reaction of thioformaldehyde with either biradical **3** or thietane. The high concentrations of both biradicals and thioformaldehyde which could be obtained by trapping these species at low temperatures might make these reactions feasible in the warmed glass even though they do not occur in the liquid phase at room temperature or in the gas phase.

This research was supported by the National Research Council of Canada for which the authors wish to express their gratitude.

1. (*a*) J. C. Hemminger, C. F. Rusbult, and E. K. C. Lee. J. Am. Chem. Soc. **93**, 1867 (1971); (*b*) H. A. J. Carless and E. K. C. Lee. J. Am. Chem. Soc. **94**, 1 (1972); (*c*) J. Metcalfe and E. K. C. Lee. J. Am. Chem. Soc. **94**, 7 (1972); (*d*) H. A. J. Carless, J. Metcalfe, and E. K. C. Lee. J. Am. Chem. Soc. **94**, 7221 (1972); (*e*) H. A. J. Carless, J. Metcalfe, and E. K. C. Lee. J. Am. Chem. Soc. **94**, 7235 (1972); (*f*) J. Metcalfe and E. K. C. Lee. J. Am. Chem. Soc. **95**, 4320 (1973); (*g*) J. C. Dalton, K. Dawes, N. J. Turro, D. S. Weiss, J. A. Barltrop, and J. D. Coyle. J. Am. Chem. Soc. **93**, 7213 (1971); (*h*) P. Dowd, A. Gold, and K. Sachdev. J. Am. Chem. Soc. **92**, 5724 (1970); (*i*) P. Dowd, G. Sengupta, and K. Sachdev. J. Am. Chem. Soc. **92**, 5726 (1970); (*j*) N. J. Turro and D. M. McDaniel. J. Am. Chem. Soc. **92**, 5727 (1970).
2. (*a*) D. I. Davies and S. J. Cristol. Adv. Free-Radical Chem. **1**, 193 (1965); (*b*) P. D. Bartlett and N. A. Porter. J. Am. Chem. Soc. **90**, 5317 (1968); (*c*) E. B. Klunder and R. W. Carr. Chem. Commun. 742 (1971); (*d*) R. J. Crawford, R. J. Dummel, and A. Mishra. J. Am. Chem. Soc. **87**, 3023 (1965); (*e*) S. D. Nowacki, P. B. Do, and F. H. Dorer. Chem. Commun. 273 (1972).
3. J. D. Margerum, J. N. Pitts, Jr., J. G. Rutgers, and S. Searles. J. Am. Chem. Soc. **81**, 1549 (1959).
4. (*a*) A. Padwa and R. Gruber. J. Org. Chem. **35**, 1781 (1970); (*b*) H. A. Wiebe and J. Heicklen. J. Am. Chem. Soc. **92**, 7031 (1970); (*c*) S. Braslavsky and J. Heicklen. Can. J. Chem. **49**, 1317 (1971); (*d*) W. E. Haines, G. L. Cook, and J. S. Ball. J. Am. Chem. Soc. **78**, 5213 (1956).
5. (*a*) D. R. Dice and R. P. Steer. Chem. Commun. 106 (1973); (*b*) D. R. Dice and R. P. Steer. J. Phys. Chem. **77**, 434 (1973); (*c*) D. R. Dice and R. P. Steer. Can. J. Chem. **52**, 3518 (1974); (*d*) D. R. Dice and R. P. Steer. J. Am. Chem. Soc. **96**, 7361 (1974).
6. G. A. Crosby and B. Pankuch. Chem. Instrum. **2**, 329 (1970).
7. J. G. Calvert and J. N. Pitts, Jr. Photochemistry. John Wiley and Sons, New York. 1966. p. 782.
8. S. Searles, Jr., H. R. Hays, and E. F. Lutz. J. Org. Chem. **27**, 2828 (1962).
9. F. G. Bordwell and W. A. Hewett. J. Org. Chem. **23**, 636 (1958).
10. (*a*) R. B. Woodward and R. Hoffmann. The conservation of orbital symmetry. Academic Press, Weinheim, Germany. 1970; (*b*) N. D. Epiotis. J. Am. Chem. Soc. **94**, 1924, 1935, 1941, 1946 (1972); (*c*) N. D. Epiotis. J. Am. Chem. Soc. **95**, 1191, 1200, 1206, 1214 (1973).
11. H. E. O'Neal and S. W. Benson. J. Phys. Chem. **72**, 1866 (1968).
12. E. L. Eliel, N. L. Allinger, S. J. Angyal, and G. A. Morrison. Conformational analysis. Interscience, New York. 1965. p. 9.
13. D. M. Golden, S. Furuyama, and S. W. Benson. Int. J. Chem. Kinet. **1**, 57 (1969).
14. (*a*) L. B. Clark and W. T. Simpson. J. Chem. Phys. **43**, 3666 (1965); (*b*) J. A. B. Whiteside and P. A. Warsop. J. Mol. Spectrosc. **29**, 1 (1969).
15. G. Herzberg. Molecular spectra and molecular structure, Vol. III. Van Nostrand, Toronto. 1966. p. 445 ff.
16. W. A. Pryor. Mechanisms of sulfur reactions. McGraw–Hill, New York. 1962. p. 84.
17. H. Mackle. Tetrahedron, **19**, 1159 (1963).

18. J. D. Cox. Tetrahedron, **19**, 1175 (1963).
19. (*a*) Kj. Rosengren. Acta Chem. Scand. **16**, 2284 (1962); (*b*) J. Fabian and R. Mayer. Spectrochim. Acta, **20**, 229 (1964); (*c*) A. Jones and F. P. Lossing. J. Phys. Chem. **71**, 4111 (1967); (*d*) N. C. Baird and J. R. Swenson. J. Phys. Chem. **77**, 277 (1973).
20. P. J. Wagner, P. A. Kelso, and R. G. Zepp. J. Am. Chem. Soc. **94**, 7480 (1972).
21. P. Rentzepis. Chem. Phys. Lett. **2**, 117 (1968).
22. P. J. Wagner and R. G. Zepp. J. Am. Chem. Soc. **94**, 287 (1972).
23. A. A. Zavitsas. J. Am. Chem. Soc. **94**, 2779 (1972).
24. A. F. Trotman-Dickenson. Adv. Free-Radical Chem. **1**, 1 (1965).
25. G. Bergson, G. Claeson, and L. Schotte. Acta Chem. Scand. **16**, 1159 (1962).

Can. J. Chem. Downloaded from www.nrcresearchpress.com by 210.87.254.6 on 09/05/12
For personal use only.

Entropy Production in Simple Chemical Reactions

HUW O. PRITCHARD

Centre for Research in Experimental Space Science, York University, Downsview, Ontario M3J 1P3

Received November 29, 1974

HUW O. PRITCHARD. Can. J. Chem. **53**, 1756 (1975).

It is shown that entropy production appears to be a completely monotonic function of time for several chemical reactions or reaction sequences taking place in closed systems at constant temperature; however this monotonicity principle does not extend to autocatalytic or oscillatory processes. Where it occurs, the complete monotonicity of entropy production stems essentially from the completely monotonic behavior of the species number densities as functions of time in the evolution of the reaction.

HUW O. PRITCHARD. Can. J. Chem. **53**, 1756 (1975).

On montre que la production d'entropie, pour plusieurs réactions chimiques ou pour des séquences de réactions se produisant en système circuit fermé et à température constante, est une fonction du temps qui est complètement monotone; toutefois cette monotonie ne s'applique pas aux processus autocatalytiques ou oscillatoires. Quand elle se produit, cette monotonie complète dans la production d'entropie dérive principalement d'un comportement complètement monotone des "densités en nombres des espèces" en fonction du temps lors de l'évolution de la réaction. [Traduit par le journal]

Can. J. Chem. Downloaded from www.nrcresearchpress.com by 210.87.254.40 on 09/05/12
For personal use only.

Introduction

We have shown recently that there appear to exist certain chemically reacting systems for which the time derivatives of the total entropy production have the following property

$$[1] \qquad (-1)^n \mathrm{d}^n S/\mathrm{d}t^n \leqslant 0$$

known as "complete" monotonicity; the process for which this apparent behavior was established was the vibrational relaxation and dissociation of a dilute diatomic gas at constant enthalpy in a shock wave, and eq. 1 was found to hold whether the system was considered to be isolated or whether there was a constant rate of loss of energy or mass from the flowing gas (1). Such a system is obviously far too complex to disentangle, and the origin of this special kind of monotonic behavior is not clear. This paper therefore presents the results of a ranging investigation intended to establish some limits on the validity of eq. 1 using a selection of simple chemical reactions or reaction sequences taking place isothermally and in closed systems.

The approach we have taken is a rather empirical one. No theorems exist for determining whether a given function is monotonic in the sense of eq. 1, nor does proof by induction appear to be possible (except for certain very simple cases, see *e.g.* eq. 16 below and discussion thereof). Thus, as we did before (1), we have chosen to work out numerically the derivatives of the entropy with respect to time to see whether their signs alternate. This is very time-consuming and so we chose only to inspect the first four derivatives, the expectation being that if the first four derivatives have the appropriate signs, all succeeding derivatives *may* also behave. In saying this, we recognize that examples exist in physics of functions which either converge or alternate up to a given order, and then the pattern suddenly breaks down; thus, our inspection of only the first four derivatives really can do no more than establish that this kind of monotonicity is not impossible. From a practical point of view, it is hard to imagine that derivatives of the entropy beyond the third could have any observational effect, and so from this point of view, inspection of four derivatives is plenty. However, from a theoretical point of view, had it been the case that eq. 1 had wide validity, it would have been very important, not only for its curiosity value, but as a stringent test of the correctness of the solutions of complex reaction sequences, in particular oscillating reaction sequences.

Elementary Processes

The rate equations for certain simple reactions *i.e.*

$$[2] \qquad \mathrm{A} \rightleftarrows \mathrm{B}$$

$$[3a] \qquad \mathrm{A} \rightleftarrows \mathrm{B} + \mathrm{C}$$

$$[3b] \qquad \mathrm{A} \rightleftarrows 2\mathrm{B}$$

$$[4] \qquad \mathrm{A} + \mathrm{B} \rightleftarrows \mathrm{C} + \mathrm{D}$$

Can. J. Chem. Downloaded from www.nrcresearchpress.com by 210.87.254.40 on 09/05/12
For personal use only.

can be integrated analytically (2) and it is therefore possible to write down successive derivatives of the entropy production with respect to time, *ad infinitum*. The following analysis of reaction 2 can be extended easily to reactions 3 and 4, and in fact exemplifies the problem perfectly. Starting from the Sackur–Tetrode equation it follows quite simply that at constant temperature

$$[5] \qquad \frac{1}{R}\frac{dS}{dt} = \frac{dN_A}{dt}\ln\left(\frac{\tilde{P}_A P_B}{P_A \tilde{P}_B}\right)$$

where S is the *total* entropy, P_A and P_B are the actual pressures of the species, and $\tilde{P}_A$ and $\tilde{P}_B$ refer to their pressures at equilibrium; the well-known result (3) that

$$[6] \qquad dS/dt \geqslant 0$$

falls out because

(*a*) dN_A/dt is negative when $P_A > \tilde{P}_A$ and $P_B < \tilde{P}_B$

(*b*) dN_A/dt is positive when $P_A < \tilde{P}_A$ and $P_B > \tilde{P}_B$

(*c*) dN_A/dt is zero when $P_A = \tilde{P}_A$ and $P_B = \tilde{P}_B$

Differentiation of eq. 5 then gives

$$[7] \qquad \frac{1}{R}\frac{d^2S}{dt^2} = \frac{d^2N_A}{dt^2}\ln\left(\frac{\tilde{P}_A P_B}{P_A \tilde{P}_B}\right) + \frac{dN_A}{dt}\left(\frac{d\ln P_B}{dt} - \frac{d\ln P_A}{dt}\right)$$

$$= \frac{d^2N_A}{dt^2}\ln\left(\frac{\tilde{P}_A P_B}{P_A \tilde{P}_B}\right) - \left(\frac{dN_A}{dt}\right)^2\left(\frac{1}{N_A} + \frac{1}{N_B}\right)$$

signs: (+ve) (−ve) − (−ve)^2 (+ve)

whence

$$[8] \qquad d^2S/dt^2 \leqslant 0$$

the signs shown under each term in eq. 7 relate to the process going from A → B *i.e.* condition (*a*); this is all well-known, since eqs. 5 and 7 are familiar equations (3) cast in the specific form appropriate to reaction 2. Continuing in the same fashion

$$[9] \qquad \frac{1}{R}\frac{d^3S}{dt^3} = \frac{d^3N_A}{dt^3}\ln\left(\frac{\tilde{P}_A P_B}{P_A \tilde{P}_B}\right) - 3\left(\frac{d^2N_A}{dt^2}\right)\left(\frac{dN_A}{dt}\right)\left(\frac{1}{N_A} + \frac{1}{N_B}\right) + \left(\frac{dN_A}{dt}\right)^3\left(\frac{1}{N_A{}^2} - \frac{1}{N_B{}^2}\right)$$

signs: (−ve) (−ve) − (+ve) (−ve) (+ve) + (−ve)^3 (?)

and

$$[10] \qquad \frac{1}{R}\frac{d^4S}{dt^4} = \frac{d^4N_A}{dt^4}\ln\left(\frac{\tilde{P}_A P_B}{P_A \tilde{P}_B}\right) - \left[4\left(\frac{d^3N_A}{dt^3}\right)\left(\frac{dN_A}{dt}\right) + 3\left(\frac{d^2N_A}{dt^2}\right)^2\right]\left(\frac{1}{N_A} + \frac{1}{N_B}\right)$$

signs: (+ve) (−ve) − [(−ve) (−ve) + (+ve)^2] (+ve)

$$- 2\left(\frac{dN_A}{dt}\right)^4\left(\frac{1}{N_A{}^3} + \frac{1}{N_B{}^3}\right) + 6\left(\frac{d^2N_A}{dt^2}\right)\left(\frac{dN_A}{dt}\right)^2\left(\frac{1}{N_A{}^2} - \frac{1}{N_B{}^2}\right)$$

− (−ve)^4 (+ve) + (+ve) (−ve)^2 (?)

both of which are unambiguously in conformity with the monotonicity principle, eq. 1, provided that $N_A \geqslant N_B$ if the reaction is proceeding from A → B *or* that $N_A \leqslant N_B$ if the reaction is proceeding in the opposite direction; this is because the last term in each expression contains the difference between N_A and N_B.

However, numerical examination of eqs. 9 and 10 suggests (within the limitations outlined earlier) that they do conform to the monotonicity principle for all N_A and N_B. Given a pair of forward and reverse rate constants and an initial concentration of one of the reactants, the standard form of the rate law (2) enables us to write down N_A, N_B, and dN_A/dt at any time t, in analytic form; simple differentiation of the latter leads to d^nN_A/dt^n, again in analytic form. Thus, assigning a self-consistent set of arbitrary

Can. J. Chem. Downloaded from www.nrcresearchpress.com by 210.87.254.40 on 09/05/12
For personal use only.

numerical magnitudes to the constants associated with reaction 2, *i.e.* equilibrium constant, temperature, energy change, standard entropy change, and so on, eqs. 9 and 10, can be computed exactly, and for a very wide range of sets of trial values, the third derivative of the total entropy with respect to time was always found to be positive, and the fourth was always negative. This implies that the last term in either eq. 9 or eq. 10, whose sign is indefinite, must be relatively unimportant, and examination of the numerical magnitudes reveals in fact that the dominant term is the first one in each of the eqs. 7, 9, or 10. The domination of the entropy derivatives d^nS/dt^n by the corresponding derivative of the number density d^nN_A/dt^n means therefore that since N_A is an exponential function (thus having alternating derivatives with respect to time) the derivatives of the entropy must also alternate; it is not surprising therefore to find that for those simple reaction systems, plots of $\ln|d^nS/dt^n|$ against time for $n = 1, 2, 3$, and 4, whilst not exactly so, are very close to being linear.

Consecutive Reactions

The behavior of the total entropy as a function of time was then investigated for a number of simple reaction schemes which are not amenable to analytic integration, *viz.*

[11] $A \rightleftarrows B \rightleftarrows C$

[12] $A \rightleftarrows B; \quad A + B \rightleftarrows C$

[13] $A \rightleftarrows B; \quad 2B \rightleftarrows C$

all taking place at constant volume, constant mass, and constant temperature. The technique used in these cases was a simple extension of the numerical work described for reaction 2 in the preceding paragraph. A complete self-consistent set of numerical rate constants and thermodynamic parameters was assigned to each reaction scheme, and the rate law was integrated by standard Runge–Kutta methods to give the concentrations of A, B, and C at any time t, starting from an arbitrary set of initial concentrations; such integrations can be performed to any desired numerical accuracy. Expressions analogous to eq. 5 were then constructed for the total rate of entropy production, and were differentiated analytically. Evaluation of these entropy derivatives then only required the knowledge of the successive derivatives of the concentrations d^nN_A/dt^n etc., and once N_A, N_B, and N_C have been determined numerically, these may be obtained analytically by differentiating the rate expression. For example, for reaction 11 we would have

$$\frac{dN_A}{dt} = -k_{1_f}N_A + k_{1_r}N_B$$

whence

$$\frac{d^2N_A}{dt^2} = -k_{1_f}\frac{dN_A}{dt} + k_{1_r}\frac{dN_B}{dt}$$
$$= -k_{1_f}(-k_{1_f}N_A + k_{1_r}N_B) + k_{1_r}(k_{1_f}N_A - [k_{1_r} + k_{2_r}]N_B + k_{2_r}N_C)$$

and so on; thus, once the actual concentrations are known, all their time derivatives follow automatically, and there is no need for numerical differentiations such as we were forced to use in our earlier work (1), and which are very difficult to perform with high precision. Again, the first four time derivatives of the total entropy alternated in sign in conformity with eq. 1; however, for reactions 12 and 13 only one set of arbitrary parameters was examined, and in view of other discussions of these reactions (4), it would seem prudent not to infer at this stage that these two processes could obey eq. 1 under all conditions.

Autocatalytic Processes

Two autocatalytic processes are commonly invoked in discussions of oscillatory phenomena (5), namely

[14] $A + B \rightleftarrows 2A$

[15] $2A + B \rightleftarrows 3A$

Applying the same techniques to these two reactions with a few sets of trial parameters, it is soon found that $dS/dt \geqslant 0$ always, but $d^3S/dt^3 < 0$ often, and $d^2S/dt^2 > 0$ sometimes; as before, the reactions are considered to be taking place at constant volume, mass, and temperature. The following empirical observation is strongly indicative that this failure to obey eq. 1 results from the fact that the rate law itself is no longer predominantly exponential. Reaction 14 can be considered as nothing more than reaction 2 with a time-dependent rate law, and in fact reaction 2 with a factor of $(1 + at)$ multiplying both forward and reverse rate constants could well be used to simulate the early stages of reaction 14. A logical step in developing the algorithm for this hypothetical process is to take

Can. J. Chem. Downloaded from www.nrcresearchpress.com by 210.87.254.40 on 09/05/12
For personal use only.

the numerical integration algorithm for reaction 2 and superimpose upon it the time dependence of the rate constants, and when this is done the (incorrectly) computed entropies actually conform to eq. 1. However, when the additional terms arising from the rate of change of the rate constant with time are added into the expressions for the entropy derivatives, eq. 1 fails; since each individual step of the numerical integration is piecemeal exponential in character, it is only through the inclusion of these terms that the nonexponential behavior of the rate law is carried through into the entropy derivatives in the numerical procedures.

At the time these calculations were performed, we were unaware that the rate equation for reaction 14 can be integrated analytically (5), and the segments of the trajectory for which $d^2S/dt^2 > 0$ can be located rigorously, obviating our trial-and-error numerical techniques.[1]

Tossing Coins

An interesting analog to reaction 2 can be constructed in the following way. Consider a tray containing a large number N of coins, all the same way up. A number a of the coins is then selected at random and thrown down, and the process repeated t times, always taking a coins each time. If the coins are loaded with a bias factor $\mathscr{H}/\mathscr{T}$ such that $\mathscr{H} + \mathscr{T} = 1$, then the information theory result for entropy production is

$$[16] \quad \frac{dS}{dt} = \frac{k}{N} e^{-at/N} \ln \left(\frac{a\mathscr{H} + e^{-at/N}}{a\mathscr{T} - e^{-at/N}} \right)$$

This expression is rather similar to eq. 5, and if the coins are unbiased, *i.e.* $\mathscr{H} = \mathscr{T} = \frac{1}{2}$, it is easily shown to be monotonic in the sense of eq. 1; if $\mathscr{H} \neq \mathscr{T}$, a term of indefinite sign appears in the third derivative and persists, as in the molecular case.

Developing further, if in using unbiased coins the handful is not constant in size, but is of the form $a = a_0(1 + bt)$, a situation closely similar to the autocatalytic reaction case is found. The first derivative of the entropy is unambiguously positive, but the second and successive derivatives contain terms of both signs and monotonicity is dependent upon the magnitudes of the various terms. However, it if is assumed that the signs of successive derivatives of the head or tail counts alternate in sign, the entropy derivatives can be shown also to alternate.

[1]J. Keizer. Personal communication.

Conclusions

The numerical experiments undertaken in this investigation show that for a number of simple reactions or reaction schemes, namely reactions 2, 3, 4, 11, and perhaps 12 and 13, taking place at constant volume, mass, and temperature, the time derivatives of the total entropy are probably completely monotonic in the sense of eq. 1; autocatalytic reaction steps like [14] and [15] however may have positive second derivatives, and subsequent calculations show that this quality persists in some parts of the path of the oscillatory reaction scheme

$$A \rightleftarrows X$$
$$B + X \rightleftarrows Y + D$$
$$2X + Y \rightleftarrows 3$$
$$X \rightleftarrows E$$

(treated as being a closed system with all reactions reversible; note also that under these conditions no trial sets of parameters were found which led to a cycling of the concentrations of the X and Y intermediates, see also ref. 7).

Moreover, several indications have been found that when monotonic behavior occurs, it is in a sense accidental, arising because the approach to equilibrium in simple reaction systems follows a monotonic path. Thus, as far as chemical kinetics is concerned, there seems to be no fundamental thermodynamic "meaning" to the monotonicity principle, eq. 1, despite the fact that many physical examples have been established (see refs. 3–11 of ref. 1). Such monotonicity will arise whenever the signs of d^nN_A/dt^n etc. alternate *and* these terms dominate numerically the expressions for the successive derivatives of the entropy with respect to time. Consequently, we have to assume that in our two previous observations of monotonic behavior (1, 6) for calculations on the vibration–dissociation coupling of a diatomic gas, essentially

$$A \rightleftarrows B \rightleftarrows 2C$$

the entropy production resembled that of a coupled pair of monotonic chemical processes, (rather like reaction 11, admittedly with very different time constants for the two steps) and that the accompanying changes in temperature, pressure, etc., were either themselves virtually

monotonic, or otherwise unimportant. Thus, whilst there seems to be no new principle of fundamental importance for entropy production in chemistry, there are aspects of the problem which are intriguing and worthy of further investigation, most of which can be approached analytically or semi-analytically using reactions 2, 11, and 14, and possibly some simple coin tossing analogs.

This work was supported by the National Research Council of Canada, and owes much to a great deal of careful algebraic and numerical work by Miss Peggy R. Hill.

1. H. O. PRITCHARD, N. I. LABIB, and D. L. S. MCELWAIN. Can. J. Chem. **52**, 2618 (1974).
2. S. GLASSTONE. Textbook of physical chemistry, 2nd ed. Macmillan & Co., London. 1946. pp. 1069–1073.
3. I. PRIGOGINE. Thermodynamics of irreversible processes, 3rd ed. John Wiley & Sons, Inc., New York. 1967.
4. R. J. TYKODI. Physica, **72**, 341 (1974).
5. J. KEIZER and R. F. FOX. Proc. Natl. Acad. Sci. U.S.A. **71**, 192 (1974).
6. D. L. S. MCELWAIN and H. O. PRITCHARD. J. Am. Chem. Soc. **91**, 7693 (1969).
7. B. F. GRAY and L. J. AARONS. Faraday Symposium on the Physical Chemistry of Oscillatory Phenomena, Royal Institution, London. December, 1974.

Can. J. Chem. Downloaded from www.nrcresearchpress.com by 210.87.254.40 on 09/05/12
For personal use only.

Properties of Concentrated Solutions of Indium Chloride

ALAN N. CAMPBELL

Department of Chemistry, University of Manitoba, Winnipeg, Manitoba R3T 2N2

Received January 13, 1975

ALAN N. CAMPBELL. Can. J. Chem. **53**, 1761 (1975).

Certain properties of concentrated solutions of indium trichloride, ranging in strength from 9.889 to 0.4070 *m*, have been investigated. These properties are: density, molar volume, specific and equivalent conductance, degree of ionization, ionization constant, relative viscosity, activities, and activity coefficients of solvent water and of solute. Two interesting results emerge, *viz.*, the specific conductance passes through a maximum at 3.5 *m*, and, if the ionization of indium chloride is treated as that of a binary electrolyte, the expression $\alpha^2 c/(1 - \alpha)$ is constant within 10% over the range 6.267 to 0.7363 *m* (13.90 to 2.122 *N*).

ALAN N. CAMPBELL. Can. J. Chem. **53**, 1761 (1975).

On a examiné certaines propriétés de solutions concentrées (de 9.889 à 0.4070 *m*) de trichlorure d'indium. Ces propriétés sont les densités, les volumes molaires, les conductivités spécifiques et équivalentes, les degrés d'ionisation, les constantes d'ionisation, les viscosités relatives, les activités et les coefficients d'activité de l'eau agissant comme solvant et des solutés. On note deux résultats intéressants: la conductivité spécifique passe par un maximum à 3.5 *m* et si l'on considère que le chlorure d'indium est un électrolyte binaire, l'expression $\alpha^2 c/(1 - \alpha)$ est une constante à 10% près entre 6.267 à 0.7363 *m* (13.90 à 2.122 *N*).

[Traduit par le journal]

Introduction

In previous communications (1–4) such properties as conductance, heats of solution and dilution, e.m.f.'s and activities, change of volume on dilution, etc., of relatively dilute solutions of indium trichloride ($m < 1$) have been studied. Because indium trichloride is very soluble, it appeared that it would be interesting to study the corresponding properties in the concentrated range, just as Campbell and Kartzmark, some years ago, studied the conductances of silver nitrate and of ammonium nitrate (5).

The properties reported in this paper are: density, specific and equivalent conductance, relative viscosity, and activity. The range of composition is from 9.889 to 0.4070 *m*, corresponding to 19.93 *N* (equivalent normal) down to 1.152 *N*.

Experimental

Materials

The indium chloride used consisted partly of a very pure strong (58 wt.%) solution, supplied gratuitously by Cominco, and of a solid prepared in the following way. Metallic indium was refluxed with excess of concentrated hydrochloric acid until all the indium had dissolved, a process requiring about 12 h. The product was evaporated on the water bath to syrupy consistency; on cooling, it solidified. Analysis at this point showed that the product contained slightly less chlorine (about 2%) than corresponded to $InCl_3 . 3H_2O$, *i.e.*, the product was slightly damp, but contained no free HCl. The salt was then dissolved in water and the crystallization repeated. Provided excess of concentrated hydrochloric acid is used in the preparation, the sole product is the trichloride, uncontaminated by the mono- or dichloride.

Anhydrous indium chloride cannot be otained by heating the trihydrate in a drying oven at 110°, because of the occurrence of the hydrolysis reaction

$$InCl_3 . 3H_2O \rightarrow In(OH)_3 + 3HCl$$

followed, no doubt, by dehydration to the oxide. The product of the above treatment is not more than 50% anhydrous chloride. The anhydrous chloride can, however, be obtained by heating in high vacuum at 70°.

Anhydrous chloride was used only in the preparation of solutions lying between 9.889 and 6.919 *m*; otherwise, the pure concentrated solution obtained from Cominco was used. Each individual solution was analyzed gravimetrically by precipitation as silver chloride.

Apparatus and Procedure

All measurements, except those of boiling point, were made at 25 °C. All the methods are standard and have been described elsewhere (1–3). A few words should be said about the determination of activity. This was done by the boiling point method, using a Cottrell apparatus. It was found that by sealing a stout platinum wire vertically through the bottom of the boiling tube, allowing about ¼ in. of wire to project on each side, bumping and superheating were entirely eliminated; boiling points were constant to ± 0.01°. The procedure was first to read the barometer (p). From this and tables of vapor pressure, the boiling point of water on the Centigrade scale was obtained. The apparatus was then charged with conductance water and the boiling point observed on the Beckman thermometer of the apparatus.

Can. J. Chem. Downloaded from www.nrcresearchpress.com by 210.87.254.40 on 09/05/12
For personal use only.

Can. J. Chem. Downloaded from www.nrcresearchpress.com by 210.87.254.40 on 09/05/12
For personal use only.

The apparatus was then charged with a solution of known concentration and the boiling point observed. This gave the vapor pressure of water at the boiling temperature of the solution ($p°$). The activity of the solvent water was then taken as $p/p°$ and from this, knowing the composition, the activity coefficient of the solvent was obtained. The activity coefficient of the solute results from the Gibbs–Duhem theorem, using the procedure described in Glasstone's *Thermodynamics for Chemists* (6). Since the measurements were made in the neighborhood of 100°, the results are not strictly comparable with those made at 25°. An objection might also be raised that since individual measurements were made over a range of 18°, they are not really comparable with one another, but it is known that activity coefficients are not very sensitive to temperature change.

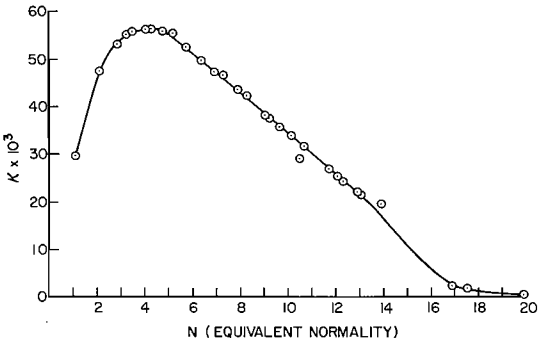

FIG. 1. Specific conductance κ, at 25°, *vs.* equivalent normality.

Results and Discussion

The numerical results are to be found in the Depository of Unpublished Data.[1] For the general reader, they are here represented graphically.

The densities of solutions can be calculated from the expression, derived from the experimental results, $d_4^{25} = 0.99707 + \alpha m^{1/2} + \beta m$ where m is the molality and α and β have the values 0.06374 and 0.09957 respectively. The molar volumes are readily calculated from the density data, when it is found that they decrease smoothly from a value of 22.74 ml mol^{-1} for a concentration of 9.889 m to 18.44 ml mol^{-1} at 0.5533 m. Since densities were determined with a pycnometer, and are therefore only accurate to the fourth decimal, at best, the figures for the apparent molar volume of the solute have no quantitative significance.

It is known theoretically that the specific conductance should pass through a maximum at some high concentration but this phenomenon is rarely realised because of the limited solubility in water. The reason for such a maximum is discussed by Campbell *et al.* (7). Figure 1, a plot of κ *vs.* concentration, shows very clearly that the specific conductance of indium trichloride passes through a maximum at 3.5 m.

The most interesting result is that, in the range of concentration 6 to 0.5 m, indium chloride behaves as a binary electrolyte

$$AB \rightleftarrows A^+ + B^-$$

having an ionization constant of $14.5 \times 10^{-2} \pm 0.5 \times 10^{-2}$, calculated on the basis of $\Lambda° = 132.6\ \Omega^{-1}\ cm^2\ equiv.^{-1}$. In the calculation of the ionization constant ($k = \alpha^2 c/(1 - \alpha)$), α was evaluated as $\alpha = \Lambda\eta/\Lambda°$, where η is the relative viscosity and Λ° the limiting equivalent conductance. This corresponds to the procedure used, for lack of a better, to reconcile calculated values of Λ with observed values; obviously the viscosity must have the effect of reducing Λ. Such a procedure is incorrect, since the Λ° used corresponds to the sum of $\lambda°In^{3+}/3$ and $\lambda°Cl^-$, whereas the binary ionization, corresponding to something like

$$InCl_3 \rightleftarrows InCl_2^+ + Cl^-$$

would require for its limiting conductance the sum of the ionic conductances of the products of the binary ionization. Nevertheless, since the ionization constant can be written

$$k = \frac{\Lambda^2 c}{\Lambda°(\Lambda° - \Lambda)}$$

it is apparent that, while the numerical value of k changes with the assumed value of Λ°, its constancy does not. Moreover, since the limiting conductances of most salts are constant within ~20 mho, even the numerical value of k should be acceptable as to order of magnitude.

The old formula of Ostwald, used in the calculation of k, is not accurate. The true "thermodynamic" dissociation constant K is connected with the conventional k by the formula

$$K = k f_{M^+} f_{A^-} / f_{MA}$$

where the f's represent the activity coefficients of ions and of undissociated salt. In very dilute

[1]Complete set of tabular data is available, at a nominal charge, from the Depository of Unpublished Data, CISTI, National Research Council of Canada, Ottawa, Canada K1A 0S2.

TABLE 1. Thermodynamic dissociation constant*

m	$K \times 10^2$	m	$K \times 10^2$	m	$K \times 10^2$	m	$K \times 10^2$
6.267	0.98	4.869	1.10	3.105	1.33	1.924	1.60
5.750	1.01	4.579	1.17	3.277	1.49	2.484	1.81
5.259	0.99	4.175	1.18	2.779	1.25	2.022	1.82
5.858	1.04	3.957	1.18	2.692	1.62	1.718	1.99
5.409	1.06	3.755	1.22	2.424	1.72	1.580	2.45
5.066	0.99	3.686	1.36	2.132	1.82	1.470	2.35
						1.247	2.34

*$t = 25$ °C.

solutions the above formula can be reduced to

$$\log K = \log k - 2A\sqrt{ac}$$

where A represents the Debye–Hückel slope. This formula will not be applicable to the concentrated solutions of this paper but if it can be assumed that A is a constant, any constant, then the above formula should be a test of constancy. At all events, it is worth trying. When this is done, the deviation from constancy is so slight that it cannot be shown on the graph used for plotting k (Fig. 2). The figures are therefore given in Table 1. Over the range of concentration for which k is roughly constant, *viz.* 1 to 6 m, K approaches much closer to constancy, but does show a small but steady increase from 0.98×10^{-2}, most of the increase occurring below 2 m. It is difficult to believe that such constancy is purely fortuitous.

Ferri (8) assumes the existence in solution of both $InCl_2^+$ and $InCl^{2+}$ ions.

The relative viscosity of the most concentrated solution (Fig. 3) is very high, 203.3 for 9.889 m, but it drops rapidly to 9.46 for 6.267 m, after which the decrease in viscosity with dilution is more normal. The region of abnormally high viscosity is also the region of low conductance. Ionization of any kind must be small in this region.

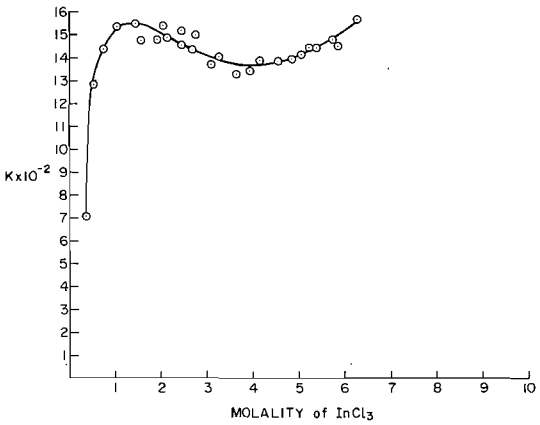

FIG. 2. Ionization constant k *vs.* molality, at 25°.

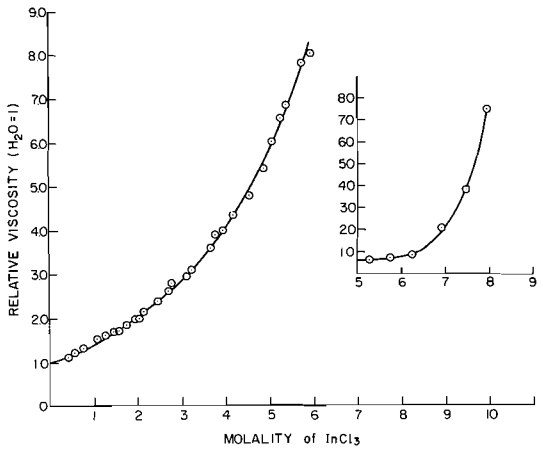

FIG. 3. Relative viscosity ($H_2O = 1$), at 25°, *vs.* molality.

The boiling points are not given because, since the barometric pressure in this region varies between 730 and 760 mm, they are not comparable. Table 2 reproduces the mean molal activities of the solvent water, as well as the activity coefficients of the solvent and of the solute. The latter are not comparable with the activity coefficients previously obtained (3) for the more dilute range because the present figures are calculated on the basis of $\nu = 2$ (binary ionization) but the former figures on the basis of $\nu = 4$, reasonable assumptions in both cases. Perhaps it is merely coincidental that the numerical values are not greatly different for the two regions.

Can. J. Chem. Downloaded from www.nrcresearchpress.com by 210.87.254.40 on 09/05/12
For personal use only.

TABLE 2. Activities of solvent and of solute

Solvent			Solute	
Molality of $InCl_3$	Activity a_w	Osmotic coefficient*	Activity	Activity coefficient $\gamma^{\pm}$ ($\nu = 2$)
6.267	0.5189	2.906	6.76	0.0129
5.858	0.5727	2.641	5.76	0.04657
5.409	0.5908	2.700		
5.066	0.6411	2.436		
4.869	0.6727	2.260	4.84	0.05102
4.579	0.6964	2.194		
4.175	0.7293	2.099		
3.957	0.7399	2.113	4.00	0.05344
3.755	0.7516	2.111		
3.686	0.7554	2.113		
3.277	0.8115	1.769	3.24	0.06788
2.779	0.8591	1.517		
2.692	0.8670	1.472		
2.424	0.8708	1.584	2.56	0.07664
2.132	0.9044	1.308	1.96	0.09381
1.924	0.9212	1.184		
2.484	0.8860	1.353		
2.022	0.9211	1.128		
1.718	0.9223	1.307		
1.580	0.9352	1.177	1.44	0.1194
1.470	0.9437	1.094		
1.247	0.9543	1.041	1.00	0.1624
1.071	0.9603	1.050		
1.039	0.9641	0.977	0.64	0.2314
0.7393	0.9869	0.495		
0.5533	0.9878	0.616		
0.4070	0.9935	0.445		

*$\phi = -55.51 (\ln a_w)/2m$.

1. A. N. CAMPBELL. Can. J. Chem. **51**, 3006 (1973).
2. A. N. CAMPBELL, E. M. KARTZMARK, and O. N. BHATNAGAR. Can. J. Chem. **52**, 1954 (1974).
3. A. N. CAMPBELL. Can. J. Chem. **52**, 3769 (1974).
4. A. N. CAMPBELL and S. Y. LAM. Can. J. Chem. **51**, 4005 (1973).
5. A. N. CAMPBELL and E. M. KARTZMARK. Can. J. Chem. **30**, 128 (1952).
6. S. GLASSTONE. Thermodynamics for chemists. 1st ed. Van Nostrand, New York. 1947.
7. A. N. CAMPBELL, A. P. GRAY, and E. M. KARTZMARK. Can. J. Chem. **31**, 617 (1953).
8. D. FERRI. Acta Chem. Scand. **26**, 747 (1972).

Can. J. Chem. Downloaded from www.nrcresearchpress.com by 210.87.254.40 on 09/05/12
For personal use only.

Complexes of Dimethylaminophosphazenes with Metal Ions

H. P. CALHOUN,[1] N. L. PADDOCK,[2] AND J. N. WINGFIELD[3]

Department of Chemistry, University of British Columbia, Vancouver, British Columbia V6T 1W5

Received December 20, 1974

H. P. CALHOUN, N. L. PADDOCK, and J. N. WINGFIELD. Can. J. Chem. **53**, 1765 (1975).

The preparation of complexes DDPN.$2MCl_2$ (M = Mn, Fe, Co, Zn), DDPN.$M(NO_3)_2$, (M = Mn, Co, Ni, Cu, Zn), (DDPN = $N_6P_6(NMe_2)_{12}$), and $N_9P_9(NMe_2)_{18}.2CoCl_2$ is described. All the complexes of the hexamer are of the high spin type and contain the cations $DDPNMX^+$ (X = Cl, NO_3). Their infrared and electronic spectra show that their molecular structures are essentially the same as those established crystallographically for the chlorocations (M = Co, Cu), in which, as a consequence of steric interactions, the metal has a distorted trigonal–bipyramidal environment. The complex with $Cu(NO_3)_2$ is exceptional in that the $DDPNCu^{2+}$ ion is formed in ionizing solvents, with a change in the stereochemistry of the metal. Coordination localizes π-electrons in nitrogen, weakens the ring bonds, and strengthens the exocyclic P—N bonds, as expected theoretically. Approximate values of ligand field parameters of the $Co(NO_3)_2$ and $Ni(NO_3)_2$ complexes are similar to those of complexes formed by simple amines; the phosphazenes act as σ-donors, their acceptor levels not being used significantly.

H. P. CALHOUN, N. L. PADDOCK et J. N. WINGFIELD. Can. J. Chem. **53**, 1765 (1975).

On décrit la préparation de complexes DDPN.$2MCl_2$ (M = Mn, Fe, Co, Zn), DDPN.$M(NO_3)_2$ (M = Mn, Co, Ni, Cu, Zn), (DDPN = $N_6P_6(NMe_2)_{12}$) et $N_9P_9(NMe_2)_{18}.2CoCl_2$. Tous les complexes de l'hexamère sont du type à haut spin et contiennent les cations $DDPNMX^+$ (X = Cl, NO_3). Les spectres électroniques et infrarouges montrent que leurs structures moléculaires sont pratiquement les mêmes que celles déterminées par cristallographie pour les chlorocations (M = Co, Cu) dans lesquels le métal est dans un environnement trigonal–bipyramidal à cause des interactions stériques. Considérant que l'ion $DDPNCu^{2+}$ se forme dans des solvants ionisants avec un changement de stéréochimie au niveau du métal, on peut considérer que le complexe avec $Cu(NO_3)_2$ est exceptionnel. Comme on peut le prédire sur une base théorique, la coordination localise les électrons π sur l'azote, affaiblit les liens du cycle et renforcit les liens P—N exocycliques. Les valeurs approximatives des paramètres de la théorie des champs de ligand pour les complexes de $Co(NO_3)_2$ et $Ni(NO_3)_2$ sont semblables à celles de complexes formés par des amines simples; les phosphazènes agissent comme donneurs d'électrons σ alors que leurs niveaux accepteurs ne sont pas utilisés d'une façon importante.

[Traduit par le journal]

Introduction

Cyclic phosphazenes $(NPX_2)_n$ act as donors to many types of acceptor, such as the proton (1), neutral (2) or cationic (3) metals, alkyl halides (4, 5), molecules such as iodine (3*a*, 6), and even phosphazenes themselves (7). In solution the alkyl and alkylamino derivatives are the strongest bases (8).

The effect of the substituent in the alkylphosphazenes is primarily to facilitate electron localization on nitrogen, by reducing the electronegativity of the phosphorus atom (5). The origin of the base properties of the dimethylaminophosphazenes $N_nP_n(NMe_2)_{2n}$ is different. The exocyclic groups are moderately electronegative, the donor properties now being a result of conjugative electron release by the substituents. Coordination may now occur at the ring atoms (normally), at the exocyclic nitrogen atoms (9), or at both ring and exocyclic sites (10); the dimethylaminophosphazenes are clearly more versatile ligands than the methylphosphazenes. We have studied some of their complexes with transition metal ions to find out, from their stereochemistry, magnetism, and spectra, how the metal and ligand interact.

Qualitatively, it was found easier to obtain complexes of the hexamer $N_6P_6(NMe_2)_{12}$ than of $[NP(NMe_2)_2]_{3-5}$, possibly because the cations can fit inside the larger ring, which then acts as a macrocyclic ligand (3*i*, 11). Most of the work reported concerns the complexes of

[1]Present address: Department of Chemistry, University of Alberta, Edmonton, Alberta T6G 2G2.

[2]To whom correspondence should be addressed.

[3]Present address: Rothamsted Experimental Station, Harpenden, Herts, England, AL5 2JQ.

Can. J. Chem. Downloaded from www.nrcresearchpress.com by 210.87.254.105 on 09/05/12
For personal use only.

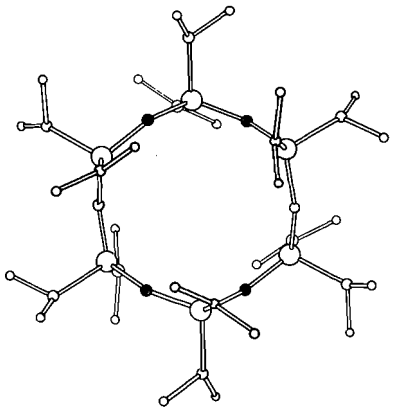

FIG. 1. The molecular structure of $N_6P_6(NMe_2)_{12}$. The shaded nitrogen atoms are those coordinated to metal.[4]

the hexameric dimethylamide (Fig. 1) with the chlorides MCl_2 (M = Mn, Fe, Co, Zn) and nitrates $M(NO_3)_2$ (M = Mn, Co, Ni, Cu, Zn). Complexes such as $N_9P_9(NMe_2)_{18}.2CoCl_2$ were formed with ligands of greater ring size, but they were harder to purify, and were not investigated systematically.

Experimental

Manganese(II) chloride, cobalt(II) chloride, and nickel(II) chloride were dehydrated by heating them with thionyl chloride under reflux. Iron(II) chloride was prepared by heating iron(III) chloride in boiling chlorobenzene (12). Zinc chloride was dried by heating it *in vacuo* at 200°; copper(II) chloride (Fisher) was used as received. Acetonitrile was distilled from calcium hydride, and diethyl ether, benzene, and petroleum ether from lithium aluminum hydride. Triethylamine was dried with calcium oxide. Dodecachlorocyclohexaphosphazene (13) and octadecafluorocyclonaphosphazene (14) were prepared by standard methods.

Ligands

Dodeca(dimethylamino)cyclohexaphosphazene(DDPN) was prepared as described (15). The nonameric dimethylamide was prepared from the fluoride. Dimethylamine (5.0 g, 0.11 mol) in 50 ml diethyl ether was added to an ice-cold solution of butyllithium in pentane (2.37 *N*, 34 ml) and stirred under reflux at −78° for 30 min. The excess of dimethylamine was allowed to evaporate and a solution of octadecafluorocyclononaphosphazene $N_9P_9F_{18}$ (2.0 g, 2.68 mmol) in 30 ml diethyl ether was added dropwise with stirring. The reaction mixture was stirred for 7 d at room temperature and then heated under reflux for a further 48 h. After extraction with water, the ether was removed. Elution of a solution of the product in petroleum ether (30–60°) on a silica column gave white crystals of octadeca(dimethylamino)cyclononaphosphazene, $N_9P_9(NMe_2)_{18}$, m.p. 232–234° (2.0 g, 62%).

Anal. Calcd. for $C_{36}H_{108}N_{27}P_9$: C, 36.1; H, 9.0; N, 31.6. Found: C, 36.2; H, 9.0; N, 31.7.

Complexes of DDPN with Metal Chlorides

Cobalt(II) chloride (0.136 g, 1.05 mmol) and DDPN (0.83 g, 1.04 mmol) were heated under reflux in acetonitrile for 84 h. The blue color became steadily darker as all the ligand went into solution. Removal of the solvent gave a pale blue solid which was washed with petroleum ether and recrystallized from $CHCl_3/CCl_4$ as blue crystals of $DDPN.2CoCl_2.CHCl_3$.

Anal. Calcd. for $C_{25}H_{73}Cl_7Co_2N_{18}P_6$: C, 25.5; H, 6.2; N, 21.4. Found: C, 25.6; H, 6.4; N, 21.2.

Other solvents used for recrystallization, such as benzene, were also incorporated into the lattice.

In a similar experiment with iron(II) chloride, attempted crystallization of the product from mixtures, including acetonitrile/toluene and methylene chloride/cyclohexane, gave semicrystalline products which contained solvent, which was removed *in vacuo* at 135° to give $DDPN.2FeCl_2$ as a brown powder.

Anal. Calcd. for $C_{24}H_{72}Cl_4Fe_2N_{18}P_6$: C, 27.4; H, 6.9; Cl, 13.5; Fe, 10.6; N, 24.0; P, 17.7. Found: C, 27.3; H, 7.0; Cl, 13.5; Fe, 10.7; N, 24.1; P, 17.3.

Similar complexes, of the general formula $DDPN.2MX_2$ were obtained with $MnCl_2$, $NiCl_2$, $NiBr_2$, and, $ZnCl_2$, but analyses, especially of the nickel complexes, showed variable and irreproducible incorporation of solvent, which could not be completely removed by heating *in vacuo*, though for the $MnCl_2$, $ZnCl_2$ complexes it did not interfere with the infrared spectra. This difficulty, probably arising from the presence in the crystal of bulky polynuclear anions, was avoided by the use of metal nitrates.

Complexes of DDPN with Metal Nitrates

Silver nitrate (0.17 g, 1 mmol) was added with stirring to a solution of cobalt(II) chloride (0.064 g, 0.49 mol) in 20 ml acetonitrile. A slight excess of DDPN (0.4 g, 0.5 mmol) was added to the filtered red solution and the reaction mixture was heated under reflux for 18 h. The solution was filtered from a small amount of brown precipitate and the solvent removed to give a purple solid. The product was washed with light petroleum (30–60) to remove the excess of DDPN, the yield of $DDPN.Co(NO_3)_2$ being quantitative. It was recrystallized from acetonitrile/toluene as blue air-stable crystals which appeared purple in reflected light.

Anal. Calcd. for $C_{24}H_{72}CoN_{20}O_6P_6$: C, 29.4; H, 7.4; Co, 6.0; N, 28.5; P, 18.9. Found: C, 29.5; H, 7.5; Co, 5.6; N, 28.6; P, 18.9.

A similar method was used to prepare $DDPN.Mn(NO_3)_2$, a buff powder, DDPN $Ni(NO_3)_2$, green crystals, $DDPN.Cu(NO_3)_2$, a green powder, and $DDPN.Zn(NO_3)_2$, a buff powder.

Anal. Calcd. for $C_{24}H_{72}MnN_{20}O_6P_6$: C, 29.5; H, 7.4; Mn, 5.6; N, 28.7; P, 19.0. Found: C, 29.3; H, 7.7; Mn, 5.3; N, 28.9; P, 19.1.

Anal. Calcd. for $C_{24}H_{72}N_{20}NiO_6P_6$: C, 29.4; H, 7.4; N, 28.5. Found: C, 29.1; H, 7.2; N, 28.5.

Anal. Calcd. for $C_{24}H_{72}CuN_{20}O_6P_6$: C, 29.2; H, 7.4; Cu, 6.4; N, 28.4; P, 18.8. Found: C, 29.0; H, 7.4; Cu, 6.1; N, 28.5; P, 19.0.

[4]Reproduced, by permission, from Wagner and Vos (21).

Can. J. Chem. Downloaded from www.nrcresearchpress.com by 210.87.254.105 on 09/05/12
For personal use only.

Can. J. Chem. Downloaded from www.nrcresearchpress.com by 210.87.254.105 on 09/05/12
For personal use only.

Anal. Calcd. for $C_{24}H_{72}N_{20}O_6P_6Zn$: C, 29.2; H, 7.3; N, 28.4; P, 18.8; Zn, 6.6. Found: C, 28.9; H, 7.4; N, 28.5; P, 19.0; Zn, 5.9.

Only the cupric nitrate complex appeared to be sensitive to air and moisture.

Complexes of the Nonameric Dimethylamide

Cobalt(II) chloride (0.026 g, 0.2 mmol) was treated under reflux with $N_9P_9(NMe_2)_{18}$ (0.24 g, 0.2 mmol) in acetonitrile for 20 h. Removal of solvent from the clear blue solution gave a blue solid which, after washing with petroleum ether, was reextracted with acetonitrile. The complex $N_9P_9(NMe_2)_{18}.2CoCl_2$ was obtained as a blue solid.

Anal. Calcd. for $C_{36}H_{108}Cl_4N_{27}P_9$: C, 29.7; H, 7.4; N, 25.9. Found: C, 29.6; H, 7.3; N, 25.9.

Reactions with $NiCl_2$, $NiBr_2$, gave similar products, but containing variable amounts of solvent. A complex with $Ni(NO_3)_2$ was obtained as an impure sticky brown solid.

Physical Measurements

Electrical conductivities of solutions of the complexes in acetonitrile and (in one case) in nitroethane were determined at room temperature, using a Wayne Kerr Universal Conductivity Bridge, Model B 221A (Table 1). The magnetic susceptibilities (Table 2) of the complexes DDPN.$M(NO_3)_2$ were measured at room temperature by the Gouy method. Corrections for the diamagnetism of the metal nitrate and the ligand were made by using Pascal's constants (16), combined with the result of a direct measurement on $N_6P_6Cl_{12}$ (17). Their electronic spectra were determined at frequencies less than 29 000 cm^{-1} (Table 3) using a Cary Model 14 spectrophotometer. Infrared spectra of all the complexes were obtained on a Perkin–Elmer Model 457 instrument, using mulls with either Nujol or hexachlorobutadiene, and a Perkin–Elmer Model 301 for the range 300–100 cm^{-1}. Figure 2 shows the spectrum of DDPN for the region 250–1350 cm^{-1}. Higher frequencies are given in Table 4 for the ligand and its complex with $Mn(NO_3)_2$, typical of all. The spectra of all the complexes are complicated but very similar, the lines falling into the groups shown in Fig. 3; detailed frequencies are given in Table 5.

Discussion

Conductivities

Crystal structure determinations (3*i*, 11) show that two DDPN complexes are ionic, the cation being of the form DDPN.MCl^+, the metal being 5-coordinated. If the metal:ligand ratio in the complex cation is assumed to be 1:1 in the other complexes, the nitrate complexes in solution can then (18) be assigned the formulae (DDPN.$MNO_3)^+NO_3^-$, (M = Mn, Co, Ni, Zn) and (DDPN.$M)^{2+}(NO_3^-)_2$, (M = Cu). The nitratonickel cation also appears to be partially dissociated. Although nitrogen ligands are known to displace oxygen ligands increasingly in the series Mn^{2+}–Cu^{2+} (19), the high conductivities are unlikely to be a result of solvolysis, since

TABLE 1. Molar conductances of the complexes in acetonitrile

Complex	Concentration ($M \times 10^2$)	Λ_M (cm^2 ohm^{-1} mol^{-1})
DDPN.$Mn(NO_3)_2$	1.02	124
DDPN.$Co(NO_3)_2$	1.00	120
DDPN.$Ni(NO_3)_2$	1.00	147
DDPN.$Cu(NO_3)_2$	1.02	245
DDPN.$Cu(NO_3)_2$	0.11	315
DDPN.$Cu(NO_3)_2$	0.26*	140
DDPN.$Zn(NO_3)_2$	0.99	126
DDPN.$2FeCl_2$	0.96	140
DDPN.$2CoCl_2.CHCl_3$	0.34	132

*In nitroethane.

TABLE 2. Magnetic susceptibilities of DDPN.$M(NO_3)_2$

M	μ_{eff} (B.M.)
Mn	5.74
Co	4.55
Ni	3.04
Cu	1.79

TABLE 3. Electronic spectra of DDPN.$M(NO_3)_2$ complexes[a]

M	Solvent	ν_{max}, cm^{-1} (ε_{max}, l cm^{-1} mol^{-1})	Assignment[b]
Co	$CHCl_3$[c]	7 090(15)	$4A_1'' + {}^4A_2''$(F)
		10 470(11)	$^4E''$(F)
		15 270(14)	$^4E'$(F)
		18 350(45)	$^4A_2'$(P)
		20 000(37)sh	$^4E''$(P)
Ni	CH_3CN[d]	8 620(17)	$^3E''$(F)
		13 900(26)	$^3A_1''$(F), $^3A_2''$(F), $^3A_2'$(F)
		22 200(60)	$^3E''$(P)
		23 900(92)	$^3A_2'$(P)
Cu	$CHCl_3$[e]	8 890(99)sh	$^2E'$
		11 425(138)	$^2E''$
		28 600(2930)	CT[f]
Cu	CH_3CN[g]	17 200–19 000(76)	(centered at 18 000)
		28 000	CT

[a]No absorption found for DDPN.$Zn(NO_3)_2$, or for DDPN.$Mn(NO_3)_2$ (10^{-2} *M*), in which the transitions are spin-forbidden.
[b]The strict symmetry of all the complexes is low. The symmetry labels given are those of the D_{3h} states which correspond most closely to those in the complexes.
[c]Ground state $^4A_2'$(F). In CH_3CN, bands are at: 7090(14), 10 470(6), 14 140(5), 18 280(31), 20 000(20)sh. Alternative assignments to the two lowest frequency bands are possible (46) and were used for the estimation of ligand field parameters. Those given are based on calculations by Ciampolini and Bertini (47).
[d]Ground state $^3E'$(F). Assignments based on ref. 48.
[e]Ground state $^2A_1'$.
[f]Charge transfer.
[g]In $MeNO_2$, bands are at 17 400–19 600, centered at 18 350(87).

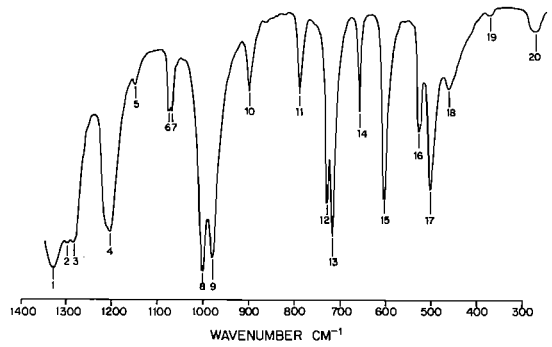

FIG. 2. The infrared spectrum of DDPN. Frequencies (cm^{-1}). *1*, 1323; *2*, 1290; *3*, 1280; *4*, 1198; *5*, 1143; *6*, 1071; *7*, 1063; *8*, 993; *9*, 972; *10*, 893; *11*, 783; *12*, 720; *13*, 711; *14*, 652; *15*, 593; *16*, 518; *17*, 493; *18*, 453; *19*, 376; *20*, 290.

TABLE 4. Methyl stretching and deformation frequencies (cm^{-1})*

DDPN	DDPN.$Mn(NO_3)_2$
3010(m)	3014(m, br)
2973(m)	—
2930–2840(vs, br, pr)	2934–2874(vs, br, pr)
2830(s)	2844(s)
2790(s)	2800(m)
1484(m)	1487(m)†
1460(s)	1457(s)†
1404(m)	1403(m)

*vs, very strong; m, medium; br, broad; pr, poorly relsoved.
†Broadened and split in all complexes, especially DDPN.$Cu(NO_3)_2$.

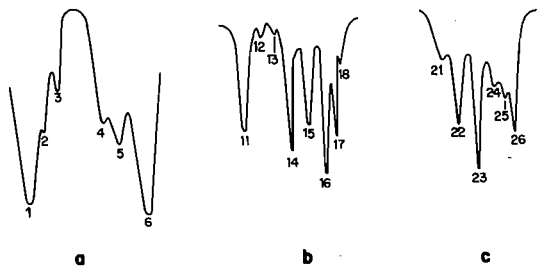

FIG. 3. Groups of bands in the infrared spectra of DDPN complexes; band numbers and frequencies are given in Table 5.

the conductance of the cupric nitrate complex in the less strongly coordinating solvent nitroethane is also about that expected for a 1:2 electrolyte (20). Solvent effects on the electronic spectra are referred to later. The chloride complexes have a different stoichiometry, consistent with the occurrence of metal in both cation and anion. In the crystal, the cobalt chloride complex is $(DDPNCoCl^+)_2.Co_2Cl_6^{2-}$, but a single conductance measurement cannot rule out dissociation of the anion; the nature of the anion in the ferrous chloride complex is similarly undecided. There is, however, no sign of dissociation in the cation, and it seems likely that the metal is always 5-coordinated in the crystal, and always in solution with the exception of the cupric (and possibly the nickel) nitrate complex.

Infrared Spectra

The infrared spectra of the complexes confirm that they all have the same structural pattern. The simplicity of the spectrum of the free ligand (Fig. 2) indicates a high symmetry (possibly as high as the S_6 found in the crystal (21)) which is entirely lost on complex formation. Only a few bands (Table 5, *7–10*) are related in an obvious way to the spectrum of the free ligand. The remainder of the lines now fall into well-defined groups (Fig. 3), and within each group not only the frequencies but also the relative intensities vary little between the different complexes.

There are some exceptions to these general statements. All the nitrate complexes have a band at 1343–1344 cm^{-1} attributed to the E' asymmetric stretching vibration of the free nitrate ion (22). The nitrate complexes also have an additional band at 1241–1251 cm^{-1}, and the band near 1295 cm^{-1} is much more intense than it is in the chloride complexes. Both bands may arise from interaction between the A_1 symmetric stretching vibration of a coordinated nitrate ion and a ring vibration. The band corresponding to the asymmetric stretching mode, which is found in nitrato tetraamino complexes of nickel at 1420–1495 cm^{-1} (23), may be obscured by $\delta(CH_3)$; the A_2'' out of plane bending vibration of the free nitrate ion may contribute to the weak band at $\sim$830 cm^{-1}. Bands specific to the chloride complexes are found below 400 cm^{-1} and are mostly weak and poorly resolved. No metal–ligand vibrations could be detected with certainty (some possibly obscured by the strong $\tau(CH_3)$ band at 315–333 cm^{-1}, 290 cm^{-1} in the free ligand); the distinctive low frequency bands in the spectra of the $FeCl_2$, $CoCl_2$, and $ZnCl_2$ complexes may reflect differences in anion structure or arrangement.

The stretching and deformation frequencies of the methyl groups (Table 4) are similar in range

Can. J. Chem. Downloaded from www.nrcresearchpress.com by 210.87.254.105 on 09/05/12
For personal use only.

TABLE 5. Frequencies of infrared bands of complexes DDPN.nMX$_2$ (cm^{-1})[a]

nMX$_2$	Mn(NO$_3$)$_2$	Co(NO$_3$)$_2$	Ni(NO$_3$)$_2$	Cu(NO$_3$)$_2$	Zn(NO$_3$)$_2$	2MnCl$_2$	2FeCl$_2$	2CoCl$_2$	2ZnCl$_2$
Band number									
1	1284	1294	1296	1297	1295	1292	1287	1291	1292
2	1261	1256	1273	1272	1259	1267	1268	1267	1268
3	1249	1243	1255	1252	1241	—	—	—	—
4	1193	1193	1193	1190	1190	1178	1207	1184	1220
5	1177	1174	1173	1171	1177	1172	1183	1169	1185
6	1154	1133	1143	1134	1134	1144	1141	1126	1133
7[b]	1064	1065	1064	1063	1062	1063	1063	1064	1063
8	1017sh	1018sh	1020	1015	1014	1014	1014	1014	1016
9	993	991br	991	993	991	992	990br	990	989br
10	978	—	979	980	979	979	—	977	—
11	855	860	858	860	856	855	855	855	854
12	831	830	815	831	829	833[c]	834[c]	832[c]	834[c]
13	813	814	804	819	811	812	810	814	815
14	794	792	794	792	792	794	793	793	794
15	770	770	771	769	769	770	769	771	772
16	746	747	747	746	746	746	744	748	745
17	732	733	741	731	731	731	730	730	731
18[d]	724	725	730	724	724	723	722	722	719
19[e]	634	633	636	632	631	633	632	632	631
20[e]	602	605sh	607	—	605	662	608(sh)	612	604
21	584	599	591	617	588	588	595	599	593
22	564	571	570	574	569	565	568	564	566
23	544	541	543	549	541	542	540	534	536
24	520	523	515	504	521	522	521	521	520
25	508	510	511	491	515	505	504	502	504
26	494	496	494	480	493	494	496	493	493
27[f]	463	464	462	472	466	463	462	464	461
28	439	436	435	434	436	440	436	439	436
29	402	409	—	404	406	404	409	411	406
30[g]	313	315	315	318	315	321	323	333	324

[a]Additional weak bands: Mn(NO$_3$)$_2$, 417; Co(NO$_3$)$_2$, 187, 274; Zn(NO$_3$)$_2$, 258; MnCl$_2$, 225, 247; FeCl$_2$, 357, 374(m); CoCl$_2$, 106, 242, 253; ZnCl$_2$, 111, 130, 226 cm^{-1}.
[b]See text. Band *7* is of medium intensity, *8* and *10* are weaker shoulders on the very strong band *9*.
[c]Weaker than in the nitrate complexes.
[d]Some contribution from a Nujol band.
[e]Both *19* and *20* weak, except for DDPN.Cu(NO$_3$)$_2$, which has medium absorption.
[f]Bands 27–29 vw, 30w–m.
[g]Broadened to low frequency, with component ~290 cm^{-1}.

to those in the free ligand, in dimethylamine itself (24), and in Me_2NPSF_2 and $(Me_2N)_2PSF$ (25). There are shifts in individual frequencies and intensities, especially for the Cu(NO$_3$)$_2$ complex, but the band at 2790 cm^{-1}, although weakened, does not disappear, as it does when an Me_2N group is complexed through nitrogen (26). The bands at 1198, 1071/1063, and 993/972 cm^{-1} in the spectrum of the free ligand are characteristic of NC_2 stretching and methyl rocking modes of the NMe_2 group in $N_3P_3Cl_5NMe_2$ (1173, 1063, 998 cm^{-1}) (27) and $N_4P_4Cl_7NMe_2$ (28), though detailed assignments differ (25, 29). In the complexes the lowest frequency bands are broadened and split (Table 5, bands *8–10*), and the bands at 1064 cm^{-1} are sufficiently broadened to obscure the doublet structure without change of frequency. Again, there is no indication of coordination of the exocyclic nitrogen atoms to the metal.

The skeletal modes are hard to assign and are in any case greatly changed on complex formation; the band which occurs at 652 cm^{-1} in the spectrum of the free ligand disappears completely. The free ligand has a very strong band at 1323 cm^{-1}, arising from a degenerate asymmetric stretching vibration. On complex formation its frequency is reduced (upper limit ~1295 cm^{-1}) and probably split, though possible lower frequency components could not be distinguished from $\nu(NC_2)$ and $\rho(CH_3)$. The lower frequency ranges (Fig. 3*b* and *c*) are very similar for all the complexes, only the Cu(NO$_3$)$_2$ complex showing some variation (Table 5). The general qualita-

Can. J. Chem. Downloaded from www.nrcresearchpress.com by 210.87.254.105 on 09/05/12
For personal use only.

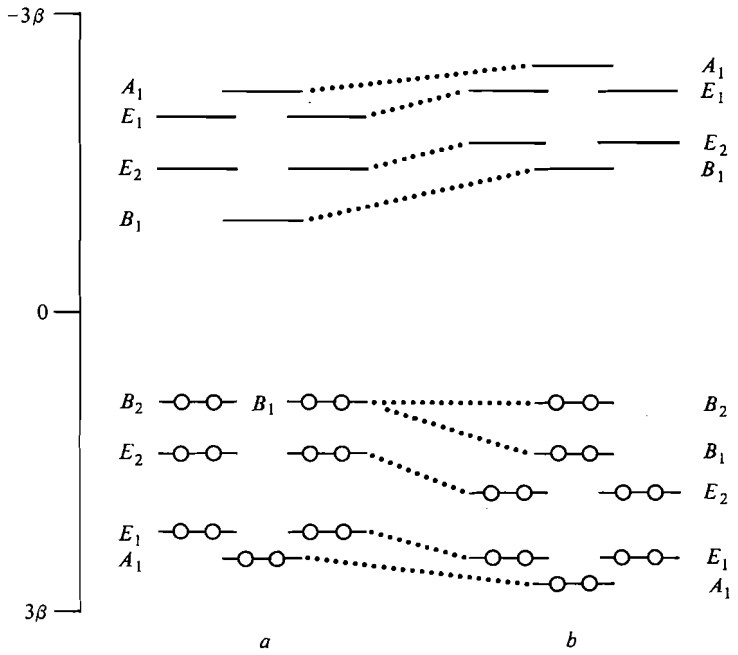

FIG. 4. The π-electron levels of homomorphic N_6P_6 ring (*a*) without (*b*) with exocyclic conjugation. Assumptions: symmetry C_{6v}, one interacting Me_2N group at each phosphorus atom, $\alpha_N = \alpha_P + 2\beta$, all β's equal. For both (*a*) and (*b*), there are additional nonbonding levels ($E = \alpha + \beta$) of species A_1, E_1, E_2. These are localized on the exocyclic groups in (*a*), shared with the ring nitrogen atoms in (*b*).

tive result is that, although the high symmetry of the ligand is lost on complex formation, the conformational changes are very similar for all the complexes. Conclusions drawn from the detailed study of the molecular structure of one of them, specifically $DDPNCoCl^+$, are therefore likely to be general.

Molecular Structures

Phosphazenes differ from most other cyclic ligands (30) in that reaction with acceptors localizes π-electrons and changes bond orders and bond lengths within the ring. The interpretation of several methylphosphazene structures in these terms (5) requires extension for the dimethylaminophosphazenes, because the exocyclic groups now form part of the conjugated system. Figure 4 shows the results of an HMO calculation on a simple model. Bond orders (in parentheses) and charge densities for the unconjugated (above) and conjugated (below) repeating units are:

2.000 (0) 0.356 (0.516) 1.644
N (*exo*)——————P——————N (*endo*)
1.815 (0.527) 0.473 (0.456) 1.712

Electron release from the exocyclic group strengthens the molecule as a whole, appreciable exocyclic π-bonding being attained partly at the expense of the ring bonds. If both π-systems are included, the exocyclic:endocyclic bond orders are in the ratio 0.58:1, in satisfactory agreement with typical bond lengths, P—N (*exo*) 1.67, (*endo*) 1.60 Å. Electron density is increased at phosphorus, diminishing its sensitivity to nucleophilic attack, and at nitrogen, where a reduction in the two-electron localization energy corresponds to an increased base strength as a consequence of conjugation. A less obvious result is the raising of the first unoccupied level through mixing of the B_1 exocyclic lone pair combination with the formally nonbonding phosphorus orbital, making it less accessible to metal back-bonding orbitals.

In spite of the large structural changes which take place on complex formation, the simple model is still useful, principally because the two π-systems tend to compensate each other as the molecule is deformed. If two electrons are localized at each complexed nitrogen, the expected bond orders and charge densities (for the

Can. J. Chem. Downloaded from www.nrcresearchpress.com by 210.87.254.105 on 09/05/12
For personal use only.

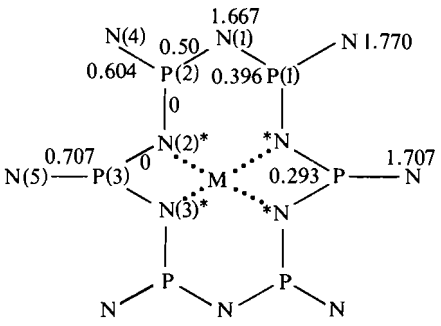

FIG. 5. Bond orders (l.h.s.) and charge densities (r.h.s.) for DDPN ring (assumptions as Fig. 4), two electrons localized at each N*.

perturbed π-system) are as shown in Fig. 5. The mean geometry of DDPN.$CoCl^+$ is given in Table 6, compared with that of the free ligand. The theoretical treatment accounts successfully for (*1*) the increase of mean ring bond length, the bonds to the coordinated nitrogen atoms being the longest, and (*2*) the strengthening (previously recognized (1*b*)) of the exocyclic P—N bonds, P(3)N(5) more than P(2)N(4). The expected slight strengthening of P(2)N(1) is not found, however, possibly because electron repulsion is not directly included in the HMO method. Apart from this, the conjugative model gives a good qualitative account of the structural features of both the free and complexed ligand. Quantitatively, the lengths of such bonds as P(2)N(2) (1.618 Å) show, by comparison with the 1.669 Å found for the bonds to the protonated center in $N_3P_3(NMe_2)_6H^+$ (1*d*) that the $CoCl^+$ group localizes electrons less effectively than H^+; a similar conclusion was reached for a copper(II) complex of $N_4P_4Me_8$ (5).

TABLE 6. Comparative mean geometry[a] of DDPN,[b] DDPN.$CoCl^+$[c]

	DDPN	DDPN.$CoCl^+$
P—N(ring) (Å)	1.563	1.602[d]
NPN(ring) (deg)	120.0	109.4[e]
PNP(ring) (deg)	147.5	135.0[f]
P—N(*exo*) (Å)	1.669	1.647[g]
NPN(*exo*) (deg)	102.9	105.1
Σ(angles at *exo* N)	353.1	356.3

[a]Numbering as Fig. 5.
[b]Reference 21.
[c]Reference 11*b*. The geometry of DDPNCuCl$^+$(3*i*) is almost identical.
[d]P(2)N(1) 1.570 Å, P(2)N(2), P(3)N(2) 1.618 Å.
[e]N(2)P(3)N(3) 100.9°, N(2)P(2)N(1) 113.8°.
[f]P(2)N(2)P(3) 135.1°, P(2)N(1)P(1) 134.7°.
[g]P(2)N(4) 1.652, P(3)N(5) 1.637 Å.

The 5-coordination of the central atom is principally a steric effect. Planar coordination by four nitrogen atoms, necessary for the normal octahedral coordination, is prevented by repulsive interactions between the fifth ligand and near dimethylamino groups, typically those at P(3) and its symmetrically related atom. The molecule bends about the axis N*MN*, excluding a sixth ligand, but allowing the attainment of normal van der Waals distances on both sides of the molecule. The coordination polyhedron of the metal is then a strongly distorted trigonal bipyramid, like that of the aluminum atom in a structurally similar aluminosiloxane (31), and of the iron atom in $[Fe(C_6H_{32}N_4)Cl]I$, (coordinating atoms N_4Cl) in which the steric constraints of the macrocyclic ligand do not allow 6-coordination (32).

Although steric interactions are important (as they are in the neutral ligand (21)) they do not obscure the characteristic stereochemical differences between the metal ions in the two complexes of known structure. The immediate environments of the metals are shown in Fig. 6. For the Cu^{2+} ion, the lengthening of axial bonds by steric repulsion (33, 34) is more than offset by an equatorial elongation arising from the filled $d_{x^2-y^2}$, and d_{xy} orbitals; in DDPN.$CuCl^+$, as in most other 5-coordinated Cu(II) compounds (34–36) axial bonds are the shorter. In high spin Co(II), the $d_{x^2-y^2}$, d_{xy}, and d_{z^2} orbitals are occupied equally, no equatorial expansion is expected, and axial elongation occurs instead (37, 38); it is exceptionally and unexpectedly large (0.2 Å) in the present case. Low spin TBP Co(II), on the other hand, shows axial contraction (39). DDPN is evidently a weak field donor to Co(II), in agreement with the magnetic results discussed below. Similar inequalities in apical and equatorial bond lengths occur in such complexes as $[M(Me_6tren)Br]^+Br^-$, in which the ligand [Me_6tren = tris(2-dimethylaminoethyl)amine] is a simple amine (40).

Magnetism and Electronic Spectra

Measurements of magnetic susceptibility on the nitrate complexes (Table 2) confirm both the weak-field nature of the ligand and the 5-coordination. The moments all correspond to high-spin behavior, but only those of the Co(II) and Ni(II) complexes are stereochemically sensitive. For Co(II) the moment is raised above the spin-only value (3.87 B.M.) by spin–orbit coupling,

Can. J. Chem. Downloaded from www.nrcresearchpress.com by 210.87.254.105 on 09/05/12
For personal use only.

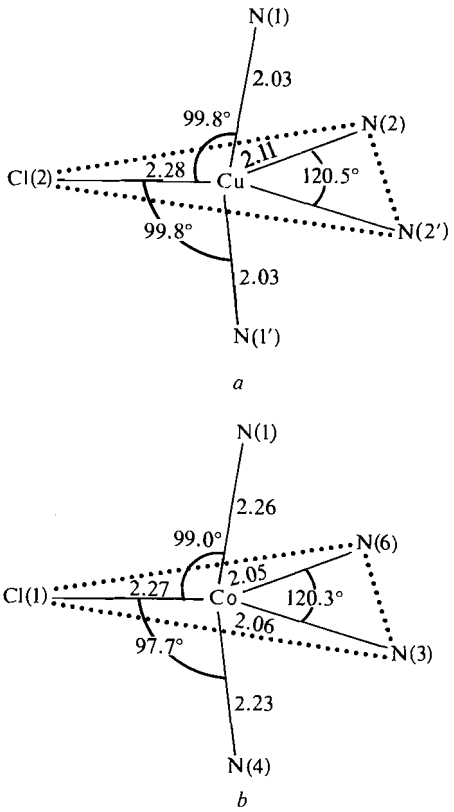

FIG. 6. Environments of the metal in (*a*) DDPNCuCl$^+$, (*b*) DDPNCoCl$^+$.

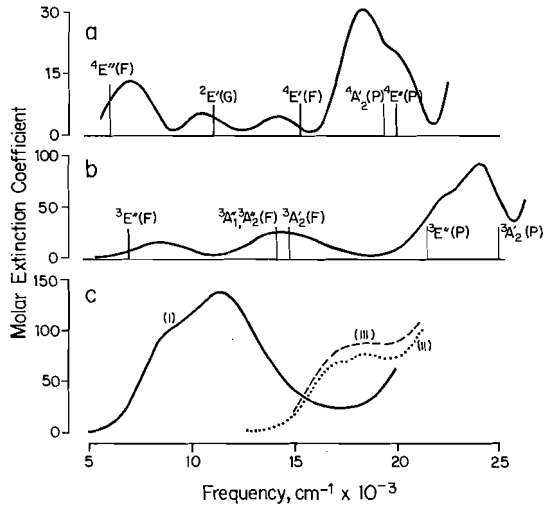

FIG. 7. Electronic spectra of (*a*) [DDPN.Co(NO$_3$)]-NO$_3$ in CH$_3$CN, (*b*) [DDPN.Ni(NO$_3$)]NO$_3$ in CH$_3$CN, (*c*) (*i*) DDPN.Cu(NO$_3$)$_2$ in CHCl$_3$, (*ii*) in CH$_3$CN, (*iii*) in MeNO$_2$. The vertical lines in (*a*) and (*b*) correspond to frequencies calculated for a model of D_{3h} symmetry, using parameters given in the text.

but it is still less than moments typical of octahedral coordination (4.9–5.3 B.M.) (41), since the ground state is nondegenerate. It is near that (4.45 B.M.) of the complex [Me$_6$trenCoCl$^+$]-Cl$^-$ (20), in which the set of donor atoms (N$_4$Cl) has crystallographic C_{3v} symmetry. Five-coordinate high-spin nickel complexes have lower moments (3.1–3.4 B.M.) than tetrahedral complexes (3.6–4.0 B.M.), and the value obtained for DDPN.Ni(NO$_3$)$_2$ is fully consistent with five-coordination, though octahedral coordination cannot be ruled out by the magnetic measurements alone.

The electronic spectra of the cobalt, nickel, and cupric nitrate complexes (Table 3), provide more detailed information on the interaction of the metal with the ligand. Qualitatively, the spectrum of DDPN.Co(NO$_3$)$_2$ is quite different from those of octahedral or tetrahedral complexes of Co(II), but it is generally similar (42) to those of 5-coordinate complexes of known structure, such as [Co(Me$_6$tren)Br]Br (C_{3v}) (43) or [Co(OAsMePh$_2$)$_4$ClO$_4$]ClO$_4$ (C_{4v}) (44). The same is true of the nickel and copper complexes.

Estimates of ligand field parameters can only be approximate, even for the ideal symmetries D_{3h} or C_{4v} (45), but the results, though crude, are of comparative value even when the symmetry is lower. Adjustment of the ligand field and interelectron repulsion parameters (46) to fit the observed spectrum of DDPN.Co(NO$_3$)$_2$ gave Dq 1240 cm^{-1}, B 738 cm^{-1}, β 0.66. The degree of correspondence between the observed and calculated spectra is shown in Fig. 7*a*. Another calculated band (4410 cm^{-1}) is presumably of too low a frequency to be observed. Application of the same method to the spectrum of [Co(Me$_6$tren)Cl]Cl (47) gave Dq 1130 cm^{-1}, B 783 cm^{-1}, β 0.70; Dq = 1100 cm^{-1} if interelectron repulsion is neglected (47). The values of Dq are typical of simple amine ligands, suggesting that DDPN and Me$_6$tren are similar and typical weak-field donors, the former being slightly the stronger. The values obtained for the nephelauxetic parameter β indicate that neither ligand accepts electron density from the metal, a conclusion which agrees with the low intensities of the bands.

No theoretical treatment of the d^8 case which includes interelectron repulsion appears to have

Can. J. Chem. Downloaded from www.nrcresearchpress.com by 210.87.254.105 on 09/05/12
For personal use only.

Can. J. Chem. Downloaded from www.nrcresearchpress.com by 210.87.254.105 on 09/05/12
For personal use only.

been carried out. Band frequencies calculated from the energy diagram of ref. 48 (*Dq* 1390 cm^{-1}) are compared with the observed spectrum in Fig. 7*b*. The spectrum of [Ni(Me_6tren)Br]Br, in which the cation is known to have the symmetry C_{3v} (49), was matched by using *Dq* 1250 cm^{-1} (42, 48).

The spectrum of DDPN.$Cu(NO_3)_2$ differs from those of the cobalt and nickel complexes in being strongly dependent on the solvent. In chloroform (Fig. 7*c*(*i*)) two d–d bands are observed (Table 3) as for $CuCl_5^{3-}$, (8300, 10 400 cm^{-1}) (50), which has D_{3h} symmetry (34). The complexes [Cu(Me_6tren)X]X (X = Br, ClO_4, NO_3) also have two bands, at 10 300, 13 500 cm^{-1} for X = Br (20). It is therefore most likely that the DDPN complex in chloroform is properly formulated as [Cu(DDPN)NO_3]NO_3, analogously to the cobalt and nickel complexes. Since the band assignments are still controversial (42) no estimate of *Dq* is made.

In acetonitrile the spectrum is quite different (Fig. 7*c*(*ii*)), its single broad peak being similar in position to that of [Cu(dach)$_2NO_3$]NO_3 (18 700 cm^{-1}) (51) (dach = 1,4-diazacycloheptane), in which the metal has square pyramidal coordination, the nitrate ion being apical (52). The spectrum of DDPN.$Cu(NO_3)_2$ is almost unaltered in the less strongly coordinating solvent nitromethane (Fig. 7*c*(*iii*)), and is very much like that of the 4-coordinate Cu(dach)$_2(ClO_4)_2$ in the same solvent (ν_{max} 19 800 cm^{-1}, ε_{max} 172 l cm^{-1} mol^{-1}) (51). It is clear that the ionization of the second nitrate ion which occurs as the solvent is changed from chloroform to either acetonitrile or nitromethane is accompanied by a significant change in coordination, the four nitrogen atoms becoming more nearly coplanar. These results confirm the conclusion from the conductivity measurements that the dissociation in acetonitrile is electrolytic, and not a result of the displacement of a nitrate ion by a solvent molecule.

Conclusion

Cations in the series Mn^{2+}–Zn^{2+} are coordinated by four nitrogen atoms of DDPN. The molecule is folded about one NMN axis by repulsive interactions between the dimethylamino groups and the anionic fifth ligand, so preventing the coordination of a sixth group. In the solid state, the metal in the complex cation [DDPN.MX]$^+$ has a distorted trigonal bipyramidal environment; further dissociation of the cupric nitrate complex takes place in ionizing solvents, the cation [DDPN.Cu]$^{2+}$ probably having four coplanar nitrogen atoms. The magnetic moments and electronic spectra of the complexes show that DDPN acts as a weak-field donor, similar to, but rather stronger than, tetradentate amines. It is possible that ligands of the same type, but of sufficiently large ring size to allow planar coordination, might cause spin pairing (53). DDPN does not act as a π-acceptor (although this is not precluded by the trigonal bipyramidal coordination (54)), because the difference of orbital electronegativities of phosphorus and nitrogen is too great to allow appreciable mixing of metal and ligand antibonding orbitals. In contrast, the bonding levels are significantly perturbed by the partial localization of π-electrons by the metal. The significant bond length inequalities induced in this way extend, through conjugation, to the exocyclic groups.

1. (*a*) H. Bode, K. Butow, and G. Lienau. Chem. Ber. **81**, 547 (1948); (*b*) N. V. Mani and A. J. Wagner. Acta Cryst. B**27**, 51 (1971); (*c*) J. Trotter and S. H. Whitlow. J. Chem. Soc. A, 460 (1970); (*d*) H. R. Allock, E. C. Bissell, and E. T. Shawl. Inorg. Chem. **12**, 2963 (1973); (*e*) H. P. Calhoun and J. Trotter. J. Chem. Soc. Dalton, 382 (1974).
2. (*a*) N. L. Paddock, T. N. Ranganathan, and J. N. Wingfield. J. Chem. Soc. Dalton, 1578 (1972); (*b*) F. A. Cotton, G. A. Rusholme, and A. Shaver. J. Coord. Chem. **3**, 99 (1973).
3. (*a*) T. Moeller and S. G. Kokalis. J. Inorg. Nucl. Chem. **25**, 875 (1963); (*b*) R. Ratz, E. Kober, C. Grundmann, and G. Ottmann. Inorg. Chem. **3**, 757 (1964); (*c*) M. F. Lappert and G. Srivastava. J. Chem. Soc. A, 210 (1966); (*d*) T. Chivers and N. L. Paddock. J. Chem. Soc. A, 1687 (1969); (*e*) G. E. Coxon and D. B. Sowerby. J. Chem. Soc. A, 3012 (1969); (*f*) J. Trotter, S. H. Whitlow, and N. L. Paddock. Chem. Commun. 695 (1969); (*g*) W. C. Marsh, N. L. Paddock, C. J. Stewart, and J. Trotter. Chem. Commun. 1190 (1970); (*h*) J. Trotter and S. H. Whitlow. J. Chem. Soc. A, 455 (1970); (*i*) W. C. Marsh and J. Trotter. J. Chem. Soc. A, 1482 (1971).
4. G. Allen, J. Dyson, and N. L. Paddock. Chem. Ind. 1832 (1964).
5. H. T. Searle, J. Dyson, T. N. Ranganathan, and N. L. Paddock. J. Chem. Soc. Dalton. 203 (1975).
6. S. K. Das, R. A. Shaw, B. C. Smith, W. A. Last, and F. B. G. Wells. Chem. Ind. 866 (1963).
7. (*a*) S. K. Das, R. A. Shaw, and B. C. Smith. Chem. Commun. 176 (1965); (*b*) S. K. Das, D. Feakins, W. A. Last, S. N. Nabi, S. K. Ray, R. A. Shaw, and B. C. Smith. J. Chem. Soc. A, 616 (1970).
8. D. Feakins, W. A. Last, N. Neemuchwala, and R. A. Shaw. J. Chem. Soc. 2804 (1965).

9. J. N. RAPKO and G. FEISTEL. Inorg. Chem. **9**, 1401 (1970).
10. H. P. CALHOUN, N. L. PADDOCK, and J. TROTTER. J. Chem. Soc. Dalton, 2708 (1973).
11. (*a*) W. HARRISON, N. L. PADDOCK, J. TROTTER, and J. N. WINGFIELD. Chem. Commun. 23 (1972); (*b*) W. HARRISON and J. TROTTER. J. Chem. Soc. Dalton, 61 (1973).
12. P. KOVACIC and N. O. BRACE. *In* Inorganic syntheses. Vol. 6. *Edited by* E. G. Rochow. McGraw Hill, New York. 1960. p. 172.
13. L. G. LUND, N. L. PADDOCK, J. E. PROCTOR, and H. T. SEARLE. J. Chem. Soc. 2542 (1960).
14. A. C. CHAPMAN, N. L. PADDOCK, D. H. PAINE, H. T. SEARLE, and D. R. SMITH. J. Chem. Soc. 3608 (1960).
15. G. ALLEN, D. J. OLDFIELD, N. L. PADDOCK, F. RALLO, J. SERREQI, and S. M. TODD. Chem. Ind. 1032 (1965).
16. B. N. FIGGIS and J. LEWIS. *In* Modern coordination chemistry. *Edited by* J. Lewis and R. G. Wilkins. Interscience, New York. 1960. p. 400.
17. D. P. CRAIG, M. L. HEFFERNAN, R. MASON, and N. L. PADDOCK. J. Chem. Soc. 1376 (1961).
18. R. A. WALTON. Q. Rev. **19**, 126 (1965); W. J. GEARY. Coord. Chem. Rev. **7**, 81 (1971).
19. F. J. C. ROSSOTTI. *In* Modern coordination chemistry. *Edited by* J. Lewis and R. G. Wilkins. Interscience, New York. 1960. p. 1.
20. M. CIAMPOLINI and N. NARDI. Inorg. Chem. **5**, 41 (1966).
21. A. J. WAGNER and A. VOS. Acta Cryst. B**24**, 1423 (1968).
22. B. O. FIELD and C. J. HARDY. Q. Rev. **18**, 361 (1964); C. D. GARNER, D. SUTTON, and S. C. WALLWORK. J. Chem. Soc. A, 1949 (1967).
23. N. F. CURTIS and Y. M. CURTIS. Inorg. Chem. **4**, 804 (1965).
24. J. R. BARCELÓ and J. BELLANATO. Spectrochim. Acta, **8**, 27 (1956).
25. R. G. CAVELL. Can. J. Chem. **46**, 613 (1968).
26. D. A. BALDWIN and G. J. LEIGH. J. Chem. Soc. A, 1431 (1968); R. J. MUREINIK and W. ROBB. Spectrochim. Acta, **24**A, 377 (1968).
27. R. STAHLBERG and E. STEGER. Spectrochim. Acta, **23**A, 2005 (1967).
28. R. STAHLBERG and E. STEGER. J. Inorg. Nucl. Chem. **30**, 737 (1968).
29. M. A. FLEMING, R. J. WYMA, and R. C. TAYLOR. Spectrochim. Acta, **21**, 1189 (1965).
30. M. R. TRUTER. Struct. Bonding. **16**, 71 (1973).
31. M. BONAMICO and G. DESSY. J. Chem. Soc. A, 291 (1968).
32. V. L. GOEDKEN, J. MOLIN-CASE, and G. G. CHRISTOPH. Inorg. Chem. **12**, 2894 (1973).
33. R. J. GILLESPIE. J. Chem. Soc. 4679 (1963).
34. K. N. RAYMOND, D. W. MEEK, and J. A. IBERS. Inorg. Chem. **7**, 1111 (1968).
35. P. C. JAIN and E. C. LINGAFELTER. J. Am. Chem. Soc. **89**, 6131 (1967).
36. S. A. GOLDFIELD and K. N. RAYMOND. Inorg. Chem. **10**, 2604 (1971).
37. B. A. COYLE and J. A. IBERS. Inorg. Chem. **9**, 767 (1970).
38. J. L. SHAFER and K. N. RAYMOND. Inorg. Chem. **10**, 1799 (1971).
39. T. L. BLUNDELL, H. M. POWELL, and L. M. VENANZI. Chem. Commun. 763 (1967).
40. M. DI VAIRA and P. L. ORIOLI. Inorg. Chem. **6**, 955 (1967); Acta Cryst. B**24**, 595, 1269 (1968); P. L. ORIOLI. Coord. Chem. Rev. **6**, 285 (1971).
41. V. L. GOEDKEN, J. V. QUAGLIANO, and L. M. VALLARINO. Inorg. Chem. **8**, 2331 (1969).
42. M. CIAMPOLINI. Struct. Bonding, **6**, 52 (1969).
43. M. DI VAIRA and P. L. ORIOLI. Inorg. Chem. **6**, 955 (1967).
44. P. PAULING, G. B. ROBERTSON, and G. A. RODLEY. Nature, **207**, 73 (1965).
45. M. GERLOCH, J. KOHL, J. LEWIS, and W. URLAND. J. Chem. Soc. A, 3269, 3283 (1970).
46. J. S. WOOD. Inorg. Chem. **7**, 852 (1968).
47. M. CIAMPOLINI and I. BERTINI. J. Chem. Soc. A, 2241 (1968).
48. M. CIAMPOLINI. Inorg. Chem. **5**, 35 (1966).
49. M. DI VAIRA and P. L. ORIOLI. Acta Cryst. B**24**, 595 (1968).
50. G. C. ALLEN and N. S. HUSH. Inorg. Chem. **6**, 4 (1962).
51. W. K. MUSKER and M. S. HUSSAIN. Inorg. Chem. **8**, 528 (1969).
52. M. S. HUSSAIN and H. HOPE. Acta Cryst. B**25**, 1866 (1969).
53. E. K. BAREFIELD and D. H. BUSCH. Inorg. Chem. **10**, 1216 (1971).
54. B. B. CHASTAIN, E. A. RICK, R. L. PRUETT, and H. B. GRAY. J. Am. Chem. Soc. **90**, 3994 (1968).

Can. J. Chem. Downloaded from www.nrcresearchpress.com by 210.87.254.105 on 09/05/12
For personal use only.

Synthetic Studies in the *Veratrum* Alkaloid Series. I.[1] Introduction and the Total Synthesis of Appropriate C-Nor-D-homo Steroid Derivatives

JAMES P. KUTNEY, ARNOLD BY, JOHN CABLE, WILLIAM A. F. GLADSTONE, TADANOBU INABA, SIM Y. LEONG, PETER ROLLER, EDWARD J. TORUPKA, AND WILLIAM D. C. WARNOCK

Department of Chemistry, University of British Columbia, Vancouver, British Columbia V6T 1W5

Received May 22, 1974[2]

JAMES P. KUTNEY, ARNOLD BY, JOHN CABLE, WILLIAM A. F. GLADSTONE, TADANOBU INABA, SIM Y. LEONG, PETER ROLLER, EDWARD J. TORUPKA, and WILLIAM D. C. WARNOCK. Can. J. Chem. **53**, 1775 (1975).

An introduction to the synthetic approach leading to the total synthesis of various *Veratrum* alkaloids is presented. The total synthesis of a series of C-nor-D-homo steroid derivatives is described. These substances are important intermediates in the laboratory synthesis of these natural products.

JAMES P. KUTNEY, ARNOLD BY, JOHN CABLE, WILLIAM A. F. GLADSTONE, TADANOBU INABA, SIM Y. LEONG, PETER ROLLER, EDWARD J. TORUPKA et WILLIAM D. C. WARNOCK. Can. J. Chem. **53**, 1775 (1975).

On présente une introduction à l'approche d'une synthèse menant à la synthèse totale de divers alkaloides du *Veratrum*. On décrit la synthèse totale d'une série de dérivés de C-nor D-homo stéroides. Ces substances sont des intermédiaires importants dans la synthèse au niveau du laboratoire de ces produits naturels. [Traduit par le journal]

The *Veratrum* alkaloid family (1, 2) occupies a position of importance among the various groups of steroidal alkaloids mainly because many of its members possess a rearranged C-nor-D-homo steroidal skeleton and some of them exhibit interesting pharmacological activities. For example, their application in the control of hypertension is well known (3) and some interest in the insecticidal area (4) and their teratogenic activity (5) has been noted.

The division of the *Veratrum* alkaloids into the *Jerveratrum* and *Ceveratrum* groups originally proposed by Fieser and Fieser (6) is now generally accepted. Examples of the former group, which are directly relevant to the present discussion, are verarine (**1**), veratramine (**2**), and jervine (**3**) while verticine (**4**) is cited as an example of the latter group.

There are now several published syntheses of various members of this family. Johnson *et al.* (7) have described a synthesis of veratramine while Masamune *et al.* (8) have completed a synthesis of jervine. Both groups have employed

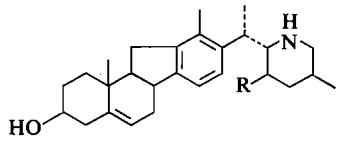

1 R = H
2 R = OH

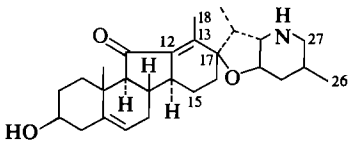

3

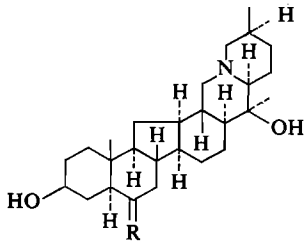

4 R =

[1]Part IV in the series entitled "Total synthesis of steroidal derivatives." For preliminary reports on a portion of this work, see ref. 44.

[2]Revision received February 4, 1975.

Can. J. Chem. Downloaded from www.nrcresearchpress.com by 210.87.254.5 on 09/05/12
For personal use only.

Can. J. Chem. Downloaded from www.nrcresearchpress.com by 210.87.254.5 on 09/05/12
For personal use only.

the same 17-acetyl-5α-etiojervane derivative for the steroidal unit but different pathways for the elaboration of the heterocyclic portion of the molecule. The Johnson synthesis involves a sequence of reactions in which the piperidine system is attained via a cyclization of an appropriately functionalized acyclic unit initially attached to the carbonyl side chain of the etiojervane analog. In the Masamune approach, an enamine derivative of the appropriate piperidine is attached directly onto the side chain of the C-nor-D-homo steroidal unit. Our own approach, also published in preliminary form (4), is rather different and this as well as the accompanying publication (9) provide a more detailed description of the overall strategy which we have employed.

An analysis of the structural features inherent in these natural systems reveals that they possess two main structural units: (*i*) the interesting C-nor-D-homo steroid unit and (*ii*) an appropriate heterocyclic system attached in a variety of ways to ring D of the steroidal component. A schematic representation is shown in **5**.

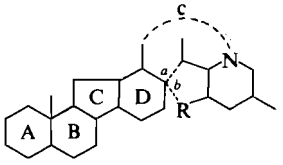

5

a veratranine bases
a + *b* jervanine bases
a + *c* cevanine bases

Thus for the synthesis of verarine (**1**) and veratranine (**2**) according to this analysis, a requisite piperidine unit must be attached at position *a* in **5** whereas the jervine system requires bond formation at both *a* and *b*. The hexacyclic *Ceveratrum* group involves the attachments of such a unit at *a* and *c*. This overall plan was adopted in our laboratory investigations and these provided the synthesis of various members within the *Veratrum* family.

To accommodate this overall strategy, it is essential to direct the investigations at several distinct phases. These are (*i*) synthesis of the required C-nor-D-homo steroid intermediates; (*ii*) synthesis of the appropriately substituted heterocyclic unit; (*iii*) attachment of the latter to ring D of the steroidal template; and (*iv*) elaboration of the coupled product to the final natural product. The results in this and the accompanying publication will be presented in this manner.

In previous studies (10–12) we reported stereospecific syntheses of certain hydrochrysene analogs via multistep sequences starting from β-naphthol. As already noted (10–12), the crucial steps in the synthesis of these molecules involved application of the "hydrochrysene approach" originally developed by Johnson and co-workers (7). The *trans-anti-trans* acetate, **6**, was chosen as the intermediate for elaboration to the C-nor-D-homo steroid system. For this purpose we considered the introduction of a suitable functional group into ring C of the hydrochrysene skeleton to provide an entry into synthetic intermediates where ring C had been opened. A brief discussion of the various experiments in this direction has been presented previously (11) but a more detailed description of our more recent investigations is now in order.

The introduction of substituents at C_{12} (see **6**), the desired site of reaction, is not a straightforward process. It must be recognized that another benzylic center C_{4b}, by virtue of its *para* relationship to the methoxyl function, would be expected to provide serious competition. Indeed electronic considerations would favor substitution at this position while steric factors would tend to favor the secondary center (C_{12}). It was felt that ultimate success could be achieved by the use of a sterically large oxidant such as *tert*-butyl chromate and this proved to be the case. A number of other reagents met with failure (11).

Reaction of *trans-anti-trans* acetate **6** with *tert*-butyl chromate provided a complex reaction mixture from which four products could be isolated and characterized. Fortunately the major product was the desired keto acetate (**7**) mentioned previously (11), while the three minor components (**8**–**10**) were clearly the result of further oxidation. In each instance the spectroscopic properties were very instructive (see Experimental) and provided strong evidence in favor of aromatization of ring C as well as further reaction in ring B in two of the compounds. Chemical correlations between the various products were performed to establish their structures. A summary of these experiments is provided in Fig. 1.

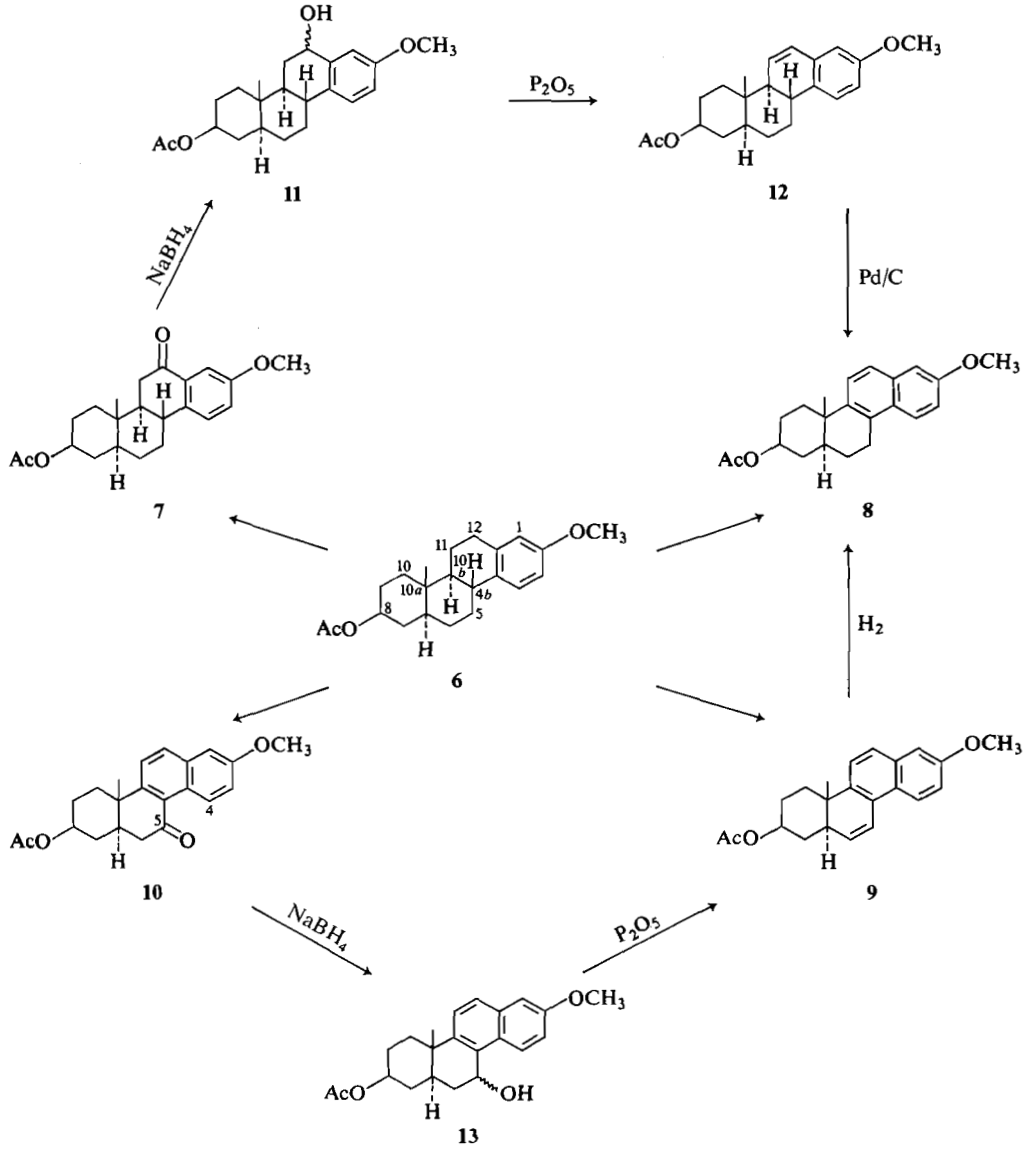

FIG. 1. Oxidation studies on *trans-anti-trans* acetate (**6**) and interrelationships between the various products.

It was now clear from this detailed investigation that, as previously mentioned (12), the oxidation pathway in the *trans-anti-trans* series is substantially different from the corresponding *cis-syn-cis* series. In the latter, the formation of hydrochrysene derivatives analogous to **10** (A/B *cis*) represents the predominant course of reaction. The reasons for this difference are readily apparent from molecular models (12).

The keto acetate (**7**) was selected as the crucial intermediate for ultimate conversion to the C-nor-D-homo series and the successful sequence is outlined in Fig. 2. For this purpose a more detailed investigation of the carbonyl reduction at C_{12} was essential in order to obtain optimum conditions and/or yields in the subsequent steps. When **7** was reduced with sodium borohydride at room temperature, a high yield of a mixture of the expected C_{12}-hydroxy compounds (**11**) was obtained. The major isomer could be obtained crystalline and on the basis of the spectral data, could be assigned the 12β

Can. J. Chem. Downloaded from www.nrcresearchpress.com by 210.87.254.5 on 09/05/12
For personal use only.

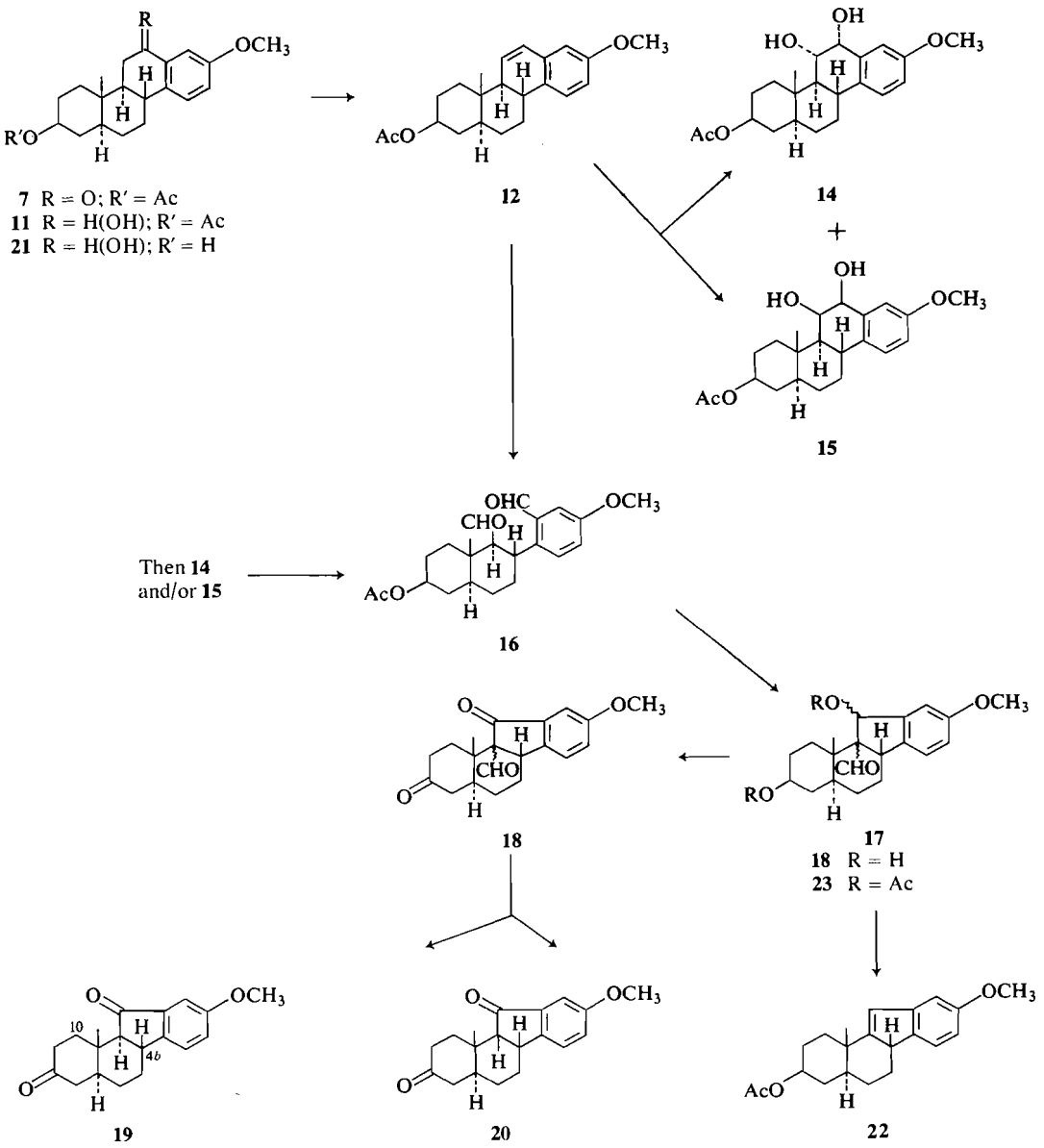

FIG. 2. The synthesis of C-nor-D-homo steroid intermediates from the hydrochrysene analog (7).

configuration (**11**, $C_{12}\beta$-OH). Analysis of the n.m.r. spectrum revealed a two-proton multiplet centered at τ 5.3 due to the C_{12} and C_8 protons. Acetylation of the C_{12} hydroxyl function resolved these signals into two distinct multiplets (τ 5.35, septet, C_8H; τ 4.09, quartet, $J_{11e,12a}$ = 6 Hz, $J_{11a,12a}$ = 9 Hz, $C_{12}\alpha$-H) and allowed the stereochemical assignment at C_{12}.

If the sodium borohydride reduction mixture is refluxed, not only is the 12-keto group reduced but hydrolysis of the C_8 acetoxy function is also observed and the diol **21** ($C_{12}\beta$-OH) is obtained in good yield.

The olefin (**12**) obtained by dehydration of the mixture of alcohols or the pure 12β-alcohol, was utilized for the ring opening studies. Our initial investigations on the transformation of olefin **12** to the secodialdehyde (**16**) involved ozonolysis under various conditions followed by reductive cleavage of the resulting ozonide.

Can. J. Chem. Downloaded from www.nrcresearchpress.com by 210.87.254.5 on 09/05/12
For personal use only.

Can. J. Chem. Downloaded from www.nrcresearchpress.com by 210.87.254.5 on 09/05/12
For personal use only.

In all instances the yield of **16** was very low. On the other hand, hydroxylation with osmium tetroxide proceeded smoothly to provide both possible 11,12-diols (**14** and **15**). The yield in this reaction was very sensitive to the reaction conditions. Initially a trace of pyridine was used since it was felt that this compound might catalyze the reaction but subsequent experiments showed that the yield was higher if no pyridine was present. The optimum yield of the mixture of diols was achieved by keeping the amount of ethyl ether used and the time required for the reaction work-up to a minimum. Although the reaction produced two isomeric diols, one of these (**15**) is by far the predominant isomer and its characterization will be discussed. The minor component was not isolated in pure state.

The n.m.r. spectrum of **15** (in pyridine) showed no absorption in the olefinic region but now new signals at τ 5.24 ($C_{12}H$, $J_{12,11}$ = 4 Hz) and τ 5.61 ($C_{11}H$, triplet, $w_{1/2}$ = 9 Hz) confirmed the structural assignment for the diol. Furthermore, the β orientation for the hydroxyl functions was clear from two points of view: (*a*) the small coupling constant, $J_{10b,11}$ = 4.5 Hz, revealing coupling of the C_{10b} axial proton with an equatorial C_{11} proton and (*b*) the downfield shift of the angular methyl group (for example, τ 9.26 in **6** $\rightarrow$ τ 9.13 in **15**) (13, 14). It should be noted here that in a related hydrochrysene series, Johnson *et al.* (15) also observed β-hydroxylation in the osmium tetroxide reaction.

The conversion of either diol to dialdehyde **16** was performed in a straightforward manner with periodic acid in methanol. For preparative purposes, the mixture resulting directly from the hydroxylation reaction was immediately treated with this reagent. The extent of the conversion could be conveniently followed by u.v. spectroscopy (λ_{max} 225, 255.5, and 321 nm) while the i.r. spectrum with three carbonyl absorptions (5.79, 5.87, and 5.97 μ) as well as a band at 3.63 μ for the aldehydic C—H stretching vibration and the n.m.r. spectrum confirmed the presence of equatorial aliphatic (0.50, doublet, $J_{11,10b}$ = 4.5 Hz, $J_{10b,4b}$ = 12 Hz) and aromatic (−0.27, singlet) aldehydic functions demanded by structure **16**. The stereochemistry of this product with respect to centers C_{10b} and C_{4b} was established by spin decoupling experiments. Thus irradiation at the frequency of the aliphatic aldehydic proton (τ 0.50) caused collapse of the quartet at τ 7.63 (α-H at C_{10b}) to a doublet (J = 12 Hz) while irradiation at τ 5.5 (β-H at C_{4b}) similarly caused collapse of this signal to a doublet (J = 4.5 Hz). The n.m.r. data confirm the *trans* stereochemistry of the C_{10b} and C_{4b} positions since the coupling constant, $J_{10b,4b}$ = 12 Hz, is only consistent with diaxial coupling.

The synthesis of the desired C-nor-D-homo skeleton was accomplished by an internal aldol condensation using alcoholic sodium hydroxide. Again the u.v. spectrum, now typical of the anisole-type chromophore (λ_{max} 284 and 289sh, nm), already well known from our previous studies, could be used to recognize the desired cyclization product (**18**). The i.r. spectrum with absorptions at 2.80, 2.89, 3.64, and 5.90 μ was in accord with the presence of only hydroxyl and saturated aldehyde functions.

Confirmatory evidence to support the desired cyclization became available from the crystalline diacetate derivative (**23**). The n.m.r. spectrum of the latter showed singlets at τ 9.02 (C_{10a} methyl), 8.02 (C_8 acetate), 7.84 (C_{11} acetate), and 6.35 (OCH_3). A quartet, which was assigned to the single C_{4b} benzylic proton appeared at τ 6.58. Axial–axial ($J_{4b,5\alpha}$ = 12 Hz) as well as axial–equatorial ($J_{4b,5\beta}$ = 7 Hz) couplings are observed between this proton and the pair of C_5 protons, giving rise to the above mentioned quartet. This confirms that the C_{4b} proton is axial and thereby β oriented.

The diol aldehyde on oxidation with Jones' reagent (16) provided the unstable diketo aldehyde **18**. Purification of this product was complicated by its facile loss of the aldehyde function so that spectral data could only be obtained on the crude product. For example, chromatography on neutral alumina converted **18** to a mixture of ketones which proved to be identical with diketones **19** and **20** as obtained in subsequent studies.

Although removal of the aldehydic function in **18** could be accomplished by contact with alumina, it proved more convenient to utilize alkaline conditions for this reaction. While our studies were in progress, Johnson and coworkers (17) described their results in a related series where an alkaline medium had also been employed in a deformylation reaction. Thus treatment of **18** with potassium hydroxide in refluxing dioxane provided an approximate 1:1 mixture of two compounds for which the struc-

Can. J. Chem. Downloaded from www.nrcresearchpress.com by 210.87.254.5 on 09/05/12
For personal use only.

tures **19** and **20** were deduced. Separation of these latter isomers proved extremely difficult and all attempts at separation by chromatography failed. Fractional crystallization allowed the eventual separation into two crystalline components whereupon complete spectral and analytical data could be obtained. The n.m.r. spectra of **19** and **20** showed some interesting differences. Of particular note was the angular methyl group region which showed singlets at τ 8.85 and 8.74 for **19** and **20**, respectively, thereby allowing assignment of the *trans-anti-trans* stereochemistry to the diketone **19** and the *trans-syn-cis* stereochemistry to isomer **20**.

It is well known (18) that the influence of the carbonyl group on protons in close proximity to it depends on the relative orientation of these protons to the plane in which the carbonyl group resides. Molecular models of **19** and **20** reveal that in the former the angular methyl group lies in a plane perpendicular to that of the carbonyl group whereas in the latter this group lies essentially in the plane of the trigonal carbon atom. Johnson and co-workers (19) have arrived at similar conclusions in their studies on a closely analogous system.

Finally to confirm the isomeric nature of the above diketones, a mass spectroscopic analysis was carried out. The mass spectra of **19** and **20** reveal the virtually complete identity in the region *m/e* 80–225. Minor intensity differences occur in the region *m/e* 225–280 while one significant difference is noted above *m/e* 280. Only the *trans-anti-trans* diketone **19** possesses a significant $M - 15$ peak (*m/e* 283) which indicates loss of the angular methyl group. It is interesting to compare the fragmentation process of the *trans-anti-trans* ketone in the normal hydrochrysene series which also reveals significant $M - 15$ and $M - 18$ fragments. It seems clear that the loss of the angular methyl group is a more significant process when the normal steroid stereochemistry prevails in the above hydrochrysene analogs. These results are in good agreement with the detailed investigations of Djerassi and collaborators (ref. 20, Chapt. 20) on steroidal ketones. In steroid 11-ketones, for example, fragmentation of bonds 9,10 and 6,7 occurs readily to provide the fragment ions normally observed. By analogy, cleavage of bonds 10a, 10b and 5,6 in the above compounds would be expected. Indeed plausible mechanistic pathways

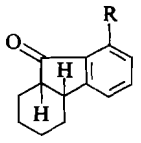

24 R = H
25 R = CH_3

similar to those presented by Djerassi and co-workers (ref. 20, Chapt. 20) can be presented to explain the formation of the various fragments.

Before proceeding to the next series of reactions, it is appropriate to discuss the interesting problem of *cis–trans* isomers in the indanone series and to compare these results with the above C-nor-D-homo ketones. House *et al.* (21) have shown that the *cis*-fused benzindanone (**24**) is more stable than the *trans* isomer. Under equilibrating conditions it was established that the equilibrium lies 85% in favor of the *cis* system. In a further study (22) these workers found that the methyl substituted *cis* indanone (**25**) was stable to refluxing methanolic sodium methoxide. Other workers (23–27) have made observations in favor of *cis* configuration in the hydrindanone series. There are also examples in the literature (28–32) where *trans*-fused hydrindanones are more stable. With respect to somewhat more complicated examples, Johnson and co-workers (19) have synthesized the *cis-anti-trans* diketone (**26**) and its *cis-syn-cis* epimer (**27**) and have shown that at equilibrium the ratio of *cis*:*trans* was about 7:3. On the other hand, 11-ketoveratramine (**28**) (19) is very stable in the *trans* B/C ring fused system.

The above workers explain their observations by stating that the most unstable isomer is obviously the one which has the most steric interactions. With this in mind, the models of 11-ketoveratramine (**26** and **27**) as well as our diketones **19** and **20** were examined. It was apparent that two interactions, apart from the usual types associated with these molecules, seemed to require consideration. These are as follows: (*a*) The interaction between the oxygen atom of the carbonyl group and the hydrogen atoms on C_{10} (hydrochrysene numbering) and (*b*) the interaction between the angular methyl group and the hydrogen atom on C_{4b}. In the case of **28**, which can exist with rings A and B in a nonsteroidal conformation (angular methyl group is equatorial to ring B), these interactions are not appreciable. On the other

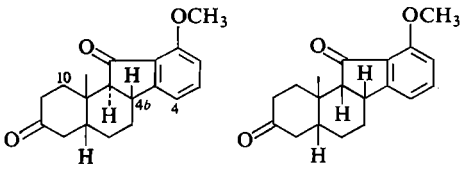

26 27

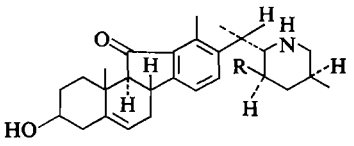

28 R = OH

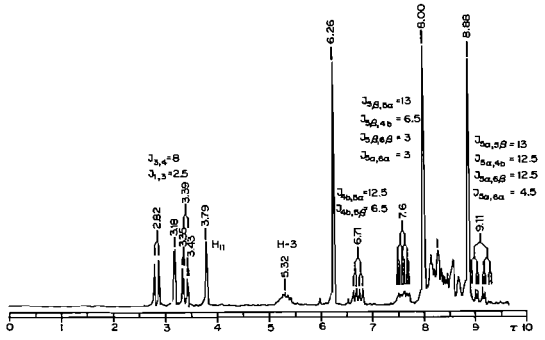

FIG. 3. Nuclear magnetic resonance spectrum of olefin **22**.

hand **26** shows the *b* type interaction. Therefore the ratio observed by Johnson is explicable in these terms. In *trans-anti-trans* diketone **19** the *b* type interaction is also present but in *trans-syn-cis* isomer **20**, where no such interaction exists, a more serious *a* type interaction is noticed. Thus the approximate ratio of 1:1 observed in our experiments is in good agreement with what one would expect from molecular models. In the case of 11-ketoveratramine the 5,6-double bond decreases the interaction of the methyl group with the C_{4b} proton thus making the B/C *trans* isomer more stable with respect to the *cis* one.

Another approach to the removal of the oxygen functionality in ring C of the aldol product **17** was considered and this proved to be highly successful. It was envisaged that the acetate derivative (**23**) mentioned previously might undergo elimination in the manner indicated, **23** → **29** → **22**, and the latter could also prove useful in its subsequent elaboration to the desired C-nor-D-homo steroidal template.

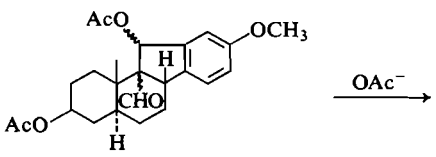

23

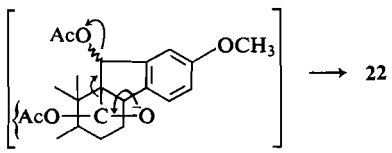

29

Johnson and co-workers (17) had employed a similar reaction in their studies.

Upon heating **23** for 8 days in a sodium acetate – acetic acid mixture an 80% yield of crystalline olefin **22** was obtained. Extensive n.m.r. studies (Fig. 3) were performed on this compound to establish its structure and, in particular, the stereochemistry at C_{4b}, the latter information being vital to the subsequent use of this intermediate in further studies. A few features are worthy of note at this point.

The C_{4b} hydrogen appeared at τ 6.71 as a quartet while the $C_{5\alpha}$ and β hydrogen were evident at τ 9.1 and 7.60, respectively, as multiplets. A possible explanation for the observed deshielding of the $C_{5\beta}$ hydrogen was provided in our studies as well as those of Nagata *et al.* (33). This latter group in studying a series of hydrophenanthrene derivatives noted that a strong deshielding of the aromatic C_4 protons had occurred. They attributed this result as being due to the steric effect of an equatorial C_5 proton. The degree of this deshielding was correlated to the van der Waals compression between the C_4 and C_5 protons which is determined by the interatomic distance between them. A conformational structure of **22** (see **22***a*) clearly reveals the significant difference in the relative orientations of the $C_{5\beta}$ and $C_{5\alpha}$ hydrogens, the latter being in the ring current of the aromatic ring.

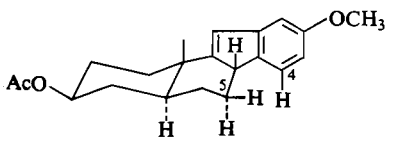

22*a*

Can. J. Chem. Downloaded from www.nrcresearchpress.com by 210.87.254.5 on 09/05/12
For personal use only.

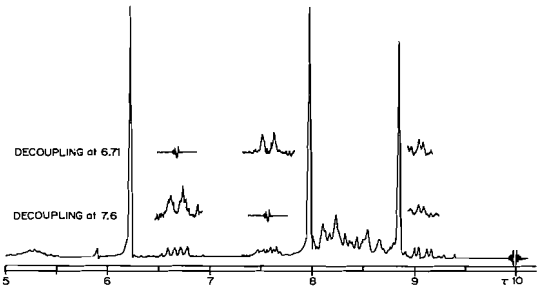

FIG. 4. Nuclear magnetic resonance decoupling studies of olefin **22**.

In all the previously studied compounds no C_5 proton resonances had been observed and thus olefin **22** provided a unique opportunity to evaluate stereochemistry by means of n.m.r. spectroscopy. Decoupling studies (Fig. 4) established the above assignments and provided the essential coupling constants.

Thus irradiation at τ 6.71 caused a collapse of the multiplet at τ 7.60 to a pair of triplets ($J_{5\alpha,5\beta}$ = 13 Hz, $J_{6\alpha,5\beta} = J_{6\beta,5\beta}$ = 3 Hz). Irradiation at τ 7.60 caused a collapse of the quartet at τ 6.71 to a doublet (J = 12 Hz). In each of the above experiments changes were observed at τ 9.1, thus establishing conclusively the identity of the proton resonating at τ 9.1. As for the stereochemistry at C_{4b} the second experiment shows that a *trans–trans* coupling exists. This could only be possible if the C_{4b} proton was β oriented.

The above studies completed the synthesis of several types of C-nor-D-homo steroid intermediates and their elaboration to the requisite unit for the *Veratrum* alkaloids was now considered. The ultimate objective was the synthesis of C-nor-D-homo derivatives bearing a carbonyl function in ring D since this functional group could serve as the site of reaction with the appropriate heterocyclic unit.

Previous investigations (11, 35) had revealed that in the Birch reduction of various hydrochrysene analogs, it was possible to control conditions so as to provide intermediates in which the aromatic ring D is maintained (11) or in which an α,β-unsaturated ketone was present (35). Thus reduction of olefin **22** with lithium metal in anhydrous ammonia and tetrahydrofuran provided a good yield of a crystalline product possessing a conjugated carbonyl chromophore (λ_{max} 242 nm; τ 4.07, 1H) and clearly lacking any other olefinic protons. Thus both the olefin and aromatic functions had been reduced and structure **30** could be assigned to this product. It was tempting, on the basis of the results obtained in the hydrochrysene series (11, 35) to assign the *trans-anti-trans-anti* stereochemistry, to this reduction product. However, the obvious importance of establishing, beyond doubt, the correct stereochemistry particularly at C_{10b}, demanded additional investigations in this direction. For this purpose olefin **22** was hydrogenated and the resultant sharp-melting product was carefully evaluated by various spectroscopic techniques. Of particular relevance to the present discussion are the n.m.r. spectral data since direct comparison could be made with the extensive results already available for the starting olefin as discussed previously (see Figs. 3 and 4). A quintet (J = 6.5 and 12.5 Hz) which appeared at τ 7.00 was attributed to the C_{4b} axial proton. Molecular models show that the conformation of the molecule is not significantly altered by removal of the double bond. On this basis it was possible to conclude that the coupling constant between the C_{4b} and C_{10b} protons is 6.5 Hz, hence the C_{10b} proton must be β. Similarly, an ABX type pattern was observed for the C_{10b}, $C_{11\alpha}$, and $C_{11\beta}$ protons in which the resonance for the C_{10b} proton also appeared as a quintet consistent with $J_{10b,11\alpha}$ = 12.5 Hz, $J_{10b,11\beta}$ = 6.5 Hz, complementing the above conclusion about the C_{10b} stereochemistry. These results left little doubt that hydrogenation of **22** had proceeded from the β face of the molecule and the reduction product could be assigned structure **31**. When the latter substance was exposed to Birch reduction conditions it yielded a product *identical* in every respect with **30**, obtained directly from the reduction of olefin **32**. It was now clear that in the C-nor-D-homo series, the Birch reduction procedure was providing the undesired stereochemistry at C_{10b} and the resultant fusion of rings A, B, and

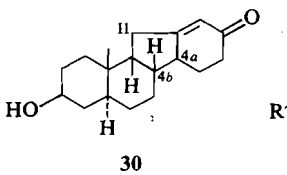

30

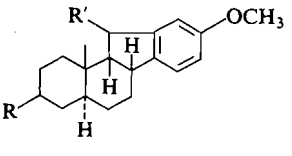

31 R = OAc; R' = H
32 R = R' = OH

Can. J. Chem. Downloaded from www.nrcresearchpress.com by 210.87.254.5 on 09/05/12
For personal use only.

Can. J. Chem. Downloaded from www.nrcresearchpress.com by 210.87.254.5 on 09/05/12
For personal use only.

C was *trans-syn-cis* rather than the required *trans-anti-trans* backbone obtained in the hydrochrysene compounds. Unambiguous confirmation of the above stereochemical assignments was obtained in later studies, as described below, when the desired intermediate was synthesized and compared with the above compounds.

An alternative approach to the generation of the desired stereochemistry at C_{10b} was considered in terms of electrophilic addition to the double bond of olefin **22**. Hydroboration of **22** in diglyme, followed by addition of propionic acid under reflux, gave a complex mixture. This mixture was simplified somewhat by hydrolysis in aqueous methanolic potassium carbonate followed by reacetylation. Column chromatography followed by preparative layer chromatography gave a poor yield (14%) of a compound identical with that of the product obtained in the catalytic reduction of **22**. On the other hand, hydroboration of **22** followed by an oxidative treatment allowed isolation of a crystalline product in much higher yield (68%). This product was the expected alcohol **32** again indicating *cis* attack from the β face of the molecule. Again n.m.r. spectroscopy could be utilized to establish stereochemistry at C_{10b} and C_{11} ($J_{4b,10b} = 12.5$; $J_{10b,11\alpha} = 10$ Hz). It was now clear that olefin **22** could not be utilized effectively in any of these ways to generate the desired stereochemistry at C_{10b} and an alternative approach must be developed.

Consideration of the conformational structure **33** for the olefin does reveal some preference for β attack since approach from the α side of the bent backbone receives interference particularly from the axial α hydrogen atoms at C_5, C_{6a}, and C_{10}. On the other hand the axial methyl group and the hydrogen atom at C_{4b} provide some steric hindrance for β approach. Alteration in molecular shape, in particular with respect to rings C and D, may encourage α approach of reactants to the olefinic linkage and for this purpose the unsaturated ketone **34**

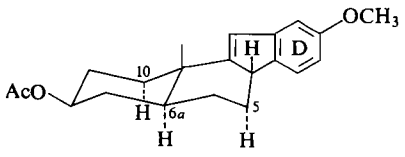

33

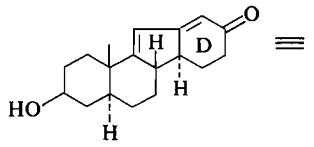

34

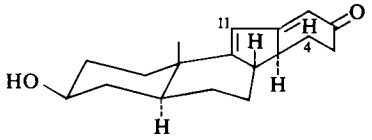

34*a*

was selected as a possible intermediate. The latter, with a nonplanar ring D (**34***a*), reveals increased hindrance to β attack at C_{10b}—C_{11}. One possible route to **34** is presented by the sequence **32** → **35** → **34** and the requirement for retaining the oxygen function in ring C during Birch reduction of the aromatic system in **32** became obvious.

When the C-nor-D-homo intermediate **32** was reacted with lithium in ammonia, dioxane, and isopropanol, a crystalline product could be obtained which revealed interesting spectroscopic characteristics. The i.r. spectrum indicated a conjugated carbonyl absorption (6.12 μ) while the u.v. spectrum (λ_{max} 295 nm) and the n.m.r. signals (broad singlets at τ 4.05 and 4.25) demanded a dienone chromophore as shown in **34**. It was clear that the desired reduction had occurred and the resultant intermediate **35** was dehydrated under the reaction conditions to provide the desired C-nor-D-homo intermediate **34**.

Catalytic hydrogenation of **34** provided a product mixture of the saturated ketone **36**

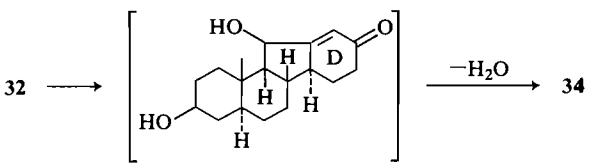

35

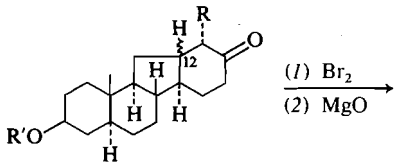

36 R = R′ = H
38 R = CH_3; R′ = Ac

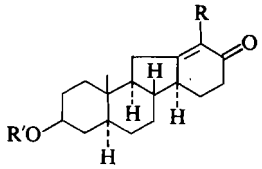

37 R = R′ = H
39 R = CH_3; R′ = Ac

(no stereochemistry implied at C_{12}) and the conjugated ketone **37**. These compounds proved difficult to separate and since **37** was the desired compound it was found convenient to react the hydrogenation mixture initially with bromine and then magnesium oxide so as to transform **36** to **37** thereby permitting isolation of the latter. Comparison of **37** with **30** discussed previously, clearly established that they were different substances and allowed the assignment of the sought for *trans-anti-trans-anti* stereochemistry shown in **37**. The correctness of this assignment was established unambiguously as will be shown below.

The veratramine–jervine series of alkaloids, as already noted, carry a methyl substituent at C_{13} in the C-nor-D-homo steroidal component and it was now essential to develop methods for the introduction of this substituent into the available substances. More specifically the synthesis of intermediates **38** and **39** became the next requirement in the synthetic pathway.

The substance utilized in the initial investigations was the α,β-unsaturated ketone **40** since it was available in larger quantity from previous studies (11). The first method evaluated involved the enamine alkylation technique (36) since it could be shown that **40** undergoes essentially quantitative conversion to the dienamine derivative **41** (λ_{max} 276 nm) by reaction with pyrrolidine in refluxing benzene. Subsequent treatment of **41** with methyl iodide, alkaline hydrolysis, and finally rearrangement of the double bond under acidic conditions provided a product which exhibited spectral characteristics in accord with the desired alkylation product **42**. Thus the u.v. spectrum (λ_{max} 250 nm) showed the expected bathochromic shift of 10 nm relative to that of the starting ketone **40**, while the n.m.r. spectrum clearly revealed a vinyl methyl group (τ 8.22). In addition to this signal, a very interesting doublet was observed at τ 7.10 (J = 12 Hz). The starting conjugated ketone has no peaks in the region τ 6.7–7.3 and it was obvious that this absorption must be characteristic of the alkylation product. Pertinent to this last observation, another group (37) has noted a doublet at about τ 7.21 (J = 14.5 Hz) in the n.m.r. spectrum of 4-methyl-cholest-4-en-3-one and were able to assign this absorption to the $C_{6\alpha}$ equatorial proton. They indicated that a spatial interaction between the C_4 methyl group and the $C_{6\alpha}$ proton is the cause of the deshielding. A comparison with the system shown in **42** reveals that the $C_{12\beta}$ equatorial proton is identically oriented with respect to the methyl group at C_1. On this basis we assign our low-field doublet to this proton.

Finally, a comparison of the mass spectra of **40** and **42** also supported the structure of

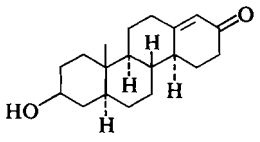

40

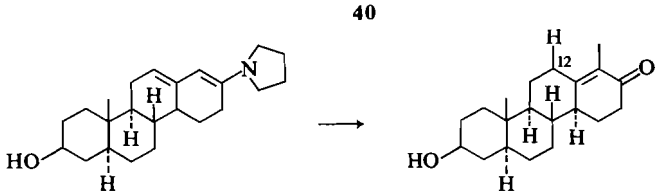

41 **42**

Can. J. Chem. Downloaded from www.nrcresearchpress.com by 210.87.254.5 on 09/05/12
For personal use only.

Can. J. Chem. Downloaded from www.nrcresearchpress.com by 210.87.254.5 on 09/05/12
For personal use only.

the latter molecule. First of all, the molecular ion peak at *m/e* 302 in the mass spectrum of **42** relative to the corresponding peak at *m/e* 288 for **40** established an additional methyl group in the former compound. Moreover, the $M - 42$ peaks (*m/e* 246 and 260, respectively) are due to the loss of ketene, $CH_2{=}C{=}O$, and are indicative of a compound having the system, —C=CR—CO—CH_2 (ref. 20 pp. 87–91 and ref. 28). Steroids bearing the Δ^4-3-keto chromophore and their corresponding 19-nor analogs have prominent peaks at *m/e* 124 and 110, respectively (ref. 20, pp. 87–91 and refs. 37–39). These fragments are due to cleavage of the 9,10 and 6,7 bonds (steroidal nomenclature) plus the transfer of two protons to the charged fragment. In the mass spectrum of **42** an intense peak is observed at *m/e* 124, whereas in that of **40** one is noted at *m/e* 110. It is seen that these latter facts are in excellent agreement with the steroid series and offer further confirmation that the relationship between **42** and **40** is as suggested above.

Unfortunately, although the desired substance was now clearly available from the above approach, the observed low yields (about 10%) were discouraging. Various attempts to improve this reaction failed and this approach was abandoned.

Stork *et al.* (40) developed an interesting method which involves the trapping of an enolate anion formed during the Birch reduction of an α,β-unsaturated ketone and subsequent alkylation thereby providing introduction of the alkyl group at the α-olefinic carbon atom. Utilization of this technique proved successful in both the normal hydrochrysene and C-nor-D-homo series.

When the unsaturated ketone **40** in the form of its C_8-tetrahydropyranyl ether, prepared *in situ*, was reacted with lithium in ammonia followed by treatment with methyl iodide, a crystalline product was obtained. The mass spectrum of the latter revealed a molecular ion peak at *m/e* 304 thereby indicating introduction of a methyl group into the system, while the n.m.r. spectrum with a new secondary methyl signal (doublet, τ 9.02) and the saturated carbonyl absorption in the i.r. suggested entry of this substituent at C_1 of the tetracyclic skeleton. Confirmatory evidence was obtained when this alkylation product was first brominated and then dehydrobrominated to provide a conjugated ketone identical in all respects with **42** obtained and characterized previously in the pyrrolidine enamine studies.

The C-nor-D-homo unsaturated ketone **37** was now reacted with lithium, in a mixture of ammonia and dioxane followed by addition of methyl iodide. The amorphous product thus formed was acetylated directly to yield a crystalline acetate, m.p. 169–171.5°, which exhibited spectral properties (n.m.r. signal at τ 9.02, $J = 12$ Hz; i.r. at 5.85 μ) in accord with the desired alkylation product. The unambiguous proof of structure and stereochemistry of this substance was obtained when it was shown to be identical with 3β-acetoxy-5α-etiojervan-17-one (**38**, α-H at C_{12}) prepared from hecogenin as mentioned below.

Introduction of the 12,13 olefinic linkage into **38** was achieved by the bromination and dehydrobromination procedure used previously. The crystalline product thus obtained could be readily assigned the desired structure **39** and, as indicated below, this substance was subsequently resolved into an optically active isomer identical with 3β-acetoxy-5α-etiojerv-12(13)-en-17-one (**39**) obtained from the hecogenin degradation sequence.

At this stage of the investigations it was important to substantiate the structural and stereochemical assignments in the above C-nor-D-homo compounds since heavy reliance on spectroscopic data had been made. An unambiguous correlation could be made with compounds derived from a degradation of the steroid sapogenin hecogenin acetate (**43**) according to the scheme developed by Johns and Laos (41) and outlined in Fig. 5. In several instances, minor modifications in the sequence, **43** → **44** → **45** → **38**, originally presented (41) were made and these are documented in the experimental portion. Comparison of both **38** and **39** (i.r., n.m.r., t.l.c.) obtained in racemic form with the optically active isomers derived from the hecogenin series established their complete identity.

Resolution of racemic **39** was achieved by one of us (G.V.N.) during subsequent studies with Fried (42). During these latter investigations microbiological resolution involving the steroid dehydrogenase of *Arthrobacter simplex* was performed and the isolated substance was identical in every respect with 3β-acetoxy-5α-

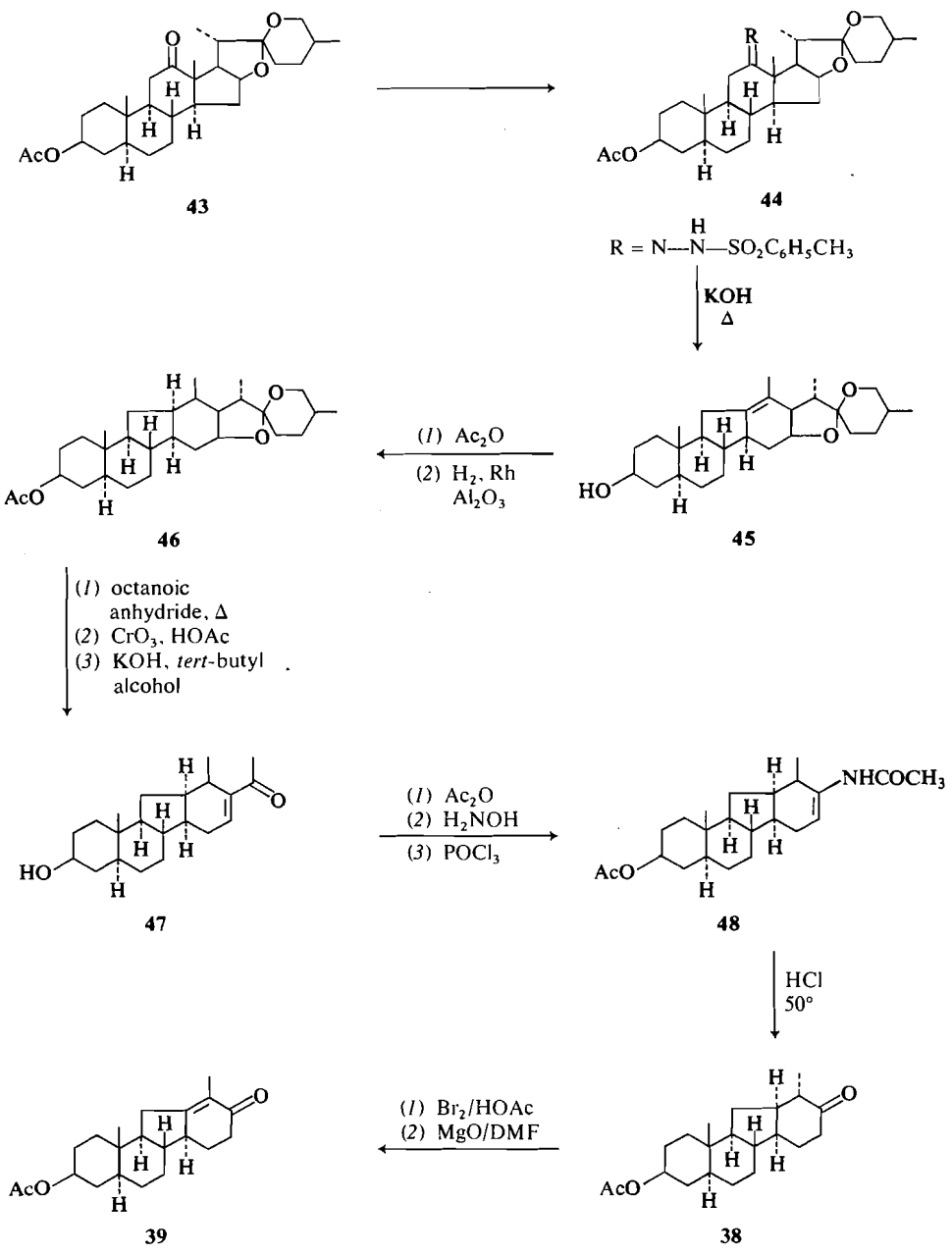

FIG. 5. Degradation scheme of hecogenin acetate (**43**) to 3β-acetoxy-5α-etiojerv-12(13)-en-17-one (**39**).

etiojerv-12(13)-en-17-one (**39**) as obtained from the sequence in Fig. 5.

In summary, the above discussion presents the completion of a crucial phase in the *Veratrum* alkaloid synthesis. The C-nor-D-homo steroid derivatives now available can be effectively employed for the further elaboration to the natural series and experiments in this direction are presented in the accompanying publication.

Experimental

The melting points were determined on a Kofler block unless otherwise stated and are uncorrected. The u.v. spectra were recorded in 95% ethanol on a Cary 11 or 14

Can. J. Chem. Downloaded from www.nrcresearchpress.com by 210.87.254.5 on 09/05/12
For personal use only.

Can. J. Chem. Downloaded from www.nrcresearchpress.com by 210.87.254.5 on 09/05/12
For personal use only.

recording spectrophotometer and the i.r. spectra were taken on a Perkin-Elmer Model 21 spectrometer as potassium bromide pellets unless otherwise stated. The n.m.r. spectra were measured at 60 or 100 MHz on Varian A60, HA 100, or XL100 spectrometers. The centers of multiplets or positions of singlets are given in the Tiers τ scale with reference to tetramethylsilane as the internal standard. The type of protons, integrated area, multiplicity, half-height width ($W_{1/2}$) in Hz, the spin–spin coupling constant (J) in Hz, and peak positions in Hz are indicated in parentheses. Deuteriochloroform was used as the solvent unless otherwise stated. The analyses were performed by Dr. A. Bernhardt and his associates, Mulheim (Ruhr) Germany, and by Mrs. Aldridge, Mrs. C. Jenkins, and Mr. P. Borda, University of British Columbia. Every molecular weight quoted was determined on either the AEI MS9 or the Atlas CH-4 mass spectrometer.

*Oxidation of trans-anti-trans-2-Methoxy-8β-acetoxy-10a-methyl-4b,5,6,6a,7,8,9,10,10a,10b,11,12-dodecahydrochrysene (**6**)*

A solution of *tert*-butyl chromate in carbon tetrachloride was prepared according to the procedure of Heusler and Wettstein (34) except the final solution was concentrated to 600 ml instead of 1000 ml. Aliquots of this solution were then used for the various experiments.

The methoxy acetate (**6**; 6.70 g) was dissolved in carbon tetrachloride (180 ml) and the *tert*-butyl chromate solution (90 ml), which was mixed with acetic anhydride (15 ml), was added. The mixture was stirred under reflux for 4 h and the excess oxidant was then destroyed by stirring with a solution of oxalic acid (75 g) in water (500 ml) for 2 h. The carbon tetrachloride layer was separated and the solvent was removed *in vacuo*. The residue was taken up in ether. The ether solution was washed with aqueous sodium bicarbonate to remove any residual acetic acid and then washed with a 1:1 mixture of a saturated aqueous sodium bicarbonate and a 1 *N* potassium carbonate solution. The organic layer was dried over anhydrous magnesium sulfate and, after removal of the solvent, provided 6.25 g of a crude neutral product. The material was purified by chromatography on alumina (300 g, grade III). Elution with 7:3 benzene – petroleum ether provided starting material (3.74 g, 56%) and further elution with 9:1 benzene–ether yielded the desired ketone **7** (1.16 g, 16%) as described previously (11).

The mother liquor from the recrystallization of the 12-keto compound **7** was investigated in more detail. After evaporating the solvent the gummy product was purified by another alumina chromatography (Woelm, grade I). Elution with 15:1 benzene–chloroform yielded a very small amount of crystalline fraction. Fractional crystallization from 95% ethanol gave two compounds: *First*, less soluble component, *trans*-2-methoxy-8β-acetoxy-10a-methyl-5,6,6a,7,8,9,10,10a-octahydrochrysene (**8**; 65 mg), m.p. 169–172.5°; i.r.: 5.82 μ; u.v.: λ_{max} 227 (4.74), 256 (3.54), 266 (3.64), 276 (3.66), 287 (3.46), 307 (2.96), 314 (3.04), 319 (3.18), 328 (3.10), and 334 nm (3.27); λ_{min} 254 (3.53), 259 (3.54), 271 (3.60), 284 (3.29), 302 (2.91), 309 (2.96), 324 (3.06) and 331 nm (2.09); n.m.r.: 8.81 (angular methyl, 3H), 6.11 (CH_3O—, 3H), broad signal centered at 5.2 (H—C—OAc, 1H) multiplet centered at 2.5 (aromatic H, 5H).

Anal. Calcd. for $C_{22}H_{26}O_3$: C, 78.01; H, 7.69; O, 14.20. Found: C, 77.89; H, 8.02; O, 14.76.

Second, more soluble component, *trans*-2-methoxy-8β-acetoxy-10a-methyl-6a,7,8,9,10,10a-hexahydrochrysene (**9**; 40 mg), m.p. 158.5–160.5°; i.r.: 5.82 μ; u.v.: λ_{max} 244 (4.59), 276 (3.57), 288 (3.65), 301 (3.82), 314 (3.89), 335 (3.53), and 351 nm (3.54); λ_{min} 273 (3.56), 281 (3.55), 293 (3.64), 307 (3.73), 327 (3.38), and 342 nm (3.41); n.m.r.: 8.93 (angular methyl, 3H), 7.94 (CH_3COO—, 3H), 6.10 (CH_3O—, 3H), broad signal centered at 5.2 (H—C—OAc, 1H), quartet centered at 4.2 (C_6 olefinic H, 1H), multiplet centered at 2.4 (aromatic H, C_5 olefinic H, 6H).

Anal. Calcd. for $C_{22}H_{24}O_3$: C, 78.54; H, 7.69; O, 13.72. Found: C, 78.55; H, 7.67; O, 13.64.

Further elution with 8:2 benzene–chloroform provided a mixture of two compounds, one of which was found to be 12-keto compound 7. Since the other compound was less soluble than the 12-keto compound (**7**), the former was purified by fractional crystallization from ether to give an analytical sample of *trans*-2-methoxy-8β-acetoxy-5-keto-10a-methyl-5,6,6a,7,8,9,10,10a-octahydrochrysene (**10**), m.p. 156–157.5°; i.r.: 5.82 and 6.02 μ; u.v.: λ_{max} 219.5 (4.66), 248 (4.43), and 315 nm (3.79), broad shoulder at 348 nm (3.48); λ_{min} 233 (4.23) and 278 nm (3.02); n.m.r.: 8.76 (angular methyl, 3H), 7.94 (CH_3COO—, 3H), 6.10 (CH_3O—, 3H), broad signal centered at 5.3 (H—C—OAc, 1H), multiplet centered at 2.5 (aromatic H, 4H), doublet centered at 0.93 (C_4H, aromatic H, 1H).

Anal. Calcd. for $C_{22}H_{24}O_4$: C, 74.97; H, 6.86; O, 18.16. Found: C, 75.10; H, 7.25; O, 17.82.

*Synthesis of trans-anti-trans-2-Methoxy-8β-acetoxy-10a-methyl-12-hydroxy-4b,5,6,6a,7,8,9,10,10a,10b,11,12-dodecahydrochrysene (**11**)*

The 12-keto acetate (**7**; 3.2 g) was dissolved in methanol (400 ml) and a solution of sodium borohydride (1.0 g) in methanol (400 ml) and water (20 ml) was added. The mixture was stirred at room temperature for 3.5 h. Acetic acid (15 ml) was added and the solution was stirred for a further ½ h. The reaction mixture was partitioned between water and ethyl ether then washed with sodium bicarbonate solution and water. After drying the organic layer over magnesium sulfate (anhydrous) and removal of the liquid, a gum (3.2 g) was isolated. On t.l.c. two spots of ratio 2:1 were observed. The product of lower R_f value crystallized from ethanol or benzene – high boiling petroleum ether gave an analytical sample of *trans-anti-trans*-2-methoxy-8β-acetoxy-10a-methyl-12β-hydroxy-4b,5,6,6a,7,8,9,10,10a,10b,11,12-dodecahydrochrysene (**11**), m.p. 147.5–149°; i.r.: 2.86, 5.85, 6.22, 6.65 μ; u.v.: λ_{max} 226 (3.86), 281 (3.33), 288 nm (3.31); λ_{min} 247 (2.77), 286 nm (3.27); n.m.r.: 9.15 (angular methyl, 3H, singlet), 8.03 ($C_{8\beta}$ acetoxyl, 3H, singlet), 7.93 ($C_{12\beta}$ hydroxyl, 3H, singlet removed by D_2O exchange), 6.29 (C_2 methoxyl, 3H, singlet), 5.3 ($C_{8\alpha}$, $C_{12\alpha}$H, 2H, multiplet), 3.30 (C_3, 1H, quartet, $J_{1,3}$ = 3 Hz), 2.96 (C_1, 1H, doublet, $J_{1,4}$ = 0 Hz), 2.90 (C_4, 1H, doublet, $J_{3,4}$ = 9 Hz); mass spectrometry: *m/e* 358 (M^+) prominent peaks at *m/e* 158, 159, 171, 172, 173, 174, 185, 265, 280, 296, 316, 340, 342, 356.

Anal. Calcd. for $C_{22}H_{30}O_4$: C, 73.71; H, 8.44; O, 17.85. Found: C, 73.91; H, 8.31; O, 17.70.

If the above sodium borohydride reaction mixture is refluxed for as little as 1 h the major product is a

Can. J. Chem. Downloaded from www.nrcresearchpress.com by 210.87.254.5 on 09/05/12
For personal use only.

mixture of C_{12} epimeric diols, *trans-anti-trans*-2-methoxy-8β,12β-dihydroxy-10a-methyl-4b,5,6,6a,7,8,9,10,10a,10b,11,12-dodecahydrochrysene, m.p. 190°; i.r.: 2.80, 3.02, 6.19, 6.36, 6.69, 11.3 μ; u.v.: λ_{max} 224 (3.81), 280 (3.24), 288 nm (3.21); λ_{min} 247 (2.05), 286 nm (3.18); n.m.r.: (in pyridine) 9.22 (angular methyl, 3H, singlet), 6.38 (C_2 methoxyl, 3H, singlet), 6.24 ($C_{8\alpha}$, 1H, septet, $J_{7,8} = J_{8,9} = 5.5$ Hz, $J_{7,8} = J_{8,9} = 11$ Hz), 5.00 ($C_{12\alpha}$, 1H, quartet, $J_{11\beta,12\beta} = 10$ Hz, $J_{11\alpha,12\alpha} = 5$ Hz); mass spectrometry: *m/e* 316 (M^+) prominent peaks at *m/e* 298, 185, 175, 174, 173, 159, 158, 150, 149.

Anal. Calcd. for $C_{20}H_{28}O_3$: C, 75.91; H, 8.92; O, 15.17. Found: C, 76.02; H, 8.97; O, 15.16.

The diacetate of the above compound was synthesized in the usual manner, *trans-anti-trans*-2-methoxy-8β,12β-diacetoxy-10a-methyl-4b,5,6,6a,7,8,9,10,10a,10b,11,12-dodecahydrochrysene, m.p. 175°; i.r.: 5.78, 5.81, 6.22, 6.64, 7.26 μ; u.v.: λ_{max} 226 (3.84), 281 (3.33), 288 nm (3.30); λ_{min} 246 (2.18), 286 nm (3.28); n.m.r.: 9.16 (angular methyl, 3H, singlet), 8.03 ($C_{8\beta}$ acetoxyl, 3H, singlet), 7.92 ($C_{12\beta}$ acetoxyl, 3H, singlet), 6.30 (C_2 methoxyl, 3H, singlet), 5.35 ($C_{8\alpha}$, 1H, septet, $J_{7e,8} = J_{8,9e} = 5$ Hz, $J_{7a,8} = J_{8,9a} = 10$ Hz), 4.09 ($C_{12\alpha}$, 1H, quartet, $J_{11e,12a} = 6$ Hz, $J_{11a,12a} = 9$ Hz), 3.35 (C_1, 1H, doublet, $J_{1,4} = 0$ Hz), 3.28 (C_3, 1H, quartet, $J_{1,3} = 3$ Hz), 2.86 (C_4, 1H, doublet, $J_{3,4} = 8.5$ Hz); mass spectrometry: *m/e* 400 (M^+), prominent peaks at *m/e* 158, 159, 171, 172, 173, 174, 184, 185, 265, 280, 325, 340, 358.

Anal. Calcd. for $C_{24}H_{32}O_5$: C, 71.91; H, 8.05; O, 19.98. Found: C, 71.72; H, 7.91; O, 20.20.

Dehydration of Crude Alcohol **11**

The crude alcohol (3.2 g) was dissolved in anhydrous benzene (150 ml) and phosphorus pentoxide (3.2 g) was added. After 2 h of reflux the reaction mixture was cooled in ice water then transferred into another flask. A small amount of ice was added and the yellow-green fluorescent solution was swirled occasionally while most of the residue in the reaction flask was dissolved in ice water. To the suspension in the reaction flask, ethyl ether and saturated sodium chloride solution were added. Sodium bicarbonate was added in small portions until the solution became basic. At this point it was as difficult to destroy the emulsions formed as it was to dissolve the residue completely. The aqueous layer was extracted several times with ether and combined with the decanted solution. The organic phase was washed with sodium bicarbonate, water, and dried over magnesium sulfate. On removal of solvent the crude material (2.7 g) was isolated. Purification by column chromatography on alumina (grade III, 100 g) gave the desired olefin **12** (2.2 g) with benzene – petroleum ether (1:1). Recrystallization from ethanol gave pure *trans-anti-trans*-2-methoxy-8β-acetoxy-10a-methyl-4b,5,6,6a,7,8,9,10,10a,-10b-decahydrochrysene (**12**), m.p. 105–106.5°; i.r.: 5.80, 6.14, 6.25, 6.39, 6.73 μ; u.v.: λ_{max} 221 (4.44), 262.5 (3.84), 270 (3.88), 302 (3.51), 312 nm (3.40); λ_{min} 247 (3.83), 284 nm (3.48); n.m.r.: 9.11 (angular methyl, 3H, singlet), 8.15 (C_{10a}, 1H, multiplet), 8.04 (C_8 acetoxyl, 3H, singlet), 6.32 (C_2 methoxyl, 3H, singlet), 5.33 ($C_{8\alpha}$, 1H, septet, $J_{7e,8a} = J_{8a,9e} = 5.5$ Hz, $J_{7a,8a} = J_{8a,9a} = 11$ Hz), 4.11 (C_{12}, 1H, quartet, $J_{10a,12} = 2$ Hz), 3.67 (C_{11}, 1H, quartet, $J_{11,12} = 10$ Hz, $J_{10b,11} = 3$ Hz), 3.49 (C_1, 1H, doublet, $J_{1,4} = 0$ Hz), 3.39 (C_3, 1H, quartet, $J_{1,3} = 2.5$ Hz, $J_{3,4} = 8$ Hz), 2.98 (C_4, 1H, doublet); mass spectrometry: *m/e* 340 (M^+), prominent peaks at *m/e* 158, 159, 160, 161, 171, 172, 173, 184, 185, 197, 263, 265, 280, 325, 338.

Anal. Calcd. for $C_{22}H_{28}O_3$: C, 77.61; H, 8.29; O, 14.10. Found: C, 77.48; H, 8.23; O, 14.44.

*Synthesis of trans-2-Methoxy-8β-acetoxy-10a-methyl-5,6,6a,7,8,9,10,10a-octahydrochrysene (**8**)*

The olefinic methoxy acetate (7; 286 mg) was mixed and powdered with 10% palladium-on-charcoal (215 mg) in a 50 ml Erlenmeyer flask. The flask was then heated for 3 min at 240–245° with nitrogen passing over the mixture. Some acetic acid was evolved near the end of the heating period. After the flask had cooled to room temperature, the residue was treated with chloroform, the catalyst was filtered, and the solvent was removed *in vacuo* to yield 232 mg of product. This material was dissolved in benzene and chromatographed on alumina (14 g Woelm, activity grade I). Elution with 10:1 benzene–chloroform yielded first a solid material (140 mg) which, after three recrystallizations from 95% ethanol, gave an analytical sample of *trans*-2-methoxy-8β-acetoxy-10a-methyl-5,6,6a,7,8,9,10,10a-octahydrochrysene (**8**), m.p. 169–172.5°. This compound was completely identical with one of the *tert*-butyl chromate oxidation products (mixture m.p., u.v. and i.r. spectra).

*Catalytic Hydrogenation of Hexahydrochrysene Analog (**9**)*

The naphthalene olefin (**9**; 10 mg or 29.7 mmol) was dissolved in chloroform (3 ml). Palladium-on-charcoal (10%; 3 mg) was put into a microhydrogenation apparatus. After the absorption of an equimolar amount of hydrogen, the catalyst was filtered off. Evaporating the solvent *in vacuo* yielded 10 mg of oily product (**8**). When petroleum ether was poured into the oil, it solidified and gave a m.p. 169–172°. The melting point on admixture with the dehydrogenation product of the styrene compound (**12**) gave no depression. The u.v. and i.r. spectra were also identical.

*Synthesis of trans-2-Methoxy-8β-acetoxy-10a-methyl-6a,7,8,9,10,10a-hexahydrochrysene (**9**)*

A solution of the ketone (**10**; 100 mg) in methanol (50 ml) was treated with a solution of sodium borohydride (100 mg) in 80% methanol – 20% water (50 ml) and the mixture was stirred at room temperature for 2 h. The mixture was then treated with 10% acetic acid (5 ml). The solution was concentrated *in vacuo* to a volume of 10 ml, water and ether were added, and the ether layer was separated. The ether layer was washed with water, aqueous sodium bicarbonate, and water, and then dried over anhydrous magnesium sulfate. Removal of the solvent provided an oily product (**13**; 101 mg). The i.r. spectrum showed no conjugated carbonyl band but had an intense hydroxyl absorption (2.78 μ). The u.v. spectrum showed typical complex peaks for the saturated naphthalene chromophore (λ_{max} 227, 256, 266, 276, 287, 307, 314, 319, 328, and 334 nm). This oil (**13**) was dissolved in dry benzene (50 ml, dried over sodium) and phosphorus pentoxide (100 mg) was added. After refluxing for 2 h, the mixture was poured onto crushed ice. Ethyl ether was added and the ether layer was separated. The ether layer was washed with water, with

Can. J. Chem. Downloaded from www.nrcresearchpress.com by 210.87.254.5 on 09/05/12
For personal use only.

aqueous sodium bicarbonate, and finally with water. After drying over anhydrous magnesium sulfate, the solvent was removed to yield an oily material (94 mg). The material was purified by chromatography on alumina (10 g, Woelm activity grade 1). Elution with petroleum ether – benzene yielded the desired olefin (**9**) (61 mg) which melted at 158.5–160.5° after recrystallization from cyclohexane. This compound was identical with one of the minor components of the *tert*-butyl chromate oxidation reaction (mixture m.p., i.r., u.v.).

*Synthesis of trans-anti-trans-11,12-Seco-2-methoxy-8β-acetoxy-10a-methyl-11,12-dioxo-4b,5,6,6a,7,8,9,-10,10a,10b,11,12-dodecahydrochrysene (**16**) by Ozonolysis*

The olefinic compound (7; 485 mg) was dissolved in dry ethyl acetate (40 ml) and ozonized oxygen was passed through the solution at −78° over a period of 20 min. When the reaction was over, the solution was pale blue in color. The ozonide was catalytically cleaved by shaking with hydrogen and 10% palladium-on-charcoal under a pressure of about 3 atm (Parr instrument). After shaking for 20 h, the catalyst was removed. The solvent was evaporated off *in vacuo* to yield a crude product (609 mg). This material was purified by chromatography (30 g silica gel, B.D.H.). Elution with chloroform yielded the desired dialdehyde **16** (243 mg). Purification and characterization data for this compound are presented in the periodate cleavage experiment given below.

*Synthesis of trans-anti-trans-2-Methoxy-8β-acetoxy-11β,12β-dihydroxy-10a-methyl-4b,5,6,6a,7,8,9,-10,10a,10b,11,12-dodecahydrochrysene (**15**)*

The olefin (**12**; 600 mg) was dissolved in dry ethyl ether (10 ml). Osmium tetroxide (500 mg, 12% excess) was dissolved in dry ethyl ether (10 ml) and latter and former solutions were rapidly mixed. The osmium tetroxide container was rinsed with more ether (10 ml) and added. The solution was allowed to stand at room temperature in the dark for 57 h. The dark precipitate which separated was treated with methanol (6 ml) and water (1 ml). Hydrogen sulfide gas was passed into the solution for 5 min, the solution was stirred for a further 5 min, and the precipitate filtered in a sintered glass funnel. The precipitate was washed with methanol then removed and subjected to the hydrogen sulfide treatment twice more to insure decomposition of the osmate ester. When for some unknown reason the osmium sulfide did not aggregate sufficiently and was passed through the sintered glass funnel, it was found that only centrifugation was able to remove this impurity. When the solvent was removed from the filtrate solution a crude solid product (0.688 g) was obtained. This substance was refrigerated until purified by chromatography. Elution of the product (590 mg), from Woelm silica gel was accomplished with 5% methanol in chloroform. Thin-layer chromatography showed two isomers with R_f values 0.17 and 0.13, the latter being the major constituent. Recrystallization of the polar fractions from chloroform and petroleum ether (65–110°) produced an analytical sample m.p. 225–226°; i.r.: 2.90, 5.86, 6.12, 6.31 μ; u.v.: λ_{max} 276 (3.21), 282 nm (3.19); λ_{min} 244.5 (2.13), 280 nm (3.16); n.m.r.: 9.05 (angular methyl, 3H, singlet), 8.48 (C_{11} or C_{12} hydroxyl, 1H, doublet, removed by D_2O exchange), 8.02 ($C_{8\beta}$ acetoxyl, 3H, singlet), 7.22 (C_{11} or C_{12} hydroxyl, 1H, doublet, removed by D_2O exchange), 6.24 (C_2 methoxyl, 3H, singlet), 5.94 (C_{11}, 1H, multiplet, to triplet on D_2O addition), 5.60 (C_{12}, 1H, quartet, to doublet on D_2O addition), 5.3 (C_8, 1H, multiplet), 3.25 (C_3, 1H, quartet, $J = 2.5$ Hz), 2.94 (C_4, 1H, doublet, $J_{3,4} = 8.5$ Hz), 290 (C_1, 1H, doublet).

Anal. Calcd. for $C_{22}H_{30}O_5$: C, 70.56; H, 8.08; O, 21.36. Found: C, 70.18; H, 7.99; O, 21.83.

*Acetylation of Diol Acetate **15***

The above diol acetate (**15**) was acetylated in the usual manner to give the triacetate, *trans-anti-trans*-2-methoxy-8β,11β,12β-triacetoxy-10a-methyl-4b,5,6,6a,7,8,9,10,10a,-10b,11,12-dodecahydrochrysene, m.p. 194–195.5°; i.r.: 5.77, 6.20, 6.68 μ; u.v.: λ_{max} 283 (3.32), 277 (3.33), 225 nm (3.88); λ_{min} 280 (3.30), 243 nm (2.48); n.m.r.: 8.95 (angular methyl, 3H, singlet), 8.11 (C_{11} acetoxyl, 3H, singlet), 8.00 ($C_{8\beta}$ acetoxyl, 3H, singlet), 7.87 (C_{12} acetoxyl, 3H, singlet), 6.22 (C_2 methoxyl, 3H, singlet), 5.33 ($C_{8\alpha}$, 1H, septet), 4.33 (C_{11}, C_{12}, 2H, multiplet), 3.19 (C_3, 1H, quartet), 3.13 (C_1, 1H, doublet), 2.87 (C_4, 1H, doublet); mass spectrometry: *m/e* 458 (M^+), prominent peaks at *m/e* 149, 159, 161, 171, 174, 175, 176, 187, 188, 230, 263, 279, 296, 313, 338, 356, 372, 383, 398, 416, 443.

Anal. Calcd. for $C_{26}H_{34}O_7$: C, 68.10; H, 7.47; O, 24.43. Found: C, 68.89; H, 7.24; O, 23.87.

*Synthesis of trans-anti-trans-11,12-Seco-2-methoxy-8β-acetoxy-10a-methyl-11,12-dioxo-4b,5,6,6a,7,8,9,10,-10a,10b,11,12-dodecahydrochrysene (**16**) by Periodate Cleavage*

The above diol mixture (166.7 mg) obtained directly from the osmium tetroxide reaction was dissolved in methanol (77.5 ml) and a solution of periodic acid in water (24 ml; 0.0219 *M* in acid) was added to the reaction mixture. A 10% increase in temperature was noted. The reaction, which was followed by u.v. spectroscopy proceeded rapidly. After 2 h in the dark at room temperature ethylene glycol (0.39 ml) was added and mixed. On standing for 1 h the reaction mixture was partitioned between aqueous sodium bicarbonate and benzene, washed with water, and dried over anhydrous sodium sulfate. After removing the solvent the expected acetoxy dialdehyde (**16**; 173.4 mg) was obtained. Thin-layer chromatography showed one spot. Recrystallization from benzene – petroleum ether (65–110°) produced an analytical sample of *trans-anti-trans*-11,12-seco-2-methoxy-8β-acetoxy-10a-methyl-11,12-dioxo-4b,5,6,6a,7,-8,9,10,10a,10b,11,12-dodecahydrochrysene (**16**), m.p. 135–137°; i.r.: 3.64, 5.78, 5.83, 5.96, 6.24, 6.66 μ; u.v.: λ_{max} 225 (4.33), 255.5 (3.86), 321 nm (3.50); λ_{min} 242.5 (3.75), 281 nm (2.70); n.m.r.: 8.87 (angular methyl, 3H, singlet), 8.01 (C_8 acetoxyl, 3H, singlet), 7.63 (C_{10b}, 1H, quartet, $J_{10b,11} = 6.5$ Hz, $J_{10b,4b} = 12$ Hz), 6.23 (C_2 methoxyl, 3H, singlet), 5.5 (C_{4b}, 1H, multiplet), 5.3 (C_8, 1H, multiplet), 2.98 (C_3, 1H, quartet, $J_{1,3} = 2.5$ Hz), 2.74 (C_1, 1H, doublet), 2.74 (C_4, 1H, doublet, $J_{3,4} = 9$ Hz), 0.05 (C_{11}, 1H, doublet, $J_{10b,11} = 6.5$ Hz), −0.27 (C_{12}, 1H, singlet).

Anal. Calcd. for $C_{22}H_{28}O_5$: C, 70.94; H, 7.58; O, 21.44. Found: C, 70.96; H, 7.46; O, 21.84.

Since chromatography of this compound gave a very

Can. J. Chem. Downloaded from www.nrcresearchpress.com by 210.87.254.5 on 09/05/12
For personal use only.

poor recovery it was used directly for the next reaction, both these reactions being carried out on the same day.

Aldol Condensation of Dialdehyde **16**

A solution of crude dialdehyde (**16**; 480 mg) in methanol (110 ml) was added to a solution of sodium hydroxide (100 mg in 1.4 ml water). Reflux was continued for 3 h, after which time the reaction mixture was partitioned between chloroform and water several times. After drying over sodium sulfate and removing the solvent, a crude orange reaction product was obtained (397 mg). Thin-layer chromatography of the latter showed an intense orange fluorescent spot when sprayed with antimony trichloride – acetic acid (1:1) and heated in the oven. Recrystallization from benzene – petroleum ether (65–110°) gave an analytical sample of C-nor-2-methoxy-8β,11ξ-dihydroxy-10a-methyl-10bξ-formyl-4b,5,6,6a,7,8,9,10,10a,10b,11-undecahydrochrysene (**17**), m.p. 192°; i.r.: 2.96, 3.65, 5.84, 5.90, 6.19, 6.30, 6.75 μ; u.v.: λ_{max} 284 (3.36), 2.89 nm (3.32); λ_{min} 257 nm (2.74); n.m.r.: 8.91 (angular methyl, 3H, singlet), 6.6 (C_{4b}, 1H, quartet), 6.35 ($C_{8\alpha}$, 1H, multiplet—obscured), 6.27 (C_2, methoxyl, 3H, singlet), 4.6 (C_{11}, 1H, doublet), 3.08 (C_4, 1H, doublet—overlaps with C_1), 3.02 (C_1, 1H, doublet), 0.30 (C_{10b} formyl, 1H, doublet); mass spectrometry: *m/e* 330 (M^+) prominent peaks at *m/e* 158, 171, 172, 173, 174, 175, 186, 204, 213, 225, 235, 251, 269, 279, 284, 297, 312, 328.

Anal. Calcd. for $C_{20}H_{26}O_4$: C, 72.70; H, 7.93; O, 19.37. Found: C, 72.66; H, 7.85; O, 19.49.

Synthesis of C-Nor-2-methoxy-8,11-diketo-10bξ-formyl-10a-methyl-4bβ,5,6,6aα,7,8,9,10,10a,10b,11-undecahydrochrysene (18)

Jones' reagent (16) (0.6 ml; 3 at. O per molecule) was added rapidly with stirring to a solution of diol aldehyde (260 mg, m.p. 175–182°) in acetone (20 ml). After stirring at room temperature for 30 min, the excess chromic acid was decomposed with a small amount of methanol. The solvent was removed *in vacuo* on a steam bath and to the residue, water and benzene were added. The aqueous solution was extracted three times with benzene and the combined benzene extract was washed with water and then dried over anhydrous magnesium sulfate. Evaporation of the solvent yielded a pale yellow gummy product (260 mg) which had the desired u.v. (λ_{max} 220, 255, 326 nm; λ_{min} 244, 282 nm) and i.r. spectra (CCl_4 film, 5.82, 5.91 μ). Two recrystallizations from benzene and cyclohexane gave crystals melting at 140–152°; n.m.r.: 0.32 (—CHO, 1H, singlet), 8.78 (angular methyl, 3H, singlet), 6.19 (CH_3O—, 3H, singlet), 6.17 (C_{10}, 1H, doublet), 6.71 (C_{4b}, 1H, multiplet). This crystalline material was chromatographed on a plate in a manner somewhat different from conventional thin-layer chromatography. In this instance Woelm neutral alumina suitable for column chromatography was placed in dry powder form on a flat plate of glass which was held in an almost horizontal position. This chromatoplate was then developed with chloroform as eluant. The solvent was allowed to run to the top of the plate; the latter was removed from the chromatography tank and allowed to dry after which time it was placed back into the tank and redeveloped with chloroform. This operation was repeated twice and at this time four distinct bands were noted on the chromatoplate. The bands were cut out and eluted with methanol to yield four fractions (order of decreasing R_f; 69, 17, 44, 21 mg). The largest fraction gave a n.m.r. spectrum identical to that of a 1:1 mixture of the diketo isomers **19** and **20** obtained by deformylation of **18** with potassium hydroxide as mentioned below. This isomeric mixture on recrystallization from benzene and cyclohexane provided a crystalline material which was obviously still a mixture (m.p. 150–205°). No further characterization was performed due to lability of this substance.

The other major fraction (44 mg) also showed no aldehyde proton absorption in the n.m.r. spectrum (angular methyl protons at 8.74) as well as only one carbonyl peak in the i.r. spectrum. The most polar fraction (21 mg) had a R_f 0 and therefore was not examined. Since the second fraction (17 mg) was a mixture of compounds and in small quantity, it was not investigated.

The amount of acidic material (extractable with sodium bicarbonate solution) obtained from this oxidation was always very low (less than 10% of total reaction mixture).

Potassium Hydroxide Deformylation of C-Nor-2-methoxy-8,11-diketo-10bξ-formyl-10a-methyl-4bβ,5,6,6aα,7,8,9,10,10a,10b,11-undecahydrochrysene

The crude diketo aldehyde **18** obtained directly from the Jones' oxidation mixture (147 mg) was taken up in dioxane (37 ml) and water (3.7 ml) and to this solution potassium hydroxide (214 mg) was then added. The mixture was refluxed for 100 min after which time most of the dioxane was removed *in vacuo*. The residue was treated with water and benzene and dilute hydrochloric acid was added until the mixture was acidic. The aqueous solution was extracted three times with benzene. Thereafter the combined benzene extract was washed twice with water. After drying over anhydrous magnesium sulfate and evaporating the solvent, a neutral product (94 mg) was obtained. The yellow basic aqueous solution from the sodium bicarbonate washings was acidified with hydrochloric acid and then extracted three times with benzene. The benzene solution was washed with water until neutral, dried over anhydrous magnesium sulfate, and then evaporated to give the acidic material (24 mg). The acidic product had λ_{max} 308 nm and λ_{min} 273 nm in its u.v. spectrum.

The n.m.r. spectrum on the neutral product showed no low-field protons due to a formyl group but two angular methyl peaks in an intensity ratio of about 1:1 were evident at high field. It was therefore obvious that two compounds were in fact present. All attempts to separate these compounds (shown later to be the isomers **19** and **20**) on silica gel or alumina chromatography met with failure. These substances possess a slightly larger R_f value than the starting material **18** but all three compounds show the same behavior towards 20% antimony pentachloride in carbon tetrachloride on thin-layer chromatoplates. Prior to heating the spots slowly turn from yellow to tan color but when heated to 110° they become pink in colour. From thin-layer chromatography on the neutral product it was possible to exclude the presence of any unreacted starting material. Ultraviolet spectra on the reaction mixture showed that the reaction was essentially completed in 30 min; a change in the maxima from 329 to 318 nm occurred in this time.

Can. J. Chem. Downloaded from www.nrcresearchpress.com by 210.87.254.5 on 09/05/12
For personal use only.

Fortunately, the *trans-anti-trans* isomer (**19**) was less soluble than the *trans-syn-cis* isomer (**20**) and thus these two compounds could be separated by careful fractional crystallization. Since these compounds crystallized in different crystal types, hand separation of these crystals greatly facilitated purification on a small scale. To remove trace impurities which hampered crystallization, the crude reaction product was first chromatographed on neutral Woelm alumina and the fractions (60 mg) containing **19** and **20** were combined. Recrystallization from benzene and petroleum ether (65–110°) or cyclohexane gave orange needles and colorless plates. A mixture of these crystals, m.p. 137–150 and 175–195°, was used for microanalysis.

Anal. Calcd. for $C_{19}H_{22}O_3$: C, 76.48; H, 7.43; O, 16.09. Found: C, 76.30; H, 7.35; O, 16.48.

After several more recrystallizations the pure *trans-anti-trans* diketone (**19**) was obtained as orange needles, m.p. 198.5–201.5° (dec.); i.r.: 5.85, 6.22, 6.32, 6.71 μ; u.v.: λ_{max} 219 (4.44), 249 (3.92), 319 nm (3.59); λ_{min} 237 (3.83), 273 nm (2.98); n.m.r.: 8.85 (angular methyl, 3H, singlet), 6.23 (CH_3O—, 3H, singlet), 7.06 (C_{10b} and C_{4b}, 2H, multiplet), 2.74–2.96 (aromatic H, 3H, multiplet); n.m.r.: (C_6H_6): 9.20 (angular methyl, 3H, singlet), 6.70 (CH_3O—, 3H, singlet), 7.16 (C_{10b} and C_{4b}, 2H, broad multiplet).

Three crystallizations from benzene and cyclohexane produced an analytical sample of the *trans-syn-cis* diketone (**20**) as colorless plates, m.p. 140–142° (no decomposition); i.r.: 5.87, 6.20, 6.70 μ; u.v.: λ_{max} 218 (4.47), 249 (3.98), 318 nm (3.58); λ_{min} 236 (2.88), 272 nm (2.09); n.m.r.: 8.74 (angular methyl, 3H, singlet), 6.18 (CH_3O—, 3H, singlet), 6.57 ($C_{10\alpha}$ and C_{4b}, 2H, broad multiplet), 2.81 (aromatic, 3H, singlet); n.m.r.: (C_6H_6): 9.24 (angular methyl, 3H, singlet), 6.69 (CH_3O—, 3H, singlet), 6.40 ($C_{10\alpha}$, 1H, quintet), 7.08 (C_{4b}, 1H, quintet).

Both isomers decompose at about 200° to give rise to new maxima at about 234, 270, and 281 nm in the u.v. spectra in addition to the other three maxima already mentioned.

Acetylation of Dihydroxy Aldehyde ***17***

Upon acetylating the analytical sample of the above C-nordihydroxy aldehyde (**17**) under the usual conditions an 85% yield of C-nor-2-methoxy-8β,11ξ-diacetoxy-10a-methyl-10bξ-formyl-4b,5,6,6a,7,8,9,10,10a,10b,11-undecahydrochrysene (**23**) was obtained, m.p. 158.5–159.5°; u.v.: λ_{max} 222 (3.91), 286 (3.50), 291 nm (3.44); λ_{min} 252 nm (2.57); n.m.r.: 9.02 (angular methyl, 3H, singlet), 8.02 ($C_{8\beta}$ acetoxyl, 3H, singlet), 7.84 (C_{11}, acetoxyl, 3H, singlet), 6.58 (C_{4b}, 1H, quartet, $J_{4b\alpha,5\alpha}$ = 7 Hz, $J_{4b\alpha,5\beta}$ = 12 Hz), 6.35 (C_2 methoxyl, 3H, singlet), 5.30 ($C_{8\alpha}$, 1H, multiplet), 2.51 (C_1, 1H, doublet), 2.32 (C_3, 1H, quartet), 2.26 (C_{11}, 1H, singlet), 2.00 (C_4, 1H, doublet), 0.10 (C_{10b} formyl, 1H, singlet); mass spectrometry: parent peak, not visible, prominent peaks at *m/e* 158, 172, 251, 266, 211, 324, 326, 356.

Anal. Calcd. for $C_{24}H_{30}O_6$: C, 69.54; H, 7.30; O, 23.16. Found: C, 69.81; H, 7.40; O, 22.79.

*Synthesis of trans-C-Nor-2-methoxy-8β-acetoxy-10a-methyl-4b,5,6,6a,7,8,9,10,10a-nonahydrochrysene (****22****)*

The diacetate (**23**) was dissolved in glacial acetic acid (15.0 ml) containing sodium acetate (50 g, 4 *M*) and acetic anhydride (3 ml) and refluxed for 20 h. The reaction mixture was poured into water, partitioned between aqueous sodium bicarbonate – benzene, washed with water, and dried over sodium sulfate. After removal of the solvent the crude product was chromatographed on 50 g of alumina. Elution with benzene–hexane (1:9) gave olefin **22** (621 mg, 57.6% yield). Elution with chloroform gave a polar material (521 mg) which was reacted once more and worked-up in the above manner to give more olefin **22** (293 mg). The overall yield was 84.8%. Crystallization of this compound from hexane–benzene gave an analytical sample of **22** in the form of large plates, m.p. 140–141°; i.r.: 5.78, 6.21, 6.36, 6.75, 6.80, 6.91 μ; u.v.: λ_{max} 227 (4.41), 239 (4.21), 263 (3.88), 293 (3.54), 305 nm (3.51); λ_{min} 248 (3.75), 289 (3.47), 301 nm (3.42); n.m.r.: 9.11 ($C_{5\alpha}$, 1H, multiplet, by spin decoupling), 8.89 (angular methyl, 3H, singlet), 8.02 ($C_{8\beta}$ acetoxyl, 3H, singlet), 7.61 ($C_{5\beta}$, 1H, multiplet, $J_{5\alpha,5\beta}$ = 13 Hz, $J_{4b,5\beta}$ = 6.5 Hz, $J_{5\beta,6\beta}$ = $J_{5\beta,6\alpha}$ = 3 Hz), 6.72 (C_{4b}, 1H, quartet, $J_{4b,5\beta}$ = 6.5 Hz, $J_{4b,5\alpha}$ = 12.5 Hz), 6.27 (C_2 methoxyl, 3H, singlet), 3.80 (C_{11}, 1H, singlet), 3.40 (C_3, 1H, quartet), 3.19 (C_1, 1H, doublet), 2.86 (C_4, 1H, doublet); mass spectrometry: *m/e* 326 (M^+), prominent peaks at *m/e* 158, 172, 249, 251, 311, 324.

Anal. Calcd. for $C_{21}H_{26}O_3$: C, 77.27; H, 8.03; O, 14.71. Found: C, 77.55; H, 7.97; O, 14.48.

*Synthesis of trans-syn-cis-trans-C-Nor-2-keto-8β-hydroxy-10a-methyl-3,4,4a,4b,5,6,6a,7,8,9,10,10a,10b,11-tetradecahydrochrysene (****30****)*

The olefin (**22**; 350 mg) was dissolved in *tert*-butyl alcohol (15 ml) and tetrahydrofuran (20 ml). Dry ammonia was condensed into the three-necked flask and lithium (1 g) was added. After refluxing for 5 h the blue color disappeared, ammonia was evaporated in a stream of nitrogen, and the residue was partitioned between benzene and water. The dry solvent was evaporated to give a crystalline product. The product was dissolved in methanol (100 ml) and 12 *N* hydrochloric acid (5 ml). The mixture was heated under reflux for 3 h and then partitioned between the ethyl ether and water. Removal of the solvent provided the crude product (290 mg). Chromatography on alumina (30 g, activity III) gave a mixture (248 mg) when the eluent was benzene – ethyl acetate (9:1). Several crystallizations gave an analytical sample (235 mg) of **30**, m.p. 178–180°; i.r.: 5.79, 6.17, 6.31, 6.71, 6.78 μ; u.v.: λ_{max} 242 nm (4.19); n.m.r.: 8.99, (angular methyl, 3H, singlet) 7.78 (C_8 hydroxyl, 1H, singlet, removed by D_2O), 6.45 ($C_{8\alpha}$, 1H, septet), 4.07 (C_1, 1H, broad singlet).

Anal. Calcd. for $C_{18}H_{26}O_2$: C, 78.79; H, 9.55; O, 11.66. Found: C, 78.51: H, 9.58; O, 11.91.

Catalytic Hydrogenation of C-Nor-D-homo Olefin ***22***

The olefin (47 mg) dissolved in ethanol (10 ml) was hydrogenated over palladium-on-charcoal (100 mg) at slightly over 1 atm for 24 h. The reaction mixture was diluted with ethanol (40 ml) and filtered. The filtrate was evaporated and the residue dissolved in chloroform and the solution filtered again to leave a clear gum. The n.m.r. spectrum showed that no olefinic proton was present. On crystallization from methanol an analytical sample (40 mg) of *trans-syn-cis*-C-nor-2-methoxy-8β-acetoxy-10a-methyl-4b,5,6,6a,7,8,9,10,10a,11-undecahydrochrysene (**31**), m.p. 98.5–100°; i.r.: 5.79, 6.17,

Can. J. Chem. Downloaded from www.nrcresearchpress.com by 210.87.254.5 on 09/05/12
For personal use only.

6.31, 6.71, 6.78 μ; u.v.: λ_{max} 207 (3.97), 219 (3.88), 282 (3.45), 288 nm (3.41); λ_{min} 214 (3.86), 245 (2.11), 286 nm (3.38); n.m.r.: 8.99 (angular methyl, 3H, singlet), 8.03 ($C_{8\beta}$ acetoxyl, 3H, singlet), 7.89 ($C_{10b\beta}$, 1H, quintet, $J_{10b\beta,11\beta}$ = 6.5 Hz, $J_{10b\beta,11\alpha}$ = 12.5 Hz), 7.43 ($C_{11\beta}$, 1H, quartet, $J_{11\alpha,11\beta}$ = 15 Hz), 7.26 ($C_{11\alpha}$, 1H, quartet), 7.00 ($C_{4b\alpha}$, 1H, quintet, $J_{4b\beta,10b\beta} = J_{4b\beta,5\beta}$ = 6.5 Hz, $J_{4b\beta,5\alpha}$ = 12.5 Hz), 6.31 (C_2 methoxyl, 3H, singlet), 5.33 ($C_{8\alpha}$, 1H, multiplet), 3.43 (C_3, 1H, quartet), 3.29 (C_4, 1H, doublet), 3.05 (C_1, 1H, doublet); mass spectrometry: *m/e* 328 (M^+), prominent peaks at *m/e* 146, 158, 159, 160, 173, 186, 197, 214, 225, 227, 253, 268.

Anal. Calcd. for $C_{21}H_{28}O_3$: C, 76.79; H, 8.59; O, 14.61. Found: C, 76.52; H, 8.81; O, 14.67.

Birch Reduction of C-Nor-D-homo Hydrochrysene Analog 31

Reduction of **31** under exactly the conditions mentioned above in the conversion, **22** → **30**, gave an 80% yield of **30**, identical in every respect with the sample obtained and characterized above.

Reductive Hydroboration of C-Nor-D-homo Olefin 22

Diborane generated by the slow addition of sodium borohydride (0.6 g) in diglyme (30 ml) to boron trifluoride etherate (5 ml) in diglyme (20 ml) was passed in a stream of nitrogen into a solution of the olefin (225 mg) in diglyme (30 ml). Generation of the diborane took 2 h and the solution of olefin was allowed to stand overnight in contact with the gas. One drop of water was added followed by propionic acid (7 ml) and the mixture was heated under reflux for 5 h, poured into water, and extracted with ethyl ether. The ether extract was washed with dilute aqueous sodium chloride solution and dried over magnesium sulfate. The solvent was removed to give a brown gum (290 mg). This material showed several blue spots on t.l.c. when sprayed with antimony trichloride. This material (290 mg) was dissolved in a mixture of methanol (35 ml), water (15 ml), and potassium carbonate (1 g). Reflux was maintained for 2 h. The product was partitioned between chloroform and water and dried over sodium sulfate. The residue was reacetylated in the usual manner. The usual work-up gave an oil (236 mg) which was chromatographed on alumina (50 g, activity III). Elution with hexane–benzene (17:3) gave (69 mg) a material with R_f comparable to that of the previous Birch reduction products of the reaction mentioned above. Further elution with hexane–benzene (3:1) gave a complex mixture (121 mg) not further investigated. The major product (32 mg, 14%), after two preparative layer chromatographs of the first fractions, was submitted to n.m.r. spectroscopy. The product consisted of two isomers in a ratio of 5:1 with the major component being *trans-syn-cis*-C-nor-2-methoxy-8β-acetoxy-10a-methyl-4b,5,6,6a,7,8,9,10,10a,10b,11-undecahydrochrysene (**31**).

Oxidative Hydroboration of C-Nor-D-homo Olefin 22

The olefin (130 mg) and the ethyl ether adduct of boron trifluoride (0.5 ml) were dissolved in ethyl ether (10 ml) and stirred under nitrogen at 0°. Sodium borohydride (130 mg) in ether (15 ml) was added gradually over 45 min. Stirring was continued for 2 h during which time the temperature was allowed to rise to 20°. The solution was worked up in the usual manner and 70% ethanol (10 ml) containing sodium hydroxide (0.25 g) was added to the residue. Hydrogen peroxide solution (3 ml, 20%) was added dropwise. When effervescence subsided the solution was heated to 70°. Further effervescence was observed for 10 min. The solution was cooled, diluted, and neutralized with acid. This solution was partitioned between water and chloroform. The product (125 mg) was purified by preparative t.l.c. on silica gel GF (0.5 mm thick, developed with ethyl acetate – petroleum ether (2:1)) and bands were located by water spray. The main band was removed and extracted to give a 68% yield (98 mg) of *trans-syn-cis*-C-nor-2-methoxy-8β,11β-dihydroxy-10a-methyl-4b,5,6,6a,7,8,9,10,10a,10b,11-undecahydrochrysene (**32**), m.p. 180–181°; n.m.r. 8.97 (angular methyl, 3H, singlet), 8.39 (C_8 and C_{11} hydroxyls, 2H, singlets, removed by D_2O exchange), 6.86 (C_{4b}, 1H, quintet, $J_{4b,10b}$ = 12.5 Hz, $J_{4b,5\alpha} = J_{4b,5\beta}$ = 6 Hz), 6.3 ($C_{8\alpha}$, 1H, multiplet), 6.24 (C_2 methoxyl, 3H, singlet), 4.91 (C_{11}, 1H, doublet, $J_{10b,11}$ = 10 Hz), 3.27 (C_3, 1H, quartet, $J_{1,3}$ = 2.5 Hz), 3.07 (C_1, 1H, doublet, $J_{3,4}$ = 8 Hz), 2.98 (C_4, 1H, doublet).

Anal. Calcd. for $C_{19}H_{26}O_3$ (mol. wt. 302.1881): C, 75.46; H, 8.67. Found (high resolution mass measurement, 302.1878): C, 75.46; H, 8.58.

Modified Birch Reduction of trans-syn-cis-C-Nor-D-homo Diol 32

Small pieces of lithium metal (500 mg) were added cautiously with stirring to a solution of **32** (500 mg) in dry dioxane (25 ml), isopropanol (25 ml), and ammonia (100 ml). The mixture was then stirred under reflux for 6 h. Removal of the solvents in a stream of nitrogen provided a residue (497 mg) which was taken up in methanol (50 ml) and 12 *N* hydrochloric acid (5 ml) and refluxed for 3 h. The resultant mixture was partitioned between ethyl ether and water. Removal of the ether provided a colorless gum (450 mg). Chromatography on alumina (40 g, activity III) using benzene – ethyl acetate (9:1) provided 400 mg of a white solid. Crystallization from methanol–water gave A/B *trans*-C-nor-2-keto-8β-hydroxy-10a-methyl-3,4,4a,4b,5,6,6a,7,8,9,10,10a-dodecahydrochrysene (**34**; 350 mg), m.p. 199–203°; i.r.: 6.12 μ; u.v.: λ_{max} 295 nm (4.38); n.m.r.: 8.97 (angular methyl, 3H, singlet), 4.25 and 4.05 (C_{11} and C_1, 2H, broad singlets).

Anal. Calcd. for $C_{18}H_{24}O_2$ (mol. wt. 272.1776): C, 79.37; H, 8.88; O, 11.75. Found (high resolution mass measurement, 272.1754): C, 79.29; H, 8.74; O, 11.51).

Catalytic Reduction of C-Nor-D-homo Dienone 34

The dienone (**34**; 350 mg) was taken up in ethanol and hydrogenated over a 10% platinum-on-charcoal catalyst (150 mg). After 1 h, during which time 1.5 mol of hydrogen had been absorbed, the hydrogenation was terminated. Evaporation of the solvent provided the crude product (345 mg) which on t.l.c. was a mixture of two main components. These compounds proved extremely difficult to separate and for preparative purposes the total mixture was subjected to the bromination–dehydrobromination sequence as noted below.

In one experiment, extensive column chromatography on alumina (activity III) followed by high vacuum distillation, did provide a small sample of saturated ketone (**36**, epimeric mixture at C_{12}) as a clear glass, b.p.

Can. J. Chem. Downloaded from www.nrcresearchpress.com by 210.87.254.5 on 09/05/12
For personal use only.

125°/0.1 mm; i.r.: ($CHCl_3$) 5.89 μ; no u.v. absorption; n.m.r.: 9.22 (angular methyl, 3H, singlet) 6.45 (C_8, 1H, multiplet).

Anal. Calcd. for $C_{18}H_{28}O_2$ (mol. wt. 276.2089): C, 78.21; H, 10.21. Found (high resolution mass measurement, 276.2110): C, 78.08; H, 10.21.

The crude product mixture (345 mg) was treated with a solution of bromine in acetic acid (10 ml, 0.19 *M*) at room temperature. Decolorization of the bromine was immediate. The solution was diluted with water and extracted with benzene. The extract was washed with water, the solvent removed, and the residue taken up in dimethylformamide (10 ml) and treated with magnesium oxide (700 mg). After refluxing for 1 h, the mixture was diluted with water and extracted with benzene. Removal of the solvent provided a crude product mixture (300 mg). Chromatography of the latter on alumina (30 g, activity III) and elution with benzene – ethyl acetate (9:1) provided A/B *trans*-C-nor-2-keto-8β-hydroxy-10a-methyl-3,4,4a,4b,5,6,6a,7,8,9,10,10a,10b,11-tetradecahydrochrysene (**37**; 260 mg). Purification of **37** for analytical purposes was achieved by high vacuum distillation whereupon **37** was obtained as a clear glass, b.p. 142°/0.1 mm; i.r.: ($CHCl_3$) 6.06 μ; u.v.: λ_{max} 238 nm (4.20); n.m.r.: 9.22 (angular methyl, 3H, singlet), 4.13 (C_1, 1H, broad singlet).

Anal. Calcd. for $C_{18}H_{26}O_2$ (mol. wt. 274.1932): C, 78.79; H, 9.55; O, 11.66. Found (high resolution mass measurement, 274.1928): C, 78.61; H, 9.47; O, 11.54.

Synthesis of trans-anti-trans-2-Keto-8β-hydroxy-1,10a-dimethyl-2,3,4,4a,5,6,6a,7,8,9,10,10a,10b,11,12-hexadecahydrochrysene (42) via Enamine Alkylation

The conjugated ketone (**40**; 251 mg) was dissolved in a mixture of benzene (10 ml) and pyrrolidine (0.4 ml). The reaction mixture was heated under reflux for 190 min during which time water was gradually removed from the reaction by azeotropic distillation with benzene with the help of a Dean–Stark apparatus. After this time all the solvent was evaporated *in vacuo* and the residual product showed in its u.v. spectra a strong maximum at 276 nm in methanol and at 274.5 nm in a mixture of hydrochloric acid and methanol. The dienamine was refluxed under a dry nitrogen atmosphere with anhydrous methanol (6 ml) and methyl iodide (0.9 ml) for 47 h. On addition of methyl iodide to the methanolic solution of the dienamine a white precipitate formed immediately but it dissolved when the solution was heated. After this reflux period, the solvent was evaporated *in vacuo* on a steam bath. The reaction product was then refluxed under nitrogen with methanol (4 ml), water (1 ml), acetic acid (0.4 ml), and sodium acetate (500 mg, anhydrous) for 4 h. After removal of the solvent, the residue was treated with water and chloroform. The chloroform extract, after drying over anhydrous sodium sulfate, was concentrated to yield an orangish-brown solid glassy product (272 mg). This material showed a maximum at 242 nm (methanol) in the u.v. spectrum as well as a small band due to a saturated carbonyl group in its i.r. spectrum. The product was then dissolved in methanol (15 ml) and refluxed for 1.5 h with dilute hydrochloric acid (2 ml of concentrated acid in 3 ml of water). After this period, the solvent was removed and the residue was extracted with chloroform. The chloroform extract was then washed with water until neutral to p*H* paper, dried over anhydrous sodium sulfate, filtered, and evaporated to dryness to give 240 mg of crude product. The i.r. spectrum of the latter showed that this product contained less unconjugated ketonic material than from the previous work-up. Chromatography on alumina (20 g, activity II–III) with a mixture of chloroform and benzene (1:4) gave four fractions (62 mg) which contained the desired **42** (about 40 mg, 15% yield). The earlier fractions of the chromatography yielded 29 mg of a substance while the later fractions contained 143 mg. The latter fractions possessed mostly starting ketone **40**. The desired material could be easily identified on thin-layer chromatography, since it behaved differently from starting ketone **40**. The methylated compound (**42**) formed an orange spot on silica gel G chromatoplates when sprayed with a mixture of antimony trichloride and acetic acid (1:1) followed by heating to 110°. Its R_f value of about 0.25 (ethyl acetate – chloroform (1:10) as eluant) was slightly greater than that of **40** which gave a red spot with this spray reagent. Further purification of the fractions (62 mg) on preparative silica gel (0.5 mm thick 50 g) chromatoplates (eluant was ethyl acetate – chloroform (1.5:10), run three times) gave 25 mg of **42** (10% yield). Recrystallization from benzene and cyclohexane gave crystals, m.p. 170–183°; i.r.: (CCl_4) 6.05 μ; u.v.: λ_{max} 250, 309 nm; λ_{min} 287 nm; n.m.r.: 9.25 (angular methyl, 3H, singlet), 8.22 (C_1 methyl, singlet), 6.38 ($C_{8\alpha}$, 1H, broad multiplet), 8.11 (HO—, singlet), 7.10 ($C_{12\beta}$, 1H, doublet).

Anal. Calcd. for $C_{20}H_{30}O_2$: C, 79.42; H, 10.00; O, 10.58. Found: C, 79.21; H, 9.87; O, 10.31.

Synthesis of 42 via Enolate Trapping and Alkylation

The tetrahydropyranyl ether derivative of ketone **40** was prepared by dissolving the ketone (624 mg) in freshly distilled tetrahydropyran (10 ml) along with several milligrams of *p*-toluenesulfonic acid. After 16 h powdered potassium carbonate was added. Stirring was continued for 6 h. The mixture was diluted with ether, filtered, and the filtrate evaporated to leave a gum (1.04 g). A solution containing the tetrahydropyranyl ether in dry tetrahydrofuran (25 ml) was added to scrupulously dry solution of ammonia (50 ml) containing lithium (49 mg) and a further amount of lithium (20 mg) was added to maintain the blue color. The solution was allowed to evaporate slowly while more tetrahydrofuran (50 ml) was added. When the ammonia was completely removed, methyl iodide (20 ml), which had been freshly distilled, was added and the solution refluxed for 3 h. Most of the solvent was removed and the rest partitioned between benzene and water. The dried benzene layer was evaporated and replaced with 3% aqueous oxalic acid (20 ml) in ethanol (25 ml). After the usual work-up the residue (890 mg) was chromatographed on alumina (85 g, activity III). Benzene–chloroform (4:1) gave a ketone fraction (393 mg) which was then rechromatographed on alumina (60 g, activity III). The center fractions (278 mg) were crystalline. Recrystallization from acetone–hexane gave an analytical sample of *trans-anti-trans*-1-methyl-2-keto-8-hydroxy-10a-methyl-1,3,4,4a,4b,5,6,6a,7,8,9,10,10a,10b,11,12,13-heptadecahydrochrysene (**42**, no double bond), m.p. 182–183°; n.m.r.: 9.26 (angular methyl, 3H, singlet),

Can. J. Chem. Downloaded from www.nrcresearchpress.com by 210.87.254.5 on 09/05/12
For personal use only.

9.02 (C_1 methyl, 3H, doublet), 8.24 (C_8 hydroxyl, 1H, singlet, removed by D_2O) 6.43 ($C_{8\alpha}$, 1H, septet); mass spectrometry: *m/e* 304 (M^+), prominent peaks at *m/e* 149, 232, 247, 271, 272, 286, 290.

Anal. Calcd. for $C_{20}H_{32}O_2$: C, 78.89; H, 10.59; O, 10.51. Found: C, 78.62; H, 10.41; O, 10.40.

This ketone (213 mg) was treated with a solution of bromine in acetic acid (7 ml, 0.19 *M*) at room temperature. An immediate decolorization of bromine was observed. The mixture was diluted with water and extracted with benzene. The extract was washed with water, the solvent removed, and the residue taken up in dimethylformamide (25 ml) and treated with magnesium oxide (2 g). After refluxing for 1 h, the mixture was diluted with water and extracted with benzene. Removal of the solvent provided a crude product (197 mg). Chromatography on alumina (35 g, activity III) and elution with petroleum ether – benzene provided a product identical with **42** as obtained above in the enamine alkylation reaction.

Synthesis of C-Nor-D-homo Ketone 38 via Enolate Trapping and Alkylation

The C-nor-D-homo enone (**36**; 300 mg) was reacted with lithium (70 mg) in ammonia (50 ml) and dioxane (25 ml), then methyl iodide (15 ml), in exactly the manner described above in the synthesis of **42**. The crude product (280 mg) was acetylated directly with pyridine and acetic anhydride to yield after chromatography on alumina (40 g, activity III) and crystallization (methanol–water) an analytical sample (190 mg) of **38**, m.p. 169–171.5°; i.r. 5.85 μ; n.m.r.: 9.02 (C_{18}, methyl, 3H, doublet, $J = 12$ Hz), 9.20 (angular methyl, 3H, singlet).

Anal. Calcd. for $C_{21}H_{32}O_3$ (mol. wt. 332.2331): C, 75.86; H, 9.70. Found (high resolution mass measurement, 332.2349): C, 75.71; H, 9.75.

This compound was found identical (t.l.c., i.r., n.m.r., and mass spectra) with 3β-acetoxy-5α-etiojervan-17-one (**38**) obtained in the hecogenin degradation sequence as described below.

Synthesis of 3β-Acetoxy-5α-etiojerv-12(13)-en-17-one (39) via Hecogenin Degradation

Throughout the entire project this compound occupied a position of prime importance since it provided the etiojervane portion of most of the compounds synthesized. It was prepared from hecogenin acetate employing degradation procedures well documented by Johns (41). Details of the quantities used and the yields obtained in this work for the various steps are given below. Wherever modifications in the experimental procedure or additional data were obtained, for characterization of the intermediates in the degradation, these are included.

Hecogenin p-Toluenesulfonylhydrazone (44)

A solution of hecogenin acetate (400 g) in glacial acetic acid yielded hecogenin *p*-toluenesulfonylhydrazone (560 g) when treated with *p*-toluenesulfonylhydrazine hydrochloride as outlined by Hirschmann *et al.* (43). The product was not further purified but subjected to the next reaction.

13-Methyl-C-nor-D-homo-18-nor-5α,22α-spirost-12(13)-en-3β-ol (45)

A solution of hecogenin *p*-toluenesulfonylhydrazone (560 g) in potassium hydroxide – ethylene glycol was heated under nitrogen as outlined by Johns (41). The product was obtained crystalline from ethanol–water as colorless needles, m.p. 108–111° (lit. (41) m.p. 108–118°); n.m.r.: 9.28 (angular methyl, 3H, singlet), 9.24 (C_{26} methyl, 3H, doublet, $J = 6$ Hz), 8.91 (C_{21} methyl, 3H, $J = 6$ Hz), 8.40 (C_{18} methyl, 3H, broad singlet); mass spectrometry: *m/e* 414 (M^+) prominent peaks at *m/e* 300, 271, 263.

13-Methyl-C-nor-D-homo-18-nor-5α,22α-spirostan-3β-ol Acetate (46)

13-Methyl-C-nor-D-homo-18-nor-5α,22α-spirost-12(13)-en-3β-ol acetate (280 g), which had been prepared by treatment of the olefin-3β-ol with pyridine – acetic anhydride overnight, was hydrogenated in acetic acid over 5% rhodium-on-alumina as outlined by Johns (41). The product was readily obtained crystalline (from methanol) as needles, m.p. 168–173° (220 g) (lit. (41) m.p. 173–177°); n.m.r.: 9.20 (C_{19} methyl, 3H, singlet), 8.01 (acetoxy, 3H, singlet); mass spectrometry: *m/e* 458 (M^+) base peak at *m/e* 342.

17-Acetyl-5α,13β-etiojerv-16-en-3β-ol (47)

The hydrogenation product (110 g) was subjected to ring opening by octanoic anhydride, oxidation with chromic acid, and elimination employing potassium hydroxide in *tert*-butyl alcohol, according to the procedures outlined by Johns (41). Chromatography of the product on alumina (2 kg, activity III) eluting with 20% chloroform in benzene gave 17-acetyl-5α,13β-etiojerv-16-en-3β-ol (34 g) which was crystallized from acetone – petroleum ether, m.p. 162–165° (lit. (41) m.p. 164–168°); n.m.r.: 9.22 (C_{19} methyl, 3H, singlet), 9.19 (C_{18} methyl, 3H, doublet, $J = 7$ Hz), 7.0 (C_{13}, 1H, quintet), 3.1 (C_{16}, 1H, two doublets, $J = 3$ and 7.5 Hz).

Conversion to 17-acetyl-5α,13β-etiojerv-16-en-3β-ol acetate was accomplished by dissolving the product in acetic anhydride – pyridine (1:1) and allowing the solution to stand at 20° for 12 h. Recrystallization of the product from acetone – petroleum ether gave needles (34.2 g), m.p. 143–144°.

17-Acetyl-5α,13β-etiojerv-16-en-3β-ol 3-Acetate 20-Oxime

A solution of 17-acetyl-5α,13β-etiojerv-16-en-3β-ol acetate (33 g) in pyridine was treated with hydroxylamine hydrochloride according to the procedure of Johns (41). The product was obtained crystalline from acetone as needles (33.5 g), m.p. 198–202° (lit. (41) m.p. 205–210°); n.m.r.: 9.18 (C_{19} methyl, 3H, singlet), 9.07 (C_{18} methyl, 3H, doublet, $J = 7$ Hz), 8.0 (*O*-acetate and enamide methyl, 6H, singlet) 7.03 (C_{13}, 1H, quintet), 3.82 (C_{16}, 1H, two doublets, $J = 7$ Hz); mass spectrometry: *m/e* 373 (M^+), prominent peaks at *m/e* 358, 296, and 255.

3β-Acetoxy-5α-etiojervan-17-one (38)

A solution of 17-acetyl-5α,13β-etiojerv-16-en-3β-ol acetate 20-oxime (33.0 g) in pyridine (400 ml) was treated with phosphorus oxychloride following the procedure of Johns (41). The product, obtained by filtration after pouring the reaction mixture into aqueous hydrochloric acid at 60°, was chromatographed on alumina (700 g, activity III). Elution with 15% chloroform in benzene gave pure 3β-acetoxy-5α-etiojervan-17-one (24.8 g) which was crystallized from methanol–water giving colorless needles, m.p. 169–171.5° (lit. (41) m.p. 175–177°). This

compound was compared with the product obtained via enolate trapping and alkylation of **36**. Both were shown to be identical.

3β-Acetoxyetiojerv-12(13)-en-17-one (39)

Bromination of 3β-acetoxy-5α-etiojervan-17-one (**38**) using an equimolar quantity of bromine followed by dehydrobromination as outlined by Johns (41) gave a mixture of compounds. Chromatography on alumina (400 g, activity III) eluting with 15% chloroform–benzene gave 3β-acetoxyetiojervan-17-one while further elution with the same solvent provided 3β-acetoxyetiojerv-12(13)-en-17-one (**39**), m.p. 167–168°; i.r.: 6.06 μ; u.v.: λ_{max} 246 nm (4.19); n.m.r.: 9.18 (C_{19} methyl, 3H, singlet), 8.31 (C_{18} methyl, 3H, singlet), 8.01 (acetate, 3H, singlet); mass spectrometry: *m/e* 330 (M^+), prominent peaks at *m/e* 288, 272, 270, and 255.

Financial aid from the National Research Council of Canada and the B.C. Heart Foundation is gratefully acknowledged. We would also wish to express our thanks to Syntex S.A., G. D. Searle and Company, and Smith Miller and Patch Inc., for supplying generous samples of hecogenin and hecogenin acetate.

1. S. M. KUPCHAN and A. W. BY. *In* The alkaloids. Vol. 10. *Edited by* R. H. F. Manske. Academic Press, New York. 1968. pp. 193–285; J. TOMKO and Z. VOTICKY. *In* The alkaloids. *Edited by* R. H. F. Manske. Academic Press, New York. 1973. pp. 1–79.
2. C. R. NARAYANAN. *In* Progress in chemistry of organic natural products. Vol. 20. *Edited by* L. Zechmeister. Springer-Verlag, Vienna. 1962. pp. 298–371.
3. S. M. KUPCHAN and W. E. FLACKE. *In* Antihypertensive agents. *Edited by* E. Schlittler. Academic Press, New York. 1967. pp. 429–458.
4. D. G. CROSBY. *In* Naturally occurring insecticides. *Edited by* M. Jacobson and D. G. Crosby. Marcel Dekker, New York. 1971. pp. 186–235.
5. R. F. KEELER. Steroids, **18**, 741 (1971).
6. L. F. FIESER and M. FIESER. Steroids. Reinhold Publishing Corp., New York. 1959. p. 867.
7. W. S. JOHNSON, H. A. P. DE JONGH, C. E. COVERDALE, J. W. SCOTT, and U. BURCKHARDT. J. Am. Chem. Soc. **89**, 4523 (1967).
8. T. MASAMUNE, M. TAKASUGI, A. MURAI, and K. KOBAYASHI. J. Am. Chem. Soc. **89**, 4521 (1967).
9. J. P. KUTNEY, J. CABLE, W. A. F. GLADSTONE, H. W. HANSSEN, G. V. NAIR, E. J. TORUPKA, and W. D. C. WARNOCK. Can. J. Chem. This issue.
10. J. P. KUTNEY, W. MCCRAE, and A. BY. Can. J. Chem. **40**, 982 (1962).
11. J. P. KUTNEY, J. WINTER, W. MCCRAE, and A. BY. Can. J. Chem. **41**, 470 (1963).
12. J. P. KUTNEY and A. BY. Can. J. Chem. **42**, 591 (1964).
13. K. TORI and K. AONO. Ann. Rep. of Shionogi Res. Lab. **14**, 136 (1964).
14. N. S. BHACCA and D. H. WILLIAMS. Application of NMR spectroscopy in organic chemistry. Holden-Day Inc., San Francisco, California. 1964. Chapt. 2.
15. W. S. JOHNSON, A. D. KEMP, R. PAPPO, J. ACKERMAN, and W. F. JOHNS. J. Am. Chem. Soc. **78**, 6312 (1956).
16. J. BOWDEN, I. M. HEILBRON, E. R. H. JONES, and B. C. L. WEEDON. J. Chem. Soc. 39 (1946).
17. P. W. SCHIESS, D. M. BAILEY, and W. S. JOHNSON. Tetrahedron Lett. 549 (1963).
18. L. M. JACKMAN and S. STERNHELL. Applications of nuclear magnetic resonance spectroscopy in organic chemistry. Pergamon Press, London. 1969. p. 88.
19. D. M. BAILEY, D. P. G. HAMON, and W. S. JOHNSON. Tetrahedron Lett. 555 (1963).
20. H. BUDZIKIEWICZ, C. DJERASSI, and D. H. WILLIAMS. Structure elucidation of natural products by mass spectrometry. Vol. 2. Holden-Day, Inc., San Francisco, California. 1964. Chapt. 20.
21. H. O. HOUSE, V. PARAGAMIAN, R. S. RO, and D. J. WLUKA. J. Am. Chem. Soc. **82**, 1457 (1960).
22. H. O. HOUSE and R. G. CARLSON. J. Org. Chem. **29**, 74 (1964).
23. G. QUINKERT. Experientia, **13**, 381 (1957).
24. J. BIELLMANN, P. CRABBE, and G. OURISSON. Tetrahedron, **3**, 303 (1958).
25. J. BIELLMANN, D. FRANCETIC, and G. OURISSON. Tetrahedron Lett. 4 (1960).
26. Y. MORISAWA. Chem. Pharm. Bull. Jap. **12**, 1066 (1964).
27. C. W. SHOPPEE and R. E. LACK. J. Chem. Soc. 3619 (1964).
28. D. H. R. BARTON and G. F. LAWS. J. Chem. Soc. 52 (1954).
29. J. WINTER, M. RAJIC, and G. OURISSON. Bull. Soc. Chim. Fr. 1213 (1961).
30. H. O. HOUSE and G. RASMUSSON. J. Org. Chem. **28**, 31 (1963).
31. O. WINTERSTEINER and M. MOORE. Tetrahedron, **20**, 1947 (1964).
32. Y. MORISAWA. Chem. Pharm. Bull. Jap. **12**, 1060 (1964).
33. W. NAGATA, T. TERASAWA, and K. TORI. J. Am. Chem. Soc. **86**, 3746 (1964).
34. K. HEUSLER and A. WETTSTEIN. Helv. Chim. Acta, **35**, 284 (1952).
35. W. NAGATA, S. HIRAI, T. TERASAWA, and K. TAKEDA. Chem. Pharm. Bull. Jap. **9**, 569 (1961).
36. J. L. JOHNSON, M. E. HERR, J. C. BABCOCK, A. E. FONKEN, J. E. STAFFORD, and F. W. HEYL. J. Am. Chem. Soc. **78**, 430 (1956).
37. M. TOMOEDA, M. INUZUKA, and T. FURUTA. Tetrahedron Lett. 1233 (1964).
38. R. H. SHAPIRO, J. M. WILSON, and C. DJERASSI. Steroids, **1**, 1 (1963).
39. L. PETERSON. Anal. Chem. **34**, 1781 (1962).
40. G. STORK, P. ROSEN, N. GOLDMAN, R. V. COOMBS, and J. TSUJI. J. Am. Chem. Soc. **87**, 275 (1965).
41. W. F. JOHNS and I. LAOS. J. Org. Chem. **30**, 123 (1965).
42. J. FRIED, M. J. GREEN, and G. V. NAIR. J. Am. Chem. Soc. **92**, 4136 (1970).
43. R. HIRSCHMANN, C. S. SNODDY, C. F. HISKEY, and N. L. WENDLER. J. Am. Chem. Soc. **76**, 4013 (1954).
44. J. P. KUTNEY, A. BY, T. INABA, and S. Y. LEONG. Tetrahedron Lett. 2911 (1965); J. P. KUTNEY, J. CABLE, W. A. F. GLADSTONE, H. W. HANSSEN, E. J. TORUPKA, and W. D. C. WARNOCK. J. Am. Chem. Soc. **90**, 5333 (1968).

Can. J. Chem. Downloaded from www.nrcresearchpress.com by 210.87.254.5 on 09/05/12
For personal use only.

Synthetic Studies in the *Veratrum* Alkaloid Series. II.[1] The Total Synthesis of Verarine, Veratramine, Jervine, and Veratrobasine

JAMES P. KUTNEY, JOHN CABLE, WILLIAM A. F. GLADSTONE, HARALD W. HANSSEN, G. VIJAY NAIR, EDWARD J. TORUPKA, AND WILLIAM D. C. WARNOCK

Department of Chemistry, University of British Columbia, Vancouver, British Columbia V6T 1W5

Received May 22, 1974[2]

JAMES P. KUTNEY, JOHN CABLE, WILLIAM A. F. GLADSTONE, HARALD W. HANSSEN, G. VIJAY NAIR, EDWARD J. TORUPKA, and WILLIAM D. C. WARNOCK. Can. J. Chem. **53**, 1796 (1975).

Coupling of 3β-acetoxy-5α-etiojerv-12(13)-en-17-one (**1**) with the lithio derivative of 2-ethyl-5-methylpyridine provides the crucial intermediate (**3**) for the subsequent elaboration to verarine. Aromatization of **3** to **4** and reduction of the latter provides a mixture from which *N*-acetyl-5α,6-dihydroverarine (**11**) was isolated. Subsequent introduction of the 5,6-double bond in the latter and removal of the *N*-acetate function completed the synthesis of verarine (**31**). In a similar sequence of reactions employing **1** and the lithio derivative of 2-ethyl-3-methoxy-5-methylpyridine, the resultant intermediate (**54**), was elaborated to 5α,6-dihydroveratramine (**56**). Due to known conversions of the latter to veratramine (**14**), jervine (**32**), veratrobasine (**33**), and 11-deoxojervine (**34**), the formal total synthesis of these natural products is complete.

JAMES P. KUTNEY, JOHN CABLE, WILLIAM A. F. GLADSTONE, HARALD W. HANSSEN, G. VIJAY NAIR, EDWARD J. TORUPKA et WILLIAM D. C. WARNOCK. Can. J. Chem. **53**, 1796 (1975).

Le couplage de l'acétoxy-3β(5α)-étiojervène-12(13) one-17 (**1**) avec le dérivé lithié de l'éthyl-2 méthyl-5 pyridine fournit l'intermédiaire (**3**) crucial pour l'élaboration subséquente de la véranine. L'aromatisation de **3** en **4** et la réduction de ce dernier dérivé fournit un mélange duquel on peut isoler la *N*-acétyldihydro-5α,6 véranine (**11**). L'introduction subséquente d'une double liaison en position 5,6 et l'élimination de la fonction *N*-acétate, complète la synthèse de la véranine (**31**). Utilisant une séquence semblable de réactions faisant appel à **1** et au dérivé lithié de l'éthyl-2 méthoxy-3 méthyl-5 pyridine, on a obtenu l'intermédiaire (**54**) qui a été transformé en dihydro-5α,6 vératramine (**56**). En se basant sur le fait que ce dernier composé peut être transformé, à l'aide de séquences connues, en vératramine (**14**), en jervine (**32**), en vératrobasine (**33**) et en déoxo-11 jervine (**34**), on peut considérer que la synthèse totale formelle de ces produits naturels est maintenant complète. [Traduit par le journal]

In the previous publication (26) we described the total synthesis of various C-nor-D-homo steroidal analogs to be employed as intermediates in the synthesis of *Veratrum* alkaloids. We also outlined a synthetic plan which envisages the *Veratrum* skeleton as consisting of a C-nor-D-homo steroid or etiojervane portion to which is attached at the 17-position, an appropriate heterocyclic unit. We would now like to present the experiments which demonstrate the application of this plan to the total synthesis of the alkaloid verarine (**31**) (1, 2).

The structure of verarine reveals that the required heterocyclic unit attached to the steroid portion is a 2,5-disubstituted piperidine and it was felt that the latter is readily available from the appropriate pyridine by well known reduction methods. On this basis, the essential features of the synthetic plan, as outlined in Fig. 1, were to couple the pyridine system at C_{17} of the already available 3β-acetoxy-5α-etiojerv-12(13)-en-17-one (**1**)[1] and the resultant product **3** could, hopefully by aromatization of ring D (**4**) and subsequent reduction, lead to the desired 5,6-dihydroverarine (**5**, R = R′ = H) system. It should be noted here that *both* racemic and optically active forms of **1** are available from total synthesis, the former from our previous work (26, 27) and the latter from that of Sondheimer and co-workers (3) who presented a total synthesis of optically active hecogenin from isoandrosterone. For the purposes of the synthetic experiments discussed here we have employed optically active **1** obtained via degradation of hecogenin acetate as outlined in Part I of this series.[1]

To evaluate the feasibility of the approach

[1]For part I, see ref. 26. For preliminary reports on a portion of this work, see ref. 27.

[2]Revision received February 4, 1975.

Can. J. Chem. Downloaded from www.nrcresearchpress.com by 210.87.254.5 on 09/05/12
For personal use only.

Can. J. Chem. Downloaded from www.nrcresearchpress.com by 210.87.254.5 on 09/05/12
For personal use only.

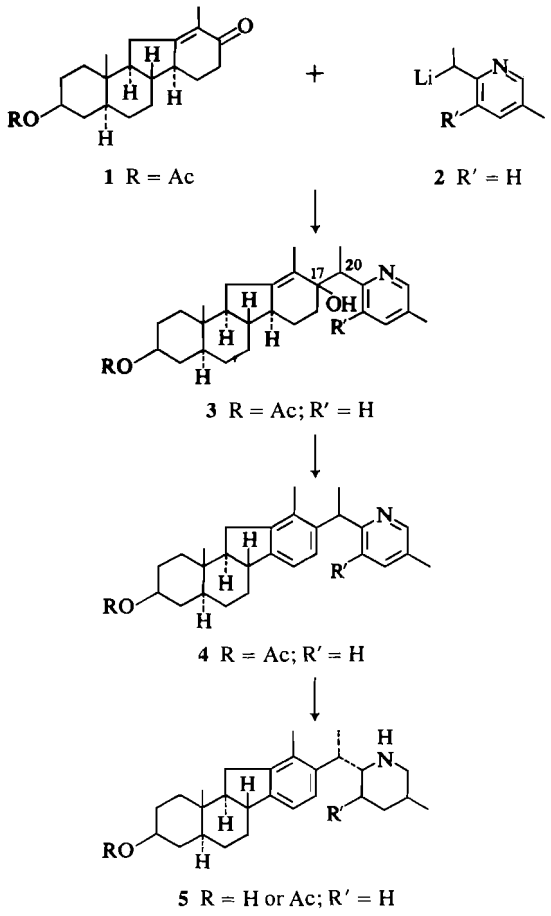

FIG. 1. General outline of synthetic plan for the synthesis of verarine (**31**).

presented in Fig. 1, the readily available (26, 27) hydrochrysene derivative **6** was utilized as the model substance and this was condensed with the lithio derivative of 2-ethylpyridine (**7**).

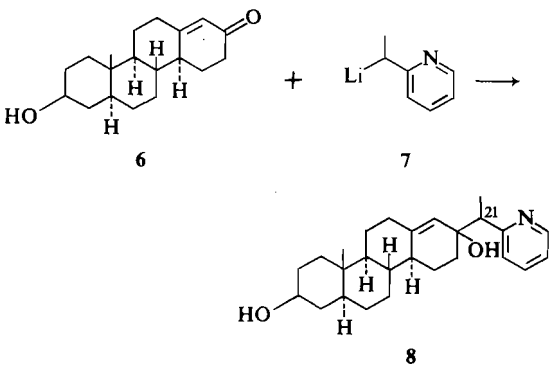

Addition of **6** to the red solution of 2-ethylpyridine and methyl lithium provided a reaction mixture which after chromatographic purification yielded the desired product. Its u.v. spectrum showed peaks at 257, 262, and 270 nm corresponding to the pyridine chromophore while the mass spectrum exhibited a peak at *m/e* 395 corresponding to the parent ion for compound **8**. The absence of a carbonyl peak in the i.r. supported the 1,2-addition of the organolithium derivative to the α,β-unsaturated carbonyl compound as opposed to any 1,4 addition.

This procedure was then extended to the reaction of **7** with 3β-acetoxy-5α-etiojerv-12(13)-en-17-one (**1**). Column chromatography of the products from this reaction gave primarily some material which appeared as one compound on t.l.c. The spectroscopic properties of the reaction product (λ_{max} 257, 262, and 269 nm; *m/e* 395) were again in accord with the desired coupling product although the n.m.r. spectrum (two doublets in the region τ 8.84) revealed that a mixture of two isomers, most likely epimeric at C_{20}, had been obtained (**9**).

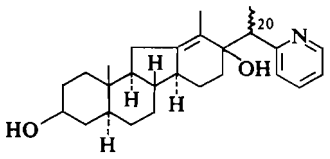

These model studies indicated that the required attachment of a heterocyclic unit at C_{17} of the C-nor-D-homo compound could be achieved and our efforts turned to the consideration of substituted 2-ethylpyridines which would allow entry to the skeleton of some of the naturally occurring *Veratrum* alkaloids.

Methylation of 2,5-lutidine employing phenyl lithium and methyl iodide afforded the known (4) 2-ethyl-5-methylpyridine and this in the form of its lithium salt (**2**) was condensed with the etiojervene derivative (**1**). The resultant product mixture upon t.l.c. examination, revealed two major components with similar R_f values but attempts to separate these proved fruitless. Conversion to the C_3-acetate derivatives did allow purification of this mixture.

It is to be noted that the coupling reaction creates two new asymmetric centers and consequently there exists the possibility of obtaining

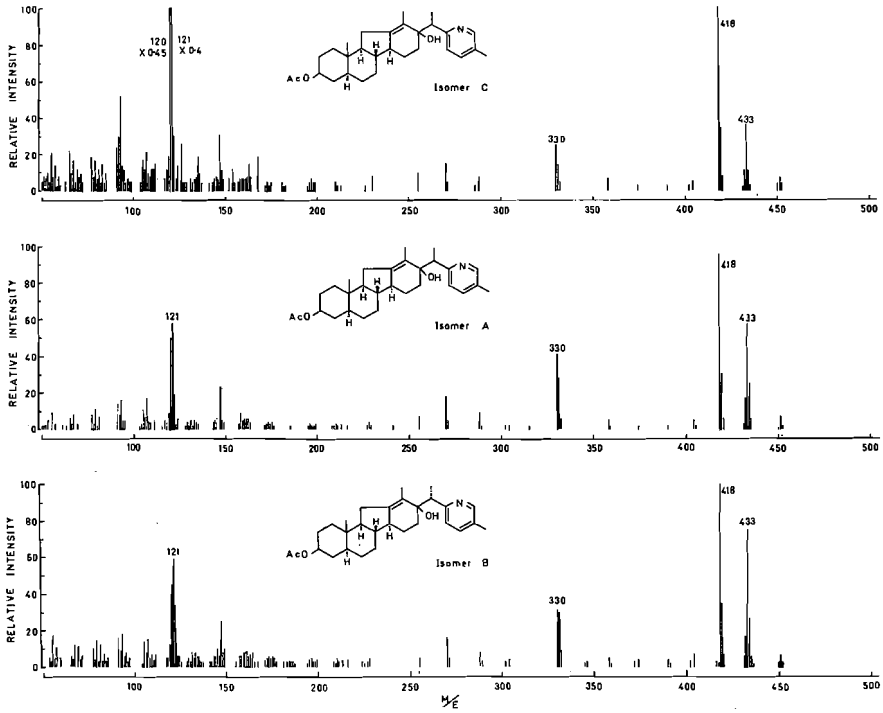

FIG. 2. Mass spectra of isomers **A**, **B**, and **C**.

four compounds possessing the gross structure **3** and differing in stereochemistry at C_{17} and/or C_{20}. All of these could be obtained in pure form.

One of the major components which could be obtained crystalline, m.p. 189–190°, was designated compound **A**. Spectral data allowed the assignment of structure **3** to this substance. Apart from the pyridine chromophore in the u.v., the n.m.r. spectrum was particularly instructive. A quartet occurring at τ 6.71 was assigned to the proton at C_{20} since a decoupling experiment showed this signal to be coupled to the C_{21} methyl doublet at τ 8.79. The C_{19} methyl signal appeared as a sharp three-proton singlet at τ 9.21. The pyridine protons were readily discernible in the aromatic region of the spectrum with a one-proton doublet at τ 2.82, $J = 8$ Hz, corresponding to $C_{23}H$ whereas $C_{24}H$ gave rise to two doublets at τ 2.52 ($J = 8$ and 2 Hz) and $C_{25}H$ appeared as a broad singlet at τ 1.67. The mass spectrum of **A** (Fig. 2) revealed the desired molecular ion (*m/e* 451) and expected fragmentation pattern.

Column chromatography of the mother liquors from the crystallization of compound **A** gave a second crystalline component, m.p. 191–192°, designated as compound **B** which also revealed spectral data in accord with structure **3**. The isomeric nature of **B** and **A** is seen from the close similarity in the mass (Fig. 2) and n.m.r. spectra of these compounds. In general the n.m.r. features already noted for **A** also appear in **B** although there are some differences in the chemical shifts. The largest differences are seen in the positions of the C_{18} and C_{21} methyl group signals and the pyridine protons (see Experimental).

Additional purification of chromatography fractions, obtained during isolation of **B** by means of preparative layer chromatography, allowed the isolation of two minor components, **C** and **D**, which constituted about 4 and 1% of the total product mixture. Neither of these could be induced to crystallize but satisfactory spectral data could also be accumulated for these substances and again the gross structure **3** could be assigned. At this stage of the investigations no assignments of stereochemistry at C_{17} and/or C_{21} could be made to these four coupling products but evidence in this direction was obtained during later studies as discussed below.

Can. J. Chem. Downloaded from www.nrcresearchpress.com by 210.87.254.5 on 09/05/12
For personal use only.

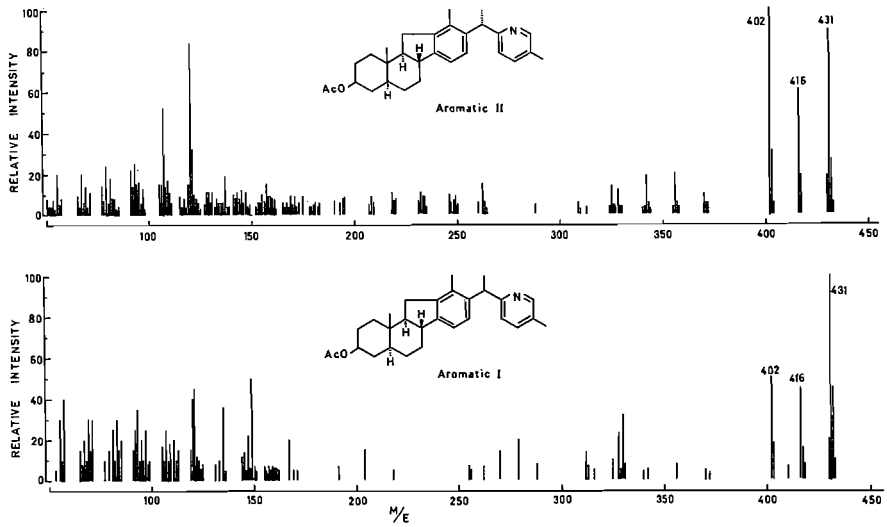

FIG. 3. Mass spectra of aromatic **I** and **II**.

The further extension of this sequence to the ring D aromatized series only involved the compounds **A** and **B** as the small amounts of **C** and **D** which were available precluded any useful reactions.

Compound **B** was ground with 10% palladized charcoal until the two substances were thoroughly mixed and then the powder was heated at 200° for 10 min. Examination of the reaction product mixture by t.l.c. indicated that compound **B** had been converted to a new compound possessing a similar R_f value. Separation by preparative layer chromatography indicated this new compound, which was designated 'aromatic **II**', had been produced in 80% yield. The u.v. spectrum showed no qualitative difference from that of compound **B** but the extinction coefficient at 270 nm increased from 4130 in the latter to 5400 in this compound. The mass spectrum exhibited a peak at *m/e* 431 corresponding to the molecular ion for a compound of structure **4**. The mass spectrum (Fig. 3) shows a completely different pattern to that observed with the series of compounds **A** to **D**. The n.m.r. spectrum was particularly useful in confirming that the desired ring **D** aromatization had occurred. The most significant feature is the appearance of a second pair of doublets in the downfield region of the spectrum corresponding to the expected AB system for the protons at C_{15} and C_{16}. In addition the broad three-proton singlet which corresponds to the C_{18} methyl in the starting material has disappeared but a new sharp singlet appears at τ 7.89 in the product in accord with the aromatization of ring **D**.

Isomer **A** was similarly treated with 10% Pd/C at 200° and the residue examined by t.l.c. Three compounds could be isolated in pure form by thick-layer chromatography. Two of these could be identified as the α,β-unsaturated ketone (**1**) and 2-ethyl-5-methylpyridine. The third compound which was formed in 25% yield appeared similar in properties to the aromatic compound from isomer **B** and was designated 'aromatic **I**'. The mass spectrum exhibited a peak at *m/e* 431 corresponding to the molecular ion for a compound of structure **4** and, in general, the fragmentation pattern was very similar to that of aromatic **II** (Fig. 3). This and other data suggested that these two aromatic substances were merely isomeric at C_{20} and support for this postulate came forth from further experiments as noted below.

In view of the different extent of ring D aromatization encountered with isomers **A** and **B**, the relative stability of these two compounds was further investigated. The C_{17}—C_{20} bond cleavage, which occurs with isomer **A** under the conditions for the D ring aromatization, appears to be very facile since this cleavage also occurs slowly in methanol or ethanol. The cleavage is slightly enhanced when the compound is dissolved in 0.1 *N* methanolic potassium hydroxide. Isomer **A** is stable in dimethylformamide or benzene but is converted to 3β-acetoxy-5α-etiojerv-12(13)-en-

Can. J. Chem. Downloaded from www.nrcresearchpress.com by 210.87.254.5 on 09/05/12
For personal use only.

Can. J. Chem. Downloaded from www.nrcresearchpress.com by 210.87.254.5 on 09/05/12
For personal use only.

17-one and 2-ethyl-5-methylpyridine when dissolved in aqueous dimethylformamide containing potassium hydroxide (p*H* 9).

Isomer **B** is stable under the above conditions and shows no C_{17}—C_{20} bond cleavage. Dehydration of the tertiary alcohol appears to be the main process for both isomers **A** and **B** in acidic methanol solution.

Thus two compounds of structure **4** had been prepared and the selective reduction of the pyridine to a piperidine ring was investigated. One of these aromatic compounds should lead to an isomeric mixture of 5α,6-dihydroverarines while the other would lead to a mixture of isomers of similar structure but differing in configuration at C_{20} from the naturally occurring alkaloid verarine.

Catalytic reduction (5) of aromatic compound **II** provided a reaction mixture, which upon examination by t.l.c. indicated that four new compounds possessing very similar R_f values had been formed. These compounds, which were numbered **i** to **iv** in order of decreasing R_f values on silica gel, were separated by careful preparative layer chromatography. These compounds were suspected to be isomers of 3-*O*-acetyl-5α,6-dihydroverarine (**10**). However, preparation of a sample of this compound from verarine for comparison purposes is difficult since acetylation of verarine yields *N*-acetylverarine or 3-*O*,*N*-diacetylverarine.

None of the four compounds from the hydrogenation of aromatic compound **II** could be induced to crystallize but it was found from other investigations that *N*-acetyl-5α,6-dihydroverarine (**11**) crystallizes readily from an ethereal solution. Consequently it was decided to convert the four compounds obtained above to the *N*-acetyl derivatives (gross structure **12**) via acetylation to the 3-*O*,*N*-diacetates (**13**) followed by selective hydrolysis of the 3-acetoxyl group. The conversion to the respective diacetates was accomplished with acetic anhydride–pyridine (1:1) while hydrolysis of the 3-acetoxyl group was achieved with 0.1 *M* potassium hydroxide in methanol.

The appropriate verarine derivatives required for the above comparison were prepared from the more readily available alkaloid veratramine (**14**) essentially according to the scheme developed by Masamune (1) with modifications at appropriate stages (**14** → **15** → **16** → **17**).

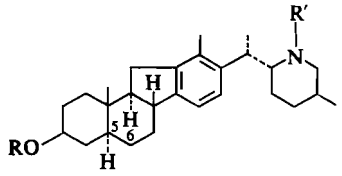

10 R = Ac; R′ = H
11 R = H; R′ = Ac

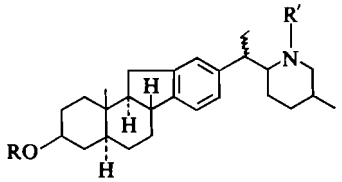

12 R = H; R′ = Ac
13 R = R′ = Ac

The diacetate **17** was identified by t.l.c. comparison with an authentic sample[3], melting point, rotation, mass spectrum, and n.m.r., all of which were in accord with the published data (6). Subsequent hydrolysis of the 3-acetoxyl compound gave *N*-acetylverarine.

Hydrogenation of the 5,6-double bond in veratramine employing Adams' catalyst in acetic acid had been reported to give mainly the 5α,6-dihydroveratramine (7). By analogy it was expected that the hydrogenation of the 5,6-double bond in 3-*O*,*N*-diacetylverarine (**17**) using these conditions would provide mainly the desired 3-*O*,*N*-diacetyl-5α,6-dihydroverarine. This hydrogenation was carried out and careful examination of the product by t.l.c. indicated that only one compound had been formed. However, a close examination of the n.m.r. spectrum particularly in the region τ 8.5–9.5 indicated that both the 5α and the 5β compounds had been formed.

The n.m.r. spectrum of 3-*O*,*N*-diacetylverarine exhibited a three-proton doublet at τ 9.02 which was attributed to the C_{26} methyl while the C_{19} methyl appeared as a three-proton singlet at 8.85.

The n.m.r. spectrum of the hydrogenation product exhibited a sharp singlet at 8.92 and a doublet at 9.03. The upfield half of the doublet centered at 9.03 was, however, very intense and the integral of this doublet corresponded to 4.5 protons. From the excellent n.m.r. study of 22,27-

[3]We are grateful to Dr. J. Tomko, Slovak Academy of Sciences, Bratislava, Czechoslovakia, for a gift of this sample.

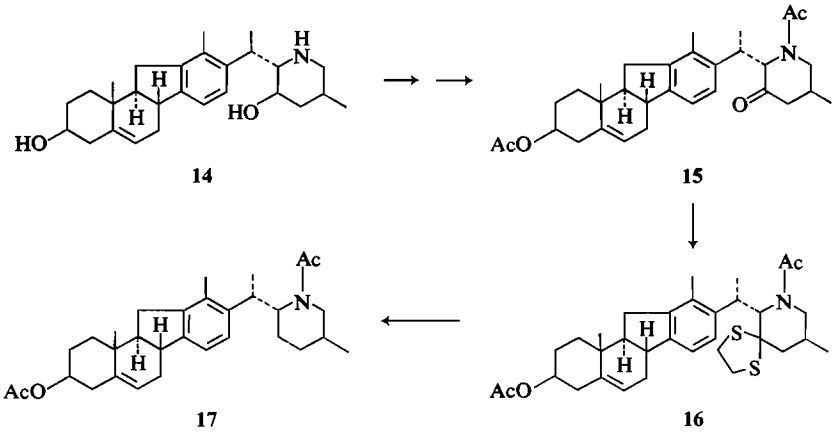

14 15 16 17

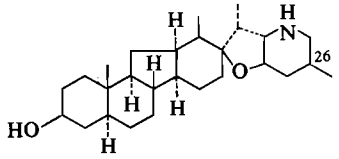

18

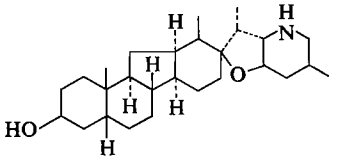

19

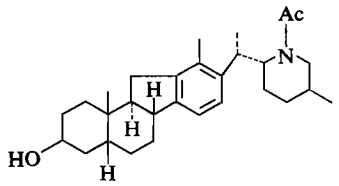

20

imino-17,23-oxidojervane derivatives by Masamune *et al.* (8) one would expect the C_{19} methyl signal for the 5α compound to be at a higher field position than in the 5β compound. This difference is due to the shielding of the C_{19} methyl group by the ring A protons which are in close proximity in the 5α derivatives but removed to a large extent in the 5β derivatives. This effect has been noted in various steroids (9) where the stereochemistry of the molecule is fixed.

The difference in chemical shift between the singlet at 8.92 and the upfield half of the doublet due to the C_{26} methyl group was 13 Hz and it was informative to compare this difference with the C_{19} methyl resonances in compounds **18** and **19**.

The n.m.r. spectra of these two compounds have been studied by Masamune *et al.* (8) who found the C_{19} methyl resonance in **18** to occur at τ 9.19 whilst in **19** the three proton-singlet is observed at τ 9.07, a separation of 12 Hz.

It therefore appeared that the hydrogenation of 3-*O*,*N*-diacetylverarine had given both the 5α and 5β compounds. In an attempt to obtain some separation of these two compounds and verify their existence the product was converted to the monoacetate by hydrolysis of the 3-acetoxyl group by means of 0.1 *N* potassium hydroxide in methanol. A t.l.c. examination of the resulting *N*-acetyl-5,6-dihydroverarines showed clearly that two compounds (**11** and **20**) were present. The n.m.r. spectra of the two compounds after separation by thick-layer chromatography, supported the analysis of the C_{19} methyl group positions outlined above.

Additional support for the configurational differences at C_5 was evident from the C_3 proton signals (τ 5.97, narrow multiplet in **11**, equatorial H; 6.3–6.5, broad multiplet in **20**, axial H).

It was vital to provide additional data which establish more firmly the identity and stereochemistry of these compounds. The o.r.d. curves of 3-keto steroids with the 5α and 5β configuration have been extensively studied and Masamune *et al.* (8) have recorded the o.r.d. curves of compounds **21** and **22**. These latter substances provide a very good analogy with the compounds under consideration.

Compound **21** exhibits a strong positive Cotton

Can. J. Chem. Downloaded from www.nrcresearchpress.com by 210.87.254.5 on 09/05/12
For personal use only.

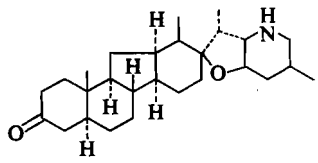

21

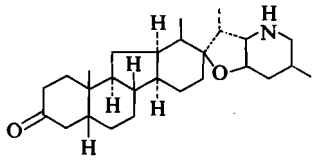

22

effect curve with values of $[\phi]_{304}^{peak}$ +2740° and $[\phi]_{265}^{trough}$ −1180° whereas **22** exhibits a negative Cotton effect curve with values of $[\phi]_{304}^{trough}$ +265° and $[\phi]_{265}^{peak}$ +2340°.

The hydrogenation products which had tentatively been assigned the 5α (**11**) and 5β (**20**) configurations were converted to the respective 3-keto compounds (**23** and **24**) using Jones' reagent as the oxidizing agent. The presence of the *N*-acetyl group tended to complicate the o.r.d. curves to some extent since it had a strong absorption at 230 nm but the absorption at 300 nm was not sufficient to affect the curve in this region. Compound **23** showed a strong positive Cotton effect curve with a peak at 305 nm while compound **24** showed only a very weak trough at 305 nm.

After this work had been completed, a publication (10) appeared in which the hydrogenation of veratramine employing Adams' catalyst in acetic acid has been more closely examined. Saito (7) had reported only the formation of the 5α-6,

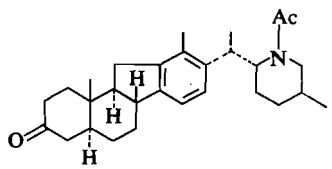

23

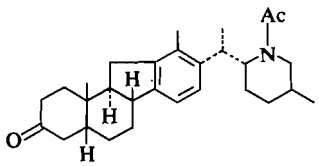

24

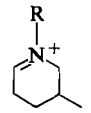

25 R = H
26 R = Ac

dihydroveratramine but the recent work indicates that a mixture of 5α,6-dihydroveratramine (41%) and 5β,6-dihydroveratramine (44%) is produced. It is interesting to note that these workers also distinguished the two compounds on the basis of the chemical shifts of the C_{19} methyl resonances in the n.m.r. spectra.

Having established the identity of the desired *N*-acetyl-5α,6-dihydroverarine (**11**) the comparison of this compound with the *N*-acetyl derivatives of the four compounds obtained from the hydrogenation of aromatic compound **2** was now undertaken. These crystalline acetates of compounds **i–iv** were compared in the usual manner (m.p., t.l.c., i.r., n.m.r., and mass spectra) with authentic **11**. It was established that **i**, *N*-acetate, was identical in every respect with **11** as prepared above.

Careful analysis of the mass spectra of all five compounds (**11** and **i–iv**) reveals an essentially identical fragmentation pattern with very intense peaks at *m/e* 140 and 98. Budzikiewicz (11) has examined the mass spectra of veratramine, *N*-acetylveratramine, and verarine and has postulated cleavage of the benzylic C_{20}—C_{22} bond which, in the present instance, would allow the fragments **25** and **26** to account for strong peaks at *m/e* 98 and 141, respectively.

Aromatic compound **I** which was obtained in 25% yield from isomer **A** was subjected to hydrogenation under the same conditions as applied to aromatic compound **II**. Examination of the product by t.l.c. indicated that four new compounds of similar R_f values had been formed. For the sake of convenience these were designated **v–viii** in order of decreasing R_f values on a thin-layer chromatoplate. These compounds were separated by thick-layer chromatography and then converted via the diacetates to the respective *N*-acetyl derivatives. A t.l.c. comparison of the four *N*-acetates with *N*-acetyl-5α,6-dihydroverarine (**11**) indicated that only compounds **v** and **vi** had a similar R_f value. Surprisingly none of these *N*-acetyl derivatives could be induced to crystallize from ether in contrast to *N*-acetyl-5α,6-dihy-

Can. J. Chem. Downloaded from www.nrcresearchpress.com by 210.87.254.5 on 09/05/12
For personal use only.

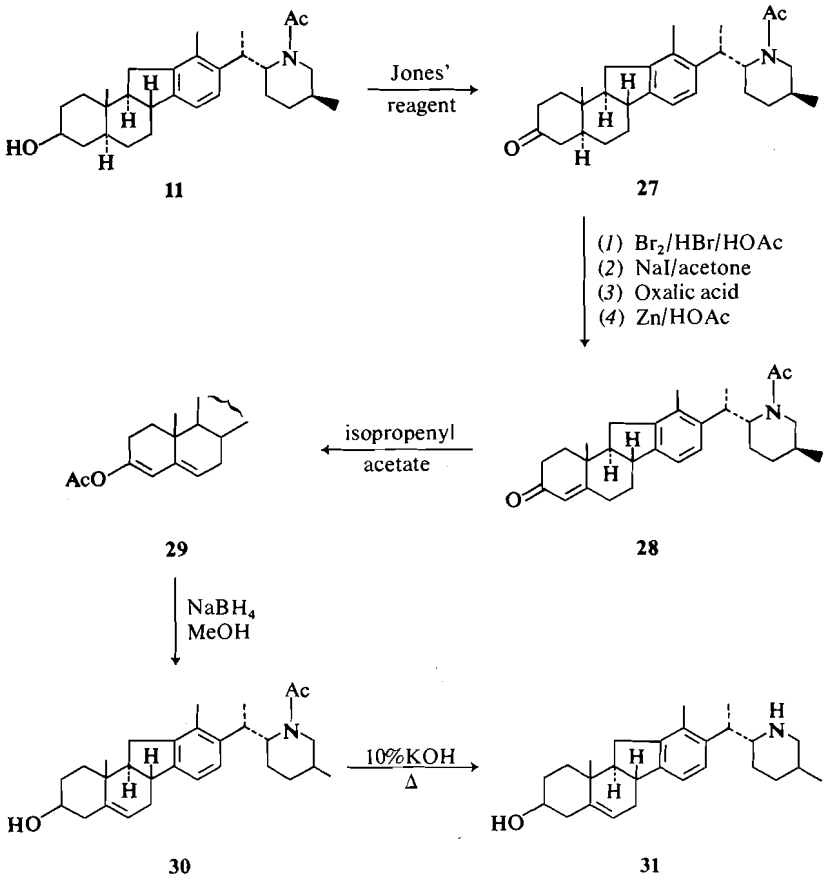

FIG. 4. Conversion of *N*-acetyl-5α,6-dihydroverarine (**11**) to verarine (**31**).

droverarine and the *N*-acetates of compounds **i–iv** which all crystallize very readily from this solvent. The mass spectra of the compounds **v–viii** exhibited a peak at *m/e* 437 corresponding to the molecular ion for *N*-acetyl-5α,6-dihydroverarine as well as prominent peaks at *m/e* 98 and 140.

To complete the synthesis of verarine (**31**) it was necessary to introduce the 5,6-double bond and remove the *N*-acetate function in *N*-acetyl-5α,6-dihydroverarine (**11**). The steps involved in achieving these goals are outlined in Fig. 4. The procedure for introduction of the double bond is taken from the investigations of Evans *et al.* (12) in the cortisone series. A similar pathway has been employed by Johnson *et al.* (13) in the conversion of 23-*O*,*N*-dibenzoyl-5α,6-dihydroveratramine to veratramine.

Having completed the synthesis of the simplest member of the *Veratrum* series, it was decided to extend the above strategy to encompass some of the more oxygenated *Veratrum* alkaloids and 5α,6-dihydroveratramine (**56**) became the target compound. Since the latter had already been converted to veratramine (**14**) (13), jervine (**32**) (14, 15), veratrobasine (**33**) (15, 16), and 11-deoxojervine (**34**) (17), a synthesis of this intermediate represents in a formal sense the total synthesis of these natural products.

Analysis of the structure of veratramine, for

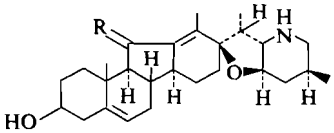

32 R = O

33 R = 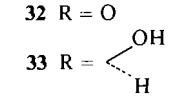

34 R = H_2

Can. J. Chem. Downloaded from www.nrcresearchpress.com by 210.87.254.5 on 09/05/12
For personal use only.

Can. J. Chem. Downloaded from www.nrcresearchpress.com by 210.87.254.5 on 09/05/12
For personal use only.

example, reveals that the substituents attached to the three chiral centers (C_{22}, C_{23}, and C_{25}) involving the piperidine ring are in equatorial orientations. It was thus felt that reduction of an appropriately substituted pyridinium system, under equilibrating conditions, should lead predominantly to the desired stereochemistry in the resultant product (see **35** → **36** + **37** → **38** → **39**).

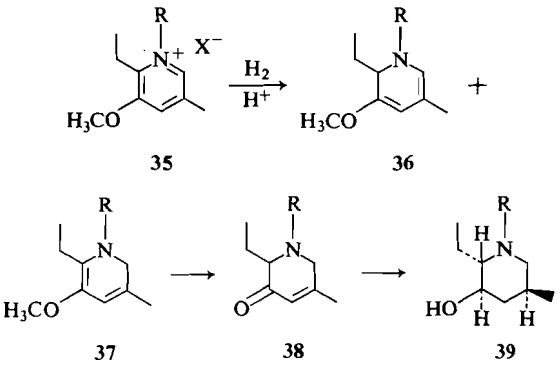

35 **36** **37** **38** **39**

The obvious heterocyclic unit required for achieving the synthesis in this direction was an unknown pyridine derivative, 2-ethyl-3-hydroxy-5-methylpyridine, and its synthesis was first considered. We chose an approach which made use of the reaction of furyl ketones with ammonia (18) since it seemed to be more direct and suitable for our purposes. In this connection we have developed two independent sequences for the synthesis of the desired pyridine. In effect, both sequences depend on the availability of crucial furan intermediates and therefore the synthesis of these substances was initially considered. Figures 5 and 6 outline the reactions involved in the preparation of these materials. Figure 5 reveals the preparation of 2-propionyl-4-methylfuran (**44**) via a Friedel–Crafts reaction on 3-methylfuran.

A survey of the literature at this time indicated that there had been no work on the Friedel–Crafts reaction of 3-methylfuran. In fact only limited data on the electrophilic substitution of 3-alkylfurans in general was available and the data indicated that the substitution takes place exclusively at the 2-position (19–21). However, we did not rule out the possibility of substitution at the 5-position and hence decided to investigate this further. The desired starting material, 3-methylfuran (**42**), was prepared according to the procedure of Cornforth (22, 23) as outlined in Fig. 5.

Reaction of 3-methylfuran with propionic anhydride and orthophosphoric acid as the catalyst at 60° provided a product which upon examination by v.p.c. indicated that it was a mixture of two compounds in the ratio 70:30. Separation of the mixture by means of preparative v.p.c. using a FFAP column allowed the isolation of 2-propionyl-3-methylfuran (**43**) and 2-propionyl-4-methylfuran (**44**).

It is noteworthy that indeed substitution takes place at both C_2 and C_5 positions of 3-methylfuran and this was the first demonstrated example of electrophilic substitution at the C_5 position of

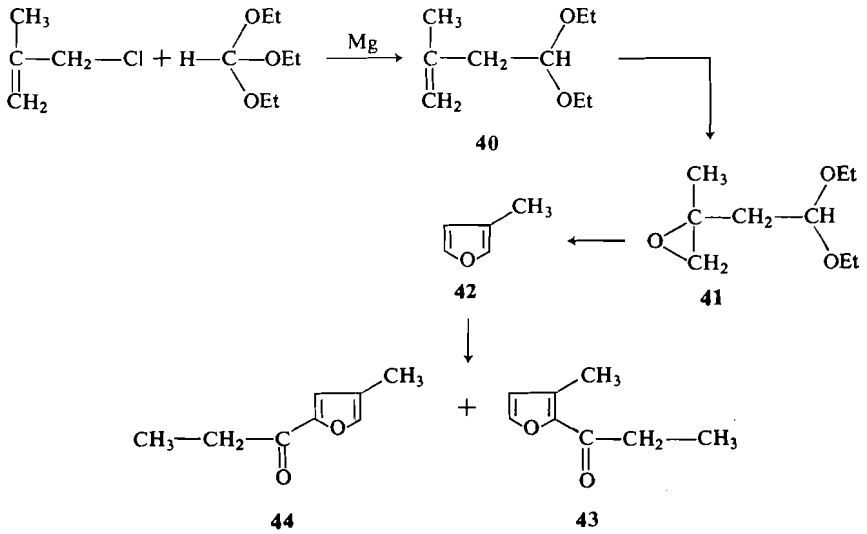

40 **42** **41** **44** **43**

FIG. 5. Synthesis and propionylation of 3-methylfuran.

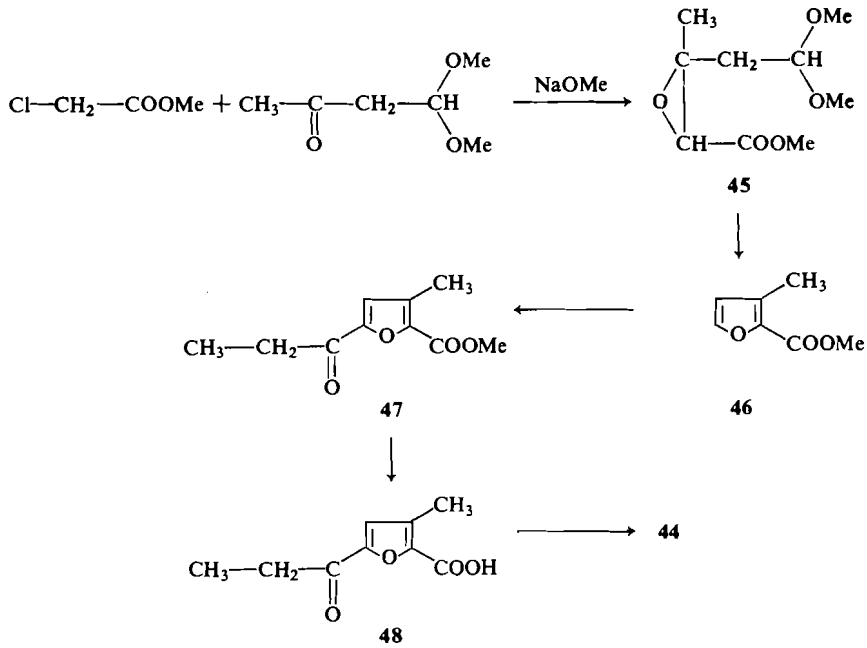

FIG. 6. Synthesis of 2-propionyl-4-methylfuran (**44**).

a 3-alkylfuran unsubstituted at the 2-position. Documented data indicate that only furans with electron-withdrawing substituents (*e.g.*, —COOR group) at C_3 can direct substitution to C_5 whereas the presence of electron-donating substituents invariably direct the substitution to C_2 (20). A more detailed investigation is now reported from our laboratory (24).

The difficulties encountered in the separation of the reaction mixture as well as the poor yield of the desired ketone **44** compelled us to discard the above sequence in favor of an alternate direct route to the preparation of this compound.

This latter route makes use of methyl 3-methyl-2-furoate (**46**) as the starting material. The preparation of this compound by a known procedure (25) and the subsequent reactions leading to 2-propionyl-4-methylfuran are schematically presented in Fig. 6.

The next stage in the synthesis was the conversion of 2-propionyl-4-methylfuran to 2-ethyl-3-hydroxy-5-methylpyridine (**49**). This conversion was effected by a known procedure (18). The resultant product (**49**) was crystalline and revealed spectral data in agreement with the assigned structure (λ_{max} 287 nm; τ 8.75, triplet, CH_3CH_2; 7.8, singlet, C_5—CH_3; 2.9 and 2.1, singlets, C_4 and C_6H).

In our initial studies on the coupling of the substituted pyridine with the steroidal enone, it was decided to use the lithio derivative of 2-ethyl-3-*O*-benzyl-5-methylpyridine (**50**). This compound was prepared by heating a solution of 2-ethyl-3-hydroxy-5-methylpyridine in aqueous

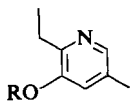

49 R = H
50 R = $CH_2C_6H_5$
51 R = CH_3

sodium hydroxide with benzyl chloride. However these investigations were unsuccessful and hence we discarded the use of the *O*-benzyl ether in favor of the corresponding *O*-methyl ether (**51**) which was readily available from the reaction of **49** with diazomethane.

Thus with the desired steroidal enone, 3β-acetoxy-5α-etiojerv-12(13)-en-17-one (**1**), and the appropriately substituted pyridine, 2-ethyl-3-methoxy-5-methylpyridine (**51**), in hand the stage was set for the coupling reaction of these units. The actual reaction sequence employed for the synthesis of 5α,6-dihydroveratramine (**56**) is

Can. J. Chem. Downloaded from www.nrcresearchpress.com by 210.87.254.5 on 09/05/12
For personal use only.

Can. J. Chem. Downloaded from www.nrcresearchpress.com by 210.87.254.5 on 09/05/12
For personal use only.

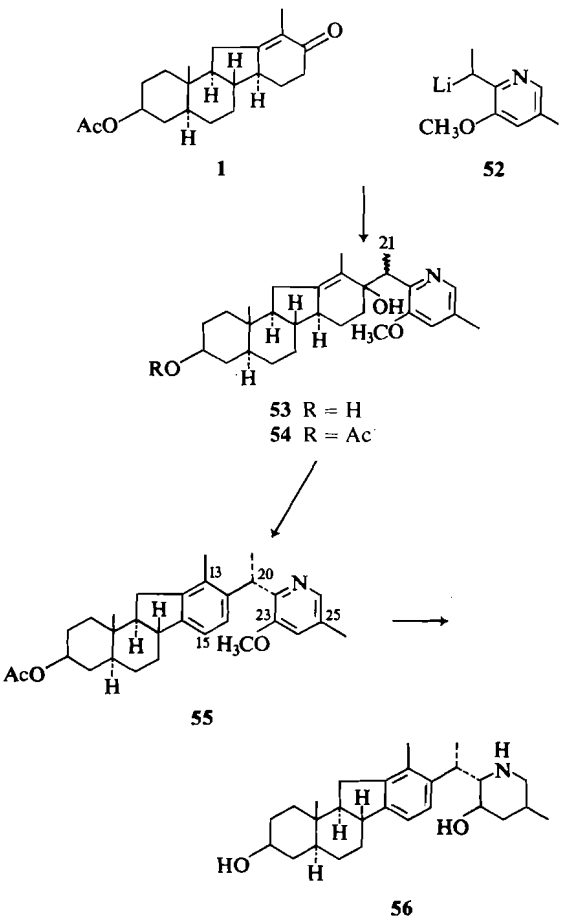

FIG. 7. Synthesis of 5α,6-dihydroveratramine (**56**).

shown in Fig. 7 and follows the strategy outlined previously.

Coupling of the lithio derivative **52** and **1** provided a reaction product which in the u.v. spectrum (λ_{max} 283 nm) showed a pyridine chromophore while the mass spectrum exhibited a peak at *m/e* 439 corresponding to the parent ion for a substance bearing the gross structure **53**.

That the material obtained above, although homogeneous on t.l.c., was a mixture of two compounds was indicated by the n.m.r. spectrum which exhibited two sharp singlets at τ 6.21 and 6.24 due to the presence of two methoxyl groups. Two doublets were also seen at τ 8.81 and 8.84 which were probably due to the C_{21} methyl group in each of the two compounds. Attempts at the separation of this mixture by chromatographic techniques were unsuccessful since both the compounds had identical R_f values on t.l.c. in numerous solvent systems.

In an attempt to achieve separation of these two compounds the mixture was subjected to acetylation by means of acetic anhydride and pyridine. The resulting reaction mixture on t.l.c. examination showed the presence of two compounds possessing very different R_f values. These were separated by column chromatography on alumina. For the sake of discussion the more polar compound is referred to as compound **E** while the less polar one is designated as compound **F**.

Examination of compound **E** revealed the following spectral data. The u.v. spectrum showed a peak of 283 nm with a shoulder at 225 nm indicative of the pyridine chromophore while the mass spectrum exhibited the parent peak at *m/e* 463 which indicated that dehydration of the coupled product (**54**) has occurred in the mass spectrometer. The n.m.r. spectrum of **E** was particularly instructive and a detailed analysis was carried out. Thus a sharp singlet at τ 9.22 with a three-proton integral was assigned to the C_{19} methyl resonance. The doublet at 8.82 was attributed to the C_{21} methyl protons, which were coupled with the C_{20} proton, $J_{20,21}$ = 7.0 Hz. The sharp singlets at τ 8.79, 8.0, and 7.7 were due to C_{18} methyl, C_3 acetate, and C_{26} methyl protons, respectively, while the three proton signal at 6.22 was easily recognized as due to the C_{23} methoxyl protons. The protons on the pyridine ring appeared as sharp singlets at τ 3.08 (C_{24}H) and 2.0 (C_{27}H).

The u.v. spectrum of compound **F** was similar to that of **E** while the mass spectrum exhibited the parent peak at *m/e* 461 corresponding to an ion which accounts for the loss of 20 units from the desired compound of gross structure **54**. In the n.m.r. spectrum, the C_{18} methyl signal was shifted downfield (τ 7.7) and was in the position expected for a methyl group on an aromatic ring. Further evidence in support of aromatization of ring D came from an examination of the low field (τ 4–2) region in the spectrum where, in

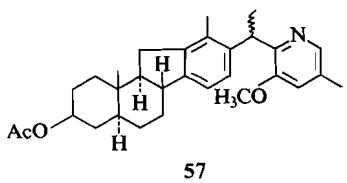

57

addition to the pyridine proton signals, an AB quartet centered at τ 3.05 was noted. This signal is clearly due to the C_{15} and C_{16} protons in a ring D aromatic compound with the expected large *ortho* coupling ($J = 7$ Hz).

Since the above spectral data was consistent for the structure **57**, it was clear that compound **F** arises via dehydration of the C_{17} hydroxyl function in the condensation product (**53**) followed by aromatization of the resulting diene.

It can be seen from Fig. 7 that the coupling reaction generates two chiral centers and consequently there exists the possibility of obtaining four compounds possessing structure **53**. However in our studies only two compounds could be isolated and characterized.

The above results suggest that the coupling reaction afforded a mixture of alcohols of gross structure **53** and that one of them fortuitously underwent dehydration followed by aromatization during the subsequent work-up. There existed the possibility of this sequence of reactions occurring either during acetylation of the reaction mixture or during the chromatographic separation on alumina.

We set out to explore this phenomenon by monitoring a typical experiment by n.m.r. spectroscopy. The product obtained in the coupling reaction was subjected directly to acetylation with acetic anhydride and pyridine at room temperature. After allowing the reaction mixture to stand overnight followed by the usual work-up, the n.m.r. spectrum of this material displayed the low field AB quartet noted earlier. The results of the experiment allowed us to conclude that one of the two alcohols undergoes dehydration and aromatization to **F** (**57**) during the acetylation step.

In our subsequent studies we have been able to convert the alcohol acetate **54** (compound **E**) to an aromatic compound isomeric with **F**. In a typical experiment, compound **E** was reacted with palladized charcoal at 200° and three compounds, the α,β-unsaturated ketone **1**, 2-ethyl-3-methoxy-5-methoxypyridine (**52**), and a new substance designated as compound **G**, were isolated in a pure state. The spectral properties of **G** were remarkably similar to those of **F** and it was clear that these compounds were diastereoisomeric at C_{20}, the chiral center created during the coupling reaction.

Since in subsequent experiments the aromatic compound **F** gave rise to compounds in the natural series, the stereochemistry at C_{20} in this compound is known and is indicated in **55**. This leads to the conclusion that compound **G** is the C_{20} epimer of **F** and has the stereochemistry as indicated in **58**.

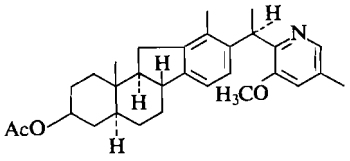

58

After having established that the condensation product of 2-ethyl-3-methoxy-5-methylpyridine and 3β-acetoxy-5α-etiojerv-12(13)-en-17-one is a mixture of epimeric alcohols **53** and that one of these alcohols undergoes dehydration and aromatization to give compound **F** during the subsequent work-up, we set out to assign the stereochemistry of the condensation products. One of the several rational interpretations of the results is advanced in the following paragraphs. We wish to emphasize that we are unable at this time to distinguish clearly between several alternative explanations.

It is clear that several important factors must be considered in proposing any stereochemical assignments to the condensation products possessing the gross structure **53**. (*i*) Is the stereochemistry at C_{20} determined during the approach of the anion to form the C_{17}—C_{20} bond or is the product composition a result of equilibration *after* the initial reaction has occurred? It is well known that protons adjacent to a pyridine ring (as at C_{20}) are readily removed by strong base. (*ii*) Is the approach of the anion equally favorable from the 'equatorial' and 'axial' sides of the molecule since this factor determines the stereochemistry at C_{17}? With regard to the latter, an investigation of molecular models quickly revealed that no distinct preference for either approach is apparent. In other words, one would expect the epimers at C_{17} as the most likely course of events. In the explanation given below we have assumed that such is the case, *i.e.*, the two condensation products differ in stereochemistry at C_{17} but not at C_{20}. In actual fact the discussion below indicates that the results obtained are explicable, regardless whether a definite stereochemistry is initially assigned to C_{20} in the condensation products. For the sake of clarity the

Can. J. Chem. Downloaded from www.nrcresearchpress.com by 210.87.254.5 on 09/05/12
For personal use only.

Can. J. Chem. Downloaded from www.nrcresearchpress.com by 210.87.254.5 on 09/05/12
For personal use only.

particular stereochemistry chosen for C_{20} was the one which is present in the natural *Veratrum* series. The reasons for the latter choice are twofold: (*a*) there is a minimal interaction between the various groups on ring D and the heterocyclic portion when this stereochemistry is considered and (*b*) one of the above condensation products leads to 5α,6-dihydroveratramine.

Once a tentative assignment of the stereochemistry at C_{20} in the condensation products is advanced one is left with the task of advancing a reasonable explanation for the difference in the stability of the alcohols and the observed facile dehydration followed by aromatization in one case as opposed to the sluggishness in the other. An acceptable explanation for the difference in their behaviour is given in the following paragraphs. Here again, it should be emphasized that there can be alternate explanations but the one chosen appears to be the most reasonable.

If we consider the 'axial' alcohol (**58***a*) and its possible conversion to the ring D aromatic derivative (**55**) it is clear that the allylic hydroxyl can undergo 1,4-elimination making use of the C_{14} proton, or alternatively a 1,2-elimination involving the α-(axial) proton at C_{16} is also a feasible process. Either of these eliminations would yield a highly strained cyclohexadiene system (with regard to ring D) which would be expected to aromatize rapidly to yield a compound of structure **55**.

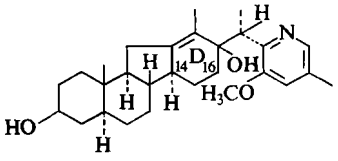

58*a*

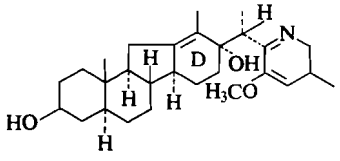

69

On the other hand, examination of molecular models for the 'equatorial' alcohol (**69**) reveals that in this compound there are no ring D protons which are *trans* and coplanar to the hydroxyl group. The desired stereochemistry for the elimination can be attained at C_{20} by rotation around the C_{17}—C_{20} bond but such a process leads to an eclipsing of the C_{18} and C_{21} methyl groups and an increase in nonbonded interactions between ring D (particularly C_{16}) and the substituents on the heterocyclic ring. Hence the sluggishness of this alcohol to dehydrate may be related to the energy required to force the molecule into this sterically unfavorable conformation. The higher temperature (200°) as noted above, under which this alcohol converts to a substance possessing an aromatic D ring would then provide the necessary energy. Dehydration in this event will lead to a diene **70**, which via

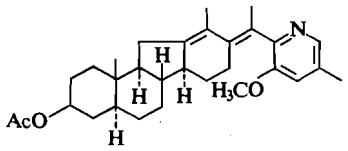

70

double bond rearrangement and aromatization would provide the aromatic compound **57**. Obviously such a process can lead to epimerization at C_{20}. In fact the aromatic compound (**G**) isolated in this reaction is isomeric with compound **F** and must therefore be its C_{20} epimer (*i.e.* **58**).

Now that the desired D ring aromatized compound had been obtained, it was essential to find suitable methods to reduce the pyridine ring to the appropriately functionalized piperidine moeity present in veratramine. For this purpose catalytic hydrogenation was selected as the method of choice. Compound **F** when subjected to hydrogenation in ethanol at pressures ranging from 40–65 p.s.i. did not undergo any change. However, it was found that this substance undergoes hydrogenation in an acid–alcohol medium (Pt as catalyst). Thin-layer chromatography examination of the reaction product revealed the presence of three major compounds along with trace amounts of several other components. One of the major compounds had the same R_f value as 5α,6-dihydroveratramine. Indeed, separation of the mixture afforded an 18% yield of 5α,6-dihydroveratramine (**56**), identical with the natural sample prepared by the hydrogenation of veratramine (7, 10) (i.r., n.m.r., mass spectra, mixture m.p.).

The two other compounds isolated in the hydrogenation experiment were found to be extremely unstable and the limited quantities of these available prevented any meaningful investigation. However, a preliminary inspection of the n.m.r. spectra of the impure compounds

Can. J. Chem. Downloaded from www.nrcresearchpress.com by 210.87.254.5 on 09/05/12
For personal use only.

revealed that in both instances the pyridine ring was only partially reduced (to the dihydro or tetrahydropyridine stage) while the methoxyl group was still intact.

As mentioned earlier, the synthesis of 5α,6-dihydroveratramine was sufficient for our purpose because this material has already been converted to veratramine (**14**), jervine (**32**), veratrobasine (**33**), and 11-deoxojervine (**34**).

Experimental

All details concerning spectral measurements, chromatographic separations, etc., are described in part I of this series.

18-Nor-C-homo-26-nor-22,27-iminojerva-12α(13),22,24,27-tetraene-3β,17-diol (8)

An ether solution of 1.88 *M* methyl lithium (1.0 ml) was added to anhydrous tetrahydrofuran (4 ml) in a round-bottom flask which had been flame dried and flushed with dry nitrogen. A tetrahydrofuran solution of 2.0 *M* 2-ethylpyridine (1 ml) was added immediately and the mixture refluxed under nitrogen for 30 min. During this time the solution developed a deep red color. After the period of reflux the α,β-unsaturated ketone (**6**) in the form of a fine powder was added slowly until the color faded (120 mg) and the reaction mixture refluxed for a further 30 min while the flask was still under nitrogen. Water was then added cautiously to destroy any alkyl lithium remaining and the resulting mixture diluted with ether (10 ml). The organic phase was separated and washed with water (4 × 10 ml), before drying over anhydrous sodium sulfate. Evaporation of the ether gave a light oil (100 mg) which appeared as one major and several minor components when examined by thin-layer chromatography. The major component was obtained pure by preparative thin-layer chromatography on Woelm neutral alumina (20 × 20 cm, 0.4 mm, 2% methanol in chloroform). Spectral data indicated this was the desired condensation product (**8**) although the n.m.r. indicates the material is probably a mixture of two isomers; i.r.: 6.3, 6.4 (pyridine), 3.1 μ (hydroxyl); u.v.: λ_{max}: 257 (3.55), 262 (3.58), 270 nm (3.45); n.m.r.: 9.26 (angular methyl, 3H, singlet), 8.8, 8.75 (two overlapping doublets due to the presence of two isomers in the product (CH_3—C—H, J=7 Hz, 3H), 6.53 (CH_3CH, 1H, J = 7 Hz, quartet), 5.1 (C_{13}, 1H, singlet), 2.0, 3.0 (pyridine, 3H, multiplet), 1.5 (pyridine, 1H, multiplet).

26-Nor-22,27-iminojerva-12(13),22,24,27-tetraene-3β,17-diol (9)

An ether solution of 1.88 *M* methyl lithium (1.0 ml) was added to anhydrous tetrahydrofuran in a dry round-bottom flask under nitrogen. A solution of 2-ethylpyridine (1.0 ml of 2.0 *M*) in tetrahydrofuran was added immediately and the mixture refluxed for 30 min during which time a deep red color developed. Addition of 3β-acetoxy 5α-etiojerv-12(13)en-17-one (**1**) in the form of a finely ground dry solid was continued until the color faded (90 mg added) and the mixture stirred for a further 30 min, while the flask was still under nitrogen. Water was added to quench the reaction and the mixture diluted with ether (10 ml). The organic phase was separated and then washed with water (4 × 10 ml) before drying over anhydrous sodium sulfate. Examination of the ethereal extract by thin-layer chromatography indicated one major component which appeared as a bright yellow spot when the chromatoplate was developed with 1:1 antimony pentachloride – carbon tetrachloride (1:1) spray reagent. Column chromatography on alumina (Shawinigan, activity III, 25 g) eluting with benzene–chloroform (4:1) enabled purification of this component which was crystallized from benzene–ether as needles (42 mg), m.p. 204–206°; i.r. ($CHCl_3$): 6.30, 6.41 μ (pyridine); u.v.: λ_{max} 257sh, 262.5 (3.58), 269sh nm; n.m.r.: 9.26 (angular methyl, 3H, singlet), 8.84 (C_{21} methyl, 3H, $J_{20,21}$ = 7 Hz, doublet), 8.26 (C_{18} methyl, 3H, singlet), 2.8 (pyridine, 2H, multiplet), 2.34 (pyridine, 1H, multiplet), 1.5 (pyridine, 1H, multiplet) mass spectrometry: *m/e* 395 (M^+), prominent peaks at *m/e* 377, 362, 288.

Anal. Calcd. for $C_{26}H_{37}O_2N$: C, 78.94; H, 9.43; N, 3.54. Found: C, 78.85;, H, 9.50; N, 3.50.

2-Ethyl-5-methylpyridine

An anhydrous ether solution (250 ml) of bromobenzene (31.4 g, 0.2 mol) was added slowly to a dry round-bottom flask which had been flushed with nitrogen and which contained lithium wire (2.8 g, 0.4 mol). When the lithium had largely dissolved an ethereal solution (100 ml) of 2,5-lutidine (21 g, 0.2 mol) was added and the mixture refluxed for 30 min, during which time a deep red color developed in the solution. Methyl iodide (14.2 g, 0.1 mol) in ether (40 ml) was added slowly to this red solution over a period of 15 min and the mixture stirred for 10 min. The excess lithium and phenyl lithium were removed by the careful addition of water (100 ml) to the reaction mixture while the flask was still under nitrogen. A further 200 ml of water was then added and the organic phase separated, and washed with water (2 × 50 ml). The ethereal solution was reduced in volume to 40 ml by use of a rotary evaporator. This 40 ml was then carefully distilled at a pressure of 10 mm, employing a spinning band column. The first fraction, distilling at 50–55° was shown by n.m.r. to be recovered 2,5-lutidine whereas that distilling at 62–63° was shown to be 2-ethyl-5-methylpyridine; i.r. (film): 6.3, 6.4, 6.8, 7.02 μ; u.v.: λ_{max} 265sh (3.54), 269 (3.60), 276 nm (3.48); n.m.r.: 8.70 (CH_3CH_2, 3H, J = 7.5 Hz, triplet), 7.72 (CH_3—C, 3H, singlet), 7.20 (CH_2CH_3, 2H, J = 7.5 Hz, quartet), 2.93 (C_3, 1H, $J_{3,4}$ = 8 Hz, doublet), 2.59 (C_4, 1H, $J_{4,3}$ = 8.0 and $J_{4,6}$ = 2.0 Hz, two doublets), 1.63 (C_6, 1H, $J_{6,4}$ = 2.0 Hz, doublet). Picrate derivative from acetone, m.p. 143–144° (lit. (7) m.p. 144°).

3β-Acetoxy-22,27-iminojerva-12(13),22,24,27-tetraene-17-ol (3)

A 2.05 *M* ethereal solution of methyl lithium (25 ml, 0.051 mol) was added to a flame dried round-bottom flask containing anhydrous tetrahydrofuran (40 ml) under nitrogen. A mixture of anhydrous tetrahydrofuran (10 ml) and 2-ethyl-5-methylpyridine (6 g, 0.05 mol) was added immediately and the reaction mixture refluxed for 1½ h. During this period a deep red color developed in the solution. A faint pink color persisted after 3β-acetoxy-5α-etiojerv-12-en-17-one (**1**) (2.0 g, 0.006 mol) was added as a fine powder to the cooled solution and the mixture stirred for 10 min. Water (50 ml) was added cautiously to the reaction mixture while still under nitrogen, followed by ether (50 ml) prior to separation of the organic and

Can. J. Chem. Downloaded from www.nrcresearchpress.com by 210.87.254.5 on 09/05/12
For personal use only.

aqueous phases. The organic phase was washed with water (3 × 25 ml) and then dried over anhydrous sodium sulfate. Removal of the solvent *in vacuo* gave a light oil (2.3 g) which appeared to consist of two new components when examined by thin-layer chromatography. Attempts to obtain these compounds in a pure state were unsuccessful. However a small scale investigation indicated that the compounds could be separated more readily as the C_3 acetates rather than as the C_3 alcohols which were formed in the reaction.

Conversion to the C_3 acetates was achieved by dissolving the crude product from the reaction in acetic anhydride – pyridine (1:1, 20 ml) and allowing the solution to stand at room temperature for 12 h. The solution was then poured onto crushed ice and the resultant flocculant solid extracted into ether. The combined ethereal extracts were washed with saturated aqueous sodium hydrogen carbonate solution and then several times with water before drying over anhydrous sodium sulfate. The volume of the ethereal solution was reduced *in vacuo* to 20 ml and then allowed to stand whereupon colorless needles were deposited, m.p. 187–189° (370 mg). Examination of the crystals by thin-layer chromatography indicated only one compound was present and recrystallization from ether gave an analytical sample, m.p. 189–190°. This compound was designated **A** and the physical and spectral data are in accord with structure **3**; i.r. ($CHCl_3$): 5.83 (OAc) 6.25, 6.37 (pyridine) μ; u.v.: λ_{max} 270 nm (3.61); $[\alpha]_D$ +83° (*c*, 1.24); n.m.r.: 9.21 (angular methyl, 3H, singlet), 8.79 (C_{21} methyl, 3H, $J_{21,20}$ = 7.0 Hz, doublet), 8.40 (C_{18} methyl, 3H, singlet), 8.01 (acetate, 3H, singlet), 7.70 (C_{26} methyl, 3H, singlet), 6.71 (C_{20}H, 1H, $J_{20,21}$ = 7.0 Hz, quartet), 3.89 (OH, 1H, broad multiplet, disappears on D_2O addition), 2.82 (C_{23}, 1H, $J_{23,24}$ = 8 Hz, doublet), 2.52 (C_{24}, 1H, $J_{24,23}$ = 8 and $J_{24,27}$ = 2 Hz, two doublets), 1.67 (C_{27}, 1H, $J_{27,24}$ = 2 Hz, doublet); mass spectrometry: *m/e* 451 (M^+), prominent peaks at *m/e* 433, 330, 147, and 121.

Anal. Calcd. for $C_{29}H_{41}O_3N$: C, 77.12; H, 9.15; O, 10.63; N, 3.10. Found: C, 76.92; H, 8.95; O, 10.46; N, 3.21.

Examination by thin-layer chromatography of the mother liquors from the crystallization of compound **A** indicated the presence of a further compound of similar color reaction when sprayed with antimony pentachloride – carbon tetrachloride reagent. These mother liquors were combined and chromatographed on alumina (60 g, activity III). Elution with benzene yielded unreacted 2-ethyl-5-methylpyridine initially, while further elution provided an additional compound (350 mg) which was obtained crystalline from a small volume of ether, m.p. 190–192°. Recrystallization from acetone – petroleum ether gave an analytical sample (250 mg), m.p. 190–192°. This compound was designated compound **B** and was slightly less polar than compound **A** on a silica gel chromatoplate developed with 2% methanol in chloroform; i.r. ($CHCl_3$): 5.83 (OAc), 6.25, 6.37 (pyridine) μ, u.v.: λ_{max} 265sh (3.57), 270 (3.61), 276sh nm (3.51); $[\alpha]_D$ −126° (*c*, 1.26); n.m.r.: 9.23 (angular methyl, 3H, singlet), 8.88 (C_{21} methyl, 3H, $J_{20,21}$ = 7.0 Hz, doublet), 8.28 (C_{18} methyl, 3H, singlet), 8.02 (CH_3CO, 3H, singlet), 7.72 (C_{26} methyl, 3H, singlet), 6.71 (C_{20}, 1H, $J_{20,21}$ = 7.0 Hz, quartet), 4.20 (OH, 1H, broad signal, disappears on D_2O addition), 2.92 (C_{23}, 1H, $J_{23,24}$ = 8.0 Hz, doublet), 2.70 (C_{24}, 1H, $J_{24,23}$ = 8 and $J_{24,27}$ = 2.0 Hz), 1.75 (C_{27}, 1H, $J_{27,24}$ = 2.0 Hz, doublet); mass spectrometry: *m/e* 451 (M^+), prominent peaks at *m/e* 433, 418, 330, 147, and 121.

Anal. Calcd. for $C_{29}H_{41}O_3N$: C, 77.12; H, 9.15; N, 3.10. Found: C, 77.19; H, 9.21; N, 3.19.

Elution with 20% ether in benzene gave additional compound **A** (150 mg) while two fractions appeared to contain two further compounds of similar reaction to the spray reagent when examined by thin-layer chromatography. Separation by preparative layer chromatography (20 × 20 cm, 0.3 mm, 1% methanol in chloroform, chromatoplate developed twice) yielded 35 mg and 8 mg of these compounds which were designated **C** and **D**, respectively. Compound **C** could not be induced to crystallize and an analytical sample was prepared by sublimation at 190°/0.1 mm which gave a clear glass. The spectral data were consistent with this compound being isomeric with **A** and **B**; i.r.: 5.8 (—OAc), 6.25, 6.39 (pyridine) μ; u.v.: λ_{max} 270 nm (3.60); n.m.r.: 9.26 (angular methyl, 3H, singlet), 8.77 (C_{21} methyl, 3H, $J_{21,20}$ = 7.02 Hz, doublet), 8.43 (C_{18} methyl, 3H, broad singlet), 8.01 (CH_3CO, 3H, singlet), 7.73 (C_{26} methyl, 3H, singlet), 6.90 (C_{20}H, 1H, $J_{20,21}$ = 7.0 Hz, quartet), 2.97 (C_{23}, 1H, $J_{23,24}$ = 8.0 Hz, doublet), 2.65 (C_{24}, 1H, $J_{24,23}$ = 8.0 and $J_{24,27}$ = 2.0 Hz, two doublets), 1.72 (C_{27}H, 1H, $J_{27,24}$ = 2.0 Hz, doublet); mass spectrometry: *m/e* 451 (M^+), prominent peaks at *m/e* 433, 418, 330, and 120.

Anal. Calcd. for $C_{29}H_{41}O_3N$: C, 77.12; H, 9.15. Found: C, 77.05; H, 9.33.

Compound **D** could not be induced to crystallize but the n.m.r. and mass spectrum indicate this compound is probably isomeric with the three characterized above; i.r. ($CHCl_3$): 5.83 (OAc), 6.25, 6.37 (pyridine) μ; u.v.: λ_{max} 270 nm (3.62); n.m.r. 9.21 (angular methyl, 3H, singlet), 8.63 (C_{21} methyl, 3H, $J_{21,20}$ = 7.0 Hz, doublet), 8.27 (C_{18} methyl, 3H, singlet), 8.01 (CH_3CO, 3H, singlet), 7.74 (C_{26} methyl, 3H, singlet), 6.89 (C_{20}, 1H, $J_{20,21}$ = 7.0 Hz, quartet), 3.08 (C_{23}, 1H, $J_{23,24}$ = 8.0 Hz, doublet), 2.62 (C_{24}, 1H, $J_{24,23}$ = 8.0 and $J_{24,27}$ = 2.0 Hz, two doublets), 1.70 (C_{27}, 1H, $J_{27,24}$ = 2.0 Hz, doublet); mass spectrometry: *m/e* 451 (M^+), prominent peaks at *m/e* 433, 418, and 121.

3β-Acetoxy-22,27-iminojerv-12(13),14(15),16,22,24,27-hexaene (4)

Aromatic I

Compound **A** (118 mg) was thoroughly ground with 10% palladized charcoal (30 mg) until a homogeneous powder was obtained. This powder was heated at 200° for 7 min and the resultant solid residue washed several times with chloroform. Thin-layer chromatography of the chloroform extract indicated the product contained three major components and these were separated by preparative layer chromatography (20 × 20 cm, 0.4 mm, 2% methanol in chloroform). One of these three components was shown to be 2-ethyl-5-methylpyridine by n.m.r. The band which exhibited a strong fluorescence when the chromatoplate was viewed under u.v. light was extracted and yielded a light oil which crystallized from acetone – petroleum ether as needles, m.p. 167°. This compound was identified as 3β-acetoxy-5α-etiojerv-12(13)-en-17-one (**1**) by its u.v. spectrum and by mixture melting point with an authentic sample. The third compound which appeared as a light orange spot when the chromatoplate was sprayed with

Can. J. Chem. Downloaded from www.nrcresearchpress.com by 210.87.254.5 on 09/05/12
For personal use only.

antimony pentachloride – carbon tetrachloride reagent was extracted to yield a light oil which could not be induced to crystallize. An analytical sample of this compound which was designated aromatic **1** was obtained as a clear glass after sublimation at 185°/0.1 mm. Spectral data indicated this compound possessed structure **4**; i.r.: 5.82, 6.26, 6.39 μ; u.v.: λ_{max} 265sh, 269 (3.73) 277 nm (3.62); $[\alpha]_D$ +13° (*c*, 0.84); n.m.r.: 9.10 (angular methyl, 3H, singlet), 8.41 (C_{21} methyl, 3H, $J_{21,20}$ = 7.0 Hz, doublet), 8.03 (CH_3CO, 3H, singlet), 7.90 (C_{18} methyl, 3H, singlet), 7.80 (C_{26} methyl, 3H, singlet), 5.61 (C_{20}, 1H, $J_{20,21}$ = 7.0 Hz, quartet), 3.22–3.0 (C_{15} or C_{16} and C_{23}, 2H, two overlapping doublets), 2.94 (C_{15} or C_{16}, 1H, J = 8 Hz, doublet), 2.72 (C_{24}, 1H, $J_{24,23}$ = 8.0 and $J_{24,27}$ = 2 Hz, two doublets), 1.7 (C_{27}H, 1H, $J_{27,24}$ = 2 Hz, doublet); mass spectrometry: *m/e* 431, prominent peaks at 416, 402.

Mol. Wt. Calcd. for $C_{29}H_{37}O_2N$: 431.2824. Found (high resolution mass measurement): 431.2809.

Aromatic II

Compound **B** (80 mg) was ground with 10% palladized charcoal (20 mg) until a homogeneous powder was formed. This powder was heated at 200° for 7 min and the solid residue washed several times with chloroform. Thin-layer chromatographic examination of the chloroform extract indicated the major component was a new compound which appeared as a light orange spot when the chromatoplate was sprayed with antimony pentachloride – carbon tetrachloride reagent. This compound was separated from the reaction mixture by preparative layer chromatography (20 × 20 cm, 0.4 mm, 1% methanol in chloroform, developed twice) as a light oil (60 mg) which could not be induced to crystallize. An analytical sample of the compound, which was designated 'aromatic **II**', was obtained as a clear glass after sublimation at 185°/0.01 mm; i.r.: 5.82, 6.26, 6.39 μ; u.v.: λ_{max} 265sh, 269 (3.73), 277 nm (3.62); n.m.r.: 9.10 (angular methyl, 3H, singlet), 8.40 (C_{21} methyl, 3H, $J_{21,20}$ = 7 Hz, doublet), 8.02 (CH_3CO, 3H, singlet), 7.89 (C_{18} methyl, 3H, singlet), 7.80 (C_{26} methyl, 3H, singlet), 5.58 (C_{20}, 1H, $J_{20,21}$ = 7.0 Hz, quartet), 3.14 (C_{23}, 1H, $J_{23,24}$ = 8 Hz, doublet), 3.09 (C_{15} or C_{16}, 1H, J = 8 Hz, doublet), 2.91 (C_{15} or C_{16}, 1H, J = 8 Hz, doublet), 2.75 (C_{24}, 1H, $J_{24,23}$ = 8 and $J_{24,27}$ = 2 Hz, two doublets), 1.73 (C_{27}, 1H, $J_{27,24}$ = 2 Hz, doublet); mass spectrometry: *m/e* 431 (M^+), prominent peaks at *m/e* 416, 402.

Mol. Wt. Calcd. for $C_{29}H_{37}O_2N$: 431.2824. Found (high resolution mass measurement): 431.2809.

N-Acetyl-22,27-iminojerva-12(13),14(15),16-triene-3β-ol (5)

Isomers i–iv

Aromatic compound **II** (50 mg) was dissolved in glacial acetic acid (10 ml) and the solution hydrogenated at 20° and 45 p.s.i. over Adams' catalyst (PtO_2, 20 mg) for 3 h. The mixture was filtered to remove the catalyst which was carefully washed with additional acetic acid (5 ml). The combined filtrates were reduced in volume to 2 ml *in vacuo*, then diluted with water (20 ml) and made basic with ammonia solution. The resultant suspension was extracted with methylene chloride (3 × 10 ml) before drying over anhydrous sodium sulfate. Thin-layer chromatography revealed the presence of four compounds of similar R_f value and color reaction with various spray reagents. These compounds were designated **i–iv** in order of decreasing R_f value, (silica gel G, 5% methanol in chloroform) and were separated by careful preparative layer chromatography (20 × 20 cm, 0.3 mm, 1% methanol in chloroform, plates developed three times). The bands corresponding to the four compounds were delineated by inspection of the developed plates under u.v. light. Extraction of the various bands and removal of the solvent (methanol–chloroform 1:1) gave each of the compounds as a clear oil. None of the compounds could be induced to crystallize.

All four compounds were separately converted via the 3-*O*,*N*-diacetates (**13**) to the *N*-acetyl derivatives **12** (since a sample of *N*-acetyl-5α,6-dihydroverarine was available for comparison) as outlined for one of the isomers below.

Compound **ii** was dissolved in pyridine – acetic anhydride (2 ml, 1:1) and allowed to stand for 12 h at 20°. The solution was then poured into ice water (5 ml) and the resulting suspension extracted with methylene chloride (3 × 3 ml). The combined extracts were washed with saturated aqueous sodium hydrogen carbonate (10 ml) and then with water (2 × 5 ml), before drying over anhydrous sodium sulfate. Removal of the methylene chloride *in vacuo* gave a light oil which crystallized from ether (the diacetates of compounds **i**, **iii**, and **iv** were not obtained crystalline) as needles, m.p. 203–205°; i.r. ($CHCl_3$): 5.80 (OAc), 6.19 (NAc) μ; u.v.: λ_{max} 268 (2.7), 277 nm (2.7).

The diacetate (20 mg) was refluxed with 0.1 *M* potassium hydroxide in methanol (5 ml) for 1 h, the solution cooled, and diluted with water (20 ml). The aqueous suspension was extracted with methylene chloride (3 × 5 ml) and the combined extracts washed with water (2 × 5 ml) prior to drying over anhydrous sodium sulfate. Evaporation of the solvent *in vacuo* gave a light oil which was readily crystallized from anhydrous ether. (All four *N*-acetyl derivatives were obtained crystalline via this procedure.)

The *N*-acetyl derivatives of compounds **i** and **ii** had R_f values comparable with that of *N*-acetyl-5α,6-dihydroverarine whereas those of the *N*-acetyl derivatives of compounds **iii** and **iv** were slightly smaller. All compounds showed similar color reactions when the chromatoplate was sprayed with various reagents. The *N*-acetyl derivatives were characterized as follows.

*Compound **i**, N-acetate;* prisms, m.p. 249–250° (6 mg); i.r. ($CHCl_3$): 6.20 9.70 μ; u.v.: λ_{max} 268 (2.68), 277 nm (2.66); $[\alpha]_D$ +36° (*c*, 0.605); n.m.r.: 9.07 (angular methyl, 3H, singlet), 8.19 (CH_3CON, 3H, singlet), 7.74 (C_{18} methyl, 3H, singlet), 3.15 (C_{15} or C_{16}, J = 8 Hz, doublet), 2.96 (C_{15} or C_{16}, J = 8 Hz, doublet); mass spectrometry: *m/e* 437 (M^+), prominent peaks at *m/e* 297, 140, 98.

Mol. Wt. Calcd. for $C_{29}H_{43}O_2N$: 437.329. Found (high resolution mass measurement): 437.325.

*Compound **ii**, N-acetate;* prisms, m.p. 263–264° (17 mg); i.r. ($CHCl_3$): 6.19, 9.70 μ; u.v.: λ_{max} 268 (2.65), 277 nm (2.61); $[\alpha]_D$ +26° (*c*, 1.71); mass spectrometry: *m/e* 437 (M^+), prominent peaks at *m/e* 298, 297, 140, 98.

*Compound **iii**, N-acetate;* rosettes, m.p. 270–274° (5 mg); i.r. ($CHCl_3$): 6.20, 9.70 μ; u.v.: λ_{max} 268, 277 nm; mass spectrometry: *m/e* 437 (M^+), prominent peaks at *m/e* 297, 140, 98.

*Compound **iv**, N-acetate;* long needles, m.p. 260–261° (10 mg); i.r. ($CHCl_3$): 6.20, 9.70, 9.80 μ; u.v.: λ_{max} 268, 277 nm; mass spectrometry: *m/e* 437 (M^+), prominent peaks at *m/e* 298, 297, 140, 98.

Can. J. Chem. Downloaded from www.nrcresearchpress.com by 210.87.254.5 on 09/05/12
For personal use only.

Isomers v–viii

Aromatic compound **I** (50 mg) was dissolved in glacial acetic acid (10 ml) and the solution shaken with Adams' catalyst (PtO_2, 20 mg) in an atmosphere of hydrogen at 45 p.s.i. and 20° for a period of 3 h. The mixture was filtered to remove the catalyst which was washed with a further 10 ml of glacial acetic acid and the filtrates combined. The volume of the acetic acid was reduced to 2 ml by use of a rotary evaporator before dilution with water (20 ml). The aqueous acid solution was made basic with dilute ammonia and the resulting suspension extracted several times with methylene chloride (3 × 10 ml) prior to drying over anhydrous sodium sulfate. Thin-layer chromatographic investigation of the light oil (45 mg) obtained by removal of the methylene chloride indicated the presence of four compounds, of similar R_f value and color reaction to the spray reagent. These compounds were numbered **v–viii** in order of decreasing R_f value and were separated by careful preparative layer chromatography (silica gel G 20 × 20 cm, 0.3 mm, 1% methanol in chloroform, plates developed three times). The compounds were obtained as colorless oils which could not be crystallized. Conversion of these compounds via the 3-*O*,*N*-diacetates to the *N*-acetyl derivatives was accomplished as outlined above for the 3β-acetoxy-22,27-iminojerva-12(13),14(15),16-triene isomers **i–iv** obtained from aromatic compound **II**. None of the *N*-acetyl derivatives of compounds **v–viii** could be induced to crystallize although compounds **v** and **vi** had R_f values comparable with *N*-acetyl-5,6-dihydroverarine. These compounds were not fully characterized but their spectral properties were in accord with structure **5**.

Compound v, N-acetate: i.r.: 6.19, 9.28 μ; u.v.: λ_{max} 267, 276 nm; mass spectrometry: *m/e* 437 (M^+), prominent peaks at *m/e* 298, 297, 98.

Spectral properties for the *N*-acetyl derivatives of compounds **vi–viii** are virtually the same as for the acetate of ***v*** and no additional data were obtained for any of these compounds.

Hydrogenation of 3-O,N-Diacetylverarine

The 3-*O*,*N*-diacetylverarine utilized in this reaction was prepared from veratramine (1) and had the following physical constants, m.p. 189–190° (lit. (1) m.p. 189–190°); $[\alpha]_D$ −23 ±2° (ethanol).

A solution of 3-*O*,*N*-diacetylverarine (190 mg) in glacial acetic acid (5 ml) was stirred with Adams' catalyst (PtO_2, 60 mg) in an atmosphere of hydrogen at 20°. After 14 h, 9.1 ml of hydrogen had been consumed and the mixture was filtered to remove the catalyst which was washed with a further 10 ml of acetic acid. The combined filtrates were reduced in volume (to 2 ml) *in vacuo* and diluted with water (30 ml) to give a white precipitate which was taken up in ether. The ethereal phase was washed with water (3 × 10 ml) before drying over anhydrous sodium sulfate. Thin-layer chromatographic examination on both silica gel and alumina using a variety of solvents indicated that a single new compound had been formed.

Removal of the ether *in vacuo* gave an oil which could not be induced to crystallize. A small scale investigation revealed that after selective hydrolysis of the 3-*O*-acetate the product appeared as two components of similar R_f value on a silica gel chromatoplate. Consequently 3-*O*,*N*-diacetyl-5,6-dihydroverarine (170 mg) was refluxed with 0.1 *N* methanolic potassium hydroxide (5 ml) for 1 h, the solution cooled, and then diluted with water (20 ml). The resulting aqueous suspension was extracted with methylene chloride (3 × 10 ml) and the combined extracts washed with water (3 × 10 ml) before drying over anhydrous sodium sulfate. Removal of the solvent *in vacuo* gave a light oil which on trituration with ether gave crystals, m.p. 190–225°. Thin-layer chromatography showed the crystalline product to consist of two compounds which were separated by preparative layer chromatography on silica gel (20 × 20 cm, 0.4 mm, 2% methanol in chloroform). The least polar compound (75 mg) was tentatively assigned the 5β configuration on the basis of its n.m.r. spectrum. Recrystallization from ether gave an analytical sample of *N*-acetyl-5β,6-dihydroverarine (**20**), m.p. 198–199°; i.r. ($CHCl_3$): 6.21 (—NC(=O)—CH) μ; u.v.: λ_{max} 267 (2.74), 276 nm (2.74); n.m.r.; 9.02 (C_{26} methyl, 3H, $J_{26,25}$ = 7 Hz, doublet), 8.94 (angular methyl, 3H, singlet), 8.82 (C_{21} methyl, 3H, $J_{21,20}$ = 8 Hz, doublet) 8.14 (CH_3CON, 3H, singlet), 7.71 (C_{18} methyl, 3H, singlet), 6.45 (C_{20}, 1H, $J_{20,21}$ = 8 and $J_{20,22}$ = 10 Hz, multiplet), 5.97 (*H*—C—OAc, 1H, multiplet), 3.12 (C_{15} or C_{16}, 1H, J = 8 Hz, doublet), 2.96 (C_{15} or C_{16}, J = 8 Hz, doublet); mass spectrometry: *m/e* 437 (M^+), prominent peaks at *m/e* 297, 140, 98.

Anal. Calcd. for $C_{29}H_{43}O_2N$: C, 79.58; H, 9.90; N, 3.20. Found: C, 79.51; H, 10.02; N, 3.25.

The more polar compound was crystallized from ether as prisms, m.p. 249–250°. This compound was tentatively assigned the 5α configuration on the basis of its n.m.r. spectrum and an analytical sample of *N*-acetyl-5α,6-dihydroverarine (**11**) was prepared by sublimation at 220°/0.01 mm, as prisms, m.p. 249–250°; i.r.: 6.22 (N—C(=O)CH_3), 12.23 μ; u.v.: λ_{max} 267 (2.69), 276 nm (2.68); $[\alpha]_D$ +41° (*c*, 0.961); n.m.r.: 9.06, 9.02 (angular and C_{26} methyl, 6H, singlet and doublet), 8.19 (CH_3CON, 3H, singlet), 7.72 (C_{18} methyl, 3H, singlet), 3.13 (C_{15} or C_{16}, 1H, J = 8 Hz, doublet), 2.99 (C_{15} or C_{16}, 1H, J = 8 Hz, doublet); mass spectrometry: *m/e* 437 (M^+), prominent peaks at *m/e* 394, 297, 140.

Anal. Calcd. for $C_{29}H_{43}O_2N$: C, 79.58; H, 9.90. Found: C, 79.32; H, 9.99.

*N-Acetyl-3-keto-5α,6-dihydroverarine (**23**)*

A solution of *N*-acetyl-5α,6-dihydroverarine (**11**; 212 mg) in acetone (75 ml) was treated with Jones' reagent (0.3 ml) and allowed to stand at 20° for 2 min. Isopropanol (2 ml) was added to remove the excess oxidant and the mixture diluted with water (600 ml). The aqueous acetone solution was extracted with methylene chloride (3 × 30 ml) and the combined extracts washed with water (3 × 30 ml) before drying over anhydrous sodium sulfate. Evaporation of the methylene chloride gave a colorless oil (191 mg) which could not be crystallized but appeared homogeneous when examined by thin-layer chromatography. An analytical sample was obtained as a clear glass after sublimation at 185°/0.01 mm; i.r.: 5.89 (saturated carbonyl), 6.14 (N—C(=O)—CH_3) μ; u.v.: λ_{max} 267 (2.73), 276

Can. J. Chem. Downloaded from www.nrcresearchpress.com by 210.87.254.5 on 09/05/12
For personal use only.

nm (2.71); $[\alpha]_D$ +66° (*c*, 1.15); o.r.d. $[\phi]^{peak}_{305}$ +1090°, $[\phi]^{trough}_{270}$ +115°, $[\phi]^{peak}_{230}$ +3910°; n.m.r.: 9.03 (C_{26} methyl, 3H, $J_{26,25}$ = 7.0 Hz, doublet), 8.88 (angular methyl, 3H, singlet), 6.45 (C_{20}, 1H, $J_{20,21}$ = 7.5, $J_{20,22}$ = 9.0 Hz, multiplet), 3.13 (C_{15} or C_{16}, 1H, J = 8 Hz, doublet), 2.95 (C_{15} or C_{16}, 1H, J = 8 Hz, doublet); mass spectrometry: *m/e* 435 (M^+), prominent peaks at *m/e* 392, 295, 140, 98.

Mol. Wt. Calcd. for $C_{29}H_{41}O_2N$: 435.313. Found (high resolution mass measurement): 435.312.

*N-Acetyl-Δ⁴-3-keto-5,6-dihydroverarine (**28**)*

A solution of *N*-acetyl-3-keto-5α,6-dihydroverarine (162 mg, 0.372 mmol) in acetic acid (6 ml) containing hydrogen bromide (60 mg, 0.744 mmol) was placed in a dry round-bottom flask. Bromine (130 mg, 0.8 mmol) in acetic acid (5 ml) was added slowly and the mixture stirred at 20° for 20 min and then diluted with water (25 ml). The resulting heavy white precipitate was taken up in methylene chloride and the extract washed with water (3 × 10 ml) prior to drying over anhydrous sodium sulfate. Removal of the solvent *in vacuo* gave a colorless gum (225 mg) which was shown by thin-layer chromatography to consist of one major compound. This crude product was immediately subjected to the conditions of Evans (12) for introduction of the 4,5-double bond as outlined below. Bromine (0.26 ml) was added to acetone (7.5 ml) at 0° and the solution stirred until the color disappeared. Sodium carbonate (0.7 g) was then added and the mixture was stirred for a further 30 min, then filtered directly into hot acetone containing sodium iodide (7.0 g). This solution was refluxed for 15 min during which time a precipitate of sodium bromide was formed.

A portion (6 ml) of the supernatant of this hot solution was added to a round bottom-flask containing 2,4-dibromo ketone (220 mg) and the solution refluxed for 2½ h. During this time more sodium bromide precipitated, indicative of the exchange of the 2-bromine for an iodine atom. Oxalic acid (220 mg) was added as a fine powder and the solution refluxed for a further hour before cooling. The reaction mixture was diluted with ethyl acetate (20 ml) and filtered. This filtrate was washed with water (2 × 10 ml), saturated aqueous sodium hydrogen carbonate (2 × 10 ml), and water (2 × 10 ml). The ethyl acetate was decolorized by adding zinc dust (600 mg) and acetic acid (0.2 ml) and then shaking. When the solution had attained a light yellow color the zinc dust was removed by filtration and the ethyl acetate filtrate washed with water (2 × 10 ml), sodium hydrogen carbonate solution (2 × 10 ml), and water (2 × 10 ml) before drying over anhydrous sodium sulfate.

Removal of the ethyl acetate *in vacuo* gave a light yellow gum (158 mg) which was examined by thin-layer chromatography. The spot on the chromatoplate corresponding to the major product exhibited an intense fluorescence under u.v. light and appeared purple when the plate was sprayed with antimony pentachloride – carbon tetrachloride reagent. Preparative layer chromatography on silica gel (20 × 60 cm, 0.4 mm, developed twice with 1% methanol in chloroform) gave this compound as a light gum (110 mg, 50% yield) which was not crystallized. An analytical sample was prepared by sublimation at 180°/0.01 mm which gave a light yellow glass; i.r.: 6.03 (α,β-unsaturated carbonyl), 6.14 (N—Ac) μ; $[\alpha]_D$ +74° (*c*, 1.26); n.m.r.: 9.02 (C_{26} methyl, 3H, $J_{26,25}$ = 7 Hz, doublet), 8.72 (angular methyl, 3H, singlet), 8.18 (CH_3C—N, 3H, singlet), 6.45 (C_{20}, 1H, $J_{20,21}$ = 7.5, $J_{20,22}$ = 10 Hz, multiplet), 4.22 (C_4, 1H, singlet), 3.10 (C_{15} or C_{16}, 1H, J = 8Hz, doublet), 2.94 (C_{15} or C_{16}, 1H, J = 8Hz, doublet); mass spectrometry: *m/e* 433 (M^+), prominent peaks at *m/e* 390, 293, 140, 98.

Mol. Wt. Calcd. for $C_{29}H_{39}O_2N$: 433.2980. Found (high resolution mass measurement): 433.2974.

*N-Acetylverarine (**30**)*

A solution of *N*-acetyl-Δ⁴-3-keto-5,6-dihydroverarine (100 mg) in isopropenyl acetate (3 ml) containing 0.5% sulfuric acid was refluxed for 1 h. Anhydrous sodium acetate (60 mg) was then added and most of the isopropenyl acetate removed by use of a rotary evaporator. The residue was diluted with methylene chloride (10 ml) and then filtered. Thin-layer chromatography of the filtrate indicated the complete absence of (**23**) and the formation of a less polar compound. Evaporation of the methylene chloride gave an oil (100 mg) the i.r. spectrum of which exhibited a carbonyl band at 5.75 μ indicative of an enol acetate.

This oil was dissolved in a mixture of methanol (10 ml) and ether (3 ml) and heated to reflux. During the refluxing a methanolic solution of sodium borohydride (150 mg in 5 ml) was added slowly over a period of 15 min. The solution was refluxed for a further 1 h and then concentrated hydrochloric acid (1 ml) was added and the refluxing continued with stirring for 30 min. During this final period vigorous stirring was necessary to overcome severe bumping.

The reaction mixture was cooled and then diluted with ether (50 ml). The ethereal solution was washed with water and then dried over anhydrous sodium sulfate. Removal of the solvent gave a light oil (70 mg) which was shown to contain a compound of identical R_f value to that of *N*-acetylverarine. Separation by preparative layer chromatography (20 × 20 cm, 0.3 mm, 2% methanol in chloroform) and extraction of the band corresponding to this product yielded an oil (30 mg). This compound was shown to be identical with *N*-acetylverarine by thin-layer chromatography and superimposable i.r. and n.m.r. spectra; i.r. ($CHCl_3$): 6.19 ($NC(=O)CH_3$) μ; u.v.: λ_{max} 268 (2.76) 277 nm (2.65); n.m.r.: 9.03 (C_{26} methyl, 3H, $J_{26,25}$ = 7 Hz, doublet), 8.87 (angular methyl, 3H, singlet), 8.18 (CH_3CON, 3H, singlet), 4.56 (C_6 1H, multiplet), 3.12 (C_{15} or C_{16}, 1H, J = 8 Hz, doublet,), 2.94 (C_{15} or C_{16}, 1H, J = 8 Hz, doublet); mass spectrometry: *m/e* 435 (M^+), prominent peaks at *m/e* 295, 140, 98.

*Verarine (**31**)*

A solution of *N*-acetylverarine (20 mg) in ethylene glycol (5 ml) containing 10% potassium hydroxide was refluxed for 12 h. The reaction mixture was cooled, diluted with water (20 ml), and extracted with methylene chloride (3 × 5 ml). Examination of the extract by thin-layer chromatography indicated the presence of *N*-acetylverarine and a more polar compound which had the same R_f value and color reaction to the spray reagent, as an authentic sample of verarine. The more polar compound was separated by preparative layer chromatography (20 × 20 cm, 0.3 mm, 5% methanol in chloroform) as a light oil

Can. J. Chem. Downloaded from www.nrcresearchpress.com by 210.87.254.5 on 09/05/12
For personal use only.

(8 mg) which crystallized from ether. This compound was shown to be identical with verarine by thin-layer chromatography, i.r., and n.m.r. comparison; i.r. ($CHCl_3$): 9.57 μ; u.v.: λ_{max} 267 (2.74) 276 nm (2.73); n.m.r.: 9.15 (C_{26} methyl, 3H, $J_{26,25}$ = 6 Hz, doublet), 8.88 (angular methyl, 3H, singlet), 7.73 (C_{18} methyl, 3H, singlet), 4.55 (C_6, 1H, broad doublet), 3.02 (C_{15} and C_{16}H, 2H, singlet); mass spectrometry: *m/e* 393 (M^+), prominent peaks at *m/e* 392, 376, 295, 284, 256, 98.

Mol. Wt. Calcd. for $C_{27}H_{39}ON$: 392.2953. Found (high resolution mass measurement): 392.2922.

*3-Methylbut-3-enal Diethyl Acetal (**40**)*

This compound was prepared according to the procedure of Cornforth and Firth (23) with small modifications as indicated. The additional data obtained in our investigations in this and the next few experiments are also provided. Triethyl orthoformate (45 g) and magnesium (17.5 g) were stirred and heated at 60°. 2-Methylallyl chloride (24.5 g) was then added gradually (about 2.5 h) and the reaction mixture left overnight. The flask was cooled in ice and saturated aqueous ammonium chloride (20 ml) was added dropwise until the mixture set solid; the cake was filtered and washed well with ether. The filtrate on work-up afforded the acetal (**40**, 19 g), b.p. 60–61°/20 mm (lit. (25) b.p. 60°/19 mm). The compound was found to be pure by v.p.c. examination using a FFAP column; i.r. (film): 6.25 μ; n.m.r. 8.85 (2 × CH_3—CH_2, 6H, triplet), 8.25 (C_2—CH_3, 3H, singlet), 7.7 (C_3—CH_2, 2H, doublet, J = 6.0 Hz), 6.5 (CH_2's of —O—CH_2—CH_3, 4H, multiplet), 5.4 (C_4H, 1H, triplet), 5.2 (CH_2=C<, 2H, singlet).

*3,4-Epoxy-3-methylbutanal Diethyl Acetal (**41**)*

A solution of 3-methylbut-3-enal diethyl acetal (**40**, 6.6 g) in anhydrous ether (10 ml) was cooled in ice and treated gradually with a solution of *m*-chloroperbenzoic acid (9 g) in ether (30 ml). The reaction mixture was then allowed to warm up and kept at 30° by occasional cooling until the reaction subsided. Next day the reaction mixture was washed repeatedly with saturated sodium bicarbonate solution until the whole of *m*-chlorobenzoic acid was removed. The ether layer was separated and dried over magnesium sulfate. The solvent was removed under reduced pressure and distillation of the residual liquid afforded the epoxide (**41**) as a colorless oil (4.1 g), b.p. 82–86°/18 mm (lit. (22) b.p. 83–84°/17 mm). The compound was found to be homogeneous by v.p.c. examination; i.r. (film): 10.0, 10.5, 12.5 μ (epoxide); n.m.r.: 8.85 (2 × CH_3—CH_2—O—, 6H, triplet), 8.7 (C_3—CH_3, 3H, singlet), 8.2 (C_2—CH_2, 2H, doublet, J = 7.0 Hz), 7.5 (O<, 2H, AB quartet, $J_{A,B}$ = 5.5 Hz), 6.5 (CH_2's of —O—CH_2—CH_3, 4H multiplet), 5.4 (C_1H, 1H, triplet).

*3-Methylfuran (**42**)*

A mixture of 3,4-epoxy-3-methylbutanal diethyl acetal (**41**, 5.0 g) and 0.1 *N* sulfuric acid (500 ml) were heated under a fractionating column for 3 h, the methylfuran and ethanol being removed intermittently by distillation. The distillate was washed once with half-saturated aqueous calcium chloride (10 ml) and twice with saturated aqueous ammonium chloride, dried over sodium, and redistilled to give pure 3-methylfuran (1.1 g); b.p. 65–66° (lit. (22) b.p. 65–65.5°); i.r. (chloroform): 6.67, 8.33, 11.2 μ; n.m.r.: 8.0 (C_3—CH_3, 3H, singlet), 3.85 (C_4H, 1H, singlet), 2.87 (C_2H, 1H, broad singlet), 2.75 (C_5H, 1H, broad singlet).

Propionylation of 3-Methylfuran

3-Methylfuran (1 g) and propionic anhydride (1.6 g) were mixed and to the mixture 2 drops of orthophosphoric acid (85%) were added. The mixture was stirred vigorously and the heat generated was removed by cooling. Gradually the reaction mixture acquired a dark red color. It was then heated to 60–65° and maintained at this temperature for 2 h. The reaction mixture was then cooled and stirred with water (2 ml) for 1 h. The dark organic layer was separated and again stirred with saturated sodium carbonate solution (5 ml) for 24 h. It was then washed thoroughly with water, extracted with ether (2 × 5 ml), and dried over magnesium sulfate. The solvent was removed under reduced pressure and the residual reddish brown oil obtained was distilled *in vacuo* in a hot box. A colorless fragrant liquid (0.5 g) was collected, b.p. 125–130°/25 mm. The i.r. spectrum (film) of the product showed a double carbonyl absorption (~5.88 μ). Examination of this material by v.p.c. using a FFAP column (172°) indicated that it was a mixture of two compounds in the ratio 70:30, with retention times 1.8 and 2.8 min, respectively. These were separated by v.p.c. using a FFAP column (172°). The major component was characterized as 2-propionyl-3-methylfuran (**43**), b.p. 77–80°/5 mm; i.r. (film): 5.99, 6.65, 11.3 (furan) μ; u.v.: λ_{max} 278, 230 nm; n.m.r.: 8.85 (CH_3—CH_2—, 3H, triplet), 7.65 (C_3—CH_3, 3H, singlet), 7.2 (—CO—CH_2—CH_3, 2H, quartet), 3.65 (C_4H, 1H, doublet, $J_{4,5}$ = 2.5 Hz), 2.65 (C_5H, doublet, $J_{4,5}$ = 2.5 Hz); mass spectrometry: *m/e* 138 (M^+), prominent peak at *m/e* 109.

Anal. Calcd. for $C_8H_{10}O_2$: C, 69.56; H, 7.24. Found: C, 69.71; H, 7.27.

The second component was characterized as 2-propionyl-4-methylfuran (**44**), b.p. 78–82°/5 mm; i.r. (film): 5.97, 6.65, 11.3 μ; u.v.: λ_{max} 280, 230 nm; n.m.r.: 8.85 (CH_3—CH_2—, 3H, triplet), 7.9 (C_4CH_3, 3H, singlet), 7.2 (—CO—CH_2—CH_3, 2H, quartet), 3.05 (C_3H, 1H, singlet), 2.75 (C_5H, 1H, broad singlet); mass spectrometry: *m/e* 138 (M^+), prominent peak at *m/e* 109.

Anal. Calcd. for $C_8H_{10}O_2$: C, 69.56; H, 7.24. Found: C, 69.68; H, 7.26.

*Methyl 5,5-Dimethoxy-3-methyl-2,3-epoxypentanoate (**45**)*

This compound was prepared according to the procedure of Burness (25).

*Methyl 3-Methyl-2-furoate (**46**)*

This compound was prepared according to the procedure of Burness (25); i.r. (chloroform): 5.80 μ; u.v.: λ_{max} 252 nm; n.m.r.: 7.65 (C_3—CH_3, 3H, singlet), 6.2 ($COOCH_3$, 3H, singlet), 3.68 (C_4H, 1H, doublet, J = 2.0 Hz), 2.6 (C_5H, 1H, doublet, J = 2.0 Hz).

*Methyl 3-Methyl-5-propionyl-2-furoate (**47**)*

Methyl 3-methyl-2-furoate (25.6 g, 0.2 mol) was dissolved in propionic anhydride (75 ml) and orthophosphoric acid (7.0 g) was added to it with vigorous stirring. The heat generated was removed by cooling with ice. The reaction mixture was then stirred at 65–70° for 48 h. It

Can. J. Chem. Downloaded from www.nrcresearchpress.com by 210.87.254.5 on 09/05/12
For personal use only.

was then cooled and stirred into water. The dark brown organic layer was extracted with chloroform and the chloroform extract was washed with bicarbonate solution until neutral to litmus and dried over sodium sulfate. The solvent was distilled off under reduced pressure. The unreacted starting materials were removed by distillation *in vacuo* and the semisolid residue was distilled at 120°/0.3–4 mm. A pale yellow crystalline material was collected in the receiver (23.5 g), m.p. 109–111°. It was recrystallized from aqueous ethanol (70%), colorless shining needles, m.p. 113–114°; i.r. (chloroform): 5.73, 5.88 μ; u.v.: λ_{max} 280, 285sh, 212 nm; n.m.r.: 8.8 (—CH_2—CH_3, 3H, triplet), 7.65 (C_3CH_3, 3H, singlet), 7.2 (—CO—CH_2—, 2H, quartet), 6.1 (—$COOCH_3$, 3H, singlet), 3.0 (C_5H, 1H, singlet); mass spectrometry: *m/e* 196 (M^+), prominent peaks at *m/e* 167, 138, 123, 109.

Anal. Calcd. for $C_{10}H_{12}O_4$: C, 61.22; H, 6.12. Found: C, 61.01; H, 5.97.

*3-Methyl-5-propionyl-2-furoic Acid (**48**)*

A solution of methyl 3-methyl-5-propionyl-2-furoate (**47**, 9.8 g) in aqueous sodium hydroxide (10%, 100 ml) was heated under reflux for 1.5 h. The solution was then cooled and acidified with concentrated hydrochloric acid and stirred for a few minutes. The product which separated as a brown granular solid was collected by filtration. It was washed with a little ice cold water and dried *in vacuo*. Crystallization from methanol afforded pale yellow shining prisms (7.6 g), m.p. 179–181°; i.r. (chloroform): 5.67, 5.88 μ; u.v.: λ_{max} 282, 212 nm; n.m.r.: 8.8 (CH_3—CH_2—, 3H, triplet), 7.6 (C_3CH_3, 3H, singlet), 7.0 (—CH_2—CO—, 2H, quartet), 2.85 (C_4H, 1H, singlet), −0.2 (—COOH, 1H, singlet); mass spectrometry: *m/e* 182 (M^+), prominent peak at *m/e* 137.

Anal. Calcd. for $C_9H_{10}O_4$: C, 59.33; H, 5.49. Found: C, 59.21; H, 5.50.

*2-Propionyl-4-methylfuran (**44**)*

A mixture of 3-methyl-5-propionyl-2-furoic acid (9.1 g, 0.05 mol), anhydrous quinoline (20 ml), and powdered copper (2.0 g) was heated 200–210° under a nitrogen atmosphere for 3 h. The evolution of carbon dioxide ceased by this time and the reaction mixture was extracted with chloroform (50 ml). The chloroform extract was filtered to remove the copper powder and washed successively with 1 *N* hydrochloric acid (3 × 50 ml), water (100 ml), and finally with sodium bicarbonate solution until neutral to litmus. It was then dried over sodium sulfate and the solvent was distilled off under reduced pressure. The residual dark oil was distilled using a short fractionating column. The fraction boiling at 78–82°/5 mm was collected as a colorless fragrant liquid (5.4 g). Examination of the compound by t.l.c. and v.p.c. indicated that it was pure. The physical and spectral data of the compound were identical with those of **44** obtained by the propionylation of 3-methylfuran.

*2-Ethyl-3-hydroxy-5-methylpyridine (**49**)*

2-Propionyl-4-methylfuran (**44**; 1.0 g) and aqueous ammonia (11 *N*, 25 ml), were heated in a sealed tube for 20 h (18). The reaction mixture was filtered off the residual solid matter and the filtrate was evaporated to dryness under a stream of nitrogen. The residue was extracted with chloroform and dried. The solvent was removed under reduced pressure and the dark brown semisolid residue distilled at 150°/0.3–5 mm. A small quantity of pale yellow liquid which collected in the receiver soon solidified into shining prisms (202 mg), m.p. 140–144°. Crystallization from chloroform provided an analytical sample as colorless shining prisms, m.p. 145–147°; i.r. (chloroform): 3.11, 6.29 μ; u.v.: λ_{max} (log ε): 287 (3.95), 225sh nm; n.m.r.: 8.75 (CH_3—CH_2—, 3H, triplet), 7.8 (C_5CH_3, 3H, singlet), 7.1 (—CH_2—CH_3, 2H, quartet), 2.9 (C_4H, 1H, singlet), 2.1 (C_6H, 1H, singlet), 1.0 (C_3OH, 1H, multiplet); mass spectrometry: *m/e* 137 (M^+), prominent peaks at *m/e* 136, 121, 94, 93.

Anal. Calcd. for $C_8H_{11}NO$: C, 70.07; H, 8.02. Found: C, 70.11; H, 8.10.

*2-Ethyl-3-O-benzyl-5-methylpyridine (**50**)*

2-Ethyl-5-methyl-3-hydroxypyridine (274 mg, 0.002 mol) was dissolved in aqueous sodium hydroxide (5%, 10 ml) and benzyl chloride (240 mg, 0.002 mol) was added to it. The mixture was heated at 100° for 2.5 h. During this time the benzyl chloride gradually dissolved and a pale yellow oil separated in the flask. The reaction mixture was cooled and extracted with chloroform (2 × 10 ml). The chloroform extract was washed with water until neutral to litmus and dried over sodium sulfate. The residual oil obtained after the removal of the solvent was distilled *in vacuo*. A colorless oil collected in the receiver (228 mg), b.p. 118–120°/0.4–5 mm. Thin-layer chromatography on alumina indicated that the compound was pure; i.r. (film): 6.27, 7.87, 9.52 μ; u.v.: λ_{max} 285, 225sh nm; n.m.r.: 8.8 (CH_3—CH_2—, 3H, triplet), 7.75 (C_5CH_3, 3H, singlet), 7.2 (—CH_2—CH_3, 2H, quartet), 5.0 (—O—CH_2—C_6H_5, 2H, singlet), 3.15 (C_4H, 1H, singlet), 2.65 (C_6H_5—CH_2—O—, 5H, singlet), 2.1 (C_6H, 1H, singlet).

*2-Ethyl-3-methoxy-5-methylpyridine (**51**)*

A solution of 2-ethyl-3-hydroxy-5-methylpyridine (2.74 g, 0.02 mol) in methanol (40 ml) containing 10% water was chilled in an ice-salt bath. To this was added a solution of diazomethane (4.2 g, 0.1 mol) in ether (175 ml) with constant swirling from a dropping funnel, the stem of which projected below the surface of the liquid. A brisk effervescence accompanied the addition which was interrupted several times in order to boil off the accumulated ether. The latter procedure serves to keep the polarity of the solution at a maximum. After being allowed to stand overnight, the methanolic solution was acidified with hydrochloric acid and most of the ether and methanol removed by concentration on the steam bath. The resulting syrup was diluted with water and the solution exhausted with ether. It was then made alkaline with sodium hydroxide pellets and again extracted with ether (3 × 100 ml). This second extract was dried over potassium carbonate, the ether removed by distillation, and the residual oil distilled *in vacuo*. The product (2.01 g) was a colorless oil, b.p. 100°/10 mm.

Some of the starting material was recoverable by the following procedure. The alkaline solution after exhaustion with ether was neutralized and evaporated to dryness followed by extraction with chloroform. Removal of the chloroform afforded a dark brown solid (480 mg) which was identified as 2-ethyl-3-hydroxy-5-methylpyridine (**49**).

The methyl ether was characterized as follows; i.r. (film): 6.26, 6.41, 7.91, 9.52 μ; u.v.: λ_{max} (log ε): 283 (3.86), 2.25sh nm; n.m.r.: 8.8 (CH_3—CH_2—, 3H, triplet),

Can. J. Chem. Downloaded from www.nrcresearchpress.com by 210.87.254.5 on 09/05/12
For personal use only.

7.7 (C_5CH_3, 3H, singlet), 7.25 (—CH_2—CH_3, 2H, quartet), 6.25 (—OCH_3, 3H, singlet), 3.2 (C_4H, 1H, singlet), 2.15 (C_6H, 1H, singlet).

Anal. Calcd. for $C_9H_{13}NO$: C, 71.52; H, 8.60. Found: C, 71.47; H, 8.64.

*23-Methoxy-22,27-iminojerva-12(13),22,24,27-tetraene-3β-17-diol(s) (**53**)*

An ether solution (7.0 ml) of 2.0 *M* methyl lithium was added to anhydrous tetrahydrofuran (50 ml) in a dry round bottom flask which had been flushed with nitrogen. A solution of 2.0 *M* 2-ethyl-3-methoxy-5-methylpyridine (6.9 ml) was added immediately and the mixture refluxed for 1 h. A deep red color slowly developed in the solution. It was then cooled and 3β-acetoxy-5α-etiojerv-12(13)-en-17-one (**1**) was added as a fine powder until the color faded (800 mg). The mixture was stirred under reflux for a period of 20 min. Saturated ammonium chloride solution (20 ml) was added cautiously while the mixture was still under nitrogen. Ether (50 ml) was added to the reaction mixture and the organic phase washed with water before drying over sodium sulfate. Evaporation of the solvent *in vacuo* gave a pale yellow oil (1.1 g) which appeared primarily as one spot when examined by thin-layer chromatography; (canary yellow spot when the chromatoplate is developed with antimony pentachloride – carbon tetrachloride spray reagent). Column chromatography on alumina (55 g, activity III) eluting with 50% ligroin in benzene removed the unreacted pyridine (**51**). Continued elution with benzene removed the unreacted enone (**1**). The desired condensation product was eluted with 5% chloroform in benzene. Evaporation of the solvent afforded 23-methoxy-22,27-iminojerva-12(13),22,24,27-tetraene-3β,17-diol(s) as a pale yellow oil which crystallized from 5% chloroform in ether (700 mg), m.p. 209–214°. The spectral data indicated that the product is a mixture of two compounds of gross structure, **53**; i.r. (chloroform): 3.05, 6.27 μ; u.v.: λ_{max} (log ε) 283.5 nm (3.86); n.m.r.: 9.22 ($C_{19}CH_3$, 3H, singlet), 8.84, 8.81 ($C_{21}CH_3$, 3H, two overlapping doublets $J_{20,21}$ = 7.0 Hz), 6.24, 6.21 (—OCH_3, 3H, two singlets), 3.10 ($C_{24}H$, 1H, singlet), 2.04 ($C_{27}H$, 1H, singlet); mass spectrometry: *m/e* 421 (M^+), prominent peaks at *m/e* 406 and 288.

*Acetylation of 23-Methoxy-22,27-iminojerva-12(13),22,24,27-tetraene-3β,17-diols (**53**)*

A mixture of acetic anhydride and pyridine (1:1, 5 ml) was added to the condensation product (**53**; 390 mg) obtained in the above experiment and left overnight at room temperature. The solution was then poured into crushed ice and the resultant oil was extracted with ether (3 × 20 ml). The combined ether extracts were washed with saturated sodium bicarbonate solution and several times with water before drying over sodium sulfate. The solvent was distilled off *in vacuo* when a pale yellow semisolid residue (330 mg) was obtained. Thin-layer chromatographic examination of the product revealed the presence of two compounds with very different R_f values. The less polar compound appeared as an orange-yellow spot when the chromatoplate was developed with antimony pentachloride reagent, while the second component appeared as a canary yellow spot. This mixture of acetates was separated by column chromatography on alumina (30 g, activity III). Elution with benzene afforded the less polar compound (designated as compound **F**) in essentially pure state (125 mg). Further elution with 5% chloroform afforded the second component (designated as compound **E**, 191 mg).

An analytical sample of **E** was prepared by crystallization from 5% chloroform in ether whereupon colorless shining prisms were obtained, m.p. 181–182°; i.r.: 3.05, 5.84, 6.25, 6.39 μ; u.v.: λ_{max} (log ε) 284 nm (3.86); n.m.r.: 9.22 ($C_{19}CH_3$, 3H, singlet), 8.82 ($C_{21}CH_3$, 3H, doublet, $J_{20,21}$ = 7.0 Hz), 8.79 ($C_{18}CH_3$, 3H, singlet), 8.0 ($OCOCH_3$, 3H, singlet), 7.7 ($C_{26}CH_3$, 3H, singlet), 6.22 (OCH_3, 3H, singlet), 3.90 ($C_{17}OH$, 1H, broad multiplet, disappears on D_2O addition), 3.08 ($C_{24}H$, 1H, singlet), 2.0 ($C_{27}H$, 1H, singlet); mass spectrometry: *m/e* 463 (*M* − 18), prominent peaks at *m/e* 448, 330, 288, 255, 146.

Anal. Calcd. for $C_{30}H_{41}NO_3$: C, 74.84: H, 8.94. Found: C, 74.65; H, 8.97.

Compound **F**, on the other hand, could not be induced to crystallize. An analytical sample of this material was prepared by subliming a small amount of **B** at 170°/0.2 mm, when a colorless glassy solid was obtained; i.r.: 5.83, 6.27, 6.39 μ; u.v.: λ_{max} (log ε) 283.5 nm (4.03); n.m.r.: 9.08 ($C_{19}CH_3$, 3H, singlet), 8.45 ($C_{21}CH_3$, 3H, doublet, $J_{20,21}$ = 7.0 Hz), 8.0 ($OCOCH_3$, 3H, singlet), 7.7 ($C_{18}CH_3$ and $C_{26}CH_3$, 6H, singlet), 6.3 ($C_{23}OCH_3$, 3H, singlet), 3.05 ($C_{15}H$ and $C_{16}H$, 2H, AB quartet, $J_{15,16}$ = 7.0 Hz), 3.16 ($C_{24}H$, 1H, singlet), 2.0 ($C_{27}H$, 1H, singlet); mass spectrometry: *m/e* 461 (*M* − 20), prominent peaks at *m/e* 461, 446, 432, 298, 150.

Anal. Calcd. for $C_{30}H_{39}NO_3$ (mol. wt. 461.293): C, 78.09; H, 8.45. Found (high resolution mass measurement, 461.291): C, 77.78; H, 8.47.

*3β-Acetoxy-23-methoxy-22,27-iminojerv-12(13),14(15),16(17),22,24,27-hexaene: Compound **G** (**57**)*

Compound **E** (**54**; 150 g) was thoroughly ground with 10% palladized charcoal (37 mg) until a homogeneous powder was obtained. This powder was heated at 200° under nitrogen for 7 min and the resultant solid residue washed several times with chloroform. Thin-layer chromatography of the chloroform extract indicated that the product contained three major components and these were separated on preparative layer plates (20 × 20 cm, 0.4 mm, chloroform). One of these three components was shown to be 2-ethyl-3-methoxy-5-methylpyridine (**51**) by n.m.r. The second band on extraction yielded a light oil which crystallized from acetone – petroleum ether as needles, m.p. 167°. This compound was identified as 3β-acetoxy-5α-etiojerv-12(13)-en-17-one (**1**) by its u.v. spectrum and mixture m.p. with an authentic sample. The third component which appeared as a light orange yellow spot when the chromatoplate was developed with antimony pentachloride – carbon tetrachloride reagent was extracted to yield a light oil which could not be induced to crystallize. An analytical sample of this compound, designated as compound **G** was obtained as a clear glass after distillation at 170°/0.1 mm; i.r.: 5.84, 6.27, 6.39 μ; u.v.: λ_{max} (log ε) 283.5 nm (4.04); n.m.r.: 9.07 ($C_{19}CH_3$, 3H, singlet), 8.4 ($C_{21}CH_3$, doublet, $J_{20,21}$ = 7.0 Hz), 8.0 ($OCOCH_3$, 3H, singlet), 7.74 ($C_{18}CH_3$ and $C_{26}CH_3$, 6H, singlet), 6.3 (OCH_3, 3H, singlet), 3.1 ($C_{15}H$ and $C_{16}H$, AB quartet, $J_{15,16}$ = 8.0 Hz), 3.18 ($C_{24}H$, 1H, singlet), 2.02 ($C_{27}H$, 1H, singlet); mass spectrometry: *m/e* 461 (M^+), prominent peaks at *m/e* 461, 446, 432, 298, 150.

Anal. Calcd. for $C_{30}H_{39}O_3$ (mol. wt. 461.293): C,

78.09; H, 8.45. Found (high resolution mass measurement, 461.293): C, 77.80; H, 8.46.

5α,6-Dihydroveratramine (56)

A solution of compound **F** (45 mg) in 95% ethanol (10 ml) containing 2% 12 *N* hydrochloric acid was stirred with Adams' catalyst (PtO_2, 20 mg) at 20° for 18 h. The mixture was filtered to remove the catalyst which was carefully washed with additional ethanol (5 ml). The combined extracts were neutralized with sodium bicarbonate solution and then reduced in volume to 2 ml *in vacuo*. It was diluted with water and extracted with chloroform (3 × 10 ml) before drying over sodium sulfate. Thin-layer chromatography on silica gel G (6% methanol in chloroform) revealed the presence of three major compounds. The two less polar components had similar R_f values, while the third compound had an R_f value identical with that of 5α,6-dihydroveratramine. Besides these three compounds, there were several other compounds present in the product mixture in trace amounts. The three major components were separated by thick-layer chromatography on neutral alumina (20 × 20 cm, 0.4 mm, 3% methanol in chloroform, plates developed three times). Extraction of the bands followed by the usual work-up afforded the two less polar compounds as pale yellow oils. The third compound, with an R_f value corresponding to that of 5α,6-dihydroveratramine, was obtained crystalline from 5% methanol in chloroform as colorless fluffy crystals (8 mg), m.p. 198°. This material was characterized as 5α,6-dihydroveratramine; undepressed m.p. (197–198°) and identical i.r., n.m.r., and mass spectra with an authentic sample.

The two less polar components obtained (17 and 13 mg, respectively) were found to be very unstable and hence no detailed investigation of these were carried out. A preliminary examination of the n.m.r. spectra revealed that the pyridine ring was only partially reduced in both the compounds (signals at 3.8 and 4.2) while the 23-methoxyl group was intact (signal at 6.3).

Financial aid from the National Research Council of Canada and Smith Miller and Patch, Inc., is gratefully acknowledged. Two of us (J. C. and G. V. N.) would like to thank the University of British Columbia for University Graduate Scholarships during the period of this study.

1. T. MASAMUNE, I. YAMAZAKI, and M. TAKASUGI. Bull. Chem. Soc. Jap. **39**, 1090 (1966).
2. S. M. KUPCHAN and M. E. SUFFNESS. J. Am. Chem. Soc. **90**, 2730 (1968).
3. Y. MAZUR, N. DANIELI, and F. SONDHEIMER. J. Am. Chem. Soc. **82**, 5889, (1960).
4. W. A. JACOBS and L. C. CRAIG. J. Biol. Chem. **124**, 659 (1938).
5. R. L. AUGUSTINE. Catalytic hydrogenation – techniques and applications in organic synthesis. Marcel Dekker Inc., New York. 1965. p. 104.
6. J. TOMKO and S. BAUER. Coll. Czech. Chem. Commun. **29**, 2570 (1964).
7. K. SAITO. Bull. Chem. Soc. Jap. **15**, 22 (1940).
8. T. MASAMUNE, N. SATO, K. KOBAYASHI, I. YAMAZAKI, and Y. MORI. Tetrahedron, **23**, 1591 (1967).
9. N. S. BHACCA and D. H. WILLIAMS. Application of NMR spectroscopy in organic chemistry. Holden-Day, San Francisco. 1964. p. 14.
10. T. MASAMUNE, K. KOBAYASHI, M. TAKASUGI, Y. MORI, and A. MURAI. Tetrahedron, **24**, 3461 (1968).
11. H. BUDZIKIEWICZ. Tetrahedron, **20**, 2267 (1964).
12. R. M. EVANS, J. C. HAMLET, J. S. HUNT, P. G. JONES, A. G. LONG, J. F. OUGHTON, L. STEPHENSON, T. WALKER, and B. M. WILSON. J. Chem. Soc. 4356 (1956).
13. W. S. JOHNSON, H. A. P. DE JONGH, C. E. COVERDALE, J. W. SCOTT, and U. BURCKHARDT. J. Am. Chem. Soc. **89**, 4523 (1967).
14. T. MASAMUNE, M. TAKASUGI, A. MURAI, and K. KOBAYASHI. J. Am. Chem. Soc. **89**, 4521 (1967).
15. S. M. KUPCHAN and M. I. SUFFNESS. J. Am. Chem. Soc. **90**, 2730 (1968).
16. B. M. ISELIN, M. MOORE, and O. WINTERSTEINER. J. Am. Chem. Soc. **78**, 403 (1956).
17. T. MASAMUNE, Y. MORI, M. TAKASUGI, A. MURAI, S. OUCHI, N. SATO, and N. KATSUI. Bull. Chem. Soc. Jap. **38**, 1374 (1965).
18. W. GRUBER. Can. J. Chem. **31**, 564 (1953).
19. A. P. DUNLOP and F. N. PETERS. The furans. Reinhold, New York. 1953.
20. P. BOSSHARD and C. H. EUGSTER. *In* Advances in heterocyclic chemistry. Vol. 7. *Edited by* A. R. Katritzky and A. J. Boulton. Academic Press, New York. 1966. p. 377.
21. L. A. PAQUETTE. Principles of modern heterocyclic chemistry. W. A. Benjamin, New York. 1968. p. 124.
22. J. W. CORNFORTH. J. Chem. Soc. 1310 (1958).
23. J. W. CORNFORTH and M. FIRTH. J. Chem. Soc. 1098 (1958).
24. J. P. KUTNEY, H. W. HANSSEN, and G. V. NAIR. Tetrahedron, **27**, 3323 (1971).
25. D. M. BURNESS. *In* Organic syntheses. Vol. 39. *Edited by* M. Tishler. John Wiley and Sons, Inc., New York. 1959. p. 49.
26. J. P. KUTNEY, A. BY, J. CABLE, W. A. F. GLADSTONE, T. INABA, S. Y. LEONG, P. ROLLER, E. J. TORUPKA, and W. D. G. WARNOCK. Can. J. Chem. This issue.
27. J. P. KUTNEY, J. CABLE, W. A. F. GLADSTONE, H. W. HANSSEN, E. J. TORUPKA, and W. D. C. WARNOCK. J. Am. Chem. Soc. **90**, 5333 (1968); Chem. Rep. 4, 265 (1970).

Can. J. Chem. Downloaded from www.nrcresearchpress.com by 210.87.254.5 on 09/05/12
For personal use only.

The 7-Cycloheptatrienylmethyl/7-Norcaradienylmethyl Cation System[1]

IVAN PIKULIK AND RONALD F. CHILDS[2]
Department of Chemistry, McMaster University, Hamilton, Ontario L8S 4M1
Received November 11, 1974

IVAN PIKULIK and RONALD F. CHILDS. Can. J. Chem. 53, 1818 (1975).

Reaction of 7-carbomethoxycycloheptatriene with either BCl_3 or BBr_3 gave a 1:1 complex in which the Lewis acid was complexed to the carbonyl oxygen. The low temperature p.m.r. and u.v. spectra of these zwitterions indicated that they existed almost entirely in the norcaradiene forms **10** and **14**, respectively. In contrast, reaction of *N,N*-dimethyl-1,3,5-cycloheptatriene-7-carboxamide with BCl_3 was found to result in the formation of a mixture of the cycloheptatriene **12** (65%) and norcaradiene **13** (35%). Comparison of the chemical shifts of the cyclopropyl proton resonances of **10** and **14** with model compounds showed that their positions were anomolous, the C_7 protons resonating at much higher and the C_1 and C_6 protons resonating at much lower field than expected and to account for this it is suggested that these norcaradienes are aromatic systems. Both **10** and **14** were thermally unstable and underwent an irreversible rearrangement to form the complex of methyl phenylacetate, the phenylmethylacylium cation and the appropriate counterion, $CH_3O\bar{B}Cl_3$ or $CH_3O\bar{B}Br_3$, respectively. The rate of these rearrangements and the product distribution was found to be dependent upon both the ratio of Lewis acid to ester used and the nature of the Lewis acid.

IVAN PIKULIK et RONALD F. CHILDS. Can. J. Chem. 53, 1818 (1975).

La réaction du carbométhoxy-7 cycloheptatriène avec soit le BCl_3 soit le BBr_3 donne un complexe 1:1 dans lequel l'acide de Lewis est complexé à l'oxygène du carbonyle. Les spectres r.m.n. et u.v. à basse température de ces ions hermaphrodites indiquent qu'ils existent presque entièrement dans les formes respectives **10** et **14** du norcaradiène. Par opposition avec ces résultats, la réaction de la *N,N*-diméthylcycloheptatriène-1,3,5 carboxamide-7 avec BCl_3 conduit à la formation d'un mélange de cycloheptatriène **12** (65%) et de norcaradiène **13** (35%). La comparaison des déplacements chimiques des résonances des protons du cyclopropyle de **10** et **14** avec ceux de composés modèles montrent que leurs positions sont anormales; les protons C_7 présentent une résonance à des champs beaucoup plus haut et les protons en C_1 et C_6 présentent des résonances à des champs beaucoup plus bas que ceux attendus et pour tenir compte de ces résultats, on suggère que ces norcaradiènes sont des systèmes aromatiques. Les composés **10** et **14** sont thermiquement instables et subissent des réarrangements irréversibles pour former respectivement le complexe du phénylacétate de méthyle, le cation phénylméthylacylium et l'ion antagoniste approprié $CH_3O\bar{B}Cl_3$ ou $CH_3O\bar{B}Br_3$. On a trouvé que les vitesses de ces réarrangements et la distribution des produits dépendent à la fois du rapport d'acide de Lewis l'ester utilisé et de la nature de l'acide de Lewis. [Traduit par le journal]

Just as the monocyclic $(CH)_n^+$ cations, such as the cyclopropenium (1), cyclopentadienyl (2), and tropylium (3) cations, have been important in the development of the concept of aromaticity, so their monohomo counterparts, **1**, **2**, and **3**, have been of consequence in the evolution of the concepts of homoaromaticity (4). More recently, following the observation of a degenerate circumambulation of the cyclopropane around the periphery of the five-membered ring of **2** and its derivatives (5), cations **1**, **2**, and **3** have taken on a new significance in terms of the importance of orbital symmetry control of a molecular rearrangement. The degenerate rearrangement exhibited by **2**, which can be regarded as a 1,4 sigmatropic shift, takes place with a very high stereoselectivity in just that mode demanded by the dictates of orbital symmetry (6). The transition state for the rearrangement can be regarded as the cyclopentadienylmethyl cation **4**, in which, despite the overlap of the formally vacant p orbital on C_6 with the diene unit, a substantial fraction of the positive charge is localized on this carbon (5).

While comparable rearrangements of **1** and **3** have been considered from a theoretical viewpoint, as yet they have not been detected experimentally (7, 8). For example, with **3** and its

[1]Presented in part at the 57th Canadian Chemical Conference of the Chemical Institute of Canada, June, 1974, Abstract 145.

[2]Author to whom correspondence should be addressed.

Can. J. Chem. Downloaded from www.nrcresearchpress.com by 210.87.254.42 on 09/05/12
For personal use only.

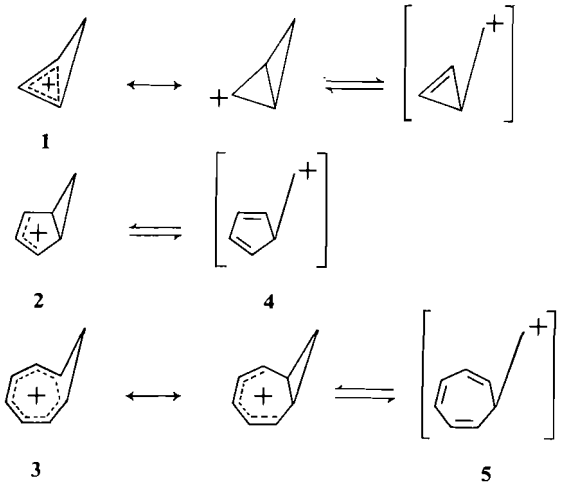

derivatives, competing reactions such as ring contraction or decomposition set in before the onset of any degenerate rearrangement. By analogy with the circumambulatory isomerization of **2**, a cycloheptatrienyl cation might well be expected to be involved in a degenerate rearrangement of **3**. However, as yet no consideration has been given to the importance of the structure and properties of a cation such as **5** in determining the possible occurrence of a degenerate isomerization of a homotropylium cation.

Information about the cycloheptatrienylcarbinyl cation, available at the outset of this work, derived very largely from the results of a solvolytic study of **6** reported by Sargent *et al.* (9), and a number of others (10).[3] It was suggested by Sargent that the cation involved in this solvolysis was **7** rather than **5** and that no products derived from the homotropylium cation, which could have been formed by rearrangement of **5**, could be detected. Factors affecting the position of the equilibrium between cycloheptatriene and norcaradiene valence tautomers, such as **5** and **7**, have recently been considered by both Hoffmann (11) and Günther (12) and it was pointed out that a carbonium ion center attached to C_7 should very effectively stabilize the bicyclic form.

To examine the question of the structure of **5** and whether degenerate migrations of C_8 of a homotropylium cation can occur or not, we have attempted the preparation of some 7-cycloheptatrienylmethyl cations. As previously it had been shown to be possible to prepare derivatives of **4** by reaction of a 5-acylcyclopentadiene with strong Lewis acids (12), the extension of these techniques to cycloheptatriene derivatives has been investigated. We report here on the preparation of derivatives of **5** and **7**, on the role of the C_7 substituents in determining the equilibrium position, on the thermal rearrangement of these cations, and on the possible aromatic nature of **7**. Recently in a series of papers Betz and Daub (14) have reported the preparation of some differently substituted derivatives of these cations and in some respects our results parallel their findings.

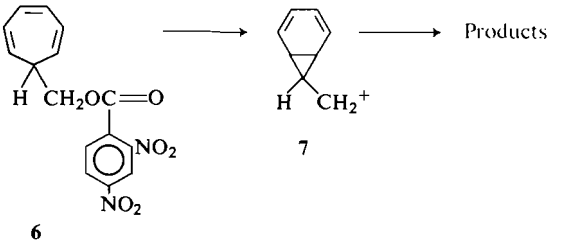

6 7

Results and Discussion

Treatment of a CD_2Cl_2 solution of 7-carbomethoxycycloheptatriene, **8**, with BCl_3 in CD_2Cl_2 at $-60°$ resulted in the quantitative formation of a 1:1 complex of the ester and Lewis acid. The low temperature p.m.r. spectrum of the complex was independent of the ratio of the Lewis acid to ester used provided that there was at least a molar equivalent of the acid present. The complex was found to be stable at low temperatures and could be reacted with dimethylamine to regenerate **8** in high yield.

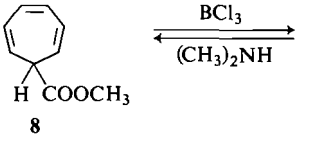

8

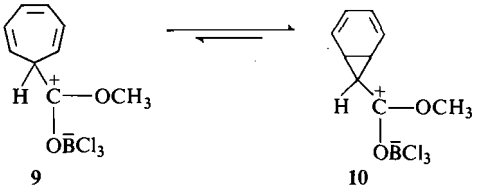

9 10

[3]The acetolysis of (7-cycloheptatrienyl)methyl tosylate at 24° proceeds with a first-order rate constant of 5.2 ± 0.1 s^{-1}. The only product detected was styrene (>93% recovery). (Unpublished results of R. F. Childs and S. Winstein, University of California at Los Angeles, 1968.)

Can. J. Chem. Downloaded from www.nrcresearchpress.com by 210.87.254.42 on 09/05/12
For personal use only.

TABLE 1. Proton chemical shifts of cycloheptatrienes and zwitterions

Compound	Temperature (°C)	Proton chemical shifts* H_1/H_6	H_2/H_5	H_3/H_4	H_7	Other
8	37	5.43	6.24	6.63	2.48	3.72
10	−40	3.41	6.14–6.54	6.14–6.54	1.60	4.14
14	−40	3.48	6.2–6.6	6.2–6.6	1.65	4.14
11	37	5.46	6.25	6.68	2.40	2.85, 2.95
12 + **13**	−40	4.81	6.35	6.52	3.20	3.43
15†	37	5.78	5.78	1.98–2.52	4.23	3.69
16†	−40	5.58	6.13	2.37	5.31	4.28

*In p.p.m. from TMS using $CHCl_3$ (taken as 7.30) as a secondary standard for the solutions of the zwitterions.
†Numbering schemes of cycloheptatriene maintained so as to facilitate comparison (ester grouping is then assumed to be attached to C_7).

The p.m.r. spectrum of the complex (Table 1 and Fig. 1) was completely consistent with the formation of a zwitterion in which the Lewis acid has reacted with the carbonyl oxygen of the ester. For example, the resonance attributable to the methoxy group is deshielded by the appropriate amount on reaction with BCl_3 and the signals due to the ring protons retain their plane of symmetry. It is also clear from the resonance position of the ring protons that the complex cannot be simply regarded as having the structure **9** but must be very largely in the norcaradiene form **10**. Thus the signals of the hydrogens in C_1, C_6, and C_7 all occur at considerably higher field than those of **8** and appear in similar regions to those encountered for other norcaradienes (14, 15).

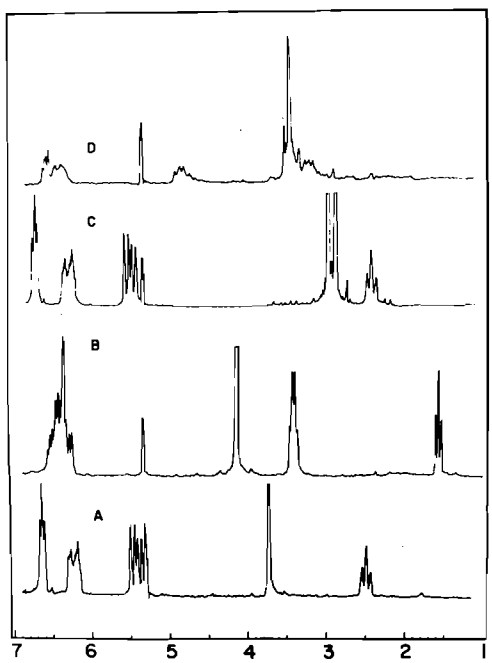

FIG. 1. Proton magnetic resonance spectra of cycloheptatrienes and their BCl_3 complexes in CD_2Cl_2. 7-Carbomethoxycycloheptatriene, **8**, spectrum *A*, and its BCl_3 complex **10**, spectrum *B*. *N*,*N*-Dimethylcycloheptatriene-7-carboxamide, **11**, spectrum *C*, and its BCl_3 complexes **12** and **13**, spectrum *D*. (Resonance at 5.38 due to $CHDCl_2$.)

Ciganek (16) has shown the rate of interconversion of a substituted cycloheptatriene and norcaradiene to be slow enough at −110° to enable them to be observed as separate species by p.m.r. No additional p.m.r. signals could be detected when a CD_2Cl_2/CF_2ClH solution of the complex was cooled to −135°, indicating that the zwitterion exists predominantly in one form.

The low temperature u.v. spectrum of the complex in CH_2Cl_2 exhibited a single, fairly intense band at λ_{max} 284 (log ε 4.3). The position of this absorption is again indicative of the structure of the zwitterion being **10**, the absorption being at too long a wavelength to be attributable to a structure such as **9**.

Formally, two stereoisomers of **10** are possible in which the C_7 substituent can be either in the *exo* or *endo* position, **10***a*, and **10***b*, respectively. From the n.m.r. spectrum obtained, it is clear that only one of these two isomers is present. Comparison of the magnitude of the coupling constant between the protons on C_7 and C_1/C_6 (J = 3.1 Hz) with that reported for other cyclopropylcarbinyl cations, would indicate that the isomer formed is **10***a* (17). Stohrer and Daub have found a similar preference for the formation of the *exo* isomer and this has been attributed to unfavorable secondary interactions in the *endo* isomer, **10***b*, between the p orbital on C_7 and the diene molecular orbitals (18).

Can. J. Chem. Downloaded from www.nrcresearchpress.com by 210.87.254.42 on 09/05/12
For personal use only.

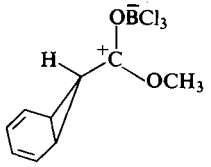

10*a*

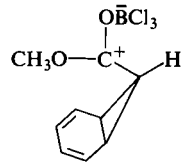

10*b*

The dimethylamide **11** when reacted with BCl_3 in CD_2Cl_2, gave a zwitterion with a p.m.r. spectrum at $-40°$ that indicated complexation had occurred with the carbonyl oxygen (19). However, the chemical shifts of the ring proton resonances (Table 1, Fig. 1) were now intermediate between those observed for **10** and **11**. It would appear that both **12** and **13** are being produced on reaction of **11** with BCl_3 and that these valence tautomers are interconverting sufficiently rapidly at $-40°$ for their p.m.r. spectra to be averaged. The low solubility of these amide complexes prevented p.m.r. spectra from being obtained at sufficiently low temperatures to stop this interconversion. Reaction of **12** and **13** with dimethylamine regenerated **11** in high yield.

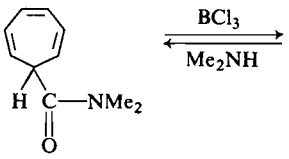

11

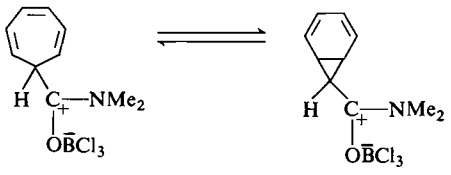

12 13

As a dimethylamino group is known to be more effective at stabilizing a positive charge than is a methoxy group (20), it would appear that the position of the equilibrium between the norcaradiene and cycloheptatriene forms of these zwitterions is dependent on the electron deficiency of C_8. The more electron deficient C_8 becomes, the greater is the amount of norcaradiene present.

Confirmation that the complex derived from **8** existed almost entirely in the norcaradiene form **10** was obtained by reaction of **8** with BBr_3. The zwitterion so obtained, which was stable at low temperatures and could be reacted with dimethylamine to give back **8**, exhibited a p.m.r spectrum that was directly comparable to that of **10**, suggesting that its structure can be regarded as **14**. Complexation of the oxygen atom of a carbonyl group with BBr_3 results in the accumulation of a larger fraction of the positive charge on the carbon atom of the group than similar BCl_3 complexes (13, 21). Thus replacement of the BCl_3 in the complexes derived from **8** by BBr_3 would be expected to result in an increase in the amount of norcaradiene present and unless the equilibrium mixture of **9** and **10** was almost completely in favor of **10** with BCl_3, a net upfield shift of C_1/C_6 and C_7 protons would occur. As no such change was observed (Table 1) it is clear that the complexes of **8** with both BCl_3 and BBr_3 must exist almost completely in the norcaradiene forms **10** and **14**, respectively.

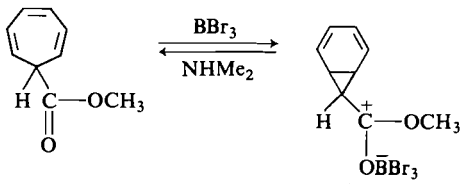

8 14

To evaluate the position of the equilibrium between **12** and **13**, it is necessary to know the resonance positions of the signals of some of the protons in unaveraged spectra of **12** and **13**. An estimate for the position of the C_7 and C_1/C_6 proton resonances of **12** can be obtained by adding to the values found for the corresponding protons of the uncomplexed cycloheptatriene, the appropriate changes in chemical shifts observed on complexation of the model compound **15**.[4] As the zwitterion formed from reaction of **8** with BCl_3 has been shown to be in the norcaradiene form, the resonance positions of the C_1/C_6 and C_7 protons of **13** were taken to be those observed for **10**. On this basis the amount of norcaradiene **13** present in the equilibrium mixture of **12** and **13** was found to be 35%.

[4]Compound **15** was prepared by the addition of 4-phenyl-1,2,4-triazoline-3,5-dione to 7-carbomethoxycycloheptatriene, reduction of the so formed adduct with H_2/Pd and subsequent hydrolysis, oxidation, nitrogen elimination, and esterification. Experimental details will be given in a forthcoming full paper.

Can. J. Chem. Downloaded from www.nrcresearchpress.com by 210.87.254.42 on 09/05/12
For personal use only.

Can. J. Chem. Downloaded from www.nrcresearchpress.com by 210.87.254.42 on 09/05/12
For personal use only.

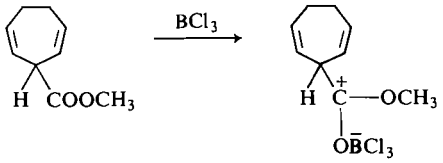

15 16

The Structure of Norcaradienes 10 and 14

It is instructive to compare the position of the C_7 and C_1/C_6 proton resonances of **10** and **14** with that generally encountered for the comparable protons of cyclopropylcarbinyl cations. Frequently, the ring proton resonances of a protonated cyclopropyl ketone or carboxylic ester are observed as overlapping multiplets; however, typically the range over which the α-proton resonates is at lower field than that of the β-protons. For example the α-proton signal is usually found in the range 1.9 to 3.4 p.p.m. whereas the β-proton signal is found between 1.75 and 2.40 p.p.m. (25). This is quite the reverse of the situation encountered with the cyclopropyl proton resonances of **10** and **14**, in which the signal attributable to the α-proton is found to be more than 1.8 p.p.m. upfield from that of the β-protons. To ensure that these seemingly anomolous positions of the proton resonances of **10** (and **14**) cannot be attributed to the use of a boron halide rather than proton to induce the positive charge, complexes of some model cyclopropylcarbonyl compounds were prepared.

Reaction of the cyclopropyl ester **17** with BCl_3 in CD_2Cl_2 gave the zwitterion **18**. The p.m.r. spectrum of **18** exhibited a single, sharp, three proton resonance at 4.10 δ, a four proton signal at 1.65 δ, and a single proton resonance at 2.76 δ which is similar to that encountered for comparable protonated species and is quite different from that of **10** (17).

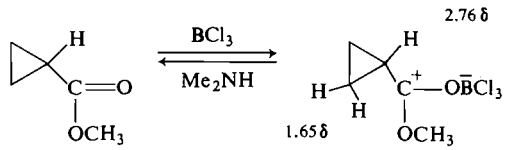

17 18

As the cyclopropane of **10** bears vinyl substituents, perhaps a better model for the expected chemical shifts of the protons is provided by the zwitterion **19**. This complex, which was readily formed by reaction **20** (22) with BCl_3 in CD_2Cl_2, was stable at temperatures below 0° and gave back **20** on reaction with dimethylamine. The p.m.r. spectrum of the complex was consistent with its structure being that shown for **19**. The cyclopropyl proton resonances of **19** occurred as an overlapping multiplet in the range 2.56 to 2.83 δ and individual α- and β-proton resonances could not be assigned. However, it is apparent that the vinyl groups on the β-carbons do deshield the β-protons to some extent.

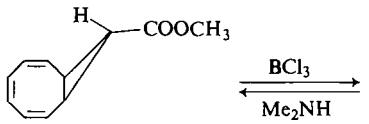

20

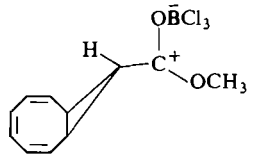

19

While neither **18** nor **19** is a perfect model for **10**, they do suggest that the position of the cyclopropyl proton resonances of **10** cannot be adequately described by the effect of the adjacent positively charged group. Clearly the six-membered ring of **10** must be influencing the cyclopropyl protons in some different way to the effect of the eight-membered ring of **19**. The complexes **10** and **19** differ in two respects. Firstly the geometry of these two systems is expected to be different, the six-membered ring of **10** being almost flat (23) while the eight-membered ring of **19** would be expected to exist preferentially in a tub conformation with the cyclopropane ring being in a pseudo-equatorial position. Secondly, **10** and **19** differ in the number of π electrons in the unsaturated ring.

A major consequence of the first factor is that the cyclopropyl protons of **10** could be affected by the diamagnetic anisotropy of the carbon–carbon double bonds (24). However using the

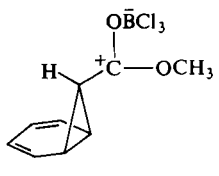

10

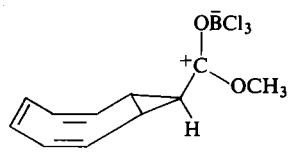

19

Can. J. Chem. Downloaded from www.nrcresearchpress.com by 210.87.254.42 on 09/05/12
For personal use only.

values of either Tillieu (25) or Pople (26) for the long range shielding of a double bond, the effect on the C_7 proton is found to be very small. With the data of Tillieu, the C_7 proton was found to be shielded by less than 0.1 p.p.m. and with that of Pople a deshielding of 0.1 p.p.m. was estimated. In either case the effect is very much smaller than the observed *ca.* 1 p.p.m. upfield shift of the resonance of this proton as compared to the corresponding proton of **19**. Similarly, the downfield position of the C_1/C_6 proton signals cannot be accounted for on this basis.

Both Hoffmann (11) and Günther (12) have suggested a way in which an electron withdrawing substituent on C_7 of a cycloheptatriene can affect the equilibrium between this and its norcaradiene valence tautomer. In essence, the lowest unoccupied molecular orbital of a π electron withdrawing substituent, and a carbonium ion is such a group 'par excellence', can interact with the antisymmetric, highest occupied Walsh molecular orbital of the cyclopropane ring of a norcaradiene, resulting in electron transfer from the three membered ring to its substituent. The net effect is that the C_1/C_6 antibonding component is weakened and this bond should become stronger.

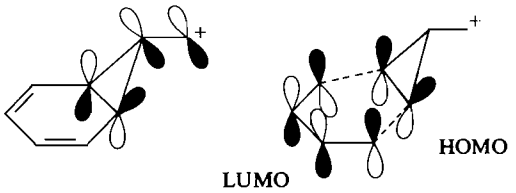

The remaining symmetric Walsh orbital of the cyclopropane, which is bonding between C_1 and C_6 and contains two electrons, has the correct symmetry to interact with the lowest unoccupied orbital of the diene component of the norcaradiene (27). Moreover, the symmetry of the highest occupied molecular orbital of the diene is the same as the antisymmetric Walsh orbital from which electron transfer to the C_7 substituent has occurred. Such interactions should lead to a net stabilization of the norcaradiene structure.

It is of importance to note that this involvement of the diene with the cyclopropane results in an aromatic system. Viewed from the Hückel–Möbius viewpoint, in these norcaradienes there are formally six electrons contained in a Hückel array of atomic p orbitals (8, 28). One result of this should be that in a magnetic field, a diamagnetic ring current should be induced which would shield the *endo* C_7 proton and deshield the C_1 and C_6 bridgehead protons, *just as is observed with both* ***10*** *and* ***14*** (4).

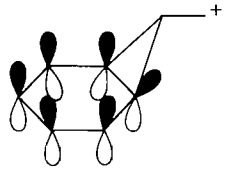

Hückel array: 6π electrons, aromatic.

We would suggest then that the norcaradienes **10** and **14** can be regarded as homoaromatic molecules and that to some degree such cyclic delocalization is required to account for their p.m.r. spectra. It is interesting that Sargent *et al.* (9) in their initial communication recognized that formulating the cyclopropylcarbinyl portion of these cations in the usual way imparted partial benzenoid character to the norcaradiene six-membered ring.

Thermal Rearrangement of Zwitterions

While the norcaradiene complexes were stable at low temperatures, on heating they underwent a ring contraction to give benzenoid compounds. Thus **10** at temperatures above 0° gave three products, one of which was identified as the methyl phenylacetate complex **21** by its p.m.r. spectrum (resonances at 4.19, 4.62, and 7.4 δ) and by the recovery of **22** when the solution containing the rearranged product was reacted with dimethylamine. Reaction of **22** with BCl_3 in CD_2Cl_2 gave **21**, with a p.m.r. spectrum identical to that obtained by the rearrangement of **10**.

The p.m.r. spectrum of the rearrangement products of **10** contained resonances over and above those attributable to **21** (Table 2). In particular, signals at 3.87, 4.16 δ and part of the multiplet of aromatic protons remained to be accounted for. Reaction of a solution of the rearranged products with ethanol gave rise to two esters which were isolated and characterized as **22** and the ethyl ester **23**. On this basis and by comparison with the results obtained with the BBr_3 complexes (*vide infra*), it is suggested that the additional products formed on the rearrangement of **10** are the acylium cation **24** and its counterion **25**. The methyl resonance of **25** occurs in a very similar region to that of the BCl_3 complex of methanol (3.95 δ). Comparable

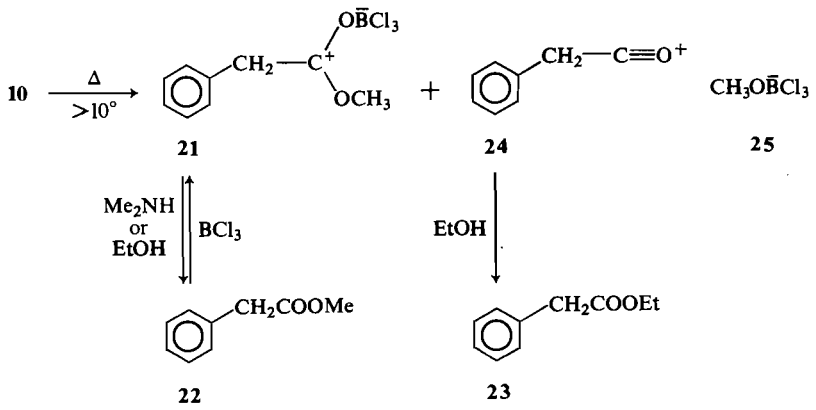

anions to **25** involving BF_3 have been described (29).

While the formation of acylium cations from protonated carboxylic acid derivatives is well known (30), in this case **24** is not being formed directly from **21**. On heating a solution of **21**, prepared by reacting **22** with BCl_3, at 50° for 1 h, no formation of **24** and **25** could be detected by p.m.r. Thus **21**, **24**, and **25** must be primary products of the rearrangement of **10**.

The rate of rearrangement of **10** and the distribution of products was found to be dependent on the ratio of the Lewis acid to ester used. Increase in the ratio of BCl_3 to **8** resulted both in an increase in the rate of rearrangement of **10** and also an increase in the amount of the acylium cation **24**, formed (Tables 3 and 4).

A possible reaction sequence which can account for these observations is shown in Scheme 1. In its simplest form the cyclobutyl cation **26**, which can be considered to be in equilibrium with **10** (31), undergoes a 1,2 hydride shift to give **27**. This hydride shift could well be the slow step in the rearrangement for two reasons. Firstly, the free energy difference between **26** and **27** might not be all that great in that the hexadienyl cation in **27** is forced to be twisted by the fused cyclobutane ring. Secondly, the rigidity of the system makes it difficult for the appropriate geometry for this hydride shift to be attained (32). Comparable cyclobutyl cations have been suggested to be involved in the ring contraction reactions of certain homotropylium cations (33).

In the cyclobutyl cation **26**, the positive charge has been formally removed from the oxygen atoms and further reaction of the ether oxygen with additional BCl_3 could take place. The extra positive charge so induced in the system could result in an enhancement of the rate of the 1,2 hydride shift to give **28**, which could then give the acylium ion **24** or complex **21** as indicated. Comparable ring openings of

TABLE 2. Proton chemical shift data of norcaradiene rearrangement products

Product	Chemical shift*		
	ArH	CH_2	OCH_3
21	7.2–7.6	4.71	4.30
30	7.2–7.6	4.75	4.48
24 + **25**	7.2–7.6	4.16	3.87
24 + $CH_3O\bar{B}Br_3$	7.2–7.6	4.27	3.96

*In p.p.m. from TMS using $CHCl_3$ as internal standard.

TABLE 3. Rate constants for rearrangement of norcaradiene complexes*

Complex	Ester to Lewis acid ratio	k (s^{-1})	Temperature (°C)
10	1:1.1	4.6×10^{-5}	0
10	1:10	$>2.8\times10^{-4}$	0
14	1:2	2.7×10^{-4}	−43

*Rate constants obtained by following the reaction by p.m.r.

TABLE 4. Products of rearrangement of **10**

Ester to Lewis acid ratio	Temperature (°C)	Products*	
		%**21**	%**24**
1:0.9	20	93	7
1:2	20	77	23
1:8	20	42	58

*Product composition determined by integration of p.m.r. spectra.

Can. J. Chem. Downloaded from www.nrcresearchpress.com by 210.87.254.42 on 09/05/12
For personal use only.

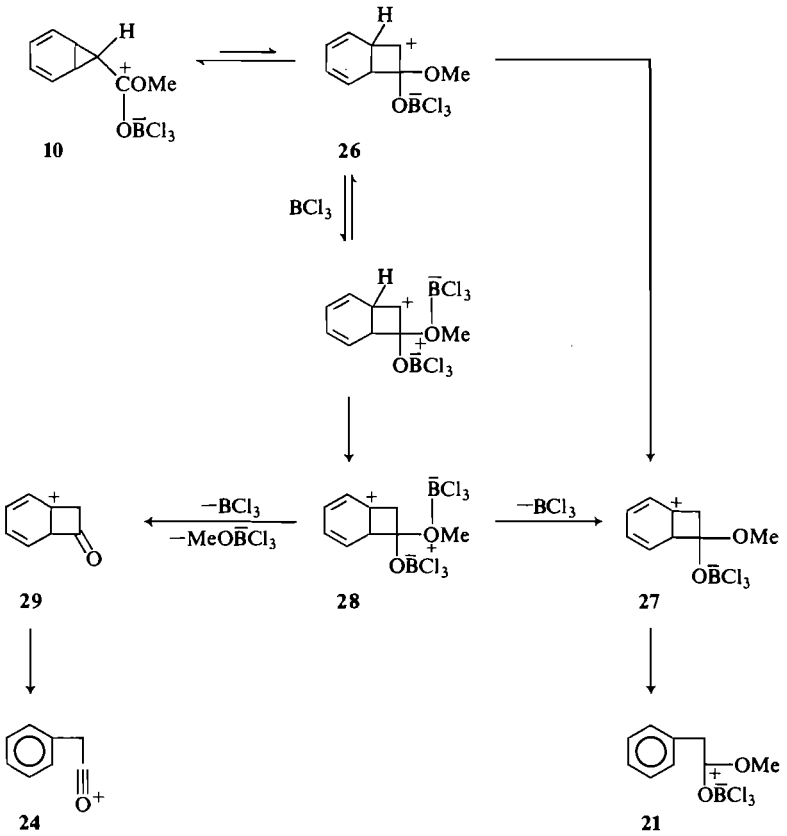

SCHEME 1

cyclobutanone cations such as **29** have been reported (34).

The BBr_3 complex **14** rearranged in an analogous manner to that described for **10** to give the BBr_3 complex of methylphenylacetate, **30**, **24** and $MeO\bar{B}Br_3$, however in this case, **30** was slowly converted into **24** and its counterion under the isomerization conditions. The formation of the acylium cation on rearrangement of **14** was confirmed by examination of its i.r. spectrum when an absorption at 2270 cm^{-1} was found. Acylium cations typically exhibit a carbonyl absorption in this region, the phenylmethylacylium cation with a SbF_6^- counterion being reported to absorb at 2279 cm^{-1} (30). The temperature at which this rearrangement of **14** occurred was found to be much lower than that required for **10**. With a two-fold excess of BBr_3, **14** rearranged at $-43°$ with a half-life of 40 min. The amide complex mixture of **12** and **13** did not rearrange until heated to above $+20°$, the BCl_3 adduct of *N*,*N*-dimethylphenylacetamide being the major product. Clearly, both the amount of norcaradiene present in these tautomeric mixtures and also the ease of their rearrangement to aromatic systems are directly related to the ability of the C_8 substituents to stabilize the positive charge.

The existence of these complexes almost entirely in the norcaradiene form does not necessarily preclude the migration of C_8 around the periphery of the system. This could either occur in the norcaradiene form in a comparable manner to that found by Berson *et al.* for related systems (35) or by intervention of a homotropylium cation species as outlined at the start of this paper. However, at the temperatures at which the thermal ring contraction reaction occurred, no line broadening could be detected in the p.m.r. spectra of either **10** or **14**, indicating that no degenerate rearrangement was occurring at those temperatures with a sufficiently high rate to cause averaging of the p.m.r. signals.

Based on the characteristics of the analogous migrations observed with derivatives of **4** (13), one way to lower the energy barrier for the

Can. J. Chem. Downloaded from www.nrcresearchpress.com by 210.87.254.42 on 09/05/12
For personal use only.

Can. J. Chem. Downloaded from www.nrcresearchpress.com by 210.87.254.42 on 09/05/12
For personal use only.

degenerate rearrangement of these norcaradienyl/cycloheptatrienyl methyl cations would be to decrease the ability of the C_8 substituents to stabilize positive charge. However, as has been shown, this would also result in an increase in the rate of the collapse of these cations to benzenoid systems. Indeed, in the limit, it is known that the rearrangement of the unsubstituted ion **7** to styrene under acetolysis conditions is sufficiently rapid to completely exclude either collapse of **7** with solvent to give cycloheptatriene derivatives or formation of the homotropylium ion and its subsequent products.[3] We are then in a dilemma, as changes made with these systems intended to enhance the rate of the degenerate migration, also increase the rate of their collapse to benzene derivatives and it would appear that we are unlikely to be able to devise a system in which the degenerate rearrangement can compete with this facile ring contraction. Taking this further, it would also seem that the production of a cycloheptatrienylmethyl cation as the first step of a degenerate rearrangement of a homotropylium cation would lead irreversibly to a benzenoid cation and not to the regeneration of the homotropylium cation. Perhaps, indeed, the often encountered ring contraction reactions of homotropylium cations involve just such a pathway.

Experimental

Proton magnetic resonance spectra were recorded on a Varian HA-100 spectrometer fitted with a variable temperature probe controlled by a Varian V-6040 temperature controller. The probe temperature was measured with a copper–constantan thermocouple and Leeds and Northrup 8692 potentiometer. The thermocouple was mounted at the appropriate depth in a nonrotating sample tube. Chemical shifts are referred to TMS or $CHCl_3$ (taken as 7.30 δ) for the zwitterions. Vapor phase chromatographic separations were performed with either an Aerograph A-90P3 instrument (preparative) using a 10 ft × ¼ in. column with 15% carbowax on chromosorb W, or with a Varian-Aerograph 204-1B instrument (analytical) using a 10 ft × ⅛ in. column with 5% carbowax on chromosorb W. Ultraviolet spectra were measured with a Carry 14 spectrometer.

CD_2Cl_2, BCl_3, and BBr_3 were purified by distillation, stored over P_2O_5 and further distilled immediately before use. All manipulations were carried out on a vacuum line. $CHCl_3$ was washed with H_2O, H_2SO_4, 0.1 *N* $NaHCO_3$, and H_2O, dried over P_2O_5 and distilled twice. CF_2ClH was doubly distilled before use.

*7-Carbomethoxycycloheptatriene (**8**)*

7-cyanocycloheptatriene (10 g) was refluxed under N_2 in MeOH (150 ml) containing concentrated H_2SO_4 (30 g) for 30 h. The bulk of the solvent was removed *in vacuo* and the residue poured into H_2O (400 ml). The solution was extracted with petroleum ether (30–60°) (3 × 100 ml), the extract dried over $MgSO_4$, and the solvent removed *in vacuo* to give the crude ester. Distillation gave 9.0 g (80%) of **8** (b.p. 60° at 0.5 mm) containing a small amount of methyl phenylacetate (~2%). Pure material was obtained by preparative v.p.c. at a temperature below 130°.

*N,N-Dimethyl-1,3,5-cycloheptatriene-7-carboxamide (**11**)*

An excess of gaseous dimethylamine was added to a 10% solution of 7-chlorocarbonylcycloheptatriene in anhydrous ether. The dimethylamine hydrochloride formed was filtered off and the filtrate concentrated *in vacuo* to give a brown oil. This was chromatographed on neutral alumina eluting with ether to give a colorless solid. Recrystallization from pentane gave **11** as colorless crystals (m.p. 64.5°) which slowly became colored on standing. Nuclear magnetic resonance spectral data are given in Table 1.

*9-Carbomethoxybicyclo[6.1.0]nona-2,4,6-triene (**20**)*

Compound **20**, prepared by ester exchange of the corresponding ethyl ester, had properties identical to those previously reported (22).

Preparation of Complexes, General Procedure

All manipulations were carried out under high vacuum conditions. The starting organic compound (*ca.* 30 mg) was weighed into a small reaction vessel which contained a magnetic stirrer, was fitted with a sealed on n.m.r. tube, and could be attached to a vacuum line through a suitable high vacuum stopcock. The reactor was cooled and CD_2Cl_2 (1 ml) was transferred from a reservoir where it had been stored over P_2O_5. The organic material was dissolved and then a weighed amount of the appropriate Lewis acid was slowly distilled in while the solution was being stirred and maintained at −78°. On completion of the addition, the reactor was separated from the vacuum line and the appropriate amount of the solution transferred to the n.m.r. tube which was then sealed. During this transfer the apparatus was kept at −78°.

For the u.v. determinations, a similar technique was used except that a larger reaction vessel with an attached 0.2 cm u.v. cell was employed.

Infrared spectra of **24** and its counterion were obtained as Nujol mulls of the residue left after evaporation of the solvent *in vacuo*.

Quenching of Complexes

An excess of gaseous $(CH_3)_2NH$ was passed into the CD_2Cl_2 solution of the zwitterions at −78°. The resulting mixture was treated with water and the organic material was extracted three times with ether. The combined ether extracts were dried over $MgSO_4$ and the solvent removed *in vacuo* prior to analysis by g.l.p.c. and n.m.r. Hexamethylbenzene was used as an internal standard in some of the reactions in order to quantitatively measure the recovery of the starting compounds. The results of these quenches are shown in Table 5.

*Reaction of the Rearrangement Products of **10** with EtOH*

Ethanol (2 ml) was slowly added to a CD_2Cl_2 solution

TABLE 5. Products obtained on quenching zwitterions

Complex(es)	Quenching agent	Product (%recovery)*
10	Me_2NH	**8** (100%)
21 (58%) + **24** (42%)	Me_2NH	**22** (70%)
21 (60%) + **24** (40%)	EtOH	**22** (58%) + **23** (42%)
24 + $MeO\bar{B}Br_3$	EtOH	**22** (13%) + **23** (87%)
12 + **13**	Me_2NH	**11**†
19	Me_2NH	**20**†
16	Me_2NH	2-methoxycarbonyl-1,3-cycloheptatriene†

*Yield determined by comparison with internal hexamethylbenzene.
†No other products detected by p.m.r.

of the rearrangement products of **10** at −78°. Water (10 ml) was added, the mixture extracted with ether (3 × 5 ml), and the extract dried over $MgSO_4$. Evaporation of the ether gave an oil which was analyzed by both p.m.r. and also analytical g.l.p.c. using authentic samples of **22** and **23** for comparison purposes. The two esters, **22** and **23** in the quenched material were separated by preparative g.l.p.c. and the p.m.r. spectra of the isolated compounds were identical in all respects to that of the authentic samples.

We thank the National Research Council of Canada and the Research Corporation (Frederick Gardner Cottrell Grant) for financial support.

1. R. BRESLOW, J. T. GROVES, and G. RYAN. J. Am. Chem. Soc. **89**, 5048 (1967). A. W. KREBS. Angew. Chem. Int. Ed. **4**, 10 (1965).
2. M. SAUNDERS, R. BERGER, A. JAFFE, J. M. MCBRIDE, J. O'NEILL, R. BRESLOW, J. M. HOFFMAN, JR., C. PERCHONOCK, E. WASSERMAN, R. S. HUTTON, and V. J. KUCK. J. Am. Chem. Soc. **95**, 3017 (1973).
3. W. VON E. DOERING and L. H. KNOX. J. Am. Chem. Soc. **76**, 3203 (1954). K. M. HARMON. *In* Carbonium ions. Vol. 4 *Edited by* G. A. Olah and P. von R. Schleyer. Wiley Interscience, New York. 1973. p. 1579.
4. S. WINSTEIN. Q. Rev. Chem. Soc. **23**, 141 (1969).
5. D. W. SWATTON and H. HART. J. Am. Chem. Soc. **89**, 5075 (1967). P. VOGEL, M. SAUNDERS, N. M. HASTY, JR., and J. A. BERSON. J. Am. Chem. Soc. **93**, 1551 (1971). R. F. CHILDS, and S. WINSTEIN. J. Am. Chem. Soc. **96**, 6409 (1974). I. S. ISAEV, V. I. MAMATYUK, L. I. KUZUBOVA, T. A. GORDYMOVA, and V. A. KOPTYUG. Zh. Org. Khim. **6**, 2482 (1970) and references cited therein.
6. R. B. WOODWARD and R. HOFFMANN. The conservation of orbital symmetry. Academic Press, New York, N.Y. 1969.
7. J. A. BERSON and J. A. JENKINS. J. Am. Chem. Soc. **94**, 8907 (1972). S. WINSTEIN, C. G. KREITER, and J. I. BRAUMAN. J. Am. Chem. Soc. **88**, 2047 (1966).
8. W. J. HEHRE. J. Am. Chem. Soc. **96**, 5207 (1974).
9. G. D. SARGENT, N. LOWRY, and S. D. REICH. J. Am. Chem. Soc. **89**, 5985 (1967).
10. S. KOHEN and S. J. WEININGER. Tetrahedron Lett. 4403 (1972). P. WARNER and S. LU. Tetrahedron Lett. 3455 (1974); J. Am. Chem. Soc. **95**, 5099 (1973). G. L. THOMPSON, W. E. HEYD, and L. A. PAQUETTE. J. Am. Chem. Soc. **96**, 3177 (1974). L. A. PAQUETTE and G. L. THOMPSON. J. Am. Chem. Soc. **95**, 2364 (1973).
11. R. HOFFMANN. Tetrahedron Lett. 2907 (1970).
12. H. GÜNTHER. Tetrahedron Lett. 5173 (1970).
13. R. F. CHILDS and M. ZEYA. J. Am. Chem. Soc. **96**, 6418 (1974).
14. W. BETZ and J. DAUB. Chem. Ber. **107**, 2095 (1974); Angew. Chem. Int. Ed. **10**, 269 (1971). J. DAUB and W. BETZ. Tetrahedron Lett. 3451 (1972).
15. G. MAIER. Angew. Chem. Int. Ed. **6**, 402 (1967). E. CIGANEK. J. Am. Chem. Soc. **87**, 652 (1965); **89**, 1454 (1967). G. E. HALL and J. D. ROBERTS. J. Am. Chem. Soc. **93**, 2203 (1971).
16. E. CIGANEK. J. Am. Chem. Soc. **93**, 2207 (1971).
17. H. G. RICHEY, JR. *In* Carbonium ions. Vol. 3. *Edited by*, G. A. OLAH and P. VON R. SCHLEYER. Wiley Interscience, N.Y. 1972. p. 1201.
18. W. STOHRER and J. DAUB. Angew. Chem. Int. Ed. **13**, 86 (1974).
19. S. J. KUHN and J. S. MCINTYRE. Can. J. Chem. **43**, 375 (1965).
20. S. CLEMENTI and P. LINDA. J. Chem. Soc. Perkin II, 1887 (1973).
21. R. G. PEWS, Y. TSUNO, and R. W. TAFT. J. Am. Chem. Soc. **89**, 2391 (1967). R. W. TAFT and J. W. CARTEN. J. Am. Chem. Soc. **86**, 4199 (1964).
22. K. F. BANGERT and V. BOEKELHIDE. J. Am. Chem. Soc. **86**, 905 (1964).
23. C. J. FRITCHIE, JR. Acta Cryst. **20**, 2766 (1966).
24. L. M. JACKMAN and S. STERNHELL. *In* Applications of nuclear magnetic resonance spectroscopy in organic chemistry. Pergamon, Oxford. 1969. p. 85.
25. J. TILLIEU. Ann. Phys. **2**, 471 (1957); **2**, 631 (1957).
26. J. A. POPLE. J. Chem. Phys. **37**, 60 (1962).
27. R. HOFFMANN and W. STOHRER. J. Am. Chem. Soc. **93**, 6941 (1971).
28. E. HEILBRONNER. Tetrahedron Lett. 1923 (1964). M. J. S. DEWAR. Angew. Chem. Int. Ed. **10**, 761 (1971). H. E. ZIMMERMAN. Acc. Chem. Res. **4**, 272 (1971).
29. V. L. KOLDITZ and C. LUNG. Z. Anorg. Allg. Chem. **360**, 23 (1968). I. G. Ryss and V. N. PLAKHOTNIK. Z. Inorg. Khim. **13**, 1535 (1968).
30. G. A. OLAH, W. S. TOLGYESI, S. J. KUHN, M. E. MOFFAT, J. BASTIEN, and E. B. BAKER. J. Am. Chem. Soc. **85**, 1328 (1963). N. C. DENO, C. U. PITTMAN, JR.,

Can. J. Chem. Downloaded from www.nrcresearchpress.com by 210.87.254.42 on 09/05/12
For personal use only.

and M. J. WISOTSKY. J. Am. Chem. Soc. **86**, 4370 (1964).
31. K. B. WIBERG, B. A. HESS, JR., and A. J. ASHE, III. *In* Carbonium ions. Vol. 3. *Edited by* G. A. Olah and P. von R. Schleyer. Wiley Interscience, New York, N.Y. 1972. p. 1295.
32. D. M. BROUWER and H. HOGEVEEN. Recl. Trav. Chim. Pays-Bas, **89**, 211 (1969).
33. M. S. BROOKHART and M. A. M. ATWATER. Tetrahedron Lett. 4399 (1972). M. BROOKHART, M. OGLIARUSO, and S. WINSTEIN. J. Am. Chem. Soc. **89**, 1965 (1967).
34. E. LEE-RUFF. Can. J. Chem. **50**, 952 (1972).
35. J. A. BERSON, P. W. GRUBB, R. A. CLARK, D. R. HARTTER, and M. R. WILLCOTT. III. J. Am. Chem. Soc. **89**, 4076 (1967).

Can. J. Chem. Downloaded from www.nrcresearchpress.com by 210.87.254.42 on 09/05/12
For personal use only.

Carbon-13 Nuclear Magnetic Resonance Spectra of Carcinogenic Polynuclear Hydrocarbons. II. Benzo[*a*]pyrene

GERALD W. BUCHANAN AND RICHARD S. OZUBKO[1]

Department of Chemistry, Carleton University, Ottawa, Canada K1S 5B6

Received December 31, 1974

GERALD W. BUCHANAN and RICHARD S. OZUBKO. Can. J. Chem. **53**, 1829 (1975).

^{13}C n.m.r. signal assignments are presented for the carcinogenic polynuclear hydrocarbon benzo[*a*]pyrene. In addition to selective ^{1}H decoupling, valuable information is obtained from the magnitudes of the α-, β-, and "*peri*" deuterium isotope shifts in the 1,3,6-trideuterio analog. The applicability of the model compound approach to signal assignment is explored in detail.

GERALD W. BUCHANAN et RICHARD S. OZUBKO. Can. J. Chem. **53**, 1829 (1975).

On présente les attributions de signaux en r.m.n. du ^{13}C pour l'hydrocarbure polynucléaire cancérigène benzo[*a*]pyrène. On obtient des informations intéressantes par découplage sélectif du ^{1}H et aussi à partir de l'amplitude des déplacements isotopiques du deutérium pour les positions α, β, et "*peri*" des analogues trideutério-1,3,6. On examine en détail la possibilité d'appliquer l'approche du composé modèle pour l'attribution des signaux.

[Traduit par le journal]

Introduction

Considerable effort has been directed toward the elucidation of the ^{1}H n.m.r. spectra of polynuclear hydrocarbons. For the potent carcinogen benzo[*a*]pyrene, precise analysis has been accomplished only by utilization of 220 MHz instruments and iterative computer fitting due to the complex nature of the ^{1}H spectrum (1, 2).

Molecules such as benzo[*a*]pyrene are the objects of intense theoretical interest, and several theories attempting to relate electronic structure with carcinogenic activity have been advanced (3 and references therein). It is in connection with the electronic properties of these systems, however, that the ^{13}C n.m.r. parameters are of greatest interest, since the carbon shieldings should give more valuable information regarding local electronic properties at carbon than those for the bonded protons. Furthermore, an earlier report from these laboratories (4) has demonstrated the utility of ^{13}C n.m.r. for analysis of related systems such as 3-methylcholanthrene and the benzanthracenes.

Results and Discussion

The numbering scheme (5) and structures for the five compounds included in the present study are illustrated in Fig. 1.

Assignments of resonances were accomplished using several methods. Initially, reduced intensities for all quaternary centers were evident, permitting ready distinction between these resonances and those due to carbons bearing hydrogen. Increased relative intensities for quaternary carbons were observed in the presence of 5×10^{-2} molar-equiv. of the relaxation reagent Cr(acac)$_3$, which is known to attenuate greatly the spin–lattice relaxation times (6). In cases where the ^{1}H spectra have been assigned, selective ^{1}H decoupling at low r.f. power (4) was employed. Model compounds, empirical chemical shift additivity correlations and deuterium substitution were also utilized. All spectra were recorded using $CDCl_3$ solutions and the chemical shifts are presented in Table 1.

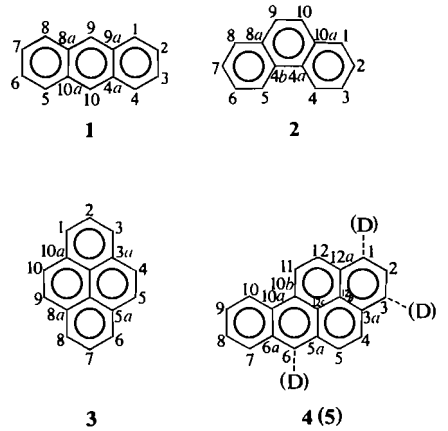

FIG. 1. Numbering scheme for polynuclear hydrocarbons.

[1]NRCC Postgraduate Scholar 1972–present.

Can. J. Chem. Downloaded from www.nrcresearchpress.com by 210.87.254.105 on 09/05/12
For personal use only.

Can. J. Chem. Downloaded from www.nrcresearchpress.com by 210.87.254.105 on 09/05/12
For personal use only.

TABLE 1. ^{13}C chemical shifts for **1–5** (δ_C from TMS)

Position	1	2	3	4	5
1	128.3	128.5	124.6	124.61d	124.30d
2	125.2	126.5	125.5	125.78	125.67
3	125.2	126.5	124.6	124.68d	124.37d
3a			130.9	131.21f	131.14f
4	128.3	122.6	127.0	127.33	127.28
4a	131.6	130.3			
4b		130.3			
5	128.3	122.6	127.0	127.66	127.61
5a			130.9	129.71	129.62
6	125.2	126.5	124.6	125.38	125.06
6a				131.46	131.39
7	125.2	126.5	125.5	128.77	128.71
8	128.3	128.5	124.6	125.88e	125.88e
8a	131.6	132.0	130.9		
9	126.1	126.9	127.0	125.91e	125.91e
9a	131.6				
10	126.1	126.9	127.0	122.87	122.87
10a	131.6	132.0	130.9	127.22	127.21
10b			124.6	128.10	128.10
10c			124.6		
11				122.00	122.00
12				128.00	127.95
12a				131.27f	131.20f
12b				125.27	not obs'd
12c				123.58	not obs'd

NOTE: d, e, f, denote possible interchange of assignments.

Results for anthracene **1** and phenanthrene **2** are included from our earlier work (4) since these will be used as model compounds. Shieldings for pyrene **3** are in good agreement with those reported for a $CDCl_3$ solution (7). The ^{13}C Fourier transform spectrum of benzo[*a*]pyrene **4**, obtained under conditions of complete ^1H noise decoupling is shown in Fig. 2. Preliminary inspection indicates 8 quaternary carbon resonances and 12 CH resonances as expected. Addition of $Cr(acac)_3$ verified the reality of the low intensity absorptions.

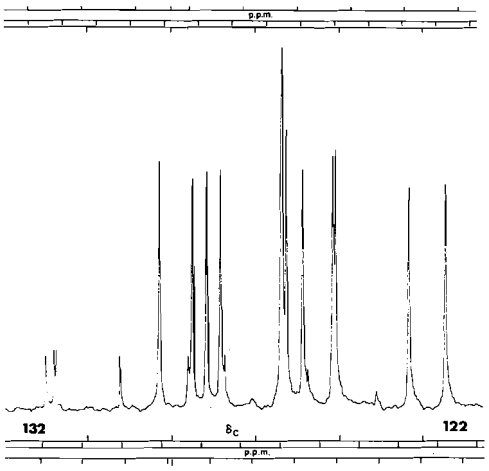

FIG. 2. ^{13}C n.m.r. spectrum of benzo[*a*]pyrene.

In the ^1H spectrum of **4** (2) only the protons at C-10, C-11, and C-6 are sufficiently separated to allow selective decoupling. Resonances for the remaining protons appear at higher field and take the form of overlapping multiplets. Selective ^1H decoupling at δ 8.9 sharpens carbons at 122.00 and 122.87, corresponding to C-11 and C-10, respectively, which are shielded from the well known "γ" steric shift (8, 9). Due to its similarity with C-4,5 of phenanthrene **2**, C-10 is assigned as 122.87. Irradiation at δ 8.3, the C-6 proton shift, selectively sharpens the carbon resonance at δ 125.38.

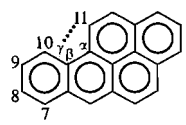

The majority of the remaining carbons of **4** were assigned using simple model compounds and additivity. To check the predicted values, compound **5** with 99% selective deuteration at

Can. J. Chem. Downloaded from www.nrcresearchpress.com by 210.87.254.105 on 09/05/12
For personal use only.

C-1,3 and 6 (10, 11) was examined. Deuterium isotope shifts at various carbons were compared with our earlier findings (4) and those recently reported by Martin *et al.* (12).

Employing C-1,3 of pyrene **3** as models for C-1,3 of **4**, shifts near 124.6 p.p.m. are predicted for the latter carbons. Careful study of the 1,3,6-trideuterio system **5** verified these predictions, since resonances at 124.61 and 124.68 in **4** were absent in **5** and in their place are two triplets, each shielded by 0.31 p.p.m. These spectral changes are consistent with previously observed α-deuterium isotope effects on carbon spectra of related compounds (12–14).

Similarly, C-2 of **4** is expected to resonate near C-2 of **3**, which appears at δ 125.5. After deuteration, the resonance at δ 125.78 in **4** broadens and shifts upfield by 0.11 p.p.m., indicative of β-deuterium substitution. Martin *et al.* (12) have found that the β-deuterium isotope shift is *ca.* 0.12 p.p.m. for carbons bearing a proton but only 0.07 p.p.m. for carbons lacking directly bonded hydrogens. Interestingly, although there are two deuteriums β to C-2 of **5** the observed effect indicates that these isotope shifts cannot be considered additive.

A further important observation of Martin *et al.* (12) is the "*peri*" deuterium isotope shift. The γ carbon bearing a hydrogen *peri* to deuterium is shielded by *ca.* 0.04 p.p.m. and such shifts in **5** permit assignment of resonances for carbons 4, 5, 7, and 12 of **4**. For C-4 of **4**, C-4 of **3**, resonating

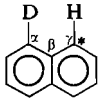

at δ 127.0, was used as a model. The 127.33 p.p.m. resonance in **4** shifts to 127.28 p.p.m. in **5** consistent with *peri* deuterium incorporation.

A shift for C-5 of **4** was predicted in the following way: using C-5 of **3** as a starting point (δ 127.0) one must then consider the effect due to addition of the extra benzenoid function, *i.e.*

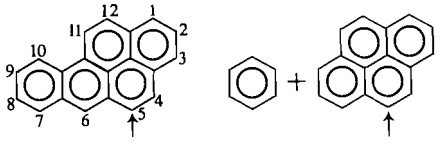

An estimation of the annelation effect is available by comparison of C-1,4,5,8 of **1** (δ 128.3) with C-1,4,5,8 of naphthalene (δ 127.7). Thus, one predicts a shift of 127.0 + 0.6 = 127.6 for C-5 of **4**. The resonance at δ 127.66 in **4** shifts to 127.61 in **5** indicating a *peri* deuterium and lending support to this method of analysis.

For C-7 of benzo[*a*]pyrene again the C-1,4,5,8 resonance of **1** serves as a model, as does C-8 of benz[*a*]anthracene (4). Accordingly a shift near δ 128.3 is predicted. In **4** the resonance at δ 128.77 shifts to 128.71 in **5** mirroring the influence of the γ deuterium and supporting the model compound approach.

Now, with respect to carbons bearing hydrogens, we are left with C-8,9, and -12 of **4** to assign, and resonances at δ 125.88, 125.91, and 128.00, respectively. One would expect that C-8,9 of **4** should be rather similar to C-2,3,6,7 of **1** (δ 125.2) and thus we assign resonances at 125.88 and 125.91 to C-8,9 of **4**. Support for this comes from the absence of any observable changes in these resonances in the trideuterio derivative **5**. The remaining resonance at δ 128.00 in **4** is attributed to C-12 and in **5**, the expected γ deuterium isotope shift to 127.95 is found.

Quaternary Carbons

For carbons lacking bonded protons in aromatic hydrocarbons, Martin *et al.* (12) have observed shielding β-deuterium isotope effects of *ca.* 0.07 p.p.m. In **5** there are four quaternary centers (3a, 5a, 6a, and 12a) which are β to deuterium. The resonance at δ 131.46 in **4** is shifted to δ 131.39 in **5**. Employing C-4a of **1** as a model (δ 131.6) for C-6a of **4** allows an assignment to be made with a reasonable degree of confidence. Carbon 3a of **3** (δ 130.9) furnishes a good model for positions 3a and 12a of **4**. Accordingly the peaks at δ 131.27 and 131.21 in **4**, which shift to 131.20 and 131.14 respectively in **5**, are assigned to 3a and 12a. No distinction between these, however, is possible. By elimination, the quaternary resonance at 129.71 in **4** which shifts to 129.62 in **5** must correspond to position 5a.

Employing C-10b and -10c of **3** as models (δ 124.6), it is clear that resonances for C-12b and -12c of **4** will be the most shielded of those arising from quaternary centers. In **5**, resonances for 12b and 12c are not visible. Vicinal coupling to the deuteriums on C-1 and C-3 will extensively broaden the C-12b resonance, whereas the resonance for 12c, in addition to its vicinal coupling with the deuterium on C-6, is obscured by the triplet for C-6 centered at δ 125.06.

Differentiation between the remaining quaternary resonances for C-10a and -10b is made on

the basis of observed broadening of the C-10a resonance at δ 127.22 in **4** on becoming vicinal to the deuterium at C-6 of **5**. Thus the remaining resonance at δ 128.10 of **4** is attributed to C-10b. No recognizable difference in position or linewidth of this resonance is observed in **5** *vs.* **4**.

To conclude, it is clear that Fourier transform ^{13}C n.m.r. represents a valuable addition to the available physical methods for the study of polynuclear hydrocarbons. For cases where unambiguous assignments are not possible due to peak overlap or insufficient sensitivity, it can be envisaged that high field spectrometers utilizing larger sample tubes will be valuable.

Experimental

Materials

The compound benzo[*a*]pyrene was purchased from K & K Laboratories Inc., Plainview, New York. The 1,3,6-trideuterio derivative was prepared according to the method of Cavalieri and Calvin (10, 11).

Spectra

Nuclear magnetic resonance spectra of ^{13}C in natural abundance were obtained by the pulsed Fourier transform technique at 25.16 MHz on a Varian XL-100-15 spectrometer. The free-induction decays were stored in a Varian 620/L computer (16K memory) and were Fourier transformed after a sufficient number had been accumulated. Before transformation all interferograms were smoothed with an exponential function to enhance signal-to-noise. The maximum number of data points used in accumulating the interferograms was 8192.

Samples were studied in tubes of 12 mm outer diameter with concentrations at 0.24 *M* in $CDCl_3$. The deuterium of the solvent was used as a field-frequency lock and all chemical shifts are expressed as downfield from internal TMS. Routinely, spectra were recorded with complete proton noise decoupling at a probe temperature of 32 °C. For the selective decoupling experiments, proton irradiation was carried out at low decoupler power with no noise modulation. The decoupler was calibrated by irradiating the protons of TMS (in $CDCl_3$) under low power conditions.

The isotope shifts observed in 1,3,6-trideuteriobenzo[*a*]pyrene were obtained by comparing its spectrum with that of benzo[*a*]pyrene run under identical experimental conditions. Both compounds were 0.24 *M* in $CDCl_3$ and each spectrum was obtained using a 1000 Hz sweep width, 8192 data points, and the same sweep offset (as verified with the spectrometer's digital frequency counter). The line positions (as measured in Hz from the carrier frequency) of the folded back $CDCl_3$ triplet were found to be the same in the two spectra, a further proof for the experimental conditions being identical.

Financial support from the National Cancer Institute of Canada and the National Research Council of Canada is gratefully recognized.

1. R. H. Martin, M. Defay, F. Geerts Evrard, and S. Delavarenne. Tetrahedron, **20**, 1073 (1964).
2. C. W. Haigh and R. B. Mallion. J. Mol. Spectrosc. **29**, 478 (1969).
3. J. C. Arcos and M. F. Argus (*Editors*). Chemical induction of cancer. Vol. II A. Academic Press, New York, N.Y. 1974.
4. R. S. Ozubko, G. W. Buchanan, and I. C. P. Smith. Can. J. Chem. **52**, 2493 (1974).
5. Definitive rules for nomenclature of organic chemistry, A. IUPAC, Butterworths, London. 1957.
6. O. A. Gansow, A. R. Burke, and W. D. Vernon. J. Am. Chem. Soc. **94**, 2550 (1972).
7. L. F. Johnson and W. C. Jankowski. Carbon-13 NMR spectra. John Wiley and Sons, New York, N.Y. 1972.
8. D. M. Grant and B. V. Cheney. J. Am. Chem. Soc. **89**, 5315 (1967).
9. J. B. Stothers. Carbon-13 NMR Spectroscopy. Academic Press, New York, N.Y. 1972.
10. E. Cavalieri and M. Calvin. Proc. Nat. Acad. Sci. U.S.A. **68**, 1251 (1971).
11. M. Calvin and E. Cavalieri. J. Chem. Soc. Perkin I, 1253 (1972).
12. R. H. Martin, J. Moriau, and N. Defay. Tetrahedron, **30**, 179 (1974).
13. R. A. Bell, C. L. Chau, and B. G. Sayer. Chem. Commun. **67** (1972).
14. W. Kitching, M. Bullpitt, D. Doddrell, and W. Adcock. Org. Magn. Reson. **6** (5), 289 (1974).

Can. J. Chem. Downloaded from www.nrcresearchpress.com by 210.87.254.105 on 09/05/12
For personal use only.

Equilibria between Palladium(II) Acetate and Olefins in Acetic Acid containing Sodium Acetate[1]

RAJ N. PANDEY AND PATRICK M. HENRY

Guelph-Waterloo Centre for Graduate Work in Chemistry, University of Guelph, Guelph, Ontario N1G 2W1

Received November 12, 1974

RAJ N. PANDEY and PATRICK M. HENRY. Can. J. Chem. **53**, 1833 (1975).

π-Complex equilibria between dimeric Pd(II) acetate and various olefins (ethylene, styrene, 3,3-dimethyl-1-butene, vinylic and allylic esters) in acetic acid solvent have been investigated by spectral means. The results indicate two π-complexes are formed. The first π-complex, which is formed rapidly, is a dimeric π-complex (ol = olefin).

$$Na_2Pd_2(OAc)_6 + ol \underset{\longleftarrow}{\overset{K_{\pi 22}}{\longrightarrow}} NaPd_2(OAc)_5(ol) + NaOAc$$

The Benesi–Hildebrand plots for these complexes are linear for all olefins and thus values of $K_{\pi 22}$ can be readily evaluated. The values of the equilibrium coefficient, $K_{\pi 22}$, do not change with solution composition or [NaOAc]. The second π-complex is formed slowly. The data are consistent only with the equilibrium

$$Na_2Pd_2(OAc)_6 + 2ol \underset{\longleftarrow}{\overset{K_{\pi 21}}{\longrightarrow}} 2NaPd(OAc)_3(ol)$$

The data are inconsistent with the equilibrium

$$Na_2Pd_2(OAc)_6 + 2ol \underset{\longleftarrow}{\overset{K'_{\pi 22}}{\longrightarrow}} Pd_2(OAc)_4(ol)_2 + 2NaOAc$$

which is analogous to that reported for the $Na_2Pd_2Cl_6$ reaction with olefins in acetic acid. Furthermore, previous assumptions as to the equilibria between ethylene and Pd(II) in the all-acetate system have proved incorrect, and so the kinetics of oxidation of ethylene in this system must be reinterpreted in view of the present results.

RAJ N. PANDEY et PATRICK M. HENRY. Can. J. Chem. **53**, 1833 (1975).

On a étudié, à l'aide de méthodes spectrales, l'équilibre dans l'acide acétique, des complexes π entre l'acétate de Pd(II) dimère et diverses oléfines (éthylène, styrène, diméthyl-3,3 butène-1, esters vinyliques et allyliques). Les résultats indiquent qu'il y a formation de deux complexes π. Le premier complexe π, qui se forme rapidement, est un complexe π dimère (ol = oléfine)

$$Na_2Pd_2(OAc)_6 + ol \underset{\longleftarrow}{\overset{K_{\pi 22}}{\longrightarrow}} NaPd_2(OAc)_5(ol) + NaOAc$$

Les courbes de Benesi–Hildebrand de ces complexes sont linéaires pour toutes les oléfines et on peut donc évaluer facilement les valeurs de $K_{\pi 22}$. Les valeurs du coefficient d'équilibre $K_{\pi 22}$, ne changent pas avec la composition de la solution ou avec [NaOAc]. Le deuxième complexe se forme lentement. Les données sont seulement en accord avec l'équilibre.

$$Na_2Pd_2(OAc)_6 + 2ol \underset{\longleftarrow}{\overset{K_{\pi 21}}{\longrightarrow}} 2NaPd(OAc)_3(ol)$$

Les données ne sont pas en accord avec l'équilibre

$$Na_2Pd_2(OAc)_6 + 2ol \underset{\longleftarrow}{\overset{K'_{\pi 22}}{\longrightarrow}} Pd_2(OAc)_4(ol)_2 + 2NaOAc$$

qui est analogue à l'équilibre suggéré pour la réaction de $Na_2Pd_2Cl_6$ avec les oléfines dans l'acide acétique. De plus on a prouvé que des hypothèses antérieures concernant l'équilibre entre l'éthylène et le Pd(II) dans des systèmes ne contenant que des acétates sont incorrectes; on doit donc réinterpréter la cinétique de l'oxydation de l'éthylène dans ce système en tenant compte des nouveaux résultats. [Traduit par le journal]

Introduction

In the past several years, the field of palladium(II) catalyzed reactions has been extensively studied (for recent reviews, see refs. 1 and 2). Important intermediates in the olefin reactions are palladium(II)–olefin π-complexes and a large number of π-complexes of mono and diolefins have been prepared and characterized (1–3). The equilibria between palladium(II)

[1]Presented in part at the 166th National meeting of the American Chemical Society, Chicago, August 1973, Abstract INDE 20(17).

Can. J. Chem. Downloaded from www.nrcresearchpress.com by 210.87.254.40 on 09/05/12
For personal use only.

Can. J. Chem. Downloaded from www.nrcresearchpress.com by 210.87.254.40 on 09/05/12
For personal use only.

chloride salts and olefins in acetic acid have also been studied by spectral means. Cruikshank and Davies (4) studied the interaction of $Na_2Pd_2Cl_6$ with allylbenzene and postulated the presence of $Na[Pd_2Cl_5(olefin)]$, $[Pd_2Cl_4(olefin)_2]$, and $[PdCl_2(olefin)_2]$. They proposed that the latter complex is the catalytically active species in olefin isomerization. Hartley and Wagner (5), using 1-hexene and 1-octene as olefins, also postulated that the first two species were formed in the following equilibria

[1] $Na_2Pd_2Cl_6 + olefin \rightleftarrows Na[Pd_2Cl_5(olefin)] + NaCl$

[2] $Na[Pd_2Cl_5(olefin)] \rightleftarrows [Pd_2Cl_4(olefin)_2] + NaCl$

but found no evidence for $PdCl_2(olefin)_2$. They postulated that Cruikshank and Davies did not take into account the presence of $Na[Pd_2Cl_5(CH_3COOH)]$. Hartley and Wagner postulated the formation of $Pd_2Cl_4(olefin)_2$ because their results required a complex with a Pd:olefin ratio of 1. However it is not clear that these workers ruled out the formation of $Na[PdCl_3(olefin)]$ which would have the same Pd:olefin ratio as $Pd_2Cl_4(olefin)_2$.

In the lithium chloride system containing excess LiCl, spectral and kinetic studies on allylic ester exchange indicated the main equilibrium between allylic esters and $Li_2Pd_2Cl_6$ was formation of the monomeric species while the kinetics

[3] $Li_2Pd_2Cl_6 + 2\ allyl\ ester \rightleftarrows 2Li[PdCl_3(allyl\ ester)]$

require that a dimeric π-complex be present in at least kinetically significant amounts.

[4] $Li_2Pd_2Cl_6 + allyl\ ester \rightleftarrows Li[Pd_2Cl_5(allyl\ ester)]$

Olefin π-complex formation in the palladium(II) acetate system has not been studied as extensively as the chloride containing system. To our knowledge the only previous study is the reaction of ethylene with palladium(II) acetate in acetic acid containing sodium acetate (7). However, the interpretation of the data was based on the assumption that in the range of sodium acetate concentrations from 0.3 to 1 *M*, the palladium was entirely in the form of the monomeric species, $Na_2Pd(OAc)_4$. As discussed below, this assumption is incorrect.

A previous report (8) from these laboratories described a study of the equilibria between palladium(II) acetate and sodium acetate. The following equilibria were found to be operative.

[5] $2Pd_3(OAc)_6 + 6NaOAc \overset{K_{32}}{\rightleftarrows} 3Na_2Pd_2(OAc)_6$

[6] $Na_2Pd_2(OAc)_6 + 2NaOAc \overset{K_{21}}{\rightleftarrows} 2Na_2Pd(OAc)_4$

The value of K_{32} was such that the trimer was completely converted to dimer at 0.2 *M* NaOAc while even at the highest [NaOAc] used (*ca.* 1.0 *M*) the conversion of dimer to monomer was incomplete.

A previous study of the analogous equilibria in the chloride system indicated that only the dimer–monomer equilibrium is important (9).

[7] $Li_2Pd_2Cl_6 + 2LiCl \rightleftarrows 2Li_2PdCl_4$

However, an even more important difference between the two systems is that the attainment of equilibria in the acetate system is a slow process while the reactions in the chloride system are instantaneous. Thus bridging acetates react slowly while bridging chlorides react fast. The lability of terminal acetates could not be determined in this study since no net chemical change occurs by terminal acetate exchange.

The present work will describe a study of the interaction of palladium(II) acetate with several olefins in the sodium acetate concentration range in which the predominant palladium(II) species is the acetate-bridged dimer $Na_2Pd_2(OAc)_6$. This study should detect differences in lability between terminal and bridging acetates. In addition, it will provide more of the basic equilibrium data required to interpret the kinetics of Pd(II) catalyzed reactions of olefins in this system.

Experimental

Materials

Palladium acetate (purchased from Engelhard Chemicals and Catalysts, New Jersey) was purified by the method of Stephenson *et al.* (10). The acetic acid (Baker Chemical Co.) was dried by refluxing over triacetylborate, $B(OAc)_3$, and distilled (11). The determination of water by Karl Fisher analysis indicated water contents of less than 0.01%. Sodium acetate (Baker Chemical Co.) was reagent grade. Allylic esters, styrene (Eastman, Rochester, N.Y.), vinylic esters (J. T. Baker Chemical Co.), 3,3-dimethyl-1-butene (Aldrich Chemical Co.), and C.P. grade ethylene (Matheson of Canada Ltd.) were used without further purification. The Pd(II) stock solutions were analyzed by the dimethylglyoxime procedure (12).

Equilibrium Measurements

The formation of π-complexes between Pd(II) species and olefins was followed spectrophotometrically. Spectra

Can. J. Chem. Downloaded from www.nrcresearchpress.com by 210.87.254.40 on 09/05/12
For personal use only.

were recorded on a Unicam S.P. 800, Cary 14, and Cary 118 spectrophotometer using cells of 1, 5, and 10 mm pathlengths. All measurements were made at 25 °C.

Solutions of palladium(II) acetate and sodium acetate were equilibrated at 25 °C for *ca.* 24 h prior to addition of olefins. Usually 2 ml of total solution was used. Aliquots (0.001 to 0.1 ml) of the pure liquid olefin were added to these solutions. In case of ethylene, a saturated solution of ethylene in acetic acid was prepared. A creased flask containing a known volume of acetic acid was placed in a constant temperature (25 °C) bath and connected to a gas burette (also at 25 °C) which was connected to a vacuum system. A magnetic stirrer was used to agitate the contents of the flask. The system was evacuated for several minutes with the stirrer running. The stirring was then turned off and the system was filled with approximately 1 atm of ethylene. The mercury in the gas burette and leveling bulb was then equalized, an initial reading taken, and the stirrer turned on to allow the ethylene to dissolve. During this time the pressure was continually kept constant by equalizing the level of mercury in the bulb and burette. The solution was considered saturated when the ethylene uptake stopped. A final burette reading was recorded. The difference (ΔV) between the initial and final volume at 1 atm was used in determining the solubility of the gas. The solubility of ethylene was found to be 0.082 *M*. The flask containing this solution was tightly stoppered and removed. A measured volume of this solution was withdrawn by means of a glass syringe and mixed in a closed container filled almost entirely by the reacting solution. This solution was then quickly transferred via glass syringe to a cell for spectral measurements.

Addition of olefins caused an instantaneous change in the spectra followed by a slow change. The slower reaction in fact took a period of hours to come to equilibrium. The initial isosbestic point observed at λ_{365nm} shifts gradually with time towards lower wavelength $\simeq\lambda_{350nm}$ as the reaction proceeds.

The equilibrium optical density for the fast reaction was reached in less than 2 min. In that period no measurable amount of the second slow reaction had taken place. The equilibrium optical density for the slow reaction was reached in several hours.

The wavelength region used for the spectral measurements was 400–275 nm. All olefins but styrene were transparent in this region. However, at 300 nm styrene has a negligible absorption so this wavelength was used in the determinations with this olefin.

The equilibrium measurements were made in the [NaOAc] range in which the main species is $Na_2Pd_2(OAc)_6$. However correction was made for the amount of dimer converted to monomer (reaction 6) using the previously determined value of K_{21}.

Method of Continuous Variation

The Job (13) method was used to determine the stoichiometry of the complexes formed by the interaction of dimeric Pd(II) and olefin. For reason of greater stability to oxidative decomposition as well as high values of the equilibrium constants for π-complex formation, allyl acetate was the olefin selected for this purpose. Solutions were prepared in which the mole fraction of metal (x) varied from 0 to 1 and in which the olefin concentration was adjusted to $1 - x$. The changes in optical density were low because of the low solubility of $Na_2Pd_2(OAc)_6$ in acetic acid (*ca.* 0.02 *M*). To increase accuracy the difference in optical density (ΔD) between the metal–olefin solution and a solution containing the same concentration of metal without olefin was measured. Solutions of 5 ml volume containing the palladium(II) acetate plus sodium acetate were allowed to come to equilibrium. Then the appropriate amount of an allyl acetate stock solution (0.1 *M*) was added followed by another period of several hours to allow complete equilibration between Pd(II) and olefin. Results are shown in Figs. 1 and 2.

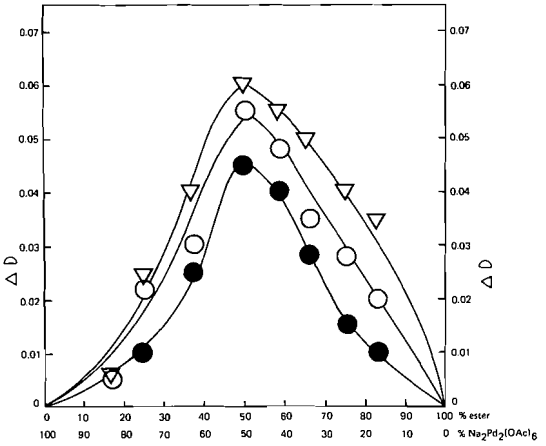

FIG. 1. Job plots for the system $Na_2Pd_2(OAc)_6$ and allyl acetate in dry acetic acid: Σ ($[Na_2Pd_2(OAc)_6]$ + [ester]) = 3.78×10^{-3} *M*. ΔD = difference in optical density (in 5 mm optical pathlength) of the two solutions differing only in that [ester] = 0 in one of them. ▽, λ = 320 nm; ○, λ = 330 nm; ●, λ = 335 nm.

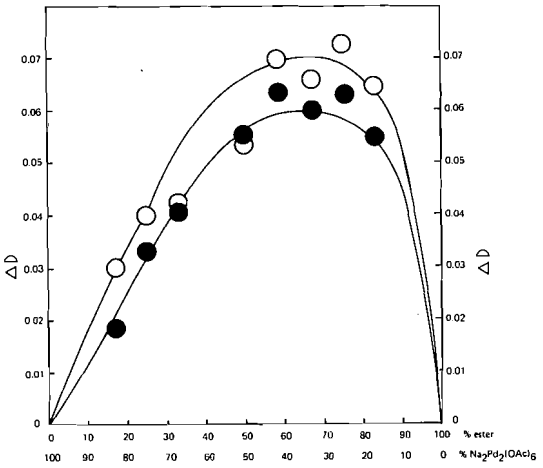

FIG. 2. Job plots for the system $Na_2Pd_2(OAc)_6$ and allyl acetate in dry acetic acid: Σ ($[Na_2Pd_2(OAc)_6]$ + [ester]) = 3.78×10^{-3} *M*. ΔD = difference in optical density (in 5 mm optical pathlength) of the two solutions differing only in that [ester] = 0 in one of them. ○, 280 nm; ●, 290 nm.

Can. J. Chem. Downloaded from www.nrcresearchpress.com by 210.87.254.40 on 09/05/12
For personal use only.

Figure 1 has a maxima corresponding to 1:1 complexing. However the curve in Fig. 2 gives a maxima when dimer to ester molar ratio is 1 to ~2. Plots of optical density *vs.* [dimer] at all wavelengths used for the Job plots were found to be linear indicating that Beer's law is obeyed.

The following equilibria must be considered on the basis of the Job plots (ol = vinyl, allyl propionate (or acetate), ethylene, styrene, and neohexene).

$$[8]\quad Na_2Pd_2(OAc)_6 + ol \underset{}{\overset{K_{\pi 22}}{\rightleftharpoons}} Na[Pd_2(OAc)_5(ol)] + NaOAc$$

$$[9]\quad Na_2Pd_2(OAc)_6 + 2ol \overset{K_{\pi 21}}{\rightleftharpoons} 2Na[Pd(OAc)_3(ol)]$$

$$[10]\quad Na_2Pd_2(OAc)_6 + 2ol \overset{K'_{\pi 22}}{\rightleftharpoons} [Pd_2(OAc)_4(ol)_2] + 2NaOAc$$

This complicated set of equilibria can be simplified since the Job plots (see Results section) indicate reaction 8 is the fast equilibrium. This 1:1 type of complex formation can be treated by the Benesi–Hildebrand type of plot (14). For reaction 8 the equilibrium can be written

$$[11]\quad K_{\pi 22} = \frac{[NaPd_2(OAc)_5(ol)][NaOAc]}{[Na_2Pd_2(Ac)_6][ol]}$$

which at constant acetate becomes

$$[12]\quad K''_{\pi 22} = \frac{[NaPd_2(OAc)_5(ol)]}{[Na_2Pd_2(OAc)_6][ol]}$$

The difference in optical density, D_i, at a given olefin concentration and that at zero olefin concentration can be expressed as follows;

$$[13]\quad \frac{D_i - D_0}{l} = \varepsilon_{\pi_2}\pi_2 + \varepsilon_{P_2}P_2 - \varepsilon_{P_2}P_{20}$$

where π_2 is the concentration of $[NaPd_2(OAc)_5(ol)]$, P_2 is the concentration of $[Na_2Pd_2(OAc)_6]$ at a given olefin concentration, and P_{20} is the concentration in the absence of olefin. ε_{π_2} and ε_{P_2} are the corresponding extinction coefficients and l is the path length of the cell. Since $\pi_2 = P_{20} - P_2$, and $D_i - D_0 = \Delta D$, eq. 13 can be rewritten as eq. 14.

$$[14]\quad \frac{\Delta D}{l} = \pi_2(\varepsilon_{\pi_2} - \varepsilon_{P_2}) = \pi_2\Delta\varepsilon$$

Substituting eq. 14 into eq. 12 and rearranging gives eq. 15.

$$[15]\quad \frac{P_{20}}{\Delta D} = \frac{1}{\Delta\varepsilon l} + \frac{1}{\Delta\varepsilon l K''_{\pi 22}[ol]}$$

Equation 15 predicts that a plot of $P_{20}/\Delta D$ *vs.* 1/[ol] should be linear. In fact such plots were linear for all the olefins studied. From the slope and intercept of these lines could be obtained values of $K''_{\pi 22}$ (and thus $K_{\pi 22}$). Some representative plots are given in Figs. 3 and 4. Values of $K_{\pi 22}$ are summarized in Table 1. At sodium acetate concentrations of over 0.2 *M* a correction was made for conversion of $Na_2Pd_2(OAc)_6$ to $Na_2Pd(OAc)_4$ via reaction 6.

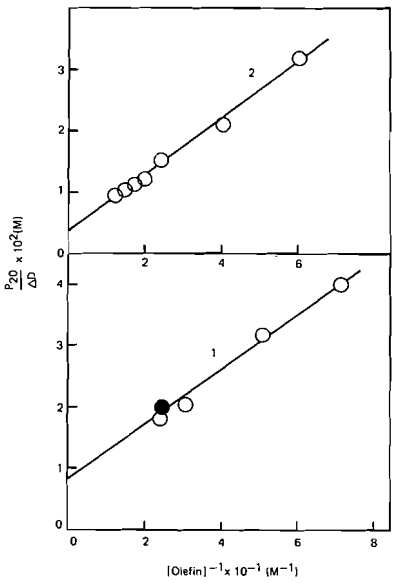

FIG. 3. Plots of $P_{20}/\Delta D$ *vs.* inverse of olefin concentration: (*1*) olefin = ethylene; ○, $[Na_2Pd_2(OAc)_6]$ = 0.0032 *M*; ●, $[Na_2Pd_2(OAc)_6]$ = 0.0016 *M*; [NaOAc] = 0.200 *M*; optical pathlength = 5 mm; (*2*) olefin = styrene; $[Na_2Pd_2(OAc)_6]$ = 0.0063 *M*; [NaOAc] = 0.400 *M*; optical pathlength = 1 mm.

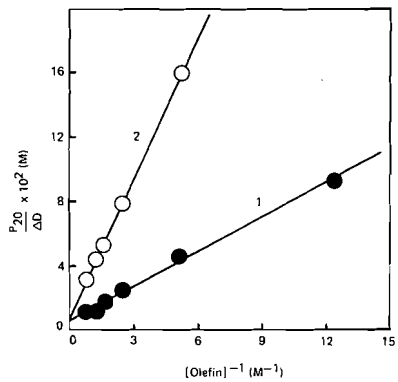

FIG. 4. Plots of $P_{20}/\Delta D$ *vs.* inverse of allylic propionate concentration. $[Na_2Pd_2(OAc)_6]$ = 0.0064 *M*; optical pathlength = 1 mm. (*1*) [NaOAc] = 0.200 *M*; (*2*) [NaOAc] = 1.00 *M*.

The second equilibrium, which took several hours to attain, was studied for vinyl acetate, allyl acetate, and allyl propionate only since the other olefins give a precipitate of Pd metal upon standing this length of time. This precipitate no doubt resulted from oxidation of the ethylene, styrene, and neohexene.

The determination of equilibrium constants for the second equilibria was simplified by the fact that the con-

Can. J. Chem. Downloaded from www.nrcresearchpress.com by 210.87.254.40 on 09/05/12
For personal use only.

TABLE 1. Calculated values of equilibrium constants $K_{\pi 22}$ ($Na_2Pd_2(OAc)_6$ + ol $\overset{K_{\pi 22}}{\rightleftharpoons}$ $NaPd_2(OAc)_5$(ol) + NaOAc) for various olefins using Benesi–Hildebrand plots at 25 °C, at 300 nm*

Olefin	Range of [Olefin] (M)	$[Na_2Pd_2(OAc)_6]_0 \times 10^2$ (M)	$[NaOAc]_0$ (M)	Intercept $= 1/\varepsilon_{\pi 2} xl \times 10^2$ (M)	Slope $= 1/l\varepsilon_{2\pi} K''_{\pi 22} \times 10^2$ (M^2)	$K''_{\pi 22} = \frac{\text{Intercept}}{\text{Slope}}$ (M^{-1})	$K_{\pi 22}(= K''_{\pi 22}$ NaOAc]) (M^0)
$H_2C{=}CH_2$	0.014–0.041	0.16–0.32	0.50	0.79 ± 0.20	0.044 ± 0.005	17.70	8.23
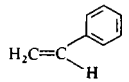	0.016–0.083	0.63	0.40	0.38 ± 0.06	0.046 ± 0.002	8.33	3.13
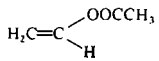	0.162–1.620	0.64	1.00	0.21 ± 0.04	2.62 ± 0.13	0.08	0.07
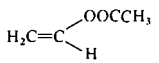	0.162–0.851	0.14	0.20	0.50 ± 0.02	1.11 ± 0.05	0.45	0.09
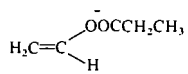	0.285–0.855	0.64	1.00	0.29 ± 0.12	3.71 ± 0.14	0.08	0.07
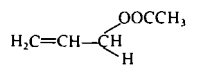	0.045–0.733	0.63	0.20	0.85 ± 0.21	0.61 ± 0.03	1.39	0.28
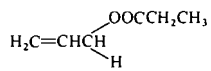	0.200–1.200	0.63	1.00	0.70 ± 0.16	3.05 ± 0.06	0.23	0.20
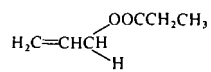	0.080–1.200	0.63	0.20	0.76 ± 0.13	0.68 ± 0.02	1.12	0.22
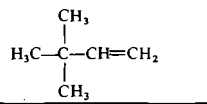	0.191–1.528	0.64	0.20	1.10 ± 0.04	0.51 ± 0.01	2.18	0.44

*The absorbance due to $Na_2Pd_2(OAc)_6$ at this wavelength is minimum ($\varepsilon_{P_2} = 94$) and the difference in absorbance (ΔD) between complex and dimer is about maximum.

Can. J. Chem. Downloaded from www.nrcresearchpress.com by 210.87.254.40 on 09/05/12
For personal use only.

TABLE 2. Typical calculation of equilibrium constants $K_{\pi 21}$ and $K'_{\pi 22}$ at 25 °C, for allyl acetate system

						$Na_2Pd_2(OAc)_6 + 2ol \underset{}{\overset{K_{\pi 21}}{\rightleftharpoons}} 2NaPd(OAc)_3(ol)$		$Na_2Pd_2(OAc)_6 + 2ol \overset{K'_{\pi 22}}{\rightleftharpoons} Pd_2(OAc)_4(ol)_2 + 2NaOAc$	
λ (nm)	$[Na_2Pd_2(OAc)_6]_0$ (*M*)	$[Olefin]_0$ (*M*)	Absorbance* D_i	$[Olefin]_{eq}$ (*M*)	$[Na_2Pd_2(OAc)_6]_{eq} \times 10^2$ (*M*)	$[NaOAc]_0$ (*M*)	$K_{\pi 21}$ (M^{-1})	$[NaOAc]_{eq}$‡ (*M*)	$K'_{\pi 22}$
340	0.0063	0	0.300	—	—	—	—	—	—
		0.0092	0.348	0.0077	0.5554	0.200	6.72	0.1888	80.52
		0.0276	0.420	0.0239	0.4452		5.36	0.1911	28.12
		0.0450	0.492	0.0391	0.3349		6.79	0.1933	21.52
		0.0966	0.598	0.0874	0.1713		6.42	0.1965	13.52
		0.1840	0.669§	0.1726	0.0615		7.05	0.1992	23.53
		0.460†	0.710†	—	—	—	—	—	—
		0.736	0.710						
300	0.0063	0	0.059						
		0.0276	0.389	0.0238	0.4408		5.72	0.1911	27.63
		0.0450	0.560	0.0392	0.3429		6.23	0.1933	20.25
		0.0966	0.874	0.0872	0.1636		6.97	0.1965	14.44
		0.1840	1.050	0.1726	0.0629		6.85	0.1992	11.93
		0.460†	1.160†	—	—	—	—	—	—
		0.736	1.160						
320	0.0032	0.0368	0.256	0.0336	0.0016		5.51	0.1967	33.65
340	0.00596	0.0368	0.438	0.0320	0.0036	0.400	6.17	0.3928	100.00
		0.0738	0.523	0.0664	0.0023		5.33	0.3954	56.79
		0.0920	0.543	0.0840	0.00197		4.56	0.3960	44.87
		0.1840	0.625	0.1735	0.00071		5.12	0 3985	38.79

*Absorbance in 1 mm pathlength.
†Data implying complete complexing, ε_{π_1} at $\lambda_{300} = 920.6$, ε_{π_1} at $\lambda_{320} = 726.9$, ε_{π_1} at $\lambda_{340} = 563.5$; corresponding values of ε_{π_2}' will be twice these values.
‡Calculated free concentration of NaOAc considering the equilibria: $2Pd_3(OAc)_6 + 6NaOAc \overset{K_{32}}{\rightleftharpoons} 3Na_2Pd_2(OAc)_6$; $Na_2Pd_2(OAc)_6 + 2ol \overset{K'_{\pi 22}}{\rightleftharpoons} Pd_2(OAc)_4(ol)_2 + 2NaOAc$.
§Data showing 90% complexing. Mean $K_{\pi 21} = 6.05 \pm 0.76$, $K'_{\pi 22} = 36.8 \pm 25.2$.

Can. J. Chem. Downloaded from www.nrcresearchpress.com by 210.87.254.40 on 09/05/12
For personal use only.

version to π-complex was complete at easily attainable olefin concentrations. Thus the extinction coefficients for both initial and final species are known. Either reaction 9 or 10 can be assumed to be the correct equilibrium and constants calculated. Whichever of $K_{\pi 21}$ or $K'_{\pi 22}$ remains constant with changing reaction conditions is correct. Sample calculations for allyl acetate are given in Table 2.

Results

Composition of Complexes, Job Plots

Plots of absorption of light (ΔD) *vs.* composition of dimer–olefin solutions, Figs. 1 and 2, show a wavelength dependence of maxima. Such a result would not be expected when only a single complex is formed. In fact for a single complex the maxima or minima in ΔD should be independent of the wavelength of light used. Similar results have been reported by Vosburgh and Cooper (15) for *o*-phenanthroline and nickel ion complexes. A critical review of the application of the method of continuous variation in the case of mixed complexes has been discussed by Rossotti and Rossotti (16). As shown below the application of this method in determining the stoichiometry of the complexes formed in the present work proved particularly simple. First under the experimental conditions of Job plots (Figs. 1 and 2) the species formed are stable. Second, the difference between the extinction coefficients of the two complexes and dimeric species in different regions of spectrum is great.

Now assume that reaction 8 and either reaction 9 or 10 are operative. Since the Job plot will not distinguish between [9] or [10] assume for simplicity that [8] and [9] are the two equilibria and designate π_2' for $[Pd_2(OAc)_4(ol)_2]$ and ε_{π_2}' its corresponding extinction coefficient. Then since ε_{ol} is negligible at the wavelength used, for sample (S) and reference (R) solutions, the optical density is given by

$$[16] \qquad D_S = l(\varepsilon_{P_2}P_2 + \varepsilon_{\pi_2}\pi_2 + \varepsilon_{\pi_2}'\pi_2')$$

$$[17] \qquad D_R = l(\varepsilon_{P_2}M(1 - x))$$

where x is the mole fraction of olefin.

Subtracting eq. 17 from eq. 16 gives eq. 18

$$[18] \quad \Delta D = D_S - D_R = l(\varepsilon_{P_2}P_2 + \varepsilon_{\pi_2}\pi_2 + \varepsilon_{\pi_2}'\pi_2' - \varepsilon_{P_2}M(1 - x))$$

The mass balance is given by eqs. 19 and 20

$$[19] \qquad P_2 = M(1 - x) - \pi_2 - \pi_2'$$

$$[20] \qquad \frac{dP_2}{dx} = -M - \frac{d\pi_2}{dx} - \frac{d\pi_2'}{dx}$$

Differentiating eq. 18 and substituting for dP_2/dx from eq. 20, eq. 21 follows:

$$[21] \quad \frac{d}{dx}(\Delta D) = l\left\{(\varepsilon_{\pi_2} - \varepsilon_{P_2})\frac{d\pi_2}{dx} + (\varepsilon_{\pi_2}' - \varepsilon_{P_2})\frac{d\pi_2'}{dx}\right\}$$

If the complex formed is assumed to be $[NaPd(OAc)_3(ol)](\pi_1)$, (reaction 10), then the corresponding relation for $d(\Delta D)/dx$ is given by

$$[22] \quad \frac{d}{dx}(\Delta D) = l\left\{(\varepsilon_{\pi_2} - \varepsilon_{P_2})\frac{d\pi_2}{dx} + (\varepsilon_{\pi_1} - \tfrac{1}{2}\varepsilon_{P_2})\frac{d\pi_1}{dx}\right\}$$

Equations 21 and 22 imply that the maxima will depend on the extinction coefficients at the wavelengths used. If $\varepsilon_{\pi_2} - \varepsilon_{P_2}$ is much greater than $\varepsilon_{\pi_2}' - \varepsilon_{P_2}$ or $\varepsilon_{\pi_1} - \frac{1}{2}\varepsilon_{P_2}$ then the maxima will occur at the 1:1 complex. This is apparently the case at λ = 320, 330, and 335 nm while at λ = 280 and 290 nm the opposite is the case and the maximum occurs at the 2-olefin:1-$Na_2Pd_2(OAc)_6$ complex.

Note that because of the lack of precision of the data (see Experimental) the Job plots cannot be treated in a quantitative fashion. Thus, the plots are not linear on either side of the maxima as would be expected from high quality Job plots. However, the maxima do occur at approximately the expected compositions.

Labile π-Complex

The wavelengths at which the 1:1 maxima appears on the Job plots are those wavelengths at which the initial rapidly formed complex absorbs strongly.

If, as this result indicates, reaction 8 represents the rapid equilibrium, then the data can be treated by the Benesi–Hildebrand method (14). This treatment predicts a linear plot of $P_{20}/\Delta D$ *vs.* 1/[olefin]. As shown in Figs. 3 and 4 linear plots were obtained for which an equilibrium constant, $K''_{\pi 22}$ (eq. 12), could be calculated at any given [NaOAc]. Since a single run does not give the [NaOAc] term in the equilibrium, runs were made in some cases at more than one [NaOAc]. As can be seen from

Can. J. Chem. Downloaded from www.nrcresearchpress.com by 210.87.254.40 on 09/05/12
For personal use only.

TABLE 3. Values of the equilibrium constants $K_{\pi 21}$ at 25 °C for various olefin complexes of Pd(II)

Olefin	$K_{\pi 21}$ (M^{-1})
$H_2C{=}C(O_2CCH_3)H$	0.51 ± 0.05*
$H_2C{=}CH{-}CH(O_2CCH_3)H$	6.7 ± 1.2
$H_2C{=}CH{-}CH(O_2CCH_2CH_3)H$	8.8 ± 2.1

*Standard deviation.

Table 1, $K''_{\pi 22}$ varies with [NaOAc] but the true equilibrium constant, $K_{\pi 22}$ does not.

Nonlabile π-complex

The wavelengths for the Job plot at which the maximum for a 2:1 olefin to $Na_2Pd(OAc)_6$ π-complex was obtained corresponded to the region in which the slowly formed complex absorbed strongly. This suggests the equilibrium is represented either by reaction 9 or 10. Sample calculations of the values of $K_{\pi 21}$ and $K'_{\pi 22}$ with allyl acetate as substrates are given in Table 2. It is apparent that $K'_{\pi 22}$ varies much more than $K_{\pi 21}$. This is particularly evident when the sodium acetate concentration is varied. This type of result was obtained with all three olefins. Thus reaction 9 must be the correct equilibrium for the slow reaction. The values of $K_{\pi 21}$ for the three olefins are given in Table 3.

Discussion

The evidence for the types of equilibrium in this system is twofold. First there are the Job plots shown in Figs. 1 and 2. Unfortunately these plots are not of the highest quality because of the limited solubility of $Na_2Pd_2(OAc)_6$ (see Experimental) and are only semiquantitative indications of the compositions of the complexes. However, it is interesting that both the rapidly and slowly formed π-complexes could be detected and their approximate stoichiometry determined.

The second type of evidence involves the Benesi–Hildebrand plots for the labile complex (Figs. 3 and 4) and the calculation of equilibrium constants from spectral data at final equilibrium (Table 2). This second type of evidence is certainly the most quantitative and conclusive evidence for the correct modes of complexing since the accuracy of the data is not limited by $Na_2Pd_2(OAc)_6$ solubility.

In any case both types of results are in agreement and clearly indicate that replacement of terminal acetates on palladium(II) acetate by olefins is a fast reaction while breaking of acetate bridges is a slow reaction. The nonlability of bridging

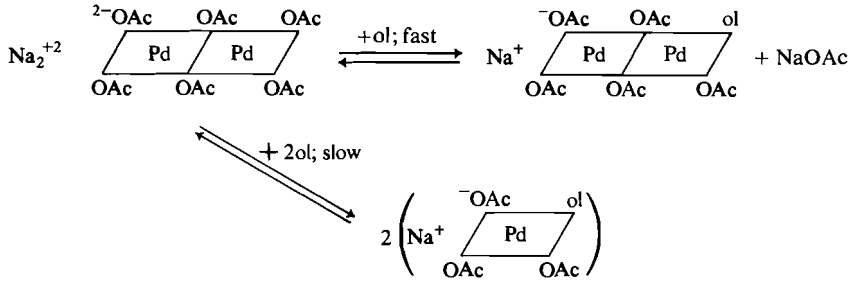

[23]

acetates was demonstrated by the previous study on reaction of palladium(II) acetate with sodium acetate in acetic acid (8) but the demonstration of lability of terminal acetates is new. The exact reason for the nonlability of bridging acetates is not known. It could be that the acetate in the bridging form is particularly stable or it could be related to the fact that two acetate bridges must be broken simultaneously to give the monomer π-complexes. A kinetic study of the interaction of $Na_2Pd_2(OAc)_6$ with allyl acetate, presently in progress,[2] could shed some light on this question.

The two equilibria found in the all-acetate

[2]R. N. Pandey. Unpublished results.

Can. J. Chem. Downloaded from www.nrcresearchpress.com by 210.87.254.40 on 09/05/12
For personal use only.

system are analogous to those found for allylic esters in the chloride system containing lithium chloride (6). In that system only the dimeric to monomeric π-complex was observed by equilibrium measurements (reaction 3) but small amounts of dimeric π-complex (reaction 4) were inferred from kinetic measurements on allylic ester exchange. In the present study the amount of dimeric π-complex at equilibrium was also much smaller than the monomeric π-complex. However the dimeric π-complex could be detected in the all-acetate system only because it was formed much more rapidly than monomeric π-complex. The formation of $[Pd_2(OAc)_4(ol)_2]$ which would be analogous to one of the species postulated in the sodium chloride containing system (4, 5) was not found. However it may well be formed in the sodium chloride system since sodium chloride is sparingly soluble (0.013 *M*) in acetic acid and the form of $[Pd_2Cl_4(ol)_2]$ would be strongly inhibited by free chloride. In the present study a sodium acetate level of at least 0.2 *M* had to be used to maintain the palladium(II) acetate in the dimeric state.

As was pointed out previously (8) the fact that sodium acetate equilibrates with palladium(II) acetate slowly complicates kinetic studies of Pd(II) catalysis in this system. The present results indicate further complications. For fast Pd(II) catalyzed reactions of olefins only the formation of dimeric π-complex will be important while for slow reactions the monomeric species will predominate. For systems in which the rate of catalysis is about equal to the rate of formation of $NaPd(OAc)_3(ol)$ the kinetics will be very complicated. Previous studies in the chloride system indicated the dimer was catalytically active while the monomer was not and preliminary results in this laboratory (17) indicate the same is true in the all-acetate system. Thus an olefin will inhibit its own reaction with Pd(II) by forming unreactive monomeric π-complex. In the acetate system the rate will change with time as reactive $NaPd_2(OAc)_5(ol)$ is slowly converted to unreactive $NaPd(OAc)_3(ol)$. In any case previous work on ethylene oxidation in this system (7) must be reinterpreted in light of the present results.

The fact that both monomeric and dimeric π-complexes were detected by the Job plots deserves brief comment. Since the formation constants for the monomeric π-complexes are much higher than those for the dimeric complexes one might expect that only the former be produced at complete equilibrium and in fact at the olefins concentrations used in most of the equilibrium work this is by far the predominate species. However because of the limited solubility of $Na_2Pd_2(OAc)_6$ the olefin concentration also had to be very low. Because of the nature of the equilibria (reactions 8 and 9), lower olefin concentrations favor $[NaPd_2(OAc)_5(ol)]$ more than $[NaPd(OAc)_3(ol)]$ and it was fortuitous that at the olefin concentrations used both were formed in sufficient amounts for detection.

The authors thank the National Research Council of Canada for financial support of this work.

1. P. M. MAITLIS. The organic chemistry of palladium, Vols. I and II. Academic Press, New York, N.Y. 1971.
2. F. R. HARTLEY. The chemistry of platinum and palladium. John Wiley and Sons, New York. 1973.
3. F. R. HARTLEY. Chem. Rev. **69**, 799 (1969).
4. B. I. CRUIKSHANK and N. R. DAVIES. Aust. J. Chem. **25**, 919 (1972).
5. F. R. HARTLEY and J. L. WAGNER. J. Organometal. Chem. 395 (1973).
6. P. M. HENRY. J. Am. Chem. Soc. **94**, 1527 (1972).
7. I. I. MOISEEV, A. P. BELOV, V. A. IGNOSHIV, and YA. K. SYRKIN. Dokl. Akad. Nauk SSSR, **173**, 863 (1967).
8. R. N. PANDEY and P. M. HENRY. Can. J. Chem. **52**, 1241 (1974).
9. P. M. HENRY and O. W. MARKS. Inorg. Chem. **10**, 373 (1971).
10. T. A. STEPHENSON, S. M. MOREHOUSE, A. R. POWELL, J. P. HEFFER, and G. WILKINSON. J. Chem. Soc. 3632 (1965).
11. W. C. EICHELBERGER and V. K. LAMER. J. Am. Chem. Soc. **55**, 3633 (1933).
12. W. W. SCOTT. Standard methods of chemical analysis, Vol. I, 6th ed. Van Nostrand, Princeton, N.J. 1962. p. 883.
13. P. JOB. Ann. Chim. Paris, **9**, 113 (1928); Chem. Abstr. **22**, 2120 (1928).
14. H. A. BENESI and J. H. HILDEBRAND. J. Am. Chem. Soc. **71**, 2703 (1949).
15. W. C. VOSBURGH and G. R. COOPER. J. Am. Chem. Soc. **63**, 437 (1941).
16. F. J. C. ROSSOTTI and H. ROSSOTTI. The determination of stability constants. McGraw-Hill, New York. 1961. p. 47–51.
17. P. M. HENRY and R. N. PANDEY. Adv. Chem. Ser. **132**, 33 (1974).

The *trans*-Effect in Octahedral Complexes. VI. Base Hydrolysis of *trans*-Hydroxybromo and *trans*-Hydroxychlorobis(ethylenediamine)-rhodium(III) Complexes

ANTHONY POË AND CAROL VUIK

Erindale College and the Department of Chemistry, University of Toronto, Mississauga, Ontario L5L 1C6

Received January 22, 1975

ANTHONY POË and CAROL VUIK. Can. J. Chem. **53**, 1842 (1975).

The kinetics of base hydrolysis of the complexes *trans*-$[Rh(en)_2(OH)X]^+$ (X = Br or Cl) follow the pseudo first order rate equation $k_{obs} = k_1 + k_2[OH^-]$. The small contribution of the $[OH^-]$-dependent term is due to lower values of $\Delta S_2^* - \Delta S_1^*$ than are observed for the complexes *cis*-$[Rh(en)_2(OH)Cl]^+$ and $[Rh(NH_3)_5X]^{2+}$ (X = Cl, Br, or I). The values of ΔH_1^* are used to obtain new values of the *intrinsic kinetic trans*-effect (i.k.t.e.) of hydroxide that agree with that determined from aquation of *trans*-$[Rh(en)_2(OH)I]^+$ and place hydroxide in the i.k.t.e. series $I \gg Br > NH_3 > OH \gtrsim Cl$. The new data also allow hydroxide to be placed in a thermodynamic *trans*-effect (t.t.e.) series $I > OH > NH_3 > Br > Cl > OH_2$, and the different position of hydroxide in the two series is discussed.

ANTHONY POË et CAROL VUIK. Can. J. Chem. **53**, 1842 (1975).

La cinétique de l'hydrolyse basique des complexes $[Rh(en)_2(OH)X]^+$ *trans* (X = Br ou Cl) suit l'équation de vitesse du pseudo premier ordre: $k_{obs} = k_1 + k_2[OH^-]$. La faible contribution du terme dépendant de $[OH^-]$ est dû aux valeurs plus faibles de $\Delta S_2^* - \Delta S_1^*$ que celles observées pour les complexes $[Rh(en)_2(OH)Cl]^+$ *cis* et $[Rh(NH_3)_5X]^{2+}$ (X = Cl, Br ou I). On utilise les valeurs de ΔH_1 pour obtenir de nouvelles valeurs de l'effet *cinétique intrinsèque trans* (i.k.t.e.) de l'hydroxyde qui sont en accord avec celle déterminée à partir de l'aquation du $[Rh(en)_2(OH)I]^+$ *trans*; ces résultats indiquent que dans la série i.k.t.e. l'hydroxyde se range de la façon suivante: $I \gg Br > NH_3 > OH \gtrsim Cl$. Les nouvelles données permettent aussi de ranger l'hydroxyde dans une série d'effet thermodynamique *trans* (t.t.e.) $I > OH > NH_3 > Br > Cl > OH_2$; on discute de la position d'hydroxyde des deux séries.

[Traduit par le journal]

A kinetic study of the base hydrolysis of *trans*-$[Rh(en)_2(OH)I]^+$ has been reported (1). The reaction followed the rate equation $k_{obs} = k_1 + k_2[OH^-]$ and the value of ΔH_1^* was combined with the enthalpy of activation for the anation of *trans*-$[Rh(en)_2(OH)OH_2]^{2+}$ by iodide (2) to provide a single measure of the *intrinsic kinetic trans*-effect (i.k.t.e.) (3) of hydroxide in such complexes. Since the i.k.t.e. of any ligand is obtained in such a way that it should be independent of the particular interchange reaction used to measure it we now report kinetic studies of the base hydrolysis of the analogous hydroxybromo and hydroxychloro complexes which confirm this independence for the *trans*-hydroxy complexes. The second-order term in the rate equation for reaction of *trans*-$[Rh(en)_2(OH)I]^+$ (not previously found in such *trans*-diacido complexes (4, 5)) has also been found in these reactions.

Experimental

The complexes *trans*-$[Rh(en)_2X_2]ClO_4$ (X = Cl or Br) were prepared by standard methods (6, 7). Satisfactory analyses were obtained for carbon, nitrogen, and hydrogen and the electronic spectra (Table 1) of aqueous solutions of the complexes were in satisfactory agreement with published results (6, 8) although there are some slight differences in the extinction coefficients, particularly of the highest energy band of the dibromo complex (*cf.* $\varepsilon = 31\,000\ cm^{-1}\ l\ mol^{-1}$ (8)). Two previously unreported higher energy bands for the dichloro complex are also listed. Solutions of the *trans*-hydroxyhalogeno complexes were obtained by dissolving *ca.* 1 mmol of the *trans*-dihalogeno complexes in the minimum of hot water and refluxing with 1 cc of 0.1 *M* perchloric acid and 10 cc of *ca.* 0.1 *M* silver perchlorate (1 equiv.) for 200 min (X = Cl) or 40 min (X = Br). Curved rate plots were obtained when the base hydrolyses of such solutions were studied spectrophotometrically and it was evident that the solutions contained mixtures of complexes. Pure solutions of the hydroxyhalogeno complexes were obtained by pressure chromatography through a 12 cm-long column of Dowex 50W (100–200 mesh). Elution with 0.5 *M* sodium perchlorate

Can. J. Chem. Downloaded from www.nrcresearchpress.com by 210.87.254.105 on 09/05/12
For personal use only.

TABLE 1. Electronic absorption spectra of some *trans*-$[Rh(en)_2XY]^+$ complexes

X	Y	λ_{max} (nm)	ε (cm^{-1} l mol^{-1})
Cl	Cl	410, 289, ~240(sh), 207	82, 121, 1700, 39 600
Br	Br	431, 277, 234	115, 2900, 37 800
I	I	467, 342	271, 16 000
OH	Br	376, 290(sh)	105, 148
OH	Cl	370, 293	94, 134
OH	OH[a]	297, 347	133, 102
OH	OH[b]	297, 348	133, 100
OH	OH[c]	296, 346	128, 98
OH	OH[d]	297, 346	129, 97
OH	OH[e]	297, 346	131, 99
OH	OH[f]	298, 347	130, 97

[a]From *trans*-$[Rh(en)_2(OH)I]^+$ and 1.0 *M*- hydroxide.
[b]From *trans*-$[Rh(en)_2(OH)I]^+$ and 0.1 *M* hydroxide.
[c]From *trans*-$[Rh(en)_2(OH)Br]^+$ and 0.7 *M* hydroxide.
[d]From *trans*-$[Rh(en)_2(OH)Br]^+$ and 0.07 *M* hydroxide.
[e]From *trans*-$[Rh(en)_2(OH)Cl]^+$ and 0.7 *M* hydroxide.
[f]From *trans*-$[Rh(en)_2(OH)Cl]^+$ and 0.07 *M* hydroxide.

completely removed the *trans*-dihalogeno complexes (detected and identified by their electronic spectra) and subsequent elution with a solution 0.1 *M* in sodium hydroxide and 0.5 *M* in sodium perchlorate removed what was believed to be the *trans*-hydroxyhalogeno complexes. Reaction with acid solutions of the appropriate halide reconverted these into spectroscopically pure solutions of the corresponding *trans*-dihalogeno complexes. A knowledge of the absorbances of the particular eluate used, of the sum of the absorbances and volumes of all the eluates containing particular complexes, and of the appropriate extinction coefficients of the *trans*-dihalogeno complexes, enabled an estimate to be made of the proportion of the unreacted *trans*-dihalogeno complexes in the original solutions of the reaction products (*ca.* 15% in both cases). The concentration of hydroxyhalogeno complexes in a particular eluate was also easily obtained from the absorbances of the *trans*-dihalogeno complexes produced after anation with acid halide solutions. The spectroscopic data for the hydroxyhalogeno complexes are also reported in Table 1 together with those for the dihydroxy product of base hydrolysis. It can be seen that the latter are essentially independent of the nature of the starting complex and the hydroxide concentration. The assignment of a *trans*-structure to these complexes is made on the grounds (*a*) that the kinetic behavior (see below) shows that the solutions are "kinetically" pure, *i.e.* they contain only one species since it is highly unlikely that *cis* and *trans* complexes would react at the same rates, (*b*) the product of base hydrolysis is spectroscopically pure *trans*-$[Rh(en)_2(OH)_2]^+$ (2), and (*c*) that complete *trans* → *cis* rearrangement during the reaction of *trans*-$[Rh(en)_2X_2]^+$ with silver ions, and complete *cis* → *trans* rearrangement on anation of the aquohalogeno complexes and on base hydrolysis of the hydroxyhalogeno complexes is not in accord with the known stereochemical retention that occurs in all reactions of *trans*-dihalogeno complexes studied so far (5, 7–9). The only cases where substantial *trans* → *cis* rearrangements have been found in such diacido complexes are in base hydrolysis of the *trans*-dihalogeno complexes (10). These rearrangements were shown to be associated with the $[OH^-]$-dependent term that appears in the rate equation. The mixed *cis* and *trans* products of such reactions were easily detected by their own u.v.–visible spectra, by the spectra of the mixed dihalogeno products of their anation reactions, and by their separation by ion exchange chromatography (10).

Spectroscopic Changes During Base Hydrolysis

The spectra changed smoothly from those characteristic of the *trans*-hydroxyhalogeno complexes to that of the *trans*-dihydroxy complex. Absorbance changes in the 300–400 nm range were quite small but clear isosbestic points were observed at 301 and 360 nm (hydroxybromo reaction) and at 296 and 358 nm (hydroxychloro reaction). In both cases quite large absolute decreases in absorbance occurred below *ca.* 250 nm because of a shift in a very high intensity band to lower wavelengths, this shift being greater during reaction of the hydroxybromo complex. In the reactions of the hydroxychloro complex the spectral changes at *ca.* 250 nm depended slightly on the concentration of hydroxide, isosbestic points that appeared at 253 and 266 nm in 0.07 *M* not being evident in 0.7 *M* hydroxide.

Kinetics of Base Hydrolysis

Reactions were followed spectrophotometrically, the reacting solutions being contained in 10 mm cells in thermostatted cell holders of a Perkin–Elmer 402 or Cary 16K spectrophotometer, up to five reactions being followed simultaneously. Temperatures were measured either with a thermistor (Cary 16K) or precision thermometer (Perkin–Elmer 402). Reaction mixtures came to constant temperature within 10 min and exposure to the spectrophotometer light for different amounts of time had no effect on the rates. The kinetics were followed at 250 or 255 nm (hydroxybromo complex; absorbance decreased from *ca.* 1.2 to 0.6) and at 240 nm (hydroxy-

Can. J. Chem. Downloaded from www.nrcresearchpress.com by 210.87.254.105 on 09/05/12
For personal use only.

Can. J. Chem. Downloaded from www.nrcresearchpress.com by 210.87.254.105 on 09/05/12
For personal use only.

TABLE 2. Kinetic data for reaction of *trans*-$[Rh(en_2)OHBr]^+$ with hydroxide. [Complex] = 1.3×10^{-3} *M*. Ionic strength = 1.0 *M*

Temperature (°C)	$[OH^-]$ (*M*)	$10^5 k_{obs}$ s^{-1}	Temperature (°C)	$[OH^-]$ (*M*)	$10^5 k_{obs}$ (s^{-1})
78.94	0.0301	143	63.4	0.630	28.8
	0.230	149		0.830	32.0
	0.430	160	56.51	0.0301	10.9
	0.630	165		0.230	11.2
	0.830	171		0.430	11.9
69.72	0.0301	53.2		0.630	12.6
	0.230	53.2		0.830	13.6
	0.430	58.9	50.06	0.0301	4.86
	0.630	62.9		0.230	4.98
	0.830	65.8		0.430	5.37
63.4	0.0301	25.4		0.630	5.68
	0.230	26.1		0.830	6.02
	0.430	27.7			

TABLE 3. Kinetic data for reaction of *trans*-$[Rh(en)_2(OH)Br]^+$ with 0.032 *M* hydroxide. [Complex] = 1.3×10^{-3} *M*. Ionic strength = 1.0 *M**

Temperature (°C)	$10^5 k_{obs}$ (s^{-1})		
79.64	156	159	162
73.77	82.5	82.7	83.4
69.10	49.2	49.4	51.2
63.63	26.4	25.8	25.7
59.40	15.6	15.3	15.3
54.04	7.83	8.04	7.76
50.04	4.66	4.66	4.56

*$\Delta H_{obs}^{\ddagger} = 26.38 \pm 0.10$ kcal mol^{-1}; $\Delta S_{obs}^{\ddagger} = 3.11 \pm 0.29$ cal mol^{-1} deg^{-1}; $\sigma(k_{obs}) = \pm 2.0\%$.

chloro complex; absorbance decreased from *ca.* 1.0 to 0.6). Excellent first order rate plots were obtained (linear for three half-lives) and the dependence of the pseudo-first-order rate constants (Tables 2 and 4) on $[OH^-]$ was determined up to $[OH^-] = ca.$ 0.8 *M*, the ionic strength being maintained at 1.0 *M* with sodium perchlorate. A small but significant dependence was observed and the data were analyzed by a linear weighted least squares treatment according to the rate equation $k_{obs} = k_1 + k_2[OH^-]$, all values of k_{obs} being assumed to have the same percentage standard deviation. When values at a given temperature were considered separately there seemed to be no significant change of $\sigma(k_{obs})$ with temperature so values of k_{obs} at all temperatures were assumed to have the same standard deviation, the number of degrees of freedom being thereby greatly increased. When this pooling was applied to data for the reaction of *trans*-$[Rh(en)_2(OH)I]^+$ (1) the activation parameters previously reported were modified very slightly and the new values are given in Table 5 for comparison. Values of k_1, k_2, and $\sigma(k_{obs})$ are shown in Table 5, the uncertainties (standard deviations) having been corrected according to the number of degrees of freedom so that good estimates of 95% confidence levels can be obtained by doubling the standard deviations. Activation parameters (Table 5) were estimated by a linear weighted least squares analysis of the dependence of $\log(k_1/T)$ and $\log(k_2/T)$ on $1/T$, the uncertainties in $\log(k_1/T)$ and $\log(k_2/T)$ being derived from the uncertainties in k_1 and k_2. In the case of reactions of the *trans*-hydroxybromo complex with 0.032 *M* hydroxide (Table 3) the k_2 term contributed less than 1% to the value of k_{obs} (Table 5) and values of $\Delta H_1^{\ddagger}$ and $\Delta S_1^{\ddagger}$ for this reaction were calculated by a least squares analysis, all the rate constants in Table 3 being assumed to have the same percentage standard deviation.

Discussion

The Intrinsic Kinetic trans-Effect of Hydroxide

If the kinetic *trans*-effects of various ligands L in *trans*-$[RhA_4LX]^{n+}$ complexes (A = NH_3 or $\frac{1}{2}$en) are defined simply in terms of the relative rate constants or activation enthalpies for displacement of X by a water molecule (or for the reverse, anation reaction) then it is found that the *trans*-effect order depends on the nature of X (1–3). However, it has been shown (3) that an *intrinsic kinetic trans*-effect (i.k.t.e.) can be defined by comparing the activation enthalpy for a particular reaction with that found ($\Delta H_{ref}^{\ddagger}$) for a hypothetical reaction

[1] *trans*-$[Rh(en)_2IY]^{n+} + OH_2 \rightleftharpoons$ *trans*-$[Rh(en)_2I(OH_2)]^{(n+1)+} + Y^-$

that has the same value of ΔH^0. The latter values are obtained by interpolation of plots of $\Delta H^{\ddagger}$

TABLE 4. Kinetic data for reaction of *trans*-$[Rh(en)_2(OH)Cl]^+$ with hydroxide. [Complex] = 3×10^{-3} *M*. Ionic strength = 1.0 *M*

Temperature (°C)	$[OH^-]$ (*M*)	$10^5 k_{obs}$ (s^{-1})	Temperature (°C)	$[OH^-]$ (*M*)	$10^5 k_{obs}$ (s^{-1})
75.76	0.233	98.7	58.02	0.633	15.9
	0.433	107		0.833	16.7
	0.633	113	53.77	0.233	8.18
	0.833	119		0.433	8.98
71.80	0.233	65.5		0.633	9.50
	0.433	73.2		0.833	9.76
	0.633	77.1	49.89	0.233	5.11
	0.833	81.0		0.433	5.47
64.80	0.233	31.0		0.633	5.85
	0.433	34.2		0.833	6.22
	0.633	36.9	45.50	0.233	2.91
	0.833	37.9		0.433	3.12
58.02	0.233	14.3		0.633	3.28
	0.433	15.0		0.833	3.52

against ΔH^0 for reactions of the *trans*-iodo complexes, these being a useful reference since iodide has the strongest *trans*-effect of the ligands so far studied, and the data obtained for these complexes are among the most precise found (9, 11). The larger the value for $\Delta H_{obs}^{\ddagger} - \Delta H_{ref}^{\ddagger}$ the smaller the i.k.t.e.

Kinetic data for the reactions

[2] *trans*-$[Rh(en)_2(OH)I]^+ + OH_2 \rightleftharpoons$ *trans*-$[Rh(en)_2(OH)OH_2]^{2+} + I^-$

showed, by comparison with other reactions involving interchange of iodide and OH_2 ligands but with different groups in the position *trans* to the reaction site, that the simple kinetic *trans*-effect of hydroxide did depend on the nature of the reaction chosen to measure it (1). Derivation of the i.k.t.e. removed this ambiguity and a value very close to that for chloride was obtained. The data reported here enable a further test to be made of the conclusion that values of the i.k.t.e. should be independent of the particular reactions used to measure it since the values of $\Delta H_1^{\ddagger}$ obtained (Table 5) can be taken to be the activation enthalpies for the aquation reactions of the *trans*-hydroxybromo and *trans*-hydroxychloro complexes, the hydroxide being necessary only to drive the re-

TABLE 5. Kinetic parameters[a] derived according to the rate equation: $k_{obs} = k_1 + k_2[OH^-]$

Complex	Temperature (°C)	$10^5 k_1$ (s^{-1})	$10^5 k_2$ (l mol^{-1} s^{-1})	Parameter	Value
trans-$[Rh(en)_2(OH)Br]^+$	78.94	141.9 ±2.7	36.5 ±5.6	$\Delta H_1^{\ddagger}$	25.99±0.19 kcal mol^{-1} [b]
	69.72	51.3 ±1.0	17.3 ±2.1	$\Delta S_1^{\ddagger}$	1.91±0.57 cal mol^{-1} deg^{-1} [b]
	63.38	24.7 ±0.5	7.70±1.0	$\Delta H_2^{\ddagger}$	25.08±1.30 kcal mol^{-1}
	56.51	10.6 ±0.2	3.33±0.44	$\Delta S_2^{\ddagger}$	−3.11±3.88 cal mol^{-1} deg^{-1}
	50.06	4.73±0.09	1.50±0.19	$\sigma(k_{obs})$	±2.3%
trans-$[Rh(en)_2(OH)Cl]^+$	75.75	91.4 ±1.8	33.7 ±3.2	$\Delta H_1^{\ddagger}$	25.14±0.15 kcal mol^{-1}
	71.80	60.5 ±1.2	25.7 ±2.1	$\Delta S_1^{\ddagger}$	−0.67±0.46 cal mol^{-1} deg^{-1}
	64.80	28.6 ±0.6	12.0 ±1.0	$\Delta H_2^{\ddagger}$	25.84±0.70 kcal mol^{-1}
	58.02	13.3 ±0.3	4.03±0.45	$\Delta S_2^{\ddagger}$	−0.49±2.10 cal mol^{-1} deg^{-1}
	53.77	7.67±0.15	2.69±0.26	$\sigma(k_{obs})$	±1.3%
	49.89	4.67±0.09	1.87±0.17		
	45.50	2.69±0.05	0.98±0.09		

[a] Values of activation parameters for reaction of *trans*-$[Rh(en)_2(OH)I]^+$ are $\Delta H_1^{\ddagger} = 27.81 \pm 0.18$ kcal mol^{-1}, $\Delta S_1^{\ddagger} = 5.01 \pm 0.52$ cal mol^{-1} deg^{-1}, $\Delta H_2^{\ddagger} = 29.34 \pm 0.85$ kcal mol^{-1}, $\Delta S_2^{\ddagger} = 7.93 \pm 2.48$ cal mol^{-1} deg^{-1} ($\sigma(k_{obs}) = \pm 3.7\%$). These values are very slightly different from those in ref. 1 because $\sigma(k_{obs})$ has here been assumed to be the same at all temperatures.
[b] *Cf.* activation parameters in Table 3. Weighted average gives $\Delta H_1^{\ddagger} = 26.30 \pm 0.09$ kcal mol^{-1}, $\Delta S_1^{\ddagger} = 2.87 \pm 0.26$ cal mol^{-1} deg^{-1}.

Can. J. Chem. Downloaded from www.nrcresearchpress.com by 210.87.254.105 on 09/05/12
For personal use only.

Can. J. Chem. Downloaded from www.nrcresearchpress.com by 210.87.254.105 on 09/05/12
For personal use only.

action to completion by converting the aquo product to the hydroxy form.

Values of the activation enthalpies for the reactions

[3] *trans*-$[Rh(en)_2(OH)OH_2]^{2+} + X^- \rightarrow$ *trans*-$[Rh(en)_2(OH)X]^+$

(X = Cl or Br) are not known because, at the p*H* at which the hydroxyaquo complex exists as the preponderate species compared with the dihydroxy and diaquo complexes, the products of this reaction are the chloro and bromoaquo complexes that undergo further reaction in such a way as to make study of the first step extremely difficult (2). However, the enthalpies of activation for anation of such rhodium(III) complexes depend on the nature of the halide in a way which seems to be essentially independent of the nature of the complex. Thus $\Delta H^{\ddagger}$ for anation of *trans*-$[Rh(en)_2LOH_2]^{2+}$ by chloride is 0.9 ± 0.4, -0.3 ± 0.6, and 0.9 ± 0.1 kcal mol^{-1} greater than that for anation by bromide when L is Cl, Br, and I, respectively (11). Similarly, $\Delta H^{\ddagger}$ for anation of $[Rh(NH_3)_5OH_2]^{3+}$ by chloride, is 0.2 ± 0.6 kcal mol^{-1} greater than for anation by bromide (3). These values are not distinguishably different within the precision of the measurements. (The constancy of these differences in relative nucleophilic character, when the latter is defined in terms of $\Delta H^{\ddagger}$ for anation, is also generally implied by the fact that a plot of $\Delta H^{\ddagger}$ against ΔH^0 for anation or aquation of complexes with a particular *trans* group lies a constant value of $\Delta H^{\ddagger}$ above the corresponding plot for reactions involving a different *trans* group (3).) Quite precise values of differences in $\Delta H^{\ddagger}$ for anation of *trans*-$[Rh(en)_2IOH_2]^{2+}$ by chloride and iodide (1.4 ± 0.2 kcal mol^{-1}), and by bromide and iodide (0.6 ± 0.1 kcal mol^{-1}) were obtained directly by competition studies (11) and compare quite well with corresponding differences of 1.1 ± 0.5 and 0.9 ± 0.4 kcal mol^{-1} for anation of $[Rh(NH_3)_5OH_2]^{3+}$ for which each anation reaction was studied separately (3), thus leading to lower precision. We therefore assume that the relative nucleophilicities (in terms of $\Delta H^{\ddagger}$ for anation) of chloride, bromide, and iodide are the same for *trans*-$[Rh(en)_2(OH)OH_2]^{2+}$ as for *trans*-$[Rh(en)_2IOH_2]^{2+}$ and obtain values of $\Delta H^{\ddagger} = 25.2 \pm 0.2_5$ and $24.4 \pm 0.1_9$ kcal mol^{-1} for anation of *trans*-$[Rh(en)_2(OH)OH_2]^{2+}$ by chloride and bromide, respectively. These lead to values of -0.1 ± 0.3 (X = Cl) and 1.9 ± 0.2 (X = Br) kcal mol^{-1} for ΔH^0 for the reactions

[4] *trans*-$[Rh(en)_2(OH)X]^+ \rightarrow$ *trans*-$[Rh(en)_2(OH)OH_2]^{2+} + X^-$

The reference values $\Delta H_{ref}^{\ddagger}$ for the hypothetical reactions of *trans*-iodo complexes that have the same values of ΔH^0 as reaction 4 are 20.3 ± 0.2 and 21.4 ± 0.1 kcal mol^{-1} for X = Cl and Br, respectively, and 20.4 ± 0.2 and 19.4 ± 0.1 kcal mol^{-1} for reaction 3 with X = Cl and Br, respectively. The differences between the values of $\Delta H^{\ddagger}$ obtained for reactions of the *trans* hydroxy complexes and these $\Delta H_{ref}^{\ddagger}$ reference values are 4.8 ± 0.3, 4.9 ± 0.2, 4.8 ± 0.3, and 5.0 ± 0.3 kcal mol^{-1}, respectively, as compared with values (1) of 5.1 ± 0.3 and 5.1 ± 0.2 kcal mol^{-1} from aquation of *trans*-$[Rh(en)_2(OH)I]^+$ and anation by iodide of *trans*-$[Rh(en)_2(OH)OH_2]^{2+}$, respectively. These values are a measure of the i.k.t.e. relative to iodide as a standard, the larger the difference $\Delta H^{\ddagger} - \Delta H_{ref}^{\ddagger}$ the smaller the *trans*-effect.

It is clear, therefore, that this measure of the i.k.t.e. of hydroxide is indeed independent of the actual reaction used to study it provided appropriate reference values are used. The average of the six values obtained is $4.9_3 \pm 0.1_2$ kcal mol^{-1} which can be compared with values (3) of $5.0_2 \pm 0.1_8$, $4.7_5 \pm 0.1_5$, and $3.2_0 \pm 0.2_0$ kcal mol^{-1} for the corresponding i.k.t.e. of chloride, ammonia, and bromide, respectively, and the *trans*-effect order is therefore $I \gg Br > NH_3 > OH \gtrsim Cl$. This order correlates qualitatively with the polarizability of the *trans* group as measured by the molar refraction (12) of the free ligands. Indeed, as shown in Fig. 1, a linear relation is observed for the three halide ligands but the values for hydroxide and ammonia lie 1–2 kcal mol^{-1} below this line. A factor which could contribute to deviations of this sort is the different nature of the solvation of the complex in the vicinity of the *trans* ligand. When this is a halide ion the solvent water molecules will tend to be attracted to the ligand through H—O—H· · ·X—Rh hydrogen bonding. As the transition state is approached the halide ligand will tend to

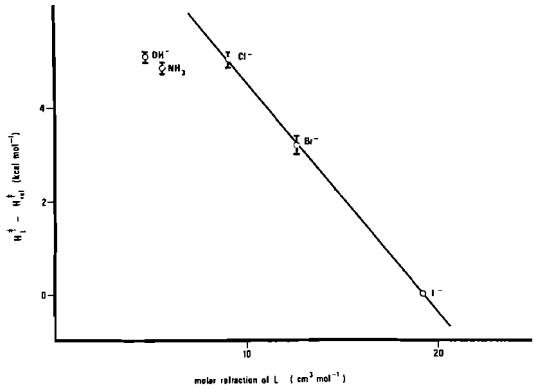

FIG. 1. The dependence of the i.k.t.e. of L on the polarizability of the *trans* ligand where i.k.t.e. = $-(\Delta H_L^{\ddagger} - \Delta H_{ref}^{\ddagger})$.

become more strongly bound to the metal as the leaving group withdraws its electrons.[1] This will tend to decrease the negative charge on the halide and decrease the strength of the H—O—H· · ·X—Rh interaction. On the other hand, when the *trans* ligands are hydroxide or ammonia the solvation will tend to involve hydrogen bonding of the type H_2O· · ·H_3N—Rh and H_2O· · ·HO—Rh so that the effect of the strengthening of the NH_3—Rh and HO—Rh bonds as the transition state is approached will be to increase the positive charge on the hydrogen atom(s) of the *trans* ligand and increase the strength of the hydrogen bonding to the solvent.

The Thermodynamic trans-Effect of Hydroxide

The new data also enable an estimate to be made of the thermodynamic *trans*-effect (t.t.e.) of hydroxide. This has been defined (3, 7, 11) in terms of the standard enthalpies of the complexes *trans*-$[Rh(en)_2LX]^{n+}$, the enthalpies increasing along the series X = Cl < Br < I, and being measured relative to that of *trans*-$[Rh(en)_2LI]^{n+}$ as standard. The thermodynamic *trans*-effect can be quantitatively expressed by the gradient of a plot of H^0(*trans*-$[Rh(en)_2LX]^{n+}$) against H^0(*trans*-$[Rh(en)_2ClX]^+$). Lower gradients are associated with higher thermodynamic *trans*-effects, the latter having been associated (3, 7) essentially with the class (*b*), or soft, nature (13) of the $[Rh(en)_2L]^{(n+1)+}$ moiety. This is not entirely arbitrary as it is the softness or polarizability of the *trans*-ligand that seems to lead to high kinetic *trans*-effects (see above and refs. 7 and 9) and also leads to high thermodynamic *trans*-effects when they are defined in this way. The relative enthalpies of the complexes *trans*-$[Rh(en)_2(OH)X]^+$ are calculated from the values of ΔH^0 for the reactions

[5] *trans*-$[Rh(en)_2(OH)Y]^+ + I^-$
$\rightleftharpoons$ *trans*-$[Rh(en)_2(OH)I]^+ + Y^-$

(Y = Cl and Br) by subtracting the enthalpy contribution due to the different hydration enthalpies of the free halides. In order to obtain values consistent with our earlier data we have used the older values (14) for the enthalpies of hydration of the halides rather than the newer ones (15) that are significantly, though not greatly, different. (The choice of values will not affect the gradients of the plots of H^0(*trans*-$[Rh(en)_2LX]^{n+}$) against H^0(*trans*-$[Rh(en)_2ClX]^+$ although the magnitude of individual relative H^0 values will be changed.) The value of the gradient for the *trans*-OH complexes is 0.77 which places the t.t.e. of hydroxide in the series I > OH > NH_3 > Br > Cl > OH_2. This order is quite different from that of the i.k.t.e. discussed above, although it is likely that the i.k.t.e. of OH_2 will also turn out to be very low, since the polarizability of H_2O is low. The t.t.e. of a ligand L has been shown to be a function both of the intrinsic *trans* bond weakening effect (t.b.w.e.) of the *trans* ligand L due to its σ donor capacity and of the susceptibility to the *trans* bond weakening effect (s.t.b.w.e.) of the halide ligands on the Rh—L bond itself (7). The latter is an effect which does not show up in the i.k.t.e. which is independent of the leaving group. A high t.t.e. can arise from a high t.b.w.e. and/or from a low s.t.b.w.e. The higher position of NH_3 in the t.t.e. series than in the i.k.t.e. series was ascribed to a low t.b.w.e. coupled with a low s.t.b.w.e. (3*b*) and this could equally well be true for the hydroxide ligand. It is interesting that the order of decreasing t.t.e. parallels the order of decreasing intensity of the first ligand field (l.f.) band of *trans*-$[Rh(en)_2LCl]^{n+}$. It is tempting to say that this correlation arises because the intensity series

[1]Although it has been suggested (19, 20) that anation reactions of $[Rh(NH_3)_5OH_2]^{3+}$ may involve some associative character it seems unlikely that this will be sufficient actually to *increase* the electron density at the metal as the transition state is approached.

Can. J. Chem. Downloaded from www.nrcresearchpress.com by 210.87.254.105 on 09/05/12
For personal use only.

measures the covalency of the Rh—L bond when it is *trans* to a halide, and therefore takes into account the susceptibility of L to *trans* bond weakening which is important in the t.t.e. series. However, the complicated nature of the factors which determine the intensity of l.f. transitions probably preclude such a simple approach. Finally, the position of NH_3 in the t.t.e. series does not correlate with the nephelauxetic ratio which has been suggested (11) as a parameter that might determine the magnitude of the t.t.e. Similarly, nephelauxetic ratios are not known for hydroxy complexes of rhodium(III) but they may be expected to be high by comparison with other anionic oxygen donor ligands (16). Clearly the t.t.e. is a complicated one for which no single simple explanation is likely to prove satisfactory.

The $[OH^-]$-dependent Reaction

The kinetic parameters for the $[OH^-]$-dependent reactions of the *trans*-hydroxybromo and *trans*-hydroxychloro complexes are very similar to those for the *trans*-hydroxyiodo complex (1). Those for other amine complexes of rhodium(III) (4, 5, 17) are characterized by values of $\Delta S_2^{\ddagger} - \Delta S_1^{\ddagger}$ of between 20 and 40 cal mol^{-1} deg^{-1} whereas these *trans* complexes have values of $\Delta S_2^{\ddagger} - \Delta S_1^{\ddagger}$ which are not significantly different from zero. The *trans* complexes have values of $\Delta H_2^{\ddagger} - \Delta H_1^{\ddagger}$ that are about the same or slightly smaller than those (4) for the complexes *cis*-$[Rh(en)_2(OH)Cl]^+$ (3.8 kcal mol^{-1}) and *cis*-$[Rh(en)_2(NO_2)Cl]^+$ (0.7 kcal mol^{-1}) so it is the entropy contribution that is decisive. In this connection it is interesting that reactions of both the *cis* complexes (4) and these *trans* complexes are stereoretentive so that the high values of $\Delta S_2^{\ddagger} - \Delta S_1^{\ddagger}$ observed for the *cis* complexes cannot be correlated with stereochemical change in the way expected from Tobe's correlation (18) in the analogous cobalt(III) complexes.

The authors are grateful to the National Research Council of Canada and to Erindale College for support of this work.

1. A. J. Poë and C. P. J. Vuik. J. Chem. Soc. Dalton, 2250 (1972).
2. A. J. Poë and K. Shaw. J. Chem. Soc. A, 393 (1970).
3. (*a*) A. J. Poë and K. Shaw. Chem. Commun. 52 (1967); (*b*) A. J. Poë, K. Shaw, and M. J. Wendt. Inorg. Chim. Acta, **1**, 371 (1967).
4. U. Klabunde. Ph.D. Thesis, Northwestern University, Evanston, Illinois. 1967.
5. S. A. Johnson, F. Basolo, and R. G. Pearson. J. Am. Chem. Soc. **85**, 1741 (1963).
6. S. A. Johnson and F. Basolo. Inorg. Chem. **1**, 925 (1962); Inorg. Synth. **7**, 214 (1963).
7. E. J. Bounsall and A. J. Poë. J. Chem. Soc. A, 286 (1966).
8. H. L. Bott and A. J. Poë. J. Chem. Soc. 5931 (1965).
9. H. L. Bott, E. J. Bounsall, and A. J. Poë. J. Chem. Soc. A, 1275 (1966).
10. C. P. J. Vuik. Ph.D. Thesis, University of London, London, England. 1974.
11. H. L. Bott and A. J. Poë. J. Chem. Soc. A, 205 (1967).
12. A. Eucken (*Editor*). Landholt-Bornstein, Auflage 6, Vol. I, Part 1. Springer Verlag, Berlin. 1950. p. 404.
13. J. E. Huheey. Inorganic chemistry. Harper and Row, New York. 1972. p. 225.
14. L. Benjamin and V. Gold. Trans. Faraday Soc. **50**, 797 (1954).
15. Technical Note 270-1, National Bureau of Standards, Washington, D.C. 1965.
16. C. K. Jørgensen. Absorption spectra and chemical bonding in complexes. Pergamon Press, Oxford. 1962. p. 138; A. B. P. Lever. Inorganic electronic spectroscopy. Elsevier, Amsterdam. 1968. p. 212.
17. G. W. Bushnell, G. C. Lalor, and E. A. Moelwyn-Hughes. J. Chem. Soc. A, 719 (1966).
18. M. L. Tobe. Inorg. Chem. **7**, 1260 (1968).
19. H. L. Bott, A. J. Poë, and K. Shaw. Chem. Commun. 793 (1968); J. Chem. Soc. A, 1745 (1970).
20. F. Monacelli. Inorg. Chim. Acta, **2**, 263 (1968).

Can. J. Chem. Downloaded from www.nrcresearchpress.com by 210.87.254.105 on 09/05/12
For personal use only.

Crystal Structure of the Glaserite Form of $BaNaPO_4$

CRISPIN CALVO AND ROMOLO FAGGIANI
Institute for Materials Research, McMaster University, Hamilton, Ontario L8S 4M1

Received November 6, 1974

CRISPIN CALVO and ROMOLO FAGGIANI. Can. J. Chem. **53**, 1849 (1975).

Crystals of $BaNaPO_4$ were grown from a $Ba_3P_2O_8$–$Na_2B_4O_7$ melt. The crystals are trigonal, space group $P\bar{3}m1$ with $a = 5.622(4)$ and $c = 7.259(5)$ Å. The structure, isotypic with that of glaserite, was refined by full-matrix least-squares methods to a final R value of 0.042 using 218 unique reflections. There are three different cation sites. Na and Ba lie at sites of $\bar{3}m$ symmetry and are coordinated to 6 and 12 oxygen atoms respectively. The Na—O bond lengths are 2.344(7) Å and the two unique Ba—O bond lengths are 2.788(7) and 3.247(9) Å. The remaining cation site has $3m$ symmetry, a coordination number of 10, and contains equal amounts of Na^+ and Ba^{2+}. The bond lengths range from 2.548(12) to 3.017(7) Å. The phosphate group also has $3m$ symmetry with mean P—O bond lengths of 1.538 Å. The underbonded apical P—O bond length is 1.520 Å.

CRISPIN CALVO et ROMOLO FAGGIANI. Can. J. Chem. **53**, 1849 (1975).

On a fait croître des cristaux de $BaNaPO_4$ à partir d'un mélange de $Ba_3P_2O_8$–$Na_2B_4O_7$ en fusion. Les cristaux trigonaux appartiennent au groupe d'espace $P\bar{3}m1$ avec $a = 5.622(4)$ et $c = 7.259(5)$ Å. La structure qui est isotypique avec celle de la glaserite a été affinée par la méthode des moindres carrés (matrice complète) jusqu'à une valeur finale de R de 0.042 utilisant 218 réflexions indépendantes. Il y a trois sites différents pour les cations. Le Na et le Ba occupent des sites de symétrie $\bar{3}m$ et sont respectivement coordonnés à 6 et 12 oxygènes. Les longueurs de liaisons Na—O sont 2.344(7) Å et les deux longueurs des liaisons Ba—O sont 2.788(7) et 3.247(9) Å. Le dernier cation occupe un site de symétrie $3m$; il possède un nombre de coordination de 10 et contient des quantités égales de Na^+ et de Ba^{2+}. Les longueurs de liaisons varient de 2.548(12) à 3.017(7) Å. Le groupe phosphate possède aussi une symétrie $3m$ avec une valeur moyenne de 1.538 Å pour la longueur du lien P—O. La longueur de la liaison P—O vers le sommet en dessous de la molécule est de 1.520 Å. [Traduit par le journal]

Introduction

Wells (1) has outlined the variety of structures available to a system with stoichiometry $ABXO_4$, where X is a tetrahedrally coordinated ion. When A and B are both small the preferred structure type is phenacite with all cations tetrahedrally coordinated. For cations of intermediate size relative to that of oxygen atoms the most common structural types are olivine and spinel with the cations in octahedral sites. Here it appears that the interplay between the radius of X and those of A and B determine which of these structure types is stable (2, 3). If either A or B has a radius comparable to that of the oxygen ion the glaserite structure is stable, at least in some temperature range.

Polymorphic transformations abound even when A and B are chemically identical. Na_2SO_4 is said to have four phases (4), K_2SO_4 has two (5), and Ca_2SiO_4 has five (6). The number of structural possibilities increase substantially if A and B are different. Phosphates with this stoichiometry have been studied for their luminescence characteristics (7). Klement and Kresse have prepared a number of vanadates and arsenates in addition to phosphates with this stoichiometry (8). A tetragonal form of $BaNaPO_4$, stable at high temperatures, in addition to a glaseritelike phase has been reported (9). It has been proposed that glaserite, $K_3Na(SO_4)_2$, has K at $0,0,\frac{1}{2}$ and $\frac{1}{2},\frac{2}{3},z$ and Na at 0,0,0 (10). Although glaserite is regarded as a solid solution of αK_2SO_4 and $NaKSO_4$ (aphthitalite) the latter structure is said to have Na in the two cation sites of $\bar{3}m$ symmetry (0,0,0, $0,0,\frac{1}{2}$) and K in the remaining site (11). The $K_3Na(SO_4)_2$ structure is compatible with the expectation that K should prefer the sites of higher coordination number leaving the octahedrally coordinated site for Na. No reliable single crystal studies have been reported concerning this site preference.

Experimental

Crystals of $BaNaPO_4$ were obtained from a mix of $Ba_3(PO_4)_2$ and $Na_2B_4O_7$ in the molar ratio of 1 to 3. This mix was chosen in an attempt to prepare a barium analog of the Sr–apatite containing BO_2 groups (12). The mix

Can. J. Chem. Downloaded from www.nrcresearchpress.com by 210.87.254.5 on 09/05/12
For personal use only.

TABLE 1. Atomic and thermal parameters for $BaNaPO_4$ with estimated standard deviations in parentheses

Atom	Site	x	y	z	U_{11}* (Å²)	U_{33} (Å²)
Na	1a	0	0	0	0.017(5)	0.017(5)
Ba	1b	0	0	1/2	0.026(1)	0.0067(7)
Y	2d	1/3	2/3	0.8419(3)	0.0145(1)	0.011(1)
P	2d	1/3	2/3	0.2816(6)	0.009(2)	0.006(2)
O(1)	2d	1/3	2/3	0.5091(17)	0.016(6)	0.010(5)
O(2)	6i	0.1849(16)	−x	0.2068(9)	0.020(4)	0.014(3)

*The thermal parameters appear in the structure factor expression as $T = \exp -2\pi^2(h^2b_1^2U_{11} + \ldots + 2hkb_1b_2U_{12} + \ldots)$ and the b_i's are reciprocal lattice vectors.

was heated to 1400 °C and slowly cooled. The resulting sample showed a few crystals on the surface of the amorphous looking mass.

A crystal with dimensions 0.1 × 0.1 × 0.4 mm was used to collect lattice parameters and intensity data. Unit cell parameters were determined by least-squares methods using 2θ values between 20 and 25°. The crystal data are as follows:

$BaNaPO_4$ f.w. = 255.30

Trigonal, $a = 5.622(5)$ Å, $c = 7.259(5)$ Å, $V = 198.7$ Å³, $Z = 2$, $\rho_x = 4.267$, $\rho_m = 4.17$ (13), space group $P\bar{3}m1$, $T = 21 \pm 2$ °C, $\lambda_{Mo\alpha} = 0.71069$ Å.

All the reflections in a hemisphere defined by $2\theta_{max} = 55°$ were scanned using a Syntex $P\bar{1}$ and graphite monochromatized Mo radiation. Peaks were scanned at a rate between 2 and 24 deg/min and backgrounds were determined at either side of the peak. Those reflections whose intensity measures were zero or less were discarded and of the remainder those with intensities less than 3σ were considered unobserved. σ was derived from the counting statistics for the peaks and backgrounds. A total of 218 reflections, 23 of them unobserved, remained after averaging symmetry equivalent reflections. The data were corrected for Lorentz and polarization effects. Absorption corrections ($\mu = 104.1$ cm^{-1}) were made assuming the crystal to be a cylinder.

The parameters reported for glaserite (10) were used as initial values in the least-squares refinement. Equal amounts of Na^+ and Ba^{2+} were assigned to each cation site. The scattering curves for Ba^{2+}, Na^+, P, and O^- were taken from the *International Tables for X-ray Crystallography* (14). Subsequent refinement indicated that the cations on the threefold axis through the origin were ordered. Thus Na^+ was placed at 0,0,0, Ba^{2+} at 0,0,½, and an equal mixture of Na^+ and Ba^{2+} at site 2d. Weights, chosen so that $\omega\Delta F^2$ would be independent of F_o, were assigned according to $[75 + 0.1F_o + 0.0003F_o^2]^{-1}$. This model refined readily to an R value of 0.042 and R_ω $(= \Sigma\omega(F_o - F_c)^2/\Sigma\omega F_o^2)^{1/2}$ of 0.052. The final values of the atomic and thermal parameters are in Table 1. The observed and calculated structure factors are in Table 2.[1]

[1]Photocopies of Table 2 are available, at a nominal charge, from the Depository of Unpublished Data, CISTI, National Research Council of Canada, Ottawa, Canada K1A 0S2.

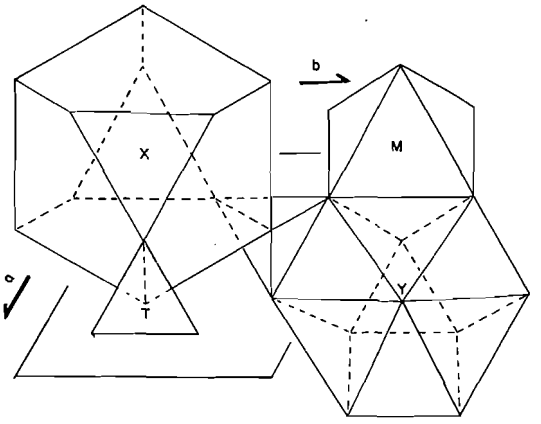

FIG. 1. A composite view of the $BaNaPO_4$ structure. Oxygen atoms are at the corners of the polyhedra enclosing the cations. The X polyhedron is at the origin. The M polyhedron is drawn displaced by a b axis length to prevent superposition and lies at 0,1,1/2. Tetrahedral groups are shown at 1/3,2/3 and 2/3,1/3 while the Y group is at 2/3,4/3.

Description of the Structure

$BaNaPO_4$ contain chains of polyhedra parallel to c. These alternately involve 6 and 12 oxygen atoms and are called the A chains. In each case six oxygen atoms, arising from six separate PO_4 groups, form a distorted octahedron about the cation (Fig. 1). The 12 coordinate site is generated by an additional long interaction $(=a/\sqrt{3})$ per phosphate group so that this cation, Ba^{2+} in the present case, shares six O(I)—O(II) edges. These edges lie in mirror planes containing the threefold axis. The six apical oxygen atoms, O(I)'s, are nearly coplanar and they together with the Ba^{2+} are said to lie in the equatorial plane of this cation. Na^+ and Ba^{2+} ions alternate in this chain sharing an octahedral face between neighbors.

The remaining cations (Y) lie at sites of $3m$ symmetry with 10 neighboring atoms in the B chains (Fig. 2). PO_4 groups and these cations alternate in a chain parallel to the c axis. The PO_4 groups share O(1) and a face composed of three O(II) atoms with alternate cations in this chain. The Y—O bond lengths to these oxygen atoms, at 3.017 Å, are long enough to indicate cationic repulsion. The remaining six arise from three edges shared with three PO_4 groups on neighboring B chains.

Can. J. Chem. Downloaded from www.nrcresearchpress.com by 210.87.254.5 on 09/05/12
For personal use only.

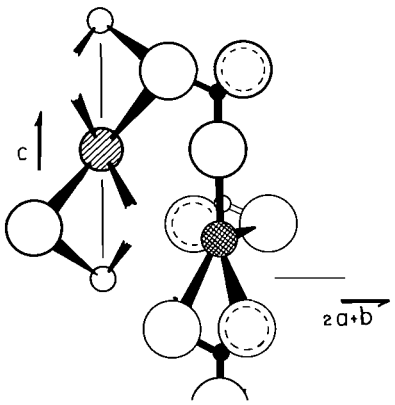

FIG. 2. The $BaNaPO_4$ structure near the plane $(1\bar{2}0)$. The large circles are oxygen atoms. The striped circle represents the X ion with the M (small open circle) on the same threefold axis. The Y ion is crosshatched. The full environment of the cations are generated by the threefold axes.

The pertinent bond lengths and angles are in Table 3. The Ba^{2+} has six nearest neighbors at 2.788 Å involving O(2) and six further interactions with O(1) type oxygen atoms at 3.247 Å. The six neighbors deviate from an ideal octahedron by a substantial elongation along the threefold axis as indicated by O(2)—Ba—O(2)′ angle of 68.0°. The NaO group is a more regular octahedron since the O(2)—Na—O(2)′ angle is 83.4°. The O(1) atoms are within 0.07 Å of coplanarity with the Ba^{2+}.

The remaining cation site contains Na^+ and Ba^{2+} randomly distributed. These cations are displaced by 2.548 Å from the apical oxygen atom lying on the same threefold axis. Since this latter oxygen atom is underbonded it also subtends the shortest P—O bond length in the PO_4 group. This group is distorted from regularity by a displacement of the phosphorus atom towards the O(1) yielding O(1)—P—O(2) bond angles of 110.6° compared to O(2)—P—O(2) bond angles of 108.4°. Alternately the repulsion between the Ba^{2+} and P atoms across the shared tetrahedral face could be responsible for these distortions since they are separated by only 3.19 Å.

Discussion

The structure of $BaNaPO_4$ is consistent with the packing constraints since the ions with the largest and smallest radii are partitioned between the sites with largest and smallest coordination numbers.

Struck and White showed that in the βK_2SO_4 form of $BaKPO_4$ K^+ lies in a site with 10-fold coordination, much like the Y site of glaserite, and Ba^{2+} in a 9-fold coordinated site (15). Since Ba^{2+} and K^+ ions have nearly the same radii some disorder between these sites might be expected but this has not been investigated. The change to the glaserite structure involves a transformation of the 9-fold coordinated site to an equal number of 6- and 12-fold coordinated sites. However, the ordered Y site in the glaserite form of $BaKPO_4$ is not compatible with the disordered Y site in the glaserite form of $BaNaPO_4$. $CaNaPO_4$ and $CaKPO_4$ (13) also have the βK_2SO_4 structure as low temperature phases and high temperature phases isotypic with glaserite. Again a disorder amongst the nearly equivalent sized Ca^{2+} and Na^+ would also not be surprising. A further reduction in the radii of one of the cations, as in $CaLiPO_4$, leads to structures isotypic with olivine (ref. 16, confirmed from single crystal measurements by Marrow in this laboratory). The correlations between ionic radii, based upon a coordination of six, and the structure type is found in Fig. 3. Both the βK_2SO_4 and glaserite structure types are stable when at least one of the cations is

TABLE 3. Bond lengths and angles in $BaNaPO_4$ with estimated standard deviations in parentheses

Bond	Distance (Å)		Bonds	Angle (deg)	
P—O(1)	1.520(13)		O(1)—P—O(2)	110.6(3)	
P—O(2)	1.544(8)	3×	O(2)—P—O(2)	108.4(4)	3×
Na—O(2)	2.344(7)	6×	O(2)—Na—O(2)′	83.4(3)	3×
			—O(2)″	96.6(3)	3×
			—O(2)‴	180.0	3×
Ba—O(2)	2.788(7)	6×	O(2)—Ba—O(2)′	68.0(2)	3×
—O(1)	3.247(9)	6×	—O(2)″	112.0(2)	3×
			—O(2)‴	180.0	3×
Y—O(1)	2.548(12)		O(1)—M—O(2)	82.8(2)	3×
—O(2)	2.840(5)	6×	—O(2)′	151.4(1)	3×
—O(2)′	3.017(7)	3×	O(2)—M—O(2)	66.6(2)	
			—O(2)′	73.3(2)	

Can. J. Chem. Downloaded from www.nrcresearchpress.com by 210.87.254.5 on 09/05/12
For personal use only.

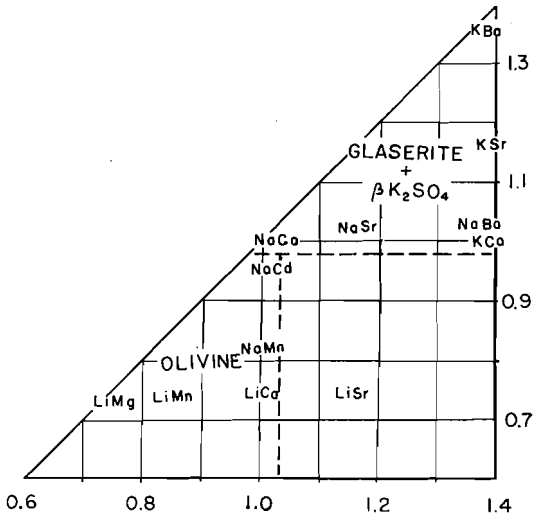

FIG. 3. Regions of structural stability of the olivine and glaserite–βK_2SO_4 *vs.* cation radius. The ion, A or B with the larger radius is plotted vertically and the other horizontally. The AB pair of the $ABPO_4$ species is shown. These data are from refs. 8, 22, or 23.

large and the olivine structure type when both cations are small.

Moore (17) has shown that the cationic coordination polyhedra found in glaserite are features common to a number of structure types. He showed that there are 13 possible ways in which six tetrahedra can be arranged at the corners of an octahedron in a pseudoglaserite arrangement. Only a few of these possibilities have been identified and these are consistent with short periodicities. In glaserite the tetrahedra about the M and X ions have an arrangement with $\bar{3}2m$ symmetry. This leads to the apical oxygen near the equatorial plane of one of the cations at the center of the octahedron. In the βK_2SO_4 structure (15) three of the tetrahedra have their apical oxygens bond pointing in the same direction leading to a site with a coordination of nine containing a crystallographic mirror plane. Distortion can yield lower coordination numbers. Olivine is based upon a close packed arrangement of oxygen atoms, in contrast to glaserite and βK_2SO_4. Although the octahedral cation site can be generated from the X sites of glaserite it would appear not to be worth pursuing this unless structures with mixed glaserite- and olivinelike arrangements are found.

The idealized glaserite structure will be defined by (*a*) perfect octahedral and tetrahedral geometries for the MO_6 and TO_4 groups and (*b*) the coplanarity of the six apical oxygen atoms O(1) with X. The perfect octahedral geometry for $XO(2)_6$ follows from condition (*a*). This also leads to the equivalence of the M—O and X—O bond lengths. The axes lengths are: $a = \sqrt{2}(\text{M—O}) + \sqrt{8/3}(\text{T—O})$ and $c = (4/\sqrt{3})(\text{M—O} = (4 \times 4/3)(\text{T—O})$. The minimum X—O(1) bond length is $a/\sqrt{3}$, whether (*b*) is true or not, and if this is equal to X—O(2) the ratio M—O/T—O is $2\sqrt{2}/(3 - \sqrt{6}) = 5.13$. This is unreasonable, suggesting that X—O(1) > X—O(2), as was concluded by Moore (17). On the other hand, (*a*) and (*b*) require that the height of the octahedron be twice that of the tetrahedron and lead to M—O/T—O $= 4/\sqrt{3} = 2.309$ and thus to $c/a = (11/32)\sqrt{6} = 1.188$. All experimental values for this ratio lie between 1.29 and 1.41 (18, 8).

The position of Y, aside from lying on the threefold axis, is unrestricted. However, $c = (4/3)(\text{T—O}) + \text{Y—O(1)} + [\text{Y—O(2)}']_{\|}$ where $[\text{Y—O(2)}']_{\|}$ is the component of the bond length between Y and the oxygens of the shared face parallel to the *c* axis. Thus, $\text{Y—O(1)} + [\text{Y—O(2)}']_{\|} \geq 4(\text{T—O})$ and since X—O(1) > X—O(2), then Y—O(1) < Y—O(2)′ in order to compensate for the otherwise underbonded O(1). The free atomic parameters then are $z_Y \simeq 0.865$, $z_p = 5/16$, $z_{O(1)} = 1/2$, $x_{O(2)} = 0.2326$, and $z_{O(2)} = 1/4$. These predictions can be improved for a particular composition using the least-squares routine developed by Meier and Villiger (19, 20). For the present qualitative considerations will suffice.

The M and X sites will be stabilized by cations of different radii with the smaller preferentially in the M site. Radii for K^+, Sr^{2+}, and Ba^{2+} in sites of 12-fold coordination are $\sim\frac{1}{4}$ Å larger than the individual "octahedral" radii. This is consistent with a difference of $\sim\frac{1}{2}$ Å between X—O(2) and X—O(1) as has been found in $BaNaPO_4$ and in $Ba_3V_2O_8$ (21). This could be used to provide another relationship between M—O and T—O. The smaller M—O bond length is achieved by a displacement of the TO_4 group resulting in a contraction of the MO_6 octahedra and a dilation of XO_6 octahedra both along the *c* axis. In $BaNaPO_4$ both groups are dilated but the latter more than the former, suggesting that the *c* axis is "abnormally" en-

Can. J. Chem. Downloaded from www.nrcresearchpress.com by 210.87.254.5 on 09/05/12
For personal use only.

larged because of the repulsion between the ions in the M and X sites.

The *a* axis also appears to be contracted leading to a greater *c*/*a* ratio than predicted. In the idealized structure the Y—O(2) length is too long relative to the Y—O(2)′ length, since these are expected to be roughly comparable in length. The Y—O(2) vector, nearly lying on the *ab* plane, can be reduced in magnitude by a contraction of the *a* and *b* axes. Y should be displaced away from the plane containing the O(2)—O(2) edges as a result of the repulsion between Y and T across the shared face. The repulsion between the oxygen atoms also plays a role in that, for example, the Y—O(2) bond length cannot be so small as to lead to the O(2)—O(2) interactions between different TO_4 equal to or smaller than an edge of the TO_4 group.

The Y ion should be of a size intermediate between that of the M and X ions. If a small ion attempted to bond strongly to the oxygen atoms of the shared face and the apical oxygen atom, this *c* length would be too small to be compatible with the requirements of M and X. Further the *ab* plane would be enlarged in order to remove the remaining six O(2) atoms from the coordination sphere of Y. Alternately, a large ion in the Y site would also enlarge this plane and in both cases result in a six coordinate X ion with an underbonded O(1) atom.

It is apparent that both the glaserite and βK_2SO_4 are pliable to a variety of ionic substitutions. Thus the investigation of systems where the M, Y, and X are chemically distinct should be fruitful in determining the limits of phase stability. The mechanism for the phase transformation needs further investigation. Systems with cations having nearly equal radii, such as $NaCoPO_4$ (22) and $NaCdPO_4$ (23) show the olivine structure in addition to structures related to those occurring in Na_2SO_4. These look particularly promising.

This research was supported by a grant from the National Research Council of Canada.

1. A. F. Wells. Structural inorganic chemistry, 3rd ed. Oxford University Press, London. 1962.
2. B. Kamb. Am. Mineral. **53**, 1439 (1968).
3. P. B. Moore and J. V. Smith. Phys. Earth Planet. Inter. **3**, 166 (1970).
4. W. Eysel. Am. Mineral. **58**, 736 (1973).
5. H. F. Fischmeister. Monatsh. Chem. **93**, 420 (1962).
6. D. K. Smith, A. J. Majumdar, and F. Ordway. J. Am. Ceram. Soc. **44**, 405 (1961).
7. W. L. Wanmaker and H. L. Spier. J. Electrochem. Soc. 109 (1962).
8. R. Klements and P. Kresse. Z. Anorg. Chem. **310**, 53 (1961).
9. R. Klements and R. Uffelmann. Naturwiss. **29**, 300 (1941).
10. Strukturbericht **1**, 378.
11. Structure Reports **9**, 232.
12. C. Calvo, N. Krishnamachari, and R. Faggiani. Acta Cryst. B**31**, 188 (1975).
13. M. A. Bredig. J. Phys. Chem. **46**, 747 (1942).
14. International tables for X-ray crystallography, Vol. III. Kynoch Press, Birmingham. 1962.
15. C. W. Struck and J. G. White. Acta Cryst. **15**, 290 (1962).
16. E. Thilo. Naturwiss. **16**, 239 (1941).
17. P. B. Moore. Am. Mineral. **58**, 32 (1973).
18. Crystal data, determinative tables, Vol. II, Inorganic compounds, 3rd ed. U.S. Department of Commerce, National Bureau of Standards and the Joint Committee on Powder Diffraction Standards, U.S.A. 1973.
19. W. M. Meier and H. Villiger. Z. Krist. **129**, 411 (1969).
20. W. Baur. Nature London, Phys. Sci. **233**, 135 (1971).
21. P. Süsse and M. J. Buerger. Z. Kristallogr. **131**, 161 (1970).
22. M.-T. Averbach. Thesis, L'Universite Scientifique et Medicale et L'Institut National Polytechnique de Grenoble. 1974.
23. M.-Th. Paques-Ledent. Rev. Chim. Miner. **10**, 785 (1973).

Can. J. Chem. Downloaded from www.nrcresearchpress.com by 210.87.254.5 on 09/05/12
For personal use only.

Erratum: Syntheses of Some Phosphino- and Phosphinatoazoles

SVEN FISCHER AND LOUIS K. PETERSON
Department of Chemistry, Simon Fraser University, Burnaby, British Columbia V5A 1S6
AND
JOHN F. NIXON
School of Molecular Sciences, University of Sussex, Brighton BN1 9QJ, Great Britain
Received April 11, 1975

(Ref.: Can. J. Chem. **52**, 3981 (1974))

The abstract contains two errors. In line 3, preparation *b* should read: (*b*) diphenylphosphinatopyrazole (**4***a*) and diphenylthiophosphinatopyrazole (**4***b*). In line 9, the identification number assigned to diphenylchlorophosphine should be (**7**).

Il y a deux erreurs dans le résumé. Dans la ligne 3, la préparation *b* doit être: (*b*) diphénylphosphinatopyrazole (**4***a*) et diphénylthiophosphinatopyrazole (**4***b*). Dans la ligne 9, le nombre d'identication assigné à diphénylchlorophosphine doit être (**7**).

Erratum: Solubility of Indium Trichloride and Some Double Salts

ELINOR M. KARTZMARK
Department of Chemistry, University of Manitoba, Winnipeg, Manitoba R3T 2N2
Received March 14, 1975
(Ref.: Can. J. Chem. **52**, 3459, (1974))

I am indebted to Whitlow and Gabe[1] for a preprint of their work on the single crystal structure analysis of compound A in Fig. 4, p. 3461, which I reported to have formula $InCl_3 \cdot 3$dioxane$\cdot 2H_2O$ (6.9% H_2O); from the X-ray analysis, the correct formula appears to be $InCl_3 \cdot 3$dioxane$\cdot 3H_2O$ (10.0% H_2O). The method of "wet rest" analysis which relies on the point of intersection of tie-lines, is subject to error in water content, because of the low molecular weight of water in comparison with the high molecular weight hydrated compound. It is also possible that the formula of B should be $InCl_3 \cdot 2$dioxane$\cdot 3H_2O$ (12% H_2O) rather than $InCl_3 \cdot 2$dioxane$\cdot 2H_2O$ (8.3% H_2O). According to Whitlow and Gabe, the water of hydration of $InCl_3 \cdot 3H_2O$ is not affected by the dioxane in the compound, which consists of "layers of distorted In octahedra which interleave with dioxane layers".

[1]S. H. Whitlow and E. J. Gabe. To be published.

Can. J. Chem. Downloaded from www.nrcresearchpress.com by 210.87.254.6 on 09/05/12
For personal use only.

Can. J. Chem. Downloaded from www.nrcresearchpress.com by 210.87.254.42 on 09/05/12
For personal use only.

Canadian Journal of Chemistry

Published by
THE NATIONAL RESEARCH COUNCIL OF CANADA

Journal canadien de chimie

Publié par
LE CONSEIL NATIONAL DE RECHERCHES DU CANADA

Volume 53 Number 13 July 1, 1975

Volume 53 numéro 13 1 juillet 1975

The ^{125}Te Mössbauer Absorption Spectra of Tellurium Complexes with Sulfur-containing Ligands

ROBERT MICHAEL CHEYNE AND COLIN HENRY WILSON JONES
Department of Chemistry, Simon Fraser University, Burnaby, British Columbia V5A 1S6
AND
STEINAR HUSEBYE
Chemical Institute, University of Bergen, Bergen, Norway

Received December 16, 1974

ROBERT MICHAEL CHEYNE, COLIN HENRY WILSON JONES, and STEINAR HUSEBYE. Can. J. Chem. **53**, 1855 (1975).

The ^{125}Te Mössbauer spectra of a number of Te(II) and Te(IV) complexes with sulfur-containing ligands have been measured. The Te(II) compounds exhibit large quadrupole splittings of 12.4 to 15.2 mm s^{-1} and isomer shifts (^{125}I/Cu) of +0.33 to +0.91 mm s^{-1}. These data are interpreted as evidence for the incorporation of some 5s character in the bonding scheme for several of the compounds, consistent with the interpretation of X-ray crystal structure data. For the Te(IV) compounds 6, 7, and 8 coordinate molecules have been studied containing tellurium in distorted octahedral, pentagonal bipyramidal, and dodecahedral coordination.

ROBERT MICHAEL CHEYNE, COLIN HENRY WILSON JONES et STEINAR HUSEBYE. Can. J. Chem. **53**, 1855 (1975).

On a mesuré les spectres Mössbauer ^{125}Te d'un certain nombre de complexes Te(II) et Te(IV) portant des ligands contenant du soufre. Les composés du Te(II) présentent de grands couplages quadrupolaires de 12.4 à 15.2 mm s^{-1} et des déplacements d'isomères (^{125}I/Cu) de +0.33 à +0.91 mm s^{-1}. On interprète ces données comme signifiant qu'il y a incorporation d'un certain caractère 5s dans les liaisons de plusieurs de ces composés; cette conclusion est en accord avec l'interprétation de données structurales dérivées d'études par rayons-X. Pour les composés du Te(IV), on a étudié des molécules hexa-, hepta- et octa coordonnées contenant du tellure dans des coordinations octaédrique, pentagonale bipyramidale et dodécaédrique déformées. [Traduit par le journal]

Introduction

In an earlier paper (1) we reported the Mössbauer data for a number of complexes of tellurium(II) and tellurium(IV) with thiourea (Tu) and related derivatives. For many of those compounds there is considerable evidence from the structural work of Foss (2) and Husebye (3) that the tellurium $5s^2$ electrons form a stereochemically inert lone-pair and that only the 5p electrons are involved in bonding. Thus the common occurrence of bond angles close to 90° and the large Te—S bond lengths, for example in the $TeTu_4^{2+}$ cation, are consistent with the presence of three-center bonds (2 electrons bonding, 2 nonbonding) in which the tellurium 5p orbitals participate.[1] The Mössbauer data for these compounds (1) were found

[1]In the previous discussion (1) these bonds were described as three-center two-electron bonds since the two nonbonding electrons are localized entirely on the sulfur atoms and only the bonding electrons directly influence the tellurium Mössbauer parameters.

TABLE 1. Mössbauer parameters

Compound	δ* (mm s^{-1}) (±0.07)	Δ (mm s^{-1}) (±0.10)	2Γ (mm s^{-1})
1 $Te[(CH_3O)_2PS_2]_2$	+0.56	15.1	6.9
2 $Na_2Te(S_2O_3)_2$	+0.33	12.4	8.4
3 $Rb_2Te(S_2O_3)_2$	+0.31	12.8	8.2
4 $Te(SCH_2CH_2CO_2H)_2$	+0.40	13.3	6.5
5 $Te(Et_2NCS_2)_2$	+0.59	15.2	7.4
6 $Te(MeOCS_2)_2$	+0.69	15.6	6.6
7 *trans*-$Te(SC[N(CH_3)_2]_2)_2(S_2O_2C_6H_5)_2$	+0.91	16.0	6.7
8 $Te(Et_2NCS_2)_4$	+1.23	0	6.9
9 $Te[(OC_4H_8NCS_2)_4]\cdot 3C_6H_6$	+1.31	0	7.6
10 $Te[(Et_2NCS_2)_3C_6H_5]$	+0.89	5.3	6.2
11 $Te[(Me_2NCS_2)_3C_6H_5]$	+0.84	5.5	6.7
12 *trans*-$TeCl_4(SC[N(CH_3)_2]_2)_2$ monoclinic	+1.52	0	8.6
13 *trans*-$TeCl_4(SC[N(CH_3)_2]_2)_2$ orthorhombic†	+1.60	0	9.5

*δ with respect to I/Cu source. For compounds 1–5 and 8 the measurements were made at 80 K, and compounds 6, 7, 9–12 at 4.2 K.
†From ref. 1.

to be consistent with the bonding scheme proposed by Foss, exhibiting relatively large, positive isomer shifts, and large quadrupole splittings, indicating the presence of a lone-pair of $5s^2$ electrons and a large imbalance in the 5p orbital populations respectively (1).

Aleksandrov *et al.* (4) have reported briefly on the ^{125}Te Mössbauer spectra of tellurium(II) thiourea complexes but these authors were evidently unaware of the work of Foss (2) and interpreted their results together with the i.r. data in terms of a tetrahedral structure for these molecules.

In the present work we have studied several other compounds where sulfur is coordinated to tellurium(II) or tellurium(IV). This investigation has included several compounds where the bond angles about the tellurium show significant deviations from 90°, this being used as a criterion to identify examples where the bonding may not be explained solely by the presence of linear 3-center bonds, and where the participation of 5s and/or 5d orbitals may be invoked.

Results

The Mössbauer parameters for the compounds investigated are reported in Table 1 and sample spectra are shown in Fig. 1. The Te(II) compounds studied were tellurium(II) bis(dimethyldithiophosphate), $Te((CH_3O)_2PS_2)_2$, tellurium(II) bis(thiopropionic acid), $Te(SCH_2CH_2CO_2H)_2$, sodium and rubidium telluropentathionate, $M_2Te(S_2O_3)_2$, bis(diethyldithiocarbomato)tellurium(II), $Te(Et_2NCS_2)_2$, tellurium di(methylxanthate), $Te(MeOCS_2)_2$, and *trans*-dibenzenethiosulfonatobis(tetramethylthiourea)tellurium(II), *trans*-$Te(SC[N(CH_3)_2]_2)_2(S_2O_2C_6H_5)_2$. The Te(IV) compounds studied included tetrakis(diethyldithiocarbamato)tellurium(IV), $Te(Et_2NCS_2)_4$, tetrakis(4-morpholinecarbodithioato)tellurium(IV) containing benzene molecules of crystallization $Te[(OC_4H_8NCS_2)_4]\cdot 3C_6H_6$, tris(diethyldithiocarbamato)phenyltellurium(IV), $Te[(Et_2NCS_2)_3C_6H_5]$, and the dimethyl analog $Te[(Me_2NCS_2)_3C_6H_5]$, and the monoclinic form of *trans*-tetrachlorobis(tetramethylthiourea)tellurium(IV), *trans*-$TeCl_4[SC(N(CH_3)_2)_2]_2$. In addition, several tellurium thiourea complexes were used as intercalibration standards and their parameters are given in Table 2.

In these experiments a $Pb^{125m}Te$ source was used rather than a ^{125}I/Cu source because it gave somewhat narrower line-widths. To facilitate comparison of the data with previous work the isomer shifts are quoted with respect to an ^{125}I/Cu source and the conversion was made using the data for the thiourea complexes given in Table 2. The spectra of the thiourea complexes were measured with the present source in connection with anisotropy studies which have previously been reported (5). The isomer shift conversion factor was found to be $\delta(^{125}I/Cu) =$

Can. J. Chem. Downloaded from www.nrcresearchpress.com by 210.87.254.42 on 09/05/12
For personal use only.

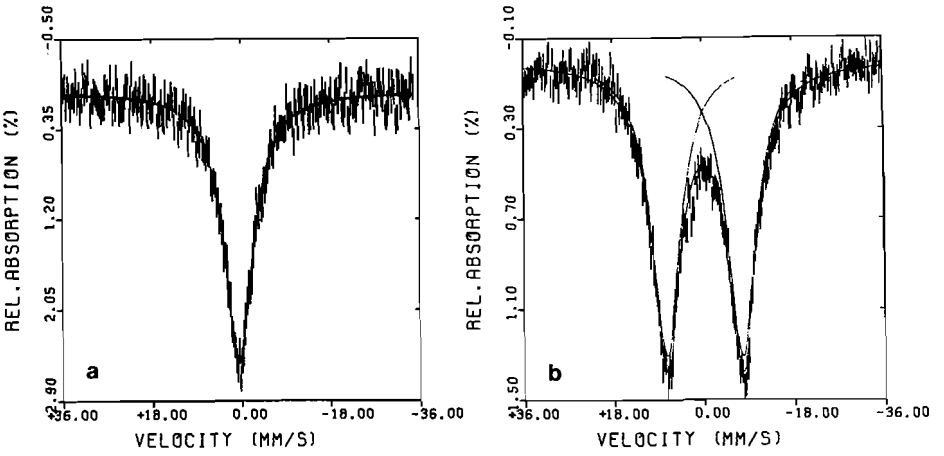

FIG. 1. Sample spectra for (*a*) $Te(Et_2NCS_2)_4$ and (*b*) $Te((CH_3O)_2PS_2)_2$.

TABLE 2. Mössbauer parameters of tellurium thiourea complexes used as intercalibration standards

Compound*	δ ($mm\,s^{-1}$) $Pb^{125}Te$	δ ($mm\,s^{-1}$) $^{125}I/Cu$	Δ ($mm\,s^{-1}$)	Reference
$TeTu_4(SCN)_2$	$+0.77 \pm 0.04$		16.2 ± 0.1	This work‡
		$+0.86 \pm 0.07$	16.11 ± 0.07	1
$TeEtu_4Cl_2$	$+0.77 \pm 0.04$		15.9 ± 0.1	This work§
		$+0.93 \pm 0.12$	16.0 ± 0.2	1
$TeTu_4Cl_2 \cdot 2H_2O$	$+0.72 \pm 0.05$		15.4 ± 0.1	This work‡
	$\pm 0.76 \pm 0.06$		15.8 ± 0.1	This work (4.2 K) (Harwell)
		$+0.93 \pm 0.06$	15.60 ± 0.06	1†

*Tu = thiourea, Etu = ethylenethiourea.
†$TeTu_4Cl_2$ in ref. 1 was in fact the dihydrate.
‡Mean of 2 independent measurements.
§Mean of 3 independent measurements.

$\delta(Pb^{125m}Te) + 0.15 \pm 0.05$. The data of Table 2 also fulfills another useful purpose in indicating the reproducibility of independent measurements.

Discussion

Tellurium(II) Compounds

As can be seen from Table 1 the general features of the results for the Te(II) compounds (**1**–**7**) are that the isomer shifts are positive and that all of these compounds exhibit large quadrupole splittings. Given that $\Delta R/R$ for the ^{125}Te transition is positive (6, 7), the isomer shifts correspond to relatively large s-electron densities at the tellurium nucleus, and this in turn implies that the $5s^2$ electrons in these compounds are predominantly nonbonding in character. The large quadrupole splittings, Δ, arise from a large imbalance in the tellurium 5p orbital populations. In all of these Te(II) compounds, the tellurium is coordinated in a planar environment and the large Δ values are consistent with the presence of a lone-pair with predominantly $5p_z$ character directed out of the plane, the $5p_x$ and $5p_y$ orbitals in the plane bonding to the ligands.

However, it is apparent from Table 1 that the isomer shifts and quadrupole splittings of the Te(II) compounds are not all the same and in some instances show very significant differences from the parameters for the thiourea complexes (Table 2). Given the above model for the bonding in these compounds, changes in the donor character of the ligands would produce changes in the population of the 5p orbitals in the *xy*

Can. J. Chem. Downloaded from www.nrcresearchpress.com by 210.87.254.42 on 09/05/12
For personal use only.

Can. J. Chem. Downloaded from www.nrcresearchpress.com by 210.87.254.42 on 09/05/12
For personal use only.

plane. In the Townes and Dailey theory (8, 9) the quadrupole splitting is directly proportional to the 5p orbital imbalance as expressed in the parameter U_p, where

$$U_p = -U_z + \frac{U_x + U_y}{2}$$

and the U terms are the 5p orbital populations. The isomer shift may be expected to show a simple linear dependence on the 5p orbital populations in analogy with ^{129}I Mössbauer data (8, 10). In the limit, when $U_x = U_y = U_z = 2$, the quadrupole splitting would be zero and the isomer shift would approach zero. From Tables 1 and 2 it can be seen that the isomer shifts for the Te(II) compounds span a range of values from 0.9 to 0.31 mm s^{-1} while the quadrupole splittings range only from 16 to 12.4 mm s^{-1}. These trends in δ and Δ cannot be explained simply in terms of changes in the tellurium $5p_x$ and $5p_y$ orbital populations as the ligand is changed, the isomer shifts showing too large a range of values in comparison with the small changes observed in Δ.

A possible explanation for the relatively small values of the isomer shifts in compounds **1–6** may lie in the direct participation of some fraction of the 5s electrons in the bonding. For several of the compounds studied here there is direct evidence from X-ray crystal structure data for considerable distortion of the S—Te—S bond angles from 90° and 180° which may indicate that the 5s electrons are stereochemically active. Thus in $Te((CH_3O)_2PS_2)_2$ (11) the S—Te—S bond angle between the strongly coordinated sulfur atoms is 98.3° while in $Rb_2Te(S_2O_3)_2$ (2) this angle is 101.1°. Such distortions are further exemplified by $Te(Et_2NCS_2)_2$ (12, 13) and $Te(MeOCS_2)_2$ (14) in which a marked tendency to 5-coordination is observed. In *trans*-$Te(SC[N(CH_3)_2]_2)_2(S_2O_2C_6H_5)_2)$ (15) the S—Te—S bond angles are found to be 79.5 and 100.5°.

Assuming, as for ^{129}I, that the removal of one 5s electron has approximately six times the influence on the isomer shift as the removal of one 5p electron (the two effects being of opposite sign) (10), then the results for compounds **1–6** of Table 1 are consistent with the presence of 5–12% s-character in the bonding scheme, the large quadrupole splittings in these compounds indicating that the number of 5p electrons involved in bonding does not change greatly. Compound **7**, however, exhibits both an isomer shift and quadrupole splitting very similar to that of the thiourea complexes, even though the molecule exhibits distortion from 90° bond angles. In this instance all four Te—S bonds are comparable in length with those observed in the linear 3-center bonds and it appears that in this instance crystal packing effects, dictated by the bulky $—S_2O_2C_6H_5$ ligands, are responsible for the molecular distortion.

Two other points which should be noted concerning the parameters of compounds **1** through **7**. Compounds **2** and **3** exhibit the smallest quadrupole splittings of the Te(II) compounds studied, and this is consistent with a greater population of the $5p_x$ and $5p_y$ orbitals in these compounds, compared with the other Te(II) complexes, as might be expected given the negative charge on the pentathionate ion. The similarity in Δ for the $Te(thiourea)_4^{2+}$ cation, the neutral molecules **1** and **4–7**, and the pentathionate anion support the general assumption that the electrostatic field gradient at the tellurium originates primarily from the valence-shell electrons and that any lattice contributions must be small.

Tellurium(IV) Compounds

In compounds **8** and **9** the tellurium is 8 coordinate and is found in a distorted dodecahedral environment (16, 17), in which two almost planar TeS_4 trapezoids interleave at approximately 90° to one another. No measurable quadrupole splitting was observed, as might be expected given the high coordination number and more or less symmetrical disposition of ligands about the tellurium. The isomer shifts are large and positive, corresponding to Te(IV) and a predominately lone-pair of $5s^2$ electrons on the tellurium. It is interesting that the isomer shifts of $Te[Et_2NCS_2]_2$ and $Te[Et_2NCS_2]_4$ appear to be a simple additive property of the ligand.

The isomer shifts of compounds **8** and **9** are not as large as those of octahedral TeX_4Tmtu_2 or TeX_6^{2-} (X = Cl, Br) (1), and this may again be explained by some small participation of the 5s electrons in the bonding, although other factors may also be involved. Thus there is a significant increase in the Te—S bond length in going from TeX_4Tmtu_2 to $Te(Et_2NCS_2)_4$ (16) and this may reflect the stronger ligand–ligand

Can. J. Chem. Downloaded from www.nrcresearchpress.com by 210.87.254.42 on 09/05/12
For personal use only.

repulsions on increasing the coordination number, together with the increasing use of high-energy d-orbitals on the tellurium, and the possible antibonding character of the lone-pair. The isomer shifts in **8** and **9** are consistent with a smaller charge on tellurium than in TeX_4Tmtu_2 which would be expected given the change in Te—S bondlengths.

The role of d-orbitals in bonding in compounds **8** and **9**, and presumably in **5** and **6**, is a point of some interest. In the interpretation of the Mössbauer parameters of ^{119}Sn, ^{121}Sb, ^{125}Te, and ^{129}I it is generally assumed that d-orbital electrons will not contribute to the quadrupole coupling and that they will not shield the 5s electrons to any great extent. Jung and Triftshäuser have estimated that d-orbital electrons will exhibit about one-third the shielding of 5p electrons (18). From the data for compounds **8** and **9** little can be said about the role of d-orbitals. However compounds **5** and **6** have very similar Δ values to those of the thiourea complexes, and this would appear to imply similar 5p orbital populations and that 5d orbitals do not play a major role, since any removal of $5p_x$ and $5p_y$ electrons into tellurium d-orbitals would be reflected in an increase in Δ and in δ.

In compounds **10** and **11** the tellurium is 7-coordinate and the geometry may be best described as distorted pentagonal bipyramidal (19), in which two of the bidentate ligand form an approximately planar TeS_5 equatorial grouping, with the second sulfur of the third ligand and the phenyl group occupying *trans* axial positions.

The positive isomer shifts again confirm that the 5s electrons are predominantly nonbonding. However the δ values are significantly smaller than those of other Te(IV) compounds and indeed overlap those of the Te(II) compounds. This must in part be attributed to the presence of the phenyl group and significant tellurium 5s character in the Te—C bond. This behavior is similar to that of triphenylstibine (20) and iodobenzene (21) where the isomer shifts for ^{121}Sb and ^{127}I are also consistent with significant 5s character in the Sb—C and I—C bonds.

The quadrupole splittings of *ca.* 5 mm s^{-1} in these compounds correspond to coupling constants, $e^2q^{125}Q$, of *ca.* 290 MHz, assuming $\eta = 0$. For IF_7, which is also pentagonal bipyramidal, $e^2q^{127}Q$ is reported to be -148 MHz, with $\eta = 0$. Expressed in units of $e^2q^{127}Q$, the coupling constants in compounds **10** and **11** are equivalent to *ca.* 1000 MHz. This very considerable difference between the magnitude of the coupling constants in pentagonal bipyramidal tellurium complexes on the one hand and IF_7 on the other is somewhat surprising.

On the basis of the available data it is possible to make a rough estimate of the orbital populations in compounds **10** and **11**. The planar TeS_5 unit in these compounds is structurally similar to that in $Te[Et_2NCS_2]_2$. For the latter, $\Delta = 15$ mm s^{-1} and taking Δ for a one p-electron imbalance as *ca.* 12 mm s^{-1} (1) and assuming the presence of a $5p_z^2$ nonbonding pair, (V_{zz} negative), this implies that in the Townes and Dailey formulation $U_x + U_y = 1.5$. Adopting this value for $U_x + U_y$ in compounds **10** and **11**, the observed Δ of *ca.* 5 mm s^{-1} (assuming $\eta = 0$) then corresponds to $U_z = 1.2$ or 0.3, depending on whether the coupling constant is positive or negative in sign respectively. The value of 1.2 for U_z seems the more realistic and this suggests that e^2qQ is probably positive (V_{zz} negative) *i.e.* there is an excess of 5p electron density along the *z* axis, this axis lying along, or close to, the axial S—Te—C bonds.

The study of compound **12** was motivated by the observation that orthorhombic *trans*-$TeCl_4$-$[SC(NCH_3)_2)_2]_2$ is converted to a monoclinic form on standing for a period of several years, or, more rapidly, an irradiation with X-rays (22). The monoclinic form (22) has been shown to exhibit quite distinct structural differences from the orthorhombic form (23). In particular the center of symmetry observed in the molecules of the orthorhombic form (A) is not observed in the monoclinic form (B). Moreover, whereas three linear three-center S—Te—S, Cl—Te—Cl systems are observed in (A), two of them are quite asymmetric in (B) both with regard to bond length and bond angle. A possible explanation for the considerable distortion from octahedral geometry observed in (B) could lie in stereochemical activity of the lone-pair in the more stable monoclinic form. However the Mössbauer parameters for the two forms were found to be the same within the errors. Thus neither the orthorhombic nor monoclinic forms exhibit a resolvable quadrupole splitting, while the isomer shifts are essentially identical. It is apparent that the distortion in the monoclinic form does not produce a sufficiently large

electrostatic field gradient to result in a measurable quadrupole coupling, while the s-electron density at the tellurium nucleus does not show the marked change that would be expected if the lone-pair were now stereochemically active.

Experimental

Most of the compounds were synthesized on the 100 scale using enriched ^{125}Te (>75%) and using methods described in the literature (2, 3, 11–17, 19, 22). However for compounds **7**, **10**, **11**, and **12** spectra were recorded on naturally abundant samples previously prepared in connection with the X-ray structural work. The compounds were identified using n.m.r., i.r., and Raman spectra and C, H, and N analyses where each was applicable.

The Mössbauer spectra were either recorded in our own laboratory at 80 K and using the methods previously described (4) (compounds **1–5** and **8**) at 4.2 K at the P.C.M.U. at Harwell (compounds **6**, **7**, **9–12**). In both instances $Pb^{125m}Te$ sources chemically prepared in our own laboratory were used and calibration using ^{125}Te-$Etu_4Cl_2 \cdot 2H_2O$ as a standard was employed. The two spectrometers gave values in very good agreement with one another for the same absorber. The spectra obtained in our own laboratory were 2 × 256 channel spectra and average values for the δ, Δ, and 2Γ values are quoted. The spectra recorded at Harwell were single spectra and such averaging was not required. In all instances the spectra gave χ_t^2/N values which lay within the 1% confidence limit.

The authors wish to thank Dr. F. Brown, Head, Solid State Research Branch, Chalk River for assisting in the production of a $Pb^{125m}Te$ source and Dr. Barry Dale of P.C.M.U. Harwell and his staff for their assistance in performing the experiments at 4.2 K. We are also grateful to Dr. O. Foss for his gift of *trans*-$Te(SC(N(CH_3)_2)_2)_2$-$(S_2O_2C_6H_5)_2$.

One of the authors (C.H.W.J.) is grateful to the National Research Council of Canada for a grant supporting this research, and Dr. A. G. Maddock for his hospitality at Cambridge University during 1973.

1. B. M. Cheyne, C. H. W. Jones, and P. Vasudev. Can. J. Chem. **50**, 3677 (1972).
2. O. Foss. Pure Appl. Chem. **24**, 31 (1970).
3. S. Husebye. Compounds of divalent selenium and tellurium with bidentate ligands: their preparation structure and bonding. Ph.D. Dissertation, University of Bergen, Bergen, Norway. 1969.
4. A. Yu. Aleksandrov, A. M. Babeshkin, V. I. Goldanskii, S. P. Ionov, V. A. Lebedev, and R. A. Lebedev. J. Struct. Chem. USSR, **12**, 302 (1971).
5. B. M. Cheyne and C. H. W. Jones. Can. J. Chem. **52**, 564 (1974).
6. K. V. Makariunas, R. A. Kalinauskas, and R. I. Davidonis. Sov. Phys. JETP, **33**, 848 (1971).
7. B. Martin and R. Schule. Phys. Lett. **46B**, 367 (1973).
8. M. Pasternak. Symp. Faraday Soc. **1**, 119 (1967).
9. C. H. Townes and B. P. Dailey. J. Chem. Phys. **17**, 782 (1949).
10. N. N. Greenwood and T. C. Gibb. *In* Mössbauer, spectroscopy. Chapman and Hall Ltd., London. 1971. pp. 455–482.
11. S. Husebye. Acta Chem. Scand. **20**, 24 (1966).
12. S. Husebye. Acta Chem. Scand. **24**, 2198 (1970).
13. C. Fabiani, R. Spagna, A. Vaciago, and L. Zambonelli. Acta Cryst. B**27**, 1499 (1971).
14. N. J. Brøndmo, S. Esperås, H. Graver, and S. Husebye. Acta Chem. Scand. **27**, 713 (1973).
15. K. Åse and I. Roti. Acta Chem. Scand. A**28**, 104 (1974).
16. S. Husebye and S. E. Svaeren. Acta Chem. Scand. **27**, 763 (1973).
17. S. Esperås and S. Husebye. Acta Chem. Scand. **27**, 706 (1973).
18. P. Jung and W. Triftshäuser. Phys. Rev. **175**, 512 (1968).
19. S. Esperås and S. Husebye. Acta Chem. Scand. **26**, 3293 (1972).
20. G. G. Long, J. G. Stevens, R. J. Tullbane, and L. H. Bowen. J. Am. Chem. Soc. **92**, 4230 (1970).
21. M. S. Lazarus and T. D. Thomas. J. Chem. Phys. **60**, 4682 (1974).
22. S. Esperås, J. W. George, S. Husebye, and O. Mikalsen. Acta Chem. Scand. **27**, 1089 (1973).
23. S. Husebye and J. W. George. Inorg. Chem. **8**, 313 (1969).

Can. J. Chem. Downloaded from www.nrcresearchpress.com by 210.87.254.42 on 09/05/12
For personal use only.

L'effet de la longueur de la chaîne et du p*H* sur la conformation de polyampholytes alternés du type (L-lysyl-L-aspartyl)$_n$

HUBERT DAOUST ET SERGE ST-PIERRE[1]

Département de chimie, Université de Montréal, C.P. 6210, Montréal, Québec H3C 3V1

Reçu le 2 juillet 1974[2]

HUBERT DAOUST et SERGE ST-PIERRE. Can. J. Chem. **53**, 1861 (1975).

Nous avons réalisé la synthèse, par la méthode en phase solide, d'une série de co-oligopeptides alternés, du type (L-lysyl-L-aspartyl)$_n$, (n = 4–10, dans le but d'étudier le comportement des polyampholytes en solution aqueuse, en fonction du p*H* et de la longueur de la chaîne peptidique. Nous avons observé que les spectres de dichroïsme circulaire variaient moins, en fonction de la longueur de la chaîne et du p*H*, que ceux observés avec des homooligoélectrolytes ne possédant pas de caractère polyampholytique. Nos résultats suggèrent une structure globulaire pour les peptides au point isoélectrique et une structure étendue en milieu fortement acide ou basique.

HUBERT DAOUST and SERGE ST-PIERRE. Can. J. Chem. **53**, 1861 (1975).

The synthesis of alternating (L-lysyl-L-aspartyl)$_n$ co-oligopeptides (n = 4–10) was realized by the solid phase method, to study the effect of chain length and p*H* on the conformation of polyampholytes in aqueous solution. The c.d. spectra do not show as important a dependance on p*H* and chain length as those observed with the nonampholytic homooligoelectrolytes. Our results suggest that the peptides are globular in shape when the p*H* of the solution is close to the isoelectric point but are extended in strong acid and base solutions.

Introduction

Depuis le début des années '50, un nombre incalculable de travaux ont été effectués dans le but d'étudier la stabilité intrinsèque de la conformation hélicoïdale des peptides et polypeptides. Pour mieux simuler la structure hélicoïdale qu'on retrouve à l'intérieur des protéines, où les segments hélicoïdaux comprennent rarement plus d'une vingtaine de résidus consécutifs, d'autres auteurs étudiaient l'influence de la longueur de la chaîne peptidique sur l'hélicité.

Une des premières études du genre fut accomplie par Brand et collaborateurs (1–3), sur les propriétés rotatoires de la poly-L-lysine (PLL) en fonction de la longueur de la chaîne. Robinson et Bott (4), utilisant un copolymère de D,L-phénylalanine et de γ-L-glutamate de benzyle de poids moléculaire variable, proposèrent une relation entre la longueur de la chaîne et son degré d'hélicité. Doty et collaborateurs (5–7) firent de même avec le poly-γ-L-glutamate de benzyle. Les polypeptides de masse moléculaire élevée formaient des hélices stables dans des solvants tel le chloroforme, alors que les chaînes de faible masse moléculaire étaient désordonnées en solution diluée et de structure-β en solution plus concentrée. Goodman et collaborateurs (8–22) effectuèrent le plus grand nombre de travaux dans le domaine, en milieu non-aqueux. Dans le cas des oligomères de γ-L-glutamate de méthyle, ils proposèrent que l'hélicité s'amorce entre l'hepta et le nonamère, utilisant b_0 comme critère d'hélicité. Les oligomères de masse moléculaire plus faible (d.p. < 12) avaient tendance à s'associer dans le dioxanne, alors que les fractions de masse moléculaire supérieure formaient plus spontanément des hélices (12). Tous les oligopeptides adoptaient la conformation désordonnée dans les acides forts, tel l'acide dicloroacétique (DCA). Pour les oligopeptides correspondants du β-L-aspartate de méthyle, la structure-β commençait à l'octamère et l'hélicité à l'undécamère, dans une solution à 3% de DCA dans le chloroforme.

Un travail similaire fut accompli avec des oligopeptides solubles dans l'eau. En 1952, Becker et Stahmann (23) mesuraient la rotation spécifique, $[\alpha]_D^{25}$, d'oligomères de longueur croissante de L-lysine·HCl. Alors que la rotation spécifique de la poly-L-lysine, de poids moléculaire élevé, atteignait −80°, celle du 22-mère se rapprochait de −70°. Schellman (24), en 1958, avait prédit que la longueur critique d'une hélice-α, en solution aqueuse, était de 15–20

[1]Adresse actuelle: Department of Chemistry, University of California, La Jolla, California.

[2]La révision reçue le 19 février 1975.

Can. J. Chem. Downloaded from www.nrcresearchpress.com by 210.87.254.105 on 09/05/12
For personal use only.

résidus, mais que les interactions entre les chaînes latérales étaient responsables d'une stabilité moindre de cette conformation. De même, les effets de bouts de chaîne, négligeables pour un polypeptide de masse moléculaire élevé, devenaient un facteur prédominant pour la stabilité des oligopeptides.

En 1971, Fasman et collaborateurs (25) publiaient les résultats d'une étude par dispersion optique rotatoire (d.o.r.) sur la relation entre la longueur de la chaîne d'oligopeptides de L-lysine et leur hélicité. Ils démontrèrent qu'une chaîne comprenant jusqu'à 22 résidus de lysine n'avait pas le même spectre d.o.r. que le polypeptide correspondant. L'hélicité s'amorçait à $n = 12$; le 22-mère ne contenait que 13% d'hélicité à p*H* 11.9. De même, une étude des oligomères de l'acide L-glutamique à p*H* 3.5, par Snipp *et al.* (26) n'attribuait que 40% d'hélicité à la chaîne de 17 résidus et 70% à la chaîne de 40 résidus.

En 1971, Schechter *et al.* (27) effectuaient une des premières études sur une série de co-oligopeptides de longueur croissante en solution aqueuse. La détermination de la conformation des homologues de la série (L-tyrosyl-L-alanyl-L-alanyl)$_n$ dans le but d'étudier l'effet de la longueur de la chaîne et de la densité de charge sur les propriétés antigéniques et immunogéniques de ces peptides.

Quoique les protéines soient avant tout des polyampholytes, aucun travail n'a été rapporté concernant l'influence de la longueur de la chaîne sur la conformation de peptides possédant cette propriété. On relève cependant plusieurs travaux relatifs à la synthèse et à l'étude conformationnelle de polypeptides possédant des propriétés ampholytiques, de séquence aléatoire (29, 30) et alternée (31–37). Une des principales limitations à ce genre d'étude est la synthèse de fractions d'oligopeptides homogènes et exempts de racémisation. Yaron et collaborateurs (25, 28) a utilisé une méthode chromatographique pour obtenir des fractions dont l'homogénéité, pour les homologues de masse moléculaire supérieure, laissait à désirer. Récemment, Bonora *et al.* (38), utilisaient la synthèse en phase solide pour obtenir des oligopeptides de longueur croissante de l'acide glutamique.

Nous avons également utilisé la méthode de synthèse en phase solide (39) pour obtenir la série de peptides (L-lysyl-L-aspartyl)$_n$ ($n = 1$–10). Les couplages ont été réalisés à l'aide du réactif de Belleau, soit le *N*-éthoxycarbonyl-éthoxy-2-dihydroquinoline-1,2 (EEDQ) (40–42). Cet agent de couplage, appliqué pour la première fois à la synthèse en phase solide par Sipos et Gaston (42), permet de former l'anhydride mixte de l'acide aminé qu'on veut ajouter à la chaîne et donne lieu à des couplages rapides, avec un rendement élevé. Ce réactif n'occasionne pas la formation de produit secondaire indésirable comme c'est le cas pour la dicyclohexylcarbodiimide (DCCI) (39); on peut par conséquent utiliser des excès moindres de dérivé Boc[3] d'acide aminé et diminuer le coût de la synthèse.

Nous avons étudié la variation des spectres de dichroïsme circulaire de ces peptides en fonction de la longueur de la chaîne et du p*H*. L'influence des bouts de chaîne sur les spectres d.c. des peptides a été évaluée par une méthode similaire à celle de Fasman et collaborateurs (25). Nous présentons également l'évaluation des fractions d'hélice-α, de structure-β et désordonnée par une méthode basée sur celle que Yang et collaborateurs (43, 44) ont mise au point pour évaluer la structure secondaire des protéines à partir de spectres d.c. Au lieu des standards protéiniques de Yang, nous avons utilisé les valeurs de Greenfield et Fasman (45) des spectres d.c. de la poly-L-lysine en solution aqueuse, sous les formes hélice-α, structure-β ou désordonnée. Nos résultats tendent à démontrer que la longueur de la chaîne est un critère de stabilité conformationnelle moins important pour les polyampholytes qu'elle ne l'est pour les homopolypeptides ioniques.

Partie expérimentale

Solvants et réactifs

Les solvants et réactifs pour la synthèse en phase solide ont été purifiés comme suit. Le dichlorométhane a été redistillé sur P_2O_5 et utilisé immédiatement après. La triéthylamine était refluée et distillée sur sodium et conservée sous atmosphère d'azote au réfrigérateur. L'acide trifluoroacétique était refluë et distillé sur P_2O_5 et conservé dans des bouteilles scellées. Tous les autres réactifs et solvants étaient de qualité réactif analytique et ont été utilisés comme tels.

La résine de Merrifield, soit un copolymère de styrène et de divinyl-benzène (1%) provenait de la compagnie Bio-Rad; elle contenait 1.25 mequiv. de chlore par gramme. Le EEDQ (Aldrich Chemicals, qualité Gold Label, +99%) a été utilisé sans purification supplémentaire.

Le *N*-α-Boc-β-L-aspartate de benzyle et le *N*-α-Boc-*N*-ε-tosyl-L-lysine furent préparés dans notre laboratoire,

[3] *t*-Butyl-oxycarbonyle.

Can. J. Chem. Downloaded from www.nrcresearchpress.com by 210.87.254.105 on 09/05/12
For personal use only.

Can. J. Chem. Downloaded from www.nrcresearchpress.com by 210.87.254.105 on 09/05/12
For personal use only.

selon des méthodes déjà décrites (39, 46–48). Le copoly (L-lysyl-L-aspartyl) a été synthétisé dans nos laboratoires et cette synthèse est rapportée dans une autre publication (49). Son poids moléculaire moyen en poids est de 31 700, tel que déterminé par approche à l'équilibre de sédimentation.

Purification et analyse des peptides

L'appareil "Osmolyser" (Bio-Rad) a été utilisé pour le dessalage des peptides. Les résines Sephadex G-10 et G-25 provenaient de la compagnie Pharmacia Canada Ltd., de Montréal.

Les chromatographies sur couche mince ont été effectuées sur des plaques de gel de silice G, de la compagnie Baker. Les mélanges de solvants suivants ont été utilisés: (*a*) butanol-1:acide acétique:eau:pyridine (15:3:12:10); (*b*) butanol-1:acide acétique: eau (4:1:1); et (*c*) pyridine:acide acétique: eau (10:6:3). Les électrophorèses ont été effectuées sur papier Whatman No. 1, en utilisant une source de courant de 1200 V, 50 mA, dans une solution tampon à p*H* 2.8, pendant 90 min. Les chromatographies sur couche mince et les électrophorèses ont été révélées indépendamment à la ninhydrine (0.2% dans l'acétone) et au réactif hypochlorite de sodium-*o*-toluidine – iodure de potassium (50).

Les analyses d'acides aminés ont été effectuées au moyen d'un appareil automatique Beckman, modèle 120 (51).

Synthèse des oligopeptides

L'attachement du premier acide aminé à la résine, soit le *N*-α-Boc-β-L-aspartate de benzyle, s'est effectué selon le procédé habituel (39), en faisant réagir 20 g de résine chlorométhylée (25 mmol de Cl) avec 6.5 g (20 mmol) de dérivé d'acide aspartique. La quantité d'acide aminé ainsi fixée a été déterminée, par analyse quantitative, à 0.37 mmol/g de résine. Au cours de toutes les opérations de la synthèse en phase solide, nous avons utilisé comme solvant le dichlorométhane. Le EEDQ (15% dans l'éthanol absolu) (42) a été utilisé comme agent de couplage. Pour chaque couplage, nous avons utilisé un triple excès molaire de dérivé d'acide aminé, en solution concentrée dans le dichlorométhane et le même excès de EEDQ dans l'éthanol. A partir du dixième résidu attaché à la chaîne, chaque couplage a été répété avec des quantités fraîches des mêmes réactifs, pour s'assurer d'un rendement quantitatif à chaque étape. La complétion de chaque couplage a été vérifiée par la méthode colorimétrique de Kaiser *et al.* (52), puis par analyse quantitative d'acides aminés, juste avant le couplage suivant.

Après chaque couplage, la résine était lavée avec de larges quantités de dichlorométhane. Après le couplage d'un dérivé de lysine, nous prélevions environ 1 g de résine et procédions ensuite à la réaction de déprotection du dérivé Boc. Cette réaction était effectuée au moyen de l'acide trifluoroacétique (TFA) à 50% dans le dichlorométhane, pendant 20 min. Après de copieux lavages au dichlorométhane, la neutralisation était effectuée au moyen d'une solution de triéthylamine à 10% (v/v) dans le dichlorométhane. Cette même série d'opérations a été répétée jusqu'à l'obtention de l'eicosapeptide.

Le clivage de chaque échantillon de peptide du support a été effectué en faisant barboter un faible courant de HBr anhydre et exempt de brome dans une suspension du complexe de résine–peptide dans le TFA. Avant d'être barboté dans la suspension, le HBr gazeux était préalablement lavé dans du tétrahydronaphtalène-1,2,3,4, puis dans de l'anisole maintenu à 30°, enfin séché sur Drierite et P_2O_5. Le groupement tosyl a été clivé au moyen d'une réduction par le sodium dans l'ammoniac liquide. Nous avons adouci les conditions de la réaction conventionnelle (39) en ajoutant goutte à goutte une solution de peptide dans l'ammoniac liquide. Nous avons ajouté la solution bleu foncé à la solution de peptide jusqu'à ce que cette dernière atteigne une couleur bleue pâle persistante; au bout de 15 s, nous arrêtions la réaction en y ajoutant brusquement de chlorure d'ammonium solide. La solution devenait alors incolore et limpide. Après évaporation de l'ammoniac et séchage sous vide, le peptide et le sel étaient dissous dans un volume minimum d'acide acétique à 2%. La solution était dessalée au moyen de l'"Osmolyser" et lyophilisée. La complétion des réactions de clivage par HBr/TFA et de détosylation était alors vérifiée par r.m.n. et spectroscopie u.v. pour la présence de groupements aromatiques résiduels. De même, les spectres i.r. des peptides ne révèlent aucune bande typique aux esters entre 1750 et 1800 cm^{-1}.

Chaque peptide a ensuite subi une première purification sur résine IRC-50, préalablement regénérée avec une solution d'acide acétique à 50% et lavée à l'eau jusqu'à neutralité. La solution de peptide était alors appliquée à la résine et le peptide était élué dans un gradient de bicarbonate d'ammonium de 0 à 0.5 *M*. Le pic principal de peptide était alors détecté par spectrophotométrie à 230 nm et la fraction lyophilisée. La purification finale de chaque peptide a été effectuée sur résine Sephadex G-10 (de l'octapeptide au dodécapeptide) ou G-25 (du tétradécapeptide à l'eicosapeptide) dans l'eau. Seules les fractions correspondant au maximum d'absorption, détecté comme précédemment, ont été conservées et lyophilisées. Dans tous les cas, un seul maximum d'absorption a été détecté.

Pureté des peptides

Le tableau 1 nous montre les résultats de l'analyse d'acides aminés des peptides et révèle des rapports respectifs lys/asp très voisins de 1. Les chromatographies sur couche mince de tous les peptides, dans les trois systèmes de solvants énumérés précédemment, ne révélaient qu'une seule tache bien définie dans tous les cas, par développement à la ninhydrine ou à l'hypochlorite de sodium-*o*-toluidine – iodure de potassium.

TABLEAU 1. Résultats de l'analyse quantitative d'acides aminés des différents peptides

Peptide $(lys–asp)_n$	Rapport théorique lys/asp	Rapport expérimental lys/asp
4	1.00	0.95
5	1.00	1.07
6	1.00	1.02
7	1.00	1.04
8	1.00	0.95
9	1.00	1.00
10	1.00	0.93

Can. J. Chem. Downloaded from www.nrcresearchpress.com by 210.87.254.105 on 09/05/12
For personal use only.

Enfin, l'électrophorèse sur papier, à p*H* 2.8, apporte les mêmes conclusions, utilisant les mêmes réactifs de développement des taches.

Il est difficile de calculer le rendement global de la synthèse jusqu'à l'obtention du peptide pur, à cause des prélèvements que nous avons effectués à chaque étape pour recueillir le peptide de longueur désirée. Nous ne pouvons qu'estimer grossièrement le poids de résine–peptide prélevé; selon nos estimations, le rendement global, basé sur le poids d'acide aspartique attaché à la résine du départ, se situe aux environs de 50% pour l'octapeptide et diminue jusqu'à environ 15% pour l'eicosapeptide.

Mesures de dichroïsme circulaire

Les spectres d.c. ont été enregistrés au moyen d'un spectropolarimètre Durrum-Jasco, de modèle ORD/UV-5, muni d'un attachement d.c. installé par Sproul Scientific (modèle SS-20). Tous les spectres ont été enregistrés à 23 ± 1°, la température étant maintenue constante au moyen d'un bain à circulation d'eau Haake. Les cellules de quartz utilisées étaient de qualité Suprasil (Hellma); les chemins optiques étaient de 1.00, 0.10 et 0.01 cm.

Le spectropolarimètre a été calibré en utilisant les valeurs standards de De Tar (53). L'acide *d*-10-camphorsulfonique nécessaire à la calibration a été préalablement recristallisé deux fois à partir du produit commercial (Aldrich Chemicals, 99%, $[\alpha]_D^{20}$ +19.9° (*c* 2, H_2O), dans l'acide acétique glacial et séché rigoureusement à 50° sous vide, sur P_2O_5. Sous ces conditions, le point de fusion est de 195° et la rotation spécifique $[\alpha]_D^{20}$ +22.1° (*c* 1, H_2O). Ces valeurs restent invariables après une cristallisation supplémentaire. Une valeur de calibration de +8216 deg cm^2 dmol^{-1} a été utilisée et revérifiée périodiquement avec une solution fraîche du standard.

L'ellipticité moyenne par résidu, [θ], exprimée en deg cm^2 dmole^{-1}, a été calculée selon la relation:

$$[1] \qquad [\theta]_\lambda = \frac{\theta_\lambda \text{p.m.r.}}{10Lc}$$

où θ_λ est l'ellipticité observée, en degrés, à la longueur d'onde λ, *L* est le chemin optique de la solution (en cm), p.m.r. est le poids moléculaire moyen d'un résidu de la chaîne et *c* la concentration de peptide en g/cm^3.

Nous avons préparé les solutions pour le dichroïsme circulaire de la façon suivante. Une quantité d'environ 5 mg de peptide était pesée dans un ballon jaugé de 5 ml et dissoute dans l'eau décarbonatée ou dans une solution de NaF 0.05 *M*. La solution était filtrée sur Millipore (type GSWPO-1300, Millipore, Bedford, Mass.). Des échantillons de 0.5 ml de cette solution stock étaient mesurés précisément dans des flacons et gardés au congélateur jusqu'à usage. Une minime fraction de cette solution était utilisée pour la détermination de la concentration par analyse quantitative d'acides aminés.

A l'exception des mesures pour déterminer l'effet de la concentration, des solutions dont la concentration variait entre 0.01 et 0.05% ont été préparées en diluant le volume requis de solution stock avec de l'eau ou la solution à 0.05 *M* de NaF. Nous avons ajusté le p*H* des solutions en y ajoutant lentement du NaOH ou du HCl 4 *N* à l'aide d'une micropipette. Le p*H* était lu avant et après l'enregistrement d'un spectre et la moyenne notée. L'effet de dilution a été étudié en utilisant une solution à 1% de peptide dans une cellule de 0.01 cm et une solution à 0.005% dans une cellule de 1 cm.

Nous avons comparé les spectres d.c. obtenus avec notre appareil avec ceux obtenus par Greenfield et Fasman (45) avec la poly-L-lysine sous les formes hélice-α, structure-β et désordonnée. L'échantillon de poly-L-lysine (Sigma Chemicals) possédait un poids moléculaire moyen de 100 000 (comparativement à 120 000 pour l'échantillon utilisé par Fasman). Nous avons reproduit exactement les conditions utilisées par ces derniers pour la préparation des échantillons et l'enregistrement des spectres, pour les trois formes de la poly-L-lysine. Les valeurs d'ellipticité moyenne par résidu sont en moyenne reproductibles à ±2% de 250 à 215 nm, ±5% de 215 à 205 nm et ±10% de 205 à 200 nm. Cette dernière différence s'explique par le bruit de fond particulièrement intense dans cette région du spectre, dû à une trop grande énergie au photomultiplicateur (0.5 kV à 200 nm, solvant seul) de notre instrument. C'est pourquoi tous nos spectres sont rapportés de 250 à 205 nm.

Pour plus de précaution, les spectres d.c. de quelques solutions de copolypeptide ont été remesurés au moyen d'un spectropolarimètre Cary 61 et ont montré une excellente reproductibilité, de 250 à 205 nm, avec les spectres enregistrés par l'appareil Durrum-Jasco.

Mesure du pH

Les valeurs de p*H* ont été mesurées au moyen d'un p*H* mètre digital Radiometer, modèle PHM52, relié à une électrode combinée Radiometer, de type GK2302G. Le p*H* mètre fut calibré à l'aide de tampons standards (Fisher Scientific Co.) à p*H* 7.00, 10.00 et 4.01, précis à ±0.02 unité de p*H*.

Méthode d'analyse conformationnelle des peptides

Pour évaluer le pourcentage relatif (f_i) d'hélice-α, de structure-β et de structure désordonnée, nous avons utilisé une méthode d'analyse comparable à celle de Yang et collaborateurs (43, 44). L'équation de base peut s'écrire comme suit, à une longueur d'onde donnée:

$$[2] \qquad \theta = f_H\theta_H + f_\beta\theta_\beta + f_R\theta_R$$

où

$$[3] \qquad f_H + f_\beta + f_R = 1$$

et

$$f_i \geq 0$$

où les θ_i représentent les ellipticités respectives des spectres standards de la poly-L-lysine (45) sous la forme hélice-α, structure-β, et désordonnée; θ est la valeur donnée par nos échantillons.

On peut tirer les paramètres f_H, f_β et f_R de la résolution des n équations, où n est le nombre de valeurs de longueur d'onde utilisées. Nous avons résolu, dans tous les cas, un système de 45 équations, incluant toutes les valeurs de θ comprises entre 250 et 205 nm, par la méthode de Cramer, au moyen d'un programme adapté à un ordinateur CDC 6400.

Enfin, le programme a été testé en effectuant le calcul des f_i pour la myoglobine et la papaïne, utilisant les

Can. J. Chem. Downloaded from www.nrcresearchpress.com by 210.87.254.105 on 09/05/12
For personal use only.

valeurs d'ellipticité et les standards de Yang et collaborateurs (43) pour ces protéines. Les valeurs de f_i respectives se comparaient bien à celles de Yang.

Résultats et discussion

La synthèse des peptides

La synthèse en phase solide s'est révélée un moyen remarquablement efficace et rapide pour obtenir des oligopeptides de longueur croissante rigoureusement homogènes. Pour cette première étude sur les oligoampholytes, nous avons préféré choisir deux acides aminés simples, tels la lysine et l'acide aspartique, pour les raisons suivantes.

Premièrement, les dérivés de la lysine sont reconnus pour n'occasionner aucun problème majeur lors de synthèse par la méthode de Merrifield, si le groupe de protection de l'amine en ε est choisi judicieusement (39). Pour une synthèse répétitive comme celle que nous rapportons ici, nous devions choisir un groupe très résistant à la présence d'acide trifluoroacétique à 50% dans le dichlorométhane, pour que la déprotection du groupe *N*-α-Boc soit vraiment sélective. Des essais préliminaires nous ont montré que le groupement carbobenzoxy ne convenait pas à nos besoins, à cause de son instabilité en milieu acide. C'est pourquoi nous avons choisi le groupement tosyle, qui est d'une stabilité remarquable à l'hydrolyse acide et qu'on peut enlever facilement par réduction par le sodium dans l'ammoniac liquide; tel que décrit dans la partie expérimentale, les conditions que nous avons utilisées pour cette déprotection nous ont donné satisfaction.

Deuxièmement, le choix de l'acide aspartique, de préférence à l'acide glutamique, a été fait dans le but d'éviter les difficultés qu'ont rencontrées d'autres chercheurs (38, 54) lors de l'utilisation de cet acide aminé en synthèse en phase solide.

Troisièmement, le choix de la lysine, de préférence à d'autres acides aminés à chaîne latérale basique, tels le tryptophane ou l'histidine par exemple, a été fait dans le but d'obtenir des spectres de dichroisme circulaire dépourvus des complications inhérentes aux acides aminés aromatiques (55–57).

Quatrièmement, la poly-L-lysine est un polypeptide ionique dont le comportement en solution aqueuse a suscité un nombre incalculable de travaux à cause des trois conformations qu'elle peut présenter, selon les paramètres de la solution. Ce polypeptide est reconnu principalement pour la stabilité de son hélice-α, donnant lieu à des spectres de dichroisme circulaire caractéristiques de cette conformation (45). Par contre, les polypeptides de l'acide aspartique et de ses esters (58–60) manifestent des propriétés particulières concernant la stabilité et la chiralité des hélices qu'ils forment en solution aqueuse ou organique. Le comportement en solution aqueuse de polypeptides alternés composés de ces deux résidus d'acides aminés, compliqué des problèmes propres aux polyampholytes, s'avère le sujet d'une étude des plus intéressantes. Dans cette première étude, nous n'avons considéré que l'effet de la longueur de la chaîne et du p*H* sur la conformation des chaînes.

Dichroïsme circulaire

Nous illustrons, dans les figs. 1–3, l'influence de la longueur de la chaîne sur l'allure des spectres de dichroïsme circulaire. Nous avons choisi d'étudier le phénomène à trois p*H* extrêmes, soient 2, 7 et 12, où la charge globale sur le peptide est respectivement positive, nulle et négative. Pour une plus grande clarté, nous n'avons présenté sur les figures que les spectres de quatre peptides. Pour faciliter la comparaison

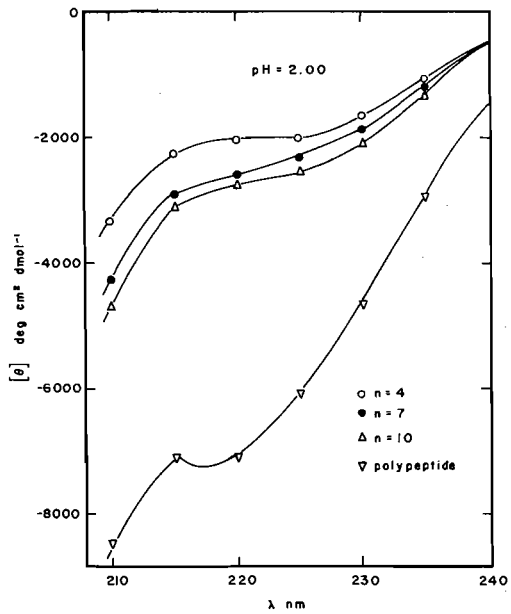

FIG. 1. Influence de la longueur de la chaîne sur le spectre d.c. de quatre peptides de la série $(lys\text{–}asp)_n$ à p*H* 2.00, à 22°, dans une solution aqueuse de NaF 0.02 *M* (concentration en peptides: 0.01% p/v).

Can. J. Chem. Downloaded from www.nrcresearchpress.com by 210.87.254.105 on 09/05/12
For personal use only.

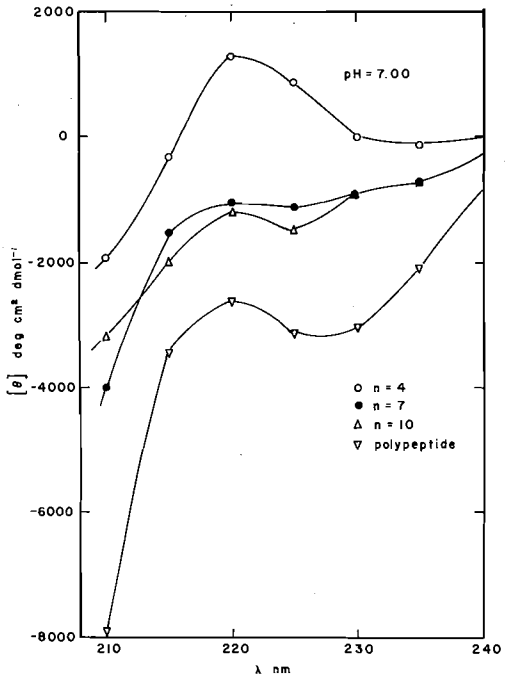

FIG. 2. Influence de la longueur de la chaîne sur le spectre d.c. de quatre peptides de la série $(lys\text{–}asp)_n$ à p*H* 7.00, à 22°, dans une solution aqueuse de NaF 0.02 *M* (concentration en peptides: 0.01% p/v).

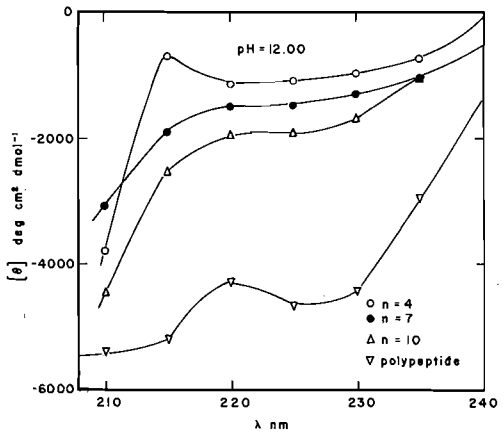

FIG. 3. Influence de la longueur de la chaîne sur le spectre d.c. de quatre peptides de la série $(lys\text{–}asp)_n$ à p*H* 12.00 à 22°, dans une solution aqueuse de NaF 0.02 *M* (concentration en peptides: 0.01% p/v).

entre les divers spectres, nous avons conservé la même échelle pour toutes les figures. Les résultats sont exprimés en degré cm^2 $dmol^{-1}$ et représentent l'ellipticité molaire par résidu d'acide aminé. Le poids moléculaire moyen par résidu a été assigné à 121.65, soit la moyenne pondéré d'un résidu lysyl (128.2) et aspartyl (115.1). On observe en premier lieu, à un p*H* donné, une légère augmentation de la bande d'ellipticité négative autour de 225 nm, de l'octapeptide au polypeptide. A p*H* 7, cependant, on observe une légère bande positive pour l'octapeptide et l'eicosapeptide. La différence d'ellipticité autour de 225 nm est nettement supérieure lorsque l'on compare l'eicosapeptide et le polypeptide. Globalement, l'ellipticité dans cette région du spectre passe, de l'octapeptide au polypeptide, de -1900 à -6700 deg cm^2 $dmol^{-1}$ à p*H* 2.0, de $+1000$ à -3000 deg cm^2 $dmol^{-1}$ à p*H* 7.0 et de -200 à -4000 deg cm^2 $dmol^{-1}$ à p*H* 12.0. Qualitativement, on peut également constater que la bande négative de dichroïsme autour de 200 nm diminue d'intensité lorsque l'on augmente la longueur de la chaîne, quelque soit le p*H*.

Afin de mieux illustrer l'influence de la longueur de la chaîne sur la conformation des peptides, nous avons choisi premièrement une méthode similaire à celle que Yaron *et al.* (25) avaient utilisée pour évaluer la longueur critique d'une hélice et l'importance des effets de bouts de chaîne dans le cas d'oligomères de longueur croissante de L-lysine. Ces derniers avaient supposé l'existence de la relation suivante entre la rotation molaire par résidu et la longueur de la chaîne:

$$[4] \qquad [m]_\lambda = [m]_{\text{interne}} + (1/n)[m]_{\text{bouts}}$$

où $[m]_\lambda$ est la rotation moyenne par résidu dans une chaîne désordonnée à une longueur d'onde λ; $[m]_{\text{interne}}$ et $[m]_{\text{bouts}}$ sont respectivement la rotation due aux résidus situés au centre de la chaîne et en bouts de chaîne; n est le nombre de résidus dans la chaîne. Toute déviation de la linéarité de cette équation devrait indiquer l'amorce d'une forme ordonnée de structure secondaire.

Nous avons supposé qu'une telle relation peut être convertie en termes d'ellipticité molaire et s'écrire:

$$[5] \qquad [\theta]_\lambda = [\theta]_{\text{interne}} + (1/n)[\theta]_{\text{bouts}}$$

où $[\theta]_\lambda$ est l'ellipticité molaire à 220 nm, calculée à partir du spectre d.c.; $[\theta]_{\text{interne}}$, $[\theta]_{\text{bouts}}$ et n correspondent aux termes semblables de l'éq. 4. A partir du graphique de $[\theta]$ en fonction de $1/n$, on doit obtenir les valeurs de $[\theta]_{\text{interne}}$ et de

Can. J. Chem. Downloaded from www.nrcresearchpress.com by 210.87.254.105 on 09/05/12
For personal use only.

$[\theta]_{bouts}$ comme étant respectivement l'ordonnée à l'origine et la pente des droites. Ces courbes, à p*H* 2.0, 7.0 et 12.0, sont représentées à la fig. 4. Comme le montre la figure, la linéarité de l'éq. 5 est respectée pour tous les oligopeptides, de l'octapeptide à l'eicosapeptide, aux trois p*H* étudiés. On remarque cependant que les trois points correspondant au polypeptide sont en dehors de leur tracé respectif. A p*H* 7.0 et 12.0, l'ellipticité du polypeptide varie d'environ 1000 deg cm^2 $dmol^{-1}$ de la linéarité. A p*H* 2.0, cependant, cette différence est d'environ 2500 deg cm^2 $dmol^{-1}$. La contribution des résidus internes à l'ellipticité est la plus faible (-2500 deg cm^2 $dmol^{-1}$) lorsque la charge globale des peptides est nulle et la plus forte (-4100 deg cm^2 $dmol^{-1}$) lorsque la charge globale est positive. Par contre, la contribution des bouts de chaîne demeure forte, soit de l'ordre de $+1600$ deg cm^2 $dmol^{-1}$, pour toutes les valeurs de p*H*. Quoique très approximative, cette valeur nous donne une excellente idée de l'importante contribution des bouts de chaîne à l'ellipticité. Elle nous permet aussi de justifier les bandes positives d'ellipticité obtenues avec les courtes chaînes. Elle explique enfin les faibles intensités des bandes négatives pour les peptides de masse moléculaire plus élevée.

En deuxième lieu, nous avons choisi de mettre en relief l'effet de la longueur de la chaîne et du p*H* sur la conformation des peptides en calculant, à partir de chaque spectre d.c., la fraction d'hélice et de structures beta et désordonnée de chaque peptide, pour une valeur de p*H* donnée. Le résultat de ce calcul est résumé dans le tableau 2. Comme on pouvait s'y attendre d'après l'allure des spectres d.c., la fraction hélicoïdale calculée est très faible sur toute la gamme des p*H* et longueurs de chaînes. Même pour le polypeptide à p*H* 2.0, qui donne

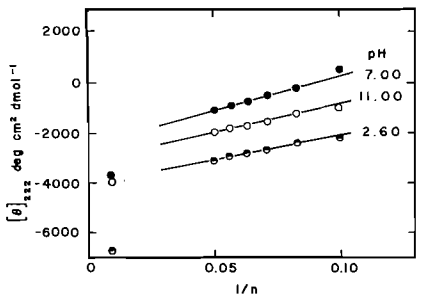

FIG. 4. Ellipticité à 222 nm en fonction de l'inverse de la longueur de la chaîne à différents p*H*.

TABLEAU 2. Calcul des fractions des trois conformations par la méthode de Yang et Martinez

$(lys\text{-}asp)_n$ valeur de n	f_H	f_β	f_R
	pH 2.00		
4	0.04	0.24	0.72
5	0.05	0.23	0.71
6	0.06	0.26	0.68
7	0.07	0.27	0.66
8	0.09	0.28	0.63
9	0.09	0.27	0.64
10	0.11	0.25	0.64
Poly	0.20	0.21	0.59
	pH 7.00		
4	0.01	0.2	0.77
5	0.03	0.12	0.85
6	0.04	0.17	0.79
7	0.03	0.26	0.71
8	0	0.24	0.76
9	0.03	0.23	0.74
10	0.02	0.24	0.75
Poly	0.10	0.13	0.77
	pH 12.00		
4	0	0.23	0.77
5	0.03	0.21	0.76
6	0.04	0.21	0.75
7	0.05	0.21	0.74
8	0.05	0.22	0.73
9	0.06	0.23	0.71
10	0.06	0.25	0.69
Poly	0.13	0.25	0.62

la bande d'ellipticité négative la plus forte autour de 220 nm, f_H ne dépasse par 20%. Par contre, f_β calculé demeure relativement constant, variant entre 10 et 30%. La fraction désordonnée demeure toujours importante, soit plus grande que 60% dans tous les cas. Il faut toutefois se rappeler que le rapport f_H/f_β est sujet à des erreurs importantes, dû à la similarité de l'emplacement de la bande d'ellipticité négative autour de 220 nm dans le spectre d.c. de ces deux conformations de polypeptide. Une autre source d'erreur importante dans l'évaluation des fractions f_H, f_β et f_R par cette méthode est l'existence de charges électrostatiques permanentes sur les chaînes à toutes les valeurs de p*H*. Il en résulte la possibilité toujours existante d'attraction électrostatique intra et intermoléculaire, dont on ne peut tenir compte en utilisant comme modèle un polypeptide ionique simple comme la poly-L-lysine. Cette particularité des polyampholytes contribue certainement à une estimation quelque peu erronée de la structure

Can. J. Chem. Downloaded from www.nrcresearchpress.com by 210.87.254.105 on 09/05/12
For personal use only.

secondaire au point isoélectrique des peptides. Cette source d'erreur est probablement négligeable aux valeurs p*H* extrêmes, 2 et 12, où les peptides se comportent essentiellement comme la poly-L-lysine ou l'acide poly-L-aspartique chargés.

En dépit des limitations que nous venons d'énumérer, nous considérons cette méthode d'analyse comme étant des plus valables. Son attrait principale est de tenir compte de tous les points d'un spectre, permettant de choisir les intervalles de longueur d'onde désirés. Dans notre cas, nous avons choisi un intervalle de 1 nm, après avoir vérifié que l'utilisation de plus petits intervalles, conséquemment, un plus grand nombre d'équations, ne modifiaient pas sensiblement la valeur des fractions obtenues.

Il ressort de cette étude que la longueur de la chaîne n'est pas un facteur prédominant de la stabilité conformationnelle des polyampholytes alternés, si nous nous basons sur la variation de leurs spectres de dichroïsme circulaire. Nous pensons que l'existence d'une charge permanente sur les chaînes, quelque soit le p*H*, joue le rôle principal dans l'organisation de la structure des molécules en solution, à cause des interactions intra et intermoléculaires qui en résultent. L'effet de la charge empêche en tout temps ces peptides d'acquérir une conformation vraiment stable et organisée, comme on retrouve chez les homopolypeptides ioniques non-chargés. Leur nature ampholytique n'exclut cependant pas une certaine rigidité de la structure. Une étude viscosimétrique, menée en parallèle avec les mesures de dichroisme circulaire, sur le polypeptide (61), jette quelque lumière sur les résultats précédents. Selon la théorie de Harris et Rice (62), la conformation des polyampholytes alternés en solution aqueuse peut être reliée d'assez près à celle des polyélectrolytes simples, lorsque le p*H* de la solution est éloigné du point isoélectrique.

L'effet du pH

A p*H* fortement acide, seuls les groupement amino de la lysine sont sous forme NH_3^+; les carboxyles de l'acide aspartique sont protonés, donc électriquement neutres. Sous ces conditions, la poly-L-lysine donne lieu à un spectre d.c. typique de chaîne étendue, selon Tiffany et Krimm (63, 64). Les spectres d.c. des oligoampholytes et du polyampholyte, en solution acide, diffèrent fortement des spectres de la poly-L-lysine chargée. C'est à ce p*H* que nos spectres d.c. manifestent les valeurs les plus négatives pour la bande d'ellipticité autour de 220 nm, de même que les pourcentages d'hélicité (f_H) les plus élevés. Le graphique de la fig. 4 nous indique également une plus grande contribution des résidus internes à l'ellipticité autour de 220 nm. On voit aussi à cette figure que la déviation à la linéarité du polypeptide à p*H* 2.0 est la plus importante.

La présence de résidus d'acide aspartique, situés à intervalles réguliers entre les résidus de lysine chargés, ne semble donc pas jouer, en solution acide, le simple rôle d'espaceur qu'on pourrait leur attribuer *a priori*. En plus de permettre l'augmentation de la distance entre les charges portées par les groupements NH_3^+, les résidus d'acide aspartique semblent contribuer à la formation de liaisons hydrogène, stabilisant la conformation du squelette du peptide. Toutefois, même pour le copolypeptide, cette conformation, si nous la supposons à tendance hélicoïdale, est fortement déformée, en se basant sur les calculs effectués; il serait logique de supposer dans ce cas une hélice étendue, d'après les constatations suivantes. La chaîne latérale portant le groupement NH_3^+ de la lysine est constituée de quatre CH_2; elle possède donc une longueur qui lui confèrent une certaine flexibilité. Toujours à cause de la longueur de cette chaîne, nous pouvons supposer négligeable l'existence d'interaction ion–dipôle entre le groupe NH_3^+ et les liaisons amide du squelette. Si cette hypothèse s'avère exacte, l'existence de liaisons hydrogène stabilisant la structure secondaire du squelette est concevable. Enfin, la flexibilité de la chaîne latérale de la lysine, relié au fait que chacun de ces résidus est séparé de l'autre par un résidu d'acide aspartique, permet, selon nous, aux groupements NH_3^+ de se placer à une distance d'interaction minimum l'un de l'autre. De cette façon, l'énergie électrostatique de répulsion est inférieure à l'énergie de stabilisation de l'hélice.

Le deuxième fait appuyant ces hypothèses est tiré des travaux de dichroïsme circulaire effectués par Brahms et Spach (58) sur l'acide poly-L-aspartique (APLA). Ces travaux ont démontré que l'APLA, comme l'acide poly-L-glutamique (APLG), forme des hélices-α en solution acide (p*H* 4.3). Toutefois, l'ellipticité manifestée par la transition n–π^* de l'APLA

Can. J. Chem. Downloaded from www.nrcresearchpress.com by 210.87.254.105 on 09/05/12
For personal use only.

est beaucoup plus faible que pour l'APLG ou la PLL, indiquant une stabilité moins grande de l'hélice en solution. Cependant, la chiralité de cette hélice est la même, soit une hélice-α droite. Nous pouvons donc, à la lumière de ces faits, suggérer pour le polypeptide en milieu fortement acide, une conformation d'hélice-α droite, étendue à cause de la répulsion électrostatique des charges positives, mais partiellement stabilisée par les liaisons hydrogène du squelette. La déformation supplémentaire peut être causée, comme dans le cas de l'APLA, par l'interaction dipôle–dipôle du groupement carboxylique avec les liaisons amides.

Les résultats viscosimétriques appuient également l'existence d'une hélice étendue, le comportement du polypeptide en solution acide ressemblant au cas d'un bâtonnet rigide. Il eut été très intéressant d'étudier le comportement des oligoampholytes par viscosimétrie. Malheureusement, leur faible masse moléculaire ne nous a pas permis d'obtenir des différences de temps d'écoulement suffisantes, même pour l'eicosapeptide. C'est pourquoi les études de structure des autres oligoampholytes en solution aqueuse ne sont basées que sur leurs spectres d.c. et les résultats obtenus avec le polypeptide. L'augmentation de l'ellipticité autour de 220 nm en fonction de la longueur de la chaîne serait imputable à la diminution progressive des effets de bouts de chaîne. On voit par contre que même avec l'eicosapeptide, la courbe en milieu acide de la fig. 4 ne dévie pas de la linéarité. Si on suppose juste l'hypothèse émise à l'éq. 5, cela signifie qu'aucune forme de structure secondaire n'est amorcée lorsque la chaîne contient jusqu'à vingt résidus.

Les spectres d.c. des peptides en solution basique ont l'allure des spectres en solution acide. Toutefois, la bande d'ellipticité autour de 220 nm est toujours moins négative, pour un peptide donné, que dans le cas de la solution acide. On voit également, à la fig. 4, que la contribution à l'ellipticité totale par les résidus internes est moindre qu'en milieu acide. En solution fortement basique, le peptide est chargé négativement, à cause de la présence des groupements carboxyl de l'acide aspartique sous forme COO^-. Les groupements amine de la lysine sont sous forme NH_2. D'une part, on note en milieu basique une plus grande viscosité intrinsèque de la solution qu'en milieu acide. Cette différence est cependant minime. D'autre part, les calculs du pourcentage de chaque forme, tirés des spectres d.c., nous montrent un pourcentage plus faible d'hélicité qu'en milieu acide et un pourcentage plus élevé de chaîne "étendue". Si le raisonnement précédent est applicable, la courte chaîne latérale de l'acide aspartique, moins flexible que celle de la lysine, ne permettrait pas aux groupements carboxyliques chargés de se maintenir à une distance suffisante l'un de l'autre pour annuler l'effet de répulsion électrostatique. De plus, il est possible à l'ion COO^- d'interagir fortement avec les liaisons polaires du squelette et nuire à la formation des liaisons hydrogène. Le niveau d'organisation des courtes chaînes en solution basique semble également moins important que précédemment.

Aux environs du point isoélectrique des peptides, nous avons affaire à un phénomène complètement différent. Les résultats de viscosimétrie indiquent une chute importante de la viscosité intrinsèque, signe d'une forte association des chaînes causée par l'attraction électrostatique d'ions de signe contraire portés par les chaînes latérales des peptides. Un fait intéressant à signaler est la diminution de l'ellipticité de la bande de dichroïsme circulaire autour de 200 nm lorsque les solutions de peptide tendent vers un p*H* neutre. Dans le cas d'homopolypeptides chargés, cette bande est très intense, de l'ordre de $-50\,000$ deg cm^2 dmol^{-1} pour la poly-L-lysine (45). Dans notre cas, l'intensité de cette bande ne dépasse pas $-15\,000$ deg cm^2 dmol^{-1} pour le polypeptide à p*H* 7.0. Ces résultats nous porte à croire à l'adoption, par les polyampholytes, d'une forme globulaire compacte au point isoélectrique. Comme la dilution ne semble pas affecter les spectres d.c. dans ces conditions, du moins dans les limites expérimentales de concentration permissibles (1–0.005%), nous croyons que l'association est surtout intramoléculaire. Des essais de variation de température sur le spectre d.c. nous portent aux mêmes conclusions. Le fait que les chaînes tendent à se replier sur elles-mêmes lorsqu'on approche du point isoélectrique aurait alors pour effet de diminuer le moment dipolaire résultant de chaque chaîne et par conséquent l'ellipticité des transitions n–π^* et π–π^*, comme on l'observe sur les spectres d.c. à p*H* 7.0. Comme le montre la fig. 4, l'effet de la longueur de la chaîne dans ces conditions semble le moins important.

Can. J. Chem. Downloaded from www.nrcresearchpress.com by 210.87.254.105 on 09/05/12
For personal use only.

A la lumière de ces résultats, il nous apparait que la conformation d'un polyampholyte alterné, composé de résidus d'acide aspartique et de lysine, diffère fortement de celles des homopolypeptides respectifs. Cette propriété de polyampholyte confère à ces peptides une ressemblance indéniable avec les protéines globulaires, pour lesquelles ils peuvent éventuellement servir de modèle. Ce travail montre également que la longueur de la chaîne n'est pas un critère primordial pour qu'un polyampholyte adopte sa conformation la plus stable en solution, contrairement aux homopolypeptides ou polyélectrolytes simples. D'autres travaux restent à faire pour déterminer exactement la structure secondaire qu'adoptent ces peptides en solution aqueuse et la raison pour laquelle ils manifestent des propriétés de dichroïsme circulaire aussi compliquées.

Nous remercions le Ministère de l'Education de la Province de Québec ainsi que le Conseil national de recherche du Canada pour l'aide financière apportée à ces travaux de recherche.

1. E. BRAND et B. ERLANGER. J. Am. Chem. Soc. **72**, 3114 (1950).
2. B. ERLANGER et E. BRAND. J. Am. Chem. Soc. **73**, 3508, 4025, 4027 (1951).
3. E. BRAND, B. ERLANGER et H. SACHS. J. Am. Chem. Soc. **74**, 1849, 1851 (1952).
4. C. ROBINSON et M. J. BOTT. Nature, **168**, 325 (1957).
5. P. DOTY, A. M. HOLTZER, J. H. BRADBURY et E. R. BLOUT. J. Am. Chem. Soc. **76**, 4493 (1954).
6. P. DOTY et R. D. LUNDBERG. J. Am. Chem. Soc. **78**, 4810 (1956).
7. R. D. LUNDBERG et P. DOTY. J. Am. Chem. Soc. **79**, 3961 (1957).
8. M. GOODMAN et E. E. SCHMITT. J. Am. Chem. Soc. **81**, 5507 (1959).
9. M. GOODMAN, E. E. SCHMITT et D. YPHANTIS. J. Am. Chem. Soc. **82**, 3483 (1960).
10. M. GOODMAN, E. E. SCHMITT et D. YPHANTIS. J. Am. Chem. Soc. **84**, 1288 (1962).
11. M. GOODMAN, I. LISTOWSKY et E. E. SCHMITT. J. Am. Chem. Soc. **84**, 1296 (1962).
12. M. GOODMAN, C. M. DEBER et A. M. FELIX. J. Am. Chem. Soc. **84**, 3771 (1962).
13. M. GOODMAN, C. M. DEBER et A. M. FELIX. J. Am. Chem. Soc. **84**, 3773 (1962).
14. M. GOODMAN et F. BOARDMAN. J. Am. Chem. Soc. **85**, 2483 (1963).
15. M. GOODMAN, F. BOARDMAN et I. LISTOWSKY. J. Am. Chem. Soc. **85**, 2483 (1963).
16. M. GOODMAN, I. LISTOWSKY, Y. MASUDA et F. BOARDMAN. Biopolymers, **1**, 33 (1963).
17. M. GOODMAN, A. M. FELIX, C. M. DEBER, A. R. BRAUSE et G. SCHWARTZ. Biopolymers, **1**, 371 (1963).
18. M. GOODMAN et Y. MASUDA. Biopolymers, **2**, 107 (1964).
19. M. GOODMAN et I. G. ROSEN. Biopolymers, **2**, 537 (1964).
20. M. GOODMAN, M. LANGSAM et I. G. ROSEN. Biopolymers, **4**, 305 (1966).
21. M. GOODMAN. J. Polym. Sci. **49**, 150 (1961).
22. M. GOODMAN, A. S. VERDINI, C. TONIOLO, W. D. PHILLIPS et F. BOVEY. Proc. Natl. Acad. Sci. **64**, 444 (1969).
23. R. R. BECKER et M. A. STAHMANN. J. Am. Chem. Soc. **74**, 38 (1952).
24. J. A. SCHELLMAN. J. Phys. Chem. **62**, 1485 (1958).
25. A. YARON, E. KATCHALSKI, A. BERGER, G. D. FASMAN et H. A. SOBER. Biopolymers, **10**, 110 (1971).
26. R. L. SNIPP, W. G. MILLER et R. E. NYLUND. J. Am. Chem. Soc. **87**, 3547 (1965).
27. B. SCHECHTER, I. SCHECHTER, J. RAMACHANDRAN, A. CONWAY-JACOBS et M. SELA. Eur. J. Biochem. **20**, 301 (1971).
28. A. YARON, E. K. DUNHAM et S. F. SCHLOSSMAN. Biochemistry, **13**, 347 (1974).
29. E. R. BLOUT et M. IDELSON. J. Am. Chem. Soc. **80**, 4909 (1958).
30. M. ATREYI et R. C. GUPTA. Bull. Chem. Soc. Jap. **46**, 2795 (1973).
31. T. VAJDA. Chem. Ind. 785 (1963).
32. T. VAJDA. Acta Chim. Acad. Sci. Hung. **46**, 221 (1965).
33. R. LEDGER et F. H. C. STEWART. Aust. J. Chem. **20**, 2509 (1967).
34. J. RAMACHANDRAN, A. BERGER et E. KATCHALSKI. Biopolymers, **10**, 1829 (1971).
35. R. D. COWELL et J. H. JONES. J. Chem. Soc. Perkin I, 1814 (1972).
36. B. J. JOHNSON et N. TSANG. J. Med. Chem. **15**, 488 (1972).
37. A. R. ZEIGER, A. LANGE et P. H. MAURER. Biopolymers, **12**, 2135 (1973).
38. G. M. BONORA, C. TONIOLO, A. FONTANA, C. DI BELLO et E. SCOFFONE. Biopolymers, **13**, 157 (1974).
39. J. M. STEWART et J. D. YOUNG. Solid phase peptide synthesis. W. H. Freeman. San Francisco. 1969.
40. B. BELLEAU et G. MALEK. J. Am. Chem. Soc. **90**, 1651 (1968).
41. H. YAJIMA et H. KAWATANI. Chem. Pharm. Bull. **19**, 1905 (1971).
42. F. SIPOS et D. W. GASTON. Synthesis, **6**, 321 (1971).
43. Y. H. CHEN, J. T. YANG et H. MARTINEZ. Biochemistry, **11**, 4120 (1972).
44. Y. H. CHEN, J. T. YANG et K. H. CHAU. Biochemistry, **13**, 3350 (1974).
45. N. J. GREENFIELD et G. D. FASMAN. Biochemistry, **8**, 4108 (1969).
46. L. BENOITON. Can. J. Chem. **40**, 570 (1962).
47. L. ZAORAL. Coll. Czech. Chem. Commun. **30**, 1853 (1965).
48. E. SCHANBEL. Justus Liebigs Ann. Chem. **702**, 188 (1967).
49. S. ST-PIERRE, C. ROUX et H. DAOUST. En préparation.
50. E. STAHL. Thin layer chromatography, a laboratory handbook. Springer-Verlag, New York, N.Y. 1965. p. 404.
51. D. H. SPACKMAN, W. H. STEIN et S. MOORE. Anal. Chem. **30**, 1190 (1958).

52. E. KAISER, R. L. COLESCOTT, C. D. BOSSINGER et P. I. COOK. Anal. Biochem. **34**, 595 (1970).
53. D. F. DE TAR. Anal. Chem. **41**, 1406 (1969).
54. D. E. NITECKI et J. W. GOODMAN. *Dans* Peptides: chemistry and biochemistry. *Redigé par* B. Winstein. M. Dekker, New York. 1970. p. 435.
55. M. GOODMAN et C. TONIOLO. Biopolymers, **6**, 1673 (1968).
56. M. GOODMAN, G. W. DAVIS et E. BENEDETTI. Acc. Chem. Res. **1**, 275 (1968).
57. A. J. ADLER, N. J. GREENFIELD et G. D. FASMAN. *Dans* Methods in enzymology. Vol. XXVII. *Redigé par* C. W. H. Hirs et S. N. Timasheff. Academic Press, New York. 1973. p. 675.
58. J. BRAHMS et G. SPACH. Nature, **200**, 72 (1963).
59. J. T. YANG. *Dans* Poly-α-amino acids. *Redigé par* G. D. Fasman. Marcel Dekker, Inc., New York. 1967. p. 239.
60. G. D. FASMAN. *Dans* Poly-α-amino acids. *Redigé par* G. D. Fasman. Marcel Dekker, Inc., New York. 1967. p. 499.
61. H. DAOUST et S. ST-PIERRE. En préparation.
62. F. E. HARRIS et S. A. RICE. J. Chem. Phys. **24**, 336 (1956).
63. M. L. TIFFANY et S. KRIMM. Biopolymers, **8**, 347 (1969).
64. M. L. TIFFANY et S. KRIMM. Biopolymers, **12**, 575 (1973).

Can. J. Chem. Downloaded from www.nrcresearchpress.com by 210.87.254.105 on 09/05/12
For personal use only.

Orientation Effects and the Sign of Two-bond ^{13}C–^{1}H Coupling[1,2]

JOSEPH A. SCHWARCZ,[3] NATSUKO CYR, AND ARTHUR S. PERLIN
Department of Chemistry, McGill University, Montreal, Quebec H3C 3G1

Received December 20, 1974

JOSEPH A. SCHWARCZ, NATSUKO CYR, and ARTHUR S. PERLIN. Can. J. Chem. **53**, 1872 (1975).

Signs of two bond (^{2}J) ^{13}C–^{1}H coupling in ^{13}C-enriched carbohydrates have been determined from proton spectra by the double irradiation technique. Instances of both positive and negative ^{2}J values are given and are characterized in terms of the relative orientations of the coupled proton and of oxygen appended to the ^{13}C nucleus; *e.g.*, an oxygen *anti* to the proton appears to make a positive contribution to ^{2}J and a *gauche* oxygen a negative one. Theoretical calculations, using ethanol and 1,1-ethanediol as model compounds, are in accord with these experimental observations.

JOSEPH A. SCHWARCZ, NATSUKO CYR et ARTHUR S. PERLIN. Can. J. Chem. **53**, 1872 (1975).

On a déterminé le signe du couplage sur deux liaisons (^{2}J) ^{13}C–^{1}H dans des carbohydrates enrichis en ^{13}C; ces attributions ont été faites à partir des spectres du proton en utilisant la technique à double irradiation. On présente des cas où les valeurs de ^{2}J sont positives et d'autres où elles sont négatives et ces valeurs sont caractérisées en terme d'orientation relative du proton couplé par rapport à l'oxygène attaché aux noyaux ^{13}C; *e.g.* un oxygène *anti* par rapport à un proton semble apporter une contribution positive à ^{2}J et un oxygène *gauche* apporterait une contribution négative. Des calculs théoriques utilisant l'éthanol et l'éthanediol-1,1 comme composés modèles sont en accord avec les observations expérimentales.

[Traduit par le journal]

The magnitude of coupling between ^{13}C and ^{1}H across two bonds ($^{2}J_{C,H}$) is dependent on the orientation of substituents appended to the ^{13}C nucleus relative to the proton. For example, C-1 of β-D-glucopyranose-*1*-^{13}C (**1**) exhibits coupling of 5.7 Hz with H-2, whereas the corresponding value for the α-anomer (**2**) is <1 Hz (1, 2).[4] Similarly, an orientational dependence has been noted for sp^2 hybridized carbon: coupling between ^{13}C-6 and H-5 is 4 Hz for 1,2-*O*-isopropylidene-α-D-glucofuranurono-6,3-lactone but none is observed (2) for the epimeric β-L-*ido* derivative. In bromoethylene (**3**) two-bond coupling with both of the vinyl protons is observed but $^{2}J_{C,H}$ for the proton *trans* to the halogen has a positive value, whereas that involving the *cis* proton is negative (4). The current study deals with the sign of coupling associated with the orientation of substituents in molecules such as **1**.

The double irradiation technique of sign determination (5) was found to be effective for the present purpose. An AMX spin system is ideal in this type of application and, in principle, should be encountered in the H-1,^{13}C-1,C-2,H-2 portion of **1** ($\nu_{H\text{-}1} - \nu_{H\text{-}2} = 150$ Hz; ^{13}C-1 is the X nucleus). However, due to signal overlap the spectrum of **1** proved to be unsuitable for the double irradiation experiment. A much more satisfactory spectrum (Fig. 1) was obtained for β-D-allopyranose-*1*-^{13}C (**4**), *i.e.*, the 3-epimer of **1**. Since in this instance $J_{H\text{-}1,H\text{-}2}$ and $J_{H\text{-}2,H\text{-}3}$ differ, and neither equals $J_{C\text{-}1,H\text{-}2}$, the H-2 signal is an octet; both the latter signal and the lower H-1 satellite signal are clearly observable in the spectrum.

When irradiation was carried out at the frequency of the upfield half of the H-2 octet (*C*), the low-field portion of the H-1 signal collapsed but it was unaffected at the frequency of the low-field half (*B*) of the H-2 signal (inset, Fig. 1). Analogously, irradiation at the frequency of the low-field half of H-1 (*A*) caused perturbation only of the upfield half of the H-2 signal. Therefore, $^{1}J_{C,H}$ and $^{2}J_{C,H}$ in this system are of opposite sign and hence, since $^{1}J_{C,H}$ is taken to be positive (5), coupling between ^{13}C-1 and H-2 in **4** may be specified as -5 Hz. By implication, the corresponding coupling in **1** is *minus* 5.7 Hz.

---

[1]This paper is dedicated to Professor C. A. Winkler of McGill University on the occasion of his sixty-fifth birthday by one of his colleagues (A.S.P.).

[2]Presented in part at the 1974 Meeting of the American Chemical Society, Atlantic City, N.J. September 8–13.

[3]NRCC Scholar, McGill University, 1969–1973.

[4]More recently, these data have also been obtained (3) with nonenriched α,β-D-glucose by ^{13}C n.m.r. spectroscopy.

Can. J. Chem. Downloaded from www.nrcresearchpress.com by 210.87.254.5 on 09/05/12
For personal use only.

Can. J. Chem. Downloaded from www.nrcresearchpress.com by 210.87.254.5 on 09/05/12
For personal use only.

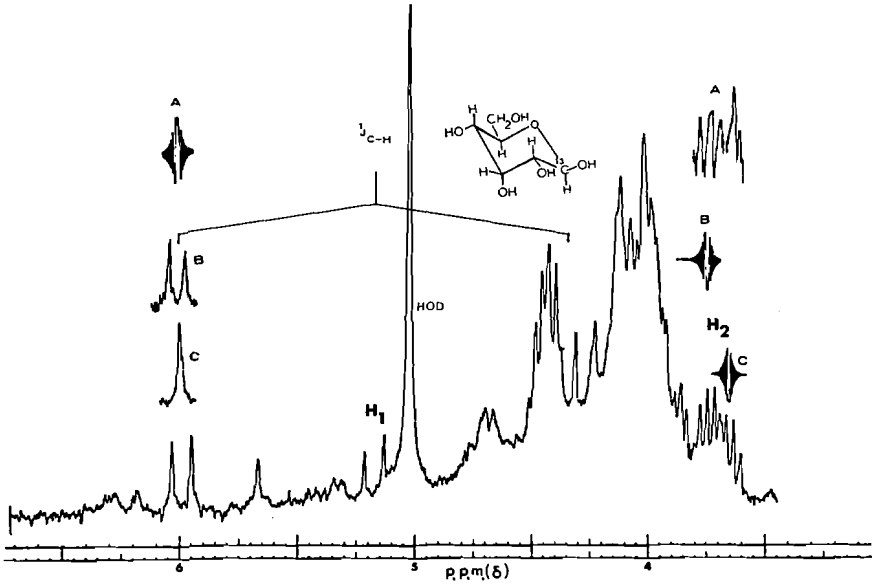

FIG. 1. Relative sign determination for $^2J_{C\text{-}1,H\text{-}2}$ of β-D-allopyranose-*1*-^{13}C (80% enriched) (**4**), by the double resonance method; *A*, *B*, and *C* refer to the individual irradiation frequencies selected and the corresponding signals observed.

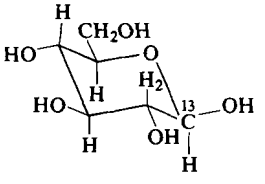

1

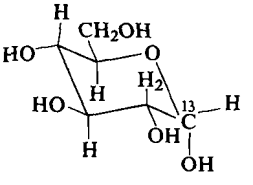

2

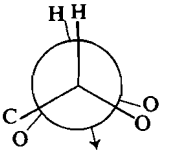

7

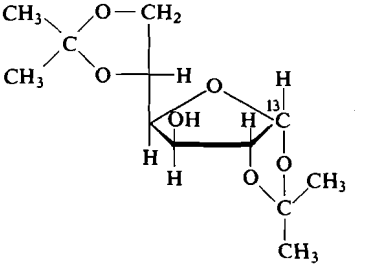

8

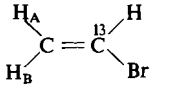

$^2J_{C\text{-}H_A} = +7.5$ Hz

$^2J_{C\text{-}H_B} = -8.5$ Hz

3

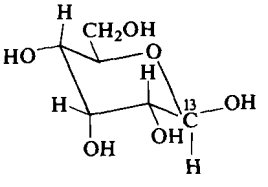

4

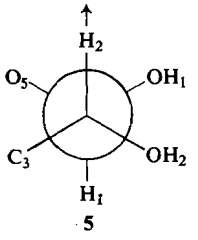

5

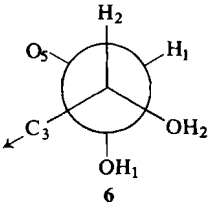

6

In comparing this result with the value of <1 Hz cited for coupling between ^{13}C-1 and H-2 of α-D-glucopyranose-*1*-^{13}C, one way to describe the relative stereochemistry of these isomers is to treat the C-1, O-1, and C-1.O-5 bonds as vectors and consider their "resultant" (v.r.), as in **5** (β-anomer) or **6** (α-anomer) with respect to the C-2, H-2 bond. Accordingly, it appears that the value of $^2J_{C,H}$ becomes more negative as the dihedral angle relating v.r. and H-2 decreases.

The sign of two-bond coupling in an analogous system (**7**) incorporating an *increase* in the angle between v.r. and H-2 was determined from the spectrum of 1,2:5,6-di-*O*-isopropylidene-α-D-glucofuranose-*1*-^{13}C (**8**). Since there is no detectable coupling of H-2 and H-3 in this molecule, the H-2, H-3 dihedral angle must be close to 90° and the furanose ring must approximate an

TABLE 1. Dependence of two-bond ^{13}C–^{1}H coupling in ethanol and ethane-1,1-diol on the relative orientations of the coupled proton and oxygen

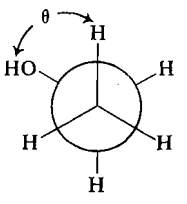

9

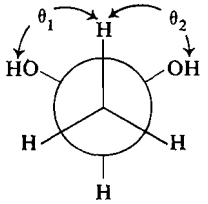

10

Ethanol (9)		Ethane-1,1-diol (10)		
θ (deg)	$\pi_{\mu v}$ (Hz)	θ_1 (deg)	θ_2 (deg)	$\pi_{\mu v}$ (Hz)
0	−3.2	60	60	−3.0
30	−3.0	30	90	−2.8
60	−2.2	0	120	−1.9
90	0	30	150	0
120	+3.9	60	180	+2.6
150	+7.2	90	150	+4.9
180	+9.3	120	120	+6.0

envelope conformation (6), which may be partially depicted by projection **7**. In this arrangement, v.r. is almost *trans* to H-2.

Double irradiation experiments with **8** showed that the sign is the same for coupling of ^{13}C-1 with H-1 as with H-2, *i.e.*, collapse of the downfield half of the H-1 signal was effected by irradiation at the frequency of the lower half of the H-2 signal; similarly, the two upfield halves of these signals were correlated. The results were confirmed by reversal of the double irradiation procedure. Hence, for the particular stereochemistry represented by **7** the value of $^{2}J_{C,H}$ is positive (+5.5 Hz).

In summary, coupling between a ^{13}C atom bearing two oxygen atoms and a proton on a neighboring carbon is negative when the dihedral angle relating the C—O bonds with the C—H bond is small. As the angle increases the coupling constant increases, then passes through zero, and its sign becomes positive. Stated alternatively, an oxygen *anti* to the coupled proton may be regarded as making a positive contribution to the coupling, whereas a *gauche* oxygen makes a negative contribution.

A theoretical approach (7) for calculating the sign and relative magnitude of two bond ^{13}C–^{1}H coupling constants has been applied to ethanol (**9**) and 1,1-ethanediol (**10**) for comparison with the observed substituent orientational dependence described above.

The results (Table 1), expressed as a function of J (*i.e.*, $\pi_{\mu v}$(8)), show that the calculated coupling constants qualitatively exhibit a stereochemical dependence analogous to that found experimentally. For ethanol, the positive contribution of an *anti* hydroxyl and the negative one of a *gauche* hydroxyl are clearly demonstrated. The results observed with the *1*-^{13}C enriched carbohydrates are also reproduced with the *gem*-ethanediol system: *i.e.*, coupling is negative when the hydroxyls are oriented 60° with respect to the coupled proton and becomes positive when the dihedral angles become 120° (Table 1).

According to these findings, two bond ^{13}C–^{1}H coupling is, in principle, a more definitive type of stereochemical descriptor than three-bond (vicinal) coupling. Hence, the absolute magnitude of $^{2}J_{C,H}$ varies in a progressive manner, increasing continuously as the dihedral angle (or v.r.) increases, whereas a given value of $^{3}J_{C,H}$ may correspond to either of two different orientational arrangements because of the U-shape of the "Karplus-type" curve for vicinal coupling (2, 9). Improvements in methodology for determining the sign of ^{2}J are needed, however, to facilitate a general application of two bond coupling to stereochemical problems.

Experimental and Calculations

Proton magnetic resonance spectra were recorded at 100 MHz with a Varian HA-100 spectrometer using D_2O

Can. J. Chem. Downloaded from www.nrcresearchpress.com by 210.87.254.5 on 09/05/12
For personal use only.

(for **4**) or $CDCl_3$ (for **8**) as solvent. The frequency sweep mode was employed in the double irradiation experiments.

1,2:5,6-Di-*O*-isopropylidene-α-D-glucofuranose-*1*-^{13}C (**8**) was synthesized as described previously (2) and β-D-allopyranose-*1*-^{13}C (**4**) from **8** (10) by the route developed (11) for synthesis of the nonenriched sugar.

The equation proposed by Pople and Santry (ref. 8 eqs. 3.4 and 3.5) was utilized for the calculation of coupling constants. Only the Fermi contact terms were considered in the calculations, as is usual (12), and orbital coefficients and energies were obtained by use of the CNDO/2 method (7). In this method the unoccupied orbital's energy (ε_j (8)) is calculated by placing one extra electron in the orbital. For the present purpose, however, the triplet state energy (ε_j (corr.)) was required and this was obtained by subtracting from ε_j the energy of repulsion between the electron in the highest occupied orbital and the remaining electrons, as follows.

$$\varepsilon_j(\text{corr.}) = \varepsilon_j - \sum_{\mu}\sum_{\nu} C^2{}_{\mu j} C^2{}_{\nu k} \gamma_{\mu\nu}$$

where μ and ν are the basic atomic orbitals, k is the highest occupied molecular orbital, and γ is the electron repulsion integral.

The authors express their gratitude to Dr. J. E. Grabenstetter for valuable discussion and to the National Research Council of Canada and the Pulp and Paper Research Institute of Canada for generous support.

1. A. S. PERLIN and B. CASU. Tetrahedron Lett. 2921 (1969).
2. J. A. SCHWARCZ and A. S. PERLIN. Can. J. Chem. **50**, 3667 (1972).
3. A. S. PERLIN, N. CYR, R. G. S. RITCHIE, and A. PARFONDRY. Carbohydr. Res. **37**, C1(1974).
4. R. M. LYNDEN-BELL. Mol. Phys. **6**, 537 (1963); F. J. WEIGERT and J. D. ROBERTS. J. Phys. Chem. **73**, 449 (1969).
5. R. FREEMAN. Mol. Phys. **4**, 385 (1961); E. D. BECKER. High resolution NMR. Academic Press, New York, N.Y. 1969. p. 192.
6. R. J. ABRAHAM, L. D. HALL, L. HOUGH, and K. A. MCLAUCHLAN. J. Chem. Soc. 3699 (1962).
7. J. A. POPLE and G. A. SEGAL. J. Chem. Phys. **43**, S136 (1965); **44**, 3289 (1966).
8. J. A. POPLE and D. P. SANTRY. Mol. Phys. **8**, 1 (1965).
9. R. U. LEMIEUX, T. L. NAGABHUSHAN, and B. PAUL. Can. J. Chem. **50**, 773 (1972).
10. J. A. SCHWARCZ. Ph.D. Thesis, McGill University, Montreal. 1974.
11. W. SOWA and G. H. S. THOMAS. Can. J. Chem. **44**, 836 (1966).
12. M. KARPLUS. J. Chem. Phys. **30**, 11 (1959).

Can. J. Chem. Downloaded from www.nrcresearchpress.com by 210.87.254.5 on 09/05/12
For personal use only.

Predicting the Most Favored Path and the Overall Rate of Multistep 2-Norbornyl Cation Rearrangements. The Assignment of a Trial Activation Energy for Each Unique Step

R. HASELTINE, E. HUANG, K. RANGANAYAKULU, T. S. SORENSEN, AND N. WONG

Department of Chemistry, University of Calgary, Calgary, Alberta T2N 1N4

Received October 31, 1974

R. HASELTINE, E. HUANG, K. RANGANAYAKULU, T. S. SORENSEN, and N. WONG. Can. J. Chem. **53**, 1876 (1975).

Observable 2-norbornyl cations undergo at least five different rearrangement reactions, all of which are known from previous work on this system. In this paper, these rearrangement categories have been subdivided to reflect secondary–tertiary energy and rate differences and a trial set of activation free energies $\Delta G^{\ddagger}$ is derived for each subdivided step. The most important of these parameters is the energy difference between secondary and tertiary (methyl) systems which was estimated as 5.5 kcal/mol. These parameters allow one, for the first time, to make a rational assessment of the overall reaction course of multistep rearrangement reactions in this system, for example, those observed in a number of bicyclo[2.2.1]heptyl(norbornyl) terpene systems.

R. HASELTINE, E. HUANG, K. RANAGNAYAKULU, T. S. SORENSEN et N. WONG. Can. J. Chem. **53**, 1876 (1975).

Les cations norbornyl-2 que l'on peut observer subissent au moins cinq réactions de réarrangement différentes et elles étaient toutes connues à partir de travaux antérieurs sur ce système. Dans ce travail, on a subdivisé ces catégories de réarrangement afin de mettre en relief les différences d'énergie et de vitesse des cations secondaires *vs.* tertiaires et on a établi des valeurs préliminaires pour les énergies libres d'activation $\Delta G^{\ddagger}$ de chaque étape des subdivisions. Le paramètre le plus important est la différence d'énergie entre les systèmes secondaires et tertiaires (du méthyle) qui serait de 5.5 kcal/mol. En utilisant ces paramètres, on peut pour la première fois faire une attribution raisonable pour l'évolution globale des réactions de réarrangement de ce système impliquant plusieurs étapes; à titre d'exemple on peut faire des attributions pour les réactions observées dans un certain nombre de systèmes terpéniques du bicyclo[2.2.1]heptyle(norbornyle). [Traduit par le journal]

Introduction

Organic molecular rearrangements occur by a variety of mechanisms but for hydrocarbons the most important class involves the intermediacy of carbocations, the actual molecular rearrangement taking place in the carbocation intermediate (eq. 1).

[1] $R_1X \rightleftharpoons [R_1^+ \xrightarrow{k} R_2^+] \rightarrow R_2X$

Working in very stong acids, it is now possible to prepare many of these carbocation "intermediates" and to directly measure the rate of the critical cation$_1$ → cation$_2$ step. For simple reactions of the eq. 1 type, this measurement is mainly of interest to the physical organic chemist since, regardless of the absolute rate of the cation step, the product remains the same. Let us consider, however, a more realistic case, given in eq. 2.

[2] $R_1X \rightleftharpoons [R_1^+ \xrightarrow{k_1} R_2^+ \xrightarrow{k_4} R_5^+;\ R_1^+ \xrightarrow{k_2} R_3^+ \xrightarrow{k_5} R_6^+;\ R_1^+ \xrightarrow{k_3} R_4^+ \xrightarrow{k_6} R_7^+] \rightarrow R_2X, R_3X, R_4X, R_5X, R_6X, R_7X$?

In this case, the product formed is critically dependent on what R_1^+ does and may also be dependent on the behavior of the primary rearrangement ions. If one knew the relative rates (or

Can. J. Chem. Downloaded from www.nrcresearchpress.com by 210.87.254.42 on 09/05/12
For personal use only.

Can. J. Chem. Downloaded from www.nrcresearchpress.com by 210.87.254.42 on 09/05/12
For personal use only.

activation barriers $\Delta G^{\ddagger}$) of the k_1–k_6 processes, one would be in a position to rationally assess what the probable product might be.

Previously, it has been verified that the products formed from the acid-catalyzed treatment of α-fenchol (which differ greatly in composition depending on the severity of the reaction) correlate with the measured rates of the various rearrangements involving the corresponding observable α-fenchyl cation (1). Since these cation → cation absolute rates were not previously known, one could not of course have predicted the actual products formed in the α-fenchol acid-catalysis reactions. However, in this paper it is suggested that one can build up from a number of these "base" measurements, a reasonably consistent set of activation energy parameters (constants), each constant being characteristic of a particular single-step rearrangement process of the kind given in eq. 2.

The choice of the 2-norbornyl cation system as an illustrative example of eq. 2 is dictated by two factors: (*i*) a given norbornyl cation has at least five different structural "chess moves", *i.e.* given by k_1, k_2, k_3, etc. in eq. 2, which it can undergo at any one stage and (*ii*) there has been an enormous amount of solvolysis and acid-catalysis work (which can be used for comparison purposes) carried out on methyl-substituted 2-norbornyl systems, including all of the monomethyl analogs (2) and a great many di- (3) and trimethyl (4) systems. Many of the di- and trimethyl systems studied (like α-fenchol) are terpenes or rearrangement products derived from these.

Although the division is somewhat artificial (see further), we will use as "base" systems, the activation energy parameters derived from the observed rearrangements of the parent 2-norbornyl cation, the 2-methyl cation, and a number of trimethyl and higher methylated norbornyl cations. One can then test the validity (predictive power) of these parameters on the rearrangement reactions involving the complete set of 10 tertiary dimethyl-2-norbornyl cations **1** (accompanying paper) (5). Six of these ions, and hence their rearrangement reactions, were completely unknown until after the formulation of the trial activation energy parameters and hence offered a genuine test of the validity of these. The other four ions and their rearrangement reactions were known and hence the treatment involving these is somewhat artificial.

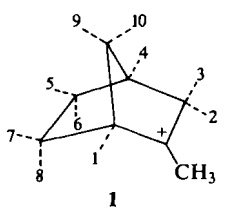

1

Results and Discussion

Rearrangement Processes Considered

In organizing this paper, it seems best to outline the various rearrangements which the 2-norbornyl system can undergo and then to consider whatever specific subdivision of these main categories which may be necessary. Following this, we will discuss the particular rearrangement (or rearrangements) which allows one to assign an activation energy value to that particular step. Some previously communicated work and procedures (1, 6) will be described in full in this paper but the focus of the presentation differs somewhat (*e.g.* one communication (1) covered a number of sequential rearrangements involving initially the α-fenchyl cation system).

The rearrangement processes considered (the first three are well known) for the 2-norbornyl cation system were the following.

(*1*) A Wagner–Meerwein shift of the C6—C1 bond to C6—C2:

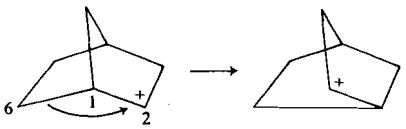

(*2*) An *exo*-3,2-substituent shift:

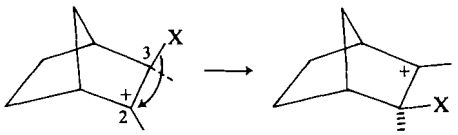

(*3*) An *endo*-6,2-hydride shift:

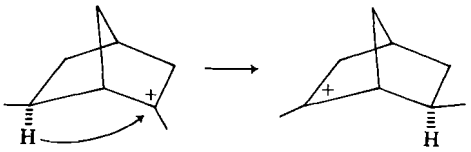

(*4*) An overall two-step process involving the shift of the C1—C7 bond to C2 to give a high energy, unobservable, 2-bicyclo[3.1.1]heptyl cation intermediate and then the shift of the original C2—C3 bond to C1. This overall sequence has been termed a double Wagner–Meerwein

(DWM) rearrangement (7):

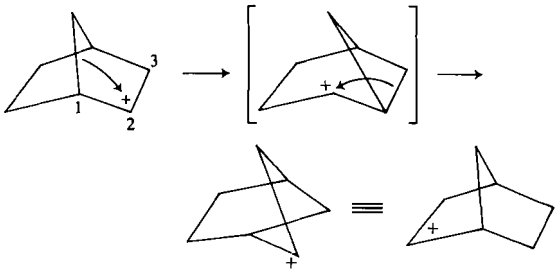

(5) An *endo*-3,2-substituent shift:

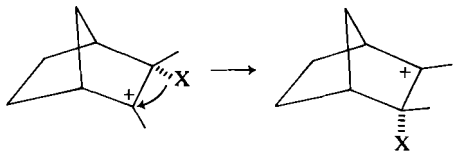

(6) Ring opening – bond rotation – ring closure processes:

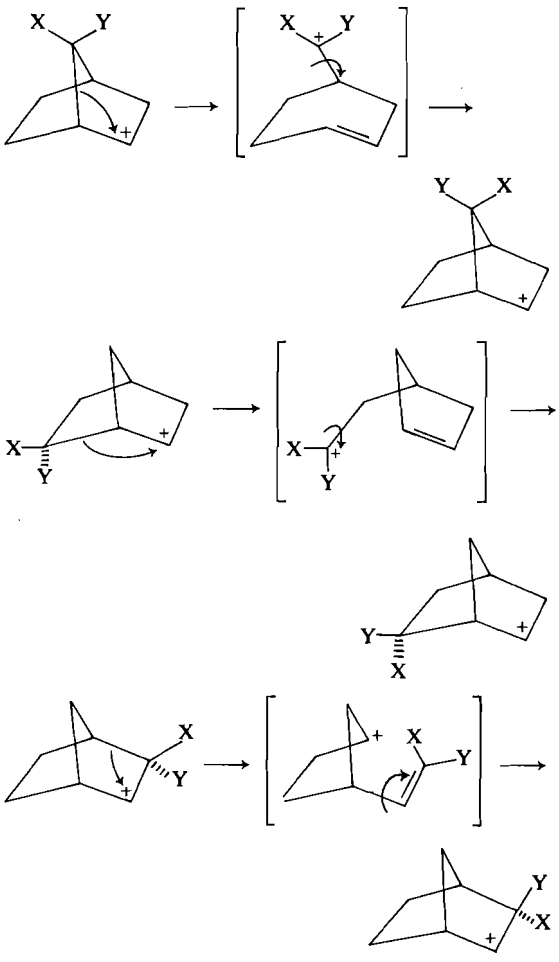

(7) In addition to the above, a process involving deprotonation–reprotonation might occur.

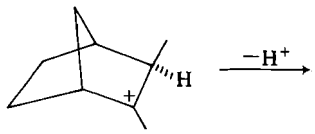

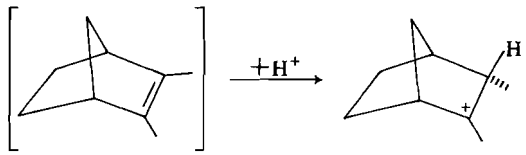

This last process is expected to differ from all of the others in that the rate of the reaction should be markedly sensitive to the strength of the strong acid solvent (8). Based on present knowledge (9), the rearrangement rates of processes *1–6* will not be appreciably affected by changes in the strong acid solvent system used.

Subdivision of the Major Categories

One could not possibly expect the rearrangement rates of the processes *1–6* to be insensitive to a variety of substituents on the basic 2-norbornyl ring system. Fortunately, much of the solvolysis and acid-catalysis work in the chemical literature involves only methyl or hydrogen as substituents (*e.g.* terpenes) and in this work, the same restriction is applied. It would also be expected that steric effects would be an important factor, particularly if one had very many methyl substituents. In setting up the "base" activation energy parameters, we have tried to avoid model systems where rearrangement rates might be seriously changed by some steric factor. Nevertheless this must remain a nagging problem.

One factor demonstrably affecting the rates and the thermodynamic stability of the ions which cannot be ignored concerns the substitution at C2, *i.e.* either an H (secondary 2-norbornyl) or CH_3 (tertiary 2-norbornyl). The other factor concerns the *exo*- and *endo*-3,2-substituent shift, *i.e.* the rate is demonstrably different for a methyl *vs.* a proton shift. These considerations lead to the following further subdivision of the major categories (Scheme 1).

Can. J. Chem. Downloaded from www.nrcresearchpress.com by 210.87.254.42 on 09/05/12
For personal use only.

Major process	*Subdivisions considered*
1	1TT 1TS 1ST 1SS
2	2HTT 2HTS 2HST 2HSS 2MTT 2MTS 2MST 2MSS
3	3TT 3TS 3ST 3SS
4	4TT 4TS 4ST 4SS
5	5HTT 5HTS 5HST 5HSS 5MTT 5MTS 5MST 5MSS

SCHEME 1. Abbreviations: T = tertiary, S = secondary, the first letter refers to the reactant ion and the second to product, H = hydrogen, M = methyl, the major rearrangement processes take the same number as was used to list them.

The ring opening – rotation – ring closure processes, *6a–c*, have been left out of Scheme 1. Although all three rearrangements, *6a* (10, 11), *6b* (12), *6c* (11), have been proposed in part for stable 2-norbornyl cations, it appears that not only is the activation energy quite high but that also, in some cases, a ring opening would lead irreversibly to cycloallyl cations (11). The deprotonation–reprotonation sequence *7* has also been left out since experimentally this process does not appear to play a significant role in the mono- , di- , or trimethyl-2-norbornyl cation rearrangements. In any case, if one uses the strongest acid systems available, *e.g.* $R^+ SbF_6(SbF_5)_n^-$ salts, the activation energy for this process could be made very high and the process effectively shunted aside. Other marginally possible processes, *e.g. endo*-5,2-hydride shifts, have not been observed and likely have a high activation energy barrier associated with them.

Obtaining the $\Delta G^{\ddagger}$ Parameters for Each Subdivided Rearrangement Process

The experimental evidence available for assigning $\Delta G^{\ddagger}$ parameters comes, as will be seen, in varying degrees of reliability. Some observable 2-norbornyl cation rearrangement processes involve a single specific step and this is then easily assigned a $\Delta G^{\ddagger}$ value. Other rearrangements involve two or more steps but the sequence can be uniquely assigned. However, in other multistep rearrangements it is not possible to assign an unique sequence or to even ascertain the particular rearrangement steps. A good discussion of this situation is given in two recent papers by Collins and co-workers (7). They show that one can bring about any overall 2-norbornyl cation transformation by using only combinations of the first three rearrangement processes given in Scheme 1, albeit the number of steps may be very large. In practice, one is forced to assign a specific mechanism sequence from among many theoretical possibilities. We will use the computerized treatment of Collins and co-workers (7), where appropriate, together with our further subdivision of each major step and then give our reasons for the choice of a specific sequence[1] in discussing an overall multistep rearrangement.

In most cases, only a $\Delta G^{\ddagger}$ activation energy value was experimentally obtained. However, in those rearrangements where both $\Delta G^{\ddagger}$ and $\Delta H^{\ddagger}$ were measured, they have turned out to be very similar, *i.e.* $\Delta S^{\ddagger} \sim 0$ and $\Delta G^{\ddagger} \sim$ constant. Also, since one is dealing with rate *comparisons*, the term $T\Delta S^{\ddagger}$ would become significant only if the temperature of the "base" measurement rearrangement and the observed rearrangement differed considerably.

Rearrangement 1TT

Only a lower limit $\Delta G^{\ddagger}$ value can be obtained for this shift since it cannot be "frozen out" in the n.m.r. spectrum of the 1,2,4-trimethyl-2-norbornyl cation **2** (1) or in higher methylated analogs (12). Cation **2** can be obtained as the

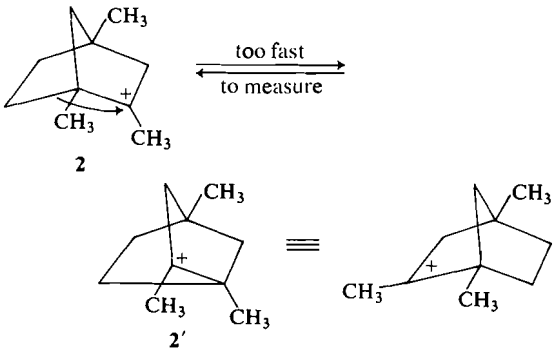

"ultimate rearrangement" product of the tertiary α-fenchenehydro cation (1) and the structure was proven from quenching experiments wherein the

[1]From basic thermodynamic principles, all sequences are probably being followed and the occasional explorer molecule may indeed complete even the most unfavorable path. In the discussion, therefore, one is concerned about the route followed by > 99% of the reactant carbocations.

Can. J. Chem. Downloaded from www.nrcresearchpress.com by 210.87.254.42 on 09/05/12
For personal use only.

two new "fenchenes" **3** and **4** were obtained and

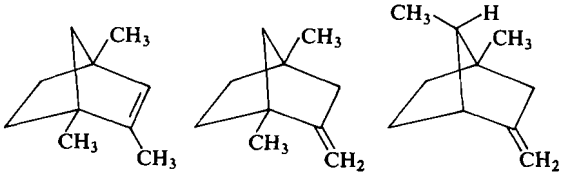

3 **4** **5**

characterized (see Experimental). In addition, a small amount of what is likely the alkene **5** was obtained. The carbon-13 n.m.r. spectrum of **2** is particularly useful for obtaining an upper limit estimate for the 1TT activation energy barrier since the process is degenerate in this ion and the C1—C2 n.m.r. peak is a composite of peaks which are expected to be separated widely in the "frozen out" structure. The rate constant for an n.m.r. averaging process needed to give a sharp coalesced peak is dependent on the intrinsic separation of the individual peaks, and if one makes a reasonable choice of a 4000 Hz separation for C1 and C2 in **2** (based on values for C1 and C2 obtained for the 2-methyl-2-norbornyl cation (ref. 13 and footnote 2)), one can show by standard n.m.r. theory that a rate constant of $>10^6$ s^{-1} (see accompanying paper (17)) is needed to produce the relatively sharp peak observed (14) for **2** at -140 °C. This leads to a maximum possible $\Delta G^{\ddagger}$ value of 4 kcal/mol. Since this barrier is so small, one may wonder whether the ion might not have a symmetrical structure and hence there would be no 1TT process involved at all. Previous work with unsymmetrical cations of this type has shown, however, that the averaged chemical shifts are temperature dependent in exactly the manner expected for an equilibrating pair of ions, where the more stable isomer becomes more dominant at low temperatures (the van't Hoff relationship) (14). Other evidence also indicates equilibrating structures (15, 16).

Rearrangement 1SS

For consistency in the computerized treatment, a secondary 2-norbornyl cation will be treated as an equilibrating structure, *i.e.* as having a 1SS process. (A discussion of the structure problem is given in an accompanying paper (17).) Olah *et al.* have recently published (18) a ^{13}C n.m.r. spectrum of the 2-norbornyl cation which shows a sharp coalesced C1—C2 peak at -150 °C. Using identical calculations to those used for the 1TT case, one calculates a maximum activation energy barrier of 4 kcal/mol.

Rearrangements 1TS and 1ST

Assuming a simple transition state model, these two processes involve the same potential energy surface. If one knew the energy difference between a secondary and a tertiary(methyl) 2-norbornyl cation and only one of the two activation energies, one could always obtain the other. This applies not only for the WM process but for all five major divisions in Scheme 1. Thus, the value assigned to this secondary–tertiary energy difference is quite critical. Fortunately, a method exists for estimating such a value. In the first (fastest rate) degenerate rearrangement of the 2-methyl-2-norbornyl cation **6** (prepared from 2-methylnorbornanol or the corresponding chloride), in a second (slower rate) degenerate rearrangement in the camphenehydro cation (6, 19)

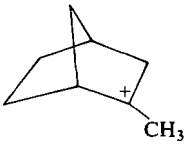

6

and in the overall process interconverting the tertiary α- and β-fenchenehydro cations (1), one has a process which can be unequivocally assigned to the three-step sequence 1TS, 3SS, 1ST. A careful matching of the observed n.m.r. line broadening in **6** with computed spectra has been carried out and from this analysis one obtains, in the usual way, $\Delta G^{\ddagger} = 11.3$ kcal/mol at -49 °C, $\Delta H^{\ddagger} = 11.0 \pm 1$ kcal/mol. Some of the experimental and calculated spectra for the line broadening in **6** are shown in Fig. 2. The activation energy for the 3SS step in the 2-norbornyl cation has been reported by Olah *et al.* (20) $\Delta G^{\ddagger} = 5.8$ kcal/mol at -141 °C, $\Delta H^{\ddagger} = 5.3$ kcal/mol. If this same value is applicable to the 3SS step in a 1-methyl secondary cation, then one can construct the transition state diagram shown in Fig. 1, leading to an estimate of 5.5 kcal/mol for the secondary–tertiary energy difference. Concerning the 1TS and 1ST processes, one would expect the activation energy for the 1ST process to be, at worst, the same as the 1SS process, *i.e.* <4 kcal/mol. This leads to a value of <9.5 kcal/mol for 1TS and, although the argument is

[2]A. J. Jones and T. S. Sorensen, unpublished results.

Can. J. Chem. Downloaded from www.nrcresearchpress.com by 210.87.254.42 on 09/05/12
For personal use only.

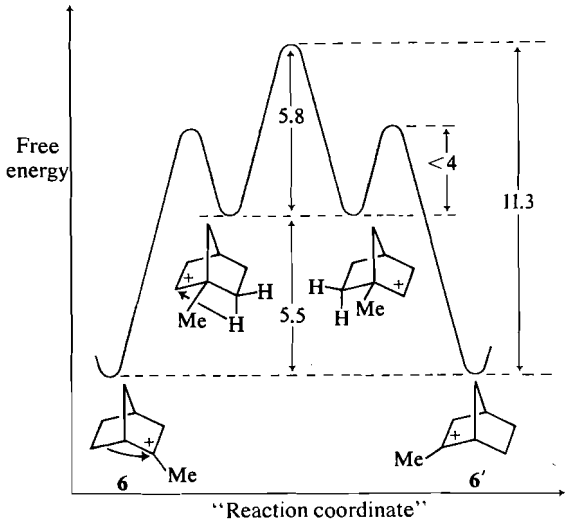

FIG. 1. "Reaction coordinate" diagram showing the derivation of the energy difference between a 1-methyl secondary norbornyl cation and a 2-methyl tertiary norbornyl cation.

circular, this confirms the assumed equilibrium kinetic treatment made in Fig. 1, *i.e.*

$$A \underset{k_{-1}}{\overset{k_1}{\rightleftarrows}} B \xrightarrow{k_2} C,$$

where

$$k_{-1} > k_2$$

and B is a steady state-intermediate.

Rearrangement 2HTT

This process can be directly measured (n.m.r. line broadening) as a single degenerate step in the 1,2-*endo*-3,4-tetramethyl-2-norbornyl cation (11), $\Delta G^{\ddagger} = 7.1$ kcal/mol, and also in even higher methylated analogs, 7.4 kcal/mol (12).

Rearrangement 2HSS

This process occurs as a degenerate rearrangement in the 2-norbornyl cation and has been analyzed by Olah *et al.* (20) $\Delta G^{\ddagger} = 11.4$ kcal/mol at -29 °C, $\Delta H^{\ddagger} = 10.2 \pm 0.6$ kcal/mol. In the analysis of the observed line broadening, one cannot distinguish between an *exo*-3,2-hydride shift and an *endo* equivalent or a mixture of both but, in the corresponding TT process, the *exo* shift is favored over the corresponding *endo* shift by at least 6.9 kcal/mol (see below). There is also much solvolysis evidence showing that *exo* shifts are highly preferred (21) in the secondary system.

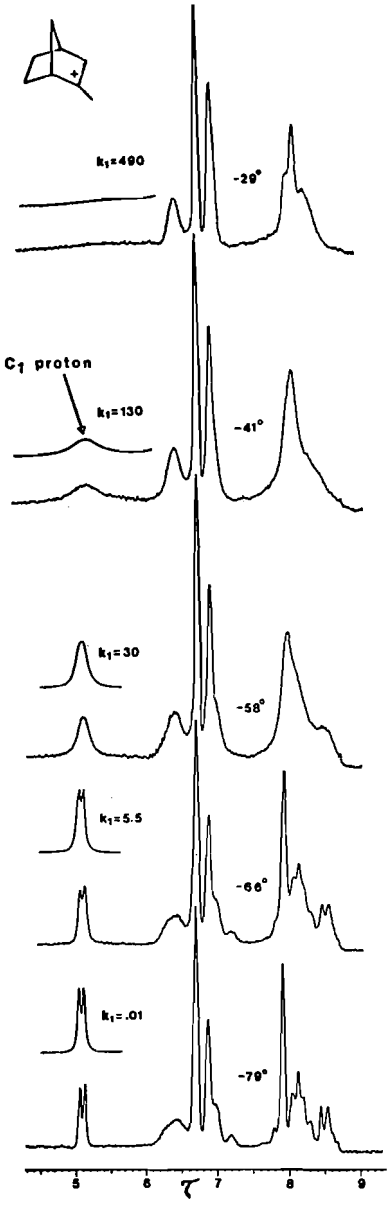

FIG. 2. ^{1}H n.m.r. spectrum of the 2-methyl-2-norbornyl cation showing the experimental line broadening due to the most rapid of two degenerate rearrangements occurring in this ion. The H1 proton at *ca.* τ 5.1 was used for the rate analysis with the calculated spectrum shown above each experimental peak. At temperatures above -40 °C, the amplitude of the H1 signal in the experimental spectra was increased considerably over that shown in this diagram.

Rearrangements 2HTS and 2HST

As explained previously, only one of these needs to be measured. This can be done from an

Can. J. Chem. Downloaded from www.nrcresearchpress.com by 210.87.254.42 on 09/05/12
For personal use only.

Can. J. Chem. Downloaded from www.nrcresearchpress.com by 210.87.254.42 on 09/05/12
For personal use only.

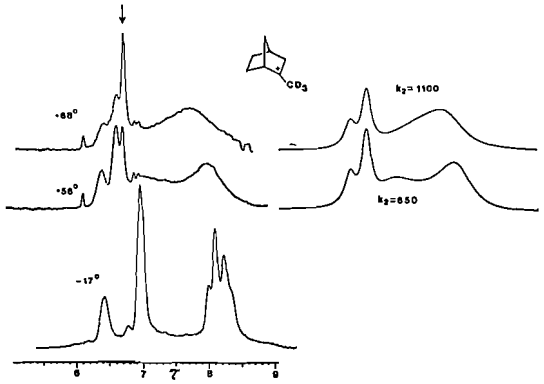

FIG. 3. ^{1}H n.m.r. spectrum of the 2-deuteriomethyl-2-norbornyl cation showing the experimental line broadening (left) due to the slower of two degenerate rearrangements occurring in this ion. At the right are two calculated spectra for this exchange, k_1 being set from the data obtained in Fig. 2. The peak designated by ↓ is the C2 deuteriomethyl group which is being exchanged with H at the higher temperatures.

analysis of the second (slower) degenerate rearrangement observed for the 2-methyl-2-norbornyl cation **6**. Examples of the actual line broadening experimentally observed at 0 °C and above for **6** are illustrated in Fig. 3. The rearrangement sequence responsible for this broadening is not immediately obvious because there appear at first sight to be several degenerate sequences which might cause the observed broadening. However, the fact that the *exo*-6 proton peak (H7 in Fig. 4) does not broaden (at least initially) allows one to assign the process as follows (Scheme 2).

The overall topology of the process is to rotate the protons A, B, C, and D one turn for each six-step sequence. The overall proton equivalences are shown in Fig. 4, together with the kinetic exchange matrix used. This matrix embodies the assumption that one will statistically partition the protons A, B, C, and D equally among the four positions available to these before returning to the tertiary ion via a 2ST step. This requires the rate of the 2ST step to be much slower than the 1SS and 3SS processes, a requirement that may not be strictly true. The calculated $\Delta G^{\ddagger}$ values are <4 and 5.8 kcal/mol for the 1SS and 3SS processes *vs.* a calculated 9.7 kcal/mol for the 2ST process. Even if there is some bias towards returning to the original configuration, as compared to the other three, the effect on the calculated $\Delta G^{\ddagger}$ value will probably not be large (the calculated value will always be on the high side). The specific proton exchanges listed in Fig. 4 were also confirmed using the D1SST technique of Forsén and Hoffmann (22). Thus, irradiation of the averaged C5—C7 protons (Fig. 3) at +15 °C, causes the overlapping C3—C4 signal to nearly disappear and *vise versa*. The *exo*-H6 proton is not appreciably affected.

Using the equivalences shown in Fig. 4, the calculated and experimental line shapes are compared in Fig. 3 for various rate constants. The approximations used in the calculations are detailed in the Experimental. Only the calculated spectra in the intermediate exchange region can validly be used for comparison to experimental spectra. From this, one obtains $\Delta G^{\ddagger}$ = 15.2

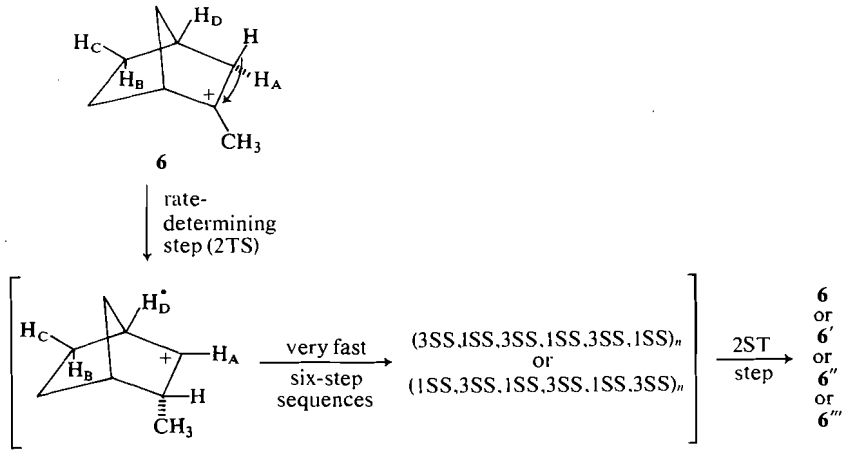

SCHEME 2

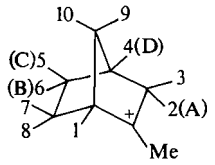

First exchange (k_1)	Second exchange (k_2)	Overall exchange
$H_1 = H_8$	$H_2 = H_4 = H_5 = H_6$	$H_1 = H_8$
$H_2 = H_3$	H_9	$H_2 = H_3 = H_4 = H_5 =$
$H_5 = H_{10}$	H_{10}	$= H_6 = H_9 = H_{10}$
$H_6 = H_9$	H_7	
H_7	H_8	H_7
H_4	H_3	
	H_1	

k_1							$-k_1$		
	$k_1+\frac{3k_2}{4}$	$-k_1$	$\frac{-k_2}{4}$	$\frac{-k_2}{4}$	$\frac{-k_2}{4}$				
	$-k_1$	k_1							
	$\frac{-k_2}{4}$		$\frac{3k_2}{4}$	$\frac{-k_2}{4}$	$\frac{-k_2}{4}$				
	$\frac{-k_2}{4}$		$\frac{-k_2}{4}$	$k_1+\frac{3k_2}{4}$	$\frac{-k_2}{4}$			$-k_1$	
	$\frac{-k_2}{4}$		$\frac{-k_2}{4}$	$\frac{-k_2}{4}$	$k_1+\frac{3k_2}{4}$				$-k_1$
$-k_1$							k_1		
				$-k_1$				k_1	
					$-k_1$				k_1

FIG. 4. Overall exchanges occurring in the 2-methyl-2-norbornyl cation and the kinetic matrix used in the exchange.

kcal/mol, using a matching just before coalescence, *i.e.* the +56 °C spectrum in Fig. 3. Subtracting 5.5 results in the $\Delta G^{\ddagger}$ value of 9.7 kcal/mol for the 2HST process.

At higher temperatures (>65 °C), there is evidence that still another degenerate process in cation **6** is beginning to show up since the *exo*-H6 proton starts to broaden. This is very likely due to the sequence 1TS,2HSS,3SS,2HSS,1ST.

Rearrangement 2MTT

This single-step process has been directly measured as a degenerate process in the camphenehydro cation (6, 19), $\Delta G^{\ddagger} = 8.3$ kcal/mol at −104 °C, $\Delta H^{\ddagger} = 8.2 \pm 1$ kcal/mol, and in two higher methylated analogs (12), $\Delta G^{\ddagger} = 9.4$ kcal/mol.

Rearrangement 2MSS

No satisfactory value could be arrived at for this process. However, we believe that the $\Delta G^{\ddagger}$ value should be as high or higher than the process 2MST (which can be determined). Tentatively, therefore, 2MSS is assigned a lower limit value, $\Delta G^{\ddagger} \geq 7.6$ kcal/mol. However in some cases, methyl shifts are slower than the corresponding proton shifts. Since the 2HSS value is 11.4 kcal/mol, it would not be unreasonable to expect a 2MSS value even higher than this.

Rearrangements 2MTS and 2MST

The best estimate for the 2MST rearrangement comes from the observed rearrangement of the tertiary α-fenchenehydro cation **7** to the 1,2-*endo*-3-trimethyl-2-norbornyl cation **8**, for which the mechanism in eq. 3 appears the most reasonable (from graph theory there are many other longer sequences possible). The overall activation energy is 13.1 kcal/mol ≡ 2MST. The reverse 2MTS step is assigned a value 13.1 − 5.5 = 7.6 kcal/mol.

Can. J. Chem. Downloaded from www.nrcresearchpress.com by 210.87.254.42 on 09/05/12
For personal use only.

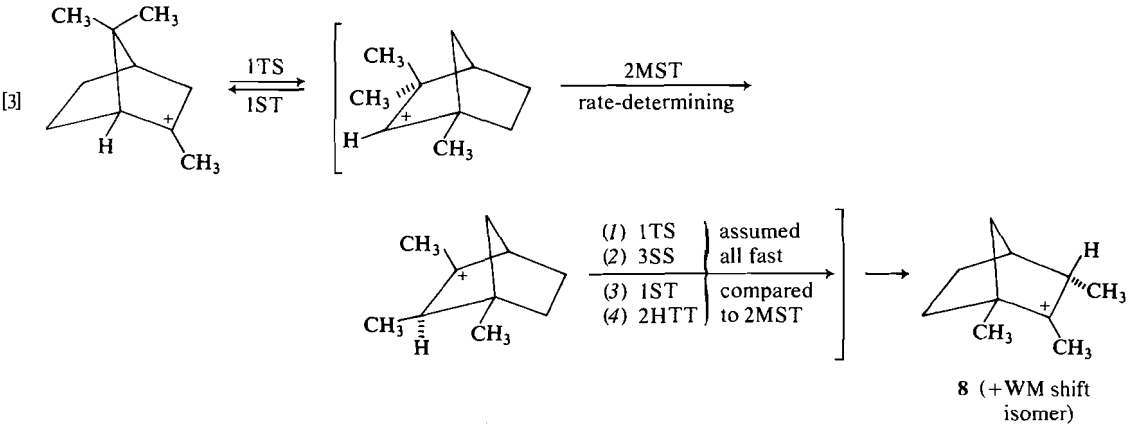

The structure of cation **8** was confirmed by an unequivocal synthesis starting from the known ketone **9** (eq. 4).

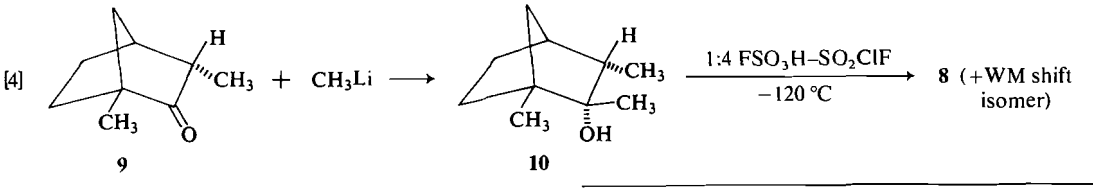

Rearrangement 3TT

No direct measurement of this parameter is available from any of the mono- or trimethyl-2-norbornyl cation rearrangements studied in this work. However a maximum $\Delta G^{\ddagger}$ value of 11.3 kcal/mol is estimated (below) for the 3TS process and the same value is tentatively used for 3TT.

Rearrangement 3SS

This degenerate process has been observed in the 2-norbornyl cation, $\Delta G^{\ddagger} = 5.8$ kcal/mol at −141 °C, $\Delta H^{\ddagger} = 5.3$ kcal/mol (20).

Rearrangements 3TS and 3ST

It seems reasonable to assume that the process 3ST will have a $\Delta G^{\ddagger}$ value of no more than the 3SS value, *i.e.* $\Delta G^{\ddagger} = 5.8$ kcal/mol is assigned. This results in a maximum value of 11.3 kcal/mol for 3TS.

Although the $\Delta G^{\ddagger}$ values assigned to the *endo*-6,2-hydride shifts (process *3*) appear rather uncertain, they are all small enough so that this step will rarely be rate determining in an overall multistep rearrangement.

Rearrangement 4

Assigning a $\Delta G^{\ddagger}$ value for this two-step process has proven difficult since, as previously mentioned, one can always find a theoretical sequence of steps for any 2-norbornyl cation rearrangement not *requiring* this process. This point is discussed in detail by Johnson and co-workers (7). There are, however, two kinds of experimental results which offer reasonably good evidence for process *4*.

(*a*) The camphenehydro cation **11** rearrangement to give **8** also yields as a side reaction the cyclohexenyl cation **12** (the ratio of **8** (+WM shift isomer) to **12** is about 62:38) (6, 19). That

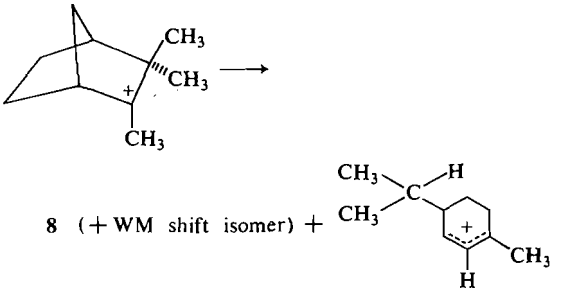

the simultaneous formation of both these ions may be indicative of the intermediacy of the 2-bicyclo[3.1.1]heptyl cation formed in process *4* is shown by protonation reactions carried out in this study on α- and β-pinene **13** and **14**. Addition of these to FSO_3H at −50 °C or 1:4

Can. J. Chem. Downloaded from www.nrcresearchpress.com by 210.87.254.42 on 09/05/12
For personal use only.

Can. J. Chem. Downloaded from www.nrcresearchpress.com by 210.87.254.42 on 09/05/12
For personal use only.

FSO_3H–SO_2ClF at −120 °C and then warming to −50 °C yields the same two cations **8** and **12**, although the ratio favors the cycloallyl cation **12** (eq. 5).

[5] 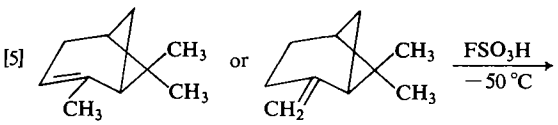

13 **14**

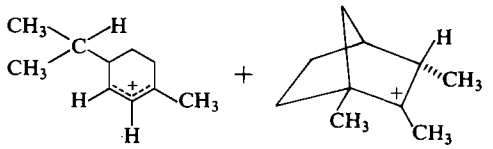

12 **8** (+WM shift isomer)

The actual ratio is somewhat difficult to determine since there is considerable polymer formation but it is about 3:1 favoring **12**. There is often some difference in the partitioning behavior of a steady-state intermediate and the partition which occurs when one attempts to directly prepare the intermediate (see refs. 8 and 23 for some previously discussed examples of this).

(*b*) The addition of α-fenchyl tosylate **15** (*endo* leaving group) to fluorosulfonic acid at −80 °C yields the same two cations **8** and **12** (eq. 6), in about the same proportions as are produced from the camphenehydro cation rearrangement.

[6] 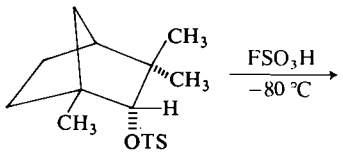

15

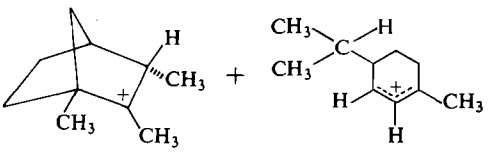

8 (+WM shift isomer) **12**

What makes this result odd is that **12** is not a normal product of the tertiary α-fenchenehydro cation **7** rearrangement sequence (which one might have expected from **15** via a WM shift) and mechanistically its formation is difficult to rationalize *unless* there is bond migration (eq. 7) in the solvolysis, to yield the 2-bicyclo[3.1.1.]-heptyl cation intermediate, which then partitions as previously noted. This same problem arises in

[7] 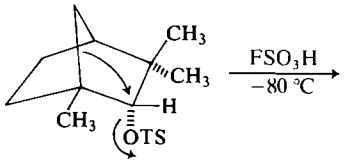

15

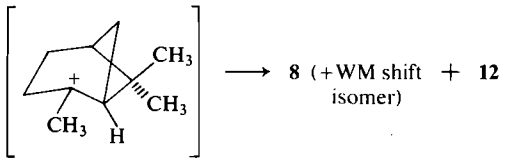

rationalizing the approximately 50% of ring-opened products produced in the deamination of α-fenchylamine (24). However this interpretation of the solvolysis of **15** is negated somewhat by the observation that borneol tosylate **16** in FSO_3H–SO_2ClF at −80 °C does not yield detectable amounts (< 10%) of **8** or **12**, which would be expected if a similar 7,1–7,2 bond migration had occurred. The sole product is the WM shift species, the camphenehydro cation **11** (eq. 8).

[8] 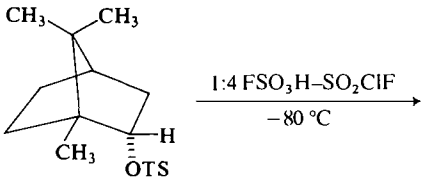

16

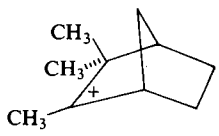

11

The deamination of bornylamine does yield ring-opened products (24); however, the percentage of these is somewhat less than in the fenchyl case, just the opposite of what might have been expected, so it may still mean that the fenchyl system for some reason is directly yielding the 2-bicyclo[3.1.1]heptyl cation system, while the bornyl is not.

On balance, we feel that there is some evidence that the 2-bicyclo[3.1.1]heptyl system is an intermediate in some observable 2-norbornyl cation rearrangements.

Can. J. Chem. Downloaded from www.nrcresearchpress.com by 210.87.254.42 on 09/05/12
For personal use only.

Considering the rearrangement *4* subcategories (Scheme 1), one finds that if C1 and C2 are substituted by identical groups, *i.e.* H or CH_3, then a rearrangement *1* process accomplishes the same permutation as a rearrangement *4* process, except that the former interchanges the C1 and C2 carbons and attached substituent while the latter does not. Since none of our labelling can distinguish such differences we can forget about these categories, the $\Delta G^{\ddagger}$ value for process *1* being much lower than that expected for process *4*.

Rearrangements 4TT and 4SS

The sequences 4TT and 1TS,4SS,1ST accomplish the same permutations (7) and cannot be distinguished. The experimental barrier for the camphenehydro cation **11** giving **8** and the ring-opened cyclohexenyl cation **12** is 17.5 kcal/mol. As explained previously, one can rationalize the formation of both products on the assumption of common bicyclo[3.1.1]heptyl cation intermediate but the evidence certainly does not require this mechanism. Tentatively, we assign a barrier $\geq$ 18 kcal/mol for either 4TT or 1TS, 4SS,1ST, whichever is less. In other words, if the actual barrier is 4TT, then the 18 kcal/mol is directly appropriate. If the 1TS,4SS,1ST sequence is lower, then the 4SS barrier would be assigned as $\geq 18 - 5.5 = \geq 12.5$ kcal/mol.

Rearrangement 5HSS

Several results (11, 21) suggest that an *exo*-3,2-hydride shift will be much faster than the *endo* shift. The process 5HSS accomplishes the same overall permutations (unless the C2 and C3 protons are labelled) as the apparently much easier 2HSS process and the former need not be considered further (*i.e.* it would represent a very minor pathway).

Rearrangement 5HTT

There is no observable n.m.r. line broadening in the 1,2-*exo*-3,4-tetramethyl-2-norbornyl cation (**17**) up to at least -10 °C, such as might have occurred from an *endo*-3,2-hydride shift (11)

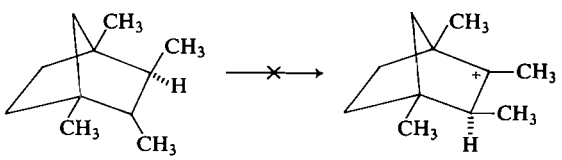

17 **17′**

and we can assign a minimum $\Delta G^{\ddagger}$ value of *ca.* 14.2 kcal/mol. The interconversion of the 1,2-*exo*-3-trimethyl-2-norbornyl cation (**18**) prepared by an unambiguous route starting from the known ketone **19** and the alcohol **20** and the 1,2-*endo*-3-trimethyl-2-norbornyl cation (**8**) (eq. 9), for which $k = 3.0 \pm 0.5 \times 10^{-4}\ s^{-1}$ at -90 °C, $\Delta G^{\ddagger} = 13.6$ kcal/mol, can be most expeditiously

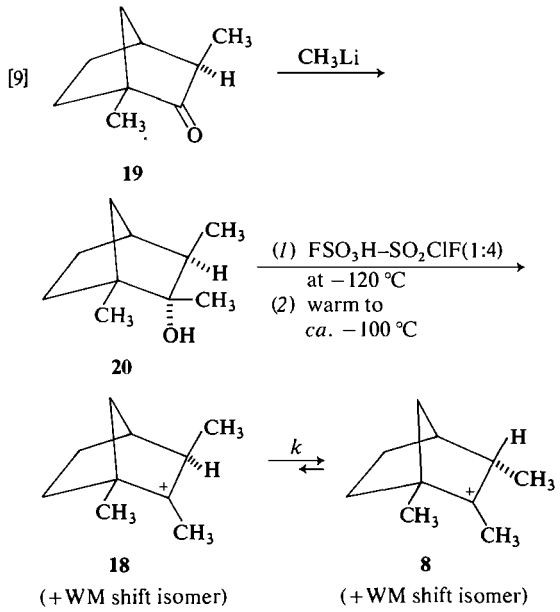

explained using an *endo*-3,2-hydride shift, a five-step sequence involving 5HTT,1TS,3SS,1ST, 2HTT. However, there are other ways that this transformation could have occurred, for example, using only the first three processes; this requires a minimum of eight steps for the lowest calculated 15.2 kcal/mol (2HST) barrier, perilously close to the observed 13.6 kcal/mol barrier. Tentatively, a $\Delta G^{\ddagger}$ value of $\leq$ 14.0 kcal/mol is assigned for 5HTT.

Rearrangements 5HTS and 5HST

Starting from a tertiary cation energy base, the 2HTS(2HST) process requires 15.2 kcal/mol. If one looks at the minimum $\Delta\Delta G^{\ddagger}$ difference between 2HTT and 5HTT, *i.e. ca.* 7 kcal/mol, and applies this difference to the 5HTS and 5HST processes, one obtains barriers in excess of 20 kcal/mol. Since these processes are never *required* in any of the overall transformations, the molecules ($\gg$99%) will always find easier routes.

Can. J. Chem. Downloaded from www.nrcresearchpress.com by 210.87.254.42 on 09/05/12
For personal use only.

Rearrangement 5MTT

The rearrangement has been observed in a hexamethyl-2-norbornyl cation system (12), $\Delta G^{\ddagger} = 19.5$ kcal/mol. Since a 2MTT process, $\Delta G^{\ddagger} = 8.9$ kcal/mol, accomplishes the same permutation of groups, unless the methyls at C2 and C3 are labelled, one need not consider 5MTT any further.

Rearrangements 5MSS, 5MST, and 5MTS

If one adds the same $\Delta\Delta G^{\ddagger}$ difference observed between 2MTT and 5MTT to the 2MSS, 2MST, and 2MTS values derived previously, one arrives at $\Delta G^{\ddagger} > 20$ kcal/mol (from a tertiary cation energy base) for the title processes. Since these processes are not *required* for any of the overall transformations they could only represent very minor pathways.

Of all the *endo*-3,2-substituent shift processes, only 5HTT appears to have a reasonable chance of being important.

Concluding Discussion

The $\Delta G^{\ddagger}$ values obtained for each of the rearrangements *1–5* represent the "best" values which can be derived from the limited number of "base" measurements investigated to date. The most unsatisfactory situation concerns the 2MSS step. The problems created by this uncertainty are readily apparent when we come to test the predictive power of the parameters (following paper). The uncertainty with process *4* is not as serious since we have some confidence that the barrier for this is quite high and sequences not requiring process *4* can usually be found.

Experimental

Carbocations and protonated alcohol solutions were prepared and referenced using previously described procedures (11, 25). Nuclear magnetic resonance spectra were obtained on a Varian Associates HA-100 equipped with a variable temperature probe. Probe temperatures were monitored by placing a thermocouple directly into the spinning n.m.r. tube. Preparative g.l.c. separations were performed using either (*A*) a 12 ft. × 3/8 in. column of 30% Carbowax 20M on Chromosorb 60–80 or (*B*) a 10 ft. × 3/8 in. column of 20% SE-30 on Chromosorb 60–80.

1,2,4-Trimethyl-2-norbornyl Cation **2**

The ^{1}H n.m.r. chemical shifts for this cation have been reported in a communication (1). The cation was obtained by protonating α-fenchene, prepared from α-fenchyl tosylate and g.l.c. separation (column *A*, 90 °C) from small amounts of ζ-fenchene and cyclofenchene (26); from β-fenchene, prepared by g.l.c. separation (column *A*) of the complex mixture obtained by dehydrating α-fenchol with solid potassium bisulfate (27) (α- and β-fenchene are the highest retention products and are only poorly resolved but by cutting the front part of this combined "peak" pure β-fenchene can be obtained); from cyclofenchene or from α-fenchol itself, obtained by lithium aluminum hydride reduction of fenchone (28). In the α- and β-, and cyclofenchene cases, one initially obtains at −120 °C a mixture of the tertiary α- and β-fenchenehydro cations, the chemical shifts of these have been reported in the communication (1). On warming the solutions one obtains first a 1,2,3-trimethyl-2-norbornyl cation system and finally at around −15 °C, cation **2**. In the case of α-fenchol, one initially obtains in FSO_3H the protonated alcohol, characterized by ^{1}H n.m.r. peaks at τ 8.67, 8.78, and 8.87 (3H each, the methyl groups) and 5.36 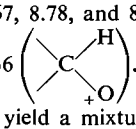 . At −18 °C, this solvolyzes within 0.5 h to yield a mixture of the 1,2,3-trimethyl species and **2**. After 0.5 h at 0 °C, only **2** is left.

On cooling a solution of **2** in 4:1 SO_2ClF–FSO_3H down to −120 °C, there is no evidence that the degenerate WM shift is being slowed down enough to see ^{1}H n.m.r. line broadening.

Structure Proof of **2**. *Isolation of Two New Fenchenes*

The structure of cation **2** is reasonably assigned from the n.m.r. spectrum but is confirmed from quenching experiments. Solutions of **2** were prepared at −80 °C using 10% w/v of α-fenchol in FSO_3H and letting the solution stand 0.5 h at 0 °C. This acid solution was then added dropwise to an ice-cold, well stirred, aqueous sodium hydroxide solution containing a small upper ether layer. The aqueous solution was extracted twice with ether and the ether dried over anhydrous potassium carbonate. The organic residue showed two "peaks" on g.l.c. analysis (column *B*): a large shorter retention peak and a more diffuse higher retention one, about 3:1 area ratio. Both were collected in quantity. Rechromatography on column *A* of the first fraction yielded three well-separated peaks. The lowest retention product was very small and not further investigated. The highest retention product was a liquid with *m/e* 136. The n.m.r. spectrum (CCl_4) showed peaks at τ 8.82 and 8.85 (3H each, methyl groups at C1 and C4), 7.94 (broad, 2H, C3 protons), 5.42 and 5.54 (1H each, t, $J = 2$, the C2 *exo*-methylene protons). This allows one to assign the structure as 1,4-dimethyl-2-methylenebicyclo[2.2.1]heptane **4**, which can also be labelled η-fenchene. The structure is further confirmed by ozonolysis of **4**, whereby the pure ketone, 1,4-dimethylbicyclo[2.2.1]heptan-2-one, was obtained by preparative g.l.c. separation (column *B*); i.r. 1750 cm^{-1}, C=O; n.m.r. (CCl_4), τ 8.74 and 8.90 (3H each, the C1 and C4 methyl groups), 8.10 (broad, 2H, the C3 protons); 2,4-DNPH derivative, m.p. 128–130 °C (lit. (29) m.p. 129–129.5 °C). Readdition of **4** to FSO_3H at −80 °C yields the cation **2**. The middle retention product was also a liquid, *m/e* 136; n.m.r. (CCl_4), τ 8.76 and 8.79 (3H each, C1 and C4 methyl groups), 8.41 (d, $J = 1.5$, 3H, C2 methyl group), 4.71 (broad, 1H, the alkene proton at C3). The m.s. fragmentation shows a large even ion at *m/e* 108 (−28 for

Can. J. Chem. Downloaded from www.nrcresearchpress.com by 210.87.254.42 on 09/05/12
For personal use only.

the reverse Diels–Alder product ethylene). These data allow one to assign the structure as 1,2,4-trimethylbicyclo-[2.2.1]hept-2-ene (**3**) which can also be labelled θ-fenchene. Readdition of **3** to FSO_3H at −80 °C gives **2**. The ratio of **4**/**3** is about 4:1. In theory, there should be no more alkenes produced from **2** but rechromatography of the second column *B* peak on column *A* yields a complex series of peaks. The largest is the highest retention peak which was collected, a liquid, *m/e* 136. From the n.m.r. spectrum (CCl_4), the compound is not pure but has major peaks at τ 9.17 (d, J = 6.75), 8.91 and 8.96, 5.34 and 5.57. Readdition of this alkene to 4:1 SO_2ClF–FSO_3H at *ca.* −120 °C yields **2** and in part a cation assigned as 2,4-*anti*-7-trimethyl-2-norbornyl cation; n.m.r. τ 5.37 (d, J = 5.5, C1 proton), 6.78 (C2 methyl), 8.59 (C4 methyl), and 8.86 (possibly an unresolved doublet, *anti*-C7 methyl). This rearranges to **2** at very low temperatures and was not further investigated. The alkene can be assigned as 4-*anti*-7-dimethyl-2-methylenebicyclo[2.2.1]heptane (**5**).

2-Methyl-2-norbornyl Cation **6**. *Degenerate Rearrangements*

Cation **6** was prepared in a number of solvent systems, FSO_3H, FSO_3H–SO_2ClF (1:4), SbF_5–SO_2, FSO_3H–SbF_5 and the rearrangement rates do not vary to any measurable extent. The cation was prepared in *ca.* 5% w/v concentration either from the tertiary alcohol, *exo*-2-methylnorbornan-2-ol or the tertiary chloride, *endo*-2-methyl-2-chloronorbornane. The 2-CD_3 alcohol was used in some cases and was prepared from norbornanone and CD_3MgI. The chemical shifts of **6** have been reported by Olah *et al.* (20) but their assignment should be corrected. Our results show that the C6-*endo* and a C5 proton assignment should be interchanged. Cation **6** undergoes two degenerate rearrangements. The rate of the faster process was obtained by matching computed spectra of the H1 proton doublet (AX) with calculated spectra assuming various exchange rates with the H6-*endo* proton (simulated as a broad singlet of half-width 24 Hz). The experimental coalesced H1–H6-*endo* proton peak appears very close to the C2 methyl peak but could be observed using the 2-CD_3 cation. No peak matchings were attempted at or beyond coalescence because the H6-*exo* and H3 protons interfere to some extent and also the very approximate line shape assigned to H6-*endo* will be a factor in the coalesced peak line shapes (but will not affect the more exact matchings done only on the C1 proton doublet prior to coalescence). The second degenerate rearrangement occurs at temperatures above 0 °C (in FSO_3H–SbF_5 (1:2)) and can be assigned to the process given in Scheme 2. The kinetic matrix used is shown in Fig. 4. Monstrous problems arise in treating this line broadening since all 10 protons are coupled in an interwoven manner, some involving second-order effects. Programs to handle such large exchanges are impossibly expensive even if one could determine all of the unknown coupling constants. The approximations used in the calculations consist in treating all protons (except C2) as uncoupled singlets, using various line widths to mimic coupling to some extent. The values used were as follows: H1, doublet, J = 7, line-width 5 Hz; *exo*-H3, 12; *endo*-H3, 12; H4, 7.5; *exo*-H5, 15; *endo*-H5, 10; *exo*-H6, 19; *endo*-H6, 24; *anti*-H7, 7; *syn*-H7, 7. In spite of these severe approximations, we expect that spectra in the intermediate exchange region should be relatively good since the exchanging protons are separated by large chemical shifts and consequently the peaks are very broad (see Fig. 3) in this region (and relatively unaffected by the exact line shape of the "frozen out" peaks.

Interconversion of the α- *and* β-*Fenchenehydro Cations*

On adding α-, β-, or cyclofenchene to FSO_3H–SO_2ClF (1:4) at *ca.* −120 °C, one obtains only the equilibrium mixture of the α- and β-cations, K being near unity. On warming very rapidly (there is also an irreversible transformation occurring rapidly as one warms the solution, next sextion) to −78 °C, the interconversion becomes rapid enough so that the DISST technique of Forsén and Hoffman (22) can be used to estimate the interconversion rate. Irradiation of the combined *endo*-H6 region (*ca.* τ 8.6) results in a 50% decrease in the combined H1 proton region. Assuming T_1 = 2 s (30), this gives an order of magnitude rate constant, k = 1 s^{-1}, $\Delta G^{\ddagger}$ = *ca.* 11.2 kcal/mol. For confirmation, this technique was also applied to the degenerate rearrangements observed for cation **6**, where both line broadening and the DISST technique can be used. For the faster of the two degenerate rearrangements in **6**, the DISST technique gives k = 1 s^{-1} at −87.0 °C, compared to the extrapolated estimate of 0.85 s^{-1} from the log k *vs.* $1/T$ plot using line-broadening data. The DISST technique was also used to confirm qualitatively the exchanges suggested for the slower degenerate rearrangement in **6**.

α- *and* β-*Fenchenehydro Cations* → *1,2-endo-3-Trimethyl-2-norbornyl Cation* **8** *(+ WM Shift Isomer)*

This rate was followed by determining the height of the growing C1 and C2 methyl peaks of **8** (+ WM shift isomer) as a function of time using a standard first-order plot. At −92 °C, $k = 5.1 \pm 0.2 \times 10^{-4}$ s^{-1}, $\Delta G^{\ddagger}$ = 13.1 kcal/mol (average of two runs).

Structure Proof of Cation **8** *(+ WM Shift Isomer)*

The ketone 1-*endo*-3-dimethylbicyclo[2.2.1]heptan-2-one (**9**), was prepared by first alkylating 1-methylbicyclo-[2.2.1]heptan-2-one using trityl sodium and methyl iodide (31). The product is mainly the *exo*-3-methyl compound **19** (g.l.c.) with traces of **9** and some starting material. Equilibration in refluxing $NaOCH_3$–CH_3OH gives an equilibrium mixture now slightly richer in **9** (*ca.* 55%) and this was isolated by preparative g.l.c. (column *A*, 155 °C). The ketone has been reported (31). Treating 0.210 g (1.52 mmol) of **9** in ether with excess methyl lithium in ether at 0 °C yields, after work-up, an oil, 0.236 g, which solidifies in the freezer; i.r., no C=O, 3420 cm^{-1} (b), OH; n.m.r. (CCl_4), τ 8.97, 9.03, 9.20 (d, J = 7 Hz, all 3H, the three methyl groups of **10**). Judging from the lack of doubling of n.m.r. peaks, the product is likely to be mainly the *exo*-2-methyl isomer. Addition of the alcohol **10** to FSO_3H–SO_2ClF (1:4) at −120 °C and warming to −100 °C gives **8** (+ WM shift isomer). The chemical shifts for **8** (+ WM isomer) have been reported previously (1). Some of these are temperature dependent, as expected (14). Solutions of **8** can be quenched (−20 °C), as for **2**, and pure 1,2,3-trimethylbicyclo[2.2.1]hept-2-ene (ε-fenchene) can be isolated by preparative g.l.c. (column *A*). There are also produced in this quenching a number of other alkenes with an exocyclic methylene group, probably corresponding in

Can. J. Chem. Downloaded from www.nrcresearchpress.com by 210.87.254.42 on 09/05/12
For personal use only.

part to elimination at the C2 methyl in **8** and also from the C2 methyl of the WM shift isomer. However, there are more products than this will account for. Cation **8** (+ WM shift isomer) is produced on adding ε-fenchene to FSO_3H–SO_2ClF (1:4) at *ca.* −120 °C.

1,2-endo-3-Trimethyl-2-norbornyl Cation 8 → 1,2,4-Trimethyl-2-norbornyl Cation 2

The rate of this reaction was measured by following the increase in the C4 methyl peak height of **2** as a function of time. The reaction was run at −15.0 °C in a cryostat and samples were periodically quenched at −78 °C and the n.m.r. spectrum determined at −50 °C. Nitromethane was used to obtain a constant reference peak height, $k = 1.1 \pm 0.2 \times 10^{-4}\ s^{-1}$, $\Delta G^{\ddagger} = 18.5$ kcal/mol (average of two determinations).

Protonation of α- and β-Pinene

α-Pinene or β-pinene was dissolved in an equal volume of $CDCl_3$ and added slowly to either pure FSO_3H with stirring at −50 °C in a 5 ml round-bottom flask or directly to an n.m.r. tube containing a 1:4 mixture of FSO_3H–SO_2ClF at *ca.* −120 °C. The spectra were reasonably clean and could be analyzed at low temperatures but on warming, broad featureless n.m.r. peaks characteristic of polymers appeared. Both products **8** and **12** are stable at these temperatures so the reason for the polymerization is not known.

α-Fenchyl Tosylate and Borneol Tosylate

These compounds were prepared by standard procedures and are both known (32).

1,2-exo-3-Trimethyl-2-norbornyl Cation 18 → 1,2-endo-3-Trimethyl-2-norbornyl Cation 8

Cation **18** (+ WM shift isomer) was prepared from the corresponding tertiary alcohol **20**. The preparation of **20** follows that of **10**, except that the 1-*exo*-3-dimethyl ketone **19**, needed in this case, had to be isolated by a double preparative g.l.c. collection of the initial alkylation mixture referred to in the preparation of **10**. On column *A*, the ketone **19** and the starting material can be separated as a single peak from the 1-*endo*-3-dimethyl ketone **9**. Reinjection on column *B* separates the starting ketone and **19**. Methylation (0.209 g, 1.51 mmol) with excess methyl lithium, as previously, yields an oily tertiary alcohol (0.226 g); i.r., no C=O, 3430 cm^{-1}, OH. The n.m.r. spectrum (CCl_4) indicates a mixture of the *exo*-2 and *endo*-2 methyl alcohols, peaks at τ 8.94, 9.00, 9.06, and 9.14 (d, $J = 7$ Hz). The 8.94 and 9.06 peaks add up to approximately 3H and presumably are the *exo*-2 and *endo*-2 methyl groups, the C1 and C3 methyls overlapping in both isomers. Both isomers yield the same cation so the stereochemistry at C2 is unimportant for our purposes. Addition of **20** to FSO_3H–SO_2ClF (1:4) at *ca.* −120 °C and then warming to −100 °C yields **18** (+ WM shift isomer). The chemical shifts for this rapidly equilibrating pair have been reported (1) and as expected (14), the C1 and C2 methyl shifts are temperature dependent. The interconversion rate was followed by determining the increase of the standardized C1 and C2 methyl peak heights of **8** (+ WM shift isomer) as a function of time. Reversible first-order kinetics were used since a small amount of **18** (+ WM shift isomer) exists at equilibrium, **8**/**18** = 6.3 ± 0.3, $k_{18\rightarrow 8} = 3.0 \pm 0.5 \times 10^{-4}\ s^{-1}$ at −90 °C, $\Delta G^{\ddagger} =$ 13.6 kcal/mol (average of three runs).

The authors wish to thank the National Research Council of Canada for generous financial support.

1. E. Huang, K. Ranganayakulu, and T. S. Sorensen. J. Am. Chem. Soc. **94**, 1779 (1972).
2. J. A. Berson, A. W. McRowe, and R. G. Bergman. J. Am. Chem. Soc. **89**, 2573 (1967).
3. S. Beckmann and R. Bamberger. Ann. **580**, 198 (153): S. Beckmann and A. Dürkop. Ann. **594**, 205 (1955); S. Beckmann and H. Geiger. Chem. Ber. **94**, 1905 (1961).
4. S. Coffey (*Editor*). Rodd's chemistry of carbon compounds, 2nd. ed. Elsevier, Amsterdam. 1969. pt. II.
5. R. Haseltine, K. Ranganayakulu, N. Wong, and T. S. Sorensen. Can. J. Chem. This issue.
6. E. Huang, K. Ranganayakulu, and T. S. Sorensen. J. Am. Chem. Soc. **94**, 1780 (1972).
7. C. K. Johnson, and C. J. Collins. J. Am. Chem. Soc. **96**, 2514 (1974); C. J. Collins, C. K. Johnson, and V. F. Raaen. J. Am. Chem. Soc. **96**, 2524 (1974).
8. T. S. Sorensen, I. J. Miller, and C. M. Urness. Can. J. Chem. **48**, 3374 (1970).
9. T. S. Sorensen. J. Am. Chem. Soc. **91**, 6398 (1969).
10. N. C. Deno and J. J. Houser. J. Am. Chem. Soc. **86**, 1741 (1964).
11. L. Huang, K. Ranganayakulu, and T. S. Sorensen. J. Am. Chem. Soc. **95**, 1936 (1973).
12. R. P. Haseltine and T. S. Sorensen. Can. J. Chem. **53**, 1067 (1975).
13. G. A. Olah, J. R. DeMember, C. Y. Lui, and A. M. White. J. Am. Chem. Soc. **91**, 3958 (1969).
14. T. S. Sorensen and K. Ranganayakulu. Tetrahedron Lett. 2447 (1972).
15. H. L. Goering and J. V. Clevenger. J. Am. Chem. Soc. **94**, 1010 (1972).
16. G. A. Olah, J. R. DeMember, C. Y. Lui, and R. D. Porter. J. Am. Chem. Soc. **93**, 1442 (1971).
17. R. Haseltine, N. Wong, T. S. Sorensen, and A. J. Jones. Can. J. Chem. This issue.
18. G. A. Olah, G. Liang, G. D. Mateescu, and J. L. Riemenschneider. J. Am. Chem. Soc. **95**, 8698 (1973).
19. R. Haseltine, E. Huang, K. Ranganayakulu, and T. S. Sorensen. Can. J. Chem. **53**, 1056 (1975).
20. G. A. Olah, A. M. White, J. R. DeMember, A. Commeyras, and C. Y. Lui. J. Am. Chem. Soc. **92**, 4627 (1970).
21. J. A. Berson, J. H. Hammons, A. W. McRowe, R. G. Bergman, A. Remanick, and D. Houston, J. Am. Chem. Soc. **89**, 2590 (1967).
22. S. Forsén and R. A. Hoffman. J. Chem. Phys. **39**, 2892 (1963).
23. T. S. Sorensen and K. Ranganayakulu. J. Am. Chem. Soc. **92**, 6539 (1970).
24. W. Hückel and H. J. Kern. Ann. **728**, 49 (1969).
25. P. H. Campbell, N. W. K. Chiu, K. Deugau, I. J. Miller, and T. S. Sorensen. J. Am. Chem. Soc. **91**, 6404 (1969).
26. M. Hanack. Chem. Ber. **94**, 1087 (1961).
27. W. Hückel and H. J. Kern. Ann. **687**, 40 (1965).

28. A. COULOMBEAU and A. RASSAT. Bull. Soc. Chim. Fr. 3338 (1965).
29. A. N. ELIZAROVA and V. A. MIRONOV. Probl. Organ. Sinteza, Akad. Nauk SSSR, Otd. Obstich. Tekhn. Khim. (1965); Chem. Abstr. **64**, 1101(d) (1966).
30. R. CONE, R. P. HASELTINE, P. KAZMAIER, and T. S. SORENSEN. Can. J. Chem. **52**, 3320 (1974).
31. E. PULKKINEN. Ann. Acad. Sci. Fennicae Ser. A, II, **74** (1956).
32. W. HÜCKEL. Chem. Ber. **77B**, 805 (1944).

Can. J. Chem. Downloaded from www.nrcresearchpress.com by 210.87.254.42 on 09/05/12
For personal use only.

A Kinetic and Thermodynamic Behavioral Comparison of Observable Secondary and Tertiary 2-Norbornyl Cations

R. HASELTINE, N. WONG, AND T. S. SORENSEN
Department of Chemistry, University of Calgary, Calgary, Alberta T2N 1N4
AND
A. J. JONES
Department of Chemistry, University of Alberta, Edmonton, Alberta
Received October 31, 1974

R. HASELTINE, N. WONG, T. S. SORENSEN, and A. J. JONES. Can. J. Chem. **53**, 1891 (1975).

By analyzing various rearrangement processes, one can deduce the relative stabilities of the following 2-norbornyl cations (kcal/mol): 1,2-dimethyl, 0; 2-methyl, 1; 1-methyl, 6.5; and the parent 2-norbornyl, 8.5. Secondary 2-norbornyl cations have been assigned a "carbonium ion" structure and tertiary a "carbenium ion" structure. Using suitable model systems, an absolute rate comparison has been made of all three common rearrangement processes in the tertiary systems ("carbenium") with those already measured for the 2-norbornyl cation ("carbonium"). The activation free energies, $\Delta G^{\ddagger}$, (in kcal/mol) were: Wagner–Meerwein (WM) shift: tertiary, <4; secondary, <4; *endo*-6,2-hydride shift: tertiary, 7.2; secondary, 5.8; *exo*-3,2-hydride shift: tertiary, 6.6; secondary, 11.4. A discussion of the structure of tertiary and secondary 2-norbornyl cations emphasizes the following points: (*i*) a rationalization of the rapid *endo*-6,2-hydride shift observed in norbornyl cations does *not* necessitate a protonated nortricyclene ("carbonium ion") postulate; (*ii*) on the basis of the results for acyclic cations and the 1,2-dimethyl-2-norbornyl cation, one would *not* expect to "freeze out" the WM shift in an equilibrating 2-norbornyl cation structure; (*iii*) the formation of nortricyclenes may be related to a partial C6—C2 bond in the ions; and (*iv*) the structure of the observable secondary 2-norbornyl cation probably involves partial C6—C2 bonding but, in our opinion, this does not require a symmetrical static formulation.

R. HASELTINE, N. WONG, T. S. SORENSEN et A. J. JONES. Can. J. Chem. **53**, 1891 (1975).

En faisant l'analyse des divers processus de réarrangements, on peut déduire les stabilités relatives des cations norbornyl-2 suivants (kcal/mol): diméthyl-1,2, 0; méthyl-2, 1; méthyl-1, 6.5; et le norbornyl-2 non-substitué, 8.5. On a attribué au cation norbornyl-2 secondaire une structure de "carbocation" et au cation tertiaire une structure d'"ion carbènium". Faisant appel à des systèmes modèles appropriés, on a fait une comparaison entre les vitesses absolues des trois processus de réarrangement commun dans les systèmes tertiaires ("carbènium") avec celles qui ont déjà été mesurées pour le cation norbornyl-2 ("carbocation"). Les énergies libres d'activation $\Delta G^{\ddagger}$ (en kcal/mol) sont: réarrangements de Wagner–Meerwein (WM): tertiaire, <4; secondaire, <4; déplacement d'hydrure 6,2-*endo*: tertiaire, 7.2; secondaire, 5.8; déplacement d'hydrure 3,2-*exo*: tertiaire, 6.6; secondaire, 11.4. Une discussion de la structure des cations norbornyl-2 tertiaires et secondaires met en évidence les points suivants: (*i*) une rationalisation du réarrangement rapide d'hydrure 6,2-*endo* observé dans les cations norbornyles n'implique pas nécessairement que l'on doive postuler l'existence d'un nortricyclène protoné ("carbocation"); (*ii*) sur la base des résultats obtenus avec des cations acycliques et ceux obtenus avec le cation diméthyl-1,2 norbornyl-2, on ne devrait pas espérer éliminer ("freeze-out") le réarrangement de WM dans la structure du cation norbornyl-2 en équilibre; (*iii*) la formation de nortricyclènes peut être reliée à la présence de lien partiel C2—C6 dans les ions; et (*iv*) la structure du cation norbornyl-2 secondaire qui peut être observée implique probablement un lien partiel C2—C6; toutefois on ne croit pas que ceci requiert une formulation statique symétrique. [Traduit par le journal]

Introduction

The postulate of a symmetrical 2-norbornyl cation **1** is mainly due to Winstein (1). Following this, Saunders *et al.* (2) first reported the observable 2-norbornyl cation. This has now been studied by ^{1}H and ^{13}C n.m.r. (3, 4), Raman spectroscopy (3), and e.s.c.a. (4, 5) and these results have also been interpreted in terms of the symmetrical static structure.

The tertiary analogs **2** and **3** are very generally regarded as having an unsymmetrical structure (5, 6). Olah has recently suggested that carboca-

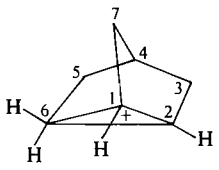

1

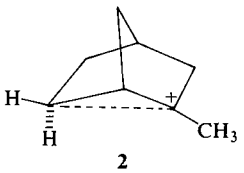

2

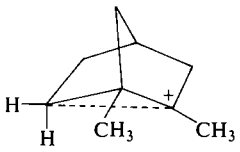

3

tions be divided into "carbonium" and "carbenium" ions (7). Accordingly, the norbornyl cation **1**, specifically the C6 carbon, becomes a member of the CH_5^+ symmetrical pentacoordinate "carbonium" ion group and **2** and **3**, while regarded as having some C6—C2 bonding, are basically trivalent "carbenium" ions.

From a study of both the degenerate and irreversible rearrangements which occur in various dimethyl-2-norbornyl cations, it is now possible (this work) to estimate with some assurance the actual energy difference between **1** and **2** or **3**. It is also possible to compare the rates of the three most characteristic rearrangement processes of norbornyl cations: (*a*) the Wagner–Meerwein (WM) shift, (*b*) the *endo*-6,2-hydride shift, and (*c*) the *exo*-3,2-hydride shift, using in the case of the tertiary ions, model systems in which each of these processes (as in **1**) is degenerate. It is then of interest to see how the structural differences, **1** *vs.* **2** or **3**, affect the rates observed for each of these rearrangements.

Results and Discussion

An Estimate of the Energy Difference Between a Secondary Norbornyl Cation with a C1 Methyl vs. a C1 Hydrogen

Let us start by deriving an estimate of the energy difference between a 1,2-di **H** (secondary) and a 1,2-di CH_3 (tertiary) norbornyl cation. A value of 5.5 kcal/mol has been previously derived (8) for the secondary–tertiary (methyl) energy difference using the activation energy for a degenerate rearrangement occurring in **2**. The 2,4-dimethyl-2-norbornyl cation **4**, likewise undergoes this same degenerate rearrangement[1] (eq. 1) and on analysis of this (see Experimental), one obtains the nearly identical value of 5.3 kcal/mol.

[1]

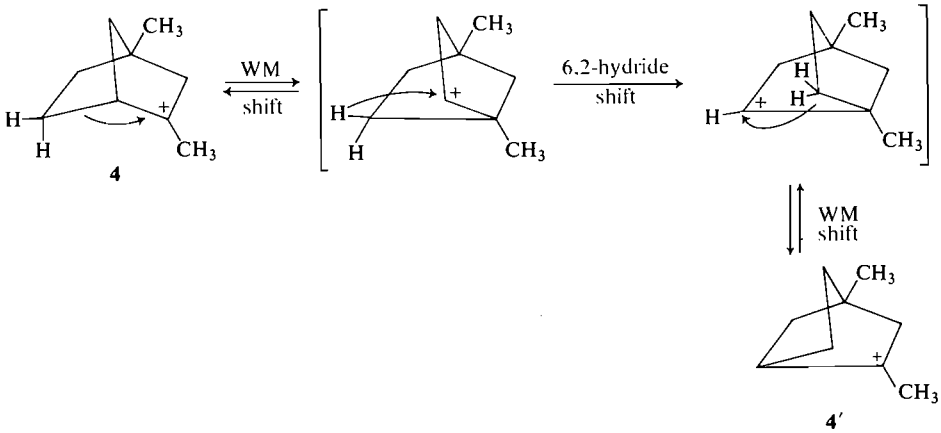

This energy difference is really the difference between a tertiary ion and a secondary ion with a C1 methyl group. The more fundamental comparison which one wants is between an ion with both C1 and C2 substituted by hydrogen, *i.e.* **1**, and a tertiary species, *i.e.* **2** or **3**. That a C1 methyl probably does increase the stability of the secondary cation was alluded to previously (9) and can be demonstrated in several ways. The following arguments are illustrative rather than comprehensive: (*a*) The activation energy barrier separating the secondary and tertiary

[1]A second degenerate process can also be observed which interconverts the two methyl groups but there are at least three reasonable mechanisms for this.

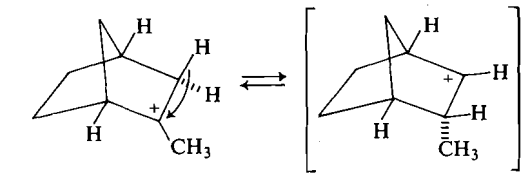

2 6

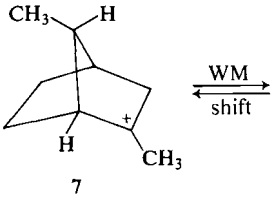

7

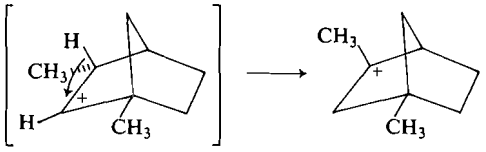

8 4

cations **2** and **6** is *ca.* 15.2 kcal/mol (8) (13.9 and 15.0 in two other structurally related cases) (9). This same barrier in the rearrangement of **7** to **4**, where one has a C1 methyl intermediate is experimentally only 12.1 kcal/mol (9). This suggests either that the C1 methyl cation **8** starts off *ca.* 2–3 kcal/mol lower in energy (than **6**) or that the activation barrier for a 3,2-hydride shift changes. We prefer the former explanation, shown schematically in Fig. 1. (*b*) The activation barrier for a 3,2-hydride shift from one secondary center to another (abbreviated previously as 2HSS) is about 11.4 kcal/mol

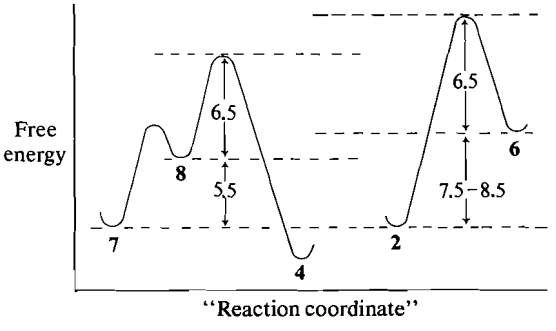

FIG. 1. Reaction coordinate diagram showing the postulated extra stability associated with cation **8** *vs.* **6**, assuming the *exo*-3,2-hydride shift barrier in both cases is 6.5 kcal/mol.

in the norbornyl cation (3). Starting from a tertiary ion, the overall barrier should be 11.4 + 5.5 = 16.9 kcal/mol. However, in the rearrangement of the 2,4-dimethyl-2-norbornyl cation **4** to the 1,2-dimethyl isomer **3**, the experimental barrier is 18.9 kcal/mol. Regardless of the actual mechanism (9), there exists a 10-step mechanism for this conversion for which one predicts, using the above value, a *ca.* 17.2 kcal/mol barrier for two rate-determining 2HSS steps. However, one of these steps involves the shift shown in eq. 2, *i.e.* a shift starting from a secondary ion having no C1 or C4 methyl group. If this were $\geq$ 2 kcal/mol less stable than a C1 methyl secondary ion, one obtains $\Delta G^{\ddagger} \geq 2 + 5.5 + 11.4 \geq 18.9$ kcal/mol, a value more in line with experiment. A barrier of this size would also be more consistent with results obtained for several other rearrangements (10).

[2] **4** —five steps→ 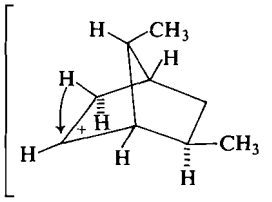 —2HSS step→

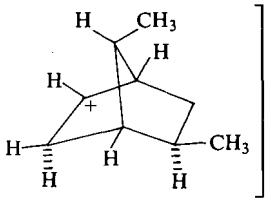 —four steps→ **3**

The Stabilizing Influence of a C1 Methyl on Tertiary 2-Norbornyl Cations

This can be quantitatively evaluated in several ways. The most direct observation is simply that all of the dimethyl-2-norbornyl cations eventually yield the 1,2-dimethyl analog **3**. Probably the best comparison here is between the 2,4-dimethyl isomer **4** and **3**. Experimentally **3** is 1.5 kcal/mol more stable (at 25 °C) than **4** (9). Cation **3** is at least 2 kcal/mol more stable than any of the others (9) but steric interactions may play a role in this. Another approach is to look at cations such as **9** and **10**. The equilibrium here (at −80 °C for example) lies most definitely ($\Delta G \geq 1$ kcal/mol) on the side of **9** and **10**, *i.e.* the isomers with the C1 methyl (10, 11).

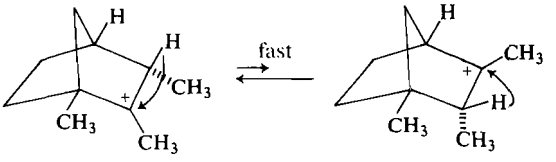

9

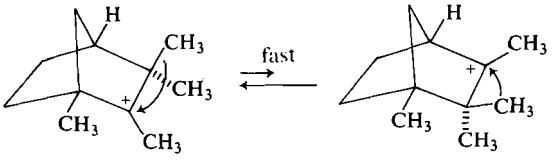

10

Overall Energy Comparison

From the foregoing, one can assign the following approximate relative energies (ΔG in kcal/mol). (In giving an energy difference for nonisomeric species one assumes, perhaps unwisely, that the extra methyl groups in "nonactive" positions are "normal" C—C and C—H bond free energies.)

The norbornyl cation energy differences are to be compared to the calculated 11–15 kcal/mol difference between the tertiary and secondary amyl cations (12). Several other estimates of the secondary–tertiary norbornyl cation energy difference have been made (4, 10, 13).

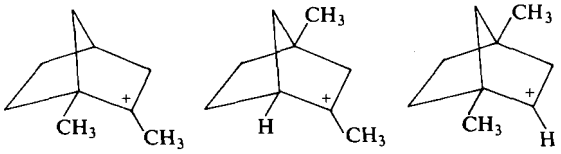

0 *ca.* 1 *ca.* 6.5

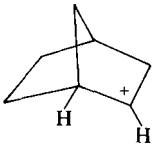

ca. 8.5

Kinetic Aspects

The WM Shift: Secondary vs. Tertiary (Methyl)

This degenerate process does not occur if the structure is symmetrical and static. However,

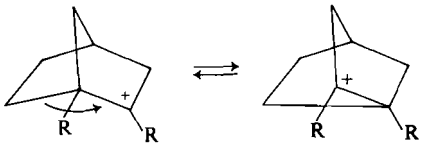

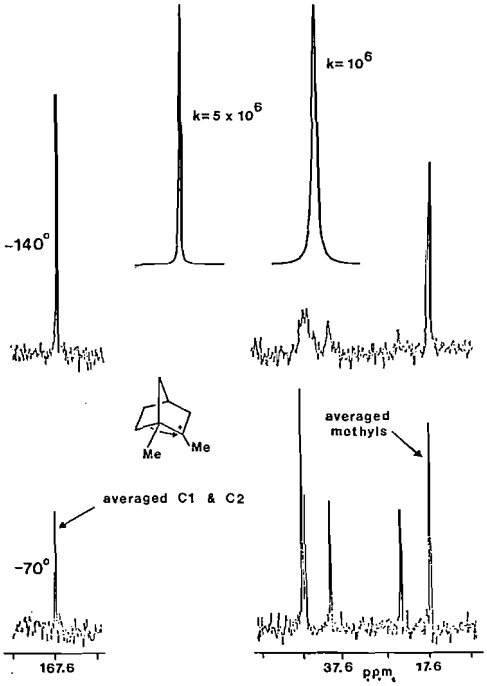

FIG. 2. ^{13}C n.m.r. spectrum of the 1,2-dimethyl-2-norbornyl cation at -70 and -140 °C in SbF_5–SO_2ClF–SO_2F_2. The feature of interest is the averaged C1 and C2 carbon signal which still remains very sharp at -140 °C. The two curves inset at the top are calculated spectra for this peak assuming the exchange rate constants shown. Both are still broader than the natural line width used in the calculations.

one can in any case put a lower limit, $\Delta G^{\ddagger} < 4$ kcal/mol, on such a hypothetical process in the secondary ion (R = H), using the recently published (4) ^{13}C n.m.r. spectrum of the 2-norbornyl cation.

The ^{13}C n.m.r. spectrum of the tertiary equivalent, the 1,2-dimethyl cation **3** (R = CH_3), measured at -70 and -140 °C, is shown in Fig. 2. Olah and Liang have previously reported ^{13}C chemical shifts for this cation at -90 °C (14). As one goes down in temperature to -140 °C, a progressive weakening of all signals, except the coalesced methyl carbons and the coalesced C1 and C2 carbons, was observed. This apparent variability in T_1 relaxation times could be related to the WM shift and is being investigated further[2] but in any case, the existence of a sharp coalesced C1, C2 signal implies a rate constant at -140 °C of $k > 10^6\ s^{-1}$,

[2]A. J. Jones, private communication.

$\Delta G^{\ddagger} < 4$ kcal/mol. Several computed spectra assuming certain exchange rates are shown in Fig. 2 for the C1,C2 carbons of **3**, using a chemical shift separation of 4000 Hz (similar to the separation of these carbons in **2**). A broadening of the magnitude shown for $k = 10^6\ s^{-1}$ would have been detectable.

The endo-6,2-Hydride Shift: Secondary vs. Tertiary (Methyl)

The rate of this process in a secondary cation (R = H) is known, $\Delta G^{\ddagger} = 5.8$ kcal/mol (3).

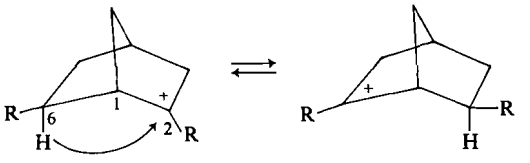

11 **11′**

Having previously prepared the 2-*exo*-6-dimethyl-2-norbornyl cation **11** (R = CH_3) (9), we were able to observe this same process in a tertiary situation. The ^1H n.m.r. spectrum of this ion is shown in Fig. 3, for various temperatures. The line broadening observed is unequivocally assigned to an *endo*-6,2-hydride shift and using the C6 and C2 methyl peaks, the computed spectra, also shown in Fig. 3, were obtained. Matching these in the usual way results in the following activation parameters, $\Delta G^{\ddagger} = 7.2$ kcal/mol at -96 °C, $\Delta H^{\ddagger} = 7.2 \pm 1$ cal/mol, $\Delta S^{\ddagger} = 0 \pm 3$ e.u.

The exo-3,2-Hydride Shift: Secondary vs. Tertiary (Methyl)

The rate for this process in the secondary cation is known, $\Delta G^{\ddagger} = 11.4$ kcal/mol (3). Using the 2-*endo*-3-dimethyl-2-norbornyl cation

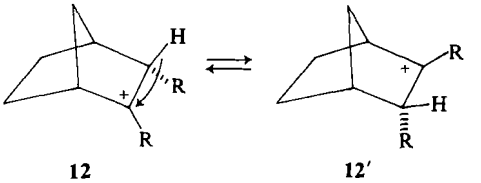

12 **12′**

12 (R = CH_3), the same process in a tertiary situation can be directly observed, yielding $\Delta G^{\ddagger} = 6.6$ kcal/mol, $\Delta H^{\ddagger} = 6 \pm 1$ kcal/mol, $\Delta S^{\ddagger} = -4 \pm 7$ e.u. (15).

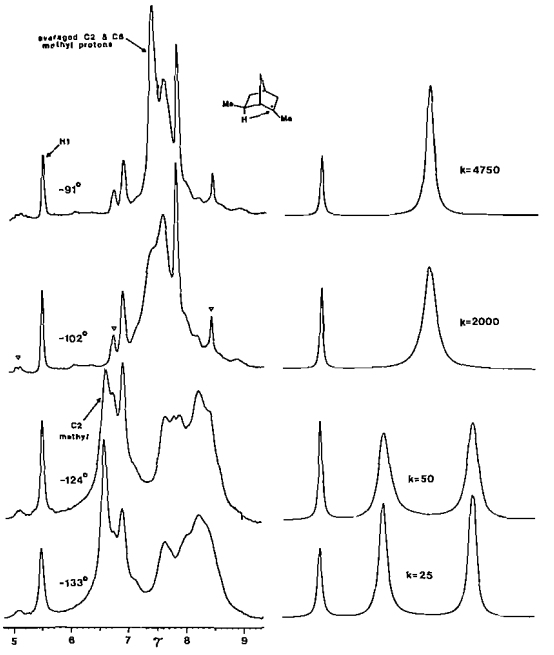

FIG. 3. ^1H n.m.r. spectrum of the 2-*exo*-6-dimethyl-2-norbornyl cation showing experimental and calculated line broadening curves. The signals designated by ▽ are peaks due to the 2,4-dimethyl-2-norbornyl cation.

The Question of "Structure" in Tertiary (Methyl) 2-Norbornyl Cations and the Relationship if any Between this and Rearrangement Rates

Tertiary norbornyl cations such as **13** and **14** exhibit typical equilibrium behavior, *i.e.* a

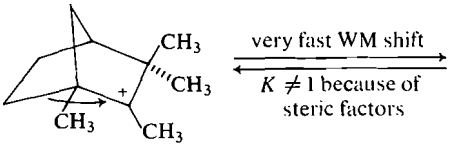

13

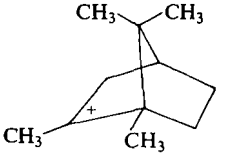

14

temperature dependent equilibrium constant (11). As in the parent 1,2-dimethyl cation **3**, one cannot "freeze out" the WM shift in the n.m.r. spectrum. Attempts to observe this same equilibrium constant behavior using the 1-ethyl-2-methyl **15** ⇄ 1-methyl-2-ethyl **16** system (this

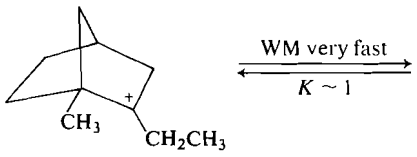

15

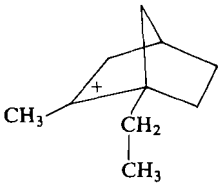

16

work) were not very successful since K was very close to 1 (see Experimental for chemical shift details).

Even though the 1,2-dimethyl parent system **3** is also very probably an equilibrating pair of enantiomeric cations, this is no reason, of course, to disregard charge delocalization within each enantiomer.

We believe there is evidence, both from thermodynamics and from a comparison of n.m.r. chemical shifts, suggesting *some* bonding interaction between C6 and C2 in the tertiary cations. Olah *et al.* (6) have reached this same conclusion from e.s.c.a. experiments and ^{13}C n.m.r. shift comparisons. The thermodynamics argument is simply that a methyl is preferred at the C1 position in the cations compared to the sterically equivalent C4 position, *i.e.* the 1,2-dimethyl-2-norbornyl cation is more stable than the 2,4-dimethyl isomer. This indicates unusual charge density at C1 since in aliphatic cations there is no particular preference for a methyl *vs.* hydrogen on the carbon alpha to the cation center.

In the ^1H n.m.r. spectra, the *exo*-6-H proton in these cations is very substantially deshielded relative to the *endo*-6-H or the 7-position protons (which are in each case methylene protons at an equivalent σ bond distance from the cation center. We believe this result is reasonably interpreted as evidence that electron density has been removed from the C to *exo*-6-H bond. However, a referee suggests that some polarizing effect of the positive charge could cause this deshielding and he would dispute that there is any evidence for a weakening of this bond.

It may not be clear that either of these observations relates to a C6—C2 bond and in a sense this is true. However, one can rationalize both observations by postulating some weak overlap of the empty p orbital on C2 with the back lobe of an sp^3 orbital on C6 (6). Geometric considerations dictate that this will be the back lobe of the particular sp^3 orbital bonding to the *exo*-6 proton. If the weak bonding does occur, there can be little doubt but what the C to *exo*-6-H bond would be weakened.

The reader is also referred to a recent paper by Wolf and Farnum (16) concerning the onset of "nonclassical" delocalization in norbornyl cations.

The partial bonding from C2 to C6 is in a way similar to hyperconjugative stabilization. Thus, in hyperconjugation, one considers resonance structure contributions related to an alkene plus H^+. Similarly, the C2,C6 partial bond description has a contributing resonance structure related to a nortricyclene + H^+.

One can now ask how the structure of these tertiary (methyl) norbornyl cations is related to the three common norbornyl cation rearrangement processes? In Table 1, we contrast the absolute rearrangement rates for the secondary and tertiary 2-norbornyl cation rearrangements with the rates of analogous tertiary–tertiary processes in simple aliphatic cations (except for a 1,2-hydride shift no suitable secondary model systems are available). In observable aliphatic cations, no evidence exists for partial 1,3-bond bridging (equivalent to C6,C2 bridging in the norbornyl systems). The Table 1 comparisons suggest to us that the rapid *endo*-6,2-hydride shift in **11** is *not particularly related* to the presence of 1,3 (or C6,C2) bridging. A similar point has been made by Saunders (17). There are of course small differences in the activation energies shown in Table 1 for this shift. In a comparison of the tertiary norbornyl system with the aliphatic system, the difference is very reasonably explained on steric grounds, *i.e.* the former is conformationally rigid while in the latter the conformation for the 1,3-hydride transfer may be only one of many. The secondary–tertiary norbornyl difference is also not unreasonable since the charge density on the cation center in the former is larger.

We envisage two completely different roles for the two C6 protons. The *endo*-proton, for steric reasons, becomes the migrating proton but is not involved in charge delocalization via

TABLE 1. Activation energies for norbornyl cation rearrangements

Rearrangement process	ΔG^* (kcal/mol) 2-Norbornyl	Tertiary 2-norbornyl	Tertiary aliphatic analog
WM shift or 1,2-dialkyl shift	<4	<4	<3.5*
endo-6,2-Hydride shift or 1,3-hydride shift	5.8	7.2	8.5†
exo-3,2-Hydride shift or 1,2-hydride shift	11.4	6.6	<4‡

*Data for the 1,2-methyl shift in the 2,3,3-trimethyl-2-butyl cation (footnote 3 and ref. 17).
†Data for the 1,3-hydride shift in the 2,4-dimethyl-2-pentyl cation (18).
‡Data for the 1,2-hydride shift in the 2,3-dimethyl-2-butyl cation (15, 19).

C2,C6 bonding. The *exo*-proton is involved in the delocalization. The stronger the C2,C6 bonding, the weaker the C—*exo*-H-6 bonding. This is predicted to be the proton lost in forming nortricyclenes, *not the migrating proton.* In aliphatic systems where 1,3-bond bridging is unimportant in ground states, one does not normally observe cyclopropane formation although 1,3-hydride shifts readily occur (Table 1).

The relationship between the mode of delocalization in a carbocation and product stability of a deprotonated species is an interesting question. The proton lost in deprotonation is normally a proton for which a hyperconjugative resonance hybrid structure can be written, *i.e.*

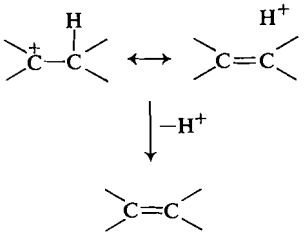

implying of course that some weakening of the bond already exists in the ion and also that some C—C double bond character is present. Assuming the deprotonation transition state occurs early in the C—H bond breaking (the Hammond postulate), then product ratios will reflect the relative ease with which various C—H bonds are broken and by implication which are the weakest. One can sometimes obtain kinetic control of products in cases involving the deprotonation of solvolytically generated carbocations but the more usual case is to obtain products of thermodynamic control under reversible protonation–deprotonation conditions. Even in this case, the observed products often appear to bear a superficial relationship to what one anticipates to be the weakest bond in the cation, *i.e.* a relationship in which breaking the weakest bond generates the thermodynamically most stable hydrocarbon. This results in the suggestion that long-lived carbocations will *tend to delocalize charge in the direction of the most stable deprotonated hydrocarbon.* Tertiary (methyl) norbornyl cations then represent an interesting group since one is assuming both significant σ-hyperconjugation (C6,C2 bonding) and π-hyperconjugation (principally the C3 protons and the C2 methyl protons). Experimentally, on the basis of the above discussion, the π-hyperconjugation is slightly dominant. In the case of 2-methyl and 1,2-dimethyl norbornyl compounds, there is experimental data relating to thermodynamic stabilities and some to kinetic control. The equilibrium percentages in the 2-methyl system have been measured at 250 °C by Maurel *et al.* (20) and are as follows.

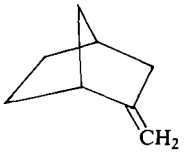

60%

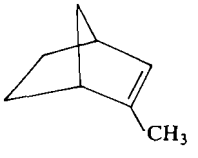

21%

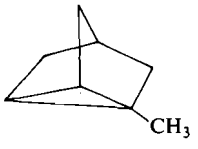

14%

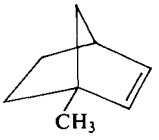

5%

For a more ambient temperature comparison, we have equilibrated (21) a pentamethyl series with the following (25 °C) results.

[3]M. Saunders, correspondence with H. C. Brown and circulated by Brown.

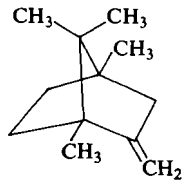
78%

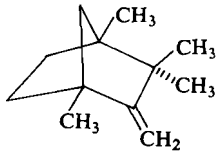
14%

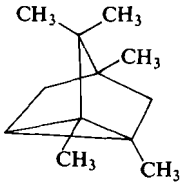
6.5%

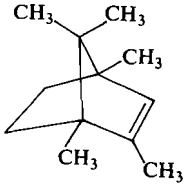
1.5%

In equilibrating a single alkene isomer in the pentamethyl series, one observes that the alkenes equilibrate faster than they form the nortricyclene (initial kinetic control).

In the parent 2-norbornyl system, Schleyer (22) has shown that the equilibrium at 105°C favors nortricyclene (77%) over norbornene (23%), whereas in solvolysis (kinetic control), there is a report (23) showing that of the hydrocarbon fraction formed, 97.5% was nortricyclene and only 2.5% norbornene.

We interpret the nortricyclene formation in the tertiary ions (previously shown to be unsymmetrical even in a 1,2-dimethyl case) in terms of this σ-hyperconjugation, *i.e.* as a further piece of evidence to go with the thermodynamic and n.m.r. chemical shift arguments cited as evidence for a weak C6—C2 bond.

Coming back to the comparisons in Table 1, one notes that the tertiary WM shift and the equivalent methyl shift in an aliphatic cation are both too fast to measure. These shifts may eventually be found to be different but on the basis of our *present data*, one cannot conclude that the rapid WM shift in the 1,2-dimethyl-2-norbornyl cation has any relation to the proposed weak C6—C2 bond (nor can one exclude such a possible relationship, although admittedly one would have only 4 kcal/mol of activation energy left to differentiate these with).

Finally, the *exo*-3,2-hydride shift in the tertiary norbornyl system is considerably slower than in aliphatic systems but much faster than in the secondary ion. One anticipates that the rate of a 3,2-hydride shift would be related to the charge density of the carbocation center and on this basis one would have to conclude that the secondary center is the most delocalized, followed by the tertiary norbornyl system. However, the steric requirements for a 1,2- (or 3,2-) hydride shift appear to be extremely important (24) and in fact this factor may be the dominant one in this case. For example, in the tertiary norbornyl system, the activation free energies for the *exo*- and *endo*-3,2-hydride shifts are 6.6 and > 14 kcal/mol. Clearly this difference is unrelated to charge delocalization at the cationic center. It seems likely that the acyclic-tertiary norbornyl difference, <4 *vs.* 6.6, is also due to steric effects.

In summary, we suggest that there is evidence for weak C6—C2 bonding in tertiary 2-norbornyl cations. Paradoxically, we suggest however that this bonding has no proven connection with the three characteristic rearrangement processes found in these cations. While one cannot exclude some future structure–reactivity correlation being established, we believe a satisfactory rationalization of these rates can be made on the basis of simple acyclic models.

The Question of "Structure" in Secondary 2-Norbornyl Cations

Although this work involves secondary cations only as intermediates, we believe there are important conclusions concerning these, derivable from the tertiary cation work. Firstly, a corner-to-corner proton shift of a protonated cyclopropane (specifically a protonated nortricyclene) is now shown to be unnecessary to rationalize the rapid *endo*-6,2-hydride shift in the secondary ion. Secondly, the fact that the WM shift in this cation (assuming equilibrating enantiomers) has not been "frozen out" is not unexpected in view of the fact that neither is the WM shift in the tertiary case (known to be equilibrating enantiomers). Thirdly, the slow 3,2-hydride shift may simply reflect a poor steric alignment of the empty orbital on C2 and the C3 proton. In this connection, an unfavorable tipping of the empty p orbital may occur as a result of the weak C6,C2 bonding, the stronger this bond, the poorer the alignment.

Therefore, as in the tertiary ions, one can reasonably rationalize the rearrangements on the basis of simple aliphatic models and need not involve any C6,C2 bonding.

The observable 2-norbornyl cation has been assigned a static, symmetrically bridged struc-

ture but it now seems to us that this is a somewhat too restrictive interpretation of the excellent data obtained by Olah and co-workers. Olah has introduced (7) the terms "carbenium" and "carbonium" to refer to trivalent, and static, symmetrical pentavalent carbocations, respectively, and wants of course to have examples. However, as admitted by Olah, charge delocalization in carbocations should be a continuous function of structure and there should exist cations at each waystop on the road from "carbenium" to "carbonium" ions. We do not exclude a symmetrical structure for the 1,2-di H cation nor perversely would we exclude a package description of the 2-norbornyl cation that included equilibrating enantiomers, each enantiomer having a weakened C—*exo*-H-6 bond, a normal C—*endo*-H-6 bond, a significant C2—C6 bond, significant positive charge at C1, and considerably less charge at C2[4] than in an aliphatic secondary cation.

In this specific case, one can construct a "graph" (Fig. 4) relating C2—C6 bond strength to structure (assume bond strength one represents equal C2—C6 and C1—C6 bond strengths). At the origin, one might place the 1,2-di-*p*-anisyl structure, further along, the 1,2-dimethyl and still further somewhere the 1,2-di H structure.

Our alternative suggestion for the secondary 2-norbornyl cation structure is really a "continuum model" as opposed to the "carbonium–carbenium" dichotomy, *i.e.* both the tertiary and secondary systems are pictured as being somewhat stabilized by the C6,C2 delocalization mode.

Perhaps one is nitpicking to worry about symmetrical *vs.* partly symmetrical structures for the norbornyl cation? Nature does not usually prefer high symmetry and there is a positive entropy factor which would result from rapidly equilibrating structures. Since it would generally be conceded that carbon does not make appreciable use of 3d and higher orbitals, the issue here really involves an explicit description of the bonding at the C6 carbon atom (and hence the resulting geometry).

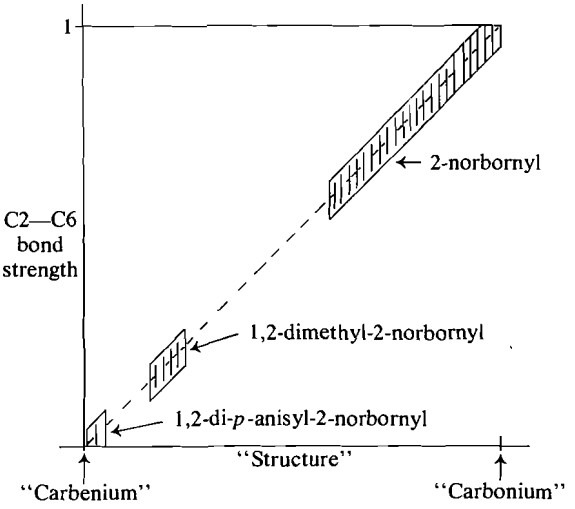

FIG. 4. Diagrammatic representation suggesting that secondary and tertiary 2-norbornyl cations should not be considered in black and white terms but as having a gradation in structure or shades of gray.

The interpretation of solvolysis results (25, 26) presents a different set of problems to those encountered in observable ion work and these have not been discussed in this paper. Solvolytically generated 2-norbornyl cation could also exist as a pair of equilibrating *R*, *S* cations with significant 6,2 bonding in each structure.

Experimental

Degenerate Rearrangement in **12**

Carbocation **12** has been reported (9). The kinetics of the degenerate *endo*-6,2-hydride shift can be best obtained using the two methyl groups. In the computed spectra, a half-width (T_2) = 8.0 Hz for C2 and for C6, a doublet, $J = 6$, was assumed with $T_2 = 4.0$ Hz. Prior to coalescence, the matching was done using the C2 methyl group. Since the upper field part of this is distorted somewhat by other absorptions, the matching was done by dividing the peak lengthwise and matching this half to computed spectra. After coalescence, a similar procedure was used, but where the peak is very broad, no matchings were attempted because of gross distortions in the line shape caused again by other peaks. Temperatures were monitored using a thermocouple directly placed in the n.m.r. tube.

Degenerate Rearrangement in **4**

Carbocation **4** has been reported (9). The kinetics of the degenerate Wagner–Meerwein shift – 6,2-hydride shift – Wagner–Meerwein shift process (line broadening) were measured in exactly the same way as described for the 2-methyl cation **2** (8).

[4]In comparing n.m.r. chemical shifts and e.s.c.a. results, Olah and co-workers have mainly been concerned with excluding structures with essentially localized charges. However, we believe the data would be equivocal if one attempted to differentiate between a symmetrical structure and, for instance, a structure where the positive charge at C1 was one-half that at C2.

Carbon-13 Nuclear Magnetic Resonance Spectrum of 3

Carbocation **3** was prepared from 3,3-dimethyl-2-*exo*-chloronorbornane (which rearranges via the 2,3-dimethyl isomer (15) eventually to **3**) dissolved in a mixture of excess SbF_5 and SO_2ClF–SO_2F_2. The concentration limit was about 10% w/v in order that precipitation did not occur at the very low temperatures. The spectrum was measured on a Bruker HFX-90 at 20° intervals from −60 to −140 °C (15). Computed ^{13}C spectra were obtained as previously described (15).

1-Methyl-exo-2-ethylbicyclo[2.2.1]heptan-2-ol

This alcohol was obtained by adding 1-methylbicyclo-[2.2.1]heptan-2-one to ethyl magnesium bromide at 0 °C, b.p. 93–96 °C/13 mm; n.m.r. (CCl_4), τ 9.02 (3H, C1 methyl), 9.115 (t, $J = 7$, 3H, C2 ethyl group).

Anal. Calcd. for $C_{10}H_{18}O$: C, 77.87; H, 11.7. Found: C, 77.98, H, 11.7.

The alcohol is probably a mixture of *exo* and *endo* hydroxyl isomers, with the latter dominant. The mixture obtained is mostly crystalline at 0 °C.

1-Methyl-2-ethyl-2-norbornyl Cation 15 and 1-Ethyl-2-methyl-2-norbornyl Cation 16

The cation mixture **15** ⇄ **16** was prepared by adding the above alcohol to FSO_3H or 1:4 FSO_3H–SO_2ClF. Relative to $TMA^+ = \tau$ 6.90, the methyl group of the rapidly equilibrating pair was located at 7.595 (−15 °C), very close to the position in the 1,2-dimethyl-2-norbornyl cation (7.58) and indicating nearly equal populations of **15** and **16**. The methyl peak moved to a lower field, 7.530 at −125 °C but this shift is too small to be significant. The CH_3 of the ethyl group, a triplet, $J = 6.75$ Hz, also moves to lower field, 8.660 at −15 °C to 8.63 at −125 °C, whereas a temperature dependent equilibrium would have suggested an upfield shift at lower temperatures if **16** really were slightly dominant.

The authors would like to thank Dr. C. J. Kim for stimulating suggestions and the National Research Council of Canada for valuable financial support.

1. S. Winstein and D. S. Trifan. J. Am. Chem. Soc. **71**, 2953 (1949).
2. M. Saunders, P. von R. Schleyer, and G. A. Olah. J. Am. Chem. Soc. **86**, 5680 (1964).
3. G. A. Olah, A. M. White, J. R. DeMember, A. Commeyras, and C. Y. Lui. J. Am. Chem. Soc. **92**, 4627 (1970).
4. G. A. Olah, G. Liang, G. D. Mateescu, and J. L. Riemenschneider. J. Am. Chem. Soc. **95**, 8698 (1973).
5. G. A. Olah, G. D. Mateescu, and J. L. Riemenschneider. J. Am. Chem. Soc. **94**, 2530 (1972).
6. G. A. Olah, J. R. DeMember, C. Y. Lui, and R. D. Porter. J. Am. Chem. Soc. **93**, 1442 (1971).
7. G. A. Olah and G. Liang. J. Am. Chem. Soc. **95**, 3794 (1973).
8. R. Haseltine, E. Huang, K. Ranganayakulu, N. Wong, and T. S. Sorensen. Can. J. Chem. This issue.
9. R. Haseltine, K. Ranganayakulu, N. Wong, and T. S. Sorensen. Can. J. Chem. This issue.
10. E. Huang, K. Ranganayakulu, and T. S. Sorensen. J. Am. Chem. Soc. **94**, 1779, 1780 (1972).
11. T. S. Sorensen and K. Ranganayakulu. Tetrahedron Lett. 2447 (1972).
12. M. Saunders and E. L. Hagen. J. Am. Chem. Soc. **90**, 2436 (1968).
13. H. Hogeveen. Recl. Trav. Chim. Pays-Bas, **89**, 74 (1970).
14. G. A. Olah and G. Liang. J. Am. Chem. Soc. **96**, 189 (1974).
15. A. J. Jones, E. Huang, R. Haseltine, and T. S. Sorensen. J. Am. Chem. Soc. **97**, 1133 (1975).
16. A. D. Wolf and D. G. Farnum. J. Am. Chem. Soc. **96**, 5175 (1974).
17. M. Saunders. Acc. Chem. Res. **6**, 53 (1973).
18. (*a*) D. M. Brouwer and J. A. van Doorn. Recl. Trav. Chim. Pays-Bas, **88**, 573 (1969). (*b*) M. Saunders and J. J. Stofko, Jr. J. Am. Chem. Soc. **95**, 252 (1973).
19. G. A. Olah and J. Lukas. J. Am. Chem. Soc. **89**, 2227 (1967); **89**, 4739 (1967).
20. R. Maurel, M. Guisnet, and Garin-Place. Bull. Soc. Chim. Fr. 4112 (1969).
21. R. P. Haseltine and T. S. Sorensen. Can. J. Chem. **53**, 1067 (1975).
22. P. von R. Schleyer. J. Am. Chem. Soc. **80**, 1700 (1958).
23. E. Vogelfanger. Ph.D. Dissertation. University of California. Los Angeles. 1963; Diss. Abstr. **24**, 982 (1963).
24. D. M. Brouwer and H. Hogeveen. Recl. Trav. Chim. Pays-Bas, **89**, 211 (1970).
25. G. D. Sargent. Chem. Rev. **20**, 301 (1966).
26. H. C. Brown. Acc. Chem. Res. **6**, 377 (1973).

Reaction Sequences Involving the Mutual Interconversion of All 10 Tertiary Dimethyl-2-norbornyl Cations. A Comparison of Predicted Products and Rates with Experiment

R. HASELTINE, K. RANGANAYAKULU, N. WONG, AND T. S. SORENSEN

The Department of Chemistry, University of Calgary, Calgary, Alberta T2N 1N4

Received October 31, 1974

R. HASELTINE, K. RANGANAYAKULU, N. WONG, and T. S. SORENSEN. Can. J. Chem. **53**, 1901 (1975).

All 10 tertiary dimethyl-2-norbornyl cations have been prepared. There are sequences of individual steps which will in theory interconvert any given two of these cations, a total of 45 permutations. All of the possible sequences (within a defined limit on the allowable total number of steps) for performing these interconversions were determined using a digital computer. Each step used in the computer generated sequence had previously been assigned a trial activation free energy value and a comparison is made in this paper between the actual experimental rearrangement results (in terms of both the kinetics of disappearance for the cation and what product is in fact formed) and the predicted results.

R. HASELTINE, K. RANGANAYAKULU, N. WONG et T. S. SORENSEN. Can. J. Chem. **53**, 1901 (1975).

On a préparé les dix cations tertiaires diméthylnorbornyl-2. Il y a des séquences d'étapes individuelles qui transformeront en théorie n'importe quelle paire de ces cations et il y a en tout 45 permutations possibles. Toutes les séquences possibles, (à l'intérieur de limites définies pour un nombre total permissible d'étapes) pour effectuer ces transformations ont été déterminées en faisant appel à un ordinateur digital. Pour chaque étape utilisée dans la séquence générée par l'ordinateur, on avait auparavant assigné une valeur d'essai pour l'énergie d'activation et une comparaison est faite dans cet article entre les valeurs expérimentales trouvées pour ces réarrangements (en terme de cinétique de disparition de ces cations et en terme de quel produit est de fait formé) et les résultats qui sont prédits. [Traduit par le journal]

Introduction

In a previous paper (1), a trial set of activation free energy parameters were deduced for all of the low energy rearrangement processes which occur in 2-norbornyl cations, using data from the rearrangements experimentally observed in the parent 2-norbornyl cation, the 2-methyl-2-norbornyl cation, and in several trimethyl and higher methylated analogs. It is now the intention to test the predictive value of these parameters using the rearrangements involved in interconversions among the complete set of tertiary dimethyl-2-norbornyl cations.

Results

There exist 55 (isomeric) dimethyl-2-norbornyl cations, **I**, if one does not differentiate *R* and *S* enantiomers. Of this total, only 10 are tertiary, **II**, *i.e.* one methyl group always at C2.

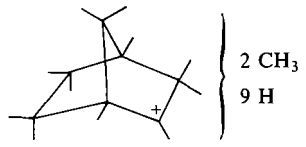

I

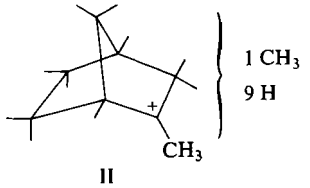

II

However, in constructing a diagram showing the rearrangements possible between any 2 of the 10 tertiary cations, the 45 secondary cation intermediates would have to be shown. Since this becomes extremely messy to depict, we have used an alternative approach, which is a modification

Can. J. Chem. Downloaded from www.nrcresearchpress.com by 210.87.254.5 on 09/05/12
For personal use only.

Can. J. Chem. Downloaded from www.nrcresearchpress.com by 210.87.254.5 on 09/05/12
For personal use only.

of the procedure described recently by Johnson and co-workers (2) and which simply consists of a computer print-out listing the combination of single steps which would bring about any given rearrangement.

Let us say one wishes to find the routes between two tertiary dimethyl-2-norbornyl cations **A** and **D** using a number of individual steps (which each result in certain permutations of the atoms). The first problem consists in delineating the various possible individual rearrangement steps; this was reported in a previous paper (1) and is historically based, of course, on the experimental results of many previous workers. The second problem consists in deciding how many steps one will allow since with 55 nodal points, it is perhaps possible that one could find a loop-free route of 50 steps or more connecting **A** and **D**. Johnson and co-workers (2) have used a weighting factor for each individual step in deciding sequence length but since we have introduced an activation energy for each step, we have simply made an arbitrary cut-off, based largely on the cost of computing time, on the number of steps considered. Any routes which regenerate starting material or in fact any other loops, are redundant and were not printed by the computer. Furthermore, certain rearrangement categories have been excluded in the computerized treatment for reasons discussed previously (1). These include process *4* steps where the two substituents on C1 and C2 are the same and also most of the *endo*-3,2-substituent shifts (process *5*). Besides printing out all the possible sequences, the computer prints out the highest activation energy for each sequence using the set of activation free energy parameters previously deduced (1).

In practice, there turn out to be thousands of predicted routes interconnecting any given tertiary dimethyl-2-norbornyl cation with any other one. When one comes to consider which route may be the one experimentally followed, one finds that one has done the absolute minimum amount of labelling, *i.e.* no isotopic substitution or enantiomeric labelling. The computerized treatment is ideally suited for telling one how many specific labels would be required to yield an unique answer regarding any particular interconversion. As an example, simply using as starting ion a single enantiomer of known absolute configuration and determining the absolute configuration of the product ion (assuming no symmetrical intermediates) would rule out approximately one-half of the computer predicted routes since it can be shown that an even number of steps keeps the same absolute configuration for the cation and an odd number reverses it (2). In solvolysis work, this sort of approach has been elegantly used by Berson *et al.* (3) in studying the much faster and much shorter overall routes involving secondary cation (intermediates) rearrangements.

Our intention is not necessarily to unequivocally decide which particular route experimentally interconnects any given pair of cations (clearly not possible nor could the required work be justified). By assigning activation energies to each step, one will find that the barrier for some routes is much smaller than for others. Therefore, one wishes to see whether the computed route showing the lowest activation energy *correlates* with the *experimentally determined* activation energy for the process.

The overall kinetic equation for multistep reactions is only simplified where one barrier is much larger than any other (a rate-determining step). Where several highest barriers of equal height are predicted, one can readily take this into account in comparing theory and experiment. In the worst cases, where nearly equal barriers might exist, it may be impossible to obtain a meaningful comparison. Such problems will be discussed in each specific case but turn out in practice not to be as bad as one might anticipate.

The activation energy parameters used in the computer print-out are listed in Table 1. Two sets of computations were carried out: (*a*) calculations using only processes *1*, *2*, and *3* (13 steps maximum) and (*b*) calculations using processes *1*, *2*, *3*, and *4* (10 steps maximum). The process 5TT can only be degenerate (corresponding to a loop) in a dimethyl-2-norbornyl cation and therefore never appears in a sequence. The two sets were computed because it is possible to bring about any overall transformation using only the first three processes (2). From this computation, one can see what the shortest sequences excluding a *4* step will be. For each set, one needs a total of 45 separate calculations to obtain all possible interconversions. Fortunately, all of these interconversions are not experimentally measurable since this might have resulted in carbocation solutions containing in the end up to ten different cations. The success of this study,

TABLE 1. Activation energies assigned to the major rearrangement categories

Major rearrangement	Abbreviated symbol used for this operator	Subdivisions considered	Assigned activation energy parameter $\Delta G^{\ddagger}$ (kcal/mol)
Wagner–Meerwein shift	1	1TT	<4
		1TS	<9.5
		1ST	<4 (<9.5)[a]
		1SS	<4 (<9.5)
exo-3,2-Substituent shift	2	2HTT	7.2
		2HTS	15.2
		2HST	9.7 (15.2)
		2HSS	11.4 (16.9)
		2MTT	8.9
		2MTS	13.1
		2MST	7.6 (13.1)
		2MSS	≥7.6 (≥13.1)
endo-6,2-Hydride shift	3	3TT	11.3
		3TS	11.3
		3ST	5.8 (11.3)
		3SS	5.8 (11.3)
Double Wagner–Meerwein shift	4	4TT	18.0
		4SS	12.5 (18.0)
endo-3,2-Substituent shift	5	5HTT	≥14.0

[a]The bracketed values refer to the barrier starting from a tertiary cation energy base and these were used in the computer treatment.

in this regard, was by no means assured at the start and we were extremely lucky in that there were never more than three different observable ions present at any one time in a particular reaction sequence (at least within the limits of experimental detection).

The Thermodynamic Stability of Tertiary Dimethyl-2-norbornyl Cations

The reason that one does not eventually see all 10 cations after all possible interconversions have occurred is that two in particular represent distinct energy minima. The end product of starting with any of the other nine tertiary dimethyl-2-norbornyl cations is the eventual formation of the 1,2-dimethyl isomer. The 2,4-dimethyl isomer however represents a distinct secondary minimum. It appears to be much more stable than any of the other eight remaining cations and indeed at higher temperatures can just be detected in equilibrium with the 1,2-dimethyl isomer, although the latter is considerably more stable. Furthermore, the barrier connecting the 1,2- and 2,4-dimethyl cations is predicted, and is found experimentally (see following), to be higher than any other observed process, *i.e.* the 2,4-dimethyl isomer is in part a minimum because of its thermodynamic stability relative to the eight other cations and partly because it is walled off from the actual true minimum by the highest barrier. The fortuitous end result of this is that if any of the other eight cations can rearrange to the 1,2- or 2,4-dimethyl isomers more easily than to any other in this group, the rearrangement sequence is essentially quenched at that stage (the billiard ball drops). Even so, it is remarkable that the observed sequences never involve more than three cations.

The Overall Rearrangement Sequences

The observed behavior of all 10 tertiary dimethyl-2-norbornyl cations is shown in Fig. 1, where only those interconversions with connecting lines shown could be experimentally measured (or verified). There are two ways in which the trial parameters used in the computed sequences can be checked against experiment: (*a*) One can directly compare the rates of the experimentally observed processes against the computed rate for this process and (*b*) one can verify in a qualitative sense whether the observed product is in fact the one expected, *i.e.* connected by the lowest barrier to the reactant ion. For example, if one experimentally observes the transformation of the 2-*endo*-6-dimethyl isomer into the 1,2-dimethyl isomer, one can compare this rate with

Can. J. Chem. Downloaded from www.nrcresearchpress.com by 210.87.254.5 on 09/05/12
For personal use only.

Can. J. Chem. Downloaded from www.nrcresearchpress.com by 210.87.254.5 on 09/05/12
For personal use only.

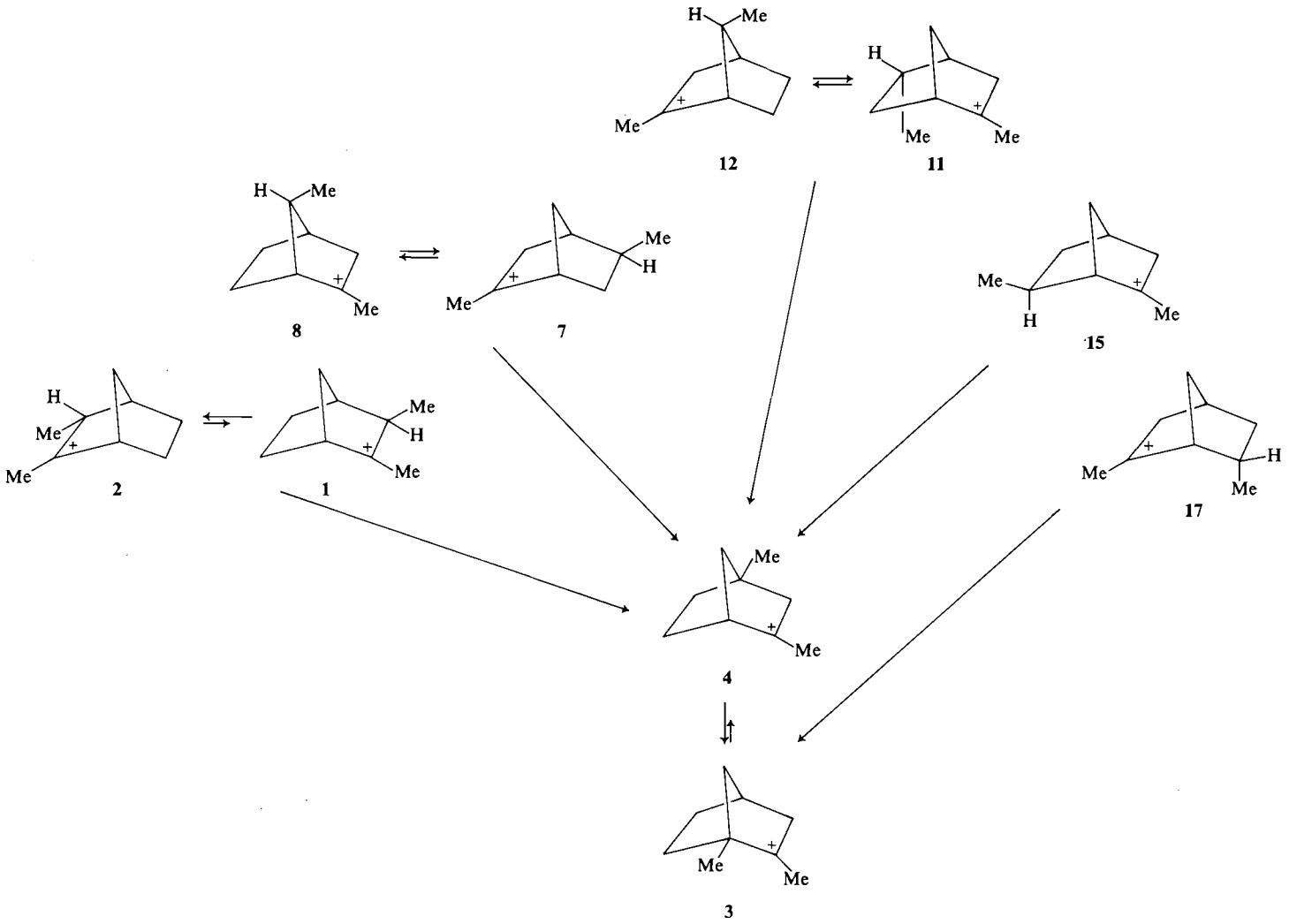

FIG. 1. The 10 possible tertiary dimethyl-2-norbornyl cations. Arrows indicate those conversions or interconversions which could be measured or at least verified.

Can. J. Chem. Downloaded from www.nrcresearchpress.com by 210.87.254.5 on 09/05/12
For personal use only.

the lowest computed rate for this process. Then one can check the computer outputs to see whether there are predicted to be any still lower energy pathways leading from the 2-*endo*-6-dimethyl isomer to any of the other eight.

2-exo-3-Dimethyl-2-norbornyl Cation 1 and 2-endo-3-Dimethyl-2-norbornyl Cation 2

The preparation of these cations has been reported in a previous publication (4). One predicts the 2-*exo*-3-dimethyl **1** and 2-*endo*-3-dimethyl isomer **2** to be interconnected by a three-step sequence 1TS,3SS,1ST with a predicted barrier of 11.3 kcal/mol. The experimentally

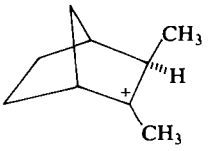

1

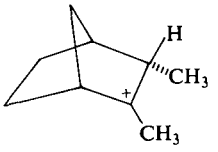

2

observed value, obtained both by n.m.r. line-broadening studies and probably by direct observation, was $\Delta G^{\ddagger} = 11.9$ kcal/mol (for **2** → **1**). The 2-*endo*-3-dimethyl cation **2** undergoes a degenerate *exo*-3,2-hydride shift (2HTT) for which $\Delta G^{\ddagger} = 6.6$ kcal/mol at -117 °C, in good agreement with the trial value for this parameter. The equilibrium constant for **2**/**1** was *ca.* 35 at -44 °C.

What else may be formed from either of these ions? Since they are interconverted by the low energy barrier of only 11.9 kcal/mol, both can be treated together, *i.e.* if another path of say $\Delta G^{\ddagger} = 15$ kcal/mol is somehow predicted for only one of the two, the other will have the same route open but the total sequence will be preceded by the three-step sequence 1TS,3SS,1ST. Unless excluded because of sequence length, this route will show up on the computer output anyhow. Equilibrium energy differences can be added to the kinetic $\Delta G^{\ddagger}$ value. It is obviously impractical to reproduce here the large number of routes interconnecting the cations **1** and **2** with all the others. It is even impractical to reproduce, in most cases, all the "lowest energy" routes. With 3 processes and 13 steps, the highest activation energy barrier mostly involves the 2HSS step (16.9 kcal/mol) or occasionally the 2HTS (or 2HST) step (15.2 kcal/mol). With the addition of process *4*, the only different routes will automatically involve the 18.0 kcal/mol barrier assigned to this. Simply for illustrative purposes, we show just one example of the fact that any one tertiary dimethyl-2-norbornyl cation, in this case **2**, can be rearranged into any one of the other nine. This is depicted in Table 2. Using only the first three processes, the shortest sequence is arbitrarily shown. If there is a still shorter sequence using process *4*, this is also shown. The highest barriers are listed together with the number of times they occur. An overall kinetic equation is very complex if two or more steps are competitive in rate. However, the higher barriers, *i.e.*, 18.0, 16.9, and 15.2 kcal/mol, are reasonably spread out and multiple steps with the same rate simply increase $\Delta G^{\ddagger}$ by the factor $RT \ln 2^{n-1}$, where n = number of like barriers. At the temperatures involved here, this will involve multiples of *ca.* 0.3 kcal/mol.

The sequences listed in Table 2 are illustrative only, since the shortest path need not involve the lowest barrier(s). However, an overall perusal of the computer output shows that one cannot do any better than shown in Table 2 except for the 2-*anti*-7-, 2-*exo*-6-, and 2,4-dimethyl isomers, where one can find single 16.9 barrier routes. If one looks at routes from the 2-*exo*-3-dimethyl isomer **1**, one finds, as expected, that the number and kind of high barriers is the same.

The actual "predicted product" results in the case of **1** and **2** are only marginally interpretable. The experimental result is the formation of the 1,2-dimethyl-2-norbornyl cation **3** with a rate constant, $k = 3 \times 10^{-4}$ s^{-1} at -39 °C, $\Delta G^{\ddagger} = 17.4$ kcal/mol. This is marginally higher than the predicted barrier for **2** → **3** of 16.9 kcal/mol.

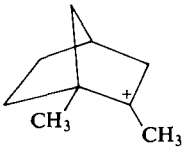

3

Of the routes with this barrier, we prefer the shortest route shown in Table 2. That one should have formed **3** is not so obvious since the predicted barrier to any of the other cations also need involve no more than a single 2HSS step (16.9 kcal/mol). However, the 2-*endo*-6-dimethyl sequences all have **3** formed in the sequence and this route would be excluded. It may be significant in the other cases that all transformations involving a single 2HSS step also require the doubtful 2MSS step *except* for the transformation to **3**. Although the 2MSS barrier (from a tertiary base) is assigned a minimum 13.1 kcal/mol value, one can rationalize an upper

Can. J. Chem. Downloaded from www.nrcresearchpress.com by 210.87.254.5 on 09/05/12
For personal use only.

TABLE 2. Summary of the shortest sequences for **2** giving any of the other nine isomeric cations

Product ion	Reaction sequences involving processes *1*, *2*, and *3*	Shorter alternative sequences involving process *4*	$\Delta G^{\ddagger}$ barrier (kcal/mol)
2-*exo*-3-Dimethyl **1**	1TS,3SS,1ST	—	11.3
2,4-Dimethyl **4**	1TS,3SS,2HSS,1SS,2MSS,3SS,2HSS,3ST	1TS,3SS,4SS,2HST	16.9(twice)
2-*exo*-5-Dimethyl **7**	1TS,2HSS,3SS,1SS,2MSS,3SS,1ST,3TS,2HST[a]	1TS,4SS,3SS,1ST[b]	16.9
2-*endo*-5-Dimethyl **11**	1TS,2HSS,3SS,1SS,2MSS,3SS,1ST	1TS,3SS,4SS,3SS,1ST[c]	16.9
2-*exo*-6-Dimethyl **15**	1TS,2HSS,1SS,3SS,2HSS,1ST	—	16.9(twice)
2-*endo*-6-Dimethyl **17**	1TS,2HSS,1SS,2HST,3TS,1ST	—	16.9
2-*anti*-7-Dimethyl **12**	1TS,3SS,2HSS,1SS,2MSS,3SS,2HSS,3ST,2HTS,1ST	4TT	16.9(twice)
2-*syn*-7-Dimethyl **8**	1TS,3SS,2HSS,1SS,2MSS,1ST	1TS,3SS,4SS,1ST	16.9
1,2-Dimethyl **3**	1TS,2HSS,1SS,2HST	—	16.9

[a]The symbol ↶↷ implies that the operations can be carried out in either order (commute).
[b]The symbol ↙R↘ implies that the operations can be carried out in either order but that a secondary–tertiary designation has to be changed.

value of perhaps 20 kcal/mol. For example, the 2MSS barrier is 11.4 kcal/mol. The 2HTT and 2MTT barriers are 7.2 and 8.9, respectively. Therefore, the 2MSS barrier could be as high as $11.4 \times 8.9/7.2 = 14$ and from a tertiary base $14 + 5.5 = 19.5$ kcal/mol. The lower limit value (13.1) will rarely be even rate determining while the upper limit value would rule out any sequences containing the 2MSS step. We will therefore keep this in mind in the subsequent discussion.

2,4-Dimethyl-2-norbornyl Cation 4

The title cation was prepared from the alcohol **5**, which was in turn obtained by hydride reduction of the ketone **6** (eq. 1). On adding **5** to the

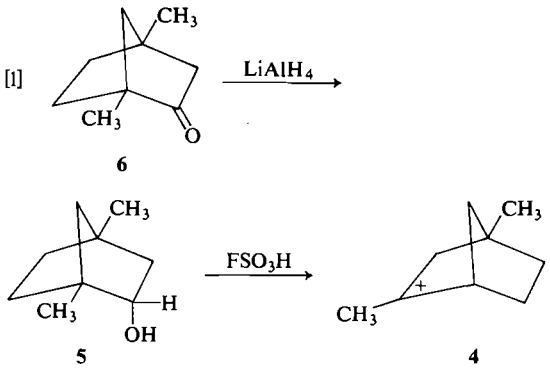

acid, one first obtains the protonated alcohol which solvolyzes at -45 °C to give **4** ($k = ca.\ 1.5 \times 10^{-4}$ s^{-1}). The chemical shifts observed for **4** are reported in Table 3. Two degenerate rearrangement processes can be observed in **4**; the faster is a 1TS,3SS,1ST sequence and the slower is an unknown sequence which interconverts the two methyl groups. The 1TS,3SS,1ST sequence is quantitatively evaluated in another paper (5) and has also been briefly communicated previously (6).

Since the ion **4** is thermodynamically more stable than all others except the 1,2-dimethyl isomer **3**, one can only observe the transformation **4** → **3**. This process is experimentally observed, $k = 1.2 \pm 0.2 \times 10^{-4}$ s^{-1} at -19 °C, $\Delta G^{\ddagger} = 18.9$ kcal/mol. A measurable equilibrium exists at 25 °C between **4** and **3**, $K = \mathbf{3}/\mathbf{4} = 13 \pm 3$, $\Delta G = 1.5 \pm 0.2$ kcal/mol. The lowest calculated barrier for **4** → **3** is $16.9 + 0.3 = 17.2$ kcal/mol (two 2HSS steps) which occurs in numerous routes. However, all are long and the shortest is 3TS,2HSS,3SS,2MSS,3SS,2HSS,3ST. If one avoids the questionable 2MSS step, the best is ten steps, one of two possibilities is

TABLE 3. Summary of observed and calculated activation energy ($\Delta G^{\ddagger}$) barriers for all of the measurable rearrangements

Rearrangement	Observed barrier (kcal/mol)	Calculated barrier (kcal/mol)
2 → **1**	11.9	11.3
2 → **3**	17.4	16.9
4 → **3**	18.9	16.9 + 0.3
7 ⇄ **8**	≤11.0	11.3
7,8 → **4**	12.1	15.2
11 ⇄ **12**	≤11.9	11.3
11,12 → **4**	13.9	15.2 + 0.3
15 → **4**	15.3	15.2 + 0.3 × 4
17 → **3**	≲11.2	11.3

3TS,2HSS,3SS,1ST,3TS,2HSS,1SS,2HST,1TS,3ST. Using a *4* process, there is a shorter path involving 2HTS,4SS,2HSS,1SS,2HST. Looking at the observed rate, we would not rule out the process *4* sequence nor can one really rule out the 10 step sequence involving two 2HSS barriers. In any case, since the barrier is nearly 2 kcal/mol higher than predicted for the two 2HSS barriers we would tentatively conclude that our trial parameter for the 2HSS process may be too low.

2-exo-5-Dimethyl-2-norbornyl Cation 7 and 2-anti-7-Dimethyl-2-norbornyl Cation 8

There is predicted to be a low energy barrier, 1TS,3SS,1ST, $\Delta G^{\ddagger} = 11.3$ kcal/mol, separating **7** and **8**. Experimentally, this is found to be the case. Cation solutions prepared from the chloride(s) of alcohol **9**, which should yield **7**, or from chlorides of the alcohol **10**, which should yield **8**, have identical n.m.r. spectra. The synthetic sequences start from known ketones and are shown in eq. 2. There are slight differences in the proton chemical shifts observed for **7** and **8** (listed in Table 3) so that one can clearly establish that two ions are present; however, it is not possible to assign which peaks are due to which particular ion. The equilibrium (close to unity) is established within 0.5 h at -120 °C (the Cl protons in **7** and **8** are separated enough so that one can clearly see both **7** and **8** at this temperature). One can estimate that the interconversion **7** ⇄ **8** must have a rate constant of greater than *ca.* 1×10^{-3} s^{-1} at -120 °C, $\Delta G^{\ddagger} \lesssim 11.0$ kcal/mol, in agreement with the predicted barrier. Since all other barriers for **7** and **8** to rearrange to anything else involve energies of 15.2 or 16.9 kcal/mol, one can treat the two

Can. J. Chem. Downloaded from www.nrcresearchpress.com by 210.87.254.5 on 09/05/12
For personal use only.

[2] 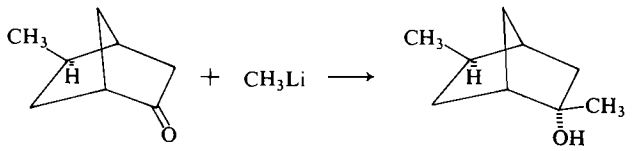

9

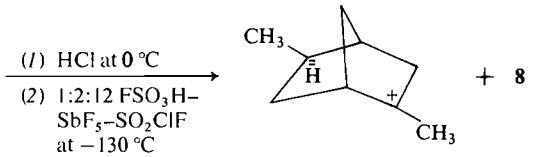

7

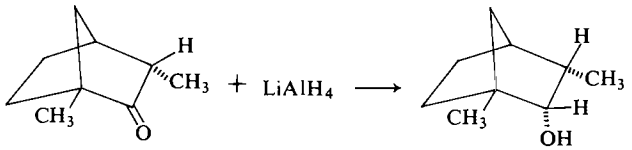

10

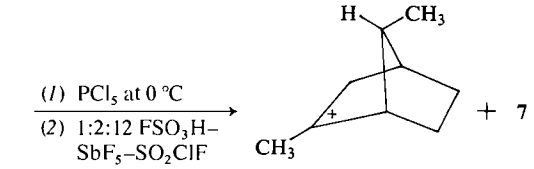

8

together (as was done with the two 3-methyl isomers).

Experimentally, **7** and **8** rearrange to the 2,4-dimethyl-2-norbornyl cation very rapidly, $k_{combined} = 1.35 \pm 0.5 \times 10^{-4}$ s^{-1} at -111 °C, $\Delta G^{\ddagger} = 12.1 \pm 0.1$ kcal/mol. Rather than looking at all possible interconversions, we will simply compare the barriers for these ions giving either the 1,2- or 2,4-dimethyl isomers. The shortest path to the 2,4-dimethyl isomer is from **8**, a two-step 1TS,2HST sequence involving a calculated 15.2 kcal/mol barrier. The shortest path to the 1,2-dimethyl isomer is again from **8** and involves the sequence 4TT,1TS,2HSS,1SS, 2HST, with a calculated high barrier of 18.0 kcal/mol. One can avoid this process *4* barrier by a number of much longer routes, the shortest being eight steps from **7**, 2HTS,3ST,1TS,3SS, 2MSS,3SS,2HSS,3ST, and a 16.9 kcal/mol barrier. Whichever one considers, the route to the 2,4-dimethyl isomer is clearly predicted but the predicted barrier is over 3 kcal/mol too high.

2-endo-5-Dimethyl-2-norbornyl Cation 11 and 2-syn-7-Dimethyl-2-norbornyl Cation 12

This pair are also predicted to be separated by the 11.3 kcal/mol barrier for the 1TS,3SS,1ST sequence and experimentally this is found to be the case. Cation solutions prepared from the chloride(s) of alcohol **13**, which should yield **11** or from chloride(s) of the alcohol **14**, which should yield **12**, have identical spectra. The synthetic sequences start from known ketones and are shown in eq. 3. The n.m.r. peaks of **11** and **12** overlap more than in the case of **7** and **8** and one has to warm the solution to -110 °C before the resolution is sufficiently good to be able to see two sets of 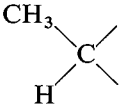 peaks. At still higher temperatures, the ratio of these does not change and therefore an equilibrium concentration of **11** and **12** has been established. It is not possible to assign the observed n.m.r. peaks to a given isomer, **11** or **12**, but in any case, the equilibrium

Can. J. Chem. Downloaded from www.nrcresearchpress.com by 210.87.254.5 on 09/05/12
For personal use only.

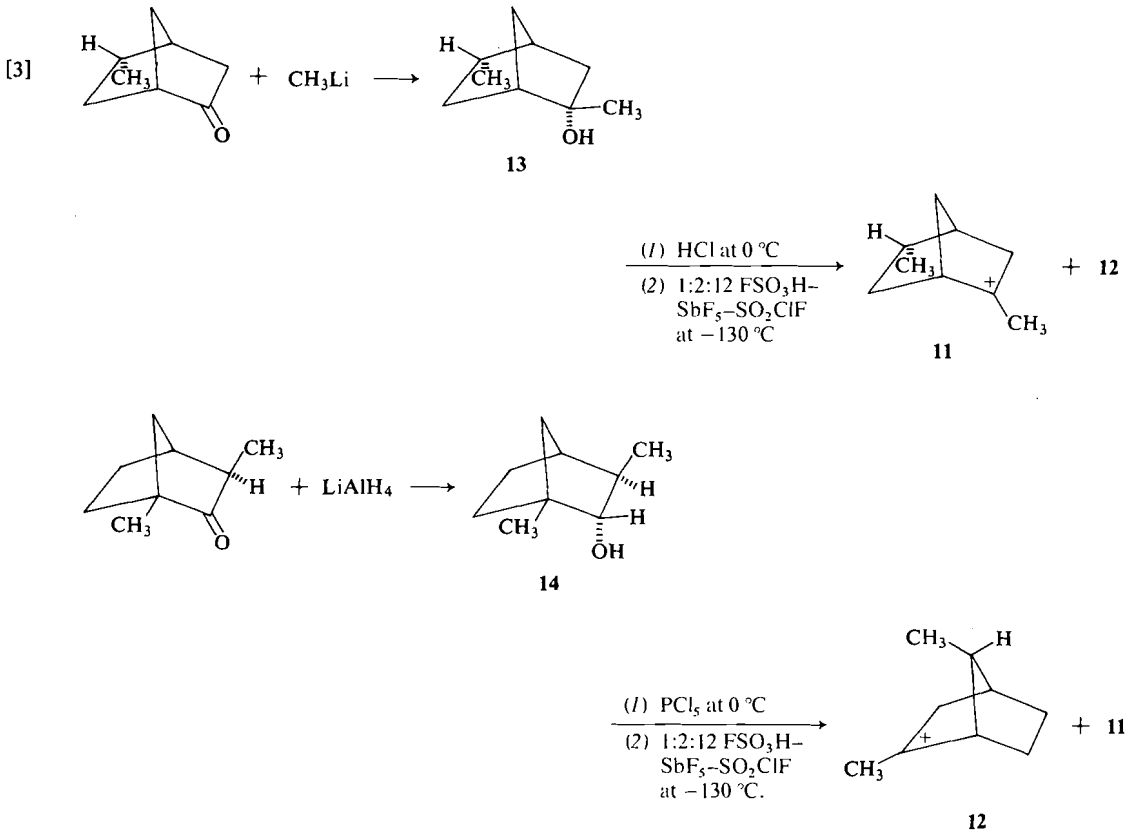

constant is near unity. The chemical shifts are listed in Table 3. One can estimate that the interconversion rate must be larger than 5×10^{-4} s^{-1} at -110 °C, $\Delta G^{\ddagger} \gtrsim 11.9$ kcal/mol, in agreement with the calculated 11.3 kcal/mol. Since all other barriers involve values of 16.9 or 15.2 kcal/mol, one can again treat the two ions together.

Experimentally, cations **11** and **12** rearrange to the 2,4-dimethyl isomers **4** with a combined rate of $4.8 \pm 0.15 \times 10^{-4}$ s^{-1} at -83 °C, $\Delta G^{\ddagger} = 13.9$ kcal/mol. Once again, we will simply look at the barriers for these ions giving either **4** or the 1,2-dimethyl isomer **3**. The shortest sequence for giving **4** starts from **11** and involves 1TS,2HSS,3ST and a barrier of 16.9 kcal/mol. The shortest sequence giving the 1,2-dimethyl isomer **3** is five steps from **12**, 1TS, 2MSS,3SS,2HSS,3ST, and once again a barrier of 16.9 kcal/mol. There are four 15.2 kcal/mol barrier routes to **3** but all involve the questionable 2MSS step.

The actual route to the 2,4-dimethyl isomer **4** is predicted to *not* be the shortest sequence in this case but to involve, starting from **11**, the sequence 3TS,2HST,1TS,3SS,2HST, with two barriers of 15.2 kcal/mol. This sequence yields the 2-*exo*-5-dimethyl cation **7** after only two steps and then follows the same route to **4** as does **7**. Experimentally, the overall barrier is about 1 kcal/mol smaller than predicted. The rate-determining step must be the first 2HST step since experimentally the 2-*exo*-5-dimethyl cation **7** rearranges to **4** even faster than **11**–**12**.

2-exo-6-Dimethyl-2-norbornyl Cation 15

Carbocation **15** was prepared according to the sequence shown in eq. 4, starting from a known ketone. On addition of the alcohol **16** to the acid, one initially obtains the protonated alcohol and on warming, this gradually solvolyzes to **15**. Cation **15** undergoes a rapid, degenerate *endo*-6,2-hydride shift (see following paper) (5) which is not of interest here except that it gives one

Can. J. Chem. Downloaded from www.nrcresearchpress.com by 210.87.254.5 on 09/05/12
For personal use only.

[4] 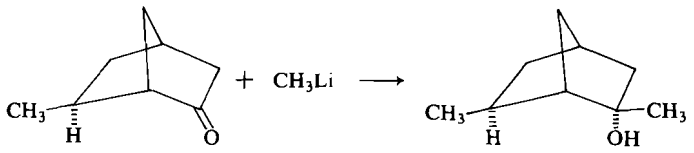

16

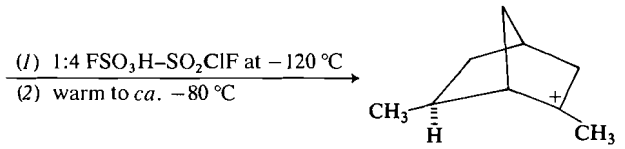

15

a definite value for the 3TT process, $\Delta G^{\ddagger} = 7.2$ kcal/mol. This had been only estimated previously as <11.3 kcal/mol.

Experimentally, cation **15** is found to rearrange to the 2,4-dimethyl isomer **4**, $k = 1.3 \pm 0.05 \times 10^{-4}$ s^{-1} at -57 °C, $\Delta G^{\ddagger} = 15.3$ kcal/mol.[1] As before, we will check to see what the predicted product would be by looking at the calculated barrier for **15** giving either the 2,4-dimethyl isomer **4** or the 1,2-dimethyl isomer **3**. The shortest sequence giving the 1,2-dimethyl isomer is three steps involving 4TT,1TS,3ST. There is, however, a sequence bypassing process *4* involving only four steps, 1TS,2HSS,3SS, 2HST, with a calculated 16.9 kcal/mol barrier. There are in fact four sequences for **15** → **3** which involve the 15.2 kcal/mol barrier (three of these barriers) but all require the doubtful 2MSS step. The shortest sequence from **15** to **4** and involving the lowest calculated barrier is the seven-step sequence 2HTS,3SS,2MSS,1SS, 3ST,1TS,2HST with two 15.2 kcal/mol barriers. Avoiding the questionable 2MSS step, one finds that there are only two sequences involving 15.2 kcal/mol barriers, both 12 steps. They actually differ only in the fifth, sixth, and seventh steps, involving 3TS,1SS,2HST in one case and 1TS,3SS,1ST in the other. The preferred sequence is (2HTS,1SS,3SS,2HST)(1TS,3SS,1ST) (3TS,2HST)(1TS,3SS,2HST). (For convenience, parentheses have been added to enclose sequences leading from one tertiary ion to another.) The sequence converts the 2-*exo*-6-dimethyl ion **15** first to the 2-*syn*-7-dimethyl isomer **12**, then to the 2-*endo*-5-dimethyl **11**, to the 2-*exo*-5-dimethyl isomer **7**, and finally to **4**. There is excellent experimental support for this sequence since we already know that the rate from the 2-*syn*-7-dimethyl isomer **12** to **4** is faster than the experimental barrier from **15**, *i.e.* the barrier involves the first five-step sequence. This involves two 2HTS steps, 15.2 + 0.3 = 15.5 kcal/mol, in good agreement with the observed 15.3 kcal/mol.

This case neatly points out the tremendous advantages of having activation energy parameters assigned to the individual steps. Without these, one might have been tempted incorrectly to predict as product the 1,2-dimethyl isomer with the short, five-step, 16.9 kcal/mol barrier. The activation energies are also indispensible in sorting out the large number of predicted routes for a given interconversion. What we believe to be the correct sequence (above) for **15** → **4** is actually well "buried" in the computer output, *i.e.* without considering barriers and using only the "three process" routes, there are 2 7-step sequences, 4 of 8 steps, 2 of 9 steps, 5 of 10 steps, 5 of 11 steps, 13 of 12 steps, and 17 of 13 steps.

2-endo-6-Dimethyl-2-norbornyl Cation 17

Carbocation **17** was not directly observed, as in fact expected. The sequence which should have generated cation **17** is shown in eq. 5, starting from a known ketone. Addition of the alcohol **18** to FSO_3H–SO_2ClF (1:4) at -130 °C yields predominantly the protonated alcohol and some **3**. The protonated alcohol solvolyzes fairly rapidly and has disappeared within 0.5 h at -90 °C. Carbocation **3** is the only observed product. Addition of the chloride at -129 °C to SbF_5–FSO_3H–SO_2ClF and running the n.m.r. spectrum at -120 °C shows only the cation **3**. The rate constant for **17** → **3** can be conservatively estimated as $> 5 \times 10^{-4}$ s^{-1} at -120 °C,

[1] At -60 °C, there appears to be an equilibrium, where $K = ca.$ 65 for **4**/**15**.

Can. J. Chem. Downloaded from www.nrcresearchpress.com by 210.87.254.5 on 09/05/12
For personal use only.

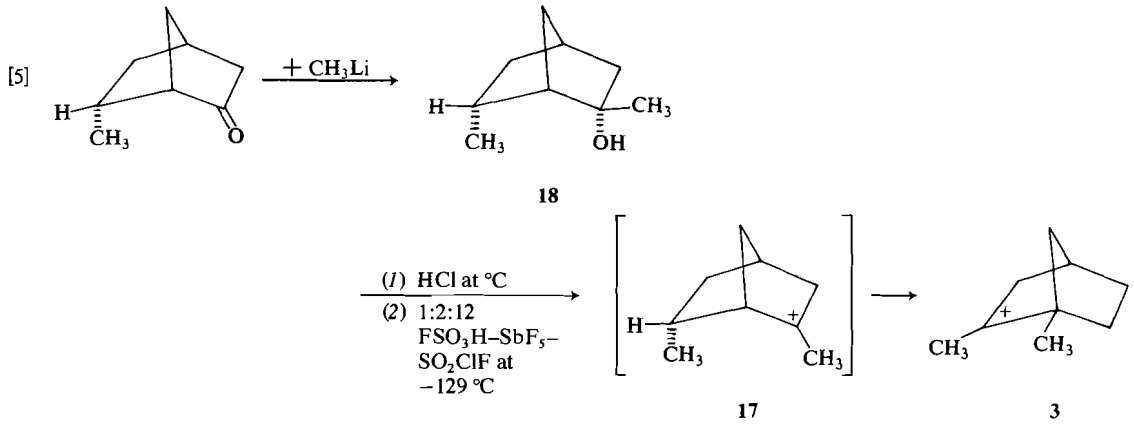

$\Delta G^{\neq} \lesssim 11.2$ kcal/mol. The predicted lowest barrier for **17** to rearrange to anything else is the 1TS,3ST sequence leading to **3**, with a predicted barrier of 11.3 kcal/mol.

Discussion

The use of a computer to enable one to look at all of the allowed paths (up to at least a predetermined number of steps) in a sense shows one too much. It would be gratifying to have one clearcut path which could be safely separated from the less likely ones. In fact, this probably occurs in pencil and paper type elucidations of the overall transformations since the writer may have a bias toward certain steps and will almost certainly be biased toward the shorter sequences. It is completely unmanageable to work out many of the numerous multistep sequences by hand.

In looking at the success of the trial parameters, which is the real point of this work, the critical ones are the highest barriers. Numerical errors in the low barriers will not affect the calculated overall rate of a process involving at some point a much higher barrier. In practice, the three critical values for the "three process" sequences are for 2HST (or 2HTS), 2HSS, and 2MSS. A comparison of calculated and observed behavior for all of the rearrangements are summarized in Table 3 and a perusal of this shows that some sizeable $\Delta G^{\neq}$ deviations exist. We believe at this time that the major error factor is probably a thermodynamic one, due to a neglect of the "special" effect of a C1 methyl group, *i.e.* just as we have clearly separated the secondary C2 H and tertiary C2 CH_3 cations, we should probably take into account the increased stability of a secondary *or* tertiary cation resulting from a C1 methyl *vs.* hydrogen substitution. To make this distinction in the computerized treatment of activation energies seems too restrictive; there is already enough subdivision of steps for a general treatment. Such subtle thermodynamic factors are relevant to questions about the molecular structure of 2-norbornyl cations and this point is explored in an accompanying paper (5). Basically, the results of this analysis suggest that the 2HSS value used in this work (16.9) is appropriate only to a C1 methyl-substituted secondary ion and that the 2HTS value of 15.2 is only appropriate to a C1 hydrogen-substituted secondary ion. Consideration of this brings both the **4** → **3** and **7,8** → **4** barriers closer to the experimental values. Furthermore, we can better rationalize our overall observations by assuming a 2MSS value near our previously derived upper limit so that sequences involving this barrier are discounted.

We have been rather surprised in this work to note the large thermodynamic ground state energy differences between some of the dimethyl cations, *i.e.* **1** and **2** or **4** and **15**. This complicates the use of trial activation energy parameters and suggests that one should be cautious about trying to make too fine a comparison between calculated and experimental rates. We implicitly recognize this in the transformations of **7** and **8** to **4**, or **11** and **12** to **4**, where we have not evaluated the few tenths of a kcal/mol associated with the fact that the concentration of the reactive member of the pair has less than unit concentration. Similar small effects were

Can. J. Chem. Downloaded from www.nrcresearchpress.com by 210.87.254.5 on 09/05/12
For personal use only.

Can. J. Chem. Downloaded from www.nrcresearchpress.com by 210.87.254.5 on 09/05/12
For personal use only.

TABLE 4. Chemical shift values[a]

Ion	Positions										
	1	2(CH_3)	3-*exo*	3-*endo*	4	5-*exo*	5-*endo*	6-*exo*	6-*endo*	7-*syn*	7-*anti*
1	*ca.*5.0[b]	6.9	—[c]	—	—	—	—	6.3	—	—	—
2	*ca.*5.1[b]	*ca.*7.0 (7.70)[d]	7.10	*ca.*8.5 (CH_3)	*ca.*7.1[e]	(7.31)[f]	(8.46)[f]	(7.31)[f]	(8.46)[f]	8.13[g]	7.99[g]
3[h]	(7.58) (CH_3)	(7.58)	(7.63)[j]	(7.49)[j]	7.07	(8.37)[k]	(8.37)[k]	(7.15)[l]	(7.15)[l]	(7.49)[j]	(7.63)[j]
4	5.11[m]	6.76	6.94[n]	7.13[n]	8.51 (CH_3)	8–8.5	8–8.5	6.32	8–8.5	8.05	8.05
7	5.33[p] or *ca.*5.14[q]	6.70	—[r]	—	7.15?	8.73[b] (CH_3)	—	6.3	—	—	—
8	*ca.*5.14[q] or 5.33[p]	6.70	—	—	7.15?	—	—	6.3	—	—	8.73[b] (CH_3)
11	5.18[s]	6.73	—	—	—	—	8.94[t] or 8.99[t]	6.08–6.41[u]	—	—	—
12	5.18[s]	6.73	—	—	—	—	—	6.08–6.41[u]	—	8.94[t] or 8.99[t]	—
17	5.44	6.64 (7.44)	(7.72 or 7.62)[v]	(7.72 or 7.62)[v]	6.92	(7.72 or 7.62)[v]	(7.72 or 7.62)[v]	8.24[h] (CH_3) (7.44)	8.02[w]	(7.86)	(7.86)

[a]Relative to tetramethylammonium cation (TMA^+) = τ 6.90.
[b]These values have been obtained at extremely low temperatures and are poorly resolved. There is also some evidence that chemical shifts change slightly with temperature.
[c]The assignments for **1** are somewhat tentative. Complete assignments were not made because the higher field region is obscured by cation **2** peaks.
[d]Values in parentheses represent averaged chemical shifts caused by a particular rearrangement (see text for these).
[e]Obtained by interpolation, knowing an averaged value and one of the "frozen out" peak values (see, however, [b]).
[f]A doublet, $J_{average} = 11$.
[g]An AB quartet, $J = 11$.
[h]The spectrum of **3** has been published (14) but several small peaks have been chopped off. Above 25 °C, this cation undergoes a second degenerate rearrangement shown from DISST experiments to be identical to the second degenerate rearrangement occurring in the 2-methyl-2-norbornyl cation (1).
[j]A 2(AB) quartet, $J = 15$.
[k]Triplet, $J = 6$.
[l]Poorly resolved triplet, $J = 6$.
[m]Doublet, $J = 6.5$.
[n]This assignment may be reversed.
[p]Doublet, $J = 5$.
[q]Partially obscured by HI of **4**.
[r]Assignments for **7** ⇄ **8** and **11** ⇄ **12** are incomplete because with two ions present, one has a very complex spectrum in the 7.5–8.5 region.
[s]Doublet, $J = 7$.
[t]Doublet, $J = 6.5$.
[u]Curiously shaped with two humps on the ends and nearly flat between these.
[v]The two peaks are not equal and are somewhat broad, possibly part of an AB quartet.
[w]This peak is broad and the assignment is somewhat uncertain.

Can. J. Chem. Downloaded from www.nrcresearchpress.com by 210.87.254.5 on 09/05/12
For personal use only.

also ignored, in general, in deriving the trial activation energy parameters.

In closing, perhaps the most valuable aspect of this study is to show how incredibly fast are many of these long rearrangement sequences. We have recently studied a pentamethyl-2-norbornyl cation rearrangement occuring at −40 °C where 15 steps (three processes) were needed to produce a single predicted sequence.

Experimental

Product purity was determined in each case by i.r., g.l.c., and n.m.r. Cation n.m.r. chemical shifts are reported relative to $TMA^+ = \tau$ 6.90 and were obtained on a Varian Associates HA-100.

1,4-Dimethylbicyclo[2.2.1]heptan-endo-2-ol **5**

Small quantities of the g.l.c. pure ketone, 1,4-dimethylbicyclo[2.2.1]heptan-2-one (**6**) were available from the ozonolysis of a 2-exomethylene hydrocarbon related to **6** (1). Reduction of this with lithium aluminum hydride gave the corresponding alcohol, which almost certainly has mainly the *endo* configuration; n.m.r. (CCl_4), 8.935 and 8.950 (both 3H, the C1 and C4 methyl groups), 6.155 and 6.250, (d, J = 10.5, each peak is further split into a doublet of doublets, J = 3.5 and 1.5, the C2 proton). Addition of the alcohol to FSO_3H or 1:4 FSO_3H–SO_2ClF at −80 °C yields only the protonated alcohol, peaks at 8.84 and 8.72 (3H each, the C1 and C4 methyl groups), 4.87 (d, J = 9, the C2 proton). Solvolysis becomes fairly rapid about −45 °C to yield the pure cation **4**. Secondary 2-norbornyl alcohols with an *exo* configuration cleave much more readily (7).

2-exo-5-Dimethylbicyclo[2.2.1]heptan-2-ol **9**

A commercial mixture of *exo*-5- and *endo*-5-methylbicyclo[2.2.1]hept-2-ene was converted to a mixture of the *exo*-5-, *endo*-5-, *exo*-6-, and *endo*-6-methylbicyclo-[2.2.1]heptan-2-ones using a literature procedure (8). Using a 20 ft × 3/8 in. column of 30% Carbowax 20M, it was possible to separate preparatively, without difficulty, the *endo*-6- and *endo*-5-methyl ketones, the shortest and longest retention peaks, respectively. Just the opposite g.l.c. behavior is reported (8) and the assignments in this paper may be in error. The *exo*-6- and the *exo*-5-methyl ketones have very similar retention times, the former marginally shorter. By cutting the longer retention side of the combined peak twice it was possible to obtain a sample of the *exo*-5-methyl ketone which was pure enough for our purposes (the same cations, **7** and **8**, in a pure form, are obtained from alcohol **10** and the *exo*-6-methyl cation impurity also produced from the impure **9** does not interfere with either our characterization of cations **7** and **8**, nor with the measurement of their rate of rearrangement). The split methyl peak in all four ketones is at a different chemical shift, in CCl_4, *endo*-6-methyl, τ 9.02; *exo*-5-methyl, 8.91; *exo*-6-methyl, 8.92; *endo*-5-methyl, 8.96; and based on this, the ketone fraction was about 75% *exo*-5-methyl and 25% *exo*-6-methyl. The pure *exo*-6-methyl ketone can be obtained by another route. The *exo*-5-methyl ketone (75.6 mg, 0.61 mmol) was treated with 1.2 mmol of methyl lithium in ether to yield 47.9 mg of alcohol. This was stirred with 1 ml of concentrated HCl at 0 °C for 30 min, the cold solution extracted with pentane, and the pentane dried and neutralized with anhydrous K_2CO_3. After pentane removal, the chloride residue (no —OH in i.r.) was used directly. From Berson's results (3), the alcohol–chloride transformation should proceed without appreciable rearrangement involving 6,2-hydride shifts.

1-exo-3-Dimethylbicyclo[2.2.1]heptan-2-ol **10**

The ketone, 1-*exo*-3-dimethylbicyclo[2.2.1]heptan-2-one, was prepared as previously described. The ketone (186.3 mg, 1.35 mmol) in 2 ml of ether was added dropwise to a solution of lithium aluminum hydride (102 mg) in 10 ml of ether. On work-up, 172.5 mg of alcohol **10** was obtained as a liquid at 25 °C; n.m.r. (CCl_4), τ 9.18 (d, J = 6.5, 3H, the C3 methyl), 8.945 (3H, the Cl methyl), 6.43 (d, J = 10, 1H, each peak is further split into a doublet, J = 1.5, the C2 proton). Judging from the n.m.r. spectrum, the alcohol is essentially a single isomer at C2, almost certainly the *endo*-2 alcohol. Using the phosphorus pentachloride – pentane procedure of Brown *et al.* (9), the alcohol was converted to the chloride, which is likely a mixture of the secondary and tertiary chlorides (*cf.* α-fenchol result (10) indicating that no 6,2-hydride shift is expected under these conditions).

2-endo-5-Dimethylbicyclo[2.2.1]heptan-2-ol **13**

The alcohol **13** was prepared as described for **9**. From 210 mg, 1.5 mmol, of ketone there was obtained 193 mg of **13** as a solid, m.p. 28–30 °C; n.m.r. (CCl_4), 9.02 (d, J = 6.5, 3H, the *endo*-5 methyl group), 8.78 (3H, the C2 methyl group).

Anal. Calcd. for $C_9H_{16}O$: C, 77.08; H, 11.5. Found: C, 77.02; H, 11.4.

Judging from the n.m.r. spectrum, the alcohol is mainly a single isomer at C2, almost certainly the *endo* alcohol. The alcohol was converted to the chloride (i.r.) by the same procedure described for **9**.

1-endo-3-Dimethylbicyclo[2.2.1]heptan-2-ol **14**

This alcohol was prepared by the same procedure used to prepare alcohol **10**, starting with the *endo*-3-methyl ketone (1). The alcohol has been reported (11). From g.l.c. and n.m.r., the alcohol is a mixture of the *exo*-2 and *endo*-2 alcohols. The major isomer (a solid) can be isolated by preparative g.l.c. The alcohol was converted to the chlorides by the same procedure described for **10**.

2-exo-6-Dimethylbicyclo[2.2.1]heptan-2-ol **16**

The ketone, *exo*-6-methylbicyclo[2.2.1]heptan-2-one was obtained using a procedure partially described by Beckmann *et al.* (12), starting with *exo*-2-methylbicyclo-[2.2.1]heptan-2-ol, converting this to the *endo*-2-methyl alcohol, heating this with formic acid and then saponifying. At this stage, the crude alcohol was oxidized with Jones' reagent to give a crude ketone mixture consisting mainly, as expected, of the 1-methyl ketone together with about 15% of the *exo*-6-methyl ketone and small amounts of others. Spinning band distillation (Nestor Faust Autoannular 30 in. column) at 14 mm effected the separation of most of the 1-methyl ketone, b.p. 57–58 °C. From the residue, a fraction consisting mainly of the *exo*-6-methyl ketone was separated by preparative g.l.c. (see **9**). This was further purified through the crystalline semicarbazone and hydrolysis of this in aqueous oxalic acid. The alcohol **14** was prepared as for **9** and after sublimation had

Can. J. Chem. Downloaded from www.nrcresearchpress.com by 210.87.254.5 on 09/05/12
For personal use only.

m.p. 38–41 °C; n.m.r. (CCl_4), τ 9.13 (d, J = 7, 3H, the *exo*-6-methyl peak), 8.79 (3H, the C2 methyl peak). The alcohol appears to be, from n.m.r. and g.l.c., a single isomer at C2, in all probability, the *endo* alcohol.

Anal. Calcd. for $C_9H_{16}O$: C, 77.08; H, 11.5. Found: C, 76.85; H, 11.98.

2-endo-6-Dimethylbicyclo[2.2.1]heptan-2-ol ***18***

The alcohol **18** was prepared as described for **9**. From 270 mg, 1.93 mmol, of the ketone, there was obtained 260 mg of alcohol, which after sublimation had a m.p. of 56–59 °C; n.m.r. (CCl_4), τ 8.77 (d, J *ca.* 6.5, 3H, the *endo*-6 methyl), 8.79 (3H, the C2 methyl). Judging from the g.l.c. and n.m.r. evidence, the alcohol is a single isomer at C2, in all probability the *endo* alcohol.

Anal. Calcd. for $C_9H_{16}O$: C, 77.08; H, 11.5. Found: C, 76.07; H, 11.2.

The alcohol was converted to the chloride (i.r.) by the same procedure described for **9**.

Rate Measurements

The preparation of the cations followed previously described procedures (13). The particular solvent system used is given under Results. Chemical shifts are given in Table 4. Plots involved a standard first-order kinetic treatment and were subject to standard least-squares analysis. The error limits represent the 90% confidence level. A given rate was run from two to five times. In the case of the lower temperatures, it was not possible to duplicate the exact temperature each time. In these cases, the best fit line is reported and the corresponding $\Delta G^{\ddagger}$ values for all runs are averaged and the deviation reported. A thermocouple was inserted directly into the n.m.r. tube and a temperature reading accompanied each time reading. The temperatures over a complete run were averaged. The specific procedures followed in each case were as follows.

Cation ***4*** → *Cation* ***3:*** (peak height of coalesced C1—C2 methyls of **3**)/2 (*a*) + C4 methyl peak height of **4** (*b*) = constant peak height (*c*). Plotted increase of (*a*)/(*c*) with time. The half-widths of (*a*) and (*b*) are nearly identical at the temperatures involved here.

Cation ***2*** → *Cation* ***3:*** followed increased peak height of coalesced C1—C2 methyls of **3** with time. The peak was standardized against a reference TMA^+ peak height.

Cations ***7*** ⇄ ***8*** → ***4:*** at the low temperatures involved, the H1 proton region shows two broad multiplet peaks. The lower field belongs to either **7** or **8** and **4**. The higher field one belongs to only one ion, either **8** or **7**. The total area of H1 protons was determined by tracing, cutting, and weighing and taken as constant. The rate was determined by plotting the decrease in the higher field H1 peak area (standardized) with time.

Cations ***11*** ⇄ ***12*** → *Cation* ***4:*** followed increased peak area of C4 methyl of **4** with time. The peak area was standardized against a reference TMA^+ peak area.

Cation ***15*** → *Cation* ***4:*** peak area of coalesced (C2—C6 methyl of **15**)/2 (*d*) + area of C4 methyl of **4** (*e*) = constant peak area (*f*). Plotted increase of (*e*)/(*f*) with time using the appropriate form of a first-order rate expression.

Program Transform

The purpose of the program is to find all possible pathways of getting from one norbornyl cation to another in N steps or less and with K different processes. A reaction sequence is represented by an integer with N digits with each digit representing a certain process and the arrangement of the digits representing the order in which they are performed. An integer is generated and the transformations are carried out, checking after each transformation to see if the product was formed. If it has been formed, then further checks are made to eliminate sequences which contain internal cycles and if the overall transformation requires less than N steps, a check is performed to eliminate identical sequences which were found previously. Finally, the sequence is printed along with complementary information concerning the nature of the intermediates, *i.e.* tertiary or secondary ions, and the energy barriers which the sequence must hurdle. The integer is incremented by one unit and the process starts over. The principle advantage of this over the elegant procedure of Johnson and co-worker (2) is that only a very limited amount of central memory is required, although our program does not execute as fast and never generates or contains the information necessary to construct a complete graph.

The authors thank the National Research Council of Canada for generous financial support and Drs. C. Collins and C. Johnson for preprints of their papers.

1. R. Haseltine, E. Huang, K. Ranganayakulu, T. S. Sorensen, and N. Wong. Can. J. Chem. This issue.
2. C. K. Johnson and C. J. Collins. J. Am. Chem. Soc. **96**, 2514 (1974); C. J. Collins, C. K. Johnson, and V. F. Raaen. J. Am. Chem. Soc. **96**, 2524 (1974).
3. J. A. Berson, R. G. Bergman, J. H. Hammons, and A. W. McRowe. J. Am. Chem. Soc. **89**, 2581 (1967).
4. A. J. Jones, E. Huang, R. Haseltine, and T. S. Sorensen, J. Am. Chem. Soc. In press.
5. R. Haseltine, N. Wong, T. S. Sorensen, and A. J. Jones. Can. J. Chem. This issue.
6. E. Huang, K. Ranganayakulu, and T. S. Sorensen. J. Am. Chem. Soc. **94**, 1780 (1972).
7. R. Haseltine, E. Huang, K. Ranganayakulu, and T. S. Sorensen. Can. J. Chem. **53**, 1056 (1975).
8. J. B. Grutzner, M. Jautelat, J. B. Dence, R. A. Smith, and J. D. Roberts. J. Am. Chem. Soc. **92**, 7107 (1970).
9. H. C. Brown, J. H. Kawakami, and S. Misumi. J. Org. Chem. **35**, 1360 (1970).
10. C. A. Bunton and T. W. Del Pesco. Org. Mass Spectros. **2**, 81 (1969).
11. S. Beckmann and R. Mezger. Chem. Ber. **90**, 1564 (1957).
12. S. Beckmann, G. Eder, and H. Geiger. Chem. Ber. **102**, 815 (1969).
13. P. H. Campbell, N. W. K. Chiu, K. Deugau, I. J. Miller, and T. S. Sorensen. J. Am. Chem. Soc. **91**, 6404 (1969).
14. G. A. Olah, J. R. DeMember, C. Y. Lui, and R. D. Porter. J. Am. Chem. Soc. **93**, 1442 (1971).

The Role of Excess Kinetic Energy in the Reactions of $O(^1D)$ Atoms [1,2]

RALPH OVEREND, GEORGE PARASKEVOPOULOS[3], JANICE R. CRAWFORD,[4] AND H. ALAN WIEBE[5]

Division of Chemistry, National Research Council of Canada, Ottawa, Canada K1A 0R9

Received February 10, 1975

RALPH OVEREND, GEORGE PARASKEVOPOULOS, JANICE R. CRAWFORD, and H. ALAN WIEBE. Can. J. Chem. **53**, 1915 (1975).

The effect of the excess kinetic energy of $O(^1D)$ atoms on their reactions with some gaseous compounds was investigated using two different experimental methods. $O(^1D)$ atoms with maximum excess kinetic energies of 41 ± 5 and 31 kcal/mol respectively, were produced by flash photolysis of N_2O (1800–2300 Å) and by photolysis of N_2O at 2139 Å, in the presence and absence of He which is a deactivator of kinetic energy. In the first method the competition between N_2O and one of CO_2, Xe, CO, and N_2 for $O(^1D)$ atoms was measured and it was found that the relative rate constants k_{CO_2}/k_{N_2O}, k_{Xe}/k_{N_2O}, k_{CO}/k_{N_2O}, and k_{N_2}/k_{N_2O} are not affected by the excess kinetic energy of the $O(^1D)$ atoms.

In the second method the competition between neopentane and one of CO_2, Xe, CO, and N_2 for $O(^1D)$ atoms was measured. The results of the second study were not entirely conclusive. However, they also indicate no effect or at best only a very small effect of excess kinetic energy.

RALPH OVEREND, GEORGE PARASKEVOPOULOS, JANICE R. CRAWFORD et H. ALAN WIEBE. Can. J. Chem. **53**, 1915 (1975).

Nous avons évalué l'effet de l'excès d'énergie cinétique des atomes $O(^1D)$ sur quelques-unes de leurs réactions en phase gazeuse en utilisant deux méthodes. Nous avons produit les atomes $O(^1D)$ avec un excès d'énergie cinétique de 41 ± 5 kcal/mol et de 31 kcal/mol, par une photolyse-éclair de N_2O (1800–2300 Å) et par une photolyse de N_2O à 2139 Å respectivement. Ceci a été fait en présence et absence de He qui agissait comme un désactivateur d'énergie cinétique.

Suivant la première méthode nous avons mesuré la compétition entre N_2O et CO_2, Xe, CO ou N_2 pour les atomes $O(^1D)$, et nous avons trouvé que les constantes relatives k_{CO_2}/k_{N_2O}, k_{Xe}/k_{N_2O}, k_{CO}/k_{N_2O} et k_{N_2}/k_{N_2O} ne sont pas influencées par l'excès d'énergie cinétique des atomes $O(^1D)$.

Suivant la deuxième méthode nous avons mesuré la compétition entre le néopentane et CO_2, Xe, CO ou N_2 pour les atomes $O(^1D)$. Les résultats de la deuxième étude n'ont pas été entièrement définitifs. Néanmoins, eux aussi n'indiquent guère d'effet ou, tout au plus un effet très faible.

Introduction

The photolysis of N_2O in the wavelength region 1800–2300 Å gives electronically excited oxygen atoms mainly in the $O(^1D_2)$ state (1, 2). The photon energy in this wavelength region is in excess of the N_2—O bond dissociation energy. The factors affecting the partition of the excess energy between the translational and internal modes of excitation of the photofragments are not well understood. The available evidence from the photodissociation of NO_2 and NOCl (3) shows that 60–70% of the excess energy appears as translational excitation of the fragments. In the light of this we assume that all the excess energy goes into translational excitation of the $O(^1D)$ and N_2 fragments and calculation on the basis of conservation of momentum yields an upper limit for the kinetic energy of the $O(^1D)$ atoms, in the range 25–47 kcal/mol for the wavelength region 2300–1800 Å. It is possible that the excess kinetic energy of the $O(^1D)$ atoms could have an effect on their reactivity, and indeed, Heicklen and co-workers (4–7) have suggested such an effect on the relative rates k_{2a}/k_{2b}, k_{CH_4}/k_{N_2O}, and k_{O_3}/k_{N_2O} of the reactions of $O(^1D)$ with N_2O, CH_4, and O_3.

[2a] $O(^1D) + N_2O \rightarrow N_2 + O_2$

[2b] $\rightarrow 2NO$

[1]This paper is dedicated to Professor C. A. Winkler of McGill University on the occasion of his sixty-fifth birthday by one of his former students (G.P.).

[2]NRCC No. 14607.

[3]Author to whom correspondence should be addressed.

[4]Summer student, 1972.

[5]NRCC Postdoctorate Fellow 1971–1972.

Can. J. Chem. Downloaded from www.nrcresearchpress.com by 210.87.254.105 on 09/05/12
For personal use only.

[3] $O(^1D) + CH_4 \rightarrow$ Products

[4] $O(^1D) + O_3 \rightarrow$ Products

On the other hand Preston and co-workers (8) found no evidence of a kinetic energy effect on the ratio k_{2a}/k_{2b}. More recently the ratio was redetermined in this laboratory by Wiebe and Paraskevopoulos (9); the value obtained agrees with that of Preston and co-workers and again it was found to be independent of the excess kinetic energy.

It should be pointed out however, that there is an inherent difficulty in all studies that attempt to detect the effect of kinetic energy on the relative rates of $O(^1D)$ atoms. Such studies involve comparisons of small differences in relative rates, measured with $O(^1D)$ atoms possessing various amounts of excess kinetic energy. This is usually accomplished by measuring the relative rates in the absence and presence of He, or other deactivators of kinetic energy. Since most of the reactions of $O(^1D)$ atoms are very fast, approaching collision efficiencies (10–13), any effect of the excess kinetic energy is likely to be small; therefore the resulting differences in relative rates due to the removal of 30–40% of it would be still smaller and difficult to distinguish from the experimental uncertainty.

The reactions of $O(^1D)$ atoms are of current interest to the chemistry of the stratosphere (14) and the present study is an attempt to further clarify the role of kinetic energy in these reactions. We have used two different methods to study the rates of deactivation of $O(^1D)$ to $O(^3P)$ by CO_2, Xe, CO, and N_2, relative to the rates of its reaction with N_2O and neopentane; the experiments were made in the absence and presence of He which is a deactivator of translational energy but does not interact in any other way with $O(^1D)$ atoms (2, 10). The deactivation reactions were chosen in this study, because in addition to their interest as a distinct class of reactions, they are generally somewhat slower than the reactions with N_2O and neopentane, and it was hoped that any effect of the kinetic energy would result in large differences in the reactivities and would be thus easier to detect. We have also discussed the present and previous results in terms of some approximate calculations of the collisional removal of kinetic energy from $O(^1D)$ by helium.

Methods

Method A

$O(^1D)$ atoms with a maximum excess kinetic energy of 41 ± 5 kcal/mol were produced by flash photolysis (1800–2300 Å) of mixtures of N_2O with CO_2, Xe, CO, and N_2, in the absence and presence of He which is a deactivator of excess kinetic energy but does not interact with $O(^1D)$ to any significant extent (2, 10). The following reactions take place:

[1] $N_2O + h\nu \rightarrow N_2 + O(^1D)$

[2a] $O(^1D) + N_2O \rightarrow N_2 + O_2$

[2b] $\rightarrow 2NO$

[5] $O(^1D) + Q \rightarrow O(^3P) + Q$

where Q = CO_2, Xe, CO, and N_2. For constant flash energy and pressures of N_2O and Q the NO or N_2 produced in the absence and presence of He should give a measure of the effect of the excess kinetic energy on the rates of the deactivation of $O(^1D)$ by Q, relative to its rate of reaction with N_2O, *i.e.*, on the ratio k_Q/k_{N_2O}.

Method B

$O(^1D)$ atoms with a maximum excess kinetic energy of 31.0 kcal/mol were produced by photolysis of N_2O at 2139 Å, and reacted subsequently with neopentane and CO_2, Xe, CO, and N_2 in the absence and presence of He. The following reactions take place:

[1] $N_2O + h\nu \rightarrow N_2 + O(^1D)$

[5] $O(^1D) + Q \rightarrow O(^3P) + Q$

[6] $O(^1D) + RH \rightarrow \alpha ROH + (1 - \alpha)(R + OH)$

[7] $O(^3P)$ + 1-butene → Products

where RH = neopentane, ROH = neopentanol, Q = CO_2, Xe, CO, and N_2, and Products are the characteristic products of the addition of $O(^3P)$ to 1-butene, *i.e.* 1,2-butene oxide, *n*-butyraldehyde, and methyl ethyl ketone (15). When the ratios (neopentane + Q)/N_2O and (neopentane + Q)/1-butene are sufficiently high, virtually all the $O(^1D)$ will react with neopentane and Q and not with N_2O or 1-butene (2, 16). The vibrationally excited neopentanol formed initially is completely stabilized and its yield becomes constant at a pressure of about 150 Torr (17). If a small amount of a scavenger of $O(^3P)$ such as 1-butene is also added, most of the $O(^3P)$ atoms formed

Can. J. Chem. Downloaded from www.nrcresearchpress.com by 210.87.254.105 on 09/05/12
For personal use only.

Can. J. Chem. Downloaded from www.nrcresearchpress.com by 210.87.254.105 on 09/05/12
For personal use only.

in the system will add to 1-butene, and the yields of the characteristic products of the addition (1,2-butene oxide, *n*-butyraldehyde, and methyl ethyl ketone) should give a measure of the deactivation of $O(^1D)$ to $O(^3P)$ by Q. This technique has been used successfully in this laboratory to identify and measure the $O(^3P)$ formed by deactivation of $O(^1D)$ and is described in detail in ref. 2. The values of the ratio $\sum O(^3P)$Products/neopentanol determined under constant conditions in the absence and presence of He should give a measure of the effect of the excess kinetic energy on the rate of deactivation of $O(^1D)$ by Q relative to its rate of reaction with neopentane.

Experimental

Method A

The flash photolysis apparatus consisted of a flash lamp reaction vessel assembly connected to a mercury free vacuum system. A 75 μF capacitor was charged to 8 kV (2400 J) and discharged in low pressure air producing a light pulse of about 20 μs duration to half-peak height. The apparatus and experimental arrangement were the same as those used in a similar study of the effect of the excess kinetic energy of the $O(^1D)$ atoms on their reaction with N_2O and have been described in ref. 9.

The NO was measured spectrophotometrically in absorption by the attenuation of the $\gamma(0, 0)$ band of NO (2267 Å line emitted by a cadmium lamp and monitored by a photomultiplier mounted at the exit slit of a 1 m scanning spectrophotometer). In order that the absorption varied linearly with NO pressure the NO γ-band was pressure broadened before measurement by addition of He to a total pressure of 1 atm. The He was added before or after the flash depending on whether the reactions took place in the absence or presence of He. The analytical arrangement and the calibration for NO have been described in detail previously (9). In a few experiments with CO_2 and Xe nitrogen was also measured as described previously (9). The N_2O and He used were the same grade and were purified in the same manner described in ref. 9. The CO_2, Xe, CO, and N_2 were Matheson research grade and were used without further purification.

Method B

The 2139 Å light was provided by two Philips 93106 E zinc lamps and were focused by Ultrasil lenses. The cylindrical photolysis cell had a volume of 195.6 ml and Suprasil quartz windows 5 cm in diameter. After photolysis the noncondensable gases were pumped off slowly through three liquid nitrogen traps; neopentanol and the other oxygenated compounds were collected, separated from the excess reactants, and measured on a 300 ft, 0.015 in. i.d. capillary column coated with β,β′-thiodipropionitrile and equipped with a flame ionization detector. The experimental and analytical techniques have been described in detail in ref. 2. The neopentane and N_2O were purified as described previously (2). The CO_2, Xe, CO, and N_2 were the same as those used in Method *A*.

Results

Method A

In the experiments with CO and N_2 as reactants only NO was determined while with CO_2 and Xe, nitrogen was also measured in some runs. The reactivity of $O(^1D)$ toward N_2O was estimated mainly from the yields of NO, assuming that the amount of $O(^1D)$ produced per flash or the light intensity delivered per flash is constant. The validity of this assumption was tested in separate experiments (9), in which 12.0 Torr of H_2O flashed at 8 kV in the presence of an excess of CO gave 16.0 mTorr ± 10% of OH per flash, as determined from the amount of CO_2 formed. Furthermore, for constant N_2O pressure and flash energy, the yields of NO and N_2 produced were reproducible to within better than 10% as may be seen in Table 1 of ref. 9. The assumption then is valid to within 10%.

The photons in our system will have energy corresponding to a wavelength of about 1900 ± 100 Å. This was estimated from the assumed blackbody intensity distribution with wavelength of the flash light, the known transmission of the quartz walls of the reaction vessel, and the absorption of N_2O in the wavelength region 2300–1700 Å (18). If we assume, as discussed in the Introduction, that all the excess energy goes into the translation of the $O(^1D)$ and N_2 fragments of the photolysis of N_2O we estimate that the $O(^1D)$ in our system will have a maximum excess kinetic energy of about 41 ± 5 kcal/mol.

The experiments were done at room temperature (25 ± 2 °C). The sequence was one experiment in the absence of He followed by one with He present. The results for CO_2 and Xe are given in Table 1 and those for CO and N_2 in Table 2. The errors in the average values reported in Tables 1 and 2, about ±15% at 1σ, were estimated from an assessment of the uncertainties in all the measurements involved (pressure, absorbance) and taking into account the propagation of errors in the calculation of the final results (19). The results show that within this error the average values of N_2 and NO, produced in the experiments with CO_2 and Xe, and of NO produced in the experiments with CO and N_2, do not change by addition of He.

Can. J. Chem. Downloaded from www.nrcresearchpress.com by 210.87.254.105 on 09/05/12
For personal use only.

TABLE 1. Yields of N_2 and NO from the flash photolysis of mixtures of N_2O with CO_2 and Xe in the absence and presence of He

Mixture (Torr)	N_2 (Torr)	NO (Torr)
$N_2O/CO_2 = 0.836$, flashed without He		
162.0	0.112	0.045
164.2	0.132	0.052
165.0	n.d.*	0.042
	Average	0.046 ± 15%
$N_2O/CO_2 = 0.836$, flashed with 594 ± 2 Torr He		
162.0	0.145	0.037
165.0	0.118	0.048
163.5	n.d.	0.045
	Average	0.043 ± 15%
$N_2O/Xe = 0.90$, flashed without He		
163.5	0.172	0.063
162.0	0.163	0.062
165.5	0.165	0.068
162.1	n.d.	0.062
	Average	0.064 ± 15%
$N_2O/Xe = 0.90$, flashed with 576 ± 5 Torr He		
163.0	0.151	0.061
162.1	0.163	0.064
159.5	n.d.	0.061
	Average	0.062 ± 15%

*n.d. = not determined.

Method B

The experiments were done at 27 ± 2 °C. The $O(^1D)$ atoms in the system have a maximum excess kinetic energy of 31.0 kcal/mol, estimated as described above. The approximate composition of the mixtures of reactants as well as the measured values of the ratio $\sum O(^3P)$Products/neopentanol in the absence and presence of He are given in Table 3. The errors in the average values of the ratio were estimated as described above and were found to be about ±20% at 1σ.

The average values of the ratio for CO_2, CO, and N_2 appear to increase slightly in the presence of He by 17, 23, and 12% respectively, while for Xe they are the same within the experimental error. The observed differences were tested by Student's t test (19) and were only significant to the $P = 0.2$ level *i.e.*, there is 80% certainty that there is a difference.

Discussion

In our previous study (9) it was found that the ratio k_{2a}/k_{2b} is independent of the excess kinetic energy of the $O(^1D)$ atoms. This finding combined with the present results of the flash photolysis of N_2O (Method *A*) indicates that k_Q/k_{N_2O} (Q = CO_2, Xe, CO, and N_2) is also independent of the excess kinetic energy of the $O(^1D)$ atoms.

The results of the second method show that addition of He produces a definite increase of the ratio k_Q/k_{neop} for CO_2, CO, and N_2, while for Xe the ratio is not affected. The results could imply that kinetically "hot" $O(^1D)$ atoms react slightly faster with neopentane or slightly slower with CO_2, CO, and N_2, than thermalized $O(^1D)$ atoms. However, they could imply, equally well, that the $O(^3P)$ atoms formed are kinetically "hot" and are responsible for the small changes in the ratio k_Q/k_{neop}. This could come about as follows. As mentioned in the section on methods, it is assumed that most of the $O(^3P)$ atoms formed will add to 1-butene to give the characteristic addition products. This assumption is valid for thermalized $O(^3P)$ which add to 1-butene about 300 times faster than they

TABLE 2. Yields of NO from the flash photolysis of mixtures of N_2O with CO and N_2 flashed in the absence and presence of He

Mixture (Torr)	NO (Torr)
$N_2O/CO = 0.89$, flashed without He	
166.0	0.065
166.2	0.063
167.5	0.078
166.2	0.077
166.2	0.081
Average	0.073 ± 15%
$N_2O/CO = 0.89$, flashed with 584 ± 5 Torr He	
166.0	0.067
166.2	0.072
166.2	0.074
167.5	0.075
166.2	0.076
Average	0.073 ± 15%
$N_2O/N_2 = 0.40$, flashed without He	
238.5	0.075
239.9	0.078
239.9	0.080
239.9	0.080
Average	0.078 ± 15%
$N_2O/N_2 = 0.40$, flashed with 506 ± 2 Torr He	
238.5	0.076
239.9	0.076
241.0	0.081
240.0	0.078
Average	0.078 ± 15%

Can. J. Chem. Downloaded from www.nrcresearchpress.com by 210.87.254.105 on 09/05/12
For personal use only.

TABLE 3. Yields of deactivation products relative to the yield of neopentanol from the reaction of O(¹D) with mixtures of neopentane with CO_2, Xe, CO, and N_2*

	$\frac{\Sigma O(^3P) \text{ products}\dagger}{\text{neopentanol}}$	
	Without He	With He 568 ± 6 Torr
Neopentane/CO_2 = 8.2	1.04	1.18
	1.06	1.14
	0.99	1.24
	0.95	1.17
Average values	1.01 ± 20%	1.18 ± 20%
Neopentane/Xe = 8.1	1.26	1.19
	1.24	1.25
	1.24	1.16
Average values	1.25 ± 20%	1.20 ± 20%
Neopentane/CO = 8.1	0.38	0.49
	0.40	0.47
	0.38	0.49
Average values	0.39 ± 20%	0.48 ± 20%
Neopentane/N_2 = 8.2	0.35	0.37
	0.34	0.38
	0.33	0.39
Average values	0.34 ± 20%	0.38 ± 20%

*The experimental conditions were: approximate composition of the photolysis mixture, 1-butene 0.5 Torr, N_2O 5 Torr, neopentane 20 Torr, (CO_2, Xe, CO, N_2) 170 Torr, pressure ≈ 195 Torr, temperature 27 ± 2 °C, reaction time ≈ 900 min.

†$\Sigma O(^3P)$ products is the total yield of products formed from addition of O(³P) to 1-butene, *i.e.*, 1,2-butene oxide, *n*-butyraldehyde, and methyl ethyl ketone.

abstract hydrogen from neopentane (2), and at the ratio of neopentane/1-butene ≈ 40 used, about 90% of the thermalized O(³P) would add to 1-butene. It is possible however, that the O(³P) atoms in our experiments may possess an appreciable amount of the kinetic energy of the O(¹D) atoms and thus be preferentially scavenged by neopentane in the absence of He. There is evidence[6] that kinetically "hot" O(³P) atoms do abstract hydrogen from some paraffins substantially faster than thermalized O(³P) atoms. It is quite likely then that the observed small increase in the ratio, $\Sigma O(^3P)$Products/neopentanol, may be due to kinetically "hot" O(³P) atoms. Since it is not possible to distinguish experimentally between the two alternatives in our system, the results for k_Q/k_{neop} are inconclusive. In view of the more definite finding that k_Q/k_{N_2O} is independent of the excess kinetic energy of the O(¹D) atoms, it seems to us more probable that k_Q/k_{neop} is also independent of such energy.

However, if we attribute variation in the ratio to a "hot" atom effect, what would be the quantitative significance of the observation?

The available theoretical treatments of "hot" atom effects range from the case discussed by Wolfgang (20) for very high energy atoms generated by nuclear reactions to the case of photolytically generated "hot" hydrogen atoms treated for example by Oldershaw and Porter (ref. 21 and references therein). In these treatments the "hot" atom has a velocity much greater than the thermal velocities of the target and moderator species. This enables a simplification in the computation of the collision density function, in that the velocity distribution of the "hot" atom is the only consideration in calculating the rate of encounter of the "hot" atom with what are considered to be stationary target and moderator molecules. In nearly all of the earlier investigations of "hot" atom reactions the velocity consideration is maintained because the reactions studied have a considerable threshold to reaction such that $E > E_0 \gg kT$, where E is the translational energy of the "hot" atom and E_0 is the threshold to reaction.

The available data for O(¹D) atom reactions have been summarized, and recommended values for the rate constants have been given by Cvetanović (14). The recommended values together with calculated values of the hard-sphere collision frequencies are given in Table 4. These indicate that both presumed "hot" and thermalized O(¹D) atoms react with close to collisional rates. This, combined with the evidence that hydrocarbon reactions with O(¹D) occur to an appreciable extent at liquid argon temperatures (22), indicates that they have negligible or very

TABLE 4. Recommended values of rate constants k, and hard-sphere collision frequencies Z, of O(¹D) reactions

Reactant	$k \times 10^{-14}$* ($cm^3\ mol^{-1}\ s^{-1}$)	$Z \times 10^{-14}$† ($cm^3\ mol^{-1}\ s^{-1}$)
N_2O	1.32	1.82
Neopentane	7.41	2.22
CO_2	1.08	1.56
Xe	0.84	1.44
CO	0.46	1.48
N_2	0.33	1.52

*The recommended values of k were taken from ref. 14.

†The atomic and molecular diameters used in the calculation of Z were taken from refs. 24 and 25.

[6]O. Kajimoto and R. J. Cvetanović. Private communication.

Can. J. Chem. Downloaded from www.nrcresearchpress.com by 210.87.254.105 on 09/05/12
For personal use only.

small activation energies. Thus theories of "hot" atom reactions are not easy to apply since $O(^1D)$ atoms react over the entire range of energies from E to kT. This complication causes the collision density function to change possibly over a factor of 2 in going from $E = 50$ kcal/mol to thermalized conditions. As an illustration of this consider a competition for $O(^1D)$ between two molecules A and B of similar collision cross sections, which react at each encounter with $O(^1D)$ though A and B have molecular weights of 16 and 50 respectively. At high translational excess energies of $O(^1D)$ the molecules A and B can be considered as stationary and the relative rate measured from the products of A and B will be

$$\frac{k_{(O(^1D)+A)}}{k_{(O(^1D)+B)}} = \frac{s^2_{(O(^1D)-A)}}{s^2_{(O(^1D)-B)}} \approx 1.0$$

(s^2 = collision cross sections) which is the ratio of collision probabilities. At thermal energies the normal collison equation will apply taking into account the Maxwell distribution of velocities of the colliding species, *i.e.*

$$\frac{k_{(O(^1D)+A)}}{k_{(O(^1D)+B)}} = 1.0\left(\frac{m_B(m_{O(^1D)} + m_A)}{m_A(m_{O(^1D)} + m_B)}\right)^{1/2} \approx 1.23$$

Thus a purely physical effect could alter the apparent rate coefficient ratio.

Notwithstanding this objection a further dilemma is in quantifying the extent of moderation in experiments where the range of moderator addition would not thermalize all the "hot" atoms. This is unfortunately the case in both our experiments and those of Heicklen and coworkers (5, 6). They compute the extent of moderation by the argument

$$\langle E \rangle = \left(\frac{E'}{E}\right)^{\alpha}$$

where, $\langle E \rangle$ is the average excess translational energy of the reacting $O(^1D)$ atoms and E'/E, the fraction of kinetic energy left to the $O(^1D)$ atom after a moderating collision is calculated from the hard-sphere, stationary target model and is equal to $(m_1^2 + m_2^2)/(m_1 + m_2)^2$, and α is the relative likelihood of collision with a moderator or reactant molecule *i.e.* $\alpha = s^2_{(mod)}/\sum s^2_{(react)}$.

We suggest that the way of determining the average energy of reaction would be developed not from the average number of collisions with moderator before meeting the reactant as above, but rather from the average energy of all the reactive encounters. This method is given in detail in the Appendix.

The objection to both models is that neither takes into account nonreactive collisions between the "hot" atom and the reactant molecule. This would reduce the mean energy of reaction.

Conclusion

On the basis of our results and the comments given above we conclude that the excess kinetic energy of the $O(^1D)$ atoms does not affect the relative rates of their reaction to any measurable extent. A possible small effect in most instances borders the experimental error when it is assessed rigorously. The interpretation of the effects of additions of moderator in any quantitative fashion is almost impossible. We suggest that studies of systems in which the reactive species reacts over the entire range of energy from E to kT be studied by means of variation in the photon energy and not by moderator addition except in the cases where moderator can be added in such an excess as to thermalize the "hot" population completely.

The authors are grateful to Dr. R. J. Cvetanović for his interest in this work, his advice, and encouragement.

Appendix

Given a gas mixture containing $O(^1D)$ atoms with excess kinetic energy E, He, and reactants A_i, the $O(^1D)$ atoms may collide with A_i and react or they may collide with He and lose some of their kinetic energy. The partially cooled $O(^1D)$ atoms may then react with A_i or be cooled further by collision with He. We are interested in calculating approximately the average kinetic energy $\langle E \rangle$ with which the $O(^1D)$ atoms will react with A_i. The "hot" $O(^1D)$ atoms have a much larger velocity than the He atoms and A_i molecules (which have a Maxwell distribution of velocities), hence, we assume the latter as stationary. Let E and E' be the kinetic energy of $O(^1D)$ before and after collision with a He atom. From the hard-sphere collision model (23) the fraction of kinetic energy transferred per collision is

$$\frac{\Delta E}{E} = \frac{E - E'}{E} = \frac{2m_1m_2}{(m_1 + m_2)^2}$$

where m_1 and m_2 are the masses of $O(^1D)$ and

Can. J. Chem. Downloaded from www.nrcresearchpress.com by 210.87.254.105 on 09/05/12
For personal use only.

He. The fraction f_e of kinetic energy left to O(¹D) after a collision is

$$f_e = \frac{E'}{E} = 1 - \frac{\Delta E}{E} = \frac{m_1^2 + m_2^2}{(m_1 + m_2)^2}$$

Let f_c be the fraction of collisions between O(¹D) and reactants A_i, $1 - f_c$ is the fraction of collisions between O(¹D) and He

$$f_c = \frac{\sum s_{A_i}^2 P_{A_i}}{s_{He}^2 P_{He} + \sum s_{A_i}^2 P_{A_i}}$$

where s_{He}^2, $s_{A_i}^2$, are the collisional cross sections of O(¹D) with He and A_i ($s_{He} = (\sigma_{O(^1D)} + \sigma_{He})/2$, σ = collision diameters) and P_{He} and P_{A_i} are the pressures of He and A_i in the gas mixture. f_c and $1 - f_c$ are the respective probabilities that O(¹D) will collide and react with A_i with kinetic energy E or that it will collide with He and be cooled to kinetic energy $f_e E$.

We have then that: f_c O(¹D) atoms react with kinetic energy E, $1 - f_c$ atoms will be cooled to $f_e E$, from these $(1 - f_c) \cdot f_c$ will react with energy $f_e E$ and $(1 - f_c - (1 - f_c)f_c) = (1 - f_c)^2$ will be cooled to $f_e^2 E$, etc. The average kinetic energy with which all the O(¹D) atoms will react is

$$\langle E \rangle = E[f_c + f_c(1 - f_c)f_e + f_c(1 - f_c)^2 f_e^2 + \ldots f_c(1 - f_c)^n f_e^n]$$

which can be rearranged by substituting the limit of the power series to

$$\langle E \rangle = f_c \cdot E[1 - f_e(1 - f_c)]^{-1}$$

For the present experiments we estimate that $\langle E \rangle$ is about 60% of E (it is 70% of E for N_2, Method A). For the experiments of ref. 6, $\langle E \rangle$ is about 77% and 61% of E at 330 and 760 Torr of He respectively. The atomic and molecular collision diameters used in these estimates were taken from the work of Rabinovitch and co-workers (24) which appear to provide a self-consistent set. The collision diameter of O(¹D), $\sigma = 2.7$ Å was taken to be between that of He and Ne. That of N_2O, $\sigma = 4.54$ Å was taken from ref. 25.

1. K. F. Preston and R. F. Barr. J. Chem. Phys. **54**, 3347 (1971).
2. G. Paraskevopoulos and R. J. Cvetanović. J. Am. Chem. Soc. **91**, 7572 (1969).
3. G. E. Busch and K. R. Wilson. J. Chem. Phys. **56**, 3626 (1972); **56**, 3655 (1972).
4. R. I. Greenberg and J. Heicklen. Int. J. Chem. Kinet. **2**, 185 (1970).
5. R. Simonaitis, R. I. Greenberg, and J. Heicklen. Int. J. Chem. Kinet. **4**, 497 (1972).
6. R. I. Greenberg and J. Heicklen. Int. J. Chem. Kinet. **4**, 417 (1972).
7. C. S. Goldman, R. I. Greenberg, and J. Heicklen. Int. J. Chem. Kinet. **3**, 501 (1971).
8. P. M. Scott, K. F. Preston, R. J. Anderson, and L. M. Quick. Can. J. Chem. **49**, 1808 (1971).
9. H. A. Wiebe and G. Paraskevopoulos. Can. J. Chem. **52**, 2165 (1974).
10. R. F. Heidner III and D. Husain. Int. J. Chem. Kinet. **6**, 77 (1974).
11. R. F. Heidner III, D. Husain, and J. R. Wiesenfeld. J. Chem. Soc. Faraday II, **69**, 927 (1973).
12. R. F. Heidner III and D. Husain. Int. J. Chem. Kinet. **5**, 819 (1973).
13. P. Michaud, G. Paraskevopoulos, and R. J. Cvetanović. J. Phys. Chem. **78**, 1457 (1974).
14. R. J. Cvetanović. Can. J. Chem. **52**, 1452 (1974).
15. R. J. Cvetanović. Adv. Photochem. **1**, 115 (1963).
16. G. Paraskevopoulos, V. B. Symmonds, and R. J. Cvetanović. Can. J. Chem. **50**, 1838 (1972).
17. G. Paraskevopoulos and R. J. Cvetanović. J. Chem. Phys. **52**, 5821 (1970).
18. K. Watanabe, M. Zelikoff, and E. C. Y. Inn. Absorption coefficients of several atmospheric gases. Geophysics Research Directorate, Air Force Cambridge Research Center, Cambridge, Mass. Technical Report No. 53–23, 1953.
19. E. M. Pugh and G. H. Winslow. The analysis of physical measurements. Addison–Wesley, Reading, Mass. 1966.
20. R. Wolfgang. Progr. React. Kinet. **3**, 97 (1965).
21. G. A. Oldershaw and D. A. Porter. J. Chem. Soc. Faraday I, **68**, 709 (1972) and references therein.
22. W. B. DeMore. J. Phys. Chem. **73**, 391 (1969).
23. H. E. Kennard. Kinetic theory of gases. McGraw Hill, New York. 1938.
24. S. C. Chan, B. S. Rabinovitch, J. T. Bryant, L. D. Spicer, T. Fujimoto, Y. N. Lin, and S. P. Pavlou. J. Phys. Chem. **74**, 3160 (1970).
25. J. O. Hirschfelder, C. F. Curtiss, and R. B. Bird. Molecular theory of gases and liquids. John Wiley and Sons, New York, 1964.

Organoselenium Chemistry. Addition of Toueneselenenyl Chloride to Ethylene: Concerning the Reported Isolation of a Stable Episelenurane

HANS J. REICH AND JOHN E. TREND
Department of Chemistry, University of Wisconsin, Madison, Wisconsin 53706

Received December 10, 1974

HANS J. REICH and JOHN E. TREND. Can. J. Chem. **53**, 1922 (1975).

The addition of ethylene to solutions of 4-toueneselenenyl chloride (ArSeCl) gives initially the selenide dichloride **5**. Only after more than 20% of the theoretical amount of ethylene has been added does the normal adduct appear. This anomaly is caused by the reversible reaction of the normal adduct **4** with ArSeCl, giving diselenide and **5**. The episelenurane **1** reported as a product of the reaction of ArSeCl with ethylene appears to be actually the dichloride **5**. Even at low temperature no evidence for the formation of a stable episelenurane was obtained. The ^{13}C n.m.r. spectra of several organoselenium compounds are reported, including a number of selenium-77 carbon-13 coupling constants.

HANS J. REICH et JOHN E. TREND. Can. J. Chem. **53**, 1922 (1975).

L'addition d'éthylène à des solutions de chlorure de *p*-toluènesélénenyle (ArSeCl) conduit tout d'abord à la formation du dichlorure de sélémine (**5**). Le produit d'addition normal ne commence à apparaitre que lorsque plus de 20% de la quantité théorique d'éthylène a été additionnée. Cette anomalie est dû à une réaction reversible entre le produit d'addition normal **4** et ArSeCl conduisant au disélémine et à **5**. Il a été rapporté que la réaction de ArSeCl sur l'éthylène conduit à l'épisélénuranne **1**; il semble toutefois que ce composé est le dichlorure **5**. On n'a pas pu mettre en évidence la formation d'un épisélénuranne stable, même à basse température. On rapporte les spectres r.m.n. du ^{13}C de plusieurs dérivés organosélénium; ces résultats comprennent un certain nombre de constantes de couplage sélénium-77 carbone-13.
[Traduit par le journal]

Garratt and Schmid (1) recently reported the isolation of the stable episelenurane **1**. Our interest in the stereochemistry of selenuranes (2) and in the addition of electrophilic selenium reagents to olefins (3) has led us to prepare a number of compounds related to **1**. The stability and

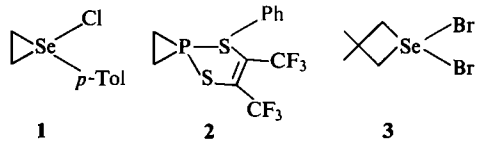

1 **2** **3**

spectral properties of **1** appear to be inconsistent with our observations and those reported by others.

Although phosphoranes in general show greater stability than sulfuranes and selenuranes, an attempted preparation of the epiphosphorane **2** resulted in rapid fragmentation to give ethylene even at low temperature (4).[1] Furthermore, the four-membered cyclic selenurane **3** (7) undergoes ring opening[2] below $-20°$, even though there are a number of isolable four-membered cyclic phosphoranes (8).

These and other related considerations prompted us to reexamine the preparation and characterization of **1**. In our hands the reaction of 4-toueneselenenyl chloride (ArSeCl) with excess ethylene gives the normal adduct **4** (3*a*, 9) with no indication of the formation of **1**. However, if ethylene is added to a solution of the selenenyl chloride and the reaction is monitored by n.m.r., a compound which we have identified as **5** initially appears as the major product of the reaction (Fig. 1). Signals which can be assigned to 4,4'-ditolyl diselenide (**6**) also appear in the n.m.r. spectrum. When about 25% of the theoretical quantity of ethylene has reacted, **4** begins to appear, and increases steadily at the expense of **5** and **6** as more ethylene is added. Addition of pentane when the concentration of **5** is at a maximum results in its crystallization in 23% yield (85% based on ethylene added). The material prepared in this way is identical in physical and chemical properties to **5** prepared by chlorination of **4** or by reaction of ethylene with 4-tolylselenium trichloride.

[1]It should be noted that episelenides (5) appear to be substantially less stable than epiphosphines (6).

[2]H. J. Reich and I. L. Reich, unpublished results.

Can. J. Chem. Downloaded from www.nrcresearchpress.com by 210.87.254.42 on 09/05/12
For personal use only.

Can. J. Chem. Downloaded from www.nrcresearchpress.com by 210.87.254.42 on 09/05/12
For personal use only.

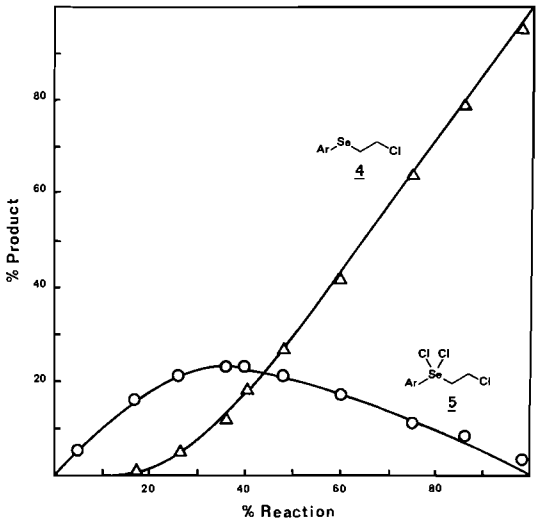

FIG. 1. Variation in product composition during the addition of ethylene to a solution of 4-tolueneselenenyl chloride (1 *M* in $CDCl_3$) at 33°; Compound **4**, △; Compound **5**, ○. The points are experimental numbers determinded by n.m.r. integration. The solid lines are calculated curves assuming the stoichiometry and mechanism of eqs. 1 and 2 with $K = k_2/k_{-2} = 13\ \mathrm{l\ mol^{-1}}$.

The product data summarized in Fig. 1 are rationalized by the following reactions:

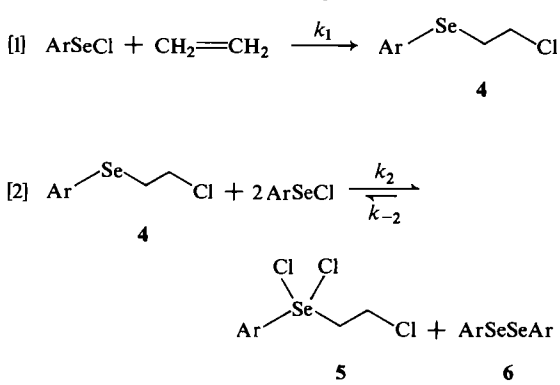

The equilibrium constant ($K = k_2/k_{-2}$) is approximately 13 $\mathrm{l\ mol^{-1}}$. Thus only **5** is detected initially. As more ethylene is added, the small equilibrium concentration of ArSeCl is maintained by the chlorination of **6**, with **5** as the chlorinating agent. Solutions of appropriate mixtures of **4** and ArSeCl, or **5** and **6** prepared from the pure compounds behave the same as equivalent solutions prepared by reaction of ethylene and ArSeCl.

At low temperature (−60°) ethylene still reacts rapidly with ArSeCl (low temperature n.m.r.) giving mixtures of **4** and **5** in variable ratio (30–60% of **4**) depending on reaction conditions, but this ratio does not change when excess ethylene is present. Apparently at this temperature k_{-2} is sufficiently small that equilibration forming more ArSeCl does not occur.

Pyrolysis of **5** neat or in solution (pentachloroethane, tetrachloroethylene) gives a mixture of products, mainly 1,2-dichloroethane and **7**. Compound **7** could not be purified since it decomposed during chromatography on silica gel or during g.l.c. It was characterized spectrally by comparison with the addition products of ArSeCl to vinyl chloride.

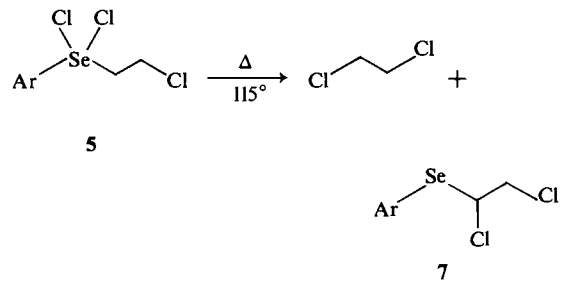

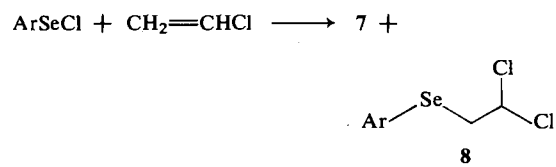

Reaction mixtures containing **5**, prepared by the reaction of ArSeCl with a deficiency of ethylene as described above, also give **7** and 1,2-dichloroethane on pyrolysis. *No additional **4** is formed during this pyrolysis.*

We have thus been unable to detect the presence of **1** during the reaction of ethylene with ArSeCl. Even at −60°, **4** is formed as a product, clearly incompatible with Schmid and Garratt's observation that **1** is stable above room temperature. Furthermore, **5** is formed in these reactions under appropriate conditions, and the detailed proton and carbon n.m.r. data reported for **1** (on which the structure assignment for **1** was largely based) are identical in every respect with the data we have obtained for **5** (Table 1). Table 2 lists the carbon-13 n.m.r. parameters for ArSeCl, **6**, **7**, **8**, and the model systems 4-tolyl propyl selenide and 4-tolyl propyl selenide dichloride. The c.m.r. parameters (chemical shifts, J_{C-H}, J_{C-Se}) of these compounds when compared with the data for **5** in Table 1 provide further verifica-

TABLE 1. Proton and carbon-13[a] n.m.r. parameters for **5**. Data reported for "**1**" in parentheses[b]

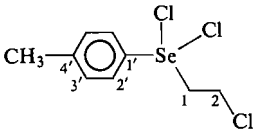

	δ_C TMS	$^1J_{CC}$	$^1J_{C-H}$	$^2J_{CCH}$	$J_{C^{77}Se}$	δ_H TMS
1	65.0(65.20)	(37.25)	152.0(152.03)	3.0(3.18)	59.4(59.25)	4.50[d](4.53)
2	38.1(38.06)		155.5(155.23)	4.0(4.38)	18.1(18.54)	4.34[d](4.37)
1′	136.9[c]				98.8[c]	
2′	129.3[c]		165[c]		12.4[c]	7.85[e](7.89)
3′	130.7[c]		162[c]		4.3[c]	7.35[e](7.38)
4′	142.8[c]				<3[c]	
CH_3	21.4[c]		127.4[c]	4.0[c]	<5[c]	2.43(2.40)

[a]Assignments were verified by undecoupled spectra.
[b]Reference 1.
[c]Data for "**1**" not reported.
[d]AA′BB′ pattern.
[e]AA′BB′ pattern with J_{AB} = 8.6 Hz (9.0 Hz).

tion for the structure assignment of **5**. We conclude that the compound identified by Schmid and Garratt as the episelenurane **1** is, in fact, the selenide dichloride **5**.

Apart from the identity of all available spectral parameters with those of **5**, there are features in the n.m.r. spectrum reported for "**1**" which are inconsistent with the episelenurane structure. The p.m.r. spectrum was reported as an AA′BB′ pattern for the ethylene fragment. Since the c.m.r. spectrum shows different carbons, the AA′ protons must be geminal. Any reasonable structure for the covalent episelenurane should have an ABCD pattern. Consideration of possible Berry pseudorotational pathways for this compound leads to the conclusion that no process exists which could average the ABCD pattern to give the proper AA′BB′ pattern while maintaining nonequivalent carbons. An episelenonium salt would have an AA′BB′ pattern but AA′ would be *cis*-vicinal rather than geminal. The pattern is, of course, exactly as expected for **5**. The unusual hybridization in three-membered rings usually results in characteristic C–C and C–H couplings.[3] The observed couplings for "**1**" are again as expected for an acyclic compound.

[3]The C–H couplings in thiirane *S*-oxide and *S*,*S*-dioxide are between 170 and 172 Hz (10). Carbon–carbon couplings have not been reported for thiiranes but cyclopropanes have internal C–C couplings of 10–16 Hz (11), as compared to 37.25 Hz for "**1**".

Experimental

Proton magnetic resonance spectra were obtained in $CDCl_3$ on a Varian XL-100, Brueker WH-270, or Jeol MH-100 spectrometer. Carbon-13 (Fourier transform) n.m.r. spectra were measured at natural abundance in $CDCl_3$ on the XL-100 system, undecoupled or using noise modulated proton decoupling, and are reported in Tables 1 and 2. Mass spectra were obtained on an AEI MS-902 spectrometer. Melting points are uncorrected.

4,4′-Ditolyl Diselenide (6)

The diselenide was prepared by published procedures from 4-tolylmagnesium bromide, m.p. 43–45° (lit. (12) 47°); p.m.r.: δ 2.33 (s, 3H), 7.07 and 7.49 (AA′BB′, J_{AB} = 8.0 Hz, 4H).

4-Tolueneselenenyl Chloride (ArSeCl)

To a solution of 1.7 g (5.0 mmol) of **6** in 15 ml chloroform was added dropwise 0.40 ml (4.9 mmol) of freshly distilled sulfuryl chloride. The mixture was stirred 5 min and purged of the SO_2 formed with a stream of nitrogen. Distillation of the dard red-orange liquid (b.p. 62°/0.07 mm) gave 1.55 g (75%) of ArSeCl; p.m.r.: δ 2.35 (s, 3H), 7.12 and 7.62 (AA′BB′, J_{AB} = 8.0 Hz, 4H).

2-Chloroethyl 4′-Tolyl Selenide (4)

A solution of 154 mg (0.75 mmol) of ArSeCl in 5 ml of $CHCl_3$ was purged with nitrogen. Ethylene was bubbled through the solution at room temperature with a glass tube until the orange-red color had faded to a light yellow and no further lightening was observed. Evaporation of solvent in a stream of nitrogen gave 175 mg (100%) of crude product. The p.m.r. spectrum showed the presence of only the adduct **4** and no others. Despite repeated purifications (low temperature crystallization from pentane or ether and sublimation) the melting point could not be raised above room temperature; however, the n.m.r. data (both ^1H and ^{13}C) were identical to those reported (1). Mass spectrum *m/e* Calcd. for $C_9H_{11}SeCl$: 233.97137. Found: 233.97157.

Can. J. Chem. Downloaded from www.nrcresearchpress.com by 210.87.254.42 on 09/05/12
For personal use only.

Can. J. Chem. Downloaded from www.nrcresearchpress.com by 210.87.254.42 on 09/05/12
For personal use only.

TABLE 2. Carbon-13 n.m.r. data[a]

Compound		$\delta_{C-Aryl}(J_{C-Se})$ 1′	2′	3′	4′	CH_3–Ar	$\delta_{C-Alkyl}(J_{C-Se})$ 1	2	3
(6)									
Ar_2Se_2	δ	127.7	132.3	129.8	137.8	21.0			
ArSeCl	δ	[b]	135.5	130.5	141.8	21.6			
	J_{CH}		dd 164.1, 5.9	dm 160.7		q 127.5			
4	δ	124.5	134.0	130.1	137.9	21.1	29.2(67.4)	43.2(<5)	
ArSePr[c]	δ	126.9	133.2	129.7	136.2	21.0	30.3(61.6)	23.6(7.1)	14.4(5.6)
	J_{CH}		dd 161.2, 6.3	dm 157.9		qm 126.3	tm 146.8		qm 120.8
Cl Cl ArSePr	δ	137.1(100.2)	129.0(12.1)	130.5(4.1)	142.3(<3)	21.3	66.8(61.4)	18.4(15.1)	13.6(12.7)
	J_{CH}		dd 162.8, 5.7	dm 153.4		qm 127.5	tm 149.0	tm 132.2	qm 126.8
7	δ	122.3	136.5	130.2	139.6	21.2	57.7(98.6)	49.4(6.3)	
	J_{CH}		dd 158.8, 6.0	dt 153.3, 5.9		qm 126.2	dm 165.0	t 153.1	
8	δ	124.6	134.3	130.2	138.1	21.1	40.3 (75.0)	71.7(8.6)	
	J_{CH}		dd 162.6, 6.5	dt 153.3, 5.9		qm 126.3	t 146.5	dt 181.2, 3.8	

[a]See Table 1 for numbering.
[b]Not observed.
[c]*p*-Tolyl *n*-propyl selenide.

Can. J. Chem. Downloaded from www.nrcresearchpress.com by 210.87.254.42 on 09/05/12
For personal use only.

2-Chloroethyl 4′-Tolyl Selenide Dichloride (5)

A solution of 595 mg (1.75 mmol) of 4,4′-ditolyl diselenide (**6**) in 10 ml of $CHCl_3$ was cooled to 0° and 750 mg (5.56 mmol) of sulfuryl chloride was added dropwise with stirring. As the reaction proceeded SO_2 was evolved and a pale yellow precipitate (4-tolylselenium trichloride) was formed. On completion of the addition, ethylene was bubbled through this slurry until the precipitate had dissolved and a nearly colorless solution was obtained. Evaporation of solvent and trituration of the residue with cold pentane followed by filtration afforded 940 mg (88%) of a faint green powder, m.p. 102–102.5° (sealed tube). Crystallization from CCl_4 and pentane gave an analytical sample, m.p. 102–102.5°.

Anal. Calcd. for $C_9H_{11}Cl_3Se$: C, 35.50; H, 3.64; Cl, 34.93; Se, 25.93. Found: C, 35.42; H, 3.72; Cl, 35.04; Se, 26.31.

The Reaction of Ethylene with 4-Tolueneselenenyl Chloride

At Room Temperature (Fig. 1)

A solution (1 *M*) of ArSeCl in $CDCl_3$ was treated at room temperature with successive aliquots of ethylene added by bubbling the gas through the solution for 10–30 s using a glass capillary. At the end of each addition the p.m.r. spectrum of the solution was measured and the relative amounts of 2-chloroethyl 4′-tolyl selenide (**4**) and its dichloride (**5**) were determined by integration of the peaks at δ 2.9–3.8 and 4.2–4.6, respectively, *vs.* the Ar–methyl peaks at δ 2.3–2.4. Initially all the ethylene was immediately consumed but as the reaction neared completion (the last 5–10% reaction) the consumption of ethylene slowed so that an ethylene resonance at δ 5.29 was observed. The integration of this resonance slowly decreased with concomitant increase in product integration.

The equilibrium constant ($K = k_2/k_{-2} = 13 \pm 3$ l mol^{-1}) was determined using the p.m.r. integration data and the following relationships.

$$[\mathbf{5}] = [\mathbf{6}]$$

$$[\mathrm{ArSeCl}] = 1 - [\mathbf{4}] - 2[\mathbf{6}] - [\mathbf{5}]$$

$$K = [\mathbf{5}][\mathbf{6}]/[\mathrm{ArSeCl}]^2[\mathbf{4}]$$

The theoretical curves in Fig. 1 were calculated by solving the following equation for X (the %**4** formed) while varying Y (the %reaction) and assuming $K = 13$. The equation is derived by assuming the stoichiometry and mechanism of eqs. 1 and 2.

$$4KX^3 + (4Ka - 1)X^2 + (Ka^2 + 2Y)X - Y^2 = 0$$

$$a = 1 - 3Y$$

$$\%\mathbf{4} = X$$

$$\%\mathbf{5} = Y - X$$

At Low Temperature

While ethylene was bubbled through 0.25 ml of $CDCl_3$ at −65° (Dry Ice – $CHCl_3$ bath) a solution of 50 mg (0.24 mmol) of ArSeCl in 0.20 ml of $CDCl_3$ was added slowly by syringe at such a rate as to allow the selenenyl chloride to react before attaining any significant concentration in the ethylene-saturated $CDCl_3$ solution (as indicated by the absence of any orange-red color). The low temperature (−60°) p.m.r. spectrum of the resulting solution showed a large excess of ethylene present and a *ca.* 5:2 ratio of **4** to **5** (selenide to selenide dichloride) by integration.

Ethylene was bubbled into a solution of 50 mg (0.24 mmol) of **6** in 0.45 ml of $CDCl_3$ at −65° until the solution decolorized. The low temperature (−65°) p.m.r. spectrum showed excess ethylene present and a *ca.* 1:1 ratio of **4** to **5**. On warming to room temperature, the excess ethylene was consumed and the product composition altered to a ratio of 5:1. By addition of more ethylene the composition of the solution was further altered so that only **4** and ethylene were observed.

Isolation of 5 and 6

Ethylene was bubbled via a glass capillary into a solution prepared from 206 mg (1 mmol) of ArSeCl and 0.40 ml of $CDCl_3$ (purified by filtration through alumina) until the p.m.r. spectrum of the solution showed the integration of the resonances attributed to 2-chloroethyl 4′-tolyl selenide dichloride (**5**) to be at a maximum (*ca.* 25% of the total ArSeX species). Resonances attributed to 2-chloroethyl 4′-tolyl selenide (**4**) were also evident to the extent of *ca.* 7% of the total ArSeX species. An equal volume of pentane was added and the solution cooled to −78° until crystals formed. The mother liquor was decanted while the remaining crystalline mass was washed with CCl_4. The crude material obtained (74 mg, 24% based on ArSeCl, 75% based on ethylene added) was recrystallized from CCl_4 to give 54 mg of nearly colorless crystals m.p. 102.5–103.5°. Further recrystallization from pentane did not improve the m.p. The n.m.r. data for this compound were identical to that of **5** (Table 1).

Anal. Calcd. for $C_9H_{11}Cl_3Se$: C, 35.50; H, 3.64. Found: C, 35.16; H, 3.40.

The combined mother liquor and washings were evaporated to dryness and the oily residue crystallized from absolute ethanol to give 65 mg of yellow crystals identified as 4,4′-ditolyl diselenide (**6**) by n.m.r. comparison and m.p. (44–46°). From the mother liquor an additional 21 mg of **6** could be obtained by thin-layer chromatography (pentane – sliica gel) to give a 51% yield based on ArSeCl, 75% based on ethylene added. From the t.l.c. a second fraction was obtained containing a small amount of **4** (identified by its p.m.r. spectrum) accompanied by other unidentified products.

The Equilibrium Behavior of Binary Mixtures of Pure Components of the ArSeCl–Ethylene Reaction

Solutions of 5 and 6

When 76 mg (0.25 mmol) of authentic **5** and 42.5 mg (0.125 mmol) of pure **6** were dissolved in 0.45 ml of $CDCl_3$, a solution was obtained which by its p.m.r. spectrum was found to contain **4** and ArSeCl in addition to **5** and **6**. By integration and by assuming the stoichiometry of eq. 2, a $K = 9$ l mol^{-1} was determined for the mixture, in good agreement with the K determined for the reaction of ArSeCl with ethylene.

Solutions of 4 and ArSeCl

When 58.4 mg (0.25 mmol) of **4** and 51.4 mg (0.25 mmol) of ArSeCl were combined in 0.45 ml of $CDCl_3$, the p.m.r. spectrum of the solution revealed the presence of **5** and **6**. The K for this mixture was found to be 14 l mol^{-1}, again in agreement with previous results.

Can. J. Chem. Downloaded from www.nrcresearchpress.com by 210.87.254.42 on 09/05/12
For personal use only.

Pyrolysis of 2-Chloroethyl 4′-Tolyl Selenide Dichloride (5)

A neat sample (305 mg, 1 mmol) of **5** was heated in a sealed tube for 30 min at 115°. The tube was cooled to −78° and the red-orange pyrolysate dissolved in 0.20 ml of $CDCl_3$. The p.m.r. spectrum of the solution showed **5** to be 45% decomposed (by integration) to a mixture of two major products: 1,2-dichloroethane and a product tentatively identified as 1,2-dichloroethyl 4′-tolyl selenide (**7**). When **5** was pyrolyzed in tetrachloroethylene or pentachloroethane solution at 115°, similar results were obtained. When samples containing **5** prepared by the addition of ArSeCl to ethylene as described above were pyrolyzed at 115° in pentachloroethane, product mixtures were obtained similar to those from the pyrolysis of authentic **5**. No additional **4** was formed. Attempts to isolate pure 7 by thin-layer chromatography and gas–liquid chromatography failed due to separation difficulties and the decomposition of **7** under these conditions. The presence of 1,2-dichloroethane was established by direct p.m.r. and c.m.r. comparison with an authentic sample. Direct n.m.r. comparison also established the presence of **6**. The identification of **7** was based on its carbon (Table 2) and p.m.r. spectra: δ 2.34 (s, 3H), 3.77, 3.87, and 5.12 (ABX, J_{AB} = 12.0 Hz, J_{AX} = 8.2 Hz, J_{BX} = 5.2 Hz, 3H), 7.16 and 7.60 (AA′BB′, J_{AB} = 8 Hz, 4H). Further evidence for the identity of **7** was provided by n.m.r. comparison with the spectra of the compound obtained as the minor adduct of the addition of ArSeCl to vinyl chloride (see below).

Addition of 4-Toluneselenenyl Chloride to Vinyl Chloride

Vinyl chloride was bubbled into a solution of 205.5 mg (1 mmol) of ArSeCl in 0.30 ml of $CDCl_3$ until the solution was completely colorless. The n.m.r. spectra (^{13}C, ^1H) of the solution showed the presence of two products identified as 1,2-dichloroethyl 4′-tolyl selenide (**7**) and 2,2-dichloroethyl 4′-tolyl selenide (**8**) in a *ca.* 2:3 ratio by integration; p.m.r. spectrum of **8**: δ 2.28 (s, 3H), 3.36 (d, J = 6.5 Hz, 2H), 5.66 (t, J = 6.5 Hz, 1H), 7.04 and 7.42 (AA′BB′, J_{AB} = 8 Hz, 4H); p.m.r. spectrum of **7**, as above.

1-Propyl 4′-Tolyl Selenide

Sodium borohydride (760 mg, 20 mmol) was added under nitrogen in small portions to a slurry of 2.55 g (7.5 mmol) of 4,4-ditolyl diselenide (**6**) in 50 ml of absolute ethanol. After the vigorous evolution of heat and hydrogen had subsided a pale orange-yellow solution was obtained and 2.46 g (20 mmol) of 1-bromopropane was added. The reaction was allowed to stir overnight and then quenched with water and a few ml of 10% HCl. The mixture was then extracted with 100 ml of pentane and 25 ml of ether, and the combined organic layers dried over sodium sulfate. Evaporation of solvent and distillation (b.p. 54°/0.1 mm) gave 2.40 g (75%) of the selenide; p.m.r.: δ 0.93 (t, J = 7.5 Hz, 3H), 1.64 (sextet, J = 7.5 Hz, 2H), 2.23 (s, 3H), 2.72 (t, J = 7.5 Hz, 2H), 6.95 and 7.35 (AA′BB′, J = 8 Hz, 4H). Mass spectrum *m/e* Calcd. for $C_{10}H_{14}Se$: 214.02598. Found: 214.02598.

1-Propyl 4′-Tolyl Selenide Dichloride

A solution of 1.07 g (50 mmol) of 1-propyl 4′-tolyl selenide in 2 ml of $CHCl_3$ was treated with 0.41 ml (51 mmol) of sulfuryl chloride. As the reagent was added the solution became bright lime green and then colorless as the addition was completed. On evaporation a quantitative yield of the crude dichloride was obtained as a faintly yellow crystalline mass. Recrystallization from CCl_4 afforded 1.20 g (85%) of colorless crystals, m.p. 79–80°; p.m.r.: δ 1.15 (t, J = 7.5 Hz, 3H), 2.26 (sextet, J = 7.5 Hz, 2H), 2.32 (s, 3H), 4.14 (t, J = 7.5 Hz, 2H), 7.21 and 7.76 (AA′BB′, J = 8.5 Hz, 4H).

Anal. Calcd. for $C_{10}H_{14}Cl_2Se$: C, 42.28; H, 4.97. Found: C, 42.28; H, 4.85.

We thank the donors of the Petroleum Research Fund, administered by the American Chemical Society, and the National Science Foundation for support of this work, and the DuPont Company for a DuPont Young Faculty Grant.

1. D. G. Garratt and G. H. Schmid. Can. J. Chem. **52**, 1027 (1974).
2. H. J. Reich. J. Am. Chem. Soc. **95**, 964 (1973).
3. (*a*) H. J. Reich. J. Org. Chem. **39**, 428 (1974). (*b*) H. J. Reich, I. L. Reich, and J. M. Renga. J. Am. Chem. Soc. **95**, 5813 (1973).
4. D. B. Denny and L. S. Shih. J. Am. Chem. Soc. **96**, 317 (1974).
5. (*a*) W. J. R. Tyerman, W. B. O'Callaghan, P. Kebarle, O. P. Strausz, and H. E. Gunning. J. Am. Chem. Soc. **88**, 4277 (1966). (*b*) T. H. Chan and J. R. Finkenbine. Tetrahedron Lett. 2091 (1974).
6. S. Chan, H. Goldwhite, H. Keyzer, D. G. Rowsell, and R. Tang. Tetrahedron, **25**, 1097 (1969).
7. H. J. Backer and H. J. Winter. Rec. Trav. Chim. **56**, 492 (1937).
8. (*a*) D. Z. Denney, D. W. White, and D. B. Denney. J. Am. Chem. Soc. **93**, 2066 (1971). (*b*) R. E. Duff, R. K. Oram, and S. Trippett. Chem. Commun. 1011 (1971).
9. (*a*) N. N. Yarovenko, V. N. Shemanina, and G. B. Gazieva. Zh. Obshch. Khim. **29**, 942 (1959). (*b*) E. G. Kataev, T. G. Mannafov, E. A. Berdnikov, and O. A. Komarovskaya. Zh. Org. Khim. **9**, 1983 (1973). (*c*) K. B. Sharpless and R. F. Lauer. J. Org. Chem. **39**, 429 (1974).
10. M. Ohtsuru, K. Tori, and M. Fukuyama. Tetrahedron Lett. 2877 (1970) M. Ueyama, K. Tori, and M. Fukuyama. Org. Magn. Reson. **4**, 441 (1972).
11. F. J. Weigert and J. D. Roberts. J. Am. Chem. Soc. **89**, 5962 (1967); **94**, 6021 (1972).
12. M. T. Rogers and T. W. Campbell. J. Am. Chem. Soc. **69**, 2039 (1947).

Horseradish Peroxidase. XVIII. The Arrhenius Activation Energy for the Formation of Compound I

W. D. HEWSON AND H. B. DUNFORD

Department of Chemistry, University of Alberta, Edmonton, Alberta T6G 2E1

Received November 15, 1974

W. D. HEWSON and H. B. DUNFORD. Can. J. Chem. **53,** 1928 (1975).

The rate of formation of compound I from the reaction of native horseradish peroxidase with hydrogen peroxide was studied from 3.7–70.0 °C. The second-order rate constants were used to construct an Arrhenius plot from which the activation energy of this reaction was calculated to be 3.5 ± 1.0 kcal/mol. The irreversibility of the reaction at 25 °C was confirmed by comparing absolute absorbance changes as recorded by the stopped-flow apparatus with the known spectra of the native enzyme and compound I.

W. D. HEWSON et H. B. DUNFORD. Can. J. Chem. **53,** 1928 (1975).

On a étudié, de 3.7 à 70.0 °C, la vitesse de formation du composé I par réaction de la peroxydase du raifort naturel avec le peroxydyde d'hydrogène. On a utilisé les constantes de vitesse du deuxième ordre pour établir une courbe d'Arrhénius à partir de laquelle on a pu établir que l'énergie d'activation de la réaction est de 3.5 ± 1.0 kcal/mol. On a pu confirmer que la réaction est irréversible à 25 °C en comparant les changements d'absorbtion absolue tels que mesurés par un appareil à flux stoppé avec le spectre connu de l'enzyme at du composé I.

[Traduit par le journal]

Introduction

The stoichiometric reaction for the formation of compound I from native horseradish peroxidase (HRP) is

[1] $$HRP + H_2O_2 \rightarrow \text{Compound I}$$

and is known to be second order over a range of substrate concentrations (1). The first temperature dependence of the rate of this reaction was undertaken in 1947, at which time there appeared to be no significantly measurable increase in rate with temperature (2, 3). The reverse rate of reaction 1 has been considered to be very small, approximately seven orders of magnitude smaller than the forward rate (1). The present paper describes experiments performed to obtain the temperature dependence of the reaction from which the activation energy for the formation of compound I can be calculated. Also, changes in absorbance measurements have been used to verify the essential irreversibility of this reaction.

Experimental

Materials

Horseradish peroxidase (Lot No. 7024524) was purchased from Boehringer-Mannheim Corp. as an ammonium sulfate precipitate and was prepared for use by extensive dialysis against triply distilled water followed by Millipore filtration. Isozyme C, using the notation of Shannon *et al.* (4) and of Paul and Stigbrand (5) has been determined to be the major component of HRP obtained from Boehringer-Mannheim Corp. (6). Despite some fairly complicated kinetics, there has never been any valid kinetic evidence for a detectable amount of a second isozyme component (7). Enzyme purity and concentration were determined from absorbance measurements at 280 and 403 nm. A purity number (PN is a ratio of absorbances, 403/280 nm) of 3.54 was obtained. Published values usually lie between 2.8 and 3.2. It was found that extensive dialysis tends to increase PN values. Triply distilled water was used throughout and buffers were made from reagent grade materials.

Apparatus

Kinetic runs were carried out on a Gibson-Durrum stopped-flow spectrophotometer model D-110 in the absorbance mode at 403 nm with a 2 cm cuvette. Steady-state spectra and absorbance measurements were made on a Cary 14 spectrophotometer, p*H* was measured with an Orion 801 p*H* meter outfitted with a Fisher combination electrode calibrated with fresh standard buffers, and solution temperatures were maintained to ±0.3 °C by circulating thermostated water. The upper limit of the temperature range was 70.0 °C because at any higher temperature a significant amount of HRP denatured during the incubation period. A check for decomposition of hydrogen peroxide and/or enzyme was carried out by incubating the solutions in the drive syringes to 70.0 °C for a period of time approximately equal to the time necessary to perform a kinetic experiment. Then the solutions were quickly cooled to 25.0 °C and a kinetic experiment performed in order to compare the absorbance change accompanying the reaction after incubation with the absorbance change expected without the incubation period. Because enzyme absorption at

Can. J. Chem. Downloaded from www.nrcresearchpress.com by 210.87.254.6 on 09/05/12
For personal use only.

403 nm decreases with denaturation, the lack of a significant decrease in the change of absorption indicated no destruction of either reactant.

Methods

Stopped-flow kinetics were performed under second-order conditions where the initial concentrations of HRP and hydrogen peroxide are equal. The concentration of hydrogen peroxide was determined as previously described (8). One drive syringe contained 2.0 μM HRP and the other contained 2.0 μM hydrogen peroxide, resulting in an initial reactant concentration of 1.0 μM for both reactants in the 2 cm cuvette. Both drive syringe solutions had phosphate buffer (pH 7.10 $\pm$ 0.02 and ionic strength 0.01) and 0.10 M potassium nitrate as common components for a total ionic strength of 0.11. The reaction resulted in a decrease in absorbance as a function of time because the molar absorptivity at 403 nm for compound I is less than for HRP (ε_{HRP} = $1.02 \times 10^5\ M^{-1}\ cm^{-1}$ (9) and $\varepsilon_{compound\ I} = 5.31 \times 10^4\ M^{-1}\ cm^{-1}$ (10, 11)[1].) Checks on the absorbance changes recorded by both instruments should be the same. In the experiments performed on a Cary 14 spectrophometer, initiation of the formation of compound I was accomplished using a few microliters of hydrogen peroxide (equimolar with respect to HRP) on the end of a Teflon plumper.

Steady-state spectra, initiated in the same fashion, were recorded with [HRP] = 2.0 μM, [I^-] = 10.0 μM, and [H_2O_2] = 4.0 μM. The steady state spectrum of such a reaction mixture is known to be that of compound I (11). To achieve the steady state for a sufficiently long period of time to record the spectrum (about 50 s), the enzyme must cycle many times, the period of the cycle depending on the rate constant of the compound I reaction with iodide ion and the concentration of iodide ion, which govern the rate-controlling step. Iodide ion was in excess of the hydrogen peroxide so that should the steady state end before the spectrum was scanned the enzyme would revert to the native form and no longer exist as compound I which would facilitate detection of the end of the steady state.

The integrated rate expression for the reaction of HRP with H_2O_2 where reactants are in equal initial concentration and combine in a 1:1 stoichiometry is

$$[2] \qquad 1/[HRP]_t = kt + 1/[HRP]_0$$

The concentration of HRP at time t was determined by

$$[3] \qquad [HRP]_t = [HRP]_0(V_t - V_\infty)/(V_0 - V_\infty)$$

where V is the stopped-flow apparatus photomultiplier voltage and V_0, V_t, and V_∞ are voltages at times 0, t, and ∞. V_∞ values were determined by retriggering the data collection system (12) about 8 s after the reaction data had been recorded. Rate constants were determined from linear least-squares analysis of plots of $1/[HRP]_t$ *vs.* t. These plots were linear for 3 to 5 half-lives.

A near neutral pH of 7.10 was chosen because the rate of formation of compound I has been shown to be virtually pH independent from pH 5 to 9 (13). Preparing solutions at this pH at room temperature served to minimize any change in rate that might be a consequence of the change in pH of the solution with temperature.

[1]The $\varepsilon_{compound\ I}$ is corrected to the new reference value for HRP at 403 nm.

Results and Discussion

The Arrhenius plot shown in Fig. 1 was constructed from the rate constants recorded in Table 1 and yields an activation energy of 3.5 $\pm$ 1.0 kcal/mol.[2] This value corresponds to isozyme C. The activation energy of compound I formation with hydrogen peroxide has recently been determined independently for isozymes A2 and C to be 4.0 and 2.2 kcal/mol, respectively. These values were obtained from measurements at three temperatures over the range of 10 to 40 °C (14). If the experimental error of $\pm$1 kcal/mol can also be applied to their measurements (14), then all three values are identical within experimental error. A small value for the activation energy is necessary if HRP is to be an efficient enzyme.

The transition state theory interprets the Arrhenius preexponential factor A as

$$[4] \qquad A = \frac{\kappa kT}{h} \exp(\Delta S^{\ddagger}/R)$$

where κ, k, h, and $S^{\ddagger}$ are, respectively the transmission coefficient (usually assumed to be unity), Boltzmann's constant, Planck's constant, and the entropy of activation. The entropy of activation obtained from eq. 4 is -12.8 ± 0.1 cal/mol-deg, the negative value indicating a reaction where the activated complex is more ordered (less random) than the two reactants in accord with the fact that the enzyme and hydrogen peroxide must combine to form compound I (15). This correlates with a small steric factor, according to collision theory, which would lower the reaction rate.

A bimolecular rate constant in the order of $10^7\ M^{-1}\ s^{-1}$ is somewhat below the value expected for diffusion control of rate unless there are rigid steric requirements for reaction (16, 17). The limit of the value for the bimolecular rate constant is approximately $10^{10}\ M^{-1}\ s^{-1}$ for molecules of small cross-sectional area (18).

[2]The activation energy error was estimated by raising the value of the rate constant of the highest temperature and lowering the value of the rate constant at the lowest temperature by half the experimental error in the average rate constant determination; a new slope was calculated using these two points and gave a new activation energy different by 1.0 kcal/mol.

Can. J. Chem. Downloaded from www.nrcresearchpress.com by 210.87.254.6 on 09/05/12
For personal use only.

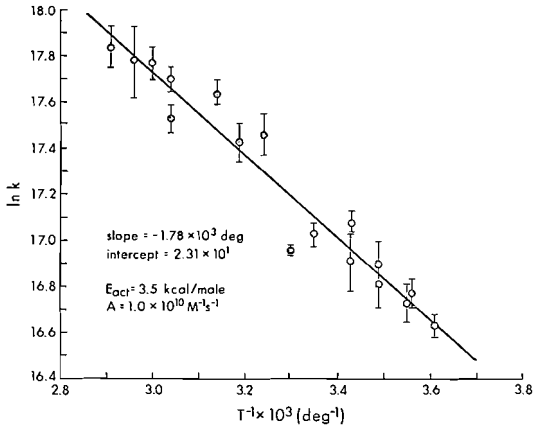

FIG. 1. Arrhenius plot of ln k *vs.* T^{-1}. Errors represent the average deviation of four to eight determinations of k at each temperature.

TABLE 1. Second-order rate constants for the formation of compound I from native HRP at pH 7.10

T (°C)	$k \times 10^{-7}$ (M^{-1} s^{-1})*	No. of determinations
3.7	1.7±0.1	8
7.4	1.9±0.1	5
8.6	1.8±0.2	5
13.0	2.0±0.2	5
13.5	2.2±0.2	5
18.1	2.6±0.1	8
18.7	2.2±0.1	6
25.0	2.5±0.1	5
30.0	2.3±0.1	7
35.0	3.8±0.4	4
40.0	3.7±0.3	6
45.0	4.6±0.3	6
55.4	4.1±0.3	5
55.6	4.8±0.3	7
60.0	5.2±0.4	7
65.0	5.3±0.8	6
70.0	5.6±0.6	7

*Errors are the average deviation from the mean.

The value might be expected to be lower for a relatively large, thus more slowly diffusing enzyme but the fact that it presents a bigger target for encounter with substrate compensates for its slower rate of diffusion. Note that this is only strictly applicable to molecules that are uniformly reactive over their entire surface, which may (19) or may not (20) be a good model for an enzyme with an active site. In an interesting publication by Schmitz and Schurr (21) it is pointed out that moderate angular constraints imposed on reactants that orient by rotational diffusion can lead to a rather drastic decrease in the maximum diffusion-controlled rate of values of 10^6 to 5×10^8 M^{-1} s^{-1}. They contend that it is plausible that reactions thought to be far removed from the diffusion-controlled rate might in fact be strongly viscosity dependent. The model used by these workers is a rotating sphere diffusing to a localized site on a plane. This appears to be an accurate model for the planar ferriprotoporphyrin IX prosthetic group which is the active site of HRP. When a reaction rate is strongly viscosity dependent, the activation energy can in large part be determined by the temperature variation of the diffusion coefficients of the reactants as the viscosity of the water changes and not solely determined by the fraction of reactant molecules with sufficient energy to form products. Other collisions between the enzyme's protein moiety and hydrogen peroxide may be ineffective (20).

Although indisputable proof that the reaction rate between HRP and hydrogen peroxide is diffusion-controlled is lacking, the conjecture is worth considering. Since superoxide dismutase is known to react with the oxygen radical anion ($O_2 \cdot^-$) at a rate of $(1.5 \pm 0.1) \times 10^9$ M^{-1} s^{-1} (22) it might be inferred that 10^7 M^{-1} s^{-1} does not represent a diffusion-controlled rate limit. However, no entropy of activation (or steric factor) has been measured for the superoxide dismutase reaction.

When the natural logarithm of the fluidity of water is plotted against T^{-1} (K^{-1}) over the same temperature range as the Arrhenius plot, a slope of $(-1.92 \pm 0.03) \times 10^3$ deg is obtained (23), which when multiplied by the gas constant, R, gives the activation energy for the fluidity of water as 3.89 ± 0.04 kcal/mol (fluidity is the reciprocal of viscosity). This is the theoretical minimum activation energy for reactions in aqueous solution (24) and is the same as the Arrhenius activation energy for compound I formation within experimental error.

The percentage error in the measurement of a second-order rate constant can be calculated according to the method of Benson (25). Percentage errors calculated with this method at several temperatures gave an average of 37 ± 5%.

The study conducted in 1947 (2) quotes rate constants of 8, 9, and 9, all times 10^6 M^{-1} s^{-1} at 3, 25, and 42 °C, respectively, which are

Can. J. Chem. Downloaded from www.nrcresearchpress.com by 210.87.254.6 on 09/05/12
For personal use only.

Can. J. Chem. Downloaded from www.nrcresearchpress.com by 210.87.254.6 on 09/05/12
For personal use only.

consistently lower than the rate constants in Table 1 measured at comparable temperatures. Dolman *et al.* (13) have measured the rate of compound I formation to be $1.84 \times 10^7\ M^{-1}\ s^{-1}$ at p*H* 7.07 and 25 °C. This value agrees more favorably with the present work.

It is interesting to compare briefly the combining rates of other heme systems with oxygen containing substrates. The rate of lactoperoxidase compound I formation has been measured at p*H* 7.17 and 25 °C by Maguire *et al.* (26) to be $1.2 \times 10^7\ M^{-1}\ s^{-1}$, and by Chance (27) at p*H* 7.0 to be $2 \times 10^7\ M^{-1}\ s^{-1}$. The rate of formation of compound I of HRP has been measured with methyl, ethyl (1), and hydroxymethyl (28) hydroperoxides and gave the respective rate constants 1.5, 3.6, and 0.5 all times $10^6\ M^{-1}\ s^{-1}$ which are much slower than for hydrogen peroxide. Bonnischsen *et al.* (2) have measured the rate of hydrogen peroxide and horse blood catalase combination at 25 °C to be $3.5 \times 10^7\ M^{-1}\ s^{-1}$.

Much of the work on the kinetics of the reaction of blood hemoglobin and myoglobin with oxygen has been compiled by Antonini and Brunori (29). Ilgenfritz and Schuster recently used the temperature-jump technique to measure the rate of oxygen binding to blood hemoglobin (30). At low oxygen saturations a fast binding step with a rate constant of $4 \times 10^7\ M^{-1}\ s^{-1}$ was found and at high oxygen saturation two steps were found, a fast and a slow step with the respective rate constants 4×10^7 and $5 \times 10^6\ M^{-1}\ s^{-1}$. They conclude that the first binding step occurs as fast as the last step, and the low affinity of deoxyhemoglobin for oxygen arises from the fast dissociation rate of Hb_4O_2, $10^3\ s^{-1}$. The two hemoproteins show many similarities in their kinetics. However, electric field jump measurements have shown a time constant of 10^{-7} s for blood hemoglobin but a correspondingly short time constant, could not be found for myoglobin, which, in the oxidized state, gave time constants of 10^{-6} s (31). The rate of reaction of horse blood catalase with hydrogen peroxide has been measured at two different temperatures and, assuming the validity of the Arrhenius equation, the activation energy was calculated to be 1.7 kcal/mol (2). This value is well below the minimum activation energy for the fluidity of water and is therefore of doubtful validity.

To test whether reaction 1 was going to completion in the stopped-flow apparatus, the absorbance change, ΔA, at 25 °C was determined several times with an average $\Delta A = 0.095 \pm 0.003$. The theoretical ΔA at this temperature for the same solution and cuvette specifications is 0.0978. Steady-state spectra of compound I reacting with iodide ion, where more than 99% of the enzyme should be in the form of compound I gave $\Delta A = 0.100$ within the reading precision of the recorded spectra. These absorbance measurements substantiate the claim that reaction 1 is essentially irreversible (1).

Steady-state spectra were attempted at higher temperatures; but the much accelerated spontaneous decay of compound I to compound II, which is a one electron reduction of the enzyme interfered with the steady state. For p*H* values slightly greater than 7, compound I is known to react with iodide ion approximately 1000 times faster than compound II (11, 12). This means that any spontaneously formed compound II will react much less readily with iodide ion and therefore accumulate in the system if it is formed spontaneously. Accumulation of some compound II occurred at 40 °C thereby making accurate absorbance measurements impossible for steady-state experiments. The ΔA for steady-state spectra at 40 and 55 °C agreed reasonably well with the ΔA as measured at the corresponding temperature in the stopped-flow apparatus but, because of the problem of compound I spontaneously forming compound II, these results should probably not be relied upon to confirm the irreversibility of reaction 1 at these temperatures.

1. B. CHANCE. Arch. Biochem. **22**, 224 (1949).
2. R. K. BONNISCHSEN, B. CHANCE, and H. THEORELL. Acta Chem. Scand. **1**, 685 (1947).
3. K. J. LAIDLER and P. S. BUNTING. The chemical kinetics of enzyme action. 2nd Ed. Clarendon Press, Oxford. 1973. pp. 199–216.
4. L. M. SHANNON, E. KAY, and J. Y. LEW, J. Biol. Chem. **241**, 2166 (1966).
5. K.-G. PAUL and T. STIGBRAND. Acta Chem. Scand. **24**, 3607 (1970).
6. C. PHELPS and E. ANTONINI. Biochem. J. **114**, 719 (1969).
7. H. B. DUNFORD and M. L. COTTON. J. Biol. Chem. **250**, 2920 (1975).
8. M. L. COTTON and H. B. DUNFORD. Can. J. Chem. **51**, 582 (1973).
9. G. R. SCHONBAUM and S. LO. J. Biol. Chem. **247**, 3353 (1971).
10. A. S. BRILL and H. E. SANDBERG. Biochemistry, **7**, 4254 (1968).

11. R. ROMAN and H. B. DUNFORD. Biochemistry, **11**, 2076 (1972).
12. R. ROMAN, H. B. DUNFORD, and M. EVETT. Can. J. Chem. **49**, 3059 (1971).
13. D. DOLMAN, G. A. NEWELL, N. D. THURLOW, and H. B. DUNFORD. Can. J. Biochem. In press.
14. S. MARKLUND, P. J. OHLSSON, A. OPARA, and K.-G. PAUL. Biochim. Biophys. Acta, **350**, 304 (1974).
15. H. B. DUNFORD. Physiol. Vég. **12**, 13 (1974).
16. G. G. HAMMES. Adv. Protein Chem. **23**, 17 (1968).
17. J. Z. HEARON, S. A. BERNHARD, S. L. FRIESS, D. J. BOTTS, and M. F. MORALES. *In* The enzymes. Vol. 1 *Edited by* P. D. Boyer, H. Lardy, and K. Myrbäck. Academic Press, New York. 1959. pp. 60–62.
18. M. V. SMOLUCHOWSKI. Z. Phys. Chem. **92**, 129 (1917).
19. S. H. KOENIG and R. D. BROWN. Proc. Natl. Acad. Sci. U.S.A. **69**, 2422 (1972).
20. S. LINDSKOG and J. E. COLEMAN. Proc. Natl. Acad. Sci. U.S.A. **70**, 2505 (1973).
21. K. S. SCHMITZ and J. M. SCHURR. J. Phys. Chem. **76**, 534 (1972).
22. M. PICH, J. RABANI, F. YOST, and I. FRIDOVICH. J. Am. Chem. Soc. **96**, 7329 (1974).
23. C. D. HODGMAN. (*Editor*). Handbook of chemistry and physics. 41st Ed. Chemical Rubber Publishing Company, Cleveland. 1960. pp. 2181.
24. E. F. CALDIN. Fast reactions in solution. John Wiley and Sons. New York. 1964. p. 12.
25. S. W. BENSON. The foundations of chemical kinetics. McGraw-Hill Book Company, Inc., Toronto. 1969. pp. 86–89.
26. R. J. MAGUIRE, H. B. DUNFORD, and M. MORRISON. Can. J. Biochem. **49**, 1165 (1971).
27. B. CHANCE. Science, **109**, 204 (1949).
28. S. MARKLUND. Acta Chem. Scand. **26**, 2128 (1972).
29. E. ANTONINI and M. BRUNORI. Hemoglobin and myoglobin in their reactions with ligands. North Holland Publishing Co., Amsterdam. 1971.
30. G. ILGENFRITZ and T. M. SCHUSTER. J. Biol. Chem. **249**, 2959 (1974).
31. T. M. SCHUSTER and G. ILGENFRITZ. Biochem. Saurest. Colloq. Ges. Biol. Chem. **19**, 53 (1968).

Can. J. Chem. Downloaded from www.nrcresearchpress.com by 210.87.254.6 on 09/05/12
For personal use only.

The Stability and Conformation of the 1,3,6,8-Tetraazatricyclo[4.4.1.1^{3,8}]dodecane System: the Structure of the Condensation Product of 1,2-Diaminocyclohexane and Formaldehyde

P. MURRAY-RUST AND F. G. RIDDELL[1]

Department of Chemistry, University of Stirling, Stirling, Scotland

Received November 22, 1974

P. MURRAY-RUST and F. G. RIDDELL. Can. J. Chem. **53**, 1933 (1975).

The condensation of *d,l-trans*-1,2-diaminocyclohexane with formaldehyde gives a pentacyclic molecule based on the 1,3,6,8-tetraazatricyclo[4.4.1.1^{3,8}]dodecane nucleus. This was shown to have S_4 symmetry by ^{1}H n.m.r. and an X-ray analysis showed crystals to be orthorhombic, *Fddd*, $a = 12.02$, $b = 19.25$, $c = 12.90$ Å. The symmetry of the compound in the crystal was D_{2d} due to a disordered arrangement and structure analysis was carried out to $R = 0.166$. When optically active diamine was used as starting material, the analogous reaction did not occur and this was attributed to strain in the tricyclic system. The conformation of the molecule is related to those of similar compounds as found by X-ray analysis.

P. MURRAY-RUST et F. G. RIDDELL. Can. J. Chem. **53**, 1933 (1975).

La condensation du *d,l-trans*-diamino-1,2 cyclohexane avec la formaldéhyde conduit à une molécule pentacyclique comportant le noyau tétraaza-1,3,6,8-tricyclo[4.4.1.1^{3,8}] dodécane. On a établi, par r.m.n. du proton que la molécule a une symétrie S_4; la diffraction des rayons-X revèle que les cristaux sont orthorhombiques, *Fddd*, $a = 12.02$, $b = 19.25$, $c = 12.90$ Å. A cause d'un arrangement désordonné la symétrie de ce composé dans le cristal est D_{2d}. La structure a été affinée jusqu'à une valeur de R de 0.166. Si une diamine optiquement active est utilisée comme produit de départ, la réaction de condensation n'a pas lieu; ceci est attribué à une tension dans le système tricyclique. La conformation de la molécule est comparée à celles établies par diffraction des rayons-X pour des composés similaires.

[Traduit par le journal]

Introduction

The 1,3,6,8-tetraazatricyclo[4.4.1.1^{3,8}]dodecane system (**1**) is of considerable conformational interest. The parent compound has been investigated both by n.m.r. (1) and X-ray single crystal (2) analysis but doubt remains as to whether the system has D_{2d} symmetry in the ground state or consists of rapidly interconverting species with the lower S_4 symmetry. The crystal structure had site symmetries for the molecule of D_{2d} but this could have been due to disordered molecules (S_4) or even inversion in the solid state. By making the aromatic derivative (**2**) and analyzing its crystal structure (3) it was shown that the nucleus could be forced into the D_{2d} arrangement (even if this is not the ground state geometry for **1**). The present study describes a similar attempt to force the nucleus into a conformation which possesses only S_4 symmetry, where the two-carbon bridge must adopt a *gauche* conformation. A simple way to do this is to make the bridge part of a cyclohexane ring which, if it adopts the chair conformation, will force the torsional angle in the 4,5 bond to be about 60°,

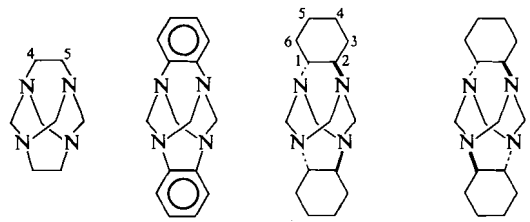

1 **2** **3** **4**

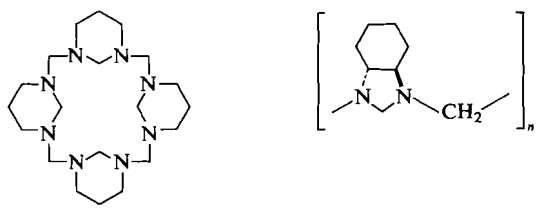

6 **5**

[1]On sabbatical leave at the Department of Chemistry, McMaster University, Hamilton, Ontario L8S 4M1.

Can. J. Chem. Downloaded from www.nrcresearchpress.com by 210.87.254.105 on 09/05/12
For personal use only.

Can. J. Chem. Downloaded from www.nrcresearchpress.com by 210.87.254.105 on 09/05/12
For personal use only.

approximately the angle predicted by Dreiding models (2). This might be accomplished by reacting *trans*-1,2-diaminocyclohexane with formaldehyde when two products could be expected. Reaction of one molecule of *d-trans*-1,2-diaminocyclohexane with one molecule of its enantiomer and four molecules of formaldehyde gives a product with S_4 symmetry[2] but if optically active diamine is used this cannot be formed. The only possible tricyclic product in this case is **4** (with D_2 symmetry) which is very highly strained and it is probable that other compounds such as **5** might be more stable. (This is analogous to the formation (4) of **6** from 1,3-diaminopropane and formaldehyde, where the tricyclic system would be severely overcrowded and has not been observed.) The preparation of **3** was therefore undertaken in an attempt to verify its existence and to produce crystals whose structure could be analyzed by X-ray crystallography.

Experimental

Condensation of 1,2-Diaminocyclohexane with Formaldehyde

1,2-Diaminocyclohexane was obtained from R. Emanuel Ltd. (stated to contain 80% of the *trans* isomer, the rest being mainly *cis*). As model building suggested that this impurity was unlikely to form a stable compound of the type required, the commercial sample was used without further treatment. The diamine (0.02 mol) was reacted with the calculated amount of formaldehyde in aqueous sodium hydroxide by a similar procedure (2) to that used for the preparation of **1**. After 3 weeks the solution was reduced in volume and the gluey residue extracted with acetone, from which small transparent rhombic bipyramidal crystals were obtained on evaporation. The molecular formula of these was confirmed by mass spectrometry (M^+ 276) and by the X-ray molecular weight determination (see below). The room temperature ^{1}H n.m.r. spectrum showed a well-resolved AB quartet at 5.9 and 6.2 τ (J = *ca.* 15 Hz) and broader resonances at *ca.* 7.5, 8.25, and 8.7 τ (Perkin Elmer R32 at 90 MHz).

The diaminocyclohexane was resolved via its hydrogen *d*-tartrate salt, treatment with base, and redistillation. This was then condensed with formaldehyde in an identical manner to that employed for the racemic diamine but no crystalline product could be isolated. The ^{1}H n.m.r. spectrum of the resulting syrup was clearly due to a mixture of products but showed no trace whatsoever of the AB quartet observed for the previous compound.

X-Ray Structure Analysis of the Crystalline Product

A rhombic bipyramid of *ca.* 0.3 × 0.2 × 0.2 mm was photographed by Weissenberg and precession techniques with MoKα radiation. The cell dimensions were found to be $a = 12.02$, $b = 19.25$, and $c = 12.90$ Å (all ±0.02 Å) and the space group was uniquely determined from systematic absences as *Fddd* (No. 70). The observed density of 1.25 g cm^{-3} (flotation) indicated eight molecules per unit cell for which the density is calculated to be 1.23 g cm^{-3}. The photographs showed considerable thermal diffuse reflection reminiscent (2) of that found for **1**. Reflection intensities were measured on a Hilger-Watts linear diffractometer with MoKα radiation for layers 0*kl* to 10*kl* (366 data) and *hk*0 to *hk*7 (277 data). Interlayer scalefactors were found by comparison of common reflections and the two sets were merged to give a unique set of 404 reflection data, all of which had $I > 2.5\sigma(I)$. Lorentz and polarization corrections (but none for extinction or absorption) were applied and the data put on an absolute scale by a Wilson plot, after which a Patterson synthesis was calculated.

The only eightfold positions in *Fddd* have D_2 (= 222) symmetry which is incompatible with the assumed molecular symmetry ($S_4 = \bar{4}$) of **3**. As the n.m.r. spectra and experiments with resolved diamine rule out the possibility of discrete molecules of D_2 symmetry, the crystal structure must consist of either a disordered arrangement of S_4 molecules or an infinite three-dimensional network quite different from the solution species. The former was strongly suggested by the similarity of the diffraction pattern to that of **1**, particularly the thermal diffuse reflection (common with highly symmetrical molecules of this type, especially when disorder may be present). Moreover, the cell dimensions were compatible with long cylindrical molecules lying on the points of D_2 symmetry in *Fddd*. Structure analysis therefore proceeded on the assumption of molecules of *average* crystallographic D_2 symmetry (but molecular symmetry S_4) lying on the Wyckoff points (*a*). (Throughout the calculations, the first setting (5) with the origin at *a* has been used.) The combination of the crystallographic and molecular symmetries will result in a structure with local D_{2d} (= $\bar{4}2m$) symmetry at these points. It is not surprising that the structure should be disordered as the molecules are highly symmetrical and have few directional intermolecular forces.

The Patterson function within 4.0 Å of the origin showed a close resemblance to that calculated for I (where the molecule has exact D_{2d} symmetry). On this basis the *average* positions of the atoms in the tricyclic nucleus were located and a subsequent Fourier synthesis revealed the *average* positions of the other atoms in the cyclohexane rings. A second Fourier synthesis showed that the molecule was wrongly orientated and after this correction three cycles of full-matrix least-squares refinement of the positional parameters (with the B_{iso} fixed at 4.0 Å^2) led to a structure with $R = 0.213$. (Scattering factors (6) were taken from International Tables for X-Ray Crystallography and the programs (7) used were our version of the CRYSTAL 69 suite. Unit weights were used throughout the least-squares analysis.) At this stage a difference synthesis was calculated but gave no clear indication of the precise position of the disordered molecules, except that there were large negative values at most atomic positions. Anisotropic temperature factors were introduced to simulate the disorder and three further cycles of refinement reduced the R value to 0.166. (No model with disordered molecules was

[2]The reader may find it helpful to build models of these compounds.

TABLE 1. The atomic parameters ($\times 10^4$) (with e.s.d.s. in parentheses) obtained for the average structure

	x/a	*y/b*	*z/c*	β_{11}	β_{22}	β_{33}	β_{12}	β_{13}	β_{23}
N	823(6)	524(4)	593(7)	45(7)	17(2)	82(7)	10(3)	6(6)	6(3)
CM(1)	0(*)	920(6)	0(*)	61(13)	12(3)	124(16)	*	24(13)	*
CM(2)	1461(13)	0(*)	0(*)	47(12)	25(4)	102(14)	*	*	12(7)
C(1,2)	413(11)	−275(7)	1587(10)	106(14)	46(5)	77(11)	43(6)	11(9)	2(6)
C(3,6)	861(13)	−577(7)	2528(12)	150(17)	57(6)	78(10)	50(8)	1(12)	−6(8)
C(4,5)	468(13)	−292(7)	3535(12)	150(18)	46(5)	101(13)	30(8)	3(12)	10(7)

NOTE: The carbon atoms in the methylene bridges are CM. The origin was taken at *a* (= 222) in the first setting for *Fddd*. The expression used for the anisotropic temperature factor was: $\exp(-(\beta_{11}H^2 + \beta_{22}k^2 + \beta_{33}l^2 + 2\beta_{12}hk + 2\beta_{13}hl + 2\beta_{23}kl))$.
*Atoms on special positions.

refined as there was no indication of their accurate geometry.) Final positional and thermal parameters are given in Table 1, where they describe the *average* positions of the disordered molecules. Bond lengths and angles for **3** cannot be accurately determined.[3]

Discussion

The ^{1}H n.m.r. spectrum of the crystalline product shows the expected AB quartet for the methylene bridge hydrogens, indicating that there is no molecular symmetry element relating these atoms. The molecular weight and crystal structure analysis then help to confirm its formulation as **3**. Although the crystallographic results do not give an accurate geometry because of the disorder the connectivity of the atoms is established with certainty. The structure (**3**) containing two diamine units of opposite absolute configuration cannot be made from optically active starting materials. Since the reaction mixture from the resolved diamine shows neither a crystalline product nor any trace of the diagnostic AB quartet, the structure (**3**) as the product from the racemic diamine is strongly supported. In any case, had the crystal consisted of equal amounts of enantiomers of D_2 symmetry (**4**) this would have become obvious from the refinement and difference syntheses.

The conformation of **3** cannot be very different from the rigid geometry produced by Dreiding models. Firstly, it is not possible for the cyclohexane rings to invert into another chair form. Secondly, any attempt to decrease the NC(1)C(2)N torsion angle from its value of *ca.* 60° leads to a similar increase in the C(6)C(1)C(2)C(3) system and causes severe angle strain in the cyclohexane ring. We can conclude from the present work that a molecule with the connectivity **1** can exist in an S_4 conformation. The present study does not allow however any estimate to be made of the magnitude of the distortion away from D_{2d} symmetry giving S_4 symmetry for **1** nor if S_4 is the ground state of **1**, can we say exactly where the minimum lies.

[3]Structure factor tables are available, at a nominal charge, from the Depository of Unpublished Data, CISTI, National Research Council of Canada, Ottawa, Canada K1A 0S2.

1. P. MURRAY-RUST and F. G. RIDDELL. Chem. Commun. 1075 (1970).
2. P. MURRAY-RUST. J. Chem. Soc. Perkin II, 1136 (1974).
3. P. MURRAY-RUST and I. SMITH. Acta Cryst. B30. In press.
4. H. KRASSIG. Makromol. Chem. 17, 77 (1956).
5. International tables for X-ray crystallography. Vol. I. Kynoch Press, Birmingham. 1968.
6. International tables for X-ray crystallography. Vol. III. Kynoch Press, Birmingham. 1969.
7. M. T. G. POWELL and A. GRIFFITHS. CRYSTAL 69 Computer Program, Portsmouth Polytechnic.

Can. J. Chem. Downloaded from www.nrcresearchpress.com by 210.87.254.105 on 09/05/12
For personal use only.

Carbon-13 Nuclear Magnetic Resonance Studies of Some *Lycopodium* Alkaloids

THOMAS T. NAKASHIMA, PETER P. SINGER, LOIS M. BROWNE, AND WILLIAM A. AYER

Department of Chemistry, University of Alberta, Edmonton, Alberta T6G 2E1

Received December 6, 1974

THOMAS T. NAKASHIMA, PETER P. SINGER, LOIS M. BROWNE, and WILLIAM A. AYER. Can. J. Chem. **53**, 1936 (1975).

The natural abundance ^{13}C magnetic resonance spectra of some *Lycopodium* alkaloids have been determined at both 25.15 and 22.63 MHz. By using standard techniques it has been possible to make self-consistent assignments of almost all of the resonances. The results suggest some interesting conclusions regarding the stereochemistry of some of the alkaloids and have been used to confirm the stereochemical assignment at C-12 in sauroxine and to assign the preferred conformation (axial) of the *N*-methyl group in the obscurines and *N*-methyllycodine.

THOMAS T. NAKASHIMA, PETER P. SINGER, LOIS M. BROWNE et WILLIAM A. AYER. Can. J. Chem. **53**, 1936 (1975).

On a déterminé, à 25.15 et 22.63 MHz, les spectres de résonance magnétique nucléaire du ^{13}C en abondance naturelle de quelques alkaloides *Lycopodium*. Utilisant les techniques habituelles, on a pu faire des attributions cohérentes de pratiquement toutes les résonances. Les résultats obtenus suggèrent quelques conclusions intéressantes concernant la stéréochimie de quelqu'uns des alkaloides et ces résultats ont été utilisés pour confirmer l'attribution stéréochimique en C-12 dans la sauroxine et pour attribuer la conformation privilégiée (axiale) du groupe *N*-méthyle des obscurines et de la *N*-méthyllycodine. [Traduit par le journal]

Introduction

A large amount of effort has been expended in the determination of the structures of the *Lycopodium* alkaloids.[1] Modern instrumental techniques such as mass spectrometry, optical rotatory dispersion and circular dichroism, X-ray crystallography, and proton magnetic resonance (p.m.r.) spectroscopy have all played a part (1, 2). Since, however, the majority of these alkaloids possess rather few functional groups and most of the protons reside on sp^3 hybridized carbons, the p.m.r. spectra are often of limited value due to the small chemical shifts and extensive spin–spin coupling involved. The majority of the signals appear as overlapping multiplets in the δ 1.0–2.5 region. Carbon-13 magnetic resonance (c.m.r.) is now emerging as a most attractive complimentary technique for structural elucidation (3, 4) of the alkaloids because of the sensitivity of the ^{13}C shielding parameter to slight geometric alterations.

We report here the ^{13}C chemical shifts for a series of *Lycopodium* alkaloids whose structures are shown below, along with the carbon numbering scheme for the parent alkaloid, lycopodine (**1**). The structures of each of these compounds have been determined previously (1, 2) utilizing many of the techniques mentioned above. This particular series of compounds offers the opportunity to examine substituent and geometric effects on the ^{13}C chemical shift parameter in a rather rigid system. Also the presence of the nitrogen atom allows the investigation of the effects of protonation on the ^{13}C chemical shielding and whether these protonation shifts are dependent upon the orientation of the nitrogen lone pair. With these general interests in mind we undertook a ^{13}C investigation of lycopodine (**1**), dihydrolycopodine (**2**), epidihydrolycopodine (**3**), flabelliformine (**4**), clavolonine (**5**), lycodoline (**6**), alkaloid L-23 (**7**), and α-lofoline (**8**).

[1]For recent reviews see refs. 1 and 2.

Results and Discussion

The ^{13}C chemical shifts of compounds **1**–**8** are listed in Table 1 and are summarized for convenience in graphical form in Fig. 1, which depicts changes in the carbon shielding with structural alterations within this set of related compounds. Table 2 summarizes the effects of *N*-protonation on the ^{13}C chemical shifts. Carbon-13 titration curves were determined on **1**, **4**, **5**, **6**, and **7**. Known amounts of CD_3CO_2D were added to the free base and the changes in the ^{13}C

Can. J. Chem. Downloaded from www.nrcresearchpress.com by 210.87.254.5 on 09/05/12
For personal use only.

TABLE 1. Carbon-13 chemical shifts[a] of some *Lycopodium* alkaloids

Carbon	1	2	3	4	5	6	7	8
1	47.2	47.1	47.2	46.2	47.2	46.2	48.0[d]	46.9
2	19.3[b]	20.7	19.9	16.9	18.7[b]	17.8[b]	25.2[h]	18.1[b]
3	20.1[b]	23.5[f]	24.1[f]	25.8[f]	19.4[b]	19.8[b,g]	18.7[g]	20.3[b]
4	43.4	32.6	37.2	79.8	43.1	43.3	52.3	31.1
5	213.4	68.5	71.5	211.0	213.2	212.1	210.5	70.2
6	43.3	34.0	36.6[e]	39.6	36.5	44.4	44.0	29.3
7	37.3	35.6	36.3[e]	36.8	43.1	40.8	40.9	42.8
8	43.1	42.0	42.2	43.0	78.9	35.8	37.5	75.2
9	47.8	47.4	47.2	49.4	47.2	46.2	48.7[d]	47.2
10	26.6[c]	26.6[f]	26.4[f]	25.8[f]	26.2[c]	20.8[g]	21.0[g]	26.4[c]
11	25.7[c]	25.0[f]	24.8[f]	27.3[f]	25.1[c]	30.3	30.3	24.2[c]
12	45.5	45.8	45.5	46.2	43.9	69.5	70.1	37.4
13	59.9	55.2	56.8	59.0	59.7	61.6	62.5	54.6
14	43.7	43.2	43.4	44.8	42.0	36.1	25.6[h]	38.3
15	25.8	23.5	28.9	25.5	33.0	24.3	24.6	27.5
16	23.3	24.1	24.1	23.2	19.4	22.6	22.6	23.0
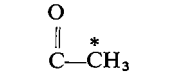								21.4
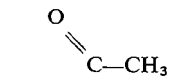								170.20

[a]Accurate to ±0.1 p.p.m. from internal TMS. Higher positive numbers indicate a decrease in shielding.
[b]C-2 and C-3 may be reversed.
[c]C-10 and C-11 may be reversed.
[d]C-1 and C-9 may be reversed.
[e]C-6 and C-7 may be reversed.
[f]C-3, C-10, and C-11 may be reversed.
[g]C-3 and C-10 may be reversed.
[h]C-14 and C-2 may be reversed.

TABLE 2. *N*-Protonation shifts[a] ($\delta^{13}C_{acid} - \delta^{13}C_{base}$)

Carbon	1[b]	2[c]	3[c]	4[d]	5[d]	6[d]	7[d]	8[c]
1	−0.8[e]	−0.9	−0.7	0.3	−0.6	−0.2	−0.1	−0.8
2	−0.8	−1.1	−0.9	−1.2	−0.7	−0.2	−3.0	−0.2
3	−1.9	−1.8	−2.2	−1.3	−1.6	−1.8	−1.1	−1.0
4	1.2	1.2	1.2	−2.1	1.1	2.4	−2.6	0.8
5	−5.4	−2.8	−1.8	−3.1	−5.0	−5.0	−2.9	−1.6
6	−0.5	−0.4	−0.8	−0.4	−0.6	−0.5	−0.4	−0.7
7	−0.7	−0.3	−0.7	−0.4	−0.6	0.5	0.9	−0.3
8	−1.6	−1.3	−1.4	−1.3	−2.2	−0.8	−0.4	−1.0
9	−0.7	−1.1	−0.9	0.6	−0.7	−0.2	−0.5	−1.1
10	−3.4	−3.2	−3.4	−2.5	−3.2	−2.7	−2.5	−2.5
11	−2.1	−1.6	−2.1	−2.3	−1.8	−2.0	−1.5	−2.9
12	−2.8	−2.4	−2.5	−1.9	−2.8	0.0	0.0	−2.2
13	3.8	6.7	6.0	3.4	3.4	4.5	4.8	4.7
14	−4.5	−4.3	−4.6	−3.1	−4.4	−3.3	3.8	−3.7
15	0.2	−0.2	−0.1	0.1	−0.4	0.3	−0.5	0.2
16	−0.8	−0.7	−0.7	−0.4	−0.7	−0.8	−0.4	−0.2
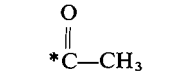								−0.2
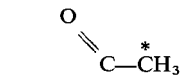								0.0

[a]Positive algebraic numbers indicate a decrease in shielding.
[b]Carbon-13 titration curve determined experimentally (0.5 *M*).
[c]Connectivity of carbon resonances of free base to the acidified solution done by analogy.
[d]Carbon-13 titration curve determined experimentally (0.22 *M*).
[e]See Table 1 for ambiguous assignments.

Can. J. Chem. Downloaded from www.nrcresearchpress.com by 210.87.254.5 on 09/05/12
For personal use only.

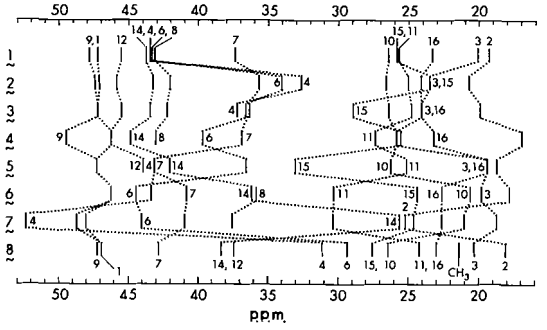

FIG. 1. Correlation of ^{13}C chemical shifts for compounds **1–8** in the 17–53 p.p.m. region.

shieldings were plotted *vs.* equivalents of acid. Such plots are shown in Fig. 2 for **7**, **1**, and **6**.

For **1**, excluding C-5 and C-13, whose resonances can be readily assigned using chemical shift theory (*5*), the carbon shieldings are grouped roughly into two regions: one occurring from 16 to 27 p.p.m. and the other from 36 to 48 p.p.m., relative to TMS. Using a simple additivity approach (5–11), one may group into the first region those ^{13}C resonances due to carbons 2, 3, 10, 11, 15, and 16, and carbons 1, 4, 6, 7, 8, 9, 12, and 14 into the second. Deuteration at C-9 and at C-4 and C-6 in **1** and **2** (coupled with the ^{1}H off-resonance spectrum in the nondeuterated compounds) allowed the unambiguous assignments for the resonances of these carbons. Carbon-16 was assigned unambiguously via ^{1}H off-resonance and selective decoupling. The similarity of the chemical environments of C-1 with respect to that of C-9 led to the assignment of C-1. Carbons 12, 14, 8, and 7 were assigned on the basis of additivity considerations, multiplicities obtained from the ^{1}H off-resonance experiments and from the expected responses of these shieldings to *N*-protonation (12). Substitution of a hydroxyl group at C-12 (**6**) in **1** is expected to decrease the shielding of C-11, C-7, and C-13 via a β-axial hydroxyl effect (13), increase the shielding of C-8, C-10, and C-14 via a γ-axial hydroxyl effect (13) and have little effect on the shieldings of the remaining carbons. On this basis C-10 and C-11, and C-2 and C-3 were assigned, though there is no unambiguous means of distinguishing between the first two carbons with the present data. A slight β deuterium isotope effect (14, 15) was noted in lycopodine-*4,6,6-d*$_3$ which led to the assignment of C-3. For lycopodine-*9,9-d*$_2$ no correlation between chemical shift change *vs.* carbon position could be observed. The assignments for

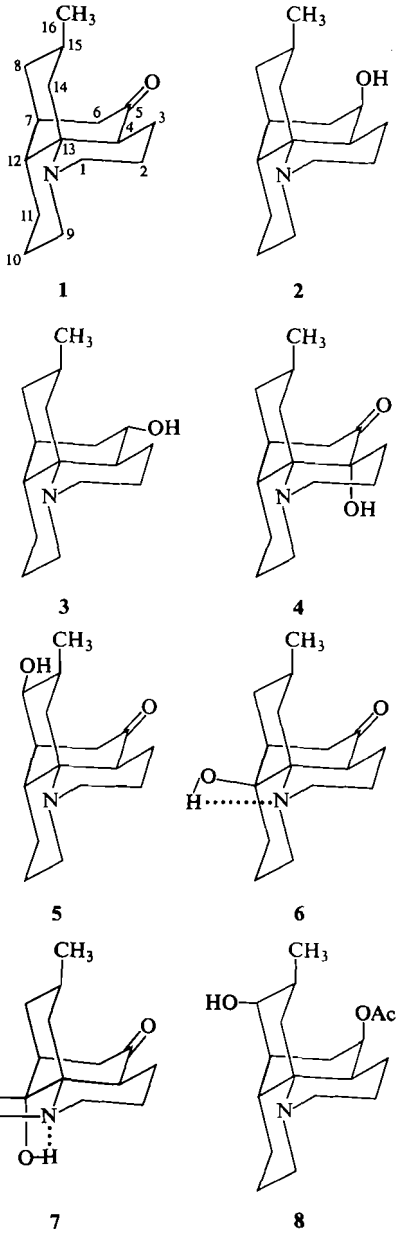

the carbons for the remainder of the compounds within this series were based on arguments similar to those just presented for the lycopodine case. While several of the assignments remain tentative, as indicated in Table 1, they all seem to be internally consistent.

There are several interesting features that emerge from the ^{13}C results for this particular series of compounds. The shielding at C-15 should reflect the steric influences generated at

Can. J. Chem. Downloaded from www.nrcresearchpress.com by 210.87.254.5 on 09/05/12
For personal use only.

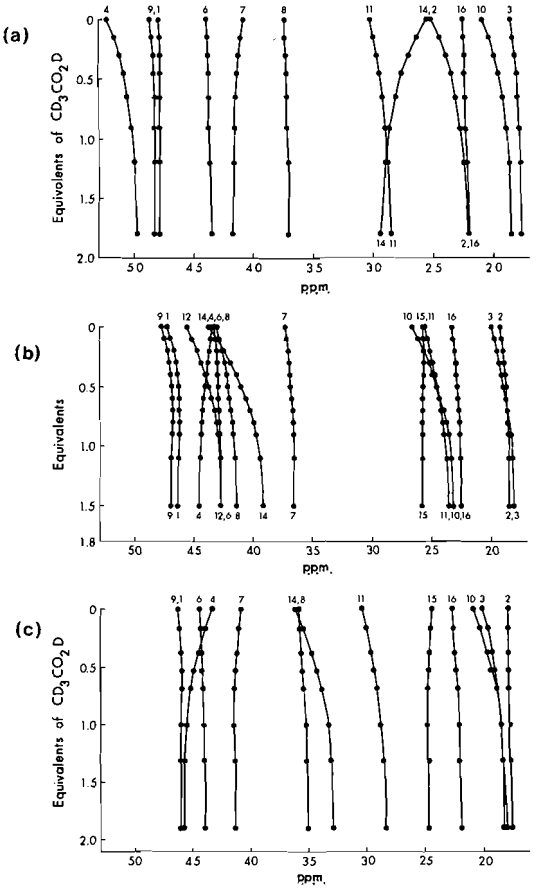

FIG. 2. Carbon-13 titration curves for (*a*) **7** (*b*) **1**, and (*c*) **6** in the 17–53 p.p.m. region.

this position via substituents attached to C-5. The shieldings found for C-15 in **1**, **2**, and **3** indicate that the steric influence of a carbonyl or an axial acetoxyl group is intermediate to that exerted by an axial hydroxyl group on one hand (shielding) and an equatorial hydroxyl group on the other (deshielding). The ε steric effect noted here may be a consequence of the proximity of C-5 to C-15 in the bicyclo[3.3.1]nonane system involved. Earlier p.m.r. studies (16) have indicated that this bicyclo[3.3.1]nonane system may be somewhat distorted from the ideal two chair form.

The shieldings of C-1 and C-9 are very similar throughout most of the series except in **4** in which there is a *syn*-axial orientation of the C-4 hydroxyl group with respect to both C-9 and C-11, which should produce a decrease in shielding for the latter two carbons. Thus, in the case of **4**, C-9 is less shielded than C-1 and C-11 deshielded with respect to C-10. The latter pair of assignments must, however, be regarded as tentative at this time. Such deshielding effects for similar geometric configurations have previously been shown to occur (17). The γ-axial effect of the hydroxyl at C-4 on C-2 in **4** is smaller than expected. This may be due to ring distortion caused by the intramolecular hydrogen bonding between the hydroxyl group and the carbonyl (18).

The most dramatic change in carbon shieldings within this set of related compounds occurs between **6** and **7** where there is a configurational change about C-12 and the nitrogen. The most notable change in shielding occurs for C-4 and C-14. The γ_{HH} and γ_{2HH} interactions (the nomenclature is that introduced by Dalling and Grant (10)) felt by C-14 in **6** from the protons of C-1 and C-3 are augmented in **7** by an additional γ_{HH} and γ_{2HH} perturbation arising from the protons of C-9 and C-11, consequently the large difference in shielding found for C-14 between the two geometrical isomers, **6** and **7**. For C-4 in **6**, a γ_{HH} and γ_{2HH} interaction is replaced in **7** by an γ-axial hydroxyl effect plus the orientational effect of the proton of the hydroxyl group in a hydrogen-bonded situation with the nitrogen lone pair. Similar changes in shielding of other carbons between the isomers may be accounted for in a like manner. These changes in shielding, especially for C-14, should prove to be a useful diagnostic tool in determining the configuration about nitrogen for compounds of related structure.

We have used these ^{13}C results to confirm the stereochemistry of sauroxine (**9**), originally assigned the configuration shown as **9***a* on the basis of a comparison of its mass spectrum and p.m.r. spectrum (19) with that of α-obscurine (**10**≡ **10***a*). The relative and absolute stereochemistry of α-obscurine, except for the configuration of the *N*-methyl group, is known through direct correlation with lycopodine (20). Since sauroxine is stereoisomeric with α-obscurine, the difference must be due to the configuration at C-12 and/or C-15. Since it is shown above that the ^{13}C shieldings are sensitive to changes in stereochemistry at C-12 (**6** *vs.* **7**), we have examined the ^{13}C spectra of these two compounds.

The ^{13}C results for **9** and **10** are summarized in Table 3 along with the results for lycodine (**11**) and *N*-methyllycodine (**12**) which were used as model compounds to aid in the chemical shift assignments. The assignments for **9**–**12** were

Can. J. Chem. Downloaded from www.nrcresearchpress.com by 210.87.254.5 on 09/05/12
For personal use only.

TABLE 3. Comparison of the carbon-13 chemical shifts[a] of α-obscurine and sauroxine

	9		10		11		12	
Carbon	δ	Δ[b,c]	δ	Δ[c]	δ	Δ[d]	δ	Δ[c]
1	171.7	0.8	171.8	0.6	147.1	0.6	146.7	0.0
2	31.1	−0.8	30.1	−0.5	121.6	1.3	121.6	1.1
3	18.7	−0.6[e]	19.5	−0.4	133.4	0.4	134.4	0.9
4	115.4	−5.6	114.2	−5.4	136.2	−3.8	138.1	−3.1
5	132.0	3.7	130.6	2.8	158.8	−0.6	158.4	−1.0
6	35.2	−0.2[f]	31.4	−0.9	35.5	−0.8	35.3	−1.2[g]
7	32.7	2.4[h]	33.7	−0.9	34.1	−0.9	34.0	−0.7
8	36.3	−0.9[f]	43.6	−0.9[i]	44.1	−1.1[k]	44.0	−0.7
9	47.7	−0.3	51.4	−0.8	41.5	−2.0[k]	50.5	−0.3
10	19.7	−0.1[e]	19.5	−1.1	26.4	−1.9[j]	19.8	−0.8
11	25.0	−1.8	26.5	−1.8	28.2	−2.5[j]	27.1	−1.4
12	33.9	−0.8[h]	36.0	0.4	44.9	−1.9	34.7	0.8[g]
13	59.6	6.8	59.0	5.7	56.2	2.8	59.7	3.7
14	35.2	−2.7[f]	43.0	−2.5[i]	51.7	−3.1	48.3	−2.1
15	27.7	0.0	27.2	−0.1	25.9	−0.8	26.5	0.0
16	22.5	−0.7	22.3	−0.6	22.1	−0.4	22.4	−0.4
17	36.6	−2.1	35.6	0.4			36.4	−0.6

[a]Chemical shifts accurate to ±0.1 p.p.m. from internal TMS. Higher positive numbers indicate a decrease in shielding.
[b]Δ represents the *N*-protonation shift in p.p.m. Higher algebraic numbers correspond to a decrease in shielding.
[c]Carbon-13 titration curve determined experimentally.
[d]Connectivity of carbon resonances of free base to the acidified solution done by analogy.
[e]C-3 and C-10 may be reversed.
[f]C-6, C-8, and C-14 may be reversed.
[g]C-6 and C-12 may be reversed.
[h]C-7 and C-12 may be reversed.
[i]C-8 and C-14 may be reversed.
[j]C-10 and C-11 may be reversed.
[k]C-8 and C-9 may be reversed.

based on additivity (21–23) (using **1**–**8** as model compounds for certain carbons), multiplicities obtained in the ^{1}H off-resonance spectra and from the expected responses of these shieldings to *N*-protonation (12). Initially the assumption was made that the *N*-methyl group would adopt an equatorial conformation. Comparison of the ^{13}C data of **11** and **12** clearly reveals that this is not the case. The increase in shielding of both C-10 (26.4 → 19.8 p.p.m.) and C-12 (44.9 → 34.7 p.p.m.) between **11** and **12**, together with the high-field position of the *N*-methyl signal (36.4 p.p.m.) (24) may only be explained if the *N*-methyl group adopts the axial configuration in **12**. It appears that the nonbonded interaction between the *N*-methyl group and the C-3 hydrogen is sufficient to cause a reversal of the normal conformational preference. The ^{13}C data for **9** and **10** indicate that in these compounds the *N*-methyl group is axially oriented as well.

Although several of the assignments in these compounds remain tentative because of the small shielding differences in several cases, it is clear that the change in shielding for C-14 between **9** and **10** (35.2 → 43.0 p.p.m.) is of the same order as that between **7** and **6** (25.6 → 36.1 p.p.m.) and indicates that sauroxine is indeed epimeric with α-obscurine at C-12 (and consequently also at nitrogen). Also, if the two differed in configuration at C-15 one would expect dramatic shielding differences for C-4, C-5, C-15, and C-16 between **9** and **10** and this is not observed experimentally.

Turning now to the effects of acidification on the ^{13}C chemical shift parameter in this series, we found them to be more complex than at first anticipated. Morishima *et al.* (12) have studied the effect of *N*-protonation on the ^{13}C chemical shieldings for a number of nitrogen containing compounds. For saturated nitrogen heterocycles, they found that in general methyl and methylene carbons become more shielded on *N*-protonation. More fully substituted carbons usually show a diminished effect and in some cases may be deshielded on protonation, as is observed here for C-13. Our acidification results agree well with Morishima's work with the exception of C-4 and C-14 in **7**. In all the compounds studied in this investigation, C-4 is deshielded[2] and C-14 is shielded on *N*-protonation except for **7** in which

[2]Excluding **4** in which there is a hydroxyl substituent at C-4.

Can. J. Chem. Downloaded from www.nrcresearchpress.com by 210.87.254.5 on 09/05/12
For personal use only.

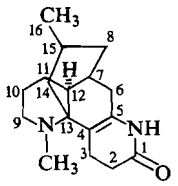

9

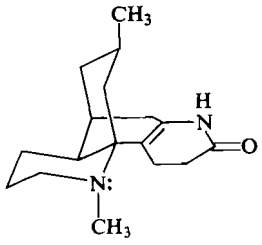

9a

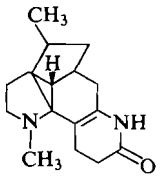

10

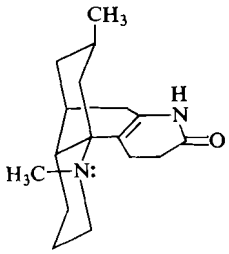

10a

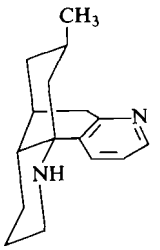

11

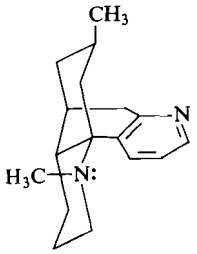

12

this tendency is reversed. The reason for this reversal in the 12-*epi* compound is not clear at this time.

It is informative to examine the effect of acidification on the shift of the C-5 carbonyl in these compounds. It has been shown that β-amino ketones, in which the unshared pair of electrons of the nitrogen, the α,β σ bond and the π orbital of the carbonyl are parallel, give rise to a non-classical e.t. (electron transfer) band in the 220–260 nm region in the u.v. (25). These bands, which disappear on *N*-protonation, are attributed to the splitting in the electronic energy levels caused by the interaction between the nitrogen lone pair and the π orbitals (referred to as a σ-coupled-p interaction) through the σ bond. All of the *Lycopodium* alkaloids with a carbonyl group situated at C-5 reported here show such e.t. bands with the exception of alkaloid L-23 in which this interaction does not exist because of the improper orientation of the nitrogen lone pair with respect to the carbonyl group (26). The details of the u.v. results, taken from ref. 26, are summarized in Table 4. The strength of the σ-coupled-p interaction for a related series is reflected by both the λ_{max} and ε values; the lower the λ_{max} (or the higher ε) values indicate a stronger interaction.

TABLE 4. Ultraviolet spectra of lycopodine type alkaloids in the region 215–230 nm (25)

Compound	Solvent	λ_{max} nm (ε value)
Lycopodine (**1**)	MeOH	217(2400)[a]
	Octane	217(2400)[a]
Clavolonine (**5**)	MeOH	218(1670)[a]
Lycodoline (**6**)	MeOH	221(1500)[a]
Flabelliformine (**4**)	MeOH	228(inf)(≃ 500)[a]
L-23 (**7**)	MeOH	No maximum

[a]Disappears on acidification of solution.

If appreciable charge transfer occurs in the ground state due to this interaction, the ^{13}C chemical shift data should reflect the amount of electron transfer and should be valuable in the investigation of such interactions. Some support for this view is found in the protonation shifts of the carbonyl carbon for which an induced shift of approximately −5 p.p.m. is observed for those compounds (**1**, **5**, and **6**) exhibiting strong e.t. bands while a smaller (−3 p.p.m.) shift is noted for those compounds (**4** and **7**) exhibiting weak or no e.t. transitions. The ^{13}C results imply that there is a greater increase in the electron density about the carbonyl carbon caused by *N*-protonation for compounds with a stronger σ-coupled-p interaction. Whether or not this is generally applicable to other such systems (27) remains to be determined. Such an interpretation should be viewed with caution as carbonyl shifts are known to be quite sensitive to other electronic influences (28).

One would also have expected the shieldings of C-13 to reflect this interaction since it occurs through this carbon. However, the *N*-protonation shifts for this carbon are almost identical for **6** and **7**, the stereochemical isomers.

Experimental

The ^{13}C spectra were obtained on natural abundance samples of approximately 0.5 *M* solution in $CDCl_3$ – 5% TMS (unless otherwise noted) at a frequency of 25.15 MHz (Varian HA-100 interfaced to a Digilab FTS/NMR-3 data system and associated pulser and proton decoupler) or at 22.628 MHz (Bruker HFX-90 interfaced to a Nicolet 1085 computer) in 10 mm tubes in the pulse Fourier mode. The deuterium resonance of $CDCl_3$ served as the lock signal for field/frequency stabilization. For the ^{13}C

Can. J. Chem. Downloaded from www.nrcresearchpress.com by 210.87.254.5 on 09/05/12
For personal use only.

titration experiments, known quantities of CD_3CO_2D–$CDCl_3$ (0.64 g of CD_3CO_2D in 1 ml solution) were syringed directly into the n.m.r. sample.

Compounds **1**–**8** were available from previous work in these laboratories (2). The deuterated compounds were prepared from the appropriate nondeuterated alkaloid as described below.

Lycopodine-4,6,6-d_2,d_3

Lycopodine (0.16 g) was dissolved in D_2O (1 ml) and PCl_5 (1 g) was added cautiously. The stoppered reaction mixture was allowed to stand at room temperature for 5 days, then basified by careful addition of anhydrous sodium carbonate. The mixture was diluted with D_2O, extracted with ether, the ether extract dried (anhydrous magnesium sulfate) and concentrated to give 0.135 g of a mixture of lycopodine-*4,6-d_2* and lycopodine-*4,6,6-d_3* (1:1) as shown by low-resolution mass spectrometry (A.E.I. MS-12 mass spectrometer).

Dihydrolycopodine-4,6,6-d_2,d_3

Lycopodine-d_2–lycopodine-d_3 (0.13 g), anhydrous sodium carbonate (trace), and sodium borohydride (0.1 g) were dissolved in deuteriomethanol. The reaction mixture was allowed to stand at room temperature overnight, then diluted with aqueous hydrochloric acid. The aqueous extract was washed with ether, basified with 10% sodium hydroxide solution, then extracted with methylene chloride. The methylene chloride extract was dried (anhydrous magnesium sulfate) and concentrated to give 0.125 g dihydrolycopodine-*4,6,6-d_2,d_3* (1:1) as shown by low-resolution mass spectrometry.

Lycopodine-9,9-d_2 was prepared by the method of MacLean and co-workers (29).

We gratefully acknowledge the financial support of the National Research Council of Canada.

1. D. B. MacLean. *In* Chemistry of the alkaloids. *Edited by* S. W. Pelletier. Van Nostrand Reinhold Company, Toronto. 1970. p. 469.
2. W. A. Ayer. *In* MTP international review of science. Series 1, Vol. 9. *Edited by* D. H. Hey and K. F. Wiesner. University Park Press, Baltimore. 1973. p. 1.
3. E. Wenkert, B. Chauncy, K. G. Dave, A. R. Jeffcoat, F. M. Schell, and H. P. Schenk. J. Am. Chem. Soc. **95**, 8427 (1973).
4. W. O. Crain, Jr., W. C. Wildman, and J. D. Roberts. J. Am. Chem. Soc. **93**, 990 (1971).
5. J. B. Stothers. Carbon-13 NMR spectroscopy. Academic Press, New York, N.Y. 1972.
6. D. M. Grant and E. G. Paul. J. Am. Chem. Soc. **86**, 2984 (1964).
7. D. M. Grant and B. V. Cheney. J. Am. Chem. Soc. **89**, 5315 (1967).
8. D. K. Dalling and D. M. Grant. J. Am. Chem. Soc. **94**, 5318 (1972).
9. L. P. Linderman and J. Q. Adams. Anal. Chem. **43**, 1245 (1971).
10. D. K. Dalling and D. M. Grant. J. Am. Chem. Soc. **96**, 1827 (1974).
11. C. G. Moreland, A. Philip, and F. I. Carroll. J. Org. Chem. **39**, 2413 (1974).
12. I. Morishima, K. Yoshikawa, K. Okada, T. Yonezawa, and K. Goto. J. Am. Chem. Soc. **95**, 165 (1973).
13. J. D. Roberts, F. J. Weigert, J. I. Kroschwitz, and H. J. Reich. J. Am. Chem. Soc. **92**, 1338 (1970).
14. R. A. Bell, C. L. Chan, and B. G. Sayer. J. Chem. Soc. Chem. Commun. 67 (1972).
15. J. B. Stothers, C. T. Tan, A. Nickon, F. Huang, R. Sridhar, and R. Weglein. J. Am. Chem. Soc. **94**, 8581 (1972).
16. W. A. Ayer and D. A. Law. Can. J. Chem. **40**, 2088 (1962).
17. S. H. Grover, J. P. Guthrie, J. B. Stothers, and C. T. Tan. J. Magn. Resonance, **10**, 227 (1973).
18. M. Curmumelli-Rodostamo and D. B. MacLean. Can. J. Chem. **40**, 1068 (1962).
19. W. A. Ayer, T. E. Habgood, V. Deulofeu, and H. R. Juliani. Tetrahedron, **21**, 2169 (1965).
20. W. A. Ayer, J. A. Berezowsky, and G. G. Iverach. Tetrahedron, **18**, 567 (1962).
21. P. C. Lauterbur. J. Am. Chem. Soc. **83**, 1838 (1961).
22. H. L. Retcofsky and R. A. Friedel. J. Phys. Chem. **72**, 290, 2619 (1968).
23. H. L. Retcofsky and R. A. Friedel. J. Phys. Chem. **71**, 3592 (1967).
24. E. L. Eliel and F. W. Vierhapper. J. Am. Chem. Soc. **96**, 2257 (1974).
25. R. C. Cookson, J. Henstock, and J. Hudec. J. Am. Chem. Soc. **88**, 1060 (1966).
26. W. A. Ayer, B. Altenkirk, R. H. Burnell, and M. Moinas. Can. J. Chem. **47**, 449 (1969).
27. A. W. J. D. Dekkers, J. W. Verhoeven, and W. N. Speckamp. Tetrahedron, **29**, 1691 (1973).
28. G. E. Maciel and J. J. Natterstad. J. Chem. Phys. **42**, 2752 (1965).
29. N. Chin-You, D. B. MacLean, A. Prakash, and C. Calvo. Can. J. Chem. **49**, 3240 (1971).

Can. J. Chem. Downloaded from www.nrcresearchpress.com by 210.87.254.5 on 09/05/12
For personal use only.

The Stereochemistry of the Reformatsky Reaction of Methyl 4-Bromo-3-methylbut-2-enoate with β-Cyclocitral and Related Compounds

R. N. GEDYE, PARKASH ARORA, AND A. H. KHALIL
Department of Chemistry, Laurentian University, Sudbury, Ontario P3E 2C6

Received October 11, 1974

R. N. GEDYE, PARKASH ARORA, and A. H. KHALIL. Can. J. Chem. **53**, 1943 (1975).

Both methyl *Z*- and *E*-4-bromo-3-methylbut-2-enoate react with β-cyclocitral in the presence of zinc to give the δ-lactone of 5-hydroxy-3-methyl-5-(2,6,6-trimethyl-1-cyclohexen-1-yl)-2-pentenoic acid as the main product, indicating an *E* to *Z* inversion during the Reformatsky reaction. Similar results were obtained in the Reformatsky reactions of the *Z*- and *E*-bromoesters with benzaldehyde and cyclohexenecarboxaldehyde. Here hydrolysis of the Reformatsky product gave, in each case, the corresponding *Z*-2,*E*-4-acids as the main products, indicating the formation of the δ-lactone as an intermediate. The synthesis of *Z*- and *E*-β-ionylideneacetic acid and the corresponding ring demethyl analogs using a Wittig reaction is also described.

R. N. GEDYE, PARKASH ARORA et A. H. KHALIL. Can. J. Chem. **53**, 1943 (1975).

Les bromo-4 méthyl-3 butène-2 oates de méthyle *Z* et *E* réagissent avec le β-cyclocitral en présence de zinc pour conduire à la δ lactone de l'acide hydroxy-5 méthyl-3 (triméthyl-2,6,6 cyclohexène-1 yl-1)-5 pentène-2 oique comme produit principal; ce résultat indique qu'il y a une interconversion de *E* et *Z* au cours de la réaction de Reformatsky. On a obtenu des résultats semblables lors de la réaction de Reformatsky des bromoesters *E* et *Z* avec le benzaldéhyde et le cyclohexènecarboxaldéhyde. Dans chacun de ces cas, l'hydrolyse du produit de Reformatsky conduit aux acides 2-*Z*,4-*E* correspondants comme produits principaux; ces résultats indiquent qu'il y a formation de la δ lactone comme intermédiaire. On décrit aussi la synthèse faisant appel à la réaction de Wittig des acides β-ionylidène acétiques *Z* et *E* ainsi que des analogues desméthyles cycliques correspondants. [Traduit par le journal]

The Reformatsky reactions between benzaldehyde, β-cyclocitral, and β-ionylideneacetaldehyde with esters of 4-bromo-3-methylbut-2-enoic acid have attracted the attention of several laboratories as a possible route to the synthesis of vitamin A and related compounds (1–8). Harper and Oughton (1) and Fuson and Southwick (2) have reported that the Reformatsky reaction between benzaldehyde and methyl 4-bromo-3-methylbut-2-enoate yields a mixture of compounds in which there is a substantial amount of the δ-lactone **3***b*. The bromoester used in these Reformatsky reactions was obtained by the allylic bromination of methyl 3-methylbut-2-enoate with *N*-bromosuccinimide. The formation of the δ-lactone was ascribed either to the presence of the *Z*-bromoester **1** or to the inversion of the *E*-bromoester **2** during the Reformatsky reaction (1).

Tanabe (5), Yoshida and Tanabe (6), and Eiter *et al.* (7) have reported that the Reformatsky reaction between β-cyclocitral and the bromoester gave an isolatable δ-lactone **3** which on subsequent hydrolysis yielded *Z*-β-ionylideneacetic acid, **4***a*. Harper and Oughton (1) on the other hand, reported the formation of the hydroxy ester **5***a* but did not mention any investigation of its stereochemistry.

It is almost certain that in all the above reports, a mixture of *Z*- and *E*-bromoesters **1** and **2** has been used (9–11). It has been suggested that the use of the pure *E*-bromoester **2** might be advantageous in the synthesis of all-*trans*-vitamin A(12) but as far as we can ascertain no attempt has been made to examine the stereochemical outcome of the Reformatsky reaction using either pure *Z-1* or *E-2* to prove or disprove that the presence of the *Z*-bromoester might be responsible for the production of the δ-lactone (1).

Our present investigations have confirmed previous reports (9, 10) that the allylic bromination of methyl 3-methylbut-2-enoate gives a mixture of the two geometrical isomers **1** and **2** in the ratio 2:3. The successful separation of **1** and **2** in stereochemically pure forms enabled us to reexamine the above mentioned Reformatsky reactions using either the pure *Z*-

Can. J. Chem. Downloaded from www.nrcresearchpress.com by 210.87.254.5 on 09/05/12
For personal use only.

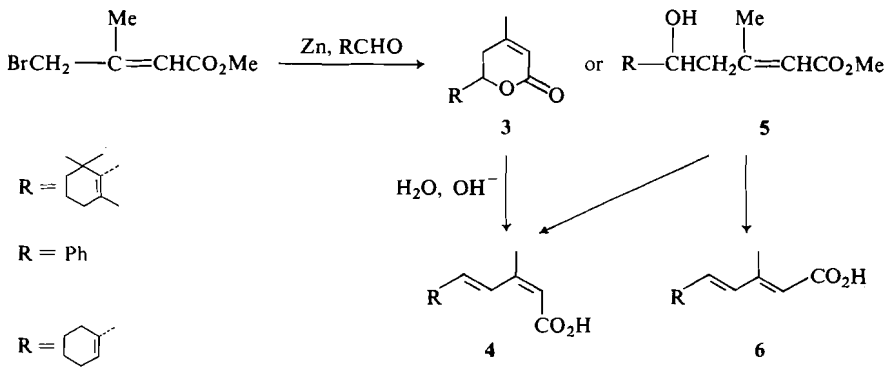

bromoester **1** or *E*-bromoester **2**. Three carbonyl substrates were used in this study: (*a*) benzaldehyde, (*b*) β-cyclocitral, and (*c*) cyclohexenecarboxaldehyde. On the basis of the identification of the products by comparison with reference compounds prepared by unequivocal procedures it was evident that the *Z*-bromoester and the *E*-bromoester afforded the same products under the same conditions. It is therefore not true that the *Z*-bromoester is solely responsible for the formation of the δ-lactone nor is there any real advantage to be gained in the use of the pure *E*-bromoester in the synthesis of vitamin A intermediates using a conventional Reformatsky reaction.

The Reformatsky reaction between benzaldehyde and the *Z*- or the *E*-bromoesters gave similar products. Although we were not successful in isolating the δ-lactone, the product showed an i.r. absorption at 1720 cm^{-1} indicative of the δ-lactone **3***b*. Alkaline hydrolysis followed by isolation of the acidic products and esterification with ethereal diazomethane gave a mixture of the *Z*-2,*E*-4 (70%) and the *E*-2,*E*-4 (30%) isomers of the methyl ester of 3-methyl-5-phenylpenta-2,4-dienoic acid. These results are in agreement with the structural assignments of the Reformatsky products made by Wiley (4), who ascribed the formation of the *Z*-2,*E*-4-isomer **4***b* to the ring opening of the δ-lactone **3***b* during the saponification process. The *E*-2,*E*-4-isomer **6***b* presumably arises, along with **4***b*, from the dehydration of the hydroxy ester **5***b*.

A similar Reformatsky reaction between cyclohexene carboxaldehyde and either the *Z*- or the *E*-bromoester showed the formation of an unsaturated δ-lactone (i.r. 1719 cm^{-1}) in all the isolated fractions. Alkaline hydrolysis of the Reformatsky product followed by isolation of the acidic product gave an acid shown to be 5-(cyclohexen-1-yl)-3-methyl-*Z*-2,*E*-4-pentadienoic acid (**4***c*). Again the acid **4***c* would be expected to arise from the ring opening of the δ-lactone **3***c* during the saponification process.

The Reformatsky reaction of β-cyclocitral and

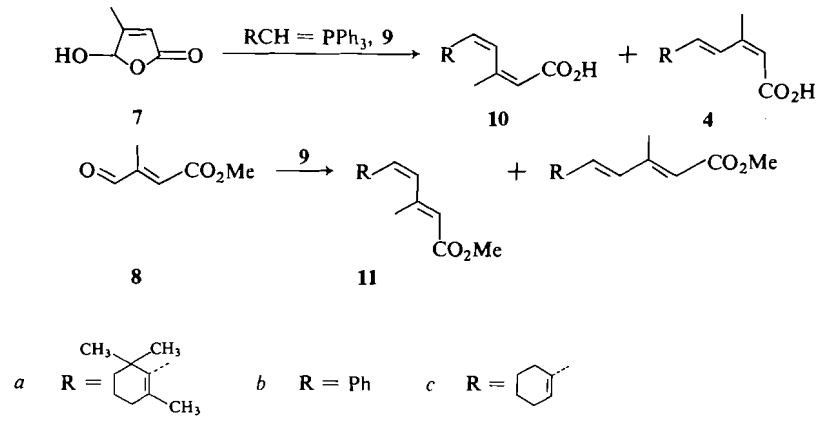

Can. J. Chem. Downloaded from www.nrcresearchpress.com by 210.87.254.5 on 09/05/12
For personal use only.

Can. J. Chem. Downloaded from www.nrcresearchpress.com by 210.87.254.5 on 09/05/12
For personal use only.

the *Z*- and *E*-bromoesters gave a product from which δ-lactone **3***a* was isolated by column chromatography on alumina. Alkaline hydrolysis of the lactone followed by acidification gave *Z*-β-ionylideneacetic acid (**4***a*).

The products in this study were determined by g.l.c. using reference compounds prepared by standard procedures, notably those of Pattenden and Weedon (13) who showed that the Wittig reaction of 4-hydroxy-3-methylbut-2-enolide (**7**) and of methyl *E*-3-formylcrotonate (**8**) with the Wittig reagent **9***b* gave a convenient method for the synthesis of the four geometrical isomers of 3-methyl-5-phenylpenta-2,4-dienoic acid (**10***b*, **4***b*, **11***b*, and **6***b*).

We have applied this method to the synthesis of *Z*- and *E*-β-ionylideneacetic acid. Only one isomer was formed in each reaction, probably due to steric factors, providing a convenient method for the preparation of these important vitamin A intermediates in stereochemically pure forms and in high yield.

Condensation of the Wittig reagent **9***a* (14) with the lactol **7** followed by isolation of the acidic product gave only *Z*-β-ionylideneacetic acid (**4***a*) in 87% yield. The Wittig reaction of **9***a* with methyl *E*-3-formylcrotonate (**8**) gave only the *E*-methyl ester **6***a* in 80% yield.

The *Z*-2,*E*-4 and *E*-2,*E*-4-isomers of 3-methyl-5-(cyclohexen-1-yl)penta-2,4-dienoic acid (**4***c* and **6***c*) were prepared in high yield by similar reactions using the Wittig reagent **9***c* with the lactol **7** and with methyl *E*-3-formylcrotonate, respectively. The n.m.r. properties of these previously unreported isomers **4***c* and **6***c* are shown in the accompanying formulae.

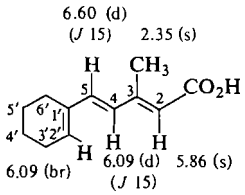

6*c*

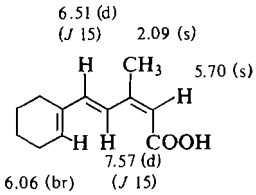

4*c*

The relative δ values for the C_3 methyl protons provides a convenient means for determining the stereochemical configuration of compounds of the β-ionylideneacetic acid series, where the absorption in the all-*trans* isomer always occurs at a lower field (11, 15).

On the basis of these experimental results the following points deserve mention. Firstly, under similar conditions in the various Reformatsky reactions the *Z*- and *E*-bromoesters afford the same products, which include the δ-lactone, and it is clear that the δ-lactone does not arise only from the *Z*-bromoester as has been suggested (1). Secondly the formation of the *Z*-2,*E*-4-isomers **4***a*, *b*, and *c*, is only explainable by the formation of δ-lactones as intermediates in the Reformatsky reactions concerned. Unsaturated lactones have been shown to open with conservation of the stereochemistry of the α,β position (16). Finally, in order to account for the formation of the δ-lactones from the *E*-bromoester the following explanations may be considered. (*i*) Excess zinc, usually used in the Reformatsky reaction, might catalyze the stereomutation of the double bond in the *E*-bromoester and result in lactonization. A similar stereomutation has been reported in the presence of iron (17). On refluxing either the pure *E*- (or pure *Z*-) bromoester in benzene with zinc for several hours, however, no stereomutation was observed using g.l.c. or n.m.r. (*ii*) Recently Coffignal and Gaudemar (18) have found that an allylic rearrangement occurs in the condensation of γ-bromocrotonates with aldehydes and ketones and suggested the reaction involved the formation of the rearranged ester **12** (R_3 = H) as the first intermediate. This undergoes equilibration with the "linear" ester **13** (R_3 = H) resulting in a mixture of the rearranged and "linear" β-hydroxy esters after hydrolysis.

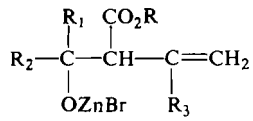

12

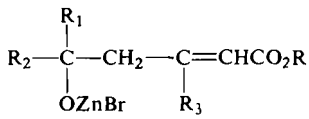

13

Although no lactone was isolated by these workers, the formation of the δ-lactone in the present study is not inconsistent with this mechanism. The same equilibrium mixture of *Z*-

Can. J. Chem. Downloaded from www.nrcresearchpress.com by 210.87.254.5 on 09/05/12
For personal use only.

and *E*-esters **13** (R_3 = Me) would be expected to result from both the *Z*- and *E*-bromoesters **1** and **2**, and the *Z* form may have lactonized during the course of the reaction.

Experimental

All boiling and melting points are uncorrected. Infrared spectra were recorded with a Beckman IR-10 double beam spectrophotometer. The n.m.r. spectra were obtained with a Varian A-60 deuteriochloroform solution unless otherwise stated, with tetramethyl silane as an internal reference. Ultraviolet spectra were recorded with a Hitachi Perkin-Elmer Model 124 double beam spectrophotometer. Gas chromatography was carried out on a Varian Aerograph Model 90-P gas chromatograph using a 160 cm × 6 mm column of 3% SE-30 silicone gum rubber on Chromosorb W with the helium as a carrier gas. Fractional distillations were carried out using a Nester-Faust annular spinning band column with 100 theoretical plates.

Methyl Z- and E-4-Bromo-3-methylbut-2-enoate (1 and 2)

A mixture of *Z*- and *E*-bromoesters was obtained from the reaction of methyl 3-methylbut-2-enoate with *N*-bromosuccinimide according to the literature procedure (9). The product, b.p. 80–88°/12 mm, n_D^{20} 1.5022, was shown by g.l.c. and n.m.r. to consist mainly of two components in the approximate ratio 2:3; the n.m.r. data for the mixture was in agreement with the literature values (9).

Fractional distillation of the isomeric mixture (40.0 g) gave (*i*) methyl *Z*-4-bromo-3-methylbut-2-enoate (**1**) (11.8 g), b.p. 63–65°/7 mm, n_D^{24} 1.4871; λ_{max} (EtOH) 215 nm (ε 11.8 × 10^3); ν_{max} (CCl_4) 1730vs, 1650s, 1440s, 1360s, 1250vs, 1160vs, 1045s, 860s, and 635 cm^{-1}; n.m.r. δ 5.80br (=CH), 4.60s (CH_2Br), 3.70s (OMe).

Anal. Calcd. for $C_6H_9BrO_2$: C, 37.3; H, 4.7; Br 41.5. Found: C, 37.1; H, 4.6; Br, 41.4.

(*ii*) Intermediate fraction (4.3 g), b.p. 65–67°/7 mm; n.m.r. and g.l.c. showed the *Z*:*E* ratio to be about 1:3. (*iii*) Methyl *E*-4-bromo-3-methylbut-2-enoate (**2**) (20.6 g), b.p. 67–8°/7 mm, n_D^{24} 1.4994; λ_{max} (EtOH) 218 nm (13.7 × 10^3); ν_{max} (CCl_4) 1730vs, 1645s, 1435s, 1355s, 1250m, 1230vs, 1210s, 1155vs, 1037s, 925w, 860w, and 620 cm^{-1}; n.m.r. 5.93br (=CH), 393s (CH_2Br), 3.70s (OMe), and 2.26d (J = 2 Hz, MeC=C).

Anal. Found: C, 37.1; H, 4.8; Br, 41.3.

Reformatsky Reaction of Benzaldehyde with Methyl Z-4-Bromo-3-methylbut-2-enoate (1)

A portion (5 ml) of a solution of the *Z*-bromoester **1** (15.0 g, 0.078 mol) and benzaldehyde (8.16 g, 0.077 mol) in dry benzene (25 ml) and dry ether (5 ml) was added dropwise to activated zinc (19) (5.23 g, 0.08 g-at.). The mixture was warmed until the reaction started. The mixture was then stirred with gentle warming and the rest of the solution added at such a rate as to maintain a slow reflux. The reaction mixture was refluxed for 30 min, cooled to 0°, and hydrolyzed with ice-cold 10% sulfuric acid (25 ml). The organic layer was separated and successively washed with water, sodium bicarbonate solution, and water and dried over anhydrous sodium sulfate. The solvent was evaporated and the residue distilled giving a pale yellow oil (8.5 g), b.p. 150–175°/3 mm. The i.r. spectrum for the fraction b.p. 169–175°/3 mm (5.9 g) showed a pronounced band at 1725 cm^{-1} indicative of the δ-lactone. Attempts to crystallize the lactone were unsuccessful. The δ-lactone band was less pronounced in the other fractions.

The fraction b.p. 169–175°/3 mm was treated with ethanolic potassium hydroxide for 12 h at 50°, diluted with water, extracted with ether, and acidified with cold 10% sulfuric acid. The white precipitate was taken up in ether, washed with water, and then dried. The ether was evaporated and the resulting crystalline material had m.p. 128–134°. A sample of this product was treated with excess ethereal diazomethane and the resulting oil was shown by g.l.c. to be a mixture of approximately 70% of the *Z*-2,*E*-4 and 30% *E*-2,*Z*-4 isomers of methyl 3-methyl-5-phenylpenta-2,4-dienoate.

Iodine-catalyzed isomerization of the isomeric mixture m.p. 128–134°, according to the directions of Pattenden and Weedon (13) gave the *E*-2,*E*-4-acid **6***b*, m.p. 156–158° (petroleum ether). The acid exhibited the spectral properties as reported (13).

Reformatsky Reaction of Benzaldehyde with Methyl E-4-Bromo-3-methylbut-2-enoate-(2)

Repetition of the preceding experiment with the *E*-bromoester **2**, gave a similar product ratio. The products from both the above reactions were identified by g.l.c. using reference compounds prepared by procedures given below (10, 13).

Reformatsky reaction of Methyl E-4-Bromo-3-methylbut-2-enoate with β-Cyclocitral

The *E*-bromoester (19.3 g, 0.1 mol) was reacted with β-cyclocitral (15.2 g, 0.1 mol) in dry benzene (85 ml) and ether (15 ml) and activated zinc (7.0 g, 0.107 g-at.) using the procedure described above for the benzaldehyde reaction. The product was distilled to give unreacted β-cyclocitral (2.5 g), b.p. 42–44°/1 mm, and a thick syrup (10.4 g), b.p. 130–153°/1 mm, which partly solidified on standing. A portion of the solid was recrystallized from 50% ethanol giving the δ-lactone **3***a*, m.p. 60–63°. Column chromatography of the syrup (2.0 g) on neutral alumina (80–200 mesh) using benzene–hexane as eluent gave the δ-lactone **3***a* (1.3 g), m.p. 60–63°. A sample obtained by recrystallization from 50% ethanol had m.p. 64–65° (lit. (5) m.p. 65–66°); λ_{max} (EtOH) 209 nm; ν_{max} ($CHCl_3$) 1716 cm^{-1} (δ-lactone). The δ-lactone (2.0 g) was hydrolyzed with ethanolic potassium hydroxide (10%, 10 ml) at room temperature, diluted with water (100 ml), extracted several times with ether, and acidified with cold 10% sulfuric acid. The precipitate was taken up in ether, washed with water, and dried over magnesium sulfate. Evaporation of the ether and recrystallization from petroleum ether (b.p. 30–60°) at 0° gave *Z*-β-ionylideneacetic acid **4***a* (0.74 g), m.p. 98–99° not depressed on admixture with an authentic sample prepared as described below. The spectral properties were also identical with those of the authentic sample.

Reformatsky Reaction of Methyl Z-4-Bromo-3-methylbut-2-enoate with β-Cyclocitral

Repetition of the preceding Reformatsky reaction using the *Z*-bromoester gave similar results. No product other than the δ-lactone was isolated.

Can. J. Chem. Downloaded from www.nrcresearchpress.com by 210.87.254.5 on 09/05/12
For personal use only.

Reformatsky Reaction of Methyl E-4-Bromo-3-methylbut-2-enoate with Cyclohexene Carboxaldehyde

The *E*-bromoester (15.0 g, 0.078 mol) was reacted with cyclohexene carboxaldehyde (20) (8.58 g, 0.077 mol) in dry benzene (25 ml) and dry ether (15 ml) and activated zinc (5.23 g, 0.08 g-at.), using the procedure described above for the benzaldehyde reaction. The product was distilled giving a pale yellow oil (7.9 g), b.p. 148–165°/6 mm. The i.r. spectrum for the fraction b.p. 150–165°/6 mm showed a pronounced band at 1719 cm^{-1} indicative of a δ-lactone. This fraction was treated with ethanolic potassium hydroxide at 50° for 12 h, diluted with water, extracted with ether, and acidified with 10% sulfuric acid. The white precipitate was evaporated and the resulting crystalline material had m.p. 158° and showed the same spectral properties as 3-methyl-5-(cyclohexen-1-yl)penta-*Z*-2,*E*-4-dienoic acid (**4***c*) prepared as described below.

Reformatsky Reaction of Methyl Z-4-Bromo-3-methylbut-2-enoate with Cyclohexene Carboxaldehyde

Repetition of the preceding Reformatsky reaction with the *Z*-bromoester gave similar results. Alkaline hydrolysis of the product gave the same *Z*-2,*E*-4-acid.

Preparation of the Reference Compounds

The 3-methyl-5-phenylpenta-2,4-dienoic acids and their methyl esters. The four isomeric acids (*Z*-2,*Z*-4, *Z*-2,*E*-4, *Z*-2,*E*-4, and *E*-2,*E*-4 isomers) were prepared using the Wittig reactions between benzyltriphenylphosphonium chloride and 4-hydroxy-3-methylbut-2-enolide and methyl *E*-3-formylcrotonate in the presence of sodium methoxide according to the method of Pattenden and Weedon (13). The methyl esters were obtained by treating the corresponding acids with ethereal diazomethane.

E-β-Ionylideneacetic Acid (6a) and its Methyl Ester

Phenyllithium (0.04 mol) in dry ether (50 ml) was added during 15 min to a well stirred suspension of triphenylcyclogeranyl bromide (14) (12 g, 0.024 mol) in dry ether (300 ml) at 10° under nitrogen. The resulting deep red solution was stirred for 20 min and methyl *E*-3-formylcrotonate (3.07 g, 0.024 mol) in dry ether (40 ml) was added during 15 min. The reaction mixture was stirred for 2 h at 10° and for 1 h at 35° and then diluted with water (300 ml). The mixture was stirred for 30 min at room temperature. The organic layer was separated, washed with water, dried, and then evaporated. The residue was diluted with petroleum ether (b.p. 30–60°), cooled to 0°, and the precipitated triphenylphosphine filtered off. The filtrate was dried over anhydrous sodium sulfate and distilled under reduced pressure giving methyl *E*-β-ionylideneacetate (5.2 g, 87%), b.p. 160–163°/5 mm (lit. (5) b.p. 110–111°/0.5 mm); g.l.c. showed only one peak; λ_{max} (EtOH) 257 and 302 nm; ν_{max} 1720vs (C=O), 1610s (C=C), 970m (CH=CH *trans*).

A sample of this ester (2.0 g) was saponified with ethanolic potassium hydroxide at room temperature and the product acidified giving *E*-β-ionylideneacetic acid (1.2 g) m.p. 125–127° (acetonitrile) (lit. (8) m.p. 126–127°), not depressed on admixture with a sample prepared according to the directions of Ishikawa (21); λ_{max} (EtOH) 258 and 290 nm.

Z-β-Ionylideneacetic Acid (4a)

Phenyllithium (0.05 mol) in dry ether (60 ml) was added during 20 min to a cooled (0°) and well stirred suspension of triphenyl-β-cyclogeranylphosphonium bromide (12.2 g, 0.026 mol) in dry ether (300 ml) under nitrogen. The resulting deep red solution was stirred for 20 min and 4-hydroxy-3-methylbut-2-enolide (3.0 g, 0.026 mol) added during 15 min. The reaction mixture was stirred for 2 h at 0° and for an additional 2 h at room temperature. It was then diluted with water (300 ml) and stirred for 30 min. The aqueous layer was separated, extracted with ether, acidified with cold 20% sulfuric acid, and the acidic product extracted several times with ether. The combined ether extracts were washed with water, dried, and evaporated leaving *Z*-β-ionylideneacetic acid (**4***a*) (5.2 g, 85%), m.p. 98–99° (petroleum ether) (lit. (8) m.p. 98.5–99.5°); λ_{max} (EtOH) 256 and 305 nm; λ_{max} 1680(s) (C=O), 1620 (C=C), and 850 cm^{-1}. The n.m.r. spectra of the *Z*- and *E*-acids were the same as reported (11). Iodine-catalyzed isomerization of *Z*-β-ionylideneacetic acid according to the procedure of Robeson *et al.* (8) gave the *E* isomer (g.l.c.). A sample of the *Z*-acid was treated with ethereal diazomethane giving the methyl ester, g.l.c. one peak; λ_{max} 257, 310 nm.

3-Methyl-5-(cyclohexen-1-yl)penta-E-2,E-4-dienoic Acid (6c) and its Methyl Ester

The reaction was carried out according to the procedure used for *E*-β-ionylideneacetic acid and its methyl ester. Methyl *E*-3-formylcrotonate (5.9 g, 0.046 mol) in dry ether (50 ml) was allowed to react with a mixture of phenyllithium (0.064 mol) in dry ether (50 ml) and triphenyl(1-cyclohexen-1-yl-methyl)phosphonium bromide (22) (20.0 g, 0.046 mol) in dry ether (300 ml). After a similar work-up procedure the product was distilled giving methyl 3-methyl-5-(cyclohexen-1-yl)-penta-*E*-2,*E*-4-dienoate (8.5 g, 89%) as a pale yellow oil, b.p. 155–158°/7 mm, n_D^{24} 1.5341; g.l.c. one peak; λ_{max} (EtOH) 207 and 318 nm; ν_{max} ($CHCl_3$) 1720vs (C=O), 1615s (C=C), 962s (CH=CH *trans*), and 880w cm^{-1}.

Anal. Calcd. for $C_{13}H_{18}O_2$: C, 75.73; H, 8.74. Found: C, 75.64; H, 8.56.

A sample of the ester (2.0 g) was saponified as described above for the preparation of **6***a* giving the *E*-2,*E*-4 acid (1.1 g), m.p. 172–175° (dec.) (benzene – petroleum ether). The acid is very sensitive to either air or light.

3-Methyl-5-(cyclohexen-1-yl)penta-Z-2,E-4-dienoic Acid (4c)

The reaction was carried out according to the procedure for *Z*-β-ionylideneacetic acid (above): 4-hydroxy-3-methylbut-2-enolide (3.4 g, 0.03 mol) in dry ether (25 ml) was reacted with a mixture of the above phosphonium salt (13.0 g, 0.03 mol) in dry ether (250 ml) and phenyllithium (0.05 mol) in dry ether (40 ml). After a similar work-up procedure the *Z*-2,*E*-4 acid **4***c* (5.2 g, 90%), m.p. 161–162° (benzene – petroleum ether) was obtained.

Anal. Calcd. for $C_{12}H_{16}O_2$: C, 75.00; H, 8.33. Found: C, 74.31; H, 7.95.

A sample of the acid was treated with excess ethereal diazomethane giving the methyl ester; g.l.c. one peak; λ_{max} (EtOH) 206 and 316 nm; ν_{max} ($CHCl_3$) 1740vs (C=O), 975s (CH=CH *trans*).

The n.m.r. spectra of these isomers (**4***c* and **6***c*) are shown in the formulae above.

1. S. H. HARPER and J. F. OUGHTON. Chem. Ind. 574 (1950).
2. R. FUSON and P. L. SOUTHWICK. J. Am. Chem. Soc. **66**, 679 (1944).
3. K. ZIEGLER, W. SCHUMANN, and E. WINKELMANN. Ann. **551**, 120 (1942).
4. R. H. WILEY. J. Chem. Soc. 3831 (1958).
5. K. TANABE. Pharm. Bull. Jap. **3**, 25 (1955).
6. S. YOSHIDA and K. TANABE. Japan Patent No. 8420 (May, 1957); Chem. Abstr. **52**, 14673d (1958).
7. K. EITER, E. TRUSCHEIT, and H. OEDIGER. Angew. Chem. **72**, 948 (1960).
8. C. D. ROBESON, J. D. CAWLEY, L. WEISLER, M. H. STERN, C. C. EDDINGER, and A. J. CHECHAK. J. Am. Chem. Soc. **77**, 4111 (1955).
9. I. L. AHMAD, R. N. GEDYE, and A. NECHVATAL. J. Chem. Soc. C, 185 (1968).
10. G. PATTENDEN and B. C. L. WEEDON. J. Chem. Soc. C, 1984 (1968).
11. P. K. KORVER, C. KRUK, P. J. VAN DER HAAK, J. L. BAAS, and H. O. HUISMAN, Tetrahedron, **22**, 277 (1966).
12. O. ISLER and P. SCHUDEL. Adv. Org. Chem. **4**, 115 (1963).
13. G. PATTENDEN and B. C. L. WEEDON. J. Chem. Soc. C, 1997 (1968).
14. H. POMMER. Angew. Chem. **72**, 811 (1960).
15. M. MOUSSERON-CANET and J. C. MANI. Bull. Soc. Chim. Fr. **10**, 3285 (1966).
16. J. A. ELVIDGE and P. D. RALPH. J. Chem. Soc. B, 243 (1966).
17. A. LOFFLER, F. NORRIS, W. TAUB, K. L. SVANHOLT, and A. S. DREIDING. Helv. Chim. Acta, **53**, 403 (1970).
18. R. COFFIGNAL and M. GAUDEMAR. J. Organometal. Chem. **60**, 209 (1973).
19. L. F. FIESER and M. FIESER. Reagents for organic synthesis. J. Wiley, New York. 1967. p. 1285.
20. I. HEILBRON, E. R. H. JONES, R. W. RICHARDSON, and F. SONDHEIMER. J. Chem. Soc. 737 (1949).
21. Y. ISHIKAWA. Bull. Chem. Soc. Jap. **36**, 1527 (1963).
22. H. H. INHOFFEN, K. BRUCKNER, G. DOMAGK, and H. M. ERDMANN. Chem. Ber. **88**, 1415 (1955).

Can. J. Chem. Downloaded from www.nrcresearchpress.com by 210.87.254.5 on 09/05/12
For personal use only.

Perchlorato, Nitrato, and Acetylacetonato Complexes of Copper(I). The Crystal and Molecular Structure of Perchloratobis(tricyclohexylphosphine)Copper(I)

RODERIC J. RESTIVO, ABRAHAM COSTIN, AND GEORGE FERGUSON[1]

Guelph-Waterloo Centre for Graduate Work in Chemistry, University of Guelph, Guelph, Ontario N1G 2W1

AND

ARTHUR J. CARTY

Guelph-Waterloo Centre for Graduate Work in Chemistry, University of Waterloo, Waterloo, Ontario

Received January 6, 1975

RODERIC J. RESTIVO, ABRAHAM COSTIN, GEORGE FERGUSON, and ARTHUR J. CARTY. Can. J. Chem. **53**, 1949 (1975).

Copper(I) perchlorate, nitrate, and acetylacetonate complexes of the types Cu(triphos)ClO_4 (triphos = $CH_3C(CH_2PPh_2)_3$), Cu$(Cy_3P)_2ClO_4$ (Cy_3P = $P(C_6H_{11})_3$), Cu(triphos)NO_3, Cu$(Cy_3P)_2$(HFac) (HFac = hexafluoroacetylacetonate), and Cu$(Cy_3P)_2$(TtFac) (TtFac = thienyltrifluoroacetylacetonate) have been synthesized by reduction of the corresponding perchlorate, nitrate, and acetylacetonates with tertiary phosphines. Infrared spectra indicate the presence of monodentate perchlorate groups in Cu(triphos)ClO_4 and in Cu$(Cy_3P)_2ClO_4$ and the crystal structure of the latter has been determined by a three-dimensional X-ray analysis using diffractometer data. The crystals are monoclinic, space group $C2/c$, with cell dimensions a = 18.159(6), b = 9.493(2), c = 22.182(3) Å, and β = 95.41(2)° and four molecules per unit cell. The structure was refined by block-diagonal least squares methods to a final R of 0.051 for 2617 reflections using anisotropic thermal parameters for the nonhydrogen atoms. The structure consists of discrete Cu$(Cy_3P)_2ClO_4$ molecules with symmetry C_2 separated by normal van der Waals distances. The copper atom is three-coordinate and the perchlorate anion is monodentate but disordered over two sites. Principal dimensions include: Cu—P 2.262(1) Å, Cu—O 2.220(7) Å, ∠P—Cu—P 144.46(6)°, ∠P—Cu—O 114.1(2)° and 99.8(2)°, and ∠Cu—O—Cl 122.4(6)°.

RODERIC J. RESTIVO, ABRAHAM COSTIN, GEORGE FERGUSON et ARTHUR J. CARTY. Can. J. Chem. **53**, 1949 (1975).

On a synthétisé les complexes du perchlorate, du nitrate et de l'acétylacétonate de cuivre(I) du type Cu(triphos)ClO_4 (triphos = $CH_3C(CH_2PPh_2)_3$), Cu$(Cy_3P)_2ClO_4$ (Cy_3P = $P(C_6H_{11})_3$), Cu(triphos)NO_3, Cu$(Cy_3P)_2$(HFac) (HFac = hexafluoroacétylacétonate) et Cu$(Cy_3P)_2$(TtFac) (TtFac = thiényltrifluoroacétylacétonate) en réduisant les perchlorates, les nitrates et les acétylacétonates correspondants par des phosphines tertiaires. Les spectres infrarouges suggèrent la présence de groupes perchlorates monodentates dans Cu(triphos)ClO_4 et dans Cu$(Cy_3P)_2ClO_4$; la structure cristalline de ce dernier composé a été établie à l'aide d'une analyse tridimentionnelle par rayons-X en faisant appel à des données diffractométriques. Les cristaux sont monocliniques appartiennent au groupe d'espace $C2/c$, et possèdent les dimensions a = 18.159(6), b = 9.493(2), c = 22.182(3) Å et β = 95.41(2)° et contiennent quatre molécules par maille. La structure a été affinée par la méthode des moindres carrés jusqu'à une valeur finale de R de 0.051 pour 2617 réflexions utilisant des paramètres thermiques anisotropes pour les atomes différents de l'hydrogène. La structure comprend des molécules discrètes de Cu$(Cy_3P)_2ClO_4$ possédant une symétrie C_2 qui sont séparés par des distances de van der Waals normales. L'atome de cuivre est tricoordonnée et l'anion perchlorate est monodentate mais désordonnée sur deux sites. Les dimensions principales sont Cu—P 2.262(1) Å, Cu—O 2.220(7) Å, ∠P—Cu—P 144.46(6)°, ∠P—Cu—O 114.1(2)° et 99.8(2)°, et ∠Cu—O—Cl 122.4(6)°.

[Traduit par le journal]

Introduction

Structural studies of several tertiary phosphine derivatives of copper(I) are in progress in our laboratories in an attempt to relate steric and electronic properties of the ligands to molecular stereochemistry. Considerable impetus for structural work in this area derives from the burgeoning interest in the chemistry of zerovalent nickel, palladium, and platinum phosphine compounds as a result of their synthetic and catalytic

[1]Author to whom correspondence should be addressed.

Can. J. Chem. Downloaded from www.nrcresearchpress.com by 210.87.254.5 on 09/05/12
For personal use only.

Can. J. Chem. Downloaded from www.nrcresearchpress.com by 210.87.254.5 on 09/05/12
For personal use only.

utility (1). In the presence of a noncomplexing anion, the stereochemistry of copper(I) might be expected to show a close resemblance to that of an isoelectronic nickel(0) species. However, whereas nickel(0)–phosphine complexes are often highly sensitive and difficult to handle, the corresponding copper(I) compounds can be synthesized with ease and are generally air-stable. X-Ray studies of several copper(I) complexes of tertiary phosphines have been summarized (2). Of interest to the present work are the results of the analysis of nitratobis(triphenylphosphine)copper(I) (3) and nitratobis(tricyclohexylphosphine)copper(I) (4), (which both contain a bidentate nitrate group giving the copper atoms a pseudotetrahedral configuration), and of the tris complex, $Cu(MePh_2P)_3NO_3$, in which the nitrate group is unidentate (5). Also of relevance to this work are the structures of $Cu(Ph_3P)_2(HFac)$, $Cu(Ph_3P)_2(TFac)$, and $Cu(Ph_3P)_2(TtFac)$ (HFac = hexafluoroacetylacetonate anion, TFac = trifluoroacetylacetonate anion, and TtFac = thienyltrifluoroacetylacetonate anion) which contain pseudotetrahedrally coordinated copper atoms (6).

A synthetic route utilizing the reduction of an appropriate copper(II) compound with a tertiary phosphine ligand has led to the preparation of several new copper(I) perchlorate, nitrate, and acetylacetonate complexes of the very bulky ligand tricyclohexylphosphine (Cy_3P) and the potentially tridentate ligand 1,1,1-tris(diphenylphosphinomethyl)ethane (triphos) (7). The single crystal X-ray structural analysis of perchloratobis(tricyclohexylphosphine)copper(I) is reported herein. This molecule is of interest because the bulky tricyclohexyl groups should exert a large steric influence on the structure. Moreover, the perchlorate ion is weakly coordinating and relatively few complexes containing coordinated ClO_4^- have been structurally characterized (8) although there are many known structures with uncomplexed ClO_4^-. (A few examples are cited in ref. 9.)

Experimental

Infrared spectra were measured on Perkin–Elmer 457 and Perkin–Elmer 180 infrared spectrometers using Nujol mulls on CsI plates.

Preparations

Perchloratobis(tricyclohexylphosphine)copper(I), $Cu(Cy_3P)_2ClO_4$

Cupric perchlorate, $Cu(ClO_4)_2.nH_2O$, was first prepared by dissolving anhydrous cupric carbonate in 66% perchloric acid, followed by careful evaporation of the filtered neutral solution to low volume until crystallization occurred. The product was dried over anhydrous $Mg(ClO_4)_2$ in a vacuum desiccator.

Cupric perchlorate (1.0 g) was dissolved in absolute ethanol (25 ml) and the solution warmed to 60°. A hot solution (50 ml) (1:1 ethanol, cyclohexane) containing sufficient tricyclohexylphosphine to give a 4:1 molar ratio of copper to phosphine, was filtered into the perchlorate solution and the mixture cooled. Colorless crystals, m.p. 180–182°, of the product which could be recrystallized from absolute ethanol, were obtained.

The same complex was obtained when 8:1 molar ratios of phosphine to copper were used.

Anal. Calcd. for $Cu(Cy_3P)_2ClO_4$: C, 59.10; H, 9.33; Cl, 4.96. Found: C, 59.82; H, 9.10; Cl, 4.42.

Perchlorato[1,1,1-tris(diphenylphosphinomethyl)-ethane]copper(I), Cu(triphos)ClO_4

Sufficient triphos to give a 1.3:1 molar ratio of phosphine to copper was added to a warm solution of cupric perchlorate dissolved in absolute ethanol. The colorless product which crystallized on cooling was washed with benzene and recrystallized (m.p. 200° (dec.) from absolute ethanol and chloroform (5:1)).

Anal. Calcd. for Cu(triphos)ClO_4: C, 62.4; H, 5.0. Found: C, 61.76; H, 5.08.

Nitrato[1,1,1-tris(diphenylphosphinomethyl)ethane]-copper(I), Cu(triphos)NO_3

The product, m.p. 255° (dec.) was prepared via the method used for Cu(triphos)ClO_4 by addition of the phosphine to cupric nitrate.

Anal. Calcd. for Cu(triphos)NO_3: C, 65.50; H, 5.25. Found: C, 65.72; H, 5.30.

Hexafluoroacetylacetonatobis(tricyclohexylphosphine)-copper(I), $Cu(Cy_3P)_2HFac$, and Thienyltrifluoro-acetylacetonatobis(tricyclohexylphosphine)copper(I), $Cu(Cy_3P)_2TtFac$

The bis chelates $Cu(HFac)_2$ and $Cu(TtFac)_2$ were prepared by published procedures (10). The Cy_3P complexes were prepared under a nitrogen atmosphere by addition of the copper(II) chelate to a solution of the phosphine, in a 3:1 molar ratio of phosphine to copper, in 1:1 absolute ethanol and degassed cyclohexane. The $Cu(HFac)_2$ and triphos reacted immediately while the $Cu(TtFac)_2$ and triphos were refluxed under nitrogen for an hour and then left to cool in a refrigerator. The yellow products were recrystallized from *n*-pentane; m.p. 140° (sub.) ($Cu(Cy_3P)_2(HFac)$) and 150° (sub.) ($Cu(Cy_3P)_2(TtFac)$).

Anal. Calcd. for $Cu(Cy_3P)_2(HFac)$: C, 59.10; H, 8.1. Found: C, 59.34; H, 8.14.

Anal. Calcd. for $Cu(Cy_3P)_2(TtFac)$: C, 62.1; H, 8.5. Found: C, 62.06; H, 8.52.

Crystal Data for Perchloratobis(tricyclohexylphosphine)-copper(I)

$C_{36}H_{66}ClCuP_2O_4$ f.w. = 723.9

Monoclinic, $a = 18.159(6)$, $b = 9.493(2)$, $c = 22.182(3)$ Å, $\beta = 95.41(2)°$, $V = 3807$ Å^3, $D_m = 1.27$ g cm^{-3}, $Z = 4$, $D_c = 1.26$ g cm^{-3}, (20 °C; $MoK_\alpha\lambda = 0.71069$ Å), $F(000) = 3240$, space group $C2/c(C_{2h}^6$, no. 15), linear

Can. J. Chem. Downloaded from www.nrcresearchpress.com by 210.87.254.5 on 09/05/12
For personal use only.

absorption coefficient for X-rays ($\lambda = 0.71069$ Å), $\mu = 7.86$ cm^{-1}, symmetry C_2 required.

Unit-cell and space group data were obtained from preliminary precession and Weissenberg photographs which indicated monoclinic symmetry with systematic absences: *hkl* when $h + k$ is odd and *h0l* when both *h* and *l* are odd, allowing the space group to be *Cc* or *C2/c*. The latter was chosen (but see below). The cell dimensions were obtained from a least squares treatment of the setting angles of 12 general reflections measured on a diffractometer. The crystal chosen for the data collection was a small rectangular plate with approximate dimensions 0.16 × 0.17 × 0.19 mm. Intensity data were collected to a maximum Bragg angle θ of 27° on a PDP8-I controlled Hilger and Watts Y290 four-circle diffractometer equipped with a graphite monochromator. The θ–2θ scan technique was used with a scan through 60 steps of 0.01° with 1 s counts at each step. Background counts of 15 s were made at the beginning and end of each scan. The maximum variation in intensity of the standard reflections was 1%. Lorentz and polarization corrections were applied but no absorption correction was made. Reflections which had a net count of less than 3σ above background, where $\sigma(I)$ is defined by $\sigma(I) = \sqrt{[S + 4(B_1 + B_2)]}$ and S, B_1, and B_2 are the scan, first background, and second background respectively, were taken as "unobserved". Of the 4159 independent reflections measured, 2617 were classified as "observed" and used in the solution and refinement of the structure.

Structure Analysis

The coordinates of the copper and phosphorus atoms were found from inspection of the three-dimensional Patterson function. The remaining atoms were located by application of the heavy atom method. The perchlorate group appeared to be disordered in such a way that the chlorine atom lay off the twofold axis slightly, and one of the two independent oxygen atoms was distributed equally over two sites; allowance was made for this disorder by giving the Cl, O(21), and O(22) atoms an occupancy factor of 0.5 while O(1) was given an occupancy factor of unity. The structure was first refined by full-matrix least square calculations using isotropic thermal parameters and finally by block-diagonal least squares allowing the Cu, P, Cl, and C atoms to vibrate anisotropically. Only the observed reflections were included in the least squares calculations, and the function minimized was $\Sigma\omega(|F_o| - |F_c|)^2$ with absolute weights based on $\sigma(F_o)$ being used. In all F_c calculations, atomic scattering factors were obtained from ref. 11.[2] Corrections for the anomalous dispersion (12) for Cu, P, and Cl were included in the final stages of the refinement. A difference map calculated when R was 0.079 revealed peaks (~0.7 e/Å^3) in positions corresponding to all 33 independent hydrogen atoms. These were then included in the structure factor calculations with fixed isotropic thermal parameters, but were not refined. The refinement converged with $R = \Sigma(|F_o| - |F_c|)/\Sigma|F_o| = 0.051$, and $R' = [\Sigma\omega(|F_o| - |F_c|)^2/\Sigma\omega(|F_o|)^2]^{1/2} = 0.059$ for the 2617 observed reflections. The final error in an observation of unit weight was 1.02. A table of final values of the structure amplitudes and $\sigma(F_o)$ is placed with the Depository of Unpublished Data.[3] The final positional parameters are listed in Table 1, the thermal parameters in Table 2, and interatomic distances and angles in Table 3.

On conclusion of the *C2/c* refinement, it was apparent that the disorder of the perchlorate group might be an artifact brought about by choosing *C2/c* instead of *Cc* as the space group. To check this point, we took the final coordinates (Table 1), generated a complete molecule with only one (nondisordered) perchlorate group, and proceeded to a *Cc* refinement. The result was that the *R*-factor rose slightly (to 0.059), the thermal parameters of the perchlorate atoms became anomalously large, and the Cl atom tended to move from $x \sim 0, z = 0.23$ back to $x = 0, z = \frac{1}{4}$ which would be the 2-fold axis location in *C2/c*. We accordingly abandoned this refinement and feel that we have indeed confirmed that the structure is best described in terms of a *C2/c* system with a disordered perchlorate group.

Discussion

The X-ray analysis shows that the crystal structure consists of discrete molecules of $Cu(Cy_3P)_2ClO_4$ separated by normal van der Waals contacts (Fig. 1). A view of a single molecule along with the labelling scheme is seen in Fig. 2 which shows that the coordination geometry of the copper atom is distorted trigonal (see also Fig. 3). The coordination number of 3 for copper is rather uncommon and only a few 3-coordinate complexes have now been characterized structurally. These include $[Cu(Me_3PS)_3]ClO_4$ (13), $Cu[(Me_3PS)Cl]_3$ (13), $Cu(Ph_3P)_2Br\cdot 0.5C_6H_6$ (14), $(Ph_3P)_3Cu_2Cl_2$ (15), and $[Cu(etu)_3]_2SO_4$ (etu = ethylenethiourea) (16).

The P—Cu—P angle (144.46(6)°) observed here for $Cu(Cy_3P)ClO_4$ is the largest P—Cu—P angle reported to date and it would appear that the bulkiness of the Cy_3P groups is responsible for this distortion. The corresponding P—Cu—P angle in $Cu(Cy_3P)_2NO_3$ (4) is 140(1)°. These angles are significantly greater than those typically reported for systems with the less bulky Ph_3P groups (*e.g.* 131.2(1)° in $Cu(Ph_3P)_2NO_3$ (3) and 123.26(6)° in $Cu(Ph_3P)_2BH_4$ (17)).

The Cu—P bond length 2.262(1) Å can be compared with the distance (2.29(1) Å) found in $Cu(Cy_3P)_2NO_3$ (4) (but that analysis is of low accuracy and the e.s.d.'s may be under-

[2]Atomic scattering functions were obtained from Cromer and Mann; the hydrogen scattering function was obtained from Stewart *et al.* (11).

[3]Complete set of tabular data is available, at a nominal charge, from the Depository of Unpublished Data, CISTI, National Research Council of Canada, Ottawa, Canada K1A 0S2.

Can. J. Chem. Downloaded from www.nrcresearchpress.com by 210.87.254.5 on 09/05/12
For personal use only.

TABLE 1

(*a*) Fractional coordinates for nonhydrogen atoms of $[P(C_6H_{11})_3]_2CuClO_4$

Atom	*x*	*y*	*z*
Cu	0.0*	0.21619(8)	0.2500*
P	0.05824(6)	0.2889(1)	0.33920(5)
Cl	0.0003(9)	−0.1243(3)	0.2379(4)
O(1)	0.0620(3)	−0.2074(4)	0.2704(2)
O(21)	0.0233(5)	−0.0058(8)	0.2268(3)
O(22)	0.0202(5)	−0.0764(11)	0.1816(4)
C(11)	0.0857(3)	0.1436(5)	0.3932(2)
C(12)	0.1063(3)	0.1832(5)	0.4591(2)
C(13)	0.1167(3)	0.0508(7)	0.4982(2)
C(14)	0.1711(3)	−0.0495(7)	0.4756(3)
C(15)	0.1523(3)	−0.0842(6)	0.4093(3)
C(16)	0.1438(3)	0.0488(5)	0.3704(2)
C(21)	0.0005(2)	0.4039(4)	0.3830(2)
C(22)	−0.0220(3)	0.5389(5)	0.3484(2)
C(23)	−0.0691(3)	0.6340(6)	0.3852(3)
C(24)	−0.1368(3)	0.5574(6)	0.4041(2)
C(25)	−0.1152(3)	0.4212(6)	0.4375(2)
C(26)	−0.0685(3)	0.3263(5)	0.4005(2)
C(31)	0.1385(2)	0.4001(5)	0.3247(2)
C(32)	0.1881(3)	0.3298(5)	0.2818(2)
C(33)	0.2474(3)	0.4303(6)	0.2628(2)
C(34)	0.2922(3)	0.4932(6)	0.3158(3)
C(35)	0.2432(3)	0.5650(6)	0.3575(2)
C(36)	0.1841(3)	0.4655(5)	0.3789(2)

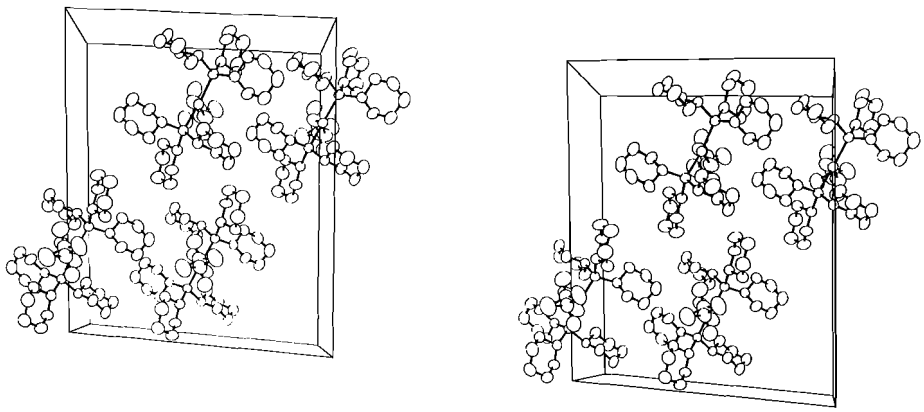

FIG. 1. The molecular packing diagram for perchloratobis(tricyclohexylphosphine)copper(I). The hydrogen atoms have been omitted for clarity.

estimated). A wide range of Cu—P bond lengths has been reported for three-coordinate copper(I) complexes (*e.g.* 2.262(2) and 2.282(2) in $Cu(Ph_3P)_2Br$ (14) and 2.183(4) Å for the three-coordinate copper atom in $(Ph_3P)_3Cu_2Cl_2$ (15)).

The perchlorate group, which is disordered about the twofold crystallograhic axis, is monodentate with a bonded Cu—O(21) length of 2.220(7) Å and a nonbonded intramolecular contact, Cu···O(22), of 3.203(10) Å. Although a number of coordination complexes purportedly containing monodentate perchlorate groups have been characterized (18), relatively few of these have been subjected to single crystal X-ray analysis. The bonded Cu—O length is considerably shorter than the Cu—O(perchlorate)

TABLE 1 (*Concluded*)

(*b*) Fractional coordinates of hydrogen atoms†

Atom	*x*	*y*	*z*
H(111)	0.033	0.089	0.389
H(121)	0.157	0.242	0.463
H(122)	0.063	0.246	0.475
H(131)	0.135	0.080	0.544
H(132)	0.064	−0.003	0.498
H(141)	0.226	−0.003	0.481
H(142)	0.172	−0.147	0.501
H(151)	0.194	−0.151	0.394
H(152)	0.099	−0.140	0.405
H(161)	0.197	0.104	0.374
H(162)	0.129	0.020	0.324
H(211)	0.035	0.431	0.423
H(221)	0.027	0.593	0.338
H(222)	−0.054	0.510	0.306
H(231)	−0.035	0.670	0.425
H(232)	−0.087	0.725	0.358
H(241)	−0.165	0.624	0.433
H(242)	−0.172	0.532	0.364
H(251)	−0.084	0.446	0.480
H(252)	−0.165	0.366	0.446
H(261)	−0.052	0.235	0.427
H(262)	−0.102	0.294	0.360
H(311)	0.107	0.482	0.301
H(321)	0.215	0.240	0.304
H(322)	0.154	0.295	0.242
H(331)	0.284	0.373	0.236
H(332)	0.221	0.514	0.236
H(341)	0.323	0.411	0.340
H(342)	0.330	0.569	0.300
H(351)	0.278	0.604	0.396
H(352)	0.216	0.653	0.334
H(361)	0.211	0.381	0.406
H(362)	0.148	0.523	0.406

*Fixed by space group *C*2/*c*.
†An isotropic *U* value of 0.057 Å was assigned to each hydrogen atom. Hydrogen atom parameters were not refined.

distances (2.546(3) Å) in $Cu\{[(CH_3)_2N]_2P(O)OP(O)[N(CH_3)_2]_2\}_2(ClO_4)_2$ (8*c*) and 2.61 Å observed in $Cu(en)_2(ClO_4)_2$ (en = ethylenediamine) (8*d*) where a monodentate perchlorate is present. However, in the latter complexes the copper is hexacoordinated and data are lacking for perchlorato complexes of low coordination number. The coordinated perchlorate group affords a Cu—O length which agrees favorably with the values obtained for $Cu(Cy_3P)_2NO_3$ (2.34(2) Å) (4) and $Cu(Ph_3P)_2NO_3$ (2.22(1) Å) (3) which contain symmetrically-bidentate nitrato groups. Thus, the apparent similarity of Cu—O distances in $Cu(Cy_3P)_2ClO_4$, $Cu(Ph_3P)_2NO_3$ (3), and $Cu(Cy_3P)_2NO_3$ (4) indicates that the Cu—O(perchlorate) interaction is stronger than might be predicted from a knowledge of the poor coordinating tendencies of ClO_4^-. The Cl—O distances in the disordered ClO_4 group are in the range 1.38–1.50 Å but the disorder precludes any meaningful discussion of these. There are two independent P—Cu—O(perchlorate) angles, 114.1(2) and 99.8(2)°, which together with the P—Cu—P angle of 144.46(6)° imply that the coordination at the copper atom is not planar; it lies 0.08 Å from the OPP′ plane.

Structures containing uncomplexed perchlorate groups have shown the same poor refinement characteristics (disorder or large thermal motion for the perchlorate) as observed in this crystal structure analysis. As Einstein and Rodley (9*c*) have pointed out, the disorder of perchlorate ions can be related to the spherical shape of the

Can. J. Chem. Downloaded from www.nrcresearchpress.com by 210.87.254.5 on 09/05/12
For personal use only.

TABLE 2. Anisotropic thermal parameters* for nonhydrogen atoms of $[P(C_6H_{11})_3]_2CuClO_4$

Atom	U_{11}	U_{22}	U_{33}	U_{12}	U_{13}	U_{23}
Cu	5.72(4)	5.03(4)	5.23(4)	0.0†	0.62(4)	0.0†
P	5.33(6)	4.24(6)	4.67(6)	0.84(6)	0.43(5)	−0.08(6)
Cl	9.6(2)	4.9(1)	11.1(7)	1.5(2)	−0.2(5)	0.1(2)
O(1)	12.0(3)	7.7(3)	16.3(4)	1.8(3)	−2.1(3)	1.7(3)
O(21)	14.2(8)	6.4(5)	9.7(7)	−1.1(5)	0.0(5)	0.2(4)
O(22)	15.0(8)	14.4(9)	11.7(7)	4.9(7)	3.6(6)	4.9(6)
C(11)	6.5(3)	5.4(3)	5.6(3)	1.6(2)	0.6(2)	0.5(2)
C(12)	9.8(4)	8.4(4)	5.3(3)	3.5(3)	1.0(3)	0.9(3)
C(13)	10.8(4)	12.1(5)	6.6(3)	4.1(4)	2.2(3)	2.6(3)
C(14)	11.1(5)	10.1(5)	9.0(4)	4.1(4)	0.8(3)	3.7(4)
C(15)	11.4(5)	6.5(4)	10.1(4)	4.0(3)	0.7(4)	1.1(3)
C(16)	7.6(3)	6.5(3)	6.5(3)	2.3(3)	0.2(2)	−0.2(3)
C(21)	5.1(2)	5.0(2)	5.3(3)	1.2(2)	0.2(2)	−0.4(2)
C(22)	8.4(4)	5.8(3)	8.3(3)	1.9(3)	2.2(3)	0.5(3)
C(23)	10.7(5)	6.5(3)	10.6(4)	3.4(3)	2.5(4)	−0.1(3)
C(24)	7.3(3)	9.6(4)	8.9(4)	3.1(3)	0.9(3)	−2.1(3)
C(25)	6.1(3)	9.2(4)	8.7(4)	1.7(3)	2.3(3)	0.0(3)
C(26)	6.6(3)	6.7(3)	8.1(3)	1.2(3)	1.9(3)	−0.1(3)
C(31)	5.4(3)	5.4(3)	5.7(3)	0.3(2)	0.1(2)	−0.7(2)
C(32)	7.8(3)	6.9(3)	6.9(3)	−1.4(3)	2.1(3)	−1.1(3)
C(33)	8.0(4)	9.3(4)	8.5(4)	−1.4(4)	2.6(3)	−0.1(3)
C(34)	6.7(3)	7.3(4)	11.2(4)	−0.8(3)	0.9(3)	1.4(3)
C(35)	8.1(4)	6.5(3)	9.7(4)	−1.9(3)	−1.3(3)	−0.9(3)
C(36)	7.1(3)	7.2(3)	6.6(3)	−0.1(3)	0.0(2)	−1.4(3)

*Expressed as exp $[-2\pi^2(U_{11}h^2a^{*2} + U_{22}k^2b^{*2} + U_{33}l^2c^{*2} + 2U_{12}hka^*b^* + 2U_{13}hla^*c^* + 2U_{23}klb^*c^*)]$, U_{ij} in Å^2 × 10^2 for all atoms.
†Fixed by space group $C2/c$.

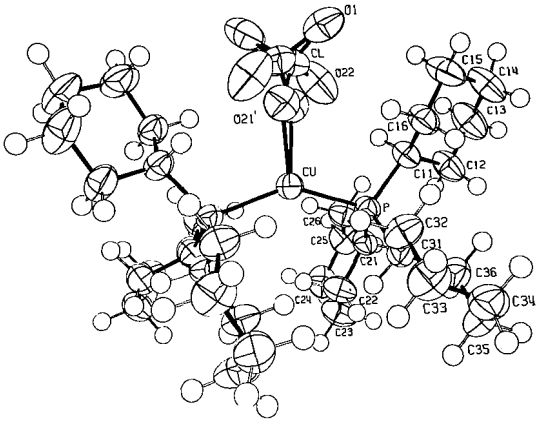

FIG. 2. A view with 50% probability ellipsoids of perchloratobis(tricyclohexylphosphine)copper(I) showing the molecular geometry and atomic numbering. The copper atom lies on a twofold axis which passes through the molecule.

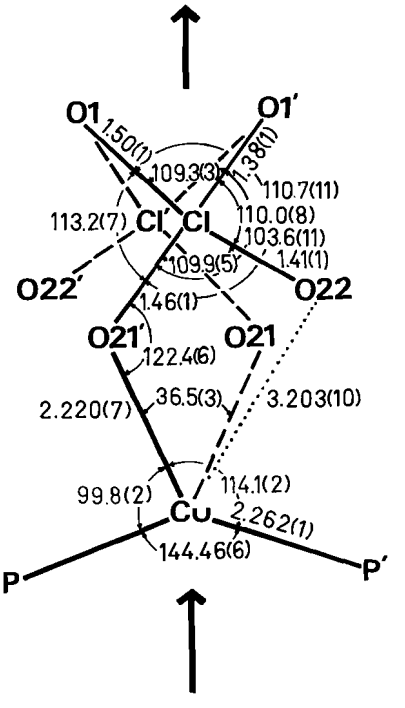

FIG. 3. The geometry about the copper atom in the perchloratobis(tricyclohexylphosphine)copper(I).

ion which allows a certain degree of freedom of orientation. However, even on complexing the perchlorate group may still show considerable motion or, in the extreme case, disorder; both of these characteristics are found in $(Ph_3BiClO_4)_2O$

Can. J. Chem. Downloaded from www.nrcresearchpress.com by 210.87.254.5 on 09/05/12
For personal use only.

TABLE 3. Interatomic distances (Å) and angles (deg) for $[P(C_6H_{11})_3]_2CuClO_4$*

(*a*) Bonded distances

Bond	Distance (Å)	Average (Å)	Bond	Distance (Å)	Average (Å)
Cl—O(1)	1.50(1)		C(11)—C(12)	1.522(6)	
Cl—O(1′)	1.38(1)		C(12)—C(13)	1.528(8)	
Cl—O(21′)	1.46(1)		C(13)—C(14)	1.492(9)	
Cl—O(22)	1.41(1)	1.44(1)	C(14)—C(15)	1.513(8)	
			C(15)—C(16)	1.529(7)	
Cu—O(21)	2.220(7)		C(16)—C(11)	1.510(7)	
Cu—P	2.262(1)		C(21)—C(22)	1.529(6)	
			C(22)—C(23)	1.532(8)	
P—C(11)	1.863(5)		C(23)—C(24)	1.521(8)	
P—C(21)	1.851(4)		C(24)—C(25)	1.523(8)	
P—C(31)	1.853(5)	1.856(5)	C(25)—C(26)	1.528(7)	
			C(26)—C(21)	1.534(7)	
			C(31)—C(32)	1.524(7)	
			C(32)—C(33)	1.528(8)	
			C(33)—C(34)	1.490(8)	
			C(34)—C(35)	1.505(8)	
			C(35)—C(36)	1.538(7)	
			C(36)—C(31)	1.524(6)	1.521(8)

(*b*) Angles

Bonds	Angle (deg)	Bonds	Angle (deg)
O(22)—Cl—O(21′)	109.9(5)	C(13)—C(14)—C(15)	111.7(5)
O(1)—Cl—O(1′)	109.3(3)	C(14)—C(15)—C(16)	111.7(5)
O(1)—Cl—O(21′)	113.2(7)	C(15)—C(16)—C(11)	109.8(4)
O(1′)—Cl—O(22)	110.0(8)	P—C(21)—C(22)	111.6(3)
O(1′)—Cl—O(21′)	103.6(11)	P—C(21)—C(26)	111.4(3)
O(1)—Cl—O(22)	110.7(11)	C(26)—C(21)—C(22)	110.1(4)
P—Cu—P′	144.46(6)	C(21)—C(22)—C(23)	111.2(4)
P—Cu—O(21)	114.1(2)	C(22)—C(23)—C(24)	111.8(4)
Cu—O(21′)—Cl	122.4(6)	C(23)—C(24)—C(25)	111.2(4)
P—Cu—O(21′)	99.8(2)	C(24)—C(25)—C(26)	111.7(4)
O(21)—Cu—O(21′)	36.5(3)	C(25)—C(26)—C(21)	111.1(4)
Cu—P—C(21)	113.4(1)	P—C(31)—C(32)	112.3(3)
Cu—P—C(31)	109.5(1)	P—C(31)—C(36)	118.2(3)
P—C(11)—C(12)	117.5(3)	C(36)—C(31)—C(32)	111.2(4)
P—C(11)—C(16)	112.3(3)	C(31)—C(32)—C(33)	111.9(4)
C(16)—C(11)—C(12)	110.6(4)	C(32)—C(33)—C(34)	112.2(4)
C(11)—C(12)—C(13)	110.4(4)	C(33)—C(34)—C(35)	110.9(4)
C(12)—C(13)—C(14)	112.6(5)	C(34)—C(35)—C(36)	112.3(4)
		C(35)—C(36)—C(31)	110.5(4)

*The coordinates of atoms marked with a prime are obtained from those of Table 1 by applying the twofold symmetry axis transformation $-x, y, \frac{1}{2} - z$.

(*9a*) which has one ordered and one disordered perchlorate group.

All of the intermolecular distances less than 3.5 Å were calculated. Most of the intermolecular contacts involve the hydrogen atoms of the bulky Cy_3P groups; however, no short intramolecular contacts were found.

The infrared spectrum of $Cu(Cy_3P)_2ClO_4$ shows the following bands due to the perchlorate group when compared to the spectrum of the free ligand Cy_3P: 1120 vs br, 1020 vs br, 910 m, 618 m, and 610 m. In the ionic, T_d ClO_4^- ion, the infrared active modes appear at 1119 s br cm^{-1} (ν_3) and 625 m cm^{-1} (ν_4) (19). Thus the splitting of the ν_3 band of ionic ClO_4^- into two strong broad bands at 1120 and 1020 cm^{-1} in $Cu(Cy_3P)_2ClO_4$, together with the appearance of ν_1, of ClO_4^- (i.r. inactive in the T_d ClO_4^- ion)

Can. J. Chem. Downloaded from www.nrcresearchpress.com by 210.87.254.5 on 09/05/12
For personal use only.

Can. J. Chem. Downloaded from www.nrcresearchpress.com by 210.87.254.5 on 09/05/12
For personal use only.

at 910 cm^{-1}, and the splitting of ν_4 into two bands at 618 and 610 cm^{-1} is indicative of coordination of the perchlorate ion to copper(I). The spectrum appears characteristic of C_{3v} monodentate perchlorate. Moers and Op Het Veld (20) have described the same compound. However, they have either misinterpreted their i.r. spectra or have not compared their spectra with the spectrum of the free Cy_3P ligand, for they propose that the perchlorate is uncomplexed and that the copper is two-coordinate and presumably linear. The possibility of their complex being structurally different from the complex described herein seems remote since the two compounds appear to have identical melting points.

The triphosphine complex, Cu(triphos)ClO_4 exhibits an infrared spectrum typical of coordinated perchlorate and very similar to that of $Cu(Cy_3P)_2ClO_4$. Thus ν_3 of ClO_4^- is resolved into two bands at 1130 and 1025 cm^{-1} while ν_1 of ClO_4^- appears at 905 cm^{-1} and ν_4 appears as a doublet at 615 and 610 cm^{-1}. These observations suggest that the complex may be structurally similar to that of $Cu(Cy_3P)_2ClO_4$, with a monodentate perchlorate and bidentate triphosphine or alternatively that all three phosphorus atoms are coordinated to a tetrahedral copper atom. Both bidentate and tridentate behavior have been established for the tritertiary phosphine $CH_3C(CH_2PPh_2)_3$ (7).

The infrared spectra of Cu(triphos)NO_3 and $Cu(Cy_3P)_2NO_3$ (4) in the NO_3^- region of the spectra are virtually identical. Cu(triphos)NO_3 has the following nitrate bands (derived from ν_3 of NO_3^-), 1437 s and 1291 m. These compare with 1452 cm^{-1} (ν_1) and 1288 cm^{-1} (ν_4) in $Cu(Cy_3P)_2NO_3$ (4). Hence, the triphos and nitrate ligands should be bidentate coordinated in Cu(triphos)NO_3 with a structure analogous to $Cu(Cy_3P)_2NO_3$ and not analogous to $Cu(MePh_2P)_3NO_3$ where the nitrate is unidentate (5).

In the ν(C=O) and ν(C=C) region of the infrared spectrum of $Cu(Cy_3P)_2$(HFac) strong bands appear at 1658, 1650, and 1513 cm^{-1}. These frequencies can be compared with the spectrum of $Cu(HFac)_2$ (21) (1644, 1614, 1565, and 1540 cm^{-1}) in the same spectral region. If the diketonate is bidentate in this complex, then considerable steric interaction between bulky tricyclohexyl groups and the acetylacetonate ligand may be expected to result from a large P—Cu—P bond angle (*vide infra*). Alternatively, a more ionic or monodentate form (22) of the diketonate may be indicated by the infrared spectrum.

For $Cu(Cy_3P)_2$(TtFac), a strong ν(C=O) + ν(C=C) band of the acetylacetonate appears at 1612 cm^{-1} with the weaker bands at 1547, 1529, and 1510 cm^{-1}. The parent complex $Cu(TtFac)_2$ exhibits bands at 1595 m, 1574 s, 1540 m, and 1508 cm^{-1}. These spectral changes favor bidentate diketonato bonding with somewhat weaker Cu—O bonds than in $Cu(TtFac)_2$.

We have recently prepared complexes with the extremely bulky phosphines (23) P(—*o*-$CH_3C_6H_4)_3$ and PBu^t_3. Structural studies of these compounds are underway in order to investigate the effect of ligand size on P—Cu—P bond angles and anion coordinating tendencies.

We are grateful to the National Research Council of Canada for operating grants (to G.F. and A.J.C.). All the calculations were performed on the University of Guelph IBM 370/155 computer system.

1. R. UGO. Coord. Chem. Rev. **3**, 319 (1968); F. A. COTTON and G. WILKINSON. Advanced inorganic chemistry, 3rd ed. Interscience, New York. 1972. pp. 903, 1042.
2. S. J. LIPPARD and G. J. PALENIK. Inorg. Chem. **10**, 1322 (1971).
3. G. G. MESSMER and G. J. PALENIK. Inorg. Chem. **8**, 2750 (1969).
4. W. A. ANDERSON, A. J. CARTY, G. J. PALENIK, and G. SCHREIBER. Can. J. Chem. **49**, 761 (1971).
5. M. MATHEW, G. J. PALENIK, and A. J. CARTY. Can. J. Chem. **49**, 4119 (1971).
6. M. BARTLETT and G. J. PALENIK. Acta Cryst. A, **25**, S173 (1969); M. BARTLETT. Ph.D. Thesis, University of Waterloo, Waterloo, Ontario. 1970.
7. W. O. SIEGL, S. J. LAPPORTE, and J. P. COLLMAN. Inorg. Chem. **10**, 2158 (1971).
8. (*a*) F. C. MARCH and G. FERGUSON. J. Chem. Soc. Dalton. In press; (*b*) G. FERGUSON, F. C. MARCH, and D. R. RIDLEY. Acta Cryst. In press; (*c*) M. S. HUSSAIN, M. D. JOESTEN, and P. G. LENHERT. Inorg. Chem. **9**, 162 (1970); (*d*) A. PAJUNE. Ann. Acad. Sci. Fenn. Ser. AII, No. 138 (1967); (*e*) F. A. COTTON and D. L. WEAVER. J. Am. Chem. Soc. **87**, 4189 (1965); (*f*) P. PAULING, G. B. ROBERTSON, and G. A. RODLEY. Nature, **207**, 73 (1965).
9. (*a*) P. T. MILLER, P. G. LENHERT, and M. D. JOESTEN. Inorg. Chem. **12**, 218 (1973); (*b*) M. D. JOESTEN, M. S. HUSSAIN, and P. G. LENHERT. Inorg. Chem. **9**, 151 (1970); (*c*) F. W. B. EINSTEIN and G. A. RODLEY. J. Inorg. Nucl. Chem. **29**, 347 (1967).
10. (*a*) H. F. HOLTZCLAW, JR. and J. P. COLLMAN. J. Am. Chem. Soc. **79**, 3318 (1957); (*b*) W. R. WALKER and N. C. LI. J. Inorg. Nucl. Chem. **27**, 411 (1965).
11. J. M. STEWART. X-Ray 72. Technical Report TR-192, 1972, University of Maryland Computer Science Center, College Park, Maryland; D. CROMER and J.

MANN. Acta Cryst. A**24**, 321 (1968); R. F. STEWART, E. R. DAVIDSON, and W. T. SIMPSON. J. Chem. Phys. **42**, 3178 (1965).
12. D. T. CROMER. Acta Cryst. **18**, 17 (1965).
13. J. A. TIETHOF, A. T. HETEY, and D. W. MEEK. Inorg. Chem. **13**, 2505 (1974); J. A. TIETHOF, J. K. STALICK, P. W. R. CORFIELD, and D. W. MEEK. J. Chem. Soc. Chem. Commun. 1142 (1972); P. G. ELLER and P. W. R. CORFIELD. J. Chem. Soc. Chem. Commun. 105 (1971).
14. P. H. DAVIS, R. L. BELFORD, and I. C. PAUL. Inorg. Chem. **12**, 213 (1973).
15. D. F. LEWIS, S. J. LIPPARD, and P. S. WELCKER. J. Am. Chem. Soc. **92**, 3805 (1970). V. G. ALBANO, P. L. BELTON, G. CIANI, and M. MANASSERO. J. Chem. Soc. Dalton, 171 (1972).
16. M. S. WEININGER, G. W. HUNT, and E. L. AMMA. J. Chem. Soc. Chem. Commun. 1140 (1972).
17. S. J. LIPPARD and K. M. MELMED. Inorg. Chem. **6**, 2223 (1967).
18. W. C. JONES and W. E. BULL. J. Chem. Soc. A, 1849 (1968) and references therein; R. S. TAYLOR and A. G. SYKES. J. Chem. Soc. Chem. Commun. 1137 (1969).
19. K. NAKAMOTO. I.R. spectra of inorganic and coordination compounds, 2nd ed. Wiley, 1972.
20. F. G. MOERS and P. H. OP HET VELD. J. Inorg. Nucl. Chem. **22**, 3225 (1970).
21. K. NAKAMOTO, Y. MORIMOTO, and A. G. MARTELL. J. Phys. Chem. **66**, 346 (1962).
22. M. A. BUSH, D. E. FENTON, R. S. NYHOLM, and M. R. TRUTER. J. Chem. Soc. Chem. Commun. 1335 (1970).
23. C. A. TOLMAN. J. Am. Chem. Soc. **92**, 2956 (1970).

Can. J. Chem. Downloaded from www.nrcresearchpress.com by 210.87.254.5 on 09/05/12
For personal use only.

^{13}C Nuclear Magnetic Resonance Studies of Methylated Anthracenes

MYRON L. CASPAR
East Carolina University, Greenville, North Carolina 27834
AND
J. B. STOTHERS
Department of Chemistry, University of Western Ontario, London, Ontario N6A 3K7
AND
NANCY K. WILSON[1]
National Institute of Environmental Health Sciences, Research Triangle Park, North Carolina 27709
Received November 20, 1974

MYRON L. CASPAR, J. B. STOTHERS, and NANCY K. WILSON. Can. J. Chem. **53,** 1958 (1975).

The ^{13}C n.m.r. spectra of anthracene and 11 methylated anthracenes have been examined. Analysis of the ^{1}H spectra allowed unequivocal assignments for most of the protonated carbons by selective proton decoupling. Parameters describing the methyl substituent effects on the aryl carbon shieldings were defined and refined by regression analysis so that the ^{13}C shieldings were predicted for 67 independent aryl positions in anthracenes without *peri*-methyls with a standard deviation of 0.12 p.p.m. *Peri* methyl–methyl interactions cause considerable deviations from the predicted substituent effects. The relationships of the ^{13}C shieldings to charge densities calculated by the CNDO/2 method were briefly examined. Syntheses of 2,7,9-trimethyl-, 1,4,5,8- and 1,4,5,9-tetramethyl-, and 1,4,5,8,9-pentamethylanthracene are described.

MYRON L. CASPAR, J. B. STOTHERS et NANCY K. WILSON. Can. J. Chem. **53,** 1958 (1975).

On a examiné les spectres de résonance magnétique nucléaire du ^{13}C de l'anthracène et de 11 dérivés méthylés de l'anthracène. L'analyse des spectres ^{1}H permet d'attribuer d'une façon non-équivoque la résonance de la plupart des carbones protonés en faisant appel au découplage sélectif du proton. On a défini des paramètres décrivant les effets d'un substituant méthyle sur le blindage des carbones aromatiques. Ces paramètres ont été affinés par une analyse de régression d'une façon telle que les blindages du ^{13}C ont pu être prédits (avec une déviation standard de 0.12 p.p.m.) pour 67 positions aromatiques indépendantes dans des anthracènes sans groupement méthyle en *péri*. Les interactions *péri* méthyle–méthyle causent des déviations considérables par rapport aux effets de substituants qui sont prédits. On a examiné brièvement les relations entre les blindages des ^{13}C par rapport aux densités de charges calculées par la méthode CNDO/2. On décrit la synthèse du triméthyl-2,7,9, des tétraméthyl-1,4,5,8 et 1,4,5,9 et du pentaméthyl-1,4,5,8,9 anthracène. [Traduit par le journal]

Introduction

Since the pioneering studies of ^{13}C spectra by Lauterbur and Burke and Lauterbur (1) in the early sixties, the utility of ^{13}C shieldings for identification of hydrocarbons (2–4) and assessment of electronic structure (5–6) has been firmly established. There is great interest in the relationships of the chemical reactivities and electronic structures to carcinogenicities of several polynuclear aromatic hydrocarbons (7–9). Thus the potential of ^{13}C n.m.r. studies to elicit information about the local electronic environments of these compounds has considerable practical as well as theoretical significance.

Detailed interpretation of the ^{13}C n.m.r. parameters of a group of compounds such as the methylated polycyclic aromatic carcinogens (10) depends to a large extent on an understanding of the influences governing ^{13}C shieldings in simpler methyl-substituted aryl systems. Methylbenzenes were carefully examined some time ago (3) and recently series of methylnaphthalenes have been examined in two separate studies (11, 12), one of which also included an investigation of the relationships of the ^{13}C shieldings to calculated charge densities (11).

To aid the further understanding of ^{13}C shieldings in aryl systems, in this study the ^{13}C spectra of anthracene and 11 methylated anthra-

[1]Author to whom correspondence should be addressed. Present address: Chemistry Branch, Pesticides and Toxic Substances Effects Laboratory, U.S. Environmental Protection Agency, Research Triangle Park, N.C. 27711.

Can. J. Chem. Downloaded from www.nrcresearchpress.com by 210.87.254.5 on 09/05/12
For personal use only.

Can. J. Chem. Downloaded from www.nrcresearchpress.com by 210.87.254.5 on 09/05/12
For personal use only.

cenes were examined. Analyses of the proton n.m.r. spectra allowed unequivocal assignments of the resonances of the proton-bearing carbons by selective proton decoupling. From the measured effects of the methyl substituents on the ^{13}C shieldings, a set of parameters describing the effect of methyl substitution at the 1-, 2-, and 9-positions was derived. Deviations from the expected substituent effects due to steric interactions of *peri*-methyl groups were found. Charge densities at the carbons calculated by the CNDO/2 method were found to correlate roughly with the ^{13}C shieldings. Two of the compounds studied, 1,4,5,9-tetramethylanthracene and 1,4,5,8,9-pentamethylanthracene, have not previously been reported in the literature. Their syntheses are described below.

Results and Discussion

Syntheses of Substrates

Polysubstituted anthracenes are commonly prepared by cyclodehydration of *o*-benzylacetophenones (13) and *o*-methylbenzophenones (14) or by reduction of the corresponding anthraquinones which are obtained by the cyclodehydration of *o*-benzoylbenzoic acids (15). These cyclodehydrations, which are carried out under vigorous pyrolytic or acid-catalyzed conditions, are subject to phenonium ion rearrangements (16), alkyl group migrations (17), and dealkylations (18). As a result of these and other unspecified side reactions, anthracenes prepared by these cyclodehydration processes are often obtained in low yields as difficult to purify mixtures (19).

In contrast to cyclodehydration leading to anthracenes and anthraquinones, anthrones can be prepared by the cyclodehydration of *o*-benzylbenzoic acids under mild conditions (80% sulfuric acid, 0 °C) and in high yields (> 90%) without rearrangement (20). Anthrones **are** particularly useful synthetic intermediates for the present study since they can be reduced by complex metal hydrides to 9,10-dihydro-9-anthranols which can then be converted to the corresponding anthracenes by mild acid-catalyzed dehydration. This route, summarized in Scheme 1, was used for the synthesis of 1,4,5,8-tetramethylanthracene (**4**).

Anthrones may also be converted conveniently to 9- or 10-alkylated anthracenes by base-catalyzed alkylation at the 10-methylene group followed by reduction and dehydration, or by Grignard addition to the carbonyl group followed by dehydration. The former route, outlined in Schemes 2 and 3, was used for the syntheses of 1,4,5,8,9-pentamethylanthracene (**6**) and 1,4,5,9-tetramethylanthracene (**12**). The latter route, shown in Scheme 4, was followed for the synthesis of 2,7,9-trimethylanthracene (**16**).

Syntheses of **4** and **16** through the anthrones confirm the structures of these anthracenes, which previously had been prepared via the anthraquinone for **4** (19) and via a modified Bradsher route for **16** (21).

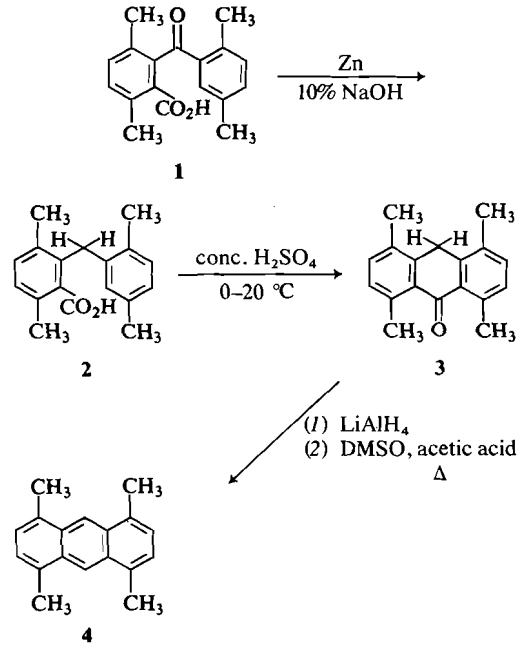

SCHEME 1. Preparation of 1,4,5,8-tetramethylanthracene (**4**).

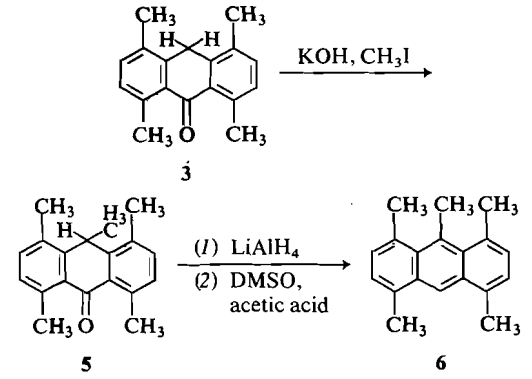

SCHEME 2. Preparation of 1,4,5,8,9-pentamethylanthracene (**6**).

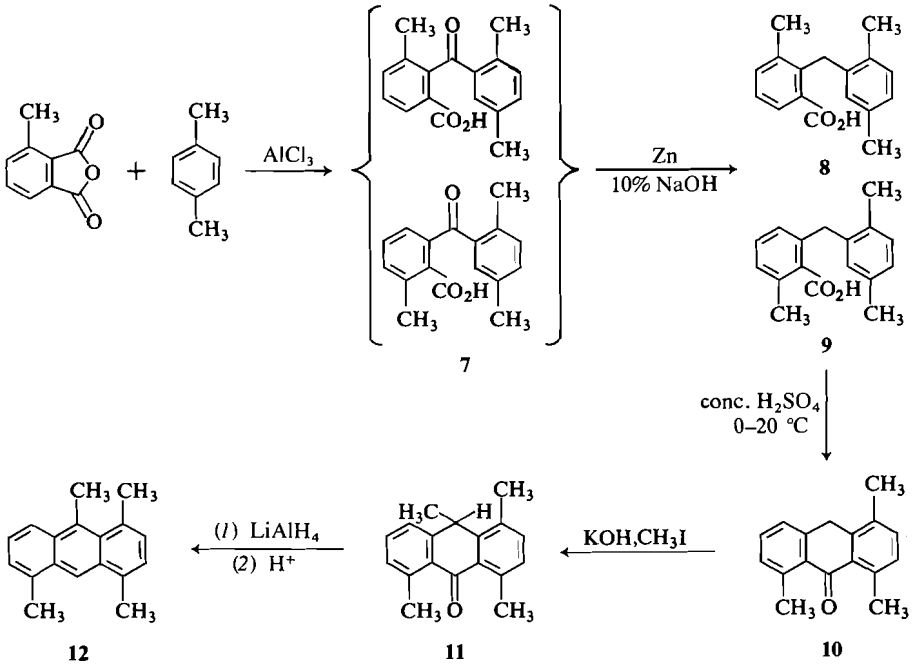

SCHEME 3. Preparation of 1,4,5,9-tetramethylanthracene (**12**).

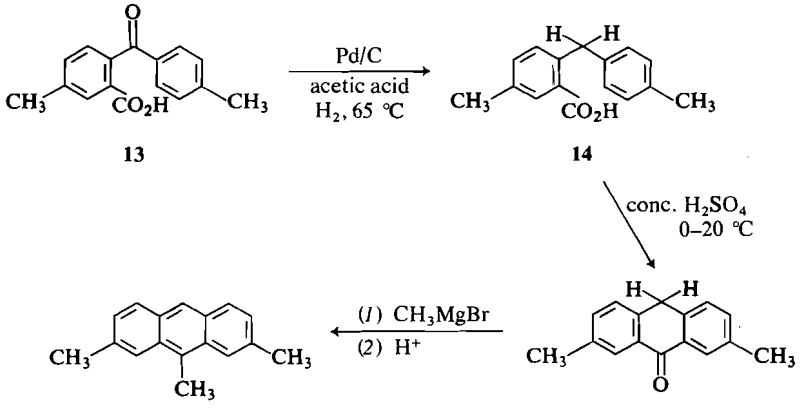

SCHEME 4. Preparation of 2,7,9-trimethylanthracene (**16**).

Nuclear Magnetic Resonance Parameters

The proton n.m.r. parameters for anthracene and 11 methylated anthracenes are given in Table 1. The deshielding effect of substitution at the 1-, 4-, 5-, 8-, 9-, or 10-positions on the *peri*-proton resonances is well established (22); thus unambiguous assignments were possible for all the proton resonances, including those giving AA′BB′ patterns, with the exception of 2-methylanthracene for which there was extensive overlap of the subspectral patterns and which also had nearly equivalent chemical shifts. Using these proton assignments, selective decoupling experiments allowed assignments of the ^{13}C resonances to specific proton-bearing carbons for all the compounds except 2-methylanthracene. Quaternary carbon signals were assigned on the basis of their relative intensities, with the assumption of approximately equal effective rotational correlation times. The nuclear Overhauser

Can. J. Chem. Downloaded from www.nrcresearchpress.com by 210.87.254.5 on 09/05/12
For personal use only.

Can. J. Chem. Downloaded from www.nrcresearchpress.com by 210.87.254.5 on 09/05/12
For personal use only.

TABLE 1. Proton n.m.r. parameters of several methylanthracenes*

Substitution	Chemical shift (δ, p.p.m. from TMS)										
	CH_3	H-1	H-2	H-3	H-4	H-5	H-6	H-7	H-8	H-9	H-10
9-Me	3.070	8.261	7.482	7.436	7.974	7.974	7.436	7.482	8.261	—	8.311
9,10-Me_2	3.086	8.316	7.500	7.500	8.316	8.316	7.500	7.500	8.316	—	—
1-Me	2.802	—	7.284	7.341	7.851	7.986	7.439	7.458	8.017	8.517	8.396
1,4-Me_2	2.768	—	7.174	7.174	—	8.018	7.456	7.456	8.018	8.520	8.520
1,8-Me_2	2.823	—	7.303	7.344	7.849	7.849	7.344	7.303	—	8.597	8.393
1,4,5,8-Me_4	2.783	—	7.189	7.189	—	—	7.189	7.189	—	8.591	8.591
1,4,9-Me_3	2.737(4) 2.940(1) 3.229(9)	—	7.130	7.130	—	7.971	7.425	7.472	8.248	—	8.390
1,4,5,9-Me_4	2.772(4) 2.819(5) 2.948(1) 3.244(9)	—	7.155	7.155	—	—	7.290	7.383	8.152	—	8.515
1,4,5,8,9-Me_5	2.762(4, 5) 2.872(1, 8) 3.093(9)	—	7.160	7.160	—	—	7.160	7.160	—	—	8.419
2-Me	2.512	7.708	—	7.271	7.874	7.945	7.399	7.407	7.938	8.269	8.334
2,7,9-Me_3	2.559(2, 7) 3.009(9)	7.978	—	7.252	7.850	7.850	7.252	—	7.978	—	8.204

Substitution	Coupling constants (*J*, Hz)											
	1,2	1,3	1,4	2,3	2,4	3,4	5,6	5,7	5,8	6,7	6,8	7,8
9-Me	8.6	0.7	0.3	6.2	1.1	8.5	8.5	1.1	0.3	6.2	0.7	8.6
9,10-Me_2	8.6	1.4	0.0	5.5	1.4	8.6	8.6	1.4	0.0	5.5	1.4	8.6
1-Me	—	—	—	6.9	0.9	8.2	8.6	1.6	0.4	7.0	1.6	8.2
1,4-Me_2	—	—	—	—	—	—	8.5	1.2	0.0	6.6	1.2	8.5
1,8-Me_2	—	—	—	6.7	1.1	8.5	8.5	1.1	—	6.7	—	—
1,4,9-Me_3	—	—	—		—	—	8.9	1.0	0.3	6.4	0.5	9.8
1,4,5,9-Me_4	—	—	—		—	—	—	—	—	8.7	1.4	8.4
2-Me	—	1.7	~0.0	—	—	8.7	7.6	1.1	0.0	6.2	1.4	9.3
2,7,9-Me_3	—	0.9	~0.0	—	—	8.0	8.0	—	~0.0	—	0.9	—

*Obtained for 5% (w/v) solutions in chloroform-*d*, using LAOCN3 program. The mean overall rms error is 0.059 Hz, with a range of 0.029–0.178 Hz, except for 2-methylanthracene, for which the r.m.s. error is 0.244 Hz.

Can. J. Chem. Downloaded from www.nrcresearchpress.com by 210.87.254.5 on 09/05/12
For personal use only.

TABLE 2. ^{13}C shieldings of several methylanthracenes*

Substitution	C-1	C-2	C-3	C-4	C-5	C-6	C-7	C-8	C-9	C-10	C-11	C-12	C-13	C-14	Me
Nil	127.9	125.1	125.1	127.9	127.9	125.1	125.1	127.9	126.0	126.0	131.5	131.5	131.5	131.5	
9-Me	124.3	(124.8)	(124.4)	128.7	128.7	(124.4)	(124.8)	124.3	129.7	124.3	129.8	131.1	131.1	129.8	13.7
9,10-Me_2	125.0	124.4	124.4	125.0	125.0	124.4	124.4	125.0	128.1	128.1	129.6	129.6	129.6	129.6	14.1
1-Me	133.9	125.4	124.9	126.5	127.7	125.1	125.0	128.3	122.5	126.6	131.2	131.7	131.4	131.2	19.7
1,4-Me_2	132.1	125.2	125.2	132.1	128.1	125.1	125.1	128.1	123.0	123.0	131.0	131.0	131.3	131.3	19.7
1,8-Me_2	134.1	125.4	124.9	126.3	126.3	124.9	125.4	134.1	118.7	127.1	130.9	131.4	131.4	130.9	19.7
1,4,5,8-Me_4	132.2	125.2	125.2	132.2	132.2	125.2	125.2	132.2	119.6	119.6	130.6	130.6	130.6	130.6	19.6
1,4,9-Me_3	133.0	128.5	125.1	132.5	128.7	124.7	124.3	124.5	131.5	122.0	131.7	132.1	130.4	131.2	19.6 (4-Me) 20.3 (9-Me) 27.1 (1-Me)
1,4,5,9-Me_4	133.1	128.8	125.0	133.0	134.6	125.3	125.0	123.0	131.7_2	118.3	131.6_8	132.2	130.2	132.0	19.9 (4-Me) 20.0 (5-Me) 20.3 (9-Me) 27.0 (1-Me)
1,4,5,8,9-Me_5	134.3	128.5	124.8	132.2	132.2	124.8	128.5	134.3	133.4	118.0	132.3	131.0	131.0	132.3	20.0 (4,5-Me) 25.9 (1,8-Me) 26.8 (9-Me)
2-Me	126.3	134.9	128.2	128.0	128.1	(124.9)	(125.2)	128.2	125.2	125.9	132.1	130.4	131.3	131.9	21.9
2,7,9-Me_3	122.7	134.3	126.9	128.7	128.7	126.9	134.3	122.7	127.5	124.5	130.3	129.4	129.4	130.3	13.7 (9-Me) 22.4 (2,7-Me)

*In p.p.m. from internal TMS in $CDCl_3$ solutions; similar values in parentheses may be interchanged.

Can. J. Chem. Downloaded from www.nrcresearchpress.com by 210.87.254.5 on 09/05/12
For personal use only.

TABLE 3. Methyl substituent effects* on anthracene ^{13}C shieldings

Substitution	C-1	C-2	C-3	C-4	C-5	C-6	C-7	C-8	C-9	C-10	C-11	C-12	C-13	C-14
1-Methyl	5.8	0.3	−0.2	−1.5	−0.2	0.0	0.0	0.4	−3.6	0.5	−0.4	0.0	−0.1	−0.3
2-Methyl	−1.5	9.6	2.9	0.0	0.2	−0.3	0.0	0.1	−1.0	0.0	0.4	−1.2	−0.4	0.2
9-Methyl	−3.6	−0.2	−0.6	0.8	0.8	−0.6	−0.2	−3.6	3.7	−1.7	−1.6	−0.3	−0.3	−1.6

*In p.p.m.; positive values denote downfield shifts.

TABLE 4. Differences between predicted and observed ^{13}C shieldings* in methylated anthracenes having *peri*-methyl groups

Substitution	C-1	C-2	C-3	C-4	C-5	C-6	C-7	C-8	C-9	C-10	C-11	C-12	C-13	C-14
1,4,9-Me_3	4.4	3.5	0.5	−0.5	−0.2	0.2	−0.6	0.0	4.6	0.8	2.2	1.3	−0.4	2.0
1,4,5,9-Me_4	4.7	3.8	0.4	−0.4	−0.1	0.5	0.3	0.0	5.1	0.7	2.3	1.5	−0.2	2.2
1,4,5,8,9-Me_5	5.5	3.5	0.2	−1.0	−1.0	0.2	3.5	5.5	9.9	−0.1	3.2	0.6	0.6	3.2

*Observed − calculated (by additivity) values in p.p.m.

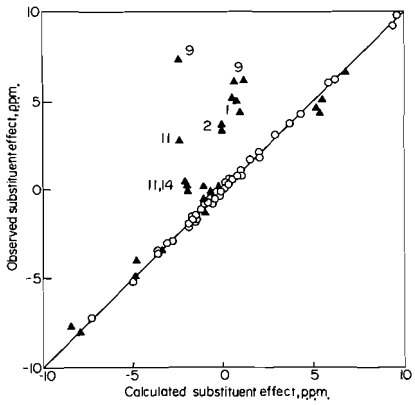

FIG. 1. Observed *vs.* calculated methyl substituent effects on aryl ^{13}C shieldings in several methylated anthracenes. ○, anthracenes without *peri*-methyl groups; ▲, anthracenes with *peri*-methyl groups. The line drawn is that for a perfect correlation with slope +1. The numbers beside groups of data points lying far off the line indicate the positions of those carbons in the anthracene molecule. Some closely clustered points have been omitted for clarity.

enhancements depend on dipolar relaxation by protons, which decreases with increases in the C–H separation, as the inverse sixth power of this separation. Thus the closer the neighboring protons, the more intense the carbon resonances, up to the maximum enhancement, which is obtained for entirely dipolar relaxation (23). The remaining resonances were assigned in a mutually consistent manner, assuming additivity of methyl group effects. The ^{13}C shieldings are collected in Table 2.

Using the results for 1-methyl-, 1,4-dimethyl-, 1,8-dimethyl-, and 1,4,5,8-tetramethylanthracene, a set of additive parameters describing the effects of a 1-methyl group on the ^{13}C shielding at all aryl positions was derived. Similarly, from the data for 9-methyl- and 9,10-dimethylanthracene, parameters for a 9-methyl substituent were obtained and from these and the data for 2-methyl- and 2,7,9-trimethylanthracene, the corresponding parameters for a 2-methyl substituent were found. After refinement of the parameters to provide the best overall fit for the set of all methylated anthracenes lacking *peri* substituents, the methyl substituent parameters given in Table 3 were obtained. These parameters predict the ^{13}C shieldings at all 67 independent aryl positions in the methylanthracenes lacking *peri*-methyl substitution with a standard error of 0.12 p.p.m. This is illustrated in Fig. 1, which compares the predicted to the observed methyl substituent effects, where the open circles correspond to data points for non-*peri*-substituted methylanthracenes. The substituent effects of a 1-methyl group on the anthracene ^{13}C shieldings are similar to those previously observed for 1-methylnaphthalenes (11). For positions which are nearly equivalent in the two systems, these agree within 0.2 p.p.m., except for the deshielding effects of the 1-methyl at C-1 and C-2, which are smaller by −0.4 and −0.5 p.p.m. in anthracene. The 2-methyl substituent effects in anthracene differ from those in naphthalene by −0.5, 0.0, 0.6, and 0.6 p.p.m., for C-1, C-2, C-3, and C-4, respectively. Although these effects are more pronounced at positions near the substituent in anthracene, at the methyl-substituted carbon C-2, they are identical, 9.6 p.p.m. in both naphthalene and anthracene.

A different picture emerges for the anthracenes with *peri* methyl–methyl interactions, 1,4,9-trimethyl-, 1,4,5,9-tetramethyl-, and 1,4,5,8,9-pentamethylanthracene. These compounds have ^{13}C shieldings which differ markedly from those predicted on the basis of the derived substituent parameters and the assumption of additivity. These differences are illustrated by the shaded triangles in Fig. 1 and are listed in Table 4.

In contrast to the increased shielding generally associated with crowded carbons separated by three bonds (24, 25) and observed for the methyl carbons with *ortho*-dimethyl substitution in naphthalenes (11), steric crowding of carbons separated by four bonds leads to deshielding of the carbons involved. This δ effect, only recently clearly recognized (26), is evident in the deshielding of the 1-methyl and 9-methyl carbons, 7.4 and 6.6 p.p.m., respectively, relative to their ^{13}C shieldings in their nonhindered counterparts. Other carbons in the sterically crowded part of the molecule likewise evince this deshielding. Thus at the methyl-substituted carbons, a single *peri*-methyl interaction results in average deshieldings of 4.9 p.p.m. at C-1 and C-9. In 1,8-dimethylnaphthalene (11) this effect was 5.1 p.p.m. at C-1. At positions *ortho* to the *peri*-methyl groups, C-2, C-11, and C-14, these effects average 3.6, 2.2, and 2.1 p.p.m., respectively. These, too, are similar to those observed in 1,8-dimethylnaphthalene, 3.0 p.p.m. at C-2 and 1.2 p.p.m. at C-9. Interestingly, the deshielding δ effects appear to be approximately additive, as is shown by comparison of the differences between

Can. J. Chem. Downloaded from www.nrcresearchpress.com by 210.87.254.5 on 09/05/12
For personal use only.

predicted and observed shieldings (Table 4) for C-9 of 1,4,5,8,9-pentamethylanthracene, which has two *peri*-methyl interactions, with those differences at the same carbon in 1,4,9-trimethyl- and 1,4,5,9-tetramethylanthracene, each of which has only one *peri*-methyl interaction. The 9-methyl carbon shieldings in these three compounds exhibit similar behavior, with two *peri*-methyl interactions giving rise to a deshielding of 13.1 p.p.m. and one a deshielding of 6.6 p.p.m. This 6.6 p.p.m. methyl carbon deshielding resulting from one *peri*-methyl interaction is exactly that observed in 1,8-dimethylnaphthalene (11). It seems likely that the deviations in Table 4 resulting from steric crowding of the methyl groups arise partially from alterations in the aryl carbon –carbon bond orders in the parts of the molecule close to the methyl groups. Other factors cannot, however, be discounted.

One contribution to the shielding of a given ^{13}C nucleus results from the electronic charge density at that nucleus (24). Several studies have indicated that charge distributions calculated by the CNDO/2 method (27) correlate reasonably well with experimental trends in ^{13}C n.m.r. data (28). To test for such correlations between the observed aryl shieldings and calculated charge densities for the methylated anthracenes, CNDO/2 calculations (29) for anthracene and its 1-methyl, 2-methyl, 9-methyl, 1,4-dimethyl, 1,8-dimethyl, 9,10-dimethyl, 2,7,9-trimethyl, and 1,4,5,8-tetramethyl derivatives were carried out. The results of these calculations are plotted in Fig. 2 *vs.* the experimental ^{13}C shieldings. The points shown are for the total charge density; the π charge density gave a similar plot but the correlation was slightly poorer. It was anticipated from the previous work on methylated naphthalenes (11), that aryl carbons in the β positions (C-2, C-3, C-6, C-7) of unsubstituted rings and these carbons when two bonds removed from the substituted carbon in substituted rings would be more shielded than the general trend for the other carbons, illustrated by the straight line in Fig. 2, would indicate. Data points for these β carbons were clustered tightly about one point, showing no trend in shielding with charge density. The *peri* effects of 1-methyl groups on the C-9 shieldings are sufficiently large that no discernible correlation of these shieldings with total charge density was found. For all carbons at ring junctions, C-11, -12, -13, and -14, the trends in both π and total charge densities successfully predicted the ordering of the ^{13}C resonances, but extension of these predictions to include all quaternary aryl carbons was unsuccessful, suggesting that the prediction of the ordering of the condensed carbon shieldings was somewhat fortuitous. The observed ^{13}C shieldings in the methylated anthracenes are related to the electronic charge distributions, but crudely, and other contributions to these shieldings, including bond orders and possibly as yet ill-defined steric effects, must be considered.

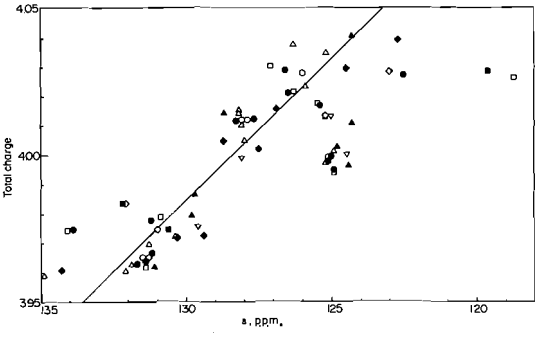

FIG. 2. Total charge densities *vs.* ^{13}C shieldings of aryl carbons in methylated anthracenes. ○, anthracene; ●, 1-methylanthracene; △, 2-methylanthracene; ▲, 9-methylanthracene; ◇, 1,4-dimethylanthracene; ◆, 2,7,9-trimethylanthracene; □, 1,8-dimethylanthracene; ■, 1,4,5,8-tetramethylanthracene; ▽, 9,10-dimethylanthracene. The total charge is given in units of *e*, the charge on the electron.

Experimental

Materials

Anthracene and 2-methyl-, 9-methyl-, and 9,10-dimethylanthracene of reagent quality were commercially obtained and used without further purification. Literature methods were followed for the syntheses of 1-methylanthracene (30), 1,4-dimethylanthracene (31), 1,8-dimethylanthracene (20), and 1,4,9-trimethylanthracene (31).

*1,4,5,8,9-Pentamethylanthracene (**6**)*

*(a) 2-(2,5-Dimethylbenzyl)-3,6-dimethylbenzoic Acid (**2**)*

To a well-stirred solution of 14.1 g (0.05 mol) of 2-(2,5-dimethylbenzoyl)-3,6-dimethylbenzoic acid (**1**) in 1500 ml of 10% sodium hydroxide heated at reflux, 50 g of zinc dust was added over a period of 48 h (19). The mixture was refluxed for an additional 24 h and then filtered. The filter cake was washed with 10% sodium hydroxide and with boiling water. The combined filtrates were strongly acidified with hydrochloric acid and extracted with benzene. The benzene extracts were dried, treated with charcoal, concentrated and then diluted with hexane. Crystallization gave 9.5 g (71%) of **2**.

Anal. Calcd. for $C_{18}H_{20}O_2$: C, 80.56; H, 7.51. Found: C, 80.72; H, 7.59.

Can. J. Chem. Downloaded from www.nrcresearchpress.com by 210.87.254.5 on 09/05/12
For personal use only.

Can. J. Chem. Downloaded from www.nrcresearchpress.com by 210.87.254.5 on 09/05/12
For personal use only.

(b) 1,4,5,8-Tetramethylanthrone (3)

A mixture of 2.68 g (0.01 mol) of finely powdered 2-(2,5-dimethylbenzyl)-3,6-dimethylbenzoic acid (**2**) and 20 ml of ice-cold concentrated sulfuric acid was stirred for *ca.* 15 min until all the solid had dissolved to give a clear lemon-yellow solution. This solution was allowed to warm to room temperature over 30 min, then poured onto ice and the resultant colorless solid was filtered and washed with hot water. The crude solid was dissolved in benzene, treated with anhydrous potassium carbonate and charcoal, and recrystallized from benzene–hexane to give 2.26 g (90%) of **3**, m.p. 198.5–199 °C.

Anal. Calcd. for $C_{18}H_{18}O$: C, 86.36; H, 7.25. Found: C, 86.35; H, 7.25.

The ^1H n.m.r. spectrum of **3** in $CDCl_3$ showed singlets for the 1- and 8-methyl (δ 2.48, 6H), the 4- and 5-methyl (δ 2.73, 6H), and the methylene (δ 3.82, 2H) protons; and an AB quartet (centered at δ 7.185, J = 8 Hz, 4H) for the aromatic protons.

(c) 1,4,5,8,10-Pentamethylanthrone (5)

To a refluxing, vigorously stirred suspension of 1.50 g (5.99 mmol) of 1,4,5,8-tetramethylanthrone (**3**) in 75 ml of 95% ethanol and 25 ml of methyl iodide, 9 g (0.15 mol) of potassium hydroxide was added over a period of 1 h. The cooled reaction mixture was poured into 1 l of water, filtered, and dried to give 1.61 g of a crude heterogeneous yellow and red solid.

This solid was dissolved in chloroform, treated with anhydrous sodium sulfate and charcoal and crystallized from chloroform – carbon tetrachloride to give 1.43 g (91%) of **5**.

Anal. Calcd. for $C_{19}H_{20}O$: C, 86.35; H, 7.63. Found: C, 86.28; H, 7.71.

The ^1H n.m.r. spectrum of **5** in $CDCl_3$ showed singlets for the 1- and 8-methyls (δ 2.44, 6H) and the 4- and 5-methyls (δ 2.65, 6H); a doublet for the 10-methyl (δ 1.33, 3H, J = 7 Hz); a quartet for the 10-methine proton (δ 4.40, 1H, J = 7 Hz); and an AB quartet (centered at δ 7.12, 4H, J = 8 Hz) for the aromatic protons. A carbonyl absorption at 1665 cm^{-1} was observed in the i.r. spectrum of **5** in a KBr pellet.

(d) 1,4,5,8,9-Pentamethylanthracene (6)

To a stirred solution of 1.0 g (26 mmol) of lithium aluminum hydride in 100 ml of absolute ether at 0 °C was added 100 mg (0.38 mmol) of 1,4,5,8,10-pentamethylanthrone (**5**). The solid dissolved rapidly to give a pale yellow-green solution which turned colorless over 15 min. The reaction was allowed to continue for 1 h at 0 °C. Stirring and cooling was continued while ice was added over a period of 1 h and while anhydrous magnesium sulfate was added over a second 1 h interval. The mixture was filtered and the filtrate evaporated to dryness under a stream of nitrogen to give 104 mg of a colorless mixture of *cis*- and *trans*-1,4,5,8,10-pentamethyl-9-anthranol (>90% *cis*).

The ^1H n.m.r. spectrum of this alcohol, 100 mg in 0.5 ml dimethyl sulfoxide-d_6, exhibited singlets for the 1- and 8-methyls (δ 2.38, 6H), the 4- and 5-methyls (δ 2.48, 6H), and the aromatic protons (δ 6.99, 4H); doublets for the 10-methyl (δ 1.42, 3H, J = 7 Hz), the carbinol proton (δ 5.97, 1H, J = 4 Hz) and the hydroxyl proton (δ 5.14, 1H, J = 4 Hz); and a quartet for the 10-methine proton (δ 4.25, 1H, J = 7 Hz).

Dehydration of the alcohol was carried out in the n.m.r. tube by the addition of 0.05 ml of acetic acid-d_4 and heating to 130 °C. After heating for 10 min the spectrum of the alcohol was completely replaced by the spectrum of 1,4,5,8,9-pentamethylanthracene (**6**), which showed singlet resonances for all protons; the 1- and 8-methyls (δ 2.82, 6H), 4- and 5-methyls (δ 2.70, 6H), and 9-methyl (δ 3.03, 3H); the 2-, 3-, 6-, and 7-aromatic protons (δ 7.16, 4H) and the 10- aromatic proton (δ 8.36, 1H).

1,4,5,8,9-Pentamethylanthracene (**6**) was isolated by dilution with water and extraction with chloroform as a slightly yellow, blue-green fluorescent solid (81 mg, 87%). Aged samples lost their fluorescence and turned yellow. Due to rapid oxygen incorporation, with formation of a photo-oxide of formula $C_{19}H_{20}O_2$, probably by oxygen addition across the 9,10 or 1,4 positions (32), satisfactory elemental analyses could not be obtained.

Vacuum sublimation of **6** at *ca.* 115 °C and 20 mm Hg gave a yellow crystalline solid, m.p. 140–148 °C. This solid was sublimed at 0.35 mm Hg and the fraction which sublimed between 110 and 150 °C was passed through a silica gel column (Woelm activity grade 1) with 5% benzene–hexane. The first-eluting component was concentrated and pumped at room temperature for 45 min at 0.15 mm Hg. The resulting very pale yellow crystalline solid had m.p. 154–157 °C. Its mass spectrum had the anticipated molecular ion at *m/e* 248 and the expected mass fragments for a pentamethylanthracene of formula $C_{19}H_{20}$. No significant impurities were observed.

1,4,5,8-Tetramethylanthracene (4)

This preparation was similar to the preparation of **6** above, but 1,4,5,8-tetramethylanthrone (**3**) was the starting material. The 1,4,5,8-tetramethylanthracene, in 87% yield from **3**, recrystallized from benzene–hexane and sublimed had m.p. 221–221.5 °C (lit. (19) m.p. 220–221 °C).

Anal. Calcd. for $C_{18}H_{18}$: C, 92.26; H, 7.74. Found: C, 92.34; H, 7.60.

1,4,5,9-Tetramethylanthracene (12)

(a) 2-(2,5-Dimethylbenzyl)-6-methylbenzoic Acid (9)

To a cooled, stirred solution of 50 g (0.31 mol) of 3-methylphthalic anhydride (33) in 400 ml of *p*-xylene was added 190 g of anhydrous aluminum chloride. The reaction mixture was heated at 60–65 °C for 4 h, poured onto ice, acidified with hydrochloric acid, and extracted with benzene. The benzene extracts were extracted with 5% sodium hydroxide. This basic solution was treated with charcoal, filtered, and acidified to give, upon filtration and washing with hot water, 56 g (68%) of a mixture of 2-(2,5-dimethylbenzoyl)-3- and 6-methylbenzoic acids (**7**). This mixture of isomeric acids was dissolved in 3 l of 10% sodium hydroxide and heated at reflux for 72 h with 250 g of zinc dust, which was added in portions over the course of the reduction. The hot mixture was filtered and the residue washed with hot 10% sodium hydroxide and hot water. The filtrates were strongly acidified with hydrochloric acid and extracted with benzene. The benzene extract was treated with charcoal, then fractionally recrystallized from benzene–hexane. From the more soluble fractions there was isolated 2.4 g of 2-(2,5-dimethylbenzyl)-6-methylbenzoic acid (**9**), m.p. 103–104.5 °C.

Anal. Calcd. for $C_{17}H_{18}O_2$: C, 80.28; H, 7.13. Found: C, 80.22; H, 7.26.

Can. J. Chem. Downloaded from www.nrcresearchpress.com by 210.87.254.5 on 09/05/12
For personal use only.

From the less soluble fractions there was obtained 15.6 g of 2-(2,5-dimethylbenzyl)-3-methylbenzoic acid (**8**), m.p. 184–185 °C.

Anal. Calcd. for $C_{17}H_{18}O_2$: C, 80.28; H, 7.13. Found: C, 80.20; H, 7.30.

The structures of the isomeric acids **8** and **9** were determined from the ^1H n.m.r. spectra. The proton *ortho* to the carboxyl group in **8** appeared as a multiplet at δ 7.8, with the remainder of the aromatic protons absorbing at δ 6.8–7.5. With a methyl group *ortho* to the carboxyl group in **9**, all of the aromatic proton resonances were at δ 6.8–7.5.

(b) 1,4,8-Trimethylanthrone (10)

A mixture of 1.5 g (5.9 mmol) of 2-(2,5-dimethylbenzyl)-6-methylbenzoic acid (**9**) and 10 ml of concentrated sulfuric acid was stirred at 0 °C for *ca.* 10 min until a clear yellow solution was obtained. This solution was allowed to stand at room temperature for 30 min, then poured onto ice. Filtration and washing with water followed by recrystallization from benzene–hexane gave 1.15 g (83%) of **10**.

Anal. Calcd. for $C_{17}H_{16}O$: C, 86.40; H, 6.83. Found: C, 86.22; H, 6.92.

The ^1H n.m.r. spectrum of **10** in $CDCl_3$ exhibited singlet absorptions for the 4-methyl (δ 2.36, 3H), the 1- and 8-methyls (δ 2.72 and 2.77, 6H), and the methylene (δ 4.06, 2H); and a multiplet for the aromatic protons (centered at δ 7.25, 5H).

(c) 1,4,8,10-Tetramethylanthrone (11)

To a refluxing solution of 500 mg (2.16 mmol) of 1,4,5-trimethylanthrone (**10**) in 75 ml of ethanol under a nitrogen atmosphere, was added 1.0 g (17 mmol) of potassium hydroxide followed by the slow addition of 14 g (0.1 mol) of methyl iodide. The reaction was heated at reflux for 30 min, cooled to room temperature, diluted with 50 ml of water, and concentrated with a rotary evaporator. Filtering and drying gave 519 mg (98%) of pale yellow 1,4,8,10-tetramethylanthrone (**11**).

The ^1H n.m.r. spectrum of **11** in $CDCl_3$ showed singlets for the 4-methyl (δ 2.41, 3H) and the 5- and 8-methyls (δ 2.67 and 2.70, 6H); a doublet for the 10-methyl (δ 1.38, 3H, $J = 7$ Hz); a quartet for the methine proton (δ 4.22, 1H, $J = 7$ Hz); and a multiplet for the aromatic protons (centered at δ 7.2, 5H).

Attempts to recrystallize this anthrone **11** from chloroform–pentane caused the formation of a colorless high melting, sparingly soluble product. The same product appeared in aged samples of the anthrone.

(d) 1,4,5,9-Tetramethylanthracene (12)

A fresh sample of 1,4,8,10-tetramethylanthrone (**11**) was prepared by the above procedure from 100 mg of 1,4,8-trimethylanthrone (**10**) and without purification was directly subjected to reduction and dehydration. The crude dried **11** was dissolved in 100 ml of ether, to which, at the boiling point, 1.0 g (26 mmol) of lithium aluminum hydride was added. The reaction was stirred at room temperature for 45 min, then poured into a vigorously stirred mixture of 250 ml of ether and 10 ml of water. After 15 min of stirring, the mixture was dried with anhydrous magnesium sulfate. The filtrate was concentrated to 100 ml and then heated at the boiling point with several crystals of *p*-toluenesulfonic acid and 1 ml of water for 10 min. The solution was cooled, dried over anhydrous potassium carbonate, and evaporated to dryness with a stream of nitrogen to give 81 mg (82%) of pale yellow crystalline 1,4,5,9-tetramethylanthracene (**12**).

The mass spectrum of **12** gave the expected molecular ion at *m/e* 234 and fragments consistent with a tetramethylanthracene $C_{18}H_{18}$. About 7% of the sample was an oxygenated impurity, $C_{18}H_{18}O_2$, probably the transannular peroxide (32). Since this oxygen adduct formed rapidly in solution, n.m.r. analyses were obtained on the directly prepared product above.

Vacuum sublimation of 2 mg of **12** recovered from the n.m.r. analyses at 115 °C and *ca.* 20 mm Hg gave pale yellow crystals, m.p. 131–135 °C.

2,7,9-Trimethylanthracene (16) (34)

(a) 2-(4-Methylbenzoyl)-5-methylbenzoic Acid (13)

To 15 ml of 100% sulfuric acid was added 16.3 g (64.2 mmol) of a mixture of 2-(4-methylbenzoyl)-4- and 5-methylbenzoic acids (35). The bright orange mixture was heated at 50 °C for 49 h.

The resulting deep brown solution was poured with rapid stirring onto a slurry of crushed ice and water. The precipitate was extracted into ether and the ether solution extracted with a saturated solution of sodium bicarbonate. The basic solution was treated with charcoal, acidified with concentrated hydrochloric acid and the precipitated keto acid was extracted into ether. The ether solution was washed with water and a saturated solution of sodium chloride. After the ether solution was dried over magnesium sulfate and evaporated to dryness, 10.6 g of product was recovered, m.p. 127–144 °C. Fractional crystallization from benzene–heptane and chloroform–heptane as alternating solvent systems yielded 1.73 g (16.3%) of 2-(4-methylbenzoyl)-5-methylbenzoic acid (**13**), m.p. 162–163 °C. The i.r. spectrum showed absorption maxima at 760, 830, and 940 cm^{-1} characteristic of **13**, with no bands at 778, 842, 858, and 963 cm^{-1} characteristic of 2-(4-methylbenzoyl)-4-methylbenzoic acid.

Anal. Calcd. for $C_{16}H_{14}O_3$: C, 75.57; H, 5.55. Found: C, 75.69; H, 5.49.

The structure of keto acid **13** was proven by decarboxylation (36) to 4,4′-dimethylbenzophenone. To 19 mg of basic cupric carbonate in a short path distillation apparatus was added 500 mg (1.97 mmol) of keto acid **13**. The mixture was heated gently with a free flame until the acid melted and neutralization was complete. Water was removed on a steam bath under reduced pressure. Decarboxylation was accomplished by heating the mixture in a sand bath at 265 °C until evolution of carbon dioxide ceased. Distillation of the residue (0.5 mm) gave 205 mg (49.7%) of a yellow oil. Pale yellow needles, m.p. 91–93 °C, were obtained after a solution of the yellow oil in 95% ethanol was allowed to cool slowly. A mixture melting point of 91–93 °C was obtained for the crystallized product and an authentic sample of 4,4′-dimethylbenzophenone, m.p. 92.5–93.5 °C (lit. (37) 95 °C). The i.r. spectra of the two samples were superimposable.

(b) 2-(4-Methylbenzyl)-5-methylbenzoic Acid (14)

To 50 ml of glacial acetic acid in a Parr bottle was added 4.65 g (18.3 mmol) of keto acid **13** and 0.6 g of 5% palladium-on-carbon. The mixture was hydrogenated on a Parr apparatus under 40 psi of hydrogen at 65 °C for 6 h. The catalyst was filtered off and the acetic acid filtrate diluted with water to give 3.95 g (90%) of 2-(4-methyl-

Can. J. Chem. Downloaded from www.nrcresearchpress.com by 210.87.254.5 on 09/05/12
For personal use only.

benzyl)-5-methylbenzoic acid (**14**), m.p. 113–115 °C. An analytical sample was prepared by recrystallization from chloroform–benzene, m.p. 116 °C.

Anal. Calcd. for $C_{16}H_{16}O_2$: C, 79.97; H, 6.71. Found: C, 79.69; H, 7.00.

(c) 2,7-Dimethylanthrone (15)

To 5 ml of 98% sulfuric acid at 0 °C was added 500 mg (2.1 mmol) of 2-(4-methylbenzyl)-5-methylbenzoic acid (**14**). The orange solution was allowed to warm to room temperature over 30 min, poured onto ice, and filtered. The dried product was recrystallized from chloroform–hexane to give 403 mg (87%) of pale yellow needles, m.p. 153–154 °C.

Anal. Calcd. for $C_{16}H_{14}O$: C, 86.45; H, 6.35. Found: C, 86.60; H, 6.25.

(d) 2,7,9-Trimethylanthracene (16)

To a chilled solution of methylmagnesium bromide (9 mmol) in 15 ml of ether was added 400 mg (1.8 mmol) of 2,7-dimethylanthrone **15**. The reaction mixture was vigorously stirred for 2 h while cooled in an ice-water bath. The mixture was then poured into dilute hydrochloric acid and extracted with ether. The ether solution was washed with water, 5% sodium bicarbonate, and saturated sodium chloride and dried over anhydrous magnesium sulfate. The dried ether solution was treated heavily with charcoal and evaporated to dryness. Recrystallization from ethanol gave 286 mg (72%) of 2,7,9-trimethylanthracene **16**, m.p. 124–126 °C (lit. 126 °C (21)).

Spectra

The ^1H n.m.r. spectra were obtained by pulsed Fourier transform operation on a Varian XL-100 spectrometer with internal deuterium lock, using 5% (w/v) solutions in chloroform-*d* containing 0.5% tetramethylsilane (TMS) at 28 °C. These spectra were examined with methyl protons and other protons decoupled as appropriate to obtain more accurate line positions by removal of line broadening due to small long-range couplings. Additional spectra in other solvents, *e.g.*, benzene-d_6 and acetone-d_6, were used to aid the interpretation of the overlapping patterns observed for some of the compounds. Analysis of the spectra was done with the aid of the iterative spectral fitting program LAOCN3 (38). Natural abundance ^{13}C spectra were obtained similarly, using 10–15% (w/v) solutions in chloroform-*d* containing a few drops of TMS at 40 °C. The individual aryl carbon shieldings were measured from noise-decoupled spectra. Definitive assignments of the protonated carbon resonances were then made by single frequency proton decoupling at relatively low decoupler power, with the decoupler frequency set at the proper value for each individual proton resonance in turn. The 500 Hz sweep widths used for the ^{13}C spectra gave precisions of ± 0.03 p.p.m., however, dilution effects are anticipated to be significant in these systems (11), although probably small at the concentrations employed (10), and the shieldings are therefore reported to ± 0.1 p.p.m., except for very closely lying signals.

Mass spectra were obtained by gas–liquid chromatography coupled with methane chemical ionization and 70 eV electron impact mass spectrometry on a Finnigan Model 1015C mass spectrometer interfaced with a Finnigan model 9500 gas chromatograph and on a Hewlett-Packard 5930 70 eV electron impact mass spectrometer interfaced with a Hewlett-Packard 5700 gas chromatograph. Single components and the expected mass fragments were observed for 1-methyl-, 1,4-dimethyl-, 1,8-dimethyl-, and 1,4,5,8-tetramethylanthracene. The 1,4,5,9 compound ($C_{18}H_{18}$) contained less than 7% of an oxygenated impurity ($C_{18}H_{18}O_2$) and the 1,4,5,8,9 compound contained approximately 4% of a similar impurity ($C_{19}H_{20}O_2$). Attempts to prepare acetate derivatives of the concentrated impurities were unsuccessful. These impurities are probably photooxides (32) formed by oxygen addition. To prevent formation of photooxides, the solid methylated anthracenes were stored in the dark in the freezer and solutions for n.m.r. analysis were made up immediately prior to the acquisition of spectra.

CNDO/2 Calculations

Standard bond lengths and bond angles as given by Pople and Beveridge (27) and planar ring systems were assumed. The CNINDO program from QCPE (29) was used without modification. Calculations were done on the IBM 370/165 computer of the Triangle Universities Computation Center.

We thank Dr. E. O. Oswald and Dr. G. W. Sovocool for obtaining and interpreting the mass spectra, Dr. R. D. Zehr and Miss Ināra Grikis for technical assistance, and the National Research Council of Canada for partial financial support of this research.

1. P. C. Lauterbur. J. Am. Chem. Soc. **83**, 1828 (1961); J. J. Burke and P. C. Lauterbur. J. Am. Chem. Soc. **86**, 1870 (1964).
2. D. M. Grant and E. G. Paul. J. Am. Chem. Soc. **85**, 1701 (1963); **86**, 2984 (1964).
3. W. R. Woolfenden and D. M. Grant. J. Am. Chem. Soc. **88**, 1496 (1966).
4. T. G. Alger, D. M. Grant, and E. G. Paul. J. Am. Chem. Soc. **88**, 5397 (1966); A. J. Jones and D. M. Grant. Chem. Commun. 1670 (1968).
5. A. J. Jones, T. D. Alger, D. M. Grant, and W. M. Litchman. J. Am. Chem. Soc. **92**, 2386 (1970).
6. A. J. Jones, P. D. Gardner, D. M. Grant, W. M. Litchman, and V. Boekelheide. J. Am. Chem. Soc. **92**, 2395 (1970).
7. P. Daudel and R. Daudel. Chemical carcinogenesis and molecular biology. Wiley, New York. 1966.
8. E. D. Bergman and B. Pullman. (*Editors*). Physico-chemical mechanisms of carcinogenesis. Proc. Int. Symp. Israel Acad. Sci. Humanities, Jerusalem. 1969.
9. E. Cavalieri and M. Calvin. Proc. Nat. Acad. Sci. U.S.A. **68**, 1251 (1971); J. H. Weisburger. *In* Cancer medicine. *Edited by* J. F. Holland and E. Frei. Lea and Febiger, Philadelphia. 1973. pp. 45–90.
10. R. S. Ozubko, G. W. Buchanan, and I. C. P. Smith. Can. J. Chem. **52**, 2493 (1974).
11. N. K. Wilson and J. B. Stothers. J. Magn. Reson. **15**, 31 (1974).
12. D. Doddrell and P. R. Wells. J. Chem. Soc. Perkin II, 1333 (1973).
13. C. K. Bradsher. J. Am. Chem. Soc. **62**, 486 (1940).
14. K. Elbs. J. Prakt. Chem. (2), **41**, 142 (1890).
15. C. Liebermann. Ber. **7**, 805 (1874).

16. (*a*) M. HAYASHI. J. Chem. Soc. 2516 (1927). (*b*) M. S. NEWMAN and K. G. IHRMAN. J. Am. Chem. Soc. **80** 3652 (1958).
17. G. BADDELEY, G. HOLT, and S. M. MAKAR. J. Chem. Soc. 2415 (1952).
18. L. F. FIESER. Organic reactions. Vol. I. Wiley, New York. 1942. p. 129.
19. W. CARRUTHERS, H. N. M. STEWART, P. S. HANSELL, and K. M. KELLY. J. Chem. Soc. 2607 (1967).
20. S. J. CRISTOL and M. L. CASPAR. J. Org. Chem. **33**, 2020 (1968).
21. J. COLOGNE and L. BONNARD. Bull. Soc. Chim. Fr. 742 (1958).
22. L. M. JACKMAN and S. STERNHELL. Applications of nuclear magnetic resonance spectroscopy in organic chemistry. 2nd ed. Pergamon Press, New York. 1969. p. 206.
23. A. J. JONES, D. M. GRANT, and K. F. KUHLMANN. J. Am. Chem. Soc. **91**, 5013 (1969).
24. J. B. STOTHERS. Carbon-13 NMR spectroscopy. Academic Press, New York. 1972.
25. N. K. WILSON and J. B. STOTHERS. *In* Topics in stereochemistry. Vol. 8. *Edited by* E. L. Eliel and N. L. Allinger. Wiley-Interscience, New York. 1974. pp. 1–158.
26. S. H. GROVER, J. P. GUTHRIE, J. B. STOTHERS, and C. T. TAN. J. Magn. Reson. **10**, 227 (1973); K. R. STEPHENS, J. B. STOTHERS, and C. T. TAN. *In* Mass spectrometry and NMR spectroscopy in pesticide chemistry. Plenum Press, New York. 1974. pp. 179–196; J. B. STOTHERS and C. T. TAN. Can. J. Chem. **52**, 308 (1974); S. H. GROVER and J. B. STOTHERS. Can. J. Chem. **52**, 870 (1974).
27. J. A. POPLE and D. L. BEVERIDGE. Approximate molecular orbital theory. McGraw-Hill, New York. 1970; J. A. POPLE. Acc. Chem. Res. **3**, 217 (1970).
28. R. J. PUGMIRE and D. M. GRANT. J. Am. Chem. Soc. **93**, 1880 (1971); P. LAZZERETTI and F. TADDEI. Org. Magn. Reson. **3**, 282 (1971); G. L. NELSON, G. C. LEVY, and J. D. CARGIOLI. J. Am. Chem. Soc. **94**, 3089 (1972); N. K. WILSON and M. ANDERSON. *In* Mass spectrometry and NMR spectroscopy in pesticide chemistry. Plenum Press, New York. 1974. pp. 197–218.
29. P. A. DOBOSH. Program 141, Quantum Chemistry Program Exchange, Indians University, Bloomington, Indiana.
30. J. O. VON BRAUN and O. BAYER. Ber. **59B**, 914 (1926).
31. E. DEB. BARNETT and J. A. LOW. Ber. **64B**, 49 (1931).
32. J. RIGAUDY, J. GUILLAUME, and D. MAURETTE. Bull. Soc. Chim. Fr., 144 (1971).
33. M. S. NEWMAN and C. D. MCCLEARY. J. Am. Chem. Soc. **63**, 1537 (1941).
34. R. C. HERMANN. M.S. Thesis. Arizona State University, Tempe, Arizona. 1966.
35. F. MEYER and H. GUNTHER. Ber. **63**, 1455 (1930).
36. G. DOUGHERTY. J. Am. Chem. Soc. **50**, 571 (1928).
37. J. FERRANTE and A. BLOOM. Am. J. Pharm. **105**, 381 (1933).
38. A. A. BOTHNER-BY and S. CASTELLANO. Program 111, Quantum Chemistry Program Exchange, Indiana University, Bloomington, Indiana.

Can. J. Chem. Downloaded from www.nrcresearchpress.com by 210.87.254.5 on 09/05/12
For personal use only.

A Facile Route to 1 → 6 Linked Disaccharides: Syntheses of 6-*O*-β-D-Glucopyranosyl-D-glucose (Gentiobiose) and of 2-Acetamido-6-*O*-(2-acetamido-2-deoxy-β-D-galactopyranosyl)-2-deoxy-D-galactose[1]

RUSSELL R. KING[2] AND CLAUDE T. BISHOP

Division of Biological Sciences, National Research Council of Canada, Ottawa, Canada K1A 0R6

Received February 4, 1975

RUSSELL R. KING and CLAUDE T. BISHOP. Can. J. Chem. **53,** 1970 (1975).

The condensation of acetohalogeno sugars with unblocked benzyl hexopyranosides gave the 1 → 6 linked disaccharides exclusively and in good yield. The utility of this "open" synthesis was demonstrated by preparation of 6-*O*-β-D-glucopyranosyl-D-glucose (gentiobiose) and of a new disaccharide, 2-acetamido-6-*O*-(2-acetamido-2-deoxy-β-D-galactopyranosyl)-2-deoxy-D-galactose.

RUSSELL R. KING et CLAUDE T. BISHOP. Can. J. Chem. **53,** 1970 (1975).

La condensation des saccharides acétohalogénés avec les glycosides benzyliques des hexoses conduit exclusivement aux disaccharides à liaison 1 → 6 en bon rendement. On a démontré l'utilité de cette synthèse "ouverte" en préparant le 6-*O*-β-D-glucopyranosyl-D-glucose (gentiobiose) et un nouveau disaccharide, le 2-acétamido-6-*O*-(2-acétamido-2-deoxy-β-D-galactopyranosyl)-2-deoxy-D-galactose.

Previous studies (1, 2) have shown that condensation of unblocked glycosides with glycosyl halides offers an attractive synthetic route to disaccharides, particularly those for which a suitably protected aglycone would be difficult to obtain. Those studies were done with a 6-deoxyhexopyranoside (benzyl α-L-rhamnopyranoside) as the aglycone, thus eliminating the possibility of reaction at the C-6 position. It was noted (2) that the greater reactivity of primary hydroxyl groups would undoubtedly lead to a predominance of 1 → 6 linked disaccharides when this method was used with hexopyranoside aglycones.

The present report confirms the utility of this "open" synthesis for β 1 → 6 linked disaccharides by describing the preparation of a known compound, 6-*O*-β-D-glucopyranosyl-D-glucose (gentiobiose), and of a new disaccharide required for structural and serological studies, 2-acetamido-6-*O*-(2-acetamido-2-deoxy-β-D-galactopyranosyl)-2-deoxy-D-galactose.

Thus, condensation of 2,3,4,6-tetra-*O*-acetyl-α-D-glucopyranosyl bromide (**1**) with benzyl β-D-glucopyranoside (**2**) in nitromethane at 24 °C in presence of silver carbonate gave a single disaccharide product in 56% yield. The p.m.r. spectrum of this compound showed the presence of one benzyl and four acetyl groups, consistent with the expected compound (**3**). Deacetylation and hydrogenolysis of the condensation product (**3**) yielded 6-*O*-β-D-glucopyranosyl-D-glucose (**4**) (gentiobiose), characterized as its crystalline octaacetate.

The formation of a 1 → 6 linked disaccharide from 2-acetamido-3,4,6-tri-*O*-acetyl-2-deoxy-α-D-galactopyranosyl chloride (**5**) and benzyl 2-acetamido-2-deoxy-β-D-galactopyranoside (**6**) required more rigorous conditions than those used with the neutral sugar derivatives. However, condensation was effected successfully by heating the two compounds under reflux in benzene–nitromethane in the presence of cadmium carbonate. The single new compound that was formed in 13% yield gave analytical values and a p.m.r. spectrum that were appropriate for the expected disaccharide derivative (**7**). The crystalline condensation product (**7**) was readily oxidized by periodate thus confirming the anticipated 1 → 6 linkage. Deacetylation of **7** yielded a crystalline benzyl glycoside (**8**), hydrogenolysis of which furnished the new disaccharide, 2-acetamido-6-*O*-(2-acetamido-2-deoxy-β-D-galactopyranosyl)-2-deoxy-D-galactose (**9**). The p.m.r. spectrum of this disaccharide showed a doublet for the internal anomeric proton with $J_{1',2'} = 7.0$ Hz, consistent with a β-linkage (3). The yield of initial condensation product (13%) in this "open" synthesis is comparable with

[1]NRCC No. 14603.

[2]NRCC Postdoctorate Fellow, 1972–1974.

Can. J. Chem. Downloaded from www.nrcresearchpress.com by 210.87.254.42 on 09/05/12
For personal use only.

Can. J. Chem. Downloaded from www.nrcresearchpress.com by 210.87.254.42 on 09/05/12
For personal use only.

those obtained (15–20%) from the reaction of acetohalogeno amino sugars with specifically blocked neutral sugars (4) and better than the 5.3% yield reported for the initial condensation step in the synthesis of 2-acetamido-6-*O*-(2-acetamido-2-deoxy-β-D-glucopyranosyl)-2-deoxy-D-glucose (5). The results show that this "open" synthesis (*i.e.* no specific blocking of the aglycone), is a practical route to β 1→6 linked disaccharides of hexopyranoses.

Experimental

Melting points were determined on a Kofler hot stage microscope and are uncorrected. Optical rotations were measured with a Perkin-Elmer 141 polarimeter and are equilibrium values unless stated otherwise. Proton magnetic resonance spectra were recorded on a Varian Anaspect EM 360 NMR spectrometer with tetramethylsilane as an internal standard except as noted. Thin-layer chromatograms were run on glass plates coated with silica gel F-254. Solvent mixtures used were (v/v): (*A*) chloroform–methanol, 5:1 and (*B*) chloroform–methanol, 7:3. Components were detected on thin-layer chromatograms by examination under u.v. light (for all benzyl glycosides) or by charring after a spray of 5% sulfuric acid in ethanol. Reducing sugars were detected by *p*-anisidine spray (6).

Benzyl 6-O-(2,3,4,6-Tetra-O-acetyl-β-D-glucopyranosyl)-β-D-glucopyranoside (3)

Benzyl β-D-glucopyranoside (**2**) (7) (0.5 g) was dissolved in nitromethane (25 ml) and the solution was stirred for 18 h with silver carbonate (1.0 g) and Drierite (2.0 g). 2,3,4,6-Tetra-*O*-acetyl-α-D-glucopyranosyl bromide (**1**) (8) (1.2 g) was added to the stirred mixture over a period of 1 h and stirring was continued for a further 18 h. The inorganic salts were removed by filtration, washed with methanol (2 × 15 ml), and the combined filtrate and washings were evaporated to dryness under diminished pressure. The condensation product was separated from unreacted monomers by preparative thin-layer chromatography (solvent *A*) which furnished pure benzyl 6-*O*-(2,3,4,6-tetra-*O*-acetyl-β-D-glucopyranosyl)-β-D-glucopyranoside (**3**), 623 mg (56% based on **2**), crystallized from acetone, m.p. 114–116 °C, $[\alpha]_D^{24}$ −38.8° (*c*, 1.0 in ethanol); p.m.r. ($CDCl_3$) τ 2.66 (5 H singlet, aromatic protons), 7.94 (12 H quartet, 4 × OAc).

Anal. Calcd. for $C_{27}H_{36}O_{15}$: C, 53.99; H, 6.04. Found: C, 53.82; H, 6.12.

6-O-β-D-Glucopyranosyl-D-glucose (4, Gentiobiose)

The tetraacetate (**3**) (450 mg) was deacetylated in methanol (10 ml) by sodium methoxide (0.1 *N*, 10 ml). The solution was deionized (Amberlite IR-120), evaporated, and the resultant benzyl glycoside was shaken overnight with palladium black (40 mg) in 95% ethanol (25 ml) under hydrogen at atmospheric pressure. The catalyst was removed by filtration and evaporation of the filtrate gave 6-*O*-β-D-glucopyranosyl-D-glucose (142 mg), $[\alpha]_D^{24}$ +9.8° (*c*, 2.0 in water), characterized as its β-octaacetate, identical with an authentic sample, m.p. and mixture m.p. 193–194 °C.

Benzyl 2-Acetamido-6-O-(2-acetamido-2-deoxy-3,4,6-tri-O-acetyl-β-D-galactopyranosyl)-2-deoxy-β-D-galactopyranoside (7)

A mixture of 2-acetamido-3,4,6-tri-*O*-acetyl-2-deoxy-α-D-galactopyranosyl chloride (**5**) (9) (2.0 g), benzyl 2-acetamido-2-deoxy-β-D-galactopyranoside (**6**, for preparation see below) (750 mg), cadmium carbonate (1 g), and Drierite (3 g), in benzene–nitromethane (30:70, 75 ml), was heated under reflux, with stirring, until complete reaction of **6** was indicated by t.l.c. (solvent *B*), 20 min. The inorganic residue was removed by filtration, washed with acetone (2 × 75 ml) and the combined filtrate and washings were evaporated to dryness under diminished pressure. Preparative t.l.c. (solvent *B*) of the residual sirup yielded benzyl 2-acetamido-6-*O*-(2-acetamido-2-deoxy-3,4,6-tri-*O*-acetyl-β-D-galactopyranosyl)-2-deoxy-β-D-galactopyranoside (**7**) (207 mg, 13.4% based on **6**) which crystallized from ethanol, m.p. 230–232 °C, $[\alpha]_D^{24}$ −34.8° (*c*, 1.0 in water); p.m.r. (D_2O, external standard) τ 2.53 (5 H singlet, aromatic protons), 7.76 (3 H singlet, OAc), 7.90 (3 H singlet, OAc), 7.98 (3 H singlet, OAc), 8.03 (3 H singlet, NAc), and 8.09 (3 H singlet, NAc).

Anal. Calcd. for $C_{29}H_{40}N_2O_{14}$: C, 54.38; H, 6.25; N, 4.37. Found: C, 54.07; H, 6.32; N, 4.06.

This compound was sensitive to oxidation by aqueous sodium metaperiodate (reaction monitored by t.l.c., solvent *B*).

Benzyl 2-Acetamido-6-O-(2-acetamido-2-deoxy-β-D-galactopyranosyl)-2-deoxy-β-D-galactopyranoside (8)

Deacetylation of compound 7 (175 mg), as described for compound **3**, yielded the benzyl glycoside (**8**) (118 mg) which crystallized from methanol, m.p. 244–246 °C, $[\alpha]_D^{24}$ −26.5° (*c*, 1.0 in water).

Anal. Calcd. for $C_{23}H_{34}N_2O_{11}$: C, 53.67; H, 6.61; N, 5.44. Found: C, 53.22; H, 6.42; N, 5.02.

2-Acetamido-6-O-(2-acetamido-2-deoxy-β-D-galactopyranosyl)-2-deoxy-D-galactose (9)

Hydrogenolysis of compound **8** (105 mg), as described for the preparation of compound **4**, yielded the disaccharide **9** (66 mg) as a sirup, $[\alpha]_D^{24}$ +42.5° (*c*, 1.0 in H_2O); p.m.r. (D_2O, external standard) τ 4.27 (½ H doublet, $J_{1,2}$ = 3.5 Hz, H-1 of α-D-form), 4.62 (½ H doublet, $J_{1,2}$ = 7.0 Hz, H-1 of β-D-form), 5.49 (1 H doublet, $J_{1',2'}$ = 7.0 Hz, H^1-1), 7.97 (6 H singlet, 2 × NAc).

Benzyl 2-Acetamido-2-deoxy-β-D-galactopyranoside (6)

A mixture of benzyl alcohol (5 ml), 2-acetamido-2-deoxy-3,4,6-tri-*O*-acetyl-α-D-galactopyranosyl chloride (**5**) (9) (4.2 g), cadmium carbonate (2.5 g), and Drierite (8.0 g) in benzene–nitromethane (30:70, 125 ml) was heated under reflux with stirring for 2 h. The inorganic residue was removed by filtration, washed with chloroform (2 × 100 ml), and the combined filtrate and washings were evaporated to dryness under reduced pressure.

The sirupy residue was redissolved in chloroform (150 ml), the solution was washed with 10% aqueous sodium chloride (150 ml) and dried over anhydrous sodium sulfate. Evaporation of the solution gave a sirup that crystallized from ether furnishing benzyl 2-acetamido-2-deoxy-3,4,6-tri-*O*-acetyl-β-D-galactopyranoside

(1.6 g), m.p. 185–186 °C, $[\alpha]_D^{24}$ −42.6° (*c*, 1.0 in methanol) (lit. (10), m.p. 180–182 °C, $[\alpha]_D^{23}$ −55° (*c*, 1.0 in chloroform).

Anal. Calcd. for $C_{21}H_{27}NO_9$: C, 57.66; H, 6.18; N, 3.20. Found: C, 57.78; H, 6.15; N, 2.96.

The foregoing triacetate was deacetylated as described for compound **3** to yield benzyl 2-acetamido-2-deoxy-β-D-galactopyranoside (**6**) (810 mg) which crystallized from methanol, m.p. 232–234 °C, $[\alpha]_D^{24}$ −22.5° (*c*, 1.0 in methanol) (lit. (10) values for the hemihydrate, m.p. 210–212 °C, $[\alpha]_D^{23}$ −3.4° (*c*, 0.5 in water).

Anal. Calcd. for $C_{15}H_{21}NO_6$: C, 57.86; H, 6.75; N, 4.50. Found: C, 57.56; H, 6.47; N, 4.03.

We are grateful to F. P. Cooper for the p.m.r. spectra and H. Seguin for the microanalyses.

1. R. R. KING and C. T. BISHOP. Carbohydr. Res. **32**, 239 (1974).
2. R. R. KING and C. T. BISHOP. Can. J. Chem. **52**, 3913 (1974).
3. J. N. C. WHYTE. Anal. Biochem. **42**, 476 (1971).
4. R. KUHN and W. KIRSCHENLOHR. Chem. Ber. **87**, 384 (1954).
5. Y. WANG and H-I. TAI. Acta Chim. Sinica, **25**, 54 (1959); Chem. Abstr. **54**, 6561a (1960).
6. L. HOUGH, J. K. N. JONES, and W. H. WADMAN. J. Chem. Soc. 1702 (1950).
7. E. FISCHER and B. HELFERICH. Ann. **71**, 383 (1911).
8. J. K. DALE. J. Am. Chem. Soc. **38**, 2187 (1916).
9. R. HEYWORTH, D. H. LEABACK, and P. G. WALKER. J. Chem. Soc. 4121 (1959).
10. K. L. MATTA, E. A. JOHNSON, and J. J. BARLOW. Carbohydr. Res. **26**, 215 (1973).

Can. J. Chem. Downloaded from www.nrcresearchpress.com by 210.87.254.42 on 09/05/12
For personal use only.

Isomerization of Bicyclic Hydrazine Monoesters to *N*-Amino-2-pyridone Esters, Precursors to Bicyclic "Isosydnones"

DONALD MACKAY AND LICHIN L. WONG

Department of Chemistry, University of Waterloo, Waterloo, Ontario N2L 3G1

Received December 23, 1974

DONALD MACKAY and LICHIN L. WONG. Can. J. Chem. **53**, 1973 (1975).

Selective aqueous alkaline hydrolysis of the diazetidine diesters **4** gives the basic monoesters **1** which isomerize quantitatively in trifluoroacetic acid or by refluxing with sodium methoxide in dioxane to the *N*-aminopyridone esters **2**. The bridged pyridazine ester **5***a* can also be selectively hydrolyzed to the presumed intermediate **10**, hydrolysis being accompanied by immediate isomerization to **2***a*. A common mechanistic pattern is proposed for these isomerizations.

Heating of **2** causes loss of alcohol to give the mesoionic "isosydnone" **3**, a fairly stable ring system slowly opened by ethanol to **2***b* and by concentrated alkali to the *N*-aminopyridone **16***a*. Oxidation of **16***a* with lead tetraacetate gives the pyridone **18***a*.

DONALD MACKAY et LICHIN L. WONG. Can. J. Chem. **53**, 1973 (1975).

L'hydrolyse alkaline aqueuse sélective des diesters de diazétidine **4** conduit au monoester basique **1** qui s'isomérise quantitativement en ester de *N*-aminopyridone **2** lorsqu'on le traite par de l'acide trifluoroacétique ou par reflux en présence de méthylate de sodium dans le dioxanne. L'ester cyclisé de pyridazine **5***a* peut aussi être hydrolysé sélectivement pour conduire à l'intermédiaire présumé **10**; l'hydrolyse est accompagnée par une isomérisation immédiate en **2***a*. On suggère que ces isomérisations procèdent par un mécanisme commun.

Le chauffage de **2** conduit à une perte d'alcool fournissant "l'isosydnone" mésoionique **3**, un système cyclique relativement stable, ouvert lentement par l'éthanol pour conduire à **2***b* et par les bases concentrées pour conduire à la *N*-aminopyridone **16***a*. L'oxydation de **16***a* par le tétraacétate de plomb conduit à la pyridone **18***a*. [Traduit par le journal]

We have recently reported that an excess of trifluoroacetic acid (TFA) isomerizes the basic diazetidine ester **1***a* to the aminopyridone ester **2***a* which cyclizes with loss of methanol to the mesoionic structure **3** (1).

We now wish to describe some aspects of the chemistry of these ring systems and in particular to show that the esters **2** can be obtained under other quite different reaction conditions, again involving deep seated skeletal rearrangements.

The diesters **4**, the precursors to **1**, were readily available in quantity as the end products of the thermal isomerization of the adducts **5** of azo esters with 2,5-dimethyl-3,4-diphenylcyclopentadienone (2). Though they are very stable to heat we have already shown that **4***a* is labile to acid, TFA causing demethylation and rearrangement to **6** (3). We were interested in trying to prepare the parent nitrogen unsubstituted 1,2-diazetidine **7**, since examples of such diazetidines are unknown.

Under varying conditions of alkaline hydrolysis it was found that one ester group in **4***a* was always easily removed. The product **1***a* was unstable to prolonged exposure to the hydrolysis conditions especially at high temperature or with high alkali concentration but when it was allowed to react completely the major end product was not the expected **7**, but the dimer of the cyclone 2,5-dimethyl-3,6-diphenylcyclopentadie-

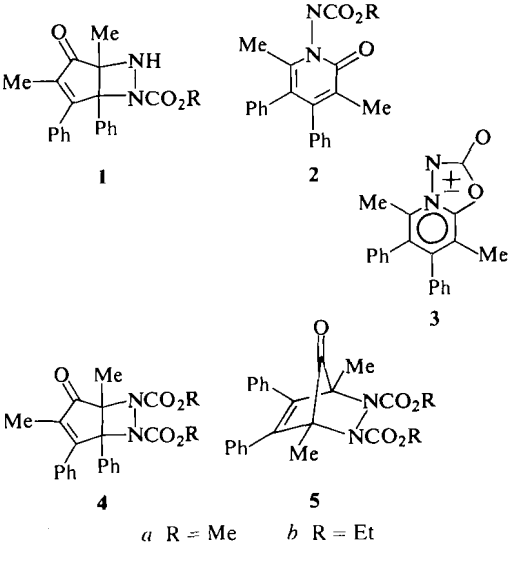

Can. J. Chem. Downloaded from www.nrcresearchpress.com by 210.87.254.5 on 09/05/12
For personal use only.

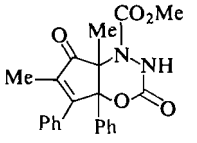

6

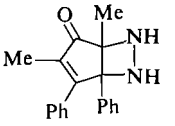

7

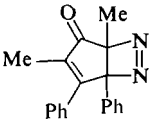

8

none. It seems likely that **7** is formed but is highly unstable and decomposes to the cyclone by direct loss of diimide or by prior hydrogen transfer[1] to give the diazetine **8** which would be expected to lose nitrogen readily.

The amino ester **1***a* was a faintly yellow solid, m.p. 159–160°. The optimum conditions for its preparation (90%) from **4***a* required the use of 1 *N* sodium hydroxide in aqueous ethanol for 12 h at room temperature or a 0.1 *N* solution for 6 h at reflux. The survival of the diazetidine ring followed from its conversion back into **4***a* with methyl chloroformate in refluxing pyridine; similarly it gave the mixed ester **9**, m.p. 189.5–190°, by treatment with ethyl chloroformate. The i.r. bands at 3250, 1726, and 1695 cm^{-1} (Nujol) for the NH, ester, and keto stretching frequencies and the β-phenyl-α-methyl enone chromophore at 281 nm (4) supported the bicyclic urethane structure but gave no information on the position of the ester group. The compelling evidence for our assignment is found in the n.m.r. spectrum. The parent diester has methoxy absorptions at 6.22 and 7.05 $\tau(CDCl_3)$, the latter being at unusually high field. The X-ray analysis of the *p,p'*-dibromo analog (5) showed clearly that the ester group on N-6 was very close to the face of the C-4 phenyl ring and it is reasonable that a powerful shielding effect would persist in solution. The ester absorption at 6.87 τ in the hydrolysis product thus completely identifies its structure as **1***a*; the greater resistance of this ester group to hydrolysis may be attributed to steric protection.

Hydrolysis of **4***b* under the same conditions gave a 75% yield of **1***b*, m.p. 129.5–130°. The n.m.r. absorptions of the methylene protons in its remaining ester group were widely separated, one at 5.96 and the other, highly shielded, at 6.55 τ, an effect observed for the corresponding ester group in **4***b* as previously noted (2).

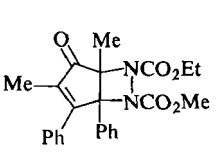

9

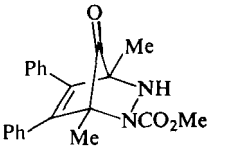

10

Isomerization of **1***a* was complete in the time (~30 s) taken to dissolve a sample in TFA in an n.m.r. tube and run the spectrum: the reaction was quantitative. An excess of acid was necessary, however, amounts less than 1 equiv. giving a complex mixture, which contained the isomer and some of the dienone dimer but which was not analyzed further.

Isolation of the isomer involved evaporation of the TFA solution and addition of a few drops of methanol to the residue. *N*-Carbomethoxy-1-amino-3,6-dimethyl-4,5-diphenyl-2-pyridone (**2***a*), m.p. 232–233° (with loss of methanol), had n.m.r. absorptions at 6.16, 7.80, and 8.06 τ assignable to the methoxy, C_6, and C_3-methyl groups, i.r. bands at 3140(NH), 1756, and 1640cm^{-1} (ester and ring CO) and strong chromophores at 245 and 317 nm (*cf.* i.r. and u.v. spectra of ring substituted 1-amino-2-pyridones (6,7)). The structure was finally confirmed by X-ray analysis.[2]

The preparation of the ethyl ester **2***b*, m.p. 218–218.5° was carried out in the same way. Its spectra were completely analogous to those of **2***a*.

Our results with the selective hydrolysis of the diester **4***a* prompted us to examine the behavior of the parent isomeric compound **5***a* with alkali. The use of 1 *N* sodium hydroxide in methanol or, as for **4***a*, aqueous methanol at room temperature caused considerable decomposition but the major product (50–60%) was again **2***a*. The pyridone ester is evidently a stable end product of both the [2.2.1] and the [3.2.0]diazabicyclo systems. This reaction which also involves monohydrolysis and decarboxylation, presumably went through the basic ester **10**, an isomer of **1***a*, but it did not involve the sequential rearrangements **10** → **1***a* → **2***a*, since **1***a* was found to be stable to the solvolysis conditions. The conversion of **10** to **2***a* thus probably occurred directly. The isomerization of **1***a* to **2***a* (70% yield) with basic catalysis could, however, be

[1]Since **7** would be sensitive to air oxidation the hydrolysis was repeated under nitrogen but without affecting the result.

[2]M. Mathew and G. J. Palenik. Centre for Molecular Structure, Department of Chemistry, University of Florida, Gainsville, Florida. Unpublished results.

Can. J. Chem. Downloaded from www.nrcresearchpress.com by 210.87.254.5 on 09/05/12
For personal use only.

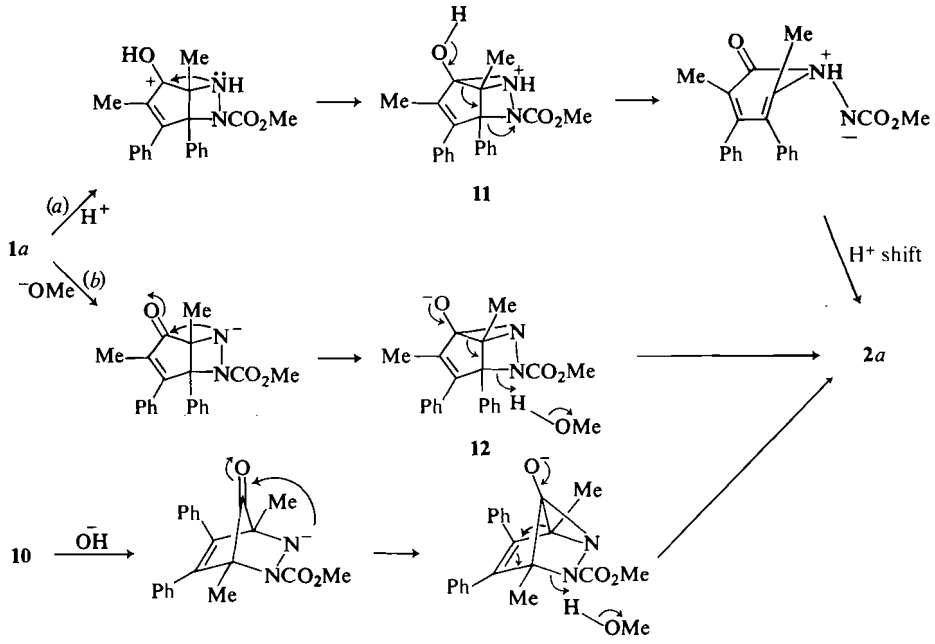

SCHEME 1

achieved with a suspension of sodium methoxide in refluxing dioxane.

These isomerizations to **2***a* involve in effect the transposition of the *tert*-methyl and the adjacent basic nitrogen. We have suggested (1) that the acid catalyzed route from **1***a* involves the tricyclic azirdinium ion **11** (Scheme 1, route *a*). In the methoxide catalyzed reaction (Scheme 1, route *b*) of **1***a* the intermediate by analogy would be **12**, the anion equivalent of **11**; similarly the alkaline isomerization of **10** would go through the tricyclic anion **13**. The acidity of the NH in **1***a* and **10** would be promoted by the adjacent electron withdrawing urethane group.

Treatment of **2***a* in dimethoxyethane with sodium hydride followed by methyl chloroformate gave the diester **14**, m.p. 217.5–219°. Its methoxy groups gave the sharp singlet in the n.m.r. spectrum expected from the symmetry of the molecule and rapid N—N rotation.

Hydrolysis of the ester group in **2***a* was slow in dilute alkali and only 65% complete after refluxing for 24 h in 4 *N* sodium hydroxide in aqueous dioxane. The product *N*-aminopyridone was more efficiently made from the bicyclic compound **3**.

Loss of alcohol from **2***a* or *b* was rapid at the m.p., the product immediately solidifying and remelting at 300–301°.[3] On a preparative scale it was conveniently made by heating a sample of **2***a* at 270° for 15 min. The n.m.r. absorptions at 7.50 and 7.77 τ showed that the methyl groups were still located on unsaturated centers but the profound changes in the u.v. spectrum, with λ_{max} at 278 with a shoulder at 305 nm, clearly originated from a quite different π bond arrangement. There was one intense carbonyl singlet at 1780 cm^{-1} in Nujol, shifted to 1755 cm^{-1} in chloroform. The high m.p., the spectra, the method of formation, and the ensuing chemical reactions are consistent only with the mesoionic ("isosydnone") structure 5,8-dimethyl-6,7-diphenyl-1,3,4,-oxadiazolo[3,2-*a*] pyridin-2(*3H*)-one (**3**).

Monocyclic analogs of this ring system have been examined (8), as well as the bicyclic parent compound **15** (9), the latter being evidently the more stable type towards nucleophilic opening of the oxadiazolone ring (10). This is presumably due to the contribution of resonance forms **15***a* and *b* involving a formal pyridinium cation, a

[3]The quantitative nature of the isomerization is emphasized by the observation that a mixture of **2***a* and *b* heated in a capillary tube gave **3** which melted sharply at 300–301°.

Can. J. Chem. Downloaded from www.nrcresearchpress.com by 210.87.254.5 on 09/05/12
For personal use only.

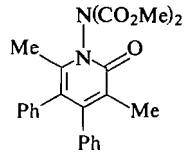

14

15

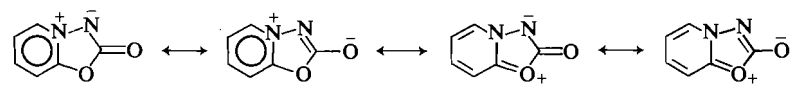

a *b* *c* *d*

source of stabilization which is unavailable to the monocyclic species and which makes the oxadiazolone ring relatively unattractive to nucleophiles. In keeping with this **3** was very slowly (17 days) cleaved by refluxing ethanol to give **2***b* and required refluxing for 3 h with 4 *N* sodium hydroxide for complete hydrolysis to 1-amino-3,6-dimethyl-4,5-diphenyl-2-pyridone (**16***a*), m.p. 217–219°, which gave a yellow benzylidene derivative, m.p. 233–233.5°.

Rees and Yelland (11, 7) found that oxidation of a series of ring substituted *N*-aminopyridones **16** with lead tetraacetate in methylene chloride proceeded with loss of carbon monoxide to give the pyridazines **17** and by deamination to give the pyridones **18** as major products, the proportions depending on the substitution pattern. Thus the tetraphenyl derivative **16***b* gave **17***b* and no **18***b*,

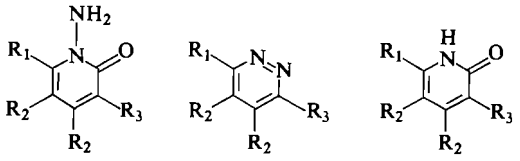

16 **17** **18**

a $R_1 = R_3 =$ Me; $R_2 =$ Ph
b $R_1 = R_2 = R_3 =$ Ph
c $R_1 = R_2 =$ Ph; $R_3 =$ H
d $R_1 =$ Me; $R_2 = R_3 =$ Ph

the triphenyl derivative **16***c* gave a little **17***c* and mostly **18***c*, whereas the triphenyl monomethyl derivative **16***d* gave only **18***d*. Predictably from these results the similar oxidation of **16***a* gave a mixture whose n.m.r. spectrum showed the main product to be the pyridone **18***a* (48%) but no low field methyl absorption which could be attributed to the pyridazine **17***a*.[4] Work-up gave **18***a* of m.p. 309.5–310.5°. Its identity followed from comparison of its properties with those published (13) for the pyridone synthesized by ring closure.

[4]All absorptions occurred above 7.5 τ. The methyl absorption in **17***a* would be expected at lower field than in 3,4,6-trimethylpyridazine in which both the C_3- and the C_6-methyl groups absorb at 7.40 τ in $CDCl_3$ (12).

Experimental

The following spectrometers were used: for i.r. a Beckman IR 10; for u.v. a Coleman EPS-3T Hitachi; for n.m.r. a Varian T-60, absorptions being given in τ values against tetramethylsilane; for m.s. an AEI MS-30.

Magnesium sulfate was used as drying agent for solutions in organic solvents; melting points are uncorrected.

1,3-Dimethyl-4,5-diphenyl-6-carbomethoxy-6,7-diazabicyclo[3.2.0]hept-3-en-2-one (1a)

A solution of the diazetidine **4***a* (2) (600 mg, 1.48 mmol) in 0.1 *N* sodium hydroxide in aqueous methanol (1:9, 30 ml) was refluxed for 6 h, neutralized with acetic acid, and evaporated to near dryness to give a solid residue (470 mg, 91%) which was washed thoroughly with water.

Alternatively **4***a* (200 mg) was allowed to stand for 12 h at room temperature in 1 *N* sodium hydroxide in aqueous methanol (1:1, 10 ml) and the solution neutralized and worked-up as above. The yield was about the same.

Crystallization from methanol and then benzene–isooctane gave faintly yellow prisms of the basic ester **1***a*, m.p. 159–160°; ν(Nujol) 3250 (NH), 1726, 1695 cm^{-1} (ester, keto C=O); λ_{max} (EtOH) 281 nm (ε 12 800); τ($CDCl_3$) 2.5–3.0 (10 phenyl H), 4.77 (s, 1 NH), 6.97 (s, 3H, OMe), 7.90 (s, 3H, vinyl Me), 8.92 p.p.m. (s, 3H *tert*-Me); *m/e* 348(P^+, 9%), 260 ($C_{19}H_{16}O^+$, 100%).

Anal. Calcd. for $C_{21}H_{20}N_2O_3$: C, 72.39; H, 5.79; N, 8.04. Found: C, 72.28; H, 5.80; N, 8.22.

Hydrolysis of 4a under Vigorous Conditions

A sample of **4***a* (100 mg, 0.25 mmol) was refluxed for 1 h in 1 *N* sodium hydroxide in aqueous ethanol (5:1, 10 ml). Neutralization, evaporation, and addition of water to the residue gave mainly the dimer of 2,5-dimethyl-3,4-diphenylcyclopentadienone, identified by i.r. and n.m.r. spectra and by its mixture m.p. of 185–186° after crystallization from aqueous ethanol. The same result was obtained when the hydrolysis was carried out under nitrogen.

Reconversion of 1a to 4a

The basic ester **1***a* (100 mg, 0.29 mmol) and methyl chloroformate (0.2 ml) were refluxed in pyridine (3 ml) for 1.5 h. The solution was evaporated, water was added,

Can. J. Chem. Downloaded from www.nrcresearchpress.com by 210.87.254.5 on 09/05/12
For personal use only.

Can. J. Chem. Downloaded from www.nrcresearchpress.com by 210.87.254.5 on 09/05/12
For personal use only.

and the solid residue (90 mg, 76%) twice crystallized from aqueous methanol to give **4***a*, m.p. 198–200°, mixture m.p. 200–201° with an authentic sample.

*Conversion of **1***a* to 1,3-Dimethyl-4,5-diphenyl-6-carbomethoxy-7-carbethoxy-6,7-diazabicyclo[3.2.0]-hept-3-en-2-one (**9**)*

A solution of **1***a* (100 mg, 0.29 mmol) in pyridine (1 ml) containing ethyl chloroformate (50 mg 0.046 mmol) was kept at room temperature for 3 days and then evaporated to dryness. Addition of water gave the mixed ester **9** (87 mg, 72%), which when twice crystallized from aqueous ethanol had m.p. 189.5–190°; ν(Nujol) 1755, 1726, 1710 cm^{-1} (ester, keto C=O); τ($CDCl_3$) 2.2–3.4 (10 phenyl H), 5.75 (q, 2 ethoxy CH_2, J = 7.0 Hz), 7.06 (s, 3 OMe H), 7.91 (s, 3H, vinyl Me), 8.71 (t, 3H, ethoxy Me), 8.82 p.p.m. (s, 3H, *tert*-Me).

Anal. Calcd. for $C_{24}H_{24}N_2O_5$: C, 68.56; H, 5.75; N, 6.66. Found: C, 68.63; H, 5.88; N, 6.93.

*1,3-Dimethyl-4,5-diphenyl-6-carbethoxy-6,7-diazabicyclo[3.2.0]hept-3-en-2-one (**1b**)*

A solution of the diazetidine **4***b* (500 mg, 1.15 mmol) in 1 *N* sodium hydroxide in aqueous ethanol (1:4, 50 ml) was kept at room temperature for 12 h and then neutralized with acetic acid and evaporated to a small volume. The residual gum crystallized on addition of water. The product (340 mg, 82%) was twice crystallized from cyclohexane giving almost colorless prisms, m.p. 129.5–130°; ν(Nujol) 3180(NH) 1704, 1682 cm^{-1} (ester, keto C=O); λ_{max} (EtOH) 282 nm (ε 13 000); τ($CDCl_3$) 2.4–3.3 (10 phenyl H), 4.7 (broad, 1 NH), 5.96 (octet, 1H, methylene A portion of ester AMX_3, J_{AM} = 10.2, J_{AX} = J_{MX} = 7.0 Hz), 6.55 (octet, 1H, broadened, M portion of AMX_3, 3H), 7.82 (s, 3H, vinyl Me), 8.84 (s, 3H, *tert*-Me), 9.11 p.p.m. (t, 3H, X_3 portion of AMX_3).

Anal. Calcd. for $C_{22}H_{22}N_2O_3$: C, 72.91; H, 6.12; N, 7.73. Found: C, 72.84; H, 6.37; N, 7.95.

*N-Carbomethoxy-1-amino-3,6-dimethyl-4,5-diphenyl-2-pyridone (**2a**)*

A solution of **1***a* (300 mg, 0.86 mmol) in TFA (3.0 ml) was kept at room temperature for 4 h and then evaporated in a stream of nitrogen. Trituration of the residue with methanol caused crystallization and the product (282 mg, 94%) was collected and washed with aqueous sodium bicarbonate. Its spectra were identical with those obtained after recrystallization from methanol as colorless prisms, m.p. 232–233°, followed by loss of methanol, solidification, and remelting at 300–301° (the m.p. of **3**); ν(Nujol) 3140(NH), 1756, 1640 cm^{-1} (ester, ring C=O); λ_{max}(EtOH) 245, 317 nm (ε 13 000, 7500); τ($CDCl_3$) 1.15 (s, 1 NH) 2.6–3.4 (10 phenyl H), 6.16 (s, 3H, OMe), 7.80 (s, 3H, C_3–Me), 8.06 p.p.m. (s, 3H, C_6-Me).

Anal. Calcd. for $C_{21}H_{20}N_2O_3$: C, 72.39; H, 5.79; N, 8.04. Found: C, 72.19; H, 5.83; N, 7.97.

When a sample of **1***a* (50 mg) was added to TFA (0.5 ml) in an n.m.r. sample tube it rapidly dissolved. The spectrum was scanned within 30 s but showed absorptions only for the product **2***a*; τ(TFA) 2.3–3.3 (10 phenyl H), 5.93 (s, 3H, OMe), 7.53 (s, 3H, C_3-Me), 7.76 p.p.m. (s, 3H, C_6-Me).

*Reaction of **1***a* with Limited Amounts of TFA*

A solution of **1***a* (200 mg, 0.58 mmol) in methylene chloride (2 ml) was treated with TFA (10 μl, 0.13 mmol) and a portion monitored by n.m.r. analysis. The spectrum slowly became very complex but showed no further change after 7 h; the amount of **2***a* was rather less than 50%. Work-up with methanol of the residue from the whole reaction gave a small amount of the sparingly soluble dimer of 2,5-dimethyl-3,4-diphenylcyclopentadienone, identified by comparison with a synthetic sample.

*N,N-Dicarbomethoxy-1-amino-3,6-dimethyl-4,5-diphenyl-2-pyridone (**14**)*

To a solution of **2***a* (348 mg, 1 mmol) in dry dimethoxyethane (10 ml) was added first a sodium hydride – paraffin oil dispersion (1:1, 72 mg, 1.5 mmol) which caused evolution of hydrogen and the formation of a yellow solution and then, immediately, methyl chloroformate (75 μl, 1 mmol). The solution rapidly became cloudy and sodium chloride precipitated. The mixture was left for 12 h and worked-up with ether and water, the organic layer being thoroughly washed with water and dried. It gave on evaporation almost pure diester **14** (326 mg, 81%), which crystallized from aqueous methanol as rods, m.p. 217.5–219°; ν(Nujol) 1821, 1668 cm^{-1} (2 ester, ring C=O); λ_{max} (EtOH) 247, 319 nm (ε 15 000, 7900); τ($CDCl_3$) 2.6–3.3 (10 phenyl H), 6.04 (sharp s, 6H, OMe), 7.98 (s, 3H, C_3-Me), 8.04 p.p.m. (s, 3H, C_6-Me).

Anal. Calcd. for $C_{23}H_{22}N_2O_5$: C, 67.97; H, 5.46; N, 6.89. Found: C, 68.06; H, 5.35; N, 7.16.

*N-Carbethoxy-1-amino-3,6-dimethyl-4,5-diphenyl-2-pyridone (**2b**)*

The basic ester **1***b* was treated with an excess of TFA exactly as described for **1***a*. The yield was nearly quantitative. Crystallization from aqueous methanol gave prisms, m.p. 218–218.5°, followed by loss of ethanol, solidification, and remelting at 299–300°; ν(Nujol) 3150 (NH), 1754, 1638 cm^{-1} (ester, ring C=O); λ_{max} (EtOH) 245, 317 nm (ε 13 000, 7300); τ($CDCl_3$) 1.25 (s, 1NH), 2.6–3.4 (10 phenyl H), 5.71 (q, 2H, ester methylene, J = 7.1 Hz), 7.82 (s, 3H, C_3-Me), 8.07 (s, 3H, C_6-Me), 8.71 p.p.m. (t, 3H, ester Me).

Anal. Calcd. for $C_{22}H_{22}N_2O_3$: C, 72.91; H, 6.12; N, 7.73. Found: C, 73.01; H, 6.30; N. 7.97.

*Reaction of 1,4-Dimethyl-5,6-diphenyl-2,3-dicarbomethoxy-2,3-diazabicyclo[2.2.1]hept-5-en-7-one (**5a**) with Sodium Hydroxide*

(a) Aqueous methanol

A solution of **5***a* (100 mg, 0.25 mmol) in 1 *N* sodium hydroxide in aqueous methanol (1:1, 5 ml) was allowed to stand at room temperature for 12 h. Most of the methanol was removed by evaporation at room temperature and the milky solution was thoroughly extracted with methylene chloride. The n.m.r. of the residue (60 mg) contained about 70% of **2***a* (overall yield 50%), determined by integration. It was identified as described in *b*.

(b) Methanol

A solution of **5***a* (200 mg) in 1 *N* sodium hydroxide in methanol (20 ml) was allowed to react at room temperature over 24 h and then reduced in volume and neutral-

Can. J. Chem. Downloaded from www.nrcresearchpress.com by 210.87.254.5 on 09/05/12
For personal use only.

ized with acetic acid. Evaporation to near dryness and addition of water gave product (103 mg) which was nearly pure **2***a* (60%). Recrystallization from carbon tetrachloride – cyclohexane gave material of m.p. 231–232°, identified by spectra and mixture m.p. The end result was the same if the alkaline solution was not neutralized.

Control Reaction: Stability of 1a to Methanolic Sodium Hydroxide

When **1***a* (50 mg) was treated under the exact conditions of reaction *b* above it was quantitatively recovered.

Sodium Methoxide Catalyzed Isomerization of 1a to 2a

A suspension of sodium methoxide (54 mg, 1 mmol) in dry dioxane (10 ml) containing **1***a* (100 mg, 0.29 mmol) was refluxed for 24 h. The mixture was evaporated to dryness and treated with methylene chloride and an excess of dilute acetic acid. The organic layer on drying afforded solid (83 mg) whose n.m.r. spectrum showed the presence of **2***a* in an overall yield of 70%. Crystallization from carbon tetrachloride – cyclohexane gave pyridone of m.p. and mixture m.p. 230–231°.

5,8-Dimethyl-6,-7-diphenyl-1,3,4-oxadiazolo[3,2-a]-pyridine-2(3H)-one (3)

The pyridone **2***a* (300 mg, 0.86 mmol) was heated at 270° for 15 min during which it melted, lost methanol, and then solidified. The product (276 mg, 100%) was twice crystallized from ethanol as long needles, m.p. 300–301°; ν(Nujol) 1780 cm^{-1} (C=O); ν($CHCl_3$) 1755 cm^{-1} (C=O); λ_{max} (EtOH) 278, sh 305 nm (ε 15 200, 8800); τ($CDCl_3$) 2.5–3.2 (10 phenyl H), 7.50 (3H, C_8-Me), 7.77 p.p.m. (3H, C_5-Me); *m/e* 316 (P^+, 100%), 288 (13%), 274 (15%), 246 (14%), 205 (14%), 115 (15%), 77(11%).

Anal. Calcd. for $C_{20}H_{16}N_2O_2$: C, 75.93; H, 5.10; N, 8.86. Found: C, 75.66; H, 5.25; N, 8.55.

Compound **3** could be similarly made in quantitative yield by elimination of ethanol from the pyridone **2***b* at 270°.

1-Amino-3,6-dimethyl-4,5-diphenyl-2-pyridone (16a)

(a) Hydrolysis of 2a

To a solution of **2***a* (100 mg, 0.29 mmol) in dioxane (1 ml) was added aqueous 4 *N* sodium hydroxide (2 ml). The two-phase system was refluxed for 24 h, the dioxane was evaporated off, and the residue, which slowly crystallized, was collected by filtration. Its n.m.r. spectrum showed it to contain 35% of starting material and 65% of the product **16***a*. Its i.r. spectrum likewise showed only bands for these two compounds. No effort was made to isolate **16***a*, a more efficient synthesis being available as described in *b*.

(b) Hydrolysis of 3

A two-phase mixture of aqueous 4 *N* sodium hydroxide (3 ml) and dioxane (1 ml) containing **3** (100 mg, 0.32 mmol) was refluxed for 3 h. Evaporation of the dioxane layer produced the crystalline hydrazine **16***a* (89 mg, 97%) whose spectra were indistinguishable from those of material obtained by recrystallization from aqueous methanol, m.p. 217–219° (dec.); ν(Nujol) 3256, 3156 (NH_2), 1630 cm^{-1} (C=O); λ_{max} (EtOH) 318, sh 245 nm (ε 7500, 13 000); τ($CDCl_3$) 2.7–3.4 (10 phenyl H), 4.55 (s, 2NH), 7.72 (3H, C_3-Me), 8.02 p.p.m. (3H, C_6-Me).

Anal. Calcd. for $C_{19}H_{18}N_2O$: C, 78.59; H, 6.25; N, 9.65. Found: C, 77.91; H, 6.34; N, 9.55.

The benzylidene derivative was prepared by refluxing **16***a* (72 mg, 0.25 mmol) and benzaldehyde (40 mg, 0.38 mmol) for 3.5 h in ethanol (3 ml) containing 3 drops of acetic acid. Evaporation and addition of water gave the product (60 mg, 63%) which was recrystallized from aqueous ethanol as yellow needles, m.p. 233–233.5°; ν(Nujol) 1637, 1610 cm^{-1} (C=O, C=N); λ_{max} (EtOH) 349 nm.

Anal. Calcd. for $C_{26}H_{22}N_2O$: C, 82.51; H, 5.86; N, 7.40. Found: C, 82.42; H, 5.95; N, 7.43.

Ethanolysis of 3

A solution of **3** (100 mg) was refluxed in ethanol (5 ml) and the progress of the reaction followed by evaporation and n.m.r. analysis of the residue. Solvolysis had occurred to the extent of 60% in 7 days and was complete in 17 days. The reaction was quantitative, and one crystallization from aqueous ethanol gave **2***b*, m.p. 216–216.5°, undepressed on admixture with authentic ester.

Oxidation of 16a with Lead Tetraacetate (7)

A solution of **16***a* (100 mg, 0.35 mmol) in dry methylene chloride (5 ml) was treated with lead tetraacetate (200 mg, 0.45 mmol) in portions. There was vigorous effervescence and the development of a yellow color. Unraacted oxidizing agent was destroyed by adding a few drops of 2-propanol and the filtered solution was washed out with water and aqueous potassium carbonate. The n.m.r. spectrum of the residue (100 mg) was complex in the methyl region, which occurred above 7.5 τ, but the major product was 3,6-dimethyl-4,5-diphenyl-2-pyridone, **18***a* (48%, determined by area measurement of its two methyl peaks as a fraction of the total). Two crystallizations from methanol gave the pale yellow pyridone **18***a*, m.p. 309.5–310.5° (lit. (13) m.p. 305–307°); ν(Nujol) 3415 (NH), 1640 cm^{-1} (C=O); λ_{max} (EtOH) 243.5, 317 nm (lit. (13) 242, 314 nm); τ($CDCl_3$) 2.5–3.3 (10 phenyl H and 1 NH, exchangeable with D_2O), 7.78 (3H, C_3-Me), 8.04 p.p.m. (3H, C_6-Me).

Anal. Calcd. for $C_{19}H_{17}NO$: C, 82.88; H, 6.22; N, 5.09. Found: C, 83.16; H, 6.18; N, 5.11.

We thank the National Research Council of Canada for financial assistance.

1. D. MACKAY and L. L. WONG. J. Chem. Soc. Chem. Commun. 621 (1974).
2. D. MACKAY, C. W. PILGER, and L. L. WONG. J. Org. Chem. **38**, 2043 (1973).
3. D. MACKAY and C. W. PILGER. Can. J. Chem. **52**, 1114 (1974).
4. C. F. H. ALLEN, T. DAVIS, D. W. STEWART, and J. A. VANALLAN. J. Org. Chem. **20**, 310 (1955).
5. P. C. CHIEH, D. MACKAY, and L. WONG. J. Chem. Soc. Perkin Trans. II, 2094 (1972).
6. I. EL-SAYED EL-KHOLY, F. K. RAFLA, and G. SOLIMAN. J. Chem. Soc. 4490 (1961); I. EL-SAYED EL-KHOLY, F. K. RAFLA, and M. M. MISHRIKEY. J. Chem. Soc. C, 1950 (1969) and 1578 (1970).
7. C. W. REES and M. YELLAND. J. Chem. Soc. Perkin Trans. I, 77 (1972).

8. M. HASHIMOTO and M. OHTA. Bull. Chem. Soc. Jap. **34**, 668 (1961); E. B. ROCHE and L. B. KIER. J. Pharm. Sci. **54**, 1700 (1965); C. AINSWORTH. Can. J. Chem. **43**, 1607 (1965); R. HUISGEN, H. GOTTHARDT, and R. GRASHEY. Ber. **101**, 536 (1968); A. R. MCCARTHY, W. O. OLLIS, A. N. BARNES, L. E. SUTTON, and C. AINSWORTH. J. Chem. Soc. B. 1185 (1969); P. B. TALUKDAR, S. BANERJEE, and A. CHAKRABORTY. Ind. J. Chem. **10**, 610 (1972).
9. K. HOEGERLE. Helv. Chim. Acta, **41**, 548 (1958).
10. M. OHTA and H. KATO. *In* "Non-benzenoid aromatics". Vol I. *Edited by* J. P. Snyder. Academic Press, New York and London. 1969, Chapt. 4, p. 220.
11. C. W. REES and M. YELLAND. Chem. Commun. 377 (1969).
12. T. TSUCHIYA, H. ASAI, and H. IGETA. Chem. Pharm. Bull. Jap. **20**, 273 (1972).
13. C. R. HAUSER and C. J. EBY. J. Am. Chem. Soc. **79**, 728 (1957).

Can. J. Chem. Downloaded from www.nrcresearchpress.com by 210.87.254.5 on 09/05/12
For personal use only.

High Resolution ^{13}C Spectrum and Long-range $^{13}C,H$ Couplings in 2-Pyrone

A. A. CHALMERS AND K. G. R. PACHLER

Chemical Physics Group, National Chemical Research Laboratory, Council for Scientific and Industrial Research, P.O. Box 395, Pretoria 0001, Republic of South Africa

Received January 21, 1975

A. A. CHALMERS and K. G. R. PACHLER. Can. J. Chem. **53**, 1980 (1975).

The natural abundance ^{13}C n.m.r. spectrum of 2-pyrone has been analyzed by the ^{13}C–$\{^1H\}$ SPI technique. The magnitudes and signs of all long-range $^{13}C,H$ couplings have been obtained and are compared with those of related compounds.

A. A. CHALMERS et K. G. R. PACHLER. Can. J. Chem. **53**, 1980 (1975).

On a analysé, par la technique SPI ^{13}C–$\{^1H\}$, les spectres r.m.n. du ^{13}C en abondance naturelle de la pyrone-2. On a obtenu les amplitudes et les signes de tous les couplages $^{13}C,H$ à longue distance et on a comparé ces valeurs avec celles de composés apparentés.

[Traduit par le journal]

Introduction

Determination of long-range $^{13}C,H$ coupling constants from natural abundance ^{13}C spectra is becoming increasingly more feasible as modern FT spectrometers make available high resolution, high sensitivity spectra. Second-order analysis of the ^{13}C spectra can give the assignment and signs of such couplings (1–3) but ^{13}C spectra commonly show only slight second-order features so that ambiguities can arise (4). Since the ^1H part of the spectrum cannot usually be observed the $J(C,H)$ assignments will depend on either ^{13}C–$\{^1H\}$ double resonance or knowledge of the magnitudes of couplings in related structures. Present knowledge is still sparse but it appears that similar values for ^2J, ^3J, and ^4J are possible (5). More data are, therefore, required if these couplings are to become of use in structural studies.

The double-resonance method used here, ^{13}C–$\{^1H\}$ SPI (6), has been employed previously in studies on three-spin systems (7, 8) and so the five-spin systems of 2-pyrone (**1**) provide a more exacting test of the method.

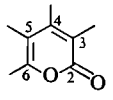

1

In **1** five differing carbons are all coupled to four nonequivalent protons and consequently 16 long-range $^{13}C,H$ couplings exist. Analysis of the $^{13}C,H$ long-range couplings requires first analysis of the usual ^1H spectrum for chemical shifts $\delta(H)$ and coupling constants $J(H,H)$. Although the ^1H spectrum of 2-pyrone has already been analyzed (9), data obtained under identical conditions (solvent, concentration, and temperature) as for the ^{13}C spectra are required. The appropriate data are given in the experimental section. In dilute solution (3 mol%) in C_6D_6 the ^1H spectrum of **1** is close to first order and a ^1H–$\{^1H\}$ INDOR study of this spectrum showed that all $J(H,H)$ have the same sign which is presumed to be positive. Assignments of the ^{13}C chemical shifts were obtained unambiguously from the ^{13}C–$\{^1H\}$ SPI experiments and agree with the assignments already reported (10).

Spectra and Method

Figure 1 shows the complete ^{13}C spectrum of **1** with expanded high-field halves of C_4, C_5, and C_6. The low-field halves are mirror images

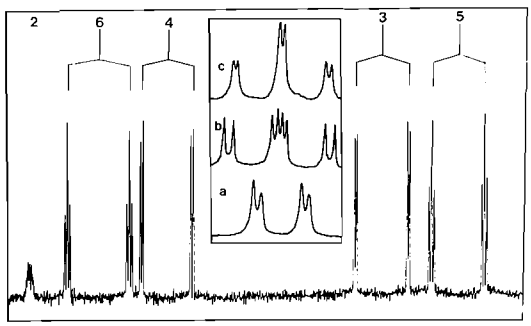

FIG. 1. Single-resonance ^{13}C spectrum of **1**. Insert expanded high-field halves of (*a*) C_4, (*b*) C_5, and (*c*) C_6.

Can. J. Chem. Downloaded from www.nrcresearchpress.com by 210.87.254.42 on 09/05/12
For personal use only.

Can. J. Chem. Downloaded from www.nrcresearchpress.com by 210.87.254.42 on 09/05/12
For personal use only.

of those shown and it is clear that the spectra are close to first order, as is the spectrum of C_3 which is displayed in Fig. 3*a*. The spectrum of C_2 is shown in Fig. 2.

In the following analysis the method is divided into making assignment experiments and sign determination experiments. An SPI irradiation in the region of a proton resonance $\delta(H_i)$ will usually cause sufficient perturbation of the ^{13}C lines for assignment of all long-range $J(C,H_i)$ provided there is no serious overlap of the H_i lines with those of other protons. This convenient procedure has been demonstrated in a previous communication (7). Irradiations at the other $\delta(H)$ regions will enable all the $J(C,H)$ to be assigned and hence theoretical ^1H spectra for every ^{13}C isotopomer can be constructed. Selective irradiations at specific ^1H lines will then give the sign information.

Figure 4*a* shows the calculated ^1H spectrum for the C_3 isotopomer and serves to illustrate the two examples of selective experiments, the results of which are displayed in Fig. 3. In Fig. 4*a* the $J(C,H)$ couplings are indicated as an aid to the understanding of the splitting pattern. Irradiation at line 2 of Fig. 4*a* gives the DSPI spectrum (7) Fig. 3*c* and can be viewed as an assignment experiment since it shows that the second smallest coupling to C_3 is $^4J(C_3,H_6)$. Another irradiation at either an H_5 or an H_4 line then allows complete assignment of the couplings to C_3. Figure 4*c* represents the lower field half of the C_3 resonance, that is the left hand part of Fig. 3*a*, and shows the assignment of the couplings as determined above. The combination of spin states shown in Fig. 4*c* comes from the sign determination experiment in which line 1 of Fig. 4*a* was irradiated. The known spin states ($^1J(C,H)$ and all $J(H,H)$ positive) give the representation of the H_3 lower field outer satellites shown in Fig. 4*b*. Thus, the DSPI spectrum Fig. 3*b* for irradiation at line 1 shows that all the long-range $J(C_3,H)$ are positive except for $^4J(C_3,H_6)$. Analogous experiments at other lines give the complete data given in Table 1.

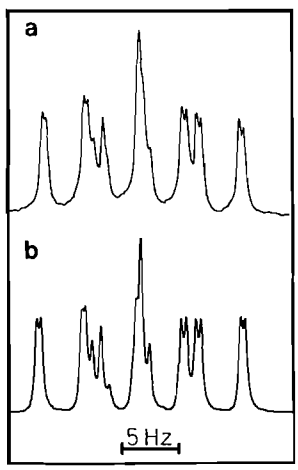

FIG. 2. (*a*) Observed and (*b*) calculated spectra of C_2.

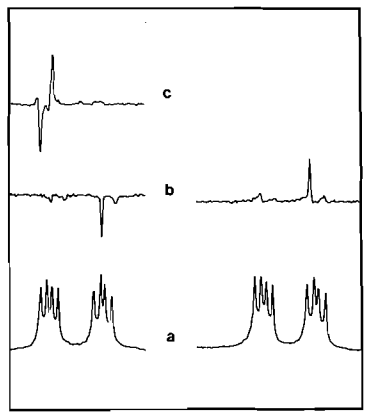

FIG. 3. (*a*) Single-resonance ^{13}C spectrum of C_3, (*b*) and (*c*) $^{13}C_3$-{^1H} DSPI spectra.

The spectrum of the C_2 isotopomer Fig. 2*a* deserves some extra comment since it shows definite second-order features which are essentially confined to the low-field half of the

TABLE 1. Long-range $^{13}C,H$ coupling constants (Hz) for 2-pyrone and related structures[a]

J	1	2	3	4	5
$^2C_2H_3$	4.7	4.1			3.1
$^3C_2H_4$	11.2	14.1			6.9
$^4C_2H_5$	−0.4				−0.9
$^3C_2H_6$	6.7				11.2
$^2C_3H_4$	0.9	1.6			0.8
$^3C_3H_5$	6.8				6.6
$^4C_3H_6$	−1.4				−1.6
$^2C_4H_3$	<0.3	−0.6			0.7
$^2C_4H_5$	1.3			4.1	0.7
$^3C_4H_6$	7.8			6.1	6.3
$^3C_5H_3$	7.9				6.6
$^2C_5H_4$	1.5				0.8
$^2C_5H_6$	7.6		9.7	13.8	8.5
$^4C_6H_3$	−0.8				−0.9
$^3C_6H_4$	7.6			7.0	6.9
$^2C_6H_5$	7.6		7.6	11.0	3.1

[a]Data for compounds 2–5 from refs. 1–3.

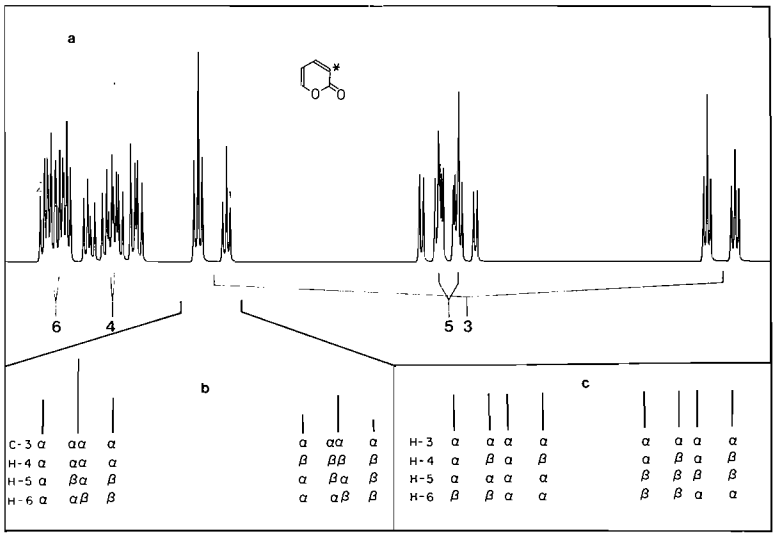

FIG. 4. (*a*) Calculated ^1H spectrum of C_3 isotopomer. (*b*) Expanded portions of *a* with spin states. (*c*) Low-field half of C_3 resonance with spin states.

spectrum. The SPI spectra are straightforward when the ^1H irradiation is located so as to perturb the high-field half of this resonance. The calculated spectrum Fig. 2*b* reproduces moderately well the second-order features although no adjustment was made for isotope effects on the ^1H chemical shifts and the J(C,H) used came directly from the SPI results. Further calculations show that the second-order features are due to interaction between the H_4 and H_6 parts of the spin system.

Discussion

The only unresolved coupling is $^2J(C_4,H_3)$ and from the overall resolution of the spectrum its absolute value must be less than 0.3 Hz. The signs of the couplings are in agreement with previous work (3, 11) on six-membered ring molecules; ^4J(C,H) negative, and ^3J(C,H) and ^2J(C,H) positive. In Table 1 the couplings are compared with literature values (1–3) of some molecules which contain structural moieties similar to **1** *viz.* acrylic acid (**2**), vinyl acetate (**3**), furan (**4**), and pyridine (**5**). The structures of these molecules are drawn below, numbered artificially for ease of comparison with **1**.

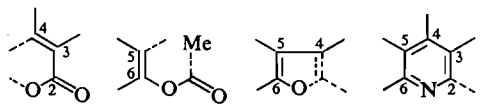

2 **3** **4** **5**

The data for **2** and **1** agree remarkably well. For **3** the couplings to the carbonyl are unfortunately not available but the couplings shown are both large as in **1**. Comparison of **1** and **5** shows that although all couplings to C_2 are very different in the two molecules and for C_6 there is a large difference between the $^2J(C_6,H_5)$ the other couplings show rather close agreement and especially so for C_3. The couplings in **4**, however, show little similarity to those of **1** reflecting the structure differences between the furan and 2-pyrone rings.

Experimental

Compound **1** was prepared from coumalic acid and purified by vacuum distillation (12); 2.5 ml of **1** containing 10% hexadeuterioacetone for internal lock was used for ^{13}C spectra. The ^1H spectrum of this solution gave the chemical shifts (δ) $H_3 = 6.40$, $H_4 = 7.58$, $H_5 = 6.45$, $H_6 = 7.77$ and J(H,H), $J(3,4) = 9.45$, $J(3,5) = 1.15$, $J(3,6) = 1.20$, $J(4,5) = 6.32$, $J(4,6) = 2.24$, $J(5,6) = 5.20$. The 25.2 MHz ^{13}C spectra were recorded in the FT mode on a Varian XL-100-15 spectrometer equipped with gated gyrocode. DSPI spectra (7) were produced using Varian Program No. 994100-D modified by Dr P. L. Wessels. The computer size was 16 K.

1. K. M. CRECELY, R. W. CRECELY, and J. H. GOLDSTEIN. J. Mol. Spectrosc. **37**, 252 (1971).
2. M. HANSEN, R. HANSEN, and H. J. JAKOBSEN. J. Magn. Reson. **13**, 386 (1974).
3. M. HANSEN and H. J. JAKOBSEN. J. Magn. Reson. **10**, 74 (1973).
4. F. J. WEIGERT and J. D. ROBERTS. J. Am. Chem. Soc. **90**, 3543 (1968).

Can. J. Chem. Downloaded from www.nrcresearchpress.com by 210.87.254.42 on 09/05/12
For personal use only.

5. J. B. STOTHERS. *In* Carbon-13 NMR spectroscopy. Academic Press, New York. 1972.
6. K. G. R. PACHLER and P. L. WESSELS. J. Magn. Reson. **13**, 387 (1974).
7. A. A. CHALMERS, K. G. R. PACHLER, and P. L. WESSELS. J. Magn. Reson. **15**, 415 (1974).
8. A. A. CHALMERS, K. G. R. PACHLER, and P. L. WESSELS. Org. Magn. Reson. **6**, 445 (1974).
9. W. H. PIRKLE and M. DINES. J. Heterocycl. Chem. **6**, 1 (1969).
10. W. V. TURNER and W. H. PIRKLE. J. Org. Chem. **39**, 1935 (1974).
11. F. J. WEIGERT, J. HUSAR, and J. D. ROBERTS. J. Org. Chem. **38**, 1313 (1973).
12. H. E. ZIMMERMAN, G. L. GRUNEWALD, and R. M. PAUDLER. Org. Synth. **46**, 101.

Can. J. Chem. Downloaded from www.nrcresearchpress.com by 210.87.254.42 on 09/05/12
For personal use only.

Reversible Inhibition of Carboxypeptidase A. III.[1] Inhibition of Specific Esterase Activity by Substituted Benzoate and Related Anions

JOHN W. BUNTING AND CHESTER D. MYERS
Department of Chemistry, University of Toronto, Toronto, Ontario M5S 1A1
Received December 16, 1974

JOHN W. BUNTING and CHESTER D. MYERS. Can. J. Chem. **53**, 1984 (1975).

The reversible inhibition of the hydrolysis of *O*-hippuryl-L-3-phenyllactic acid by bovine carboxypeptidase A, has been studied for a series of *para*-substituted benzoate ions (p-$XC_6H_4CO_2^-$) at p*H* 7.5, 25°, ionic strength 0.2. For X = H, F, CN, NH_2, CH_3 competitive inhibition occurs, whereas non-competitive inhibition occurs for X = CF_3, NO_2, Cl, Br, $(CH_3)_2N$, CH_3O, $(CH_3)_2CH$, $(CH_3)_3C$. For X = C_2H_5 mixed inhibition is observed and this can be separated into individual competitive and noncompetitive components. Uncompetitive inhibition occurs with X = I. The distinction between competitive and noncompetitive inhibition appears to depend on the size of X rather than on its chemical properties. The p-tolylacetate and 3-(p-tolyl)propanoate ions display partially competitive inhibition consistent with the formation of $E.I_2$ species. The inhibition by the 3-(p-iodophenyl)propanoate ion is complex and depends on the binding of at least two inhibitor ions per enzyme molecule.

JOHN W. BUNTING et CHESTER D. MYERS. Can. J. Chem. **53**, 1984 (1975).

On a étudié à un p*H* de 7.5, une température de 25° et une force ionique de 0.2, l'inhibition réversible, par une série d'ions benzoates substitués en *para* (p-$XC_6H_4COO^-$), de l'hydrolyse de l'acide *O*-hippuryl L-phényl-3 lactique par la carboxypeptidase A du bœuf. Une inhibition compétitive se produit avec X = H, F, CN, NH_2 et CH_3; par ailleurs, il y a une inhibition non-compétitive lorsque X = CF_3, NO_2, Cl, Br, $(CH_3)_2N$, CH_3O, $(CH_3)_2CH$, $(CH_3)_3C$. Lorsque X = C_2H_5, on observe une inhibition mélangée qui peut être séparée en composantes individuelles compétitives et non-compétitives. Une inhibition non-compétitive se produit lorsque X = I. Il semble que la distinction entre inhibition compétitive et incompétitive dépend de la grosseur plutôt que des propriétés chimiques du groupe X. Les ions p-tolylacétate et (p-tolyl)-3 propanoate sont des inhibiteurs partiellement compétitifs formant des espèces $E.I_2$. L'inhibition par l'ion (p-iodophényl)-3 propanoate est complexe et dépend de l'association d'au moins deux ions inhibiteurs par molécule d'enzyme. [Traduit par le journal]

As a part of our continuing investigation (1, 2) of the influence of the structure of the inhibiting ion on the form and extent of the reversible inhibition of bovine carboxypeptidase A, we now wish to report a study of the effect of modifications in the benzoate anion on its reversible inhibition of the enzymic hydrolysis of the specific ester substrate, *O*-hippuryl-L-3-phenyllactic acid. Benzoate ion, itself, is a competitive inhibitor for this ester substrate (1) but we have found that the introduction of certain simple substituents into the aromatic ring in a position *para* to the carboxylate group can cause the form of inhibition to become noncompetitive. On the other hand, there are other *para*-substituted benzoate anions that are competitive inhibitors of this same ester substrate, although these are usually poorer inhibitors than the unsubstituted benzoate ion. This discrimination between competitive and noncompetitive modes of inhibition by different *para* substituents in the benzoate ion appears to be related mainly to the size of the *para* substituent rather than to its chemical nature.

We have also investigated the reversible inhibition of the enzymic hydrolysis of this ester by a few higher homologs of some of these *para*-substituted benzoate ions and in these cases have observed a variety of forms of reversible inhibition.

Experimental

All carboxylic acids except 3-(p-iodophenyl)propanoic acid were obtained commercially. This latter acid was prepared by the method of Plati *et al.* (3). All acids were recrystallized to constant melting point in agreement with literature values and their identities were checked by p.m.r. spectroscopy. Stock solutions of the carboxylate inhibitors were then prepared by titration of aqueous suspensions of the acids to p*H* 7.5 with aqueous potassium hydroxide.

[1]For Part II see ref. 2.

Can. J. Chem. Downloaded from www.nrcresearchpress.com by 210.87.254.40 on 09/05/12
For personal use only.

Can. J. Chem. Downloaded from www.nrcresearchpress.com by 210.87.254.40 on 09/05/12
For personal use only.

O-Hippuryl-L-3-phenyllactic acid was purchased from Fox Chemical Co., Los Angeles, California. Stock solutions of bovine carboxypeptidase A (Worthington Biochemical Corporation (Code COA)) were prepared from a toluene-preserved suspension of the crystalline enzyme as previously described (1).

The enzymic hydrolysis of *O*-hippuryl-L-3-phenyllactic acid was followed on the p*H*-stat at p*H* 7.5, 25°, ionic strength 0.2 (adjusted with sodium chloride). All experimental techniques and data treatment were as previously described (1, 2). For the uninhibited reaction under these conditions $K_m = 7.2 \times 10^{-5}$ *M* and $k_{cat} = 2.50 \times 10^4$ min^{-1} (1). All substrate concentrations were $< 4 \times 10^{-4}$ *M*, so that substrate inhibition which intervenes at higher concentrations of this substrate could be neglected. In all cases linear Lineweaver–Burk plots were observed which is a clear indication that the Michaelis–Menten equation is a suitable description of the reaction under the present conditions.

Results

Lineweaver–Burk plots (E/v *vs.* $1/S$) for the hydrolysis of *O*-hippuryl-L-3-phenyllactic acid by carboxypeptidase A in the presence of the *para*-substituted benzoate anions **1**: X = F, NH_2, CH_3, CN are shown in Fig. 1 and indicate that these anions are competitive inhibitors for this substrate. Dixon plots (E/v *vs.* *I*) for these same anion inhibitors are linear (Fig. 2). Inhibition constants, K_i, calculated from Figs. 1 and 2, are in good agreement for each of these competitive inhibitors (Table 1).

On the other hand, for the benzoate anions **1**: X = NO_2, OCH_3, CF_3, $(CH_3)_2CH$,

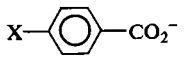

1

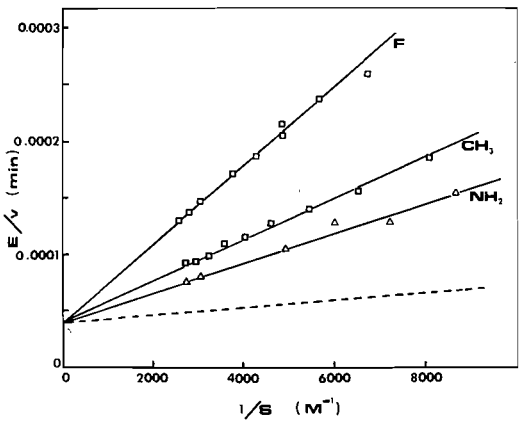

FIG. 1. Lineweaver–Burk plots for the inhibition of the hydrolysis of *O*-hippuryl-L-3-phenyllactic acid by carboxypeptidase A (p*H* 7.5, 25°, ionic strength 0.2) by *para*-substituted benzoate anions (**1**): X = F (62.6 m*M*); CH_3 (45.5 m*M*); NH_2 (143 m*M*). Data for X = CN (118 m*M*) (not shown) are almost exactly superimposable on data for X = F. Broken line indicates the uninhibited reaction.

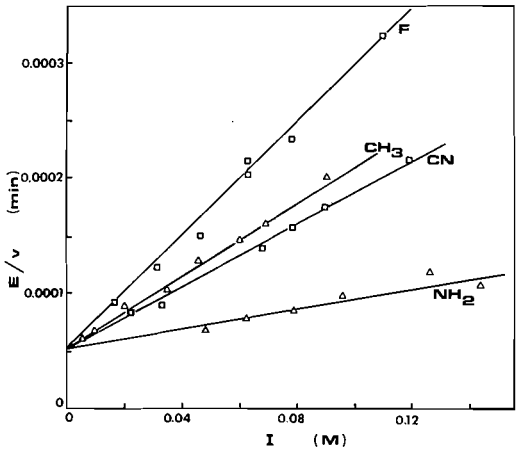

FIG. 2. Dixon plots for the inhibition of the hydrolysis of *O*-hippuryl-L-3-phenyllactic acid ($S = 0.20$ m*M*) by carboxypeptidase A (p*H* 7.5, 25°, ionic strength 0.2) by *para*-substituted benzoate anions (**1**).

TABLE 1. Reversible inhibition of esterase activity of carboxypeptidase A by $p\text{-}XC_6H_4CO_2^-$ ions[a]

X	Inhibitor concentration (m*M*)	K_I (m*M*)[b]	K_I (m*M*)[c]
	(i) Competitive inhibition		
H		6.0[d]	
F	62.6	5.5	5.8
CN	118	13	10
NH_2	143	37	37
CH_3	45.5	8.8	8.0
C_2H_5	[e]	23[e]	—
OH	[f]	21[f]	—
	(ii) Noncompetitive inhibition		
C_2H_5	[e]	24[e]	—
$(CH_3)_2CH$	19.3	6.5	10
$(CH_3)_3C$	3.49	1.4	1.3
CF_3	32.4	7.6	9.0
NO_2	42.1	22	22
Cl	52.1	15	15
Br	39.9	9.7	8.3
CH_3O	126	48	43
$(CH_3)_2N$	37.3	13	14

[a]At p*H* 7.5, 25°, ionic strength 0.2 against *O*-hippuryl-L-3-phenyllactic acid as substrate.
[b]From Lineweaver–Burk plot at indicated inhibitor concentration.
[c]From Dixon plot (at $S = 2.0 \times 10^{-4}$ *M*) assuming form of inhibition indicated by Lineweaver–Burk plot.
[d]From ref. (1).
[e]Average of values in Table 2.
[f]See text.

Can. J. Chem. Downloaded from www.nrcresearchpress.com by 210.87.254.40 on 09/05/12
For personal use only.

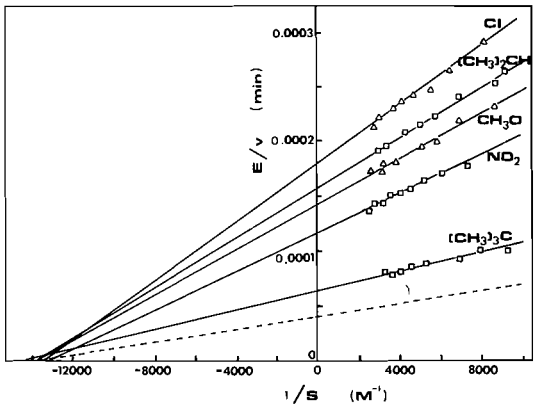

FIG. 3. Lineweaver–Burk plots for the inhibition of the hydrolysis of *O*-hippuryl-L-3-phenyllactic acid by carboxypeptidase A (p*H* 7.5, 25°, ionic strength 0.2) by *para*-substituted benzoate anions (**1**): X = Cl (52.1 m*M*); $(CH_3)_2CH$ (19.3 m*M*); CH_3O (126 m*M*); NO_2 (42.1 m*M*); $(CH_3)_3C$ (3.49 m*M*). Data not shown for other noncompetitive inhibitors: X = CF_3 (32.4 m*M*, $k_{cat}^{app} = 4.76 \times 10^3$ min^{-1}, $K_m^{app} = 6.76 \times 10^{-5}$ *M*); Br (39.9 m*M*, $k_{cat}^{app} = 4.90 \times 10^3$ min^{-1}, $K_m^{app} = 6.54 \times 10^{-5}$ *M*); $(CH_3)_2$ N (37.3 m*M*, $k_{cat}^{app} = 6.47 \times 10^3$ min^{-1}, $K_m^{app} = 7.70 \times 10^{-5}$ *M*). Broken line indicates the uninhibited reaction.

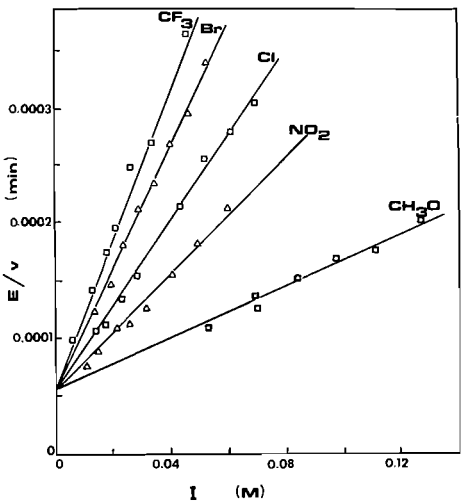

FIG. 4. Dixon plots for the inhibition of the hydrolysis of *O*-hippuryl-L-3-phenyllactic acid (*S* = 0.20 m*M*) by carboxypeptidase A (p*H* 7.5, 25°, ionic strength 0.2) by *para*-substituted benzoate anions (**1**). Linear plots were also observed for X = $(CH_3)_2N$, $(CH_3)_2CH$, $(CH_3)_3C$ (not shown).

$(CH_3)_3C$, $N(CH_3)_2$, Cl, Br, the Lineweaver–Burk plots are typical of noncompetitive inhibition (Fig. 3). Dixon plots for each of these latter anions are again linear (Fig. 4) and

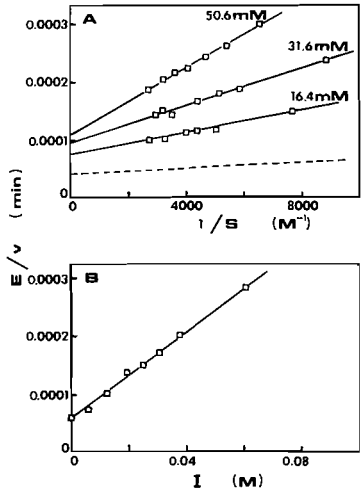

FIG. 5. Inhibition of the hydrolysis of *O*-hippuryl-L-3-phenyllactic acid by carboxypeptidase A (p*H* 7.5, 25°, ionic strength 0.2) by the *p*-ethylbenzoate anion: *A*, Lineweaver–Burk plots at indicated inhibitor concentrations; *B*, Dixon plot at *S* = 0.20 m*M*. Broken line indicates the uninhibited reaction.

inhibition constants calculated from these latter plots, assuming noncompetitive inhibition, are in close agreement with the K_i values, calculated from the Lineweaver–Burk plots for these anions (Table 1).

Unlike the above purely competitive and noncompetitive inhibitor anions, the anion **1**: X = C_2H_5 displayed mixed inhibition kinetics (Fig. 5*A*) although the Dixon plot was linear in *I* (Fig. 5*B*). Since the lower (**1**: X = CH_3) and higher (**1**: X = $(CH_3)_2CH$) homologs of this ion are competitive and noncompetitive inhibitors respectively, it seemed reasonable to assume that for **1**: X = C_2H_5, the observed mixed inhibition probably arises from a mixture of competitive and noncompetitive inhibitory modes. Such a reaction scheme is indicated in Scheme 1. Analysis of this scheme, assuming all equilibria are attained rapidly relative to k_2,

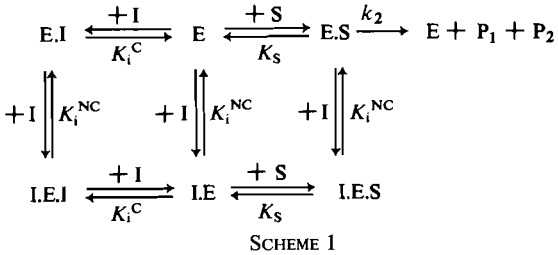

SCHEME 1

Can. J. Chem. Downloaded from www.nrcresearchpress.com by 210.87.254.40 on 09/05/12
For personal use only.

gives the dependence of initial velocity on substrate and inhibitor concentrations (for S, $I \gg E$) in eq. 1.

$$[1] \qquad \frac{v}{E} = \frac{k_2/(1 + I/K_i^{NC})}{1 + \frac{K_s}{S}(1 + I/K_i^{C})}$$

At constant inhibitor concentration, this equation has the form of the Michaelis equation having

$$K_m^{app} = K_s(1 + I/K_i^{C})$$

and

$$k_{cat}^{app} = \frac{k_2}{1 + I/K_i^{NC}}$$

Thus K_i^{C} and K_i^{NC} may be individually calculated from a Lineweaver–Burk plot at constant inhibitor concentration.

Competitive (K_i^{C}) and noncompetitive (K_i^{NC}) inhibition constants calculated in this way for the *p*-ethylbenzoate ion, using the K_m^{app} and k_{cat}^{app} values defined by the data in Fig. 5*A* are collected in Table 2. These values of K_i^{C} and K_i^{NC} are apparently independent of inhibitor concentration and so suggest that Scheme 1 is probably a reasonable representation of the mixed inhibition which is observed for this inhibitor.

Attempts to study the inhibitor **1**: X = OH were frustrated by the buffering effect of the phenolic moiety of this inhibitor on the p*H*-stat studies at the relatively high concentrations of this inhibitor that were found necessary to produce significant amounts of inhibition. It is clear, however, that this species is a much poorer inhibitor than the unsubstituted benzoate anion and we have estimated that at $I = 80$ mM this inhibitor produces 50% inhibition for $S = 2.0 \times 10^{-4}$ M. In the light of the other substituent effects observed (see later discussion), it seems likely that this species would be a competitive inhibitor, and making this assumption, we have estimated $K_i = 21$ mM from the observed 50% inhibition at $I = 80$ mM.

The *p*-iodobenzoate ion (**1**: X = I) differs from all the other substituted benzoate ions examined in displaying neither competitive nor noncompetitive inhibition. Rather, Lineweaver–Burk plots at various concentrations of this inhibitor are parallel to the uninhibited line (Fig. 6*A*); the Dixon plot is linear in I (Fig. 6*B*).

Parallel Lineweaver–Burk plots are typical of what has variously been denoted as "uncompetitive" or "coupling" inhibition (4, 5). The simplest form of such inhibition arises when an inhibitor binds to E.S to form E.S.I but will not bind (or binds only very poorly with respect to S) to the free enzyme to form E.I (Scheme 2).

$$E + S \underset{}{\overset{K_s}{\rightleftarrows}} E.S \overset{k_2}{\rightarrow} E + P_1 + P_2$$

$$E.S + I \overset{K_{si}}{\rightleftarrows} E.S.I$$

SCHEME 2

Assuming that the equilibria are established rapidly relative to k_2, this scheme generates equation (2) for the dependence of initial velocity on substrate and inhibitor concentrations. This equation is of

$$[2] \qquad \frac{v}{E} = \frac{k_2/(1 + I/K_{si})}{1 + \frac{K_s}{S(1 + I/K_{si})}}$$

the classical Michaelis form at constant I, with $k_{cat}^{app} = k_2/(1 + I/K_{si})$ and $K_m^{app} = K_s/(1 + I/K_{si})$ and hence K_{si} may be calculated from either k_{cat}^{app} or K_m^{app}. Values for K_{si} calculated in this way from the data for the *p*-iodobenzoate ion are given in Table 3 and appear to be indepen-

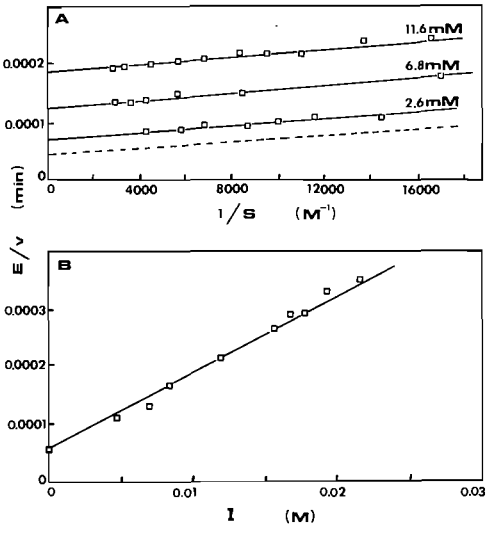

FIG. 6. Inhibition of the hydrolysis of *O*-hippuryl-L-3-phenyllactic acid by carboxypeptidase A (p*H* 7.5, 25°, ionic strength 0.2) by the *p*-iodobenzoate anion: *A*, Lineweaver–Burk plots at indicated inhibitor concentrations; *B*, Dixon plot at $S = 0.20$ mM. Broken line indicates the uninhibited reaction.

TABLE 2. Reversible inhibition of the esterase activity of carboxypeptidase A by the *p*-ethylbenzoate ion[a]

Inhibitor concentration (m*M*)	% inhibition[b]	K_m^{app} (m*M*)	k_{cat}^{app} (min^{-1})	K_I^C (m*M*)[c]	K_I^{NC} (m*M*)[c]
16.4	54	0.125	1.39×10^4	22	21
31.6	69	0.155	1.03×10^4	27	22
50.6	78	0.268	9.13×10^3	19	29

[a]At p*H* 7.5, 25°, ionic strength 0.2 against *O*-hippuryl-L-3-phenyllactic acid as substrate.
[b]At $S = 0.2$ m*M*.
[c]Calculated as described in text.

TABLE 3. Reversible inhibition of esterase activity of carboxypeptidase A by the *p*-iodobenzoate ion[a]

Inhibitor concentration (m*M*)	% inhibition[b]	k_{cat}^{app} (min^{-1})	K_{SI} (m*M*)[c]
2.60	35	1.43×10^4	3.5
6.80	61	7.87×10^3	3.1
11.6	73	5.32×10^3	3.1

[a]At p*H* 7.5, 25°, ionic strength 0.2 against *O*-hippuryl-L-3-phenyllactic acid as substrate.
[b]At $S = 0.2$ m*M*.
[c]Calculated as described in text.

dent of inhibitor concentration. Thus, Scheme 2 seems to be a reasonable representation of the reversible inhibition by the *p*-iodobenzoate ion of the hydrolysis of *O*-hippuryl-L-3-phenyllactic acid by this enzyme.

In addition to the above substituted benzoate ions, we have also investigated inhibition of ester hydrolysis by a few higher homologs of **1**. Thus, *p*-fluorophenylacetate ion (**2**: X = F) is also a competitive inhibitor ($K_i = 1.5$ m*M* from

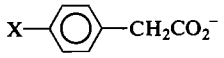

2

both Lineweaver–Burk and Dixon plots; *cf.* $K_i = 0.52$ m*M* for the phenylacetate ion (**2**: X = H) (1)). The *p*-tolylacetate (**2**: X = CH_3) and 3-(*p*-tolyl)propanoate (**3**: X = CH_3) ions

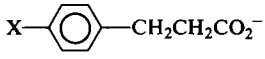

3

both appear to be competitive inhibitors in Lineweaver–Burk plots at several inhibitor concentrations (Fig. 7). However, in both these cases the calculated competitive K_i values are dependent on inhibitor concentration (Table 4) and, furthermore, the Dixon plots are nonlinear in *I*, although linear in I^2 (Fig. 8). We have previously observed similar partially competitive inhibition with other carboxylate inhibitors of the esterase activity of this enzyme (1, 2, 6) and have shown (2, 6) that such inhibition is consistent with Scheme 3. This scheme predicts that plots of $1/K_i^{app}$ *vs. I* should be linear, and such appears to be the case for **3**: X = CH_3 (Fig. 9) with values of the product $K_i' K_{ii}'$ calculated (6) from Figs. 8 and 9 independently for this inhibitor being in reasonable agreement (Table 4).

Inhibition by 3-(*p*-iodophenyl)propanoate (**3**: X = I) was of particular interest in view of the X-ray crystallographic investigations that have been made of the binding of this species to crystalline bovine carboxypeptidase A (7). Lineweaver–Burk plots for this inhibitor are displayed in Fig. 10*A* and it seems that such plots

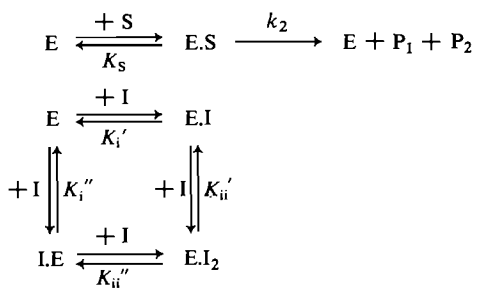

SCHEME 3

Can. J. Chem. Downloaded from www.nrcresearchpress.com by 210.87.254.40 on 09/05/12
For personal use only.

TABLE 4. Reversible inhibition of esterase activity of carboxypeptidase A by *p*-tolylacetate and 3-(*p*-tolyl)propanoate ions[a]

Inhibitor Concentration (m*M*)	% inhibition[b]	K_i^{app} (m*M*)	$K_I'K_{II}'(M^2)$[c]	$K_I'K_{II}'(M^2)$[d]
		(i) p-Tolylacetate ion		
12.1	47	3.6		
18.1	71	1.9		2.6×10^{-5}
22.3	81	1.4		
		(ii) 3-(p-Tolyl)propanoate ion		
0.74	48	0.22		
1.30	73	0.123		
1.48	78	0.116		
2.59	91	0.075	2.2×10^{-7}	1.7×10^{-7}

[a]At p*H* 7.5, 25°, ionic strength 0.2 against *O*-hippuryl-L-3-phenyllactic acid as substrate.
[b]At $S = 0.2$ m*M*.
[c]From $1/K_i^{app}$ *vs.* *I* (Fig. 9).
[d]From E/v *vs.* I^2 (Fig. 8).

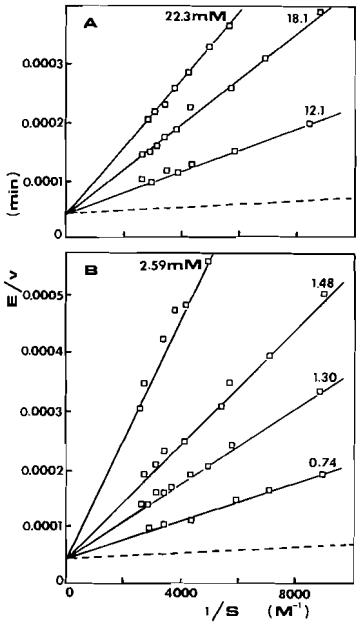

FIG. 7. Lineweaver–Burk plots for the inhibition of the hydrolysis of *O*-hippuryl-L-3-phenyllactic acid by carboxypeptidase A (p*H* 7.5, 25°, ionic strength 0.2) at indicated inhibitor concentrations: *A*, *p*-tolylacetate anion; *B*, 3-(*p*-tolyl)propanoate anion. Broken line indicates the uninhibited reaction.

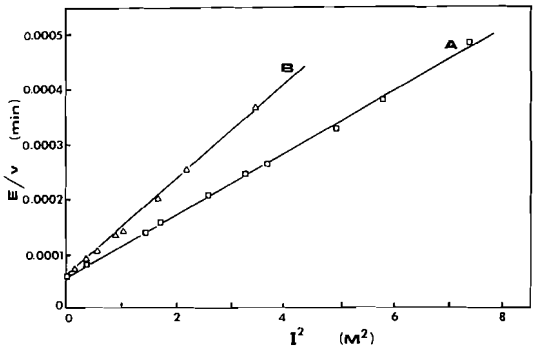

FIG. 8. Dependence of E/v on I^2 for the inhibition of the hydrolysis of *O*-hippuryl-L-3-phenyllactic acid ($S = 0.20$ m*M*) by carboxypeptidase A (p*H* 7.5, 25°, ionic strength 0.2): *A*, *p*-tolylacetate ion (I^2 scale $\times 10^{-4}$); *B*, 3-(*p*-tolyl)propanoate ion (I^2 scale $\times 10^{-6}$).

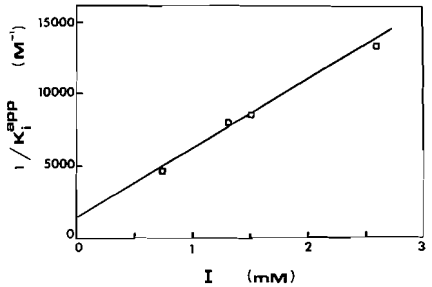

FIG. 9. Dependence of $1/K_i^{app}$ on *I* for the 3-(*p*-tolyl)propanoate anion.

become parallel at high inhibitor concentrations. Dixon plots for this inhibitor are linear in I^2 (Fig. 10*B*) and so indicate that the binding of two of these inhibitor ions per enzyme molecule occurs. As discussed above, parallel Lineweaver–Burk plots are typical of uncompetitive inhibition. In view of the observed dependence of E/v on I^2 in this case (Fig. 10*B*), it appears that uncompetitive inhibition with **3**: X = I must be superimposed on some simpler form of reversible inhibition by this same species;

Can. J. Chem. Downloaded from www.nrcresearchpress.com by 210.87.254.40 on 09/05/12
For personal use only.

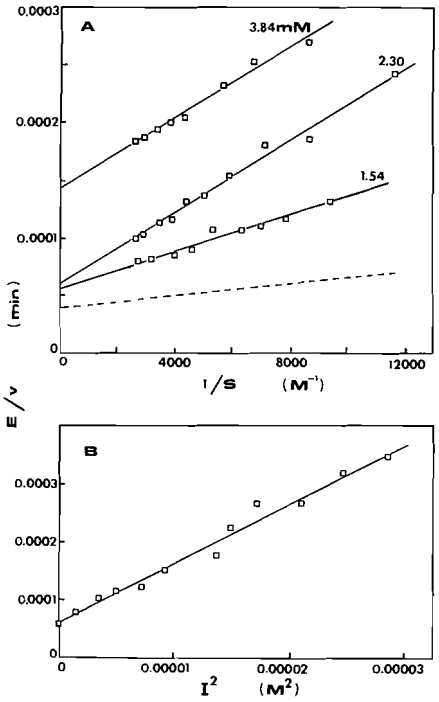

FIG. 10. Inhibition of the hydrolysis of *O*-hippuryl-L-3-phenyllactic acid by carboxypeptidase A (p*H* 7.5, 25°, ionic strength 0.2) by the 3-(*p*-iodophenyl)propanoate ion: *A*, Lineweaver–Burk plots at indicated inhibitor concentrations; *B*, dependence of E/v on I^2 at S = 0.20 m*M*. Broken line indicates the uninhibited reaction.

e.g. the binding of a second inhibitor anion to E.S.I to form E.S.I_2 much more readily than the binding of I to E.I to give E.I_2. It should be noted, that there is X-ray crystallographic evidence for multisite binding of the 3-(*p*-iodophenyl)propanoate ion to this enzyme (7).

Discussion

It is clear from the data in Table 1 that the distinction between competitive and noncompetitive modes of inhibition by *para*-substituted benzoate anions is not related to the chemical nature of the *para* substituent X. Thus, for X = F competitive inhibition is observed, whereas, for X = Cl[2] or Br the inhibition is noncompetitive.

[2]A dramatic effect from a *p*-chloro substituent also is apparent in a comparison of the hydrolysis of *O*-hippuryl-L-mandelic acid and *O*-hippuryl-L-*p*-chloromandelic acid by this enzyme. Thus K_m for the latter ester substrate is estimated to be approximately 1000 times greater than for the former (8).

Similarly, X = NH_2 leads to competitive inhibition but X = $N(CH_3)_2$ displays noncompetitive inhibition and purely hydrocarbon X moieties may produce either competitive (X = CH_3, C_2H_5) or noncompetitive inhibition (X = C_2H_5, $(CH_3)_2CH$, $(CH_3)_3C$). In each of these comparisons it is clear that the larger X substituents are associated with noncompetitive inhibition and the smaller X substituents with competitive inhibition, and perusal of all substituents in Table 1 confirms that small substituents lead to competitive inhibition, whereas noncompetitive inhibition is observed for large X.

We have previously shown (1) that for a series of carboxylate anion (RCO_2^-) competitive inhibitors for the present substrate, log K_i is linearly related to Hansch's π-parameter for the hydrophobicity of R provided that R does not become too large. When R contains a phenyl ring, the benzoate (K_i = 6 m*M* (1)), phenylacetate (K_i = 0.52 m*M* (1)) and 3-phenylpropanoate (K_i = 0.17 m*M* (1)) ions are increasingly effective competitive inhibitors. One might therefore have predicted that since **1**: X = CH_3 and **1**: X = C_2H_5 have the same π values as phenylacetate and 3-phenylpropanoate, respectively, these two substituted benzoate ions would both be stronger inhibitors than the benzoate ion itself. In fact, **1**: X = CH_3 (K_i = 8.3 m*M*) is a slightly poorer inhibitor than benzoate (K_i = 6 m*M*) and **1**: X = C_2H_5 (K_i = 23 m*M*) is an even poorer inhibitor. So it is clear that in these two cases it is not hydrophobic character alone that determines the interaction of R with the enzyme. This effect is even more magnified for X = $(CH_3)_2CH$ and $(CH_3)_3C$ such that competitive modes of inhibition are no longer observed with these inhibitors. The most obvious explanation for these observations is that these alkyl groups are too large to penetrate to that region of the hydrophobic pocket where the *para* substituent of a *para*-substituted benzoate ion would be located. The fact that this effect is apparent even for X = CH_3 suggests that the interior of the hydrophobic pocket is restricted in such a way that it is able to accept an aromatic ring but not the methyl group of **1**: X = CH_3 without some unfavorable interactions with the wall of the pocket. In support of this idea it should be noted (1) that the largest straight-chain alkanoate

Can. J. Chem. Downloaded from www.nrcresearchpress.com by 210.87.254.40 on 09/05/12
For personal use only.

Can. J. Chem. Downloaded from www.nrcresearchpress.com by 210.87.254.40 on 09/05/12
For personal use only.

ion competitive inhibitor that is acceptable in its energetically most favorable conformation is the pentanoate ion which is somewhat shorter than the 3-phenylpropanoate ion in its most extended conformation.

In light of the above suggestion that the size of the alkyl group is important in determining the binding of these *p*-substituted benzoate ions, it would be expected that other *para* substituents of the same size as, or larger than, a methyl group would also encounter accommodation problems in the hydrophobic pocket. This expectation seems to be borne out by the data in Table 1. The only substituent larger than methyl to display competitive inhibition is the ethyl group. While ethyl is larger than methyl, it is also more hydrophobic which would be expected to favor binding; even so, **1**: X = C_2H_5 is approximately a three-fold poorer inhibitor than **1**: X = CH_3.

It is quite unexpected of course, that those anions that are very poor competitive inhibitors according to the above concepts, should instead be reasonably good noncompetitive inhibitors. The observation of noncompetitive inhibition implies, of course, the existence of a second binding site for carboxylate anion inhibitors, which is quite distinct from the binding sites for the substrate and carboxylate anion competitive inhibitors. The analysis of the apparent mixed inhibition observed with the *p*-ethylbenzoate ion in terms of distinct competitive and noncompetitive inhibition modes is quite consistent with this idea.

For noncompetitive inhibition, as for competitive inhibition, there seems to be little dependence of K_i on the chemical nature of X (Table 1). The most strongly bound noncompetitive inhibitor is **1**: X = $(CH_3)_3C$ and the order $K_i(C_2H_5) > K_i((CH_3)_2CH) > K_i((CH_3)_3C)$ suggests a preference for a hydrophobic X substituent at the noncompetitive site. On the other hand, $K_i(NO_2) \approx K_i(C_2H_5)$ is not consistent with such a hypothesis. Of course, it is quite possible that there is more than one binding site which leads to noncompetitive inhibition by these benzoate anions. The observed specificity for X in noncompetitive inhibitors is probably best accommodated by postulating two noncompetitive binding sites, one of which shows a preference for hydrophobic X substituents and the other being relatively nonspecific and able to accept a variety of X substituents containing various electronegative atoms.

The details of the partially competitive inhibition that is observed for the *p*-tolylacetate and 3-(*p*-tolyl)propanoate ions are consistent with the formation of an $E.I_2$ species (Scheme 2) and are typical of the form of partially competitive inhibition that has been previously observed (1, 6) for a range of other carboxylate anions having large hydrophobic moieties. Thus, the heptanoate, octanoate, cyclohexanecarboxylate, cyclohexylacetate, 3-cyclohexylpropanoate, and 4-phenylpentanoate ions all display similar partially competitive inhibition characteristics (1, 6). This requirement for a large hydrophobic moiety for the formation of an $E.I_2$ species indicates the presence of a hydrophobic region in the enzyme that is capable of accepting such a unit.

The complicated mixed inhibition that is observed for 3-(*p*-iodophenyl)propanoate is similar to that previously observed for some carboxylate anions having very large hydrophobic moieties, *e.g.* nonanoate, 4-cyclohexylbutanoate and 6-phenylhexanoate ions (1). In each of these cases K_m^{app} seems to pass through a maximum value with increasing inhibitor concentration as in Fig. 10*A*. These data are indicative of complex mixed modes of reversible inhibition which we have not attempted to analyze further.

The examples of noncompetitive inhibition in Table 1 represent the first cases as far as we are aware of noncompetitive inhibition of the *esterase* activity of bovine carboxypeptidase A. The continuing elucidation of the reversible inhibition of this enzyme by carboxylate ions continues to provide evidence for a number of possible binding sites for carboxylate anions to this enzyme in such a way as to influence the catalytic activity of the enzyme towards ester hydrolysis. Unfortunately it is not possible at the present time to even speculate on the relationship of these various sites to one another and to the general active site region of the enzyme. The possibility that one or more of these inhibitor binding sites may be remote from the active site region and may influence catalytic activity via an important enzyme conformational change is also a distinct possibility. The totally unexpected distinction between

competitive and noncompetitive inhibitors as observed in Table 1, stresses the need for *systematic* studies of inhibitor and substrate structural effects in this and other enzymic reactions. In particular, the totally unexpected difference between the *p*-fluorobenzoate (competitive), p-chloro- and p-bromobenzoate (noncompetitive), and *p*-iodobenzoate (uncompetitive) ions as reversible inhibitors indicates that the utmost caution is required in extrapolating data for one inhibitor (or substrate) for this enzyme to even closely related species.

We appreciate the continued support of this work by the National Research Council of Canada and the award of a Walter C. Sumner Memorial Fellowship to C.D.M.

1. J. W. BUNTING and C. D. MYERS. Can. J. Chem. **51**, 2639 (1973).
2. J. W. BUNTING and C. D. MYERS. Can. J. Chem. **52**, 2053 (1974).
3. J. T. PLATI, W. H. STRAIN, and S. L. WARREN. J. Am. Chem. Soc. **65**, 1273 (1943).
4. H. R. MAHLER and E. H. CORDES. Biological chemistry. 2nd Ed. Harper and Row, New York. 1971. p. 295.
5. J. L. WEBB. Enzyme and metabolic inhibitors. Vol. 1. Academic Press, New York. 1963. pp. 59 and 160.
6. J. W. BUNTING and C. D. MYERS. Biochem. Biophys. Acta, **341**, 222 (1974).
7. T. A. STEITZ, M. L. LUDWIG, F. A. QUIOCHO, and W. N. LIPSCOMB. J. Biol. Chem. **242**, 4662 (1967).
8. J. MURPHY and J. W. BUNTING. Can. J. Chem. **52**, 3829 (1974).

Can. J. Chem. Downloaded from www.nrcresearchpress.com by 210.87.254.40 on 09/05/12
For personal use only.

Reversible Inhibition of Carboxypeptidase A. IV.[1] Inhibition of Specific Esterase Activity by Hippuric Acid and Related Species and other Amino Acid Derivatives and a Comparison with Substrate Inhibition

JOHN W. BUNTING AND CHESTER D. MYERS

Department of Chemistry, University of Toronto, Toronto, Ontario M5S 1A1

Received December 16, 1974

JOHN W. BUNTING and CHESTER D. MYERS. Can. J. Chem. **53**, 1993 (1975).

The anions of each of the following carboxylic acids exhibit uncompetitive inhibition of the hydrolysis of *O*-hippuryl-L-3-phenyllactic acid by bovine carboxypeptidase A at p*H* 7.5, 25°, ionic strength 0.2: hippuric acid, *p*-chloro- and *p*-nitrohippuric acids, hippurylglycine, carbobenzoxyglycine, phenaceturic acid, *N*-(3-phenylpropanoyl)glycine, benzoxyacetic acid, 3-benzoylpropanoic acid, and *O*-hippuryl-D-mandelic acid. In each case, this uncompetitive inhibition is consistent with the ordered binding of substrate and inhibitor to the enzyme; *i.e.* the inhibitor binds to E.S but not to the free enzyme. Evidence is presented for the binding site for uncompetitive inhibitors being the same as for inhibitory ester substrate molecules. Comparison of the specificities of uncompetitive inhibitors and esters which display substrate inhibition provides evidence for a critical conformational change which controls the binding of uncompetitive inhibitors and inhibitory substrate molecules.

D-Phenylalanine, D-leucine, D-*p*-nitrophenylalanine, glycyl-L-tyrosine, glycyl-L-phenylalanine, and glycyl-L-leucine are competitive inhibitors of the enzymic hydrolysis of *O*-hippuryl-L-3-phenyllactic acid, whereas the *N*-chloroacetyl derivatives of L-tyrosine, L-phenylalanine, and L-leucine are noncompetitive inhibitors. For the above D-amino acids, glycyl dipeptides, and *N*-chloroacetyl amino acids, the phenylalanine derivative in each case is a considerably stronger inhibitor than the corresponding leucine derivative. This preference is similar to that observed for the binding of peptide substrates but the reverse of that observed for ester substrates and simple mono- and dicarboxylate ion inhibitors.

The peptide substrates carbobenzoxyglycylglycyl-L-phenylalanine and *N*-chloroacetyl-L-phenylalanine are noncompetitive inhibitors of the enzymic hydrolysis of *O*-hippuryl-L-3-phenyllactic acid. This clearly demonstrates the presence of different ester and peptide binding sites in this enzyme, which is consistent with conclusions from recent studies in other laboratories.

JOHN W. BUNTING et CHESTER D. MYERS. Can. J. Chem. **53**, 1993 (1975).

A un p*H* de 7.5, une température de 25° et une force ionique de 0.2, les anions de chacun des acides carboxyliques suivants agissent comme inhibiteurs incompétitifs pour l'hydrolyse de l'acide *O*-hippuryl L-phényl-3 lactique par la carboxypeptidase A du boeuf: l'acide hippurique, les acides *p*-chloro- et *p*-nitrohippuriques, la hippurylglycine, la carbobenzoxyglycine, l'acide phénacéturique, la *N*-(phényl-3 propanoyl) glycine, l'acide benzoxyacétique, l'acide benzoyl-3 propanoïque et l'acide *O*-hippuryl D-mandélique. Dans chaque cas, cette inhibition incompétitive est en accord avec une association ordonnée du substrat et de l'inhibiteur à l'enzyme; *i.e.* l'inhibiteur s'associe au E.S mais non à l'enzyme libre. On présente des résultats suggérant que le site d'association des inhibiteurs incompétitifs est le même que le site pour les molécules d'esters agissant comme substrats inhibiteurs. Une comparaison des spécificités des inhibiteurs incompétitifs et des esters agissant comme substrats inhibiteurs indique qu'il y a des changements conformationnels critiques qui controlent l'association des inhibiteurs incompétitifs et des molécules de substrats inhibiteurs.

La D-phénylalanine, la D-leucine, la D-*p*-nitrophénylalanine, la glycyl L-tyrosine, la glycyl L-phénylalanine et la glycyl L-leucine sont des inhibiteurs compétitifs de l'hydrolyse enzymatique de l'acide *O*-hippuryl L-phényl-3 lactique; toutefois les dérivés *N*-chloroacétylés de la L-tyrosine, de la L-phénylalanine et de la L-leucine sont des inhibiteurs non-compétitifs. Dans le cas des acides aminés de la série D, des dipeptides contenant de la glycine et des acides aminés *N*-chloroacétylés, on remarque dans chaque cas que le dérivé de la phénylalanine est un inhibiteur beaucoup plus fort que le dérivé correspondant de la leucine. Cette préférence est semblable à celle observée pour l'association de substrats peptidiques; cet ordre est toutefois l'inverse de celui observé pour des substrats de type ester de même que pour les inhibiteurs ioniques dérivés d'acides mono- et dicarboxyliques simples.

[1]For Part III see ref. 3.

Can. J. Chem. Downloaded from www.nrcresearchpress.com by 210.87.254.6 on 09/05/12
For personal use only.

Les substrats peptidiques carbobenzoxyglycylglycyl L-phénylalanine et *N*-chloroacétyl L-phénylalanine sont des inhibiteurs non-compétitifs de l'hydrolyse enzymatique de l'acide *O*-hippuryl L-phényl-3 lactique. Ceci démontre sans ambiguité la présence, dans l'enzyme, dessites d'association différents pour les esters et les peptides; cette conclusion est en accord avec d'autres dérivées d'études récentes émanant d'autres laboratoires.

[Traduit par le journal]

Can. J. Chem. Downloaded from www.nrcresearchpress.com by 210.87.254.6 on 09/05/12
For personal use only.

Recent studies (1–3) in our laboratory of the reversible inhibition of the hydrolysis of *O*-hippuryl-L-3-phenyllactic acid by bovine carboxypeptidase A have revealed a variety of competitive, partially competitive, and noncompetitive modes of inhibition by carboxylate anions. The form of inhibition appears to be very dependent on the size and structure of the hydrophobic unit of the inhibiting anion. In a parallel investigation (4, 5), we have also been exploring the phenomenon of substrate inhibition which is displayed by some ester substrates in their hydrolysis by this enzyme and have deduced some structural features that are common to those ester substrates which exhibit this phenomenon.

Substrate inhibition of the esterase activity of this enzyme is consistent with the binding of a second substrate molecule to the catalytically productive E.S complex to give an $E.S_2$ species which is considerably less reactive ($E.S_2$ is 25-fold less reactive than E.S for hippuric acid esters) (5). Our studies on the dependence of substrate inhibition on the structure of ester substrates of general formula **1** indicate that: (*i*) the dissociation

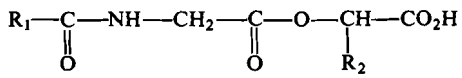

1

constant K_{ss} for $E.S_2 \rightleftarrows E.S + S$ is independent of R_2 for hydrocarbon R_2 units at least as large as isobutyl and benzyl (5); (*ii*) R_1 should be phenyl or other hydrophobic group of similar size for most effective substrate inhibition (4); and (*iii*) the integrity of the amide CONH group is essential for the formation of $E.S_2$: replacement of NH in **1** by NCH_3, O, or CH_2 results in the complete disappearance of substrate inhibition effects (4). In general, the formation and hydrolysis of E.S are much less sensitive to these same structural modifications in **1**. The fact that K_{ss} is independent of both the R_2 substituent and also of the configuration of the α-carbon atom of the terminal α-hydroxy acid unit of **1** (5) suggests that the formation of $E.S_2$ involves the interaction of only the acid unit ($R_1CONHCH_2CO_2H$) of the substrate with the enzyme at the binding site responsible for substrate inhibition. To explore this conclusion further we have now investigated the reversible inhibition of the enzymic hydrolysis of *O*-hippuryl-L-3-phenyllactic acid by a series of carboxylate anions **2** related to the acid units

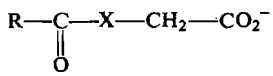

2

of the esters which we have previously surveyed for substrate inhibition. The majority of these species proved to be uncompetitive inhibitors of the hydrolysis of this ester, thus establishing that they bind at a site that does not overlap with the productive binding site for this ester substrate. Furthermore, the structural dependence of the binding of the inhibitors **2** proved to be quite different to the influence of similar structural variations in the esters **1** on the formation of an $E.S_2$ species. This leads to a modified interpretation of the dependence of substrate inhibition on the structure of the acid unit of the ester substrate.

We also report in this paper some studies of the reversible inhibition of the enzymic hydrolysis of *O*-hippuryl-L-3-phenyllactic acid by some derivatives of phenylalanine and leucine in an attempt to further explore the previously noted discrimination by the enzyme between aliphatic and aromatic hydrophobic groups in the binding of ester substrates and simple mono- and dicarboxylate anion inhibitors but not in the binding of peptide substrates (5).

Experimental

All *N*-acyl glycines and related species and *O*-hippuryl-D-mandelic acid were available from previous studies (4–6) and were recrystallized to constant melting point. Derivatives of phenylalanine, tyrosine, and leucine were purchased from Sigma Chemical Co., St. Louis, Missouri. The preparation of D-*p*-nitrophenylalanine followed the method of Houghten and Rapoport (7). The identities of all inhibitors were checked by p.m.r. spectroscopy. Stock solutions of the carboxylate inhibitors were prepared by titration of aqueous suspensions of the carboxylic acids to p*H* 7.5 with aqueous potassium

Can. J. Chem. Downloaded from www.nrcresearchpress.com by 210.87.254.6 on 09/05/12
For personal use only.

hydroxide. The stock solution of *O*-hippuryl-D-mandelic acid was prepared by the acetone solution procedure previously described for related substrates (4).

O-Hippuryl-L-3-phenyllactic acid was purchased from Fox Chemical Co., Los Angeles, California. Stock solutions of bovine carboxypeptidase A (Worthington Biochemical Corporation (Code COA)) were prepared from a toluene-preserved suspension of the crystalline enzyme as previously described (1).

The enzymic hydrolysis of *O*-hippuryl-L-3-phenyllactic acid was followed on the p*H*-stat at p*H* 7.5, 25°, ionic strength 0.2 (adjusted with sodium chloride). All experimental techniques and data treatment were as previously described (1, 2). For the uninhibited reaction under these conditions $K_m = 7.2 \times 10^{-5}$ *M* and $k_{cat} = 2.50 \times 10^4$ min^{-1} (1). All substrate concentrations were $< 4 \times 10^{-4}$ *M*, so that substrate inhibition which intervenes at higher concentrations of this substrate could be neglected. In all cases linear Lineweaver–Burk plots were observed which is a clear indication that the Michaelis–Menten equation is a suitable description of the reaction under the present conditions.

Results

Reciprocal plots (E/v *vs.* $1/S$) for the dependence of the initial velocity (v/E) on substrate concentration (S) for the hydrolysis of *O*-hippuryl-L-3-phenyllactic acid by carboxypeptidase A in the presence of various concentrations of hippuric acid anion (**2**: R = C_6H_5; X = NH) are given in Fig. 1. These data at each constant inhibitor concentration appear to describe parallel lines which are also approximately parallel to the Lineweaver–Burk plot in the absence of inhibitor. Such parallel plots are typical of a form of inhibition that has been variously referred to as "uncompetitive" or "coupling" inhibition (8, 9). The simplest reaction scheme that gives rise to this form of inhibition involves the ordered binding of substrate and inhibitor molecules as indicated in Scheme 1. Assuming that the equilibria are established rapidly relative to k_2, Scheme 1 generates eq. 1

$$\begin{array}{c} \overset{K_s}{\rightleftarrows} \quad \overset{k_2}{\rightarrow} \\ E + S \rightleftarrows E.S \rightarrow E + P_1 + P_2 \\ \\ \overset{K_i}{\rightleftarrows} \\ E.S + I \rightleftarrows E.S.I \end{array}$$

SCHEME 1

$$[1] \qquad \frac{v}{E} = \frac{k_2/(1 + I/K_i)}{1 + K_s/S(1 + I/K_i)}$$

for the dependence of initial velocity on substrate and inhibitor concentrations. Such an equation has the form of the Michaelis equation with $K_m^{app} = K_s/(1 + I/K_i)$ and $k_{cat}^{app} = k_2/(1 + I/K_i)$ and thus $k_{cat}^{app}/K_m^{app} = k_2/K_s$ independent of I. The value of K_i may be calculated from either k_{cat}^{app} or K_m^{app} at each inhibitor concentration. Since k_{cat}^{app} is determined much more accurately than K_m^{app}, we have used k_{cat}^{app} to calculate K_i from the data in Fig. 1 at each inhibitor concentration. Values for K_i are collected in Table 1 and lie in the range 10 ± 3 m*M*.

Rearrangement of eq. 1 gives eq. 2 which indicates that at constant substrate concentra-

$$[2] \qquad \frac{E}{v} = \frac{1 + K_s/S}{k_2} + \frac{I}{k_2 K_i}$$

tion plots of E/v *vs.* I (Dixon plots) should be linear and of slope $1/k_2K_i$. Such a plot for inhibition by hippurate anion is shown at $S = 0.20$ m*M* in Fig. 2 and the value of K_i calculated from the slope of this line is 8.1 m*M* which lies in the range of values obtained from the data in Fig. 1.

Lineweaver–Burk plots which were approximately parallel to the data for the uninhibited reaction were also observed (*e.g.* Fig. 3) for a number of other anions related to the hippurate anion. For each of these inhibitors, K_i values were calculated from both the Lineweaver–Burk plots and Dixon plots assuming uncompetitive inhibition as in Scheme 1. Values of K_i calculated in this way are included in Table 1. In general, there is reasonable agreement between the K_i values for any given inhibitor as evaluated from both Lineweaver–Burk and Dixon plots and this suggests that the assumption of Scheme 1 for each of these inhibitors is quite reasonable.

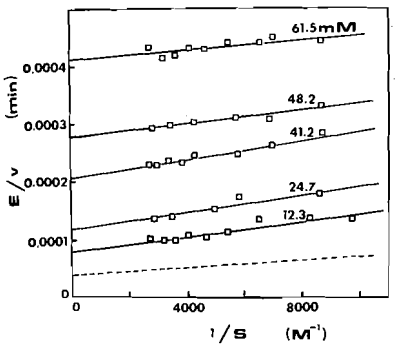

FIG. 1. Lineweaver–Burk plots for the inhibition of the hydrolysis of *O*-hippuryl-L-3-phenyllactic acid by carboxypeptidase A (p*H* 7.5, 25°, ionic strength 0.2) by the hippurate anion at indicated inhibitor concentrations. Broken line indicates the uninhibited reaction.

TABLE 1. Uncompetitive inhibition of the esterase activity of carboxypeptidase A[a]

Inhibitor	I (mM)	k_{cat}^{app} (min^{-1})	K_i (mM)[b]	K_i (mM)[c]
$C_6H_5CONHCH_2CO_2^-$	12.3	1.24×10^4	12	8.1
	24.7	8.56×10^3	13	
	41.2	4.87×10^3	10	
	48.2	3.59×10^3	8	
	61.5	2.42×10^3	7	
$C_6H_5CH_2OCONHCH_2CO_2^-$	24.6	6.53×10^3	8.7	8.2
	41.1	4.50×10^3	9.0	
$C_6H_5CONHCH_2CONHCH_2CO_2^-$	18.3	7.51×10^3	7.9	7.5
	36.6	4.40×10^3	7.8	
p-$ClC_6H_4CONHCH_2CO_2^-$	30.4	5.24×10^3	8.1	7.7
	47.5	3.94×10^3	8.9	
p-$NO_2C_6H_4CONHCH_2CO_2^-$	56.4	1.35×10^4	66	62
	112	8.70×10^3	60	
$C_6H_5CH_2CONHCH_2CO_2^-$	23.7	1.26×10^4	24	15
	39.5	7.37×10^3	17	
$C_6H_5CH_2CH_2CONHCH_2CO_2^-$	9.22	8.37×10^3	4.6	4.0
$C_6H_5CO_2CH_2CO_2^-$	16.0	4.38×10^3	3.4	3.1
$C_6H_5COCH_2CH_2CO_2^-$	6.64	6.89×10^3	2.5	2.5
	10.3	5.00×10^3	2.6	
	15.5	3.82×10^3	2.8	
D-$C_6H_5CONHCH_2CO_2CH(C_6H_5)CO_2^-$	18.8	4.76×10^3	4.4	4.4

[a]At pH 7.5, 25°, ionic strength 0.2, against O-hippuryl-L-3-phenyllactic acid as substrate.
[b]From Lineweaver–Burk k_{cat}^{app} at indicated inhibitor concentration.
[c]From Dixon plot at $S = 0.2$ mM.

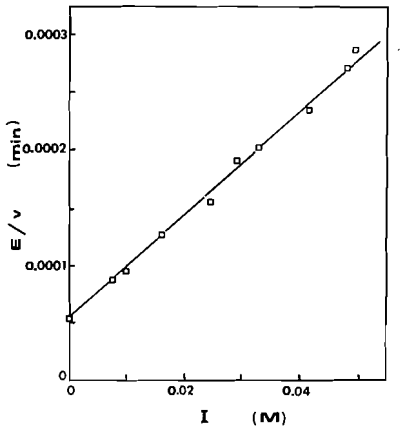

FIG. 2. Dixon plot for the inhibition of the hydrolysis of O-hippuryl-L-3-phenyllactic acid ($S = 0.20$ mM) by carboxypeptidase A (pH 7.5, 25°, ionic strength 0.2) by the hippurate anion.

For several of the inhibitors in Table 1 deviations from parallel Lineweaver–Burk plots are observed at high inhibitor concentrations; *e.g.* phenaceturate ion (**2**: R = $C_6H_5CH_2$; X = NH) in Fig. 4. The Dixon plots for these inhibitors show deviations from linearity at similar inhibitor concentrations and suggest that the binding of a second inhibitor ion per enzyme molecule is becoming important at these inhibitor concentrations. This effect appears to be particularly pronounced with hexahydrohippuric acid (**2**: R = cyclo-C_6H_{11}; X = NH) for which E/v is linear in I^2 rather than I up to greater than 80% inhibition (Fig. 5). We have, therefore, been unable to evaluate this latter species as an uncompetitive inhibitor.

The N-methylhippurate anion also displays a linear dependence of E/v on I^2 at constant substrate concentration (Fig. 5). Unlike the related inhibitors in Table 1, the Lineweaver–Burk plots in this case seem to indicate noncompetitive inhibition (Fig. 6). However, calculation of an inhibition constant from the data in Fig. 6 assuming noncompetitive inhibition gives a K_i value which appears to decrease with increasing inhibitor concentration (Table 2). A similar phenomenon of K_i decreasing with increasing inhibitor concentration has also been observed for a number of carboxylate anions which are

Can. J. Chem. Downloaded from www.nrcresearchpress.com by 210.87.254.6 on 09/05/12
For personal use only.

Can. J. Chem. Downloaded from www.nrcresearchpress.com by 210.87.254.6 on 09/05/12
For personal use only.

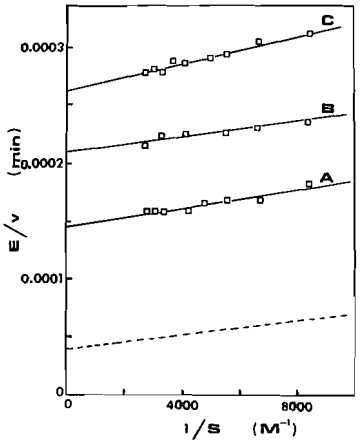

FIG. 3. Lineweaver–Burk plots for the inhibition of the hydrolysis of *O*-hippuryl-L-3-phenyllactic acid by carboxypeptidase A (p*H* 7.5, 25°, ionic strength 0.2): *A* and *C*, 3-benzoylpropanoate ion at 6.64 and 15.5 m*M*, respectively; *B*, *O*-hippuryl-D-mandelic acid at 18.8 m*M*. Broken line indicates the uninhibited reaction.

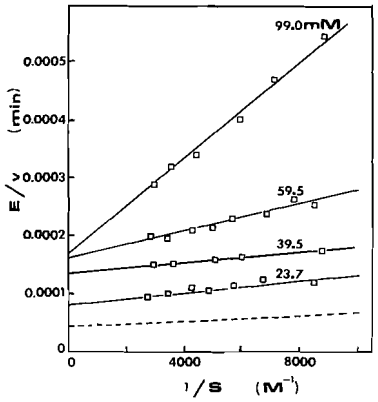

FIG. 4. Lineweaver–Burk plots for the inhibition of the hydrolysis of *O*-hippuryl-L-3-phenyllactic acid by carboxypeptidase A (p*H* 7.5, 25°, ionic strength 0.2) by the phenaceturate anion (**2**: R = $C_6H_5CH_2$; X = NH) at the indicated inhibitor concentrations. Broken line indicates the uninhibited reaction.

nominally competitive inhibitors but which also show a linear dependence of E/v on I^2 (2, 3, 10). This partially competitive inhibition has been shown to be consistent with the formation of both E.I and E.I_2 species. By analogy, the inhibition observed for the *N*-methylhippurate anion should presumably be referred to as partially noncompetitive inhibition and can be most simply described by Scheme 2. It should be noted that Scheme 2 is not the same as the most commonly postulated form of partially

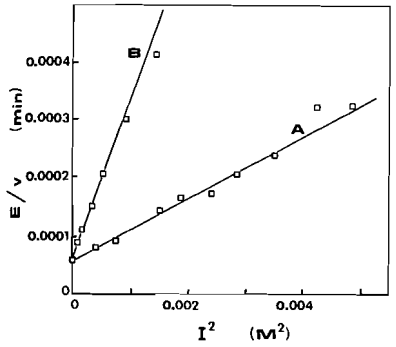

FIG. 5. Dependence of E/v on I^2 for the inhibition of the hydrolysis of *O*-hippuryl-L-3-phenyllactic acid (S = 0.20 m*M*) by carboxypeptidase A (p*H* 7.5, 25°, ionic strength 0.2): *A*, *N*-methylhippurate ion (**2**: R = C_6H_5; X = NCH_3); *B*, hexahydrohippurate ion (**2**: R = cyclo-C_6H_{11}; X = NH).

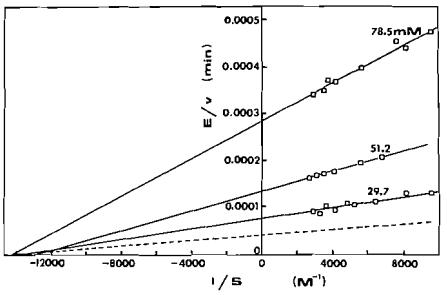

FIG. 6. Lineweaver–Burk plots for the inhibition of the hydrolysis of *O*-hippuryl-L-3-phenyllactic acid by carboxypeptidase A (p*H* 7.5, 25°, ionic strength 0.2) by the *N*-methylhippurate ion at the indicated inhibitor concentrations. Broken line indicates the uninhibited reaction.

noncompetitive inhibition (11). The presence of E.I_2 and E.I_2.S species in the present case is demanded by the dependence of E/v on I^2 rather than on I.

Amide hydrolysis results in no significant net uptake or release of protons at p*H* 7.5. While this fact makes it impossible to study amide hydrolysis on the p*H*-stat at p*H* 7.5, it may be taken advantage of to study the reversible inhibition of ester hydrolysis by amide substrates. Thus, we have investigated the inhibition of the enzymic hydrolysis of *O*-hippuryl-L-3-phenyllactic acid by carbobenzoxyglycylglycyl-L-phenylalanine which is a much studied peptide substrate of carboxypeptidase A (12–15). Reciprocal plots for the dependence of initial velocity on substrate concentration at two concentrations of cbz-gly-gly-L-phe are displayed

TABLE 2. Noncompetitive inhibition of the esterase activity of carboxypeptidase A [a]

Inhibitor	I (mM)	k_{cat}^{app} (min^{-1})	K_i (mM) [b]	K_i (mM) [c]
$C_6H_5CON(CH_3)CH_2CO_2^-$	29.7	1.30×10^4	31.9	[d]
	51.2	7.36×10^3	21.4	
	78.5	3.48×10^3	11.1	
Cbz-gly-gly-L-phe	1.21	1.27×10^4	1.3	1.1
	2.71	7.62×10^3	1.2	
N-Chloroacetyl-L-phe	1.47	6.39×10^3	0.51	0.48
N-Chloroacetyl-L-tyr	1.90	5.00×10^3	0.47	0.49
N-Chloroacetyl-L-leu	10.5	4.70×10^3	2.4	2.3

[a]At pH 7.5, 25°, ionic strength 0.2, against *O*-hippuryl-L-3-phenyllactic acid as substrate.
[b]From Lineweaver–Burk k_{cat}^{app} at indicated inhibitor concentration.
[c]From Dixon plot at $S = 0.2$ mM.
[d]Dixon plot linear in I^2 (see Fig. 5).

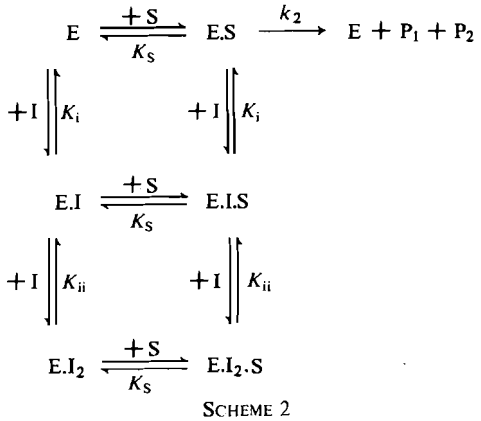

SCHEME 2

in Fig. 7*A*. Although this figure appears to indicate mixed inhibition, it is clear that the predominant contribution is from noncompetitive inhibition. Calculation of K_i values from k_{cat}^{app} at each inhibitor concentration assuming noncompetitive inhibition gives values which agree with one another (Table 2) and also with the K_i value calculated from the Dixon plot (Fig. 7*B*) for this inhibitor assuming noncompetitive inhibition.

In addition to cbz-gly-gly-L-phe, we have also studied the inhibition of ester hydrolyses by some small amide substrates for this enzyme. Thus the *N*-chloroacetyl derivatives of each of L-phenylalanine, L-tyrosine, and L-leucine proved to be noncompetitive inhibitors of specific ester hydrolysis (Fig. 8); the Dixon plots for each of these inhibitors are linear in I and there is close agreement between the K_i values calculated by both methods (Table 2). On the other hand, glycyl-L-tyrosine and glycyl-L-phenylalanine are competitive inhibitors for the same ester substrate (Fig. 9). The K_i values calculated from Fig. 9 and from linear Dixon plots for those inhibitors are in agreement (Table 3). The study of inhibition by glycyl-L-leucine was complicated by buffering effects from the free amino group of this inhibitor at the relatively high inhibitor concentrations found necessary to produce reasonable amounts of inhibition. The K_i value in Table 3 for glycyl-L-leucine is therefore estimated, assuming competitive inhibition,

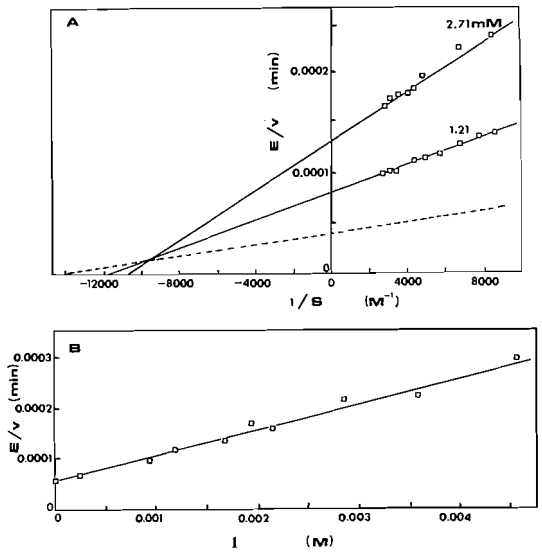

FIG. 7. Inhibition of the hydrolysis of *O*-hippuryl-L-3-phenyllactic acid by carboxypeptidase A (pH 7.5, 25°, ionic strength 0.2) by carbobenzoxyglycylglycyl-L-phenylalanine: *A*, Lineweaver–Burk plots at indicated inhibitor concentrations; *B*, Dixon plot at $S = 0.20$ mM. Broken line indicates the uninhibited reaction.

Can. J. Chem. Downloaded from www.nrcresearchpress.com by 210.87.254.6 on 09/05/12
For personal use only.

TABLE 3. Competitive inhibition of the esterase activity of carboxypeptidase A[a]

Inhibitor	I (mM)	K_m^{app} (mM)	K_I (mM)[b]	K_i (mM)[c]
$CH_3CONHCH_2CO_2^-$	179	0.647	94	63
Gly-L-tyr	1.72	1.38	0.095	0.076
Gly-L-phe	1.78	0.625	0.23	0.22
Gly-L-leu	[d]			3.4[d]
D-Phe	2.94	1.60	0.16	0.15
D-p-NO_2phe	5.40	0.642	0.68	0.64
D-Leu	18.1	0.559	2.7	3.0

[a]At pH 7.5, 25°, ionic strength 0.2, against O-hippuryl-L-3-phenyllactic acid as substrate.
[b]From Lineweaver–Burk K_m^{app} at indicated inhibitor concentration.
[c]From Dixon plot at $S = 0.2$ mM.
[d]See text.

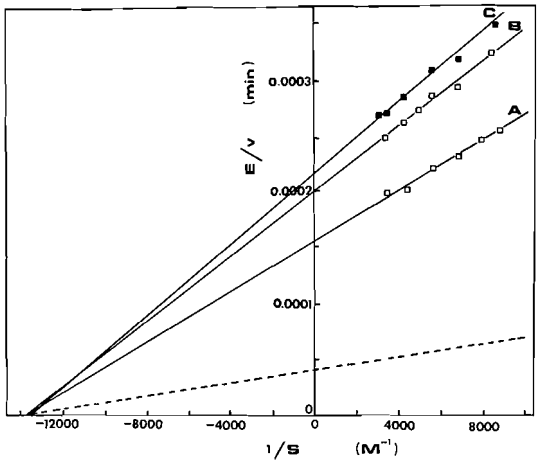

FIG. 8. Lineweaver–Burk plots for the inhibition of the hydrolysis of O-hippuryl-L-3-phenyllactic acid by carboxypeptidase A (pH 7.5, 25°, ionic strength 0.2): A, N-chloroacetyl-L-phenylalanine (1.47 mM); B, N-chloroacetyl-L-tyrosine (1.90 mM); C, N-chloroacetyl-L-leucine (10.5 mM). Broken line indicates the uninhibited reaction.

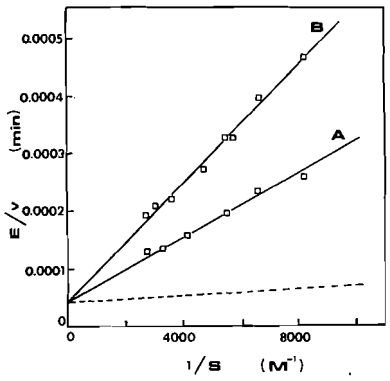

FIG. 9. Lineweaver–Burk plots for the inhibition of the hydrolysis of O-hippuryl-L-3-phenyllactic acid by carboxypeptidase A (pH 7.5, 25°, ionic strength 0.2): A, glycyl-L-phenylalanine (1.78 mM); B, glycyl-L-tyrosine (1.72 mM). Broken line indicates the uninhibited reaction.

from the observation that approximately 50% inhibition is produced by 13 mM solutions of this dipeptide at $S = 0.20$ mM.

In the light of observations (16–18) that the D-amino acids are much stronger inhibitors of the peptidase activity of this enzyme at pH 7.5 than their L-analogs, we have also examined the inhibition of the hydrolysis of O-hippuryl-L-3-phenyllactic acid by some of these species. The D-isomers of each of phenylalanine, leucine, and p-nitrophenylalanine proved to be competitive inhibitors for the hydrolysis of this ester (Fig. 10); K_i values are collected in Table 3. The corresponding L-isomers of these three amino acids proved to be at least three to five times poorer competitive inhibitors in each case.

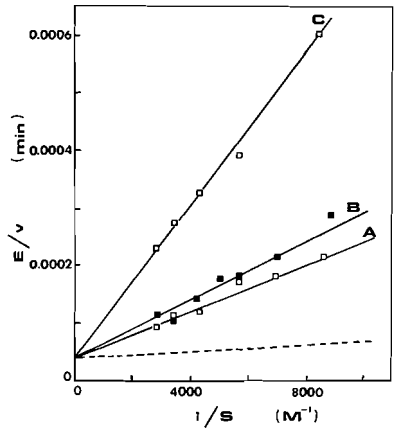

FIG. 10. Lineweaver–Burk plots for the inhibition of the hydrolysis of O-hippuryl-L-3-phenyllactic acid by carboxypeptidase A (pH 7.5, 25°, ionic strength 0.2): A, D-leucine (18.1 mM); B, D-p-nitrophenylalanine (5.40 mM); C, D-phenylalanine (2.94 mM). Broken line indicates the uninhibited reaction.

Can. J. Chem. Downloaded from www.nrcresearchpress.com by 210.87.254.6 on 09/05/12
For personal use only.

Can. J. Chem. Downloaded from www.nrcresearchpress.com by 210.87.254.6 on 09/05/12
For personal use only.

Finally, aceturic acid (**2**: R = CH_3; X = NH) also proved to be a weak competitive inhibitor (Table 3).

Discussion

The uncompetitive inhibition of the hydrolysis of *O*-hippuryl-L-3-phenyllactic acid that is observed for the inhibitors in Table 1 seems to be consistent with the ordered binding of substrate and inhibitor molecules to the enzyme which is outlined in Scheme 1. The close agreement between K_i values calculated independently from Lineweaver–Burk plots and Dixon plots for each of these inhibitors (Table 1) indicates that Scheme 1 is a reasonable expression of the inhibition observed in these cases.

We have previously shown that substrate inhibition of the hydrolysis of hippuric acid esters by carboxypeptidase A is the result of the formation of a relatively unreactive $E.S_2$ species and moreover, that the binding of substrate molecules at the catalytically productive and inhibitory sites in $E.S_2$ is either truly ordered or else closely approximates ordered binding (5). Furthermore, substrate binding at the inhibitory site depends only on the acyl unit of the ester and is independent of the alcohol moiety of these substrates (4, 5). In this light, uncompetitive inhibition by hippurate anion of the enzymic hydrolysis of *O*-hippuryl-L-3-phenyllactic acid involving ordered binding of substrate and inhibitor molecules exactly parallels the ordered binding of two substrate molecules at the catalytically productive and inhibitory sites, and strongly suggests that the hippurate anion is binding at the same site as the inhibitory substrate molecule. As further confirmation of this conclusion, it should be noted that *O*-hippuryl-D-mandelic acid, which is known (5) to be able to replace its L-isomer at the inhibitory substrate site, is an uncompetitive inhibitor of *O*-hippuryl-L-3-phenyllactic acid in the present study (Table 1). The value of K_i = 4.4 m*M* (ionic strength 0.2) found for *O*-hippuryl-D-mandelic acid in the present study is in reasonable agreement with the dissociation constant of 2.6 m*M* (ionic strength 0.5) previously found (5) for dissociation of this ester from the inhibitory site of the $E.S_2$ complex.

In recent work in our laboratory (6), it has been shown that *p*-chloro- and *p*-nitrohippuric acid esters also display marked substrate inhibition of their hydrolyses by carboxypeptidase A. Analyses of the kinetic data for these esters indicate that the presence of the chlorine substituent slightly promotes binding at the inhibitory substrate site, whereas the *p*-nitro group diminishes binding at this site approximately threefold. Phenaceturate esters are also known (4) to be bound less strongly at the inhibitory site than are hippurate esters. Comparison of the K_i values in Table 1 for *p*-chlorohippurate ion, *p*-nitrohippurate ion, and phenaceturate ion with that for hippurate ion are in qualitative agreement with the above observations of substrate affinity for the inhibitory site, and this fact further supports identical binding sites for these uncompetitive inhibitors and inhibitory substrate molecules.

In view of this satisfying relationship between uncompetitive inhibition and substrate inhibition, it comes as a surprise to find that, whereas esters of 3-benzoylpropanoic acid, benzoxyacetic acid, and hippurylglycine do not display substrate inhibition, the anions of these three acids do nevertheless act as uncompetitive inhibitors of the enzymic hydrolysis of *O*-hippuryl-L-3-phenyllactic acid (see Table 4). At first sight, this observation may seem to contradict the above postulated identical binding sites for uncompetitive inhibitors and inhibitory substrate molecules. However, it should be remembered that both uncompetitive inhibition and substrate inhibition appear to involve ordered binding, and that in each case the inhibitory effects arise from either inhibitor or substrate binding to the E.S complex. Now, 3-benzoylpropanoic acid anion is able to bind to the E.S complex when the substrate is *O*-hippuryl-L-3-phenyllactic acid (Table 1) but an ester of this same acid cannot bind to the E.S complex when the substrate is 2-(3-benzoylpropanoxy)butanoic acid (4). One might therefore conclude that the enzymic site that accepts the 3-benzoylpropanoyl unit is available in the E.S complex of the former substrate but not in the E.S complex of the latter substrate; *i.e.* the E.S complexes that these two substrates form with carboxypeptidase A are not equivalent. Since substrate inhibition is equally apparent in both *O*-hippuryl-L-3-phenyllactic acid and 2-hippuroxybutanoic acid (5), this nonequivalence cannot be related to the presence of different alcohol units in the above two substrates. Furthermore, hippuric acid and 3-benzoylpropanoic acid are isosteric so that *if* these two

TABLE 4. Comparison of uncompetitive inhibition and substrate inhibition of the esterase activity of carboxypeptidase A[a]

R	Uncompetitive inhibition by RCO_2^-	Substrate inhibition for $RCO_2CH(C_2H_5)CO_2^-$
$C_6H_5CONHCH_2$	+	+
p-$ClC_6H_4CONHCH_2$	+	+
p-$NO_2C_6H_4CONHCH_2$	+	+
$C_6H_5CH_2CONHCH_2$	+	+
$C_6H_5CONHCH_2CONHCH_2$	+	–
$C_6H_5COCH_2CH_2$	+	–
$C_6H_5CO_2CH_2$	+	–
$C_6H_5CON(CH_3)CH_2$	[b]	–
$C_6H_5CH_2CH_2CH_2$	[c]	–
$CH_3CONHCH_2$	[c]	–

[a]Data for substrate inhibition from refs. 4 and 6.
[b]Partially noncompetitive inhibitor.
[c]Competitive inhibitor.

substrates bind to the enzyme at the same site, the lack of substrate inhibition for the 3-benzoylpropanoate ester cannot be due to the substrate inhibitory site being physically blocked in the E.S complex by the presence of the substrate molecule that is bound at the catalytically productive site.

We must then conclude that one of the following situations exists: (*i*) in the E.S complexes of the two substrates presently under consideration, the substrate molecules are bound at either partially or wholly different sites and in the case of the 3-benzoylpropanoate ester the first-bound substrate molecule blocks the binding of a second substrate molecule; or (*ii*) the two substrate molecules are bound in either identical or different sites to the enzyme, but one of the E.S complexes can undergo an important conformational change which is not available to the other. This latter condition actually encompasses two separate possibilities; (*iia*) the binding of hippurate esters may cause a conformational change which makes the inhibitory site accessible to a second substrate molecule, or alternatively, (*iib*) the binding of the 3-benzoylpropanoate ester may produce a conformational change which makes the inhibitory site inaccessible. The conformational mobility of carboxypeptidase A in its interaction with substrates and inhibitors is well established on the basis of X-ray crystallographic, chemical modification, spectroscopic, and temperature-jump studies (19–24).

The observation of ordered binding by both uncompetitive inhibitors and inhibitory substrate molecules to the E.S complex for hippurate ester substrates would seem to be most readily accommodated by case *iia*. In both cases *i* and *iib*, if both binding sites preexist in the enzyme molecule, it is difficult to understand why binding should be ordered rather than random, when the enzyme is confronted with both an inhibitor ion and a hippurate ester substrate molecule. The requirement for a conformational change in the E.S complex of a hippurate ester substrate (case *iia*), which makes the binding site accessible to the uncompetitive inhibitor or inhibitory substrate molecule (or which creates such a binding site), is the situation that is most satisfactorily reconciled with the experimental observations of ordered binding.

It should be noted that K_m for the hippurate ester is a factor of 10 smaller than K_m for any of the other esters in Table 4 (4). There is evidence for other carboxypeptidase substrates (both esters and peptides) (25, 26) that K_m is a true measure of the dissociation constant (K_s) of the E.S complex provided that nonproductive binding modes are absent. Thus, the especially small K_m for the hippuric acid esters appears to reflect the importance of the NH unit of these esters in their interaction with the enzyme. Replacement of this NH by either NCH_3 or O drastically increases K_m by a factor of at least 200 and strongly suggests a role for the NH unit as a hydrogen bond donor in the interaction of hippuric acid esters with this enzyme. Since this same structural feature also appears to be essential to the display of substrate inhibition (4),

Can. J. Chem. Downloaded from www.nrcresearchpress.com by 210.87.254.6 on 09/05/12
For personal use only.

we tentatively suggest that the formation of this hydrogen bond is also related to the enzymic conformational change which is envisioned in *iia* above.

The above argument in terms of the anion and esters of 3-benzoylpropanoic acid is equally applicable to explaining the observation of uncompetitive inhibition by the anion of benzoxyacetic acid but the lack of substrate inhibition with esters of this acid. A similar argument can also formally be made for the anion and esters of hippurylglycine, although in this case the NH unit which was suggested above to be related to substrate inhibition is present. On the other hand, esters of this acid are considerably longer than the other ester substrates considered above, and it is possible that this increased size of the ester substrate may critically influence the postulated sensitive conformational change in the E.S complex.

We have previously suggested (4) in the light of our studies of substrate inhibition that the presence of a CONH unit, as in hippuric acid, is essential for binding to occur at the substrate inhibitory site. On the other hand, the data in Table 1 suggest that the replacement of the hippuric acid NH by O or CH_2 actually slightly strengthens the binding of these uncompetitive inhibitors. If, as suggested above, the binding sites for uncompetitive inhibitors and inhibitory substrate molecules are the same, it then becomes clear that the apparent essentiality of a CONH unit for substrate inhibition is actually an artifact of the requirement for the NH unit in the E.S complex to allow the conformational change which is postulated to be a prerequisite for substrate inhibition. In view of the data in Table 1, the only specificity feature that is certain for binding at the inhibitory site is the requirement for a relatively large (*e.g.* phenyl) terminal group. Aceturate anion which lacks such a group does not show uncompetitive inhibition but instead is a poor competitive inhibitor (Table 3). The requirement for the carbonyl unit of the amide moiety is uncertain at the present time, since the only inhibitor that we have studied that could illuminate this point is the 4-phenylbutanoate ion which is such a strong competitive inhibitor (K_i = 0.58 m*M* (1)) that contributions from uncompetitive inhibition similar to that for the hippurate anion would not be observable.

If, as suggested above, uncompetitive inhibitors do bind at the same site as inhibitory substrate molecules, one might also expect that the resultant E.S.I species might show the same low catalytic activity as $E.S_2$ species which are approximately 25 times less reactive than E.S for hippurate ester substrates (5). Although we have not investigated this point in detail, it should be noted that in all cases the Lineweaver–Burk plots in the presence of inhibitor are of slightly different slope than, although approximately parallel to, the uninhibited line. Such a phenomenon is consistent with the E.S.I species having a low residual activity.

The predominant noncompetitive inhibition of the hydrolysis of *O*-hippuryl-L-3-phenyllactic acid by cbz-gly-gly-L-phe is consistent with recent conclusions (26–28) of quite different productive binding sites for ester and peptide substrates. The value of K_i = 1.2 m*M* observed in the present study (at ionic strength 0.2) for cbz-gly-gly-L-phe is somewhat larger than the value of K_m = 0.25 m*M* obtained (at ionic strength 1.0) (12) for this peptide as a substrate for carboxypeptidase A. Ionic strength effects, which are known (29) to be important for this enzyme, and the slight deviation from noncompetitive inhibition apparent in Fig. 7*A* are probably responsible for this difference between K_i and K_m.

The simple amide substrate *N*-chloroacetyl-L-phenylalanine is also a noncompetitive inhibitor of specific esterase activity. The value of K_i = 0.5 m*M* for this inhibitor (ionic strength 0.2, 25°) is in reasonable agreement with K_m = 0.24 m*M* (ionic strength 0.1, 20°) (30) reported for the hydrolysis of this amide by carboxypeptidase A. Auld and Vallee (13) have established that the p*H* profiles for the enzymic hydrolysis of *N*-chloroacetyl-L-phenylalanine and cbz-gly-gly-L-phe are similar.

We have previously noted (5) that one of the manifestations of different binding modes for ester and peptide substrates is the difference in preference shown by the enzyme for aliphatic and aromatic side chains in peptide and ester substrates. Thus, although K_m for cbz-gly-gly-L-phe is about 10-fold smaller than for cbz-gly-gly-L-leu (12), comparison of corresponding hippurate esters (5) and simple carboxylate ion competitive inhibitors for hippurate esters (1) containing benzyl (*cf.* phenylalanine) and isobutyl (*cf.* leucine) groups indicates that K_m and K_i values are, respectively, eight and four times smaller for the isobutyl group than for the benzyl group. We have explored this phe-

Can. J. Chem. Downloaded from www.nrcresearchpress.com by 210.87.254.6 on 09/05/12
For personal use only.

Can. J. Chem. Downloaded from www.nrcresearchpress.com by 210.87.254.6 on 09/05/12
For personal use only.

nomenon further in the present study by comparison of the inhibition of esterase activity by several derivatives of phenylalanine and leucine and the relevant K_i values are in Tables 2 and 3. It will be noted that the phenylalanine derivatives are considerably stronger inhibitors than the corresponding leucine derivatives for the D-amino acids (competitive inhibitors), the glycyldipeptides (competitive inhibitors) and *N*-chloroacetyl-L-amino acids (noncompetitive inhibitors). This preference for a benzyl rather than an isobutyl side chain is the same as that observed in the K_m values for peptide substrates (12).

The preference for aromatic over aliphatic side chains in the D-amino acids and glycyl dipeptides which are competitive inhibitors for *O*-hippuryl-L-3-phenyllactic acid contrasts with the reverse preference expressed in mono- and dicarboxylate anions (*e.g.* $(CH_3)_2\,CHCH_2CO_2^-$, $K_i = 0.12$ m*M* and $C_6H_5CH_2CO_2^-$, $K_i = 0.52$ m*M*) (1, 2) which are also competitive inhibitors of this same ester. This difference strongly suggests that the hydrophobic side chains of these amino acid derived competitive inhibitors are not bound in the same site as similar hydrophobic groups of simple carboxylic and dicarboxylic acid competitive inhibitors. This conclusion is further strengthened by the observation that, whereas phenylacetate ion is a competitive inhibitor for ester hydrolysis but a noncompetitive inhibitor for peptide hydrolysis (26), on the other hand glycyl-L-tyrosine (and presumably also gly-L-phe and gly-L-leu) is a competitive inhibitor for *both* peptide (12) and ester hydrolyses. Since it is shown above that peptide substrates are noncompetitive inhibitors for ester substrates, it is quite reasonable that competitive inhibitors of ester hydrolysis should be noncompetitive inhibitors of peptide hydrolysis. On this same basis, it is quite unexpected that glycyl-L-tyrosine should be a competitive inhibitor for both ester and peptide hydrolyses. The K_i value for glycyl-L-tyrosine observed in the present study for inhibition of ester hydrolysis (0.085 m*M*) agrees closely with the value reported by Auld and Vallee (12) for inhibition of peptide hydrolysis (0.1 m*M*) and there can then be little doubt that the same binding mode for this inhibitor is under observation in both studies. This competitive inhibition of both ester and peptide hydrolysis by glycyl-L-tyrosine may be interpreted in one of two ways. Thus, the glycyl-L-tyrosine may bind in such a way that it bridges the peptide and ester binding sites; this in turn requires that the ester and peptide binding sites should be close together, although nonoverlapping since peptides are noncompetitive inhibitors of ester binding. Alternatively, binding of glycyl-L-tyrosine may cause an enzymic conformational change which makes inaccessible either or both of the ester and peptide binding sites. Such an "indirect" competitive inhibition is kinetically equivalent to the more usually considered competitive inhibition due to overlapping substrate and inhibitor binding sites. It should be noted that there is a large conformational change in the crystalline enzyme upon glycyl-L-tyrosine binding (19, 20) and it has recently been suggested that even larger conformational changes may occur in solution (31); the influence of glycyl-L-tyrosine on the conformational mobility of carboxypeptidase A in solution has been directly shown by temperature-jump relaxation studies (24). In view of the close relationship discussed above between the binding of glycyl dipeptide inhibitors and peptide substrates it seems reasonable to propose that competitive inhibition of peptide hydrolysis by these dipeptides results from true competition for overlapping binding sites. The competitive inhibition of ester hydrolysis would then be associated with the conformational change in the enzyme that is referred to above.

D-Phenylalanine, a competitive inhibitor of ester hydrolysis in the present study, has several times been reported (15, 16, 21) to be also a competitive inhibitor for peptide hydrolysis. However, K_i values for inhibition of peptidase activity are in the range 1.0–2.0 m*M*, which is an order of magnitude larger than we find (0.15 m*M*) for inhibition of ester hydrolysis. It is therefore not clear whether the competitive inhibitions by D-phenylalanine of ester and peptide hydrolyses arise from the same binding mode for this inhibitor. Since it seems that the productive ester and peptide binding sites are quite separate, it is clearly possible for an inhibitor to independently competitively inhibit esterase and peptidase activities provided it can bind at more than one site. Our recent studies seem to indicate that a variety of binding sites for carboxylate ion inhibitors are available in this enzyme (1–3).

Finally, we note that the presence of a *para* substituent (OH or NO_2) in the phenylalanine ring has relatively little effect on K_i in Tables

2 and 3. This contrasts with the influence of these two substituents on inhibition by benzoate ions (3). Thus *p*-hydroxybenzoate ion is a threefold weaker inhibitor than the parent benzoate ion (competitive inhibitor) for the enzymic hydrolysis of *O*-hippuryl-L-3-phenyllactic acid, whereas the *p*-nitrobenzoate ion is such a poor competitive inhibitor that noncompetitive inhibition intervenes (3). Such differences in substituent effects tend to further support more than one mode of binding for carboxylate ions which act as competitive inhibitors for the enzymic hydrolysis of *O*-hippuryl-L-3-phenyllactic acid.

We appreciate the continued support of this work by the National Research Council of Canada, and by the award of a Walter C. Sumner Memorial Fellowship to C.D.M. We thank Dr. J. Murphy and Mr. S. S-T. Chu for samples of many of the inhibitors studied.

1. J. W. BUNTING and C. D. MYERS. Can. J. Chem. **51**, 2639 (1973).
2. J. W. BUNTING and C. D. MYERS. Can. J. Chem. **52**, 2053 (1974).
3. J. W. BUNTING and C. D. MYERS. Can. J. Chem. This issue.
4. J. W. BUNTING and J. MURPHY. Can. J. Chem. **52**, 2640 (1974).
5. J. MURPHY and J. W. BUNTING. Can. J. Chem. **53**, 283 (1975).
6. S. S-T. CHU. M.Sc. Thesis, University of Toronto, Toronto, Ontario. 1974.
7. R. A. HOUGHTEN and H. RAPOPORT. J. Med. Chem. **17**, 556 (1974).
8. H. R. MAHLER and E. H. CORDES. Biological chemistry. 2nd Ed. Harper and Row, New York. 1971. p. 295.
9. J. L. WEBB. Enzyme and metabolic inhibitors. Vol. 1. Academic Press, New York. 1963. pp. 59 and 160.
10. J. W. BUNTING and C. D. MYERS. Biochem. Biophys. Acta, **341**, 222 (1974).
11. M. DIXON and E. C. WEBB. Enzymes. 2nd Ed. Longmans, Green and Co., London. 1967. p. 323.
12. D. S. AULD and B. L. VALLEE. Biochemistry, **9**, 602 (1970).
13. D. S. AULD and B. L. VALLEE. Biochemistry, **9**, 4352 (1970).
14. D. S. AULD and B. L. VALLEE. Biochemistry, **10**, 2892 (1971).
15. L. D. BYERS and R. WOLFENDEN. Biochemistry, **12**, 2070 (1973).
16. E. ELKINS-KAUFMAN and H. NEURATH. J. Biol. Chem. **175**, 893 (1948).
17. E. ELKINS-KAUFMAN and H. NEURATH. J. Biol. Chem. **178**, 645 (1949).
18. J. E. COLEMAN and B. L. VALLEE. Biochemistry, **3**, 1874 (1964).
19. W. N. LIPSCOMB, G. N. REEKE JR., J. A. HARTSUCK, F. A. QUIOCHO, P. H. BETHGE, M. L. LUDWIG, T. A. STEITZ, H. MUIRHEAD, and J. C. COPPOLA. Brookhaven Symp. Biol. **21**, 24 (1968).
20. W. N. LIPSCOMB, G. N. REEKE JR., J. A. HARTSUCK, F. A. QUIOCHO, and P. H. BETHGE. Phil. Trans. Roy. Soc. London, Ser. B, **257**, 177 (1970).
21. H. FUJIOKA and K. IMAHORI. J. Biol. Chem. **237**, 2804 (1962).
22. J. F. RIORDAN, M. SOKOLOVSKY, and B. L. VALLEE. Biochemistry, **6**, 358, 3609 (1967).
23. J. T. JOHANSEN, D. M. LIVINGSTON, and B. L. VALLEE. Biochemistry, **11**, 2584 (1972).
24. T. C. FRENCH, N-T. YU, and D. S. AULD. Biochemistry, **13**, 2877 (1974).
25. D. S. AULD, S. A. LATT, and B. L. VALLEE. Biochemistry, **11**, 4994 (1972).
26. D. S. AULD and B. HOLMQUIST. Biochemistry, **13**, 4355 (1974).
27. J. F. RIORDAN. Biochemistry, **12**, 3915 (1973).
28. L. G. LANGE III, D. S. AULD, and J. F. RIORDAN. Biochemistry, **13**, 1983 (1974).
29. W. O. MCCLURE and H. NEURATH. Biochemistry, **5**, 1425 (1966).
30. F. A. HOMMES. Arch. Biochem. Biophys. **96**, 37 (1962).
31. W. N. LIPSCOMB. Proc. Nat. Acad. Sci. U.S.A. **70**, 3797 (1973).

Can. J. Chem. Downloaded from www.nrcresearchpress.com by 210.87.254.6 on 09/05/12
For personal use only.

Lithium Aluminum Hydride Reductive Rearrangement of Allylic Acetals to Vinyl Ethers: A Synthesis of 3-Deoxy Glycals[1]

BERT FRASER-REID, STEVE Y-K. TAM,[2] AND BRUNO RADATUS[2]
Chemistry Department, University of Waterloo, Waterloo, Ontario
Received May 16, 1974[3]

BERT FRASER-REID, STEVE Y-K. TAM, and BRUNO RADATUS. Can. J. Chem. **53**, 2005 (1975).

Carbohydrate allylic acetals (hex-2-enopyranosides) are reductively rearranged to vinyl ethers (3-deoxy glycals) by treatment with lithium aluminium hydride in refluxing ethereal solvents. Under similar conditions, some allylic alcohols are also reductively rearranged to olefins, although the reaction appears to be confined to carbohydrate substrates since the reaction fails with typical carbocyclic allylic alcohols.

The results are rationalized by postulating the intermediacy of an oxygen–alane complex, this being formed more readily in the case of an hydroxyl (or ester) rather than an ethereal oxygen. An axial oxygen permits easier achievement of the reactive transition state than an equatorial oxygen. The complex normally leads to an S_N2' reductive rearrangement in which the entering hydride and departing oxygen are *syn*-related. Alternatively, and particularly when the double bond is flanked by an hydroxyl group at one allylic position and a leaving group at the other, an abnormal S_N2' process may occur so that the hydride ion is delivered vicinal and *cis* to the hydroxyl group, with ejection of the leaving group. The process is at all times stereospecific but not always regiospecific.

BERT FRASER-REID, STEVE Y-K. TAM et BRUNO RADATUS. Can. J. Chem. **53**, 2005 (1975).

Le traitement, par $LiAlH_4$ dans des solvants éthérés à reflux, permet de réduire des acétals allyliques de carbohydrates (hexèno-2 pyrannosides) avec réarrangement en éthers vinyliques (déoxy-3 glycals). Soumis à des conditions semblables, quelques alcools allyliques peuvent aussi être transformés en oléfines; il semble toutefois que la réaction ne s'applique qu'aux carbohydrates puisque la réaction ne se produit pas avec des alcools allyliques carbocycliques typiques.

On rationalise les résultats en faisant l'hypothèse qu'il y a formation d'un complexe intermédiaire oxygène–alane; ce complexe se formerait plus facilement avec un groupe hydroxyle (ou un ester) qu'avec l'oxygène d'un éther. Un oxygène axial permet plus facilement d'atteindre l'état de transition réactif qu'un oxygène équatorial. Le complexe conduit normalement à une réduction avec réarrangement impliquant un mécanisme S_N2' dans lequel l'hydrure qui approche et l'oxygène qui s'en va occupent une relation *syn*. Une alternative qui se présente, particulièrement quand la double liaison est flanquée par un groupe hydroxyle dans une position allylique et un groupe nucléofuge dans l'autre, implique un processus S_N2' anormal au cours duquel un ion hydrure s'approche en position vicinale et *cis* par rapport au groupe hydroxyle amenant l'expulsion du groupe nucléofuge. Le processus est toujours stéréospécifique mais il n'est pas toujours régiospécifique. [Traduit par le journal]

The vinyl ethers known in carbohydrate chemistry as glycals, are versatile synthons for a diverse array of saccharide derivatives (1). In a recent report from this laboratory, we reported the ready synthesis of the hitherto unknown 3-deoxy glycals (2) and, in subsequent publications, we demonstrated their synthetic utility (3) and examined some mechanistic aspects of the reaction by which they are produced (4). The present article reports in greater depth upon synthetic and mechanistic details of this reductive rearrangement.

Results

Reductive Rearrangements of Compounds 1–3.

In our first publication (2) we reported that use of high boiling ethereal solvent (dioxan > tetrahydrofuran > ether) caused remarkable improvement in the rate of the reductive rearrangements (*e.g.* **1** → **9**). The use of lithium aluminium deuteride (LAD) instead of lithium aluminium hydride (LAH) was also shown to be advantageous since it facilitated mechanistic interpreta-

[1]For preliminary reports on this topic see refs. 2–4.

[2]Taken in part from the Ph.D. Theses of B. K. Radatus and S. Y-K. Tam, University of Waterloo, 1971 and 1974, respectively.

[3]Revision received February 17, 1975.

Can. J. Chem. Downloaded from www.nrcresearchpress.com by 210.87.254.5 on 09/05/12
For personal use only.

TABLE 1. Reductive rearrangement of hex-2-enopyranosides with lithium aluminium deuteride in dioxan

Substrate	Product* C-1 control S	C-4 control T†	C-4 control U‡	Acyclic vinyl ethers
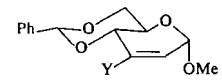 1 Y = H; 2 Y = CH_2OH	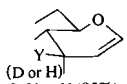 9 Y = H (95%); 10 Y = CH_2OH (87%)	—	—	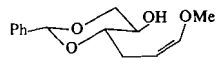 (D or H) 19 (3.9%)
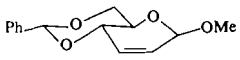 3	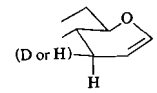 11 (82%)	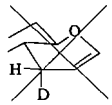 9	—	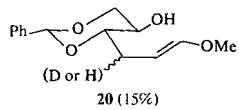 20 (15%)
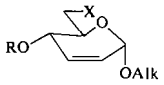 4 Alk = Me or Et	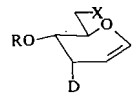 12 X = OR (90%) see footnote 6		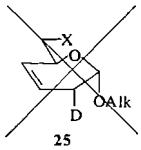 25	—
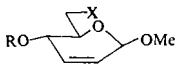 5	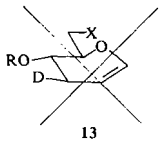 13	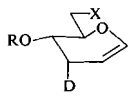 12 (35%)	—	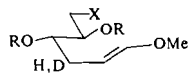 21 (21%)
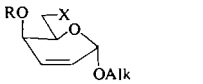 6 Alk = Me or Et	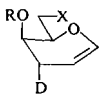 14 (22%)	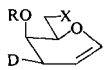 16 (22%)	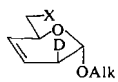 18 (10.5%)	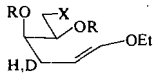 22 (9.1%)
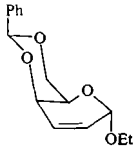 7	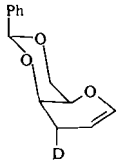 15 (11%)	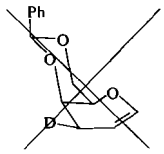 24	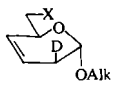 18 (77%)	—
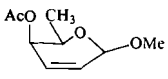 8	—	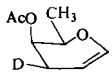 17	—	—

NOTE: *a* X = OH; R = H
b X = OAc; R = Ac
c X = H; R = Ac
d X = $OCPh_3$
e X = H; R = H
f X = OCOPh; R = H
*Percentages shown are for isolated products.
†"*M*" and "*N*" used in the preliminary publication (4) correlate with U and T, respectively.
‡See ref. 16.

tion via analysis of the n.m.r. spectra of the deuterated products. For these reasons, LAD in refluxing dioxan has been adopted for use in most of these studies. In this connection, it should be noted that reactions with LAD are usually much slower than with LAH, presumably because of isotope effects not presently understood (5).

Can. J. Chem. Downloaded from www.nrcresearchpress.com by 210.87.254.5 on 09/05/12
For personal use only.

Can. J. Chem. Downloaded from www.nrcresearchpress.com by 210.87.254.5 on 09/05/12
For personal use only.

Characterization of Products (see Table 1)

The progress of the reaction is readily followed on thin-layer chromatograms sprayed with sulfuric acid, whereupon the starting materials (*e.g.* **1–3**) char immediately in the cold to a black deposit, while the products (*e.g.* **9–11**) require heating in an oven before charring occurs. On the other hand, the products, but not the starting materials, are readily visualized by iodine vapor and the acyclic vinyl ethers such as **19** and **20** run much more slowly because of the free hydroxyl group. Hence a product running slower than the starting material, and which is visualized by iodine, is very likely to be an acyclic enol ether.

For the deuterated products **9**(D) and **11**(D) i.r. absorptions at 1645, 1233, and 1080 cm^{-1} and n.m.r. data (Table 2) provide standards for determining structural features of the other cyclic products shown in Table 1. Thus multiplets centered at τ 3.67 and 3.69, respectively, were appropriately located for H-1 of these glycals (6).

The definitive criteria for assigning the orientation of deuterium in **9**(D) and **11**(D) are the four-bond (J_{13}) and the three-bond (J_{23}) vinyl–allylic couplings. The former $|J_{13}|$ is larger and the latter $|J_{23}|$ smaller when the allylic proton is pseudoaxial than when it is pseudoequatorial. These criteria originally recognized by Garbisch (7) have been frequently supported, recently by ourselves, in a computer assisted study of a number of 3-substituted 3-deoxy glycals (8). The J_{13} values for **9**(D) and **11**(D) are -1.0 and -2.7 Hz, while the J_{23} values are 5.5 and 2.0 Hz, respectively. These are in agreement with the expected values and further support for the assigned structures is provided by the values for for J_{34} (9.5 and 6.0 Hz, respectively) which indicate diaxial and equatorial–axial relationships between the protons concerned.

Compounds **19** and **20** were also evidently vinyl ethers in view of the i.r. absorption at $\sim$1645 cm^{-1} and the presence of exchangeable protons in the n.m.r. suggested the free hydroxyl group. In the case of **19**, H-1 and H-2 were observed at τ 4.00 and 5.43, respectively, with a common coupling of 6.0 Hz indicative of *Z* arrangement. In **20**, H-1 and H-2 were at τ 3.57 and 5.10 with a common coupling of 13.0 Hz indicating *E* arrangement.

Reductive Rearrangements of Compounds 4–7

The α-D-diol **4***a* (Alk = Et) or its diacetate **4***b* (Alk = Et) gave only one product **12***a*, no trace of acyclic material being obtained. The acetylated product **12***b* was characterized by mass spectrometry and n.m.r. The anomeric β-D-olefin **5***b* gave the same cyclic ether **12***a* as well as the *trans*-triol **21***a*. The formation of **12***a* from **5***b* meant that the deuterium had added to the side of the molecule opposite to that vacated by the aglycon. Since this result was in contrast to that in substrates **1–4**, it was decided to examine other substrates having a *trans*-1,4-arrangement.

Compound **6***a* (Alk = Et) gave three cyclic products **14***a*, **16***a*, and **18***a* (Alk = Et) in 2:2:1 ratio, as well as the *trans*-triol **22**a. The products were separated by column chromatography except for the epimers **14***a* and **16***a* which travelled together. The H-1 signal in the n.m.r. spectrum of the mixture **14***a* and **16***a* was a deceptively simple doublet of doublets. H-2 was more complicated than "normal" but the prime indication of a mixture was the presence of two signals at τ 7.98 and 7.64 in the region appropriate for H-3. Confirmation was forthcoming from double irradiation of each signal which caused perturbations in the multiplets for H-1 and H-2. The signal to lower field is ascribed to the equatorial H-3 in **14***a*, in accordance with the expectation that the axial H-3 (in **16***a*) should resonate at higher field (9). The result is also in keeping with the studies of Hall and Manville (10) which show that an equatorial proton is deshielded, relative to its axial counterpart, by a vicinal hydroxyl group.

The structure of **18***a* (Alk = Et) was deduced by comparison with the analog prepared by deuterolysis of the methanesulfonate, **23** (11) followed by detritylation of the product **18***d* (Scheme 1). The alcohol so obtained, **18***a* (Alk = Me), gave superimposable n.m.r. spectra with that from the LAD reaction on **6***a* (Alk = Et) with the exception of the aglycon resonances.

The products from the benzylidenated derivative, **7**, were the previously encountered olefin **18***a* (Alk = Et) and compound **15** in a ratio of

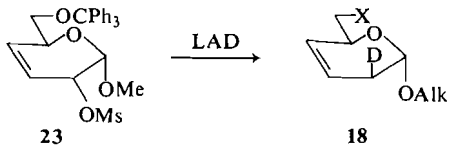

23 **18**

a X = OH
b X = OAc
d X = $OCPh_3$
Alk = Me or Et

SCHEME 1

Can. J. Chem. Downloaded from www.nrcresearchpress.com by 210.87.254.5 on 09/05/12
For personal use only.

TABLE 2. Proton magnetic resonance parameters for some 3-deuterio-3-deoxy glycals*

	Chemical shifts (τ)							J values (Hz)									
Compound	H_1	H_2	H_3	H_4	H_5	H_6	$H_{6'}$	J_{12}	J_{13}	J_{23}	J_{24}	J_{34}	J_{45}	J_{46}	J_{56}	$J_{56'}$	$J_{66'}$
9(D)	3.67	5.28	7.67	6.08	6.15–6.29		5.61	6.0	−1.0	5.5	—	6.0	9.0	—	10.0	4.5	−10.5
11(D)	3.69	5.29	7.76	6.08	6.15–6.29		5.62	6.0	−2.7	2.0	—	9.5	9.5	—	10.0	5.0	−10.5
12*a*	3.56	5.30	7.67	5.9	–	6.3		6.5	−1.0	4.0	†	†	†	†	†	†	†
12*b*	3.63	5.30	7.60	4.97	5.50–6.17			6.0	−1.0	5.0	—	7.5	8.5	†	†	†	†
14*a*	3.56	5.31	7.64	5.7	–	6.3		6.0	−1.0	5.0	†	†	†	†	†	†	†
14*b*	3.57	5.30	7.60	4.81	5.61–6.00			6.0	−1.0	4.6	1.2	1.0	small	†	†	†	†
16*a*	3.56	5.31	7.98	5.7	–	6.3		6.0	−2.1	~1.0	†	†	†	†	†	†	†
16*b*	3.57	5.30	7.60	4.81	5.61–6.00			6.0	−2.1	2.5	1.0	5.0	small	†	†	†	†
15	3.52	5.34	7.81	5.73	6.24	5.93	5.64	6.2	−1.0	5.0	1.3	1.0	1.0	0.5	1.5	1.7	−12.2

*Determined at 220 MHz in $CDCl_3$ (TMS). J values were read directly from spectra run at 250 Hz sweep width.
†Unresolved multiplet.

Can. J. Chem. Downloaded from www.nrcresearchpress.com by 210.87.254.5 on 09/05/12
For personal use only.

7:1. Benzyl alcohol-d_1 was isolated from the reaction products and identified by comparison of the n.m.r. spectrum of its acetate with that of benzyl acetate.

Discussion

Cyclic Products

The anomers **1** and **3** each gave only one cyclic product, **9** and **11**, respectively, results which seemed to suggest a classical S_N2' mechanism (12) operating through a transition state such as that depicted in **S** (2).[4] However, shortly after our preliminary report (2), Achmatowicz and Szechner (17) reported the interesting observation that with LAD in ether at room temperature, the *cis*-1,4-analogs **4***c* and **8** were readily rearranged to glycals **12***e* and **17**, respectively, whereas the *trans*-1,4-analogs **5***c* and **6***c* were unrearranged after 7 days at *room* temperature.

In view of the equatorial orientation of the methoxy group in their substrate **5***c*, failure to observe rearrangement in ether at *room temperature*[5], did not seem surprising in view of our earlier observation on the low reactivity of **3** in *boiling* diethyl ether (2). Low reactivity of these β-D-derivatives (**3**, **5**, and **8**) seemed entirely consistent with the S_N2' transition state **S**, since with these substrates the equatorial methoxy – AlH_3 complex is poorly poised for delivering the deuteride to carbon-3, an energy-demanding conformational change being required to bring the complex into axial orientation before optimal geometry is achieved. The improved reactivity of **3** in the higher boiling solvents, as reported earlier (2), is in keeping with this concept. We were therefore prompted to test the response of some *trans*-1,4-derivatives (diequatorial as well as diaxial) in boiling dioxan.

Added impetus for this study was given by the suggestion of Achmatowicz and Szechner (17) that the site for coordination of the aluminium was not the aglycon, as we had originally proposed, but the carbon-4 oxygen. In fact, this principle could not have been tested in their experiments, since the carbon-1 and carbon-4 oxygens in their reactive substrates (**4***c* and **8**) are in *cis* relationship! Clearly only with a *trans*-1,4-substrate is it possible to tell, from the orientation as well as the position of the deuterium in the product, whether the intermediate oxygen–aluminium complex had been formed at carbon-1 or carbon-4.

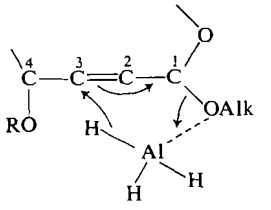

S
(classical S_N2')

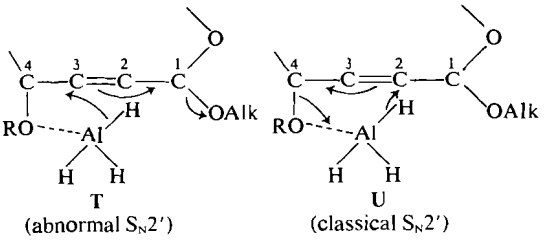

T (abnormal S_N2') U (classical S_N2')

Some observations relating the *cyclic* vinyl ethers obtained from reactions with LAD in boiling dioxan are summarized here.

(*i*) The olefinic acetals react whether the geometry of the oxygens is *cis*-1,4 or *trans*-1,4. Thus compounds **1**–**8** were all reductively rearranged (Table 1).

(*ii*) If the carbon-4 oxygen is an alcohol or ester which would be immediately converted to alkoxide by LAD, the abnormal S_N2' transition state T may be brought into operation.

[4]We have not done any experiments to determine the nature of the aluminium species in the intermediate complex. In our preliminary report (2) we suggested a pentacoordinate complex such as that favored by Eliel *et al.* (13). However, we are indebted to Professor W. Kraus (14) of the University of Tubingen, for suggesting in a private communication, that the tetracoordinate complex (*e.g.* **S**) would be more appropriate. This follows from the fact that the alane which is present in appreciable amounts in boiling solvents (15) is expected to be a better Lewis acid than AlH_4^- (15). Nevertheless it should be noted that a rearrangement (*p* to *q*) reported by Davis and Brown which is similar to those under discussion here, gives a different product (*r*) when pure alane is used as the reagent (16). *In any event, our mechanistic arguments remain the same whether the complex is pentacoordinate (with AlH_4^-) or tetracoordinate (with AlH_3).*

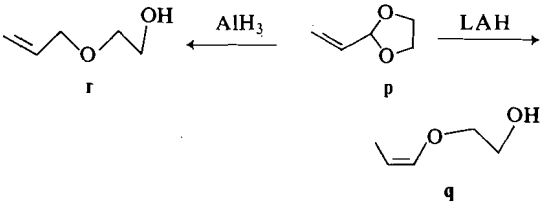

r p q

[5]In our hands, even the *cis*-1,4-derivatives **1**, **4***a*, or **4***b* do not rearrange in ether at *room temperature*, a period of heating being required to induce reaction.

Can. J. Chem. Downloaded from www.nrcresearchpress.com by 210.87.254.5 on 09/05/12
For personal use only.

(*iii*) If the carbon-4 oxygen is etherified the abnormal transition state **T** is apparently rendered inoperative. We have no explanation for this effect but two entries in Table 1 support this conclusion. Substrate **5***b* gave **12***a* but the related benzylidenated substrate **3** gave none of the corresponding product **9**. Similarly **6***a* gave **16***a* but upon benzylidenation **7** did not give any **24**.

(*iv*) An axial allylic oxygen permits easier attainment of the S_N2' transition state than does its equatorial counterpart. This conclusion follows from (*a*) the greater reactivity of substrates **1** and **2** as compared with **3** and (*b*) from the appreciable formation of **18** in the reactions of **6***a* and **7** as compared for example, with the absence of compound **25** in the reaction of **4***b*. Further support for observation *iv* is found in the course of reaction of **26** in which an axial oxygen is pitted against an equatorial oxygen (2). (Scheme 2) The reduction produces **27** via complexation at the axial oxygen (transition state **S**) but no **28** which would have arisen by complexation at the equatorial oxygen (transition state **U**).[6,7]

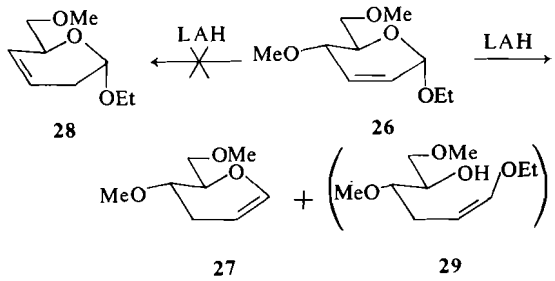

SCHEME 2

(*v*) The formation of **18***a* from **6***b* or **7** indicates that the allylic oxygen lost in the reductive rearrangement may be a simple allylic alcohol and not necessarily a member of an acetal functionality. Further support for observation *v* is found in the formation of **32** and **33** from substrates **30** and **31** respectively (Scheme 3). Under the

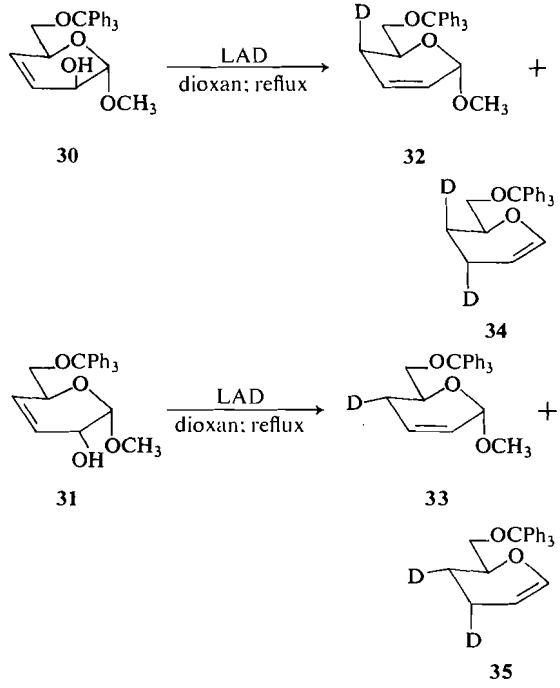

SCHEME 3

reaction conditions, the primary products react further giving dideuterated products **34** and **35**, respectively. However, neither 1- nor 4-cholesten-3-ol reacted with LAD in refluxing dioxan.

(*vi*) Considered in relation to the operative transition state, the reactions are always stereospecific, since there is a definite and exclusive correlation between the configuration of substrates and products (19). However, the reactions are not always regiospecific (20).

The transformations **1** → **9** and **3** → **11** are clearly both stereo- and regiospecific and this conclusion suggests that there is only one transition state (**S**) in operation. In the case of **6**, two of the products (**14** and **16**) are epimers which at first sight might suggest a nonstereospecific process. However, in view of the weight of evidence from the other entries in the Scheme, formation of the epimers **14** and **16** may be rationalized as occurring stereospecifically through different transition states **S** and **T**, respectively. The carbon-4 complex decomposes in a nonregiospecific manner thereby producing both **16** and **18**.

[6]This result could, however, be influenced by other forces; thus, it has been proposed that the course of hydrogenolysis of acetals is dependent on a stabilized oxocarbonium ion intermediate (18). If so, the ring-oxygen will clearly favor the development of transition state "**S**" It will be of interest in the future to pit axial against equatorial oxygens, in less equivocal circumstances.

[7]Compound **12** could be formed from **4** via either transition state **S** or T. Our present results do not allow for any distinction between the two.

Can. J. Chem. Downloaded from www.nrcresearchpress.com by 210.87.254.5 on 09/05/12
For personal use only.

Acyclic Products

With regard to the acyclic products **19–22** and **29** correlation between their geometry and those of their progenitors, is very straightforward. If the 1,4-oxygens in the substrate are *cis*-related, the acyclic enol ether produced is itself *cis*; if *trans* in the substrate, the product is *trans*. The reasons for this regularity are not currently understood and experiments are underway to determine the basis for this correlation.

The transition state **T**, whereby products **12**, **16**, and **17** are formed, is reminiscent of that (**36**) operating in the hydrogenation of phenylallyl alcohols by LAH in refluxing tetrahydrofuran (21). These rearrangements all proceed via abnormal S_N2' five-center transition states, which are successful because of the intermediacy of a resonance-stabilized benzylic carbanion **37** in one case and because of the presence of a good leaving group in the other (see **T**) (Scheme 4).

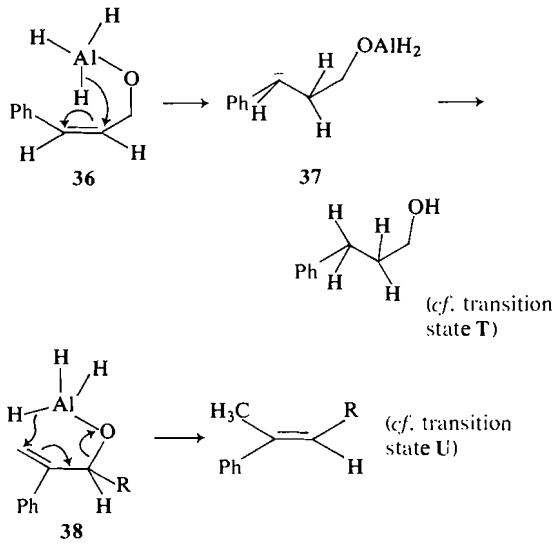

SCHEME 4

In **36**, the hydride ion is donated to the proximate end of the double bond with the formation of the benzylic carbanion which is quenched subsequently by a proton. In the case of **5*b***, **6*a***, and **8**, the double bond moves over, ejecting the aglycon.

The "normal" S_N2 transition state **38** corresponding to **U** is observed with the formation of olefins from 2-phenylallyl alcohols.

In summary reductive rearrangement of hex-2-enopyranosides by LAH or LAD in ethereal solvents is a stereospecific reaction giving rise to cyclic and/or acyclic vinyl ethers. With hex-3-enopyranosides, reductive rearrangement of the allylic alcohol also takes place. The geometry of the acyclic vinyl ether products is strictly correlated with the relative configuration of the 1,4-allylic oxygens; *i.e.* *trans*-substrate giving *trans*-enol ether and *cis* giving *cis*.

The presence of an axial substituent at C-1 or C-4 greatly facilitates the achievement of an S_N2' transition state **S** or **U**, which leads to the 1,2- or 3,4-olefin, respectively. Appropriate with this principle, equatorial oxygens at these sites either retard or inhibit completely the formation of the related transition states, as judged by slow formation or absence, of the congruent products.

An allylic alkoxide generated *in situ* from an alcohol or an acetate is a prime site for complexation with the aluminium species[4] and delivers the hydride ion in a *cis* manner to the proximate end of the double bond, via transition state "**T**".

Experimental

General

Melting points were determined on a Fischer-Johns heating stage or a Mel-Temp apparatus and are uncorrected. The n.m.r. spectra whose analyses are given in Tables 2 and 3 were recorded using a Varian T-60, a Varian HA 100, or a Varian HR 220 spectrometer and unless otherwise specified, the solvent was deuteriochloroform containing 1% tetramethylsilane as internal standard. Coupling constants (in Hz) were obtained by measuring spacings of spectra judged to be first order. All geminal and allylic (through four bonds) couplings were assigned negative signs as predicted for these systems (7, 8, 23).

Infrared spectra were determined on a Beckman model IR 5 spectrometer using 0.1 mm sodium chloride solution cells (chloroform as solvent) and silver chloride plates for smears. Mass spectra were determined on a Hitachi Mass Spectrometer model RMU-6E.

Thin-layer chromatography was performed on glass plates coated with silica gel (HF-254, E. Merck) to a thickness of 0.3 mm. The solvent systems used were (*A*) ethyl acetate and (*B*) petroleum ether (35–60 °C) – ethyl acetate (4:1). The chromatograms were first viewed under u.v. light, then exposed to iodine vapor, and finally sprayed with concentrated sulfuric acid. With the latter the starting materials char instantly in the cold to a black deposit but the products either fail to char or char very faintly to a brown residue. Heating in an oven is required for complete visualization. On the other hand, the glycal products, but not the starting materials, are rapidly visualized by iodine vapor.

For column chromatography, E. Merck Silica Gel (0.05–0.20 mm, 70–325 mesh A.S.T.M.) was used. Dioxan, diethyl ether, and tetrahydrofuran were dried with benzophenone ketyl (24).

General Experimental Procedure

The general procedure below is described for reactions

TABLE 3. Proton magnetic resonance parameters of some unsaturated sugars*

Substrate	Chemical shifts (τ) H_1	H_2	H_3	H_4	H_5	$H_6H_{6'}$	*J* values (Hz)
6*a*	4.93	4.07	3.82		5.75–6.30		$J_{12} = 2.2$
6*f*	4.93	4.07	3.79	6.09	5.20–5.80		$J_{23} = 10.0$
6*h*	4.84	3.95	3.72	4.64	5.24–5.66		$\|J_{24}\| < 0.3$
6*i*	4.84	3.91	3.74	4.69	5.32–5.66		$J_{34} = 5.0'$
							$J_{45} = 2.0$
18*a* (Alk = Et)	4.94	7.94	4.20	4.39	5.62	6.20–6.40	$J_{12} < 1$
18*a* (Alk = Me)	5.06	7.94	4.20	4.39	5.62	6.20–6.40	$J_{23} = 4.5$
18*d* (Alk = Me)	5.10	7.99	4.23 with satellites		5.67	6.60–6.90	$J_{24} = -1.5$
18*b* (Alk = Et)	4.97	7.94	4.07	4.34	5.40–6.00		$J_{34} = 10.0$
							$J_{35} = -2.0$
							$J_{45} = 1.5$
32	5.13	4.33	4.04	8.20	5.87	6.7–7.0	$J_{12} = 2.2; J_{23} = 10.0; J_{34} = 5.0;$ $J_{13} = J_{24} = -0.3; J_{45}$ unresolved
33	5.13	4.33	4.05	8.20	5.87	6.7–7.0	$J_{12} = 2.0; J_{23} = 10.00; J_{34} = 1.5;$ J_{13} small; $J_{24} = -2.0; J_{45}$ unresolved
34	3.60	5.35	8.15		5.87	6.7–7.0	$J_{12} = 6.0$
35	3.60	5.35	8.15		6.0	6.7–7.0	$J_{23} = 5.0$
							$J_{13} = -1.0$
							J_{24} unresolved

*Determined at 100 MHz in $CDCl_3$ (TMS).

using lithium aluminium deuteride (LAD) in refluxing dioxan. However LAH, ether, or tetrahydrofuran can be substituted, without changing the product composition. In general, reactions with LAH go faster than those with LAD; on the other hand, the lower boiling solvents cause the reaction to be much slower than with dioxan.

In a typical experiment, the substrate (3 mmol) was dissolved in dry dioxan (25 ml) and LAD (0.38 g, 9 mmol) was added with efficient stirring with a magnetic stirrer – hot plate. The mixture was brought to gentle reflux and the progress of the reaction was followed by t.l.c. (see General). Upon completion, the method of work up *a* or *b*, depended upon the substrate. *a*) For the benzylidenated materials the excess LAD was destroyed by addition of a minimum amount of water and the aluminium hydroxide was removed by filtration through a bed of Celite. The filtrate was dried and evaporated under reduced pressure whereupon most of the compound usually crystallized. The products were recovered by recrystallization and/or silica column chromatography as described for the individual cases below. (*b*) If the substrate was an acetate or alcohol, the excess LAD was destroyed by dropwise addition of ethyl acetate. The salts were removed by filtration through Celite and the residue washed generously with ethyl acetate. (The product sometimes adheres strongly to the aluminium salts, in which case, the filter cake was stirred overnight with ethyl acetate.) The ethyl acetate filtrate was evaporated and the residue which still contains aluminium salts, was acetylated with acetic anhydride and pyridine. The ether soluble acetylated product is then recovered in the usual way and treated as described for the individual cases below.

Reactions of Methyl 4,6-O-Benzylidene-2,3-dideoxy α-D-erythrohex-2-enopyranoside, 1

4,6-O-Benzylidene-1,2,3-trideoxy-D-erythro-hex-1-enopyranose, 9(H)

Compound **1** (2.48 g, 0 01 mol) was treated with LAH (0.15 g) in refluxing dioxan for 0.5 h. The product isolated by procedure *a* was crystalline and its t.l.c. indicated two components (R_f 0.63 (major) and 0.31 (minor)) in solvent system *B*. Upon recrystallization from ethanol, the minor component remained in the mother liquor. The mother liquor was put on a short silica column (10 cm × 1.8 cm), eluted with solvent system *B*, and both components were separated to give a total 2.08 g (95% of cyclic compound 9(H)).

Compound **9**(H) was recrystallized from ethanol, m.p. 113–114 °C; $[\alpha]_D^{23}$ + 65.9° (*c*, 10.7 in $CHCl_3$); *m/e* = 218.

Anal. Calcd. for $C_{13}H_{14}O_3$: C, 71.54; H, 6.47. Found: C, 71.74; H, 6.43.

The 220 MHz n.m.r. data for compound 9(H) are: τ 2.60 (m, 5, Ph), 4.38 (5, 1, PhC*H*), 3.65 (dt, 1, $J_{12} = 6.0$, $J_{13} = -2.7$, $J_{13'} = -1.0$, H-1), 5.27 (m, 1, $J_{23} = 2.5$, $J_{23'} = 5.5$, H-2), 7.75 (calcd.) (m, 1, $J_{34} = 9.5$, $J_{33'} = -16.0$, H-3), 7.66 (calcd.) (m, 1, $J_{3'4} = 6.0$, H-3′), 6.11 (m, 1, $J_{45} = 9.0$, H-4), 6.16–6.31 (m, 2, $J_{56a} = 10.0$, $J_{56e} = 4.5$ (assumed), H-5, −6*a*), 5.63 (m, 1, $J_{6a6e} = -10.5$, H-6*e*); $\nu_{max}(CHCl_3)$ 1645, 1233, 1080 cm^{-1}.

4,6-O-Benzylidene-2,3-dideoxy-1-O-methyl-D-erythro-cis-hex-1-enose, 19(H)

The chromatogram described above afforded 0.98 g

Can. J. Chem. Downloaded from www.nrcresearchpress.com by 210.87.254.5 on 09/05/12
For personal use only.

Can. J. Chem. Downloaded from www.nrcresearchpress.com by 210.87.254.5 on 09/05/12
For personal use only.

(3.9%) of the minor product **19**(H). The structure was assigned on the basis of its molecular ion (*m/e* = 250); i.r.: ν_{max}(CHCl$_3$) 1645 cm^{-1}; n.m.r.: τ 2.60 (m, 5, Ph), 4.57 (s, 1, PhC*H*), 6.47 (s, 3, OCH$_3$), 4.00 (bd, 1, J_{12} = 6.0, H-1), 5.43 (td, 1, J_{23} = $J_{23'}$ = 7.0, H-2), 7.47 (m, 2, H-3, −3′), 6.53–6.80 (m, 5, H-4, -5, -6, -6′, OH).

Satisfactory microanalytical data could not be obtained for compound **19**(H).

*4,6-O-Benzylidene-1,2,3-trideoxy-3-deuterio-*D*-ribo-hex-1-enopyranose, 9(D)*

When compound **1** was treated as above with LAD instead of LAH, the reaction required 5 h for completion. The product, **9**(D), was isolated as above and recrystallized from ethanol, m.p. 113–114 °C; $[\alpha]_D^{23}$ +42.5° (*c*, 7.70 in CHCl$_3$); *m/e* = 219. The n.m.r. data for **9**(D) are shown in Table 1. The i.r. shows ν_{max}(CHCl$_3$) 2153 and 1645 cm^{-1}.

*Reactions of Methyl 4,6-O-Benzylidene-2,3-dideoxy-3-C-hydroxymethyl-α-*D*-erythro-hex-2-enopyranoside, 2*

*4,6-O-Benzylidene-1,2,3-trideoxy-3-C-hydroxymethyl-*D*-arabino-hex-1-enopyranose, 10(H)*

Compound **2** (0.262 g, 0.94 mmol) was dissolved in dry ether (60 ml) and LAH (0.1 g) added. The mixture was refluxed with constant stirring for 1 h when t.l.c. indicated completion. Upon isolation by process *a* (see General), compound **10**(H) was obtained (0.204 g, 87% yield) as a crystalline substance. After recrystallization from carbon tetrachloride, m.p. 138–140 °C; $[\alpha]_D^{23}$ −57.2° (*c*, 8.6 in CHCl$_3$); n.m.r.: τ 2.60 (m, 5, Ph), 4.68 (s, 1, PhC*H*), 8.02 (bs 1, exchangeable, OH), 3.73 (q, 1, J_{12} = 7.0, J_{13} = −2.5, H-1), 5.37 (q, 1, J_{23} = 2.0, H-2), 7.35 (m, 1, J_{37} = $J_{37'}$ = 5.5, H-3), 6.03–6.23 (m, 3, H-4, -5, -6*a*), 5.58 (q, 1, J_{6a6e} = −10.5, H-6*e*), 6.26 (m, 2, H-7, -7′); i.r.: ν_{max}(CHCl$_3$) 1645 cm^{-1}.

Anal. Calcd. for $C_{14}H_{16}O_4$: C, 67.72; H, 6.50. Found: C, 67.62; H, 6.21.

*Reactions of Methyl 4,6-O-Benzylidene-2,3-dideoxy-β-*D*-erythro-hex-2-enopyranoside, 3*

*4,6-O-Benzylidene-1,2,3-trideoxy-*D*-erythro-hex-1-enopyranose, 11(H)*

Compound **3** (2.48 g, 0.01 mol) was treated with LAH (0.15 g) in dry dioxan (30 ml) under reflux for 20 h. The t.l.c. (solvent system *B*) and n.m.r. of the isolated crystalline material indicated two components. The n.m.r. indicated that compound **11**(H) (*vide supra*) accounted for 82% of the reaction product. Most of the material was recovered by fractional crystallization and the mother liquors were chromatographed using the solvent system *B*.

*4,6-O-Benzylidene-2,3-dideoxy-1-O-methyl-*D*-erythro-trans-hex-1-enose, 20(H)*

The above chromatogram afforded (410 mg) of compound **20**(H) which was recrystallized from methanol, m.p. 76–78 °C; $[\alpha]_D^{23}$ −36.2° (*c*, 3.6 in CHCl$_3$). The 220 MHz n.m.r. spectrum of compound **20**(H) afforded the following data: τ 2.60 (m, 5, Ph), 4.58 (s, 1, PhC*H*), 6.45 (s, 3, OCH$_3$), 8.03 (bs, 1, exchangeable OH), 3.57 (d, 1, J_{12} = 13.0, J_{13} = $J_{13'}$ < −0.5 H-1), 5.10 (dt, 1, J_{23} = $J_{23'}$ = 7.5, H-2), 7.64 (m, 1, J_{34} = 7.5, $J_{33'}$ = −15.0, H-3), 7.48 (m, 1, $J_{3'4}$ = 4.0, H-3′), 6.20–6.49 (m, 3, H-4, -5, -6), 5.72 (q, 1, $J_{56'}$ = 4.5, $J_{66'}$ = −10.5, H-6′).

Anal. Calcd. for $C_{14}H_{18}O_3$: C, 67.18; H, 7.25. Found: C, 67.02; H, 6.71.

*4,6-O-Benzylidene-1,2,3-trideoxy-3-deuterio-*D*-arabino-hex-1-enopyranose, 11(D)*

Compound **3** (0.250 g, 0.001 mol) was treated with LAD (0.015 g) in dry dioxan (10 ml) under reflux for 2 days. The product was isolated by procedure *a*. The n.m.r. indicated that compound **11**(D) (*vide supra*) accounted for 86% of the reaction product. Most of the material was recovered by fractional crystallization and the mother liquors were chromatographed using the solvent system *B*.

Compound **11**(D) was recrystallized from ethanol, m.p. 117–119 °C; $[\alpha]_D^{23}$ +43.5° (*c* 6.6 in CHCl$_3$); *m/e* = 219. Its n.m.r. parameters are shown in Table 2; the i.r. spectrum shows ν_{max}(CHCl$_3$) 2153, 1645 cm^{-1}.

Anal. Calcd. for $C_{13}H_{13}DO_3$: C, 71.21; H and D, 6.90. Found: C, 71.15; H and D, 6.65.

*4,6-O-Benzylidene-2,3-dideoxy-3-deuterio-*D*-arabino-hex-1-enopyranose, 20(D)*

The chromatogram described above afforded 315 mg of **20**(D) which decomposed readily. The n.m.r. parameters were: τ 2.60 (m, 5, Ph), 4.55 (s, 1, PhC*H*), 6.50 (s, 3, OCH$_3$), 3.60 (d, 1, J_{12} = 13.0, J_{13} = −1.0, H-1), 5.13 (q, 1, J_{23} = 7.0, H-2), 7.70 (m, 1, H-3), 7.60 (bs, 1, exchangeable, OH), 5.73–6.70 (m, 4, H-4, -5, -6, -6′).

*Reaction of Ethyl 2,3-Dideoxy-α-*D*-erythro-hex-2-enopyranoside, 4a, or its Diacetate, 4b*

*1,2,3-Trideoxy-3-deuterio-*D*-ribo-hex-1-enopyranose, 12a, and its Diacetate, 12b*

Compound **4***a* (1.74 g, 0.01 mol) or **4***b* (2.58 g, 0.01 mol) was treated with LAD (1.20 g) in dry dioxan (50 ml) under reflux for 24 h when t.l.c. indicated the complete absence of starting material and the presence of a single new substance. The product, **12***a*, was isolated by procedure *b* (see General) and esterified with acetic anhydride (1 ml) and pyridine (5 ml) overnight. After customary work-up the ester was purified by passage down a silica column (10 cm × 1.9 cm). The product was a syrup: $[\alpha]_D^{23}$ +115.6° (*c*, 4.05 in CHCl$_3$); *m/e* = 215. The n.m.r. data for compounds **12***a* and **12***b* are shown in Table 2. The i.r. spectrum shows ν_{max}(CHCl$_3$) 2153, 1645 cm^{-1}.

*Methyl 4,6-Di-O-acetyl-2,3-di-O-methanesulfonyl-β-*D*-glucopyranoside*

The di-*O*-methanesulfonate (11.0 g, 0.025 mol) of methyl 4,6-*O*-benzylidene-β-D-glucopyranoside (25) was stirred with a mixture of water (240 ml), dioxan (360 ml), and concentrated sulfuric acid (30 g) at 60 °C for 1.5 h. Barium sulfate was then added to neutralize the acid and after filtering the insoluble material, the filtrate was extracted with petroleum ether (30–60 °C) twice to remove benzaldehyde. Evaporation of the water afforded a thick syrup which crystallized upon trituration with methanol. A portion (5.0 g) of the product was treated with acetic anhydride (30 ml) and pyridine (30 ml) at 0 °C for 5 h. Upon customary work-up, the title compound was obtained (5.7 g, 93% yield) as a crystalline substance. After recrystallization from chloroform – petroleum ether (30–60 °C), m.p. 144 °C; $[\alpha]_D^{23}$ − 31.9° (*c*, 1.0 in CHCl$_3$); *m/e* = 434.

Anal. Calcd. for $C_{13}H_{22}O_{12}S_2$: C, 35.96; H, 5.07; S, 14.77. Found: C, 36.25; H, 5.06; S, 14.79.

Can. J. Chem. Downloaded from www.nrcresearchpress.com by 210.87.254.5 on 09/05/12
For personal use only.

Methyl 4,6-Di-O-acetyl-2,3-dideoxy-β-D-erythro-hex-2-enopyranoside, 5b

Methyl 4,6-di-*O*-acetyl-2,3-di-*O*-methanesulfonyl-β-D-glucopyranoside, (5.7 g, 0.013 mol) was added to an efficiently stirred mixture of potassium iodide (1.1 g, 0.066 mol) and zinc–copper couple (4.16 g) in 40 ml of dimethylformamide. After 1 h the product, isolated in the previously described manner (26), afforded 2.5 g of material which on thin-layer chromatography (ethyl acetate–petroleum ether (30–60 °C) (1:1) as solvent) revealed two components of R_f 0.34 (**A**) and 0.52 (**B**), the latter being the major one. Treatment of the mixture with acetic anhydride and pyridine in the usual way gave **B** as the sole component. Silica column chromatography of the acetylation products afforded 2.5 g (78% yield) of **5b** (*m/e* 244). For the corresponding di-*O*-*p*-nitrobenzoate, m.p. 132.5 °C.

Anal. Calcd. for $C_{21}H_{18}O_{10}N_2$: C, 55.03; H, 3.96; N, 6.11. Found: C, 55.33; H, 4.01; N, 6.28.

Reaction of Methyl 4,6-Di-O-acetyl-2,3-dideoxy-β-D-erythro-hex-2-enopyranoside, 5b

1,2,3-Trideoxy-3-deuterio-D-ribo-hex-1-enopyranose, 12a, and its Di-O-acetate, 12b

Compound **5b** (1 g, 0.004 mol) was treated with LAD (425 mg, 0.010 mol) in dry dioxan (20 ml) under reflux for 30 h. The reaction was then worked-up by procedure *b* and esterified with acetic anhydride (3 ml) and pyridine (6 ml) overnight. After usual work-up the mixture showed two components (R_f 0.32 and 0.25) on t.l.c. in solvent system *B*. The mixture was easily separated on a silica column to give 305 mg (35%) of the previously encountered diacetate, **12b**.

4,5,6-Tri-O-acetyl-2,3-dideoxy-1-O-methyl-D-erythro-trans-hex-1-enose, 21b

The second compound from the chromatogram described above was the acyclic product **21b** (247 mg, 21%). The structure was assigned on the basis of its peaks in the mass spectrum at 229, 169, 127 for $M^+ - (HOAc)$, $M^+ - (HOAc)_2$, and $M^+ - ((HOAc)_2 + CH_2CO)$, respectively; i.r.: $\nu_{max}(CHCl_3)$ 1645 cm^{-1}, n.m.r.: τ 6.47 (s, 3, OCH_3), 3.63 (bd, 1, $J_{12} = 13.0$, $J_{13} = -1.0$, H-1) 5.20 (dd, 1, $J_{23} = 8.0$, H-2) 7.80 (m, 1, H-3), 4.65–5.10 (m, 2, H-4 and H-5) 5.66–6.05 (m, 2, H-6 and -6′) 7.90 (3s, 9, 3-OAc).

Ethyl 2,3-Dideoxy-α-D-threo-hex-2-enopyranoside, 6a

The title compound **6a** was obtained from diol **4a** by a modification of Ferrier's procedure (27). Methanesulfonyl chloride (6.6 ml, 0.086 mol) was added slowly to a cold (0 °C) and efficiently stirred solution of the diol **4a** (5 g, 0.029 mol) in dry pyridine (60 ml). After 5 h at 0 °C, the solution was poured slowly into about 200 ml ice water with vigorous stirring. The precipitated product **4g** was filtered and washed repeatedly with water until the washings were neutral and then dried overnight in a vacuum oven at ~35 °C. The dried material weighed 6.9 g (73% yield); m.p. 68.5–69.5 °C; $[\alpha]_D^{23}$ +71.9° (*c*, 1 in $CHCl_3$); R_f 0.53 in 50% EtOAc – petroleum ether (30–60°C); n.m.r.: τ 6.90, 6.92 (2 singlets, 6, 2 × OSO_2CH_3) 4.92 (bs, 1, $J_{12} = 2.0$, H-1) 4.08 (td, 1, $J_{23} = 10.0$, $J_{24} = -2.0$, H-2) 3.88 (dd, 1, $J_{34} = 1.5$, H-3), 4.75 (m, 1, $J_{45} = 9.0$, H-4), 5.77 (m, 1, H-5) 5.52 (with satellites, 2, $J_{66'} = -9.5$, H-6, -6′).

To a warm (~80 °C) mechanically stirred solution of the dimesylate **4g** (6.9 g, 0.021 mol) in dimethylformamide (900 ml), was added slowly, sodium benzoate (14.4 g, 0.1 mol). The mixture was then heated using a heating mantle up to 115 °C. After 12 h at that temperature the reaction mixture was allowed to cool and then filtered through a bed of Celite. The filtrate was washed with methylene chloride (~400 ml). Evaporation of the filtrate and washings afforded a thick syrup, which on t.l.c. (50% EtOAc – petroleum ether), showed four spots (R_f 0.71 (**6h**) 0.49 (**6i**) 0.38 (**6j**), and 0.30 (**6f**)). However, if the reaction was kept at 80 °C for 37 h only **6h** and **6i** in a ratio 5:9, were the products. In any case, the product mixture was easily separated on a silica column using petroleum ether (30–60 °C) – ethyl acetate (1:1) as eluent. Compounds **6h** and *f* and **6i** and *j* were separately combined, weighing 3.0 and 2.7 g, respectively. The mixture of **6i** and *j* was then treated with sodium benzoate (5.2 g) in dimethylformamide (450 ml) in the same manner as described above. From this reaction, 2 g of mixture of **6h** and *f* was isolated.

The mixture (5 g) of compounds **6h** and *f* obtained from above, was treated with methanol (150 ml), triethylamine (40 ml), and water (120 ml). After stirring at room temperature for 28 h, the solvents were evaporated off leaving a solid residue (4 g). Recrystallization from ethyl acetate – petroleum ether afforded 1 g of pure **6a**, m.p. 76–77 °C; $[\alpha]_D^{23}$ −77.3 (*c*, 1.0 in $CHCl_3$). The mother liquid was mainly **6a** as judged from its n.m.r.; the data are shown in Table 3.

Anal. Calcd. for $C_8H_{14}O_4$: C, 55.16; H, 8.10. Found: C, 55.04; H, 8.27.

Reaction of Ethyl 2,3-Dideoxy-α-D-threo-hex-2-enopyranoside, 6a, or its monobenzoate, 6f

1,2,3-Trideoxy-3-deuterio-D-arabino-hex-1-enopyranose, 14a, 1,2,3-Trideoxy-3-deuterio-D-ribo-hex-1-enopyranose, 16a, and their Acetates, 14b and 16b

Compound **6a** (400 mg, 0.0023 mol) or **6f** (640 mg, 0.0023 mol) was treated with LAD (240 mg, 0.0057 mol) in refluxing dioxan for 4 h. The reaction was worked-up by procedure *b*. The product mixture showed three components (R_f 0.45, 0.20, and 0.14) on t.l.c. in solvent system *A*. After silica column chromatography with ethyl acetate as solvent, the material of R_f 0.20 was found to be a mixture of epimers **14a** and **16a** (see Discussion on reductive rearrangement of compounds **4**–**7**). Acetylation of the mixture afforded **14b**, **16b** (both have R_f 0.31 in solvent system *B*) with a total weight of 201 mg (43.5% yield).

The n.m.r. data for compounds **14a**, **16a** and their acetates, **14b** and **16b**, obtained from the analysis of the

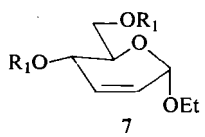

7

a R_1 = H
b R_1 = Ms

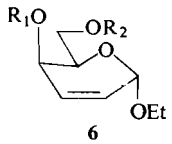

6

	R_1	R_2
a	H	H
h	PhCO	PhCO
i	PhCO	Ms
j	Ms	H
f	H	PhCO

Can. J. Chem. Downloaded from www.nrcresearchpress.com by 210.87.254.5 on 09/05/12
For personal use only.

220 MHz n.m.r. spectrum of the two mixtures, are shown in Table 2; the i.r. shows $\nu_{max}(CHCl_3)$ 1645 cm^{-1}.

*Ethyl 2,3,4-Trideoxy-2-deuterio-α-D-threo-hex-3-enopyranoside, **18a**, and its acetate, **18b***

The chromatogram described above afforded 40 mg (10.5%) of the substance of R_f 0.45. The structure **18a**, was first assigned on the basis of the similarity of its n.m.r. spectrum to that of other 3,4-unsaturated glycosides. Later it was confirmed by comparison with the methyl analog **18a** (Alk = Me) synthesised as described below. Acetylation of **18a** with acetic anhydride and pyridine gave **18b** (R_f 0.38 in solvent system *B*). The n.m.r. data for compounds **18a** and **18b** are shown in Table 3.

*2,3-Dideoxy-1-O-methyl-D-threo-trans-hex-1-enose, **22a** and its triacetate, **22b***

The slowest-running compound **22a** (R_f 0.14) from the chromatogram described above after acetylation weighed 63 mg (9.1%) **22b** (R_f 0.24 in solvent system *B*); i.r. $\nu_{max}(CHCl_3)$ 1645 cm^{-1}; n.m.r.: τ 3.73 (d, 1, J_{12} = 13.0, H-1), 5.37 (dd, 1, J_{23} = 8.0, H-2), 7.80 (m, 1, H-3), 4.98 (dd, 1, J_{34} = 7.0, J_{45} = 4.0, H-4) 4.73 (m, 1, H-5) 5.95 (dd, J_{56} = 6.5, $J_{66'}$ = −12.2, H-6) 5.70 (dd, $J_{56'}$ = 6.5 H-6′). The material was not crystalline.

*Methyl 2,3,4-Trideoxy-6-O-trityl-2-deuterio-α-D-threo-hex-3-enopyranoside, **18d***

Methyl 3,4-dideoxy-2-*O*-methanesulfonyl-6-*O*-trityl-α-D-*erythro*-hex-3-enopyranoside, **23** (11) (1 g, 2 mmol) was treated with LAD (160 mg) in refluxing dioxan (25 ml) for 7 h. The product, **18d**, isolated by procedure *a* (see General), was purified on a silica column with solvent system *B* as eluent. After recrystallization from ethanol, m.p. 102–103 °C; *m/e* 387; $[\alpha]_D^{23}$ +8.9° (*c*, 1 in $CHCl_3$). The n.m.r. data are shown in Table 3.

Anal. Calcd. for $C_{26}H_{27}O_3$: C, 80.59; H, 7.00. Found: C, 80.48; H, 6.99.

*Methyl 2,3,4-Trideoxy-2-deuterio-α-D-threo-hex-3-enopyranoside, **18a***

Chloroform (10 ml) was cooled down to about −5 °C and hydrogen chloride gas slowly bubbled through for 10 s. The cold HCl–$CHCl_3$ solution (5 ml) was then added to a solution of the compound **18d** (250 mg) in 10 ml of cold chloroform, and the resulting solution stirred at −10 °C for half an hour. After quenching with solid sodium bicarbonate and filtration, the solution was evaporated to dryness and the residue purified on a silica column with ethyl acetate – petroleum ether (30–60 °C) (1:1) as eluent. The product **18a** (Alk = Me) isolated has a superimposable n.m.r. spectrum with that of the ethyl analog **18a** (Alk = Et) except for the aglycon resonances. The n.m.r. parameters are shown in Table 3.

*Ethyl 4,6-O-Benzylidene-2,3-dideoxy-α-D-threo-hex-2-enopyranoside, **7***

Crude **6a** (3 g) was treated with α,α-dimethoxytoluene (10 ml) and dimethylformamide (75 ml). Toluenesulfonic acid was then added to the stirred solution to achieve ~p*H* 2. After 25 min, saturated sodium bicarbonate solution was added to quench the reaction. The mixture was then extracted with chloroform and the extract was washed with water and dried with anhydrous sodium sulfate. Evaporation of the solvent with a high vacuum pump left a thick syrupy residue, which was purified on a silica column with solvent system *B* to give 780 mg of pure **7** and 2 g of mixture of **7** and an unidentified side product.

Compound **7** was recrystallized from ether, m.p. 145–146. 5 °C; *m/e* 262.

Anal. Calcd. for $C_{15}H_{18}O_4$: C, 68.69; H, 6.92. Found: C, 68.57; H, 6.78.

*Reaction of Ethyl 4,6-O-Benzylidene-2,3-dideoxy-α-D-threo-hex-2-enopyranoside, **7***

*4,6-O-Benzylidene-1,2,3-trideoxy-3-deuterio-D-xylo-hex-1-enopyranose, **15***

Compound **7** (780 mg, 0.003 mol) was treated with LAD (400 mg, 0.0095 mol) in refluxing dioxan (25 ml) for 8 h. The reaction was worked-up by procedure *a* and esterified with acetic anhydride (5 ml) and pyridine (5 ml) overnight. After customary work-up, the residue was tested on t.l.c. and shown to contain two components (R_f 0.42 and 0.20 with $CHCl_3$ as solvent). Purification on a silica column with chloroform as eluent afforded 11 mg pure **15**, 350 mg of a mixture of **15** and **18a**, and 200 mg of pure **18a**. The ratio of **15** to **18a** in the total mixture was about 1:7. The n.m.r. parameters for **15** shown in Table 2, support the assigned structure (see Discussion).

Compound **15** was recrystallized from hexane, m.p. 98–99 °C; $[\alpha]_D^{23}$ +162.3° (*c*, 2 in $CHCl_3$).

Anal. Calcd. for $C_{13}H_{13}DO_3$: C, 71.21; H, 6.90. Found: C, 71.30; H, 6.87.

In addition to compounds **15** and **18a** benzyl alcohol-d_1 was isolated. It was acetylated and identified by comparison of its n.m.r. spectrum with that of benzyl acetate.

*Reaction of Methyl 2,3-Dideoxy-4,6-di-O-methyl-α-D-erythro-hex-2-enopyranoside, **26***

*4,6-Di-O-methyl-1,2,3-trideoxy-D-erythro-hex-1-enopyranose, **27***

Compound **26** was prepared from compound **4a** by methylation, (28). Compound **26** (0.20 g, 0.001 mol) was treated with LAH (0.015 g) in dry dioxan (10 ml) under reflux for 5 h. The isolated product was a syrup and the n.m.r. spectrum showed two vinyl ethers present in equal amounts, which were obtained as syrups by silica column chromatography (EtOAc – petroleum ether (35–60 °C) 1:1) and identified as **27** and **29**.

For **27** (which was also obtained by methylation of **12a**(H)); $[\alpha]_D^{23}$ +93.3 (*c*, 9.6 in $CHCl_3$); *m/e* 158; $\nu_{max}(CHCl_3)$ 1645 cm^{-1}; n.m.r. data: τ 6.60 (s, 6, 2 × OCH_3), 3.20 (dt, 1, J_{12} = 6.0, J_{13} = $J_{13'}$ = −1.5, H-1), 5.40 (m, 1, H-2), 7.57–8.03 (m, 2, H-3, -3′), 6.00–6.50 (m, 4, H-4, -5, -6, -6′).

*2,3-Dideoxy-1-O-ethyl-4,6-di-O-methyl-D-erythro-cis-hex-1-enopyranose, **29***

Compound **29** was a syrup, *m/e* 204; $\nu_{max}(CHCl_3)$ 1645 cm^{-1}; n.m.r.: τ 6.63 (s, 6, 2 × OCH_3), 8.77 (t, 3, $J_{CH_2CH_3}$ = 7.0 Hz, OCH_2CH_3), 7.0 (bs, 1, exchangeable, OH), 3.92 (dt, 1, J_{12} = 6.0, J_{13} = $J_{13'}$ = −1.5, H-1), 5.53 (m, 1, J_{23} = $J_{23'}$ = 8.5, H-2), 7.60 (m, 2, J_{34} = $J_{3'4}$ = 6.0, H-3, -3′), 6.43–6.93 (m, 4, H-4, -5, -6, -6′).

*Reaction of Methyl 3,4-Dideoxy-6-O-trityl-α-D-threo-hex-3-enopyranoside, **30***

*Methyl 2,3,4-Trideoxy-4-deuterio-6-O-trityl-α-D-threo-hex-2-enopyranoside, **32***

Compound **30** (11) (3.50 g, 8.7 mmol) was treated with LAD (910 mg, 21.8 mmol) in refluxing dioxan (100 ml)

for 19 h. The reaction was worked up in the usual way, and the product mixture showed two components (R_f 0.70 and 0.57) on t.l.c. in chloroform as solvent. After silica column chromatography, the material of R_f 0.57 was found to be crystalline **32** (909 mg, 27% yield). The n.m.r. data are shown in Table 3.

Compound **32** was recrystallized from hexane, m.p. 81.5–82.5 °C; $[\alpha]_D^{23}$ −38.4° (*c*, 1 in $CHCl_3$).

Anal. Calcd. for $C_{26}H_{27}O_3$: C, 80.57; H, 7.02. Found: C, 80.85; H, 7.03.

*1,2,3,4-Tetradeoxy-3,4-dideuterio-6-O-trityl-*D*-xylo-hex-1-enopyranose, 34*

The chromatogram described above afforded 500 mg of the substance of R_f 0.7 (16% yield). The structure **34** was assigned on the basis of n.m.r. evidence (Table 3) which showed that the material was a glycal and the expected course of reductive rearrangement of the primary product, **32**. Satisfactory elemental analysis of **34** could not be obtained.

*Reaction of Methyl 3,4-Dideoxy-6-O-trityl-*α*-*D*-erythro-hex-3-enopyranoside, 31*

Compound **31** (11) (3.0 g, 7.45 mmol) was treated with LAD (1.6 g, 38 mmol) in refluxing dioxan (200 ml) for 1 week. The reaction was worked-up by procedure *a* and the products, **33** (554 mg) and **35** (210 mg), were isolated by column chromatography as described above (R_f 0.57 and 0.70). The structures of **33** and **35** were assigned on the basis of n.m.r. evidence (Table 3).

Compound **33** was recrystallized from hexane m.p. 75–77 °C; $[\alpha]_D^{23}$ +15.5° (*c*, 0.5 in $CHCl_3$).

Anal. Calcd. for $C_{26}H_{27}O_3$: C, 80.57; H, 7.02. Found: C, 80.60; H, 7.00.

*1,2,3,4-Tetradeoxy-3,4-dideuterio-6-O-trityl-*D*-ribo-hex-1-enopyranose, 35*

The structure of **35** is assigned on the n.m.r. evidence (Table 3) which shows it to be a glycal and the expected course of reductive rearrangement of the primary product **33**. Satisfactory elemental analysis of **35** could not be obtained.

We are grateful to the National Research Council of Canada and Bristol Laboratories, Syracuse, N.Y., for financial support.

1. R. J. Ferrier. Adv. Carbohydr. Chem. **20**, 67 (1965); **24**, 199 (1969).
2. B. Fraser-Reid and B. Radatus. J. Am. Chem. Soc. **92**, 6661 (1970).
3. B. Radatus, M. Yunker, and B. Fraser-Reid. J. Am. Chem. Soc. **93**, 3086 (1971).
4. B. Fraser-Reid and S. Tam. Tetrahedron Lett. 4897 (1973).
5. E. L. Eliel and F. W. Nader. J. Am. Chem. Soc. **92**, 3045 (1970).
6. L. D. Hall and L. F. Johnson. Tetrahedron, **20**, 833 (1964).
7. E. W. Garbisch, Jr. J. Am. Chem. Soc. **86**, 5561 (1964).
8. B. Fraser-Reid, B. J. Carthy, and B. Radatus. Tetrahedron, **28**, 2741 (1972).
9. R. U. Lemieux, R. K. Kullnig, H. J. Bernstein, and W. G. Schneider. J. Am. Chem. Soc. **80**, 6098 (1958).
10. L. D. Hall and J. F. Manville. Adv. Chem. Ser. **74**, 228 (1968).
11. N. L. Holder and B. Fraser-Reid, Can. J. Chem. **51**, 3357 (1973).
12. G. Stork and W. N. White. J. Am. Chem. Soc. **78**, 4609 (1956); W. Dreuth. Rec. Trav. Chim. **86**, 318 (1967).
13. E. L. Eliel, V. G. Badding, and M. N. Rerick. J. Am. Chem. Soc. **84**, 2371 (1962).
14. W. Kraus and C. Chassin. Tetrahedron Lett. 1003, 1113, 1443 (1970).
15. E. Wiberg and E. Amberger. Hydrides. Elsevier, Amsterdam. 1971. Chapt. 5.
16. H. A. Davis and R. K. Brown. Can. J. Chem. **49**, 2563 (1971).
17. O. Achmatowicz and B. Szechner. Tetrahedron Lett. 1205 (1972).
18. B. E. Leggetter, U. E. Diner, and R. K. Brown. Can. J. Chem. **42**, 2113 (1964); U. E. Diner, H. A. Davis, and R. K. Brown. Can. J. Chem. **45**, 207 (1967); U. E. Diner and R. K. Brown, Can. J. Chem. **45**, 1297 (1967).
19. (*a*) E. L. Eliel. Stereochemistry of carbon compounds. McGraw Hill Book Co. Inc., New York. 1962. p. 434–437; (*b*) H. E. Zimmerman, L. Singer, and B. S. Thyagarajan. J. Am. Chem. Soc. **81**, 108 (1959) footnote 16.
20. A. Hassner. J. Org. Chem. **33**, 2684 (1968).
21. W. T. Borden. J. Am. Chem. Soc. **92**, 4898 (1970).
22. W. T. Borden and M. Scott. J. Chem. Soc. Chem. Commun. 381 (1971).
23. J. W. Emsley, J. Feeney, and L. H. Sutcliffe. High resolution nuclear magnetic resonance spectroscopy. Vol. 1, Pergamon Press, London 1965. pp. 172 ff.
24. M. S. Kharash and O. Reinmuth. Grignard reactions of nonmetallic substances. Prentice-Hall, Inc., New York. 1954. p. 25.
25. W. N. Haworth, C. R. Porter, and A. C. Waine. J. Chem. Soc. 2254 (1932).
26. B. Fraser-Reid and B. Boctor. Can. J. Chem. **47**, 393 (1969).
27. R. J. Ferrier and N. Vethaviyaser. J. Chem. Soc. C, 1907 (1971); D. M. Ciment, R. J. Ferrier, and W. G. Overend. J. Chem. Soc. C, 446 (1966).
28. B. Fraser-Reid, M.Sc. Thesis. Queen's University, Kingston, Ontario. 1960.

Can. J. Chem. Downloaded from www.nrcresearchpress.com by 210.87.254.5 on 09/05/12
For personal use only.

The 2- and 3-*C*-Methyl Derivatives of Methyl 2,3-Dideoxy-α-D-*erythro*-hex-2-enopyranosid-4-ulose

DAVID ROY HICKS AND BERT FRASER-REID

Department of Chemistry, University of Waterloo, Waterloo, Ontario N2L 3G1

Received December 24, 1974

DAVID ROY HICKS and BERT FRASER-REID. Can. J. Chem. **53**, 2017 (1975).

The oxirane rings of carbohydrate 2,3-anhydro sugars are opened stereospecifically by lithium dimethyl cuprate. These reactions go in high yields, without the formation of abberant side products encountered with other organometallic reagents. The alcohols produced are converted via their xanthate esters to olefins in good overall yields. The latter on hydrolysis and oxidation give the title enones.

DAVID ROY HICKS et BERT FRASER-REID. Can. J. Chem. **53**, 2017 (1975).

Les cycles oxirannes des anhydro-2,3 carbohydrates sont ouverts d'une façon stéréospecifique par le diméthyl cuprate de lithium. Ces réactions se produisent avec des rendements élevés et sans la formation des produits secondaires aberrants rencontrés avec d'autres réactifs organométalliques. Les alcools formés peuvent être transformés en oléfines par l'intermédiaire de leur xantogénate; le rendement global de ces réactions est bon. Les oléfines soumises à une hydrolyse puis une oxydation conduisent aux énones mentionnées dans le titre.

[Traduit par le journal]

Can. J. Chem. Downloaded from www.nrcresearchpress.com by 210.87.254.40 on 09/05/12
For personal use only.

In connection with synthetic projects underway in this laboratory, we need to have ready access to the conjugated enones **7** and **16**, simpler congeners of which have proved to be versatile intermediates in the synthesis of deoxy (1), amino (2), and branched-chain (3) sugars. With regard to the last category, the alkyl substituents in **7** and **16** are of particular interest since they provide an additional branching point on the saccharide annulus. We therefore report herein syntheses of these enones via intermediates which are themselves of interest as precursors to highly modified sugars.

Conceptually, an appealing method for attaching an alkyl chain to carbons-2 and -3 of the sugar ring would be by reaction of the readily available oxiranes **1** (4) and **8** (5), respectively, with an organometallic reagent. This follows from the preferred geometry of ring opening which would be expected to give the alcohols **2***a* (*7b*) and **9** (*6a*). However, the reactions of carbohydrate epoxides with organometallic reagents have been shown to yield a great variety of unwanted products such as **i**–**viii** with the desired alcohols present in unsatisfactory yields (6, 7). The formation of the unsaturated compounds **i**, **ii**, and **iii** is probably due in part to the basicity of the organometallic reagent. Johnson has recently demonstrated the virtues of lithium dimethyl cuprate (8) in oxirane cleavage (9). Hence it occurred to us that this difficulty might

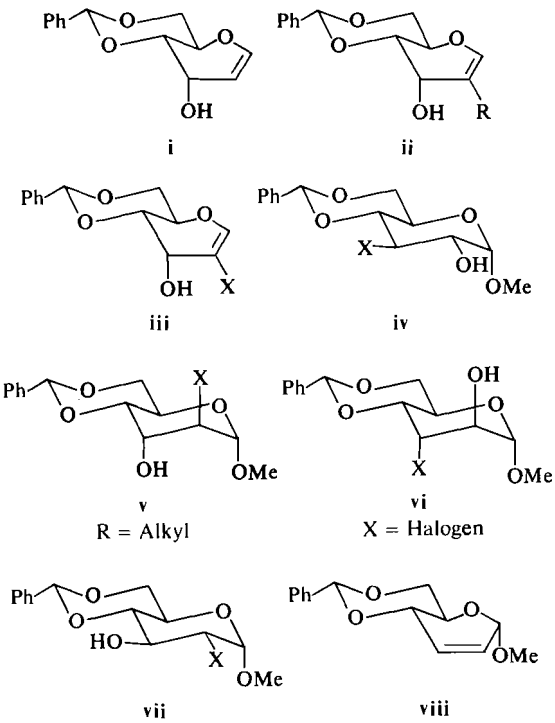

be overcome by use of this reagent which although a good nucleophile, is less prone to cause elimination than methyl lithium (see for example ref. 10).

With this in mind, reaction of the *allo*-epoxide **1** (4) with lithium dimethyl cuprate in ether at

Can. J. Chem. Downloaded from www.nrcresearchpress.com by 210.87.254.40 on 09/05/12
For personal use only.

0 °C, afforded a 1:8.5 mixture (n.m.r. estimate) of the glycal **3***a* and the desired alcohol **2***a* (*7b*). The latter could be crystallized from the mixture in about 65% yield using cold ethanol. The yield of **2***a* was increased to 75% by taking advantage of the reluctance of **2***a* to undergo esterification (*7b*). Thus treatment of the mixture (**2***a* and **3***a*) with acetic anhydride and pyridine for 5 h at 0 °C gave **2***a* and **3***b*, which were now readily separated on a silica gel column.

A method for the *cis*-elimination of the elements of water from the alcohol **2***a* to give the olefin **5** was now required. Burgess *et al.* (11) have reported the preparation and use of methyl (carboxysulfamoyl) triethylammonium hydroxide inner salt [$CH_3OCO\bar{N}SO_2\overset{+}{N}(C_2H_5)_3$] as a useful reagent for the dehydration of simple alcohols. Crabbé (12) has since extended this reaction to the preparation of steroidal olefins from the corresponding alcohols. However, when this method was applied to compound **2***a* extensive decomposition resulted due, no doubt, to the sensitive nature of the carbohydrate molecule which could not tolerate the sulfur trioxide liberated during the course of the reaction. Attempts to dehydrate **2***a* by heating with hexamethylphosphoric triamide (HMPT) (13) also failed.

Unsaturated carbohydrate derivatives have been obtained by Ferrier by application of the Chugaev elimination reaction sequence (14). Consequently the xanthate ester **4** was prepared by treatment of the alcohol **2***a* with sodium hydride, carbon disulfide, and methyl iodide in refluxing diethyl ether (14, 15). Compound **4** obtained as a light yellow syrup and used without further purification, yielded the desired olefin **5** upon pyrolysis in an equal amount of biphenyl at 235 °C for 1 h. Column chromatography of the pyrolysate mixture on silica gel using benzene as eluant afforded compound **5** in pure crystalline form.

Brief treatment of the olefin **5** with *p*-toluenesulfonic acid in dry methanol led to debenzylidenation and formation of the diol **6***a* a colorless syrup. This facile reaction made it necessary to isolate compound **5** chromatographically. Thus the crude pyrolysate was treated with methanol and *p*-toluenesulfonic acid and after neutralization and concentration the residue was partitioned between ether and water. The aqueous phase yielded **6***a* which was then oxidized using active manganese dioxide in chloroform (16) to give the desired ketone **7**.

Conceptually, conversion of the diastereomeric oxirane **8** (5) to the analogous ketone **16** should have been achieved by application of the same series of reactions employed in Scheme 1. However, several difficulties encountered when this was attempted, required several modifications (Scheme 2). First of all the *manno*-epoxide did not react with lithium dimethyl cuprate in diethyl ether at 0 °C and at room temperature three compounds were formed. Benzene or tetrahydrofuran as solvent gave equally discouraging results. However, if the reagent was prepared in dry hexane at 0 °C, the oxirane added and the reaction mixture allowed to warm to and stand at room temperature for 4 h a 70% yield of the desired alcohol **9** (*6a*) could be obtained. Unfortunately this reaction could not be adapted for large scale preparations of **9**. When the amount of **8** was greater than 0.008 mol, appreciable quantities of the iodohydrin **10** (*6c*) were formed.[1] However, the latter could be removed chromatographically using a silica gel column.

The xanthate ester **11** could be prepared in a similar manner to that used for the preparation of **4**. However, pyrolysis of **11** under identical conditions to those used for the formation of **5** did not yield the expected olefin **12** (17) but the diene **13** (18) as the only isolable product. Upon careful monitoring of the reaction on t.l.c., it was discovered that compound **13** was formed at the expense of a slower-moving material which had been formed initially. This material proved to be the desired olefin **12** which undergoes pyrolytic 1,4-elimination of methanol to form the diene **13**.[2] Optimum conditions for the formation of **12** were achieved by raising the pyrolysis temperature to 265 °C and shortening the reaction time to 15 min.

Unlike compound **4**, which is an unambiguous case, the xanthate ester **11** contained two available *cis*-hydrogens (19) and could conceivably have led to the formation of the olefin **17** on

---

[1]The formation of the iodohydrin **10** must arise from oxirane cleavage by iodide ion. However, we are unable to account for the formation of **10** since in control experiments lithium iodide was found to be insoluble in hexane at room temperature and oxirane **8** did not react with cuprous iodide in hexane at room temperature.

[2]This and other routes leading to **13** will be described in detail in a forthcoming issue of this journal.

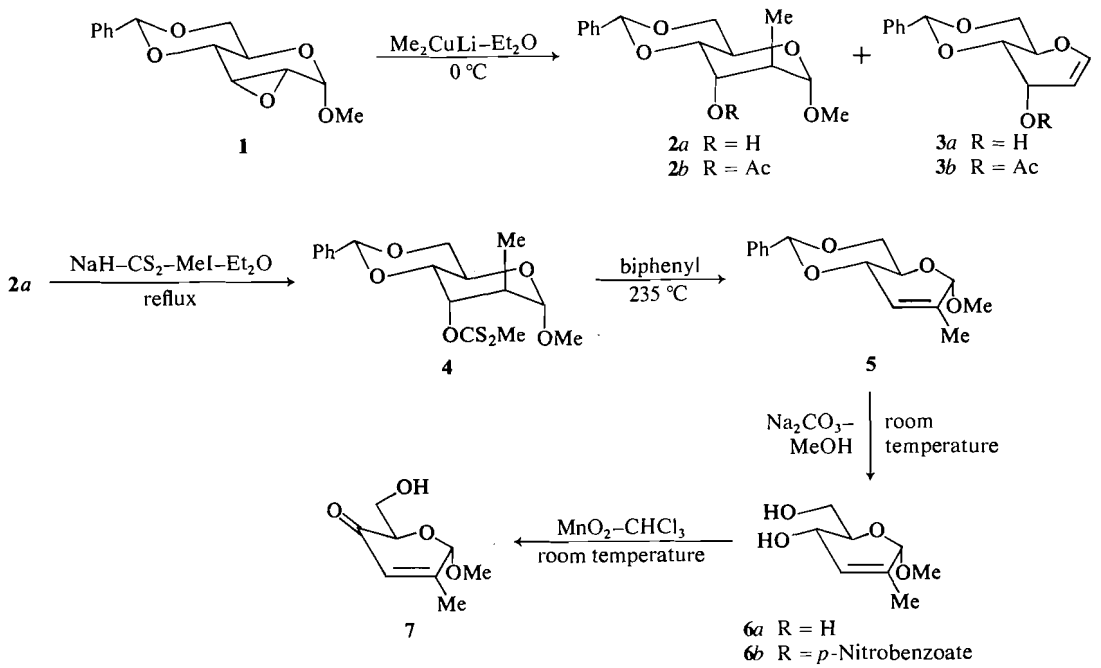

SCHEME 1

pyrolysis. The fact that none of this material was isolated supported our faith in precedents which have indicated that the hydrogen α to the two oxygens at carbon-1 would be less readily removed in the olefin forming step (14, 20).

Another difference with Scheme 1 was encountered when the acid-catalyzed debenzylidenation of **12** proved to be unworkable since the molecule appeared to be too sensitive to acid. If correct, this problem would be circumvented by using base-labile blocking groups. Therefore, with this in mind, the benzylidene group of the xanthate ester **11** was removed and the resulting diol **15***a* was converted to the diacetate **15***b*. Pyrolysis of this compound in a manner similar to that used for the analogous benzylidene derivative **11** afforded the olefin diacetate **14***b*. The diol **14***a* was then obtained upon deacetylation of the diester **14***b* with sodium carbonate and dry methanol and easily oxidized (16) as before to the required ketone **16**.

Experimental

Melting points were determined in capillary tubes in a Mel-Temp block and are uncorrected. Elemental analyses were performed by Microanalyses Laboratory, Toronto, Ontario. The n.m.r. spectra ($CDCl_3$, TMS) were determined on a Varian T-60 or a Varian HR-220 spectrometer the J values quoted being the spacing measured directly from the spectra. Infrared spectra were determined on a Beckman model IR-10 spectrometer using 0.1 mm sodium chloride solution cells (chloroform as solvent). Optical rotations were determined on a Carl Zeiss model LEP nür 370740 Lichtelektrishes Präzision polarimeter at 23 °C.

Thin-layer chromatography was performed on glass plates coated with silica gel (HF-254, E. Merck) to a thickness of 0.3 mm. The following solvent systems were used to develop the plates. (*A*) ethyl acetate – petroleum ether (30–60 °C) (1:4); (*B*) ethyl acetate – petroleum ether (30–60 °C) (1:1); (*C*) ethyl acetate; (*D*) benzene. For column chromatography E. Merck silica gel (0.063–0.20 mm 70–230 mesh A.S.T.M.) was used.

Methyl 4,6-O-Benzylidene-2-deoxy-2-C-methyl-α-D-altropyranoside (2) and 4,6-O-Benzylidene-1,2-dideoxy-D-ribo-hex-1-enopyranose (3)

Cuprous iodide (15.2 g, 0.08 mol), in anhydrous ether (90 ml), was stirred under dry nitrogen at 0 °C in a three-necked round bottom flask. A stock solution of methyl lithium (2 *M* in ether) was added to this suspension until a colorless solution was obtained, approximately 80 ml being required. Compound **1** (10.56 g, 0.04 mol) was added to this reagent and the reaction was allowed to stir at 0 °C.

After 4 h the starting material had disappeared and two new spots (R_f 0.46 and 0.38 solvent *B*) had appeared. At this time the contents of the reaction flask were transferred to a separatory funnel and the flask was washed with ether. The combined ether solutions were washed with a saturated ammonium chloride solution (2 × 20 ml) and saturated sodium bicarbonate solution (20 ml)

Can. J. Chem. Downloaded from www.nrcresearchpress.com by 210.87.254.40 on 09/05/12
For personal use only.

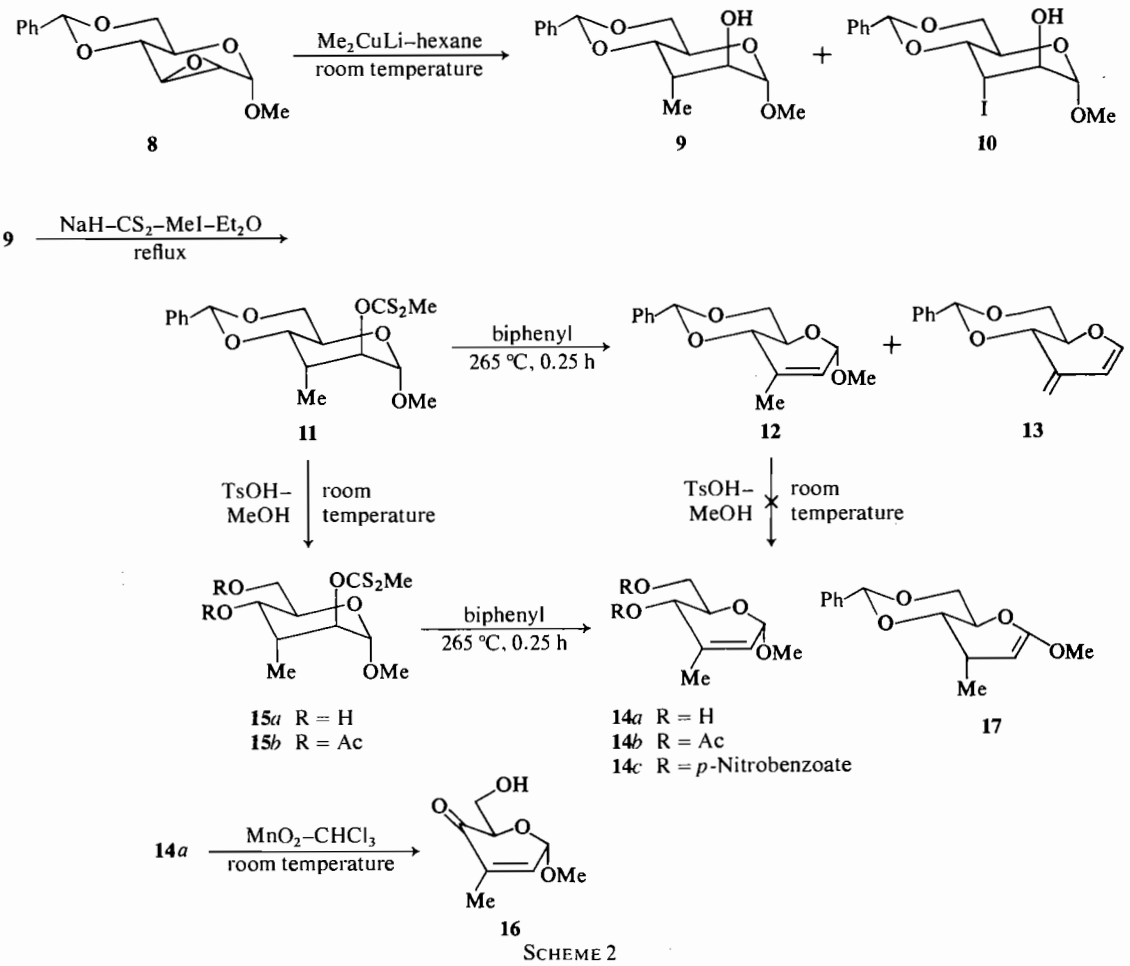

SCHEME 2

and then dried over sodium sulfate and evaporated: yield 9.7 g, 89%.

The alcohol **2** (6.9 g) was recovered when the crude product was crystallized from ethanol. A further amount of **2***a* (1.5 g) was obtained when the mother liquors were acetylated and chromatographed (see below). Compound **2***a* was recrystallized from ether–*n*-hexane, m.p. 111–113 °C; $[\alpha]_D^{23}$ +122.5° (*c*, 1 in $CHCl_3$) (lit. (7*b*) 110–111 °C; $[\alpha]_D^{23}$ +120.8° (*c*, 1 in $CHCl_3$)).

*3-O-Acetyl-4,6-O-benzylidene-1-2-dideoxy-*D*-ribo-hex-1-enopyranose (3b)*

The residue (1.0 g) obtained upon evaporation of the mother liquors from above was dissolved in dry pyridine (5 ml) and cooled in an ice bath. Acetic anhydride (3 ml) was added and the reaction stirred for 5 h at 0 °C. At this time methanol (10 ml) was added to the reaction mixture and the solution was allowed to warm up to and remain at room temperature for 1 h. The solvents were then removed on a rotary evaporator and the residue dissolved in chloroform (20 ml) washed with a 5% HCl solution (20 ml) and a saturated sodium bicarbonate solution (20 ml), dried over sodium sulfate, and evaporated. The resulting syrup was then chromatographed on a silica column using solvent *A* to yield compound **2***a* (0.55 g) and compound **3***b* (0.49 g). Compound **3***b* was recrystallized from ethanol, m.p. 120–121 °C; $[\alpha]_D^{23}$ +237° (*c*, 0.17 in ethanol) (lit. (7*c*) m.p. 121–121.5 °C; $[\alpha]_D$ +253° (*c*, 0.17 in ethanol)).

*Methyl 3-O-Acetyl-4,6-O-benzylidene-2-deoxy-2-C-methyl-*α*-*D*-altropyranoside (2b)*

Compound **2***a* (0.50 g, 1.79 mmol) was dissolved in dry pyridine (5 ml) and cooled in an ice bath to 0 °C while acetic anhydride (3 ml) was added to the stirred solution. The reaction mixture was allowed to warm to room temperature. After 24 h, t.l.c. indicated that the starting material had disappeared and a new faster-running compound (R_f 0.29, solvent *A*) had been formed. The reaction mixture was worked-up as above to yield **2***b* (5.02 g, 87%) recrystallized from hexane, m.p. 65–65.5 °C; $[\alpha]_D^{23}$ +81.2° (*c*, 1 in $CHCl_3$) (lit. (7*b*) m.p. 65–66 °C; $[\alpha]_D^{25}$ +86.5° (*c*, 1 in $CHCl_3$)).

*Methyl 4,6-O-Benzylidene-2-deoxy-2-C-methyl-3-O-((thiomethyl)thiocarbonyl)-*α*-*D*-altropyranoside (4)*

Sodium hydride (2.54 g, 0.053 mol) (50% oil dispersion) was placed in a dry 250-ml round-bottom flask fitted

Can. J. Chem. Downloaded from www.nrcresearchpress.com by 210.87.254.40 on 09/05/12
For personal use only.

Can. J. Chem. Downloaded from www.nrcresearchpress.com by 210.87.254.40 on 09/05/12
For personal use only.

with a magnetic stirrer, reflux condenser, and drying tube. The sodium hydride was then washed free of oil with pentane by stirring and decantation. Compound **2***a* (12.0 g, 0.043 mol) dissolved in dry diethyl ether (100 ml) was added to the flask and the reaction mixture was refluxed for 3 h. Carbon disulfide (5.3 ml) and methyl iodide (5.4 ml) were added dropwise to the solution after 3 and 6 h, respectively. After a total reflux period of 9 h t.l.c. indicated that the starting material had disappeared and a new faster-running material (R_f 0.60, solvent *B*) had been formed. The excess sodium hydride was destroyed by the cautious addition of water to the cooled solution. The ether layer was washed with water (3 × 50 ml), dried over sodium sulfate, and evaporated to give the xanthate ester **4** (14.82 g, 89%). Significant n.m.r. features were: δ 1.20 (d,3,J = 8.0 Hz, C—CH_3), 2.58 (s,3,S—CH_3), 3.37 (s,3,OCH_3), 3.98 (bs,1,H-1), 5.63 (s,1,H-7), 5.87 (m,1,H-3).

Methyl 4,6-O-Benzylidene-2,3-dideoxy-2-C-methyl-α-D-erythro-hex-2-enopyranoside (5)

The xanthate ester **4** (10 g, 0.057 mol) unpurified was mixed with biphenyl (10 g) in a 50-ml round-bottom flask fitted with a magnetic stirrer and an air condenser. A stream of nitrogen was passed over the reaction mixture by means of a capillary tube extending into the flask through the condenser. A preheated (240 °C) Wood's metal bath was then raised around the flask and the temperature of the bath was maintained at 235 °C for 1 h. At this time no starting material was apparent on t.l.c. only a faster running spot (R_f 0.50, solvent *A*) now remained. The crude pyrolysate was then chromatographed on a silica column using solvent *D* to yield the olefin **5** (4.45 g, 67%). The material after recrystallization from ether–hexane had m.p. 141.5–142.5 °C; $[\alpha]_D^{23}$ +105.7 (*c*, 4.72 in $CHCl_3$); n.m.r., δ 1.77 (m,3, C—CH_3), 3.50 (s, 3, OCH_3), 3.76–4.40 (m, 4, H-4, 5, 6, 6′), 4.73 (bs, 1, H-1), 5.63 (s, 1, H-7), 5.83 (m, 1, H-2).

Anal. Calcd. for $C_{15}H_{18}O_4$: C, 68.69; H, 6.92. Found: C, 68.87; H, 6.92.

Methyl 2,3-Dideoxy-2-C-methyl-α-D-erythro-hex-2-enopyranoside (6a)

Method A

The benzylidene olefin **5** (3.95 g, 0.015 mol) was placed in a round-bottom flask equipped with a magnetic stirring bar. Dry methanol (100 ml) and *p*-toluenesulfonic acid (0.100 g) were added and the reaction mixture was allowed to stir at room temperature until the reaction was complete (~20 min). The solution was neutralized by the addition of solid sodium bicarbonate and filtered. The methanol was removed on a rotary evaporator and the residue partitioned between water (50 ml) and ether (20 ml). The ether layer was extracted with water (50 ml) and the combined aqueous layers were evaporated to dryness. The resulting residue was extracted with ethyl acetate and filtered. Upon evaporation of the ethyl acetate the diol **6***a* was obtained as a light yellow syrup: yield 2.15 g, 79%.

The diol **6***a* was characterized as the di-*p*-nitrobenzoate **6***b* which after recrystallization from ethanol had m.p. 138–139 °C; $[\alpha]_D^{23}$ +158.5° (*c*, 1.18 in $CHCl_3$); n.m.r. δ 1.81 (m,3,C—CH_3), 3.53 (s,3,O—CH_3), 4.15–4.75 (m,3,H-5,6,6′), 4.83 (bs,1,H-1), 5.6–5.9 (m,2,H-3,4), 8.28 (bs,8, phenyl).

Anal. Calcd. for $C_{22}H_{20}N_2O_{10}$: C, 55.94; H, 4.27; N, 5.93. Found: C, 56.06; H, 4.22; N, 6.01.

Method B

When the total crude pyrolysis mixture was treated with methanol and *p*-toluenesulfonic acid as described above, the diol **6***a* was isolated in 47% yield from **4**.

Methyl 2,3-Dideoxy-2-C-methyl-α-D-glycero-hex-2-enopyranosid-4-ulose (7)

The olefinic diol **6***a* (2.15 g, 12.3 mmol) was dissolved in chloroform (500 ml) and active manganese dioxide (27 g) was added. The reaction mixture was stirred at room temperature and the progress of the reaction was followed on t.l.c. After 5½ h the starting material had disappeared and been replaced by a faster-moving material (R_f 0.30, solvent *B*). The reaction mixture was then filtered through Celite to remove the manganese dioxide and the filterate was evaporated to dryness. The crystalline product was recrystallized from ether–hexane to give the ketone **7**: yield 1.44 g, 68%; m.p. 94–95 °C; $[\alpha]_D^{23}$ −2.17° (*c*, 3.65 in $CHCl_3$); n.m.r. δ 2.02 (m,3,C—CH_3), 2.75 (bs,1,OH), 3.57 (s,3,OCH_3), 3.8–4.1 (m,2,H-6,6′), 4.38 (t,l,J_{56} = $J_{5'6'}$ = 5.0 Hz, H-5), 4.98 (s,1,H-1), 5.93 (m,1,H-3), i.r. ν_{max} ($CHCl_3$) 3600, 1680, 1645 cm^{-1}.

Anal. Calcd. for $C_8H_{12}O_4$; C, 55.81; H, 7.02. Found: C, 55.82; H, 7.21.

Methyl 4,6-O-Benzylidene-3-deoxy-3-C-methyl-α-D-altropyranoside (9)

Cuprous iodide (3.04 g, 0.016 mol) and dry hexane (60 ml) were placed in a dry three-necked flask equipped with nitrogen inlet, condenser, drying tube, and rubber septum. The reaction mixture was stirred at 0 °C under dry nitrogen while a stock solution of methyl lithium (2 *M* in ether) was added. After the addition of 2 equiv. of methyl lithium, the yellow precipitate formed initially had been replaced by a white precipitate of lithium dimethyl cuprate and lithium iodide. The reagent was stirred for 30 min at 0 °C and then compound **8** (2.11 g, 0.008 mol) was added and the reaction allowed to warm to room temperature. After 4 h the reaction mixture was poured into a separatory funnel and the flask was rinsed with diethyl ether (100 ml). The combined organic solutions were washed with a saturated solution of ammonium chloride (2 × 50 ml), saturated sodium bicarbonate solution (50 ml), and water (50 ml) and then dried over sodium sulfate. After evaporation of the solvents a light yellow oil was obtained which crystallized on standing to yield **9** (1.56 g, 70%). The material after recrystallization from ether–hexane had m.p. 116–117.5 °C; $[\alpha]_D^{23}$ +104.1° (*c*, 0.28 in ethanol) (lit. (*6a*) m.p. 114–115 °C; $[\alpha]_D^{24}$ +115.9° (*c*, 0.28 in ethanol)).

If the reaction was attempted on larger amounts of **8** appreciable quantities of the iodohydrin **10** were formed. This compound, when isolated by means of column chromatography (solvent *B*) and recrystallized from ethyl acetate, gave the following physical constants: m.p. 163–164.5 °C; $[\alpha]_D^{23}$ +117.0° (*c*, 4 in $CHCl_3$) (lit. (*5c*) m.p. 163–163.5 °C; $[\alpha]_D^{24}$ +111° (*c*, 4 in $CHCl_3$)).

Methyl 4,6-O-Benzylidene-3-deoxy-3-C-methyl-2-O-((thiomethyl)thiocarbonyl)-α-D-altropyranoside (11)

Sodium hydride (2.84 g, 0.06 mol) (a 50% oil dispersion) was placed in a dry round-bottom flask fitted with

Can. J. Chem. Downloaded from www.nrcresearchpress.com by 210.87.254.40 on 09/05/12
For personal use only.

a magnetic stirrer, a reflux condenser, and a calcium chloride drying tube. The sodium hydride was washed free of oil with pentane (3 × 20 ml) by stirring and decantation. Dry diethyl ether (100 ml) and the alcohol **9** (4.90 g, 0.0175 mol) were then placed in the flask and the reaction mixture was stirred and refluxed for 24 h. Carbon disulfide (4.5 ml) and methyl iodide (4.5 ml) were added to the reaction mixture after 12 and 18 h, respectively. The solution was cooled to room temperature and water was added dropwise to destroy the excess sodium hydride. The ether layer was then washed with water (3 × 50 ml) and dried over sodium sulfate. The light yellow syrup which remained upon evaporation of the solvent weighed 5.60 g (82%) and showed as one spot on t.l.c. (R_f 0.62, solvent *B*). Significant n.m.r. features were: δ 1.28 (d,3,J = 7.0 Hz, C—CH_3), 2.60 (s,3,S—CH_3), 3.40 (s,3,O—CH_3), 4.75 (bs, 1, H-1), 5.62 (bs, 2, H-2,7).

*Methyl 4,6-O-Benzylidene-2,3-dideoxy-3-C-methyl-α-D-erythro-hex-2-enopyranoside (**12**)*

The xanthate ester **11** (0.50 g, 1.28 mmol) and biphenyl (1.0 g) were placed in a 5 ml round-bottom flask fitted with a magnetic stirrer and an air condenser. The system was flushed with nitrogen by means of a capillary tube extending through the condenser. The flask was then placed in a preheated Wood's metal bath (270 °C). The temperature of the reaction mixture was maintained at 265–270 °C for 15 min. At this time t.l.c. indicated all of the starting material had been converted to a new compound (R_f 0.49, solvent *B*). The olefin **12** (16) was isolated as a crystalline solid (0.204 g, 61%) when the crude pyrolysate was chromatographed on a silica column using benzene as the eluant. The material when recrystallized from ethanol gave the following data: m.p. 138.5–139.5 °C; $[\alpha]_D^{23}$ +62.7° (*c*, 4.15 in $CHCl_3$) (lit. (16) m.p. 139–140 °C; $[\alpha]_D^{27}$ +60.6° (*c*, 4.15 in $CHCl_3$)).

*4,6-O-Benzylidene-1,2,3-trideoxy-3-C-methylene-D-erythro-hex-1-enopyranose (**13**)*

The xanthate ester **11** (0.50 g, 1.28 mmol) and biphenyl (1.0 g) were pyrolyzed in the same manner as above. After 30 min at 265 °C a t.l.c. of the reaction mixture indicated that all of the xanthate ester **11** had been converted to a faster-running compound (R_f 0.62, solvent *A*). When the crude pyrolysate was chromatographed on a silica column using benzene as eluant a compound whose n.m.r. spectrum was identical to the known diene **13** (16) was obtained (0.074 g, 25%). The compound was recrystallized from ethanol, m.p. 95–96 °C; $[\alpha]_D^{23}$ +97.7° (*c*, 3.6 in $CHCl_3$) (lit. (16) m.p. 98–100 °C; $[\alpha]_D^{23}$ +98.4° (*c*, 3.6 in $CHCl_3$)).

*Methyl 3-Deoxy-3-C-methyl-2-O-((thiomethyl)-thiocarbonyl)-α-D-altropyranoside (**15a**)*

The xanthate ester **11** (1.4 g, 3.6 mmol) was dissolved in dry methanol (60 ml) and *p*-toluenesulfonic acid (0.07 g, 0.4 mmol) was added. The reaction mixture was stirred at room temperature for 5 h. At this time t.l.c. indicated that the starting material had been consumed and a new lower-running compound (R_f 0.21, solvent *B*) had been formed. The solution was then neutralized with solid sodium bicarbonate, filtered through Celite, and evaporated to dryness. The residue was then extracted with chloroform and filtered. Compound **15a** (1.0 g, 92%) was obtained as a light yellow syrup upon evaporation of the filtrate. Significant n.m.r. features were: δ 1.21 (d, 3, J = 7.0 Hz, C—CH_3), 2.60 (s, 3, S—CH_3), 3.42 (s, 3, O—CH_3), 4.78 (bs, 1, H-1), 5.62 (m, 1, H-2).

*Methyl 4,6-Di-O-acetyl-3-deoxy-C-methyl-2-O-((thiomethyl)thiocarbonyl)-α-D-altropyranoside (**15b**)*

The diol **15a** (1.0 g, 3.32 mmol) was dissolved in dry pyridine (10 ml) and cooled to 0 °C in an ice bath. Acetic anhydride (3 ml) was added and the reaction mixture was left at 0 °C for 10 h. At this time methanol (5 ml) was added and the solution allowed to warm to room temperature. After evaporation of the solvents the residue was dissolved in chloroform (20 ml) washed with a 5% hydrochloric acid solution (20 ml), a saturated sodium bicarbonate solution (20 ml) and water (20 ml). The chloroform layer was then dried over sodium sulfate and evaporated to give **15b** as a light yellow syrup (1.06 g, 83%). Compound **15b** was homogeneous on t.l.c. (R_f 0.55, solvent *B*) and exhibited the following n.m.r. features: δ 1.18 (d, 3, J = 7.0 Hz, C—CH_3), 2.07 and 2.10 (pair of singlets, 6, —$OCOCH_3$), 2.60 (s, 3, S—CH_3), 3.43 (s, 3H, OCH_3), 4.85 (bs, 1, H-1), 5.10–5.40 (m, 1, H-4), 5.7 (m, 1, H-2).

*Methyl 4,6-Di-O-acetyl-2,3-dideoxy-3-C-methyl-α-D-erythro-hex-2-enopyranoside (**14b**)*

The diacetate **15b** (0.880 g, 2.28 mmol) and biphenyl (1.5 g) were placed in a 5 ml round-bottom flask and pyrolyzed as above at 265 °C. After 15 min a t.l.c. of the reaction mixture indicated a new compound (R_f 0.47, solvent *B*) and none of the starting xanthate. Column chromatography on the crude pyrolysate using benzene as solvent yielded the diacetate olefin **14b** (0.391 g, 66%). Significant n.m.r. features were: δ 1.63 (m, 3, C—CH_3), 2.02 and 2.07 (pair of singlets, 6, —$OCOCH_3$), 3.37 (s, 3, OCH_3), 4.78 (d, 1, J_{12}=4 Hz, H-1), 5.2–5.6 (m, 1, H-2).

*Methyl 2,3-Dideoxy-3-C-methyl-α-D-erythro-hex-2-enopyranoside (**14a**)*

The diacetate olefin (2.42 g, 11.2 mmol) was dissolved in dry methanol (175 ml) and sodium carbonate (2.68 g) was added. After 9 h at room temperature t.l.c. indicated that the reaction was complete and a new compound (R_f 0.10, solvent *B*) had been formed. The residue obtained when the reaction mixture was filtered and evaporated to dryness, was extracted with ethyl acetate, and filtered to remove residual inorganic salts. Concentration of the filtrate yielded compound **14a** (1.70 g, 87%) as a colorless syrup. The diol **14a** was characterized as the di-*p*-nitrobenzoate **14c** which after recrystallization from ethanol gave the following data: m.p. 147–148 °C; $[\alpha]_D^{23}$ +162.1° (*c*, 0.63 in $CHCl_3$); n.m.r. δ 1.75 (m, 3, C—CH_3), 3.48 (s, 3, OCH_3), 4.3–4.7 (m, 3, H-5, 6.6′), 5.0 (m, 1, H-1), 5.65–6.0 (m, 2, H-2,4), 8.3 (bs, 8, phenyl).

Anal. Calcd. for $C_{22}H_{20}N_2O_{10}$: C, 55.94; H, 4.27; N, 5.93. Found: C, 56.05; H, 4.19; N, 5.96.

*Methyl 2,3-Dideoxy-3-C-methyl-α-D-glycero-hex-2-enopyranosid-4-ulose (**16**)*

The olefinic diol **14a** (1.25 g, 7.2 mmol) was dissolved in chloroform (575 ml) and active manganese dioxide (12.5 g) was added and the mixture stirred at room temperature. After 6 h t.l.c. indicated that the starting material had disappeared and a new compound (R_f 0.24,

solvent *B*) had been formed. The manganese dioxide was removed by filtration through Celite and evaporation of the filtrate yielded a crystalline solid which was recrystallized from ether–hexane to give the ketone **16** (0.95 g, 77%), m.p. 104–105 °C; $[\alpha]_D^{23}$ +56.47° (*c*, 3.17 in $CHCl_3$); n.m.r. δ 1.83 (m, 3, C—CH_3), 2.33 (bs, 1, OH), 3.53 (s, 3, OCH_3), 4.0 (m, 2, H-6, 6′), 4.5 (t, 1, $J_{56}=J_{56'}$ = 4.0 Hz, H-5), 5.16 (d, 1, J_{12}=4.0 Hz, H-1), 6.70 (m, 1, H-2); i.r. ν_{max} ($CHCl_3$) 3600, 1685, 1650 cm^{-1}.

Anal. Calcd. for $C_8H_{12}O_4$: C, 55.81; H, 7.02. Found: C, 55.68; H, 7.14.

1. E. H. Williams, W. A. Szarek, and J. K. N. Jones. Carbohydr. Res. **20**, 49 (1971).
2. J. Cleophax, S. D. Gero, and J. Leboul. J. Chem. Soc. Chem. Commun. 710 (1973); R. M. Srivastava, B. J. Carthy, and B. Fraser-Reid. Tetrahedron Lett. 2175 (1974).
3. D. L. Walker and B. Fraser-Reid. J. Chem. Soc. Chem. Commun. 319 (1974); B. Fraser-Reid, N. L. Holder, and M. B. Yunker. J. Chem. Soc. Chem. Commun. 1286 (1972).
4. N. K. Richtymer. Methods Carbohydr. Chem. **1**, 107 (1962).
5. D. R. Hicks and B. Fraser-Reid. Synthesis, 203 (1974).
6. (*a*) T. D. Inch and G. J. Lewis. Carbohydr. Res. **15**, 1 (1970); (*b*) G. N. Richards and L. F. Wiggins. J. Chem. Soc. 2442 (1953); (*c*) G. N. Richards. J. Chem. Soc. 4511 (1954); (*d*) F. H. Newth, G. N. Richards, and L. F. Wiggins. J. Chem. Soc. 2356 (1950).
7. (*a*) R. U. Lemieux, E. Fraga, and K. A. Watanabe. Can. J. Chem. **46**, 61 (1968); (*b*) M. Sharma and R. K. Brown. Can. J. Chem. **46**, 757 (1968); (*c*) A. A. J. Feast, W. G. Overend, and N. R. Williams. J. Chem. Soc. 7378 (1965).
8. H. O. House, W. L. Respess, and G. M. Whitesides. J. Org. Chem. **31**, 3128 (1966).
9. R. W. Herr, D. M. Wieland, and C. R. Johnson. J. Am. Chem. Soc. **92**, 3813 (1970).
10. E. J. Corey and G. H. Posner. J. Am. Chem. Soc. **89**, 3911 (1967); E. J. Corey, J. A. Katzenellenbogen, and G. H. Posner. J. Am. Chem. Soc. **89**, 4245 (1967).
11. G. M. Atkins, Jr. and E. M. Burgess. J. Am. Chem. Soc. **90**, 4744 (1968); E. M. Burgess, E. A. Taylor, and H. P. Denton, Jr. 159th National Meeting of the American Chemical Society, Houston, Texas. Feb. 1970. Abstr. No. ORGN-105.
12. P. Crabbé and C. León. J. Org. Chem. **35**, 2594 (1970).
13. R. S. Monson and D. N. Priest. J. Org. Chem. **36**, 3826 (1971); R. S. Monson. Tetrahedron Lett. 567 (1971).
14. R. J. Ferrier. J. Chem. Soc. 5443 (1964).
15. R. E. Gilman, J. D. Henion, S. Shakshooki, J. I. H. Patterson, M. J. Bogdanowicz, R. J. Griffith, D. E. Harrington, R. K. Crandall, and K. T. Finley. Can. J. Chem. **48**, 970 (1970).
16. B. Fraser-Reid, A. McLean, E. W. Usherwood, and M. Yunker. Can. J. Chem. **48**, 2877 (1970).
17. B. Fraser-Reid and B. Radatus. Can. J. Chem. **50**, 2919 (1972).
18. S. Y-K. Tam, D. E. Iley, N. L. Holder, D. R. Hicks, and B. Fraser-Reid. Can. J. Chem. **51**, 3150 (1973).
19. H. R. Nace. Org. React. **12**, 57 (1962).
20. K. J. Ryan, H. Arzoumanian, E. M. Acton, and L. Goodman. J. Am. Chem. Soc. **86**, 2503 (1964).

Can. J. Chem. Downloaded from www.nrcresearchpress.com by 210.87.254.40 on 09/05/12
For personal use only.

Electric Dipole Moment Investigation of Buttressing in Alkyl Duryl Ketones

A. George Pinkus and Herman C. Custard, Jr.[1]
Department of Chemistry, Baylor University, Waco, Texas 76703

Received April 9, 1974[2]

A. George Pinkus and Herman C. Custard, Jr. Can. J. Chem. **53**, 2024 (1975).

Dipole moments (D) determined for the following alkyl duryl ketones in benzene at 30° were: Me, 2.83; Et, 2.80; *i*-Pr, 2.74; *t*-Bu, 2.65. The decrease in the series is explained by increasing rotational restriction about the carbonyl group due to an increasing interference by the *ortho* methyl groups with the alkyl group. This results in a greater twist from coplanarity between the ring and carbonyl and less π-electron delocalization and consequently a lower dipole moment as the size of the alkyl increases. The increase observed for the duryl ketone moments over those of corresponding mesityl ketones is tentatively explained as due to a higher duryl group moment relative to the mesityl moment. The interplanar angles (angles of twist) for the duryl ketones calculated with the Braude–Sondheimer equation were slightly larger than those calculated for the mesityl ketones, the magnitude depending on the method of calculation. It is tentatively concluded that evidence from dipole moment data indicates that a small buttressing effect exists in the duryl ketone system.

A. George Pinkus et Herman C. Custard, Jr. Can. J. Chem. **53**, 2024 (1975).

Les moments dipolaires (D) des alkyl duryl-cétones suivantes, tels que déterminés dans le benzène à 30°, sont: Me, 2.83; Et, 2.80; *i*-Pr, 2.74; *t*-Bu, 2.65. On explique l'abaissement des valeurs au fur et à mesure que l'on progresse dans la série en faisant l'hypothèse qu'il y a augmentation de l'empêchement à la rotation autour du groupe carbonyle dû à une augmentation de l'interférence des groupes méthyles en *ortho* avec le groupe alkyle. Cette interférence provoque un éloignement plus grand de la planéité du cycle et du groupe carbonyle et une délocalisation plus faible des électrons π; ceci amène un moment dipolaire plus faible à mesure que la grosseur du groupe alkyle augmente. On attribue l'augmentation du moment dipolaire lorsque l'on passe des mésityl-cétones aux duryl-cétones correspondantes au fait que le groupe duryle à un moment dipolaire plus élevé que celui du groupe mésityle. On a calculé les angles interplanaires (angles de torsion) des duryl-cétones à l'aide de l'équation de Braude–Sondheimer; ces valeurs sont légèrement supérieures à celles calculées pour les mésityl-cétones mais l'amplitude des différences dépend du modèle de calcul. On en conclut que les moments dipolaires suggère qu'un petit effet de compression existe dans les duryl-cétones.
[Traduit par le journal]

Introduction

The dipole moments of a series of alkyl mesityl ketones (**1**) were found (1) to decrease from methyl (2.81 D) to *t*-butyl (2.50 D). This decrease was attributed to decreasing π–π conjugation of the aromatic ring with the carbonyl group due to increasing steric interference between the alkyl group from methyl to *t*-butyl with *ortho* methyls thus increasing the angle between the aromatic ring and the C—CO—C plane. As an extension of the study on mesityl ketones, dipole moments of a corresponding series of alkyl duryl ketones (**2**) were determined to investigate whether "buttressing" of *ortho* methyl groups by adjacent methyl groups in the *meta* positions would be detectable via dipole moment data.

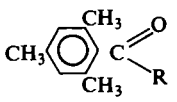

1

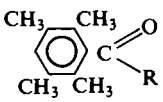

2

Experimental

Determination of Dielectric Constants

The apparatus, procedure, and method of calculation of dipole moments were described previously (1). Linear plots were obtained on extrapolation to infinite dilution.[3]

[1]Present address: Mobil Research & Development Corp., Dallas, Texas.

[2]Revision received April 3, 1975.

[3]The equation of Halverstadt and Kumler (2) which was used to calculate solute polarization ($_\infty P_2$) at infinite dilution was misprinted previously (1) and is reproduced here to correct this error:

$$_\infty P_2 = \frac{3\alpha_0 v_1 M_2}{(\varepsilon_1 + 2)^2} + M_2(v_1 + \beta)\frac{\varepsilon_1 - 1}{\varepsilon_1 + 2}$$

Can. J. Chem. Downloaded from www.nrcresearchpress.com by 210.87.254.40 on 09/05/12
For personal use only.

Can. J. Chem. Downloaded from www.nrcresearchpress.com by 210.87.254.40 on 09/05/12
For personal use only.

Preparation and Purification of Compounds and Solvents

Thiophene-free benzene was purified as described previously (1). The duryl ketones were prepared by the general method given for isopropyl duryl ketone. The compounds were checked for the presence of impurities by v.p.c.

Isopropyl Duryl Ketone

Anhydrous aluminum chloride (60 g, 0.45 mol) in a flask was cooled in an ice–salt bath. Methylene chloride (100 ml) previously cooled to 0° was added. A solution of durene (26.8 g, 0.200 mol) and isobutyryl chloride (25 g, 0.23 mol) in methylene chloride (400 ml) was added dropwise at such a rate that the temperature of the reaction mixture did not rise above 10°. The reaction mixture was poured slowly into a mixture of cracked ice and hydrochloric acid. The methylene chloride layer was washed twice with 10% sodium bicarbonate, twice with water, and dried with anhydrous sodium sulfate. On removing the solvent, a white powder was obtained which was recrystallized once from methanol and twice from cyclohexane; 25% yield; m.p. 49.8–50.0° (lit. (3) 40–41°).

Anal. Calcd. for $C_{14}H_{20}O$: C, 82.30; H, 9.80. Found:[4] C, 82.28; H, 10.01.

t-Butyl Duryl Ketone

Reagents: pivaloyl chloride; same relative amounts of other reagents. After three recrystallizations from methanol and two from cyclohexane, 20% yield; m.p. 102.8–103.2°.

Anal. Calcd. for $C_{15}H_{22}O$: C, 82.51; H, 10.16. Found:[4] C, 82.93; H, 10.28.

Methyl Duryl Ketone

Prepared in 61% yield; recrystallized from methanol, m.p. 73–74° (lit. (4) 73°; (5) 75°; (6) 74–75°).

Ethyl Duryl Ketone

Prepared in 79% yield; recrystallized from methanol, m.p. 78.0–78.5° (lit. (7) 79°; (3) 78–79°).

Results and Discussion

Weight fractions (w_2), dielectric constants (ε_{12}), and specific volumes (v_{12}) for solutions are in Table 1; molar refractions ($m.r._D$), solute polarizations at infinite dilution ($_\infty P_2$), values of α_0 and β, and dipole moments (μ) are in Table 2.

On the basis of our experience,[5] it is felt that the differences between dipole moments of the ketones reported in the present paper are significant. Thus, for example, when the dipole moment was determined for different samples of the same pure reference compound by five different workers in our laboratory at different periods of time using the same apparatus, the deviations in the dipole moment between the extreme results differed by only 0.02 D. For the same worker, the variation would be expected to be less than this. The differences in the present paper are well within this limit of error.

TABLE 1. Dielectric constants and specific volumes of alkyl duryl ketones in benzene at 30°

Ketone	$w_2 \times 10^3$	ε_{12}	v_{12}
Methyl duryl ketone	2.663	2.2763	—
	5.971	2.2924	—
	12.34	2.3226	—
	17.26	2.3452	—
	8.791	2.3082	1.1504
	12.85	2.3286	1.1499
	25.11	2.3890	1.1485
Ethyl duryl ketone	2.559	2.2747	1.1512
	6.540	2.2921	1.1507
	10.52	2.3095	1.1502
	19.82	2.3497	1.1493
Isopropyl duryl ketone	3.217	2.2761	1.1512
	8.102	2.2950	1.1507
	13.98	2.3175	1.1501
	20.57	2.3422	1.1493
t-Butyl duryl ketone	2.469	2.2720	1.1509
	6.451	2.2861	1.1506
	9.261	2.2963	1.1503
	11.50	2.3039	1.1501

The dipole moment of 2.83 obtained for methyl duryl ketone in benzene at 30° checks with the value of 2.81 D in carbon tetrachloride at 25° reported by Aroney *et al.* (8) but is higher than the value of 2.63 in benzene at 25° reported by Kadesch and Weller (9). Dipole moments for the other three ketones have not previously been reported.

The decrease in dipole moments in the series from methyl to *t*-butyl is analogous to that found previously for alkyl mesityl ketones and is explicable in terms of increasing rotational restriction about the carbonyl group with size of alkyl due to its interference with *ortho* methyl groups. Since the carbonyl group is twisted more from coplanarity with the aromatic ring the larger the alkyl group, the less π–π electron delocalization between the carbonyl group and aromatic ring and consequently the lower the dipole moment. However, the dipole moments of alkyl duryl ketones are higher than those for each of the corresponding mesityl ketones listed in Table 2 for comparison. *A priori*, on the basis that buttressing would result in enhanced restriction of rotation of

[4]Analysis by Galbraith Laboratories, Knoxville, Tennessee.

[5]Pinkus and Lin (18) and unpublished work with C. D. Moon, P. G. Waldrep, and R. Smyrl.

TABLE 2. Experimental data on alkyl duryl ketones

Alkyl group	Molar refractions (cc)	β	α_0	$_\infty P_2$ (cc)	μ(D)* Duryl	μ(D)* Mesityl	Δμ†
Methyl	52.487	−0.11988	4.85	216.33	2.83	2.81	0.02
Ethyl	56.888	−0.11100	4.39	217.42	2.80	2.76	0.04
Isopropyl	61.430	−0.10220	3.91	215.34	2.74	2.64	0.10
t-Butyl	65.972	−0.08859	3.40	209.84	2.65	2.50	0.15

*Benzene solution; 30°.
†μ(duryl) − μ(mesityl).

the carbonyl group, it might have been expected that lower moments would be obtained for the corresponding members of the duryl series. This apparent anomaly can be rationalized as follows. As was pointed out previously (1) in comparing dipole moments from one series of compounds to another, the relative group moments must be taken into account. Estimates of differences in mesityl and duryl group moments can be made from published dipole moment data for corresponding monosubstituted mesityl and duryl derivatives where the substituent exerts little or no steric influence on *ortho* methyl groups and in itself has no complicating rotational isomerism. For substituents fulfilling this criterion, data are available for only bromo, hydroxy, and amino compounds. The available data are collected in Table 3. Although some minor variations in the data may exist because of differences in temperatures and methods of calculation, the duryl values for the bromo and hydroxy derivatives are higher from 0.03 for Br to 0.32 D for OH, these being in the range of the increases for the ketone data of the present paper. On this basis, it is reasonable to attribute an appreciable component of the higher moments for the duryl ketones to a higher duryl group moment. More data on monosubstituted mesityl and duryl compounds would be desirable to decide this question more conclusively. At the present time, no other alternative explanation seems evident.

Another approach to the question as to whether buttressing is detectable from dipole moments is in a comparison of interplanar angles (angles of twist) (θ) for the duryl and mesityl ketones. These can be calculated from dipole moment data on duryl ketones using the Braude–Sondheimer equation (13)

$$\cos^2\theta = (\mu_{obs} - \mu_{90})/(\mu_0 - \mu_{90})$$

where μ_{obs} is the observed dipole moment, μ_{90} is the moment for a "completely deconjugated system" (where plane of the ring and the carbonyl group to alkyl-carbon plane are at right angles), and μ_0 is the moment for a coplanar configuration. As was pointed out in the calculations on mesityl ketones (1) the moment for a saturated ketone cannot be used for μ_{90} as suggested by Braude and Sondheimer (13). As a better standard for μ_{90}, *t*-butyl mesityl ketone was used (1) since it was assumed that maximum restriction of rotation would be present and the angle of the carbonyl group with the ring would be 90° as indicated in molecular models. This assumption is justified on the basis of a recent X-ray study (14) on 2,4,6-trimethyl-3-pivaloylbenzoic acid (15) where the mean plane through the keto group was found to make an angle of 89.9° with the mean plane of the six-membered ring. Analogously, the moment of *t*-butyl duryl ketone can be used as the standard for μ_{90} in the present calculations.

As was done for the calculations on mesityl ketones, a corrected value of 3.09 D was used for μ_0 to correct the observed dipole moment of acetophenone for influences of the methyl groups by adding 0.04 D to the value. This value is obtained by applying a correction of +0.04 D to the experimental value of 3.05 D obtained (1) for acetophenone. The correction is based on reported moments (9) of 2.96 D for mesitylaldehyde (2,4,6-trimethylbenzaldehyde) and 2.92 D for benzaldehyde (measured under the same conditions) which reflect an increase of 0.04 D for mesitylaldehyde in a comparison of mesityl and phenyl systems where the same type of carbonyl group is not sterically prevented from conjugation with the ring since there is no steric interference between the *ortho*-methyls and hydrogen and little, if any, interference with the carbonyl oxygen. A better value for μ_0 for the duryl ketones could be similarly derived;

Can. J. Chem. Downloaded from www.nrcresearchpress.com by 210.87.254.40 on 09/05/12
For personal use only.

Can. J. Chem. Downloaded from www.nrcresearchpress.com by 210.87.254.40 on 09/05/12
For personal use only.

TABLE 3. Dipole moments (μ in D) of some monosubstituted mesityl ($C_9H_{11}X$) and duryl ($C_{10}H_{13}X$) compounds in benzene solution

X	μ (mesityl)	Temperature (°C)	Method* or P_A % of P_E	References	μ (duryl)	Temperature (°C)	Method* or P_A % of P_E	References	Δμ†
Br	1.53	30	0	10‡, 11, 12, 19	1.56	25	—	10‡, 11, 12, 23	0.03
OH	1.37	30	0	10‡, 11, 19	1.69	25	—	10‡, 11, 12, 21	0.32
	1.43	30	0	10‡, 12, 20	—				0.26
NH_2	1.41	25	—	10‡, 11, 21	1.40	25	—	10‡, 11, 20	—
	1.45	25	0	10‡, 11, 12, 22	1.45	25	0	10‡, 11, 12, 22	0

*Listings as in McClellan, ref. 10, p. 5.
†$\Delta\mu$ = μ(duryl) − μ(mesityl).
‡The values listed here have been corrected to allow for changes in Avogadro's number and Boltzmann's constant and thus differ slightly from those given by the original authors and those listed in refs. 11 and 12.

Can. J. Chem. Downloaded from www.nrcresearchpress.com by 210.87.254.40 on 09/05/12
For personal use only.

TABLE 4. Interplanar angles (angles of twist) (θ in deg) of alkyl duryl and alkyl mesityl ketones

Alkyl group	θ(mesityl)			θ(duryl)		
	A(μ_0 = 3.09 D)*	B(μ_0 = 3.12 D)†	C(^{13}C n.m.r.)‡	A(μ_0 = 3.09 D)*	B(μ_0 = 3.05 D)†	C(^{13}C n.m.r.)‡
Me	44	45	51§	49	48	52 (57)§
Et	48	50	49‖	53	52	55‖
i-Pr	61	62	45‖	62	62	49‖
t-Bu	90¶	90¶	—	90¶	90¶	—

*Method of calculation in text.
†Braude-Sondheimer vectorial method (13); see text.
‡Calculated from ^{13}C n.m.r. chemical shifts of carbonyl carbon by Dhami and Stothers (3, 6); corrected values are listed as reported (3, 6).
§Reference 6. Value in parentheses as reported in ref. 24 is a typographical error as confirmed by private communication.
‖Reference 3.
¶Assumed.

Can. J. Chem. Downloaded from www.nrcresearchpress.com by 210.87.254.40 on 09/05/12
For personal use only.

however, although the corresponding duryl aldehyde (2,3,5,6-tetramethylbenzaldehyde) has recently been prepared (16) the dipole moment has not been reported. Thus, the same value of 3.09 D for μ_0 was used for the duryl series although a slight increase would be anticipated which would result in slightly larger values for the interplanar angles. The values calculated on this basis are in Table 4.

In the Braude–Sondheimer procedure of correcting for methyl substituent effects, μ_0 is calculated on the following basis. The μ_0 moment is compounded of the group moment of C=O taken as the experimental value for acetophenone or 3.05 D as previously determined (1) and C_6H_4—Me (taken as 0.40 D, the value for toluene for *o*- and *m*-methyl substituents, and as 0.54, the observed vector component in 4-methylacetophenone for *p*-methyl substituents). The vector addition is carried out assuming the carbon–carbon and carbon–oxygen bond angles to be 120°. The value for μ_0 for the mesityl ketones on this basis is 3.12 D. For the duryl ketones, since the moments of the two opposing pairs of methyl groups cancel each other, μ_0 is taken as equal to acetophenone, or 3.05 D in the present case. The interplanar angles for the mesityl and duryl ketones as calculated[6] on this basis are also listed in Table 4 for comparison.

In comparing the results by the above two methods, it can be seen that the calculated values for the interplanar angles are nearly the same in all cases. The increases in the interplanar angles for each alkyl group ($\Delta\theta$ = θ(duryl) − θ(mesityl)) are listed in Table 5 for the two methods A and B described above. For comparison the values determined by Dhami and Stothers (3, 6) using carbonyl ^{13}C n.m.r. data[7] are also listed in Tables 4 and 5. The values check very well except for the isopropyl derivative in both the mesityl and duryl series, the angles being slightly lower for the ^{13}C method. The correlation between the

TABLE 5. Differences ($\Delta\theta$ in deg) between interplanar angles (θ) of alkyl duryl and alkyl mesityl ketones from dipole moment and ^{13}C n.m.r. data

	$\Delta\theta$ = θ(duryl) − θ(mesityl), method		
Alkyl group	A*	B†	C‡
Me	5	3	1
Et	5	2	6
i-Pr	1	0	4

*Calculations with Braude–Sondheimer equation using μ_0 = 3.09 D.
†Calculations with Braude–Sondheimer equation using μ_0 = 3.12 D for mesityl ketones and μ_0 = 3.05 D for duryl ketones.
‡Calculations from ^{13}C n.m.r. data (3, 6).

^{13}C and present dipole moment methods is much better than with the values for methyl mesityl ketone of 62° calculated by Braude and Sondheimer (13) from the dipole moment determined by Bentley *et al.* (17), 63° determined by Braude and Sondheimer (13) from ultraviolet data, and 90° determined by Aroney *et al.* (8) from Kerr constants and 90° for methyl duryl ketone also by the latter workers (8).

Dhami and Stothers (3, 6) concluded that the increases ($\Delta\theta$) of 1 to 6° in interplanar angles on going from the mesityl to the corresponding duryl ketones were evidence for the operation of a buttressing effect by the additional *meta* methyl groups in the duryl ketones. In the present investigation, increases of 1 to 5° as calculated by method A and values to 3° using method B were obtained. Since the amount of increase depends on the validity of the method of calculation, it is concluded that evidence for buttressing from dipole moment data in the duryl ketone system is tentative at the present time.

The authors express appreciation to the Robert A. Welch Foundation of Houston, Texas for partial support of the work reported and to Professor J. Trotter, University of British Columbia for a copy of his paper (14) before publication.

[6]These were calculated by a referee and rechecked during the revision of the paper. The authors express appreciation to the referee for constructive comments on this and other points.

[7]The values listed are "corrected" values which are derived from "corrected" ^{13}C shielding data which were applied to correct for an *ortho* effect ascribed to a non-steric origin as observed in a significant variation in chemical shifts between *ortho* derivatives compared with *meta*- and *para*-substituted ones.

1. A. G. PINKUS and H. C. CUSTARD, JR. J. Phys. Chem. **74**, 1042 (1970).
2. I. G. HALVERSTADT and W. D. KUMLER J. Am. Chem. Soc. **64**, 2988 (1942).
3. K. S. DHAMI and J. B. STOTHERS. Can. J. Chem. **43**, 498 (1965).
4. L. I. SMITH and C. GUSS. J. Am. Chem. Soc. **59**, 804 (1937); V. MEYER. Chem. Ber. **29**, 146 (1896).
5. W. F. FORBES and W. A. MUELLER. Can. J. Chem. **33**, 1145 (1955).

6. K. S. DHAMI and J. B. STOTHERS. Can. J. Chem. **43**, 479 (1965).
7. F. BAUM and V. MEYER. Chem. Ber. **28**, 3212 (1895).
8. M. J. ARONEY, M. B. CORFIELD, and R. J. W. LE FÈVRE. J. Chem. Soc. 648 (1964).
9. R. G. KADESCH and S. W. WELLER. J. Am. Chem. Soc. **63**, 1310 (1941).
10. A. L. MCCLELLAN. Tables of experimental dipole moments. W. H. Freeman and Co., San Francisco, California. 1963.
11. J. W. SMITH. Electric dipole moments. Butterworths, London. 1955. pp. 214, 215.
12. V. I. MINKIN, O. A. OSIPOV, and Y. A. ZHDANOV. Dipole moments in organic chemistry. *Translated by* B. J. Hazard. Plenum Press, New York. 1970. p. 209.
13. E. A. BRAUDE and F. SONDHEIMER. J. Chem. Soc. 3754 (1955).
14. C. A. BEAR, A. L. MACDONALD, and J. TROTTER. Acta Cryst. B**29**, 2716 (1973).
15. A. G. PINKUS, J. I. RIGGS, JR., and S. B. BROUGHTON. J. Am. Chem. Soc. **90**, 5043 (1968).
16. V. V. MOISEEV and L. P. ZALUKAEV. Izv. Vyssh. Uchebn. Zaved. Khim. Khim. Tekhnol. **10**, 945 (1967); Chem. Abstr. **68**, 68590 (1968); W. R. WATT and C. K. FISHER. J. Polym. Sci. Part A-1, **7**, 2815 (1969); T. HORIE and M. MAUMURA. Kogyo Kagaku Zasshi, **72**, 686 (1969); Chem. Abstr., **72**, 66154 (1970).
17. J. B. BENTLEY, K. B. EVERARD, R. J. B. MARSDEN, and L. E. SUTTON. J. Chem. Soc. 2957 (1949).
18. A. G. PINKUS and E. Y. LIN. J. Mol. Struct. **24**, 9 (1975).
19. F. BROWN, J. M. A. DE BRUYNE, and P. M. GROSS. J. Am. Chem. Soc. **56**, 1291 (1934).
20. E. V. GOODE and D. A. IBBITSON. J. Chem. Soc. 4265 (1960).
21. C. E. INGHAM and G. C. HAMPSON. J. Chem. Soc. 981 (1939).
22. J. W. SMITH. J. Chem. Soc. 109 (1953).
23. R. H. BIRTLES and G. C. HAMPSON. J. Chem. Soc. 10 (1937).
24. J. B. STOTHERS. Q. Rev. **19**, 144 (1965).

Can. J. Chem. Downloaded from www.nrcresearchpress.com by 210.87.254.40 on 09/05/12
For personal use only.

Erratum: The Chemistry of Cochliodinal, a Metabolite of *Chaetomium* spp.

W. A. JERRAM, A. G. MCINNES, W. S. G. MAASS, D. G. SMITH, A. TAYLOR, AND J. A. WALTER

Atlantic Regional Laboratory, National Research Council of Canada, Halifax, Nova Scotia B3H 3Z1

Received April 30, 1975

(Ref.: Can. J. Chem. **53**, 727 (1975))

Compounds **1–4** were incorrectly arranged after proofreading and should be as indicated below:

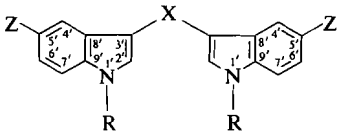

Compound **1**

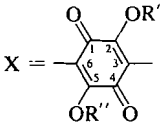

a–d Z = CH_3—C(13′CH_3)=CH—CH_2— (14′ 12′ 11′ 10′)

a R = R′ = R″ = H
b R = R′ = H; R″ = CH_3CO
c R = H; R′ = R″ = CH_3CO
d R = H; R′ = R″ = CH_3

e and *f* Z = CH_3—C(H)(CH$_3$)—CH_2—CH_2—

e R = R′ = R″ = H
f R = H; R′ = R″ = CH_3CO

Compound **2**

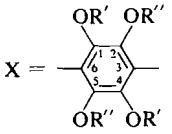

a–g Z = CH_3—C(13′CH_3)=CH—CH_2— (14′ 12′ 11′ 10′)

a R = R′ = R″ = H
b R = H; R′ = R″ = CH_3CO
c R = R′ = R″ = CH_3CO
d R = CHO; R′ = R″ = CH_3CO
e R = H; R′ = CH_3; R″ = CH_3CO
f R = R′ = H; R″ = CH_3
g R = R′ = H; R″ = CH_3CO

h–k Z = CH_3—C(H)(CH$_3$)—CH_2—CH_2—

h R = R′ = R″ = H
i R = R′ = H; R″ = CH_3CO
j R = H; R′ = R″ = CH_3CO
k R = R′ = R″ = CH_3CO

l Z = CH_3—C(OR‴)(CH$_3$)—C(OR‴)(H)—CH_2—

R = H; R′ = R″ = R‴ = CH_3CO

Compound **3**

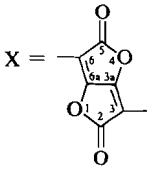

a and *b* Z = CH_3—C(13′CH_3)=CH—CH_2— (14′ 12′ 11′ 10′)

a R = H
b R = CH_3CO

c and *d* Z = CH_3—CH(CH$_3$)—CH_2—CH_2—

c R = H
d R = CH_3CO

Compound **4**

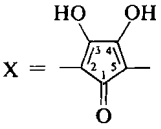

a Z = CH_3—C(13′CH_3)=CH—CH_2— (14′ 12′ 11′ 10′)

R = H

Can. J. Chem. Downloaded from www.nrcresearchpress.com by 210.87.254.42 on 09/05/12
For personal use only.

Can. J. Chem. Downloaded from www.nrcresearchpress.com by 210.87.254.5 on 09/05/12
For personal use only.

Canadian Journal of Chemistry

Published by
THE NATIONAL RESEARCH COUNCIL OF CANADA

Journal canadien de chimie

Publié par
LE CONSEIL NATIONAL DE RECHERCHES DU CANADA

Volume 53 Number 14 July 15, 1975 Volume 53 numéro 14 15 juillet 1975

Hydroboration du *tert*-butyl-4 diméthyl-2,2 méthylène-1 cyclohexane et du triméthyl-3,3,5 méthylène-1 cyclohexane. Préparation des *tert*-butyl-4 hydroxyméthyl-1 diméthyl-2,2 cyclohexanes et des hydroxyméthyl-1 triméthyl-3,3,5 cyclohexanes[1]

JEAN-CLAUDE RICHER ET CLAUDE LAMARRE[2]

Département de Chimie, Université de Montréal, B.P. 6210, Montréal, Québec H3C 3V1

Received November 4, 1974

JEAN-CLAUDE RICHER et CLAUDE LAMARRE. Can. J. Chem. 53, 2033 (1975).

On examine la stéréochimie de la réaction d'hydroboration du *tert*-butyl-4 diméthyl-2,2 méthylène-1 cyclohexane et du triméthyl-3,3,5 méthylène-1 cyclohexane. Pour fins de comparaison, la stéréochimie de la réaction d'hydroboration du *tert*-butyl-4 méthylène-1 cyclohexane a aussi été examinée. Les *tert*-butyl-4 hydroxyméthyl-1 diméthyl-2,2 cyclohexanes *cis* et *trans* ainsi que les hydroxyméthyl-1 triméthyl-3,3,5 cyclohexanes *cis* et *trans* ont été obtenus à l'état pur et leur stéréochimie respective prouvée par l'intermédiaire des acides et des esters correspondants.

JEAN-CLAUDE RICHER and CLAUDE LAMARRE. Can. J. Chem. 53, 2033 (1975).

The stereochemistry of the hydroborations of 4-*tert*-butyl-2,2-dimethyl-1-methylenecyclohexane and of 3,3,5-trimethyl-1-methylenecyclohexane has been studied for comparison with that of the hydroboration of 4-*tert*-butyl-1-methylenecyclohexane which also was examined. *cis*- and *trans*-4-*tert*-butyl-1-hydroxymethyl-2,2-dimethylcyclohexane as well as *cis*- and *trans*-1-hydroxymethyl-3,3,5-trimethylcyclohexane were obtained in a pure state and their configurations proved by means of the corresponding acids and esters. [Journal translation]

Introduction

Dans le cadre de nos travaux sur la stéréochimie des réactions d'addition sur des cyclohexanones (1) et du méthylène cyclohexane **1***a* (2) et dans le but de préparer les hydroxyméthyl-1 cyclohexanes correspondants, nous avons été amenés à examiner la stéréochimie des réactions d'hydroboration des méthylènes cyclohexanes **1***a*, **1***b* et **2**. Ce sont les résultats obtenus au cours de cette étude qui font l'objet du présent mémoire. La stéréochimie de la réaction d'hydroboration du *tert*-butyl-4 méthylène-1 cyclohexane (**1***b*) a été rapportée (3) depuis que ce travail a été complété; nous comparons les résultats obtenus avec ceux rapportés antérieurement.

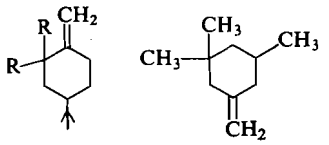

1
a R = CH_3
b R = H

2

[1]Les résultats rapportés dans ce mémoire sont tirés en partie de la thèse présentée par C. L. en vue de l'obtention du grade de Ph.D. (mars 1971).

[2]Adresse actuelle: Institut de Recherche de l'Hydro-Québec (IREQ), Varennes, Québec.

Can. J. Chem. Downloaded from www.nrcresearchpress.com by 210.87.254.5 on 09/05/12
For personal use only.

Résultats

Hydroboration du tert-butyl-4 diméthyl-2,2 méthylène-1 cyclohexane (1a)

L'hydroboration de l'alcène **1***a* dans le diglyme, selon la méthode décrite par Brown et Zweifel (4), fournit les organoboranes **3***a* et **4***a* qui, par oxydation par l'eau oxygénée alcaline, conduisent aux alcools primaires **3***b* et **4***b* accompagnés du *bis*(*tert*-butyl-4 diméthyl-2,2 cyclohexyl)-1,2 éthane (**5**). Les quantités relatives des alcools **3***b* et **4***b* ont été déterminées par chromatographie en phase gazeuse à l'aide des

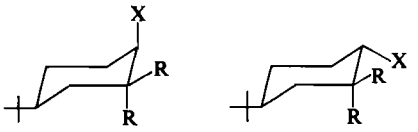

3 R = CH_3
9 R = H

4 R = CH_3
10 R = H

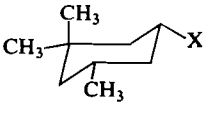

6

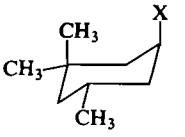

7

a X = CH_2—B<
b X = CH_2OH
c X = $CH_2OSi(CH_3)_3$
d X = COOH
e X = COOEt
f X = Br
g X = OH
h X = MgBr

éthers silylés **3***c* et **4***c* préparés selon la méthode de Sweeley *et al.* (5). On note alors la présence de 42.5% d'éther *cis* **3***c* par rapport à 57.5% d'éther *trans* **4***c*. L'oxydation du mélange des alcools **3***b* et **4***b* par de l'acide chromique selon le procédé de Brown et Garg (6) conduit avec un rendement de 50% aux acides correspondants **3***d* et **4***d*. L'estérification de ces acides en milieu acide par l'éthanol selon la méthode de Mori (7) fournit les esters éthyliques correspondants **3***e* et **4***e*. L'analyse par chromatographie en phase gazeuse de ces esters indique la présence de 22% d'ester éthylique *cis* **3***e* et 78% d'ester éthylique *trans* **4***e*. Ce résultat analytique indique qu'une épimérisation se produit au cours de la transformation des alcools primaires en esters. Les esters éthyliques **3***e* et **4***e* ont été séparés par chromatographie en phase gazeuse préparative.

TABLEAU 1. Les résultats de l'épimerisation des esters **3***e* et **4***e*

Esters	δ C*H* (COOEt) (p.p.m.)	% à l'équilibre
3*e*	2.20	9
4*e*	1.65	91

Les configurations relatives *cis* et *trans* des esters éthyliques **3***e* et **4***e* furent établies en se basant sur les deux critères suivants.

(*a*) Le déplacement chimique en r.m.n. du méthine en α du carboéthoxy: Lemieux *et al.* (8) et Eliel et Gianni (9) ont démontré que les méthines axiaux apparaissent dans la r.m.n. à des champs plus forts que les méthines équatoriaux pour les dérivés *cis* et *trans* dans le système *tert*-butyl-4 cyclohexyle du type 4-$(CH_3)_3$—C—CH—$(CH_2)_4$—CHX. Si l'on fait l'hypothèse que les groupes *tert*-butyle et *gem*-diméthyle n'affectent pas le déplacement chimique du méthine en α du groupement carboéthoxy; il est raisonnable de supposer que l'ester dont le méthine apparait au champ le plus fort possède la configuration relative *trans*. L'examen du tableau 1 permet d'attribuer la configuration relative *cis* à l'ester éthylique **3***e* et la configuration relative *trans* à l'ester éthylique **4***e*.

(*b*) La position de l'équilibre lors de l'épimérisation des esters éthyliques en présence d'une quantité catalytique de *tert*-butylate de potassium dans du DMSO à 25°: Les résultats obtenus lors de l'épimérisation de chacun des esters éthyliques **3***e* et **4***e* par une quantité catalytique de *tert*-butylate de potassium dans le DMSO à 25° sont résumés dans le tableau 1. Ils mettent en évidence la présence d'une quantité prépondérante de l'ester équatorial **4***e*. La différence d'énergie libre entre les deux esters serait de 1.39 kcal/mol et cette valeur est en accord avec la différence d'énergie libre que l'on peut calculer en faisant appel aux valeurs préconisées d'une part par Tichy et Sicher (10) pour les interactions *gauches* vicinales entre le couple CH_3 . . . COOMe et d'autre part par divers auteurs (11) pour les interactions 1,3 diaxiales entre le substituant COOEt et les hydrogènes axiaux en position 3 et 5. Cette conclusion suppose que l'on fait l'hypothèse que les valeurs de l'énergie d'interaction *gauche* vicinale du couple CH_3 . . . COOEt sont du même ordre de grandeur que celles du couple CH_3 . . . COOMe.

La connaissance des configurations relatives

Can. J. Chem. Downloaded from www.nrcresearchpress.com by 210.87.254.5 on 09/05/12
For personal use only.

des esters éthyliques **3***e* et **4***e* permet également, par réduction par l'hydrure de lithium et d'aluminium des esters obtenus à l'état pur, d'attribuer les configurations relatives *cis* et *trans* aux alcools primaires **3***b* et **4***b*.

Hydroboration du triméthyl-3,3,5 méthylène-1 cyclohexane (2)

L'hydroboration de l'alcène **2**, préparé à partir de la triméthyl-3,3,5 cyclohexanone (**12**) de la manière de Cross et Whitham (12), conduit par oxydation directe des organoboranes intermédiaires **6***a* et **7***a* aux alcools primaires **6***b* et **7***b* en plus d'un produit auquel on a attribué la structure du *bis*(triméthyl-3,3,5 cyclohexyl)-1,2 éthane (**8**) par extrapolation des résultats obtenus lors

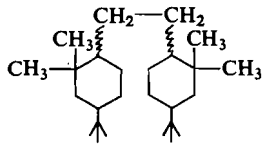

5

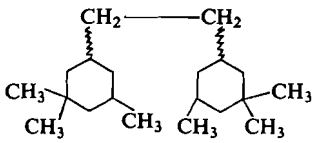

8

de l'hydroboration de l'alcène **1***a*. Le rapport *cis*/*trans* des alcools primaires **6***b* et **7***b* est de 12:88. L'alcool primaire *trans* **7***b* a été isolé de ce mélange par chromatographie en phase gazeuse préparative; on peut aussi l'obtenir par la suite des réactions décrites ci-dessous. L'oxydation du mélange des alcools primaires **6***b* et **7***b* par l'acide chromique conduit aux acides correspondants **6***d* et **7***d*. L'estérification de ce mélange avec de l'éthanol en milieu acide conduit aux esters **6***e* et **7***e*. Le triméthyl-3,3,5 cyclohexane carboxylate d'éthyle *trans* (**7***e*) a été isolé de ce mélange réactionnel par chromatographie en phase gazeuse préparative et sa réduction par l'hydrure de lithium et d'aluminium conduit au même alcool **7***b* qui a été isolé du milieu réactionnel d'hydroboration. La chromatographie en phase gazeuse préparative n'a pas permis d'isoler l'alcool primaire *cis* **6***b* formé lors de la réaction d'hydroboration. Cet alcool a été synthétisé et obtenu à l'état pur en faisant appel à la procédure expérimentale qui suit. Le dérivé bromé **7***f* est préparé par l'action du tribromure de phosphore sur le triméthyl-3,3,5 cyclohexanol-1 *cis* (**6***g*) selon les indications de Braude et Evans (13). La carbonation de l'organomagnesien (**6***h* ou **7***h*) permet d'obtenir l'acide carboxylique **6***d* et l'estérification de cet acide avec de l'éthanol en milieu acide conduit à l'ester éthylique *cis* **6***e*. La réduction de **6***e* par l'hydrure de lithium et d'aluminium permet d'obtenir l'alcool primaire *cis* **6***b* pur et son temps de rétention en c.p.g. correspond à l'alcool primaire non isolé de la réaction d'hydroboration. La détermination des configurations relatives des esters éthyliques **6***e* et **7***e* sur laquelle repose l'attribution des configurations relatives des alcools primaires **6***b* et **7***b* dépend: (*i*) de la position de l'équilibre lors de l'épimérisation des esters éthyliques **6***e* et **7***e* à l'état pur, (*ii*) des vitesses relatives de saponification de ces esters et (*iii*) du déplacement chimique des protons $\rangle CH$—COOEt tel que décrit précédemment. Les résultats consignés dans le tableau 2 montrent que l'ester équatorial *cis* **6***e* est présent en quantité prépondérante (95%) dans le mélange à l'équilibre. Ce pourcentage correspond à une différence d'énergie libre entre les deux esters de 2.06 kcal/mol. Par ailleurs la plus grande vitesse de saponification de l'ester équatorial *cis* **6***e* est en accord avec les résultats rapportés antérieurement par Eliel *et al.* (11*c*) pour l'hydrolyse des *tert*-butyl-4 cyclohexane carboxylates d'éthyle (**9***e* et **10***e*).

Hydroboration du tert-butyl-4 méthylène-1 cyclohexane (1b)

L'hydroboration de l'alcène **1***b* dans le diglyme selon la technique habituelle (4) conduit après oxydation des organoboranes intermé-

TABLEAU 2. Les résultats de l'épimerisation des esters **6***e* et **7***e*

Esters	δ *CH* (COOEt) (p.p.m.)	% à l'équilibre	Vitesse de saponification ($l\ mol^{-1}\ s^{-1}$)
6*e*	2.44	95	29.02×10^{-4}
7*e*	2.61	5	6.30×10^{-4}

diaires **9***a* et **10***a* aux alcools primaires correspondants **9***b* et **10***b* accompagnés d'un composé auquel on a attribué la structure *bis*(*tert*-butyl-4 cyclohexyl)-1,2 éthane de configuration non déterminée (**11**) par comparaison avec les résultats

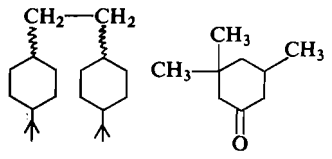

11 **12**

obtenus lors de l'hydroboration de l'alcène **1***a*. Les quantités relatives d'alcools **9***b* et **10***b* présents dans le milieu réactionnel ont été déterminées par chromatographie en phase gazeuse par l'intermédiaire de leurs éthers silylés **9***c* et **10***c*, préparés d'après la méthode de Sweeley *et al.* (5). Le produit *cis* **9***b* et le produit *trans* **10***b* seraient présents dans les proportions de 52 et de 48%. L'oxydation du mélange d'alcools par l'acide chromique selon la méthode de Brown et Garg (6) conduit aux acides correspondants **9***d* et **10***d* et leur estérification conduit aux esters éthyliques **9***e* et **10***e*; d'après la chromatographie en phase gazeuse, ils sont présents dans les proportions de 52% de **9***e* et 48% de **10***e*. Ces résultats confirmeraient ceux obtenus à l'aide des éthers silylés et indiqueraient bien que les alcools primaires **9***b* et **10***b* sont formés en quantités pratiquement égales. L'épimérisation du mélange des esters **9***e* et **10***e* a été effectuée dans les conditions classiqués, c'est à dire, dans l'éthanol absolu en présence d'éthylate de sodium à la température de 80°. Le pourcentage des différents isomères à l'équilibre a été déterminé par chromatographie en phase gazeuse et il est de 14.4% d'ester *cis* **9***e* et de 85.6% d'ester *trans* **10***e*. Ce résultat concorde avec celui d'Eliel *et al.* (11*c*) qui ont obtenu 84.7 ± 0.6% d'ester éthylique *trans* **10***e*. La réduction par $LiAlH_4$ du mélange d'esters **9***e* et **10***e* (14.4:85.6) de configuration relative connue permet d'obtenir le mélange des alcools primaires **9***b* et **10***b*. L'analyse par chromatographie en phase gazeuse, après le traitement par les réactifs de silylation, indique la présence de 15.5% d'éther silylé *cis* **9***c* et 84.5% d'éther silylé *trans* **10***c* et permet ainsi d'attribuer les configurations relatives *cis* et *trans* aux alcools primaires **9***b* et **10***b*. Ces résultats sont différents de ceux rapportés, depuis que ce travail a été terminé, par Klein et Litchtenberg (3) qui ont observé que le diborane dans le tétrahydrofuranne s'additionne à l'alcène **1***b* pour conduire à un mélange d'alcools primaires *cis* **9***b* et *trans* **10***b* dans les proportions de 68 et 32%, respectivement.

Discussion

Les résultats obtenus lors de la réaction d'hydroboration des alcènes **1***a*, **1***b* et **2** sont rapportés dans le tableau 3. Pour fins de comparaison, les résultats de l'époxydation des al-

TABLEAU 3. Les résultats de la reaction d'hydroboration des alcènes **1***a*, **1***b* et **2**

	% entrée équatoriale (réf.)				
	X = CH_2			X = O	
Composés	Hydroboration	Epoxydation	CH_3MgI	$(CH_3)_2SOCH_2$	$LiAlH_4$
	88(ce travail)	100(14)	100(14)	100(14)	55(18)
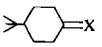	52(ce travail) 68(3)	31(15)	50(16)	100(17)	11(19)
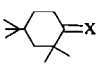	42.5(ce travail)	28(2)	40(2)	84(2)	5(20)

Can. J. Chem. Downloaded from www.nrcresearchpress.com by 210.87.254.5 on 09/05/12
For personal use only.

Can. J. Chem. Downloaded from www.nrcresearchpress.com by 210.87.254.5 on 09/05/12
For personal use only.

cènes **1***a*, **1***b* et **2**, de l'addition de l'organomagnésien CH_3MgI, de l'addition de l'hydrure de lithium et d'aluminium et de la méthylénation par l'action du méthylure de diméthylsulfonium sur les cétones correspondantes sont aussi rapportés.

On peut déduire de ces résultats que la stéréochimie de la réaction d'hydroboration sur l'alcène **2** est dirigée principalement par la présence du méthyle axial en position 3 par rapport au centre réactionnel qui provoque une réaction par la face opposée de la molécule conduisant principalement à l'alcool primaire **7***b* du type *trans*. La comparaison des résultats obtenus lors de l'hydroboration des alcènes **1***a* et **1***b* met de nouveau en évidence l'influence du groupe méthyle axial en position 2 qui empêche une attaque par cette face de la molécule et provoque l'entrée par la face axiale opposée réduisant ainsi le pourcentage d'entrée équatoriale.

La correspondance entre les résultats rapportés dans le tableau 3 pour les réactions d'hydroboration, d'époxydation, de Grignard, d'addition d'hydrure et de méthylénation montre la similitude des facteurs influençant le cours stéréochimique de ces réactions.

Partie expérimentale

Les instruments utilisés pour déterminer les propriétés physiques des produits obtenus au cours de cette étude ont été décrits dans une publication précédente (21). Les propriétés physiques sont consignées dans le tableau 4. Les poids moléculaires ont été déterminés au moyen d'un osmomètre à pression de vapeur de la compagnie Perkin-Elmer modèle 115 en utilisant le chloroforme comme solvant. La précision est de $\pm 2\%$.

Les séparations par chromatographie en phase gazeuse (c.p.g.) préparative ont été effectuées à l'aide d'un appareil Varian modèle 705 dans les conditions suivantes: (*a*) Colonne en aluminium de 20 pieds par 3/8 de pouce de diamètre remplie de Chromport XXX (80–90 mesh) supportant 20% de son poids de silicone SE-52. La colonne est maintenue à une température de 185°; le collecteur à 115°; le détecteur à 250°; l'injection est faite à 225°. Le gaz porteur est l'azote; son débit est de 165 ml/min. (*b*) Colonne en aluminium de 20 pieds par 3/8 de pouce de diamètre remplie de Chromosorb P (30–60 mesh) supportant 20% de son poids d'hyprose. La colonne est maintenue à une température de 160°; le collecteur à 135°; le détecteur à 255°; et l'injecteur à 225°. Le gaz porteur est l'azote; son débit est de 165 ml/min.

Dans le but de vérifier si tous les pourcentages relatifs d'épimères qui sont rapportés au cours de ce travail sont exacts, des mélanges connus d'épimères ont été préparés par pesée et analysée par c.p.g. Dans chaque cas, le pourcentage obtenu par c.p.g. s'est avéré exact.

Synthèse des tert-butyl-4 hydroxyméthyl-1 diméthyl-2,2 cyclohexanes cis (3b) et trans (4b)

L'hydroboration oxydative de 3 g (16 mmol) d'alcène **1***a* en solution dans le diglyme en suivant la méthode décrite par Brown et Zweifel (4) conduit à 3.6 g d'un liquide visqueux. La chromatographie de 2.83 g de ce mélange sur 200 g d'alumine Woëlm (activité 1) fournit 756 mg du dimère **5** et 1.73 g du mélange des alcools primaires **3***b* et **4***b*. L'analyse de ces alcools, sous forme d'éthers silylés (5), indique la présence de 42.5% d'éther *cis* (**3***c*) et 57.5% d'éther *trans* (**4***c*); une analyse semblable effectuée sur le produit brut de l'hydroboration montre que les composés **5**, **3***c* et **4***c* sont respectivement présents dans les proportions 20:34:46 soit un rapport 42.5:57.5 pour les alcools primaires **3***b*/**4***b*.

L'oxydation de 12 g (61 mmol) du mélange des alcools **3***b* et **4***b* (débarrassé de l'hydrocarbure **5**) selon la technique de Brown et Garg (6) conduit à 6.3 g (50% de rendement) du mélange des acides **3***d* et **4***d* se présentant sous forme de solide de p.f. 115° après recristallisation dans un mélange acide acétique - eau.

L'estérification de 14.6 g (69 mmol) du mélange des acides carboxyliques **3***d* et **4***d* en suivant la technique de Mori (7) permet d'obtenir les esters éthyliques **3***e* et **4***e* correspondants avec un rendement de 50%. Les deux esters **3***e* et **4***e* ont été obtenus à l'état pur par c.p.g. préparative sur la colonne de SE-52; leurs propriétés respectives sont résumées au tableau 4.

La réduction de chacun de ces esters **3***e* et **4***e* par le $LiAlH_4$ dans le THF conduit aux alcools correspondants **3***b* et **4***b* à l'état pur. Les propriétés de ces alcools sont aussi résumées au tableau 4.

L'épimérisation de chacun des esters **3***e* et **4***e* (45 mg, 0.18 mmol) a été effectuée à l'aide de 3.2 ml (0.22 mmol) d'une solution (0.072 *N*) de *tert*-butylate de potassium dans le DMSO; la réaction, sous atmosphère d'azote, dure 18 h.

Synthèse des hydroxyméthyl-1 triméthyl-3,3,5 cyclohexanes 6b et 7b

L'alcène **2** est obtenu avec un rendement de 70% (35 g) à partir de la cétone correspondante **12** (50 g, 0.38 mol) et du méthylène triphénylphosphine, préparé à partir de 185 g (0.5 mol) de bromure de méthyltriphénylphosphonium et de 32 g (0.5 mol) de butyllithium, selon le mode opératoire décrit par Cross et Whitham (12).

L'hydroboration oxydative de 15 g (0.11 mol) de l'alcène **2** selon la technique de Brown et Zweifel (4) conduit à un mélange réactionnel formé de 10% de l'alcool **6***b*, 75% de l'alcool **7***b* et 15% de l'hydrocarbure **8**.

L'hydroxyméthyl-1 triméthyl-3,3,5 cyclohexane *trans* (**7***b*) a été isolé par c.p.g. préparative sur la colonne d'hyprose et purifié par distillation. Ses caractéristiques sont résumées dans le tableau 4.

L'oxydation de 6.5 g du mélange des alcools **6***b* et **7***b* en suivant la procédure de Brown et Garg (6) conduit à 2.1 g (30% de rendement) des acides carboxyliques **6***d* et **7***d* correspondants; l'estérification de 1.6 g de ces acides en opérant selon la technique de Mori (7) conduit aux esters éthyliques **6***e* et **7***e* avec un rendement de 96%.

La c.p.g. préparative permet d'isoler l'ester éthylique *trans* **7***e* à l'état pur; ses caractéristiques sont résumées au

Can. J. Chem. Downloaded from www.nrcresearchpress.com by 210.87.254.5 on 09/05/12
For personal use only.

TABLEAU 4. Les propriétés physiques des produits d'hydroboration

	Point d'ébullition (°C) (mm Hg)	n_D (°C)	Infrarouge $\nu(cm^{-1})^a$	Chromatographie en phase gazeuse[b]	Résonance magnétique nucléaire (p.p.m.)[a,c] $(CH_3)_3C$	CH_3	Particularités	Spectre de masse ion moléculaire *m/e*
3*b*[d]	80	—	3650		0.80[e]	0.87	1.65 (OH)	
	(0.7)		3350(OH)			0.98	3.47 (q, J_{vic}=8.0 et $J_{gém}$=10.47) et	
			1035				3.68 (q, J_{vic}=5.19 et $J_{gém}$=10.47)	198
	(p.f. 67–69		1010				(CH_2OH: partie AB d'un système ABX)	
			990					
			975(C—O)					
4*b*[d]	88	1.4698	3670		0.80	0.74	1.68 (OH)	
	(0.4)	(26.5)	3460(OH)			0.95	3.16 (q, J_{vic}=8.06 et $J_{gém}$=10.13) et	
			1040				3.78 (q, J_{vic}=3.00 et $J_{gém}$=10.13)	198
			1025				(CH_2OH: partie AB d'un système ABX)	
			995					
			965(C—O)					
3*e*	66–68	1.4532	1720	Colonne B	0.85	0.93	1.22 et 4.02 (CH_3—CH_2—O, J=7.0)	
	(0.4)	(24.5)		Tr: 7.25 min		0.97	2.20 (massif) (C*H*—COOEt)	240
4*e*	86–88	1.4542	1725	Colonne B	0.82	0.92	1.22 et 4.04 (CH_3—CH_2—O, J = 7.0)	240
	(0.6)	(24)		Tr: 9 min		1.00	1.65 (massif) (C*H*—COOEt)	
5	140	—	1465	Colonne A	0.81[e]	0.72(1)		362
	(0.4)		1380	Tr: 8.25 min		0.88(2)		p.m.
			1365			0.95(1)		Trouvé 365
	(p.f. 95–100)		1230					Calculé 362.6
			1180					
2	109–110	1.4438	3080	Colonne C		0.88	1.85 (CH_2 en C_2)	
	(244)	(26)	1650	Tr: 14 min		0.95	(3 × CH_3) 4.56 ($>C{=}CH_2$)	138
			880					
			860					

Can. J. Chem. Downloaded from www.nrcresearchpress.com by 210.87.254.5 on 09/05/12
For personal use only.

TABLEAU 4 (*Suite en fin*)

	Point d'ébullition (°C) (mm Hg)	n_D (°C)	Infrarouge $\nu(cm^{-1})$[a]	Chromatographie en phase gazeuse[b]	Résonance magnétique nucléaire (p.p.m.)[a,c] $(CH_3)_3C$	CH_3	Particularités	Spectre de masse ion moléculaire *m/e*
6b	114	1.4568	3650	Colonne D		0.90 ($3\times CH_3$)	3.28 (d, $J = 6.0$) (CH_2OH)	
	(24)	(27.5)	3350(OH)	Tr: 4 min			3.78 (OH)	156
			1055					
			1020(C—O)					
7b	120	1.4609	3610	Colonne D		0.93 ($3\times CH_3$)	1.72 (OH)	
	(24)	(25.5)	3400(OH)	Tr: 5 min			3.57 (multiplet) (CH_2OH)	p.m.
			1025					Trouvé 159
			1005(C—O)					Calculé 156.1
			($CHCl_3$)					
6e	115	1.4424	1725	Colonne B		0.92 ($3\times CH_3$)	1.20 et 4.01 (CH_3—CH_2—O, J=6.75)	
	(21)	(26)		Tr: 17 min			2.44 (multiplet) ($>CH$—COOEt)	198
7e	120	1.4419	1725	Colonne B		0.88 ($3\times CH_3$)	1.26 et 4.14 (CH_3—CH_2—O, $J = 7.5$	
	(20)	(27)		Tr: 16 min			2.61 (multiplet) [$>CH$—COOEt]	198
11	160		1480	Colonne A	0.81			306
	(0.4)		1450	Tr: 17.5 min				p.m.
	(p.f. 60)		1365	(16.5%)				Trouvé 295
			1230	Tr: 18.75 min				Calculé 306.5
				(18%)				

[a]A moins d'indication contraire, les spectres i.r. et r.m.n. ont été déterminés dans le CCl_4.
[b]Les analyses par chromatographie en phase gazeuse (c.p.g.) ont été effectuées à l'aide des appareils suivants: colonne A: F et M (modèle 700) à ionisation de flamme: SE-30 10% – Chromport XXX 80–90, 12 pieds, diamètre 1/4 pouce (3*c*, 4*c* et 5, *T*: 200°, He: 40 ml/min et **11**, *T*: 180°, He: 30 ml/min); colonne B: "Microtek" à détection thermique: SE-52 5% – Chromport XXX 80–90, 15 pieds, diamètre 1/4 pouce (3*e* et 4*e*, *T*: 200°, He: 75 ml/min et 6*e* et 7*e*, *T*: 150°, He: 60 ml/min); colonne C: F et M (modèle 810) à ionisation de flamme: Ucon Polar 20% Chromosorb W 30–60, 15 pieds, diamètre 1/4 pouce, *T*: 160°, He: 30 ml/min; colonne D: "Microtek" à détection thermique: hyprose 15% – Chromosorb P 30–60, 10 pieds, diamètre 1/4 pouce, *T*: 150°, He: 75 ml/min.
[c]La partie AB du système ABX pour le signal du —CH_2OH est obtenue par calcul du premier ordre. Les constantes de couplage de spin, *J*, sont exprimés en Hz. Le centre de symétrie est rapporté pour le signal d'un multiplet ou d'un massif.
[d]Les temps de retention des éthers silylés 3*c* et 4*c* sont respectivement de 21 et 33 min (colonne A).
[e]Spectres r.m.n. déterminés dans $CDCl_3$.

tableau 4. Sa réduction par $LiAlH_4$ conduit à un alcool primaire *trans* **7***b* identique à celui isolé précédemment.

L'acide triméthyl-3,3,5 cyclohexane carboxylique *cis* (**6***d*) est préparé selon la technique de Braude et Evans (13); ses propriétés, identiques à celles rapportées par ces auteurs, sont résumées au tableau 4. Son estérification selon la technique de Mori (7) fournit l'ester éthylique **6***e* avec un rendement de 90%; les propriétés de cet ester sont résumées au tableau 4. Sa réduction par $LiAlH_4$–éther conduit à l'alcool primaire **6***b* à l'état pur; les propriétés de cet alcool sont aussi résumées au tableau 4.

L'épimérisation des esters **6***e* et **7***e* se fait en chauffant 2 mmol d'ester, sous atmosphère d'azote pendant 72 h, en présence de 33 mmol d'éthylate de sodium dans l'éthanol.

Les vitesses de saponification sont obtenues par mesure de conductivité dans une cellule Radiometer du type CDC 104 reliée à un conductomètre Radiometer du type CDC 2d. La cellule est immergée durant toute l'expérience dans un bain maintenu à la température constante de 35.2°. Les mesures sont effectuées en utilisant une solution aqueuse de soude et une solution éthanolique d'ester à saponifier dans des proportions équimoléculaires et les constantes de vitesse sont calculées d'après la méthode du temps infini (22) et sont analysées comme réaction du deuxième ordre. Les résultats de ces cinétiques sont rapportés dans le tableau 2.

Hydroboration du tert-butyl-4 méthylène-1 cyclohexane (1b)

L'hydroboration oxydative de 8.5 g d'alcène **1***b* en solution dans le diglyme en suivant la technique de Brown et Zweifel (4), fournit 10 g de produits réactionnels qui par chromatographie sur 400 g d'alumine Woëlm (activité 1) permet de recueillir 2.6 g du dimère **11** et 7.2 g du mélange des alcools primaires **9***b* et **10***b*. La silylation de cette dernière fraction et son analyse par c.p.g. met en évidence que les quantités relatives des éthers **9***c* et **10***c* sont 52 et 48%.

L'oxydation des alcools **9***b* et **10***b* et l'estérification des acides **9***d* et **10***d*, dont les propriétés sont discutées dans la littérature (7, 23) ont été effectuées de la façon décrite précédemment. L'épimérisation des esters éthyliques **9***e* et **10***e* a été effectuée dans les mêmes conditions que celles décrites par Eliel *et al.* (11*c*).

Les auteurs remercient vivement le Conseil national de recherches du Canada et le Ministère de l'Education de la Province de Québec pour l'aide financière apporté sous forme d'octrois de recherche (A-1295) et de bourses d'étude (C.L.).

1. J. C. Richer, J. Org. Chem. **30**, 324 (1965).
2. J. C. Richer et C. Lamarre. Can. J. Chem. **47**, 2349 (1969).
3. J. Klein et D. Litchtenberg. J. Org. Chem. **35**, 2654 (1970).
4. H. C. Brown et G. Zweifel. J. Am. Chem. Soc. **83**, 1241 (1961).
5. C. C. Sweeley, R. Bentley, M. Makita et W. W. Wells. J. Am. Chem. Soc. **85**, 2497 (1963).
6. H. C. Brown et C. P. Garg. J. Am. Chem. Soc. **83**, 2952 (1961).
7. N. Mori. Bull. Soc. Chim. Jap. **34**, 1567 (1961).
8. R. U. Lemieux, R. K. Kullnig, H. J. Bernstein et W. G. Schneider. J. Am. Chem. Soc. **80**, 6098 (1958).
9. E. L. Eliel et M. H. Gianni. Tetrahedron Lett. 97 (1962).
10. M. Tichy et J. Sicher. Coll. Czech. Chem. Commun. **33**, 68 (1968).
11. (*a*) R. J. Ouellette et G. E. Booth. J. Org. Chem. **31**, 587 (1966); (*b*) N. L. Allinger et L. A. Freiberg. J. Org. Chem. **31**, 894 (1966); (*c*) E. L. Eliel, H. Haubenstock et R. V. Acharya. J. Am. Chem. Soc. **83**, 2351 (1961).
12. B. Cross et G. H. Whitham. J. Chem. Soc. 3892 (1960).
13. E. A. Braude et E. A. Evans. J. Chem. Soc. 607 (1954).
14. S. R. Landor, P. W. O'Connor, A. R. Tatchell et I. Blair. J. Chem. Soc. Perkin I, 473 (1973).
15. R. G. Carlson et N. S. Behn. J. Org. Chem. **32**, 1363 (1967).
16. H. Favre et D. Gravel. Can. J. Chem. **39**, 1548 (1961).
17. E. J. Corey et M. Chaykovsky. J. Am. Chem. Soc. **87**, 1353 (1965).
18. E. L. Eliel et H. Haubenstock. J. Org. Chem. **26**, 3504 (1961).
19. E. L. Eliel et M. N. Rerick. J. Am. Chem. Soc. **82**, 1367 (1960).
20. J. C. Richer et G. Perrault. Can. J. Chem. **43**, 18 (1965).
21. J. C. Richer et C. Lamarre. Can. J. Chem. **53**, 556 (1975).
22. F. Daniels, J. H. Mathews, J. W. Williams, P. Bender, G. W. Murphy et R. A. Alberty (*Redacteurs*). Experimental physical chemistry. McGraw-Hill Book Co. Inc., New York. 1949. p. 143.
23. H. O. House, R. W. Giese, K. Kronberger, J. P. Kaplan et J. F. Simeone. J. Am. Chem. Soc. **92**, 2800 (1970).

Can. J. Chem. Downloaded from www.nrcresearchpress.com by 210.87.254.5 on 09/05/12
For personal use only.

The Mechanism of the Microbial Hydroxylation of Steroids. Part 2. Hydroxylation of a Δ^4-3-Ketosteroid Analog by *Rhizopus arrhizus* ATCC 11145

HERBERT L. HOLLAND AND BARBARA J. AURET

Department of Chemistry, The Queen's University of Belfast, Belfast, Northern Ireland BT9 5AG

Received February 7, 1975

HERBERT L. HOLLAND and BARBARA J. AURET. Can. J. Chem. **53**, 2041 (1975).

The Δ^4-3-ketosteroid analog (±)-4a-methyl-4,4a,5,6,7,8-hexahydro-2(3*H*)-naphthalenone (**1**) is hydroxylated at both C-8α and C-8β by *Rhizopus arrhizus* ATCC 11145. The ratio of C-8α to C-8β hydroxylation is compared with that obtained from the peracid oxidation of 2-ethoxy-4a-methyl-3,4,4a,5,6,7-hexahydronaphthalene (**4**) and a mechanism is proposed for both microbial and chemical hydroxylation in which the stereochemistry of the product is transition state controlled. The significance of this to the mechanism of microbial C-6β hydroxylation of Δ^4-3-ketosteroids is discussed.

HERBERT L. HOLLAND et BARBARA J. AURET. Can. J. Chem. **53**, 2041 (1975).

Sous l'action du *Rhizopus arrhizus* ATCC 11145, la (±)-méthyl-4a hexahydro-4,4a,5,6,7,8-(3*H*)naphtalènone-2, qui est un analogue des Δ^4 céto-3 stéroides, est hydroxylée aux positions C-8α et C-8β. On compare les quantités relatives d'hydroxylation en C-8α et en C-8β avec les résultats obtenus lors de l'époxydation de l'éthoxy-2 méthyl-4a hexahydro-3,4,4a,5,6,7 naphtalène; on propose des mécanismes pour les hydroxylations microbiologiques et chimiques indiquant que le produit est contrôlé par l'état de transition. On discute de la signification de ce mécanisme par rapport à celui de l'hydroxylation microbiologique en C-6β des Δ^4 céto-3 stéroides. [Traduit par le journal]

It has long been known (1, 2) that microbial hydroxylations at the enolizable C-2 and C-6 of Δ^4-3-ketosteroids give only axial (β) products: the corresponding equatorial (α) hydroxyketones are not available by microbial methods. Analogously, treatment of steroid enols with electrophiles leads to exclusive axial substitution (3), exemplified by the reaction of $\Delta^{3,5}$ enols with peracids to give only 6β-hydroxy-Δ^4-3-ketones (4) (Scheme 1) and controlled by a stereoelectronic effect arising from preferred interaction of reagent orbitals in the transition state leading to axial substitution (5, 6). It has been proposed (1, 2) that microbial hydroxylations of ketosteroids at enolizable positions involve enolic intermediates and that oxygenation occurs under chemical rather than enzymic control.

We have found a significant lack of stereospecificity in both microbial and chemical hydroxylation at C-8 of the Δ^4-3-ketosteroid analog (±)-4a-methyl-4,4a,5,6,7,8-hexahydro-2(3*H*)-naphthalenone (**1**). Hydroxylation of **1** at C-8 is analogous to C-6β hydroxylation of Δ^4-3-ketosteroids, a reaction performed by *Rhizopus arrhizus* ATCC 11145 (7).

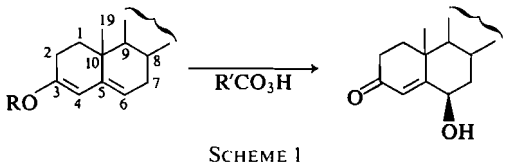

SCHEME 1

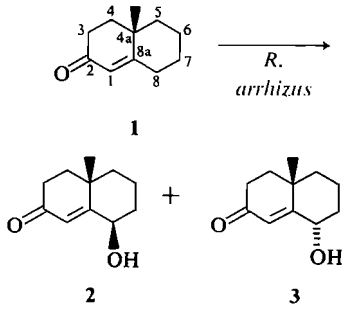

1 **2** **3**

SCHEME 2

Incubation of **1** with *R. arrhizus* gave two products, 8β-hydroxy-4a-methyl-4,4a,5,6,7,8-hexahydro-2(3*H*)-naphthalenone (**2**)[1] and 8α-hydroxy-4a-methyl-4,4a,5,6,7,8-hexahydro-2(3*H*)-naphthalenone (**3**) (Scheme 2). Their structures follow from p.m.r. data (Table 1). The position of the C-4a-methyl signal of **2** is characteristic of the presence of 1,3 diaxially disposed hydroxyl

[1]The terms α and β are used with the same connotation as that applicable to the steroid molecule.

Can. J. Chem. Downloaded from www.nrcresearchpress.com by 210.87.254.6 on 09/05/12
For personal use only.

TABLE 1. Proton magnetic resonance spectral data of compounds **1–4**

Compound	δ value		
	C-4a methyl	C-1 H	C-8 H
1	1.24	5.74	—
2	1.46	5.80	4.34
3	1.24	6.22	4.10–4.40
4	1.02	5.18–5.30	

(8) and confirmation of structure is provided by the width of the C-1 proton signal ($\omega_{1/2}$ = 1.3 Hz). The C-1 proton of **1** is, by analogy with corresponding steroids (9) coupled to the C-8β proton and appears as a broad singlet ($\omega_{1/2}$ = 3.8 Hz). The C-4a-methyl and methine proton geminal to hydroxyl of **3** show signals consistent with substitution at C-8α. Confirmation of structure comes from the C-1 proton signal at δ 6.22 (d, J = 2.0 Hz). A similar downfield shift and multiplicity is observed for the C-4 proton of C-6α substituted Δ^4-3-ketosteroids (10). The conversion of **2** to **3** has been achieved by acid catalysis.

The use of replacement culture (see Experimental) implies that the hydroxylation of **1** is performed by an enzyme which is noninduced and therefore a normal constituent of the fungus. Incubation of **1** with autoclaved *R. arrhizus* did not give transformation products and control experiments confirm that **2** is stable under the incubation conditions, excluding formation of **3** from **2**. We therefore feel that **2** and **3** are produced by the steroid C-6β hydroxylase but rigid proof of this is presently lacking.

The epimers **2** and **3** were obtained in the ratio 13 to 1. The microbial hydroxylation of **1** thus shows no stereoselectivity such as that observed for Δ^4-3-ketosteroids, where concomittant C-6α and C-6β hydroxylation has not been observed (1). Incubation of Δ^4-3-ketosteroids under conditions identical with those used for the hydroxylation of **1** does not give C-6α hydroxylated products (1, 7).[2]

The results may be rationalized by a consideration of the conformational mobility of **1** and the postulate that hydroxylation proceeds via the $\Delta^{2,8a}$ enol. Malhotra and Ringold have shown (5) that the transition state for electrophilic addition to a $\Delta^{3,5}$ enolic steroid resembles the keto form. The C-6—O bond is almost complete and the C-5—C-6 bond has lost most of its π electron density. Ring B is close to a chair conformation with the C-6β bond axial. During electrophilic addition to the bicyclic system, however, the C-8α bond may become pseudoaxial in a transition state with a twist-boat conformation of ring B. Attack of oxygen under stereoelectronic control will, favoring axial addition, form the C-8α substituted product **3** (Scheme 3, route *A*). Proceeding via a transition state with ring B in the chair conformation, the C-8β substituted product **2** will result. For the more rigid steroid molecule, only a transition state with ring B in the chair form is feasible and only C-6β substitution is observed. The proportion of **2** to **3** may therefore reflect the relative stabilities of the transition states (Scheme 3) from which C-8α or C-8β becomes axial.

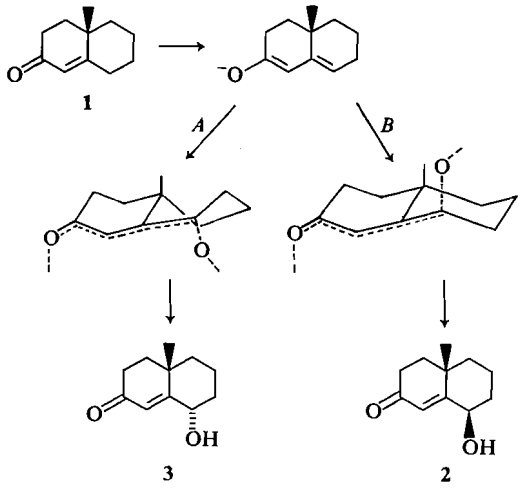

SCHEME 3

If the concurrent microbial formation of **2** and **3** is a consequence of the stereoelectronic control of oxygen addition to the enol, a parallel should exist in the chemical reaction of that enol with electrophilic oxygen. Accordingly, the enol ether **4** was prepared and its oxidation studied. The structure of **4** follows from u.v. spectral data (11) and p.m.r. analysis (Table 1) (8).

A close parallel with the microbial reaction was observed on oxidation of **4** with *m*-chloroperbenzoic acid (Scheme 4), when **2** and **3** were obtained in the ratio 4 to 1. Control experiments have shown that **2** is stable under the

[2]B. J. Auret and H. L. Holland. Unpublished data.

Can. J. Chem. Downloaded from www.nrcresearchpress.com by 210.87.254.6 on 09/05/12
For personal use only.

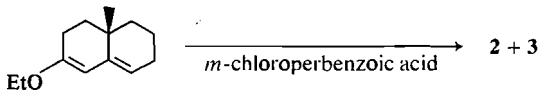

4

SCHEME 4

reaction conditions and so the formation of **3** from **2** may be discounted. The formation of both **2** and **3** indicates that, if normal stereoelectronically controlled axial addition is operative, then two reaction pathways such as those discussed above must be present. The greater degree of selectivity observed in the enzymic process may be due to some enzyme control of oxygen addition, but the microbial formation of **3** indicates that such control, if present, is not rigid.

The parallel between the peracid oxidation of **4** and the microbial hydroxylation of **1** thus suggests that prior enolization of **1** occurs in the microbial reaction but this cannot be definitively stated without further investigation.

Experimental

Apparatus, Materials, and Methods

Melting points were determined on a Kofler heating stage and are uncorrected. Infrared spectra were recorded with a Perkin-Elmer 137 and ultraviolet spectra in methanol solution with a Perkin-Elmer 402. Extinction coefficients were measured on a Unicam SP500. Proton magnetic resonance spectra were obtained at 100 MHz with a Varian HA100 or at 60 MHz on a Varian A60, using deuteriochloroform as solvent and tetramethylsilane as internal standard. Mass spectra were obtained with an AEI MS902 at an ionizing voltage of 70 eV. Accurate mass measurements were made by reference to appropriate ions of the perfluorokerosene spectrum.

Column chromatography was performed on silica gel (Woelm activity 1) and thin-layer chromatography on Merck silica $PF_{254+366}$.

Rhizopus arrhizus ATCC 11145 was obtained from the American Type Culture Collection, Washington D.C. and was maintained on 2% malt agar slopes.

Incubations with R. arrhizus

The fungus was grown in a medium consisting of a solution of glucose (250 g), peptone (100 g), and corn steep liquor (Dista Products Ltd., 15 ml) in water (5 l). One-litre Erlenmeyer flasks, each containing 150 ml of medium, were sterilized at 15 p.s.i. for 20 min and allowed to cool. A spore suspension obtained from an agar slope of the fungus by shaking with sterile glass beads in water was transferred to each flask using a sterile syringe and the flasks incubated on a rotary shaker (180 r.p.m.) at 28° for 60 h. The mycelium was then separated by centrifugation, washed by maceration with water, and resuspended in aliquots of distilled water (150 ml) in 1-l Erlenmeyer flasks. A solution of **1** (50 mg) in ethanol (3 ml) was added to each flask and shaking continued at 28° for a further 24 h; the p*H* of the suspension during this time remained constant at 5.0–5.3. The mycelium and water were separated by centrifugation and both extracted with dichloromethane. The combined organic extract was dried and evaporated to give a residue which was subjected to chromatography.

Incubation with autoclaved *R. arrhizus* was performed as follows. The washed mycelium, obtained as above, was resuspended in distilled water in 1-l Erlenmeyer flasks (150 ml per flask) and then autoclaved at 15 p.s.i. for 20 min. After cooling the suspension, the substrate was added and subsequent operations performed as above. The p*H* of the suspension of autoclaved mycelium was 5.0–5.3.

Incubation of 4a-Methyl-4,4a,5,6,7,8-hexahydro-2(3H)-naphthalene (1) (12)

Incubation of **1** (2 g) gave a residue (1.79 g) which was chromatographed by 5% stepwise elution from chloroform to dioxan to give **1** (0.32 g), b.p. 110–112°/2.5 mm, 2,4-DNP m.p. 166–169° (lit (12) b.p. 102–110°/2.5 mm, 2,4-DNP m.p. 169°).

8β-Hydroxy-4a-methyl-4,4a,5,6,7,8-hexahydro-2(3H)-naphthalenone (**2**) (0.43 g), b.p. 124–126°/0.15 mm; n^{22} 1.5362; i.r.: ν_{max} (film) 3440, 1680, 1640 cm^{-1}, u.v.: λ_{max} 234 nm (log ε 4.18), p.m.r.: included signals at δ 1.46 (3H, s, C-4a methyl), 4.34 (1H, t, J = 3, 3 Hz, C-8 H), 5.80 (1H, s, $\omega_{1/2}$ = 1.3 Hz, C-1 H); 2,4-DNP m.p. 155–157° (EtOH).

Anal. Calcd. for $C_{11}H_{16}O_2$: C, 73.29; H, 8.94. Found: C, 72.98; H, 8.82.

8α-Hydroxy-4a-methyl-4,4a,5,6,7,8-hexahydro-2(3H)-naphthalenone (**3**) (0.032 g), b.p. 100–110°/0.1 mm; M^+ 180.1158 ($C_{11}H_{16}O_2$ requires 180.1150); i.r.: ν_{max} (film) 3440, 1680, 1640 cm^{-1}; u.v.: λ_{max} 238 nm (log ε 4.20); p.m.r.: included signals at δ 1.24 (3H, s, C-4a methyl), 4.10–4.40 (1H, m, C-8 H), 6.22 (1H, d, J = 2.0 Hz, C-1 H); 2,4-DNP m.p. 234–236° (dec.) (EtOH).

Anal. Calcd. for $C_{11}H_{16}O_2$: C, 73.29; H, 8.98. Found: C, 73.12; H, 8.90.

Incubation of **2** with *R. arrhizus* resulted in the recovery on an oil which was shown by chromatographic and spectral analysis to consist of unchanged **2** only.

Epimerization of the Alcohol 2

A solution of **2** (0.4 g) in methanol (5 ml) and hydrochloric acid (37%, 0.3 ml) was stirred at room temperature for 12 h and then poured onto water (25 ml) and extracted with ether (3 × 10 ml). The extract was washed with 2 *M* sodium bicarbonate and water, and then dried and evaporated to give a residue which, on purification by passage through a short column of silica in ether, afforded an oil (0.37 g), identical in all respects with **3**.

2-Ethoxy-4a-methyl-3,4,4a,5,6,7-hexahydronaphthalene (4)

This was prepared from **1** (5 g) and ethylorthoformate (5 ml) by the method described (13). Distillation gave the title compound (3.2 g, 61%), b.p. 68–72°/0.35 mm; n^{21} 1.5190; i.r.: ν_{max} (film) 1650, 1625 cm^{-1}; u.v.: λ_{max} 240 nm (log ε 4.14); p.m.r.: included signals at δ 1.02 (3H, s, C-4a methyl), 1.30 (3H, t, J = 7, 7 Hz, $—CH_2CH_3$), 3.79 (2H, q, J = 7, 7, 7 Hz, $—CH_2CH_3$), 5.18–5.30 (2H, m, C-1 and C-8 H's).

Can. J. Chem. Downloaded from www.nrcresearchpress.com by 210.87.254.6 on 09/05/12
For personal use only.

Anal. Calcd. for $C_{13}H_{20}O$: C, 81.20; H, 10.48. Found: C, 81.29; H, 10.55.

Oxidation of 4 by m-Chloroperbenzoic Acid

A solution of m-chloroperbenzoic acid (2.59 g, 80%, 0.012 mol) and sodium hydroxide (0.24 g, 0.006 mol) in 50% aqueous dioxan (200 ml) was added over a period of 1 h to a stirred solution of **4** (1.96 g, 0.01 mol) in 50% aqueous dioxan (200 ml) at room temperature. Stirring was continued at room temperature for 12 h and then water (500 ml) was added and the mixture extracted with dichloromethane (4 × 100 ml). The extract was washed with 2 *M* sodium sulfite, 2 *M* sodium bicarbonate and water, and then dried and evaporated to give an oil which was chromatographed to give 4a-methyl-4,4a,5,6,7,8-hexahydro-2(3*H*)-naphthalenone (**1**) (0.2 g, 12%), identified by spectral and t.l.c. comparison with an authentic sample, *8β-hydroxy-4a-methyl-4,4a,5,6,7,8-hexahydro-2(3H)-naphthalenone* (**2**) (1.24 g, 64%), b.p. 120–125°/0.15 mm, 2,4-DNP m.p. 156–158° (EtOH), identical in spectral and t.l.c. comparison with a sample of **2** obtained from the incubation of **1** with *R. arrhizus*, and *8α-hydroxy-4a-methyl-4,4a,5,6,7,8-hexahydro-2(3H)-naphthalenone* (**3**) (0.3 g, 16%), b.p. 100–110°/0.1 mm, 2,4-DNP m.p. 234–236° (dec.) (EtOH), identical in spectral and chromatographic properties with a sample of **3** produced by the incubation of **1** with *R. arrhizus*.

The alcohol **2** was recovered unchanged following treatment with *m*-chloroperbenzoic acid by the above procedure.

The award of a demonstratorship (to HLH) from the Queen's University of Belfast is gratefully acknowledged, as also is the able technical assistance of Miss H. Reid with the microbiological work.

Thanks are also due to Dr. D. B. MacLean of McMaster University, Hamilton, Ontario, who read the manuscript and offered many helpful suggestions.

1. W. Charney and H. L. Herzog. Microbial transformations of steroids: a handbook. Academic Press, New York. 1967. p. 25.
2. H. L. Holland and B. J. Auret. Can. J. Chem. **53**, 845 (1975).
3. B. A. Koechlin, D. L. Garmaise, T. H. Kritchevsky, and T. F. Gallagher. J. Am. Chem. Soc. **71**, 3262 (1949); **73**, 184 (1951); V. Sanda and J. Fajkos. Coll. Czech. Chem. Commun. **26**, 2734 (1961).
4. J. Romo, G. Rosenkranz, C. Djerassi, and F. Sondheimer. J. Org. Chem. **19**, 1509 (1954).
5. S. K. Malhotra and H. J. Ringold. J. Am. Chem. Soc. **86**, 1997 (1964); G. Subramanyam, S. K. Malhotra, and H. J. Ringold. J. Am. Chem. Soc. **88**, 1332 (1966).
6. L. H. Knox, E. Velarde, S. Berger, D. Cuadriello, P. W. Landis, and A. D. Cross. J. Am. Chem. Soc. **85**, 1851 (1963); R. A. Moss, R. W. Kleinman, and K. L. Williamson. Chem. Commun. 927 (1970).
7. S. H. Eppstein, P. D. Meister, H. M. Leigh, D. H. Peterson, H. C. Murray, L. M. Reineke, and A. Weintraub. J. Am. Chem. Soc. **76**, 3174 (1954).
8. J. E. Bridgeman, P. C. Cherry, A. S. Clegg, J. M. Evans, Sir Ewart R. H. Jones, A. Kasal, V. Kumar, G. D. Meakins, Y. Morisawa, E. E. Richards, and P. D. Woodgate. J. Chem. Soc. C, 250 (1970).
9. S. K. Malhotra and H. J. Ringold. J. Am. Chem. Soc. **87**, 3228 (1965).
10. T. A. Wittstruck, S. K. Malhotra, and H. J. Ringold. J. Am. Chem. Soc. **85**, 1699 (1963).
11. H. J. Hagenmeyer and D. C. Hull. Ind. Eng. Chem. **41**, 2920 (1949).
12. M. Yanagita and K. Yamakawa. J. Org. Chem. **22**, 291 (1957).
13. A. Serini and H. Kosler. Berichte, **71B**, 1766 (1938); B. Reigel and Y. C. Liu. J. Org. Chem. **16**, 1610 (1951).

Can. J. Chem. Downloaded from www.nrcresearchpress.com by 210.87.254.6 on 09/05/12
For personal use only.

Bridged Xanthenes. I. An Intermolecular Cycloaddition Route

PETER YATES AND D. J. BICHAN

Lash Miller Chemical Laboratories, University of Toronto, Toronto, Ontario M5S 1A1

Received January 22, 1975

PETER YATES and D. J. BICHAN. Can. J. Chem. **53**, 2045 (1975).

Condensation of *o*-hydroxybenzyl alcohol (**4**) with 1,3-cyclohexanedione (**7**) in hexamethylphosphoramide gives 3,4-dihydro-1(2*H*)-xanthenone (**9**). Treatment of the tosylhydrazone of **9** with methyllithium gives 3,4-dihydroxanthene (**12**), which undergoes Diels–Alder reactions with dimethyl acetylenedicarboxylate and propiolonitrile to give the bridged xanthenes **15** and **17**, respectively. Condensation of *o*-hydroxybenzyl alcohol (**4**) with 4-carboxamido-1,3-cyclohexanedione (**29**) and 4-carbomethoxy-1,3-cyclohexanedione (**38**) gives 2-carboxamido- (**30**) and 2-carbomethoxy-3,4-dihydro-1(2*H*)-xanthenone (**39**), respectively.

PETER YATES et D. J. BICHAN. Can. J. Chem. **53**, 2045 (1975).

La condensation de l'alcool *o*-hydroxybenzylique (**4**) avec la cyclohexanedione-1,3 (**7**) dans l'hexaméthylphosphoramide conduit à la dihydro-3,4 (2*H*)-xanthènone-1 (**9**). Une réaction entre la tosylhydrazone de **9** et le méthyllithium fournit le dihydro-3,4 xanthène (**12**) qui peut subir des réactions de Diels–Alder avec l'acétylènedicarboxylate de méthyle et le propiolonitrile pour conduire respectivement aux xanthènes pontés **15** et **17**. La condensation de l'alcool *o*-hydroxybenzylique (**4**) avec la carboxamido-4 cyclohexanedione-1,3 (**29**) et la carbométhoxy-4 cyclohexanedione-1,3 (**38**) conduit respectivement aux carboxamido-2 (**30**) et carbométhoxy-2 dihydro-3,4 (2*H*)-xanthènone-1. [Traduit par le journal]

The naturally occurring coloring matters morellin (**1**) (1) and gambogic acid (**2**) (2) and their congeners have a nucleus consisting of the 2,4a-ethano-2,3,4,4a-tetrahydroxanthene system (**3**). In this and the following paper (3) we

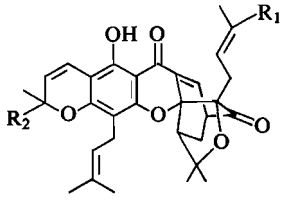

1 $R_1 = CHO; R_2 = CH_3$
2 $R_1 = CO_2H; R_2 = CH_2CH_2CH{=}C(CH_3)_2$

discuss two methods that we have developed for the synthesis of this bridged xanthene system.[1] While this work was in progress Quillinan and Scheinmann (5) reported a third route to this system.

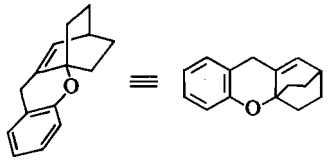

3

[1]For preliminary accounts of this work, see ref. 4.

The approach to be described here is based on the synthesis of the bicyclo[2.2.2]octene system of **3** via a Diels–Alder reaction of the corresponding 1,3-diene with an external dienophile; our other approach (3) involves an intramolecular cycloaddition reaction. The 1,3-dienes required for the intermolecular cycloadditions are 3,4-dihydroxanthenes, a class of compounds that had not been described hitherto. We therefore first addressed ourselves to developing a method for the synthesis of such compounds.

Quagliaro *et al.* (6) have shown that when *o*-hydroxybenzyl alcohol (**4**) and cyclohexanone are heated together to 200° the alcohol **5** is formed; the yield is increased by amine catalysis and *o*-quinonemethide (**6**) is considered to be an intermediate (*cf.* ref. 7). This suggested to us that the reaction of **4** with 1,3-cyclohexanedione (**7**) might provide a ready route to 3,4-dihydro-1(2*H*)-xanthenone (**9**) via dehydration of an intermediate of type **8**, analogous to **5**.

In the event, when **4** was heated with **7** in hexamethylphosphoramide (HMPA) at 195°, a crystalline product was obtained in 43% yield whose elemental composition and spectral characteristics are in accord with its formulation as **9**. Bands at 6.00 (shoulder) and 6.05 μ in its i.r. spectrum and maxima at 221 nm (ε 11 100) and 286 nm (ε 6100) in its u.v. spectrum

Can. J. Chem. Downloaded from www.nrcresearchpress.com by 210.87.254.40 on 09/05/12
For personal use only.

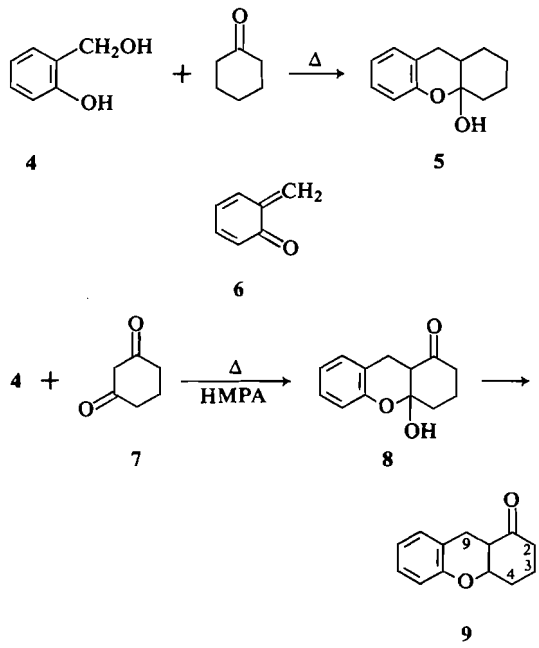

are in good accord with the presence of a β-aryloxy-α,β-enone chromophore. A broad two-proton singlet in its p.m.r. spectrum at δ 3.50 can be assigned to the methylene protons at C.9; multiplets at δ 2.03 (2 H), 2.45 (4 H), and 7.14 (4 H) are attributable to the C.3 protons, the C.2 and C.4 protons, and the aromatic protons, respectively. These data do not rigorously exclude the alternative formulation **10** for this product; however, structure **7** is much more likely on mechanistic grounds (Scheme 1) and was confirmed by subsequent transformations.[2]

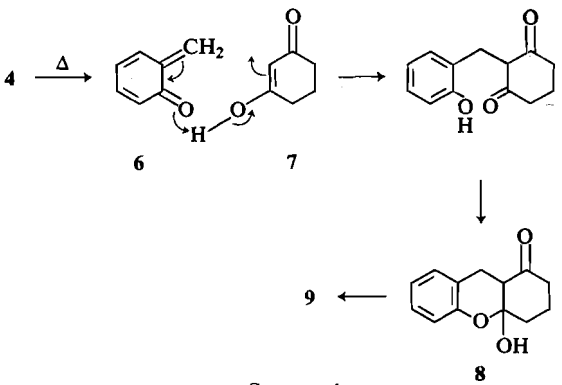

SCHEME 1

[2]For another route to 3,4-dihydro-1(2*H*)-xanthenones, see ref. 8.

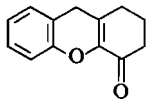

10

Compound **9** was converted via its tosylhydrazone **11** to 3,4-dihydroxanthene (**12**) by the method of Dauben *et al.* (9). The diene **12** was obtained in 76% overall yield from **9**; its elemental composition and spectral characteristics are in accord with the structural assignment but do not distinguish it from **13**, the product that would be anticipated from **10**.[3] Bands at 5.92 (m) and 6.03 (w) μ in its i.r. spectrum and maxima in its u.v. spectrum at 290 (ε 6400), 298 (sh, ε 6000), and 314 nm (sh, ε 3700) are in accord with the presence of an aryloxy-1,3-cyclohexadiene chromophore. Two one-proton signals in its p.m.r spectrum at δ 5.56 (m) and 5.68 (d, J = 9 Hz) can be assigned to the vinylic protons at C.2 and C.1, respec-

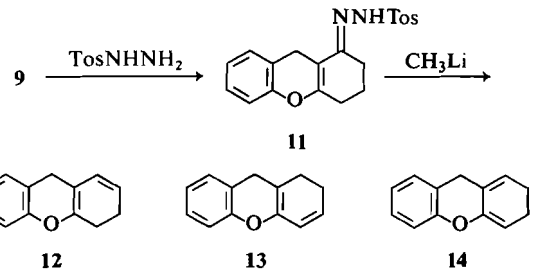

tively; a two-proton singlet at δ 3.29 and a four-proton multiplet centered at δ 6.96 are attributable to the C.9 methylene protons and the aromatic protons, respectively; the remaining protons at C.3 and C.4 give rise to a "deceptively simple" doublet at δ 2.29.

Treatment of **12** with dimethyl acetylenedicarboxylate at room temperature gave a 1:1 adduct in 95% yield. This is assigned the bridged xanthene structure **15**. Its i.r. spectrum shows the presence of two nonequivalent ester groups with carbonyl-stretching bands at 5.70 and 5.78 μ as does its p.m.r. spectrum with two three-proton singlets at δ 3.69 and 3.73. The latter spectrum shows a two-proton broad

[3]Another possible structure, **14**, may be considered to be unlikely, since diene formation from the tosylhydrazones of α,β-enones has previously been observed to occur exclusively via removal of the α′- rather than the δ-hydrogen (9).

Can. J. Chem. Downloaded from www.nrcresearchpress.com by 210.87.254.40 on 09/05/12
For personal use only.

Can. J. Chem. Downloaded from www.nrcresearchpress.com by 210.87.254.40 on 09/05/12
For personal use only.

singlet at δ 3.48 assigned to the benzylic allylic protons, broadened by slight nonequivalence and by allylic coupling with the olefinic proton. This gives rise to a doublet of triplets at δ 6.11 (1 H), owing to vicinal coupling with the bridgehead proton (J = 6 Hz) in addition to allylic coupling with the two benzylic allylic protons (J = 2 Hz). The doubly allylic bridgehead proton gives a signal at δ 4.17 (1 H), which is a doublet of triplets, attributable to coupling with the vinyl proton (J = 6 Hz) and with each of the methylene protons adjacent to it (J = 3 Hz). Examination of a molecular model indicated that the dihedral angles in this latter situation are each *ca* 60°, in accord with the magnitude of the coupling observed. The u.v. spectrum of the adduct shows absorption comparable with that of chroman (*cf.* ref. 10).

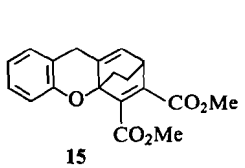

15

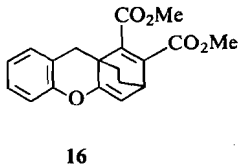

16

The formation of the adduct **15** not only confirms the presence of the 1,3-diene system in **12** but also provides evidence against the alternative diene structure **13**. The adduct of the latter with dimethyl acetylenedicarboxylate would have structure **16**, which is contraindicated by the splitting pattern of the vinylic proton signal in the p.m.r. spectrum of the adduct.[4]

A second bridged xanthene, **17**, was obtained in 93% yield by treating **12** with boiling propiolonitrile (b.p. 42.5°). A choice of structure **17** rather than its regioisomer **18** can be made on the basis of p.m.r. spectroscopy. A one-proton complex multiplet at δ 3.71 is assigned to the bridgehead proton; when double irradiation was carried out at the frequency corresponding to the signal of the adjacent methylene protons, the bridgehead proton signal collapsed to a triplet (J = 6 Hz). This is in accord with equal coupling between the bridgehead proton and the two vicinal vinylic protons of **17**; such equal coupling would not be possible in **18**, where one of the vinyl protons is vicinal and the other allylic with respect to the bridgehead proton.

[4]This spectrum excludes structure **14** for the diene.

In contrast to the case of **15**, the benzylic allylic methylene protons of **17** show a distinct difference in chemical shift, giving rise to a pair of one-proton doublets of doublets at δ 3.40

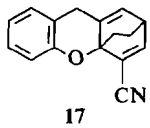

17

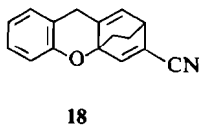

18

and 3.51. The coupling constants are 17 and 2 Hz; the former is attributable to geminal coupling between the methylene protons and the latter to coupling of each with the allylic proton. The presence of an α,β-unsaturated nitrile group in **17** was confirmed by a band at 4.54 μ in its i.r. spectrum; its u.v. spectrum resembles that of chroman (10).

Full confirmation of the foregoing assignments was accomplished by a simple degradation of **17**. When **17** was treated at 163° for 5 min, a retro-Diels–Alder reaction occurred with elimination of ethylene to give 4-cyanoxanthene (**19**). The structure of the latter was established by its hydrolysis to 4-xanthenecarboxylic acid (**20**) and the esterification of this to methyl 4-xanthenecarboxylate (**21**) (Scheme 2). The

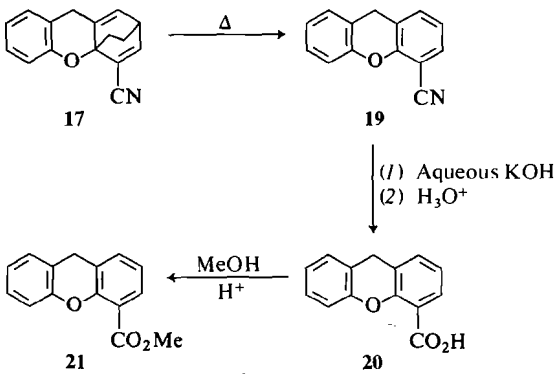

17 19 21 20

SCHEME 2

methylene proton signal in the p.m.r. spectrum of **19** occurs at δ 4.04 (*cf.* xanthene, δ 4.01) but the seven aromatic protons were not differentiable and thus the position of attachment of the nitrile group was not immediately apparent, although its presence was demonstrated by a band at 4.49 μ in the i.r. spectrum of the pyrolysis product. However, the carboxylic acid **20** is a known compound (11) and is reported to have a similar m.p. and u.v. spectrum

Can. J. Chem. Downloaded from www.nrcresearchpress.com by 210.87.254.40 on 09/05/12
For personal use only.

to that of the hydrolysis product obtained here (see Experimental). Furthermore, the carbonyl-stretching band in the i.r. spectrum of this product occurs at 5.76 μ; this is at unusually low wavelength for an aromatic carboxylic acid but is explicable in terms of strong intramolecular hydrogen bonding in the 4-xanthenecarboxylic acid (*cf.* **22**), which disrupts the dimeric structure normally assumed by carboxylic acids in solution. Related phenomena have been thoroughly documented in the i.r. spectra of other *o*-phenoxybenzoic acids (12). Finally, in accord with these structural assignments, the p.m.r. spectrum of the methyl ester **21** shows a one-proton signal at *ca* 0.6 p.p.m. downfield from the signals of the other six aromatic protons; this signal is a doublet of doublets (J = 7 and 2 Hz) and can be assigned to the C.3 proton of **21**.

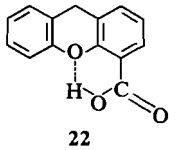

22

The determination of **19** as the structure of the pyrolysis product from **17** not only establishes the structure of the latter, but also establishes the structure of the diene **12** and, in turn, of the ketone **9**.

Some preliminary experiments were carried out on the further transformation of **17** to a compound with functionality more closely related to **1** and **2**. Epoxidation with *t*-butyl hydroperoxide and potassium *t*-butoxide in dimethyl sulfoxide (*cf.* ref. 13) gave a mixture of products that are considered to be the epimers **23** (see Experimental). These products could not be separated and were not fully characterized; treatment with aqueous alkali gave a mixture considered to consist of the epimeric amides **24**.

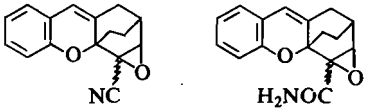

23 **24**

Since any closer approach to **1** and **2** via compounds of type **17** would require the presence of a functional group on the ethano bridge, modifications of the route to **17** were

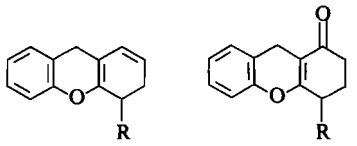

25 R = $CONH_2$ **27** R = $CONH_2$
26 R = CO_2Me **28** R = CO_2Me

undertaken in attempts to prepare compounds **25** and **26**. This required the preparation of the ketones **27** and **28**. When *o*-hydroxybenzyl alcohol (**4**) and 4-carboxamido-1,3-cyclohexanedione (**29**) (14) were heated at 185° in a mixture of HMPA and 1,5-diazabicyclo[5.4.0]undec-5-ene (DBU), one major product was formed in 67% yield. The elemental composition and spectra of this product were in accord with its formulation as either **27** or **30**, as was the fact that on treatment with boiling hydrochloric acid it gave compound **9**.

Evidence suggesting that this product is **30** rather than **27** was obtained by its reduction with sodium borohydride, which gave a dihydro compound arising from reduction of the ketonic

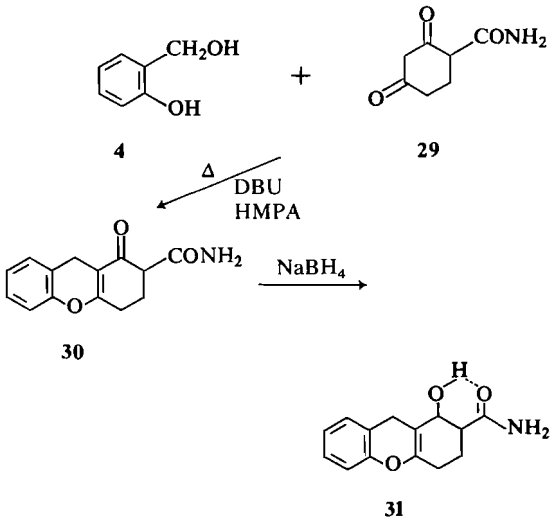

4 **29**

30

31

group. The position of the amide carbonyl-stretching band in the i.r. spectrum of this product at 6.02 μ indicates that the amide carbonyl group is hydrogen bonded with the hydroxyl group as in **31** and that the original product is **30**. This conclusion is buttressed by the observation that bisdehydration of the dihydro compound with phosphorus oxychloride and pyridine gave a product whose spectra

Can. J. Chem. Downloaded from www.nrcresearchpress.com by 210.87.254.40 on 09/05/12
For personal use only.

are in accord with its formulation as 2-cyano-3,4-dihydroxanthene (**32**). Thus its i.r. spectrum shows a band at 4.55 μ attributable to an extensively conjugated nitrile group; a high intensity maximum at 336 nm (ε 12 100) also suggests extensive conjugation. Its p.m.r. spectrum shows a single vinyl proton signal at δ 6.53 that appears as a slightly broadened singlet. These data exclude structures **33** and **34** for this product, one or both of which would have been expected to have arisen from the keto amide had it had structure **27**.

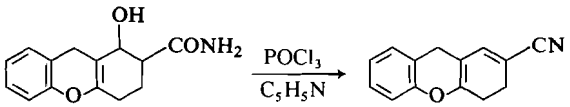

31 **32**

33 **34**

Full confirmation of these conclusions was obtained by dehydrogenation of **32** with 5% palladium-on-carbon, which afforded 2-cyanoxanthene (**35**); this in turn was hydrolyzed to the corresponding carboxylic acid **36**, which was esterified to give the methyl ester **37** (Scheme 3). Although **35** and **36** were not fully characterized, it was demonstrated that their i.r. spectra were different from those of the corresponding 4-substituted xanthenes, **19** and **20**, respectively. The ester **37** was fully characterized and shown to be different from methyl 4-xanthenecarboxylate (**21**). Furthermore, as expected in terms of the earlier considerations relating to the 4-substituted xanthene series, the carbonyl-stretching band in the i.r. spectrum of **36** occurs at 5.91 μ and the p.m.r. spectrum of **37** shows the presence of two low field aromatic proton signals. Thus structure **27** can be excluded for the keto amide and structure **30** must be assigned to it.

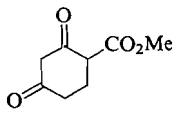

38

Attention was next turned to the case of an ester rather than an amide substituent. When *o*-hydroxybenzyl alcohol (**4**) and 4-carbomethoxy-1,3-cyclohexanedione (**38**) were heated together at 100° without solvent under reduced pressure (15 mm), one major product was formed in 51% yield. The elemental composition and spectra of this product were in accord with its formulation as either the 4-carbomethoxy derivative **28** or the 2-carbomethoxy compound **39**. Reduction, dehydration, and dehydrogenation of this product gave via **40** and **41** a compound that was identical with the ester **37** obtained from **30**; again the undesired regioisomer had been formed and the original keto ester must be **39** (Scheme 4).

Thus, although the generality of the method for the synthesis of 3,4-dihydro-1(2*H*)-xanthenones has been demonstrated[5] and the conversion of the parent compound to bridged xanthenes has been effected, a close approach to the more ramified systems of compounds **1** and **2** by this route has encountered obstacles.

[5]For other examples, see ref. 4*a*.

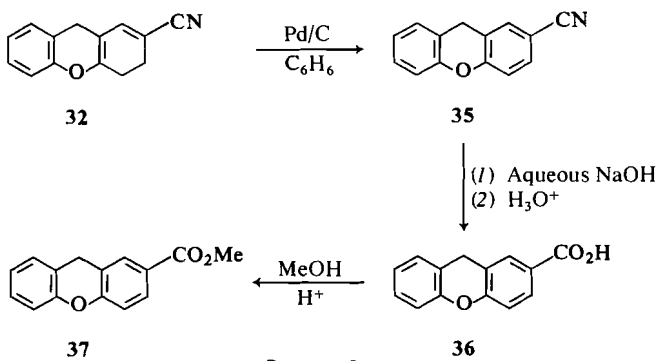

32 **35**

37 **36**

SCHEME 3

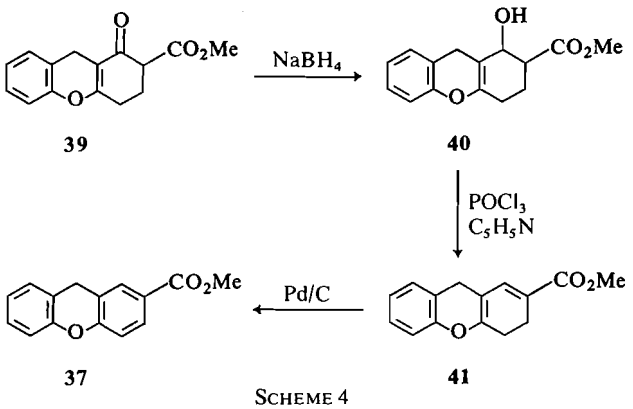

39 40 37 41

SCHEME 4

Although these may well not be insuperable, the successful outcome of an alternative approach that leads to a bridged xanthene incorporating several of the additional features of **1** and **2** (3) led us to place the present approach in abeyance.

Experimental

Melting points were determined with a Thomas Hoover Uni-Melt apparatus and are uncorrected. Infrared spectra were recorded in chloroform solution, ultraviolet spectra in methanol solution, and proton magnetic resonance spectra in deuteriochloroform, unless otherwise indicated. Solutions in organic solvents were dried over anhydrous magnesium sulfate.

3,4-Dihydro-1(2H)-xanthenone (9)

o-Hydroxybenzyl alcohol (**4**) (12.40 g, 100 mmol), 1,3-cyclohexanedione (7) (11.20 g, 100 mmol), and hexamethylphosphoramide (15 ml) were heated together to 195° for 30 min. The cooled solution was taken up in benzene (500 ml) and washed with 5% hydrochloric acid (2 × 400 ml), aqueous 10% sodium hydroxide (3 × 300 ml), and water (400 ml), dried, and evaporated to yield 8.52 g (43%) of **9**, m.p. 79–89°, which after two recrystallizations from methanol had m.p. 90.3–91.3°; $\lambda_{max}(CCl_4)$ 6.00 (sh), 6.05, 7.22 μ; λ_{max}(EtOH) (ε) 221 (11 100), 286 (6100) nm; δ 2.03 (m, 2 H), 2.45 (m, 4 H), 3.50 (br s, 2 H), 7.14 (m, 4 H); *m/e* 200.

Anal. Calcd. for $C_{13}H_{12}O_2$: C, 77.98; H, 6.04. Found: C, 77.96; H, 6.21.

3,4-Dihydro-1(2H)-xanthenone Tosylhydrazone (11)

3,4-Dihydro-1(2*H*)-xanthenone (**9**) (4.42 g, 22.1 mmol) and *p*-toluenesulfonylhydrazine (4.11 g, 22.1 mmol) were dissolved in 95% ethanol (125 ml) and the solution was stirred for 17 h at room temperature in the presence of 10% hydrochloric acid (10 drops). Filtration yielded 6.59 g (82%) of **11**, m.p. 215–216° (dec.). The filtrate was evaporated to 25 ml and allowed to crystallize to yield a further 670 mg (8%) of **11**, m.p. 212–215° (dec.). Three recrystallizations of the first crop from acetone gave material with m.p. 219–220° (dec.); λ_{max} 3.08 (w), 3.17 (w), 6.00 μ; λ_{max} (ε) 288 (16 400) nm; δ 1.86 (m, 2 H), 2.34 (m, 4 H), 2.40 (s, 3 H), 3.45 (br s, 2 H), 7.18 (m, 6 H), 7.97 (d, J = 8 Hz, 2 H); *m/e* 368.

Anal. Calcd. for $C_{20}H_{20}N_2O_3S$: C, 65.23; H, 5.45; N, 7.61; S, 8.70. Found: C, 65.14; H, 5.46; N, 7.63; S, 8.63.

3,4-Dihydroxanthene (12)

A slurry of 3,4-dihydro-1(2*H*)-xanthenone tosylhydrazone (**11**) (1.73 g, 4.70 mmol) in anhydrous ether (15 ml) was stirred in an ice bath. Ethereal 2.43 *M* methyllithium (10 ml, 24.3 mmol) was added dropwise over 20 min. Stirring was continued for 1 h until gas evolution ceased. The mixture was poured into pentane (200 ml) and water was very carefully added dropwise with stirring until two clear layers separated. The pentane layer was decanted and the aqueous layer was extracted again with pentane (150 ml). The combined extracts were dried and evaporated to yield 800 mg (93%) of **12** as an oil that after sublimation (65°, 0.1 mm) had m.p. 33–35°; $\lambda_{max}(CCl_4)$ 5.92 (m), 6.03 (w) μ; λ_{max} (ε) 290 (6400), 298 (sh, 6000), 314 (sh, 3700) nm; δ 2.29 (d, J = 2 Hz, 4 H), 3.29 (s, 2 H), 5.56 (m, 1 H), 5.68 (d, J = 9 Hz, 1 H), 6.96 (m, 4 H); *m/e* 184.

Anal. Calcd. for $C_{13}H_{12}O$: C, 84.75; H, 6.57. Found: C, 84.54; H, 6.78.

Reaction of 12 with Dimethyl Acetylenedicarboxylate: Diester 15

3,4-Dihydroxanthene (**12**) (122 mg, 0.66 mmol) and dimethyl acetylenedicarboxylate (94 mg, 0.85 mmol) were mixed and the mixture was allowed to stand at room temperature for 16 h. Deuteriochloroform (0.5 ml) was added and the solution was allowed to stand at room temperature for 33 h. The deuteriochloroform was evaporated and the residue was placed under vacuum (0.03 mm) for 19 h to yield 205 mg (95%) of **15** as a gum that solidified at −20°. Three recrystallizations from methanol gave material with m.p. 92–96°; $\lambda_{max}(CCl_4)$ 5.70, 5.78, 5.97 (w), 6.09 (w) μ; λ_{max} (ε) 269 (2100), 278 (1700), 305 (650) nm; δ 1.70 (m, 4 H), 3.48 (br s, 2 H), 3.69 (s, 3 H), 3.73 (s, 3 H), 4.17 (dt, J = 6, 3 Hz, 1 H), 6.11 (dt, J = 6, 2 Hz, 1 H), 7.04 (m, 4 H); *m/e* 326.

Anal. Calcd. for $C_{19}H_{18}O_5$: C, 69.92; H, 5.56. Found: C, 70.10; H, 5.58.

Reaction of 12 with Propiolonitrile: Nitrile 17

3,4-Dihydroxanthene (**12**) (500 mg, 2.72 mmol) was dissolved in propiolonitrile (1.0 g, 20 mmol) and the solution was boiled under reflux for 10 h. The excess propiolonitrile was distilled and the residue was taken

Can. J. Chem. Downloaded from www.nrcresearchpress.com by 210.87.254.40 on 09/05/12
For personal use only.

Can. J. Chem. Downloaded from www.nrcresearchpress.com by 210.87.254.40 on 09/05/12
For personal use only.

up in benzene and placed on a column of silica gel (12 g). Elution with benzene yielded 600 mg (93%) of **17** as an oil. Crystallization and recrystallization from methanol yielded material with m.p. 75–78°; $\lambda_{max}(CCl_4)$ 4.54 (m) μ; λ_{max} (ε) 270 (1600), 276 (1400) nm; δ 1.62 (m, 4 H), 3.40 (dd, J = 17, 2 Hz, 1 H), 3.51 (dd, J = 17, 2 Hz, 1 H), 3.71 (m, 1 H), 5.95 (dt, J = 6, 2 Hz, 1 H), 7.14 (m, 5 H); *m/e* 235.

Anal. Calcd. for $C_{16}H_{13}NO$: C, 81.68; H, 5.57; N, 5.95. Found: C, 81.82; H, 5.54; N, 6.00.

4-Cyanoxanthene (19)

Nitrile **17** (282 mg, 1.20 mmol) was heated to 163° for 5 min while a colorless gas was evolved. The residue solidified on cooling to give 248 mg (100%) of **19**. Two recrystallizations from ethanol–acetone gave material with m.p. 91–93°; $\lambda_{max}(CCl_4)$ 4.49 (w) μ; λ_{max} (ε) 252 (7000), 279 (2100), 307 (4200) nm; δ 4.04 (s, 2 H), 7.29 (m, 7 H); *m/e* 207.

Anal. Calcd. for $C_{14}H_9NO$: C, 81.14; H, 4.38; N, 6.76. Found: C, 81.24; H, 4.40; N, 6.76.

Xanthene-4-carboxylic Acid (20)

4-Cyanoxanthene (**19**) (30 mg, 0.15 mmol) and aqueous 10% potassium hydroxide (5 ml) were heated together under reflux for 1 h. The resulting solution was cooled, diluted with water (95 ml), and acidified to pH 2 with concentrated hydrochloric acid (~1.5 ml). The resulting precipitate was collected and dried to give 33 mg (100%) of **20**. One recrystallization from boiling benzene–acetone gave material with m.p. 185–186° (dec.); λ_{max} 3.04 (m), 5.76, 5.86 (sh) μ; λ_{max} (ε) 248 (8200), 279 (2400), 303 (2800) nm; *m/e* 226.

Anal. Calcd. for $C_{14}H_{10}O_3$: C, 74.33; H, 4.46. Found: C, 74.10; H, 4.36.

Methyl Xanthene-4-carboxylate (21)

Xanthene-4-carboxylic acid (**20**) (189 mg, 0.84 mmol) was dissolved in methanol (25 ml). Concentrated sulfuric acid (1 ml) was added with stirring and stirring was continued at room temperature for 21 h; the solution was poured into ether (150 ml). The ethereal solution was washed with water (2 × 100 ml) and saturated aqueous sodium bicarbonate (100 ml), dried, and evaporated to yield 176 mg (87%) of **21**, which was purified by elution with benzene from a column of silica gel (8 g) followed by crystallization from ethanol to give material with m.p. 48–49°; λ_{max} 5.82 μ; λ_{max} (ε) 248 (8200), 278 (2300), 305 (3200) nm; δ 3.94 (s, 3 H), 3.99 (s, 2 H), 7.11 (m, 6 H), 7.72 (dd, J = 7, 2 Hz, 1 H); *m/e* 240.

Anal. Calcd. for $C_{15}H_{12}O_3$: C, 74.99; H, 5.03. Found: C, 74.71; H, 5.11.

Epoxidation of 17: Cyano Epoxides 23

Nitrile **17** (472 mg, 2.01 mmol) and *t*-butyl hydroperoxide (dried by azeotropic distillation of water with benzene followed by distillation; 181 mg, 2.01 mmol) were dissolved in anhydrous dimethyl sulfoxide (5 ml). Potassium *t*-butoxide (20 mg, 0.18 mmol) was added; the solution was swirled, allowed to stand at room temperature for 5 min, and poured into ether (300 ml). The ethereal solution was washed with water (5 × 50 ml), dried, and evaporated to yield 471 mg (93%) of **23** as a gum. Partial separation of the two diastereomers was achieved by elution from a silica gel column with carbon tetrachloride – 25% methylene chloride. The mixture had $\lambda_{max}(CCl_4)$ 4.45 (w) μ; δ 1.3–2.6 (m, 7 H), 3.88 (d, J = 4 Hz, 1 H), 6.08 (t, J = 1.5 Hz, 1/2 H), 6.25 (t, J = 1.5 Hz, 1/2 H), 6.89 (m, 4 H); *m/e* 251.

Base Hydrolysis of 23: Epoxy Amides 24

Cyano epoxides **23** (91 mg, 0.36 mmol) and sodium hydroxide (92 mg, 2.30 mmol) were dissolved in aqueous 60% methanol (5 ml) and the solution was stirred at room temperature for 19 h and poured into ether (100 ml). The ethereal solution was washed with water (2 × 75 ml), dried, and evaporated to yield 45 mg (46%) of **24** as a gum, λ_{max} 2.94 (m), 3.04 (m), 5.90 μ; δ 3.88 (d, J = 4 Hz).

2-Carboxamido-3,4-dihydro-1(2H)-xanthenone (30)

o-Hydroxybenzyl alcohol (**4**) (1.24 g, 10 mmol), 4-carboxamido-1,3-cyclohexanedione (**29**) (**14**) (1.55 g, 10 mmol), 1,5-diazabicyclo[5.4.0]undec-5-ene (1.5 ml), and hexamethylphosphoramide (3 ml) were heated together in an oil bath at 190° under reflux under a vacuum of 100 mm for 30 min. The mixture was cooled briefly and poured into water (300 ml) with vigorous stirring. The solution was acidified to pH 2 with concentrated hydrochloric acid and stirred for 17 h at room temperature. The precipitate was collected and dried to yield 1.62 g (67%) of **30**, which after three recrystallizations from methanol had m.p. 217–218°; λ_{max} 2.96 (m), 3.05 (m), 5.91, 6.12, 7.20 μ; λ_{max} (ε) 221 (12 100), 291 (6800) nm; δ 2.42 (m, 4 H), 3.25 (m, 1 H), 3.52 (br s, 2 H), 5.42 (v br s, 1 H), 7.16 (m, 4 H); *m/e* 243.

Anal. Calcd. for $C_{14}H_{13}NO_3$: C, 69.12; H, 5.39; N, 5.76. Found: C, 68.98; H, 5.46; N, 5.72.

Conversion of 30 to 9

2-Carboxamido-3,4-dihydro-1(2*H*)-xanthenone (**30**) (349 mg, 1.44 mmol) and concentrated hydrochloric acid (15 ml) were heated under reflux for 20 h. The mixture was cooled, diluted with water to 200 ml, and extracted with ether (200 ml); the extract was dried and evaporated to yield 139 mg (48%) of a solid, which was recrystallized from methanol and shown (by i.r., m.p., and mixture m.p.) to be identical with **9** prepared from 1,3-cyclohexanedione.

Reduction of 30: Hydroxy Amide 31

A slurry of 2-carboxamido-3,4-dihydro-1(2*H*)-xanthenone (**30**) (538 mg, 2.21 mmol) in 2-propanol (75 ml) was stirred at room temperature. Sodium borohydride (252 mg, 6.63 mmol) was added in three equal portions at t = 0, 45, and 300 min. Ethanol (10 ml) was added after 120 min. After 9 h the solution was poured into water (250 ml) and extracted with chloroform (2 × 250 ml) and ether (2 × 200 ml). The combined extracts were dried and evaporated to yield 511 mg (94%) of **31** which after three recrystallizations from acetone–ethanol had m.p. 188–192°; λ_{max}(KBr) 6.02, 6.08 (m) μ; λ_{max} (ε) 248 (3700), 279 (1900) nm; *m/e* 245.

Anal. Calcd. for $C_{14}H_{15}NO_3$: C, 68.55; H, 6.16; N, 5.71. Found: C, 68.52; H, 6.21; N, 5.61.

2-Cyano-3,4-dihydroxanthene (32)

Hydroxy amide **31** (441 mg, 1.80 mmol) was dissolved in anhydrous pyridine (10 ml) and phosphorus oxychloride (225 mg, 1.47 mmol) was added with stirring, which was continued for 4 h at room temperature. The solution was poured into ether (150 ml) and the

Can. J. Chem. Downloaded from www.nrcresearchpress.com by 210.87.254.40 on 09/05/12
For personal use only.

ethereal extract was washed with 4% hydrochloric acid (2 × 75 ml) and water (75 ml), dried, and evaporated to yield 210 mg of a gum, which was placed on a silica gel t.l.c. plate (20 × 20 × 0.05 cm) in chloroform. Elution with ether yielded 79 mg (21%) of **32** ($R_f \simeq 0.85$), which after one recrystallization from methanol had m.p. 112–114°; λ_{max} 4.55 (m), 5.97 (m), 6.38 μ; λ_{max} (ε) 232 (4730), 245 (sh, 3500), 279 (sh, 3500), 289 (2700), 336 (12 100) nm; δ 2.52 (br s, 4 H), 3.43 (br s, 2 H), 6.53 (br s, 1 H), 7.02 (m, 4 H); *m/e* 209.

Anal. Calcd. for $C_{14}H_{11}NO$: C, 80.36; H, 5.30; N, 6.69. Found: C, 80.25; H, 5.30; N, 6.52.

Methyl Xanthene-2-carboxylate (37) (from 32)

2-Cyano-3,4-dihydroxanthene (**32**) (197 mg, 0.94 mmol) was dissolved in benzene (25 ml) and 5% palladium-on-carbon (201 mg) was added. The mixture was stirred and boiled under reflux for 16 h, cooled, filtered, and evaporated to yield 2-cyanoxanthene (**35**) ($\lambda_{max}(CHCl_3)$ 4.48 (w) μ), which was dissolved in methanol (3 ml). Water (2 ml) and sodium hydroxide (185 mg, 4.63 mmol) were added and the solution was boiled under reflux for 21 h, diluted to a volume of 50 ml with water, acidified to p*H* 2 with 4% hydrochloric acid, and extracted with ether (2 × 100 ml). The combined extracts were dried and evaporated to yield xanthene-2-carboxylic acid (**36**) (λ_{max} 3–4 (m), 5.91 μ), which was dissolved in methanol (25 ml). Concentrated sulfuric acid (951 mg) was added and the solution was stirred for 19 h at room temperature, poured into ether (125 ml), and washed with water (2 × 75 ml) and saturated aqueous sodium bicarbonate (75 ml). The organic layer was dried and evaporated to yield 43 mg (19%, from **32**) of **37**, which after crystallization from methanol had m.p. 129–130° and was shown (by i.r. and mixture m.p.) to be identical with **37** prepared from **39**.

4-Carbomethoxy-1,3-cyclohexanedione (38)[6]

Sodium hydroxide (60 g, 1.5 mol) was dissolved in water (600 ml) in a 2-l beaker. The solution was heated to 90° and the heat source was turned off. Nickel–aluminum alloy (1:1, 20 g) was added in small amounts with stirring at a rate sufficient to maintain a temperature of 90–95°. Stirring was continued for a further 30 min at 90° and during subsequent cooling to room temperature. The aqueous layer was decanted and aqueous 10% sodium hydroxide (400 ml) was added; the mixture was stirred for 10 min and the aqueous layer was decanted. This procedure was repeated three times with water. The slurry was transferred to a 500-ml roundbottomed flask (*Caution*: Raney nickel of this activity spontaneously bursts into flame in the presence of oxygen if allowed to become dry), the aqueous layer was decanted, and benzene (250 ml) was added. Azeotropic distillation of the residual water was carried out to completion. Most of the benzene was decanted and dry methanol was added. The mixture was swirled several times, the nickel was allowed to settle, and most of the methanol–benzene solution was decanted. More methanol was used to transfer the nickel to a 500 ml hydrogenation bottle where it was allowed to settle and most of the methanol was decanted. Methyl 2,4-dihydroxybenzoate (32.5 g, 193 mmol) and methanolic sodium methoxide prepared by the reaction of sodium (4.89 g, 213 mmol) with methanol (300 ml) were added to the hydrogenation bottle which was subjected to a pressure of 80 p.s.i. of hydrogen at 55° with shaking for 5 days. The mixture was cooled and filtered and the methanol was evaporated. Water (200 ml) was added followed by concentrated hydrochloric acid to p*H* 8. Saturated aqueous sodium bicarbonate (200 ml) was added and the solution was extracted with ether (400 ml) and chloroform (400 ml). The aqueous layer was acidified with concentrated hydrochloric acid to p*H* 2 and extracted with ether (400 ml) and chloroform (400 ml). The latter extracts were combined, dried, and evaporated to yield 11.5 g (35%) of **38** which after crystallization and recrystallization from boiling benzene had m.p. 81–82°; λ_{max} 2.7–4.3 (m), 5.77, 5.82, 6.21 μ; λ_{max} (ε) 257 (14 500), 286 (sh, 5730) nm; δ 2.55 (m), 3.17 (s), 2.39 (m), 3.74 (s), 3.81 (s), 5.54 (s), 8.47 (br s); *m/e* 170.

Anal. Calcd. for $C_8H_{10}O_4$: C, 56.46; H, 5.92. Found: C, 57.00; H, 5.92.

2-Carbomethoxy-3,4-dihydro-1(2H)-xanthenone (39)

o-Hydroxybenzyl alcohol (**4**) (2.17 g, 17.5 mmol) and 4-carbomethoxy-1,3-cyclohexanedione (**38**) (2.94 g, 17.5 mmol) were heated together to 100° at 15 mm for 42 h. The mixture was dissolved in hot methanol (30 ml), cooled, and poured into ether (150 ml). The ethereal solution was washed with aqueous 1% sodium hydroxide (2 × 100 ml), dried, and evaporated to yield 2.30 g (51%) of **39**, which after elution from silica gel (95 g) in benzene – 1% ether and two recrystallizations from methanol had m.p. 126–127.5°; λ_{max} 5.77, 6.00 (sh), 6.10, 7.22 μ; λ_{max} (ε) 222 (13 400), 291 (8200) nm; δ 2.35 (m, 2 H), 2.64 (m, 2 H), 3.48 (m, 1 H), 3.55 (br s, 2 H), 3.79 (s, 3 H), 7.19 (m, 4 H); *m/e* 258.

Anal. Calcd. for $C_{15}H_{14}O_4$: C, 69.75; H, 5.46. Found: C, 69.72; H, 5.55.

Methyl Xanthene-2-carboxylate (37) (from 39)

4-Carbomethoxy-3,4-dihydro-1(2*H*)-xanthenone (**39**) (463 mg, 1.80 mmol) was dissolved in methanol and cooled to 0° with stirring. Sodium borohydride (284 mg, 7.5 mmol) was added in four equal portions at 30 min intervals. Stirring was continued for 1 h after the last addition and the solution was poured into ether (125 ml). The ethereal solution was washed with water (2 × 75 ml), dried, and evaporated to yield 460 mg of a gum, which was placed on four silica gel t.l.c. plates (20 × 20 × 0.05 cm). Elution with benzene – 50% ether yielded 308 mg (66%) of the hydroxy ester **40** ($R_f \simeq 0.4$); $\lambda_{max}(CHCl_3)$ 2.87–3.20 (m), 5.78, 5.89 (sh) μ.

Hydroxy ester **40** (75 mg, 0.29 mmol) was dissolved in anhydrous pyridine (3 ml) and phosphorus oxychloride (44 mg, 0.29 mmol) was added with swirling. The solution was allowed to stand at room temperature for 19 h under a drying tube and then poured into ether (125 ml). The ethereal solution was washed with 4% hydrochloric acid (75 ml) and water (2 × 75 ml), dried, and evaporated to yield 39 mg (56%) of the diene ester **41**; λ_{max} 5.88, 6.00 (m) μ. This was dissolved in methanol (15 ml) and 5% palladium-on-carbon (103 mg) was added. The mixture was boiled under reflux for 19 h, cooled, filtered, and evaporated to yield 25 mg of a gum, which was placed on a silica gel t.l.c. plate (20 × 5 × 0.05 cm) in

[6]This procedure is a modification of that of Tomino (14).

chloroform. Elution with benzene afforded 10 mg (26%) of **37** ($R_f \simeq 0.4$); λ_{max} 5.82 μ; λ_{max} (ε) 275 (11 800), 300 (sh, 4600) nm; δ 3.98 (s, 3 H), 4.13 (s, 2 H), 7.22 (m, 5 H), 7.98 (m, 2 H); *m/e* 240.

Anal. Calcd. for $C_{15}H_{12}O_3$: C, 74.99; H, 5.03. Found: C, 74.60; H, 5.03.

We thank the National Research Council of Canada for support of this work.

1. G. KARTHA, G. N. RAMACHANDRAN, H. B. BHAT, P. M. NAIR, V. K. V. RAGHAVAN, and K. VENKATARAMAN. Tetrahedron Lett. 459 (1963); P. M. NAIR and K. VENKATARAMAN. Indian J. Chem. **2**, 402 (1964); H. B. BHAT, P. M. NAIR, and K. VENKATARAMAN. Indian. J. Chem. **2**, 405 (1964); C. G. KARANJGAONKAR, P. M. NAIR, and K. VENKATARAMAN. Tetrahedron Lett. 687 (1966).
2. P. YATES, S. S. KARMARKAR, D. ROSENTHAL, G. H. STOUT, and V. F. STOUT. Tetrahedron Lett. 1623 (1963); W. D. OLLIS, M. V. J. RAMSAY, I. O. SUTHERLAND, and S. MONGKOLSUK. Tetrahedron, **21**, 1453 (1965); S. A. AHMAD, W. RIGBY, and R. B. TAYLOR. J. Chem. Soc. C, 772 (1966); M. AMOROSA and G. GIOVANNINETTI. Ann. Chim. (Rome), **56**, 232 (1966); G. CARDILLO and L. MERLINI. Tetrahedron Lett. 2529 (1967).
3. D. J. BICHAN and P. YATES. Can. J. Chem. This issue.
4. (*a*) P. YATES, D. J. BICHAN, and J. E. MCCLOSKEY. Chem. Commun. 839 (1972); (*b*) D. J. BICHAN and P. YATES. J. Am. Chem. Soc. **94**, 4773 (1972).
5. A. J. QUILLINAN and F. SCHEINMANN. Chem. Commun. 966 (1971).
6. R. QUAGLIARO, M. MOREAU, and J. DREUX. C. R. **257**, 2843 (1963); *cf.* D. MOLHO. Bull. Soc. Chim. Fr. 1417 (1961).
7. W. R. SCHLEIGH. Eastmen Org. Chem. Bull. **43** (1), 1 (1971).
8. L. JURD. J. Org. Chem. **31**, 1639 (1966); T. RIOS. Bol. Inst. Quim. Univ. Nac. Auton. Mexico, **18**, 78 (1966); Chem. Abstr. **67**, 82037 (1967).
9. W. G. DAUBEN, M. E. LORBER, N. D. VIETMEYER, R. H. SHAPIRO, J. H. DUNCAN, and K. TOMER. J. Am. Chem. Soc. **90**, 4762 (1968).
10. G. CHATELUS. Ann. Chim. (Paris) (12), **4**, 541 (1949); BADDELEY and N. H. P. SMITH. J. Chem. Soc. 2516 (1961); J. GRIPENBERG and T. HASE. Acta Chem. Scand. **20**, 1561 (1966).
11. S. AKAGI and T. IWASHIGE. J. Pharm. Soc. Jap. **74**, 608 (1954).
12. M. ŌKI and M. HIROTA. Bull. Chem. Soc. Jap. **37**, 209 (1964).
13. G. B. PAYNE. J. Org. Chem. **26**, 663 (1961).
14. K. TOMINO. Yakugaku Zasshi, **80**, 275 (1960); Chem. Abstr. **54**, 18385 (1960).

Can. J. Chem. Downloaded from www.nrcresearchpress.com by 210.87.254.40 on 09/05/12
For personal use only.

Bridged Xanthenes. II. An Intramolecular Cycloaddition Route

D. J. BICHAN AND PETER YATES

Lash Miller Chemical Laboratories, University of Toronto, Toronto, Ontario M5S 1A1

Received January 22, 1975.

D. J. BICHAN and PETER YATES. Can. J. Chem. **53**, 2054 (1975).

Oxidation of mesitol (**8**) with lead tetraacetate in acrylic acid followed by gentle heating gives 6-hydroxy-4,6,7-trimethyl-5-oxobicyclo[2.2.2]oct-7-ene-2-carboxylic acid lactone (**13**), which is considered to be formed via intramolecular cycloaddition of 6-acryloxy-2,4,6-trimethyl-2,4-cyclohexadienone (**11**). Similar treatment of 4-methylxanthen-3-ol (**7**) gives the corresponding bridged xanthene keto lactone **5**. Ketalization of this with ethylene glycol, followed by treatment with methylmagnesium iodide, hydrolysis, and pyrolysis gives the bridged xanthene keto ether **4**, which possesses many of the structural features of the nucleus of the naturally occurring coloring matters morellin and gambogic acid.

D. J. BICHAN et PETER YATES. Can. J. Chem. **53**, 2054 (1975).

L'oxydation du mésitol (**8**) par le tétraacétate de plomb dans l'acide acrylique suivie par un léger chauffage conduit à la lactone de l'acide hydroxy-6 oxo-5 triméthyl-4,6,7 bicyclo-[2.2.2]octène-2 carboxylique; on croit que ce composé se forme par une cycloaddition intramoléculaire de l'acryloxy-6 triméthyl-2,4,6 cyclohexadiène-2,4 one (**11**). Dans des conditions similaires, le méthyl-4 xanthénol-3 conduit au xanthène céto-lactonique **5**. La cétalisation de ce composé par de l'éthylène glycol, suivie successivement par une réaction avec de l'iodure de méthylmagnésium, par une hydrolyse puis par une pyrolyse, conduit au xanthène céto-éther **4** qui possède déjà plusieurs caractéristiques importantes des noyaux de la morelline et de l'acide gambogique, deux colorants naturels. [Traduit par le journal]

In the preceding paper (1) we have adumbrated the reasons for our interest in devising methods for the synthesis of bridged xanthene systems of type **1** and have reported on the successful development of a method based on Diels–Alder reactions of 3,4-dihydroxanthene with external dienophiles. Difficulties were experienced, however, when we sought to extend this method to bridged xanthenes incorporating additional functionality related to the naturally occurring compounds morellin (**2**) and gambogic acid (**3**) that had originally stimulated these synthetic studies. We now report on an alternative route based on an intramolecular cycloaddition reaction that leads to bridged xanthenes more closely related to **2** and **3**.[1]

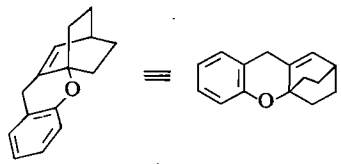

1

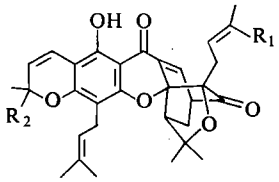

2 $R_1 = CHO$, $R_2 = CH_3$
3 $R_1 = CO_2H$; $R_2 = CH_2CH_2CH{=}C(CH_3)_2$

The goal we set ourselves was the synthesis of compound **4**, which incorporates into the bridged xanthene system **1** several of the functional features of **2** and **3**. This is clearly closely related to the keto lactone **5**, which we conceived might be formed by an intramolecular cycloaddition reaction of **6**. Compound **6** was reminiscent of the 6-acetoxy-2,4-cyclohexadienones formed by Wessely oxidation of *o*-alkylphenols with lead tetraacetate (4) and we entertained the possibility that it might be accessible via a modified Wessely oxidation of **7** with lead tetraacrylate as the effective oxidizing agent.

An investigation of this route was first undertaken in a model series. Mesitol (**8**) was chosen for this purpose since its oxidation with lead tetraacetate in acetic acid gives the 6-acetoxy-2,4-cyclohexadienone **9** in good yield; further, its oxidation with lead tetraacetate in propionic

[1]For a preliminary account of this work, see ref. 2; for another route, see ref. 3.

Can. J. Chem. Downloaded from www.nrcresearchpress.com by 210.87.254.40 on 09/05/12
For personal use only.

Can. J. Chem. Downloaded from www.nrcresearchpress.com by 210.87.254.40 on 09/05/12
For personal use only.

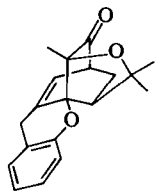

4

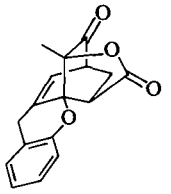

5

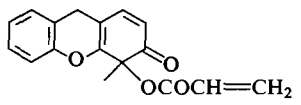

6

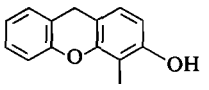

7

acid has been shown to give the 6-propionoxy-2,4-cyclohexadienone **10** (5). This latter observation suggested that lead tetraacetate in acrylic acid might serve our purpose, thus avoiding the necessity for the preparation of lead tetraacrylate.

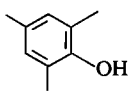

8

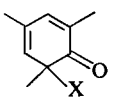

9 X = $OCOCH_3$
10 X = $OCOCH_2CH_3$

In the event, when **8** was added to a stirred solution of lead tetraacetate in acrylic acid at room temperature and stirring was continued for a few minutes, a slightly exothermic reaction occurred, and work-up gave in essentially quantitative yield a mixture of two products, which are considered to be the 6-acryloxy-2,4- and 4-acryloxy-2,5-dienones **11** and **12** (Scheme 1). The i.r. spectrum of the mixture shows carbonyl-stretching bands at 5.80, 5.96, and 6.02 μ; the first is attributable to the acrylate ester groups of both **11** and **12**, while the others are assigned to the ketonic groups of **11** and **12**, respectively. The p.m.r. spectrum of the mixture shows a complex set of signals in the region δ 5.6–6.6 attributable to the vinyl protons of **11** and **12**; it also shows singlets at δ 1.4 and 1.9 that can be assigned to methyl protons on sp^3 carbon bearing oxygen and to vinyl methyl protons, respectively.

Attempts to separate the product mixture by chromatography led to decomposition. Accordingly, a solution of the mixture in hexane was boiled under reflux overnight; on cooling the solution deposited a crystalline product that is considered to be the desired keto lactone **13**, formed by an intramolecular Diels–Alder reaction of **11** (Scheme 1). The yield from **8** was 41%.

The structural assignment **13** is based on the elemental composition and spectral characteristics of the product. Its i.r. spectrum shows carbonyl-stretching bands at 5.74 and 5.58 μ, assigned to the ketone and lactone groups, respectively. Each band appears at shorter wavelength than that normally associated with the group concerned; this can be attributed to increased strain in **13** and dipole–dipole interaction between the carbonyl groups (6). As expected for a bicyclo[2.2.2]oct-5-enone (7), **13** shows enhanced n → π* absorption in its u.v. spectrum (λ_{max} 312 nm (ε 184)). Its p.m.r. spectrum can readily be interpreted in terms of the assigned structure (Table 1); the observed coupling constants are in accord with dihedral angle measurements made on a molecular model.

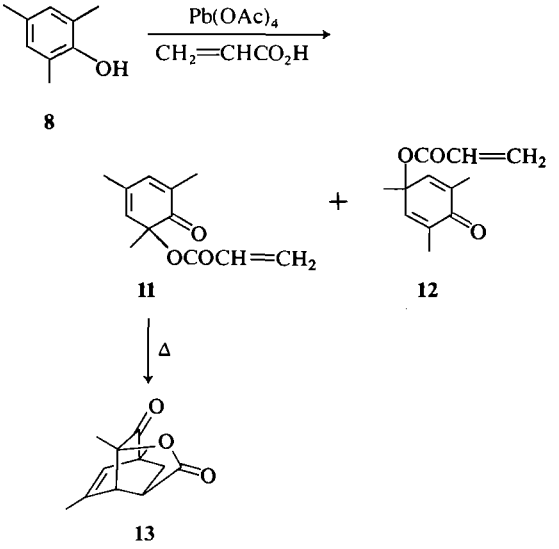

SCHEME 1

The structural assignment was corroborated by the degradation shown in Scheme 2. Treatment of **13** with aqueous base followed by acidification effected hydrolysis of the lactone and gave the corresponding hydroxy acid **14**, which is unstable and rapidly reverts to the lactone. Addition of periodic acid to the basic solution followed by acidification to p*H* 2 resulted in oxidative cleavage of the α-ketol system, accompanied by some reclosure to **13**. The resulting keto acid **15*a*** exists, at least in solution, mainly as the lactol acid **15*b***, since its i.r. spectrum shows in addition to typical carboxylic acid absorption a strong peak at 5.71 μ

TABLE 1. Proton magnetic resonance spectrum of **13**[a]

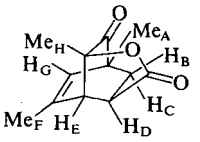

13

Assignment[b]	Chemical shift (δ)	Multiplicity	Coupling constant (Hz)
H_B,H_C	1.93	m	
H_D	2.84	ddd[c]	$J_{BD} = 2, J_{CD} = 9, J_{DE} = 5$
H_E	3.30	dd[d]	$J_{DE} = 5, J_{EG} = 2$
H_G	5.79	br s	
Me_A	1.26	s	
Me_F	1.93	d	$J_{FG} = 2$
Me_H	1.44	s	

[a]In $CDCl_3$.
[b]Signal intensities are in accord with the assignments.
[c]With irradiation at the H_B, H_C frequency, the H_D signal appears as d (J_{DE} = 5 Hz).
[d]With irradiation at the H_D frequency, the H_E signal appears as br s; with irradiation at the H_G frequency, it appears as d (J_{DE} = 5 Hz).

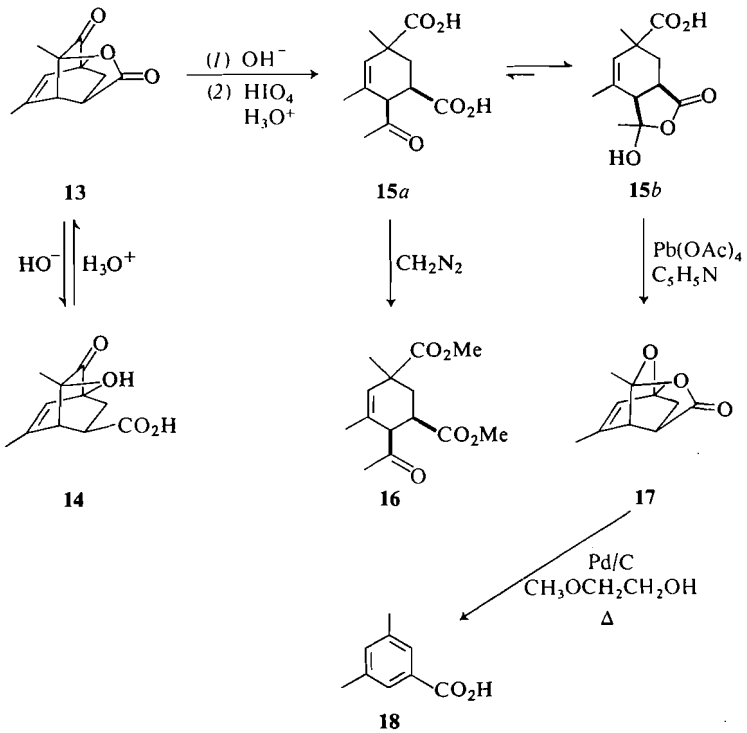

13 **15***a* **15***b*

14 **16** **17**

18

SCHEME 2

attributable to the lactol carbonyl group. That **15***b* exists in equilibrium with **15***a* was shown by treatment with diazomethane to give a product, which, although not fully characterized, shows i.r. and p.m.r. spectra in accord with the keto diester structure **16** (see Experimental). Reaction of **15***b* with lead tetraacetate and pyridine gave a product that is assigned structure **17**, which can be envisaged as arising by oxidative decarboxylation to give the allylic cation **19**, followed

Can. J. Chem. Downloaded from www.nrcresearchpress.com by 210.87.254.40 on 09/05/12
For personal use only.

Can. J. Chem. Downloaded from www.nrcresearchpress.com by 210.87.254.40 on 09/05/12
For personal use only.

by ether formation by attack of the lactol hydroxyl group at one terminus of the cation. Its i.r. spectrum shows a carbonyl-stretching band at 5.64 μ. Its p.m.r. spectrum shows

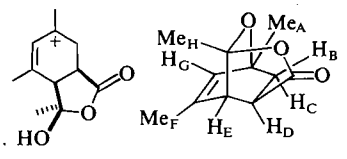

19 17

several similarities to that of **13**; although the signals attributable to H_B, H_C, and H_D overlap in the δ 2.0–2.6 region, the H_E (δ 3.19, dd, J_{DE} = 4 Hz, J_{EG} = 2 Hz), H_G (δ 6.12, br s) and Me_F (δ 1.90, d, J_{FG} = 2 Hz) signals are clearly analogous to the signals of the corresponding protons in **13**; the Me_A and Me_H signals (δ 1.40 s, 1.42 s) appear close together in the case of **17**, since each is now attached to an sp^3 carbon bearing one or more oxygen atoms.

When **17** was heated in boiling ethylene glycol monomethyl ether (b.p. 125°) with palladium-on-carbon, 3,5-dimethylbenzoic acid (**18**) was formed and identified by comparison with an authentic sample. It seems probable that the transformation involves thermal conversion of **17** to the anhydride **21** by a retro-Diels–Alder reaction or a stepwise process via **20** followed by dehydrogenation and solvolysis (Scheme 3).

Having established the practicability of the intramolecular cycloaddition route in the case of mesitol (**8**), we proceeded to apply it to the xanthene system. 3-Hydroxy-4-methylxanthone (**25**), which had previously been obtained by another method (8), was prepared by a modification of the general xanthone synthesis of Grover *et al.* (9) (Scheme 4). Treatment of salicylic acid (**22**) and 2-methylresorcinol (**23**) with zinc chloride and phosphorus oxychloride gave the benzophenone **24**. The structure of this product was corroborated by the occurrence of the carbonyl-stretching band at 6.20 μ in its i.r. spectrum as a result of hydrogen bonding with two *o*-hydroxyl groups (*cf.* 2,4-dihydroxybenzophenone: 6.13 μ (10)). The p.m.r. spectrum of **24** shows three hydroxyl proton signals at δ 5.82, 10.27, and 11.83; the last two can be assigned to the two hydroxyl groups that are intramolecularly hydrogen bonded to the carbonyl group; their chemical shifts may be compared with those recorded for the hydroxylated benzophenones **26** (δ 10.4), **27** (δ 10.2, 11.5), and **28** (δ 12.6) (11). The remainder of the p.m.r. spectrum is in good accord with the assigned structure (see Experimental). Nevertheless, a discrepancy was encountered on comparison of the u.v. spectrum of **24** (λ_{max} (MeOH) (ε) 297(12 700), 332(9600) nm) with that reported (12) for the unmethylated analog **29** (λ_{max} (MeOH) (ε) 288(25 100), 329(24 000) nm); although the small differences in band positions are not unexpected, the large differences in band intensities appear to be anomalous. However, there is reason to question the intensity values reported for **29**, since its monomethyl ether is reported to have a long wavelength maximum at 327 nm (ε 10 100) in its u.v. spectrum (13).

The general procedure (9) referred to above called for heating of **24** to 200–220° to convert

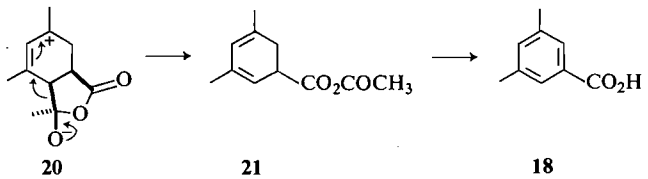

20 21 18

SCHEME 3

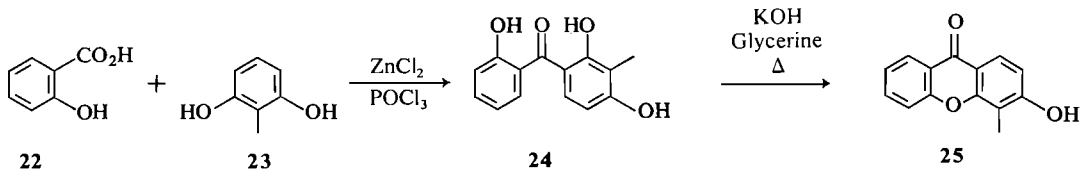

22 23 24 25

SCHEME 4

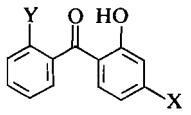

26 X = H; Y = OH
27 X = OMe; Y = OH
28 X = OMe; Y = H

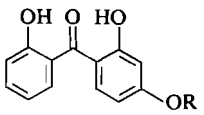

29 R = H
30 R = Me

it to the xanthone **25**. This led to low yields of very impure xanthone; however, heating **24** with a trace of potassium hydroxide in glycerol at 210–215° cleanly afforded **25** in high yield. The melting point of this product (271–272°) is close to that originally reported (8) for **25** (268°) and its i.r. spectrum is reasonably related to that reported (14) for its nonmethylated analog, 3-hydroxyxanthone. A discrepancy was encountered again when the u.v. spectrum of **25** (λ_{max} (ε) 237(40 600), 266(6300), 276(5700), 313(12 500), 332(9800) nm) was compared with that reported (15) for 3-hydroxyxanthone (λ_{max} (ε) 235(25 600), 261(5750), 270(5310), 307(9630), 333(6530) nm). As before, the discrepancy concerns the intensities rather than the positions of the maxima. However, there is again reason to question the reported intensity values since xanthone itself has λ_{max} (ε) 239(42 800), 260(12 500), 288(4400), 336(7000) nm (16).

The xanthone **25** was treated with lead tetraacetate in acrylic acid in the hope that a product analogous to **11** would be formed. One main product was obtained in high yield but this was not the desired compound as was immediately apparent from its p.m.r. spectrum. It was not fully characterized but is considered to have structure **31** on the basis of its spectra (see Experimental).

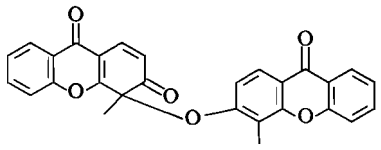

31

It appeared possible that one or both of two factors might account for the difference in the course of the reactions of the xanthone **25** and mesitol (**8**) with lead tetraacetate in acrylic acid. First, in the case of **25** but not of **8** there is a ketonic carbonyl group attached to the ring undergoing oxidation, and second, the reaction mixture with **25** did not become homogeneous until after several hours of stirring at room temperature, whereas with **8** the reaction mixture became homogeneous very rapidly and was worked-up after a few minutes. We therefore converted **25** to 4-methylxanthen-3-ol (**7**), which lacked the carbonyl group of **25** and was also expected to be more soluble (see Scheme 5).

The conversion was carried out with lithium aluminum hydride under vigorous conditions (*cf.* ref. 17). The xanthene **7** was an unstable compound, whose spectra were in accord with anticipation (see Experimental). Treatment with lead tetraacetate in acrylic acid gave a product that is considered to be a mixture of the desired cyclohexadienone **6** with the cyclohexadienones **32** and **33**. Its p.m.r. spectrum includes extensive acrylate proton absorption and three singlets in the region δ 1.5–2; the most intense of these (δ 1.62) is assigned to the methyl protons of **6**, while the others (δ 1.95, 2.05) are tentatively assigned to the vinyl methyl protons of **32** and **33**.

As in the case of mesitol, an attempt to separate the Wessely oxidation product mixture by chromatography led to decomposition. The mixture was therefore heated in boiling benzene to effect intramolecular cycloaddition of **6**. Chromatography of the resulting mixture gave the keto lactone **5** in an overall yield from **7** of 23%. Its i.r. spectrum in the carbonyl-stretching region resembled that of the keto lactone **13** with bands at 5.58 and 5.72 μ, and its u.v. spectrum showed similarly enhanced $n \rightarrow \pi^*$ absorption (λ_{max} 310 nm (ε 204)); the latter showed in addition bands attributable to a chroman-type system (λ_{max} (ε) 271(1410), 275(1380) nm) (*cf.* ref. 18). Its p.m.r. spectrum is in complete accord with the assigned structure (Table 2) and shows the expected relationship to the p.m.r. spectrum of **13** (Table 1); the observed coupling constants are in accord with dihedral angle measurements made on a molecular model.

With the structure of **5** secure, we turned to the final stage in attaining our goal, the conversion of **5** to the keto ether **4** (Scheme 6). The ketonic group of **5** was first protected by conversion of the latter to the ketal **34**. Treatment of this with a large excess of methylmagnesium iodide in boiling benzene–ether for 2 days gave the ketal diol **35**, which on treatment with dilute aqueous acid afforded the keto diol **36**. This was heated at 200° (100 mm) in a sublimation apparatus to effect dehydration; these conditions were designed to maximize dehydration and sublima-

Can. J. Chem. Downloaded from www.nrcresearchpress.com by 210.87.254.40 on 09/05/12
For personal use only.

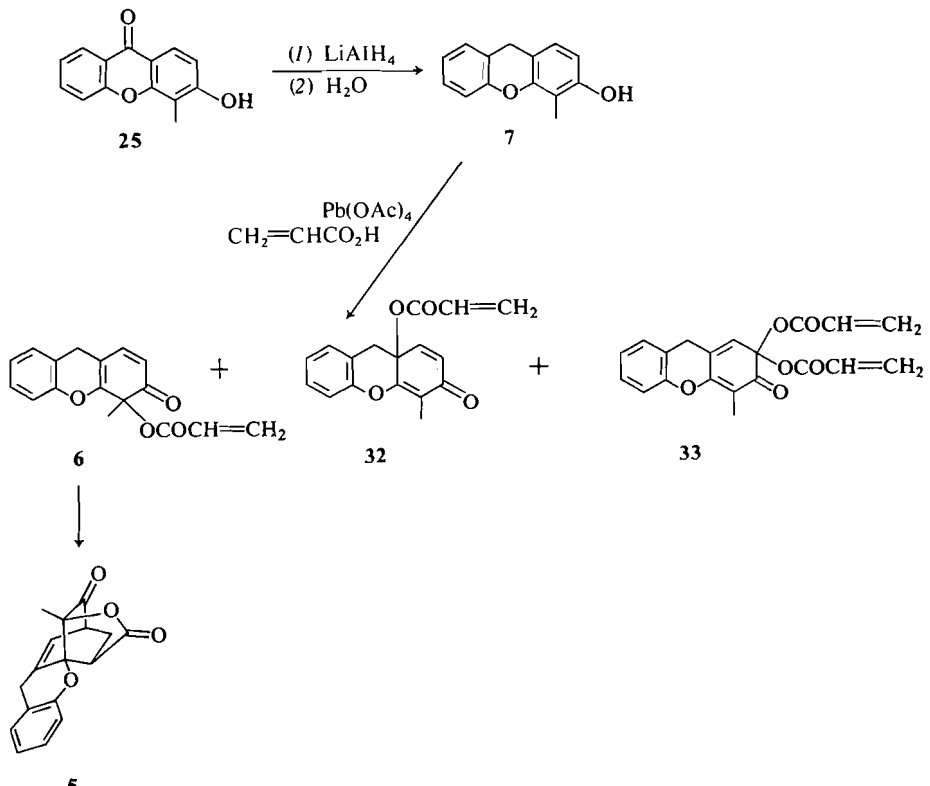

25 7 6 32 33 5

SCHEME 5

TABLE 2. Proton magnetic resonance spectrum of **5**[a]

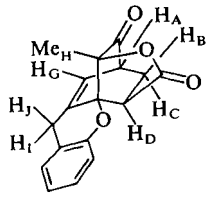

5

Assignment[b]	Chemical shift (δ)	Multiplicity	Coupling constant (Hz)
H_A	3.42	ddd[c]	$J_{AB} = 3.5, J_{AC} = 2, J_{AG} = 7$
H_B	2.26	ddd[d]	$J_{AB} = 3.5, J_{BC} = 13, J_{BD} = 1.5$
H_C	1.84	ddd[e]	$J_{AC} = 2, J_{BC} = 13, J_{CD} = 11$
H_D	2.70	dd	$J_{BD} = 1.5, J_{CD} = 11$
H_G	6.28	dt[f]	$J_{AG} = 7, J_{G(IJ)} = 2$
H_I, H_J	3.59	d[g]	$J_{G(IJ)} = 2$
Me_H	1.39	s	
Aromatic	7.14	m	

[a]In $CDCl_3$.
[b]Signal intensities are in accord with the assignments.
[c]With irradiation at the approximate frequency of H_B and H_C, the H_A signal appears at d (J_{AG} = 7Hz); with irradiation at the H_G frequency, it appears as dd (J_{AB} = 3.5, J_{AC} = 2 Hz).
[d]With irradiation at the H_A frequency, the H_B signal appears as dd (J_{BC} = 13, J_{BD} = 1.5 Hz).
[e]With irradiation at the H_A frequency, the H_C signal appears as dd (J_{BC} = 13, J_{CD} = 11 Hz).
[f]With irradiation at the H_A frequency, the H_G signal appears as br s.
[g]With irradiation at the H_G frequency, the H_I,H_J signal appears as s.

Can. J. Chem. Downloaded from www.nrcresearchpress.com by 210.87.254.40 on 09/05/12
For personal use only.

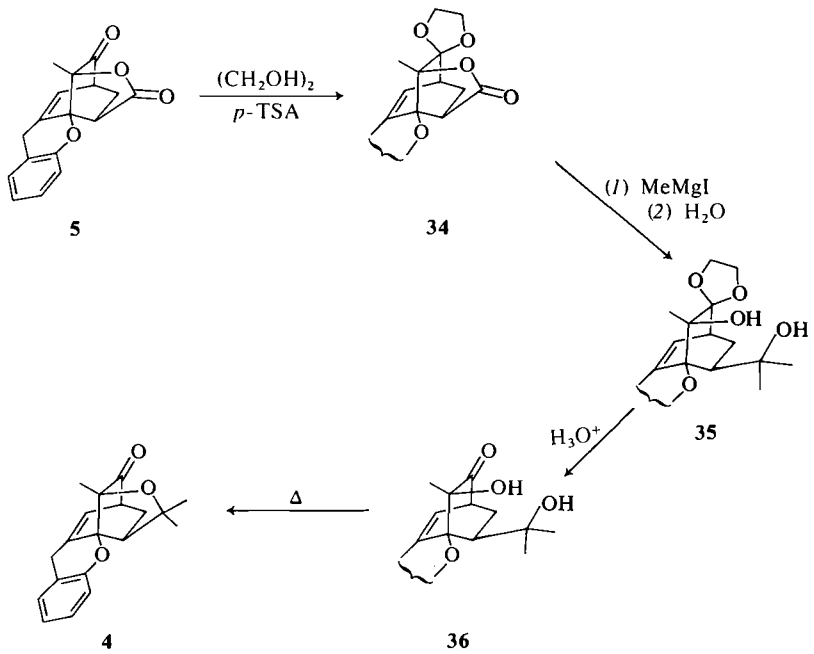

SCHEME 6

TABLE 3. Nuclear magnetic resonance spectrum of **4**[a]

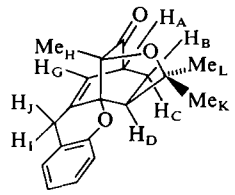

4

Assignment[b]	Chemical shift (δ)	Multiplicity	Coupling constant (Hz)
H_A	3.06	ddd	$J_{AB} = 5, J_{AC} = 1, J_{AG} = 6.5$
H_B, H_C	1.3	m	
H_D	2.2	m	
H_G	6.10	dt	$J_{AG} = 7, J_{G(IJ)} = 2$
H_I, H_J	3.45	d	$J_{G(IJ)} = 2$
Me_H	1.25[c]	s	
Me_K	1.22	s	
Me_L	1.72	s	
Aromatic	7.17	m	

[a]In $CDCl_3$.
[b]Signal intensities are in accord with the assignments.
[c]This one of the three Me signals is assigned to Me_H since it is considerably sharper than the other two; it is anticipated that the signals of the geminal Me group will be broadened by long-range coupling between the protons of one group and those of the other (20).

tion of the product while minimizing sublimation of the starting material. The sublimate consisted of a mixture of the desired keto ether **4** and the keto diol **36**; after correction for unconsumed **36**, the overall yield of **4** from **5** was *ca.* 50%.

The spectroscopic data for the intermediates **34–36** are in accord with expectation (see Experimental) and the structural assignment **4** is established by the elemental composition of the product, its spectra, and the relation of these

Can. J. Chem. Downloaded from www.nrcresearchpress.com by 210.87.254.40 on 09/05/12
For personal use only.

Can. J. Chem. Downloaded from www.nrcresearchpress.com by 210.87.254.40 on 09/05/12
For personal use only.

to the spectra of **13** and **5**. Its i.r. spectrum shows a single carbonyl-stretching band at 5.75 μ, and its u.v. spectrum (λ_{max} (ε) 271(1600), 275(1600), 312(580) nm) shows both chroman-type and enhanced n → π* absorption. The intensity of the latter is much greater than in the case of **5** (λ_{max} 310 (204) nm). This is considered to result from a change in the geometry of the bridged ring system arising from steric repulsion between the Me_L group and H_B, which examination of a molecular model shows are in very close proximity. The p.m.r. spectrum of **4** is given in Table 3. Some departure from first order coupling patterns and uncertainties regarding some assignments prevented full analysis of this spectrum. However, its relationship to that of **5** corroborates the structural assignment **4**, with changes in coupling constants interpretable in terms of the geometrical change to which reference has been made above.

In addition to its application to the synthesis of bridged xanthenes herein described, the reaction sequence of Wessely oxidation of phenols with lead tetraacetate in acrylic acid followed by intramolecular cycloaddition clearly has wider potentialities for the synthesis of bicyclo[2.2.2]octane derivatives and has been successfully applied with α,β-unsaturated carboxylic acids other than acrylic acid (19).

Experimental

Melting points were determined with a Thomas Hoover Uni-Melt apparatus and are uncorrected. Infrared spectra were recorded in chloroform solution, ultraviolet spectra in methanol solution, and proton magnetic resonance spectra in deuteriochloroform, unless otherwise indicated. Solutions in organic solvents were dried over anhydrous magnesium sulfate.

*Lead Tetraacetate Oxidation of Mesitol (**8**) in Acrylic Acid and Subsequent Intramolecular Cycloadditions: Keto Lactone **13***

Lead tetraacetate (20.1 g, 45.4 mmol) was dissolved with stirring in acrylic acid (150 ml) and the solution was stirred for 5 min at room temperature. Mesitol (**8**) (4.13 g, 30.4 mmol) was added and stirring was continued for 10 min. Ethylene glycol (25 ml) was added and the solution was stirred for 2 min and poured into hexane (400 ml). The hexane extract was washed with water (5 × 400 ml) and dried. Evaporation of a small aliquot yielded a gum with λ_{max} 5.80, 5.96, 6.02 (m) μ; δ 1.4 (s), 1.9 (s), 5.6–6.6 (m). The remainder of the solution was evaporated to a volume of 70 ml, and boiled under reflux for 21 h. The solution was evaporated to a volume of 20 ml, when crystallization yielded 2.56 g (41%) of **13** which after two recrystallizations from boiling hexane had m.p. 111–112°; λ_{max} (CCl_4) 5.58, 5.74 μ; λ_{max} (ε) 312 (184) nm; *m/e* 206.[2]

Anal. Calcd. for $C_{12}H_{14}O_3$: C, 69.88; H, 6.84. Found: C, 69.90; H, 6.85.

*Hydrolysis of **13** and Subsequent Periodic Acid Cleavage: Lactol Acids **15b***

Keto lactone **13** (1.06 g, 5.15 mmol), sodium hydroxide (450 mg, 11.3 mmol), and aqueous 50% tetrahydrofuran (63 ml) were stirred together for 23 h at room temperature. The solution was filtered and periodic acid (1.20 g, 5.26 mmol) was added. The p*H* was brought to 2 by slow dropwise addition of 4% hydrochloric acid with stirring, and stirring was continued for 20 h; the solution was poured into saturated aqueous sodium bicarbonate (60 ml) and extracted with chloroform (70 ml). The chloroform layer was dried and evaporated to give 201 mg (19%) of **13**. The aqueous layer was acidified to p*H* 2 with 4% hydrochloric acid and extracted with ether (2 × 125 ml). The extracts were dried and evaporated to yield 915 mg (74%) of **15***b*, which after crystallization from chloroform had m.p. 178–181°; λ_{max} 3–4 (m), 5.71, 5.85 μ; δ (C_5H_5N) 1.50 (s, 3 H), 1.82 (s, 3 H), 2.23 (br s, 3 H), 2.45 (m, 1 H), 3.15 (m, 2 H), 3.53 (m, 1 H), 6.07 (br s, 1 H).

Anal. Calcd. for $C_{12}H_{16}O_5 \cdot \frac{1}{4} H_2O$: C, 58.89; H, 6.75. Found: C, 58.82; H, 6.43.

*Esterification of **15**: Keto Diester **16***

Lactol acids **15***b* (64 mg, 0.27 mmol) were dissolved in ether (15 ml). Ethereal diazomethane was added slowly dropwise with stirring to the solution until a pale yellow color persisted and 4% hydrochloric acid (5 drops) was added. The solution was poured into chloroform (85 ml), washed with water (100 ml), dried, and evaporated to yield 67 mg (71%) of **16** as a gum; λ_{max} 5.79 μ; δ 1.28 (s, 3 H), 1.83 (br s, 3 H), 2–3 (m, 3 H), 2.25 (s, 3 H), 3.43 (br d, J = 4 Hz, 1 H), 3.72 (s, 6 H), 5.70 (br s, 1 H).

*Lead Tetraacetate Oxidation of **15b**: Lactone Ether **17***

Lactol acids **15***b* (217 mg, 0.90 mmol) were added to a solution of lead tetraacetate (845 mg, 1.91 mmol) in dry benzene (15 ml) and dry pyridine (158 mg, 12 drops) (*cf.* ref. 21). The solution was refluxed for 3 h under a drying tube and cooled. Ethylene glycol (1 ml) was added, and the mixture was stirred for 2 min and poured into benzene (100 ml). The benzene extract was washed with water (2 × 100 ml), dried, and evaporated to yield 156 mg (89%) of **17**, which after sublimation (55°, 0.1 mm) had m.p. 56–57.5°; λ_{max} 5.64 μ; δ 1.40 (s, 3 H), 1.42 (s, 3 H), 1.90 (d, J = 2 Hz, 3 H), 2.0–2.6 (m, 3 H), 3.19 (dd, J = 4, 2 Hz, 1 H), 6.12 (br s, 1 H); *m/e* 194.

Anal. Calcd. for $C_{11}H_{14}O_3$: C, 68.02; H, 7.27. Found: C, 68.13; H, 7.48.

*3,5-Dimethylbenzoic Acid (**18**) from Degradation of Lactone Ether **17***

Lactone ether **17** (61 mg, 0.31 mmol) was dissolved in 2-methoxyethanol (15 ml) and 5% palladium-on-carbon (106 mg) was added. The mixture was boiled under reflux for 16 h, cooled, and filtered. The filtrate was evaporated to give 42 mg of a gum, which was placed on a silica gel t.l.c. plate (20 × 10 × 0.05 cm) in chloroform. Elution with chloroform yielded 11 mg (23%) of

[2]For p.m.r. spectrum, see Table 1.

Can. J. Chem. Downloaded from www.nrcresearchpress.com by 210.87.254.40 on 09/05/12
For personal use only.

18 ($R_f \simeq 0.3$), which after recrystallization from boiling cyclohexane had m.p. 166–169° (lit. (22) m.p. 170°), which was undepressed upon admixture with authentic material. Identity was also established by comparison of i.r., n.m.r., u.v., and mass spectra.

2,2′,4-Trihydroxy-3-methylbenzophenone (24)

Salicyclic acid (**22**) (13.8 g, 100 mmol), 2-methylresorcinol (**23**) (12.4 g, 100 mmol), anhydrous zinc chloride (42 g, 310 mmol), and phosphorus oxychloride (100 ml) were heated together with stirring in an oil bath at 60–65° under dry nitrogen for 4 h. The mixture was allowed to cool for 5 min and poured into a 1500-ml beaker full of ice. The resulting mixture was stirred for several hours until it had cooled to room temperature. The aqueous layer was decanted, saturated aqueous sodium bicarbonate (1 l) was added, and the mixture was stirred at room temperature for 17 h. The aqueous layer was decanted and benzene (600 ml) was added to the residue. The mixture was boiled with stirring until the volume was reduced to 500 ml. The solution was decanted, charcoal (10 g) was added, and the mixture was boiled gently with stirring until the volume was reduced to 400 ml and filtered. The filtrate was concentrated by evaporation to a volume of 50 ml and allowed to crystallize to yield 12.3 g of **24** as a yellow solid. A second crop (1.13 g) brought the total yield to 55%. Two recrystallizations of the first crop from benzene yielded material with m.p. 145.5–147°; λ_{max} 2.88 (m), 3.0–3.4 (m), 6.20 μ; λ_{max} (ε) 241 (sh, 7300), 297 (12 700), 332 (sh, 9600) nm; δ 2.17 (s, 3 H), 5.82 (v br s, 1 H), 6.38 (d, J = 9 Hz, 1 H), 6.91 (td, J = 8, 1.5 Hz, 1 H), 7.07 (dd, J = 8, 1.5 Hz, 1 H), 7.41 (m, 3 H), 10.27 (br s, 1 H), 11.83 (s, 1 H); *m/e* 244.

Anal. Calcd. for $C_{14}H_{12}O_4$: C, 68.84; H, 4.95. Found: C, 68.55; H, 5.05.

3-Hydroxy-4-methylxanthone (25)

2,2′,4-Trihydroxy-3-methylbenzophenone (**24**) (13.9 g, 52 mmol), glycerine (100 ml), and sodium hydroxide (118 mg, 2.95 mmol) were heated together under nitrogen to 210–215° with stirring for 2 h. The solution was cooled to *ca.* 130° and poured slowly into water (400 ml) with stirring. The precipitate was collected, washed with water, and dried to give 11.5 g (89%) of **25**, which after recrystallization from boiling benzene–ethanol had m.p. 271–272° (lit. (8) m.p. 268°); λ_{max} (KBr) 6.06 (m), 6.19, 6.23 μ; λ_{max} (ε) 237 (40 600), 266 (6300), 276 (5700), 313 (12 500), 332 (sh, 9800) nm.

Lead Tetraacetate Oxidation of 25 in Acrylic Acid

3-Hydroxy-4-methylxanthone (**25**) (1.39 g, 6.15 mmol), lead tetraacetate (4.64 g, 10.5 mmol), and acrylic acid (60 ml) were stirred together at room temperature under a drying tube for 2.5 h while the mixture became homogeneous. Ethylene glycol (1.5 ml) was added and the solution was stirred for 1 min and poured into benzene (200 ml). The benzene solution was washed with water (7 × 200 ml), dried, and evaporated to yield 1.56 g of a yellow solid, which was triturated in ethanol – 17% chloroform to yield 1.31 g (95%) of **31**, m.p. 170° (dec.); λ_{max} 5.90 (m), 6.04, 6.21 μ; δ 2.00 (s, 3 H), 2.65 (s, 3 H), 6.12 (d, J = 8 Hz, 1 H), 6.48 (d, J = 10 Hz, 1 H), 7.2–8.4 (m, 10 H).

4-Methylxanthen-3-ol (7)

3-Hydroxy-4-methylxanthone (**25**) (1.01 g, 4.47 mmol), lithium aluminum hydride (700 mg, 18.4 mmol), anhydrous ether (50 ml), and anhydrous benzene (30 ml) were stirred together and heated for 3 h under reflux with protection from atmospheric moisture with a drying tube. The mixture was then stirred for 20 h at room temperature. Aqueous 10% ammonium chloride was added carefully until no further hydrogen evolution was observed. Ether (50 ml) was added followed by water (125 ml) and 3% hydrochloric acid until the aqueous layer became homogeneous. Ether (75 ml) and water (75 ml) were added, and the mixture was shaken. The organic layer was separated, dried, and evaporated to yield 835 mg (88%) of **7**, which after sublimation (90°, 0.1 mm) had m.p. 120–121°; λ_{max} 2.86 (m), 3.08 (w) μ; λ_{max} (ε) 250 (5740), 277 (3070) nm; δ 2.25 (s, 3 H), 3.94 (s, 2 H), 4.59 (br s, 1 H), 6.52 (d, J = 8.5 Hz, 1 H), 7.25 (m, 5 H); *m/e* 212.

Anal. Calcd. for $C_{14}H_{12}O_2$: C, 79.22; H, 5.70. Found: C, 78.76; H, 5.67.

Lead Tetraacetate Oxidation of 7 in Acrylic Acid and Subsequent Intramolecular Cycloaddition: Keto Lactone 5

Lead tetraacetate (15.8 g, 36.7 mmol) was dissolved in acrylic acid (100 ml) and the solution was stirred at room temperature for 5 min and placed in an ice bath. Immediately 3-hydroxy-4-methylxanthene (**7**) (5.01 g, 23.6 mmol) in acrylic acid (75 ml) was added dropwise over 2 min. The ice bath was removed and stirring was continued for 8 min more. Ethylene glycol (10 ml) was added and stirring was continued for 2 min. The solution was poured into benzene (400 ml) and the benzene extract was washed with water (4 × 400 ml) and aqueous 1% potassium bicarbonate (400 ml) and dried. Evaporation of a small aliquot gave a gum with λ_{max} ($CHCl_3$) 5.79, 5.91 (m), 5.98–6.02 μ; δ 1.62 (s), 1.95 (s), 2.05 (s), 3.62 (m), 5.6–6.6 (m). Hydroquinone (87 mg, 0.79 mmol) was added and the solution was heated under reflux for 20 h under nitrogen. Evaporation of the solvent yielded 6.13 g of a red gum, which was placed on silica gel (375 g) in benzene and eluted with benzene – 1% ether; 200-ml fractions were collected. Fractions 16–35 contained 1.51 g (23%) of **5**, which after three recrystallizations from methanol had m.p. 116–118°; λ_{max} 5.58; 5.72 μ; λ_{max} (ε) 271 (1410), 275 (1380), 310 (204) nm; *m/e* 282.[3]

Anal. Calcd. for $C_{17}H_{14}O_4$: C, 72.33; H, 5.00. Found: C, 72.15; H, 5.16.

Ketalization of 5: Lactone Ketal 34

Keto lactone **5** (219 mg, 0.78 mmol), ethylene glycol (1.5 ml), *p*-toluenesulfonic acid monohydrate (1.22 g, 6.4 mmol), and benzene (50 ml) were heated under reflux in a nitrogen atmosphere for 21 h with azeotropic removal of water. The solution was cooled and poured into ether (75 ml). The ethereal solution was washed with saturated aqueous sodium bicarbonate (70 ml), dried, and evaporated to yield 492 mg of a yellow gum, which was placed on Florisil (25 g) and eluted with benzene to yield 240 mg (95%) of **34**, which after two recrystallizations from boiling cyclohexane–benzene had m.p.

[3]For p.m.r. spectrum, see Table 2.

Can. J. Chem. Downloaded from www.nrcresearchpress.com by 210.87.254.40 on 09/05/12
For personal use only.

145.5–148°; λ_{max} 5.61 μ; λ_{max} (ε) 271 (1320), 275 (1300) nm; δ 1.33 (s, 3 H), 1.54 (ddd, J = 13, 11, 2 Hz, 1 H), 2.20 (ddd, J = 13, 3.5, 1.5 Hz, 1 H), 2.38 (dd, J = 11, 1.5 Hz, 1 H), 2.69 (ddd, J = 7, 3.5, 2 Hz, 1 H), 3.50 (d, J = 2 Hz, 2 H), 4.01 (m, 4 H), 6.19 (dt, J = 7, 2 Hz, 1 H), 7.03 (m, 4 H); *m/e* 326.

Anal. Calcd. for $C_{19}H_{18}O_5$: C, 69.92; H, 5.56. Found: C, 70.17; H, 5.63.

Keto Ether 4

Methyl iodide (1.51 g, 10.6 mmol), magnesium (270 mg, 11.3 mol), and anhydrous ether (25 ml) were stirred in a flame-dried apparatus under dry nitrogen to form methylmagnesium iodide. Anhydrous ether (35 ml) was added with stirring followed by lactone ketal **34** (295 mg, 0.91 mmol) in anhydrous benzene (5 ml). The mixture was stirred and heated under reflux for 42 h while the volume of ether was maintained by intermittent addition from a dropping funnel. The solution was cooled, 4% hydrochloric acid (10 ml) was added very carefully, and stirring was continued until both phases were clear. The solution was poured into a separatory funnel and the volume of each phase was made up to 150 ml by addition of ether and water. The organic layer was separated and washed with aqueous 1% sodium bicarbonate (125 ml), dried, and evaporated to yield 331 mg of a gum. This was placed on two silica gel t.l.c. plates (20 × 20 × 0.05 cm) in chloroform and eluted with ether to yield 286 mg (88%) of the ketal diol **35** ($R_f \simeq 0.2$); λ_{max} 2.9–3.3 (m) μ; δ 1.15 (s, 3 H), 1.25 (s, 3 H), 1.4–2.2 (m, 3 H), 1.68 (s, 3 H), 2.48 (m, 1 H), 3.49 (d, J = 2 Hz, 2 H), 3.98 (m, 4 H), 4.34 (br s, 2 H), 5.89 (dt, J = 7, 2 Hz, 1 H), 7.04 (m, 4 H).

Ketal diol **35** (286 mg, 0.80 mmol) and *p*-toluenesulfonic acid monohydrate (450 mg, 2.37 mmol) were dissolved in aqueous 80% tetrahydrofuran (15 ml) and the solution was refluxed gently for 17 h under nitrogen and poured into ether (150 ml). The ethereal extract was washed with water (50 ml) and saturated aqueous sodium bicarbonate (50 ml), dried, and evaporated to yield 228 mg (91%) of the keto diol **36** as a gum; λ_{max} 2.9–3.3 (m), 5.75 μ; δ 1.17 (s, 3 H), 1.33 (s, 3 H), 1.6–2.3 (m, 3 H), 1.73 (s, 3 H), 3.14 (m, 1 H), 3.50 (d, J = 2 Hz, 2 H), 4.34 (br s, 2 H), 5.93 (dt, J = 7, 2 Hz, 1 H), 7.10 (m, 4 H).

Keto diol **36** (51 mg, 0.17 mmol) was placed in a sublimation apparatus with a cold water cold finger and the pressure was reduced to 160 mm. The apparatus was placed in an oil bath at 200°. After 5 min the pressure was reduced to 100 mm over 5 min and sublimation was allowed to continue for 45 min. The sublimate consisted of a gum (38 mg), which was placed on a silica gel t.l.c. plate (20 × 10 × 0.05 cm) in chloroform. Elution with chloroform yielded 14 mg (27%) of starting material **36** ($R_f \simeq 0.1$) and 15 mg (31%) of the keto ether **4** ($R_f \simeq 0.6$), which after crystallization from hexane had m.p. 110–113°; λ_{max} (CCl_4) 5.75 μ; λ_{max} (ε) 271 (1600), 275 (1600), 312 (580) nm; *m/e* 296.[4]

Anal. Calcd. for $C_{19}H_{20}O_3$: C, 77.00; H, 6.80. Found: C, 76.77; H, 6.80.

We thank the National Research Council of Canada for support of this work.

1. P. YATES and D. J. BICHAN. Can. J. Chem. This issue.
2. D. J. BICHAN and P. YATES. J. Am. Chem. Soc. **94**, 4773 (1972).
3. A. J. QUILLINAN and F. SCHEINMANN. Chem. Commun. 966 (1971).
4. R. CRIEGEE. *In* Oxidation in organic chemistry. Part A. *Edited by* K. B. Wiberg. Academic Press, New York. 1965. pp. 288–291.
5. G. W. K. CAVILL, E. R. COLE, P. T. GILHAM, and D. J. MCHUGH. J. Chem. Soc. 2785 (1954).
6. R. N. JONES and C. SANDORFY. *In* Chemical application of spectroscopy. *Edited by* W. West. Interscience, New York. 1956. pp 479–481.
7. H. LABHART and G. WAGNIÈRE. Helv. Chim. Acta, **42**, 2219 (1959).
8. Y. S. AGASIMUNDIN and S. RAJAGOPAL. Monatsh. **97**, 423 (1966).
9. P. K. GROVER, G. D. SHAH, and R. C. SHAH. J. Chem. Soc. 3982 (1955).
10. W. L. DILLING. J. Org. Chem. **31**, 1045 (1966).
11. J. R. MERRILL. J. Phys. Chem. **65**, 2023 (1961).
12. J. A. VANALLAN. J. Org. Chem. **23**, 1679 (1958).
13. R. G. SCHMITT and R. C. HIRT. J. Polym. Sci. **45**, 35 (1960).
14. F. SCHEINMANN. Tetrahedron, **18**, 853 (1962).
15. A. A. LINS MESQUITA, D. DE BARROS CORRÊA, O. R. GOTTLIEB, and M. TAVEIRA MAGALHÃES. Anal. Chim. Acta, **42**, 311 (1968).
16. G. H. STOUT, V. F. STOUT, and M. J. WELSH. Tetrahedron, **19**, 667 (1963).
17. A. MUSTAFA and O. H. HISHMAT. J. Org. Chem. **22**, 1644 (1957).
18. G. CHATELUS. Ann. Chim. (Paris) (12), **4**, 541 (1949); G. BADDELEY and N. H. P. SMITH. J. Chem. Soc. 2516 (1961); J. GRIPENBERG and T. HASE. Acta Chem. Scand. **20**, 1561 (1966).
19. P. YATES and H. AUKSI. To be submitted for publication.
20. K. M. BAKER and B. R. DAVIS. Tetrahedron, **24**, 1663 (1968).
21. E. J. COREY and J. CASANOVA, JR. J. Am. Chem. Soc. **85**, 165 (1963).
22. J. R. A. POLLOCK and R. STEVENS (*Editors*). Dictionary of organic compounds. 4th ed. Eyre and Spottiswoode, London. 1965. p. 1149.

[4]For p.m.r. spectrum, see Table 3.

Refinement of the Crystal Structure of the Low-quartz Modification of Ferric Phosphate

HOK NAM NG AND CRISPIN CALVO

Institute for Materials Research, McMaster University, Hamilton, Ontario L8S 4M1

Received February 5, 1975

HOK NAM NG and CRISPIN CALVO. Can. J. Chem. **53**, 2064 (1975).

The structure of ferric phosphate at room temperature was refined on a Dauphiné-twinned crystal using full-matrix least-squares methods. The final R value was 0.078 for 487 symmetry-independent reflections whose intensities were corrected for twinning. The structure was found to be isotypic with $AlPO_4$ (berlinite) with the space group $P3_121$ and four formula units in a unit cell defined by $a = 5.036(2)$ and $c = 11.255(4)$ Å. The structure is also closely related to that of α-quartz with a nearly doubled c-axis because of the ordering of Fe and P atoms. The PO_4 tetrahedron is almost regular with a mean P—O distance of 1.526 Å. The Fe^{3+} ion is tetrahedrally coordinated with an average Fe—O distance of 1.853 Å.

HOK NAM NG et CRISPIN CALVO. Can. J. Chem. **53**, 2064 (1975).

On a raffiné la structure du phosphate ferrique tel qu'il existe à la température de la pièce en appliquant la méthode des moindres carrés (matrice complète) à un cristal Dauphiné mâclé. La valeur finale R est de 0.078 pour 487 réflexions de symétrie indépendantes dont l'intensité a été corrigée pour le mâclage. On a trouvé que la structure est isostructurale avec celle de $AlPO_4$ (berlinite) avec un groupe d'espace $P3_121$ et quatre molécules par maille définie par $a = 5.036(2)$ et $c = 11.255(4)$ Å. Cette structure ressemble beaucoup à celle de quartz α; l'axe c est toutefois le double à cause de l'alignement des atomes de Fe et de P. Le tétraèdre PO_4 est pratiquement régulier avec une distance P—O de 1.526 Å. L'ion Fe^{3+} est coordonné tétraédriquement avec une distance moyenne de 1.853 Å. [Traduit par le journal]

Introduction

Ferric phosphate ($FePO_4$) has long been known to have a structure isotypic with the berlinite structure of aluminum phosphate ($AlPO_4$). Both, in turn, are related to the α-quartz structure (1). The structures of both berlinite (2, 3) and quartz (4) have been accurately refined. They belong to the space group $P3_121$ or its enantiomorph $P3_221$, and may be considered as a three-dimensional network of corner sharing tetrahedra. The arrangements of P and Al are completely ordered in berlinite with alternate sheets of PO_4 and AlO_4 tetrahedra stacked up the c-axis. The c-axis and therefore the unit cell volume is double that of quartz to accommodate the inequivalence of P and Al. All three compounds have a characteristic "α–β" transformation and these are found at 573, 586, and 707 °C for quartz, $AlPO_4$, and $FePO_4$, respectively. In the present study we refined the room temperature structure of $FePO_4$ and compared it with those of quartz and $AlPO_4$. Accurate positional and thermal parameters for the atoms are needed in order to assess the distortions resulting from the substitution of Al^{3+} by Fe^{3+} in the electron paramagnetic resonance study of the α–β phase transformation of Fe^{3+}-doped $AlPO_4$ (5).

Experiments

$FePO_4$ was prepared by the method of Royen and Korinth (6) from an aqueous solution of $Fe(NO_3)_3 \cdot 9H_2O$ and $(NH_4)_2HPO_4$ in stoichiometric amounts. The warm solution was neutralized with 2 M ammonia solution and a pale yellow precipitate was obtained. The precipitate was filtered, washed with distilled water, and then dried at 200 °C. This material (possibly strengite $FePO_4 \cdot 2H_2O$) was heated at 600 °C for 6 h, transforming into a white crystalline powder identified as $FePO_4$ by a Debye–Scherrer pattern. This powder was melted in a platinum crucible at 1300 °C and cooled at 6°/h to 600 °C and then quenched to room temperature. Clear yellowish crystals of $FePO_4$ were obtained.

Precession photographs showed that $FePO_4$ has a primitive unit cell very similar to that of $AlPO_4$ with $00l$ reflections absent unless $l = 3n$, thus verifying the space group as $P3_121$ or $P3_221$. Lattice parameters were obtained by a least-squares fit of 15 2θ values measured with the Syntex $P\bar{1}$ automatic diffractometer ($\lambda\alpha_1 = 0.70926$ Å). The crystal data are as follows:

trigonal f.w. = 150.85

$a = 5.036(2)$, $c = 11.255(4)$ Å, $V = 247.20$ Å^3, $Z = 3$, $\rho_{calc} = 3.054$ g/cm^3, space group $P3_121$, $T = 22$ °C, $\mu = 50.18$ cm^{-1} (MoKα).

A good quality crystal was selected by using a petrographic microscope and then ground into a sphere, with a radius of 0.012 cm, for subsequent measurements of the diffracted intensity with a Syntex $P\bar{1}$ automatic diffractometer. θ/2θ scan at variable rate was employed with graphite monochromatized MoKα radiation. Reflections were labelled unobserved when the measured

Can. J. Chem. Downloaded from www.nrcresearchpress.com by 210.87.254.40 on 09/05/12
For personal use only.

Can. J. Chem. Downloaded from www.nrcresearchpress.com by 210.87.254.40 on 09/05/12
For personal use only.

intensity corrected for background was less than three times the standard deviation. A total of 828 reflections, some of which are symmetry equivalent, were collected within a sphere with $2\theta \leqslant 60°$. Lorentz, polarization, and absorption corrections were applied to the intensity data.

Refinement of the Structure

Refinement of the structure was performed on a CDC 6400 computer by using a least-squares program that minimizes the function $\Sigma\omega(|F_o| - |F_c|)^2$. The coefficients of the weighting function $\omega = (a + bF_o + cF_o^2)^{-1}$ were chosen such that the square of the difference between the observed and calculated structure factors $\omega(\Delta F)^2$ would be independent of the local average value of F_o. Unobserved reflections were given zero weight if the calculated structure factor was less than the local minimum observable value. Atomic scattering curves for Fe^{3+}, P, and O were taken from Cromer and Waber (7) and that for Fe^{3+} was corrected for anomalous scattering (8).

The final positional and thermal parameters of $AlPO_4$ (3) in the space group $P3_121$ were used as initial parameters for the refinement. After three cycles the R value was 0.28. The crystal appeared to show Dauphiné-twinning as in quartz, since the observed and calculated structure factors of $hk0$ and hhl reflections were in better agreement than the others. The Dauphiné twins are related by a 180° rotation about the c-axis. Thus reflection hkl from one component of the twin will superimpose on reflection $\bar{h}\bar{k}l$ from the other, so that the observed intensity $I(hkl)$ is a weighted sum of the intensity $I'(hkl)$ from part of the crystal and the intensity $I''(\bar{h}\bar{k}l)$ from its twin. Assuming that Friedel's law holds, we may write

$$[1] \quad |F(hkl)|^2 = f \cdot |F'(hkl)|^2 + (1 - f) \cdot |F''(hk\bar{l})|^2$$

and

$$[2] \quad |F(hk\bar{l})|^2 = f \cdot |F'(hk\bar{l})|^2 + (1 - f) \cdot |F''(hkl)|^2$$

where f is the volume fraction of the unrotated crystal. It has been shown by Young (4) that for special reflections of the type $hk0$ and hhl

$$|F'(hk0)| = |F''(\bar{h}\bar{k}0)|$$

and

$$|F'(hhl)| = |F''(\bar{h}\bar{h}l)|$$

Therefore, the intensities of these reflections are unaffected by Dauphiné-twinning.

The volume fraction is difficult to determine directly from experiment. Since all the reflections are overlapped as a result of Dauphiné-twinning, the volume fraction was treated as a parameter to be determined by an iterative method. The best structure was first obtained by using $hk0$ and hhl type data only since their intensities are independent of the volume fraction f. The R value converged to 0.033 for these 81 reflections. This structural model was then used to calculate $F_c(hkl)$ and $F_c(hk\bar{l})$. By putting these values of the F_c's on the right-hand side of eqs. 1 and 2 and the corresponding observed structure factors on the left, an initial value of f was determined as the average value over all the reflections. Equations 1 and 2 could be rewritten as

$$|F_o(hkl)|^2 = f \cdot |\bar{F}_o(hkl)|^2 + (1 - f) \cdot |\bar{F}_o(hk\bar{l})|^2$$

$$|F_o(hk\bar{l})|^2 = f \cdot |\bar{F}_o(hk\bar{l})|^2 + (1 - f) \cdot |\bar{F}_o(hkl)|^2$$

and solved for $|\bar{F}_o(hkl)|$ and $|\bar{F}_o(hk\bar{l})|$ by using the average value of f and the actually observed $|F_o(hkl)|$ and $|F_o(hk\bar{l})|$. These $|\bar{F}_o|$'s are the structure factors that would have been observed for an untwinned crystal of the same total volume as the one being studied. For a small number of reflections (10), all weak or unobserved, the $|\bar{F}_o(hkl)|^2$ values were calculated to be negative. These reflections were removed from further consideration. This set of corrected observed structure factors was used for a few more cycles of least-squares refinement of the atomic parameters. When the R value converged this second model was used to obtain a new average value of f and the process was repeated until the value of f converged to 0.64(1) and the unweighted R factor converged to 0.061. Symmetry equivalent reflections were averaged at this stage. A parameter g, for correcting the effects of secondary extinction following Larson (9), was also refined and was found to be 0.50×10^{-5}. The final weighted R value

$$R_\omega = \left[\frac{\Sigma\omega(|F_o| - |F_c|)^2}{\Sigma\omega|F_o|^2}\right]^{1/2}$$

was 0.078 for 487 symmetry independent reflections among which 445 were classified as observed. The weighting function was $\omega = [3.0 - 0.008F_o + 0.0015F_o^2]^{-1}$ with coefficients chosen so that $\omega|F_o - F_c| \sim 1$. The structure was also refined in the enantiomorphic space group $P3_221$, and the values of R and R_ω converged to 0.064 and 0.081 respectively. The space group $P3_221$, same as $AlPO_4$ (2), was then chosen for $FePO_4$. The final positional and thermal parameters are listed in Table 1. The calculated and hypothetical observed structure factors are listed in Table 2. Table 3 lists the actually observed structure factors and the structure factors calculated from eqs. 1 and 2 for $f = 0.64$.[1]

Discussion

$AlPO_4$ and $FePO_4$ are isostructural. The molecular geometries of these compounds are compared with that of quartz in Table 4. The berlinite structure has been discussed in detail by Schwarzenbach (2). These structures consist of helices of alternate FeO_4 or AlO_4 and PO_4 tetrahedra running parallel to the c-axis. In quartz, of course, the two tetrahedra are identical. Each oxygen atom is bonded to a P and a Fe in the present structure. The average Fe—O distance of 1.853 Å compares well with the value of the sum of the effective ionic radii for tetrahedrally coordinated Fe^{3+} and two-coordinated oxygen (10). The average P—O distance is 1.526 Å, as compared with 1.522 Å for P—O in $AlPO_4$. However, this difference is within one standard deviation and hardly significant. The O—P—O bond angles and O—O distances in the PO_4 group appear to be signi-

[1]Tables 2 and 3 may be obtained, at a nominal charge, from the Depository of Unpublished Data, CISTI, National Research Council of Canada, Ottawa, Canada K1A 0S2.

TABLE 1. Positional and thermal parameters of $FePO_4$ (e.s.d. in parentheses)

Atom	Position type	x	y	z	U_{11}*	U_{22}	U_{33}	U_{12}	U_{13}	U_{23}
Fe	3*a*	0.4583(3)	0	1/3	0.0132(7)	0.0096(8)	0.0103(6)	$\frac{1}{2}U_{22}$	−0.0009(6)	$2U_{13}$
P	3*b*	0.4577(6)	0	5/6	0.011(1)	0.009(1)	0.0095(8)	$\frac{1}{2}U_{22}$	0.0007(9)	$2U_{13}$
O(1)	6*c*	0.419(2)	0.318(1)	0.3963(4)	0.033(4)	0.018(3)	0.017(2)	0.015(3)	−0.008(2)	−0.010(2)
O(2)	6*c*	0.413(2)	0.264(1)	0.8749(5)	0.022(3)	0.014(3)	0.025(2)	0.011(3)	−0.002(2)	−0.009(2)

*Calculated from $\beta_{ij} = 2\pi^2 b_i b_j U_{ij}$ where $T = \exp[-(\beta_{11}h^2 + 2\beta_{12}hk + \ldots)]$ is the thermal factor appearing in the structure factor expression and b_i's are reciprocal lattice vectors.

TABLE 4. Molecular geometry of $FePO_4$ and $AlPO_4$* (e.s.d. in parentheses)

	Distance (Å)				Angle (deg)		
Bond	$FePO_4$	$AlPO_4$†	SiO_2	Bonds	$FePO_4$	$AlPO_4$†	SiO_2
MO_4 tetrahedron							
M—O(1) ×2	1.847(7)	1.728(7)	1.603(2)	O(1)—M—O(1)6	114.8(4)	113.4(5)	109.2(2)
—O(2)2 ×2	1.859(7)	1.738(7)	1.611(3)	—O(2)2	109.0(3)	108.8(6)	110.3(2)
O(1)—O(1)6	3.113(9)	2.888(6)	2.604(4)	—O(2)5	105.5(3)	108.1(6)	108.8(1)
—O(2)2	3.018(11)	2.819(9)	2.637(4)	O(2)2—M—O(2)5	113.1(4)	109.5(4)	109.5(2)
—O(2)5	2.951(13)	2.806(10)	2.614(2)				
O(2)2—O(2)5	3.101(10)	2.839(7)	2.640(5)				
PO_4 tetrahedron							
P—O(1)2 ×2	1.524(7)	1.518(5)		O(2)—PO—(2)6	108.7(5)	106.6(6)	
—O(2) ×2	1.529(7)	1.525(6)		—O(1)2	110.5(4)	111.6(6)	
O(2)—O(2)6	2.484(9)	2.446(6)		—O(1)5	108.6(4)	107.7(6)	
—O(1)2	2.508(11)	2.517(9)		O(1)2—P—O(1)5	109.9(5)	111.5(4)	
—O(1)5	2.480(13)	2.458(10)					
O(1)2—O(1)5	2.497(9)	2.509(6)					
Others							
				Fe—O(1)—P	139.2(6)	143.1(2)	144.0(2)
				P—O(2)—Fe	137.5(5)	142.0(2)	144.0(2)

*Oxygen atom position denoted by O(*m*)*n* is derived from the position of O(*m*) listed in Table 2 by the *n*th symmetry operation in the order listed in ref. 11, for space group $P3_121$.
†Reference 3.

ficantly more uniform in $FePO_4$. In contrast, the O—M—O bond angles (M = Fe, Al) have a higher dispersion in $FePO_4$ than in $AlPO_4$. Both groups are angularly more irregular than the SiO_4 groups in quartz although in all cases the M—O(1) distance is about 0.01 Å larger than the M—O(2) distance. The angular distortion of the SiO_4 tetrahedron is a result of twisting the O(1)—O(1)6 edge about the twofold axis relative to the O(2)—O(2)5 edge. In $FePO_4$ the distortion is equivalent to a compression of the FeO_4 tetrahedron along the twofold axis at both ends, which leads to O(1)—Fe—O(1)6 and O(2)—Fe—O(2)5 angles both larger than the ideal tetrahedral angle. In $AlPO_4$ only the O(1)—Al—O(1)6 end is compressed. The angular distortion of the MO_4 tetrahedron can be related to the reduction in the M—O—P angle in $FePO_4$ compared with $AlPO_4$ and quartz. This reduction in the M—O—P angle results in a stronger metal–phosphorus repulsion, which in turn leads to larger tetrahedral angles in FeO_4. However, the Al—O—P angles are only slightly smaller than the Si—O—Si angle in quartz and yet the AlO_4 tetrahedron displays considerably greater angular distortion than the SiO_4. This suggests that other factors are also playing a role, *e.g.*, the difference in covalency of the bonds of the cations with oxygen.

The question of the immediate environment of the Fe^{3+} ion substituted in $AlPO_4$ is an open one. Although the M—O(1) distance is characteristically shorter than the M—O(2) distance by about 0.01 Å for both AlO_4 and FeO_4 tetrahedra, it is uncertain what the angular distortion will be for such a substitution. We calculated

Can. J. Chem. Downloaded from www.nrcresearchpress.com by 210.87.254.40 on 09/05/12
For personal use only.

the spin Hamiltonian parameter D for Fe^{3+} in $AlPO_4$ from a point-charge model, assuming no distortion of the environment due to substitution, *vs.* FeO_4 type tetrahedron for the substituent site. The difference in the values of D is a nontrivial 400%. Thus it appears that this distortion is important and can perhaps be measured by an examination of the diffuse scattering in highly doped $AlPO_4$ crystals.

This rearch has been supported by a grant from the National Research Council of Canada.

1. V. GAGLIOTI. Atti accad, Lincei, **22**, 146 (1935); E. C. SHAFER, M. W. SHAFER, and R. ROY, Z. Krist. **107**, 263 (1956).
2. D. SCHWARZENBACH. Z. Krist. **123**, 161 (1966).
3. H. N. NG and C. CALVO. To be published.
4. R. A. YOUNG. Final Report to U.S. Air Force Office of Scientific Research, Project A-447. Solid State Sciences Division, Air Force Office of Scientific Research, Washington, D.C. 1962.
5. R. LANG, W. R. DATARS, and C. CALVO. Phys. Lett. **30**A, 340 (1969).
6. P. ROYEN and T. KORINTH. Z. Anorg. Allg. Chem. **291**, 227 (1957).
7. D. T. CROMER and J. T. WABER. Acta Cryst. **18**, 104 (1965).
8. D. T. CROMER. Acta Cryst. **18**, 17 (1965).
9. A. C. LARSON. Acta Cryst. **23**, 664 (1967).
10. R. D. SHANNON and C. T. PREWITT. Acta Cryst. B**25**, 925 (1969).
11. N. F. M. HENRY and K. LONSDALE. (*Editors*). International tables for X-ray crystallography, Vol. I. Kynoch Press, Birmingham. 1965.

Can. J. Chem. Downloaded from www.nrcresearchpress.com by 210.87.254.40 on 09/05/12
For personal use only.

The Two-step Synthesis and Crystal and Molecular Structure of Tetracyclo[6.4.0.0^{2,11}.0^{4,9}]dodec-6-ene-3,10-dione

YUEN-MUI NGAN, STEVEN J. RETTIG, JOHN R. SCHEFFER, AND JAMES TROTTER

Department of Chemistry, University of British Columbia, Vancouver, British Columbia V6T 1W5

Received January 27, 1975

YUEN-MUI NGAN, STEVEN J. RETTIG, JOHN R. SCHEFFER, and JAMES TROTTER. Can. J. Chem. **53**, 2068 (1975).

The photochemistry of the *trans*-1,3,5-hexatriene-*p*-benzoquinone Diels–Alder adduct has been investigated. Irradiation of this material in its long wavelength n → π* absorption band leads to a single photoproduct in high yield. A single crystal X-ray structure determination shows this product to be tetracyclo[6.4.0.0^{2,11}.0^{4,9}]dodec-6-ene-3,10-dione, the result of a novel regiospecific intramolecular 2+2 photoaddition between the side chain vinyl group and the ene-dione double bond. Crystals of tetracyclo[6.4.0.0^{2,11}.0^{4,9}]dodec-6-ene-3,10-dione are monoclinic, a = 7.5290(7), b = 19.072(1), c = 6.7237(4) Å, β = 107.918(6)°, Z = 4, space group $P2_1/n$. The structure was solved by direct methods and was refined by full-matrix least-squares procedures to a final R of 0.041 for 1603 reflections with $I \geq 3\sigma(I)$. The structure consists of well-separated molecular units. Bond distances are: C=O, 1.216 and 1.219(2), C=C, 1.318(2), mean C(sp^3)—C(sp^2), 1.508, mean C(sp^3)—C(sp^3), 1.560 in the four-membered ring and 1.544 elsewhere, mean C(sp^3)—H, 0.99, and mean C(sp^2)—H, 0.95 Å. Bond distances between nonhydrogen atoms have been corrected for thermal motion. A possible rationalization for the observed photoprocess is discussed in terms of conformational and radical stability effects.

YUEN-MUI NGAN, STEVEN J. RETTIG, JOHN R. SCHEFFER et JAMES TROTTER. Can. J. Chem. **53**, 2068 (1975).

On a étudié la photochimie du produit provenant de la réaction de Diels–Alder entre l'hexatriène-1,3,5 *trans* et la *p*-benzoquinone. L'irradiation de ce produit, a une longueur d'onde correspondant à la bande d'absorption n → π*, conduit à un seul produit avec un excellent rendement. La structure de ce produit a été établie par diffraction de rayons-X sur un cristal unique; il s'agit de la tétracyclo[6.4.0.0^{2,11}.0^{4,9}]dodécène-6 dione-3,10 qui provient d'une nouvelle réaction de photoaddition 2+2 intramoléculaire et régiospécifique impliquant le groupe vinyle de la chaine latérale et la double liaison de la portion ènedione. Les cristaux de cette dicétone sont monocliniques, a = 7.5290(7), b = 19.072(1), c = 6.7237(4) Å, β = 107.918(6)°, Z = 4, groupe d'espace $P2_1/n$. On a résolu sa structure par des méthodes directes et on l'a affinée par la méthode des moindres carrés (matrice complète) jusqu'à une valeur finale de R de 0.041 pour 1603 réflexions avec $I \geq 3\sigma(I)$. La structure comprend des unités moléculaires bien définies. Les longueurs des liaisons sont: C=O, 1.216 et 1.219(2); C=C, 1.318(2); valeur moyenne des C(sp^3)—C(sp^2), 1.508; valeur moyenne des C(sp^3)—C(sp^3), 1.560 dans le cycle à quatre chainons et 1.544 ailleurs; valeur moyenne C(sp^3)—H, 0.99 et valeur moyenne C(sp^2)—H, 0.95 Å. On a corrigé les longueurs des liaisons entre atomes autres que l'hydrogène afin de tenir compte des mouvements thermiques. On discute d'une rationalisation possible du photoprocessus observé en termes d'effets conformationnels et de stabilité du radical. [Traduit par le journal]

Introduction

The photochemistry of Diels–Alder adducts of *p*-benzoquinone with 1,3-dienes has proven to be a remarkably rich source of interesting and unusual polycyclic ring systems. Among the ring systems so produced are derivatives of tricyclo[4.4.0.0^{2,8}]decane (1–4), tricyclo[4.4.0.0^{2,9}]decane (3, 4), tricyclo[4.4.0.0^{3,9}]decane (1–3), and tricyclo[5.3.1.0^{2,7}]undecane (2, 3) as well as "cage" photoproducts possessing the basic tetracyclo[4.4.0.0^{3,9}.0^{4,8}]decane ring system[1] and their 7,10-bridged analogs (5).

In this paper we report a derivative of another novel ring system which may easily be obtained in this way in good yield, namely tetracyclo-[6.4.0.0^{2,11}.0^{4,9}]dodec-6-ene-3,10-dione (2) via intramolecular 2+2 cycloaddition in the benzoquinone-*trans*-1,3,5-hexatriene Diels–Alder adduct **1**.

[1]J. R. Scheffer and B. Jennings. Unpublished results.

Diels–Alder adduct **1** is unreported in the literature, although two substituted derivatives are known (6). Adduct **1** may be prepared as a light yellow solid, m.p. 58–60°, in 40–50% yield simply by warming *p*-benzoquinone with a threefold molar excess of *trans*-1,3,5-hexatriene. The stereochemistry of **1** shown is that expected from concerted *cis-endo* addition and is the only configuration capable of giving the observed photoproduct **2**. The n → π* u.v. spectrum of **1** (λ_{max} (EtOH) 355 nm, ε 75) is essentially identical to that of the parent butadiene–benzoquinone Diels–Alder adduct (1) thus indicating no ground state interaction between the side chain vinyl group and the ene–dione double bond.

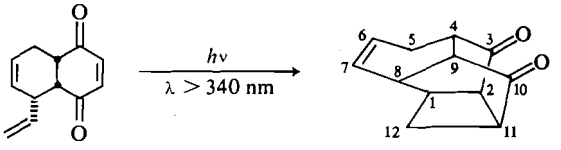

1 **2**

Diels–Alder adduct **1** (200 mg in 200 ml of benzene or *tert*-butyl alcohol) was irradiated in its n → π* absorption band with light of λ > 340 nm (Corning 7380 glass filter) and the reaction followed by t.l.c. This showed the formation of essentially only one photoproduct which could be isolated in 60–70% yield by column chromatography on alumina. The recrystallized photoproduct (50% yield) was a colorless solid, m.p. 91.5–92.5°, whose spectra (see Experimental section) indicated that it had been formed by intramolecular vinyl–ene-dione 2+2 cycloaddition. However these data were incapable of distinguishing between structure **2** and its alternative, **3**, shown below. For example, the i.r. data, which were expected to be of help in distinguishing between structures **2** and **3**, were equivocal, showing carbonyl stretching frequencies of 1715 and 1735 cm^{-1} in KBr and 1725 cm^{-1} in carbon tetrachloride. For this reason, and because the photoproduct promised to have an interesting and unusual strained polycyclic ring skeleton, an X-ray crystal structure investigation was undertaken.

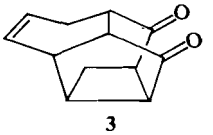

3

X-Ray Crystal Structure Determination

The crystal chosen for study was mounted with *b* parallel to the goniostat axis and had dimensions of *ca.* 0.8 × 0.5 × 1.0 mm. Unit-cell and space group data were obtained from film and diffractometer measurements. The unit-cell parameters were refined by a least-squares treatment of $\sin^2\theta$ values for 24 reflections measured on a diffractometer with CuK_α radiation. Crystal data are:

$C_{12}H_{12}O_2$ f.w. = 188.2

Monoclinic, a = 7.5290(7), b = 19.072(1), c = 6.7237(4) Å, β = 107.918(6)°, V = 918.6(1) $Å^3$, ρ_m = 1.359 (flotation in aqueous KI), Z = 4, ρ_c = 1.3609(2) g cm^{-3}, $F(000)$ = 400 (22 °C, CuK_α, λ = 1.5418 Å, μ = 7.5 cm^{-1}). Absent reflections: $0k0$, $k \neq 2n$, and $h0l$, $h + l \neq 2n$ define uniquely the space group $P2_1/n$ (C_{2h}^5, No. 14).

Intensities were measured on a Datex-automated General Electric XRD 6 diffractometer, with a scintillation counter, CuK_α (nickel filter and pulse height analyzer), and a θ–2θ scan at 2 deg min^{-1} over a range of (1.80 + 0.86 tan θ)° in 2θ, with 10 s background counts being measured at each end of the scan. Data were measured to 2θ = 146° (minimum interplanar spacing 0.81 Å). The intensity of the check reflection remained constant to within ±1.5% of its initial value throughout the data collection. Lorentz and polarization

TABLE 1. Final positional parameters (fractional × 10^5, H × 10^4, equivalent positions: ±[x, y, z; ½ − x, ½ + y, ½ − z]) with estimated standard deviations in parentheses

Atom	x	y	z
O(1)	56045(15)	28319(6)	9770(18)
O(2)	13325(17)	48210(6)	−15800(19)
C(1)	14229(18)	32681(8)	21853(23)
C(2)	23926(19)	30751(7)	5120(21)
C(3)	44167(18)	32547(7)	10372(18)
C(4)	48801(18)	40124(7)	16969(21)
C(5)	64176(21)	40492(10)	37948(26)
C(6)	56793(23)	38212(9)	55041(24)
C(7)	38890(22)	37591(9)	52826(21)
C(8)	23408(20)	39353(7)	33259(20)
C(9)	30697(19)	43691(7)	18000(21)
C(10)	17252(19)	43290(7)	−3875(21)
C(11)	9896(19)	36037(8)	−9477(21)
C(12)	−3336(20)	34532(10)	3669(26)
H(1)	1372(22)	2917(9)	3159(29)
H(2)	2100(22)	2597(9)	−27(27)
H(4)	5314(25)	4244(10)	604(30)
H(5a)	7408(26)	3727(9)	3733(28)
H(5b)	6888(31)	4512(12)	3972(36)
H(6)	6614(31)	3718(10)	6802(34)
H(7)	3480(24)	3581(9)	6373(31)
H(8)	1379(24)	4202(9)	3715(29)
H(9)	3327(22)	4852(9)	2226(24)
H(11)	550(26)	3519(9)	−2508(33)
H(12a)	−1050(30)	2980(12)	−223(38)
H(12b)	−1188(26)	3819(10)	543(28)

TABLE 2. Final thermal parameters and their estimated standard deviations

(*a*) Anisotropic thermal parameters ($U_{ij} \times 10^4$ Å^2)

Atom	U_{11}	U_{22}	U_{33}	U_{12}	U_{13}	U_{23}
O(1)	578(7)	645(8)	624(7)	189(5)	245(5)	−43(5)
O(2)	831(9)	609(8)	659(8)	172(6)	258(6)	306(6)
C(1)	415(7)	512(8)	502(8)	−23(5)	171(6)	141(6)
C(2)	466(7)	353(7)	470(7)	−27(5)	105(5)	−26(5)
C(3)	455(7)	450(7)	318(6)	57(5)	148(5)	8(5)
C(4)	430(7)	462(8)	443(7)	−64(5)	172(5)	24(5)
C(5)	451(8)	644(10)	587(9)	−107(7)	85(7)	−83(7)
C(6)	578(9)	655(10)	407(7)	54(7)	33(6)	−84(7)
C(7)	628(9)	685(10)	331(7)	100(7)	175(6)	−4(6)
C(8)	463(7)	518(8)	402(7)	87(6)	194(5)	22(5)
C(9)	518(7)	324(7)	468(7)	2(5)	166(6)	1(5)
C(10)	468(7)	470(8)	462(8)	90(5)	207(6)	116(6)
C(11)	443(7)	539(9)	399(7)	6(6)	72(5)	18(6)
C(12)	396(7)	669(10)	602(9)	−44(7)	126(6)	84(7)

(*b*) Isotropic thermal parameters ($U \times 100$)

Atom	U (Å^2)	Atom	U (Å^2)
H(1)	5.8(5)	H(7)	6.3(5)
H(2)	5.2(4)	H(8)	6.0(5)
H(4)	6.8(5)	H(9)	5.2(4)
H(5*a*)	6.0(5)	H(11)	6.7(5)
H(5*b*)	8.4(6)	H(12*a*)	8.5(6)
H(6)	7.8(6)	H(12*b*)	6.4(5)

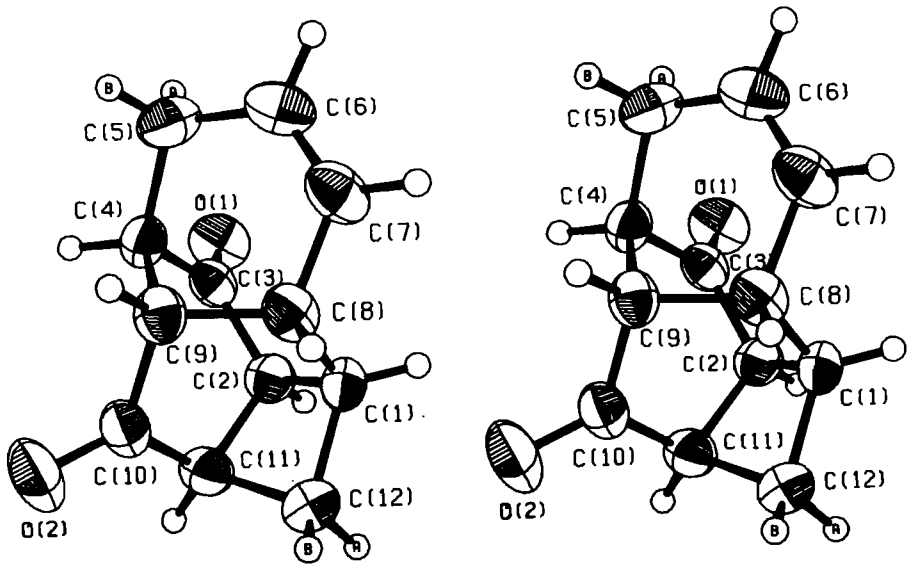

FIG. 1. Stereoscopic view of the tetracyclo[6.4.0.0^{2,11}.0^{4,9}]dodec-6-ene-3,10-dione molecule showing the atom numbering scheme and 50% probability thermal ellipsoids for the nonhydrogen atoms.

corrections and check reflection scaling were applied, and the structure amplitudes were derived. No absorption correction was made in view of the low value of μ. Of the 1856 independent reflections measured, 230 had intensities less than $3\sigma(I)$ above background where $\sigma^2(I) = S + B + (0.06S)^2$ with S = scan count and B = time averaged background count. These reflections were given zero weight in the refinement but were included in the structure factor calculations.

Structure Analysis

The structure was solved by direct methods. Sixteen sets of signs for 236 reflections with $|E| \geq 1.50$ were determined by a computer program which uses Sayre relationships in an iterative procedure (7). One set of signs was outstanding in that it converged in 6 cycles to a set having the highest consistency index (7), 0.80, with 126 positive and 110 negative signs. The 14 nonhydrogen atoms accounted for the 14 highest peaks on the E-map computed from the 236 signed values of E from this set.

Three cycles of isotropic followed by two cycles of anisotropic full-matrix least-squares refinement of the overall scale factor and the O and C atoms gave R 0.091. A difference map at this point clearly gave the positions of the 12 hydrogen atoms which were included in all subsequent cycles of refinement with isotropic thermal parameters. The entire structure was refined for six cycles giving a final R of 0.041 and R_w 0.056 for 1603 reflections with $I \geq 3\sigma(I)$ (23 reflections which had $|F_o - F_c| > 3\sigma(F)$ were removed from the data set in the final stages of refinement).

The least-squares refinement was based on the minimization of $\Sigma w |F_o| - |F_c/(1 + gI)|]^2$ where g is the extinction parameter and I the uncorrected intensity. The final value of g was 1.89×10^{-7}. The scattering factors of ref. 8 were used for the nonhydrogen atoms and those of ref. 9 for the hydrogen atoms. Anomalous scattering factors from ref. 10 were used for the oxygen and carbon atoms. The anisotropic thermal parameters employed in the refinement are U_{ij} in the expression

$$f = f^0 \exp[-2\pi^2(U_{11}h^2a^{*2} + U_{22}k^2b^{*2} + U_{33}l^2c^{*2} + 2U_{12}hka^*b^* + 2U_{13}hla^*c^* + 2U_{23}klb^*c^*)]$$

where f^0 is the tabulated scattering factor and f is that corrected for thermal motion. The weighting scheme: $w = 1$ if $|F_o| < 6.0$ and $w = (6.0/|F_o|)^2$ if $|F_o| \geq 6.0$ gave uniform average values of $w(|F_o| - |F_c|)^2$ over ranges of $|F_o|$ and was employed in the final stages of refinement.

On the final cycle of refinement the greatest parameter shift was 0.31 σ and the mean parameter shift was 0.06 σ. A final difference map showed maximum fluctuations of ±0.27 e Å^{-3}. The final positional and thermal parameters appear in Tables 1 and 2 respectively. Measured and calculated structure factors have been placed in the Depository of Unpublished Data.[2]

[2]The structure factor table is available, at a nominal charge, from the Depository of Unpublished Data, CISTI, National Research Council of Canada, Ottawa, Canada K1A 0S2.

Thermal Motion and Correction of Molecular Geometry

The ellipsoids of thermal motion for the nonhydrogen atoms are shown in Fig. 1. The thermal motion has been analyzed in terms of the rigid-body modes of translation (**T**), libration (**L**), and screw (**S**) motion (11) using the computer program MGTLS. The r.m.s. standard deviation in the temperature factors U_{ij} is 0.00074 Å^2 indicating that the thermal motion of the 14 nonhydrogen atoms of the molecule is reasonably described by the rigid-body thermal parameters in Table 3 (r.m.s. ΔU_{ij} = 0.0021 Å^2). The unique origin lies close to the center of gravity. The orientation of the principal axes

TABLE 3. Rigid-body thermal parameters*

All nonhydrogen atoms			
	217(10)	−55(7)	57(8)
L (× 10 deg^2)		143(8)	−40(7)
			226(10)

Principal axes of **L**

r.m.s. amplitude	Direction cosines (× 10^3)		
5.5°	655	−380	653
4.1	626	−210	−751
3.4	423	901	101

Principal axes of reduced **T**

r.m.s. amplitude	Direction cosines (× 10^3)		
0.20 Å	−758	−142	−637
0.18	−385	885	262
0.17	527	444	−725

Displacement of axes from intersecting (Å)

Parallel to L_1	0.054
Parallel to L_2	−0.075
Parallel to L_3	0.278

Effective screw translations (Å)

Parallel to L_1	−0.003
Parallel to L_2	−0.008
Parallel to L_3	0.015

Fractional coordinates of unique origin (× 10^4)

x	3195
y	3645
z	1712

Fractional coordinates of center of gravity (× 10^4)

x	3146
y	3759
z	1593
r.m.s. ΔU_{ij} (Å^2)	0.0021

*Axes of reference are orthogonal angstrom axes. E.s.d.'s of components of **L** are given in parentheses in units of the last places shown.

TABLE 4. Bond lengths (Å) with estimated standard deviations in parentheses

(*a*) Nonhydrogen atoms

Bond	Distance (Å)		Bond	Distance (Å)	
	Uncorrected	Corrected		Uncorrected	Corrected
O(1)—C(3)	1.214(2)	1.219	C(4)—C(9)	1.544(2)	1.551
O(2)—C(10)	1.210(2)	1.216	C(5)—C(6)	1.487(2)	1.493
C(1)—C(2)	1.562(2)	1.569	C(6)—C(7)	1.315(2)	1.318
C(1)—C(8)	1.536(2)	1.543	C(7)—C(8)	1.503(2)	1.507
C(1)—C(12)	1.541(2)	1.544	C(8)—C(9)	1.544(2)	1.552
C(2)—C(3)	1.494(2)	1.501	C(9)—C(10)	1.509(2)	1.515
C(2)—C(11)	1.568(2)	1.572	C(10)—C(11)	1.495(2)	1.503
C(3)—C(4)	1.520(2)	1.529	C(11)—C(12)	1.549(2)	1.554
C(4)—C(5)	1.526(2)	1.530			

(*b*) Bonds involving hydrogen atoms

Bond	Distance (Å)	Bond	Distance (Å)
C(1)—H(1)	0.95(2)	C(7)—H(7)	0.94(2)
C(2)—H(2)	0.98(2)	C(8)—H(8)	0.98(2)
C(4)—H(4)	0.99(2)	C(9)—H(9)	0.97(2)
C(5)—H(5*a*)	0.98(2)	C(11)—H(11)	1.01(2)
C(5)—H(5*b*)	0.95(2)	C(12)—H(12*a*)	1.06(2)
C(6)—H(6)	0.96(2)	C(12)—H(12*b*)	0.98(2)

of **L** is as expected: L_1 lies roughly along the long axis of the molecule, L_2 is 6° from the C(1)—C(2) vector, and L_3 is 11° from the C(11)—C(10) vector.

The appropriate bond distances and angles have been corrected for libration (12, 13), using shape parameters q^2 of 0.08 for all atoms involved. Independent motion corrections based on the ΔU_{ij} (14, 15) have also been applied. Both corrected and uncorrected bond distances appear in Table 4. The changes in the bond angles were insignificant, thus only the uncorrected values appear in Table 5.

Discussion

Figure 1 shows a general view of the molecule and the atom numbering scheme. Dihedral angles are given in Table 6 and selected intra- and intermolecular nonbonded distances are listed in Table 7.

The structure analysis has shown that the major product, which has the structure **2**, is formed from **1** by the formation of the C(1)—C(2) and C(11)—C(12) bonds and has provided accurate details of the geometry of this unusual tetracyclic system. The cage structure may be thought of as being derived from bicyclo[2.2.2]octa-2,5-diene by addition of a one atom bridge between C(1) and C(11) and a three atom bridge from C(4) to C(8) (numbering of Fig. 1).

Both carbonyl groups are slightly, but significantly, nonplanar. C(3) and C(10) are displaced 0.008 (6σ) and 0.017 Å (23σ) from the O(1)C(2)C(4) and O(2)C(9)C(11) planes. The grouping about the C(6)—C(7) double bond is also nonplanar, the dihedral angle C(5)[C(6)—C(7)]C(8) being 2.7(1)°. The nonplanarity of these groups is presumably a result of strain in the polycyclic system.

There are five six-membered rings in the structure. Those three which form the bicyclo[2.2.2]octadiene subgroup have distorted conformations which are best described as intermediate between the boat and twist-boat conformations. The fourth six-membered ring, C(1) and C(8)—C(12), has a distorted chair conformation. These distortions are hardly surprising since each of the four rings mentioned above has 2 or 3 atoms in common with a four-membered ring. The last six-membered ring, which contains the double bond, shows only a small amount of strain. The conformation of this ring is close to the average of those calculated for the minimum energy conformations of 4,5- and 3,4-disubstituted cyclohexenes (16), also shown in Table 6. Dihedral angles in the eight membered ring, C(1)—C(8), are also given, but understandably do not correspond to any of the usual minimum energy conformations (17, 18).

The four-membered ring [C(1),C(2),C(11), C(12)] is nonplanar, the dihedral angles in the

TABLE 5. Bond angles (deg) with estimated standard deviations in parentheses

(*a*) Nonhydrogen atoms

Bonds	Angle (deg)	Bonds	Angle (deg)
C(2)—C(1)—C(8)	108.5(1)	C(6)—C(7)—C(8)	124.8(1)
C(2)—C(1)—C(12)	87.7(1)	C(1)—C(8)—C(7)	111.1(1)
C(8)—C(1)—C(12)	110.5(1)	C(1)—C(8)—C(9)	108.0(1)
C(1)—C(2)—C(3)	116.4(1)	C(7)—C(8)—C(9)	111.3(1)
C(1)—C(2)—C(11)	85.7(1)	C(4)—C(9)—C(8)	107.0(1)
C(3)—C(2)—C(11)	116.3(1)	C(4)—C(9)—C(10)	105.7(1)
O(1)—C(3)—C(2)	123.2(1)	C(8)—C(9)—C(10)	110.6(1)
O(1)—C(3)—C(4)	122.4(1)	O(2)—C(10)—C(9)	124.1(1)
C(2)—C(3)—C(4)	114.4(1)	O(2)—C(10)—C(11)	123.7(1)
C(3)—C(4)—C(5)	110.7(1)	C(9)—C(10)—C(11)	112.2(1)
C(3)—C(4)—C(9)	107.8(1)	C(2)—C(11)—C(10)	108.1(1)
C(5)—C(4)—C(9)	111.5(1)	C(2)—C(11)—C(12)	87.2(1)
C(4)—C(5)—C(6)	110.1(1)	C(10)—C(11)—C(12)	106.3(1)
C(5)—C(6)—C(7)	123.5(1)	C(1)—C(12)—C(11)	87.1(1)

(*b*) Angles involving hydrogen atoms

Bonds	Angle (deg)	Bonds	Angle (deg)
C(2)—C(1)—H(1)	117(1)	C(6)—C(7)—H(7)	121(1)
C(8)—C(1)—H(1)	110(1)	C(8)—C(7)—H(7)	114(1)
C(12)—C(1)—H(1)	120(1)	C(1)—C(8)—H(8)	108(1)
C(1)—C(2)—H(2)	113(1)	C(7)—C(8)—H(8)	109(1)
C(3)—C(2)—H(2)	113(1)	C(9)—C(8)—H(8)	110(1)
C(11)—C(2)—H(2)	110(1)	C(4)—C(9)—H(9)	110(1)
C(3)—C(4)—H(4)	108(1)	C(8)—C(9)—H(9)	113(1)
C(5)—C(4)—H(4)	110(1)	C(10)—C(9)—H(9)	111(1)
C(9)—C(4)—H(4)	109(1)	C(2)—C(11)—H(11)	119(1)
C(4)—C(5)—H(5*a*)	108(1)	C(10)—C(11)—H(11)	113(1)
C(4)—C(5)—H(5*b*)	108(1)	C(12)—C(11)—H(11)	120(1)
C(6)—C(5)—H(5*a*)	109(1)	C(1)—C(12)—H(12*a*)	108(1)
C(6)—C(5)—H(5*b*)	113(1)	C(1)—C(12)—H(12*b*)	120(1)
H(5*a*)—C(5)—H(5*b*)	109(2)	C(11)—C(12)—H(12*a*)	107(1)
C(5)—C(6)—H(6)	115(1)	C(11)—C(12)—H(12*b*)	120(1)
C(7)—C(6)—H(6)	122(1)	H(12*a*)—C(12)—H(12*b*)	112(2)

ring having a mean magnitude of 26.0°. The bond lengths in the ring are divided into two groups, those involving the "free" C(12) atom (C(1)—C(12), 1.544(2), and C(11)—C(12), 1.554(2) Å) being significantly shorter than the other two bonds (C(1)—C(2), 1.569(2), and C(2)—C(11), 1.572(2) Å). Bond distances in gaseous cyclobutane (19) and in the four-membered ring of bicyclo[3.1.1]heptane (20) are 1.548 and 1.553 Å respectively. Mean C—C distances in the four-membered rings of gaseous bicyclo[2.2.0]hexane (21) and gaseous *anti*- and *syn*-tricyclo[4.2.0.$0^{2,5}$]octane (22) are 1.556, 1.557, and 1.566 Å compared to a mean bond length of 1.560 Å in the four-membered ring of the present structure. Bond angles in the four-membered ring range from 85.7(1)° at C(2) to 87.7(1)° at C(1). These values are similar to those in related molecules, *e.g.* 84.9 and 87.1° in bicyclo[3.1.1]heptane (20).

Bond distances and angles in the remainder of the molecule are normal. The C=C distance of 1.318(2) Å is the same as that in the related molecule tricyclo[4.4.0.$0^{2,8}$]dec-3-ene-7,10-dione (1, 23). Other mean bond distances are C=O, 1.218, C(sp^2)—C(sp^3), 1.508, C(sp^3)—C(sp^3), (not in the four-membered ring), 1.544, C(sp^3)—H, 0.99, and C(sp^2)—H, 0.95 Å.

The crystal structure consists of well-separated molecular units. The shortest intermolecular contacts, listed in Table 7, correspond to normal van der Waals contacts.

The observation that the photocyclization of **1** leads exclusively to **2** is interesting particularly in view of the fact that **2** undoubtedly incorporates more ring strain than **3**. One possible

TABLE 6. Intraannular dihedral angles (deg)

(*a*) Six-membered rings

Bond	Angle	Bond	Angle	Bond	Angle Observed	Angle Calculated
C(2)—C(3)	52.1(1)	C(2)—C(3)	−46.6(1)	C(4)—C(5)	−48.7(1)	−47.0
C(3)—C(4)	−4.6(1)	C(3)—C(4)	−4.6(1)	C(5)—C(6)	14.5(1)	16.3
C(4)—C(9)	−56.5(1)	C(4)—C(9)	61.3(1)	C(6)—C(7)	2.7(1)	0.0
C(9)—C(8)	76.6(1)	C(9)—C(10)	−73.2(1)	C(7)—C(8)	14.2(1)	14.8
C(8)—C(1)	−28.8(1)	C(10)—C(11)	22.0(1)	C(8)—C(9)	−45.6(1)	−44.5
C(1)—C(2)	−32.3(1)	C(11)—C(12)	36.9(1)	C(9)—C(4)	65.2(1)	63.5
C(2)—C(1)	84.9(1)	C(1)—C(8)	65.8(1)			
C(1)—C(8)	−28.8(1)	C(8)—C(9)	−38.0(1)			
C(8)—C(9)	−38.0(1)	C(9)—C(10)	42.2(1)			
C(9)—C(10)	42.2(1)	C(10)—C(11)	−70.4(1)			
C(10)—C(11)	22.0(1)	C(11)—C(12)	81.9(1)			
C(11)—C(2)	−80.5(1)	C(12)—C(1)	−82.6(1)			

(*b*) Eight and four-membered rings

Bond	Angle	Bond	Angle
C(1)—C(2)	−32.3(1)	C(1)—C(2)	−26.0(1)
C(2)—C(3)	52.1(1)	C(2)—C(11)	25.8(1)
C(3)—C(4)	−126.8(1)	C(11)—C(12)	−26.2(1)
C(4)—C(5)	71.3(1)	C(12)—C(1)	26.2(1)
C(5)—C(6)	14.5(1)		
C(6)—C(7)	2.7(1)		
C(7)—C(8)	14.3(1)		
C(8)—C(1)	93.5(1)		

rationalization for this regiospecificity can be made in terms of arguments based on conformational analysis and radical stability. Mono-C_5-substituted 4a,5,8,8a-tetrahydro-1,4-naphthoquinones (*e.g.*, **1**) possess six well-defined conformations only two of which, in the case of **1**, are capable of vinyl–ene-dione cycloaddition. These are the conformations **1***a* and **1***b* shown below. If, as seems likely (24), the cycloaddition is a two-step process, then initial bonding in the case of **1** should occur preferentially between C_2 or C_3 and the terminal carbon of the vinyl group so as to give the more stable (presumably diradical) intermediate. In both **1***a* and **1***b* however, the terminal carbon of the vinyl group can approach C_3 much more closely than C_2 without serious nonbonded interactions; hence photoproduct **2** is eventually formed in preference to **3**. This argument, ignoring as it does the likely intermediacy of twisted ene–dione excited states and/or intramolecular exciplex intermediates, should be regarded as tentative.

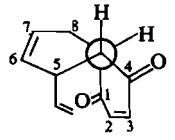

1*a*

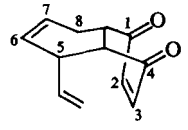

1*b*

Experimental

Preparation of the trans-1,3,5-Hexatriene-p-benzoquinone Diels–Alder Adduct **1**

A mixture of 4.0 g (0.05 mol) of 1,3,5-hexatriene (prepared by the method of Hwa and Sims (25)) and 1.6 g (0.014 mol) of freshly recrystallized *p*-benzoquinone was stirred at 60° for 2 h during which time the benzoquinone slowly dissolved. The solution was then stirred for 4 h at room temperature and the hexatriene removed *in vacuo* to leave a yellow solid. Two recrystallizations of this material from petroleum ether afforded 1.2 g (43%) of light yellow crystals, m.p. 58–60°; i.r. ($CHCl_3$) 1695 (C=O) and 1610 (weak, C=C) cm^{-1}; n.m.r. ($CDCl_3$) τ 3.3 (d, 2, AB quartet, J = 10 Hz, C_2 and C_3 vinyls), 4.1–4.6 (m, 3), 4.9–5.1 (m, 2, methylene vinyls), and 6.5–8.0 (m, 5); n → π* u.v. max (EtOH) 355 nm, ε 75; mass spectrum parent (70 eV) *m/e* 188.

Anal. Calcd. for $C_{12}H_{12}O_2$: C, 76.59; H, 6.39. Found: C, 76.51; H, 6.30.

Photolysis of Diels–Alder Adduct **1**

Numerous photolyses were carried out in either benzene or *tert*-butyl alcohol with identical results; the following description is typical. A solution of 200 mg of adduct **1** in 200 ml of anhydrous distilled benzene was situated external (6 in.) to a standard immersion well

TABLE 7. Selected intra- and intermolecular contacts

Intramolecular		Intermolecular*	
Atoms	Distance (Å)	Atoms	Distance (Å)
O(1)...C(5)	2.939(2)	O(1)...C(11)[1]	3.389(2)
C(1)...C(11)	2.129(2)	O(2)...C(5)[2]	3.359(2)
C(2)...C(12)	2.149(2)	O(2)...C(10)[3]	3.399(2)
C(2)...H(12*a*)	2.49(2)	O(1)...H(1)[4]	2.58(2)
C(3)...H(5*a*)	2.58(2)		
C(5)...H(9)	2.71(2)		
C(7)...H(1)	2.56(2)		
C(10)...H(4)	2.58(2)		
C(10)...H(12*b*)	2.65(2)		
C(12)...H(2)	2.53(2)		
C(12)...H(8)	2.64(2)		
H(4)...H(5*b*)	2.27(3)		
H(6)...H(7)	2.30(3)		

*Superscripts refer to atoms at positions: [1] $\frac{1}{2}+x, \frac{1}{2}-y, \frac{1}{2}+z$; [2] $\frac{3}{2}-x, \frac{1}{2}+y, \frac{1}{2}-z$; [3] $\frac{1}{2}-x, \frac{1}{2}+y, \frac{1}{2}-z$; [4] $\frac{1}{2}+x, \frac{1}{2}-y, z-\frac{1}{2}$.

apparatus and thoroughly degassed with nitrogen. Using a 450 W Type L Hanovia lamp the solution was irradiated with light of $\lambda > 340$ nm by means of an interposed 17 × 17 × 0.2 cm plate of Corning #7380 glass. The reaction was followed by alumina/ethyl acetate t.l.c. which showed the disappearance of starting material after 2.5 h and the development of only one significant new spot. Removal of benzene *in vacuo* and column chromatography (alumina – ethyl acetate) afforded a 60% yield of crude solid photoproduct **2**. Recrystallization from petroleum ether – ether mixtures afforded colorless crystals, m.p. 91.5–92.5°, in 50% overall yield. Spectral data for **2** include: i.r. (CCl_4) 1725 (C=O) cm^{-1}; i.r. (KBr) 1715 and 1735 (C=O) cm^{-1}; n.m.r. ($CDCl_3$) τ 4.2 (m, 2, vinyls) and 6.8–8.4 (complex multiplet, 10); $n \rightarrow \pi^*$ u.v. max (EtOH) 283 nm, ε 30; and mass spectrum parent (70 eV) *m/e* 188.

Anal. Calcd. for $C_{12}H_{12}O_2$: C, 76.59; H, 6.39. Found: C, 76.28; H, 6.40.

Acknowledgment is made to the donors of the Petroleum Research Fund, administered by the American Chemical Society, for partial support of this research. We thank the National Research Council of Canada for financial support, and the University of British Columbia Computing Centre for assistance.

1. J. R. SCHEFFER, J. TROTTER, R. A. WOSTRADOWSKI, C. S. GIBBONS, and K. S. BHANDARI. J. Am. Chem. Soc. **93**, 3813 (1971).
2. J. R. SCHEFFER, K. S. BHANDARI, R. E. GAYLER, and R. H. WIEKENKAMP. J. Am. Chem. Soc. **94**, 285 (1972).
3. J. R. SCHEFFER, K. S. BHANDARI, R. E. GAYLER, and R. A. WOSTRADOWSKI. J. Am. Chem. Soc. **97**, 2178 (1975).
4. J. R. SCHEFFER, J. TROTTER, R. E. GAYLER, and C. A. BEAR. Tetrahedron Lett. 2871 (1973).
5. (*a*) R. C. COOKSON, E. CRUNDWELL, R. R. HILL, and J. HUDEC. J. Chem. Soc. 3062 (1964); (*b*) P. E. EATON and S. A. CEREFICE. Chem. Commun. 1494 (1970); (*c*) J. C. BARBORAK, L. WATTS, and R. PETTIT. J. Am. Chem. Soc. **88**, 1328 (1966).
6. E. W. J. BUTZ and L. W. BUTZ. J. Org. Chem. **7**, 199 (1942).
7. R. E. LONG. Ph.D. Thesis, University of California at Los Angeles, 1965.
8. D. T. CROMER and J. B. MANN. Acta Cryst. A**24**, 321 (1968).
9. R. F. STEWART, E. R. DAVIDSON, and W. T. SIMPSON. J. Chem. Phys. **42**, 3175 (1965).
10. D. T. CROMER and D. LIBERMAN. J. Chem. Phys. **53**, 1891 (1970).
11. V. SCHOMAKER and K. N. TRUEBLOOD. Acta Cryst. B**24**, 63 (1968).
12. D. W. J. CRUICKSHANK. Acta Cryst. **14**, 896 (1961).
13. D. W. J. CRUICKSHANK. Acta Cryst. **9**, 747 (1956); **9**, 754 (1956).
14. W. R. BUSING and H. A. LEVY. Acta Cryst. **17**, 142 (1964).
15. C. K. JOHNSON. *In* Crystallographic computing. Munksgaard, Copenhagen. 1970. pp. 207–226.
16. R. BUCOURT and D. HAINAUT. Bull. Soc. Chim. Fr. 1366 (1965).
17. J. B. HENDRICKSON. J. Am. Chem. Soc. **89**, 7036 (1967); **89**, 7043 (1967); **89**, 7047 (1967).
18. E. M. ENGLER, J. D. ANDOSE, and P. V. R. SCHLEYER. J. Am. Chem. Soc. **95**, 8005 (1973).
19. A. ALMENNINGEN, O. BASTIANSEN, and P. N. SKANCKE. Acta Chem. Scand. **15**, 711 (1961).
20. G. DALLINGA and L. H. TONEMAN. Recl. Trav. Chim. Pays-Bas, **88**, 185 (1969).
21. B. ANDERSEN and R. SRINIVASAN. Acta Chem. Scand. **26**, 3468 (1972).
22. B. ANDERSEN and L. FERNHOLT. Acta Chem. Scand. **24**, 445 (1970).
23. C. S. GIBBONS and J. TROTTER. J. Chem. Soc. Perkin II, 737 (1972).
24. (*a*) G. KAUPP, Justus Liebigs Ann. Chem. 844 (1973); (*b*) R. O. LOUTFY, P. DE MAYO, and N. A. FARID. Can. J. Chem. **50**, 3465 (1972); (*c*) R. M. BOWMAN, C. CALVO, J. J. MCCULLOUGH, P. W. RASMUSSEN, and R. F. SNYDER. J. Org. Chem. **37**, 2084 (1972); (*d*) P. DE MAYO. Acc. Chem. Res. **4**, 41 (1971).
25. J. C. H. HWA and H. SIMS. Org. Syn. **41**, 49 (1961).

Metastable Ion Studies. V. The Identification of $C_2H_4O^{+\cdot}$ Ion Structures from their Characteristic Kinetic Energy Releases

JOHN L. HOLMES AND JOHAN K. TERLOUW[1]

Chemistry Department, University of Ottawa, Ottawa, Canada K1N 6N5

Received March 6, 1975

JOHN L. HOLMES and JOHAN K. TERLOUW. Can. J. Chem. **53**, 2076 (1975).

Metastable ion peaks for the fragmentation $C_2H_4O^{+\cdot} \rightarrow C_2H_3O^+ + H^\cdot$ have been studied in the first field-free region of a double focussing mass spectrometer under conditions of good energy resolution. Three isomeric $C_2H_4O^{+\cdot}$ ions were generated, (a) $CH_2—CH_2^{+\cdot}$ (O), (b) $CH_3CHO^{+\cdot}$, and (c) $CH_2{=}CHOH^{+\cdot}$ from ethylene oxide, acetaldehyde, and ethyl vinyl ether respectively, each fragment producing a different $^1m^*$ peak having a characteristic shape and kinetic energy release. The above ions do not therefore interconvert prior to fragmentation and their characteristic $^1m^*$ peaks permit their unequivocal identification, thus providing a powerful method for ion structure determination.

In agreement with some recent collisional activation data it was found that the unbranched aldehydes, cyclic alcohols, and 2-haloethanols investigated generated (c) type $C_2H_4O^{+\cdot}$ ions. These are also produced by glycidol and α-furfuryl alcohol. Some compounds generated composite $^1m^*$ peaks, *e.g.* 1,3-dioxolane produces (a) and (c) ions, while compounds which produce prominent $C_2H_5O^+$ ions having the protonated acetaldehyde structure, generate *m/e* 44 ions of structures (b) and (c). In isopropanol these components were separated by a deuterium labelling experiment. Contrary to earlier proposals, pyruvic acid does not generate (b) type ions but produces predominantly ions of structure (c).

JOHN L. HOLMES et JOHAN K. TERLOUW. Can. J. Chem. **53**, 2076 (1975).

On a étudié les pics des métastables de la fragmentation $C_2H_3O^{+\cdot} \rightarrow C_2H_3O^+ + H^\cdot$ dans la première région libre de champ d'un spectromètre de masse à double focalisation dans des conditions où l'on peut observer une bonne résolution des énergies. On a produit respectivement les trois ions isomères $C_2H_4O^{+\cdot}$ suivants (a) $CH_2—CH_2^{+\cdot}$ (O), (b) $CH_3CHO^{+\cdot}$ et (c) $CH_2{=}CHOH^{+\cdot}$ à partir de l'oxyde d'éthylène, de l'acétaldehyde et de l'éther vinylique. Chaque ion se fragmente pour conduire à un pic $^1m^*$ différent tant par sa forme que par l'émission d'énergie cinétique. Les ions mentionnés plus haut ne se transforment donc pas les uns dans les autres avant leur fragmentation et leurs pics $^1m^*$ caractéristiques permet donc de les identifier sans ambiguïté; cette propriété fournit donc une méthode puissante pour déterminer la structure des ions.

On a trouvé, en accord avec des données récentes sur l'activation collisionnelle, que les aldéhydes en chaîne droite, que les alcools cycliques et que les halogéno-2 éthanols étudiés fournissent tous des ions $C_2H_4O^{+\cdot}$ du type (c). Ces ions se forment aussi à partir du glycidol et de l'alcool α-furfurylique. Quelques composés conduisent à des pics $^1m^*$ composés; par exemple le dioxolanne-1,3 fournit des ions du type (a) et du type (c) alors que des composés qui produisent pour $C_2H_5O^+$ des ions importants de structure acétaldehyde protoné, donnent naissance à des ions de $m/e = 44$ ayant les structures (b) et (c). Dans l'isopropanol, on a séparé ces constituants à l'aide d'expériences impliquant un marquage au deutérium. Contrairement à ce qui a été proposé antérieurement, l'acide pyruvique ne conduit pas à des ions du type (b) mais principalement à des ions de structure (c). [Traduit par le journal]

Introduction

Three methods have been widely used in recent years to try to establish ion structures and fragmentation mechanisms. These are (*i*) the metastable ion peak abundance ratio test (for competing fragmentations of a given ion) originally proposed by Shannon and McLafferty (1). This well-known approach is a comparative method and applies to *ions fragmenting in the microsecond time frame* and having a range of internal energies of several eV; (*ii*) ion cyclotron

[1]Permanent address: Analytical Chemistry Laboratory, University of Utrecht, Croesestraat 77A, Utrecht, The Netherlands.

resonance (i.c.r.) spectroscopy, which identifies *ions having insufficient energy to fragment in the millisecond time frame*, by examining their reaction with various neutral substrate molecules; (*iii*) collisional activation spectrometry (c.a.) identifies *ions which have insufficient energy to dissociate within the microsecond time frame* (the first field-free region of a reversed geometry double-focussing mass spectrometer) by inducing their dissociation with a neutral collision gas and then examining the ion kinetic energy spectrum of the products.

Application of these methods to small heteroatom containing ions such as $C_2H_5O^+$ (1–4), $C_2H_6N^+$ (5–7), $C_3H_8N^+$ (5–7), $C_3H_7O^+$ (8, 9), and small hydrocarbon ions $C_3H_6^{+\cdot}$ (10, 11) has certainly advanced our knowledge of these systems. These methods are however not unambiguous and because of the wide range of ion internal energies and lifetimes involved they should be considered as complementary. Moreover the abundance ratio test and c.a. approaches are most useful for ion identification by comparison with selected reference ions of known or assumed structure.

Another method, which has mainly been pioneered by Beynon and co-workers (12), is based upon measurement of the kinetic energy released in the dissociation of metastable ions. This technique, which relies on the recording of ^{1}m* peaks under conditions of good energy resolution, has not been widely practised, possibly because of the level of electronic stability required for reproducible ^{1}m* measurements with a very narrow β-slit setting. Without additional measurements this too is only a comparative technique, but when combined with appropriate accurate thermochemical measurements, unequivocal precursor and daughter ion structures may confidently be assigned (13, 14).

We have undertaken a study of ^{1}m* peaks for $C_2H_4O^{+\cdot}$ fragmentations under conditions of high energy resolution. This ion, *m/e* 44, which is a prominent fragment ion in the mass spectra of many organic oxycompounds has been studied by both the metastable peak abundance method (15) and by c.a. (16). In the present work the chosen probe reaction was H atom loss because the associated ^{1}m* peak was found clearly to be characteristic of the $C_2H_4O^{+\cdot}$ ion structure. A discussion of the energetics of this fragmentation as a function of $C_2H_4O^{+\cdot}$ structure and their relationship with ^{1}m* observations will be described in a future publication (17).

Results and Discussion

Choice of Reference Ions and the Probe Reaction

The following structures can be envisaged for $C_2H_4O^{+\cdot}$ ions

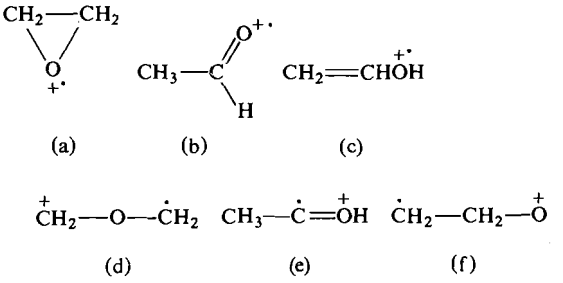

(a) (b) (c)

(d) (e) (f)

(a) and (b) are directly related to stable neutral species, whereas (c), ionized vinyl alcohol, has no known neutral counterpart. The remaining three ions may not be stable observable entities although (e) has been postulated as an intermediate in the formation of $C_2H_4O^{+\cdot}$ ions from pyruvic acid (18). Ion (d) might be generated by loss of H_2 from the molecular ion of dimethyl ether and (f) is a ring opened form of (a). These will be discussed later.

In their c.a. study of $C_2H_4O^{+\cdot}$, Van de Sande and McLafferty (16) only considered (a), (b), and (c) as possible structures.[2] They selected ethylene oxide, acetaldehyde, and a series of unbranched aldehydes as reference compounds for the generation of (a), (b), and (c) respectively, and found that their c.a. spectra were markedly different. They concluded therefore that (a), (b), and (c) represent stable species with lifetimes of $>10^{-5}$ s. With the above as reference spectra they compared the behavior of a number of *m/e* 44 ions derived from a variety of oxygen containing molecules and were able in every case to identify the ions as being either of class (a) or (b) or (c) or in a few instances as a mixture thereof.

In order to classify $C_2H_4O^{+\cdot}$ ions by examination of their ^{1}m* energy release characteristics, a suitable probe reaction is required which produces a metastable ion peak of good abundance from each isomeric structure. Accordingly the 70 eV metastable ion spectra of ethylene

[2]Our notation (a), (b), and (c) is the same as that of Van de Sande and McLafferty (16).

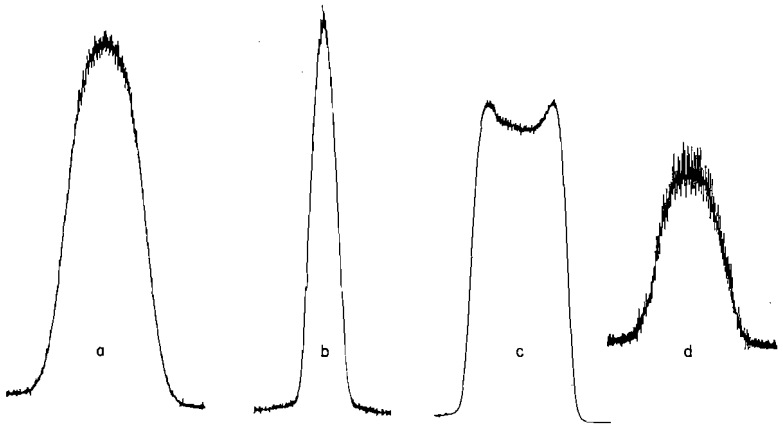

FIG. 1. $^1m^*$ peaks for $C_2H_4O^{+\cdot} \rightarrow C_2H_3O^+ + H^\cdot$, precursor molecule (*a*) ethylene oxide; (*b*) acetaldehyde; (*c*) ethyl vinyl ether; (*d*) dimethyl ether.

oxide (a), acetaldehyde (b), and (c) which is very probably generated from ethyl vinyl ether (16, 19), were examined first by use of a scintillation photomultiplier detector (see Experimental) and then by separation from the main ion beam by the acceleration potential scan method. Of the four possible primary fragmentations of interest, namely loss of $H^\cdot$, H_2, $CHO^\cdot$, and $CH_3^\cdot$ only H atom loss was accompanied by an intense $^1m^*$ in each case. For H_2 elimination only a weak $^1m^*$ is generated, loss of $HCO^\cdot$ is absent in (a) and of only moderate intensity (partly collision induced) in (b) and (c). Formation of HCO^+ from ethylene oxide produced a strong $^1m^*$, for (b) it was weak and it was barely detectable in (c). Pritchard (15) compared the $^2m^*$ for the latter reaction with that for the dissociation which generates CH_3^+ in the mass spectra of (a) and (b) and acetaldehyde-d_4. His intent was to use the $^2m^*$ abundances to characterize the fragmenting ions; however the results for acetaldehyde (d_0 and d_4) were difficult to interpret and we have not been able to repeat his observations (see below). In any case, the presence of only one metastable ion peak of appreciable intensity makes structure identification by comparing peak abundances a hazardous undertaking. Because of its good intensity in (a), (b), and (c) we chose H atom loss as the probe reaction and the corresponding $^1m^*$ peaks are shown in Fig. 1, together with that derived from *m/e* 44 in the mass spectrum of dimethyl ether (d). As can be seen, these $^1m^*$ are markedly different in appearance under the energy resolution conditions employed (see Experimental). The $T_{0.5}$ values are (a) 430 meV, (b) 43 meV, (d) 320 meV, and for (c) 580 meV; the latter is a dished flat-top peak and $T_h = 300$ meV represents all or a fraction of the reverse activation energy of this fragmentation.[3] It could be argued that the $^1m^*$ for (a) is either made up of a mixture of (b) and (c) or that it represents (b) ions having a different range of internal energy contents. The former is certainly not the case, it proving impossible to reproduce the shape of (a) by summing (b) and (c) in various proportions. The latter possibility is effectively ruled out by thermochemical data (17) and in any case differences in kinetic energy release in noncomposite $^1m^*$ peaks due to internal energy content effects are usually found to be small (20, 21). Furthermore, as will be shown below, $T_{0.5}$ values for this fragmentation produced from a wide range of precursor molecules vary very little from those of the "model" compounds.

The shape of the ethylene oxide peak deserves comment; it is neither a dished flat-top peak (as would normally be expected for a fragmentation having so large a $T_{0.5}$ and such steep sides (14)) nor does it have the Gaussian profile so commonly observed. Note the similarity of (a) to (d); the latter has a *smaller* $T_{0.5}$ than (a); it is possible that they are both composite peaks in which different proportions of two (or more) isomeric daughter ions are generated; this and related matters will be discussed elsewhere (17).

[3] T_h is the energy release calculated from the peak width at its upper extremities or "horns" (14).

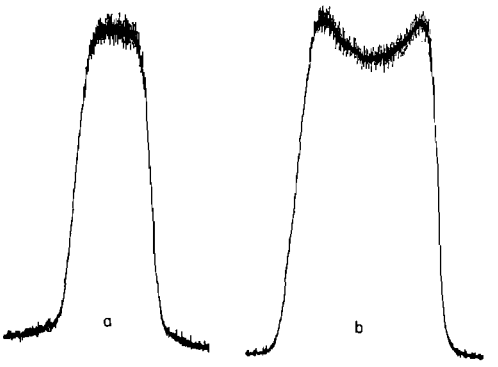

FIG. 2. (*a*) ^{1}m* peak for $CH_3CDO^{+\cdot} \rightarrow CH_3CO^+ + D^\cdot$; (*b*) ^{1}m* peak for $C_2H_3DO^{+\cdot} \rightarrow C_2H_3O^+ + D^\cdot$ generated from cyclobutanol-OD.

The observations described thus far parallel those of the recent c.a. study (16) and these ^{1}m* peaks should permit a clear distinction to be made between fragmenting *m/e* 44 daughter ions.

It is evident from these results and the c.a. data (16) that (b) and (c) are easily differentiated both as fragmenting and nonfragmenting ions. This is contrary to the proposal of Pritchard (15) that (b) and (c) undergo a facile tautomerization. This suggestion arose from the observation that whereas generation of CDO^+ from CD_3CDO yielded a weak ^{2}m*, the unlabelled compound produced no detectable metastable ion peak. In order to explain this observation a large kinetic isotope effect was invoked and it was proposed that methyl loss was preceded by a tautomeric hydrogen shift. We have reexamined the ^{2}m* spectra of CH_3CHO, CD_3CDO, and CH_3CDO, and were unable to observe any significant difference in the intensities of the weak ^{2}m* for the CHO^+, CDO^+ generating fragmentations. Furthermore CH_3CDO yielded only CDO^+ daughter ions both in the normal mass spectrum (fragmentations in the ion source) and in the ^{2}m*. These observations rule out the tautomeric change proposed by Pritchard.

The H loss (probe reaction) provides further evidence that (b) ions do not rearrange prior to fragmentation either in the ion source or field-free regions. $CH_3CDO^{+\cdot}$ loses exclusively the D atom and the ^{1}m* peak is shown as Fig. 2*a*. It is noteworthy that $T_{0.5} = 104$ meV[4] is appreciably larger than in unlabelled (b), thus $T_H/T_D = 0.4$. This result, $T_H/T_D < 1$, is an uncommon observation (22) and its significance will be discussed elsewhere (17).

The H atom lost from (c) is exclusively the hydroxyl hydrogen. This is borne out by observations on cyclobutanol partially exchanged with D_2O in the mass spectrometer's inlet system. This molecule yields (c) without mechanistic complexity by a simple elimination of C_2H_4 from the molecular ion (23); this too is in accord with the c.a. results (16). In the mass spectrum of the partially labelled compound, ions of *m/e* 45 $C_2H_3DO^{+\cdot}$, lost exclusively D and the ^{1}m* peak is shown in Fig. 2*b*. $T_{0.5}$ for this dissociation was 640 meV, close to that for the unlabelled counterpart, $T_{0.5}^H = 609$ meV.

Structure Assignments of $C_2H_4O^{+\cdot}$ Fragment Ions (Table 1)

Compounds Producing (c) Type Ions ($CH_2{=}\overset{+\cdot}{C}HOH$)

In order to compare our method with the c.a. investigation (16) we have examined molecules representative of four of the classes of compounds reported therein (see Table 1, **4–9**). Results from the two experimental methods agree and thus for these compounds both the fragmenting and nonfragmenting $C_2H_4O^{+\cdot}$ ions retain their structural identity in the microsecond time frame.

$C_2H_4O^{+\cdot}$ ions of structure (c) were also found to be generated from α-furfuryl alcohol (**10** in Table 1) and glycidol (**11**). Partial deuterium exchange in these compounds produced the same observations as obtained with cyclobutanol. The potential scope of this method of ion identification is well exemplified by the glycidol result; this molecule contains an ethylene oxide ring in addition to a $-CH_2OH$ moiety and the generation of two *m/e* 44 ion structures could well be envisaged. The present method easily and clearly establishes ion structure, a result not achieved by conventional e.i. labelling experiments.

1,3-Dioxolane

This compound is of special interest because in the c.a. study it was shown to generate a mixture of (a) and (c) the proportions of which varied with ionizing electron energy (16) (5:1 at 70 eV and 2:1 at 20 eV respectively). It was proposed that (a) was generated directly from

[4]The same value was found for D$^\cdot$ loss from $C_2D_4O^{+\cdot}$ ions.

the molecular ion as shown below

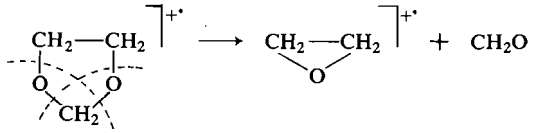

The generation of (c) type ions is difficult to envisage but they may arise by H loss from *m/e* 45, $C_2H_5O^+$, a fragmentation accompanied by a ^{1}m*. $C_2H_5O^+$ is generated from the $[M—H]^+$ ion with an intense ^{2}m*. The elucidation of the route for the formation of these ions awaits a deuterium labelling experiment. It is worth noting that the mass spectrum of this compound also contains an intense ^{2}m* for *m/e* 44 → *m/e* 29, again supporting the (a) structure for the $C_2H_4O^{+\cdot}$ ions. The ^{1}m* peak for the probe reaction in 1,3-dioxolane is shown as item (a) in Fig. 3*a*. Superficially it indeed closely resembles that shown in Fig. 1*a*, however the $T_{0.5}$ value, 480 meV, is significantly higher than that observed in the ethylene oxide fragmentation. Following the c.a. results, the extra broadening can be attributed to a contribution from (c) type ions. Trial and error summations of peaks 1*a* and 1*c* allowed duplication of peak 3*a* using relative abundances of 2(a):1(c). This ratio is different from that reported in the c.a. experiments but it must be remembered that the two methods deal with ions having different initial internal energy contents. Furthermore, the accuracy with which relative contributions of metastable peaks in a composite signal can be assigned, decreases with decrease in the difference between their $T_{0.5}$ values. A more accurate assessment can be made by an overall peak-shape analysis rather than by using a single parameter (*e.g.* the half-height width).

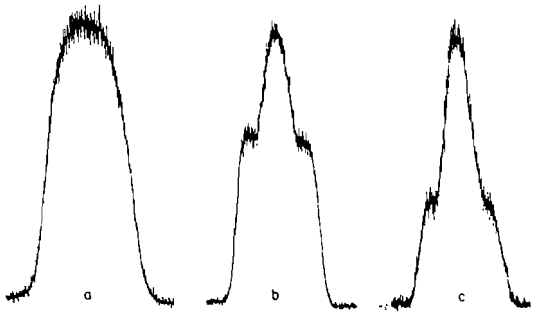

FIG. 3. ^{1}m* ion peaks for $C_2H_4O^{+\cdot} \rightarrow C_2H_3O^+ + H^\cdot$ generated from (*a*) 1,3-dioxolane; (*b*) isopropanol; and (*c*) diisopropyl ether.

Composite ^{1}m Peaks of (b) plus (c) Type*

From the i.c.r. experiments of Beauchamp and Dunbar (4) it was concluded that $C_2H_5O^{+\cdot}$ ions generated from ethanol, isopropanol, diethyl ether, and diisopropyl ether had either the protonated acetaldehyde or protonated ethylene oxide structure. A later c.a. study (2) showed that protonated acetaldehyde was the more probable structure for the above compounds and acetal. The $C_2H_5O^+$ ions in the mass spectra of the above five compounds are prominent and are accompanied by relatively weak *m/e* 44, $C_2H_4O^{+\cdot}$ ions. The latter are largely (but not exclusively) generated by H loss from the former and so we investigated the corresponding ^{1}m*'s for $C_2H_4O^{+\cdot} \rightarrow C_2H_3O^+$. In every case a (b) plus (c) composite peak was observed (see Table 1 and Figs. 3*b* and 3*c*). This is in keeping with the proposed protonated acetaldehyde structure for $C_2H_5O^+$ ions, which can lose H in two ways

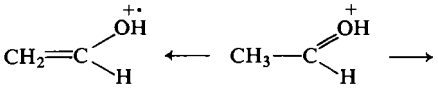

(c)

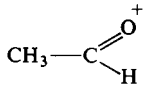

(b)

to yield (c) and (b) as shown. (The oxirane type of $C_2H_5O^+$ ion might be expected to generate (a).) This suggestion is further supported by observations on isopropanol-OD. The *m/e* 46 ions of proposed structure[5] 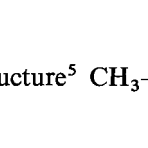 lose both H$^\cdot$ and D$^\cdot$ with accompanying ^{1}m* peaks. The label retaining ion *m/e* 45, of proposed structure (c) *exclusively* lost D$^\cdot$ with a $T_{0.5}$ of 635 meV, and the peak shape was closely similar to that observed for cyclobutanol (see Fig. 4*b*). The ion generated by D loss from *m/e* 46, generated a ^{1}m* peak with a shape and $T_{0.5}$ characteristic of acetaldehyde. This result is shown in Fig. 4*a*. Note that there is a residual (c) (vinyl alcohol) component in the *m/e* 44 → *m/e* 43 ^{1}m*, Fig.

[5]In completely deuterated isopropanol-OD, *m/e* 45 (unlabelled compound) is completely shifted to *m/e* 46 (3).

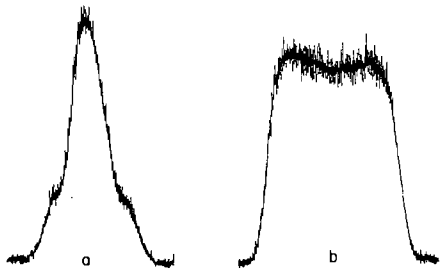

FIG. 4. (*a*) ^{1}m* peak for $C_2H_4O^{+\cdot} \rightarrow C_2H_3O^+ + H^\cdot$ generated from $CH_3CH(OD)CH_3$; (*b*) ^{1}m* peak for $C_2H_3DO^{+\cdot} \rightarrow C_2H_3O^+ + D^\cdot$ generated from $CH_3CH(OD)CH_3$.

4*a*, but that is entirely due to the presence of unlabelled material. The unlabelled compound also accounts for the markedly reduced dish in the $C_2H_3OD^+ \rightarrow C_2H_3O^+ + D^\cdot$ ^{1}m* (Fig. 4*b*); here the dish is partly filled by the weak flat-topped ^{1}m* corresponding to the fragmentation $C_2H_5O^+ \rightarrow C_2H_3O^+ + H_2$. Closely similar results were obtained with ethanol. As can be seen in Table 1, the relative proportions of the (b) and (c) components depend upon the precursor molecules but the $T_{0.5}$ values are essentially precursor independent. These differences arise from the possibility of additional routes for the generation of *m/e* 44 and/or the production of *m/e* 44 ions having different internal energy distributions.

Tetrahydrofuran provided a surprising result in that (b) and (c) type *m/e* 44 ions were generated therefrom. This result negates the earlier proposal (24), that they have an ethylene oxide (a) structure. Although some deuterium labelled tetrahydrofurans have been examined (25, 26), it is still not possible to propose sound mechanisms for the formation of $C_2H_4O^{+\cdot}$ daughter ions.

Ethylene Glycol Dimethyl Ether, a Composite of (a)/(d), (b) Type

Ion cyclotron resonance, c.a., and thermochemical evidence indicate that there is another stable $C_2H_5O^+$ ion, of structure $CH_3—\overset{+}{O}=CH_2$, which can be generated for example, from ethylene glycol dimethyl ether, $CH_3—O—CH_2—CH_2—O—CH_3$. This compound displays a prominent *m/e* 45 peak in its mass spectrum but only a very weak *m/e* 44. However there is a weak ^{1}m* for the fragmentation *m/e* 45 → *m/e* 44 and since this may herald the production of $C_2H_4O^{+\cdot}$ ions of structure (d), the probe reaction for this compound was duly measured. The ^{1}m* is shown in Fig. 5*a*. It contains at least two components, one of which can be identified as ion (b) (generated by an unknown pathway) while the broad component arises from either or both of (a) and (d) ions. Unfortunately, the weak signal renders difficult an accurate analysis of the peak shape. However the broad component certainly is not ion (c) because the estimated $T_{0.5}(= 410$ meV) is too small and also because under the optimum energy resolution conditions employed no clearly defined shoulder can be seen.

For example in Fig. 3*b* the isopropanol (b) and (c) composite peak shows clearly defined shoulders under optimum resolution conditions (these are only poorly seen when moderate resolution is employed, Fig. 5*b*). In the present case *no* shoulder was apparent even under the best experimental conditions; such a peak can be produced by summation of (a) with (b) or (d).

1,4-Dioxane and Pyruvic Acid

Both of these precursor molecules generated *m/e* 44 ions consisting mainly of ion (c) and the ^{1}m* peaks are shown in Fig. 5. For 1,4-dioxane, the dish in (c) (Fig. 5*c*) appears to be filled in presumably by an (a) and a (b) component. The $C_2H_4O^{+\cdot}$ ions are formed by at least two different routes, directly from the molecular ion and via the intense *m/e* 45 ions, since both fragmentations exhibit the appropriate ^{1}m* peaks. Additional experiments with labelled compounds would probably provide the answers.

The pyruvic acid fragmentation has been discussed previously by Turro *et al.* (18) who used the gas-phase photolytic behavior of this com-

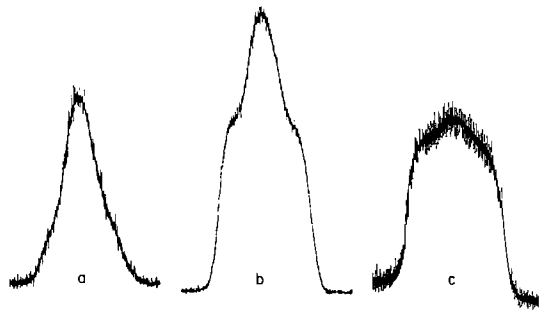

FIG. 5. (*a*) ^{1}m* peak for $C_2H_4O^{+\cdot} \rightarrow C_2H_3O^+ + H^\cdot$ generated from $CH_3OCH_2CH_2OCH_3$; (*b*) ^{1}m* peak for $C_2H_4O^{+\cdot} \rightarrow C_2H_3O^+ + H^\cdot$ generated from isopropanol under conditions of moderate energy resolution (see text); (*c*) ^{1}m* peak for $C_2H_4O^{+\cdot} \rightarrow C_2H_3O^+ + H^\cdot$ generated from 1,4-dioxane.

TABLE 1. $T_{0.5}$ values (meV) for H· loss from $C_2H_4O^{+\cdot}$ ions generated from various precursor molecules. Relative abundances of components are evaluated from peak areas. Reproducibility of the $T_{0.5}$ values was within 5%

Compound	Ion type	$T_{0.5}$	Compound	Ion type	$T_{0.5}$
1 Acetaldehyde	b	43	**12** 1,3-Dioxolane	a/c 2:1	480
2 Ethylene oxide	a	430			
3 Dimethyl ether	d	320	**13** Ethanol	b/c 1:8*	40 (b), 560 (c)
4 Ethyl – vinyl ether	c	580	**14** Isopropanol	b/c 1:6*	49 (b), 560 (c)
			15 Diethyl ether	b/c 1:6	47 (b), 583 (c)
5 *n*-Butanal	c	580	**16** Diisopropyl ether	b/c 1:2	49 (b), 545 (c)
6 *n*-Hexanal	c	577	**17** Acetal	b/c 1:4	52 (b), 605 (c)
7 Cyclobutanol	c*	609	**18** Tetrahydrofuran	b/c 1:4	48 (b), 615 (c)
8 Cyclopentanol-D-1	c	600			
9 2-Chloroethanol	c*	620	**19** Ethylene glycol dimethyl ether	b/a, d 2:1	46 (b), 410 (a, d)
10 α-Furfuryl alcohol	c*	615	**20** 1,4-Dioxane	c†	580 (c)
11 Glycidol	c	618	**21** Pyruvic acid	c*†	500

In compounds 7, 9, 10, 13, 14, and 21 the hydroxylic hydrogen atom was partially exchanged with D_2O in the inlet system of the mass spectrometer. In all cases a similar flat-topped ^{1}m peak associated with an energy release $T_{0.5} = 637 \pm 10$ meV, was observed for the transition $45 \rightarrow 43 + 2(C_2H_3OD^{+\cdot} \rightarrow C_2H_3O^+ + D\cdot)$.
†See text for discussion.

pound to provide an analogy for the fragmentation mechanism. They proposed that an ion of structure (e), $CH_3\dot{C}{=}\overset{+}{O}H$, was formed via a five-centered intermediate. This ion was then supposed to isomerize to an acetaldehyde

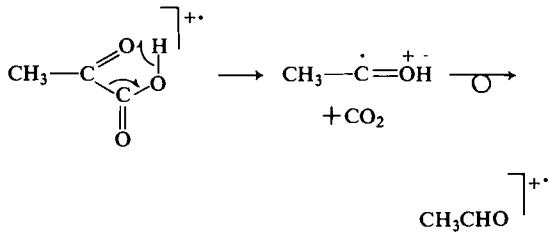

structure. Bentley and Johnstone (27) suggested an alternative four-centered mechanism

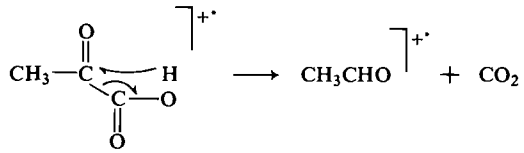

The ^{1}m* for *m/e* 44 → *m/e* 43 in pyruvic acid was of shape type (c) but the $T_{0.5}$ value, 500 meV, was significantly less than that found for all other (c) producing species (see Table 1). However, it was found that in pyruvic acid-OD,[6] the $C_2H_3DO^{+\cdot}$ ions lost D with a pure (c)-type ^{1}m*, $T_{0.5} = 640$ meV. In addition, and unlike all the other $C_2H_3DO^{+\cdot}$ ions discussed above, there was a small ^{1}m* corresponding to H loss therefrom. This was a flat-topped peak with $T_{0.5} = 460$ meV, an energy release appreciably smaller than that found in unlabelled (c) ions. Possibly this result indicates the generation of a hitherto unobserved isomeric form of $C_2H_4O^{+\cdot}$ ions. It is quite clear however that acetaldehyde (b)-type ions are *not* involved in the fragmentation of pyruvic acid and the photochemical analogy remains uncertain. The five-centered mechanism however provides the simplest route to ion (c) possibly via ion (e) as intermediate. As will be described elsewhere (17), the vinyl alcohol molecular ion is the most stable form of $C_2H_4O^{+\cdot}$ and this may explain the nonrearrangement of (e) to (b).

This last example particularly clearly illustrates how metastable ion studies of this kind can readily provide detailed information concerning ion structures of fragmenting ions of relatively low internal energy content. These experiments can be performed with a double-focussing mass spectrometer provided that it is equipped with an energy resolving β-slit. For $C_2H_4O^{+\cdot}$ ions the method is at least the equal of the c.a. technique which examines ions with insufficient internal energy to dissociate in the microsecond time frame. It seems possible however that the present method may prove less successful when applied to larger ions where the greater variety of isomeric species are less likely to be noninterconverting in the energy ranges appropriate for generating ^{1}m* peaks.

[6]The compound was deuterated by exchange with D_2O in the mass spectrometer. There was some small uptake of a *second* D atom presumably by enol exchange.

Experimental

All metastable ion peak measurements were performed with an A.E.I.-G.E.C. MS902S instrument. The peaks were separated from the main ion beam by the acceleration sweep method. Instrument parameters were: source slit 0.002 in.; β-slit 0.005 in. (for lower energy resolution 0.025 in.); collector slit *ca.* 90% transmission; acceleration potential for transmitted ions *ca.* 6200 V; electron energy 70 V. Compounds were admitted to the ion source via a Granville–Phillips variable leak; sample pressures *ca.* 5×10^{-7} Torr. Second field-free region metastable ion peaks were examined using a scintillator photomultiplier detector of the type described by Daly *et al.* (28). Energy release values were calculated in the usual way having first corrected the half-height widths for the main beam energy spread by subtracting the limiting main beam width (as the β-slit is narrowed a point is reached at which the main beam width no longer changes; this width corresponds to *ca.* 1.3 acceleration volts at *ca.* 6 kV). For most of the measurements recorded here this represents *ca.* 5% of the $^1m^*$ peak width.

Compounds were obtained commercially and purified where necessary.

We wish to thank Dr. F. P. Lossing for many valuable discussions. We also thank Prof. F. W. McLafferty for permission to quote his results (16) prior to publication. This work was financially supported by the National Research Council of Canada. One of us (J.K.T.) thanks the Netherlands Organisation for the Advancement of Pure Research (Z.W.O.) for a Fellowship during the tenure of which this work was completed.

1. T. W. Shannon and F. W. McLafferty. J. Am. Chem. Soc. **88**, 5951 (1967).
2. F. W. McLafferty, R. Kornfeld, W. F. Haddon, K. Levson, P. F. Bente III, S. C. Tsai, and H. D. R. Schuddemage. J. Am. Chem. Soc. **95**, 3886 (1973).
3. B. G. Keyes and A. G. Harrison. Org. Mass Spectrom. **9**, 221 (1974).
4. J. L. Beauchamp and R. C. Dunbar. J. Am. Chem. Soc. **92**, 1477 (1970).
5. N. A. Uccella, I. Howe, and D. H. Williams. J. Chem. Soc. B, 1933 (1971).
6. K. B. Tomer. Org. Mass Spectrom. **9**, 686 (1974).
7. K. Levsen and F. W. McLafferty. J. Am. Chem. Soc. **96**, 139 (1974).
8. C. W. Tsang and A. G. Harrison. Org. Mass Spectrom. **3**, 647 (1970).
9. F. W. McLafferty and I. Sakai. Org. Mass Spectom. **7**, 971 (1973).
10. M. L. Gross and P. H. Lin. Org. Mass Spectrom. **7**, 795 (1973).
11. M. L. Gross. J. Am. Chem. Soc. **93**, 3744 (1972).
12. R. G. Cooks, J. H. Beynon, R. M. Caprioli, and G. R. Lester. Metastable ions. Elsevier Scientific Publishing Company, Amsterdam. 1973. Chapts. 4 and 6.
13. J. L. Holmes and G. M. Weese. Org. Mass Spectrom. **9**, 618 (1974).
14. J. L. Holmes, A. D. Osborne, and G. M. Weese. Int. J. Mass Spectrom. Ion Phys. In press.
15. J. G. Pritchard. Org. Mass Spectrom. **8**, 103 (1974).
16. C. C. Van de Sande and F. W. McLafferty. J. Am. Chem. Soc. In press.
17. J. L. Holmes, F. P. Lossing, and J. K. Terlouw. To be published.
18. N. J. Turro, D. S. Weiss, W. F. Haddon, and F. W. McLafferty. J. Am. Chem. Soc. **89**, 3370 (1967).
19. S. Meyerson and J. D. McCollum. *In* Advances in analytical chemistry. *Edited by* C. N. Reilley. Interscience, New York. 1963. p. 211.
20. E. G. Jones, L. E. Baumann, R. G. Cooks, and J. H. Beynon. Org. Mass Spectrom. **7**, 185 (1973).
21. J. L. Holmes and J. K. Terlouw. Org. Mass Spectrom. In press.
22. R. G. Cooks, J. G. Beynon, R. M. Caprioli, and G. R. Lester. Metastable ions. Elsevier Scientific Publishing Company, Amsterdam. 1973. pp. 120–121, 238–240.
23. J. L. Holmes and R. T. B. Rye. Can. J. Chem. **51**, 2342 (1973).
24. J. E. Collin and G. Condé-Caprace. Int. J. Mass Spectrom. Ion Phys. **1**, 213 (1968).
25. R. Smakman and Th. J. de Boer. Org. Mass Spectrom. **1**, 403 (1968).
26. A. M. Duffield, H. Budzikiewicz, and C. Djerassi. J. Am. Chem. Soc. **87**, 2920 (1965).
27. T. W. Bentley and R. A. W. Johnstone. Adv. Phys. Org. Chem. **8**, 247 (1970).
28. N. R. Daly, A. McCormick, and R. E. Powell. Rev. Sci. Instrum. **39**, 1163 (1968).

Conformations of Bridged Diphenyls. VII. Crystal Structure of 2-(4′-Carbomethoxy-2′-nitrophenoxy)-1,3,5-trimethylbenzene

SIMON P. N. VAN DER HEIJDEN, ELIZABETH A. H. GRIFFITH, W. DAVID CHANDLER, AND BEVERLY E. ROBERTSON[1]

Faculty of Science, University of Regina, Regina, Saskatchewan S4S 0A2

Received November 22, 1974

SIMON P. N. VAN DER HEIJDEN, ELIZABETH A. H. GRIFFITH, W. DAVID CHANDLER, and BEVERLY E. ROBERTSON. Can. J. Chem. **53**, 2084 (1975).

The structure of 2-(4′-carbomethoxy-2′-nitrophenoxy)-1,3,5-trimethylbenzene, $C_{17}H_{17}NO_5$, has been determined by X-ray diffraction. The crystals are monoclinic, $a = 8.352(4)$, $b = 17.892(10)$, $c = 10.966(6)$ Å, $\beta = 100.59(3)°$, $P2_1/c$ with $Z = 4$. The intensities of 3877 independent reflections were measured on a four circle diffractometer; 2272 of these reflections were used to obtain a final least-squares residual of 0.053 and traditional R factor of 0.054. The general conformation is similar to that found earlier for differently substituted diphenyl ethers. Comparison of this structure with those previously determined indicates that distortions in ring angles are primarily a result of electronic rather than steric effects.

SIMON P. N. VAN DER HEIJDEN, ELIZABETH A. H. GRIFFITH, W. DAVID CHANDLER et BEVERLY E. ROBERTSON. Can. J. Chem. **53**, 2084 (1975).

On a déterminé la structure cristalline du (carbométhoxy-4′ nitro-2′ phénylate)-2 triméthyl-1,3,5 benzène, $C_{17}H_{17}NO_5$, par diffraction de rayons-X. Les cristaux sont monocliniques, $a = 8.352(4)$, $b = 17.892(10)$, $c = 10.966(6)$ Å, $\beta = 100.59(3)°$, $P2_1/c$ avec $Z = 4$. On a mesuré les intensités de 3877 réflexions indépendantes à l'aide d'un diffractomètre à quatre cercles. On a utilisé 2272 de ces réflexions pour affiner la structure jusqu'à une valeur de R pondérée de 0.053 et une valeur de R conventionnelle de 0.054. La conformation générale de cette molécule se rapproche de celle observée antérieurement pour des diphényléthers substitués dans diverses positions. Une comparaison de cette structure avec d'autres déterminées antérieurement indique que les distorsions dans les angles du cycle sont dues principalement à des effets électroniques plutôt que stériques. [Traduit par le journal]

Introduction

The structures determined previously in this series (2-(3′-methyl-4′-nitrophenoxy)-1,3-diisopropylbenzene (1), 2-(2′,4′-dinitrophenoxy)-1,3,5-tri-*t*-butylbenzene (2), 2-(2′-carbomethoxy-4′-nitrophenoxy)-1,3,5-trichlorobenzene(3)) show a common general conformation which appears to be related both to the presence of two *ortho* substituents on one ring and the electronic character of the substituents. The compound whose structure is reported here is one of a series of structures of substituted diphenyl ethers with no more than one *ortho* substituent on the phenyl ring containing electron-withdrawing substituents. It is also one of a series of studies of bridged diphenyls identically substituted but with variation in the nature of the bridging group.

Previously determined structures in this series have shown deviations from the ideal value of 120° in the internal ring angles at the substituted carbon atoms, which may be related to either the electronic or steric character of the substituents. If the decrease in internal ring angles at the carbon atoms bonded to alkyl groups in the previously reported structures of 2-(3′-methyl-4′-nitrophenoxy)-1,3-diisopropylbenzene (1) and 2-(2′,4′-dinitrophenoxy)-1,3,5-tri-*t*-butylbenzene (2) as opposed to the increase in similar angles at ring carbon atoms bonded to chlorine atoms in 2-(2′-carbomethoxy-4′-nitrophenoxy)-1,3,5-trichlorobenzene (3), from the expected 120° for a hexagonally symmetric ring, is due to electronic rather than steric (substituent size) effects, one would expect a similar decrease in the case of a trimethyl-substituted ring. As has been discussed previously (4), ring distortions limit the accuracy with which conformational parameters can be determined from ring-current shielding measurements. Hope (5) made the observation that in aromatic chlorine compounds the internal ring angle at the carbon atom carrying the chlorine group is greater than 120°. This effect has also been observed by

[1]Author to whom correspondence should be addressed.

Can. J. Chem. Downloaded from www.nrcresearchpress.com by 210.87.254.40 on 09/05/12
For personal use only.

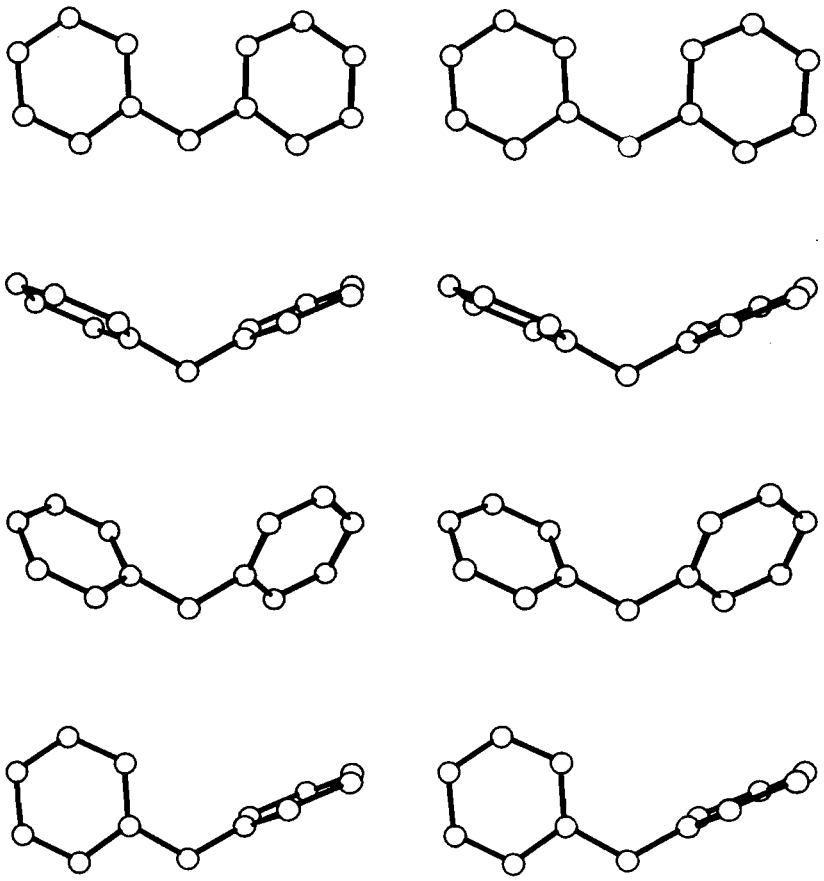

FIG. 1. Stereoscopic view of the four basic conformations for bridged diphenyl compounds. From top to bottom; planar, butterfly, twist, and skew.

Carter *et al.* (6) in aromatic nitro compounds and has been linked to the electron-withdrawing ability of these substituents. The van der Waals radius of CH_3 (2.00 Å) is similar to that of Cl (1.80 Å) (7) and therefore would be expected to show a similar effect if it is determined by steric factors.

Nomenclature

Several systems of nomenclature are currently being used to describe the conformation of bridged diphenyl compounds. We attempt here to establish a uniform nomenclature based upon those currently in use and further we will suggest guidelines for assigning this nomenclature. The basic conformations were first discussed by Higgasi and Smyth (8).

The conformations of bridged diphenyls may be divided conveniently into four general categories, idealized examples of which are shown in Fig. 1. The names assigned to these by most authors (some exceptions exist) are respectively planar, butterfly, twist, and skew.

As a result of the various orientations of the phenyl rings, caused by rotation around their bonds to the bridging group, intermediate conformations are possible. The conformations which deviate only slightly from the basic ones are usually assigned the same name as the basic conformation. However, no limits have been set on the conformational parameters which are associated with a given conformational type. The suggested classification scheme is illustrated in Fig. 2. The horizontal axis represents the largest of the two dihedral angles which the phenyl rings make with the central plane. The vertical axis represents the dihedral angle between the other ring and the central plane.

Can. J. Chem. Downloaded from www.nrcresearchpress.com by 210.87.254.40 on 09/05/12
For personal use only.

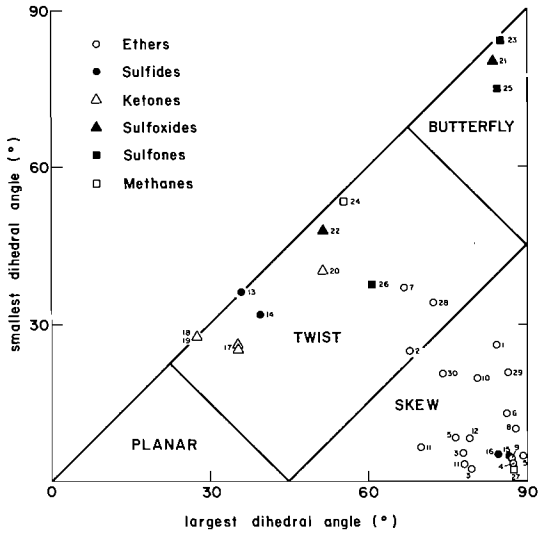

FIG. 2. Density plot of the conformations of bridged diphenyl compounds as determined by X-ray diffraction. The numbers refer to those in Table 1.

Both dihedral angles are taken between 0° and 90°. The lines within the triangle in Fig. 2 define the four basic conformations. The diagram indicates that, for example, a conformation is still considered to be planar when one ring is coplanar with the central plane and the other is allowed to deviate up to 45°. However, if the first ring is allowed to deviate from coplanarity, the allowable range for the second ring decreases. Other conformations have similar constraints. Points representing the conformations of structures reported in this series and others related to them are also shown in Fig. 2.

In a molecule which is not distorted from idealized geometry the dihedral angle between the bridging plane and the plane of the phenyl ring corresponds to the torsional angle about the bond to the bridging group. A number of choices are possible for the definitions of these angles. In order to avoid the establishment of a convention to choose the end of the molecule from which the torsional angles will be viewed, we will define each angle as viewed from the opposite ring. Since the sense of rotation is not dependent on this choice, the signs given for the angles may be compared directly with those given for thyroid hormones where the angles are both viewed from the end of the molecule bearing the amino acid group.

We will choose, in our definition of the torsional angle, the ring atom adjacent to the atom bonded to the bridging atom so that the magnitude of the torsional angle is less than 90°. This implies that when both torsional angles are zero one of the two *ortho* positions is *distal* and the other is *proximal*. The configuration of the planar molecule, corresponding to both torsional angles being placed at their zero values, will be specified by labeling unsymmetrically substituted *ortho* or *meta* substituents as *distal* or *proximal*. We shall use in determining the magnitudes of the torsional angles the least-squares planes fitted to the entire ring in question because this is a more accurate indicator of the relative orientation of the parts of the molecule than the torsional angles based on planes formed by only three atoms.

All of the structures studied to date in this series contain a center of symmetry, Thus the torsional angles must appear in either the pairs (+ +),(− −) or (+ −),(− +). In cases of the butterfly and twist conformations, the combinations of signs (+ −),(− +) would lead to steric problems even in unsubstituted molecules, and no such combination of signs is known to exist. No planar bridged diphenyl compounds have been identified but steric interactions would clearly favor the (+ +),(− −) combinations of signs. In the case of the skew conformation, a rotation of the *proximal ortho* hydrogen atom or a *proximal ortho* substituent towards one of the *ortho* hydrogen atoms or substituents on the other ring clearly favors a rotation of the other ring which moves that *ortho* position away from the *proximal* hydrogen atom or substituent. This leads again to the (+ +),(− −) combination of signs.

In summary then, the conformations of all bridged diphenyl compounds would be expected to show a (+ +) or (− −) conformation of signs, and in the case of centrosymmetric structures both of these combinations would be present. The only observed exception to this prediction is the conformation of the second molecule in the asymmetric unit of 2-(2′-carbomethoxy-4′-nitrophenoxy)-1,3,5-trichlorobenzene (3) where the angles are −89.7° and 4.6°; *i.e.*, a decrease in the former angle greater than 0.3° would lead to a change in the choice of torsional angle such that the prediction would be followed.

Figure 3 shows two of the four possible conformations for a substituted bridged diphenyl compound with a substituent R on the right

Can. J. Chem. Downloaded from www.nrcresearchpress.com by 210.87.254.40 on 09/05/12
For personal use only.

Can. J. Chem. Downloaded from www.nrcresearchpress.com by 210.87.254.40 on 09/05/12
For personal use only.

TABLE 1. Bridged diphenyls in Fig. 2

No. in Fig. 2	Compound	Reference
1	2-(2′,4′-Dinitrophenoxy)-1,3-diiodo-5-methylbenzene	9
2	1-(2′,4′-Dinitro-6′-bromophenoxy)-napthalene	9
3	2-(3′-Methyl-4′-nitrophenoxy)-1,3-diisopropylbenzene	1
4	2-(2′,4′-Dinitrophenoxy)-1,3,5-trimethyl-*t*-butylbenzene	2
5	2-(2′-Carbomethoxy-4′-nitrophenoxy)-1,3,5-trichlorobenzene	3
6	3,5,3′-Triodo-L-thyronine, HCl	10
7	Thyronine·HCl ethyl ester monohydrate	11
8	Triiodothyropropionic acid ethyl ester	12
9	3,5,3′-Triiodothyroacetic acid	13
10	3,5-Diiodo-L-thyronine	14
11	2-(2′,6′-Dinitrophenoxy)-1-*t*-butylbenzene	15
12	2-(4′-Carbomethoxy-2′-nitrophenoxy)-1,3,5-trimethylbenzene	This work
13	4,4′-Dibromodiphenyl sulfide	17
14	Di-*p*-tolyl sulfide	18
15	4-Diethylaminodiphenyl sulfide	19
16	2-(4′-Carbomethoxy-2′-nitrothiophenyl)-1,3,5-trimethylbenzene	20
17	*p,p*′-Dimethoxybenzophenone	21
18	Benzophenone	22
19	3,3′-Dibromobenzophenone	23
20	2-(4′-carbomethoxy-2′-nitrobenzoyl)-1,3,5-trimethylbenzene	24
21	Diphenyl sulfoxide	25
22	2-(4′-Carbomethoxy-2′-nitrophenylsulfinyl)-1,3,5-trimethylbenzene	26
23	4,4-Dichlorodiphenyl sulfone	27
24	2,2′,4,4′,6,6′-Hexamethyldiphenyl sulfone	28
25	4,4′-Diaminodiphenyl sulfone	29
26	2-(4′-Carbomethoxy-2′-nitrophenylsulfonyl)-1,3,5-trimethylbenzene	30
27	2-(4′-Carbomethoxy-2′-nitrobenzyl)-1,3,5-trimethylbenzene	31
28	3,5,3′-Triiodo-L-thyronine methyl ester	42
29	3′-Isopropyl-3,5-diiodo-L-thyronine	43
30	3,5,3′-Triiodo-L-thyronine	44

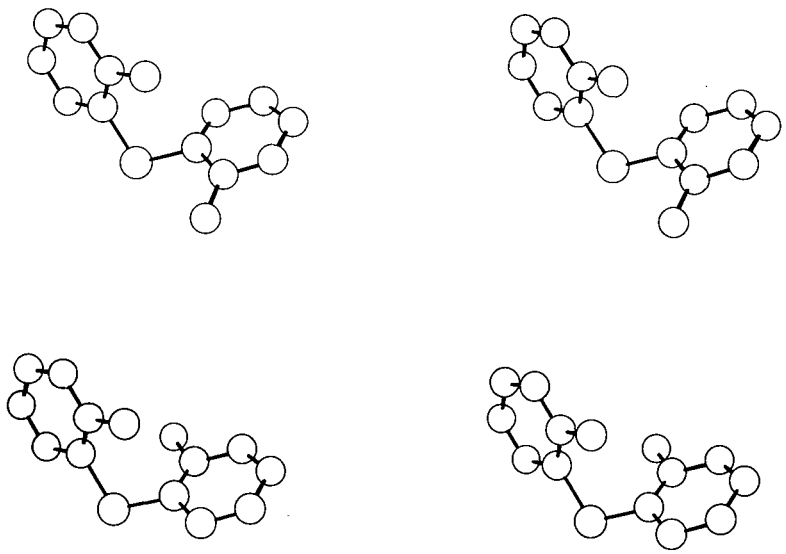

FIG. 3. Stereoscopic view of a twist-2-R-*distal*-1′-X-*proximal* conformation (upper) and a twist-2-R-*proximal*-1′-X-*proximal* conformation (lower).

Can. J. Chem. Downloaded from www.nrcresearchpress.com by 210.87.254.40 on 09/05/12
For personal use only.

phenyl ring and a substituent X on the left phenyl ring. Both molecules have the (− −) combination of torsional angles. The conformation of the upper molecule in Fig. 3 would then be a twist-2-R-*distal*-1′-X-*proximal* conformation, while that of the lower would be a twist-2-R-*proximal*-1′-X-*proximal* conformation.

Experimental

The synthesis of 2-(4′-carbomethoxy-2′-nitrophenoxy)-1,3,5-trimethylbenzene, $C_{17}H_{17}NO_5$, has been reported earlier (33). It was recrystallized from 95% ethanol, m.p. 104–106 °C. A sample with dimensions of 0.6 × 0.4 × 0.5 mm was used for data collection. The systematic absences ($h0l$, $l = 2n + 1$; $0k0$, $k = 2n = 1$) and the Laue symmetry as determined by film methods, gave the space group $P2_1/c$. The crystal was then mounted on a Picker FACS I four circle automatic diffractometer equipped with a graphite monochromator. Twenty-four reflections with 2θ values between 35 and 45°, where the MoKα_1 and Kα_2 diffraction peaks were resolved, were used to calculate the cell constants by least squares. The cell constants are given below with the estimated errors calculated as three times the estimated standard deviations given by the least-squares procedure.

The crystal data are as follows:

$C_{17}H_{17}NO_5$ f.w. = 315.33

Monoclinic, $P2_1/c$: $a = 8.352(4)$, $b = 17.892(10)$, $c = 10.966(6)$ Å, $\beta = 100.59(3)°$, $\rho_o = 1.28$ g cm^{-3} (flotation), $\rho_c = 1.32$ g cm^{-3}, $Z = 4$, $F(000) = 664e$, λ(MoKα_1) = 0.70926 Å, μ(MoKα) = 1.05 cm^{-1}, $T = 22 \pm 2$ °C. The angle settings of 12 of the centered reflections were used to determine the orientation of the crystal on the diffractometer. The integrated intensities of 3877 independent reflections with 2θ values between 3.5 and 55° were collected with MoKα radiation. The θ–2θ scan mode was used with a 1 deg min^{-1} scan rate, a minimum base width of 3.2°, and 40 s background counts at each limit of the scan. The intensities of three standard reflections were measured every 100 reflections, and were not found to vary significantly. The data were reduced to observed structure factors using standard procedures. No corrections were made for absorption or extinction effects. A Wilson statistical calculation gave an overall temperature factor of 4.4 Å^2. The scattering factors for oxygen, nitrogen, and carbon were taken from the series coefficients given by Cromer and Mann (34). The scattering factors for the hydrogen atoms were those given by Stewart *et al.* (35). The 397 reflections with $|E| > 1.62$ were used to solve the structure by the logical symbolic addition method.[2] The solution with the highest figures of merit gave an *E*-map showing all 23 nonhydrogen atom positions. Full-matrix least-squares refinement with unit weights and individual anisotropic temperature factors reduced the weighted residual R_w, defined as $R_w = \{\Sigma w(|F_o| - |F_c|)^2 / \Sigma w|F_o|^2\}^{1/2}$; $w = \sigma^{-2}$, to 0.114 A difference map at this point revealed all 17 hygrogen atoms. The final least-squares weights were calculated from $w^{-1/2} = 0.5962 - 0.02640|F_o| + 0.000848|F_o|^2$. The 2272 reflections for which $|F_o| > 2.0w^{-1/2}$ were used in the final cycles of refinement. The final values of R_w and the conventional R factor were 0.053 and 0.054 respectively. The observed and calculated structure factors have been placed in the Depository of Unpublished Data.[3] The final positional and thermal parameters are listed in Table 2. The estimated errors are the estimated standard deviations from the least-squares analysis. The bond lengths and angles and the atomic numbering are given in Figs. 4 and 5. The numbering of the atoms is based upon standard crystallographic practice; *i.e.*, atoms of the same chemical species will be differentiated by arabic numbers enclosed in parentheses. This implies that the crystallographic designation will be quite different from the chemical designation of the same atom. Primes will be used to differentiate between equivalent atoms belonging to separate molecules within the asymmetric unit.

Past practice in this series has been to report errors as three times the estimated standard deviations determined by the least-squares refinement. The errors in the bond lengths and angles have also been multiplied by the factor 3. The degree of consistency between equivalent bond lengths and angles in related structures in the series suggests that this method of reporting errors is unnecessarily conservative. Therefore in this and succeeding papers, the errors in least-squares determined structural parameters and in parameters derived from them will be given as the estimated standard deviations with no modifications.

In the case of the errors in lattice constants, our experience indicates that significant differences often occur between lattice constants obtained by least-squares refinements of the positions of different sets of reflections from the same crystal, even when the zero settings of the angle encoders are not fixed and are included as least-squares variables. We assume that these differences arise from imperfections in alignment settings such as those associated with the positioning of the crystal, the geometry of the rotation axes of the goniostat, or the positioning of the X-ray source. Errors in lattice constants will therefore be multiplied by three as before.

Discussion

The molecular packing diagram is shown in Fig. 6.

The crystal structure shows no unusual intermolecular contacts. Bond lengths to hydrogen atoms range from 0.86(4) to 1.00(5) Å and the isotropic hydrogen temperature factors, B, range from 5 to 15 Å^2.

[2]The direct methods program LSAM, written by Germain and Woolfson (36) was used for structure solution. Fourier calculations were carried out with the Zalkin program FORDAP (37). Least-squares refinement was done with the Busing *et al.* program ORFLS (38). The molecular geometry and associated e.s.d's were determined with the Busing and Levy program ORFFE (39). Stereograms were prepared with the aid of the Johnson Program ORTEP (40).

[3]Complete set of tabular data is available, at a nominal charge, from the Depository of Unpublished Data, CISTI, National Research Council of Canada, Ottawa, Canada K1A 0S2.

TABLE 2. Structural parameters (e.s.d.'s) for 2-(4′-carbomethoxy-2′-nitrophenoxy)-1,3,5-trimethylbenzene

(*a*) Fractional atomic coordinates ($\times 10^4$) and thermal parameters U_{ij} ($\times 10^3$), t.f. = exp $\{-2\pi^2(a^{*2}h^2U_{11} + \ldots + 2a^*b^*hkU_{12} + \ldots)\}$

Atom	*x*	*y*	*z*	U_{11}	U_{22}	U_{33}	U_{12}	U_{13}	U_{23}
C(1)	3249(3)	1509(1)	1869(2)	54(2)	37(1)	50(2)	0(1)	6(1)	−2(1)
C(2)	4269(3)	902(1)	2248(2)	44(1)	42(1)	47(1)	−1(1)	5(1)	2(1)
C(3)	4102(3)	236(2)	1601(2)	52(2)	41(1)	50(2)	2(1)	10(1)	4(1)
C(4)	2956(3)	171(1)	531(2)	56(2)	41(1)	47(2)	−2(1)	10(1)	−2(1)
C(5)	2004(4)	783(2)	116(3)	66(2)	57(2)	51(2)	4(1)	−5(2)	−5(1)
C(6)	2134(4)	1444(2)	774(3)	72(2)	49(2)	57(2)	14(2)	−8(2)	−3(1)
C(7)	2679(3)	−540(2)	−176(3)	65(2)	47(2)	60(2)	−5(1)	15(2)	−7(1)
C(8)	3222(8)	−1833(2)	−145(5)	148(4)	42(2)	93(3)	−6(2)	46(3)	−13(2)
C(9)	2235(3)	2702(1)	2322(2)	55(2)	40(1)	47(2)	4(1)	−2(1)	−8(1)
C(10)	2705(3)	3333(1)	1753(2)	55(2)	46(2)	53(2)	2(1)	8(1)	−7(1)
C(11)	1587(3)	3916(2)	1538(3)	69(2)	46(2)	52(2)	5(1)	7(2)	−2(1)
C(12)	74(3)	3873(2)	1862(3)	60(2)	63(2)	49(2)	16(1)	−2(1)	−11(1)
C(13)	−328(4)	3228(2)	2429(3)	47(2)	78(2)	59(2)	1(2)	6(2)	−15(2)
C(14)	734(3)	2626(2)	2685(2)	55(2)	56(2)	49(2)	−7(1)	2(1)	−8(1)
C(15)	4343(5)	3381(2)	1372(5)	72(2)	63(2)	106(3)	3(2)	35(2)	−1(2)
C(16)	−1091(6)	4527(3)	1622(5)	83(3)	96(3)	84(3)	45(2)	−6(2)	−10(3)
C(17)	289(6)	1938(2)	3336(4)	92(3)	75(2)	77(3)	−22(2)	20(2)	3(2)
N	5536(3)	949(1)	3359(2)	61(2)	52(1)	57(2)	9(1)	−2(1)	−6(1)
O(1)	6266(3)	1531(1)	3578(2)	65(1)	72(2)	102(2)	−6(1)	−16(1)	−20(1)
O(2)	5800(3)	390(1)	3985(2)	135(2)	74(2)	78(2)	17(2)	−35(2)	11(1)
O(3)	1863(3)	−600(1)	−1179(2)	114(2)	68(2)	80(2)	5(1)	−16(2)	−27(1)
O(4)	3460(3)	−1109(1)	450(2)	106(2)	41(1)	67(1)	4(1)	17(1)	−5(1)
O(5)	3392(2)	2123(1)	2612(2)	65(1)	41(1)	64(1)	9(1)	−10(1)	−9(1)

(*b*) Fractional atomic coordinates ($\times 10^3$) and isotropic temperature factors for hydrogen atoms

Atom	*x*	*y*	*z*	*B* (Å²)
H(3)	485(3)	−15(2)	193(2)	5(1)
H(5)	120(3)	74(2)	−63(3)	6(1)
H(6)	137(3)	183(2)	52(3)	6(1)
H(11)	194(3)	436(1)	116(2)	4(1)
H(13)	−135(4)	319(2)	268(3)	6(1)
H(8,1)	222(5)	−198(2)	−11(4)	10(2)
H(8,2)	387(5)	−214(2)	41(4)	10(1)
H(8,3)	358(4)	−185(2)	−90(4)	8(1)
H(15,1)	439(4)	303(2)	70(4)	9(1)
H(15,2)	451(4)	388(2)	105(3)	9(1)
H(15,3)	512(5)	317(3)	188(4)	10(2)
H(16,1)	−90(6)	489(3)	224(5)	15(2)
H(16,2)	−213(6)	438(3)	156(4)	11(2)
H(16,3)	−108(6)	473(3)	90(5)	12(2)
H(17,1)	3(5)	155(2)	281(4)	10(1)
H(17,2)	127(6)	172(3)	389(4)	12(2)
H(17,3)	−50(5)	203(2)	378(4)	10(1)

The C(9)—O(5) bond length is 0.053(5) Å longer than the C(1)—O(5) bond length. A comparison of this value for the difference in lengths to the ether oxygen atom with those found earlier shows that the difference in these bond lengths increases as the difference in total electron-withdrawing ability of the substituents on the two rings increases.

The deviation from coplanarity of the electron-withdrawing ring (the ring containing the nitro group) with the central C—O—C′ plane in the tri-*ortho*-substituted compounds ranges from 8.8° to 2.1° (1–3), with the present value being 8.7°.

The trimethyl-substituted ring is nearly perpendicular to the central plane, the general

Can. J. Chem. Downloaded from www.nrcresearchpress.com by 210.87.254.40 on 09/05/12
For personal use only.

Can. J. Chem. Downloaded from www.nrcresearchpress.com by 210.87.254.40 on 09/05/12
For personal use only.

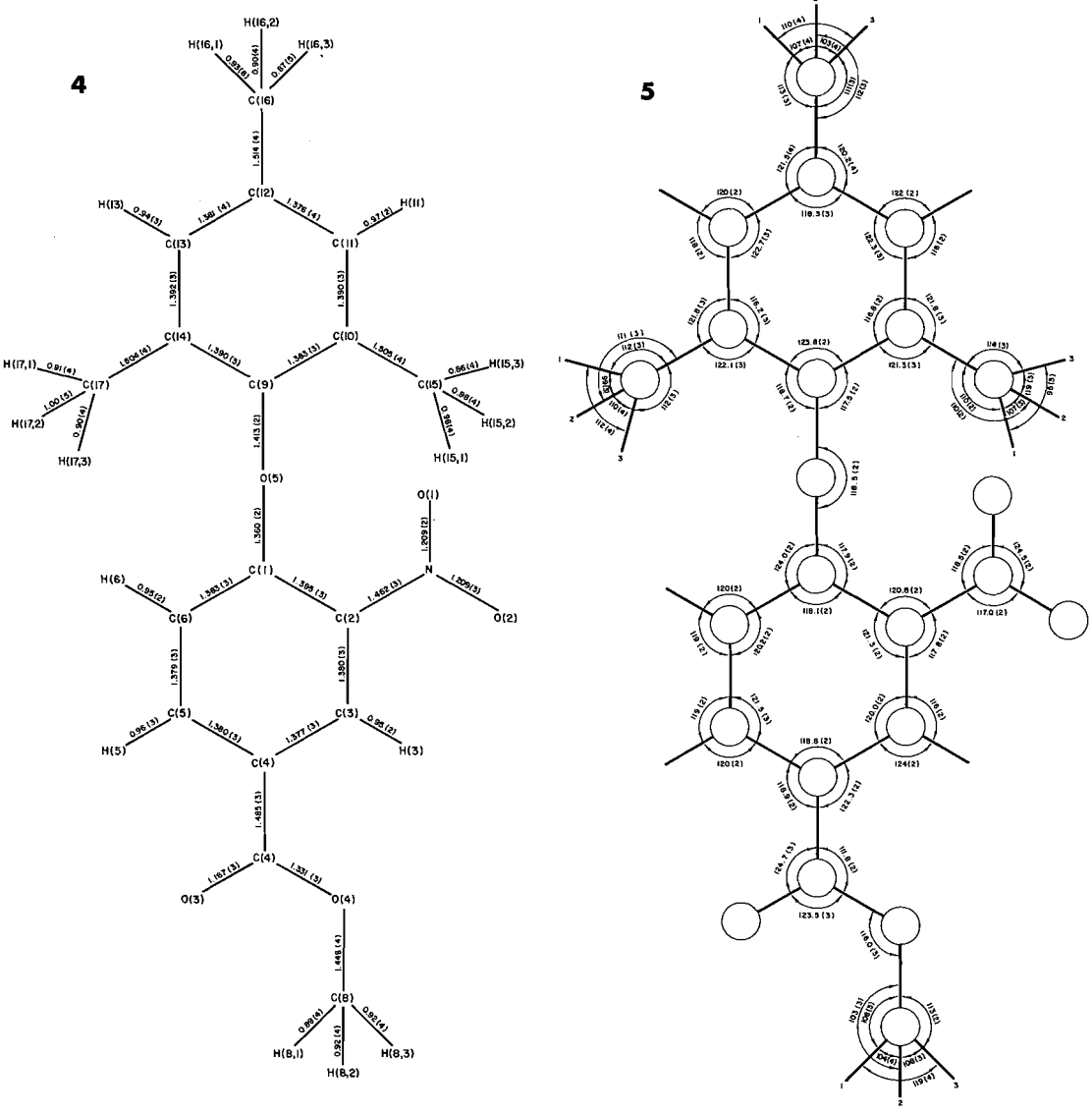

FIG. 4. Bond lengths and atom labeling. Numbers in parentheses are estimated errors.
FIG. 5. Bond angles. Numbers in parentheses are estimated errors.

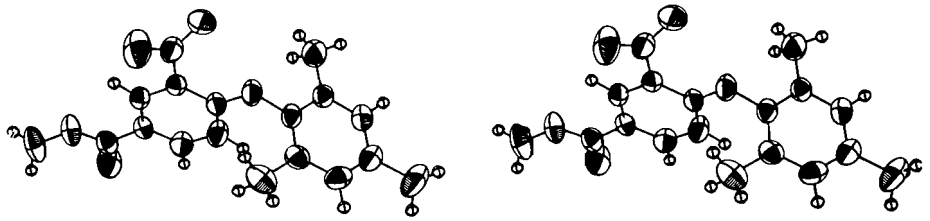

FIG. 6. Stereoscopic view of 2-(4′-carbomethoxy-2′-nitrophenoxy)-1,3,5-trimethylbenzene. The thermal ellipsoids for the nonhydrogen atoms are drawn at the 50% probability level. The hydrogen atoms are given arbitrary temperature factors.

Can. J. Chem. Downloaded from www.nrcresearchpress.com by 210.87.254.40 on 09/05/12
For personal use only.

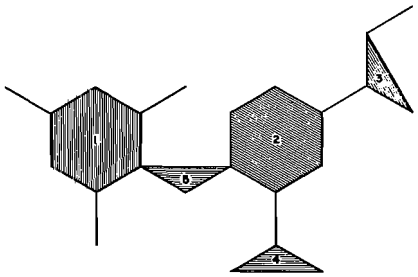

FIG. 7. Labeling of the least-squares planes.

conformation being skew-nitro-*distal* as suggested by p.m.r. data for the same compound (41). The dihedral angles between the normals to the molecular planes, which are labeled in Fig. 7, are given in Table 3. The torsional angles ϕ[C(9)—O(5)—C(1)—C(6)] and ψ[C(1)—O(5)—C(9)—C(14)], corresponding to the dihedral angles between the planes 2,5 and 1,5, occur in (+ +) and (− −) pairs as expected. In 2-(4′-carbomethoxy-2′-nitrophenoxy)-1,3,5-trimethylbenzene the O(5)—C(1)—C(6) angle is 6.1° larger than the O(5)—C(1)—C(2) angle, because of a bending of the nitro-substituted ring away from the mesityl ring by 3.05(15)°. A stereoscopic view of the molecule is given in Fig. 8. This type of distortion has also been observed in other nitro-substituted compounds and varies from 4.2° in 2-(3′-methyl-4′-nitrophenoxy)-1,3-diisopropylbenzene to 2.5° in 2-(2′,4′-dinitrophenoxy)-1,3,5-tri-*t*-butylbenzene. The bending at the bridgehead carbon atom is probably a result of steric interaction between the H(6) hydrogen atom and the mesityl ring.

TABLE 3. Least-squares planes

(*a*) Equations of planes $Ax + By + Cz = D$. Coordinates refer to the directions of the $\boldsymbol{a}$, $\boldsymbol{c}^*\boldsymbol{x}\boldsymbol{a}$, and $\boldsymbol{c}^*$ axes. The planes are defined in Fig. 7

Plane	*A*	*B*	*C*	*D*
1	−0.2174	−0.3900	−0.8948	−4.4325
2	0.7860	0.3201	−0.5271	1.6691
3	0.8911	0.1857	−0.4141	1.9250
4	0.7799	−0.2982	−0.5504	0.5796
5	0.6944	0.4362	−0.5723	1.6475

(*b*) Dihedral angles

Planes	Angle (deg)
1,2	79.9
1,5	79.0
2,3	11.9
2,4	36.2
2,5	8.7

The nitro group is bent away from the ether oxygen atom by 1.5(2)°. A similar bending (3)° is observed for the *ortho*-nitro group of 2-(2′,4′-dinitrophenoxy)-1,3,5-tri-*t*-butylbenzene.

In the present study the nitro group is rotated by 36.2° from the plane of the phenyl ring, which is greater than any of the values found previously. Holden and Dickenson (16) observed a rotation of 75° and 37° for the 2- and 4,6-nitro groups respectively of 1,3-dichloro-2,4,6-trinitrobenzene. This suggests that the twist of the nitro groups is due to repulsive interaction of the ether oxygen and one of the nitro group oxygen atoms. The intramolecular nitro oxygen,

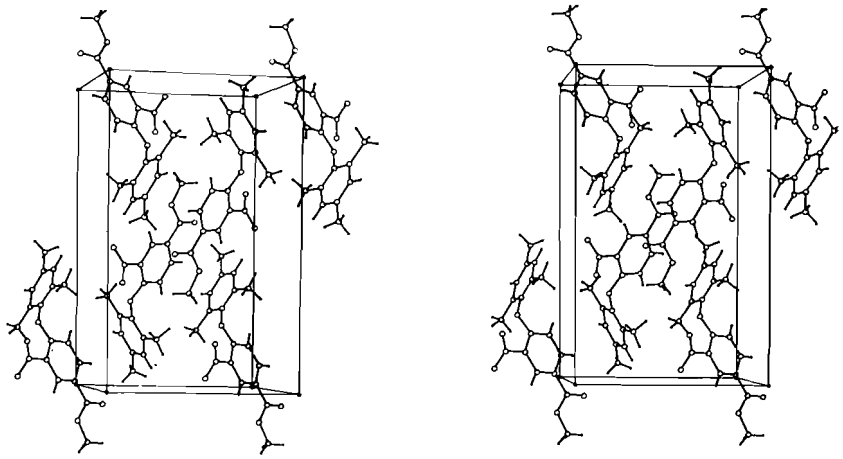

FIG. 8. Stereoscopic view of the molecular packing.

O(1), to ether oxygen distance is 2.659 Å, which is similar to the ether oxygen distance of 2.570 Å in 2-(2′,4′-dinitrophenoxy)-1,3,5-tri-*t*-butylbenzene (2) and the average carbonyl oxygen to ether oxygen distance of 2.703 Å in 2-(2′-carbomethoxy-4′-nitrophenoxy)-1,3,5-trichlorobenzene (3).

The internal ring angles at the carbon atoms bonded to the methyl group are decreased from the 120° expected for a hexagonally symmetric ring. This deviation is the same as for the isopropyl and *t*-butyl groups but opposite in sign to that of the chlorine-substituted benzene ring in 2-(2′-carbomethoxy-4′-nitrophenoxy)-1,3,5-trichlorobenzene. We therefore conclude that the distortions in the internal ring angles are primarily a result of electronic rather than steric effects.

The research was supported by grants from the National Research Council of Canada.

1. E. A. H. Griffith, W. D. Chandler, and B. E. Robertson. Can. J. Chem. **50**, 2963 (1972).
2. E. A. H. Griffith, W. D. Chandler, and B. E. Robertson. Can. J. Chem. **50**, 2972 (1972).
3. E. A. H. Griffith, W. D. Chandler, and B. E. Robertson. Can. J. Chem. **50**, 2979 (1972).
4. J. J. Bergman, E. A. H. Griffith, B. E. Robertson, and W. D. Chandler. Can. J. Chem. **51**, 162 (1973).
5. H. Hope. Acta Cryst. B**25**, 78 (1969).
6. O. L. Carter, A. T. McPhail, and G. A. Sim. J. Chem. Soc. A, 822 (1966).
7. L. Pauling. The nature of the chemical bond. Cornell University Press, New York. 1960.
8. K. Higgasi and C. P. Smyth. J. Am. Chem. Soc. **82**, 4759 (1960).
9. P. A. F. Lehmann and E. Shefter. Rev. Latinoam. Quim. **3**, 91 (1972).
10. N. Camerman and A. Camerman. Science, **175**, 764 (1972).
11. A. Camerman and N. Camerman. Can. J. Chem. **52**, 3042 (1974).
12. N. Camerman and A. Camerman. Can. J. Chem. **52**, 3048 (1974).
13. V. Cody and W. L. Duax. Biochem. Biophys. Res. Commun. **52**, 430 (1973).
14. V. Cody, W. L. Duax, and D. A. Norton. Acta. Cryst. B**28**, 224 (1972).
15. K. Gurtu, W. Chandler, and B. E. Robertson. Can. J. Chem. **53**, 2093 (1975).
16. J. R. Holden and C. Dickinson. J. Phys. Chem. **71**, 1129 (1967).
17. J. Toussaint. Bull. Soc. Chim. Belg. **54**, 319 (1945).
18. W. R. Blackmore and S. C. Abrahams. Acta Cryst. **8**, 329 (1955).
19. C. Panattoni, G. Bandoli, D. A. Clemente, A. Dondoni, and A. Mangini. J. Cryst. Mol. Struct. **3**, 65 (1973).
20. S. P. N. van der Heijden, W. D. Chandler, and B. E. Robertson. Can. J. Chem. **53**, 2102 (1975).
21. H. G. Norment and I. L. Karle. Acta Cryst. **15**, 873 (1962).
22. E. Fleiser, N. Sung, and S. Hawkinson. J. Phys. Chem. **72**, 4311 (1968).
23. V. Pattabhi and K. Vankatesan. J. Cryst. Mol. Struct. **3**, 25 (1973).
24. S. P. N. van der Heijden, W. D. Chandler, and B. E. Robertson. Can. J. Chem. **53**, 2127 (1975).
25. S. C. Abrahams. Acta Cryst. **10**, 417 (1957).
26. S. P. N. van der Heijden, W. Chandler, and B. E. Robertson. Can. J. Chem. **53**, 2108 (1975).
27. J. G. Sime and S. C. Abrahams. Acta Cryst. **13**, 1 (1960).
28. S. A. Chawdhury and A. Hargreaves. Acta Cryst. B**27**, 548 (1971).
29. C. Dickinson, J. M. Stewart, and H. L. Ammon. J. Chem. Soc. D, 920 (1970).
30. S. P. N. van der Heijden, W. D. Chandler, and B. E. Robertson. Can. J. Chem. **53**, 2115 (1975).
31. S. P. N. van der Heijden, W. D. Chandler, and B. E. Robertson. Can. J. Chem. **53**, 2121 (1975).
32. V. Cody and W. L. Duax. Science, **181**, 757 (1973).
33. W. D. Chandler, J. J. Bergman, and G. H. Haas. Can. J. Chem. **49**, 583 (1971).
34. D. T. Cromer and J. B. Mann. Acta Cryst. A**24**, 321 (1968).
35. R. F. Stewart, E. R. Davidson, and W. T. Simpson. J. Chem. Phys. **42**, 3175 (1965).
36. G. Germain and M. M. Woolfson. Acta Cryst. B**24**, 91 (1968).
37. A. Zalkin. FORDAP, A Fortran program for Fourier calculations. University of California, Berkeley, California. 1965.
38. W. R. Busing, K. O. Martin, and H. A. Levy. ORFLS, Report ORNL-TM-305. Oak Ridge National Laboratory, Oak Ridge, Tennessee. 1962.
39. W. R. Busing and H. A. Levy. ORFFE, Report ORNL-TM-306. Oak Ridge National Laboratory, Oak Ridge, Tennessee. 1964.
40. C. K. Johnson. ORTEP, Report ORNL-3794. Oak Ridge National Laboratory, Oak Ridge, Tennessee. 1965.
41. H. Benjamins and W. D. Chandler. Can. J. Chem. **52**, 597 (1974).
42. V. Cody. J. Med. Chem. **18**, 126 (1975).
43. J. K. Fawcett and A. Camerman. Biochem. Biophys. Res. Commun. **52**, 407 (1973).
44. V. Cody. J. Am. Chem. Soc. **96**, 6720 (1974).

Can. J. Chem. Downloaded from www.nrcresearchpress.com by 210.87.254.40 on 09/05/12
For personal use only.

Conformations of Bridged Diphenyls. VIII. Crystal Structure of 2-(2′,6′-Dinitrophenoxy)-*t*-butylbenzene

KAPIL GURTU, W. DAVID CHANDLER, AND BEVERLY E. ROBERTSON[1]

Faculty of Science, University of Regina, Regina, Saskatchewan S4S 0A2

Received November 22, 1974

KAPIL GURTU, W. DAVID CHANDLER, and BEVERLY E. ROBERTSON. Can. J. Chem. **53**, 2093 (1975).

The crystal structure of 2-(2′,6′-dinitrophenoxy)-*t*-butylbenzene, $C_{16}H_{15}N_2O_5$, has been determined by X-ray diffraction. The crystals are monoclinic, space group $P2_1/c$: a = 13.949(9), b = 9.652(6), c = 23.806(12) Å, β = 93.82(5), Z = 8. The integrated intensities of 6811 reflections were recorded with a four circle automated diffractometer at 20 °C; 3334 of these reflections were used in the refinement of the structure to a least-squares weighted residual of 0.057 and a traditional R factor of 0.057.

The two crystallographically independent molecules both have the skew-*t*-butyl-*distal* conformation, suggesting that the steric effects of the two *ortho*-nitro groups play a greater role in determining the conformation than does conjugation with the bridging oxygen atom.

KAPIL GURTU, W. DAVID CHANDLER et BEVERLY E. ROBERTSON. Can. J. Chem. **53**, 2093 (1975).

On a déterminé la structure cristalline du (dinitro-2′,6′-phénylate)-2 *t*-butyl benzène, $C_{16}H_{15}N_2O_5$, par diffraction de rayons-X. Les cristaux sont monocliniques, groupe d'espace $P2_1/c$: a = 13.949(9), b = 9.652(6), c = 23.806(12) Å, β = 93.82(5)°, Z = 8. On a mesuré, à 20 °C, les intensités de 6811 réflexions indépendantes à l'aide d'un diffractomètre à quatre cercles. On a utilisè 3334 de ces réflexions pour affiner la structure jusqu'à une valeur de R pondérée de 0.057 et une valeur de R conventionnelle de 0.057.

Les deux molécules cristallographiquement indépendantes adoptent chacune une conformation *t*-butyl-*gauche distal* impliquant que les effets stériques des deux groupes nitro en *ortho* jouent, par opposition à la conjugaison avec l'atome d'oxygène du pont, un rôle plus grand dans la détermination de la conformation. [Traduit par le journal]

Introduction

In the *ortho*-substituted diphenyl ethers whose structures have been reported previously in this series (1–4) one benzene ring has been di-*ortho*-substituted with halogen atoms or electron-donating groups. Each of these compounds was found to adopt the skew-H-*proximal* conformation. This conformation has also been predicted on the basis of p.m.r. studies of the same compounds. (5). The notation used here to indicate the conformation was introduced previously in this series of papers (4).

The skew conformation for molecules of this sort allows the steric repulsion between the *ortho* substituents on the di-*ortho*-substituted ring and the rest of the molecule to be minimized while keeping the more electron-withdrawing ring in the C—O—C plane. Montaudo *et al.* (6) have discussed the conformational effect of double bond character arising out of the overlap of π electrons in the phenyl rings and the unshared electrons on the bridging oxygen atom. This effect tends to favor a conformation which is planar. Steric interactions appear, however, to discourage the planar conformation. Then the ring which contains the more electron-withdrawing substituents would be expected to be more nearly coplanar with the central C—O—C plane than the other ring, as has been observed to be the case (1–4).

In all compounds reported previously in this series, both the *ortho* substituent steric effect and the conjugation effect have favored the same conformation, and it has not been possible to estimate the relative importance of these two effects in determining the conformation of diphenyl ethers. In the compound whose structure is reported here, the electron-withdrawing phenyl ring is di-*ortho*-substituted. If steric effects are overriding, the molecular conformation will be skew-*t*-butyl-*distal*; if mesomeric effects predominate, a skew-NO_2-*distal* (or *proximal*) conformation will result; if the two effects are of nearly equal weight one would

[1]Author to whom correspondence should be addressed.

expect a twist-*t*-butyl-*distal* conformation. Lehmann (7) and Lehmann and McEachern (8) have used dipole moment studies and p.m.r. to investigate the conformation of di-*ortho*-nitro-substituted compounds and have concluded that the conjugation between the electron-withdrawing ring and the ether oxygen atom will lead either to a skew- or twist-nitro-*proximal* conformation with the *proximal* nitro group rotated to near coplanarity with the adjacent ring. For the sake of clarity it should be pointed out here that the above conformations could equally be labeled skew-nitro-*distal* or twist-nitro-*distal* because of the presence of identical *ortho*-nitro substituents.

Experimental

The method of Wright and Jorgensen (9), as modified by Bergman (10), was used to synthesize 2-(2′,6′-dinitrophenoxy)-*t*-butylbenzene, ($C_{16}H_{16}N_2O_5$). The ether was recrystallized from methanol as small light yellow crystals, m.p. 115–118 °C. Another recrystallization from a petroleum ether – acetone (1:1) mixture aided by slow evaporation yielded monoclinic crystals suitable for diffraction studies. A crystal of approximate dimensions 0.3 × 0.5 × 0.7 mm was first examined by film methods. The Laue symmetry and systematic extinctions ($h0l$, $l = 2n \pm 1$, $0k0$, $k = 2n + 1$) indicated the space group $P2_1/c$.

The crystal was mounted on a Picker FACS I diffractometer. The crystal orientation was determined by a least-squares fit to the positions of 12 strong reflections centered with MoKα_1 radiation. Accurate cell parameters were determined later by fitting to the positions of 30 reflections.

Crystal data are as follows:

$C_{16}H_{16}N_2O_5$ f.w. = 326.34

Monoclinic, $P2_1/c$: $a = 13.949(3)$, $b = 9.652(2)$, $c = 23.806(4)$ Å, $\beta = 93.82(4)°$, $Z = 8$, $\rho_o = 1.32$ g cm^{-3}, $\rho_c = 1.34$ g cm^{-3}, $F(000) = 1328e$, μ(MoKα) = 1.35 cm^{-1}, λ(MoKα_1) = 0.70926 Å, $T = 20$ °C.

The integrated intensities of 6811 reflections were recorded using the θ–2θ scan mode for 2θ values between 3° and 50° with a scan rate of 1 deg min^{-1}. The background was counted for 20 s at each limit of the scan. The intensities of three standard reflections were recorded after every 50 reflections and their intensities were not observed to change significantly. The data were reduced to observed structure factors using standard procedures. A Wilson statistical calculation gave an overall temperature factor of 4.8 Å^2.

The scattering factors for nonhydrogen atoms were taken from Cromer and Mann (11). The scattering factors for the hydrogen atoms were from Stewart *et al.* (12). The structure was solved by direct methods using the logical symbolic addition method.[2] An *E*-map calculated with the set of nontrivial signs with the highest figure of merit revealed 50 peaks. Forty-three of these were used to construct two independent molecules. The structure was then refined through one cycle of least squares. All reflections were initially assigned equal weighting. Most of the hydrogen atoms and the three missing nonhydrogen atoms were located using a difference map. The structure was further refined to a least-squares residual, defined by $R_w = (\Sigma w(|F_o| - |F_c|)^2/\Sigma w|F_o|^2)^{1/2}$, of 0.12.

It was observed at this point that one of the four NO_2 substituents showed irregular geometry. A new difference map was calculated and it indicated that both NO_2 groups on one of the two independent molecules were disordered by rotation about the C—N bond. Four additional oxygen atoms were then introduced into the structure, and each of the eight NO_2 oxygen atoms were assigned an occupation number of $\frac{1}{2}$. The occupation numbers and positions of the eight disordered oxygen atoms were allowed to vary in the least-squares refinement and the occupation numbers refined to values which did not differ significantly from $\frac{1}{2}$. They were therefore fixed at $\frac{1}{2}$. The positions of four of the hydrogen atoms were still undetermined at this point. Peaks for these atoms were found in the difference maps but attempts to refine their positions led to unreasonable molecular geometry. Their positional parameters were therefore not varied in the final least-squares process. The temperature factors for these atoms were set equal to the isotropic temperature factor of the carbon atoms to which they were bonded, as determined by averaging over the three axes of the thermal ellipsoid of the carbon atoms.

In the final stages of full-matrix least squares the weights were calculated as $w = \sigma^{-2}$ where $\sigma = 1.0313 - 0.00914|F_o| + 0.00015|F_o|^2$. The 3334 reflections for which $|F_o| > 2.3\sigma$ were used in the final cycles of least squares. The final value of the least-squares residual and the conventional *R* factor were both 0.057.

The observed and calculated structure factors have been placed in the Depository of Unpublished Data.[3] The final positional and thermal parameters are listed in Table 1. The estimated errors are the estimated standard deviations given by the least-squares analysis. The bond lengths and angles, and the atom numbering for both of the two independent molecules in the asymmetric unit of the structure are given in Figs. 1 and 2. In the case of oxygen or hydrogen atoms labeled with a double subscript, the first subscript refers to the atom to which it is bonded. In the disordered molecule, indicated as molecule **2** in Table 1 and in Fig. 1*b*, the subscripts 3 and 4 on oxygen or nitrogen atoms refer to the disordered nitro groups associated with the nitro groups labeled 1 and 2 respectively. The atoms N′(3) and N′(4) are assumed to be identical with N′(1) and N′(2).

Discussion

All of the hydrogen atoms except four of those belonging to the *t*-butyl substituents on molecule **2** are in reasonable positions with bond

[2]The Germain and Woolfson program LSAM (13) was used for structure solution. The Busing *et al.* program ORFLS (14) was used for least-squares refinement. The Johnson program ORTEP (15) was used to prepare the stereograms.

[3]Complete set of tabular data is available, at a nominal charge, from the Depository of Unpublished Data, CISTI, National Research Council of Canada, Ottawa, Canada K1A 0S2.

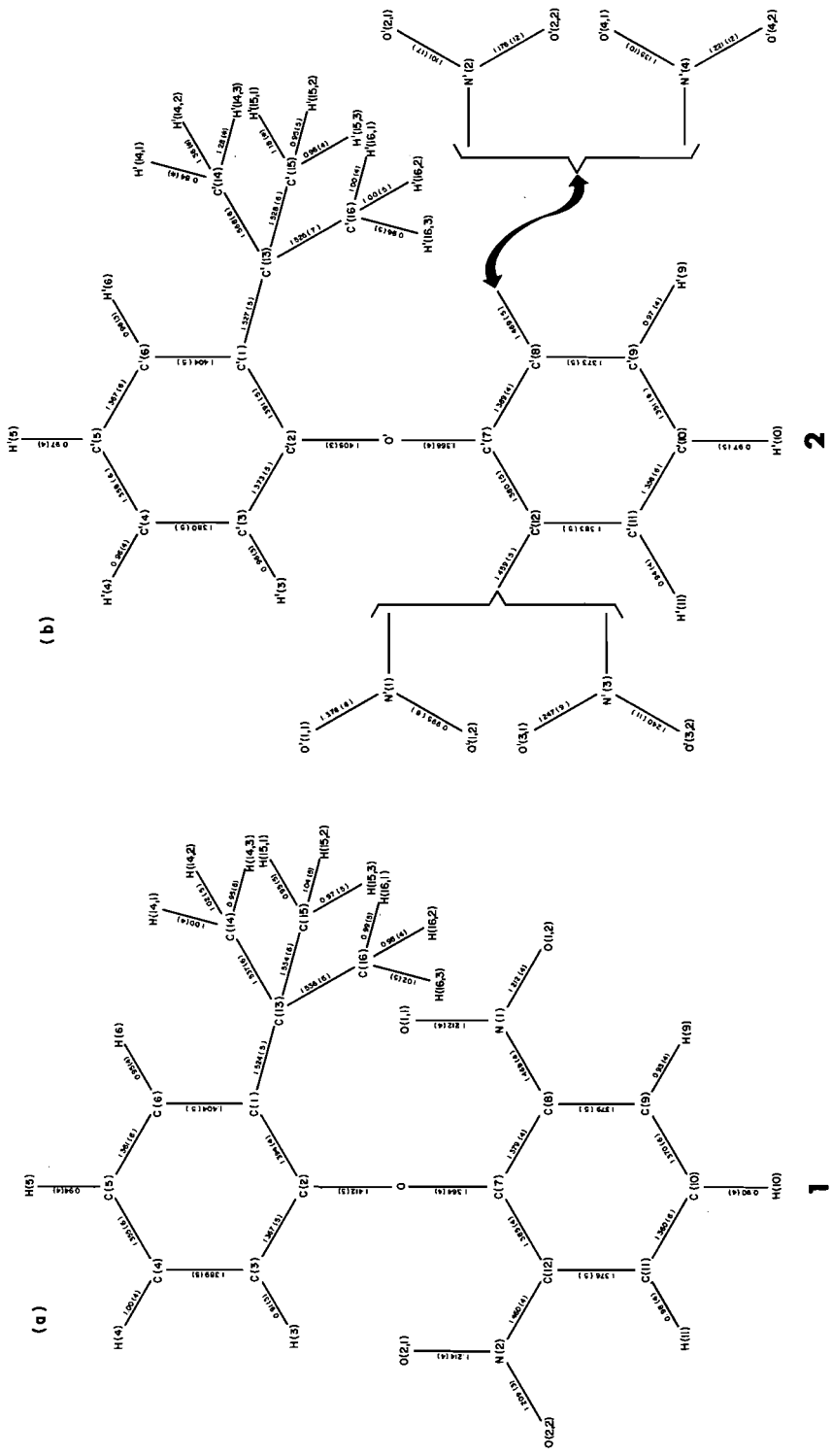

FIG. 1. (*a*) Bond lengths (Å) and atom labeling in molecule **1**. (*b*) Bond lengths (Å) and atom labeling in molecule **2**. The numbers in parentheses are the estimated standard deviations in the bond lengths. The asterisks indicate that the estimated standard deviation of the bond length was not determined.

TABLE 1. Structural parameters (e.s.d.'s) for 2-(2′,6′-dinitrophenoxy)-*t*-butylbenzene

(*a* Fractional atomic coordinates ($\times 10^4$) and thermal parameters U_{ij} ($\times 10^3$), t.f. = exp $\{-2\pi^2(a^{*2}h^2U_{11} + \ldots + 2a^*b^*hkU_{12} + \ldots)\}$

Atom	*x*	*y*	*z*	U_{11}	U_{22}	U_{33}	U_{12}	U_{13}	U_{23}
Molecule **1**									
C(1)	3236(3)	3252(4)	949(2)	52(2)	71(3)	46(2)	15(2)	3(2)	5(2)
C(2)	3714(2)	1984(4)	943(1)	38(2)	68(3)	35(2)	4(2)	2(2)	−1(2)
C(3)	3291(3)	772(5)	762(2)	42(2)	76(3)	53(2)	6(2)	2(2)	−2(2)
C(4)	2327(3)	758(6)	574(2)	51(2)	100(4)	55(3)	−6(3)	3(2)	−4(3)
C(5)	1834(3)	1968(7)	574(2)	44(3)	132(5)	69(3)	2(3)	−4(2)	5(3)
C(6)	2264(3)	3166(6)	757(2)	51(3)	107(4)	64(3)	38(3)	3(2)	7(3)
C(7)	5210(2)	797(4)	1160(2)	38(2)	51(2)	51(2)	−2(2)	−6(2)	−3(2)
C(8)	5143(2)	−149(4)	1590(2)	42(2)	59(2)	63(3)	0(2)	1(2)	2(2)
C(9)	5739(3)	−1287(5)	1650(2)	75(3)	60(3)	74(3)	6(2)	−9(3)	8(3)
C(10)	6443(3)	−1457(5)	1281(2)	75(3)	70(3)	95(4)	35(3)	−8(3)	−8(3)
C(11)	6541(3)	−555(5)	850(2)	61(3)	81(3)	71(3)	18(2)	0(2)	−13(3)
C(12)	5908(2)	537(5)	787(2)	48(2)	57(2)	49(2)	−1(2)	2(2)	−6(2)
C(13)	3725(3)	4605(4)	1132(2)	77(3)	61(3)	65(3)	19(2)	5(2)	3(2)
C(14)	4151(5)	4498(6)	1743(2)	110(4)	76(4)	85(4)	19(4)	−16(3)	−19(3)
C(15)	4513(5)	4974(7)	738(3)	108(4)	69(4)	112(5)	−3(4)	24(4)	10(4)
C(16)	3008(6)	5815(7)	1116(3)	125(5)	80(4)	113(5)	47(4)	−3(4)	−2(4)
N(1)	4432(2)	58(5)	2010(2)	55(2)	98(3)	63(2)	0(2)	2(2)	24(2)
N(2)	5985(3)	1453(4)	304(2)	62(2)	75(2)	62(2)	−6(2)	12(2)	−10(2)
O	4703(2)	2004(2)	1113(1)	40(1)	54(2)	61(2)	7(1)	−4(1)	−2(1)
O(1,1)	4327(3)	1210(4)	2198(2)	109(3)	113(3)	80(2)	24(2)	37(2)	2(2)
O(1,2)	4011(2)	−970(4)	2153(2)	83(2)	136(3)	120(3)	−18(2)	23(2)	51(3)
O(2,1)	5251(2)	1721(3)	22(1)	82(2)	103(3)	67(2)	−2(2)	0(2)	16(2)
O(2,2)	6777(2)	1839(4)	197(2)	79(2)	131(3)	101(3)	−30(2)	30(2)	2(2)
Molecule **2**									
C′(1)	1690(3)	8247(4)	3641(2)	50(2)	65(3)	71(3)	−12(2)	−2(2)	15(2)
C′(2)	1151(2)	7136(4)	3422(2)	39(2)	63(3)	65(3)	−2(2)	5(2)	12(2)
C′(3)	1497(3)	6180(5)	3059(2)	57(3)	73(3)	70(3)	4(2)	9(2)	−1(3)
C′(4)	2427(3)	6284(6)	2897(2)	62(3)	103(4)	76(3)	22(3)	23(3)	27(3)
C′(5)	2980(3)	7353(6)	3102(2)	47(3)	115(4)	84(4)	8(3)	13(3)	47(3)
C′(6)	2627(3)	8303(6)	3460(2)	55(3)	83(3)	88(3)	−20(3)	−8(3)	26(3)
C′(7)	−352(2)	5931(4)	3415(2)	38(2)	65(2)	57(2)	−7(2)	7(2)	−9(2)
C′(8)	−1088(3)	6102(4)	2999(2)	55(2)	65(3)	60(3)	−3(2)	3(2)	8(2)
C′(9)	−1735(3)	5066(5)	2861(2)	59(3)	89(4)	71(3)	−8(3)	−7(2)	−8(3)
C′(10)	−1660(4)	3827(6)	3124(2)	76(3)	80(4)	88(4)	−18(3)	1(3)	−20(3)
C′(11)	−953(4)	3622(5)	3535(2)	95(4)	51(3)	93(4)	−3(3)	12(3)	−1(3)
C′(12)	−306(3)	4666(4)	3685(2)	56(2)	53(3)	71(3)	6(2)	−1(2)	1(2)
C′(13)	1305(4)	9305(5)	4046(2)	81(3)	68(3)	102(4)	−24(3)	−1(3)	−14(3)

TABLE 1 (*Concluded*)

Atom	x	y	z	U_{11}	U_{22}	U_{33}	U_{12}	U_{13}	U_{23}
C′(14)	405(4)	10041(5)	3751(3)	120(4)	72(3)	161(5)	15(3)	−2(4)	−25(4)
C′(15)	2051(6)	10424(9)	4202(4)	132(6)	119(6)	171(7)	−64(5)	21(6)	−45(6)
C′(16)	1044(5)	8614(7)	4592(3)	87(4)	109(5)	92(4)	−10(4)	13(3)	−27(4)
N′(1)	404(4)	4415(6)	4152(2)	102(4)	85(4)	108(4)	26(3)	−36(3)	7(3)
N′(2)	−1192(4)	7409(5)	2685(2)	87(3)	90(3)	91(3)	−3(3)	−9(3)	20(3)
O′	207(2)	7031(3)	3591(1)	42(1)	67(2)	77(2)	−8(1)	11(1)	−15(2)
O′(1,1)	1(6)	3560(9)	4536(3)	120(6)	176(8)	117(6)	−38(6)	−32(5)	92(6)
O′(1,2)	1077(7)	4755(16)	4210(6)	50(5)	186(15)	133(9)	−36(7)	−25(5)	86(10)
O′(2,1)	−576(13)	8118(21)	2668(8)	248(19)	179(16)	254(17)	−99(14)	−172(19)	134(13)
O′(2,2)	−1934(10)	7992(18)	2670(8)	139(11)	172(13)	307(18)	111(11)	127(12)	149(24)
O′(3,1)	1006(8)	3487(9)	4081(5)	113(7)	89(6)	209(10)	31(6)	−55(6)	9(7)
O′(3,2)	670(10)	5392(11)	4463(5)	144(10)	105(7)	141(9)	27(6)	−83(7)	−15(6)
O′(4,1)	−471(8)	7955(15)	2523(5)	93(7)	113(9)	148(9)	22(7)	80(7)	68(7)
O′(4,2)	−1905(9)	7639(18)	2445(7)	138(11)	164(11)	263(15)	−32(9)	−153(12)	88(11)

(*b*) Fractional atomic coordinates ($\times 10^3$) and isotropic temperature factors for the hydrogen atoms

Atom	x	y	z	B (Å^2)	Atom	x	y	z	B (Å^2)
Molecule **1**					Molecule **2**				
H(3)	361(2)	−5(3)	78(1)	3(1)	H′(3)	112(2)	549(3)	290(2)	4(1)
H(4)	204(3)	−14(4)	45(2)	7(1)	H′(4)	264(3)	563(5)	263(2)	9(2)
H(5)	119(3)	196(4)	42(2)	7(1)	H′(5)	363(3)	743(4)	299(2)	7(1)
H(6)	193(3)	402(4)	79(2)	6(1)	H′(6)	298(3)	909(4)	361(2)	5(1)
H(9)	562(3)	−190(4)	194(2)	6(1)	H′(9)	−221(3)	531(4)	257(2)	7(1)
H(10)	680(3)	−222(4)	133(2)	6(1)	H′(10)	−210(3)	310(5)	300(2)	10(2)
H(11)	704(3)	−62(5)	58(2)	9(2)	H′(11)	−88(3)	280(4)	375(2)	7(1)
H(14,1)	467(3)	380(5)	178(2)	8(1)	H′(14,1)	22(*)	1060(*)	399(*)	8(*)
H(14,2)	362(4)	418(5)	199(2)	11(2)	H′(14,2)	92(*)	1072(*)	337(*)	8(*)
H(14,3)	437(3)	538(5)	187(2)	9(2)	H′(14,3)	−20(*)	910(*)	360(*)	8(*)
H(15,1)	500(3)	429(5)	74(2)	9(2)	H′(15,1)	242(*)	1087(*)	381(*)	11(*)
H(15,2)	420(3)	502(5)	33(2)	10(2)	H′(15,2)	176(4)	1103(6)	445(3)	10(2)
H(15,3)	475(4)	589(6)	83(2)	11(2)	H′(15,3)	264(3)	1004(5)	436(2)	9(2)
H(16,1)	247(4)	559(5)	136(2)	10(2)	H′(16,1)	50(3)	795(5)	452(2)	9(2)
H(16,2)	334(3)	667(5)	124(2)	7(2)	H′(16,2)	160(4)	809(6)	478(2)	12(2)
H(16,3)	273(3)	598(5)	72(2)	10(2)	H′(16,3)	86(3)	932(5)	485(2)	9(2)

*Errors were not calculated for these hydrogen atoms.

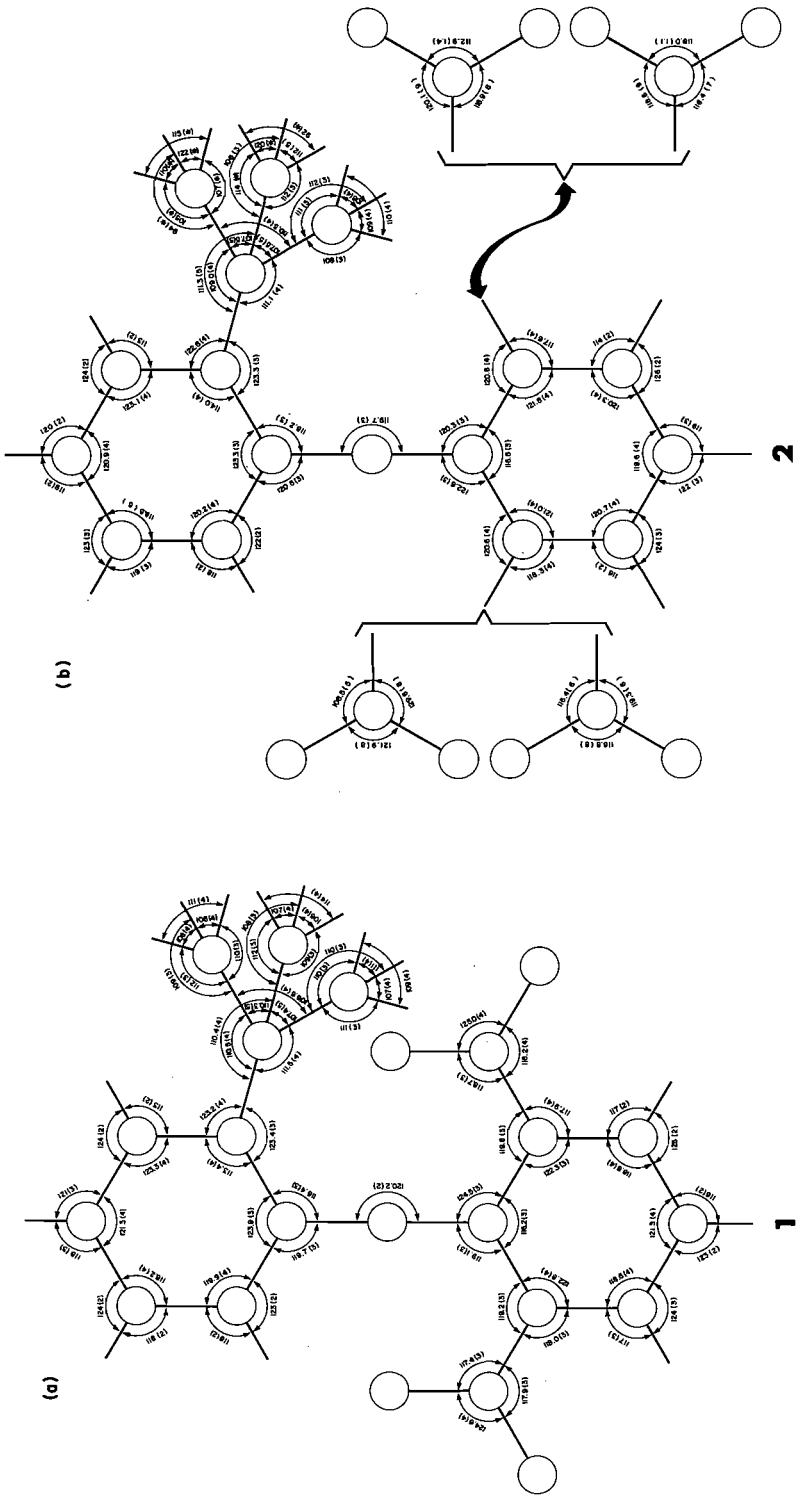

FIG. 2. (*a*) Bond angles (deg) in molecule **1**. (*b*) Bond angles (deg) in molecule **2**. The numbers in parentheses are estimated standard deviations in the angles. The asterisks indicate that the estimated standard deviation of the angle was not determined.

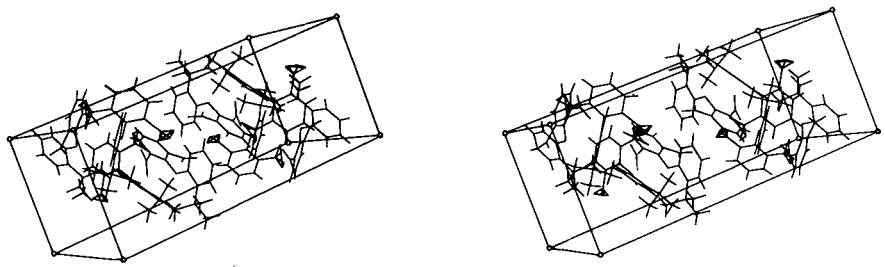

FIG. 3. Stereoscopic view of the molecular packing. The *a* axis points out of the paper, the *b* axis points up, and the *c* axis points to the lower left.

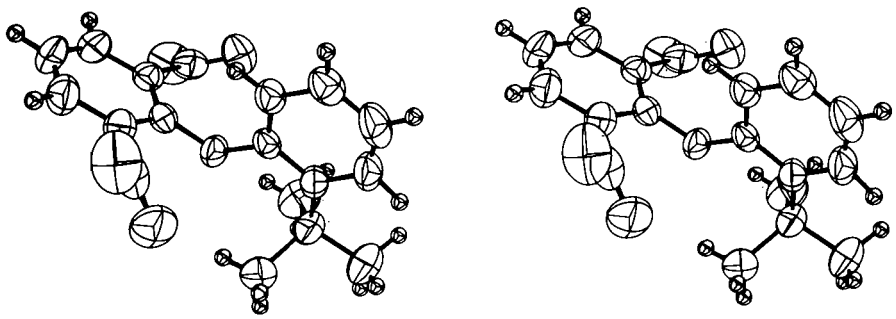

FIG. 4. Stereogram of molecule **1**. The thermal ellipsoids are scaled to include 50% probability.

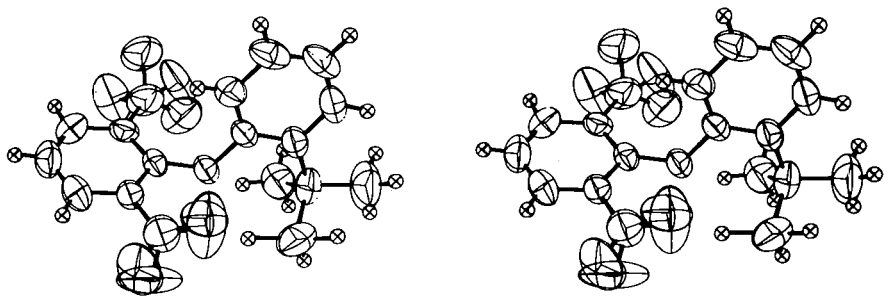

FIG. 5. Stereogram of molecule **2**. The thermal ellipsoids of the disordered nitro oxygen atoms are superimposed.

distances varying from 0.90 to 1.05 Å. The four hydrogen atoms in question, H′(14,1), H′(14,2), H′(14,3), and H′(15,1), are those whose coordinates were not refined by least squares. The difficulty in placing these hydrogen atoms and the abnormal C—H bond lengths, marked by an asterisk in Fig. 2, are presumably related to the high values of the anisotropic thermal parameters for those carbon atoms as shown in Table 1.

A stereoscopic view of the molecular packing is shown in Fig. 3. The packing diagram suggests that the molecules pack in loosely associated pairs, with the *t*-butyl-substituted ring of molecule **2** lying roughly parallel and relatively close to the dinitro-substituted ring of molecule **1**.

Stereoscopic views of the conformation of molecule **1** and molecule **2** are shown in Figs. 4 and 5 respectively. The large ellipsoids of the terminal *t*-butyl carbon atoms are evident in the stereograms. Also the thermal ellipsoids of the nitro oxygen atoms on molecule **2** clearly suggest that those nitro substituents may be undergoing hindered rotation about the C—N bonds.

Table 2 shows the dihedral angles between

TABLE 2. Least-squares planes

(*a*) Coefficients of planes $Ax + By + Cz = D$. The coordinates refer to the directions of the ***a***, ***c***xa***, and ***c****** axes. The planes are defined in Fig. 6

Plane	*A*	*B*	*C*	*D*
Molecule **1**				
1	0.3147	0.1882	−0.9304	−0.1374
2	0.2845	0.0799	−0.9554	−0.5559
3	−0.6009	−0.5481	−0.5819	−6.2702
4	−0.6827	0.1768	−0.7090	−7.3781
5	0.1527	−0.8260	−0.5426	−0.2822
Molecule **2**				
1	−0.2724	0.5634	−0.7800	−2.7466
2	−0.2808	0.5160	−0.8093	−3.3213
3	0.6488	−0.3353	−0.6831	−8.1372
4	0.3541	−0.8011	−0.4826	−8.2062
5	−0.0023	−0.0650	−0.9979	−6.8248
6	0.3603	0.4949	−0.7908	−5.7239
7	0.1760	−0.7808	−9.5995	−9.7753

(*b*) Angles between normals to planes

	Angle (deg)	
Planes	Molecule **1**	Molecule **2**
1,2	6.6	3.2
2,3	70.1	78.6
1,3	75.6	80.4
3,4	47.4	34.1
3,5	43.5	45.5
3,6		57.8
3,7		38.2
4,6		83.5
5,7		49.6

the planes of the two molecules. The planes are labeled in Fig. 6. The dihedral angles 1,2 and 2,3 and the conformations as shown in Figs. 4 and 5 clearly indicate that the conformation is skew-*t*-butyl-*distal*, in contrast to the predictions made by other workers (7, 8). These latter conclusions were based in part on the observation of a large chemical shift for the H(6) hydrogen atom. It seems quite clear that this shielding arises from its proximity to the *other* ring rather than a *proximal* nitro group as has been suggested by Lehmann (7). It also seems quite clear that the dipole moment method of predicting conformations of bridged diphenyls is somewhat unreliable since this was the method used originally to assess the conformation (7, 8).

The conformation determined for both molecules indicates that the steric effects of the *ortho* substituents are more important than mesomeric electronic effects in determining the conformations of bridged diphenyls. However, Fig. 1 shows that the O—C bond lengths to the dinitro-substituted ring are 0.048(7) and 0.039(7) Å shorter than the O—C bond length to the *t*-butyl-substituted ring on molecules **1** and **2** respectively. These values are approximately one-half those observed for rings containing two electron-withdrawing substituents where steric factors allow the electron-withdrawing ring to be coplanar with the central plane. The angles of 70.1° and 78.6° between the normals to planes 2 and 3 in the two molecules hardly allow for any significant conjugation effects even if the unshared electron pair on the oxygen atom is in a nonpure p orbital. In both of the two independent molecules the angles ϕ[C(7)—O—C(2)—C(3)] and ψ[C(2)—O—C(7)—C(8)] occur in (+ +) pairs in one enantiomer and (− −) pairs in the other, as would be expected.

The structures of the two independent mole-

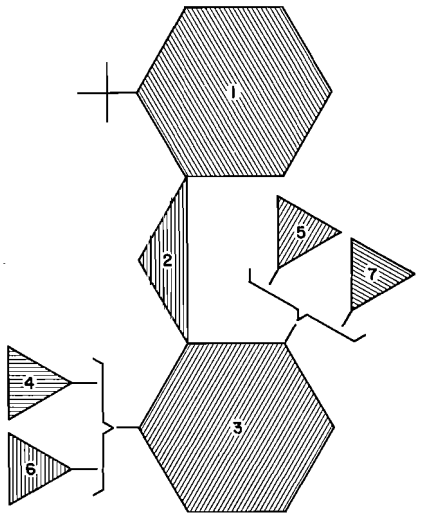

FIG. 6. Numbering of the molecular planes. The planes labeled 6 and 7 appear only in molecule **2**.

cules show deviations from idealized geometry which are consistent with observations made earlier. The internal ring angles at the carbon atoms bonded to the electron-donating *t*-butyl group are 113.4(4)° and 114.0(4)°. The internal ring angles at the carbon atoms bonded to the electron-withdrawing nitro groups average 122°. The internal ring angles at C(2) are *ca.* 3.5° greater than 120° and *ca.* 3.5° less than 120° at C(7). The *t*-butyl-substituted ring is bent 1.6° and 2.2° away from the dinitro-substituted ring. The *t*-butyl terminal carbon atom lying closest to the plane of the phenyl ring bearing the *t*-butyl substituent is rotated through a torsional angle of 3.5° about the C(1)—C(13) bond towards the *proximal* nitro group from the plane of the phenyl ring in molecule **1** and 2.0° away from the *proximal* nitro group in molecule **2**.

This research was supported by grants from the National Research Council of Canada.

1. E. A. H. GRIFFITH, W. D. CHANDLER, and B. E. ROBERTSON. Can. J. Chem. **50**, 2963 (1972).
2. E. A. H. GRIFFITH, W. D. CHANDLER, and B. E. ROBERTSON. Can. J. Chem. **50**, 2972 (1972).
3. E. A. H. GRIFFITH, W. D. CHANDLER, and B. E. ROBERTSON. Can. J. Chem. **50**, 2979 (1972).
4. S. P. N. VAN DER HEIJDEN, E. A. H. GRIFFITH, W. D. CHANDLER, and B. E. ROBERTSON. Can. J. Chem. **53**, 2084 (1975).
5. J. J. BERGMAN. E. A. H. GRIFFITH, B. E. ROBERTSON, and W. D. CHANDLER. Can. J. Chem. **51**, 162 (1973).
6. G. MONTAUDO, P. FINOCCHIARO, E. TRIVELLONE, F. BOTTINO, and R. MARAVIGNA. Tetrahedron, **27**, 2125 (1971).
7. P. A. LEHMANN F. Org. Magn. Reson. **2**, 467 (1970).
8. P. A. LEHMANN F. and D. M. MCEACHERN B. J. Mol. Struct. **7**, 277 (1971).
9. J. WRIGHT and E. G. JORGENSEN. J. Org. Chem. **33**, 1245 (1968).
10. J. J. BERGMAN. Ph.D. Thesis, University of Regina, Regina, Saskatchewan. 1971.
11. D. T. CROMER and J. B. MANN. Acta Cryst. A**24**, 321 (1969).
12. R. F. STEWART, E. R. DAVIDSON, and W. T. SIMPSON. J. Chem. Phys. **42**, 3175 (1965).
13. G. GERMAIN and M. M. WOOLFSON. Acta Cryst. B**24**, 31 (1968).
14. W. R. BUSING, K. O. MARTIN, and H. A. LEVY. ORFLS, Report ORNL-TM-305. Oak Ridge National Laboratory, Oak Ridge, Tennessee. 1962.
15. C. K. JOHNSON. ORTEP, Report ORNL-3794. Oak Ridge National Laboratory, Oak Ridge, Tennessee. 1965.

Conformations of Bridged Diphenyls. IX. Crystal Structure of 2-(4′-Carbomethoxy-2′-nitrothiophenyl)-1,3,5-trimethylbenzene

SIMON P. N. VAN DER HEIJDEN, W. DAVID CHANDLER, AND BEVERLY E. ROBERTSON[1]

Faculty of Science, University of Regina, Regina, Saskatchewan S4S 0A2

Received November 22, 1974

SIMON P. N. VAN DER HEIJDEN, W. DAVID CHANDLER, and BEVERLY E. ROBERTSON. Can. J. Chem. **53**, 2102 (1975).

The structure of 2-(4′-carbomethoxy-2′-nitrothiophenyl)-1,3,5-trimethylbenzene, $C_{17}H_{17}NO_4S$, has been determined by X-ray diffraction. The crystals are monoclinic, $a = 18.616(15)$, $b = 5.739(8)$, $c = 15.712(14)$ Å, $\beta = 101.97(3)°$, $P2_1/c$ with $Z = 4$. The intensities of 3820 independent reflections were measured on a four circle diffractometer; 2825 reflections were used in the refinement of the structure to give a final least-squares weighted residual of 0.059 and a traditional R factor of 0.054. The presence of electron-withdrawing groups on one of the phenyl rings increases the conjugation between the ring and the sulfur atom in a similar manner as that observed in diphenyl ethers. The mesityl ring is nearly orthogonal to the C—S—C plane.

SIMON P. N. VAN DER HEIJDEN, W. DAVID CHANDLER et BEVERLY E. ROBERTSON. Can. J. Chem. **53**, 2102 (1975).

On a déterminé la structure cristalline du (carbométhoxy-4′ nitro-2′ thiophényl)-2 triméthyl-1,3,5 benzène, $C_{17}H_{17}NO_4S$, par diffraction de rayons-X. Les cristaux sont monocliniques, $a = 18.616(15)$, $b = 5.739(8)$, $c = 15.712(14)$ Å, $\beta = 101.97(3)°$, $P2_1/c$ avec $Z = 4$. On a mésure les intensités de 3820 réflexions indépendantes à l'aide d'un diffractomètre à quatre cercles. On a utilisé 2825 de ces réflexions pour affiner la structure jusqu'à une valeur de R pondérée de 0.059 et une valeur de R conventionnelle de 0.054. La présence de groupes électroaffinitaires sur un des groupes phényle augmente, d'une façon similaire à celle observée dans les diphényl éthers, la conjugaison entre le cycle et l'atome de soufre. Le cycle mésityle est presque perpendiculaire au plan C—S—C. [Traduit par le journal]

Introduction

This is the first study in this series of a compound having an atom other than oxygen as a bridging atom. From previous studies on diphenyl ethers it has been shown that the conformation for this type of compound is in general determined by steric rather than electronic effects (1–5). In order to be able to describe changes in conformation due to changes in the bridging group the compound chosen is identically substituted to one of the diphenyl ethers (4) studied previously.

Few crystallographic studies of diphenyl sulfides are reported in the literature (6–8) and none of these carried any *ortho* substituents. Both di-*p*-tolyl sulfide (6) and di-*p*-bromophenyl sulfide (7) show a twist conformation, while 4-dimethylaminodiphenyl sulfide (8) is a skew conformation with the *ortho* hydrogen of the substituted ring *proximal, i.e.* the unsubstituted ring is coplanar with the central C—S—C plane and almost perpendicular to the substituted ring. The nomenclature used here has been defined earlier (4).

Experimental

The synthesis of 2-(4′-carbomethoxy-2′-nitrothiophenyl)-1,3,5-trimethylbenzene, $C_{17}H_{17}NO_4S$, has been reported earlier (9). It was recrystallized from 95% ethanol, m.p. 125–126 °C. A sample with well-defined faces and approximate dimensions of $0.6 \times 0.4 \times 0.5$ mm (mounted with the long axis parallel to the fiber axis) was used for data collection. The systematic absences ($h0l$, $l = 2n + 1$; $0k0$, $k = 2n + 1$) and the Laue symmetry ($2/m$) as determined by film methods gave the space group $P2_1/c$.

The intensity data were collected on a Picker FACS I automated diffractometer using monochromatic MoKα radiation (graphite monochromator). The θ–2θ scan mode was used with a scan rate of 1 deg min^{-1}, covering a minimum scan width of 3°, in 2θ. Background counts (40 s) were measured at each limit of the scan. The centered positions of 24 reflections with 2θ values between 35 and 45° as determined using MoKα_1 radiation were used to calculate the cell parameters. Twelve of these reflections were used to determine the orientation of the crystal on the diffractometer. The errors in the lattice constants are given as three times the estimated standard deviations

[1]Author to whom correspondence should be addressed.

Can. J. Chem. Downloaded from www.nrcresearchpress.com by 210.87.254.6 on 09/05/12
For personal use only.

Can. J. Chem. Downloaded from www.nrcresearchpress.com by 210.87.254.6 on 09/05/12
For personal use only.

given by the least-squares procedures. Errors in atomic coordinates and derived quantities will be presented as unmodified estimated standard deviations. The rationale for this convention has been presented earlier (4).

Crystal data are as follows:

$C_{17}H_{17}NO_4S$ f.w. = 331.39

Monoclinic, $P2_1/c$; $a = 18.616(15)$, $b = 5.739(8)$, $c = 15.712(14)$ Å, $\beta = 101.97(3)°$, $\rho_o = 1.36$ g cm^{-3} (flotation), $\rho_c = 1.34$ g cm^{-3}, $Z = 4$, $F(000) = 696e$, $\lambda(MoK\alpha_1) = 0.70926$ Å, $\mu(MoK\alpha) = 2.17$ cm^{-1}, $T = 22 \pm 2$ °C. The integrated intensities of 3820 independent reflections between 3.5 and 55° in 2θ were collected with MoKα radiation. The data were reduced to the observed structure factors using standard procedures. No corrections were made for the effects of extinction or absorption. The scattering factors for the nonhydrogen atoms were taken from Cromer and Mann (10). The scattering factors for the hydrogen atoms were taken from Stewart *et al.* (11). A Wilson statistical calculation gave an overall temperature factor of 3.52 Å^2. The 447 reflections with $|E| > 1.58$ were used to solve the structure by the logical symbolic addition method.[2] An *E*-map calculated from the solution with the highest figures of merit, yielded all nonhydrogen positions. The weighted residual, R_w, of the full-matrix least squares was lowered to 0.109, using individual anisotropic temperature factors and unit weights. The weighted residual is defined as: $R_w = \{\Sigma w(|F_o| - |F_c|)^2 / \Sigma w|F_o|^2\}^{1/2}$. The least-squares process minimizes R_w^2. A difference Fourier map at this point revealed all hydrogen atom positions; 2825 reflections, for which $|F_o| > 1.0w^{-1/2}$, were used in the final refinement cycles using full-matrix least squares and weights calculated from $w^{-1/2} = 0.7042 - 0.01168|F_o| + 0.000360|F_o|^2$. The final values of R_w and the conventional R factor were 0.059 and 0.054 respectively. The final observed and calculated structure factors have been placed in the Depository of Unpublished Data.[3] The final positional and thermal parameters are given in Table 1 with estimated standard deviations. The bond lengths and angles and the atomic numbering are given in Figs. 1 and 2.

Discussion

The dihedral angles between the planes labeled in Fig. 3 are given in Table 2. The sulfide, 2-(4′-carbomethoxy-2′-nitrothiophenyl)-1,3,5-trimethylbenzene has a skew-nitro-*distal* conformation similar to that observed for the corresponding ether (4), in agreement with p.m.r. studies of the same compound (9). The notation used here has been introduced earlier (4). The conformation is also similar to that of 4-dimethylaminodiphenyl sulfide (8) where the dimethylamine-substituted ring is 7.8° from being orthogonal to the C—S—C plane compared with an angle of 3.6° here for the mesityl ring. The unsubstituted ring in the former is 4.9° from being coplanar with the C—S—C plane compared with 4.2° here for the nitro-substituted ring.

In both cases the ring bearing the electron-donating substituents is nearly perpendicular to the C—S—C plane. We have shown that in the case of diphenyl ethers, steric factors associated with the *ortho* substituents may make this conformation (*i.e.* coplanarity of the C—O—C plane with the plane of the electron-withdrawing side of the molecule) unfavorable. The conformation of diphenyl ethers and sulfides suggests, however, that in the absence of steric hindrances, the conjugation effect leads to this particular skew conformation, despite the tendency to the twist conformation for unsubstituted or symmetrically substituted compounds. The torsional angles φ[C(9)—S—C(1)—C(6)] and ψ[C(1)—S—C(9)—C(10)] occur in (+ +) pairs in one enantiomer and (− −) pairs in the other, as would be expected.

The structures of both 2-(4′-carbomethoxy-2′-nitrothiophenyl)-1,3,5-trimethylbenzene and 4-dimethylaminodiphenyl sulfide show C—S bonds from the electron-withdrawing ring shorter (0.026(4) and 0.017(11) Å) than C—S bonds from the other ring. This effect was also observed for the diphenyl ethers but the differences are smaller in the sulfides. The average C—S bond length, 1.772 Å, is shorter than the sum of Pauling single bond covalent radii of 1.812 Å (16). The C—S—C bond angle of 102.9(1)° is slightly smaller than the values observed for other diphenyl sulfides (6, 8) but is within the range observed for C—S—C bonds.

The nitro-substituted ring appears to be bent 0.6(2)° towards the mesityl ring. The value of the bending is calculated from [∠(S—C(1)—C(2)) − ∠(S—C(1)—C(6))]/2. The direction of the bending is opposite from that observed in the corresponding ether (4). However, because of the fact that the C—S bonds are *ca.* 0.40 Å longer than the C—O bonds, the *proximal* hydrogen atom, H(6), remains 2.38 Å from the plane of the mesityl ring which is not significantly different from 2.43 Å in the ether despite the op-

[2]The structure was solved using the Germain and Woolfson program LSAM (12). All Fourier calculations were carried out with the Zalkin program FORDAP (13). The Busing *et al.* program ORFLS (14) was used for least-squares refinement. Stereograms were prepared with the aid of the Johnson program ORTEP (15).

[3]Complete set of tabular data is available, at a nominal charge, from the Depository of Unpublished Data, CISTI, National Research Council of Canada, Ottawa, Canada K1A 0S2.

Can. J. Chem. Downloaded from www.nrcresearchpress.com by 210.87.254.6 on 09/05/12
For personal use only.

TABLE 1. Structural parameters (e.s.d.'s) for 2-(4′-carbomethoxy-2′-nitrothiophenyl)-1,3,5-trimethylbenzene

(*a*) Fractional atomic coordinates ($\times 10^4$) and thermal parameters U_{ij} ($\times 10^3$), t.f. = exp $\{-2\pi^2(a^{*2}h^2U_{11} + ... + 2a^*b^*hkU_{12} + ...)\}$

Atom	x	y	z	U_{11}	U_{22}	U_{33}	U_{12}	U_{13}	U_{23}
C(1)	2265(2)	2287(5)	−48(2)	39(1)	40(2)	39(1)	3(1)	5(1)	−2(1)
C(2)	1829(2)	1669(5)	−858(2)	45(2)	44(2)	42(2)	3(1)	8(1)	−9(1)
C(3)	1196(2)	2842(5)	−1228(2)	45(2)	54(2)	41(2)	1(2)	−1(1)	−9(1)
C(4)	968(2)	4717(5)	−805(2)	45(2)	48(2)	46(2)	5(1)	4(1)	−2(1)
C(5)	1388(2)	5387(6)	−4(2)	53(2)	53(2)	52(2)	15(2)	3(1)	−12(2)
C(6)	2017(2)	4205(6)	360(2)	52(2)	54(2)	41(2)	10(2)	−2(1)	−12(2)
C(7)	278(2)	5938(6)	−1231(2)	48(2)	58(2)	52(2)	8(2)	2(1)	−1(2)
C(8)	−484(3)	9192(9)	−1177(3)	74(3)	85(3)	76(3)	40(3)	−2(2)	−2(3)
C(9)	3418(2)	2441(5)	1384(2)	40(1)	43(2)	36(1)	9(1)	3(1)	−1(1)
C(10)	3897(2)	4301(5)	1341(2)	46(2)	44(2)	39(1)	8(1)	13(1)	5(1)
C(11)	4214(2)	5404(5)	2110(2)	47(2)	54(2)	53(2)	−8(2)	15(1)	−5(2)
C(12)	4072(2)	4747(6)	2907(2)	47(2)	60(2)	42(2)	0(2)	6(1)	−8(2)
C(13)	3587(2)	2916(6)	2921(2)	51(2)	63(2)	36(2)	4(2)	10(1)	2(2)
C(14)	3249(2)	1746(5)	2173(2)	41(2)	46(2)	44(2)	2(1)	10(1)	2(2)
C(15)	4061(2)	5123(7)	495(2)	76(3)	63(2)	47(2)	5(2)	22(2)	11(2)
C(16)	4421(3)	5985(10)	3731(3)	82(3)	105(4)	53(2)	−22(3)	9(2)	−26(2)
C(17)	2710(2)	−168(7)	2230(3)	71(2)	67(2)	64(2)	−19(2)	16(2)	7(2)
N	2038(2)	−293(5)	−1351(2)	58(2)	70(2)	54(2)	13(2)	0(1)	−27(2)
O(1)	2527(2)	−1572(4)	−1005(2)	85(2)	62(2)	61(2)	26(1)	2(1)	−19(1)
O(2)	1727(2)	−519(7)	−2098(2)	138(3)	194(4)	91(2)	100(3)	−59(2)	−95(3)
O(3)	−117(2)	5288(5)	−1884(2)	70(2)	79(2)	79(2)	21(2)	−28(1)	−20(2)
O(4)	164(1)	7852(4)	−804(2)	66(2)	74(2)	62(2)	32(1)	−7(1)	−14(1)
S	3069(1)	775(2)	429(1)	51(1)	47(1)	41(1)	15(1)	1(1)	−7(1)

(*b*) Fractional atomic coordinates ($\times 10^3$) and isotropic temperature factors for the hydrogen atoms

Atom	x	y	z	B (Å^2)
H(3)	94(2)	237(5)	−176(2)	4(1)
H(5)	122(2)	671(6)	28(2)	4(1)
H(6)	228(2)	462(5)	92(2)	4(1)
H(11)	454(2)	663(6)	209(2)	4(1)
H(13)	350(2)	242(6)	348(2)	5(1)
H(8,1)	−43(2)	998(7)	−172(3)	9(1)
H(8,2)	−56(3)	1015(10)	−78(3)	11(2)
H(8,3)	−88(3)	821(9)	−133(3)	9(2)
H(15,1)	441(2)	636(8)	59(3)	8(1)
H(15,2)	365(2)	569(6)	11(2)	6(1)
H(15,3)	424(2)	393(7)	19(3)	7(1)
H(16,1)	431(3)	761(11)	365(4)	13(2)
H(16,2)	493(3)	586(9)	383(3)	11(2)
H(16,3)	426(3)	545(9)	420(3)	11(2)

Can. J. Chem. Downloaded from www.nrcresearchpress.com by 210.87.254.6 on 09/05/12
For personal use only.

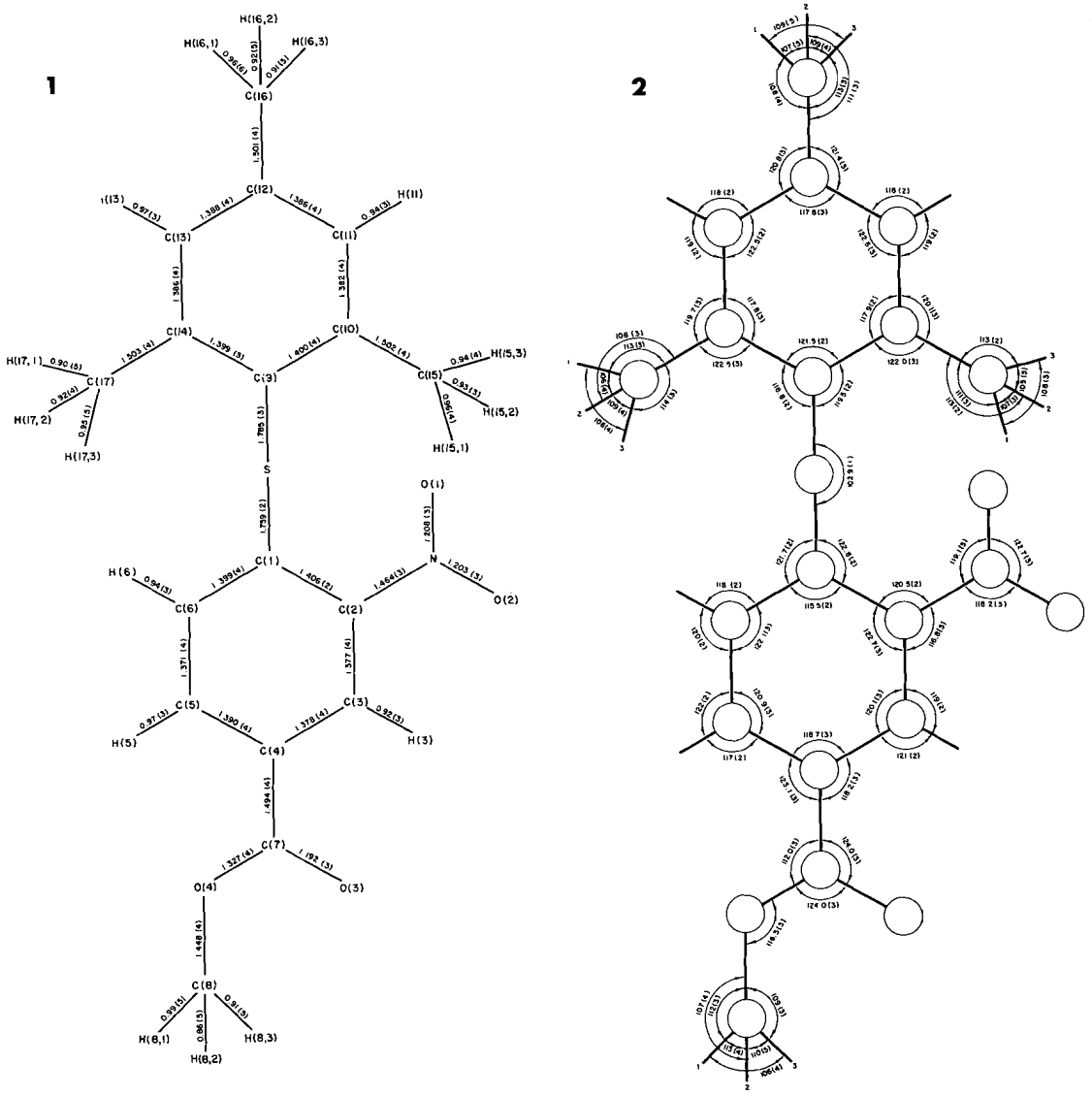

FIG. 1. Bond lengths and atom numbering. The numbers in parentheses are the estimated errors based on the errors in Table 1 and the errors in the lattice constants.

FIG. 2. Bond angles. The numbers in parentheses are the estimated errors.

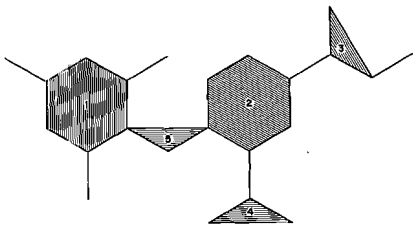

FIG. 3. Labeling of the least-squares planes.

posite sign of the bending. The repulsion between the *proximal* atom H(6) and the mesityl ring is counteracted by the contact between the *distal ortho*-nitro group and the sulfur atom. The S—O(1) distance is 2.639(4) Å. Since there is no bulky substituent in the *distal ortho* position of the unsubstituted ring in 4-dimethylaminodiphenyl sulfide, the phenyl ring is bent away by 4.0° from the substituted ring. A bending of 4.2°

TABLE 2. Least-squares planes

(*a*) Equations of planes $Ax + By + Cz = D$. Coordinates refer to the directions of the *a*, *c*xa*, and *c** axes. The planes are defined in Fig. 3

Plane	*A*	*B*	*C*	*D*
1	−0.7538	0.6441	−0.1302	−3.8218
2	0.6412	0.6134	−0.4612	3.5556
3	0.6537	0.5312	−0.5389	3.4312
4	0.7455	0.6022	−0.2856	3.6484
5	0.6453	0.5636	−0.5157	3.5083

(*b*) Dihedral angles

Planes	Angle (deg)
1,2	88.4
1,5	86.8
2,3	6.5
2,4	11.7
2,5	4.2

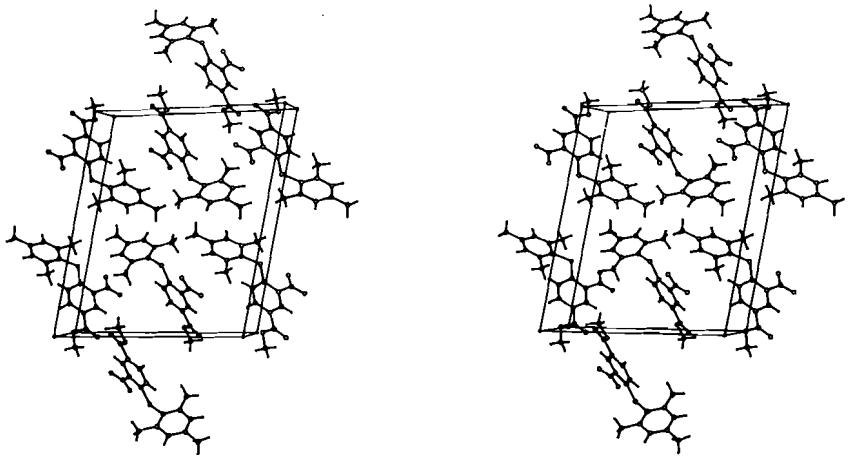

FIG. 4. Stereoscopic view of the molecular packing.

has also been observed for the skew conformation of 2-(3′-methyl-4′-nitrophenoxy)-1,3-diisopropylbenzene (1) which also lacks a bulky *ortho* substituent in the *distal ortho* position.

The longer C—S bonds also require the *ortho*-nitro group to twist only through 11.7° from coplanarity with the ring to which it is bonded in order to accommodate steric repulsion between the nitro oxygen atom and the sulfur atom. The O(1)—S distance is 2.64 Å which is similar to the O(1)—O distance of 2.66 Å in the identically substituted ether where the twist about the C—N bond is 36.7°.

All of the hydrogen atoms appear to be in reasonable positions. The bonds to hydrogen atoms range in length from 0.92(2) to 0.97(3) Å for the phenyl hydrogen atoms and from 0.86(5) to 0.96(6) Å for the methyl hydrogen atoms on the methyl group. The isotropic temperature factors range from 4(1) to 5(1) $Å^2$ for the phenyl hydrogen atoms and 7(1) to 13(2) $Å^2$ for the methyl hydrogen atoms. A stereoscopic view of the packing of the molecules is shown in Fig. 4. The packing of the molecules produces no unusually short intermolecular contacts.

A stereogram of details of the molecular con-

Can. J. Chem. Downloaded from www.nrcresearchpress.com by 210.87.254.6 on 09/05/12
For personal use only.

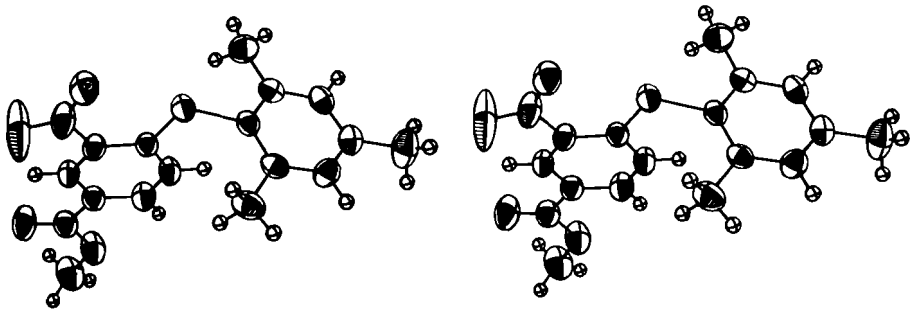

FIG. 5. Stereoscopic view of 2-(4′-carbomethoxy-2′-nitrothiophenyl)-1,3,5-trimethylbenzene. The thermal ellipsoids for the nonhydrogen atoms are drawn at the 50% probability level. The hydrogen atoms are given arbitrary temperature factors.

formation is shown in Fig. 5. The nitro oxygen atom further from the sulfur atom shows an anomalous thermal ellipsoid suggesting either large motion normal to the phenyl plane or disorder. Similar anomalous thermal ellipsoids have been observed previously in these compounds (1) but have not been satisfactorily explained.

This research was supported by grants from the National Research Council of Canada.

1. E. A. H. GRIFFITH, W. D. CHANDLER, and B. E. ROBERTSON. Can. J. Chem. **50**, 2963 (1972).
2. E. A. H. GRIFFITH, W. D. CHANDLER, and B. E. ROBERTSON. Can. J. Chem. **50**, 2972 (1972).
3. E. A. H. GRIFFITH, W. D. CHANDLER, and B. E. ROBERTSON. Can. J. Chem. **50**, 2979 (1972).
4. S. P. N. VAN DER HEIJDEN, E. A. H. GRIFFITH, W. D. CHANDLER, and B. E. ROBERTSON. Can. J. Chem. **53**, 2084 (1975).
5. K. GURTU, W. D. CHANDLER, and B. E. ROBERTSON. Can. J. Chem. **53**, 2093 (1975).
6. W. R. BLACKMORE and S. C. ABRAHAMS. Acta Cryst. **8**, 329 (1955).
7. J. TOUSSAINT. Bull. Soc. Chem. Belg. **54**, 319 (1945).
8. C. PANATTONI, G. BANDOLI, D. A. CLEMENT, A. DONDONI, and A. MANGINI. J. Cryst. Mol. Struct. **3**, 65 (1973).
9. H. BENJAMINS and W. D. CHANDLER. Can. J. Chem. **52**, 597 (1974).
10. D. T. CROMER and J. B. MANN. Acta Cryst. A**24**, 321 (1968).
11. R. F. STEWART, E. R. DAVIDSON, and W. T. SIMPSON. J. Chem. Phys. **42**, 3175 (1965).
12. G. GERMAIN and M. M. WOOLFSON. Acta Cryst. B**24**, 91 (1960).
13. A. ZALKIN. FORDAP, A Fortran program for Fourier calculations. University of California, Berkeley, California. 1965.
14. W. R. BUSING, K. O. MARTIN, and H. A. LEVY. ORFLS, Report ORNL-TM-305. Oak Ridge National Laboratory, Oak Ridge, Tennessee. 1962.
15. C. K. JOHNSON. ORTEP, Report ORNL-3794. Oak Ridge National Laboratory, Oak Ridge, Tennessee. 1965.
16. L. PAULING. The nature of the chemical bond. Cornell University Press, New York. 1960.

Can. J. Chem. Downloaded from www.nrcresearchpress.com by 210.87.254.6 on 09/05/12
For personal use only.

Conformations of Bridged Diphenyls. X. Crystal Structure of 2-(4′-Carbomethoxy-2′-nitrophenylsulfinyl)-1,3,5-trimethylbenzene

SIMON P. N. VAN DER HEIJDEN, W. DAVID CHANDLER, AND BEVERLY E. ROBERTSON[1]

Faculty of Science, University of Regina, Regina, Saskatchewan S4S 0A2

Received November 22, 1974

SIMON P. N. VAN DER HEIJDEN, W. DAVID CHANDLER, and BEVERLY E. ROBERTSON. Can. J. Chem. **53**, 2108 (1975).

The crystal structure of 2′-(4′-carbomethoxy-2′-nitrophenylsulfinyl)-1,3,5-trimethylbenzene, $C_{17}H_{17}NO_5S$, has been determined by X-ray diffraction. The crystals are triclinic, $a = 9.848(11)$, $b = 7.654(10)$, $c = 12.513(15)$ Å, $\alpha = 107.33(8)$, $\beta = 100.73(8)$, $\gamma = 106.53(8)°$, $P\bar{1}$ with $Z = 2$. The intensities of 3850 independent reflections were measured on a four circle diffractometer; 2985 reflections were used in the refinement to give a final least-squares residual of 0.053 and a traditional R factor of 0.052.

Repulsion between the sulfoxide oxygen atom and the nitro oxygen atoms forces the molecule into the twist-nitro-*proximal* conformation as opposed to the nitro-*distal* conformation which has been observed for other bridged diphenyls in this series.

SIMON P. N. VAN DER HEIJDEN, W. DAVID CHANDLER et BEVERLY E. ROBERTSON. Can. J. Chem. **53**, 2108 (1975).

On a déterminé la structure cristalline du (carbométhoxy-4′ nitro-2′ phénylsulfinyl)-2 triméthyl-1,3,5 benzène, $C_{17}H_{17}NO_5S$, par diffraction de rayons-X. Les cristaux sont tricliniques: $a = 9.848(11)$, $b = 7.654(10)$, $c = 12.513(15)$ Å, $\alpha = 107.33(8)$, $\beta = 100.73(8)$, $\gamma = 106.53(8)°$, $P\bar{1}$ avec $Z = 2$. On a mesuré les intensités de 3850 réflexions indépendantes à l'aide d'un diffractomètre à quatre cercles. On a utilisé 2985 de ces réflexions pour affiner la structure jusqu'à une valeur de R pondérée de 0.053 et une valeur de R conventionnelle de 0.052.

La répulsion entre l'atome d'oxygène du sulfoxyde et les atomes d'oxygène du groupe nitro force la molécule à adopter une conformation nitro-croisé "*proximal*" et ceci par opposition avec la conformation nitro-*distal* qui est observée pour d'autres diphényles pontés de cette série.

[Traduit par le journal]

Introduction

This is the third report in this series of studies by X-ray diffraction of the conformations of similarly substituted bridged diphenyl compounds, each with a different bridging group (1, 2). It is also the first structure reported in this series of a compound in which the bridging group is not a single atom (1–6). Based on p.m.r. studies of the shielding of ring currents within the molecule, the conformation of this compound has been predicted to be in the twist-nitro-*proximal* conformation (7). The nomenclature used here has been discussed earlier (1). This method for predicting conformations and also its validity have been discussed previously (8, 9). The conformation of diphenyl sulfoxide itself is reported to be butterfly (10).

Experimental

The synthesis of 2-(4′-carbomethoxy-2′-nitrophenylsulfinyl)-1,3,5-trimethylbenzene, $C_{17}H_{17}NO_5S$, has been reported earlier (7). It was recrystallized from absolute ethanol, m.p. 168–169 °C. A sample of approximate dimensions 0.41 × 0.32 × 0.36 mm was chosen for data collection.

The crystal was mounted on a Picker FACS 1 four circle automated diffractometer, equipped with a graphite monochromator. Twenty-four reflections with 2θ values between 35 and 45°, where the MoKα_1 and Kα_2 diffraction peaks were resolved, were used to calculate the cell constants by least squares. The estimated errors shown below are calculated as three times the estimated standard deviations given by the least-squares procedure. Errors in atomic coordinates and derived quantities will be presented as unmodified estimated standard deviations. The rationale for the convention has been presented earlier (1).

The crystal data are as follows:

$C_{17}H_{17}NO_5S$ f.w. = 347.39

Triclinic $P\bar{1}$; $a = 9.848(11)$, $b = 7.654(10)$, $c = 12.513(15)$ Å, $\alpha = 107.33(8)$, $\beta = 100.73(8)$, $\gamma = 106.53(8)°$, $\rho_o = 1.43$ g cm^{-3} (flotation), $\rho_c = 1.40$ g cm^{-3}, $Z = 2$, $F(000) = 364$e, $\lambda(\text{MoK}\alpha_1) = 0.70926$ Å, $\mu(\text{MoK}\alpha) = 2.24$ cm^{-1}, $T = 22 \pm 2$ °C. The angle settings of 12 reflections were used to determine the orientation of the crystal on the diffractometer. The integrated intensities of 3850 independent reflections with 2θ values between 3.5 and 55° were collected with MoKα radiation. The θ–2θ scan mode was used with a 1 deg min^{-1} scan rate, a base

[1]Author to whom correspondence should be addressed.

Can. J. Chem. Downloaded from www.nrcresearchpress.com by 210.87.254.5 on 09/05/12
For personal use only.

Can. J. Chem. Downloaded from www.nrcresearchpress.com by 210.87.254.5 on 09/05/12
For personal use only.

width of 3.2° and 40 s background counts at each limit of the scan.

The intensities of three standard reflections were measured every 100 reflections and were not found to vary significantly. The data were reduced to the observed structure factors using standard procedures. No corrections were made for absorption or extinction effects. The standard deviation of each reflection was calculated as $\sigma = 1.0 + 0.01|F_o| + \sigma'$ where σ' is based entirely on counting statistics. A Wilson statistical calculation gave an overall temperature factor of 3.02 Å^2. The scattering factors for the sulfur, oxygen, nitrogen, and carbon atoms were taken from the series coefficients of Cromer and Mann (11). The scattering factors for the hydrogen atoms were those given by Stewart *et al.* (12). The average values of $|E|$ and $|E^2 - 1|$ were determined to be 0.788 and 0.981 respectively, indicating the centrosymmetric triclinic space group. The lattice parameters for the sulfoxide were similar to those observed for 2-(4′-carbomethoxy-2′-nitrobenzoyl)-1,3,5-trimethylbenzene (13), the structure of which has been determined previously but will appear later in this series. An examination of the larger normalized structure factors of the ketone and the sulfoxide showed a considerable degree of similarity in their values. It was therefore apparent that crystals of the two compounds were isostructural. The coordinates of all the nonhydrogen atoms except the sulfoxide oxygen atom were taken directly from those of the equivalent atom in the refined structure of 2-(4′-carbomethoxy-2′-nitrobenzoyl)-1,3,5-trimethylbenzene (13). The isotropic temperature factors were set at 3.0 Å^2. An electron density Fourier map calculated with the phases from these atoms revealed all the nonhydrogen atoms, including the sulfoxide oxygen atom.

The structure was refined by full-matrix least squares to a weighted residual R_w of 0.083 using individual anisotropic temperature factors and weights calculated from $w^{-1/2} = \sigma$. The least-squares refinement, in effect, minimizes R_w^2 where R_w is defined by $R_w = (\Sigma w(|F_o| - |F_c|)^2 / \Sigma w|F_o|^2)^{1/2}$. A difference Fourier map revealed all 17 hydrogen atoms.[2] The strongest peak in the difference map was located 1.2 Å from the sulfur atom on the side of the C—S—C plane opposite to the oxygen atom. The 2985 reflections for which $|F_o| > 2.5w^{-1/2}$ were used in the final cycles. The weights in the final cycles of refinement were calculated from $w^{-1/2} = 0.6406 - 0.0368|F_o| + 0.00113|F_o|^2$. The final values of the conventional R factor and R_w were 0.052 and 0.053 respectively.

The observed and calculated structure factors have been placed in the Depository of Unpublished Data.[3] The final positional and thermal parameters are listed in Table 1. The estimated standard deviations are given in parentheses and are taken directly from the least-squares refinement. The bond lengths, bond angles, and the atom numbering are given in Figs. 1 and 2.

[2]The program FORDAP written by Zalkin (14) was used for all Fourier calculations. The program ORFLS written by Busing *et al.* (15) was used for least-squares refinement. The program ORTEP written by Johnson (16) was used to prepare the stereographic drawings.

[3]Complete set of tabular data is available, at a nominal charge, from the Depository of Unpublished Data, CISTI, National Research Council of Canada, Ottawa, Canada K1A 0S2.

Discussion

The angles between the planes of 2-(4′-carbomethoxy-2′-nitrophenylsulfinyl)-1,3,5-trimethylbenzene, as labeled in Fig. 3, are given in Table 2. The angles between the planes of the two phenyl rings and the central C—S—C plane are 51.6° and 48.1°. The stereogram of the molecule as shown in Fig. 4 shows that the *ortho*-nitro substituent is pointed towards the other ring. The conformation is then twist-nitro-*proximal* in agreement with the p.m.r. studies (7). The angle between the mesityl ring and the C—S—C plane is only slightly outside the range of values predicted for that angle (7). The torsional angles ϕ[C(9)—S—C(1)—C(2)] and ψ[C(1)—S—C(9)—C(10)] occur in (+ +) pairs in one enantiomer and in (− −) pairs in the other as is implied by the definition of the twist conformation (1).

The *proximal* conformation observed here is in marked contrast to the *distal* conformations observed previously in this series. The only other *proximal* conformation observed for a bridged diphenyl is that of 3,5,3′-triiodothyronine where the *proximal* iodine substituent is in the *meta* position (17). Although this conformation may be affected by the solvent used to crystallize the compound (17), we would assume that the *proximal* conformation is related to the interactions between the nitro oxygen atoms and the sulfoxide oxygen atom that would result if the molecule adopted the *distal* conformation. It would appear, however, upon examination of Fig. 4, that by suitable adjustment of the dihedral angles between the nitro-substituted ring and the C—S—C plane and the plane of the NO_2 group, a twist-nitro-*distal* conformation could be accommodated sterically. The coulombic interaction between the oxygen atoms therefore plays an important role in determining the conformation.

The nitro-*proximal* conformation leads to a number of distortions within the molecule. A survey of the C—S—C angles in sulfoxides (18) gives an average C—S—C angle of 97.1°, which is 4.3° less than the value observed here. The nitro-substituted ring is bent 6.1(2)° away from the mesityl ring at the bridging carbon atom C(1′). The nitro group is rotated through 41.4° from coplanarity with the phenyl ring to which it is bonded leaving it 35.5° from coplanarity with the mesityl ring. All of these factors accommodate the steric interactions between the nitro group and the mesityl ring. The nearest nitro

Can. J. Chem. Downloaded from www.nrcresearchpress.com by 210.87.254.5 on 09/05/12
For personal use only.

TABLE 1. Structural parameters (e.s.d.'s) for 2-(4′-carbomethoxy-2′-nitrophenylsulfinyl)-1,3,5-trimethylbenzene

(*a*) Fractional atomic coordinates ($\times 10^4$) and thermal parameters U_{ij} ($\times 10^3$), t.f. = exp $\{-2\pi^2(a^{*2}h^2U_{11} + ... + 2a^*b^*hkU_{12} + ...)\}$

Atom	x	y	z	U_{11}	U_{22}	U_{33}	U_{12}	U_{13}	U_{23}
C(1)	5055(3)	4242(3)	3391(2)	40(1)	33(1)	29(1)	15(1)	8(1)	12(1)
C(2)	4597(3)	2310(3)	3323(2)	34(1)	31(1)	31(1)	9(1)	5(1)	10(1)
C(3)	5483(3)	1614(3)	3944(2)	38(1)	29(1)	36(1)	11(1)	8(1)	14(1)
C(4)	6862(3)	2917(3)	4699(2)	35(1)	36(1)	31(1)	13(1)	8(1)	13(1)
C(5)	7325(3)	4866(4)	4812(2)	36(1)	34(1)	34(1)	6(1)	3(1)	10(1)
C(6)	6436(3)	5525(4)	4156(2)	44(2)	30(1)	37(1)	10(1)	7(1)	12(1)
C(7)	7796(3)	2135(4)	5369(2)	38(1)	42(1)	35(1)	14(1)	7(1)	16(1)
C(8)	10097(4)	2843(6)	6683(4)	45(2)	83(3)	77(1)	24(2)	−1(2)	44(2)
C(9)	3444(3)	3582(3)	1125(2)	41(1)	34(1)	31(1)	15(1)	6(1)	13(1)
C(10)	4436(3)	2976(3)	563(2)	38(1)	39(1)	39(1)	16(1)	10(1)	23(1)
C(11)	3851(3)	1629(4)	−579(2)	44(2)	46(2)	39(1)	22(1)	16(1)	17(1)
C(12)	2349(3)	910(4)	−1179(2)	46(2)	43(1)	33(1)	15(1)	10(1)	14(1)
C(13)	1418(3)	1593(4)	−614(2)	35(1)	46(2)	38(1)	13(1)	4(1)	16(1)
C(14)	1931(3)	2947(4)	532(2)	39(1)	42(1)	37(1)	18(1)	10(1)	19(1)
C(15)	6085(3)	3754(5)	1120(3)	37(2)	56(2)	51(2)	17(1)	10(1)	22(2)
C(16)	1769(4)	−534(5)	−2423(3)	58(2)	64(2)	38(2)	21(2)	7(2)	6(2)
C(17)	846(4)	3689(5)	1052(3)	49(2)	66(2)	50(2)	32(2)	16(2)	22(2)
N	3101(2)	932(3)	2593(2)	38(1)	37(1)	44(1)	7(1)	−1(1)	15(1)
O(1)	2096(2)	1553(3)	2618(2)	36(1)	60(1)	63(1)	15(1)	5(1)	26(1)
O(2)	2937(3)	−736(3)	2030(2)	64(2)	38(1)	93(2)	12(1)	−22(1)	−5(1)
O(3)	7399(3)	495(3)	5343(2)	67(2)	44(1)	71(2)	13(1)	−11(1)	29(1)
O(4)	9130(2)	3477(3)	5994(2)	36(1)	55(1)	65(1)	11(1)	−3(1)	29(1)
O(5)	5173(3)	7167(3)	2704(2)	80(2)	33(1)	55(1)	13(1)	−4(1)	20(1)
S	4025(1)	5334(1)	2601(1)	54(1)	35(1)	34(1)	22(1)	4(1)	11(1)

TABLE 1 (*Concluded*)

(*b*) Fractional atomic coordinates ($\times 10^3$) and isotropic temperature factors for the hydrogen atoms

Atom	*x*	*y*	*z*	*B* (Å²)
H(3)	515(3)	30(4)	384(3)	4(1)
H(5)	827(3)	575(4)	536(2)	3(1)
H(6)	680(3)	688(4)	425(3)	4(1)
H(11)	451(3)	125(4)	−95(3)	4(1)
H(13)	34(3)	109(4)	−102(3)	4(1)
H(8,1)	1094(5)	399(6)	709(4)	7(1)
H(8,2)	962(4)	230(5)	716(3)	7(1)
H(8,3)	1029(4)	177(6)	610(4)	7(1)
H(15,1)	648(5)	508(6)	164(4)	8(1)
H(15,2)	658(4)	337(5)	58(3)	7(1)
H(15,3)	639(4)	319(6)	165(4)	7(1)
H(16,1)	228(5)	5(6)	−293(4)	9(1)
H(16,2)	196(5)	−171(6)	−252(4)	8(1)
H(16,3)	74(5)	−87(6)	−275(4)	8(1)
H(17,1)	−13(5)	304(6)	43(4)	7(1)
H(17,2)	112(4)	505(6)	122(3)	7(1)
H(17,3)	79(4)	344(5)	171(4)	7(1)

TABLE 2. Least-squares planes

(*a*) Equations of planes $Ax + By + Cz = D$. Coordinates refer to the directions of the ***a***, ***c***xa***, and ***c****** axes. The planes are labeled in Fig. 3

Plane	*A*	*B*	*C*	*D*
1	0.2703	0.9047	−0.3293	1.5995
2	0.6588	−0.1394	−0.7393	−0.5965
3	0.6044	−0.1751	−0.7772	−1.0134
4	0.3713	0.5956	−0.7788	−2.1244
5	0.9225	0.3566	−0.1477	2.9272

(*b*) Dihedral angles

Planes	Angle (deg)
1,2	72.8
1,5	51.6
2,3	4.3
2,4	41.4
2,5	48.1
1,4	35.5

oxygen atom, O(1), is 2.64 Å from the plane of the mesityl ring.

The length of the C(9)—S and C(1)—S bonds are 1.798(3) and 1.819(2) Å respectively. The difference of 0.021(4) Å is opposite to that observed in the corresponding ether (1) and sulfide (2), where the bond to the nitro-substituted ring was the shorter. This shortening effect has been explained in terms of conjugation between the electron-withdrawing ring and the unshared electrons on the bridging atom. The effect persists even when the plane of the electron-withdrawing ring is nearly orthogonal to the C—X—C plane where X is the bridging atom (4).

The reverse of the effect here is related to the fact that the sulfoxide group is itself slightly electron-withdrawing, which results in a shortening of the bond to the electron-donating mesityl ring rather than the electron-withdrawing nitro-substituted ring.

Can. J. Chem. Downloaded from www.nrcresearchpress.com by 210.87.254.5 on 09/05/12
For personal use only.

Can. J. Chem. Downloaded from www.nrcresearchpress.com by 210.87.254.5 on 09/05/12
For personal use only.

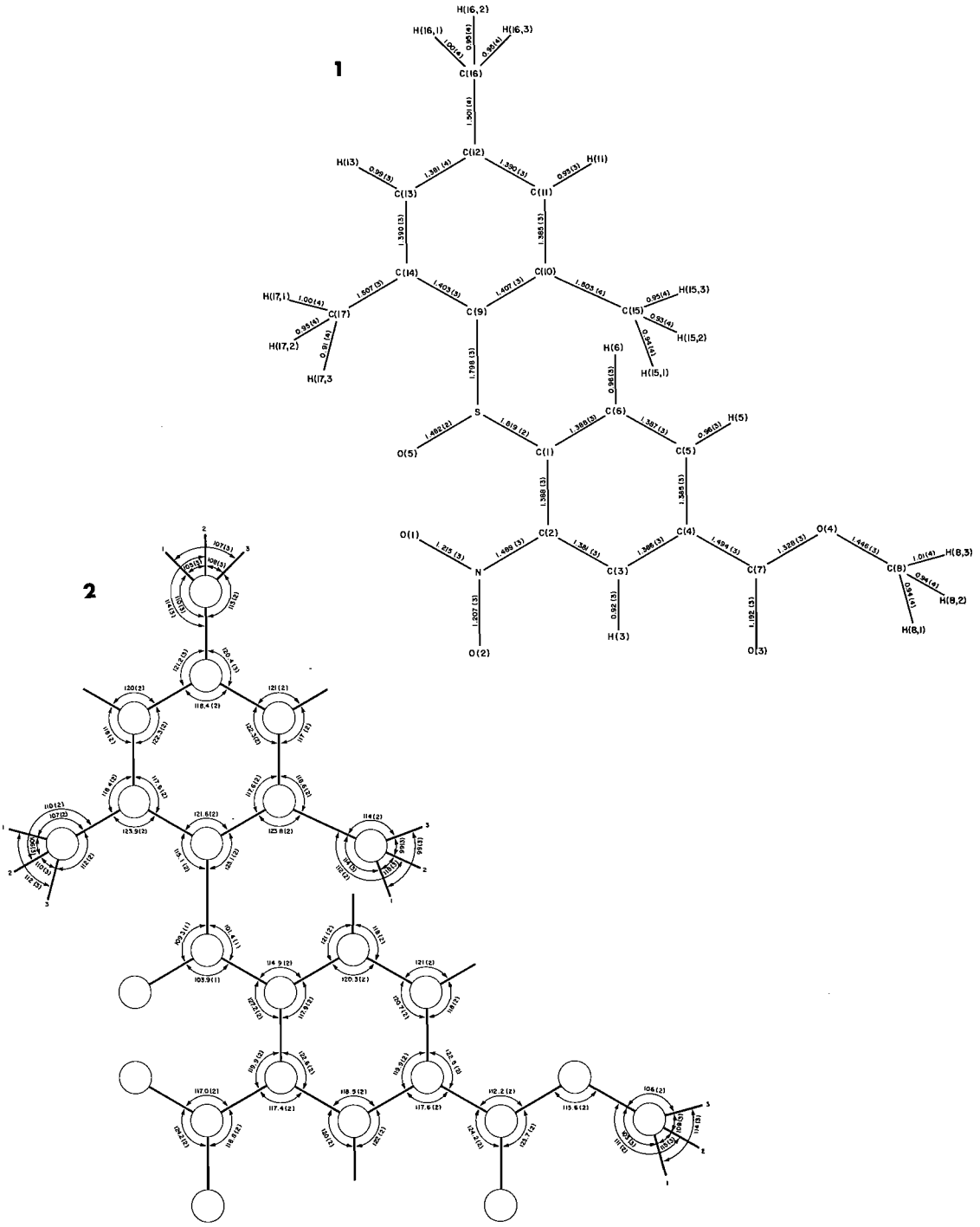

FIG. 1. Bond lengths and atom labeling for 2-(4′-carbomethoxy-2′-nitrophenylsulfinyl)-1,3,5-trimethylbenzene. Numbers in parentheses are the estimated errors based on the errors in Table 1 for the atom positions and the errors in the lattice constants.

FIG. 2. Bond angles. The numbers in parentheses are the estimated errors.

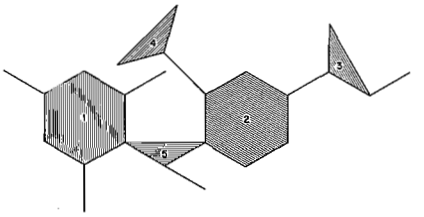

FIG. 3. Labeling of the planes of the molecule.

The sulfoxide oxygen atom does not lie in the C—S—C plane but is removed 1.32 Å from it. The second strongest density peak (0.52 electrons $Å^{-3}$) observed in the difference Fourier map used to locate the hydrogen atoms was located 1.2 Å from the sulfur atom on the opposite side of the C—S—C plane to the oxygen atom. The average density corresponding to the five ring hydrogen atoms was 0.45 electrons $Å^{-3}$. The angle between the plane formed by this peak, the oxygen and sulfur atoms, and the C—S—C plane, is 87°. This peak then corresponds to the lone pair electrons on the sulfur atom.

The bonds to hydrogen atoms range from 0.91 to 1.01 Å in length. The isotropic temperature factors for the hydrogen atoms attached to the phenyl ring range from 3 to 4 $Å^2$ and for methyl hydrogen atoms the temperature factors range from 7 to 9 $Å^2$. There are no unusual intermolecular contacts in the structure. The molecular packing is shown in Fig. 5.

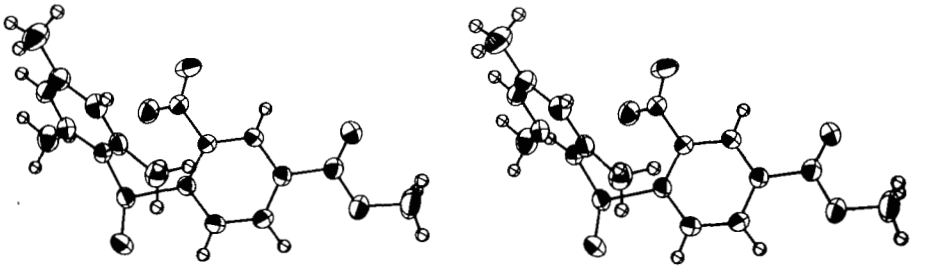

FIG. 4. Stereoscopic view of 2-(4′-carbomethoxy-2′-nitrophenylsulfinyl)-1,3,5-trimethylbenzene. The thermal ellipsoids for the nonhydrogen atoms are drawn at the 50% probability level. The hydrogen atoms are given arbitrary temperature factors.

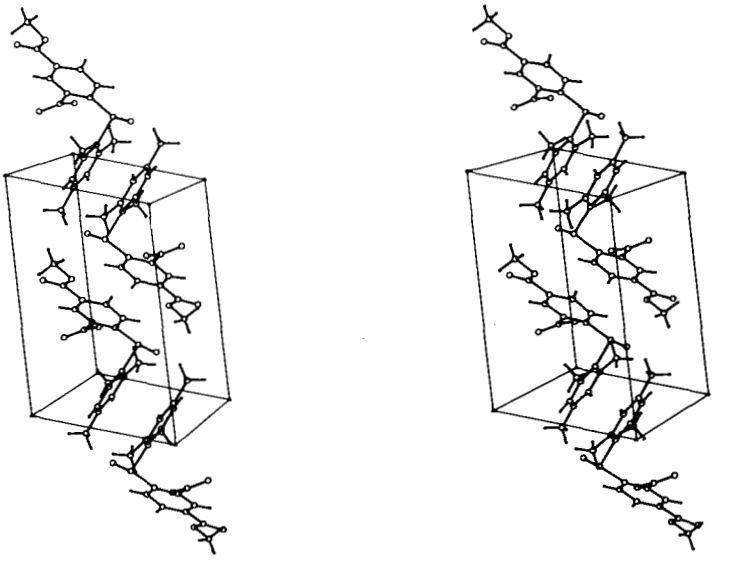

FIG. 5. Stereoscopic view of the packing.

Can. J. Chem. Downloaded from www.nrcresearchpress.com by 210.87.254.5 on 09/05/12
For personal use only.

This research was supported by grants from the National Research Council of Canada.

1. S. P. N. VAN DER HEIJDEN, E. A. H. GRIFFITH, W. D. CHANDLER, and B. E. ROBERTSON. Can. J. Chem. **53**, 2084 (1975).
2. S. P. N. VAN DER HEIJDEN, W. D. CHANDLER, and B. E. ROBERTSON. Can. J. Chem. **53**, 2102 (1975).
3. E. A. H. GRIFFITH, W. D. CHANDLER, and B. E. ROBERTSON. Can. J. Chem. **50**, 2963 (1972).
4. E. A. H. GRIFFITH, W. D. CHANDLER, and B. E. ROBERTSON. Can. J. Chem. **50**, 2972 (1972).
5. E. A. H. GRIFFITH, W. D. CHANDLER, and B. E. ROBERTSON. Can. J. Chem. **50**, 2979 (1972).
6. K. GURTU, W. D. CHANDLER, and B. E. ROBERTSON. Can. J. Chem. **53**, 2093 (1975).
7. H. BENJAMINS and W. D. CHANDLER. Can. J. Chem. **52**, 597 (1974).
8. J. J. BERGMAN, W. D. CHANDLER, and R. Y. MOIR. Can. J. Chem. **49**, 225 (1971).
9. J. J. BERGMAN, E. A. H. GRIFFITH, B. E. ROBERTSON, and W. D. CHANDLER. Can. J. Chem. **51**, 162 (1973).
10. S. C. ABRAHAMS. Acta Cryst. **10**, 417 (1957).
11. D. T. CROMER and J. B. MANN. Acta Cryst. A**24**, 321 (1960).
12. R. F. STEWART, E. R. DAVIDSON, and W. T. SIMPSON. J. Chem. Phys. **42**, 3175 (1965).
13. S. P. N. VAN DER HEIJDEN, W. D. CHANDLER, and B. E. ROBERTSON. Can. J. Chem. **53**, 2127 (1975).
14. A. ZALKIN. FORDAP, A Fortran program for Fourier calculations, University of California, Berkeley, California. 1965.
15. W. R. BUSING, K. O. MARTIN, and H. A. LEVY. ORFLS, Report ORNL-TM-305. Oak Ridge National Laboratory, Oak Ridge, Tennessee. 1962.
16. C. K. JOHNSON. ORTEP, Report ORNL-3794. Oak Ridge National Laboratory, Oak Ridge, Tennessee. 1965.
17. N. CAMERMAN and A. CAMERMAN. Science, **175**, 764 (1972).
18. S. P. N. VAN DER HEIJDEN. Ph.D. Thesis, University of Regina, Regina, Saskatchewan. 1974.

Can. J. Chem. Downloaded from www.nrcresearchpress.com by 210.87.254.5 on 09/05/12
For personal use only.

Conformations of Bridged Diphenyls. XI. Crystal Structure of 2-(4′-Carbomethoxy-2′-nitrophenylsulfonyl)-1,3,5-trimethylbenzene

SIMON P. N. VAN DER HEIJDEN, W. DAVID CHANDLER, AND BEVERLY E. ROBERTSON[1]

Faculty of Science, University of Regina, Regina, Saskatchewan S4S 0A2

Received December 20, 1974

SIMON P. N. VAN DER HEIJDEN, W. DAVID CHANDLER, and BEVERLY E. ROBERTSON. Can. J. Chem. **53**, 2115 (1975).

The crystal structure of 2-(4′-carbomethoxy-2′-nitrophenylsulfonyl)-1,3,5-trimethylbenzene, $C_{17}H_{17}NO_6S$, has been determined by X-ray diffraction. The crystals are triclinic, a = 12.907(13), b = 7.577(5), c = 9.1808(9) Å, α = 105.82(3), β = 112.81(5), γ = 93.97(4)°, $P\bar{1}$ with Z = 2. The integrated intensities of 3792 independent reflections were measured on a four circle diffractometer and 2985 reflections were used in the refinement to give a least-squares residual of 0.046 and a conventional R factor of 0.057.

The molecule shows a twist-nitro-*proximal* conformation. However, the dihedral angles made by the mesityl ring and the nitro-substituted ring with the central C—S—C plane are dissimilar in contrast to the nearly equal angles found for the similarly substituted sulfinyl compound.

SIMON P. N. VAN DER HEIJDEN, W. DAVID CHANDLER et BEVERLY E. ROBERTSON. Can. J. Chem. **53**, 2115 (1975).

On a déterminé la structure cristalline du (carbométhoxy-4′ nitro-2′ phenylsulfonyl)-2 triméthyl-1,3,5 benzène, $C_{17}H_{17}NO_6S$, par diffraction de rayons-X. Les cristaux sont tricliniques, a = 12.907(13), b = 7.577(5), c = 9.1808(9) Å, α = 105.82(3), β = 112.81(5), γ = 93.97(4)°, $P\bar{1}$ avec Z = 2. On a mesuré les intensités de 3792 réflexions indépendantes à l'aide d'un diffractomètre à quatre cercles. On a utilisé 2985 de ces réflexions pour affiner la structure jusqu'à une valeur de R pondérée de 0.046 et une valeur de R conventionnelle de 0.057.

La molécule existe dans une conformation nitro croisé "*proximal*". Toutefois, par opposition avec les résultats obtenus avec des composés sulfinyles substitués d'une manière similaire, les angles dièdres des noyaux mésityle et nitrobenzène avec le plan C—S—C central ne sont pas semblables. [Traduit par le journal]

Introduction

This is the fourth in a series of reports of the structures of similarly substituted bridged diphenyls with variation in the bridging group (1–3). The present compound represents an increase in the bulkiness of the bridging group over those in the structures reported previously.

In 1951 Koch and Moffit observed that in diphenyl sulfones the sulfur 3d and 3p orbitals may overlap with the π orbitals of the phenyl rings if the dihedral angles between the rings and the C—S—C plane are both 90°, thus making the butterfly conformation favorable (4). The structures of 4,4′-dichlorodiphenyl sulfone (5) and 4,4′-diaminodiphenyl sulfone (6) are consistent with the predictions made by Koch and Moffit. However, in 2,2′,4,4′,6,6′-hexamethyldiphenyl sulfone (7) steric hindrances between the four *ortho* substituents lead to a twist conformation with dihedral angles near 55°. The present study involves a compound which is tri-*ortho*-substituted. The notation used here has been discussed in detail previously (1).

Benjamins and Chandler (8) have studied this compound using ring-current shielding effects and have concluded that the conformation is near butterfly although this conformation brings the NO_2 group and a CH_3 group into close proximity.

Experimental

The synthesis of 2-(4′-carbomethoxy-2′-nitrophenylsulfonyl)-1,3,5-trimethylbenzene, $C_{17}H_{17}NO_6S$, has been reported earlier (8). The sample was recrystallized from 95% ethanol, m.p. 169–170 °C. A crystal with dimensions 0.59 × 0.32 × 0.28 mm was prepared for data collection with the long axis parallel to the axis of the fiber with which it was mounted on a Picker FACS I four circle automated diffractometer equipped with a graphite monochromator. The orientation of 23 reflections with 2θ values between 30° and 40° was determined using MoKα_1 radiation. These were used to obtain accurate lattice constants by least squares. Twelve of these reflections were used to orient the crystal on the diffractometer.

[1]Author to whom all correspondence should be addressed.

Can. J. Chem. Downloaded from www.nrcresearchpress.com by 210.87.254.6 on 09/05/12
For personal use only.

Can. J. Chem. Downloaded from www.nrcresearchpress.com by 210.87.254.6 on 09/05/12
For personal use only.

TABLE 1. Structural parameters (e.s.d.'s) for 2-(4′-carbomethoxy-2′-nitrophenylsulfonyl)-1,3,5-trimethylbenzene

(*a*) Fractional atomic coordinates ($\times 10^4$) and thermal parameters U_{ij} ($\times 10^3$), t.f. = exp $\{-2\pi^2(a^{*2}h^2U_{11} + ... + 2a^*b^*hkU_{12} + ...)\}$

Atom	*x*	*y*	*z*	U_{11}	U_{22}	U_{33}	U_{12}	U_{13}	U_{23}
C(1)	1659(2)	991(3)	1935(3)	27(1)	27(1)	40(2)	1(2)	9(1)	10(1)
C(2)	1769(2)	−869(3)	1485(3)	28(1)	29(1)	30(1)	5(1)	10(1)	8(1)
C(3)	1138(2)	−2265(3)	1658(3)	31(1)	25(1)	35(2)	6(1)	10(1)	9(1)
C(4)	339(2)	−1821(4)	2247(3)	29(1)	32(1)	36(2)	3(1)	11(1)	10(2)
C(5)	190(2)	8(4)	2652(4)	31(2)	38(2)	51(2)	8(1)	21(1)	9(1)
C(6)	851(2)	1401(4)	2517(4)	36(2)	26(1)	62(2)	8(1)	20(2)	9(1)
C(7)	−337(2)	−3369(4)	2408(3)	32(1)	40(2)	38(2)	6(1)	11(1)	18(1)
C(8)	−1711(5)	−4163(7)	3266(6)	81(3)	71(3)	83(3)	−3(2)	57(3)	24(3)
C(9)	3917(2)	2575(3)	2482(3)	25(1)	28(1)	35(2)	1(1)	6(1)	11(1)
C(10)	4479(2)	2399(3)	3975(3)	33(1)	25(1)	36(2)	0(1)	15(1)	7(1)
C(11)	5579(2)	2035(4)	4409(3)	35(2)	33(1)	32(2)	2(1)	10(1)	11(1)
C(12)	6138(2)	1881(4)	3438(3)	30(1)	33(1)	41(2)	3(1)	13(1)	9(1)
C(13)	5573(3)	2115(4)	2002(3)	38(2)	41(2)	39(2)	2(1)	19(1)	11(1)
C(14)	4467(2)	2471(4)	1475(3)	38(2)	33(1)	35(2)	−2(1)	12(1)	11(1)
C(15)	3998(3)	2643(5)	5179(4)	43(2)	42(2)	44(2)	6(2)	22(2)	12(2)
C(16)	7339(2)	1533(1)	3973(5)	36(2)	65(2)	59(2)	15(2)	20(2)	23(2)
C(17)	3985(3)	2785(6)	−90(4)	49(2)	67(2)	43(2)	5(2)	15(2)	27(2)
N	2547(2)	−1454(3)	753(3)	42(1)	29(1)	53(2)	1(1)	27(1)	5(1)
O(1)	2446(2)	−1001(3)	−378(3)	76(2)	63(2)	58(2)	10(1)	43(2)	21(1)
O(2)	3220(2)	−2389(4)	1300(3)	69(2)	69(2)	105(2)	42(2)	59(2)	42(2)
O(3)	−300(2)	−4985(3)	1937(3)	56(2)	37(1)	94(2)	14(1)	43(1)	31(1)
O(4)	−982(2)	−2736(3)	3144(3)	61(2)	49(1)	58(2)	1(1)	40(1)	11(1)
O(5)	2024(2)	3072(3)	367(3)	41(1)	57(1)	62(2)	1(1)	6(1)	36(1)
O(6)	2478(2)	4535(3)	3136(3)	39(1)	25(1)	78(2)	3(1)	19(1)	7(1)
S	2500(1)	2992(1)	1926(1)	27(1)	25(1)	50(1)	2(1)	8(1)	15(1)

(*b*) Fractional coordinates ($\times 10^3$) and isotropic temperature factors for hydrogen atoms

Atom	*x*	*y*	*z*	*B* (Å²)
H(3)	123(3)	−352(4)	134(3)	3(1)
H(5)	−35(3)	30(4)	306(3)	4(1)
H(6)	74(3)	260(4)	277(3)	3(1)
H(11)	591(3)	192(4)	538(3)	3(1)
H(13)	598(3)	203(4)	136(3)	3(1)
H(8,1)	−214(5)	−357(7)	367(6)	10(3)
H(8,2)	−119(4)	−483(7)	396(6)	9(3)
H(8,3)	−217(4)	−505(6)	225(5)	7(2)
H(15,1)	331(4)	189(5)	484(4)	6(2)
H(15,2)	448(4)	232(6)	608(5)	7(2)
H(15,3)	389(3)	387(6)	554(4)	6(2)
H(16,1)	787(5)	250(7)	495(6)	10(3)
H(16,2)	763(4)	146(7)	326(6)	9(3)
H(16,3)	740(4)	42(7)	420(5)	8(2)
H(17,1)	326(3)	191(5)	−77(4)	6(2)
H(17,2)	453(3)	258(5)	−50(4)	5(2)
H(17,3)	388(3)	416(6)	9(4)	6(2)

The crystal data are as follows:

$C_{17}H_{17}NO_6S$ f.w. = 363.38

Triclinic $P\bar{1}$, a = 12.907(13), b = 7.577(5), c = 9.808(9) Å, α = 105.82(3), β = 112.81(5), γ = 93.97(4)°, ρ_o = 1.40 g cm^{-3} (flotation), ρ_c = 1.44 g cm^{-3}, Z = 2, $F(000)$ = 380e, $\lambda(MoK\alpha_1)$ = 0.70926 Å, $\mu(MoK\alpha)$ = 2.29 cm^{-1}, T = 20 ± 1 °C.

The integrated intensities of 3792 independent reflections between the 2θ values of 3.5° and 55° were collected using the θ–2θ scan mode with a scan rate of 1 deg min^{-1}, a minimum base width of 3.2° in 2θ, MoKα radiation, and background times of 40 s. Three standard reflections were used to monitor changes in the apparatus or crystal. Two of the standard reflections did not change in intensity during the period of the data collection but

Can. J. Chem. Downloaded from www.nrcresearchpress.com by 210.87.254.6 on 09/05/12
For personal use only.

the intensity of the third decreased by 10%. The data were reduced to observed structure factors using standard procedures. No corrections were made for extinction or absorption. The scattering factors for the sulfur, oxygen, nitrogen, and carbon atoms were taken from Cromer and Mann (9). The scattering factors for the hydrogen atoms were taken from Stewart *et al.* (10). Reflections below background were assigned zero intensity.

A Wilson statistical calculation gave an overall temperature factor of 2.51 Å^2. The average values of $|E^2 - 1|$ and $|E|$ were 1.022 and 0.768 indicating the centrosymmetric space group $P\bar{1}$. The 429 reflections with $|E| > 1.62$ were used to solve the structure using the logical symbolic addition method.[2] An *E*-map generated from the nontrivial set having the highest figures of merit yielded all nonhydrogen atom positions.[3]

A difference Fourier map calculated at this point revealed all 17 hydrogen positions and refinement was completed with anisotropic temperature factors assigned to the nonhydrogen atoms and isotropic temperature factors assigned to the hydrogen atoms.

The least-squares weights were calculated from $w^{-1/2} = 0.4013 - 0.01237|F| + 0.000676|F|^2$. The 2985 reflections for which $|F_o| > 2.6w^{-1/2}$ were used in the final cycles of refinement. The final values of R_w and the conventional R factor were 0.046 and 0.057. The observed and calculated structure factors have been placed in the Depository of Unpublished Data.[4] The final positional and thermal parameters are listed in Table 1. The estimated errors are taken directly from the least-squares analysis. The bond lengths with estimated standard deviations and the atomic numbering are given in Fig. 1. The bond angles are given in Fig. 2.

[2]The direct methods program LSAM written by Germain and Woolfson (11) was used for structure solution. The program FORDAP written by Zalkin (12) was used for all Fourier calculations. The Busing *et al.* program ORFLS (13) was used for least-squares refinement. Stereoscopic drawings were prepared with the aid of the program ORTEP written by Johnson (14).

[3]The least-squares refinement revealed that the accuracy of the data collected last (that with $2\theta < 40°$) was less accurate than that collected at the beginning of the data collection, indicating some loss of alignment precision had occurred during the data collection. The original crystal was therefore placed on the diffractometer and realigned. The data between $2\theta > 3.5°$ and $2\theta > 42°$ were collected again. The agreement between the two sets of data in the region $40° < 2\theta < 42°$ was within the counting statistics. The final cycles of refinement used the first set of data for $2\theta > 42°$ and the second set of data for $2\theta < 42°$. We are obliged to point out that the final parameters therefore suffer from any systematic errors which may arise from the use of two sets of alignment parameters. However, a comparison of the bond lengths in all identically substituted bridged diphenyls in this series, including this one, shows that the r.m.s. deviation of equivalent bonds not affected by the bridging group is less than (or equal to) the average e.s.d.'s of those bond lengths.

[4]Complete set of tabular data is available, at a nominal charge, from the Depository of Unpublished Data, CISTI, National Research Council of Canada, Ottawa, Canada K1A 0S2.

Discussion

The angles between the planes of 2-(4′-carbomethoxy-2′-nitrophenylsulfonyl)-1,3,5-trimethylbenzene, as labeled in Fig. 3, are given in Table 2. The molecule shows the twist-nitro-*proximal* conformation as does the identically substituted sulfoxide compound (3). However the angles made by the mesityl ring and the nitro-substituted ring with the central C—S—C plane in the present compound are dissimilar at 60.6° and 38.2°, while in the sulfinyl compound they are nearly identical at 51.7° and 48.3° respectively. The torsional angles ϕ[C(9)—S—C(1)—C(2)] and ψ[C(1)—S—C(9)—C(10)] occur in (+ +) pairs in one enantiomer and in (− −) pairs in the other, as is implied by the twist conformation. A stereogram of the molecule is shown in Fig. 4.

The conformation observed here is not the one predicted on the basis of p.m.r. studies of the ring-current shielding of phenyl hydrogen atoms (8). In view of the rigidity of the molecule it does not seem likely that the conformation in solution and in the solid state are markedly different. We conclude that because of the small values of the "other ring" shielding parameters and thus the lack of sensitivity of the p.m.r. method in the case of the diphenyl sulfones, the conformation predicted by that method may have been erroneous.

TABLE 2. Least-squares planes

(*a*) Equations of planes $Ax + By + Cz = D$. Coordinates refer to the directions of the ***a***, ***c***x**a***, and ***c**** axes. The planes are defined in Fig. 3

Plane	*A*	*B*	*C*	*D*
1	−0.2206	−0.8876	−0.4042	−2.599
2	−0.3348	0.1724	−0.9264	−1.964
3	−0.4206	0.2304	−0.8775	−1.949
4	−0.4790	−0.6443	−0.5962	−0.8242
5	0.2211	−0.1716	−0.9600	−1.3016
6	−0.9171	−0.3689	−0.1511	−3.0586

(*b*) Dihedral angles

Planes	Angle (deg)
1,2	72.8
1,5	60.6
2,3	6.6
2,4	53.0
2,5	38.2
5,6	89.7
1,4	23.3

Can. J. Chem. Downloaded from www.nrcresearchpress.com by 210.87.254.6 on 09/05/12
For personal use only.

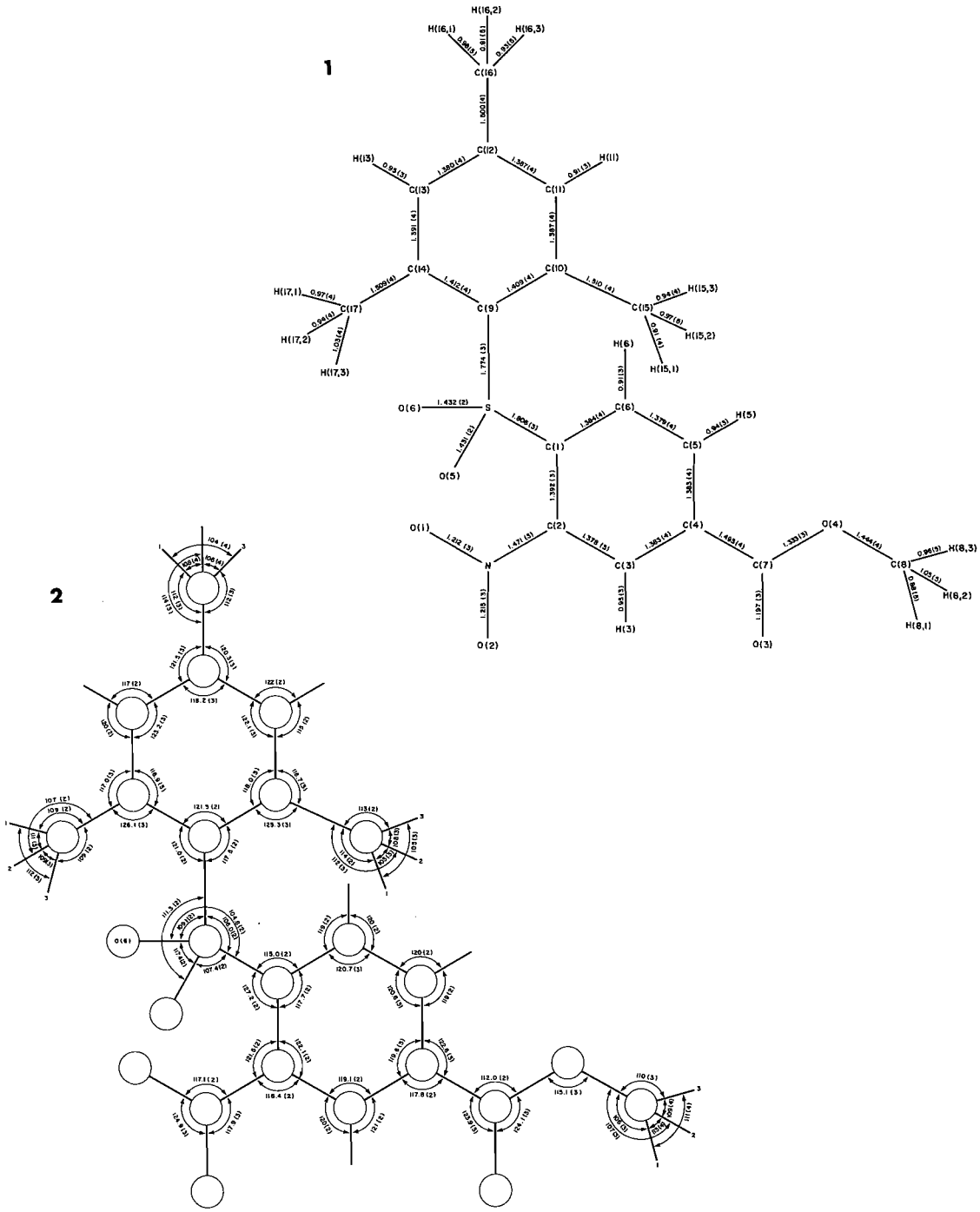

FIG. 1. Bond lengths and atom labeling. The numbers in parentheses are the estimated errors based on the estimated errors in the coordinates and the lattice constants.

FIG. 2. Bond angles. The numbers in parentheses are the estimated errors.

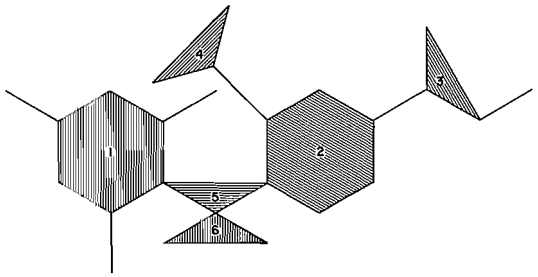

FIG. 3. Labeling of the least-squares planes.

The molecule shows deviations from idealized geometry similar to those which have been observed previously. The nitro-substituted ring is bent 6.1(2)° away from the mesityl ring at C(1) as it was in the sulfoxide. The mesityl ring is bent 1.8(2)° away from the nitro-substituted ring compared to a bending 4.0(2)° in the sulfoxide. The larger value for the bending of the mesityl ring in the sulfoxide may be related to the asymmetric nature of the sulfinyl bridging group. The C(9)—S bond length is 0.032(5) Å shorter than the C(1)—S bond length. The difference is opposite in sign to that observed for ethers and in 2-(4′-carbomethoxy-2′-nitrothiophenyl)-1,3,5-trimethylbenzene and is of the same sign as in the corresponding sulfoxide but it is slightly greater because of the greater electron-withdrawing character of the sulfonyl over the sulfinyl moiety.

The S—O bond lengths in the sulfone are 0.051 Å shorter than is the S—O bond length in the sulfoxide, and are in agreement with

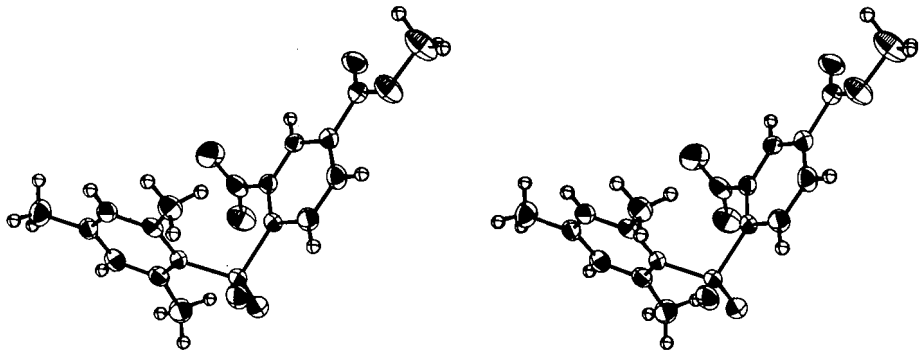

FIG. 4. Stereoscopic view of 2-(4′-carbomethoxy-2′-nitrophenylsulfonyl-1,3,5-trimethylbenzene. The thermal ellipsoids for the nonhydrogen atoms are drawn at the 50% probability level. The hydrogen atoms are given arbitrary temperature factors.

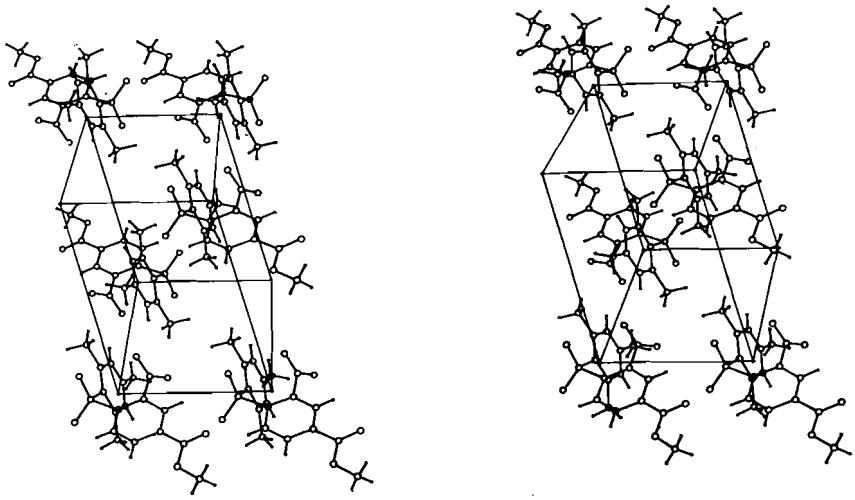

FIG. 5. Stereoscopic view of the molecular packing.

Can. J. Chem. Downloaded from www.nrcresearchpress.com by 210.87.254.6 on 09/05/12
For personal use only.

values observed in other sulfones (15). Bent (16) has predicted a value of 1.43 Å with a deviation of up to 0.03 Å depending on the electronegativity of the substituents of the sulfur. The O—S—O angle of 117.4(2)° is typical of other sulfones.

The packing of the molecules is shown in Fig. 5. The structure shows no unusual intermolecular contacts. Bond lengths to phenyl hydrogen atoms range from 0.91(3) to 0.95(2) Å with isotropic temperature factors from 3(1) to 4(1) Å^2. The bond lengths to methyl hydrogen atoms range from 0.88(5) to 1.03(5) Å with isotropic temperature factors from 5(2) to 10(3) Å^2.

This research was supported by grants from the National Research Council of Canada.

1. S. P. N. VAN DER HEIJDEN, E. A. H. GRIFFITH, W. D. CHANDLER, and B. E. ROBERTSON. Can. J. Chem. **53**, 2084 (1975).
2. S. P. N. VAN DER HEIJDEN, W. D. CHANDLER, and B. E. ROBERTSON. Can. J. Chem. **53**, 2102 (1975).
3. S. P. N. VAN DER HEIJDEN, W. D. CHANDLER, and B. E. ROBERTSON. Can. J. Chem. **53**, 2108 (1975).
4. H. P. KOCH and W. E. MOFFIT. Trans. Faraday Soc. **47**, 7 (1951).
5. J. G. SIME and S. C. ABRAHAMS. Acta Cryst. **13**, 1 (1960).
6. C. DICKINSON, J. M. STEWART, and H. L. AMMON. J. Chem. Soc. D, 920 (1970).
7. S. A. CHAWDHURY and A. HARGREAVES. Acta Cryst. **B27**, 548 (1971).
8. H. BENJAMINS and W. D. CHANDLER. Can. J. Chem. **52**, 597 (1974).
9. D. T. CROMER and J. B. MANN. Acta Cryst. **A24**, 321 (1968).
10. R. F. STEWART, E. R. DAVIDSON, and W. T. SIMPSON. J. Chem. Phys. **42**, 3175 (1965).
11. G. GERMAIN and M. M. WOLFSON. Acta Cryst. **B24**, 91 (1968).
12. A. ZALKIN. FORDAP, A Fortran program for Fourier calculations. University of California, Berkeley, California. 1965.
13. W. R. BUSING, K. O. MARTIN, and H. A. LEVY. ORFLS, Report ORNL-TM-305. Oak Ridge National Laboratory, Oak Ridge, Tennessee. 1962.
14. C. K. JOHNSON. ORTEP, Report ORNL-3794. Oak Ridge National Laboratory, Oak Ridge, Tennessee. 1965.
15. S. P. N. VAN DER HEIJDEN. Ph.D. Thesis, University of Regina, Regina, Saskatchewan. 1974.
16. H. BENT. Organic sulfur compounds, Vol. 2. Pergamon Press, London. 1965.

Can. J. Chem. Downloaded from www.nrcresearchpress.com by 210.87.254.6 on 09/05/12
For personal use only.

Conformations of Bridged Diphenyls. XII. Crystal Structure of 2-(4′-Carbomethoxy-2′-nitrobenzyl)-1,3,5-trimethylbenzene

SIMON P. N. VAN DER HEIJDEN, W. DAVID CHANDLER, AND BEVERLY E. ROBERTSON[1]

Faculty of Science, University of Regina, Regina, Saskatchewan S4S 0A2

Received December 20, 1974

SIMON P. N. VAN DER HEIJDEN, W. DAVID CHANDLER, and BEVERLY E. ROBERTSON. Can. J. Chem. **53**, 2121 (1975).

The crystal structure of 2-(4′-carbomethoxy-2′-nitrobenzyl)-1,3,5-trimethylbenzene, $C_{18}H_{19}NO_4$, has been determined by X-ray diffraction. The crystals are triclinic, $a = 9.534(5)$, $b = 11.887(7)$, $c = 7.431(6)$ Å, $\alpha = 101.62(3)$, $\beta = 97.25(3)$, $\gamma = 88.61(3)°$, $P\bar{1}$ with $Z = 2$. The integrated intensities of 3789 independent reflections were measured on a four circle diffractometer; 2448 reflections were used in a full-matrix refinement to a least-squares residual of 0.067 and a conventional R factor of 0.055.

The molecule is in the skew-nitro-*distal* conformation. The angle between the di-*ortho*-substituted ring and the central C—CH_2—C plane is 87.6° and the angle between the nitro-substituted ring and the C—CH_2—C plane is 2.2°.

SIMON P. N. VAN DER HEIJDEN, W. DAVID CHANDLER et BEVERLY E. ROBERTSON. Can. J. Chem. **53**, 2121 (1975).

On a déterminé la structure cristalline du (carbométhoxy-4′ nitro-2′ benzyl)-2 triméthyl-1,3,5 benzène, $C_{18}H_{19}NO_4$, par diffraction de rayons-X. Les cristaux sont tricliniques, $a = 9.534(5)$, $b = 11.887(7)$, $c = 7.431(6)$ Å, $\alpha = 101.62(3)$, $\beta = 97.25(3)$, $\gamma = 88.61(3)°$, $P\bar{1}$ avec $Z = 2$. On a mesuré les intensités de 3789 réflexions indépendantes à l'aide d'un diffractomètre à quatre cercles. On a utilisé 2448 de ces réflexions pour affiner la structure par la méthode des moindres carrés (matrice complète) jusqu'à une valeur de R pondérée de 0.067 et une valeur de R conventionnelle de 0.055.

La molécule existe dans une conformation avec le nitro-*gauche* "*distal*". L'angle entre le cycle *ortho*-disubstitué et le plan du C—CH_2—C central est de 87.6°; l'angle entre le cycle substitué par le groupe nitro et le plan C—CH_2—C est de 2.2°.

[Traduit par le journal]

Introduction

In diphenylmethanes one would expect little overlap, if any, between the π orbitals of the phenyl rings and the orbitals of the bridging carbon atom. The methylene group can carry only a small charge and there are no unshared electrons present. Therefore coulombic repulsion would not be expected to be an important factor in determining the conformation of diphenylmethanes. The factors that remain then, are the steric interactions associated with the *ortho* substituents, both among themselves and with the bridging group. In the nitro *distal* conformation the nitro group must be accommodated between the methylene hydrogen atoms and an adjacent hydrogen atom on the ring. Other structures determined in this series would indicate that in the *proximal* conformation the nitro group would be rotated out of coplanarity with the ring on which it is substituted through contact with the π electrons of the mesityl ring (1, 2). The notation used here has been discussed in detail previously (13).

The conformation of the compound reported here, 2-(4′-carbomethoxy-2′-nitrobenzyl)-1,3,5-trimethylbenzene, has been studied by n.m.r. and was predicted to have a skew-nitro-*distal* conformation (3) similar to the ether and sulfide analogs. The structure of 3,3′-dichloro-4,4′-dihydroxydiphenylmethane has been studied by X-ray diffraction and has the twist conformation with both chlorine substituents *proximal* (4).

Experimental

The syntheses of 2-(4′-carbomethoxy-2′-nitrobenzyl)-1,3,5-trimethylbenzene, $C_{18}H_{19}NO_4$, has been reported earlier (3). It was recrystallized from absolute ethanol, m.p. 104–105 °C. A sample with dimensions 0.42 × 0.28 × 0.34 mm was chosen for data collection. It was mounted on a Picker FACS I four circle diffractometer equipped with a graphite monochromator. The centered positions of 27 reflections with 2θ values between 35° and

[1]Author to whom all correspondence should be addressed.

Can. J. Chem. Downloaded from www.nrcresearchpress.com by 210.87.254.6 on 09/05/12
For personal use only.

Can. J. Chem. Downloaded from www.nrcresearchpress.com by 210.87.254.6 on 09/05/12
For personal use only.

45° were determined using MoKα_1 radiation. These reflections were used to determine accurate cell parameters by a least-squares calculation. Twelve of these reflections were used to determine the orientation of the crystal on the diffractometer.

The crystal data are as follows:

$C_{18}H_{19}NO_4$ f.w. = 313.35

Triclinic $P\bar{1}$, $a = 9.534(5)$, $b = 11.887(7)$, $c = 7.431(6)$ Å, $\alpha = 101.62(3)$, $\beta = 97.25(3)$, $\gamma = 88.6(3)°$, $\rho_o = 1.30$ g cm^{-3} (flotation), $\rho_c = 1.27$ g cm^{-3}, $Z = 2$, $F(000) = 332e$, $\lambda(\text{MoK}\alpha_1) = 0.70926$ Å, $\mu(\text{MoK}\alpha) = 0.97$ cm^{-1}, $T = 20 \pm 1$ °C.

The integrated intensity of 3789 independent reflections with 2θ values between 3.5° and 55° were collected using the θ–2θ scan mode with a scan rate of 1 deg min^{-1}, a minimum base width of 2.7°, and 40 s background counts at each limit of the scan. The intensities of three standard reflections were measured after every 30 reflections and were not found to vary significantly. The data were reduced to observed structure factors using standard procedures. Corrections were not made for absorption or extinction effects. The scattering factors for the carbon, nitrogen, and oxygen atoms were taken from Cromer and Mann (5). The scattering factors for the hydrogen atoms were taken from Stewart *et al.* (6). A Wilson statistical calculation gave an overall temperature factor of 4.38 Å^2. The average values of $|E|$ and $|E^2 - 1|$ were 0.741 and 1.075 respectively, indicating the centrosymmetric space group $P\bar{1}$.

The 369 reflections with normalized structure factors, $|E|$, greater than 1.63 were used to solve the structure using the logical symbolic addition method.[2] The solution of the structure proved to be other than straightforward. Attempts were made to solve the structure by using Patterson methods directly but the lowest least-squares residual, R_w, that could be obtained with any model was 0.44. Unsuccessful attempts to solve the structure were also made using noncentrosymmetric programs.

The normalized structure factors were modified to provide proper scaling for subsets of the data and a new electron density map was obtained. This yielded a 15 atom solution which could be fitted to a model of the molecule. However, it was too close to a center of symmetry and the space group symmetry was therefore lowered to $P1$. The complete structure was found in this space group and a true center of symmetry was then identified between similar molecules. The structure was now easily refined in the space group $P\bar{1}$ and the hydrogen atoms were found from difference Fourier maps. The least-squares weights were calculated from $w^{-1/2} = 0.3106 - 0.00926|F_o| + 0.000912|F_o|^2$; 2448 reflections with $|F_o| > 2.6w^{-1/2}$ were used in the final cycles of refinement. The final values of the least-squares residual and the conventional R factor were 0.067 and 0.055 respectively.

The observed and calculated structure factors have been placed in the Depository of Unpublished Data.[3] The final positional and thermal parameters are listed in Table 1 with estimated standard deviations taken from the least-squares analysis. The bond lengths, bond angles, and the atom labeling are given in Figs. 1 and 2.

Discussion

The compound 2-(4′-carbomethoxy-2′-nitrobenzyl)-1,3,5-trimethylbenzene adopts the skew-nitro-*distal* conformation. The dihedral angles between the planes labeled in Fig. 3 are given in Table 2. They show that the conformation has very small deviations from the idealized skew conformation. The result is consistent with predictions based on n.m.r. ring shielding measurements (3). Since conjugation effects and coulombic repulsion are not important here, the skew conformation is clearly determined by the steric interactions of the *ortho* substituents. The nitro-substituted ring adopts the *distal* conformation to avoid contact between the nitro oxygen atoms and the π electrons of the mesityl ring. The mesityl ring is forced to be orthogonal to the nitro-substituted ring to avoid contact between its *ortho* substituents and the nitro substituent. The torsional angles ϕ[C(9)—C(18)—C(1)—C(6)] and ψ[C(1)—C(18)—C(9)—C(10)] occur in (+ +) pairs in one enantiomer and (− −) pairs in the other. The observed C—CH_2 bond lengths to the bridging methane group are nearly equal at 1.514(3) and 1.522(3) Å and are slightly shorter than the length of single C—C bonds. The C—CH_2—C bond angle at 114.3(2)° is larger than the tetrahedral angle as is the case for 3,3′-dichloro-4,4′-dihydroxydiphenylmethane where the reported value is 119(6)° (4).

The NO_2 group is rotated through 16.8° from coplanarity with the phenyl ring on which it is substituted. This rotation brings the nitro oxygen to methane hydrogen contact distance, H(18,1)—O(1), to 2.38(3) Å in comparison with an H(18,2)—O(1) contact distance of 2.55(2) Å. The contact distance between the other nitro

[2]The direct methods programs LSAM written by Germain and Woolfson (7) and MULTAN written by Germain *et al.* (8), were used for structure solution in centrosymmetric and noncentrosymmetric space groups respectively. The program FORDAP, written by Zalkin (9), was used for all Fourier calculations. The program ORFLS, written by Busing *et al.* (10), was used for least-squares refinement. The stereograms were prepared with the aid of the Johnson program ORTEP (11).

[3]Complete set of tabular data is available, at a nominal charge, from the Depository of Unpublished Data, CISTI, National Research Council of Canada, Ottawa, Canada K1A 0S2.

TABLE 1. Structural parameters (e.s.d.'s) for 2-(4′-carbomethoxy-2′-nitrobenzyl)-1,3,5-trimethylbenzene

(*a*) Fractional atomic coordinates ($\times 10^4$) and thermal parameters U_{ij} ($\times 10^3$), t.f. = exp $\{-2\pi^2(a^{*2}h^2U_{11} + ... + 2a^*b^*hkU_{12} + ...)\}$

Atom	*x*	*y*	*z*	U_{11}	U_{22}	U_{33}	U_{12}	U_{13}	U_{23}
C(1)	9108(2)	7069(2)	6308(3)	45(1)	56(2)	53(2)	0(1)	2(1)	20(1)
C(2)	9899(2)	6214(2)	7021(3)	38(1)	63(2)	50(1)	4(1)	4(1)	17(1)
C(3)	9291(3)	5305(2)	7532(3)	51(1)	51(1)	49(1)	10(1)	10(1)	16(1)
C(4)	7840(3)	5216(2)	7371(3)	50(1)	47(1)	50(1)	3(1)	11(1)	12(1)
C(5)	7013(3)	6049(2)	6698(4)	43(1)	59(2)	69(2)	3(1)	8(1)	22(1)
C(6)	7649(3)	6944(2)	6179(4)	44(1)	58(2)	72(2)	6(1)	3(1)	29(1)
C(7)	7233(3)	4212(2)	7931(4)	60(2)	48(2)	67(2)	5(1)	19(1)	14(1)
C(8)	5164(5)	3408(4)	8575(8)	75(2)	76(3)	138(4)	−13(2)	39(3)	36(3)
C(9)	8644(2)	8846(2)	4888(4)	42(1)	51(1)	64(2)	−4(1)	6(1)	25(1)
C(10)	8110(3)	8597(2)	3020(4)	47(1)	53(2)	61(2)	2(1)	11(1)	19(1)
C(11)	7106(3)	9319(3)	2334(4)	51(2)	69(2)	61(2)	−1(1)	4(1)	27(2)
C(12)	6619(3)	10284(2)	3443(4)	46(1)	59(2)	93(2)	5(1)	14(2)	34(2)
C(13)	7157(3)	10521(2)	5280(5)	64(2)	49(2)	93(2)	2(1)	30(2)	11(2)
C(14)	8157(3)	9816(2)	6040(4)	60(2)	58(2)	59(2)	−14(1)	12(1)	14(1)
C(15)	8582(4)	7554(3)	1715(5)	74(2)	70(2)	83(2)	9(2)	21(2)	9(2)
C(16)	5521(4)	11053(4)	2647(9)	57(2)	86(3)	171(4)	19(2)	9(2)	64(3)
C(17)	8676(6)	10111(4)	8070(5)	113(3)	100(3)	66(2)	−34(3)	11(2)	8(2)
C(18)	9733(3)	8066(3)	5666(5)	44(1)	71(2)	84(2)	−4(1)	1(2)	40(2)
N	11466(2)	6216(2)	7241(3)	45(1)	90(2)	80(2)	1(1)	−2(1)	43(2)
O(1)	12065(2)	7078(3)	7246(6)	49(1)	171(3)	339(5)	−25(2)	−35(2)	186(4)
O(2)	12085(2)	5356(2)	7459(4)	53(1)	93(2)	128(2)	22(1)	6(1)	23(2)
O(3)	7908(2)	3417(2)	8319(4)	77(2)	66(1)	135(2)	16(1)	37(1)	49(1)
O(4)	5849(2)	4314(2)	7963(3)	56(1)	65(1)	110(2)	0(1)	22(1)	35(1)

(*b*) Fractional atomic coordinates ($\times 10^3$) and isotropic temperature factors for the hydrogen atoms

Atom	*x*	*y*	*z*	*B* (Å²)
H(3)	989(3)	475(2)	797(4)	5(1)
H(5)	599(3)	599(2)	653(4)	5(1)
H(6)	704(3)	748(2)	567(3)	16(4)
H(11)	676(3)	914(2)	103(4)	6(1)
H(13)	687(3)	1118(3)	611(4)	7(1)
H(8,1)	561(6)	336(5)	975(8)	11(3)
H(8,2)	517(5)	275(4)	765(6)	11(2)
H(8,3)	427(5)	364(4)	864(6)	11(2)
H(15,1)	957(4)	759(3)	167(5)	9(2)
H(15,2)	802(4)	751(3)	46(6)	9(2)
H(15,3)	839(3)	682(3)	214(5)	7(2)
H(16,1)	463(5)	1074(4)	245(6)	11(2)
H(16,2)	554(5)	1179(5)	358(7)	12(3)
H(16,3)	576(6)	1131(5)	150(8)	14(3)
H(17,1)	853(4)	947(3)	864(1)	8(2)
H(17,2)	970(5)	1027(4)	829(6)	10(2)
H(17,3)	822(5)	1074(4)	866(6)	11(3)
H(18,1)	1038(3)	851(3)	667(4)	7(1)
H(18,2)	1039(4)	777(3)	473(4)	7(1)

oxygen atom and the adjacent hydrogen atom H(3) is 2.33(2) Å. It would appear that the nitro group is wedged between the methane hydrogen atoms and the adjacent hydrogen atom H(3) on the ring and rotates out of plane in order to fit between them. A similar situation was shown to arise in 2-(3′-methyl-4′-nitrophenoxy)-1,3,5-diisopropylbenzene and there the nitro groups

Can. J. Chem. Downloaded from www.nrcresearchpress.com by 210.87.254.6 on 09/05/12
For personal use only.

Can. J. Chem. Downloaded from www.nrcresearchpress.com by 210.87.254.6 on 09/05/12
For personal use only.

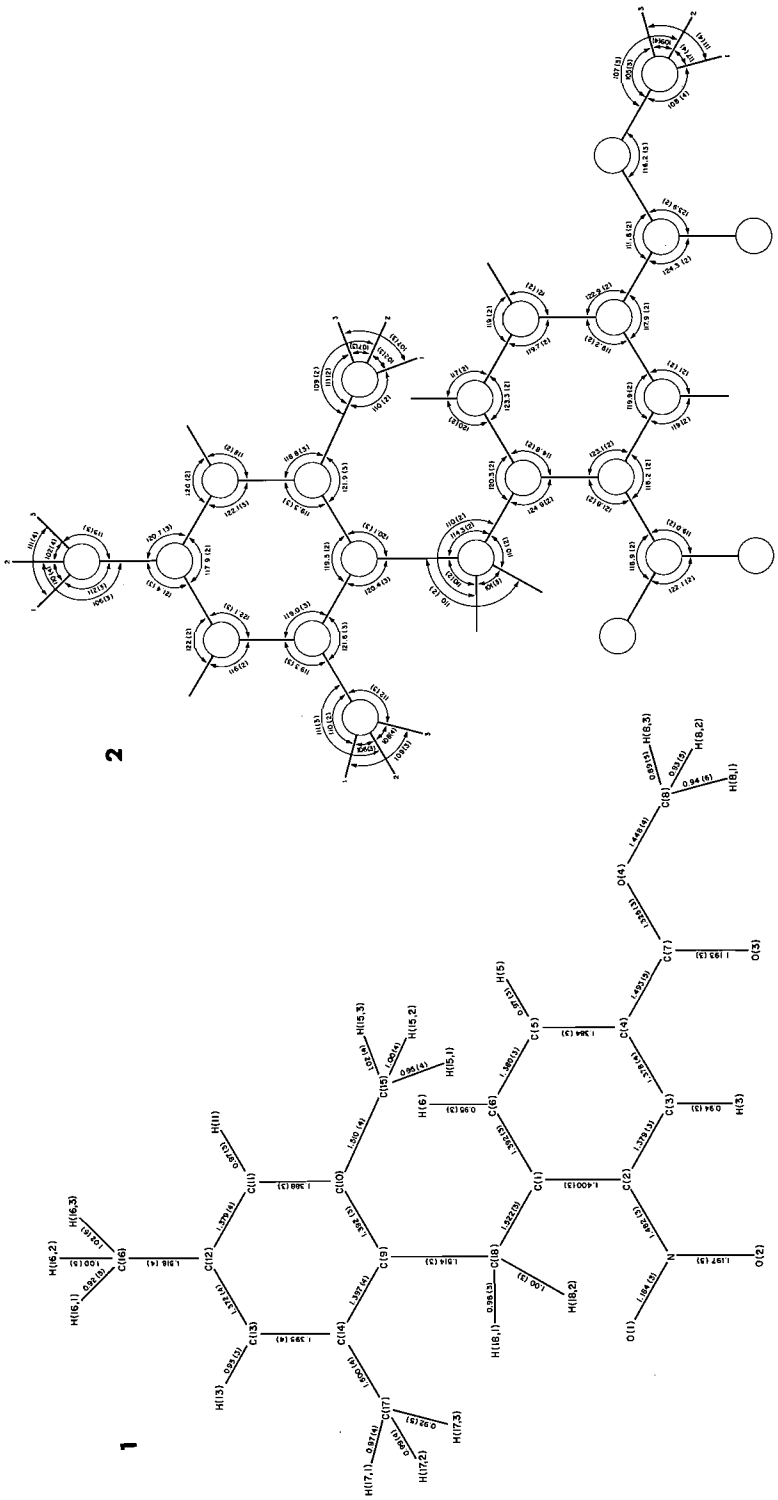

FIG. 1. Bond lengths and atom labeling. The numbers in parentheses are the estimated standard deviations.
FIG. 2. Bond angles.

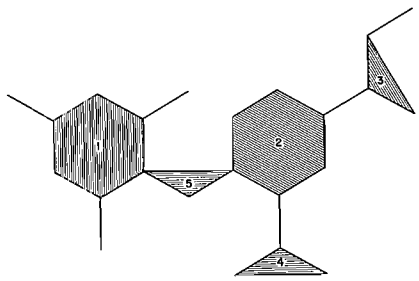

FIG. 3. Labeling of the least-squares planes.

are rotated by 11.7° and 4.8° in the two independent molecules (12). The bendings of the C—CH_3 and C—NO_2 bonds at the ring carbon atoms in the ether and the C—CH_2 and C—NO_2 bonds in the methane are similar in the two structures.

The nitro-substituted ring is bent 2.3(2)°

TABLE 2. Least-squares planes

(a) Equations of planes $Ax + By + Cz = D$. Coordinates refer to the directions of the a, c^*xa, and c^* axes. The planes are defined in Fig. 3

Plane	A	B	C	D
1	0.7619	0.6145	−0.2049	11.3491
2	0.1072	−0.3564	−0.9282	−6.0960
3	−0.0370	−0.2937	−0.9552	−6.8750
4	0.1401	−0.0730	−0.9875	−4.2042
5	0.1221	−0.3878	−0.9136	−6.1455

(b) Dihedral angles

Planes	Angle (deg)
1,2	87.0
1,5	87.6
2,3	9.1
2,4	16.8
2,5	2.2

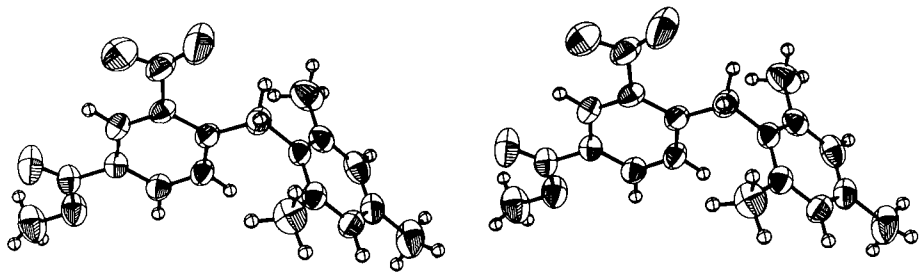

FIG. 4. Stereoscopic view of 2-(4′-carbomethoxy-2′-nitrobenzyl-1,3,5-trimethylbenzene.

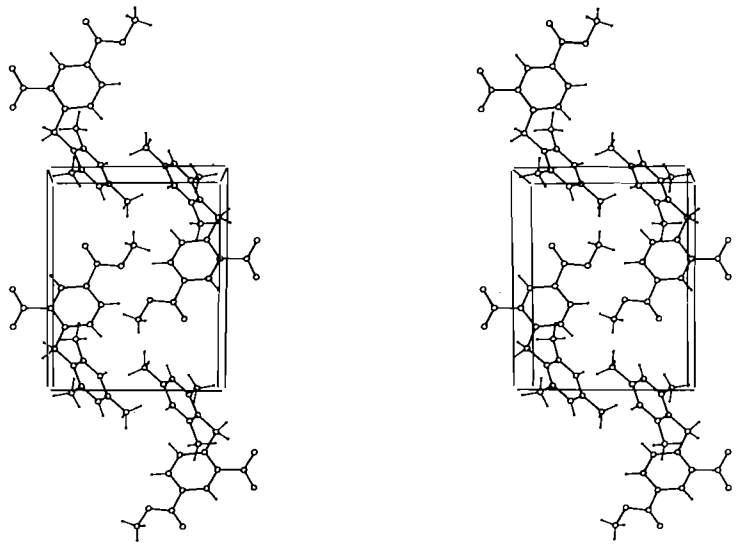

FIG. 5. Stereoscopic view of the molecular packing.

Can. J. Chem. Downloaded from www.nrcresearchpress.com by 210.87.254.6 on 09/05/12
For personal use only.

towards the mesityl ring. The similarly substituted ether and thioether and other ethers reported in this series which have a similar conformation to that of the methane are bent in the opposite sense. The difference here is caused by the contacts between the methylene hydrogen atoms and the atom O(1). This bending brings the atom H(6) closer to the π electrons of the mesityl ring but, because the C—CH_2 bond lengths here are longer than the C—O bond lengths in the ethers, the distance from the mesityl plane to the atom H(6) is not unusually short at 2.43 Å. Figure 4 shows a stereoscopic view of the molecule and Fig. 5 shows the molecular packing.

This research was supported by grants from the National Research Council of Canada.

1. S. P. N. VAN DER HEIJDEN, W. D. CHANDLER, and B. E. ROBERTSON. Can. J. Chem. **53**, 2108 (1975).
2. S. P. N. VAN DER HEIJDEN, W. D. CHANDLER, and B. E. ROBERTSON. Can. J. Chem. **53**, 2115 (1975).
3. H. BENJAMINS and W. D. CHANDLER. Can. J. Chem. **52**, 597 (1974).
4. E. WHITTAKER. Acta Cryst. **6**, 714 (1953).
5. D. T. CROMER and J. B. MANN. Acta Cryst. A**24**, 321 (1968).
6. R. F. STEWART, E. R. DAVIDSON, and W. T. SIMPSON. J. Chem. Phys. **42**, 3175 (1965).
7. G. GERMAIN and M. M. WOOLFSON. Acta Cryst. B**24**, 91 (1968).
8. G. GERMAIN, P. MAIN, and M. M. WOOLFSON. Acta Cryst. B**26**, 274 (1970).
9. A. ZALKIN. FORDAP, A Fortran program for Fourier calculations. University of California, Berkeley, California. 1965.
10. W. R. BUSING, K. O. MARTIN, and H. A. LEVY. ORFLS, Report ORNL-TM-305. Oak Ridge National Laboratory, Oak Ridge, Tennessee. 1962.
11. C. K. JOHNSON. ORTEP, Report ORNL-3794. Oak Ridge National Laboratory, Oak Ridge, Tennessee. 1965.
12. E. A. H. GRIFFITH, W. D. CHANDLER, and B. E. ROBERTSON. Can. J. Chem. **50**, 2963 (1972).
13. S. P. N. VAN DER HEIJDEN, E. A. H. GRIFFITH, W. D. CHANDLER, and B. E. ROBERTSON. Can. J. Chem. **53**, 2084 (1975).

Can. J. Chem. Downloaded from www.nrcresearchpress.com by 210.87.254.6 on 09/05/12
For personal use only.

Conformations of Bridged Diphenyls. XIII. Crystal Structure of 2-(4′-Carbomethoxy-2′-nitrobenzoyl)-1,3,5-trimethylbenzene

SIMON P. N. VAN DER HEIJDEN, W. DAVID CHANDLER, AND BEVERLY E. ROBERTSON[1]

Faculty of Science, University of Regina, Regina, Saskatchewan S4S 0A2

Received December 20, 1974

SIMON P. N. VAN DER HEIJDEN, W. DAVID CHANDLER, and BEVERLY E. ROBERTSON. Can. J. Chem. **53**, 2127 (1975).

The structure of 2-(4′-carbomethoxy-2′-nitrobenzoyl)-1,3,5-trimethylbenzene, $C_{18}H_{17}NO_5$, has been determined by X-ray diffraction. The crystals are triclinic, $a = 10.266(5)$, $b = 7.672(5)$, $c = 11.975(8)$ Å, $\alpha = 105.11(3)$, $\beta = 100.08(3)$, $\gamma = 111.50(3)°$, $P\bar{1}$ with $Z = 2$. The integrated intensities of 3732 independent reflections were measured on a four circle diffractometer; 2784 of these reflections were used in the refinement to give a final least-squares weighted residual of 0.046 and a conventional R factor of 0.053.

The molecule adopts the twist-nitro-*proximal* conformation similar to the conformation in the corresponding sulfoxide and sulfone. The angle subtended at the bridging carbon atom is 118.5(2)° and its bond lengths to phenyl carbon atoms are 1.502(2) and 1.503(2) Å.

SIMON P. N. VAN DER HEIJDEN, W. DAVID CHANDLER et BEVERLY E. ROBERTSON. Can. J. Chem. **53**, 2127 (1975).

On a déterminé la structure du (carbométhoxy-4′ nitro-2′ benzoyl)-2 triméthyl-1,3,5 benzène, $C_{18}H_{17}NO_5$, par diffraction de rayons-X. Les cristaux sont tricliniques, $a = 10.266(5)$, $b = 7.672(5)$, $c = 11.975(8)$ Å, $\alpha = 105.11(3)$, $\beta = 100.08(3)$, $\gamma = 111.50(3)°$, $P\bar{1}$ avec $Z = 2$. On a mesuré les intensités de 3732 réflexions indépendantes à l'aide d'un diffractomètre à quatre cercles. On a utilisé 2784 de cas réflexions pour affiner la structure jusqu'à une valeur de R pondérée de 0.046 et une valeur de R conventionnelle de 0.053.

Les molécules existent dans une conformation nitro-croisé "*proximal*" semblable à celle des sulfoxydes et des sulfones correspondantes. L'angle sous-tendu à l'atome de carbone de pont est de 118.5(2)° et les longueurs de liaisons avec les atomes de carbone des groupes phényles sont de 1.502(2) et 1.503(2) Å. [Traduit par le journal]

Introduction

This is the sixth and final detailed report of the structures of a series of similarly substituted bridged diphenyls in which the bridging group is varied (1–5). The conformation of this structure also has been studied by p.m.r., using the effect of ring-current shielding (6). The results of that study were not conclusive because of complications produced by the magnetic anisotropy of the carbonyl functional group. By comparison of the results with those obtained for the corresponding sulfoxide it was inferred, however, that the conformation was probably twist-nitro-*proximal*.

The results of the X-ray diffraction study of the sulfoxide and sulfone suggest that the coulombic repulsion between the nitro oxygen atoms and the carbonyl oxygen atom would promote a nitro-*proximal* conformation for this compound. The effect of possible conjugation between the bridging group and π electrons on either of the two rings is not important here and both the skew and twist conformation would seem possible based on this consideration. The notation used here has been discussed in detail previously (1).

The structures of three benzophenones have been determined previously by X-ray diffraction. Benzophenone and 3,3′-dibromobenzophenone both adopt the twist conformation (7, 8). The dihedral angles made by both phenyl rings and the central C—CO—C plane being *ca.* 27.5° in each case. 4,4′-Dimethoxybenzophenone (9) has two molecules per asymmetric unit with dihedral angles ranging from 24.2° to 35.4°. This conformation is presumably influenced by the steric interaction between the *ortho* hydrogen atoms and the carbonyl oxygen atom. The twist conformations thus seem to be preferred in diphenyl ketones.

Experimental

The synthesis of 2′-(4′-carbomethoxy-2′-nitrobenzoyl)-1,3,5-trimethylbenzene, $C_{18}H_{17}NO_5$, has been reported earlier (6). It was recrystallized from absolute ethanol, m.p. 121–122 °C. A sample with approximate dimensions 0.60 × 0.28 × 0.24 mm was examined by film techniques.

The crystal orientation and cell constants were deter-

[1]Author to whom correspondence should be addressed.

Can. J. Chem. Downloaded from www.nrcresearchpress.com by 210.87.254.5 on 09/05/12
For personal use only.

Can. J. Chem. Downloaded from www.nrcresearchpress.com by 210.87.254.5 on 09/05/12
For personal use only.

mined on a Picker FACS 1 automated four circle diffractometer, equipped with a graphite monochromator. The cell constants were determined by least squares. The errors in the cell constants are calculated as three times the estimated standard deviations obtained from the least-squares analysis. Twenty-three reflections centered at 2θ values between 35 and 45° were used in the calculation.

The crystal data are as follows:

$C_{18}H_{17}NO_5$ f.w. = 327.34

Triclinic, $P\bar{1}$, $a = 10.226(5)$, $b = 7.672(5)$, $c = 11.975$ (8) Å, $\alpha = 105.11(3)$, $\beta = 100.08(3)$, $\gamma = 111.50(3)°$, $\rho_o = 1.39$ g cm^{-3} (flotation), $\rho_c = 1.35$ g cm^{-3}, $Z = 2$, $F(000) = 344e$, $\mu(MoK\alpha) = 1.06$ cm^{-1}, $\lambda(MoK\alpha_1) = 0.70926$ Å, $T = 22 \pm 2$ °C.

The integrated intensities of 3732 independent reflections with 2θ values between 3.5 and 55° were collected with MoKα radiation using the θ–2θ scan mode, a minimum base width of 3.0° in 2θ, and 20 s background counts at each limit of the scan. The data were reduced to structure factors using standard procedures. No corrections were made for extinction or absorption.

A Wilson statistical calculation gave an overall temperature factor of 3.32 Å^2. The scattering factors for carbon, oxygen, and nitrogen atoms were taken from those given by Cromer and Mann (10). The scattering factors for the hydrogen atoms were taken from Stewart *et al.* (11). The average values of $|E|$ and $|E^2 - 1|$ were 0.767 and 1.044 indicating the centrosymmetric space group $P\bar{1}$. The 411 reflections with $|E| > 1.58$ were used to solve the structure using the logical symbolic addition method.[2] The *E*-map calculated from the solution with the second highest figures of merit yielded all 24 non-hydrogen atom positions. Using individual anisotropic temperature factors and unit weights, the weighted residual, R_w, of the full-matrix least squares was lowered to 0.116.[3]

The hydrogen atoms were found by difference Fourier calculations. The 2784 reflections for which $|F_o| > 1.0w^{-1/2}$ were used in the final cycles of refinement with the least-squares weights now calculated from $w^{-1/2} = 0.3907 - 0.05003|F_o| + 0.002630|F_o|^2$.

The final values of R_w and the conventional R factor were 0.046 and 0.053 respectively. The observed and calculated structure factors have been placed in the Depository of Unpublished Data.[4] The final positional and thermal parameters are listed in Table 1, with errors taken directly from the least-squares analysis. The bond lengths, bond angles, and atomic numbering are given in Figs. 1 and 2.

Discussion

The angles between the planes of 2-(4′-carbomethoxy-2′-nitrobenzoyl)-1,3,5-trimethylbenzene, as defined in Fig. 3, are given in Table 2. The molecule has the twist-nitro-*proximal* conformation as predicted. The larger dihedral angles made by the phenyl rings with the central plane than in the case of other reported benzophenones are caused, at least in part, by the larger van der Waals radius of the methyl groups as compared with hydrogen atoms in the benzophenone structures reported previously (7–9). The dihedral angles found here are in fact similar to those of the identically substituted sulfoxide and sulfone (3, 4). The torsional angles φ[C(9)—C(18)—C(1)—C(2)] and ψ[C(1)—C(18)—C(9)—(C10)] occur in (+ +) pairs in one enantiomer and in (− −) pairs in the other as is inferred by the twist conformation.

Buchanan *et al.* (16) have used ^{13}C n.m.r. as a tool in studying the conformations of benzophenones. They are able, however, to predict only the value of $\cos^2 \phi + \cos^2 \psi$. The only tri-*ortho*-substituted benzophenone which they considered contained three methyl groups. They concluded that the di-*ortho*-substituted ring is perpendicular to the central plane and the other is rotated through 30°. Although no predictions were made for compounds of the type reported here, it seems reasonable that the charges on the oxygen atoms of the nitro group might lead to a different conformation for 2-(4′-carbomethoxy-2′-nitrobenzoyl)-1,3,5-trimethylbenzene. A stereogram of the molecule is shown in Fig. 4.

The molecule shows no unusual intermolecular contacts and the hydrogen atoms show bond lengths ranging from 0.87(3) to 1.03(3) Å. The

[2]The direct methods program LSAM, written by Germain and Woolfson (12), was used for structure solution. The program FORDAP written by Zalkin (13) was used for all Fourier calculations. The program ORFLS, written by Busing *et al.* (14), was used for least-squares refinement. Stereograms were prepared with the aid of the program ORTEP, written by Johnson (15).

[3]During the data collection the angular setting of one of the Teflon coated arcs of the gonimeter head changed causing a drop in the intensity of the standard reflections. The crystal was realigned and data collection was resumed at a point such that all the data affected by the arc slippage were assumed to have been collected again. However, during the structure refinement it became apparent that this assumption was not correct and that some of the data not recollected were inaccurate. Therefore all of the data (approximately 400 reflections) in the shell of data including the inaccurate data were excluded from the final stages of refinement. We are obliged to point out, then, that the results of this analysis suffer from any systematic errors associated with either the use of two sets of alignment parameters for data collection or the exclusion of a shell of data from the least-squares refinement. However, a comparison of the bond lengths in all identically substituted bridged diphenyls in this series, including this one, shows that the r.m.s. deviation in the bonds not affected by the bridging group is less than (or equal to) the average e.s.d.'s of that bond length.

[4]Complete set of tabular data is available, at a nominal charge, from the Depository of Unpublished Data, CISTI, National Research Council of Canada, Ottawa, Canada K1A 0S2.

TABLE 1. Structural parameters (e.s.d.'s) for 2-(4′-carbomethoxy-2′-nitrobenzoyl)-1,3,5-trimethylbenzene

(*a*) Fractional atomic coordinates ($\times 10^4$) and thermal parameters U_{ij} ($\times 10^3$), t.f. = exp $\{-2\pi^2(a^{*2}h^2U_{11} + \ldots + 2a^*b^*hkU_{12} + \ldots)\}$

Atom	x	y	z	U_{11}	U_{22}	U_{33}	U_{12}	U_{13}	U_{23}
C(1)	5046(2)	4229(2)	3249(2)	38(1)	33(1)	35(1)	15(1)	6(1)	12(1)
C(2)	4623(2)	2251(2)	3192(2)	33(1)	32(1)	34(1)	11(1)	5(1)	13(1)
C(3)	5478(2)	1676(3)	3892(2)	36(1)	34(1)	33(1)	13(1)	7(1)	16(1)
C(4)	6808(2)	3129(3)	4715(2)	36(1)	39(1)	33(1)	16(1)	9(1)	15(1)
C(5)	7225(2)	5126(3)	4841(2)	38(1)	37(1)	36(1)	8(1)	0(1)	9(1)
C(6)	6354(2)	5660(3)	4119(2)	45(1)	31(1)	41(1)	12(1)	5(1)	12(1)
C(7)	7733(2)	2455(3)	5437(2)	39(1)	45(1)	34(1)	18(1)	8(1)	15(1)
C(8)	9997(3)	3391(5)	6836(3)	45(1)	81(2)	77(2)	29(2)	0(1)	36(2)
C(9)	3577(2)	3532(2)	1070(2)	37(1)	33(1)	39(1)	14(1)	8(1)	18(1)
C(10)	2106(2)	2985(2)	486(2)	40(1)	39(1)	42(1)	18(1)	11(1)	19(1)
C(11)	1487(2)	1667(3)	−712(2)	38(1)	47(1)	47(1)	15(1)	6(1)	21(1)
C(12)	2299(2)	958(3)	−1348(2)	52(1)	42(1)	40(1)	16(1)	10(1)	15(1)
C(13)	3767(2)	1588(3)	−773(2)	49(1)	44(1)	49(1)	23(1)	20(1)	20(1)
C(14)	4433(2)	2846(2)	437(2)	39(1)	36(1)	48(1)	16(1)	13(1)	23(1)
C(15)	1151(3)	3736(4)	1087(3)	50(1)	63(2)	65(2)	32(1)	20(1)	24(1)
C(16)	1591(4)	−454(5)	−2655(2)	76(1)	75(2)	44(1)	29(2)	9(2)	6(1)
C(17)	6048(2)	3490(3)	977(2)	39(1)	56(1)	59(1)	21(1)	16(1)	26(1)
C(18)	4234(2)	4860(2)	2384(2)	43(1)	34(1)	41(1)	16(1)	7(1)	16(1)
N	3163(2)	714(2)	2412(2)	41(1)	37(1)	46(1)	10(1)	2(1)	22(1)
O(1)	2125(2)	1109(2)	2495(1)	36(1)	64(1)	70(1)	16(1)	8(1)	32(1)
O(2)	3065(2)	−862(2)	1756(2)	69(1)	33(1)	77(1)	14(1)	−10(1)	4(1)
O(3)	7352(2)	758(2)	5401(1)	61(1)	49(1)	62(1)	23(1)	4(1)	28(1)
O(4)	9039(2)	3936(2)	6108(1)	38(1)	55(1)	57(1)	16(1)	−2(1)	23(1)
O(5)	4152(2)	6429(2)	2764(1)	86(1)	43(1)	56(1)	39(1)	5(1)	13(1)

(*b*) Fractional atomic coordinates ($\times 10^3$) and isotropic temperature factors for the hydrogen atoms

Atom	x	y	z	B (Å^2)
H(3)	517(2)	28(3)	379(2)	4(1)
H(5)	815(2)	609(3)	542(2)	4(1)
H(6)	667(2)	707(3)	424(2)	4(1)
H(11)	47(2)	120(3)	−111(2)	4(1)
H(13)	439(2)	119(3)	−118(2)	4(1)
H(8,1)	1078(3)	451(4)	724(3)	8(1)
H(8,2)	949(3)	274(4)	739(3)	10(2)
H(8,3)	1020(3)	237(5)	626(3)	10(2)
H(15,1)	15(3)	296(4)	63(2)	7(1)
H(15,2)	128(3)	367(4)	188(3)	7(1)
H(15,3)	138(3)	507(4)	118(2)	7(1)
H(16,1)	69(5)	−70(5)	−306(3)	12(2)
H(16,2)	184(4)	−154(5)	−278(3)	11(2)
H(16,3)	212(3)	6(4)	−314(3)	9(2)
H(17,1)	623(3)	270(4)	147(2)	8(1)
H(17,2)	652(3)	327(4)	42(2)	7(1)
H(17,3)	655(2)	489(4)	150(2)	6(1)

packing of the molecules is shown in Fig. 5, and is the same as for the similarly substituted sulfoxide. The packing scheme assumed by both compounds shows an association of phenyl rings of adjacent molecules as was the case for 2-(2′,6′-dinitrophenoxy)-*t*-butylbenzene (17), although the actual packing in the latter case was not the same as that reported here.

The bond lengths to the central carbon atom are virtually identical at 1.503(2) and 1.502(2) Å. They are slightly shorter than in the identically substituted diphenylmethane (1.514(3) and 1.522(3) Å for the mesityl and nitro-substituted ring respectively) (5). The angle subtended at the bridging carbon atom is 118.5(2)°, which is smaller than in the reported structures of other

Can. J. Chem. Downloaded from www.nrcresearchpress.com by 210.87.254.5 on 09/05/12
For personal use only.

Can. J. Chem. Downloaded from www.nrcresearchpress.com by 210.87.254.5 on 09/05/12
For personal use only.

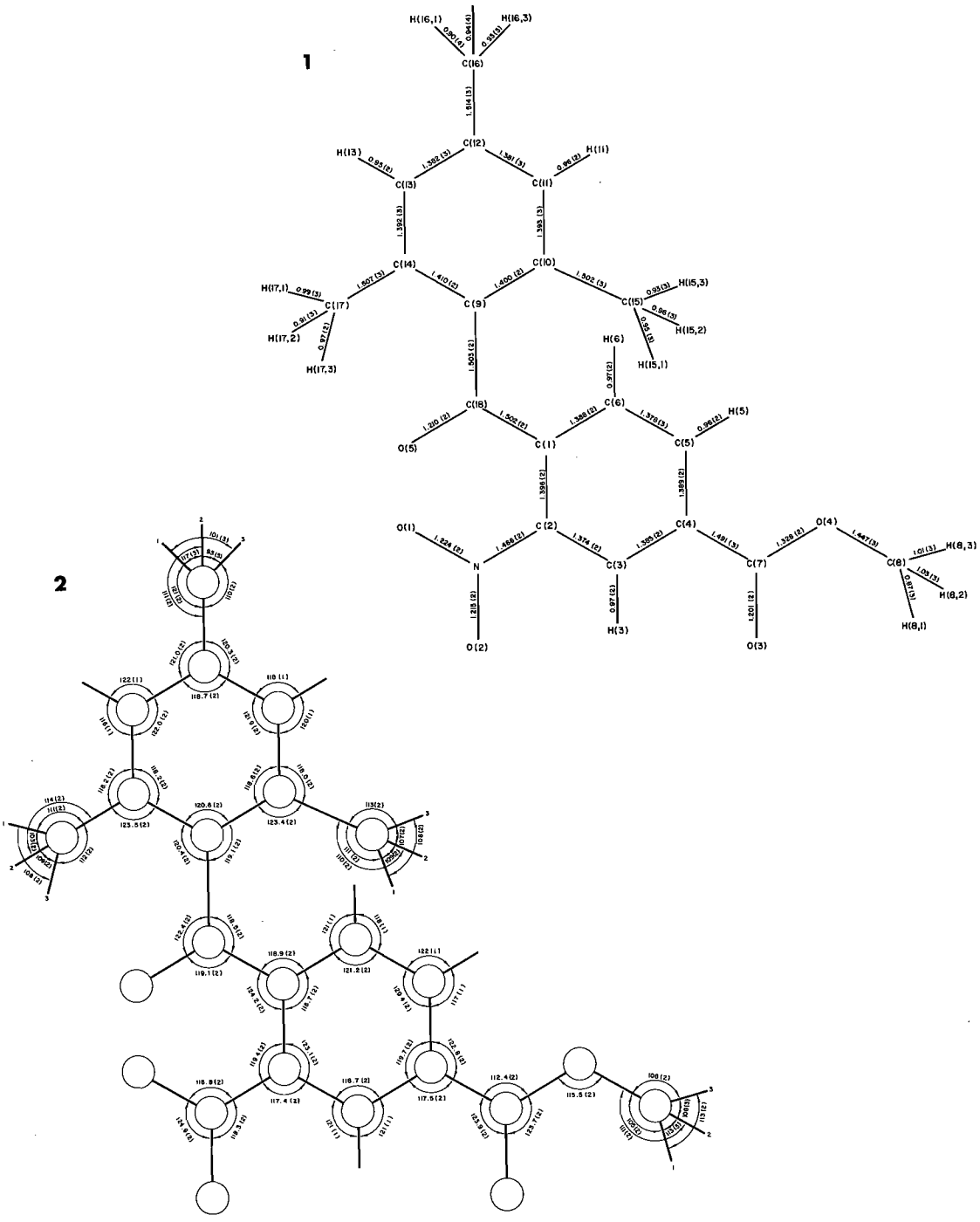

FIG. 1. Bond lengths and atom labeling. The numbers in parentheses are the estimated standard deviations.
FIG. 2. Bond angles.

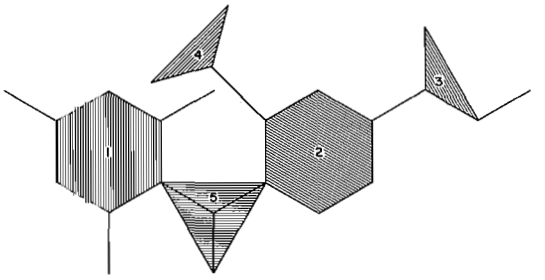

FIG. 3. Labeling of the least-squares planes.

TABLE 2. Least-squares planes

(*a*) Equations of planes $Ax + By + Cz = D$. Coordinates refer to the directions of the ***a***, ***c***xc***, and ***a****** axes. The planes are defined in Fig. 3

Plane	*A*	*B*	*C*	*D*
1	0.3632	0.8829	−0.2977	1.6782
2	0.7107	−0.1399	−0.6895	0.0803
3	0.6273	−0.1649	−0.7611	−0.6663
4	0.3216	0.5940	−0.7374	−2.0876
5	0.9504	0.2546	−0.1788	2.9450

(*b*) Dihedral angles

Planes	Angle (deg)
1,2	70.1
1,5	51.5
2,3	6.7
2,4	49.1
2,5	40.2

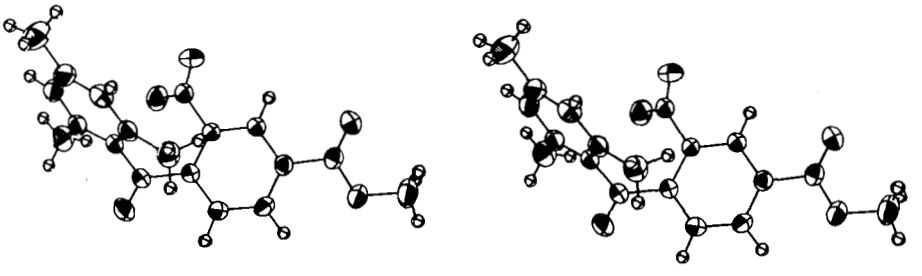

FIG. 4. Stereoscopic view of 2-(4′-carbomethoxy-2′-nitrobenzoyl)-1,3,5-trimethylbenzene.

Can. J. Chem. Downloaded from www.nrcresearchpress.com by 210.87.254.5 on 09/05/12
For personal use only.

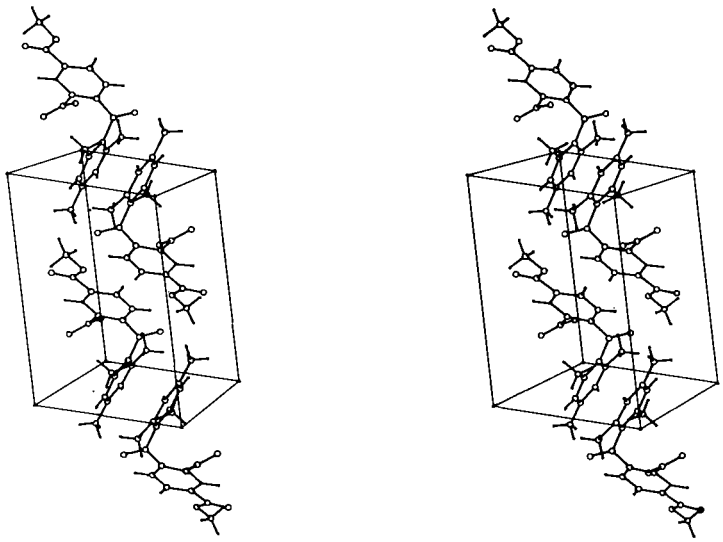

FIG. 5. Stereoscopic view of the molecular packing.

diphenyl ketones. The nitro-substituted ring is bent 2.7(2)° away from the mesityl ring at the atom C(1) and the nitro group is rotated through 49.1° from the plane of the ring to which it is bonded in order to fit over the mesityl ring.

This research was supported by grants from the National Research Council of Canada.

1. S. P. N. VAN DER HEIJDEN, E. A. H. GRIFFITH, W. D. CHANDLER, and B. E. ROBERTSON. Can. J. Chem. **53**, 2084 (1975).
2. S. P. N. VAN DER HEIJDEN, W. D. CHANDLER, and B. E. ROBERTSON. Can. J. Chem. **53**, 2102 (1975).
3. S. P. N. VAN DER HEIJDEN, W. D. CHANDLER, and B. E. ROBERTSON. Can. J. Chem. **53**, 2108 (1975).
4. S. P. N. VAN DER HEIJDEN, W. D. CHANDLER, and B. E. ROBERTSON. Can. J. Chem. **53**, 2115 (1975).
5. S. P. N. VAN DER HEIJDEN, W. D. CHANDLER, and B. E. ROBERTSON. Can. J. Chem. **53**, 2121 (1975).
6. H. BENJAMINS and W. D. CHANDLER. Can. J. Chem. **52**, 597 (1974).
7. E. FLEISER, N. SUNG, and S. HAWKINSON. J. Phys. Chem. **72**, 4311 (1968).
8. V. PATTABHI and K. VANKATESAN. J. Cryst. Mol. Struct. **3**, 25 (1973).
9. H. G. NORMENT and I. L. KARLE. Acta Cryst. **15**, 873 (1962).
10. D. T. CROMER and J. B. MANN. Acta Cryst. A**24**, 321 (1968).
11. R. F. STEWART, E. R. DAVIDSON, and W. T. SIMPSON. J. Chem. Phys. **42**, 3175 (1965).
12. G. GERMAIN and M. M. WOLFSON. Acta Cryst. B**24**, 91 (1968).
13. A. ZALKIN. FORDAP, A Fortran program for Fourier calculations. University of California, Berkeley, California. 1965.
14. W. R. BUSING, K. O. MARTIN, and H. A. LEVY. ORFLS, Report ORNL-TM-305. Oak Ridge National Laboratory, Oak Ridge, Tennessee. 1962.
15. C. K. JOHNSON. ORTEP, Report ORNL-3794. Oak Ridge National Laboratory, Oak Ridge, Tennessee. 1965.
16. G. W. BUCHANAN, G. MONTAUDO, and P. FINOCCHIARO. Can. J. Chem. **51**, 1053 (1973).
17. K. GURTU, W. D. CHANDLER, and B. E. ROBERTSON. Can. J. Chem. **53**, 2093 (1975).

Can. J. Chem. Downloaded from www.nrcresearchpress.com by 210.87.254.5 on 09/05/12
For personal use only.

Phosphorescence Lifetime of SO_2 in the $\tilde{a}^3B_1$ State at Low Pressure

J. PHILIP BRIGGS,[1] ROBERT B. CATON,[2] AND MICHAEL J. SMITH[3]

Department of Chemistry and Scarborough College, University of Toronto, West Hill, Ontario M1C 1A4

Received December 11, 1974

J. PHILIP BRIGGS, ROBERT B. CATON, and MICHAEL J. SMITH. Can. J. Chem. **53**, 2133 (1975).

The emission decay rate (inverse lifetime) of the optically-excited $\tilde{a}^3B_1$ electronic state of SO_2 vapor at approximately 25 °C has been measured in a 35 cm diameter spherical container over the pressure range $1 < P < 500$ mTorr in pure SO_2 and in mixtures of SO_2 with He, Ar, or Xe. The Stern–Volmer rate constant for quenching by SO_2 ($\tilde{X}^1A_1$) was determined to be $(4.46 \pm 0.11) \times 10^8$ l mol^{-1} s^{-1}, and the extrapolated, zero-pressure decay rate was calculated to be $(3.75 \pm 0.58) \times 10^2$ s^{-1}. The latter quantity implies a considerably greater proportionate contribution by radiative, as opposed to nonradiative, relaxation of this state than has been reported previously.

J. PHILIP BRIGGS, ROBERT B. CATON et MICHAEL J. SMITH. Can. J. Chem. **53**, 2133 (1975).

On a mesuré le taux d'émission de dégénérescence (inverse du temps de vie) de l'état électronique $\tilde{a}^3B_1$ du SO_2 sous forme vapeur excité optiquement; ces mesures ont été effectuées à environ 25 °C, dans un récipient sphérique de 35 cm de diamètre, à des pressions allant de 1 à 500 mTorr de SO_2 pur et dans des mélanges de SO_2 avec He, Ar ou Xe. On a déterminé que la constante de vitesse de Stern–Volmer pour le piégage du SO_2 ($\tilde{X}^1A_1$) est $(4.46 \pm 0.11) \times 10^8$ l mol^{-1} s^{-1} et on a calculé, par extrapolation, que le taux de dégénérescence à pression zéro est $3.75 \pm 0.58 \times 10^2$ s^{-1}. Contrairement à ce qui avait été rapporté antérieurement, cette dernière valeur suggère que la relaxation de cet état evolue relativement plus par des processus radiatifs que par des processus non-radiatifs. [Traduit par le journal]

Introduction

Recent theories of radiationless transitions (1) predict that for small molecules, which possess relatively few vibrational degrees of freedom, the experimental phenomenon of nonradiative relaxation should be absent in an isolated molecule. The variety of attempts which have been made both to measure and to calculate the zero-pressure, or collision-free lifetime of the $\tilde{a}^3B_1$ electronic state of sulfur dioxide vapor have not demonstrated convincingly whether this system behaves as predicted by theory.

Recent experimental measurements of the decay rate of SO_2 phosphorescence by flash lamp excitation (2), by pulsed laser excitation (3), and by a Becquerrel phosphoroscope technique (4) have led to the conclusion that there is a dominant nonradiative contribution to the relaxation rate. This conclusion, however, is based, in part, on a long extrapolation of the linear portion of τ^{-1} *vs.* P plots from a minimum 70 mTorr to obtain the value of the intercept, τ_0^{-1}, the collision-free relaxation rate constant.

Such behavior is, of course, at odds with theory (1) and with the fact that the discrete rotational structure of the transitions to the first few levels of the $\tilde{a}^3B_1$ state, whose lifetime was measured in these studies, can be assigned line-by-line and shows no major perturbations (5). If these levels decay by primarily nonradiative channels, the lines should be severely inhomogeneously broadened (1) or should exhibit severe perturbations (6), neither of which is observed.

We felt it worthwhile to reinvestigate the transient decay characteristics of optically-excited SO_2 in its $\tilde{a}^3B_1$ state, specifically to measure the $^3SO_2$ lifetime at considerably lower pressures than had been reached previously. The SO_2 triplets in our study, as in refs. 2 and 4, were produced by intersystem crossing from the electronically-excited singlet manifold of the 290 nm absorption system. We have also examined the effect of rare gas collision partner on the lifetime of $^3SO_2$.

[1]Present address: Department of Chemical Engineering, University of Waterloo, Waterloo, Ontario.

[2]Present address: Ontario Ministry of the Environment, 880 Bay St., Toronto, Ontario M5S 1Z8.

[3]Present address: Dow Chemical Co. of Canada Ltd., Sarnia, Ontario.

Can. J. Chem. Downloaded from www.nrcresearchpress.com by 210.87.254.6 on 09/05/12
For personal use only.

TABLE 1. Measured pseudo first-order rate constants for the decay of $^3SO_2$ in pure SO_2

k ($s^{-1} \times 10^{-3}$)	P (mTorr)	λ_{exc} (nm)	k ($s^{-1} \times 10^{-3}$)	P (mTorr)	λ_{exc} (nm)
11.70	481.2	313	0.870	19.4	313
6.17	245.9	313	0.800	18.2	313
5.04	181.6	313*	0.666	16.8	313
3.88	157.6	313	0.760	16.5	313
4.16	157.6	313	0.660	15.5	313
4.05	138.5	313*	0.857	14.8	313
3.35	124.0	313	0.900	14.8	313
2.84	98.0	313*	0.690	14.0	313
2.50	81.5	289	0.630	13.8	297
1.77	70.0	313*	0.670	11.9	313
1.84	56.4	313*	0.644	11.2	289
1.84	56.4	313*	0.600	11.2	297
1.46	47.1	313	0.600	11.2	313
1.29	46.7	313	0.580	10.1	313
1.50	46.3	313	0.560	8.9	297
1.50	46.3	289	0.730	8.0	313
1.05	38.0	289	0.585	6.25	313
0.985	32.0	313	0.600	5.9	297
1.35	31.3	313	0.775	4.8	313
1.09	30.6	313	0.665	4.0	297
0.993	29.2	313*	0.717	3.35	313
1.14	28.3	313	0.755	3.05	313
1.04	26.2	313	0.840	2.60	313
0.930	24.4	313	0.842	2.10	297
0.819	23.7	289	0.886	2.05	297
0.915	23.5	313	1.35	1.31	313
0.860	21.0	313	1.24	1.2	313
1.05	20.7	313	1.31	1.15	313
0.820	19.4	297			

*NOTE: Emission detected at 415 nm.

Experimental

SO_2 gas (Anhydrous Grade, 99.995%) and the rare gases He, Ar, and Xe (Research Grade, 99.995 to 99.9995%) were supplied by Matheson of Canada and were used without further purification.

SO_2 at about 25 °C in a spherical, 35 cm diameter cell was excited by the 289, 297, or 313 nm pressure-broadened lines of a 200 W Hg/Xe compact arc lamp, which were selected by a ½ m monochromator having a bandpass of about 2.4 nm. The number density of $^3SO_2$ in the cell and the collection of the emission were enhanced by means of a multi-pass optical system described by Parmenter and Schuyler (7).

The detector, an EMI 6256S PMT, was interfaced with the cell either directly via a Jena WG-1 cutoff filter (1% transmission at 350 nm) or via a Spex ¾ m spectrometer. The latter arrangement allowed the decay characteristics of individual vibronic features of the emission spectrum to be monitored.

Modulation of the exciting light was achieved mechanically by means of a sectored disk rotated at 1750 r.p.m. The time-dependent $^3SO_2$ (or in some cases $^1SO_2$) emission was measured as follows. A phototransitor mounted behind the entrance slit of the ½ m monochromator was part of a Schmitt trigger circuit whose output fed a Tektronix 2101 pulse generator. The delayed trigger from this pulse generator activated the coincidence gate of an Ortec photon-counting unit for a time period equal to the width of the pulse. The output signals from both the phototransitor and the pulse generator were displayed on a Tektronix 547 dual-trace oscilloscope. The counting period (normally 20 μs) and delay time, which were set with the 2101 pulse generator, could be observed and measured with the oscilloscope. The time bases of the oscilloscope and pulse generator were recently calibrated.

The pressure of SO_2 (or of gas mixtures) over the entire pressure range was measured with an M.K.S. Baratron capacitance manometer which was attached directly to the cell. The accuracy of this instrument was checked between 1 and 500 mTorr by calibrating it against an H.S. Martin and Son McLeod gauge. Helium was used as the calibrating gas to prevent error due to pumping by the stream of mercury vapor flowing from the gauge to the isolating cold trap (8). The M.K.S. specification of 1% accuracy was found to be satisfactory above 30 mTorr, whereas, the agreement was within 5% below this pressure.

Photon counts were normally accumulated for 200 s on a digital scaler, and the emission intensity as a function of the gate delay time was recorded manually. Inverse lifetimes were computed from the exponential

Can. J. Chem. Downloaded from www.nrcresearchpress.com by 210.87.254.6 on 09/05/12
For personal use only.

Can. J. Chem. Downloaded from www.nrcresearchpress.com by 210.87.254.6 on 09/05/12
For personal use only.

decay curves according to the usual relationship: $\ln (I_0/I) = \tau^{-1}t$ by a linear least-squares method. Ten to twelve data points, corrected for background, were used for each inverse lifetime calculation.

The graph of these τ^{-1} values plotted *vs.* pressure was in turn fitted by an unweighted linear least-squares method to obtain its slope and intercept, the desired Stern–Volmer bimolecular quenching rate constant and inverse collision-free lifetime, respectively. The calculation assumed no error in the independent variable, namely pressure at a given time. The validity of this assumption was established by the calibration procedures described above.

Results

The measured emission decay pseudo-first-order rate constants at each pressure are presented for pure SO_2 in Table 1, and for SO_2/rare gas mixtures in Table 2, along with the excitation wavelengths.

These data show that the $^3SO_2$ decay rate was insensitive to variations in the exciting wavelength at a given pressure, which suggests that the observed rate is characteristic of $^3SO_2$ and not of the rate process which populates $^3SO_2$ from $^1SO_2$. Decay rates measured for the $\tilde{a}^3B_1$ (000)–$\tilde{X}^1A_1$ (110) vibronic band at 415 nm were indistinguishable from those for the integrated $^3SO_2$ emission passed by the cutoff filter. Because of low signal, the 415 nm band could be monitored only at pressures greater than about 30 mTorr; thus, the low-pressure rates refer only to integrated emission passed by the WG-1 filter.

The least-squares equation for τ^{-1} as a function of pressure for the linear portion of this

TABLE 2. Measured pseudo first-order rate constants for the decay of $^3SO_2$ in SO_2/rare gas mixtures excited at 313 nm

He		Ar		Xe	
k ($s \times 10^{-3}$)	P_{total} (mTorr)*	k ($s \times 10^{-3}$)	P_{total} (mTorr)*	k ($s \times 10^{-3}$)	P_{total} (mTorr)*
1.14	241.0	0.678	198.8	1.18	240.0
1.00	241.0	0.669	197.8	0.885	150.0
0.728	218.0	0.665	197.8	0.505	71.6
0.793	218.0	0.405	103.0	0.360	33.8
0.767	174.8	0.443	103.0	0.423	33.8
0.997	174.8	0.433	50.0	0.345	17.6
0.760	137.6	0.347	24.3	0.329	17.6
0.553	120.0	0.370	24.3	0.396	9.8
0.600	120.0	0.500	10.2	0.419	9.8
0.599	115.0	0.542	10.2	0.441	6.6
0.561	79.5	0.576	10.2	0.457	6.6
0.549	79.5	0.735	3.2	0.611	4.0
0.561	77.5	0.760	3.2	0.524	4.0
0.421	61.0				
0.476	61.0				
0.501	48.6				
0.635	42.2				
0.650	40.8				
0.460	40.0				
0.507	40.0				
0.566	29.2				
0.548	29.2				
0.664	20.8				
0.580	20.0				
0.556	20.0				
0.696	10.2				
0.716	10.0				
0.747	5.8				
0.874	4.0				
0.748	4.0				
0.882	4.0				
0.668	3.0				

*NOTE: Partial pressure of SO_2 = 2 mTorr in all experiments.

TABLE 3. Summary of decay rate constants for optically excited $^3SO_2$ in pure SO_2 compared with literature values

k_q (l mol^{-1} s^{-1} × 10^{-8})*	$k_p + k_{nr}$ (s^{-1} × 10^{-3})*	Reference
4.46 ± 0.11	0.375 ± 0.058	This work
4.52 ± 0.18	1.12 ± 0.20	4
	2.0 ± 0.8	4
3.9 ± 0.1	0.98 ± 0.68	2
3.9 ± 0.7	1.13 ± 0.18	3

*NOTE: Errors quoted are 2 standard deviations in most cases.

function, that is, for the 43 points in the pressure range 10 to 480 mTorr, is

$$[1]\quad \tau^{-1} = (3.75 \pm 0.58) \times 10^2 + (23.8 \pm 0.6) \times P_{SO_2}\ \text{mTorr s}^{-1}$$

Thus, the rate constants for processes 2, 3, and 4 in the usual Stern–Volmer quenching scheme:

$$[2]\quad {}^3SO_2 + SO_2 \xrightarrow{k_q} 2SO_2$$

$$[3]\quad {}^3SO_2 \xrightarrow{k_p} SO_2 + h\nu_p$$

$$[4]\quad {}^3SO_2 \xrightarrow{k_{nr}} SO_2$$

may be computed to be

$$[5]\quad k_q = (4.46 \pm 0.11) \times 10^8\ \text{l mol}^{-1}\ \text{s}^{-1}$$

and

$$[6]\quad (k_p + k_{nr}) = (3.75 \pm 0.58) \times 10^2\ \text{s}^{-1}$$

The errors noted are two standard deviations.

These values of k_q and $(k_p + k_{nr})$ are compared with literature values in Table 3. The zero-pressure rate constant [6] is barely within the uncertainty limits of the pulsed laser experiments of Calvert and co-workers (3) and is nearly a factor of three smaller than that of Otsuka and Calvert (2) and Strickler *et al.* (4).

There is no noticeable curvature of the τ^{-1} *vs.* P plot at low pressure which might have led to this considerable disagreement. The 17 values of τ^{-1} for pressures greater than 35 mTorr give essentially the same slope and intercept (23.7 mTorr^{-1} s^{-1} and 400 s^{-1}, respectively) as the 26 values corresponding to pressures between 10 and 35 mTorr (24.8 mTorr^{-1} s^{-1} and 357 s^{-1}, respectively). Thus, vibrational relaxation effects which were observed by Caton and Gangadharan (9) at pressures less than approximately 35 mTorr did not influence the present results appreciably.

The heterogeneous quenching reaction

$$[7]\quad {}^3SO_2 + \text{wall} \rightarrow SO_2 + \text{wall}$$

has prevented previous investigators from making accurate measurements of inverse lifetime below 100 mTorr pressure. Both Calvert and co-workers (2, 3) and Strickler *et al.* (4) have used containers of small diameter (~5 cm) to make $^3SO_2$ lifetime measurements below 100 mTorr, which may have influenced their results.

The slope of the τ^{-1} *vs.* P plot, k_q, is essentially identical to the values reported by Calvert (2, 3) and Strickler (4). The disagreement between the present and previous results concerns only the intercept, which is, of course, extremely sensitive to small deviations in the slope and to extrapolation. The smallest measured value of τ^{-1} for pure SO_2 in this work, 580 s^{-1} at 10.1 mTorr, is already a factor of two smaller than Strickler's intercept, and the minimum value of τ^{-1} measured in an SO_2/Xe mixture was about 330 s^{-1}. These facts suggest that our extrapolated value of τ^{-1} is more significant than that of Calvert and co-workers (2, 3) and of Strickler *et al.* (4).

The analogs of eq. 1 for SO_2 (2 mTorr partial pressure) in the presence of the added gases He, Ar, or Xe are

$$[8]\quad \tau^{-1}(\text{He}) = (304 \pm 28) + (2.70 \pm 0.18) \times P_{\text{total}}\ \text{mTorr s}^{-1},\ P > 60\ \text{mTorr}$$

$$[9]\quad \tau^{-1}(\text{Ar}) = (301 \pm 17) + (1.78 \pm 0.14) \times P_{\text{total}}\ \text{mTorr s}^{-1},\ P > 24\ \text{mTorr}$$

$$[10]\quad \tau^{-1}(\text{Xe}) = (262 \pm 11) + (3.88 \pm 0.10) \times P_{\text{total}}\ \text{mTorr s}^{-1},\ P > 17\ \text{mTorr}$$

The quenching rate constants for these three gases with respect to reaction 11:

$$[11]\quad {}^3SO_2 + M \xrightarrow{k_q'} SO_2 + M$$

are then

$$k_q'(\text{He}) = (5.06 \pm 0.34) \times 10^7\ \text{l mol}^{-1}\ \text{s}^{-1}$$

$$k_q'(\text{Ar}) = (3.34 \pm 0.26) \times 10^7\ \text{l mol}^{-1}\ \text{s}^{-1}$$

$$k_q'(\text{Xe}) = (7.27 \pm 0.19) \times 10^7\ \text{l mol}^{-1}\ \text{s}^{-1}$$

For comparison, Sidebottom *et al.* (10) measured k_q' for He, Ar, and Xe, respectively, to be $(6.8 \pm 0.7) \times 10^7$, $(5.2 \pm 0.5) \times 10^7$, and $(7.1 \pm 1.1) \times 10^7$ l mol^{-1} s^{-1} for direct laser excitation of the $\tilde{a}^3B_1$ state. Wampler *et al.* (11)

Can. J. Chem. Downloaded from www.nrcresearchpress.com by 210.87.254.6 on 09/05/12
For personal use only.

found $k_q'(Ar)$ to be $(4.75 \pm 0.96) \times 10^7$ l mol^{-1} s^{-1} for broadband excitation of the singlet manifold or $(5.58 \pm 0.56) \times 10^7$ l mol^{-1} s^{-1} for direct laser excitation of the triplet state. These data were obtained at much higher pressure than the present results.

As a check on the instrumentation, the long-lived $^1SO_2$ emission discovered by Brus and McDonald (12) was monitored at 351 nm at pressures between 0.5 and 5 mTorr in pure SO_2. For excitation at 297 nm, τ_0 was 140 μs, and at 313 nm, 200 μs. The Stern–Volmer quenching rate constants were 1.6×10^{-10} and 2.0×10^{-10} cm^3 s^{-1}, respectively. These values are to be compared with Brus and McDonald's values (12) for τ_0 of 184 μs (296 nm excitation) and 308 or 532 μs (304 or 320 nm excitation, respectively). Brus and McDonald's quenching constants were 1.09×10^{-10} and 1.47×10^{-10} or 1.53×10^{-10} cm^3 s^{-1}, respectively. The agreement is satisfactory, considering the severe wavelength and bandwidth dependence of the $^1SO_2$ lifetime.

Discussion and Conclusions

The Effect of Container Diameter on the Measured Decay Rate of $^3SO_2$

The data reported in Table 1 are represented in Fig. 1 along with the analogous results of Otsuka and Calvert (2) and Strickler *et al.* (4). Comparison of these data reveals the effect of container size on the measured decay rates. Otsuka and Calvert (2), as well as Strickler *et al.* (4), attributed the curvature in their $^3SO_2$ τ^{-1} *vs.* P graphs to the boundary process [7]. Our data support this explanation of the earlier investigators. Detection geometry may also influence the measured decay rates (13), and deviation from the linear Stern–Volmer relation at low pressure can occur if $^3SO_2$ diffuses from the monitored volume element (2). Such diffusion apparently explains the decrease in $^3SO_2$ lifetime below 10 mTorr in pure SO_2. If the decay rates for pressures of pure SO_2 less than 10 mTorr are plotted as $(\tau_{obs}^{-1} - \tau_{calc}^{-1})$ *vs.* P^{-1}, where τ_{calc}^{-1} is calculated from eq. 1, by analogy with Fig. 3 of ref. 2, a linear relationship is found. Such a linear relationship is to be expected if either diffusion-controlled wall deactivation or diffusion from the field of view of the detector is important (2). Analysis of our data indicates that diffusion alters the measured decay rates by less than 10% above 10 mTorr

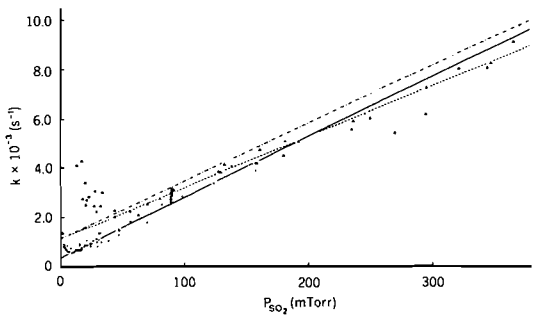

FIG. 1. Plot of τ^{-1} *vs.* P for pure SO_2: ● and —, present work; ▲ and ---, data from Table 1 of ref. 2; △ and –·–, data reconstructed from Fig. 1 of ref. 4.

in pure SO_2 and by only 20% at 10 mTorr, the lowest pressure which was used in obtaining eq. 1.

Caton and Gangadharan (9) have demonstrated the influence of vibrational relaxation on the population of $^3SO_2$ from $^1SO_2$ at pressures less than 5 mTorr. Vibrational relaxation (cascade) effects, such as emission from possibly shorter-lived vibrationally-excited levels of $^3SO_2$, might be indistinguishable from diffusion-loss effects. This point is discussed further in ref. 9.

In any case, the emission collection geometry and the large cell which were employed in the present work have clearly extended, by an order of magnitude, the pressure range over which diffusion-free decay constants could be measured.

The Effect of He, Ar, and Xe on the Measured Decay Rates of $^3SO_2$

The diffusion coefficient of SO_2, in mixtures with the rare gases at a given total pressure should decrease monotonically from He to Xe, as predicted by the usual gas kinetic formulae. Deviations from Stern–Volmer behavior are thus to be expected at higher pressures in SO_2/He mixtures than in SO_2/Ar and SO_2/Xe mixtures, respectively. Figure 2, in which the data of Table 2 are plotted for pressures less than 50 mTorr, shows clearly that at low pressures the inverse lifetimes do in fact increase in the order $\tau^{-1}(Xe) < \tau^{-1}(Ar) < \tau^{-1}(He)$ at a given pressure. Furthermore, curvature in the Stern–Volmer plot appears at a much higher pressure in He mixtures (about 50 mTorr) than in Xe mixtures (about 15 mTorr), as expected if diffusional loss is responsible.

The slopes of eqs. 8, 9, and 10 are also expected to increase monotonically in the order

Can. J. Chem. Downloaded from www.nrcresearchpress.com by 210.87.254.6 on 09/05/12
For personal use only.

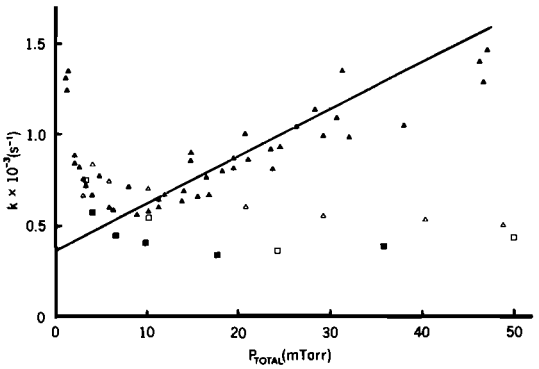

FIG. 2. Plot of τ^{-1} *vs.* P for pure SO_2 and for mixtures of SO_2 with He, Ar, or Xe in the low pressure region. Partial pressure of SO_2 in each mixture = 2 mTorr. △, He; □, Ar; ■, Xe; ▲, SO_2. The solid line is the least-squares fit to the pure SO_2 data between 10 and 480 mTorr, eq. 1.

$k_q'(\text{He}) < k_q'(\text{Ar}) < k_q'(\text{Xe})$, since both the polarizability (14) and spin–orbit coupling (external heavy atom effect) increase in this order. On the basis of the present data, Xe is clearly somewhat more effective than Ar and He, but a more quantitative theoretical treatment on the basis of these three isolated data does not seem justifiable. Our values of k_q' for He, Ar, and Xe agree reasonably well with the values reported in refs. 10 and 11. The fact that $k_q'(\text{He})$ and $k_q'(\text{Ar})$ are slightly smaller for initial excitation into the singlet manifold than for direct triplet excitation may be a real effect of intersystem crossing and vibrational relaxation.

The intercepts of eqs. 8, 9, and 10 should not be taken very seriously because of the uncertainty of extrapolating graphs with such shallow slopes, but they are nearly within the error limits of the pure SO_2 (eq. 1) intercept and serve to support our contention that τ_0^{-1} is considerably less than the value reported by other investigators.

Calculated Values of the Zero-pressure Decay Rate of $^3SO_2$

The purely radiative rate constant for reaction 3 has been calculated from absorption spectroscopic data (4) and found to be (79 ± 5) s^{-1}.

In calculating this value Strickler *et al.* made use of the formula

$$A_{u\to l} = 2.880 \times 10^{-9} n^2 \langle \bar{\nu}_e^{-3} \rangle_{Av}^{-1} g_l/g_u \times \frac{\langle M^2 \rangle_u}{\langle M^2 \rangle_l} \int \varepsilon \, d \ln \bar{\nu}$$

for the radiative transition probability, where the ratio of the degeneracies of the lower and upper states ($\tilde{X}^1A_1$ and $\tilde{a}^3B_1$, respectively) was taken as $g_l/g_u = 1/3$. Strickler and Berg (15) pointed out in their development of the above equation that a triplet state should be given a degeneracy of three only if all possible transitions between the spin components of the triplet state and the ground singlet state are equally allowed or if "... there is a rapid equilibrium established between molecules in the different component states of each degenerate level." Brand *et al.* (5) have shown that 80 to 90% of the intensity in the $\tilde{a}^3B_1$–$\tilde{X}^1A_1$ transition of SO_2 is carried by the z-spin component (b-axis polarization), which does not satisfy the first criterion of Strickler and Berg and implies that g_u should be near unity.

If the rapid equilibrium hypothesis is valid at pressures greater than about 10 mTorr (70 mTorr in previous studies), then the linearly-extrapolated, zero-pressure value of τ^{-1} would correspond to $g_u = 3$ as claimed by Strickler *et al.* (4). Since Strickler and Berg (15) intended this criterion to be applied to the condensed phase, the existence of a rapid equilibrium amongst the three spin levels, under conditions of low pressure in the gas-phase, is only hypothetical in the absence of an experimental test. A rough calculation indicates that a $^3SO_2$ molecule undergoes about 150 collisions during its measured lifetime at 10 mTorr in pure SO_2 and about 100 collisions during that time in the 1:5 SO_2/Xe mixture at 10 mTorr. These collision numbers are probably sufficient to bring about equilibration of the spin level populations, since the available data for polyatomic molecules suggest that only a few collisions are necessary to bring about randomization of rotational angular momentum from an initially nonequilibrium distribution. This fact, combined with the fact that the spin–spin and spin–rotation coupling constants are of the same magnitude as the spin–orbit splitting in the $\tilde{a}^3B_1$ state (5), argues in favor of the rapid equilibration model.

If the value of (79 ± 5) s^{-1} is to be used for k_p ($g_u = 3$), $\tilde{a}^3B_1$ relaxation is about 20% radiative, rather than 6% as found by Calvert *et al.* (2, 3) and Strickler *et al.* (4).

If the rapid equilibration model is incorrect, the calculated value of k_p should be multiplied by a factor of 3, such that the predicted zero-pressure intercept of τ^{-1} *vs.* P would be (237 ±

Can. J. Chem. Downloaded from www.nrcresearchpress.com by 210.87.254.6 on 09/05/12
For personal use only.

Can. J. Chem. Downloaded from www.nrcresearchpress.com by 210.87.254.6 on 09/05/12
For personal use only.

15) s^{-1}. Comparing this revised calculated value with the present experimental value of (375 ± 58) s^{-1}, it appears that $\tilde{a}^3B_1$ would be predominantly radiative, rather than predominantly nonradiative as suggested in refs. 2–4.

Several arguments can be put which support the reliability of the present results. The reasonable agreement between our values for the lifetimes and quenching constants of long-lived $^1SO_2$ and those of Brus and McDonald (12) and the fact that we measured our pressures with a single, reliable gauge over the entire pressure range (which had not been the case previously) imply that a systematic error should not be invoked to explain the large difference in intercept between our Stern–Volmer plots and those of previous investigators. The loss of precision associated with our use of 10 or 12 manually-set scaler channels as compared with 100 electronically scanned channels of Strickler *et al.* should not be critical, since the statistical significance is related to the square root of the sample size.

General Discussion

All of the results of experiments in which optical excitation was used (this work and refs. 2–4) should be compared with those of the only other study in which the emission decay characteristics of SO_2 were monitored to a pressure of 1 mTorr (16). Caton and Duncan (16) reported the parameters $\tau(^3SO_2)$, $k_q(SO_2)$, and $k_q'(He)$ as derived from an analysis of transient decay traces produced by a pulsed electrodeless electrical discharge. Their values of $\tau_0^{-1} = (1.4 \pm 0.2) \times 10^2\ s^{-1}$ and of both $k_q(SO_2)$ and $k_q'(He) \approx 0$ are far outside the experimental uncertainty of those from the optical studies. One can conclude with some caution that the electrically-excited emission processes are not the same as those processes described in this paper and in the other reports on optical experiments. A source of the vast difference between these two sets of results may be the significant degree of dissociation of the SO_2, which occurred in the discharge and the consequent uncertainty of the nature of the emitting species. It is possible of course, that these results refer to sublevels of $^3SO_2$ which are not populated by optical processes.

In summary, the present study demonstrates that electronic relaxation of optically-excited $^3SO_2$ has a significantly greater radiative contribution than has been reported earlier. The data suggest that radiative decay occurs with between 20 and 60% efficiency, depending upon the argument outlined in the previous section of this Discussion. This conclusion, which remains unexplained on theoretical grounds, should be tested further, perhaps by molecular beam magnetic resonance techniques. Some attempt, as well, should be made to elucidate the differences between the characteristics of optically-excited and electrically-excited emission processes in SO_2.

We thank Professor S. J. Strickler for helpful discussions and correspondence.

1. M. Bixon and J. Jortner. J. Chem. Phys. **50**, 3284 (1969); W. M. Gelbart and K. F. Freed. Chem. Phys. Lett. **18**, 470 (1973).
2. K. Otsuka and J. G. Calvert. J. Am. Chem. Soc. **93**, 2581 (1971).
3. H. W. Sidebottom, C. C. Badcock, J. G. Calvert, G. W. Reinhardt, B. R. Rabe, and E. K. Damon. J. Am. Chem. Soc. **93**, 2587 (1971).
4. S. J. Strickler, J. P. Vikesland, and H. D. Bier. J. Chem. Phys. **60**, 664 (1974).
5. J. C. D. Brand, V. T. Jones, and C. DiLauro. J. Mol. Spectrosc. **40**, 616 (1971); **45**, 404 (1973).
6. A. E. Douglas. J. Chem. Phys. **45**, 1007 (1966).
7. C. S. Parmenter and M. W. Schuyler. J. Chem. Phys. **52**, 5366 (1970).
8. N. G. Utterback and T. Griffith. Rev. Sci. Instrum. **37**, 866 (1966).
9. R. B. Caton and A. R. Gangadharan. Can. J. Chem. **52**, 2389 (1974).
10. H. W. Sidebottom, C. C. Badcock, G. E. Jackson, J. G. Calvert, G. W. Reinhardt, and E. K. Damon. Environ. Sci. Technol. **6**, 72 (1972).
11. F. B. Wampler, K. Otsuka, J. G. Calvert, and E. K. Damon. Int. J. Chem. Kinet. **5**, 669 (1973).
12. L. Brus and J. R. McDonald. Chem. Phys. Lett. **21**, 283 (1973); J. Chem. Phys. **61**, 97 (1974).
13. P. B. Sackett and J. T. Yardley. J. Chem. Phys. **57**, 152 (1972).
14. H. D. Mettee. J. Phys. Chem. **73**, 1071 (1969); J. I. Steinfeld. Acc. Chem. Res. **3**, 313 (1970).
15. S. J. Strickler and R. A. Berg. J. Chem. Phys. **37**, 814 (1962).
16. R. B. Caton and A. B. F. Duncan. J. Am. Chem. Soc. **90**, 1945 (1968).

On the Construction of Delphinine-type Alkaloids via the Rearrangement of Substituted Denudatine Derivatives

KAREL WIESNER, PAK-TSUN HO, WING-CHEONG LIU, AND MADHAV N. SHANBHAG

Natural Products Research Center, University of New Brunswick, Fredericton, New Brunswick E3B 5A3

Received January 23, 1975

KAREL WIESNER, PAK-TSUN HO, WING-CHEONG LIU, and MADHAV N. SHANBHAG. Can. J. Chem. **53**, 2140 (1975).

A simple and stereospecific conversion of compound **1** to the aconite alkaloid model **25** is described.

KAREL WIESNER, PAK-TSUN HO, WING-CHEONG LIU et MADHAV N. SHANBHAG. Can. J. Chem. **53**, 2140 (1975).

On décrit une transformation simple et stéréospécifique du composé **1** en composé **25** qui est un modèle pour l'alcaloide de l'aconite. [Traduit par le journal]

Can. J. Chem. Downloaded from www.nrcresearchpress.com by 210.87.254.40 on 09/05/12
For personal use only.

Introduction

About a year ago we have completed (1) the synthesis of the delphinine-type alkaloid talatisamine **V** by a route which proceeded via the main stages **I**, **II**, **III**, and **V** and included the "biogenetic" rearrangement (*cf.* ref. 2) of the substituted atisine derivative **II** (Scheme 1). In spite of this success it became quite clear that this route has two built-in fundamental disadvantages which cannot be remedied by development work.

(*i*) In the rearrangement of the atisine derivative **II** the desired product **III** is accompanied by an equal quantity of the useless compound **IV**.

(*ii*) The formation of the last carbon ring, the ring B bridge, in the final stages of the synthesis is a poor yield reaction (40%).

It is obvious that a modification of the approach which would introduce the ring B bridge at the very beginning of the synthesis might be completely free of both these defects. Consequently, we have projected a synthesis of a delphinine-type alkaloid[1] which would proceed via the main stages **VI** through **IX** (Scheme 2).

The relatively simple and stereospecific synthesis of the starting material **VI** may be accomplished by the use of our aziridine rearrangement method (5).[2]

The crucial step of the synthesis is the rearrangement of the polysubstituted denudatine derivative **VII**. It is expected to produce compound **VIII** as the only product and to proceed with greater ease than the similar rearrangement **II** → **III**. The bicyclooctane C/D ring system in compound **VII** (unlike the same system in compound **II**) is twisted and strained. The relief of this strain should provide additional driving force for the rearrangement **VII** → **VIII**.

In spite of the efficiency which we have now developed in the synthesis of compounds of the type **VI**, it would be quite expensive to produce a quantity of this material large enough to try out experimentally all the conceivable variations of the process **VI** → **VII** → **VIII** → **IX**. For this reason we have worked out a simple and efficient conversion of the model starting material **1** to the product **26** (Scheme 3).

We believe that the experience obtained in this model work will be applicable without any major changes to compound **VI**. This last material while structurally complex is operationally as simple as the model compound **1**. The entire system of **VI** is saturated and very stable and it is expected to survive easily all the reaction conditions which we have employed in the conversion **1** → **26**.

Discussion

The model starting material **1** (6) was first converted to the α,β-unsaturated ketone **2** by Birch reduction followed by treatment with dilute aqueous hydrochloric acid at room temperature. The ketone **2** was oily but homogeneous in thin-layer (t.l.c.) and gas–liquid (g.l.c.) chromatog-

[1]The formula **IX** represents the alkaloid chasmanine. It has been shown recently (3) that the ring A methoxyl configuration in this compound originally assigned (4) anti to the nitrogen was incorrect and has to be reversed.

[2]We have already prepared and characterized the ring A methoxy epimer of compound **VI**. This product is now useless as a starting material for chasmanine. The synthesis of compound **VI** by the same method is in progress.

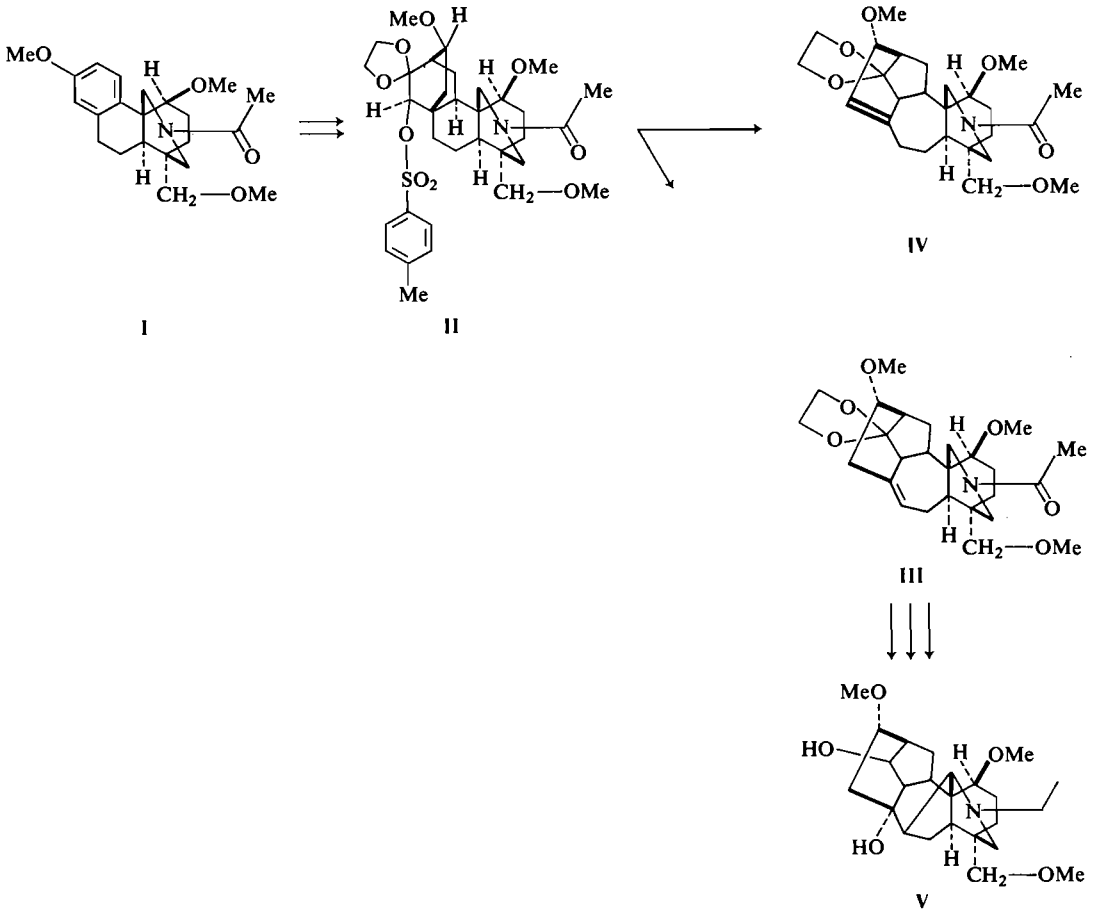

SCHEME 1

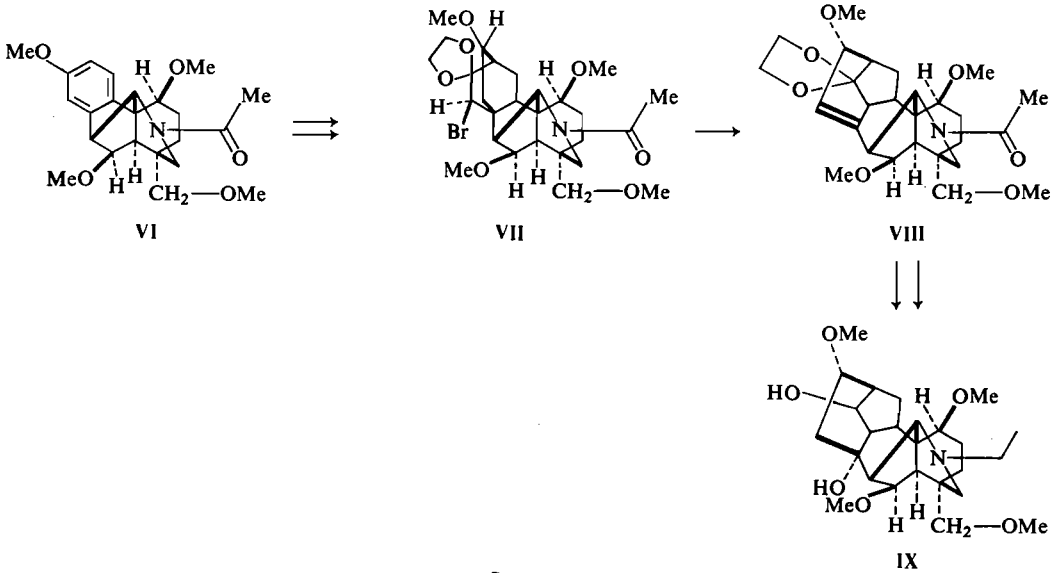

SCHEME 2

Can. J. Chem. Downloaded from www.nrcresearchpress.com by 210.87.254.40 on 09/05/12
For personal use only.

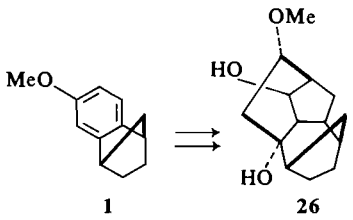

SCHEME 3

raphy in several systems. The nuclear magnetic resonance spectrum (n.m.r.)[3] of the product showed the allylic proton as a multiplet at 7.04 p.p.m.

In a kinetically controlled acid hydrolysis of the dihydrobenzenoid derivative obtained in the Birch reduction of **1** a stereoselective formation of **2** is expected, because of the well-known (7) preference of bicycloheptene derivatives for *exo* protonation. Compound **2** was now subjected to equilibration in methanolic hydrochloric acid – dioxane under reflux and the mixture was periodically examined by g.l.c. After 6 days the equilibrium was reached and the final ratio of compound **2** and the epimer **3** was 2.7:1. A similar equilibrium ratio (2.4:1) was obtained in *t*-butyl alcohol – potassium *t*-butoxide at 155 °C in a sealed tube.

The isomer **3** was separated in a preparative (acid-catalyzed) run by careful column chromatography on silica gel. The recovery of both products **2** and **3** was practically quantitative. Thus, the synthesis of compound **3** was somewhat laborious but it was accomplished in a very good yield.

The product **3** was an oil and its spectral data were very similar to those of compound **2**. The allylic hydrogen in the n.m.r. spectrum of **3** was shifted slightly upfield and appeared as a multiplet at 7.16 p.p.m. While it was not quite clear why the epimer **2** predominated in the equilibrium (the identical equilibrium ratio was also reached starting with **3**), the assignment of configuration to the two isomers seemed unambiguous.

The photoaddition of allene to the α,β-unsaturated ketone **3** was predicted to yield stereospecifically the adduct **5**. The stereochemistry of such additions (8, 9) is controlled by the stability of the excited state. The β-carbon of this (presumably n–π*) excited state is pyramidal and carries a σ orbital which can swing through the plane of the substituents and select the more stable configuration. If we assume that the β-carbon has an excess of negative charge with respect to the α-carbon, the excited state of the ketone **3** may be represented as **4**. It is clear that this stereoisomer with a *cisoid exo* ring junction is more stable than its *transoid* epimer.

Thus, it was possible to make the superficially unlikely prediction, that allene addition will take place from the distinctly more sterically hindered *endo* side. In fact, a single oily adduct homogeneous in t.l.c. and g.l.c. was obtained in a yield of 90%.

To prove that the configuration of this product corresponded indeed to the formula **5** the ketone was reduced by lithium aluminum hydride and the oily alcohol **6** was converted to the crystalline (m.p. 101 °C) *p*-bromobenzoate **7**. The structure of this ester was determined by Przybylska and Ahmed (10) by single crystal X-ray analysis and was found to agree with our expectations.

The conversion of the adduct **5** to the substituted "denudatine model" **16** proceeded in principle along the lines of our talatisamine synthesis (1). There were, however, differences between the two processes which originated (*a*) in the reversed configurations of the two allene adducts and (*b*) in the fact, that the strain of the denudatine system which is absent from the atisine system required special measures to be applied in the former case.

The adduct **5** was first converted to the ketal **8** and this compound gave by ozonolysis, sodium borohydride reduction and acid treatment the ketoaldehyde **9** in a yield of 92%. Analogous ketoaldehydes in the atisine series were never isolated since they underwent immediate ring closure of the 2.2.2-bicyclooctane system by aldol condensation. In the present case the equilibrium of the reversible internal aldol – retroaldol reaction favors the open keto aldehyde **9** and no amount of base or acid treatment can bring about ring closure.

However, the aldol condensation may be forced if it is performed under acetylating conditions (*cf.* ref. 11). Presumably the trace of the energetically unfavorable strained aldol condensation product, which is in equilibrium with the keto aldehyde **9** is removed by acetylation. In

[3]All spectra of all compounds were recorded and are given in the Experimental. In the Discussion only specially significant spectral results are mentioned to conserve space

Can. J. Chem. Downloaded from www.nrcresearchpress.com by 210.87.254.40 on 09/05/12
For personal use only.

Can. J. Chem. Downloaded from www.nrcresearchpress.com by 210.87.254.40 on 09/05/12
For personal use only.

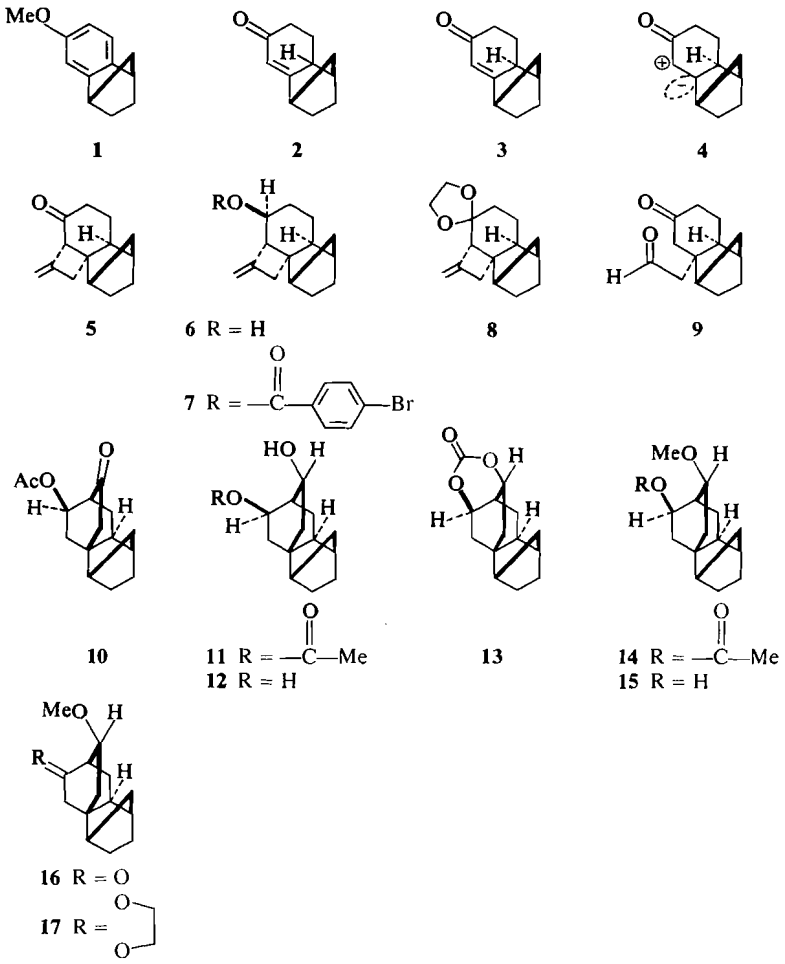

this manner the equilibrium is disturbed and new aldol is formed and acetylated until the entire amount of the starting material is converted to the product **10**. The acetoxy ketone **10** was a homogeneous sharply melting (m.p. 112 °C) compound and it was thus clear, that the condensation was stereospecific with respect to the new asymmetric center created in this process.

In order to prove the configuration of the acetoxy ketone **10**, this compound was reduced with sodium borohydride in absolute methanol. The oily but homogeneous acetoxy alcohol **11** was obtained in a quantitative yield. Saponification of this material yielded quantitatively the crystalline sharply melting (m.p. 99 °C) diol **12**. Finally treatment of compound **12** with phosgene and pyridine in absolute benzene gave a quantitative yield of the cyclic carbonate **13** (m.p. 185 °C; i.r.: 1740 cm^{-1} (carbonate carbonyl)).

The acetoxy alcohol **11** was now methylated with diazomethane and BF_3 etherate to the oily methoxy derivative **14**. The acetoxy group of this material was saponified and the resulting oily alcohol **15** was oxidized with chromium trioxide in pyridine to the oily ketone **16** in a quantitative yield. Finally, the ketone **16** was converted by heating under reflux with ethylene glycol and *p*-toluenesulfonic acid in benzene to the crystalline ketal **17** (m.p. 115 °C) in a quantitative yield.

The substitution of the model system may now be completed by the introduction of a β-oriented leaving group next to the ketal. Here we encounter a further advantage of the "denudatine route" as opposed to the "atisine route" utilized by us previously in the synthesis of talatisamine (1). Several steps were required in this last case to introduce the necessary β-tosyloxy function.

The greater ease of rearrangement of the denu-

Can. J. Chem. Downloaded from www.nrcresearchpress.com by 210.87.254.40 on 09/05/12
For personal use only.

datine system makes it possible to use bromine as a leaving group and it can be introduced in a single step in the correct configuration.

The ketal **17** was brominated in tetrahydrofuran with pyridine hydrobromide perbromide. The oily but homogeneous bromo derivative **18** was isolated in a yield of 65% by chromatography on silica gel. The configuration of the bromine atom in compound **18** followed mainly from the clean and unique outcome of the subsequent rearrangement step, which requires antiplanarity of the leaving group and the migrating bond. The n.m.r. spectrum of compound **18** showed a narrow doublet at 5.72 p.p.m. for the proton deshielded by the bromine atom. This was consistent with the assigned configuration but of course did not prove it.

A number of methods were tried to bring about the crucial rearrangement of the bromo ketal **18**. It turned out that the most efficient one was heating under reflux in absolute benzene with 1,5-diazabicyclo[3.4.0]nonene (as base) for several days. Chromatography of the reaction mixture yielded 90% of the pure oily rearranged product **19**. The n.m.r. spectrum of this material showed the vinylic proton as a doublet at 4.53 p.p.m.

To prove the structure of compound **19** we have attempted to liberate the keto group under mild acidic conditions. However, treatment with dilute hydrochloric acid in tetrahydrofuran at room temperature yielded the allylic rearrangement product **20** with the ketal group still intact.

This compound was oily but homogeneous in t.l.c. and its n.m.r. spectrum showed clearly the loss of the methoxyl and the acquisition of two vinylic protons which appeared as a quartet at 4.01 and doublet at 4.49 p.p.m. Allylic rearrangements of so called "pyroderivatives" of delphinine type alkaloids, which have the same functional group system as **19**, have been recognized by us (12) many years ago and it is with some satisfaction that we have observed the same reactivity in our synthetic system.

Deketalization of compound **20** in 60% acetic acid at 70 °C yielded the corresponding crystalline (m.p. 115 °C) ketone **21**. The i.r. spectrum of this material showed a carbonyl peak at 1760 cm^{-1} in agreement with our expectation based on i.r. spectra of diterpene alkaloid derivatives with a keto group in the same position.

Hydrogenation of the rearrangement product

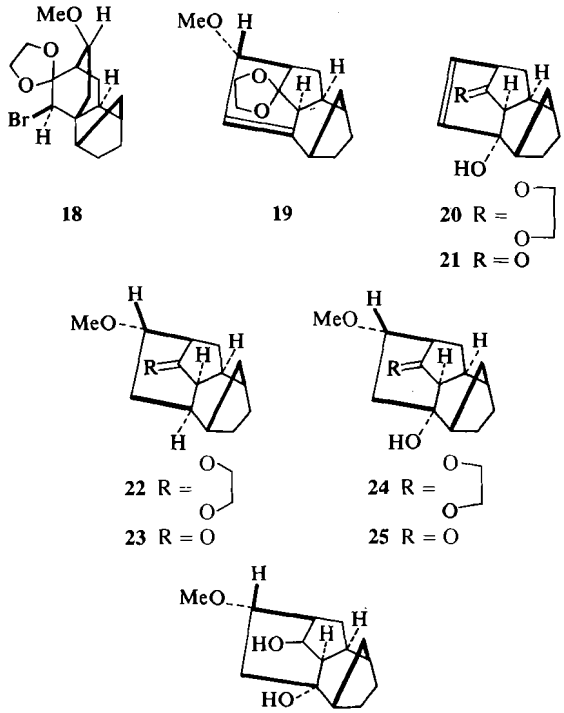

19 with palladium–charcoal in methanol gave a quantitative yield of the dihydro derivative **22**. This material was now deketalized with 60% acetic acid at 70 °C and the corresponding ketone **23** was obtained as an oil homogeneous in t.l.c. Compound **23** showed again in the i.r. spectrum the expected carbonyl maximum at 1760 cm^{-1}.

All these transformations left no doubt that the structure assigned to compound **19** is indeed correct. The stage was now set for the final modification of the functional groups.

Compound **19** was stirred at room temperature with mercuric acetate in 50% aqueous acetone. Chromatography of the reaction mixture yielded 70% of the oily oxymercuration product **24**. This material was deketalized to the crystalline (m.p. 104 °C) ketone **25** in a yield of 98% by heating with 50% acetic acid at 70 °C.

The i.r. spectrum of compound **25** showed hydroxyl peaks at 3600, 3475 cm^{-1} and a carbonyl peak at 1755 cm^{-1}. The n.m.r. spectrum showed a methoxyl peak at 6.63 p.p.m. A high resolution mass spectrum confirmed the precise molecular weight.

For further characterization crystals of the

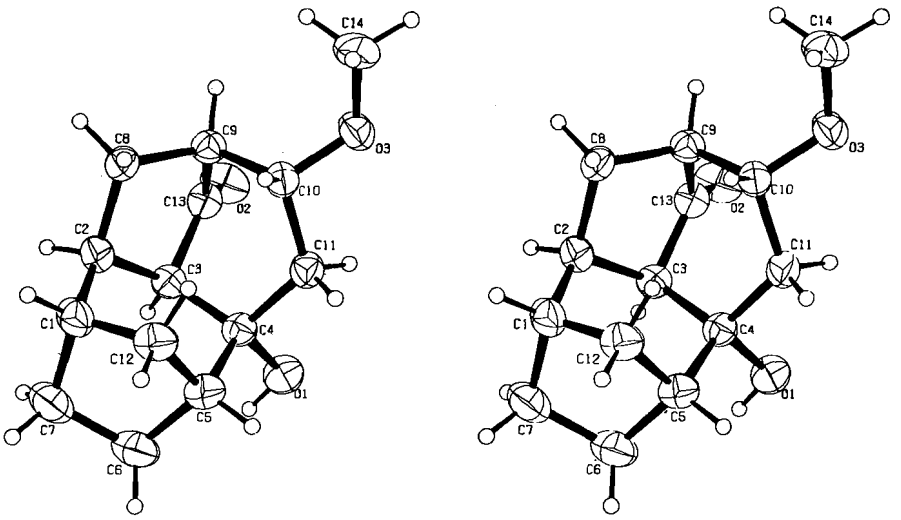

FIG. 1. Stereoscopic view of ketone **25**.

ketone **25** were submitted to Dr. John F. Blount, (Hoffmann–La Roche Inc, Nutley, New Jersey) who has kindly agreed to determine the structure of the material by single crystal X-ray crystallography. The structure derived by Dr. Blount in a remarkably short time is given in the Fig. 1 and fully confirms our expectations.

Reduction of the ketone **25** with sodium borohydride in methanol gave the alcohol **26** (m.p. 79 °C) in a yield of 80% after recrystallization. Diterpene alkaloid ketones analogous to **25** are known (1) to undergo stereospecific hydride reduction to yield alcohols with the hydroxy group in the "natural" configuration. Consequently we may safely assume that the reduction of our model ketone followed the same steric course.[4]

The present work clearly demonstrates that the synthesis of (say) chasmanine **IX** from the starting material **VI** is not only feasible but a practically solved problem. Whether or not it will be carried out depends on several nonchemical factors which are not under our control.

Experimental

Preparation of the α,β-Unsaturated Ketone 2

A solution of compound **1** (6) (32.7 g) in anhydrous tetrahydrofuran (190 ml) and *t*-butyl alcohol (190 ml) was added dropwise over a period of 30 min to a stirred solution and extracted with ether. The extract was washed with water, dried, and evaporated to dryness. The resulting residue was purified by chromatography on silica gel to give the oily α,β-unsaturated ketone **2** (23.8 g, 77%) homogeneous by t.l.c. in several solvent systems.

Mol. Wt. Calcd. for $C_{11}H_{14}O$: 162.1044. Found (high resolution mass spectroscopy): 162.1043.

Infrared (CCl_4): 1675 (conjugated six-membered ketone), 1655 cm^{-1} (double bond); u.v.: λ_{max}(EtOH) 245 nm (log ε 4.24); n.m.r. ($CDCl_3$): τ 4.30 (d, J = 1.5 Hz, 1H, vinylic proton), 7.04 p.p.m. (m, 1H, allylic proton).

Isomerization of 2 to 3

(*A*) The α,β-unsaturated ketone **2** (20.5 g) was dissolved in dioxane (600 ml) and saturated methanolic hytion of lithium metal (13.2 g) in distilled liquid ammonia (700 ml). The mixture was stirred at acetone – Dry Ice temperature for 2½ h. Absolute methanol was added until the blue color disappeared and the reaction mixture was allowed to stand to evaporate the ammonia. After workup by the standard procedure, the product (30 g) was treated with 5% aqueous hydrochloric acid (400 ml) and methanol (500 ml) at room temperature for 2 days. The mixture was neutralized with aqueous sodium bicarbonate drogen chloride (500 ml) was added. The mixture was heated under reflux in a nitrogen atmosphere. The reaction was examined by g.l.c. (15% Carbowax 20 M on Chromosorb W at 180 °C) and after 6 days it appeared that the equilibrium was reached (ratio of **2** to **3** about 2.7:1). The cooled reaction mixture was poured into a saturated sodium chloride solution and extracted with methylene dichloride. The extract was washed with water and dried over anhydrous magnesium sulfate. Evaporation of the solvent gave 20 g of an oily mixture of the ketones **2** and **3**. This mixture was separated by careful column chromatography on silica gel. Elution with 3% ethyl acetate in *n*-hexane resulted in the isolation of pure **3** (5.4 g) as an oil. Further elution yielded the starting material **2** (14.5 g).

[4]In the unlikely event that "natural" and model derivatives would be reduced with opposite stereospecificity our method would nevertheless yield the correct final product if applied to the synthesis of a natural alkaloid.

Can. J. Chem. Downloaded from www.nrcresearchpress.com by 210.87.254.40 on 09/05/12
For personal use only.

Can. J. Chem. Downloaded from www.nrcresearchpress.com by 210.87.254.40 on 09/05/12
For personal use only.

(*B*) The α,β-unsaturated ketone **2** (133 mg) was heated in a sealed tube at 155 °C with potassium *t*-butoxide (100 mg) in *t*-butyl alcohol (8 ml) in an inert atmosphere for 8 days. Under these conditions the final ratio of **2** to **3** was about 2.4:1.

Mol. Wt. Calcd. for $C_{11}H_{14}O$: 162.1044. Found (high resolution mass spectroscopy): 162.1041.

The entire mass spectra of **2** and **3** were practically identical; i.r. (CCl_4): 1675 (conjugated six-membered ketone), 1655 cm^{-1} (double bond); u.v.: λ_{max}(EtOH) 241 nm (log ε 4.12); n.m.r. ($CDCl_3$): τ 4.36 (broad s, 1H, vinylic proton), 7.16 p.p.m. (m, 1H, allylic proton).

Photoaddition of Allene to Compound 3

Compound **3** (5 g) was dissolved in anhydrous tetrahydrofuran (500 ml) and cooled to −70 °C. Allene was added in excess (60 g) and the reaction mixture was irradiated by a 200 W Hanovia Mercury lamp with a Pyrex filter for 8 h under nitrogen. After evaporation of the solvent and the excess allene, the photoadduct **5** was purified by chromatography on silica gel. The yield was 6.2 g (90%).

Mol. Wt. Calcd. for $C_{14}H_{18}O$: 202.1358. Found (high resolution mass spectroscopy): 202.1351.

Infrared (CCl_4): 1710 cm^{-1} (six-membered ketone); n.m.r. (CCl_4): τ 5.14 p.p.m. (sextet, 2H, vinylic protons).

Preparation of Bromo Compound 7 for X-Ray Analysis

A solution of the photoadduct **5** (23 mg) in anhydrous ether (5 ml) was added dropwise to a cold stirred suspension of $LiAlH_4$ (10 mg) in anhydrous ether (5 ml). The reaction mixture was stirred for 20 min at room temperature and work-up in the usual manner gave the alcohol **6** (22 mg, 96%) as a colorless oil homogeneous in t.l.c.

Mol. Wt. Calcd. for $C_{14}H_{20}O$: 204. Found (mass spectroscopy): 204.

Infrared (CCl_4): 3560, 3400 cm^{-1} (hydroxyl); n.m.r. (CCl_4): τ 5.07 (m, 2H, vinylic protons), 6.43 p.p.m. (m, 1H, proton unshielded by hydroxyl).

The alcohol **6** (80 mg) was dissolved in anhydrous benzene (10 ml) and *p*-bromobenzoyl chloride (150 mg) and anhydrous sodium carbonate (15 mg) were added. The mixture was heated under reflux for 3 days. After cooling the reaction mixture was diluted with ether (100 ml), washed with water, dried over anhydrous magnesium sulfate, and evaporated to dryness. Chromatography of the crude product by preparative t.l.c. on silica gel yielded the crystalline compound **7** (82 mg, 54%). A sample of **7** for X-ray analysis (m.p. 101 °C) was prepared by recrystallization from pentane.

Anal. Calcd. for $C_{21}H_{23}O_2Br$: C, 65.26; H, 5.97. Found: C, 65.24; H, 6.04.

Infrared (CCl_4): 1720 cm^{-1} (ester); n.m.r. ($CDCl_3$): τ 2.00, 2.34 (two d, J = 9 Hz, 4H, aromatic protons), 5.17 p.p.m. (m, 3H, vinylic protons and proton deshielded by benzoate).

Preparation of the Ketal 8

The photoadduct **5** (6 g) was dissolved in anhydrous benzene (500 ml) to which ethylene glycol (5 ml) and *p*-toluenesulfonic acid (600 mg) were added. The reaction mixture was heated under reflux for 3½ h with a water separator. The crude product was chromatographed on a column of basic alumina (grade II). The ketal **8** was eluted with 2% ether in *n*-hexane as an oil homogeneous in t.l.c. The yield was 5.15 g (72%).

Mol. Wt. Calcd. for $C_{16}H_{22}O_2$: 246.1620. Found (mass spectroscopy): 246.1615.

Nuclear magnetic resonance (CCl_4): τ 4.94 (q, 1H, vinylic proton), 5.20 (m, 1H, vinylic proton), 6.13 p.p.m. (broad s, 4H, dioxolane protons).

Preparation of the Keto Aldehyde 9

Compound **8** (3.5 g) was dissolved in methanol (150 ml) and cooled to −70 °C. A stream of ozone was slowly passed through the solution until it acquired a permanent blue color. Sodium borohydride (3 g) was then added in portions and the reaction mixture was stirred for an additional 20 min at 0 °C. The solution was acidified with 5% aqueous hydrochloric acid and stirred for 6 h at room temperature. The reaction mixture was then diluted with saturated aqueous sodium chloride (250 ml) and extracted with methylene dichloride. The extract was washed with water and dried over anhydrous magnesium sulfate. Removal of the solvent *in vacuo* gave the unstable oily keto aldehyde **9** (2.7 g, 92%) which had to be used immediately without purification.

Mol. Wt. Calcd. for $C_{13}H_{18}O_2$: 206. Found (mass spectroscopy): 206.

Infrared (CCl_4): 2840, 2730 (aldehyde), 1720 cm^{-1} (aldehyde and six-membered ketone); n.m.r. ($CDCl_3$): τ 0.32 p.p.m. (t, 1H, aldehyde).

Cyclization of Compound 9 to the Keto Acetate 10

A solution of the keto aldehyde **9** (4.7 g) in acetic acid (15 ml) was added dropwise under nitrogen at −10 °C to a stirred mixture of boron trifluoride etherate (50 ml), acetic anhydride (50 ml), and acetic acid (85 ml). The stirring was continued at room temperature under nitrogen for 5 days. The solvents were removed *in vacuo*, the dark residue was dissolved in ice water (300 ml), and the solution was extracted with methylene dichloride (3 × 150 ml). The combined extracts were washed with water, dilute aqueous sodium bicarbonate, then water again, dried over anhydrous sodium sulfate, and evaporated to dryness. Chromatography of the brown residue on silica gel and elution with 5% ether in *n*-hexane yielded the crystalline keto acetate **10**. The compound melted at 112 °C after one recrystallization from *n*-hexane (3.5 g, 62%).

Anal. Calcd. for $C_{15}H_{20}O_3$: C, 72.55; H, 8.12. Found: C, 72.30; H, 8.24.

Infrared (CCl_4): 1734 cm^{-1} (acetate and six-membered ketone); n.m.r. (CCl_4): τ 4.86 (heptet, J = 7, 5, and 2 Hz, 1H, proton unshielded by acetoxyl), 8.01 p.p.m. (s, 3H, acetoxy methyl).

Reduction of Compound 10 to the Alcohol 11

The keto acetate **10** (1.6 g) was dissolved in absolute methanol (60 ml) and sodium borohydride (600 mg) was added to the solution at 0 °C. The reaction mixture was maintained at this temperature for an additional 30 min. After this time the solution was neutralized with aqueous acetic acid and extracted with methylene dichloride. The extract was washed with water, dried over anhydrous magnesium sulfate, and evaporated to dryness. The alcohol **11** was obtained in a quantitative yield as a colorless oil, homogeneous in t.l.c.

Mol. Wt. Calcd. for $C_{15}H_{22}O_3$: 250.1575. Found (high resolution mass spectroscopy): 250.1569.

Infrared (CCl_4): 3620 (hydroxyl), 1748 cm^{-1} (acetate); n.m.r. (CCl_4): τ 4.98 (broad quintet, 1H, proton un-

Can. J. Chem. Downloaded from www.nrcresearchpress.com by 210.87.254.40 on 09/05/12
For personal use only.

shielded by acetoxyl), 6.23 (m, 1H, proton unshielded by hydroxyl), 8.06 p.p.m. (s, 3H, acetoxy methyl).

Preparation of the Diol **12**

A solution of compound **11** (45 mg) in 1% methanolic potassium hydroxide (4 ml) was stirred at room temperature for 3½ h and worked-up in the usual manner. The product **12** was recrystallized from ether to a m.p. of 99 °C. The yield was quantitative.

Anal. Calcd. for $C_{13}H_{20}O_2$: C, 75.01; H, 9.61. Found: C, 75.08; H, 9.58.

Infrared (CCl_4): 3540, 3345 cm^{-1} (hydroxyl); n.m.r. (CCl_4): τ 5.84 p.p.m. (m, 2H, protons unshielded by hydroxyls).

Preparation of the Carbonate **13**

A solution of phosgene (10 drops) in anhydrous benzene was added to a stirred solution of the diol **12** (21 mg) and pyridine (15 drops) in the same solvent (3 ml). The resulting mixture was stirred at room temperature for 4 h. The solution diluted with benzene (50 ml) was washed with water, dried, and evaporated to dryness. The crude product was crystallized from ether and gave the pure carbonate **13** (m.p. 185 °C) in quantitative yield.

Anal. Calcd. for $C_{14}H_{18}O_3$: C, 71.77; H, 7.74. Found: C, 71.46; H, 7.64.

Infrared ($CHCl_3$): 1740 cm^{-1} (carbonate); n.m.r. ($CDCl_3$): τ 5.26 p.p.m. (m, 2H, protons deshielded by carbonate).

Preparation of the Methyl Ether **14**

An excess of diazomethane in ether was added dropwise to a stirred solution of the alcohol **11** (500 mg) and boron trifluoride etherate (40 mg) in methylene dichloride (30 ml) at 0 °C. The reaction mixture was stirred at this temperature for a further 30 min, after which time it was poured into 5% aqueous sodium bicarbonate and extracted with ether. The combined extracts were washed with water, dried and evaporated to dryness. The crude product was purified by chromatography in silica gel and yielded the pure oily methyl ether **14** (350 mg, 70%,) homogeneous in t.l.c.

Mol. Wt. Calcd. for $C_{16}H_{24}O_3$: 264.1726. Found (mass spectroscopy): 264.1734.

Infrared (CCl_4): 1730 cm^{-1} (acetate); n.m.r. (CCl_4): τ 5.03 (broad, t, 1H, proton unshielded by acetoxyl), 6.80 (s, 3H, methoxyl), 8.03 p.p.m. (s, 3H, acetoxy methyl).

Hydrolysis of Compound **14** *to the Alcohol* **15**

A solution of **14** (350 mg) in 2% methanolic potassium hydroxide (10 ml) was stirred at room temperature for 24 h and worked-up in the usual manner. The alcohol **15** (300 mg) was obtained as an oil homogeneous in t.l.c. The yield was quantitative.

Mol. Wt. Calcd. for $C_{14}H_{22}O_2$: 222. Found (mass spectroscopy): 222.

Infrared (CCl_4): 3545 cm^{-1} (hydroxyl); n.m.r. (CCl_4): τ 6.67 p.p.m. (s, 3H, methoxyl).

Preparation of the Ketone **16**

The alcohol **15** (206 mg) in methylene dichloride (5 ml) was added dropwise to a stirred solution of the chromium trioxide – pyridine complex (1.5 g) in methylene dichloride (30 ml). The mixture was stirred at room temperature for 1 h. It was then dissolved in ether (100 ml) and the brown precipitate was removed by filtration. The filtrate was washed with dilute hydrochloric acid, dilute aqueous sodium bicarbonate, and finally with water. The ether solution was dried over anhydrous magnesium sulfate and filtered through a short neutral alumina column (grade II). The pure ketone **16** was obtained as a thick oil in quantitative yield. It behaved homogeneously in t.l.c.

Mol. Wt. Calcd. for $C_{14}H_{20}O_2$: 220.1463. Found (high resolution mass spectroscopy): 220.1462.

Infrared (CCl_4): 1730 cm^{-1} (six-membered ketone); n.m.r. (CCl_4): τ 6.43 (q, 1H, proton unshielded by methoxyl), 6.83 p.p.m. (s, 3H, methoxyl).

Preparation of the Ketal **17**

The ketone **16** (330 mg) was dissolved in anhydrous benzene (60 ml) to which ethylene glycol (0.3 ml) and *p*-toluenesulfonic acid (30 mg) were added. The solution was heated under reflux with a water separator for 1½ h and worked-up by the usual procedure. The ketal **17** was crystallized from *n*-hexane and melted at 115 °C. The yield was quantitative.

Anal. Calcd. for $C_{16}H_{24}O_3$: C, 72.72; H, 9.09. Found: C, 72.54; H, 9.18.

Mol. Wt. Calcd. for $C_{16}H_{24}O_3$: 264.1725. Found (high resolution mass spectroscopy): 264.1718.

Nuclear magnetic resonance ($CDCl_3$): τ 6.13 (m, 4H, dioxolane protons), 6.61 (m, 1H, proton deshielded by methoxyl), 6.71 p.p.m. (s, 3H, methoxyl).

Preparation of the Bromo Ketal **18**

The ketal **17** (300 mg) was dissolved in anhydrous tetrahydrofuran (10 ml). A solution of pyridine hydrobromide perbromide (450 mg) in anhydrous tetrahydrofuran was added dropwise to the stirred solution at room temperature. After 2 h of stirring the solution was poured into 5% aqueous sodium bicarbonate in an ice-water bath and extracted with methylene dichloride. The extract was washed with water, dried over anhydrous magnesium sulfate, and evaporated to dryness. The residue was chromatographed on silica gel and elution with ether–*n*-hexane (1 : 1, v/v) yielded the oily bromo ketal **18** (250 mg, 65%) homogeneous in t.l.c. in several solvent systems.

Mol. Wt. Calcd. for $C_{16}H_{23}O_3Br$: 342.0830. Found (high resolution mass spectroscopy): 342.0825.

Nuclear magnetic resonance ($CDCl_3$): τ 5.72 (d, J = 2.2 Hz, 1H, proton deshielded by bromine atom), 6.03 (m, 4H, dioxolane protons), 6.51 (q, 1H, proton deshielded by methoxyl), 6.68 p.p.m. (s, 3H, methoxyl).

Preparation of the Rearranged Product **19**

A solution of the bromo ketal **18** (300 mg) and 1,5-diazabicyclo[3.4.0]nonene, (DBN) (2 ml) in anhydrous toluene (20 ml) was heated under reflux in a nitrogen atmosphere for 4 days. The cooled solution was diluted with ether (200 ml) and washed with 1% cold aqueous acetic acid (3 × 100 ml), 5% aqueous sodium bicarbonate, and finally with water. Drying over anhydrous magnesium sulfate and evaporating to dryness gave an unstable oil which was purified immediately by preparative t.l.c. on silica gel using *n*-hexane–ether (2 : 3, v/v) as solvent. The oily rearranged olefin **19** (207 mg, 90%) was isolated as the sole product and was a very unstable compound which could be characterized only by methods available in our own laboratory. It behaved homogeneously in t.l.c.

Mol. Wt. Calcd. for $C_{16}H_{22}O_3$: 262. Found (mass spectroscopy): 262.

Can. J. Chem. Downloaded from www.nrcresearchpress.com by 210.87.254.40 on 09/05/12
For personal use only.

Infrared (CCl_4): 1630 cm^{-1} (weak; double bond); n.m.r. ($CDCl_3$): τ 4.53 (d, J = 6 Hz, 1H, vinylic proton), 6.03 (broad s, 4H, dioxolane protons), 6.53 (q, J = 6 and 2 Hz, 1H, proton unshielded by methoxyl), 6.65 p.p.m. (s, 3H, methoxyl).

*Rearrangement of Compound **19** to the Tertiary Allylic Alcohol **20***

Compound **19** (30 mg) was dissolved in tetrahydrofuran (2 ml) to which 1 *N* aqueous hydrochloric acid (1 ml) was added. The mixture was stirred at room temperature for 30 min, after which time it was poured into water (50 ml) and extracted with ether. The extract was worked-up by the usual procedure. Evaporation of the solvent yielded quantitatively the oily product **20** which behaved homogeneously in t.l.c.

Mol. Wt. Calcd. for $C_{15}H_{20}O_3$: 248. Found (mass spectroscopy): 248.

Infrared (CCl_4): 3560 cm^{-1} (tertiary alcohol); n.m.r. ($CDCl_3$): τ 4.01 (q, J = 10 and 6 Hz, 1H, vinylic proton), 4.49 (d, J = 10 Hz, 1H, vinylic proton), 6.03 p.p.m. (broad s, 4H, dioxolane protons).

*Deketalization of **20** to **21***

Compound **20** (25 mg) was dissolved in 60% aqueous acetic acid (5 ml) and the solution was heated to 70 °C for 1 h. The solvent was removed *in vacuo*, ether (50 ml) was added, and the solution was washed, dried, and evaporated to dryness. The product **21** was crystallized from ether to a m.p. of 115 °C. The yield was quantitative.

Mol. Wt. Calcd. for $C_{13}H_{16}O_2$: 204.1150. Found (high resolution mass spectroscopy): 204.1140.

Infrared (CCl_4): 3600 (tertiary hydroxyl), 1760 cm^{-1} (five-membered ketone). n.m.r. ($CDCl_3$): τ 3.80 (q, J = 9 and 6 Hz, 1H, vinylic proton), 4.46 p.p.m. (d, J = 9 Hz, 1H, vinylic proton).

*Hydrogenation of Compound **19** to the Dihydro Derivative **22***

Compound **19** (17 mg) was hydrogenated in methanol (3 ml) with 10% palladium-on-charcoal (10 mg) overnight. The catalyst was filtered off and the methanolic solution was evaporated to dryness. The product **22** was obtained as a colorless oil in a quantitative yield. It was homogeneous in t.l.c.

Mol. Wt. Calcd. for $C_{16}H_{24}O_3$: 264. Found (mass spectroscopy): 264.

Nuclear magnetic resonance ($CDCl_3$): τ 6.07 (broad s, 4H, dioxolane protons), 6.53 (m, 1H, proton unshielded by methoxyl), 6.70 p.p.m. (s, 3H, methoxyl).

*Deketalization of Compound **22** to the Ketone **23***

A solution of compound **22** (17.5 mg) in 60% aqueous acetic acid (5 ml) was heated to 70 °C for 1½ h and worked-up in the usual manner. Purification of the crude product by preparative t.l.c. on silica gel yielded the pure ketone **23** (12 mg, 81%) as a thick oil, homogeneous in t.l.c.

Mol. Wt. Calcd. for $C_{14}H_{20}O_2$: 220.1462. Found (high resolution mass spectroscopy): 220.1463.

Infrared (CCl_4): 1760 cm^{-1} (five-membered ketone); n.m.r. ($CDCl_3$): τ 6.06 (broad t, J = 8 Hz, 1H, proton deshielded by methoxyl), 6.70 p.p.m. (s, 3H, methoxyl).

*Preparation of the Tertiary Alcohol **24***

A solution of the olefin **19** (130 mg) and mercuric acetate (acetic acid free) (320 mg) in 50% aqueous acetone (30 ml) was stirred at room temperature for 44 h. The reaction mixture was cooled in an ice bath and an excess of 0.5 *M* sodium borohydride in 3 *M* aqueous sodium hydroxide (10 ml) was added dropwise to it. The mixture was stirred for 30 min, poured into saturated aqueous sodium chloride (80 ml), and extracted with ether (4 × 50 ml). The combined extracts were washed with 2% aqueous hydrochloric acid, water, and dried over anhydrous magnesium sulfate. Evaporation of the solvent gave a yellow crude product. Purification by preparative t.l.c. (ether–hexane, 3 : 2) gave the pure alcohol **24** (88 mg, 70%) as a colorless oil homogeneous in t.l.c.

Mol. Wt. Calcd. for $C_{16}H_{24}O_4$: 280.1675. Found (high resolution mass spectroscopy): 280.1683.

Infrared (CCl_4): 3585 cm^{-1} (tertiary hydroxyl); n.m.r. ($CDCl_3$): τ 6.05 (broad s, 4H, dioxolane protons), 6.67 (s, 3H, methoxyl), 6.70 p.p.m. (broad t, 1H, proton unshielded by methoxyl).

*Deketalization of **24** to **25***

A solution of the hydroxy ketal **24** (34 mg) in 50% aqueous acetic acid (4 ml) was heated to 70 °C for 3 h. The reaction mixture was worked-up in the usual manner. The ketone **25** was crystallized from ether–chloroform and melted at 104 °C. The yield was quantitative.

Mol. Wt. Calcd. for $C_{14}H_{20}O_3$: 236.1412. Found (high resolution mass spectroscopy): 236.1402.

Infrared (CCl_4): 3600, 3475 (hydroxyl), 1755 cm^{-1} (five-membered ketone); n.m.r. ($CDCl_3$) : τ 6.24 (sextet, J = 7, 6, and 2 Hz, 1H, proton unshielded by methoxyl), 6.63 p.p.m. (s, 3H, methoxyl).

*Reduction of the Ketone **25** to the Alcohol **26***

The ketone **25** (30 mg) was dissolved in methanol (5 ml) and sodium borohydride (15 mg) was added in portions at room temperature. The reaction mixture was stirred at room temperature for 1 h and poured into saturated aqueous sodium chloride (10 ml). The product **26** was isolated by extraction with methylene dichloride, purified by preparative t.l.c. on silica gel and recrystallized from ether to a constant m.p. of 79 °C. The yield was 80%.

Anal. Calcd. for $C_{14}H_{22}O_3$: C, 70.58; H, 9.24. Found: C, 70.32; H, 9.33.

Mol. Wt. Calcd.: 238.1564. Found (high resolution mass spectroscopy): 238.1569.

Infrared (CCl_4): 3575, 3480 cm^{-1} (hydroxyls); n.m.r. ($CDCl_3$): τ 5.81 (t, 1H, proton unshielded by secondary hydroxyl), 6.63 (m, 1H, proton unshielded by methoxyl), 6.65 p.p.m. (s, 3H, methoxyl).

We wish to express our gratitude to Dr. M. Przybylska and F. R. Ahmed (the National Research Council of Canada, Ottawa) and Dr. John F. Blount, Hoffmann–La Roche, Inc., Nutley, New Jersey (U.S.A.) for the X-ray structure determination of our compounds.

We also thank the National Research Council of Canada, Ottawa, and the Hoffmann–La Roche Company, Vaudreuil, Quebec, for financial support of this study.

1. K. Wiesner, T. Y. R. Tsai, K. Huber, S. E. Bolton, and R. Vlahov. J. Am. Chem. Soc. **96**, 4990 (1974).
2. K. Wiesner and Z. Valenta. *In* Progress in the chemistry of organic natural products. Vol XVI.

Edited by L. Zechmeister. Springer-Verlag, Wien. 1958. p. 26.
3. S. W. PELLETIER, Z. DJARMATI, and S. LAJSIC. J. Am. Chem. Soc. **96**, 7817 (1974).
4. O. ACHMATOWICS, Y. TSUDA, L. MARION, T. OKAMOTO, M. NATSUME, H. H. CHANG, and K. KAJIMA. Can. J. Chem. **43**, 825 (1965).
5. (*a*) K. WIESNER, P. T. HO, R. C. JAIN, S. F. LEE, S. OIDA, and A. PHILIPP. Can. J. Chem. **51**, 1448 (1973); (*b*) K. WIESNER, P. T. HO, D. CHANG, Y. K. LAM, C. S. J. PAN, and W. Y. REN. Can. J. Chem. **51**, 3978 (1973).
6. H. TANIDA, R. MUNEYUKI, and T. TSUJI. Bull. Chem. Soc. Jap. **37**, 40 (1964).
7. P. VON R. SCHLEYER. J. Am. Chem. Soc. **89**, 699 (1967); **89**, 701 (1967).
8. K. WIESNER, L. POON, I. JIRKOVSKY, and M. FISHMAN. Can. J. Chem. **47**, 433 (1969).
9. K. WIESNER. Tetrahedron. In press.
10. M. PRZYBYLSKA and F. R. AHMED. Acta Cryst. B**30**, 2338 (1974).
11. A. BELANGER, Y. LAMBERT, and P. DESLONGCHAMPS. Can. J. Chem. **47**, 795 (1969).
12. K. WIESNER, F. BICKELHAUPT, D. R. BABIN, and M. GOTZ, Tetrahedron, **9**, 254 (1960).

Can. J. Chem. Downloaded from www.nrcresearchpress.com by 210.87.254.40 on 09/05/12
For personal use only.

General Base Catalysis of β Elimination by a Steroidal Enzyme Model

J. PETER GUTHRIE AND STELLA O'LEARY
Department of Chemistry, University of Western Ontario, London, Ontario N6A 3K7
Received October 30, 1974

J. PETER GUTHRIE and STELLA O'LEARY. Can. J. Chem. **53**, 2150 (1975).

The water soluble steroid **1** acts as a catalyst for the enolization of the ketones **2***a–c*. The rate enhancement for **1**-catalyzed reaction relative to imidazole-catalyzed reaction (*R*), increases as the size of the aromatic ring system of the substrate increases; a plot of log *R vs.* π has a slope of 0.43. This is interpreted in terms of hydrophobic binding between steroid α-surface and aromatic ring system which lowers the free energy level of the transition state for steroid-catalyzed enolization.

J. PETER GUTHRIE et STELLA O'LEARY. Can. J. Chem. **53**, 2150 (1975).

Le stéroide **1** soluble dans l'eau agit comme catalyseur pour l'énolisation des cétones **2***a–c*. L'augmentation de la vitesse de la réaction catalysée par **1** par rapport à celle catalysée par l'imidazole (*R*) varie en fonction de l'augmentation de la grosseur du système cyclique aromatique du substrat; une courbe de log *R* en fonction de π a une pente de 0.43. On interprète ce résultat en fonction d'une liaison hydrophobe entre la face α du stéroide et le système cyclique aromatique; ceci à comme effet d'abaisser l'énergie libre de l'état de transition de l'énolisation catalysée par les stéroides. [Traduit par le journal]

Introduction

Numerous enzyme model systems showing rate enhancements due to noncovalent binding of substrate to catalyst have been reported in recent years (1–13). Almost invariably (1–9) these have involved hydrolytic reactions, normally of aryl esters, which are sensitive to nucleophilic catalysis. We have prepared a steroidal enzyme model **1** (14, 15) which is water soluble by virtue of its two ionic substituents and has a hydrophobic binding surface as well as a catalytic group, the 17β-imidazolyl substituent. This compound was shown to be a catalyst for the hydrolysis of active esters with hydrophobic substituents, with a marked specificity for phenanthrene derivatives (15). However, it became evident that nucleophilic attack by the steroidal imidazole upon ester carbonyl groups was subject to steric and conformational constraints which limited its catalytic potential (16). Therefore, we sought a reaction, subject to catalysis by imidazole, which would be less sterically and conformationally demanding, in hopes of seeing larger catalytic effects. We wish to report experiments demonstrating the activity of **1** as a general base catalyst for the enolization of suitable ketones. This reaction turns out to have some definite advantages for enzyme model studies and in particular can be considered a more "specific" reaction for the enzyme model **1**.

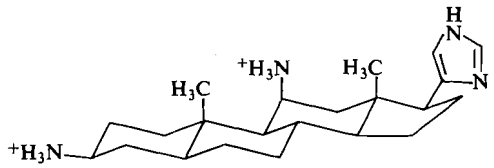

1

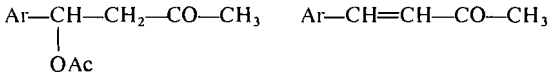

2 **3**

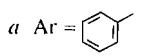

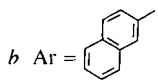

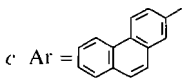

Results

Elimination of acetic acid from **2***a–c* is readily followed spectrophotometrically because of the strongly absorbing chromophore which develops. Our kinetics results for this elimination are found in Tables 1 and 2. Exploratory studies were conducted with **2***b*: the elimination reaction was shown to be subject to catalysis by hydroxide ion and by buffers. The buffer catalysis observed for carbonate–bicarbonate buffer is due to carbonate alone. This behavior

Can. J. Chem. Downloaded from www.nrcresearchpress.com by 210.87.254.6 on 09/05/12
For personal use only.

TABLE 1. Buffer-catalyzed reaction of **2b***

pH	Catalyst	$10^3 \times$ concentration† (M)	$10^5 \times k_{obs}$ (s^{-1})	k_2‡ ($M^{-1}\ s^{-1}$)
10.07	CO_3^{2-}	4.97	79.6	
		24.9	96.5	
		49.7	107	
				0.0097±0.0078
9.01	CO_3^{2-}	8.45	9.64	
		42.3	12.2	
		42.3	14.0	
		84.5	15.5	
				0.0084±0.0036
8.00	HPO_4^{2-}	3.50	0.965	
		17.4	1.49	
		35.0	2.06	
				0.00042±0.00010

*In aqueous solution at 25.5°.
†Total buffer concentration.
‡Calculated from the slope of k_{obs} *vs.* concentration of free base.

parallels that reported for other β-acetoxy ketones (17–18). A Brønsted plot of the data for simple buffers assuming that only general base catalysis occurs gives a β value of *ca.* 0.5; there is an indication that nitrogen bases are slightly more effective than oxygen bases but the overall pattern is of general base catalysis.

The products of the eliminations, **3***a–c*, are expected to be unstable to retroaldol cleavage; however, the rate constants for this process are such that it is much slower than the elimination: for **2***b* the rate constant for hydroxide-catalyzed decomposition is 8.2 $M^{-1}\ s^{-1}$; for **3***b* the corresponding rate constant is $2.1 \times 10^{-4}\ M^{-1}\ s^{-1}$ or 40 000-fold slower.

The rate constants for the imidazole-catalyzed elimination reaction of **2***a–c* show an increase in rate with increasing size of the aromatic ring. Since these rate constants are independent of amine or ketone concentration, they must reflect an electronic effect upon the rate by changing the size of the ring system. No value of σ* for phenanthryl appears to be available but from literature values of σ* for phenyl (19) and 2-naphthyl (19), one can calculate an approximate ρ* of 0.8 for the elimination reaction.

The rate constants for **1**-catalyzed elimination reaction of **2***a–c* are consistently larger than those for imidazole-catalyzed elimination and show a much more marked increase with increasing ring size. Since the imidazole group of **1** has a pK_a virtually identical to that of imidazole itself (16), this rate enhancement must result from a favorable interaction of steroid and substrate in the transition state. To isolate this effect we calculate relative rates, $k_{rel} = k_2^{steroid}/k_2^{imidazole}$. A plot of log k_{rel} *vs.* π (the Hansch hydrophobicity parameter (20)) is shown in Fig. 1. The plot gives a good straight line,

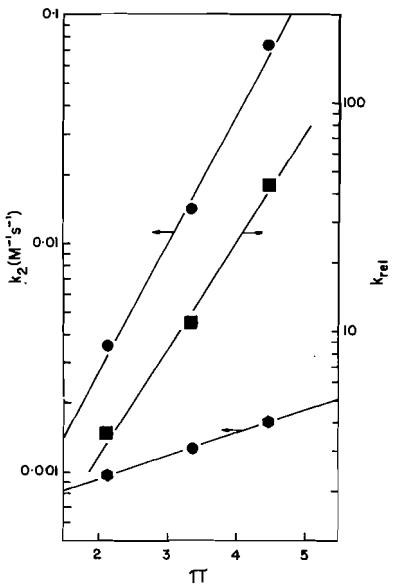

FIG. 1. Dependence upon π, the Hansch hydrophobicity parameter, of the logarithms of the second-order rate constants for imidazole- (●) and **1**- (●) catalyzed elimination reactions (left ordinate) and of the logarithms of the relative rate constants, $k_{rel} = k_2^{1}/k_2^{imidazole}$, (■) (right ordinate).

Can. J. Chem. Downloaded from www.nrcresearchpress.com by 210.87.254.6 on 09/05/12
For personal use only.

TABLE 2. Imidazole- and **1**-catalyzed elimination reactions*

Substrate	$10^{-5} \times$ concentration (M)	Catalyst	Concentration† (M)	$10^{-5} \times k_{obs}$ (s^{-1})	k_2 ($M^{-1}\,s^{-1}$)
2*a*	5.0	—		0.87	
	1.0	Imidazole	0.01	2.04	0.00117
	1.0	Imidazole	0.01	1.77	0.00090
	5.0	Imidazole	0.01	1.85	0.00098
	5.0	Imidazole	0.01	1.77	0.00090
	10.0	Imidazole	0.01	1.77	0.00090
					Average 0.00097 ± 0.00012
	1.0	**1**	0.005	2.72	0.00370
	5.0	**1**	0.001	1.25	0.0038
	5.0	**1**	0.005	2.57	0.00340
	10.0	**1**	0.01	4.20	0.00343
	10.0	**1**	0.005	2.57	0.00340
					Average 0.00355 ± 0.00019
2*b*	5.0	—		0.904	
	1.0	Imidazole	0.05	8.48	0.00152
	5.0	Imidazole	0.01	2.07	0.00117
	5.0	Imidazole	0.01	2.07	0.00117
					Average 0.00129 ± 0.00022
	1.0	**1**	0.005	7.84	0.0139
	1.0	**1**	0.01	14.1	0.0132
	1.0	**1**	0.001	5.07	0.0417
	1.0	**1**	0.001	2.50	0.0160
	1.0	**1**	0.001	2.22	0.0132
	5.0	**1**	0.001	2.32	0.0142
					Average 0.0141 ± 0.0011
2*c*	0.1			1.28	
	0.2	Imidazole	0.01	3.04	0.00176
	0.1	Imidazole	0.01	2.96	0.00168
	0.1	Imidazole	0.05	9.25	0.00159
					Average 0.00168 ± 0.00009
	0.2	**1**	0.00033	4.20	0.0824
	0.1	**1**	0.00033	3.50	0.0673
	0.1	**1**	0.00066	6.08	0.0727
					Average 0.0741 ± 0.0077

*All reactions in aqueous solution at 25°, pH = 8.0 with .01 M Tris buffer; μ = 0.1 M (KCl).
†Total catalyst concentration.

implying that the rate enhancement resulting from steroid–substrate interactions is dependent upon the hydrophobicity of the substrate. The slope is 0.43 ± 0.05, suggesting that rather less than half the hydrophobic surface of the aromatic ring systems is being removed from contact with water, which is consistent with the observed 1:1 stoichiometry of reaction. If the geometries of the transition states for **1**- and imidazole-catalyzed enolization were identical except for the presence of the steroid, then for $\pi = 0$, k_{rel} should be 1.0, since there would then be no stabilizing interaction to make the transition state for **1**-catalyzed reaction distinguishable from that for imidazole-catalyzed reaction. In fact the graph of log k_{rel} *vs.* π extrapolates to $k_{rel} = 0.4$; if the deviation from $k_{rel} = 1$ is real it suggests that in fact the geometry appropriate for hydrophobic interaction of the aryl group with the steroid is not quite optimal for the general base catalyzed reaction so that a small conformational destabilization must be introduced to gain the larger hydrophobic stabilization. Since the values of log k_{rel} increase

Can. J. Chem. Downloaded from www.nrcresearchpress.com by 210.87.254.6 on 09/05/12
For personal use only.

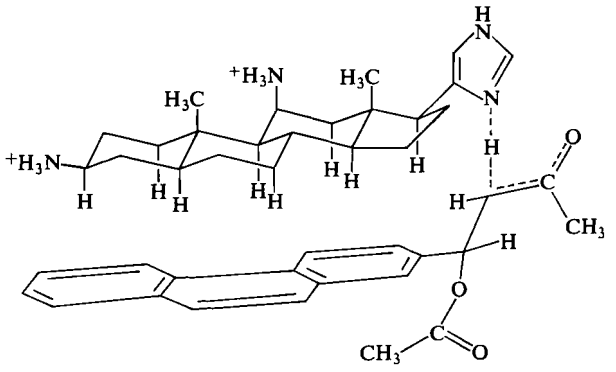

linearly with π, it appears reasonable to conclude that the transition state geometry is the same for all three substrates, with only the amount of contact changing. For $\pi = 0$, k_{rel} reflects the relative rate appropriate for this geometry. The magnitude of the hydrophobic rate enhancement should then be estimated as the rise from the intercept at $\pi = 0$ to the observed value for a given aryl group. Values so calculated are: phenyl, 9.0; naphthyl, 27; phenanthryl, 110.

Discussion

The mechanism of general base catalyzed elimination of acetic acid from β-acetoxy ketones is believed to be that of eq. 1 (17, 18).

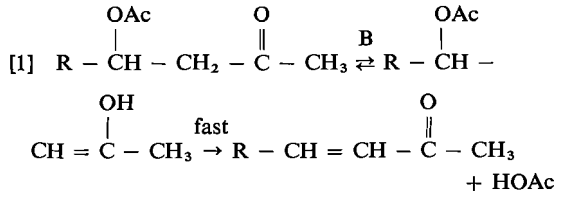

[1] $R-CH(OAc)-CH_2-C(=O)-CH_3 \overset{B}{\rightleftarrows} R-CH(OAc)-CH(OH)=C(CH_3)-CH_3 \xrightarrow{\text{fast}} R-CH=CH-C(=O)-CH_3 + HOAc$

with the rate determining step being the enolization. It is difficult to rule out unequivocally the alternative one-step process where loss of acetate is simultaneous with loss of proton. For the present purposes the uncertainty as to detailed mechanism is not important, since in either case, the transition state geometry is quite suitable for contact of the 17β-imidazole with the enolizable hydrogen *and* of the α-surface of the steroid with the aryl substituent of the ketone. The enolization–elimination reaction is far more convenient for kinetics experiments than is simple enolization, since it can be followed spectrophotometrically at very low concentrations. The techniques which have been employed to study kinetics of enolization (hydrogen isotope exchange or halogenation)[1] would be difficult or impossible in the present case, where the concentration of substrate had to be extremely low.

The origin of the rate enhancement for **1**-(compared to imidazole) catalyzed eliminations must now be considered. The pK_a's of **1** (7.2, (16*a*)) and imidazole (7.1 (16*b*)) are essentially identical, so catalyst basicity is not responsible. The imidazole group in **1** has a bulky substituent which should if anything retard reaction of **1**. If the inherent reactivity of the catalytic group is not responsible for the rate of enhancements, then some favorable interaction of the rest of the steroid with the substrate must be involved. Since the imidazole of **1** is abstracting a proton from the substrate at the transition state and the substrates **2***a–c* show progressively greater rate enhancements, the conformation of the transition state must be such that the aromatic rings of the substrate interact with the steroid. The monotonic increase in rate enhancement as the size of the aromatic ring system increases suggests strongly that the conformation of the transition state is the same for all substrates. The environment of the reaction center in such a conformation will have rather less polar character than for the imidazole-catalyzed reaction because one side of the developing double bond will be shielded from water by the steroid but this solvent effect will be constant for **2***a–c*.[2] The only noncovalent interaction

[1]For a discussion of the experimental problems associated with these techniques, see ref. 21.

[2]A referee has suggested that a local solvent effect of this sort may be responsible for some of the rate effects which we observe. This appears quite possible but we feel that any such effect should be essentially constant for the series **2***a–c*.

Can. J. Chem. Downloaded from www.nrcresearchpress.com by 210.87.254.6 on 09/05/12
For personal use only.

Can. J. Chem. Downloaded from www.nrcresearchpress.com by 210.87.254.6 on 09/05/12
For personal use only.

between an aromatic hydrocarbon and an alicyclic system which would explain the observed rate effect is hydrophobic bonding (22). The magnitude of the interaction to be expected can be estimated after Némethy and Scheraga (23), although there is some uncertainty about the proper way to estimate the number of water molecules released from contact with hydrocarbon as the two molecules come together. Our estimate of the free energy of hydrophobic interaction for phenanthrene plus perhydrophenanthrene is -2.4 kcal mol^{-1} or a potential rate factor of 56-fold, which is relatively close to the observed value. (It should be noted that Némethy and Scheraga used unitary free energies, corresponding to a standard state of hypothetical unit mole fraction, while we use a standard state of hypothetical unit molarity, so that it is necessary to apply a suitable correction to the values derived from their equations.)

The elimination reaction of β-acetoxy ketones can clearly be used in enzyme model studies: it has the advantage of relatively small steric requirements but suffers from the disadvantages of being inherently rather slow and of having a rather small selectivity for imidazoles as catalysts, compared with nucleophilic reactions of aryl esters. The uncatalyzed enolization of **2***c* at p*H* 8 and 25° has a half-life of *ca.* 15 h; in the presence of 0.01 *M* imidazole, **2***c* has a half-life of *ca.* 6 h or twofold faster; in the presence of 0.01 *M* **1**, **2***c* would have a half life of *ca.* 15 min. By contrast, uncatalyzed hydrolysis of *p*-nitrophenyl acetate in aqueous solution at p*H* 8 and 25° has a half-life of *ca.* 14 h (24); in the presence of 0.01 *M* imidazole the half-life is *ca.* 3 min (24) or 280-fold faster.

Inherently slow reactions are more convenient for enzyme model studies *if* the enzyme model is an efficient catalyst but not if the catalysis is modest. We conclude that as enzyme model systems with stronger substrate binding abilities than **1** are developed, elimination reactions such as that reported above will become more suitable than hydrolysis of active esters, since large catalytic effects will not compel the use of stopped-flow techniques to measure the rates of reaction and uncatalyzed reactions will be negligibly slow.

The experiments reported above were conducted under second-order conditions, *i.e.* at low concentrations of both substrate and catalyst. The observed second-order rate constants were demonstrated to be independent of both substrate and catalyst concentrations. These values permit a discussion of the difference in free energy between isolated completely solvated reactions and the overall transition state, in which we believe that the hydrophobic groups of substrate and catalyst are in contact with each other, and partially desolvated. We believe that it is probable that this transition state is reached by a two-step process,

$$\text{Substrate} + \text{Catalyst} \overset{K}{\rightleftarrows} (\text{Substrate–catalyst}) \overset{k}{\rightarrow} \text{Product} + \text{Catalyst}$$

analogous to the Michaelis–Menton mechanism for enzymic catalysis. It would be of immense interest to evaluate the k and K parameters if this mechanism truly applies; however, this is unlikely to be attainable with the present system, since the equilibrium constant for substrate–catalyst binding which is useful for interpreting the kinetics is the one corresponding to formation of the reactive conformation, *i.e.* productive binding, whereas any measured equilibrium constant would include all possible modes of nonproductive binding.[3] Until an enzyme model with a more specific binding site, which would constrain the substrate to bind in only one mode can be prepared, it is better to use the second-order rate constants (specificity constants (25)) since these can be interpreted in a straightforward way.

Experimental

Materials

Imidazole and tris-hydroxymethylaminomethane were recrystallized before use. KCl, NaOH, $NaHCO_3$, and KH_2PO_4 were reagent grade chemicals, used without further purification. Compound **1** was prepared and purified as described previously (14). Acetonitrile (Eastman spectrograde) was passed through a column of grade I neutral alumina (Woelm) to remove nucleophilic impurities.

4-Acetoxy-4-(2-phenanthryl)-2-butanone, 2c

2-Acetylphenanthrene (Aldrich), m.p. 139–141° (lit. (26) m.p. 143°) was converted to 2-phenanthroic acid, m.p. 260–262° (lit. (26) m.p. 258–260°) by hypochlorite oxidation (26). 2-Phenanthroic acid (2.25 g in 22.5 ml

[3]For the simple scheme, involving one productive $(ES)_P$ and one nonproductive, $(ES)_{NP}$, complex:

$$(ES)_{NP} \overset{K_{NP}}{\rightleftarrows} E + S \overset{K_P}{\rightleftarrows} (ES)_P \overset{k_{cat}}{\rightarrow} E + P$$

it may readily be shown that Michaelis–Menton kinetics will be followed with $K_{m_{app}} = (1/K_P + 1/K_{NP})^{-1}$.

Can. J. Chem. Downloaded from www.nrcresearchpress.com by 210.87.254.6 on 09/05/12
For personal use only.

dry THF) was added to $LiAlH_4$ (0.56 g in 22.5 ml dry THF); the mixture was refluxed for 2½ h, cooled, and treated with saturated aqueous sodium potassium tartarate. The mixture was acidified and extracted with ether. The combined extracts were washed with saturated aqueous NaCl, dried over $MgSO_4$, and evaporated. Crystallization of the residue (benzene – petroleum ether) gave 1.36 g of 2-phenanthryl carbinol, m.p. 123–127° (lit. (27) m.p. 125–125.5°). 2-Phenanthryl carbinol (1.36 g in 35 ml dry CH_2Cl_2) was added dropwise to a solution of 4.05 g CrO_3 and 5.4 ml pyridine in 100 ml dry CH_2Cl_2. After 40 min at room temperature, the solution was poured into water in a separatory funnel and the tarry residue was rinsed with CH_2Cl_2 and with ether. These rinsings were added to the separatory funnel and shaken well. The aqueous layer was washed with CH_2Cl_2; the combined organic layers were washed with aqueous HCl, water, and saturated aqueous NaCl. After drying the solution ($MgSO_4$) and removing the solvent a brown oil remained. This was partially purified by treating with methanol, centrifuging to remove insoluble material, and evaporating the supernatant. The aldehyde was at best a semicrystalline gum; (lit. (27) m.p. 59–59.5°); n.m.r. δ ($CDCl_3$): 7.3–9.05 (9 H, complex multiplet), 10.10 (0.74 s, 1H, Ar—C*H*O). Crude 2-phenanthraldehyde (0.55 g in acetone (1.92 ml)) was cooled in an ice bath and added to 0.055 *N* NaOH (27 ml, in 1.5:1 acetone–water) cooled in an ice bath. The solution was stirred (ice bath) for 1.5 h, neutralized (*N* HCl), and extracted three times with ether; the extracts were washed with saturated aqueous NaCl, dried ($MgSO_4$), and evaporated to give 0.62 g of a white solid. Crystallization (ethyl acetate – petroleum ether) gave 0.188 g of 4-hydroxy-4-(2-phenanthryl)-2-butanone, m.p. 82–87°; n.m.r. δ ($CDCl_3$): 2.2 (s, 3H, *C*H_3—CO—), 2.9 (multiplet, 2H, —CH_2—CO—), 5.3 (multiplet, 1H, —C*H*(OH)—), 7.2–8.9, (complex, aromatic H).

4-Hydroxy-4-(2-phenanthryl)-2-butanone (0.188 g, in 4:1 glacial acetic acid – acetic anhydride, 5.15 ml, containing 4 mg of *p*-toluenesulfonic acid) was stirred at room temperature for 2 h, neutralized by addition of sodium acetate, and partitioned between water and ether. The combined ether extracts were washed with saturated aqueous $NaHCO_3$ (five times), water, and saturated aqueous NaCl. Evaporation gave 0.214 g of a white solid which on crystallization from benzene–cyclohexane gave 0.046 g of 4-acetoxy-4-(2-phenanthryl)-2-butanone, m.p. 92–95°; n.m.r. δ ($CDCl_3$): 2.04 (s, *C*H_3—CO—O—), 2.12 (s, *C*H_3—CO—CH_2—), 3.02 (t, CO—*C*H_2—), 6.38 (multiplet, —C*H*(OAc)—), 7.4–8.8 (complex, aromatic H).

Anal. Calcd. for $C_{20}H_{10}O_3$: C, 78.66; H, 5.99. Found, C, 78.37; H, 5.92.

4-Acetoxy-4-(2-naphthyl)-2-butanone, 2b

By the same procedures, 2-naphthaldehyde (Aldrich) was converted into 4-hydroxy-4-(2-naphthyl)-2-butanone, m.p. 60–61° (benzene–cyclohexane); n.m.r. δ ($CDCl_3$): 2.1 (s, 3H, *C*H_3—CO—), 2.8 (m, 2H, CO—*C*H_2—), 2.8 (m, 2H, CO—*C*H_2—), 3.6 (br s, 1H, —CH(O*H*)—), 5.2 (m, 1H, —C*H*(OH)—), 7.0–7.8 (complex, 7H, aromatic H). Acetylation gave 4-acetoxy-4-(2-naphthyl)-2-butanone, m.p. 40–41° (absolute ethanol); n.m.r. δ ($CDCl_3$): 2.0_2 (s, *C*H_3—CO—O), 2.1_2 (s, *C*H_3—CO—CH_2), 3.0 (m, CO—*C*H_2—), 6.3 (m, —C*H*(OAc)—), 7.2–7.9 (complex, aromatic H).

Anal. Calcd. for $C_{16}H_{16}O_3$: C, 74.95; H, 6.29. Found: C, 74.89; H, 6.41.

4-Acetoxy-4-phenyl-2-butanone, 2a

By the same procedures, benzaldehyde was converted into 4-hydroxy-4-phenyl-2-butanone, m.p. 33–36° (lit. (29) m.p. 34–36°); n.m.r. δ ($CDCl_3$): 2.1 (s, 3H, *C*H_3—CO—), 2.8 (m, 2H, CO—*C*H_2—), 3.5 (s, 1H, —CH(O*H*)—), 5.1 (m, 1H, —C*H*(OH)—), 7.2 (s, 5H, aromatic H). Acetylation gave 4-acetoxy-4-phenyl-2-butanone as an oil which was purified by preparative-layer chromatography (Merck silica gel PF 254, eluting with 2:1 petroleum ether – ether). Analysis was performed by injecting a known amount into aqueous sodium hydroxide. Comparison of the absorbance at 295 nm (extrapolated to zero time to correct for slow retroaldol reaction) with that of an authentic sample of benzalacetone, m.p. 40° (lit. (28) m.p. 42°) showed that **2a** was 98% pure; n.m.r. δ ($CDCl_3$): 1.9_4 (s, 3H, *C*H_3—CO—O), 2.0_6 (s, 3H, *C*H_3—CO—CH_2), 2.9 (t, 2H, —CO—*C*H_2—), 6.1 (m, 1H, —C*H*(OAc)—), 7.2 (s, 5H, aromatic H).

Kinetic Procedures

Reactions were initiated by adding a small portion of a stock solution of substrate in purified acetonitrile to temperature equilibrated buffer in a spectrophotometer cell. Changes in absorbance were followed using a Gilford Model 240 spectrophotometer. p*H* values were measured at the end of the reaction using a Radiometer p*H* Meter 25SE with a GK 2301C combined electrode. For the slower reactions, secondary reactions became significant at long times, so that it was not possible to determine infinity points for the elimination reactions by following to 8 or 10 half-lives. In these cases, data to 4 or 5 half-lives were fitted to the equation

$$\text{Absorbance} = a + be^{-ct}$$

using a nonlinear least-squares (30, 31) program.

1. H. R. L. Van Etten, J. F. Sebastion, G. A. Clowes, and M. L. Bender. J. Am. Chem. Soc. **89**, 3242 (1967); **89**, 2253 (1967).
2. C. Aso, T. Kunitake, and S. Shinkai. Chem. Commun. 1983 (1968); Bull. Chem. Soc. Jap. **43**, 1109 (1970); **43**, 2581 (1970).
3. R. G. Shorenstein, C. S. Pratt, C. J. Hsu, and T. E. Wagner. J. Am. Chem. Soc. **90**, 6199 (1968).
4. R. Breslow and L. E. Overman. J. Am. Chem. Soc. **92**, 1075 (1970).
5. C. A. Blyth and J. R. Knowles. J. Am. Chem. Soc. **93**, 3017 (1971); **93**, 3021 (1971).
6. T. Maugh, II and T. C. Bruice. J. Am. Chem. Soc. **93**, 6584 (1971).
7. D. E. Tutt and M. A. Schwartz. J. Am. Chem. Soc. **93**, 767 (1971).
8. R. Herschfield and M. L. Bender. J. Am. Chem. Soc. **94**, 1376 (1972).
9. D. Oakenfull. J. Chem. Soc. Perkin II, 1006 (1973).
10. F. Cramer and W. Kampe. J. Am. Chem. Soc. **87**, 1115 (1965).

11. N. HENNRICH and F. CRAMER. J. Am. Chem. Soc. **87**, 1121 (1965).
12. R. BRESLOW and P. CAMPBELL. J. Am. Chem. Soc. **91**, 3085 (1969).
13. T. W. STRAUB and M. L. BENDER. J. Am. Chem. Soc. **94**, 8875 (1972); **94**, 8881 (1972).
14. J. P. GUTHRIE. Can. J. Chem. **50**, 3993 (1972).
15. J. P. GUTHRIE and Y. UEDA. Chem. Commun. 898 (1973).
16. (*a*) J. P. GUTHRIE and Y. UEDA. In preparation. (*b*) W. P. JENCKS and J. REGENSTEIN. *In* Handbook of biochemistry. 1st. Ed. Chemical Rubber Publishing Co., Cleveland. 1968.
17. L. R. FEDOR and W. R. GLOVE. J. Am. Chem. Soc. **93**, 985 (1971) and previous papers in this series.
18. D. J. HUPE, M. C. R. KENDALL, and T. A. SPENCER. J. Am. Chem. Soc. **94**, 254 (1972).
19. G. B. BARLIN and D. D. PERRIN. Q. Rev. Chem. Soc. **92**, 5194 (1970).
20. T. FUJITA, J. IWASA, and C. HANSCH. J. Am. Chem. Soc. **86**, 5175 (1964); M. S. TUTE. Adv. Drug. Res. **6**, 1 (1971).
21. J. K. COWARD and T. C. BRUICE. J. Am. Chem. Soc. **91**, 5339 (1969).
22. W. P. JENCKS. Catalysis in chemistry and enzymology. McGraw-Hill, N.Y. 1969. pp. 393–395.
23. G. NÉMETHY and H. A. SCHERAGA. J. Chem. Phys. **36**, 3382 (1962); **36**, 3401 (1962); J. Phys. Chem. **66**, 1773 (1962).
24. W. P. JENCKS and M. GILCHRIST. J. Am. Chem. Soc. **90**, 2622 (1968).
25. M. L. BENDER and F. J. KEZDY. Ann. Rev. Biochem. **34**, 65 (1965).
26. E. MOSETTIG and J. VAN DE KAMP. J. Am. Chem. Soc. **52**, 3704 (1930).
27. E. MOSETTIG and J. VAN DE KAMP. J. Am. Chem. Soc. **55**, 2995 (1935).
28. A. H. COOK, H. M. BUNBURY, and D. H. HEY. (*Editors.*) Dictionary of organic chemistry. 5th Ed. Eyre and Spottiswoode, London. 1965.
29. D. S. NOYCE and W. L. REED. J. Am. Chem. Soc. **80**, 5539 (1958).
30. W. E. WENTWORTH. J. Chem. Educ. **42**, 96 (1965); **42**, 162 (1965).
31. W. E. DEMING. Statistical adjustment of data. Dover, New York, N.Y. 1964.

Can. J. Chem. Downloaded from www.nrcresearchpress.com by 210.87.254.6 on 09/05/12
For personal use only.

The Use of Magnesium and its Salts in the Reaction of α,β-Unsaturated Carbonyl Compounds with Sodium Acetylide

JOHN NICHOLSON GARDNER

Technical Development Department, Hoffmann-La Roche Inc., Nutley, New Jersey 07110

Received December 30, 1974

JOHN NICHOLSON GARDNER. Can. J. Chem. **53**, 2157 (1975).

Conditions are described for the preparation in anhydrous ammonia of a magnesium–acetylene complex. In the presence of this complex, the addition of sodium acetylide to the carbonyl groups of some α,β-unsaturated aldehydes and ketones is shown to be a much more efficient reaction than when sodium acetylide alone is employed.

JOHN NICHOLSON GARDNER. Can. J. Chem. **53**, 2157 (1975).

On décrit les conditions permettant de préparer, dans l'ammoniac liquide, un complexe magnésium–acétylène. On démontre qu'en présence de ce complexe l'addition de l'acétylure de sodium sur les groupes carbonyles de certains aldéhydes et cétones α,β-non-saturés est une réaction beaucoup plus efficace que la réaction de l'acétylure de sodium seul.

[Traduit par le journal]

The addition of the monoanion of acetylene to the carbonyl functions of aldehydes and ketones, as shown in [1], is an important synthetic method. For example, the reaction in

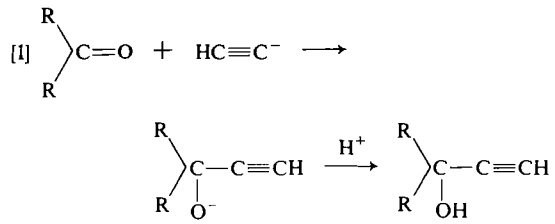

liquid ammonia of sodium acetylide with such carbonyl groups plays a major role in syntheses of vitamin A and β-carotene (see for example ref. 1) and yields in excess of 90% are not uncommon when the substrate is a saturated ketone. However, with α,β-unsaturated aldehydes and ketones, the reaction with sodium acetylide takes a less felicitous course. Thus, Hennion and Lieb (2) reported yields of 20–27% for the ethynylcarbinols prepared from methyl vinyl ketone (MVK), ethylidenacetone, mesityl oxide, and benzalacetone by this reaction, whereas with crotonaldehyde the reaction went in only 46% yield. This last case was examined in detail by other workers (3) who concluded that, to obtain yields of 72–77%, it was necessary to use carefully purified reagents at a temperature of −80°. Without these precautions, they recorded yields as low as 55%. Yet another group (4) examined the reaction of MVK with sodium acetylide in liquid ammonia at reflux and found that the yield of the corresponding ethynylcarbinol could be raised to 40% if 4.5 g-at. of sodium was used per mole of MVK.

Because of the problems encountered in reacting sodium acetylide with α,β-unsaturated ketones, Oroshnik and Mebane (5) explored the use of the acetylides of potassium, lithium, and calcium. They reported that the first of these was no better than sodium but with lithium and calcium they obtained superior results. For example, with MVK, calcium acetylide gave the ethynylcarbinol in 71% yield and with lithium acetylide the figure was 68%. Thus, these acetylides provide a satisfactory method for the addition of acetylene to α,β-unsaturated carbonyl groups but the high costs of lithium and calcium have discouraged the use of these reactions on an industrial scale.

The fact that lithium and calcium acetylides react with α,β-unsaturated carbonyl groups in high yield led us to consider the possibility that magnesium, which is chemically somewhat similar but less expensive, might yield an acetylide which would react in the same way. A report in the literature (6) encouraged the belief that magnesium could be made to dissolve in liquid ammonia although it might be necessary to have another reactant present. It was quickly established that magnesium does not dissolve in liquid ammonia in the presence of acetylene but if magnesium metal is added

Can. J. Chem. Downloaded from www.nrcresearchpress.com by 210.87.254.6 on 09/05/12
For personal use only.

Can. J. Chem. Downloaded from www.nrcresearchpress.com by 210.87.254.6 on 09/05/12
For personal use only.

TABLE 1. Data for the reaction

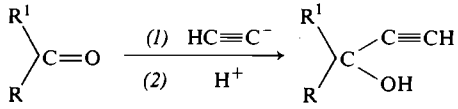

Carbonyl compound	Na–Mg		Na–$MgSO_4$		Na*		Li†		Ca†	
	Yield	Conversion‡	Yield	Conversion	Yield	Conversion	Yield	Conversion	Yield	Conversion
MVK	69	100	70	100	21§	100	68	100	71	100
Mesityl oxide	59	72	95	46	24	55	48	54	75	61
Benzalacetone	46	89	82	83	20	100	85	84	96	100
Crotonaldehyde	77	100	74	100	46¶	100	—	—	—	—

NOTE: All the numbers cited are percentages
*From ref. 2.
†From ref. 5.
‡Conversion = (weight carbonyl compound consumed)/(weight carbonyl compound charged).
§A yield of 40% has been reported when a large excess of sodium acetylide is used (4).
¶A yield of 72–77% has been reported when highly purified reagents are used at −80° (3).

Can. J. Chem. Downloaded from www.nrcresearchpress.com by 210.87.254.6 on 09/05/12
For personal use only.

to a solution of sodium acetylide in ammonia which contains excess acetylene, dissolution of the magnesium occurs with concomitant formation of a white precipitate. A few trials demonstrated that the resultant suspension gave encouraging yields of the ethynylcarbinol from MVK and an investigation of the phenomena involved was undertaken.

When sodium and magnesium in a ratio of 1:9 by weight were stirred in anhydrous ammonia under reflux with acetylene passing through the mixture, dissolution of the magnesium was essentially complete in 15–18 h. The resultant white precipitate was isolated by centrifugation and proved to be sufficiently stable to air and moisture for these operations to be performed without the need for any special precautions. After drying over phosphorus pentoxide, the precipitate was analyzed for sodium, magnesium, ammonia, and acetylene. Small amounts of sodium and ammonia were detected but the analysis showed that the solid was essentially a complex of magnesium and acetylene with the approximate composition $Mg(C{\equiv}CH)_{1.2}$. This result is consistent with the observation that, when the complex was prepared in liquid ammonia as described and was reacted *in situ* with a large excess of 6-methyl-5-hepten-2-one, the amount of ketone converted to ethynylcarbinol was in agreement with each magnesium atom being associated with one molecule of acetylene available for reaction.

The reaction of the complex with MVK was then explored. Addition, to the acetylides in liquid ammonia, of the MVK as a solution in ether at $-20°$ gave the optimum yield. Ether proved to be the preferred solvent and better results were obtained with it than with diisopropyl ether or toluene. It was found that, up to a ratio of about 4.5:1 of sodium to magnesium, the ethynylcarbinol could be obtained in 67–70% yield but with more sodium present the yield fell.

Using the conditions which had been optimized for MVK, experiments were run with other α,β-unsaturated carbonyl compounds. These results, together with figures from the literature for reactions using sodium, lithium, and calcium, are set forth in Table 1. In most cases the results with sodium–magnesium mixtures compare favorably with those from the other methods.

When magnesium metal is added to a solution of sodium acetylide in liquid ammonia which contains no excess acetylene and the mixture is stirred for several hours, a white precipitate forms and the blue color characteristic of solutions of metals in liquid ammonia may be seen faintly. Addition of acetylene discharges the color but it will return on further stirring. These results suggest that an equilibrium such as

$$Mg + xNaC{\equiv}CH \rightleftharpoons Mg(C{\equiv}CH)_x + xNa^+ + xe^- \text{ (solvated)}$$

is involved and only when the sodium ions are converted to the acetylide is the equilibrium displaced in favor of $Mg(C{\equiv}CH)_x$. This hypothesis led to the supposition that sodamide might function in the same manner as sodium acetylide and it was found that, if sodamide is prepared in liquid ammonia, using iron as a catalyst, magnesium will dissolve in the suspension. The resultant suspension, of what is presumably sodium and magnesium amides, may be reacted with acetylene and then with MVK to give the ethynylcarbinol in as high yield as when sodium acetylide is used to attack the magnesium.

From the data already cited, it seems quite certain that it is the presence of $Mg(C{\equiv}CH)_x$ in the reaction mixture which results in improved yields in reactions with α,β-unsaturated ketones. Therefore, we sought to devise alternative methods for the formation of this species. In anhydrous ammonia, the equilibrium between sodium acetylide and a soluble magnesium salt on the one hand and insoluble $Mg(C{\equiv}CH)_x$ and a sodium salt on the other should favor the formation of $Mg(C{\equiv}CH)_x$ and thus yield an effective reagent for conversion of α,β-unsaturated ketones and aldehydes to the corresponding ethynylcarbinols. That this hypothesis is correct was shown by addition of ethyl magnesium bromide in ether to a solution of sodium acetylide in anhydrous ammonia. Reaction of this mixture with MVK yielded the ethynylcarbinol in 67% yield. The other salts shown in Table 2 were therefore screened for their influence upon the reaction. It will be noted that, in addition to ethyl magnesium bromide, magnesium chloride and sulfate gave yields of the carbinol close to those obtained with magnesium metal. Because of its vigorous reaction with

Can. J. Chem. Downloaded from www.nrcresearchpress.com by 210.87.254.6 on 09/05/12
For personal use only.

TABLE 2. Effect of anhydrous magnesium salts on the reaction of MVK with sodium acetylide

Salt	Yield of ethynylcarbinol (%)
$MgBr_2$	—*
$Mg(OMe)_2$	—*
MgO	31*
Mg_3N_2	—*
MgAcac†	21*
$MgSO_4$	70
$MgCl_2$	59
MgF_2	46
C_2H_5MgBr	67

*Tar formation occurred.
†Acac = acetonylacetonate.

ammonia, magnesium chloride is less convenient to use than is magnesium sulfate.

Results obtained using magnesium sulfate are given in Table 1. Only the reaction with MVK was optimized, a yield of 70% being achieved. Our experiences with different grades of magnesium sulfate strongly suggest that its surface properties are important in the reaction, but a finely divided, reagent grade material usually works well. Magnesium sulfate has little, if any, solubility in anhydrous ammonia and so, in its case, the hypothesis of a metathetical reaction in solution with sodium acetylide is very likely an oversimplification. However, although the mechanism of the reaction is not understood, the procedure is a useful one and is attractive as it avoids the lengthy stirring period which is required when magnesium metal is used.

Experimental

Materials

Methyl vinyl ketone was fractionated at atmospheric pressure through a 12 in. Goodloe column. The distillate was stabilized by addition of 0.1% of acetic acid and 0.1% of hydroquinone. It assayed 96–98% by gas chromatography. The other α,β-unsaturated carbonyl compounds were flash distilled and assayed 92–100%. The structures of the alcohols obtained from the α,β-unsaturated carbonyl compounds were confirmed by n.m.r. spectroscopy. Anhydrous magnesium sulfate (reagent grade) was purchased from the J. T. Baker Chemical Company or made as described below. Yields were calculated on the basis of the assays of the starting materials and products.

Analysis of the Magnesium–Acetylene Complex

The acetylene content was determined gasometrically, the complex being decomposed with dilute acid because water gave incomplete decomposition. The gas evolved was identified as acetylene by i.r. spectroscopy. Magnesium was determined by titration with ethylenediamine tetraacetic acid and sodium by precipitation with zinc uranyl acetate. Ammonia, which was entrained with nitrogen from the surface of the solid and from a solution in alkali, was absorbed in dilute acid and determined by back titration.

Determination of Water in Magnesium Sulfate

A known amount of dry methanol was added to the weighed sample and the mixture was agitated in an ultrasonic bath for 3 h. The water content of the methanol was then determined gas chromatographically by comparison with mixtures of water and methanol of known composition.

Procedure for the Precipitation and Drying of Magnesium Sulfate

Magnesium sulfate (300 g, anhydrous) was dissolved in deionized water (1050 ml) and this solution, after filtration, was added with vigorous stirring to acetone (5000 ml). The precipitated solid was isolated by filtration and dried for 18 h at 60–80°. Drying was continued for 3.5 days, the temperature being raised to 140° over 1.5 days and maintained at this value for 1 day. The solid was then held at 400° for 1 day. The water content of the product was 0.28% and the particle size was *ca.* 200 mesh.[1] Drying at too high an initial temperature causes the magnesium sulfate to dissolve in its water of crystallization.

Procedure for Reaction of MVK with Acetylene using Sodium and Magnesium Metals

Sodium (60 g, 2.61 mol) and magnesium turnings (20 g, 0.83 mol) were added to anhydrous ammonia (1500 ml) and acetylene was passed rapidly through the solution until the blue color was discharged. The gas flow was reduced to a slow, steady rate and the mixture was stirred for 15–18 h, at the end of which almost all the magnesium had reacted and a white precipitate had formed. Ether (200 ml) was added and, while agitating as rapidly as possible, a solution of MVK (189 g, 97%, 2.62 mol) in ether (600 ml), precooled to −10 to −20°, was introduced over 20–30 min. The acetylene was shut off, the ammonia was evaporated by warming the reaction flask with steam, and when the temperature of the residue reached −15 to −20°, the contents of the flask were added over about 20 min to a solution of sulfuric acid (200 ml) in water (1200 ml) maintained at 0–15°. The aqueous phase, which had p*H ca.* 2, was separated and extracted with ether (2 × 200 ml). The combined organic phases were washed with a mixture of saturated sodium bicarbonate solution (20 ml) and saturated brine (80 ml), and dried over sodium sulfate. The ether was removed by distillation through a 12 in. Goodloe column and the residue (254 g) was distilled through a 12 in. Vigreux column to yield 3-methylpent-1-en-4-yn-3-ol (182 g, assay 93%, 1.76 mol), b.p. 46–57°/48 Torr. A forerun (12 g, assay 51%, 0.06 mol) was also obtained. The yield was thus 69%.

[1]When drying was stopped at a water content of 2.5%, the product resulted in reduced yields when used in the reaction of MVK with acetylene.

Procedure for the Reaction of MVK with Acetylene using Sodamide and Magnesium Metal

Anhydrous ferric chloride (0.2 g) was dissolved in anhydrous ammonia (1500 ml) and sodium (60 g) was added in pieces (1–2 g), each being allowed to react to form sodamide before the next was added. Magnesium turnings (20 g) were then introduced and the mixture was stirred for 15–18 h, at the end of which most of the magnesium had reacted and a pale grey precipitate had formed. Acetylene was passed through the mixture for 1 h and its color darkened until it was almost black. Ether and MVK were added in exactly the same manner as in the previous experiment and the product was isolated as before. The yield was the same within experimental error.

Procedure for Reaction of Crotonaldehyde with Acetylene using Sodium Metal and Magnesium Sulfate

Sodium (80 g, 3.48 mol) was added to anhydrous ammonia (1500 ml) and acetylene was passed rapidly through the solution until the blue color was discharged. While continuing slow passage of acetylene, anhydrous magnesium sulfate (100 g, 0.83 mol) was added and the mixture was stirred for 30 min.[2] Ether (200 ml) was added and then a solution, at −10 to −20°, of crotonaldehyde (170 g, 99%, 2.40 mol) in ether (600 ml) was introduced over 20 min. The ether was evaporated and the product isolated as described for the reaction using MVK. Hex-4-en-1-yn-3-ol (186 g, assay 92%, 1.78 mol), b.p. 58–65°/20 Torr, was obtained in 74% yield.

[2]Use of less magnesium sulfate resulted in lower yields, as did a shorter stirring time.

Isolation of the Magnesium–Acetylene Complex

Sodium (5 g) and magnesium turnings (45 g) were reacted with acetylene in anhydrous ammonia (1500 ml) as already described. The resultant white suspension was decanted from a little unreacted magnesium. The suspended solid was isolated by centrifugation, resuspended in anhydrous ammonia, and again centrifuged. After drying over phosphorus pentoxide under vacuum, it was analyzed.

Anal. Found: Mg, 37.9; Na, 1.3; C_2H_2, 49; NH_3, 6.7 (4.3% surface NH_3 and 2.4% combined NH_3).

The ratio of $Mg:C_2H_2$ corresponds to a complex of empirical formula $Mg(C{\equiv}CH)_{1.2}$.

The author wishes to thank Prof. George M. Whitesides for many helpful discussions during the course of this work. He is grateful to Dr. V. S. Venturella, Dr. A. V. Holmgren, and Mr. P. DePaolo for the analytical data and to Mr. F. E. Dyer and Miss O. Abril for much of the experimental work.

1. O. Isler. Carotenoids. Birkhauser Verlag, Basle. 1971.
2. G. F. Hennion and D. J. Lieb. J. Am. Chem. Soc. **66**, 1289 (1944).
3. J. M. Shackelford and W. A. Michalowicz. J. Org. Chem. **27**, 1631 (1962).
4. J. Cymerman, I. H. Heilbron, and E. R. H. Jones. J. Chem. Soc. 90 (1945).
5. W. Oroshnik and A. D. Mebane. J. Am. Chem. Soc. **71**, 2062 (1949).
6. A. G. Loomis. J. Am. Chem. Soc. **44**, 8 (1922).

Can. J. Chem. Downloaded from www.nrcresearchpress.com by 210.87.254.6 on 09/05/12
For personal use only.

Linear Free Energy Relationships. IV.[1] Synthesis and Spectral Characterization of Some New Solvatochromics. *N*-(*p*-Substituted)benzyl-2′-hydroxy-4-stilbazolium Betaines

HARRY W. GIBSON AND F. C. BAILEY

Webster Research Center, Xerox Corporation, Webster, N.Y. 14580

Received November 20, 1974

HARRY W. GIBSON and F. C. BAILEY. Can. J. Chem. **53**, 2162 (1975).

The spectral data for the present series of compounds indicate that the long wavelength $\pi \rightarrow \pi^*$ transition in each case involves transfer of negative charge from the phenol–quinone moiety to the pyridyl ring. Two separate features bear on this point: the transition energy dependence on (*i*) substituent and (*ii*) solvent. The plots of transition energy *vs.* Hammett substituent constant for the salts and the betaines have negative slopes as expected for such a transition. The plots of transition energy for the betaines *vs.* the solvent polarity parameter have large positive slopes, which are evidence for a large decrease in dipole moment upon excitation, consistent with such a transition. Through study of the p*H* dependence of the spectrum, the pK_a of the parent compound was found to be 8.37 at 22°. From this pK_a the apparent σ_{ortho} for the *N*-benzylstilbazolium substituent was estimated to be 0.75.

HARRY W. GIBSON et F. C. BAILEY. Can. J. Chem. **53**, 2162 (1975).

Les données spectrales concernant la nouvelle série de composés indiquent que dans chaque cas la transition $\pi \rightarrow \pi^*$ observée à grande longueur d'onde implique un transfert d'une charge négative de la position phénol–quinone vers le cycle pyridyl. Il y a deux caractéristiques principales qui suggèrent cette conclusion: la dépendance de l'énergie de transition sur (*i*) les substituants et (*ii*) le solvant. Les courbes montrant l'énergie de transition en fonction des constantes de Hammett pour des substituants sous formes de sels ou de bétaines possèdent des pentes négatives telles que l'on pourrait les prédire pour de telles transitions. Les courbes de l'énergie de transition pour les bétaines en fonction du paramètre pour la polarité du solvant montrent de fortes pentes positives; ceci indique qu'il y a un fort abaissement du moment dipolaire lors de l'excitation et ceci est en accord avec une telle transition. A l'aide d'études sur l'influence du p*H* sur le spectre, on a pu évaluer que le pK_a du composé de base est 8.37 à 22°. En se basant sur ce pK_a, on a pu estimer que la valeur apparente du σ_{ortho} pour le substituant *N*-benzylstilbazolium est de 0.75. [Traduit par le journal]

Introduction

Solvatochromic compounds undergo changes in 'color' with changes in solvent (1). In valence bond terminology this is ascribed to the variation in relative contribution of two resonance forms to the hybridized structure and molecular orbital calculations support this picture (2). Compounds which show the largest solvatochromic effects are those possessing extreme resonance forms: a polarized or zwitterionic one and a delocalized or quinoidal one. Increasing polarity of the solvating medium thus shifts the electron distribution of the ground state continuously toward the polar resonance from while the structure of the excited state is affected negligibly (Franck–Condon principle); this results in a change in energy difference and absorption wavelength (3). Such compounds have, therefore, served as empirical solvent polarity indicators (1, 3, 4).

Our interest in solvatochromics arises from our work relating molecular orbital energy levels and structure by means of linear free energy relationships (5–7). In a previous report (6) the synthesis and absorption spectra of solvatochromic compounds **1** were described. In this series the energy of the longest wavelength band is linearly related to the substituent constant in all five solvents examined (6). This is in contrast to the generally limited success of such correlations in substituted benzenes (8). Part of this latter difficulty may arise from crossover of energy levels as substituents are changed and the resultant problem of proper assignment of transitions. However, such linear correlations of *hν* and substituent constant are observed in dyes (9–12),

[1]For parts I–III, see refs. 5–7. For part V, see ref. 34.

Can. J. Chem. Downloaded from www.nrcresearchpress.com by 210.87.254.42 on 09/05/12
For personal use only.

Can. J. Chem. Downloaded from www.nrcresearchpress.com by 210.87.254.42 on 09/05/12
For personal use only.

where the identity of the absorption is readily assigned to a given transition for the entire series due to its isolation in the visible portion of the spectrum, and in donor–acceptor complexes of both inter-(13–15) and intramolecular (14) types. In intermolecular charge transfer transitions, it also is known that to a good approximation $h\nu = I - A + C$ (16), where I is the ionization potential of the donor, A is the electron affinity of the acceptor, *i.e.*, the energy levels of the orbitals involved, and C is a constant containing solvation, polarization, and nonbonding terms. Thus, a linear relationship between I and σ, and A and σ may be inferred.

Although not generally thought of in these terms, intramolecular charge transfer transitions can be similarly considered. Thus, attachment of a substituent at a particular site causes a larger perturbation of the energy levels in that moiety than in the other portion of the charge transfer couple. Thus, the primary effect is to vary the highest occupied orbital (ionization potential) of the donor moiety or the lowest unoccupied orbital (electron affinity) of the acceptor portion. In series **1**, as X becomes more electron withdrawing, the long wavelength transition energy increases. On the basis of these substituent and solvent effects on the absorption spectra, it was concluded that the long wavelength absorption transition involves transfer of electron density from the phenol–quinone moiety to the pyridyl ring, *i.e.*, excitation involves conversion of a ground state resembling **1***a* to an excited state more like **1***b*. Thus, the effect of substituent is primarily to alter the energy of the highest occupied molecular orbital associated with the phenolate–quinone moiety. The fact that this energy is lowered (ionization potential raised) by electron withdrawing groups is consistent with substituent effects on ionization potentials in other aromatic systems (5, 7).[2]

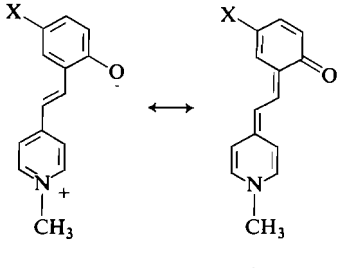

a *b*

1

To corroborate this picture of the long wavelength transition of these compounds, we chose to examine *N*-(*p*-substituted)benzyl-2′-hydroxy-4-stilbazolium betaines (**2**). In this series of compounds, the substituent is attached to the pyridyl portion of the molecule. Since this is the acceptor portion of the molecule in the model deduced previously, the primary effect of the substituent is expected to be a result of alteration of the lowest unoccupied molecular orbital. By study of series **1** and **2**, substituent effects on the donor and acceptor portions can be discerned to some extent independently, in addition to the effects of solvent on the resultant electronic transitions.

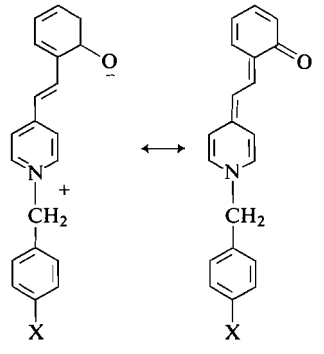

a *b*

2

Discussion

Synthesis

The synthesis of this new solvatochromic series is analogous to our previous work (6). 4-Picoline (**3**) and the *p*-substituted-benzyl bromides (**4**) react in tetrahydrofuran(THF) to yield the quaternary salts (**5**) in ~90% yields. The yields, melting points, and elemental analyses are given in Table 1.

Condensation of the quaternary salts **5** with salicylaldehyde (**6**) in the presence of piperidine led to the (*p*-substituted)benzyl-2′-hydroxy-4-stilbazolium bromides (**7**) in variable yields. The synthesis and characterization data are summarized in Table 2. As expected all of these com-

[2]For example the first four ionization potentials of substituted pyridine-*N*-oxides (data of Maier and Muller (33)) are linearly correlated (correlation coefficients r = 0.994, 0.995, 0.945, 0.935, respectively) with positive slopes by sums of σ^+_{para} substituent constants.

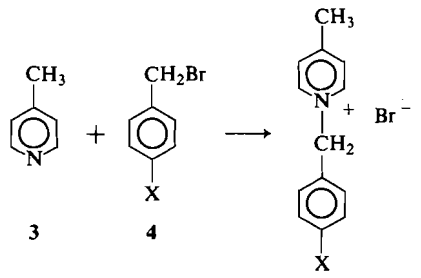

3 4 5

pounds are more soluble in organic solvents than the corresponding methiodides of series **1**. Significantly, none of the 1 : 1 complexes of **2** and **7** was observed; these compounds differ in this respect from series **1**, which form such complexes with the corresponding hydriodide salts.

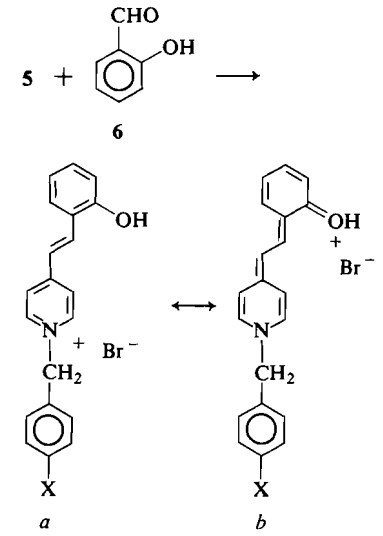

6

a b

7

In addition to the compounds listed in Table 2, the syntheses of **7**, X = CN, NO_2, were also pursued. Though these compounds were believed to have been prepared, they could not be isolated in pure form even by column chromatography.

Similarly attempts to isolate and purify the solvatochromic series **2** after their generation by base treatment of **7** were unsuccessful. Attempted recrystallization led to formation of intractable gums. These may be polymers arising from intermolecular electron transfer reactions. This proclivity for gum formation was also observed in the previously studied **1**, X = OCH_3.

Spectral Characterization

The ultraviolet–visible spectrum of the salt **7**, X = H, in water is shown in Fig. 1. Compounds **2** were generated *in situ* by addition of NaOH to solutions of the salts **7**. The spectra were then recorded within a few minutes time. The spectrum of **2**, X = H, in water is shown in Fig. 2. As can be seen by comparison of Figs. 1 and 2, the major spectral change is a shift of the long wavelength band from 372 to 458 nm. The spectra of other salts **7** and solvatochromics **2** were recorded in a

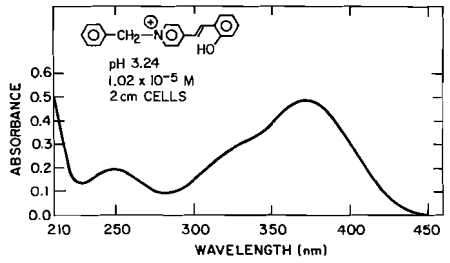

FIG. 1. Ultraviolet–visible absorption spectrum of *N*-benzyl-2′-hydroxy-4-stilbazolium bromide (**1**, X = H) in H_2O (borate, phosphate, acetate buffer (24), p*H* 3.243).

TABLE 1. (*p*-Substituted)benzyl-4-picolinium bromides (**5**)

X	Yield (%)	Melting point[a] (°C)	Analyses (%) Calculated C	H	N	Br	Found C	H	N	Br
OCH_3	86	155.5–156.0	57.15	5.48	4.76	27.17	57.19	5.48	4.75	27.22
CH_3	89	159.0–160.5	60.44	5.80	5.04	28.73	60.36	5.71	5.05	28.79
H	90	158.5–159.5	59.10	5.34	5.30	30.25	59.60	5.26	5.08	30.18
Br	89	168.5–169.0	45.51	3.82	4.08	46.59	45.58	3.77	4.12	46.64
CN	87	217.0–218.5	58.14	4.53	9.69	27.64	57.90	4.78	9.65	27.64
NO_2	94	184.5–186.0[b]	49.28[c]	5.02	8.21	23.42	48.88	4.44	8.37	24.07

[a]Recrystallized from ethanol–benzene unless noted otherwise.
[b]Recrystallized from methanol–benzene.
[c]Calculated for methanolate.

Can. J. Chem. Downloaded from www.nrcresearchpress.com by 210.87.254.42 on 09/05/12
For personal use only.

TABLE 2. *N*-(*p*-Substituted)benzyl-2′-hydroxy-4-stilbazolium bromides (7)

X	Yield (%)	Melting point[a] (°C)	Analyses (%) Calculated C	H	N	Br	Found C	H	N	Br
OCH_3	80	221.5–222.5	63.32	5.06	3.52	20.07	63.26	5.07	3.55	20.12
CH_3	39	99–101	65.98	5.27	3.66	20.90	65.64	5.55	3.69	20.94
H	56	211–213	65.23	4.93	3.80	21.70	64.88	5.28	3.76	21.76
Br	44	167–171	53.72	3.83	3.13	35.74	53.55	4.01	3.03	35.60

[a]Recrystallized from methanol.

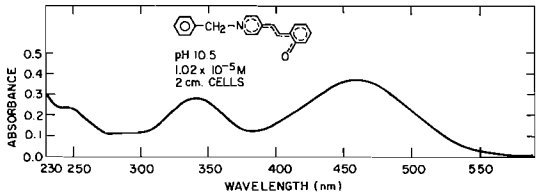

FIG. 2. Ultraviolet–visible absorption spectrum of *N*-benzyl-2′-hydroxy-4-stilbazolium betaine (**2**, X = H) in H_2O (borate, phosphate, acetate buffer (24), p*H* 10.484).

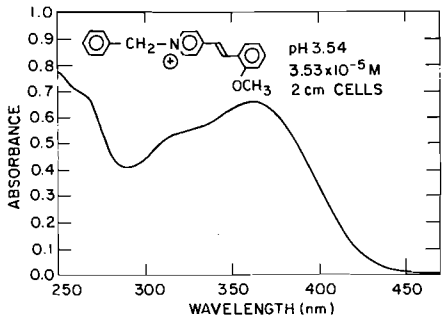

FIG. 3. Ultraviolet–visible absorption spectrum of *N*-benzyl-2′-methoxy-4-stilbazolium bromide (**9**) in H_2O (citric acid, sodium citrate buffer (31), p*H* 3.544).

variety of other solvents as well and similar changes occur.

To demonstrate unequivocally that the solvatochromic species do have structure **2** and not that of the ylid **8** (and associated resonance forms) resulting from removal of a benzylic proton from **7**, the *O*-methyl derivative (**9**) of **2**, X = H, was synthesized and examined. The m.p., n.m.r. spectrum, and solution properties of **9** are very similar to those of **2**, X = H. The u.v.–visible spectrum of **9** in aqueous acid is shown in Fig. 3; its λ_{max}(362 nm) and ε (9.55×10^3) are very similar to those of **2**, X = H (Fig. 1; 372; 9.55×10^3). The spectrum is unchanged in solutions of p*H* up to 10.5 (Fig. 4). Thus, the benzylic protons of **9** are not sufficiently acidic to be removed at this p*H*. It is, therefore, concluded that the structure of the solvatochromic compounds under discussion is indeed **2**.

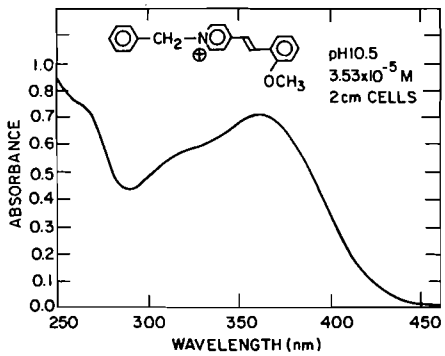

FIG. 4. Ultraviolet–visible spectrum of *N*-benzyl-2′-methoxy-4-stilbazolium bromide (**9**) in H_2O (sodium hydroxide, sodium bicarbonate buffer (32), p*H* 10.484).

The long wavelength transition energies of salts **7** and the solvatochromics **2** are displayed as a function of substituent constant, σ_X, in Figs. 5 and 6, respectively. It is significant that

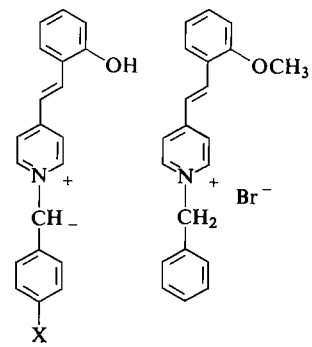

8 **9**

Can. J. Chem. Downloaded from www.nrcresearchpress.com by 210.87.254.42 on 09/05/12
For personal use only.

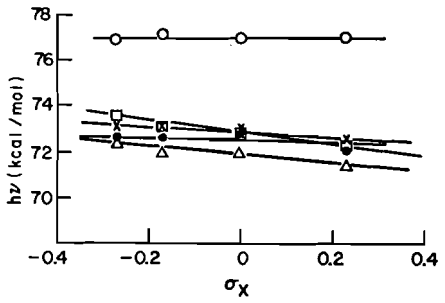

FIG. 5. Energy of longest wavelength transition *vs.* Hammett substituent constant for *N*-(*p*-substituted)-benzyl-2′-hydroxy-4-stilbazolium bromides (**7**): ○ H_2O: $h\nu = -0.164\sigma_X + 76.9$ ($r = 0.358$); □ 95% EtOH: $h\nu = -2.64\sigma_X + 72.8$ ($r = 0.986$); △ *i*-PrOH: $h\nu = -1.94\sigma_X + 71.8$ ($r = 0.942$); × *t*-BuOH: $h\nu = -1.33\sigma_X + 72.8$ ($r = 0.943$); ● $CHCl_3$: $h\nu = -0.955\sigma_X + 72.4$ ($r = 0.614$).

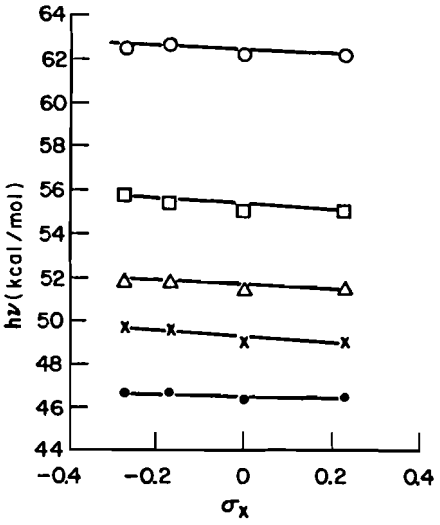

FIG. 6. Energy of longest wavelength transition *vs.* Hammett substituent constant for *N*-(*p*-substituted)-benzyl-2′-hydroxy-4-stilbazolium betaines (**2**): ○ H_2O: $h\nu = -0.708\sigma_X + 62.4$ ($r = 0.907$); □ 95% EtOH: $h\nu = -1.28\sigma_X + 55.3$ ($r = 0.968$); △ *i*-PrOH: $h\nu = -1.02\sigma_X + 51.6$ ($r = 0.938$); × *t*-BuOH: $h\nu = -1.40\sigma_X + 49.3$ ($r = 0.993$); ● $CHCl_3$: $h\nu = -0.466\sigma_X + 46.5$ ($r = 0.884$).

straight lines result and that the slopes are all negative, in contrast to the highly positive slopes for the series **1** and the corresponding hydriodide salts (6). Results for series **1** are shown in Fig. 7 for direct comparison.

As pointed out above the substituents in **2** and **7** are attached to the acceptor portion of the molecule and their effect is primarily a consequence of changes in the lowest unoccupied orbital. It has been demonstrated both by 'charge transfer' spectroscopy (13–15, 17) and electrochemistry (15, 18–20) that the electron affinity increases with σ_X in aromatic compounds; that is, the energy of the lowest unoccupied orbital level decreases. On this basis for both of the present series **2** and **7** then, increasing the electron withdrawing power should cause a decrease in transition energy. This is what is observed (Figs. 3 and 4).

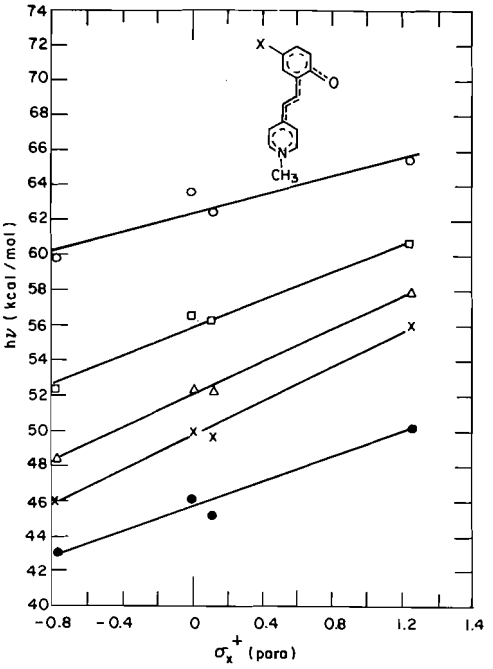

FIG. 7. Energy of longest wavelength transition *vs.* electrophilic substituent constant for *N*-methyl-5′-substituted-2′-hydroxy-4-stilbazolium betaines (**1**): ○ H_2O: $h\nu = +2.66\sigma^+ + 62.4$ ($r = 0.949$); □ 95% EtOH: $h\nu = +3.98\sigma^+ + 55.8$ ($r = 0.990$); △ *i*-PrOH: $h\nu = +4.70\sigma^+ + 52.0$ ($r = 0.998$); × *t*-BuOH: $h\nu = +4.96\sigma^+ + 49.7$ ($r = 0.995$); ● $CHCl_3$: $h\nu = +3.47\sigma^+ + 45.6$ ($r = 0.983$).

A further point is that while the results for series **1** were fit better by σ^+ (the electrophilic substituent constant) than by σ (the normal Hammett substituent constant), with the present compounds σ fits better than σ^+ as judged on the basis of the correlation coefficient, r (*e.g.*, **2** in H_2O, 0.907 *vs.* 0.696; **2** in 95% EtOH, 0.968 *vs.* 0.959; **2** in *i*-PrOH, 0.938 *vs.* 0.736). Again, this is consistent with the nature of the transition. In series **1** and the corresponding salts, σ^+ fits better since the substituent X is on the phenolate–

Can. J. Chem. Downloaded from www.nrcresearchpress.com by 210.87.254.42 on 09/05/12
For personal use only.

Can. J. Chem. Downloaded from www.nrcresearchpress.com by 210.87.254.42 on 09/05/12
For personal use only.

quinone moiety which becomes positively (or less negatively) charged; in series **2** and **7** the substituent is nearer the pyridyl ring which becomes negatively (or less positively charged) and hence σ would be expected to describe the energetics better than σ^+.

A word should be said regarding the relative magnitudes of the slopes of *hν vs.* σ for series **1** and **2**. For series **1** slopes using σ (not σ^+ as reported (6)) range from +1.7 to +8.7, whereas in the present case (**2**) the range is −0.5 to −1.4, as shown in Fig. 6. The larger slopes in **1** are due to the fact that the substituents are directly attached to the chromophore, whereas in **2** they are not in conjugation with the chromophore because of the presence of the insulating methylene group.

Thus, the negative slopes of Figs. 5 and 6 and the better fit by σ support the previous conclusion regarding the nature of the electronic transitions in compounds **1** and **2** and the corresponding salts. The transition involves conversion from a ground state structure resembling **2***a* (and **7***a*) to an excited state structure more like **2***b* (and **7***b*). The transitions are most certainly of $\pi \rightarrow \pi^*$ type on the basis of recent molecular orbital calculations for compound **10** (2, 23) and the large extinction coefficients ($\sim 10^4$).

In Fig. 8 the transition energy of **7** is plotted as a function of the solvent polarity parameter, E_T (21). These plots are all nonlinear but the degree of solvatochromism is relatively small ($\Delta h\nu \sim 5$ kcal/mol). For comparison, nitrobenzene's ^1L_a band suffers a 2.5 kcal/mol decrease in energy when the solvent is changed from water to ethanol (22). The magnitudes are similar to those observed previously as are the shapes of the curves

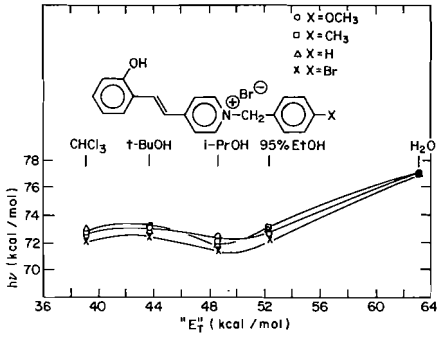

FIG. 8. Energy of longest wavelength transition *vs.* solvent polarity parameter for *N*-(*p*-substituted)benzyl-2′-hydroxy-4-stilbazolium bromides (**7**).

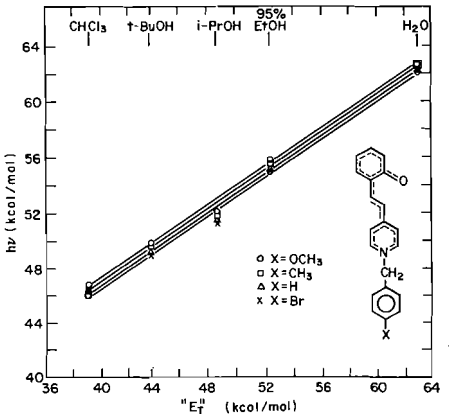

FIG. 9. Energy of longest wavelength transition *vs.* solvent polarity parameter for *N*-(*p*-substituted)benzyl-2′-hydroxy-4-stilbazolium betaines (**2**): X = OCH_3: $h\nu = 0.699E_T + 20.2$ ($r = 0.996$); X = CH_3: $h\nu = 0.687E_T + 19.2$ ($r = 0.998$); X = H: $h\nu = 0.673E_T + 19.8$ ($r = 0.997$); X = Br: $h\nu = 0.670E_T + 19.7$ ($r = 0.996$).

(6). The nonlinearity of these plots indicates that on a molecular level these salts are not solvated in the same manner as the reference compound used to evaluate E_T. This could be due to variations in the extent of ion pairing or degree of solvation because of the steric effect of the counter ion.

Figure 9 is a plot of the transition energy of **2** as a function of the solvent polarity parameter, E_T. As with **1**, large positive slopes are observed. The slopes of the lines are very similar to each other (0.67–0.69) and to those of **1**, X = OCH_3, H, Cl (0.71–0.73) (6). The range of solvatochromism ($\Delta h\nu$) in the present compounds **2** is about the same as observed in compounds **1** (6). Like the situation with **1**, the large positive slope of Fig. 9 is indicative of a large decrease in dipole moment (charge distribution) with excitation (1). This result corroborates the conclusion that light absorption converts a ground state resembling **1***a* or **2***a* to an excited state which resembles **1***b* or **2***b* to a greater extent.

Acidity

It was deemed of interest to ascertain the acidity of the stilbazolium salts **7** as a measure of the relative electron distribution in **7** and the corresponding 'anion' **2**. In view of the small spectral changes encountered in both of these series, the acidity of **7**, X = H, alone was determined in the belief that changes in acidity would also be small across the series.

Can. J. Chem. Downloaded from www.nrcresearchpress.com by 210.87.254.42 on 09/05/12
For personal use only.

A series of aqueous buffer solutions comprised of sodium hydroxide, boric, phosphoric, and acetic acids covering a pH range from 3.2 to 10.5 was prepared (24). Solutions of **7**, X = H, at 10^{-5} M were prepared using these buffer solutions, so as to eliminate the possibility of associative phenomena. By comparison of the ratio of the long wavelength peak due to **2**, X = H, at 458 nm (see Fig. 2) to that at 372 nm due to **7**, X = H, (see Fig. 1) and taking into account the extinction coefficients measured at the extreme high and low pH's ,the pK_a of **7**, X = H, at 22° was determined to be 8.37 ($\pm$0.01 standard deviation, three different buffer solutions).

Recently, the pK_a of the conjugate acid of **10** (as the hydriodide salt) was similarly evaluated by spectroscopic means and found to be 8.57 at room temperature (23). Thus **7**, X = H, is somewhat more acidic than the salt of **10**. The increase in acidity must be due to the substitution of an *N*-benzyl group for an *N*-methyl group inasmuch as the conjugate acid of **10** and its 2′-hydroxyl analog (**1**, X = H) (6) have identical pK_a's within experimental error (25). The *N*-benzyl group is expected to be more electron withdrawing than the *N*-methyl substituent on the basis of the Hammett substituent constants of $CH_2C_6H_5$ and CH_3 (−0.09 and −0.16, respectively) as well as those of C_6H_5 and H (0.02 and 0.00, respectively) (26). Thus the benzyl group would cause a larger net positive charge on the pyridinium ring and the rest of the conjugated system and in this way enhance the acidity.

Furthermore, it is interesting to note that the pK_a of salicylaldehyde (**6**) is reported to be 8.37 (27) and 8.34 (28) at 25°, virtually identical to that of **7**, X = H. Salicylaldehyde is significantly less acidic than the isomeric *p*-hydroxybenzaldehyde (pK_a 7.62 (27, 28)); this difference is attributed to hydrogen bonding in the former in concert with the mesomeric effect in the latter (28). Nonetheless, the identity of the acidities of **6** and **7**, X = H, is very striking. The net effects of the *N*-benzylstilbazolium and formyl substituents on the acidity of *ortho* substituted phenol are identical. Thus, one can assign to the *N*-benzylstilbazolium substituent a value of +0.75 for the apparent *ortho* substituent constant (σ_{ortho}) based on that of the CHO group (29). In view of the known complexity in treatment of the effects of *ortho* substituents (30), detailed discussion of the observed results seems unwarranted at this time.

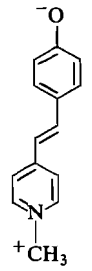

10

In conclusion, the spectral examination of a new series of *N*-(*p*-substituted)benzyl-2′-hydroxy-4-stilbazolium betaines (**2**) substantiates our previous conclusion based on the related *N*-methyl-5′-substituted-2′-hydroxy-4-stilbazolium betaines (**1**) (6). The conclusion was that the long wavelength transition in **1**, **2**, and their salts involves the $\pi \rightarrow \pi^*$ excitation of a predominantly zwitterionic ground state to a more delocalized or quinoidal excited state, *i.e.*, **1***a* → **1***b*, **2***a* → **2***b*, and **7***a* → **7***b* in valence bond terms. The experimental evidence in support of this is the dependence of the transition energy on (*i*) substituent and (*ii*) the polarity of the solvent. The first point bears on the effect of substituents on molecular orbital energy levels; in the present series the energy of the lowest unoccupied orbital was effectively varied while in the former that of the highest occupied orbital was effectively varied, both by substituent changes. The second point relates to the large changes in dipole moments (or electron distributions) upon excitation, which are negative in both systems. The solvatochromism of this new series **2** is similar in magnitude to that of the previous series (**1**), while the dependence of the transition energy on substituent is much less striking in the present series.

The pK_a of the parent salt **7**, X = H, at 22° is 8.37. This compound is slightly more acidic than the conjugate acid of **10** whose pK_a is 8.57 (23). This increase in acidity is attributed to the electron withdrawing effect of the *N*-benzyl group relative to the *N*-methyl group. From the pK_a a value for the apparent σ_{ortho} of the *N*-benzylstilbazolium substituent in phenols is found to be 0.75.

Experimental

General

Melting points are corrected. Analyses are by Spang Microanalytical Laboratory, Ann Arbor, Michigan.

Can. J. Chem. Downloaded from www.nrcresearchpress.com by 210.87.254.42 on 09/05/12
For personal use only.

(p-Substituted)benzyl-4-picolinium Bromides (5)

To a solution of 18.6 g (0.200 mol) of 4-picoline (**3**) in 150 ml THF was added 0.205 mol of the *p*-substituted benzyl bromide (**4**). The mixture was refluxed for 2.5 h and filtered. The solid was washed with *n*-hexane and recrystallized from ethanol–benzene. The results are summarized in Table 1.

(p-Substituted)benzyl-2′-hydroxy-4-stilbazolium Bromides (7)

To a solution of 0.100 mol of the quaternary salt **5** in a minimum amount of methanol (50–100 ml) was added 15.3 g (0.125 mol) of salicylaldehyde (**6**) and 2.5 ml piperidine. After 3.5 h reflux the solution was concentrated, cooled, and filtered. The solid was recrystallized from methanol. Table 2 summarizes the results. The n.m.r. spectrum of **7**, X = H, in CD_3SOCD_3 was typical: δ 3.38 (s, 1H, O*H*), 5.78 (s, 2H, CH_2), 6.6–8.0 (m, 11H, aromatic *H*), 8.20 (d, 2H, H_3, H_5, J = 6 Hz), 9.05 (d, 2H, H_2, H_6, J = 6 Hz).

N-Benzyl-2′-methoxy-4-stilbazolium Bromide (9)

This was prepared by the above procedure using *o*-anisaldehyde and **5**, X = H. The desired product, isolated in about 30% yield by elution from acidic alumina with chloroform, was recrystallized three times from isopropanol: yellow plates, m.p. 187.0–187.5°.

Anal. Calcd. for $C_{21}H_{20}NBrO$: C, 65.97; H, 5.27; N, 3.66; Br, 20.90. Found: C, 65.11; H, 5.10; N, 3.72; Br, 21.44.

Its u.v.–visible spectra in aqueous acid and base are shown in Figs. 3 and 4: λ_{max} 362, ε 9.55 × 10^3 in base and 9.25 × 10^3 in acid; n.m.r. (CD_3SOCD_3): δ 3.88 (s, 3H, OCH_3), 5.84 (s, 2H, CH_2), 6.8–8.0 (m, 11H, aromatic), 8.21 (d, 2H, H_3, H_5, J = 6 Hz), 9.11 (d, 2H, H_2, H_6, J = 6 Hz). **9** was also prepared in 79% yield by reaction of benzyl bromide and 2′-methoxy-4-stilbazole, which was synthesized by condensation of 4-picoline and σ-anisaldehyde. 2′-Methoxy-4-stilbazole has b.p. 163°/0.5 mm; n.m.r. ($CDCl_3$) δ 3.71 (s, 3H, OCH_3), 6.7–7.8 (m, 4H, H_3, H_4, H_5, H_6), 7.29 (d of d, 2H, H_3, H_5, J = 2, 6 Hz), 8.51 (d of d, 2H, H_2, H_6, J = 2, 6 Hz).

Anal. Calcd. for $C_{14}H_{13}NO$: C, 79.59; H, 6.20; N, 6.63. Found: C, 79.00; H, 6.61; N, 6.39.

Ultraviolet–Visible Spectra

These were recorded on a Cary 15 instrument in quartz cells using matched reference cells containing solvent. Triply distilled water, commercial 95% ethanol (U.S. Industrial Chemicals), spectrophotometric grade 2-propanol (Baker), chloroform (Baker), and reagent grade *t*-butyl alcohol (Baker) were used.

The spectra of the salts **7** were determined first. Then a drop of 10% aqueous sodium hydroxide was added to 5 ml of the solution to generate the solvatochromic **2**. These stoppered solutions were stirred for a few minutes prior to spectral determination. Concentrations were 10^{-4}–10^{-5} *M*.

Determination of pK_a of 7, X = H

Buffer solutions were prepared from sodium hydroxide, boric acid, phosphoric acid, and acetic acid (24); these were not of constant ionic strength. The p*H* values were determined at 22° on a Beckman Research p*H* meter calibrated using standard buffer solutions. An aqueous 1.02 × 10^{-4} *M* solution of **7**, X = H, was then diluted to 1.02 × 10^{-5} *M* with each of the following buffer solutions: p*H* 3.243, 8.293, 8.629, 8.866, and 10.484. Spectra were determined at 22° as before in 2-cm cells using the appropriate buffer as reference. From the lowest p*H* solution the extinction coefficient of the 372 nm peak due to **7**, X = H, was found to be 9.55 × 10^3 while that of the 458 nm peak of **2**, X = H from the highest p*H* solution was 7.42 × 10^3. Due to the fact that there was absorption at 372 nm in **2**, X = H, the absorption at this wavelength at the intermediate p*H*'s was corrected in direct proportion to the 458 absorption. The pK_a of **7**, X = H, was then determined for these solutions by the equation:

$$pK_a = pH - \log\left[\frac{A_{458}\varepsilon_{372}}{A_{372}\varepsilon_{458}}\right]$$

which is derived from

$$K_a = \frac{[H^+][2, X = H]}{[7, X = H]}$$

The average pK_a value of the three intermediate buffer solutions was 8.37 with a standard deviation of 0.01.

The authors wish to acknowledge helpful discussion with Dr. James Kuder, the encouragement of Dr. Wolfgang Gunther, and the suggestions of a referee.

1. C. Reichardt. Angew Chem. Int. Ed. Eng. **4**, 29 (1965).
2. H. G. Benson and J. N. Murrell. J. Chem. Soc. Far. Trans II, 137 (1972).
3. E. M. Kosower. J. Am. Chem. Soc. **80**, 3253 (1958).
4. P. Suppan. J. Chem. Soc. A, 3125 (1968).
5. H. W. Gibson. Can. J. Chem. **51**, 3065 (1973).
6. H. W. Gibson and F. C. Bailey. Tetrahedron, **30**, 2043 (1974).
7. J. E. Kuder, H. W. Gibson, and D. Wychick. J. Org. Chem. **40**, 875 (1975).
8. A. R. Katritzky and R. D. Topsom. *In* Advances in linear free energy relationships. *Edited by* N. B. Chapman and J. Shorter. Plenum Press, New York. 1972. p. 129.
9. M. Day and A. Y. Peters. J. Soc. Dyers Colourists, **85**, 8 (1967).
10. Yu. E. Gerasimenko and V. A. Shigalevskii. Zh. Org. Khim. **2**, 1294 (1966).
11. T. Hayashi and R. Shibata. Bull. Chem. Soc. Jap. **34**, 1116 (1961).
12. L. Yagupolskii and L. Z. Gandelsman. Zh. Obshch. Khim. **35**, 1252 (1965).
13. E. M. Kozower, D. Hofmann, and K. Wallenfels. J. Am. Chem. Soc. **84**, 2755 (1962).
14. P. R. Hammond. J. Chem. Soc. 471 (1964).
15. K. M. C. Davis, P. R. Hammond, and M. E. Peover. Trans. Far. Soc. **61**, 1516 (1965).
16. F. Gerson and E. Heilbronner. Helv. Chim. Acta, **42**, 1877 (1959).
17. L. J. Andrews and R. M. Keefer. Molecular complexes in organic chemistry. Holden-Day, San Francisco. 1964.
18. M. E. Peover. Trans. Far. Soc. 1656 (1962); 2370 (1962).

19. R. N. ADAMS. Electrochemistry at solid electrodes. Marcel Dekker, New York. 1969. p. 327.
20. P. ZUMAN. Substituent effects in organic polarography. Plenum Press, New York. 1967.
21. K. DIMROTH, C. REICHARDT, T. SIEPMAN, and F. BOHLMANN. Ann. Chem. **661**, 1 (1963).
22. H. H. JAFFE and M. ORCHIN. Theory and applications of ultraviolet spectroscopy. Wiley, New York. 1962. p. 266.
23. J. E. KUDER and D. WYCHICK. Chem. Phys. Lett. **24**, 69 (1973).
24. J. HEYROVSKÝ and P. ZUMAN. Practical polarography. Academic Press, New York. 1968. p. 179.
25. H. W. GIBSON and F. C. BAILEY. To be published.
26. O. EXNER. *In* Advances in linear free energy relationships. *Edited by* N. B. Chapman and J. Shorter. Plenum Press, New York. 1972. p. 28.
27. R. A. ROBINSON and H. K. KIANG. Trans. Far. Soc. **52**, 327 (1956).
28. L. B. MAGNUSSON, C. POSTMUS, JR., and C. A. CRAIG. J. Am. Chem. Soc. **85**, 1711 (1963).
29. G. B. BARLIN and D. D. PERRIN. Q. Rev. **20**, 75 (1966).
30. J. SHORTER. *In* Advances in linear free energy relationships. *Edited by* N. B. Chapman and J. Shorter. Plenum Press, New York. 1972. pp. 103–110.
31. R. M. C. DAWSON, D. C. ELLIOT, W. H. ELLIOT, and K. M. JONES. Data for biochemical research. Clarendon Press, Oxford, England. 1959. p. 196.
32. R. C. WEAST (*Editor*). Handbook of chemistry and physics. 55th ed. Chemical Rubber Co., Cleveland, Ohio. 1974. p. D-113.
33. J. P. MAIER and J. F. MULLER. Tetrahedron Lett. 2987 (1974).
34. H. W. GIBSON. J. Am. Chem. Soc. In press.

Can. J. Chem. Downloaded from www.nrcresearchpress.com by 210.87.254.42 on 09/05/12
For personal use only.

Base-catalyzed Degradations of Carbohydrates. VII. Alkaline Degradation of 3,6-Di-*O*-substituted Hexoses

GERALD O. ASPINALL[1] AND THINNAYAM N. KRISHNAMURTHY
Department of Chemistry, York University, Downsview, Toronto, Ontario M3J 1P3
AND
IVAN FURDA AND RIAZ KHAN
Department of Chemistry, Trent University, Peterborough, Ontario K9J 7B8
Received March 18, 1975

GERALD O. ASPINALL, THINNAYAM N. KRISHNAMURTHY, IVAN FURDA, and RIAZ KHAN. Can. J. Chem. **53**, 2171 (1975).

6-*O*-β-D-Glucopyranosyl-3-*O*-methyl-D-glucose (**4**) has been synthesized as a model compound for regions of branching in polysaccharides. Alkaline degradation of the disaccharide affords an epimeric pair of *O*-glycosyl metasaccharinic acids which have been characterized by reduction to 3-deoxy-6-*O*-β-D-glucopyranosyl-D-*ribo*-hexose (**6**) and 3-deoxy-6-*O*-β-D-glucopyranosyl-D-*arabino*-hexose (**7**). Alkaline degradation of the branched β-D-glucan from *Sclerotium rolfsii* followed by reduction of the derived metasaccharinic acids furnishes 3-deoxy-D-*ribo*-hexose (**8**), 3-deoxy-D-*arabino*-hexose (**9**), and the two disaccharides (**6** and **7**).

GERALD O. ASPINALL, THINNAYAM N. KRISHNAMURTHY, IVAN FURDA et RIAZ KHAN. Can. J. Chem. **53**, 2171 (1975).

On a synthétisé le 6-*O*-β-D-glucopyrannosyl-3-*O*-méthyl-D-glucose (**4**) comme produit de référence pour les positions de branchement dans les polysaccharides. La dégradation alcaline du disaccharide fournit une paire d'acides *O*-glycosyl métasaccharinques épimères, caractérisés par réduction en 3-déoxy-6-*O*-β-D-glucopyrannosyl-D-*ribo*-hexose (**6**) et en 3-déoxy-6-*O*-β-D-glucopyrannosyl-D-*arabino*-hexose (**7**). La dégradation alcaline du β-D-glucane ramifié provenant du *Sclerotium rolfsii* suivie d'une réduction des acides métasaccharinques dérivés, conduit au 3-déoxy-D-*ribo*-hexose (**8**), au 3-déoxy-D-*arabino*-hexose (**9**) et aux deux disaccharides (**6** et **7**).

3-*O*-Substituted reducing sugars are degraded by alkali with elimination of the 3-*O*-substituent and with the formation of an epimeric pair of metasaccharinic acids (3-deoxyhexonic acids) (1). In (1 → 3)-linked polysaccharides, stepwise degradation occurs from the reducing end by the 'peeling' mechanism (2) and branched glycans with (1 → 3)-linked interior chains carrying side chains at 0–6 would be expected to give *O*-glycosyl metasaccharinic acids. Some years ago (3) exploratory investigations were carried out on larch arabinogalactan (4) and the resulting saccharinic acids were treated with hypochlorite at p*H* 5 (5) to give the corresponding 2-deoxy-5-*O*-glycosylpentoses. The desired products, however, were formed in less than satisfactory yield and were accompanied by a parallel series of oligosaccharides lacking the reducing 2-deoxypentose residues. We have therefore reexamined the alkaline degradation giving an epimeric pair of *O*-glycosyl metasaccharinic acids using (*a*) the disaccharide 6-*O*-β-D-glucopyranosyl-3-*O*-methyl-D-glucose (**4**) as a model compound for regions of branching in polysaccharides and (*b*) the branched β-D-glucan from *Sclerotium rolfsii* (6, 7) in which a (1 → 3)-linked chain carries at 0–6 of every third residue a side chain of a single β-D-glucopyranosyl residue. Attempted degradations of the *O*-glycosyl saccharinic acids to give a single transformation product, namely the disaccharide 2-deoxy-5-*O*-β-D-glucopyranosyl-D-*erythro*-pentose (**5**), were again unsuccessful and the saccharinic acids have been characterized by reduction to neutral disaccharides.

1,2,4-Tri-*O*-acetyl-6-*O*-(2,3,4,6-tetra-*O*-acetyl-β-D-glucopyranosyl)-3-*O*-methyl-β-D-glucopyranose (**3**) was prepared (*a*) by the Koenigs–Knorr condensation of 2,3,4,6-tetra-*O*-acetyl-α-D-glucopyranosyl bromide and 1,2,4-tri-*O*-acetyl-3-*O*-methyl-β-D-glucopyranose (**2**) or (*b*) by the Bredereck condensation (8) of the glycosyl halide

[1]To whom enquiries should be addressed at York University.

Can. J. Chem. Downloaded from www.nrcresearchpress.com by 210.87.254.6 on 09/05/12
For personal use only.

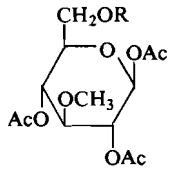

1 R = Trityl
2 R = H

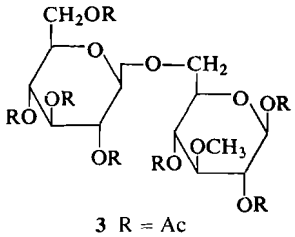

3 R = Ac
4 R = H

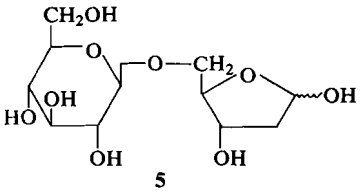

5

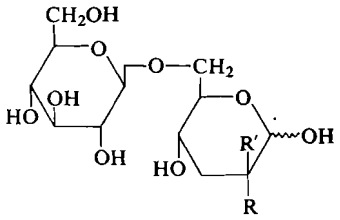

6 R = OH; R′ = H
7 R = H; R′ = OH

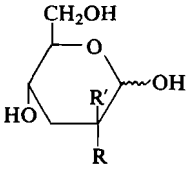

8 R = OH; R′ = H
9 R = H; R′ = OH

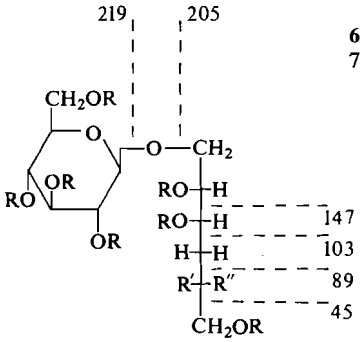

SCHEME 1. Major fragment ions in the mass spectra of methylated disaccharide alditols (R = CH_3; R′ = OCH_3 (or H); R″ = H (or OCH_3)) formed from disaccharides **6** and **7**.

and 1,2,4-tri-*O*-acetyl-3-*O*-methyl-6-*O*-trityl-β-D-glucopyranose (**1**). De-*O*-acetylation of the hepta-*O*-acetyl derivative furnished the disaccharide, 6-*O*-β-D-glucopyranosyl-3-*O*-methyl-D-glucose (**4**), which afforded a crystalline hexa-*O*-acetyl-*N*-*p*-nitrophenylglycosylamine.

Degradation of disaccharide **4** with oxygen-free lime water gave a mixture of *O*-glycosyl saccharinic acids. Treatment of the saccharinic acids with hypochlorite at p*H* 5 (5) gave some of the desired disaccharide **5** but glucose was formed in a similar amount. A similar mixture of products was formed on Ruff degradation (9) of the saccharinic acids. In a later experiment the mixture of saccharinic acids from alkaline degradation of the β-D-glucan was converted into the corresponding saccharinamides which were treated with sodium hypochlorite at p*H* 13 (Hofmann rearrangement) (10). Whereas the unsubstituted metasaccharinic acids furnished 2-deoxy-D-*erythro*-pentose, the 6-*O*-glycosyl saccharinic acids gave only glucose and no disaccharide **5** was formed. In the following paper (11) other syntheses of 2-deoxy-5-*O*-β-D-glycopyranosyl-D-*erythro*-pentose (**5**) are reported and the observation that the disaccharide is readily degraded by base with the liberation of glucose provides an explanation for the present results.

The *O*-glycosyl saccharinic acids from disaccharide **4** were lactonized and then reduced with sodium borohydride at p*H* 3–4 (12) to give two epimeric disaccharides. The disaccharides were separated by chromatography on cellulose and g.l.c. – mass spectrometry of the derived methylated *O*-glycosylalditols (13) (Scheme 1) confirmed that both disaccharides were 3-deoxy-6-*O*-hexosylhexoses. One disaccharide gave glucose and 3-deoxy-*ribo*-hexose on hydrolysis and was characterized as 3-deoxy-6-*O*-β-D-glucopyranosyl-D-*ribo*-hexose (**6**) by conversion into the

Can. J. Chem. Downloaded from www.nrcresearchpress.com by 210.87.254.6 on 09/05/12
For personal use only.

Can. J. Chem. Downloaded from www.nrcresearchpress.com by 210.87.254.6 on 09/05/12
For personal use only.

crystalline heptaacetate which was identical with a synthetic sample (11). The second disaccharide, which gave glucose and 3-deoxy-*arabino*-hexose on hydrolysis, yielded a crystalline hexa-*O*-acetyl-*N*-*p*-nitrophenylglycosylamine, and was assigned the structure 3-deoxy-6-*O*-β-D-glucopyranosyl-D-*arabino*-hexose (**7**).

The β-D-glucan from *Sclerotium rolfsii* was heated at 56° in oxygen-free sodium hydroxide until no further degradation took place. Degraded alkali-stable polysaccharide was separated by precipitation and the soluble metasaccharinic acids were lactonized and reduced with sodium borohydride at p*H* 3–4 to give a mixture of neutral sugars. Chromatographic fractionation afforded 3-deoxy-D-*ribo*-hexose (**8**), 3-deoxy-D-*arabino*-hexose (**9**), and the two above-mentioned disaccharides (**6** and **7**), each sugar being characterized by conversion into a crystalline derivative.

The alkaline degradations of 3,6-di-*O*-substituted hexoses described here result in metasaccharinic acid formation diagnostic for the 3-*O*-substituent and with retention of the 6-*O*-substituent. The formation of an epimeric pair of metasaccharinic acids and thence, after reduction, of the corresponding 3-deoxyhexoses, from the degradation of each type of 3-*O*-substituted structural unit would be an obvious disadvantage in the extension of this degradative procedure to more complex polysaccharides. Additional factors, however, must be taken into account when the degradation of a polysaccharide proceeds in stepwise manner from a single reducing group, as in the case of the β-D-glucan when degradation came to a halt before complete erosion of the (1 → 3)-linked chains had taken place. The isolation of an alkali-stable polysaccharide may have resulted from a number of causes, *e.g.* (*i*) from the presence in the polysaccharide preparation of two types of molecule, one of which contained natural nonreducing end groups, *cf.* the mannitol-terminated chains in laminaran (14), whilst alkaline degradation of the reducing chains proceeded to completion; (*ii*) by the exposure of an alkali-insensitive reducing group arising from some unrecognized minor structural feature; or (*iii*) by the interception of a 'stopping' reaction giving rise to a nonreducing end group. Methylation analyses of the β-D-glucan and the alkali-degraded β-D-glucan showed no detachable differences between the polysaccharides. The results were consistent with the previously proposed structure (6, 7) but also revealed the presence of *ca.* 2.4% of (1 → 6)-linkages at other than branch points. Since the native and degraded polysaccharides contained the same proportion of these structural units it is probable that they are distributed at regular intervals along the chain. The exposure of an unbranched 6-*O*-substituted unit after erosion of the (1 → 3)-linked chain would provide occasion for intervention by a 'stopping' reaction to give an alkali-stable metasaccharinic acid (3-deoxy-

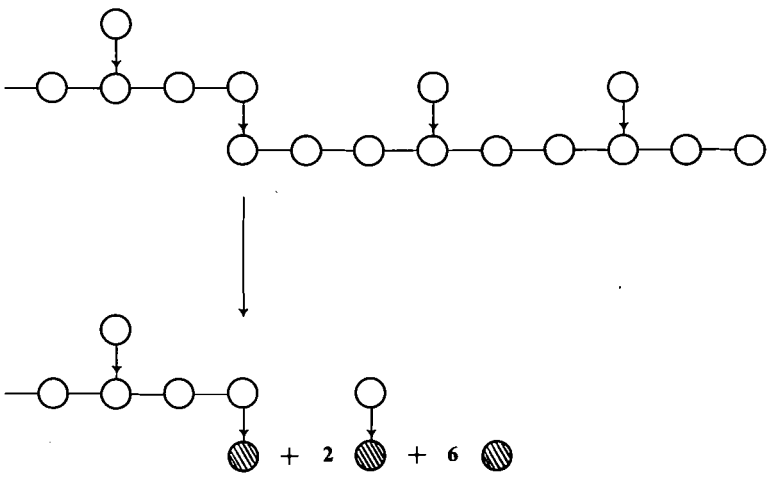

SCHEME 2. Alkaline degradation of β-D-glucan: ○ = β-D-glucopyranose residue, ▨ = 3-deoxyhexonic acid (metasaccharinic acid) residue, — = (1→3)-linkage, → = (1 → 6)-linkage.

Can. J. Chem. Downloaded from www.nrcresearchpress.com by 210.87.254.6 on 09/05/12
For personal use only.

hexonic acid) end group (Scheme 2) as shown by Burns and Somers (15) during the alkaline degradation of isomaltooligosaccharides.

We conclude that alkaline degradations of branched polysaccharides initiated at the single reducing groups are liable to provide only limited information on detailed structure since the stepwise 'peeling' reaction, like other chain reactions, is susceptible to premature termination with the consequent formation of saccharinic acids or other degradation products from only part of the polysaccharide structure. However, oligosaccharides of relatively low molecular weight will undergo degradation reactions diagnostic for substitution pattern in satisfactory yield with few detectable side reactions. Where *O*-glycosyl saccharinic acids are formed these may be separated by anion-exchange chromatography (15). A more generally satisfactory approach in polysaccharide studies would be to expose reducing groups by the selective cleavage of interior glycosidic linkages, *e.g.* by base-catalyzed β-elimination of 4-*O*-substituted hexuronate residues (16–18), and to submit the resulting oligosaccharides to alkaline degradation.

Experimental

Melting points are uncorrected. Optical rotations were measured with a Perkin–Elmer model 141 polarimeter at 20 ± 2°. The i.r. and u.v. spectra were measured on Unicam SP 200 and SP 800A spectrophotometers. The n.m.r. spectra were recorded on JEOL C-60H and Varian A-60 and HA-100 spectrophotometers, usually with tetramethylsilane as internal standard. Mass spectra were recorded on an Hitachi-Perkin-Elmer RMU-6 mass spectrometer with an ionization potential of 70 eV. The g.l.c. was performed with a Hewlett-Packard model 5750 chromatograph using columns of dichlorodimethylsilane-treated Celite coated with (*a*) 5% of neopentylglycol adipate polyester (operating temperature 160–185°), (*b*) 3% of silicone gum OV-225 (operating temperature 200–240°), and (*c*) 3% of silicone gum ECNSS-M (operating temperature 180°). Retention times (*T*) are quoted relative to methyl 2,3,4,6-tetra-*O*-methyl-β-D-glucopyranoside for methyl glycosides, to 2,3,4,6-tetra-*O*-methyl-D-glucitol diacetate for methylated alditol acetates, and to maltitol nonamethyl ether for methylated disaccharide alditols. For g.l.c. – mass spectrometry columns *b* and *c* were used in a Perkin–Elmer 990 chromatograph which was attached to the mass spectrometer via a Watson–Biemann separator.

The t.l.c. was performed with Kieselgel HF 254 as the adsorbent and the dried plates were sprayed with ethanol containing 5% of sulfuric acid and heated at about 150°. Solvent systems used for t.l.c. were chloroform–acetone (4:1), benzene–acetone (4:1), and light petroleum – acetone (5:1). Column chromatography was carried out on silica gel (Davison grade 950, 60–200 mesh) and microgranular cellulose powder (Whatman No. CC 31). Paper chromatography was carried out on Whatman filter paper No. 1 using the following solvent systems (v/v): (*A*) butanone–1-propanol–water (14:3:3), (*B*) ethyl acetate – acetic acid – formic acid – water (18:3:1:4). Light petroleum refers to the fraction of b.p. 30–60°. Solutions were concentrated below 50° under reduced pressure. Microanalyses were determined by A. B. Gygli, Toronto, Ontario, and by F. and E. Pascher, Bonn, West Germany.

1,2,4-Tri-O-acetyl-3-O-methyl-6-O-trityl-β-D-glucopyranose (1) and 1,2,4-Tri-O-acetyl-3-O-methyl-β-D-glucopyranose (2)

Reaction of 3-*O*-methyl-D-glucose (19) (10 g) with chlorotriphenylmethane in pyridine under standard conditions (20) followed by normal work-up and chromatography on silica gel furnished syrupy 3-*O*-methyl-6-*O*-trityl-D-glucose (16.7 g), $[\alpha]_D$ +32° (*c*. 1,2 in dichloromethane). The trityl ether (10 g) was acetylated with acetic anhydride and anhydrous sodium acetate, and normal work-up followed by crystallization from methanol furnished 1,2,4-tri-*O*-acetyl-3-*O*-methyl-6-*O*-trityl-β-D-glucopyranose (**1**) (8 g), m.p. 169–170°, $[\alpha]_D$ +27° (*c*, 1.0 in dichloromethane) (lit. (21) m.p. 173–175° $[\alpha]_D$ +18° (chloroform)). Concentration of the filtrate from the above crystallization afforded 1,2,4-tri-*O*-acetyl-3-*O*-methyl-6-*O*-trityl-α-D-glucopyranose (3.5 g), m.p. 143–144°, $[\alpha]_D$ +102° (*c*, 1.1 in dichloromethane) (lit. (21, 22) m.p. 145°, $[\alpha]_D$ +92.2° (chloroform)). As reported by Perlin (21, 22) acetylation with acetic anhydride and pyridine gave relatively more of the α-anomer.

The trityl ether (**1**) (5 g) was reacted with hydrogen bromide in acetic acid in the usual way and recrystallization of the product from ether afforded 1,2,4-tri-*O*-acetyl-3-*O*-methyl-β-D-glucopyranose (**2**) (2.4 g), m.p. 117–119°, $[\alpha]_D$ −2.5° (*c*, 1.1 in chloroform) (lit. (22) m.p. 121–122°, $[\alpha]_D$ +13.2° (chloroform)).

1,2,4-Tri-O-acetyl-6-O-(2,3,4,6-tetra-O-acetyl-β-D-glucopyranosyl)-3-O-methyl-β-D-glucopyranose (3)

(*a*) Iodine (450 mg) and 2,3,4,6-tetra-*O*-acetyl-α-D-glucopyranosyl bromide (2.5 g) were added to 1,2,4-tri-*O*-acetyl-3-*O*-methyl-β-D-glucopyranose (1.5 g) in benzene (50 ml) in the presence of silver carbonate (2.5 g) and Drierite (7.5 g) and the mixture was stirred for 48 h at room temperature. The mixture was filtered and concentration of the filtrate afforded a crystalline residue which was recrystallized from methanol to give the acetylated disaccharide (**3**) (1.5 g), m.p. 174–175°, $[\alpha]_D$ −15.8° (*c* 1.3 in chloroform); n.m.r. data ($CDCl_3$): τ 6.45 (3-proton singlet, OCH_3), 7.8–8.05 (21 protons, 7 × $OCOCH_3$).

Anal. Calcd. for $C_{27}H_{38}O_{18}$: C, 49.84; H, 5.84. Found: C, 49.86; H, 6.08.

(*b*) Tetra-*O*-acetyl-α-D-glucopyranosyl bromide (4.11 g) and the trityl ether (**1**) (5.63 g) were condensed in nitromethane (20 ml) in the presence of Drierite (1.5 g) and silver perchlorate (2.2 g) and the mixture was heated at 80° for 10 min. The mixture was filtered, the filtrate was washed with cold saturated aqueous sodium hydrogen carbonate and filtered, and concentration of the filtrate furnished a syrup which crystallized in methanol and on recrystallization from ethanol gave the acetylated disaccharide (**3**) (3.9 g), m.p. 174–175°, $[\alpha]_D$ −15.1° (*c*, 1.2 in

Can. J. Chem. Downloaded from www.nrcresearchpress.com by 210.87.254.6 on 09/05/12
For personal use only.

chloroform), whose n.m.r. spectrum was identical to that of the previously prepared sample.

6-O-β-D-Glucopyranosyl-3-O-methyl-D-glucose (4)

The acetylated disaccharide (**3**) (2.5 g) was de-*O*-acetylated with sodium methoxide in methanol (23) and the product was chromatographed on cellulose in solvent *A* to give the disaccharide (**4**) (0.9 g) as a semicrystalline solid, m.p. 80°, $[\alpha]_D$ +1° (*c*, 1.5 in water).

Anal. Calcd. for $C_{13}H_{24}O_{11}$: C, 43.75; H, 6.79. Found: (after drying at 80°): C, 43.83; H, 7.08.

A sample (100 mg) of the disaccharide (**4**), glacial acetic acid (0.1 ml), and *p*-nitroaniline (50 mg) were heated under reflux in ethanol–water (4:1) (2 ml) for 1 h (24). After removal of solvent the residue was chromatographed on cellulose (20 × 2.5 cm) using solvent *A* to give syrupy glycosylamine (60 mg) which was reacted with acetic anhydride and pyridine. Recrystallization of the product from ethanol–chloroform (7:3) afforded 6-*O*-β-D-glucopyranosyl-3-*O*-methyl-*N*-*p*-nitrophenyl-D-glucosylamine hexaacetate (70 mg), m.p. 139–140°, $[\alpha]_D$ −105° (*c*, 2.0 in chloroform); ν_{max}(chloroform) 1470, 1310 (NO_2), 1720 (acetate C=O) 3500 cm^{-1} (NH); n.m.r.: τ 1.85, 3.34 (2 × 2-proton doublets, splitting 9 Hz, 4 aromatic H's) 4.32 (1-proton doublet, splitting 8 Hz, H-1), 6.51 (3-proton singlet, OCH_3), 7.8–8.1 (18 protons, 6 × $OCOCH_3$).

Anal. Calcd. for $C_{31}H_{40}N_2O_{18}$: C, 51.10; H, 5.34; N 3.84. Found: C, 51.23; H, 5.55; N, 3.78.

Alkaline Degradation of Disaccharide 4 and Reduction of Metasaccharinolactones

Disaccharide **4** (1.2 g) was kept in oxygen-free saturated lime-water (250 ml) at room temperature for 144 h, after which time paper chromatography showed complete disappearance of starting material. The solution was passed through a column of Amberlite resin IR-120(H) and freeze-dried to give a mixture of saccharinolactones (0.9 g); ν_{max} (film) 1708 cm^{-1} (lactone C=O). A solution of the lactones (0.9 g) in water (10 ml) at 0–3° was adjusted to p*H* 3–4 by dropwise addition of 0.5 *M* sulfuric acid, sodium borohydride (100 mg) in water (0.75 ml) was added dropwise during 15 min with maintenance of p*H* and temperature, and the solution was kept for 1 h (12). The solution was neutralized with barium carbonate, stirred with Amberlite resin IR-120(H), filtered, and repeatedly evaporated with methanol to remove boric acid. Paper chromatography of the resulting syrup (0.8 g) in solvent *A* showed two reducing disaccharides, $R_{glucose}$ 0.68 and 0.85, with smaller amounts of unchanged lactones and neutral alditols. The syrup was passed through a column of diethylaminoethyl-Sephadex A-25 (formate form), elution with water giving the neutral components (0.6 g). The neutral components were chromatographed on cellulose using solvent *A* to give disaccharides **6** (0.27 g), $R_{glucose}$ 0.68, $[\alpha]_D$ −8° (*c*, 1.1 in water) and **7** (0.16 g), $R_{glucose}$ 0.85, $[\alpha]_D$ −1° (*c*, 1.8 in water).

Hydrolysis of disaccharide **6** gave glucose and 3-deoxy-*ribo*-hexose. A sample (5 mg) of the disaccharide was reduced with sodium borohydride (5 mg) in water (1 ml) and the resulting disaccharide alditol was methylated with methyl iodide and sodium hydride in *N*,*N*-dimethylformamide (25). Gas–liquid chromatography of the methylated disaccharide alditol on column *b* at 240° showed a single peak, *T* 1.20, and g.l.c. – mass spectrometry showed characteristic fragment ions at *m/e* 219(10), 205(26), 147(23), 103(15), 89(95), 88(100), and 45(75). The disaccharide (40 mg) was characterized by reaction with acetic anhydride and sodium acetate to give 1,2,4-tri-*O*-acetyl-3-deoxy-6-*O*-(2,3,4,6-tetra-*O*-acetyl-β-D-glucopyranosyl)-D-*ribo*-hexopyranose (45 mg), m.p. and mixture m.p. 195–196°, $[\alpha]_D$ −14° (*c*, 1.0 in chloroform), whose n.m.r. spectrum was identical with that of a synthetic sample (11).

Hydrolysis of disaccharide **7** gave glucose and 3-deoxy-*arabino*-hexose. A sample of the disaccharide alditol was methylated as described above and g.l.c. of the methylated derivative on column *b* at 240° showed a single peak, *T* 1.12, and g.l.c. – mass spectrometry showed characteristic fragment ions at *m/e* 219(9), 205(24), 147(21), 103(14), 89(85), 88(100), and 45(70). The disaccharide was characterized by reaction with *p*-nitroaniline, followed by acetylation in acetic anhydride and pyridine, to give 2,4-di-*O*-acetyl-3-deoxy-6-*O*-(2,3,4,6-tetra-*O*-acetyl-β-D-glucopyranosyl)-*N*-*p*-nitrophenyl-D-*arabino*-hexopyranosylamine, m.p. 214–215°, $[\alpha]_D$ −47° (*c*, 0.6 in chloroform); ν_{max} (chloroform) 1340 (NO_2), 1720 (ester C=O), 3500 cm^{-1} (NH); n.m.r.: τ 1.85, 3.34 (2 × 2-proton doublets, splitting 9 Hz, 4 aromatic H's), 4.32 (1-proton doublet, splitting 8 Hz, H-1), 7.8–8.1 (18 protons, 6 × $OCOCH_3$).

Anal. Calcd. for $C_{30}H_{38}N_2O_{17}$: C, 51.57; H, 5.48; N, 4.01. Found: C, 51.87; H, 5.41; N, 3.98.

Alkaline Degradation of β-D-Glucan

An oxygen-free solution of β-D-glucan (5 g) in water (1 l) containing sodium hydroxide (4 g) was maintained in an atmosphere of nitrogen at 56°. Aliquot portions were withdrawn at intervals and analyzed for metasaccharinic acid by thiobarbituric acid assay of the periodate oxidation products (26) and for carbohydrate content by the phenol – sulfuric acid procedure (27). No further change (metasaccharinic acid, 56%; undegraded glucose residues, 44%) occurred after 10 days and the cooled solution was passed through a column of Amberlite resin IR-120(H), concentrated to 100 ml, and poured into acetone (750 ml). The precipitated polysaccharide was separated by centrifugation and the supernatant liquid was concentrated again, poured into acetone, centrifuged to remove further precipitate, and concentrated to a syrup (2.7 g) which contained saccharinic acid and nonreducing sugar residues in the proportions of 2.6:1. The combined degraded polysaccharide precipitates (2.0 g) contained saccharinic acid and nonreducing sugar residues in the proportions of 1:12.

A portion (1.8 g) of the above syrup (as saccharinolactones) was reduced with sodium borohydride at p*H* 3–4 as described previously and furnished a mixture of neutral sugars (1.2 g) after passing through a column of diethylaminoethyl-Sephadex A-25 (formate form). Paper chromatography in solvent *A* showed the presence of four reducing sugars and a nonreducing fraction ($R_{glucose}$ 0.31), and column chromatography on cellulose afforded homogeneous samples of the reducing sugars. Fraction 1 (0.25 g), $R_{glucose}$ 2.85, $[\alpha]_D$ −17.5° (*c*, 1.0 in water), was chromatographically indistinguishable from 3-deoxy-D-*arabino*-hexose (**9**) and was characterized by conversion into 3-deoxy-D-*arabino*-hexitol pentabenzoate, m.p. 102–104°, $[\alpha]_D$ −34° (*c*, 0.5 in chloroform) (lit. (28) m.p. 104–105°, $[\alpha]_D$ −33.6° (chloroform)). Fraction 2 (0.35 g), $R_{glucose}$

Can. J. Chem. Downloaded from www.nrcresearchpress.com by 210.87.254.6 on 09/05/12
For personal use only.

2.45, $[\alpha]_D$ +32° (*c*, 1.0 in water), was chromatographically indistinguishable from 3-deoxy-D-*ribo*-hexose (**8**) and was characterized by conversion into the β-D-tetraacetate which was identical (m.p. and mixture m.p. 129–130°, $[\alpha]_D$ −16° (*c*, 1.0 in chloroform), and n.m.r. spectrum) to an authentic sample. Fraction 3 (0.16 g), $R_{glucose}$ 0.85, $[\alpha]_D$ −1° (*c*, 1.0 in water), was chromatographically indistinguishable from the previously characterized disaccharide **7**, and its identity was further established by g.l.c.–mass spectrometry of the methylated disaccharide alditol and by conversion into the *N*-*p*-nitrophenyl-glycosylamine hexaacetate which was identical (m.p. and mixture m.p., $[\alpha]_D$, i.r. and n.m.r. spectra) to the previous sample. Fraction 4 (0.12 g), $R_{glucose}$ 0.68, was chromatographically indistinguishable from disaccharide **6** and was characterized by g.l.c. – mass spectrometry of the methylated disaccharide alditol and by conversion into the β-D-heptaacetate which was identical (m.p. and mixture m.p., $[\alpha]_D$, i.r. and n.m.r. spectra) to previous samples.

Methylation of β-D-*Glucan and Alkali-degraded* β-D-*Glucan*

β-D-Glucan (200 mg) was methylated with methyl iodide and sodium hydride in dimethyl sulfoxide (29) to give methylated β-D-glucan (160 mg), $[\alpha]_D$ —30° (*c*, 1.5 in chloroform) (found: OMe, 45.1%). Similarly degraded polysaccharide (50 mg) isolated from the above alkaline degradation furnished methylated degraded β-D-glucan (40 mg), $[\alpha]_D$ −21° (*c*, 1.2 in chloroform) (found: OMe, 44.8%). Samples of both methylated polysaccharides were hydrolyzed, reduced with sodium borohydride, and acetylated to give mixtures of partially methylated alditol acetates which were estimated and identified by g.l.c. on column *c*. In both cases derivatives of the component sugars, 2,3,4,6-tetra-(*T* 1.00), 2,4,6-tri-(*T* 1.95), and 2,4-di-*O*-methylglucose (*T* 5.1) were present in the molar ratio of 1:2:1. In addition small amounts (~2.4%) of a 2,3,4-tri-*O*-methylglucose derivative (*T* 2.51) were present. This minor component was further identified by analysis of the methyl glycosides formed on methanolysis of the methylated glucan.

Degradations of Saccharinic Acids

(*a*) The mixture (0.6 g) of saccharinic acids from the alkaline degradation of β-D-glucan was kept in methanolic 5% hydrogen chloride for 20 min at room temperature to ensure complete esterification or lactonization. Removal of acid by repeated evaporation with methanol afforded a mixture of esters and lactones (0.6 g); ν_{max} (film) 1780 (γ-lactone) and 1750 cm^{-1} (ester C=O). The syrup was treated with saturated methanolic ammonia for 24 h and concentration furnished a mixture of amides (0.57 g); ν_{max} (film) 1650 cm^{-1} (amide C=O). Sodium hypochlorite solution (0.5 *M*, 20 ml) was added to the amides (0.5 g) in water at 0°, the solution was maintained at p*H* 13 for 1 h, and acetic acid was added to p*H* 5 and the solution was left overnight at room temperature. The solution was deionized by passage through columns of Amberlite resins IR-120(H) and IR-45(OH) and concentrated to a syrup. The syrup was chromatographed on charcoal–Celite (1:1) and elution with water and water containing 2% of butanone gave (*i*) D-glucose (0.10 g), identified by t.l.c. of the sugar and g.l.c. of glucitol hexaacetate, and (*ii*) 2-deoxy-D-*erythro*-pentose (0.15 g), identified by conversion into the *N*-phenyl glycosylamine, m.p. and mixture m.p. 172–173°. No 2-deoxy-5-*O*-β-D-glucopyranosyl-D-*erythro*-pentose (**5**) (11) could be detected.

(*b*) The mixture (50 mg) of *O*-glycosylsaccharinic acids from the alkaline degradation of disaccharide **4** was treated with sodium hypochlorite at p*H* 5 as described by Whistler and Schweiger (5) and the reaction mixture was worked-up to give a syrup which was examined by paper chromatography in solvents *A* and *B* and shown to contain approximately equal amounts of glucose, disaccharide **5** ($R_{glucose}$ 1.9 in solvent *A*), and unchanged saccharinic acids.

(*c*) The mixture (100 mg) of *O*-glycosyl saccharinic acids from the alkaline degradation of disaccharide **4** was submitted to a Ruff degradation by the modified procedure of Haga *et al.* (9). The reaction mixture was worked-up to give a syrup which was shown by paper chromatography to contain approximately equal amounts of glucose and disaccharide **5** together with some unchanged saccharinic acid.

The authors wish to acknowledge financial support from the National Research Council of Canada and a grant from the Institute of Paper Chemistry, Appleton, Wisconsin, under the Pioneering Research Program. We thank Dr. Milton H. Fischer of The Pillsbury Company, Minneapolis, for a generous supply of the β-D-glucan.

1. W. PIGMAN and E. F. J. L. ANET. *In* The carbohydrates. 2nd ed. Vol. 1A. *Edited by* W. Pigman and D. Horton. Academic Press, New York, 1972. Chapt. 4.
2. R. L. WHISTLER and J. N. BEMILLER. Advan. Carbohydr. Chem. **13**, 289 (1958).
3. G. O. ASPINALL and J. P. MCKENNA. Abstracts 152nd Am. Chem. Soc. Meeting, Sept. 1966. p. 14E; J. P. MCKENNA. Ph.D. Thesis, University of Edinburgh, Edinburgh. 1967.
4. G. O. ASPINALL, R. M. FAIRWEATHER, and T. M. WOOD. J. Chem. Soc. C, 2174 (1968).
5. R. L. WHISTLER and R. SCHWEIGER. J. Am. Chem. Soc. **81**, 5190 (1959).
6. J. JOHNSON, S. KIRKWOOD, A. MISAKI, T. E. NELSON, J. V. SCALETTI, and F. SMITH. Chem. Ind. London, 820 (1963).
7. T. E. NELSON, J. JOHNSON, E. JANTZEN, and S. KIRKWOOD. J. Biol. Chem. **244**, 5972 (1969).
8. H. BREDERECK, A. WAGNER, D. GEISSEL, P. GROSS, U. HUTTEN, and H. OTT. Chem. Ber. **95**, 3064 (1962) and earlier papers.
9. M. HAGA, M. TAKANO, and S. TEJIMA. Carbohydr. Res. **21**, 440 (1972).
10. N. K. KOCHETKOV, O. S. CHIZHOV, and A. F. SVIRIDOV. Carbohydr. Res. **14**, 277.
11. G. O. ASPINALL, T. N. KRISHNAMURTHY, and I. FURDA. Can. J. Chem. This issue.
12. J. NEMEC and J. JARY. Coll. Czech. Chem. Commun. **34**, 843 (1969).
13. J. KÄRKKÄINEN. Carbohydr. Res. **14**, 27 (1970).
14. T. E. NELSON and B. A. LEWIS. Carbohydr. Res. **33**, 63 (1974).
15. R. F. BURNS and P. J. SOMERS. Carbohydr. Res. **31**, 191 (1973).
16. B. LINDBERG, J. LÖNNGREN, and J. L. THOMPSON. Carbohydr. Res. **28**, 351 (1973).

17. G. O. ASPINALL, T. N. KRISHNAMURTHY, W. MITURA, and M. FUNABASHI. Can. J. Chem. This issue.
18. G. O. ASPINALL and A. S. CHAUDHARI. Can. J. Chem. This issue.
19. W. L. GLEN, G. S. MYERS, and G. A. GRANT. J. Chem. Soc. 2568 (1951).
20. G. R. BARKER, Methods Carbohydr. Chem. **1**, 168 (1962).
21. A. S. PERLIN. Can. J. Chem. **42**, 2365 (1964).
22. D. M. MACKIE and A. S. PERLIN. Carbohydr. Res. **24**, 67 (1972).
23. A. THOMPSON, M. L. WOLFROM, and E. PACSU. Methods Carbohydr. Chem. **2**, 215 (1963).
24. S. ADACHI. Carbohydr. Res. **10**, 165 (1969).
25. J. S. BRIMACOMBE. Methods Carbohydr. Chem. **6**, 376 (1972).
26. L. WARREN. J. Biol. Chem. **234**, 1971 (1959).
27. M. DUBOIS, K. A. GILLES, J. K. HAMILTON, P. A. REBERS, and F. SMITH. Anal. Chem. **31**, 1199 (1959).
28. H. B. WOOD and H. G. FLETCHER, JR. J. Org. Chem. **26**, 1969 (1961).
29. P. A. SANDFORD and H. E. CONRAD. Biochemistry, **5**, 1508 (1966).

Can. J. Chem. Downloaded from www.nrcresearchpress.com by 210.87.254.6 on 09/05/12
For personal use only.

Base-catalyzed Degradations of Carbohydrates. VIII. Disaccharide Syntheses

GERALD O. ASPINALL[1] AND THINNAYAM N. KRISHNAMURTHY
Department of Chemistry, York University, Downsview, Toronto, Ontario M3J 1P3
AND
IVAN FURDA
Department of Chemistry, Trent University, Peterborough, Ontario K9J 7B8

Received March 18, 1975

GERALD O. ASPINALL, THINNAYAM N. KRISHNAMURTHY, and IVAN FURDA. Can. J. Chem. **53**, 2178 (1975).

Acetylated derivatives (**3** and **10**) of the disaccharides 6-*O*-β-D-glucopyranosyl-3-*O*-mesyl-D-glucose and 3-deoxy-6-*O*-β-D-glucopyranosyl-D-*ribo*-hexose have been synthesized. The parent disaccharides have been degraded to give 2-deoxy-5-*O*-β-D-glucopyranosyl-D-*erythro*-pentose (**4**) which has been characterized as the methylated disaccharide alditol.

GERALD O. ASPINALL, THINNAYAM N. KRISHNAMURTHY et IVAN FURDA. Can. J. Chem. **53**, 2178 (1975).

On a synthétisé les dérivés acétylés (**3** et **10**) des disaccharides 6-*O*-β-D-glucopyrannosyl-3-*O*-mésyl-D-glucose et 3-déoxy-6-*O*-β-D-glucopyrannosyl-D-*ribo*-hexose. Les disaccharides mères ont été dégradés produisant ainsi le 2-déoxy-5-*O*-β-D-glucopyrannosyl-D-*érythro*-pentose (**4**) qui a été identifié comme le disaccharide méthylé de l'alditol.

In part VII (1) attempts to degrade an epimeric pair of 3-deoxy-6-*O*-β-D-glucopyranosylhexonic acids (*O*-glycosyl metasaccharinic acids) to a single transformation product, 2-deoxy-5-*O*-β-D-glucopyranosyl-D-*erythro*-pentose (**4**), were less than fully successful due to the susceptibility of the disaccharide (**4**) to further degradation. In addition to degradation of 3-deoxyhexonic acids (metasaccharinic acids), *e.g.* by the Ruff procedure (2), 2-deoxy-D-*erythro*-pentose is conveniently prepared by alkaline degradation of 3-*O*-methanesulfonyl (mesyl)- or 3-*O*-*p*-toluenesulfonyl (tosyl)-D-glucose (3) or by reaction of 3-deoxy-D-*ribo*-hexose with 1 mol of periodate (4). We describe here syntheses of the peracetates of 6-*O*-β-D-glucopyranosyl-3-*O*-mesyl-D-glucose and 3-deoxy-6-*O*-β-D-glucopyranosyl-D-*ribo*-hexose from which the parent disaccharides have been obtained for further degradation to disaccharide **4**.

Reaction of 3-*O*-mesyl-D-glucose (5) with chlorotriphenylmethane in pyridine furnished 3-*O*-mesyl-6-*O*-trityl-α-D-glucopyranose (**1**) as a crystalline pyridine complex which gave 1,2,4-tri-*O*-acetyl-3-*O*-mesyl-6-*O*-trityl-α-D-glucopyranose (**2**) on acetylation. Bredereck condensation (6,7) of 2,3,4,6-tetra-*O*-acetyl-α-D-glucopyranosyl bromide with the trityl ether (**2**) afforded the β-heptaacetyl derivative (**3**) of 6-*O*-β-D-glucopyranosyl-3-*O*-mesyl-D-glucose. The parent disaccharide was formed on de-*O*-acetylation and was used directly for conversion into disaccharide **4**. Further treatment of the 3-*O*-mesyl disaccharide under controlled conditions gave 2-deoxy-5-*O*-β-D-glucopyranosyl-D-*erythro*-pentose (**4**) but in confirmation of previous observations (1) it was noted that the disaccharide **4** on prolonged contact with base underwent degradation with the liberation of glucose. Accordingly disaccharide **4** was not isolated but its formation was confirmed by reduction with sodium borohydride and conversion into 2-deoxy-5-*O*-(2,3,4,6-tetra-*O*-methyl-β-D-glucopyranosyl)-1,3,4-tri-*O*-methyl-D-*erythro*-pentitol (**5**). The methylated disaccharide alditol (**5**) showed characteristic fragment ions in the mass spectrum and methanolysis gave components with the retention times of 2-deoxy-1,3,4-tri-*O*-methyl-D-*erythro*-pentitol and the methyl glycosides of 2,3,4,6-tetra-*O*-methyl-D-glucose.

Acetylation of the 6-*O*-trityl derivative (**6**) of 3-deoxy-D-*ribo*-hexose (8) gave a mixture of 1,2,4-tri-*O*-acetyl-3-deoxy-6-*O*-trityl-β-D-*ribo*-hexopyranose (**7**) and 1,2,5-tri-*O*-acetyl-3-deoxy-6-*O*-D-*ribo*-hexofuranose (**8**). The formation of appreciable quantities of the furanose acetate is not surprising since n.m.r. studies (9) have shown

[1]To whom enquiries should be addressed at York University.

Can. J. Chem. Downloaded from www.nrcresearchpress.com by 210.87.254.5 on 09/05/12
For personal use only.

Can. J. Chem. Downloaded from www.nrcresearchpress.com by 210.87.254.5 on 09/05/12
For personal use only.

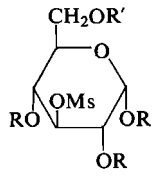

1 R = H; R′ = Tr
2 R = Ac; R′ = Tr

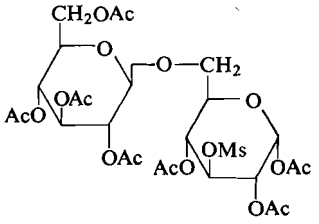

3

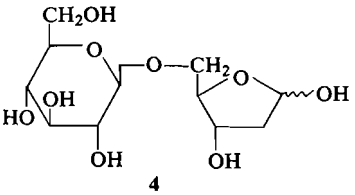

4

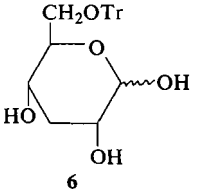

6

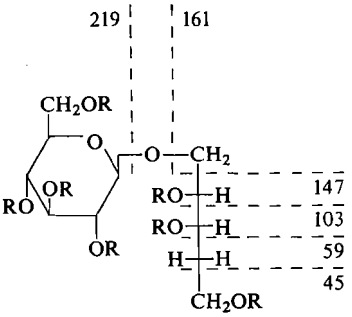

5 (R = CH_3) with characteristic fragment ions in the mass spectrum

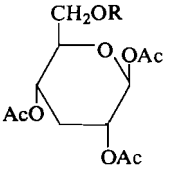

7 R = Tr
9 R = H

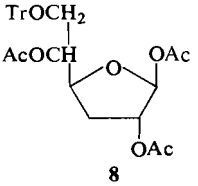

8

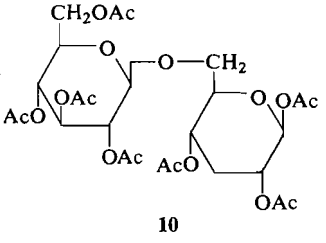

10

the presence of *ca.* 25% of furanose isomers in aqueous solutions of 3-deoxy-D-*ribo*-hexose. In like manner Zinner *et al.* (10) have shown that acetylation of 3-deoxy-D-*xylo*-hexose gives isolable quantities of the furanose acetate. The β-heptaacetyl derivative (**10**) of 3-deoxy-6-*O*-β-D-glucopyranosyl-D-*ribo*-hexose was prepared (*i*) by Bredereck condensation of trityl ether **7** with tetra-*O*-acetyl-α-D-glucopyranosyl bromide and (*ii*) by the de-*O*-tritylation of the trityl ether **7** to give 1,2,4-tri-*O*-acetyl-3-deoxy-β-D-*ribo*-hexopyranose (**9**) followed by Koenigs–Knorr condensation with tetra-*O*-acetyl-α-D-glucopyranosyl bromide. The parent disaccharide formed on de-*O*-acetylation of the heptaacetate **10** was oxidized with periodic acid and furnished 2-deoxy-5-*O*-β-D-glucopyranosyl-D-*erythro*-pentose (**4**). The disaccharide **4** was characterized by conversion into the methylated disaccharide alditol **5**, whose identity was established by g.l.c. – mass spectrometry.

No detailed explanation is yet available for the alkali lability of 2-deoxy-5-*O*-β-D-glucopyranosyl-D-*erythro*-pentose (**4**). The alkaline degradation of 2-deoxy-D-*erythro*-pentose is discussed in a recent review (11) and it is noteworthy that derivatives of this sugar which are also present in the furanose form in deoxyribonucleic acid derivatives are readily degraded by alkali (12).

Experimental

Unless otherwise stated experimental conditions were as described in part VII (1).

*3-O-Mesyl-6-O-trityl-*D*-glucose (1)*

Reaction of 3-*O*-mesyl-D-glucose (3) (25 g) with chlorotriphenylmethane in pyridine under standard conditions (13), followed by extraction with chloroform and concentration by repeated distillation with toluene to remove excess of pyridine, furnished 3-*O*-mesyl-6-*O*-trityl-D-glucose (**1**) as a crystalline pyridine complex (53 g), which after recrystallization from toluene had m.p. 112–118° (slow heating on the hot stage), 129–131° (rapid heating in a capillary), and $[\alpha]_D$ +38.6° (constant during 4 h) (*c*, 1.0 in chloroform); n.m.r. ($CDCl_3$): τ 2.55–2.62 (2 protons, α-H of pyridine residue, *cf.* τ 2.40 of pyridine), 2.40–3.00 (18 protons, trityl and β- and γ-H of pyridine residue), 4.79 (1-proton doublet, $J_{1,2}$ = 3.8 Hz, H-1), 6.93 (3-proton singlet, mesyl).

Anal. Calcd. for $C_{26}H_{28}O_8S \cdot C_5H_5N$: C, 64.10; H, 5.74; S, 5.51; N, 2.42. Found: C, 64.42; H, 5.69; S, 5.70; N, 2.45.

*1,2,4-Tri-O-acetyl-3-O-mesyl-6-O-trityl-*α*-*D*-glucopyranose (2)*

Reaction of the trityl ether **1** as the pyridine complex (24 g) with acetic anhydride (170 ml) containing anhydrous sodium acetate (12 g) at 125° for 3 h, followed by normal work-up and recrystallization from ethanol afforded the triacetate **2** (27 g), m.p. 120–122°, $[\alpha]_D$ +95° (*c*, 1.0 in chloroform); n.m.r. ($CDCl_3$): τ 4.67 (1-proton doublet, $J_{1,2}$ = 3.7 Hz, H-1), 7.08 (3-proton singlet, mesyl), 7.88, 7.95, 8.22 (3 × 3-proton singlets, 3 × $OCOCH_3$).

Anal. Calcd. for $C_{32}H_{34}O_{11}S$: C, 61.31; H, 5.47; S, 5.10. Found: C, 60.83; H, 5.36; S, 5.45.

*1,2,4-Tri-O-acetyl-6-O-(2,3,4,6-tetra-O-acetyl-*β*-*D*-glucopyranosyl)-3-O-mesyl-*α*-*D*-glucopyranose (3)*

2,3,4,6-Tetra-*O*-acetyl-α-D-glucopyranosyl bromide (8.22 g) and the trityl ether **2** (12.5 g) were condensed in nitromethane (20 ml) in the presence of Drierite (5 g) and silver perchlorate (4.5 g), and the mixture was kept at

Can. J. Chem. Downloaded from www.nrcresearchpress.com by 210.87.254.5 on 09/05/12
For personal use only.

room temperature for 10 min. The reaction mixture was worked-up in the usual way (1), crystallization from methanol removed most of the tritanol, and further crystallization gave acetylated disaccharide **3** (4.7 g), m.p. 149–151°, $[\alpha]_D$ +46° (*c*, 1.0 in chloroform); n.m.r. ($CDCl_3$): τ 3.80 (1-proton doublet, $J_{1,2}$ = 4 Hz, H-1), 7.07 (3-proton singlet, mesyl), 7.87–8.30 (21 protons, 7 × $OCOCH_3$).

Anal. Calcd. for $C_{27}H_{38}O_{20}S$: C, 45.34; H, 5.35; S, 4.48. Found: C, 45.22; H, 5.36; S, 4.85.

Alkaline Degradation of 1,2,4-Tri-O-acetyl-6-O-(2,3,4,6-tetra-O-acetyl-β-D-glucopyranosyl)-3-O-mesyl-α-D-glucopyranose (3)

Methanolic sodium methoxide was added to the acetylated disaccharide **3** (500 mg) in methanol (25 ml) in order to maintain permanent alkalinity and the solution was stirred for 5 min in an atmosphere of nitrogen. The major product had $R_{glucose}$ 1.15 on paper chromatography in solvent *A*. Oxygen-free lime-water (250 ml) was added to the methanolic solution during 1 h and reaction was continued for 3 h in an atmosphere of nitrogen. At this point paper chromatography showed a major component, $R_{glucose}$ 1.9, which gave a positive staining reaction with the perchloric acid – acetone spray for 2-deoxy sugars (14), together with glucose as a minor component. Prolonged reaction resulted in the formation of increasing amounts of glucose. The reaction mixture was treated with cation and anion exchangers and concentrated to a syrup which was treated with sodium borohydride (250 mg) in water (5 ml) and worked-up in the usual way to give the corresponding mixtures of alditols (140 mg). The mixture of alditols was methylated with methyl iodide and sodium hydride in *N*,*N*-dimethylformamide (15) and g.l.c. on column *b* showed hexa-*O*-methylglucitol (*T* 0.24) as a minor component and a major component with *T* 0.48. Methanolysis of the methylated alditols and examination of the products by g.l.c. on column *a* at 150° showed components with the retention times of 2-deoxy-1,3,4-tri-*O*-methyl-D-*erythro*-pentitol (*T* 0.69; a reference sample was prepared from 2-deoxy-5-*O*-trityl-D-*erythro*-pentose (16) by reduction, methylation, and de-*O*-tritylation) and the methyl glycosides of 2,3,4,6-tetra-*O*-methyl-D-glucose (*T* 1.00 and 1.49). Examination of the major component by g.l.c. – mass spectrometry showed characteristic fragment ions at *m/e* 219(5), 161(30), 147(21), 103(53), 59(16), and 45(100). Preparative-layer chromatography of the mixture of methylated alditols on silica gel using chloroform–ethanol (9:1) afforded a sample of 2-deoxy-5-*O*-(2,3,4,6-tetra-*O*-methyl-β-D-glucopyranosyl)-1,3,4-tri-*O*-methyl-D-*erythro*-pentitol (**5**), $[\alpha]_D$ −18° (*c*, 0.4 in methanol).

Anal. Calcd. for $C_{18}H_{36}O_9$: OMe, 54.8. Found: OMe, 54.3.

3-Deoxy-6-O-trityl-D-ribo-hexose (6) and Acetylated Derivatives (7 and 8)

3-Deoxy-D-*ribo*-hexose (8) (2.65 g) was reacted with chlorotriphenylmethane in pyridine under standard conditions (13) and normal work-up followed by chromatography on silica gel furnished with syrupy trityl ether **6** (3.5 g).

Anal. Calcd. for $C_{25}H_{26}O_5$: C, 73.87; H, 6.45. Found: (after drying at 80°): C, 73.89; H, 6.56.

Reaction of the trityl ether **6** (3.5 g) with acetic anhydride (40 ml) containing anhydrous sodium acetate (2 g) at 130° for 3 h, followed by normal work-up and fractional crystallization from ethanol gave (*i*) 1,2,4-tri-*O*-acetyl-3-deoxy-6-*O*-trityl-β-D-*ribo*-hexopyranose (**7**) (1.4 g), m.p. 200°, $[\alpha]_D$ +14° (*c*, 3.0 in chloroform); n.m.r. ($CDCl_3$): τ 2.43–2.86 (15-proton multiplet, trityl), 4.28 (1-proton doublet, $J_{1,2}$ = 8 Hz, H-1), 7.90, 7.96, 8.20 (3 × 3-proton singlets, 3 × $OCOCH_3$); and (*ii*) 1,2,5-tri-*O*-acetyl-3-deoxy-6-*O*-trityl-β-D-*ribo*-hexofuranose (8) (1.2 g), m.p. 137° $[\alpha]_D$ −39.5° (*c*, 2.0 in chloroform), −33.7° (*c*, 1.0 in pyridine); n.m.r. ($CDCl_3$): τ 2.50–2.84 (15-proton multiplet, trityl), 3.90 (1-proton broad singlet, separation < 1 Hz, H-1), 7.87, 7.92, 8.05 (3 × 3-proton singlets, 3 × $OCOCH_3$).

Anal. Calcd. for $C_{31}H_{32}O_8$: C, 69.90; H, 6.05. Found: (**7**): C, 70.25; H, 5.80. Found (**8**): C, 69.66; H, 5.89.

1,2,4-Tri-O-acetyl-3-deoxy-β-deoxy-β-D-ribo-hexopyranose (9)

Treatment of the trityl ether **7** (2.2 g) in acetic acid (20 ml) with hydrogen bromide (45%) in acetic acid (1.1 ml) at 0° for 3 min, followed by normal work-up and crystallization from ether – light petroleum afforded the triacetate **9** (580 mg), m.p. 86–88°, $[\alpha]_D$ −7.2° (*c*, 1.0 in chloroform); n.m.r. ($CDCl_3$): τ 4.40 (1-proton doublet, $J_{1,2}$ = 8 Hz, H-1), 7.90, 7.94, 7.96 (3 × 3-proton singlets, 3 × $OCOCH_3$).

Anal. Calcd. for $C_{12}H_{18}O_8$: C, 49.65; H, 6.20. Found: C, 49.54; H, 6.30.

1,2,4-Tri-O-acetyl-3-deoxy-6-O-(2,3,4,6-tetra-O-acetyl-β-D-glucopyranosyl)-β-D-ribo-hexopyranose (10)

(*a*) Condensation of 2,3,4,6-tetra-*O*-acetyl-α-D-glucopyranosyl bromide (386 mg) and trityl ether **7** (500 mg) in nitromethane (15 ml) in the presence of Drierite (0.3 g) and silver perchlorate (0.58 g) at 80° for 10 min, followed by work-up as described previously (1) and crystallization from ethanol furnished the disaccharide derivative **10** (250 mg), m.p. 185–187°, $[\alpha]_D$ −14° (*c*, 1.0 in dichloromethane); n.m.r. ($CDCl_3$): τ 4.33 (1-proton doublet, $J_{1,2}$ = 8 Hz, H-1), 7.87–8.05 (7 × 3-proton singlets, 7 × $OCOCH_3$).

(*b*) Condensation of tetra-*O*-acetyl-α-D-glucopyranosyl bromide (1.1 g) and the triacetate **9** (0.59 g) in benzene (20 ml) in the presence of silver carbonate (0.9 g) and Drierite (2.5 g) for 48 h at room temperature, followed by filtration and concentration, afforded a crystalline product, which was recrystallized from methanol to give the acetylated disaccharide **10** (780 mg), m.p. 195–196°, $[\alpha]_D$ −15° (*c*, 1.0 in chloroform), whose n.m.r. spectrum was indistinguishable from that of the previous sample.

Anal. Calcd. for $C_{26}H_{36}O_{17}$: C, 50.32; H, 5.85. Found: C, 60.60; H, 5.70.

2-Deoxy-5-O-β-D-glucopyranosyl-D-erythro-pentose (4)

Reaction of the acetylated disaccharide **10** (50 mg) in methanol (5 ml) with 0.1 *M* methanolic sodium methoxide (1 ml) for 45 min, followed by treatment with Amberlite resin IR-120(H) and concentration furnished 3-deoxy-6-*O*-β-D-glucopyranosyl-D-*ribo*-hexose, $[\alpha]_D$ −8° (*c*, 1.0 in water). The disaccharide (20 mg) was oxidized in aqueous 0.05 *M* periodic acid (25 ml) at 5° for 3 h (1 mol of reagent was consumed per mole of disaccharide (17)), the solution was neutralized with barium hydroxide, and precipitated barium salts were removed by filtration. The solution was

treated with cation and anion exchangers and concentrated to a syrup, which was shown by paper chromatography to contain only disaccharide **4**, $R_{glucose}$ 1.9 in solvent *A*. The disaccharide was reduced with sodium borohydride, as described previously, and the resulting disaccharide alditol was methylated (15). The methylated disaccharide alditol (**5**) gave a single peak on examination by g.l.c. on column *b* (*T* 0.48) and its mass spectrum was identical with that of the previously prepared sample.

The authors acknowledge financial support from the National Research Council of Canada and a grant from the Institute of Paper Chemistry, Appleton, Wisconsin, under the pioneering Research Program.

1. G. O. ASPINALL, T. N. KRISHNAMURTHY, I. FURDA, and R. KHAN. Can. J. Chem. This issue.
2. G. N. RICHARDS. Methods Carbohydr. Chem. **1**, 180 (1962).
3. E. HARDEGGER. Methods Carbohydr. Chem. **1**, 177 (1962).
4. G. REMBARZ. Chem. Ber. **93**, 622 (1960).
5. B. HELFERICH, H. DRESSLER, and R. GRIEBEL. J. Prakt. Chem. [2] **153**, 285 (1939).
6. H. BREDERECK, A. WAGNER, G. FABER, H. OTT, and J. RAUTHER. Chem. Ber. **92**, 1135 (1959).
7. H. BREDERECK, A. WAGNER, D. GEISSEL, and H. OTT. Chem. Ber. **95**, 3064 (1962).
8. E. VIS and P. KARRER. Helv. Chim. Acta, **37**, 378 (1957).
9. S. J. ANGYAL and V. A. PICKLES. Aust. J. Chem. **25**, 1711 (1972).
10. H. ZINNER and G. WULF. J. Prakt. Chem. **312**, 192 (1970).
11. M. S. FEATHER and J. F. HARRIS. Adv. Carbohydr. Chem. Biochem. **28**, 161 (1973).
12. A. S. JONES, A. M. MIAN, and R. T. WALKER. J. Chem. Soc. C, 2042 (1968).
13. G. R. BARKER. Methods Carbohydr. Chem. **1**, 168 (1962).
14. G. WEIDEMANN and W. FISCHER. Z. Physiol. Chem. **336**, 192 (1964).
15. J. S. BRIMACOMBE. Methods Carbohydr. Chem. **6**, 376 (1972).
16. R. K. NESS and H. G. FLETCHER, JR. J. Am. Chem. Soc. **82**, 3434 (1960).
17. G. O. ASPINALL and R. J. FERRIER. Chem. Ind. London, 1216 (1957).

Can. J. Chem. Downloaded from www.nrcresearchpress.com by 210.87.254.5 on 09/05/12
For personal use only.

Base-catalyzed Degradations of Carbohydrates. IX. β-Eliminations of 4-*O*-Substituted Hexopyranosiduronates[1]

GERALD O. ASPINALL,[2] THINNAYAM N. KRISHNAMURTHY, WALTER MITURA,
Department of Chemistry, York University, Downsview, Toronto, Ontario M3J 1P3

AND

MASUO FUNABASHI
Department of Chemistry, Trent University, Peterborough, Ontario K9J 7B8

Received March 18, 1975

GERALD O. ASPINALL, THINNAYAM N. KRISHNAMURTHY, WALTER MITURA, and MASUO FUNABASHI. Can. J. Chem. **53**, 2182 (1975).

Two methylated disaccharides, methyl [methyl 4-*O*-(2,3,4,6-tetra-*O*-methyl-α-D-glucopyranosyl)-2,3-di-*O*-methyl-β-D-glucopyranosid]uronate (**9**) and methyl 6-*O*-(methyl 2,3,4-tri-*O*-methyl-α-D-galactopyranosyluronate)-2,3,4-tri-*O*-methyl-β-D-glucopyranoside (**15**) have been synthesized and used as model compounds for the study of the base-catalyzed β-elimination of 4-*O*-substituted hexopyranosiduronates without degradation of exposed reducing sugars and of the selective acid hydrolysis of hex-4-enopyranosiduronates.

GERALD O. ASPINALL, THINNAYAM N. KRISHNAMURTHY, WALTER MITURA et MASUO FUNABASHI. Can. J. Chem. **53**, 2182 (1975).

On a synthétisé deux disaccharides méthylés, le méthyl [méthyl 4-*O*-(2,3,4,6-tétra-*O*-méthyl-α-D-glucopyrannosyl)-2,3-di-*O*-méthyl-β-D-glucopyrannoside]uronate (**9**) et le méthyl 6-*O*-(méthyl-2,3,4-tri-*O*-méthyl-α-D-galactopyrannosyluronate)-2,3,4-tri-*O*-méthyl-β-D-glucopyrannoside (**15**). On s'en est ensuite servi comme produits de référence pour l'étude de la β-élimination par catalyse basique des hexopyrannoside uronates *O*-substitués en position 4 sans dégradation des sucres réducteurs exposés. Ces deux composés servent aussi à l'aide de l'hydrolyse acide sélective des hex-4 énopyrannosiduronates.

4-*O*-Substituted hexuronate residues, which are readily formed on esterification of many acidic polysaccharides, are susceptible to base-catalyzed degradation with the formation of unsaturated hexuronates and with the exposure of new reducing groups (1, 2). The reactions outlined in Scheme 1 must be considered if this degradation is to be used effectively to isolate fragments both exterior and interior to points of cleavage, and thus to obtain new structural information on polysaccharides. The first requirement is that the reaction is performed in a nonaqueous solvent using a base of low nucleophilicity towards ester functions ($k_1 \gg k_2$) so that the driving force of the carboalkoxy group is maintained. It is also desirable that protecting groups for hydroxyl functions are stable to the reaction conditions. Since β-elimination results in the exposure of reducing sugar residues the isolation of fragments exterior to the points of cleavage requires that reducing sugars should be either stable under the reaction conditions or protected against further degradation ($k_3 \ll k_4$). The fragments interior to the points of cleavage will be terminated by hex-4-enopyranosyluronate residues and should be amenable to characterization either directly or after selective hydrolysis of the acid-labile hex-4-enopyranosiduronate residues with minimum cleavage of other glycosidic linkages. We report here syntheses of the methylated disaccharides **9** and **15** as model compounds for an examination of these reaction requirements.

The methylated disaccharides **9** and **15** were chosen as model compounds since they would be expected to furnish known compounds on degradation. Attempts to synthesize methyl 2,2′,3,3′,4,6′-hexa-*O*-methyl-β-maltoside (**8**) from 1,6-anhydro-2,2′,3,3′,4,6′-hexa-*O*-methylmaltose involving ring opening by acetolysis, conversion into the glycosyl halide, and glycosidation were unsuccessful due to the acid-lability of the interresidue glycosidic linkage during formation of

[1]Presented in part at the Canadian Chemical Conference of the Chemical Institute of Canada, Regina, Saskatchewan June 3–5, 1974, and at the VII International Symposium on Carbohydrate Chemistry, Bratislava, Czechoslovakia, August 5–9, 1974.

[2]To whom enquiries should be addressed at York University.

Can. J. Chem. Downloaded from www.nrcresearchpress.com by 210.87.254.105 on 09/05/12
For personal use only.

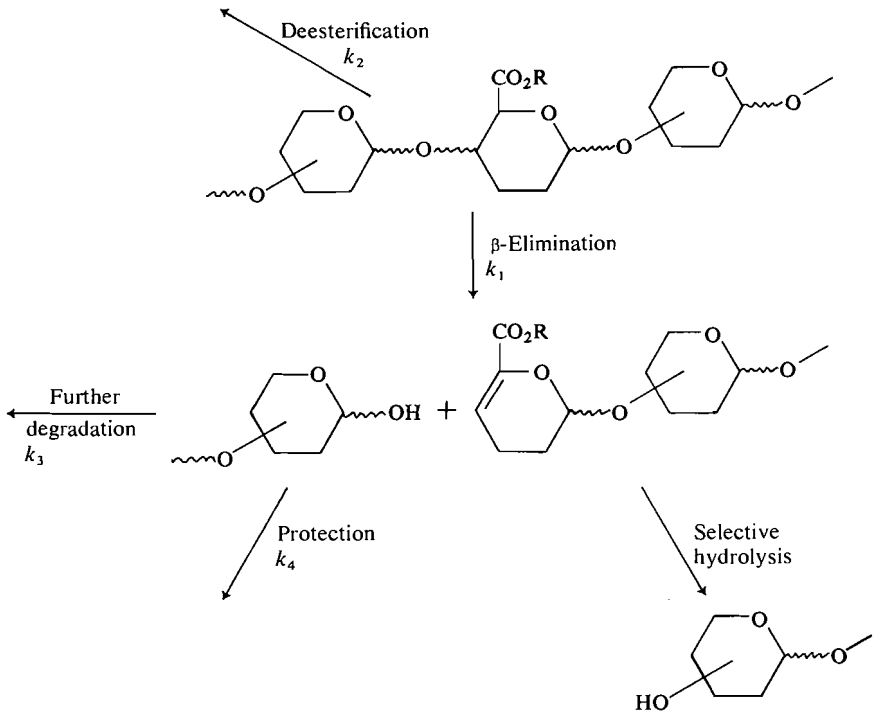

SCHEME 1. Base-catalyzed β-elimination of 4-*O*-substituted hexuronate residues.

the glycosyl halide. The disaccharide derivative **8** was then prepared from methyl β-maltoside in a rather lengthy series of reactions involving *O*-benzylidenation to give **1**, acetylation (to **2**), de-*O*-benzylidenation (to **3**), methylation using diazomethane – boron trifluoride in order to retain base-labile substituents (3) (to **4**), de-*O*-acetylation (to **5**), selective tritylation (to **6**), methylation (to **7**), and de-*O*-tritylation. Oxidation of the hexamethyl ether **8** with chromium trioxide and sulfuric acid in acetone (4) followed by esterification with diazomethane furnished methyl [methyl 4-*O*-(2,3,4,6-tetra-*O*-methyl-α-D-glucopyranosyl)-2,3-di-*O*-methyl-β-D-glucopyranosid]uronate (**9**).

In the above series of reactions it was essential to ensure that 0–6′ was alkylated during the formation of the dimethyl ether **4** and that the process was not accompanied by acetyl migration. Examination of the mass spectrum (5, 6) of the disaccharide derivative provided evidence for the location of the methoxyl substituents. Although the mass spectra of acetylated disaccharides show relatively weak peaks in the high mass range, the following observations (see Scheme 2) supported the proposed structure: (*i*) only a weak molecular ion at *m/e* 594 was observed but fragment ions at *m/e* 563 ($M - CH_3O\cdot$), 562 ($M - CH_3OH$), 535 ($M - CH_3CO_2\cdot$), 534 ($M - CH_3CO_2H$), 503 ($M - CH_3O\cdot - CH_3CO_2H$), 502 ($M - CH_3OH - CH_3CO_2H$), and 475 ($M - CH_3CO_2\cdot - CH_3CO_2H$) provided indirect confirmation of the molecular weight; (*ii*) the fragment ion at *m/e* 549 ($M - CH_3OCH_2\cdot$) pointed to the presence of a primary methoxy substituent; (*iii*) fragment ions of high relative intensity from cleavage of the different bonds at the glycosidic linkage were observed at *m/e* 275 and 303 (*cf.* those from other maltose derivatives (7)); (*iv*) the formation of the fragment ion at *m/e* 275 indicated that the nonreducing residue in the disaccharide **4** contained two methoxyl groups and the successive formation of ions at *m/e* 215 and 173, which was supported by the appearance of the relevant metastable peaks, was consistent with the proposed location of *O*-methyl and *O*-acetyl substituents.

Reaction of the methylated disaccharide **9** with DBU (1,5-diazabicyclo[5.4.0]undec-5-ene) in benzene resulted in β-elimination but under these conditions the liberated 2,3,4,6-tetra-*O*-

Can. J. Chem. Downloaded from www.nrcresearchpress.com by 210.87.254.105 on 09/05/12
For personal use only.

Can. J. Chem. Downloaded from www.nrcresearchpress.com by 210.87.254.105 on 09/05/12
For personal use only.

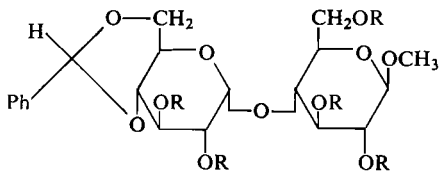

1 R = H
2 R = Ac

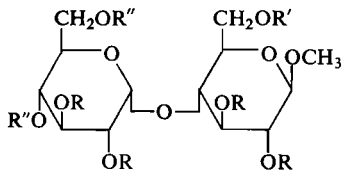

3 R = R′ = Ac; R″ = H
4 R = R′ = Ac; R″ = CH_3
5 R = R′ = H; R″ = CH_3
6 R = H; R′ = Tr; R″ = CH_3
7 R = R″ = CH_3; R′ = Tr
8 R = R″ = CH_3; R′ = H

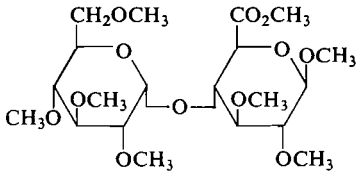

9

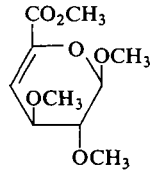

10

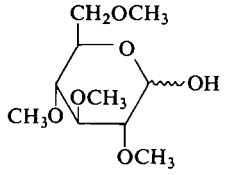

11

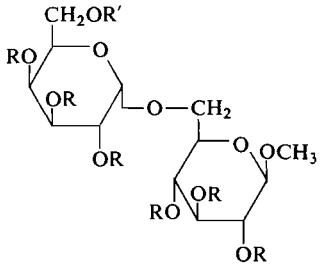

12 R = H; R′ = Tr
13 R = CH_3; R′ = Tr
14 R = CH_3; R′ = H

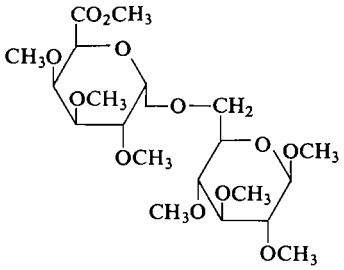

15

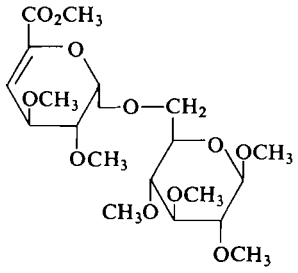

16

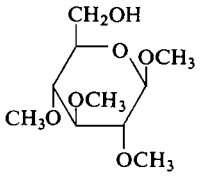

17

methyl-D-glucose (**11**) was further degraded, probably with formation of 3-deoxy-2,4,6-tri-*O*-methyl-D-*erythro*-hex-2-enopyranose (8, 9). However, similar reaction in the presence of added acetic anhydride resulted in protection of the reducing sugar, and chromatography of the products furnished methyl (methyl 4-deoxy-2,3-di-*O*-methyl-α-L-*threo*-hex-4-enopyranosid)uronate (**10**) (10) and a mixture of 1-acetates from which 2,3,4,6-tetra-*O*-methyl-D-glucose (**11**) was isolated after de-*O*-acetylation.

Methyl 6-*O*-(methyl 2,3,4-tri-*O*-methyl-α-D-galactopyranosyluronate)-2,3,4-tri-*O*-methyl-β-D-glucopyranoside (**15**) was prepared from methyl β-melibioside in a sequence of reactions involving *O*-tritylation to give **12**, methylation (to **13**), de-*O*-tritylation (to **14**), and oxidation with chromium trioxide and sulfuric acid in acetone followed by esterification with diazomethane. Reaction of the methylated disaccharide **15** in boiling benzene with DBU – acetic anhydride or DBU alone afforded the unsaturated di-

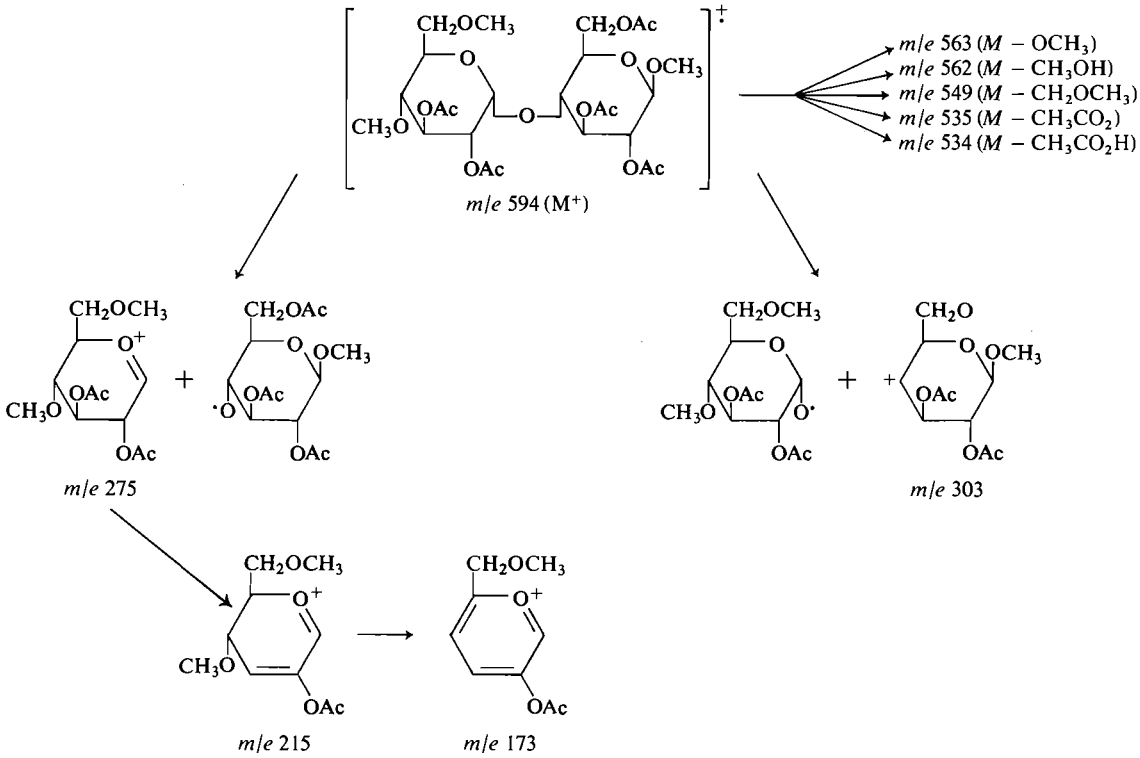

SCHEME 2. Mass spectral fragmentation of methyl 2,2′,3,3′,6-penta-*O*-acetyl-4′,6′-di-*O*-methyl-β-maltoside (**4**).

saccharide, methyl 6-*O*-(methyl 4-deoxy-2,3-di-*O*-methyl-β-L-*threo*-hex-4-enopyranosyluronate)-2,3,4-tri-*O*-methyl-β-D-glucopyranoside (**16**). Selective hydrolysis of the hex-4-enopyranosiduronate with no detectable cleavage of the methyl glycosidic linkage occurred on heating with cation exchanger in aqueous acetone at 70° or with aqueous acetic acid at 100° and methyl 2,3,4-tri-*O*-methyl-β-D-glucopyranoside (**17**) was isolated. These latter conditions have been used by Lindberg *et al.* (2) for the selective cleavage of unsaturated hexuronate residues from methylated acidic polysaccharides after degradation with methylsulfinyl carbanion in methyl sulfoxide.

An application of the reactions described here to polysaccharide structure determination is reported in the following paper (11).

Experimental

Unless otherwise stated experimental conditions were as described in part VII (12).

Methyl 4′,6′-O-Benzylidene-β-maltoside (1) and Derived Pentaacetate (2)

Dry methyl β-maltoside (20 g) and freshly crushed zinc chloride sticks (40 g) were shaken in freshly distilled benzaldehyde (200 ml) for 24 h and the reaction mixture was poured into ether. The precipitate was removed by filtration and washed twice with ether to give a powdery residue, a portion of which was recrystallized from ether–methanol to give methyl 4′,6′-*O*-benzylidene-β-maltoside (**1**), m.p. 140–141°, $[\alpha]_D$ +47.6° (*c*, 2.0 in ethanol).

Anal. Calcd. for $C_{20}H_{28}O_{11}$: C, 53.77; H, 6.62; OCH_3, 6.86. Found: C, 54.04; H, 6.35; OCH_3, 7.01.

Powdery **1** was treated with acetic anhydride (300 ml) in pyridine (600 ml) for 2 days, the reaction mixture was worked-up in the usual way, and recrystallization from ethanol furnished methyl 2,2′,3,3′,6-penta-*O*-acetyl-4′,6′-*O*-benzylidene-β-maltoside (**2**) (20 g), m.p. 200–201°, $[\alpha]_D$ +25.4° (*c*, 1.9 in chloroform); M^+, 654; n.m.r. ($CDCl_3$): τ 2.45–2.70 (5-proton multiplet, phenyl), 4.30 (1-proton singlet, benzylidene-methine), 6.50 (3-proton singlet, OCH_3), 7.85–8.22 (15-protons, 5 × $OCOCH_3$).

Anal. Calcd. for $C_{30}H_{38}O_{16}$: C, 55.04; H, 5.85; OCH_3, 4.73. Found: C, 54.94; H, 5.77; OCH_3; 4.66.

Methyl 2,2′,3,3′,6-Penta-O-acetyl-β-maltoside (3)

The benzylidene derivative **2** (20 g) was heated in acetic acid – water (7:3, 250 ml) on the boiling water bath for 30 min. The reaction mixture was diluted with water (2 volumes), extracted with light petroleum, and repeatedly concentrated after addition of water to a residue (14 g) which crystallized in ether. Recrystallization from ether – ethyl acetate afforded the pentaacetate (**3**) (10 mg), m.p. 152–153°, $[\alpha]_D$ +41° (*c*, 1.0 in dichloromethane); n.m.r. ($CDCl_3$): τ 4.75 (1-proton doublet, $J_{1',2'}$ = 4 Hz, H-1′), 5.60 (1-proton doublet, $J_{1,2}$ = 7.6 Hz, H-1), 6.60 (3-proton singlet, OCH_3), 7.93, 7.97, 8.00, 8.03, 8.06 (3-proton singlets, 5 × $OCOCH_3$).

Can. J. Chem. Downloaded from www.nrcresearchpress.com by 210.87.254.105 on 09/05/12
For personal use only.

Can. J. Chem. Downloaded from www.nrcresearchpress.com by 210.87.254.105 on 09/05/12
For personal use only.

Anal. Calcd. for $C_{23}H_{34}O_{16}$: C, 48.76; H, 6.63. Found: C, 49.04; H, 6.25.

Methyl 2,2′,3,3′,6-Penta-O-acetyl-4′,6′-di-O-methyl-β-maltoside (4)

Diazomethane in ether was added gradually to the pentaacetate (**3**) (5 g) in chloroform (50 ml) containing boron trifluoride etherate (50 mg) until a pale yellow color persisted. Methanol was added to destroy diazomethane and the solution was concentrated to a syrup which was dissolved in chloroform, washed with sodium hydrogen carbonate solution, and concentrated. The resulting syrup crystallized from methanol to give the dimethyl ether **4** (3 g), m.p. 131–132°; n.m.r. ($CDCl_3$): τ 4.67 (1-proton doublet, $J_{1',2'}$ = 4 Hz, H-1′), 5.70 (1-proton doublet, $J_{1,2}$ = 8 Hz, H-1), 6.62–6.66 (3-proton singlets, 3 × OCH_3), 7.95–8.10 (3-proton singlets, 5 × $OCOCH_3$); mass spectrum *m/e* (% relative abundance) 594(0.01) (M^+), 563(0.03) ($M - CH_3O$)$^+$, 562(0.01) ($M - CH_3OH$)$^+$, 549(0.2) ($M - CH_3OCH_2$)$^+$, 535(0.02) ($M - CH_3CO_2$)$^+$, 534(0.02) ($M - CH_3CO_2H$)$^+$, 503(0.1) ($M - CH_3OH - CH_3CO_2$)$^+$, 502(0.07) ($M - CH_3OH - CH_3CO_2H$), 475(4.2) ($M - CH_3CO_2H - CH_3CO_2$)$^+$, 303(64), 275(73), 215(86), 173(93), 43(100) $(CH_3CO)^+$.

Anal. Calcd. for $C_{25}H_{38}O_{16}$: C, 50.49; H. 6.44. Found: C, 50.82; H, 6.54.

Methyl 4′,6′-Di-O-methyl-β-maltoside (5)

The penta-*O*-acetyl dimethyl ether **4** (5 g) in methanol (50 ml) was de-*O*-acetylated by reaction with sodium methoxide (from 0.1 g sodium) in methanol (3 ml) for 16 h. The solution was shaken with Dowex 50(H) resin and concentration of the filtrate gave a syrup (3 g) which crystallized from ether–methanol to give the dimethyl ether **5** (2.1 g), m.p. 154–155°, $[\alpha]_D$ +70.5° (*c*, 1.4 in methanol); n.m.r. ($CDCl_3$): τ 4.65 (1-proton doublet, $J_{1',2'}$ = 4 Hz, H-1′), 5.65 (1-proton doublet, $J_{1,2}$ = 8 Hz, H-1), 6.42 (6-proton singlet, 2 × OCH_3), 6.62 (3-proton singlet, OCH_3).

Anal. Calcd. for $C_{15}H_{28}O_{11}$: C, 46.87; H, 7.34. Found: C, 47.14; H, 7.31.

Methyl 4′,6′-Di-O-methyl-6-O-trityl-β-maltoside (6)

The foregoing dimethyl ether **5** (5 g) in pyridine (50 ml) containing chlorotriphenylmethane (5.5 g) was heated on the boiling water bath for 1 h and kept at room temperature for 24 h. The reaction mixture was poured into ice water to give a syrupy mass which was extracted with chloroform and the chloroform layer was washed with water, dried, and concentrated to a syrup (10 g). Chromatography on silica gel using chloroform–acetone (9:1) as eluant furnished a syrup (7.7 g) which crystallized from methanol to give the dimethyl trityl ether **6** (4.5 g), m.p. 105°, $[\alpha]_D$ +49° (*c*, 2.1 in chloroform); n.m.r. ($CDCl_3$): τ 2.30–2.80 (15-proton multiplet, 3 × phenyl), 6.38, 6.50, 6.70 (3 × 3-proton singlets, 3 × OCH_3).

Anal. Calcd. for $C_{34}H_{42}O_{11}$: OMe, 14.85. Found: OMe, 14.59.

Methyl 2,2′,3,3′,4′,6′-Hexa-O-methyl-6-O-trityl-β-maltoside (7)

Sodium hydride (1 g) was added to the dimethyl trityl ether **6** (4.1 g) in *N*,*N*-dimethylformamide (50 ml) at 0°, the mixture was stirred for 0.5 h, methyl iodide (6 g) was added during 20 min, and the mixture was stirred with cooling for 2 h, and kept at room temperature overnight. Methanol was added to destroy excess of sodium hydride, the mixture was filtered, and the filtrate was concentrated to a syrup which was diluted with chloroform, washed with water, and concentrated again. The resulting hexamethyl trityl ether **7** (4.0 g) was chromatographically pure and had $[\alpha]_D$ +46.5° (*c*, 1.0 in chloroform); n.m.r. ($CDCl_3$): τ 2.40–2.80 (15-proton multiplet, 3 × phenyl), 5.75 (1-proton doublet, $J_{1,2}$ = 8 Hz, H-1), 6.25–6.65 (3-proton singlets, 7 × OCH_3).

Anal. Calcd. for $C_{38}H_{50}O_{11}$: C, 66.84; H, 7.38. Found: C, 66.83, H; 7.51.

Methyl 2,2′,3,3′,4′,6′-Hexa-O-methyl-β-maltoside (8)

The foregoing hexamethyl trityl ether **7** (4 g) in acetic acid – water (100 ml, 7:3) was heated on the boiling water bath for 1 h. The cooled solution was diluted with water, filtered to remove precipitated triphenylmethanol, concentrated to remove acetic acid, diluted again with water, and the whole procedure was repeated twice. The final syrup was dissolved in methanol and the solution was filtered through charcoal and concentrated to give methyl 2,2′,3,3′,4′,6′-hexa-*O*-methyl-β-maltoside (**8**) (2.3 g), $[\alpha]_D$ +67° (*c*, 5.25 in chloroform); n.m.r. ($CDCl_3$): τ 5.75 (1-proton singlet, $J_{1,2}$ = 8 Hz, H-1), 6.30–6.60 (3-proton singlets, 7 × OCH_3).

Anal. Calcd. for $C_{19}H_{36}O_{11}$: C, 51.81; H, 8.24. Found: C, 52.11; H, 8.34.

Methyl [Methyl 4-O-(2,3,4,6-Tetra-O-methyl-β-D-glucopyranosyl)-2,3-di-O-methyl-β-D-glucopyranosid]uronate (9)

Chromium trioxide (3 g) in 3.75 *N* sulfuric acid was added dropwise to methyl hexa-*O*-methyl-β-maltoside (**8**) (2.3 g) in acetone (5 ml) at 5°. Reaction was complete after 12 h and the mixture was chromatographed on a column of silica gel (20 g) using chloroform–acetone (7:3) as eluant to give chromatographically pure acidic disaccharide (2 g). Diazomethane in ether was added with stirring to the acidic disaccharide in ether until t.l.c. showed that esterification was complete. Concentration of the solution afforded chromatographically pure methylated acidic disaccharide **9** (2 g), $[\alpha]_D$ +71° (*c*, 1.0 in chloroform); n.m.r. ($CDCl_2$); τ 5.75 (1-proton doublet, $J_{1,2}$ = 7 Hz, H1), 6.25 (3-proton singlet, ester OCH_3), 6.38–6.60 (3-proton singlets, 7 × OCH_3).

Anal. Calcd. for $C_{20}H_{36}O_{12}$: C, 51.81; H, 8.24. Found: C, 52.11; H, 8.34.

Action of Base on Methyl [Methyl 4-O-(2,3,4,6-Tetra-O-methyl-α-D-glucopyranosyl)-2,3-di-O-methyl-β-D-glucopyranosid]uronate

A sample of methylated acidic disaccharide **9** was heated under reflux in benzene containing 1,5-diazabicyclo[5.4.0]undec-5-ene (DBU). Thin-layer-chromatography indicated the formation of the unsaturated hexuronate **10** and 2,3,4,6-tetra-*O*-methylglucose (**11**) but when reaction was prolonged to ensure disappearance of starting compound a further product with the mobility of 3-deoxy-2,4,6-tri-*O*-methyl-D-*erythro*-hex-2-enopyranose was formed.

Methylated acidic disaccharide **9** (250 mg) was heated under reflux for 24 h in benzene (10 ml) containing DBU (1.6 g) and acetic anhydride (0.9 g). The reaction mixture was separated by preparative-layer chromatography on

Can. J. Chem. Downloaded from www.nrcresearchpress.com by 210.87.254.105 on 09/05/12
For personal use only.

silica gel with chloroform–acetone (9:1) to give (*i*) methyl (methyl 4-deoxy-2,3-di-*O*-methyl-α-L-*threo*-hex-4-enopyranosid)uronate (**10**) (61 mg), m.p. and mixture m.p. 51–52°, whose n.m.r., u.v., and mass spectra were identical with those of an authentic specimen; (*ii*) a mixture of α- and β-acetates of 2,3,4,6-tetra-*O*-methyl-D-glucose (98 mg); and (*iii*) an incompletely separated mixture of the compounds in *i* and *ii*. Treatment of the mixed acetates with methanolic sodium methoxide in the usual way furnished 2,3,4,6-tetra-*O*-methyl-D-glucose (**11**), m.p. and mixture m.p. 92–93°, $[\alpha]_D$ +80.5° (*c*, 1.2 in water).

Methyl 6′-O-Trityl-β-melibioside (12)

Reaction of methyl β-melibioside (13) (5 g) with chlorotriphenylmethane in pyridine under standard conditions (14) followed by normal work-up and recrystallization from toluene furnished methyl 6′-*O*-trityl-β-melibioside (**12**), m.p. 211–212°, $[\alpha]_D$ +26° (*c*, 1.0 in methanol); n.m.r. ($CDCl_3$): τ 2.52–2.97 (15-proton multiplet, 3 × phenyl), 6.45 (3-proton singlet, OCH_3).

Anal. Calcd. for $C_{32}H_{38}O_{11}$: C, 64.21; H, 6.35. Found: C, 64.12; H, 6.42.

Methyl 2,2′,3,3′,4,4′-Hexa-O-methyl-6′-O-trityl-β-melibioside (13)

The trityl ether **12** (5 g) was methylated with methyl iodide and sodium hydride in *N,N*-dimethylformamide (15), as described previously, and the desired hexamethyl trityl ether **13** (5.1 g), after recrystallization from ethanol, had m.p. 133–135°, $\alpha[_D]$ +39.6° (*c*, 1.9 in chloroform); n.m.r. ($CDCl_3$): τ 2.52–2.97 (15-proton multiplet, 3 × phenyl), 5.87 (1-proton doublet, $J_{1,2}$ = 7 Hz, H-1), 6.36–6.61 (3-proton singlets, 7 × OCH_3).

Anal. Calcd. for $C_{38}H_{50}O_{11}$: C, 66.84; H, 7.38. Found: C, 67.10; H, 7.31.

Methyl 2,2′,3,3′,4,4′-Hexa-O-methyl-β-melibioside (14)

The foregoing compound **13** (5 g) in acetic acid – water (75 ml, 4:1) was heated on the boiling water bath for 1 h. Normal work-up gave a syrup (ν_{max} (film) 1730 cm^{-1}, ester C=O) in which t.l.c. showed a major product with a small amount of a compound of higher mobility. De-*O*-acetylation of the syrup with methanolic sodium methoxide gave a single product which was recrystallized from ethanol gave the hexamethyl ether **14** (2.6 g), m.p. 110–111°, $[\alpha]_D$ +80° (*c*, 1.1 in chloroform); n.m.r. ($CDCl_3$): τ 4.83 (1-proton doublet, $J_{1',2'}$ = 3.5 Hz, H-1′), 5.83 (1-proton doublet, $J_{1,2}$ = 7.5 Hz, H-1), 6.34, 6.38, 6.40, 6.43, 6.44, 6.46, 6.47 (3-proton singlets, 7 × OCH_3).

Anal. Calcd. for $C_{19}H_{36}O_{11}$: C, 51.81; H, 8.24. Found: C, 51.49; H, 8.36.

Methyl 6-O-(Methyl 2,3,4-Tri-O-methyl-α-D-galactopyranosyluronate)-2,3,4-tri-O-methyl-β-D-glucopyranoside (15)

Chromium trioxide (1.2 g) in 3.75 *N* sulfuric acid was added dropwise to methyl hexa-*O*-methyl-β-melibioside (**14**) (2 g) in acetone (7 ml) at 5°. Reaction was complete after 16 h and the mixture was chromatographed on a column of silica gel using benzene as eluant to give syrupy aldobiouronic acid (1.75 g) (ν_{max} (film) 2800, 1710 cm^{-1} (CO_2H)). Diazomethane in ether was added with stirring to the acidic disaccharide (1.6 g) in ether until t.l.c. showed that reaction was complete. Concentration of the solution followed by crystallization from light petroleum afforded methylated aldobiouronic ester **15** (1.6 g), m.p. 97–98°, $[\alpha]_D$ +82° (*c*, 1.2 in chloroform); ν_{max} (film) 1750 cm^{-1} (ester C=O); n.m.r. ($CDCl_3$): τ 4.83 (1-proton singlet, $J_{1',2'}$ = 3 Hz, H-1′), 5.82 (1-proton singlet, $J_{1,2}$ = 7.5 Hz, H-1), 6.16 (3-proton singlet, ester OCH_3), 6.37–6.46 (3-proton singlets, 7 × OCH_3).

Anal. Calcd. for $C_{20}H_{36}O_{12}$: C, 51.30; H, 7.69. Found: C, 51.52; H, 7.70.

Action of Base on Methyl 6-O-(Methyl 2,3,4-Tri-O-methyl-α-D-galactopyranosyluronate)-2,3,4-tri-O-methyl-β-D-glucopyranoside

Methylated aldobiouronic ester **15** (250 mg) was heated with DBU (0.5 g) in benzene (2 ml) in a sealed tube at 95–100° for 20 h. Thin-layer chromatography showed complete disappearance of starting compound. The solution was chromatographed on a silica gel column and elution with benzene afforded methyl 6-*O*-(methyl 4-deoxy-2,3-di-*O*-methyl-β-L-*threo*-hex-4-enopyranosyluronate)-2,3,4-tri-*O*-methyl-β-D-glucopyranoside (**16**) (185 mg), $[\alpha]_D$ +94° (*c*, 1.4 in chloroform); ν_{max} (film) 1740 (ester C=O), 1660 cm^{-1}; λ_{max} (MeOH) 238 nm (ε 6540); n.m.r. ($CDCl_3$): τ 3.90 (1-proton doublet, $J_{3',4'}$ = 4 Hz, H-4′), 4.75 (1-proton doublet, $J_{1',2'}$ = 3 Hz, H1′), 6.22 (3-proton singlet, ester OCH_3), 6.40–6.55 (6 × 3-proton singlets, 6 × OCH_3). The same reaction took place when methylated aldobiouronic ester **15** was heated with DBU and acetic anhydride in benzene.

Anal. Calcd. for $C_{19}H_{32}O_{11}$: C, 52.30; H, 7.34. Found: C, 51.98; H, 7.25.

Hydrolysis of the Unsaturated Disaccharide 16

Unsaturated disaccharide **16** (30 mg) in 6.7% aqueous acetic acid (3 ml) was heated on the boiling water bath for 1 h. Thin-layer chromatography showed complete disappearance of starting compound with the formation of a single detectable product. Concentration of the solution with repeated additions of water afforded a syrup which crystallized from light petroleum – ethanol to give methyl 2,3,4-tri-*O*-methyl-β-D-glucopyranoside (**17**) (11 mg), m.p. and mixture m.p. 92–93°, $[\alpha]_D$ −23° (*c*, 1.0 in chloroform), which gave a single peak on g.l.c. The unsaturated disaccharide **16** also underwent complete hydrolysis with formation of the glucoside **17** when heated at 70° with stirring with Amberlite resin IR-120(H) in acetone–water (7:3) for 4 h.

The authors acknowledge financial support from the National Research Council of Canada.

1. J. Kiss. Adv. Carbohydr. Chem. Biochem. **29**, 230 (1974).
2. B. Lindberg, J. Lonngren, and J. L. Thompson. Carbohydr. Res. **28**, 351 (1973).
3. I. O. Mastronardi, S. M. Flematti, J. O. Deffer-rari, and E. G. Gros. Carbohydr. Res. **3**, 177 (1966). (1966).
4. E. Zissis and H. G. Fletcher, Jr. Carbohydr. Res. **12**, 361 (1970).
5. N. K. Kochetkov and O. S. Chizhov. Adv. Carbohydr. Chem. **21**, 39 (1966).
6. N. K. Kochetkov, O. S. Chizhov, and A. F. Bochkov. *In* MTP international review of science, organic chemistry series 1. Vol. 7. *Edited by* G. O. Aspinall. Butterworths, London and University Park Press, Baltimore. 1973.

7. J. GUERRERA and C. E. WEILL. Carbohydr. Res. **27**, 471 (1973).
8. A. KLEMER, H. LUKOWSKI, and F. ZERHUSEN. Chem. Ber. **96**, 1515 (1963).
9. E. F. J. L. ANET. Aust. J. Chem. **18**, 837 (1965).
10. G. O. ASPINALL and P. E. BARRON. Can. J. Chem. **51**, 388 (1972).
11. G. O. ASPINALL and A. S. CHAUDHURI. Can. J. Chem. This issue.
12. G. O. ASPINALL, T. N. KRISHNAMURTHY, I. FURDA, and R. KAHN. Can. J. Chem. This issue.
13. P. A. LEVENE and E. JORPES. J. Biol. Chem. **86**, 403 (1930).
14. G. R. BARKER. Methods Carbohydr. Chem. **1**, 168 (1962).
15. J. S. BRIMACOMBE. Methods Carbohydr. Chem. **6**, 376 (1972).

Can. J. Chem. Downloaded from www.nrcresearchpress.com by 210.87.254.105 on 09/05/12
For personal use only.

Base-catalyzed Degradations of Carbohydrates. X. Degradation by β-Elimination of Methylated Degraded Leiocarpan A[1]

GERALD O. ASPINALL[2] AND ATMARAM S. CHAUDHARI

Department of Chemistry, York University, Downsview, Toronto, Ontario M3J 1P3

Received March 18, 1975

GERALD O. ASPINALL and ATMARAM S. CHAUDHARI. Can. J. Chem. **53**, 2189 (1975).

Treatment of methylated degraded leiocarpan A with 1,5-diazabicyclo[5.4.0]undec-5-ene and acetic anhydride, followed by mild acid hydrolysis and de-*O*-acetylation, furnishes 3,4,6-tri-*O*-methyl-D-mannose and 3,4-di-*O*-methyl-6-*O*-(2,3,4-tri-*O*-methyl-β-D-xylopyranosyl)-D-mannose. The characterization of the methylated disaccharide provides evidence for the site of attachment and anomeric configuration of the D-xylopyranose end groups in the parent polysaccharide.

GERALD O. ASPINALL et ATMARAM S. CHAUDHARI. Can. J. Chem. **53**, 2189 (1975).

Le traitement de la forme méthylée du léiocarpan A dégradé avec le diaza-1,5 bicyclo[5.4.0]-undécène-5 et l'anhydride acétique, suivie d'une hydrolyse acide douce et d'une *O*-déacétylation, conduit aux composés 3,4,6-tri-*O*-méthyl-D-mannose et 3,4-di-*O*-méthyl-6-*O*-(2,3,4-tri-*O*-méthyl-β-D-xylopyrannosyl)-D-mannose. La caractérisation du disaccharide méthylé donne la preuve de la position d'attachement et de la configuration anomérique des groupes terminaux du *D*-xylopyrannose dans la polysaccharide mère.

Leiocarpan A, the major polysaccharide component of the gum exudate from *Anogeissus leiocarpus* contains interior chains of alternating 4-*O*-substituted β-D-glucuronic acid and 2-*O*-substituted α-D-mannopyranose residues (1–3). Previous studies on this polysaccharide showed that side chains of single D-xylopyranose and L-arabinofuranose are probably linked to 0–6 and 0–3, respectively, of some of the D-mannopyranose residues but the evidence was indirect and no information was available on the configuration of the glycosidic linkages. Since partial acid hydrolysis of leiocarpan A (1) and acetolysis of the carboxy-reduced polysaccharide (2) were shown to cause preferential liberation of the pentose sugars in the side chains we have now examined base-catalyzed degradation as an alternative approach to the isolation of oligosaccharides with intact side chains. Using procedures developed using model compounds (4) we describe here the base-catalyzed degradation of methylated degraded leiocarpan A.

Autohydrolysis of leiocarpan A has been shown to be a convenient procedure for the selective cleavage of L-arabinofuranose residues with only partial removal of D-xylopyranose end groups (2). Previous studies (2) established the identity of the component sugars of methylated degraded leiocarpan A. Quantitative analyses of the methylated sugars formed from reduced methylated degraded leiocarpan A (**1**) and from this reduced polysaccharide after remethylation of exposed hydroxyl groups by g.l.c. of the partially methylated alditol acetates (5) have now shown that the major components, 2,3,4-tri-*O*-methyl-D-xylose, 2,3-di-*O*-methyl-D-glucuronic acid, 3,4,6-tri- and 3,4-di-*O*-methyl-D-mannose, are present in the molar ratio of 2:5:3:2. Methylated degraded leiocarpan A was heated with DBU (1,5-diazabicyclo[5.4.0]undec-5-ene) and acetic anhydride in benzene in a sealed tube, the unsaturated hexuronate residues were cleaved by heating with aqueous acetic acid and de-*O*-acetylation gave two neutral sugar fractions which were separated chromatographically to give 3,4,6-tri-*O*-methyl-D-mannose (**2**) and the partially methylated disaccharide, 3,4-di-*O*-methyl-6-*O*-(2,3,4-tri-*O*-methyl-β-D-xylopyranosyl)-D-mannose (**3**) (Scheme 1). The structure of disaccharide **3** was assigned on the basis of the following observations: (*i*) methanolysis gave methyl glycosides of 2,3,4-di-*O*-methylxylose and and 3,4-di-*O*-methylmannose; (*ii*) hydrolysis, followed by reduction with borohydride and acetylation gave peracetates of 2,3,4-tri-*O*-methylxylitol and 3,4-di-*O*-methylmannitol; (*iii*)

[1]Presented in part at the Canadian Chemical Conference of the Chemical Institute of Canada, Regina, Saskatchewan June 3–5, 1974, and at the VII International Symposium on Carbohydrate Chemistry, Bratislava, Czechoslovakia, August 5–9, 1974.

[2]To whom enquiries should be addressed.

Can. J. Chem. Downloaded from www.nrcresearchpress.com by 210.87.254.105 on 09/05/12
For personal use only.

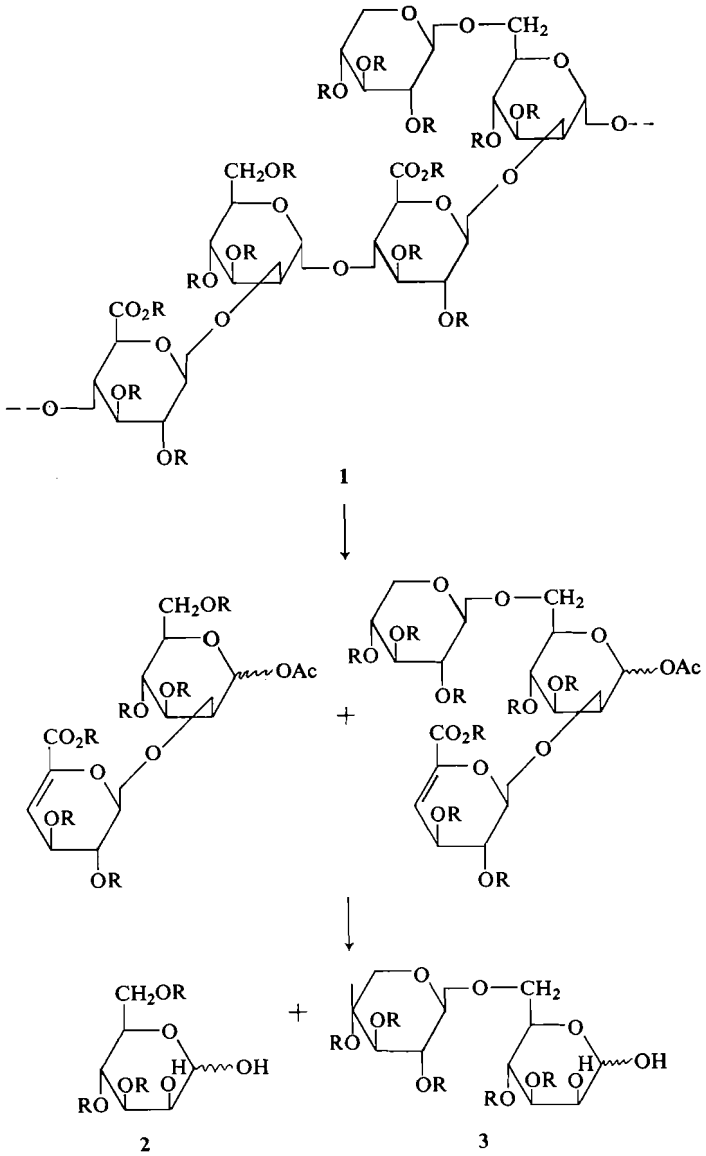

SCHEME 1. Degradation of methylated degraded leiocarpan A (R = CH_3).

reduction with borohydride, methanolysis, and acetylation gave methyl glycosides of 2,3,4-tri-*O*-methylxylose and 3,4-di-*O*-methylmannitol tetraacetate; (*iv*) reduction with borohydride gave a crystalline disaccharide alditol (**4**) which afforded a methylated derivative (**5**) whose n.m.r. spectrum showed a doublet (τ 5.70, J = 7 Hz) characteristic for H-1′ of a β-D-xyloside; (*v*) the mass spectra of methylated (**5**), trideuteriomethylated (**6**), and acetylated (**7**) derivatives whose mass spectra showed primary fragments (Scheme 2) and ions of the type **8**–**10** (6) which were consistent with the assigned structure. Of these derivatives the methylated (**5** and **6**) but not the acetylated (**7**) were sufficiently stable for examination by g.l.c. – mass spectrometry.

These experiments provide direct evidence for the site of attachment and for the glycosidic configuration of the D-xylopyranose end groups in leiocarpan A. The degradative procedure should be applicable to other similar structural problems in polysaccharide chemistry which have so

Can. J. Chem. Downloaded from www.nrcresearchpress.com by 210.87.254.105 on 09/05/12
For personal use only.

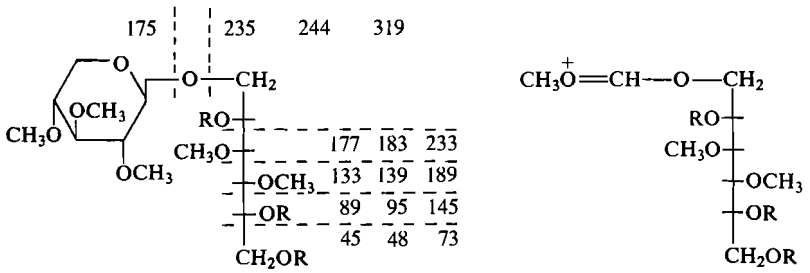

4 R = H
5 R = CH_3
6 R = CD_3
7 R = $COCH_3$

8 R = CH_3 *m/e* 295
9 R = CD_3 *m/e* 304
10 R = $COCH_3$ *m/e* 379

SCHEME 2. Mass spectral fragmentations of derivatives of 3,4-di-*O*-methyl-6-*O*-(2,3,4-tri-*O*-methyl-β-D-xylopyranosyl)-D-mannitol; *m/e* values are for ions from derivatives **5**, **6**, and **7**, respectively.

far resisted solution and relevant experiments are in progress. In the event that in some instances only limited quantities of methylated acidic polysaccharides might be available, the degradation was repeated using 30 mg[3] of methylated degraded leiocarpan A and the results gave clear information on the type, *i.e.* 1 → 6, but not on the configuration of the intact linkage in the disaccharide (**3**). The crude mixture of products from the methylated polysaccharide, without further purification, was reduced with sodium borohydride, portions of the derived alditols were methylated with (*a*) methyl iodide and (*b*) trideuteriomethyl iodide, and the resulting mixtures were analyzed directly by g.l.c. – mass spectrometry. The two major components gave mass spectra with characteristic fragment ions for hexa-*O*-methylmannitol (or its isotopically labelled derivative) and the methylated disaccharide alditol (**5** or **6**).

Experimental

Unless otherwise stated experimental conditions were as described in part VII (7).

Quantitative Analysis of Sugars from Reduced Methylated Degraded Leiocarpan A and its Remethylated Derivative

Reduced methylated degraded leiocarpan A (**2**) (20 mg) was further methylated with methyl iodide and sodium hydride in methyl sulfoxide (8) to give methylated reduced degraded leiocarpan A (16 mg), $[\alpha]_D$ −1° (*c*, 1.0 in chloroform) (Found: OMe, 42.5%), whose i.r. spectrum showed no hydroxyl absorption. Samples of both methylated polysaccharide derivatives were hydrolyzed, reduced with sodium borohydride, and acetylated to give mixtures of partially methylated alditol acetates (5) which were estimated and identified by g.l.c. on column *c* (see Table 1). Qualitative identification of the sugar components was also obtained by g.l.c. on column *a* of the methyl glycosides formed on methanolysis.

Base-catalyzed Degradation of Methylated Degraded Leiocarpan A

Methylated degraded leiocarpan A (300 mg) in benzene (12 ml) containing DBU (6 ml) and acetic anhydride (3 ml) was heated in a sealed tube at 100° for 24 h. A sample of the reaction product was washed with *M* hydrochloric acid and the benzene layer was washed with water, dried, and concentrated. The resulting syrup was methanolyzed and examination of the mixture of methyl glycosides by g.l.c. on column *a* showed the almost complete absence of derivatives of 2,3-di-*O*-methyl-glucuronic acid. The major part of the reaction product was chromatographed on a column of silica gel with chloroform–ethanol (9:1) as eluant. Coloring matter and much of the DBU was retained on the column, and the eluate was shaken with Amberlite resins IR-120(H) and IR-45(OH) and concentrated to a syrup (610 mg). The crude syrup was heated in aqueous 10% acetic acid at 100° for 1 h, acetic acid was removed by repeated evaporations after addition of water, and the residue was extracted with chloroform, dried, and concentrated. Methanolic sodium methoxide was added dropwise to the syrup (530 mg) in methanol until a permanent alkalinity was maintained and the solution was kept for 4 h, neutralized by treatment with Amberlite resin IR-120(H), and concentrated. The crude syrup (450 mg) was purified by preparative-layer chromatography to give a mixture (180 mg) of reducing sugars in which two major components were present. The syrup was adsorbed on a column (15 × 2.5 cm) of charcoal–Celite (1:1) and the column was eluted with water containing increasing proportions (up to 15%) of butanone. Although complete separation was not achieved subsequent preparative-layer chromatography on silica gel using chloroform–ethanol (9:1) as eluant gave chromatographically homogeneous samples of (*i*) 3,4,6-tri-*O*-methyl-D-mannose (45 mg), which was characterized by g.l.c. of the methyl glycoside on column *a* and of the derived alditol acetate on column *c*, and (*ii*) disaccharide **3** (42 mg), $[\alpha]_D$ −17° (*c*, 1.0 in methanol).

[3]Substantially smaller quantities could be used.

Can. J. Chem. Downloaded from www.nrcresearchpress.com by 210.87.254.105 on 09/05/12
For personal use only.

TABLE 1. Gas-liquid chromatography of methylated sugar derivatives from methylated polysaccharides

Sugar	Retention times: Methyl glycosides (column *a*)	Retention times: Alditol acetates (column *c*)	Methylated alditol acetates (mol%): Reduced methylated leiocarpan A	Methylated alditol acetates (mol%): Methylated reduced leiocarpan A
2,3,4-Me_3-xylose	0.42 0.56	0.65	14.9	15.1
2,3,4,6-Me_4-glucose	1.00 1.34	1.00		7.1
3,4,6-Me_3-mannose	2.48	1.98	25.4	22.8
2,3,4-Me_3-glucose	2.20 2.90	2.50	3.0	
2,3,6-Me_3-glucose	2.76 3.60			39.6
2,3-Me_2-glucose	7.6 9.8	5.50		
			56.3	
3,4-Me_2-mannose	5.1	5.50		15.5

TABLE 2. Relative abundances of fragment ions in the mass spectra of derivatives of partially methylated disaccharide alditol **4**

O-Methyl derivative **5**		*O*-Trideuteriomethyl derivative **6**		*O*-Acetyl derivative **7**	
m/e	Relative abundance*	*m/e*	Relative abundance*	*m/e*	Relative abundance*
295	6	304	5	379	4
235	18	244	13	319	22
177	8	183	7	233	4
175	30	175	30	175	30
133	12	139	13	189	19
89	36	95	48	145	7
45	35	48	51	73	13

*Relative abundances are quoted with reference to that of the 2,3,4-tri-*O*-methyl-D-xylopyranosyl ion (*m/e* 175) which is common to each spectrum.

Characterization of 3,4-Di-O-methyl-6-O-(2,3,4-tri-O-methyl-β-D-xylopyranosyl)-D-mannose (3)

Methanolysis of the disaccharide gave compounds which had the retention times of methyl glycosides of 2,3,4-tri-*O*-methylxylose (*T* 0.48, 0.55) and 3,4-di-*O*-methylmannose (*T* 5.53) on column *a*. Hydrolysis of the disaccharide, followed by reduction with sodium borohydride and acetylation, gave compounds with the retention times of the peracetates of 2,3,4-tri-*O*-methylxylitol (*T* 0.65) and 3,4-di-*O*-methylmannitol (*T* 5.5) on column *c*. Reduction of the disaccharide with sodium borohydride, followed by methanolysis and acetylation, furnished compounds with the retention times of methyl glycosides of 2,3,4-tri-*O*-methylxylose (*T* 0.48, 0.55 on column *a*) and 3,4-di-*O*-methylmannitol tetraacetate (*T* 5.5 on column *c*).

Reduction of disaccharide **3** (30 mg) with sodium borohydride followed by normal work-up furnished 3,4-di-*O*-methyl-6-*O*-(2,3,4-tri-*O*-methyl-β-D-xylopyranosyl)-D-mannitol (**4**) (27 mg), m.p. 116–118°, $[\alpha]_D$ −20° (*c*, 1.0 in methanol).

Anal. Calcd. for $C_{16}H_{32}O_{10}$: OMe, 40.37. Found: OMe, 40.66.

The disaccharide alditol **4** (20 mg) was methylated with methyl iodide and sodium hydride in *N,N*-dimethylformamide (9) to give 1,2,3,4,5-penta-*O*-methyl-6-*O*-(2,3,4-tri-*O*-methyl-β-D-xylopyranosyl)-D-mannitol (**5**) (19 mg), $[\alpha]_D$ −17° (*c*, 1.0 on methanol); n.m.r. ($CDCl_3$): τ 5.75 (1-proton doublet, $J_{1',2'}$ = 8 Hz, H-1'), 6.37–6.55 (overlapping 3-proton singlets, 8 × OCH_3). The disaccharide alditol **4** was similarly converted into the 1,2,5-tri-*O*-(trideuteriomethyl) derivative **6**. Treatment of the disaccharide alditol **4** with acetic anhydride in pyridine under standard conditions furnished the 1,2,5-tri-*O*-acetyl derivative **7**. The relative intensities of the structurally significant fragment ions (see Scheme 2) observed in the mass spectra of the *O*-methyl (**5**), *O*-trideuteriomethyl (**6**), and *O*-acetyl (**7**) derivatives are shown in Table 2.

Base-catalyzed Degradation of Methylated Degraded Leiocarpan A and Direct Characterization of Products by Gas-Liquid Chromatography – Mass Spectrometry

Methylated degraded leiocarpan A (30 mg) in benzene (1.2 ml) containing DBU (0.6 ml) and acetic anhydride (0.3 ml) was heated in a sealed tube at 100° for 24 h. The reaction product was washed with *M* hydrochloric acid and the benzene layer was washed with water, dried, and concentrated. The resulting syrup was heated with aqueous acetic acid, de-*O*-acetylated with sodium methoxide, and reduced with sodium borohydride as described previously. One portion of the product was methylated with methyl iodide and sodium hydride in *N,N*-dimethylformamide (9) and a second portion was similarly treated

Can. J. Chem. Downloaded from www.nrcresearchpress.com by 210.87.254.105 on 09/05/12
For personal use only.

with trideuteriomethyl iodide. Examination of each reaction produced by g.l.c. – mass spectrometry using column *b* showed two major components with the retention times of hexa-*O*-methylmannitol and the methylated disaccharide alditol **5** (and 6). The former gave mass spectra with characteristic fragment ions and the mass spectra of the methylated disaccharide alditols **5** and **6** were indistinguishable from those of the previously examined samples.

The authors acknowledge financial support from the National Research Council of Canada.

1. G. O. ASPINALL, J. J. CARLYLE, J. M. MCNAB, and A. RUDOWSKI. J. Chem. Soc. C, 840 (1969).
2. G. O. ASPINALL and J. M. MCNAB. J. Chem. Soc. C, 845 (1969).
3. G. O. ASPINALL and J. J. CARLYLE. J. Chem. Soc. C, 851 (1969).
4. G. O. ASPINALL, T. N. KRISHNAMURTHY, W. MITURA, and M. FUNABASHI. Can. J. Chem. This issue.
5. H. BJÖRNDAL, C. G. HELLERQVIST, B. LINDBERG, and S. SVENSSON. Angew. Chem. Internat. Ed. **9**, 610 (1970).
6. O. S. CHIZHOV, L. A. POLYAKOVA, and N. K. KOCHETKOV. Doklady Akad. Nauk SSSR, **158**, 685 (1964).
7. G. O. ASPINALL, T. N. KRISHNAMURTHY, I. FURDA, and R. KHAN. Can. J. Chem. This issue.
8. P. A. SANDFORD and H. E. CONRAD. Biochemistry, **5**, 1508 (1966).
9. J. S. BRIMACOMBE. Methods Carbohydr. Chem. **6**, 376 (1972).

Can. J. Chem. Downloaded from www.nrcresearchpress.com by 210.87.254.105 on 09/05/12
For personal use only.

The Stereochemical Basis of Anticonvulsant Drug Action. V. The Crystal and Molecular Structure of Sulthiame[1]

ARTHUR CAMERMAN
Departments of Medicine (Neurology) and Pharmacology, University of Washington, Seattle, Washington 98195
AND
NORMAN CAMERMAN
Department of Biochemistry, University of Toronto, Toronto, M5S 1A8

Received January 30, 1975

ARTHUR CAMERMAN and NORMAN CAMERMAN. Can. J. Chem. **53**, 2194 (1975).

The crystal and molecular structure of sulthiame, (*N*-[4′-sulfamylphenyl]-1,4-butansultam), one of a series of carbonic anhydrase inhibitors that have gained wide use as antiepileptic agents, has been determined in order to compare the stereochemistry of this compound to that of other antiepileptics. Crystals of sulthiame are orthorhombic, space group $Pca2_1$, with cell dimensions $a = 8.267$, $b = 17.750$, $c = 8.651$ Å. The structure was determined by Patterson and Fourier methods and refined to a final R value of 0.039.

Sulthiame molecular conformation differs markedly from that of diphenylhydantoin and other anticonvulsant drugs, suggesting a different mechanism of action for this compound. If the sulfonamide group is removed from sulthiame, however, the resulting molecule, although no longer a carbonic anhydrase inhibitor, does retain weak antiepileptic activity and does bear a weak conformational resemblance to the other noncarbonic anhydrase inhibitor anticonvulsant drugs.

ARTHUR CAMERMAN et NORMAN CAMERMAN. Can. J. Chem. **53**, 2194 (1975).

On a déterminé la structure cristalline et moléculaire du sulthiame (*N*-[sulfamyl-4 phényl]-butanesultame-1,4), l'un des inhibiteurs de l'anhydrase carbonique qui a connu un gain d'intérêt comme agent antiépileptique; nos études ont été entreprises afin de comparer la stéréochimie de ce composé avec celle d'autres antiépileptiques. Les cristaux de sulthiame sont orthorhombiques, groupe d'espace $Pca2_1$; les dimensions de la maille sont: $a = 8.267$, $b = 17.750$ et $c = 8.651$ Å. La structure, déterminée par les méthodes de Patterson et Fourier, a été affinée jusqu'à une valeur de R de 0.039.

La configuration moléculaire du sulthiame diffère considérablement de celle de la diphénylhydantoine et d'autres médicaments anticonvulsifs; cette différence suggère que le mécanisme d'action de ce composé est différent. Si l'on enlève le groupe sulfonamide du sulthiame, la molécule qui en résulte n'est plus un inhibiteur de l'anhydrase carbonique; toutefois elle possède encore une faible activité comme antiépileptique et ressemble vaguement, au point de vue conformationnel, aux autres médicaments anticonvulsifs qui ne sont pas des inhibiteurs d'anhydrase carbonique. [Traduit par le journal]

Introduction

Sulthiame, (*N*-[4′-sulfamylphenyl]-1,4-butansultam) (Ospolot, Conadil; Fig. 2), is one of a group of sulfonamide carbonic anhydrase inhibitors that have been shown to possess anticonvulsant activity. It has been widely and successfully used in Europe, particularly for the treatment of psychomotor epilepsy, usually as an adjunct medication with other antiepileptic drugs. A recent double-blind clinical study (2) suggests, however, that sulthiame is much less useful than diphenylhydantoin (DPH) as a primary anticonvulsant and is of questionable value as a second agent in mixed drug therapy.

It has been demonstrated that the antiepileptic activities of sulfonamide compounds such as acetazolamide and sulthiame are due to inhibition of brain carbonic anhydrase (3–5) with a possible mechanism involving a buildup of excess carbon dioxide which inhibits nerve conduction (6). If this is so, then these compounds act differently from antiepileptic drugs such as diphenylhydantoin and phenobarbital which do not inhibit carbonic anhydrase.

Hansen *et al.* (7) found that when sulthiame is administered to patients already receiving DPH it elevates serum levels of DPH. Olesen

[1]For part IV see ref. 1.

Can. J. Chem. Downloaded from www.nrcresearchpress.com by 84.22.46.98 on 09/08/12
For personal use only.

Can. J. Chem. Downloaded from www.nrcresearchpress.com by 84.22.46.98 on 09/08/12
For personal use only.

and Jensen (8) confirmed these findings but found no alteration in the rate of degradation of DPH. They suggest that a possible cause of the rise of DPH serum levels may be displacement by sulthiame of DPH from storage depots in the erythrocytes.

As part of our investigations of the stereochemistries of antiepileptic drugs (1, 9–11) we have elucidated the crystal structure of sulthiame so that we may compare the three-dimensional molecular conformation of this compound with those of other anticonvulsant agents.

Methods

Sulthiame powder was dissolved in water, NaOH was added to attain a basic p*H*, and colorless lath-shaped crystals were obtained by solvent evaporation. Cell dimensions and space group information were determined from X-ray photographs and diffractometer measurements; crystal data are listed in Table 1. Intensities were measured on a four-circle automated diffractometer using $\omega/2\theta$ scan technique and Nb-filtered Mo radiation on a crystal approximately $0.10 \times 0.17 \times 0.30$ mm in size. The intensities of all independent reflections with $0 < 2\theta$ (MoKα) $\leq 55°$, corresponding to an interplanar spacing of 0.77 Å, were recorded; of the 1566 reflections in this range, 1333 had intensities-above-background greater than twice their standard deviations. These were classified as observed and subsequently used in structure refinement. Structure amplitudes were obtained in the usual fashion; weights were taken as $w^{1/2} = 1/\sigma_F$. No absorption corrections were applied.

Structure Determination

One sulfur atom was located in a three-dimensional origin-removed sharpened Patterson map and a Fourier synthesis phased from that atomic position showed the locations of the second sulfur and one oxygen atom. The rest of the nonhydrogen atoms were iteratively located from additional Fourier maps phased from successively determined atom positions. The first postulated structure gave a discrepancy factor, *R*, of 0.33 which decreased to 0.14 after two cycles of full-matrix least-squares refinement with individual isotropic thermal parameters and to 0.07 in two cycles with anisotropic thermal parameters. The function minimized was $\sum w(|F_o| - |F_c|)^2$. The 14 hydrogen atoms were located from difference electron-density maps and further least-squares refinement of all atoms with anisotropic thermal parameters for the nonhydrogen atoms and isotropic ones for the hydrogens reduced *R* to 0.039 and $(\sum w(\Delta F)^2/(m - n))^{1/2}$ to 1.58.

Atomic parameters for the nonhydrogen atoms are listed in Table 2, in which the U_{ij}'s are coefficients in the expression

$$\exp[-2\pi^2(h^2U_{11}a^{*2} + \ldots + 2klU_{23}b^*c^*)]$$

Atomic parameters for the hydrogen atoms are listed in Table 3. The table of observed and calculated structure factors is available.[2] Scattering factors used for sulfur (13), hydrogen (14), and the other atoms (15), are as cited. Anomalous dispersion corrections were applied to the sulfur scattering factors.

TABLE 1. Crystal data for sulthiame

Formula	$C_{10}H_{14}N_2O_4S_2$
Molecular weight	290.37
Crystal system	Orthorhombic
a (Å)	8.267 ± 0.002
b (Å)	17.750 ± 0.004
c (Å)	8.651 ± 0.002
V (Å^3)	1269.44
Z	4
D_x (g cm^{-3})	1.52
F(000)	608
Space group	$Pca2_1$
μ (for MoKα) (cm^{-1})	4.1
λ (MoKα) (Å)	0.7107

Results and Discussion

Molecular Structure

The three-dimensional conformation of sulthiame in the crystal is shown by a stereoscopic drawing in Fig. 1. The saturated heterocyclic ring is in the chair conformation and the phenyl ring is planar. Bond lengths and angles are displayed in Fig. 2. Estimated standard deviations are 0.003–0.006 Å and 0.2–0.4° for the bonds and angles, respectively. There are two bond distances in sulthiame which are significantly short and bear special comment. The N(2)—C(9) distance of 1.431 Å suggests there is some double bond character in that bond. There does not appear to be extension of phenyl ring electron delocalization to include S(15); the C(12)—S(15) distance of 1.773 Å is a normal single bond and matches the value for the S(1)—C(6) bond. The second short bond distance is S(15)—N(18) (1.611 Å). This length is considerably shorter than the normal single bond value of 1.67–1.68 Å and indicates electron delocalization within the sulfonamide group. In contrast, the S(1)—N(2) bond distance is 1.670 Å, indicating no double bond character between those atoms.

Comparison with Other Anticonvulsants

In earlier studies in this series we have shown that the molecular conformations of diphenyl-

[2]Tables of final observed and calculated structure factors are available, at a nominal charge, from the Depository of Unpublished Data, CISTI, National Research Council of Canada, Ottawa, Canada K1A 0S2.

TABLE 2. Fractional coordinates and anisotropic thermal parameters ($\times 10^2$)[a]

Atom	x	y	z	U_{11}	U_{22}	U_{33}	U_{12}	U_{13}	U_{23}
S(1)	0.1102(1)	0.1060(1)	0.0	3.95	3.15	3.29	0.10	0.29	−0.13
N(2)	0.1078(4)	0.1898(2)	0.0881(4)	3.04	3.26	4.01	0.29	0.24	−0.72
C(3)	−0.0598(5)	0.2168(2)	0.1191(6)	3.62	4.54	5.87	−0.10	0.43	−1.45
C(4)	−0.1415(5)	0.1649(2)	0.2342(6)	3.87	6.11	5.95	−0.27	1.41	−1.33
C(5)	−0.1559(5)	0.0842(3)	0.1785(6)	5.34	5.57	4.80	−1.17	0.22	−0.39
C(6)	0.0096(5)	0.0510(2)	0.1425(6)	4.38	4.12	3.97	−0.63	0.16	0.48
O(7)	0.2761(3)	0.0835(1)	−0.0159(4)	4.12	3.92	6.38	0.97	1.08	−0.22
O(8)	0.0130(3)	0.1077(1)	−0.1369(3)	6.39	5.51	3.00	−0.14	−0.41	−0.26
C(9)	0.2242(4)	0.2439(2)	0.0360(5)	3.51	3.26	3.53	0.40	0.07	−0.82
C(10)	0.1807(5)	0.3065(2)	−0.0503(5)	3.47	4.53	4.75	0.26	−1.12	−0.09
C(11)	0.2955(5)	0.3596(2)	−0.0914(5)	5.50	3.41	3.98	0.54	−0.31	0.73
C(12)	0.4538(5)	0.3496(2)	−0.0460(5)	4.28	3.42	3.44	−0.32	0.22	0.18
C(13)	0.4978(5)	0.2879(2)	0.0410(5)	3.47	5.33	4.55	0.07	−0.52	0.38
C(14)	0.3838(5)	0.2344(2)	0.0835(5)	4.30	3.69	4.13	−0.01	−0.46	0.59
S(15)	0.6063(1)	0.4140(1)	−0.1032(2)	5.56	4.66	4.12	−1.24	0.90	0.15
O(16)	0.5406(5)	0.4620(2)	−0.2170(4)	9.11	10.07	7.68	−3.68	−2.47	5.10
O(17)	0.7480(5)	0.3720(2)	−0.1399(5)	6.32	6.76	12.27	−0.71	4.51	−1.40
N(18)	0.6509(6)	0.4654(3)	0.0441(5)	7.50	5.47	6.12	−2.13	0.43	−0.39

[a]Estimated standard deviations are given in parentheses.

TABLE 3. Hydrogen atom fractional coordinates and isotropic thermal parameters ($\times 10^2$)[a]

Atom	x	y	z	U	Atom	x	y	z	U
H(3.1)	−0.117(4)	0.211(2)	0.024(5)	4.8	H(6.2)	0.083(5)	0.049(2)	0.237(6)	5.8
H(3.2)	−0.039(5)	0.274(3)	0.158(5)	7.0	H(10)	0.086(4)	0.310(2)	−0.084(4)	3.1
H(4.1)	−0.070(4)	0.170(2)	0.343(5)	5.4	H(11)	0.269(5)	0.400(2)	−0.148(5)	4.6
H(4.2)	−0.248(5)	0.184(2)	0.265(4)	3.7	H(13)	0.583(5)	0.278(3)	0.067(6)	7.3
H(5.1)	−0.208(5)	0.048(2)	0.267(5)	4.6	H(14)	0.412(3)	0.192(2)	0.141(3)	2.5
H(5.2)	−0.214(4)	0.083(2)	0.081(5)	3.7	H(18.1)	0.564(5)	0.495(3)	0.031(6)	7.4
H(6.1)	0.004(5)	0.006(3)	0.093(5)	4.9	H(18.2)	0.705(8)	0.433(3)	0.104(8)	11.4

[a]Estimated standard deviations are given in parentheses.

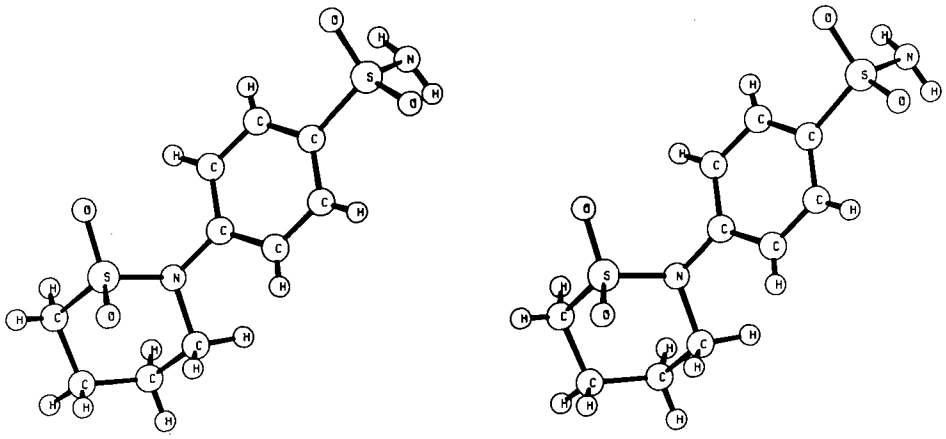

FIG. 1. Three-dimensional molecular conformation of sulthiame illustrated by a stereoscopic drawing.

Can. J. Chem. Downloaded from www.nrcresearchpress.com by 84.22.46.98 on 09/08/12
For personal use only.

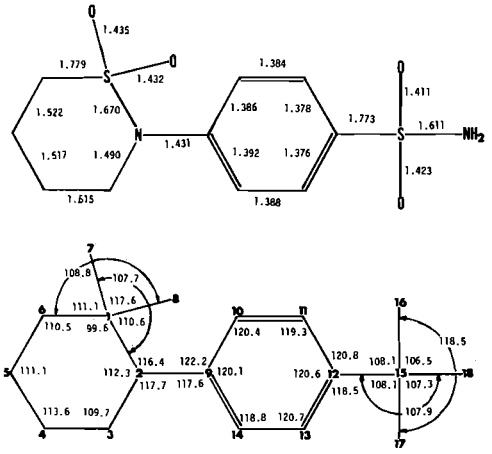

FIG. 2. Bond distances (Å) and valency angles (deg) in sulthiame.

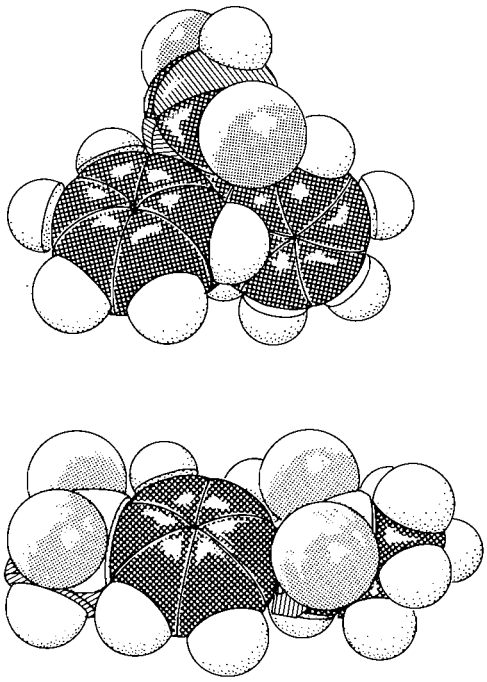

FIG. 3. Space filling models of sulthiame and diphenylhydantoin (top).

hydantoin, diazepam, procyclidine, and trihexyphenidyl bear specific structural resemblances to one another. They all contain two hydrophobic rings (phenyl or cyclohexyl) and two electron-donating or hydrogen-bondable atoms (oxygen or nitrogen). When the drugs' three-dimensional structures are compared these chemical groups occupy similar orientations and positions in space: thus these are conformational features which may be necessary for anticonvulsant activity (12).

The three-dimensional molecular conformation of sulthiame, as a whole, is not strikingly similar to the conformations of the other drugs studied in this series and thus is not suggestive of a mechanism of anticonvulsant action for sulthiame similar to that of the diphenylhydantoin type of antiepileptic. These results are wholly consistent with the accumulated evidence that links the anticonvulsant properties of sulthiame and other sulfonamides with their ability to inhibit brain carbonic anhydrase, a property not shared by diphenylhydantoin and the other anticonvulsant drugs we have studied. Figure 3 shows a comparison of a space-filling model of sulthiame constructed from the crystallographic structure with a similar model constructed for diphenylhydantoin. Although it is obvious that the structural features common to the other antiepileptic drugs we have previously studied are not found in sulthiame, it is equally noticeable that if the sulfonamide group were removed from sulthiame, similarity to diphenylhydantoin would be increased: there is then a slight similarity between the location and orientation in space of the phenyl and saturated heterocyclic groups (both hydrophobic) and one of the oxygen atom positions between them of sulthiame, and the two (hydrophobic) phenyl rings with the ketonic oxygen between them of DPH. Removal of the sulfonamide group from sulthiame destroys the carbonic anhydrase inhibitory properties of the molecule, of course, and therefore its anticonvulsant properties via the brain carbonic anhydrase inhibition mechanism. Tanimukai *et al.* (5) compared carbonic anhydrase inhibitory effect and anticonvulsant activity of four aromatic compounds, including sulthiame, with and without the sulfonamide group. They found that sulthiame alone exhibits a weak anticonvulsant effect when the sulfonamide group is removed. As this effect can no longer be ascribed to inhibition of carbonic anhydrase and because of the slight resemblances (Fig. 3) in molecular conformation between diphenylhydantoin and phenylbutansultam (sulthiame with the sulfonamide group removed) it is possible that the weak anticonvulsant

Can. J. Chem. Downloaded from www.nrcresearchpress.com by 84.22.46.98 on 09/08/12
For personal use only.

Can. J. Chem. Downloaded from www.nrcresearchpress.com by 84.22.46.98 on 09/08/12
For personal use only.

TABLE 4. Distances (Å) between cyclic group centroids and oxygen atoms in diphenylhydantoin (DPH) and phenylbutansultam (PBS)

	DPH	PBS
Ring(1)–Ring(2)	4.84	4.29
Ring(1)–Atom(1)	5.68	4.46
Ring(1)–Atom(2)	3.97	3.83
Ring(2)–Atom(1)	5.51	2.35
Ring(2)–Atom(2)	4.23	2.91
Atom(1)–Atom(2)	4.56	2.45

activity of this latter compound is achieved through a mechanism similar to that of the diphenylhydantoin type of antiepileptic drug. We have calculated the distances between the centroids of the two ring groups in phenylbutansultam and the oxygen atoms bonded to the ring sulfur and compared them with distances between phenyl ring centroids and ketonic oxygens in diphenylhydantoin. The comparison is shown in Table 4. There is moderate similarity between the two compounds in those distances involving the phenyl ring of phenylbutansultam but not in those involving the other ring. Since, however, compounds with only one phenyl group such as 5-phenyl-5-ethylhydantoin possess some anticonvulsant activity, it is likely that the moderate conformational similarities involving one ring and the oxygen atoms between DPH and phenylbutansultam, without the large stereochemical dissimilarity caused by the sulfonamide group, are enough to effect phenylbutansultam's weak anticonvulsant properties.

The slight resemblance in stereochemical features between phenylbutansultam and DPH may also be responsible for sulthiame's action in elevating serum DPH levels in patients receiving both drugs. A hypothesis wherein conformational similarities allow a metabolite of sulthiame without the sulfonamide moiety (or even sulthiame itself with the sulfonamide adding increasing binding by interaction with additional parts of the receptor) to diplace DPH from a storage receptor in the erythrocytes or tissues is consistent with the conclusions of Olesen and Jensen (8).

To summarize, we have found little similarity in three-dimensional molecular conformation between sulthiame and the diphenylhydantoin type of antiepileptic. These findings reinforce the pharmacological evidence for different mechanisms for the anticonvulsant activities of these drugs and are consistent with the close parallels between anticonvulsant activity and brain carbonic anhydrase inhibition properties of the sulfonamide drugs. However, the fact that phenylbutansultam is a weak anticonvulsant and our findings that this molecule shares some of the conformation properties we have found in common among other antiepileptics bolsters our previous evidence that these stereochemical features are important for a drug to possess activity against grand mal epilepsy.

This work was supported in part by U.S.P.H.S. research grant NS 09-839-02 BBCA from the N.I.N.D.S. and in part by a grant from the Epilepsy Foundation of America. A.C. is the recipient of a Research Career Development Award from the National Institutes of Health.

1. N. CAMERMAN and A. CAMERMAN. J. Am. Chem. Soc. **94**, 8553 (1972).
2. J. R. GREEN, A. S. TROUPIN, L. M. HALPERN, P. FRIEL, and P. KANAREK. Epilepsia. In press.
3. J. G. MILLICHAP, D. M. WOODBURY, and L. S. GOODMAN. J. Pharmacol. **115**, 251 (1955).
4. T. NISHIMURA. Psychiat. Neurol. Jap. **65**, 523 (1963).
5. H. TANIMUKAI, M. INUI, S. HARIGUCHI, and Z. KANEKO. Biochem. Pharmacol. **14**, 961 (1965).
6. T. NISHIMURA, H. TANIMUKAI, and K. NICHINUMA. J. Neurochem. **10**, 257 (1963).
7. J. M. HANSEN, M. KRISTENSEN, and L. SKOVSTED. Epilepsia, **9**, 17 (1968).
8. O. V. OLESEN and O. N. JENSEN. Dan. Med. Bull. **16**, 154 (1969).
9. A. CAMERMAN and N. CAMERMAN. Acta Cryst. B **27**, 2205 (1971).
10. A. CAMERMAN and N. CAMERMAN. J. Am. Chem. Soc. **94**, 268 (1972).
11. N. CAMERMAN and A. CAMERMAN. Mol. Pharmacol. **7**, 406 (1971).
12. A. CAMERMAN and N. CAMERMAN. Science, **168**, 1457 (1970).
13. B. DAWSON. Acta Cryst. **13**, 403 (1960).
14. R. F. STEWART, E. R. DAVIDSON, and W. T. SIMPSON. J. Chem. Phys. **42**, 3175 (1965).
15. J. BERGHUIS, I J. HAANAPPELL, M. POTTERS, B. O. LOOPSTRA, C. A. MACGILLAVRY, and A. L. VEENENDAAL. Acta Cryst. **8**, 478 (1955).

Autoxidation and Photooxidation of 1,3-Diphenylisobenzofuran: A Kinetic and Product Study[1]

JAMES A. HOWARD AND G. DAVID MENDENHALL[2]

Division of Chemistry, National Research Council of Canada, Ottawa, Canada K1A 0R9

Received January 20, 1975

JAMES A. HOWARD and G. DAVID MENDENHALL. Can. J. Chem. 53, 2199 (1975).

Photooxidation of 1,3-diphenylisobenzofuran (DPBF) in aromatic solvents at 30° gives a monomeric peroxide along with minor amounts of *o*-benzylphenyl benzoate, whereas in CCl_4 *o*-dibenzoylbenzene is the principal reaction product. 1,3-Diphenylisobenzofuran is very susceptible to autoxidation at this temperature $(k_p/(2k_t)^{1/2} = 4\ M^{-1/2}\ s^{-1/2}$, $k_p \sim 10^5\ M^{-1}s^{-1}$, $2k_t \sim 5 \times 10^8\ M^{-1}s^{-1})$ yielding a polyperoxide (50%) and *o*-dibenzoylbenzene (35%). Clearly, in the absence of appropriate control experiments, neither rapid disappearance of DPBF nor production of *o*-dibenzoylbenzene are sufficient to prove the intermediacy of singlet delta oxygen during molecular oxygen oxidations.

JAMES A. HOWARD et G. DAVID MENDENHALL. Can. J. Chem. 53, 2199 (1975).

La photo-oxydation du diphényl-1,3 isobenzofuranne (DPBF) dans les solvants aromatiques à 30° conduit à un peroxyde monomère ainsi qu'à une faible quantité de benzoate de *o*-benzylphényle, tandis que dans le CCl_4 le produit principal de la réaction est le *o*-dibenzoylbenzène. A cette température, le diphényl-1,3 isobenzofuranne est sensible à l'autoxidation $(k_p/(2k_t)^{1/2} = 4\ M^{-1/2}\ s^{-1/2}$, $k_p \sim 10^5\ M^{-1}\ s^{-1}$, $2k_t \sim 5 \times 10^8\ M^{-1}s^{-1})$ ce qui conduit à un polyperoxyde (50%) et au *o*-dibenzoylbenzène (35%). Clairement, en l'absence d'un contrôle approprié, ni la disparition rapide du DPBF ni la production de *o*-dibenzoylbenzène suffisent à démontrer qu'il se forme un intermédiaire oxygène dans l'état singulet delta au cours des oxydations par l'oxygène moléculaire. [Traduit par le journal]

Introduction

1,3-Diphenylisobenzofuran (DPBF) is a popular substrate for photooxidation studies in the liquid phase because of the rapidity with which it reacts with electronically excited singlet delta oxygen ($^1\Delta_g$). There have been several determinations of absolute rate constants for this reaction and it would appear that the 'best' values lie in the range 6–8 × $10^8\ M^{-1}s^{-1}$ (1). It is generally accepted that $^1O_2$ undergoes a 1,4-addition to DPBF to give the *endo*-peroxide **1** which decomposes at ambient temperature to give *o*-dibenzoylbenzene (ODB) (2–7).

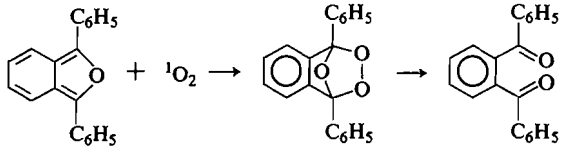

DPBF **1** ODB

Chemical evidence for the intermediacy of $^1O_2$ during photooxidation is based, with the appropriate control experiments, on the rapid disappearance of DPBF and/or the production of ODB.

We have recently conducted a thorough kinetic and product study of the autoxidation and photooxidation of DPBF at 30° in the liquid phase. The results of this work and its relevance to diagnostic tests for the intermediacy of singlet oxygen during molecular oxygen oxidations are reported here.

Experimental

1,3-Diphenylisobenzofuran (Aldrich) was purified by recrystallization or zone refining. The solvents (CCl_4, C_6H_6, and *tert*-butylbenzene) were distilled before use.

Oxygen absorptions were followed with the automatic recording apparatus described previously (8). All reactions were performed in solution at 30°. Autoxidations were initiated by thermal decomposition of α,α′-azobisisobutyronitrile (AIBN). Photooxidations were carried out in the presence of the radical scavenger 2,6-di-*tert*-butyl-4-methylphenol with light of a λ > 500 nm.

Polyperoxides were isolated by slow addition of autoxidized DPBF to *n*-pentane and yields were determined by weight. The composition of the polymer depended on the autoxidation chain length (v). For example, autoxidation of DPBF (0.015 *M*) initiated by AIBN (0.036 *M*), v = 1300, gave a polyperoxide with a molecular weight of 1350 ± 50, a m.p. of 127.5–128.5°, and an elemental

[1]NRCC No. 14661.

[2]NRCC Postdoctorate Fellow, 1971–1973. Present address: Battelle, Columbus Laboratories, 505 King Avenue, Columbus, Ohio 43201.

Can. J. Chem. Downloaded from www.nrcresearchpress.com by 210.87.254.42 on 09/05/12
For personal use only.

TABLE 1. Kinetic data for autoxidation of DPBF at 30° and 710 Torr

$[DPBF]_0$ (M)	[AIBN] (M)	$10^8 R_i$ ($M\ s^{-1}$)	$10^6(-d[O_2]/dt)_0$ ($M\ s^{-1}$)	ν	$k_p/(2k_t)^{1/2}$ ($M^{-1/2}\ s^{-1/2}$)
0.015	0.012	0.10	1.55	1550	3.3
0.015*	0.012	0.10	1.55	1550	3.3
0.015	0.036	0.3	4.0	1300	4.9
0.015	0.12	1.0	6.65	665	4.4
0.0004	0.085	0.77	—	—	4.0†

*P_{O_2} = 363 Torr.
†This ratio was obtained by following the disappearance of DPBF spectrophotometrically (λ = 413 nm) in the presence of a large excess of oxygen ($\sim 10^{-2}$ M).

analysis of C = 80.54, H = 4.98, and N = 0.62. Yields of *o*-dibenzoylbenzene and *o*-benzoylphenyl benzoate were determined from the intensities of the carbonyl absorptions in the i.r.

Attempts to prepare an analytically pure sample of DPBF endoperoxide were unsuccessful. An elemental analysis of a fraction with a measured molecular weight of 290 ± 10 gave C = 81.1, H = 5.15 whereas the theoretical analysis is C = 79.4, H = 4.67.

The absolute termination rate constant for autoxidation of DPBF was determined from the steady-state peroxy radical concentration and the rate of chain initiation by electron spin resonance techniques (9).

Results and Discussion

Autoxidation

Le Berre and Ratsimbazafy (10) reported that the self-initiated autoxidation of DPBF in the dark at ambient temperatures yielded a polymeric peroxide with a molecular weight of 2630. We found that solutions of DPBF did not absorb oxygen in the dark in the absence of a free radical initiator at 30°. Kinetic chain lengths were, however, very long when autoxidation was initiated by AIBN. Overall rates of autoxidation were found to fit the general kinetic expression for hydrocarbon autoxidation

$$\frac{-d[O_2]}{dt} = \frac{k_p[RH]R_i^{1/2}}{(2k_t)^{1/2}}$$

where k_p and $2k_t$ are the rate controlling propagation and termination rate constants, R_i is the rate of chain initiation, and [RH] is the substrate concentration. Kinetic data for autoxidation are given in Table 1. The oxidizability of DPBF at 30° is 4 $M^{-1/2}\ s^{-1/2}$ and since $2k_t$ is $\sim 5 \times 10^8$ $M^{-1}\ s^{-1}$ the reactivity of DPBF to its own peroxy radical is $\sim 10^5$ $M^{-1}\ s^{-1}$. Solutions of DPBF are, therefore, susceptible to autoxidation because of the high reactivity of this substrate to peroxy radicals (*cf.* cyclohexa-1,3-diene which has a homopropagation rate constant of 800 $M^{-1}\ s^{-1}$ at 30° (11)).

DPBF (0.015 M) in *t*-butylbenzene containing AIBN (0.036 M) absorbed 0.012 M of O_2 to give a polyperoxide (50%) and *o*-dibenzoylbenzene (35%). Molecular weight determinations and elemental analyses indicated that the polymer had structure **2** with n = 4–5. The

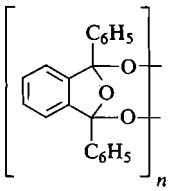

2

low molecular weight of the polyperoxide relative to the kinetic chain length is probably the result of 0—0 bond cleavage during autoxidation, a common characteristic of polymerizable olefin autoxidation (12). This was supported by the observation that a sample of polyperoxide dissolved in benzene had a half-life of ~72 h at 50° and thermolyzed to give ODB (1 mol per mol of polymer).

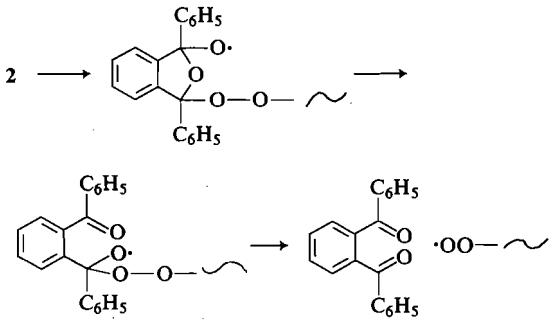

Photooxidation

Dufraisse and Ecary (13) reported that photooxidation of DPBF yielded a crystalline *endo*-peroxide which was stable for several hours at −78° but which exploded when the temperature

Can. J. Chem. Downloaded from www.nrcresearchpress.com by 210.87.254.42 on 09/05/12
For personal use only.

Can. J. Chem. Downloaded from www.nrcresearchpress.com by 210.87.254.42 on 09/05/12
For personal use only.

was raised to 18°. We found, however, that the principal stable photooxidation products at 30° depend on the nature of the solvent.

In aromatic solvents, such as benzene and *tert*-butylbenzene, less than 10% of the reaction product contained the carbonyl function(s). The principal product was a white crystalline material which liberated 1 equiv. of iodine from acidified KI and was reduced to ODB by 1 equiv. of triphenylphosphine. The molecular weight of this material and the stoichiometry of the reaction were consistent with a 1 : 1 adduct between oxygen and DPBF. We feel confident that this compound is the *endo*-peroxide **1** although elemental analyses were unsatisfactory. Thermal decomposition of **1** in *tert*-butylbenzene at 20° indicated that it had a $t_{1/2}$ of 100 h at this temperature in this solvent.

The principal minor product was *o*-benzoylphenyl benzoate which is believed to arise by 0—0 bond cleavage of **1** followed by rearrangement (6).

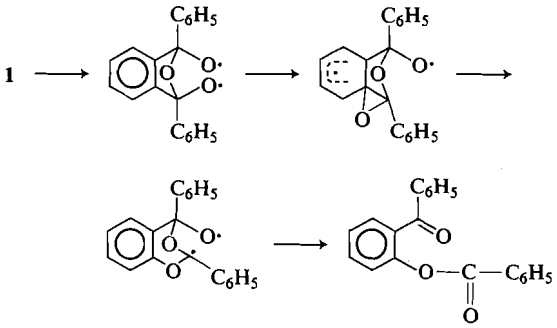

When photooxidation was performed in CCl_4 or when **1**, prepared in benzene, was dissolved in CCl_4, ODB was produced quantitatively. The loss of an oxygen atom from **1** is not easily explained. However, if **1** is considered to be an ozonide it may exist as the zwitterion **3** which would be readily hydrolyzed to ODB, *e.g.*,

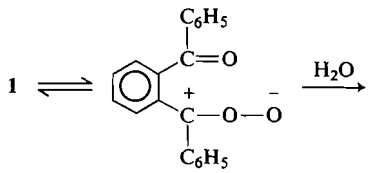

3

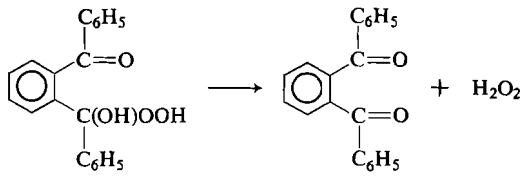

Conclusions

It is quite clear from this work that DPBF can react very rapidly with ground state triplet oxygen in the presence of a free radical initiator to give ODB. Great care should, therefore, be exercised to ensure that the disappearance of DPBF or the production of ODB during photooxidation is not due to adventitious autoxidation.

We thank Mr. J. H. B. Chenier for assistance with the experimental work, Mr. H. Seguin for elemental analyses and molecular weights determinations, and a referee for valuable comments.

1. P. B. Merkel and D. R. Kearns. J. Am. Chem. Soc. **97**, 462 (1975).
2. J. A. Bell and J. D. MacGillvray. J. Chem. Ed. **51**, 677 (1974).
3. E. J. Corey and W. C. Taylor. J. Am. Chem. Soc. **86**, 3881 (1964).
4. J. R. Scheffer and M. D. Ouchi. Tetrahedron Lett. 223 (1970).
5. H. H. Wasserman, J. R. Scheffer, and J. L. Cooper. J. Am. Chem. Soc. **94**, 4991 (1972).
6. F. Nahavandi, F. Razmara, and M. P. Stevens. Tetrahedron Lett. 301 (1973).
7. W. R. Adams. *In* Oxidation. Vol. 2. *Edited by* R. L. Augustine and D. J. Trecker. Marcel Dekker Inc., New York. 1971.
8. J. A. Howard and K. U. Ingold. Can. J. Chem. **47**, 3809 (1969).
9. J. E. Bennett, J. A. Eyre, and R. Summers. J. Chem. Soc. Perkin II, 797 (1974).
10. A. Le Berre and R. Ratsimbazafy. Bull. Chem. Soc. Fr. 229 (1963).
11. J. A. Howard. Adv. Free Radical Chem. **4**, 49 (1972).
12. F. R. Mayo. Acc. Chem. Res. **1**, 193 (1968).
13. Ch. Dufraisse and S. Ecary. C.R. Acad. Sci. **223**, 735 (1946).

Polar Radicals. VIII. Kinetic Studies on the Mechanism of the Vapor Phase Bromination of 1-Chlorobutane. The Role of Reversible Hydrogen Abstraction[1]

DENNIS D. TANNER, TONY PACE, and TAMEICHI OCHIAI[2]
Department of Chemistry, University of Alberta, Edmonton, Alberta T6G 2G2
Received February 13, 1975

DENNIS D. TANNER, TONY PACE, and TAMEICHI OCHIAI. Can. J. Chem. 53, 2202 (1975).

A general method for the evaluation of the kinetics of the vapor phase brominations of alkanes and substituted alkanes is presented. The method is applied to the bromination of 1-chlorobutane.

The hydrogen abstraction reaction and its reversal are both found to be deactivated by the polar influence of the substituent; the effect, as predicted, falls off as the distance of the substituent from the C—H bond involved increases. In the vapor phase bromination of 1-chlorobutane, because of this deactivated reversal, transfer with hydrogen bromide cannot compete (< 10%) with transfer with molecular bromine.

There was no evidence for anchimeric assistance by the neighboring chlorine atom during hydrogen abstraction.

DENNIS D. TANNER, TONY PACE et TAMEICHI OCHIAI. Can. J. Chem. 53, 2202 (1975).

On présente une méthode générale d'évaluation des cinétiques de la bromation en phase vapeur d'alkanes substitués et non substitués. La méthode est appliquée à la bromation du chloro-1 butane.

La réaction d'abstraction d'un proton ainsi que la réaction inverse sont toutes les deux désactivées par l'influence polaire du substituant; comme prévu l'effet décroît à mesure que la distance du substituant au lien C—H impliqué s'accroît. Dans le cas de la bromation en phase vapeur du chloro-1 butane, la réaction inverse étant désactivée, le transfert avec l'acide bromhydrique ne peut pas entrer en compétition (< 10%) avec le transfert de brome moléculaire.

Il n'y a pas de preuve d'assistance anchimère par l'atome de chlore voisin au cours de l'abstraction d'un proton. [Traduit par le journal]

Introduction

Hydrogen abstraction from alkanes by bromine atoms has long been recognized by gas phase kinetesists as a reversible reaction (2). The values obtained for the relative rates of substitution and isomer distributions of various alkanes and substituted alkanes by molecular bromine, in general, have been obtained ignoring the effect of the reversibility of the abstraction reaction (3).[3] Attempts to take into account reversible abstraction have recently demonstrated that these reactions cannot be ignored (ref. 4 and references therein) and further, that in solution the reversal reaction is enhanced by the rapid transfer reactions of an alkyl radical with the complex species HBr_3, that is formed during the reaction (5). The mechanism of bromination in solution has been found to be further complicated since cage filtering of radicals by cage reversal can play a significant part in determining the rates observed and products formed in the bromination (6).

In order to obtain meaningful values for the relative rates of abstraction by bromine atoms from alkanes or substituted alkanes, a comparison of the vapor phase and solution kinetics must be obtained (5, 6). In this report a general method for the evaluation of the kinetics for the vapor phase bromination of alkanes and substituted alkanes is presented. The method is applied to the bromination of 1-chlorobutane.

The isomer distributions obtained from the homolytic substitution reactions of electronegatively substituted alkanes are influenced by the electron withdrawing substituent. The molecule is deactivated toward hydrogen abstraction, the effect falling off with the distance of the substituent from the carbon–hydrogen bond involved. The carbon–hydrogen bond strength, in opposition to the former effect, is lowered by electron withdrawal. By a combination of these effects, appropriately weighted to account for the substrates involved, the observed isomer distributions have been rational-

[1]For part VII, see ref. 1.
[2]Postdoctoral Fellow, University of Alberta, 1973–1974.
[3]For a discussion of this problem see ref. 4.

Can. J. Chem. Downloaded from www.nrcresearchpress.com by 210.87.254.40 on 09/05/12
For personal use only.

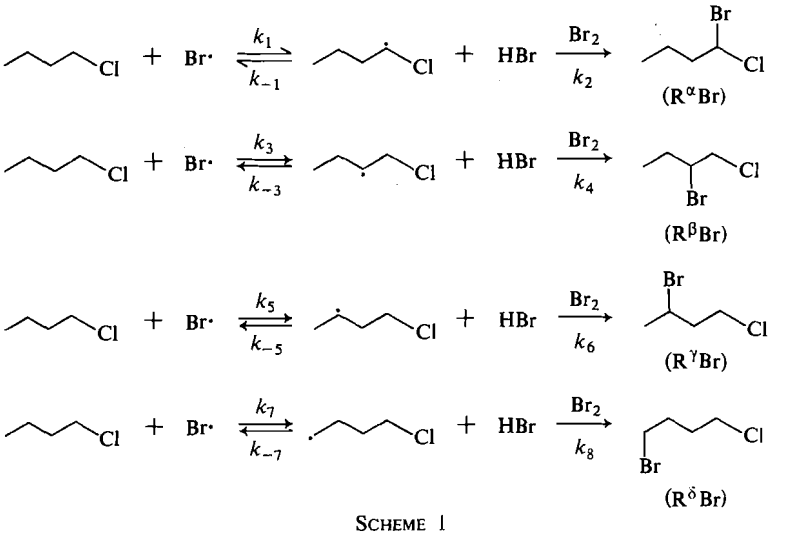

SCHEME 1

ized (7–9). An understanding of the factors governing the isomer distribution obtained in the bromination of haloalkanes is complicated by the proposal that a halogen, bromine (10, 11), or chlorine (3*d*, 12, 13), accelerates by anchimeric assistance the abstraction of the hydrogen located β to these substituents.

The substrate chosen, 1-chlorobutane, tests the method fully, since on bromination it yields four possible isomeric bromides whose distribution is effected by polar interactions, reversible abstraction, and presumably by anchimeric assistance.

Discussion and Results

If one assumes the simplest mechanism to explain the formation of the products formed in the vapor phase bromination of 1-chlorobutane, Scheme 1, then the relative rate of the production of two of the bromo chlorides is given by [1].

$$[1]\quad \frac{d[R^{\alpha}Br]/dt}{d[R^{\gamma}Br]/dt} = \frac{k_1}{k_5}\cdot\frac{k_2}{k_6}\cdot\frac{k_{-5}}{k_{-1}}\left[\frac{1+\dfrac{k_6\ [Br_2]}{k_{-5}\ [HBr]}}{1+\dfrac{k_2\ [Br_2]}{k_{-1}\ [HBr]}}\right]$$

We have been able to evaluate this expression by carrying out the bromination of perdeuterio-1-chlorobutane in the presence of high concentrations of hydrogen bromide and molecular bromine. The relative rates of production of 2-brominated, ($R^{\beta}Br$), to 2-protiated, ($R^{\beta}H$), substrate are given by [2].

$$[2]\quad \frac{d[R^{\beta}Br]/dt}{d[R^{\beta}H]/dt} = \frac{k_4[Br_2]}{k_{-3}[HBr]}$$

At high concentrations of $[Br_2]^0$ and $[HBr]^0$, if the reaction is taken to low conversion, where concentrations do not change appreciably, [2] may be integrated and the value of k_4/k_{-3} can be obtained by an analysis of the ratio of the final concentrations of the two products, [3].

$$[3]\quad \frac{[R^{\beta}Br]}{[R^{\beta}H]-[R^{\beta}H]^0}\cdot\frac{[HBr]^0}{[Br_2]^0} = \frac{k_4}{k_{-3}}$$

A similar operation allowed us to evaluate the k_2/k_{-1} and k_6/k_{-5} ratios by an examination of the substitution products for the reactions in the α- and γ-positions of perdeuterio-1-chlorobutane.

At constant values of $[Br_2]^0$ and $[HBr]^0$ [1], and a similar expression 4 for $(d[R^{\beta}Br]/dt)/(d[R^{\gamma}Br]/dt)$

$$[4]\quad \frac{d[R^{\beta}Br]/dt}{d[R^{\gamma}Br]dt} = \frac{k_3}{k_5}\cdot\frac{k_4}{k_6}\cdot\frac{k_{-5}}{k_{-3}}\left[\frac{1+\dfrac{k_6\ [Br_2]}{k_{-5}\ [HBr]}}{1+\dfrac{k_4\ [Br_2]}{k_{-3}\ [HBr]}}\right]$$

can be evaluated knowing the ratios of 1/3-brominated and 2/3-brominated chlorobutanes.

Can. J. Chem. Downloaded from www.nrcresearchpress.com by 210.87.254.40 on 09/05/12
For personal use only.

Can. J. Chem. Downloaded from www.nrcresearchpress.com by 210.87.254.40 on 09/05/12
For personal use only.

TABLE 1. Photobromination of perdeuterio-1-chlorobutane with excess bromine and hydrogen bromide in the vapor phase (22 l) (concentration mol/l × 10^5)

	Run			
	1	2	3	
Reactant*				
$[RD(H)]^0$	21.34	23.68	22.34	
$[Br_2]^0$	40.23	42.82	40.82	
$[HBr]^0$	306.06	359.92	325.65	
$[R^{\alpha}H]^0$	0.89	0.97	0.91	
$[R^{\beta}H]^0$	0.34	0.37	0.34	
$[R^{\gamma}H]^0$	1.04	1.14	1.09	
$[R^{\delta}H]^0$	1.58	1.74	1.63	
Products†				
[RD(H)]	19.72	20.54	18.71	
$[R^{\alpha}H]$	0.91	1.02	0.97	
$[R^{\beta}H]$	0.41	0.60	0.63	
$[R^{\gamma}H]$	1.31	1.93	1.68	
$[R^{\delta}H]$	1.60	1.85	1.69	
$[R^{\alpha}Br]$	0.17	0.46	0.41	
$[R^{\beta}Br]$	0.16	0.50	0.40	
$[R^{\gamma}Br]$	0.27	0.74	0.66	
$[R^{\delta}Br]$‡	0.00	0.00	0.00	
Relative rate constants				Average
k_2/k_{-1}	64.7	77.3	54.5	65.5 ± 7.9
k_4/k_{-3}	17.4	18.3	11.0	15.6 ± 3.0
k_6/k_{-5}	7.6	7.9	8.9	8.1 ± 0.5
k_1/k_5	0.33	0.33	0.37	0.34 ± 0.02
k_3/k_5	0.43	0.48	0.55	0.49 ± 0.04
k_7/k_5§	0.03	0.05	0.03	0.04 ± 0.01
Temperature (°C)	22.7	22.8	23.1	

*[RD(H)] refers to the concentration of perdeuterio-1-chlorobutane, and $[R^iH]$ is the average concentration of the residual protium at position i.
†The values for $[R^iH]$ at the end of the reaction were calculated as: $[R^iH]^0 + 1/2([RD(H)]^0 + [RD(H)]) \times$ (fractional incorporation of H at position i).
‡Not detected by g.l.p.c.
§Per H atom.

By substituting into [1] and [4] the values previously obtained for k_2/k_{-1}, k_6/k_{-5}, and k_4/k_{-3} the values for the relative rates of k_1/k_5 and k_3/k_5 can be calculated. Equation 5

$$[5] \qquad \frac{k_7}{k_5} = \frac{[R^{\delta}H] - [R^{\delta}H]^0}{[R^{\gamma}H] - [R^{\gamma}H]^0 + [R^{\gamma}Br]}$$

was derived to calculate the ratio k_7/k_5, since an expression of the form of [1] could not be evaluated for the δ-position, due to the negligible amount of 4-bromo-1-chlorobutane formed.

The ratio of rate constants for the abstraction of a deuterium atom from perdeuterio-1-chlorobutane in the α-, β-, and γ-positions can be equated to the same ratio of rate constants in the undeuterated substrate if the assumption is made that analogous ratios of rate constants for the two substrates are the same, [6].

$$[6] \qquad k_i^H/k_j^H = k_i^D/k_j^D$$

The photobrominations of perdeuterio-1-chlorobutane were carried out in a 22 l reaction vessel at ambient temperature. The concentrations and values obtained for the kinetic analyses are listed in Table 1.

The reactions were carried out to low conversion where multiple exchange reactions will be negligible. The reaction mixture was condensed, diluted with Freon 113, and an internal standard (*o*-dichlorobenzene) was quantitatively added. The mixture was then freed from hydrogen bromide and molecular bromine by washing with ice-cold aqueous sodium bisulfite. After

Can. J. Chem. Downloaded from www.nrcresearchpress.com by 210.87.254.40 on 09/05/12
For personal use only.

drying the mixture was subjected to g.l.p.c. analysis. Gas-liquid partition chromatography analysis (see Table 1) showed the presence of only the perdeuterio analogs of 1-bromo-1-chlorobutane, 2-bromo-1-chlorobutane, 3-bromo-1-chlorobutane, and the unbrominated substrate. A synthetic mixture, whose composition corresponded to the mixture of reactants and products obtained from reaction 2 (Table 1) with the addition of 4-bromo-1-chlorobutane (7.95×10^{-6} *M*) and a 1:2.7 mixture of 1,2-dibromo-3-chlorobutane and 2,3-dibromo-1-chlorobutane (3.43×10^{-6} *M*) was introduced, in the absence of light, into the reaction vessel and was subjected to the same isolation and analysis procedures. The yield of the recovered brominated chlorides was >97% for all four of the monobrominated materials and for the trihalides was >99%. The ratio of all the products was the same within the limits of the g.l.p.c. analysis (±2%).

The unbrominated substrate was collected by preparative g.l.p.c. and the amount of incorporated protium at each position (see Table 1) was determined from a comparison of the H^1 100 MHz spectrum of the residual protium in the (Merck, Sharp and Dohme, 98.3 atom% D) starting perdeuterio-1-chlorobutane and the spectrum of the recovered unbrominated substrate (see Fig. 1). The total amount of protium was determined by mass spectrometry for reactions 2 and 3. The n.m.r. method of determining the total protium content of the starting material and the recovered unbrominated substrate was used for reaction 1 (see Table 1).

A test of the kinetics of the bromination of 1-chlorobutane under "normal" conditions, *i.e.*, without excess bromine or added hydrogen bromide, could be achieved. Since the ratio of $[Br_2]/[HBr]$ is a monotonic function of time, $d[R^iBr]/dt = (d[R^iBr]/dx)(dx/dt)$. Using this substitution [1] can be rewritten as [7], where $x = [Br_2]/[HBr]$.

$$[7]\quad \frac{d[R^\alpha Br]/dx}{d[R^\gamma Br]/dx} = \frac{k_1}{k_5}\cdot\frac{k_2}{k_6}\cdot\frac{k_{-5}}{k_{-1}}\cdot\frac{\left(1+\frac{k_6}{k_{-5}}(x)\right)}{\left(1+\frac{k_2}{k_{-1}}(x)\right)} = f^{\alpha/\gamma}$$

A similar expression, [8], can be written for $d[R^\beta Br]/dx/d[R^\gamma Br]/dx = f^{\beta/\gamma}$. Making use of the relative rate constants obtained from the perdeuterio-1-chlorobutane brominations, [7] or [8] may be employed to calculate the ratios of the derivatives $f^{\alpha/\gamma}$ or $f^{\beta/\gamma}$ for any value of x. The consistency of the mechanism used to derive [1], the accuracy of the kinetic values obtained for the bromination of perdeuterio-1-chlorobutane, and their applicability to "normal brominations", can be tested by comparing the calculated ratios of these derivatives with those obtained experimentally. Mixtures of bromine and 1-chlorobutane ("normal brominations") were photolyzed in the vapor phase to varying percentages of reaction and the products of bromination were isolated and analyzed (see Table 2).

From these analyses (see Table 2) plots of the concentration of 2-bromo-1-chlorobutane, $[R^\beta Br]$, 1-bromo-1-chlorobutane, $[R^\alpha Br]$, and 3-bromo-1-chlorobutane, $[R^\gamma Br]$ *vs.* x, $[Br_2]/[HBr]$, could be constructed. The experimental values obtained for the "normal" brominations were fitted manually or by a least squares method to an exponential function $[R^\beta Br]$, $[R^\alpha Br]$, or $[R^\gamma Br] = ae^{-bx} + ce^{-2bx} + de^{-3bx} + fe^{-4bx}$ and the ratios of slopes obtained (graphical differentiation) from these synthesized curves gave the values $d[R^\beta Br]/dx/d[R^\gamma Br]/dx$ and $d[R^\alpha Br]/dx/d[R^\gamma Br]/dx$. A comparison of the calculated values for these functions, $f^{\beta/\gamma}$ and $f^{\alpha/\gamma}$, with those of the experimentally derived values is shown in Figs. 2 and 3.

The error limits shown in Figs. 2 and 3 for the calculated values of $f^{\beta/\gamma}$ and $f^{\alpha/\gamma}$ were obtained using the maximum and minimum values reported for the relative rates of transfer at each position (see Table 1). When the error limits were included for the data (±2%, g.l.p.c. error)

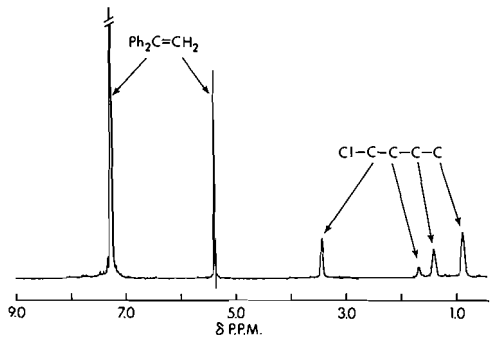

FIG. 1. 100 MHz H^1 spectrum of perdeuterio-1-chlorobutane (Freon 113, TMS reference), before reaction.

Can. J. Chem. Downloaded from www.nrcresearchpress.com by 210.87.254.40 on 09/05/12
For personal use only.

TABLE 2. Photobromination of 1-chlorobutane (8.080×10^{-4} *M*) with molecular bromine (8.262×10^{-5} *M*) in the vapor phase (5 l)

% reaction	Temperature (°C)	Products* $R^{\alpha}Br$	Products* $R^{\beta}Br$	Products* $R^{\gamma}Br$	$[Br_2]/[HBr]$	$f^{\alpha/\gamma}$ Observed	$f^{\alpha/\gamma}$ Calculated	$f^{\beta/\gamma}$ Observed	$f^{\beta/\gamma}$ Calculated
4.5	23.9	0.078	0.098	0.218	21.13	0.363	0.352	0.466	0.481
9.2	24.2	0.152	0.190	0.420	9.910	0.358	0.354	0.424	0.483
20.0	24.8	0.324	0.402	0.880	3.998	0.397	0.359	0.489	0.487
27.4	24.6	0.480	0.588	1.250	2.649	0.402	0.364	0.504	0.491
43.6	25.0	0.742	0.926	2.592	1.296	0.406	0.379	0.517	0.500
60.9	24.8	1.232	1.032	2.752	0.6415	0.441	0.407	0.512	0.519
71.0	23.8	1.422	1.248	3.162	0.4086	0.491	0.439	0.538	0.539
82.7	23.8	1.652	1.482	3.582	0.2092	0.626	0.516	0.584	0.583
90.3	22.8	1.818	1.628	3.824	0.1069	0.748	0.672	0.622	0.648

*Concentration in mol/l, $\times 10^5$.

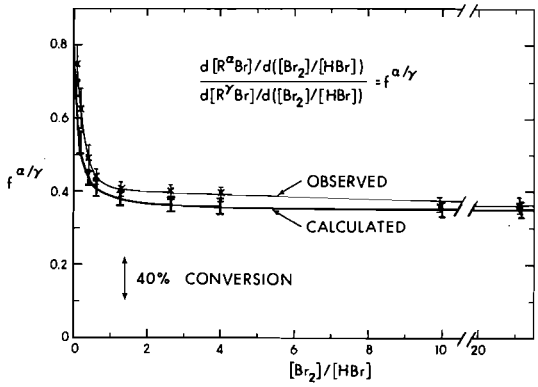

FIG. 2. Plot of the observed and calculated $f^{\alpha/\gamma}$ *vs.* $[Br_2]/[HBr]$ for the bromination of 1-chlorobutane.

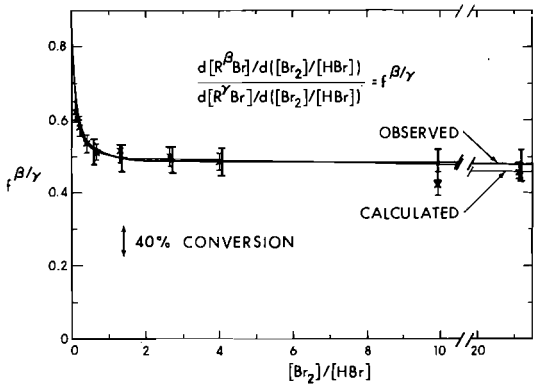

FIG. 3. Plot of the observed and calculated $f^{\beta/\gamma}$ *vs.* $[Br_2]/[HBr]$ for the bromination of 1-chlorobutane.

used to determine the observed values of $f^{\beta/\gamma}$ and $f^{\alpha/\gamma}$ (see Table 2) the observed and calculated functions were coincident within the experimental limits (see Figs. 2 and 3).

The coincidence of the calculated values of $f^{\beta/\gamma}$ and $f^{\alpha/\gamma}$ with those of the experimentally determined values demonstrates that the relative rate data obtained for perdeuterio-1-chlorobutane describes adequately the kinetic behavior of the "normal" vapor phase bromination of 1-chlorobutane, and shows that the assumption proposed in [6] must hold.

Mechanistic Conclusions

The relative rates of hydrogen abstraction/H, which include reversible hydrogen transfer, are found to follow the order predicted for the reaction of a selective radical whose reactivity is strongly affected by the polar influence of the electronegative chlorine substituent, *i.e.* α-H, $0.34 <$ β-H, $0.49 <$ γ-H, $1.00 >$ the primary δ-H, 0.04. The relative reactivity of the β/γ hydrogens (0.49/1.00) determined in these brominations is similar to that reported for other substitution reactions, carried out under irreversible conditions, on electronegatively substituted substrates, where the substituent does not have the ability to anchimerically assist in hydrogen abstraction (8). The normality of the β/γ relative reactivity fortifies the conclusion that a neighboring chlorine atom does not accelerate the rate of abstraction of hydrogen by a bromine atom.

The effect of the polar substituent upon the energy of the transition state for hydrogen abstraction will be the same as for reversible transfer of the polar radical with polar hydrogen bromide (microscopic reversibility).

$$[ClC_4H_8\text{---}H\text{---}Br]\cdot\ddagger$$

If the assumption is made that polar interactions are negligible for transfer of the polar radical with a nonpolar molecule of molecular bromine, the order found for competitive transfer of the polar radical with bromine and hydrogen bromide, k_2/k_{-1} (α-position) $> k_4/k_{-3}$ (β-position) $> k_6/k_{-5}$ (γ-position) $> k_8/k_{-7}$ (δ-position), can be rationalized. The magnitude of the rate constant for reversal will increase as the distance from the substituent is increased while the polar influence of the substituent on the rate of transfer with molecular bromine will be negligible.

In the "normal" vapor phase bromination, reversible reactions between the chlorobutyl radicals and hydrogen bromide are small, due to polar deactivation, $k_{Br_2}/k_{HBr} = 9.1$ for the whole molecule, and only 9.0% of the radicals formed will transfer with hydrogen bromide. This value can be compared with the competitive transfer rates determined for the vapor phase bromination of the nonpolar cyclohexyl radical (5), $k_{Br_2}/k_{HBr} = 2.81$, where a significantly higher fraction, 26%, of the radicals transfer with hydrogen bromide.

Experimental

Materials

1-Chlorobutane (BDH) was washed with concentrated sulfuric acid, water, dried over sodium sulfate, and distilled. Gas–liquid partition chromatography (10 ft × 1/4 in. 10% UCON 50 LB 550X) showed it to be >99.9% pure. Perdeuterio-1-chlorobutane was obtained from Merck, Sharp and Dohme, Ltd. Gas–liquid partition chromatography analysis showed it to be 99.5%

Can. J. Chem. Downloaded from www.nrcresearchpress.com by 210.87.254.40 on 09/05/12
For personal use only.

Can. J. Chem. Downloaded from www.nrcresearchpress.com by 210.87.254.40 on 09/05/12
For personal use only.

pure. Mass spectral analysis (AEI MS9, 15.8 eV) showed it to contain 98.3 atom% D, and n.m.r. spectroscopy, using 1,1-diphenylethylene as standard (see below), showed it to contain 98.0 atom% D.

Molecular bromine (McArthur Chemical Co., reagent grade) was washed with concentrated sulfuric acid and distilled twice from phosphorus pentoxide.

Hydrogen bromide (Matheson) was passed over molecular sieve 4A, degassed, and distilled twice prior to use.

1,1-Diphenylethylene (Aldrich) was distilled prior to use: b.p. 136.5–137.0° (9 mm), n_D^{20} 1.6088 (lit. (14) b.p. 139° (11 mm), n_D^{20} 1.6085); n.m.r. spectroscopy and g.l.p.c. analysis showed it to have no detectable impurities.

A mixture of 1-bromo-, 2-bromo-, and 3-bromo-1-chlorobutane was obtained by preparative g.l.p.c. collection (10 ft × 1/4 in. 10% UCON 50 LB 550X) of the products of the liquid phase bromination of 1-chlorobutane with molecular bromine (3*e*). The products were identified by a comparison of their g.l.p.c. retention times with those of the authentic materials (15). 4-Bromo-1-chlorobutane (Aldrich) was purified by g.l.p.c. collection.

A mixture of 2,3-dibromo-1-chlorobutane and 1,2-dibromo-3-chlorobutane was prepared by the addition of a carbon tetrachloride solution of bromine to commercial crotyl chloride (Aldrich technical grade, containing 20% 3-chloro-1-butene; g.l.p.c. showed the presence of these two compounds in a ratio of 3.0:1.0) in carbon tetrachloride at 0°. The crude product was purified by distillation: b.p. 78–79° (8.7 mm), n_D^{25} 1.5385. The n.m.r. spectrum showed two doublets (τ 8.13, J = 6.3 Hz; τ 8.19, J = 6.6 Hz, 3H) in the ratio of 2.7:1 centered at τ 6.02 (2H) and τ 5.59 (2H). The mixture did not give a parent peak in the mass spectrum (70 eV), but gave peaks at *m/e* 173, 171 (base peak), 169 (P—Br, ratio 3:4:1), 217, 215, 213 (P—Cl), 135, 133 (ratio 1:1) and 91, 89 (ratio 3:1). The two compounds were not separated by g.l.p.c. (10 ft 10% UCON 50 LB 550X), but the g.l.p.c. showed the mixture to be >99.9% pure.

Anal. Calc. for $C_4H_7Br_2Cl$: C, 19.20; H, 2.82. Found: C, 18.93; H, 2.85.

Determination of Relative Rates

1-Chlorobutane-d_9 (~0.5 g) was carefully weighed in a Pyrex breakseal, degassed three times by the freeze-thaw method, and finally sealed. Bromine (about 1.5 g) was weighed into another breakseal, degassed, and sealed. Hydrogen bromide was degassed and distilled in a vacuum line, measured, distilled into a breakseal, and the breakseal sealed. The three breakseals were attached to a 22 l reaction bulb, and the system was degassed. The bulb was isolated from the vacuum line and the breakseals broken in the absence of light (in the order C_4D_9Cl, HBr, Br_2, with 30 min intervals between each breakseal). The mixture of the three substrates was allowed to equilibrate for about 30 min in the absence of light, and then the reaction vessel was irradiated (1 × 100 W incandescent lamp). The contents of the reaction vessel were condensed and an internal standard (*o*-dichlorobenzene) added. The excess bromine and hydrogen bromide were destroyed with cold (0°) sodium bisulfite solution. The organic substrates were dissolved in Freon 113 (about 30 ml), and the Freon solution washed with cold water and dried ($MgSO_4$). The solution was analyzed by g.l.p.c. (6 ft × 1/4 in. 10% UCON 50 LB 550X on Chromosorb P AW, glass column) for starting material and products. The solution was concentrated on a 24 in. Teflon spinning band column to approximately 4 ml, and the unbrominated perdeuterio-1-chlorobutane was collected and then recollected by preparative g.l.p.c. (20 ft × 1/4 in. 10% Carbowax 20 M TPA on Chromosorb P AW, glass column, 50°).

In a control experiment, 5.530×10^{-3} mol 1-chlorobutane, 8.425×10^{-5} mol 1-bromo-1-chlorobutane, 1.005×10^{-4} mol 2-bromo-1-chlorobutane, 1.748×10^{-4} mol 3-bromo-1-chlorobutane, 4.422×10^{-5} mol 4-bromo-1-chlorobutane, 7.550×10^{-5} mol of a mixture of 2,3-dibromo-1-chloro- and 1,2-dibromo-3-chlorobutane, 9.466×10^{-3} mol bromine and 7.484×10^{-2} mol hydrogen bromide were introduced into the reaction bulb (22 l), in the absence of light, and condensed after 2 h. After isolation of the organic material, in the above manner, the mixture was analyzed by g.l.p.c. The material balance was 97.7% for 1-bromo-, 96.9% for 2-bromo-, 97.4% for 3-bromo-, 95.5% for 4-bromo-1-chlorobutane, and 102.2% for the trihalide.

Determination of Residual Protium in 1-Chlorobutane-d_9

Accurately prepared solutions of perdeuterio-1-chlorobutane (150–300 mg) and 1,1-diphenylethylene (3–10 mg) in Freon 113 (~0.3 ml) were analyzed by n.m.r. spectroscopy using a Varian HR 100 spectrometer. Two spectra were run (normal and D decoupled) with the phenyl protons as lock and reference. A small amount of TMS was added, and two more spectra, normal and D decoupled, were run, with TMS as lock and reference. Each spectrum was integrated at least five times, and the average values for the integrated areas were again averaged for the four spectra. Both decoupled and undecoupled spectra gave the same integration values, within experimental error, showing the absence of any experimentally important Overhauser effects. From the relative areas of the chlorobutane protons (τ 9.12, 8.59, 8.32, 6.58) and the olefinic protons of 1,1-diphenylethylene (τ 4.63), the amount of protium in each position of the perdeuterio-1-chlorobutane could be determined. This method was used for reaction 1.

The total protium content was also calculated by mass spectrometry (AEI MS9, 13 eV, slow magnetic scanning) by the method of Biemann (16). The amount of protium in each position was determined using the ratio of the α:β:γ:δ-H^1 signals from the n.m.r. spectra. This method was used for runs 2 and 3 (Table 1), and gave more accurate results than the n.m.r. method described above.

Photobromination of 1-Chlorobutane with Molecular Bromine

Aliquots (0.500 ml) of a solution of 1-chlorobutane (7.447 g, 8.045×10^{-2} mol) and bromine (1.315 g, 8.226×10^{-3} mol) were transferred into each of 12 breakseals. Each breakseal was in turn attached to the 5 l reaction vessel, degassed, and its contents were introduced into the reaction vessel. After equilibration in the dark (30 min), the reaction bulb was photolyzed (100 W incandescent lamp) for the appropriate time, and the contents were condensed. To the isolated mixture was added 20 ml of a 5% potassium iodide solution and an

aliquot of a Freon 113 solution containing a known amount of an internal standard (*o*-dichlorobenzene). The mixture was titrated iodometrically for bromine and hydrogen bromide (17). The organic layer was separated, dried over magnesium sulfate, and analyzed by g.l.p.c. (10% UCON 50 LB 550X). Only 1-bromo-, 2-bromo-, and 3-bromo-1-chlorobutane were observed; the material balance (based on bromine) was always greater than 98.7%.

The authors wish to thank the National Research Council of Canada and the University of Alberta for their generous support of this work.

1. D. D. TANNER, R. J. ARHART, E. V. BLACKBURN, N. C. DAS, and N. WADA. J. Am. Chem. Soc. **96**, 829 (1974).
2. (*a*) G. B. KISTIAKOWSKY and E. R. VAN ARTSDALEN. J. Chem. Phys. **12**, 469 (1944); (*b*) H. C. ANDERSEN and E. R. VAN ARTSDALEN. J. Chem. Phys. **12**, 479 (1944); (*c*) B. H. ECKSTEIN, H. A. SCHERAGA, and E. R. VAN ARTSDALEN. J. Chem. Phys. **22**, 28 (1954); (*d*) E. I. HORMATS and E. R. VAN ARTSDALEN. J. Chem. Phys. **19**, 778 (1951); (*e*) H. R. ANDERSON, H. A. SCHERAGA, and E. R. VAN ARTSDALEN. J. Chem. Phys. **21**, 1258 (1953); (*f*) J. H. SULLIVAN and N. DAVIDSON, J. Chem. Phys. **19**, 143 (1951).
3. (*a*) M. S. KHARASCH, W. S. ZIMMT, and W. NUDENBERG. J. Org. Chem. **20**, 1430 (1955); (*b*) H. SINGH and J. M. TEDDER. J. Chem. Soc. B, 608 (1966); (*c*) P. S. SKELL, D. L. TULEEN, and P. D. READIO. J. Am. Chem. Soc. **85**, 2849 (1963); (*d*) J. C. TRAYNHAM and W. G. HINES. J. Am. Chem. Soc. **90**, 5208 (1968); (*e*) W. THALER. J. Am. Chem. Soc. **85**, 2607 (1963); (*f*) P. S. SKELL and P. D. READIO. J. Am. Chem. Soc. **86**, 3334 (1964); (*g*) B. BLOURI, C. CERCEAU, and G. LANCHEC. Bull. Soc. Chim. Fr. 304 (1963); (*h*) S. J. CRISTOL, M. A. IMHOFF, and D. C. LEWIS. J. Org. Chem. **35**, 1722 (1970); (*i*) P. W. STORMS and G. B. MILLER. J. Org. Chem. **31**, 2705 (1966).
4. D. D. TANNER, J. E. ROWE, T. PACE, and Y. KOSUGI. J. Am. Chem. Soc. **95**, 4705 (1973).
5. D. D. TANNER, T. PACE, and T. OCHIAI. J. Am. Chem. Soc. In press.
6. D. D. TANNER, T. OCHIAI, and T. PACE. J. Am. Chem. Soc. In press.
7. J. M. TEDDER. Q. Rev. **14**, 336 (1960).
8. G. A. RUSSELL. *In* Free radicals, Vol. 1. *Edited by* J. K. Kochi. Wiley, New York, N.Y. 1973. Chapt. 7.
9. A. F. TROTMAN-DICKENSON. Advances in free-radical chemistry, Vol. 1. *Edited by* G. H. Williams. Academic Press, London. 1965. p. 1.
10. W. A. THALER. Methods in free-radical chemistry, Vol. 2. *Edited by* E. S. Huyser. Dekker, New York, N.Y. 1969.
11. L. KAPLAN. Bridged free radicals. Dekker, New York, N.Y. 1972.
12. H. SCHIVERNSBERG and J. G. TRAYNHAM. Abstracts, 158th National Meeting of the American Chemical Society, New York, N.Y. Sept. 1969.
13. P. S. SKELL. Chem. Soc. Spec. Publ. No. **19**, 137 (1964).
14. C. F. H. ALLEN and S. CONVERSE. Org. Synth. **1**, 226 (1951).
15. J. E. ROWE. Ph.D. Thesis. The University of Alberta, Edmonton, Alberta. 1973.
16. K. BIEMANN. Mass spectrometry, applications to organic chemistry. McGraw-Hill, New York, N.Y. 1962.
17. G. H. CADY. Inorg. Synth. **5**, 156 (1957).

Can. J. Chem. Downloaded from www.nrcresearchpress.com by 210.87.254.40 on 09/05/12
For personal use only.

Erratum: Water-soluble Lysine-containing Polypeptides. II. The Interaction of Several Sequential Lysine–Glycine Polypeptides with DNA. A Circular Dichroism Study of DNA Conformation in Annealed Complexes

ROSS E. WILLIAMS AND SANDRA L. KIELLAND
Division of Biological Sciences, National Research Council of Canada, Ottawa, Canada K1A 0R6
Received March 18, 1975
(Ref.: Can. J. Chem. **53**, 542 (1975))

In the caption for Fig. 2 the experimental conditions should read: DNA-phosphate concentration 1.76×10^{-4} *M*; 0.15 *M* sodium chloride, sodium cacodylate, 0.001 *M*, p*H* 7.0.

Can. J. Chem. Downloaded from www.nrcresearchpress.com by 210.87.254.105 on 09/05/12
For personal use only.

Can. J. Chem. Downloaded from www.nrcresearchpress.com by 210.87.254.6 on 09/05/12
For personal use only.

Base-catalyzed Exchange of Cyclic Diketones under Homoenolization Conditions; Facile Exchange at the Bridgehead and C-7 in 3,3,6,6-Tetramethyl Bicyclo[2.2.1]heptan-2,5-dione

NICK HENRY WERSTIUK

Department of Chemistry, McMaster University, Hamilton, Ontario L8S 4M1

Received March 25, 1975

NICK HENRY WERSTIUK. Can. J. Chem. **53**, 2211 (1975).

Treatment of 3,3,6,6-tetramethyl bicyclo[2.2.1]heptan-2,5-dione (**1**) under mild homoenolization conditions (*t*-BuO$^-$, 175°, 28 h) results in unusually facile exchange at the bridgehead and C-7. 1,4-Homoenolization to an *endo* methyl group, converts **1** into 2,2,5-trimethyl bicyclo[3.2.1]octan-3,8-dione (**3**).

NICK HENRY WERSTIUK. Can. J. Chem. **53**, 2211 (1975).

Dans des conditions douces d'homoénolisation (*t*-BuO$^-$, 175°, 28 h), la tétraméthyl-3,3,6,6 bicyclo[2.2.1.] heptadione-2,5 (**1**) s'échange très facilement au niveau de l'atome de pont et du C-7. Une homoénolisation-1,4 impliquant une groupe méthyle *endo* transforme **1** en triméthyl-2,2,5 bicyclo[3.2.1.] octanedione-3,8 (**3**). [Traduit par le journal]

There are presently chronicled in the literature (1–11) a number of reports on base-catalyzed H–D exchange of C—H bonds situated 1,3 (homoenolization) from a solitary carbonyl group. The studies have quantified the degree of 1,3 or β-homoenolization and the propensity for rearrangement. Several examples of 1,4 or γ-homoenolization (4, 5, 10) have also been documented. However, homoenolization via in concert activation by two or more carbonyl groups has not been observed. Also, in the studies carried out thus far, 1,3-homoenolization to C-7 in bicyclo[2.2.1] heptyl ketones, such as camphenilone (**2***a*) and fenchone (**2***b*), has not been observed. Presumably, this is a consequence of the strain in the homoenolate anion and/or the improper alignment of the C—H bonds at C-7 with the π system of the carbonyl group at C-2. For example, fenchone (**2***b*) resists exchange (<1%) at C-7 even under the forcing conditions of 0.7 *M* *t*-BuO$^-$ maintained at 185° for 2½ weeks (8, 11). Another point of interest is the apparent ease at which bridgehead exchange, α to the carbonyl group, occurs under homoenolization conditions (7, 9, 12–14). However, most of the systems examined thus far do not possess the constraints against bridgehead exchange imposed by the bicyclo[2.2.1]-heptyl system. That is, formal conjugation of the anion at C-1 to a carbonyl group at C-2 in camphenilone (**2***a*) or C-7 in norbornan-7-one is rigorously denied because of strain and the fact that the dihedral angle between the anion and the carbonyl π system is essentially 90°. Only the exchange study on norbornan-7-one and nortricyclanone[1,2] undertaken by Gassman and Zalar (13) presents data on bridgehead exchange in [2.2.1]-ketones. To gain information on the extent of, and the factors which control bridgehead exchange in these systems is important, since such exchange would not be detected directly in camphenilone (**2***a*)[1,2] (1) and the isocamphanone–camphor (8) system and would add to the deuterium incorporated at C-1 and C-6.

To expand the research on the chemistry of

[1]Although there is a good correlation between $J_{^{13}C-H}$ (% s character) and the kinetic acidity of C—H bonds, an exception has recently been reported (15). However, it has not yet been established conclusively (16) whether $J_{^{13}C-H}$ is a good measure of hybridization α to a carbonyl group although Ellis and Maciel (17) have shown that $J_{^{13}C-H}$ α to the carbonyl group in 2,2-dimethyl cyclopropanone (160), cyclobutanone (134.8), and cyclopentanone (129.5) are essentially identical to $J_{^{13}C-H}$ in the corresponding hydrocarbons.

[2]Gassman and Zalar (13) have shown that norbornan-7-one ($J_{^{13}C_1-H}$, 152 ± 1 Hz) (16) and nortricyclanone ($J_{^{13}C_4-H}$, 159 ± 1 Hz) (16) exchange 25% (49 h) and 75% (29 h) of C—H at the bridgehead α to the carbonyl group under homoenolization conditions, what would be expected qualitatively from the magnitudes of $J_{^{13}C-H}$. **2***a* has a $J_{^{13}C_1-H}$ of 152 ± 1 Hz (16).

Can. J. Chem. Downloaded from www.nrcresearchpress.com by 210.87.254.6 on 09/05/12
For personal use only.

TABLE 1. Reaction of 3,3,6,6-tetramethyl bicyclo[2.2.1]heptan-2,5-dione (**1**) with *t*-BuO$^-$–*t*-BuOH(D)

Entry (Run)	Conditions*	Relative yield (%)†		Excess D‡		Deuterium position	
		1 (isolated yield)	**3** (isolated yield)	**1**	**3**	**1**§	**3**‖
1	5 ml KO*t*-Bu–*t*-BuOD (0.9 *M*) 0.30 g **1** (0.17 *M*) 160±5°, 28 h	95±1 (0.25 g)	5±1 Not determined	0.75	Not determined	0.4 ±0.1 at C-1, C-4 0.1 ±0.05 at C-7	Not determined
2	5 ml KO*t*-Bu–*t*-BuOD (0.9 *M*) 0.26 g **1** (0.15 *M*) 175±5°, 28 h	87±2 (0.20 g)	13±2 (0.025 g)	2.3	5.6	1.35±0.05 at C-1, C-4 0.85±0.05 at C-7 0.1 ±0.05 at C-8, 9, 10, 11	3.5±0.2 at C-1, C-4, C-6, C-7 and 2.6±0.2 at C-9
3	5 ml KO*t*-Bu–*t*-BuOH (0.9 *M*) 0.26 g **1** (0.15 *M*) 175±5°, 52 h	80±4 (0.21 g)	20±4 (0.020 g)				
4	3.5 ml KO*t*-Bu–*t*-BuOD (71.0 *M*) 0.20 g **1** (0.11 *M*) 180±5°, 15 h	75±5% (0.10 g)	25±5 (0.012 g)	2.5	6.6	1.35±0.05 at C-1, C-4 1.00±0.05 at C-7 0.15±0.05 at C-8, 9, 10, 11	Not determined

*The base was prepared by dissolving K in the appropriate alcohol in a dry box.
†The relative yields of 1 and 3 were determined by g.l.p.c. with electronic integration. The isolated yields are the actual yields obtained after recrystallization of 1 and preparative v.p.c. of 3.
‡Determined mass spectrometrically at low voltage. 1 contained up to d_4 species, 3 contained up to d_9–d_{10} species.
§Determined by ^1H and ^2H n.m.r.
‖Determined by ^1H n.m.r.

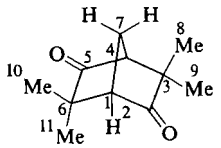

1

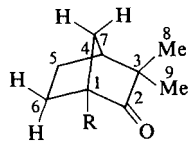

2

2*a*, R = H

b, R = Me

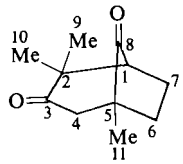

3

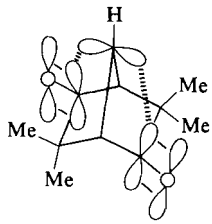

4

bicyclic diketones (16, 18) a study was undertaken to establish the propensity of exchange in 3,3,6,6-tetramethyl bicyclo[2.2.1]heptan-2,5-dione (**1**)[3] under "mild" homoenolization conditions (175°, 28 h).

The results in Table 1 establish (*a*) the stability of diketone **1** in strongly basic medium, (*b*) that the exchange at the bridgehead and especially C-7 is unusually facile, (*c*) that 1,4-homoenolization to an *endo* methyl converts[4] **1** into 2,2,5-trimethyl bicyclo[3.2.1]octan-3,8-dione (**3**),[3] and (*d*) one of the methyl groups, likely C-9, in **3** undergoes very rapid H–D exchange.

The high degree of exchange at the bridgehead in **1** is remarkable, when compared to norbornan-7-one and nortricyclanone, since $J_{^{13}C_1-H}$ in **1** is normal at 152 ± 2 Hz. Also, s character effects cannot be the source of the facile exchange at C-7, compared to fenchone, since $J_{^{13}C_7-H}$ in **1** is 138 ± 2 Hz. Is bis-1,3-homoconjugation therefore, as depicted in **4**, responsible for the enhanced reactivity at C-7? The unusual kinetic acidity at the bridgehead perhaps can be ascribed to a decrease in the diheral angle, through a synchro-twist,[5] between the anionic center at C-1 and the π system at C-2. Unfortunately no studies, either experimental or theoretical, have yet been carried out to establish quantitatively the stabilization of an anionic center by a carbonyl group as a function of dihedral angle and hybridization at the anionic site. Possibly the enhanced acidity at C-7 results from *cyclic* delocalization of the developed negative charge through the carbonyl groups conjugated either through three σ bonds (19–22) or through space beneath the bicyclic system.

The 1,4-homoenolization to the *endo* methyl in **1** provides a convenient route to the bicyclo-[3.2.1]octan-3,8-dione system. The facile exchange of the C-9 methyl in **3** likely results from in concert 1,3 and 1,4 activation by the carbonyl groups at C-3 and C-8, the second example (*vide supra*) of bis-activation. It is expected, therefore, that 1,3 and 1,4 multi-activation of remote C—H bonds by three or four carbonyl groups should provide for an enormous increase in kinetic acidity.

Financial assistance by the National Research Council of Canada is gratefully acknowledged. The author wishes to thank Ms. Valerie Meng for preliminary work on the synthesis of **1** and Professor J. B. Stothers who very kindly obtained the ^2H n.m.r. spectra for exchanged **1**.

1. A. Nickon and J. L. Lambert. J. Am. Chem. Soc. **84**, 4604 (1962).
2. A. Nickon, J. L. Lambert, and J. E. Oliver. J. Am. Chem. Soc. **88**, 2287 (1966).
3. A. Nickon, H. Kwasnik, T. Swartz, R. O. Williams, and J. B. DiGiorgio. J. Am. Chem. Soc. **87**, 1615 (1965).
4. R. Howe and S. Winstein. J. Am. Chem. Soc. **87**, 915 (1965).
5. T. Fukunaga. J. Am. Chem. Soc. **87**, 916 (1965).
6. R. M. Coates and J. P. Chen. Chem. Commun. 1481 (1970).
7. K. W. Turnbull, S. J. Gould, and D. Arigoni. Chem. Commun. 597 (1972).
8. D. H. Hunter, A. L. Johnson, J. B. Stothers, A. Nickon, J. L. Lambert, and D. F. Covey. J. Am. Chem. Soc. **94**, 8582 (1972).
9. J. B. Stothers and C. T. Tan. J. Chem. Soc. Chem. Commun. **738** (1974).
10. A. L. Johnson, N. W. Petersen, M. B. Rampersad, and J. B. Stothers. Can. J. Chem. **52**, 4143 (1974).
11. A. J. Johnson, J. B. Stothers, and C. T. Tan. Can. J. Chem. **53**, 212 (1975).

[3]The diketone **1** was prepared by tetramethylation of norbornan-2,5-dione with MeI and KO*t*-Bu in ether. **1** had a m.p. of 114–115° and spectroscopic properties consistent with its structure. **3** had a m.p. of 48–50°; ^1H n.m.r. (60 MHz, $CDCl_3$) σ 2.25 (bs, 3H, C-1, C-3—H), 2.25–1.6 (m, 4H, C-6, C-7—H), 1.20 (s, 3H, CH_3—), 1.05 (s, 3H, CH_3), 1.00 (s, 3H, CH_3—); m.s. (80 eV) *m/e* (M^+) 180; i.r. γ_{max} ($CDCl_3$) C=O, 1740, 1725 cm^{-1}.

[4]That approximately 15% rearrangement to **3** is observed with only 1% exchange in the methyl groups indicates that 1,4-homoenolization results in predominate rearrangement with little return to **1**.

[5]A synchro-twist (23) that places the ends of the π systems in close proximity, and alters the alignment of the C—H bonds at C-7 and C-1 with the C=O group, relative to **2***a* or **2***b*, is possible in **1**.

Can. J. Chem. Downloaded from www.nrcresearchpress.com by 210.87.254.6 on 09/05/12
For personal use only.

12. D. H. BOWEN and J. MACMILLAN. Tetrahedron Lett. **40**, 4111 (1972).
13. P. G. GASSMAN and F. V. ZALAR. J. Am. Chem. Soc. **88**, 3070 (1966).
14. A. NICKON, D. F. COVEY, F. HUANG, and Y.-N. KUO. J. Am. Chem. Soc. **97**, 904 (1975).
15. T. Y. LUH and L. M. STOCK. J. Am. Chem. Soc. **96**, 3712 (1974).
16. N. H. WERSTIUK, R. J. TAILLEFER, R. A. BELL, and B. SAYER. Can. J. Chem. **51**, 3010 (1973).
17. P. D. ELLIS and G. E. MACIEL. J. Am. Chem. Soc. **92**, 5829 (1970).
18. N. H. WERSTIUK and R. TAILLEFER. Can. J. Chem. **48**, 3966 (1970).
19. R. C. COOKSON, J. HENSTOCK, and J. HUDEC. J. Am. Chem. Soc. **90**, 1059, 1060 (1966).
20. R. HOFFMANN, A. IMAMIERA, and W. J. HEHRE. J. Am. Chem. Soc. **90**, 1499 (1968).
21. R. HOFFMANN, E. HEILBRONNER, and R. GLEITER. J. Am. Chem. Soc. **92**, 706 (1970).
22. R. HOFFMANN. Acc. Chem. Res. **4**, 1 (1971).
23. C. ALTONA and M. SUNDARALINGAM. J. Am. Chem. Soc. **92**, 1995 (1970).

Can. J. Chem. Downloaded from www.nrcresearchpress.com by 210.87.254.6 on 09/05/12
For personal use only.

Can. J. Chem. Downloaded from www.nrcresearchpress.com by 210.87.254.6 on 09/05/12
For personal use only.

Canadian Journal of Chemistry

Published by
THE NATIONAL RESEARCH COUNCIL OF CANADA

Journal canadien de chimie

Publié par
LE CONSEIL NATIONAL DE RECHERCHES DU CANADA

Volume 53 Number 15 August 1, 1975 Volume 53 numéro 15 1 août 1975

1,4-Dioxane Hydrate: Dielectric Absorption by a Nondipolar Enclathrated Molecule[1]

S. R. GOUGH, J. A. RIPMEESTER, AND D. W. DAVIDSON
Division of Chemistry, National Research Council of Canada, Ottawa, Canada K1A 0R9

Received March 21, 1975

S. R. GOUGH, J. A. RIPMEESTER, and D. W. DAVIDSON. Can. J. Chem. **53**, 2215 (1975).

X-Ray, continuous-wave and pulsed n.m.r., and dielectric relaxation studies show the hydrate of 1,4-dioxane (D) to be a normal clathrate hydrate of von Stackelberg's structure II with composition $D\cdot\sim 17H_2O$. The reorientation rate of the relatively large D molecule is slower and the effective activation energy (1.6 kcal/mol) larger than for other guest molecules previously studied in hydrates of the same structure. Weak dielectric absorption associated with reorientation of nondipolar D molecules is attributed mainly to the induction of a total dipole moment of ~0.2 D in the 28 water molecules of the large structure II cage by two equal and opposed dipoles in the chair form of D.

S. R. GOUGH, J. A. RIPMEESTER et D. W. DAVIDSON. Can. J. Chem. **53**, 2215 (1975).

Les études par diffraction des rayons X, r.m.n. par ondes continues et par impulsion, et relaxation diélectrique, indiquent que l'hydrate de dioxanne-1,4 (D) est un hydrate de clathrate normal ayant la structure II de von Stackelberg et la composition $D\cdot\sim 17H_2O$. La vitesse de réorientation de cette molécule D relativement grande est plus lente et l'énergie d'activation effective (1.6 kcal/mol) est plus grande que dans le cas des autres molécules encagées déjà étudiées pour des hydrates de même structure. La faible absorption diélectrique associée à la réorientation des molécules D non dipolaires, est attribuée en grande partie à l'induction d'un moment dipolaire total de ~0.2 D dans les 28 molécules d'eau de la grande cage de structure II par deux dipôles égaux et opposés dans la forme chaise de D. [Traduit par le journal]

Formation of a high hydrate of 1,4-dioxane which melts incongruently at −13 °C has recently been reported from thermal analysis and differential scanning calorimetry (1, 2). Its high water content, estimated as 34 (1) or more (2) water molecules per molecule of dioxane, has been said to indicate a structure II-like clathrate hydrate in which the 16-hedral cages are only half-occupied (1) or, alternatively, a hydrate of an entirely different structure (2).

We present here X-ray, n.m.r., and dielectric evidence that 1,4-dioxane forms a type II clathrate hydrate of the usual kind. The dielectric and n.m.r. behavior of this hydrate presents special interest because dioxane is perhaps the largest molecule known to form a simple type II hydrate. At the same time, the absence of a permanent dipole moment in the 1,4-dioxane molecule makes it necessary to devise a mechanism to account for the dielectric absorption observed in this hydrate at low temperatures.

Experimental Methods and Results

Purity of Samples

Because of the presence of weak dielectric absorption in 1,4-dioxane hydrate at low temperatures (see below), it is important to establish the purity of the Eastman Kodak *p*-dioxane

[1]NRCC No. 14664.

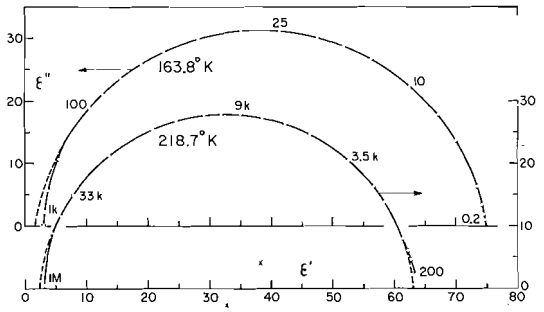

FIG. 3. Cole–Cole plots of the water relaxation region of 1,4-dioxane hydrate.

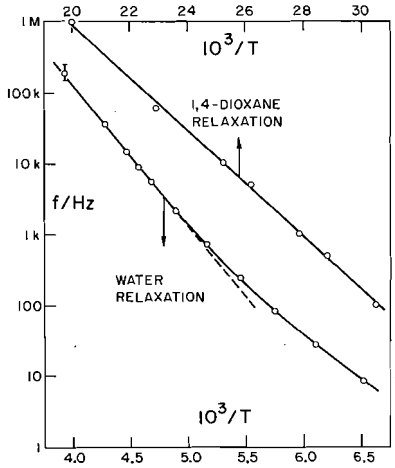

FIG. 4. Temperature dependence of frequencies of maximum dielectric absorption by host and guest molecules of 1,4-dioxane hydrate.

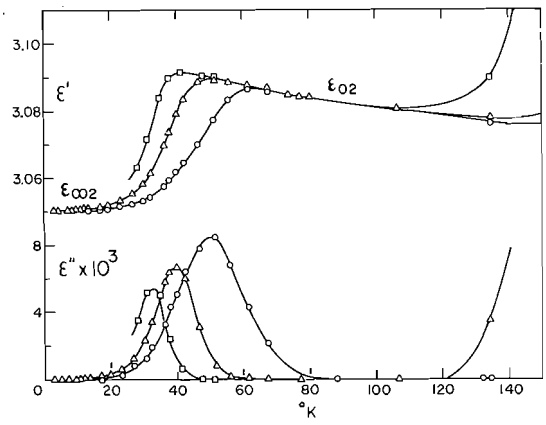

FIG. 5. Low-temperature permittivity and loss curves of 1,4-dioxane hydrate: □, 100 Hz; △, 10 kHz; ○, 1 MHz.

high-temperature side of minimum T_1 (*i.e.*, between 80 and 170 K) is considerably higher (1.55 kcal/mol) than the value (0.92 kcal/mol) obtained for the corresponding region of tetrahydrofuran deuterate. The smaller and temperature-dependent slope to the low-temperature side of minimum T_1 (*e.g.*, ~0.52 kcal/mol between 50 and 35 K) may again (9) be formally associated with a broad and asymmetric distribution of reorientational correlation times with a long tail extending to shorter times. The distribution required is less broad than in the tetrahydrofuran case, the β of the approximate skewed arc representation being about 0.33 in the region of minimum T_1 rather than 0.21 (9).

Dielectric Measurements

Permittivity and loss measurements were made at frequencies between 0.2 Hz and 1 MHz and at temperatures between 3 and 253 K with techniques already described (11). Results are shown in Figs. 3 to 5 for a sample of composition $C_4H_8O_2 \cdot 14.68H_2O$, excess dioxane having been employed to promote hydrate formation (slow for hydrates which form from ice (12)) and to suppress the amount of unreacted ice. After a day of conditioning at −14 °C the dielectric behavior of this sample showed no features which could be identified with the presence of ice.

The complex permittivity loci illustrated in Fig. 3 have the shapes characteristic of the relaxation of water molecules in the structure II hydrate lattice (11, 13). The cell "filling factor" is good for a hydrate which forms incongruently from ice, the static permittivity of 57 at 253 K comparing favorably with the value of 62 expected (11) at this temperature for a type II hydrate of a nonpolar molecule. At least part of the difference may be attributed to the presence of excess solid dioxane of permittivity 2.3 (see below). The increase of permittivity with decrease of temperature (to about 77 at 153 K) is less rapid than expected for complete filling of the interelectrode region. This result is formally attributable to development of an air gap in series with the sample which increased in thickness to about 0.012 of the interelectrode spacing as the temperature fell to 153 K.

The activation energy for reorientation of the water molecules, as derived from the temperature dependence of the frequency of maximum loss (Fig. 4), is 9.1 ± 0.2 kcal/mol for tempera-

Can. J. Chem. Downloaded from www.nrcresearchpress.com by 210.87.254.6 on 09/05/12
For personal use only.

Can. J. Chem. Downloaded from www.nrcresearchpress.com by 210.87.254.6 on 09/05/12
For personal use only.

tures above 200 K. At lower temperatures the rate plot is no longer linear, but shows the smaller dependence on temperature which is generally found in the relaxation behavior of clathrate hydrates at low temperatures (11, 13). As in ice itself, the relaxation may be controlled at low temperatures by extrinsic or impurity-related Bjerrum defects.

A second region of dielectric relaxation, associated with relatively small but easily measurable absorption and dispersion (Fig. 5), occurs below 80 K. The amplitude of this dispersion ($\varepsilon_{02} - \varepsilon_{\infty 2}$) is about 1% of that found for the low-temperature dispersion of structure II hydrates containing such polar guest molecules as tetrahydrofuran and acetone (11) where the relaxation is associated with reorientation of the guest dipoles. As in the latter cases, the absorption is very broad and asymmetric. The "activation energy" which corresponds to the dependence on temperature of the frequency of maximum absorption (see plot in Fig. 4) is 1.72 ± 0.04 kcal/mol (*cf.* 0.91, 1.25, and 1.44 kcal/mol for the corresponding absorption in the hydrates of tetrahydrofuran (11), isoxazole (14), and cyclobutanone (11), respectively).

Discussion

Nature of the Hydrate

The X-ray, n.m.r., and dielectric results all go to establish that 1,4-dioxane hydrate is a normal structure II clathrate hydrate. Despite the X-ray indication that the lattice may be somewhat "stretched" by the presence of the large guest molecule, the stability of the lattice as measured by the slowness of reorientation of the water molecules and the associated activation energy is only exceeded by one (SF_6 hydrate) of the nine structure II hydrates for which such information is available (11, 14). At the same time the narrow distribution of water-molecule reorientation times reflected in the shape of the complex permittivity locus is, to good experimental accuracy, the same in all these cases.

Although no hydrate composition studies were made, it may be inferred that the value of n in $C_4H_8O_2 \cdot nH_2O$ is much closer to the normal structure II value of 17 (15) than to the value of 34 or more previously suggested (1, 2). For complete equilibration, values of n of 17 and 34 correspond to the presence of 3.4 and 22.7 wt.%, respectively, of excess solid dioxane in the sample of composition $C_4H_8O_2 \cdot 14.68H_2O$. Expressed as a linear function of the permittivities and volume fractions of the two phases, the anticipated static permittivity at 253 K is about 60 in the first case and 48 in the second. Since incomplete filling also lowers the permittivity, the experimental permittivity of 57 is not consistent with any great departure from the normal structure II composition.

A supporting indication is the absence of spurious lines from solid dioxane in the X-ray diffraction patterns.

Origin of the Low-temperature Dielectric Absorption

The dielectric absorption and dispersion shown in Fig. 5 may formally be attributed to reorientation of an encaged molecule which possesses[2] a dipole moment of about 0.19 D. However, there is an accumulation of evidence to show that, at room temperature and below, 1,4-dioxane exists exclusively in the nondipolar chair conformation. See, for example, the results of studies of vapor-phase (17) and liquid-phase (18) electric polarization, liquid-phase infrared and Raman spectra (19), electron diffraction (8), and conformation energies (20). Measurement of a finite dielectric loss at microwave frequencies in liquid dioxane at 20 °C cannot be taken as evidence of a permanent dipole moment of ~0.1 D (21, 22) since this absorption is continuous with the far infrared absorption which reaches a maximum value of ε'' around 40 cm^{-1} (23) and is of the same kind as occurs in such nondipolar liquids as benzene. Moreover, the Boltzmann factor which may permit polar conformations to occur above 473 K (17) is very unfavorable to their existence below 80 K.

Likewise, it does not seem possible to ascribe the present dielectric absorption to polar impurity in the dioxane. Such an impurity would have to consist of relatively large, but still encageable, molecules. For a dipole moment of ~2 D, the concentration would need to be two orders of magnitude larger than the impurity concentrations shown in Table 1.

[2]This estimate is based on the assumption that ($\varepsilon_{02} - \varepsilon_{\infty 2}$), measured at a temperature high enough that reorientation is effectively isotropic, is linear in (dipole moment)^2 of the guest molecule. This relationship adequately applies to the experimental data at 168 K for structure II hydrates of many polar guest molecules (16).

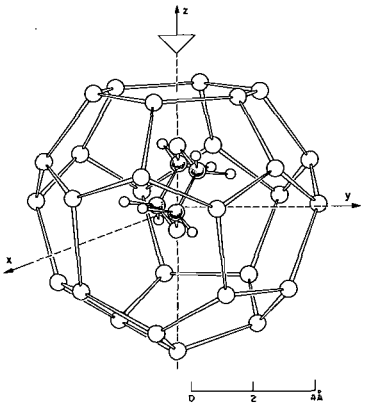

FIG. 6. The 16-hedral cage of water molecules containing a 1,4-dioxane molecule at the position used to estimate the induced dipole moment.

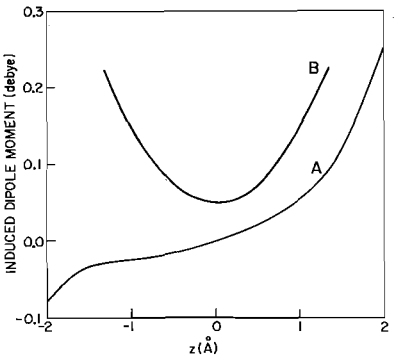

FIG. 7. Total dipole moment induced in the water molecules of the cage by a dipole of 1 D aligned with (*A*) a 3-fold axis of a 16-hedral cage and (*B*) the $\bar{4}$ axis of a 14-hedral cage, as a function of displacement of the dipole along the axis.

It is therefore concluded that the dielectric absorption must originate with the reorientation of the chair form of 1,4-dioxane itself. This conclusion is supported by the good agreement (see below) between the n.m.r. and dielectric information about the reorientation kinetics of the guest molecules.

Mechanism of Dielectric Absorption by 1,4-Dioxane

The most likely mechanism of this absorption is to be found in the dipole moments induced in the water molecules of the cage by the dioxane molecule. To a first approximation the charge distribution of dioxane may be represented by two equal and opposed dipoles, each associated with a C—O—C group. To calculate the magnitude of the total dipole moment induced in the 28 water molecules of the 16-hedral cage, we use a simplified model in which the O--O vector of dioxane is assumed to coincide with one of four 3-fold axes of symmetry of the (average) $\bar{4}3m$ cage which passes through the center of a hexagonal ring of water molecules (see Fig. 6). It has previously been suggested (24) that guest ether molecules tend to have preferred configurations in which the O atoms approach the centers of hexagonal rings to the extent determined by the repulsion between the water molecules and the H atoms on the α C atoms. We further consider only the major component of each C—O—C group dipole which lies along the O--O direction.

We first evaluate the total dipole moment induced in the 28 water molecules of the cage by a single dipole which lies on, and points along, a 3-fold axis of cage symmetry, hereafter called the Z axis. By symmetry, the induced moment has only a Z component which is given by summation of the 28 terms of the form $\alpha m(1 - 3z_i^2)R_i^{-3}$, where α is the polarizability (assumed isotropic) of a water molecule, R_i is the distance of a water molecule from the dipole, and z_i the component of a unit vector in the direction of R_i. The sign is chosen for a negative dipole moment of magnitude m with the hexagonal ring taken at positive Z (Fig. 6).

Figure 7 (curve *A*) shows the variation of induced dipole moment with displacement of a unit guest dipole moment ($m = 1$ D) along the Z axis, with[3] $\alpha = 3.44$ Å^3. It is seen that the sign of the induced moment changes at $Z = 0$, which means that the magnitude of the moment induced by a dipole at a positive Z adds to that induced by an opposite dipole at a negative Z.

To apply the model to dioxane we must estimate the Z coordinates of the two dipoles. An O atom can approach to within about 1.75 Å of the center of a hexagonal ring before the equatorial protons of the adjacent CH_2 groups

[3]This polarizability is derived from an estimated permittivity of the empty structure II lattice of 2.81 (11) and the Clausius–Mossotti equation. It includes full contributions from rotational and translational vibrations of the lattice.

Can. J. Chem. Downloaded from www.nrcresearchpress.com by 210.87.254.6 on 09/05/12
For personal use only.

Can. J. Chem. Downloaded from www.nrcresearchpress.com by 210.87.254.6 on 09/05/12
For personal use only.

come into van der Waals contact (at about 2.4 Å) with the water molecules. This places one O atom at Z = 2.0 Å and the other at $Z = -0.8$ Å (Fig. 6). The C—O—C dipoles are probably somewhat displaced from the O atoms toward the center of the molecule; we take their positions as $Z = 1.7$ and -0.5 Å. From $m =$ 1.4 D, the Z component of a C—O—C group dipole moment of 1.6 D (the experimental moment of tetrahydropyran), and inspection of Fig. 7 (curve *A*), the induced moment is $1.4 \times (0.16 + 0.02)$ or 0.25 D.

The model is too specific for the result to be of great accuracy. However, it is good enough to show that the observed dielectric absorption may be attributed to relaxation of the dipole moments induced in the water molecules of the lattice.

The magnitude of the total induced moment depends on the symmetry of the arrangement of the water molecules of the cage. Thus, curve *B* of Fig. 7 shows the moment induced in the 24 water molecules of the 14-hedral cage of the structure I lattice by a unit dipole aligned along the $\bar{4}$ axis. Since this curve is symmetric about $Z = 0$, no induced moment or dielectric absorption is expected for a molecule like CO_2 whose charge distribution can be represented by an opposed dipole pair or linear quadrupole located at the cage center and aligned along the $\bar{4}$ axis.

Reorientation of Encaged Dioxane

The shapes of the complex permittivity curves given by the low-temperature dielectric measurements are approximately skewed arcs, with, for example, $\beta \sim 0.14$ at 35 K and ~ 0.17 at 40 K. Shapes of this kind are also found for polar guest molecules (7, 11). Another resemblance to the behavior of hydrates of polar guests is to be found in the failure of ε_{02} (Fig. 5) to increase as $1/T$ at low temperatures, a clear indication of reorientation between energetically nonequivalent sites. In the case of dioxane, the gradients of the electrostatic fields of the water molecules, along with short-range dispersion and overlap forces, may well act to favor some orientations of the opposed-dipole axis at the expense of others. The extent of this distortion of the (average) tetrahedral cage symmetry is expected to vary greatly from cage to cage as a result of the disorder in the orientations of the water molecules and to result in a broad distribution of reorientational jump rates.

The relatively sharp fall in line width of the proton resonance absorption which begins at about 30 K (Fig. 1) requires frequencies of relative proton motion of the order of 50 kHz. Since this frequency is several orders of magnitude higher than the frequency of maximum dielectric absorption at a comparable temperature, the initial narrowing is caused by motions to which the dielectric absorption is not strongly sensitive. This is generally also true of previous results[4] for polar ether and ketone guest molecules and one may infer in these cases that the faster motional process corresponds, roughly speaking, to reorientation about the polar axis in which the O atom tends to be held by its affinity to a hexagonal ring (16, 25). Relatively fast motion of this kind is also expected for dioxane and, to the extent that the model of dielectric absorption presented in the last section is a realistic one, only minor dielectric absorption is expected from reorientation about an axis close to the O--O vector.

At higher temperatures the n.m.r. results show a broad and asymmetric distribution of slower reorientational correlation times similar to those responsible for dielectric relaxation. Thus the value of the distribution parameter β (~ 0.33) suggested by the behavior of T_1 (Fig. 2) in the vicinity of its minimum value is consistent with the value expected from extrapolation of the dielectric β's to considerably higher temperatures. The agreement between the "activation energies" given by the high-temperature T_1 slope (1.55 kcal/mol) and by the temperature dependence of maximum dielectric absorption (1.72 kcal/mol) is sufficiently good as to confirm that both relate to essentially the same reorientational processes. The agreement would have been improved if the effects of variation of β with temperature had been incorporated into the experimental activation energies.

A comparison of dielectric and n.m.r. kinetic parameters for dioxane hydrate is given in Table 2, along with earlier results for tetra-

[4]The case of cyclobutanone hydrate is particularly noteworthy; in it line narrowing begins below 15 K but dielectric absorption reaches a maximum at 50 kHz only at 38 K (11, 25).

TABLE 2. Relaxation parameters at temperature (T_m) of minimum T_1

Parameter	Guest	
	1,4-Dioxane	Tetrahydrofuran
Larmor frequency (MHz)	9.2	10.0
T_m (K)	63.3	43
Approximate β	0.33	0.21
τ_0 (diel.) at T_m (s)	1.0×10^{-8}	1.5×10^{-8}
τ_0 (n.m.r.) at T_m (s)	2.8×10^{-8}	4.6×10^{-8}
Minimum T_1 (exptl.) (ms)	18	36
Minimum T_1 (calcd.) (ms)	10	16

hydrofuran hydrate (9). The value of τ_0, the long-time cut-off value of the dielectric distribution, is estimated by extrapolation of the low-temperature dielectric data to the temperature of minimum T_1, where $\beta = 0.33$ is assumed. For the same value of β it may be shown (9) that $\omega\tau_0 = 1.61$ at the temperature of minimum T_1, with ω the Larmor frequency. Values of τ_0 estimated in this way are seen (Table 2) to be about three times as large for n.m.r. relaxation as for dielectric relaxation in both the dioxane and tetrahydrofuran cases. The difference is probably due to the basic differences in the way individual molecular reorientation processes contribute to the two kinds of relaxation when they are widely distributed (9). The same model predicts values of T_1 at the minimum which are within a factor of about two of the experimental values (Table 2). Here the difference probably arises from a basic weakness of the assumption that the mean square fluctuating local field associated with each relaxation process may be identified with the full value of the second moment (15 G^2) which is removed by motional narrowing.

We are greatly indebted to M. E. Bednas for gas chromatography measurements and to Mrs. F. Lee for X-ray photographs.

1. J. C. Rosso and L. Carbonnel. C.R. Acad. Sci. Paris, Ser. C, **272**, 136 (1971).
2. H. Nakayama and M. Tahara. Bull. Chem. Soc. Jap. **46**, 2965 (1973).
3. D. F. Sargent and L. D. Calvert. J. Phys. Chem. **70**, 2689 (1966).
4. M. von Stackelberg and H. R. Müller. Z. Elektrochem. **58**, 25 (1954).
5. M. von Stackelberg and W. Jahns. Z. Electrochem. **58**, 162 (1954).
6. S. K. Garg and D. W. Davidson. J. Chem. Phys. **58**, 1898 (1973).
7. S. K. Garg, B. Morris, and D. W. Davidson. J. Chem. Soc. Faraday Trans. II, **68**, 481 (1972).
8. M. Davis and O. Hassell. Acta Chem. Scand. **17**, 1181 (1963).
9. S. K. Garg, D. W. Davidson, and J. A. Ripmeester. J. Magn. Reson. **12**, 295 (1974).
10. S. K. Garg and D. W. Davidson. Chem. Phys. Lett. **4**, 585 (1970).
11. S. R. Gough, R. E. Hawkins, B. Morris, and D. W. Davidson. J. Phys. Chem. **77**, 2969 (1973).
12. B. Morris and D. W. Davidson. Can. J. Chem. **49**, 1243 (1971).
13. D. W. Davidson. *In* Water: a comprehensive treatise, Vol. 2. *Edited by* F. Franks. Plenum Press, New York. 1973. p. 115.
14. S. R. Gough, S. K. Garg, J. A. Ripmeester, and D. W. Davidson. Can. J. Chem. **52**, 3193 (1974).
15. S. R. Gough and D. W. Davidson. Can. J. Chem. **49**, 2691 (1971).
16. S. R. Gough and D. W. Davidson. *In* Physics and chemistry of ice. *Edited by* E. Whalley, S. J. Jones, and L. W. Gold. Royal Society of Canada, Ottawa. 1973. p. 51.
17. R. S. Armstrong, R. J. W. Le Fèvre, and J. Yates. Austr. J. Chem. **11**, 147 (1958).
18. M. Yasumi and M. Shirai. Bull. Chem. Soc. Jap. **28**, 193 (1955).
19. F. E. Malherbe and H. J. Bernstein. J. Am. Chem. Soc. **74**, 4408 (1952).
20. H. M. Pickett and H. L. Strauss. J. Am. Chem. Soc. **92**, 7281 (1970).
21. S. K. Garg, H. Kilp, and C. P. Smyth. J. Chem. Phys. **43**, 2341 (1965).
22. J. Crossley, A. Holt, and S. Walker. Tetrahedron, **21**, 3141 (1965).
23. M. Davies, G. W. F. Pardoe, J. Chamberlain, and H. A. Gebbie. Chem. Phys. Lett. **2**, 411 (1968).
24. D. W. Davidson. Can. J. Chem. **49**, 1224 (1971).
25. S. K. Garg and D. W. Davidson. *In* Physics and chemistry of ice. *Edited by* E. Whalley, S. J. Jones, and L. W. Gold. Royal Society of Canada, Ottawa. 1973. p. 56.

Can. J. Chem. Downloaded from www.nrcresearchpress.com by 210.87.254.6 on 09/05/12
For personal use only.

Palladium(II) Catalyzed Exchange Reactions. XI. Vinyl Propionate Exchange with Acetic Acid Catalyzed by Palladium(II) Acetate[1]

RAJ N. PANDEY AND PATRICK M. HENRY

Guelph–Water Centre for Graduate Work in Chemistry, University of Guelph, Guelph, Ontario N1G 2W1

Received January 30, 1975

RAJ N. PANDEY and PATRICK M. HENRY. Can. J. Chem. 53, 2223 (1975).

The kinetics of the palladium(II) acetate catalyzed exchange of vinyl propionate with acetic acid solvent to give vinyl acetate has been studied in the sodium acetate concentration range from 0 to 1 *M*. The exchange rate first sharply increases as [NaOAc] increases, reaches a maximum at about 0.2 *M* and then gradually decreases as the sodium acetate concentration is increased to 1.0 *M*. Using previous results on the equilibrium between palladium(II) acetate and sodium acetate in acetic acid it can be shown that the rate expression for exchange is: rate = $(k_o + k_t[Pd_3(OAc)_6] + k_d[Na_2Pd_2(OAc)_6])$ $[CH_2{=}CHO_2CC_2H_5]$ where $k_o = 2 \times 10^{-4}$ s^{-1}, $k_t = 0.045\ M^{-1}$ s^{-1}, and $k_d = 0.089\ M^{-1}$ s^{-1}. A monomeric palladium(II) species, $Na_2Pd(OAc)_4$, formed at high [NaOAc] is unreactive. Since the rate expression does not contain a term in [NaOAc], the sodium acetate serves only to convert one palladium(II) species to another. The lack of a [NaOAc] term in the rate expression for the $Na_2Pd_2(OAc)_6$ catalyzed reaction is believed to result from cancellation of an inhibitory term for π-complex formation by a catalytic term in [NaOAc] in the rate determining conversion of π-complex to σ-complex (acetoxypalladation). Stereochemical studies indicate that acetoxypalladation is nonstereospecific. This result is expected since in the chloride free system acetate is both a ligand and a reactant. Thus it can attack from both inside and outside the coordination sphere of Pd(II).

RAJ N. PANDEY et PATRICK M. HENRY. Can. J. Chem. 53, 2223 (1975).

Les cinétiques de l'échange du propionate de vinyle avec l'acide acétique, catalysée par l'acétate de palladium(II), sont étudiées dans l'acétate de sodium pour des concentrations de 0 à 1 *M*. Au début la vitesse d'échange croît rapidement à mesure que [NaOAc] croît, elle atteint un maximum à environ 0.2 *M*, puis décroit progressivement lorsque la concentration en acétate de sodium augmente jusqu'à 1.0 *M*. Utilisant les résultats antérieurs concernant l'équilibre entre l'acétate de palladium(II) et l'acétate de sodium dans l'acide acétique on peut montrer que l'expression de la vitesse d'échange est: vitesse = $(k_o + k_t[Pd_3(OAc)_6] + k_d[Na_2Pd_2(OAc)_6])$ $[CH_2{=}CHO_2CC_2H_5]$ où $k_o = 2 \times 10^{-4}$ s^{-1}, $k_t = 0.045\ M^{-1}$ s^{-1} et $k_d = 0.089\ M^{-1}$ s^{-1}. Une espèce monomérique du palladium(II), $Na_2Pd(OAc)_4$, formée à haute concentration en NaOAc n'est pas réactive. Puisque l'expression de la vitesse ne contient pas le terme en [NaOAc], l'acétate de sodium sert uniquement à la conversion d'une espèce du palladium(II) en une autre. L'absence du terme [NaOAc] dans l'expression de la vitesse pour la réaction catalysée par $Na_2Pd_2(OAc)_6$ pourrait résulter de l'annulation d'un terme inhibiteur dans la formation d'un complexe π par un terme catalytique en [NaOAc] dans la vitesse déterminante de la conversion du complexe π en un complexe σ (acétoxypalladation). Les études stéréochimiques indiquent que l'acétoxypalladation n'est pas stéréospécifique. Ce résultat est attendu puisque dans le système exempt de chlorure, l'acétate est à la fois ligand et réactif. Ainsi, il peut attaquer de l'intérieur et de l'extérieur de la sphère de coordination du Pd(II).

[Traduit par le journal]

Introduction

Previous papers of this series reported studies of exchange of vinylic and allylic groups with solvent containing chloride ion catalyzed by palladium(II) chloride in acetic acid. The groups exchanged were either chloride or various carboxylic acid groups. These studies indicate that exchange proceeded by an addition elimination mechanism illustrated in reactions 1 and 2 (X, Y = Cl or OOCR).

[1] $Pd(II) + Y^- + CH_2{=}CHX \rightarrow$

$$Pd(II)\text{—}CH_2\text{—}\underset{\displaystyle X}{\overset{\displaystyle Y}{CH}} \rightarrow Pd(II) + X^- + CH_2{=}CHY$$

[1]Presented in part at the 166th National Meeting of the American Chemical Society, Chicago, August, 1973, Abstract INDE 20.

Can. J. Chem. Downloaded from www.nrcresearchpress.com by 210.87.254.40 on 09/05/12
For personal use only.

Can. J. Chem. Downloaded from www.nrcresearchpress.com by 210.87.254.40 on 09/05/12
For personal use only.

[2] $Pd(II) + Y^- + CH_2{=}CH{-}CHX \rightarrow YCH_2{-}\underset{\displaystyle Pd(II)}{\underset{|}{CH}}{-}CHX \rightarrow YCH_2{-}CH{=}CH_2 + Pd(II) + X^-$

Since the addition and elimination reactions are basic reactions in Pd(II) catalytic chemistry these studies offer a convenient way of elucidating the detailed mechanism of these reactions. This work has recently been reviewed (1).

For present purposes the important results of this study are the following.

The reactive species is a dimeric olefin π-complex formed by reaction 3 (ol = olefin).

[3] $Li_2Pd_2Cl_6 + ol \overset{K_1}{\leftrightharpoons} LiPd_2Cl_5(ol) + LiCl$

A monomeric π-complex formed by reaction 4 can sometimes be detected but is unreactive.

[4] $Li_2Pd_2Cl_6 + 2ol \overset{K_2}{\leftrightharpoons} 2LiPdCl_3(ol)$

With some olefins such as allylic esters π-complex formation can be detected by spectral measurements. In such cases it is found that K_2 is much larger than K_1 so the predominant species is unreactive monomeric π-complex. Also of interest in regard to the present study, is the fact that attainment of equilibrium in this system is very rapid.

This is the first paper of the series to describe a study of exchange in the chloride free system in acetic acid. A study of the equilibria between palladium(II) acetate and sodium or lithium acetate has been published (2). The equilibria operative in this system are given in reactions 5 and 6 (M = Na or Li).

[5] $Pd_3(OAc)_6 + 6MOAc \overset{K_{32}}{\leftrightharpoons} 3M_2Pd_2(OAc)_6$

[6] $M_2Pd_2(OAc)_6 + 2MOAc \overset{K_{21}}{\leftrightharpoons} 2M_2Pd(OAc)_4$

The conversion of trimer to dimer (reaction 5) is complete at [NaOAc] = 0.2 *M* and [LiOAc] = 0.5 *M*. The conversion of dimer to monomer (reaction 6) is not complete even in solutions saturated in NaOAc or LiOAc. One important feature of these equilibria, as opposed to the chloride containing system, is that the reactions are slow, taking of the order of hours to come to equilibrium. This indicates that acetate bridges are nonlabile.

The interaction of olefins with the dimer, $Na_2Pd_2(OAc)_6$, has also been studied (3). In this case two equilibria were detected, one which attained equilibrium rapidly and a second slow equilibrium. The rapid equilibrium is represented by reaction 7 while the slow equilibrium is given by reaction 8 (ol = $CH_2{=}CHO_2CC_2H_5$, $CH_2{=}CHCH_2O_2CC_2H_5$, $PhCH{=}CH_2$, $(CH_3)_3CCH{=}CH_2$).

[7] $Na_2Pd_2(OAc)_6 + ol \overset{K'_{22}}{\rightleftharpoons} Na^+ \begin{bmatrix} {}^-OAc{-}OAc{-}ol \\ | \quad Pd \quad | \quad Pd \quad | \\ OAc{-}OAc{-}OAc \end{bmatrix} + NaOAc$

[8] $Na_2Pd_2(OAc)_6 + 2ol \overset{K'_{21}}{\rightleftharpoons} 2\left(Na^+ \begin{bmatrix} {}^-OAc{-}ol \\ | \quad Pd \quad | \\ OAc{-}OAc \end{bmatrix} \right)$

This study demonstrates that, while bridging acetates are nonlabile in agreement with the palladium(II) acetate – MOAc study, the terminal acetates are quite labile.

The kinetics of the vinyl ester exchange in the chloride free system described in this paper must be interpreted in light of these two equilibrium studies.

Experimental

Materials

The sources and methods of purification of most reagents, as well as preparation of stock solutions, has been described previously (2, 3). The vinyl propionate (Aldrich Chemical Company) was distilled before use. The mixture of *cis*- and *trans*-propen-1-yl propionate was prepared by procedures analogous to those used for preparation of the corresponding acetates (4). Pure samples of the *cis*- and *trans*-isomers were obtained by preparative vapor phase chromatography (v.p.c.) using a 20 ft 20% Carbowax 20M on 60–80 mesh Chromasorb W column. The column temperature was 120° and the helium flow rate was 60 ml/min. The two isomers were identified by their n.m.r. spectra using the assignments previously determined for the corresponding acetate esters (5).

The enol propionate of cyclopentanone was prepared by refluxing cyclopentanone with propionic anhydride using potassium propionate as catalyst. Pure samples were obtained by preparative v.p.c. using the same Carbowax column at 160°.

Can. J. Chem. Downloaded from www.nrcresearchpress.com by 210.87.254.40 on 09/05/12
For personal use only.

Kinetic Runs

All kinetic runs were followed by v.p.c. analysis. The reaction mixture was prepared by mixing known amounts of the palladium(II) acetate and sodium or lithium stock acetate solutions and diluting with acetic acid to the final volume. They were thermostated at 25° and allowed to equilibrate for more than 10 half-lives to obtain complete equilibrium between Pd(II) and acetate (reactions 5 and 6) before the run was started by adding neat vinyl propionate. Usually 10–25 μl of vinyl ester for 2–5 ml of reaction mixture was used. Samples of 10–25 μl were withdrawn periodically for v.p.c. analysis. The vinyl propionate concentration was monitored using a 6 ft 20% Carbowax 20M on 60–80 mesh Chromosorb W column at 80°. Helium flow rate was 60 ml/min. In the [NaOAc] range where dimer was the predominant species, the data gave good first order plots for the entire reaction when the data were plotted as a first-order reaction in vinyl propionate. Since all other reagents remain constant for a given run, the rate constant, k_{ex}, for a given run is a pseudo first-order rate constant in vinyl propionate. The rates of reaction were fast enough so that the reaction was over before appreciable amounts of monomeric π-complex were formed (reaction 8). In the [NaOAc] range in which $Pd_3(OAc)_6$ is the major species, the kinetics displayed an induction period before first-order kinetics were observed. The rate constants were obtained from the region of first-order kinetics.

The propenyl propionate reaction mixtures were also analyzed without workup. However, the acetic acid peak had about the same retention time as cyclopentenyl propionate so for these runs aliquots were removed, diluted with CH_2Cl_2, and washed with water and saturated aqueous $NaHCO_3$ to remove the acetic acid and inorganic salts. After the CH_2Cl_2 was dried with anhydrous $MgSO_4$ an aliquot was analyzed using a 20 ft 20% Lac-2R-446 on 60-80 mesh Chromosorb W column at 160°. Helium flow rate was 60 ml/min.

Saponification (6) and oxidation were side reactions in all exchanges so the yield of vinylic acetates was always less than quantitative. With vinyl propionate these side reactions were not serious. With the propenyl propionates the reaction mixture deposited palladium metal after 1 h, at which time the exchange was about 10% complete. The run was always discontinued after Pd(0) precipitated.

Results

All kinetic measurements were made at 25° in dry acetic acid solvent. The effect of vinyl propionate concentration was tested both in the presence and absence of added sodium acetate. As shown in Table 1, the pseudo first-order rate constant in vinyl propionate remains constant in both cases so the reaction is strictly first order in vinyl propionate.

The determination of order in palladium(II) acetate and sodium acetate is complicated since, as mentioned in the introduction, Pd(II) can exist in three forms (see reactions 5 and 6) and sodium acetate can not only be a potential reactant but also acts as a ligand which converts one Pd(II) species to another. Furthermore, because of the complicated nature of the equilibria at a given [NaOAc], the ratios of the three Pd(II) species will not be the same at different total Pd(II) concentrations ($[Pd(II)]_t$). In initial studies it was found that at a given [NaOAc], the value of k_{ex} increased approximately linearly with increasing $[Pd(II)]_t$.

At a given $[Pd(II)]_t$ the rate first increased sharply with increasing [NaOAc], reached a maximum at *ca.* 0.2 *M* [NaOAc] and then decreased slightly with further increase in [NaOAc]. A typical plot is shown in Fig. 1. This type of profile suggests that less reactive trimer is being converted to more reactive dimer which at higher [NaOAc] is converted to unreactive monomer. Since at low [NaOAc] (<0.02 *M*) the trimer is the only species present in appreciable amounts, while at [NaOAc] = 0.2 *M* over 95% of the Pd(II) is in the dimer form, the rate constants for these two species can be readily estimated. With these values and the values of the

TABLE 1. Effect of vinyl propionate concentration on the experimental rate constant

$[Pd_3(OAc)_6] \times 10^3$ (*M*)	[NaOAc] (*M*)	$[H_2C{=}CHO_2C_3H_5]$ (*M*)	$k_{ex} \times 10^4$ (s^{-1})
4.71	0.644	0.064	4.20
4.71	0.644	0.096	4.70
4.71	0.644	0.191	4.22
6.90	0.0	0.028	1.60
6.90	0.0	0.047	1.48
6.90	0.0	0.085	1.62
6.90	0.0	0.095	1.60
6.90	0.0	0.190	1.38

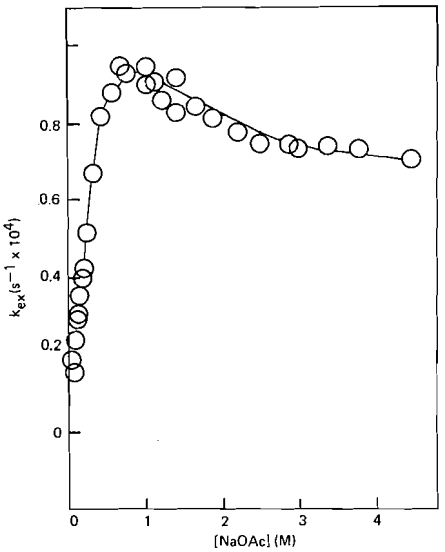

FIG. 1. Dependence of first-order rate constant on sodium acetate concentration: [Pd(II)] = 0.0128 M; [vinyl ester] = 0.095 M.

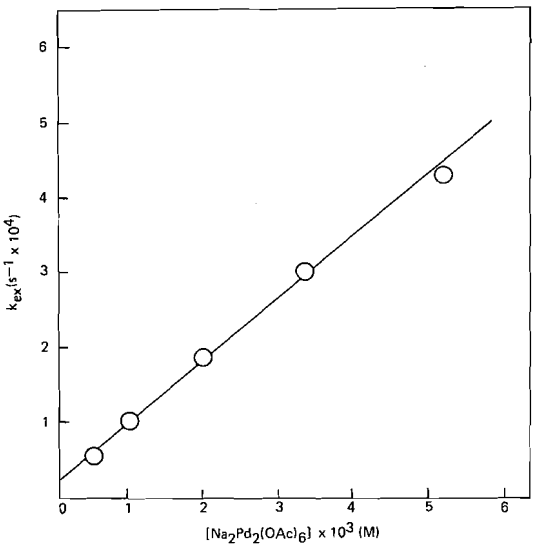

FIG. 2. Plot of exchange rate *vs.* concentration of dimeric Pd(II) acetate [vinyl propionate] = 0.095 M; [NaOAc] = 0.20 M.

equilibrium constants K_{32} in reaction 5 (7.77×10^4 M^{-5} for NaOAc) and K_{21} in reaction 6 (7.6×10^{-4} M^{-1} for NaOAc), the values of k_{ex} at all values of [NaOAc] can be calculated. These calculations were carried out assuming various orders for sodium acetate in the rate expression. Agreement between calculated and

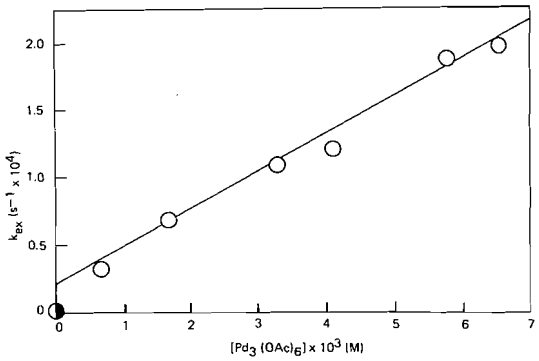

FIG. 3. Plot of exchange rate *vs.* concentration of trimeric Pd(II) acetate: [vinyl ester] = 0.095 M; [NaOAc] = 0. ◑ = Rate in absence of Pd(II). (No measurable exchange in 24 h, some exchange did occur in 7 d.)

observed values of k_{ex} was obtained only if it was assumed that [NaOAc] did not appear in the rate expression. Its only role is thus to convert one Pd(II) species to another. The solid line in Fig. 1 is the calculated rate profile for one value of $[Pd(II)]_t$. At other values of $[Pd(II)]_t$ similar agreement is obtained.

The orders in trimer and dimer can now be checked by varying the Pd(II) concentrations in sodium acetate concentration ranges where either trimer or dimer are the predominant species. The plot for trimer is given in Fig. 2 and the plot for dimer in Fig. 3. In both cases first-order dependence is observed but, surprisingly, each give a positive intercept. This rate might be expected to be the uncatalyzed exchange rate but it can be shown that in the absence of any Pd(II) the exchange rate is much slower than the rate given by the intercept.

TABLE 2. Effect of [NaOAc] on the trimer exchange rate: [vinyl ester] = 0.095 M and $[Pd(II)]_t = 0.0195$ M*

[NaOAc] (M)	$k_{ex} \times 10^4$ (s^{-1})
Nil	1.80
5.0×10^{-5}	4.15
1.0×10^{-4}	3.85
2.0×10^{-4}	4.10
5.0×10^{-4}	3.80
2.0×10^{-3}	3.75
2.0×10^{-3}	3.70
2.0×10^{-2}	4.20

*Using $K_{32} = 7.8 \times 10^4$ M^{-5} for the equilibrium in reaction 5 (M = Na), it can be shown that Pd(II) is practically all trimer (>95%).

Can. J. Chem. Downloaded from www.nrcresearchpress.com by 210.87.254.40 on 09/05/12
For personal use only.

Can. J. Chem. Downloaded from www.nrcresearchpress.com by 210.87.254.40 on 09/05/12
For personal use only.

TABLE 3. Calculated and experimental pseudo first-order rate constants for the vinyl ester exchange reaction catalyzed by the $Pd(OAc)_2$–LiOAc system, $[Pd_3(OAc)_6]_0 = 4.26 \times 10^{-3}$ *M*, $T = 25$ °C

$[Pd_3(OAc)_6]_{eq}$* $\times 10^2$ (*M*)	$[Li_2Pd_2(OAc)_6]$* $\times 10^2$ (*M*)	$[LiOAc]_{eq}$ (*M*)	k_t(calcd) $\times 10^4$ (s^{-1})	k_d(calcd) $\times 10^4$ (s^{-1})	$k_{ex}(=k_t + k_d)$(calcd) $\times 10^4$ (s^{-1})	k_{ex}(exptl) $\times 10^4$ (s^{-1})
0.3850	0.0624	0.0673	1.73	1.23	2.96	2.50 ± 0.09
0.2200	0.3099	0.1808	0.99	6.13	7.12	7.56 ± 0.25
0.0720	0.5319	0.3437	0.32	10.53	10.85	8.87 ± 0.21
0.0400	0.5799	0.4365	0.18	11.48	11.66	10.98 ± 0.11
0.0177	0.6371	1.3173	0.08	12.61	12.69	12.59 ± 0.32

*The concentrations of these species were calculated using the value of equilibrium constant, $K'_{32}(= 1.76 \times 10^2\ M^{-5})$ for reaction 6 (M = Li) from ref. 2.

Can. J. Chem. Downloaded from www.nrcresearchpress.com by 210.87.254.40 on 09/05/12
For personal use only.

Another unexpected result is that addition of even traces of NaOAc causes the rate of exchange to jump to about twice the rate in the absence of any sodium acetate. Data are given in Table 2. Thus, a sodium acetate concentration of 5×10^{-5} M, much less than trimer concentration, causes the rate to rise from 1.80×10^{-4} s^{-1} to *ca.* 4×10^{-4} s^{-1}. Addition of more sodium acetate does not change the rate any further, indicating a zero-order dependence on [NaOAc].

The complete rate expression is thus given by

$$[9] \quad \frac{-d[C_2H_3O_2C_3H_5]}{dt} = [C_2H_3O_2C_3H_5](k_0 + k_t[Pd_3(OAc)_6] + k_d[Na_2Pd_2(OAc)_6])$$

where k_0 is *ca.* 2×10^{-4} s^{-1}, k_t is 0.045 M^{-1} s^{-1}, and k_d is 0.089 M^{-1} s^{-1}. The lithium acetate system was studied in somewhat less detail but gave an analogous rate expression. Sample data are given in Table 3. The average value of k_d in this system is 0.18 M^{-1} s^{-1}.

A few words concerning π-complex formation are in order. As mentioned in the introduction and discussed in other papers of this series (7, 8), the first-order dependence indicates the reactive π-complex is the dimeric π-complex formed by equilibrium shown in reaction 7, rather than the monomeric π-complex formed by the equilibrium shown in reaction 8. In fact when the monomeric π-complex is formed in appreciable amounts, as in the allylic ester exchange in the chloride containing system (8), the rate of exchange is actually inhibited. The previously determined (3) values of K'_{22} (reaction 7) and K'_{21} (reaction 8) are 0.07 and 0.51 M^{-1} respectively. The value of K'_{21} is such that at 0.1 M vinyl propionate at complete equilibrium, about one-third of the Pd(II) would be in the form of unreactive $NaPd(OAc)_3(ol)$, so the rate would only be two-thirds that at low vinyl propionate concentrations. However, the rate of exchange is about five times faster than formation of monomeric π-complex according to reaction 8, so the inhibition does not appreciably affect the value of k_{ex}, especially if the data for the early part of the run is used to calculate k_{ex}.

The value of K'_{22} is such that at [NaOAc] = 0.2 M and [vinyl propionate] = 0.2 M about 7% of the $Na_2Pd_2(OAc)_6$ is in the form of $NaPd_2(OAc)_5(VP)$ (VP = vinyl propionate) while at [NaOAc] = 1.0 M and [VP] = 0.2 M about 1.4% is in the form of π-complex. Thus, slight deviations from the dependencies on [NaOAc] and [VP] from that expected if π-complex formation were insignificant should be found. If the data is treated in the usual fashion, assuming rate of exchange = $k[NaPd_2(OAc)_5(VP)]$, [10] is obtained for the region in which dimer is the only reactive species ($[Na_2Pd_2(OAc)_6]_0$ is concentration of dimer before addition of VP). This rate expression was used in

$$[10] \quad \text{rate} = \frac{k_d K'_{22}[Na_2Pd_2(OAc)_6]_0[VP]}{[NaOAc] + K'_{22}[VP]}$$

calculating the curve in Fig. 1. Better agreement with experiment is obtained when this expression is used.

The effect of enol propionate structure on rate was tested by measuring the rate of exchange of *cis*- and *trans*-1-propen-1-yl propionate, and cyclopentyl propionate. Data are listed in Table 4. It was hoped to obtain the exact rate constants for conversion of *cis*- and *trans*-propenyl propionate to *cis*-propenyl acetate and to *trans*-propenyl acetate. However, side reactions such as saponification and oxidation of the ester were more serious than in the chloride containing system so a complete kinetic analysis could not be carried out. However, qualitatively *trans*-propenyl propionate gave mainly *trans*-propenyl acetate while the *cis* isomer gave mainly *cis*-propenyl acetate.

TABLE 4. Values of k_{ex} for various vinylic esters under one set of experimental conditions*

Vinylic ester	$k_{ex} \times 10^5$ (s^{-1})
$H_2C{=}CHOOCC_2H_5$	58.0
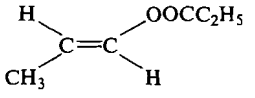	2.2
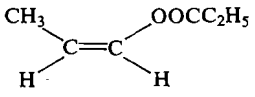	1.4
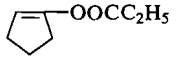	1.30

*$[Na_2Pd_2(OAc)_6] = 6.4 \times 10^{-3}$ M; [NaOAc] = 0.20 M.

Can. J. Chem. Downloaded from www.nrcresearchpress.com by 210.87.254.40 on 09/05/12
For personal use only.

Discussion

The rate expression given by [9] contains three independent terms, all of which are zero order in [NaOAc]. Each term will be considered separately in order of importance.

k_d Term

This term represents the exchange catalyzed by the dimeric species, $Na_2Pd_2(OAc)_6$. This term is analogous to the $Li_2Pd_2Cl_6$ catalysis in the chloride system. The two features of this contribution by this term which is different from $Li_2Pd_2Cl_6$ catalysis are (*1*) the lack of a sodium acetate term and (*2*) the stereochemical results. The rate expression for the exchange in the chloride system is given by [11].

[11] $$\text{rate} = \frac{k[Li_2Pd_2Cl_6][VP](k' + k''[LiOAc])}{[LiCl]}$$

Furthermore in the chloride system *cis*-propenyl propionate gave only *trans*-propenyl acetate, and the *trans*-isomer gave *cis*-acetate. Also cyclopentyl propionate did not exchange as a detectable rate. The rate of exchange of the propenyl propionates was at least 10^4 times faster than that for cyclopentyl propionate. The results provided conclusive evidence that acetoxypalladation–deoxypalladation is a very stereospecific process, which other evidence indicated is exclusively *trans* (9). For instance, as shown in reaction 12, cyclopentyl propionate would not be expected to exchange if acetoxypalladation–deacetoxypalladation is stereospecific (A = addition; E = elimination).

[12]

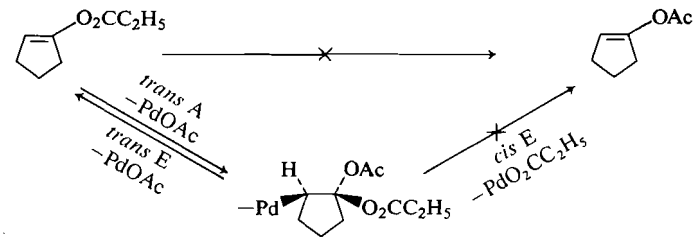

These differences between the two systems are not too surprising in light of the fact that in the chloride system acetate does not effectively compete with chloride as a ligand for Pd(II). As a result it is only a reactant. In the chloride free system acetate is both a ligand and reagent. A better comparison with acetate exchange catalyzed by $Na_2Pd_2(OAc)_6$ might thus be vinyl chloride exchange with radioactive lithium chloride catalyzed by $Li_2Pd_2Cl_6$ (10).

[13] $$CH_2{=}CHCl + LiCl^* \xrightarrow{Li_2Pd_2Cl_6} CH_2{=}CHCl^* + LiCl$$

In this case chloride is also both a ligand and reactant, and the rate expression is analogous to acetate exchange by $Na_2Pd_2(OAc)_6$ in that it does not contain a term in [LiCl]. Also in this case stereochemical studies indicate that chloropalladation, as opposed to acetoxypalladation in this system, is a nonstereospecific process.

[14] $$\text{rate} = k[Li_2Pd_2Cl_6][C_2H_3Cl]$$

The lack of a [LiCl] term must result from the cancellation of an inhibitory term in the π-complex formation step (reaction 3) by a catalytic term in the chloropalladation step. The lack of stereospecificity is explained by the fact chloride can attack from either inside or outside the coordination sphere. Note that both modes of attack require a catalytic term in [LiCl] since the chloride coordinated to Pd(II) cannot complete its transfer to carbon until a chloride from solution fills the incipient vacant coordination site on Pd(II) (1, 10).

[15]

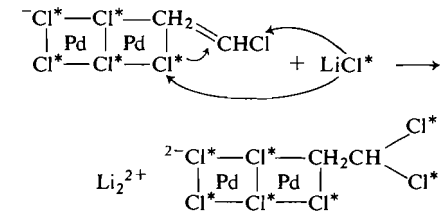

An analogous situation would exist in the chloride free system with acetate now taking the role of chloride. The inhibitory term in reaction 16 would be cancelled by a catalytic term from reaction 17, where acetoxypalladation can now

Can. J. Chem. Downloaded from www.nrcresearchpress.com by 210.87.254.40 on 09/05/12
For personal use only.

[16] $Na_2Pd_2(OAc)_6 + VP \rightleftharpoons NaPd_2(OAc)_5(VP) + NaOAc$

[17] 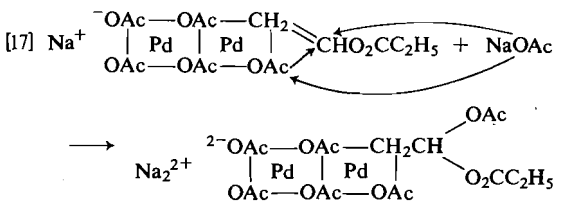

occur from either inside or outside the coordination sphere of Pd(II). This is consistent with the stereochemical results which indicate acetoxy palladation is nonstereospecific in this system.

The present results provide further evidence that addition of Pd(II) and nucleophiles to double bonds is not always stereospecific but depends on reagent, reaction conditions, and probably other more subtle factors such as olefin structure and solvent (11). Thus, a phenyl ligand is convalently bonded to Pd(II) and is constrained to add *cis* to olefin (12). Hydride probably adds *cis* for the same reason. However, reagents such as chloride and acetate can add *cis* or *trans* depending on their ability to coordinate to Pd(II) under the reaction conditions.

k_t Term

Somewhat less is known about this term than the k_d. One problem in defining this term is that no interaction between the trimer and vinyl propionate could be detected spectroscopically so equilibrium studies could not be carried out. This follows from the fact that vinyl esters are poor at complexing Pd(II) as compared with allylic esters or ordinary monosubstituted olefins such as styrene (3).

The reaction is zero-order [NaOAc] and requires an induction period to form a catalytically active species which is presumably an olefin π-complex. It is not suprising there is an induction period since to form a π-complex, acetate bridges must be broken, and it is known (2, 3) that bridging acetates are nonlabile.

Although the data provides little evidence for the exact nature of the reactive intermediate, the two most likely possibilities are given by reactions 18 and 19.

[18] $Pd_3(OAc)_6 + 2VP \rightleftharpoons$ 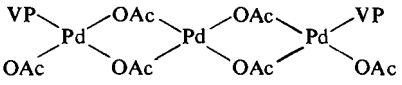

[19] $Pd_3(OAc)_6 + VP \rightleftharpoons$ 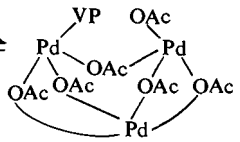

The first has some analogy in formation of π-allylic complexes (13).

[20] $Pd_3(OAc)_6 + R_1CH_2CH{=}CHR_2 \longrightarrow$ 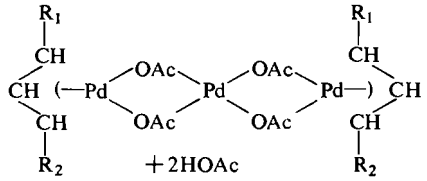

In both cases a [NaOAc] dependent term in the rate expression arising from attack of acetate on the π-complex, might be expected. It is possible that acetate is behaving as a bidentate ligand and reagent in the acetoxypalladation step. With the intermediate formed via reaction 19 the scheme would be given by reaction 21.

[21] 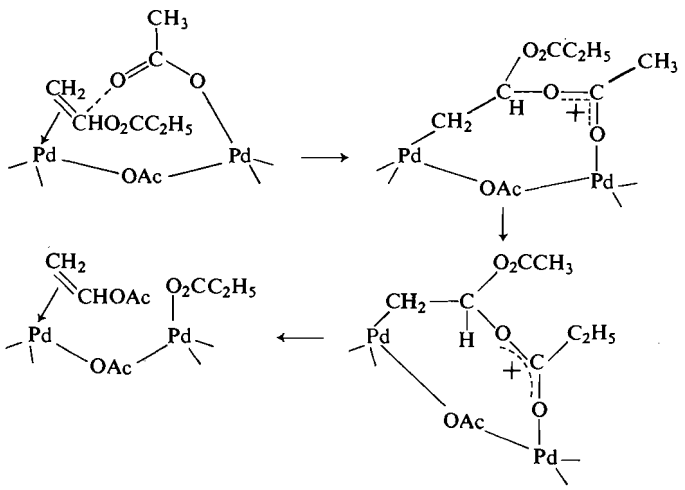

Such internal attack would be expected to give specific *cis* addition. Unfortunately because of the slowness of exchange and the induction time as compared with rates of side reactions, stereochemical studies are experimentally very difficult with the trimer and were not attempted.

The reason the rate jumps by a factor of about two when trace amounts of sodium acetate are added is not clear but does appear to be a real effect since it is reproducible. Perhaps the sodium acetate catalyzes the formation of the active π-complex.

k_0 Term

This term is the most mysterious of all since it is zero order in Pd(II). There is a temptation to dismiss it as an experimental artifact but the positive intercepts in Figs. 2 and 3 appear to be outside of experimental error. A possible scheme which would give a reaction catalyzed by Pd(II) yet zero order in Pd(II) would be that shown in reaction 22.

$$[22]\quad CH_2{=}CHO_2CC_2H_5 \xrightarrow{\text{slow}} \text{intermediate} \xrightarrow[\text{Pd(II)}]{\text{fast}} \text{products}$$

In any case this term is small and further speculation as to its origin, if in fact it is real, seems unwarranted.

Conclusions

There have been a number of very interesting studies of catalysis by palladium(II) acetate in acetic acid and some intriguing stereochemical and kinetic results have been reported (13–18). The present kinetic study as well as the two preceding equilibria studies (2, 3) demonstrate the complexity of this system with three different Pd(II) species to consider and equilibria which may be either slow or fast. Thus, if the vinyl propionate exchange were slower, the complication of formation of unreactive π-complexes (reaction 8) would arise. This complication actually does arise in allylic propionate exchange and is probably present in olefin oxidation (15). Thus, in order to understand completely the various observations in this system, the various equilibria and rates of attainment of equilibria must be taken into account.

Acknowledgment is made to the National Research Council of Canada and to the Donors of The Petroleum Research Fund, administered by the American Chemical Society, for support of this research.

1. P. M. Henry. Acc. Chem. Res. **6**, 16 (1973).
2. R. N. Pandey and P. M. Henry. Can. J. Chem. **52**, 1241 (1974).
3. R. N. Pandey and P. M. Henry. Can. J. Chem. **53**, 1833 (1975).
4. D. Y. Curtin and M. J. Hurwitz. J. Am. Chem. Soc. **74**, 5381 (1952).
5. M. O. House and V. Kramer. J. Org. Chem. **28**, 3362 (1963).
6. P. M. Henry. J. Org. Chem. **38**, 3596 (1973).
7. P. M. Henry. J. Am. Chem. Soc. **93**, 3853 (1971).
8. P. M. Henry. J. Am. Chem. Soc. **94**, 1527 (1972).
9. P. M. Henry and G. A. Ward. J. Am. Chem. Soc. **93**, 1494 (1971).
10. P. M. Henry. J. Org. Chem. **37**, 2443 (1972).
11. P. M. Henry. Adv. Organomet. Chem. **13**, 363 (1975).
12. P. M. Henry and G. A. Ward. J. Am. Chem. Soc. **94**, 673 (1972).
13. R. G. Brown and J. M. Davidson. Adv. Chem. Ser. **132**, 49 (1974).
14. W. Kitching, Z. Rappoport, S. Winstein, and W. G. Young. J. Am. Chem. Soc. **88**, 2054 (1966).
15. I. I. Moiseev, A. P. Belov, W. A. Igoshin, and Ya K. Syrkin. Dokl. Akad. Nauk SSSR, **173**, 863 (1967).
16. R. G. Schultz and D. G. Gross. Adv. Chem. Ser. **70**, 97 (1968).
17. D. Clark, P. Hayden, and R. D. Smith. Discuss. Faraday Soc. **45**, 98 (1968).
18. J. E. McCaskie. Ph.D. Thesis, University of California, Los Angeles, California. 1971.

Can. J. Chem. Downloaded from www.nrcresearchpress.com by 210.87.254.40 on 09/05/12
For personal use only.

Monosubstituted Derivatives of $(L–L)Fe_2(CO)_6$ (L–L = fluorocarbon bridged ligand)

LIAN SAI CHIA, WILLIAM R. CULLEN, JOHN R. SAMS, AND JAMES C. SCOTT

Chemistry Department, University of British Columbia, Vancouver, British Columbia V6T 1W5

Received January 31, 1975

LIAN SAI CHIA, WILLIAM R. CULLEN, JOHN R. SAMS, and JAMES C. SCOTT. Can. J. Chem. **53**, 2232 (1975).

The reaction of the ditertiary arsines and phosphines $f_n$fars, $f_n$fos, and f_nAsP, (L–L), with $Fe(CO)_5$ at 150° is a superior route to the complexes $(L–L)Fe_2(CO)_6$. Two are reported for the first time (L–L = $f_6$fars, $f_8$fars). The complexes react with monodentate and certain potentially bidentate ligands on u.v. irradiation to afford the monosubstituted derivatives $L(L–L)Fe_2(CO)_5$ and $(L–L)'(L–L)Fe_2(CO)_5$. Spectroscopic studies, in particular magnetically perturbed Mössbauer spectra, indicate that the site of substitution is *trans* to the Fe^A—Fe^B bond and *cis* to the two group V atoms (on Fe^A). Disubstitution seems to result in further displacement of CO from either Fe^A or Fe^B.

LIAN SAI CHIA, WILLIAM R. CULLEN, JOHN R. SAMS et JAMES C. SCOTT. Can. J. Chem. **53**, 2232 (1975).

La réaction des arsines et phosphines ditertiaires $f_n$fars, $f_n$fos et f_nAsP, (L–L), avec $Fe(CO)_5$ à 150° est une excellente manière d'arriver aux complexes $(L–L)Fe_2(CO)_6$. Deux complexes sont décrits pour la première fois (L–L = $f_6$fars, $f_8$fars). Les complexes réagissent avec des ligands monodentates et certains ligands potentiellement bidentates sous irradiation u.v., pour conduire aux dérivés mono-substitués $L(L–L)Fe_2(CO)_5$ et $(L–L)'(L–L)Fe_2(CO)_5$. Les études spectroscopiques, en particulier le spectre Mössbauer magnétiquement perturbé, indiquent que la position de substitution est *trans* par rapport au lien Fe^A—Fe^B et *cis* par rapport aux deux atomes du groupe V (sur Fe^A). La disubstitution semble résulter d'un déplacement ultérieur du CO soit de Fe^A, soit de Fe^B. [Traduit par le journal]

Introduction

The fluorocarbon-bridged ligands $f_n$fars $[(CH_3)_2AsC{=}CAs(CH_3)_2(CF_2)_{n/2}]$, $f_n$fos $[(C_6H_5)_2PC{=}CP(C_6H_5)_2(CF_2)_{n/2}]$, and f_nAsP $[(C_6H_5)_2PC{=}CAs(CH_3)_2(CF_2)_{n/2}]$ have an almost unique ability to form complexes of formula $(L–L)Fe_2(CO)_6$ in which the two group V donor atoms and the double bond of the bridging group are coordinated to the iron atoms (1, 2). The solid state structure of $f_4farsFe_2(CO)_6$ (3) is seen in Fig. 1.

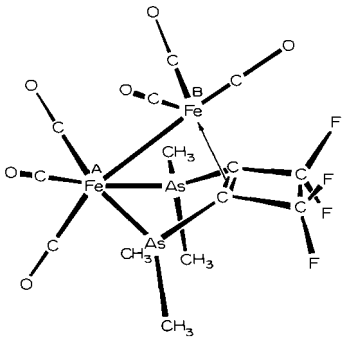

FIG. 1. The solid state structure of $f_4farsFe_2(CO)_6$.

The present investigation describes the preparation of two new $(L–L)Fe_2(CO)_6$ complexes where L–L = $f_6$fars and $f_8$fars and some substitution reactions of the complexes using a variety of Lewis bases, L, which afford $L(L–L)Fe_2(CO)_5$. Magnetically perturbed Mössbauer spectra have been used as an aid in establishing the site of substitution (4).

Experimental

All volatile chemicals were manipulated using a conventional vacuum system. The Carius tubes used in this work, with volumes of about 80 ml, were constructed of thick-walled Pyrex glass. All chromatography was carried out on Florisil columns under a nitrogen atmosphere using nitrogen saturated solvents. The petroleum ether was the 30–60° boiling fraction.

Infrared spectra were recorded on a Perkin–Elmer 457 spectrophotometer and calibrated using polystyrene and cyclohexane. Unless otherwise stated, all n.m.r. spectra were run on a Varian T-60 spectrometer with chemical shifts given in p.p.m. downfield from internal TMS for ^1H, and upfield from internal $CFCl_3$ for ^{19}F spectra. Ultraviolet and visible spectra were run in methylene chloride solution using a Cary 15 spectrophotometer. Mass spectra were measured with an AEI MS-9 mass spectrometer with direct introduction of solid samples. All molecular weights were measured with a Mechrolab

Can. J. Chem. Downloaded from www.nrcresearchpress.com by 210.87.254.42 on 09/05/12
For personal use only.

Can. J. Chem. Downloaded from www.nrcresearchpress.com by 210.87.254.42 on 09/05/12
For personal use only.

vapor pressure osmometer using benzene as a solvent. Melting points were determined in evacuated capillaries and are uncorrected. Most microanalyses were performed by P. Borda of this department, and some by Pascher Mikroanalytisches Laboratorium, Bonn, Germany.

The Mössbauer spectrometer has been described (2, 4). Spectra in zero applied field were recorded with the $^{57}Co(Cu)$ source at room temperature and the finely powdered absorbers at 80 K in transmission geometry. The data were least-squares fitted to Lorentzian components using unconstrained fitting parameters, and isomer shifts are quoted relative to the centroid of the sodium nitroprusside spectrum. Magnetic perturbation Mössbauer spectra were obtained as described elsewhere (4), employing longitudinal magnetic fields of up to 50 kG.

The iron pentacarbonyl and the more common ligands were obtained commercially and used without further purification. The fluorocarbon-bridged ligands f_nAsP ($n = 4, 6$), and f_nfos and f_nfars ($n = 4, 6, 8$) were prepared using published procedures (2, 5).

Preparation of $(L–L)Fe_2(CO)_6$ Complexes

The method used to obtain $f_6farsFe_2(CO)_6$ is given as an example. A benzene solution (10–15 ml) containing 2.0 mmol of f_6fars and 5 to 10 g of $Fe(CO)_5$ was heated at 150° in an evacuated Carius tube for 1 d. At the end of the reaction period the initially yellow solution had become deep red. The tube was cooled in liquid nitrogen and opened. The volatile contents were removed at reduced pressure. The resulting red residue was dissolved in a minimum amount of methylene chloride and chromatographed on a Florisil column. A 5% diethyl ether – 95% petroleum ether mixture eluted the more soluble iron carbonyl complexes (*e.g.* $(L–L)Fe(CO)_4$, $(L–L)Fe(CO)_3$, etc.). The desired product was eluted with diethyl ether/petroleum ether (1:9) and was obtained as an orange-red solid m.p. 225° in 70% yield. ^1H n.m.r.; singlets at 1.55 and 2.40 p.p.m.

Anal. Calcd. for $C_{15}H_{12}As_2F_6Fe_2O_6$: C, 27.5; H, 2.3. Found: C, 26.8; H, 2.3.

In the same way $f_8farsFe_2(CO)_6$ was obtained as an orange-red solid m.p. 210° in 45% yield after 1 d. ^1H n.m.r.; singlets at 1.57 and 2.53 p.p.m.

Anal. Calcd. for $C_{16}H_{12}As_2F_8Fe_2O_6$: C, 26.9; H, 1.7. Found: C, 27.0; H, 1.9.

Other known $(L–L)Fe_2(CO)_6$ complexes could also be prepared by this new method, *e.g.* $f_4farsFe_2(CO)_6$, reaction time 1 d, yield 20%; $f_4AsPFe_2(CO)_6$, 2 d, 90%; $f_4fosFe_2(CO)_6$, 2 d, 80%; $f_6AsPFe_2(CO)_6$, 1 d, 50%; $f_6fosFe_2(CO)_6$, 2 d, 10%.

Preparation of Monosubstituted Derivatives of $(L–L)Fe_2(CO)_6$

The general procedure was as follows, specific details are given in Table 1. The $(L–L)Fe_2(CO)_6$ complex (1.0 mmol), an equimolar amount of ligand, and acetone (15–20 ml) were sealed under vacuum in a Carius tube. After irradiation for several days with a 100 W u.v. lamp (20 cm from the tube) the tube was opened and the volatile contents were removed. The residue was dissolved in a small amount of methylene chloride and chromatographed on Florisil. The excess ligand and the unreacted $(L–L)Fe_2(CO)_6$ were removed by eluting with diethyl ether/petroleum ether (1:9). The desired product was eluted with the solvent indicated in Table 1. Analytical data for these complexes are also given in Table 1 and some spectroscopic data are listed in Table 2.

Use of a 450 W lamp in a quartz jacket inserted into the reaction solution gave the same products but much shorter reaction times were needed.

The di- and trisubstituted derivatives were obtained by irradiating $(L–L)Fe_2(CO)_6$, $L(L–L)Fe_2(CO)_5$, or $L_2(L–L)Fe_2(CO)_4$ in the presence of excess monodentate ligand, L.

Results and Discussion

$(L–L)Fe_2(CO)_6$ Complexes

The ligands f_6fars and f_8fars react with $Fe(CO)_5$ at 150° to give high yields of $f_6farsFe_2(CO)_6$ and $f_8farsFe_2(CO)_6$. Previously the best method of preparing this type of complex was from the more expensive $Fe_3(CO)_{12}$ (6). The new method is superior in terms of yields and ease of workup.

The two new $(L–L)Fe_2(CO)_6$ complexes have spectroscopic properties which are very similar to those of the others of the same formula and hence are assumed to have an analogous structure (Fig. 1).

During initial studies on the preparation of the $(L–L)Fe_2(CO)_6$ complexes of f_nfos (2) and f_nAsP (6), it was found that the yields decrease with increased ring size (compounds with $n = 8$ are not known). This was originally taken as an indication that as the ring becomes less strained there is less tendency for the double bond to coordinate to Fe^B. However, the good yields of f_6fars and f_8fars derivatives (70% and 45% respectively) suggest that ring strain is not the only factor and that steric hindrance (possibly by bulky $P(C_6H_5)_2$ groups) plays some part. The related unstrained acyclic ligand *cis*-$(CH_3)_2AsC(CF_3)=C(CF_3)As(CH_3)_2$ also forms a $Fe_2(CO)_6$ derivative (7).

The infrared carbonyl bands of the known $(L–L)Fe_2(CO)_6$ complexes are listed in Table 3. Three of the six carbonyl stretching frequencies $\sim$2061, $\sim$2023, and $\sim$1983 cm^{-1}, are relatively insensitive to ligand substitution, the variation in frequency, $\Delta\nu(CO)$, being less than 7 cm^{-1}, while the other three, at $\sim$1997, $\sim$1966, and $\sim$1954 cm^{-1}, vary markedly with ligand substitution ($\Delta\nu(CO) = 12$ to 22 cm^{-1}). Provided no coupling occurs between carbonyl groups on Fe^A and those on Fe^B (Fig. 1), then the three $\nu(CO)$ bands at $\sim$2061, $\sim$2023, and $\sim$1983 cm^{-1} can be assigned to CO groups on Fe^B. The $\nu(CO)$ of the other three carbonyl groups on Fe^A increase in the order $(L–L) = f_nfars < f_nAsP < f_nfos$. This order is expected on the

Can. J. Chem. Downloaded from www.nrcresearchpress.com by 210.87.254.42 on 09/05/12
For personal use only.

TABLE 1. Preparative and analytical data for derivatives of $(L\text{–}L)Fe_2(CO)_6$*

Complex	Color†	Melting point (°C)	Reaction time (d)	Eluent‡	Yield (%)	Analyses (%) C Calcd.	C Found	H Calcd.	H Found	Molecular weight Calcd.	Molecular weight Found
$Ph_3Pf_4AsPFe_2(CO)_5$	d.r.	208	7	A	24	53.0	52.9	3.4	3.4	928	915
$(PhO)_3Pf_4AsPFe_2(CO)_5$	o.r.	190	10½	A	20	50.4	50.8	3.2	3.4	976	934
$Ph_3Asf_4AsPFe_2(CO)_5$	r.	180	20	A,B	5	50.6	50.7	3.2	3.4		
$Ph_3Sbf_4AsPFe_2(CO)_5$	o.r.	110	40	A	5	48.3	48.5	3.1	3.2		
$Ph_3Sbf_4fosFe_2(CO)_5$	o.r.	145	30	A	30	55.6	57.4	3.2	4.8		
$(PhO)_3Pf_4farsFe_2(CO)_5$	d.b.	175	15	A	40	41.5	41.9	3.0	3.4		
$f_4fars^mf_4AsPFe_2(CO)_5$	o.r.	105	20	C,D	~5	37.2	37.0	2.8	2.8	1000	949
$dpae^mf_4AsPFe_2(CO)_5$	o.r.	160	12	C,D	6	51.0	50.8	3.5	3.7	1152	1170
$dppp^mf_4AsPFe_2(CO)_5$	o.r.	155	10½	C,D	18	55.7	56.1	3.9	4.2	1078	1004
$f_4AsP^mf_4farsFe_2(CO)_5$	o.r.	168	21½	C,D	30	37.2	37.0	2.8	2.8	1000	976
$(Ph_3As)_2f_4AsPFe_2(CO)_4$	r.	184	105	A,B	10	55.7	54.3	3.7	3.8	1250	1005
$[(PhO)_3P]_2f_4AsPFe_2(CO)_4$	d.b.	130	40	A,B	10	55.3	55.0	3.7	4.7		
$(Ph_3Sb)_3f_4fosFe_2(CO)_3$	r.	115	90	B	5	73.1	68.5	4.7	5.2	1749	1578

*In general a bidentate ligand (L–L) gave two or three types of complexes from the same reaction. Only the monodentate ones designated by m are listed here. The following abbreviations are used in this and subsequent tables: Ph = C_6H_5; dpae = $(C_6H_5)_2AsCH_2CH_2As(C_6H_5)_2$; dppp = $(C_6H_5)_2P(CH_2)_3P(C_6H_5)_2$; $f_4$fars etc. see Introduction.

†d.b. = dark brown, d.r. = dark red, r. = red, o.r. = orange red.

‡Solvent key: A: 10–20% diethyl ether – 90–80% petroleum ether mixture; B: 20–50% diethyl ether – 80–50% petroleum ether mixture; C: CH_2Cl_2; D: acetone. The chromatographic column was eluted with the solvent in the following order: petroleum ether, A. B, C, and then D.

TABLE 2. Spectroscopic data for derivatives of (L–L)$Fe_2(CO)_6$*

Complex	$\nu_{CO}(CH_2Cl_2)$ (cm^{-1})†			$\lambda_{max}(CH_2Cl_2)$ (nm) (ε_{molar})‡
$Ph_3Pf_4AsPFe_2(CO)_5$	2034(10)	1979(9)	1960(8)	386(10 922)
$(PhO)_3Pf_4AsPFe_2(CO)_5$	2044(10)	1990(9)	1970(9)	382(9 610)
$Ph_3Asf_4AsPFe_2(CO)_5$	2035(10)	1977(9)	1958(9)	387(3 900)
$Ph_3Sbf_4AsPFe_2(CO)_5$	2036(10)	1976(9)	1954(9)	385(9 782)
$Ph_3Sbf_4fosFe_2(CO)_5$	2037(10)	1984(10)	1969(10)	388(6 170)
$(PhO)_3Pf_4farsFe_2(CO)_5$	2035(10)	1987(8)	1965(8)	391(8 272)
$f_4fars^mf_4AsPFe_2(CO)_5$	2037(10)	1977(9)	1957(8)	386(8 467)
$dpae^mf_4AsPFe_2(CO)_5$	2035(10)	1976(9)	1957(9)	382(11 232)
$dppp^mf_4AsPFe_2(CO)_5$	2036(10)	1979(9)	1960(8)	386(8 842)
$f_4AsP^mf_4farsFe_2(CO)_5$	2035(10)	1980(9)	1958(9)	397(15 100)
$(Ph_3As)_2f_4AsPFe_2(CO)_4$	1985(9)	1948(10)	1923(7),1904(6)	432(5 813)
$[(PhO)_3P]_2f_4AsPFe_2(CO)_4$	2013(10)	1966(9)	1907(5)	402(11 762)
$(Ph_3Sb)_3f_4fosFe_2(CO)_3$	1968(6.5)	1944(10)	1913(7)	515(3 210)

*See footnote * Table 1.
†Integers in parentheses refer to relative peak height.
‡ε_{molar} = molar extinction coefficient.

TABLE 3. Infrared CO bands of (L–L)$Fe_2(CO)_6$ complexes

(L–L)	$\nu_{CO}(C_6H_{12})$ (cm^{-1})*					
f_4fars†	2059(s)	2022(vs)	1992(s)	1982(s)	1965(w)	1950(m)
f_4AsP‡	2062(7)	2024(10)	1996(8)	1982(5)	1969(4)	1952(3)
f_4fos†	2062(s)	2024(vs)	2001(s)	1984(m)	1971(m)	1965(m)
f_6fars	2060(8)	2019(10)	1992(9)	1980(9)	1953(6)	1942(7)
f_6AsP‡	2062(8)	2026(10)	2000(8)	1986(7)	1973(4)	1955(4)
f_6fos†	2063(s)	2026(vs)	2004(m)	1985(m)	1973(m)	1968(m, sh)
f_8fars	2061(7)	2020(10)	1994(8)	1985(7)	1958(4)	1946(4)

*Symbols or figures in parentheses refer to relative peak height.
†From ref. 2.
‡From ref. 6.

basis of phosphines being better π-acceptors than arsines (8).

The electronic spectra of the (L–L)$Fe_2(CO)_6$ complexes (Table 4) show two strong bands. Gray and co-workers (9, 10) have assigned an intense band at 244 nm in $Fe(CO)_5$ to the lowest allowed metal-to-ligand charge transfer transition. It is likely that the bands at ~230 nm in the (L–L)$Fe_2(CO)_6$ complexes have the same origin. The other strong bands at ~375 nm are similar, both in energy and extinction coefficient, to the σ–σ* band in $Mn_2(CO)_{10}$ which involves orbitals from the metal–metal bond (11, 12). If this assignment is carried over to the (L–L)$Fe_2(CO)_6$ derivatives then the observed order of λ_{max} $f_nfosFe_2(CO)_6$ < $f_nAsPFe_2(CO)_6$ < $f_nfarsFe_2(CO)_6$ could be an indication that the better donors increase the electron density on Fe^A allowing it to become a better donor in turn to Fe^B thus increasing the strength of the Fe—Fe bond.

^{57}Fe Mössbauer parameters for the (L–L)$Fe_2(CO)_6$ complexes are given in Table 5. In each case the spectra in zero applied magnetic field consist of four lines, and in principle there are three ways of assigning these lines to the two iron atoms. Previously, line assignments in such compounds have been based on known crystallographic data and predicted effects on the Mössbauer parameters of changes in ligand structure. We have recently shown (4) that magnetically perturbed Mössbauer spectra can pro-

TABLE 4. Electronic spectra of (L–L)$Fe_2(CO)_6$ complexes

(L–L)	$\lambda_{max}(CH_2Cl_2)$ (nm) (ε_{molar})*	
f_4fars	382(8235)	232(12 500)
f_4AsP	375(8536)	229(16 500)
f_4fos	361(6482)	226(9 850)
f_6fars	382(8549)	233(25 050)
f_6AsP	375(5952)	229(11 040)
f_6fos	360(5521)	226(10 500)
f_8fars	381(7701)	232(15 000)

*ε_{molar} = molar extinction coefficients.

Can. J. Chem. Downloaded from www.nrcresearchpress.com by 210.87.254.42 on 09/05/12
For personal use only.

TABLE 5. Mössbauer parameters at 80 K for $(L\text{–}L)Fe_2(CO)_6$ complexes*

(L–L)	δ (mm/s)	ΔE_Q (mm/s)	Γ (mm/s)	η	Iron atom
$f_4$fos	0.23	−0.66	0.26	0.6	A
	0.32	+1.32	0.26	0.6	B
$f_6$fos	0.22	0.65	0.23		A
	0.32	1.19	0.23		B
f_4AsP	0.27	−0.83	0.23	0.8	A
	0.31	+1.45	0.23	0.6	B
f_6AsP	0.26	0.73	0.30		A
	0.32	1.19	0.24		B
$f_4$fars	0.28	0.64	0.25		A
	0.32	1.44	0.25		B
$f_6$fars	0.30	−0.67	0.26	0.0	A
	0.33	+1.41	0.27	0.6	B
$f_8$fars	0.28	0.62	0.28		A
	0.32	1.38	0.27		B

*For δ, ΔE_Q, and Γ the experimental uncertainty is ±0.01 mm/s. Isomer shifts are relative to sodium nitroprusside. η values and signs of ΔE_Q were determined with source and absorber at 4.2 K.

vide completely unequivocal assignments of the spectral lines to the two iron atoms in binuclear complexes of this type. Three of the present compounds (L–L = $f_4$fos, f_4AsP, $f_6$fars) have been studied in applied magnetic fields, and the results have confirmed our earlier assignments (2) based on semi-intuitive arguments.

As expected in view of the coordination geometry about the two iron atoms in $f_4farsFe_2(CO)_6$ (Fig. 1), Fe^A shows a smaller quadrupole splitting $|\Delta E_Q|$ than does Fe^B in all the $(L\text{–}L)Fe_2(CO)_6$ complexes. There are two other interesting trends in the $|\Delta E_Q|$ values in Table 5. Firstly, for Fe^A $|\Delta E_Q|$ in the compounds $f_nAsPFe_2(CO)_6$ are larger than the values observed in the derivatives $f_nfosFe_2(CO)_6$ and $f_nfarsFe_2(CO)_6$, where both group V atoms bonded to Fe^A are the same. This behavior presumably reflects differences in σ-donor and π-acceptor abilities of the phosphine and arsine groups in the "mixed" ligands.

Secondly for Fe^B $|\Delta E_Q|$ decreases as the value of n increases in each series of compounds containing $f_n$fos, $f_n$fars, and f_nAsP. The coordination about Fe^B may be regarded as distorted trigonal bipyramidal if the double bond of the ligand is considered as a single entity forming a π-bond with the iron moiety (3). It may also be regarded as distorted octahedral if the carbon atoms at each end of the double bond are considered to form two normal σ-bonds with Fe^B (1). The trend in $|\Delta E_Q|$ for Fe^B may indicate a change from the former bond type to the latter as n increases, since an opening of the angles at the double-bonded carbon atoms would facilitate the formation of σ-bonds to Fe^B.

In all the $(L\text{–}L)Fe_2(CO)_6$ complexes the isomer shift δ of Fe^B is greater than that of Fe^A, showing a smaller s-electron density at the former nucleus. To satisfy the effective atomic number rule, Fe^A can be viewed as forming a dative bond to Fe^B, so it is not surprising that the s-electron density at Fe^B remains somewhat less than that at Fe^A. Although the electronic spectra suggest that the iron–iron bond may be slightly stronger in the phosphine derivatives than in the arsine ones, this is not reflected in the isomer shift data, where δ for Fe^B is constant within experimental error and independent of the nature of the ligand. It is possible, of course, that the admixture of electron density in the $Fe^A \rightarrow Fe^B$ bond is such that any increase in 4s electron donation is effectively counterbalanced by an additional shielding from enhanced 3d donation, leaving the isomer shift of Fe^B constant. On the other hand, δ of Fe^A is fairly sensitive to the nature of the ligand, being lowest for the $f_n$fos derivatives and increasing when arsenic replaces phosphorus as the donor atom. This is the trend usually observed in similar iron carbonyl complexes (2, 13) and reflects the fact that phosphines are better σ-donors and π-acceptors than arsines (8).

For the three $(L\text{–}L)Fe_2(CO)_6$ complexes studied in applied magnetic fields, we find that

Can. J. Chem. Downloaded from www.nrcresearchpress.com by 210.87.254.42 on 09/05/12
For personal use only.

Can. J. Chem. Downloaded from www.nrcresearchpress.com by 210.87.254.42 on 09/05/12
For personal use only.

the quadrupole coupling constants e^2qQ are negative at Fe^A and positive at Fe^B. Since the quadrupole moment eQ is positive for ^{57m}Fe, e^2qQ carries the same sign as $V_{zz}(= eq)$, the principal component of the electric field gradient (e.f.g.) tensor. Thus, our results indicate that there is an excess of electron density along the z-axis at Fe^A and a deficiency of electron density along the z-axis at Fe^B. Although one does not know the relative orientations of the molecular axes and the principal e.f.g. axes at either site, it does not seem unreasonable to assume that the z-axis of the e.f.g. lies roughly along the iron–iron bond direction in both cases (*vide infra*). If this is so, the signs of V_{zz} at each site are at least consistent with the formulation of an $Fe^A \rightarrow Fe^B$ dative bond.

In fitting the magnetic perturbation spectra we have also attempted to estimate the asymmetry parameters η at each site. Theoretical spectra were computed with $\eta = 0.0$, 0.6, and 0.8 for each iron atom, and all possible combinations of these η values were examined. The preferred solution was that which yielded the smallest value of χ^2. We should stress that this procedure does not necessarily provide the best possible value of η, especially since the computed spectra are rather insensitive to η values less than about 0.5, but merely serves to indicate whether η is large or small at each site. In the three cases examined, best agreement was obtained with $\eta = 0.6$ at Fe^B, although η at Fe^A appears to vary from compound to compound. For $f_6farsFe_2(CO)_6$, $\eta(Fe^A)$ is small (4), but it is large for the other two complexes (see Fig. 2). This is perhaps not surprising for $f_4AsPFe_2(CO)_6$ since the two group V donor atoms differ, but we might have expected $f_4fosFe_2(CO)_6$ to be more like the f_6fars complex. It may be that geometrical factors are quite important in determining η at Fe^A.

Substitution Reactions

All the above (L–L)$Fe_2(CO)_6$ complexes react with various arsines and phosphines under u.v. irradiation to give a number of derivatives which can be classified into eight groups (14). Only those derivatives of monodentate ligands, including potentially bidentate acting in a monodentate fashion, will be considered in this paper (Table 1).

Most of the derivatives are monosubstituted and have the formula (L)(L–L)$Fe_2(CO)_5$. Their

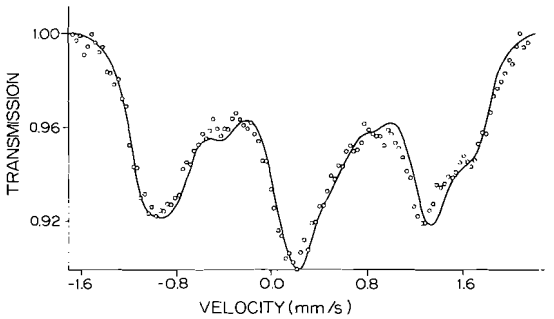

FIG. 2. ^{57}Fe Mössbauer spectrum of $f_4AsPFe_2(CO)_6$ in a parallel magnetic field of 50 kG. Site A, $\Delta E_Q = -0.83$ mm/s, $\eta = 0.8$; site B, $\Delta E_Q = +1.45$ mm/s, $\eta = 0.6$.

infrared spectra show only three ν(CO) bands suggesting a structure with a plane of symmetry. This is confirmed by the ^1H n.m.r. spectra of $(PhO)_3Pf_4farsFe_2(CO)_5$ and $(f_4AsP)^mf_4farsFe_2(CO)_5$ (m indicates monodentate) where the arsenic methyl groups of the f_4fars moiety appear as two singlets at 1.60 and 2.07 p.p.m., and 1.03 and 2.35 p.p.m. respectively. ($f_4farsFe_2(CO)_6$ absorbs at 1.50 and 2.21 p.p.m. (2).)

The f_4AsP compound also has an arsenic methyl singlet at 1.01 p.p.m. indicating that this particular —$As(CH_3)_2$ group is "dangling" so that, not unexpectedly, it is the phosphorus end of the ligand which is coordinating.[1] These results indicate that monosubstitution occurs at one of the "axial" carbonyl groups in Fig. 1 *i.e.* a carbonyl group *trans* to the Fe—Fe bond.

The solid state structure of $(f_4AsP)f_4AsPFe_2(CO)_4$ (15) (Fig. 3) shows that one f_4AsP ligand has displaced two carbonyl groups from $f_4AsPFe_2(CO)_6$ and that the ligand is chelated to Fe^A with the $P(C_6H_5)_2$ moiety *trans* to the Fe—Fe bond. This result also indicates that monosubstitution would take place on Fe^A and that the axial CO group would be displaced. Further substitution of the $Fe_2(CO)_6$ skeleton can be achieved using $(C_6H_5O)_3P$ and $(C_6H_5)_3E$ (E = As, Sb). The trisubstituted complexes are not very stable and are difficult to characterize. The disubstituted derivative $[(C_6H_5O)_3P]_2(f_4AsP)Fe_2(CO)_4$ has an infrared spectrum very similar to that of the chelate derivative $f_4AsP(f_4AsP)Fe_2(CO)_4$. Hence both ligands are prob-

[1]The "dangling" ligand could absorb at 1.03 p.p.m. and the f_4fars at 1.01. The following argument is valid in either case.

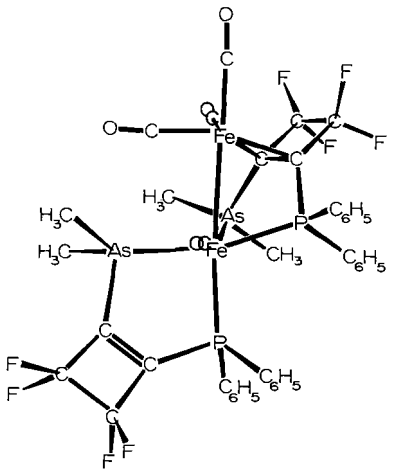

FIG. 3. The solid state structure of $(f_4AsP)f_4AsPFe_2(CO_4)$.

ably attached to Fe^A. Monosubstitution of $f_4AsPFe_2(CO)_6$ by $(C_6H_5O)_3P$ on Fe^A lowers the frequency of ν(CO)(max) on Fe^B by 25 cm^{-1}. Further substitution to give $((C_6H_5O)_3P)_2f_4AsPFe_2(CO)_4$ results in a further drop of ν(CO)(max) by ~27 cm^{-1}. However on substituting $f_4AsPFe_2(CO)_6$ by $(C_6H_5)_3As$, monosubstitution (on Fe^A) lowers ν(CO)(max) by ~25 cm^{-1} but on disubstitution, ν(CO)(max) is decreased by a further ~52 cm^{-1}, indicating that the second ligand is substituting on Fe^B where it can have a more direct effect on the frequency. The resulting spectrum is also very similar to compounds of the type $(L—L)^b(L—L)Fe_2(CO)_4$ where $(L—L)^b$ is believed to be bridging Fe^A and Fe^B.[2]

Mössbauer spectra have been determined for several $(L)(L–L)Fe_2(CO)_5$ derivatives and are similar in appearance to those of the $(L–L)Fe_2(CO)_6$ complexes. A magnetic perturbation Mössbauer spectrum of $(C_6H_5O)_3Pf_4AsPFe_2(CO)_5$ confirmed that the inner pair of lines arise from Fe^A and the outer pair from Fe^B. Using this as a basis the spectral parameters for the monosubstituted derivatives have been deduced and are given in Table 6.

Examination of the data in Tables 5 and 6 shows that the isomer shift of Fe^A increases on going from $(L–L)Fe_2(CO)_6$ to $(L)(L–L)Fe_2(CO)_5$, whereas that of Fe^B shows a very slight decrease. Since substitution of CO by a group V donor atom has always been found to increase δ of the substituted iron atom (2, 13), these results clearly confirm that substitution occurs at Fe^A. Usually, the increase in isomer shift found on replacing CO by an arsine or stibine is greater than that for replacement of CO by a phosphine (16). In going from $f_4farsFe_2(CO)_6$ to $(f_4AsP)^mf_4farsFe_2(CO)_5$ δ of Fe^A increases by 0.06 mm/s, compared to an increase of 0.08 mm/s for $(C_6H_5)_3Pf_4AsPFe_2(CO)_5$ relative to $f_4AsPFe_2(CO)_6$, while the increase for the $(C_6H_5)_3Sb$ derivative is 0.15 mm/s. This supports the previous conclusion that in $(f_4AsP)^m$-$f_4farsFe_2(CO)_5$ the f_4AsP ligand is bonded through phosphorus.

The magnetic perturbation result for $(C_6H_5O)_3Pf_4AsPFe_2(CO)_5$ shows that the signs of e^2qQ at the two iron sites are the same as in the $(L–L)Fe_2(CO)_6$ complexes (Table 6). In general the magnitude of the quadrupole splitting for Fe^A is smaller than that in the corresponding $(L–L)Fe_2(CO)_6$ derivatives, and in particular the reduction in $|\Delta E_Q|$ is very large for the $(C_6H_5)_3$-Sb complex. These results imply that the change in $|\Delta E_Q|$ for Fe^A on substitution arises chiefly from differences in σ- and π-bonding abilities of the substituents relative to CO. Although geometry changes which follow on ligand substitution may play some role in determining the precise value of $|\Delta E_Q|$, they are clearly not the major factor. For most of the monosubstituted derivatives $|\Delta E_Q|$ for Fe^B is somewhat smaller than in the corresponding $(L–L)Fe_2(CO)_6$ complexes. The fact that V_{zz} is opposite in sign at the two sites and that substitution at Fe^A tends to decrease the magnitude of the e.f.g. at both sites, suggests that V_{zz} is directed more or less along the iron–iron bond, as assumed above.

The Mössbauer data, in particular the negative V_{zz} at Fe^A, appear to confirm that substitution in the $(L)(L–L)Fe_2(CO)_5$ complexes occurs *trans* to the Fe—Fe bond. In the $(L–L)^b(L–L)$-$Fe_2(CO)_4$ compounds mentioned above, where the bite of the bridging ligand insures "equatorial" substitution, e^2qQ for Fe^A is dramatically increased in magnitude and is positive in sign.[2] Since ΔE_Q remains small and negative in the $(L)(L–L)Fe_2(CO)_5$ complexes, *trans* substitution seems far more likely.

The electronic spectra of the derivatives of $(L–L)Fe_2(CO)_6$ also have an intense band near 380 nm which is at longer wavelength than in the parent. In the monosubstituted $L(L–L)Fe_2$-

[2]L. S. Chia, W. R. Cullen, J. R. Sams, and J. C. Scott. Unpublished results.

Can. J. Chem. Downloaded from www.nrcresearchpress.com by 210.87.254.42 on 09/05/12
For personal use only.

TABLE 6. Mössbauer parameters at 80 K for (L)(L–L)$Fe_2(CO)_5$ complexes*

(L)(L–L)	δ (mm/s)	ΔE_Q (mm/s)	Γ (mm/s)†	Iron atom
Ph_3Pf_4AsP	0.35 ± 0.02	0.56 ± 0.03	0.29	A
	0.30 ± 0.02	1.38 ± 0.03	0.29	B
$dppp^mf_4AsP$	0.32 ± 0.02	0.59 ± 0.04	0.34	A
	0.31 ± 0.02	1.28 ± 0.04	0.32	B
$(PhO)_3Pf_4AsP$‡	0.29 ± 0.02	−0.58 ± 0.03	0.30	A
	0.29 ± 0.02	+1.51 ± 0.03	0.30	B
$(PhO)_3Pf_4fars$	0.32 ± 0.02	0.64 ± 0.03	0.27	A
	0.31 ± 0.02	1.45 ± 0.03	0.26	B
$f_4AsP^mf_4fars$	0.34 ± 0.01	0.44 ± 0.02	0.25	A
	0.30 ± 0.01	1.35 ± 0.02	0.24	B
$(PhO)_3Pf_8fars$§	0.29 ± 0.01	0.50 ± 0.02	0.24	A
	0.31 ± 0.01	1.26 ± 0.02	0.25	B
Ph_3Sbf_4fos	0.38 ± 0.02	0.17 ± 0.03	0.27	A
	0.30 ± 0.01	1.27 ± 0.02	0.24	B

*See footnote *, Table 1. Isomer shifts are relative to sodium nitroprusside.
†Experimental uncertainty ± 0.02 mm/s.
‡Signs of ΔE_Q determined with source and absorber at 4.2 K. The η values are 0.0 for Fe^A and 0.8 for Fe^B.
§Analytical data were not obtained for this complex.

$(CO)_5$ complexes the red shift is not particularly sensitive to the nature of the ligand, L. (The range of the red shifts in derivatives of $Mn_2(CO)_{10}$ is wider (17)[3].) The λ_{max} of di- and trisubstituted derivatives increases as the degree of substitution. The considerable difference in λ_{max} for $L_2f_4AsPFe_2(CO)_4$ where L = $(C_6H_5O)_3P$ (402 nm) and $(C_6H_5)_3As$ (432 nm) may be a further indication of substitution at Fe^A and Fe^B in the case of the arsine derivative.

The authors are grateful to the National Research Council of Canada for financial assistance. L.S.C. thanks the International Nickel Company of Canada for a scholarship.

1. W. R. CULLEN. Adv. Inorg. Chem. Radiochem. **15**, 323 (1972).
2. W. R. CULLEN, D. A. HARBOURNE, B. V. LIENGME, and J. R. SAMS. Inorg. Chem. **8**, 95 (1969).
3. F. W. B. EINSTEIN and J. TROTTER. J. Chem. Soc. A, 824 (1967).

[3]W. R. Cullen and F. L. Hou. Unpublished results.

4. J. R. SAMS and J. C. SCOTT. J. Chem. Soc. Dalton Trans. 2265 (1974).
5. L. S. CHIA and W. R. CULLEN. Can. J. Chem. **50**, 1421 (1972).
6. L. S. CHIA, W. R. CULLEN, and D. A. HARBOURNE. Can. J. Chem. **50**, 2182 (1972).
7. W. R. CULLEN and L. MIHICHUK. Can. J. Chem. **51**, 936 (1973).
8. E. W. ABEL and F. G. A. STONE. Q. Rev. **23**, 325 (1969).
9. N. A. BEACH and H. B. GRAY. J. Am. Chem. Soc. **90**, 5713 (1968).
10. M. DARTIQUENAVE, Y. DARTIQUENAVE, and H. B. GRAY. Bull. Soc. Chim. Fr. 4223 (1969).
11. R. A. LEVENSON, H. B. GRAY, and G. P. CEASAR. J. Am. Chem. Soc. **92**, 3653 (1970).
12. B. BOSNICH, W. G. JACKSON, and S. T. D. LO. Inorg. Chem. **13**, 2598 (1974).
13. J. A. DE BEER, R. J. HAINES, R. GREATREX, and N. N. GREENWOOD. J. Chem. Soc. A, 3271 (1971).
14. L. S. CHIA. Ph.D. Thesis, University of British Columbia, Vancouver, British Columbia. 1974.
15. F. W. B. EINSTEIN and R. D. G. JONES. Inorg. Chem. **12**, 255 (1972).
16. J. C. SCOTT. Ph.D. Thesis, University of British Columbia, Vancouver, British Columbia. 1973.
17. J. P. FAWCETT, A. J. POË, and M. V. TWIGG. Chem. Commun. 267 (1973).

Can. J. Chem. Downloaded from www.nrcresearchpress.com by 210.87.254.42 on 09/05/12
For personal use only.

Constantes d'association de quelques éthers de polyéthylène glycols avec Na^+, K^+, Cs^+ et Tl^+

GÉRARD CHAPUT ET GEORGES JEMINET

Laboratoire de Chimie Organique Biologique E.R.A. n°392 du C.N.R.S.

ET

JEAN JUILLARD

Laboratoire d'Etude des Interactions Solutés-Solvants, U.E.R. des Sciences Exactes et Naturelles,

[Université de Clermont-Fd, Complexe Universitaire des Cézeaux, B.P. 45, 63170, Aubière, France]

Reçu le 7 janvier 1975

GÉRARD CHAPUT, GEORGES JEMINET ET JEAN JUILLARD. Can. J. Chem. **53**, 2240 (1975).

Les constantes d'association 1:1 avec des cations monovalents d'un certain nombre d'éthers de polyéthylène glycols préparés ici ont été mesurées par potentiométrie avec des électrodes sélectives (Na^+, K^+) et par conductométrie (Cs^+, Tl^+) dans le méthanol à 25 °C.

On montre que l'augmentation du nombre de sites coordinants (oxygènes) entraine un accroissement de la constante d'association K_A et de la sélectivité K^+/Na^+.

Le remplacement de deux groupements méthoxy terminaux dans la chaine par des groupements amide primaire ou ester réduit les propriétés complexantes des ligandes.

La stéréochimie de la coordination des polyéthers biphényliques est discutée.

GÉRARD CHAPUT, GEORGES JEMINET, and JEAN JUILLARD. Can. J. Chem. **53**, 2240 (1975).

We report data concerning the association of monovalent cations with some polyethyleneglycol ethers that we have prepared.

1:1 association constants K_A have been obtained in methyl alcohol at 25 °C using selective glass electrode potentiometric measurements for Na^+ and K^+ and conductimetric measurements for Cs^+ and Tl^+.

The values obtained for K_A and for the selectivity ratio $K_A(K^+)/K_A(Na^+)$ increase with the number of coordinating sites.

Replacement of the two methoxy terminal groups in the chain by primary amide or ester groups reduces the complexing properties of the ligand.

The stereochemistry of the coordination is discussed in the case of some biphenylic polyethers.

Introduction

Dans un travail précédent, nous avons déterminé les constantes d'association des sels neutres formés par la grisorixine (1), un antibiotique polyéther monoacide, en chaîne ouverte, isolé au laboratoire (2). Son mode d'action[1] le situe dans les composés ionophores[2] du groupe de la nigéricine qui induisent un transport cationique à travers les membranes cellulaires.

L'étude de modèles accessibles par la synthèse chimique constituait un prolongement possible et normal du travail entrepris dans le cadre de la recherche d'ionophores nouveaux.

Au cours de cette première investigation, nous nous sommes intéressés aux associations de faible stabilité qui existent entre les polyéthers éthyléniques acycliques sans fonction dissociable et les cations monovalents Na^+, K^+, Cs^+ et Tl^+. Ces molécules simples présentent l'enchaînement structural —O—C—C—O— que l'on rencontre dans les antibiotiques carboxyliques.

Pour quelques éthers méthyliques de polyéthylène glycols ou glymes, des constantes d'association ont été déterminées dans le méthanol (4, 5) ou le tétrahydrofuranne (6). Nous avons étendu ce travail à une série de polyéthers aliphatiques, aromatiques ou fonctionnalisés en bout de chaîne. Les mesures ont été effectuées dans le méthanol anhydre, les effets relatifs sont comparables à ceux obtenus dans l'eau mais les constantes mesurées sont plus élevées.

L'équilibre de l'association 1:1 du polyéther P et du cation M^+ s'écrit:

[1] $$P_{MeOH} + M_{MeOH}^+ + A_{MeOH}^- \rightleftarrows (PM^+)_{MeOH} + A_{MeOH}^-$$

[2] $$K_A = \frac{c_{PM^+}}{c_P c_{M^+}} \frac{y_{PM^+}}{y_P y_{M^+}}$$

y coefficients d'activité, c concentrations.

[1] Travail non publié de R. Durand.

[2] Nomenclature de Pressman et Harris (3).

On a choisi des sels MA présentant une dissociation la plus complète possible dans le milieu. La constance des valeurs K_A obtenues pour des concentrations relatives en P et en M^+ variables montre que la formation des complexes d'ordre supérieur 2P, M^+ ... n'influence pas l'équilibre 1.

Pour la connaissance de l'activité de M^+, seuls les cations Na^+ et K^+ donnent des réponses stables et reproductibles des électrodes de verre sélectives utilisées, en présence des polyéthers. Aussi, une deuxième série de mesures a été effectuée par conductométrie avec Cs^+ et Tl^+.

Partie expérimentale

Produits

Sels et solvants

Le méthanol utilisé est distillé une première fois à l'aide d'une colonne à remplissage, il est traité ensuite à reflux sur du magnésium en présence d'iode. Après une nouvelle distillation, on obtient un solvant présentant les caractéristiques suivantes, $\kappa < 5 \times 10^{-7}\ \Omega^{-1}\ cm^{-2}$, teneur en eau inférieure à 0.1% en poids.

Les sels commerciaux utilisés sont des produits "pour analyses". Avant emploi, NaCl, KI sont séchés 24 h à l'étuve à 200 °C; CsCl et $TlNO_3$ à l'étuve à vide à 100 °C.

Préparation et purification des polyéthers

Composés 1 à 4: A partir des éthers monométhyliques de glycols $CH_3O—(CH_2CH_2O)_nCH_2CH_2OH$, **17**, décrits, on prépare les chlorures $CH_3O—(CH_2CH_2O)_n-CH_2CH_2Cl$, **18**, par la méthode de Pedersen (11) ($SOCl_2$/pyridine).

Composé **18**: $n = 1$ p.é.$_{10}$ 54–55 °C, $n = 2$ p.é.$_1$ 89–90 °C, $n = 3$ p.é.$_{0.8}$ 112–113 °C.

Les glymes sont obtenus par *O*-alcoylation de **17** avec **18** (solvant diméthoxy-1,2 éthane, NaH); rendements moyens 80%.

Composé **1**: produit commercial redistillé p.é.$_{0.3}$ 87–88 °C.

Composé **2**: réaction **17** ($n = 1$) + **18** ($n = 2$), p.é.$_{0.3}$ 108–113 °C, r.m.n.: 3.54 (20H, m), 3.26 (6H, s).

Composé **3**: réaction **17** ($n = 2$) + **18** ($n = 2$), p.é.$_{0.6}$ 145–149 °C, r.m.n.: 3.54 (24H, m), 3.36 (6H, s).

Composé **4**: réaction **17** ($n = 3$) + **18** ($n = 3$), p.é.$_{0.5}$ 160–168 °C, r.m.n.: 3.64 (28H, m), 3.36 (6H, s).

Composé 5: On fait réagir deux molécules du chloroéther **18** ($n = 1$) sur l'hexanediol-1,6.

Composé **5**: huile transparente, r.m.n.: 1.40 (8H, m), 3.39 (6H, s), 3.65 (20H, m).

Composés 6 à 9, 10–11 et 15–16: Nous avons suivi les conditions opératoires décrites par Pedersen (11) (butanol-1, NaOH), en faisant réagir les chloroéthers **18** soit sur le dihydroxy-1,2 benzène, soit sur le dihydroxy-2,2′ biphényle. Le rendement en chacun des produits purs ne dépasse pas 30%. Tous les composés étudiés sont des huiles transparentes.

Composé **6**: r.m.n.: 6.81 (4H, m), 4.10 (4H, m), 3.62 (12H, m), 3.33 (6H, s).

Composé **7**: r.m.n.: 6.85 (4H, m), 4.11 (4H, m), 3.65 (12H, m), 3.53 (4H, q), 1.17 (6H, t).

Composé **8**: r.m.n.: 6.88 (4H, m), 4.11 (4H, m), 3.65 (20H, m), 3.35 (6H, s).

Composé **9**: r.m.n.: 6.85 (4H, m), 4.11 (4H, m), 3.65 (28H, m), 3.35 (6H, s).

Composé **10**: r.m.n.: 7.06 (8H, m), 4.06 (4H, m), 3.40 (12H, m), 3.28 (6H, s).

Composé **11**: r.m.n.: 7.05 (8H, m), 4.05 (4H, m), 3.45 (20H, m), 3.29 (6H, s).

Composé **15**: r.m.n.: 6.88 (5H, m), 4.11 (2H, m), 3.65 (10H, m), 3.35 (3H, s).

Composé **16**: r.m.n.: 6.85 (5H, m), 4.11 (2H, m), 3.65 (14H, m), 3.35 (3H, s).

Composé 14: Par dicyanoéthylation du tétraéthylèneglycol par l'acrylonitrile (19), le dinitrile $CN—(CH_2-CH_2O)_5CH_2CH_2CN$ est obtenu, p.é.$_{0.5}$ 175–185 °C. Il est ensuite soumis à une alcoolyse acide (H_2SO_4/EtOH) pour obtenir le diester éthylique **14**.

Composé **14**: r.m.n.: 4.15 (4H, q), 3.65 (20H, m), 2.56 (4H, t), 1.25 (6H, t).

Composés 12–13: Par une méthode identique à celle utilisée pour la préparation du dinitrile précédent, en substituant l'acrylamide à l'acrylonitrile on récupère un solide blanc parfaitement cristallisé. Cette méthode de préparation, vraisemblablement non décrite, des diamides cristallisés des polyéthylènes glycols peut constituer le point de départ de systèmes polyfonctionnels plus complexes. Le rendement est voisin de 85% après recristallisation.

Composé **12**: p.f. 94–95° (acétone–chloroforme (6:4)), r.m.n.: 7.42 (2H, m), 6.30 (2H, m), 3.65 (16H, m), 2.50 (4H, m).

Composé **13**: p.f. 82–83° (acétone), r.m.n.: 6.96 (2H, m), 6.16 (2H, m), 3.65 (20H, m), 2.48 (4H, m).

La purification finale des composés **1** à **11** et **14–16** a été effectuée en utilisant successivement la chromatographie sur colonne (gel de silice 60 Merck) puis sur plaque de verre (support de 1 à 2 mm d'épaisseur; gel de silice PF Merck).

Les spectres de r.m.n. sont enregistrés à l'aide des appareils Varian A-60 et Perkin Elmer R-24. Le solvant utilisé est $CDCl_3$. Les déplacements chimiques sont donnés en p.p.m. par rapport au TMS pris comme référence interne.

Tous les composés étudiés donnent des analyses centésimales satisfaisantes.

Mesures potentiométriques

Les mesures sont effectuées à l'aide d'un p*H*-mètre Radiometer-4 utilisé en millivoltmètre. La lecture est faite à ± 0.5 mV.

La détermination des constantes est basée sur la mesure de la tension réversible d'une cellule galvanique formée de deux électrodes: une électrode de référence de tension constante et une électrode de verre spécifique aux cations monovalents. L'électrode de référence est une électrode au calomel avec une jonction liquide constituée par une solution 0.1 *M* d'iodure de tétraéthylammonium dans le méthanol. Les électrodes indicatrices sont des électrodes de verre spécifiques d'une part de Na^+ (Beckman n° 39278) d'autre part des cations monovalents (Beckman n° 39137) pour K^+.

Les électrodes sont immergées dans une cellule de 25 ml thermorégulée à 25.0 ± 0.1 °C. Une agitation magnétique est assurée pendant toute la manipulation. Le domaine de travail le plus convenable se situe entre 10^{-2}

et 10^{-3} M en électrolyte. On procède par dilution d'une solution de sel AM environ 0.1 M dans la solution de polyéther environ 0.05 M. Après chaque addition, le potentiel d'électrode est mesuré.

La tension réversible de la cellule utilisée est:

$$[3] \qquad E = E^0 + k \log a_{M^+}$$

avec $k = 0.05916$ V à 25 °C.

$$[4] \qquad a_{M^+} = c_{M^+} y_{M^+}$$

La deuxième loi de Debye–Hückel où l'on utilise comme paramètre de distance le paramètre q de Bjerrum permet d'exprimer le facteur d'activité

$$[5] \qquad \log y_{M^+} = \frac{A\sqrt{c_s}}{1 + Bq\sqrt{c_s}}$$

c_s concentration analytique

En solution diluée, le facteur d'activité de la molécule P est très voisin de 1; $y_P = 1$ et pour les ions $y_{PM^+} = y_{M^+}$, d'où

$$[6] \qquad K_A = \frac{c_{PM^+}}{c_P c_{M^+}}$$

L'ensemble des équations de conservation de la matière et des équations précédentes permet de calculer K_A.

Mesures conductométriques

On utilise une sonde Tacussel CM-02 reliée à un conductomètre Beckman RC 18A permettant la mesure des conductances avec une précision au moins égale à 1 pour 1000. La sonde est immergée dans une cellule de 25 ml thermorégulée au centième de degré.

On opère par dilution à l'aide d'une burette gravimétrique, les pesées étant effectuées à 0.1 mg, d'une solution contenant le polyéther (environ 0.1 M) et le sel AM, dans une quantité pesée de la même solution de sel AM environ 0.005 M. Cette méthode nous permet ainsi de conserver constante la concentration en sel et supprimer le paramètre provenant de la dilution de celui-ci.

L'expression de la constante thermodynamique d'équilibre en fonction de α, coefficient de dissociation est:

$$[7] \qquad K_A = \frac{(1 - \alpha)c}{\alpha(c' - c + \alpha c)}$$

Dans laquelle c est la concentration en sel maintenue constante et c' la concentration variable en polyéther.

Pour chaque valeur de c', nous déterminons la conductivité équivalente Λ qui peut s'écrire:

$$[8] \qquad \Lambda = \alpha\Lambda_{(M^+,A^-)} + (1 - \alpha)\Lambda_{(PM^+,A^-)}$$

d'où

$$[9] \qquad \alpha = \frac{\Lambda - \Lambda_{(PM^+,A^-)}}{\Lambda_{(M^+,A^-)} - \Lambda_{(PM^+,A^-)}}$$

$\Lambda(M^+,A^-)$ est la conductivité équivalente de la solution pure de sel que l'on obtient avant toute addition. $\Lambda(PM^+,A^-)$ est la conductivité équivalente à déterminer du complexe.

On résoud le système d'équations 8 et 9 par itérations en ajustant les deux paramètres α et $\Lambda(PM^+,A^-)$ jusqu'à obtenir une valeur de K_A constante.

Les différences entre $\Lambda_{(PM^+,A^-)}$ et $\Lambda_{(M^+,A^-)}$ sont par exemple pour le composé **4** de 10.6 pour Tl^+ et 18.6 pour Cs^+.

Evans *et al.* (7) ont utilisé récemment une méthode conductométrique semblable pour l'étude de deux polyéthers "couronne".

Résultats

Des exemples détaillés de mesures et de calculs ont été donnés par ailleurs (18). L'ensemble des résultats obtenus se trouve réuni dans les tableaux 1 et 2.

Pour une série de mesures, les valeurs moyennes sont calculées sur 12 à 24 points en potentiométrie et 7 points en conductométrie: pour $0.1 < \log K_A < 1$, l'écart moyen est ± 0.04; pour $1 < \log K_A < 3$, l'écart moyen est ± 0.02.

La reproductibilité entre plusieurs séries de mesures se situe entre les limites 0.01–0.07. Nous estimons toutefois que les résultats obtenus en potentiométrie sont plus faibles que ceux obtenus en conductométrie; en effet, l'hypothèse d'additivité des conductivités équivalentes des électrolytes (éq. 8) n'est qu'une approximation.

Discussion

Polyéthers vrais

Influence du nombre de sites

Nous avons porté sur les graphes de la fig. 1 $\log K_A$ en fonction du nombre d'atomes d'oxygènes présents dans la chaîne. Les courbes obtenues montrent que l'effet coopératif dans la coordination est très comparable entre les deux séries de polyéthers **1–4** et **6–9**. La séquence d'association demeure constante, $K^+ > Tl^+ \simeq Cs^+ > Na^+$.

Dans l'équilibre étudié la relation entre l'enthalpie libre de complexation du cation dans le solvant ΔG_A et les potentiels chimiques μ^0 des différentes espèces s'écrit:

$$\Delta G_A = -RT \log K_A = \mu^0(P,M^+) - \mu^0(P) - \mu^0(M^+)$$

Pour un cation considéré, on peut attendre que la différence $\mu^0(P,M^+) - \mu^0(P)$ augmente en fonction du nombre d'oxygènes pour des raisons purement statistiques.

Une observation très analogue a été faite par Smid et collaborateurs (6) au cours de l'étude de la séparation des paires d'ions fluorényl$^-$, Li^+ et Na^+ par les glymes dans le THF. Ces auteurs

TABLEAU 1. Association des polyéthers vrais dans le méthanol à 25 °C (log K_A)

Composés		Potentiométrie		Conductométrie	
		Na^+(1.12 Å)*	K^+(1.44 Å)*	Tl^+(1.54 Å)	Cs^+(1.84 Å)*
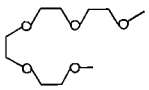	**1**	1.28	1.72	1.57	1.45
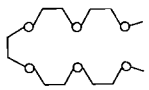	**2**	1.47 1.52† 1.0‡	2.20 2.20† 2.1‡	1.90	1.85
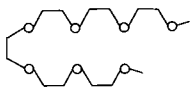	**3**	1.60	2.55	2.30	2.17
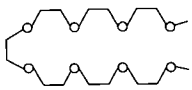	**4**	1.67	2.87	2.55	2.41
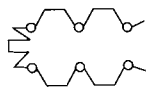	**5**	<0.1	<0.1		
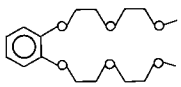	**6**	1.44	2.15	1.73	1.66
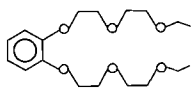	**7**	1.29	1.78		
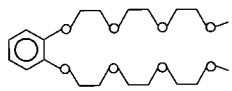	**8**	1.61	2.83	2.45	2.29
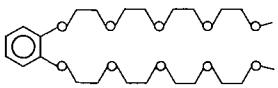	**9**	1.74	3.30	2.80	2.66
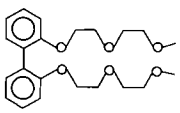	**10**	<0.1	0.90	1.13	
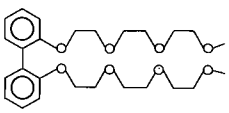	**11**	<0.1	1.45	1.81	1.43

*Rayon ionique.
†D'après réf. 4.
‡D'après réf. 5.

ont discuté en détail les raisons de cet accroissement de stabilité.

Les possibilités d'un examen approfondi des résultats sont limitées par la méconnaissance de l'influence de la solvatation sur la différence $\mu^\theta(PM^+) - \mu^\theta(P)$; de même les valeurs des indices de coordination des cations demeurent un objet de discussions (8, 9). L'intervention d'un effet statistique est cependant l'explication la plus vraisemblable (6, 10).

TABLEAU 2. Association des polyéthers fonctionalisés en bout de chaîne dans le méthanol à 25 °C (log K_A)

Composés		Potentiométrie		Conductométrie	
		Na^+(1.12 Å)*	K^+(1.44 Å)*	Tl^+(1.54 Å)*	Cs^+(1.84 Å)*
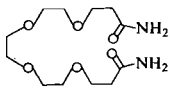	**12**	1.03	1.17	1.35	
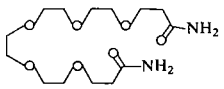	**13**	1.25	1.89	1.82	1.60
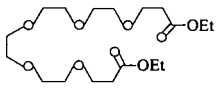	**14**	1.34	1.78	1.44	1.56
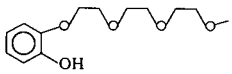	**15**	1.35	1.45		
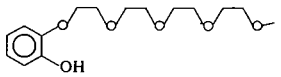	**16**	2.19	2.08		

*Rayons ioniques.

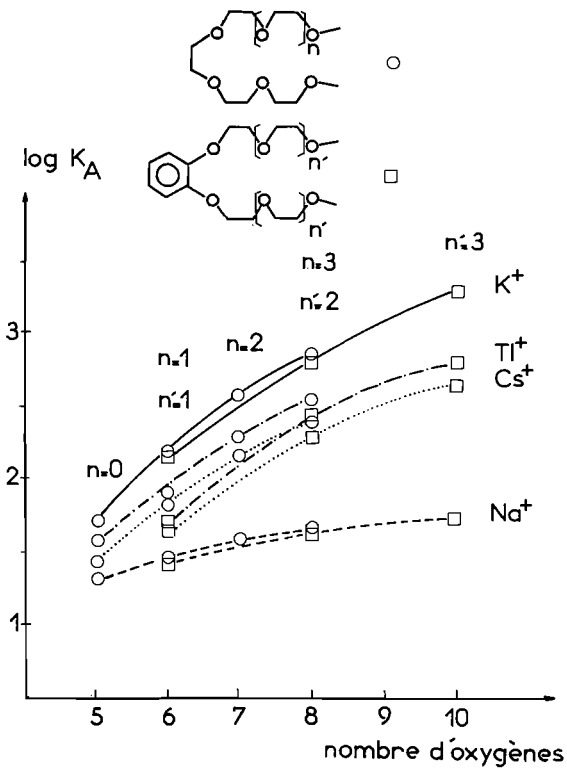

FIG. 1. Variation de l'association des éthers de polyéthylène glycols avec les cations monovalents, en fonction du nombre d'oxygènes de la chaine.

Discrimination K^+/Na^+

Les courbes de la fig. 1 mettent en évidence la discrimination croissante K^+/Na^+ qui s'opère en fonction de la longueur de la chaîne, indépendamment des énergies de solvatation des cations qui demeurent constantes d'une série à l'autre.

Pour le décaéther aromatique **9** la sélectivité K^+/Na^+ atteint 36. Ce composé peut être rapproché du dibenzo-30 couronne-10 préparé par Pedersen (11) étudié récemment par Chock (12) qui donne les constantes suivantes (MeOH, 25 °C, $K^+/Na^+ \sim 280$):

Cation	log K_A
Na^+	2.11
K^+	4.57
Cs^+	4.23
Tl^+	4.50

La conformation repliée adoptée par le macrocycle dans le complexe PM^+ (13) permet une meilleure protection du cation non solvaté, ce qui explique les valeurs supérieures obtenues pour K_A. En outre, il existe un effet macrocyclique qui est essentiellement un changement entropique défavorable pour le polyéther linéaire, si l'on se réfère aux constantes thermo-

dynamiques données par Fruh et Simon (5) pour le pentaglyme **2** et son homologue cyclique le dibenzo-18 couronne-6. Cet effet est cependant beaucoup moins important pour les deux décaéthers comparés ci-dessus. Il est vraisemblable de supposer que les conformations des deux ligandes libres changent nettement pendant la complexation.

Pour ces deux composés, le mécanisme de la discrimination K^+/Na^+ est identique; il est dû à l'impossibilité stérique de construire une couche de coordination à une distance convenable pour Na^+ dont le faible rayon ionique tend à contracter la cavité complexante et introduire ainsi des répulsions entre les sites (5, 14). Ceci est mis en évidence par l'étude des systèmes acycliques.

La sélectivité K^+/Cs^+ et Tl^+ est faible comme cela pouvait être prévu pour ces ligandes flexibles (14).

Stéréochimie dans la chaîne

Dans les polyéthers biphényliques **10** et **11** la présence de substituants en 2,2′ entraîne la non planéité des cycles aromatiques.

Pour ce type de substitution, une forme croisée est généralement postulée (15), avec un angle θ inférieur à 90°, plutôt qu'une forme où les substituants sont en opposition.

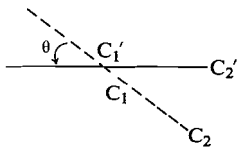

Les constantes d'association mesurées pour ces composés sont favorables à une stéréochimie croisée des cycles, sinon elles seraient nulles, comme on peut l'observer avec **5** où les sites sont séparés en deux groupes par une chaîne hydrocarbonée.

La différence de stabilité marquée des associations cationiques entre les polyéthers aromatiques et biphényliques correspondants est attribuable à la position dans l'espace des oxygènes en 2,2′ sur les cycles. A ce niveau, le processus d'association est perturbé dans le cas des biphényliques par le fait que direction et distance entre paires libres sur O et O′ ne sont pas fixées; l'effet prépondérant n'est pas connu.

Dans la structure cristalline du complexe tétraglyme **1**-$HgCl_2$ publiée récemment (16), la chaîne adopte une conformation à demi-ouverte et les atomes O sont pratiquement dans un même

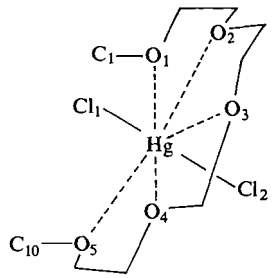

plan; ils entourent l'atome Hg et les interactions entre les méthyles terminaux sont faibles.

Les complexes des cations monovalents ne sont pas strictement comparables avec ceux de $HgCl_2$; néanmoins la possibilité d'une stéréochimie plane de la coordination, lorsque le cation est totalement associé aux oxygènes du ligande dans les complexes PM^+, n'est pas infirmée par nos résultats. Nous nous proposons de préciser ce problème par l'étude de nouveaux modèles.

Polyéthers fonctionnalisés en bout de chaîne

Le remplacement des groupements $—OCH_3$ terminaux par des sites oxygénés présentant des moments dipolaires plus élevés entraîne dans tous les cas une décroissance marquée des constantes d'association, sauf pour Na^+ avec les composés **15** et **16** ayant une fonction OH terminale.

On a observé récemment par r.m.n. (17) que Li^+ provoque une augmentation de la barrière de rotation dans le diméthylacétamide par une association avec l'oxygène alors que Ag^+ diminue cette barrière en se coordinant à l'azote. Il est possible de retenir une explication du même type pour l'inversion $Tl^+ > K^+$ dans **12** et **13**. K^+ aurait tendance à s'associer au site peu polarisable C=O tandis que Tl^+ avec ses orbitales f vacantes donnerait préférentiellement une coordination forte avec l'azote.

Conclusion

Ce travail avait un double but: l'étude de l'aspect structural et analytique de la complexation des cations monovalents par des systèmes en chaîne ouverte.

La préparation d'un certain nombre d'éthers de polyéthylène-glycols nous a permis de mettre en évidence la sélectivité K^+/Na^+ qui s'opère en fonction du nombre d'oxygène présents. La stéréochimie de la coordination autour du cation a également été discutée. Pour les polyéthers fonctionnalisés en bout de chaîne aucun des

sites étudiés n'augmente les propriétés complexantes des ligandes par rapport aux polyéthers vrais. Cependant, la précision obtenue pour les mesures potentiométriques et conductométriques développées dans ce domaine des faibles associations très peu étudiées, permettra de poursuivre le travail sur des modèles polyfonctionnels nouveaux. Cette méthode d'investigation peut permettre d'étudier la basicité de différents sites polaires vis-à-vis des cations, d'étudier l'influence de la lipophilie des chaînes, dans le but de définir de nouveaux systèmes ionophores.

1. P. GACHON, G. CHAPUT, G. JEMINET, J. JUILLARD et J. P. MOREL. J. Chem. Soc. Perkin II, Sous presse.
2. P. GACHON, A. KERGOMARD, H. VESCHAMBRE, C. ESTEVE et T. STARON. J. Chem. Soc. Chem. Commun. 1421 (1970).
3. B. C. PRESSMANN et E. J. HARRIS. Membranes models and the formation of biological membranes. *Rédigé par* E. Bolis et B. A. Pethica. North Holland, Amsterdam. 1968. pp. 247–263.
4. H. K. FRENDSDORFF. J. Am. Chem. Soc. **93**, 600 (1971).
5. P. U. FRUH et W. SIMON. Protides of the biological fluids. Tome 20. *Rédigé par* H. Peeter. Pergamon Press, Oxford. 1972. p. 505.
6. L. L. CHAN, K. H. WONG et J. SMID. J. Am. Chem. Soc. **92**, 1955 (1970).
7. D. F. EVANS, S. L. WELLINGTON, J. A. NADIS et E. L. CUSSLER. J. Sol. Chem. **1**, 499 (1972).
8. W. E. MORF et W. SIMON. Helv. Chim. Acta, 2683 (1971).
9. R. J. P. WILLIAMS. Q. Rev. **24**, 331 (1970).
10. J. UGELSTAD et O. A. ROKSTAD. Acta. Chem. Scand. **18**, 474 (1964).
11. C. J. PEDERSEN. J. Am. Chem. Soc. **89**, 2495 (1967); **89**, 7017 (1967).
12. P. B. CHOCK. Proc. Natl. Acad. Sci. U.S.A. **69**, 1939 (1972).
13. C. J. PEDERSEN et H. K. FRENDSDORFF. Angew. Chem. Int. Ed. **84**, 16 (1972) et références citées.
14. J. M. LEHN. Structure and bonding, Tome 16. Springer Verlag, Berlin. 1973. p. 54.
15. J. GRUNDY. Stereochemistry. Butterworths, London. 1964. p. 185.
16. R. IWAMOTO. Bull. Chem. Soc. Jap. **46**, 114(1973); **46**, 118(1973); **46**, 1123 (1973).
17. W. EGAN, T. E. BULL et S. FORSEN. J. Chem. Soc. Chem. Commun. 1099 (1972).
18. G. CHAPUT. Thèse de spécialité. Université de Clermont–Ferrand, France. 1973.
19. H. A. BRUSON et T. W. RIENER. J. Am. Chem. Soc. **65**, 26 (1943).

The Microwave Spectrum, Dipole Moment, and Structure of Glycidol

W. V. F. BROOKS
Department of Chemistry, University of New Brunswick, Fredericton, New Brunswick E3B 5A3
AND
K. V. L. N. SASTRY
Department of Physics, University of New Brunswick, Fredericton, New Brunswick E3B 5A3

Received February 27, 1975

W. V. F. BROOKS and K. V. L. N. SASTRY. Can. J. Chem. 53, 2247 (1975).

The microwave spectra of glycidol ($\overline{CH_2—O—CH}—CH_2OH$) and its deuterated (—OD) form have been studied in the range 8–40 GHz. The rotational (in MHz) and centrifugal distortion constants (in kHz) of glycidol are: $A = 10\,347.87$, $B = 4102.36$, $C = 3781.95$; $\Delta_J = 2.38$, $\Delta_{JK} = -311$, $\Delta_K = 5.2$, $\delta_J = 0.3159$, $\delta_K = -9.76$. The rotational constants and distortion constants of glycidol (OD) are $A = 10\,010.31$, $B = 4056.73$, $C = 3717.02$; $\Delta_J = 2.53$, $\Delta_{JK} = 197$, $\Delta_K = 7.7$, $\delta_J = 0.3532$, $\delta_K = -7.19$. The dipole moment components of the normal molecule in Debye units are $\mu_a = 0.61$, $\mu_b = 1.20$, $\mu_c = 0.52$, and the total dipole moment is 1.44 D.

A structure is derived with the alcoholic hydrogen atom close (2.5 Å) to the ring oxygen. The structure and the absence of signs of free or hindered rotation, can be accounted for by hydrogen bonding between the proton and the ring oxygen.

W. V. F. BROOKS et K. V. L. N. SASTRY. Can. J. Chem. 53, 2247 (1975).

On a étudié le spectre microonde de l'hydroxy-1 époxy-2,3 propane ($\overline{CH_2—O—CH}—CH_2OH$) ainsi que sa forme deutériée (—OD) dans la région de 8 à 40 GHz. Les constantes de distortion rotationnelles (en MHz) et de distortion par centrifugation (en kHz) de l'hydroxy-1 époxy-2,3 propane sont: $A = 10\,347.87$, $B = 4102.36$, $C = 3781.95$; $\Delta_J = 2.38$, $\Delta_{JK} = -311$, $\Delta_K = 5.2$, $\delta_J = 0.3159$, $\delta_K = -9.76$. Pour l'hydroxy-1 époxy-2,3 propane (OD) ces constantes sont: $A = 10\,010.31$, $B = 4056.73$, $C = 3717.02$; $\Delta_J = 2.53$, $\Delta_{JK} = 197$, $\Delta_K = 7.7$, $\delta_J = 0.3532$, $\delta_K = -7.19$. Les composantes du moment dipolaire d'une molécule normale en Debye sont $\mu_a = 0.61$, $\mu_b = 1.20$, $\mu_c = 0.52$, et le moment dipolaire total est 1.44 D.

On déduit une structure où l'atome d'hydrogène alcoolique se trouve près (2.5 Å) du cycle oxyrannique. La structure ainsi que l'absence d'indications montrant une rotation libre ou empêchée, peuvent être expliqués par une liaison hydrogène entre le proton et le cycle oxyrannique. [Traduit par le journal]

Introduction

In an earlier paper (1) we reported the microwave spectrum of cyclopropyl carbinol ($\overline{CH_2—CH_2—CH}—CH_2OH$) and the structural interpretation of the data. We found no evidence of internal rotation, and proposed that this is because the electrons of the strained cyclopropyl ring bonds attract the hydroxyl hydrogen atom with sufficient strength to prevent rotation. Glycidol ($\overline{CH_2—O—CH}—CH_2OH$) is similar in geometry to cyclopropyl carbinol, but the presence of an oxygen atom in the ring provides an alternative attraction for the alcoholic hydrogen. If the strained bonds and one of the unshared electron pairs of the oxygen attract the hydrogen to roughly the same degree, then two or possibly three structures might be observed; but if one conformation is considerably more stable than the others, then only that one will be observed. Chemical experience suggests that the hydroxyl proton will be attracted more strongly to an unshared electron pair on the ring oxygen than to the electrons in a strained ring bond.

We have measured the microwave spectra of glycidol and its deuterated (—OD) species in order to investigate the geometry of the molecule in the gas phase.

Experimental

Glycidol was purchased from the Aldrich Chemical Company; the makers described it as 95% pure, and mass, infrared, and n.m.r. spectra all showed the features expected for glycidol. We used the sample without further purification.

The spectra were recorded at room temperature in the pressure range 0.02 to 0.08 Torr. Most lines were measured in this laboratory on a conventional 85 kHz

Can. J. Chem. Downloaded from www.nrcresearchpress.com by 210.87.254.6 on 09/05/12
For personal use only.

TABLE 1. Rotational constants, and quartic centrifugal distortion constants of glycidol and deuterated (OD) glycidol (A, B, C in MHz, Δ and δ in kHz)

Parameter	$\overbrace{CH_2—O—CH_2}—OH$	$\overbrace{CH_2—O—CH_2}—OD$
A	10 347.871 ± 0.005*	10 010.314 ± 0.008
B	4 102.360 ± 0.002	4 056.734 ± 0.004
C	3 781.950 ± 0.002	3 717.023 ± 0.003
κ	−0.90240212	−0.89204029
Δ_J	2.38 ± 0.04	2.53 ± 0.05
Δ_{JK}	−311 ± 4	−197 ± 4
Δ_K	5.2 ± 6	7.7 ± 4
δ_J	0.3159 ± 0.0004	0.3532 ± 0.0005
δ_K	−9.76 ± 0.05	−7.19 ± 0.04

*Error limits are one standard deviation.

Stark modulated spectrometer with oscilloscope display. Some measurements were made on a Hewlett–Packard spectrometer at Harvard University and the spectrometer at the University of Kiel. The accuracy of most frequency measurements is ±0.1 MHz or better except for very weak lines or cases of interference by nearby lines.

The deuterated (—OD) species was generated in the cell by saturating the Stark cell with D_2O vapor, pumping off, and then admitting glycidol vapor which exchanges rapidly with the D_2O remaining on the walls.

The Stark field for the dipole moment measurements was calibrated by measuring Stark shifts of the OCS $1 \leftarrow 0$ line (2).

Spectra

Since no conformation of glycidol has any planes or axes of symmetry; a-, b-, and c-type lines are possible and preliminary calculations predicted a rich spectrum. The first observations confirmed the prediction and showed no obvious regularities or easily resolved Stark lobes. However, after a few trials, some of the stronger lines were assigned by Q-branch plotting to a series of Q_b transitions. Assigning an R-branch transition was more difficult since the low J lines are relatively weak, but once one was correctly assigned the spectrum presented no further problems.

At each stage, the assigned lines were used as input to a least squares fitting program which calculates the best rotational constants (including quartic and sextic centrifugal constants if desired) and then prints out a predicted spectrum with relative intensities. By following series of lines, and adding quartic constants as the rigid rotor predictions became less accurate we finally assigned more than 275 lines.[1] The rotational constants, moments of inertia, and quartic distortion constants are given in Table 1. At the highest J values assigned, ($J = 60$), consistent errors of about 1 MHz indicate that sextic constants are needed to improve the accuracy, but there did not seem to be sufficient data to determine these higher constants accurately. The quartic constants are not all well determined since most of the high J lines belong to only a few series of Q_c and Q_b transitions.

The fitting and prediction procedure accounts for most of the stronger lines in the range (8 to 40 GHz) studied. While there remain numerous unassigned lines, this is to be expected from excited vibrational states and higher J transitions. Other forms of glycidol and impurities may contribute lines also, but we have found no features that lead to possible assignments.

The deuterated species (—OD) spectrum[1] was analyzed in essentially the same way as the normal molecule, but only 125 lines have been assigned. The constants are also given in Table 1. The spectrum shows the same general features as the normal molecule, and again there are no clear indications that more than one absorbing species is present.

Stark displacements were measured only for the normal molecule. The Stark coefficients and the dipole components as determined by a least squares fitting to the measured coefficients are given in Table 2.

Structure

The six measured rotation constants of the two isotopic species were combined with data from related molecules to construct a model of glycidol. The epoxy ring and attached hydrogens

[1]The assigned and measured lines are available from the Depository of Unpublished Data, CISTI, National Research Council of Canada, Ottawa K1A 0S2.

Can. J. Chem. Downloaded from www.nrcresearchpress.com by 210.87.254.6 on 09/05/12
For personal use only.

TABLE 2. Observed and calculated Stark coefficients and dipole components of glycidol (OH)

Transition	Frequency (MHz)	M	$\Delta\nu \times 10^4/E^2$ (MHz × cm²/V²) Observed	Calculated
$3_{03} \leftarrow 2_{11}$	16 706.3	1	−8.66	−7.76
		2	−38.0	−36.05
$3_{21} \leftarrow 3_{12}$	18 323.4	2	151	162.1
		3	360	354.2
$4_{04} \leftarrow 3_{13}$	25 920.5	2	−9.45	−5.90
		3	−19.8	11.78
$5_{14} \leftarrow 5_{05}$	9 135.1	4	24.9	27.49
		5	40.2	43.10
$5_{24} \leftarrow 5_{15}$	16 866.8	2	−5.4	−5.89
		3	−12.2	−13.78
		4	−21.7	−24.84
		5	−34.3	−39.05
$5_{23} \leftarrow 5_{15}$	22 078.9	4	25.1	14.96
		5	34.15	23.39

$\mu_a = 0.61 \pm 0.02$ D
$\mu_b = 1.20 \pm 0.09$ D
$\mu_c = 0.51 \pm 0.12$ D
$\mu_{total} = 1.44 \pm 0.08$ D

were assumed to have the same geometry as ethylene oxide (3). The C_{ring}—$C_{carbinol}$ distance and the carbinol configuration were taken from the propylene oxide model (4). The $C_{carbinol}$—O distance was taken from methanol (5). With these assumptions, the remaining angles and distances can be adjusted to give a best least squares fit to the observed rotational constants. The structural coordinates and the least squares procedure are based on the coordinate system of Thompson (6).

The variables (to be adjusted) were taken as: (*1*) the angle between the C_{ring}—$C_{carbinol}$ bond and a perpendicular to the epoxy ring plane; (*2*) the C—C—C angle; (*3*) a "torsion" coordinate defining rotation about the C_{ring}—$C_{carbinol}$ bond; (*4*) a "torsion" coordinate for rotation of the hydroxyl hydrogen about the C—O bond; (*5*) the C—O—H angle; (*6*) the O—H distance.

Since the relations between rotational constants and the variables are nonlinear, it is necessary to fit a small number of variables (usually two or three) at a time; by a series permutations of variables, all the variables can be determined. This choice of variables gave reasonable results except that the O—H distance was not very well determined; the value tended to be larger than seems reasonable (1.1 to 1.2 Å at various stages of the fitting) but the final error sum was relatively insensitive to the O—H bond length. The O—H bond must certainly be greater than the 0.9451 Å of methanol (5) and a distance close to 1.0 Å seems reasonable. Therefore, we set the O—H distance to 1.0 Å and fitted only the other five variables.

The transfer of distances and angles must introduce errors. Thus the asymmetric attachment of the carbinol group destroys the symmetry of the epoxy ring, and therefore the two ring C—O distances will not be exactly the same nor will the three ring hydrogens be exactly equivalent. Similarly, the carbinol hydrogens are not equivalent in the final structure and so this group will be less symmetrical than assumed. After a satisfactory structure had been achieved, we tested various other factors as possible variables to see if the goodness of fit might be significantly improved. In all cases, the improvement was insignificant or else (as with ring hydrogen positions) a somewhat better fit could be achieved, but with an unreasonable structure. There is of course no reason to expect that the data should agree perfectly with the proposed structure since the model is a static one while the data are averaged or effective constants of dynamic systems; the data are also subject to errors of measurement. The alcoholic hydrogen position may be particularly ill-determined since

Can. J. Chem. Downloaded from www.nrcresearchpress.com by 210.87.254.6 on 09/05/12
For personal use only.

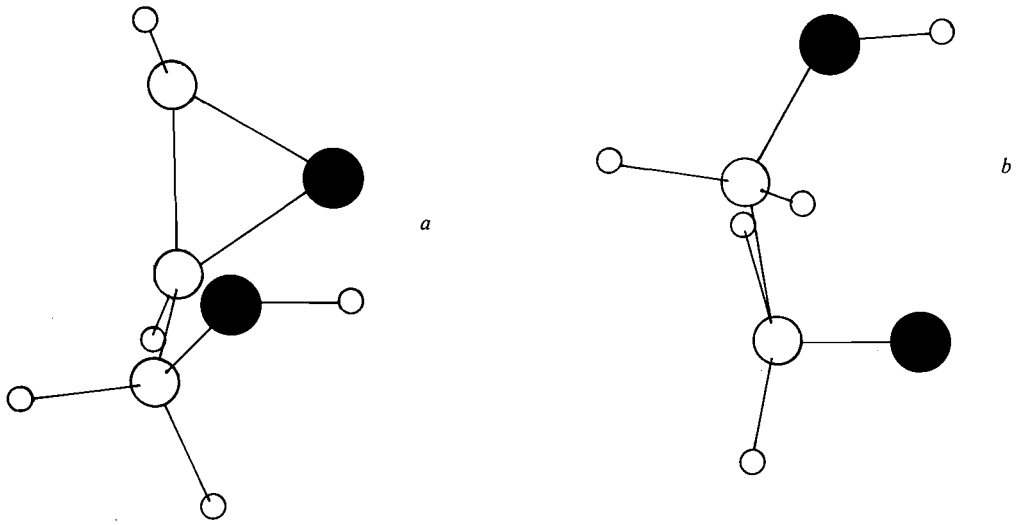

FIG. 1. Projection of glycidol structure: (*a*) on the plane of the ring; (*b*) on a plane perpendicular to the C_{ring}—C_{ring} bond.

TABLE 3. Structural data of glycidol molecular model

Bond	Distance (Å)	Source	Bonds	Angle (deg)	Source
C_{ring}—C_{ring}	1.471	Ethylene oxide	$(C—O—C)_{ring}$	61.62	Ethylene oxide
C_{ring}—O_{ring}	1.436	Ethylene oxide	H—C_{ring}—H	116.25	Ethylene oxide
H—C_{ring}	1.082	Ethylene oxide	C_{ring}—C_{ring}—H	119.34	Ethylene oxide
C_{ring}—$C_{carbinol}$	1.513	Propylene oxide	C_{ring}—C_{ring}—$C_{carbinol}$	124.15	Calculated
H—$C_{carbinol}$	1.09	Propylene oxide	CC⊥*	35.35	Calculated
C—$O_{carbinol}$	1.426	Methanol	C_{ring}—C—X	109.475	Propylene oxide
O—H	1.0	Assumed	H—C—H	109.468	Propylene oxide
			H—C—O	109.468	Propylene oxide
			C—O—H	108.24	Calculated
			O_{ring}—C_{ring}—C—O†	30.63	Calculated
			C_{ring}—C—O—H†	−72.55	Calculated

*Angle between the C_{ring}—C bond and a line perpendicular to the plane of the ring.
†The angle is zero when the four atoms are in a coplanar, *cis* configuration.

TABLE 4. Rotational constants and moments of inertia as measured and as calculated from geometry of Table 3

	$\overline{CH_2—O—CH}—CH_2OH$		$\overline{CH_2—O—CH}—CH_2OD$	
Parameter	Observed	Calculated	Observed	Calculated
A	10 347.87	10 362.47	10 010.31	10 009.83
B	4 102.36	4 136.52	4 056.73	4 057.63
C	3 781.95	3 781.17	3 717.02	3 690.85
I_a*	48.8386	48.7699	50.4855	50.4881
I_b	123.1915	122.1744	124.5772	124.5498
I_c	133.6284	133.6562	135.9627	136.9271

*In u.Å². Conversion factor from rotational constants is 505 376 MHz u.Å².

Can. J. Chem. Downloaded from www.nrcresearchpress.com by 210.87.254.6 on 09/05/12
For personal use only.

it is a light atom and its amplitude of vibration is large.

The proposed structure is shown in Fig. 1 and the angles and distances are given in Table 3; calculated and measured rotational constants and moments of inertia are given in Table 4. Because of the indeterminate model errors and the arbitrariness involved in the variable choice, no error limits are given. We estimate that the determined angles are probably useful to the nearest degree and the O—H distance lies within the range 0.95 to 1.05 Å.

The feature of greatest interest in the glycidol structure is the position of the OH hydrogen atom. The hydrogen in our proposed model is apparently in a situation appropriate for hydrogen bond formation. The H---O distance is 2.49 Å, the O---O distance is 2.67 Å, and the O—H---O angle is 89.5°. These may be compared to O---O distances from 2.55 to 2.96 Å for a series of intermolecular hydrogen bonds in alcohols (7) and the evidence that linear or approximately linear configurations are more stable (7, 8). However, the molecular geometry of glycidol imposes constraints that make it impossible to form a linear O—H---O configuration; and the hydrogen is presumably attracted, not to the center of the oxygen, but to the unshared pair of electrons which are on the same side of the plane of the ring as the carbinol group. The potential minimum holding the hydrogen (and thus, the entire carbinol group) in position is probably much shallower than the minima of more favorable hydrogen bonds (intermolecular bonds). However, for glycidol to change to another rotational configuration, a motion of the entire carbinol group may be required with the hydrogen moving several angstroms. Thus a shallow but wide barrier for a large group can restrict motion as effectively as a higher but narrower barrier.

We propose that the structure as given here is a good approximation to the most stable molecular configuration. Other rotamers, if present, do not give spectral lines of comparable intensity (due to smaller permanent dipoles or smaller concentrations or both) and have not been identified. Since no form of glycidol is likely to have a much smaller dipole moment, we think it probable that this configuration is the predominant one.

We are grateful to the National Research Council of Canada for financial support. We also wish to thank Professors E. B. Wilson and Helmut H. Dreizler and their research groups for their hospitality and help in running spectra.

1. A. BHAUMIK, W. V. F. BROOKS, S. C. DASS, and K. V. L. N. SASTRY. Can. J. Chem. **48**, 2949 (1970).
2. S. A. MARSHALL and J. WEBER. Phys. Rev. **105**, 1502 (1957).
3. G. L. CUNNINGHAM, JR., A. W. BOYD, R. J. MYERS, W. D. GWINN, and W. I. LEVAN. J. Chem. Phys. **19**, 676 (1951); T. E. TURNER and J. A. HOWE. J. Chem. Phys. **24**, 929 (1956).
4. J. D. SWALEN and D. R. HERSCHBACH. J. Chem. Phys. **27**, 100 (1957).
5. R. M. LEES and J. G. BAKER. J. Chem. Phys. **48**, 5249 (1968).
6. H. B. THOMPSON. J. Chem. Phys. **47**, 3407 (1967).
7. G. C. PIMENTEL and A. L. MCCLELLAN. The hydrogen bond. Freeman, San Francisco. 1960. pp. 263, 271.
8. C. N. R. RAO. *In* Water, a comprehensive treatment, Vol. I. *Edited by* F. Franks. Plenum Press, New York. 1972. p. 93.

Can. J. Chem. Downloaded from www.nrcresearchpress.com by 210.87.254.6 on 09/05/12
For personal use only.

Dielectric Models for Porous Adsorbent – Adsorbate Systems

M. J. DIGNAM AND B. RAO
Department of Chemistry, University of Toronto, Toronto, Ontario M5S 1A1
Received December 10, 1974

M. J. DIGNAM and B. RAO. Can. J. Chem. **53**, 2252 (1975).

Equations are derived for the dielectric constant of porous adsorbent – adsorbate systems based on several geometrical models and taking account of both adsorbate molecular orientation and the special geometrical relationship which exists between adsorbed and substrate phases. Isotropic distributions of coated spheres, rods, disks, and their cavity counterparts are treated. Although the equations are based on the above idealized physical models, unlike many previous derivations, no additional intuitive postulates are involved. Furthermore, the equations are correct in the various limiting cases in which two of the three phases are absent, again in contrast with some earlier equations. Some implications of the equations are discussed, particularly as they apply to molecular orientation. The question of a break in the curve of composite dielectric constant *vs.* volume adsorbed at monolayer coverage is also investigated.

M. J. DIGNAM et B. RAO. Can. J. Chem. **53**, 2252 (1975).

On a dérivé des équations pour calculer la constante diélectrique de systèmes adsorbants poreux/adsorbés; ces équations sont basées sur plusieurs modèles géométriques qui tiennent compte à la fois de l'orientation moléculaire de la molécule adsorbée et de la relation geométrique spéciale qui existe entre les phases adsorbées et le substrat. On traite des distributions isotropiques de sphères, de bâtonnets et de disques recouverts de même que leur contrepartie creuse. Quoique les équations soient basées sur les modèles physiques idéalisés mentionnés plus haut, elles ne font appel à aucun autre postulat intuitif et ce, contrairement à plusieurs dérivations antérieures. De plus, les équations sont correctes dans divers cas limites dans lesquels deux des trois phases sont absentes et ceci encore une fois en opposition avec des équations antérieures. On discute de quelques implications de ces équations en particulier en ce qui a trait à l'orientation moléculaire. On examine aussi la question d'un bris dans la courbe reliant la constante diélectrique globale en fonction du volume adsorbé par une couche monomoléculaire.
[Traduit par le journal]

(1) Introduction

There exists in the literature a considerable body of data concerned with the dielectric properties of porous adsorbent – adsorbate systems (1). In the preface to his book (1), McIntosh states that although much data has been amassed, little progress has been made in describing the dielectric properties of the adsorbate, due mainly to the difficulty of analyzing the internal fields which exist within a heterogeneous dielectric. In this paper, an attempt is made to take account of these in a more realistic way than heretofore.

To illustrate the nature of the difficulties which have plagued previous attempts to develop models for the dielectric behavior of porous adsorbent – adsorbate systems, we examine here one of the more successful ones developed by McIntosh *et al.* (2, 3), and based on a method for treating powders due to Böttcher (4). The main assumptions upon which the treatment is based are listed below.

(*1*) The average internal field acting to polarize the material comprising any of the phases making up the composite dielectric is the so-called spherical cavity field, *i.e.* $(\varepsilon_i + 2)/3$ times the mean macroscopic or Maxwell field with the *i*th phase, where ε_i is the dielectric constant of the *i*th phase.

(*2*) The mean internal field, averaged over the entire heterogeneous dielectric, is given by $(\varepsilon + 2)/3$, where ε is the effective dielectric constant of the composite.

(*3*) The field within the void spaces is that for spherical voids within an isotropic continuum of dielectric constant ε.

(*4*) The average internal field within the substrate phase is independent of adsorbate concentration.

This set of postulates contains a number of rather obvious shortcomings. Since they are not based on a specific geometrical model, it is difficult to know under what conditions, if any, they will be valid approximations. Some features of the model upon which the postulates depend im-

Can. J. Chem. Downloaded from www.nrcresearchpress.com by 210.87.254.40 on 09/05/12
For personal use only.

Can. J. Chem. Downloaded from www.nrcresearchpress.com by 210.87.254.40 on 09/05/12
For personal use only.

plicitly, however, are apparent. Postulates *1* and *2* imply that all three phases, but in particular the substrate and adsorbed phases, take up the same sort of geometrical configurations within the composite dielectric. Up to one monolayer, however, such an assumption is invalid, since the adsorbed phase will exist as a convoluted layer one molecule in thickness, while the substrate phase will in general have a quite different geometry. The use of the spherical cavity field for the field polarizing the adsorbed species is also clearly inappropriate when they are present as a unimolecular layer. Furthermore, in general the molecules will be partially oriented with respect to the local surface plane, introducing complications which the above set of postulates do not handle. Finally, the set of assumptions is not self-consistent, a fact most easily demonstrated by considering the expression for ε obtained for no adsorbate, and the dielectric constant of the voids set to unity:

$$[1]\quad \frac{\varepsilon + 2}{3} - \frac{3\varepsilon(1 - v_s)}{2\varepsilon + 1} = \frac{(\varepsilon - 1)(\varepsilon_s + 2)}{3(\varepsilon_s - 1)}$$

where ε_s and v_s are the dielectric constant and volume fraction, respectively, of the substrate. For $v_s = 1$, [1] correctly gives $\varepsilon = \varepsilon_s$; however for $v_s = 0$ it gives $\varepsilon = -\varepsilon_s/2$, whereas the correct relation is clearly $\varepsilon = 1$.

Other models have been proposed based on different sets of assumptions, and having in general different shortcomings. Common to all previous models, however, is their failure to take account of the special geometrical relationship that exists between the adsorbed and substrate phases, arising from the fact that one coats the other. In the present paper this geometrical relationship is taken explicitly into account using the procedure developed earlier by Dignam *et al.* (5) in connection with the interpretation of the i.r. absorption spectrum of species adsorbed within porous media. This procedure will be described in relation to a particular model treated there, namely that of a random, isotropic, distribution of spherical particles uniformly coated with the adsorbed phase. On the assumption that monolayers and submonolayers will in general consist of molecules partially oriented with respect to the local surface normal, but isotropically oriented with respect to rotation about this normal, the dielectric tensor for the adsorbed phase was assumed to possess uniaxial symmetry, with the local axis directed normal to the surface of the substrate particle, *i.e.* radially.

The procedure then involved obtaining an expression for the effective polarizability of an isolated coated sphere immersed in a dielectric continuum, by solving the appropriate problem in electrostatics, to obtain

$$[2]\quad \frac{\alpha^{(1)}}{R_2{}^3} = \frac{[(S' + 1)\varepsilon_n + \varepsilon_3][S'\varepsilon_n + \varepsilon_1]q^{2S'+1} - [S'\varepsilon_n - \varepsilon_3][\varepsilon_1 + (S' + 1)\varepsilon_n]}{[(S' + 1)\varepsilon_n + \varepsilon_3][2\varepsilon_1 + S'\varepsilon_n]q^{2S'+1} + [2\varepsilon_1 - (S' + 1)\varepsilon_n][S'\varepsilon_n - \varepsilon_3]}$$

where $S' = (2\varepsilon_t/\varepsilon_n + 1/4)^{1/2} - 1/2$, $q = R_2/(R_2 - d)$, and $\alpha^{(1)}$ is the effective polarizability of a coated sphere of total radius R_2 immersed in a continuum of dielectric constant ε_1, with d the thickness, and ε_n and ε_t the principal components of the dielectric tensor for the film corresponding to directions normal and tangent to the particle surface respectively, and ε_3 the dielectric constant of the particles.

In the limit of small d/R_2, [2] reduces in the case of a coated spherical particle to

$$[3]\quad \alpha^{sp} = R_{sp}{}^3 \frac{\varepsilon_s/\varepsilon_a - 1}{\varepsilon_s/\varepsilon_a + 2} + 3R_{sp}{}^2 \frac{2\gamma_t + (\varepsilon_s/\varepsilon_a)^2\gamma_n}{(\varepsilon_s/\varepsilon_a + 2)^2}$$

where R_{sp} is the radius of the spherical particle, ε_s and ε_a the dielectric constant of the substrate and ambient, respectively, while γ_u, with u = n or t, is 4π times the mean polarization per unit area of the adsorbate in the u-direction relative to the ambient, divided by the field in the u-direction in the absence of the adsorbate, and is given by (6)

$$[4]\quad \gamma_n = (1 - \varepsilon_a/\varepsilon_n)d$$

$$[5]\quad \gamma_t = (\varepsilon_t/\varepsilon_a - 1)d$$

As the concept of an effective polarizability is used throughout this paper, we take some pains at this point to clarify its meaning and use. $\alpha^{(1)}$ is defined through the relationships (5)

Can. J. Chem. Downloaded from www.nrcresearchpress.com by 210.87.254.40 on 09/05/12
For personal use only.

$$[6] \quad \mu^{(1)} = \alpha^{(1)} E^{(1)}$$

$$[7] \quad \psi_1{}^{(1)} = (-E^{(1)} r + \mu^{(1)}/r^2) \cos \theta$$

where $\psi_1{}^{(1)}$ is the electrostatic potential in the ambient phase resulting from the superposition of the homogeneous polarizing field $E^{(1)}$ (*i.e.* the Maxwell field that would exist in the ambient medium in the absence of the coated sphere being treated) and the field due to the induced dipole moment of the coated sphere. The polar coordinates of the center of the spherical particle are r, θ, and ϕ with $E^{(1)}$ pointing in the $\phi = 0$ direction (making $\psi_1{}^{(1)}$ independent of ϕ). If $E^{(1)}$ were inhomogeneous, then eq. 7 would have to be modified to include higher order multipole contributions from the polarized coated sphere, a point to which we return later. Neglecting moments higher than the dipole moment (*i.e.* neglecting possible field inhomogeniety) it is apparent from the form of eq. 7 that a point dipole of dipole moment $\varepsilon_1 \mu^{(1)}$ in a continuum of dielectric constant ε_1 will produce precisely the same potential distribution in medium 1 (outside the region occupied by the coated sphere) and precisely the same total polarization (in a volume containing the coated sphere) as does the coated sphere. This realization simplifies enormously the calculation of the dielectric constant of an assembly of coated spheres, immersed in a dielectric continuum, which, of course, is the aim of this exercise.

From the above, it follows that the polarization per unit volume for such a dispersion of particles, P, is given by

$$[8] \quad P = \sum \varepsilon_1 \mu_j{}^{(1)} + (\varepsilon_1 - 1) E^{(1)}/4\pi$$

where $\mu_j{}^{(1)}$ is the value of $\mu^{(1)}$ for the jth particle, and the sum is over unit volume. Note also that because of the above noted equivalence, we may immediately identify $E^{(1)}$ as the Maxwell field strength in the dispersion. The field polarizing the jth species *i.e.* the field to use in eq. 6 is $E^{(1)}$ plus the contribution from the other point dipoles. If the particles are isotropically and randomly distributed, the mean polarizing, or local, field is given by (7) $E^{(1)} + (4\pi/3)\sum \mu_j{}^{(1)}$, so that

$$[9] \quad \sum \mu_j{}^{(1)} = [E^{(1)} + (4\pi/3)\sum \mu_j{}^{(1)}] \sum \alpha_j{}^{(1)}$$

Combining eqs. 8 and 9 with the definition of dielectric constant for the dispersion, $\varepsilon = 1 + 4\pi P/E^{(1)}$, then gives

$$[10] \quad \varepsilon/\varepsilon_1 = 1 + \frac{4\pi \sum \alpha_j{}^{(1)}}{1 - (4\pi/3) \sum \alpha_j{}^{(1)}}$$

For the ambient medium vacuum, $\varepsilon_1 = 1$ and $\alpha_j{}^{(1)}$ is the conventional vacuum polarizability of the jth species, so that eq. 10 becomes identically the Lorenz–Lorentz or Clausius–Mossotti equation. Thus through the use of effective polarizabilities, problems relating to polarizable species immersed in dielectric continua can be treated as readily as those involving vacuum. (Note that $\alpha^{(1)}$ as given in eq. 2 is zero for $\varepsilon_n = \varepsilon_t = \varepsilon_3 = \varepsilon_1$.)

As the analysis leading to eq. 10 is not trivial to follow in depth, we offer the following empirical evidence for its essential correctness. Equation 10 combined with eq. 2 leads to the obviously correct result, for any two of the three phases absent (*i.e.* for only phase 3 present, $\varepsilon = \varepsilon_3$ etc.) and also, for all the phases present having the same dielectric constant. The treatment is nevertheless approximate in that it fails to take account of the quadripole and higher moments induced in the coated particles as a result of inhomogenieties in the polarizing field. Just how important these higher moments are is difficult to estimate and we make no attempt to do so here.

Combining eqs. 3 and 10 and setting $\varepsilon_1 = \varepsilon_a$, $\varepsilon_3 = \varepsilon_s$, and $\varepsilon = \varepsilon^{sp}$ then gives (5)

$$[11] \quad \frac{\varepsilon^{sp}/\varepsilon_a - 1}{\varepsilon^{sp}/\varepsilon_a + 2} = v_s \left(\frac{\varepsilon_s/\varepsilon_a - 1}{\varepsilon_s/\varepsilon_a + 2} \right) + a \frac{2\gamma_t + (\varepsilon_s/\varepsilon_a)^2 \gamma_n}{(\varepsilon_s/\varepsilon_a + 2)^2}$$

where a is the surface area per unit volume.

It is apparent that [2] applies equally well to the case of an internally coated spherical cavity, so that for small d/R_2 it becomes in this case

$$[12] \quad \alpha^{sc} = R_{sc}{}^3 \frac{1 - \varepsilon_s/\varepsilon_a}{1 + 2\varepsilon_s/\varepsilon_a} + 3R_{sc}{}^2 \frac{(\varepsilon_s/\varepsilon_a)(2\gamma_t + \gamma_n)}{(1 + 2\varepsilon_s/\varepsilon_a)^2}$$

where R_{sc} is the radius of the spherical cavity. This in turn leads to the following expression for the dielectric constant of a porous body containing a random, isotropic, distribution of coated spherical cavities

$$[13] \quad \frac{\varepsilon^{sc}/\varepsilon_s - 1}{\varepsilon^{sc}/\varepsilon_s + 2} = v_c \frac{1 - \varepsilon_s/\varepsilon_a}{1 + 2\varepsilon_s/\varepsilon_a} + a \frac{(\varepsilon_s/\varepsilon_a)(2\gamma_t + \gamma_n)}{(1 - 2\varepsilon_s/\varepsilon_a)^2}$$

Can. J. Chem. Downloaded from www.nrcresearchpress.com by 210.87.254.40 on 09/05/12
For personal use only.

where v_c is the volume fraction of the empty cavities.

Note that the relative weighting of the adsorbate dielectric parameters, γ_t and γ_n, is different for the cavity and particle models, being 2:1 for the cavity model, while $2:(\varepsilon_s/\varepsilon_a)^2$ for the particle model. When dealing with oriented molecular layers, it is thus apparent that the choice of geometry for the porous adsorbent can have important consequences for the predicted dielectric behavior of the system. Therefore, before considering further these expressions and others which follow directly from them, we will first develop analogous equations for porous systems based on cylindrical, rather than spherical symmetry. Fibrous adsorbates, such as paper, might be modelled more closely by an assembly of cylindrical rods, rather than spherical particles, and porous glass by cylindrical cavities, rather than spherical cavities. Of course, many other particle and cavity shapes are possible. In this paper, however, we shall treat only spherical, cylindrical, and disk-shaped particles and cavities, and admixtures of these, mainly because these are the easiest to treat, but also because by themselves they provide a wide variety of predicted dielectric behavior.

The problem of evaluating the dielectric constant of an assembly of coated rods begins with the determination of the polarizability of an isolated coated rod. To obtain this we first require solutions to div $\boldsymbol{D} = 0$, where $\boldsymbol{D}$ is the electric displacement vector, in all three media, the rod, the film, and the ambient. As this equation reduces to Laplace's for isotropic media, solutions for such media are well-known. We look therefore for acceptable solutions within the oriented film, from which the polarizability problem can be solved by applying the appropriate boundary conditions.

(2) Solution to div $\boldsymbol{D} = 0$ for Uniaxial Medium of Cylindrical Symmetry

Choosing the z-axis to coincide with the axis of the cylindrical rod of infinite length, we assume that the oriented molecular film can be treated as a uniaxial medium with the local optic axis being directed radially, *i.e.* normal to the z-axis. This should be a good representation of an actual film provided that the molecules are isotropically oriented with respect to rotation about a radial axis, and are isotropically distributed in the surface plane (6).

Expansion of div $\boldsymbol{D}$ in cylindrical coordinates yields

$$[14] \quad \text{div } \boldsymbol{D} = \frac{1}{r}\frac{\partial}{\partial r}(rD_r) + \frac{1}{r}\frac{\partial D_\theta}{\partial \theta} + \frac{\partial D_z}{\partial z}$$

where D_r, D_θ, and D_z are the components of $\boldsymbol{D}$ with respect to a set of unit orthogonal vectors directed along a radial line, directed normal to it in the direction of increasing θ, and directed along the z-axis, respectively. We may therefore write[1]

$$[15] \quad D_r = -\varepsilon_n\frac{\partial \psi}{\partial r}$$

$$D_\theta = \frac{-\varepsilon_t}{r}\frac{\partial \psi}{\partial \theta}$$

$$D_z = -\varepsilon_t\frac{\partial \psi}{\partial z}$$

where ψ is the electrostatic potential and ε_n and ε_t the principal components of the dielectric constant tensor for the uniaxial medium. Substituting [15] into [14] and equating div $\boldsymbol{D}$ to zero gives

$$[16] \quad \frac{\partial^2\psi}{\partial r^2} + \frac{1}{r}\frac{\partial \psi}{\partial r} + \frac{s^2}{r^2}\frac{\partial^2\psi}{\partial \theta^2} + s^2\frac{\partial^2\psi}{\partial z^2} = 0$$

where

$$[17] \quad s = \sqrt{\varepsilon_t/\varepsilon_n}$$

Although the general solution of [16] is readily obtained, we require only solutions for which $\partial\psi/\partial z = 0$. Solving [16] by the method of separation of variables for $\partial\psi/\partial z = 0$ yields for the general solution

$$[18] \quad \psi = \sum_{l=0}^{\infty} \psi_l$$

where

$$[19] \quad \psi_l = (a_l r^{ls} + b_l/r^{ls})(c_l \cos \theta l + d_l \sin \theta l)$$

(3) Polarizability per Unit Length of an Isotropic Infinitely Long Cylinder with an Oriented Molecular Film

Taking the direction of the homogeneous field to be normal to the axis of the cylinder in the $\theta = 0$ direction, the appropriate form for the potential in the three phases is obtained from [19] on setting $l = 1$. The validity of this assumption rests on whether or not the boundary conditions can be satisfied on the basis of the assumption.

Identifying the ambient phase, film phase, and

[1]We employ unrationalized e.s.u. throughout.

Can. J. Chem. Downloaded from www.nrcresearchpress.com by 210.87.254.40 on 09/05/12
For personal use only.

rod phase as media 1, 2, and 3 respectively, we have then from [19] for $l = 1$, and noting that by symmetry $d_l = 0$

$$[20]\quad \psi_1^{(1)} = (-E_\perp^{(1)} r + 2\mu_\perp^{(1)}/r)\cos\theta$$

$$[21]\quad \psi_1^{(2)} = (-E_\perp^{(2)} r^s + 2\mu_\perp^{(2)}/r^s)\cos\theta$$

$$[22]\quad \psi_1^{(3)} = (-E_\perp^{(3)} r + 2\mu_\perp^{(3)}/r)\cos\theta$$

where $E_\perp^{(1)}$ and $E_\perp^{(3)}$ are the homogeneous field strengths in media 1 and 3 respectively, $\mu_\perp^{(1)}$ the effective dipole moment per unit length of the coated rod immersed in medium 1, and $E_\perp^{(2)}$, $\mu_\perp^{(2)}$, and $\mu_\perp^{(3)}$ parameters to be evaluated from the boundary conditions.

Since there are no free charges, ψ_1 must be everywhere finite, so that $\mu_\perp^{(3)} = 0$. ψ_1 must also be continuous, leading to

$$[23]\quad -E_\perp^{(1)} R_2 + 2\mu_\perp^{(1)}/R_2 = -E_\perp^{(2)} R_2^s + 2\mu_\perp^{(2)}/R_2^s$$

$$[24]\quad -E_\perp^{(2)} R_3^s + 2\mu_\perp^{(2)}/R_3^s = -E_\perp^{(3)} R_3$$

where R_3 is the radius of the isotropic rod, and R_2 that of the film covered rod.

Applying the condition that the normal component of $\boldsymbol{D}$ (*i.e.* $D_r = -\varepsilon_n \partial\psi/\partial r$) is continuous across the boundaries gives

$$[25]\quad \varepsilon_1 E_\perp^{(1)} + 2\varepsilon_1 \mu_\perp^{(1)}/R_2^2 = s\varepsilon_n E_\perp^{(2)} R_2^{s-1} + 2s\varepsilon_n \mu_\perp^{(2)}/R_2^{s+1}$$

$$[26]\quad s\varepsilon_n E_\perp^{(2)} R_3^{s-1} + 2s\varepsilon_n \mu_\perp^{(2)}/R_3^{s+1} = \varepsilon_3 E_\perp^{(3)}$$

where ε_1 and ε_3 are the dielectric constants of the isotropic media 1 and 3 respectively.

Equations 23 to 26 are four linearly independent linear equations in the four unknown parameters, $\mu_\perp^{(1)}$, $\mu_\perp^{(2)}$, $E_\perp^{(2)}$, and $E_\perp^{(3)}$, which can be solved to yield a solution to the problem satisfying all requirements. Solving for $\mu_\perp^{(1)}$ and setting $\mu_\perp^{(1)} = \alpha_\perp^{(1)} E_\perp^{(1)}$ leads to the following expression for $\alpha_\perp^{(1)}$, the normal component of the effective polarizability-per-unit-length tensor for the film covered rod immersed in a medium of dielectric constant ε_1.

$$[27]\quad \frac{2\alpha_\perp^{(1)}}{R_2^2} = \frac{(s\varepsilon_n + \varepsilon_3)(s\varepsilon_n - \varepsilon_1)q^{2s} - (s\varepsilon_n - \varepsilon_3)(s\varepsilon_n + \varepsilon_1)}{(s\varepsilon_n + \varepsilon_1)(s\varepsilon_n + \varepsilon_3)q^{2s} - (s\varepsilon_n - \varepsilon_3)(s\varepsilon_n - \varepsilon_1)}$$

where $q = R_2/R_3$.

On setting $q = 1$, eq. 27 reduces to the well-known expression for the polarizability per unit length (specific polarizability) for an uncoated rod placed normal to the external field, *viz.*

$$[28]\quad \alpha_\perp^{(1)} = \frac{1}{2} R_2^2 \frac{\varepsilon_3 - \varepsilon_1}{\varepsilon_3 + \varepsilon_1}$$

In the limit $q \to \infty$, [27] reduces to an expression for the specific polarizability of a rod composed entirely of oriented molecular layers, the result being given by

$$[29]\quad \alpha_\perp^{(1)} = \frac{1}{2} R_2^2 \frac{s\varepsilon_n - \varepsilon_1}{s\varepsilon_n + \varepsilon_1}$$

For the isotropic case, (*i.e.* $s = 1$), [29] in turn reduces to a form equivalent to [28], as indeed it must.

Finally, on setting $q = (R_r + d)/R_r$, and $R_2 = R_r + d$, where d is the thickness of the oriented molecular layer and $R_r = R_3$, the radius of the rod, [27] may be expanded in powers of d/R_r to give, on retaining up to first order terms

$$[30]\quad \alpha_\perp^{rp} = \frac{1}{2} R_{rp}^2 \frac{\varepsilon_s/\varepsilon_a - 1}{\varepsilon_s/\varepsilon_a + 1} + R_{rp} \frac{\gamma_t + (\varepsilon_s/\varepsilon_a)^2 \gamma_n}{(\varepsilon_s/\varepsilon_a + 1)^2}$$

where, as before, ε_s and ε_a are the dielectric constant of the substrate and ambient, respectively, and have been substituted for ε_3 and ε_1, and γ_n and γ_t are defined in Section 1. The first term in [30] is the contribution due to the uncoated rod, the second being that due to the coating.

To obtain an expression from [27] for the specific polarizability of a cylindrical cavity with an internally adsorbed oriented molecular film, the substitutions $q = R_{rc}/(R_{rc} - d)$, $\varepsilon_1 = \varepsilon_s$, $\varepsilon_3 = \varepsilon_a$ are made, which on expanding in powers of d/R_{rc} and retaining up to first order terms gives

$$[31]\quad \alpha_\perp^{rc} = \frac{1}{2} R_{rc}^2 \frac{1 - \varepsilon_s/\varepsilon_a}{1 + \varepsilon_s/\varepsilon_a} + R_{rc} \frac{(\varepsilon_s/\varepsilon_a)(\gamma_t + \gamma_n)}{(1 + \varepsilon_s/\varepsilon_a)^2}$$

where $R_{rc} = R_2$ is the radius of the empty cavity.

Can. J. Chem. Downloaded from www.nrcresearchpress.com by 210.87.254.40 on 09/05/12
For personal use only.

As before, the first term in [31] is the contribution to $\alpha_\perp^{(1)}$ made by the empty cavity, the second, that made by the film.

To calculate the parallel component of the effective specific polarizability of a coated rod immersed in a medium of dielectric constant ε_1 is straightforward, since the Maxwell field strengths in all the media must be the same, and only the component ε_t of the film dielectric tensor is involved. Thus the incremental polarizations of media 3 and 2 relative to medium 1 are given by

$$[32] \qquad \Delta P_\parallel^{(3)} = E_\parallel^{(3)}(\varepsilon_3 - \varepsilon_1)/4\pi$$

$$[33] \qquad \Delta P_\parallel^{(2)} = E_\parallel^{(2)}(\varepsilon_t - \varepsilon_1)/4\pi$$

The effective specific polarizability of the coated rod is then given by

$$[34] \quad \varepsilon_1\alpha_\parallel^{(1)} = (V_3/l)(\Delta P_\parallel^{(3)}/E_\parallel^{(1)}) + (V_2/l)(\Delta P_\parallel^{(2)}/E_\parallel^{(1)})$$

where V_3 and V_2 are the volumes of the phases, and l the length of the rod. Substituting appropriately for V_3, V_2, $\Delta P_\parallel^{(3)}$, and $\Delta P_\parallel^{(2)}$ and setting $E_\parallel^{(3)} = E_\parallel^{(2)} = E_\parallel^{(1)}$ then gives

$$[35] \quad \alpha_\parallel^{(1)} = \tfrac{1}{4}R_3^2[(\varepsilon_3/\varepsilon_1 - 1) + (q^2 - 1)(\varepsilon_t/\varepsilon_1 - 1)]$$

Expanding R_3^2 and q^2 as before, gives for the case of a coated rodlike particle.

$$[36] \quad \alpha_\parallel^{rp} = \tfrac{1}{4}R_{rp}^2(\varepsilon_s/\varepsilon_a - 1) + \tfrac{1}{2}R_{rp}\gamma_t$$

while for an internally coated rodlike cavity

$$[37] \quad \alpha_\parallel^{rc} = \tfrac{1}{4}R_{rc}^2(\varepsilon_a/\varepsilon_s - 1) + \tfrac{1}{2}R_{rc}(\varepsilon_a/\varepsilon_s)\gamma_t$$

(4) Dielectric Constant for a Medium Consisting of a Set of Parallel Coated Rods

In order to calculate the dielectric constant for a set of parallel rods, we must take into account the contribution of the polarization of the medium to the field polarizing the rods. This we do in the manner of Lorentz (8), that is by considering the polarizable species to lie within an appropriately shaped cavity within a continuous dielectric, the field within the cavity being taken as the local field polarizing the species. Following the procedure outlined in Section 1, with however the mean polarizing field given by $E^{(1)}[1 + \omega(\varepsilon/\varepsilon_1 - 1)]$ rather than $E^{(1)} + (4\pi/3)\sum\mu_j^{(1)}$, leads to the result

$$[38] \qquad \varepsilon/\varepsilon_1 = 1 + \frac{4\pi\sum\alpha_j^{(1)}}{1 - 4\pi\omega\sum\alpha_j^{(1)}}$$

The term $E^{(1)}\omega(\varepsilon/\varepsilon_1 - 1)$ is the contribution to the polarizing field made by the polarization of the medium, ω being the depolarization factor appropriate to the cavity shape. For spherical cavities, $\omega = 1/3$ and eq. [38] reduces precisely to eq. [10], which is essentially the Lorenz–Lorentz or Clausius–Mossotti expression. For the problem at hand, the cavities must be chosen to be cylindrical in shape. For fields normal to and parallel to the cylinder axis respectively, $\omega = 1/2$ and 0 respectively (8), leading to the result

$$[39] \qquad \varepsilon_\perp/\varepsilon_1 = 1 + \frac{4\pi L\langle\alpha_\perp^{(1)}\rangle}{1 - 2\pi L\langle\alpha_\perp^{(1)}\rangle}$$

$$[40] \qquad \varepsilon_\parallel/\varepsilon_1 = 1 + 4\pi L\langle\alpha_\parallel^{(1)}\rangle$$

where L is the total length of rod per unit volume and $\langle\alpha_\perp^{(1)}\rangle$ the mean effective polarizability per unit length normal to the cylinder axes, etc. Thus using the expressions for $\alpha^{(1)}$ presented in Section 3, we have for a collection of parallel rodlike particles

$$[41] \quad \left(\frac{\varepsilon_\perp^{rp}/\varepsilon_a - 1}{\varepsilon_\perp^{rp}/\varepsilon_a + 1}\right) = v_s\left(\frac{\varepsilon_s/\varepsilon_a - 1}{\varepsilon_s/\varepsilon_a + 1}\right) + a\frac{\gamma_t + (\varepsilon_s/\varepsilon_a)^2\gamma_n}{(\varepsilon_s/\varepsilon_a + 1)^2} = x^{rp}$$

$$[42] \quad (\varepsilon_\parallel^{rp}/\varepsilon_a - 1) = v_s(\varepsilon_s/\varepsilon_a - 1) + a\gamma_t$$

while for a collection of parallel, internally coated rodlike cavities

$$[43] \quad \left(\frac{\varepsilon_\perp^{rc}/\varepsilon_s - 1}{\varepsilon_\perp^{rc}/\varepsilon_s + 1}\right) = v_c\left(\frac{1 - \varepsilon_s/\varepsilon_a}{1 + \varepsilon_s/\varepsilon_a}\right) + a\frac{(\varepsilon_s/\varepsilon_a)(\gamma_t + \gamma_n)}{(1 + \varepsilon_s/\varepsilon_a)^2} = x^{rc}$$

$$[44] \quad (\varepsilon_\parallel^{rc}/\varepsilon_s - 1) = v_c(\varepsilon_a/\varepsilon_s - 1) + a(\varepsilon_a/\varepsilon_s)\gamma_t$$

These expressions take the correct form for the various limiting cases. Thus for example on setting $\gamma_n = 0 = \gamma_t$ (*i.e.* no adsorbed species), then for $v_s = 1$ (or $v_c = 0$), $\varepsilon_\perp^{rp} = \varepsilon_\parallel^{rp} = \varepsilon_\perp^{rc} = \varepsilon_\parallel^{rc} = \varepsilon_s$, while for $v_s = 0$ (or $v_c = 1$), $\varepsilon_\perp^{rp} = \varepsilon_\parallel^{rp} = \varepsilon_\perp^{rc} = \varepsilon_\parallel^{rc} = \varepsilon_a$. It is interesting to note that for any other choices for the depolarization factors (or local polarizing fields) the above conditions are not all satisfied.

Can. J. Chem. Downloaded from www.nrcresearchpress.com by 210.87.254.40 on 09/05/12
For personal use only.

(5) Dielectric Constant for a Medium Consisting of a Set of Isotropically Distributed, Coated Rods

There are many ways in which a set of rods can be distributed to yield overall an isotropic distribution. We will exclude regular arrangements from consideration, and treat two limiting cases of a random, isotropic, distribution.

The first is that in which the rods are considered to be randomly oriented with respect to their immediate neighbors. To treat this case, we begin by considering the dipole moment of a typical rod lying within the isotropic dispersion. Since its immediate surround is on average isotropic, we do this by assuming the rod to lie within a cylindrical cavity in an isotropic medium of dielectric constant ε. If the axis of our typical rod, the jth rod, is oriented parallel to the field $E^{(1)}$, its effective dipole moment per unit length will be given by

$$[45] \qquad \mu_{\parallel j}{}^{(1)}/E^{(1)} = \alpha_{\parallel j}{}^{(1)}$$

while if it is oriented normal to $E^{(1)}$ by

$$[46] \quad \mu_{\perp j}{}^{(1)}/E^{(1)} = [1 + \tfrac{1}{2}(\varepsilon/\varepsilon_1 - 1)]\alpha_{\perp j}{}^{(1)}$$

where the term $\frac{1}{2}(\varepsilon/\varepsilon_1 - 1)$ allows for the contribution to the polarizing field made by the polarization of the isotropic medium, $\frac{1}{2}$ being the depolarization factor. The depolarization factor in [45] is of course zero.

Since the dielectric constant for the dispersion is given by

$$[47] \qquad \varepsilon/\varepsilon_1 - 1 = 4\pi\sum\mu_j{}^{(1)}l_j/E^{(1)}$$

where the sum is over unit volume, and the rods are isotropically oriented over unit volume, we may replace $\mu_j{}^{(1)}$ in [47] by its average over all angular orientations of the rod, *i.e.* by $\bar{\mu}_j{}^{(1)}$ where

$$[48] \qquad \bar{\mu}_j{}^{(1)} = (2\mu_{\perp j}{}^{(1)} + \mu_{\parallel j}{}^{(1)})/3$$

Combining [45] with [48] then gives

$$[49] \quad (\varepsilon/\varepsilon_1 - 1) = \frac{4\pi L\langle\bar{\alpha}^{(1)}\rangle}{1 - (4\pi/3)L\langle\alpha_\perp{}^{(1)}\rangle}$$

where $\bar{\alpha}^{(1)} = (2\alpha_\perp{}^{(1)} + \alpha_\parallel{}^{(1)})/3$ and is the polarizability per unit length of a coated rod averaged over all orientations. Although eq. 49 looks rather like the Lorenz–Lorentz (or Clausius–Mossotti) equation, it in fact differs from it since $\langle\bar{\alpha}^{(1)}\rangle$ appears in the numerator while $\langle\alpha_\perp{}^{(1)}\rangle$ appears in the denominator. Substituting for $\alpha^{(1)}$ using the expressions in Section 3 then gives for a random distribution of coated rodlike particles

$$[50] \quad (\varepsilon^{rp}/\varepsilon_a - 1) = \frac{[4x^{rp} + v_s(\varepsilon_s/\varepsilon_a - 1) + a\gamma_t]}{(3 - 2x^{rp})}$$

while for a random distribution of internally coated rodlike cavities

$$[51] \quad (\varepsilon^{rc}/\varepsilon_s - 1) = \frac{[4x^{rc} + v_c(\varepsilon_a/\varepsilon_s - 1) + a(\varepsilon_a/\varepsilon_s)\gamma_t]}{(3 - 2x^{rc})}$$

where x^{rp} and x^{rc} are given by eqs. 41 and 43. Once again eqs. 50 and 51 give the correct results in the limits $v_c = 1$, and $v_s = 1$, $v_c = 0$ respectively, providing support for the results.

The second distribution which we shall consider is that in which the dispersion can be broken up into domains, within each of which the rods may be regarded as essentially straight and parallel, their lengths being much larger than their diameters. For simplicity, we shall take the domains to be spherical in shape, and shall fill all space with such domains. Other possibilities, of course, exist.

The effective polarizability of the ith domain oriented with its optic axis $\parallel$ to the mean Maxwell field within the composite dielectric is given by

$$[52] \qquad \alpha_{\parallel j}{}^{(1)} = R_j{}^3\frac{\varepsilon_\parallel/\varepsilon_1 - 1}{\varepsilon_\parallel/\varepsilon_1 + 2}$$

while if it is oriented $\perp$ to the mean Maxwell field by

$$[53] \qquad \alpha_{\perp j}{}^{(1)} = R_j{}^3\frac{\varepsilon_\perp/\varepsilon_1 - 1}{\varepsilon_\perp/\varepsilon_1 + 2}$$

Proceeding now as for the previous case, except that the depolarization factor is 1/3 for both the parallel and perpendicular orientations, we obtain

$$[54] \quad \frac{\varepsilon/\varepsilon_1 - 1}{\varepsilon/\varepsilon_1 + 2} = 1/3\left(\frac{\varepsilon_\parallel/\varepsilon_1 - 1}{\varepsilon_\parallel/\varepsilon_1 + 2}\right) + 2/3\left(\frac{\varepsilon_\perp/\varepsilon_1 - 1}{\varepsilon_\perp/\varepsilon_1 + 2}\right)$$

Other assumptions concerning the shapes and distribution of the domains will of course lead to different expressions for ε, so that eq. 54 can be considered no more than a particular example.

Can. J. Chem. Downloaded from www.nrcresearchpress.com by 210.87.254.40 on 09/05/12
For personal use only.

(6) Dielectric Constant for a Medium Consisting of a Set of Isotropically Distributed, Coated Disks

As the procedure for obtaining the effective polarizability of a coated thin disk immersed in a medium of dielectric constant ε_1 is straight forward, we present here only the results:

$$[55]\quad \alpha_\perp^{(1)} = (V_3/4\pi)(1 - \varepsilon_1/\varepsilon_3) + (V_2/4\pi)(1 - \varepsilon_1/\varepsilon_n)$$

$$[56]\quad \alpha_\parallel^{(1)} = (V_3/4\pi)(\varepsilon_3/\varepsilon_1 - 1) + (V_2/4\pi)(\varepsilon_t/\varepsilon_1 - 1)$$

where $\alpha_\perp^{(1)}$ and $\alpha_\parallel^{(1)}$ are the effective polarizability components in the principal directions perpendicular and parallel to the plane of the disk respectively, and V_3 and V_2 the volumes of the disk and adsorbed film respectively.

We consider now only the case in which the disks are randomly oriented with respect to their immediate neighbors. Proceeding precisely as for the corresponding case involving rods, we obtain

$$[57]\quad (\varepsilon/\varepsilon_1 - 1) = \frac{4\pi \sum \bar{\alpha}_j^{(1)}}{1 - (4\pi/3)\sum \alpha_{\perp j}^{(1)}}$$

where $\bar{\alpha}_j^{(1)} = (\alpha_{\perp j}^{(1)} + 2\alpha_{\parallel j}^{(1)})/3$. Substituting eqs. 55 and 56 into eq. 57 then gives for an isotropic distribution of disk-shaped particle

$$[58]\quad \frac{\varepsilon^{dp}}{\varepsilon_a} - 1 = \frac{v_s(2\varepsilon_s/\varepsilon_a - \varepsilon_a/\varepsilon_s - 1) + a(2\gamma_t + \gamma_n)}{3 - v_s(1 - \varepsilon_a/\varepsilon_s) + a\gamma_n}$$

while for an isotropic distribution of disk-shaped cavities it gives

$$[59]\quad \frac{\varepsilon^{dc}}{\varepsilon_s} - 1 = \frac{v_c(2\varepsilon_a/\varepsilon_s - \varepsilon_s/\varepsilon_a - 1) + a(2\gamma_t\varepsilon_a/\varepsilon_s + \gamma_n\varepsilon_s/\varepsilon_a)}{3 - v_c(1 - \varepsilon_s/\varepsilon_a) + a\gamma_n\varepsilon_s/\varepsilon_a}$$

Again both these equations give the correct results in the limits $v_s = 0$, $v_c = 1$, and $v_s = 1$, $v_c = 0$.

(7) Discussion

It is apparent from the foregoing, that the dielectric behavior of porous adsorbent – adsorbate systems depends not only on the geometry of the particles and/or cavities which make up the porous adsorbent, but also on the spatial and orientational distribution of these. It would therefore appear to be extremely difficult to model effectively a real system. On the other hand, one can clearly build considerable flexibility into a model using only spherical, cylindrical, and disk-shaped particles and their cavity counterparts, and this may be sufficient to duplicate reasonably well phenomena observed for real systems. Combining spherical, cylindrical, and disk-shaped particles (or cavities) into a single model is straight forward using the procedures of Section 5, though it leads to rather unwieldy expressions. Combining both cavities and particles in a single model presents difficulties and would seem to require one to consider the composite dielectric divided into particle and cavity domains. We do not plan to investigate here the many ramifications resulting from the choice of particle and cavity shapes, their relative proportions, and their spatial and orientational distribution, but will restrict attention to two effects which are predicted by all such models, and are not taken into account by any previous models for porous adsorbent – adsorbate systems. These are: effects of molecular orientation on dielectric properties, and the change in the apparent dielectric properties of the adsorbate on going from the zero-to-one-monolayer region, to the region of capillary condensation. We examine the case of molecular orientation first.

When a polar molecule is adsorbed within a porous adsorbent, its polarizability in the adsorbed state will depend upon the extent to which the molecule is free to orient its permanent dipole along the field direction. This phenomenon is well-known (1) and has been used to attempt to gain information on the nature of the adsorbed state. It is not this orientational effect we discuss here, but rather another which will exist whenever the adsorbed species has an anisotropic polarizability. In investigating this effect, as well as that associated with the transition between monolayer coverage and capillary condensation, we will treat only the random, rodlike cavity model (eq. 51). Similar conclusions arise, however, from treating the other models.

Can. J. Chem. Downloaded from www.nrcresearchpress.com by 210.87.254.40 on 09/05/12
For personal use only.

From eq. 51, on substituting for x^{rc} from eq. 43, and for γ_n and γ_t from eqs. 4 and 5 we obtain

$$[60] \quad \varepsilon_m' \equiv \left(\frac{d\varepsilon^{rc}}{dv_f}\right)_{v_f \to 0} = A(\varepsilon_t - 1/\varepsilon_n) + B(\varepsilon_t - 1)$$

where A and B are positive, real-valued, coefficients (for ε_s real valued) characteristic of the adsorbent and are given by

$$[61] \quad A = \frac{2\varepsilon_s[6\varepsilon_s - v_c(\varepsilon_s - 1)]}{[3(\varepsilon_s + 1) + 2v_c(\varepsilon_s - 1)]^2}$$

$$[62] \quad B = \frac{\varepsilon_s + 1}{3(\varepsilon_s + 1) + 2v_c(\varepsilon_s - 1)}$$

and $v_f = ad$ is the volume of adsorbate per unit volume of adsorbent. In obtaining eq. 60, ε_a has been set equal to unity and it has been assumed that ε_t and ε_n are independent of coverage (*i.e.* of v_f) in the range zero to one monolayer, which will be the case only if adsorption occurs in the form of 2-dimensional condensed patches (6).

From the form of eq. 60, it is apparent that the differential dielectric constant for the adsorbed species will in general depend on molecular orientation. Before pursuing this further, however, we shall obtain the expression for the region of capillary condensation, corresponding to eq. 60. To do this, we assume that all subsets of the capillaries, characterized by a particular range of diameters, are randomly oriented and distributed both in relation to members of the set, and to members of any other set. This allows us to break up the sum over polarizabilities in eq. 38 into two sums, one over empty capillaries, the other over full capillaries. The resulting expression for ε^{rc} is thus obtained from eq. 51 on making the following substitutions:

$$\gamma_n = 0 = \gamma_t$$

$$x^{rc} \to [(v_c - v_L)/v_c]x_0^{rc} + [v_L/v_c]x_c^{rc}$$

$$v_c(\varepsilon_a/\varepsilon_s - 1) \to (v_c - v_L)(1/\varepsilon_s - 1) + v_L(\varepsilon_L/\varepsilon_s - 1)$$

where $x_0^{rc} = x^{rc}(\gamma_n = 0 = \gamma_t,\ \varepsilon_a = 1)$, $x_c^{rc} = x^{rc}(\gamma_n = 0 = \gamma_t, \varepsilon_a = \varepsilon_L)$, and v_c is the total volume fraction of the capillaries, v_L that of the filled capillaries, and ε_L the dielectric constant of the adsorbate condensed in the capillaries. In this treatment, we have neglected the effect of the adsorbed layer, as it will not contribute significantly to $d\varepsilon^{rc}/dv_f$ in the region of capillary condensation, and have assumed that the adsorbate molecules condensed within the capillaries are isotropically oriented and distributed. Making the above substitutions, we then obtain for the initial slope in the capillary condensation region

$$[63] \quad \varepsilon_c' \equiv \left(\frac{d\varepsilon^{rc}}{dv_L}\right)_{v_L \to 0} = 2A\frac{(\varepsilon_s + 1)(\varepsilon_L - 1)}{(\varepsilon_s + \varepsilon_L)} + B(\varepsilon_L - 1)$$

where A and B are defined as before. A comparison of eqs. 60 and 63 now allows us to determine the direction of the change in slope on going from the premonolayer region to the capillary condensation region. Various possible cases are considered below.

If the adsorbed film is isotropic, then $\varepsilon_t = \varepsilon_n \simeq \varepsilon_L$ from which we deduce the following:

$$[64] \quad \begin{aligned} &\varepsilon_c'/\varepsilon_m' > 1 \text{ for } (1 - \varepsilon_L/\varepsilon_s) > 0 \\ &\varepsilon_c'/\varepsilon_m' < 1 \text{ for } (1 - \varepsilon_L/\varepsilon_s) < 0 \\ &\varepsilon_c'/\varepsilon_m' = 1 \text{ for } (1 - \varepsilon_L/\varepsilon_s) = 0 \end{aligned}$$

Thus for a nonpolar adsorbate of isotropic polarizability in the adsorbed state, this model predicts in general a change of slope at completion of a monolayer, the sign of the change being given by the sign of $(1 - \varepsilon_L/\varepsilon_s)$. No previous model predicts a change in slope for such circumstances, yet data showing such changes are common (1), and unaccounted for in any quantitative sense except in those instances where polar adsorbates give rise to an increase of slope following completion of a monolayer. The many examples in which a decrease in slope accompanies completion of a monolayer are accounted for by this model, not only for cases in which $\varepsilon_L > \varepsilon_s$, but also for those in which $\varepsilon_s > \varepsilon_L$, since even then ε_c' can be less than ε_m' if the adsorbed species has an anisotropic polarizability. Thus it is easily shown that even for $\varepsilon_s/\varepsilon_L \to \infty$, $\varepsilon_c' < \varepsilon_m'$ provided that $(\varepsilon_t - 1)/(\varepsilon_L - 1) > 9/5$, so that a decrease in slope can occur for $\varepsilon_s/\varepsilon_L > 1$ if the molecules adsorb with their major polarizability axes parallel to the surface.

All of these effects arise, of course, as a result of variations in the local field within the composite dielectric, both with position in the composite dielectric, and with field direction relative to the normal to the local surface element. The advantage of the present treatments of porous adsorbent – adsorbate systems is that for the first time they provide a basis for exploring the

possible range of such local field effects. How well the models can account quantitatively for dielectric measurements remains to be seen. That they can account qualitatively for hitherto surprising results (such as the decrease in slope following monolayer completion) has, however, already been established. A more detailed examination of the consequences of the various models, and the relationship of the models to real systems, is the subject of a current investigation.

The authors are grateful to Dr. T. McMullen of St. Francis Xavier University who provided helpful comments on the first draft of this paper, and to the National Research Council of Canada for supporting this research.

1. R. L. McIntosh. Dielectric behavior of adsorbed species. Marcel Dekker, Inc., New York, 1966.
2. R. L. McIntosh, E. K. Rideal, and J. A. Snelgrove. Proc. R. Soc. Lond. A**208**, 292 (1951).
3. E. W. Channen and R. L. McIntosh. Can. J. Chem. **33**, 172 (1955).
4. C. J. F. Böttcher. Rec. Trav. Chim. **64**, 47 (1945).
5. M. J. Dignam, B. Rao, and J. Roth. J. Chem. Soc. Faraday II, **69**, 804 (1973).
6. M. J. Dignam and M. Moskovits. J. Chem. Soc. Faraday II, **69**, 56 (1973).
7. H. C. Van de Hulst. Light scattering by small particles, 2nd ed. Wiley, London. 1962. Chapt. 2.
8. A. R. von Hippel. Dielectrics and waves. Wiley, London. 1954.

Can. J. Chem. Downloaded from www.nrcresearchpress.com by 210.87.254.40 on 09/05/12
For personal use only.

A Micrometer Syringe Dilatometer: Application to the Measurement of the Excess Volumes of some Ethylbenzene Systems at 298.15 K[1]

REIJI TANAKA,[2] OSAMU KIYOHARA,[3] PATRICK J. D'ARCY, AND GEORGE C. BENSON
Division of Chemistry, National Research Council of Canada, Ottawa, Canada K1A 0R6

Received February 25, 1975

REIJI TANAKA, OSAMU KIYOHARA, PATRICK J. D'ARCY, and GEORGE C. BENSON. Can. J. Chem. **53**, 2262 (1975).

A dilatometer using a micrometer syringe to measure small changes in volume at constant pressure is described. Excess volumes determined for cyclohexane + benzene at 298.15 K are in reasonable agreement with values from the literature. Results are also reported for the excess volumes of mixtures of ethylbenzene with benzene, toluene, and the isomeric xylenes.

REIJI TANAKA, OSAMU KIYOHARA, PATRICK J. D'ARCY et GEORGE C. BENSON. Can. J. Chem. **53**, 2262 (1975).

On décrit un dilatomètre constitué d'une micro-seringue pour mesurer de petites variations de volume à pression constante. Les excès de volume déterminés pour un mélange cyclohexane et benzène à 298.15 K sont en bon accord avec les valeurs de la littérature. On rapporte aussi les resultats concernant les excès de volume des mélanges éthylbenzène avec le benzene, le toluène ou les isomères du xylène. [Traduit par le journal]

The volume change accompanying the mixing of nonelectrolytes is often obtained from observations of the position of a meniscus of mercury confining the liquids. In cases where the displacement of the meniscus has a vertical component, it is important to consider the effect of variations in pressure on the observed volumes of the system. For a dilution type dilatometer containing about 100 cm^3 of liquid confined by mercury having a meniscus in a vertical capillary with a 1 mm internal diameter, neglect of the compressibility of the liquid will lead to an error of about 1.5% in the values of the excess volume, V^E. Furthermore, if the liquid is not adequately degassed, pressure variations may cause bubble formation which also obscures the interpretation of the observed changes in volume. Thus for accurate determinations of V^E, it is desirable to maintain constant pressure.

Dilatometers using a micrometer screw to measure the change in volume at constant pressure have been described by Pardo (1) and by Chareyron (2). Recently we constructed a similar dilatometer of somewhat simpler design. Studies of the mixing of cyclohexane with benzene and also of ethylbenzene with benzene, toluene, and the isomeric xylenes indicate that the apparatus is capable of a good accuracy and is well suited to the routine determination of excess volumes.

Experimental

Apparatus

The dilatometer was made of heavy walled Pyrex glass and was securely mounted on a brass frame. A schematic drawing of the dilatometer is given in Fig. 1. The total volume of the mixing cell F is about 120 cm^3. The feed system consists of a 50 cm^3 reservoir E and a 5 cm^3 burette D. The feed liquid enters the cell through a capillary tube H immersed in a cup G containing mercury to prevent diffusion. The cross-sectional area of the burette was determined to an accuracy of $\pm 0.025\%$ by measuring the delivery of mercury. The filling port of the feed system is closed by a Teflon stopper J expanded by a tapered steel core V to ensure a tight seal (see insert in Fig. 1).

The volume of mixing is obtained from readings of the micrometer Q and observations of the level of the mercury in the capillary tube N. The micrometer is attached to a syringe by a brass collar R and surrounded by a plastic tube O to protect it from the bath water. A steel rod extension of the micrometer spindle is keyed to a Teflon tip T which fits snugly into a 3 mm i.d. Tru-bore tube S. Before incorporating the syringe in the dilatometer, its delivery was calibrated by weighing the mercury displaced by manipulations of the micrometer. The calibration constant was determined within an error of $\pm 0.05\%$ and its value was independent of the position of the piston. The capillary N was then calibrated *in situ*, using the micrometer syringe.

Loading and Operation

After the dilatometer has been cleaned and dried, a light coating of silicone grease is applied to the stopcocks

[1]NRCC No. 14680.
[2]NRCC Postdoctorate Fellow 1973–1975.
[3]NRCC Postdoctorate Fellow 1971–1973. Present address: Department of Chemistry, Université de Sherbrooke, Sherbrooke, Québec J1K 2R1.

Can. J. Chem. Downloaded from www.nrcresearchpress.com by 210.87.254.105 on 09/05/12
For personal use only.

Can. J. Chem. Downloaded from www.nrcresearchpress.com by 210.87.254.105 on 09/05/12
For personal use only.

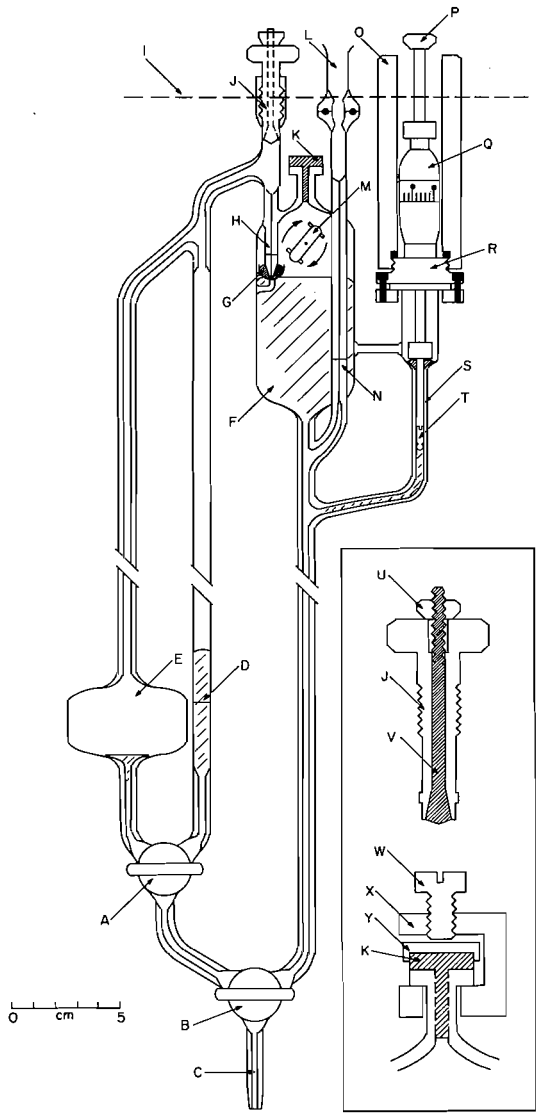

FIG. 1. Schematic diagram of the dilatometer. A and B, three-way taps (Eck and Krebs A-5032); C, drain tube; D, burette with fiducial line (approximately 0.5 cm i.d., volume 5 cm^3); E, feed reservoir (volume 50 cm^3); F, mixing cell (volume 120 cm^3); G, cup for mercury; H, Tru-bore capillary feed tube with fiducial line (approximately 0.05 cm i.d.); I, level of water in thermostat; J and K, Teflon stoppers (see inserts for details); L, extension tube with spherical O-ring joint; M, magnetic stirrer; N, Tru-bore capillary tube with fiducial line (approximately 0.05 cm i.d.); O, Lucite tube; P, extension rod to control micrometer; Q, micrometer (2.5 cm stroke, vernier reading to 10^{-4} cm); R, brass collar for attaching micrometer; S, syringe with barrel made from Tru-bore tube (approximately 0.3 cm i.d.); T, Teflon tip on piston; U and V, brass nut and tapered stainless steel core to tighten stopper J; W, X, and Y, stainless steel screw, yoke and cap to clamp stopper K.

of the taps A and B. A tube with a small tap is attached to the spherical O-ring joint on N and the opening at the top of the mixing cell is connected to a vacuum pump. The two remaining openings are sealed with temporary stoppers and the dilatometer is evacuated, taking care to remove pockets of air trapped in the grease of the stopcocks. Degassed mercury is sucked up slowly through the drain tube C into the feed system and mixing cell until the latter is filled above the level of the cup. Air is then admitted slowly through the cell opening, forcing mercury into the upper parts of the feed system, syringe and capillary.

Sufficient mercury is removed from the cell through the drain tube to make room for the addition of about 35 cm^3 of one component which is introduced from a weighing burette. All weighings are corrected to *vacuo*; the uncertainty in the amount of the cell component due to vapor loss is estimated to be less than 0.01 g. The level of the liquid in the cell is readjusted by adding mercury and/or warming–cooling operations in order to eliminate any air space when the cell is closed with the Teflon stopper K.

The stopper on the syringe opening is removed and mercury is drained out to adjust the level to a suitable position. After a little ethanol is added to the surface of the mercury in the syringe, the micrometer piston is pushed into place and the protective plastic tube installed. The alcohol acts as a lubricant and facilitates removal of air from the surface of the piston as it is inserted.

The top of the feed system is opened and the second component is introduced as mercury is drained from the feed reservoir and burette. The feed system is then sealed with the Teflon stopper J. Finally the small stopcock attached to the capillary N is opened. After the mercury level has been lowered to an appropriate position below the joint, the stopcock is removed and replaced by a glass extension tube L. Before starting a run, tap A is closed and tap B is opened from the cell toward A.

The loaded dilatometer is immersed in a water bath operated at 298.15 $\pm$ 0.01 K and controlled to better than $\pm$0.001 K during a run. The magnetic stirrer in the cell is operated continuously at about 200 r.p.m. After thermal equilibrium is reached, the level of the mercury in H is set close to the reference mark by manipulating A and J. The micrometer is then used to adjust the level in the capillary N to the same height as the meniscus in the cell. By turning tap A, some of the feed component is added slowly to the cell, displacing mercury. During the mixing, the micrometer is readjusted to maintain the mercury level in N close to that in the cell, and the final difference of levels is less than $\pm$0.05 cm. The positions of the menisci in the tubes D, H, and N, relative to the reference lines, are observed through a window in the bath. They are read by means of a cathetometer within an error of $\pm$0.003 cm. The excess volume is calculated from the micrometer readings and differences of the levels in the feed burette and capillary N. A small correction is made for the volume of the mercury in H before the first addition.

During a run, the temperature of the bath was monitored continuously with a quartz crystal thermometer. Cathetometer readings before and after a mixing were always taken within $\pm$0.0005 K of each other, which corresponds to an uncertainty of $\pm$0.00001 cm^3 in the volume.

Bottomley and Scott (3) reported that operations of a greased tap controlling the mercury in a dilution dilatom-

TABLE 1. Properites of component liquids at 298.15 K

Component	Density ρ/g cm^{-3}		Refractive index n_D	
	Experiment	Literature (4)	Experiment	Literature (4)
Cyclohexane	0.77374	0.77387	1.42340	1.42354
Benzene	0.87366	0.87368	1.49790	1.49792
Toluene	0.86224	0.86228	1.49410	1.49414
o-Xylene	0.87582	0.87594	1.50252	1.50295
m-Xylene	0.85976	0.85988	1.49416	1.49464
p-Xylene	0.85678	0.85667	1.49318	1.49325
Ethylbenzene	0.86258	0.86262	1.49312	1.49320

TABLE 2. Molar excess volume (V^E) of mixtures at 298.15 K

x_1	V^E (cm^3 mol^{-1})	x_1	V^E (cm^3 mol^{-1})	x_1	V^E (cm^3 mol^{-1})
Cyclohexane (1) + benzene (2)					
0.0222	0.0556	0.3913	0.6186	0.5424	0.6509
0.0358	0.0887	0.3914	0.6177	0.5585	0.6473
0.0472	0.1156	0.3958	0.6198	0.5981	0.6336
0.0623	0.1506	0.4143	0.6298	0.6147	0.6249
0.0808	0.1915	0.4241	0.6342	0.6684	0.5881
0.0929	0.2171	0.4310	0.6375	0.6848	0.5733
0.1197	0.2716	0.4312	0.6384	0.7583	0.4909
0.1342	0.2983	0.4456	0.6428	0.7612	0.4864
0.1668	0.3584	0.4569	0.6459	0.8186	0.3991
0.1672	0.3582	0.4651	0.6490	0.8247	0.3894
0.2038	0.4185	0.4661	0.6487	0.8691	0.3073
0.2323	0.4594	0.4817	0.6513	0.8727	0.3007
0.2393	0.4700	0.4950	0.6534	0.9247	0.1886
0.2939	0.5367	0.4957	0.6527	0.9306	0.1753
0.2941	0.5358	0.4963	0.6529	0.9652	0.0909
0.3463	0.5868	0.5114	0.6532	0.9676	0.0852
0.3468	0.5859	0.5208	0.6536		
Ethylbenzene (1) + benzene (2)					
0.0226	0.0135	0.3210	0.1162	0.5798	0.1167
0.0475	0.0280	0.3525	0.1205	0.6499	0.1060
0.0835	0.0464	0.3775	0.1226	0.7364	0.0877
0.1166	0.0613	0.4051	0.1242	0.7985	0.0714
0.1598	0.0780	0.4382	0.1249	0.8515	0.0542
0.2122	0.0944	0.4768	0.1246	0.8947	0.0397
0.2711	0.1081	0.5232	0.1223	0.9423	0.0230
Ethylbenzene (1) + toluene (2)					
0.0440	−0.0025	0.4360	−0.0142	0.6413	−0.0128
0.0949	−0.0049	0.4606	−0.0144	0.7123	−0.0110
0.1312	−0.0063	0.4696	−0.0144	0.7701	−0.0092
0.1764	−0.0080	0.4949	−0.0144	0.8272	−0.0072
0.2362	−0.0099	0.4990	−0.0144	0.8753	−0.0054
0.2976	−0.0120	0.5362	−0.0143	0.9166	−0.0040
0.3507	−0.0132	0.5823	−0.0138	0.9565	−0.0024
0.3952	−0.0137				

Can. J. Chem. Downloaded from www.nrcresearchpress.com by 210.87.254.105 on 09/05/12
For personal use only.

TABLE 2. (*Concluded*)

x_1	V^E (cm^3 mol^{-1})	x_1	V^E (cm^3 mol^{-1})	x_1	V^E (cm^3 mol^{-1})
		Ethylbenzene (1) + o-xylene (2)			
0.0386	0.0060	0.4182	0.0356	0.6167	0.0335
0.0665	0.0101	0.4582	0.0360	0.6730	0.0312
0.1076	0.0156	0.4588	0.0356	0.7433	0.0275
0.1722	0.0226	0.4901	0.0357	0.8006	0.0224
0.2102	0.0258	0.4935	0.0362	0.8439	0.0180
0.2506	0.0289	0.5231	0.0357	0.8979	0.0128
0.3157	0.0324	0.5258	0.0355	0.9457	0.0074
0.3704	0.0345	0.5671	0.0349		
		Ethylbenzene (1) + m-xylene (2)			
0.0374	0.0082	0.4345	0.0565	0.6664	0.0504
0.0692	0.0155	0.4749	0.0571	0.7337	0.0445
0.1062	0.0230	0.5089	0.0571	0.7934	0.0376
0.1484	0.0300	0.5269	0.0564	0.8427	0.0304
0.2012	0.0380	0.5396	0.0568	0.8892	0.0225
0.2674	0.0460	0.5671	0.0554	0.9276	0.0150
0.3328	0.0517	0.6120	0.0537	0.9604	0.0080
0.3876	0.0549				
		Ethylbenzene (1) + p-xylene (2)			
0.1098	−0.0007	0.4870	−0.0017	0.7206	−0.0014
0.2043	−0.0011	0.5211	−0.0017	0.7987	−0.0010
0.2806	−0.0009	0.5606	−0.0016	0.8461	−0.0008
0.3437	−0.0014	0.6042	−0.0017	0.8930	−0.0006
0.3978	−0.0016	0.6576	−0.0017	0.9431	−0.0004
0.4426	−0.0015				

eter increased the apparent volume of the system by up to 0.00005 cm^3 per turn, even though the mercury was not flowing through the tap. Similar volume changes were associated with the operation of tap A in our dilatometer when no mixing occurred, but both increases and decreases of the order of 0.00002 cm^3 were observed. During a run, unnecessary movements of the tap were avoided to reduce to a minimum the uncertainty due to this effect. From dummy measurements in which the cell and burette contained the same liquid, it was found that the volume decreased by (0.00008 ± 0.00006) cm^3 for each mixing. This result appeared to be characteristic of the tap and a correction was added in calculating the volume changes during a run.

Measurements

The dilatometer was tested by measuring the standard system cyclohexane (1) + benzene (2) at 298.15 K. To investigate its performance further, measurements were also made for mixtures of ethylbenzene with benzene, toluene, and isomeric xylenes. The component liquids were commercial reagents (purity >95 mol%) which were further purified chromatographically. Values of the densities and refractive indices characterizing the final materials used for the measurements are given in Table 1, along with values from the literature (4) for comparison. In some cases, our results are averages for several samples prepared during the course of the work. The variations between the samples were less than ±0.00005 g cm^{-3} for the density and ±0.00003 for the refractive index.

Results and Discussion

The experimental results for V^E at 298.15 K are summarized in Table 2. For each system, x_1 denotes the mole fraction of the first named component. The equation

$$[1] \quad V^E = x_1(1 - x_1) \sum_{j=1}^{n} a_j(1 - 2x_1)^{j-1}$$

was fitted to each set of results by the method of least squares, assigning equal weights to all points. Values of the coefficients a_j obtained from the analysis are listed in Table 3, along with the standard error σ for each representation.

The systematic error in the value of V^E was attributed to uncertainties in the weight of the cell component, and in the calibrations of the micrometer syringe, burette, and capillary N. Sources of random error were cathetometer and micrometer readings, temperature fluctuations, and operation of the tap A. The effects of these

Can. J. Chem. Downloaded from www.nrcresearchpress.com by 210.87.254.105 on 09/05/12
For personal use only.

TABLE 3. Coefficients and standard errors for least-squares representations of V^E(cm^3 mol^{-1})

System	a_1	a_2	a_3	a_4	a_5	σ
$C_6H_{12}(1) + C_6H_6(2)$	2.61286	−0.10103	0.06444	0.02751	−0.03163	0.00043
$C_8H_{10}(1) + C_6H_6(2)$	0.49465	0.10097	0.02671	0.01440		0.00024
$C_8H_{10}(1) + C_7H_8(2)$	−0.05730	−0.00344	0.00842			0.00018
$C_8H_{10}(1) + o\text{-}C_8H_{10}(2)$	0.14370	0.01295	0.01272			0.00026
$C_8H_{10}(1) + m\text{-}C_8H_{10}(2)$	0.22838	0.00792	0.00921			0.00032
$C_8H_{10}(1) + p\text{-}C_8H_{10}(2)$	−0.00652					0.00013

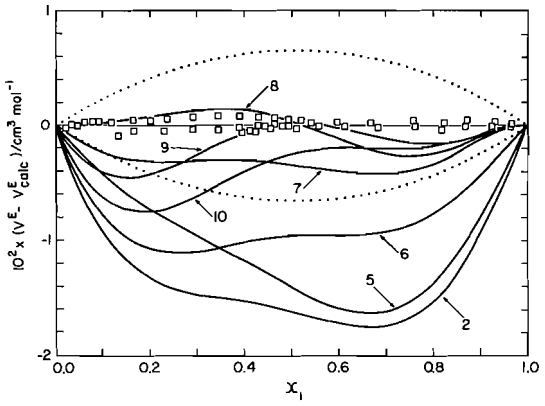

FIG. 2. Comparison of experimental results for the molar excess volume of cyclohexane (1) + benzene (2) mixtures at 298.15 K. Points and curves represent deviations from eq. 1. □, present work. The solid curves represent the smoothed results of other investigations and are labelled with their reference numbers. The dotted curves correspond to deviations of ±1%.

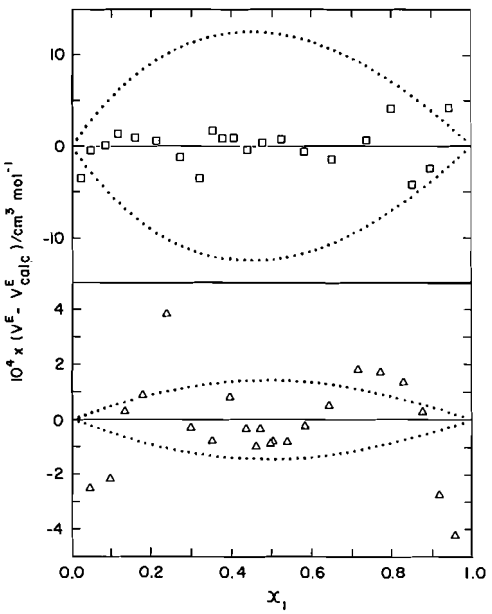

FIG. 3. Molar excess volumes of mixtures at 298.15 K. Points represent deviations of experimental results from eq. 1. □, ethylbenzene (1) + benzene (2); △, ethylbenzene (1) + toluene (2). The dotted curves correspond to deviations of ±1%.

uncertainties were examined directly by inserting their estimates into the computer program used to calculate the results from the experimental observations. The systematic error in V^E was independent of the mole fraction and was about 0.1% for systems with large excess volumes like cyclohexane + benzene and ethylbenzene + benzene, and about 0.25% for systems with small excess volumes like ethylbenzene + *m*-xylene. The random error depended on the mole fraction and was about 0.0003 cm^3 mol^{-1} for an equimolar mixture. This value agrees reasonably well with the standard errors given in Table 3.

Figure 2 gives a comparison between our results for cyclohexane + benzene and a number of the smoothed representations of V^E for this system reported in the recent literature (2, 5–10). The results in references 2, 5, and 6 were obtained with dilution dilatometers of various designs, and none were corrected for pressure changes. They are much lower than our results over the entire range of mole fractions. The data of Chareyron and Clechet (2), whose dilatometer was most similar to ours, show the largest deviations.[4] Our results agree with the other sets (7–10) within 1% over most of the mole fraction range. Quite different techniques were employed in each of these investigations. Stokes *et al.* (7) and Stookey *et al.* (10) used continuous dilution and single point (V-shaped) dilatometers respectively. Corrections for changes of pressure were applied in both studies. In the other two investigations, which were carried out in our laboratory, V^E was

[4]We have assumed that the sign of the coefficient A_1 given in ref. 2 is inappropriate for the authors' use of x for the mole fraction of benzene. The negative value of A_1 would lead to deviations larger than those indicated for $x_1 > 0.5$ in Fig. 2.

Can. J. Chem. Downloaded from www.nrcresearchpress.com by 210.87.254.105 on 09/05/12
For personal use only.

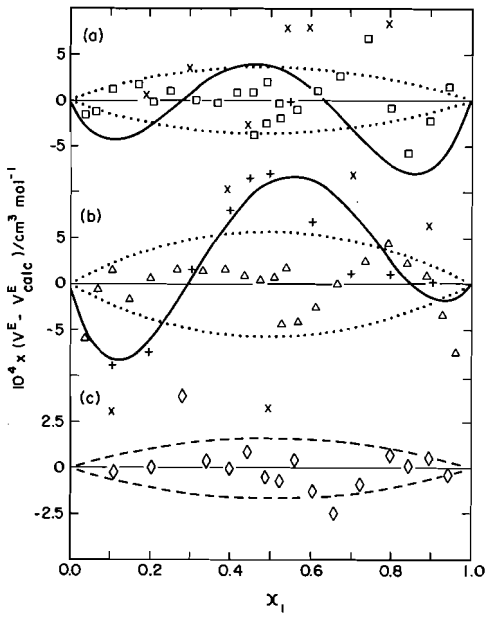

FIG. 4. Molar excess volumes of mixtures at 298.15 K. Points and curves represent deviations from eq. 1. (*a*) Ethylbenzene (1) + *o*-xylene (2): □, present work; ×, Stookey and Smith (12). (*b*) Ethylbenzene (1) + *m*-xylene (2): △, present work; +, Stookey and Smith (12). (*c*) Ethylbenzene (1) + *p*-xylene (2): ◇, present work. The solid curves are smoothed results from ref. 12. The dotted curves correspond to deviations of ±1%, the broken curves to ±10%.

obtained from determinations of density by a float method (8) and by an Anton Paar densimeter (9). It is interesting to note that the present results are in excellent agreement with the float data and are systematically slightly higher than those of Stokes *et al.* (7) which are frequently used as a basis for comparison. The discrepancy is larger than the estimated uncertainty of the determinations and must be attributed to differences in the component liquids or to some other unidentified source of systematic error.

Deviations of the experimental results for the five ethylbenzene systems from their smoothed representations by [1] are shown in Figs. 3 and 4. There is very little information about the volume properties of these systems in the literature. Densities of mixtures of ethylbenzene with benzene and toluene at 293.15 and 303.15 K have been reported by Mamedov and Panchenkov (11). However, their precision is too low to allow reliable estimates of V^E. Thus, although it appears that their results for ethylbenzene + benzene agree roughly with ours, their densities for ethylbenzene + toluene lead to values of V^E which differ in sign from our results.

The values of V^E for mixtures of ethylbenzene with toluene and with the xylenes are small and the effect of changes of pressure is relatively unimportant compared to the random error of the measurements. Figure 4 shows that our results for the *o*-xylene and *m*-xylene systems are in good agreement with the smoothed results of Stookey and Smith (12). However, their experimental points are more widely scattered than ours. The excess volumes of ethylbenzene + *p*-xylene are very small and are only about 10 times greater than their standard error. They are therefore subject to much higher percentage uncertainties than those of the other systems.

We wish to thank Mr. J. C. van den Hoff for help in the design and construction of the glass part of the dilatometer, and Mr. C. J. Halpin for preparing the solvents used in our experimental studies.

1. F. PARDO. M. Ch.E. Thesis, Rensselaer Polytechnic Institute, Troy, N.Y. 1964; F. PARDO and H. C. VAN NESS. J. Chem. Eng. Data, **10**, 163 (1965).
2. R. CHAREYRON. Ph.D. Thesis, Université de Lyon, Lyon, France 1970; R. CHAREYRON and P. CLECHET. Bull. Soc. Chim. Fr. 2853 (1971).
3. G. A. BOTTOMLEY and R. L. SCOTT. J. Chem. Thermodyn. **6**, 973 (1974).
4. American Petroleum Institute Research Project 44. Chemical Thermodynamics Properties Center, Texas A & M University, College Station, Texas. (See Table 5a dated October 31, 1950 and Table 23a dated October 31, 1952).
5. R. J. POWELL and F. L. SWINTON. J. Chem. Eng. Data, **13**, 260 (1968).
6. L. A. BEATH, S. P. O'NEILL, and A. G. WILLIAMSON. J. Chem. Thermodyn. **1**, 293 (1969).
7. R. H. STOKES, B. J. LEVIEN, and K. N. MARSH. J. Chem. Thermodyn. **2**, 43 (1970).
8. I. A. WEEKS and G. C. BENSON. J. Chem. Thermodyn. **5**, 107 (1973).
9. O. KIYOHARA and G. C. BENSON. Can. J. Chem. **51**, 2489 (1973).
10. D. J. STOOKEY, H. M. SALLAK, and B. D. SMITH. J. Chem. Thermodyn. **5**, 741 (1973).
11. A. A. MAMEDOV and G. M. PANCHENKOV. Zhur. Fiz. Khim. **29**, 1204 (1955); Chem. Abstr. **50**, 7533f (1956).
12. D. J. STOOKEY and B. D. SMITH. J. Chem. Thermodyn. **5**, 753 (1973).

Can. J. Chem. Downloaded from www.nrcresearchpress.com by 210.87.254.105 on 09/05/12
For personal use only.

Pyrolysis of $C_2H_7^+$ and other Ion–Molecule Reactions in Methane containing Traces of Ethane[1]

MARGARET FRENCH AND PAUL KEBARLE
Chemistry Department, University of Alberta, Edmonton, Alberta T6G 2E1
Received February 6, 1975

MARGARET FRENCH and PAUL KEBARLE. Can. J. Chem. **53**, 2668 (1975).

The major reactions in methane containing traces of ethane were studied with a pulsed electron beam high ion source pressure mass spectrometer. The CH_4:C_2H_6 ratios were changed from 50:1 to 100 000:1 at reaction temperatures between 28–210 °C. The reaction 1: $CH_5^+ + C_2H_6 = CH_4 + C_2H_7^+$ still proceeded from left to right even at the highest dilution ratios. Measurement of the $C_2H_7^+/CH_5^+$ ratio under these conditions leads to a lower limit of the proton affinity difference $PA(C_2H_6) - PA(CH_4) > 10$ kcal/mol. This result is in agreement with measurements by Bohme.

It was observed that $C_2H_7^+$ decomposes slowly at 30 °C. The decomposition becomes more rapid at higher temperature. Measurements of the temperature dependence of the thermal reaction 2: $C_2H_7^+ + CH_4 = C_2H_5^+ + H_2 + CH_4$, and an Arrhenius plot of k_2 led to the activation energy $E_2 = 10.5$ kcal/mol and preexponential factor $A_2 = 8.3 \times 10^{-8}$ (cm^3 molecule^{-1} s^{-1}). Assuming $E_2 = \Delta H_2$ one obtains $\Delta H_f(C_2H_7^+) = 208.5 \pm 2$ kcal/mol and $PA(C_2H_7^+) = 137.4 \pm 2$ kcal/mol. This is close to the proton affinity $PA(C_2H_7^+) = 139 \pm 2$ kcal/mol that can be deduced from Bohme's results.

At higher dilution ratios the ion $C_2H_5^+$ was observed to react not only with ethane but also with methane by reaction 6: $C_2H_5^+ + CH_4 = C_3H_7^+ + H_2$, $k_6 \approx 1 \times 10^{-14}$ cm^3 molecule^{-1} s^{-1} at 86 °C. The reaction has positive temperature dependence.

MARGARET FRENCH et PAUL KEBARLE. Can. J. Chem. **53**, 2668 (1975).

On a étudié les réactions principales du méthane contenant des traces d'éthane à l'aide d'un spectromètre de masse à faisceau d'électrons pulsés ayant une source d'ion à haute pression. Les rapports CH_4:C_2H_6 furent variés de 50:1 à 100 000:1 pour des températures de réaction entre 28–210 °C. La réaction 1: $CH_5^+ + C_2H_6 = CH_4 + C_2H_7^+$ a toujours lieu de gauche à droite même aux plus hauts taux de dilution. Dans ces conditions la mesure du rapport $C_2H_7^+/CH_5^+$ conduite à une limite inférieure de la différence d'affinité du proton $AP(C_2H_6) - AP(CH_4) > 10$ kcal/mol. Ce résultat est en accord avec les mesures faites par Bohme.

On a observé que $C_2H_7^+$ se décompose lentement à 30 °C. La décomposition devient plus rapide à plus haute température. Les mesures de la dépendance thermique de la réaction 2: $C_2H_7^+ + CH_4 = C_2H_5^+ + H_2 + CH_4$, ainsi que le graphique d'Arrhénius pour k_2 conduisent à une énergie d'activation $E_2 = 10.5$ kcal/mol et à un facteur pré-exponentiel $A_2 = 8.3 \times 10^{-8}$ (cm^3 molécules^{-1} s^{-1}). En supposant que $E_2 = \Delta H_2$ on obtient $\Delta H_f(C_2H_7^+) = 208.5 \pm 2$ kcal/mol et $AP(C_2H_7^+) = 137.4 \pm 2$ kcal/mol. Ceci est près de la valeur de l'affinité du proton $AP(C_2H_7^+) = 139 \pm 2$ kcal/mol, déduite des résultats de Bohme.

A des taux de dilution plus élevés on a remarqué que l'ion $C_2H_5^+$ réagissait non seulement avec l'éthane mais aussi avec le méthane selon la réaction 6: $C_2H_5^+ + CH_4 = C_3H_7^+ + H_2$, $k_6 \approx 1 \times 10^{-14}$ cm^3 molécules^{-1} s^{-1} à 86 °C. La réaction a une dépendance thermique positive. [Traduit par le journal]

Introduction

The present work, which is based on measurements of ion–molecule reactions of methane containing known traces of ethane, was initiated following the report of Chong and Franklin (1) on the proton transfer equilibrium 1 for which these authors found $\Delta G_1^0 = -1$ kcal/mol ($\sim$340 K). Such a very small difference between

[1] $CH_5^+ + C_2H_6 = CH_4 + C_2H_7^+$

the proton affinity of methane and ethane seemed very unlikely. Considering that a considerable change of structure occurs between CH_5^+ structure **1** and $C_2H_7^+$ structure **2**, a difference as high as 15 kcal/mol would have seemed more likely (2). Therefore we set out to remeasure the equilibrium 1. Before the work was completed Bohme *et al.* (3) showed that $PA(C_2H_6) > PA(CO) = 136$ kcal/mol. Since $PA(CH_4) \approx$

[1]Experimental work represents part of Ph.D. dissertation of M.F.

Can. J. Chem. Downloaded from www.nrcresearchpress.com by 210.87.254.40 on 09/05/12
For personal use only.

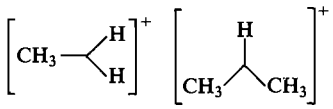

1 2

127 kcal/mol (4) this meant that the proton affinity difference between methane and ethane is larger than 9 kcal/mol in agreement with the theoretical predictions (2).

With such a large proton affinity difference the measurement of K_1 obviously becomes very difficult and possible only in methane containing only traces of ethane. Investigation of the ion–molecule reactions and their temperature dependence under such concentration conditions proved quite rewarding. Apart from information on the equilibrium 1, one other interesting reaction could be studied. This was the pyrolysis of $C_2H_7^+$ formed by reaction 1. Information on the heat of formation of $C_2H_7^+$ and thus on the $PA(C_2H_6)$ could be obtained since the activation energy E_2 for reaction 2

[2] $$C_2H_7^+ = C_2H_5^+ + H_2$$

could be related to ΔH_2.

Experimental

The measurements were made with the pulsed electron beam high pressure ion source reaction chamber shown in Fig. 1. The design is very similar to that used with other high pressure ion sources in our laboratory (5). The only difference is that the filament and associated electrode system are mounted on a small tower and flange which is screwed to the ion source. The filament is sufficiently far away from the ion source as to be ef-

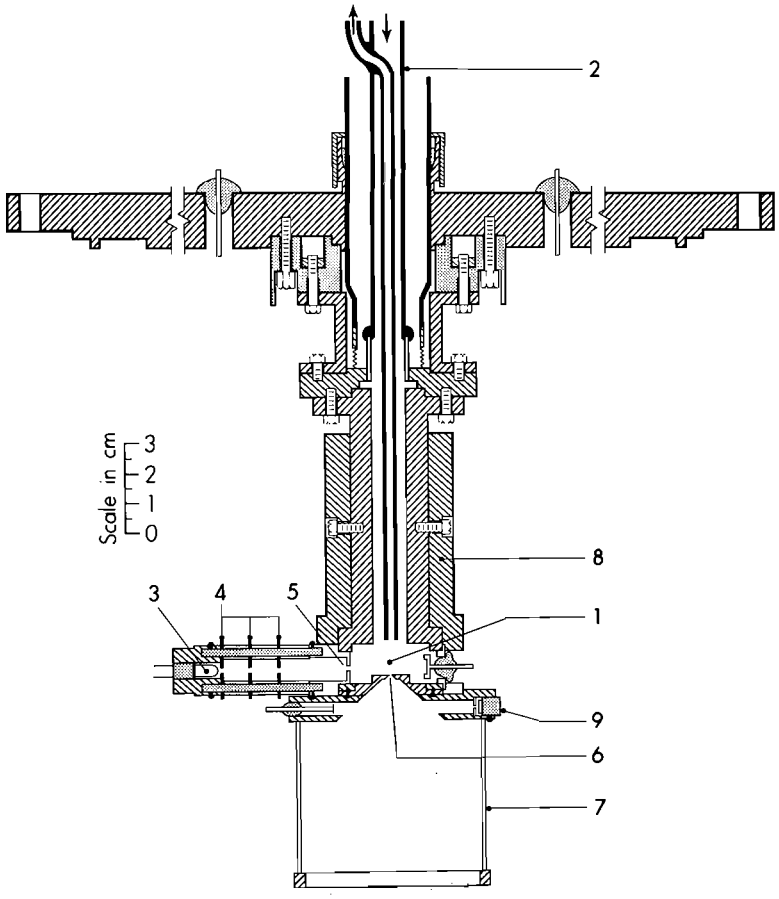

FIG. 1. Pulsed electron beam high pressure ion source: *1*, ion–molecule reaction chamber; *2*, slow flow reactant gas supply; *3*, electron filament; *4*, pulsed electron beam electrodes; *5*, electron entrance slit; *6*, ion exit slit; *7*, high transparency grid for electric field shielding; *8*, heater block; *9*, auxiliary electron beam for low pressure ionization used in purity checks of reactant gases.

Can. J. Chem. Downloaded from www.nrcresearchpress.com by 210.87.254.40 on 09/05/12
For personal use only.

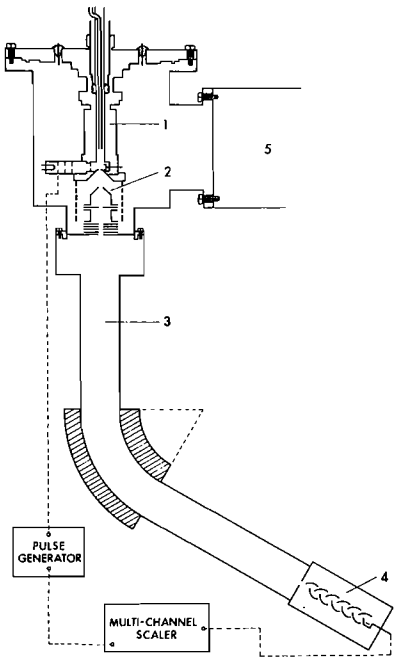

FIG. 2. Pulsed electron beam high pressure ion source mass spectrometer: *1*, ion source; *2*, ion accelerating and focussing electrodes; *3*, Atlas CH4 mass analyzer tube and magnet; *4*, electron multiplier followed by amplifier and multiscalar; *5*, to 6 in. vapor trap and diffusion pump.

fectively at the pressure of the vacuum chamber. Also the ion source heating effect by the filament is minimal.

The large flange-lid carrying the ion source bolts on to an 8 in. diameter vacuum housing pumped by a 6 in. diffusion pump via a 6 in. vapor trap. An Atlas CH4 magnetic mass spectrometer with a modified ion acceleration system is bolted to the vacuum housing as shown in Fig. 2.

The ion signal was detected with an electron multiplier and ion counting system. A multiscaler whose sweep was synchronized with the electron pulse was used for the determination of the time dependence of ions with a given mass.

Mixtures of methane and ethane were made in the gas handling vacuum system by filling a 5 l glass bulb with 1 atm ultrahigh purity methane. The required volume of ethane was then injected into the bulb and allowed to mix for several hours. Removal of traces of water was achieved by repeated bakeouts of the gas handling system and mass spectrometer and by passage of the methane through a molecular sieve maintained at −78 °C. The gas mixture was passed in slow flow through the ion source. The ion source pressures were generally varied between 1–3.5 Torr but most experiments were done at 2.5 Torr. The pressure was measured with a capacitance manometer. The ethane partial pressures in the ion source were selected between 0.07 to 50 mTorr. Some 47 experiments were made and analyzed in the temperature range 30–210 °C.

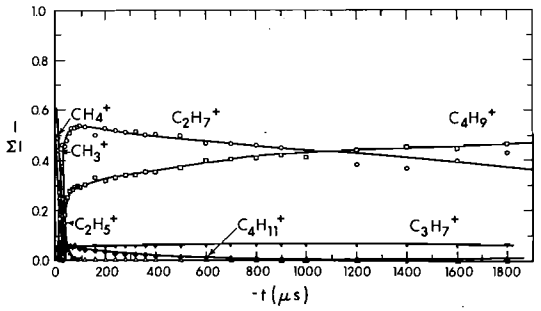

FIG. 3. Time dependence of normalized ion intensities after electron pulse: 32 °C, CH_4 2.7 Torr, C_2H_6 54 mTorr, CH_4:C_2H_6 = 50, ◐, CH_3^+; ◑, CH_4^+; ●, CH_5^+; ○, $C_2H_7^+$; △, $C_2H_5^+$; ◇, $C_4H_{11}^+$; □, $C_4H_9^+$; ▼, $C_3H_7^+$.

Results and Discussion

Major Reactions in Mixture CH_4:C_2H_6 = 50:1 near Room Temperature

The observed concentration changes of the major ions with time at ~30 °C for methane containing traces of ethane are shown in Fig. 3. The methane to ethane ratio in Fig. 3 is 50:1. Under these conditions the primary ions produced by electron impact are almost exclusively due to methane. These are CH_4^+ and CH_3^+ in an expected ratio 5:4. In the present system these ions react very rapidly with methane by the well-known reactions 3 and 4

[3] $$CH_4^+ + CH_4 = CH_5^+ + CH_3$$

[4] $$CH_3^+ + CH_4 = C_2H_5^+ + H_2$$

The resulting CH_5^+ transfers a proton to ethane forming $C_2H_7^+$ by reaction 1. This reaction is also essentially complete in 100 μs, (Fig. 3). The $C_2H_5^+$ reacts with ethane by reaction 5. This reaction has been observed in many previous studies of ethane (6–8).

[5] $$C_2H_5^+ + C_2H_6 = (C_4H_{11}^+)^* \begin{cases} \xrightarrow{d_1} C_4H_9^+ + H_2 \\ \xrightarrow{d_2} C_3H_7^+ + CH_4 \\ \xrightarrow{M} C_4H_{11}^+ \end{cases}$$

The two decomposition products $C_4H_9^+$ and $C_3H_7^+$ in a ratio 3:1 are observed in Fig. 3. Similar ratios were obtained in earlier work (8). The intermediate $C_4H_{11}^+$, stabilized by the third body M, is a minor product at this pressure and temperature.

Can. J. Chem. Downloaded from www.nrcresearchpress.com by 210.87.254.40 on 09/05/12
For personal use only.

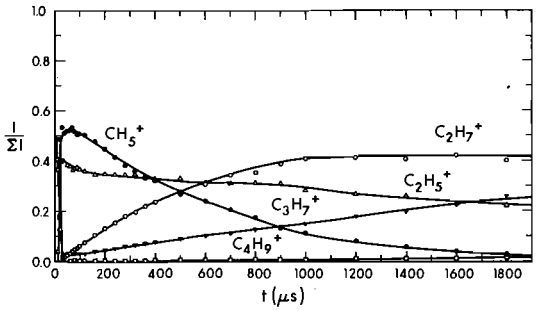

FIG. 4. Time dependence of normalized ion intensities after electron pulse: 28 °C, CH_4 2.3 Torr, CH_4:C_2H_5 = 100 000:1. Same reactant symbols as in Fig. 3.

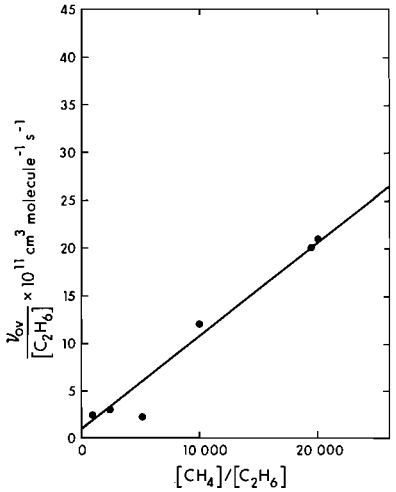

FIG. 5. Plot of pseudo first-order rate constant $\nu_{ov}/[C_2H_6]$ for overall disappearance of $C_2H_5^+$ by reactions, $C_2H_5^+ + C_2H_6 \rightarrow$ products [5], and $C_2H_5^+ + CH_4 = C_3H_7^+ + H_2$ [6]. Slope of straight line leads to k_6 while intercept with y axis equals k_5.

The Equilibrium $CH_5^+ + C_2H_6 = CH_4 + C_2H_7^+$

The ion time profiles for a much higher dilution ratio CH_4:$C_2H_6 \approx 100\,000$:1 at 30 °C are shown in Fig. 4. Even at this dilution, proton transfer from CH_5^+ to C_2H_6 by reaction 1 is still occurring over the total period of observation. The observed $C_2H_7^+/CH_5^+$ ratio at the longest reaction time (1900 μs) is 20. This leads to a low limit for the equilibrium constant $K_1 > 20 \times 100\,000 = 2 \times 10^6$. Chong and Franklin obtained $K_1 = 4.9$ at 67 °C. Assuming $\Delta S_1^0 \approx 0$ this corresponds to $K_1 \approx 5.9$ at 30°C. Evidently the present result, $K_1 > 2 \times 10^6$ at 30°C, is many orders of magnitude higher than the Franklin value. The above K_1 leads to a lower limit of 8.7 kcal/mol for the difference between the proton affinity of ethane and methane. Several experiments with larger dilution ratios were made in an attempt to observe the equilibrium 1. However, this proved impossible since some ethane (~1–10 p.p.m.) was already present in the purified ultrahigh purity methane. This allowed one to set only an approximate lower limit of ~10 kcal/mol for the proton affinity difference. Another difficulty was the slow disappearance of $C_2H_7^+$ by thermal decomposition to $C_2H_5^+ + H_2$, *i.e.* reaction 2 whose temperature dependence will be discussed below. Recently Bohme (9) using the equilibrium

$$HCO^+ + C_2H_6 = CO + C_2H_7^+$$

in combination with other sequential equilibria was able to determine $PA(C_2H_6) - PA(CH_4) = 12 \pm 1$ kcal/mol. This, combined with $PA(CH_4) = 127$ kcal/mol (4) leads to $PA(C_2H_6) = 139 \pm 2$ kcal/mol. The present results for the equilibrium 1 are consistent with these values.

The Reactions: $C_2H_5^+ + CH_4 = C_3H_7^+ + H_2$ and $C_2H_5^+ + C_2H_6 =$ products

It can be noted in Fig. 4 that the ratio of the ion products $C_4H_9^+/C_3H_7^+$ is only about 0.06. The same product ratio was equal to 3 in Fig. 3 which gave results at the same temperature but for a higher ethane concentration. This drastic change can be explained by a slow reaction of $C_2H_5^+$ with methane to give $C_3H_7^+$. At very low ethane concentrations (as in Fig. 4) such a reaction will dominate over the reaction of $C_2H_5^+$ with ethane [5]. Indeed recently the occurrence of the slow reaction 6 was observed in pure methane in our laboratory (10).

[6] $$C_2H_5^+ + CH_4 = C_3H_7^+ + H_2$$

The present observation is thus a confirmation of the earlier finding. The pseudo first-order rate constant ν_{ov} for the overall disappearance of $C_2H_5^+$ by reactions 5 and 6 is given by [7]

[7] $$\nu_{ov} = k_5[C_2H_6] + k_6[CH_4]$$

A plot of $\nu_{ov}/[C_2H_6]$ *vs.* $[CH_4]/[C_2H_6]$ should give a straight line with a slope equal to k_6 and an intercept with the y axis equal to k_5. Such a plot is shown in Fig. 5. The ν_{ov} were obtained from plots of log $[C_2H_5^+]$ *vs.* t.

Can. J. Chem. Downloaded from www.nrcresearchpress.com by 210.87.254.40 on 09/05/12
For personal use only.

Can. J. Chem. Downloaded from www.nrcresearchpress.com by 210.87.254.40 on 09/05/12
For personal use only.

These experiments were performed above room temperature (86 °C) where reaction 6, which has a positive temperature coefficient (10), is faster and thus more noticeable. The slope obtained is $k_6 \approx 1 \times 10^{-14}$ cm^3 molecule^{-1} s^{-1} which is in fair agreement with $k_6 = 1.6 \times 10^{-14}$ obtained for the same temperature in pure methane (10). The plot in Fig. 5 is obviously not suitable for an accurate determination of k_5 since the line passes close to the origin and there is considerable experimental scatter exactly in this range. The plot indicates $k_5 \approx 1 \times 10^{-11}$ cm^3 molecule^{-1} s^{-1}. An additional complication is the occurrence of the temperature dependent decomposition of $C_2H_7^+$ to $C_2H_5^+ + H_2$, *i.e.* reaction 2 discussed in the next section. The rate of this reaction which is negligible at room temperature becomes significant at 86 °C such that $C_2H_5^+$ is produced by [2] while it reacts by [5] and [6]. This has the effect of lowering the apparent rates of [5] and [6] under conditions where the rates of [2] and of [5] and [6] are comparable.

A more accurate determination of k_5 could be obtained at 300 K with methane to ethane ratios 50:1. Under these conditions both [2] and [6] are much slower than [5]. Plots of log $[C_2H_5^+]$ *vs.* time gave $k_5 = 5 \pm 1 \times 10^{-11}$ cm^3 molecule^{-1} s^{-1} at 300 K. This is in close agreement with a value of $k_5 = 5.1 \pm 1 \times 10^{-11}$ at 300 K reported recently by Bohme *et al.* (11) but lower than the value 2.8×10^{-10} cm^3 molecule^{-1} s^{-1} obtained earlier by Harrison and co-workers (7).

The Pyrolysis of $C_2H_7^+$

The $C_2H_7^+$ ion concentration is found to decrease slowly with time even at room temperature (Fig. 3). At higher temperatures this decrease was observed to become progressively more rapid. A comparison between 32° and 96° is shown in Figs. 6 and 7, where the CH_4:C_2H_6 dilution ratio is 500:1. Under these conditions proton transfer from CH_5^+ to C_2H_6 by [1] is still sufficiently fast so that the $C_2H_7^+$ formation is very rapid. As can be noticed from Figs. 6 and 7, the decrease of $C_2H_7^+$ at the higher temperature is considerably faster. On the other hand the $C_2H_5^+$ ion decreases more slowly at the higher temperature than at the lower temperature. These features can be explained by assuming the occurrence of reaction 2. Since [2] is endothermic it should have

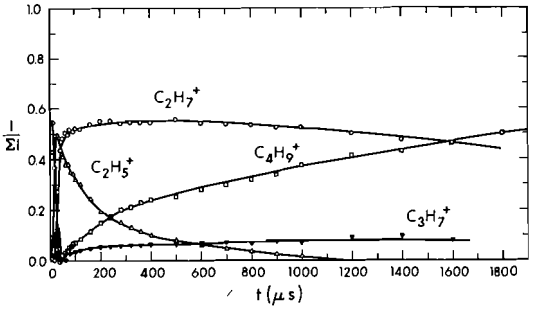

FIG. 6. Time dependence of normalized ion intensities after electron pulse. 32 °C, CH_4 2.3 Torr, CH_4:C_2H_6 = 500:1, ◐, CH_4^+; ◑, CH_3^+; ●, CH_5^+; ○, $C_2H_7^+$; ▽, $C_2H_5^+$; ◇, $C_4H_{11}^+$; □, $C_4H_9^+$; ▼, $C_3H_7^+$.

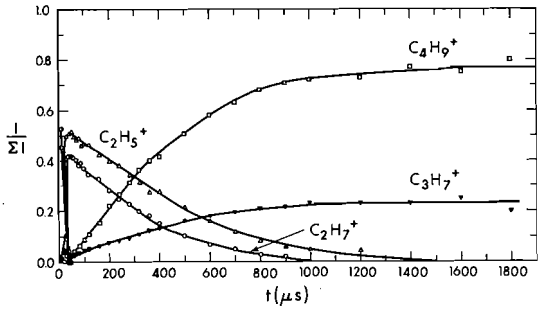

FIG. 7. Approximately the same conditions as in Fig. 6 but at 92 °C. Thermal decomposition of $C_2H_7^+$ by reaction 2, $C_2H_7^+ = C_2H_5^+ + H_2$ very noticeable.

a positive temperature coefficient. The $C_2H_5^+$ formed by [2] reacts with C_2H_6 via [5] to give $C_4H_9^+$ and some $C_3H_7^+$. The disappearance of $C_2H_5^+$ in the high temperature run (Fig. 7) is much slower than in the low temperature run (Fig. 6) since the rate of production of $C_2H_5^+$ by [2] is faster at high temperatures. Furthermore reaction 5 by which $C_2H_5^+$ is removed is faster at lower temperatures (8). This further slows down the disappearance of $C_2H_5^+$ at higher temperatures.

The rate constant k_2 for disappearance of $C_2H_7^+$ could be obtained by plotting log $[C_2H_7^+]$ *vs.* time. Since the pressure of CH_4 could not be varied over a wide enough margin it was assumed that reaction 2 depends on a third body (CH_4) for thermal activation. Reaction 2 in the present pressure regime should be second order and should be written

[2s] $C_2H_7^+ + CH_4 = C_2H_5^+ + H_2 + CH_4$

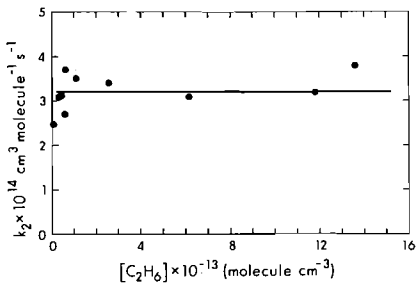

FIG. 8. Plot of k_2 for reaction 2s, $C_2H_7^+ + CH_4 = C_2H_5^+ + H_2 + CH_4$, (where major gas CH_4 involved in thermal activation) *vs.* C_2H_6 concentration. Plot shows k_2 independent of C_2H_6 concentration. Temperature 86 °C.

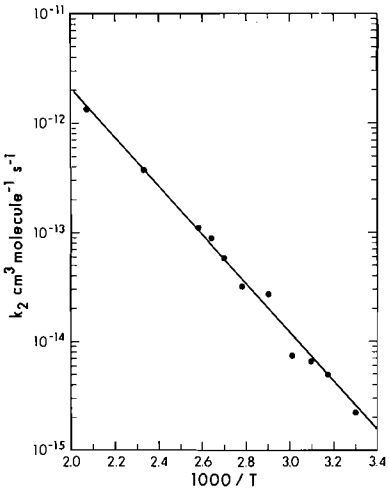

FIG. 9. Arrhenius plot of k_2 for reaction $C_2H_7^+ + CH_4 = C_2H_5^+ + H_2 + CH_4$. Straight line obtained leads to $E_{2s} = +10.5$ kcal/mol and preexponential factor $A_2 = 8.3 \times 10^{-8}$ cm^3 molecule^{-1} s^{-1}.

Experiments at constant temperature and different C_2H_6 concentrations showed that [2] is independent of ethane concentration in agreement with the assumptions. Figure 8 summarizes such results for one temperature.

The rate constants k_2 obtained at different temperatures were used to obtain the Arrhenius plot in Fig. 9. The straight line obtained defines the relationship [8].

$$[8] \quad k_2 = 8.3 \times 10^{-8}(\text{cm}^3\ \text{molecule}^{-1}\ \text{s}^{-1}) \times \exp\left(\frac{-10.5}{RT}\ \text{kcal/mol}\right)$$

It is interesting that the preexponential factor of k_2 is almost 10^{-7} and thus appreciably larger than the normal Langevin rate constant 10^{-9}. This is an expected result for bimolecular thermal activation and comes about from the fact that the colliding molecules can exchange not only translational but also internal energy. A recent determination (12) of the temperature dependence for the reaction 9 led to an even larger preexponential factor of 9×10^{-6}.

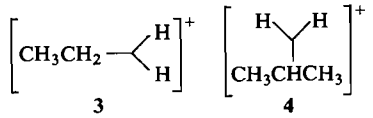

3 4

[9] $\quad H_5^+ + H_2 = H_3^+ + 2H_2$

Theoretical calculations by Pople and coworkers (2) have shown that structure **2** of $C_2H_7^+$ is some 11 kcal/mol more stable than structure **3**. Since one expects that the dehydrogenation of $C_2H_7^+$ proceeds through a rearrangement from **2** to **3** the activation energy $E_2 = 10.5$ kcal/mol appears of the right magnitude assuming the calculation (2) to be approximately correct and the dissociation from **3** to $C_2H_5^+ + H_2$ to be near thermoneutral. Recent investigations (10) of the dissociation of protonated propane to *sec*-$C_3H_7^+ + H_2$ indicate that the dissociation of the analogous three center bond structure **4** is exothermic. The assumption that the dissociation of H_2 from **3** is near thermoneutral is therefore reasonable. Assuming that the reverse of reaction 2 proceeds without activation energy $E_2 = \Delta H_2 = 10.5$ kcal/mol.

[−2] $\quad H_2 + C_2H_5^+ \rightarrow C_2H_7^+$ (2)

Combined with $\Delta H_f(C_2H_5^+) = 219$ kcal/mol (13) this leads to $\Delta H_f(C_3H_7^+) = 208.5$ kcal/mol and $PA(C_2H_6) = 137.4$ kcal/mol. We estimate the error in the above values to be ± 2 kcal/mol. This proton affinity is close to $PA(C_2H_6) = 139 \pm 2$ kcal/mol that can be deduced from Bohme's (9) measurements quoted earlier.

We believe that the study of thermal decomposition of ions as exemplified by the study of reaction 2 might prove to be a useful source of thermochemical and kinetic data.

The fact that $C_2H_7^+$ decomposes slowly even at room temperature suggests that protonated propane may also be thermally unstable. This is in agreement with findings of a recent study (14) of this species according to which even the most stable form of protonated propane

Can. J. Chem. Downloaded from www.nrcresearchpress.com by 210.87.254.40 on 09/05/12
For personal use only.

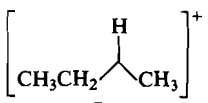

5

(structure **5**) decomposes to CH_4 and $C_2H_5^+$ already below room temperature.

1. S. L. CHONG, and J. L. FRANKLIN. J. Am. Chem. Soc. **94**, 6347 (1972).
2. W. A. LATHAN, W. J. HEHRE, and J. A. POPLE. J. Am. Chem. Soc. **93**, 808 (1971).
3. D. K. BOHME, P. FENELLY, R. S. HEMSWORTH, and H. I. SCHIFF. J. Am. Chem. Soc. **95**, 7512 (1973).
4. W. A. CHUPKA and J. BERKOWITZ. J. Chem. Phys. **54**, 4256 (1971).
5. A. J. CUNNINGHAM, J. D. PAYZANT, and P. KEBARLE. J. Am. Chem. Soc. **94**, 7627 (1972); J. D. PAYZANT, A. J. CUNNINGHAM, and P. KEBARLE. J. Chem. Phys. **59**, 5615 (1973).
6. P. AUSLOOS, R. E. REBBERT, and L. W. SIECK. J. Chem. Phys. **54**, 2612 (1971); S. WEXLER and L. G. POBO. J. Am. Chem. Soc. **93**, 1327 (1971).
7. A. S. BLAIR, E. J. HESLIN, and A. G. HARRISON. J. Am. Chem. Soc. **94**, 2935 (1972).
8. S. L. BENNETT, S. G. LIAS, and F. H. FIELD. J. Phys. Chem. **76**, 3919 (1972).
9. D. K. BOHME. Interactions between ions and molecules. *Edited by* P. Ausloos. Plenum Press Corp., New York. 1975.
10. K. HIRAOKA and P. KEBARLE. J. Chem. Phys. In press.
11. D. K. BOHME, R. A. VANE, F. C. FEHSENFELD, and E. E. FERGUSON. Seventeenth Annual Conference on Mass Spectrometry and Allied Topics, Dallas, Texas. 1969.
12. K. HIRAOKA and P. KEBARLE. J. Chem. Phys. In press.
13. F. P. LOSSING and G. P. SEMELUK. Can. J. Chem. **48**, 555 (1970).
14. K. HIRAOKA and P. KEBARLE. Can. J. Chem. **53**, 970 (1975).

Can. J. Chem. Downloaded from www.nrcresearchpress.com by 210.87.254.40 on 09/05/12
For personal use only.

2-Hydroxy-2,5,5-trimethyl-Δ^3-1,3,4-oxadiazoline. Novel Induced Decomposition by Radical Attack at the Hydroxyl Group

PETER KNITTEL AND JOHN WARKENTIN

Department of Chemistry, McMaster University, Hamilton, Ontario L8S 4M1

Received December 23, 1974

PETER KNITTEL and JOHN WARKENTIN. Can. J. Chem. **53**, 2275 (1975).

Synthesis of 2-hydroxy-2,5,5-trimethyl-Δ^3-1,3,4-oxadiazoline (**3**) is described. It decomposes readily in solution at moderate temperatures, forming nitrogen and isopropyl acetate. Evidence for a concerted, radical-chain, induced decomposition by attack at hydroxyl hydrogen includes trapping of 2-acetoxy-2-propyl radicals by nitrosobenzene and by alkenes, inhibition of decomposition by $(C_6H_5)_3SnH$, and initiation of decomposition by 'stable' free radicals. The novel chain decomposition of **3** is attributed to a concerted mechanism, which brings the heats of formation of nitrogen and of a carbonyl group into play to lower the free energy of activation.

Synthetic utility of **3** is discussed together with a general principle pointing to new reagents for radical-chain additions to unsaturated systems.

PETER KNITTEL et JOHN WARKENTIN. Can. J. Chem. **53**, 2275 (1975).

On décrit la synthèse de l'hydroxy-2 triméthyl-2,5,5 Δ^3-oxadiazoline-1,3,4 (**3**). Ce composé se décompose facilement en solution, à des températures moyennes, pour conduire à de l'azote et à de l'acétate d'isopropyle. Les données indiquent qu'il y a une décomposition induite concertée, impliquant un processus radicalaire en chaîne, commençant par une attaque sur l'hydrogène de l'hydroxyle; la décomposition impliquerait le piégage des radicaux acétoxy-2 propyl-2 par le nitrosobenzène et par les alcènes, une inhibition de la décomposition par $(C_6H_5)_3SnH$ et une initiation de la décomposition par des radicaux libres 'stables'. On attribue la nouvelle décomposition en chaîne de **3** à un mécanisme concerté qui amène les chaleurs de formation de l'azote et du groupe carbonyle en jeu afin d'abaisser l'énergie libre d'activation.

On discute de l'utilité synthétique de **3** en fonction d'un principe général indiquant l'existence de nouveaux réactifs menant à des additions radicalaires en chaîne sur des systèmes monosaturés. [Traduit par le journal]

Azo compounds play an important role in chemistry as sources of free radicals, which are generated from them either thermally or photolytically together with molecular nitrogen. An important feature characterizing such azo chemistry is the rarity of induced decomposition of the parent by its radical offspring. Potential mechanisms for induced decomposition of azo compounds include radical substitution at an atom situated α (eq. 1) or γ (eq. 2) to azo nitrogen.[1] On thermochemical grounds, those processes could be facile if concerted with the formation of N_2

[1] $$R\cdot + X{-}N{=}N{-}R \rightarrow RX + N_2 + R\cdot$$

[2] $$R\cdot + X{-}Y{-}Z{-}N{=}N{-}R \rightarrow RX + Y{=}Z + N_2 + R\cdot$$

(and of YZ, eq. 2). Azo systems which are reported to react according to eq. 1 or 2 are rare. An important reason for this, presumably, is the fact that many common, stable, azo compounds do not have a center (X, eq. 1) that is highly susceptible to radical substitution (S_R) reactions. Although the number of atoms at which S_R reactions have been demonstrated is increasing steadily (3) there are still no examples of such substitution at unstrained, saturated carbon and few, if any, examples of S_R reactions at sp^3 nitrogen (3).

Radical substitution at hydrogen is often a facile process and it is not surprising that diimides (X = H) can decompose according to eq. 1 (4, 5). Other examples that may involve the same reaction are: X = RCO (6), RSO_2 (7), RCO_2 (8), ArS (9), OCH_3 (10*a*), and Cl (10*b*). In some of the latter systems there are other major reactions and radical substitution was not established or suggested as a competitive process. With X = Cl and R = aryl (eq. 1), for

[1]Discussion is restricted here to those induced decompositions of azo compounds which lead to formation of N_2. Induced decomposition by radical substitution at azo nitrogen, to form a new azo compound, is known (1, 2) but will not be considered further in this article.

Can. J. Chem. Downloaded from www.nrcresearchpress.com by 210.87.254.40 on 09/05/12
For personal use only.

example, the yield of ArCl is higher in photochemical than in thermal decomposition (10*b*), possibly, but by no means necessarily because of induced decomposition by aryl radicals in the photochemical process.

Few cases of induced decomposition by radical substitution γ to azo nitrogen (eq. 2) have been reported. Benson and co-workers (11) observed that HCl accelerates the thermal decomposition of azo isobutane and suggested the sequence of reactions in eq. 3. The ready decomposition of

[3] $(CH_3)_3C\cdot + HCl \rightarrow (CH_3)_3CH + Cl\cdot$

$Cl\cdot + (CH_3)_3CN{=}NC(CH_3)_3 \rightarrow HCl + \dot{C}H_2(CH_3)_2CN{=}NC(CH_3)_3$

$\cdot CH_2(CH_3)_2CN{=}NC(CH_3)_3 \rightarrow CH_2{=}C(CH_3)_2 + N_2 + (CH_3)_3C\cdot$

1,1′-dihydroxyazocyclohexane (12) to cyclohexanone, cyclohexanol, hydrazine, and nitrogen may involve induced, chain decomposition as

[4] 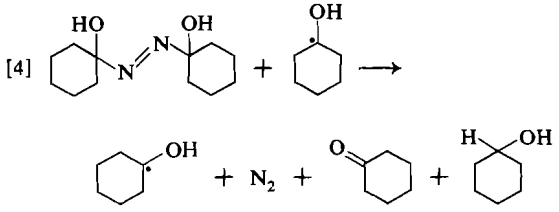

one mechanism (eq. 4). Alternatively, cyclohexanol could arise from radical decomposition of 1-hydroxycyclohexyl diimide; the mechanism suggested by the authors (12). It is noteworthy that other α-hydroxyazo systems are more easily isolated and stored (13, 14), possibly because their induced decomposition is not a chain process at all or because the chains are very short.

In this article we report the synthesis of 2-hydroxy-2,5,5-trimethyl-Δ^3-1,3,4-oxadiazoline (**3**) and its radical-chain, induced decomposition to N_2 and isopropyl acetate. That reaction appears to be the first recognized case of induced decomposition of an α-hydroxyazo compound (α-azocarbinol) by radical abstraction of hydroxyl hydrogen.

Results and Discussion

Treatment of 5,5-dimethyl-Δ^3-1,3,4-oxadiazolinone (**1**) (15) with methyl lithium in ether at 0° leads to the lithium salt (**2**), which could be isolated and stored or hydrolyzed directly to **3** (eq. 5). Unlike most acyclic esters or lactones, **1** consumes only 1 equiv. of CH_3Li, even if the latter is added in large excess. We attribute that result to the inductive effect of the azo group which serves to make ring opening of **2**, to form **4**, unusually endothermic. The strong electron withdrawing effect of the azo function is indicated by the high carbonyl stretching frequency (1835 cm^{-1}) of **1** (15) and of other azocarbonyl systems (13*a*). Substituent constants ($\sigma_p = 0.35$ and $\sigma_p^- \simeq 0.70$) for the phenylazo group (16) also attest to the same polar effect of the azo substituent.

[5] 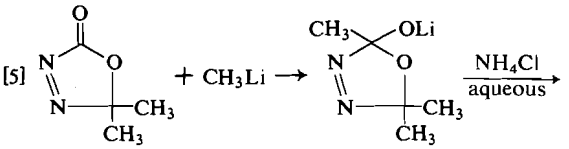

1 **2**

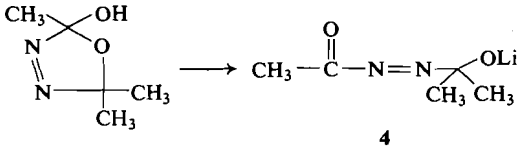

3 **4**

Product **3** is too unstable to be isolated analytically pure but the structure was readily established from its spectra and from the products of its decomposition. The ^1H n.m.r. spectrum consists of three sharp, high-field singlets (3H each) and a broader singlet (1H) which disappears on addition of D_2O. The i.r. spectrum of **3** in benzene includes a sharp band near 3550 cm^{-1} (free OH), a broad, strong band near 3350 cm^{-1} (bonded OH), and a weak band at 1565 cm^{-1} attributable to the *cis* azo group (13*a*, 17). In benzene solution **3** decomposed at room temperature, with gas evolution, to produce isopropyl acetate in quantitative yield (n.m.r.). A radical process was inferred from the following observations. Some fresh solutions of **3** in benzene were stable at room temperature for some time while others started to decompose spontaneously. Heating an aliquot of a stable solution briefly to 60° started decomposition, which could not be stopped by cooling the aliquot to the temperature of the original solution. Instead the material in the aliquot was totally converted to isopropyl acetate during a time in which the rest of the solution had lost very little of **3**. Such behavior is characteristic of radical chain pro-

Can. J. Chem. Downloaded from www.nrcresearchpress.com by 210.87.254.40 on 09/05/12
For personal use only.

Can. J. Chem. Downloaded from www.nrcresearchpress.com by 210.87.254.40 on 09/05/12
For personal use only.

cesses. A radical process was confirmed by adding nitrosobenzene, a spin trap (18), to a solution of **3** in benzene. The strong e.s.r. signal from the resulting solution[2] was a triplet with $g = 2.007$ and $a_N = 11.78$ G. Splitting by nitrogen only is consistent with trapping of a tertiary radical to form the nitroxide radical, $C_6H_5N(O\cdot)C(CH_3)_2O_2CCH_3$. Clean decomposition of **3** to isopropyl acetate in the absence of a spin trap is consistent with a chain-carrying 2-acetoxy-2-propyl radical intermediate (eq. 6). Moreover, **3** in benzene solution could be stabilized

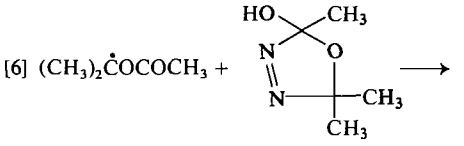

against decomposition by addition of triphenylstannane, a known H donor. Finally, various alkenes added to benzene solutions of **3** are converted to adducts of the type **5** shown in eq. 7.

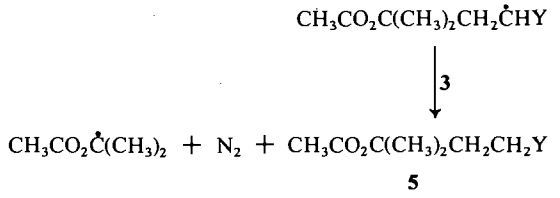

Loss of N_2 must be concerted with H abstraction to account for the ready decomposition of **3**, for abstraction of hydroxyl hydrogen from alcohols by free radicals, although known (19), is not a favored process in solution.[3] Relatively stable radicals like 2-acetoxy-2-propyl (eq. 6) or α-cyanoalkyl (eq. 7, Y = CN) cannot be expected to abstract hydroxylic hydrogen from **3** unless some driving force from the heat of formation of nitrogen becomes available to lower the free energy of the transition state. Support for concerted H—O and C—N bond ruptures came from experiments in which 2,6-di-*t*-butyl-4-methylphenol (**6**) was added to benzene solutions of **3**. Instead of inhibiting decomposition, **6** acts as an initiator and mild accelerator of the conversion of **3** to isopropyl acetate. We assume that initiation is caused by traces of aryloxy radicals from oxidation of the phenol and that those radicals are efficient chain carriers for the induced decomposition of **3**. Addition of di-*t*-butyl nitroxide to a benzene solution of **3** also initiated gas evolution. Again, the observation that 'stable' free radicals attack **3** is consistent only with concerted HO and C—N bond homolyses.

The chemistry of **3** and other members of the family may be of considerable synthetic utility. First, direct radical addition of esters to olefins (21) involves bond formation primarily α to the acyl carbon, whereas **3** provides an indirect path for adding an ester cleanly through its ether function (eq. 7). Many unsaturated systems have been successfully functionalized via **3** (eq. 7), including Y = CN, COR, CO_2R, OR, and NR_2. Details of most of those experiments will be reported separately. More important, probably, is a general principle regarding radical pathways in synthesis that emerges from those results. *Radical chain addition of the reagent X—Y to unsaturated systems, if impractical because of adverse thermochemisty of the chain-carrying abstraction step, can be made more favorable by using a new reagent which delivers the fragments X and Y, in a chain reaction, by virtue of the altered thermochemistry that results from the formation of stable co-products.*

Reagent **3**, which delivers the fragments $CH_3CO_2C(CH_3)_2$ and H by virtue of the combined heats of formation of N_2 and of a carbonyl group, is just one of many that can be envisioned. The list of potential fragments, X and Y, is very long and other likely, stable co-products include, for example, CO_2, CO, R_2CO, SO_2, aromatic molecules, and those products in combination. Exploratory work is in progress.

Experimental

2-Hydroxy-2,5,5-trimethyl-Δ³-1,3,4-oxadiazoline (3)

To an ice-cooled solution of 5,5-dimethyl-Δ³-1,3,4-oxadiazolin-2-one (**1**) (15) (2.0 g, 18 mmol) in 30 ml of anhydrous ether was added, gradually and with stirring, a solution of methyl lithium (10 ml, *ca.* 1.9 *M*) in ether until the solution in the flask just turned yellow. The addition can be performed like a titration using that

[2]Individual solutions of **3** or of nitrosobenzene in benzene did not themselves give e.s.r. signals.

[3]Exceptional in this respect are cyclopropanols, which are attacked by radicals at hydroxyl hydrogen, with concerted ring opening, in reactions analogous to that of **3** except for the different force (strain relief) that drives the former process (20).

Can. J. Chem. Downloaded from www.nrcresearchpress.com by 210.87.254.40 on 09/05/12
For personal use only.

color change as the end point. Stirring was continued for 10 min more at 0° before ice-cold $(NH_4)_2SO_4$ solution (50 ml, 20%) was added slowly. Cold H_2SO_4 (3 *M*) was then added until the aqueous layer was acidic to litmus. Separation of the ether layer, extraction of the residual aqueous layer twice with ether, drying the combined ether extracts over $MgSO_4$, filtration, addition of 2 drops of triphenylstannane, and evaporation of the ether with a rotary evaporator at room temperature, until the flask became defrosted and had regained room temperature, left **3** as an oil (80% yield, based on **1**). Its p.m.r. spectrum (benzene, TMS) consisted of three singlets (3H each) at δ 1.41, 1.57, and 1.80 as well as a broad singlet (1H) at δ 4.83. The i.r. spectrum (benzene) included bands at 3580 (sharp), 3400 (broad), and 1565 (weak) cm^{-1}.

The n.m.r. spectrum of the same sample, left for 96 h at room temperature, showed that 53% of the original **3** was still present.

Effects of 2,6-Di-t-butyl-4-methylphenol and of Di-t-butylnitroxide

A solution of **3** in benzene, prepared as described above but without added triphenylstannane, was separated into equal portions. One portion was made 0.01 *M* in the phenol and aliquots of both portions were scanned by n.m.r. The initial rate of loss of **3** from the phenol-containing portion was about twice that of the phenol-free portion.

To a solution of **3** in benzene, from which gas was evolving slowly at room temperature, was added a small amount (to make *ca.* 0.01 *M* solution) of di-*t*-butyl nitroxide. An immediate substantial increase in the rate of bubbling resulted. On the other hand, addition of corresponding molar quantities of either triphenyl or tri-*n*-butyl stannane decreased and eventually stopped such bubbling.

Spin Trapping by Nitrosobenzene

To a saturated solution of nitrosobenzene in benzene (0.5 ml) was added 20 mg of **3**. The e.s.r. spectrum of the resulting solution was obtained with a JEOLCO Model JES-3BS-X, e.s.r. instrument, using Mn^{2+} marker. A strong, triplet signal was recorded, with $g = 2.007$ and $a_N = 11.78$ *G*. A portion of the nitrosobenzene solution without added **3** did not produce an e.s.r. signal at the same instrument settings.

Trapping with Crotonaldehyde

A solution of **3** (2.0 g, 0.015 mol) in benzene (30 ml), cooled with ice, was stirred vigorously with a magnetic stirrer. Crotonaldehyde (3.0 g, 0.043 mol) was added all at once, a condenser and a drying tube were fitted to the flask, and the reaction mixture was heated at 40–50°, with constant stirring, until the n.m.r. spectrum of an aliquot showed that all **3** was consumed (about 4 h). Excess crotonaldehyde and the benzene were removed by distillation leaving crude 4-acetoxy-3,4-dimethyl pentanal (80–85%) as an oil. Analytically pure material was obtained by g.l.p.c. (SE 30, 15%, 5 ft × ¼ in., 150° 60 ml min^{-1}): p.m.r. (Varian HA 100, CCl_4) δ 0.95 (d, 3, $J = 7$ Hz), 1.38 (s, 3), and 1.46 (s, 3, diastereotopic *gem*-dimethyl), 1.92 (s, 3, CH_3CO), 1.99–2.75 (m, 3, $\rangle CH—CH_2—$), 9.66 (t, 1, $J = 2.5$ Hz, CHO); i.r. (CCl_4), 2725 (CH of CHO), 1735 (both C=O, unresolved) 1375 + 1362 ($C(CH_3)_2$), and 1255 cm^{-1} (C—O—C).

Anal. Calcd. for $C_9H_{16}O_3$: C, 62.79; H, 9.30. Found: C, 61.92; H, 9.32.

1. (*a*) J. L. Kice and R. S. Gabrielsen. J. Org. Chem. **35**, 1004 (1970). (*b*) J. L. Kice and R. S. Gabrielsen. J. Org. Chem. **35**, 1010 (1970).
2. (*a*) M. S. Kharasch, M. Zimmerman, W. Zimint, and W. Nudenberg. J. Org. Chem. **18**, 1045 (1953). (*b*) W. A. Pryor and H. Guard. J. Am. Chem. Soc. **86**, 1150 (1964). (*c*) H. Lui and J. Warkentin. Can. J. Chem. **51**, 1148 (1973).
3. K. U. Ingold and B. P. Roberts. Free-radical substitution reactions. Wiley-Interscience, New York. 1971.
4. (*a*) P. C. Huang and E. M. Kosower. J. Am. Chem. Soc. **90**, 2354 (1968). (*b*) E. M. Kosower. Acc. Chem. Res. **4**, 193 (1971).
5. A. J. M. Jimenez. Diss. Abstr. Int. B, **31**, 5878 (1971).
6. T. Imamoto. Bull. Chem. Soc. Jap. **45**, 2216 (1972).
7. J. F. Bunnett and D. A. R. Happer. J. Org. Chem. **32**, 2701 (1967).
8. L. A. Kazitsyna and N. B. Dzegilenko. Dokl. Akad. Nauk. SSSR, **192**, 570 (1970. Chem. Abstr. **73**, 121516p (1970).
9. H. van Zwet and E. C. Kooyman. Rec. Trav. Chim. Pays-Bas, **86**, 1143 (1967).
10. (*a*) J. F. Bunnett and H. Takayama. J. Org. Chem. **33**, 1924 (1968). (*b*) E. S. Lewis, R. E. Holliday, and L. D. Hartung. J. Am. Chem. Soc. **91**, 430 (1969).
11. D. F. McMillen, D. M. Golden, and S. W. Benson. J. Am. Chem. Soc. **94**, 4403 (1972).
12. E. Schmitz, R. Ohme, and S. Schramm. Liebigs' Ann. Chem. **702**, 131 (1967).
13. (*a*) J. P. Freeman and C. P. Rathjen. Chem. Commun. 538 (1969). (*b*) J. P. Freeman and C. P. Rathjen. J. Org. Chem. **37**, 1686 (1972). (*c*) E. Schmitz, R. Ohme, and S. Schramm. Angew. Chem. **75**, 208 (1963). (*d*) E. Schmitz, R. Ohme, and S. Schramm. Liebigs' Ann. Chem. **702**, 131 (1967).
14. (*a*) W. Nagata and S. Kamata. J. Chem. Soc. C, 540 (1970). (*b*) S. Hünig and J. Cramer. Angew. Chem. Int. Ed. **7**, 943 (1968). (*c*) S. Hünig and G. Büttner. Chem. Ber. **104**, 1104 (1971).
15. P. Knittel, S. L. Lee, and J. Warkentin. Can. J. Chem. **50**, 3248 (1972).
16. M. Syz and H. Zollinger. Helv. Chim. Acta, **48**, 383 (1965).
17. D. H. Williams and I. Fleming. Spectroscopic methods in organic chemistry. McGraw-Hill Publishing Co. Ltd., Berkshire, England. 1966. p. 65.
18. E. G. Janzen. Acc. Chem. Res. **4**, 31 (1971).
19. D. Griller and K. U. Ingold. J. Am. Chem. Soc. **96**, 630 (1974).
20. (*a*) C. H. DePuy, H. L. Jones, and D. H. Gibson. J. Am. Chem. Soc. Soc. **90**, 5306 (1968). (*b*) C. H. DePuy, H. L. Jones, and D. H. Gibson. J. Am. Chem. Soc. **94**, 3924 (1972).
21. (*a*) J. C. Allen, J. I. G. Cadogen, and D. H. Hey. Chem. Ind. 1621 (1962). (*b*) D. Elad and R. D. Youssefyeh. Chem. Commun. 7 (1965).

3,4-Dihydro-*2H*-1,5-benzodioxepins. A Novel Class of β-Adrenergic Stimulants

C. S. ROONEY, R. S. STUART, B. K. WASSON, AND H. W. R. WILLIAMS

Medicinal Chemistry Department, Merck Frosst Laboratories, P.O. Box 1005, Pointe Claire/Dorval, Quebec H9R 4P8

Received January 23, 1975

C. S. ROONEY, R. S. STUART, B. K. WASSON, and H. W. R. WILLIAMS. Can. J. Chem. **53**, 2279 (1975).

A series of 3-substituted-aminomethyl-3-hydroxy-3,4-dihydro-*2H*-1,5-benzodioxepins is described. Members of the series constitute a unique class of β-adrenergic stimulants and possess interesting bronchial dilator activity.

C. S. ROONEY, R. S. STUART, B. K. WASSON et H. W. R. WILLIAMS. Can. J. Chem. **53**, 2279 (1975).

On a préparé une série d'aminométhyl-3 hydroxy-3-dihydro-3,4 (*2H*)-benzodioxepines-1,5 substitué sur l'azote. Les membres de cette série constituent une classe unique de stimulants β-adrénergiques et possèdent une activité broncho-dilatatrice intéressante.

Can. J. Chem. Downloaded from www.nrcresearchpress.com by 210.87.254.40 on 09/05/12
For personal use only.

As an extension of an interest in 1-phenoxy-3-amino-2-propanols with β-adrenergic blocking activity, it was decided to prepare as analogs 3,4-dihydro-*2H*-1,5-benzodioxepins (**A**) containing hydroxyl and amino functions in a similar vicinal relationship. Instead of the expected β-adrenergic blocking properties, a number of the compounds displayed β-adrenergic stimulant activity.

A practical preparative method was devised for the key intermediate, 3-oxo-3,4-dihydro-*2H*-1,5-benzodioxepin (**3**) (1), in the syntheses of the desired amino derivatives. Thorpe cyclization of 1,2-di(cyanomethoxy)benzene (**1**) afforded an enamino nitrile (**2**) which was hydrolyzed to the ketone (**3**) in acceptable overall yield. Three similar syntheses have been published recently (2).

From the ketone (**3**), two routes to the final products were developed. The ketone (**3**) was converted to the cyanohydrin (**4**) which, upon reduction, either catalytically or with lithium aluminum hydride, gave the amino alcohol (**5**). Various *N*-alkyl and *N*-aralkyl derivatives of this amine were obtained by reductive alkylations in the presence of aldehydes or ketones and by amide formation followed by lithium aluminum hydride reduction. Alternatively, conversion of the ketone (**3**) to the epoxide (**6**) by treatment with dimethyl sulfoxonium methylide and then reaction of the epoxide with a primary amine afforded an *N*-substituted amino alcohol (**A**). The latter route is more versatile in that the products are not limited to those bearing a primary or secondary alkyl group on the nitrogen atom. Treatment of the amino alcohol (**5**) with nitrous acid provided a convenient method for the large scale preparation of the epoxide (**6**). A small amount of the glycol (**7**) was obtained along with the epoxide but the Tiffeneau–Demjanov ring-expanded product (**8**) was not observed.

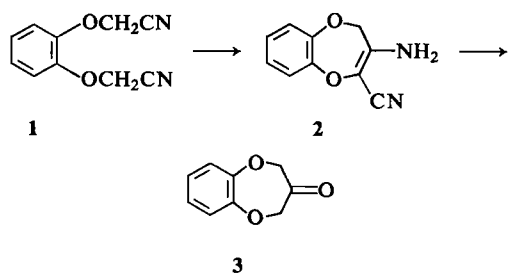

1 **2** **3**

SCHEME 1

Interesting pharmacological activity shown by some of the initial compounds of formula **A** that were made, especially R = *i*-Pr, necessitated the preparation of more highly substituted derivatives (**B**).

A number of readily available substituted catechols served as starting materials for syntheses based on the routes in Schemes 1 and 2. Although cyclization of a 1,2-di(cyanomethoxy)-benzene derived from a mono-substituted catechol could give rise to two isomeric enamino nitriles, in no case were two isolated, neither did

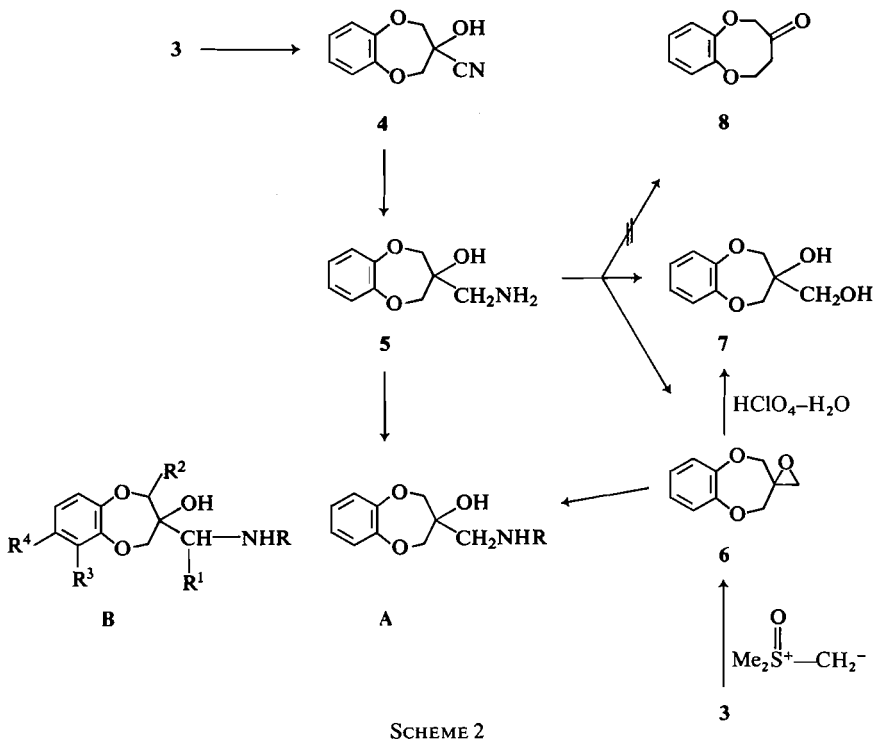

SCHEME 2

thin-layer chromatography nor n.m.r. spectrum suggest the presence of two products. The direction of cyclization of these compounds would be difficult to establish but structural ambiguity disappears when they are hydrolyzed to the ketones. Examples of substituted derivatives of **1–5** are given in Tables 1–5, respectively, and compounds of general formula **B** in Table 6.

Compound **B** (R = *t*-Bu; R^3 = OH; R^1 = R^2 = R^4 = H) was made by demethylating the corresponding 6-methoxy compound with boiling 48% HBr. The stability of the dioxepin system under these conditions is noteworthy, as also is the survival of the 3-hydroxyl group.

Compound **B** (R = *i*-Pr; R^4 = OH; R^1 = R^2 = R^3 = H) was made from **9** (**A**; R = *i*-Pr) as follows. The amino and hydroxyl functions were protected by incorporation into an oxazolidone ring; this derivative (**10**) was nitrated under mild conditions to give **11**, which was converted by conventional reactions to the required hydroxy derivative (**14**). Cleavage of the oxazolidone ring in either **11** or **13** required unusually vigorous conditions.

Access to compounds with a branched side chain (*e.g.* **B**, R^1 = Me—) was achieved by condensation of the ketone (**3**) with a nitro alkane followed by reduction of the nitro group and reductive alkylation.

Introduction of a methyl group into the dioxepin ring (**B**, R^2 = Me—) was effected by partial hydrolysis if the enamino nitrile (**2**) to the keto nitrile (**15**) which was methylated via its thallium salt. This latter procedure did not show its usual

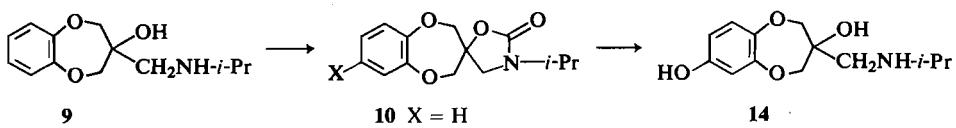

SCHEME 3

Can. J. Chem. Downloaded from www.nrcresearchpress.com by 210.87.254.40 on 09/05/12
For personal use only.

TABLE 1. Analyses of compound **1** and its derivatives

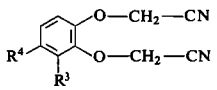

Compound	R^3	R^4	Crystallization solvent	Yield (%)	Melting point (°C)	Formula	Analyses
1	H	H	MeOH	73	85–85.5	$C_{10}H_8N_2O_2$	C, H, N
26	H	Cl	C_6H_6	13	125–127	$C_{10}H_7ClN_2O_2$	C, H, Cl, N
27	H	CH_3	MeOH	64	85–86.5	$C_{11}H_{10}N_2O_2$	C, H, N
28	CH_3O	H	MeOH	72	70–72	$C_{11}H_{10}N_2O_3$	C, H, N

TABLE 2. Analyses of compound **2** and its derivatives

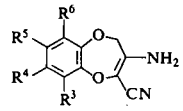

Compound	R^3 or R^6	R^4 or R^5	Crystallization solvent	Yield (%)	Melting point (°C)	Formula	Analyses
2	H	H	$CHCl_3$	62	168–169	$C_{10}H_8N_2O_2$	C, H, N
29	H	Cl	Glyme–$CHCl_3$	56	218.5–219.5	$C_{10}H_7ClN_2O_2$	C, H, Cl, N
30	H	CH_3	$CHCl_3$	52	170.5–172	$C_{11}H_{10}N_2O_2$	C, H, N
31	CH_3O	H	MeCN	78	216–218	$C_{11}H_{10}N_2O_3$	C, H, N

high degree of regiospecificity (3) and gave a significant amount of the enol ether (**17**) in addition to the desired keto nitrile (**16**). Hydrolysis and decarboxylation of **16** afforded **18**, which was converted to the oxirane (**19**) by the sulfoxonium methylide procedure. The yield and quality of the oxirane were poor but treatment of the crude product with *t*-butylamine afforded **20** in low yield.

The unusual stability of the oxazolidone system

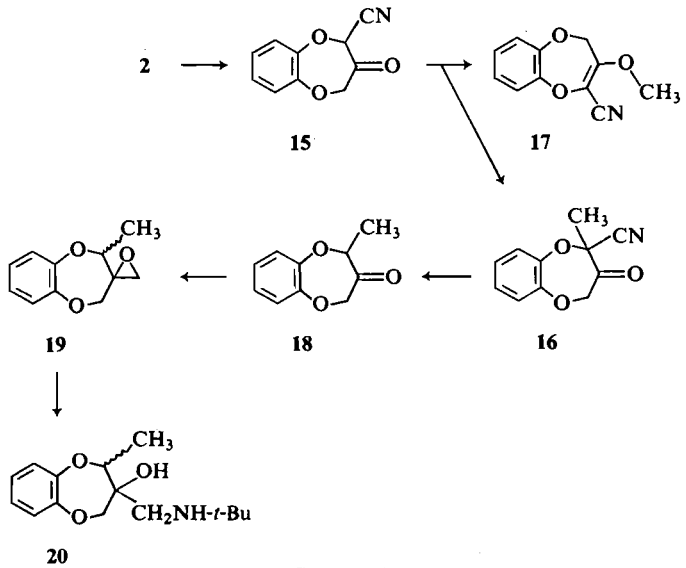

SCHEME 4

Can. J. Chem. Downloaded from www.nrcresearchpress.com by 210.87.254.40 on 09/05/12
For personal use only.

TABLE 3. Analyses of compound **3** and its derivatives

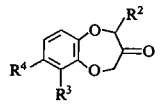

Compound	R^2	R^3	R^4	Method	Yield (%)	Crystallization solvent	Boiling or melting point (°C)	Formula	Analyses
3	H	H	H	*A*	51	—	64–68/0.35 Torr	$C_9H_8O_3$	
18	CH_3	H	H	*B*	67	—	100–105/0.15 Torr (46.5–48)	$C_{10}H_{10}O_3$	C, H[a]
32	H	H	Cl	*A*	50	Hexane	97/0.15 Torr (54–56)	$C_9H_7ClO_3$	C, H, Cl
33	H	H	CH_3	*A*	43	—	71–82/0.01 Torr	$C_{10}H_{10}O_3$	C, H
34	H	CH_3O	H	*A*	25	Et_2O	(101–102)	$C_{10}H_{10}O_4$	C, H
				B	83				

[a]H: calcd.: 5.66; found: 6.09.

TABLE 4. Analyses of compound **4** and its derivatives

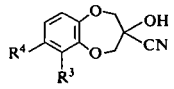

Compound	R^3	R^4	Crystallization solvent	Yield[a] (%)	Melting point (°C)	Formula	Analyses
4	H	H	CCl_4	43.5	108.5–110	$C_{10}H_9NO_3$	C, H, N
35	H	Cl	CH_2Cl_2–CCl_4	68	117–118.5	$C_{10}H_8ClNO_3$	C, H, Cl, N
36	H	CH_3	CCl_4	47	127–129	$C_{11}H_{11}NO_3$	C, H, N
37	CH_3O	H	CCl_4	39	115–117	$C_{11}H_{11}NO_4$	C, H, N

[a]Yield of recrystallized product. However, crude product was usually used in the next step.

precluded its use as a protective group during synthesis of aryl acyl amido derivatives of **B**. For the synthesis of the methanesulfonamido derivative **25**, the more readily hydrolyzable oxazolidine ring derived from benzaldehyde was employed. A few tertiary amines are described in Table 7.

Biological Activity

In recent years there has been a search for β-adrenergic stimulants showing selective action on the β_2-adrenergic receptors which mediate relaxation of bronchial muscle, rather than action on the β_1-adrenergic receptors which mediate responses of heart muscle.[1] The structures of most of the new β-stimulants described, have been based upon the observation that the 3-phenolic group of the catecholamine molecule can be replaced by a variety of other substituents with retention of pharmacological activity and improved selectivity. In addition, because the modified molecules are not substrates for catechol-*O*-methyltransferase, they exhibit longer duration

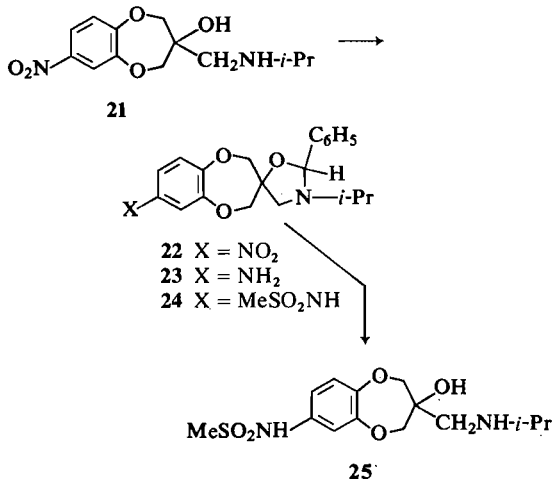

SCHEME 5

[1]For more detailed information about the classification of adrenergic receptors see the publication of Lands and Brown (4).

Can. J. Chem. Downloaded from www.nrcresearchpress.com by 210.87.254.40 on 09/05/12
For personal use only.

Can. J. Chem. Downloaded from www.nrcresearchpress.com by 210.87.254.40 on 09/05/12
For personal use only.

TABLE 5. Analyses of compound **5** and its derivatives

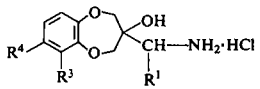

Compound	R^1	R^3	R^4	Method	Crystallization solvent	Yield[a] (%)	Melting point (°C)	Formula	Analyses
5	H	H	H	*C*	EtOH	79	235–240	$C_{10}H_{13}NO_3 \cdot HCl$	C, H, N
38	CH_3	H	H	*D*	*i*-PrOH–Et_2O EtOH	36	204–206	$C_{11}H_{15}NO_3 \cdot HCl$	C, H, Cl, N
39	C_2H_5	H	H	*D*	*i*-PrOH	31	197–198	$C_{12}H_{17}NO_3 \cdot HCl$	C, H, Cl, N
40	H	CH_3O	H	*C*	MeOH	62	227–229.5	$C_{11}H_{15}NO_4 \cdot HCl$	C, H, Cl, N
41	H	H	Cl	*C*	*i*-PrOH	40	Sinters at *ca.* 198, dec. > 240	$C_{10}H_{12}ClNO_3 \cdot HCl$	C, H, Cl, N
42	H	H	CH_3	*C*	*i*-PrOH	24	Sinters at *ca.* 217	$C_{11}H_{15}NO_3 \cdot HCl$	C, H, Cl, N

[a]Yields of **5**, **40**, **41**, and **42** are overall yields from the ketone of recrystallized product, obtained by reduction of crude cyanohydrin. Yields of **38** and **39** are based on crude nitro compound.

Can. J. Chem. Downloaded from www.nrcresearchpress.com by 210.87.254.40 on 09/05/12
For personal use only.

TABLE 6. Analyses of compounds of general formula **B**

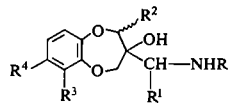

Compound	R	R^1	R^2	R^3	R^4	Method	Crystallization solvent	Yield (%)	Melting point (°C)	Formula	Analyses
43	CH_3	H	H	H	H		EtOH	33	217–219	$C_{11}H_{15}NO_3 \cdot HCl$	C, H, Cl, N
44	C_2H_5	H	H	H	H		EtOH	47	181.5–183	$C_{12}H_{17}NO_3 \cdot HCl$	C, H, Cl, N
45	$(CH_3)_2N$	H	H	H	H	*F*	*i*-PrOH	50	186–188	$C_{12}H_{18}N_2O_3 \cdot HCl$	C, H, N, Cl[a]
9	$(CH_3)_2CH$	H	H	H	H	*E*	*i*-PrOH	83	174.5–175.5	$C_{13}H_{19}NO_3 \cdot HCl$	C, H, N
46	$(CH_3)_2CH$	CH_3	H	H	H		EtOH–Et_2O	76	215–217	$C_{14}H_{21}NO_3 \cdot HCl$	C, H, Cl, N
47	$(CH_3)_2CH$	H	H	H	Cl	*E*	*i*-PrOH	70	171–172.5	$C_{13}H_{18}ClNO_3 \cdot HCl$	C, H, Cl, N
48	$(CH_3)_2CH$	H	H	H	CH_3	*E*	EtOH	76	175–177	$C_{14}H_{21}NO_3 \cdot HCl$	C, H, Cl, N
21	$(CH_3)_2CH$	H	H	H	NO_2		*i*-Pr_2O	62	97.5–98.5	$C_{13}H_{18}N_2O_5$	C, H, N
							EtOH		195–196dec.	$C_{13}H_{18}N_2O_5 \cdot (COOH)_2$	C, H, N
49	$(CH_3)_2CH$	H	H	H	NH_2		C_6H_6	74	95.5–97.5	$C_{13}H_{20}N_2O_3$	C, H, N
14	$(CH_3)_2CH$	H	H	H	HO		C_6H_6	39	133.5–134	$C_{13}H_{19}NO_4$	C, H, N

Can. J. Chem. Downloaded from www.nrcresearchpress.com by 210.87.254.40 on 09/05/12
For personal use only.

TABLE 6. (*Concluded*)

Compound	R	R¹	R²	R³	R⁴	Method	Crystallization solvent	Yield (%)	Melting point (°C)	Formula	Analyses
25	$(CH_3)_2CH$	H	H	H	CH_3SO_2NH			47	214–215dec.	$C_{14}H_{22}N_2O_5S\cdot(COOH)_2$	H, N, S, C[b]
50	$(CH_3)_2CH$	H	H	CH_3O	H	*E*	EtOH–Et_2O	56	155–157	$C_{14}H_{21}NO_4\cdot C_4H_4O_4$[c]	C, H, N
51	$(CH_3)_2CH$	H	H	HO	H		MeOH–EtOAc	80	196–197	$C_{13}H_{19}NO_4\cdot HBr$	C, H, Br, N
52		H	H	H	H	*F*	EtOH	55	187–189	$C_{13}H_{17}NO_3\cdot HCl$	C, H, Cl, N
53		H	H	H	H	*E*	*i*-PrOH	74	183–184	$C_{14}H_{21}NO_3\cdot HCl$	C, H, Cl, N
54	$(CH_3)_3C$	H	H	H	H	*F*	*i*-PrOH	75	186.5–188	$C_{14}H_{21}NO_3\cdot HCl$	C, H, Cl, N
20	$(CH_3)_3C$	H	CH_3	H	H	*F*	EtOH–*i*-PrOH	3	229–230dec.	$C_{15}H_{23}NO_3\cdot(COOH)_2$	C, H, N
55	$(CH_3)_3C$	H	H	CH_3O	H	*F*	EtOH	81	193–195dec.	$C_{15}H_{23}NO_4\cdot C_4H_4O_4$	C, H, N
56		H	H	H	H	*F*	*i*-PrOH	62	192–193	$C_{14}H_{19}NO_3\cdot HCl$	C, H, Cl, N
57		H	H	H	H	*F*	EtOH	66	190.5–192.5	$C_{15}H_{19}NO_3\cdot HCl$	C, H, Cl, N
58		H	H	H	H	*F*	*i*-PrOH	55	138.5–140	$C_{14}H_{21}NO_4\cdot C_4H_4O_4$[c]	C, H, N
59		H	H	H	H	*F*	*i*-Pr_2O MeOH	40	122–124 267–276	$C_{20}H_{27}NO_3$ $C_{20}H_{27}NO_3\cdot HCl$	 C, H, Cl, N
60	$HO(CH_2)_2O(CH_2)_2$	H	H	H	H	*F*	EtOH–Et_2O	63	155–158	$C_{14}H_{21}NO_5\cdot HCl$	C, H, Cl, N
61	$-(CH_2)_6-$[d]	H	H	H	H	*F*	MeOH	44	274–277	$C_{26}H_{36}N_2O_6\cdot 2HCl$	C, H, Cl, N
62	$C_6H_5CH_2$	H	H	H	H	*E*	EtOH	46	214–216	$C_{17}H_{19}NO_3\cdot HCl$	C, H, Cl, N
63	$C_6H_5CH_2CH_2$	H	H	H	H	*E*	EtOH	11	229–231	$C_{18}H_{21}NO_3\cdot HCl$	C, H, Cl, N
64	$C_6H_5CH(OH)CH_2$	H	H	H	H	*F*	EtOH	44	200–202	$C_{18}H_{21}NO_4\cdot HCl$	C, H, Cl, N
65	$C_6H_5CH_2CH(CH_3)$	H	H	H	H	*E*	EtOH	49	170–174	$C_{19}H_{23}NO_3\cdot HCl$	C, H, Cl, N
66	$C_6H_5CH_2CH_2CH(CH_3)$[e]	H	H	H	H	*E*	*i*-PrOH	26	180–183	$C_{20}H_{25}NO_3\cdot HCl$	C, H, Cl, N
67	4-$ClC_6H_4CH_2CH(CH_3)$	H	H	H	H	*E*	EtOH	52	163–165	$C_{19}H_{22}ClNO_3\cdot HCl$	C, H, Cl, N
68	4-$HOC_6H_4CH_2CH(CH_3)$	H	H	H	H	*E*	$CHCl_3$	50	129.5–130.5	$C_{19}H_{23}NO_4$	C, H, N
69	3,4-$(CH_2O_2)C_6H_3CH_2CH(CH_3)$	H	H	H	H	*E*	EtOH MeOH	64 62	127–129dec. 188–189.5	$C_{19}H_{23}NO_4\cdot H_3PO_4\cdot H_2O$ $C_{20}H_{23}NO_5\cdot HCl$	C, H, N, P[f] C, H, Cl, N
70	3,4,5-$(CH_3O)_3C_6H_2CH_2CH(CH_3$	H	H	H	H	*E*	MeOH	72	220–221.5	$C_{22}H_{29}NO_6\cdot HCl$	C, H, Cl, N
71	3-Indolyl-$CH_2CH(CH_3)$	H	H	H	H	*E*	EtOH–Et_2O	60	190–191dec.	$C_{21}H_{24}N_2O_3\cdot HCl$	C, H, Cl, N
72	4-$(CH_3)_2NC_6H_4CH_2CH(CH_3)$	H	H	H	H	*F*	*i*-PrOH	50	226–228	$C_{21}H_{28}N_2O_3\cdot 2HCl$	C, H, Cl, N
73	2-Furyl-$CH_2CH(CH_3)$	H	H	H	H	*F*	EtOH	66	166.5–168	$C_{17}H_{21}NO_4\cdot HCl$	C, H, N

[a]Cl: calcd.: 12.90; found: 13.35.
[b]C: calcd.: 45.70; found: 45.08.
[c]Maleate.
[d]A bis-compound.
[e]The ketone reactant was benzalacetone.
[f]P: calcd.: 6.95; found: 7.38

TABLE 7. Analyses of some tertiary amines

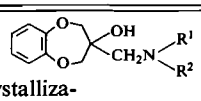

Compound	R^1	R^2	Method	Crystallization solvent	Yield (%)	Melting point (°C)	Formula	Analyses
74	CH_2—	CH_2	*F*	*i*-Pr_2O	71	98–99.5	$C_{12}H_{15}NO_3$	C, H, N[a]
75	CH_3	CH_3		*i*-PrOH	38	118–120	$C_{12}H_{17}NO_3$·HCl	C, H, Cl, N
76	$CH_2CH_2OCH_2CH_2$		*F*	EtOH	72	173–176	$C_{14}H_{19}NO_4$·HCl	C, H, Cl, N

[a]N: calcd.: 6.33; found: 6.81.

TABLE 8. Adenyl cyclase assay[a]

Activity	Compound
Active (40% increase in glycerol release)	**44, 9, 49, 14[b], 52, 53, 54, 58, 60, 62, 63, 65, 66, 67, 68, 71**
Moderately active (25% increase in glycerol release)	**43, 47, 50, 55, 56, 57, 59, 61, 64, 69, 70, 72, 74, 75**
Inactive	**20[c], 45, 46, 48, 21, 25, 51, 73, 76**

[a]Based upon the procedures of Rodbell (12) and Korn (13).
[b]Subsequently found to be not very active in the *in vivo* assays.
[c]However, the compound showed activity *in vivo*.

of action. The active compounds described in this paper constitute a novel class of β-stimulants in that there is no functionality present to mimic the phenolic groups of the catecholamines.

The compounds were tested for their ability to stimulate the enzyme adenyl cyclase as evinced by enhanced release of glycerol from rat epididymal adipose tissue (Table 8) and as inhibitors of histamine-induced bronchial constriction in the dog. Bronchial dilator data for some of the more interesting compounds are given in Table 9. As far as the substituent (R) on the nitrogen atom is concerned, the structure activity relationship in this series parallels that observed in other classes of β-stimulants (and in β-adrenergic blocking agents). The most active members of the series are secondary amines (**B**, $R^1 = R^2 = R^3 = R^4 =$ H) in which R is an alkyl or aralkyl group of the type that confers greatest activity on compounds of the catecholamine series (4). Primary or tertiary amines are generally inactive.

Comparison of the dihydrobenzodioxepin compounds with the isomeric benzodioxan derivatives indicates marked differences in pharmacological behavior because the latter are claimed to be β-adrenergic blocking agents (5).

There have been speculations about the molecular mechanism for β-stimulant activity which suggest that the two hydroxyl groups in the catechol nucleus are involved in chelation with a divalent metal ion (*6a*) or that the agonist molecule may bring about a conformational change in the enzymic (or receptor) protein and its associated shell of water molecules by hydrogen bonding at a specific site adjacent to an aromatic binding site (*6b*). While these possibilities could apply to the benzodioxepins also, the different location of the two ether oxygen atoms relative to the side chain, plus their lack of acidity means that significant differences must exist in their interactions at the receptor level. Introduction of acidic substituents on the aromatic ring of the dihydrobenzodioxepins (**14, 25, 51**), in order to increase their resemblance to the catecholamines, resulted in a reduction in biological activity. This was particularly surprising in the case of **51** which, on the basis of a comparison of molecular models, seemed most likely to be capable of interacting like a catecholamine at a receptor site. In view of the difficulty of displacing the 3-hydroxyl group in these compounds, the β-adrenergic agonist theory of Larsen (7) does not seem applicable to this series of β-stimulants.

Can. J. Chem. Downloaded from www.nrcresearchpress.com by 210.87.254.40 on 09/05/12
For personal use only.

TABLE 9. Inhibition of histamine-induced bronchial constriction in the anesthetized dog

Compound	Structure	Route of administration[a]	ED_{50}[b] (μg/kg)	No. of animals	ΔHR[c] (b.p.m.)	ΔBP[d] (Torr)
43	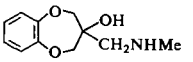	i.v.	650	1	+30	−20
44	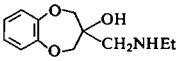	i.v.	220	1	+38	−40
9	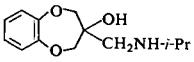	i.v.	29	1	+75	−50
54	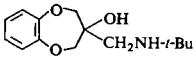	i.v. i.d.	14 66	3 5	+22 +41	−25 −34
68		i.v.	37	1	+27	−45
71	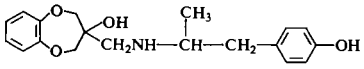	i.v.	58	1	+39	−39
Salbutamol (11)	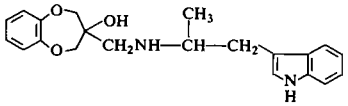	i.v. i.d.	4 29	3 5	+68 +67	−70 −55
Isoproterenol		i.v. i.d.	0.08 240	8 5	+76 +37	−57 −35

NOTE: Mongrel dogs were anaesthetized with vinbarbital (60 mg/kg i.v., supplemented by 20 mg/kg intramuscularly). Bronchoconstriction was induced at 15-min intervals by intravenous injection of 20 μg of histamine acid phosphate. Following stabilization of the bronchoconstrictor responses, test substances were injected i.v. cumulatively in threefold increments either 1- (isoproterenol) or 2 min (other compounds) before challenge until a greater than 50% inhibition of bronchoconstriction was observed. In the case of i.d. administration, three dose levels (*e.g.* 10, 30, and 100 μg/kg) calculated to produce 16–84% inhibition of the induced bronchoconstrictor response were used for each compound and five dogs were used at each dose level.

[a]Intravenous (i.v.) or intraduodenal (i.d.).
[b]Effective dose (50).
[c]Change in heart rate (beats per minute).
[d]Change in blood pressure. Results for heart rate and blood pressure are the maximal changes seen over the dose range.

Compound **54**, like salbutamol,[2] shows good absorption from the duodenum (indicated by a low ratio of i.d.[3] activity/i.v. activity in Table 9) and thereby makes up for its lack of intrinsic activity relative to isoproterenol which is very poorly absorbed. Duration of action is good and the moderate chronotropic activity at bronchial dilator dose levels is indicative of a degree of specificity for β_2-receptors.

Experimental

Melting points (uncorrected) up to 220° were taken in a Thomas Hoover capillary melting point apparatus and those above 220° were taken in an Electrothermal apparatus. The i.r. spectra were recorded with a Perkin Elmer 157 spectrometer and n.m.r. spectra with a Varian A60A spectrometer with TMS as internal reference. Mass spectra were provided by Morgan Schaffer Corporation, and microanalyses by Organic Microanalyses Laboratories (Dr. C. Daesslé), both of Montreal. Analyses are within 0.4% of theory unless otherwise stated. A table of analytical data is provided as supplementary material.[4]

1,2-Di-(cyanomethoxy)benzene (1)

To a stirred mixture of catechol (99 g, 0.9 mol), finely powdered K_2CO_3 (168 g, 1.22 mol), and acetone (600 ml) was added chloroacetonitrile (90.6 g, 1.2 mol) over 5 min. The mixture was heated slowly to reflux, then after 1½ h under reflux, the mixture was treated with more K_2CO_3

[2]2-*t*-Butylamino-1-(4-hydroxy-3-hydroxymethylphenyl) ethanol, a selective β-stimulant (11).

[3]Note, i.d. is used as an abbreviation for intraduodenal in this paper, not intradermal.

[4]A complete set of tabular data is available, at a nominal charge, from the Depository of Unpublished Data, CISTI, National Research Council of Canada, Ottawa, Canada K1A 0S2.

Can. J. Chem. Downloaded from www.nrcresearchpress.com by 210.87.254.40 on 09/05/12
For personal use only.

Can. J. Chem. Downloaded from www.nrcresearchpress.com by 210.87.254.40 on 09/05/12
For personal use only.

(84 g, 0.61 mol) and chloroacetonitrile (45.3 g, 0.6 mol). After a further 3½ h under reflux the mixture was filtered, the inorganic solid was washed with acetone (150 ml), and the combined filtrate evaporated to an oil that crystallized and was recrystallized from MeOH–H_2O (400 ml : 50 ml) giving 138 g (73%) of **1**, m.p. 85–85.5°; ν_{max} (KBr) 1500, 1080, 680, no ν CN; δ (CD_3CN) 7.20 (4H, s, aryl H), 4.98 (4H, s, OCH_2); analyzed (C, H, N) for $C_{10}H_8N_2O_2$.

3-Amino-4-cyano-2H-1,5-benzodioxepin (2)

A solution of **1** (9.4 g, 0.05 mol) in dry DMSO (20 ml) was added dropwise to potassium *t*-butoxide (12.3 g, 0.11 mol) in dry DMSO (30 ml) under dry N_2, with external cooling (water bath at room temperature). The mixture was stirred for 2 h and then poured into dilute acetic acid (6.6 ml AcOH in 20 ml H_2O). The crude product was collected, washed with water, dried, and recrystallized from chloroform giving 5.8 g (62%) of **2**, m.p. 162–164°. Pure **2** has m.p. 168–169°; ν_{max} (KBr) 3463, 3360, 2192, 1656, 747, (*cf.* ref. 8); δ (DMSO-d_6) 6.97–6.93 (4H, m, aryl H), 6.58 (2H, bs, NH_2), 4.93 (2H, s, OCH_2). Analyzed (C, H, N) for: $C_{10}H_8N_2O_2$.

3-Oxo-3,4-dihydro-2H-1,5-benzodioxepin (3)

Method A, Table 3

A mixture of **2** (29.75 g, 0.158 mol), water (20 ml), and acetic acid (300 ml) was heated under reflux for ½ h. Phosphoric acid (85%; 120 ml) was added slowly and the mixture refluxed overnight. The solution was cooled to room temperature, poured into ice water (250 ml) and saturated with ammonium sulfate, before continuously extracting with ether for 48 h. The ethereal solution was evaporated, the oily residue dissolved in ether, and the solution treated with charcoal, filtered, extracted with 10% Na_2CO_3 solution, dried ($MgSO_4$), and distilled to give **3** as a colorless oil, 13.15 g (51%), b.p. 64–68°/0.35 Torr, that crystallized on standing, m.p. 33–36°; ν_{max} (CCl_4) 1745, 1490, 1257, 1049 (l); δ ($CDCl_3$) 6.98 (4H, s, aryl H), 4.68 (4H, s, OCH_2).

6-Methoxy-3-oxo-3,4-dihydro-2H-1,5-benzodioxepin (34)

Method B, Table 3

To methanol (450 ml) saturated with HCl was added **31** (61.3 g, 0.28 mol) and the suspension was stirred until solution occurred. The solution was allowed to stand at room temperature for 6 days, then methanol (450 ml) and water (900 ml) were added, and the mixture was heated under reflux for 10 h. Evaporation of the mixture gave 19.1 g (83%) of **34**, m.p. 101–102°; ν_{max} (KBr) 1743, 1500, 1105; δ ($CDCl_3$) 7.07–6.55 (3H, m, aryl H), 4.78, 4.72 (2H and 2H, 2s, OCH_2), 3.87 (3H, s, OCH_3). Analyzed (C, H) for $C_{10}H_{10}O_4$.

3-Cyano-3-hydroxy-3,4-dihydro-2H-1,5-benzodioxepin (4)

A solution of KCN (13.5 g, 0.208 mol) in water (27 ml) was added dropwise to a solution of **3** (18.7 g, 0.114 mol) in acetic anhydride (19.6 ml) with stirring and cooling (ice bath). The mixture was stirred at room temperature overnight and then basified with 10% Na_2CO_3 solution. Ether extraction of the basified mixture gave **4** as a pale yellow oily solid, 24.3 g (> 100%). This crude material was used in the next step because recrystallization of the solid gave a poor recovery. Crude **4** on recrystallization from CCl_4 (4 parts v/w) afforded a 43% yield of colorless platelets, m.p. 108.5–110°; ν_{max} (KBr) 1505, 1255, 1126, no ν CN. Analyzed (C, H, N) for $C_{10}H_9NO_3$.

3-Aminomethyl-3-hydroxy-3,4-dihydro-2H-1,5-benzodioxepin Hydrochloride (5)

Method C, Table 5

A solution of crude **4** (4.92 g, 30 mmol) in dry ether (100 ml) was added dropwise with stirring to a slurry of lithium aluminum hydride (3.8 g, 100 mmol) in ether (100 ml) under N_2 during ¾ h. Then the mixture was stirred under reflux for 2¾ h before quenching with water (3.8 ml), followed by 10% NaOH solution (5.7 ml) and more water (11.4 ml). The inorganic solid was filtered off, washed with ether (50 ml), and the combined filtrate was dried ($MgSO_4$) and evaporated to afford crude base **5**, 5.13 g (87%), m.p. 60–63°. This can be recrystallized from benzene to afford platelets, m.p. 66–68°, but the solid appears to absorb water and CO_2 from the air. Accordingly a solution of the base in ether was treated with ethanolic HCl solution to give the hydrochloride, m.p. 235–240° (*i*-PrOH); ν_{max} (KBr) 1499, 1300, 1099, 750. Analyzed (C, H, N) for $C_{10}H_{13}NO_3 \cdot HCl$)

3-Hydroxy-3-isopropylaminomethyl-3,4-dihydro-2H-1,5-benzodioxepin Hydrochloride (9)

Method E, Table 6

A mixture of **5** (3.47 g, 15 mmol), anhydrous sodium acetate (1.23 g, 15 mmol), and ethanol (40 ml) was stirred under N_2 for 10 min. Acetone (960 mg, 16.5 mmol) was added and stirring was continued for 20 min. Hydrogenation of the mixture at 26° and atmospheric pressure in the presence of platinium oxide was carried out until uptake of H_2 was complete. The catalyst was filtered off and the filtrate evaporated to a syrup. Dry ether (60 ml) was added, followed by a slight excess of ethanolic HCl to afford **9**, 3.91 g (95%), m.p. 173–175°. Recrystallization of the solid from isopropanol (75 ml) gave pure **9**, 3.43 g (83%), m.p. 174.5–175.5°; ν_{max} (KBr) 3340, 3295, 1497, 1253, 1055. Analyzed (C, H, N) for $C_{13}H_{19}NO_3 \cdot HCl$.

3,4-Dihydro-2H-1,5-benzodioxepin-3-spirooxirane (6)

Procedure a

Sodium hydride (132 mg, 5.5 mmol) was suspended in dry DMSO (2 ml) and trimethyl sulfoxonium iodide (1.25 g; 5.68 mmol) was added. When H_2 evolution had abated (*ca.* 30 min), a solution of **3** (820 mg, 5 mmol) in DMSO (1.2 ml) was added dropwise and with stirring at room temperature. Stirring was continued for 2 h at 26° and then for 1 h at 50°. The mixture was poured into water (30 ml) and **6** was isolated by extraction with CH_2Cl_2 (2 × 20 ml), 456 mg (51%), m.p. 147–149° (MeOH).

Procedure b

A solution of $NaNO_2$ (6.9 g, 0.1 mol) in water (50 ml) was added slowly with stirring during ½ h to a solution of **5**·HCl (23.17 g, 0.1 mol) in water (200 ml) containing acetic acid (0.1 ml) at −4 to 0°. Then the solution was stirred at room temperature for ½ h and the crude **6** was collected, 14.84 g, m.p. 132–144°. Recrystallization of the solid from MeOH (*ca.* 450 ml) gave 11.65 g (65%) of **6**, m.p. 147–149°; ν_{max} (KBr) 1494, 1242, 1006; δ (DMSO-d_6) 6.98 (4H, s, aryl H), 4.35 and 3.99 (2H and 2H, 2d, OCH_2, J = 13 Hz), 2.89 (2H, s, oxirane H). Analyzed (C, H) for $C_{10}H_{10}O_3$.

Can. J. Chem. Downloaded from www.nrcresearchpress.com by 210.87.254.40 on 09/05/12
For personal use only.

Extraction of the aqueous filtrate with ether afforded an oil (1.3 g) that crystallized from $CHCl_3$ and was recrystallized from water to give 254 mg of **7**, m.p. 124.5–125.5°. This glycol can be obtained by hydrolyzing **6** with dilute $HClO_4$; ν_{max} (KBr) 3420, 1499, 1048; *m/e* 196 (M^+). Analyzed (C, H) for $C_{10}H_{12}O_4$.

6-Methoxy-3,4-dihydro-2H-1,5-benzodioxepin-3-spirooxirane (79)

This was prepared in 28% yield by procedure *a* above, m.p. 106–110° (MeOH) (pure **79** has m.p. 110.5–111.5°); ν_{max} (KBr) 1489, 1472, 1092, 1079; δ (DMSO-d_6) ~7.1–6.5 (3H, m, aryl H), 4.35 and 3.98 (1H and 1H, 2d, OCH_2, J = 13½ Hz), 4.30 and 3.98 (1H and 1H, 2d, OCH_2, J = 13½ Hz), 3.75 (3H, s, OCH_3), 2.89 (2H, s, oxirane H). Analyzed (C, H) for $C_{11}H_{12}O_4$.

3-t-Butylaminomethyl-3-hydroxy-3,4-dihydro-2H-1,5-benzodioxepin Hydrochloride (54)

Method F, Table 6

A mixture of **6** (1.78 g, 10 mmol), *t*-butylamine (3.2 ml, ~30 mmol), and methanol (25 ml) was stirred at room temperature for 42 h. Evaporation of the solvent, dissolution of the oily residue in ether, and treatment with excess ethanolic HCl solution afforded 3.0 g of **54**, m.p. 169–177°. Recrystallization of the crude product from isopropanol gave 2.15 g (75%) of **54**, m.p. 186.5–188°; ν_{max} (KBr) 3265, 1491, 1253, 1050; δ (DMSO-d_6) ~9.0 (2H, bs, NH_2^+), 7.03 (4H, s, aryl H), 6.37 (1H, bs, OH), 4.46 and 4.12 (2H and 2H, 2d, OCH_2, J = 6 Hz), 3.45 (2H, s, CH_2N), 1.36 (9H, s, *t*-Bu). Analyzed (C, H, Cl, N) for $C_{14}H_{21}NO_3 \cdot HCl$.

3-Formamidomethyl-3-hydroxy-3,4-dihydro-2H-1,5-benzodioxepin (77)

To a solution of **5** (5.86 g, 30 mmol) in dry ether (60 ml) was added formic acetic anhydride (9) (31.5 mmol) dropwise and the mixture was stirred overnight. The solution was washed successively with water, 10% Na_2CO_3 solution, and water. The product was not completely soluble in ether at this point: after separating the ether layer, an extraction with chloroform was performed. The combined extract yielded 6.1 g (91%) of waxy solid, used without purification in the next step.

3-Methylaminomethyl-3-hydroxy-3,4-dihydro-2H-1,5-benzodioxepin Hydrochloride (43)

Reduction of **77** (5.80 g, 26 mmol) with lithium aluminum hydride (2.0 g, 52 mmol) in dry ether (110 ml), followed by isolation of the product as the hydrochloride, gave 2.14 g (33%) of **43**, m.p. 217–219° (EtOH); ν_{max} (KBr) 3259, 1500, 1259. Analyzed (C, H, Cl, N) for $C_{11}H_{15}NO_3 \cdot HCl$.

3-Acetamidomethyl-3-hydroxy-3,4-dihydro-2H-1,5-benzodioxepin (78)

To a solution of **5** (3.20 g, 15.9 mmol) and triethylamine (1.68 g, 16.7 mmol) in dry chloroform was added dropwise acetic anhydride (1.70 g, 16.7 mmol) in dry chloroform. After 1 h at room temperature, the reaction mixture was washed with water, 3.6 *N* sulfuric acid, water, 10% Na_2CO_3 solution, and water. Evaporation of the organic layer yielded 3.41 g (89%) of **78**, m.p. 98–100° ($CHCl_3$); ν_{max} (KBr) 3312, 1635 (br), 1497. Analyzed (C, H, N) for $C_{12}H_{15}NO_4$.

3-Ethylaminomethyl-3-hydroxy-3,4-dihydro-2H-1,5-benzodioxepin Hydrochloride (44)

Reduction of **78** with lithium aluminum hydride in ether gave 47% of **44**, m.p. 181.5–183° (EtOH); ν_{max} (KBr) 3235, 1497, 1055. Analyzed (C, H, Cl, N) for $C_{12}H_{17}NO_3 \cdot HCl$.

2-Cyano-3-oxo-3,4-dihydro-2H-1,5-benzodioxepin (15)

A mixture of **2** (30.0 g, 0.16 mol), concentrated HCl (90 ml), water (90 ml), and ethanol (450 ml) was heated under reflux for 1¾ h. After evaporation of the mixture, water was added to dissolve NH_4Cl, and the product was extracted with ether (4 × 200 ml). The dried ethereal solution (Na_2SO_4 followed by $CaSO_4$) was evaporated to an oil at 50°/15 Torr and further stripping at 50°/0.1 Torr induced crystallization; 29.2 g (96%) of slightly waxy solid, m.p. 134–136° was obtained. Recrystallization of the crude material either from benzene or from diisopropyl ether containing 5% ethyl acetate gave pure **15**, m.p. 135–136°, but recovery was low; ν_{max} (KBr) 1752, 1489, 1260; no ν CN. Analyzed (C, H, N) for $C_{10}H_7NO_3$.

2-Cyano-2-methyl-3-oxo-3,4-dihydro-2H-1,5-benzodioxepin (16)

To a warm, stirred, solution of **15** (7.95 g, 42 mmol) in benzene (80 ml) was added a solution of thallous ethoxide (10.0 g, 40 mmol) in benzene (40 ml). After 30 min, the solid was collected, washed with benzene, and added to methyl iodide (60 ml). The suspension was heated under reflux for 6 h, filtered, and evaporated to an oil (8.2 g). Chromatography of the oil on 480 g of Baker 3405 silica gel by the dry column technique (10) gave 1.07 g (12%) of enol ether (**17**) as an oil; ν_{max} (neat) 2208 (medium intensity), 1650, 1495, 1240; δ (CCl_4), ~7.1–6.75 (4H, m, aryl H), 4.77 (2H, s, CH_2), 3.97 (3H, s, OCH_3).

The cyano ketone **16** was obtained as a low-melting solid, 5.71 g (67%), m.p. 71–72° ($CHCl_3$–CCl_4); ν_{max} (KBr) 2245 (very small), 1760, 1495, 1251; δ (CCl_4) 6.98 (4H, s, aryl H), 4.70 and 4.65 (2H, 2s, OCH_2), 1.86 (3H, s, CH_3). Analyzed (C, H, N) for $C_{11}H_9NO_3$.

2-Methyl-3-oxo-3,4-dihydro-2H-1,5-benzodioxepin (18)

Hydrolysis of **16** by method *B*, Table 3, gave **18** in 67% yield; ν_{max} (KBr) 1750, 1495, 1265; δ (CCl_4) 6.89 (4H, s, aryl H), 4.95 (1H, quartet, OCH, J = 6½ Hz), 4.76 and 4.40 (2H, 2d, OCH_2, J = 15 Hz), 1.43 (3H, d, CH_3, J = 6½ Hz).

Anal. Calcd. for $C_{10}H_{10}O_3$: H, 5.66. Found: H, 6.09.

3-t-Butylaminomethyl-3-hydroxy-2-methyl-3,4-dihydro-2H-1,5-benzodioxepin Oxalate (20)

On treating **18** (891 mg, 5 mmol) with dimethyl sulfoxonium methylide as described in procedure *a*, there was obtained a very crude product from which **19** could not be isolated. The crude product (672 mg) in methanol (10 ml) was treated with *t*-butylamine (1 ml) and the mixture was allowed to stand for 5 days, then evaporated to dryness. The residue was treated with CH_2Cl_2 (25 ml) and extracted with *N* HCl (10 ml + 5 ml). The acid extract was washed with CH_2Cl_2 (10 ml) and with ether (20 ml); then it was basified with 5 *N* NaOH solution (5 ml) and extracted with ether (2 × 20 ml), giving **20** (free base) as a colorless gum, 119 mg (9%). This material appeared to be homogeneous by t.l.c. but some impurity was evident in the n.m.r. spectrum; δ ($CDCl_3$) ~7.0–6.95 (4H, m,

Can. J. Chem. Downloaded from www.nrcresearchpress.com by 210.87.254.40 on 09/05/12
For personal use only.

aryl H), 4.32–3.97 (3H, m, OCH and OCH_2), 1.33 (3H, d, CH_3, J = 6 Hz), 1.10 (9H, s, *t*-Bu). The CH_2N signal was obscured by impurity. The base was treated with oxalic acid to give **20**, m.p. 229–230° dec. (*i*-PrOH). Analyzed (C, H, N) for $C_{15}H_{23}NO_3 \cdot (COOH)_2$.

*3'-Isopropyl-3,4-dihydro-2H-1,5-benzodioxepin-3-spiro-5'-oxazolidin-2'-one (**10**)*

To a stirred solution of phosgene (15.5 g, 0.157 mol) in chloroform (100 ml) cooled to 5–8° was added dropwise a solution of **9** (24.8 g, 0.105 mol) in chloroform (100 ml). The resulting suspension was treated dropwise with triethylamine (44.7 ml, *ca.* 0.32 mol) at 5–8° and then the reaction mixture was stirred for 1 h at room temperature before being poured into water (200 ml). The chloroform layer was separated and washed in succession with 10% HCl (25 ml), water (25 ml), 5% NaOH solution (25 ml), and water (2 × 25 ml). The solution was dried ($MgSO_4$) and evaporated to give a solid, which was recrystallized from carbon tetrachloride (90 ml) to yield 23.1 g (84%) of **10**, m.p. 118–120° (pure **10** has m.p. 121–122° (*i*-Pr_2O)); ν_{max} (KBr) 1721, 1263, 1051; δ (DMSO-d_6) 6.98 (4H, s, aryl H), 4.25 (4H, s, OCH_2), 3.90 (1H, septet, methine, J = 6½ Hz), 3.43 (2H, s, CH_2N), 1.13 (6H, d, CH_3, J = 6½ Hz). Analyzed (C, H, N) for $C_{14}H_{17}NO_4$.

*3'-Isopropyl-7-nitro-3,4-dihydro-2H-1,5-benzodioxepin-3-spiro-5'-oxazolidin-2'-one (**11**)*

A solution of **10** (24.8 g, 94.2 mmol) in acetic acid (100 ml) was cooled to the freezing point in an ice bath and a mixture of 90% HNO_3 and concentrated H_2SO_4 (54 ml containing 1.2 ml of HNO_3 (*d* 1.5) to each 10 ml of H_2SO_4) was added dropwise with stirring over 10 min. The mixture was stirred for 2 h at 26° and poured into water (400 ml). The crude product was taken up in methylene chloride (3 × 100 ml) and the extract was washed with water (100 ml), 10% Na_2CO_3 (75 ml), water (100 ml), and dried ($MgSO_4$). Evaporation of the solvent and recrystallization of the residue twice from alcohol afforded 16.4 g (56%) of **11** which was used in the next stage (pure **11** has m.p. 148–148.5° (alcohol)); ν_{max} (KBr) 1746, 1357, 1040; δ (DMSO-d_6) ~7.97–7.78 and 7.25–7.11 (2H and 1H, 2m, aryl H), 4.42 and 4.38 (2H and 2H, 2s, OCH_2), 3.89 (1H, septet, methine, J = 6½ Hz), 3.46 (2H, s, CH_2N), 1.12 (6H, d, CH_3, J = 6½ Hz). Analyzed (C, H, N) for $C_{14}H_{16}N_2O_6$.

*7-Amino-3'-isopropyl-3,4-dihydro-2H-1,5-benzodioxepin-3-spiro-5'-oxazolidin-2'-one (**12**)*

A mixture of **11** (960 mg, 3.12 mmol), ethanol (30 ml), and 5% palladium-on-charcoal was hydrogenated at 50 p.s.i. and 26° in a Parr apparatus. Work-up of the reaction mixture afforded 445 mg (51%) of **12**, m.p. 163–164° (alcohol); ν_{max} (KBr) 3450, 3360, 1745, 1510; δ (DMSO-d_6) ~6.78–6.60 and 6.25–6.07 (1H and 2H, 2m, aryl H), 4.79 (2H, s, NH_2), 4.13 and 4.05 (2H and 2H, 2s, OCH_2), 3.88 (1H, septet, methine, J = 6½ Hz), 3.36 (2H, s, CH_2N), 1.10 (6H, d, CH_3, J = 6½ Hz). Analyzed (C, H, N) for $C_{14}H_{18}N_2O_4$.

*7-Hydroxy-3'-isopropyl-3,4-dihydro-2H-1,5-benzodioxepin-3-spiro-5'-oxazolidin-2'-one (**13**)*

A solution of **12** (3.27 g, 11.75 mmol) in 10% H_2SO_4 (65 ml) was diazotized at 0–5° with 20% $NaNO_2$ solution (4.05 ml, 11.75 mmol). After stirring the mixture for 30 min at room temperature, a little urea was added to destroy excess HNO_2 (starch iodide paper as indicator) and the solution was poured into a well-stirred suspension of Baker 3405 silica gel (15 g) in boiling 10% H_2SO_4 (130 ml) during a period of 10 min. The mixture was stirred at the b.p. until a negative alkaline β-naphthol test was obtained (*ca.* 30 min). When cool, the solid was collected, washed with a little water, and dried. The solid was suspended in boiling alcohol (100 ml) and then evaporated to dryness in a rotary evaporator. It was placed on top of a column (18 × 1¼ in.) of Baker silica gel and chromatography was carried out by the dry column technique using 1:1 ether–chloroform. The first 300 ml of eluate contained 1.62 g of crude **13**, which on recrystallization from alcohol (20 ml) afforded 1.41 g of **13** of m.p. 215–217° (pure **13** separates from alcohol in prisms, m.p. 216.5–217.5°); ν_{max} (KBr) 3260 (br), 1710, 1507, 1060, 1051; δ (DMSO-d_6) ~7.02–6.75 and 6.52–6.3 (1H and 2H, 2m, aryl H), 4.17 and 4.13 (2H and 2H, 2s, OCH_2), 3.91 (1H, septet, methine, J = 6½ Hz), 3.39 (2H, s, CH_2N), 1.12 (6H, d, CH_3, J = 6½ Hz). Analyzed (C, H, N) for $C_{14}H_{17}NO_5$.

*3-Hydroxy-3-isopropylaminomethyl-7-nitro-3,4-dihydro-2H-1,5-benzodioxepin (**21**)*

A mixture of **11** (7.98 g, 25.9 mmol), dioxane (60 ml), and 45% KOH solution (16 ml) was heated in a N_2-filled stainless steel bomb at 150–160° for 16 h. When cool, the reaction mixture was extracted with ether (2 × 100 ml) and the extract was washed with saturated NaCl solution (2 × 100 ml) and then with water (100 ml). The ethereal solution was extracted with 2.75 *N* HCl (40 ml) and then with water (2 × 40 ml). Basification of the combined aqueous extract with 2.5 *N* NaOH (70 ml) and extraction with ether (2 × 100 ml), afforded a yellow solid, 6.33 g, m.p. 95–96.5°. Recrystallization of the crude product from diisopropyl ether (63 ml) gave 4.56 g (62%) of **21**, m.p. 97.5–99°; ν_{max} (KBr) 3295, 3080, 1520, 1290, 1275; δ (DMSO-d_6) ~7.90–7.74 and 7.17–7.0 (2H and 1H, 2m, aryl H), 4.23 and 3.56 (2H and 2H, 2s, OCH_2), 2.79 (2H, s, CH_2N), 0.9 (6H, d, CH_3, J = 6½ Hz). The signal for the methine proton was largely obscured by the CH_2—N and DMSO signals, and the OH and NH gave a broad signal centered on 3.5 p.p.m. Analyzed (C, H, N) for $C_{13}H_{18}N_2O_5$.

*7-Amino-3-isopropylaminomethyl-3-hydroxy-3,4-dihydro-2H-1,5-benzodioxepin (**49**)*

Hydrogenation of **21** (1.5 g, 5.32 mmol) in ethanol (25 ml) at 40 p.s.i. and room temperature in the presence of 5% palladium-on-charcoal (400 mg) gave 990 mg (74%) of **49**, m.p. 96.5–97.5° (benzene); ν_{max} (KBr) 3440, 3358, 1513, 1225, 1067; δ ($CDCl_3$) 6.78–6.63 and 6.35–6.12 (1H and 2H, 2m, aryl H), 4.03 and 3.77 (2H and 2H, 2s, OCH_2), 3.32 (4H, bs, OH, NH and NH_2), 2.91 (2H, s, CH_2N), 2.76 (1H, septet, methine, J = 6 Hz), 1.05 (6H, d, CH_3, J = 6 Hz). Analyzed (C, H, N) for $C_{13}H_{20}N_2O_3$.

*3,7-Dihydroxy-3-isopropylaminomethyl-3,4-dihydro-2H-1,5-benzodioxepin (**14**)*

A mixture of **13** (200 mg, 0.716 mmol), $Ba(OH)_2 \cdot 8H_2O$ (1.08 g, 3.42 mmol), and water (3.2 ml) in an evacuated glass pressure tube was heated at 160–165° for 16 h. The reaction mixture was poured into boiling water (60 ml) with stirring and CO_2 was passed through, until all Ba^{2+} ions had been precipitated. The suspension was filtered

Can. J. Chem. Downloaded from www.nrcresearchpress.com by 210.87.254.40 on 09/05/12
For personal use only.

through Celite and evaporated to a pale brown scale (187 mg). This solid was chromatographed by the dry column technique on Baker 3405 silica gel using 3% methanol in ether as the solvent, affording 70.5 mg (39%) of **14** as the second component to be eluted. After drying in air at 60° the solid has m.p. 108–110° but drying at 80° (0.1 Torr) raises the m.p. to 133–134.5° (pure **14** had m.p. 133.5–135° (benzene)); ν_{max} (KBr), for solid of m.p. 108–110°, 3465, 3360, 3300, 3285, 1510, 1209, 1158; ν_{max} (KBr), for solid of m.p. 133.5–135°, 3450–3260 (v br), 1509, 1470, 1155; δ (CD_3CN) ~6.79–6.61 and 6.36–6.19 (1H and 2H, 2m, aryl H), 4.0 (5H, superimposed singlets, OH, NH, OCH_2), 3.54 (2H, s, OCH_2), 2.84 (2H, s, CH_2N), 2.72 (1H, septet, methine, J = 6 Hz), 1.02 (6H, d, CH_3, J = 6 Hz). Analyzed (C_9H, N) for $C_{13}H_{19}NO_4$.

3,6-Dihydroxy-3-isopropylaminomethyl-3,4-dihydro-2H-1,5-benzodioxepin Hydrobromide (51)

A solution of **50** free base (600 mg, 2.24 mmol) in 48% HBr (10 ml) was heated under reflux for 10 h, then evaporated to dryness at 50–55° (10 Torr). A solution of the residue in alcohol was treated with charcoal, filtered, and evaporated to dryness. Recrystallization of the solid from methanol – ethyl acetate yielded 596 mg (80%) of **51**, m.p. 193–195° (pure **51** has m.p. 196–197° (MeOH–EtOAc)); ν_{max} (KBr) 3430, 3350 (both broad), 1485, 1224, 1059. Analyzed (C, H, Br, N) for $C_{13}H_{19}NO_4 \cdot HBr$.

3-Hydroxy-3-(1-nitroethyl)-3,4-dihydro-2H-1,5-benzodioxepin (80)

Nitroethane (6.32 ml, 88 mmol) was added to a mechanically stirred slurry of potassium *t*-butoxide (8.98 g, 80 mmol) in dry ether (165 ml). To the thick suspension, cooled below 10°, was added a solution of **3** (13.12 g, 80 mmol) in ether (40 ml) slowly over ½ h. After 3 h at room temperature, the reaction mixture was acidified with acetic acid (4.80 g, 80 mmol) in dry ether (40 ml); more ether (500 ml) was added and the mixture filtered. Evaporation of the filtrate gave 16.1 g (83%) of crude **80** used in the next stage.

3-(1-Aminoethyl)-3-hydroxy-3,4-dihydro-2H-1,5-benzodioxepin Hydrochloride (38)

Method D, Table 5

Crude **80** (16.1 g, 67.3 mmol) in ethanol (100 ml) was hydrogenated in a Parr low pressure hydrogenerator in the presence of 5% palladium-on-charcoal. Hydrogen uptake was about 85% of theory. After filtration and evaporation, the crude product was taken up in ether (125 ml) and extracted with 5 *N* HCl (3 × 15 ml). Basification (20% NaOH solution) of the acid extract and extraction with ether gave an oil which was converted to a hydrochloride salt with HCl in ethanol; 6.0 g (36%) of crude **38** m.p. 192–203° was obtained. Upon recrystallization from ethanol the m.p. was raised to 204–206°; ν_{max} (KBr) 3300, 1492, 1251, 1040, 751; δ (DMSO-d_6) 6.84 (4H, s, aryl H), 4.52 and 4.33 (2H, 2d, OCH_2, J = 12½ Hz), 4.10 and 4.06 (2H, 2d, OCH_2, J = 12½ Hz), 3.60 (1H, quartet, methine, J = 7 Hz), 1.37 (3H, d, CH_3, J = 7 Hz). Analyzed (C, H, Cl, N) for $C_{11}H_{15}NO_3 \cdot HCl$.

3-Hydroxy-3-(1-nitropropyl)-3,4-dihydro-2H-1,5-benzodioxepin (81)

Compound **81** was prepared from **3** and 1-nitropropane by the method described for **80** and was used without purification.

3-(1-Aminopropyl)-3-Hydroxy-3,4-dihydro-2H-1,5-benzodioxepin Hydrochloride (39)

Hydrogenation of **81** at atmospheric pressure in the presence of Raney nickel yielded 31% of **39**, m.p. 197–198°; ν_{max} (KBr) 3305(b), 1502, 1267, 1050, 770. Analyzed (C, H, Cl, N) for $C_{12}H_{17}NO_3 \cdot HCl$.

3-Dimethylaminomethyl-3-hydroxy-3,4-dihydro-2H-1,5-benzodioxepin Hydrochloride (75)

A mixture of **5** free base (3.20 g, 16.4 mmol), 88% formic acid (43 g), and 37% formalin (3.0 ml) was heated under reflux for 17 h. Basification of the reaction mixture with 20% NaOH (10 ml) and extraction with ether (2 × 50 ml) afforded an oil (3.4 g) which was converted to a hydrochloride salt, 2.84 g, m.p. 119–230°. The crude product was recrystallized twice from isopropanol to give 1.64 g (38%) of **75**, m.p. 118–120°, clearing at *ca.* 210°; ν_{max} (KBr) 3225(br), 1501, 1260, 761. Analyzed (C, H, Cl, N) for $C_{12}H_{17}NO_3 \cdot HCl$.

3'-Isopropyl-7-nitro-2'-phenyl-3,4-dihydro-2H-1,5-benzodioxepin-3-spiro-5'-oxazolidine (22)

A mixture of **21** (1.41 g, 5 mmol), benzaldehyde (530 mg, 5 mmol), acetic acid (1 drop), and isopropanol (10 ml) was distilled slowly and isopropanol was added to keep the volume constant. After 3 h, the mixture was set aside at 5° overnight. The product was collected and recrystallized from isopropanol, giving 620 mg of solid, m.p. 151–152°. Further distillation of the mother liquors and work-up as before gave another 490 mg of product, m.p. 150–151° (for a total of 60%) and 430 mg (30%) of **21** was recovered (pure **22** has m.p. 152.5–153.5°); ν_{max} (KBr) 1522, 1347, 1282; δ ($CDCl_3$) 7.95–7.5 (2H, m, aryl H), 7.42 (5H, s, phenyl), 7.03–6.85 (1H, dd, aryl H), 4.88 (1H, s, OCHN), 4.51 (2H, s, OCH_2), 4.07 (1H, dd, 1H of OCH_2, J = 11 Hz, J' = 2 Hz), 3.63 (1H, d, 1H of OCH_2), 3.23 (1H, dd, 1H of CH_2N, J = 10½ Hz, J' = 2 Hz), ~2.75 (1H, septet, methine, J = 7 Hz), 2.68 (1H, d, 1H of CH_2N, J = 10½ Hz), 0.98 (3H, d, CH_3, J = 7 Hz), 0.84 (3H, d, CH_3, J = 7 Hz). The two doublets for CH_3 overlap to form a triplet.[5] Analyzed (C, H, N) for $C_{20}H_{22}N_2O_5$.

7-Amino-3'-isopropyl-2'-phenyl-3,4-dihydro-2H-1,5-benzodioxepin-3-spiro-5'-oxazolidine (23)

A solution of **22** (92.5 mg, 0.25 mmol) in ethyl acetate (5 ml) was hydrogenated at atmospheric pressure in the presence of 5% palladium-on-charcoal (20 mg) until the theoretical amount of hydrogen had been absorbed. Work-up afforded 104 mg of oil. The product was too labile for purification but t.l.c. (silica gel – $CHCl_3$) showed the presence of a trace of **22** as the only impurity in the product.

3-Hydroxy-3-isopropylaminomethyl-7-methanesulfonamido-3,4-dihydro-2H-1,5-benzodioxepin Oxalate (25)

Crude **23** (352 mg, obtained from **22** (376 mg, 1.015 mmol)) was dissolved in dry ether and 1,4-diazabicyclo-

[5]The long-range coupling of one of the dioxepin protons with one of the oxazolidine protons (due to a W arrangement) gives an insight into the conformation of the spiro-fused ring system. This spectrum was recorded at the 220 MHz NMR Centre, Sheridan Park, Ontario.

[2.2.2]octane (118 mg, 1.065 mmol) was added. Methanesulfonyl chloride (105 mg, 1.065 mmol) in dry ether (5 ml) was added dropwise with stirring, and after 1 h the solid was filtered off and discarded. Evaporation of the filtrate afforded crude **24**, 387 mg (91%). Thin-layer chromatography on Eastman silica gel showed the presence of one major and two minor constituents but preparative t.l.c. on a 2-mm silica gel plate did not give a good separation, possibly because of hydrolysis of the product. The crude material from the plate (227 mg, 0.54 mmol) in methanol (3 ml) was treated with oxalic acid dihydrate (70 mg, 0.55 mmol) and the solution was chilled thereby yielding 108 mg (47%) of **25**, m.p. 207–209° dec. (pure **25** has m.p. 214–215° dec.); ν_{max} (KBr) 1500, 1315, 1146; m/e = 330 (M^+).

Anal. Calcd. for $C_{14}H_{22}N_2O_5S\cdot(COOH)_2$: C, 45.70. Found: C, 45.08.

The authors would like to express their thanks to Drs. J. G. Atkinson and C. H. Yates for their advice on various aspects of the chemistry contained in this paper, to Dr. N. N. Share, Mr. R. A. Hall, and (in part) to Drs. R. Robson and H. M. Guirgis and their colleagues for the biological results, to Mr. S.-C. Ho and his colleagues for n.m.r. spectral data, and particularly to Mrs. Evelyn Robbins for her substantial contribution to the synthetic work.

1. V. Rosnati and F. De Marchi. Tetrahedron, **18**, 289 (1962).
2. (*a*) A. W. Archer, P. A. Claret, and D. F. Hayman. J. Chem. Soc. B, 1231 (1971). (*b*) J. J. Beereboo, D. P. Cameron, and C. R. Stephens. U.S. Patent No. 3,517,031. (*c*) W. Schroth and B. Werner. Z. Chem. **10**, 382 (1970).
3. E. C. Taylor and A. McKillop. J. Am. Chem. Soc. **90**, 2421 (1968); Acc. Chem. Res. **3**, 338 (1970).
4. A. M. Lands and T. G. Brown, Jr. *In* Drugs affecting the peripheral nervous system. *Edited by* A. Burger. Dekker, New York. 1967. pp. 431–440.
5. R. Howe, B. S. Rao, and M. S. Chodnekar. J. Med. Chem. **13**, 169 (1970).
6. (*a*) B. M. Bloom and I. M. Goldman. Adv. Drug Res. **3**, 121 (1966). (*b*) R. T. Brittain, D. Jack, and A. C. Ritchie. Adv. Drug Res. **5**, 243 (1970).
7. A. A. Larsen. Nature, **224**, 25 (1969).
8. S. Baldwin. J. Org. Chem. **26**, 3288 (1961).
9. W. Stevens and A. Van Es. Rec. Trav. Chim. **83**, 1287. (1964); 1294 (1964).
10. B. Loev and M. M. Goodman. Chem. Ind. 2026 (1967).
11. D. Hartley, D. Jack, L. H. C. Lunts, and A. C. Ritchie. Nature, **219**, 861 (1968).
12. M. Rodbell. J. Biol. Chem. **239**, 375 (1964).
13. E. Korn. J. Biol. Chem. **215**, 1 (1955).

Can. J. Chem. Downloaded from www.nrcresearchpress.com by 210.87.254.40 on 09/05/12
For personal use only.

Effect of the *N*-Phenyl Substituent on the Pyrolyses of 1-Phenyl-2-benzothiazolinone and 1-Phenyl-2-benzothiazolinethione

DENIS C. K. LIN, MICHAEL L. THOMSON, AND DON C. DEJONGH[1]

Département de chimie, Université de Montréal, Montréal, Québec H3C 3V1

Received February 5, 1975

DENIS C. K. LIN, MICHAEL L. THOMSON, and DON C. DEJONGH. Can. J. Chem. **53**, 2293 (1975).

Results from the pyrolyses of 1-phenyl-2-benzothiazolinone (**7**) and 1-phenyl-2-benzothiazolinethione (**8**) are reported and compared with those obtained previously from the corresponding compounds without the *N*-phenyl group. The mass spectra of **7** and **8** are reported, also. The major fragmentation in the mass spectrum of **7** is the loss of CO, followed by loss of S or H·. Pyrolysis of **7** at 750° in a stream of nitrogen gives phenothiazine (**9**, 31%) and carbazole (**10**, 28%), by loss of CO and of CO and S, respectively. Pyrolysis of **9** yields **10**. The major fragmentation in the mass spectrum of **8** is the loss of H·. Pyrolysis of **8** at 750° produces 2-(phenylthio)benzothiazole (**11**, 87%), which is an isomer of **8**, resulting from phenyl migration, and 2-phenylbenzothiazole (**12**, 3%). Pyrolysis of **11** gives **12**.

DENIS C. K. LIN, MICHAEL L. THOMSON et DON C. DEJONGH. Can. J. Chem. **53**, 2293 (1975).

On rapporte les produits de pyrolyse de la phényl-1 benzothiazolinone-2 (**7**) et de la phényl-1 benzothiazolinethione (**8**) et on compare ces résultats avec ceux obtenus et déjà rapportés, des composés sans le groupe phényle. On rapporte aussi les spectres de masse des composés **7** et **8**, tel qu'obtenus par impact électronique. Le patron majeur de fragmentation trouvé dans le spectre de masse du composé **7** résulte de la perte de CO, suivie par perte de S ou de H·. La pyrolyse du composé **7** à 750° dans un courant d'azote conduit à la formation de phénothiazine (**9**, 31%) et de carbazole (**10**, 28%), par perte de CO et de CO et S. La pyrolyse du composé **9** rend le composé **10**. Dans le spectre de masse du composé **8**, le pic de base se forme par perte de H·. Les produits de la pyrolyse du composé **8** à 750° sont le phénylthio-2 benzothiazole (**11**, 87%), qui est un isomère du composé **8** dû à la migration d'un groupe phényle, et le phényl-2 benzothiazole (**12**, 3%). Le composé **11** résulte de la pyrolyse du composé **12**.

Introduction

We have reported the mass spectra and pyrolyses of a number of molecules related to the general *o*-phenylene structure **1**. For example, in the case of *o*-phenylene sulfite (a, b, d = O; c = S), the first molecule eliminated is SO (1, 2), whereas in the case of *o*-phenylene carbonate (a, b, d = O; c = C), the major fragmentation pathway involves elimination of CO_2 (3, 4).

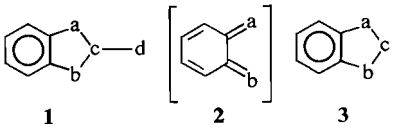

1 **2** **3**

Two other series of compounds described by **1** which we have studied are the 2-ones (d = O) (5) and 2-thiones (d = S) (6) of benzothiazole (a = NH; b = S; c = C), benzimidazole (a = NH; b = NH; c = C), and benzoxazole (a = NH; b = O; c = C). The decompositions of the 2-ones proceed by an elimination of CO giving, initially, intermediate **2** from which the final products form. However, the 2-thiones behave differently: the major products result from desulfurization, yielding compounds of the general structure **3**. Since the products of desulfurization of the 2-thiones are stable molecules (**3**), whereas the primary products (**2**) from the decarbonylation of the 2-ones are unstable under the reaction conditions, the yields from the pyrolyses are much higher in the first case, 40–80% *vs.* 14–23%.

We were able to trap intermediate **2** internally in the pyrolysis of benzimidazolinone (**4**) by placing a phenyl group on one of the nitrogens, in place of hydrogen (7). In the pyrolysis of **4** at 1000°, we recovered 10.2% of starting material and we isolated 14% of $C_6H_4N_2$ isomers, as shown in eq. 1 (5). However, when 1-phenyl-2-

[1]To whom correspondence should be addressed at Case postale 6210, Succursale A, Montréal, Québec H3C 3V1.

Can. J. Chem. Downloaded from www.nrcresearchpress.com by 210.87.254.40 on 09/05/12
For personal use only.

Can. J. Chem. Downloaded from www.nrcresearchpress.com by 210.87.254.40 on 09/05/12
For personal use only.

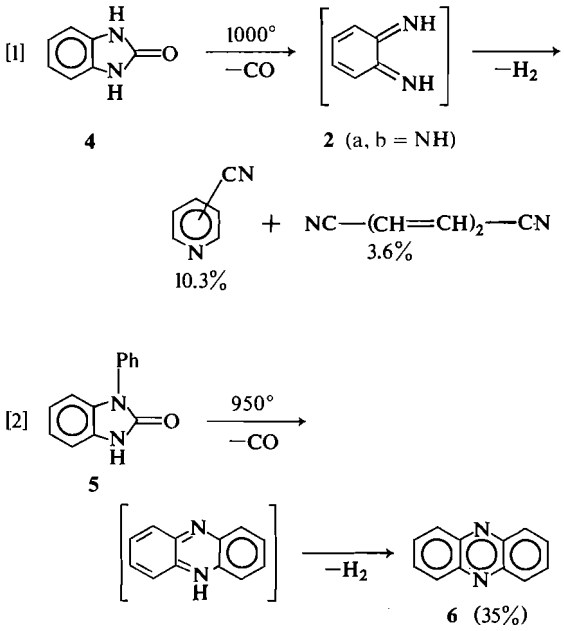

benzimidazolinone (**5**) was pyrolyzed at 950°, 16.3% of **5** was recovered and the major product isolated was phenazine (**6**), as shown in eq. 2 (7). Carbazole was also isolated from the pyrolysis of **5**, in 14% yield. Thus, the *o*-quinoid intermediate cyclized, giving phenazine.

The pyrolysis of 2-benzothiazolinone (**1**, a = NH; b = S; c = C; d = O) presented a special problem (5): no products were isolated that could be related to intermediate **2** (a = NH; b = S). This is probably due to the fact that sulfur is retained and the loss of CO followed by HCN gives products such as cyclopentadienethione which polymerize.

The object of this report is to present results obtained from the study of 1-phenyl-2-benzothiazolinone (**7**) and 1-phenyl-2-benzothiazolinethione (**8**). These results are compared with those obtained from the corresponding molecules without the *N*-phenyl group.

Pyrolyses were performed by sublimation of the samples into a stream of nitrogen which passed through an unpacked quartz tube surrounded by a furnace (8). In general, a flow rate of 0.25 l/min and a system pressure of approximately 1 Torr were used. The pyrolysis of each compound was repeated several times at the same temperature; however, the pyrolyses were first performed at various temperatures to find the one at which the best results were obtained. Where possible, products were isolated and identified by physical and spectroscopic characteristics.

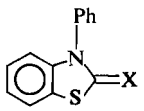

7 X = O
8 X = S

Results

1-Phenyl-2-benzothiazolinone (7)

The 70-eV mass spectrum of **7** is summarized in Scheme 1. The peak at *m/e* 198 is the base peak at 70 eV. At voltages lower than 20 eV the molecular ion forms the base peak at *m/e* 227. The only other ions present at 15 eV are found at *m/e* 199 (19), 198 (9.5), and 167 (0.8). These ions can still be observed at 10 eV with relative intensities of 16, 8, and 0.6%, respectively.

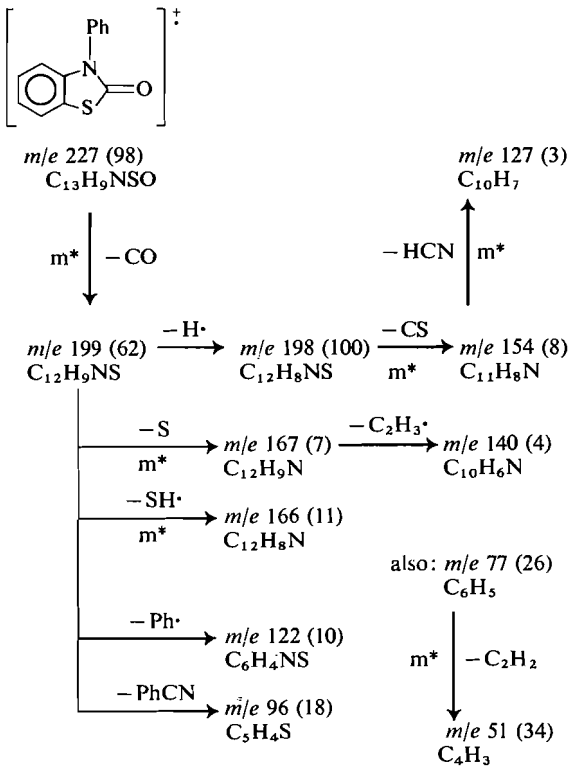

SCHEME 1[2]

[2]The elemental compositions are the result of exact-mass measurements. The values in parentheses are relative intensities and m* denotes the presence of a metastable peak.

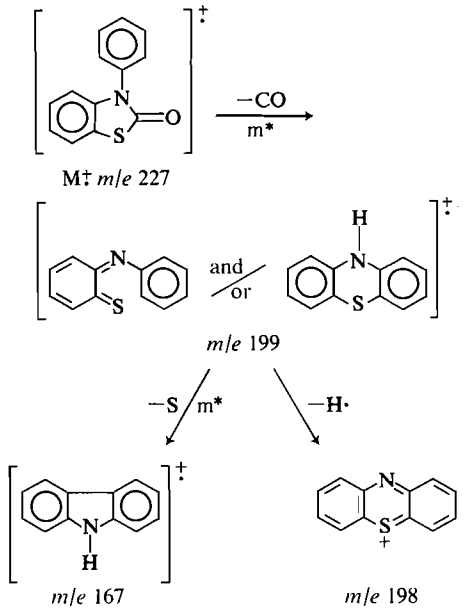

SCHEME 2

The formation of these ions can be rationalized as illustrated in Scheme 2. One of the structures proposed for *m/e* 199 is that of phenothiazine (**9**). The other has the basic *o*-quinoid structure (**2**). The ions at *m/e* 167 and 198 are formed from *m/e* 199 by the loss of S and H·, respectively. The structure shown for the ion at *m/e* 167 corresponds to ionized carbazole (**10**).

Compound **7** was pyrolyzed at 650, 750, 850, and 950°. At 750°, the two major products were **9** and **10** and the yield of each compound, based on the unrecovered starting material, is given in eq. 3. At 650°, the only product formed was phenothiazine (**9**), with 90.0% of **7** being recovered. From the pyrolyses at 850°, neither

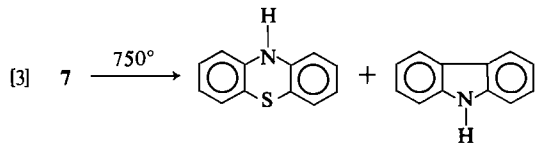

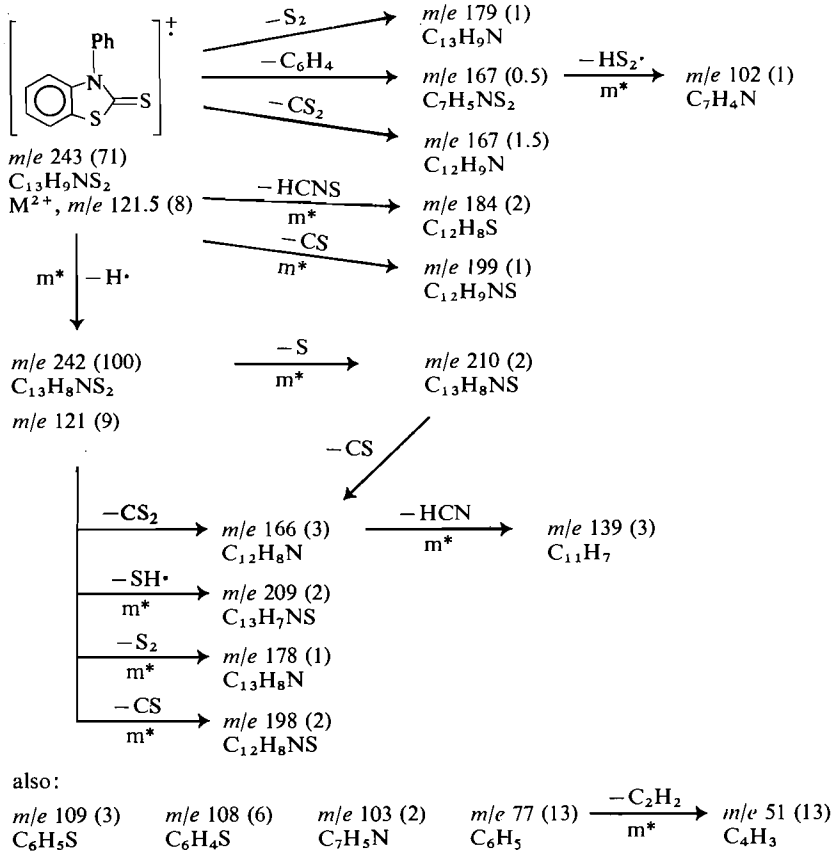

SCHEME 3[2]

Can. J. Chem. Downloaded from www.nrcresearchpress.com by 210.87.254.40 on 09/05/12
For personal use only.

Can. J. Chem. Downloaded from www.nrcresearchpress.com by 210.87.254.40 on 09/05/12
For personal use only.

7 nor **9** was isolated; the only product found was **10**. At an even higher temperature, 950°, the percentage of material accounted for was reduced and the only product was carbazole (**10**).

These results indicate that upon pyrolysis, as upon electron impact, the initial decomposition of **7** is the loss of CO which, in turn, is followed by the loss of S. To test this possibility, we pyrolyzed **9** at 650, 750, and 850°. Only starting material was recovered at 650°. However, at 750° carbazole (**10**) was formed in 38% yield, based on unrecovered starting material. No starting material was recovered at 850° and **10** was isolated in 57% yield.

In summary, the major fragmentation in the mass spectrum of **7** consists of the loss of CO from the molecular ion, followed by the loss of S or H·. Pyrolysis of **7** at 750° results in the formation of phenothiazine (**9**) and carbazole (**10**) by the loss of CO and of CO and S, respectively. Carbazole is a pyrolysis product of phenothiazine.

1-Phenyl-2-benzothiazolinethione (8)

The 70-eV mass spectrum of **8** is summarized in Scheme 3. At ionizing voltages ranging from 70 to 10 eV, the molecular ion and $(M - H\cdot)^+$ ion dominate the spectrum. At 70 eV they account for 52% of the total ion current. All the other ions in the spectrum are of much lower intensity; however, many of them persist at reduced ionizing voltages. For example, at 10 eV ions are still found at *m/e* 243 (100), 242 (50), 210 (0.3), 209 (trace), 199 (0.2), 198 (trace), 184 (0.1), 179 (0.2), 167 (0.5), 166 (trace), and 103 (0.7).

The formation of the most prominent fragment ion, at *m/e* 242, can be visualized as shown in eq. 4. The formation of most of the other fragment ions can be explained by losses of H·, S, S_2, CS, and HCN or combinations of these, from the major ions. It is interesting to note that one of the members of the doublet at *m/e* 167 has the composition $C_7H_5NS_2$. This is either due to the loss of C_6H_4 from the molecular ion of **8** or it could result from the presence of an impurity. However, we attempted to detect 2-benzothiazolinethione, a possible impurity of formula $C_7H_5NS_2$, in the sample of **8** but were unsuccessful. Moreover, the molecular ion of 2-benzothiazolinethione loses S_2 (6), whereas loss of $HS_2\cdot$ occurs from the ion at *m/e* 167 (both with appropriate metastable peaks).

[4]

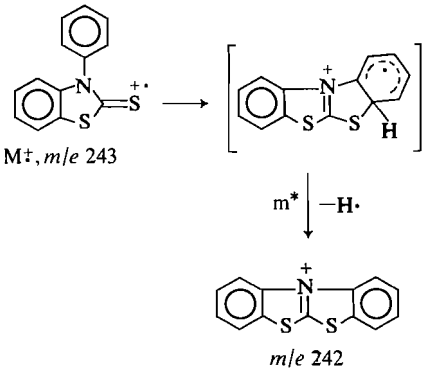

Pyrolyses of compound **8** were performed at 650, 750, 850, and 950°. At 650°, other than starting material, a trace of 2-(phenylthio)-benzothiazole (**11**) was found. At 750°, there were two products, **11** and 2-phenylbenzothiazole (**12**); the yield of each product, based on unrecovered starting material, is given in eq. 5. At 850°, the yield of **11** decreased to 60%

[5]

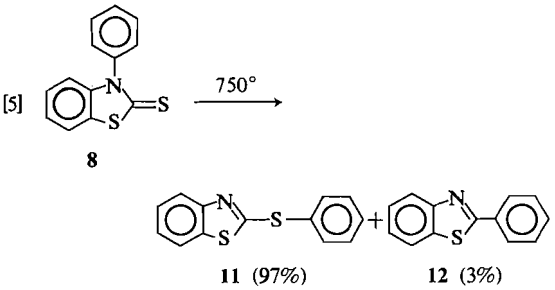

while that of **12** increased to 10%. At this temperature there were other products, 2-cyanophenyl phenyl sulfide, dibenzothiophene, phenyl sulfide, benzothiazole, and cyanobenzene. The total percentage of starting material accounted for was 82.4%. At 950° this percentage dropped to 43.6% the two major products being **12** and cyanobenzene. Two other minor products were isolated at 950°: 2-cyanobiphenyl and biphenyl. Traces of cyanodibenzothiophene, carbazole, and acridine were present, also.

Since the yield of **11** drops off with increasing temperature and the yields of the secondary products increase, we pyrolyzed **11** to demonstrate that it was the precursor of **12** and of the minor products. At 850°, 11% of **11** was recovered and the major products were cyanobenzene (10.5%) and 2-phenylbenzothiazole

Can. J. Chem. Downloaded from www.nrcresearchpress.com by 210.87.254.40 on 09/05/12
For personal use only.

(**12**, 10%). The minor products were 2-cyanophenyl phenyl sulfide (4%), dibenzothiophene (1%), phenyl sulfide (2%), benzothiazole (3%), and a trace of 2-cyanobiphenyl. Therefore, we can conclude that **12** is a pyrolysis product of **11**, although we cannot exclude the possibility that **12** also forms directly from **8**.

Upon pyrolysis at 950°, 2-phenylbenzothiazole (**12**) can be recovered almost quantitatively. The only other compound present is cyanobenzene, in trace amounts.

In summary, the 70-eV mass spectrum of **8** contains many fragment ions but is dominated by the $M^{+\cdot}$ and $(M - H\cdot)^+$ ions. Pyrolysis of **8** at 750° produces two products due to phenyl rearrangement: 2-(phenylthio)benzothiazole (**11**) and 2-phenylbenzothiazole (**12**). The latter is also a pyrolysis product of the former.

Discussion

In the 15-eV mass spectrum of 2-benzothiazolinethione (**1**, a = NH; b and d = S; c = C), the elimination of S is the only fragmentation observed, eq. 6 (6). Sulfur is also lost when this

[6] 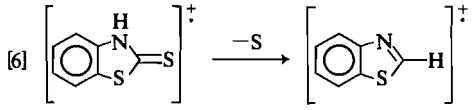

m/e 167 *m/e* 135

compound is pyrolyzed, resulting in the formation of benzothiazole. The only other product isolated was cyanobenzene, a pyrolysis product of benzothiazole. Yields are of the order of 40–45% from the pyrolyses.

There is only one major fragmentation path in the mass spectrum of 2-benzothiazolinone, eq. 7 (5), the loss of CO followed by HCN. However, upon pyrolysis at 950°, no products which could be directly related to intermediate

[7] 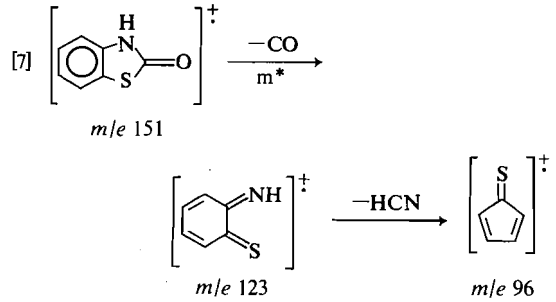

m/e 151 *m/e* 123 *m/e* 96

2 (a = NH; b = S) were isolated: 8.7% of starting material was recovered and 14.4% of products was isolated and identified. The products were cyanonaphthalenes, naphthalene, aniline, cyanobenzene, phenylisocyanate, and 2-thiophenecarbononitrile, each one in less than 3% yield.

We have made the conjecture that the pyrolysis of 2-benzothiazolinone does indeed follow a path involving intermediate **2** but that the major products polymerize and are not isolated. By placing a phenyl group on position 1, we proposed to internally trap the *o*-quinoid intermediate, as was done in the case of 2-benzimidazolinone, eqs. 1 and 2, thereby establishing its formation. This approach turned out to be successful. The results obtained from 1-phenyl-2-benzothiazolinone (**7**) can be explained by initial loss of CO, eq. 8, giving an

[8] 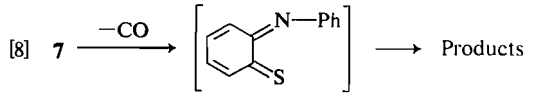

o-quinoid intermediate which rearranges to phenothiazine (**9**). Phenothiazine is then the precursor of carbazole (**10**). Thus, the *N*-phenyl group alters the fate of the *o*-quinoid intermediate via an internal cyclization process.

In the case of 1-phenyl-2-benzothiazolinethione (**8**) the *N*-phenyl group also plays an important role in determining the paths of fragmentation, both under conditions of pyrolysis and of electron impact. The stability of the $(M - H\cdot)^+$ ion at *m/e* 242 is probably due to the tetracyclic structure formed by reaction of the *N*-phenyl group with the ionized thione group, eq. 4.

The major pyrolysis product of 1-phenyl-2-benzothiazolinethione (**8**), 2-(phenylthio)benzothiazole (**11**), is the result of a phenyl rearrangement from N to S, perhaps through an intermediate such as the one shown in eq. 9. In

[9] 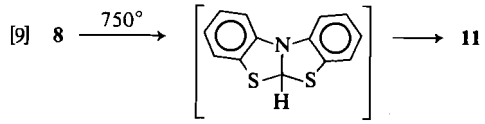

support of this possibility we can cite (7) the example of the pyrolysis of 1-phenyl-2-benzimidazolinethione (**13**), which at 950° gives a 24% yield of benzimidazo[2,1-*b*]benzothiazole

Can. J. Chem. Downloaded from www.nrcresearchpress.com by 210.87.254.40 on 09/05/12
For personal use only.

[10] 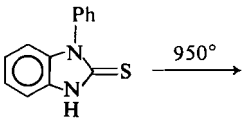

13

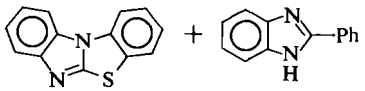

14 ($13 - H_2$) 15 ($13 - S$)

(**14**) and an 11% yield of 2-phenylbenzimidazole (**15**), eq. 10. In the formation of **14**, a molecule of hydrogen is lost from an NH group and from a rearranged hydrogen atom, a path not possible from the intermediate shown in eq. 9. The formation of **15** is the result of a phenyl rearrangement and desulfurization.

Another possible path for an intramolecular phenyl rearrangement is a spiro intermediate, eq. 11. The suggestion of this possibility is

[11] **8** 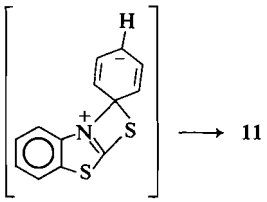 **11**

based on an analogy with the phenothiazine rearrangement which has been explained via a spirodienyl intermediate (9).

Phenyl rearrangements have been previously observed under pyrolytic conditions. For example, a S to N phenyl rearrangement occurs when anhydro-*S*-phenylphenothiazinium hydroxide is heated in toluene, eq. 12 (10). The authors proposed that the rearrangement was intramolecular. Also, an intramolecular phenyl migration has been invoked to explain the product of the pyrolysis of *o*-diazoniophenyl-*o*-phenoxyphenyl sulfide, eq. 13 (11). The oxonium salt initially formed supposedly rearranges into a sulfonium salt. Phenyl rearrangements have also been observed upon electron impact (12, 13).

[12] 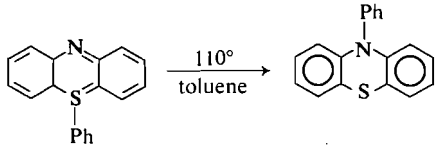

[13] 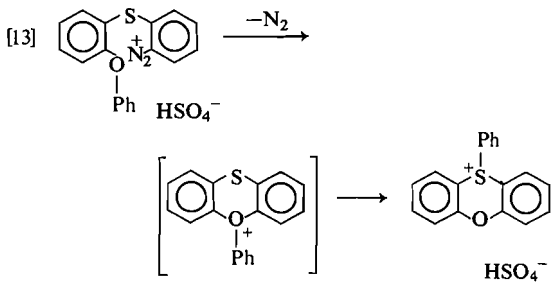

As part of a general study of the relationship between the reactivity of the thiocarbonyl group and its electronic structure, the photoelectron spectra of three compounds related to structure **16** have been reported (14). In each

16 X = O, S, and N—CH_3

case, the first band (of lowest eV) corresponds to the ionization of a π-electron localized on the extracyclic S atom. Thus, the interaction of the *N*-phenyl group with the S atom of the thiocarbonyl group in **8** and **13** can be explained as a result of initial excitation of the S atom.

In summary, the formation of phenothiazine (**9**) from 1-phenyl-2-benzothiazolinethione (**7**) is best explained as passing through an *o*-quinoid intermediate (eq. 8). This lends support to the suggestion that the pyrolysis of 2-benzothiazolinone gives an *o*-quinoid intermediate also, even though products related to it are not isolated. Even though the major product from the pyrolyses of 1-phenyl-2-benzothiazolinethione (**8**) is 2-(phenylthio)benzothiazole (**11**), comparison with results from the pyrolysis of 1-phenyl-2-benzimidazolinethione (**13**) suggests that **11** forms from a tetracyclic intermediate which further rearranges and is not isolated (eq. 9). The phenyl rearrangement that we have observed provides an alternate synthetic route to 2-(phenylthio)benzothiazole (**11**). Previous syntheses used as starting materials, 2-iodobenzothiazole (15), and 2-chlorobenzothiazole (16).

Basically, pyrolysis and mass spectrometric fragmentation are not similar processes. However, in the series of compounds described by structure **1**, we have found that the species eliminated in the two processes are similar

Can. J. Chem. Downloaded from www.nrcresearchpress.com by 210.87.254.40 on 09/05/12
For personal use only.

for a particular molecule. We find that this observation is noteworthy and that the mass spectrum of compounds related to structure **1** can be useful, in an empirical sense, for predicting and interpreting results obtained from the pyrolyses.

Experimental

Melting points were determined by the open capillary method using a MEL-TEMP apparatus and were corrected. Infrared spectra were recorded with a Beckman IR8 spectrometer and a Perkin-Elmer Infracord. Nuclear magnetic resonance spectra were taken on a Varian T-60 spectrometer using 1% TMS as an internal standard. Ultraviolet spectra (1 cm path) were determined on a Bausch and Lamb Spectronic 505. Low-resolution mass spectra were obtained from a Hitachi RMU-6D mass spectrometer. Electron voltage readings were taken directly from the dial since more precise values were not needed.

Exact-mass data were obtained from an AEI MS-902 mass spectrometer linked to a PDP-8 computer. All experimental values agreed with the calculated values within ± 0.0015 mass units. Metastable peaks were observed in the low-resolution spectra.

The ion source of the RMU-6D was maintained at 250° and the MS-902 at 150°. Since pyrolysis of the compounds studied does not begin until approximately 600°, pyrolysis in the source cannot account for the fragmentations observed.

The gas chromatographic (g.c.) work was carried out using a Hewlett-Packard 5752B Research Chromatograph with a thermal conductivity detector. Columns were prepared with 0.25 in. copper tubing and 60–80 mesh Chromosorb W as a solid support unless otherwise stated. A total of five g.c. columns were used during the initial stages of analysis of the pyrolysis mixtures. However, only the column that gave the best separations is reported for each analysis. Comparison of the areas under the peaks of the pyrolysis products with the areas under the peaks of solutions of known concentrations of the same compound was used to determine yields. Analyses were performed by Midwest Microlab, Inc., Indianapolis, Indiana.

Chemicals

The following chemicals were purchased and used directly or after recrystallization: 2-aminothiophenol, 2-aminobiphenyl, thiophenol, acridine, phenothiazine (**9**), dibenzothiophene, benzothiazole, and biphenyl (Aldrich); carbazole (**10**) (Fisher); 1,1-diphenylthiourea (Eastman); and phenyl sulfide (Baker).

1-Phenyl-2-benzothiazolinone (7)

Compound **7** was prepared from 1,1-diphenylthiourea by the method of Passing (17). Recrystallization was done in petroleum ether (30–60°): yield, 30%; m.p., 79–80° (lit. (17) m.p. 81–82°). The i.r. spectrum ($HCCl_3$) exhibits strong absorption bands at 1700 and 1680 cm^{-1}. The mass spectrum is summarized in Scheme 1 and discussed in the text.

Anal. Calcd. for $C_{13}H_9NOS$: C, 68.70; H, 3.99. Found: C, 68.66; H, 4.09.

1-Phenyl-2-benzothiazolinethione (8)

Compound **8** was prepared from compound **7** by reaction with P_2S_5 (18). The crude product was recrystallized with ethanol: yield, 40.9%; m.p. 94–95° (lit. (18) m.p. 98–99°). The i.r. spectrum ($HCCl_3$) consists of bands at 2950, 1570, 1485, 1450, 1305, 1255, 1140, and 680 cm^{-1}. The mass spectrum is summarized in Scheme 3 and discussed in the text.

Anal. Calcd. for $C_{13}H_9NS_2$: C, 64.16; H, 3.73. Found: C, 64.46; H, 3.59.

2-(Phenylthio)benzothiazole (11)

Compound **11** was synthesized from 2-iodobenzothiazole using the method of Todesco and Vivarelli (15). It was also synthesized by the pyrolysis of compound **8** at 720°. In the former case, the 2-iodobenzothiazole was prepared from an ethereal solution of 2-benzothiazlyllithium (19, 20). The 2-iodobenzothiazole was then allowed to react with thiophenol for 5 days. The resulting oil was distilled and the portion that came over at 186–187° (3 Torr) was collected (15, 16): yield, 23.3%; m.p. of picrate 107–108° (lit. (15) m.p. of picrate 108–109°); λ_{max} (EtOH) 299.5, 289.5, 281, 247sh, and 238 nm; i.r. (neat) 3100, 1458, 1432, 1313, 1268, 993, 758, and 693 cm^{-1}; δ ($CDCl_3$), 7.73 multiplet; mass spectrum, 70 eV, *m/e* 243 ($C_{13}H_9NS_2$, 44), 242 ($C_{13}H_8NS_2$, 100), 211 ($C_{13}H_9NS$, 2), 210 ($C_{13}H_8NS$, 1), 209 ($C_{13}H_7NS$, 2), 199 ($C_{12}H_9NS$, 1), 198 ($C_{12}H_8NS$, 2), 184 ($C_{12}H_8S$, 1), 179 ($C_{13}H_9N$, 1), 178 ($C_{13}H_8N$, 1), 167 ($C_{12}H_9N$, 1), 166 ($C_{12}H_8N$, 1), 135 (C_7H_5NS, 1), 121.5 ($C_{13}H_9NS_2$ (doubly charged) 4), 121 ($C_{13}H_8NS_2$ (doubly charged) 6), 109 (C_6H_5S, 6), 108 (C_6H_4S, 8), 77 (C_6H_5, 6) and 51 (C_4H_3, 8); molecular ion, *m/e* 243.0176 (calcd. for $C_{13}H_9NS_2$: 243.0176).

In using the pyrolysis method for synthesis of compound **11**, compound **8** was pyrolyzed at 720° to avoid secondary products. Details of the pyrolysis of compound **8** will be given later under that heading; however, the work up procedure in this case is different. Five grams of starting material was used in two portions. Only the products in the first trap and in the quartz tube immediately after the pyrolysis zone were collected. Unreacted starting material was crystallized from a concentrated ethanolic solution of the products and repyrolyzed. The procedure was repeated until there was no starting material left. The crude product of **11** was then vacuum distilled as in the other synthesis. The overall yield was 1.9 g (38.0%).

2-Phenylbenzothiazole (12)

Compound **12** was synthesized from 2-aminothiophenol and benzoic acid with polyphosphoric acid, using the method of Hein *et al.* (21): yield, 46.0%; m.p. 112–113° (lit. (21) m.p. 112.7–113.9°); u.v., n.m.r., and mass spectra were identical to those given in ref. 22. Molecular ion, *m/e* 211.046 (calcd. for $C_{13}H_9NS$: 211.0455).

2-Cyanophenyl Phenyl Sulfide

2-Cyanophenyl phenyl sulfide was synthesized by reacting the diazotized salt of 2-aminophenyl phenyl sulfide with cuprous cyanide (23). 2-Aminophenyl phenyl sulfide was synthesized from aniline and 2-aminothiophenol using the conditions reported by Miller *et al.* (24). The crude product was distilled and the portion that

Can. J. Chem. Downloaded from www.nrcresearchpress.com by 210.87.254.40 on 09/05/12
For personal use only.

came over at 175–178° (1 Torr) was collected. The liquid crystallized on standing and the crystals were washed sparingly with methanol. The overall yield was 11.2%; m.p. 55°; i.r. ($HCCl_3$) 3080, 2940, 2250, 1585, 1460, 1430, 1275, 1135, 1060, 1017, and 675 cm^{-1}; λ_{max} (EtOH) 239sh, 255, 274sh, 284sh, and 314 nm; δ ($CDCl_3$) multiplet 7.2; mass spectrum, 50 eV, *m/e* 211 ($C_{13}H_9NS$, 100), 210 ($C_{13}H_8NS$, 24), 209 ($C_{13}H_7NS$, 9), 184 ($C_{12}H_8S$, 42), 139 ($C_{11}H_7$, 7), 109 (C_6H_5S, 7), 105.5 ($C_{13}H_9NS$ (doubly charged) 3), 105 ($C_{13}H_8NS$ (doubly charged) 4), 92 ($C_{12}H_8S$ (doubly charged) 11) 77 (C_6H_5, 19), and 51 (C_4H_3, 24); molecular ion *m/e* 211.045 (calcd. for $C_{13}H_9NS$: 211.0455).

2-Cyanobiphenyl

2-Cyanobiphenyl was synthesized by diazotization of 2-aminobiphenyl, followed by reaction with cuprous cyanide (23). The crude product was extracted with ether and decolorized with activated carbon. The ether was evaporated under a vacuum. The product was then distilled and the portion from 98–100° (0.1 Torr) was collected. This light yellow oil crystallized on standing; yield 54.5%; m.p. 35–36°; i.r. spectrum (neat), 3090, 2249, 1600, 1478, 1435, 750, and 695 cm^{-1}; λ_{max} (EtOH) 227, 249, and 287 nm; δ ($CDCl_3$) multiplet 7.55; mass spectrum, 50 eV, *m/e* 179 ($C_{13}H_9N$, 100), 178 ($C_{13}H_8N$, 27), 177 ($C_{13}H_7N$, 15), 152 ($C_{12}H_8$, 17), 151 ($C_{12}H_7$, 16), 150 ($C_{12}H_6$, 7), 89.5 ($C_{13}H_9N$ (doubly charged), 7), 89 ($C_{13}H_8N$ (doubly charged) 7) and 76 (C_6H_4, 15); molecular ion *m/e* 179.073 (calcd. for $C_{13}H_9N$: 179.0734).

Pyrolysis Apparatus and Procedure

The pyrolysis apparatus and procedure were similar to those used in our previous reports (6, 8). The sample (approximately 1 g) was sublimed smoothly into a stream of nitrogen which passed through a hollow quartz tube heated by a 12 in. electric furnace. The flow rate was adjusted to 0.25 l/min at 1 Torr. The vacuum was maintained by a rotary pump. A series of traps were placed between the pyrolysis zone and the pump. It takes approximately an hour for each half gram of sample to be sublimed through the zone. A solution was made in a volumetric flask of the material in the traps; g.c. and t.l.c. were used to separate the compounds in this solution.

Pyrolysis of 1-Phenyl-2-benzothiazolinone (7)

In Table 1 the results and conditions of the pyrolyses of compound 7 are listed. The percentages shown are averages of different trials at the same temperature; good agreement was obtained among the different runs. Approximately 1 g of sample was used for each pyrolysis.

Three traps were used in each pyrolysis; the first one was maintained at room temperature, whereas the next two were cooled by liquid nitrogen. The traps were washed with acetone and chloroform. The g.c. column used to separate the three components was 6 ft 3% OV 225 on Chromosorb W 80–100. The temperature was programmed from 180 to 265° (5 min) at 8°/min. The products were identified by comparison with authentic samples.

TABLE 1. Pyrolyses of 1-phenyl-2-benzothiazolinone (7)*

	% found at:			
	650°	750°	850°	950°
1-Phenyl-2-benzothiazolinone (7) (recovered)	90.0	30.2	—	—
Phenothiazine (9)	8.3	19.4	—	—
Carbazole (10)	—	21.9	51.0	32.5
Total	98.3	71.5	51.0	32.5

*A N_2 flow rate of 0.2–0.25 l/min and a system pressure of 0.5–1.5 Torr were used.

TABLE 2. Pyrolyses of phenothiazine (9)*

	% found at:			
	650°	750°	780°	850°
Phenothiazine (9) (recovered)	92.2	20.7	3.7	—
Carbazole (10)	—	29.7	45.1	56.9
Total	92.2	50.4	48.8	56.9

*Same conditions as given in the footnote of Table 1.

TABLE 3. Pyrolyses of 1-phenyl-2-benzothiazolinethione (8)*

	% found at:			
	650°	750°	850°	950°
1-Phenyl-2-benzothiazolinethione (8) (recovered)	95.0	38.6	7.8	2.6
2-(Phenylthio)-benzothiazole (11)	—	53.3	54.9	0.6
2-Phenylbenzothiazole (12)	—	1.9	9.3	11.4
2-Cyanophenyl phenyl sulfide	—	—	3.6	1.1
Dibenzothiophene	—	—	0.7	2.8
Phenyl sulfide	—	—	2.4	0.5
Benzothiazole	—	—	1.1	1.1
Cyanobenzene	—	—	2.6	21.5
2-Cyanobiphenyl	—	—	—	1.2
Biphenyl	—	—	—	0.8
Total	95.0	93.8	82.4	43.6

*Same conditions as given in the footnote to Table 1.

Pyrolysis of Phenothiazine (9)

The pyrolyses of compound 9 were performed under the same conditions as those of 7. The same g.c. column and conditions were used. The average percentages are listed in Table 2 along with the pyrolytic conditions. There was good agreement on different runs at the same temperature.

Pyrolysis of 1-Phenyl-2-benzothiazolinethione (8)

The conditions for the pyrolyses of compound 8 were the same as those for compound 7. The g.c. column used was 6 ft 10% SE30. The temperature was programmed from 100 to 245° (hold) at 8°/min. The results are shown in Table 3. The agreement on different runs was

Can. J. Chem. Downloaded from www.nrcresearchpress.com by 210.87.254.40 on 09/05/12
For personal use only.

TABLE 4. Pyrolyses of 2-(phenylthio)benzothiazole (**11**)*

	% found at:	
	850°	950°
2-(Phenylthio)benzothiazole (**11**)	11.1	—
2-Phenylbenzothiazole (**12**)	9.9	7.9
2-Cyanophenyl phenyl sulfide	4.2	trace
Dibenzothiophene	1.1	1.5
Phenyl sulfide	2.0	trace
Benzothiazole	2.7	trace
Cyanobenzene	10.5	24.7
2-Cyanobiphenyl	trace	0.5
Biphenyl	—	trace
Total	41.5	34.6

*Same conditions as given in the footnote to Table 1.

good. The presence of acridine, carbazole (**10**), and cyanodibenzothiophene was detected at 850° and 950°, but they were present in trace quantities. In the case of cyanodibenzothiophene, the position of cyano substitution was not determined. There were two isomers but neither gave the same u.v. spectrum as 2-cyanodibenzothiophene (25). Except for cyanodibenzothiophene, all the other products were identified by comparison with authentic materials.

Pyrolysis of 2-(Phenylthio)benzothiazole (11)

Due to the small amount of **11** available, its pyrolyses were done on a smaller scale (0.5 g). The conditions used were the same as in the cases given above. The g.c. column and conditions used were the same as those for compound **8**. The results are listed in Table 4.

Pyrolysis of 2-Phenylbenzothiazole (12)

Compound **12** (1.04 g) was pyrolyzed at 950° using the same conditions as given for previous cases. The g.c. column and conditions used were the same as above. Only a trace of cyanobenzene was detected. The percentage of starting material recovered was 94%.

We thank the National Research Council of Canada for its financial support.

1. D. C. DEJONGH, R. Y. VAN FOSSEN, and C. F. BOURGEOIS. Tetrahedron Lett. 271 (1967).
2. D. C. DEJONGH and R. Y. VAN FOSSEN. J. Org. Chem. **37**, 1129 (1972).
3. D. C. DEJONGH and D. A. BRENT, J. Org. Chem. **35**, 4204 (1970).
4. D. C. DEJONGH, D. A. BRENT, and R. Y. VAN FOSSEN. J. Org. Chem. **36**, 1469 (1971).
5. M. L. THOMSON and D. C. DEJONGH. Can. J. Chem. **51**, 3313 (1973).
6. D. C. DEJONGH and M. L. THOMSON. J. Org. Chem. **38**, 1356 (1973).
7. D. C. K. LIN, M. L. THOMSON, and D. C. DEJONGH. Can. J. Chem. **52**, 2359 (1974).
8. D. C. DEJONGH, D. C. K. LIN, and M. L. THOMSON. *In* Advances in mass spectrometry. Vol. 6. *Edited by* A. R. West. Applied Science Publishers, Barking, England. 1974. Chapt. 12.
9. J. I. G. CADOGAN. Acc. Chem. Res. **5**, 303 (1972).
10. A. N. NESMEYANOV, T. P. TOLSTAYA, A. V. GRIB, and S. R. KIRGIZBAEVA. Bull. Acad. Sci. USSR, **22**, 1639 (1973).
11. A. N. NESMEYANOV, T. P. TOLSTAYA, I. N. LISICHKINA, and N. S. OVCHAROVA. Proc. Acad. Sci. USSR, **209**, 336 (1973).
12. W. D. WERINGA. Tetrahedron Lett. 273 (1969).
13. W. D. WERINGA, H. J. M. SINNIGE, and M. J. JANSSEN. Org. Mass Spectrom. **5**, 1399 (1971).
14. C. GUIMON, G. PFISTER-GUILLOUZO, M. ASHELOT, and M. CHANON. Tetrahedron, **30**, 3831 (1974).
15. P. E. TODESCO and P. VIVARELLI. Gazz. Chim. Ital. **94**, 435 (1964).
16. L. G. S. BROOKER, E. L. WHITE, G. H. KEYES, C. P. SMYTH, and P. F. OESPER. J. Am. Chem. Soc. **63**, 3192 (1941).
17. H. PASSING. J. Prakt. Chem. **153**, 1 (1939).
18. L. G. S. BROOKER, G. H. KEYES, and W. W. WILLIAMS. J. Am. Chem. Soc. **64**, 199 (1942).
19. P. E. IVERSEN. Acta Chem. Scand. **22**, 1690 (1968).
20. H. GILMAN and J. A. BEEL. J. Am. Chem. Soc. **71**, 2328 (1949).
21. D. W. HEIN, R. J. ALHEIM, and J. J. LEAVITT. J. Am. Chem. Soc. **79**, 427 (1957).
22. G. RABILLOUD, B. SILLION, and G. DEGAUDEMARIS. Makromol. Chem. **146**, 215 (1971).
23. A. I. VOGEL. Practical organic chemistry. Spottiswoode, Ballantyne and Co. Ltd., London. 1964. p. 608.
24. E. MILLER, F. S. CROSSLEY, and M. L. MORRE. J. Am. Chem. Soc. **64**, 2322 (1942).
25. M. KUROKI. Nippon Kagaku Zasshi, **186**, 681 (1968).

Reaction of 1,2-Dichlorohexafluorocyclopentene with Phenol and *p*-Nitrothiophenol

RICHARD F. STOCKEL

Hydron Laboratories, Inc., New Brunswick, New Jersey 08902

Received May 8, 1974[1]

RICHARD F. STOCKEL. Can. J. Chem. 53, 2302 (1975).

The reaction of phenol with 1,2-dichlorohexafluorocyclopentene gave two major components. These have been identified as 1-chloro-2-phenoxy-3,3,4,4,5,5-hexafluorocyclopentene (**1**) and 1-chloro-3,3,4,4-tetrafluoro-2,5,5-triphenoxycyclopentene (**2**). A third component was detected by g.c. and assumed to be **3**.

With *p*-nitrothiophenol as the reactant only 1,2-bis(*p*-nitrophenylthio)-3,3,4,4,5,5-hexafluorocyclopentene (**4**) was isolated in excellent yields.

RICHARD F. STOCKEL. Can. J. Chem. 53, 2302 (1975).

La réaction du phénol avec le dichloro-1,2 hexafluorocyclopentène conduit à deux produits principaux. On a pu démontrer qu'il s'agit du chloro-1 phénoxy-2 hexafluoro-3,3,4,4,5,5 cyclopentène (**1**) et du chloro-1 tétrafluoro-3,3,4,4 triphénoxy-2,5,5 cyclopentène (**2**). On a détecté par c.p.g. la présence de traces d'un troisième composé et l'on fait l'hypothèse qu'il s'agit de **3**.

Utilisant le *p*-nitrothiophénol comme réactif, on n'isole que le bis(*p*-nitrophénylthio)-1,2 hexafluoro-3,3,4,4,5,5 cyclopentène avec d'excellents rendements. [Traduit par le journal]

Results

A variety of nucleophiles reacting with 1,2-dichlorohexafluorocyclopentene has been extensively studied (1). Despite this versatility the reactions of phenol and thiophenol derivatives have remained virtually unreported for these type alicyclic olefins. This article conclusively shows the diversity of products, which is primarily dependent on the attacking nucleophile and to a lesser extent the reaction conditions.

The results of reacting phenol under basic conditions with 1,2-dichlorohexafluorocyclopentene is analogous to this haloolefin and its homologs reacting with methoxide ion (2). Both the mono- (**1**) and trisubstituted (**2**) unsaturated ethers are formed in 50.8 and 45.8% yields, respectively. Employing milder reaction conditions it was reported (3) that perfluorocyclobutene reacts with phenol to give only the corresponding monounsaturated ether. In fact, with alicyclic olefins of the 1,2-dichloro type, no case has been reported to date whereby saturated ethers are formed. In contrast acyclic perfluoro- and chlorofluoroolefins give both saturated and unsaturated ethers (4, 5).

One other minor product in about 3.4% was

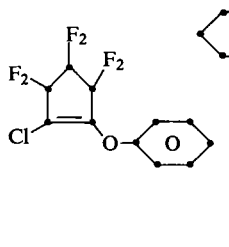

1

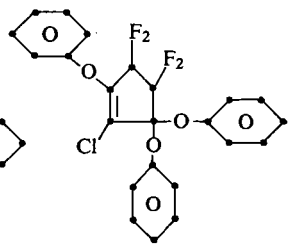

2

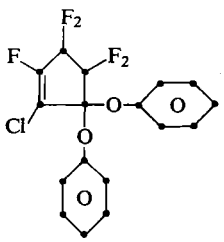

3

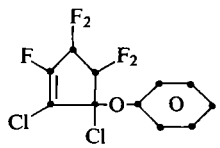

4

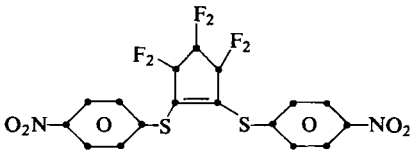

5

[1]Revision received March 23, 1975.

Can. J. Chem. Downloaded from www.nrcresearchpress.com by 210.87.254.40 on 09/05/12
For personal use only.

quantitative conversion of phenol based on the product distribution. Gas chromatography of the crude using a 2′-polyphenylether 3% on 100/120 GIS Chromosorb Q gave the following composition: **1**, 58.8%; **2**, 45.8%; and **3**, 3.4%. Each of the major peaks was checked using authentic samples and comparing retention times. Upon vacuum distillation **1** distilled at 46–48 °C/6 Torr, while **2** distills at 138–139°/0.1 Torr with a melting range of 56–57 °C. Compound **2** was reported (19); however, the method of preparation was not disclosed. Only the ^{19}F n.m.r. and melting point were reported.

Anal. Calcd. for $C_{11}H_5ClF_6O$ (**1**): C, 43.63; H, 2.17; Cl, 11.73. Found: C, 43.85; H, 1.96; Cl, 12.05.

Anal. Calcd. for $C_{23}H_{15}ClF_4O_3$ (**2**): C, 61.26; H, 3.30; Cl, 7.88. Found: C, 60.93; H, 3.16; Cl, 8.02.

Under similar reaction conditions when 3 equiv. of phenol and base were reacted with 1 equiv. of olefin a 91% yield of **2** was obtained with no other products found.

Preparation of 1,2-Bis(p-nitrophenylthio)-3,3,4,4,5,5-hexafluorocyclopentene (5)

A solution of 1,2-dichlorohexafluorocyclopentene (24.5 g, 0.1 mol), *p*-nitrothiophenol (15.1 g, 0.1 mol), and potassium hydroxide (5.6 g, 0.1 mol) was stirred and heated at *55 °C* for 15 h. The contents were then poured into 1 l of water. The bottom organic layer was separated and washed several times with water and finally dried over anhydrous sodium sulfate to give 25.1 g for an overall yield of 91%. This was recrystallized from isopropanol to give a sharp melting range 126–126.5 °C.

Anal. Calcd. for $C_{17}H_8F_6S_2N_2O_4$ (**4**): C, 42.31; H, 1.66; S, 13.27; N, 5.80. Found C, 42.60; H, 1.38; S, 13.27; N, 5.80.

1. J. D. Park, R. J. McMurtry, and J. H. Adams, *In* Fluorine chemistry reviews. Vol. 2. *Edited by* P. Tarrant. Marcel Dekker, Inc., New York. 1968. Chapt. 2.
2. J. D. Park, C. M. Snow, and J. R. Lacher. J. Am. Chem. Soc. **73**, 2342 (1951).
3. J. T. Barr, K. E. Rapp, R. L. Pruett, C. T. Bahner, J. D. Gibson, and R. H. Lafferty, Jr. J. Am. Chem. Soc. **72**, 4480 (1950).
4. W. T. Miller, E. W. Fager, and P. H. Griswold. J. Am. Chem. Soc. **70**, 431 (1948).
5. J. D. Park, W. M. Sweeney, S. L. Hopwood, and J. A. Lacher. J. Am. Chem. Soc. **78**, 1685 (1956).
6. E. T. McBee, D. L. Crain, R. D. Crain, L. R. Beholov, and H. P. Braendlin. J. Am. Chem. Soc. **84**, 3557 (1962).
7. A. B. Clayton, J. Roylance, D. R. Sayers, R. Stephens, and J. C. Tatlow. J. Chem. Soc. 7358 (1965).
8. N. B. Cotthup, L. H. Daly, and S. E. Wiberley. Introduction to infrared and Raman spectroscopy. Academic Press, Inc., New York. 1964.
9. A. Ferretti and G. Tesi. Chem. Ind. 1987 (1964).
10. J. D. Park, M. L. Sharrah, and J. R. Lacher. J. Am. Chem. Soc. **71**, 2337 (1949).
11. R. F. Stockel, M. T. Beachem, and F. H. Megson. Can. J. Chem. **42**, 2880 (1964).
12. K. E. Rapp, R. L. Pruett, J. T. Barr, C. T. Bahner, J. D. Gibson, R. H. Lafferty, Jr. J. Am. Chem. Soc. **72**, 3642 (1950).
13. C. G. Krespan and D. C. England. J. Org. Chem. **33**, 1850 (1968).
14. A. W. Frank. J. Org. Chem. **30**, 3663 (1965).
15. A. W. Frank. J. Org. Chem. **31**, 1917 (1966).
16. T. Mill, J. O. Rodin, R. M. Silverstein, and C. Woolf. J. Org. Chem. **28**, 836 (1963).
17. R. F. Stockel. Can. J. Chem. **47**, 867 (1968).
18. R. F. Stockel. Can. J. Chem. **46**, 2625 (1967).
19. V. W. Gash and D. J. Bauer. J. Org. Chem. **31**, 3602 (1966).

Can. J. Chem. Downloaded from www.nrcresearchpress.com by 210.87.254.40 on 09/05/12
For personal use only.

Can. J. Chem. Downloaded from www.nrcresearchpress.com by 210.87.254.40 on 09/05/12
For personal use only.

detected by g.c. It is suspected that it is the extremely reactive diether (**3**), which is seldom isolated under basic conditions due to the vinylic fluorine (6). However, a 3-phenoxide (**4**) derivative, resulting from an outward elimination (7) could conceivably be formed, because of a competitive reaction path between the electronically favored inward elimination (**1**) *vs.* the stereochemically favored *trans*-outward elimination (**4**). However, the latter route is very much less influential in the cyclopentene system than in the cyclohexene system. The diether structure is also preferred because its retention time on the g.c. is approximately midway between the mono- and trisubstituted ethers.

Structure proofs are based on physical and analytical data. For structure **1** the ^1H n.m.r. shows only a complex aromatic pattern while the ^{19}F n.m.r. spectrum shows three multiplets of equal intensities at 112.6, 115.9, and 130.4 ϕ. The i.r. gives characteristic bands at 6.02 (C=C stretch), 6.28 (phenyl), 7.80, 8.39, and 8.70 μ (due to CF_2 and C—O—C asymmetric stretch) (8).

The ^1H n.m.r. of the trisubstituted ether **2** shows complex aromatic absorption, while the ^{19}F n.m.r. spectrum gives two identical triplets at 115.5 and 123.6 ϕ with $J_{FF} = 6.2$ Hz. The i.r. gives comparable bands as for **1** with bands at 6.02 (C=C stretch), 6.28 (phenyl), 7.88, 8.38, and 8.80 μ (for CF_2 and C—O—C). Elemental analyses agree for both compounds. No physical data were accumulated on the minor component.

The reaction of 1,2-dichlorohexafluorocyclopentene with *p*-nitrothiophenol proceeds similarly to the previously reported reaction of this same haloolefin with cuprous benzylmercaptide (12, 13). In either case the 1,2-bisthio ethers (**5**) are formed. Interestingly, if the alicyclic olefin is a perfluorocycloalkene substrate, the 1,2-disubstituted products are formed regardless whether the nucleophile is an alkoxide ion (7, 10, 11) or a mercaptide ion (9, 12, 13). In addition to the bisthioether perfluorocyclobutene is reported to give the monosaturated and unsaturated ethers (12). It was found in this study that 1,2-dichlorohexafluorocyclopentene gives the bisether (**5**) exclusively. This same result was true even in the absence of base emphasizing the strong nucleophilic character of bivalent sulfur.

Fairly recent papers illustrate a generalized reaction path leading to the formation of 1,2-disubstituted derivatives on 1,2-dichlorohexafluorocyclopentene with phosphites, phosphonites, and phosphinite esters (14, 15). The explanation why the monosubstituted derivative is not formed with these phosphorus compounds was rationalized by a reversal of the polarization of the double bond due to the P=O moiety. Therefore carbon atom-2 becomes partially positive and subsequently becomes susceptible to nucleophilic attack. This same type of conjugative ability has been postulated in an earlier paper involving a carboxamide group (16). However, this hypothesis does not explain why some 1,2-disubstituted derivatives are obtained in the reactions of secondary phosphines with 1,2-dichlorotetrafluorocyclobutene and 1,2-dichlorohexafluorocyclopentene (17, 18).

It is obvious from this work and those references mentioned in this text, that no single unifying postulate exists to predict *a priori* the exact product formation. Although a recent attempt has been made in this direction (1) the diversity of the haloolefin and attacking nucleophile probably precludes a single working hypothesis.

The ^1H n.m.r. for **5** shows A_2B_2 pattern characteristics of a *p*-disubstituted phenyl compound. The ^{19}F n.m.r. spectrum gives a triplet at 107.6 ϕ and a quintuplet at 130.3 ϕ with a corresponding 2:1 ratio suggesting a symmetrical structure. The i.r. gives bands at 6.22 (phenyl), 6.66 (asymmetric NO_2), 7.44 (symmetric NO_2) with other large absorptions at 8.02, 8.80, 9.21, 9.89, 11.38, 11.7 (shoulder), and 13.50 μ.

Experimental

All reagents were purchased from commercial sources. Analytical results were obtained by our own microanalytical laboratory. Infrared spectra were run as mineral oil mulls or films on a Perkin-Elmer Model 317 spectrophotometer. Nuclear magnetic resonance spectra were recorded with Varian HR-60, ^1H n.m.r. reported as δ values using tetramethylsilane as internal standard, ^{19}F n.m.r. reported as ϕ values using trichlorofluoromethane as an external standard.

Preparation of 1-Chloro-2-phenoxyhexafluorocyclopentene (1) and 1-Chloro-3,3,4,4-tetrafluoro-2,5,5-triphenoxy-1-cyclopentene (2)

Phenol (9.4 g, 0.1 mol), 1,2-dichlorohexafluorocyclopentene (24.5 g, 0.1 mol), and 85% potassium hydroxide (5.6 g, 0.1 mol) were added to 200 ml of dimethylformamide. The solution was stirred at 55 °C for 15 h. The contents were then poured into 1 l of water. The bottom organic layer was separated, washed several times with water, and dried over anhydrous sodium sulfate. Approximately 23.5 g of crude were isolated, which is essentially

Some Reactions of 1-Lithio-2-phenyl-1,2-dihydropyridine. IV. Synthesis of β-Substituted Pyridines[1]

C. S. GIAM, E. E. KNAUS,[2] R. A. LOCKHART,[3] AND I. G. KEENER
Department of Chemistry, Texas A & M University, College Station, Texas 77843
Received February 19, 1975

Can. J. Chem. Downloaded from www.nrcresearchpress.com by 210.87.254.40 on 09/05/12
For personal use only.

C. S. GIAM, E. E. KNAUS, R. A. LOCKHART, and I. G. KEENER. Can. J. Chem. **53**, 2305 (1975).

Alkylation of the ambident anion 1-lithio-2-phenyl-1,2-dihydropyridine (**1***a*) has been investigated. A direct method for introducing an alkyl or arylalkyl group into the β-position of pyridine is described. Reaction of **1***a* with styrene oxide or ethylene oxide afforded 2-(2-phenyl-5-pyridyl)-1-phenylethanol (**10**) and 2-(2-phenyl-5-pyridyl)ethanol (**11**), respectively. With *N*-benzylideneaniline the unexpected 2-phenyl-5-benzylpyridine (**7**) was obtained. When **1***a* was allowed to react with perhalomethanes, conditions conducive to carbene formation, bis(6-phenyl-3-pyridyl)methane (**12**) and 6,6′-diphenyl-3,3′-dipyridyl (**13**) were obtained. Mechanisms for the formation of **7**, **12**, and **13** are discussed. Reactions of **1***a* with other electrophilic substrates are described.

C. S. GIAM, E. E. KNAUS, R. A. LOCKHART et I. G. KEENER. Can. J. Chem. **53**, 2305 (1975).

On a étudié l'alkylation d'un anion bidentate, le lithio-1 phényl-2 dihydro-1,2 pyridine **1***a*. On décrit une méthode d'introduction directe d'un groupe alkyle ou aryle en position β de la pyridine.

La réaction de **1***a* avec l'oxyde de styrène ou l'oxyde d'éthylène conduit respectivement au (phényl-2 pyridyl-5)-2 phényl-1 éthanol (**10**) et (phényl-2 pyridyl-5)-2 éthanol (**11**). Avec la *N*-benzylidènaniline un produit inattendu le phényl-2 benzyl-5 pyridine (7) est obtenu. Lorsque **1***a* est mis à réagir avec les perhalogénométhanes, c'est-à-dire dans des conditions favorables à la formation de carbènes, du bis(phényl-6 pyridyl-3) méthane (**12**) et du diphényl-6,6′ dipyridyl-3,3′ (**13**) se produisent. Les mécanismes pour la formation de **7**, **12** et **13**, sont discutés. On décrit la réaction de **1***a* avec d'autres substrats électrophiles. [Traduit par le journal]

Although β- or 3-substituted pyridines and their derivatives find important applications in biological studies (2), as intermediates in organic synthesis, and in mechanistic studies (3), the synthesis of these compounds has been a problem. The direct introduction of alkyl groups having functional moieties into the 3- or 5-position of the pyridine ring has not been reported. Alkylation and arylation of pyridine by the nucleophilic organolithium or Grignard reagents give 2- or 4-substituted pyridines rather than the 3-substituted derivatives. Free radical substitution, on the other hand, gives a mixture of all three isomers; the 3-substituted isomer is usually the minor component. Finally, alkylation via electrophilic substitution, *e.g.*, Friedel–Crafts reaction, has not been effected in the pyridine series (3, 4).

Recently, we showed that alkyl or aralkyl substituents can be directly introduced into the β-position of pyridines by reacting pyridine with lithium aluminum hydride followed by an alkyl or aralkyl halide. This simple and direct method gave very high yields of β-alkyl and aralkyl pyridines (5). In another study (6), we showed that the σ-intermediates, 1-lithio-2-substituted 1,2-dihydropyridines (**1**) isolated from the reactions of organolithium compounds with pyridine (7), reacted with alkyl, aralkyl, and aryl halides to produce 2,5-disubstituted pyridines (**2**). Although these reactions may be carried out in one step by adding the different organolithium reagents to pyridine followed by the addition of the organic halides, our investigations have concentrated on using the iso-

[1]Presented in part at the XXIII International Congress of Pure and Applied Chemistry, July, 1971, Boston, Massachusetts (1). Also presented in part at the Fourth International Heterocyclic Congress, July, 1973, Salt Lake City, Utah. (1).

[2]Medical Research Council of Canada Postdoctoral Fellow.

[3]National Defense Education Association Predoctoral Fellow.

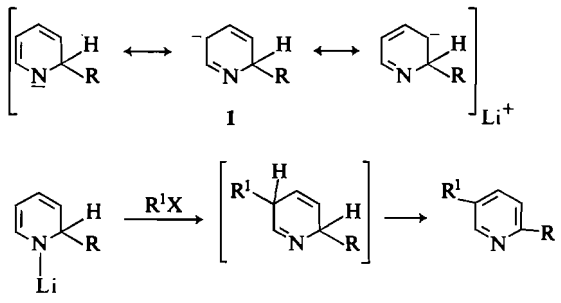

1 2

a R = Phenyl
b R = Alkyl

lated 1-lithio-2-phenyl-1,2-dihydropyridine **1***a*. While other 2,5-disubstituted pyridines can be prepared using similar reactions (8, 9), alkyl or arylalkyl substituents with functional groups such as an amino or hydroxyl have not been reported. We wish to present several interesting observations made in our studies to introduce such substituents directly into the β-position of pyridine using crystalline **1***a*.

The reaction of *N*-lithio-2-phenyl-1,2-dihydropyridine with Schiff bases was investigated as a method to introduce substituted alkyl amines into the β-position of pyridine. Treatment of **1***a* with *N*-benzylideneaniline (**3**) afforded aniline (**4**; 38.5%), 2-phenylpyridine (**5***a*; 49.3%), *N*-benzylaniline (**6***a*; 26.5%), 2-phenyl-5-benzylpyridine (**7***a*; 48.8%), and 2-phenyl-5-(α-anilinobenzyl)pyridine (**8**; 1.1%). Although **8** was

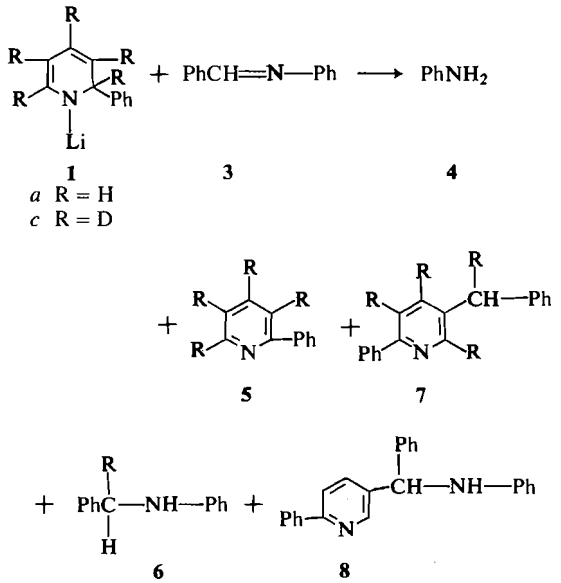

1 3 4

a R = H
c R = D

5 7

6 8

indeed formed the isolation of 2-phenyl-5-benzylpyridine (**7***a*) as one of the major products was quite unexpected. In a similar reaction, treatment of 1-lithio-2-phenyl-1,2-dihydropyridine-d_5 (**1***c*) with **3** gave rise to **4** (71.5%), 2-phenylpyridine-d_4 (**5***c*; 53.5%), *N*-benzyl-d_1-aniline (**6***c*; 22.4%), and 2-phenyl-5-benzyl-d_1-pyridine-d_3 (**7***c*; 44.5%). None of the deuterated product corresponding to **8** was detected by t.l.c.

One possible pathway for the formation of **7** may involve aromatization of **9** followed by nucleophilic hydride or deuteride attack and elimination of anilide anion to afford **7**. *N*-Benzylaniline (**6***a*) and *N*-benzyl-d_1-aniline (**6***c*) may arise in part or totally from reduction

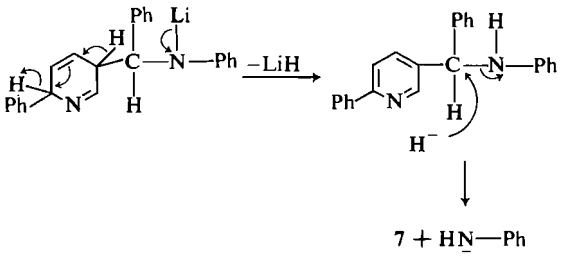

of the active Schiff base **3** by **1***a* and **1***c*, respectively, since these agents are known to selectively reduce active ketones (10, 11). Support for the proposed pathway leading to the formation of **7** is given by the observation that the combined yields of **6** and **7** exceed that of **5** and to the formation of **6***c* and **7***c*. On the other hand if **4** and **7** share the common precursor **9** their yields should correspond. This observation suggests there may be a second pathway involved whereby **9** is also cleaved to yield **5** and **6**.

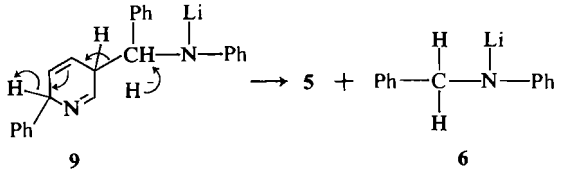

9 6

Treatment of **1***a* with styrene oxide gave **5***a* (31.2%), 2-(2-phenyl-5-pyridyl)-1-phenylethanol (**10**; 21%), and a polymeric product which exhibited a molecular weight (osmetric determination) of 506. In an attempt to reduce the amount of polymeric product, the inverse addition of **1***a* to a solution of styrene oxide

Can. J. Chem. Downloaded from www.nrcresearchpress.com by 210.87.254.40 on 09/05/12
For personal use only.

Can. J. Chem. Downloaded from www.nrcresearchpress.com by 210.87.254.40 on 09/05/12
For personal use only.

afforded **5***a* (29.7%) and **10** (24.9%). Similarly, reaction with ethylene oxide gave rise to **5***a* (31.2%) and 2-(2-phenyl-5-pyridyl)ethanol (**11**; 17.9%). Inverse addition afforded **5***a* (30.2%) and **11** (25.4%).

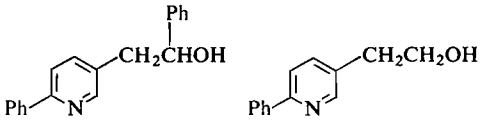

10 **11**

The reaction of **1***a* with methyl bromide provided a useful method for the preparation of 3-methylpyridine (6). In contrast, reaction with trifluoromethyl bromide gave rise to **5***a* (38.4%), a product which exhibits spectral data consistent with that expected for bis(6-phenyl-3-pyridyl)methane **12** (40.5%) and 6,6′-diphenyl-3,3′-dipyridyl **13** (1%). The presence of 2-phenyl-5-trifluoromethylpyridine was not detected by t.l.c. or g.l.c. The structure assigned to **12** was based on its mass, n.m.r., and i.r. spectra. The high resolution mass spectrum exhibited a molecular ion at *m/e* 322.146344; (mass calcd. for $C_{23}H_{18}N_2$: 322.146990 (2 p.p.m.)). The n.m.r. spectrum (CCl_4) was characteristic of a symmetric 2-phenyl-5-substituted pyridine: a 2H doublet ($J_{2,4}$ = 2 Hz) at δ 8.54 due to the C_2-H, a 4H multiplet at δ 8.0 due to the *ortho*-phenyl hydrogens, a 2H doublet ($J_{4,5}$ = 8 Hz) at δ 7.62 attributed to the C_5-H, an 8H multiplet at δ 7.2–7.5 due to the C_4-H, *meta*- and *para*-phenyl hydrogens, and a 2H singlet at δ 4.0 due to the $-CH_2-$ group. Reaction of **1***a* with trifluoromethyl iodide afforded **5***a* (39.4%), **12** (18%), and **13** (1.7%).

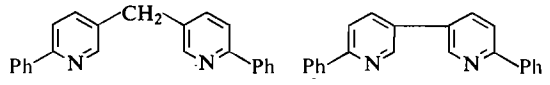

12 **13**

The mechanism of this reaction appears typical of the known reactions of trifluoromethyl halides with organolithium reagents (12–15) *viz.* carbene reactions. The formation of **13** must involve the initial formation of 2-phenyl-5-bromo-2,5-dihydropyridine (**14**) and the unstable trifluoromethyl anion (16) which decomposes to difluorocarbene with loss of fluoride. Further reaction of **14** with **1***a* and subsequent aromatization would give **13**. One pathway for the formation of **12** may involve reaction of highly

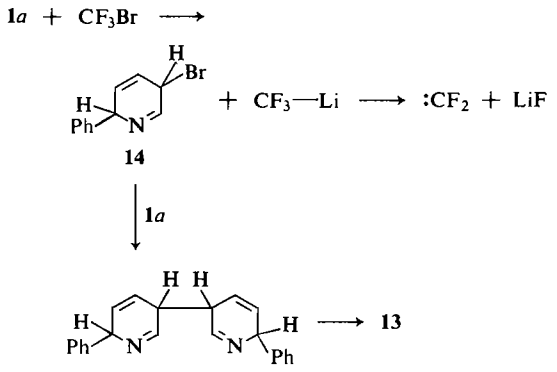

reactive and electrophilic difluorocarbene with **1***a* to yield **15**. Abstraction of the active C-3 proton by base such as 2-phenylpyridine (some of which is always obtained), elimination of fluoride anion and subsequent aromatization would ultimately yield **12**.

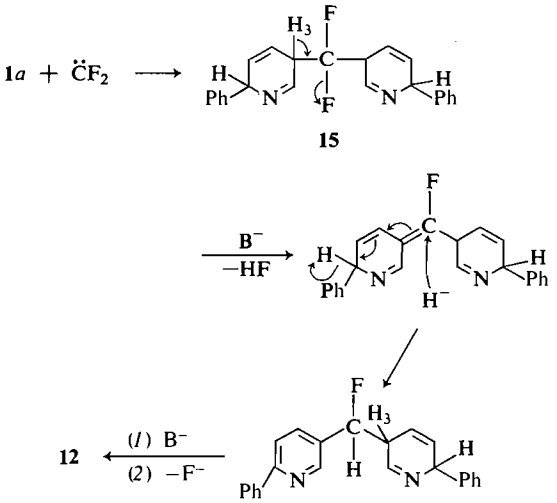

Products resulting from lithium–fluoride exchange, which would afford **12** upon hydrolysis, were eliminated since quenching the reaction mixture with deuterium oxide failed to yield deuterated **12**. Further details of this reaction are currently being investigated and will be reported later.

Addition of *N*-bromosuccinimide to **1***a* gave rise to **5***a* (74%) and 6,6′-diphenyl-3,3′-dipyridyl (**13**; 15.9%). Although **13** undoubtedly arises from reaction of **14** with **1***a*, 2-phenyl-5-bromopyridine was not detected (6).

The reaction of **1***a* with pyridines was also studied with the intention of preparing 2,3′-dipyridyls. When **1***a* was allowed to react with a

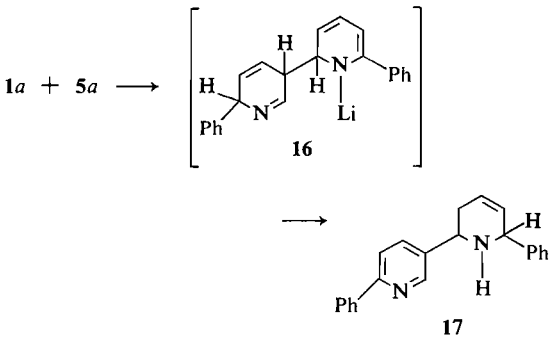

solution of **5***a* the unexpected tetrahydro product **17** (33.2%) was obtained. The intermediate product **16** must undergo further reduction rather than disproportionation to **17** since 6,6′-diphenyl-2,3′-dipyridyl was not detected.

No *N*-substitution product was detected in any of the reactions described (17). Further studies of organolithium–pyridine adducts and their derivatives are in progress in these laboratories.

Experimental

Melting points were determined with a Büchi capillary apparatus and are uncorrected. Nuclear magnetic resonance spectra were determined for solutions in deuteriochloroform or carbon tetrachloride with tetramethylsilane as an internal standard with a Varian HA-100 spectrometer. Mass spectra were measured with a CEC-21-110 mass spectrometer. Infrared spectra were recorded with a Beckman IR-8 spectrometer. Quantitative g.l.c. analyses were effected with a Hewlett-Packard 5750 or a Varian-Aerograph 1520 dual column gas chromatograph.

1-Lithio-2-phenyl-1,2-dihydropyridine (1a)

Pyridine (7.9 g, 0.1 mol) was carefully added to an ice-cold solution of phenyl lithium (8.4 g, 0.1 mol) in 200 ml of anhydrous ether under a nitrogen atmosphere. The yellow precipitate that formed was redissolved by repeated shaking. Upon cooling to 0°, **1***a* was obtained as a yellow crystalline solid. After washing with 30 ml of dry ether, the crystals were taken up in 100 ml of anhydrous tetrahydrofuran. A 2 ml aliquot of the above solution was decomposed with 10 ml of water and the concentration determined by titration with hydrochloric acid (18).

Aniline (4), 2-Phenylpyridine (5a), N-Benzylaniline (6a) 2-Phenyl-5-benzylpyridine (7a), and 2-Phenyl-5-(α-anilinobenzyl)pyridine (8)

General Procedure

N-Benzylideneaniline (0.82 g, 0.004535 mol) in 2 ml of dry tetrahydrofuran was added dropwise with shaking to a solution of 1-lithio-2-phenyl-1,2-dihydropyridine (0.74 g, 0.004535 mol) in 10 ml of dry tetrahydrofuran under an atmosphere of nitrogen at 0°. The resulting dark green solution was allowed to stand at room temperature for 1 h and then 10 ml of water was added. Extraction with chloroform (5 × 5 ml), drying (Na_2SO_4), and evaporation of the solvent gave an orange oil. Gas–liquid chromatographic analysis of a 5 ft × 1/8 in. column packed with 10% SE-30 on Anakrom ABS (60–80 mesh) with a helium flow rate of 60 ml/min at 102° gave 0.162 g (38.5%) of **4***a*, retention time of 3.25 min; at 162° gave 0.346 g (49.3%) of **5***a*, retention time of 6 min, and 0.22 g (26.5%) of **6***a*, retention time of 16 min; and at 238° gave 0.545 g (48.8%) of **7***a*, retention time of 10.75 min: m.p. 62° (lit. (19), m.p. 63–63.5°); n.m.r. ($CDCl_3$) δ 8.58 (1H, d($J_{4,6}$ = 1.5 Hz), C_6-H), 7.96 (2H, m, $C_{2',6'}$-H), 7.60 (2H, m, $C_{3,4}$-H), 7.42 (3H, m, $C_{3',4',5'}$-H), 7.25 (5H, m, —CH_2—C_6H_5), 3.98 (2H, s, —CH_2—). Aniline and *N*-benzylaniline showed i.r. and n.m.r. spectra identical to those of authentic compounds.

Isolation of 2-Phenyl-5-(α-anilinobenzyl)pyridine (8)

The residue from the above reaction was chromatographed on a 2 × 11 cm alumina column. Elution with hexane–benzene (1:1, v/v) (1000 ml) gave a mixture of **4**, **5**, **6**, and **7**. Further elution with the same solvent (600 ml) and then benzene (500 ml) gave an oil which was subjected to preparative t.l.c. on an 8 × 8 in. silica gel G plate, 0.2 mm film thickness, with benzene as the developing solvent. Extraction of the fraction with R_f of 0.6 gave 0.017 g (1.1%) of **8**: m.p. 46–48°; i.r. (KBr) 3390 cm^{-1} (NH); n.m.r. ($CDCl_3$) δ 8.7 (1H, d ($J_{4,6}$ = 2 Hz), C_6-H), 7.98 (2H, m, $C_{2'}$-H), 7.0–7.7 (11H, m, $C_{3,4}$-H and phenyl hydrogens), 6.5–6.8 (4H, m, phenyl hydrogens), 5.59 (1H, broad s, —C*H*—), 4.24 (1H, broad s, —NH—, exchanges with deuterium).

Mass Calcd. for $C_{24}H_{20}N_2$: 336.162640. Found: 336.161672.

Aniline (4), 2-Phenylpyridine-d_4 (5c), N-Benzyl-d_1-aniline (6c), and 2-Phenyl-5-benzyl-d_1-pyridine-d_3 (7c)

N-Benzylideneaniline (0.82 g, 0.00489 mol) in 2 ml of dry tetrahydrofuran was added to a solution of 0.80 g (0.00489 mol) of **1***c* in 10 ml of dry tetrahydrofuran at −65°. The reaction was completed and the g.l.c. analysis was effected as above to yield compound **4**, 0.326 g (71.5%), retention time of 2.8 min; 0.42 g (53.5%) of **5***c*, retention time of 5.25 min: b.p. 98°/0.8 Torr; n.m.r. (CCl_4) δ 8.02 (2H, m, *o*-phenyl hydrogens), 7.41 (3H, m, *m*- and *p*-phenyl hydrogens).

Mass Calcd. for $C_{11}H_5D_4N$: 159.09857. Found: 159.098936.

Compound **6***c*, 0.020 g (22.4%), retention time of 14 min: b.p. 119°/0.8 Torr; i.r. (film) 3400 cm^{-1} (NH); n.m.r. (CCl_4) δ 7.25 (5H, s, —CH—C_6H_5), 7.05 (2H, d ($J_{5,6}$ = $J_{2,3}$ = 7 Hz), $C_{2,6}$-H), 6.60 (3H, d ($J_{3,4}$ = 9 Hz) of d ($J_{2,3}$ = 7 Hz) of d ($J_{2,4}$ = $J_{4,6}$ = 2 Hz), $C_{3,4,5}$-H), 4.3 (1H, s, C_6H_5—C*H*—), 3.8 (1H, broad s, N—H, exchanges with deuterium).

Mass Calcd. for $C_{13}H_{12}DN$: 184.11101. Found: 184.110495.

Compound **7***c*, 0.544 g (44.5%), retention time 9.2 min: m.p. 54°; n.m.r. ($CDCl_3$) δ 7.98 (2H, m, *o*-phenyl hydrogens), 7.44 (3H, m, *m*- and *p*-phenyl hydrogens), 7.26 (5H, m, —CH—C_6H_5), 4.0 (1H, s, C_6H_5—C—*H*).

Mass Calcd. for $C_{18}H_{11}D_4N$: 249.14549. Found: 249.145042.

Can. J. Chem. Downloaded from www.nrcresearchpress.com by 210.87.254.40 on 09/05/12
For personal use only.

Can. J. Chem. Downloaded from www.nrcresearchpress.com by 210.87.254.40 on 09/05/12
For personal use only.

2-Phenylpyridine (5a) and 2-(2-Phenyl-5-pyridyl)-1-phenylethanol (10)

Styrene oxide (0.49 g, 0.004047 mol) in 2 ml of dry tetrahydrofuran was added to a solution of **1a** (0.66 g, 0.004047 mol) in 10 ml of dry tetrahydrofuran at −65° and the reaction was completed as above. Gas–liquid chromatographic analysis on a 2 ft × 1/8 in. column packed with 10% OV-17 on Gas Chrom P (60–80 mesh) at 200°, helium flow rate of 60 ml/min, afforded 0.196 g (31.2%) of **5a**, retention time of 3 min; and at 280° gave 0.234 g (21%) of **10**, retention time of 8.8 min: m.p. 140–142°; i.r. (KBr) 3200 cm^{-1} (OH); n.m.r. ($CDCl_3$) δ 8.41 (1H, d ($J_{4,6}$ = 2 Hz), C_6-H), 7.92 (2H, m, $C_{2',6'}$-H), 7.4 (10H, m, $C_{3',4',5'}$-H and $C_{3,4}$-H and —CH—C_6H_5), 4.83 (1H, t (J = 6 Hz), C_6H_5—C*H*), 2.98 (2H, d (J = 6 Hz), —CH_2—), 2.76 (1H, s, —OH, exchanges with deuterium).

Anal. Calcd. for $C_{19}H_{17}NO$: C, 82.88; H, 6.22; N, 5.09. Found: C, 82.63; H, 6.45; N, 5.00.

Isolation of Polymeric Product

Styrene oxide (0.8 g, 0.006712 mol) was added to **1a** (1.09 g, 0.006712 mol) as above to give an orange oil which was chromatographed on a 2.5 × 20 cm alumina column. Elution with benzene (600 ml) gave **5a**. Further elution with benzene–ether (3:1, v/v) (1200 ml) gave **10**. Elution with ether (400 ml), ether–methanol (3:1, v/v) (400 ml), and then methanol (300 ml) gave 0.5 g of a polymeric product: m.p. 60–90° (after precipitation from benzene by addition of hexane).

Mol. Wt. Found (osmetric determination): 506.

Anal. Found: C, 78.23; H, 7.00; N, 3.47. No structure was assigned to this polymer.

Similarly, the inverse addition of **1a** (1.09 g, 0.006712 mol) to styrene oxide (0.8 g, 0.006712 mol) in 5 ml of dry tetrahydrofuran afforded 0.186 g (29.7%) of **5a** and 0.275 g (24.9%) of **10** when subjected to g.l.c. analysis as described above.

2-Phenylpyridine (5a) and 2-(2-Phenyl-5-pyridyl)ethanol (11)

Ethylene oxide (0.18 g, 0.004047 mol) in 5 ml of dry tetrahydrofuran was added to a solution of **1a** (0.66 g, 0.004047 mol) in 10 ml of dry tetrahydrofuran at −65°. The reaction was completed and the g.l.c. analysis was effected as above at 200° to give 0.2 g (32.1%) of **5a**, and at 220° yielded 0.144 g (17.9%) of **11**, emergence time of 13.75 min: b.p. 188°/1.2 Torr; i.r. (film) 3300 cm^{-1} (OH); n.m.r. (CCl_4) δ 8.31 (1H, s, C_6-H), 7.82 (2H, m, *o*-phenyl hydrogens), 7.36 (5H, m, $C_{3,4}$-H and *m*- and *p*-phenyl hydrogens), 3.96 (1H, s, OH, exchanges with deuterium), 3.64 (2H, t (J = 6 Hz), HOC*H*$_2$—), 2.66 (2H, t (J = 6 Hz), —CH_2—).

Mass Calcd. for $C_{13}H_{13}NO$: 199.09964, Found: 199.099245.

Similarly, the inverse addition of **1a** (0.66 g, 0.004047 mol) in 10 ml of dry tetrahydrofuran to ethylene oxide (0.18 g, 0.004047 mol) in 5 ml of dry tetrahydrofuran at −65° afforded 0.188 g (30.2%) of **5a** and 0.205 g (25.4%) of **11** when subjected to g.l.c. analysis as described above.

2-Phenylpyridine (5a), Bis(6-phenyl-3-pyridyl)methane (12), and 6,6'-Diphenyl-3,3'-dipyridyl (13)

Trifluoromethyl bromide was bubbled slowly into a solution of **1a** (0.452 g, 0.002764 mol) in 10 ml of dry tetrahydrofuran at −65° until the dark brown color disappeared and the solution turned a yellow color. The reaction was completed as above and the reaction mixture was chromatographed on a 2.5 × 20 cm silica gel column. Elution with hexane–benzene (1:1, v/v) (900 ml) and then benzene (600 ml) gave 0.165 g (38.4%) of **5a**. Elution with benzene–ether (2:1, v/v) (300 ml) gave an oil which was purified further by t.l.c. using silica gel G plates (1.0 mm film thickness) and benzene–ether (5:1, v/v) as the developing solvent. Extraction of the fraction having an R_f of 0.25–0.55 afforded 0.18 g (40.5%) of **12**: m.p. 137–139°. Extraction of the fraction with R_f of 0.6 gave 0.004 g (1%) of **13**: m.p. 221–223°; n.m.r. ($CDCl_3$) δ 9.02 (2H, d ($J_{2,4}$ = 2 Hz), $C_{2,2'}$-H), 7.7–8.2 (8H, m, $C_{4,4',5,5'}$-H) and *o*-phenyl hydrogens), 7.4–7.6 (6H, m, *m*- and *p*-phenyl hydrogens).

Mass Calcd. for $C_{22}H_{16}N_2$: 308.131340. Found: 308.130428.

Similarly, the addition of trifluoromethyl iodide to **1a** (0.452 g, 0.002764 mol) in 10 ml of dry tetrahydrofuran and then isolation of the products as described above gave 0.169 g (39.4%) of **5a**; 0.08 g (18%) of **12**; and 0.007 g (1.7%) of **13**.

2-Phenylpyridine (5a) and 6,6'-Diphenyl-3,3'-dipyridyl (13)

N-Bromosuccinimide (0.91 g, 0.0051 mol) in 12 ml of dry tetrahydrofuran was added to **1a** (0.83 g, 0.0051 mol) in 10 ml of dry tetrahydrofuran at −65° and the reaction was completed as above. Recrystallization of the reaction mixture from 95% EtOH afforded 0.125 g (15.9%) of **13**: m.p. 221–223°; identical (i.r., n.m.r., and mass spectrum) with the same product obtained previously. The residue from the mother liquor was chromatographed on a 2.5 × 20 cm alumina column. Elution with benzene (800 ml) gave 0.566 g (75%) of **5a**.

2-Phenylpyridine (5a) and 6,6'-Diphenyl-1,2,3,6-tetrahydro-2,3'-dipyridyl (17)

2-Phenylpyridine (1.03 g, 0.00663 mol) was added to **1a** (1.08 g, 0.00663 mol) in 10 ml of dry tetrahydrofuran at 0°. The reaction was completed as above and the residue was chromatographed on a 2.5 × 25 cm silica gel column. Elution with benzene (1200 ml) gave 1.082 g (52.7%) of **5a**. Elution with benzene–ether (2:1, v/v) (700 ml) afforded 0.683 g (33.2%) of **17**: m.p. 61–63°; n.m.r. ($CDCl_3$) δ 8.74 (1H, d ($J_{2',4'}$ = 2 Hz), $C_{2'}$-H), 7.2–8.1 (12H, m, $C_{4',5'}$-H and phenyl hydrogens), 5.9 (2H, m, $C_{4,5}$-H), 4.76 (1H, m, C_6-H), 4.2 (1H, d ($J_{2,3}$ = 8.75 Hz) of d ($J_{1,2}$ = 5.75 Hz), C_2-H), 2.34 (2H, m, C_3-H), 2.18 (1H, broad s, N–H, exchanges with deuterium).

Mass Calcd. for $C_{22}H_{20}N_2$: 312.162640. Found: 312.161591.

We are grateful to the Robert A. Welch Foundation for support of this work.

1. C. S. GIAM, E. E. KNAUS, R. A. LOCKHART, and I. G. KEENER. XXIII Int. Congr. Pure Appl. Chem. July, Boston, 1971. Abstr. ORG 156; Fourth Int. Heterocycl. Congr. July, 1973, Salt Lake City. Abstr. p. 236.

2. T. C. BRUICE and S. BENKOVIC. *In* Bio-organic mechanisms. Vol. 2. W. A. Benjamin, Inc., New York, N.Y. 1966.
3. R. A. ABRAMOVITCH and J. G. SAHA. *In* Advances in heterocyclic chemistry. Vol. 6. *Edited by* A. R. Katritzky and A. J. Boulton. Academic Press, New York, N.Y. 1966. p. 229.
4. K. SCHOFIELD. *In* Hetero-aromatic nitrogen compounds. Plenum Press, New York, N.Y. 1967. Chapt. 5, p. 163.
5. C. S. GIAM and S. D. ABBOTT. J. Am. Chem. Soc. **93**, 1294 (1971).
6. C. S. GIAM and J. L. STOUT. Chem. Commun. 478 (1970).
7. C. S. GIAM and J. L. STOUT. Chem. Commun. 142 (1969).
8. P. DOYLE and R. YATES. Tetrahedron Lett. 3371 (1970).
9. R. LEVINE and W. KADUNCE. Chem. Commun. 921 (1970).
10. R. A. ABRAMOVITCH and B. VIG. Can. J. Chem. **41**, 1961 (1963).
11. C. S. GIAM and S. D. ABBOTT. Unpublished results. S. D. ABBOTT. Ph.D. Thesis, Texas A & M University, College Station, Texas, August, 1971.
12. W. T. MILLER and C. S. Y. KIM. J. Am. Chem. Soc. **81**, 5008 (1959).
13. C. L. CLOSS and L. E. CLOSS. J. Am. Chem. Soc. **82**, 5723 (1960).
14. U. FRANZEN and L. FIKENTHSCHER. Ber. **95**, 1958 (1962).
15. U. FRANZEN. Ber. **95**, 1964 (1962).
16. C. BURGESS, G. COOLEY, P. FEATHER, and U. PETROW. Tetrahedron, **23**, 4111 (1967).
17. C. S. GIAM, E. E. KNAUS, and F. M. PASUTTO. J. Org. Chem. **39**, 3565 (1974).
18. H. GILMAN and A. H. HAUBEIN. J. Am. Chem. Soc. **66**, 1515 (1944).
19. E. BENARY and H. PSILLE. Ber. B, **57**, 828 (1924); Chem. Abstr. **18**, 2896 (1924).

Can. J. Chem. Downloaded from www.nrcresearchpress.com by 210.87.254.40 on 09/05/12
For personal use only.

The Infrared Spectrum and Force Field of Matrix Isolated *cis*-Thionylimide (HNSO)

PETER O. TCHIR AND RICHARD D. SPRATLEY

Department of Chemistry, University of British Columbia, Vancouver, British Columbia V6T 1W5

Received December 3, 1974

PETER O. TCHIR and RICHARD D. SPRATLEY. Can. J. Chem. **53**, 2311 (1975).

Infrared spectra of *cis*-HNSO and several deuterium, ^{15}N, and ^{34}S isotopically substituted homologs have been obtained in argon and nitrogen matrices. The Fermi resonance between ν_4 and $2\nu_5$ is discussed. A force field has been calculated.

PETER O. TCHIR et RICHARD D. SPRATLEY. Can. J. Chem. **53**, 2311 (1975).

On a obtenu les spectres infra-rouges du HNSO *cis* et de ses homologues isotopiques ^{2}H, ^{15}N et ^{34}S dans des matrices d'argon et d'azote. On discute de la résonnance de Fermi entre ν_4 et $2\nu_5$. On a calculé le champ de force. [Traduit par le journal]

Introduction

A detailed study of the photolysis of matrix-isolated *cis*-thionylimide (HNSO) has been carried out in this laboratory (1). During the course of this work it became necessary to be able to interpret the infrared spectrum of HNSO under the high-resolution conditions provided by the matrix-isolation technique. It was also necessary to have available a reliable force field for HNSO to allow the transfer of force constants to similar molecules formed on photolysis.

Force fields based on the gas phase spectra of HNSO and DNSO have been published (2) but these are unsatisfactory for several reasons. Firstly, the molecular parameters assumed in these calculations differ significantly from those determined more recently by microwave spectroscopy (3). Secondly, and more important, Eysel (2) employed a computational technique devised by Becher and Mattes (4) which must be regarded with suspicion. Although a perfect frequency fit is guaranteed at each stage of their calculation, the problem is underdetermined; seven force constants are calculated from the six observed frequencies (HNSO and DNSO are treated separately). Thus the force fields reported represent only one choice from among the infinity of possibilities generated by their method. A detailed and incisive critique of this approach has been published by Averbukh *et al.* (5).

In this work an 11 constant force field has been adjusted by a conventional least squares technique (6) to fit 29 observed frequencies from HNSO and six isotopically substituted homologs containing deuterium, ^{15}N and ^{34}S.

Experimental

The experiments were performed in an Andonian Dewar (Model MND-3L-15N) cooled with liquid helium. Samples were isolated in argon and nitrogen matrices (Matheson prepurified grades). Mole ratios of matrix gas to HNSO (M/R) ranged from 200 to 1000 in different experiments. Deposition was carried out from a mercury free vacuum system at rates averaging 2 mmol total sample per hour. Spectra were recorded on a Perkin-Elmer Model 225 infrared spectrometer with a frequency accuracy of $\pm 2\ cm^{-1}$ on survey scans and $\pm 0.5\ cm^{-1}$ under high resolution conditions. Spectral slit widths ranged from 0.2 to 0.5 cm^{-1} for high resolution scans.

HNSO was prepared in the gas phase by the method of Schenk (7)

$$3NH_3(g) + SOCl_2(g) \rightarrow HNSO(g) + 2NH_4Cl(s)$$

Since monomeric HNSO polymerizes on condensation, samples were stored in the gas phase at room temperature. Over a period of a few weeks, a slight decomposition of HNSO was observed indicated by an increase in SO_2, the only infrared active impurity present in measurable amounts. Deuterium and ^{15}N substitution were achieved using ND_3 (Merck, Sharp and Dohme) and $^{15}NH_3$ (Isomet Corporation, 95% purity) respectively.

Results

Sample Isolation and ^{34}S Absorption

Because HNSO is polymeric as a low temperature solid, it was essential to find matrix conditions which guaranteed isolation of the monomeric species. Fortunately, as is discussed below, the NH stretching mode of HNSO proved to be an excellent indicator of monomer isolation. Figure 1 shows a survey of HNSO deposited in argon at relatively high dilution ($M/R = 800$). All the absorptions can be assigned to either HNSO (12) or the SO_2 impurity.

The two sharp, weak absorptions at 1233.4 and

Can. J. Chem. Downloaded from www.nrcresearchpress.com by 210.87.254.42 on 09/05/12
For personal use only.

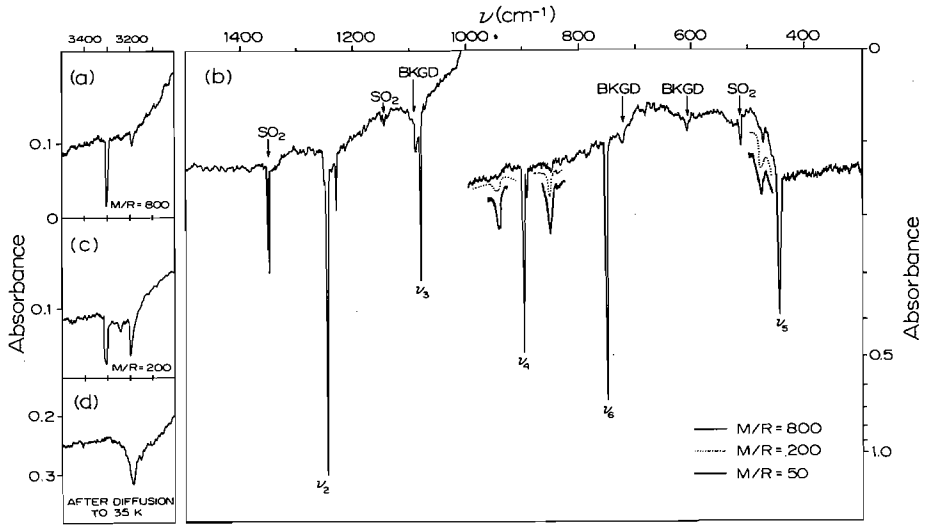

FIG. 1. The infrared spectrum of *cis*-HNSO in argon matrices.

895.7 cm^{-1} shifted slightly to low frequency of the ν_2 and ν_4 absorptions of HNSO are due to molecules containing ^{34}S in natural abundance. From the high resolution spectrum the estimated integrated intensity ratio for the 1233.4 cm^{-1} ($HN^{34}SO$) peak to the 1248.7 cm^{-1} ($HN^{32}SO$) peak is about 7%. The natural abundance of ^{34}S is 4%. Difficulties in estimating intensities are assumed to account for the discrepancy. Figure 2 shows a high resolution scan of the 900 cm^{-1} region. The 895.7 cm^{-1} absorption appears together with an overlapping peak at 893.8 cm^{-1}. The ratio of the combined intensities of these two peaks to that of the 900.4 cm^{-1} peak is about 12%. To account for this large difference from 4% the two peaks are assigned separately, the 895.7 cm^{-1} to the ^{34}S molecule and the 893.8 cm^{-1} to the overtone of ν_5 which is observed because of a slight Fermi resonance with the ν_4 vibrational level. This resonance is further discussed in the next section. An estimated intensity for the single 895.7 cm^{-1} peak gives a ratio of about 6% to the 900.4 cm^{-1} peak.

In the region above 3000 cm^{-1} Fig. 1*a* reveals a broad, weak absorption at 3200 cm^{-1}, 100 cm^{-1} below the NH stretch at 3308.5 cm^{-1}. At lower dilution the intensity of this feature is greatly enhanced as shown in Fig. 1*c* for $M/R = 200$. The spectrum in Fig. 1*d* resulted when this sample was warmed to about 35 K and recooled. The absorption at 3200 cm^{-1}, favored at low dilution, has broadened and gained intensity while the feature at 3308.5 cm^{-1} has disappeared. This behavior is characteristic of aggregation in a matrix and suggests that the 3308.5 cm^{-1} peak

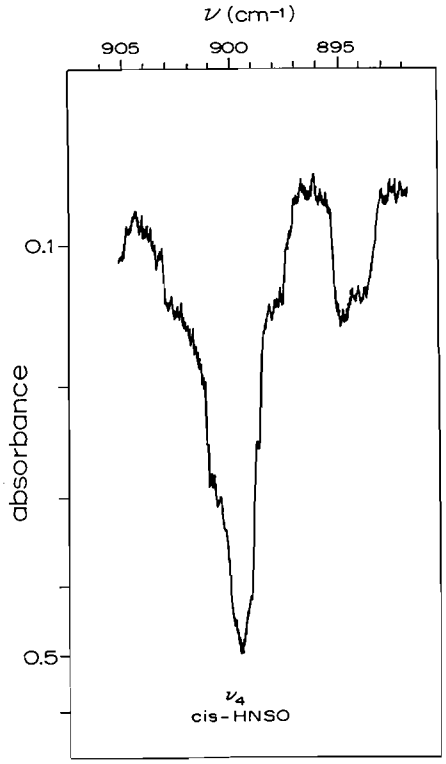

FIG. 2. The high resolution spectrum of ν_4 of *cis*-HNSO showing both the ^{34}S isotopic splitting and the $2\nu_5$ overtone.

Can. J. Chem. Downloaded from www.nrcresearchpress.com by 210.87.254.42 on 09/05/12
For personal use only.

TABLE 1. The gas phase and matrix frequencies and the matrix shifts, Δ, for *cis*-HNSO in argon and nitrogen matrices. The frequencies of *cis*-HNSO dimer in argon are included. All frequencies are in cm^{-1}

	Gas*	Ar matrix			N_2 matrix	
	ν	ν	Δ†	Dimer	ν	Δ†
ν_1	3345	3308.5	−37	3200	3303	−42
ν_2	1261	1248.7	−12	1245	1252	−9
ν_3	1090	1082.7	−7	1080	1094	+4
ν_4	911	900.4	−11	945	923	+12
ν_5	453	447.4	−6	478	455	+2
ν_6	759	754.7	−4	852	774	+15

*From ref. 12.
†Δ = ν(matrix) − ν(gas).

can be identified with the monomer and the 3200 cm^{-1} peak with the dimer or higher aggregates of HNSO. It is tempting to consider the HNSO dimer as a hydrogen bonded eight membered ring.

It has been pointed out by Pimentel and McClellan (8) that hydrogen stretching modes are most strongly affected by hydrogen bonding. Large decreases in stretching frequencies and broadening of peaks coupled with dramatic intensity enhancements are generally observed. The 3200 cm^{-1} feature shows the necessary shift and broadening. Therefore, the intensity enhancement suggests that even though the 3200 and 3308.5 cm^{-1} absorptions are of near equal intensity at $M/R = 200$, the actual concentration of dimer is still quite small. Thus this peak is a sensitive measure of isolation.

The above conclusions then allow the assignment of other weaker, but still broad and concentration dependent, features in the $M/R = 200$ spectrum to the same dimer. These are shown as a broken line in Fig. 1*b* at 945, 852, and 478 cm^{-1}. On dimerization the SO and NS stretches at 1248.7 and 1082.7 cm^{-1}, since they are least involved in the hydrogen bonding, show only slight broadening to low frequencies while the other absorptions show large shifts. The peak at 945 cm^{-1} is the HNS bend shifted up from 900.4 cm^{-1}, at 852 cm^{-1} is the torsion, or out of plane mode, shifted up from 754.7 cm^{-1}, and at 478 cm^{-1} is the NSO bend shifted down from 447.4 cm^{-1}. These absorptions show shifts that are characteristic for each type of mode (8). They also show the characteristic broadening for hydrogen bonded dimer absorptions.

A spectrum at $M/R = 50$ shows these absorptions to be still more intense and also contains numerous other broad features that can likely be assigned to higher aggregates or to aggregation with SO_2. The 945, 852, and 478 cm^{-1} peaks at $M/R = 50$ are shown in Fig. 1*b* as heavy lines. Although this aspect was not further pursued, the absorptions assigned to the HNSO dimer are listed in Table 1.

Using the relatively large intensity of the concentration dependent feature at 3200 cm^{-1} as a measure of aggregation, a dilution of $M/R = 400$ was found to provide satisfactory isolation and was used for most of the experiments reported here.

Matrix Splitting

The HN stretch, ν_1, the torsion, ν_6, and the asymmetric stretch of SO_2 appear as doublets in argon matrices. The splittings are 5.1 cm^{-1} for ν(HN), 1.7 cm^{-1} for ν(torsion), and 4.1 cm^{-1} for ν_3 of SO_2. These doublets do not show the characteristics of splittings that are due to association. The possibility that these splittings are due to rotation within a matrix cannot be ruled out without careful temperature studies which were not possible in this work. However, it is generally felt that molecules as large as HNSO will not rotate in a matrix and the rotational splitting of ν_3 of SO_2, only 0.5 cm^{-1} in krypton matrices (10), is not expected to be as large as 4.1 cm^{-1}.

Therefore, the observed splittings have been ascribed to the occupancy of different sites within the argon lattice. This type of matrix splitting is characteristic of argon matrices (11).

Matrix Shifts: Ar and N_2 Matrices

Table 1 gives the observed frequencies of HNSO in argon and nitrogen matrices and the shifts from the gas phase values (12). These results are consistent with other observations of matrix effects (14): the average absolute shift is

Can. J. Chem. Downloaded from www.nrcresearchpress.com by 210.87.254.42 on 09/05/12
For personal use only.

Can. J. Chem. Downloaded from www.nrcresearchpress.com by 210.87.254.42 on 09/05/12
For personal use only.

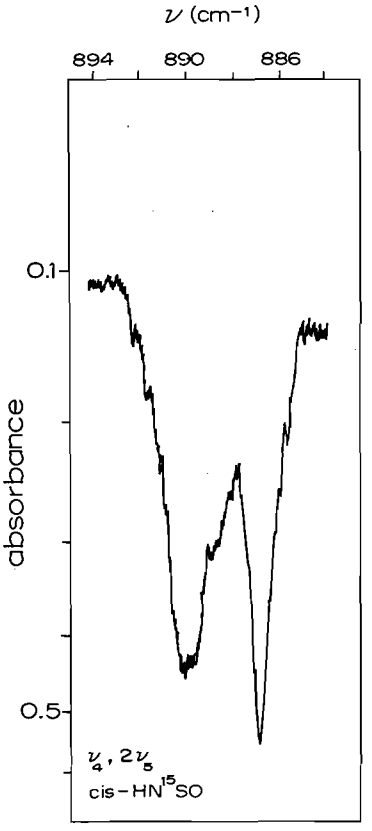

FIG. 3. The Fermi resonance doublet of ν_4 and $2\nu_5$ of *cis*-$H^{15}NSO$.

slightly less in argon (13 cm^{-1}) than in nitrogen (16 cm^{-1}); the argon frequencies are consistently lower than the gas phase frequencies whereas both positive and negative shifts are found in nitrogen; and modes involving hydrogen show particularly large shifts in nitrogen.

A comparison of the matrix shifts of HNSO and DNSO in argon reveals that ν_2, ν_3, and ν_5 have almost identical shifts for H and D; ν_1, ν_4, and ν_6 show significantly smaller shifts for D than for H. The latter modes, which involve a large hydrogen displacement, decrease in amplitude upon substitution of deuterium; therefore, the interaction with the matrix is decreased.

The results of photolysis of HNSO in solid N_2 were greatly confused by the apparent interaction of the photolysis products with the matrix. For this reason argon was chosen as the most suitable matrix material and the majority of the results were obtained in solid argon.

Fermi Resonance of ν_4 *and* $2\nu_5$

A weak absorption at 893.8 cm^{-1} in the $H^{14}NSO$ spectrum has been assigned above to the overtone of ν_5, the NSO bend. The peak is seen only because it has gained a small amount of intensity from ν_4 as a result of a Fermi resonance interaction. In $H^{15}NSO$ the effect becomes much larger and a near equal intensity doublet results as is seen in Fig. 3. Since the doublet components are of near equal intensity, the mixing of the $v_4 = 1$ and $v_5 = 2$ states resulting from the interaction is complete and the value of ν_4 must be taken as an average of the 890.6 and 887.7 cm^{-1} peaks. This is 889.2 cm^{-1}.

Table 2 shows the differences between ν_4 and $2\nu_5$ for the various isotopes of HNSO in argon and nitrogen matrices. For the ^{15}N substituted molecule in argon the separation is only 0.4 cm^{-1} and thus a strong resonance occurs while for the ^{14}N molecule the difference is 5.6 cm^{-1} and there is a weak interaction. For the deuterated species and for nitrogen matrices no resonance was seen.

Of interest is the closeness of the observed overtone to two times the fundamental which suggests a low anharmonicity in the ν_5 mode. Fermi resonance, which results from a breakdown of the harmonic oscillator approximation, also depends on anharmonicity. Perturbation theory shows that the separation of the resonance doublet depends on the cubic force constant in normal coordinates, K_{455} (9). For $H^{15}NSO$, where the zero order separation is estimated at 0.4 cm^{-1} and the intensities suggest a complete mixing of the zero order states, the resonance only causes a splitting of 2.9 cm^{-1}. By comparison, in CO_2 where a strong resonance is observed the separation of the doublet is 102.8 cm^{-1}. Thus it is evident that the resonance between $2\nu_5$ and ν_4 of HNSO is very weak. This requires that the cubic force constant K_{455} be small, *i.e.* the anharmonicity is small. Thus the frequency of the overtone and the extent of the resonance both suggest that the ν_5 potential function is nearly harmonic.

Force Field

Table 3 lists the frequencies measured for *cis*-HNSO and its isotopic homologs isolated in solid argon. Complete spectra were recorded for molecules containing ^{15}N and deuterium while for ^{34}S only peaks with large enough separation from ^{32}S peaks and with sufficient intensity to be seen in natural abundance (4%) were observed.

TABLE 2. A study of Fermi resonance in *cis*-HNSO. Separations of unperturbed ν_4 and $2\nu_5$(calcd.) levels

Isotope and matrix	ν_4 (cm^{-1})	$2\nu_5$(calcd.)(cm^{-1})	$\nu_4 - 2\nu_5$ (cm^{-1})
HNSO/Ar	900.4	894.8 (obsvd. 893.8)	5.6
$HNSO/N_2$	923	910	13
$H^{15}NSO/Ar$	889.2*	888.8 (obsvd. 887.7)	0.4
$H^{15}NSO/N_2$	911	904	7
DNSO/Ar	751.5	800.6	−49.1

*Average of doublet.

TABLE 3. Observed and calculated frequencies for several isotopic homologs of *cis*-HNSO in argon matrices. The average error in the calculated frequencies is 1.8 cm^{-1} (0.18%)

		$\nu \pm 0.5$ (cm^{-1})						
		HNSO	$HN^{34}SO$	DNSO	$DN^{34}SO$	$H^{15}NSO$	$H^{15}N^{34}SO$	$D^{15}NSO$
ν_1	Obsvd.	3308.5		2453.1		3301.4		2441†
	Calcd.	3308.8	3308.8	2452.6	2452.6	3301.1	3301.1	2441.5
ν_2	Obsvd.	1248.7	1233.4	1244.8	1230.1	1243.3	1228.4	1239.4
	Calcd.	1250.8	1236.1	1246.4	1224.6	1244.8	1223.1	1241.5
ν_3	Obsvd.	1082.7		1048.0		1072.4		1030†
	Calcd.	1086.3	1083.7	1049.2	1042.2	1069.0	1065.6	1028.4
ν_4	Obsvd.	900.4	895.7	751.5	749.6	889.2*		750.0
	Calcd.	899.5	892.9	754.8	747.0	892.9	882.7	749.1
ν_5	Obsvd.	754.7		593.8		750.9		587.6
	Calcd.	755.7	754.6	591.9	590.0	751.8	750.3	587.0
ν_6	Obsvd.	447.4		400.3		444.4		398.8
	Calcd.	447.4	444.9	400.6	398.4	443.9	440.3	399.1

*Average of Fermi doublet.
†Accuracy of ±2 cm^{-1}.

These 29 frequencies were fitted with a harmonic potential energy expression using 11 constants by means of the least squares refinement program FPERT written by Schachtschneider (6). The structural parameters used were those determined by Kirchhoff (3): $r_{NH} = 1.03$ Å, $r_{NS} = 1.51$ Å, $r_{SO} = 1.45$ Å, $\alpha_{HNS} = 116°$, $\alpha_{NSO} = 120°$, $\tau = 0°$ (*i.e.* planar).

While calculating the modified force field for this molecule, the following criteria were used: reasonable force constants with small errors; good agreement between observed and calculated data; a sensible vibrational assignment revealed through the potential energy distribution (13). The first two criteria are quite easily satisfied for a force field where many interaction constants are set equal to zero; the third is often a sensitive indication of the relative success or failure of a particular calculation.

Once calculations were begun, it soon became apparent that a single force field would not be able to fit both the hydrogen containing molecules and their deuterium homologs. The results gave poor frequency fits for ν_1 and peculiar potential energy distributions for the strongly interacting modes near 1000 cm^{-1} (*viz.* ν_2, ν_3, and ν_4). The problem stems, of course, from the use of observed rather than harmonic frequencies in the calculations. The effects of anharmonicity are greatest in the high amplitude hydrogen modes ν_1 and ν_4. Assignments indicate that ν_1 involves almost completely the HN stretching coordinate while ν_4 has a large contribution from the HNS bend. On deuteration, these vibrations sample significantly different parts of the potential energy surface, hence their force constants are not isotopic invariants. Thus the "effective" force constants for these modes will change on deuteration. Bearing these points in mind we permitted refinement of different values of the diagonal force constants f_{HN}, f_{HNS}, and $f_{torsion}$ for H- and D-containing molecules. Given this

Can. J. Chem. Downloaded from www.nrcresearchpress.com by 210.87.254.42 on 09/05/12
For personal use only.

TABLE 4. Force field for *cis*-HNSO including least squares error estimates

Constant	Value (aJ/Å², aJ/Å rad, aJ/rad²)	Error
f_{HN}	6.05	0.01
f_{DN}	6.20	0.01
f_{NS}	6.47	0.06
f_{SO}	9.01	0.10
f_{HNS}	0.457	0.009
f_{DNS}	0.469	0.012
f_{NSO}	1.66	0.04
$f_{torsion}$	0.225	0.001
f_{HNS-SO}	−0.14	0.03
f_{HNS-NS}	−0.15	0.02
$f_{HNS-NSO}$	−0.18	0.01

TABLE 5. Potential energy distribution and assignment resulting from the force field in Table 4

	ν(calcd.) (cm^{-1})	Potential energy distribution						Assignment
		f_{HN}	f_{NS}	f_{SO}	f_{HNS}	f_{NSO}	f_{τ}	
ν_1	3308.8	0.998	0.001	0.0	0.0	0.001		HN stretch
ν_2	1250.8	0.0	0.240	0.711	0.046	0.004		SO stretch
ν_3	1086.3	0.0	0.401	0.262	0.253	0.002		NS stretch
ν_4	899.5	0.001	0.320	0.013	0.528	0.116		HNS bend
ν_6	755.7						1.000	Torsion
ν_5	447.4	0.0	0.046	0.019	0.234	0.925		NSO bend

TABLE 6. Thermodynamic functions for HNSO calculated from vibrational frequencies, cal mol^{-1} K^{-1}

Temperature (K)	S	C_p	$-\frac{(G - H_0)}{T}$	$\frac{(H - H_0)}{T}$
273.15	65.95	10.57	57.22	8.72
298.10	66.89	11.01	57.99	8.90
100.00	56.94	8.08	48.97	7.96
200.00	62.86	9.30	54.57	8.29
300.00	66.96	11.04	58.05	8.91
400.00	70.37	12.65	60.71	9.65
500.00	73.33	13.90	62.95	10.38
600.00	75.96	14.84	64.90	11.05
700.00	78.30	15.55	66.65	11.65
800.00	80.42	16.11	68.24	12.17
900.00	82.34	16.57	69.70	12.64
1000.00	84.11	16.95	71.06	13.05
1100.00	85.74	17.27	72.32	13.42
1200.00	87.26	17.55	73.50	13.75
1300.00	88.67	17.78	74.61	14.05
1400.00	90.00	17.99	75.66	14.33
1500.00	91.24	18.17	76.66	14.58

freedom, the problem soon converged. The best set of force constants so obtained is given in Table 4.

It should be noted that the force constants quoted in Table 4 are not bond length weighted but are in the convenient m.k.s. system of units: aJ/Å² (10^5 dynes/cm) for stretches, aJ (10^{-11} ergs) for bends, and aJ/Å (10^{-3} ergs/cm) for bend–stretch interactions. The potential energy distribution (hence vibrational assignment) for the

Can. J. Chem. Downloaded from www.nrcresearchpress.com by 210.87.254.42 on 09/05/12
For personal use only.

common isotopic homolog of HNSO is given in Table 5. The calculated frequencies are listed for all the isotopic species of *cis*-HNSO in Table 3. The average frequency error using the force constants in Table 4 is 1.8 cm^{-1}.

The values of f_{DN} and f_{DNS} are, as expected, slightly larger (by 2%) than their hydrogenic counterparts; the deuterium vibrations are sampling a lower portion of the potential function which when fitted to a harmonic function results in a more steeply curved parabola. The torsion constant for DNSO did not differ significantly from that of HNSO so only one value was allowed in later refinements. This presumably indicates a low anharmonicity in the torsional coordinate. Every off-diagonal force constant (except those involving the HN stretching coordinate) was tried in the calculation at one time or another. Only those to which the results were significantly sensitive were retained.

Thermodynamic Functions

The thermodynamic functions calculated for *cis*-HNSO over the temperature range 100 to 1500 K are given in Table 6. These calculations were made using the vibrational frequencies taken from the argon matrix experiments.

1. P. O. TCHIR and R. D. SPRATLEY. Can. J. Chem. **53**, 2318 (1975); **53**, 2331 (1975).
2. H. H. EYSEL. J. Mol. Struct. **5**, 257 (1970).
3. W. H. KIRCHHOFF. J. Am. Chem. Soc. **91**, 2437 (1969).
4. H. J. BECHER and R. MATTES. Spectrochim. Acta, **23A**, 2449 (1967).
5. B. S. AVERBUKH, L. S. MAYANTS, and G. B. SHALTUPER. J. Mol. Spectrosc. **30**, 310 (1969).
6. J. H. SCHACHTSCHNEIDER. Shell Development Company, Tech. Rep. 263–62. 1962.
7. P. W. SCHENK. Ber. **65**, 94 (1942).
8. G. C. PIMENTEL and A. L. MCCLELLAN. The hydrogen bond. W. H. Freeman and Co., San Fransisco. 1960. pp. 67–141.
9. G. HERZBERG. Infrared and Raman spectra. D. Van Norstrand Co. Inc., New York. 1945. pp. 215–218.
10. M. ALLAVENA, R. RUSNIK, D. WHITE, V. CALDER, and D. E. MANN. J. Chem. Phys. **50**, 3399 (1969).
11. A. J. BARNES and H. E. HALLAM. Q. Rev. **23**, 392 (1969).
12. H. RICHERT. Z. Anorg. Allg. Chem. **309**, 171 (1961).
13. Y. MORINO and K. KUCHITSU. J. Chem. Phys. **20**, 1809 (1952).
14. G. C. PIMENTEL and S. W. CHARLES. Pure Appl. Chem. **7**, 111 (1963).

Can. J. Chem. Downloaded from www.nrcresearchpress.com by 210.87.254.42 on 09/05/12
For personal use only.

The Photolysis of Matrix Isolated *cis*-Thionylimide. 1. The Identification and Infrared Spectra of *cis*-HOSN, HSNO, and SNO

PETER O. TCHIR AND RICHARD D. SPRATLEY

Department of Chemistry, University of British Columbia, Vancouver, British Columbia V6T 1W5

Received December 3, 1974

PETER O. TCHIR and RICHARD D. SPRATLEY. Can. J. Chem. 53, 2318 (1975).

cis-HNSO has been photolyzed in argon matrices using a medium pressure mercury lamp. Examination of the infrared spectra has revealed the presence of four photolysis products. With the aid of isotopic substitution these species have been identified as *cis*-HOSN, *cis*-HSNO, *trans*-HSNO, and SNO, all previously unknown. Assignments have been made for all four products and force fields calculated for *cis*-HOSN and *trans*-HSNO. The following reaction scheme has been postulated for the photolysis induced process: *cis*-HNSO → *cis*-HOSN → *cis*-HSNO + *trans*-HSNO → SNO. The extent of this reaction sequence has been found to depend on reaction time and photolysis energy.

PETER O. TCHIR et RICHARD D. SPRATLEY. Can. J. Chem. 53, 2318 (1975).

On a photolysé le HNSO *cis* dans une matrice d'argon à l'aide d'une lampe à mercure de pression moyenne. L'examen du spectre infra-rouge révèle la présence de quatre produits de photolyse. Utilisant le remplacement isotopique, ces espèces son identifiées comme étant le HOSN *cis*, le HSNO *cis*, le HSNO *trans* et le SNO, tous jusqu'ici inconnues. Les attributions sont faites pour les quatre produits et les champs de force calculés pour le HOSN *cis* et HSNO *trans*. La séquence réactionnelle suivante, est proposée pour le processus photolytiques induit: HNSO *cis* → HOSN *cis* → HSNO *cis* + HSNO *trans* → SNO. L'importance de ce cheminement réactionnel dépend du temps de réaction et de l'énergie requise pour la photolyse.

[Traduit par le journal]

Introduction

In the ultraviolet spectrum of *cis*-HNSO only one diffuse absorption and one continuum were observed (1). From this observation it was deduced that photolysis of the molecule was occurring. Since it was possible that the hydrogen was being removed to give the NSO radical, this photolysis appeared to be an ideal system for a study utilizing the matrix isolation technique. In this technique a hydrogen atom can diffuse away through the matrix to leave behind the isolated, stabilized radical. On the other hand, if the product or products were unstable isomers of *cis*-HNSO, they might also be stabilized at the low temperature of the matrix.

In this paper we describe the results of the mercury arc photolysis of *cis*-HNSO in argon matrices: in part I the infrared results are presented and four new molecular species are identified; in part II the reactions taking place in the matrix are considered.

Experimental

The production of *cis*-HNSO, the matrix isolation apparatus, and the infrared spectrometer (Perkin-Elmer 225) have been described previously (2). Photolysis was carried out using a 100 W PEK medium pressure mercury lamp (#112-2118) powered by a PEK model 401 power supply.

In some special cases photolysis was done with a vacuum ultraviolet lamp similar to that of Davis and Braum (3). Using a discharged flow of 1 part hydrogen to 9 parts helium at a pressure of approximately 0.5 Torr this lamp gave good yields of 1216 Å radiation (3). In this study it was used for photolysis with simultaneous deposition of the *cis*-HNSO/Ar sample. This lamp and its use are further described by Tchir (4).

I. Identification of Products

The mercury lamp photolysis of *cis*-HNSO isolated in an argon matrix ($M/R = 400$) resulted in 17 new absorptions in the infrared spectrum. Obviously several new molecules were being produced. The intensities of these absorptions were studied as a function of photolysis time to determine which absorptions belonged to each molecule. It was found that all the absorptions followed one of the three growth curves shown in Fig. 1 and on this basis, all observed absorptions were grouped as shown in Table 1.

The groups of absorptions were then considered separately and, for the purpose of identification and normal coordinate analysis,

Can. J. Chem. Downloaded from www.nrcresearchpress.com by 210.87.254.5 on 09/05/12
For personal use only.

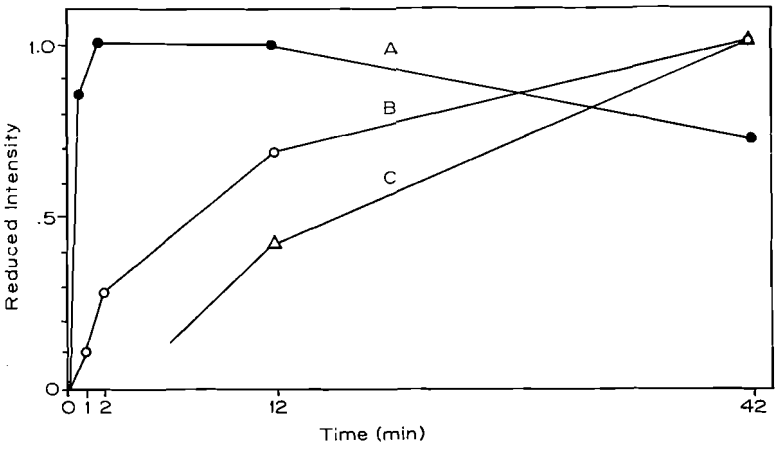

FIG. 1. Growth curves of the three different groups of peaks resulting from Hg lamp photolysis.

TABLE 1. Infrared frequencies, isotopic shifts, intensities, and assignments for three molecules produced on u.v. photolysis of *cis*-HNSO in argon matrices. Frequencies in cm^{-1}

	ν						
Molecule	Normal	D	Shift	^{15}N	Shift	Intensity*	Assignment
A (HOSN)	3519.8	2597.1	922.7	3519.3	0.5	m	HN stretch
	1320.8	1319.0	1.8	1294.3	26.5	w	SN stretch
	991.8			991.1	0.7	w	HOS bend
	673.9	671.3	2.6	673.3	0.6	vs	SO stretch
	417.5	325.2	92.3	416.5	1.0	m	torsion
	374			368	6	vw	OSN bend
B† (HSNO)	1596.8	1595.1	1.7	1569.4	27.4	vs	NO stretch
	(1595.0)	(1593.5)		(1568.0)			
	(1591.1)	(1592.4)		(1564.2)			
		(1587.8)					
	1571.0	1568.8	2.2	1544.4	26.6	s	NO stretch
	(1576.0)	(1574.1)		(1549.3)			
	876	722.7	153	872.8	3	m	HSN bend
		(725.9)		(876.2)			
		(724.0)		(874.2)			
	858			850	8	vvw	HSN bend?
	542	488?	54	533.0	9	m	NS stretch
				(536.9)			
				(535.5)			
	500	488?	12	495	5	w	torsion
	385			380	5	vvw	?
	306	304	2	304.1	2	w	?
	298	294	4	294.9	3	m	SNO bend
C (SNO)	1523.0	1523.0	0.0	1498.1	24.9	s	NO stretch
	789.7	789.7	0.0	777.6	12.1	m	SNO bend

*s = strong, m = medium, w = weak, v = very.
†For molecule B where multiplets occur all the peaks are given with the most intense selected for calculations.

isotopic substitution was carried out. Table 1 also lists the frequencies and frequency shifts observed on deuteration and ^{15}N substitution.

The observed vibrational frequencies and their shifts on isotopic substitution were used to identify the product species. Structures were proposed using bond lengths and angles from analogous molecules and vibrational analyses were carried out using the programs of Schachtschneider (5). In the following sections the

Can. J. Chem. Downloaded from www.nrcresearchpress.com by 210.87.254.5 on 09/05/12
For personal use only.

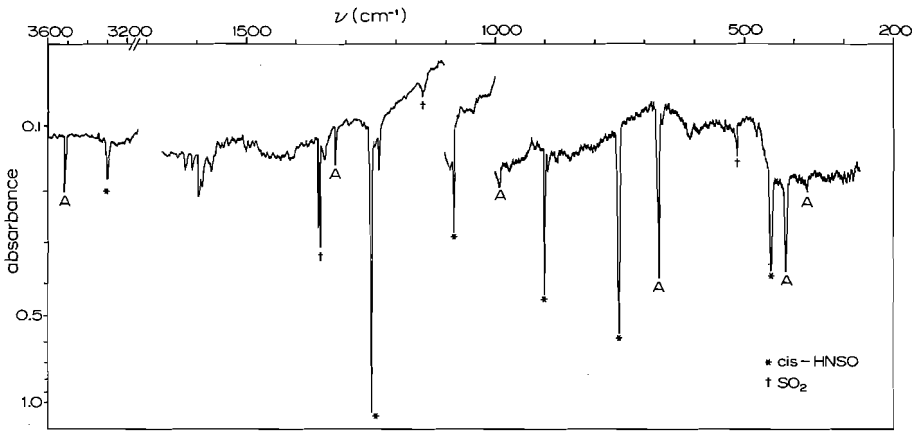

FIG. 2. Spectrum following the 1 min Hg lamp photolysis of *cis*-HNSO in argon (M/R = 400).

identification and force field calculations for each of the new molecules are discussed.

Molecule A

Identification

Figure 2 shows the spectrum of a sample of *cis*-HNSO in argon (M/R = 400) following 1 min photolysis. The peaks labelled A and grouped in Table 1 have grown very rapidly, 1 min is a very short photolysis time by matrix isolation standards where times of several hours are usual. The substitution of ^{15}N and deuterium resulted in the frequencies and shifts given in Table 1. Since the spectrum of molecule A contains 6 absorptions, molecule A is most likely tetraatomic, probably a simple isomer of *cis*-HNSO.

The first structure to come to mind is *trans*-HNSO. However, this possibility is quickly discredited when one tries to make an assignment consistent with the observed frequencies of *cis*-HNSO, the intensities, and the isotopic shifts. Firstly, the ^{15}N shift of the 3520 cm^{-1} absorption is only 0.5 cm^{-1}. This is too low for an HN stretch if one considers that the shift in *cis*-HNSO is 7.4 cm^{-1}. Also, the comparison with *cis*-HNSO requires that the 1321 cm^{-1} absorption be the SO stretch. But whereas the SO stretch in *cis*-HNSO is by far its most intense absorption, the 1321 cm^{-1} absorption is one of the weakest in the spectrum of molecule A. Similarly it is not possible to make meaningful assignments of the four low frequency absorptions to the molecule *trans*-HNSO.

A careful examination of the frequency, the intensity, and the isotopic shifts of each absorption is necessary. The absorption at 3519.8 cm^{-1} must be either an HN or HO stretch. HS stretches are always much lower (~2600 cm^{-1}) and even HN stretches are seldom this high. On substitution with ^{15}N, the mode shows almost no shift, thus demonstrating that it is an HO rather than an HN stretch.

The absorption at 1320.8 cm^{-1} may be a multiply bonded SO, SN, or NO stretch or possibly a hydrogen bend. The deuterium shift of 1.8 cm^{-1} removes the possibility of a hydrogen bend and the ^{15}N shift of 26.5 cm^{-1} eliminates an SO stretch. The possibility that it is either a low energy NO stretch or a high energy SN stretch still remains. However, it is generally found that NO stretches are very intense because of the large contribution made by this polar bond to the overall dipole moment of the molecule. Because S and N have similar electronegativities, their bonds are less polar and usually give lower intensities. Since the 1320.8 cm^{-1} absorption has a low intensity compared with the other absorptions of molecule A it is assigned to an SN stretch. By comparison, for the molecule FSN the stretching frequency of the SN triple bond is 1372 cm^{-1} (6). Thus molecule A seems to have an SN triple bond.

The next peak is at 991.8 cm^{-1}. It has a shift of only 0.7 cm^{-1} on ^{15}N substitution which suggests that the mode does not involve much nitrogen displacement. The absorption is in the appropriate region for a hydrogen bending mode but since it is not observed on deuterium substitution nothing definite can be said at this stage.

The 673.9 cm^{-1} absorption, the most intense

Can. J. Chem. Downloaded from www.nrcresearchpress.com by 210.87.254.5 on 09/05/12
For personal use only.

TABLE 2. Comparison of the fit of the *cis* and *trans* forms of HOSN to the observed torsional frequencies. Frequencies in cm^{-1}

	*cis**			*trans*†		
	Obsvd.	Calcd.	Δ	Obsvd.	Calcd.	Δ
HOSN	417.5	419.3	−1.8	417.5	421.7	−4.2
$HOS^{15}N$	416.5	418.9	−2.4	416.5	421.3	−4.8
DOSN	325.2	319.6	5.6	325.2	312.1	13.1

*f_τ = 0.0782 aJ.
†f_τ = 0.0854 aJ.

in the spectrum of molecule A, shows little ^{15}N or D shift (0.6 and 2.6 cm^{-1} respectively). These small shifts eliminate all possibilities except an SO stretch. This assignment fits the intensity observation for a polar SO bond would be expected to give an intense stretching absorption. As well, it is in the frequency range expected for an SO single bond stretch.

The next peak, 417.5 cm^{-1}, has medium intensity. It shows a large D shift of 92.3 cm^{-1} but a small ^{15}N shift of 1.0 cm^{-1}. This large D shift requires a large hydrogen movement on vibration and for the frequency to be this low, it can only be a torsional type of mode.

The remaining peak is very weak and is not observed in the D experiments because of the small quantities of sample. However, its low frequency and the medium ^{15}N shift of 6 cm^{-1} suggest assignment to a bending vibration involving a nitrogen atom.

The above discussion shows that the molecule possesses an HO bond, an SO single bond, and an SN triple bond. Molecule A must be HOSN. The assignments discussed above are given along with the frequencies in Table 1. Unfortunately, this data alone does not allow for the choice of the *cis*, *trans*, or out of plane configuration.

Normal Coordinate Analysis

Based upon comparisons with similar molecules the structure of HOSN was approximated with the following parameters (4): r_{HO} = 0.96 Å, r_{OS} = 1.62 Å, r_{SN} = 1.46 Å, α_{HOS} = 100°, and α_{OSN} = 115°. The choice of dihedral angle is very important. If the molecule is planar the torsional coordinate is of a different symmetry than the other coordinates and thus will not mix with the OSN bend which is of similar energy. In the nonplanar case the mixing of these internal coordinates will result in complicated normal coordinates and a more difficult calculation.

Accordingly, using the above structure attempts were made to fit the observed frequencies to *cis*, *trans*, and 90° out of plane molecules. In all models the four high energy modes could be well fit. However, in the out of plane molecule the fit to the 417.5 and 374 cm^{-1} absorptions had large errors without a torsion – OSN bend interaction constant while with this constant the least squares iteration would not converge. These results appear to rule out a nonplanar molecule. This is not surprising since isoelectronic molecules such as HONO and HNSO are all planar. In both the *cis* and *trans* planar models convergence and good fit could be obtained. The best source of comparison between the two is the torsional mode. Since it is the only out of plane mode of the molecule, isotopic substitution results in as good a comparison as it does for diatomic molecules. Table 2 gives the observed and best calculated frequencies for the torsional mode using *cis* and *trans* forms of HOSN. Assuming that errors in the structure have not resulted in bad G matrix elements, the fit is better for the *cis* isomer. For this reason it is felt that the molecule is *cis*-HOSN. Some further evidence favoring the *cis* structure is presented in part II of this paper.

Table 3 gives the force constants and their least squares estimated errors for *cis*-HOSN and

TABLE 3. Force field for *cis*-HOSN

Constant	Value (aJ/coord²)	Error
f_{HO}	6.91	0.00
f_{DO}	7.10	0.01
f_{OS}	2.97	0.02
f_{SN}	9.90	0.01
f_{HOS}	0.500	0.001
f_{OSN}	1.03	0.01
f_{HOS-OS}	0.259	0.021
f_τ	0.0782	0.0006

Can. J. Chem. Downloaded from www.nrcresearchpress.com by 210.87.254.5 on 09/05/12
For personal use only.

TABLE 4. The calculated frequencies and their differences from the observed frequencies for *cis*-HOSN*

HOSN		HOS^{15}N		DOSN	
ν (cm^{-1})	Δ	ν (cm^{-1})	Δ	ν (cm^{-1})	Δ
3519.6	0.2	3519.5	−0.2	2597.5	0.0
1321.5	−0.7	1291.4	2.9	1321.1	−2.1
991.6	0.2	991.3	−0.2	741.8	
673.9	0.0	673.4	−0.1	671.2	0.1
373.8	0.2	368.2	−0.2	362.8	
419.3	−1.8	418.9	−2.4	319.6	5.6

*Average frequency error = 1.1 cm^{-1} (0.21%).

TABLE 5. Potential energy distribution and assignments for *cis*-HOSN

ν(calcd.) (cm^{-1})	Potential energy distribution						Assignment
	f_{HO}	f_{OS}	f_{SN}	f_{HOS}	f_{OSN}	f_τ	
3519.6	1.000	0.0	0.0	0.0	0.0		HO stretch
1321.5	0.0	0.009	0.985	0.007	0.004		SN stretch
991.6	0.0	0.002	0.005	1.005	0.005		HOS bend
673.9	0.0	0.991	0.006	0.034	0.047		OS stretch
373.8	0.0	0.046	0.005	0.002	0.944		OSN bend
419.3						1.0	Torsion

TABLE 6. The principal moments of inertia and thermodynamic functions (cal mol^{-1} K^{-1}) for *cis*-HOSN. Principal moments: 52.197, 11.945, 6.141 (uÅ^2)

Temperature (K)	S	C_p	$-\frac{(G - H_0)}{T}$	$\frac{(H - H_0)}{T}$
273.15	67.18	11.89	57.77	9.40
298.10	68.24	12.31	58.60	9.63
100.00	57.22	8.40	49.19	8.02
200.00	63.69	10.52	54.95	8.73
300.00	68.31	12.34	58.66	9.64
400.00	72.06	13.71	61.56	10.50
500.00	75.24	14.71	63.99	11.25
600.00	77.99	15.45	66.09	11.89
700.00	80.41	16.01	67.97	12.44
800.00	82.58	16.46	69.66	12.91
900.00	84.54	16.83	71.21	13.33
1000.00	86.33	17.14	72.63	13.70
1100.00	87.98	17.41	73.96	14.02
1200.00	89.51	17.65	75.19	14.31
1300.00	90.93	17.86	76.35	14.58
1400.00	92.26	18.04	77.43	14.82
1500.00	93.51	18.21	78.47	15.04

Table 4 gives the calculated frequencies and differences from observed frequencies for the various isotopes. The p.e.d. and resulting assignments are given in Table 5.

In these calculations the HO and DO force constants were fitted separately while the constraint that the DOS bend constant was 1.03 times the HOS bend constant was used. Both of these conditions were used to account for differences in anharmonicity. The latter constraint was needed because the DOS bending absorption was not observed so insufficient data

Can. J. Chem. Downloaded from www.nrcresearchpress.com by 210.87.254.5 on 09/05/12
For personal use only.

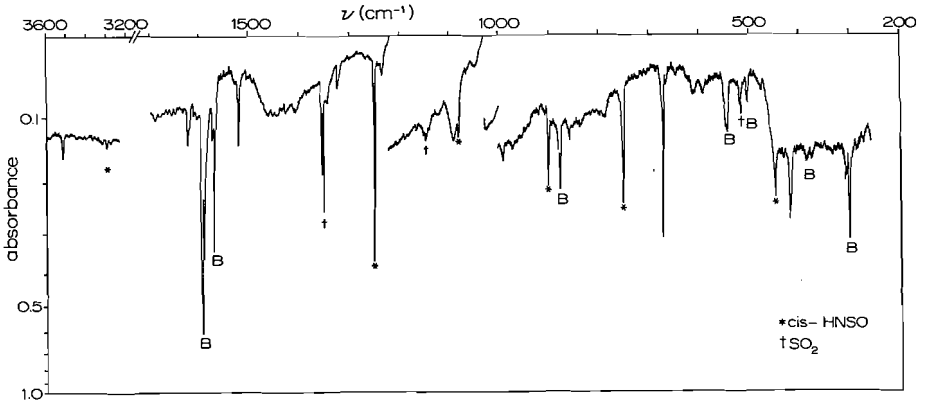

FIG. 3. Spectrum following the 42 min Hg lamp photolysis of *cis*-HNSO in argon (M/R = 400).

was available to calculate f_{DOS}. It was also found that an HOS bend – OS stretch interaction constant was necessary to obtain a good fit of the 991.8 and 673.9 cm^{-1} absorptions. Therefore eight constants were calculated from 16 observed frequencies.

Thermodynamic Functions

The availability of a complete set of frequencies allowed the calculation of the thermodynamic functions S, C_p, $-(G - H_0)/T$, and $(H - H_0)/T$. The principal moments of inertia were calculated from the approximated structure for *cis*-HOSN. These moments and the thermodynamic functions from 100 to 1500 K are given in Table 6.

Discussion

In Fig. 2 a weak absorption can be seen at 1342 cm^{-1}. It is assigned to the overtone of the SO stretching fundamental of *cis*-HOSN ($2\nu_{SO}$ = 1348 cm^{-1}). For this absorption to be seen the overtone must be in Fermi resonance with the SN stretching fundamental at 1321 cm^{-1}.

In the photolysis of isocyanic acid, HNCO, in a matrix, Jacox and Milligan (7) observed the formation of HOCN. This reaction is similar to the one suggested above, *i.e.* HNSO → HOSN, and thus provides additional support for the identification of molecule A as *cis*-HOSN.

Molecule B

Identification

Figure 3 shows the sample seen in Fig. 2 following a further 41 min photolysis with the mercury lamp. The peaks between 1500 and 1600 cm^{-1} have gained considerable intensity while those belonging to *cis*-HNSO and *cis*-HOSN have decreased. Several absorptions at lower frequencies have also grown. By careful study of these absorptions at intermediate photolysis times and in particular by looking at Fig. 1 it is seen that the 1523 and 790 cm^{-1} absorptions belong to a separate species which is discussed later. The remaining absorptions, which all follow curve B, are listed for all isotopes in Table 1.

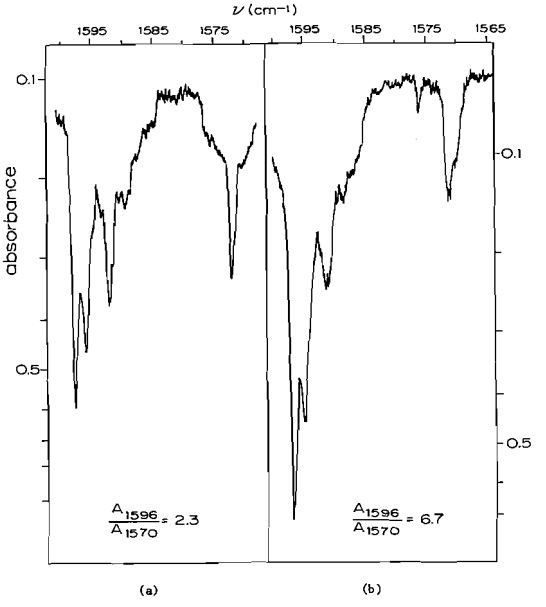

FIG. 4. The 1596 and 1570 cm^{-1} absorptions: (*a*) Hg lamp photolysis; (*b*) hydrogen resonance lamp photolysis with spray on.

The problem of at least two absorptions near 1600 cm^{-1} must first be resolved, for it would not

Can. J. Chem. Downloaded from www.nrcresearchpress.com by 210.87.254.5 on 09/05/12
For personal use only.

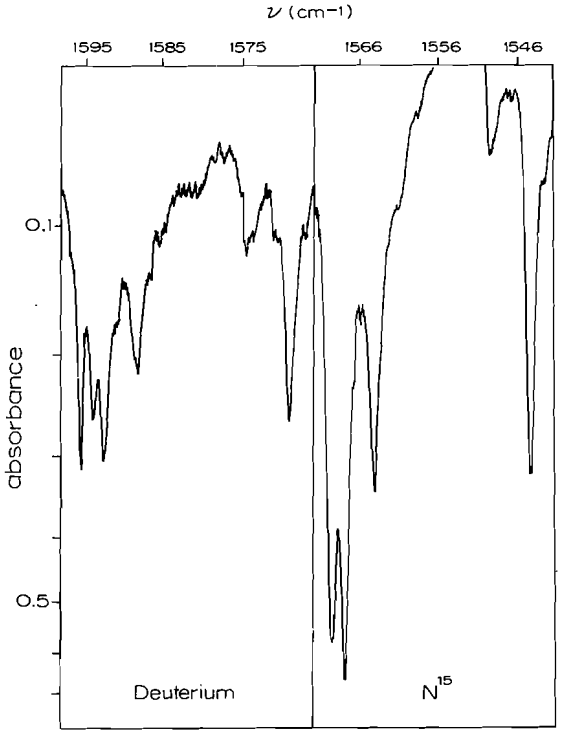

FIG. 5. Spectra of the NO stretching region for DSNO and HS^{15}NO.

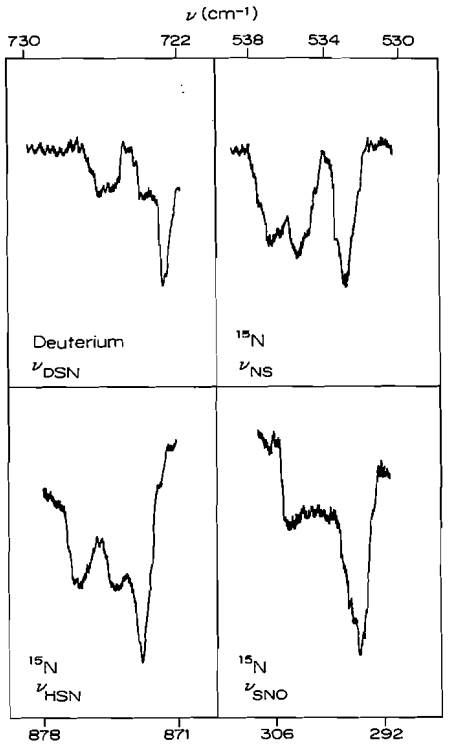

FIG. 6. The high resolution spectra of several *trans*-HSNO absorptions showing the complex splitting.

be expected that one molecule, isolated in a matrix and containing only an H, an S, an N, and an O atom, could give two absorptions in this region. Not surprisingly, a comparison of the two spectra of products produced by mercury lamp photolysis after isolation and by hydrogen resonance lamp photolysis during spray on (Fig. 4) shows that 1597 and 1571 cm^{-1} belong to different absorbers. Figures 4 and 5, showing these absorptions under high resolution for the various isotopes, demonstrate their complexity. These spectra also show that although peak heights suggest similar intensities, integrated intensities of the 1597 cm^{-1} multiplet are always much greater than those of the 1571 cm^{-1} multiplet.

The remaining absorptions of molecule B are weak and broad. High resolution of some of those absorptions in experiments where enough intensity was obtained to give good spectra show that they possess complex splitting similar to that of the 1597 cm^{-1} peak, principally a triplet structure and splittings of 3 to 10 cm^{-1} (Fig. 6). Excluding peaks labeled very, very weak in Table 1, all absorptions except 500 cm^{-1} definitely show this similarity with 1597 cm^{-1}. Unfortunately low intensity of the 500 cm^{-1} absorption made high resolution spectra unobtainable. Further, as was pointed out above, the 1597 cm^{-1} peak is much more intense than the 1571 cm^{-1} peak so that one might expect to see absorptions associated with it long before those associated with 1571 cm^{-1}. For these reasons, except for the v.v.w. peaks, all the absorptions listed for molecule B in Table 1, including 500 cm^{-1}, will be associated with the 1597 cm^{-1} absorption.

Now that the grouping is established, it is necessary to make the assignments and identification. Both the 1597 and 1571 cm^{-1} absorptions are very intense and show similar shifts of about 2 cm^{-1} on deuteration and 27 cm^{-1} on ^{15}N substitution. The frequencies, intensities, and isotopic shifts are all compatible with doubly bonded NO stretching modes. The next absorption, at 876 cm^{-1} for the common isotopes, shows a large shift of 153 cm^{-1} on deuteration so it must be a hydrogen bend. However, since no other high frequency absorptions are seen, it is felt that besides the NO double bond, no other

Can. J. Chem. Downloaded from www.nrcresearchpress.com by 210.87.254.5 on 09/05/12
For personal use only.

Can. J. Chem. Downloaded from www.nrcresearchpress.com by 210.87.254.5 on 09/05/12
For personal use only.

multiple bonds are present in this molecule. For this to be so, sulfur must be divalent and this can only happen if it is bonded to a hydrogen atom. Therefore, since the ^{15}N shift of 3 cm^{-1} requires the involvement of nitrogen in the bend, it must be of an HSN angle. An HSN bend and an NO double bond stretch would require the molecule to be HSNO, either *cis* or *trans*. Again, by comparison with isoelectronic molecules, HSNO is expected to be planar.

Following the *cis–trans* correlations of the similar molecule HONO which has ν_{NO} of 1699 cm^{-1} for the *trans* and 1640 cm^{-1} for the *cis* (8), it is not unlikely that the 1597 cm^{-1} and associated absorptions belong with *trans*-HSNO while the 1571 cm^{-1} absorption belongs to *cis*-HSNO. However, because the remaining peaks associated with 1597 cm^{-1} are very close together, complex normal coordinates are expected making assignments difficult. Even the isotopic shifts are of little help. Therefore, intuitive assignments were made by taking the SNO bend to be the lowest, 298 cm^{-1}, and the NS stretch to be the highest, 542 cm^{-1}, with the torsion at 500 cm^{-1}. These assignments are given in Table 1. It was hoped that the force field calculation might resolve the uncertainty. For *cis*-HSNO the only absorption that can be assigned with any certainty is the 1571.0 cm^{-1} to the NO stretch.

Normal Coordinate Analysis

Although uncertainties in the spectrum of HSNO exist, attempts were made to fit the assignments suggested in Table 1. A structure was approximated with the following parameters obtained by comparison with similar molecules (4): r_{HS} = 1.33 Å, r_{NS} = 1.70 Å, r_{NO} = 1.15 Å, α_{HSN} = 95°, and α_{SNO} = 115°. Fits were attempted for only the *cis* and *trans* planar forms since the similar molecule HONO is known to be planar.

For the *trans* molecule the calculation converged with the use of one interaction constant, f_{HSN-SN}. The HS stretch constant was held fixed since ν_{HS} was not observed, and the value for the DSN bend constant was constrained to 1.03 times the HSN bend constant to account for anharmonicity differences. Thus, six constants were used to fit 14 observed frequencies. The force constants are listed in Table 7. The observed frequencies and calculated frequencies of *trans*-HSNO are given in Table 8. The potential energy distribution and assignments are given in Table 9.

Attempts at fitting a *cis* structure to the same data were unsuccessful even with additional interaction constants. It is felt that this is because the approximated *cis* structure is not compatible with the observed isotopic shifts. This could be as a result of poorly chosen parameters, incorrect or insufficient data, or the inacceptability of the *cis* form. The fact that the *trans* isomer did fit the data suggests the last reason thus supporting the *trans*-HSNO identification.

Discussion

As is discussed above, many of the absorptions assigned to *trans*-HSNO and *cis*-HSNO are not single peaks but complex multiplets. It is most

TABLE 7. Force field for *trans*-HSNO

Contrast	Value (aJ/coord²)	Error
f_{HS}	4.0	Held fixed
f_{SN}	1.79	0.02
f_{NO}	11.04	0.04
f_{HSN}	0.671	0.004
f_{SNO}	0.562	0.003
f_{τ}	0.200	0.001
f_{HSN-NS}	−0.230	0.006

TABLE 8. The observed and calculated frequencies of *trans*-HSNO in argon matrices. Frequencies in cm^{-1}*

	HSNO		HS^{15}NO		DSNO		
	Obsvd.	Calcd.	Obsvd.	Calcd.	Obsvd.	Calcd.	Assignment
ν_1		2636.9		2336.9		1893.8	HN stretch
ν_2	1596.8	1597.0	1569.4	1567.7	1595.1	1596.7	NO stretch
ν_3	876	877.0	872.8	873.6	722.7	721.3	HSN bend
ν_4	542	543.9	533.0	532.2	488	487.0	SN stretch
ν_6	500	498.6	495	496.3		390.7	Torsion
ν_5	298	295.2	294.9	293.9	294	294.8	SNO bend

*Average frequency error = 1.1 cm^{-1} (0.19%).

TABLE 9. Potential energy distribution and assignments for *trans*-HSNO

ν (calcd.) (cm^{-1})	Potential energy distribution						Assignment
	f_{HS}	f_{SN}	f_{NO}	f_{HSN}	f_{SNO}	f_t	
2636.9	1.0						HS stretch
1597.0		0.009	0.983	0.008	0.004		NO stretch
877.0		0.075	0.002	0.799	0.021		HSN bend
543.9		0.707	0.004	0.227	0.230		SN stretch
498.6						1.0	Torsion
295.2		0.256	0.011	0.012	0.745		SNO bend

likely that the multiplets result from matrix splitting. It would not be surprising to find that a reaction involving the complex rearrangement that yields *trans*-HSNO from *cis*-HOSN would also result in local disruptions of the argon lattice and thus the creation of multiple trapping sites.

Molecule C

Identification

On continuing photolysis two more peaks were observed to grow in intensity after the rate of production of HSNO had decreased. This can be seen from a comparison of curves B and C in Fig. 1. However, the greatest intensity for these peaks was observed when the high-energy vacuum u.v. photolysis source was used. The two peaks were in the same positions (1523.0 and 789.7 cm^{-1}) when both HNSO and DNSO were photolyzed and at 1498.1 and 777.6 cm^{-1} when $H^{15}NSO$ was used.

The molecule appears to be a triatomic containing no hydrogen. There are three possibilities: SON, NSO, and SNO. SON is unlikely because the much more electronegative oxygen is not expected to be found in the middle. The 1523.0 cm^{-1} absorption shows an ^{15}N shift of 25 cm^{-1}, compatible with either an NS or NO stretch. However, a frequency this high would not be expected for an NS stretch (*e.g.* the SN triple bond of FSN absorbs at only 1372 cm^{-1} (6)) and it is felt that molecule C is not NSO. On the other hand, the observed frequencies are compatible with the radical SNO.

An NO stretching frequency of 1523.0 cm^{-1} is reasonable and the ^{15}N shift is appropriate. The high intensity observed is consistent with an NO stretch and the low intensity expected for the SN stretch accounts for it not being seen. The frequency of 789.7 cm^{-1} and the ^{15}N shift of

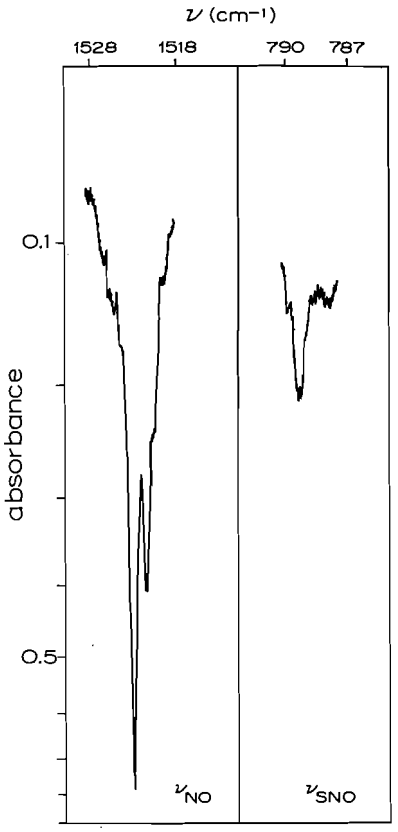

FIG. 7. The NO stretch and SNO bend of SNO.

12 cm^{-1} are reasonable for an SNO bend. Also, since the radical is produced late in the photolysis reaction, it is likely formed from HSNO. Since sulfur–hydrogen bonds are relatively weak, the removal of a hydrogen to give SNO would not be unexpected.

Both the 1523.0 and 789.7 cm^{-1} absorptions are shown in Fig. 7. The doublet character of the 1523.0 cm^{-1} absorption is characteristic of the

Can. J. Chem. Downloaded from www.nrcresearchpress.com by 210.87.254.5 on 09/05/12
For personal use only.

Can. J. Chem. Downloaded from www.nrcresearchpress.com by 210.87.254.5 on 09/05/12
For personal use only.

splittings of the asymmetric stretching modes of bent triatomics in argon matrices (4). The remaining absorption, probably the symmetric stretch consisting largely of NS stretching coordinate, is expected to be weak and has not been observed. The observed frequencies and assignments for SNO are given in Table 1.

Normal Coordinate Analysis

Because of the lack of an NS stretching frequency, it was not possible to obtain a force field for SNO. Since a great deal of mixing of internal coordinates is expected, not even approximate force constants based on characteristic frequencies would be meaningful.

Discussion

The removal of the hydrogen from *trans*-HSNO to give SNO has resulted in a shift of the NO stretching frequency from 1597 to 1523 cm^{-1}. In a similar system, going from *trans*-HONO to NO_2 shifts this stretch from 1696 to 1618 cm^{-1} (8). The similarity in shift supports the identification of SNO. The lower NO frequency can be explained by the following simple scheme. The removal of the hydrogen atom releases sulfur electron density into the delocalized π orbitals of the new SNO system. The SN bond thus increases in strength. At the same time, electrons that were in localized π bonding orbitals in the double NO bond of *trans*-HSNO now also become delocalized. Since only one of the π orbitals occupied in SNO is a bonding orbital, the NO bond order decreases with an accompanying decrease in vibrational frequency.

II. The Reactions

In part I it was shown that the u.v. photolysis of *cis*-HNSO in argon matrices results in the production of *cis*-HOSN, *cis*-HSNO, *trans*-HSNO, and SNO. The infrared absorptions associated with each of the new species were grouped by observing the rates of growth of the absorption peaks as a function of photolysis times and energies. In this section the growth-rate data will be further discussed. A mechanism for the reactions taking place on photolysis will be proposed on the basis of the kinetic information thus revealed.

Results

Figure 8 is a plot of the absorbance of the 447 cm^{-1} peak of *cis*-HNSO, the 674 cm^{-1} peak of *cis*-HOSN, the 1597 cm^{-1} peak of *trans*-HSNO, and the 1523 cm^{-1} peak of SNO as a function of photolysis time during a single experiment. In the case of the products the most intense absorption in each spectrum was chosen. For ease of presentation the intensities have been normalized to their own maximum absorption within the experiment. Figure 9 is a similar plot of the *cis*-HOSN and *trans*-HSNO absorptions when photolysis was carried out through a Corning 0-54 filter with low wavelength cut-off of 3000 Å. This in effect expanded the time scale by slowing the reactions and allowed a careful study of the product growth rates in the early stages of photolysis.

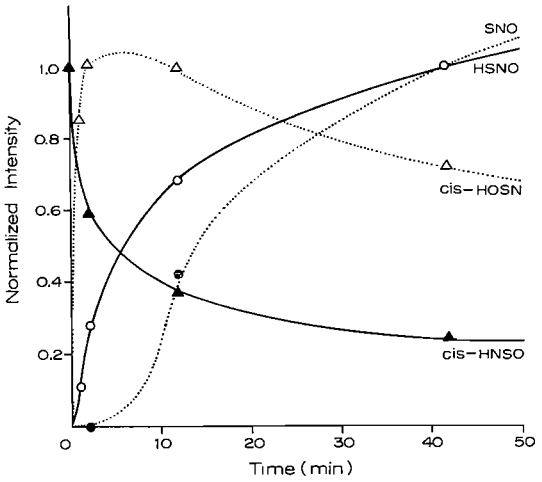

FIG. 8. Intensity of absorptions as a function of photolysis time for $\lambda > 2000$ Å.

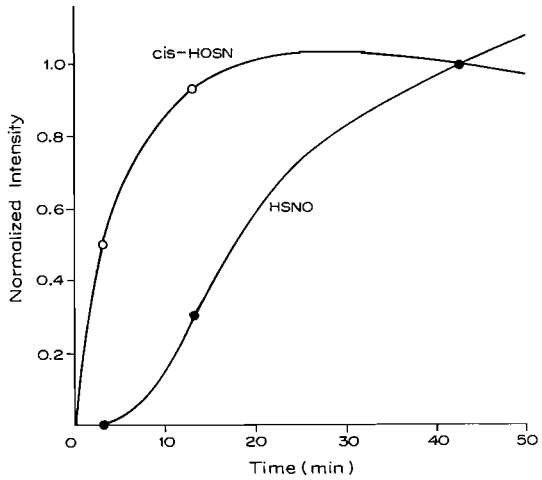

FIG. 9. Intensity of absorptions as a function of photolysis time for $\lambda > 3000$ Å.

Can. J. Chem. Downloaded from www.nrcresearchpress.com by 210.87.254.5 on 09/05/12
For personal use only.

Since the molecules involved in the reactions are isolated in the matrix, they cannot react with one another and since the film is very thin ($<10^{-2}$ cm) and the concentration very low ($\sim 5 \times 10^{-3}$ *M*), the amount of the light absorbed should be nearly proportional to the concentration of the absorbing species. Therefore, the reactions should be nearly first order, *i.e.* rate α [reactant]. The following analysis will be based upon this assumption.

Two features of the plots in Figs. 8 and 9 are important: (*1*) *cis*-HOSN is produced very quickly, reaches a maximum concentration, and is then removed by further photolysis; (*2*) both HSNO and SNO show inflection points in their growth curves. The presence of inflection points in concentration *vs.* time plots is an indication of consecutive reactions (9). Since the inflection point in the HSNO curve falls near the maximum in *cis*-HOSN concentration, it must be produced from *cis*-HOSN. Since the inflection point of SNO comes later, it must be produced from HSNO. The reactions can thus be written in the following sequence:

[1] *cis*-HNSO $\rightarrow$ *cis*-HOSN ($\xrightarrow{\text{reaction } 1a}$) $\rightarrow$ *cis*-HSNO ($\xrightarrow{\text{reaction } 1b}$) + *trans*-HSNO $\rightarrow$ SNO ($\xrightarrow{\text{reaction } 1c}$)

Each of these proposed reactions will be discussed.

Reaction 1a

Observations

(*i*) This reaction is very fast on the time scale of matrix photolysis reactions which commonly require several hours.

(*ii*) Only *cis*-HOSN has been observed in this reaction; neither *trans*-HOSN nor the dissociation product NSO appears to be formed by the u.v. photolysis of *cis*-HNSO.

(*iii*) The reaction is very fast with light of $\lambda > 2000$ Å but considerably slower when only light of $\lambda > 3000$ Å is used. The photolysis takes place over a fairly large wavelength region, most of which is under 3000 Å. It has also been observed by Allegretti and Merer (1) that *cis*-HNSO has a strong electronic absorption at 2700 Å which involves excitation of electrons occupying orbitals centered in the NSO part of the molecule.

(*iv*) While *cis*-HNSO is easily synthesized at room temperature using NH_3 and $SOCl_2$, *cis*-HOSN has not been produced and isolated. Glemser and Richert (10) have studied the room temperature hydrolysis of FSN. Although the product was entirely *cis*-HNSO, they proposed the existence of HOSN as a reaction intermediate.

[2] $H_2O + FSN \rightarrow [HF + HOSN] \rightarrow$ *cis*-HNSO

Thus if their mechanism is correct, HOSN is unstable with respect to *cis*-HNSO at room temperature with only a small activation energy. At 4 K in a matrix, however, *cis*-HOSN could be stabilized.

Discussion

From observation *iii* it is certain that the 2700 Å absorption of *cis*-HNSO leads to the formation of *cis*-HOSN. Since no *trans*-HOSN nor NSO is produced, it is most likely that the pathway is not via a dissociation of the hydrogen followed by a recombination at a new site, but rather by a concerted transfer of the hydrogen from the nitrogen to the oxygen. This simple pathway would be favored by the interaction between H and O, very likely present in *cis*-HNSO (11) and possibly enhanced in the excited state, and explain why reaction 1*a* is so fast. This reaction would yield *cis*-HOSN rather than *trans*-HOSN and thus support the earlier identification.

Since *cis*-HNSO is more stable than *cis*-HOSN at room temperature, at 4 K this rearrangement must be prevented by the lack of sufficient thermal energy. However, Fig. 10 shows a plot of the log of the intensity of a *cis*-HNSO absorption *vs.* time. The fact that this plot is not linear, as would be expected for a first-order reaction, suggests a reverse photolytic reaction yielding *cis*-HNSO is occurring as follows:

[3] 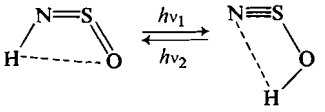

Reaction 1b

Observations

(*i*) The photolysis of *cis*-HOSN yields HSNO.

(*ii*) Within the limits of the measurements it appears that both the *trans* and *cis* isomers of HSNO are produced at the same time but at different rates.

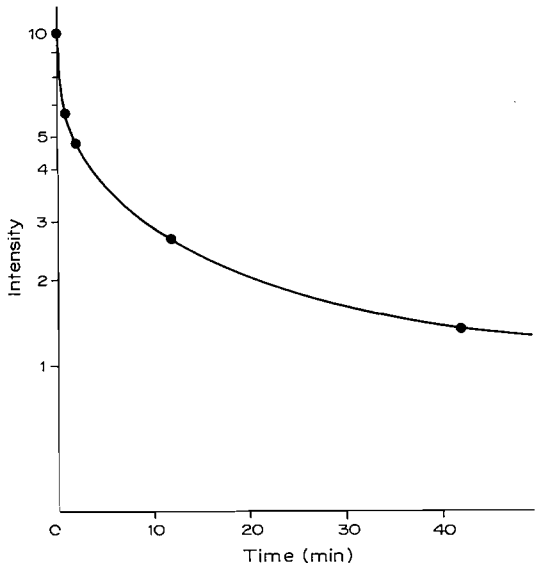

FIG. 10. Disappearance of *cis*-HNSO on photolysis with $\lambda > 2000$ Å.

(*iii*) The rearrangement is complex; two bonds are broken and two new ones are formed.

(*iv*) The i.r. absorptions of *trans*-HSNO show complex matrix splittings possibly from the occupancy of different sites in the matrix.

(*v*) No OSN resulting from the mercury lamp photolysis of *cis*-HOSN has been observed nor have the diatomic fragments HO and SN been observed in any experiments.

(*vi*) The OS force constant of *cis*-HOSN, 2.97 aJ/Å^2, indicates an OS single bond. With a probable bond energy of 60–70 kcal/mol, this is the weakest bond in the molecule.

(*vii*) The use of light of $\lambda > 3000$ Å for photolysis results in slower reactions. However, the maximum amount of *cis*-HOSN produced was much less with $\lambda > 3000$ Å than with $\lambda > 2000$ Å. This suggests that reaction 1*a* was slowed more by the use of the filter than was reaction 1*b*.

(*viii*) The use of vacuum u.v. photolysis with simultaneous spray on increases the ratio of *cis*-HSNO to *trans*-HSNO.

(*ix*) Attempts to carry out the photolysis of *cis*-HNSO in a nitrogen matrix failed. Although reaction 1*a* proceeded without complication, the further photolysis resulted in the complete disappearance of all i.r. absorptions (those of *cis*-HNSO and those of *cis*-HOSN) without the appearance of any new absorptions. Identical results were obtained in three separate experiments. However, data was not sufficient to hazard an explanation.

Discussion

From observation *vii* it appears that an electronic transition of *cis*-HOSN centered in the wavelength region just below 3000 Å results in its photolysis to give *cis*- and *trans*-HSNO. The reaction is complex; observation *iii* suggests several steps and observations *v* and *vi* show that the initial step is probably the rupture of the SO bond rather than the HO bond. It is felt that in the matrix cage the two fragments, unable to separate (a fact attested to by the absence of OH and NS i.r. absorptions), would recombine to give both *cis*- and *trans*-HSNO and possibly *cis*-HOSN and *cis*-HNSO as well. Since *cis*- and *trans*-HSNO would be produced simultaneously, the requirement of observation *ii* would be met.

[4] *cis*-HOSN → [HO + SN] → HSNO, HOSN, HNSO

The increase in *cis* to *trans* ratio when vacuum u.v. photolysis with simultaneous spray on is used, observation *viii*, could be due either to the greater light energy or to the photolysis, as a result of this technique, of more loosely trapped molecules in the not yet completely cooled surface layer. Either reason could feasibly lead to a new ratio.

Reaction 1c

The third reaction of the sequence is

$$\text{[5]} \qquad \text{HSNO} \xrightarrow{h\nu} \cdot\text{SNO} + \text{H}$$

The HS bond is probably of the order of 80 kcal/mol and so is weak enough to be broken with radiation from a mercury lamp leaving the hydrogen atom with sufficient kinetic energy to break from the matrix cage. This type of diffusion reaction is often found in matrix photolysis and is usually slow, accounting for the relatively slow production of SNO. When vacuum u.v. photolysis with simultaneous spray on is used, more energy is available for the diffusion process, and more SNO is observed. On low energy photolysis ($\lambda > 3000$ Å) very little SNO is observed; few H atoms have sufficient kinetic energy to escape the cage.

Conclusions

In part I the identification of *cis*-HOSN, *cis*-HSNO, *trans*-HSNO, and SNO resulting from the photolysis of *cis*-HNSO in argon matrices

Can. J. Chem. Downloaded from www.nrcresearchpress.com by 210.87.254.5 on 09/05/12
For personal use only.

was made from the i.r. spectroscopic data alone. The kinetic information and the proposed mechanisms presented in part II are consistent with the identifications. This consistency provides an affirmation of both the identifications and the mechanisms.

1. J. M. ALLEGRETTI and A. J. MERER. Can. J. Chem. **50**, 404 (1972).
2. P. O. TCHIR and R. D. SPRATLEY. Can. J. Chem. **53**, 2311 (1975).
3. D. DAVIS and W. BRAUM. Appl. Opt. **7**, 2071 (1968).
4. P. O. TCHIR. Ph.D. Thesis, University of British Columbia, Vancouver, British Columbia. 1972.
5. J. H. SCHACHTSCHNEIDER. Shell Development Company, Tech. Rep. 263–62. 1962.
6. O. GLEMSER and H. RICHERT. Z. Anorg. Allg. Chem. **307**, 328 (1961).
7. M. E. JACOX and D. E. MILLIGAN. J. Chem. Phys. **40**, 2457 (1964).
8. L. D'OR and P. TARTE. Bull. Soc. R. Sci. Liège **8**, 478 (1951).
9. W. J. MOORE. Physical chemistry. Prentice-Hall, Englewood Cliffs, N.J. 1962. p. 226.
10. O. GLEMSER and H. RICHERT. Z. Anorg. Allg. Chem. **307**, 313 (1961).
11. P. O. TCHIR and R. D. SPRATLEY. Can. J. Chem. **53**, 2331 (1975).

Can. J. Chem. Downloaded from www.nrcresearchpress.com by 210.87.254.5 on 09/05/12
For personal use only.

The Photolysis of Matrix Isolated *cis*-Thionylimide. 2. The Identification and Infrared Spectra of *trans*-HNSO and NSO

PETER O. TCHIR AND RICHARD D. SPRATLEY

Department of Chemistry, University of British Columbia, Vancouver, British Columbia V6T 1W5

Received December 3, 1974

PETER O. TCHIR and RICHARD D. SPRATLEY. Can. J. Chem. **53**, 2331 (1975).

It is shown that the low energy ($\lambda > 3000$ Å) photolysis of *cis*-HNSO in an argon matrix leads to formation of *trans*-HNSO. Four i.r. absorptions are observed and assigned for *trans*-HNSO and an approximate partial force field is calculated using data from isotopic substitutions. A comparison is made of the i.r. spectra of *cis*- and *trans*-HNSO using the intramolecular hydrogen bond of the *cis* form as a basis for explanation of the differences. Photolysis of *cis*-HNSO in argon matrices using vacuum u.v. light (1216 Å) has resulted in a single i.r. absorption at 1195 cm^{-1} which has been assigned to the radical, NSO.

PETER O. TCHIR et RICHARD D. SPRATLEY. Can. J. Chem. **53**, 2331 (1975).

On a montré que la photolyse à faible énergie ($\lambda > 3000$ Å) du HNSO *cis* dans une matrice d'argon conduit à la formation du HNSO *trans*. Quatre absorptions i.r. sont observées et attribuées au HNSO *trans*. On a calculé un champ de force partiel, approximatif, en utilisant les résultats des remplacements isotopiques. On a fait une comparaison des spectres i.r. du HNSO *cis* et *trans*. On explique les différences en faisant appel à une liaison hydrogène intramoléculaire dans la forme *cis*. La photolyse du HNSO *cis* dans une matrice d'argon par une lampe u.v. à vide (1216 Å), ne donne qu'une seule absorption i.r. à 1195 cm^{-1} que l'on attribue au radical NSO. [Traduit par le journal]

Introduction

In a previous paper (1) we have described the results of the photolysis of *cis*-HNSO in argon matrices using a medium pressure mercury arc as a source; that is with light of $\lambda > 2000$ Å. The products *cis*-HOSN, *trans*-HSNO, *cis*-HSNO, and SNO were identified from their i.r. spectra and, where enough vibrations were observed, approximate force fields were calculated. The kinetics and the mechanisms of the photolysis reactions were discussed.

Investigation of the i.r. absorptions produced on photolysis with high energy (1216 Å) or lower energy ($\lambda > 3000$ Å) light permitted the identification of two further molecules. This paper presents the results of this study.

Experimental

The matrix isolation apparatus (2), the i.r. spectrometer (Perkin-Elmer 225) (2), and the photolysis apparatus (1) have been described previously. To obtain low energy radiation ($\lambda > 3000$ Å) a Corning #0-54 filter was used in conjunction with a 100 W PEK medium pressure mercury lamp (#112-2118). High energy radiation (1216 Å) was obtained from a microwave discharge of a flow of a hydrogen–helium mixture (1:9).

Results

trans-HNSO

Identification

The photolysis of matrix isolated *cis*-HNSO with light limited to wavelengths greater than 3000 Å resulted in a slow reaction yielding numerous absorptions. If a period of this low energy photolysis was followed by higher energy photolysis ($\lambda > 2000$ Å), most of the absorptions grew rapidly (1). However, four of the weak absorption peaks decreased in intensity with this secondary photolysis. Figure 1 shows new peaks produced by the photolysis of *cis*-$H^{14}NSO$ for 45 min using a mercury lamp and filter ($\lambda > 3000$ Å) as well as their disappearance on further photolysis for 5 min without the filter ($\lambda > 2000$ Å). Figure 1 also shows similar results (1 h at $\lambda > 3000$ Å followed by 3 min at $\lambda > 2000$ Å) for ^{15}N substituted *cis*-HNSO. The use of ^{15}N proved that the doublet absorptions at 986 and 881 cm^{-1} in the ^{14}N sample were indeed caused by overlapping absorptions of two separate molecules. On photolysis without filter one component of each doublet decreased in intensity along with the *cis*-HNSO absorptions while the other component increased.

Can. J. Chem. Downloaded from www.nrcresearchpress.com by 210.87.254.42 on 09/05/12
For personal use only.

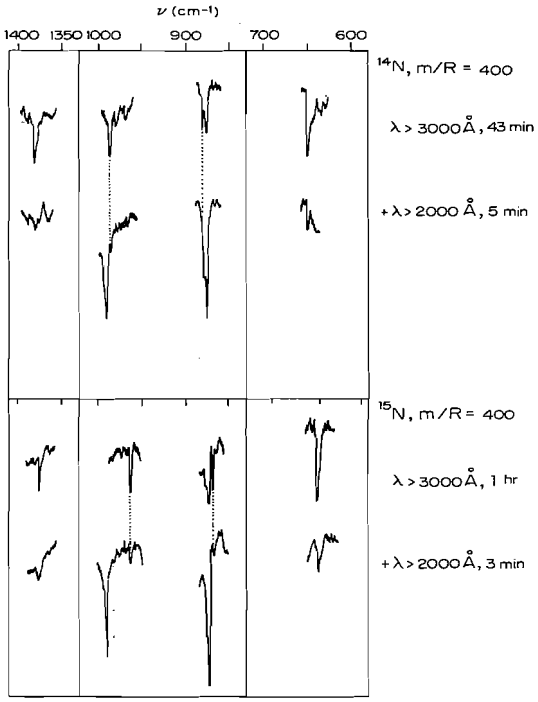

FIG. 1. The four observed absorptions of *trans*-HNSO, production with photolysis using $\lambda > 3000$ Å and disappearance using $\lambda > 2000$ Å.

Table 1 lists the measured frequencies of these four vibrations when starting with *cis*-$H^{14}NSO$, *cis*-$H^{15}NSO$, and *cis*-$D^{14}NSO$. Since four absorptions are observed apparently belonging to a single species, the molecule cannot be triatomic and, since it shows shifts of absorptions on deuterium and ^{15}N substitution, both these atoms are constituents. Since the peaks, though weak, are fairly sharp, it is assumed that isolation was maintained during the reaction. The M/R of 400 had been found to be adequate for the initial isolation of *cis*-HNSO (2). The absorbing species is most likely a simple isomer of *cis*-HNSO and it must be assumed that its two remaining absorptions are not observed due to low intensity or overlapping with intense absorptions.

Consider first the 1382 cm^{-1} absorption. This region suggests either an S=O stretch, an S≡N stretch, or a hydrogen bend. The ^{15}N shift of 3 cm^{-1} is too small for an SN stretch and the deuterium shift of 2 cm^{-1} shows that it is not a hydrogen bend. The peak at 1382 cm^{-1} must then be assigned to an S=O stretch.

TABLE 1. The observed absorption frequencies (cm^{-1}) of *trans*-HNSO in an argon matrix

HNSO	$H^{15}NSO$	DNSO	Assignment
1382	1379	1380	SO stretch
986	963	951	SN stretch
881	868		HNS bend
651	650		Torsion

Numerous vibrations could absorb in the region of the next peak, 986 cm^{-1}. The two major possibilities are an S=N stretch and a hydrogen bend. The ^{15}N shift of 23 cm^{-1} is reasonable for an S=N stretch while the D shift of 13 cm^{-1} is consistent with an S=N stretch but is certainly too small for a hydrogen bending mode. The peak at 986 cm^{-1} is assigned to an S=N stretch.

Similarly, numerous vibrations can occur at 881 cm^{-1} although multiple bonded sulfur, oxygen, and nitrogen stretches would probably be at higher frequency and single bonds involving these atoms would probably be lower; a hydrogen bend is most likely. The ^{15}N shift of 13 cm^{-1} is similar to that found for the HNS bend of *cis*-HNSO (11 cm^{-1}). The fact that this peak was not observed on deuteration suggests both a shift to another region where it could not be seen and a lowering of intensity. These observations are consistent with assignment of the 881 cm^{-1} absorption to a hydrogen bend in which hydrogen is attached to a nitrogen.

The remaining peak, at 651 cm^{-1}, is consistent with a single bond stretch, a bend, or a torsion. The small ^{15}N shift of 1 cm^{-1} suggests that it is not a bending or stretching mode involving nitrogen. Since the molecule has only four atoms, this excludes the majority of the bends and stretches. The disappearance of the peak on deuteration is probably due to a large shift to a different region. For this reason the vibration must be a torsion about a multiple bond involving large hydrogen displacements.

With a weak NS stretch, a strong SO stretch, an HNS bend and a torsion, the molecule is likely an isomer of HNSO, presumably the *trans* planar configuration:

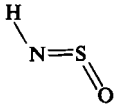

Can. J. Chem. Downloaded from www.nrcresearchpress.com by 210.87.254.42 on 09/05/12
For personal use only.

Can. J. Chem. Downloaded from www.nrcresearchpress.com by 210.87.254.42 on 09/05/12
For personal use only.

TABLE 2. Comparison of *cis–trans* frequency shifts (cm^{-1}) for HNSO and HONO

HNSO		HONO*	
Mode	Shift	Mode	Shift
ν_{SO}	−133	$\nu_{N=O}$	−61
ν_{SN}	97	ν_{N-O}	62
ν_{HNS}	19	ν_{HON}	97
ν_{τ}	104	ν_{τ}	93

*HONO frequencies from ref. 3.

The assignments are indicated in Table 1; the HN stretch and the NSO bend are not observed. It is assumed that a large mixing will be found for the 986 and 881 cm^{-1} absorptions, thus confusing their assignments. However, from the data available, the given assignments are most probable.

As a further piece of evidence for this identification, a comparison of *cis–trans* frequency shifts for HNSO and the structurally similar molecule HONO is made in Table 2. The HONO values are taken from D'Or and Tarte (3). Since both molecules are planar and might be expected to have similar bonded and nonbonded interactions, it is believed that they should show comparable *cis–trans* shifts. The similarities in the shifts shown in Table 2 are consistent with the assignments made for *trans*-HNSO.

Normal Coordinate Analysis

An attempt to fit a force field to the data in Table 1 has been made using the program of Schachtschneider (4). The structure used was that of *cis*-HNSO (2) taking the dihedral angle at 180°. The shortage of data, especially the absence of any NSO bend frequency, restricts the quality of the calculation. Only two deuterium modes are observed which, due to low intensity, have large uncertainties. However, an approximate force field has been obtained which gives a good frequency fit and reasonable potential energy distribution.

TABLE 3. Force field for *trans*-HNSO with that of *cis*-HNSO included for comparison (2). Constants in units of aJ/coordinate^2

	trans-HNSO		
Constant	Value	Error	*cis*-HNSO
f_{HN}	6.05	Held fixed	6.05
f_{NS}	5.30	0.04	6.47
f_{SO}	11.60	0.03	9.01
f_{HNS}	0.476	0.005	0.457
f_{NSO}	1.66	Held fixed	1.66
f_{τ}	0.193	0.001	0.225
f_{HNS-NS}	0.190	0.005	−0.15

TABLE 4. Calculated frequencies and differences from observed frequencies, Δ, for *trans*-HNSO*

HNSO		H^{15}NSO		DNSO	
ν (cm^{-1})	Δ	ν (cm^{-1})	Δ	ν (cm^{-1})	Δ
3308		3301		2422	
1381	1	1380	−1	1380	0
982	4	966	−3	951	0
878	3	870	−2	687	
651	0	650	0	484	
496		491		474	

*Average frequency error = 1.4 cm^{-1} (0.16%).

Because of the absence of the corresponding frequencies, the HN stretch and NSO bend force constants were held fixed to values obtained for *cis*-HNSO (2). The DNS bend force constant was constrained to 1.03 times the HNS bend constant to improve the fit by taking into account the difference in anharmonicity of this coordinate for the two isotopes. As expected, the closeness of the 986 and 881 cm^{-1} absorptions resulted in a

TABLE 5. Potential energy distribution and assignments for *trans*-HNSO

	Potential energy distribution						
ν(calcd.) (cm^{-1})	f_{HN}	f_{NS}	f_{SO}	f_{HNS}	f_{NSO}	f_{τ}	Assignment
3308	0.998	0.001	0.0	0.0	0.001		HN stretch
1381	0.0	0.037	0.951	0.004	0.005		SO stretch
982	0.0	0.548	0.005	0.531	0.045		NS stretch
879	0.001	0.401	0.034	0.460	0.001		HNS bend
651						1.0	Torsion
496	0.001	0.028	0.009	0.020	0.948		NSO bend

Can. J. Chem. Downloaded from www.nrcresearchpress.com by 210.87.254.42 on 09/05/12
For personal use only.

great deal of mixing so that an HNS bend – NS stretch interaction constant was required. This meant that five force constants were adjusted to fit 10 frequencies. Table 3 lists the force constants and their least squares estimated errors obtained for *trans*-HNSO along with their corresponding values for *cis*-HNSO (2). Table 4 gives the calculated frequencies and differences between calculated and observed frequencies for the various isotopes while the diagonal constant potential energy distribution is given for each vibration of *trans*-$H^{14}NSO$ in Table 5.

Discussion

(*i*) The shift in the SO stretching frequency from 1248.7 to 1382 cm^{-1} in going from *cis*-HNSO to *trans*-HNSO has resulted in a change of SO force constant from 9.0 to 11.6 aJ/Å^2. At the same time the NS stretch constant has decreased from 6.5 to 5.3 aJ/Å^2. This suggests a change in the bonding has occurred, an increase in bonding between sulfur and oxygen and a decrease between sulfur and nitrogen. A possible explanation is the following. In the *cis* form there is a hydrogen bond type interaction between hydrogen and oxygen. This would account for the *cis* isomer's apparent greater stability which results in the absence of any *trans* isomer in the gas phase. This could also be one reason for the larger torsional constant for the *cis* compared to the *trans* isomer (0.225 and 0.193 aJ). This hydrogen bonding shifts some oxygen electron density away from the SO bond, thus weakening the bond and releasing sulfur electrons for greater NS bonding. In the *trans* form the oxygen electrons are released, in the absence of hydrogen bonding, into the SO bond, thus strengthening it. The increased availability of the oxygen electrons attracts sulfur electrons away from the NS bond, which is weakened. This is also reflected in the lower torsional constant and lower NS stretching constant for the trans isomer.

Following the formulation of the above interaction scheme, Cox *et al.* (5) presented a similar explanation to account for the structural differences found in *cis*- and *trans*-HONO. Further work by Finnigan *et al.* (6) has also yielded a similar force constant relationship for *cis* and *trans*-HONO. This interaction has been discussed in the previous paper on the photolysis of *cis*-HNSO to *cis*-HOSN (1).

(*ii*) The lack of an NSO bending mode may result in some error in the force constants which would not be reflected in the least squares error estimates. In *cis*-HNSO (2), some interaction does take place between the HNS bend and the NSO bend so that their interaction constant was important. The other problem is the assignment of the 986 and 881 cm^{-1} absorptions. The assignment of these two modes is reversed in the p.e.d. of the ^{15}N and ^{14}N molecules. However, in the deuterated molecule, where the separation of these modes is much larger and thus their interaction is less, the assignment in Tables 1 and 5 is followed. This is the assignment chosen here for *trans*-HNSO.

(*iii*) Because this molecule is produced with low energy light and because no NSO is observed as a result of this photolysis, it is consistent to postulate a *cis–trans* rotation rather than an HN bond cleavage. The disappearance of this molecule with higher energy photolysis follows the disappearance of *cis*-HNSO. This would, of course, be expected for *trans*-HNSO. An equilibrium between the *cis* and *trans* isomers would account for the limited amount of the *trans* isomer that is produced in these experiments.

The 1195 cm^{-1} Doublet, NSO

Identification

Photolysis with the hydrogen 1216 Å emission during sample deposition resulted in the formation of a new absorption at 1195 cm^{-1}. This feature was broad under low resolution but easily resolved into a doublet. Figure 2 shows this absorption for the photolysis of *cis*-HNSO, *cis*-DNSO, and *cis*-$H^{15}NSO$. Since deuterium substitution did not cause a frequency shift, the molecule probably does not contain hydrogen. Absorption at 1195 cm^{-1} suggests either an SO or NS bond stretch. In fact it has the correct frequency to be the diatomic molecule NS (observed at 1205 cm^{-1} in the gas phase (7)), but the ^{15}N shift of 9.4 cm^{-1} is too small. Since this would be true for any NS stretch, this absorption is probably due to an SO stretching mode.

The remaining evidence for this molecule is that it was only produced with vacuum u.v. photolysis and that following its production, short exposure (2 min) to mercury lamp radiation caused it to disappear. This is shown in Fig. 2*a*. Milligan and Jacox (8) have shown the same

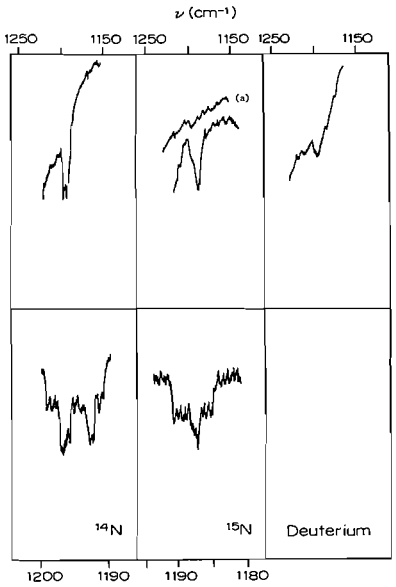

FIG. 2. The SO stretching mode of NSO produced by vacuum u.v. photolysis of *cis*-HNSO. The upper spectra under normal resolution and the lower spectra under high resolution. The spectrum marked (a) shows the disappearance of the absorption following mercury lamp photolysis.

behavior for the 1240 cm^{-1} absorption resulting from the vacuum u.v. photolysis of NO_2 which was assigned to the NO_2^- ion. Therefore, the possibility that the 1190 cm^{-1} band is due to the SNO^- ion with this absorption assigned to the NO stretch has been considered. However, the low ^{15}N shift makes this unlikely since the observed shift is 25 cm^{-1} in the neutral SNO molecule (1).

The most likely alternative is that the absorption is due to the SO stretching mode of NSO which is produced by the photodissociation of *cis*-HNSO. Further photolysis in the 2000–4000 Å region then causes the NSO to rearrange to SNO (1) or to decompose to some other fragments not seen. The other possibility that the species is the NSO^- ion is unlikely because its disappearance would require the appearance of new absorptions due to NSO. This is not observed.

The position of the absorption and the ^{15}N shift are both compatible with assignment to the NSO radical. As in the case of HSNO–SNO and HONO–ONO (1), the removal of the hydrogen from HNSO tends to increase the bonding between the nitrogen and sulfur and weaken that between the sulfur and oxygen, shifting the SO stretching vibration to lower frequency. The resulting proximity of the NS and SO (or symmetric and asymmetric) stretching frequencies would increase the mixing of these coordinates and allow the SO stretch to have a shift of 9.4 cm^{-1} on ^{15}N substitution. The SO stretch would have the greatest intensity so it is reasonable the NS stretch and NSO bend are not observed.

Discussion

The above arguments suggest that NSO is formed on vacuum u.v. photolysis of *cis*-HNSO. This would require breaking the HN bond and giving the hydrogen enough energy to escape the cage, certainly possible with 1216 Å radiation. The loose trapping in the surface layer, the layer in which most of the photolysis occurs in this technique, would also aid in the hydrogen escape and thus favor NSO production. However, since the reaction rate would still be controlled by diffusion of the hydrogen atoms, it would be slow in comparison to the fast rearrangement reaction giving *cis*-HOSN. Subsequent photolysis with lower energy radiation, $\lambda > 2000$ Å, results in the disappearance of NSO and it is suggested on little evidence that SNO is produced. The reaction can be written as follows:

$$[1] \quad \textit{cis}\text{-HNSO} \xrightarrow{\lambda = 1216\,\text{Å}} \text{NSO} \xrightarrow{\lambda > 2000\,\text{Å}} \text{SNO}$$

A reaction in which NSO is removed would further account for the small amount of NSO observed even with hydrogen resonance lamp photolysis. No NSO is observed with only mercury lamp photolysis.

Conclusions

It has thus been shown that the photolysis of matrix isolated *cis*-HNSO with low energy u.v. light leads to the production of *trans*-HNSO while with vacuum u.v. light the NSO radical is formed. These then compliment the previously published results (1) of the photolysis of *cis*-HNSO using a mercury lamp in which *cis*-HOSN, *trans*-HSNO, *cis*-HSNO, and SNO were identified.

1. P. O. TCHIR and R. D. SPRATLEY. Can. J. Chem. **53**, 2318 (1975).
2. P. O. TCHIR and R. D. SPRATLEY. Can. J. Chem. **53**, 2311 (1975).
3. L. D'OR and P. TARTE. Bull. Soc. R. Liège **8**, 478 (1951).

Can. J. Chem. Downloaded from www.nrcresearchpress.com by 210.87.254.42 on 09/05/12
For personal use only.

4. J. H. SCHACHTSCHNEIDER. Shell Development Company, Tech Rep. 263–62. 1962.
5. A. P. COX, A. H. BRITTAIN, and D. J. FINNIGAN. Trans. Faraday Soc. **67**, 2179 (1971).
6. D. J. FINNIGAN, A. P. COX, A. H. BRITTAIN, and J. G. SMITH. J. Chem. Soc. Faraday Trans. 2, **68**, 548 (1972).
7. G. HERZBERG. Spectra of diatomic molecules. D. Van Nostrand, New York. 1950. p. 558.
8. D. E. MILLIGAN and M. E. JACOX. J. Chem. Phys. **51**, 1952 (1969).

Can. J. Chem. Downloaded from www.nrcresearchpress.com by 210.87.254.42 on 09/05/12
For personal use only.

The Photolyses of Fully Aromatic Amides[1,2]

D. J. CARLSSON, L. H. GAN,[3] AND D. M. WILES
Division of Chemistry, National Research Council of Canada, Ottawa, Canada K1A 0R9

Received January 16, 1975

D. J. CARLSSON, L. H. GAN, and D. M. WILES. Can. J. Chem. **53**, 2337 (1975).

The 254 nm photolyses of ethanol solutions of four fully aromatic amides were followed by liquid chromatography and u.v. spectroscopy, and quantum yields for the major products calculated. The photolysis of benzanilide was examined in detail at various wavelengths and in several solvents, both in the presence and absence of oxygen. Quantum yields for 2- and 4-aminobenzophenones and products from free radical precursors decreased with increasing solvent polarity and with increasing incident wavelength of irradiation. Oxygen had no affect on aminobenzophenone formation but produced benzoic acid from free radical fragments which escaped the solvent cage. The results are tentatively interpreted in terms of an energy dependent radiationless conversion to a reactive $^1\pi^*$-carbonyl which then cleaves the N—C bond to give caged free radicals, rather than by a concerted, nonradical rearrangement.

D. J. CARLSSON, L. H. GAN et D. M. WILES. Can. J. Chem. **53**, 2337 (1975).

On a suivie par chromatographie liquide et par spectroscopie u.v. les photolyses à 254 nm de solutions éthanoliques de quatre amides entièrement aromatiques. Les rendements quantiques des produits majeurs sont calculés. La photolyse de la benzanilide est examinée en détail à différentes longeurs d'onde et dans plusieurs solvants en présence et en absence d'oxygène. Les rendements quantiques pour les amino-2 et amino-4 benzophénones et les produits provenant des radicaux libres précurseurs, décroissent avec une augmentation de la polarité du solvant et augmentent avec la longueur d'onde d'irradiation. L'oxygène n'affecte pas la formation d'aminobenzophénone, mais produit de l'acide benzoïque à partir des fragments à radicaux libres qui s'échappent de l'enceinte du solvant. Les résultats sont provisoirement interprétés en termes d'une conversion sans émission de radiation, mais dépendant de l'énergie, en une espèce réactive carbonyle-$^1\pi^*$ laquelle scinde la liaison N—C pour donner des radicaux libres piégés dans la cage à solvant, plutôt que par un réarrangement concerté non-radicalaire.

[Traduit par le journal]

Introduction

Some of the photolysis products from benzanilide have been previously reported (1, 2), although product analyses were only made after prolonged irradiation, with no control over second photolysis (1), and few quantitative data were reported (2). A detailed understanding of the photolyses of fully aromatic amides in strongly hydrogen bonding environments is relevant to the photodegradation of commercially important aromatic polyamides such as poly(1,3-phenylene isophthalamide) (3, 4). In this work we report an investigation of the photolyses of the amides **1–4** (which are models for some commercial polymeric materials), with a detailed investigation of the products from **1** and **2** produced by photolysis in the absence and presence of O_2.

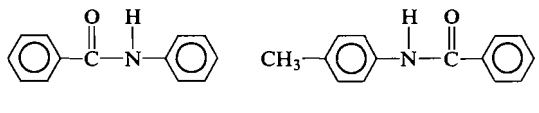

1

2

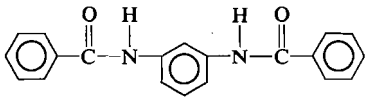

3

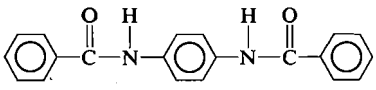

4

[1]Issued as NRCC No. 14662.

[2]This paper is dedicated to Professor C. A. Winkler of McGill University on the occasion of his sixty-fifth birthday by one of his former students (D.M.W.).

[3]NRCC Postdoctorate Fellow, 1972–1974. Present address: Department of Chemistry, University of Malaya, Kuala Lumpur, Malaysia.

Can. J. Chem. Downloaded from www.nrcresearchpress.com by 210.87.254.42 on 09/05/12
For personal use only.

Can. J. Chem. Downloaded from www.nrcresearchpress.com by 210.87.254.42 on 09/05/12
For personal use only.

Experimental

The amides were prepared from their respective amines and the appropriate acid chlorides in methylene chloride, and recrystallized from ethanol (**1**, **2**, and **3**) or aqueous *N*,*N*-dimethylacetamide (for **4**). Melting points were 162 °C (**1**), 159 °C (**2**), 245 °C (**3**), and 333 °C (**4**) which agreed well with published values (*5a*). Spectroscopic methods and liquid chromatography (l.c.) indicated the absence of impurities. Phenanthridone was prepared by the method of Walls (*5b*). Other standards for l.c. were recrystallized commercial products. Absolute alcohols and spectro grade solvents were used throughout.

Ethanol solutions in 0.1 cm path quartz cells were irradiated with a 254 ± 10 nm beam from a Bausch and Lomb High Intensity Monochrometer (200 W SP mercury lamp). Some irradiations were performed in these cells with an unfiltered, collimated 500 W Osram super pressure mercury lamp. Incident light intensities were measured with a calibrated Eppley thermopile. Ultraviolet changes accompanying irradiation were measured on a Cary 15 spectrometer.

Most irradiation products were separated by high speed l.c. on a Waters Associates ALC 201, equipped with a Varian septumless injector, a Pharmacia u.v. detector (254 nm), and a 5-μ Si-60 Lichrosorb (SiO_2) column (25 cm × 2.1 mm i.d.). The eluent was a 10 vol% ethanol–hexane mixture. At a flow rate of 0.3 ml min^{-1}, retention times (min) were 2.4 (solvent front), 3.8 (benzene), 4.1 (ethyl benzoate), 5.5 (2-aminobenzophenone), 6.4 (phenanthridone), 7.5 (aniline), 9.8 (benzanilide), 19.5 (4-aminobenzophenone), and 21.0 (benzamide). The retention times for the methyl analogs of the compounds listed above were identical to those of the unsubstituted compounds. Benzoic acid did not elute from the Lichrosorb column and was estimated by a separate analysis using reverse phase l.c., with a 2 ft C-18 Bondapak column (Water Associates) and elution with an aqueous solution (p*H* 4.0) of 9 wt.% acetonitrile, 0.013 wt.% sodium acetate, and 0.072 wt.% acetic acid. At a flow rate of 0.50 ml min^{-1}, retention times (min) were 1.3 (solvent front, amides, amines, and aminobenzophenones) and 2.6 (benzoic acid). The products separated by l.c. were identified by comparison of retention times with those of standards and by the analysis of fractions collected immediately after the u.v. detector of the chromatograph, using u.v. spectroscopy in semimicro cells and (in the few cases possible) by mass spectrometry.

Emission spectra were recorded on a Farrand MK1 spectrofluorometer, fitted with a xenon arc source, IP 28 photomultiplier, a low temperature attachment, and fixed speed light chopper. Samples were dissolved in EPA (ethyl ether – isopentane – ethanol in 5:5:2 ratio by volume). Excitation and emission band widths were set at 5 nm. Spectra at 77 K were measured on 1 cm path quartz cells.

Results

Ultraviolet irradiation at 254 ± 10 nm of **1**, **2**, or **3** in O_2-free ethanol solutions (evacuated, or under N_2) resulted in the u.v. absorption changes shown in Fig. 1, with sharp isosbestic points, except in the case of **3**. Separations of the photolysis products from **1** by l.c. showed that 2- and 4-aminobenzophenones and aniline accounted for 90–100% of the photolyzed **1** (Fig. 2). Small l.c. peaks eluted with the retention times expected for benzene and ethyl benzoate but could not be further characterized (very weak u.v. absorptions and too volatile for concentration and mass spectrometry). Reverse phase l.c. indicated the absence of benzoic acid (<10% of **1** photolyzed; low sensitivity because of low molar extinction coefficient (ε) at the detector wavelength).

Quantum yields for product formation and amide loss calculated from the l.c. data for **1**, are shown in Table 1. Only 2- and 4-aminobenzophenones contribute to the u.v. absorption changes above 330 nm (Fig. 1*a*), so that yields of these products can also be calculated from their overlapping spectra (ε_{375} 5.70 × 10^3 and ε_{335} 2.5 × 10^3 for 2-aminobenzophenone and ε_{375} 4.48 × 10^3 and ε_{335} 1.71 × 10^4 M^{-1} cm^{-1} for 4-aminobenzophenone in ethanol). These u.v. changes (at <10% conversion) were also used to calculate quantum yield values as listed in Table 1. Quantum yields for the consumption of **1** (up to 10% conversion) were also calculated from u.v. changes at its 265 nm absorption maximum (ε 1.25 × 10^4 M^{-1} cm^{-1}) and are in good agreement with values calculated from the l.c. analyses (Table 1). This agreement is consistent with the small absorption expected at 265 nm from the products (all have ε values at 265 nm below that of **1**).

The u.v. changes for **2** (Fig. 1*b*) are consistent with the formation of only the 2-aminobenzophenone product (absorption maximum ~385 nm) with no 4-amino detectable (absorption maximum ~340 nm) and this was confirmed by l.c. Quantum yields (Φ) calculated from l.c. and u.v. data for the photolysis of **2** are shown in Table 1. Values for 2-amino-5-methylbenzophenone were calculated from u.v. data using the ε value of unsubstituted 2-aminobenzophenone. The quantum yield for the loss of amide **2** calculated from u.v. changes is significantly less than the value from l.c. data, possibly due to the formation of trace products absorbing strongly at the u.v. maximum of **2** (270 nm).

The u.v. changes for **3** (Fig. 1*c*) are consistent

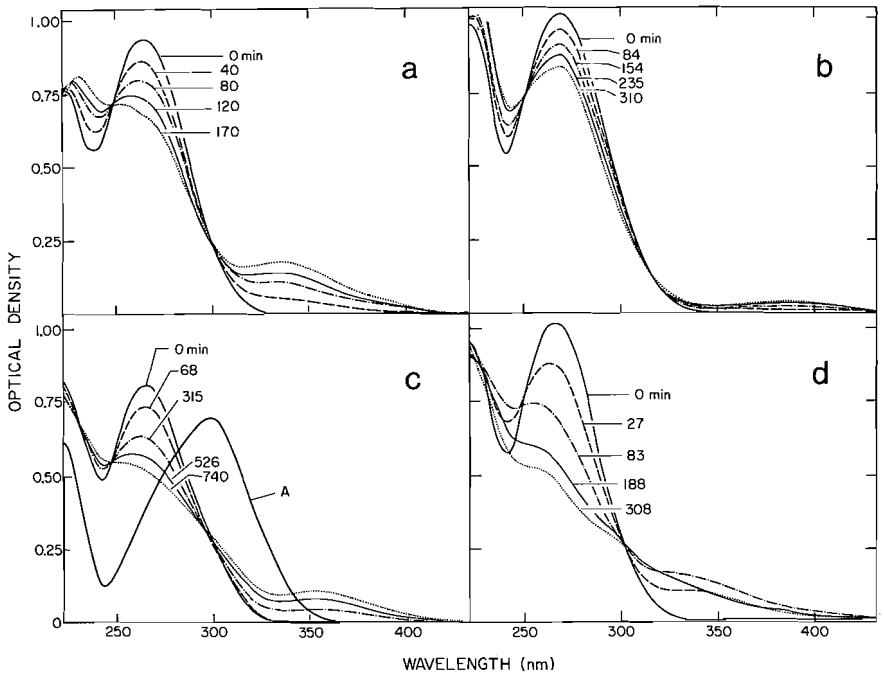

FIG. 1. Ultraviolet absorption changes during the photolysis of amide solutions. Ethanol solutions 24 °C, 254 ± 10 nm irradiation of amide (initial concentration): (*a*) **1** (7.4×10^{-4} *M*); (*b*) **2** (7.5×10^{-4} *M*); (*c*) **3** (3.4×10^{-4} *M*) curve *A*: **4** (3.0×10^{-4} *M*) (after 0 h and 10 h full mercury arc irradiation); (*d*) full mercury arc irradiation of amide **1** (8.3×10^{-4} *M*).

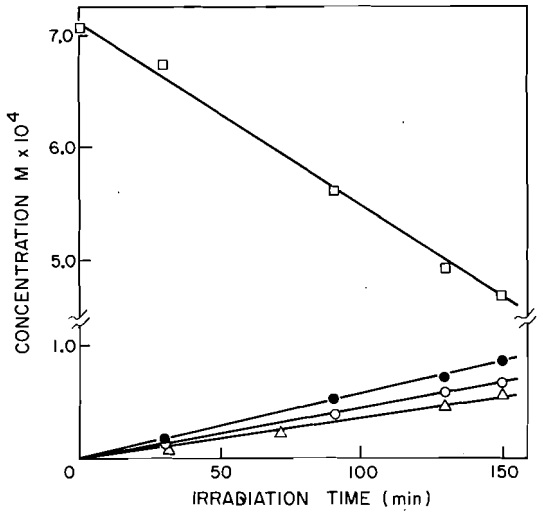

FIG. 2. Photolysis products from benzanilide (**1**). O_2-free ethanol solution, irradiated at 254 ± 10 nm, 24 °C. Incident intensity 6.9×10^{-9} einstein s^{-1} ml^{-1}. Concentrations from l.c. analysis: □, benzanilide; ●, 4-aminobenzophenone; ○, 2-aminobenzophenone; △, aniline.

with 2- and 4-aminobenzophenone formation but the poor isosbestic point probably indicates extensive secondary photolysis of the aminobenzoyl products so that quantum yields cannot be derived from these u.v. data. The general u.v. sensitivity of **3** should, however, be compared with the behavior of **4** where negligible change in u.v. absorption (curve *A*, Fig. 1*c*) was detected after 10 h of 254 nm irradiation.

For all four amides, 254 ± 10 nm irradiation of O_2- or air-saturated ethanol solutions resulted in u.v. changes identical to those found in O_2-free solutions. However, l.c. analysis of solutions of **1** and **2** indicated the presence of only small amounts of benzene, ethyl benzoate, aniline, or *p*-toluidine, but much benzoic acid. Some quantum yields in the presence of O_2 are shown in Table 1. Prolonged (~40 h) irradiation at 254 nm of 2- and 4-aminobenzophenone solutions in ethanol ($\sim 1 \times 10^{-3}$ *M*) resulted in no detectable changes of the u.v. spectra of the solutions.

The effects of incident wavelength and solvent on the photolysis of **1** in the presence of air

Can. J. Chem. Downloaded from www.nrcresearchpress.com by 210.87.254.42 on 09/05/12
For personal use only.

TABLE 1. Quantum yields (Φ) for Amide Photolysis[a]

Amide Conditions	Φ × 10³ (mol einstein⁻¹)				
	2-NH_2-5-RφCOφ[b]	4-NH_2φCOφ	4-RφNH_2[b]	φCOOH	Amide loss
1 O_2 free	1.5±0.2 (1.6±0.3)	1.6±0.2 (1.7±0.3)	0.9±0.2	<0.4	4.1±0.4 (4.0±0.4)
1 O_2 saturated	1.5±0.2 (1.4±0.3)	1.6±0.3 (1.7±0.3)	<0.2	1.0±0.2	4.0±0.4 (3.9±0.4)
2 O_2 free	0.9±0.1 (1.0±0.1)	<0.02 (<0.05)	0.9±0.2	<0.4	2.5±0.3 (1.6±0.1)
2 O_2 saturated	1.0±0.1 (1.0±0.1)	<0.02 (<0.05)	0.12±0.04	0.8±0.2	2.6±0.3 (1.6±0.1)

[a]In absolute ethanol, amide concentration 7×10^{-5}–1×10^{-3} *M*. Incident intensity of 254 ± 10 nm radiation ~7.0×10^{-9} einstein s^{-1} ml^{-1}. Calculated from l.c. analysis data at < 10% conversion; values in parentheses from u.v. changes. Error limits largely determined by scatter in product concentrations from l.c.
[b]For 1, R = H; for 2, R = CH_3.

are shown by the quantum yield data in Table 2. Liquid chromatographic analysis showed that the quantum yields for aniline production from O_2-free solutions were 0.9 (254 nm) and 0.04 (300 nm), respectively.

Irradiation of O_2-saturated or O_2-free ethanol solutions of **1** with the unfiltered mercury arc resulted in the u.v. changes shown in Fig. 1*d*. After ~350 min of irradiation of an air-saturated solution, l.c. analysis indicated the presence of trace amounts of 2- and 4-aminobenzophenones (<3% of **1** photolyzed), some nitrobenzene (~5% of **1** photolyzed), much benzoic acid (~50% of **1** photolyzed) and the absence of aniline. The differences between 254 nm and the full arc irradiations of **1** could result from the photolysis of the primary products. This was confirmed when O_2-saturated and O_2-free ethanol solutions of both 2- and 4-aminobenzophenone were found to photolyze rapidly themselves on full arc irradiation. The initial concentrations of $\sim 1 \times 10^{-3}$ *M* were reduced to virtually zero in ~100 min (4-aminobenzophenone $\Phi \sim 1 \times 10^{-4}$ mol einstein^{-1}) and ~400 min (2-aminobenzophenone $\Phi \sim 2.5 \times 10^{-5}$ mol einstein^{-1}). In each case, O_2-saturated solutions gave 20–25% benzoic acid, with none detectable from O_2-free irradiated solutions. The approximate quantum yields for aminobenzophenone losses were calculated from the known spectral output of the mercury arc and the low Φ values are con-

TABLE 2. Effect of wavelength on benzanilide photolysis in various solvents[a]

Solvent	Irradiation wavelength (nm)	Absorbed intensity × 10⁹ (einstein ml^{-1} s^{-1})	Quantum yield (mol. einstein⁻¹) × 10³		
			2NH_2φCOφ	φCONHφ loss	4NH_2φCOφ
EtOH	240±10	3	1.9	5.0	1.6
	254±10	4	1.5	4.0	1.6
	280±10	4	0.34	0.73	0.27
	300±10	16	0.092	0.22	0.06
	Full arc	400	—	0.15[b]	
MeOH	254±10	5	1.6	3.0	1.3
	300±10	12	0.095	0.20	0.07
cyC_6H_{12}[c]	254±10	1.8	5.6	11	3.9
	300±10	2.8	2.0	6.0	1.7
DMSO[d]	290±10	1.4	0.12[b]	—	0.09[b]

[a]Benzanilide concentration 8×10^{-4} *M*; values from l.c. data with ±20% certainty unless otherwise stated. Air saturated solutions 0.1 cm path.
[b]From u.v. changes.
[c]Benzanilide concentration, 1.5×10^{-4} *M* (saturated solution); ±30% certainty on quantum yield values.
[d]Dimethyl sulfoxide.

Can. J. Chem. Downloaded from www.nrcresearchpress.com by 210.87.254.42 on 09/05/12
For personal use only.

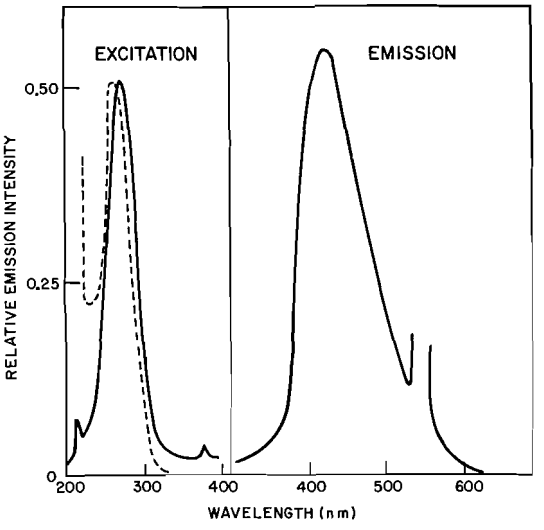

FIG. 3. Emission and excitation spectra of benzanilide. Benzanilide (4.3×10^{-6} *M*) in EPA at 77 K. Excitation spectra measured with emission at 435 nm; — uncorrected; --- corrected. Emission spectrum with excitation at 278 nm.

sistent with the reported absence of the reactive n–π* triplet state in ethanolic solutions (6).

Uncorrected emission and excitation spectra from EPA solutions of benzanilide (**1**) are shown in Fig. 3. No fluorescence was detected, and the phosphorescence emission at ~435 nm (half-life $\sim 10^{-3}$ s) was only observed at 77 K. A corrected excitation spectrum was calculated from the observed phosphorescence, the xenon arc intensity distribution, the u.v. absorption of the EPA solution, and the excitation monochromator transmission efficiency at selected wavelengths. This corrected excitation spectrum is shown in Fig. 3 and coincides well with the u.v. absorption spectrum (Fig. 1*a*).

Discussion

N-Aryl amides, aryl esters, and various other carboxylic acid derivatives are known to undergo the photo Fries rearrangement on u.v. irradiation (1, 2, 7, 8). Both a scission to give caged free radicals (reaction 1) and a concerted

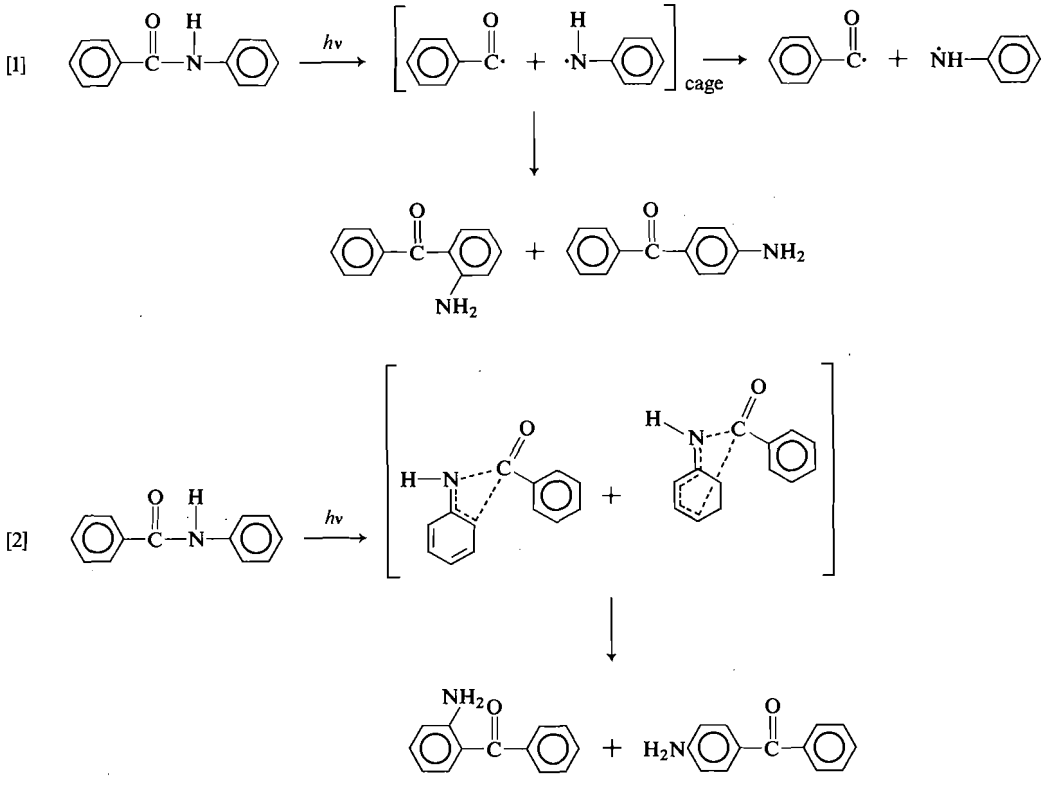

Can. J. Chem. Downloaded from www.nrcresearchpress.com by 210.87.254.42 on 09/05/12
For personal use only.

Can. J. Chem. Downloaded from www.nrcresearchpress.com by 210.87.254.42 on 09/05/12
For personal use only.

rearrangement (reaction 2) have been proposed to lead to the major photo Fries products (8). For aryl esters, the reaction analogous to reaction 1 was suggested by Bellus (7) to proceed from a higher excited state than reaction 2. From flash photolysis data, Humphrey and Roller (9) have suggested that the reaction analogous to [2] proceeds from the aryloxy $^1\pi^*$ state, whereas homolysis [1] results from the $^1\pi^*$-carbonyl state of diaryl carbonates.

The analytical results obtained under our experimental conditions for amides **1** and **2** can be interpreted in terms of processes 1 and possibly also 2. The formation of aniline and *p*-toluidine (in the absence of O_2) and benzoic acid (from O_2-containing solutions, discussed below) can only result from amide homolysis (reaction 1). The importance of aminobenzophenones from the concerted process (as well as cage recombination in reaction 1) cannot be established in the absence of direct evidence for the cyclic intermediate (from, say, flash photolysis). However, the approximate constancy in the ratios of aminobenzophenones to aniline (on average ~1.2:1.0:0.6 for 2-amino–4-amino–aniline) with irradiation wavelength and the roughly constant proportions of 2- and 4-aminobenzophenones (~1.2:1.0, Table 2) at all wavelengths and in all solvents might indicate the predominance of reaction via the homolysis 1, after conversion to the $^1\pi^*$-carbonyl state of amide **1**, as suggested for carbonate photo rearrangement (9). Reaction from the excited singlet has also been suggested by Shizuka and Tanaka (8) for acetanilide photo Fries rearrangement and the absence of an effect of O_2 on the quantum yields for 2- and 4-aminobenzophenones (Table 1) is consistent with this.

Sensitization of amide photoreactions by low concentrations of benzene (a common impurity in ethanol) has been reported (8) but deliberate doping of ethanol solutions of **1** with $5 \times 10^{-3}\,M$ of benzene resulted in identical quantum yields at 254 and 300 nm as benzene 'free' ($< 1 \times 10^{-5}\,M$ by u.v.) solution. This implies that sensitization by trace benzene impurities was negligible under our experimental conditions.

The pronounced wavelength dependence of the product quantum yields for amide **1** shown in Table 2 is apparent in all of the solvents studied, was unaffected by repeated recrystallization of **1**, and so would appear to be genuine. The strong (ε $1.25 \times 10^4\,M^{-1}\,cm^{-1}$) absorption of **1** centered at 265 nm in ethanol is probably a π–$^1\pi^*$ transition localized on a phenyl group, although a small red shift was observed in cyclohexane (λ_{max} 267 nm). By analogy with the carbonate data of Humphrey and Roller (9), the wavelength dependence can be tentatively interpreted in terms of an enhanced radiationless conversion to a reactive $^1\pi^*$-carbonyl state at shorter wavelengths. Relative quantum yields for phosphorescence at 435 nm calculated from the excitation spectrum in Fig. 3 are 0.9 (240 nm), 1.0 (260 nm), 0.7 (280 nm), and 0.3 (310 nm). This wavelength dependence roughly parallels the wavelength dependence of the product quantum yields, although the absence of fluorescence prevents the more meaningful correlation between fluorescence quantum yield and product quantum yields.

Shizuka (10) has previously observed a solvent polarity effect on the photo Fries rearrangement of acetanilide similar to that shown in Table 2 for amide **1**. The drop in quantum yield with increased solvent polarity was then interpreted to indicate the photolysis products resulted from an initial dissociation at the C—N bond into radical fragments.

Our data indicate that O_2 cannot prevent the cage recombination of the primary radicals from process 1 to give aminobenzophenones but can only react with radicals which escape the cage (from reaction 1). In particular, benzoyl radicals will be scavenged by O_2 to give benzoic acid, probably via the u.v.-unstable perbenzoic acid (reaction 3) as suggested by Kan and Furey (2).

[3] $C_6H_5\dot{C}O + O_2 \longrightarrow$

$$C_6H_5C(=O)-OO\cdot \xrightarrow{\text{solvent}} C_6H_5C(=O)-OOH \xrightarrow{h\nu}$$

$$C_6H_5C(=O)-O\cdot \xrightarrow{\text{solvent}} C_6H_5C(=O)-OH$$

Oxygen has been reported to have no effect on the formation of 2- and 4-aminoacetophenones during the photo Fries rearrangement of acetanilide (8) and no effect on the photo Fries rearrangement in general (7). In the absence of oxygen $C_6H_5\dot{C}O$ radicals which escape the cage

Can. J. Chem. Downloaded from www.nrcresearchpress.com by 210.87.254.42 on 09/05/12
For personal use only.

probably eliminate CO (11, 12) and give phenyl radicals which will hydrogen abstract from the solvent to give benzene (13). In the presence of dissolved oxygen, aniline and *o*-toluidine are probably destroyed by the attack of peroxy radicals generated from the solvent after benzoyl or anilino radical attack (14).

Previous work has indicated that the prolonged photolysis of **1** with a full mercury arc in N_2-saturated ethanol gave only low yields of the 2- and 4-aminobenzophenones (~14% of each based on the amount of **1** consumed), together with a trace amount of aniline and a higher yield of benzoic acid (27% of **1** consumed) for a 32% loss of **1** (1). This earlier work can be reconciled with our data if trace amounts of O_2 were present in the previous workers' system, so that $C_6H_5\dot{C}O$ interception by O_2 to give benzoic acid as a final product could have occurred, together with extensive secondary photolysis of the aminobenzophenones. Kan and Furey (2) have also attributed benzoic acid formation to the presence of O_2 and have observed products similar to those identified in our work when ethanolic solutions of **1** were irradiated in the presence of O_2. However, only low yields of aminobenzophenones (<10%) were reported by Kan and Furey and the benzamide detected in their work by g.p.c. was not found in our reaction products after 254 nm irradiation in the presence or absence of O_2. Phenanthridone has been detected as the major product from irradiation of benzene solutions of **1** in the presence of iodine (15) but none was detected under our irradiation conditions.

The prevention of photo Fries rearrangement to the 4-position by the presence of a blocking methyl group (amide **2**) has previously been observed with substituted acetanilides (16). The much greater photostability of **4** in comparison to **3** may result from increased conjugation through

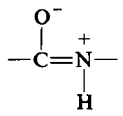

forms of the amide groups of **4** as suggested by Belyakov *et al.* (17) promoting greater delocalization of the absorbed u.v. energy. The u.v. absorption maxima of **4** (300 nm) and **3** (267 nm) are consistent with increased conjugation in the all-*para* isomer.

In conclusion, the photolysis of fully aromatic amides under controlled conditions at low conversions has been shown to yield 2- and 4-aminobenzophenone products via a photo Fries rearrangement. Formation of these products is not affected by the presence of O_2, whereas aniline which probably results from free radical scission products is only detected in O_2 free solutions. Only in the presence of O_2, is benzoic acid observed, again presumably from scission products. Meaningful quantum yields for these products are reported for the first time. Previously reported products and product yields (1) are shown to result from extensive secondary photolyses of the primary products in the presence of O_2.

Amide **3**, a model for poly(1,3-phenylene isophthalamide) (Nomex, Du Pont trade name) was found to undergo a similar photo Fries rearrangement to benzanilide (**1**) although extensive secondary photo rearrangement and cleavage of the amino products made quantitative comparison difficult. Amide **4**, a model for poly(1,4-phenylene terephthalamide) (Kevlar B, Du Pont trade name) was found to be extremely photostable. The importance of these results in the unravelling of the photooxidative degradation mechanisms of these two commercially important polymers will be discussed in a future communication (18).

1. D. ELAD, D. V. RAO, and V. I. STENBERG. J. Org. Chem. **30**, 3252 (1965); V. I. STENBERG. *In* Organic photochemistry. Vol. 1. *Edited by* O. L. Chapman. Marcel Dekker, New York. 1967. Chapt. 3, p. 143.
2. R. O. KAN and R. L. FUREY. Tetrahedron Lett. 2573 (1966).
3. D. J. CARLSSON, R. D. PARNELL, and D. M. WILES. J. Polym. Sci. Polym. Lett. Ed. **11**, 149 (1973).
4. D. J. CARLSSON, L. H. GAN, R. D. PARNELL, and D. M. WILES. J. Polym. Sci. Polym. Lett. Ed. **11**, 683 (1973).
5. (*a*) Dictionary of Organic Compounds. 4th revision. *Edited by* I. M. Heilbron. Eyre and Spottiswoode Ltd., London. 1965. (*b*) L. P. WALLS. J. Chem. Soc. 1405 (1935).
6. G. PORTER and P. SUPPAN. Trans. Faraday Soc. **61**, 1644 (1965); S. G. COHEN, M. D. SALTSMAN, and J. B. GUTTENPLAN. Tetrahedron Lett. 4321 (1969).
7. D. BELLUS. Advan. Photochem. **8**, 109 (1971).
8. H. SHIZUKA and I. TANAKA. Bull. Chem. Soc. Jap. **41**, 2343 (1968).
9. J. S. HUMPHREY and R. S. ROLLER. Mol. Photochem. **3**, 35 (1971).
10. H. SHIZUKA. Bull. Chem. Soc. Jap. **42**, 52 (1969).

11. R. M. SMITH and J. G. CALVERT. J. Am. Chem. Soc. **78**, 2345 (1956).
12. M. J. PERKINS and B. P. ROBERTS. J. Chem. Soc. Perkin II, 297 (1974).
13. G. A. RUSSELL. *In* Free radicals. Vol. 1. *Edited by* J. K. Kochi. John Wiley, New York. 1973. Chapt. 7.
14. J. A. HOWARD. *In* Free radicals Vol. 1. *Edited by* J. K. Kochi. John Wiley, New York. 1973. Chapt. 12.
15. B. S. THYAGARAJAN, N. KHARASCH, H. B. LEWIS, and W. WOLF. Chem. Commun. 614 (1967).
16. H. SHIZUKA. Bull. Chem. Soc. Jap. **42**, 57 (1969).
17. V. K. BELYAKOV, G. I. KAGAN, V. A. KOSOBUTSKII, G. A. KUZNETSOV, and L. B. SOKOLOV. Vysokomol. Soedin. Ser. B, **14**, 657 (1972).
18. D. J. CARLSSON, L. H. GAN, and D. M. WILES. To be published.

Can. J. Chem. Downloaded from www.nrcresearchpress.com by 210.87.254.42 on 09/05/12
For personal use only.

Crystal Structure of Adeninium Trichloromercurate(II), $(C_5H_6N_5)HgCl_3 \cdot 1\frac{1}{2}\ H_2O$

MONIQUE AUTHIER-MARTIN AND ANDRÉ L. BEAUCHAMP

Département de Chimie, Université de Montréal, Montréal, Québec H3C 3V1

Received March 14, 1975

MONIQUE AUTHIER-MARTIN and ANDRÉ L. BEAUCHAMP. Can. J. Chem. **53**, 2345 (1975).

The title compound belongs to space group $P2_1/c$ with $a = 23.99(1)$, $b = 4.245(2)$, $c = 25.98(1)$ Å, $\beta = 117.58(7)°$, and $Z = 8$. The structure was solved by the heavy-atom method and refined by block-diagonal least squares on 2589 independent observed reflections. All non-hydrogen atoms were refined anisotropically and some of the hydrogen atoms were located but their parameters were not refined. The final values of R and R_w were 0.042 and 0.047, respectively.

The two nonequivalent mercury atoms have very similar environments. Two short Hg—Cl bonds (2.34–2.38 Å) at ~165° define a quasi-molecular $HgCl_2$ unit. Overall octahedral coordination is completed with two chloride ions at 2.76–2.84 Å and two chlorine atoms at 3.19–3.26 Å on neighboring $HgCl_2$ quasi-molecules. $HgCl_6$ octahedra share edges to form twofold ribbons in the b direction. This pattern of octahedra is identical with the one reported for β-NH_4HgCl_3. The cations are pairs of N(1)-protonated adenine molecules linked by two N(10)—H(10) . . . N(7) hydrogen bonds and stacked in the b direction. Water molecules act as acceptors in moderately strong hydrogen bonds with acidic protons H(1) and H(9) of adeninium ions. Other generally weaker hydrogen bonds exist between the various parts of the structure.

MONIQUE AUTHIER-MARTIN et ANDRÉ L. BEAUCHAMP. Can. J. Chem. **53**, 2345 (1975).

Le composé cristallise dans le groupe $P2_1/c$ et les paramètres de maille sont: $a = 23.99(1)$, $b = 4.245(2)$, $c = 25.98(1)$ Å, $\beta = 117.58(7)°$ et $Z = 8$. La structure a été résolue par la méthode de l'atome lourd et affinée par moindres carrés (matrice à blocs diagonaux) au moyen de 2589 réflexions observées non-équivalentes. Certains des atomes d'hydrogène ont été repérés sur la carte de Fourier, mais leurs paramètres n'ont pas été affinés. L'affinement anisotrope de tous les autres atomes a été effectué et les valeurs finales de R et R_w sont 0.042 et 0.047 respectivement.

La maille renferme deux atomes de mercure indépendants, non-équivalents ayant des environnements très semblables. Deux liens courts (2.34–2.38 Å) à ~165° l'un de l'autre définissent une quasi-molécule $HgCl_2$. La coordination effective octaédrique du métal comporte en outre deux ions chlorures à 2.76–2.84 Å, ainsi que deux atomes de chlore à 3.19–3.26 Å appartenant à des quasimolécules voisines. Les octaèdres $HgCl_6$ ont des arêtes communes et forment une double chaîne parallèle à l'axe b. La disposition des octaèdres est semblable à celle de la forme β de NH_4HgCl_3. Les cations du composé sont des molécules d'adénine protonées en N(1) et réunies par paires grâce à deux ponts hydrogène N(10)—H(10) . . . N(7). Ces paires d'ions adéninium sont empilées dans la direction de l'axe b. Les molécules d'eau jouent le rôle d'accepteur dans des ponts hydrogène modérément forts avec les protons acides H(1) et H(9) des ions adéninium. Plusieurs autres ponts hydrogène souvent assez faibles existent entre les diverses espèces présentes dans la structure.

Introduction

Adenine or 6-aminopurine (HAd), a constituent of DNA and RNA, is known to react with various metal ions (1). A recent crystallographic work (2) has shown that the ligand is N(7)-coordinated in the zwitterionic complex $(H_2Ad)ZnCl_3$ obtained from dilute hydrochloric acid solutions. We have investigated the reactions of mercuric chloride with the same molecule and isolated under similar conditions the corresponding compound $(H_2Ad)HgCl_3 \cdot 1\frac{1}{2}H_2O$. The structure of this compound is reported in the present paper.

Experimental

Crystal Data

$C_5H_6N_5Cl_3Hg \cdot 1\frac{1}{2}H_2O$ f.w. = 470.12

Monoclinic, space group $P2_1/c$, $a = 23.99(1)$, $b = 4.245(2)$, $c = 25.98(1)$ Å, $\beta = 117.58(7)°$, $V = 2344$ Å^3, $Z = 8$, $D_c = 2.66$ g cm^{-3}, $D_o = 2.57(1)$ g cm^{-3} (flotation in CH_2Br_2–$CHBr_3$ mixture). μ(MoKα) = 126 cm^{-1}; λ(MoK$\bar{\alpha}$) = 0.71068 Å (graphite monochromator).

Preparation

Hot aqueous solutions of adenine (Aldrich Co.) and mercuric chloride are mixed together (molar ratio 1:3) and 0.5 M HCl is added to redissolve the precipitate initially formed. On cooling at room temperature, a colorless precipitate $(HAd)_2Hg_3Cl_6$ is obtained. This com-

Can. J. Chem. Downloaded from www.nrcresearchpress.com by 210.87.254.40 on 09/05/12
For personal use only.

Can. J. Chem. Downloaded from www.nrcresearchpress.com by 210.87.254.40 on 09/05/12
For personal use only.

pound is dissolved in a warm 1:1 mixture of acetone and 0.1 *M* aqueous HCl. By slow evaporation at room temperature, crystals of the title compound are obtained as very thin needles elongated along the *b* axis. They are stable in air. A crystal of dimensions 0.006 × 0.003 × 0.8 mm was selected for crystallographic work.

Crystallographic Measurements

Space group $P2_1/c$ was established from precession and Weissenberg photographs. Accurate cell parameters and intensity measurements were obtained with a Picker FACS-1 automatic diffractometer. Experimental details are given elsewhere (3). A total of 7470 measurements (standards included) were collected (*hkl*, $hk\bar{l}$, $\bar{h}kl$, and $\bar{h}k\bar{l}$) in a sphere $2\theta \leqslant 46°$. Three standard reflections ($01\bar{5}$, 604, $10\,1\,\bar{3}$) measured every 30 reflections showed maximum fluctuations of ±5% during data collection. Preliminary calculations indicated that the transmission factor varies from 0.93 to 0.96. Therefore, no absorption correction was applied. The data were reduced to two octants (*hkl* and $hk\bar{l}$) by averaging equivalent reflections. All reflections with net intensities $I < 2\sigma(I)$ (3) were considered as unobserved. The reduced set of data consisted of 2589 observed and 689 unobserved reflections.

Resolution of the Structure

Two general positions of group $P2_1/c$ are needed to hold the eight mercury atoms of the unit cell. The coordinates of the two nonequivalent mercury atoms were calculated from a three-dimensional Patterson map. At this stage, particular values (0 or ½) for the *y* coordinates introduced pseudo-mirrors in the unit cell. The starting model corresponded to group $A2/m$ and the phases of all reflections with $k + l \neq 2n$ were undefined. On the Fourier map calculated with phased reflections only, all six independent chlorine atoms were easily recognized, but they were very close to the pseudo-mirrors and the pseudo-symmetry problem still remained. The structure was solved as follows: the *x* and *z* coordinates and isotropic temperature factors *U* for the two mercury and the six chlorine atoms were first refined by full-matrix least squares using the reflections originally phased. The *y* coordinate of Hg(1) was then shifted arbitrarily from 0 to 0.001, which fixed the origin along the *b* axis. Parameters *x*, *y*, *z*, and *U* were refined for Hg(1) and Hg(2) in the first step, then for all mercury and chlorine atoms. Refinement converged to $R = \Sigma||F_o| - |F_c||/\Sigma|F_o| = 0.243$. The carbon, nitrogen, and oxygen atoms were located on the next Fourier map. Isotropic refinement of all nonhydrogen atoms converged to $R = 0.069$.

Anisotropic refinement was carried out by block-diagonal least squares. The real and imaginary contributions to anomalous dispersion were included for mercury and chlorine (4). Hydrogen atoms attached to N(1), C(2), C(8), and N(9) were fixed at the calculated positions on both adenine rings (C—H or N—H distances of 0.92 Å).

TABLE 1. Refined fractional coordinates (× 10^4) and anisotropic temperature factors (× 10^4), t.f. = exp $\{-(U_{11}a^{*2}h^2 + U_{22}b^{*2}k^2 + U_{33}c^{*2}l^2 + 2U_{12}a^*b^*hk + 2U_{13}a^*c^*hl + 2U_{23}b^*c^*kl)\}$

Atom	*x*	*y*	*z*	U_{11}	U_{22}	U_{33}	U_{12}	U_{13}	U_{23}
Hg(1)	842.3(3)	245.9(1.7)	2793.5(3)	43.4(4)	39.2(4)	40.8(4)	−0.8(3)	28.3(3)	−0.9(3)
Hg(2)	4241.2(3)	5378.4(1.6)	2469.0(3)	36.6(3)	36.2(4)	39.5(4)	−0.7(3)	15.4(3)	0.9(3)
Cl(1)	8472(2)	161(10)	1502(2)	47(2)	30(2)	43(2)	1(2)	22(2)	4(2)
Cl(2)	6701(2)	281(11)	3402(2)	47(2)	49(3)	42(2)	2(2)	15(2)	−5(2)
Cl(3)	1001(2)	226(10)	3161(2)	38(2)	45(2)	41(2)	1(2)	25(2)	−1(2)
Cl(4)	4698(2)	434(11)	1822(2)	40(2)	46(3)	37(2)	0(2)	17(2)	1(2)
Cl(5)	3878(2)	469(10)	2960(2)	57(3)	33(2)	42(2)	−2(2)	29(2)	−2(2)
Cl(6)	1311(2)	4725(11)	7181(2)	65(3)	46(3)	59(3)	−2(2)	49(2)	0(2)
N(1)	3261(6)	7418(33)	8810(6)	47(8)	40(8)	38(8)	14(7)	19(7)	−6(7)
C(2)	2863(8)	5476(43)	8912(8)	47(10)	39(10)	59(11)	3(9)	23(9)	−14(9)
N(3)	3004(6)	4199(35)	9415(6)	46(8)	47(9)	51(9)	2(7)	25(7)	4(7)
C(4)	3579(8)	5002(38)	9824(7)	50(9)	29(9)	42(9)	2(8)	22(8)	−7(8)
C(5)	4018(7)	6948(34)	9759(6)	45(9)	24(8)	22(8)	8(7)	13(7)	−2(7)
C(6)	3851(8)	8244(36)	9213(7)	49(10)	24(8)	37(9)	17(8)	16(8)	−6(7)
N(7)	4559(7)	7203(30)	10274(6)	61(9)	27(7)	39(8)	−5(7)	27(7)	0(6)
C(8)	4443(8)	5428(45)	10623(6)	55(11)	55(11)	27(8)	8(10)	18(8)	−9(9)
N(9)	3867(6)	4059(33)	10383(6)	52(9)	35(8)	53(9)	6(7)	27(7)	5(7)
N(10)	4206(6)	10224(37)	9080(6)	50(8)	57(10)	42(8)	−17(8)	20(7)	−3(8)
N(1)′	1297(6)	7185(34)	−502(5)	39(8)	52(9)	33(7)	−9(7)	16(6)	0(7)
C(2)′	1789(8)	5220(43)	−194(7)	52(10)	42(10)	50(10)	−8(9)	32(9)	1(9)
N(3)′	1912(7)	3899(38)	307(6)	42(8)	64(10)	44(8)	−2(8)	22(7)	−1(8)
C(4)′	1482(8)	4825(39)	492(7)	52(10)	29(9)	38(9)	0(8)	19(8)	−2(8)
C(5)′	966(7)	6774(37)	201(6)	59(10)	30(9)	23(8)	−9(8)	25(8)	−3(7)
C(6)′	864(8)	8028(39)	−337(7)	56(11)	33(9)	44(10)	−5(8)	32(9)	−5(8)
N(7)′	632(7)	7129(31)	515(5)	65(9)	33(8)	33(8)	−3(7)	30(7)	−2(6)
C(8)′	960(8)	5352(41)	974(6)	66(11)	37(10)	31(9)	7(9)	23(8)	0(8)
N(9)′	1466(6)	3945(31)	982(5)	53(8)	31(7)	36(7)	2(7)	24(7)	4(6)
N(10)′	388(7)	9945(34)	−666(5)	68(9)	38(8)	30(7)	7(8)	18(7)	11(7)
O(1)	2389(6)	4740(36)	6820(6)	54(8)	80(10)	83(9)	−17(8)	40(7)	−20(9)
O(2)	3059(6)	5077(33)	5551(5)	81(9)	58(9)	63(8)	4(8)	41(7)	−5(7)
O(3)	2553(6)	5224(31)	2663(5)	68(8)	55(8)	47(7)	−1(7)	22(6)	−5(7)

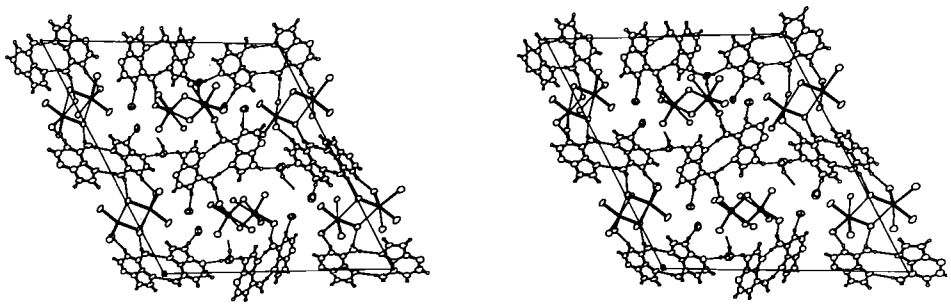

FIG. 1. Projection of the unit cell down the *b* axis. The origin is represented by a black dot. The *a* axis is horizontal, *c* is vertical, and *b* is perpendicular to the drawing, away from the reader. The mercury atoms are dark spheres surrounded with octahedra of chlorine atoms. The oxygen atoms of the water molecules are represented by darker ellipsoids.

Constant temperature factors (6 Å^2) were used. Their coordinates were not varied, but the shifts on the corresponding carbon or nitrogen coordinates were applied to the hydrogen atoms as well. Anisotropic refinement of mercury and chlorine atoms and isotropic refinement of the remaining nonhydrogen atoms reduced R to 0.048. At the latest stage of the refinement, individual weights $w = 1/\sigma_F^2$ (5) were applied to each reflection. Anisotropic refinement of all nonhydrogen atoms converged to $R = 0.042$ and $R_w = \{\Sigma w(|F_o| - |F_c|)^2/\Sigma w|F_o|^2\}^{1/2} = 0.047$ (observed reflections only). On the final difference–Fourier map, four peaks of ± 0.8 e/Å^3 were found close to mercury, all other peaks were lower than ± 0.5 e/Å^3. The refined parameters are given in Table 1 and the list of structure factors is available upon request.[1] The form factors used in this work were those of Cromer and Waber (6) and the computer programs utilized are listed elsewhere (7).

The final difference–Fourier map was examined for possible locations of the missing hydrogen atoms. Electron density of 0.4 e/Å^3 was found close to the positions expected for amino hydrogens, assuming that the groups are planar and in the plane of the adeninium rings. For water molecules, the lines joining oxygen to all possible hydrogen-bond acceptors were carefully searched. Peaks were found at reasonable positions around O(2), but no indications concerning the hydrogen atoms of O(1) and O(3) could be found. The list of hydrogen coordinates is included in the unpublished material.[1]

Results and Discussion

Figure 1 shows a projection of the unit cell down the *b* axis. The compound is a salt and adenine is not coordinated to mercury. The anionic part $(HgCl_3)_x^{x-}$ is located in layers parallel to the *ab* plane at $c = \frac{1}{4}$ and $\frac{3}{4}$. Other layers at $c = 0$ and $\frac{1}{2}$ contain adeninium cations linked in pairs via hydrogen bonding.

[1]The structure factor table and the list of hydrogen coordinates are available, at a nominal charge, from the Depository of Unpublished Data, CISTI, National Research Council of Canada, Ottawa, Canada K1A 0S2.

Mercury Coordination

The two independent mercury atoms are similarly surrounded with chlorine atoms. Bond lengths and angles are given in Fig. 2. Two short bonds (2.34–2.38 Å) at 164–165° define a quasi-molecular $HgCl_2$ unit. An approximate octahedron is completed with two chloride ions at 2.76–2.84 Å and two longer contacts (3.19–3.26 Å) involving chlorine atoms of neighboring quasi-molecules. Other examples of this type of coordination are found in mercury chemistry (8), for instance, in double salts $MHgCl_3$ and M_2HgCl_4, where M is an alkali cation or NH_4^+. $HgCl_6$ octahedra share edges to form twofold ribbons in the direction of the *b* axis. The pattern of octahedra observed here is similar to the one reported for the β form of NH_4HgCl_3 (9).

Adeninium Ions

The two independent adeninium ions have identical geometries within experimental errors (Fig. 3). In both cases, pairs of symmetrically equivalent ions are linked by hydrogen bonding and the middle of the dimer is an inversion center of the unit cell. Mean planes were calculated through the carbon and nitrogen atoms of either individual adeninium ions or ion pairs. Deviations from planarity were within 2σ (or 0.030 Å), except for amino nitrogen N(10)′, where the distance (0.049(14) Å) is more significant.

Although the presence of the extra proton on N(1) (and N(1)′) could not be ascertained from the electron density map, protonation of that position is highly probable for the following reasons: (*i*) protons were found on N(1) in adeninium hydrochloride (10) and nucleosides containing protonated 9-adenylyl groups (11, 12). It is also the protonation site in $(H_2Ad)ZnCl_3$ (2), $(9\text{-}CH_3HAd)PtCl_3$ (13), $(H_2Ad)_2Cu_3Cl_8$ ·

Can. J. Chem. Downloaded from www.nrcresearchpress.com by 210.87.254.40 on 09/05/12
For personal use only.

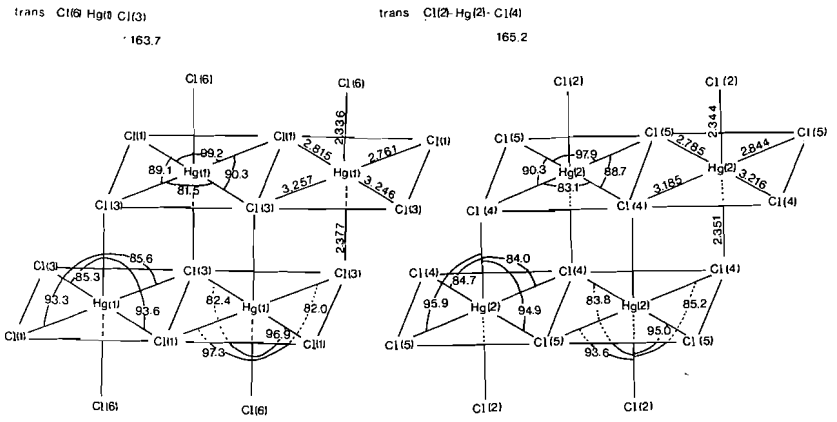

FIG. 2. Bond lengths and angles around mercury. The standard deviations are 0.005 Å on the bond lengths and 0.1° on the angles.

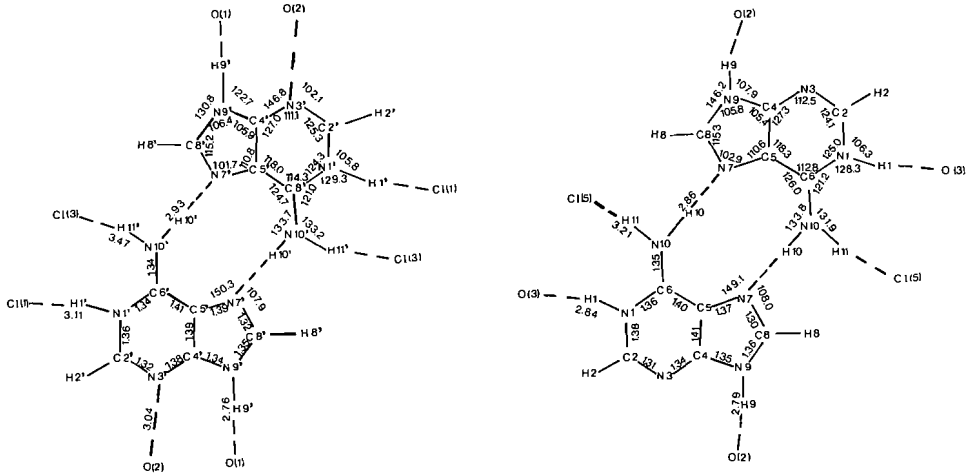

FIG. 3. Bond lengths and angles in the adeninium ions. The standard deviations are 0.02 Å on the bond lengths and 1.7° on the angles. When hydrogen bonds (X—H . . . Y) are involved, X—Y distances are given and X—Y vectors were used in angle calculations.

TABLE 2. Comparison of bond angles in the pyrimidine rings of adenine moieties

	Angle (deg)			
Bonds	Neutral*	N(1)-protonated*	This work	
C(2)—N(1)—C(6)	118.9	123.2	125.0	124.3
N(1)—C(2)—N(3)	128.8	125.2	124.1	125.3
C(2)—N(3)—C(4)	111.0	112.1	112.5	111.1
N(3)—C(4)—C(5)	126.8	127.6	127.3	127.0
C(4)—C(5)—C(6)	116.7	117.7	118.3	118.0
C(5)—C(6)—N(1)	117.7	114.0	112.8	114.3

*Reference 16.

$4H_2O$ (14), and $[(HAd)_2Co(H_2O)_4](H_2Ad)_2(SO_4)_2 \cdot 6H_2O$ (15); (*ii*) potential hydrogen-bond acceptors O(3) and Cl(1) suggest that acidic hydrogens are present on N(1) and N(1)′ (Fig. 3); (*iii*) Sundaralingam and co-worker (11) have noted significant structural differences between the N(1)-protonated and the neutral forms. Average values for bond lengths and

Can. J. Chem. Downloaded from www.nrcresearchpress.com by 210.87.254.40 on 09/05/12
For personal use only.

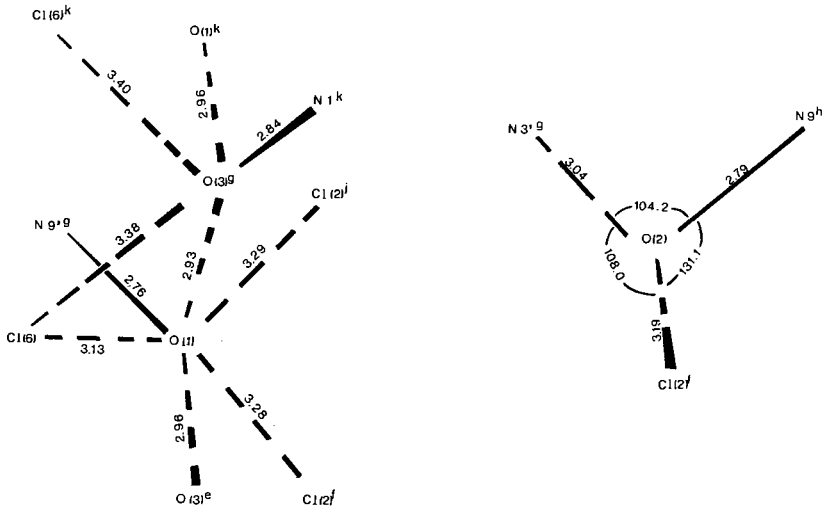

FIG. 4. Environments of the water molecules. N—H . . . O bonds are represented by solid sticks and potential bonds involving hydrogen atoms of water molecules are shown as dashed sticks. Evidence for the pattern around O(2) was obtained from the electron density map, but no unique pattern could be found around O(1) and O(3). The superscripts are explained in Table 3.

TABLE 3. Selected angles around O(1) and O(3)*

Bonds	Angle (deg)	Bonds	Angle (deg)
N(9)′^{g}—O(1)—Cl(6)	76.3	N(1)^k—O(3)^g—O(1)	147.6
N(9)′^{g}—O(1)—Cl(2)^j	81.4	N(1)^k—O(3)^g—Cl(6)^k	99.3
N(9)′^{g}—O(1)—Cl(2)^f	125.7	O(1)—O(3)^g—Cl(6)^k	112.7
Cl(6)—O(1)—Cl(2)^j	139.3	N(1)^k—O(3)^g—O(1)^k	109.4
Cl(6)—O(1)—Cl(2)^f	139.8	N(1)^k—O(3)^g—Cl(6)	127.2
		O(1)^k—O(3)^g—Cl(6)	112.6

*e.s.d. = 0.5°; ^{e} = $x, 1\frac{1}{2} - y, \frac{1}{2} + z$; ^{f} = $1 - x, 1 - y, 1 - z$; ^{g} = $x, \frac{1}{2} - y, \frac{1}{2} + z$; ^{h} = $x, \frac{1}{2} - y, -\frac{1}{2} + z$; ^{j} = $1 - x, -y, 1 - z$; ^{k} = $x, -1 + y, z$.

angles have been recalculated including more recent data (16). No significant conclusions can be drawn from bond lengths, because the two forms are expected to show maximum differences of 0.02 Å, which correspond to 1σ in the present structure. Bond angles appear to be more sensitive to protonation. Differences attaining 4.3°, or 2.5 times our standard deviations, are expected. Comparison of the angles in the pyrimidine rings (Table 2) shows a better agreement with the N(1)-protonated pattern.

Hydrogen Bonds

Ion-pairing in the adeninium dimers involves two N(10)—H(10) . . . N(7) (or N(10)′—H(10)′ . . . N(7)′) hydrogen bonds (Fig. 3). Identical pairing has been observed in other adenine derivatives (15, 17) with similar N . . . N distances. The second amino hydrogens interact more weakly with chlorine atoms at 3.21 Å (N(10) . . . Cl(5)) and 3.47 Å (N(10)′—Cl(3)).

One of the acidic ring protons, H(1)′, forms a moderately strong bond to Cl(1) (N . . . Cl = 3.11 Å), whereas the other three (H(1), H(9), and H(9)′) bind to oxygen atoms of water molecules with N . . . O distances in the range 2.76–2.84 Å. Hydration of acidic protons appears to be the primary purpose of the water molecules, since their own hydrogen atoms are not involved in strong hydrogen bonding. For instance, the hydrogen atoms attached to O(2) (Fig. 4) interact only moderately with Cl(2) (O . . . Cl = 3.19 Å) and very weakly with N(3)′(3.04 Å). The pattern around O(1) and O(3) was not determined unambiguously (Fig. 4 and Table 3). In spite of the small N(9)′—O(1)—Cl(6) angle (76°), the short Cl(6) . . . O(1) distance (3.13 Å) is probably indicative of some hydrogen bonding. Two Cl(2)

Can. J. Chem. Downloaded from www.nrcresearchpress.com by 210.87.254.40 on 09/05/12
For personal use only.

atoms at 3.28 and 3.29 Å from O(1) may be considered as potential acceptors. Around O(3), which is already attached to H(1), two reasonable pairs of acceptors are found: O(1) and Cl(6)^k or O(1)^k and Cl(6). On the basis of the oxygen-acceptor distances and the set of angles, both alternatives are equally reasonable. Such pairs of hydrogen-bonding patterns might result in crystal disorder, which would explain that no indications concerning those particular hydrogen atoms could be obtained from the electron density map.

Conclusion

In contrast with zinc and platinum, for which N(7)-coordination has been obs rved in (9-CH_3HAd)$PtCl_3$ (13) and (H_2Ad)$ZnCl_3$ (2), mercury is surrounded only with chlorine atoms and adenine is not coordinated in the present compound. This effect undoubtedly results from a delicate balance of many factors, but it is worth mentioning that such a behavior is consistent with the relative affinities of the above metals for chlorine and nitrogen donors respectively, as measured from solution equilibrium data. Formation constants β_{Cl} and β_{NH_3} are available for the $[MCl_4]^{2-}$ and $[M(NH_3)_4]^{2+}$ complexes (18, 19) and the displacement reaction

$$[MCl_4]^{2-} + 4NH_3 \rightleftarrows [M(NH_3)_4]^{2+} + 4Cl^-$$

can be characterized by the ratio $K = \beta_{NH_3}/\beta_{Cl}$:Pt = 10^{18}, Zn = 10^9, Hg = 10^3. The lower value of K for mercury suggests that replacement of chlorine by a nitrogen donor may not take place even though it does occur with platinum and zinc under similar conditions. This does not imply that mercury is devoid of affinity for adenine. A lower chloride concentration (to shift the above equilibrium to the right) and a higher pH (to deprotonate adenine) should favor interactions with mercury. Work on such systems is now in progress in this laboratory.

1. W. WESER. Struct. Bonding, **5**, 41 (1968); R. M. IZATT, J. J. CHRISTENSEN, and J. H. RYTTING. Chem. Rev. **71**, 439 (1971).
2. M. R. TAYLOR. Acta Cryst. B**29**, 884 (1973).
3. A. SAKHRI and A. L. BEAUCHAMP. Inorg. Chem. **14**, 740 (1975).
4. D. T. CROMER. Acta Cryst. **18**, 17 (1965).
5. G. H. STOUT and L. H. JENSEN. X-Ray structure determination. Macmillan, New York, 1969. p. 456.
6. D. T. CROMER and J. T. WABER. Acta Cryst. **18**, 104 (1965).
7. A. TERZIS, A. L. BEAUCHAMP, and R. RIVEST. Inorg. Chem. **12**, 1166 (1973).
8. D. GRDENIC. Q. Rev. **19**, 303 (1965).
9. R. M. BARR and M. GOLDSTEIN. J. Chem. Soc. Dalton Trans. 1180 (1973).
10. T. J. KISTENMACHER and T. SHIGEMATSU. Acta Cryst. B**30**, 166 (1974).
11. S. T. RAO and M. SUNDARALINGAM. J. Am. Chem. Soc. **92**, 4963, (1970).
12. P. L. JOHNSON, J. K. FRANK, and I. C. PAUL. J. Am. Chem. Soc. **95**, 5377 (1973); J. KRAUT and L. H. JENSEN. Acta Cryst. **16**, 79 (1963).
13. A. TERZIS, N. HADJILIADIS, R. RIVEST, and T. THEOPHANIDES. Inorg. Chim. Acta **12**, L5 (1975).
14. P. DE MEESTER and A. C. SKAPSKI. J. Chem. Soc. 2400 (1972).
15. P. DE MEESTER and A. C. SKAPSKI. J. Chem. Soc. 1596 (1973).
16. M. AUTHIER-MARTIN. Thèse de Maîtrise, Université de Montréal, Montréal, Québec. 1974.
17. T. F. LAI and R. E. MARSH. Acta Cryst. B**28**, 1982 (1972); H. STERNGLANZ and C. E. BUGG. Biochim. Biophys. Acta, **308**, 1 (1973); D. G. WATSON, D. J. SUTOR, and P. TOLLIN. Acta Cryst. **19**, 111 (1965); D. V. D. HELM. J. Cryst. Mol. Struct. **3**, 249 (1973).
18. F. A. COTTON and G. WILKINSON. Advanced inorganic chemistry, 2nd ed. Interscience, New York. 1966. pp. 600–622.
19. A. J. THOMSON, R. J. P. WILLIAMS, and S. RESLOVA. Struct. Bonding, **11**, 1 (1972).

Can. J. Chem. Downloaded from www.nrcresearchpress.com by 210.87.254.40 on 09/05/12
For personal use only.

The Use of the *n*-Propylammonium and *n*-Butylammonium Salts of *d*-10-Camphorsulfonic Acid for the Calibration of Spectropolarimeters: Circular Dichrometer Calibration[1]

MICHAEL F. GILLEN AND ROSS E. WILLIAMS[2]

Division of Biological Sciences, National Research Council of Canada, Ottawa, Canada K1A 0R6

Received February 28, 1975

MICHAEL F. GILLEN and ROSS E. WILLIAMS. Can. J. Chem. 53, 2351 (1975).

Two, easily prepared, nondeliquescent salts of *d*-10-camphorsulfonic acid have been used to improve the precision of the calibration of circular dichrometers.

MICHAEL F. GILLEN et ROSS E. WILLIAMS. Can. J. Chem. 53, 2351 (1975).

Deux sels non-déliquescents de l'acide *d*-camphresulfonique-10 qui sont facilement préparés ont été employés pour améliorer la précision de la calibration des dichromètres circulaires.

Can. J. Chem. Downloaded from www.nrcresearchpress.com by 210.87.254.6 on 09/05/12
For personal use only.

During a recent attempt at calibrating a circular dichrometer it became obvious to us that one of the compounds used for calibration purposes, namely *d*-10-camphorsulfonic acid, was troublesome to purify and, in addition, did not possess adequate criteria of chemical purity. These two inadequacies were mainly associated with the compound's extremely deliquescent nature. Indeed, the disparity of ellipticities quoted for use in calibration of circular dichrometers is likely, in part, a reflection of this deliquescent behavior (1–5). In this communication we wish to describe two easily prepared, water-soluble, derivatives of *d*-10-camphorsulfonic acid, both of which overcome the problems associated with use of the parent compound as a chiroptical standard.

We reasoned that the deliquescent nature of *d*-10-camphorsulfonic acid (CSA) was associated with the presence of the free sulfonic acid group in the compound and that neutralization of this group by salt formation would stop the deliquescent behavior. Preparation of the ammonium salt of CSA gave a water-soluble derivative in which the deliquescent behavior was blocked. However, the melting point of this derivative was high (m.p. 245–246 °C) and considerable decomposition, as evidenced by browning, occurred upon melting, thus making a satisfactory determination of chemical purity by this method difficult. Since it might be expected that the crystal lattice forces in simple alkyl ammonium salts of CSA would be less than those in the unsubstituted ammonium salt, such derivatives ought to have lower melting points and might also melt without decomposition. In fact, we found that the *n*-propyl- and *n*-butylammonium salts of CSA possessed desirably low melting points without apparent decomposition (*i.e.* no browning). In addition, these derivatives exhibited no observable deliquescent behavior. These salts were easily formed in high yield as follows. A slight molar excess of the *n*-alkylamine was mixed with crystallized (ethyl acetate), dehydrated CSA in methanol solution at room temperature. Evaporation of the methanol gave the desired salt which was crystallized from methanol solution (2 ml per gram) by the addition of at least 10 volumes of diethyl ether. The physical constants, which may be used for characterization of the compounds, are found in Table 1.

So that the compounds might be used to calibrate circular dichrometers comparison of their chiroptical properties was made with a sample of purified, but hydrated, CSA. This CSA sample was obtained as follows. CSA (Aldrich Chemical Co., U.S.A. Lot No. 121137) was crystallized twice from ethyl acetate. The resulting material was dried and dehydrated (80 °C, high vacuum, 24 h) and then analyzed 4.5 min after removal from the vacuum oven. The analytical figures (Table 1) implied that a slight impurity was present in the sample. If, however, these figures were corrected for the experimentally determined weight gain (assumed to be H_2O) which occurred during the 4.5 min before analysis they indicated that the compound was chemically pure (Table 1). This CSA sample was

[1]NRCC No. 14622.

[2]To whom correspondence should be addressed.

Can. J. Chem. Downloaded from www.nrcresearchpress.com by 210.87.254.6 on 09/05/12
For personal use only.

TABLE 1. Physical constants[a] and elemental analyses of *d*-10-camphorsulfonic acid (CSA), its *n*-propylammonium (*n*-PrA CSA), and *n*-butylammonium (*n*-BuA CSA) salts

Compound	Melting point (uncorr.)[b] (°C)	$[\alpha]_D^{25}$ (deg)[d]	Elemental analysis (%)[h] Calculated C	H	N	S	Found C	H	N	S
CSA (anhydrous)	—	+22.4[e]	51.70	6.94	—	13.80	51.72[j]	7.03[j]	—	—
CSA (hydrated)	198–199 (dec.) (G)[c]	+20.8(*c*, 4.30)[f]	48.18[i]	7.23[i]	—	12.86[i]	48.20	7.40	—	12.74
n-PrA CSA	140.5–141.5(F-J,G)	+17.6(*c*, 5.00)[g]	53.58	8.65	4.81	11.00	53.37	8.73	4.66	10.79
n-BuA CSA	140.0–141.0(F-J,G)	+16.6(*c*, 5.29)[g]	55.05	8.91	4.59	10.50	54.93	8.92	4.58	10.32

[a]Physical constants were determined to be constant after three crystallizations and drying at 60 °C under high vacuum.
[b]Determined either on a heated block (Fisher–Johns apparatus) (F-J) or in an open capillary tube (Gallenkamp apparatus) (G).
[c]Literature m.p. 195–197 °C (dec.) (2), 191–192 °C (dec.) (7).
[d]Determined on a sucrose-calibrated Perkin-Elmer spectropolarimeter, model 141, (1 dm tube). Error limits, expressed as standard deviations and calculated from three measurements were ±0.1 deg in all cases.
[e]Calculated from the hydrate assuming 7.3% by weight H_2O. Literature values, $[\alpha]_D^{25}$ 22.1 (*c* 1.0, H_2O) (2), 21.63 (T = 16 °C), 23.11 (T = 20 °C) (6).
[f]Measurements made in glass distilled water.
[g]Measurements made in 0.1 *N* HCl and unaffected by twofold dilution.
[h]Microanalyses were performed by M. Hector Seguin of these laboratories. Combustion analyses for C, H, and N were done on a Perkin-Elmer analyzer, model 240 and for S by a standard oxygen flask technique (8).
[i]Calculated assuming CSA contained 7.3% H_2O by weight.
[j]Calculated from the analytical figures (C, 51.47; H, 7.08) determined 4.5 min after removal of a dehydrated sample from the vacuum oven. Account has been taken of the observed water gain during this time (0.49% by weight).

TABLE 2. Chiroptical properties of *d*-10-camphorsulfonic acid (CSA), its *n*-propylammonium (*n*-PrA CSA), and *n*-butylammonium (*n*-BuA CSA) salts

Compound	Ellipticity $[\theta]_\lambda$[a,b] (deg-cm^2 per decimole)	
	$[\theta]_{290}$	$[\theta]_{192}$
CSA (hydrated)	7400 ± 150[c]	14 400 ± 700[c]
CSA (anhydrous)	7900 ± 200[c,d]	15 500 ± 800[c,d]
n-PrA CSA	8180 ± 50	15 800 ± 300
n-BuA CSA	8130 ± 60	15 800 ± 300

[a]All measurements were made on a Cary-Varian circular dichrometer, model 61, serial No. 53. Sample concentrations in glass distilled water were either 75 mg (approximately) per 50.0 ml (solution A) or 3 mg (approximately) per 50.0 ml (solution B). Solution B was derived from solution A by volumetric dilution (10.0 → 250 ml). In all cases commercially available volumetric glassware was used without recalibration. Quartz cells (Pyrocell Manufacturing Co., U.S.A.) of the following path lengths were used: 1.0 cm path (350–235 nm, solution A; 250–185 nm, solution B), 10.0 cm path (350–235 nm, solution B), 2.0 cm (350–185 nm, solution B). The temperature of all solutions was maintained by a thermostat at 27.0 ± 0.1 °C. The ellipticities given are either an average of at least three determinations (CSA hydrate) or an average of at least eight determinations (CSA salts). For conversion of molar ellipticity value to $E_L - E_R$ (cm^{-1} M^{-1}) divide values given by 3298 (5).

[b]Error limits given are standard deviations.

[c]Literature values: At 290 nm: 8219 (2); 7775 (3); 7840 (5); 7300 (estimated) (4); 7260 (1). At 192 nm: 15 620 (3); 14 500 (estimated.(4).

[d]Calculated from the CSA (hydrate) values assuming 7.3% H_2O by weight.

then allowed to hydrate for 3 d at room temperature (60% relative humidity) until no further weight gain was observed. Reanalysis (Table 1) showed that the water gain (7.3% by weight) was identical to that found previously (3). The chiroptical properties of this hydrated sample were measured and corrected for this water content (Table 2). The corrected ellipticity (290 mm) was similar to that which had been reported for two samples of pure, dry CSA (3, 5). The chiroptical properties of the two pure, dry *n*-alkylammonium salts of CSA were then measured under conditions identical to those used to measure the chiroptical properties of CSA. The results are reported in Table 2. At both 290 and 192 nm the specific ellipticities, [θ], were similar to those associated with the pure parent compound. The ellipticities at 290 nm were also apparently unaffected by 25-fold dilution of the sample since the results obtained using either sample A (1.0 cm path) or sample B (10 cm path) (see footnote [a], Table 2) were the same within the determined experimental error (0.6%). It should also be noted that an improvement in the precision with which the ellipticities can be determined results from the use of these nondeliquescent salts, perhaps because errors associated with the determination of sample purity now no longer play an important part in the determination of the overall experimental error associated with the measurements.

Finally, the ease of preparation, purification and characterization of the *n*-propyl- and *n*-butylammonium salts of *d*-10-camphorsulfonic acid, the retention by these salts of the desirable aqueous solubility and chiroptical properties associated with the parent compound and the improvement in the precision of circular dichrometer calibrations resulting from the use of these salts all suggest that either of these two nondeliquescent salts could profitably be used in place of the parent compound for the calibration of circular dichrometers.

1. J. Y. CASSIM and J. T. YANG. Biochemistry, **8**, 1947 (1969).
2. D. F. DETAR. Anal. Chem. **41**, 1406 (1969).
3. W. C. KREUGER and L. M. PSCHIGODA. Anal. Chem. **43**, 675 (1971).
4. K. H. CHAN and J. T. YANG. Anal. Biochem. **46**, 616 (1972).
5. A. J. ADLER, N. J. GREENFIELD, and G. D. FASMAN. *In* Methods in enzymology. Vol. XXVII. *Edited by* C. H. W. Hirs and S. N. Timasheff. Academic Press, New York. 1973. p. 675.
6. P. LIPP and H. KNAPP. Chem. Ber. B, **73**, 915 (1940).
7. W. J. POPE and C. S. GIBSON. J. Chem. Soc. **97**, 2211 (1910).
8. L. H. SCROGGINS. J. Assoc. Off. Agric. Chem. **56**, 892 (1973).

Can. J. Chem. Downloaded from www.nrcresearchpress.com by 210.87.254.6 on 09/05/12
For personal use only.

Models for the Role of Magnesium in Enzymic Catalysis. The Effect of Magnesium Ion on the General Base Catalyzed Enolization of Methyl Acetonylphosphonate

RONALD KLUGER AND ANDREA WAYDA

Department of Chemistry, University of Toronto, Toronto, Ontario M5S 1A1

Received January 21, 1975

RONALD KLUGER and ANDREA WAYDA. Can. J. Chem. 53, 2354 (1975).

Magnesium ion promotes the general base catalyzed iodination of methyl acetonylphosphonate (MAP), **1**. Although the concentration of complex is very low, definite rate constant increases are observed. The rate determining step under the experimental conditions is enolization of the substrate. Acceleration is observed for both charged and uncharged bases. The acceleration for charged bases is about twice that for uncharged bases. Thus, electrostatic effects are probably important but not exclusive. It is proposed that efficient catalysis by magnesium ion in related enzymic reactions is a consequence of the ability of magnesium ion to form a stabilizing complex with an enolate-like transition state and to reduce repulsive electrostatic interactions of the substrate and a catalytic base.

RONALD KLUGER et ANDREA WAYDA. Can. J. Chem. 53, 2354 (1975).

L'ion de magnésium favorise la catalyse basique de l'iodation de l'acétonylphosphonate de méthyle (MAP), **1**. Bien que la concentration en complexe soit très faible, on note un accroissement non négligeable de la constante de vitesse. Dans ces conditions expérimentales l'étape déterminante est l'énolisation du substrat. On observe une accélération pour les bases chargées et neutres. Pour les bases chargées, l'accélération est environ le double de celle des bases neutres. Ainsi les effets électrostatiques sont probablement importants, mais ne sont pas les seuls. L'efficacité de l'ion magnésium comme catalyseur dans les réactions de type enzymatique serait une conséquence de la capacité de cet ion à former un complexe stabilisateur dans un état de transition du genre énolate et à réduire les intéractions électrostatiques répulsives du substrat et d'une base catalytique. [Traduit par le journal]

Magnesium ion plays an important role in many reactions subject to enzymic catalysis. A major function for magnesium ion in most enzymic reactions involves facilitation of electrophilic addition reactions, such as phosphorylation (1). Another important but less well-known function proposed for magnesium ion involves the stabilization of transition states leading to formation of enolate ions in condensation (2) and decarboxylation processes (3). To obtain an understanding of the mechanism whereby metal ions facilitate the latter class of reactions, we have examined several factors controlling the effectiveness of magnesium ion catalysis of enolization.

It has been demonstrated that magnesium ion promotes the enolization of acetonylphosphonate in reactions involving anionic bases (4). A mechanism similar to that proposed by Pedersen (5), for the copper-catalyzed bromination of ethyl acetoacetate, stabilization of an incipient enolate as the metal ion complex, was considered likely. Similar conclusions for related systems have been reached by Schellenberger's group (6), who have studied the enolization of α-keto acids and recently by Cox (7), who investigated the reactions of 2-acetylpyridine. All these studies have concentrated on catalysis of enolization by metal ions in reactions involving a few anionic bases.

It has been suggested (4) that the function of the metal ion can be divided further into two general functions, Lewis acid or 'superacid' catalysis where the metal ion fulfills a role analogous to that of a proton in specific acid catalysis, and electrostatic attraction (or minimization of repulsions) of a charged base to the substrate. Since catalytic bases of enzymes are not necessarily anionic and enolates result from decarboxylation without base, it would be of interest to determine in one magnesium-catalyzed system the relative magnitudes of these two roles.

Since the enolization of ketones catalyzed by uncharged bases has been studied thoroughly (8), we have incorporated methods used in those studies to evaluate the role of magnesium ion in catalysis of the enolization of methyl acetonyl-

Can. J. Chem. Downloaded from www.nrcresearchpress.com by 210.87.254.6 on 09/05/12
For personal use only.

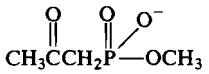

1

phosphonate (MAP), **1** (9). This compound binds magnesium definitely but weakly ($K_{assoc} \sim 1\ M^{-1}$(10)) as is necessary for efficient turnover in a catalytic system. The rather low affinity of MAP for magnesium ion keeps the effective concentration of active complex low. Fortunately, since MAP is a very weak base (pK_a of methyl acetonylphosphonic acid $\simeq 2$(10)), its reactions are not complicated by bimolecular reactions of the substrate as are the enolization reactions of the unesterified compound, acetonylphosphonate (4).

Experimental

Materials

Methyl acetonylphosphonate (sodium salt) was prepared and carefully purified as previously reported (10). All pyridine bases were obtained from the Aldrich Chemical Company or from Eastman Kodak and were distilled. Purity of the bases was determined by gas chromatography (Hewlett Packard 5700 dual flame ionization detector, 0.125 in. × 12 ft diisodecyl phthalate on bentone 34, 140°).

Other organic chemicals and all inorganic materials were of highest commercial purity grades and were used as obtained. Water was redistilled in a Corning redistillation unit. Magnesium ion was introduced as anhydrous magnesium sulfate.

Methods

The p*H* of solutions was estimated by means of a Radiometer PHM26 expanded scale meter with a GK202C electrode. No correction for ionic strength was made in p*H* measurements. Sodium ion corrections were made for alkaline solutions as described in the Radiometer manual. Solutions of sodium hydroxide and hydrogen chloride were used to adjust the p*H* of reaction mixtures.

Enolization of MAP was followed by a procedure based on the methods of Feather and Gold (11) and of Bell and co-workers (12–14). An equilibrium of triiodide with iodine and iodide was established using potassium iodide and iodine. This minimizes formation of complexes between iodine and pyridines (11, 14), taking advantage of the rapid equilibrium attained between iodide, iodine, and triiodide. We found that in our experiments addition of iodide, at the ionic strength of our experiments, did not affect the observed rate of iodine consumption. Therefore sufficient iodine was readily available from the equilibrium system. The iodine–triiodide solution was always added fresh to the solution of base followed by addition of substrate. This avoided the complication that could be introduced due to the tendency of alkyl pyridines to undergo halogenation slowly (14). In no instance was a background rate due to reaction of iodine with pyridine base observed before substrate was added. Initial rate conditions were used (*vide infra*), minimizing the possibility of our results being affected by back reactions of the products.

A solution of p*H*-adjusted base was combined with an iodine–triiodide solution. The solution was brought to reaction temperature (35°) in a cuvette held in the well-thermostatted cell compartment of a Unicam SP1800A spectrophotometer equipped with a program controller and an AR25 recorder. Absorbance at 353 nm due to triiodide in the iodine–triiodide equilibrium was recorded. Sodium MAP in a small volume of water was then added. The rate of decrease of absorbance was determined to be zero order in iodine in all cases since changing iodine concentration by factors of 1.5 and 0.5 in both the slowest and fastest reactions studied gave no change in observed rate. This assures that iodination occurs after rate-determining enolization (see Results). Furthermore, the requirement that the reaction be first order in substrate and first order in base was also confirmed by doubling those concentrations and observing that initial rates of iodine disappearance doubled.

We employed initial rate procedures since we used rather dilute solutions of substrate, due to its high reactivity. Bell and Barnes (14) discuss the high reactivity of the related β-keto acid, acetonylsulfonate, and the similar requirement for dilute solutions in that system. The reaction therefore becomes pseudo first order in substrate, requiring either that first order methods or initial rate methods be used. The initial rate approximation (15) appears to be most convenient for our system and is valid since the substrate is pure as well as highly reactive. Our results are reproducible within ±5% using this method.

Typically, a run without magnesium ion was done with 2.75 ml of 0.1 *M* potassium iodide, 0.1 ml of p*H*-adjusted base (1 *M* and less), 0.1 ml of 1.56×10^{-3} *M* iodine in 0.3 *M* potassium iodide solution, and 0.05 ml of 0.05 *M* MAP. A run with magnesium ion contained typically 2.65 ml of 0.1 *M* potassium iodide, 0.1 ml p*H*-adjusted base (1 *M* and less), 0.1 ml 1.56×10^{-3} *M* iodine in 0.3 *M* potassium iodide, 0.1 ml of 0.5 *M* magnesium sulfate, and 0.05 ml of 0.05 *M* MAP. The p*H* was checked at the end of each run. A brief induction period (11) was observed in a few cases before a linear decrease in absorbance at 353 nm was recorded; the initial linear portion (between absorbances of 1.5 and 1.0) was used to obtain initial rates. A slightly hyperbolic decay followed until nearly all iodine was depleted (below 0.1 o.d.) at which time, a sharply curved plot occurred presumably due to the low iodine concentration causing iodination of the enol to become rate limiting. The observed zero-order rate constant for the initial linear portion of triiodide disappearance was obtained from the equation (11):

$$[1] \qquad k_{obs} = (\Delta A/\Delta t)(1/\varepsilon_{353}) = \Delta[I_2]/\Delta t = \mathrm{d}[I_2]/\mathrm{d}t$$

A value of ε_{353} 26 768 was used. Beer's law was found to be obeyed in this system although it has been shown to be disobeyed in cases involving iodination of nitropropanes (16). Apparent second-order rate constants for the reaction of MAP with bases both in the presence and absence of magnesium were determined from eq. 2. The second-

Can. J. Chem. Downloaded from www.nrcresearchpress.com by 210.87.254.6 on 09/05/12
For personal use only.

[2] $k_2 = k_{obs}/[\text{free base}][\text{MAP}]$

order rate constants, corrected for reaction due to catalysis by water and by hydroxide, were use to generate Brønsted plots. General acid catalyzed processes were assumed to be insignificant under our experimental conditions based on findings for other β-keto acid derivatives (8). Water and hydroxide catalysis rate constants were determined by taking results obtained at a particular pH over a range of four buffer concentrations and extrapolating the linear plot to the point corresponding to a buffer concentration of zero (17).

In analyzing our data, we have assumed that as in the case of other β-keto acid derivatives (12, 18), only one atom of iodine is added at the 2 position (between carbonyl and ester) and this occurs prior to any significant reaction at the 4 position. We used low concentrations of magnesium ion to avoid complications arising from multiple metal ion binding as found in related systems (19). This precaution, however, also leads to low monomeric concentrations of magnesium–MAP since the affinity of the two species is rather low (10). In addition, we cannot determine what fraction of the stoichiometric complex is in an array that will promote enolization. Therefore we have only considered the effect of magnesium ion on the apparent second-order rate constants for enolization of MAP due to general bases.

Titration of pyridine and picolines in the presence and absence of large amounts of magnesium sulfate gave apparently identical pK_a values at comparable ionic strength (using potassium chloride). Therefore no apparent affinity for pyridines of magnesium ion is considered. Although acetate binds weakly to magnesium ion, magnesium acetate should account for less than 10% of magnesium present, based on published values of K_{assoc} (20). Whether catalysis is in fact due partially to $MgOAc^+$ or a transition state arising from magnesium and acetate which arrive separately cannot be distinguished by our kinetics and does not affect our use of apparent second-order rate constants.

Results and Discussion

Background Rates

As discussed in the experimental section, a pH–rate profile was determined in order to allow for corrections due to water and hydroxide catalyzed processes. The bases used for the Brønsted plots (to be described) and tris(hydroxymethylamino)methane were used. The data obtained are plotted in Figs. 1 and 2. The rate constants obtained from fitting k(extrapolated) = $k_{OH^-} + k_{H_2O}$ are summarized in Table 1.

Brønsted Plots

Data obtained as described under Methods was used to obtain the Brønsted plot in Fig. 3. Only results for 'well behaved' monofunctional bases (8, 16) are included. Pyridines alkylated in the 2 position show negative deviations from Brønsted plots for enolization (8, 16) due to steric effects and have therefore been omitted

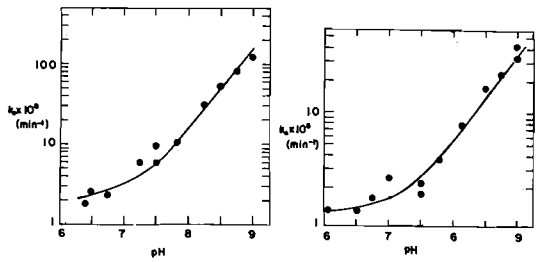

FIG. 1. The pH – rate constant profile for the iodination of (8.3×10^{-4} M) MAP at 35°. Plotted points were obtained from extrapolation to zero buffer of buffer-dependent kinetic data. The curve follows the expression $k_{obs} = k_{H_2O} + k_{OH^-}[OH^-]$ using the appropriate values in Table 1.

FIG. 2. The pH – rate constant profile for the iodination of (8.3×10^{-4} M) MAP in the presence of (1.7×10^{-2} M) magnesium sulfate. Plotted points were obtained by extrapolating buffer dependent results. The curve follows the expression $k_{obs} = k_{H_2O} + k_{OH^-}[OH^-]$ using the appropriate values in Table 1.

TABLE 1. Apparent rate constants for iodination of MAP (8.3×10^{-4} M) at 35°, 0.5 M ionic strength where enolization is rate limiting

$MgSO_4$ (M)	k_{OH^-} ($M^{-1}\,min^{-1}$)	$k_{H_2O} \times 10^6$ (min^{-1})
0.000	40	1
0.017	160	2

(a study of the steric sensitivity of magnesium ion catalysis is in progress). The plots for k_2 and k_2' (see Kinetic Equations) are nearly parallel (slope ~0.4) through the substituted pyridines. The plot for the reaction in the presence of magnesium ion (k_2') reflects an enhancement of about 1.7 compared to the reaction in the absence of magnesium (k_2). The points for acetate and propionate, the anionic bases tested, show negative deviations from the Brønsted plot of k_2 for the uncharged bases with the anionic substrate, MAP. For the reaction in the presence of magnesium ion, smaller deviations occur (from the Brønsted plot for k_2'). A discussion of these deviations is presented under Acceleration Factors.

Kinetic Equations

We assume that the enhanced rate of enolization of MAP in the present of magnesium ion results from complex formation leading to a lowering of the energy of the transition state for proton removal by a base. It is probable that any stoichiometric complex of magnesium and MAP

Can. J. Chem. Downloaded from www.nrcresearchpress.com by 210.87.254.6 on 09/05/12
For personal use only.

Can. J. Chem. Downloaded from www.nrcresearchpress.com by 210.87.254.6 on 09/05/12
For personal use only.

TABLE 2. Apparent acceleration due to presence of magnesium ion ($1.7 \times 10^{-2} M$) on rate constant for general base-catalyzed iodination of MAP ($8.3 \times 10^{-4} M$) at 35°

Base	pK*	k_2(no Mg) (M^{-1} min^{-1})	k_2'(+Mg) (M^{-1} min^{-1})	Acceleration k_2'/k_2
Pyridine	5.17	0.17	0.24	1.4
3-Picoline	5.97	0.30	0.43	1.4
4-Picoline	6.02	0.50	0.62	1.3
3,5-Lutidine	6.14	0.47	0.79	1.7
3,4-Lutidine	6.52	0.72	1.21	1.7
Acetate	4.75	0.013	0.043	3.2
Propionate	4.88	0.016	0.053	3.3

*pK_a of conjugate acid.

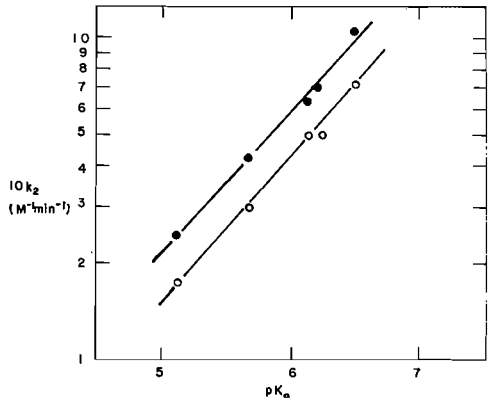

FIG. 3. Base catalysis rate constants (see Table 2) for iodination of MAP in presence (●) and absence (○) of magnesium ion as function of the pK_a of the conjugate acid of the catalytic base. Slopes are approximately 0.4.

will consist of a distribution of species. That component of the stoichiometric array which is catalytically active [(MgMAP$^+$)*] should be related to bulk concentrations by the (unknown) equilibrium constant, K_c (eq. 3),

$$[3] \quad K_c = [(MgMAP^+)^*]/[Mg^{2+}][MAP^-]$$

In the absence of magnesium ion, the system obeys the kinetic scheme of eq. 4, where B is a

$$[4] \quad MAP^- + B \xrightarrow{k_1} MAP^{2-}(\text{enolate}) + BH^+ \xrightarrow{k_0 I_2} MAPI^- + I^-$$

general base. In the presence of magnesium, the reaction of eq. 5 coexists with that of [4].

$$[5] \quad (MAPMg^+)^* + B \xrightarrow{k_1'} MAPMg(\text{enolate}) + BH^+ \xrightarrow[\text{fast}]{k_0' I_2} MAPI^- + I^- + Mg^{2+}$$

Therefore, in general, when rates due to catalysis by water and hydroxide are eliminated:

$$[6] \quad -d[I_2]/dt = k_{obs} = k_1[B][MAP^-] + k_1'[B][(MgMAP^+)^*]$$

$$[7] \quad k_{obs} = (k_1 + k_1'K_c[Mg^{2+}])[B][MAP^-]$$

The acceleration due to magnesium of iodine disappearance is given by eq. 8, the ratio of k_2' and k_2, where k_2' and k_2 result from dividing k_{obs} by [MAP] and [B].

$$[8] \quad \text{Acceleration} = k_2'/k_2 = (k_1 + k_1'K_c[Mg^{2+}])/k_1 = 1 + (k_1'K_c[Mg^{2+}])/k_1$$

We assume K_c is small since K_{assoc} is small. Therefore $[(MgMAP^+)^*] \ll [MAP^-]$. To observe acceleration, $k_2'/k_2 > 1$; therefore k_1' must be $\gg k_1$. If as an upper limit $K_c = K_{assoc}$, which is about 1 M^{-1} (10), then k_2'/k_2 is about 200 when an acceleration of 3 (see Table 2) is observed under the conditions of our experiments.

Acceleration Factors

Table 2 contains a summary of observed enhancements due to the presence of magnesium ion of rate constants for enolization of MAP (k_2'/k_2) in the presence of basic catalysts. The acceleration observed for anionic bases is about twice that observed for reactions with uncharged bases. This indicates that the electrostatic effect of magnesium ion in this system is separable from the 'Lewis acid' effect (4) which is independent of charge, suggesting the approximate simplified equation for the effect of magnesium:

$$[9] \quad \Delta\Delta G^{\ddagger}_{Mg^{2+}} = \Delta\Delta G^{\ddagger}(\text{electrostatic}) + \Delta\Delta G^{\ddagger}(\text{Lewis acid})$$

In conclusion our results indicate that the base-catalyzed enolization of MAP is enhanced by the addition of magnesium ion whether the catalytic base is charged or uncharged. It is therefore likely that a major function of magnesium ion is analogous to that of a proton in specific acid-catalyzed enolization (21): coordination of the carbonyl group by the metal ion (*vs.* hydrogen bonding to hydronium ion) stabilizes the transition state leading to formation of the enolate. Since it is likely that MAP coordinates initially to magnesium ion principally through the phosphonate functional group (10), catalysis probably results from a minor complex, $(MgMAP^+)^*$ of eqs. 3 and 5, in which bidentate coordination occurs (eq. 10). Mag-

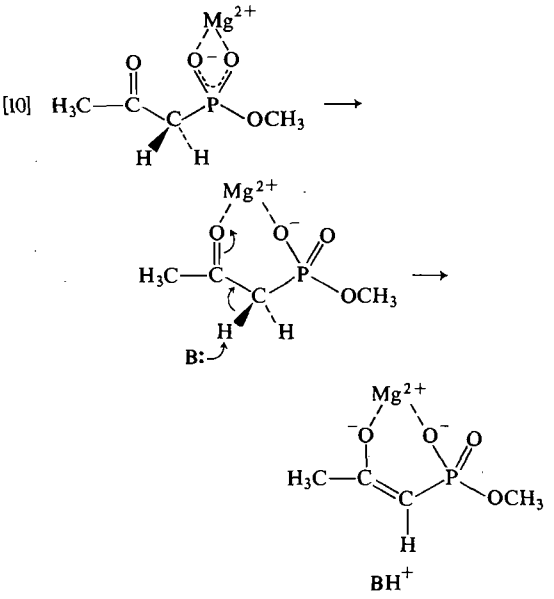

nesium ion also enhances enolization of MAP that is catalyzed by anionic bases by reducing electrostatic repulsions between the base and substrate. The optimal position for magnesium ion in this function is affected by the location of the anionic portion of MAP.

In an enzymic reaction, the site of association of magnesium ion and substrate is affected by forces introduced by the enzymic environment. Therefore, the metal ion can be bound in a position relative to the substrate which is most effective for catalysis, rather than in that which is thermodynamically defined in the absence of enzyme. In the case of an enolization reaction which is catalyzed by an uncharged base such as the histidine residue of a protein, the metal should function most effectively as a Lewis acid if it associates with the carbonyl group of the substrate to stabilize the enolate-like transition state. If the base component is negatively charged, such as the carboxylate moiety of a glutamate or aspartate residue, the optimal site for coordination of a metal ion will depend on the location of charges within the substrate as well as on the location of the potential enolate. Magnesium ion can be particularly effective in both roles because of its high positive charge density. Furthermore, since magnesium ion associates weakly with many substrates in the absence of enzyme (10), the directing effects of the enzymic environment need not operate against large preassociative barriers.

This work was initiated as a continuation of a project begun by R. K. at the University of Chicago under the sponsorship of the National Science Foundation. The work described in this paper was performed at the University of Toronto where support was from unrestricted funds awarded to R. K. by the Alfred P. Sloan Foundation.

1. A. S. MILDVAN. Enzymes, **2**, 445 (1970).
2. H. EGGERER. Biochem. Z. **343**, 111 (1965).
3. G. W. KOSICKI. Biochemistry, **7**, 4310 (1968).
4. R. KLUGER and P. WASSERSTEIN. J. Am. Chem. Soc. **95**, 1071 (1973).
5. K. J. PEDERSEN. Acta Chem. Scand. **2**, 252 (1948).
6. A. SCHELLENBERGER, G. OEHME, and G. HUBNER. Chem. Ber. **98**, 1938 (1965).
7. B. G. COX. J. Am. Chem. Soc. **96**, 6823 (1974).
8. R. P. BELL. The proton in chemistry. 2nd ed. Cornell University Press, Ithaca, New York. 1973. pp. 171–183.
9. R. KLUGER. J. Org. Chem. **38**, 2721 (1973).
10. R. KLUGER, P. WASSERSTEIN, and K. NAKAOKA. J. Am. Chem. Soc. In press.
11. J. A. FEATHER and V. GOLD. J. Chem. Soc. 1752 (1965).
12. R. P. BELL and G. A. WRIGHT. Trans. Faraday Soc. **57**, 1386 (1961).
13. R. P. BELL and H. L. GOLDSMITH. Proc. Roy. Soc. A, **210**, 322 (1952).
14. R. P. BELL and D. J. BARNES. Proc. Roy. Soc. A, **318**, 421 (1970).
15. J. F. BUNNETT. *In* Techniques of chemistry. Vol. 6. *Edited by* E. S. Lewis. John Wiley and Sons, Inc., New York, New York. 1974. pp. 133–135.
16. E. S. LEWIS and L. H. FUNDERBURK. J. Am. Chem. Soc. **89**, 2322 (1967).
17. W. P. JENCKS. Catalysis in chemistry and enzymology. McGraw-Hill Book Company, New York, N.Y. 1969. pp. 163–168.
18. R. P. BELL and E. GELLES. Proc. Roy. Soc. A, **210**, 310 (1952).
19. J. P. KLINMAN and D. SAMUEL. Biochemistry, **10**, 2126 (1971).
20. J. W. BUNTING and K. M. THONG. Can. J. Chem. **48**, 1654 (1970).
21. M. L. BENDER. Mechanisms of homogeneous catalysis from protons to proteins. John Wiley and Sons, Inc., New York, N.Y. 1971. pp. 232–235.

Can. J. Chem. Downloaded from www.nrcresearchpress.com by 210.87.254.6 on 09/05/12
For personal use only.

Erratum: Application of Carbon-13 Nuclear Magnetic Resonance to Conformational Analysis of Trimethylene Sulfites

GERALD W. BUCHANAN
Department of Chemistry, Carleton University, Ottawa, Canada K1S 5B6
J. B. STOTHERS
Department of Chemistry, University of Western Ontario, London, Ontario
AND
GORDON WOOD
Department of Chemistry, University of Windsor, Windsor 11, Ontario
Received May 16, 1975
(Ref.: Can. J. Chem. **51**, 3746 (1973))

In Table 1, the chemical shifts for R^1 and R^2 of compounds **7** and **8** should be interchanged. Thus for **7**, R^1 should read 32.2 and R^2 28.8. For **8**, R^1 should read 26.4 and R^2 31.5.

Can. J. Chem. Downloaded from www.nrcresearchpress.com by 210.87.254.42 on 09/05/12
For personal use only.

Can. J. Chem. Downloaded from www.nrcresearchpress.com by 210.87.254.5 on 09/05/12
For personal use only.

Canadian Journal of Chemistry

Published by
THE NATIONAL RESEARCH COUNCIL OF CANADA

Journal canadien de chimie

Publié par
LE CONSEIL NATIONAL DE RECHERCHES DU CANADA

Volume 53 Number 16 August 15, 1975

Volume 53 numéro 16 15 août 1975

An Electron Spin Resonance Study of Some Reactions of Pentafluorosulfuranyl (SF_5)[1]

JOHN CHARLES TAIT[2] AND JAMES ANTHONY HOWARD

Division of Chemistry, National Research Council of Canada, Ottawa, Canada K1A 0R9

Received March 14, 1975

JOHN CHARLES TAIT and JAMES ANTHONY HOWARD. Can. J. Chem. **53**, 2361 (1975).

A kinetic electron spin resonance study of the self-reaction of SF_5 and a spectroscopic and kinetic e.s.r. study of the reaction of SF_5 with 1,1-di-*t*-butylethylene are reported. This radical undergoes self-reaction by a second-order process and the rate constants are given by the Arrhenius equation $\log 2k_1(M^{-1}\,s^{-1}) = (10.3 \pm 0.5) - (1.7 \pm 0.5)/\theta$ where $\theta = 2.303RT$ kcal mol^{-1}. It adds to 1,1-di-*t*-butylethylene to give $(t\text{-Bu})_2\dot{C}CH_2SF_5$ which decomposes by a first-order process with rate constants that obey the expression $\log k_2\,(s^{-1}) = (13 \pm 0.4) - (10 \pm 0.2)/\theta$. Both these rate constants are pertinent to kinetic studies of the photoinduced addition of SF_5Cl to olefins.

JOHN CHARLES TAIT et JAMES ANTHONY HOWARD. Can. J. Chem. **53**, 2361 (1975).

On décrit l'étude cinétique par résonance paraélectronique de l'auto-réaction de SF_5 ainsi que l'étude spectroscopique et cinétique par r.p.e. de la réaction de SF_5 avec le di-*t*-butyl-1,1 éthylène. Ce radical réagit avec lui-même par un processus du second ordre. Les constantes de vitesse sont données par l'équation d'Arrhénius $\log 2k_1\,(M^{-1}\,s^{-1}) = (10.3 \pm 0.5) - (1.7 \pm 0.5)/\theta$ où $\theta = 2.303RT$ kcal mol^{-1}. Le radical s'additionne aussi sur le di-*t*-butyl-1,1 éthylène conduisant ainsi au $(t\text{-Bu})_2\dot{C}CH_2SF_5$. Ce produit se décompose par un processus du premier order dont les constantes de vitesse obéissent à l'expression $\log k_2\,(s^{-1}) = (13 \pm 0.4) - (10 \pm 0.2)/\theta$. Ces deux constantes de vitesse sont pertinentes aux études cinétiques de l'addition photo-induite du SF_5Cl sur les oléfines. [Traduit par le journal]

Introduction

Pentafluorosulfuranyl (SF_5) is one of the intermediates involved in the light induced and peroxide initiated addition of SF_5Cl to olefins (1–4), in the radiolysis of SF_6 (5–7), and reaction of alkali metal atoms with SF_6 (8–10).

The electron spin resonance spectrum of SF_5 has recently been detected during liquid-phase photolysis of SF_5Cl and by reaction of photochemically generated F· with SF_4 (11). This radical is a particularly interesting species from a theoretical standpoint (12) because the isotropic e.s.r. spectrum shows a hyperfine pattern due to the interaction of four equivalent fluorine atoms, the fifth fluorine showing no detectable isotropic hyperfine interaction.

Apart from some relative reactivity data obtained in the gas phase (2–4) little is known about the kinetics of reactions of SF_5 (and for that matter other sulfur centered radicals). We have, therefore, measured absolute rate constants for the self reaction of SF_5 in solution and rate constants for the β-scission of 1,1-di-*t*-butyl-2-pentafluorosulfuranylethyl, $(t\text{-Bu})_2\dot{C}CH_2SF_5$. The results of this work are reported here.

Experimental

Pentafluorosulfuranyl was prepared *in situ* in the cavity of a Varian E-4 EPR spectrometer either by photolysis of

[1]NRCC No. 14686.
[2]NRCC Postdoctorate Fellow, 1974–1975.

Can. J. Chem. Downloaded from www.nrcresearchpress.com by 210.87.254.5 on 09/05/12
For personal use only.

pentafluorosulfur chloride (Chemicals Procurement Laboratories Inc.) in a deoxygenated solvent (isopentane, dichlorodifluoromethane, and cyclopropane)

$$SF_5Cl \xrightarrow{h\nu} SF_5 + Cl$$

or by photolysis of pentafluorosulfur peroxide (13) in the presence of phosphorus trifluoride in deoxygenated CF_2Cl_2.[3]

$$SF_5OOSF_5 \xrightarrow{h\nu} 2SF_5O\cdot$$

$$SF_5O\cdot + PF_3 \rightarrow [SF_5O\dot{P}F_3] \rightarrow SF_5 + OPF_3$$

Absolute rate constants for self-reaction of SF_5 were determined by kinetic electron spin resonance spectroscopy, k.e.s.r., (15) with the aid of a rotating sector and a Fabri-Tek 1072 Signal Averager. Steady state SF_5 concentrations were determined by comparing the doubly integrated first derivative spectrum with a similarly integrated spectrum of a standard solution of DPPH.

1,1-Di-*t*-butyl-2-pentafluorosulfuranylethyl radical was prepared by photolysis of SF_5Cl in isopentane or cyclopropane containing 1,1-di-*t*-butylethylene. Decays of this species were followed by k.e.s.r. using the X-Y recorder provided with the spectrometer.

Results and Discussion

SF_5 + SF_5

The concentration of SF_5 rapidly attained a steady state when the radical was generated by either of the methods described above. Steady-state radical concentrations were proportional to the square-root of the light intensity, indicating that the disappearance of SF_5 in these systems followed second-order kinetics, *i.e.*

$$[1] \qquad \frac{-d[SF_5]}{dt} = 2k_1[SF_5]^2$$

The order of this reaction was confirmed by the linearity of plots of $1/[SF_5]$ as a function of time after the initiating light was shuttered (Fig. 1).

Values of $2k_1$ were determined in three solvents, isopentane, cyclopropane, and dichlorodifluoromethane from 153 to 233 K. The values in cyclopropane and CF_2Cl_2 were identical, within experimental error, and were independent of the method of radical generation (see Table 1). The rate constants were found to fit the equation

$$\log 2k_1\,(M^{-1}\,s^{-1}) = (10.3 \pm 0.6) - (1.7 \pm 0.5)/\theta$$

where $\theta = 2.303RT$ kcal mol^{-1}, as determined from a least-squares fitting procedure on the Arrhenius plot.

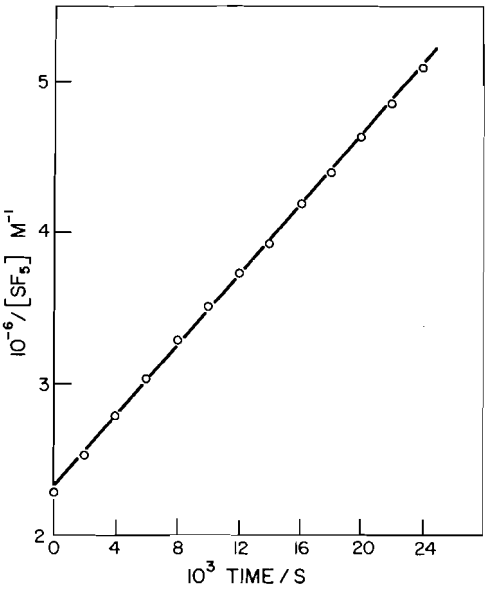

FIG. 1. The reciprocal radical concentration as a function of time for the self-reaction of SF_5 in cyclopropane at 183 K.

These Arrhenius parameters are very similar to the values of $A_1 = 10^{10}\,M^{-1}\,s^{-1}$ and $E_1 = 0$ predicted by Siddebottom *et al.* (2) and used by these workers to calculate Arrhenius parameters for addition of SF_5 to olefins.

Rate constants determined in isopentane were not reproducible and radical decays often deviated from second-order. The reason for poor kinetic data in isopentane is not clear at present and rate constants obtained in this solvent were not included in the Arrhenius plot.

Extrapolation of the Arrhenius equation gives a value of $2k_1 = 1 \times 10^9\,M^{-1}\,s^{-1}$ at 298 K somewhat less than the calculated diffusion-controlled limit for simple radicals in solution (16). A comparison of this value with absolute rate constants for self-reaction of other small radicals reveals that $2k_1$ is about 10 times smaller than the rate constant for CH_3 and about 10 times larger than the rate constant for CCl_3 (16). This difference between SF_5 and CCl_3 does, however, seem unreasonable. Relative rate constant measurements (17), which are inherently more accurate for comparing rate constants than individual rate constant measurements, indicate that the rate constant for self-reaction of CCl_3 is about $2 \times 10^9\,M^{-1}\,s^{-1}$ which implies that

[3]Photolysis of other peroxides in the presence of PF_3 gave alkoxytrifluorophosphoranyls, $ROPF_3$, (14). However, $SF_5O\dot{P}F_3$ is apparently too unstable to detect and SF_5 was the only species that could be detected.

TABLE 1. Rate constants for the self-reaction of SF_5

Radical source	Solvent	Temperature (°C)	$[SF_5]_0 \times 10^7$ (M)	$2k_1 \times 10^{-8}$ (M^{-1} s^{-1})
SF_5OOSF_5/PF_3	CCl_2F_2	−104	2.5	1.3
SF_5Cl	CCl_2F_2	−120	2.2	1.2
SF_5Cl	CCl_2F_2	− 90	2.2	3.7
SF_5Cl	CCl_2F_2	− 40	2.2	9.5
SF_5Cl	c-C_3H_6	−120	6.0	0.52
SF_5Cl	c-C_3H_6	−104	6.6	0.48
SF_5Cl	c-C_3H_6	− 90	1.6	0.94
SF_5Cl	c-C_3H_6	− 90	4.8	1.3
SF_5Cl	c-C_3H_6	− 90	5.2	1.1
SF_5Cl	c-C_3H_6	− 40	4.6	3.2

CCl_3 and SF_5 have termination rate constants of a similar magnitude.

Values of $2k_1$ that can be calculated from the Arrhenius equation should be applicable to gas-phase systems involving SF_5 since there is no reason to believe that going from the liquid to the gas-phase would significantly influence the magnitude of this rate constant.

$(t\text{-Bu})_2\dot{C}CH_2SF_5$

Griller and Ingold (18, 19) have shown that persistent 1,1-di-*t*-butyl-2-substituted-ethyl radicals are readily obtained when a variety of free radicals are generated in the presence of 1,1-di-*t*-butylethylene, **1**. Photolysis of SF_5Cl in the presence of **1** (5%) in isopentane from 133 to 173 K gave a 15-lined e.s.r. spectrum which could be interpreted as arising from the interaction of two equivalent hydrogen atoms with four equivalent fluorine atoms, consistent with the radical structure $(t\text{-Bu})_2\dot{C}CH_2SF_5$, **2**. The agreement between the observed and computer simulated spectra with $a_H(2) = 9.75 \pm 0.05$ G, $a_F(4) = 14.12 \pm 0.05$ G, $g = 2.0032$, and a linewidth of 3 G was excellent.

The absence of a hyperfine coupling from the fluorine *trans*- to the C—S bond is not surprising as it has been shown in several cases that the hyperfine coupling from this fluorine is very small (<0.5 G) (11, 20). It was also possible to observe the ^{33}S hyperfine coupling ($a^{33}S = 91.7$ G) in natural abundance. Only the $\pm\frac{3}{2}$ transitions were observable, the $\pm\frac{1}{2}$ transitions being hidden beneath the main spectrum. This coupling, when compared with the $8\pi/3\gamma_e\gamma_N\psi_{3s}(O)^2$ for ^{33}S of 969 G, represents a 10% contribution from the sulfur 3s orbital to the unpaired electron orbital.

The magnitude of the β-proton hyperfine coupling can be attributed to two effects. The steric effect of the SF_5 substituent will force the groups around the β-carbon into a locked conformation in which the SF_5 group is eclipsed with the α-carbon p-orbital containing the unpaired electron as is the case with other radicals of this type (21). This will tend to decrease the β-proton coupling from that which would be expected if there was free rotation about the C_α—C_β bond. The further effect of an electron-withdrawing group on the β-carbon will withdraw electron density from these protons further decreasing the proton coupling. The large ^{33}S hyperfine coupling observed is consistent with this explanation.

The steady-state concentration of **2** had an intensity exponent of 1.0 and radical decays were first order when the initiating light was shuttered, *i.e.*

$$\frac{-d[\mathbf{2}]}{dt} = k_2[\mathbf{2}]$$

$(t\text{-Bu})_2\dot{C}CH_2SF_5$ must, therefore, decay by the unimolecular β-scission process

[2] $$\mathbf{2} \rightarrow (t\text{-Bu})_2C{=}CH_2 + SF_5$$

rather than by the bimolecular disproportionation

[3] $$\mathbf{2} \rightarrow (t\text{-Bu})_2CHCH_2SF_5 + (t\text{-Bu})_2C{=}CHSF_5$$

Absolute values of k_2 were measured from 133 to 173 K and are summarized in Table 2. An Arrhenius plot of this data yielded the expression

$$\log k_2\,(s^{-1}) = (13 \pm 0.4) - (10 \pm 0.2/\theta)$$

The magnitude of A_2 is consistent with a unimolecular β-scission process and the low value of E_2 is in keeping with the reversible addition of sulfur centered radicals to olefins (22, 23). Sidde-

Can. J. Chem. Downloaded from www.nrcresearchpress.com by 210.87.254.5 on 09/05/12
For personal use only.

TABLE 2. Rate constants for the unimolecular decay of $(t\text{-Bu})_2\dot{C}CH_2SF_5$ in isopentane

Temperature (°C)	k_2 (s^{-1})
−140	0.000315
−130	0.00316
−125	0.0118
−120	0.0437
−115	0.118
−110	0.35
−105	0.91
−100	1.34

bottom *et al.* have in fact had to invoke the reversibility of the addition of SF_5 to olefins to account for the product distribution found for addition of SF_5Cl to olefins (2–4).

SF_5Cl was also photolyzed in the presence of ethylene and isobutylene. An e.s.r. signal could not be detected in isobutylene and although a signal was detected in ethylene it was too weak to permit analysis. The low intenisty of the e.s.r. signals in these olefins is probably because SF_5Cl is rapidly consumed by a chain reaction. The overall rate of reaction must be rapid at these low temperatures because even after a few minutes photolysis, SF_5Cl and the olefin were converted almost quantitatively to $SF_5CH_2CH_2Cl$ and $SF_5CH_2C(CH_3)_2Cl$, as shown by the correspondence of the ^{19}F and ^1H n.m.r. spectra of the products with those analyzed previously by Boden *et al.* (24). In the case of di-*t*-butylethylene, no ^{19}F resonance was observable, indicating that **2** is too sterically hindered to abstract a chlorine atom from SF_5Cl.

1. R. E. BANKS, R. N. HASZELDINE, and W. D. MORTON. J. Chem. Soc. C, 1947 (1969).
2. H. W. SIDDEBOTTOM, J. M. TEDDER, and J. C. WALTON. Trans. Faraday Soc. **65**, 2103 (1969).
3. H. W. SIDDEBOTTOM, J. M. TEDDER, and J. C. WALTON. J. Chem. Soc. D, 253 (1970).
4. H. W. SIDDEBOTTOM, J. M. TEDDER, and J. C. WALTON. Trans. Faraday Soc. **66**, 2038 (1970).
5. K.-D. ASMUS, W. GRUNBEIN, and J. H. FENDLER. J. Am. Chem. Soc. **92**, 2625 (1970).
6. K.-D. ASMUS and J. H. FENDLER. J. Phys. Chem. **72**, 4285 (1968).
7. J. GAWLOWSKI and J. A. HERMAN. Can. J. Chem. **52**, 3631 (1974).
8. H. C. COWEN, F. RIDING, and E. WARHURST. J. Chem. Soc. 4168 (1953).
9. F. M. FREUND, G. A. FISK, D. R. HERSCHBACH, and W. KLEMPERER. J. Chem. Phys. **54**, 2510 (1971).
10. S. J. RILEY and D. R. HERSCHBACH. J. Chem. Phys. **58**, 27 (1973).
11. J. R. MORTON and K. PRESTON. Chem. Phys. Lett. **18**, 98 (1973).
12. A. R. GREGORY. Chem. Phys. Lett. **28**, 552 (1974).
13. C. I. MERRILL and G. H. CADY. J. Am. Chem. Soc. **83**, 298 (1961).
14. A. J. COLUSSI, J. R. MORTON, and K. F. PRESTON. J. Phys. Chem. **79**, 651 (1975).
15. K. ADAMIC, D. F. BOWMAN, T. GILLAN, and K. U. INGOLD. J. Am. Chem. Soc. **93**, 903 (1971).
16. K. U. INGOLD. Free radicals, Vol. 1. *Edited by* J. K. Kochi. Wiley, New York. 1973. Chapt. 2.
17. D. GRILLER and K. U. INGOLD. Int. J. Chem. Kinet. **6**, 453 (1974).
18. D. GRILLER and K. U. INGOLD. J. Am. Chem. Soc. **95**, 6459 (1973).
19. G. D. MENDENHALL, D. GRILLER, D. LINDSAY, T. T. TIDWELL, and K. U. INGOLD. J. Am. Chem. Soc. **96**, 2441 (1974).
20. J. R. MORTON and K. F. PRESTON. J. Chem. Phys. **58**, 2657 (1973).
21. D. GRILLER and K. U. INGOLD. J. Am. Chem. Soc. **96**, 6715 (1974).
22. C. WALLING, Free radicals in solution. Wiley, New York, New York. 1957.
23. W. A. PRYOR. Free radicals. McGraw-Hill, New York, New York. 1966.
24. N. BODEN, J. W. EMSLEY, J. FEENEY, and L. H. SUTCLIFFE. Trans. Faraday Soc. **59**, 620 (1963).

Can. J. Chem. Downloaded from www.nrcresearchpress.com by 210.87.254.5 on 09/05/12
For personal use only.

The Equilibrium $SH^- + HCN \rightleftarrows CN^- + H_2S$ and the Determination of D_0^0(H—CN)

DON BETOWSKI, GERVASE MACKAY, JOHN PAYZANT, AND DIETHARD BOHME

Department of Chemistry and Centre for Research in Experimental Space Science, York University, Downsview, Ontario M3J 1P3

Received January 7, 1975

DON BETOWSKI, GERVASE MACKAY, JOHN PAYZANT, and DIETHARD BOHME. Can. J. Chem. **53**, 2365 (1975).

The rate constants and equilibrium constant for the proton transfer reaction $SH^- + HCN \rightleftarrows CN^- + H_2S$ have been measured at 296 ± 2 K using the flowing afterglow technique: $k_{forward} = (2.9 \pm 0.6) \times 10^{-9}$ cm^3 molecule^{-1} s^{-1}, $k_{reverse} = (1.8 \pm 0.4) \times 10^{-10}$ cm^3 molecule^{-1} s^{-1}, and $K = 16 \pm 2$. The measured value of K corresponds to a standard free energy change, ΔG_{296}^0, of −1.6 0.1 kcal mol^{-1} which provides values for the standard enthalpy change, $\Delta H_{298}^0 = -1.0$ 0.2 kcal mol^{-1}. the bond dissociation energy, D_0^0(H—CN) = 124 2 kcal mol^{-1}, and the proton affinity, p.a.(CN^-) = 350 1 kcal mol^{-1}.

DON BETOWSKI, GERVASE MACKAY, JOHN PAYZANT et DIETHARD BOHME. Can. J. Chem. **53**, 2365 (1975).

Les constantes de vitesse et la constante d'équilibre de la réaction du transfert de proton, $SH^- + HCN \rightleftarrows CN^- + H_2S$, ont été mesurées à 296 ± 2 K par la technique "flowing afterglow": $k_{droite} = (2.9 \pm 0.6) \times 10^{-9}$ cm^3 molécule^{-1} s^{-1}, $k_{gauche} = (1.8 \pm 0.4) \times 10^{-10}$ cm^3 molécule^{-1} s^{-1} et $K = 16 \pm 2$. La valeur de K mesurée correspond à une variation de l'énergie libre standard ΔG_{296}^0, de -1.6 ± 0.1 kcal mol^{-1} qui permet de calculer la variation de l'enthalpie standard, $\Delta H_{298}^0 = -1.0 \pm 0.2$ kcal mol^{-1}, l'énergie de dissociation de liaison, D_0^0 (H—CN) = 124 ± 2 kcal mol^{-1}, et l'affinité du proton, a.p.(CN^-) = 350 ± 1 kcal mol^{-1}. [Traduit par le journal]

Introduction

Recent experimental investigations carried out in this laboratory (1, 2) and elsewhere (3–6) of the equilibria of proton transfer reactions of the type

[1] $$X^- + YH \rightleftarrows Y^- + XH$$

proceeding in the gas phase, have indicated that such studies provide a valuable new method for the determination or corroboration of fundamental thermochemical properties of both charged and uncharged molecular species, *viz.* heats of formation (ΔH_f^0), electron affinities (e.a.), proton affinities (p.a.), and bond dissociation energies (D^0). The method involves the determination of the exothermicity (ΔH^0) of the proton transfer reaction from rate and/or equilibrium constant measurements at one or more temperatures. The value established for ΔH^0 is then combined with reliable values for thermochemical properties of one or more of the individual reacting species to arrive at the desired thermochemical property. The accuracies of the thermochemical quantities determined in this way often supersede those attained with other, more established, methods. In this paper we report measurements of rate and equilibrium constants at 296 ± 2 K for the proton transfer reaction

[2] $$SH^- + HCN \rightleftarrows CN^- + H_2S$$

and the derivation of values for D_0^0(H—CN) and p.a.(CN^-).

This study also provides an (as yet rare) opportunity to compare rate and equilibrium constants obtained for reactions of type 1 proceeding under quite different conditions of ion and neutral concentrations, total pressure, reaction time, ion history, and ambient electric fields. Reaction 2 has been previously investigated by McIver and Eyler (4) with the pulsed ion – cyclotron resonance (i.c.r.) technique. The gaseous ions are formed by electron impact and reaction proceeds at low pressures ($< 10^{-5}$ Torr) while the ions are trapped in an analyzer cell by the combined effects of magnetic and electric fields for periods as long as 1 s. In the present investigation reaction 2 proceeds in a flowing plasma containing HCN, H_2S, and an excess of He at total pressures of *ca.* 0.3 Torr and at a fixed reaction time of a few ms. In the determination of rate and/or equilibrium constants for reactions of type 1 using either technique it is important to establish that the reactant ions are thermalized to the ambient temperature prior to

Can. J. Chem. Downloaded from www.nrcresearchpress.com by 210.87.254.105 on 09/05/12
For personal use only.

TABLE 1. Summary of experimental results for the reaction $SH^- + HCN \rightleftarrows H_2S + CN^-$ AT 296 ± 2 K

Direction studied	N*	$\frac{k_2}{k_{-2}}$	Accuracy	N	K_2	Accuracy
Forward	3	17.8 ± 0.7†	±20%	1	18	±20%
Reverse	2	14.6 ± 1.9	±25%	2	14.3 ± 2.6	±25%

*N is the number of experiments.
†Best estimate of the precision.

reaction in either direction and consequently that the observed rate constants correspond to Maxwell–Boltzmann energy distributions and that the observed steady-state ion signals are a true measure of equilibrium concentrations.

Experimental

The experiments were performed using the flowing afterglow (f.a.) technique. The details of the apparatus and the methods of data analysis have been described previously (7, 8). Reactant ions are produced in a flowing plasma either by electron impact or by secondary ionization or ion–molecule reactions. In these experiments the plasma was generated with ionizing electrons having energies of *ca.* 60 eV. The filament emission of the electron gun was 0.5 mA. The neutral reactant is introduced sufficiently downstream of the ion production region to ensure that the reactant ions have undergone enough collisions with the carrier gas (helium was used in the experiments reported here) to become thermalized at the ambient room temperature (296 ± 2 K). The plasma communicates with a quadrupole mass spectrometer through a small orifice mounted at the tip of a sampling nose cone. Rate constants and equilibrium constants for reactions of ions with molecules are determined by measuring changes in ion signals as a function of the addition of neutral reactant molecules.

The gases used were He (Linde, Prepurified Grade, 99.995% He), H_2S (Matheson, C.P. Grade, 99.5% H_2S), $C_2H_5NH_2$ (Matheson, 98.5% $C_2H_5NH_2$), and HCN prepared in this laboratory from the action of sulfuric acid on an aqueous solution of KCN (9). The HCN was dried over anhydrous $CaCl_2$ and purified further by distillation *in vacuo*.

Results

Reaction 2 was investigated independently in both directions. The ratio of rate constants, k_2/k_{-2}, and the equilibrium constant, K_2, were determined in each direction. The results are summarized in Table 1. The sources of error have been described previously (7). The individual rate constants at 296 ± 2 K were determined to be $k_2 = (2.9 \pm 0.6) \times 10^{-9}$ cm^3 molecule^{-1} s^{-1} and $k_{-2} = (1.8 \pm 0.4) \times 10^{-10}$ cm^3 molecule^{-1} s^{-1}.

In the remainder of this section the best estimate of a true value is taken to be the mean of a series of measurements. The limits given along with the mean value represent the best estimate of the precision (10).

$$SH^- + HCN \rightleftarrows CN^- + H_2S$$

In the study of the attainment of equilibrium for reaction 2 in the forward direction, H_2S was added to the helium buffer upstream of the electron gun and was ionized directly according to one or more of the following processes:

$$[3a] \qquad H_2S + e \rightarrow SH^- + H$$

$$[3b] \qquad \rightarrow SH^- + H^+ + e$$

$$[4] \qquad He(2^3S, 2^1S) + H_2S \rightarrow SH^- + H^+ + He$$

In addition to SH^-, the mass spectrum of the negative ions sampled downstream contained several multisulfur ions of the type S_n^- or S_nH^-. The mode of formation of these ions remains unclear and will be the subject of a separate study. Only the SH^- ions were observed to react with HCN upon addition of the latter into the reaction region. The concomitant appearance of only one ion signal at *m/e* 26 dictated that the reaction of SH^- with HCN proceeded entirely via proton transfer. There was no indication that other competing reactions were occurring. Figure 1 shows the behavior observed for the SH^- and CN^- ion signals as HCN is added into the reaction region. The curvature of the SH^- decay can be attributed to the occurrence of the reverse reaction −2. The solid curve drawn through the data points for the SH^- decay represents the best fit obtained using Analysis B of ref. 7. and provides a measure of the ratio of rate constants, k_2/k_{-2}. The determination of unique values for k_2 and k_{-2} was precluded in this case since reaction 2 was observed to be in equilibrium already at low additions of HCN. This is demonstrated by the ratio plot shown in Fig. 2 which is linear over almost the entire range of HCN flows. The slope of this line affords a direct determination of the equilibrium constant from equilibrium concentrations (ref. 7, Analysis C). The ratio of ion signals, $I(CN^-)$/

Can. J. Chem. Downloaded from www.nrcresearchpress.com by 210.87.254.105 on 09/05/12
For personal use only.

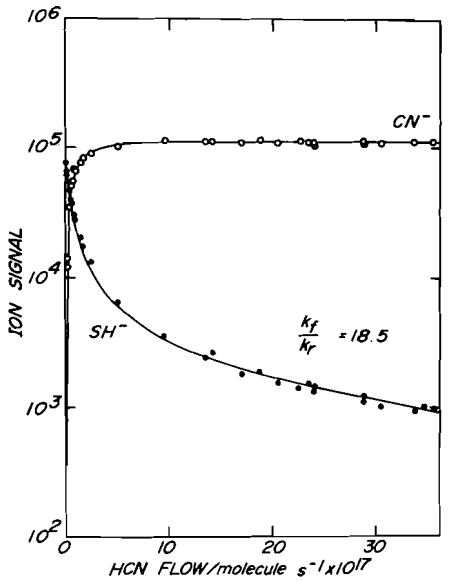

FIG. 1. The determination of the ratio of rate constants for the reaction $SH^- + HCN \rightleftarrows CN^- + H_2S$ from a fit (solid line) to the observed decay (solid points) of the SH^- signal upon addition of HCN at a constant flow of the neutral back-reactant, H_2S. H_2S flow = 8.4×10^{17} molecule s^{-1}, $T = 296$ K, $P = 0.329$ Torr, $\bar{v} = 8.7 \times 10^3$ cm s^{-1}, and $L = 59$ cm.

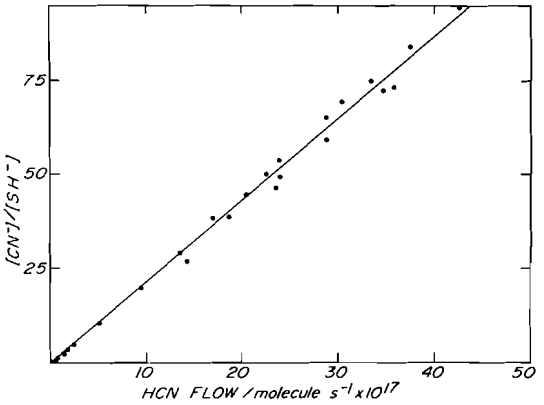

FIG. 2. The observed variation (solid points) of the ratio of the product to the reactant ion signals (corrected for mass discrimination) for the reaction $SH^- + HCN \rightleftarrows CN^- + H_2S$ with the flow of HCN at a constant flow of the neutral back-reactant, H_2S. H_2S flow = 8.4×10^{17} molecule s^{-1}. The least squares fit (solid line) provides a value for the equilibrium constant, $K = 18$. $T = 296$ K, $P = 0.329$ Torr, $\bar{v} = 8.7 \times 10^3$ cm s^{-1}, and $L = 59$ cm.

$I(SH^-)$, corrected for mass discrimination, provides a measure of the ratio of ion concentrations, $[CN^-]/[SH^-]$. An equilibrium constant, K_2, of 18 was obtained from the data shown in Fig. 2.

In two other experiments the amounts of H_2S and HCN added were lowered sufficiently to prevent attainment of equilibrium. In these cases the best fits to the SH^- decays provided unique values for k_2 and k_{-2} of $(2.9 \pm 0.3) \times 10^{-9}$ and $(1.8 \pm 0.2) \times 10^{-10}$ cm^3 molecule^{-1} s^{-1}, respectively.

The additions of H_2S in the three experiments ranged from 4.39 to 8.6×10^{17} molecule s^{-1}. The effective reaction length, L, was always 59 cm, the total gas pressure, P, was 0.329 Torr, and the gas velocity, $\bar{v}$, was 8.7×10^3 cm s^{-1}. The three experiments resulted in an average value for the ratio of rate constants, k_2/k_{-2}, of 17.8 ± 0.7.

$CN^- + H_2S \rightleftarrows SH^- + HCN$

In the studies of reaction 2 in the reverse direction the reactant ion, CN^-, was generated from HCN which was added to the helium buffer upstream of the electron gun. The processes which lead to the formation of CN^- under these conditions include one or more of the following:

[6a] $$HCN + e \rightarrow CN^- + H$$

[6b] $$\rightarrow CN^- + H^+ + e$$

[7] $$He(2^3S, 2^1S) + HCN \rightarrow CN^- + H^+ + He$$

H_2S was added into the reaction region downstream of the electron gun and the decay of the CN^- signal was recorded along with the rise of the SH^- signal at various additions of H_2S. There was no evidence for the further reaction of SH^- with H_2S which suggests that the reaction

[8] $$SH^- + H_2S \rightarrow S_2H^- + H_2$$

is endothermic, in which case $\Delta H_{f298}{}^0(S_2H^-)$ should be $\geqslant 25 \pm 4$ kcal mol^{-1}. (Values for $\Delta H_{f298}{}^0(SH)$ and $\Delta H_{f298}{}^0(H_2S)$ were taken from ref. 11 and the electron affinity of SH was taken from ref. 12.)

Figure 3 shows the behavior observed for the CN^- and SH^- ion signals as H_2S is added into the reaction region at a flow of back reactant, HCN, of 2.01×10^{17} molecule s^{-1}. The experiment was repeated at a slightly lower addition of HCN of 1.03×10^{17} molecule s^{-1}. In both experiments the effective reaction length, L, was 85 cm, $P = 0.344$ Torr, and $\bar{v} = 8.3 \times 10^3$ cm s^{-1}. Figure 4 demonstrates that under these conditions equilibrium is attained already at the lowest additions of H_2S which again precludes the determination of unique values for k_2 and k_{-2} from a fit to the decay of CN^-. The value for the ratio of rate constants, $k_2/k_{-2} = 14.6 \pm 1.9$,

Can. J. Chem. Downloaded from www.nrcresearchpress.com by 210.87.254.105 on 09/05/12
For personal use only.

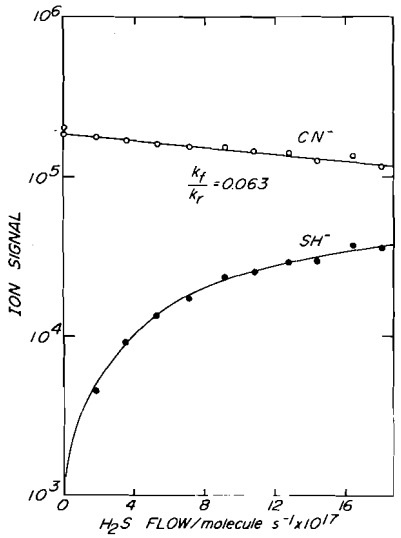

FIG. 3. The determination of the ratio of rate constants for the reaction $CN^- + H_2S \rightleftarrows SH^- + HCN$ from a fit (solid line) to the observed decay (open circles) of the CN^- signal upon addition of H_2S at a constant flow of the neutral back-reactant, HCN. HCN flow = 2.01×10^{17} molecule s^{-1}, $T = 297$ K, $P = 0.344$ Torr, $\bar{v} = 8.3 \times 10^3$ cm s^{-1}, and $L = 85$ cm.

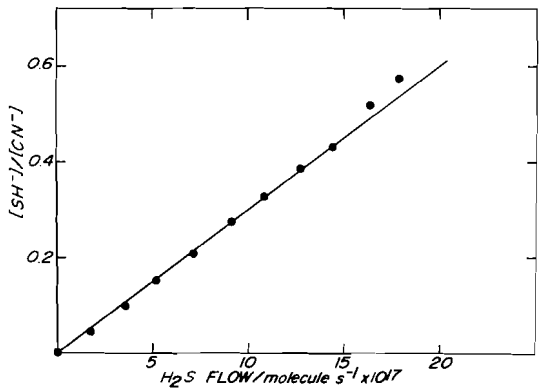

FIG. 4. The observed variation (solid points) of the ratio of the product to the reactant ion signals (corrected for mass discrimination) for the reaction $CN^- + H_2S \rightleftarrows SH^- + HCN$ with the flow of H_2S at a constant flow of neutral back-reactant, HCN. HCN flow = 2.01×10^{17} molecule s^{-1}. The least squares fit (solid line) provides a value for the equilibrium constant, $K = 0.062$. $T = 297$ K, $P = 0.344$ Torr, $\bar{v} = 8.3 \times 10^3$ cm s^{-1}, and $L = 85$ cm.

derived from the CN^- decays was found to agree with the value for the equilibrium constant, $K_2 = 14.3 \pm 2.6$, obtained from an analysis of the corresponding ratio plots. The latter determination again involves a correction for mass discrimination in the sampling region between the CN^- and SH^- ions (7).

Reaction -2 was also investigated in the absence of significant amounts of back reaction to provide an independent measure of k_{-2}. In this case CN^- was generated from $C_2H_5NH_2$ rather than HCN under otherwise similar operating conditions. Three experiments provided a value for k_{-2} of $(1.8 \pm 0.2) \times 10^{-10}$ cm^3 $molecule^{-1}$ s^{-1} which is in good agreement with the value for k_{-2} determined from the study of reaction 2 in the forward direction.

Discussion

The true equilibrium constant for the elementary reaction 2 should be independent of time, total pressure, direction of approach to equilibrium, and concentration of the reacting species if these behave as ideal gases. Furthermore, since the thermodynamic equilibrium constant relates to Maxwell–Boltzmann (M–B) energy distributions for both reactants and products, K_2 will be equal to the ratio of rate constants, k_2/k_{-2}, if the individual rate constants also correspond to such energy distributions. In the present experiments the spatial separation of the ion production and reaction regions ensures that the ions undergo many collisions (primarily with the buffer gas atoms) prior to reaction (7). The neutral reactant is added already in thermal equilibrium at the ambient (room) temperature. Consequently, both reacting species are expected to possess room temperature M–B distributions of translational and internal energies. Such a condition will not exist immediately after the reaction has occurred. However, in the presence of a large excess of buffer gas, the rate of relaxation of the product ions initially formed in disequilibrium exceeds the rate of proton transfer in the reverse direction. Furthermore, the neutral product is added in thermal equilibrium at room temperature in large excess to that generated by reaction. Under these conditions k_{-2} should also correspond to M–B energy distributions (7). The results obtained in the present study for reaction 2 are consistent, within experimental error, with these expectations:

(*1*) The ratio of rate constants, k_2/k_{-2}, was observed to be equal to the equilibrium constant determined from equilibrium concentrations, K_2, in both directions of approach to equilibrium. We would like to emphasize here that the determination of k_2/k_{-2} in the manner described does not require the correction for mass discrimination necessary in the determination of K_2 from equilibrium concentrations.

Can. J. Chem. Downloaded from www.nrcresearchpress.com by 210.87.254.105 on 09/05/12
For personal use only.

Can. J. Chem. Downloaded from www.nrcresearchpress.com by 210.87.254.105 on 09/05/12
For personal use only.

(*2*) k_2/k_{-2} and K_2 were observed to be independent of the concentrations of the two neutral constituents within the range of experimental operating conditions.

(*3*) k_2/k_{-2} and K_2 were observed to be independent of the direction of approach to equilibrium at different reaction times.

(*4*) The value of k_{-2} determined from an equilibrium study of reaction 2 in the forward direction was in agreement with the value of k_{-2} obtained in an independent study of reaction -2 in the absence of reverse reaction.

The values of k_2/k_{-2} and K_2 determined independently in both directions of reaction 2 provide a best estimate (9) of the true value (a weighted mean) of the equilibrium constant at 296 ± 2 K of 16 with a standard error of ±2.

Reaction 2 has been previously investigated by McIver and Eyler (4) with the pulsed i.c.r. technique under considerably different conditions of ion and neutral concentrations, total pressure, reaction time, ion history, and ambient electric fields. The ions CN^- and SH^- were produced either directly by electron impact (in the case of SH^-) or indirectly by the reaction of F^- (produced by electron impact on NF_3) with HCN and H_2S respectively. Steady-state ion signals measured at large reaction times (>200 ms) in various mixtures of HCN and H_2S (both pure and diluted with NF_3) at total pressures $\leqslant 2 \times 10^{-6}$ Torr were believed to be proportional to equilibrium ion concentrations. Accordingly McIver and Eyler reported a value for K_2 at 298 K of 9.5 ± 1.5 which was observed to be consistent with the value for k_2/k_{-2} of 8.9 ± 0.5 determined from rate constant measurements involving selective ion ejection (5). Values for the individual rate constants were not reported. Concerns have been expressed both by these authors (5) and others[1] (13) regarding the extent of thermalization of ions prior to reaction in experiments of this type, *i.e.* the extent to which the observed steady-state ion signals are a measure of true equilibrium concentrations and the extent to which the observed rate constants correspond to M–B energy distributions. Bowers[1] has estimated the i.c.r. relative velocity distribution in the limit of zero collisions and found it to have a high velocity tail greater than the room-temperature Maxwellian. One might therefore expect to observe that K_2(i.c.r.) < K_2(f.a.) even in the presence of several collisions. In fact, a comparison of the values for K_2 obtained with these two techniques should provide some indication of the extent to which the room-temperature Maxwellian is perturbed. For example, if one can characterize the i.c.r. equilibrium state in terms of an "effective" temperature, then a Van't Hoff calculation using $K_2 = 16$ at 296 K and the value for $\Delta H^0 = -1.0$ kcal mol^{-1} obtained in this study predicts a value for $K_2 = 9.5$ at an effective temperature of 427 K.

An equilibrium constant of 16 ± 2 for reaction 2 leads to a standard free energy change, $\Delta G_{296}{}^0 = -1.6 \pm 0.1$ kcal mol^{-1}. The standard entropy change, $\Delta S_{298}{}^0$, may be estimated from the reported values of the standard entropies of HCN, H_2S, CN^-, and HCl (12). $S_{298}{}^0(SH^-)$ is assumed to be equal to the standard entropy of the isoelectronic species HCl. The resulting value for $\Delta S_{298}{}^0 = +2.1$ e.u. is estimated to be uncertain to ±0.5 e.u. and can be combined with the value of $\Delta G_{296}{}^0$ determined in this study to provide a value for $\Delta H_{298}{}^0$ of -1.0 ± 0.2 kcal mol^{-1}.

The combination of the value obtained for $\Delta H_{298}{}^0$ with the most reliable values currently available for e.a.(CN), e.a.(SH) and $D_0{}^0$(H—CN) according to the equation:

$$[9] \quad D_0{}^0(\text{H—CN}) = D_0{}^0(\text{H—SH}) + \text{e.a.(CN)} - \text{e.a.(SH)} + \Delta H_{298}{}^0 - \int_0^{298} \Delta C_p \mathrm{d}T$$

where ΔC_p is the change in heat capacity for reaction 2 at constant pressure. A value for $D_0{}^0$(H—CN) of 124 ± 2 kcal mol^{-1} is obtained when the values for $D_0{}^0$(H—SH) = 90 ± 1 kcal mol^{-1} (14), e.a.(CN) = 88.1 ± 0.5 kcal mol^{-1} (15), and e.a.(SH) = 53.50 ± 0.23 (13) are adopted and the integral is neglected.[2] Darwent has selected a slightly larger value for $D_0{}^0$(H—CN) of 127 ± 5 kcal mol^{-1} in his compilation of bond dissociation energies (14). The values for $\Delta H_{f0}{}^0$-(H, CN, HCN) adopted in the JANAF tables (11) provide a value for $D_0{}^0$(H—CN) of 123.2 ± 4.5 kcal mol^{-1} which is in good agreement with the value determined in this study.

The exothermicity of reaction 2 is a measure of the difference in the proton affinities of CN^- and SH^-, *viz.*

[1]M.T. Bowers. Private communication.

[2]A comparison of $\Delta H_{298}{}^0$ with $\Delta H_0{}^0$ for the analogous reaction: SH + HCN → CN + H_2S indicates a value for $\int_0^{298} \Delta C_p \mathrm{d}T < 0.1$ kcal mol^{-1}.

[10] ΔH_{298}^{0} = p.a.(CN^-) − p.a.(SH^-) = -1.0 ± 0.2 kcal mol^{-1}

A value for p.a.(SH^-) of 351 ± 1 kcal mol^{-1} may be calculated from the available thermochemical data for D_{298}^{0}(H—SH), e.a.(SH), and i.p.(H^+), all of which have been established to within an uncertainty ⩽1 kcal mol^{-1}. Consequently p.a.(CN^-), which is a measure of the gas-phase acidity of HCN, is equal to 350 ± 1 kcal mol^{-1}.

The authors are not aware of any previous report of the rate constant for reaction 2. The value obtained in the present study at 296 K, *viz.* $(2.9 \pm 0.6) \times 10^{-9}$ cm^3 $molecule^{-1}$ s^{-1} is in excellent accord with the value predicted on the basis of the average-dipole-orientation theory of Su and Bowers (16, 17), *viz.* 2.84×10^{-9} cm^3 $molecule^{-1}$ s^{-1}. We have adopted a value for α(HCN) = 2.59 $Å^3$ (18) and μ_D(HCN) = 2.98 D (19).

The financial assistance of the National Research Council is gratefully acknowledged. We thank both referees for their useful comments.

1. D. K. Bohme, R. S. Hemsworth, and H. W. Rundle. J. Chem. Phys. **59**, 77 (1973).
2. D. K. Bohme, G. I. Mackay, H. I. Schiff, and R. S. Hemsworth. J. Chem. Phys. **61**, 2175 (1974).
3. M. T. Bowers, D. H. Aue, H. M. Webb, and R. T. McIver, Jr. J. Am. Chem. Soc. **93**, 4314 (1971).
4. R. T. McIver, Jr. and J. R. Eyler. J. Am. Chem. Soc. **93**, 6335 (1971).
5. R. T. McIver, Jr. and J. S. Miller. J. Am. Chem. Soc. **96**, 4323 (1974).
6. T. B. McMahon and P. Kebarle. J. Am. Chem. Soc. **96**, 5940 (1974).
7. D. K. Bohme, R. S. Hemsworth, H. W. Rundle, and H. I. Schiff. J. Chem. Phys. **58**, 3504 (1973).
8. P. F. Fennelly, R. S. Hemsworth, H. I. Schiff, and D. K. Bohme. J. Chem. Phys. **59**, 6405 (1973).
9. G. Brauer. (*Editor*). Handbook of preparative inorganic chemistry. Academic Press, New York. 1965.
10. N. C. Barford. Experimental measurements: precision, error and truth. Addison-Wesley, London. 1967.
11. JANAF Thermochemical Tables, Vol. 37. Second Edition, Natl. Stand. Ref. Data Ser., Nat. Bur. Stand. 1971.
12. L. M. Branscomb. Phys. Rev. **148**, 11 (1966).
13. M. Henchman. Ion–Molecule reactions. Vol. 1. *Edited by* J. L. Franklin. Plenum Press, New York. 1972. p. 165.
14. B. deB. Darwent. Natl. Stand. Ref. Data Ser., Natl. Bur. Stand. **31** (1970).
15. J. Berkowitz, W. A. Chupka, and T. A. Walter. J. Chem. Phys. **50**, 1497 (1969).
16. T. Su and M. T. Bowers. J. Chem. Phys. **58**, 3027 (1973).
17. T. Su and M. T. Bowers. Int. J. Mass Spectrom. Ion Phys. **12**, 347 (1973).
18. J. O. Hirschfelder, C. F. Curtiss, and R. B. Bird. Molecular theory of gases and liquids. John Wiley & Sons, Inc., New York, N.Y. 1954.
19. R. D. Nelson, D. R. Lide, and A. A. Maryott. Natl. Stand. Ref. Data Ser., Natl. Bur. Stand. **10** (1967).

Can. J. Chem. Downloaded from www.nrcresearchpress.com by 210.87.254.105 on 09/05/12
For personal use only.

The Crystal Structure of *cis*-Dichlorobis(dimethylsulfoxide)platinum(II)

ROBERT MELANSON AND FERNANDE D. ROCHON

Département de Chimie, Université du Québec à Montréal, C.P. 8888, Montréal, Québec H3C 3P8

Received March 5, 1975

ROBERT MELANSON and FERNANDE D. ROCHON. Can. J. Chem. **53**, 2371 (1975).

The molecular and crystal structure of *cis*-dichlorobis(dimethylsulfoxide)platinum(II), *cis*-$[PtCl_2(DMSO)_2]$, has been studied by X-ray diffraction. The compound belongs to the monoclinic $P2_1/c$ space group and the cell parameters are: $a = 8.653$, $b = 13.580$, $c = 10.914$ Å, $\beta = 123.43°$, and $Z = 4$. The refinement of the positional and anisotropic thermal parameters, carried out by full matrix least-squares calculations, converged to $R = 0.029$ and $R_w = 0.027$.

The coordination around the platinum atom is planar. As expected, the DMSO molecules are bonded to the platinum atom through sulfur. The bond distances found are: Pt—Cl = 2.306, 2.312 Å; Pt—S = 2.244, 2.229 Å; S—O = 1.469, 1.454 Å, and S—C = 1.77 to 1.79 Å. The crystal consists of layers of molecules parallel to the *ac* plane.

ROBERT MELANSON et FERNANDE D. ROCHON. Can. J. Chem. **53**, 2371 (1975).

La structure moléculaire et cristalline du complexe *cis*-$[PtCl_2(DMSO)_2]$ (DMSO = diméthylsulphoxyde) a été étudiée par diffraction des rayons X. Le composé cristallise dans le groupe spatial $P2_1/c$ du système monoclinique. Les paramètres de maille sont: $a = 8.653$, $b = 13.580$, $c = 10.914$ Å, $\beta = 123.43°$ et $Z = 4$. Les coordonnées atomiques et les facteurs thermiques anisotropes ont été affinés par moindres carrés (matrice entière) jusqu'à $R = 0.029$ et $R_w = 0.027$.

La coordination autour de l'atome de platine est plane. Comme prévu, les molécules DMSO sont liées au platine par les atomes de soufre. Les distances entre les atomes formant des liaisons sont: Pt—Cl = 2.306, 2.312 Å; Pt—S = 2.244, 2.229 Å; S—O = 1.469, 1.454 Å et S—C = 1.77 à 1.79 Å. Le cristal est formé de couches de molécules parallèles au plan *ac*.

Introduction

$PtCl_2(DMSO)_2$, obtained as yellow crystals from the reaction between K_2PtCl_4 and dimethylsulfoxide has variously been assigned the *cis* (1, 2) and the *trans* (3) configuration. The complex is not isomorphous with the corresponding Pd(II) complex which is known, from X-ray diffraction studies, to have a *trans* configuration (4). Although the infrared spectrum indicates a *cis* configuration, the chemical behavior is more in keeping with a *trans* configuration (ref. 5, a note added in proof, confirmed the assignment of a *cis* configuration since the authors had just synthesized the *trans* isomer). There is general agreement that in the platinum(II) complexes with one or two dimethylsulfoxide molecules, the ligands are bonded to platinum through sulfur. A strong peak around 1125 cm^{-1} in the infrared spectrum has been assigned to the S—O stretching vibration, indicating bonding through sulfur (6), since it is shifted to higher frequency than the corresponding vibration in the free ligand.

Recently, we have decided to study the reactions between $PtCl_2(DMSO)_2$ and some nucleosides. In order to know the exact nature of $PtCl_2(DMSO)_2$, we have undertaken the study of the crystals by X-ray diffraction.

Experimental Section

Crystal Data

$PtCl_2C_4H_{12}S_2O_2$ f.w. = 422.26

Monoclinic $P2_1/c$, $a = 8.653(3)$, $b = 13.580(5)$, $c = 10.914(4)$ Å, $\beta = 123.43(3)°$, $Z = 4$, $V = 1070.3(7)$ Å^3, $\rho_o = 2.59(3)$ g/cm^3 (flotation), $\rho_c = 2.620$ g/cm^3, λMoKα = 0.71069 Å, μMoKα = 143.28 cm^{-1}, $T = 22°$.

Crystals of *cis*-dichlorobis(dimethylsulfoxide)platinum(II) were obtained directly from the reaction of K_2PtCl_4 in aqueous dimethylsulfoxide as previously described (1). A set of precession photographs indicated that the $h0l$, $l = 2n + 1$ and $0k0$, $k = 2n + 1$ reflections are systematic absences indicating the $P2_1/c$ space group. The cell parameters were calculated by least-squares refinement from the setting angles of 15 automatically centered reflections (MoKα radiation) on a Syntex P$\bar{1}$ diffractometer equipped with a graphite monochromator.

Collection and Reduction of Intensity Data

The intensity data were collected from a crystal of dimensions 0.106 × 0.120 × 0.434 mm. A total of 3461 independent reflections were measured in the region of $2\theta < 60°$ by the $2\theta/\theta$ scan technique using MoKα radiation. The data collection was done at a variable speed (24° to 1 deg/min) depending on the intensity of the reflection (Syntex $2\theta/\theta$ autocollection program). The majority of the reflections were measured at a speed of 1 deg/min. A 2θ scan range of 1.2 below Kα_1 and 1.2 over Kα_2 was se-

Can. J. Chem. Downloaded from www.nrcresearchpress.com by 210.87.254.5 on 09/05/12
For personal use only.

TABLE 1. Final structure parameters* and estimated standard deviations† ($\times 10^4$)

Atom	x	y	z	β_{11}	β_{22}	β_{33}	β_{12}	β_{13}	β_{23}
Pt	2398.2(3)	152.0(2)	2137.2(2)	108.3(4)	28.5(1)	68.4(3)	3.1(2)	53.3(2)	0.5(1)
Cl_1	4389(2)	−70(1)	1377(2)	152(3)	61(1)	126(2)	−4(1)	105(2)	−14(1)
Cl_2	1429(3)	−1453(1)	1415(2)	216(4)	30(1)	141(2)	−13(1)	119(3)	−16(1)
S_1	672(2)	324(1)	3079(2)	116(2)	32(1)	71(1)	−4(1)	57(2)	−5(1)
S_2	3475(2)	1681(1)	2807(2)	133(3)	28(1)	70(2)	−6(1)	56(2)	2(1)
O_1	1779(7)	537(4)	4649(5)	185(10)	60(3)	79(5)	−18(14)	67(6)	−19(3)
O_2	2529(7)	2327(3)	3250(6)	236(12)	36(2)	170(8)	−3(4)	140(9)	−11(3)
C_1	−1079(10)	1247(5)	2136(9)	170(15)	51(4)	146(11)	23(6)	98(11)	−2(5)
C_2	−738(11)	−713(5)	2782(9)	217(17)	48(4)	154(11)	−35(6)	144(12)	−23(5)
C_3	3566(12)	2296(5)	1408(8)	280(21)	53(4)	115(10)	−26(8)	118(13)	15(5)
C_4	5839(10)	1615(6)	4276(8)	151(15)	61(5)	111(10)	−18(7)	23(10)	−9(5)

*The anisotropic thermal parameters are in the form $\exp(-h^2\beta_{11} - k^2\beta_{22} - l^2\beta_{33} - 2hk\beta_{12} - 2hl\beta_{13} - 2kl\beta_{23})$.
†Standard deviations are given in parentheses.

lected. The background time to scan time ratio was 0.30. During the data collection, three standard reflections (0, 6, 1; 3, 1, −1; and 0, 1, −3) were measured after every 47 reflections. Their variations were less than 2% from their respective means. The 3461 independent measurements reduced to a set of 3307 independent reflections after taking out the systematically absent reflections. The 703 reflections for which the intensity was less than 2.5 $\sigma(I)$ were considered as unobserved. The standard deviation $\sigma(I)$ was calculated in the following manner.

$$\sigma^2(I) = \frac{1}{\tau}\left\{\left(T + \frac{B}{(\mathrm{BSR})^2}\right)\mathrm{SCRT}^2 + (pN)^2\right\}$$

τ = transmission coefficient, T = total count, B = total background count, N = net count, BSR = background to scan time ratio, SCRT = scan rate, p = 0.04 long term instability constant. Finally, 2622 independent observed reflections remained. An absorption correction based on the equations of the crystal faces was then applied. The transmission factors varied from 0.2123 to 0.2988. The data were finally corrected for the Lorentz and polarization effects. The scattering factors for platinum, chlorine, sulfur, oxygen, and carbon were those of Cromer and Waber (7). The anomalous dispersion terms of platinum ($\Delta f' = -2.05$, $\Delta f'' = 8.43$), chlorine ($\Delta f' = +0.15$, $\Delta f'' = 0.19$), and sulfur ($\Delta f' = +0.13$, $\Delta f'' = 0.16$) (8) were included in the calculations.

Structure Determination

The platinum atom was easily located from the three-dimensional Patterson map. The positions of all other atoms except the hydrogen atoms, were obtained by structure factor and Fourier map calculations. The refinement of the parameters was carried out by full matrix least-squares calculations. In the early stages of refinement, unit weight was assigned to all observed reflections. Individual weights w according to the equation $1/w = a + bF_o + cF_o^2$ were later calculated. a, b, and c were adjusted to make the distribution of $w|\Delta F|^2$ constant with respect to $|F_o|$ and $\sin\theta/\lambda$ ($a = 35.0$, $b = -0.52$, and $c = 0.022$). An isotropic secondary extinction correction (9) was also introduced. The hydrogen atoms on the terminal methyl groups could not be localized. The refinement of the scale factor, the coordinates, and anisotropic temperature factors of all nonhydrogen atoms converged to $R = \Sigma(|F_o| - |F_c|)/\Sigma|F_o|$ of 0.029 and a weighted residual $R_w = [\Sigma w(|F_o| - |F_c|)^2/\Sigma w|F_o|^2]^{1/2}$ of 0.027.[1] The standard deviation of an observation of unit weight is 0.809. The final difference Fourier map using all observed reflections did not show peaks higher than ±1 e/Å^3. The refined parameters are given in Table 1.

The calculations were performed with a CDC 6400 computer. The following programs were used: NRC crystallographic programs (10), NUCLS, a modified version of ORFLS, and Zalkin (FORDAP).

Results and Discussion

As expected, the analyzed complex is the *cis* compound and the dimethylsulfoxide molecules are bonded to the platinum atom through sulfur. A stereoscopic view of the molecule is shown in Fig. 1. Two chlorine and two sulfur atoms form the square planar coordination expected for Pt(II) complexes. The weighted best plane was calculated through the platinum, the two chlorine, and the two sulfur atoms. The deviations from this plane are: Pt, 0.0038 (3); Cl_1, −0.120 (2); Cl_2, −0.012 (3); S_1, −0.077 (2); and S_2, −0.007 (2).

The bond distances and angles are listed in Table 2. The angles around the platinum atom are close to the expected 90 and 180°, but there seems to be some slight deviation from the ideal square planar coordination (angles Cl_1—Pt—S_1 = 174.84° and Cl_2—Pt—S_2 = 176.29°).

The Pt—Cl bonds (2.306 and 2.312 Å) are of normal lengths (11–13). The Pt—S bonds (2.244 and 2.229 Å) seem also normal. To our knowledge, this is the first crystal structure work on a platinum complex with DMSO. Two similar structures in which DMSO is complexed to

[1]The structure factor table is available from the Depository of Unpublished Data, CISTI, National Research Council of Canada, Ottawa, Canada K1A 0S2.

Can. J. Chem. Downloaded from www.nrcresearchpress.com by 210.87.254.5 on 09/05/12
For personal use only.

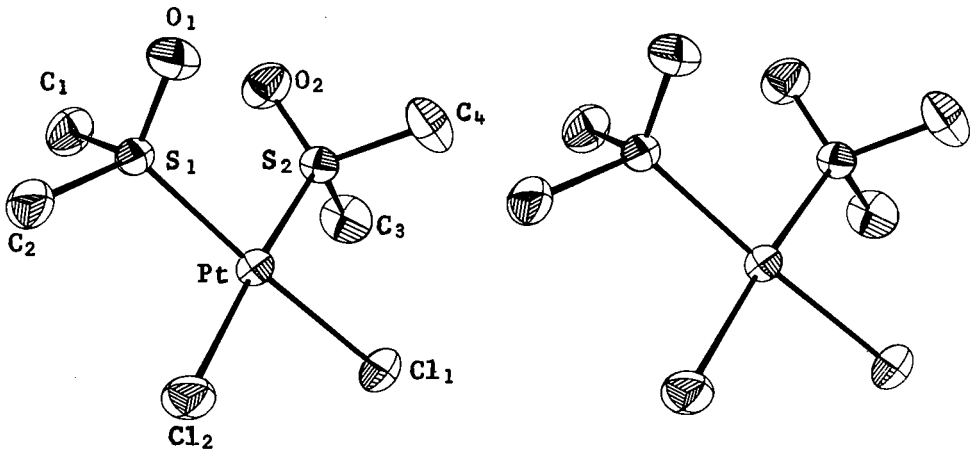

FIG. 1. Stereoscopic view of the molecule *cis*-[$PtCl_2(DMSO)_2$].

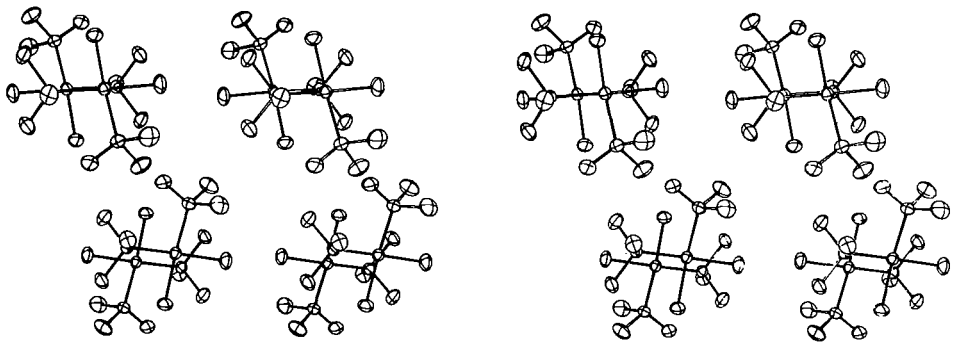

FIG. 2. Stereoscopic view of the packing in the *cis*-[$PtCl_2(DMSO)_2$] crystal.

TABLE 2. Bond distances and bond angles in [$PtCl_2(DMSO)_2$]

Bond	Distance (Å)	Bonds	Angle (deg)
Pt—Cl_1	2.306(3)	Cl_1—Pt—Cl_2	87.58(9)
Pt—Cl_2	2.312(2)	Cl_1—Pt—S_2	88.75(9)
Pt—S_1	2.244(2)	Cl_2—Pt—S_1	92.59(9)
Pt—S_2	2.229(2)	S_1—Pt—S_2	91.03(8)
S_1—O_1	1.469(6)	Cl_1—Pt—S_1	174.84(9)
S_1—C_1	1.786(11)	Cl_2—Pt—S_2	176.29(8)
S_1—C_2	1.767(11)	Pt—S_1—O_1	112.4(3)
S_2—O_2	1.454(9)	Pt—S_1—C_1	111.8(4)
S_2—C_3	1.783(11)	Pt—S_1—C_2	113.5(4)
S_2—C_4	1.790(12)	Pt—S_2—O_2	117.3(3)
		Pt—S_2—C_3	111.4(4)
		Pt—S_2—C_4	108.2(4)
		O_1—S_1—C_1	110.3(5)
		O_1—S_1—C_2	108.5(5)
		C_1—S_1—C_2	99.5(5)
		O_2—S_2—C_3	107.6(5)
		O_2—S_2—C_4	107.9(5)
		C_3—S_2—C_4	103.3(5)

palladium have been reported (4, 14). The Pt—S distances are identical to the Pd—S distances found for *cis*-[$Pd(NO_3)_2(DMSO)_2$] (2.231 and 2.253 Å) (14) and slightly shorter than the Pd—S bonds found for *trans*-[$PdCl_2(DMSO)_2$] (2.299 and 2.291 Å) (4).

The sulfur atoms in the DMSO molecules are in an approximate tetrahedral environment with angles ranging from 99.5 to 110.3°. The structure of the coordinated molecules is very similar to the structure of DMSO itself. Two determinations of the crystal structure of free DMSO have yielded S—O distances of 1.471 Å (ref. 15, determined at −60°) and 1.531 Å (ref. 16, determined at +5°). It has been suggested (4) that the latter value is more reliable for comparison with structures determined at room temperature. The S—O distances for the platinum complex are 1.469 and 1.454 Å. These distances are very similar to the S—O distances found for *trans*-

Can. J. Chem. Downloaded from www.nrcresearchpress.com by 210.87.254.5 on 09/05/12
For personal use only.

$[PdCl_2(DMSO)_2]$ (1.476 and 1.46 Å) (4), for *cis*-$[Pd(NO_3)_2(DMSO)_2]$ (1.463 Å) (14), and for *cis*-$[Ir(DMSO)_2Cl_2(C_{15}H_{13}O)]$ (1.44 and 1.47 Å) (17), but are shorter than those found for $[Ru(NH_3)_5DMSO]^{2+}$ $2PF_6^-$ (1.527 Å) (18). The S—C distances ranging from 1.767 to 1.790 Å are in good agreement with the values found in other DMSO complexes (1.75 to 1.84 Å) (4, 14, 17, 18).

Figure 2 illustrates the packing in the *cis*-$[PtCl_2(DMSO)_2]$ crystal. The latter consists of layers of molecules parallel to the *ac* plane.

Grateful acknowledgement is made to the National Research Council of Canada for financial support and to Dr. Pi-Chang Kong for the synthesis of the analyzed compound.

1. J. H. Price, A. N. Williamson, R. F. Schramm, and B. B. Wayland. Inorg. Chem. **11**, 1280 (1972).
2. W. Kitching, C. J. Moore, and D. Doddrell. Inorg. Chem. **9**, 541 (1970).
3. Y. N. Kukushkin, Y. E. Vyazmenskii, L. I. Zorina, and Y. L. Pazukhina. Russ. J. Inorg. Chem. **13**, 835 (1968).
4. M. J. Bennett, F. A. Cotton, D. L. Weaver, R. J. Williams, and W. H. Watson. Acta Cryst. **23**, 788 (1967).
5. P. D. Braddock, R. Romeo, and M. L. Tobe. Inorg. Chem. **13**, 1170 (1974).
6. F. A. Cotton, R. Francis, and W. D. Horrocks, Jr. J. Phys. Chem. **64**, 1534 (1960).
7. D. T. Cromer and J. T. Waber. Acta Cryst. **18**, 104 (1965).
8. D. T. Cromer. Acta Cryst. **18**, 17 (1965).
9. P. Coppens and W. C. Hamilton. Acta Cryst. A**26**, 71 (1970).
10. F. R. Ahmed, S. R. Hall, M. E. Pippy, and C. P. Huber. NRC Crystallographic Programs. NRC2 and 2A Data Reduction Programs, NRC-3 Absorption Correction and Angles Calculations. World List of Crystallographic Computer Programs. 2nd ed., Appendix, Utrecht, Oasthoek. p. 52.
11. R. H. B. Mais, P. G. Owston, and A. M. Wood. Acta Cryst. B**28**, 393 (1972).
12. J. A. J. Jarvis, B. T. Kilbourn, and P. G. Owston. Acta Cryst. B**27**, 366 (1971).
13. W. E. Davies, W. Hewertson, R. H. B. Mais, P. G. Owston, and C. G. Patel. J. Chem. Soc. 1873 (1970).
14. D. A. Langs, C. R. Hare, and R. G. Little. Chem. Commun. 1080 (1967).
15. M. A. Viswamitra and K. K. Kannan. Nature, **209**, 1016 (1966).
16. R. Thomas, C. B. Shoemaker, and K. Eriks. Acta Cryst. **21**, 12 (1966).
17. M. McParltin and R. Mason. Chem. Commun. 545 (1967).
18. F. C. March and G. Ferguson. Can. J. Chem. **49**, 3590 (1971).

Can. J. Chem. Downloaded from www.nrcresearchpress.com by 210.87.254.5 on 09/05/12
For personal use only.

Cinétique de la formation de la métalloporphyrine Cu(II) – hématoporphyrine IX dans l'acide acétique aqueux

GUY PAQUETTE ET MIKLOS ZADOR

Département de Chimie, Université de Montréal, C.P. 6210, Station A, Montréal, Québec H3C 3V1

Reçu le 28 février, 1975

GUY PAQUETTE et MIKLOS ZADOR. Can. J. Chem. **53**, 2375 (1975).

La cinétique de l'interaction de l'hématoporphyrine IX avec le Cu(II) a été étudiée dans un mélange acide acétique – eau (50%–50% v/v). La réaction est d'ordre un par rapport à la porphyrine et d'ordre inférieur à un par rapport au perchlorate cuivrique. Ceci est expliqué en tenant compte de l'interaction de l'ion Cu^{2+} avec l'acide acétique. Les espèces réactives sont Cu^{2+}, $CuOAc^{+}$ et la porphyrine libre. Le mécanisme de la réaction est comparé à ceux proposés pour d'autres systèmes similaires.

GUY PAQUETTE and MIKLOS ZADOR. Can. J. Chem. **53**, 2375 (1975).

The kinetics of interaction of hematoporphyrin IX with Cu(II) has been studied in an acetic acid – water solvent (50%–50% v/v). The reaction is of first order with respect to the porphyrin whereas the order with respect to copper(II) perchlorate is smaller than one. This is explained by taking into account the interaction between Cu^{2+} and acetic acid. The reactive species are Cu^{2+}, $CuOAc^{+}$, and free porphyrin. The mechanism of the reaction is compared to those proposed for similar systems.

Can. J. Chem. Downloaded from www.nrcresearchpress.com by 210.87.254.42 on 09/05/12
For personal use only.

Introduction

Les métalloporphyrines jouent un rôle important dans les organismes vivants, aussi bien animaux (*e.g.* l'hémoglobine dans le sang) que végétaux (*e.g.* la chlorophylle des plantes vertes). Le mécanisme de formation des métalloporphyrines n'est pas encore connu avec certitude (1). En général leur vitesse de formation est de plusieurs ordres de grandeur plus faible que celle de complexes impliquant des bases azotées simples.

Dans l'étude du mécanisme de formation des métalloporphyrines, un des problèmes principaux vient du fait qu'en général les porphyrines sont très peu solubles dans l'eau; l'utilisation d'autres solvants entraîne des problèmes quant à la nature des espèces réactives. Il est difficile, par exemple, de comparer les résultats obtenus dans l'eau, avec une porphyrine soluble, avec ceux obtenus dans l'acide acétique glacial; dans ce dernier solvant la porphyrine (telle l'hématoporphyrine IX) porte deux charges positives et, en plus, les ions métalliques se trouvent souvent sous forme de dimères (2–8).

Dans ce travail, les résultats concernant l'interaction de l'hématoporphyrine IX avec le Cu(II) dans l'acide acétique aqueux (50% v/v), sont présentés. Un des aspects de cette réaction qui a été approfondi concerne l'influence des interactions acide acétique – Cu(II) sur la cinétique de la réaction étudiée.

Partie expérimentale

Réactifs

La solution de perchlorate cuivrique a été obtenue en additionnant la quantité requise d'acide perchlorique (J. T. Baker) à la solution du sel double $CuCO_3 \cdot Cu(OH)_2$ (B.D.H.) en amenant le p*H* final à 4. L'hématoporphyrine IX (Nutritional Biochemicals) a été utilisée sans purification.

Les solutions finales sont constituées d'eau et d'acide acétique (C-I-L, Reagent) 50%–50% (v/v).

Méthode cinétique

Les réactions sont étudiées à 45° par spectrophotométrie en enregistrant la diminution de l'absorption de la bande Soret de l'hématoporphyrine ($\lambda = 407$ nm), due à la formation de la métalloporphyrine. Un spectrophotomètre Zeiss PMQ II, avec un compartiment à cellules thermostaté a été utilisé. La température à l'intérieur des cellules a été mesurée à l'aide d'un thermocouple. Les résultats ont été enregistrés sur un enregistreur logarithmique Sargent Welsh modèle SRLG. La concentration en porphyrine utilisée était de 4.0×10^{-6} *M*, tandis que celle de Cu(II) variait de 2.5×10^{-4} à 2.5×10^{-2} *M*. Les constantes de vitesse ont été obtenues à partir de la relation $kt = \ln [(D_0 - D_\infty)/(D - D_\infty)]$ où D_0, D et D_∞ représentent les densités optiques au temps 0, t et infini, respectivement. On obtenait des relations linéaires sur plus de trois demi-réactions. La force ionique des solutions a été maintenue constante ($\mu = 0.5$ *M*) à l'aide de perchlorate de lithium (Alpha Inorganics). Ceci est indispensable, étant donné que les expériences ont montré que l'augmentation de la force ionique entraîne une diminution de la vitesse de réaction.

Can. J. Chem. Downloaded from www.nrcresearchpress.com by 210.87.254.42 on 09/05/12
For personal use only.

Résultats et discussion

La réaction de l'hématoporphyrine IX (PH_2) avec le Cu(II) se fait d'après l'équation:

[1] $$PH_2 + Cu(II) \rightarrow P \cdot Cu(II) + 2H^+$$

Quand la réaction est réalisée en présence d'un grand excès de Cu(II), on obtient une cinétique d'ordre un par rapport à la porphyrine.

$$d[P \cdot Cu(II)]/dt = k_{exp}[PH_2]_{total}$$

La constante de vitesse expérimentale, k_{exp} varie linéairement avec la concentration en Cu(II) aux basses concentrations; à plus haute concentration en Cu(II) on observe un écart important à la linéarité, comme l'indique la fig. 1.

Un ordre de réaction inférieur à un par rapport au sel métallique a souvent été observé dans l'acide acétique glacial (2–6); on l'a expliqué de manière satisfaisante en admettant une dimérisation prononcée du sel utilisé. La concentration du monomère réactif est donnée par la relation $[Me(OAc)_2] = \sqrt{K[(Me(OAc)_2)_2]}$, ce qui conduit à un ordre $\frac{1}{2}$. Dans un solvant, contenant 50% (v/v) d'eau et 50% (v/v) d'acide acétique, on ne peut pas retenir cette explication. En effet les données concernant l'acide acétique aqueux, indiquent (7, 8) que dans nos conditions, même à la concentration la plus élevée, il y a moins de 10% de dimère.

On peut expliquer nos résultats en tenant compte de l'interaction du Cu(II) avec le solvant, soit l'acide acétique. L'ion Cu^{2+}, provenant du perchlorate cuivrique utilisé, réagit avec l'acide acétique pour donner les espèces $Cu(OAc)^+$ et $Cu(OAc)_2$.[1]

[2] $$Cu^{2+} + HOAc \rightleftharpoons CuOAc^+ + H^+$$
$$K_1 = [CuOAC^+]/[Cu^{2+}][OAc^-]$$

[3] $$CuOAc^+ + HOAc \rightleftharpoons Cu(OAc)_2 + H^+$$
$$K_2 = [Cu(OAc)_2]/[CuOAc^+][OAc^-]$$

Les protons libérés dans les réactions 2 et 3 déplacent l'équilibre de protonation de la porphyrine vers la formation de PH_4^{2+}, d'après la réaction 4.

[4] $$PH_2 + 2H^+ \rightleftharpoons PH_4^{2+}$$
$$K_3 = [PH_4^{2+}]/[PH_2][H^+]^2$$

Déjà dans l'acide acétique – eau 50%–50% (v/v), correspondant à une concentration en $H^+ = 1.5 \times 10^{-2}$ M d'après la constante dissociation de l'acide acétique obtenue par interpolation des valeurs de la littérature (9), l'équilibre 4 est déplacé vers la droite. En effet, la solution de l'hématoporphyrine présente deux bandes dans le visible, ce qui est caractéristique du diacide, PH_4^{2+}; les résultats de la littérature (10) indiquent une constante de protonation ($pK_a = 4.7$) qui serait en accord avec cette hypothèse.

La quantité de protons libérés augmente avec la concentration en Cu(II), contribuant ainsi à diminuer la concentration de la forme réactive de la porphyrine, PH_2. Ceci explique qualitativement l'ordre un à basse concentration en Cu(II) et l'écart subséquent à la linéarité à la fig. 1.

Pour confirmer ces hypothèses on a étudié l'influence de l'acide perchlorique à basse concentration en Cu(II) (5×10^{-4} M). Dans ces conditions, la quantité de protons libérés dans [2] et [3] est négligeable. Les résultats sont montrés à la fig. 2.

La concentration en H^+ représente celle à l'équilibre, calculée en tenant compte de l'acide fort ajouté et de la dissociation de l'acide acétique. Il y a une inhibition marquée, correspondant à un ordre approximatif -2 par rapport à H^+. De plus, à haute concentration en $HClO_4$, (1 M) la vitesse de réaction est négligeable; à une concentration en Cu(II) de 2.5×10^{-2} M il y a moins de 1% de réaction en deux jours. Ceci indique que pour l'hématoporphyrine IX la pro-

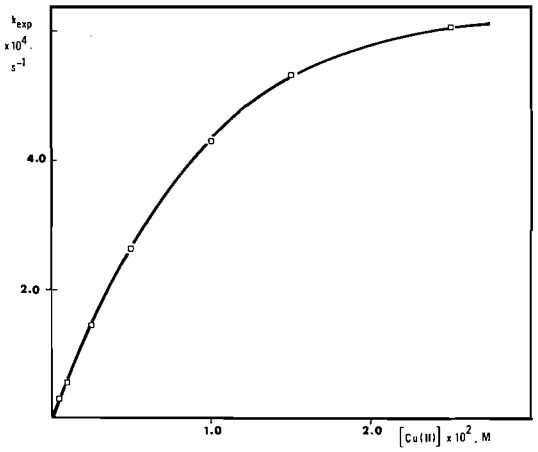

FIG. 1. Influence de la concentration en Cu(II) sur k_{exp}. $T = 45°$, $[PH_2] = 4.0 \times 10^{-6}$ M; solvant: CH_3COOH–H_2O 50%–50% (v/v).

[1]La constante d'équilibre des réactions 2 et 3 est reliée aux constantes de stabilité des complexes $CuOAc^+$ et $Cu(OAc)_2$ en tenant compte de la dissociation de l'acide acétique.

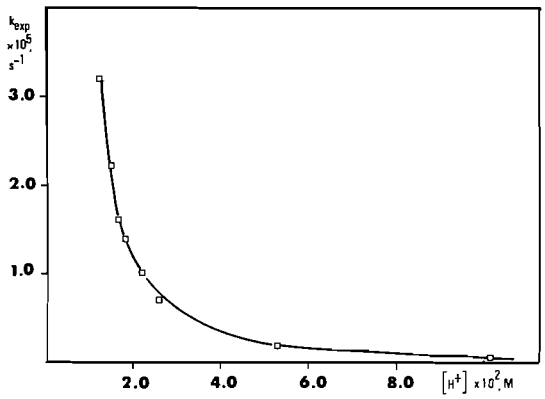

FIG. 2. Influence de l'acidité sur k_{exp} à basse concentration en Cu(II). $T = 45°$, $[PH_2] = 4.0 \times 10^{-6}$ M, [Cu(II)] $= 5.0 \times 10^{-4}$ M; solvant: CH_3COOH–H_2O 50%–50% (v/v).

tonation conduit à une espèce (PH_4^{2+}) très peu réactive dont la contribution à la vitesse peut être négligée, même à une acidité de 0.1 M.

L'espèce monoprotonée, PH_3^+ ne semble pas avoir une contribution. Cette espèce a été observée dans l'acide acétique glacial en présence d'ions métalliques, mais disparaît immédiatement lors de l'addition d'eau au solvant (11). Dans notre cas les spectres observés sont ceux de PH_4^{2+}, et ceci même en présence de Cu^{2+}. Si PH_3^+ contribuait à la vitesse de manière importante, l'inhibition par H^+ devrait correspondre à un ordre -1, au lieu de l'ordre -2 qui a été observé.

Quand on étudie la réaction à cette acidité de 0.1 M la contribution des protons libérés lors de l'interaction du Cu(II) avec l'acide acétique est moins importante; l'ordre par rapport au Cu(II) est alors très près de un dans toute la gamme de concentration (5×10^{-4} à 2.5×10^{-2} M). L'interprétation quantitative des résultats est donc basée sur les hypothèses suivantes: (*i*) PH_2 est la seule forme réactive de la porphyrine; (*ii*) les espèces réactives du Cu(II) sont Cu^{2+}, $CuOAc^+$ et $Cu(OAc)_2$; ceci conduit à l'éq. 5.

$$[5]\quad d[P \cdot Cu(II)]/dt = (k_1[Cu^{2+}] + k_2[CuOAc^+] + k_3[Cu(OAc)_2])[PH_2]$$

En tenant compte des éqs. 1–4 on obtient l'éq. 6.

$$[6]\quad k_{exp} = \frac{k_1 + k_2K_1K_a[HOAc]/[H^+] + k_3K_1K_2K_a^2[HOAc]^2/[H^+]^2}{(1 + K_3[H^+]^2)(1 + K_1K_a[HOAc]/[H^+] + K_1K_2K_a^2[HOAc]^2/[H^+]^2)}\,[Cu(II)]_{total}$$

Evidemment, pour que l'éq. 6 puisse être utilisée à haute concentration en Cu(II), il faut tenir compte, dans le calcul de la concentration en H^+ à l'équilibre, de la contribution des protons libérés dans les réactions 2 et 3. Malheureusement, on ne connait pas la valeur des constantes d'équilibre K_a, K_1 et K_2 dans le solvant utilisé et à la force ionique de 0.5 M.

On a donc procédé par une méthode itérative, en prenant, comme première approximation, les valeurs de constantes dans l'eau, c'est-à-dire $K_1 = 46$ et $K_2 = 10$ (12), et $K_a[HOAc] = 2.25 \times 10^{-4}$ donnée pour ce solvant à force ionique nulle (9). De plus, on a négligé 1 devant $K_3[H^+]^2$, ce qui est justifié comme on l'a vu plus haut.

Pour pouvoir obtenir des valeurs significatives des paramètres, les constantes de vitesse ont été déterminées à huit acidités différentes; à chaque acidité on a étudié sept concentrations en Cu(II). L'ajustement final des paramètres a été effectué par ordinateur.[2]

On a obtenu les valeurs suivantes des paramètres $k_1/K_3 = 8.2 \times 10^{-6}$ $M\,s^{-1}$, $k_2/K_3 = 1.2 \times 10^{-5}$ $M\ s^{-1}$, $K_a[HOAc] = 1.6 \times 10^{-4}$ M, $K_1 = 100\ M^{-1}$, $K_2 = 2\ M^{-1}$. L'accord entre les résultats expérimentaux et calculés est satisfaisant, comme on peut le constater sur le tableau 1. Il est significatif que, dans un domaine où les constantes de vitesse varient d'un facteur de plus de mille, on obtienne un bon accord. Compte tenu de l'erreur expérimentale, la valeur de k_3/K_3 est négligeable devant les autres valeurs; $Cu(OAc)_2$ n'a donc pas de contribution à la vitesse dans nos conditions. De plus, $Cu(OAc)_2$ n'est pas une espèce dominante, ce qui rend impossible la détermination de k_3/K_3, déjà petit.

[2]Le programme consiste à résoudre l'équation de quatrième degré donnant la concentration en H^+ à l'équilibre pour l'ensemble des paramètres K_a, K_1 et K_2; la concentration en H^+ et les paramètres sont introduits dans l'éq. 6 et les valeurs de k_1/K_3, k_2/K_3 et k_3/K_3 sont obtenues par une méthode de régression. L'écart entre les valeurs des constantes de vitesse calculées à l'aide de l'éq. 6, et expérimentales est minimisé par une méthode d'itération. Le programme a été mis au point par le professeur Urs Maag, du département d'informatique de l'Université de Montréal.

Can. J. Chem. Downloaded from www.nrcresearchpress.com by 210.87.254.42 on 09/05/12
For personal use only.

Can. J. Chem. Downloaded from www.nrcresearchpress.com by 210.87.254.42 on 09/05/12
For personal use only.

TABLEAU 1. Variation de la constante de vitesse d'ordre 1 avec la concentration en Cu(II) à diverses concentrations en acide perchlorique*

	$[HClO_4] = 0$		$[HClO_4] = 5 \times 10^{-3}\ M$		$[HClO_4] = 7.5 \times 10^{-3}\ M$		$[HClO_4] = 1.0 \times 10^{-2}\ M$	
[Cu(II)] (M)	k_{exp} (s^{-1})	k_{calc} (s^{-1})	k_{exp} (s^{-1})	k_{calc} (s^{-1})	k_{exp} (s^{-1})	k_{calc} (s^{-1})	k_{exp} (s^{-1})	k_{calc} (s^{-1})
5.0×10^{-4}	3.2×10^{-5}	3.13×10^{-5}	2.2×10^{-5}	2.08×10^{-5}	1.6×10^{-5}	1.70×10^{-5}	1.4×10^{-5}	1.41×10^{-5}
1.0×10^{-3}	5.7×10^{-5}	6.12×10^{-5}	4.3×10^{-5}	4.08×10^{-5}	2.9×10^{-5}	3.35×10^{-5}	2.8×10^{-5}	2.83×10^{-5}
2.5×10^{-3}	1.45×10^{-4}	1.43×10^{-4}	9.7×10^{-5}	9.62×10^{-5}	7.0×10^{-5}	7.92×10^{-5}	6.6×10^{-5}	6.57×10^{-5}
5.0×10^{-3}	2.6×10^{-4}	2.57×10^{-4}	1.9×10^{-4}	1.75×10^{-4}	1.3×10^{-4}	1.45×10^{-4}	1.3×10^{-4}	1.20×10^{-4}
1.0×10^{-2}	4.3×10^{-4}	4.20×10^{-4}	3.2×10^{-4}	2.93×10^{-4}	2.2×10^{-4}	2.47×10^{-4}	2.2×10^{-4}	2.08×10^{-4}
1.5×10^{-2}	5.3×10^{-4}	5.27×10^{-4}	4.0×10^{-4}	3.75×10^{-4}	2.7×10^{-4}	3.20×10^{-4}	2.6×10^{-4}	2.73×10^{-4}
2.5×10^{-2}	6.1×10^{-4}	6.45×10^{-4}	5.2×10^{-4}	4.78×10^{-4}	3.6×10^{-4}	4.13×10^{-4}	3.3×10^{-4}	3.60×10^{-4}

	$[HClO_4] = 1.5 \times 10^{-2}\ M$		$[HClO_4] = 2.0 \times 10^{-2}\ M$		$[HClO_4] = 5.0 \times 10^{-2}\ M$		$[HClO_4] = 1.0 \times 10^{-1}\ M$	
[Cu(II)] (M)	k_{exp} (s^{-1})	k_{calc} (s^{-1})	k_{exp} (s^{-1})	k_{calc} (s^{-1})	k_{exp} (s^{-1})	k_{calc} (s^{-1})	k_{exp} (s^{-1})	k_{calc} (s^{-1})
5.0×10^{-4}	1.0×10^{-5}	9.75×10^{-6}	7.2×10^{-6}	6.97×10^{-6}	1.8×10^{-6}	1.61×10^{-6}	4.2×10^{-7}	4.22×10^{-7}
1.0×10^{-3}	2.0×10^{-5}	1.92×10^{-5}	1.4×10^{-5}	1.38×10^{-5}	3.5×10^{-6}	3.20×10^{-6}	8.3×10^{-7}	8.43×10^{-7}
2.5×10^{-3}	4.6×10^{-5}	4.60×10^{-5}	3.4×10^{-5}	3.32×10^{-5}	6.8×10^{-6}	7.90×10^{-6}	2.1×10^{-6}	2.10×10^{-6}
5.0×10^{-3}	8.9×10^{-5}	8.6×10^{-5}	6.1×10^{-5}	6.27×10^{-5}	1.3×10^{-5}	1.55×10^{-5}	4.2×10^{-6}	4.17×10^{-6}
1.0×10^{-2}	1.7×10^{-4}	1.51×10^{-4}	1.1×10^{-4}	1.13×10^{-4}	2.5×10^{-5}	2.98×10^{-5}	8.2×10^{-6}	8.23×10^{-6}
1.5×10^{-2}	2.1×10^{-4}	2.03×10^{-4}	1.5×10^{-4}	1.54×10^{-4}	3.8×10^{-5}	4.30×10^{-5}	1.2×10^{-5}	1.22×10^{-5}
2.5×10^{-2}	2.7×10^{-4}	2.65×10^{-4}	2.1×10^{-4}	2.15×10^{-4}	6.1×10^{-5}	6.67×10^{-5}	2.0×10^{-5}	1.98×10^{-5}

*$T = 45°$; $[PH_2] = 4.0 \times 10^{-6}\ M$; solvant: acide acétique – eau 50%–50% (v/v).

Can. J. Chem. Downloaded from www.nrcresearchpress.com by 210.87.254.42 on 09/05/12
For personal use only.

Ceci n'exclue cependant pas la possibilité que $Cu(OAc)_2$ soit l'espèce responsable de l'incorporation dans l'acide acétique glacial, tel que suggéré par plusieurs auteurs (5, 6); dans ces conditions les concentrations en Cu^{2+} et $CuOAc^+$ seraient de loin inférieures à celle de $Cu(OAc)_2$, et malgré une constante de vitesse plus faible, $Cu(OAc)_2$ peut contribuer de manière prépondérante à la réaction dans ce solvant.

Il faut également ajouter que la valeur de la constante de vitesse calculée est relativement peu sensible à la valeur de K_2; cette constante est donc entachée d'une erreur assez grande ($\pm 100\%$).

L'écart entre résultats expérimentaux et valeurs calculées dépend de manière très sensible des valeurs de K_1 et de K_a[HOAc]; ces constantes sont obtenues avec beaucoup moins d'incertitude ($\pm 20\%$); ceci est également valable pour k_1/K_3 et k_2/K_3. Il est regrettable que K_3 ne puisse pas être connu, mais dans le solvant, l'hématoporphyrine est déjà protonée. De plus, la valeur absolue obtenue dans l'eau, ou dans l'eau contenant 10% (v/v) d'éthanol (10) ne peut pas être utilisée dans notre solvant, d'autant plus que la possibilité de formation de dimères, aux concentrations relativement élevées utilisées par les auteurs, ne peut pas être exclue.

Il est intéressant de comparer nos résultats avec ceux de Hambright et collaborateurs (13) qui ont étudié l'incorporation du Cu(II) dans la tétra(*p*-sulfophényl)porphine, en présence d'acide acétique et d'ions acétate dans l'eau.

Tout d'abord on constate quelques analogies; dans les deux cas on a, comme espèces réactives, l'ion Cu^{2+} et le complexe $CuOAc^+$. La constante de vitesse de ces deux espèces est identique chez les auteurs ($k_1 = k_2$), tandis que nous trouvons une différence, $k_2 > k_1$; les deux constantes sont toutefois du même ordre de grandeur. Il est à noter que ceci est probablement le résultat de la différence de charge entre les deux porphyrines. Dans notre cas, la porphyrine réagissant n'est pas chargée et $CuOAc^+$ est le plus réactionnel; les quatre charges négatives des groupes $-SO_3^-$ de la tétra(*p*-sulfophényl)-porphine, devraient favoriser, sur la base d'interactions électrostatiques, l'espèce ayant la charge la plus élevée, c'est-à-dire le Cu^{2+}; ceci explique donc qualitativement les différences observées.

Il y a toutefois des différences considérables entre les deux systèmes. Hambright et collaborateurs trouvent une contribution importante à la vitesse d'incorporation, de l'espèce diprotonée, correspondant à PH_4^{2+}. En effet la constante de vitesse d'incorporation du $CuOAc^+$ ne diminue que d'un facteur d'environ 40 quand on passe de PH_2 à PH_4^{2+} (13).[3] Ceci amène les auteurs à proposer que l'acide acétique est un bon solvant pour la formation des métalloporphyrines, parce que l'ion acétate présent catalyse la réaction du Cu(II) avec les porphyrines diprotonées.

Dans notre cas la réactivité de PH_4^{2+} n'est pas mesurable. Si l'on tient compte du fait que $CuOAc^+$ représente environ 16% du Cu(II) à une concentration en $HClO_4$ de 0.1 *M* il est clair que l'absence de contribution d'une réaction entre PH_4^{2+} et $CuOAc^+$ est due au fait que la forme diprotonée de l'hématoporphyrine IX est inerte. D'ailleurs c'était également la conclusion d'une étude précédente de Hambright et James sur cette porphyrine (6). La réactivité relativement élevée de la forme diprotonée de la tétra(*p*-sulfophényl)porphine est facile à comprendre, si l'on tient compte de la délocalisation des charges dans ce système conjugué; en effet, la charge totale est de -2 (entre p*H* 3.5 et 5), si l'on tient compte des quatre charges négatives; il est normal alors qu'elle soit réactive. Il est normal aussi que, relativement au cas de la forme non-protonée, l'ion $CuOAc^+$ soit plus réactif que l'ion Cu^{2+}. Evidemment, il n'est pas facile d'expliquer pourquoi la réactivité tombe à zéro pour le Cu^{2+} (13).

La comparaison de nos résultats avec ceux impliquant d'une part l'hématoporphyrine IX dans l'acide acétique glacial (5, 6) et, d'autre part, la tétra(*p*-sulfophényl)porphine dans l'eau (13) indique qu'il n'est pas possible de faire des généralisations quant au mécanisme d'incorporation du métal. Notamment la nature exacte des espèces réactives dépend de la porphyrine considérée et du solvant utilisé.

Les auteurs remercient le Conseil national de recherches du Canada pour la subvention accordée (M.Z.) et pour la bourse d'études post-graduées (G.P.). Le Ministère de l'Education du Québec est remercié pour la subvention accordée (M.Z.). Le professeur Urs Maag, du département d'informatique, de l'Université de Montréal est remercié pour avoir mis au point le programme utilisé.

[3]L'explication originale des auteurs (12) implique une réaction avec Cu^{2+}, catalysée par l'ion OAc^-, qui ne peut pas être distinguée cinétiquement d'une réaction impliquant $CuOAc^+$.

1. P. HAMBRIGHT. Coord. Chem. Rev. **6**, 247 (1971).
2. E. B. FLEISCHER et E. I. CHOI. Inorg. Chem. **2**, 94 (1963).
3. D. A. BRISBIN et R. J. BALAHURA. Can. J. Chem. **44**, 2157 (1966).
4. D. A. BRISBIN et D. J. KINGHAM. Inorg. Chem. **9**, 2034 (1970).
5. D. A. BRISBIN et G. D. RICHARDS. Inorg. Chem. **11**, 2849 (1972).
6. P. HAMBRIGHT et J. JAMES. Inorg. Chem. **12**, 474 (1973).
7. J. K. KOCHI et R. V. SUBRAMANIAN. Inorg. Chem. **4**, 1527 (1965).
8. A. T. A. CHENG et R. A. HOWALD. Inorg. Chem. **7**, 2100 (1968).
9. H. S. HARNED et B. B. OWEN. J. Am. Chem. Soc. **52**, 5079 (1930).
10. R. C. SRIVASTANA, V. D. ANAND et W. R. CARPER. Appl. Spectrosc. **27**, 444 (1973).
11. D. A. BRISBIN et R. J. BALAHURA. Can. J. Chem. **46**, 3431 (1968).
12. L. G. SILLEN et A. E. MARTELL. (Rédacteurs). Stability constants. Special Publication No. 17, The Chemical Society, London. 1964. p. 365.
13. N. JOHNSON, R. KHOSROPOUR et P. HAMBRIGHT. Inorg. Nucl. Chem. Lett. **8**, 1063 (1972).

Can. J. Chem. Downloaded from www.nrcresearchpress.com by 210.87.254.42 on 09/05/12
For personal use only.

Iminosulfuranes (Sulfilimines) Infrared and Ultraviolet Spectroscopic Studies

JITENDRA J. SHAH

Woodson-Tenent Laboratories, Inc., P.O. Box 2135, Memphis, Tennessee 38101

Received February 10, 1975

JITENDRA J. SHAH. Can. J. Chem. **53**, 2381 (1975).

This paper reports the i.r. and u.v. spectra of several *N*-*p*-tolylsulfonylsulfilimines and several new *N*-*p*-ethylbenzenesulfonylsulfilimines have been examined.

JITENDRA J. SHAH. Can. J. Chem. **53**, 2381 (1975).

On a étudié plusieurs *N*-*p*-toluènesulfonyl et *N*-*p*-éthylbenzènesulfonylsulfilimines par spectroscopie infra-rouge et ultraviolette. [Traduit par le journal]

Introduction

Sulfilimines are known as sulfur–nitrogen ylides or ylenes. The *N*-acyl derivatives are especially well known compounds and i.r. (1), u.v. (2), and X-ray data (3) of these have been accumulated in recent years. Four characteristic i.r. absorption bands due to both sulfonyl and sulfilimino groups have been observed and those due to both N—S (IV) and N—S (VI) stretching vibrations appear at nearly the same positions and overlap each other. The configuration of *N*-sulfonylsulfilimine is not established, though the S—N bond has been postulated from an i.r. spectroscopic study (1) to have a double bond character. The u.v. spectra suggest that the sulfilimino group is not an electron donor but an electron acceptor group when conjugated with a phenyl ring.

We have found the amino acids L-methionine and L-cysteine, thioxanthone, diphenylenemethane sulfide, phenothiazine, and phenarsazine chloride to react with chloramine-B, chloramine-T, and a new reagent *N*-chloro-*N*-sodio-*p*-ethylbenzenesulfonamide to obtain the corresponding sulfilimines. We have examined i.r. and u.v. spectra of various sulfilimines and P, As, and Sb analogs.

This paper describes some new data and their relation to structures of different types of sulfilimines.

Experimental

Preparation of Sulfilimines (4)

All the sulfilimines were prepared from the corresponding sulfides and chloramines in the presence of ethyl alcohol. The melting points of sulfilimines are listed in Table 1.

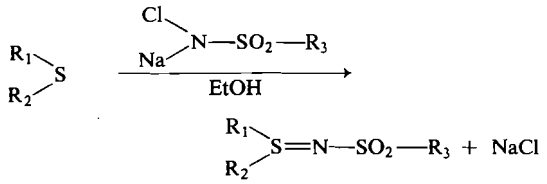

Preparation of Arsinimines and Stibinimines (5)

All the arsinimines and stibinimines were prepared from the reaction of corresponding arsines or stibines with chloramines in the presence of alcohol. The melting points of arsinimines and stibinimines are listed in Table 1.

Results and Discussion

Infrared Spectra

The general *N*-sulfonylsulfilimines may be formulated by either the ylide structure, the ylene structure, or by the resonance hybrid of both.

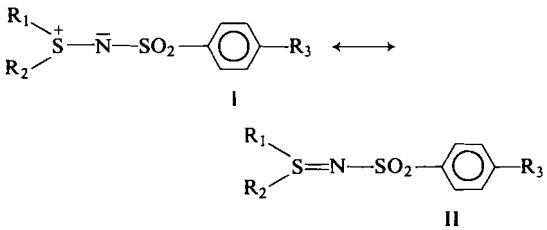

All the sulfilimines have four strong characteristic i.r. absorption bands at around 930–970, 1070–1090, 1130–1140, and 1260–1280 cm^{-1}, respectively. Tsujihara (6) and others have recently examined i.r., u.v., and n.m.r. spectra of various *N*-sulfonylsulfilimines. The two bands 1130–1140 and 1260–1280 cm^{-1} are assigned to symmetrical and asymmetrical stretching vibrations of the SO_2 group. The first band 939–

Can. J. Chem. Downloaded from www.nrcresearchpress.com by 210.87.254.5 on 09/05/12
For personal use only.

Can. J. Chem. Downloaded from www.nrcresearchpress.com by 210.87.254.5 on 09/05/12
For personal use only.

TABLE 1. Infrared and ultraviolet spectra of sulfilimines

Component No.	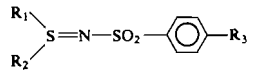 R_1	R_2	R_3	Melting point (°C)	Infrared ν S=N	Infrared ν SO_2 Symmetrical	Infrared ν SO_2 Asymmetrical	Ultraviolet λ_{max} (CH_3OH)
1	$-CH_3$	$-C_4H_8O_2N-$	$-H$	138–139	925	1170	1027, 1210	255.5, 262 267.5, 242.5
2	$-C_3H_6O_2N-$	$-C_6H_6SO_2N-$	$-H$	136–136.5	932	1168	1040, 1220	256, 262 268, 273
3		$-C_{13}H_8OS-$	$-H$	167	932	1135	1032, 1048 1210	255, 285.5 297
4		$-C_{13}H_{10}S-$	$-H$	165	922	1135	1025, 1040 1200	253
5		$-C_{12}H_9NS-$	$-H$	168	923	1132	1035, 1200	244, 302.5
6		$-C_{17}H_{20}N_2S-$	$-H$	—	926	1136	1045, 1199	221
7		$-C_{19}H_{22}N_2S-$	$-H$	—	928	1137	1042, 1200	221.5
8	$-CH_3$	$-C_4H_8O_2N-$	$-CH_3$	134–135	928	1167	1030, 1205	256, 262 267.5, 273
9	$-C_3H_6O_2N-$	$-C_7H_8SO_2N-$	$-CH_3$	138	930	1167	1038, 1218	256, 262 268, 273
10		$-C_{13}H_8OS-$	$-CH_3$	169	952	1158	1052, 1068 1230	255.5, 286 297
11		$-C_{13}H_{10}S-$	$-CH_3$	168	928	1137	1035, 1044 1205	255.5
12		$-C_{12}H_9NS-$	$-CH_3$	122	932	1140	1035, 1049	254, 306
13		$-C_{17}H_{20}N_2S-$	$-CH_3$	—	923	1136	1040, 1196	222
14		$-C_{19}H_{22}N_2S-$	$-CH_3$	—	922	1135	1035, 1198	221
15	$-CH_3$	$-CH_2C_6H_5$	$-C_2H_5$	114–115	945	1132	1088, 1270	269(C_2H_5OH)
16	$-C_2H_5$	$-CH_2C_6H_5$	$-C_2H_5$	152–153	965	1129	1085, 1265	272(C_2H_5OH)
17	$-C_3H_7$	$-CH_2C_6H_5$	$-C_2H_5$	125–126	970	1135	1088, 1268	271(C_2H_5OH)
18	$-C_4H_9$	$-CH_2C_6H_5$	$-C_2H_5$	108–109	965	1160	1095, 1290	273(C_2H_5OH)
19	$-C_5H_{11}$	$-CH_2C_6H_5$	$-C_2H_5$	189–190 (b.p.)	970	1135	1080, 1285	275(C_2H_5OH)
20	$-C_6H_{13}$	$-CH_2C_6H_5$	$-C_2H_5$	200–201 (b.p.)	965	1140	1085, 1288	274(C_2H_5OH)
21	$-C_9H_{19}$	$-CH_2C_6H_5$	$-C_2H_5$	209–210 (b.p.)	930	1170	1090, 1290	275(C_2H_5OH)
22	$-C_2H_5$	$-C_2H_5$	$-C_2H_5$	171	965	1168	1088, 1293	273(C_2H_5OH)

Can. J. Chem. Downloaded from www.nrcresearchpress.com by 210.87.254.5 on 09/05/12
For personal use only.

TABLE 1 (*Concluded*)

Component No.	R_1	R_2	R_3	Melting point (°C)	Infrared: ν S=N	Infrared: ν SO_2 Symmetrical	Infrared: ν SO_2 Assymmetrical	Ultraviolet: λ_{max} (CH_3OH)
23	$-C_3H_7$	$-C_3H_7$	$-C_2H_5$	71–72	960	1170	1095, 1290	273(C_2H_5OH)
24	$-C_4H_9$	$-C_4H_9$	$-C_2H_5$	77–78	965	1168	1095, 1295	274(C_2H_5OH)
25	$-CH_3$	$-C_4H_8O_2N$	$-C_2H_5$	98–99	930	1166	1032, 1203	(CH_3OH) 254.5, 261.5 267, 272.5
26	$-C_3H_6O_2N-$	$-C_8H_{10}SO_2N-$	$-C_2H_5$	107–108	921	1160	1030, 1211	254.5, 261.5 267, 272.5
27		$-C_{13}H_8OS-$	$-C_2H_5$	173	935	1143	1040, 1050 1212	255, 285 296.5
28		$-C_{13}H_{10}S-$	$-C_2H_5$	182	925	1134	1040, 1200	250
29		$-C_{12}H_9NS-$	$-C_2H_5$	120	925	1135	1030, 1040 1205	256.5, 306
30		p-$C_2H_5-C_6H_4-SO_2NH_2$		106–107	935	1175	1098, 1310	274(C_2H_5OH)
31		(p-$C_2H_5-C_6H_4-SO_2NCl)^-Na^+$		185–186	935	1145	1090, 1250	276(C_2H_5OH) 277

Component No.	R_1	M	R_2	Melting point (°C)	Infrared: ν M=N	Infrared: ν SO_2 Symmetrical	Infrared: ν SO_2 Assymmetrical	Ultraviolet: λ_{max} (CH_3OH)
32	$C_{12}H_9AsClN$	As	—H	115	922	1135, 1155	1035, 1195	272, 296, 305
33	$-(C_6H_5)_3-$	Sb	—H	198	920	1135, 1158	1042, 1190	256, 261 266.5
34	$C_{12}H_9AsClN$	As	$-CH_3$	122	925	1135, 1160	1042, 1198	272, 305
35	$-(C_6H_5)_3-$	Sb	$-CH_3$	180	925	1138, 1160	1045, 1200	256, 261.5 266
36	$C_{12}H_9AsClN$	As	$-C_2H_5$	90	920	1133, 1157	1022, 1038 1195	272.5, 302
37	$-(C_6H_5)_3-$	Sb	$-C_2H_5$	190	921	1132	1037, 1195	251, 267

NOTE: All wave numbers in cm^{-1} and λ_{max} in nm.

Can. J. Chem. Downloaded from www.nrcresearchpress.com by 210.87.254.5 on 09/05/12
For personal use only.

980 cm^{-1} has been assigned to the stretching vibration of the N—S(IV) group by Kucsman *et al.* (1) though there are controversies in the assignment of the absorption of S—N stretching vibrations (7, 8).

In the i.r. spectra of *N*-sulfonylsulfilimines ($R_1R_2SNSO_2C_6H_4R_3$, R_1,R_2 = alkyl or aryl group; R_3 = —H, —CH_3, —C_2H_5) the S—N band appears at 930–1012 cm^{-1}. The R_3 groups exert on the S—N and SO_2 groups an inductive effect whereas the R_1 and R_2 groups exert on the S—N group both inductive and conjugative effects. In some of these *N*-*p*-tolyl- and *N*-benzylsulfonylsulfilimines the S—N band appears in the narrow range at 935–987 cm^{-1} (slightly higher wave numbers for the *N*-benzyl derivatives) suggesting the S—N double bond of structure **II** rather than the semipolar bond of structure **I**. The exact position of the band shifts with the nature of R_1 and R_2, generally to lower wave numbers with donor groups and to higher wave numbers with acceptors. In a series of dihaloacetyl sulfilimines ($X_2CHCON{=}SR_1R_2$, where X = Cl,Br) the S—N band is shifted to about 800 cm^{-1} and its position is not influenced by the nature of R_1 and R_2.

The formation of S=N bond is connected with a band near 974 cm^{-1} in the spectra of *S*,*S*-diallyl-*N*-*p*-tolylsulfonylsulfilimines and the spectra of *N*-allyl-*N*-allylthio-*p*-tolylsulfonylsulfilimines. Migration of the allyl absorption appears to have occurred out of the region (9) and instead of this a new band at 830 cm^{-1} appears which corresponds to the $-\overset{+}{S}-\bar{N}-$ single bond. In the spectrum of *S*,*S*-diallyl-*N*-*p*-tolylsulfonylsulfilimine the S—N band is obtained at 974 cm^{-1} between two other bands at 933 and 985 cm^{-1}.

The latter are the wagging vibrations of the hydrogen atoms of the $CH_2{=}CH{-}CH_2$— group. Kucsman argued that the SO_2* band in sulfilimine appears at a wave number considerably higher than that in sulfonate although it might be predicted that both SO_2 bands in the system $-SO_2-\bar{N}$ and $-SO_2-\bar{O}$ would appear in the same region. In the reactions (10) of sulfur dichloride with aromatic and heterocyclic amines and with carboxyamides and sulfamides containing substituents that are stable to chlorination, the corresponding *N*-substituted-*S*,*S*-dichlorosulfilimines are obtained. These sulfilimines have a higher frequency for the S=N band than for other sulfilimines.

$$SO_2^* = \tfrac{1}{2}(\nu_{sym}\,SO_2 + \nu_{asym}\,SO_2)$$

Chloramine-T has four characteristic bands at (ν_{asym} SO_2) 1255 cm^{-1}, (ν_{sym} SO_2) 1130, 1083 cm^{-1}, (ν S=N) 929 cm^{-1}, while a new *N*-chloro-*N*-sodio-*p*-ethylbenzenesulfonamide has also four characteristic bands at (ν_{asym} SO_2) 1250 cm^{-1}, (ν_{sym} SO_2) 1145, 1090 cm^{-1}, (ν S=N) 935 cm^{-1}.

The characteristic i.r. spectra of several sulfilimines, a new *N*-chloro-*N*-sodio-*p*-ethylbenzenesulfonamide and other related compounds are listed in Table 1.

Ultraviolet Spectra

In the u.v. spectra there is practically no shift of λ_{max} when R_1 and R_2 change from dialkyl to alkylphenyl or diphenyl. The resonance interaction between the lone pair of electrons on the sulfur atom with the phenyl ring is well known in sulfides (11*a* and 11*b*, p. 474). The u.v. spectra of a series of oxysulfilimines have been reported (12) and claimed to provide evidence for the use of 3d orbitals of sulfur. The sulfoximines have been assigned a near tetrahedral configuration (13, 14), and by analogy with the known sulfone geometry (15), a coplanar conformation of the two phenyl rings has a low probability.

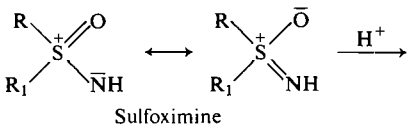

Sulfoximine

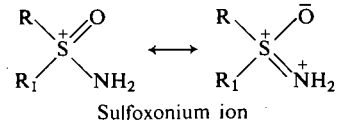

Sulfoxonium ion

The conjugation mechanism indicated is donation of carbon p orbitals into suitable unoccupied sulfur d orbitals (11*b*, p. 466). The sulfur atom again acts as an acceptor. This postulated donor–acceptor mechanism is strengthened by the enhanced bathochromic shift of when R = $H_2N{-}C_6H_4$— and R_1 = C_6H_5. In aqueous solution the spectra are very similar to those in ethanol, but in acid the sulfoximines showed slight

bathochromic shifts. It is known that the spectra of 4-*p*-aminophenyl methyl sulfone (16) and 4-aminophenyl sulfone (17) revert precisely to that of the parent sulfone in acid solution, the added proton forming the corresponding anilium ions. The spectra of the aminophenyl sulfoximines show that the site of attachment of the proton is the sulfoximine nitrogen. This will increase the formal charge near or on the sulfur and the bathochromic shifts observed are thus due to this enhancement in the acceptor capacity of the sulfur. The improved interaction of d orbitals with p or π orbitals with increased positive charge on the element containing the d orbital has been discussed theoretically (18).

The characteristic u.v. spectra of several sulfilimines, a new *N*-chloro-*N*-sodio-*p*-ethylbenzenesulfonamide and other related compounds are listed in Table 1.

From these i.r. and u.v. spectroscopic studies, *N*-sulfonylsulfilimine is considered to be represented better by the ylide structure in which the charges on the S atom and the N atom are considerably delocalized with strong dπ conjugation into S(IV)—N—S(VI) bondings. Therefore the S—N bond of the sulfilimino group is considered to be essentially semipolar.

The author wishes to thank Woodson-Tenent Laboratories, Inc., for their cooperation and research facilities.

1. A. KUCSMAN, I. KAPOVITS, and F. RUFF. Acta Chim. Acad. Sci. Hung. **40**, 75 (1964); Tetrahedron, **22**, 1575 (1966).
2. A. KUCSMAN, F. RUFF, and I. KAPOVITS. Acta Chim. Acad. Sci. Hung. **50**, 325 (1966).
3. A. KALMAN. Acta Crystallogr. **22**, 501 (1967).
4. M. A. MCCALL, D. S. TARBELL, and MARY ANN HAVILL. J. Am. Chem. Soc. **73**, 4477 (1951).
5. F. A. MANN. J. Chem. Soc. 958 (1932).
6. K. TSUJIHARA, N. FURUKAWA, and SHIGERU OAE. Bull. Chem. Soc. Jap. **43**, 2153 (1970).
7. J. N. BAXTER, J. CYMORNAN CRAIG, and J. B. WILLS. J. Chem. Soc. 669 (1955). W. AUGUS, A. H. LECKIE, and J. T. WILLIAMS. Trans Faraday Soc. **34**, 793 (1938).
8. Y. TANAKA and Y. TANAKA. Chem. Pharm. Bull. (Tokyo), **13**, 399 (1965); 13, 858 (1965).
9. A. S. F. ASH, F. CHALLENGER, and D. GREENWOOD. J. Chem. Soc. 1877 (1951).
10. L. N. MASKOVSKII, Z. I. SHAKOL, and E. S. LERCHENKP. J. Org. Chem. U.S.S.R. **6**, 496 (1970).
11. (*a*) C. C. PRICE and S. OAE. Sulfur bonding. Ronald Press, N.Y. 1962. (*b*) H. H. JAFFE and M. ORCHIN. Theory and application of ultraviolet spectroscopy. J. Wiley & Sons, N.Y. 1962.
12. M. BARASH. Chem. Ind. 1261 (1964).
13. M. BARASH. Nature, **187**, 591 (1960).
14. G. KRESZE and B. WUSTROW. Ber. Dtsch. Chem. Ges. **45**, 2652 (1962).
15. S. C. ABRAHAM and J. G. SIME. Acta Crystallogr. **13**, 1 (1960).
16. E. A. FEHNEL and H. CARMACK. J. Am. Chem. Soc. **72**, 1292 (1950).
17. A. MANGINI and R. PASSERINI. Bull. Sci. Fac. Chim. Ind. Bologna, **8**, 133 (1950).
18. D. P. CRAIG *et al.*: J. Chem. Soc. 332 (1954), D. P. CRAIG. J. Chem. Soc. 4895 (1956).

Can. J. Chem. Downloaded from www.nrcresearchpress.com by 210.87.254.5 on 09/05/12
For personal use only.

Thione Photochemistry: The *Peri* Cyclization of some Polycyclic Aromatic Thiones[1,2]

A. Cox,[3] D. R. Kemp, R. Lapouyade,[4] P. de Mayo, J. Joussot-Dubien,[5] and R. Bonneau[5]

Photochemistry Unit, Department of Chemistry, The University of Western Ontario, London N6A 5B7

Received March 10, 1975

A. Cox, D. R. Kemp, R. Lapouyade, P. de Mayo, J. Joussot-Dubien, and R. Bonneau. Can. J. Chem. **53**, 2386 (1975).

A number of polycyclic aromatic thiones have been prepared from the corresponding ketones. Several of the thiones in which there is a free *peri* position cyclize, on excitation in the $\pi^* \leftarrow n$ band, to give thiophene derivatives. The structures of these were proven by application of physical methods and by desulfurization to the corresponding benzyl derivatives. The formal hydrogen 1,3 migration involved was, in one case, shown to be intermolecular by the incorporation of deuterium, from deuterium oxide, during the irradiation. In the case of the α-naphthyl derivative, the mechanism of the reaction has been investigated and it has been concluded that the n,π^* singlet is the responsible entity.

A. Cox, D. R. Kemp, R. Lapouyade, P. de Mayo, J. Joussot-Dubien et R. Bonneau. Can. J. Chem. **53**, 2386 (1975).

On a préparé un nombre de thiones polycycliques aromatiques à partir des cétones correspondantes. Plusieurs des thiones, ayant une position *péri* libre, cyclisent par excitation de la bande $\pi^* \leftarrow n$ et conduisent ainsi à des dérivés du thiophène. La preuve de la structure de ces dérivés est obtenue par des méthodes physiques et par désulfurisation jusqu'au dérivés benzyliques correspondants. On a démontré, en incorporant un deutérium par l'eau deutériée pendant l'irradiation, que la migration 1,3 impliquée, dans un cas, se fait par un mécanisme intermoléculaire. Le mécanisme de la réaction est étudié sur le dérivé α-naphtyl; on en déduit que l'état singulet, n,π^* est l'entité responsable. [Traduit par le journal]

The literature records extensive preoccupation over the last 50 years with the photochemistry of the carbonyl group. Only much more recently has the thiocarbonyl group attracted attention and then for a very limited selection of environmental situations.[6]

Up to the present, studies of aromatic thiones have been restricted, essentially, to that of thiobenzophenone and, indeed, with the exception of certain substituted thiobenzophenones and of 1-thiobenzoylnapthalene (2), no other simple substituted aryl thiones were known. We have shown that for the former the lowest triplet state was most probably n,π^*[7] and it is this state that has been generally invoked in the photochemical cycloadditions of most aromatic thiones (4, 5).[8]

We report here the preparation of some polycyclic aromatic thiones and a photocyclization of these substances proceeding through the n,π^* singlet state.

Results and Discussion

The thiones **1***b*–**9***b* were prepared by benzoylation of the appropriate aromatic hydrocarbon, followed by conversion of the ketone to thione with hydrogen chloride and hydrogen sulfide. The ketones, with the exception of **7***a* were known substances. The position of the functional group had, however, not been unambiguously established in the cases of **5***a* and **6***a* (7, 8) and confirmation was obtained as follows. Compound **5***a* was prepared by an alternative route from 3-bromofluoranthene by reaction with cuprous cyanide, followed by Grignard reaction with phenylmagnesium bromide. The structure of 3-bromofluoranthene appeared to be assured

[1]Photochemical Synthesis Part 61. This is the 19th of a series on thione photochemistry.

[2]Publication No. 131 from the Photochemistry Unit, University of Western Ontario.

[3]On leave from Department of Molecular Sciences, University of Warwick, Coventry, England.

[4]NATO Postdoctoral Fellow, 1971–1972.

[5]Laboratoire de Chimie Physique, 33 Talence, France.

[6]For a review, see ref. 1.

[7]For a discussion of the absorption and emission spectroscopy of thioketones see ref. 3.

[8]An exception is the addition of thiobenzophenone to acrylonitrile (6) which proceeds through an upper singlet.

Can. J. Chem. Downloaded from www.nrcresearchpress.com by 210.87.254.40 on 09/05/12
For personal use only.

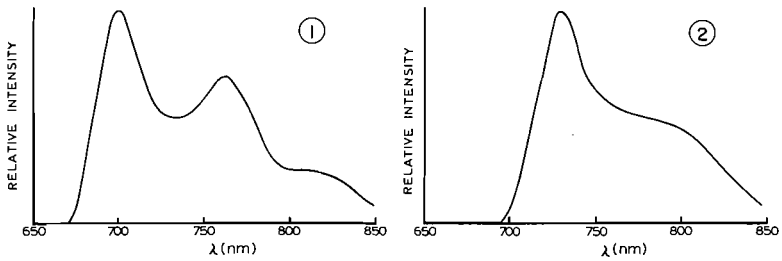

FIG. 1. Emission from 2-thiobenzoylnaphthalene (EPA) at 77 K.
FIG. 2. Emission from 1-thiobenzoylnaphthalene (EPA) at 77 K.

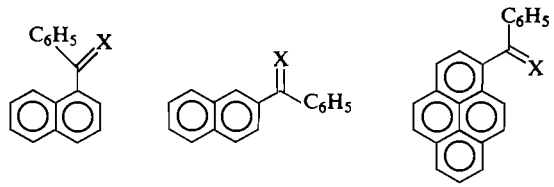

1*a*,*b*

2*a*,*b*

3*a*,*b*

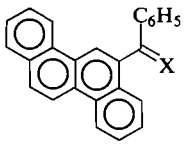

4*a*,*b*

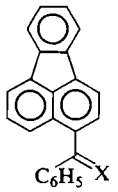

5*a*,*b*

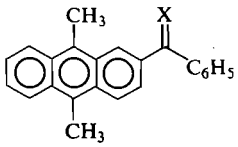

6*a*,*b*

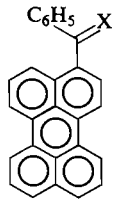

7*a*,*b*

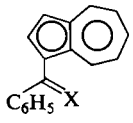

8*a*,*b*

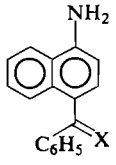

9*a*,*b*

1*a* through 9*a*, X = O
1*b* through 9*b*, X = S

(9, 10). Compound **6***a* was shown to have the indicated structure by oxidation to the known 2-benzoylanthraquinone. Compound **7***a* was not known and assignment of the position of the benzoyl group rests on the known preferred position of attack in perylene and the co-formation of 3,9-dibenzoylperylene.

The salient features of the absorption spectra of the thiones are listed in Table 1. At room temperature all compounds exhibit a relatively weak, structureless, long wavelength absorption which (except for **2***b*) shows a blue shift with increasing solvent polarity (Table 1). This band is characteristic of aromatic thiocarbonyl compounds and has been assigned to the n,π* state (11, see also footnote 7). The absorption spectrum of **1***b* has been previously reported (12).

At 77 K in a rigid matrix of EPA (ether–isopentane–ethanol, 5:5:2), the first absorption band is partially resolved into vibronic bands as has been observed for a number of thioketones and, assuming that the first resolved band is the O—O band, the singlet energies are given in Table 1 together with the spacings between the vibronic bands. In the case of **1***b*, **2***b*, and possibly also in **4***b*, a weak band appeared on the long wavelength side of the (n,π*) band at 77 K. A similar band had previously been observed for a number of thiocarbonyl compounds (13) and has been tentatively assigned to the singlet → triplet transition. Attempts to observe a similar band in the other compounds using more concentrated solutions proved unsuccessful owing to their low solubility.

The luminescent properties of all the compounds have also been measured. These were determined at 77 K in EPA, with the exception of **7***b* where, due to its low solubility, methyl acetate – ether (2:3) was used as solvent. The emission spectrum of **2***b*, observed following excitation at 390 or 550 nm, is shown in Fig. 1, (τ 66 μs). The emission from compound **1***b* is similar to that from **2***b* (see Fig. 1). Compounds **3***b*, **4***b*, and **5***b* show rather weak luminescence, the shape of which is similar to **1***b*, but no lifetime measurements were possible. No thione

Can. J. Chem. Downloaded from www.nrcresearchpress.com by 210.87.254.40 on 09/05/12
For personal use only.

TABLE 1. Absorption spectra and triplet energies of the thiones

Compound	Absorption spectra at room temperature λ_{max}, nm (log ε)		Absorption spectra at 77 K		E_T (kJ/mol)
	In cyclohexane	In ethanol ether (1:1)	O—O band (nm) and E_s (kJ/mol)	Band spacing (cm^{-1})	
1*b*	618 (2.18), 385 sh (3.43) 371 (3.47), 316 (4.19)	609 (2.21), 375 (3.49) 317 (4.20)	635 (188.4)	1087	164.0
2*b*	610 (2.34), 384 (3.73) 367 (3.82), 318 (4.28)	609 (2.37), 387 sh (3.80) 322 (4.31)	627 (190.8)	1087	172.4
3*b*	622 (2.56), 442 (3.79) 424 (3.79), 383 (3.62) 330 (4.46)	612 (2.62), 436 (3.79) 382 (3.59), 345 sh (4.39) 329 (4.47)	640 (186.9)	959	160.7
4*b*	622 (2.31), 397 (3.64) 327 sh (4.35), 317 (4.38)	610 (2.38), 403 (3.66) 330 sh (4.37), 316 (4.38)	632 (189.3)	928	164.0
5*b*	621 (2.52), 387 (4.10) 318 (4.27)	613 (2.55), 390 (4.09) 340 sh (4.21), 323 (4.28)	641 (186.6)	1121	159.4
6*b*	614 (2.23), 483 (3.71) 455 (3.66), 428 (3.51) 395 (3.74), 374 (3.94) 345 (4.37)	607 (2.36), 451 (3.79) 457 sh (3.72), 394 (3.79) 374 (4.04), 344 (4.46)	628 (190.5)	970	
7*b* (in benzene)	616 (2.74), 471 (4.29) 444 (4.31), 329 (3.77)		—	—	—
8*b*	612 (2.83), 567 (2.86) 441 (4.27), 324 (4.16)	600 (2.89), 448 (4.23) 325 (4.12)	635 (188.4)	1059	
9*b*	615 (2.37), 425 (3.70) 318 (4.00)	590 (2.85), 465 (3.98) 321 (3.98)	620 (192.9)	849	

luminescence could be detected from **6***b*, **7***b*, and **8***b*. The spectral position and general similarity to the emission observed from other thioketones[7] suggests that the emission is phosphorescence from a $^3(n,\pi^*)$ state. Assuming this to be true, the triplet energies (E_T) are given in Table 1.

All the thiones were excited by irradiation (>520 nm) into the long wavelength (n,π*) band. Products were found for thiones **1***b*, **3***b*, **4***b*, and **7***b*, whereas irradiation 5–10 times longer of the others, led only to recovery of starting material. All the reactive compounds had free *peri* positions, (and were derived from alternant hydrocarbons) and the structures of the products, **1***c*, **3***c*, and **4***c*, indicated that cyclization had occurred at this position; that in **7***c* is assumed by analogy. The structures of the cyclized products followed from their constitutions, their Raney nickel desulfurization to the corresponding known benzyl derivatives and the observation of a signal for a benzylic proton in their n.m.r. spectra close to 6.2 p.p.m. (14) (except in the case of **7***c*, which was found too insoluble for n.m.r. spectrum determination). Compound

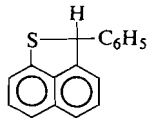

1*c*

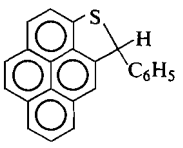

3*c*

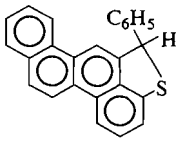

4*c*

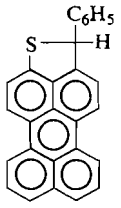

7*c*

1*c* has been obtained by a multistep synthesis previously (15) and the physical data obtained are in agreement with the present observations.

A plausible reaction pathway is that indicated in Scheme 1, where the asterisks may represent zero, one, or two electrons.

Along the reaction pathway at some point a

Can. J. Chem. Downloaded from www.nrcresearchpress.com by 210.87.254.40 on 09/05/12
For personal use only.

TABLE 2. Transients observed on flash photolysis

Compound	Concentration[a] (M)	Monitoring λ (nm)	Decay rate[b]
1*b*	8.9×10^{-4}	550	1.41×10^{7}
2*b*	7.4×10^{-4}	550	5×10^{6}
3*b*	2.5×10^{-5}; 6.2×10^{-6}	No transients detected	
4*b*	3.2×10^{-5}	450	7.7×10^{6}
5*b*	5.9×10^{-5}	470	6.85×10^{7}
6*b*	2.7×10^{-4}	540	2.5×10^{6}
7*b*	1.18×10^{-4}	No transients detected	
8*b*	2.8×10^{-5}		
9*b*	9.1×10^{-4}; 5.7×10^{-4}		

[a]In cyclohexane.
[b]A combination, most probably, of unimolecular and bimolecular rate processes.

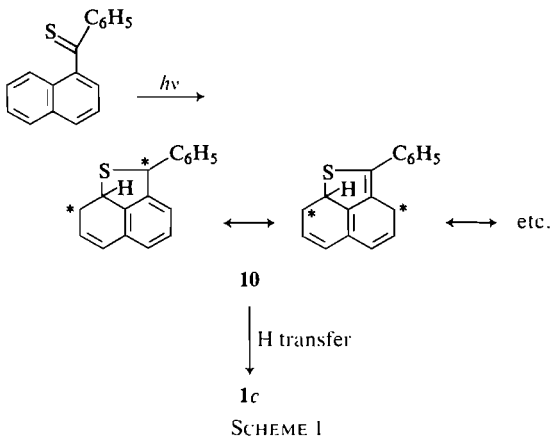

SCHEME 1

hydrogen atom must be transferred. This could be, in principle, a photochemical 1,3-proton shift (suprafacial) or a two-step intermolecular process. We were able to demonstrate that the transfer could involve a discrete intermediate by showing that the hydrogen transfer could be intermolecular. Irradiation of **1***b* in acetonitrile containing deuterium oxide led, essentially quantitatively, to the incorporation of one deuteron at the benzylic position. We conclude tentatively that the species represented by the formalism **10** is a singlet and dipolar. This, in itself, does not require that the reaction pathway only include singlets since intersystem crossing along the reaction coordinate, facilitated by the presence of the sulfur atom, is not to be excluded.

The multiplicity of the reaction was then studied. The number of triplet quenchers available having suitable energies, chemical and spectroscopic properties are few: two, of different types, were selected. The quantum yield of the reaction in benzene is 1.2×10^{-3} (excitation ~577 nm). In the presence of 1.2×10^{-2} M perylene (E_T = 150.5 kJ/mol) a value of 1.29×10^{-3} was obtained: identical with the unquenched reaction within experimental error. In the presence of cyclooctatetraene (0.29 M) the quantum yield remained at 1.28×10^{-3} and increase of quencher concentration to 0.59 M produced no change. Now, in the case of quenching by perylene, assuming the quenching to be diffusion controlled, then it should have been observed with a species of lifetime of the order of 10^{-8} s, or longer. With the same assumption for cyclooctatetraene, quenching should have been observed for a triplet of lifetime $> 10^{-9}$ s. Some doubt is attached to the use of cyclooctatetraene since its triplet energy is not known exactly. It has been shown, however, that it will quench the lowest triplets of thiobenzophenone and Michler's thione at slightly lower than diffusion controlled rates (16).

It was, thus, necessary to show that the triplet of **1***b* had, indeed, a lifetime which would have permitted quenching.

Several of the compounds were studied by flash photolytic techniques. Using a doubled ruby laser (16) the triplet decay rates determined in cyclohexane at the concentrations used are given in Table 2. A more detailed study was made of compound **1***b* using a tripled neodymium laser (λ 353 nm).[9] In benzene solution and using concentrations up to 1.5×10^{-3} M, a plot was obtained, monitoring the transient at 550 nm, of reciprocal lifetime against concentration. A

[9]The technique used has already been described: see ref. 17.

Can. J. Chem. Downloaded from www.nrcresearchpress.com by 210.87.254.40 on 09/05/12
For personal use only.

TABLE 3. Quantum yields of cyclization of **1***b*

Concentration ($M \times 10^3$)	Solvent	Quantum yield ($\Phi \times 10^3$)
4.8	Benzene	1.20±0.1
4.4	Benzene–MeOH (4:1)	1.80±0.1
4.3	Benzene–HOAc (4:1)	1.47
4.4	CH_3CN	2.61
4.4	CH_3CN–HOAc (4:1)	3.0
4.8	Benzene (1.2×10^{-2} perylene)	1.29
4.8	Benzene (0.29 *M* COT)	1.28
4.8	Benzene (0.588 COT)	1.30

unimolecular decay rate of $1.0 \pm 0.1 \times 10^7\ s^{-1}$ resulted, together with a bimolecular rate constant for quenching of the triplet by ground state thione of $1.8 \pm 1 \times 10^9\ M^{-1}\ s^{-1}$. The latter as observed with the triplets of other aromatic thiones (16) and of adamantanethione (18) was close to diffusion controlled. The large error in these determinations is a consequence of the limited concentration range possible.

The lifetime of $\sim 10^{-7}$ s should have permitted quenching and it was indeed shown that in $10^{-3}\ M$ solution in benzene, the transient could be quenched by cyclooctatetraene with a bimolecular rate constant of $2.2 \pm 1 \times 10^9\ M^{-1}\ s^{-1}$, also close to diffusion controlled. Since no quenching was observed in the quantum yield of cyclization measurements one must conclude that the triplet is not involved in this transformation and that the responsible species is the n,π* singlet.

The mechanism as formulated involves charge separation and so might be thought to be facilitated by a polar solvent. Small increases were indeed observed (Table 3) but in the most polar system used, which contained the proton donor acetic acid, the quantum yield was rather more than 2½ times that in benzene, yet nevertheless remained very small. The inefficiency of the process may be due to at least two factors. In the first place the intermediate **10** may be formed inefficiently, the greater part of the singlet energy being lost in rapid intersystem crossing. Alternatively, it may be that the intermediate **10** is formed efficiently but reverts almost equally efficiently to the ground state, the overall process being an intramolecular chemical quenching. Under such circumstances the intersystem crossing yield would be low and this would be compatible with the weak emissions observed and in particular with the important difference in intensity of emission between **1***b* and **2***b*.

The question arises as to why a similar reaction is not observed for ketones. The explanation may be, aside from geometrical changes caused by changing oxygen for sulfur, that a lowest n,π* state is required, and that in virtually all polycyclic aromatic ketones in which this might be observed the lowest energy singlet state is π,π*. The exception is that of the 1-benzoylnaphthalene but even here the n,π* and π,π* states may be close enough to perturb each other.

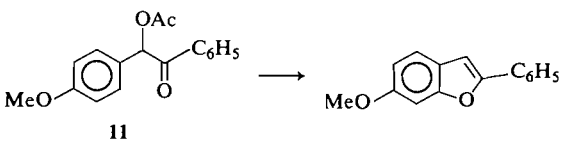

11

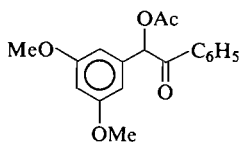

12

To induce the cyclization with a ketone it is required that the aromatic nucleus be separated from the ketone by a saturated carbon to provide both the equivalent of a *peri* position, and to maintain a lowest n,π* singlet state. Such a process has, in fact, been realized by Sheehan *et al.* (19). In their case, however, that of **11**, the reaction is completely quenchable whilst that of **12** is not. As discussed by the authors this either indicates a change of state, or a lifetime $> 10^{-10}$ s for a reactive triplet in the second case.

Can. J. Chem. Downloaded from www.nrcresearchpress.com by 210.87.254.40 on 09/05/12
For personal use only.

Can. J. Chem. Downloaded from www.nrcresearchpress.com by 210.87.254.40 on 09/05/12
For personal use only.

Experimental Section

General

Melting points were determined on a Kofler block and are uncorrected. Mass spectra were obtained on a Varian M66 spectrometer.

The apparatus used for the recording of emission spectra has been described elsewhere.[7] For the present work an RCA C31034 photomultiplier was used cooled to $-35°$. Samples for emission studies or flash photolysis were degassed by the freeze–pump–thaw method to a residual pressure of $< 5 \times 10^{-5}$ Torr.

The apparatus for nanosecond flash photolysis incorporated a pulsed ruby laser, frequency doubler, a model 82-410 Jarrell-Ash monochromator, together with a Xe arc pulsing unit (Northern Precision). The microsecond flash apparatus utilized a Spex monochromator equipped with an EMI 6256B photomultiplier.

Materials

1-Benzoylnaphthalene (**1***a*) was prepared as described previously (20), m.p. 75° (lit. (20) m.p. 76°) and shown to be free of the 2-benzoyl derivative by t.l.c. The 2-benzoylnaphthalene (**2***a*) (Pfalz and Bauer) was crystallized from MeOH, m.p. 80° (lit. (21) m.p. 81°). 1-Benzoylpyrene (**3***a*), prepared by a reported method (22) was obtained (from ethanol) in two crystalline forms m.p. 127–128° (lit. (22) m.p. 126°) and 118°. The latter on melting and resolidifying had m.p. 127–128° and the latter form was also obtained on sublimation. 6-Benzoylchrysene (**4***a*) (23) had m.p. 191° (lit. (23) m.p. 192°) from benzene–alcohol. 3-Benzoylfluoranthene (**5***a*) (24) was purified by chromatography and crystallized from ethanol, m.p. 128–129° (lit. (24) m.p. 129–130°). 1-Benzoylazulene (**8***a*) (25), 1-amino-4-benzoylnaphthalene (**9***a*) (26), and 1-thiobenzoylnaphthalene (**2***c*) (12) were prepared by reported methods.

3-Cyanofluoranthene

3-Bromofluoranthene (6 g) and CuCN (5 g) in *N*-methylpyrrolidone (50 ml) was maintained at 180° for 5 h and the product poured into aqueous ammonia. Isolation with benzene and chromatography on alumina gave the cyanide, m.p. 114° (lit. (24) m.p. 112°).

3-Benzoylfluoranthene

3-Cyanofluoranthene (2 g) in anhydrous benzene (50 ml) was added to the Grignard reagent from bromobenzene (7.9 g) and magnesium turnings (1.2 g) in 100 ml ether. The mixture was refluxed (4 h) and then decomposed with aqueous sulfuric acid (100 ml, 10 *N*) followed by 5 h further reflux. Isolation with benzene followed by chromatography on alumina gave **5***a* (47%) identical in all respects with that obtained by the previously described procedure.

2-Benzoyl-9,10-dimethylanthracene (8)

This compound (**6***a*) was obtained in two crystalline forms, m.p. 141–142° and 131° (lit. (8) m.p. 145°) from benzene–ethanol. Oxidation with chromic acid in acetic acid gave the anthraquinone, m.p. 217° (lit. (8) m.p. 216–217°).

3-Benzoylperylene (7a)

Anhydrous aluminum chloride (1 g) was added to a solution of perylene (1.8 g) and benzoyl chloride (1 g) in CS_2 (100 ml) and stirred for 3 h at room temperature. After decomposition with water and chromatography of the product on alumina, perylene (67%), **7***a* (20%), and 3,9-dibenzoylperylene (1.5%) (m.p. 291–292°; lit. (27) m.p. 293°) were obtained. The monobenzoyl derivative had m.p. 208°.

Anal. Calcd. for $C_{27}H_{16}O$: C, 90.98; H, 4.53; O, 4.49. Found: C, 90.84; H, 4.57; O, 4.80.

2-Thiobenzoylnaphthalene (2b)

2-Benzoylnaphthalene (1.1 g) was dissolved in 100 ml methanol at $-5°$ (N_2) and HCl and H_2S passed through for 4 h, H_2S passage being continued for a further 4 h. The blue crystals were filtered, dried, and sublimed to give **2***b* (0.9 g) m.p. 79°, whose i.r. spectrum showed no carbonyl band.

Anal. Calcd. for $C_{17}H_{12}S$: C, 82.24; H, 4.87; S, 12.89. Found: C, 82.01; H, 4.76; S, 12.21.

1-Thiobenzoylpyrene (3b)

1-Benzoylpyrene (2 g) was dissolved in a mixtue of 20 ml benzene and 100 ml alcohol, and HCl–H_2S passed through for 5½ h at 0°. After neutralization ($NaHCO_3$) the product was chromatographed on Florisil. Elution with CCl_4 – light petroleum gave black crystals (1.46 g), m.p. 141° (methanol).

Anal. Calcd. for $C_{23}H_{14}S$: C, 85.70; H, 4.38; S, 9.93. Found: C, 85.34; H, 4.56; S, 9.99.

6-Thiobenzoylchrysene (4b)

6-Benzoylchrysene was converted into the thione as described for (**2***b*). The green crystals (2 g, 94%; m.p. 184–185° (benzene–methanol)) showed carbonyl stretch in the i.r.

Anal. Calcd. for $C_{25}H_{16}S$: C, 86.18; H, 4.43; S, 9.19. Found: C, 86.21; H, 4.57; S, 9.48.

3-Thiobenzoylfluoranthene (5b)

This was prepared as was **3***b* in 90% yield and the green crystals had m.p. 142° (benzene–ethanol).

Anal. Calcd. for $C_{23}H_{14}S$: C, 85.70; H, 4.38; S, 9.93. Found: C, 85.85; H, 4.38; S, 10.01.

9,10-Dimethyl-2-thiobenzoylanthracene (6b)

This was prepared as described for **3***b*. It was obtained as black crystals (methanol), m.p. 144–146° (86%). The continuing presence of ketone (i.r.) made it impossible to obtain satisfactory analyses for this compound.

3-Thiobenzoylperylene (7b)

The ketone was treated, in methanol–benzene solution, as for **3***b*. The precipitate which formed (95%) as brown crystals, insoluble in the usual solvents, had m.p. 258°.

Anal. Calcd. for $C_{27}H_{16}S$: C, 81.08; H, 4.33; S, 8.59. Found: C, 81.21; H, 4.43; S, 8.30.

1-Thiobenzoylazulene (8b)

The ketone (560 mg) in 80 ml MeOH was treated at 0° with HCl–H_2S for 4 h (HCl) and 6 h (H_2S). After neutralization ($NaHCO_3$) and isolation with chloroform the product was chromatographed on Florisil. Light petroleum elution gave **8***b* as black crystals (98 mg, 16%), m.p. 68° (light petroleum).

Anal. Calcd. for $C_{17}H_{12}S$: C, 82.24; H, 4.87; S, 12.89. Found: C, 81.60; H, 5.07; S, 12.70.

1-Amino-4-thiobenzoylnaphthalene (9b)

The ketone (3 g) was dissolved in MeOH (100 ml) and HCl and H_2S passed through for 4 and 8 h, respectively, at 0°. The crystalline precipitate was collected, being the hydrochloride (2.8 g).

Can. J. Chem. Downloaded from www.nrcresearchpress.com by 210.87.254.40 on 09/05/12
For personal use only.

Anal. Calcd. for $C_{17}H_{14}NSCl$: C, 68.10; H, 4.66; N, 4.66; S, 10.68; Cl, 11.85. Found: C, 67.78; H, 4.73; N, 4.60; S, 10.72; Cl, 11.95.

The hydrochloride (1.4 g) in MeOH was neutralized with aqueous sodium bicarbonate and, after isolation, the product was crystallized from methanol (0.91 g, 74%) in brown crystals, m.p. 74°.

Anal. Calcd. for $C_{17}H_{13}NS$: C, 77.56; H, 4.94; N, 5.32. Found: C, 77.86; h, 5.22; N, 5.26.

Cyclizations

These were performed using a 450 W medium pressure lamp in conjunction with a Corning filter C53-68 to absorb wavelengths below 520 nm. Solutions were degassed and irradiated until decolorized.

2-Phenyl-2H-naphtho[1,8bc]thiophene (1c)

The thione (240 mg) in 15 ml benzene was irradiated for 26 h. The product was chromatographed through Florisil to give pale yellow crystals (51%; m.p. 101°; lit. (15*c*) m.p. 100–101°).

Anal. Calcd. for $C_{17}H_{12}S$: C, 82.24; H, 4.87; S, 12.89. Found: C, 82.25; H, 4.42; S, 12.42.

The same product was obtained using MeCN as solvent (20 ml) containing 1 ml MeOH or water. In the presence of 1 ml D_2O, 2-phenyl-2*D*-naphtho [1,8*bc*] thiophene was obtained. The n.m.r. was identical in all respects with the protium compound except for the complete absence of a singlet at δ 6.18; mol. wt. (mass spectrum) 249.

The possibility of H/D exchange occurring in the final product was excluded by the appropriate control.

2-Phenyl-2H-pyreno[1,10bc]thiophene (3c)

This was obtained in 59% yield, after similar irradiation, as pale yellow crystals, m.p. 155° (methanol); $\lambda_{max}(C_6H_{12})$ 386, 367, 361, 349, 292, 230 nm (ε 5400, 1500, 13 800, 15 300, 12 350, 42 500); *m/e* (M^+) 322; singlet at 6.25 p.p.m. in the n.m.r. spectrum.

Anal. Calcd. for $C_{23}H_{14}S$: C, 85.70; H, 4.38; S, 9.93. Found: C, 86.14; H, 4.42; S, 9.47.

2-Phenyl-2H-chryseno[1,2bc]thiophen (4c)

This was similarly obtained in 58% yield, m.p. 183–184° (benzene); $\lambda_{max}(C_6H_{12})$ 377, 360, 344, 316, 275, 267 nm (ε 5000, 9700, 10 800, 6400, 44 450, 45 000); *m/e* 348 (M^+); singlet at 6.2 p.p.m. in the n.m.r. spectrum.

Anal. Calcd. for $C_{25}H_{16}S$: C, 86.18; H, 4.63; S, 9.19. Found: C, 86.18; H, 4.95; S, 9.02.

2-Phenyl-2H-peryleno[1,12bc]thiophen (7c)

The thione (28 mg) was suspended in 20 ml benzene and irradiated for 3 h with shaking after which all the material was in solution. After chromatography on silica the product was obtained as brown crystals (60%) m.p. > 350°; $\lambda_{max}(C_6H_{12})$ 473, 445, 422, 357, 338, 240, 228, 218 nm (ε 18 600, 16 200, 10 000, 11 000, 13 800, 5900, 7700, 90 000); *m/e* 372.09823 (M^+) (calcd. 372.09726).

Desulfurization of the Thiophene Derivatives

A solution of the thiophene in ethanol was refluxed with Raney nickel previously deactivated by heating for 3 h with acetone. The reactions were followed by t.l.c. and interrupted before the appearance of over-reduction compounds. The results are given in Table 4.

Oxidation of 2-Phenyl-2H-naphtho[1,8bc]thiophen

The thiophen (264 mg) *m*-chloroperbenzoic acid (0.48 g) and sodium carbonate (800 mg) were stirred in 10 ml ethylene dichloride for 2 h at room temperature. Isolation of the product after dilution with water and washing gave the corresponding sulfoxide (97%), m.p. 167–168° (lit. 168–169° (15*c*)).

Quantum Yields

For irradiations ~577 nm the light from a mercury source (HBO 200 W) was passed through a potassium dichromate–copper sulfate filter solution (29). The actinometric solution was Reinecke's salt (30). For the 366 nm line Corning filter CS-52 and CS-7-60 were employed and ferrioxalate actinometry (31). Solutions of **1***b* were degassed. After irradiation the solution was evaporated under nitrogen and a solution of 100 mg hydroxylamine hydrochloride in 20 ml methanol containing 5 drops of pyridine was added and with the disappearance of the thione color the solvent was evaporated below 40° under nitrogen. The residue was dissolved in benzene and filtered through 20 g silica gel.

A solution of known concentration of fluoranthene was added to the eluent after evaporation and analysis performed by vapor phase chromatography using a glass column packed with 3% SE 30 on Chromasorb W at 180°.

Control experiments indicated that the maximum error introduced by this treatment was ±6%. The above sequence was necessary since no means was found of separating the thione and cyclized material by v.p.c.

The authors wish to thank Ms. J. Pereyre for assistance with the neodymium flash photolyses and the National Research Council of Canada and CNRS (France) for funds under an exchange travel agreement.

TABLE 4. Raney nickel desulfurizations of thiophenes

Thiophene	Time (h)	Yield of benzyl derivative (%)	Recovered thiophene (%)	Melting point (°C)	
				Experiment	Literature (ref. no.)
1*c*	12	39	45	55–56	55(28)
3*c*	24	37	44	89	89(22)
4*c*	24	60	27	200	200–203(23)
7*c*	24	42	36	177	*(present work)

*Anal. Calcd. for $C_{27}H_{18}$: C, 94.70; H, 5.30. Found: C, 94.66; H, 5.33. This substance was also obtained by refluxing 3-benzoylperylene, 99% hydrazine hydrate and potassium hydroxide in diethylene glycol.

1. D. PAQUER. Int. J. Sulfur Chem. **8**, 173 (1973). See also D. S. L. BLACKWELL and P. DE MAYO. Chem. Commun. 130 (1973); W. KUSTERS and P. DE MAYO. J. Am. Chem. Soc. **96**, 3502 (1974); P. DE MAYO and R. SUAU. J. Am. Chem. Soc. **96**, 6807 (1974); D. S. L. BLACKWELL, P. DE MAYO, and R. SUAU. Tetrahedron Lett. 91 (1974).
2. E. CAMPAIGNE. Chem. Rev. **39**, 1 (1946); N. LOZACH and G. GUILLOUZO. Bull. Soc. Chim. Fr. 1221 (1957); R. H. ABELES, R. F. HUTTON, and F. H. WESTHEIMER. J. Am. Chem. Soc. **79**, 712 (1957); R. W. BOST and B. O. COSBY. J. Am. Chem. Soc. **57**, 1404 (1935).
3. D. S. L. BLACKWELL, C. C. LIAO, R. O. LOUTFY, P. DE MAYO, and S. PASZYC. Mol. Photochem. **4**, 171 (1972).
4. D. R. KEMP, A. H. LAWRENCE, C. C. LIAO, R. O. LOUTFY, P. DE MAYO, A. A. NICHOLSON, and S. PASZYC. Pure Appl. Chem. 367 (1971).
5. A. OHNO, N. KITO, and T. KOIZUMI. Tetrahedron Lett. 2421 (1971); A. OHNO, T. KOIZUMI, and Y. OHNISHI. Bull. Soc. Chim. Jap. **44**, 2511 (1971); Y. OMOTE, M. YOSHIOKA, K. YAMADA, and N. SUGIYAMA. J. Org. Chem. **32**, 3676 (1967); A. OHNO, Y. OHNISHI, M. FUKUYAMA, and G. TSUCHIHASHI. J. Am. Chem. Soc. **90**, 7038 (1968); A. OHNO, Y. OHNISHI, and G. TSUCHIHASHI. J. Am. Chem. Soc. **91**, 5038 (1969); H. GOTTHARDT. Ber. **105**, 2008 (1972); T. S. CANTRELL. J. Org. Chem. **39**, 853 (1974); P. DE MAYO and H. SHIZUKA. Mol. Photochem. **5**, 339 (1973).
6. P. DE MAYO and H. SHIZUKA. J. Am. Chem. Soc. **95**, 3942 (1973); A. OHNO, Y. OHNISHI, and G. TSUCHIHASHI. Tetrahedron Lett. 161 (1969).
7. N. CAMPBELL and W. W. EASTON. J. Chem. Soc. 340 (1949).
8. P. DE BRUYN. C. R. **228**, 1809 (1949).
9. E. VON BRAUN and W. MANZ. Ann. **488**, 111 (1931).
10. S. H. TUCKER and M. WHALLEY. Chem. Rev. **50**, 483 (1952).
11. O. KORVER, J. U. VEENLAND, and T. J. DE BOER. Rec. Trav. Chim. **84**, 289 (1965).
12. J. C. D. BRAND and J. R. DAVIDSON. J. Chem. Soc. 15 (1956).
13. C. A. EMEIS, L. J. OOSTERHOFF, and G. DE VRIES. Proc. Roy Soc. London, Ser. A, **297**, 54 (1967); C. A. EMEIS and L. J. OOSTERHOFF. J. Chem. Phys. **54**, 4809 (1971).
14. P. DE MAYO and A. A. NICHOLSON. Israel J. Chem. **20**, 341 (1972).
15. D. G. HAWTHORNE and Q. N. PORTER. Aust. J. Chem. **19**, 1909 (1966); D. G. HAWTHORNE and Q. N. PORTER. Aust. J. Chem. **21**, 171 (1968); A. G. SCHULTZ and R. H. SCHLESSINGER. Chem. Commun. 1294 (1970).
16. D. R. KEMP and P. DE MAYO. Chem. Commun. 233 (1972).
17. R. BONNEAU, J. FAURE, J. JOUSSOT-DUBIEN, L. LINDQVIST, and C. BARTHELEMY. C. R. Ser. B, 412 (1968).
18. A. H. LAWRENCE, P. DE MAYO, R. BONNEAU, and J. JOUSSOT-DUBIEN. Mol. Photochem. **5**, 361 (1973).
19. J. C. SHEEHAN, R. M. WILSON, and A. W. OXFORD. J. Am. Chem. Soc. **93**, 7222 (1971).
20. G. PERRIER. Bull. Soc. Chim. Fr. **31**, 859 (1904).
21. A. SPILKER and W. SCHADE. Ber. **65**, 1686 (1932).
22. R. O. C. NORMAN, G. A. THOMPSON, and W. A. WATERS. J. Chem. Soc. 175 (1958).
23. P. MABILLE and N. P. BUU-HOI. J. Org. Chem. **25**, 1092 (1960).
24. N. CAMPBELL and W. W. EASTON. J. Chem. Soc. 340 (1949).
25. K. HAFNER and C. BERNHARD. Ann. **625**, 108 (1959).
26. K. DRIEWENSKI and L. STERNBACH. Bull. Int. Acad. Polon. Sci. Math. Ser. A, **146** (1933).
27. A. ZINKE, F. LINNER, and O. WOLFBAUER. Ber. **58**, 323 (1925). G. A. OLAH (*Editor*). Friedel–Crafts and related reactions. Vol. III. pt. 1. Interscience, New York. 1961. p. 81.
28. F. A. VINGIELLO, S.-G. QUO, and J. SHERIDAN. J. Org. Chem. **26**, 3202 (1961).
29. J. CALVERT and J. N. PITTS, JR. Photochemistry. J. Wiley and Sons, Inc. New York. 1966. p. 740.
30. E. E. WEGNER and A. W. ADAMSON. J. Am. Chem. Soc. **88**, 394 (1966).
31. C. G. HATCHARD and C. A. PARKER. Proc. Roy. Soc. London, Ser. A, **235**, 518 (1956).

Can. J. Chem. Downloaded from www.nrcresearchpress.com by 210.87.254.40 on 09/05/12
For personal use only.

The Ultrasonic Degradation of Thymine[1]

ERIC L. MEAD, RONALD G. SUTHERLAND, AND RONALD E. VERRALL
Department of Chemistry and Chemical Engineering, University of Saskatchewan, Saskatoon, Saskatchewan S7N 0W0
Received March 6, 1975

ERIC L. MEAD, RONALD G. SUTHERLAND, and RONALD E. VERRALL. Can. J. Chem. **53**, 2394 (1975).

Sonolysis at 450 kHz degrades an aqueous solution of thymine into at least six products of which four, 5-hydroxymethyluracil, *cis*- and *trans*-5,6-dihydroxy-5,6-dihydrothymine, and urea have been identified and a fifth tentatively assigned as *N*-formyl-*N'*-pyruvylurea. A mechanism of sonolytic degradation is proposed.

ERIC L. MEAD, RONALD G. SUTHERLAND et RONALD E. VERRALL. Can. J. Chem. **53**, 2394 (1975).

La sonolyse à 450 kHz dégrade une solution aqueuse de thymine en au moins six produits dont quatre sont identifiés comme étant l'hydroxy-5 méthyluracile, le dihydroxy-5,6 dihydro-5,6 thymine *cis* et *trans* et l'urée; le cinquième a été tentativement identifié à la *N*-formyl *N'*-pyruvylurée. On propose un mécanisme de la dégradation sonolytique.
[Traduit par le journal]

Chemical reactions that occur in liquids subjected to ultrasonic irradiation (insonation) of sufficient intensity to induce cavitation, have been attributed (1) to a number of processes; the reactive species produced in water and aqueous solutions during cavitation are hydroxyl radicals (2), hydrated electrons (3), hydroperoxyl radicals (4), and hydrogen atoms (5). These species are also produced during the radiolysis of water and in this paper we show that the sonolysis of thymine may be correlated with its radiolytic degradation.

The radiolysis of aqueous thymine solutions has been the subject of numerous investigations and studies by Teoule and co-workers (6–11) identified more than 26 products formed during ^{60}Co-γ irradiation. Hydroxyl radicals produced by ionizing radiation react with thymine to give 6-hydroxy-5,6-dihydro-5-thyml and 5-hydroxy-5,6-dihydro-6-thymyl radicals; hydrogen atoms (or $e_{aq}^- + H_3O^+$) react with thymine to give (5-uracyl)methyl, 5,6-dihydro-5-thyml, and 5,6-dihydro-6-thyml radicals (11). These radicals react very rapidly with dissolved oxygen (*e.g.* $K(\dot{T}OH + O_2) = 1.5 \times 10^9\ M^{-1}\ s^{-1}$ (12) to produce hydroperoxide radicals which are reduced to the hydroperoxyhydroxydihydro products (Fig. 1) (**5** and **6**) and the hydroperoxide products (**7**, 5-hydroperoxy-5,6-dihydrothymine, *cis*- and *trans*-6-hydroperoxy-5,6-dihydrothymine). The peroxide products are relatively unstable (11) and decompose to give various alcohols (*cis*- and *trans*-**9**, **8**, 5-hydroxy-5,6-dihydrothymine, *cis*- and *trans*-6-hydroxy-5,6-dihydrothymine). In addition, the hydroxyhydroperoxides decompose to give 5-hydroxy-5-methylbarbituric acid and *N*-formyl-*N'*- pyruvylurea and the remaining products result from decomposition of *N*-formyl-*N'*-pyruvylurea to give pyruvylurea, urea, and formylurea.

El'piner (1) was the first to investigate the effect of ultrasound on purine and pyrimidine bases. He insonated (500 kHz) aqueous solutions of the bases at an intensity of 5 W cm^{-2} in the presence of various gases. In the u.v. spectra of the insonated bases, the absorption maxima were reduced and the minima shifted to longer wavelengths. Uracil was found to be the most sensitive, adenine and guanine less so. In a later study, El'piner and Sokol'skaya (13) insonated aqueous solutions of cytosine, uracil, thymine, and adenine and investigated the products of sonolysis chromatographically but no degradation products were identified. The reduction in intensity of the u.v. absorption band of the various purines and pyrimidines was attributed to ring cleavage (1). Since the effect was considerably reduced in the presence of gases other than oxygen, it was suggested that molecular oxygen played an important role and a smaller oxidative role was assigned to hydroxyl radicals.

This study was undertaken to reinvestigate the sonolysis of aerated aqueous thymine solutions

[1]For a preliminary communication see ref. 27.

Can. J. Chem. Downloaded from www.nrcresearchpress.com by 210.87.254.105 on 09/05/12
For personal use only.

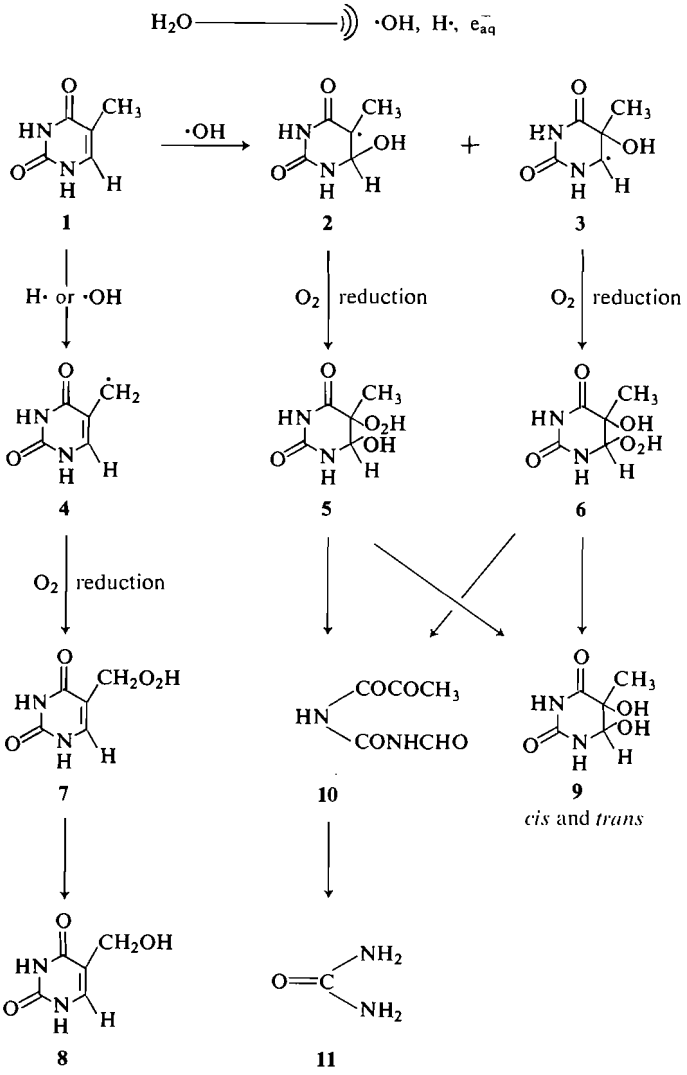

FIG. 1. Proposed sonolytic mechanism of degration of aqueous thymine solutions.

in light of the mechanism proposed for the radiolysis of thymine.

Experimental

Ultrasonic irradiation was carried out using a Multisons MC500-1 (Macrosonics Corporation, Cartaret, N.J.) broad band generator coupled to a cobalt barium titanate transducer operated at 447.5 ± 0.6 kHz with an average power output of 5 W cm^{-2} based on calorimetric measurements. The total acoustic power absorbed is not a useful measure of the energy available for chemical reactions since only a very small fraction is used in the formation of free radicals (14).

Aliquots (50 ml) of aqueous thymine solutions were insonated in a glass cell equipped with a Mylar 500A plastic window, similar to the design of Spurlock and Reifsneider (15). The temperature inside the cell was kept relatively constant at 25 °C by circulating the coupling water, transmitting the acoustic energy to the cell, through a constant temperature (25 ± 0.5 °C) bath.

The water used in this study was prepared by distillation of previously deionized water from alkaline permanganate. Thymine (Aldrich Chemical Co.) was recrystallized from distilled water. 5-Hydroxymethyluracil (16) and 5,6-dihydroxy-5,6-dihydrothymine (17) were prepared by literature procedures. These procedures give the *cis* isomer only (18). A mixture of isomers was obtained by refluxing an aqueous solution of the *cis* isomer at 90 °C for 4 h (18). Reagent grade urea was used without further purification. Chromatography was carried out on commercially prepared silica gel G and MN300 cellulose thin-layer (250 μm, 20 × 20 cm) plates and Whatman No. 1 paper.

Thymine and derivatives that retain the 5,6-double bond were located using a u.v. lamp with a maximum

Can. J. Chem. Downloaded from www.nrcresearchpress.com by 210.87.254.105 on 09/05/12
For personal use only.

Can. J. Chem. Downloaded from www.nrcresearchpress.com by 210.87.254.105 on 09/05/12
For personal use only.

emission band at 254 nm. The dihydrothymine derivatives urea, and substituted ureas were detected by spraying the chromatograms with 0.5 *N* aqueous sodium hydroxide, air drying for 30 min, and respraying with a solution of *p*-dimethylaminobenzaldehyde (PDAB) (1 g in 100 ml 95% ethanol plus 10 ml concentrated hydrochloric acid), after the method of Fink *et al.* (19). Iodine vapor was used to detect products on silica gel plates.

Ultraviolet spectra of aqueous thymine and insonated thymine solutions were obtained on a Cary 14 recording spectrophotometer using a variable path length cell (model BC14, Research and Industrial Instruments Company, London).

The following methods were used in the quantitative analyses of products. The *cis* and *trans* isomers of compound **9** were determined by a modification (20) of the method of Roberts and Friedkin (21). The original method determined thymine levels by hypobromination of the heterocyclic ring, followed by base hydrolysis to give the glycol. Continued base hydrolysis of the glycol yielded acetol which was condensed with *o*-aminobenzaldehyde to form 3-hydroxyquinaldine. Elimination of the hypobromination step in this work permitted the quantitation of thymine glycol in the presence of thymine. The fluorescence was measured at 440 nm (excitation at 310 nm) in a 1.0 cm quartz cell using an Aminco-Bowman spectrophotofluorimeter.

Total peroxides were measured as hydrogen peroxide using the molybdate catalyzed oxidation of iodide to the triiodide anion (22) which was measured spectrophotometrically at 350 nm in a 1.0 cm quartz cell. Hydrogen peroxide was determined spectrophotometrically following the method of Schumb *et al.* (23) using acidic titanium sulfate. Although not as sensitive as the triiodide anion method, it is specific for hydrogen peroxide in the presence of organic peroxides (24). Both methods for the determination of peroxide obeyed Beer's law in the concentration range 0–1 $\times 10^{-3}$ *M*.

Urea was determined spectrophotometrically by measuring the visible absorption at 420 nm arising from the reaction of urea with *p*-dimethylaminobenzaldehyde (25).

Results

Aqueous thymine solutions (2×10^{-3} to 2×10^{-2} *M*) showed a linear decrease with time in the u.v. absorption maximum at 264 nm during insonation at constant ultrasonic intensity. The characteristic changes observed were reduction of the band at 264 nm; reduction and shift to longer wavelengths of the minimum; increase and shift to shorter wavelengths of the band at 204 nm.

Semiquantitative data on the rate of degradation of thymine and relative yields of products were obtained. Figure 2 shows that the degradation rate, measured spectrophotometrically for three different initial concentrations, was constant over at least a 2-h insonation period. However, one of the products (**8**) (Fig. 1) has a molar extinction coefficient (ε 8.00 $\times 10^3$ M^{-1} cm^{-1}, λ_{max} 261 nm, 0.01 *N* HCl (16)) comparable to that of thymine and contributes to the measured absorption at 264 nm as the degradation proceeds. Attempts to determine the yield of **8** and unreacted thymine by spectrophotometric measurements of solutions, obtained by eluting the separated compounds from chromatograms, did not give accurate data. Table 1 contains some data on the product yields for two initial thymine concentrations. The methods used for the analysis were previously outlined in the experimental section.

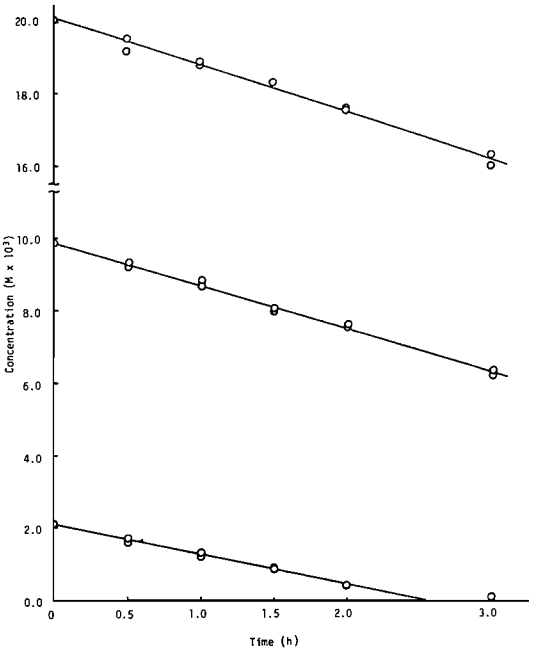

FIG. 2. Rate of degradation of aqueous thymine solutions at 447.5 kHz.

The products were separated and identified by cochromatography with synthetic samples and by their reaction to spraying with *p*-dimethylaminobenzaldehyde. The products separated and positively identified are *cis*- and *trans*-5,6-dihydroxy-5,6-dihydrothymine (thymine glycol), 5-hydroxymethyluracil, and urea. At least two more products, one tentatively identified as *N*-pyruvyl-*N'*-formylurea and the other unidentified, have also been isolated. Table 2 tabulates the R_f values measured for each of the above products on a variety of stationary and mobile phases.

The formation of 5-hydroxymethyluracil during sonolysis was verified by cochromatography with synthetic samples. As well, samples were

TABLE 1. Product yields* from two initial thymine concentrations

Time (h)	Thymine ($M \times 10^3$)	Thymine glycol ($M \times 10^3$)	Total peroxide ($M \times 10^3$)	Hydrogen peroxide ($M \times 10^3$)	Urea ($M \times 10^3$)	Thymine decomposed ($M \times 10^3$)
0.0	2.093	—	—	—	—	—
1.0	1.356	0.397	0.362	0.321	0.147	0.737
2.0	0.673	0.508	0.510	0.445	0.038	1.420
0.0	10.001	—	—	—	—	—
0.5	9.34	0.147	0.178	0.103	0.099	0.657
1.0	8.73	0.393	0.336	0.253	0.042	1.265
2.0	7.34	0.701	0.535	0.378	0.086	2.652
3.0	7.08	1.049	0.607	0.389	0.058	2.925

*Arithmetic average of at least two determinations for each product.

eluted from developed chromatograms for spectral comparison by the method of Cline *et al.* (16). The ratio of the absorbances at 280/260 and 250/260 were calculated; for the eluted sample, the ratios were 280/260 = 0.40 and 250/260 = 0.74, whereas for the synthetic mixture the ratios were 0.38 and 0.77, respectively, in methanol.

The *cis* and *trans* isomeric glycols were identified by cochromatography and by their reaction to spraying with PDAB after base hydrolysis, which gave a blue-green color for each.

Urea was also identified by cochromatography and by the bright lemon color obtained by spraying the chromatogram with PDAB without prior base hydrolysis.

The product T.1 is thought to probably be *N*-pyruvyl-*N'*-formylurea due to its color reaction (yellow-red) after spraying with PDAB after base hydrolysis while the R_f values for this product on systems II and VI were similar to those reported by Teoule and Cadet (6). The product T.2 has not yet been identified.

Discussion

The results of this work have shown that sonolysis of aqueous thymine solutions in the concentration range 2×10^{-3} to 2×10^{-2} *M* gives rise to products identical to those produced by radiolysis. The degradation of thymine was found to vary linearly with insonation time with a small dependence on initial concentration as was observed for the radiolysis of thymine (6).

Analysis of the initial rate data shown in Fig. 2 was carried out for all but the highest initial concentration of thymine. If the initial rate of reaction, *r*, is related to the reactant concentration, *c*, by the relation $r = k\,[c]^n$, then a value of the order of reaction, *n*, can be calculated from two initial rate conditions. The value obtained was 0.1 ± 0.15 and within experimental error the decomposition follows apparent zero-order kinetics. The large error in *n* includes some estimate of error arising out of the interference by product **8** in the spectrophotometric determination of thymine. A value of $1.8 \pm 0.3 \times 10^{-5}$ *M* min^{-1} was obtained for the zero-order rate constant.

The data in Table 1 are insufficient to carry out any meaningful kinetic analysis. However, some general observations can be made. After one hour of insonation approximately the same amounts of the thymine glycols, *cis*- and *trans*-**9**, were found for two different intial thymine concentrations. The method used in this study to determine the amounts of **9** appeared to be free from interference from thymine on monohydroxythymine derivatives. The initial yields of hydrogen peroxide are in agreement with those previously reported (2, 15) for air-saturated water insonated at approximately the same frequency. An estimate of the organic peroxide concentration was obtained from the difference between total peroxide and hydrogen peroxide concentrations. The organic peroxide precursors of the stable products of thymine degradation appear to never form more than *ca.* 5% of the total amount of thymine decomposed. Teoule and Cadet (6) found that at a high dose of ^{60}Co-γ irradiation, the total peroxide radiochemical yield G(peroxide) = 0.5 as compared to $G(-T) = 3.05$.

The amounts of urea formed during sonolysis of aqueous thymine solutions did not exceed 20% of the amount of decomposed thymine and appeared to decrease with increasing insonation time. This small amount of urea formed is in agreement with the radiochemical yield of urea,

Can. J. Chem. Downloaded from www.nrcresearchpress.com by 210.87.254.105 on 09/05/12
For personal use only.

Can. J. Chem. Downloaded from www.nrcresearchpress.com by 210.87.254.105 on 09/05/12
For personal use only.

TABLE 2. Chromatographic R_f values of products on a variety of stationary and mobile phases

Stationary phase*	Mobile phase†	R_f						
		Thymine	Urea	5-Hydroxymethyl-uracil	*trans*-5,6-Dihydroxy-5,6-dihydrothymine	*cis*-5,6-Dihydroxy-5,6-dihydrothymine	T.1	T.2
I	*1*	0.69	0.50	0.59	0.69	0.63	0.86	0.78
II	*2*	0.63	0.31	0.50	0.67	0.58	0.94	0.86
III	*3*	0.74		0.56				
IV	*4*	0.65		0.44				
V	*1*	0.57		0.27	0.48	0.34		
VI	*5*	0.52		0.26			0.68	0.41
VII	*6*	0.64		0.40				
VIII	*7*	0.64		0.41				

*Stationary phases: I, II: silica gel G; III, IV: MN 300 cellulose; V–VII: Whatman No. 1 paper.
†Mobile phases: *1*, acetonitrile – phosphate buffer (0.2 *M* Na_2HPO_4 and 0.2 *M* NaH_2PO_4) (85:15, v/v); *2*, ethyl acetate – isopropyl alcohol – water (75:16:9); *3*, *n*-propyl alcohol – water (10:3); *4*, *n*-butyl alcohol – methanol – water – ammonium hydroxide (60:20:20:1); *5*, *n*-butyl alcohol – water (86:14); *6*, *tert*-butyl alcohol – methyl ethyl ketone – water – formic acid (40:30:15:15); *7*, *tert*-butyl alcohol – methyl ethyl ketone – water – ammonium hydroxide (40:30:15:15). All proportions of the mobile phases are by volume.

G(urea) = 0.075 (10). The decrease in urea concentration with increasing insonation time may be accounted for in this work by further reaction of urea with nitrous acid, which is a product of the insonation of air-saturated water (26).

Although the amount of **8** could not be measured quantitatively it was possible, by visual comparison of the fluorescence intensity under u.v. illumination of chromatographic spots from aliquots of standard solution and insonated solutions, to estimate the maximum concentration of **8** to be 1×10^{-3} M.

From the results obtained in this work it appears that the radiolysis mechanism of thymine destruction proposed by Teoule *et al.* (10) may be adapted to the sonolytic degradation of thymine (Fig. 1). Cavitation produces the reactive species ·OH, H·, and e_{aq}^-; all of the sonolytic products may be accounted for by reaction of hydroxyl radicals and/or hydrogen atoms with thymine. Hydroxyl radicals undergo additional reactions with thymine to produce 6-hydroxy-5,6-dihydro-5-thymyl (**2**) and 5-hydroxy-5,6-dihydro-6-thyml (**3**) radicals; hydrogen atoms (or hydroxyl radicals) undergo abstraction reactions with thymine to give (5-uracyl)methyl radicals (**4**). These radicals react very rapidly with dissolved oxygen to produce the hydroperoxy radicals which are reduced to the hydroperoxide products, **5**, **6**, and **7**. The hydroperoxide products decompose to 5-hydroxymethyluracil (**8**) and *cis*- and *trans*-5,6-dihydroxy-5,6-dihydrothymine (**9**). In addition, the *cis*- and *trans*-5 (or 6)hydroperoxy-6(or 5)-dihydrothymines (**5** and **6**) probably undergo ring opening to give *N*-formyl-*N'*-pyruvylurea (**10**) which decomposes to urea (**11**).

The above mechanism accounts for all of the identified products in this study.

The authors acknowledge financial support of this work from the Research Corporation and the National Research Council of Canada.

1. I. E. El'piner. Ultrasound: physical, chemical and biological effects. Consultants Bureau, New York, N.Y. 1964.
2. A. Weissler. J. Am. Chem. Soc. **81**, 1077 (1959). M. Anbar and I. Pecht. J. Phys. Chem. **68**, 352 (1964). M. Haissinsky and R. Klein. J. Chem. Phys. Physico-chim. Biol. **65**, 326 (1968).
3. M. A. Margulis and A. N. Mal'tsev. Russ. J. Phys. Chem. **42**, 1412 (1968). (English translation of Zh. Fiz. Khim. **42**, 2660 (1968)).
4. B. Lippitt, J. M. McCord, and I. Fridovich. J. Biol. Chem. **247**, 4688 (1972).
5. R. Rivayrand and M. Haissinsky. J. Chim. Phys. **59**, 623 (1962). M. Anbar and I. Pecht. J. Phys. Chem. **68**, 1460 (1968).
6. R. Teoule and J. Cadet. Bull. Soc. Chim. Fr. 927 (1970).
7. J. Cadet and R. Teoule. Int. J. Appl. Radiat. Isot. **22**, 273 (1971).
8. R. Teoule, J. Cadet, and J. Ulrich. C.R. Ser. C, **270**, 362 (1970).
9. R. Teoule and J. Cadet. Chem. Commun. 1269 (1971).
10. R. Teoule, J. Cadet, M. Polverelli, and A. Cier. Peaceful uses of atomic energy. Vol. 13. U.N., New York. Intl. At. En. Agency, Vienna. 1972.
11. J. Cadet and R. Teoule. Biochim. Biophys. Acta, **238**, 8 (1971).
12. H. Loman and M. Ebert. Int. J. Radiat. Biol. **18**, 369 (1970).
13. I. E. El'piner and A. V. Sokol'skaya. Dokl. Akad. Nauk S.S.S.R. **153**, 200 (1963).
14. M. A. Margulis. Sov. Phys. Acoust. **15**, 135 (1969).
15. L. A. Spurlock and S. B. Reifsneider. J. Am. Chem. Soc. **92**, 6112 (1970).
16. R. E. Cline, R. M. Fink, and K. Fink. J. Am. Chem. Soc. **81**, 2521 (1959).
17. O. Baudisch and D. Davidson. J. Biol. Chem. **64**, 233 (1925).
18. J. Ulrich, R. Teoule, R. Massot, and A. Cornu. Org. Mass Spectrom. **2**, 1183 (1969).
19. R. M. Fink, R. E. Cline, C. McGaughey, and K. Fink. Anal. Chem. **28**, 4 (1956).
20. M. Daniels and M. Grimison. Biochim. Biophys. Acta, **142**, 293 (1967).
21. D. Roberts and M. Friedkin. J. Biol. Chem. **233**, 483 (1958).
22. A. O. Allen, C. J. Hochanadel, J. A. Ghormley, and T. W. Davis. J. Phys. Chem. **56**, 575 (1952).
23. W. C. Schumb, C. N. Satterfield, and R. L. Wentworth. Hydrogen peroxide. Reinhold Publishing Corp., New York, N.Y. 1965.
24. G. Nettesheim. Z. Anal. Chem. **191**, 45 (1962).
25. G. W. Watt and J. D. Chrisp. Anal. Chem. **26**, 452 (1954).
26. E. L. Mead, R. G. Sutherland, and R. E. Verrall. To be published.
27. E. L. Mead, R. G. Sutherland, and R. E. Verrall. Chem. Commun. 414 (1973).

Can. J. Chem. Downloaded from www.nrcresearchpress.com by 210.87.254.105 on 09/05/12
For personal use only.

Charge Distributions and Chemical Effects. IX. On the Charge Dependence of C-13 Chemical Shifts in Alkylcyclohexanes and Cyclopropane

RÉAL ROBERGE AND SÁNDOR FLISZÁR

Département de Chimie, Université de Montréal, Montréal, Québec H3C 3V1

Received February 7, 1975

RÉAL ROBERGE and SÁNDOR FLISZÁR. Can. J. Chem. **53**, 2400 (1975).

The analysis of *ab initio* charge distributions in cyclohexane and selected methylcyclohexanes indicates that no effect other than that described by the relationship $\delta_C = -237.1q_C + 242.64$ between C-13 chemical shifts and C net charges (as determined for the alkanes) contributes to any significant extent to the shielding of the carbon atoms. This is no longer true for cyclopropane.

RÉAL ROBERGE et SÁNDOR FLISZÁR. Can. J. Chem. **53**, 2400 (1975).

L'analyse des distributions de charges *ab initio* du cyclohexane et de quelques méthylcyclohexanes montre qu'aucun effet particulier, autre que celui décrit par l'équation déduite pour les alcanes $\delta_C = -237.1q_C + 242.64$ reliant les déplacements chimiques aux charges nettes, ne participe de manière significative à l'écran des atomes de carbone. Tel n'est pas le cas pour le cyclopropane.

A theory has been recently developed (1) for calculating charge distributions in simple alkanes from the knowledge of the inductive effects of alkyl groups. These 'inductive' charges were found to be in agreement with those derived from both semiempirical and *ab initio* quantum mechanical methods. With *optimized* STO-3G results (2), the agreement is virtually perfect. On a scale of relative units defined by setting the C net charge of ethane equal to 1 arbitrary unit, the carbon and hydrogen net (*i.e.*, nuclear minus gross) charges are functions of a parameter, n.[1] The various quantum chemical results simply correspond to different values for n. For example, comparisons which were made with theoretical charges satisfying Mulliken's scheme indicated that $n = 1.3325$ generates the *optimized* STO-3G charges, whereas the 'standard' STO-3G results correspond to $n \simeq 1$ (1). Multiplication of charges relative to q_C(ethane) = 1 by a unity factor, β = C net charge of ethane, yields charge distributions in charge units. The β value also differs from theoretical method to method (1).

The n value is critical in any comparison of a property with C charges: the use of any theoretical set of charge distributions corresponding to an n value other than the 'proper' one is bound to fail in showing the expected property–charge correlation (1). Postulating that in alkane molecules the various C atoms of the set are as similar as possible, it is found (3) that $n \simeq -4.4$. This n value appears to correspond to real physical situations. Indeed, from C-13 chemical shifts it was found that $n = -4.4122$, whereas adiabatic ionization potentials (4) lead to $n = -4.4083$. Similarly, the enthalpies of formation of the alkanes can be calculated using charges derived from the relation between C-13 chemical shifts

$$[1] \quad \delta_C = -237.1q_C + 242.64 \text{ p.p.m. from TMS}$$

and relative net charges, q_C (5).

The accuracy of [1] can best be evaluated by observing that a 1% error in q_C corresponds to an error of ~2.4 p.p.m., while the standard deviation is only 0.3 p.p.m. (3). Here, this relation between charges and C-13 chemical shifts is used for determining, in the case of cycloalkanes, whether any special effect due to the ring structure contributes to the C-13 shieldings which are observed.

Basic Formulas for Comparing Chemical Shifts with Net Charges

Any choice of a particular theoretical method for calculating charges was shown (1) to define a particular value for n, *i.e.*, that corresponding to the method selected. Let n^0, β^0, and q_C^0 be the quantities which correspond to a particular theoretical method and n, β, q_C those which are deduced from the former under the assumption of a nonequal partitioning of the overlap populations between bonded C and H atoms, along

[1]For example, $q_C(CH_4) = 4(n + 1)/3n$, $q_C(C_2H_6) = 1$, $q_C(C_3H_8,\text{sec}) = (2n - 3.8)/3n$, $q_C(\text{iso-}C_4H_{10}, \text{tert}) = (n - 7.7)/3n$, and $q_C(\text{neo-}C_5H_{12},\text{quat}) = -4/n$ (1).

Can. J. Chem. Downloaded from www.nrcresearchpress.com by 210.87.254.6 on 09/05/12
For personal use only.

Can. J. Chem. Downloaded from www.nrcresearchpress.com by 210.87.254.6 on 09/05/12
For personal use only.

TABLE 1. Standard and optimized carbon net charges, q_C (me)

Molecule	Atom	Net charge*	
		Standard	Optimized
Methane	C	−72	−48.92
Ethane	C	−26	−20.96
Propane	C_{prim}	−31	−23.81
	C_{sec}	+19	+5.94
Isobutane	C_{prim}	−35	−26.39
	C_{tert}	+57	+33.36
Neopentane	C_{prim}	−39	−28.66
	C_{quat}	+93	+62.92
Cyclohexane	C	+3.4	+2.76

*The results for the acyclic alkanes are those of ref. 2.

the lines described in ref. 3. The following equations enable a simple calculation of the charges corresponding to any n value of our choice from the original theoretical charges q_C^0.

$$[2] \qquad \beta/n = \beta^0/n^0$$

$$[3] \qquad p = (\beta-\beta^0)/3$$

$$[4] \qquad q_C = q_C^0 + Np$$

where N = number of H atoms bonded to C.

$$[5] \qquad q_C \text{ (rel)} = q_C \text{ (charge units)}/\beta$$

It has been stated above that calculated C-13 chemical shifts are very sensitive to small errors in q_C. Therefore, to obtain accurate results for the δ_C values, it is important to use accurate charges q_C^0 for calculating the q_C values. It was shown for alkanes that the *optimized* STO-3G charges (2) qualify as 'excellent' since the modified set which is deduced from the original STO-3G results by an appropriate mode of partitioning C-H overlap populations [2–4] exhibit a virtually perfect correlation with carbon chemical shifts [1]. Unfortunately, it appears that the STO-3G calculations implying optimization of all variational parameters are practically not feasible for methylcyclohexanes.[2] We are, therefore, forced to extract useful information from the less precise standard[3] STO-3G calculations for these molecules.

This, indeed, can be done under the following premises: if the set of the standard exponents, ζ_{st}, is not too different from the corresponding optimized exponents, ζ_{opt}, then we can apply, in a limited range (which, however, is difficult to define precisely), a Taylor series:

$$[6] \quad q_{opt} = q_0 + (q_{st}-q_0)\, dq_{opt}/dq_{st} + (\tfrac{1}{2})\,(q_{st}-q_0)^2 d^2q_{opt}/dq_{st}^2 + \ldots$$

The advantage resulting from the use of such a relation can be inferred from a comparison between the optimized and standard charges calculated for the alkanes (Table 1, Fig. 1).

Of course, no perfect linear relationship between these two sets of results should be expected, as the divergences between optimized and standard exponents are not the same for the various atoms involved in this comparison (2). On the contrary, we feel that this correlation is even better than what would have been hoped for *a priori*. We can, therefore, take advantage of this property in the present study of the methylcyclohexanes.

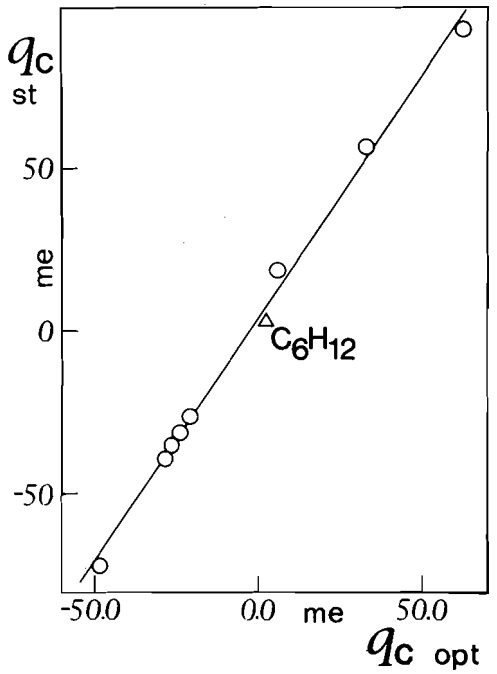

FIG. 1. Comparison between carbon net charges deduced from standard and optimized STO-3G calculations.

Results

Cyclohexane

The standard STO-3G calculation according to Pople's recipe (6), using r_{CC} = 1.540 Å, r_{CH} = 1.091 Å, ∠CCC = ∠HCH = 109.47°, ζ_C-

[2]For example, one single standard calculation of 1-*cis*-3-*cis*-5-trimethylcyclohexane requires ~10 h computer time, using the CDC CYBER 74 computer.

[3]The 'standard' STO-3G mode of calculation is defined in ref. 6. Details about the differences between standard and optimized results are given in ref. 2.

TABLE 2. Comparison between the optimized and experimental geometry of cyclohexane

		Experimental			
		From electron diffraction			From Raman spectroscopy
Coordinate	Calculated	Ref. 12	Ref. 13	Ref. 14	Ref. 15
r(CC) (Å)	1.532	1.528±0.005	1.528±0.003	1.5317	1.535±0.001
r(CHe) (Å)	1.1022	1.104±0.005	1.119±0.004	1.1037	1.102±0.001
r(CHa) (Å)	1.1029				
∠CCC (deg)	110.57	111.5±0.15	111.05±0.12	111.4±0.2	
∠HCH (deg)	107.33		110.0 ±2.5	107.5±1.5	110.0±0.3
∠CCHa (deg)	109.14		108.8 ±0.5		111.4±0.3
∠CCHe (deg)	110.30				
∠ZCHa (deg)	1.52				2.8

(s_K) = 5.67, $\zeta_C(s_L,p)$ = 1.76, and ζ_H = 1.18, yields the following net charges (in 10^{-3} electron units): q_C = 3.39, q_H(axial) = −2.61, and q_H(equatorial) = −0.77. For this molecule, the optimization was carried out following the scheme which was applied earlier for the alkanes (2). First, the geometry was optimized using the above standard scale factors (Table 2).

Next, the scale factors were optimized using the optimized geometry given in Table 2, until stable charges were obtained. In this optimization, the total energy drops from −231.4943057 (standard) to −231.504629 a.u. The net charges deduced from the optimized geometry and the optimized scale factors $\zeta_C(s_K)$ = 5.705, $\zeta_C(s_L,p)$ = 1.75375, ζ_H(e) = 1.1736, and ζ_H(a) = 1.16986 are (in 10^{-3} electron units): q_C = 2.76, q_H(e) = 1.76, and q_H(a) = −4.52. These optimized charges which were deduced following Mulliken's population analysis (7), correspond, in principle, to those calculated for the alkanes (2), for which n = 1.3325.

The carbon-13 chemical shift can now be calculated from [1–5], which involve the modified population analysis (3) for deducing the C charge corresponding to n = − 4.4122 from that corresponding to n = 1.3325. First, $\beta(n = -4.4122)$ is calculated by means of [2]: β = −4.4122 (−20.96/1.3325) = 69.40 me. Then (eq. 3), it is found that p = 30.12 me and (eq. 4) $q_C = 2.76 + 2p$ = 63.00 me. In the scale of relative units, this charge is q_C(rel) = 63.00/β = 0.9078 (eq. 5). Finally, inserting this q_C charge in [1], yields δ_C = 27.4, which compares favorably with the experimental value (8) δ_C = 27.7 p.p.m. from TMS.

This result indicates clearly that for cyclohexane the same relation holds between carbon net charges and C-13 n.m.r. shifts as that observed for the alkanes (3). Hence, no special effect seems to contribute significantly to the chemical shift, specifically because of the cyclic structure of cyclohexane. This good charge–δ_C correspondence further indicates that no special importance should be attributed to the fact that the direct comparison between standard and optimized charges yields for cyclohexane a point which is slightly off the best line shown for the alkanes in Fig. 1.

Alkyl-substituted Cyclohexanes

Table 3 reports the STO-3G results for methyl-, 1-*cis*-3-*cis*-5-trimethyl-, and 1,1,3-trimethylcyclohexane obtained from the use of standard geometries and exponents. Since it is virtually not feasible to calculate the corresponding optimized charges, the latter are estimated from the carbon-13 n.m.r. shifts by performing in reversed order the operations just described for cyclohexane. Clearly, the latter charges are those to be expected from optimized calculations, *unless the chemical shifts for cyclohexanes depend also on an effect which is not accounted for in the simple* δ_C*–charge relation* [1].

The optimized charges thus calculated from C-13 n.m.r. data are compared in Fig. 2 with the standard charges in the same way that the optimized and standard charges of the alkanes were compared in Fig. 1.

The comparison presented in Fig. 2 indicates that between these two sets of charges the same relation holds as between the standard and the STO-3G optimized charges. Therefore, within the precision of the present type of analysis, there is no indication that any effect other than that described by [1] contributes to any signifi-

Can. J. Chem. Downloaded from www.nrcresearchpress.com by 210.87.254.6 on 09/05/12
For personal use only.

TABLE 3. Standard charges and charges deduced from C-13 n.m.r. shifts for $n = 1.3325$

Molecule	Atom		δ_C (p.p.m., from TMS)*	C net charge (me) From δ_C	C net charge (me) STO-3G
Cyclohexane	C	(1)†	27.7	2.7	3.4
Me-C_6H_{11}	C-1	(2)	33.7	31.0	42.5
	C-2,6	(3)	36.4	0.1	−1.4
	C-3,5		27.2	2.8	3.5
	C-4		27.0	2.9	3.4
	C(Me)	(4)	23.3	−26.2	−34.4
1-*cis*-3-*cis*-5-Me_3-C_6	C-1,3,5		33.3	31.2	42.6
	C-2,4,6	(5)	44.8	−2.3	−6.1
	$C(CH_3)$		23.4	−26.2	−34.5
1,1,3-Me_3-C_6	C-1	(6)	31.4	61.8	75.6
	C-2		50.0	−3.9	−11.1
	C-3	(7)	28.9	32.4	39.6
	C-4		36.1	0.2	−2.0
	C-5		23.2	4.0	0.6
	C-6		40.1	−1.0	−6.3
	CH_3(e)	(8)	34.3	−29.4	−38.1
	CH_3(a)	(9)	25.5	−26.8	−43.8
	CH_3(3)		23.7	−26.3	−34.2

*Extracted from ref. 8.
†The numbers in parentheses refer to the points in Fig. 2.

TABLE 4. Results from the optimization of cyclopropane (STO-3G)

Parameter	Value: STO-3G	Value: Experimental (ref. 16)
r(CC) (Å)	1.4934	1.510 ± 0.002
r(CH) (Å)	1.0874	1.089 ± 0.003
∠HCH (deg)	113.4	115.1 ± 1.0
ζ_H	1.2031	
$\zeta_C(s_L,p)$	1.7314	
$\zeta_C(s_K)$	5.7047	
q_C (me)	−87.67	
q_H (me)	43.84	

cant extent to the C-13 n.m.r. shifts of these cyclohexanes.

Present results indicate clearly that no effects other than those described for the acyclic alkanes participate in determining charge distributions and carbon n.m.r. shifts in methylcyclohexanes. This raises the obvious question about cyclopropane.

Cyclopropane

The comparison of the standard carbon net charge (−19.01 m*e*) with the optimized one (Table 4) yields a point which is far off the lines given in Figs. 1 and 2. Moreover, the calculation of the C-13 shift from the optimized C charge (−87.67 m*e*) by means of [1–5] yields δ_C =336 p.p.m. from TMS, which is grossly in error, the experimental value (9) being −2.6 p.p.m. from TMS.

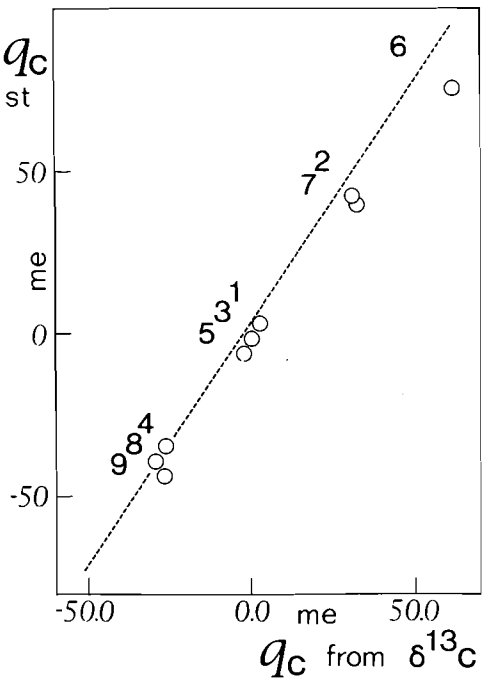

FIG. 2. Comparison of standard net C charges (STO-3G) with charges deduced from n.m.r. shifts, for $n = 1.3325$. The dotted line is that of Fig. 1.

Can. J. Chem. Downloaded from www.nrcresearchpress.com by 210.87.254.6 on 09/05/12
For personal use only.

TABLE 5. Comparison of optimized population analyses

Molecule	Electron populations $2p_x$	$2p_y$	$2p_z$	Total 2p	Net charge q_C (me)
Cyclohexane	0.94816	0.95092	0.95182	2.85090	2.76
Ethane	0.96794	0.96794	0.94891	2.88479	−20.96
Cyclopropane	1.03090	0.93092	0.99852	2.96034	−87.67
Ethylene	1.00000	1.00185	0.98752	2.98937	−135.46

TABLE 6. Comparison of optimized scale factors

Molecule	ζ_H	$\zeta_C(s_{L,p})$	$\zeta_C(s_K)$
Cyclohexane	1.1736†	1.75375	5.705
Ethane*	1.176	1.7591	5.706
Cyclopropane	1.2031	1.7314	5.70474
Ethylene*	1.226	1.709	5.703

*Extracted from ref. 2.
†Equatorial.

The unusual properties of this molecule have been the object of a number of studies (10). Present results support the view that cyclopropane possesses some characters of unsaturation. This is indicated by the comparison of population analyses given in Table 5 and the behavior of the optimized scale factors (Table 6). Moreover, the C—C overlap population in cyclopropane (0.60663 *e*) is significantly lower than those calculated for cyclohexane (0.73602), ethane (0.74682), and ethylene (1.22014 *e*) (2).[4] It is then not surprising that the δ_C–q_C relationship [1] for alkane molecules is not obeyed by cyclopropane.

Conclusions

STO-3G calculations without optimization of all variational parameters are not sufficiently precise for calculating C-13 n.m.r. shifts via the simple δ_C–q_C relationship. Nevertheless, present results suggest that no special effect, for which the six-membered ring structure could be held responsible, participates to the shielding of the carbon atoms, at least not to any significant extent. This is clearly confirmed by the optimized calculation on cyclohexane. These results do not contradict current arguments in terms of spatial proximity of neighboring atoms on C-13 shieldings, *gauche* γ interactions, etc., but tend to indicate that all these effects are ultimately reflected in the electron populations which, in turn, are simply related to the n.m.r. shifts by the same equation which applies to the acyclic alkanes. Chemical shift is a property of the interaction of the charge density with an external magnetic field. Therefore, it depends not only on the value of the integrated charge density (or 'charge') in the neighborhood of a nucleus but also on the magnetic susceptibility of that charge density. This is why the δ_C–q_C correlation used here is perforce limited to a set of very similar molecules. It is then not surprising that cyclopropane has a totally different behavior from what would be expected from [1].

[4]These results are in agreement with those given in ref. 11.

The most generous support given by the Centre de Calcul de l'Université de Montréal and the financial aid received from the National Research Council of Canada are gratefully acknowledged.

1. S. FLISZÁR, G. KEAN, and R. MACAULAY. J. Am. Chem. Soc. **96**, 4353 (1974).
2. G. KEAN and S. FLISZÁR. Can. J. Chem. **52**, 2772 (1974).
3. S. FLISZÁR, A. GOURSOT, and H. DUGAS. J. Am. Chem. Soc. **96**, 4358 (1974).
4. H. HENRY and S. FLISZÁR. Can. J. Chem. **52**, 3799 (1974).
5. H. HENRY and S. FLISZÁR. In preparation.
6. W. J. HEHRE, R. F. STEWART, and J. A. POPLE. J. Chem. Phys. **51**, 2657 (1969).
7. R. S. MULLIKEN. J. Chem. Phys. **23**, 1833, 1841, 2338, 2343 (1955).
8. D. K. DALLING and D. M. GRANT. J. Am. Chem. Soc. **89**, 6612 (1967).
9. J. J. BURKE and P. C. LAUTERBUR. J. Am. Chem. Soc. **86**, 1870 (1964).
10. C. A. COULSON and W. E. MOFFITT. Philos. Mag. **40**, 1 (1949); A. D. WALSH. Trans. Faraday Soc. **45**, 179 (1949); R. J. BUENKER and S. D. PEYERIMHOFF. J. Phys. Chem. **73**, 1299 (1969); E. KOCHANSKI and J. M. LEHN. Theor. Chim. Acta, **14**, 304 (1969).

Can. J. Chem. Downloaded from www.nrcresearchpress.com by 210.87.254.6 on 09/05/12
For personal use only.

11. R. M. STEVENS, E. SWITKES, E. A. LAWS, and W. N. LIPSCOMB. J. Am. Chem. Soc. **93**, 2603 (1971); R. M. STEVENS. J. Chem. Phys. **52**, 1397 (1970); J.-M. ANDRÉ, M. C. ANDRÉ, and G. LEROY. Bull. Soc. Chim. Belges, **80**, 265 (1971).
12. M. DAVIS and O. HASSEL. Acta Chem. Scand. **4**, 17 (1963).
13. H. J. GEISE, H. R. BUYS, and F. C. MIJLHOFF. J. Mol. Struct. **9**, 447 (1971).
14. O. BASTIANSEN, L. FERNHOLT, H. M. SEIP, HIDEKI KAMBARA, and K. KUCHITSU. J. Mol. Struct. **18**, 163 (1973).
15. R. A. PETERS, W. J. WALKER, and A. WEBER. J. Raman Spectrosc. **1**, 159 (1973).
16. O. BASTIANSEN, F. N. FRITSCH, and K. HEDBERG. Acta Cryst. **17**, 538 (1964).

Can. J. Chem. Downloaded from www.nrcresearchpress.com by 210.87.254.6 on 09/05/12
For personal use only.

Carbon-13 Nuclear Magnetic Resonance Studies of Compounds of the Vitamin B_6 Group and Related Pyridine Derivatives[1]

ROY D. LAPPER[2]

The Robert Robinson Laboratories, University of Liverpool, Liverpool, England L69 3BX

AND

HENRY H. MANTSCH[3] AND IAN C. P. SMITH[4]

Division of Biological Sciences, National Research Council of Canada, Ottawa, Canada K1A 0R6

Received January 28, 1975

ROY D. LAPPER, HENRY H. MANTSCH, and IAN C. P. SMITH. Can. J. Chem. **53**, 2406 (1975).

The ^{13}C chemical shifts and ^{13}C–^{31}P spin–spin couplings (where applicable) are reported for pyridoxine, pyridoxamine, pyridoxal, pyridoxamine phosphate, and pyridoxal phosphate. Resonance assignments are made by consideration of substituent chemical shift effects, as tested on an analogous series of pyridine derivatives. Increased shielding of the C4′ and C5′ methylene groups of the vitamin B_6 compounds and the methyl groups of 3,4-dimethylpyridine relative to the predicted values are attributed to steric compression. In aqueous solution pyridoxal exists as the hemiacetal form, although at high p*H* it is in rapid equilibrium with a significant amount of the aldehyde form. Pyridoxal phosphate exists as the aldehyde at high p*H*, as the hydrated aldehyde at low p*H*, and in a slow equilibrium between detectable amounts of both species at p*H* 4. The ^{13}C–^{31}P couplings through two bonds lie in the range 4.5 ± 0.5 Hz found for a variety of other organic phosphates. The couplings through three bonds indicate a preference for a *trans* arrangement of the phosphorus and ring carbon-5.

ROY D. LAPPER, HENRY H. MANTSCH et IAN C. P. SMITH. Can. J. Chem. **53**, 2406 (1975).

On a mesuré les déplacements chimiques du ^{13}C et les constantes de couplage spin–spin entre ^{13}C et ^{31}P (dans les phosphates) pour la pyridoxine, pyridoxamine, pyridoxal, phosphate de pyridoxamine et phosphate de pyridoxal. Les attributions sont faites en considérant les effets des substituants sur le déplacement chimique dans une série analogue des pyridines substituées. L'accroissement du blindage des carbones méthyléniques 4′ et 5′ des composés de la vitamine B_6 et des groupes méthyles du diméthyl-3,4 pyridine par rapport aux valeurs calculées, est attribué à une compression stérique. En solution aqueuse le pyridoxal existe sous la forme hémiacétale bien qu'à p*H* élevé l'hémiacétale soit en équilibre rapide avec une quantité importante d'aldéhyde. A p*H* élevé, le phosphate de pyridoxal existe sous la forme aldéhyde, à p*H* faible sous forme aldéhyde hydraté, et à p*H* 4 on a un équilibre lent entre des quantités décelables des deux espèces. Les constantes de couplage de ^{13}C–^{31}P à travers deux liaisons, se situent aux alentours de 4.5 ± 0.5 Hz. Cette valeur correspond aux valeurs trouvées pour divers phosphates organiques. Les couplages à travers trois liaisons suggèrent une forte préférence pour un arrangement *trans* du phosphore par rapport au carbone-5 du cycle.

[Traduit par le journal]

Introduction

The vitamin B_6 group of compounds consists of pyridoxine, pyridoxamine, and pyridoxal and their phosphates.[5] Of these various forms the most active and effective over a large range of organisms appears to be pyridoxal 5′-phosphate, also known as codecarboxylase or cotransaminase. This compound represents the coenzyme form of vitamin B_6 and is essential for a series of reactions involving amino acids, *e.g.* transamination, decarboxylation, and racemization. The unphosphorylated forms of the vitamin owe their activity mainly to the ability of organisms to convert them through enzymatic pathways to the coenzyme form although pyridoxamine phosphate itself is known to 'catalyze' certain transaminase reactions.

[1]NRCC No. 14679.

[2]NRCC Postdoctoral Fellowship 1970–1972. Present address: Organon Laboratories Ltd., Newhouse, Lanarkshire, Scotland ML1 5SH

[3]NRCC visiting scientist 1971, 1973. Present address: Institute of Chemistry, Str. Donath 65, Cluj, Romania.

[4]To whom correspondence should be addressed.

[5]Names and numbering schemes for the vitamin B_6 derivatives are in accordance with the recommendations of the IUPAC-IUB Commission on biochemical nomenclature (34).

Can. J. Chem. Downloaded from www.nrcresearchpress.com by 210.87.254.6 on 09/05/12
For personal use only.

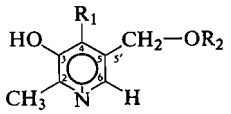

	R_1	R_2
Pyridoxine	$-CH_2OH$	$-H$
Pyridoxamine	$-CH_2NH_2$	$-H$
Pyridoxamine 5′-phosphate	$-CH_2NH_2$	$-PO_3H_2$
Pyridoxal	$-CHO$	$-H$
Pyridoxal 5′-phosphate	$-CHO$	$-PO_3H_2$

The general theory of the mechanism of action of enzymes using pyridoxal 5′-phosphate as a coenzyme has been put forward by Braunstein *et al.* (1, 2) and by Snell and co-workers (3–5). It involves reaction of the aldehyde function and the amino group of an amino acid to form a Schiff base. The electronic aspects of how such a Schiff base can then give rise to a series of different reaction products has been given by Pullman and co-workers (6, 7). However, the important first step in such reactions is always the formation of the Schiff base. In pyridoxal, formation of an internal hemiacetal occurs, reducing the amount of free aldehyde present, and thus decreasing the reactive nature of this compound. Pyridoxal phosphate, however, cannot form such a hemiacetal and hence is most active.

The effect of p*H* on vitamin B_6 compounds has been studied by ^1H n.m.r. (8, 9) and by u.v. absorption spectroscopy (10–15). We have undertaken this study by carbon-13 nuclear magnetic resonance (n.m.r.) spectroscopy to study the effect of p*H* on the conformation of the 5-carbinol phosphate side chain relative to the pyridine ring and, since ^{13}C chemical shifts are known to reflect electron densities in aromatic ring systems, to study the influence of p*H* on the pyridine ring. The ^{13}C spectra are indicative of the state of the aldehyde group at different p*H* values. This study serves as a necessary prelude to those in which the coenzyme is interacting with the apoenzyme.

Experimental

The compounds studied were obtained from Sigma Chemical Co., St. Louis, Missouri, and from Koch-Light Laboratories, Colnbrook, England, and were used as received. Samples were made up in D_2O solution and p*D* adjusted using NaOD and DCl solutions. Solutions were 0.3–0.5 *M* where solubility allowed and otherwise saturated solutions. Proton noise-decoupled carbon-13 spectra were run on Varian XL-100-15 n.m.r. spectrometers with 8K or 16K Varian 620L computers. Chemical shifts are accurate to ± 0.05 p.p.m. and coupling constants to ± 0.2 Hz. Tetramethylsilane (Me_4Si) in a tube of 5 mm o.d. concentric with the 12 mm sample tube was used as a chemical shift reference. The probe temperature was 32°.

Results and Discussion

To aid the assignment of the carbon-13 resonances in the vitamin B_6 compounds the ^{13}C n.m.r. spectra of some monosubstituted pyridines and benzenes at acid, neutral, and alkaline p*H* values were run. Assignment of the resonances in these latter compounds (Table 1) was made by use of literature substituent chemical shift (s.c.s.) effects for pyridine and benzene derivatives (16–18). Additivity of aromatic s.c.s. effects was then used to aid assignments in the vitamin B_6 derivatives.

In all the spectra of the derivatives studied the C6 carbon resonance was clearly recognizable by its high intensity relative to the others. This is because the quaternary carbons have long spin–lattice relaxation times owing to the lack of a directly-attached proton and are partially saturated under conditions of rapid acquisition. In the case of pyridoxal and pyridoxamine phosphates the C5 resonances could be recognized by the presence of a coupling to phosphorus. A further assignment which could be made throughout the series was that of the resonance due to C3, the carbon with a directly-bonded hydroxy group; predicting the shifts on the basis of additivity of s.c.s. effects clearly indicates that at all p*H* values this resonance is to lowest field in the range 150–170 p.p.m. Comparisons of the expected shift changes from derivative to derivative and especially from acid to alkaline p*H* based on the s.c.s. additivity principle allowed the final assignments given in Table 2 although some ambiguities were evident where chemical shifts were similar.

The additivity of the s.c.s. effects obtained from Table 1, applied to predicting the ^{13}C chemical shifts in the vitamin B_6 derivatives, yields a fairly good fit to the observed chemical shifts in the cases of acid and alkaline solution. The fit is often not good in the case of the solutions at about p*H* 7 because of the varying pK_a values in the compounds studied and the uncertainty as to which position in the equilibria one is observing. In the former cases the calculated shifts are within ± 2 p.p.m. of the observed

Can. J. Chem. Downloaded from www.nrcresearchpress.com by 210.87.254.6 on 09/05/12
For personal use only.

Can. J. Chem. Downloaded from www.nrcresearchpress.com by 210.87.254.6 on 09/05/12
For personal use only.

TABLE 1. ^{13}C chemical shifts[a] of pyridine and benzene derivatives at various p*H* values

	p*H*	C2	C3	C4	C5	C6	Other	
Pyridine	2.0	142.20	128.55	148.30	128.55	142.20	—	
	6.8	149.40	124.85	137.55	124.85	149.40	—	
	12.8	149.50	124.80	137.50	124.80	149.50	—	
2-Methylpyridine	1.8	(154.40)	128.90	147.40	125.30	141.20	20.40[e]	
	7.3	(158.00)	124.20	137.85	121.75	148.35	23.85	
	12.8	(158.10)	124.20	137.70	121.60	148.45	23.85	
3-Hydroxypyridine	2.0	130.30	(156.80)	134.45	129.15	133.95	—	
	7.2	135.35	(159.80)	130.50	127.20	134.55	—	
	12.4	141.60	(163.85)	127.20	125.90	135.25	—	
4-Pyridylcarbinol	1.9	141.60	124.90	(164.15)	124.90	141.60	63.00[f]	
	7.1	149.35	122.60	(151.95)	122.60	149.35	63.10	
	12.5	149.35	122.60	(152.25)	122.60	149.35	63.20	
3-Pyridylcarbinol	2.0	139.90	(142.40)	146.00	128.10	140.80	61.00[f]	
	7.0	148.35	(137.10)	137.10	125.00	148.05	62.20	
	12.7	148.35	(137.30)	137.05	124.90	148.05	62.20	
4-Pyridylaldehyde[b]	1.7[d]	142.40	125.40	(161.90)	125.40	142.40	88.75[g]	
	6.5[d]	149.45	121.95	(151.95)	121.95	149.45	89.75	
		150.85	123.55	(142.30)	123.55	150.85	195.25	
Phenol	1.2	116.55	(156.55)	116.55	131.10	121.80	—	
	6.7	116.50	(156.55)	116.50	131.05	121.75	—	
	12.8	120.10	(167.45)	120.10	131.05	115.65	—	
Benzylalcohol	1.7	129.95	(141.45)	129.95	128.65	129.00	65.10[f]	
	7.0	129.95	(141.45)	129.95	128.65	129.05	65.10	
	12.6	129.85	(141.60)	129.85	128.60	128.90	65.05	
Benzylamine	0.6	130.35	130.65	(133.90)	130.65	130.35	44.65[f]	
	7.0	130.05	129.90	(133.70)	129.90	130.05	44.15	
	11.6	129.85	128.70	(144.30)	128.70	129.85	46.65	
3-Methylpyridine	1.2	141.10	(139.50)	148.25	127.40	138.70	18.85[h]	
	7.0	148.45	(134.65)	138.50	124.35	145.35	18.45	
	12.7	149.05	(134.25)	137.70	124.00	145.95	18.40	
4-Methylpyridine	1.2	140.60	128.50	(162.10)	128.50	140.60	22.95[i]	
	7.0	148.15	125.60	(149.60)	125.60	148.15	21.15	
	12.8	148.55	125.40	(149.05)	125.40	148.55	21.15	
3,4-Dimethylpyridine[c]	1.2	141.30	(137.30)	(158.15)	127.60	139.70	17.00[h]	20.65[i]
	6.0	145.95	(134.95)	(151.20)	126.15	143.85	16.60	19.65

[a]Chemical shifts in p.p.m. (±0.05) downfield from external Me_4Si; parentheses indicate substituted ring carbons.
[b]At alkaline p*H* values 4-pyridylaldehyde undergoes the Cannizaro reaction and cannot be studied.
[c]Insoluble above p*H* 6.0.
[d]Hydrated form of 4-pyridylaldehyde.
[e]2-CH_3.
[f]CH_2.
[g]CHO.
[h]3-CH_3.
[i]4-CH_3.

Can. J. Chem. Downloaded from www.nrcresearchpress.com by 210.87.254.6 on 09/05/12
For personal use only.

TABLE 2. ^{13}C chemical shifts[a] of some vitamin B_6 derivatives

	p*H*	C6	C5	C4	C3	C2	CH_3	CH_2(C5′)	CH_2(C4′)	CHO
Pyridoxine	2.3	130.95	137.90	141.70	153.80	143.80	15.50	58.05[b]	59.20[b]	—
	6.8	126.70	136.40	139.45	160.85	145.30	16.70	57.25[b]	59.85[b]	—
	12.5	133.50	133.50[b]	133.85[b]	161.60	151.25	19.95	58.55[b]	60.85[b]	—
Pyridoxamine	1.5	132.35	139.30	137.35	154.60	144.15	16.35	59.85	35.85	—
	6.5	124.45	137.00	133.50	164.05	146.00	16.35	60.20	37.70	—
	7.0	124.65	137.00	133.50	164.05	146.10	16.50	60.30	37.85	—
	12.7	133.80	133.80	137.75	161.35	151.05	20.35	61.40	37.45	—
Pyridoxal	1.8	126.70	139.25	141.05	150.15	145.10	15.35	71.00	—	99.60
	6.2	118.75	[c]	[c]	[c]	[c]	16.30	71.25	—	100.70
	12.5	127.30	134.95	131.80	162.20	153.35	19.70	67.65	—	134.00
Pyridoxamine phosphate	1.6	132.85	136.35	138.20	154.70	144.45	16.30	62.95	36.05	—
	7.0	125.10	135.80	134.00	163.65	145.95	16.35	62.85	37.55	—
	12.5	134.10	132.20	137.45	161.20	151.05	20.25	63.80	37.55	—
Pyridoxal phosphate	1.7	131.20	[c]	[c]	[c]	[c]	16.00	62.65	—	88.85
	4.0	129.20	[c]	[c]	[c]	[c]	15.60	62.45	—	89.00
		126.50[d]	136.00	126.95	163.65	152.80	16.95	63.45	—	197.00
	6.2	125.85	136.65	126.95	164.65	152.35	17.10	63.10	—	197.25
	12.4	129.40	133.80	125.20	168.35	157.50	20.10	63.60	—	197.65

[a]Chemical shifts in p.p.m. downfield from external Me_4Si.
[b]Pairs of resonances whose assignments may be reversed.
[c]Compound too insoluble to detect these quaternary carbons.
[d]Two species present at p*H* 4.0, the hydrated (δ_{CHO} 89.0 p.p.m.) and unhydrated aldehydes.

Can. J. Chem. Downloaded from www.nrcresearchpress.com by 210.87.254.6 on 09/05/12
For personal use only.

shifts except noticeably in the case of the C4 carbon where the calculated shifts are about 7 p.p.m. greater than the observed shifts in pyridoxine and pyridoxamine. It is also of note that the C4 and C5 side-chain CH_2 carbons in these derivatives are more shielded than the corresponding carbons in the monosubstituted benzene and pyridine derivatives. This must reflect a considerable change in the environment of the groups at C4 and to a lesser extent at C5 in the vitamin B_6 derivatives over those in the monosubstituted compounds. Stereochemically these side chains in the former cases are much more crowded than in the monosubstituted derivatives, and part of these shift anomalies may well be due to steric compression shifts. Why the C4 and side-chain carbons should reflect this more than the neighboring C5 carbon and CH_2 side-chain carbon remains speculative in the absence of a clear cut theory for such effects (19).

To investigate the applicability of steric compression shifts especially between C4 and C5 substituents of the vitamin B_6 derivatives, the ^{13}C n.m.r. spectra of the corresponding pyridine derivatives, 3-methyl-, 4-methyl-, and 3,4-dimethylpyridine, were studied at selected p*H* values. The lack of solubility of the dimethylpyridine at p*H* values greater than 6.0 made the study only possible at low p*H* values but the results obtained appear to be generally applicable (similar conclusions were reached for chloroform solutions). If the ^{13}C chemical shifts are calculated for 3,4-dimethylpyridine at p*H* 1.2, on an additivity basis from the methyl s.c.s. effects obtained from the monomethylpyridines, discrepancies from the observed shifts of up to 4 p.p.m. are evident. These steric compression effects are as expected from earlier work (20–23), *i.e.* greater shielding at 4-CH_3 (−2.3 p.p.m.), 3-CH_3 (−1.8 p.p.m.), C4 (−3.8 p.p.m.), and C3 (−2.1 p.p.m.), and effects of a smaller magnitude and either sign on the other ring carbons. It is interesting to note that the effects are largest on C4 and the 4-CH_3. The unsymmetrical nature of steric compression shifts in nitrogen heterocycles has been observed previously (23). A lack of reciprocity in steric shifts has been observed recently in 3-methylcholanthrene (24). Although the corresponding carbons (C4 and C5) in the side chains are not methyl groups but methylene functions in the vitamin B_6 derivatives, such sizeable steric compression shifts would be expected, perhaps of slightly smaller magnitude (23). Taking into account such effects in the calculations to predict the chemical shifts of the vitamin B_6 compounds yields a better fit between observed and calculated shifts thus reinforcing the assignments made (Table 2).

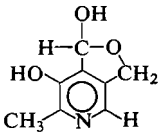

The major problem encountered in obtaining studies over the complete p*H* range was that pyridoxal at neutral p*H* and pyridoxal phosphate below p*H* 4.0 were virtually insoluble; even protracted accumulation (>24 h) of spectra did not yield measurable resonances for the quaternary ring carbons. Nevertheless it was clear from the ^{13}C spectra obtained for these compounds that at all p*H* values pyridoxal does not exist as the free aldehyde but as the hemiacetal form. This is indicated by the chemical shift of the 'aldehydic' carbon C4′ (100 p.p.m.). At p*H* 12.5 no resonance for the aldehydic carbon exists in either the normal range (~195 p.p.m.) nor in the hemiacetal region (~90 p.p.m.). A small peak does occur at 134.0 p.p.m. This may be a time average chemical shift for this carbon, in which case its position would indicate that the aldehyde to hemiacetal equilibrium is rapid and at alkaline p*H* values more free aldehyde form is present than at acid or neutral p*H* values. This is consistent with the results found from ^1H n.m.r. (8, 9) and u.v. spectroscopy (10), as discussed in detail by Korytnyk and Ahrens (8).

Pyridoxal phosphate clearly cannot form an intramolecular hemiacetal and the ^{13}C n.m.r. spectra are consistent with this; the aldehydic carbon resonance is at 197 p.p.m. However, although this compound is very insoluble at acid p*H* values it was possible to observe two forms of the aldehyde carbon at p*H* 4.0 and only one form at p*H* 1.7 which was different from that at neutral or alkaline p*H* values. At the former p*H* of 4.0 the free aldehyde and a hydrated form exist whereas at p*H* 1.7 only the hydrated form (δ 88.85 p.p.m.) is present in solution (*cf.* ref. 10).

The three-bond phosphorus–carbon couplings in the 5′-phosphates of pyridoxamine and pyri-

Can. J. Chem. Downloaded from www.nrcresearchpress.com by 210.87.254.6 on 09/05/12
For personal use only.

doxal contain conformational information. It has been shown in nucleotides (25–27) that vicinal $^{31}POC^{13}C$ couplings depend on the dihedral angle θ between the ^{31}POC and $OC^{13}C$ planes. An approximate relationship that can be used qualitatively for such compounds is (28):

$$^3J_{^{31}POC^{13}C} = J_0 \cos^2 \theta,$$

where J_0 was estimated from rigid cyclic nucleotides to be 8 Hz. Thus a large coupling (7–9 Hz) can be taken to indicate an average dihedral angle of 0° (eclipsed) or 180° (*trans* or *anti*) whereas a small coupling (1–2 Hz) is indicative of a 60° angle (*gauche*). Couplings between these extreme values are less straightforward to interpret, being possibly due to rapid interconversions between classical staggered rotamers or simply to a nonclassical dihedral angle. Also, the relationship above was tested only for nucleotides, and one cannot expect the same J_0 values when one carbon atom of the path is sp^2 hybridized. Nevertheless, the large values of the couplings observed for the vitamin B_6 derivatives strongly suggest that the phosphate group has a strong preference for the rotamer about the O—C5′ bond in which the phosphorus atom is *trans* to ring carbon C5. The eclipsed rotamer is excluded on steric grounds. The *trans* or extended rotamer has also been found to be preferred for the exocyclic phosphate groups of nucleotides (25, 27, 29), polynucleotides (25, 27, 29, 30), hexose 6-phosphates (31, 32), and polysaccharides (33). The small variation of the $^{31}POC^{13}C$ couplings with p*H* is similar to that found for nucleotides (29); it is due to effects of ionization of the phosphate group on the coupling constants and/or small changes in equilibrium conformation. Nevertheless, the strong preference for the *trans* rotamer is still evident at all p*H* values reported in Table 3.

The values of the two bond couplings, $^2J_{^{31}PO^{13}C}$, lie within the range 4.5 ± 0.5 Hz found for nucleotides (25, 27, 29) and hexose phosphates (31, 32). They thus provide valuable information in the case of difficult assignments.

In conclusion, substituent chemical shifts can be used to assign the ^{13}C resonances of substituted pyridines and vitamin B_6 derivatives. Changes in chemical shift are observed towards high field (low frequency, smaller chemical shift with respect to Me_4Si) due to steric interaction between the C4′ and C5′ methylene groups of the vitamin B_6 derivatives and the methyl groups of 3,4-dimethylpyridine. Pyridoxal exists in aqueous solution principally in the hemiacetal form; at high p*H* this is in rapid equilibrium with an appreciable population of the aldehyde form. Pyridoxal phosphate shows a preference for the free aldehyde form at high p*H*, a mixture of free and hydrated aldehydes at p*H* 4, and the hydrated aldehyde at p*H* 1.7. The phosphate groups of pyridoxamine 5′-phosphate and pyridoxal 5′-phosphate have a strong preference for the rotamer with the phosphorus atom *trans* to the ring carbon-5 at all p*H* values.

TABLE 3. ^{31}P–^{13}C coupling constants[a]

	p*H*	$^2J_{POC}$	$^3J_{POCC}$
Pyridoxamine phosphate	1.6	4.6	7.3
	7.0	4.1	7.6
	12.5	4.7	9.1
Pyridoxal Phosphate	1.7	[b]	[b]
	4.0	[b]	[b]
		5.0[c]	8.0[c]
	6.2	4.0	7.9
	12.4	4.3	7.6

[a]In Hz.
[b]Undetected.
[c]Two species present at p*H* 4.0, the hydrated and unhydrated aldehydes. The measurable couplings are for the latter species.

One of us (R.D.L.) would like to thank the Department of Organic Chemistry, University of Liverpool for facilities to complete this study.

1. A. E. BRAUNSTEIN and M. M. SHEMYAKIN. Biokhimiya, **18**, 393 (1953).
2. A. E. BRAUNSTEIN. *In* The enzymes. Vol. II. *Edited by* Boyer, Lardy, and Myrback. Academic Press, Inc., New York. 1960.
3. D. E. METZLER, M. IKAWA, and E. E. SNELL. J. Am. Chem. Soc. **76**, 648 (1954).
4. E. E. SNELL. Vitam. Horm. **16**, 77 (1958).
5. E. E. SNELL and W. T. JENKINS. J. Cellular Comp. Physiol. **54**, 161 (1959).
6. A-M. PERAULT, B. PULLMAN, and C. VALDEMORO. Biochim. Biophys. Acta, **46**, 555 (1961).
7. B. PULLMAN, C. SPANJAARD, and C. VALDEMORO. C. R. **248**, 2413 (1959).
8. W. KORYTNYK and H. AHRENS. *In* Methods in enzymology. Vol. XVIII, pt. A. *Edited by* S. P. Colwick and N. O. Kaplan. Academic Press, Inc., New York. 1970. p. 745.
9. K. F. TURCHIN, V. F. BYSTROV, M. YA. KARPEISKY, A. S. OLKHOVOY, V. L. FLORENTIER, and YU. N. SHEINKER. *In* Pyridoxal catalysis: enzymes and model systems. *Edited by* E. E. Snell, A. E. Braunstein, E. S. Severin, and Yu. M. Torchinsky. John Wiley-Interscience, New York. 1968. p. 67.
10. D. E. METZLER and E. E. SNELL. J. Am. Chem. Soc. **77**, 2431 (1955).
11. S. A. HARRIS, T. J. WEBB, and K. FOLKERS. J. Am. Chem. Soc. **62**, 3198 (1940).

12. D. MELNICK, M. HOCHBERG, H. W. HIMES, and B. L. OSER. J. Biol. Chem. **160**, 1 (1945).
13. E. A. PETERSON and H. A. SOBER. J. Am. Chem. Soc. **76**, 169 (1954).
14. D. HEYL, E. LUZ, S. A. HARRIS, and K. FOLKERS. J. Am. Chem. Soc. **73**, 3430 (1951).
15. A. K. LUNN and R. A. MORTON. Analyst, **77**, 718 (1952).
16. G. C. LEVY and G. L. NELSON. Carbon-13 nuclear magnetic resonance for organic chemists. Wiley-Interscience, New York. 1972.
17. J. B. STOTHERS. Carbon-13 NMR spectroscopy. Academic Press, New York. 1972.
18. L. F. JOHNSON and W. C. JANKOWSKI. Carbon-13 NMR spectra. Wiley-Interscience, New York. 1972.
19. E. LIPPMAA, T. PEHK, and J. PAASIVIRTA. Org. Magn. Reson. **5**, 277 (1973).
20. W. R. WOOLFENDEN. Ph.D. Thesis. University of Utah. 1965.
21. W. R. WOOLFENDEN and D. M. GRANT. J. Am. Chem. Soc. **88**, 1496 (1966).
22. D. M. GRANT and B. V. CHENEY. J. Am. Chem. Soc. **89**, 5315 (1967).
23. R. J. ABRAHAM, R. D. LAPPER, K. M. SMITH, and J. F. UNSWORTH. J. Chem. Soc. Perkin II, 1004 (1974).
24. R. OZUBKO, G. BUCHANAN, and I. C. P. SMITH. Can. J. Chem. **52**, 2493 (1974).
25. H. H. MANTSCH and I. C. P. SMITH. Biochem. Biophys. Res. Commun. **46**, 808 (1972).
26. R. D. LAPPER, H. H. MANTSCH, and I. C. P. SMITH. J. Am. Chem. Soc. **94**, 6243 (1972).
27. I. C. P. SMITH, H. H. MANTSCH, R. D. LAPPER, R. DESLAURIERS, and T. SCHLEICH. *In* Conformation of biological molecules and polymers. *Edited by* B. Pullman and E. D. Bergmann. Academic Press, New York. 1973. p. 381.
28. R. D. LAPPER, H. H. MANTSCH, and I. C. P. SMITH. J. Am. Chem. Soc. **95**, 2878 (1973).
29. T. SCHLEICH, B. CROSS, B. J. BLACKBURN, and I. C. P. SMITH. *In* Proceedings of the Steenbock Symposium, 1974. *Edited by* M. Sundaralingam. University Press, Baltimore, Md. In press.
30. G. GOVIL and I. C. P. SMITH. Biopolymers, **12**, 2589 (1973).
31. P. A. J. GORIN. Can. J. Chem. **51**, 2105 (1973).
32. D. R. BUNDLE, H. J. JENNINGS, and I. C. P. SMITH. Can. J. Chem. **51**, 3812, (1973).
33. D. R. BUNDLE, I. C. P. SMITH, and H. J. JENNINGS. J. Biol. Chem. **249**, 2275 (1974).
34. IUPAC-IUB. Biochem. J. **137**, 417 (1974).

Can. J. Chem. Downloaded from www.nrcresearchpress.com by 210.87.254.6 on 09/05/12
For personal use only.

The Crystal and Molecular Structure of the Dihydrochloride of 2-*trans*-6-Diethyl-2,4,4,6,8,8-hexamethylcyclotetraphosphazene

HARRY P. CALHOUN,[1] RICHARD T. OAKLEY, NORMAN L. PADDOCK,[2] AND JAMES TROTTER

Department of Chemistry, University of British Columbia, 2075 Wesbrook Place, Vancouver, British Columbia V6T 1W5

Received March 11, 1975

HARRY P. CALHOUN, RICHARD T. OAKLEY, NORMAN L. PADDOCK, and JAMES TROTTER. Can. J. Chem. **53**, 2413 (1975).

Octamethylcyclotetraphosphazene is deprotonated by methyllithium to form carbanions, which react with methyl iodide to give ethyl derivatives $N_4P_4Me_{8-n}Et_n$, $n \neq 4$; the structure of the dihydrochloride of the diethyl derivative, $N_4P_4Me_6Et_2 \cdot 2HCl$ has been determined. Its crystals are monoclinic, $a = 9.928(5)$, $b = 15.482(6)$, $c = 6.329(2)$ Å, $\beta = 103.29(2)°$, space group $P2_1/n$. The structure was determined from diffractometer X-ray data and refined by full-matrix least squares methods to R 0.079 for 715 observed reflections. The $N_4P_4Me_6Et_2H_2^{2+}$ ion lies on a crystallographic center of symmetry and the eight-membered phosphazene ring has the "chair" conformation. There are two significantly different P—N bond lengths, 1.665(6) and 1.572(7) Å, and two significantly different P—N—P angles, 126.7(6) and 139.8(6)°. The mean P—C bond length is 1.801(7) Å, and the mean N—P—N and C—P—C angles are 112.2(4) and 107.6° respectively. Bond lengths and angles in the phosphazene ring show the characteristic effects of π-electron localization found in other protonated phosphazene derivatives. The two ethyl groups are in *trans*-antipodal positions, corresponding to the least intramolecular electrostatic repulsion in the carbanion.

HARRY P. CALHOUN, RICHARD T. OAKLEY, NORMAN L. PADDOCK et JAMES TROTTER. Can. J. Chem. **53**, 2413 (1975).

L'octaméthylcyclotétraphosphazène est déprotoné par le méthyllithium formant ainsi des carbanions qui réagissent ensuite avec l'iodure de méthyle pour conduire à des dérivés éthylés $N_4P_4Me_{8-n}Et_n$, $n \neq 4$; on a déterminé la structure du chlorhydrate du dérivé diéthylé, $N_4P_4Me_6Et_2 \cdot 2HCl$. Les cristaux sont monocliniques $a = 9.928(5)$, $b = 15.482(6)$, $c = 6.329(2)$ Å, $\beta = 103.29(2)°$; groupe spatial $P2_1/n$. La structure a été déterminée par diffraction de rayons X à partir de mesures faites au diffractomètre. L'affinement par moindres carrés (matrice entière) conduit au facteur de reliabilité $R = 0.079$ pour 715 réflexions observées. L'ion $N_4P_4Me_6Et_2H_2^{2+}$ possède un centre de symétrie cristallographique et le cycle à huit membres du phosphazène à la conformation chaise. Il y a deux sortes de liens P—N significativement différents (1.665(6) et 1.572(7) Å) les uns des autres, et deux sortes d'angles P—N—P (126.7(6) et 139.8(6)°). La longueur moyenne du lien P—C est 1.801(7) Å, et les valeurs moyennes des angles N—P—N et C—P—C sont respectivement de 112.2(4) et de 107.6°. Les distances et les angles entre atomes du cycle phosphazénique montrent bien les effets caractéristiques de la localisation des électrons π tels qu'on les observe dans d'autres dérivés protonés du phosphazène. Les deux groupes éthyles sont en position *trans* et diamétralement opposés; cet arrangement correspond au minimum des répulsions électrostatiques intramoléculaires du carbanion. [Traduit par le journal]

Introduction

The substituent groups in the cyclic methylphosphazenes $(NPMe_2)_n$ are not inert, but react with methyllithium to form carbanions. The tetramer gives $N_4P_4(CH_3)_4(CH_2^-)_4$, from which such derivatives as $N_4P_4Me_4(CH_2XMe_3)_4$ (X = Si, Ge, Sn) are produced by reaction with Me_3XCl (1). Treatment of the carbanion with methyl iodide gives mainly the tetraethyl derivative $N_4P_4Me_4Et_4$, but a small amount of the diethyl derivative is also found. The structure of its dihydrochloride $N_4P_4Me_6Et_2 \cdot 2HCl$ is the first to have been determined of a diprotonated cyclotetraphosphazene, and is informative about the stereochemical course of carbanion formation in this series.

Experimental

Crystals of $N_4P_4Me_6Et_2 \cdot 2HCl$ were obtained from acetonitrile/benzene as colorless cubes. A crystal of approximate dimensions 0.20 × 0.20 × 0.35 mm was sealed in a thin-walled glass capillary tube. Crystal data:

[1]Present address: Chemistry Department, University of Alberta, Edmonton, Alberta T6T 2G2.

[2]To whom correspondence should be addressed.

Can. J. Chem. Downloaded from www.nrcresearchpress.com by 210.87.254.42 on 09/05/12
For personal use only.

Can. J. Chem. Downloaded from www.nrcresearchpress.com by 210.87.254.42 on 09/05/12
For personal use only.

$C_{10}H_{30}Cl_2N_4P_4$ f.w. = 401.18

Monoclinic, $a = 9.928(5)$, $b = 15.482(6)$, $c = 6.329(2)$ Å, $\beta = 103.29(2)°$, $U = 946.8(7)$ Å^3, $Z = 2$, $D_c = 1.407(1)$ g cm^{-3}, $F(000) = 424$. Space group $P2_1/n$ (C_{2h}^5). MoK_α radiation, $\lambda = 0.71069$ Å, $\mu(MoK_\alpha) = 6.8$ cm^{-1}.

A preliminary survey by film and diffractometer methods indicated that the crystal was suitable for data collection. Unit-cell parameters were obtained by least-squares refinement of 17 $\sin^2\theta$ (hkl) values measured on a General Electric XRD 6 diffractometer. Intensity data were measured on a Datex-automated General Electric XRD 6 diffractometer with zirconium filtered MoK_α radiation. All reflections with $2\theta(MoK_\alpha) < 45°$ were measured by use of a θ–2θ scan at 2 deg min^{-1} in 2θ over a range in 2θ of $(1.80 + 0.86 \tan\theta)°$, with 20 s background counts taken on either side of every scan. A check reflection, monitored every 30 reflections, was used to place the data on the same relative scale. The intensity of the check reflection showed only small fluctuations and was *ca.* 4% greater than its starting value at the end of the data collection. Of 1220 independent reflections measured 716 (59%) had intensities $> 3\sigma(I)$ above background, where $\sigma^2(I) = S + B + (0.05S)^2$, with S = scan count and B = background count (corrected to the time of the scan). These reflections were classified as observed. Lorentz and polarization corrections were applied and structure amplitudes derived. No corrections were made for absorption.

Structure Analysis

The molecule is required to have C_i symmetry. The structure was solved by direct methods. Sixteen sets of signs for 167 reflections with $|E| > 1.50$ were determined by a computer program which uses Sayre relationships in an iterative procedure (2). The starting set of reflections is given in Table 1.[3] One set of signs converged in 3 cycles and had the highest consistency index (2) (0.97) with 83 positive signs and 84 negative signs. An E map was computed using the 167 signed values of E from this set, and the positions of the chlorine atom and the two phosphorus atoms were obtained from the map. The two nitrogen and five carbon atoms were then located from a difference map. The structure was refined by full-matrix least-squares methods, initially with isotropic temperature factors and finally with anisotropic temperature factors for all nonhydrogen atoms. Hydrogen atoms could not be located with certainty from difference syntheses calculated at various stages of the refinement, and were not included in the calculations; a final difference map showed no exceptional features. Convergence was reached at R 0.079 for 715 observed reflections (one reflection, 101, was omitted from the refinement because of a suspected extinction error). On the last cycle of refinement no parameter shift was $> 0.4\sigma$.

Least-squares refinement was based on the minimization of $\Sigma w(|F_o| - |F_c|)^2$. Scattering factors were obtained from ref. 3. During the final stages of refinement, a weighting scheme of the form $w = [A + B|F_o| + C|F_o|^2 + D|F_o|^3]^{-1}$ was employed. The coefficients A, B, C, and D were adjusted to give uniform values of $\Sigma w(|F_o| - |F_c|)^2$ as a function of $|F_o|$, and this led also to uniformity with respect to $\sin\theta/\lambda$ and Miller indices; the values used in the final cycle were -2.719, 0.7890, -0.0359, and 0.00071, respectively. Unobserved reflections were given a weight of zero.

Final positional and thermal parameters are given in Table 2. A list of measured and calculated structure factors has been placed in the Depository of Unpublished Data.[3]

Results and Discussion

Bond lengths and angles (no thermal motion corrections) are given in Table 3, with their standard deviations. General views of its structure are shown in Figs. 1 and 2, a stereoview of the unit cell in Fig. 3.

The crystal structure consists of a $N_4P_4Me_6Et_2H_2^{2+}$ ion joined to two Cl^- ions by N^+—H. . .Cl^- hydrogen bonds. The geometry involving hydrogen bonded atoms is given in Table 4. The N(1). . .Cl distance, 3.06(1) Å, is quite short for a N^+—H. . .Cl^- hydrogen bond (4) and indicates that strong hydrogen bonds are formed in the present structure. Apart from the close contacts between hydrogen-bonded atoms the intermolecular distances are of the normal van der Waals type. Cl. . .C distances less than 3.8 Å include:[4] Cl. . .C(3) 3.69, Cl. . .C(1) 3.70, Cl. . .C(3)^{I} 3.76, Cl. . .C(4)^{II} 3.78, Cl. . .C(5)^{III} 3.79 Å. The shortest C. . .C intermolecular contact is C(1). . .C(4)^{II}, 3.79 Å. The structure of the cation can therefore be considered in isolation.

The $N_4P_4Me_6Et_2H_2^{2+}$ ion has exact C_i symmetry, both the protonated ring nitrogen atoms and the PMeEt groups being antipodal. In addition, C_i symmetry requires the ethyl groups to be in the *trans* configuration. Bond length and angle variations in the phosphazene ring and close N. . .Cl contacts indicate that the protonated atoms are N(1), N(1′). Six of the ring atoms, P(2), P(2′), N(1), N(1′), N(2), and N(2′), are nearly coplanar (Table 5), the deviations from their unweighted mean plane being 0.05–0.07 Å. The other two ring atoms, P(1) and P(1′), lie 0.74 Å above and below this plane. The "chair" conformation of the phosphazene ring can be seen in Fig. 2.

The centrosymmetrical structure is not un-

[3]Table 1 and the structure factor table are available, at a nominal charge, from the Depository of Unpublished Data, CISTI, National Research Council of Canada, Ottawa, Canada K1A 0S2.

[4]Roman numeral superscripts denote the following translations of atoms, relative to the reference atoms at x, y, z: I, $x - \frac{1}{2}, \frac{1}{2} - y, z - \frac{1}{2}$; II, $x - \frac{1}{2}, \frac{1}{2} - y, \frac{1}{2} + z$; III, $\frac{1}{2} + x, \frac{1}{2} - y, \frac{1}{2} + z$.

Can. J. Chem. Downloaded from www.nrcresearchpress.com by 210.87.254.42 on 09/05/12
For personal use only.

TABLE 2. Final positional parameters (fractional × 10^4) and thermal parameters[a] (anisotropic U_{ij}, Å^2 × 10^3) with standard deviations in parentheses. The molecular center is at ($\frac{1}{2}$, 0, 0)

Atom	x	y	z
Cl	4281(3)	3213(2)	808(6)
P(1)	3238(3)	610(2)	−222(5)
P(2)	5848(3)	1124(2)	−1444(5)
N(1)	4463(9)	1315(6)	−441(15)
N(2)	3801(9)	−136(6)	1435(15)
C(1)	2082(12)	1284(8)	839(21)
C(2)	2389(13)	267(8)	−2925(20)
C(3)	7170(12)	1835(8)	60(21)
C(4)	5497(14)	1488(9)	−4215(19)
C(5)	886(22)	805(14)	1257(39)

Atom	U_{11}	U_{22}	U_{33}	U_{12}	U_{13}	U_{23}
Cl	56(2)	37(2)	78(2)	−3(2)	32(2)	−13(2)
P(1)	32(2)	29(2)	56(2)	5(1)	28(1)	1(2)
P(2)	34(2)	27(2)	52(2)	0(1)	25(1)	2(1)
N(1)	37(5)	27(5)	67(6)	0(4)	32(5)	−2(5)
N(2)	38(6)	37(6)	60(6)	1(5)	33(4)	−3(5)
C(1)	47(7)	38(8)	86(10)	17(6)	44(7)	−3(7)
C(2)	43(7)	46(8)	73(9)	−6(6)	15(6)	−1(7)
C(3)	42(7)	43(8)	76(9)	−11(6)	24(6)	−8(6)
C(4)	71(10)	53(8)	48(7)	−4(7)	28(6)	6(6)
C(5)	112(16)	118(19)	175(20)	39(14)	87(15)	23(15)

[a]Thermal parameters are in the form: $\exp[-2\pi^2(U_{11}a^{*2}h^2 + U_{22}b^{*2}k^2 + U_{33}c^{*2}l^2 + 2U_{12}a^*b^*hk + 2U_{13}a^*c^*hl + 2U_{23}b^*c^*kl)]$. Equivalent positions are: $\pm(x, y, z; \frac{1}{2} + x, \frac{1}{2} - y, \frac{1}{2} + z)$.

TABLE 3. Bond lengths (Å) and angles (deg), with standard deviations in parentheses (σ for the mean values is the larger of the least-squares value and the r.m.s. deviation from the mean)

Bond	Length (Å)	Bonds	Angle (deg)
P(1)—N(1)	1.664(9)	P(1)—N(1)—P(2)	126.7(6)
P(2)—N(1)	1.667(9)	P(2′)—N(2)—P(1)	139.8(6)
Mean	1.665(6)		
		N(2)—P(1)—N(1)	112.5(5)
P(1)—N(2)	1.577(10)	N(1)—P(2)—N(2′)	111.9(5)
P(2)—N(2′)	1.567(9)	Mean	112.2(4)
Mean	1.572(7)		
		C(1)—P(1)—C(2)	109.1(6)
P(1)—C(1)	1.792(10)	C(3)—P(2)—C(4)	106.1(6)
P(1)—C(2)	1.805(12)		
P(2)—C(3)	1.808(12)	C(1)—P(1)—N(2)	109.7(5)
P(2)—C(4)	1.798(12)	C(1)—P(1)—N(1)	101.1(6)
Mean	1.801(7)	C(2)—P(1)—N(1)	107.8(5)
		C(2)—P(1)—N(2)	115.6(6)
C(1)—C(5)	1.48(3)	C(3)—P(2)—N(1)	104.7(5)
		C(3)—P(2)—N(2′)	117.2(5)
		C(4)—P(2)—N(1)	108.9(6)
		C(4)—P(2)—N(2′)	107.6(6)
		C(5)—C(1)—P(1)	112.7(11)

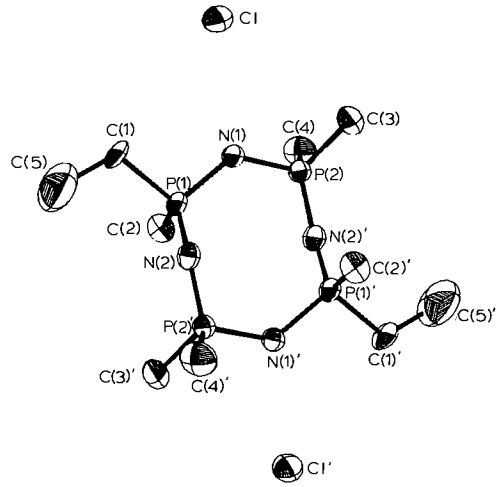

FIG. 1. General view of the $N_4P_4Me_6Et_2 \cdot 2HCl$ structure. Fifty percent probability thermal ellipsoids are shown.

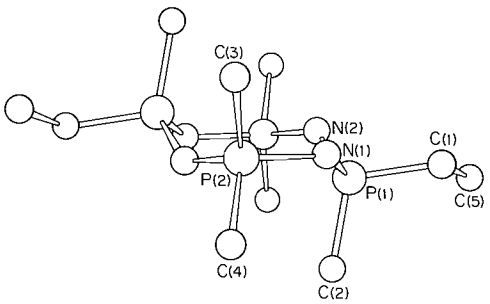

FIG. 2. General view of the $N_4P_4Me_6Et_2H_2^{2+}$ ion showing the chair conformation of the phosphazene ring.

common in phosphazene chemistry. Its occurrence in this molecule can be understood in terms of electrostatic repulsion between the CH_2^- groups of the carbanion, with the assumption that the further reaction with methyl iodide does not induce proton migration. Model calculations on molecules with the conformations found in 8-membered phosphazene rings (saddle, D_{2d}; tub, S_4; chair, C_{2h}; crown, C_{4v}) show that, for normal values of bond angles, repulsion in the dicarbanion is least in the *trans*-antipodal chair conformation, as found in the diethyl derivative. Coordination of lithium ions to both the methylene groups and the ring nitrogen atoms would also be especially easy for the chair conformation.

The more detailed structure can usefully be considered in relation to that of certain other

TABLE 4. Geometry about hydrogen bonded atoms

Parameter	Value
$Cl^-\ldots N(1)$	3.06(1) Å
$Cl^-\ldots N(1)P(1)$	121.4(4)°
$Cl^-\ldots N(1)P(2)$	111.8(4)°
P(1)N(1)P(2)	126.7(6)°

TABLE 5. Unweighted mean planes $lX + mY + nZ = p$[a]

	Plane	
	1[b]	2[c]
l	−0.4676	−0.2980
m	−0.1977	−0.2974
n	−0.8615	−0.9071
p	−2.3212	−1.4791
Distance from plane (Å)[d]		
P(1)	0.735	0.356
P(2)	−0.069	−0.024
N(1)	0.051	−0.219
N(2)	−0.065	−0.322

[a] X, Y, Z orthogonal coordinates (Å) with respect to a, b, c^*.
[b] Plane defined by P(2), N(1), N(2), P(2'), N(1'), N(2').
[c] Plane defined by all ring atoms.
[d] σ = 0.003 Å for P, 0.01 Å for N.

phosphazenes (Table 6). Structures **1**–**6** have exact C_i symmetry; the present structure resembles **4** and **5** most closely. All three deviate from $2/m$ (C_{2h}) symmetry, as shown in Table 7; for $2/m$ symmetry the torsion angles about the two bonds meeting at a given phosphorus atom are required to be numerically equal. The deviation from equality is greatest in $N_4P_4Me_6Et_2H_2^{2+}$, partly because of the bond length inequalities induced by protonation. Nevertheless, the conformations of the three molecules are very similar, probably for steric reasons. At N(1) only the p_z orbital is available for π-bonding, and, because of the large difference in the dihedral angles about P(1)N(1) and N(1)P(2), it overlaps different d-orbital combinations at P(1) and P(2). The two bond lengths are nevertheless equal within experimental error, so that any difference between the d-orbitals is too small to have an observable structural effect. A similar result was found for $N_4P_4Me_8H^+$ (12), and justifies the separate consideration of bond lengths and conformation.

There are two distinct P—N bond lengths in the phosphazene ring. The bonds meeting at the

Can. J. Chem. Downloaded from www.nrcresearchpress.com by 210.87.254.42 on 09/05/12
For personal use only.

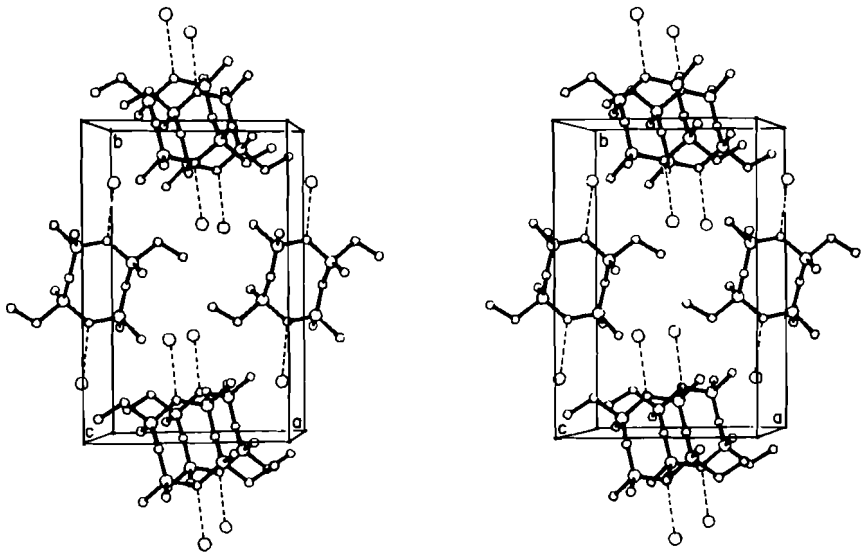

FIG. 3. Stereoview of the unit-cell. The origin is at the back lower left. Hydrogen bonds are indicated by dashed lines.

TABLE 6. Reference structures

Number	Compound	Reference	Number	Compound	Reference
1	T-$N_4P_4Cl_8$	5	**7**	$N_3P_3Cl_2(NHPr^i)_4 \cdot HCl$	11
2	$N_4P_4Cl_4Ph_4$	6	**8**	$(N_4P_4Me_8H)_2CoCl_4$	12
3	$N_4P_4(NHMe)_4Ph_4$	7	**9**	$(N_4P_4Me_8H)CuCl_3$	13
4	$N_4P_4Cl_2(NMe_2)_6$	8	**10**	$(N_5P_5Me_{10}H_2)CuCl_4 \cdot H_2O$	14
5	$N_4P_4Cl_6(NMe_2)_2$	9	**11**	$[N_3P_3(NMe_2)_6H]_2Mo_6O_{19}$	15
6	$N_4P_4F_4(NMe_2)_4$	10			

TABLE 7. Dihedral angles[a] (deg) in $N_4P_4X_6Y_2$ derivatives with C_i symmetry

Molecule	Bond			
	N(2)P(1)	P(1)N(1)	N(1)P(2)	P(2)N(2′)
$N_4P_4(NMe_2)_6Cl_2$ (**4**)	76	−61	19	44
$N_4P_4Cl_6(NMe_2)_2$ (**5**)	77	−65	26	41
$N_4P_4Me_6Et_2 \cdot 2HCl$	108	−66	20	69

[a]Angles between normals to the two successive PNP, NPN planes having the stated bond in common. The numbering scheme is that used for $N_4P_4Me_6Et_2H_2^{2+}$ (Fig. 1).

protonated nitrogen atoms, mean 1.665(6) Å, are significantly longer than the other P—N bonds, mean 1.572(7) Å. Some of the difference can be attributed to σ-hybridization effects, since the P(2′)N(2)P(1) angle, 139.8(6)°, is much larger than the P(1)N(1)P(2) angle, 126.7(6)°, indicating greater s-character in the hybrid orbitals at N(2), N(2′), but a substantial inequality remains after correction. The results are qualitatively consistent with a simple model, in which four electrons of one π-system are localized by the protonation of two antipodal nitrogen atoms. The bond lengths to these nitrogen atoms (1.665(6) Å) are similar to those in other protonated phosphazenes (Table 6): **7**, 1.666(5) Å; **8**, 1.695(15) Å; **9**, 1.670(14) Å; **10**, 1.671(12) Å; **11**, 1.669(6) Å. All correspond quite closely to the length of a PN bond in which only one π-system is operative. Calculations of bond order based on this model show that the

Can. J. Chem. Downloaded from www.nrcresearchpress.com by 210.87.254.42 on 09/05/12
For personal use only.

Can. J. Chem. Downloaded from www.nrcresearchpress.com by 210.87.254.42 on 09/05/12
For personal use only.

bonds to N(2) (1.572(7) Å) should be shorter than those in the neutral compound (1.596(5) Å in $N_4P_4Me_8$ (16)). The localization of π-electrons is expected, nevertheless, to increase the mean PN bond length, and it is consistent (since $CuCl_3^-$ is a poorer acceptor than H^+) that the mean bond length should increase in the series $N_4P_4Me_8$, $N_4P_4Me_8H^+$ (1.607 Å (12)), $N_4P_4Me_8HCuCl_3$ (1.614 Å (13)), $N_4P_4Me_6Et_2H_2^{2+}$ (1.620 Å).

The PNP bond angles, 126.7(6) and 139.8(6)° are significantly different from that in $N_4P_4Me_8$, 132.0(3)°. The angle at the protonated nitrogen atom is small, as in other protonated tetrameric and pentameric phosphazenes (**8**, mean 126.2°; **9**, 127.3(14)°; **10**, 129.0(4)° and 127.3(5)°). The NPN angles are equal within experimental error, the mean value, 112.2(4)°, being significantly smaller than the NPN angle in $N_4P_4Me_8$(119.8(2)°). Phosphazenes **8**–**10** also have small mean values for NPN angles; **8**, 115.5; **9**, 114.0; **10**, 112.7°. In a general way the results suggest a drift of electrons from phosphorus to nitrogen, to form either a localized pair or a stronger π-bond. The exocyclic CPC angles increase, ($N_4P_4Me_8$, 104.1(2)°); **8**, mean 106.4°; **9**, mean 106.6°; **10**, mean 107.4°; $N_4P_4Me_6Et_2H_2^{2+}$, 107.6°, to compensate the changes of NPN angle, so that the σ-bond structure is also changed as a result of protonation.

The P—C bonds are all equal to within experimental error, and the mean value, 1.801(7) Å, is similar to the P—C bond length in $N_4P_4Me_8$, mean value 1.805(8) Å. The C—C length, 1.48(3) Å, is shorter than expected. However, the anisotropic temperature factors for atom C(5) are approximately twice as large as those for the other atoms in the structure (Table 2). Some lengthening of the C(1)C(5) bond can be expected if correction for thermal motion is applied. Using a riding model, with C(5) riding on C(1) (which may not be completely valid because of the omission of hydrogen atoms), the C(1)C(5) bond is lengthened to 1.53(3) Å, close to the expected value for a $C(sp^3)$—$C(sp^3)$ single bond.

Conclusion

The electronic effects discussed above are similar to those found in many other phosphazene derivatives, and are compatible with models developed previously (17, 18) in which electrons of the ring nitrogen atoms and of the exocyclic groups compete for the acceptor orbitals of the phosphorus atoms, forming a double cyclic π-system. It is already known that the dimethylamino-group releases electrons conjugatively to the ring, and it can be expected that the CH_2^- group will do so even more strongly. The resultant spreading of the charge may well be a contributory cause of the stability of the multiply-charged carbanions; the electrostatic control of the stereochemistry shows that a substantial part of the charge is still localized on carbon.

We are grateful to the National Research Council of Canada for financial support, and for N.R.C.C. scholarships (to H.P.C., R.T.O.).

1. H. P. Calhoun, R. H. Lindstrom, R. T. Oakley, N. L. Paddock, and S. M. Todd. Chem. Commun. 343 (1975).
2. R. E. Long. Ph.D. Thesis. University of California at Los Angeles, Los Angeles, California. 1965.
3. D. T. Cromer and J. B. Mann. Acta Cryst. A**24**, 321 (1968).
4. G. C. Pimentel and A. L. McClellan. The hydrogen bond. Freeman, London, 1960.
5. A. J. Wagner and A. Vos. Acta Cryst. B**24**, 707 (1968).
6. G. J. Bullen, P. R. Mallinson, and A. H. Burr. Chem. Commun. 691 (1969).
7. G. J. Bullen and P. R. Mallinson. J. Chem. Soc. Dalton, 1412 (1972).
8. G. J. Bullen and P. E. Dann. J. Chem. Soc. Dalton, 705 (1974).
9. G. J. Bullen and P. E. Dann. J. Chem. Soc. Dalton, 1453 (1973).
10. D. Millington, T. J. King, and D. B. Sowerby. J. Chem. Soc. Dalton, 396 (1973).
11. N. V. Mani and A. J. Wagner. Acta Cryst. B**27**, 51 (1971).
12. J. Trotter and S. H. Whitlow. J. Chem. Soc. A, 460 (1970).
13. J. Trotter and S. H. Whitlow. J. Chem. Soc. A, 455 (1970).
14. H. P. Calhoun and J. Trotter. J. Chem. Soc. Dalton, 382 (1974).
15. H. R. Allcock, E. C. Bissell, and E. T. Shawl. Inorg. Chem. **12**, 2963 (1973).
16. M. W. Dougill. J. Chem. Soc. 5471 (1961).
17. D. P. Craig and N. L. Paddock. J. Chem. Soc. 4118 (1962).
18. D. W. J. Cruickshank. J. Chem. Soc. 5486 (1961).

Emission from Electronically Excited C_2

S. J. ARNOLD, G. H. KIMBELL, AND D. R. SNELLING

Defence Research Establishment Valcartier, P.O. Box 880, Courcelette, Quebec G0A 1R0

Received February 25, 1975

S. J. ARNOLD, G. H. KIMBELL, and D. R. SNELLING. Can. J. Chem. **53**, 2419 (1975).

Chemiluminescence attributable to the Swan, Phillips, and Ballik–Ramsay bands of C_2 was observed when halomethanes of the form $CH_{2-n}X_{2+n}$ (X = Cl, Br, I) were introduced into a stream of hydrogen atoms. The relative population of the $v' = 0$ levels of the $A\,^3\Pi_g$, $b\,^1\Pi_u$, and $A'\,^3\Sigma_g^-$ states are 10:400:1000 with the total rate of formation into all three states being approximately equal. The principal step for the formation of C_2^* is believed to be

$$C + CX \rightarrow C_2^* + X \text{ (X = halogen or hydrogen)}$$

S. J. ARNOLD, G. H. KIMBELL et D. R. SNELLING. Can. J. Chem. **53**, 2419 (1975).

La chimiluminescence attribuable aux bandes de Swan, Philipps et Ballik–Ramsay du C_2 est observée lorsque les méthanes halogénés de composition $CH_{2-n}X_{2+n}$ (X = Cl, Br, I) sont introduits dans un courant d'atomes d'hydrogène. La population relative des niveaux $v' = 0$ de chacun des états $A\,^3\Pi_g$, $b\,^1\Pi_u$, et $A'\,^3\Sigma_g^-$ est 10:400:1000, la vitesse totale de formation dans les trois états étant à peu près la même. On croit que l'étape déterminante de la formation de C_2^* est:

$$C + CX \rightarrow C_2^* + X \text{ (X = halogène ou hydrogène)}$$

[Traduit par le journal]

Introduction

Recently infrared chemiluminescence from the reactions of oxygen atoms with chloromethanes (1) and chloroethylenes (2) was reported. In the present study visible and infrared chemiluminescence from the reactions of hydrogen atoms with chloro, bromo, and iodomethanes is discussed. In 1952 Gaydon and Wolfhard (3) briefly discussed the visible chemiluminescence (250–600 nm) from the reaction of hydrogen atoms with CCl_4, $CHCl_3$, and $CHBr_3$. They observed strong emission attributable to the Swan ($A\,^3\Pi_g$–$X'\,^3\Pi_u$) system of C_2 as well as CH. In the present study C_2 emission from the Swan, Phillips ($b\,^1\Pi_u$–$X'\,^1\Sigma_g^+$), and Ballik–Ramsay ($A'\,^3\Sigma_g^-$–$X'\,^3\Pi_u$) systems was observed when hydrogen atoms reacted with CCl_4, $CHCl_3$, CH_2Cl_2, CBr_4, and $CHBr_3$ and from the Swan system when hydrogen atoms reacted with CH_2Br_2, CHI_3, and CH_2I_2.

Experimental

The experimental assembly is essentially identical to that shown in Fig. 1 of ref. 4. The reaction cell consisted of a 1.5 in. glass "tee" equipped with either an NaCl or quartz window and pumped by an Edwards 660 l/min two-stage pump. Hydrogen atoms, produced by passage of a hydrogen–helium mixture through a 2450 MHz microwave discharge, entered the cell through the center tube of the concentric mixer inlet jet. The organic halide in a helium buffer entered through five holes in the outer tube of the concentric mixer.

Initial low resolution spectroscopic studies of the wavelength region 1500–4000 nm were made with a McPherson Model 218, 0.3-m, *f*/5.3 monochromator equipped with a 300 lines/mm grating blazed at 3000 nm, a Dry Ice – acetone cooled PbS detector and PAR Model HR-8 amplifier. High resolution spectra were recorded using a Czerny–Turner 1.3-m *f*/7.5 spectrometer of local construction equipped with a 600 lines/mm grating blazed at 1600 nm. Mercury lines from a low pressure mercury lamp were used to obtain the wavelength calibration. The detectors, used with a phase-sensitive PAR Model HR-8 amplifier, were a Dry Ice – acetone cooled PbS, an R.C.A. liquid-nitrogen-cooled intrinsic germanium detector and a cooled EMI 9558 photomultiplier with an extended S-20 response. This assembly permitted spectroscopic study of the region 450–2000 nm, depending on the detector and filters used. The relative intensity of each band was determined by calibrating the detection system with a standard quartz–iodine lamp supplied by Eppley Laboratories Inc. (lamp number EPI 1057).

All gases were of the highest purity available from Matheson and were used without further purification. The CCl_4, $CHBr_3$, CHI_3, and CH_2I_2 were supplied by the J.T. Baker Chemical Co., the CHI_3 and CH_2Cl_2 by Fisher Scientific Co., and the CBr_4 by Matheson, Coleman and Bell.

The pressure for all experiments was (5.9 ± 0.1) Torr. The flow rates of inert buffer, He, of H_2, and of halomethane were 3.07, 1.88×10^{-1}, and 1.0×10^{-2} mmol s^{-1} respectively.

Results

When halomethanes of the form $CH_{2-n}X_{2+n}$ (X = Cl, Br, I) were introduced into a hydrogen atom stream, chemiluminescence attributable to the C_2 molecule was observed. Depending on the

Can. J. Chem. Downloaded from www.nrcresearchpress.com by 210.87.254.40 on 09/05/12
For personal use only.

TABLE 1. Swan, Phillips, and Ballik–Ramsay bands of C_2 observed from H-atom C_nX_{4-n} (X = Cl, Br, I) systems

	Ballik–Ramsay bands	Phillips bands	Swan bands
CCl_4	$\Delta v = -1\,(v' = 0, 1, 2)$ $\Delta v = 0\,(v' = 0, 1, 2)$ $\Delta v = +1\,(v' = 1, 2, 3, 4, 5)$ $\Delta v = +2\,(v' = 2, 3, 4, 5, 6, 7)$ $\Delta v = +3\,(v' = 3, 4, 5, 6, 7)$	$\Delta v = -1\,(v' = 0, 1)$ $\Delta v = 0\,(v' = 0, 1)$ $\Delta v = +1\,(v' = 1, 2)$ $\Delta v = +2\,(v' = 2, 3, 4, 5, 6)$ $\Delta v = +3\,(v' = 3, 4, 5)$ $\Delta v = +4\,(v' = 4, 5, 6, 7, 8)$ $\Delta v = +5\,(v' = 5, 6)$	$\Delta v = +1\,(v' = 1, 2, 3, 4)$ $\Delta v = 0\,(v' = 0, 1, 2)$ $\Delta v = -1\,(v' = 0, 1, 2, 3, 4)$
$CHCl_3$	$\Delta v = 0\,(v' = 0, 1, 2)$ $\Delta v = +1\,(v' = 1, 2, 3, 4, 5)$ $\Delta v = +2\,(v' = 2, 3, 4, 5, 6, 7)$ $\Delta v = +3\,(v' = 3, 4, 5, 6, 7, 8)$	$\Delta v = -1\,(v' = 0, 1)$ $\Delta v = 0\,(v' = 0, 1)$ $\Delta v = +1\,(v' = 1, 2)$ $\Delta v = +2\,(v' = 2, 3)$ $\Delta v = +3\,(v' = 3, 4, 5)$ $\Delta v = +4\,(v' = 4, 5)$ $\Delta v = +5\,(v' = 5, 6)$	$\Delta v = +1\,(v' = 1, 2, 3, 4)$ $\Delta v = 0\,(v' = 0, 1, 2)$ $\Delta v = -1\,(v' = 0, 1, 2, 3)$
CH_2Cl_2	$\Delta v = 0\,(v' = 0, 1, 2)$ $\Delta v = +1\,(v' = 1, 2, 3, 4)$ $\Delta v = +2\,(v' = 2, 3, 4, 5, 6, 7)$ $\Delta v = +3\,(v' = 3, 4, 5, 6)$	$\Delta v = -1\,(v' = 0)$ $\Delta v = 0\,(v' = 0, 1)$ $\Delta v = +1\,(v' = 1, 2)$ $\Delta v = +2\,(v' = 2, 3)$ $\Delta v = +3\,(v' = 3, 4, 5)$ $\Delta v = +4\,(v' = 4, 5)$ $\Delta v = +5\,(v' = 5, 6)$	$\Delta v = +1\,(v' = 1, 2, 3, 4)$ $\Delta v = 0\,(v' = 0, 1, 2)$ $\Delta v = -1\,(v' = 0, 1, 2)$
CBr_4	$\Delta v = 0\,(v' = 0, 1, 2)$ $\Delta v = +1\,(v' = 1, 2, 3, 4, 5)$ $\Delta v = +2\,(v' = 2, 3, 4, 5, 6, 7)$ $\Delta v = +3\,(v' = 3, 4, 5, 6, 7, 8)$	$\Delta v = -1\,(v' = 0, 1)$ $\Delta v = 0\,(v' = 0, 1)$ $\Delta v = +1\,(v' = 1, 2)$ $\Delta v = +2\,(v' = 2, 3, 4, 5, 6)$ $\Delta v = +3\,(v' = 3, 4, 5, 6)$ $\Delta v = +4\,(v' = 4, 5, 6, 7, 8, 9, 10)$ $\Delta v = +5\,(v' = 5, 6, 7, 8)$	$\Delta v = +1\,(v' = 1, 2, 3, 4)$ $\Delta v = 0\,(v' = 0, 1, 2)$ $\Delta v = -1\,(v' = 0, 1, 2, 3, 4)$ $\Delta v = -2\,(v' = 0, 1, 2, 3, 4, 5)$ $\Delta v = -3\,(v' = 0, 1, 2)$
$CHBr_3$	$\Delta v = 0\,(v' = 0, 1, 2)$ $\Delta v = +1\,(v' = 1, 2, 3, 4)$ $\Delta v = +2\,(v' = 2, 3, 4, 5, 6)$ $\Delta v = +3\,(v' = 3, 4, 5, 6, 7, 8)$	$\Delta v = -1\,(v' = 0, 1)$ $\Delta v = 0\,(v' = 0, 1)$ $\Delta v = +1\,(v' = 1, 2)$ $\Delta v = +2\,(v' = 2, 3, 4, 5, 6)$ $\Delta v = +3\,(v' = 3, 4, 5, 6)$ $\Delta v = +4\,(v' = 4, 5, 6, 7, 8, 9, 10)$ $\Delta v = +5\,(v' = 5, 6, 7, 8)$	$\Delta v = +1\,(v' = 1, 2, 3, 4)$ $\Delta v = 0\,(v' = 0, 1, 2)$ $\Delta v = -1\,(v' = 0, 1, 2, 3)$ $\Delta v = -2\,(v' = 0, 1, 2, 3, 4)$ $\Delta v = -3\,(v' = 0, 1, 2)$
CH_2Br_2			$\Delta v = +1\,(v' = 1, 2, 3, 4)$ $\Delta v = 0\,(v' = 0, 1, 2)$ $\Delta v = -1\,(v' = 0, 1, 2, 3)$
CHI_3			$\Delta v = +1\,(v' = 1, 2, 3, 4)$ $\Delta v = 0\,(v' = 0, 1, 2)$ $\Delta v = -1\,(v' = 0, 1, 2, 3, 4)$
CH_2I_2			$\Delta v = +1\,(v' = 1, 2, 3, 4)$ $\Delta v = 0\,(v' = 0, 1, 2)$ $\Delta v = -1\,(v' = 0, 1, 2, 3, 4)$

halomethane used, emission was observed from the Swan ($A\,^3\Pi_g$–$X'\,^3\Pi_u$), Phillips ($b\,^1\Pi_u$–$X\,^1\Sigma_g^+$), and Ballik–Ramsay ($A'\,^3\Sigma_g^-$–$X'\,^3\Pi_u$) systems of C_2. The observed bands are given in Table 1.

A portion of the spectra showing the $\Delta v = 1$ sequence of the Ballik–Ramsay bands is shown in Fig. 1. Rotational structure of the (1,0), (2,1), and (3,2) bands is clearly visible. Analysis of the band structure can be made by direct comparison with the more completely resolved spectra of Ballik and Ramsay (5). Values of J up to about 30 can clearly be identified as well as the characteristic triplet P, Q, R structure of the $^3\Sigma$–$^3\Pi$ transition.

Figure 2 shows a portion of the $\Delta v = 2$ sequence of the Phillips bands. The rotational structure of the (2,0), (3,1), and (4,2) bands has

Can. J. Chem. Downloaded from www.nrcresearchpress.com by 210.87.254.40 on 09/05/12
For personal use only.

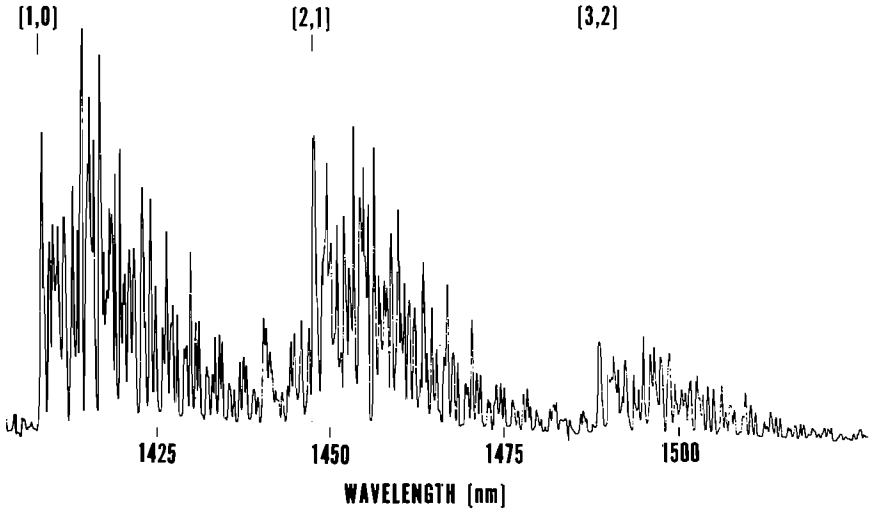

FIG. 1. A portion of the emission spectrum observed from the reaction of $CHBr_3$ with hydrogen atoms showing the $\Delta v = 1$ sequence of the Ballik–Ramsay ($A'\,^3\Sigma_g^- - X'\,^3\Pi_u$) system, recorded using a Czerny–Turner 1.3 m *f*/7.5 spectrometer.

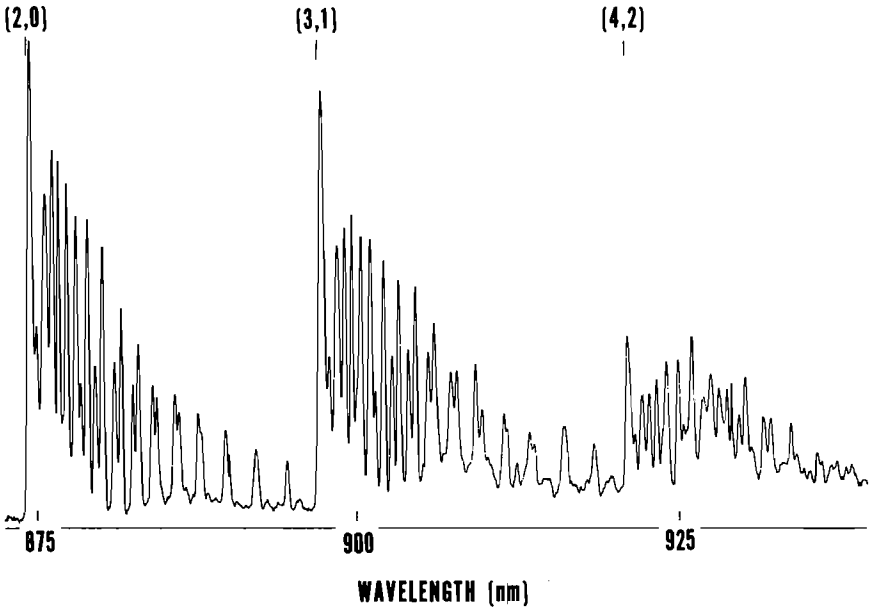

FIG. 2. A portion of the emission spectrum observed from the reaction of $CHBr_3$ with hydrogen atoms showing the $\Delta v = 2$ sequence of the Phillips ($b\,^1\Pi_u - X\,^1\Sigma_g^-$) system, recorded using a Czerny–Turner 1.3 m *f*/7.5 spectrometer.

been partially resolved. Band assignments were made by comparison with the data of Ballik and Ramsay (6).

The Swan bands were identified by comparison of the wavelengths of the band heads with those given by Tyte *et al.* (7).

Discussion

Jansson (8) has claimed that the C_2 Swan bands observed by Gaydon and Wolfhard in CCl_4 – H atom, $CHCl_3$ – H atom, and $CHBr_3$ – H atom flames were due to oxygen atoms originating from water vapor present in the hydrogen.

Can. J. Chem. Downloaded from www.nrcresearchpress.com by 210.87.254.40 on 09/05/12
For personal use only.

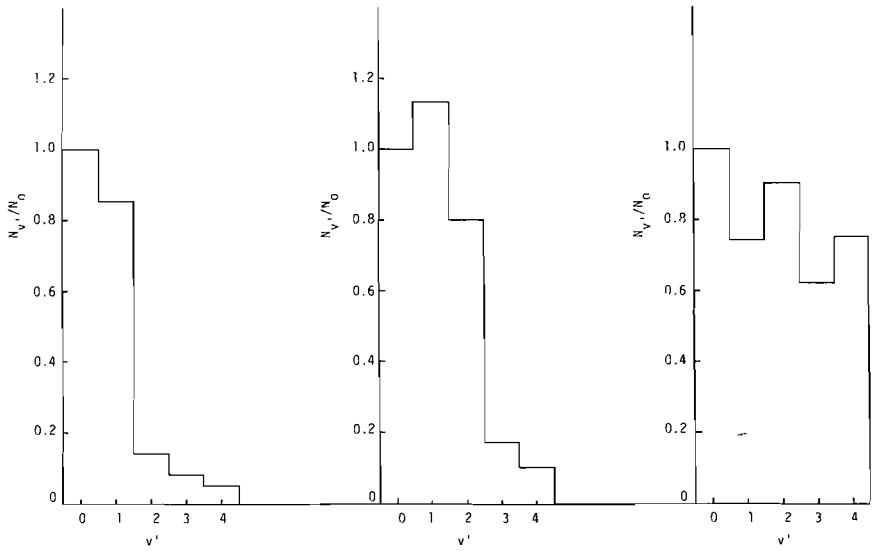

FIG. 3. Relative population distributions of C_2 in vibrational levels of the $A^3\Pi_g$ state, left to right CCl_4 – H atom system, $CHBr_3$ – H atom system, CH_2I_2 – H atom system.

In the present experiments the hydrogen–helium mixture was passed through three liquid nitrogen traps prior to passing through the microwave discharge. Contrary to Jansson's observations in a similar experiment, C_2 emission was observed in all three systems. It was not observed, however, when the hydrogen atoms were replaced by oxygen atoms. These observations suggest that the work of Jansson is in error.

Swan System

Emission of the C_2 Swan system was observed from each of the halomethane–hydrogen atom systems studied. The most intense emission for each halomethane was from the tetrahalide and the least intense from the dihalide. The maximum degree of excitation of C_2 was up to $v' = 5$ for the CBr_4–H system with excitation to $v' = 4$ being observed in all other systems.

The relative population distribution of C_2 in the vibrational levels $v' = 0$ to $v' = 4$ of the $A\,^3\Pi_g$ state is given for the CCl_4 – H atom system, the $CHBr_3$ – H atom system, and the CH_2I_2 – H atom system in Fig. 3. The population distributions were determined from the relative intensity measurements made on the $\Delta v = -1$ sequence of the Swan bands, corrected for differences in the spectral sensitivity of the detection system. The relative population ($N_{v'}/N_0$ = number of molecules in v'/number of molecules in $v' = 0$) was calculated from the expression:

$$[1] \qquad \frac{N_{v'}}{N_0} = \frac{I(v'v'')}{I(0v'')} \times \frac{\lambda(v'v'')}{\lambda(0v'')} \times \frac{A(0v'')}{A(v'v'')}$$

where I = intensity, λ = wavelength, A = Einstein A factor, as determined by Danylewych and Nicholls (9), and ($v'v''$) designates the band. The intensities were obtained from band area measurements, with ten data sets being measured in each case. The λ is included to convert the relative intensities from power units to photon units.

The relative population distribution appears to be a function of the halogen atom, with markedly different distributions being observed for the CCl_4 – H atom, $CHBr_3$ – H atom, and CH_2I_2 – H atom systems. For the CCl_4 – H atom system there is no indication of a population inversion with the maximum population being in the $v' = 0$ level. For the $CHBr_3$ – H atom system, there is an apparent population inversion with the $v' = 1$ level being preferentially populated. For the CH_2I_2 – H atom system, population maxima occur for $v' = 0$, $v' = 2$, and $v' = 4$. These distributions appear to be independent of the number of halogen atoms in the halomethane, *e.g.* there is no significant difference in the distribution obtained from the CBr_4–H atom system and from the $CHBr_3$–H atom system.

Can. J. Chem. Downloaded from www.nrcresearchpress.com by 210.87.254.40 on 09/05/12
For personal use only.

Can. J. Chem. Downloaded from www.nrcresearchpress.com by 210.87.254.40 on 09/05/12
For personal use only.

Assuming steady state conditions in the viewed region of the reaction vessel, the rate of formation of C_2 into a given vibrational level, R_v is given by

$$[2] \quad R_v = N_v \sum_{n=0}^{n} A(v, n) + N_v \sum_i k_v{}^i Q_i$$

where the second term represents the loss due to collisional deactivation ($k_v{}^i$ is the quenching rate constant and Q_i the concentration of the quencher). The radiative lifetime for molecules in the $A\,^3\Pi_g$ state is $\sim 1.5 \times 10^{-7}$ s. Under experimental conditions (pressure <6 Torr) a C_2 molecule in this state will undergo less than 10 collisions before radiating. In this and subsequent calculations hard sphere collision rates with helium as the predominant collision partner are quoted. Collision diameters used are 2.16 Å for helium and 3.72 Å for C_2, the latter being an assumed value by analogy with N_2 and CO. Collisional quenching is unlikely to proceed at the hard sphere collision rate. Thus the collisional quenching term can probably be neglected for molecules in the $A\,^3\Pi_g$ state. The loss term due to pumping of the excited molecules out of the reaction vessel has been neglected since this process is much slower than the radiative removal of excited species for all the bands considered. The values of N_v/N_1 ($v = 0$ to 4) obtained as in [1] were used in [2] to obtain the relative R_v's shown in Table 2. Collisional quenching has been neglected.

TABLE 2. Rate of formation of C_2 into vibrational levels of the $A\,^3\Pi_g$ state

	v				
System	0	1	2	3	4
CH_2I_2–H	1	0.72	0.84	0.55	0.65
$CHBr_3$–H	1	1.10	0.74	0.15	0.09
CCl_4–H	1	0.84	0.13	0.07	0.05

Phillips and Ballik–Ramsay Bands

Emission of the C_2 Phillips and Ballik–Ramsay systems was observed when hydrogen atoms were added to CH_2Cl_2, $CHCl_3$, CCl_4, $CHBr_3$, and CBr_4. No emission from either system could be detected when hydrogen atoms were added to CH_2Br_2, CH_2I_2, or CHI_3. This observation is consistent with the generally weaker emission observed from these chemical systems. The expected emission intensity would be below that capable of being detected by the experimental assembly employed. As in the case of the C_2 Swan system the most intense emission was from the tetrahalide.

The relative population of C_2 in each state was calculated from [1]. The required Einstein A factors were determined from the Franck–Condon factors calculated by Nicholls (10) and the electronic transition moments measured by Cooper and Nicholls.[1] The calculation of the relative populations for the Phillips and Ballik–Ramsay bands is less exact than the corresponding calculations for the Swan system. This results from the fact that the variation of the electronic transition moment with internuclear separation is not known for the Ballik–Ramsay and Phillips systems. When the additional errors arising from the band intensity measurements are taken into account the error in the relative populations of the Ballik–Ramsay and Phillips systems is probably of the order of $\pm 20\%$. For the $A'\,^3\Sigma_g{}^-$ state, the relative populations in the levels $v' = 0$ to $v' = 3$ were 1:0.8:0.9:0.5 for the CCl_4 – H atom system with a similar distribution being observed for the $CHBr_3$ – H atom system. For the $b\,^1\Pi_u$ state, the relative populations in levels $v' = 0$ to $v' = 8$ were 1:0.5:0.5:0.4:0.3:0.2:0.1:0.1 for the $CHBr_3$ – H atom system. A similar distribution was observed for the CCl_4 – H atom system.

For the $b\,^1\Pi_u$ state the radiative lifetime is $\sim 5 \times 10^{-6}$ s. Under experimental conditions a C_2 molecule in this state undergoes ~ 300 collisions before radiating. For the $A'\,^3\Sigma_g{}^-$ state the radiative lifetime is $\sim 1.5 \times 10^{-5}$ s with a molecule undergoing ~ 900 collisions before radiating. The assumption that collisional deactivation can be neglected when calculating the rate of formation into these states is not as justified as in the case of the $A\,^3\Pi_g$ state. However, when this assumption is made, the rate of formation into levels $v = 0$ to $v = 8$ of the $b\,^1\Pi_u$ state for the $CHBr_3$ – H atom system is 1:0.6:0.7:0.7:0.6:0.5:0.4:0.3:0.2 and into levels $v = 0$ to $v = 3$ of the $A'\,^3\Sigma_g{}^-$ state 1:1:1.1:0.7.

Since it was possible to measure bands from two different electronic transitions under identical experimental conditions, an estimate of the relative steady state populations of the $v' = 0$ levels of the $A\,^3\Pi_g$, $b\,^1\Pi_u$, and $A'\,^3\Sigma_g{}^-$ states

[1]D. M. Cooper and R. W. Nicholls. Private communication.

Can. J. Chem. Downloaded from www.nrcresearchpress.com by 210.87.254.40 on 09/05/12
For personal use only.

could be made. The relative populations are 10:400:1000 with the relative rates of formation into the $v' = 0$ level being 1.5:0.9:1.0 for the $CHBr_3 - H$ atom system. The overall rate of formation of the three states

$$\sum_{v=0}^{v(\max)} R_v$$

is approximately equal. The overall rate of formation into the $A'\,^3\Sigma_g^-$ and $b\,^1\Pi_u$ states may be underestimated because of the increased importance of collisional deactivation for these states.

Mechanism

The chemistry of these systems is sufficiently ill-defined to allow only a certain amount of speculation on the nature of the mechanism.

The initial step is most likely abstraction of a halogen atom by hydrogen

[3] $$H + CH_{2-n}X_{2+n} \rightarrow HX + CH_{2-n}X_{1+n}$$

Subsequent abstraction reactions from the parent compound or free radical intermediate by hydrogen or halogen atoms, formed via H + HX, lead to formation of CH and/or CX radicals (see refs. 1 and 11 for a discussion of these reactions). Atomic carbon can be formed by

[4] $$CX_1 + CX_2 \rightarrow C + CX_1X_2$$
(X_1, X_2 = halogen or hydrogen)

There is no evidence for the formation of $C(^1D)$ atoms from this reaction although the reaction is sufficiently exothermic to permit their formation. C_2 can then be formed in a variety of ways:

[5] $$C + C + M \rightarrow C_2 + M + 141.5 \text{ kcal/mol}$$

[6] $$C + CX \rightarrow C_2^* + X$$

[7] $$C + CH \rightarrow C_2^* + H + 60.5 \text{ kcal/mol}$$

[8] $$CX_1 + CX_2 \rightarrow C_2^* + X_1X_2$$

[9] $$CH + CH \rightarrow C_2^* + H_2 + 83.8 \text{ kcal/mol}$$

The principal step in the formation of C_2^* must be sufficiently exothermic to populate the highest observed level of the $A\,^3\Pi_g$ state and be capable of explaining the differences in the observed population maxima as a function of halogen for the $A\,^3\Pi_g$ state. The three-body association of C atoms, reaction 5, although certainly occurring, is not favored by the low pressures in the experimental system. It can also be rejected as the principal reaction for the formation of C_2 because it would lead to identical population distributions in all chemical systems. The four centered reactions 8 and 9 are probably less likely than the corresponding disproportionation reaction 4. Reaction 9 can also be rejected because it would lead to identical population distributions with varying halogen. Reaction 8 for $X_1 = X_2 =$ halogen is also ruled out because only in the case of X = I is it sufficiently exothermic to populate the $A\,^3\Pi_g$ state. For $X_1 = H$ and $X_2 =$ halogen, reaction 8 is sufficiently exothermic to populate up to $v' = 5$ for X = Cl ($\Delta H = -84$ kcal/mol), $v' = 2$ for X = Br ($\Delta H = -72 \pm 15$ kcal/mol), and $v' = 3$ for X = I ($\Delta H = -76$ kcal/mol). Reaction 7 can populate the $v' = 0$ level of the $A\,^3\Pi_g$ state and reaction 6 the $v' = 0$ level for X = Cl ($\Delta H \approx -61.8$ kcal/mol), up to $v' = 1$ for X = Br ($\Delta H = -66$ kcal/mol), and up to $v' = 5$ for I ($\Delta H = -85$ kcal/mol). Thus it appears that reaction 6 is the dominant reaction for the formation of C_2^* with a possible small contribution from reaction 8 when $X_1 = H$.

Palmer *et al.* (12) have observed emission from the C_2 Swan system in alkali metal atom – halomethane flames. The population distributions for the C_2 Swan bands observed in these flames are substantially different from those reported in Fig. 3. Palmer stated that the levels $v' \geq 6$ were populated by the C_2 molecule crossing from the $A'\,^3\Sigma_g^-$ state to the $A\,^3\Pi_g$ state. He claimed that if the contribution from these high pressure bands ($v' \geq 6$) (as observed in the alkali metal atom – CCl_4 flame) was subtracted from the distribution observed for the alkali metal atom – CBr_4 and the alkali metal atom – CI_4 flames, the resulting distribution was characteristic of reaction 6 with small contributions from the reaction sequence

[10] $$C + A_2 \rightarrow CA + A \quad (A = \text{alkali metal})$$

[11] $$CA + C \rightarrow C_2 + A$$

Palmer's resulting distribution for the alkali metal atom – CBr_4 flame is similar to that observed for the $CHBr_3 - H$ atom system with the differences being accounted for by the sequence 10 to 11.

Summary and Conclusions

When halomethanes of the form $CH_{2-n}X_{2+n}$ (X = Cl, Br, I) are added to a hydrogen atom stream chemiluminescence attributable to C_2^* is observed. Depending on the halomethane used, emission can be detected from just the Swan system or from the Swan, Phillips, and Ballik–Ramsay systems.

The relative population of vibrational levels of the $A\,^3\Pi_g$ state of C_2 is dependent upon the halogen atom present.

The relative population of the $v' = 0$ levels of the $A\,^3\Pi_g$, $b\,^1\Pi_u$, and $A'\,^3\Sigma_g^-$ states are 10:400:1000 with the total rate of formation into all three states being approximately equal.

The principal step for the formation of C_2* is believed to be

$$C + CX \rightarrow C_2 + X \quad (X = \text{halogen or hydrogen})$$

with contributions from

$$CH + CX \rightarrow C_2 + HX \quad (X = \text{halogen})$$

1. S. J. ARNOLD, G. H. KIMBELL, and D. R. SNELLING. Can. J. Chem. **52**, 271 (1974).
2. S. J. ARNOLD, G. H. KIMBELL, and D. R. SNELLING. Can. J. Chem. **52**, 2608 (1974).
3. A. G. GAYDON and H. G. WOLFHARD. Proc. R. Soc. Lond. A**213**, 366 (1952).
4. S. J. ARNOLD and G. H. KIMBELL. Can. J. Chem. **51**, 451 (1973).
5. E. A. BALLIK and D. A. RAMSAY. Astrophys. J. **137**, 61 (1963).
6. E. A. BALLIK and D. A. RAMSAY. Astrophys. J. **137**, 84 (1963).
7. D. C. TYTE, S. H. INNANEN, and R. W. NICHOLLS. Identification atlas of molecular spectra. 5. York University, Toronto. 1967.
8. R. E. W. JANSSON. Chem. Commun. **14**, 320 (1965).
9. L. L. DANYLEWYCH and R. W. NICHOLLS. Proc. R. Soc. Lond. A**339**, 197 (1974).
10. R. W. NICHOLLS. J. Res. Natl. Bur. Stand. **69**A, 397 (1965).
11. D. T. CLARK and J. M. TEDDER. Trans. Faraday Soc. **62**, 405 (1966).
12. H. B. PALMER, A. TEWARSON, D. W. NAEGELI, and C. M. PATHAK. Molecular luminescence. *Edited by* E. C. Lim. W. A. Benjamin, Inc., New York. 1969. pp. 493–507.

Can. J. Chem. Downloaded from www.nrcresearchpress.com by 210.87.254.40 on 09/05/12
For personal use only.

Metal Halide Ammines. III. Thermal Analyses and Calorimetry of Fluorosilicate Ammines and Hydrates of Bivalent Metals. Infrared Spectra of the Ammines

KASHINATH C. PATIL AND ETALO A. SECCO[1]

Department of Chemistry, St. Francis Xavier University, Antigonish, Nova Scotia B0H 1C0

Received March 10, 1975

KASHINATH C. PATIL and ETALO A. SECCO. Can. J. Chem. **53**, 2426 (1975).

Bivalent metal fluorosilicate ammines have been prepared. The thermal analyses of the dodecammines reveal the decomposition to occur via the pentammine and/or tetrammine. The final ammonia loss is concomitant with fluorosilicate decomposition. Calorimetric data are given for the decomposition reactions. Some fluorosilicate hydrates are included for comparison purposes.

The infrared spectral data of the ammines are presented with their assignments.

KASHINATH C. PATIL et ETALO A. SECCO. Can. J. Chem. **53**, 2426 (1975).

On a préparé des fluorosilicates d'ammines de métaux bivalents. Les analyses thermiques des dodécammines montrent que la décomposition se fait en passant par une pentammine et/ou une tétrammine. La perte finale d'ammoniac se fait en même temps que la décomposition du fluorosilicate. On présente les données calorimétriques des réactions de décomposition. On a inclus quelques fluorosilicates hydratés à des fins de comparaison.

On présente l'interprétation des spectres infra-rouge des ammines.

[Traduit par le journal]

Introduction

The physico-chemical properties and the infrared spectra of metal fluorosilicate hydrates have been described in the literature (1–4). The crystal structures of Fe(II) and Co(II) fluorosilicate hydrates indicate strong H-bonding (5, 6). To our knowledge no study of fluorosilicate ammines is recorded since their preparation is precluded by the instability of SiF_6^{2-} in an alkaline medium (3).

Recently, we prepared fluorosilicate ammines by the simple displacement reaction reported earlier (7), *i.e.* reacting fluoride hydrates with liquid ammonia. The purpose of this paper is to report on the thermal decomposition, heat of decomposition, relative stability, and infrared spectra of fluorosilicate ammines of some bivalent metals; the analogous hydrates were also reinvestigated and included for comparison purposes.

Experimental

All the metal fluorosilicate hydrates studied were prepared by the reaction of the corresponding oxide or carbonate with fluorosilicic acid (1). The fluorosilicates of Mg, Mn, Fe, Co, Ni, Zn, Cu, and Cd crystallized as hexahydrates; Ca and Sr formed dihydrates whereas Ba precipitated as the anhydrous salt.

Transition metal fluorosilicate hexahydrates refluxed with anhydrous liquid ammonia (7) yielded dodecammines; magnesium fluorosilicate hexahydrate formed hexammine while Ca and Sr hydrates converted to diammines. The ammines were characterized by their infrared spectra, Table 1, and thermogravimetric data, Table 3.

All our measurements were done with freshly prepared samples; the dodecammines were observed to decompose on prolonged storage at room temperature.

The heating traces were recorded on a duPont Thermal Analyzer DTA-900 and TGA-950 described earlier (8); the heats of decomposition were determined using a duPont calorimeter cell (9). X-ray diffraction patterns of solid specimens were obtained using CuK_α and MoK_α radiation (10). Infrared spectra were recorded on a Perkin-Elmer Model-180 spectrophotometer using the standard pellet technique with KBr as the matrix material.

Results and Discussion

Thermal Analyses

The thermogravimetric (t.g.) and differential thermal analysis (d.t.a.) results for the hydrates are presented in Table 2. The results for the transition metal compounds are consistent with a single step decomposition, *viz.*

[1] $$MSiF_6 \cdot 6H_2O_{(s)} \rightarrow MF_{2(s)} + SiF_{4(g)} + 6H_2O_{(g)}$$

where M = Mn, Fe, Co, Ni, Cu, Zn, Cd, and Mg. The metal fluoride residue in each case was confirmed by X-ray diffraction. The alkaline earth metal fluorosilicate hydrates undergo strict dehydration followed by decomposition of the fluorosilicate at a higher temperature,

[1]To whom correspondence should be addressed.

Can. J. Chem. Downloaded from www.nrcresearchpress.com by 210.87.254.6 on 09/05/12
For personal use only.

TABLE 1. Infrared absorption frequencies of metal fluorosilicate ammines (cm^{-1})*

Compound	$\nu_{(NH)_{as}}$	$\nu_{(NH)_s}$	$\delta_{(NH_3)_d}$	$\delta_{(NH_3)_s}$	$\rho_{(NH_3)}$	$\nu_{(M-F)}$	$\nu_{(M-N)}$	SiF_6^{2-} ν_3	SiF_6^{2-} ν_4
$MnSiF_6 \cdot 12NH_3$	3300–3000(vb)		1650(m) 1400(s)	1050(s,sp)	—	420(sh)	—	740(vs)	485(s,sp)
$CoSiF_6 \cdot 12NH_3$	3400–3100(vb)		1620(m) 1400(s)	1325(w) 1175(s) 1050(w)	650(m)	—	320(m)	740(vs)	485(s,sp)
$NiSiF_6 \cdot 12NH_3$	3380(s) 3300(s,sp)	3220(w)	1625(s) 1400(m)	1225(w) 1210(s) 1185(s)	660(w)	420(w)	340(m)	745(vs)	485(s,sp)
$CuSiF_6 \cdot 12NH_3$	3340(s) 3250(s)	3270(w)	1605(m) 1430 1410(s)	1255(s,sp)	—	—	—	740(vs)	584(s,sp)
$ZnSiF_6 \cdot 12NH_3$	3360(s) 3300(s)	3210(w) 3160(w)	1640 1620(s) 1430 1400(s)	1270(s) 1230(s)	590(w)	435(w)	—	740(vs)	485(s,sp)
$CdSiF_6 \cdot 12NH_3$	3440(s) 3260(s)	3180(sh)	1570(s) 1430 1400(s)	1200(s) 1095(m)	580(m) 560(m)	—	—	740(vs)	485(s,sp)
$MgSiF_6 \cdot 6NH_3$	3350(s,b)	3100(sh)	1625(m) 1440 1410(w)	1265(s) 1245(s) 1050(w)	—	420(sh)	—	740(vs)	485(s,sp)
$CaSiF_6 \cdot 2NH_3$	3350(b)	3125(w)	1650(m) 1410(s)	1200(s) 1100(s)	—	—	—	750(vs)	485(s,sp)
$SrSiF_6 \cdot 2NH_3$	3340(s)	3100(b)	1650(m) 1405(s)	1200(s) 1100(s)	—	—	—	750(vs)	485(s,sp)

*vs—very strong, s—strong, m—medium, w—weak, b—broad, sh—shoulder, sp—sharp.

TABLE 2. Thermogravimetric and differential thermal analysis data of $MSiF_6 \cdot 6H_2O$

	Thermogravimetric analysis				Differential thermal analysis	
			% total weight lost			
M	Step number	Temperature (°C)	Observed	Calculated	Reaction	Peak temperature (°C)*
Mn	1	80–275	69.05	69.46	[1]	185
Fe	1	90–250	68.66	69.32	[1]	200
Co	1	100–250	67.07	68.66	[1]	230
Ni	1	100–300	67.87	68.66	[1]	240
Zn	1	90–260	66.17	67.20	[1]	195
Cd	1	90–200	58.35	58.49	[1]	200
Cu	1	110–300	67.20	67.30	[1]	250
Mg	1	80–250	76.87	77.27	[1]	185
$Ca(2H_2O)$	1	100–155	16.36	16.46	[2*a*]	165
	2	225–325	63.03	63.24	[2*b*]	325
$Sr(2H_2O)$	1	110–165	13.47	13.50	[2*a*]	155
	2	300–425	52.75	52.75	[2*b*]	420
Ba†	1	410–525	35.60	37.20	[2*b*]	535

*All endotherms.
†Anhydrous $BaSiF_6$.

Can. J. Chem. Downloaded from www.nrcresearchpress.com by 210.87.254.6 on 09/05/12
For personal use only.

TABLE 3. Thermogravimetric and differential thermal analysis data of $MSiF_6 \cdot 12NH_3$

	Thermogravimetric analysis					Differential thermal analysis		
			% total weight lost					
M	Step number	Temperature (°C)	Observed	Calculated	Reaction	Peak number	Peak temperature (°C)	Reaction
Mn	1	25–150	34.32	33.91	[3*a*]	1	115	[3*a*]
	2	150–300	77.08	76.80	[3*c*]	2	300	[3*c*]
Co	1	25–130	28.55	29.37	[3*a*]	1	145	[3*a*]
	2	150–310	76.00	75.68	[3*b*,3*c*]	2	220	[3*b*]
						3	325	[3*c*]
Ni	1	25–100	28.50	29.37	[3*a*]	1	150	[3*a*]
	2	150–300	75.13	75.73	[3*b*,3*c*]	2	320	[3*b*]
						3	360	[3*c*]
Cu	1	25–130	29.07	29.04	[3*a*]	1	115	[3*a*]
	2	180–340	74.35	75.18	[3*b*,3*c*]	2	340	[3*b*]
						3	355	[3*c*]
Zn	1	25–180	28.72	28.92	[3*a*]	1	120	[3*a*]
	2	200–320	74.83	74.86	[3*b*,3*c*]	2	250	[3*b*]
						3	320	[3*c*]
Cd	1	25–140	29.38	29.65	[3*a*]	1	110	[3*a*]
	2	190–325	66.38	67.16	[3*c*]	2	300	[3*c*]
$Mg(6NH_3)$*	1	25–180	26.99	25.33	$4NH_3$ loss	1	115, 170	$4NH_3$ loss
	2	180–330	76.57	76.79	[4]	2	275	[4]
$Ca(2NH_3)$*	1	150–300	63.00	62.88	[4]	1	275	[4]
$Sr(2NH_3)$*	1	150–300	60.57	61.25	[4]	1	300	[4]

*$(6NH_3)$ and $(2NH_3)$ indicate fluorosilicate hexammine and diammine, respectively.
†All endotherms.

[2*a*] $MSiF_6 \cdot 2H_2O_{(s)} \rightarrow MSiF_{6(s)} + 2H_2O_{(g)}$ M = Ca, Sr

[2*b*] $MSiF_{6(s)} \rightarrow MF_{2(s)} + SiF_{4(g)}$ M = Ca, Sr, and Ba

The solids from [2*a*] and [2*b*], $MSiF_6$ and MF_2, were identified by infrared and X-ray diffraction.

The decomposition temperatures of the fluorosilicates observed in this work are higher than those reported elsewhere (3).

The t.g. and d.t.a. results for the ammines are summarized in Table 3. The transition metal dodecammines decompose via the pentammine and/or tetrammine intermediate, *i.e.*

[3*a*] $MSiF_6 \cdot 12NH_{3(s)} \rightarrow MSiF_6 \cdot xNH_{3(s)} + (12 - x)NH_{3(g)}$

[3*b*] $MSiF_6 \cdot 5NH_{3(s)} \rightarrow MSiF_6 \cdot 4NH_{3(s)} + NH_{3(g)}$

[3*c*] $MSiF_6 \cdot 4NH_{3(s)} \rightarrow MF_{2(s)} + SiF_{4(g)} + 4NH_{3(g)}$

where $x = 5$ for Co, Ni, Cu, and Zn and $x = 4$ for Mn and Cd. The NH_3 molecules are so strongly bound to SiF_6 in the tetrammine that the release of NH_3 effects a breakdown of the SiF_6 unit. The evolved gases were identified as NH_3 and SiF_4; the solids were identified by infrared and X-ray diffraction.

$MgSiF_6 \cdot 6NH_3$ decomposes via the diammine intermediate to the fluoride according to [4],

[4] $MSiF_6 \cdot 2NH_{3(s)} \rightarrow MF_{2(s)} + SiF_{4(s)} + 2NH_{3(g)}$

where M = Mg, Ca, and Sr. Assuming the N—H. . .F hydrogen bond analog of O—H. . .F is present, the release of the final NH_3 effects a concomitant rupture of the SiF_6^{2-} unit suggesting increased overlap by the NH_3 molecules with SiF_6 relative to H_2O in the hydrates for Ca and Sr compounds.

Calorimetric Studies

The calorimetric results along with related enthalpic values for the decomposition of metal fluorosilicate hydrates and ammines are given in Table 4; the calculated enthalpy of formation values for the compounds are also included.

Can. J. Chem. Downloaded from www.nrcresearchpress.com by 210.87.254.6 on 09/05/12
For personal use only.

TABLE 4. Calorimetric results of fluorosilicate hydrates and ammines

Reaction	Compound	Temperature (°C)	ΔH of decomposition (kcal/mol)*	$-\Delta H_f^\circ$ (kcal/mol)†
$MSiF_6 \cdot 6H_2O_{(s)} \rightarrow MF_{2(s)} + SiF_{4(g)} + 6H_2O_{(g)}$	$MnSiF_6 \cdot 6H_2O$	80–190	98.0 ± 0.5	1004
	$FeSiF_6 \cdot 6H_2O$	105–210	106.0 ± 0.5	990
	$CoSiF_6 \cdot 6H_2O$	120–240	107.0 ± 0.5	983
	$NiSiF_6 \cdot 6H_2O$	130–250	107.5 ± 0.5	984
	$CuSiF_6 \cdot 6H_2O$	150–250	91.5 ± 0.5	936
	$ZnSiF_6 \cdot 6H_2O$	80–225	98.0 ± 0.5	988
	$CdSiF_6 \cdot 6H_2O$	80–190	107.0 ± 0.2	993
	$MgSiF_6 \cdot 6H_2O$	95–220	93.0 ± 0.2	1074
$MSiF_6 \cdot 2H_2O_{(s)} \rightarrow MSiF_{6(s)} + 2H_2O_{(g)}$	$CaSiF_6 \cdot 2H_2O$	130–200	20.5 ± 0.1	811
	$SrSiF_6 \cdot 2H_2O$	100–170	26.0 ± 0.2	824
$MSiF_{6(s)} \rightarrow MF_{2(s)} + SiF_{4(g)}$	$CaSiF_6$	225–325	15.0 ± 0.1	675
	$SrSiF_6$	350–450	22.0 ± 0.2	682
$MSiF_6 \cdot 4NH_{3(s)} \rightarrow MF_{2(s)} + SiF_{4(g)} + 4NH_{3(g)}$	$MnSiF_6 \cdot 4NH_3$	200–325	68.3 ± 0.3	670
	$CoSiF_6 \cdot 4NH_3$	215–315	66.0 ± 0.5	640
	$NiSiF_6 \cdot 4NH_3$	200–325	65.6 ± 0.1	640
	$ZnSiF_6 \cdot 4NH_3$	200–325	63.0 ± 0.5	650
	$CdSiF_6 \cdot 4NH_3$	215–300	53.0 ± 0.3	632
$CuSiF_6 \cdot 5NH_{3(s)} \rightarrow CuF_{2(s)} + SiF_{4(g)} + 5NH_{3(g)}$	$CuSiF_6 \cdot 5NH_3$	205–330	98.0 ± 0.2	650
$MSiF_6 \cdot 2NH_{3(s)} \rightarrow MF_{2(s)} + SiF_{4(g)} + 2NH_{3(g)}$	$MgSiF_6 \cdot 2NH_3$	200–325	45.5 ± 0.2	700
	$CaSiF_6 \cdot 2NH_3$	200–310	47.5 ± 0.2	740
	$SrSiF_6 \cdot 2NH_3$	200–300	40.5 ± 0.5	722

*All determinations done in duplicate; ΔH values with average deviation.
†These values calculated using ΔH_f° values of $MF_{2(s)}$, $H_2O_{(g)}$, $NH_{3(g)}$, and $SiF_{4(g)}$ given in N.B.S. circular 500 (1952, Technical Notes 270-3 (1968) and 270-4 (1969), Washington, D.C.

Infrared Spectral Data

The infrared absorption frequencies of the fluorosilicate ammines in Table 1 show the characteristic frequencies of coordinated ammonia and SiF_6^{2-}. The observed frequency $\sim 320\ cm^{-1}$ for Co and Ni fluorosilicate ammines is assigned to $\nu_{(M-N)}$ mode. While we are prompted to assign the band $\sim 420\ cm^{-1}$ to $\nu_{(M-F)}$ as in the fluoride ammines (7), this assignment may be inconsistent with some fluorosilicate hydrates (6) where no direct M—F interaction is observed.

Grateful acknowledgment is made to the National Research Council of Canada and the University Council for Research for financial support of this research program.

1. J. W. MELLOR. A comprehensive treatise of inorganic and theoretical chemistry, Vol. 6, Longmans, Green and Co., New York. 1925. p. 940.
2. H. REMY. Treatise on inorganic chemistry, Vol. 1. Elsevier Publishing Co., New York. 1956. p. 481.
3. I. G. RYSS. The chemistry of fluorine and its inorganic compounds. U.S. Atomic Energy Commission Translation Series, AEC tr. 3927 Part 1. 1960. p. 370.
4. R. B. BADACHHAPE, G. HUNTER, L. D. MCCORY, and J. L. MARGRAVE. Inorg. Chem. **5**, 929 (1966).
5. W. C. HAMILTON. Acta Cryst. **15**, 353 (1962).
6. H. LYNTON and P. Y. SIEW. Can. J. Chem. **51**, 227 (1973).
7. K. C. PATIL and E. A. SECCO. Can. J. Chem. **50**, 567 (1972).
8. O. K. SRIVASTAVA and E. A. SECCO. Can. J. Chem. **45**, 579 (1967).
9. P. RAMAMURTHY and E. A. SECCO. Can. J. Chem. **46**, 3605 (1968).
10. E. A. SECCO. Can. J. Chem. **42**, 2143 (1964).

Can. J. Chem. Downloaded from www.nrcresearchpress.com by 210.87.254.6 on 09/05/12
For personal use only.

The Charge Transfer Photochemistry of the Hexaaquoiron(III) Ion, the Chloropentaaquoiron(III) Ion, and the μ-Dihydroxo Dimer Explored with *tert*-Butyl Alcohol Scavenging[1]

COOPER H. LANGFORD[2] AND JOHN H. CAREY

Department of Chemistry, Carleton University, Ottawa, Canada K1S 5B6

Received February 21, 1975

COOPER H. LANGFORD and JOHN H. CAREY. Can. J. Chem. **53**, 2430 (1975).

There have been several studies of the charge transfer photochemistry of aqueous Fe^{3+} but the complexity of hydrolytic equilibria and the requirement for scavengers to render the primary photochemical processes observable has left several issues moot as recent reports show. Using *tert*-butyl alcohol as a scavenger, it is shown that (at 35 °C), charge transfer irradiation at 254 nm of $Fe(OH_2)_6^{3+}$ gives free ·OH with a quantum yield of 0.065, charge transfer irradiation of $Fe(OH_2)_5Cl^{2+}$ at 350 nm gives free Cl· with a quantum yield of 0.093, and that as a result of the combined patterns of extinction coefficients and hydrolytic equilibria it is difficult to make $Fe(OH_2)_5OH^+$ the main absorbing species at either wavelength. The dihydroxo-bridged dimer gives only a small radical yield. The scavenger, *tert*-butyl alcohol, appears to react with ·OH or Cl· to give $\cdot CH_2—C(CH_3)_2OH$ which, on reaction with a second $Fe(OH_2)_6^{3+}$ gives $HOCH_2C(CH_3)_2OH$.

COOPER H. LANGFORD et JOHN H. CAREY. Can. J. Chem. **53**, 2430 (1975).

Il existe plusieurs études sur le transfert de charge photochimique de Fe^{3+} en solution aqueuses. La complexité de l'équilibre hydrolytique et la nécessité pour les agent piégeurs de rendre les processus photochimiques primaires observables ont laissé plusieurs questions controversées comme le montrent des communications récentes. Utilisant l'alcool *tert*-butylique comme piège, on montre qu'à 35 °C le transfert de charge de $[Fe(OH_2)_6]^{3+}$ par une irradiation à 254 nm donne le radical libre ·OH avec un rendement quantique de 0.065; l'irradiation à 350 nm de $[Fe(OH_2)_5Cl]^{2+}$ produit le radical libre Cl· avec un rendement quantique de 0.093. En conséquence de la combinaison des variations des coefficients d'extinction et des équilibres hydrolytiques en peut difficilement affirmer que $[Fe(OH_2)_5OH]^+$ est l'absorbant principal à l'une ou l'autre des longueurs d'onde. Le dimère ponté dihydroxo donne seulement un faible rendement en radicaux. L'agent piégeur (l'alcool *tert*-butylique) semble réagir avec ·OH ou ·Cl pour donner $\cdot CH_2—C(CH_3)_2OH$, qui par réaction avec un autre $[Fe(OH_2)_6]^{3+}$ conduit à $HOCH_2C(CH_3)_2OH$. [Traduit par le journal]

Introduction

When the $Fe(OH_2)_6^{3+}$ ion is irradiated at 254 nm, excitation corresponds, in first approximation, to promotion of an electron from a ligand centered orbital to a metal centered orbital. This is a so-called l.m.c.t. transition. Such transitions are frequently associated with a photochemistry of metal reduction and ligand oxidation (1). In the chemistry of Fe(III), reduction produces Fe(II) and ligand oxidation which in the absence of scavengers leads to liberation of O_2. The quantum yield for Fe(II) formation is quite small in the absence of scavengers ($\sim 10^{-4}$), but it is not immediately clear what is the significance of a small yield since a primary process producing Fe(II) and hydroxyl radicals would be subject to thermal reversal. To determine the primary yield for Fe(III) reduction to Fe(II) various workers have explored iron isotope exchanges between the two oxidation states (1), radical initiation of polymerization (2), and alcohol scavenging (3). Unfortunately, the role of scavengers has not been fully interpreted over wide concentration ranges and ambiguity remains.

In another area, there are also serious outstanding ambiguities connected with the nature of the absorbing species responsible for photoreactions. A recent communication (4) in which Fe(II) yields were examined as a function of p*H* and chloride ion concentration concluded that reaction followed on absorption by $Fe(OH_2)_5OH^{2+}$ but *not* $Fe(OH_2)_5Cl^{2+}$. Since polymerization initiated in chloride-containing solutions produces polymers with both —Cl and —OH terminal groups, there is reason to consider both

[1]We thank the National Research Council of Canada for financial support.

[2]To whom correspondence should be addressed.

Can. J. Chem. Downloaded from www.nrcresearchpress.com by 210.87.254.40 on 09/05/12
For personal use only.

Can. J. Chem. Downloaded from www.nrcresearchpress.com by 210.87.254.40 on 09/05/12
For personal use only.

hydroxyl radicals and chlorine atoms as products of the primary photo process.

In this paper, the use of *tert*-butyl alcohol as a scavenger is explored. It is shown to be a scavenger with "simple" behavior in that its *only* reaction is with free ·OH and ·Cl radicals in solution. With the aid of *tert*-butyl alcohol scavenging, the reactivities of $Fe(OH_2)_6^{3+}$, $Fe(OH_2)_5Cl^{2+}$, and the dihydroxo-bridged dimer are elucidated. We note that although the hydroxo monomer $Fe(OH_2)_5OH^{2+}$ is known to have an absorption maximum at 300 nm (5) this species could not be selectively irradiated in our cells. At concentrations required for near total absorbance, the monomer is predominantly converted to the dimer and the dimer is the strongest absorbing species in the solution.

Results and Discussion

The absorption spectra of iron(III) species irradiated in this study are as follows. The spectrum of $Fe(H_2O)_6^{3+}$, obtained in strongly acidic media, agrees well with that previously reported (5). There is only one major peak, occurring at $\lambda = 240$ nm ($\varepsilon = 4350$) corresponding to the water to iron charge transfer band. This transition was excited using 254 nm light. The spectrum obtained in weakly acidic solutions exhibits another band at 335 nm ($\varepsilon = 8300$) which is attributed to the dihydroxo-bridged dimer (6). Irradiations performed at 350 nm excite this band since $Fe(H_2O)_6^{3+}$ absorbs very weakly at this wavelength. Although the hydroxo monomer, $Fe(H_2O)_5OH^{2+}$ is known to have a maximum at 300 nm (5), this species could not be selectively irradiated since at the high concentrations needed to assure total absorbance over short path lengths, most of the hydroxo monomer underwent dimerization and the dimer was the strongest absorbing species in solution.

The absorption spectra of iron(III) solutions in 2.25 *M* $HClO_4$ containing varying concentrations of Cl^- are shown in Fig. 1. The chloride dependent peak at 335 nm ($\varepsilon = 1490$) is assigned as the chloride to metal charge transfer band. Irradiations performed at 350 nm allowed examination of the photochemistry of chloride to metal excitation.

The irradiation of $Fe(H_2O)_6^{3+}$ at 254 nm in the absence of scavengers produced Fe(II) as a product at a rate which initially was not constant but after several minutes attained a constant value. This behavior has been observed

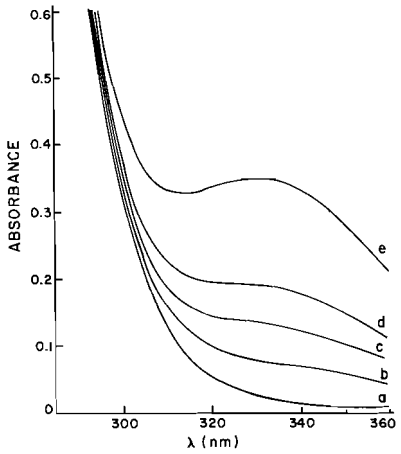

FIG. 1. Absorption spectra for ferric perchlorate in (*a*) 0, (*b*) 0.0020, (*c*) 0.0040, (*d*) 0.0060, (*e*) 0.0100, HCl; 2.10 *M* $HClO_4$, and 0.80 *M* $NaClO_4$. Cell path length is 0.10 cm.

in the photochemistry of Fe(II) where the initially increased rate is due to impurities acting as scavengers (7). The net quantum yield is determined from the slope in the region where production of Fe(II) is linear with time of irradiation after the impurities have been consumed (after 5 min of irradiation). The quantum yield calculated from the slope, $\Phi_{Fe(II)}$, is 0.0012.

As observed in other studies, the addition of organic compounds caused an increase in the rate at which Fe(II) was produced. The quantum yields observed at various scavenger concentrations for a variety of organic scavengers are given in Table 1. The largest increases in quantum yields were observed using alcohols and formic acid as scavengers. *tert*-Butyl alcohol was particularly interesting since a plateau was reached after which $\Phi_{Fe(II)}$ became independent of alcohol concentration. The value of the quantum yield on this plateau, $\Phi_{Fe(II)} = 0.130$, is taken to be twice the primary quantum yield for free ·OH. The value agrees well with the Fe isotope exchange estimate of Dainton and co-workers (1) for this primary yield of 0.07 ± 0.03 at 25 °C ($2 \times 0.07 = 0.14$).

The assignment of the limiting yield for Fe(II) as being twice the primary yield for OH is based on the following reaction path.

$$[1] \quad Fe_{aq}^{3+} \xrightarrow{h\nu} {}^*Fe_{aq}^{3+} \xrightarrow[k_1]{H_2O} Fe^{2+} + \cdot OH + H^+$$

Can. J. Chem. Downloaded from www.nrcresearchpress.com by 210.87.254.40 on 09/05/12
For personal use only.

[2] $H^+ + \cdot OH + Fe_{aq}^{2+} \xrightarrow{k_2} Fe^{3+} + OH^-$

[3] $\cdot OH + HS \xrightarrow{k_3} \cdot S + H_2O$

[4] $\cdot S + Fe^{3+} \xrightarrow{k_4} Fe^{2+} + SOH + H^+$

[5] $\cdot S + Fe^{2+} \xrightarrow{k_5} Fe^{3+} + HS + OH^-$

There exists a competition, as indicated in reactions 4 and 5, between Fe(III) and Fe(II) for S·. In the initial stages of irradiation, the high concentration of Fe(III) compared to Fe(II) ensures that reaction 4 will predominate over reaction 5. Therefore, reaction 5 may be omitted for low conversions. Reactions 2 and 3 indicate there is also a competition between Fe(II) and HS for the hydroxyl radicals. Applying a steady state treatment to this scheme gives the following kinetics:

[6] $\Phi_{Fe(II)} = V/I \times d[Fe(II)]/dt$

[7] $= \left(\frac{V}{I} \frac{2k_1k_3[Fe^{3+}][HS]}{k_2[Fe^{2+}] + k_3[HS]}\right)$

where V represents volume and I light intensity in einstein s^{-1}. If I, V, and $[Fe^{3+}]$ are assumed constant

[8] $\Phi_{Fe(II)} = \frac{c[HS]}{k_2[Fe^{2+}] + k_3[HS]}$

It can be seen from this expression that if the Fe^{2+} is kept low (limited irradiation), and the scavenger concentration is increased, a point will be reached where $k_3[HS] \gg k_2[Fe^{2+}]$ and the expression will simplify to $\Phi_{Fe(II)}$ = constant. The quantum yield becomes independent of scavenger concentration giving rise to the observed plateau. Since there are two iron ions reduced for each ·OH scavenged, this limiting quantum yield represents twice the primary yield of free ·OH.

The results from the irradiation of $Fe(OH_2)_6^{3+}$ in the presence of various organic scavengers clearly suggest that *tert*-butyl alcohol is the scavenger of choice for the determination of primary yields for hydroxyl radical formation. Fe(II) yields for methanol, 2-propanol, and formic acid scavenging continue to increase at high scavenger concentration in a way indicative of reactions above and beyond those of reactions 1 to 5. This is discussed in an accompanying paper (8). Degassing had no measurable effect. Moderate concentrations of acetone, acetic acid, and malonic acid each caused a small increase in quantum yield but the limiting plateau was not attained. This seems reasonable since hydroxyl radical attack on acetic acid and acetone produced radicals which are not oxidized further, even in the presence of added cupric ion, but are reduced back to starting material by ferrous ion (9). In view of this limitation, acetone, acetic acid, and malonic acid were dropped from the study. On the basis of its simple behavior, *tert*-butyl alcohol is selected for elucidation of the primary photochemistry of the other Fe(III) species.

The organic product of the *tert*-butyl alcohol scavenging was somewhat difficult to determine.

TABLE 1. Quantum yields as a function of scavenger concentration. Irradiation 2537 Å. T = 35 °C

Scavenger	Scavenger concentration (M)	$\Phi_{Fe(II)}$
Methanol[a]	0.0494	0.123
	0.0988	0.126
	0.988	0.154
	1.482	0.170
	1.976	0.167
	2.470	0.197
Isopropyl alcohol[a]	0.0262	0.123
	0.118	0.134
	0.131	0.134
	0.262	0.137
	0.524	0.140
	0.786	0.154
	1.048	0.167
	2.358	0.198
	2.620	0.212
	0.262 degassed	0.122
	2.620 degassed	0.208
tert-Butyl alcohol[b]	0.0212	0.100
	0.0424	0.116
	0.106	0.131
	0.212	0.134
	0.424	0.129
	0.636	0.130
	1.060	0.129
	2.120	0.132
Formic acid[c]	0.691	0.152
	1.414	0.172
	2.231	0.216
	3.257	0.230
Acetic acid[b]	0.914	0.023
	1.148	0.025
Malonic acid[b]	0.630	0.031

[a]For this scavenger, uncertainty in $\Phi_{Fe(II)}$ is ±0.002.
[b]For this scavenger, uncertainty in $\Phi_{Fe(II)}$ is ±0.003.
[c]For this scavenger, uncertainty in $\Phi_{Fe(II)}$ is ±0.004.

Can. J. Chem. Downloaded from www.nrcresearchpress.com by 210.87.254.40 on 09/05/12
For personal use only.

Neither acetone nor methanol were produced indicating that elimination of a methyl radical was not a reaction pathway. There was a small yield of isobutyraldehyde which was identified by g.c. in comparison with a known sample. Neutralization, filtration, and evaporation of both an irradiated and an unirradiated sample left a white solid (mainly $NaClO_4$). Carbon tetrachloride extracts of this solid showed the presence of organic material for the irradiated sample but not for the unirradiated one. There were two peaks in the n.m.r. in the 2–2.5 p.p.m. region of approximate 3:1 intensity.

The high boiling nature of this organic product as well as the nature of the other product, isobutyraldehyde, are indications that it is isobutylene glycol. This is, in fact, the expected product. Walling and Kato (10) reported it in the *tert*-butyl alcohol scavenging of ·OH in the presence of Fe^{3+} and Cu^{2+}. In an experiment suggested by Walling's results, solutions 0.5 *M* alcohol, 0.020 *M* Fe^{3+}, 2 *M* $HClO_4$ with and without 0.002 *M* Cu^{2+} were irradiated to 5% conversion (based on Fe^{2+}). CCl_4 extracts from these solutions were injected onto a Chromosorb 101 column at 250 °C. A product was found which has a retention time longer than ethylene glycol, which is oxidizable by dilute $KMnO_4$. These results support isobutylene glycol. It is important to note that the simple combination of two *tert*-hydroxybutyl radicals would not produce an intercept of 0.130 for $\Phi_{Fe(II)}$. The production of two Fe(II) for each hydroxyl radical scavenged indicates that the reaction of hydroxyl radicals with *tert*-butyl alcohol produces a radical which is capable of being further oxidized by Fe(III). The reaction path is most probably

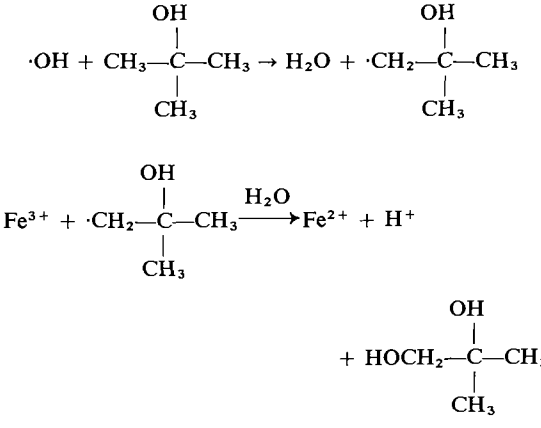

TABLE 2. Quantum yields irradiation of the dihydroxo-bridged dimer at 3500 Å

Scavenger	Scavenger concentration (*M*)	$\Phi_{Fe(II)}$
Methanol	0	0.010
	0.988	0.030
	1.975	0.035
t-Butyl alcohol	0.408	0.014
	0.816	0.013

with the isobutyraldehyde resulting from a pinacol type rearrangement of the glycol or some rearrangement of the radical prior to reaction with Fe^{3+}. We would underline for the reader the lack of quantitative accounting of organic product in these results.

Results of irradiations performed on solutions containing the dihydroxo-bridged dimer at 350 nm are given in Table 2. The yield observed in the presence of *tert*-butyl alcohol is close to the yield for unscavenged dimer irradiation. The primary yield of hydroxyl radical as indicated by *tert*-butyl alcohol scavenging is 0.007 at 350 nm. The reduced yield for the bridged dimer (as compared to the aquo monomer) is analogous to behavior reported for Fe(III) complexes of nitrilotriacetic acid (11) and ethylenediaminetetraacetic acid (12).

The irradiation of solutions of Fe(III) in 2.25 *M* $HClO_4$ with added Cl^- at 350 nm in the absence of scavengers results in photoreduction with a net quantum yield near 0.002. The results of the irradiation of $Fe(H_2O)_5Cl^{2+}$ in *tert*-butyl alcohol solutions are listed in Table 3. There is a complicated dependence of $\Phi_{Fe(II)}$ upon both concentration of scavenger and concentration of chloride. This suggests competition between the two species for the photoproduced radicals since increase in *tert*-butyl alcohol at constant chloride concentration results in an increased yield while increasing chloride for a constant *tert*-butyl alcohol concentration decreases the yield. In order to explain this behavior, the following reactions are considered:

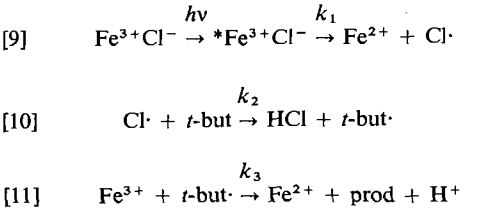

Can. J. Chem. Downloaded from www.nrcresearchpress.com by 210.87.254.40 on 09/05/12
For personal use only.

[12] $$Cl\cdot + Cl^- \xrightarrow{k_4} Cl_2^-$$

[13] $$Cl_2^- + Fe^{2+} \xrightarrow{k_5} Fe^{3+}Cl^- + Cl^-$$

where but = *tert*-butyl alcohol and prod = the oxidized organic product.

This scheme gives the following kinetics from a steady state treatment:

$$[14]\quad \Phi_{Fe(II)} = V/I \times d[Fe(II)]/dt = \left(\frac{V}{I}\frac{2k_1k_2[Fe^{3+}Cl^-][t\text{-but}]}{k_2[t\text{-but}] + k_4[Cl^-]}\right)$$

$$[15]\quad \frac{1}{\Phi_{Fe(II)}} = \frac{I}{V}\frac{k_2[t\text{-but}]}{2k_1k_2[Fe^{3+}Cl^-][t\text{-but}]} + \frac{k_4[Cl^-]}{2k_1k_2[Fe^{3+}Cl^-][t\text{-but}]}$$

If I, V, and $[Fe^{3+}Cl^-]$ are constant then [15] has the form of [16].

$$[16]\quad \frac{1}{\Phi_{Fe(II)}} = C_1 + \frac{C_2[Cl^-]}{[t\text{-but}]}$$

A plot of $1/\Phi$ *vs.* $[Cl^-]$ should be linear and have a slope dependent on each *tert*-butyl alcohol concentration. The intercept obtained from extrapolation to zero chloride concentration would represent the limiting quantum yield since contributions from reaction 12 (and reaction 13) would be eliminated. If the limiting quantum yield is independent of *tert*-butyl alcohol concentration, a plot of $1/\Phi$ *vs.* $[Cl^-]/[t\text{-but}]$ would be linear.

These plots are shown in Figs. 2 and 3 and are in excellent agreement with the above predictions. The limiting yield of Fe(II) is 0.186 from the extrapolation and thus the primary yield of chlorine atoms is 0.093 (*i.e.* 0.186/2). As a confirmation, the chloride concentration may be lowered relative to the *tert*-butyl alcohol concentration. The chloride dependent term will then become smaller and the quantum yield may be determined directly. Irradiations of this system in 0.01 *M* NaCl and 0.424, 0.636, and 0.848 *M* *tert*-butyl alcohol gave $\Phi_{Fe(II)}$ of 0.186, 0.182, and 0.182 respectively.

Finally, it may be useful to summarize some

TABLE 3. Quantum yields at 3500 Å as a function of scavenger and chloride concentrations. $[Fe]^{3+} = 0.0248$ *M*

[*tert*-Butyl alcohol] (*M*)	$[Cl^-]$	$\Phi_{Fe(II)}$[a]
0.424	0.01	0.186
0.636	0.01	0.182
0.816	0.08	0.140
0.816	0.16	0.104
0.816	0.24	0.084
0.816	0.32	0.070
0.848	0.01	0.182
1.224	0.16	0.120
1.224	0.24	0.100
1.224	0.32	0.092
1.632	0.16	0.135
1.632	0.24	0.118
1.632	0.32	0.102
2.04	0.08	0.162
2.04	0.16	0.139
2.04	0.24	0.123

[a] ± 0.003.

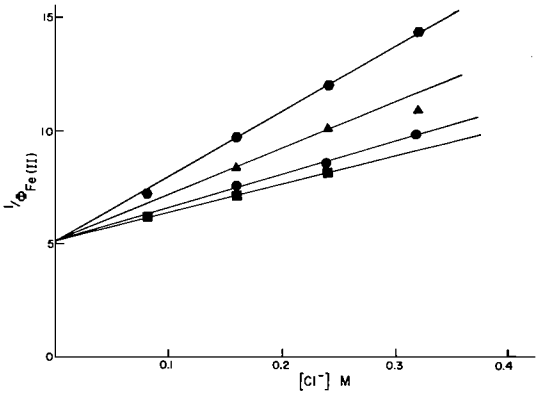

FIG. 2. The reciprocal of quantum yield for production of Fe(II) as a function of concentration of chloride on irradiation of $Fe(OH_2)_5Cl^{2+}$ using *tert*-butyl alcohol as a scavenger. The various lines are for increasing *tert*-butyl alcohol concentrations as indicated in Table 3.

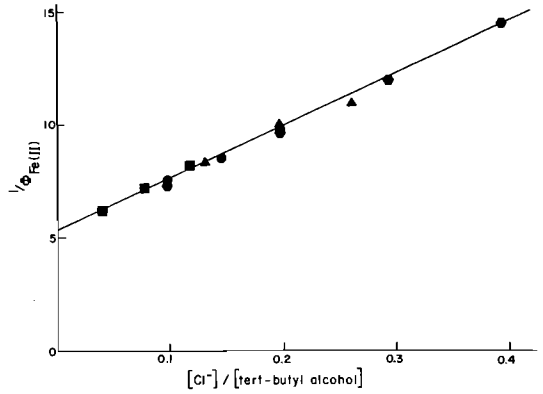

FIG. 3. The reciprocal of the quantum yield for production of Fe(II) as a function of the concentration ratio chloride/*tert*-butyl alcohol.

Can. J. Chem. Downloaded from www.nrcresearchpress.com by 210.87.254.40 on 09/05/12
For personal use only.

general conclusions about Fe(III) c.t. photochemistry. (*1*) Alcohol scavenging in general may prove complicated and methanol and 2-propanol are to be avoided in attempts to determine primary free radical quantum yields. (*2*) *tert*-Butyl alcohol scavenging of hydroxy radicals is simple and indicates primary quantum yields in good agreement with those from iron isotope exchange studies. (*3*) $Fe(OH_2)_5Cl^{2+}$ is reactive on excitation of the chloride to metal charge transfer band at 350 nm. The primary yield of ·Cl is higher than the hydroxyl radical yield from irradiation of $Fe(OH_2)_6^{3+}$ at 254 nm. Confusions have arisen previously (4) from neglect of the role of Cl^- in reactions 12 and 13. (*4*) The dihydroxo-bridged dimer is relatively unreactive in the lowest c.t. band. This may result from initial formation of an ·OH radical in a bridging position where it remains coordinated to a relatively nonlabile Fe^{3+} and is neighbor to an Fe(II) center. Such circumstances should certainly favor a reaction analogous to reaction 2.

Experimental

Materials

The source of iron was ferric sulfate. Ferric perchlorate solutions were prepared by precipitation with NaOH, thorough washing, and dissolution in $HClO_4$. Iron content of stock solutions was determined by two methods. In the first, an excess of EDTA was added and absorbance at 260 nm was measured (13). In the second, reduction was effected by prolonged irradiation at 2537 Å. After a thiocyanate test indicated absence of Fe(III), Fe(II) was determined with *o*-phenanthroline (14). Other materials were best available commercial reagents used without further purification.

Irradiation Procedures

Solutions for irradiation were prepared freshly from stock solutions. Deaeration, when desired, was accomplished by freeze–thaw cycles or bubbling free nitrogen (introduced through a serum cap with stainless steel needles) through the solution for 20 min. Irradiation at 2537 Å was carried out in a cylindrical quartz vessel in a Rayonnet photoreactor (Southern New England Ultraviolet Co., Middletown, Conn.). Ulfiltered light from medium pressure Hg lamps in this apparatus is approximately 98% at 2537 Å. The temperature in the irradiation zone stabilized at 35 °C. Irradiations at 3500 Å were similar except that lamps were changed to Rayonnet fluorescent-coated Hg lamps with peak intensity at 3500 Å. Irradiations for quantum yield determination were limited to less than 5% conversion. Concentrations were chosen to assure large excesses over the minima required for >99% absorption of light at the desired wavelengths. Actinometry was carried out with ferrioxalate (15).

Analytical Procedures

The most common analysis was that for Fe(II) carried out with *o*-phenanthroline (phen) (14). In several cases, large excesses of acid had to be neutralized before the normal procedure was carried out. Direct neutralization of irradiated solutions caused precipitation. As an alternative, 2.5 ml of 1.00 *M* NaOH per ml of photolyte and 2 ml of buffered phenanthroline, which was a more concentrated version of that used by Hatchard and Parker (15), were added to 90 ml of distilled water in a 100 ml volumetric flask. Photolyte (1 or 2 ml) was added and the solution made up to 100 ml. The solution was stored in the dark for 30 min prior to recording absorbance at 510 nm. It was verified that ClO_4^- did not interfere in the analysis.

Gas chromatographic identification of isobutyraldehyde by retention time comparison with an authentic sample was carried out on CCl_4 or $CHCl_3$ extracts using a Beckmann GC2 equipped with a 5 ft, 10% ethofat on Chromosorb W column operated at room temperature. Other organic analyses were described above.

1. M. G. Adamson, D. L. Baulch, and F. S. Dainton. Trans. Faraday Soc. **58**, 1388 (1962).
2. M. G. Evans and N. Uri. Nature, **164**, 404 (1949).
3. J. H. Baxendale and J. Magee. Trans. Faraday Soc. **51**, 205 (1955).
4. P. G. David. J. Chem. Soc. Chem. Commun. 1294 (1972).
5. G. V. Buxton, S. P. Wilford, and R. J. Williams. J. Chem. Soc. 4957 (1962).
6. L. N. Mulay and P. W. Selwood. J. Am. Chem. Soc. **77**, 2693 (1955).
7. J. Jortner and G. Stein. J. Phys. Chem. **66**, 1258 (1962).
8. J. H. Carey and C. H. Langford. Can. J. Chem. This issue.
9. C. Walling and G. L. Taliawi. J. Am. Chem. Soc. **95**, 844 (1973).
10. C. Walling and S. Kato. J. Am. Chem. Soc. **93**, 4275 (1971).
11. T. Trott, R. W. Henwood, and C. H. Langford. Environ. Sci. Tech. **6**, 367 (1972).
12. C. H. Langford and J. H. Carey. Can. J. Chem. **51**, 3665 (1973).
13. Y. Uzumasa, M. Nishimura, and T. Seo. Bull. Soc. Chem. Jap. **30**, 438 (1957).
14. M. L. Miss and M. G. Mellan. Ind. Eng. Chem. **14**, 862 (1942).
15. C. G. Hatchard and A. C. Parker. Proc. R. Soc. A, **235**, 518 (1956).

Outer Sphere Oxidations of Alcohols and Formic Acid by Charge Transfer Excited States of Iron(III) Species[1]

JOHN H. CAREY AND COOPER H. LANGFORD[2]
Department of Chemistry, Carleton University, Ottawa, Canada K1S 5B6
Received February 21, 1975

JOHN H. CAREY and COOPER H. LANGFORD. Can. J. Chem. **53**, 2436 (1975).

When methanol, 2-propanol, and formic acid are used as scavengers in the ligand to metal charge transfer (l.m.c.t.) photolysis of $Fe(OH_2)_6^{3+}$, $Fe(OH_2)_5Cl^{2+}$, $Fe_2(OH_2)_8(OH)_2^{4+}$, or FeEDTA, there is a linear relationship between quantum yield for Fe(II) production and scavenger concentration, [S], at higher [S] values. Extrapolation of the linear portions to [S] = 0 gives an intercept corresponding to the limiting yields observed for scavenging with *tert*-butyl alcohol. Butanol scavenging at the limit has been shown to give the primary free radical yields from photolysis of aquo iron(III) species. Nuclear magnetic resonance relaxation time studies show that alcohols do not coordinate to Fe(III) and calculations from known stability constants indicate that formic acid does not coordinate under the experimental conditions. The increase of Fe(II) yields with [S] is attributed to an outer sphere oxidation of noncoordinated organic species by the charge transfer excited states of Fe(III) species. There is no discrimination among the organic reductants. The results may be understood without postulating a long lifetime for the Fe(III) l.m.c.t. states if the reaction is assumed to occur only with organic molecules in encounter with the Fe(III) complex at the time of excitation. Organic products were formaldehyde from methanol oxidation and acetone from 2-propanol oxidation. The Fe(II):formaldehyde stoichiometry was 2:1.

JOHN H. CAREY et COOPER H. LANGFORD. Can. J. Chem. **53**, 2436 (1975).

La photolyse du transfert de charge du ligand au métal (t.c.l.m.) de $Fe(OH_2)_6^{3+}$, $Fe(OH_2)_5Cl^{2+}$, $Fe(OH_2)_8(OH)_2^{4+}$ ou de FeEDTA est étudiée en se servant du méthanol, du propanol-2 et de l'acide formique comme agents piégeurs. On observe une relation linéaire entre le rendement quantique de la formation de Fe(II) et la concentration [S] en agent piégeur, pour les fortes concentrations en [S]. L'extrapolation à [S] = 0 des portions linéaires permet de retrouver les rendements limites observés dans le cas du piégeage par l'alcool *tert*-butylique. Il a été montré qu'à la limite, le piégeage par l'alcool *tert*-butylique conduit aux rendements en radical libre primaire, à partir de la photolyse d'espèces aquo fer(III). Les études du temps de relaxation par r.m.n. montrent que les alcools ne se coordonnent pas au Fe(III). Les calculs basés sur les constantes de stabilité connues indiquent que l'acide formique ne se coordonne pas non plus dans ces conditions expérimentales. L'augmentation du rendement en Fe(II) avec [S] est attribué à une oxydation externe, par transfert de charge des états excités des espèces Fe(III), de composés organiques non coordonnés. Il n'y a pas de distinction entre les réducteurs organiques. Ces résultats peuvent être interprétés sans avoir à postuler une longue durée de vie pour les états t.c.l.m. de Fe(III) si l'on admet que la réaction se fait seulement entre des molécules organiques rencontrant un complexe de Fe(III) au moment de l'excitation. Les produits organiques étaient la formaldéhyde provenant de l'oxydation du méthanol et l'acétone venant de l'oxydation du propanol-2. La stoechiométrie de Fe(II):formaldéhyde est 2:1.
[Traduit par le journal]

Introduction

In many photochemical reactions, those of charge transfer excited states of metal complexes included, identification of radicals produced in primary photo processes and determination of primary quantum yields requires introduction of scavengers. Frequently, rather large scavenger concentrations (large [S]) are required to achieve complete scavenging of the desired radical. But, there is a special feature of large scavenger concentrations. The scavengers may frequently be the encounter partner in the solvent cage of the molecule absorbing light, a phenomenon described in an organic photochemical example by Waits and Hammond (1). Encounter with scavengers can be important at surprisingly low concentration. Modeling encounter equilibrium between a complex ion and a molecule using the Eigen–Fuoss equation which is successful in the description of complex formation reactions (2), assumption of a center to center

[1]We thank the National Research Council of Canada for financial support.
[2]To whom correspondence should be addressed.

Can. J. Chem. Downloaded from www.nrcresearchpress.com by 210.87.254.42 on 09/05/12
For personal use only.

Can. J. Chem. Downloaded from www.nrcresearchpress.com by 210.87.254.42 on 09/05/12
For personal use only.

encounter distance of only 5 Å gives an equilibrium constant, K_E, of 0.3. To see the implication of this value, consider a dilute aqueous solution of $Fe(OH_2)_6^{3+}$, containing 1 *M* CH_3OH. In this circumstance, 25% of the complex ions $Fe(OH_2)_6^{3+}$ have an alcohol molecule in encounter (in the second coordination sphere or solvation sphere) at any time. This means that ¼ of all $Fe(OH_2)_6^{3+}$ complexes absorbing photons from the 254 nm line of a mercury lamp may be expected to arrive in the ligand to metal charge transfer (l.m.c.t.) excited state with an alcohol molecule as a nearest neighbor. Under these circumstances there is *no need* to assume that the l.m.c.t. excited state has a substantial lifetime in order to account for a direct reaction between that state and the alcohol.

In this report we describe the reaction at high [S] between the l.m.c.t. excited states of several Fe(III) species and oxidizable organic scavengers which do not penetrate the primary coordination sphere. We will analyze the results for these outer sphere redox processes in terms of the encounter model described above because they do not become prominent except at high [S] and because this model does not require a long life for the l.m.c.t. excited states. The treatment is analogous to "static" quenching of emission (3). We note here that the alternative of "dynamic" quenching and a long-lived l.m.c.t. excited state is not excluded. It simply seems less likely.

Results and Discussion

In the preceding paper (4), we noted that the quantum yield for the reaction shown in reaction 1 could be determined simply by using *tert*-butyl alcohol as a scavenger. When methanol,

$$[1] \qquad Fe^{3+} + H_2O \xrightarrow[254\text{ nm}]{h\nu} Fe^{2+} + \cdot OH + H^+$$

2-propanol, and formic acid are employed as scavengers, the quantum yield for Fe^{2+} production does not approach a limit at high [S]. Instead, it becomes linearly dependent upon [S]. This behavior is illustrated in Fig. 1 for acid solution of $Fe(OH_2)_6^{3+}$ irradiated at 254 nm and for $Fe(OH_2)_5Cl^{2+}$ irradiated at 350 nm. Corresponding results for $Fe_2(OH_2)_8(OH)_2^{4+}$ irradiated at 350 nm and $Fe(EDTA)OH_2^-$ irradiated at 350 nm are shown in Figs. 2 and 3. The [S] = 0 intercept of the line in Fig. 1 is seen to be 0.125. This is within experimental

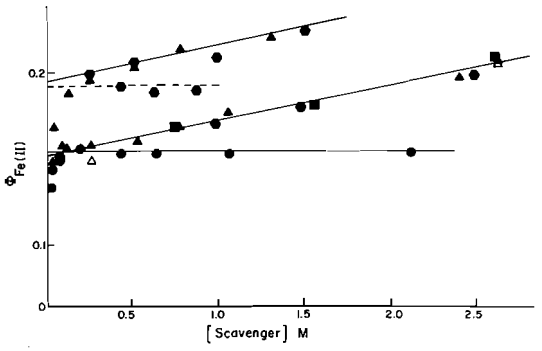

FIG. 1. Quantum yields for production of Fe(II) as a function of scavenger concentration using (●) *tert*-butyl alcohol, (■) formic acid, (▲) isopropyl alcohol, and (⬢) methanol as scavengers. Deoxygenated runs with isopropyl alcohol are shown by (△). The upper two curves refer to $Fe(OH_2)_5Cl^{2+}$. The lower two curves refer to $Fe(OH_2)_6^{3+}$.

error of the yield of Fe(II) determined with *tert*-butyl alcohol scavenging in the limit of high alcohol concentration (0.130) where all hydroxyl radicals escaping the solvent cage are scavenged and none react with Fe^{2+} to regenerate the initial complex. The increase in quantum yield for Fe(II) production above this intercept involves a process not included in the kinetic schemes of the preceding paper. An immediate possibility is that methanol, 2-propanol, and formic acid form complexes with $Fe(OH_2)_6^{3+}$ and that we observe photochemistry of these new species. (It is more difficult to entertain this suggestion for FeEDTA.) The idea may be tested easily in the case of formic acid and $Fe(OH_2)_6^{3+}$. The stability constant of the formatoiron(III) complex is known (5) and is 8.5×10^{-4} at 25°. Less than 0.1% of the formate

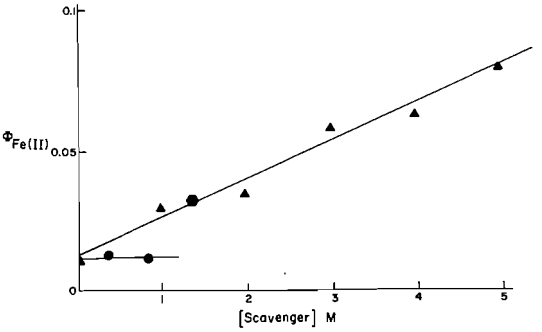

FIG. 2. Quantum yields for production of Fe(II) as a function of scavenger concentration for irradiation of the dihydroxo-bridged dimer. Symbols for scavengers as in Fig. 1.

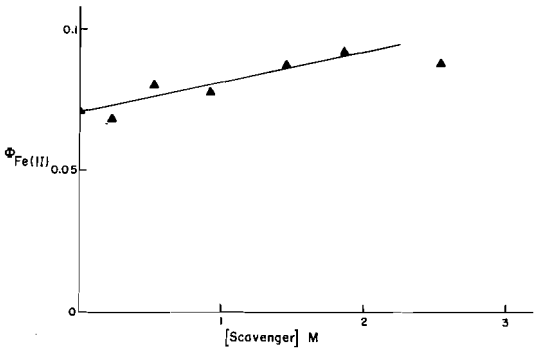

FIG. 3. Quantum yields for Fe(II) as a function of scavenger concentration (symbols as in Fig. 1) for irradiation of FeEDTA.

would be coordinated at unit hydrogen ion activity. The medium in the photolysis experiments is 2.25 *M* $HClO_4$. Formic acid is reacting in an outer sphere reaction in the sense that the effective photons cannot be exciting formato complexes. The similarity of behavior between formic acid and the alcohols suggests a similar assignment, but it is possible to be somewhat more specific.

The $Fe(OH_2)_6^{3+}$ ion is paramagnetic and its hydroxyl protons are exchanging rapidly with hydroxylic protons in the bulk solvent in this acidic medium. There is a single n.m.r. hydroxyl proton signal which is moderately broadened by the paramagnetic center. Now, as the alcohol is introduced, if alcohol molecules are *excluded* from the first coordination of Fe(III), the number of bulk hydroxylic sites will decrease without a corresponding decrease in the number of hydroxylic sites in the *paramagnetic* neighborhood of Fe(III). The result will be enhanced paramagnetic broadening of the hydroxylic protons. In other words, if Fe(III) is "preferentially solvated" in the coordination sphere by H_2O, the hydroxylic proton n.m.r. signal will become broader as alcohol concentration increases. (This discussion has neglected broadening arising from protons in the secondary solvation shell which may be as large as 5–10% of that from the primary coordination sphere.) Quantitative treatment of this effect has been given several times (6–8) and is moderately lengthy. Using the procedures indicated in the references, hydroxy proton line widths were calculated on the assumption that $Fe(OH_2)_6^{3+}$ was the only iron complex present in solutions containing alcohols. In Fig. 4, experimental

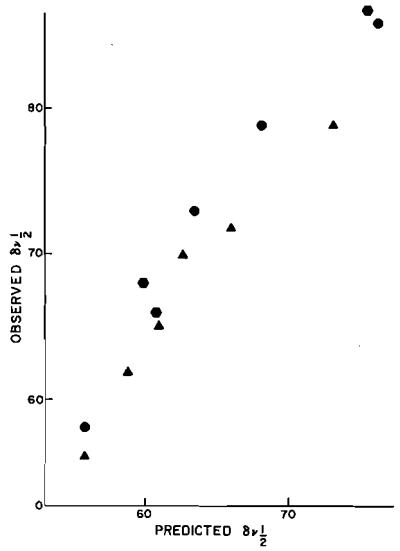

FIG. 4. Observed n.m.r. linewidths *vs.* predicted linewidths for (▲) methanol, (●) *tert*-butyl alcohol, and (⬣) isopropyl alcohol.

linewidths are plotted against calculated linewidths. Any disagreement is in the direction of lines too broad which is inconsistent with alcohol coordination and probably explained by the neglect of outer sphere broadening. Like the formic acid reactions, reactions with methanol and 2-propanol do not arise from excitation of the inner sphere complexes of the substrate undergoing oxidation.

The next result to which attention should be drawn is the similarity of the dependence of quantum yields for Fe(II) production on [S] in various cases. When $Fe(OH_2)_6^{3+}$ is excited at 254 nm, slopes for methanol, 2-propanol, and formic acid are *indistinguishable*! In turn, this value is indistinguishable from the slope describing experiments in which $Fe(OH_2)_5Cl^{2+}$ is irradiated at 350 nm.

The simplest interpretation of an equality of reactivity over several systems is the assumption that all have reached an "upper limit" of some sort. That is, we wish to test the assumption that all of the three organic molecules are oxidized with a quantum yield approaching unity (the theoretical upper limit) for the reactive excited state, not necessarily the primary one. Looking back at the argument in the introduction, it is apparent that the entity reacting with a quantum yield of unity cannot be the one-to-one encounter species (or outer sphere

Can. J. Chem. Downloaded from www.nrcresearchpress.com by 210.87.254.42 on 09/05/12
For personal use only.

Can. J. Chem. Downloaded from www.nrcresearchpress.com by 210.87.254.42 on 09/05/12
For personal use only.

complex) involving the primary excited state if the Fuoss–Eigen equation is approximately correct. According to that equation, the species with one alcohol (or formic acid) molecule in the solvation shell of $Fe(OH_2)_6^{3+}$ would account for 25% of all $Fe(OH_2)_6^{3+}$ species at 1 *M* alcohol. The implication would be a primary radical quantum yield of the order of 0.25 rising to nearly 0.5 at 2 *M* alcohol[3] and approaching a limit shortly thereafter contrary to the results in Fig. 1. To see the weakness of this simple conception, it is useful to consider $Fe(OH_2)_5Cl^{2+}$ first.

In the case of $Fe(OH_2)_5Cl^{2+}$ the c.t. transition occurs primarily between Cl^- and Fe^{3+} leading to a "chlorine atom" center as oxidant at least in so far as the release of Cl atoms to the solution (4) implies the nature of the primary excited state. If a molecule of an oxidizable substance, *e.g.* methanol, is in encounter with (or solvates) $Fe(OH_2)_5Cl^{2+}$ on the side away from the Cl, it is unlikely to be oxidized by a short-lived excited state. The quantum yield for oxidation will not be expected to approach unity until *all* outer sphere sites are occupied by the oxidizable species (*e.g.* methanol). Thus, before we can estimate the limiting reactivity of an excited state of $Fe(OH_2)_5Cl^{2+}$ we need to estimate a statistical factor for the chance that an alcohol molecule in encounter occupies the reactive site. On the assumption that the reactive site is unique and that distribution of alcohol molecules over outer sphere sites is random, the correct statistical factor is simply the outer sphere solvation number which has been variously estimated as lying between 4 and 12. A similar statistical factor was introduced by Langford and Muir and considered by Pearson and Ellgen in discussion of the interchange mechanism of thermal ligand substitution at Co(III) and Ni(II) centers (9). The factor which seems to apply in thermal reactions is between 5 and 10. On this basis, the 1.0 *M* value of the primary radical yield, or the slope of the primary radical quantum yield – alcohol concentration function should lie between 0.025 and 0.050. If these are correct, the experimental slopes for Fe(II) production (2 × primary radical) should lie between 0.050 and 0.100. In other words, we estimate a slope for a reaction of unit efficiency nearly *twice* the experimental value in Fig. 1.

It is important to recall that there was a strong reason to look for a way of regarding the slopes in Fig. 1 as representing unit efficiency. There is a very significant *lack* of discrimination among a fairly wide variety of oxidizable organic species. If the calculations of the previous paragraph are correct, they represent a limiting efficiency of about 50%. This could be rationalized if the state reacting with unit efficiency is not the primary excited state but some successor reached with comparable efficiency in all cases. Such a proposal was made by Endicott (10) to explain the behavior of acetatopentaamminecobalt(III) on c.t. excitation. Co(II) yields (but not acetate decomposition yields) increased in this case on addition of isopropyl alcohol approaching a limiting value of 0.5. *However*, the calculations in the previous paragraph depend upon the Fuoss–Eigen equation. That equation is based on a simple hard sphere encounter theory and a factor of two error is not unexpected. If the Fe(III) complexes are preferentially solvated by water to a slight extent, the observed slope could well correspond to a limiting yield of unity.

We note that the alternative of a dynamic mechanism (as opposed to the static encounter mechanism outlined above) requires that the rate constant for reaction of a longer lived excited state with a scavenger must be the same for excited states of at least two Fe(III) complexes of different structure and for the several different scavengers. The relative implausibility of this is one reason for focusing attention on encounter.

Returning to $Fe(OH_2)_6^{3+}$, we ask what is the geometrically suitable site corresponding to that of $Fe(OH_2)_5Cl^{2+}$? This is not a major difficulty. The six water molecules are equivalent only in the geometry of the ground state. It was to be expected (although there has not been experimental evidence before) that the vibrationally equilibrated excited state would be distorted in such a way that a particular water molecule has become the electron deficient one which might be visualized as "on its way toward oxidation".

Having speculated on the excited state responsible for the outer sphere oxidation, its scope is worth comment. The reaction has appeared following excitation of the c.t. transitions of all iron(III) species we have irradiated at either

[3]Recall that a primary radical yield of 0.25 implies an experimental Fe(II) yield of 0.50.

Can. J. Chem. Downloaded from www.nrcresearchpress.com by 210.87.254.42 on 09/05/12
For personal use only.

2537 or 3500 Å. The list includes $Fe(OH_2)_6^{3+}$, $Fe(OH_2)_5Cl^{2+}$, $Fe_2(OH_2)_8(OH)_2^{4+}$, and Fe(EDTA). (We shall present evidence elsewhere that the reaction extends to Co(EDTA).) It is not without precedent. In alcohol glasses, irradiation of cyano (11) and nitrosyl (12) complexes of Fe(III) has been shown by e.s.r. to produce radicals derived by removal of α-hydrogens and Fe(II). The present examples differ mainly in that net reactions are observable in fluids near room temperature. This probably indicates that recombination reactions of Fe(II) species and radicals dominate the other systems.

Oxidizable organic species so far appear to include methanol, 2-propanol, and formic acid, but not *tert*-butyl alcohol. It seems likely that an H on the carbon bearing the oxygen is a requirement.[4] The reaction scheme may be written as follows.

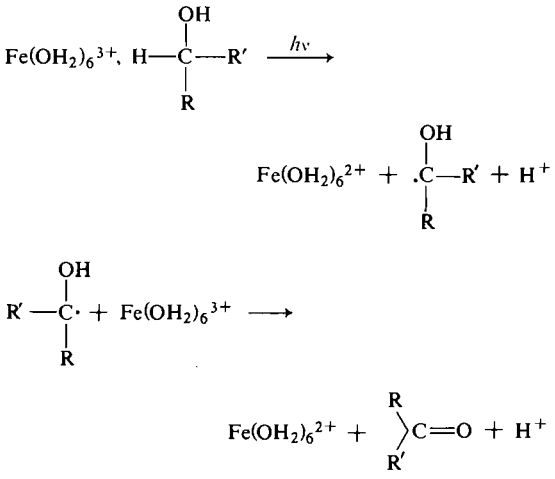

[4]A referee has suggested the following intermediate structure for a scavenger assisted reaction:

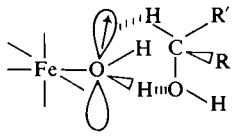

i.e. minimum strain via six member ring. Obviously *tert*-BuOH cannot form such a structure. We thank the referee.

In agreement with this scheme gas chromatography on CCl_4 or $CHCl_3$ extracts from irradiation of $Fe(OH_2)_6^{3+}$ identified as organic products only formaldehyde from methanol and acetone from 2-propanol. 2,4-Dinitrophenylhydrazone derivatives of these were also isolated. Spectrophotometric determination of the formaldehyde yield via the examination of the 2,4-dinitrophenylhydrazone in basic media (12) indicates a stoichiometry of two moles Fe(II) per mole of formaldehyde (±10%) for irradiations in presence of methanol, as required.

Experimental

Materials and solutions were prepared as described in ref. 4. Irradiation procedures were also indicated there. The temperature was 35 °C in the reaction vessels. Analyses were carried out as before (4) except that assay of formaldehyde produced was by the spectrophotometric procedures of Lappin and Clark (13). The n.m.r. procedures for preferential solvation studies have been extensively described (6–8). The treatment is lengthy and will not be reproduced here. Spectra used here were recorded on a Varian T-60 at 25 °C at an $Fe(OH_2)_6(ClO_4)_3$ concentration of 0.0200 *M* and an alcohol concentration range corresponding to that in irradiation experiments, 0.5 to 3.5 *M*.

1. H. P. Waits and G. S. Hammond. J. Am. Chem. Soc. **86**, 1911 (1964).
2. M. Eigen. Pure Appl. Chem. **6**, 97 (1963); Z. Phys. Chem. Frankfurt am Main, **1**, 176 (1954).
3. P. J. Wagner. *In* Creation and detection of the excited state, Vol. 1, Part A. *Edited by* A. A. Lamola, Marcel Dekker, New York. 1971.
4. C. H. Langford and J. H. Carey. Can. J. Chem. This issue.
5. J. H. Baxendale and N. K. Bridge. J. Phys. Chem. **59**, 783 (1955).
6. L. S. Frankel, T. R. Stengle, and C. H. Langford. Can. J. Chem. **46**, 3183 (1968).
7. L. S. Frankel, T. R. Stengle, and C. H. Langford. J. Phys. Chem. **74**, 1645 (1970).
8. V. S. Sastri, R. W. Henwood, S. Behrendt, and C. H. Langford. J. Am. Chem. Soc. **94**, 753 (1972).
9. C. H. Langford and W. R. Muir. J. Am. Chem. Soc. **89**, 3141 (1967).
10. J. F. Endicott. Israel J. Chem. **8**, 209 (1970).
11. M. C. R. Symons, D. X. West, and J. G. Wilkinson. J. Phys. Chem. **78**, 1335 (1974).
12. M. C. R. Symons, D. X. West, and J. G. Wilkinson. J. Chem. Soc. Chem. Commun. 917 (1973).
13. G. R. Lappin and L. C. Clark. Anal. Chem. **23**, 541 (1951).

Synthesis of *cis*-9-Cyano-1,10-dimethyl-6-ethylenedioxy-1-octalin and its Conversion into an Intermediate for a Synthesis of Thelepogine

RONALD B. KELLY, SANDRA J. ALWARD, AND JIRI ZAMECNIK
Department of Chemistry, University of New Brunswick, Saint John, New Brunswick E2L 4L5

Received April 10, 1975

RONALD B. KELLY, SANDRA J. ALWARD, and JIRI ZAMECNIK. Can. J. Chem. **53**, 2441 (1975).

The synthesis of *cis*-9-cyano-1,10-dimethyl-6-ethylenedioxy-1-octalin, the structure of which has been determined by X-ray crystallography, is described. Also described is the conversion of this compound into an octalone having the functionality and stereochemistry appropriate to its use as an intermediate in a total synthesis of thelepogine.

RONALD B. KELLY, SANDRA J. ALWARD et JIRI ZAMECNIK. Can. J. Chem. **53**, 2441 (1975).

On décrit la synthèse du cyano-9 diméthyl-1,10 éthylènedioxy-6 octaline-1 *cis* dont la structure a été déterminée par diffraction de rayons X. On décrit aussi la conversion de ce composé en une octalone dont la fonctionalité et la stéréochimie permettent son emploi comme intermédiaire dans la synthèse totale de la thélépogine. [Traduit par le journal]

Very recently, Lynton and Siew (1) described the structure determination of the octalin **1** by X-ray crystallographic analysis. We are prompted by the appearance of this publication to describe the synthesis of **1** which was the source of the crystals used for the X-ray study (1). At the same time we wish to report some related work.

The octalone **2** constitutes a moiety of the novel structure (**3**) assigned to the diterpenoidal alkaloid thelepogine (2). Because of this we undertook a synthesis of **2** as part of some work directed towards the total synthesis of thelepogine (**3**). We now wish to describe a synthesis of **2** through the intermediacy of **1**.

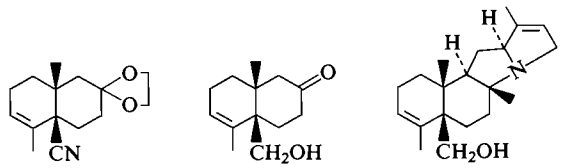

1 **2** **3**

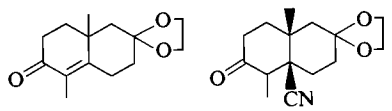

4 **5**

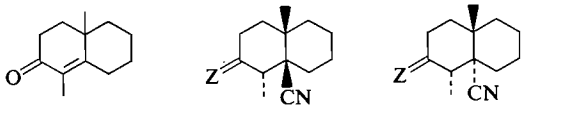

6 **7** Z = O **8** Z = O

9 Z = $O(CH_2)_2O$ **10** Z = $O(CH_2)_2O$

Our plan for the synthesis of the octalin **2** required, at the outset, a stereospecific conjugate cyanation of the ketal octalone **4** (3) to give the *cis*-cyano keto ketal **5**. Before attempting the cyanation of **4**, we carried out model cyanation studies on the octalone **6** (4) because the products (**7** and **8**) of conjugate cyanation are known (5) and are readily distinguishable by n.m.r. spectroscopy (5, 6). It has been shown (5, 6) that, with 9-cyano-10-methyl-2-decalones, the n.m.r. singlet for the angular methyl group of the *cis* isomer is deshielded by 13–15 Hz relative to the corresponding singlet for the *trans* isomer (see first two entries in Table 1). The conversion of **6** into two cyano ketones with potassium cyanide and the identification of these cyano ketones as the *cis*- (**7**) and the *trans*-decalone (**8**) has been reported but the reported yield of the *cis* isomer was only 18% (5).

By employing diethylaluminum cyanide (7) as cyanating agent and by adjusting the reaction conditions, we were able to convert **6**, at will, into either the *cis*-cyano decalone **7** in 64% yield or the *trans* isomer **8** in 67% yield.[1] Thus, treatment of **6** in benzene with diethylaluminum cyanide for 16 h at room temperature, followed by 1 h at 45°, afforded **7** (5). On the other hand,

[1]The i.r. and n.m.r. spectra of all compounds are consistent with assigned structures (see Experimental).

Can. J. Chem. Downloaded from www.nrcresearchpress.com by 210.87.254.42 on 09/05/12
For personal use only.

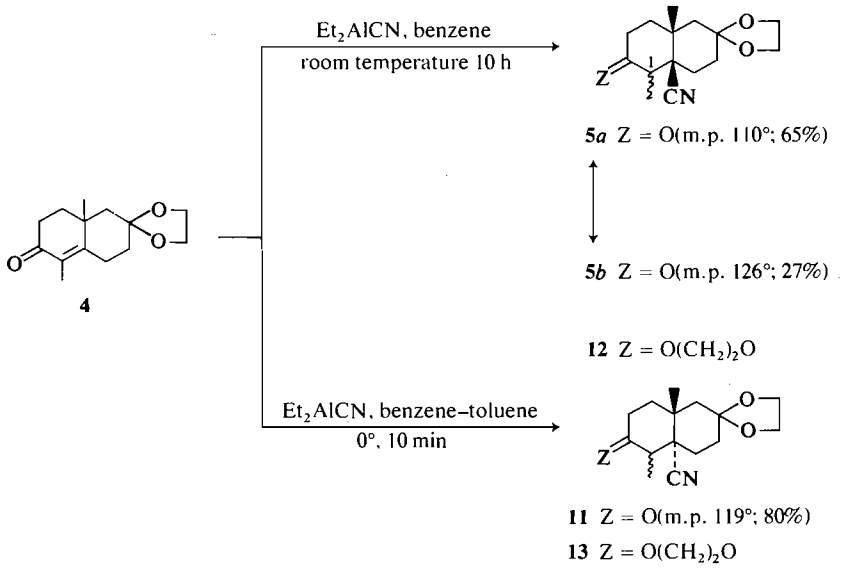

SCHEME 1

TABLE 1. Comparison of chemical shifts of angular methyl groups

Compounds (Chemical shifts* in parentheses)				Difference in chemical shift (Hz)
7	(1.48)	**8**	(1.24)	14.4
9	(1.24)	**10**	(1.02)	13.2
5*a*	(1.50)	**11**	(1.35)	9.0
5*b*	(1.39)	**11**	(1.35)	2.4
12	(1.23)	**13**	(1.15)	4.8

*In p.p.m. downfield from TMS as internal standard.

treatment of 6 in benzene–toluene with the same reagent at 0° for 10 min afforded **8** (5). These results could, to a certain extent, be anticipated from the work of Nagata *et al.* (7).

The cyano decalones **7** and **8** were converted into their respective ketals **9** and **10** for comparison of their n.m.r. spectra. The data in Table 1 show that the method (*vide supra*) for distinguishing between such *cis* and *trans* isomers by comparison of the chemical shifts of the angular methyl groups is applicable in this instance; the pertinent signal for the *cis* isomer is 13.2 Hz downfield relative to the corresponding signal for the *trans* isomer.

Having worked out satisfactory procedures for stereospecific conjugate cyanations by model studies, we now applied these procedures to the cyanation of the ketal octalone **4** (see Scheme 1). Treatment of **4** with diethylaluminum cyanide in benzene for 10 h at room temperature afforded two crystalline isomeric cyano ketones. A major isomer (**5***a*, m.p. 110°) was obtained in 65% yield while a minor isomer (**5***b*, m.p. 126°) was obtained in 27% yield. Since either of these isomers could be converted by base to the same equilibrium mixture of **5***a* and *b*, it would appear that they are C-1 epimers and that they are both either *cis* or *trans* isomers. It will be shown in the sequel that, as expected by analogy with the model experiments (*vide supra*), the former is the case.

Treatment of **4** with diethylaluminum cyanide in benzene–toluene at 0° for 10 min afforded a single crystalline cyano ketone (**11**, m.p. 119°) in 80% yield. This cyano ketone was distinctly different from those previously encountered (**5***a* and *b*). Since **5***a* and *b* proved to be *cis* isomers (*vide infra*), **11** must be a *trans* isomer as would be expected by analogy with the model experiments.

By analogy with the model experiments (*vide supra*) we suspected that **5***a* and *b* were *cis* isomers. But, since a *cis*-cyano ketone or a mixture of epimeric *cis*-cyano ketones was required, we sought assurance on this point by comparison of the chemical shifts of the angular methyl groups of the isomeric cyano ketones. This method (*vide supra*) failed to provide the assurance we sought.

A comparison of the data in Table 1 for **5***a*

Can. J. Chem. Downloaded from www.nrcresearchpress.com by 210.87.254.42 on 09/05/12
For personal use only.

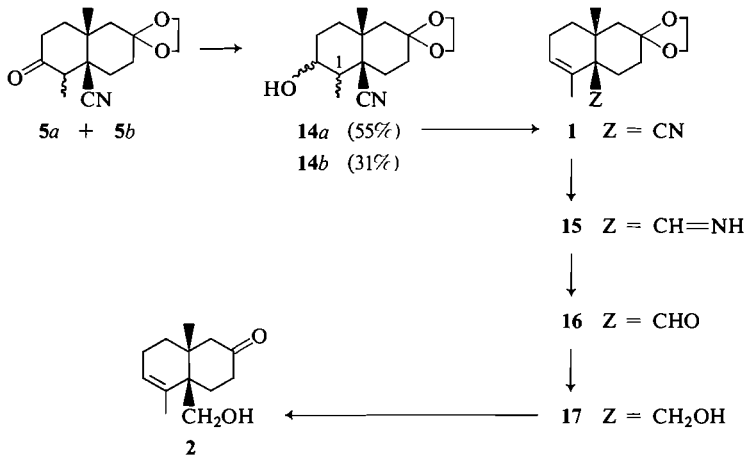

SCHEME 2

and **11** suggested that the former was indeed a *cis* isomer but, since the difference in chemical shifts was only 9 Hz, we felt that corroborative evidence was necessary. We therefore compared the pertinent n.m.r. data (Table 1) for **5***b* and **11** and finally for the ketals **12** and **13** which were derived from **5***a* and **11**, respectively. In neither case could any reliable conclusions be drawn because of the even smaller differences (less than 5 Hz) in the chemical shifts of the angular methyl groups. Consequently, it was decided to proceed with the synthesis on the assumption that **5***a* and *b* were *cis* isomers, hoping for an opportunity to test this assumption at a later stage.

The conversion of **5***a* and *b* into the desired octalone **2** is outlined in Scheme 2. Reduction of either **5***a* or a mixture of **5***a* and *b* with lithium aluminum hydride afford a crystalline alcohol **14***a* (m.p. 146°; 55%) and an oily mixture of epimers (**14***b*). Dehydration of the alcohol (**14***a*) with phosphorus oxychloride in pyridine smoothly converted it into the crystalline olefinic nitrile **1** in 76% yield. The mixture (**14***b*) failed to dehydrate satisfactorily under a variety of conditions.

An X-ray crystallographic study of the olefinic nitrile showed that it had structure **1** with the required *cis* ring fusion (1). This structure determination afforded assurance that the final product **2** would also have the desired *cis* ring fusion and provided proof that **5***a* and *b*, as suspected, were *cis*-cyano ketones and that, consequently, **11** was a *trans* isomer.

Partial reduction of the cyano group of **1** with lithium aluminum hydride to the imine **15** followed by hydrolysis in buffered solution afforded the aldehyde **16** in 71% yield. Reduction of **16** with lithium aluminum hydride gave the alcohol **17** (77%). Finally, treatment of **17** with acid afforded the desired compound **2** (86%) having the required *cis* ring fusion.

Experimental

Methods and Materials

The n.m.r. chemical shifts are expressed in parts per million (δ values) downfield from the signal for tetramethylsilane which is used as an internal standard.

Reaction products were isolated by the following procedure. The product was extracted into the specified solvent and the extract was washed three times with appropriate aqueous solutions as indicated. The original aqueous layer (if any) and the aqueous washings were extracted three times with the solvent and the combined extracts were dried over anhydrous magnesium sulfate, filtered, and evaporated *in vacuo* on a rotary evaporator.

Petroleum ether refers to the fraction with b.p. range 30–60°.

Brine refers to a saturated solution of sodium chloride.

cis-Cyano Decalone 7

A solution of 2.3 g of the octalone **6** (4) in 100 ml of benzene under a dry nitrogen atmosphere was treated with 3.5 g of diethylaluminum cyanide (7) in 27 ml of benzene. The reaction solution was left at room temperature for 16 h then heated at 45° for 1 h. The reaction solution was diluted with a mixture of 1250 g of ice and water containing 50 g of dissolved sodium hydroxide. The alkaline solution was extracted with chloroform and the extract evaporated *in vacuo*. Crystallization of the residue from ether afforded 1.70 g (64%) of **7**, m.p. 109° (lit. (5) m.p. 107–108.5°); ν_{max} (KBr) 2228 (CN) and 1710 cm^{-1} (ketone); n.m.r. ($CDCl_3$), δ 1.16 (d, J = 6.5 Hz, 3H, secondary methyl), 1.48 (s, 3H, angular methyl), 3.05 (q, J = 6.5 Hz, 1H, methine coupled to methyl). The i.r. and n.m.r. spectra were identical with

Can. J. Chem. Downloaded from www.nrcresearchpress.com by 210.87.254.42 on 09/05/12
For personal use only.

Can. J. Chem. Downloaded from www.nrcresearchpress.com by 210.87.254.42 on 09/05/12
For personal use only.

the spectra[2] of a cyano ketone of established (5) stereostructure as represented by 7.

Anal. Calcd. for $C_{13}H_{19}NO$: C, 76.06; H, 9.33; N, 6.82. Found: C, 76.26; H, 9.55; N, 6.83.

cis-Cyano Ketal ***9***

A solution of 600 mg of the *cis*-cyano ketone 7, 48 mg of *p*-toluenesulfonic acid monohydrate, and 1.40 g of ethylene glycol in 100 ml of benzene was refluxed under a nitrogen atmosphere for 20 h. The solution was cooled to room temperature and treated, with stirring, with 150 mg of solid sodium bicarbonate. The benzene solution was washed with saturated sodium bicarbonate solution and with brine. The aqueous washings were extracted with ether. Evaporation of the dried extracts gave an oil which, on crystallization from ether – petroleum ether afforded 528 mg (81%) of **9**, m.p. 75–76°; ν_{max} (Nujol) 2220 cm^{-1} (CN); n.m.r. ($CDCl_3$), δ 1.00 (d, J = 6.5 Hz, 3H, secondary methyl), 1.24 (s, 3H, angular methyl) 2.37 (q, J = 6.5 Hz, 1H, methine coupled to methyl), 3.84 (m, 4H, ethylene of ketal).

Anal. Calcd. for $C_{15}H_{23}NO_2$: C, 72.25; H, 9.30; N, 5.62. Found: C, 72.75; H, 9.47; N, 5.50.

trans-Cyano Decalone ***8***

A solution of 461 mg of the octalone **6** (4) in 16 ml of benzene and 8.5 ml of toluene was cooled on an ice bath to 0° and treated with 1.73 g of diethylaluminum cyanide (7) in 22 ml of benzene. The reaction solution was kept at 0° for 10 min then poured into 250 g of a mixture of ice and water containing 10 g of dissolved sodium hydroxide. The cold aqueous solution was worked up with chloroform and brine in the usual manner. Crystallization of the crude product, an oil, from ether – petroleum ether afforded 356 mg (67%) of **8**, m.p. 100.5° (lit. (5) m.p. 101–102°); ν_{max} (KBr) 2225 (CN) and 1705 cm^{-1} (ketone); n.m.r. ($CDCl_3$), δ 1.16 (d, J = 6.5 Hz, 3H, secondary methyl), 1.24 (s, 3H, angular methyl), 2.50 (q, J = 6.5 Hz, methine coupled to methyl). The i.r. and n.m.r. spectra[2] were identical with the spectra of a cyano ketone of established (5) stereostructure represented by **8**.

Anal. Calcd. for $C_{13}H_{19}NO$: C, 76.06; H, 9.33; N, 6.82. Found: C, 75.69; H, 9.31; N, 6.68.

trans-Cyano Ketal ***10***

The *trans*-cyano ketone **8** (2.85 g) was converted to the ketal **10** by the same procedure as was used in the case of the *cis*-cyano ketone (*vide supra*). Chromatography of the crude product on a column of 140 g of basic alumina (grade III) with 0.5% of ether in benzene as solvent and crystallization of the eluted product from ether–pentane afforded 2.74 g (78%) of **10**, m.p. 101–102°; ν_{max} (Nujol) 2220 cm^{-1} (CN); n.m.r. ($CDCl_3$), δ 0.93 (d, J = 6.5 Hz, 3H, secondary methyl), 1.02 (s, 3H, angular methyl), 3.96 (m, 4H, ethylene of ketal).

Anal. Calcd. for $C_{15}H_{23}NO_2$: C, 72.25; H, 9.30; N, 5.62. Found: C, 72.40; H, 9.49; N, 5.75.

cis-Cyano Keto Ketals 5a and b

The keto ketal **4** (3) (236 mg) was dissolved in 10 ml of dry benzene in a nitrogen atmosphere. A benzene solution (2.5 ml) of diethylaluminum cyanide (333 mg) was added and the reaction mixture was stirred at room temperature for 10 h. The reaction solution was diluted with a mixture of 125 ml of ice and water containing 5 g of dissolved sodium hydroxide. The resulting aqueous solution was extracted with chloroform and the extract evaporated *in vacuo*. Purification of the residue by silica gel preparative t.l.c. with 10% of ether in benzene as solvent, gave 170 mg (65%) of epimer ***5a***, m.p. 110°; ν_{max} (KBr) 2225 (CN) and 1720 cm^{-1} (ketone); n.m.r. ($CDCl_3$), δ 1.19 (d, J = 6.0 Hz, 3H, secondary methyl), 1.50 (s, 3H, angular methyl), 2.97 (q, J = 6.0 Hz, 1H, methine coupled to methyl), 3.89 (m, 4H, ethylene of ketal).

Anal. Calcd. for $C_{15}H_{21}NO_3$: C, 68.42; H, 8.03; N, 5.32. Found: C, 68.25; H, 7.72; N, 5.34.

There was also obtained 70 mg (27%) of epimer ***5b***, m.p. 126°; ν_{max} (KBr) 2225 (CN) and 1720 cm^{-1} (ketone); n.m.r. ($CDCl_3$) δ 1.19 (d, J = 6.0 Hz, 3H, secondary methyl), 1.39 (s, 3H, angular methyl), 2.72 (q, J = 6.0 Hz, 1H, methine coupled to methyl), 3.93 (m, 4H, ethylene of ketal).

Anal. Calcd. for $C_{15}H_{21}NO_3$: N, 5.32. Found: N, 5.50.

Treatment of either ***5a*** or ***b*** with 0.1 *N* methanolic potassium hydroxide at room temperature resulted in a mixture of both isomers as shown by t.l.c. on silica with ether as solvent.

trans-Cyano Keto Ketal ***11***

A solution of 236 mg of the keto ketal **4** (3) in 7 ml of benzene and 4 ml of toluene was cooled on an ice bath to 0° and treated with 555 mg of diethylaluminum cyanide in 4.2 ml of benzene. The reaction solution was kept at 0° for 10 min then poured into 125 g of a mixture of ice and water containing 5 g of dissolved sodium hydroxide. The cold aqueous solution was worked up with chloroform and brine in the usual manner. Evaporation of the chloroform extracts *in vacuo* yielded 250 mg of crystalline material which was recrystallized from ether – petroleum ether to give 210 mg (80%) of **11**, m.p. 118–120°; ν_{max} (KBr) 2220 (CN) and 1715 cm^{-1} (ketone); n.m.r. ($CDCl_3$), δ 1.18 (d, J = 5.5 Hz, 3H, secondary methyl), 1.35 (s, 3H, angular methyl), 2.47 (q, J = 5.5 Hz, 1H, methine coupled to methyl), 3.91 (m, 4H, ethylene of ketal).

Anal. Calcd. for $C_{15}H_{21}NO_3$: C, 68.42; H, 8.03; N, 5.32. Found: C, 68.27; H, 7.83; N, 5.27.

cis-Cyano Diketal ***12***

A solution of 376 mg of *cis*-cyano keto ketal ***5a***, 56 mg of *p*-toluenesulfonic acid monohydrate, and 2.4 ml of ethylene glycol in 60 ml of benzene was refluxed under a nitrogen atmosphere for 24 h. The benzene solution was washed with saturated sodium bicarbonate solution and with brine. The aqueous washings were extracted with ether. Evaporation of the dried extracts gave 441 mg of an oil which when purified by silica gel preparative t.l.c., with 5% of ether in benzene as solvent, gave 368 mg (83%) of **12**, m.p. 152–153°; ν_{max} (CCl_4) 2210 cm^{-1} (CN); n.m.r. (CCl_4) δ 1.04 (d, J = 6.0 Hz, 3H, secondary methyl), 1.23 (s, 3H, angular methyl), 2.33 (q, J = 6.0 Hz, 1H, methine coupled to methyl), 3.82 (m, 8H, ethylene of ketals).

Anal. Calcd. for $C_{17}H_{25}NO_4$: C, 66.43; H, 8.20: N, 4.56. Found: C, 66.27; H, 8.31; N, 4.41.

trans-Cyano Diketal ***13***

The *trans*-cyano keto ketal **11** (94 mg) was converted to the *trans*-cyano diketal **13** by the procedure given in the

[2]The i.r. and n.m.r. spectra were provided by N. J. Johnston (see ref. 5).

Can. J. Chem. Downloaded from www.nrcresearchpress.com by 210.87.254.42 on 09/05/12
For personal use only.

preceding experiment. This yielded 120 mg of a crystalline compound which was recrystallized from ether – petroleum ether to give 100 mg (91%) of **13**, m.p. 157–158°; ν_{max} (CCl_4) 2210 cm^{-1} (weak CN); n.m.r. (CCl_4) δ 0.98 (d, J = 6.0 Hz, 3H, secondary methyl), 1.15 (s, 3H, angular methyl), 3.83 (m, 8H, ethylene of ketals).

Anal. Calcd. for $C_{17}H_{25}NO_4$: C, 66.42; H, 8.20; N, 4.56. Found: C, 66.79; H, 8.60; N, 4.55.

*Cyano Alcohols **14a** and **b***

A mixture of 248 mg of **5***a* and *b*, 10 ml of tetrahydrofuran, 120 mg of sodium borohydride, and 0.8 ml of water was stirred at room temperature for 4.5 h. Then 100 ml of water was added and the mixture stirred for another 3 h. The reaction mixture was worked up with chloroform and brine in the usual manner to yield 225 mg of a mixture of isomeric cyano alcohols. Purification of the product by silica gel preparative t.l.c., with ether as solvent, gave 137 mg (55%) of the faster moving isomer **14***a*, m.p. 144–148°. Spectral data showed **14***a* to be a single epimer, thus, ν_{max} ($CHCl_3$) 3600 and 3475 (OH) and 2215 cm^{-1} (CN); n.m.r. ($CHCl_3$) δ 1.17 (s, 3H, angular methyl), 1.22 (d, J = 5.5 Hz, 3H, secondary methyl), 3.88 (m, 4H, ethylene of ketal).

Anal. Calcd. for $C_{15}H_{23}NO_3$: C, 67.90; H, 8.73; N, 5.28. Found: C, 67.77; H, 8.92; N, 5.10.

The slower moving material (78 mg of **14***b*) was still a mixture of isomers as shown by a complex methyl signal in the n.m.r. spectrum ($CDCl_3$); ν_{max} 3350 (OH) and 2215 cm^{-1} (CN).

*Olefinic Nitrile **1***

A solution of 106 mg of **14***a* in 2.4 ml of pyridine was cooled in an ice bath and treated with 0.2 ml of phosphorus oxychloride. After stirring for 1.5 h at room temperature in the dark, the mixture was diluted with a mixture of ice and water and stirred for 15 min. The cold aqueous mixture was extracted with chloroform and the extracts were worked-up in the usual manner with cold 1 *M* hydrochloric acid and cold saturated sodium bicarbonate solution. Evaporation of the dried extracts afforded 100 mg of an oil which crystallized from ether – petroleum ether to give 75 mg (76%) of **1**, m.p. 68–69°; ν_{max} ($CHCl_3$), 2215 cm^{-1} (CN); n.m.r. ($CDCl_3$) δ 1.18 (s, 3H, angular methyl), 1.85 (d, J = *ca.* 2 Hz, 3H, vinylic methyl), 3.90 (m, 4H, ethylene of ketal), 5.55 (m, 1H, vinylic proton).

Anal. Calcd. for $C_{15}H_{21}NO_2$: C, 72.84; H, 8.56; N, 5.66. Found: C, 72.54; H, 8.55; N, 5.48.

*Olefinic Alcohol **17***

The olefinic nitrile **1** (266 mg) was refluxed in 50 ml of dry tetrahydrofuran with 250 mg of lithium aluminum hydride under a nitrogen atmosphere for 1 h. After cooling to room temperature and addition of 110 ml of ether, 0.1 ml of a saturated solution of sodium sulfate was added. The mixture was stirred for 1 h then 1 g anhydrous sodium sulfate was added and stirring was continued for another 30 min. The solid material was filtered off and the solvent evaporated to give 268 mg of olefinic imine **15**; ν_{max} (neat) 1625 cm^{-1} (C=N).

The imine **15** (268 mg) was dissolved in 8 ml of tetrahydrofuran and 8 ml of methanol. Then 660 mg of sodium acetate trihydrate and 10 ml of 5% aqueous acetic acid was added and the mixture was refluxed for 20 min. The cooled reaction mixture was extracted with chloroform and the extracts were worked up in the usual manner with 2 *M* sodium hydroxide and brine. Evaporation of the dried extracts afforded 190 mg of the aldehyde **16**; ν_{max} (neat) 2700 and 1720 (aldehyde) and 1650 cm^{-1} (olefin); n.m.r. ($CDCl_3$) δ 1.10 (s, 3H, angular methyl), 1.55 (d, J = *ca.* 2 Hz, 3H, vinylic methyl), 3.90 (s, 4H, ethylene of ketal), 5.88 (m, 1H, vinylic proton), 9.58 (s, 1H, aldehyde).

A mixture of 190 mg of the aldehyde **16**, 50 ml of ether, and 125 mg of lithium aluminum hydride was refluxed for 30 min. The cooled mixture was treated with 0.1 ml of saturated sodium sulfate solution, stirred for 1 h, and treated with 1 g sodium sulfate. The solid material was removed by filtration and washed with ether. Evaporation of the combined filtrate and washings gave 193 mg of oil. Purification of the product by silica gel t.l.c., with 50% of ether in benzene as solvent, gave 148 mg of the olefinic alcohol **17** as an oil (55% yield from the olefinic nitrile **1**); ν_{max} (neat) 3460 (OH) and 1650 cm^{-1} (olefin); n.m.r. ($CDCl_3$) δ 1.12 (s, 3H, angular methyl), 1.67 (d, J = *ca.* 2 Hz, 3H, vinylic methyl), 3.30 and 3.57 (doublets, J = 12 Hz, 1H each, CH_2—OH), 3.88 (m, 4H, ethylene of ketal), 5.73 (m, 1H, vinylic proton).

*Octalone **2***

A solution of 252 mg of the olefinic alcohol **17**, 10 ml of tetrahydrofuran, and 6 ml of 1 *M* aqueous hydrochloric acid was left at room temperature under nitrogen atmosphere for 1.5 h. The reaction mixture was worked up with chloroform, saturated sodium bicarbonate, and brine in the usual manner to give 247 mg of an oil. Purification of the product on silica gel preparative t.l.c. with 50% of ether in benzene as solvent, yielded 178 mg (86%) of octalone **2**, m.p. 102–103°; ν_{max} ($CHCl_3$) 3600 and 3545 (OH) and 1720 cm^{-1} (ketone); n.m.r. ($CDCl_3$) δ 1.05 (s, 3H, angular methyl), 1.80 (d, J = *ca.* 2 Hz, 3H, vinylic methyl), 3.53 (s, 2H, CH_2OH), 5.85 (m, 1H, vinylic proton).

Anal. Calcd. for $C_{13}H_{20}O_2$: C, 74.97; H, 9.67. Found: C, 74.91; H, 9.73.

We are grateful to Dr. H. Lynton, University of New Brunswick, for determining the structure of compound **1** by X-ray crystallographic analysis, and to Dr. N. J. Johnston for assistance in establishing the structures of compounds **7** and **8**. Also, we wish to thank the National Research Council of Canada for financial support and for the Postgraduate Scholarship awarded to S.J.A.

1. H. Lynton and P-Y. Siew. Can. J. Chem. **53**, 192 (1975).
2. J. Fridrichson and A. M. Mathieson. Tetrahedron Lett. 18 (1960); W. D. Crow. Aust. J. Chem. **15**, 159 (1962).
3. S. A. Narang and P. C. Dutta. J. Chem. Soc. 2842 (1960).
4. J. K. Chakrabarti, P. Dutt, and P. C. Dutta. J. Chem. Soc. 4978 (1956); M. Yanagita, M. Hirakura, and F. Seki. J. Org. Chem. **23**, 841 (1958).
5. O. R. Rodig and N. J. Johnston. J. Org. Chem. **34**, 1942 (1969).
6. P. N. Rao and J. E. Burdett. J. Org. Chem. **34**, 1090 (1969).
7. W. Nagata, M. Yoshioka, and S. Hirai. J. Am. Chem. Soc. **94**, 4635 (1972) and papers immediately following.

A Photoelectron Investigation of Acyl Silanes: The Photoelectron Spectra of Trimethylsilyl Phenyl Ketone and Phenyl *tert*-Butyl Ketone

R. S. BROWN

Department of Chemistry, University of Alberta, Edmonton, Alberta T6G 2E1

Received February 13, 1975

R. S. BROWN. Can. J. Chem. **53**, 2446 (1975).

The photoelectron spectra of trimethylsilyl phenyl ketone and phenyl *tert*-butyl ketone are presented and analyzed in terms of their constituent orbitals. A hyperconjugative interpretation for the low energy ionization potentials of the acyl silanes is postulated. A combination of p.e. spectroscopy and u.v. data are used to infer the level of the LUMO in these systems and to construct a partial energy level diagram.

R. S. BROWN. Can. J. Chem. **53**, 2446 (1975).

On présente l'analyse du spectre photoelectronique de la triméthylsilyl phényl cétone et *tert*-butyl phényl cétone en termes de leurs orbitales constituantes. En se basant sur l'hyperconjugaison, on propose une interprétation des potentiels d'ionisation à faible énergie des acylsilanes. Une combinaison des données spectroscopiques p.e. et u.v. est utilisée pour déduire le niveau de LUMO dans ces systèmes et pour construire un diagramme partiel des niveaux d'énergie. [Traduit par le journal]

Can. J. Chem. Downloaded from www.nrcresearchpress.com by 210.87.254.5 on 09/05/12
For personal use only.

During the course of a study initiated to investigate the photoelectron spectra (p.e.) of acyl silanes (1), we became aware of an article by Ramsey *et al.* (2*a*) offering a reinterpretation of the mechanism (2*b*, *c*) by which the trimethylsilyl group interacts with β nonbonding orbitals as in **1***b*.

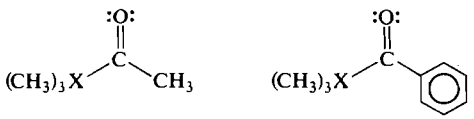

1
a X = C
b X = Si

2
a X = C
b X = Si

The above study prompted us to reveal our findings concerning **1** and the analogous series **2**. Compounds **1***b* and **2***b* are similar but differ in the following way. In both series, the n_0 orbital and the C—Si$(CH_3)_3$ σ bond are coplanar but **2***b* possesses an additional set of β orbitals in its phenyl group which are *potentially* capable of a similar interaction. If such an interaction is present, p.e. spectroscopy should detect it.

The p.e. spectra for compounds **1** and **2** are presented in Figs. 1 and 2, respectively, while the corresponding vertical ionization potentials and the interpretation of the orbitals which gave rise to these ionizations are presented in Tables 1 and 2.

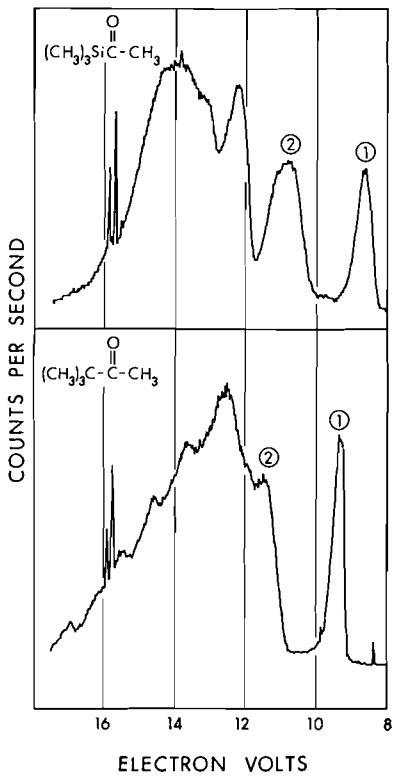

FIG. 1. Photoelectron spectra of methyl *tert*-butyl ketone (**1***a*) and methyl trimethylsilyl ketone (**1***b*) using argon as a calibrating gas.

Can. J. Chem. Downloaded from www.nrcresearchpress.com by 210.87.254.5 on 09/05/12
For personal use only.

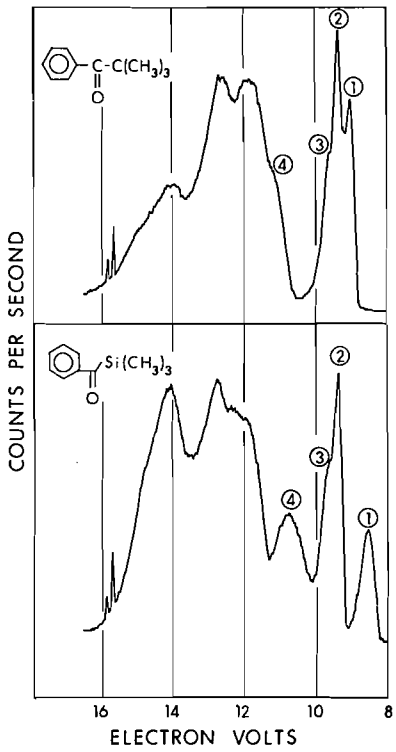

FIG. 2. Photoelectron spectra for *tert*-butyl phenyl ketone (**2***a*) and trimethylsilyl phenyl ketone (**2***b*) using argon as a calibrating gas.

TABLE 1. Vertical ionization potentials of methyl *tert*-butyl ketone (**1***a*) and methyl trimethylsilyl ketone **1***b*

Band	Vertical i.p. (eV) **1***a*	**1***b*	Assignment
1[a]	9.24	8.64	"n_0"
2	11.44	10.94	*e* symmetry orbital of $X(CH_3)_3$
3	11.86	12.26	
4	12.59	12.56	

[a]The onset potential of band 1 is 9.00 eV for **1***a* and 8.09 eV for **1***b*.

Since the spectrum of **1***b* has been presented (2*a*) only the following points need be made. Band 1 can most certainly be assigned to ionization of an electron residing in a nonbonding orbital (n_0) primarily located on oxygen. The large half-width of band 1 in **1***b* tentatively implies a large difference in the geometry of the unionized and ionized states, usually indicative of the removal of a strongly bonding or antibonding electron (3). Calculations on this system (2*a*) indicate that this orbital possesses components of both the localized n_0 and C—Si$\lessdot$ orbitals and is antibonding. The high resolution p.e. spectra indicate no discernible vibrational fine structure for band 1 and hence cannot experimentally confirm the 'antibonding' nature.

TABLE 2. Vertical ionization potentials for *tert*-butyl phenyl ketone (**2***a*) and trimethylsilyl phenyl ketone (**2***b*)

Band	Vertical i.p. (eV) **2***a*	**2***b*	Assignment
1[a]	8.98	8.41	"n_0"
2	9.33	9.29	phenyl b_1
3	9.61	9.59	phenyl a_2
4	11.16	10.71	*e* orbital of $X(CH_3)_3$
5	11.89	11.96	
6	12.66	12.34	
7		12.76	

[a]Onset of band 1 is 8.70 and 7.96 eV for **2***a* and **2***b*, respectively.

We visualize, as do others (2*a* and *c*, 4) that the raising of the n_0 orbital in the acyl silanes relative to the α-*tert*-butyl ketones can best be visualized as a hyperconjugative interaction between the coplanar carbon–silicon bond and the adjacent n_0 orbital. The C—Si$\lessdot$ bond is of net higher energy than the analogous C—C$\lessdot$ bond[1] and hence is closer in energy to an isolated n_0 orbital, allowing a greater interaction in the α-trimethylsilyl ketones than in the α-*tert*-butyl ketones and a correspondingly lower i.p. in the former.

A hyperconjugative interaction, like all conjugative interactions requires coplanarity of orbitals for maximum effect. Interestingly, the results of Hanstein *et al.* (7) clearly demonstrate this requirement since the charge-transfer absorption frequency for **3** is much lower than **4**, whereas the charge-transfer frequencies of **5** and **6** are equal (Scheme 1).[2]

While the geometry of **1***b* is such that the n_0

[1]Using Koopman's theorem (5), one can assign a value of 10.6 eV to the C—Si$\lessdot$ bond based upon the average vertical i.p. for the $3t_2$ level of tetramethylsilane (6). Similarly a value of 11.2 eV can be obtained for the C—C$\lessdot$ bond based upon tetramethylmethane (6).

[2]The above results were obtained with the trimethyltin analogs, however it is expected that the corresponding trimethylsilicon compounds will show similar trends only differing in magnitude.

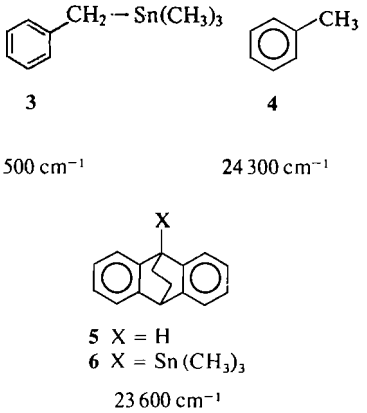

SCHEME 1. Charge-transfer frequencies for compounds **3**–**6**.

orbital and the C—Si< bond are syncoplanar, **2***b* contains a phenyl group whose π system is perpendicular to the C—Si< bond. If the mechanism of the interaction is indeed conjugative in nature, one would expect that the only differences in perturbation of the phenyl orbitals in series **2** will be due to electronegativity differences between the trimethylsilylacyl and the *tert*-butylacyl substituents.

Ultraviolet Data

The u.v. absorption data for ketones **1***a* and **1***b* have been extensively reviewed (1*f*) and are presented in Table 3 for convenient reference.

Using Table 3 one can quickly determine that $\Delta(n \rightarrow \pi^*) = 0.98$ eV for compounds **1***a* and **1***b*.

TABLE 3.[a] Ultraviolet absorption maxima for $n \rightarrow \pi^*$ and $\pi \rightarrow \pi^*$ transitions of ketones **1***a* and **1***b*

	$n \rightarrow \pi^*$		$\pi \rightarrow \pi^*$	
Ketone[b]	ν_{max} (cm^{-1})	ΔE (eV)	ν_{max} (cm^{-1})	ΔE (eV)
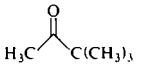	34 800	4.32	53 800	6.68
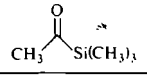	26 900	3.34	51 200	6.35

[a]Reference 1*f*.
[b]Determined in *n*-heptane.

The p.e. data are presented in Table 1. A difference in the n_0 orbital of 0.60 eV is noticed in passing from **1***a* to **1***b*. Since this difference does not fully account for the $\Delta(n \rightarrow \pi^*)$ absorption between these two ketones, it is evident that π^* in **1***b* must be lowered in energy by 0.38 eV relative to π^* in **1***a*. In accordance with Pitt (2*c*) and Bock *et al.* (2*b*), we suggest that the C=O π^* orbital is stabilized by interaction with d and/or σ^* orbitals located primarily on the trialkyl silicon moiety. CNDO/2 calculations in similar systems (2*c*) reveal that the highest occupied σ-bonding orbital contains significant Si 3p contributions while the LUMO contains both Si 3p and Si 3d components.

Phenyl Ketones 2a and 2b

Inspection of Fig. 2 indicates that the low binding energy regions of the spectra exhibit four well-defined bands which can be assigned as follows. Band I in the p.e. spectrum of **2***a* and **2***b* appears at 8.98 and 8.41 eV, respectively, and can be assigned (as in series **1**) to an orbital comprised of the n_0 orbital and the adjacent C—X(CH$_3$)$_3$ σ bond. Substitution of the trimethylsilyl group for a *tert*-butyl group raises this orbital by 0.57 eV, identical within experimental error to the raising in passing from **1***a* to **1***b*.

Bands 2 and 3 located at 9.31 ± 0.02 and 9.60 ± 0.01 eV, respectively, in both **2***a* and **2***b* can without doubt be assigned to ionizations arising primarily from orbitals located on the aromatic ring. According to CNDO/2 calculations on similar systems (8), these two orbitals are assigned to be of b_1 and a_2 symmetry, b_1 being of lower ionization energy than a_2. It is interesting to see that these phenyl bands appear to be unperturbed in changing from **2***a* to **2***b*.

The source for this coincidence may arise from the fact that the phenyl π system being orthogonal to the C—Si< bond has no conjugative interaction with it, and therefore remains unperturbed in passing from **2***a* to **2***b*. Alternatively, π donation of the entire trimethylsilylacyl group may exactly compensate an inductive σ withdrawal of the group leaving no difference in perturbation of the aromatic ring between **2***a* and **2***b*. This study then provides corroborative experimental evidence for the calculations of Yates *et al.* (1*f*) who concluded that there is little or no perturbation of the phenyl orbitals in changing from **2***a* to **2***b*.

Band 4 apears at 11.16 eV in **2***a* and 10.76 eV in **2***b* and can be assigned to ionization arising from an *e* symmetry orbital located on the *tert*-

Can. J. Chem. Downloaded from www.nrcresearchpress.com by 210.87.254.5 on 09/05/12
For personal use only.

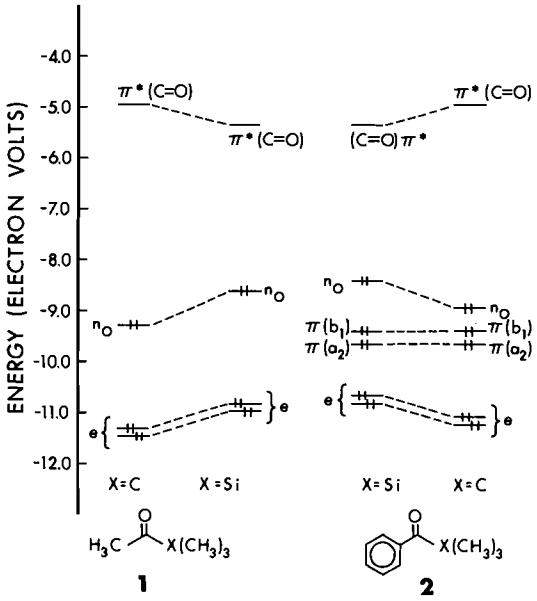

FIG. 3. Partial energy level diagrams for ketones **1** and **2**, assuming the validity of Koopman's theorem (5). Note that the above diagram differs slightly from that presented in ref. 1*f*, in that extended Hückel calculations predict another σ orbital between n_O and $\pi(b_1)$ in ketones **2**.

butyl and trimethylsilyl groups, respectively (6, 10).

Utilizing a combination of p.e. spectroscopy and u.v. data, we can now draw a partial energy level diagram for these ketones based entirely upon experimental results. Such a diagram is illustrated in Fig. 3.[3]

[3]Another related yet different example of this type of interaction is that evident in the p.e. spectrum of α-picoline (**7**) and α-trimethylsilylpyridine (**8**) (9). The n_N orbital of **7** is obscured and assumed to lie under the bands

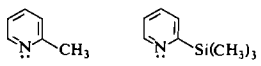

7 ($E(n_N)$ = 9–10 eV) **8** ($E(n_N)$ = 8.5 eV)

arising from the ionization of π electrons but is strongly raised in energy in **8**. While this fact was interpreted as being due to a (+)-inductive effect of the trimethylsilyl group, it is also consistent with a hyperconjugative interaction (2*a* and *c*, 4).

Experimental

Literature procedures were used to prepare derivatives **1***a* (11), **1***b* (1*c*), **2***a* (12), and **2***b* (1*b*). Photoelectron spectra were obtained using a McPherson Model 36 ESCA spectrometer equipped with a He(I) ionization source. Under optimum conditions the resolution of the $Ar_{1/2}$–$Ar_{3/2}$ doublet was 16 meV at 60 000 counts per second but was found to be between 24 and 28 meV while recording spectra.

The author would like to acknowledge the financial support of the University of Alberta, and the National Research Council of Canada.

1. (*a*) A. G. BROOK. J. Am. Chem. Soc. **79**, 4373 (1957). (*b*) A. G. BROOK, M. A. QUIGLEY, G. J. D. PEDDLE, N. V. SCHWARTZ, and C. M. WARNER. J. Am. Chem. Soc. **82**, 5102 (1960). (*c*) A. G. BROOK, J. M. DUFF, P. F. JONES, and N. R. DAVIES. J. Am. Chem. Soc. **89**, 431 (1967). (*d*) E. J. COREY, D. SEEBACH, and R. FREEDMAN. J. Am. Chem. Soc. **89**, 434 (1967). (*e*) K. YATES and F. AGOLINI. Can. J. Chem. **44**, 2229 (1960). (*f*) F. AGOLINI, S. KLEMENKO, J. G. CSIZMADIA, and K. YATES. Spectrochim. Acta A, **24**, 169 (1968) and references therein.
2. (*a*) B. G. RAMSEY, A. BROOK, A. R. BASSENDALE, and H. BOCK. J. Organometal. Chem. **74**, C41 (1974). (*b*) H. BOCK, H. ALT, and H. SEIDL. J. Am. Chem. **91**, 355 (1969). (*c*) C. G. PITT. J. Organometal. Chem. **61**, 49 (1973).
3. D. W. TURNER, C. BAKER, A. D. BAKER, and C. R. BRUNDEL. Molecular photoelectron spectroscopy, Wiley Interscience, London. 1970.
4. (*a*) T. G. TRAYLOR, W. HANSTEIN, H. J. BERWIN, N. A. CLINTON, and R. S. BROWN. J. Am. Chem. Soc. **93**, 5715 (1971). (*b*) W. H. HANSTEIN, H. J. BERWIN, and T. G. TRAYLOR. J. Am. Chem. Soc. **92**, 7476 (1970).
5. T. KOOPMANS. Physica, **1**, 104 (1934).
6. S. EVANS, J. C. GREEN, P. J. JOACHIN, A. F. ORCHARD, D. W. TURNER, and J. P. MAIER. J. Chem. Soc. Faraday Trans. II, **68**, 905 (1972).
7. W. HANSTEIN, H. J. BERWIN, and T. G. TRAYLOR. J. Am. Chem. Soc. **92**, 7476 (1970).
8. J. W. RABALAIS and R. J. COTTON. J. Electron Spectrosc. **1**, 83 (1972–1973).
9. E. HEILBRONNER, H. BOCK, and H. ALT. Angew. Chem. Internat. Ed. **8**, 524 (1969).
10. G. BIERI, F. BROGLI, E. HEILBRONNER, and E. KLOSTER-JENSEN, J. Electron Spectrosc. **1**, 67 (1972–1973).
11. G. A. HILL and E. W. FLOSDORF. Org. Syn. Coll. **1**, 462 (1932).
12. J. H. FORD, C. D. THOMPSON, and C. S. MARVEL. J. Am. Chem. Soc. **57**, 2619 (1935).

Can. J. Chem. Downloaded from www.nrcresearchpress.com by 210.87.254.5 on 09/05/12
For personal use only.

Alkaline Hydrolysis Products of *N*-Substituted Phthalimides

S. KHAQAN HASAN AND S. AHMAD ABBAS

Chemical Research Division, P.C.S.I.R. Laboratories, Karachi-39, Pakistan

Received March 27, 1975

S. KHAQAN HASAN and S. AHMAD ABBAS. Can. J. Chem. **53**, 2450 (1975).

Products of alkaline hydrolysis of *N*-substituted phthalimides are described. Five isomeric compounds, 1,6-diketo-3,4,5,6-tetrahydro-1*H*-2,5-benzoxazocine (**1**), 2-(*o*-carboxyphenyl)-Δ^2-oxazoline (**7**), 2-phthalimidoethanol (**3**), *N*-vinylphthalamic acid (**8**), and *N*-(*o*-carboxybenzoyl)-aziridine (**9**), are possible from the alkaline hydrolysis of 2-bromoethylphthalimide (**2**). Gabriel claimed in 1905 that **1** was formed on alkaline hydrolysis of **2** but later structure **7** was suggested for the product. The interest in the synthesis of **1** has led to a reinvestigation of this hydrolysis and structure **7** is confirmed for the initial product of the hydrolysis but it converts on warming during recrystallization into **1** which affords **3** on heating above melting point.

Hydrolysis of 2-chloroethylphthalimide (**4**) and 2-phthalimidoethyl-*p*-toluenesulfonate (**5**) also afforded **7**. Attempted preparation of **1** from intramolecular cyclization of 2-hydroxyethylphthalamic acid (**11**) was not successful and only **3** was obtained.

Reaction of phthalic anhydride with 2-aminoethylsulfuric acid (**14**) at 150° afforded diphthalimidoethyl phthalate (**13**) instead of 2-phthalimidoethylsulfuric acid (**6**). Isolation of **13** indicates formation of **3** as an intermediate product in this reaction.

S. KHAQAN HASAN et S. AHMAD ABBAS. Can. J. Chem. **53**, 2450 (1975).

On décrit les produits résultants de l'hydrolyse alkaline des phtalimides *N*-substituées. L'hydrolyse alkaline du bromo-2 éthylphtalimide (**2**) peut conduire à cinq isomères qui sont: la dioxo-1,6 tétrahydro-3,4,5,6 1*H*-benzoxazocine-2,5 (**1**), (*o*-carboxyphényl)-2 Δ^2-oxazoline (**7**), phtalimido-2 éthanol (**3**), acide *N*-vinylphtalamique (**8**) et la *N*-(*o*-carboxybenzoyl) aziridine (**9**). Gabriel déclara en 1905 que **1** se forme par l'hydrolyse basique de **2**. Plus tard, la structure **7** fut proposée pour le produit. L'intérêt de la synthèse de **1** nous a amené à réexaminer cette hydrolyse. La structure **7** est confirmée pour le produit initial de l'hydrolyse, mais le composé **7** se transforme en **1** par chauffage au cours de la recristallisation. Ce dernier se transforme en **3** par chauffage au delà du point de fusion.

L'hydrolyse du chloro-2 éthylphtalimide (**4**) et du phtalimido-2 éthyl *p*-toluènesulfonate (**5**) conduit aussi à **7**. La préparation de **1** par cyclisation intramoléculaire de l'acide hydroxy-2 éthylphtalamique (**11**) n'a pas été réussie. Seulement **3** a été obtenu.

La réaction de l'anhydride phtalique avec l'acide amino-2 éthylsulfurique (**14**) à 150° produit le diphtalimidoéthyl phtalate (**13**) au lieu de l'acide phtalimido-2 éthylsulfurique (**6**). La séparation de **13** indique que **3** est un intermédiaire dans cette réaction.

[Traduit par le journal]

Synthesis of 1,6-diketo-3,4,5,6-tetrahydro-1*H*-2,5-benzoxazocine (**1**) appeared to us interesting because of the reported pharmacological activity of the derivatives of benzoxazocines (1–4). Gabriel (5) in 1905 claimed the synthesis of **1** by alkaline hydrolysis of 2-bromoethylphthalimide (**2**) but it was shown later (6) that this hydrolysis afforded 2-(*o*-carboxyphenyl)-Δ^2-oxazoline (**7**) instead of **1**.

In view of these conflicting reports, this hydrolysis has been repeated to determine structures of the products by modern spectrometric methods and we wish to report here our results from the hydrolysis of **2** and other related *N*-substituted phthalimides.

Hydrolysis of **2** is also interesting owing to the possibility of the formation of three other isomeric products, 2-phthalimidoethanol (**3**), *N*-vinylphthalamic acid (**8**), and *N*-(*o*-carboxybenzoyl)aziridine **9** in addition to **1** and **7**. These products could be formed after the initial hydrolysis of **2** to bromoethylphthalamic acid (**10**). Nucleophilic displacement of bromo group by carboxyl oxygen could yield **1** while **7** could be obtained by displacement of leaving group by amide oxygen. Elimination of hydrogen bromide could give **8** while nucleophilic displacement of bromo group by amide nitrogen could afford **9**. The aziridine **9** could also rearrange to **7** and such rearrangements are known (7). The suggested isomers could also rearrange to **1** and then to **3**.

Treatment of **2** with aqueous potassium hydroxide solution followed by acidification resulted in the precipitation of a product whose

Can. J. Chem. Downloaded from www.nrcresearchpress.com by 210.87.254.40 on 09/05/12
For personal use only.

Can. J. Chem. Downloaded from www.nrcresearchpress.com by 210.87.254.40 on 09/05/12
For personal use only.

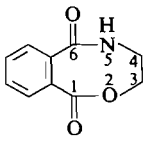

1

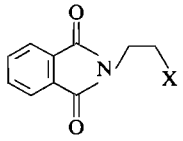

2 X = Br
3 X = OH
4 X = Cl
5 X = OTs
6 X = OSO_3H

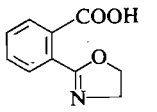

7

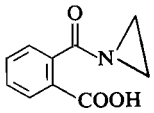

9

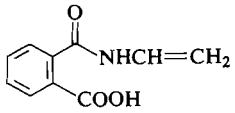

8

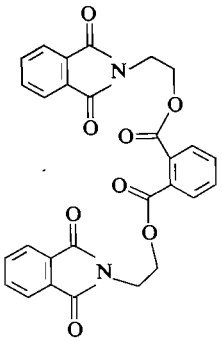

13

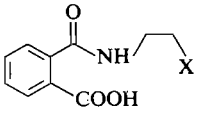

10 X = Br
11 X = OH
12 X = OSO_3H

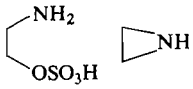

14

15

i.r. spectrum was the same as published earlier (8) for the material isolated from this hydrolysis. It shows carboxyl group absorption at 1700 cm^{-1} and another absorption at 1625 cm^{-1}. Cyclic conjugated compounds show C=N stretching absorption at 1575–1630 cm^{-1} (9) indicating **7** as the structure of the isolated product. The n.m.r. spectrum of this compound in alkaline deuterium oxide solution (p*H* 8) shows methylene triplets at δ 3.91 (J = 8.0 Hz) and 4.46 (J = 8.0 Hz) and aromatic protons at δ 7.28–7.71 as a multiplet.

Warming during recrystallization of **7** from 95% ethanol converted it into a rearranged product which shows ester carbonyl group absorption at 1740 cm^{-1} and secondary amide absorption at 1640 and 1540 cm^{-1} suggesting **1** as the structure of the compound. The n.m.r. spectrum of **1**, taken under the same conditions as utilized for **7**, shows two methylene triplets at δ 3.21 (J = 5.0 Hz) and 4.41 (J = 5.0 Hz) and aromatic protons at δ 7.31–7.86 as a multiplet. Both **1** and **7** show methylene and aromatic protons also in their n.m.r. spectra in deuterium oxide and deuterated dimethyl sulfoxide solutions.

Heating **1** and **7** above their melting points afforded **3** but **7** also gave a small amount of diphthalimidoethyl phthalate (**13**) which was not detected in the residue obtained on melting **1**. Isolation of **13** indicated formation of a small amount of phthalic anhydride on heating **7** as condensation of phthalic anhydride with **3** affords **13** (10).

Rearrangement of **7** to **1** appears to occur by the nucleophilic attack of carboxyl oxygen on C-5 of oxazoline in **7** resulting in the ring enlarged compound **1** which could further rearrange to **3** by nucleophilic attack of amide nitrogen on the ester carbonyl group.

Isolation of **13** from **7**, however, indicates nucleophilic attack of carboxyl oxygen on C-2 of oxazoline also resulting in the production of phthalic anhydride and elimination of the elements of aziridine but this attack on C-2 appears to be less favored in comparison to the attack on C-5 as evident by the small yield of **13** in comparison to the yield of **3** obtained on heating **7**.

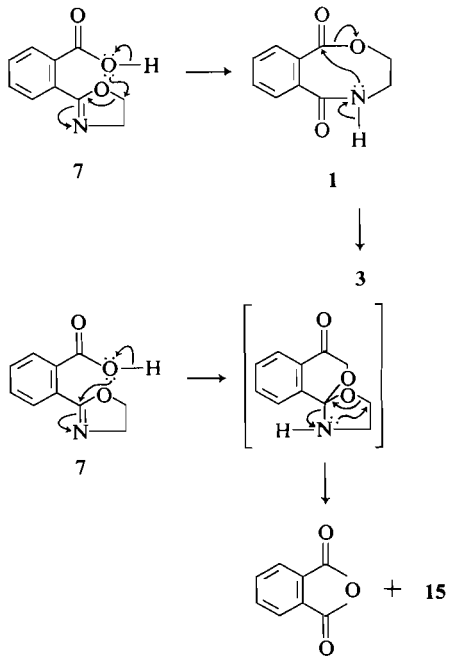

SCHEME 1

Can. J. Chem. Downloaded from www.nrcresearchpress.com by 210.87.254.40 on 09/05/12
For personal use only.

Alkaline hydrolysis of 2-chloroethylphthalimide **4** and 2-phthalimidoethyl *p*-toluenesulfonate (**5**) also afforded initially **7** indicating its preferential formation in comparison to **1** from *N*-substituted ethylphthalimides.

Another route for the synthesis of **1** appeared to be the cyclization of 2-hydroxyethylphthalamic acid (**11**) which was isolated from the alkaline hydrolysis of **3**. It cyclized to the starting material on heating above melting point. Treatment of **11** with diazomethane or an ethanolic solution of hydrogen chloride only afforded **3**. It is known that esters of phthalamic acids easily cyclize to phthalimides (11, 12). Dicyclohexylcarbodiimide is also used for esterification (13) but only **3** was isolated on the treatment of **11** with this reagent indicating a preference for the formation of five-membered phthalimide ring over eight-membered benzoxazocine ring systems.

Synthesis of another possible isomer **9** from the hydrolysis of **2** was also attempted by the hydrolysis of 2-phthalimidoethylsulfuric acid **6**. It is known that alkaline hydrolysis of 2-aminoethylsulfuric acid (**14**) yields aziridine **15** (14). Synthesis of **6** was attempted by the condensation of phthalic anhydride with **14**. This reaction should initially afford **12** but phthalamic acids cyclize to phthalimides on heating (15–17) therefore **6** could be expected as the product of the condensation. Hydrolysis of **6** could afford **9** or **7** as a result of the rearrangement of **9** or nucleophilic displacement of sulfuric acid group by carbonyl oxygen. Product **3** could also be expected in the condensation as a result of the initial rearrangement of **7** to **1** followed by its further rearrangement to **3**.

Interestingly, only diphthalimidoethyl phthalate (**13**) was obtained instead of **6** on heating phthalic anhydride with **14** at 150°. It indicated thus intermediate formation in the reaction of **3** followed by its condensation with phthalic anhydride to yield **13**.

This work thus confirms Gabriel's suggestion of the formation of a benzoxazocine **1** which appears to be an interesting compound easily available from the hydrolysis of **2**.

Experimental

The i.r. spectra were recorded on a Perkin-Elmer i.r. model 137E spectrometer and calibrated against the 6.238 μm peak of polystyrene. Ultraviolet spectra were recorded on a Beckman DB instrument. The n.m.r. spectra were obtained on a Varian A-60 analytical spectrometer. Mass spectra were determined on an Associated Electrical Industries MS-9 double focusing high resolution mass spectrometer. Microanalyses were performed by the microanalytical section of PCSIR Laboratories at Karachi. Melting points were determined on a Gallenkamp melting point apparatus and are uncorrected.

Reported procedures were used for the preparation of 2-bromoethylphthalimide (**2**) (18), 2-phthalimidoethanol (**3**) (19), 2-chloroethylphthalimide (**4**) (19), 2-phthalimidoethyl *p*-toluenesulfonate (**5**) (20), diphthalimidoethyl phthalate (**13**) (10), and 2-aminoethylsulfuric acid (**14**) (14).

Hydrolysis Products of 2-Bromoethylphthalimide (2)

2-Bromoethylphthalimide (2.0 g, 0.008 mol) was dissolved in 15% potassium hydroxide solution (15 ml, 0.04 mol) by heating on a water bath. Acidification of this reaction mixture to p*H* 2 with 4 *N* hydrochloric acid at 0° gave a precipitate of **7** (840 mg, 55%), m.p. 137–139° (lit. (6) m.p. 141–142°); λ_{max} in 95% EtOH (log ε) 206 (3.97), 277 (3.03) nm; ν_{max} (KBr): 2860–2120, 1700, 1625 cm^{-1}; n.m.r. (D_2O) δ: 4.21 (m, 2H), 5.06 (m, 2H), 7.5–7.83 (m, 4H); (D_2O, K_2CO_3, p*H* 8) δ: 3.91 (t, 2H, J = 8.0 Hz), 4.46 (t, 2H, J = 8.0 Hz), 7.28–7.71 (m, 4H); (DMSO-d_6) δ: 4.15 (m, 4H), 7.41–7.8 (m, 4H).

Anal. Calcd. for $C_{10}H_9NO_3$ (mol. wt. 191.0582): C, 62.8; H, 4.7; N, 7.3. Found (mass spectrum, 191.0574): C, 62.7; H, 4.9; N, 7.6.

Recrystallization of this product (1.0 g, 0.005 mol) from 95% ethanol afforded **1** (770 mg, 77%), m.p. 139–141° (lit. (5) m.p. 139°); λ_{max} in 95% EtOH (log ε): 202 (4.16), 275 (3.04) nm; ν_{max} (KBr): 3330–2500, 1740, 1640, 1540 cm^{-1}; n.m.r. (D_2O) δ: 3.38 (m, 2H), 4.53 (m, 2H), 7.33–7.86 (m, 4H); (D_2O, K_2CO_3, p*H* 8) δ: 3.21 (t, 2H, J = 5.0 Hz), 4.41 (t, 2H, J = 5.0 Hz), 7.31–7.86 (m, 4H); (DMSO-d_6) δ: 3.2 (m, 2H), 4.48 (m, 2H), 7.33–7.8 (m, 4H).

Anal. Calcd. for $C_{10}H_9NO_3 \cdot H_2O$ (mol. wt. 191.0582): C, 57.4; H, 5.2; N, 6.6. Found (mass spectrum, 191.0578): C, 57.6; H, 4.7; N, 7.0.

Action of Heat on 7

Compound **7** (643 mg, 0.0033 mol) was heated at 150° for 15 min and the reaction mixture was chromatographed on a column of silica gel (10 g). The column was eluted by 45 ml fractions of petroleum ether, benzene and chloroform. Evaporation of petroleum ether fraction gave a solid (378 mg) which, on crystallization from 95% ethanol, afforded diphthalimidoethyl phthalate (**13**) (39 mg), m.p. 160–161° (lit. (10) m.p. 161–162°); identified from its m.p., mixture m.p., and i.r. spectrum.

Evaporation of the mother liquor and crystallization of the residue from chloroform – petroleum ether gave **3** (254 mg). 2-Phthalimidoethanol obtained from other fractions was also combined and this material gave purer product (153 mg) on recrystallization from chloroform – petroleum ether, m.p. 125–126° (lit. (20) m.p. 127–128°); identified from its m.p., mixture m.p., and i.r. spectrum.

Action of Heat on 1

Compound **1** (490 mg, 0.0023 mol) was heated at 150–160° for 15 min. Thin-layer chromatography of the residue (developing solvent: chloroform – ethyl acetate 1:1) indicated formation of only one product. Chro-

Can. J. Chem. Downloaded from www.nrcresearchpress.com by 210.87.254.40 on 09/05/12
For personal use only.

matography on silica gel (12 g) by progressive elution with solvents, as used for the residue obtained on heating **7**, gave the product (435 mg, 99%; m.p. 128°) on elution with chloroform – ethyl acetate 1:1 (50 ml). Recrystallization of this material from 95% ethanol afforded **3** (269 mg; m.p. 127–128°) identified from its m.p. and i.r. and n.m.r. spectra.

Hydrolysis of 2-Chloroethylphthalimide (4)

2-Chloroethylphthalimide (1.0 g, 0.004 mol) was dissolved in 15% potassium hydroxide solution (4 ml, 0.01 mol), filtered and acidification of the filtrate to p*H* 5 at 0° with 4 *N* hydrochloric acid afforded the product (792 mg, 86%), m.p. 123–126°, whose i.r. spectrum was the same as that of **7**.

Hydrolysis of 2-Phthalimidoethyl p-Toluenesulfonate (5)

2-Phthalimidoethyl *p*-toluenesulfonate (1.0 g, 0.0035 mol) was dissolved in 15% aqueous potassium hydroxide solution (8.5 ml, 0.021 mol) by heating on a flame and the aqueous solution was then filtered and the filtrate was acidified at 0° to p*H* 2 by 4 *N* hydrochloric acid. Extraction with three 50 ml portions of chloroform followed by the evaporation of the dried extract gave a residue (555 mg, 72%), m.p. 120–128°, whose i.r. spectrum was the same as that of **7**.

2-Hydroxyethylphthalamic Acid (11)

2-Phthalimidoethanol (20 g, 0.1 mol) was dissolved in 10% potassium hydroxide solution (100 ml, 0.17 mol). A few crystals remained insoluble and were removed by decantation. A crystalline substance appeared on scratching the sides of the flask after acidification of the solution to p*H* 2 at 0° with 4 *N* hydrochloric acid. It was collected and dried. Recrystallization from methanol–ether afforded **11** (14.7 g, 67%) as colorless crystals, m.p. 113°, λ_{max} in 95% EtOH (log ε): 214 (3.99), 270 (3.04) nm; ν_{max} (KBr): 3450, 3330, 1725, 1665, 1560 cm^{-1}; n.m.r. (D_2O) δ: 3.6–4.1 (m, 4H), 7.45–7.9 (m, 4H).

Anal. Calcd. for $C_{10}H_{11}NO_4$: C, 57.4; H, 5.2; N, 6.6; Found: C, 57.6; H, 5.5, N, 6.5.

Attempted Preparation of the Esters of 11

Methyl Ester

2-Hydroxyethylphthalamic acid (1.0 g) was dissolved in dry methanol and the solution was esterified by diazomethane. Evaporation of the reaction mixture and crystallization of the residue from ethanol gave **3**, m.p. 124–126°.

Ethyl Ester

2-Hydroxyethylphthalamic acid (110 mg) was added to a saturated solution of hydrogen chloride in ethanol (6 ml) and the reaction mixture was evaporated. The i.r. spectrum of the residue was the same as that of **3**.

Cyclization of 2-Hydroxyethylphthalamic Acid (11)

With Dicyclohexylcarbodiimide

To a solution of **11** (200 mg) in dry dioxane (10 ml) was added a solution of dicyclohexylcarbodiimide (320 mg) in dry dioxane (25 ml). The reaction mixture was stirred for 2 h and then filtered to remove dicyclohexylurea (200 mg). Evaporation of the reaction mixture gave a residue which was triturated with acetone twice to remove more dicyclohexylurea. The insoluble residue on recrystallization from ethanol gave a product (51 mg), m.p. 114–124°. Further trituration with acetone raised the m.p. of this material to 120–124°. The i.r. spectrum, m.p. and mixture m.p. of the product indicated that it was 2-phthalimidoethanol (**3**).

By Heating

2-Hydroxyethylphthalamic acid (10.0 mg) was heated at 150° for 3 min. The i.r. spectrum of the heated material, m.p. 123–126°, was the same as that of **3**.

Reaction of Phthalic Anhydride with 2-Aminoethylsulfuric Acid (14)

2-Aminoethylsulfuric acid (12.5 g, 0.11 mol) and phthalic anhydride (14.8 g, 0.1 mol) were powdered and mixed together. The reaction mixture was then heated for 1 h at 130–150° and extracted with hot ethanol on cooling. A white solid (2.3 g) was obtained on keeping the ethanol extract overnight. Recrystallization of this material from ethanol afforded **13** (358 mg, 1.4%), m.p. 157–160° (lit. (10) m.p. 161–162°) identified from its m.p. and i.r. spectrum.

The authors are grateful to Prof. S. Wolfe (Queen's University, Kingston, Canada) and Prof. J. W. Lown (Univ. of Alberta, Edmonton, Canada) for their assistance in obtaining n.m.r. and mass spectra and to Mr. Moiz A. Warsi (PCSIR Laboratories, Karachi) for his technical assistance in the study of the reaction of phthalic anhydride with 2-aminoethylsulfuric acid.

1. H. L. YALE and E. R. SPITZMILLER. German Patent No. 1,919,092 (1969); Chem. Abstr. **72**, 31865b (1970).
2. Rexall Drug and Chemical Co. Netherlands Patent No. 6,606,390 (1966); Chem. Abstr. **66**, 55535w (1967).
3. J. J. LAFFERTY. U.S. Patent No. 3,470,154 (1969); Chem. Abstr. **72**, 31863z (1970).
4. Usines Chimiques des Laboratories Francais, S. A. and L. Francois, Paris. French Patent No. 848,386 (1939); Chem. Abstr. **35**, 6066^5 (1941).
5. S. GABRIEL. Ber. **38**, 2389 (1905).
6. K. KÖRMENDY and J. VOLFORD. Acta. Chim. Hung. **32**, 115 (1962).
7. A. A. GOLDBERG and W. KELLY. J. Chem. Soc. 1919 (1948).
8. K. KÖRMENDY, P. SOHAR, and J. VOLFORD. Acta Chim. Hung. **39**, 93 (1963).
9. L. J. BELLAMY. The infrared spectra of complex molecules. Methuen and Co., London. 1958. p. 263.
10. M. L. WOLFROM and A. CHANEY. J. Org. Chem. **26**, 1319 (1961).
11. J. A. SHAFER and H. MORAWETZ. J. Org. Chem. **28**, 1899 (1963).
12. S. WOLFE and S. K. HASAN. Can. J. Chem. **48**, 3572 (1970).
13. S. NEELAKANTAN, R. PADMASANI, and T. R. SESHADRI. Tetrahedron, 3531 (1965).
14. H. WENKER. J. Am. Chem. Soc. **57**, 2328 (1935).
15. J. B. TINGLE and H. F. ROLKER. J. Am. Chem. Soc. **30**, 1882 (1908).
16. F. S. SPRING and J. C. WOODS. J. Chem. Soc. 625 (1945).
17. M. L. BENDER, Y. L. CHOW, and F. L. CHLOUPEK. J. Am. Chem. Soc. **80**, 5380 (1958).
18. R. T. ARNOLD (*Editor*). Organic syntheses. Vol. 32. John Wiley and Sons, Inc., London. 1952. p. 18.
19. H. WENKER. J. Am. Chem. Soc. **59**, 422 (1937).
20. D. H. PEACOCK and U. C. DUTTA. J. Chem. Soc. 1303 (1934).

Structure cristalline de Tl_2CO_3

RENÉ MARCHAND, YVES PIFFARD ET MICHEL TOURNOUX

Laboratoire de Chimie Minérale B, Equipe de Recherche associée au C.N.R.S., U.E.R. de Chimie, Faculté des Sciences de Nantes, B.P. 1044, 44 037, Nantes Cedex, France

Reçu le 17 juillet 1974[1]

RENÉ MARCHAND, YVES PIFFARD et MICHEL TOURNOUX. Can. J. Chem. **53**, 2454 (1975).

Le carbonate de thallium Tl_2CO_3 cristallise dans le système monoclinique (groupe spatial $C2/m$). Les paramètres de la maille sont $a = 12.486$ Å, $b = 5.382$ Å, $c = 7.530$ Å et $\beta = 122.35°$; $Z = 4$. La structure a été déterminée à partir de 655 réflexions indépendantes mesurées à l'aide d'un diffractomètre automatique.

Le doublet solitaire du thallium(I) manifeste une activité stéréochimique dans cette structure. Il se dispose dans des tunnels parallèles à [010]. Les groupements plans CO_3 sont parallèles à [100].

RENÉ MARCHAND, YVES PIFFARD, and MICHEL TOURNOUX. Can. J. Chem. **53**, 2454 (1975).

Thallium carbonate, Tl_2CO_3, crystallizes in the monoclinic system, space group $C2/m$. The parameters of the unit cell are $a = 12.486$ Å, $b = 5.382$ Å, $c = 7.530$ Å, and $\beta = 122.35°$; $Z = 4$. The structure was determined using 655 independent reflections which were measured on an automatic diffractometer.

The lone pair of thallium(I) shows a stereochemical influence in this structure. It is arranged in tunnels parallel to [010]. The planar carbonate groups are parallel to [100].

[Journal translation]

Introduction

Les structures cristallines des carbonates Li_2CO_3 (1), Na_2CO_3-α, Na_2CO_3-γ (2) et K_2CO_3 (3) ont été déterminées. Gatehouse et Lloyd (3) ont récemment montré que les structures des carbonates de sodium et de potassium pouvaient se décrire en termes d'empilement hexagonal compact légèrement distordu d'ions carbonate: un ion M^+ est au centre d'un octaèdre, l'autre au centre d'une bipyramide trigonale, les sommets de ces polyèdres sont occupés par des ions carbonate.

La détermination de la structure cristalline de Tl_2CO_3 a été entreprise dans le cadre d'une étude très générale portant sur la comparaison entre les composés oxygénés du thallium(I) et ceux du potassium.

Partie expérimentale

Le cristal étudié est représenté sur la fig. 1 avec l'indexation des faces et leurs dimensions en centimètres. Il a été obtenu par recristallisation du produit commercial.

Données cristallographiques de:
Tl_2CO_3 p.m. = 468.8
monoclinique, $C2/m$, $a = 12.486(3)$ Å, $b = 5.382(2)$ Å, $c = 7.530(2)$ Å, $\beta = 122.35°(2)$, $V = 425.4$ Å^3, $\rho_{mes} = 7.25$ g/cm^3, $\rho_{rx} = 7.32$ g/cm^3, $Z = 4$, $\mu = 770$ cm^{-1} (20 °C, MoK$_\alpha$, $\lambda = 0.70926$ Å).

[1]Révision reçue le 10 avril 1975.

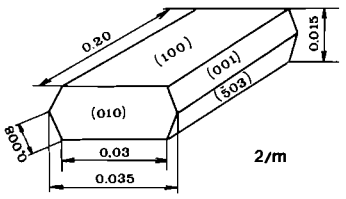

FIG. 1. Indexation et dimensions en cm des faces du cristal étudié.

Les paramètres ont été affinés à partir du diagramme de poudre. La condition d'existence observée sur les clichés de Weissenberg hkl, $h + k = 2n$, est compatible avec les groupes spatiaux $C2/m$, $C2$, Cm. Les tests physiques: piézoélectricité et doublage de fréquence laser effectués au C.N.E.T. de Lannion se sont avérés négatifs. La maille élémentaire définie par les vecteurs $\boldsymbol{a}$, $\boldsymbol{b}$, et $\boldsymbol{c}$ se déduit de celle de type I proposée par des auteurs antérieurs (4, 5), par les relations $\boldsymbol{a} = \boldsymbol{a}_1 + \boldsymbol{c}_1$, $\boldsymbol{b} = \boldsymbol{b}_1$ et $\boldsymbol{c} = -\boldsymbol{a}_1$.

L'enregistrement des intensités diffractées a été effectué au moyen d'un diffractomètre automatique Nonius CAD-3, utilisant le rayonnement MoK$_\alpha$, dans la demi-sphère réciproque comprise entre $\theta = 3.5°$ et $\theta = 40°$, les intensités de 3340 réflexions ont été mesurées avec un balayage θ–2θ. Elles correspondent à 1437 réflexions indépendantes. Après correction de Lorentz et de polarisation, des tests statistiques ont été effectués pour tenter de lever l'ambiguïté au niveau du groupe spatial. Le test portant sur la distribution des facteurs de structure normalisés n'est pas assez significatif, par contre la valeur moyenne de la quantité M définie par $|\overline{F_o}^2|/|\overline{F_o}|^2$ (6), égale à 0.610 est proche de la valeur théorique caractérisant les groupes centrosymétriques

Can. J. Chem. Downloaded from www.nrcresearchpress.com by 210.87.254.6 on 09/05/12
For personal use only.

Can. J. Chem. Downloaded from www.nrcresearchpress.com by 210.87.254.6 on 09/05/12
For personal use only.

TABLEAU 1. Distribution $N(z)$ pour Tl_2CO_3

z	$N(z)$
0.1	0.34
0.2	0.41
0.3	0.44
0.4	0.49
0.5	0.52
0.6	0.55
0.7	0.58
0.8	0.60
0.9	0.64
1.0	0.67

($M = 0.637$), de plus l'étude de la répartition de $N(z)$ (7), tableau 1, confirme la centrosymétrie. L'affinement a été conduit dans le groupe $C2/m$.

Les écarts-type sont évalués par application de la statistique de Poisson régissant les mesures de comptage. Le rapport $\sigma(I)/I$ est donné par la relation

$$\sigma(I)/I = \frac{[T + \tau^2(F_1' + F_2')]^{1/2}}{T - \tau(F_1' + F_2')}$$

où T est l'intensité brute de la réflexion, F_1' et F_2' les intensités des fonds continus de part et d'autre et $\tau = t/2t'$ le rapport des temps de comptage de la réflexion et des fonds continus est égal à 1/2 pour ce travail.

Détermination de la structure

Une fonction de Patterson tridimensionnelle a été calculée avec les 755 réflexions répondant au critère $\sigma(I)/I \leqslant 0.50$. Son interprétation a permis de retenir deux positions $4i$ pour les atomes de thallium et pour les atomes d'oxygène une position générale $8j$ et une position $4i$.

L'affinement des paramètres atomiques et des coefficients d'agitation thermique a été réalisé par la méthode des moindres carrés (matrice complète) en minimisant la quantité $s = \Sigma w(|F_o| - Z|F_c|)^2$ où Z est le facteur d'échelle et w le facteur de pondération qui s'exprime en fonction de la variance σ par la relation $w = 1/\sigma^2$. Le facteur de reliabilité classique et le facteur de reliabilité pondéré s'écrivent respectivement:

$$R = \Sigma(|F_o| - Z|F_c|)/\Sigma|F_o|$$

et

$$Rw = [\Sigma w(|F_o| - Z|F_c|)^2/\Sigma w(|F_o|)^2]^{1/2}$$

Seules les 655 réflexions telles que $\sigma(I)/I \leqslant 0.25$ ont été retenues pour l'affinement. Les facteurs de reliabilité R et Rw sont respectivement 0.151 et 0.174 après quatre cycles d'affinement des coordonnées atomiques et des facteurs d'agitation thermique isotrope des deux thallium. A ce niveau, une projection de la synthèse de Fourier a confirmé la position des groupements carbonate. L'affinement de tous les paramètres atomiques et des facteurs d'agitation thermique isotrope conduit à $R = 0.139$ et $Rw = 0.158$.

L'introduction des coefficients d'agitation thermique anisotrope sur les thallium conduit à $R = 0.105$ et $Rw = 0.127$. Jusqu'à ce stade nous avons utilisé des facteurs de pondération unitaires ($w = 1$). L'examen des facteurs de structure calculés et observés indiquait l'influence de l'absorption, cette correction a été faite à l'aide du programme DATA P1 (8). Après quatre cycles d'affinement avec les valeurs corrigées, les facteurs de reliabilité s'abaissent à $R = 0.046$ et $Rw = 0.061$. La pondération des taches faibles selon le schéma de Hughes (9) avec les bornes $F_1 = 33$, $F_2 = 34$, $F_3 = 1000$, $F_4 = 2000$ et la correction de l'extinction secondaire (10) amènent R et Rw à, respectivement, 0.033 et 0.045. Un calcul effectué en prenant en considération les 1437 réflexions indépendantes mesurées conduit pour R et Rw à 0.088 et 0.051. Pour ce calcul les réflexions dont la mesure n'a pas été significative ont été affectées d'une intensité égale à la moitié de la plus faible mesurée.

Ces calculs ont été effectués à l'aide du programme SFLS-5 sur IBM 370 (11). Les facteurs de diffusion atomique sont tirés des tables de Moore (12). La liste des facteurs de structure observés et calculés a été versée au dépôt des données non publiées.

Les valeurs des différents paramètres atomiques sont données dans le tableau 2.

Description de la structure

La fig. 2 représente la projection de la structure selon l'axe [010]. Les principaux angles et distances interatomiques sont rassemblés dans le tableau 3.

Tous les atomes, à l'exception des atomes d'oxygène notés O(2) en position générale, sont situés dans les plans miroirs correspondant à la position $4i$ du groupe $C2/m$.

Le calcul de la distance entre l'atome C(1) et le plan formé par ses trois proches voisins oxygène conduit à une valeur qui peut être considérée comme nulle (0.006 Å (0.010)). Il en est de même pour le calcul de l'angle entre le plan [100] et celui des groupements CO_3 (1° (1.5)). Ces groupements se disposent en files parallèles à [010]. L'atome Tl (1) relie trois groupements CO_3 appartenant à deux files différentes, chacun des deux groupements appartenant à une même file est lié par deux liaisons Tl—O alors que le troisième groupement n'exerce qu'une liaison de ce type. L'atome Tl(2) relie trois groupements CO_3 appartenant à deux files différentes. Il exerce une liaison Tl—O avec chacun des deux groupements d'une même file et deux liaisons de ce type avec le troisième groupement.

Sur les figs. 3 et 4 ces environnements sont complétés par de faibles liaisons correspondant à des distantes Tl—O supérieures à 3.20 Å.

Les cinq plus proches voisins oxygène de Tl(1) sont situés d'un même côté par rapport au cation. Trois des distances Tl—O sont voisines de la somme des rayons ioniques: 2.80 Å (13),

Can. J. Chem. Downloaded from www.nrcresearchpress.com by 210.87.254.6 on 09/05/12
For personal use only.

TABLEAU 2. Coordonnées atomiques et coefficients d'agitation thermique*

Atome	Position	x	y	z	B (Å^2)	β_{11}	β_{22}	β_{33}	β_{12}	β_{13}	β_{23}
Tl(1)	4*i*	0.08568(8)	0	0.30620(14)	2.25†	591(9)	1576(29)	1685(24)	0	645(12)	0
Tl(2)	4*i*	0.36365(8)	0	0.23661(13)	2.30†	478(8)	2198(35)	1237(20)	0	351(10)	0
O(1)	4*i*	0.6652(16)	0	0.3605 (26)	2.75†	710(116)	2235(415)	1290(250)	0	430(145)	0
O(2)	8*j*	0.1601(11)	0.2941(24)	0.1055 (18)	2.95†	854(86)	1502(230)	2337(226)	328(121)	868(122)	18(200)
C(1)	4*i*	0.6613(19)	0	0.1925 (30)	2.05(30)						

*Le facteur de température de chaque atome s'exprime sous la forme: $\exp -(\beta_{11}h^2 + \beta_{22}k^2 + \beta_{33}l^2 + 2\beta_{12}hk + 2\beta_{13}hl + 2\beta_{23}kl)$ ou $\exp -B(\sin^2\theta)/\lambda^2$. Dans le tableau, les coefficients du tenseur d'anisotropie ont été multipliés par 10^5.
†Ces quantités représentent la valeur isotrope B qui correspond au tenseur β_{ij} d'anisotropie.

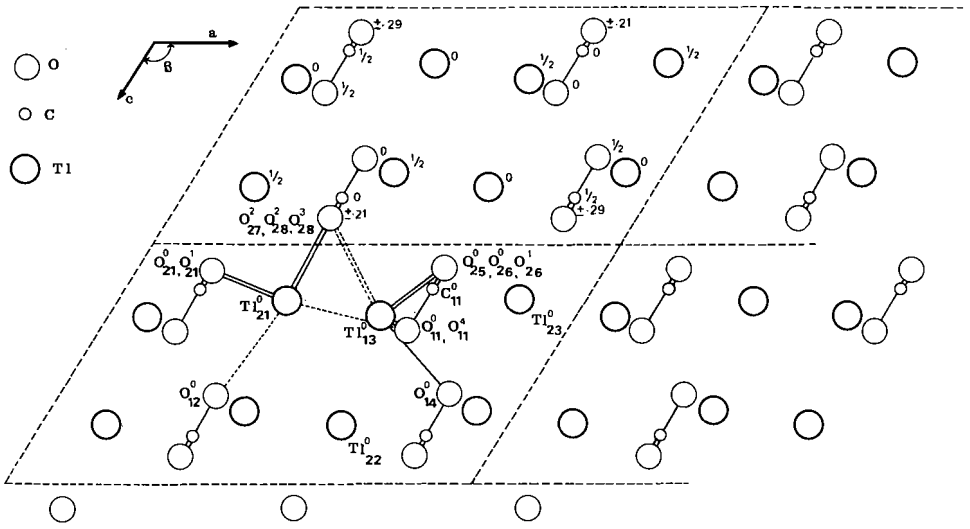

FIG. 2. Projection de la structure selon [010].

TABLEAU 3. Principales distances (en Å) et principaux angles de valence (en degré)*

Liaison	Distance (Å)	Atomes	Angle (deg)
$Tl^0_{(13)}$—$Tl^0_{(23)}$	3.777(2)	$O^0_{(11)}$—$Tl^0_{(13)}$—$O^4_{(11)}$	145.1(4)
$Tl^0_{(13)}$—$Tl^0_{(21)}$	3.693(1)†	$O^0_{(26)}$—$Tl^0_{(13)}$—$O^0_{(25)}$	72.5(4)
$Tl^0_{(21)}$—$Tl^0_{(22)}$	3.588(1)	$O^0_{(11)}$—$Tl^0_{(13)}$—$O^0_{(14)}$	74.5(4)
$Tl^0_{(13)}$—$O^0_{(14)}$	2.765(14)	$O^0_{(26)}$—$Tl^0_{(13)}$—$O^0_{(14)}$	87.2(4)
$Tl^0_{(13)}$—$O^0_{(11)}$	2.820(5)†	$O^0_{(11)}$—$Tl^0_{(13)}$—$O^0_{(26)}$	46.8(4)
$Tl^0_{(13)}$—$O^0_{(25)}$	2.677(16)†	$O^0_{(21)}$—$Tl^0_{(21)}$—$O^1_{(21)}$	72.0(4)
$Tl^0_{(13)}$—$O^2_{(27)}$	3.370(10)†	$O^2_{(28)}$—$Tl^0_{(21)}$—$O^3_{(28)}$	49.1(4)
$Tl^0_{(21)}$—$O^0_{(21)}$	2.690(13)†	$O^0_{(21)}$—$Tl^0_{(21)}$—$O^2_{(28)}$	78.8(4)
$Tl^0_{(21)}$—$O^2_{(28)}$	2.670(15)†	$O^0_{(26)}$—$C^0_{(11)}$—$O^1_{(26)}$	119.5(1.5)
$Tl^0_{(21)}$—$O^0_{(11)}$	3.360(20)	$O^0_{(26)}$—$C^0_{(11)}$—$O^0_{(11)}$	120.2(1.5)
$Tl^0_{(21)}$—$O^0_{(12)}$	3.240(20)		
$C^0_{(11)}$—$O^0_{(11)}$	1.24(3)		
$C^0_{(11)}$—$O^0_{(26)}$	1.28(2)†		

*Dans ce tableau chaque atome est affecté d'indices inférieurs et supérieurs. Le premier indice inférieur correspond à celui donné dans le tableau 2, le second indice est attribué conformément à l'ordre des positions équivalentes des tables internationales de cristallographie. L'indice supérieur 0, 1, 2, 3 ou 4 a la signification suivante: 0, l'atome est dans la maille; 1, l'atome a subi une réflexion dans un miroir situé en cote $y = 0$; 2, l'atome a subi une translation de $-c$; 3, l'atome a subi les deux opérations précédentes; 4, l'atome a subi une translation de b.

†Ces distances interviennent deux fois dans la coordinence.

les deux autres sont nettement inférieures, ce qui traduit une participation covalente plus importante.

Les quatre plus proches voisins oxygène de Tl(2) sont situés d'un même côté par rapport à celui-ci et à des distances peu différentes: 2.67 et 2.69 Å. Deux autres atomes d'oxygène situés de l'autre côté du cation et à grande distance de celui-ci: 3.24 et 3.36 Å, participent à l'environnement de deux Tl(2).

Dans cette structure le doublet du thallium au degré d'oxydation un présente un début d'activité stéréochimique. En effet, certaines distances Tl—O sont inférieures à la somme des rayons ioniques et les atomes d'oxygène fortement liés au thallium sont tous situés d'un même côté par rapport à celui-ci conformément aux prévisions de la théorie de Gillespie et Nyholm (14). Les atomes de thallium délimitent dans la structure des tunnels parallèles à [010] à l'intérieur desquels se disposent les doublets solitaires. Dans les structures telles que celles de Tl_3BO_3 (15), Tl_3PO_4 (16), Tl_4O_3 (17), Tl_2TiO_3 (18) et Tl_2SnO_3 (19) où l'activité

Can. J. Chem. Downloaded from www.nrcresearchpress.com by 210.87.254.6 on 09/05/12
For personal use only.

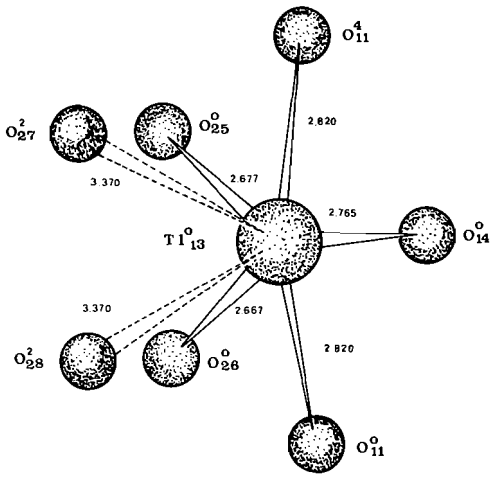

FIG. 3. Environnement oxygéné du Tl(1).

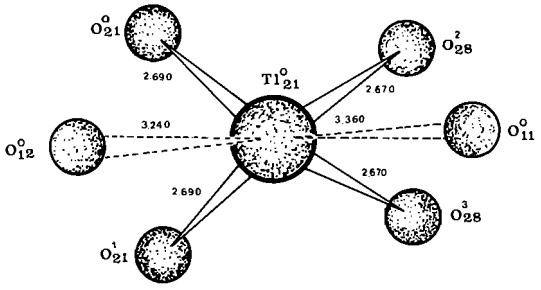

FIG. 4. Environnement oxygéné du Tl(2).

stéréochimique du doublet se manifeste nettement le thallium n'est souvent lié qu'à trois atomes d'oxygène et les distances Tl—O sont comprises entre 2.40 et 2.50 Å, au contraire lorsque le doublet est stéréochimiquement inactif la coordinence du thallium(I) est élevée. C'est le cas pour les composés oxygénés pauvres en thallium qui sont souvent isotypes des composés des alcalins de même formulation.

Le comportement cristallochimique du thallium(I) dans les composés riches en thallium est bien illustré par la structure cristalline de Tl_2CO_3 qui est très différente de celle des carbonates de sodium et de potassium.

1. ZEMANN. Acta Cryst. **10**, 664 (1957).
2. G. C. DUBBELDAM et P. M. DE WOLFF. Acta Cryst. B**25**, 2665 (1969).
3. B. M. GATEHOUSE et D. J. LLOYD. J. Chem. Soc. Dalton Trans. 70 (1973).
4. A. TRANQUARD, C. LACASSAGNE, M. J. BOINON, L. CAPELLA et R. COHEN-ADAD. C. R. Acad. Sc. Paris, sér. C, **264**, 1111 (1967).
5. R. S. MITCHELL. Z. Krist. **123**, 399 (1966).
6. A. J. C. WILSON. Acta Cryst. **2**, 318 (1949).
7. E. R. HOWELLS, D. C. PHILLIPS et D. ROGERS. Acta Cryst. **3**, 210 (1950).
8. B. G. BRANDT et A. G. NORD. DATA P1: An absorption correction program. Institute of inorganic and physical chemistry, Stockholm. 1970.
9. E. W. HUGHES. J. Am. Chem. Soc. **63**, 1737 (1941).
10. W. H. ZACHARIASEN. Acta Cryst. **16**, 1139 (1963).
11. C. T. PREWITT. Fortran IV full matrix crystallographic least squares program SFLS-5, 1966.
12. F. H. MOORE. Acta Cryst. **16**, 1169 (1963).
13. R. D. SHANNON et C. T. PREWITT. Acta Cryst. B**25**, 925 (1969).
14. R. J. GILLESPIE et R. NYHOLM. Q. Rev. Chem. Soc. **11**, 339 (1957).
15. R. MARCHAND, Y. PIFFARD et M. TOURNOUX. C. R. Acad. Sc. Paris, sér. C, **276**, 177 (1973).
16. M. GANNE et M. TOURNOUX. C. R. Acad. Sc. Paris, sér. C, **276**, 1755 (1973).
17. R. MARCHAND et M. TOURNOUX. C. R. Acad. Sc. Paris, sér. C, **277**, 863 (1973).
18. A. VERBAERE, M. DION et M. TOURNOUX. J. Solid. State Chem. **11**, 60 (1974).
19. A. VERBAERE, M. DION et M. TOURNOUX. J. Solid. State Chem. **11**, 184 (1974).

Can. J. Chem. Downloaded from www.nrcresearchpress.com by 210.87.254.6 on 09/05/12
For personal use only.

Chemically Induced Dynamic Nuclear Polarization During Irradiation of Phenol in the Presence of Amides

SHIV P. VAISH, HOLGER E. CHEN, MICHA TOMKIEWICZ, ROBERT D. MCALPINE, AND MICHAEL COCIVERA

Department of Chemistry, University of Guelph, Guelph, Ontario N1G 2W1

Received February 26, 1975

SHIV P. VAISH, HOLGER E. CHEN, MICHA TOMKIEWICZ, ROBERT D. MCALPINE, and MICHAEL COCIVERA. Can. J. Chem. **53**, 2459 (1975).

Irradiation of D_2O solutions containing various phenols with aliphatic amides at p*H* values between 9 and 12 results in nuclear spin polarization which is observed as n.m.r. emission signals during irradiation. No polarization is observed for the phenols which include tyrosine, cresol, *p*-hydroxybenzoic acid, phenol, and others. For the amides which include acetamide, propionamide, *N*-methylacetamide, and *N*,*N*-dimethylacetamide, polarization was observed for only the protons on the carbon bonded to the carbonyl group. Because excited phenolate ions are known to eject electrons, it is proposed that the radical $R\dot{C}(O^-)NR_2$ is formed by reaction of the amide with the hydrated electron. The polarization observed for the amides can be explained by reaction of $R\dot{C}(O^-)NR_2$ with a benzosemiquinone radical via a radical pair.

SHIV P. VAISH, HOLGER E. CHEN, MICHA TOMKIEWICZ, ROBERT D. MCALPINE et MICHAEL COCIVERA. Can. J. Chem. **53**, 2459 (1975).

L'irradiation de solutions dans D_2O de différents phénols avec des amides aliphatiques à des p*H* se situant entre 9 et 12, produit une polarisation du spin nucléaire. Ce phénomène est observable par une émission de signaux r.m.n. pendant l'irradiation. On n'observe pas de polarisation pour les phénols tels que la tyrosine, le crésol, l'acide *p*-hydroxybenzoïque, le phénol et autres. Une polarisation est observée seulement pour les protons du carbone lié au groupe carbonyle pour les amides telles que l'acétamide, le propionamide, la *N*-méthylacétamide et la *N*,*N*-diméthylacétamide. Sachant que les ions phénolate excités émettent des électrons, on propose que le radical $R\dot{C}(O^-)NR_2$ résulte de la réaction de l'amide avec un électron hydraté. On peut expliquer la polarisation observée pour les amides, par la réaction de $R\dot{C}(O^-)NR_2$ avec un radical benzosemiquinone par l'intermédiaire d'une paire radicalaire.

[Traduit par le journal]

Introduction

Radiation induced electron transfer from phenol and substituted phenols to water has been the subject of a number of studies (1–3). Studies into the details of the electron transfer process are of particular interest in view of the role played by tyrosine in the photochemistry of some proteins (4–6). The nature of the precursor leading to the electron transfer step is of interest for this reason.

Jortner *et al.* (2*b*) have argued against a charge transfer to solvent transition in the case of phenolate ion. In the case of the β-naphthoate anion whose fluorescence could be studied, electron transfer to water appears to occur via an excited singlet state (7). More recently in a study of the phenolate anion, it was concluded that electron transfer to water occurred via an excited triplet state since 2,4-hexadiene reduces the concentration of phenoxyl radical (3*a*). Compounds containing disulfide linkages can act as electron acceptors, also. The data for the tyrosine–lipoate system have been used as evidence for electron transfer via an excited triplet state of tyrosine (8). The present paper presents results of a chemically induced dynamic nuclear polarization (c.i.d.n.p.) study which indicates that aliphatic amides may act as electron acceptors, too. The nature of the nuclear spin polarization observed by proton n.m.r. can be interpreted to mean that the mechanism which is responsible for the polarization probably involves hydrated electron formation followed by capture by the amide. Thus, the present c.i.d.n.p. results seem to provide no information concerning interaction of amide with excited phenolate ion.

Experimental

The chemicals and their suppliers are: β-naphthol, *p*-hydroxybenzyl alcohol, and *p*-methoxybenzyl alcohol (Aldrich); aniline, $K_4Fe(CN)_6$, *p*,*p*′-biphenol, and *p*-

Can. J. Chem. Downloaded from www.nrcresearchpress.com by 210.87.254.42 on 09/05/12
For personal use only.

bromophenol (Baker); *p*-cresol, tyrosine, ascorbic acid, and acetophenone (BDH); N_2O (Canox); *N*-acetyltyrosine (Cyclochemical); *N*-methylacetamide, *N*,*N*-dimethylacetamide, propionamide, and *p*-hydroxybenzoic acid (Eastman); pyridine and benzoic acid (Fisher); acetamide, phenol, and KI (Mallinckrodt); and D_2O (Stohler). Where possible the chemicals were reagent grade. Purification of the compounds by distillation or recrystallization was done when deemed necessary.

The proton n.m.r. spectra at 100 MHz were obtained using a Varian HA-100-15 spectrometer which we have modified; details are given elsewhere (9).

While the temperature of the probe was maintained at 15°, the sample was at a somewhat higher temperature at the spot of irradiation. The spectra were obtained before, during, and after irradiation. The radiation source is a 1000 W Hanovia mercury xenon lamp. Except when a Pyrex plate was used as a filter, the sample was irradiated with the full spectrum of the lamp.

Results

During irradiation of D_2O solutions containing acetamide plus phenol or substituted phenols at p*H* greater than 9.0, the n.m.r. spectrum differs from the spectrum in the absence of radiation in that the CH_3-proton resonance appears as an emission signal. Examples of the types of spectra obtained during irradiation are given in Fig. 1. These spectra were obtained at 100 MHz using air saturated solutions. Figure 1*A* was obtained using a solution containing 0.1 *M* phenol and 0.1 *M* acetamide at p*H* 11.8. The sweep-width was 10 p.p.m. starting at the tetramethylsilane, TMS, signal. The field strength increases from left to right. The dashed lines indicate the signal heights after irradiation for about 60 s. The assignment of signals relative to TMS is: ring protons of phenolate ion 6.85 p.p.m.; HDO, 4.55 p.p.m.; and CH_3-protons of acetamide, 2.00 p.p.m. As indicated by the emission signal, only the signal due to the CH_3 of acetamide is affected during irradiation. This system was studied under a variety of conditions. Phenolate concentration was usually 0.05 *M*. The effect of the presence of O_2 in the solution was checked by degassing the solution to less than 2 μ. Under these conditions the spectrum appeared similar to Fig. 1*A*. The p*H* was varied from 7 to 12, and below p*H* 9 no polarization was observed. At p*H* 9 the polarization was small and increased with increase in p*H* to a maximum at p*H* 11.5. Saturating the solution with N_2O quenches the polarization. The polarization returns when the solution is purged with N_2. This process was repeated several times. When a Pyrex plate was used to remove light having wavelength less than 300 nm

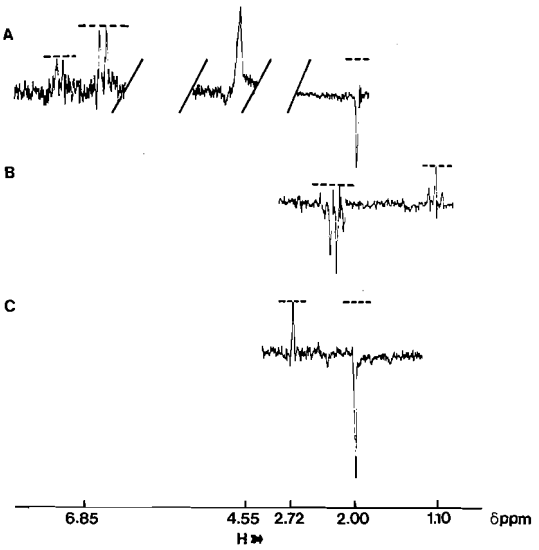

FIG. 1. Proton n.m.r. spectra obtained at 100 MHz for irradiation of D_2O solutions of phenolate ion plus amide at p*H* 11.5. (*A*) Acetamide: CH_3-protons, 2.00 p.p.m.; HDO, 4.55 p.p.m.; and phenyl ring protons, 6.85 p.p.m. (*B*) Propionamide: CH_3-protons, 1.10 p.p.m.; CH_2-protons, 2.23 p.p.m. (*C*) *N*-Methylacetamide: CH_3CO-protons, 2.00 p.p.m.; *N*-methyl protons, 2.72 p.p.m. As indicated by the signal to noise ratios, different gains were used to record the signals.

no polarization was observed. No polarization was observed during the irradiation of a solution containing only 0.1 *M* acetamide at p*H* 11.5.

Polarization of the CH_3 of acetamide was observed for a number of acetamide solutions containing various substituted phenols at p*H* values around 11.5. The list of phenols which gave polarization included: *p*,*p*′-biphenol, 2,4,6-trimethylphenol, *p*-cresol, *p*-hydroxybenzoic acid, *p*-hydroxybenzyl alcohol, tyrosine, and *N*-acetyl tyrosine. In addition, polarization was observed during the irradiation of a solution containing 0.05 *M* aniline plus 0.1 *M* acetamide at p*H* 7.0 and 10.5. On the other hand, no polarization of the CH_3 of acetamide was observed during irradiation of solutions of acetamide plus a number of other compounds including: *p*-methoxybenzyl alcohol, pyridine, benzoic acid, *p*-bromophenol, acetophenone, $K_4Fe(CN)_6$, KI, β-naphthol, and ascorbic acid.

Since the emission signal of the CH_3-proton of acetamide indicates the formation of a radical from acetamide, additional experiments were performed to identify the site of the unpaired electron. These experiments involved the study

Can. J. Chem. Downloaded from www.nrcresearchpress.com by 210.87.254.42 on 09/05/12
For personal use only.

Can. J. Chem. Downloaded from www.nrcresearchpress.com by 210.87.254.42 on 09/05/12
For personal use only.

of solutions at p*H* 11.5 containing 0.05 *M* phenol plus 0.1 *M* *N*-methylacetamide or *N*,*N*-dimethylacetamide or propionamide. In the case of propionamide, only the CH_2-protons are polarized. This can be seen in Fig. 1*B* which illustrates the spectrum obtained during irradiation of an air saturated aqueous solution containing phenol plus propionamide. The emission quartet at 2.23 p.p.m. is due to the CH_2-protons, and the absorption triplet at 1.1 p.p.m. is due to the CH_3-protons. The dashed lines indicate the signal heights of the largest lines of the multiplets after irradiation. Thus no polarization is observed for the CH_3-protons of propionamide. For both *N*-methyl- and *N*,*N*-dimethylacetamide no polarization was observed for the *N*-methyl protons whereas emission was still observed for the CH_3CO-protons as illustrated in Fig. 1*C* for the *N*-methylacetamide (*N*-methyl proton resonance at 2.72 p.p.m.).

Discussion

The emission signals observed for the amides are indicative of non-Boltzmann nuclear spin polarization. The radical pair model used to explain the occurrence of such polarization has been described in detail (9, 10) and only a general description will be presented in this paper. According to the radical pair model, non-Boltzmann nuclear spin polarization occurs as a result of reaction via a radical pair in which the singlet and triplet electronic spin states are mixed. Because of scalar interactions (electron–nuclear hyperfine coupling), the spin states of the nuclei on the radicals affect the mixing. The probability for product formation depends on the singlet character of the radical pair electronic spin state. Consequently, since the singlet character depends in part on the nuclear spin state, the nuclear spin states of the product can have non-Boltzmann populations. Thus, according to the radical pair model, the emission signals of the amides are indicative of the formation of radicals.

The nature of the radical(s) formed by the amides can be decided by comparing the polarization observed for each amide. For acetamide the CH_3-proton is observed to be polarized. For, *N*-methyl- and *N*,*N*-dimethylacetamide, only the CH_3CO-protons are polarized; no polarization is observed of *N*-methyl protons of either amide. On the basis of this information, we conclude that the electron–nuclear hyperfine coupling between the unpaired electron and the *N*-methyl protons is too small to cause nuclear spin polarization. Since α and β hyperfine coupling constants are usually not small (11), the *N*-methyl protons cannot be α or β to the site of the unpaired electron. Therefore radicals for which the nitrogen is the site of the unpaired electron (such as $R\dot{C}ONR$ and $\dot{N}R_2$) can be ruled out. Likewise since only the CH_2-protons of propionamide are polarized, the CH_3-protons cannot be α or β to the site of the unpaired electron, and radicals such as $CH_3\dot{C}HCONH_2$, $\dot{C}H_3$, and $CH_3\dot{C}H_2$ can be precluded. Thus, it seems unlikely that the amides are undergoing bond rupture or losing a hydrogen atom as a result of irradiation.

Since the methyl-protons of acetamide and the CH_2-protons of propionamide are polarized, they must be β to the site of the unpaired electron. Because of the structures of these molecules and the arguments presented above, these protons cannot be γ to the site. Furthermore, they cannot be α since the radicals, $CH_3\dot{C}H_2$ and $CH_3\dot{C}HCONH_2$, have been ruled out. Since phenolate ions and aniline are known to undergo radiation induced electron ejection (1–3) we suggest that the radical is either $R\dot{C}(O^-)NR_2$ or $R\dot{C}(OH)NR_2$. These structures have been suggested for the transients detected during the pulse radiolysis of aqueous solutions containing amides (12, 13). Furthermore, the structure $CH_3\dot{C}(O^-)NH_2$ has been assigned to a radical detected at 77 K by e.s.r. after u.v. irradiation of H_2O solid containing $K_4Fe(CN)_6$ and acetamide (14).

The other substituted phenolate ions which cause polarization of acetamide are sufficiently similar to the phenolate ion to suspect that they also undergo electron ejection when irradiated. An alternative mechanism which we also have considered involves electronic excitation of the phenolate ion followed by electron transfer from excited phenolate ion to the amide. From the arguments given below, the former mechanism seems preferable.

We will consider the electron ejection mechanism first. As indicated above nuclear polarization occurs as a result of irradiation of a number of compounds which are known to undergo electron ejection. On the other hand, a number of compounds such as KI, $K_4Fe(CN)_6$, β-naphthol, benzoic acid, and ascorbic acid did not cause polarization even though they are known to undergo photoelectron ejection (1, 2*a*, 15). How-

Can. J. Chem. Downloaded from www.nrcresearchpress.com by 210.87.254.42 on 09/05/12
For personal use only.

ever, these results do not rule out the proposed mechanism since the absence of polarization can be explained either by spin–orbit coupling or the presence of more reactive hydrated electron scavengers. Thus, heavy atoms such as I and Fe can either prevent or reduce the polarization via spin–orbit coupling. For acetamide, benzoate, and naphthoate ions at $pH \geqslant 10.9$, the rate constants for reaction with hydrated electrons are 1.7×10^7, 3.6×10^9, and 9.5×10^9 (16), respectively. Thus the benzoate and naphthoate ions can compete effectively with acetamide for the hydrated electron. For ascorbic acid, a similar mechanism may be in operation; however, the rate constant does not appear to be available.

The main aspect to consider is that polarization is observed for only the amide. According to the radical pair model, no nuclear polarization of the amide would occur as a result of the addition of the hydrated electron to the amide. Consequently, the polarization would have to occur via a subsequent reaction of $R\dot{C}(O^-)NR_2$ with another radical having a different *g*-factor. Since only the amide protons are observed to be polarized, the other radical must result in a diamagnetic compound having little or no nuclear polarization. This possibility can occur either if the radical has a structure in which the protons are coupled only very weakly to the unpaired electron, and/or if the polarization is removed more rapidly than the rate of excitation (by a relaxation process). The phenoxyl radical does not satisfy either of these conditions. The hyperfine coupling constants for the ring protons are not small (17, 18), and the phenoxide ion which would result from the phenoxyl radical should not have proton relaxation rates which are competitive with the rate of excitation. Therefore, we conclude that the amide polarization probably does not occur via the radical pair $[Ph\dot{O}\ R\dot{C}(O^-)NR_2]^F$ where F indicates a free radical precursor.

In previous work (19), we have found that the irradiation of phenolate ion in water results in the formation of a variety of semiquinone radicals: *ortho*-, *para*-, oxy-, and dioxybenzosemiquinones. Reaction of $R\dot{C}(O^-)NR_2$ with any or all of these radicals could account for the amide nuclear polarization and for the absence of any detectable polarization in any other compound. The reaction would involve disproportionation via the radical pair $[\dot{S}\ R\dot{C}(O^-)NR_2]^F$ in which $\dot{S}$ indicates the semiquinone. This reaction results in the formation of the amide and an anion of the hydroquinone derived from the semiquinone. The resultant polarization for the protons of this anion is expected to be smaller than that for the amide protons since the hyperfine coupling constants for the semiquinones are smaller. However, this polarization for the anion would not be negligible relative to the amide polarization. The fact that no polarization is detected could be caused by nuclear relaxation effects resulting from an equilibration between the anion of hydroquinone and the remaining semiquinone radicals. Thus, with this mechanism it is possible to account for the detection of polarization for only the amide.

The quenching of the amide nuclear polarization by N_2O, chloroform, and acetone provides support for the mechanism involving reaction of the amide with the hydrated electron. All of the compounds have rate constants for reaction with the hydrated electron which are substantially higher than that for the amide. For example, the value of the rate constant for N_2O is 5.6×10^9 *vs.* 1.7×10^7 for acetamide (16). Since the concentration of N_2O was 2.4×10^{-2} *M vs.* 0.1 *M* for acetamide, N_2O reacts with the hydrated electron about 100 times faster than does acetamide under these conditions. Thus, the quenching of the amide polarization by N_2O and the other compounds is consistent with the proposed mechanism. Of course, this conclusion presupposes that these compounds do not quench an excited state of the phenolate ion. This seems to be a reasonable assumption since Stein (2*a*) has found that N_2O did not affect directly the fluoresence yield of the naphthoate ion. Furthermore while Feitelson and Hayon (8) report that the lipoate anion quenches the fluorescence of tyrosine, they apparently did not detect any quenching by N_2O. Thus in view of the evidence and arguments presented above, we propose the following mechanism, Scheme 1.

$$ArO^- \xrightarrow{h\nu} {}^*ArO^-$$

$${}^*ArO^- \rightarrow Ar\dot{O} + e_{aq}$$

$$RCONR_2' + e_{aq} \rightarrow R\dot{C}(O^-)NR_2'$$

$$R\dot{C}(O^-)NR_2' + \dot{S} \rightleftharpoons [R\dot{C}(O^-)NR_2'\ \dot{S}]^F$$

$$RCONR_2' + S^- \leftarrow$$

SCHEME 1

Can. J. Chem. Downloaded from www.nrcresearchpress.com by 210.87.254.42 on 09/05/12
For personal use only.

In this mechanism, ArO^- is the phenolate ion (with or without substitution) and $\dot{S}$ is a benzosemiquinone radical which is formed as suggested previously (19). According to this mechanism, electron ejection from an electronically excited phenolate ion results in the formation of the hydrated electron which reacts with the amide to form $R\dot{C}(O^-)NR_2'$ which subsequently reacts with $\dot{S}$ via the radical pair $[R\dot{C}(O^-)NR_2'\ \dot{S}]^F$ to give the amide and the anion of the hydroquinone S^-. Although $R\dot{C}(O^-)NR_2'$ is specified in the mechanism, it is quite possible that $R\dot{C}(OH)NR_2'$ may be involved since its pK_a was measured to be $\geqslant 13.5$ (13) and the pH of our solutions was usually 11.5 or lower.

For the CH_3-protons of acetamide, emission is calculated for reaction via this radical pair, in agreement with the observed spectrum. This polarization was calculated from equations derived using the Closs Kaptein Oosterhoff theory (10). For this calculation, the g-factor and CH_3 hyperfine coupling constant for the radical $CH_3\dot{C}(O^-)NH_2$ are 2.0030 and $+13.5$ G, respectively (14). We do not expect that these values would change appreciably for the protonated species. A positive sign is chosen for the coupling constant since the protons are bonded to a β-carbon (17) as in the case of the analogous ketyl radicals produced during the photolysis of aliphatic aldehydes (20, 21). The g-factors for *o*- and *p*-benzosemiquinones are 2.0047 and 2.0044, respectively (22). The other semiquinones observed under these conditions have similar g-factors (19).

Another possibility involves electronic excitation of the phenolate ion followed by electron transfer to ground state amide. An analogous mechanism has been proposed for a reaction involving tyrosine and the lipoate ion (8). In the case of the amide, this mechanism would involve the formation of the radical pair $[Ar\dot{O}\ R\dot{C}(O^-)NR_2']$. Disproportionation of this radical pair would result in nuclear polarization for both the amide and the phenolate ion. Since no polarization could be detected for the ring protons of the phenolate ion, this path requires an additional step, *i.e.* dissociation of the radical pair followed by trapping of $R\dot{C}(O^-)NR_2$ before the nuclear polarization is lost. This mechanism is less attractive for several reasons. First, emission is calculated for the amide only if the radical pair has a singlet precursor. Feitelson and Hayon (3*b*, 8) have concluded that electron transfer from excited phenolate ion to both water and lipoate ion occurs via the triplet state. Second, the quenching of polarization by N_2O could not be explained unless quenching of the excited singlet state is postulated. As discussed above, this path seems unlikely. Third, this mechanism could not account for the absence of amide polarization when β-naphthoate and benzoic acid are excited. Consequently, the reaction of amide with the hydrated electron seems more attractive.

The polarization results for the aniline plus amide system are somewhat different from the phenolate ion results in that polarization is observed for the ring protons of the aniline in addition to the acetamide CH_3-protons. Thus, reaction with the hydrated electron need not necessarily be invoked. The analysis of this system has not been attempted. In addition, it seems likely that the results for the other amides may be explained by the same mechanism (Scheme 1) used for acetamide. Although the e.s.r. spectra do not appear to be available for the radical anions derived from these amides, there is no reason to expect that the g-factors and the sign of the appropriate hyperfine coupling constant for each of these radicals should differ from those for $CH_3\dot{C}(O^-)NH_2$. Furthermore, since a Pyrex filter prevents polarization, the process does not involve direct excitation of an amide – phenolate ion complex having an absorption spectrum above 300 nm. This conclusion is supported by the observation that amide–phenol complexes have been detected in nonpolar solvents but not in water (23). Finally in the absence of amide, irradiation of a D_2O solution of phenolate ion results in emission for HDO and the ring protons (19). In the presence of amide, the intensity of the HDO signal is reduced but the ring protons appear unaffected. Presumably, the amide causes additional reactions which compete with those proposed in its absence.

This work was supported in part by the National Research Council of Canada and the Petroleum Research Fund administered by the American Chemical Society.

1. (*a*) L. I. GROSSWEINER, G. W. SWENSEN, and E. F. ZWICKER. Science, **141**, 805 (1963); **141**, 1042 (1963); (*b*) L. I. GROSSWEINER and H. I. JOSCHEK. Adv. Chem. Ser. 50, 279 (1965); (*c*) H. I. JOSCHEK and L. I. GROSSWEINER. J. Am. Chem. Soc. **88**, 3261 (1966); (*d*) G. DOBSON and L. I. GROSSWEINER. Trans. Faraday Soc. **61**, 708 (1965); (*e*) L. I. GROSSWEINER. Photo-

physiology, Vol. 5. Academic Press, New York, New York 1970. p. 1.
2. (*a*) G. STEIN. Adv. Chem. Ser. **50**, 230 (1965); (*b*) J. JORTNER, M. OTTOLENGHI, and G. STEIN. J. Am. Chem. Soc. **85**, 2712 (1963).
3. (*a*) J. FEITELSON, E. HAYON, and A. TREININ. J. Am. Chem. Soc. **95**, 1025 (1973); (*b*) J. FEITELSON and E. HAYON. J. Phys. Chem. **77**, 10 (1973).
4. (*a*) G. STEIN. Energetics and mechanisms in radiation biology. *Edited by* G. O. Phillips. Academic Press, New York, New York 1968. p. 467; (*b*) R. SHAPIRA and G. STEIN. Science, **162**, 1489 (1968); (*c*) S. ARIAN, M. BENJAMINI, J. FEITELSON, and G. STEIN. Photochem. Photobiol. **12**, 481 (1970).
5. K. DOSE. Photochem. Photobiol. **8**, 331 (1968).
6. J. LONGWORTH. Photochem. Photobiol. **7**, 587 (1968).
7. C. GOLDSCHMIDT and G. STEIN. Chem. Phys. Lett. **6**, 299 (1970).
8. J. FEITELSON and E. HAYON. Photochem. Photobiol. **17**, 265 (1973).
9. M. TOMKIEWICZ, A. GROEN, and M. COCIVERA. J. Chem. Phys. **56**, 5850 (1972).
10. A. R. LEPLEY and G. L. CLOSS (*Editors*). Chemically induced dynamic nuclear polarization. J. Wiley and Sons, New York. 1973. Chapts. 3 and 4.
11. B. BIELSKY and J. GEBICKI. Atlas of electron spin resonance spectra. Academic Press, New York, New York 1967.
12. J. HOLLIAN and W. GARRISON. J. Phys. Chem. **72**, 4721 (1968).
13. M. SIMIC and E. HAYON. J. Phys. Chem. **77**, 996 (1973).
14. M. SEVILLA. J. Phys. Chem. **74**, 669 (1970).
15. R. MCALPINE, M. COCIVERA, and H. CHEN. Can. J. Chem. **51**, 1682 (1973).
16. M. ANBAR and P. NETA. Int. J. Appl. Rad. Isot. **18**, 493 (1967).
17. J. POPLE, D. BEVERIDGE, and P. DOBOSH. J. Am. Chem. Soc. **90**, 4201 (1968).
18. K. SCHEFFLER and H. STEGMANN. Electron spin resonance. Springer-Verlag, Berlin. 1970.
19. M. COCIVERA, M. TOMKIEWICZ, and A. GROEN. J. Am. Chem. Soc. **94**, 6598 (1972).
20. H. CHEN, S. VAISH, and M. COCIVERA. J. Am. Chem. Soc. **95**, 7586 (1973).
21. B. BLANK and H. FISCHER. Helv. Chim. Acta, **56**, 506 (1973).
22. M. ADAMS, M. BLOIS, and R. SANDS. J. Chem. Phys. **28**, 774 (1958).
23. R. COWGILL. Biochem. Biophys. Acta, **109**, 536 (1965).

Can. J. Chem. Downloaded from www.nrcresearchpress.com by 210.87.254.42 on 09/05/12
For personal use only.

Conformational Analysis of *N*-Nitrosopiperidines by ^{13}C Nuclear Magnetic Resonance. The Orientation Preference of an α-Methyl Group

ROBERT R. FRASER AND T. BRUCE GRINDLEY[1]

Department of Chemistry, University of Ottawa, Ottawa, Canada K1N 6N5

Received February 19, 1975

ROBERT R. FRASER and T. BRUCE GRINDLEY. Can. J. Chem. **53**, 2465 (1975).

The ^{13}C shielding parameters for *N*-nitroso-4-phenylpiperidine and four α-methyl derivatives have been measured. From these data a number of methyl substituent parameters have been obtained. A comparison of the observed spectra of *syn*- and *anti*-*N*-nitroso-2-methylpiperidines with those calculated from the substituent parameters and the shieldings in *N*-nitrosopiperidine established the *syn* isomer to exist exclusively in the conformation having the methyl group axial; the *anti* isomer has the methyl group predominantly axial (59%). It is proposed that the large differential shielding between α carbons *syn* and *anti* to the nitroso group is caused by steric compression at the *syn* carbon. Large dilution effects on the carbon shieldings (up to 1.3 p.p.m.) have been encountered in these nitrosamines.

ROBERT R. FRASER et T. BRUCE GRINDLEY. Can. J. Chem. **53**, 2465 (1975).

Les paramètres d'écran du ^{13}C de la *N*-nitroso phényl-4 pipéridine et de quatre dérivés α méthylés ont été déterminés. Un certain nombre de paramètres pour les substituants méthyles ont été déduits à partir de ces données. La comparaison des spectres observés des *N*-nitroso méthyl-2 pipéridines *syn* et *anti* et des spectres calculés à l'aide des paramètres des substituants et des paramètres d'écran de la *N*-nitroso pipéridine, démontre que l'isomère *syn* adopte uniquement la conformation où le groupe méthyle est axial et que 59% de l'isomère *anti* adopte cette même conformation. La grande différence de blindage entre les carbones α *syn* ou *anti* et le groupe nitroso serait due à l'encombrement stérique au niveau du carbone *syn*. Les paramètres d'écran de ces nitrosamines sont fortement affectés par la dilution (jusqu'à 1.3 p.p.m.).

[Traduit par le journal]

Currently, ^{13}C n.m.r. spectroscopy (c.m.r.) constitutes an informative and important method of conformational analysis. The shielding parameters for carbons have been shown to be very sensitive to environment (1) so that shifts for the axial *vs.* equatorial conformers are usually distinctively different. Our interest in the reactions of anions α to the nitrosoamino function (2, 3) has led to the need for increased knowledge of the conformational properties of a methyl group in the α position of *N*-nitrosopiperidines. In this paper we wish to examine a series of methylated nitrosopiperidines of known conformation with a view to establishing a correlation between shifts and conformation. Such data would then provide information on conformational equilibria in mobile systems.

Previous studies of the c.m.r. spectra of nitrosamines by Pregosin and Randall (4) and by Ellis *et al.* (5) have dealt primarily with the gross characteristics of the shielding parameters. Pregosin and Randall noted a large difference (6–10 p.p.m.) in the shieldings of the *syn* and *anti* α carbons in simple dialkyl nitrosamines. The more recent work of Ellis *et al.* (5) included the examination of nitrosamines of 2-, 3-, and 4-methylpiperidine, *cis*-2,6-dimethylpiperidine, and several piperazines. Their attention was focussed on an assessment of the contribution of the electric field and anisotropy effects to the differential shieldings of the α carbons. Their calculations of shifts, however, were in poor agreement with the spectral parameters. Our studies provide additional data pertaining to the cause of *syn vs. anti* differential shieldings.

Model Compounds: Configurational and Conformational Properties

The models used in this study are *N*-nitroso-4-phenylpiperidine (**1**) and its mono- and dimethyl derivatives (**2**–**5**). Methylation of **1** produces a 45:55 mixture of the *syn* and *anti* isomers **2** and **3**. These compounds, like most nitrosamines (6), have a barrier to interconversion of about 23 kcal/mol (3). Methylation of this mixture produced **4** which was then isomerized with base

[1]Present address: Department of Chemistry, Dalhousie University, Halifax, Nova Scotia.

Can. J. Chem. Downloaded from www.nrcresearchpress.com by 210.87.254.5 on 09/05/12
For personal use only.

Can. J. Chem. Downloaded from www.nrcresearchpress.com by 210.87.254.5 on 09/05/12
For personal use only.

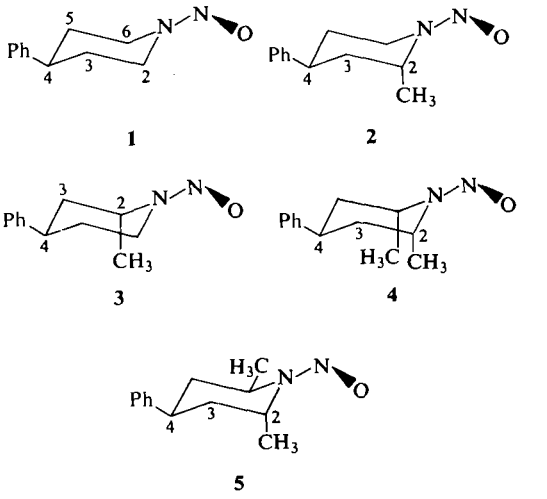

1 2 3 4 5

to give **5**. The accompanying paper (3) describes the details of their synthesis and some of the ^{1}H n.m.r. (p.m.r.) characteristics of these derivatives upon which their stereochemical assignments are based. The axial orientation (*trans* to phenyl) of the methyl group in **2** and **3** is indicated by the magnitudes of the vicinal splittings for the methine proton at C-2 with the methylene protons at C-3. Couplings of 3.5 and <1 Hz indicate an equatorial methine, hence an axial methyl group. For compound **4**, the configurations of both methyls are assigned *trans* to the phenyl at C-4 and the molecule exists in the conformation having both methyls axial. Although this conformation is highly strained by the 1,3-diaxial methyl–methyl interaction, *N*-nitroso-*cis*-2,6-dimethylpiperidine was also found to exist 'predominantly' in the chair form having both methyls axial (7,8) and the strain due to this diaxial orientation has been estimated to be 3.9 kcal/mol (8). To confirm unambiguously the conformational and configurational assignments for **4**, a detailed analysis of its p.m.r. spectrum was carried out.

The 220 MHz spectrum of **4** was measured in $CDCl_3$.[2] That portion of the spectrum showing all but the aromatic and methine absorptions appears in Fig. 1*A*. The theoretical spectrum for the seven protons on the piperidine ring was calculated using the LAOCN3 program and the parameters listed in Table 1. The resultant

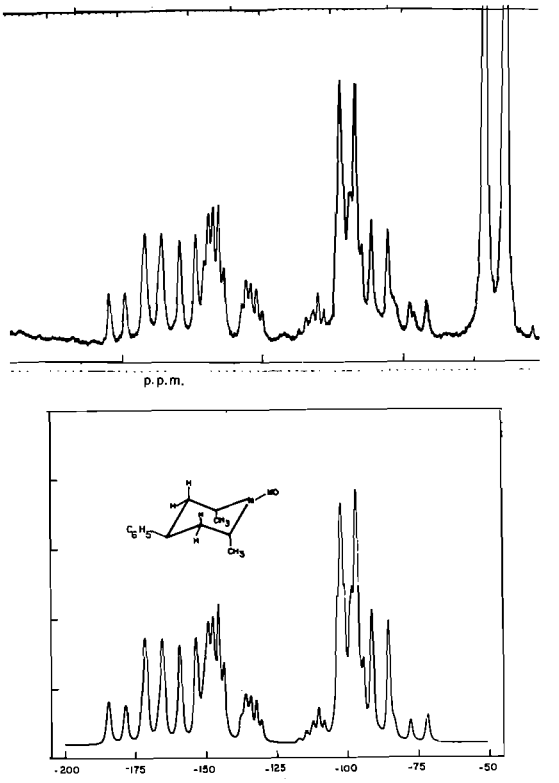

FIG. 1. (*A*) The absorption of the protons at C-3 and C-5 in **4** measured at 220 MHz. (*B*) The absorption of these protons calculated from the parameters in Table 1.

spectrum for the protons at C-3 and C-5 is shown in Fig. 1*B*. An iterative method of fitting by the computer could not be employed, as the assignment of peaks to be matched was complicated by the presence of unresolved long-range couplings. Instead, trial and error calculations were employed until agreement between all experimental and calculated line positions was $\leqslant 0.1$ Hz. Included in the calculation was a first-order perturbation by the two methyl groups on both the vicinal (methine) protons and the next nearest protons.

It can be seen in Table 1 that coupling constants between protons at carbons 3, 4, and 5 have values typical of protons on a cyclohexane ring. However, couplings between protons on carbons 2 and 3 (and 5 and 6) are not normal for a piperidine ring, *i.e.*, J_{ae} should be 3–3.5 Hz (9) and one can estimate, by considering effects of electronegativity and their orientation dependence (10), a value for J_{ee} of 2.2 Hz. The observed J_{ee} (1.5) and J_{ae} values (6.3, 6.5), indicate

[2]The authors thank the 220 MHz Centre at Sheridan Park for measurement of this spectrum.

TABLE 1. Theoretical parameters for the seven protons on the piperidine ring

Proton	Shifts (Hz from TMS at 220 MHz)	Coupling constants to other protons*							
		2	3e	3a	4	5e	5a	6	CH_3
2(*syn*)†	1150.5		1.5	6.5				1.0	7.0
3e	402.5			−13.7	3.2	2.3			0.2
3a	390.9				13.0				0.3
4	733.0					3.2	12.6		
5e	442.2						−13.3	1.5	0.2
5a	467.4							6.3	0.5
6	1143.5								7.0
CH_3(*syn*)†	272.0								
CH_3(*anti*)	341.1								

*The effects of unresolved long range couplings were simulated by the use of a line-width of 1 Hz for the print-out shown in Fig. 1*B*.
†The assignments for protons at C-2 and C-6 and at the methyl carbons were made on the basis of LIS_H produced by addition of $Eu(fod)_3$.

TABLE 2. The carbon-13 chemical shifts* and LIS values† for 4-phenylpiperidinenitrosamines‡

Compound	Parameter	C-2	C-3	C-4	C-5	C-6	CH_3(*syn*)	CH_3(*anti*)
1	δ_C	39.2	32.0	42.2	33.6	50.2		
	LIS_C	4.7	2.6	1.3	1.9	2.8		
	LIS_H	5.0				2.5		
2	δ_C	42.8	(36.7)	(37.0)	33.4	46.6	15.3	
	LIS_C	4.0	1.8	1.0	1.4	2.2	2.5	
3	δ_C	54.4	38.3	(37.6)	32.0	35.1		18.2
	LIS_C	2.3	1.4	0.7	2.0	4.1		1.5
4	δ_C	43.7	37.1	32.1	37.8	54.6	18.7	22.4
	LIS_C	3.1	1.6	1.0	1.0	2.0	2.3	1.6
	LIS_H	3.7		0.8		1.5		
5	δ_C	42.9	36.9	37.4	43.2	53.6	15.9	19.2

*Chemical shifts in p.p.m. from TMS; LIS values in p.p.m.; all spectra run on *M* solutions in $CDCl_3$.
†LIS shifts for protons are numbered according to the carbon to which they are attached; shifts were measured on solutions in $CDCl_3$ and $CDCl_3$ + $Eu(fod)_3$.
‡The numbering of the ring carbon atoms is given in the formulae.

the presence of a distortion because of the severe repulsive 1,3-diaxial methyl–methyl interaction. Should this distortion produce a 10° increase in the dihedral angle between the two equatorial protons (ϕ_{ee}) and a concomitant decrease in ϕ_{ea}, the predicted values for J_{ee} and J_{ea} would change to 1.0 and 5.2 Hz. Thus, a distortion of this type can account, at least qualitatively, for the observed vicinal coupling constants.

The conclusion that the nitrosamine **4** exists in a distorted chair conformation having two methyl groups axial, substantiates the similar proposals of Harris and Spragg (7) and Chow *et al.* (8) for the nitrosamine of *cis*-2,6-dimethylpiperidine. Furthermore, the parameters obtained for **4** rule out the presence of boat conformations to greater than a few percent for this molecule.[3]

Since compound **5** is thermodynamically more stable than **4** (3), it, too, will exist exclusively in a chair conformation.

^{13}C Spectra of 1–5

The ^{13}C chemical shifts for all ring and methyl carbons in **1–5** are listed in Table 2. Since all spectra were measured in the FT mode with complete proton decoupling, it was necessary to obtain unambiguous evidence regarding peak assignments. For this reason, the spectrum of

[3]Specifically, the axial proton at C-4 shows vicinal splittings of 3.2, 3.2, 12.6, and 13.0 Hz, which magnitudes are very close to those found in cyclohexane, *i.e.* J_{ae} = 3.7, J_{aa} = 13.1 Hz (23).

Can. J. Chem. Downloaded from www.nrcresearchpress.com by 210.87.254.5 on 09/05/12
For personal use only.

TABLE 3. Methyl substituent effects in the α position of *N*-nitrosopiperidines

Stereochemistry at methyl group	α	β	γ	δ
syn-Axial	$2^2 - 1^2 = 3.6$	$2^3 - 1^3 = 4.7$	$2^6 - 1^6 = -3.6$ $2^4 - 1^4 = -5.2$	$2^5 - 1^5 = -0.2$
syn-Axial*	$4^2 - 3^6 = 8.6$	$4^3 - 3^5 = 5.1$	$4^4 - 3^4 = -4.6$ $4^6 - 3^2 = 0.2$	$4^5 - 3^3 = -0.5$ $4^{CH_3(anti)} - 3^{CH_3(anti)} = 4.2$
anti-Axial	$3^2 - 1^6 = 4.2$	$3^3 - 1^5 = 4.7$	$3^4 - 1^4 = -5.5$ $3^6 - 1^2 = -4.1$	$3^5 - 1^3 = 0.0$
anti-Axial*	$4^6 - 2^6 = 8.0$	$4^5 - 2^5 = 4.4$	$4^4 - 2^4 = -4.9$ $4^2 - 2^2 = 0.9$	$4^3 - 2^3 = 0.4$ $4^{CH_3(syn)} - 2^{CH_3(syn)} = 3.4$
anti-Equatorial*	$5^6 - 2^6 = 7.0$	$5^5 - 2^5 = 9.8$	$5^4 - 2^4 = 0.4$ $5^2 - 2^2 = 0.1$	$5^3 - 2^3 = 0.2$ $5^{CH_3(syn)} - 2^{CH_3(syn)} = 0.6$

*These classes, involving substitution in a highly hindered position, are not comparable with normal substitution effects.

each of compounds **1**–**4** was also measured in the presence of $Eu(fod)_3$. The downfield shifts of the carbon resonances caused by the added shift reagent are also given in Table 2 under the heading LIS_C. The possibility exists that some contribution to the observed carbon shifts by a contact mechanism might be present, as in the case of amines (11). For this reason, the effects of a shift reagent on the α protons shifts (LIS_H) were also determined in the case of **1** and **4**. A comparison of the LIS_C and LIS_H values shows their magnitudes to be consistent with their relative distances from the shift reagent, thus excluding any significant contact contribution. For the purpose of arriving at our shift assignments, we need only rely on the well-established distance-dependent effect of the shift reagent (12) in a qualitative fashion. Thus, the possible limitations in the accuracy of LIS values as summarized by Horrocks and Sipe (13) will not affect the conclusions made here.

In a few instances where LIS_C values alone could not distinguish between two possible assignments, other considerations frequently permitted an unambiguous conclusion. For example, in **1**, although C-3 and C-6 might have the reverse assignments on the basis of LIS_C values, the fact that a carbon *anti* to the nitroso group occurs at much lower field than the *syn* (4) removes any ambiguity in this case. In the spectra of **2** and **3** not all carbons could be assigned with certainty. Those signals at δ 36.7 and 37.0 for which several alternative assignments are possible, are given in parentheses. Assignments for **5** were made by assuming negligible δ or γ effects (<1 p.p.m.) of an equatorial methyl group. That C-2 and C-5 or C-3 and C-4 might have reverse assignments is not too important, as the shifts for each pair are very similar and none of the conclusions to follow would be altered by a reversal.

Methyl Substituent Parameters

The data in Table 2 can be used to obtain a set of substituent effects caused by replacement of hydrogen by a methyl group having three different orientations. These effects, classified as α, β, γ, or δ effects in the standard way (1), are listed in Table 3. The following example illustrates how they have been obtained. If one substitutes a methyl group at the *anti* carbon (C-6) of **1** an upfield shift is produced at the *syn* α carbon atom (C-6 in **3**, abbreviated as $\mathbf{3}^6$) relative to the same carbon (C-2) in **1**. From Table 2, this γ effect is seen to be $3^6 - 1^2 = -4.1$ p.p.m.

The α effects in Table 3 are all larger (3.6–8.6 p.p.m.) than the same effect in cyclohexanes and piperidines, normally, 1–2 p.p.m. (14, 15) for an axial methyl. In **4**, where the methyls are *syn* diaxial, the α effect is double that found in an unstrained chair. Similarly, the γ effects involving **4** also differ from the norm while the β effects appear to be comparable to those in cyclohexanes. Other than in **4**, both γ and δ effects also have magnitudes similar to those in methyl cyclohexanes. The δ effects of one *syn* axial methyl on the other is deshielding and the magnitude is similar (3–4 p.p.m.) but slightly larger than that observed by Stothers and

Can. J. Chem. Downloaded from www.nrcresearchpress.com by 210.87.254.5 on 09/05/12
For personal use only.

TABLE 4. Carbon shieldings for *N*-nitrosopiperidine and its methyl derivatives

Compound	Shifts	C-2	C-3	C-4	C-5	C-6	CH_3(*syn*)	CH_3(*anti*)
8	δ_C	40.0	24.9	24.3	26.6	51.0		
	LIS_C	3.3	1.9	0.8	1.5	2.0		
6	δ_C	43.1	29.7	19.3	26.2	46.9	15.1	
7	δ_C	56.4	33.1	21.3	25.0	37.8		18.3
9	δ_C	60.7	41.8	16.5	39.2	62.1	26.3	31.9
	LIS_C	10.1	2.9	2.3	2.0	6.6	6.1	4.4
	LIS_H						5.2	3.3

co-workers (16) (~2.3 p.p.m.) in methylated cyclohexanones.

N-Nitroso-2-methylpiperidine

The *syn* (**6**) and *anti* (**7**) isomers of this nitrosamine have been reported to exist in the ratio 23:77 at equilibrium in $CDCl_3$ (7); (repeated integrations of the same spectrum on our instrument gave a ratio of 33:67). The conformation properties of these two isomers are both intriguing and controversial. On the basis of proton chemical shifts, Harris and Spragg (7) and later Chow *et al.* (8), concluded that the methyl group in the *syn* isomer existed exclusively in the axial orientation. The *anti* isomer was also estimated to have at least a 50% population for the axial methyl conformer (7). In conflict with this assessment, measurement of the LIS_H values in *N*-nitroso-2-methylpiperidine compared with those of the rigid *N*-nitroso-4-*t*-butylpiperidine led Forrest *et al.* (17) to conclude that the *syn* isomer **6** contained 85% of the conformer having an axial methyl group and that the *anti* isomer **7** was a 50:50 mixture of conformers. In view of the known limitations in the accuracy of LIS data[4], the conclusions thus derived remain in doubt.[5]

We have measured the c.m.r. spectrum of this nitrosamine in $CDCl_3$ and the parameters obtained are recorded in Table 4, along with those for *N*-nitrosopiperidine (**8**). Distinction between peaks from **6** *vs.* those from **7** was readily provided by the consistent 1:2 intensity

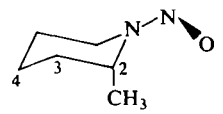

6

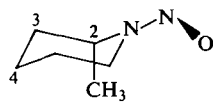

7a

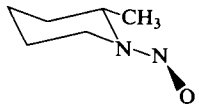

7e

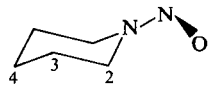

8

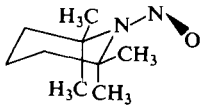

9

ratio. Individual resonances were assigned using the data in Table 2 and assuming that the phenyl would exert a negligible γ effect and equal β effects at C-3 and C-5 (the equality of the differential shieldings at C-3 and C-5 in **1** and **8** support the latter assumption). The assignments for **8**, substantiated by the LIS_C values, are also recorded in Table 4.

Two of our assignments for **7** differ from those of Ellis and co-workers (5) in that the shifts for C-4 and C-5 are reversed. From their data, the γ effect of the *anti* CH_3 on C-4 is +0.9 p.p.m. (deshielding), whereas our assignments and data give a value of −3.0 (shielding) for the γ effect, which is the normal effect (1). Further support for our assignment comes from the agreement between all three calculated conformational equilibrium constants for **7** (see Table 5).

[4]In the application in question, the greatest weakness would appear to be the possibility that the conformational populations in the complex differ from those of the free nitrosamine, as has been found for several other shift reagent–substrate complexes (18).

[5]An additional argument can be made against the likelihood of a significant proportion of the *syn*-equatorial conformer of **6**. If the *anti* methyl has little conformational preference and the *syn* methyl does adopt the equatorial configuration, then the *trans* derivative **5** should contain a measurable amount of the isomer with a *syn*-equatorial methyl. None could be seen in the p.m.r. spectrum of **5**.

Can. J. Chem. Downloaded from www.nrcresearchpress.com by 210.87.254.5 on 09/05/12
For personal use only.

Can. J. Chem. Downloaded from www.nrcresearchpress.com by 210.87.254.5 on 09/05/12
For personal use only.

TABLE 5. Predicted shieldings for axial and equatorial conformers

Carbon	Calculated		Observed
	Axial	Equatorial	
	(a) Compound **6**		
C-2	C-2 in **8** (40.0) + $\alpha_{syn\text{-axial}}$ (3.6) = 43.6		43.2
C-3	C-3 in **8** (24.9) + $\beta_{syn\text{-axial}}$ (4.7) = 29.6		29.7
C-4	C-4 in **8** (24.3) + $\gamma_{syn\text{-axial}}$ (−5.2) = 19.1	C-4 in **8** (24.32) + $\gamma_{syn\text{-equatorial}}$ (<1 p.p.m.) ≈ 24	19.3
C-6	C-6 in **8** (51.0) + $\gamma_{syn\text{-axial}}$ (−3.6) = 47.4	C-6 in **8** (51.0) + $\gamma_{syn\text{-equatorial}}$ (<1 p.p.m.) ≈ 51	46.9
CH_3	CH_3 in **2** = 15.3	CH_3 at C-6 in **5** (19.2) + δ effect (< 1) ≈ 19	15.1
	(b) Compound **7**		
C-2	C-6 in **8** (51.0) + $\alpha_{anti\text{-axial}}$ (4.2) = 55.2	C-6 in **8** (51.0) + $\alpha_{anti\text{-equatorial}}$ (7.0) = 58.0	56.4 (43% equatorial)
C-3	C-5 in **8** (26.6) + $\beta_{anti\text{-axial}}$ (4.4) = 31.0	C-5 in **8** (26.6) + $\beta_{anti\text{-equatorial}}$ (9.8) = 36.4	33.1 (39% equatorial)
C-4	C-4 in **8** (24.3) + $\gamma_{anti\text{-axial}}$ (−5.5) = 18.8	C-4 in **8** (24.3) + $\gamma_{anti\text{-equatorial}}$ (0.4) = 24.7	21.3 (42% equatorial)

Can. J. Chem. Downloaded from www.nrcresearchpress.com by 210.87.254.5 on 09/05/12
For personal use only.

A close examination of the shieldings for **6** reveals evidence against any significant amount of equatorial conformation. For example, one can predict the shieldings for each conformer utilizing the measured shieldings of nitrosopiperidine (**8**) and the substitution effects in Table 4. These predicted shieldings and their derivations are presented in Table 5. The shieldings for three of the carbons, C-4, C-6, and the methyl carbon can be estimated for both conformers. In each case, the observed shieldings agree to 0.4 p.p.m. or less with those predicted for the axial isomer and in two of the cases, are not even intermediate between the predicted axial and equatorial shieldings. It can be concluded that no signficant amount (<2%) of the equatorial conformer is present.

For three of the carbons of **7**, the shieldings in both conformers can be predicted. The data in Table 5 show a very good agreement, all three sets of data indicating the presence of 41 ± 2% of the equatorial conformer. This isomer distribution supports the conclusions of Harris and Spragg (7) but is not too different from the percentage estimated by Forrest *et al.* (17). Nevertheless, for **7** as well as **6**, we feel certain the results derived from c.m.r. are considerably more accurate than those derived on the basis of quantitative use of lanthanide induced shifts.

A further example of the utility of c.m.r. when applied to nitrosamines is provided by the spectral data for **9**, *N*-nitrosotetramethylpiperidine. Most striking is the Δ_{sa} of 1.7 p.p.m. for the α carbons of this compound. Clearly, the molecule must exist in a nonchair conformation as was proposed by Harris and Spragg (7).

Syn–anti Differential Shielding (Δ_{sa})

Both previous papers on nitrosamines (4, 5) have suggested that the large difference in shieldings of the *syn* and *anti* α carbons is due primarily to an electric field effect, although attempts to substantiate this with calculations failed (5). Currently, the accepted cause of the related Δ_{sa} values in amides (19, 20) and oximes (19, 21) is steric compression. The same should be true for nitrosamines. This view is strongly supported by the fact that the Δ_{sa} values given in Table 6 are about 11 p.p.m. for each rigid nitrosamine, but of reduced magnitude in the more flexible dialkyl nitrosamines studied by Pregosin and Randall (4). It is simply another example of a γ effect, equivalent in magnitude to that recently described by Tori *et al.* (22) in a highly rigid norbornene.

TABLE 6. The difference in ^{13}C shieldings for α carbons *syn* and *anti* to the oxygen atoms

Model	δ_{syn}	δ_{anti}	Δ_{sa}
1	39.2	50.2	11.0
4	43.7	54.6	10.9
C-2 in **2** and **3**	42.8	54.4	11.6
C-6 in **2** and **3**	35.1	46.4	11.5
		Average Δ_{sa}	11.2

Solvent Effects on Shielding Parameters

We have examined the spectrum of *N*-nitrosopiperidine both as a 5 *M* and as a 1 *M* solution in $CDCl_3$. There was a significant difference in the carbon shieldings in that all resonances appeared at higher fields in the 5 *M* solutions by 0.9–1.3 p.p.m. For this reason, all data reported in this paper were obtained using 1 *M* solutions in $CDCl_3$. It is to be noted that the spectra reported by Ellis *et al.* (5) were run on either neat liquids or 'concentrated solutions.' Their failure to specify the conditions under which each of their spectra was measured means that there is an uncertainty of at least 1 p.p.m. in their shift data and undoubtedly accounts for the differences in their data and ours for compounds **6**, **7** and **8**.

Experimental

Spectra were obtained on 1 *M* solutions of the nitrosamine in $CDCl_3$, using either a Varian XL-100 equipped with a **TT-100** accessory or a Varian CFT-20 instrument. Pulse angles of 55° and pulse delays of 4 s were employed. All peaks are reported in δ units (TMS = 0) and were referenced with respect to the central peak of $CDCl_3$ (δ 77.3).

The authors thank the National Research Council of Canada for financial support. We also wish to thank Dr. I. C. P. Smith of NRCC for use of the CFT-20.

1. J. B. STOTHERS. Carbon-13 NMR spectroscopy. Academic Press, New York. 1972. Chapt. 11.
2. R. R. FRASER, G. BOUSSARD, I. D. POSTESCU, J. WHITING, and Y. Y. WIGFIELD. Can. J. Chem. **51**, 1109 (1973).
3. R. R. FRASER, T. B. GRINDLEY, and S. PASSANNANTI. Can. J. Chem. This issue.
4. P. S. PREGOSIN and E. W. RANDALL. Chem. Commun. 399 (1971).
5. G. E. ELLIS, R. G. JONES, and M. G. PAPADOPOULOS. J. Chem. Soc. Perkin II, 1381 (1974).

6. J. D. COONEY, S. K. BROWNSTEIN, and J. W. APSIMON. Can. J. Chem. **52**, 3028 (1974).
7. R. K. HARRIS and R. A. SPRAGG. J. Mol. Spectrosc. **23**, 158 (1967).
8. Y. L. CHOW, C. J. COLON, and J. N. S. TAM. Can. J. Chem. **46**, 282 (1968).
9. R. J. ABRAHAM and G. GATTI. J. Chem. Soc. B, 961 (1969).
10. T. P. FORREST. Org. Magn. Reson. **6**, 355 (1974).
11. D. J. CHADWICK and D. H. WILLIAMS. J. Chem. Soc. Perkin II, 1202 (1974).
12. R. A. PERRY and Y. L. CHOW. Can. J. Chem. **52**, 315 (1974).
13. W. DEW. HORROCKS, JR. and J. P. SIPE, III. J. Am. Chem. Soc. **93**, 6800 (1971).
14. D. K. DALLING and D. M. GRANT. J. Am. Chem. Soc. **89**, 6612 (1967); **94**, 5318 (1972).
15. A. J. JONES, A. F. CASEY, and K. M. J. MCERLANE. Can. J. Chem. **51**, 1782 (1973).
16. J. B. STOTHERS and C. T. TAN. Can. J. Chem. **52**, 308 (1974).
17. T. P. FORREST, D. L. HOOPER, and S. RAY. J. Am. Chem. Soc. **96**, 4286 (1974).
18. R. R. FRASER and Y. Y. WIGFIELD. Chem. Commun. 1471 (1970); W. G. BENTRUDE, H.-W. TAN, and K. C. YEE. J. Am. Chem. Soc. **94**, 3264 (1972).
19. G. C. LEVY and G. L. NELSON. J. Am. Chem. Soc. **94**, 4897 (1972).
20. D. A. TORCHIA, J. R. LYERLA, JR., and C. M. DEBER. J. Am. Chem. Soc. **96**, 5009 (1974).
21. G. E. HAWKES, K. HERWIG, and J. D. ROBERTS. J. Org. Chem. **39**, 1017 (1974).
22. K. TORI, M. UEYAMA, T. TSUJI, H. MATSAMURA, H. TANIDA, and H. IWANURA. Tetrahedron Lett. 327 (1974).
23. E. W. GARBISCH, JR. and M. G. GRIFFITH. J. Am. Chem. Soc. **90**, 6543 (1968).

Can. J. Chem. Downloaded from www.nrcresearchpress.com by 210.87.254.5 on 09/05/12
For personal use only.

Stereoselectivity in the Reactions of Nitrosopiperidine Carbanions. Steric *vs*. Stereoelectronic Control

ROBERT R. FRASER, T. BRUCE GRINDLEY, AND SALVATORE PASSANNANTI
Department of Chemistry, University of Ottawa, Ottawa, Canada K1N 6N5

Received February 19, 1975

ROBERT R. FRASER, T. BRUCE GRINDLEY, and SALVATORE PASSANNANTI. Can. J. Chem. **53**, 2473 (1975).

The anion of *N*-nitroso-4-phenylpiperidine reacts with methyl iodide, carbon dioxide, and benzophenone to give solely the axial substitution product. A second methylation of the monomethyl derivative gave the 2,6-diaxial derivative. None of the isomer having *trans* methyl groups could be detected. This *trans* isomer dominates over *cis* by 75:25 at equilibrium. From a consideration of the steric interactions present in these nitrosamines, it can be concluded that they alone cannot explain the observed high stereoselectivity. It is proposed that stereoelectronic control contributes significantly to the exclusive axial attack.

ROBERT R. FRASER, T. BRUCE GRINDLEY et SALVATORE PASSANNANTI. Can. J. Chem. **53**, 2473 (1975).

L'anion du *N*-nitroso phényl-4 pipéridine réagit avec l'iodure de méthyle, le dioxyde de carbone et la benzophénone et conduit exclusivement au produit de substitution axial. Une seconde méthylation du dérivé monométhylé conduit au dérivé diaxial-2,6. Aucun isomère ayant un groupe méthylé *trans* n'a pu être détecté. A l'équilibre, le rapport isomère *trans* : isomère *cis* est de 75:25. La haute stéréospécificité observée ne peut pas être expliquée en considérant seulement les interactions stériques présentes dans ces nitroamines. On propose que le contrôle stéréoélectronique contribue notablement à l'attaque exlusive en axial.

[Traduit par le journal]

Evidence that a carbanion in the α position of a nitrosamine exhibits appreciable stability was provided by two independent studies (1, 2). In each case base-catalyzed H–D exchange was observed α to the nitrosamino function. In addition, Keefer and Fodor (1) reported that α alkylation using ethyl iodide and base was also possible, albeit in poor yield (15%). Subsequently, extensive work by Seebach and Enders (3) demonstrated the synthetic potential of nitrosamino carbanions. These authors reported high yields in the reaction of the anions of *N*-nitrosodimethylamine (3) and many additional nitrosamines (4) with a wide range of electrophiles.[1] Concurrent with their studies, work in this laboratory showed similar results for the reactions of the anion of *N*-nitrosodibenzylamine (6).

An interesting aspect of these carbanions α to nitrogen is their stereochemical behavior. We have shown that the base-catalyzed H–D exchange of the *N*-nitrosoazepine **1** is remarkably stereoselective (6). The four α protons all reside

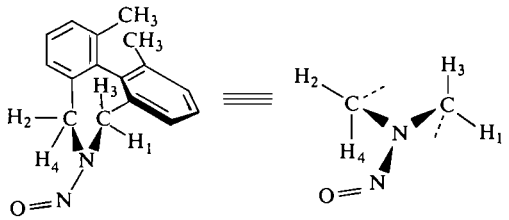

1

FIG. 1. Environments of the four α protons in *N*-nitroazepine **1**.

in the different environments shown in Fig. 1, since the barrier to rotation about the N—N bond is high (23 kcal/mol). The relative rates of exchange of the protons H_1, H_2, H_3, H_4 in *t*-butyl alcohol O-*d* and potassium *t*-butoxide are in the ratio $1:10^3:10^2:10^5$ (6). Thus, removal of the *syn*-axial proton (H_4) is a highly stereoselective process.[2] Although the stereoselectivity of proton abstraction may be the result of several factors, evidence was presented (6) that the enhanced stability of the carbanion due to nitrosation of

[1]A comprehensive review of the preparation, properties, and reactions of nitrosamines, with emphasis on anionic reactions has recently appeared (5).

[2]The preliminary account (6) of this work set only a lower limit to the selectivity. The more accurate measurements quoted above will be published shortly (8).

Can. J. Chem. Downloaded from www.nrcresearchpress.com by 210.87.254.42 on 09/05/12
For personal use only.

Can. J. Chem. Downloaded from www.nrcresearchpress.com by 210.87.254.42 on 09/05/12
For personal use only.

the nitrogen atom results from a contribution of structure *c* to the hybrid anion of **1** (see *a*, *b*, *c*).

When the anion of **1** was formed by treatment with lithium diisopropylamide (LDA) in THF at −78°, subsequent methylation and carboxylation produced *syn*-axial substitution only (7). In view of the synthetic potential of these anions, it seemed important to broaden our studies of their stereoselectivity. We now wish to report the stereochemical course of several reactions of *N*-nitroso-4-phenylpiperidine (**2**). This molecule, being conformationally homogeneous, should provide useful information on the stereoselectivity of these anion reactions.

Reactions of 2

The anion of **2** was generated by reaction with LDA in THF at −78° for 4–30 min (see Experimental). Subsequent addition of the electrophile followed by a reaction time of up to 1 h, then work-up, gave good yields of α-substituted products. For example, carboxylation, methylation and condensation with benzophenone proceeded in yields of 76, 79, and 72%, respectively. The important feature of all three reactions is the exclusive formation of *trans* products, **3**, **4**, and **5** (axial substitution only).

We can estimate that more than 1% of *cis* product would have been detected by n.m.r. or the careful t.l.c. search. Thus, these three reactions of **2** are highly stereoselective.[3]

We next examined the reactions of *N*-nitroso-*r*-2-methyl-*t*-4-phenylpiperidine (**4**). Methylation by the standard procedure gave the dimethyl derivative (**6**) in 62% yield and carboxylation of **4** gave **7** in 33% yield. Again, in both reactions, substitution gave only axial product. Owing to the greater complexity in the methyl region of the p.m.r. spectrum of **6**, as much as 2% of **8**, the product of equatorial attack, might be undetected. The fact that no trace of **8** could be found by t.l.c. indicates that <1% is a more probable upper limit.

Equilibration of 6

To further our understanding of the stereoselective methylation, information on product stabilities was sought. A sample of **6** was subjected to isomerization conditions (potassium *t*-butoxide in DMSO at 90° for 24 h). At the end of this time, the proportion of **8** to **6** was 74:26. Pure **8** was then isolated and subjected to the same isomerization conditions. A *trans* to *cis* ratio of 75:25 was produced. Some darkening of the solution occurred during both equilibrations, indicative perhaps of decomposition. However, 63% of material was recovered after isomerization. We can conclude that the observed proportion of *trans* to *cis* is quite close to the equilibrium value.

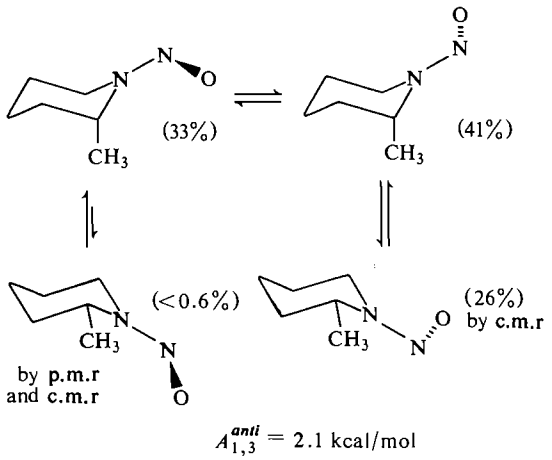

FIG. 2. The conformational properties of *N*-nitroso-2-methylpiperidine.

In the accompanying paper (9), both ^1H and ^{13}C spectral evidence established the chair conformation and the orientation for the methyl groups of the three nitrosamines **4**, **6**, **8**. Using these ^{13}C data, it was possible to determine the conformational properties of *N*-nitroso-2-methylpiperidine, with a degree of certainty which previous work in the literature lacked (10, 11). Our c.m.r. analysis coupled with a careful integration of the p.m.r. methyl region (*syn*:*anti* ratio, 33:67) established the distribution of stereoisomers of this nitrosamine as 33% *syn*-axial, 41% *anti*-axial, and 26% *anti*-equatorial, as depicted in Fig. 2. No evidence of the *syn*-equatorial isomer could be found. These results allow us to assign 0.2 kcal/mol of greater strain energy[4] to

[3]Since methylation of **1** was shown to be exclusively *syn*, we have not attempted to verify the *syn* selectivity in the reactions of **2**. We have observed a predominance of *syn* isomer in the methylation of **2** and assume the small amount of *anti* results from rotation about the N—N bond during work-up. The half-life for this process, as measured by equilibration of the dominant *syn* isomer **4**, is 2 h.

[4]We consider only strain energy, as defined by Westheimer (13), since it is highly unlikely that other factors would contribute to the stability of a methyl group in the various conformers.

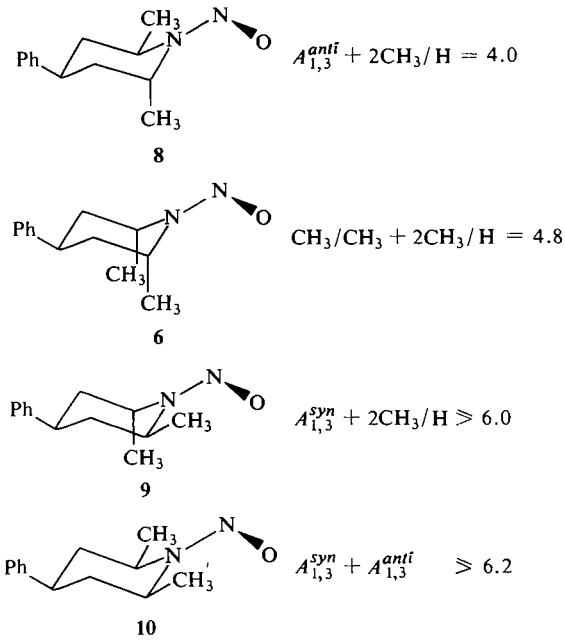

FIG. 3. Strain energies (kcal/mol) of the four isomeric 2,6-dimethyl derivatives of *N*-nitroso-4-phenylpiperidine.

the *anti*-equatorial conformer than its *anti*-axial partner. We have recently (12) determined the strain energy for an axial methyl group in the 2 position of *N*-acetylpiperidine (relative to the strain-free equatorial conformation in the transition state for amide rotation) to be 1.9 kcal/mol. If we assume the strain in this model[5] to be equal to the strain in the axial conformer of *anti*-*N*-nitroso-2-methylpiperidine, then the strain in the equatorial conformer will be 0.2 kcal/mol greater *i.e.*, 2.1 kcal/mol, (calculated from the equilibrium constant K = [equatorial]/[average axial]).

The strain in the *anti*-equatorial conformer is a type of $A_{1,3}$ strain (14) involving repulsion between the methyl group and the nitrogen 'lone pair'. It is interesting that this interaction should be so much greater than its analog involving a methyl group and the lone pair of a carbonyl oxygen (essentially zero (15)).

From this data the strain energies (in kcal/mol) of the four isomeric 2,6-dimethyl derivatives of *N*-nitroso-4-phenylpiperidine can be estimated. The results presented in Fig. 3 are arrived at in the following way. Compound **8** will possess strain because of (*a*) an axial methyl = 1.9 and (*b*) an $A_{1,3}$ strain for the *anti*-equatorial methyl = 2.1 for a total of 4.0. From the position of the equilibrium between **6** and **8** at 80°, **6** is calculated to possess 0.8 kcal/mol more strain, total = 4.8. Since **8** and **9** can interconvert by rotation about the *N*-nitroso bond, yet no trace of **9** could be detected by n.m.r. (<3% at 30°), **9** must be less stable than **8** by at least 2 kcal/mol, *i.e.* total strain ⩾6.0. Since **10** differs from **9** by encountering $A_{1,3}$ strain while removing the axial methyl interaction (difference, 0.2) it must be 0.2 kcal less stable than **9**, total ⩾6.2.

The above values are consistent with related evidence in the literature. For example, Chow *et al.* (16) estimated the strain in the 1,3-diaxial conformation of *cis*-2,6-dimethylpiperidine to be 3.9 kcal/mol, the difference in activation energies for the barrier to rotation of its nitrosamine (19.4) relative to that of dimethylnitrosamine (23.3). A better model for comparison is now available from the detailed study of Cooney *et al.* (17). Using their result of 23.8 kcal/mol for $\Delta G^{\ddagger}_{373}$, the value for the strain of the 1,3-diaxial methyl groups changes to 4.4 which agrees within experimental error with our estimate of 4.8 kcal/mol.[6] A corollary to the assignment of ⩾6.0 for the strain in **9**, is the requirement that the $A_{1,3}$ strain for a *syn*-equatorial methyl group be >4.1 kcal/mol. This agrees favorably with the estimate of >3.7 kcal/mol for the originally defined $A_{1,3}$ strain between two methyls (14).

Origin of Pronounced Stereoselectivity

Highly stereoselective organic reactions are only rarely encountered, particularly in the case of alkylations. Eliel *et al.* (20) recently disclosed that the reaction of a 2-lithio-1,3-dithiane belongs in this category in that methylation occurs in the equatorial position exclusively (>99%). Another example is provided by the work of Durst *et al.* (21) who report that methylation of benzyl *t*-butyl sulfoxide gives only one diastereomer (>99%). Methylation of other sulfoxides are often less selective (22, 23). In systems more

[5]The use of the *N*-acetyl derivative as a model for the *N*-nitrosamine can be justified on the basis of the similarity in hybridization at the nitrogen atom (both have high rotational barriers about the exocyclic nitrogen bond) and similar exclusive axial orientation of the alpha methyl group *syn* to oxygen, (9, 12).

[6]It is to be noted that the strain of 4.8 kcal/mol is made up of two axial CH_3–H and one 1,3-diaxial CH_3–CH_3 interactions. It follows that the magnitude of the CH_3–CH_3 interaction is 4.8–1.9 = 2.9 kcal/mol. This value is slightly larger than that of 2.2 kcal/mol reported for a 1,3-diaxial interaction in cyclohexane (18). In 2-bromo-2,6,6-trimethylcyclohexanone, Allinger *et al.* estimated the 1,3-diaxial interaction to be >2.0 kcal/mol (19).

Can. J. Chem. Downloaded from www.nrcresearchpress.com by 210.87.254.42 on 09/05/12
For personal use only.

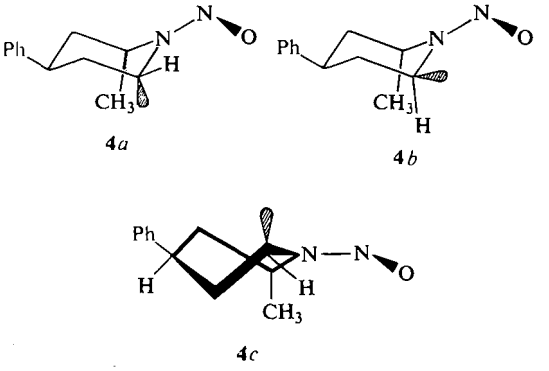

FIG. 4. Possible anion configurations of **4**.

closely related to the nitrosamino carbanions, marked stereoselectivity is lacking. For example, ethylation of lithio-4-*t*-butylcyclohexanone gives 51% axial attack by ethyl iodide (24). The pyrrolidine enamine of the same ketone showed some stereoselectivity in its alkylation, the proportion of axial product being 70, 90, and 93% in the reactions with methyl, propyl, and allyl halides, respectively (25). In view of the synthetic potential of these reactions, it is of considerable practical as well as theoretical importance to ascertain the reasons behind the abnormally high stereoselectivity.

These variations in stereoselectivity must, in some way, reflect differences in transition state geometry. Since the six-membered ring of the cyclic enolate has a half-chair conformation, the experimental results strongly imply that the nitrosamino carbanion does not, but rather retains some sp^3 character at the carbon bearing the negative charge (see Fig. 4). This seems reasonable since there would be an increase in steric repulsion between the remaining α hydrogen and the *syn* oxygen atom in a planar form. The large difference in the shieldings of the *syn* and *anti* α carbons of **6** is a strong indication that this interaction is appreciable even in the staggered chair conformation (9). It then becomes obvious that of two possible anions (**4***a* and *b*), anion **4***a* would be much more stable, since it possesses proper alignment for overlap with the π system of the N—N—O function. Such overlap is geometrically restricted in *b*. Although effective interaction would also be achievable in the twist-boat form *c*, this conformation should be less stable by at least 2.7 kcal/mol, as calculated by Allinger *et al.* (26).[7] The intermediate stereoselectivity in the enamine alkylation (25) is consistent with a finite but lesser degree of steric inhibition of co-planarity. And, as House points out (24), since the enolate is planar, the transition state for protonation or alkylation will not differ greatly from this configuration, in which the stereoelectronic effect is the same for either axial or equatorial attack. Thus, steric influences can determine the dominant stereochemical result.

The above argument is essentially a reapplication of the principle of stereoelectronic control put forward many years ago by Corey and Sneen (28). Several years ago, Bordwell and Scamehorn (29) pointed out that evidence in support of the principle has been equivocal in that the influences of steric and stereoelectronic effects have been difficult to separate. Indeed, arguments in favor of dominant steric factors in H–D exchanges of cyclohexanones have been made (30). A recent communication on the H–D exchange of 4-*t*-butylcyclohexanone ($k_a/k_e = 5.1$) again attributed the stereoselectivity to stereoelectronic control (31).

Obviously, interpretation of our results could also be made on the basis of steric effects. Since methylation of the anion **4***b* would yield **9**, and **9** is at least 1.2 kcal/mol less stable than the actual product **6**, predominant formation of **6** is to be expected; *i.e.*, the factors destabilizing **9** must also be present in the transition state for its formation. Let us suppose that the $A_{1,3}$ strain in **9** could be as high as 5.1 kcal/mol and that **9** is then 2.2 kcal/mol less stable than **6**. Even the most generous estimate of the amount of this strain present in the transition states would be < 1.3 kcal/mol.[8] In such a case, there should have been at least 3% of **9** formed but none could be detected. While these arguments are admittedly speculative, they do suggest that some factor besides the steric one contributes to the stereoselectivity in the methylation of **4**. In our view, stereoelectronic control is that factor.

[7]Recent work of Anet *et al.* (27) reinforces the validity of Allinger's calculations, in that they found the barrier ring inversion of cyclohexanone to be 4.0 kcal/mol, 0.1 kcal/mol more than predicted (26).

[8]Steric repulsive interactions fall off rapidly with increasing distance, so that a more realistic estimate would be < 1 kcal/mol for the transition state free energy differences.

Can. J. Chem. Downloaded from www.nrcresearchpress.com by 210.87.254.42 on 09/05/12
For personal use only.

Can. J. Chem. Downloaded from www.nrcresearchpress.com by 210.87.254.42 on 09/05/12
For personal use only.

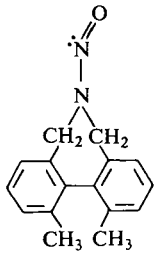

1

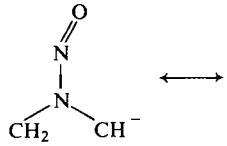

a

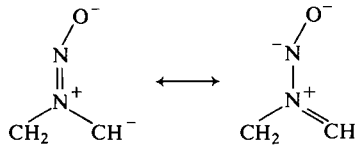

b *c*

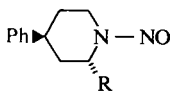

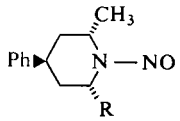

2 R = H
3 R = CO_2H
4 R = CH_3
5 R = $C(OH)Ph_2$

6 R = CH_3
7 R = COOH

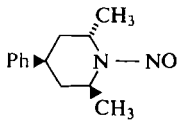

8

A Cautionary Note: The Source of Alkyllithium

Considerable difficulties have been encountered in obtaining reproducible yields in the methylation of the anions of dibenzylbenzamide (7) and *N*-nitroso-4-phenylpiperidine. The difficulties began after our supply of 2.2 *M* solution of CH_3Li in ether (Ventron) was exhausted. Thereafter, using a 1.82 *M* solution of CH_3Li in ether (Ventron), yields were variable and lower. After eliminating other reagents from consideration, it was concluded that the new CH_3Li must be at fault, probably due to the presence of LiBr (soluble in ether). Durst and Molin have reported large differences in the stereoselectivity of lithiation, then deuteration of benzyl methyl sulfoxide as a function of the amount of LiBr present (32). We suspect our original supply of CH_3Li had been made from CH_3Cl and was thus free of LiCl (insoluble in ether). Subsequently, successful methylations of both substrates were achieved by using *either* CH_3Li from Foote Corp. (made from CH_3Cl) *or* butyllithium in hexane from Ventron (no LiBr, since it is insoluble in hexane). Table 1 summarizes these results. No effects on stereoselectivity were encountered.

Experimental

General Methods

Melting points were measured on a Gallenkamp melting point apparatus and are corrected. The n.m.r. spectra were recorded on either a Varian T-60 or HA-100 spectrometer, using deuteriochloroform as solvent unless otherwise noted. Chemical shifts are expressed in δ units (p.p.m. downfield from tetramethylsilane).

All reactions involving methyllithium were carried out under an atmosphere of dry nitrogen using carefully dried equipment and reagents. The term hexanes indicates the isomeric mixture, b.p. 65.1–67.3° of Fisher Scientific. Tetrahydrofuran was distilled from lithium aluminum hydride just before use. Methyllithium, obtained from Alpha Inorganics, Inc., as a 2.2 *M* solution in ether was injected by needle and syringe into the reaction vessel through a rubber septum. The volume of methyllithium solution used per millimole of substrate was the minimum volume required to convert 1 mmol *N*-benzoyldibenzylamine to its anion in >90% yield as measured by the yield of carboxylation described earlier (7) and the methyllithium solution was checked periodically in this fashion.

N-Nitroso-4-phenylpiperidine-2-carboxylic acid (3)

Method I

To a solution of *N*-nitroso-4-phenylpiperidine (**2**, m.p. 64.5–65.5° (lit. (33) 61.5–62.5°); 190 mg, 1 mmol) stirred in THF (30 ml) at −78° was added diisopropylamine (0.15 ml, 1.05 mmol) then the methyllithium solution (1 equiv.) After the solution was stirred for a period (see Table 2) at −78°, dry carbon dioxide was bubbled through it for 10 min, and it was stirred a further 10 min at −78°. The solution was quenched with moist ether (60 ml) and concentrated to a syrup which was taken up in a 5% aqueous sodium carbonate solution (30 ml). This solu-

TABLE 1. Experimental details of anion methylation

Compound	Source of RLi*	Yield of methylation (%)
DBBA	Ventron (2.2 *M* in ether)	>90
DBBA	Ventron (1.82 *M* in ether)	<50
DBBA	Foote (1.8 *M* in ether)	>90
NPP	Ventron (2.2 *M* in ether)	79
NPP	Ventron (1.82 *M* in ether)	0–25
NPP	Foote (1.82 *M* in ether)	75
NPP	Butyllithium from Ventron (1.82 *M* in hexane)	85

*RLi represents methyllithium except in last entry; method III was used throughout; DBBA, dibenzylbenzamide; NPP, *N*-nitroso-4-phenylpiperidine.

Can. J. Chem. Downloaded from www.nrcresearchpress.com by 210.87.254.42 on 09/05/12
For personal use only.

tion was washed with chloroform (3 × 20 ml), neutralized (5% HCl solution) and extracted with chloroform (3 × 30 ml). The chloroform extracts were combined, dried, and concentrated to a syrup which solidified on standing; for yield, see Table 2. The solid was recrystallized from petroleum ether and gave m.p. 120–122° (dec.).

Method II

To THF (30 ml) stirred under nitrogen at −78° was added diisopropylamine (0.165 ml, 1.15 mol), then the methyllithium solution (1 equiv.). Ten minutes later, a solution of compound **2** (1 ml of a 1 mmol/ml solution) was injected and the solution was stirred for a further period at −78° as described in Table 2. The remainder of this procedure was as in method I.

Method III

To THF (30 ml) stirred at room temperature, was added diisopropylamine (0.165 ml, 1.15 mol), then the methyllithium solution. After being stirred 5 min at room temperature, the solution was cooled to −95° and stirred for 10 min to allow temperature equilibration.

Then a solution of compound **2** (1 mmol/ml) was injected and stirring was continued for the period stated in Table 2. The remainder of this procedure is as in method I; n.m.r. of **3**: 1.40–3.10 (m, H_3, H_4, and H_5 and *anti*[9] H_6 axial), 4.05 (triplet of doublets, J's = 3.6, 12.8, 12.8 Hz, *syn* H_6 axial), 4.85–5.25 (m, *syn* and *anti* H_6 equatorial), 5.71 (d, J = 5.7 Hz, *anti* H_2 equatorial), 5.93 (d, J = 6.0 Hz, *syn* H_2 equatorial), (ratio of *syn* to *anti* is 6:4), 7.00–7.42, phenyl protons; i.r. (CCl_4), 3040, 2930, 3300–2450 br, 1723 (C=O), 1452 (NNO).

This product (**3**) (295 mg) was cleaved as described earlier (7) by bubbling dry hydrogen chloride gas through a stirred benzene solution (100 ml). The amorphous product was recrystallized from ethanol–hexane, then from ethanol to give *trans*-2-carboxy-4-phenylpiperidine hydrochloride, m.p. 230–233° (dec.).

Anal. Calcd. for $C_{12}H_{16}ClNO_2$: C, 59.63; H, 6.67; N, 5.79. Found: C, 59.48; H, 6.58; N, 5.67.

N-Nitroso-trans-2-methyl-4-phenylpiperidine (4)

The anion of **2** (1.456 g, 7.64 mmol) was generated at −95° as in method III. Then after 10 min methyl iodide (3 ml, 5 equiv.) was added and the solution was stirred 40 min at −95°, 30 min at −78°, and allowed to warm up over 15 min. It was quenched with water (0.2 ml) then concentrated to a syrup. The syrup was taken up in methylene chloride (50 ml) which was washed with water (2 × 50 ml). The combined aqueous washings were extracted with methylene chloride (30 ml) and the combined methylene chloride fractions were dried (Na_2SO_4) and concentrated. Column chromatography using hexanes – ethyl acetate (3:1) as eluent yielded pure syrup, *N*-nitroso-*trans*-2-methyl-4-phenylpiperidine (**3**), yield 1.24 g, (79%). The product crystallized on standing and was recrystallized from ethanol–water, m.p. 53–55°; i.r. (film) 3070, 3030, 3020, 2960, 2920, 2840, 1590, 1570, 1485, 1450 (NNO); n.m.r. 1.19 (d, J = 7.0 Hz, *syn* CH_3), 1.50 (d, J = 7.0 Hz, *anti* CH_3), 1.5–2.2 (complex multiplets), 2.72 (triplet of doublets, J = 4.0, 12.5, 12.5 Hz, H_6^a in *anti*), 3.11 (m, H_4), 3.86 (triplet of doublets, J = 4.0, 12.5, 12.5 Hz, H_6^a in *syn*), 4.76 (octet, J = 12.7, 2.1, 4.5 Hz, H_6^e in *syn*), 5.07 (octet, J = 13.0, 2.0, 4.5 Hz, H_6^e in *anti*), 5.41 (m, H_2^e in *syn* and *anti*), 7.08–7.42 (m, ArH).

This reaction was carried out exactly as before, except that the column chromatography was carried out rapidly at 5° instead of room temperature. The ratio of *syn* to *anti* after this process was ~75% *syn*, 25% *anti* and confirms the proton assignments in the n.m.r. spectra. After 2 days at room temperature, the ratio of *syn* to *anti* isomers at equilibrium was 45:55.

2-Methyl-4-phenyl-N-p-toluenesulfonylpiperidine

Into a solution of compound **4** (95 mg) in dry benzene (30 ml) was bubbled dry hydrogen chloride for 15 min, then dry nitrogen for 10 min. The solution was washed with a 10% NaOH solution (2 × 30 ml) which was in turn washed with methylene chloride (15 ml). The benzene and methylene chloride layers were combined, dried (Na_2SO_4), and concentrated to a syrup (80 mg). This syrup, in 2.5 ml of 10% NaOH solution and ethanol (2.5 ml) was treated with recrystallized toluenesulfonyl chloride (104 mg, 1.2 equiv.) and stirred for 4 h. The solid product **4** was removed by filtration (150 mg, 98%) and recrystallized twice from ethanol–water to give 2-methyl-4-phenyl-*N*-toluenesulfonylpiperidine (**4**), yield 110 mg, 72%, m.p. 72–74°.

Anal. Calcd. for $C_{14}H_{23}NO_2S$: C, 69.82; H, 7.04; N, 4.25. Found: C, 69.48; H, 7.06; N, 4.17.

N-Nitroso-trans-2-(hydroxydiphenylmethyl)-4-phenylpiperidine (5)

The anion was generated from **2** (380 mg, 2 mmol) by method I. After 4 min, a solution of benzophenone (455 mg, 2.5 equiv.) in THF (5 ml) was added and the reaction was stirred 1 h at −78°, then allowed to warm to room temperature over 1 h. Water was added (0.1 ml) and the reaction mixture was concentrated to dryness and taken up in methylene chloride (40 ml) which was washed with water (2 × 30 ml). The methylene chloride layer was dried (Na_2SO_4) and concentrated. Thin-layer chromatography in hexanes – ethyl acetate 2:1 showed one compound in the concentrate besides starting materials and this product was isolated using column chromatography and the same eluent; yield 505 mg, 54%. The product was recrystallized from EtOH–water and from benzene – petroleum ether (60–80°) to give a solid, m.p. 185–187°; n.m.r. (acetone-d_6) 1.6–2.3 (complex multiplets) 3.4 (m, H_4), 4.0 (H_6^a in *syn*), 4.8 (H_6^e), 5.2 (H_6^e), 6.0 (d, J = 6.5 Hz, H_2^e in *syn*), 6.38 (d, J = 6.5 Hz, H_2^e in *anti*), 7.0–7.4 (m, ArH), *syn*:*anti* ratio is 1:2.

TABLE 2. Experimental details for the formation of *N*-nitroso-4-phenylpiperidine-2-carboxylic acid

Time for anion formation (min)	Yield (%)		
	Method I	Method II	Method III
4	64, 69	63, 65	59
7	64	56	73
10	62	44	73
30	46		76
120			59

[9]Throughout this paper, the terms *syn* and *anti* are used to designate the configuration of the isomers. Proton assignments are designated by the number of the ring carbon to which the protons are attached.

Can. J. Chem. Downloaded from www.nrcresearchpress.com by 210.87.254.42 on 09/05/12
For personal use only.

Anal. Calcd. for $C_{24}H_{24}N_2O_2$: C, 77.39; H, 6.50. Found: C, 77.44; H, 6.51.

N-Nitroso-r-2,c-6-dimethyl-t-4-phenylpiperidine (6)

To freshly distilled THF (35 ml) was added diisopropylamine (0.25 ml, 1.15 equiv.) and methyllithium solution (1 equiv.). The solution was stirred 8 min at −78°, then a solution of **4** (306 mg) in THF (1.5 ml) was added and it was stirred a further 4 min at −78°. Methyl iodide (0.7 ml, 5 equiv.) was added and the solution stirred 2 h at −78°, then 2 h at −45°. Water (0.1 ml) was added and the solution was concentrated to dryness and taken up in methylene chloride (30 ml) which was washed with water (3 × 30 ml). The combined aqueous layers were extracted with methylene chloride and the combined methylene chloride layers were dried (Na_2SO_4) and concentrated to a syrup (351 mg). The products were separated on a column of silica gel using petroleum ether (60–80°) – ethyl acetate 5:1 as eluent. The compounds obtained were 203 mg (62%) of **6**, R_f 0.44; 85 mg (26%) of starting material R_f 0.34; and minor amounts of two slower moving impurities. The major product **6** crystallized on standing and was recrystallized from ethanol–water, m.p. 63–65°; i.r. (CCl_4) 3095, 3065, 3030, 2975, 2940, 2860, 1595, 1485, 1440 (NNO); n.m.r. described in detail in ref. 9.

N-p-Toluenesulfonyl-r-2,c-6-dimethyl-t-4-phenylpiperidine

Through a solution of **6** (65 mg) in dry benzene (20 ml) was bubbled dry hydrogen chloride for 15 min and dry nitrogen for 5 min. The benzene solution was washed with 10% NaOH solutions (2 × 20 ml) which were combined and extracted with methylene chloride. The combined methylene chloride and benzene layers were dried (Na_2SO_4) and concentrated to a syrup. The syrup in ethanol (1 ml) and 10% NaOH solution (1 ml) was treated with *p*-toluenesulfonyl chloride (65 mg, 1.5 equiv.) and stirred for 3 h. The solution was extracted with chloroform (3 × 5 ml) and the combined extracts were washed with water (5 ml) and concentrated. The product, after purification from *p*-toluenesulfonyl anhydride by preparative t.l.c. chromatography on silica gel using *p*-dioxane–hexanes, 1:5 as eluent; crystallized (27 mg) and was recrystallized twice from ethanol–water to give needles (22 mg), m.p. 96–97°.

Anal. Calcd. for $C_{20}H_{25}NO_2S$: C, 69.94; H, 7.34; N, 4.08. Found: C, 69.97; H, 7.43; N, 4.02.

Equilibration of 6

To a solution of the above compound (252 mg) in DMSO (1.5 ml) was added potassium *t*-butoxide (300 mg) and the mixture was magnetically stirred 60 h at 90° under nitrogen. Preparative t.l.c. chromatography using silica gel plates and hexanes – ethyl acetate 3:1 as eluent yielded a mixture of 150 mg, (60%) *cis*-**6** and *trans* **8** isomers. Integration of n.m.r. signals indicated that the mixture contained 74% *trans*. The following absorptions were clearly attributable to the *trans* isomer; 1.18 (d, J = 7.0 Hz, *syn* CH_3), 1.68 (3H, d, J = 6.1 Hz, *anti* CH_3), 2.99–3.46 (complex multiplet, H_4), 4.13 (12-line pattern, J = 12.3, 6.1, 3.3 Hz, H_2^a), 5.51 (octet, J = 7.1, 4.1 Hz, H_6^e), 7.04–7.40 (5H m, ArH).

Through a solution of this mixture in dry benzene (30 ml), bubbled dry hydrogen chloride for 30 min and then dry nitrogen for 5 min. The product was washed with 10% NaOH solutions (2 × 20 ml) which were, in turn, washed with methylene chloride. The combined benzene and methylene chloride layers were dried (Na_2SO_4) and concentrated to a syrup which was separated into two components using preparative t.l.c. on silica gel with cyclohexane–chloroform–diethylamine 5:4:1 as eluent.

The faster moving spot was collected from the plate, isolated (37 mg), and identified as *cis* by n.m.r. (one type CH_3 absorption). The slower moving spot (89 mg, showing two CH_3 doublets in its n.m.r.) was converted to its hydrochloride using HCl in benzene. Crystallization was induced by addition of ether. Recrystallization from ethanol–water gave 65 mg of solid, m.p. 252–254°.

Anal. Calcd. for $C_{13}H_{20}NCl$: C, 69.16; H, 8.92; N, 6.20. Found: C, 68.98; H, 8.91; N, 6.11.

Equilibration of N-Nitroso-r-2,t-6-dimethyl-C-4-phenylpiperidine 8

The above *trans* amine (40 mg) was nitrosated and subjected to the same equilibration treatment as for the *cis* isomer **6**. From the n.m.r. of the isolated mixture, it was estimated by integration that the proportion of *cis* to *trans* was 25:75.

N-Nitroso-r-2-carboxy-c-6-methyl-4-t-phenylpiperidine 7

Diisopropylamine (0.08 ml, 0.5 mmol) and methyllithium (1 equiv.) were added to freshly distilled THF stirred at −78°. After 12 min, a solution of **4** (87 mg, 0.43 mmol) in THF (0.85 ml) was added and the solution stirred a further 10 min at −78°. Dry carbon dioxide was bubbled in for 10 min and then the reaction was stirred a further 10 min at −78°, then allowed to warm to room temperature over 15 min. It was concentrated to a syrup which was taken up in 5% Na_2CO_3 solution (30 ml), which was washed wih methylene chloride (2 × 20 ml), made slightly acidic with HCl (0.5 *N*) ,and extracted with methylene chloride (3 × 20 ml). The latter methylene chloride extracts were combined, dried (Na_2SO_4) and concentrated to a yellow (30 mg, 30%) solid which was recrystallized from ethanol–water, m.p. 128–129° (dec.); n.m.r. 1.21 (d, J = 7.5 Hz, *syn* CH_3), 1.56 (d, J = 7.5 Hz, *anti* CH_3), 1.6–2.8 (unresolved m), 3.22 (m, H_4), 5.33 (br, m, H_6 *syn* and *anti*), 5.67 (d, J = 5.8 Hz, H_2^e *syn* or *anti*), 5.78 (d, J = 6.1 Hz, H_2^e), 7.26 (s, Ar H). Conversion to the amine hydrochloride gave a solid which, after three recrystallizations from ethanol–acetone, had m.p. 268–270° (dec.).

Anal. Calcd. for $C_{13}H_{18}NO_2Cl$: C, 61.06; H, 7.10; N, 5.47. Found: C, 61.23; H, 7.19; N, 5.45.

The authors thank the National Research Council of Canada for financial support of this research.

1. L. K. KEEFER and C. H. FODOR. J. Am. Chem. Soc. **92**, 5747 (1970).
2. P. RADEMACHER and W. LUTTKE. Spectrochim. Acta, **27**, 715 (1971).
3. D. SEEBACH and D. ENDERS. Angew. Chem. **84**, 350 (1972).
4. D. SEEBACH and D. ENDERS. Angew. Chem. **84**, 1186 (1972).
5. D. SEEBACH and D. ENDERS. Angew. Chem. **87**, 1 (1975).
6. R. R. FRASER and Y. Y. WIGFIELD. Tetrahedron Lett. 2515 (1971).

7. R. R. FRASER, G. BOUSSARD, I. D. POSTESCU, J. J. WHITING, and Y. Y. WIGFIELD. Can. J. Chem. **51**, 1109 (1973).
8. R. R. FRASER and L. K. NG. Unpublished results.
9. R. R. FRASER and T. B. GRINDLEY. Can. J. Chem. This issue.
10. R. K. HARRIS and R. A. SPRAGG. J. Mol. Spectrosc. **23**, 158 (1967).
11. T. P. FORREST, D. L. HOOPER, and S. RAY. J. Am. Chem. Soc. **96**, 428 (1974).
12. R. R. FRASER and T. B. GRINDLEY. Tetrahedron Lett. 4169 (1974).
13. F. H. WESTHEIMER. Steric effects in organic chemistry. John Wiley and Sons, Inc., New York, N.Y. 1956, p. 523.
14. F. JOHNSON and S. K. MALHOTRA. J. Am. Chem. Soc. **87**, 5492 (1965).
15. B. RICKBORN. J. Am. Chem. Soc. **84**, 2414 (1962); W. D. COTTERILL and M. J. T. ROBINSON. Tetrahedron, **20**, 765 (1964); **20**, 777 (1964).
16. Y. L. CHOW, C. J. COLON, and J. N. S. TAM. Can. J. Chem. **46**, 2821 (1968).
17. J. D. COONEY, S. K. BROWNSTEIN, and J. W. APSIMON. Can. J. Chem. **52**, 3028 (1974).
18. H. WERNER, G. MANN, M. MUHLSTADT, and H. J. KOHLER. Tetrahedron Lett. 3563 (1970).
19. N. L. ALLINGER, J. ALLINGER, L. W. CHOW, and G. L. WANG. J. Org. Chem. **32**, 522 (1967).
20. E. L. ELIEL, A. A. HARTMANN, and A. G. ABATJOGLU. J. Am. Chem. Soc. **96**, 1807 (1974).
21. T. DURST, R. VIAU, and M. R. MCCLORY. J. Am. Chem. Soc. **93**, 3077 (1971).
22. T. DURST, R. R. FRASER, M. R. MCCLORY, R. B. SWINGLE, R. VIAU, and Y. Y. WIGFIELD. Can. J. Chem. **48**, 2148 (1970).
23. S. BORY and A. MARQUET. Tetrahedron Lett. 4155 (1973); S. BORY, R. LETT, B. MOREAU, and A. MARQUET. Tetrahedron Lett. 4921 (1972).
24. H. O. HOUSE, B. H. TERFERTILLER, and H. D. OLMSTEAD. J. Org. Chem. **33**, 935 (1968).
25. S. KARADY, M. L. ENFANT, and R. E. WOLFF. Bull. Soc. Chem. Fr. 2472 (1965).
26. N. L. ALLINGER, M. TRIBBLE, and M. A. MILLER. Tetrahedron, **28**, 1173 (1972).
27. F. A. L. ANET, G. N. CHMURNY, and J. KRANE. J. Am. Chem. Soc. **95**, 4423 (1973).
28. E. J. COREY and R. A. SNEEN. J. Am. Chem. Soc. **78**, 6269 (1956).
29. F. G. BORDWELL and R. G. SCAMEHORN. J. Am. Chem. Soc. **90**, 6749 (1968).
30. J. A. FEATHER and V. GOLD. J. Chem. Soc. 1752 (1965).
31. G. B. TRIMITSIS and E. M. VAN DAM. Chem. Commun. 610 (1974).
32. T. DURST and M. MOLIN. Tetrahedron Lett. 63 (1975).
33. N. J. HARPER, C. W. T. HUSSEY, M. E. PEEL, A. C. RITCHIE, and J. M. WARING. J. Med. Chem. **10**, 819 (1967).

Can. J. Chem. Downloaded from www.nrcresearchpress.com by 210.87.254.42 on 09/05/12
For personal use only.

Studies of β-Diketone Complexes of Rhenium. VIII. The Reaction of β-Diketones with Chloropentacarbonylrhenium(I), and the Preparation of Complexes of the Type $Re(CO)_4(dik)$, $Re_2(CO)_6(dik)_2$, $Re_2(CO)_6Cl_2(dikH)_2$, $Re(CO)_3L(dik)$, and $Re(CO)_2(dik)L_2$ [1]

MAURICE CONRAD FREDETTE AND COLIN JAMES LYNE LOCK[2]

Institute for Materials Research, McMaster University, Hamilton, Ontario L8S 4M1

Received February 11, 1975

MAURICE CONRAD FREDETTE and COLIN JAMES LYNE LOCK. Can. J. Chem. **53**, 2481 (1975).

The reaction of β-diketones with $Re(CO)_5Cl$ gave compounds of stoichiometries $Re_2(CO)_6dik_2$ or $Re_2Cl_2(CO)_6(dikH)_2$. Reaction of the former compounds with carbon monoxide at high pressure gave $Re(CO)_4dik$, while with donor ligands such as pyridine or triphenylphosphine they gave compounds of stoichiometry $Re(CO)_3dikL$. With triphenylphosphine further reaction gave $Re(CO)_2dik[P(C_6H_5)_3]_2$. Compounds were investigated by infrared spectroscopy and mass spectroscopy, and a Cotton–Kraihanzel analysis was made of the carbonyl vibrational spectra in order to get an estimate of the π-acceptor ability of the β-ketoenolate ligands.

MAURICE CONRAD FREDETTE et COLIN JAMES LYNE LOCK. Can. J. Chem. **53**, 2481 (1975).

La réaction des β-dicétones avec $Re(CO)_5Cl$ donne des composés de stoechiométries $Re(CO)_6dik_2$ ou $Re_2Cl_2(CO)_6(dikH)_2$. La réaction des composés précédents avec le monoxyde de carbone à pression élevée donne $Re(CO)_4dik$, alors qu'avec un ligand donneur comme la pyridine ou la triphénylphosphine les composés précédents conduisent à des produits de stoechiométrie $Re(CO)_3dikL$. Avec la triphénylphospine, une réaction ultérieure conduit au composé $Re(CO)_2dik[P(C_6H_5)_3]_2$. Ces composés ont été étudiés par spectroscopie infrarouge et par spectrométrie de masse. Une analyse Cotton–Kraihanzel a été faite sur le spectre vibratoire du carbonyle dans le but d'évaluer la propriété π-accepteur des ligands β-cétoénolate.

[Traduit par le journal]

Introduction

Because of the difficulty (1) of obtaining $Re(acac)_3$ by the published method (2, 3) we considered the possibility of obtaining the compound by the reaction of $Re_2(CO)_{10}$ and acetylacetone. Molybdenum, chromium, and iron trisacetylacetonates had been prepared from the simple carbonyls (4, 5). Little if any reaction was observed, however, between $Re_2(CO)_{10}$ and acetylacetone up to 373 K and so further reactions were attempted with diketones and $Re(CO)_5Cl$. The desired product, $Re(acac)_3$, was never obtained, but two series of compounds were isolated, which were clearly different in type from $Mn(CO)_4hfac$ isolated from the reaction of $Mn(CO)_5Cl$ and hexafluoroacetylacetone (6). In this paper we describe the preparation and physical properties of the two series of compounds and some of their chemical reactions.

Experiments

Analyses for carbon, hydrogen, nitrogen, fluorine, chlorine, and sulfur were done by Galbraith Laboratories Inc., Knoxville, Tennessee and A.B. Gygli, Toronto, Ontario. Rough rhenium and chlorine percentages and accurate rhenium–chlorine atom ratios were determined by neutron activation analysis (7). Infrared spectra were recorded for solid samples ground into a mull with Nujol. The Nujol had been dried by refluxing with phosphorus pentoxide followed by vacuum distillation. The mull samples were mounted between potassium bromide or polyethylene plates and spectra were recorded on Perkin–Elmer 337, 521, and 301 spectrometers. Magnetic susceptibility measurements were carried out on 10 cm length powdered sample packed into 3 mm (o.d.) tubes. Calibrations were made using mercury–thiocyanatecobaltate. The measurements were made by the Gouy method and the apparatus has been described

[1]The following abbreviations are used in this paper: L, monodentate ligand; py, pyridine, C_5H_5N; Ph, phenyl, $\cdot C_6H_5$; dik, β-ketoenolate anion; dikH, corresponding neutral β-diketone or β-ketoenol tautomer; acac, pentane-2,4-dionate anion, $C_5H_7O_2^-$; tfac, 1,1,1-trifluoropentane-2,4-dionate anion, $C_5H_4F_3O_2^-$; hfac, 1,1,1,5,5,5-hexafluoropentane-2,4-dionate anion; ttfa, 4,4,4-trifluoro-1-thienylbutane-1,3-dionate anion, $C_8H_4F_3SO_2^-$; tfba, 4,4,4-trifluoro-1-phenylbutane-1,3-dionate anion, $C_{10}H_6F_3O_2^-$; bam, 1-phenylbutane-1,3-dionate anion, $C_{10}H_9O_2^-$; dbm, dibenzoylmethanate anion, $C_{15}H_{11}O_2^-$.

[2]To whom correspondence should be addressed.

Can. J. Chem. Downloaded from www.nrcresearchpress.com by 210.87.254.42 on 09/05/12
For personal use only.

Can. J. Chem. Downloaded from www.nrcresearchpress.com by 210.87.254.42 on 09/05/12
For personal use only.

TABLE 1. Analysis of compounds

Compound	C (%)		H (%)		Other (%)		Molecular weight		Melting point (°C)*
	Calcd.	Found	Calcd.	Found	Calcd.	Found	Calcd.	Found†	
$Re_2(CO)_6(acac)_2$	26.0	25.8	1.9	2.1			738	738	260
$Re_2(CO)_6(dbm)_2$	43.8	44.0	2.2	2.2			988	> 820	420
$Re_2(CO)_6(tfba)_2$	32.2	33.6	1.3	1.6	11.7F‡	10.7F			124
$Re_2(CO)_6(ttfa)$	26.9	27.7	0.8	1.5	6.2S	6.5S			173
$Re_2(CO)_6(tfac)_2$	22.8	22.6	1.0	1.4	13.4F	12.2F	846	846	180
$Re_2(CO)_6(hfac)_2$	20.1	19.2	0.2	0.5	23.9F	22.6F	954	954	185
$Re_2(CO)_6Cl_2bamH_2$	33.4	33.2	1.9	2.2	7.6Cl	7.6Cl			161
$Re_2(CO)_6Cl_2(acacH)_2$	23.7	22.7	1.7	1.8	8.8Cl	9.8Cl			—
$Re(CO)_4acac$	27.2	27.1	1.5	1.6					§
$Re(CO)_4dbm$	43.7	43.7	2.1	2.1					§
$Re(CO)_4tfba$	32.7	31.5	1.2	1.3	11.1F	10.2F			§
$Re(CO)_4ttfa$	27.2	28.3	1.0	0.2	11.0F	12.0F			
					6.2S	6.2S			§
$Re(CO)_4tfac$	24.9	24.0	0.9	0.9	12.6F	11.4F			§
$Re(CO)_4hfac$	21.4	21.3	0.2	0.2	22.6F	22.7F			103
$Re(CO)_3(dbm)(py)$	48.3	48.3	2.8	2.9	2.4N	2.5N	572	572	189
$Re(CO)_3(dbm)Ph_3P$	57.3	47.1	3.4	3.5	4.1P	4.2P			186
$Re(CO)_2tfac(Ph_3P)_2$	56.1	56.1	3.7	3.5	6.7P	6.6P	919	> 656	206
					6.2F	6.1F			
$Re(CO)_2dbm(Ph_3P)_2$	64.3	64.3	4.1	4.6	6.3P	6.3P	989	> 726	272

*Actually decomposition temperatures except for compounds with dbm and $Re(CO)_4hfac$.
†Molecular weights were determined by mass spectroscopy using a Consolidated Electrodynamics Corp., Model 21-110B mass spectrometer.
‡Fluorine analyses were generally unsatisfactory and lower than the calculated values. Repeated crystallization to give purer samples or changing analysts did not improve the results.
§These compounds do not melt but return to the corresponding dimer upon heating.

Can. J. Chem. Downloaded from www.nrcresearchpress.com by 210.87.254.42 on 09/05/12
For personal use only.

previously (8). As all samples were diamagnetic, or had very low paramagnetism, measurements were made only at 296 and 77 K. Corrections for the diamagnetism of the ligand were taken from Selwood (9) and Foëx *et al.* (10). The value for Re(I) was obtained by comparison with other metals and extrapolation of data for other rhenium oxidation states and was assumed to be -56×10^{-6} cm^3 mol^{-1}. Mass spectra were recorded on a Consolidated Electrodynamics Corp. Model 21-110B instrument. All solvents and reagents used were reagent grade and were not purified further.

Yields are not reported for the reactions described below as they varied from one experiment to the next. Some unreacted $Re(CO)_5Cl$ was usually recovered from each preparation in which it was used as a starting material. Yields based on the amount of $Re(CO)_5Cl$ which had reacted were usually at least 50%. Derivatives made by further reaction of new compounds reported here usually had yields of about 80%. Analyses and melting points of new compounds are given in Table 1.

Bis(μ-O-pentane-2,4-dionato)tricarbonylrhenium(I)) (1)

Chloropentacarbonylrhenium(I) (1 mmol) and acetylacetone (3 mmol) were refluxed in benzene (~75 ml) for 2 weeks. The pale yellow solution gradually turned dark brown. Evaporation of the solvent (~20°, ~15 mm), followed by addition of ether (~100 ml) and filtration, served to remove any unreacted chloropentacarbonylrhenium(I). The filtrate was evaporated and the residues were dissolved in the minimum amount of chloroform or ether. Addition of enough petroleum ether (30–60°) to cause cloudiness produced a brown powder which was collected on a filter and recrystallized from dichloromethane or ether, giving small white needles.

Bis(μ-O-1,3-diphenylpropane-1,3-dionato)tricarbonylrhenium(I)) (2)

Chloropentacarbonylrhenium(I) (1 mmol) and dibenzoylmethane (3 mmol) were refluxed for 3–4 weeks in benzene (~75 ml). Bright orange crystals of the product were removed on a filter and washed with hot benzene. More product was sometimes obtained by heating the dried residues *in vacuo* with a heat lamp for 2–3 h and then washing the melt with hot benzene.

Bis(μ-O-4,4,4-trifluoro-1-phenyl-1,3-butanedionato)tricarbonylrhenium(I)) (3)

Chloropentacarbonylrhenium(I) (0.5 g) and trifluorobenzoylacetone (1 g) were refluxed in benzene (50 ml) for 1 week. The solution was cooled, filtered, and evaporated to dryness. The residues were dissolved in ether and the solution was filtered and evaporated to dryness. These procedures served to remove any unreacted $Re(CO)_5Cl$. The brown residues from the ether solution were stirred with a minimum amount of chloroform or dichloromethane for a few seconds. A brown solution was formed as the residues dissolved, leaving the yellow product as a powder in the bottom of the flask. The solid yellow product was collected on a filter as rapidly as possible because it would also dissolve within a few minutes. The brown filtrate usually contained a fair amount of the yellow product which had dissolved in the chloroform. Thus, the filtrate could be evaporated to dryness to give a brown residue from which more yellow solid could be obtained, by repeating the process of stirring with a minimum amount of solvent and filtering.

Bis(μ-O-4,4,4-trifluoro-1-thienylbutane-1,3-dionato)tricarbonylrhenium(I)) (4)

This yellow compound was prepared by the same method as **3** using chloropentacarbonylrhenium(I) and thenoyltrifluoroacetone as starting materials.

Bis(μ-O-1,1,1-trifluoropentane-2,4-dionato)tricarbonylrhenium(I)) (5)

This yellow compound was prepared by the same method as (**1**) using chloropentacarbonylrhenium(I) and trifluoroacetylacetone as starting materials.

Bis(μ-O-1,1,1,5,5,5-hexafluoro-2,4-pentanedionato)tricarbonylrhenium(I))

This yellow-orange compound was prepared by the same method as **1** using chloropentacarbonylrhenium(I) and hexafluoroacetylacetone as starting materials.

Bis(μ-chlorotricarbonyl(1-phenyl-1-hydroxobut-1-ene-3-one)rhenium(I))

Chloropentacarbonylrhenium(I) (2 g) and benzoylacetone (1.5 g) were refluxed in benzene (~150 ml) for 1 d. The pale yellow solution gradually turned green. The solution was evaporated to near dryness, dichloromethane (20 ml) was added and the solution was filtered, and the filtrate evaporated to near dryness. A mixture (1:1 v/v) of dichloromethane and petroleum ether (40–60°) was added and the resulting solution allowed to evaporate slowly over a few days to give a yellow-green powder. The powder was recrystallized from dichloromethane – petroleum ether to give crystals of the title compound which were usually six-sided plates or occasionally rhomb-shaped needles.

Bis(μ-chlorotricarbonyl(2-hydroxopent-2-ene-4-one)rhenium(I))

Chloropentacarbonylrhenium(I) (1 mmol) and acetylacetone (3 mmol) were refluxed in benzene (~75 ml) for 5 h and the white product was filtered off. We have been unable to repeat this preparation.

Pentane-2,4-dionatotetracarbonylrhenium(I) (6)

Compound **1** (0.5 g) was sealed in a stainless steel pressure vessel with 200 atm of carbon monoxide and was heated to 150 °C for 24 h. The pressure vessel was cooled, dismantled, and washed out with ether. Evaporation of the ether gave the white product.

1,3-Diphenylpropane-1,3-dionatotetracarbonylrhenium(I)

The green-yellow compound was prepared similarly to **6** using compound **2** as starting material.

4,4,4-Trifluoro-1-phenyl-1,3-butanedionatotetracarbonylrhenium(I)

The green-yellow compound was prepared similarly to **6** using compound **3** as starting material.

4,4,4-Trifluoro-1-thienylbutane-1,3-dionatotetracarbonylrhenium(I)

The green-yellow compound was prepared similarly to **6** using compound **4** as starting material.

1,1,1-Trifluoropentane-2,4-dionatotetracarbonylrhenium(I)

This pale yellow compound was prepared similarly to **6** using compound **5** as starting material.

1,1,1,5,5,5-Hexafluoro-2,4-pentanedionatotetracarbonylrhenium(I)

Chloropentacarbonylrhenium(I) (1 mmol) and hexa-

Can. J. Chem. Downloaded from www.nrcresearchpress.com by 210.87.254.42 on 09/05/12
For personal use only.

fluoroacetylacetone (3 mmol) were refluxed in benzene (~75 ml) for 12 h. The resulting solution was then treated as for compound **1** giving yellow crystals of the product (0.2 g).

1,3-Diphenylpropane-1,3-dionatotricarbonylpyridine-rhenium(I)

Compound **2** and an excess of pyridine (1 ml) were refluxed in benzene (50 ml). The orange solution turned yellow-green overnight. The solution was then evaporated to dryness. The residues were dissolved in methanol and petroleum ether (30–60°), producing an orange solution. Partial evaporation and cooling of this solution produced orange crystals which were recrystallized from ether and petroleum ether (30–60°).

1,3-Diphenylpropane-1,3-dionatotricarbonyltriphenyl-phosphinerhenium(I)

Stoichiometric quantities of compound **2** (0.5 g) and triphenylphosphine (0.27 g) were refluxed in benzene (100 ml) for 1½ h. The hot solution was filtered and then evaporated to dryness. The residues were washed with methanol and the impure solid orange product was captured on a filter and washed with ether. These crystals were dissolved in acetone and the solution was filtered. The filtrate was allowed to evaporate slowly over 2–3 d and orange crystals of the pure product were obtained.

1,1,1-Trifluoropentane-2,4-dionatodicarbonylbis(triphenylphosphine)rhenium(I)

Compound **5** (0.5 g) and an excess of triphenylphosphine (1.0 g) were refluxed in benzene (50 ml). The green solution turned yellow-green overnight. The solution was then evaporated to dryness. The residues were dissolved in methanol and petroleum ether (30–60°). Partial evaporation and cooling of this solution produced orange crystals of the product. The product was recrystallized from ether.

1,3-Diphenylpropane-1,3-dionatodicarbonylbis(triphenylphosphine)rhenium(I)

Compound **2** (0.5 g) and an excess of triphenylphosphine (1.0 g) were refluxed in benzene (50 ml) for 12 h. The orange solution turned orange-red within the first 2 h. The solution wss evaporated to dryness and the residues were washed with methanol, which left orange crystals of the product in the bottom of the flask. These crystals were collected on a filter and washed with ether.

Other Reactions

$Re_2(CO)_6Cl_2(bamH)_2$ (0.5 g) was sealed in a 1 l bomb with 200 atm of carbon monoxide and was heated to 150 °C for 24 h. The products were identified by infrared spectroscopy and were $(Re(CO)_4Cl)_2$ and bamH.

$$Re_2(CO)_6Cl_2(bamH)_2 \xrightarrow{2CO} Re_2(CO)_8Cl_2 + 2bamH$$

$Re_2(CO)_6Cl_2(bamH)_2$ (0.5 g) was refluxed in benzene (50 ml) with sodium carbonate (2.0 g) for 3 d in an attempt to remove HCl and form $Re_2(CO)_6bam_2$. The infrared spectrum of the dried residues showed that no change had taken place.

$Re_2(CO)_6Cl_2(bamH)_2$ was heated *in vacuo* up to 135 °C in a sublimation apparatus fitted with a water cooled cold finger. Initially, some bamH condensed on the cold finger. Later, some light yellow unidentified species condensed on the cold finger; it showed some C≡O and various other bands in an infrared spectrum. A brown glass was left in the bottom of the sublime and this could be purified to give mainly the original $Re_2(CO)_6Cl_2(bamH)_2$. No $Re_2(CO)_6(bam)_2$ was formed.

$Re_2(CO)_6(dbm)_2$ (0.5 g) was sealed in a bomb with 200 atm of nitrogen and was heated to 150 °C for 24 h. $Re_2(CO)_6(dbm)_2$ was recovered unchanged.

$Re(CO)_4dbm$ (0.5 g) was sealed in a bomb with 200 atm of nitrogen and was heated to 150 °C for 24 h. $Re_2(CO)_6(dbm)_2$ was the only product found.

$Re(CO)_2(dbm)(Ph_3P)_2$ was heated to 185 °C *in vacuo* in a sublimation apparatus fitted with a water cooled cold finger. The residue in the bottom was mainly $Re(CO)_2(dbm)(Ph_3P)_2$ and there were traces everywhere in the apparatus of other decomposition products, but it was not possible to obtain enough sample to identify them.

$[Ph_2SRe(CO)_3Cl]_2$ and $[(Ph—S—CH_2—Ph)Re(CO)_3Cl]_2$ were prepared by Hieber's method (ref. 11 and references therein). $[Ph_2SRe(CO)_3Cl]_2$ was heated to 185 °C *in vacuo* in a sublimation apparatus but no $[Re(CO)_3Cl]_x$ (11) could be isolated. The starting product was found unchanged in all parts of the apparatus. $[(Ph—S—CH_2—Ph)Re(CO)_3Cl]_2$ was heated to 230 °C *in vacuo* in a sublimation apparatus. Again, no $[Re(CO)_3Cl]_x$ was formed and the starting material was recovered everywhere in the sublimation apparatus. $[Ph_2SRe(CO)_3Cl]_2$ was melted at 140 °C *in vacuo* overnight together with some bamH. Only the starting products were recovered.

Results and Discussion

Two types of compounds could be obtained by the reaction of $Re(CO)_5Cl$ and a diketone in benzene at elevated temperatures. Six were of stoichiometry $Re_2(CO)_6dik_2$ and two of stoichiometry $Re_2Cl_2(CO)_6(dikH)_2$. X-Ray diffraction studies have shown the structures to be those in Fig. 1 (12, 13).

The structure of $Re_2(CO)_6(dik)_2$ was similar to that of $(Re(CO)_4Cl)_2$ if one end of the β-ketoenolate group replaced the halogen atom and the other end a carbonyl group. The structural similarity suggested it should be possible to cleave the bridge bonds with either carbon monoxide or donor ligands as can be done for $[Re(CO)_4X]_2$ (14).

$$[Re(CO)_4X]_2 \underset{-2CO}{\overset{+2CO}{\rightleftharpoons}} 2Re(CO)_5Cl$$

$$[Re(CO)_4X]_2 \xrightarrow{2L} 2L\ Re(CO)_4X$$

In the second reaction it was possible to proceed further and replace another CO group to give $ReL_2(CO)_3X$.

A series of $Re(CO)_4dik$ compounds was prepared by the action of carbon monoxide on the dimers at high pressure. The $Re(CO)_4dik$

Can. J. Chem. Downloaded from www.nrcresearchpress.com by 210.87.254.42 on 09/05/12
For personal use only.

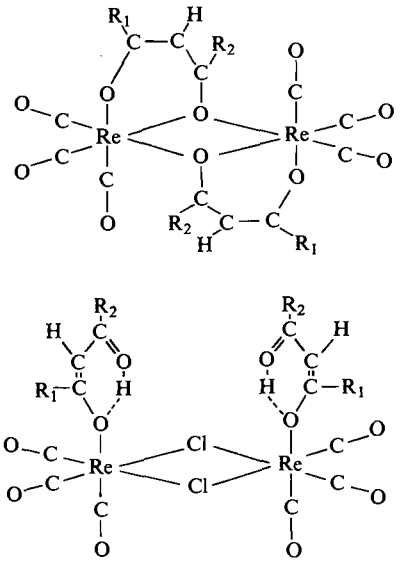

FIG. 1. The molecular structures of $Re_2(CO)_6dik_2$ and $Re_2(CO)_6Cl_2(dikH)_2$.

complexes were relatively unstable and readily lost CO (complete decomposition in 15 min in boiling benzene) to regenerate the dimers. The infrared spectra were very similar, in the carbonyl region, to $Mn(CO)_4hfac$ (6). Ligands such as triphenylphosphine and pyridine readily cleaved the dimer giving monomeric $Re(CO)_3dikL$, and in the case of triphenylphosphine it was possible to displace a CO group to give $Re(CO)_2dik(PPh_3)_2$. For donor oxygen and phosphine ligands it was relatively difficult to prepare metal complexes with less than three carbonyl groups using displacement methods, because the relatively poor π-acceptor ligands added tend to strengthen the M—CO bond for the remaining groups (15). The ease with which one could make $Re(CO)_2dikL_2$ suggests that our picture of dik being equivalent to a halogen and a CO group is qualitatively correct (*vide infra*). Despite the ease of reaction with CO and donor ligands it was not possible to react any of the compounds with dinitrogen.

The question arose early in this work as to why we obtained the dimer compounds, $Re_2(CO)_6(dik)_2$. Under the reaction conditions (refluxing benzene for almost 2 weeks) two likely pathways are

$$[1]\quad 2Re(CO)_5Cl + 2\,dikH \xrightarrow{\text{slow}} 2Re(CO)_4dik + 2HCl$$
$$\downarrow \text{fast}$$
$$Re_2(CO)_6dik_2 + 2CO$$

$$[2]\quad 2Re(CO)_5Cl \xrightarrow{12\,h} [Re(CO)_4Cl]_2 + 2CO$$
$$\downarrow 2dikH$$
$$Re_2Cl_2(CO)_6(dikH)_2$$
$$\downarrow$$
$$Re_2(CO)_6(dik)_2 + 2HCl$$

The reaction of $Mn(CO)_5Cl$ and hfacH gave only $Mn(CO)_4hfac$ (6) which is similar to the first step in reaction 1. Very careful reactions conducted for short times allowed isolation of small amounts of $Re(CO)_4hfac$, although no similar compound could be isolated for any other β-diketone. However, other $Re(CO)_4dik$ compounds lost CO very easily in boiling benzene to give the dimeric compounds and thus [1] is clearly an acceptable pathway. One cannot rule out pathway [2] because we have shown that the first step occurred in 12 h in boiling benzene and also that $[Re(CO)_4Cl]_2$ gave $Re_2(CO)_6(dik)_2$ when reacted with a β-diketone. We have not established the intermediate step since the only chloro compound we have fully characterized, $Re_2(CO)_6Cl_2(bamH)_2$, does not undergo decomposition to $Re_2(CO)_6(bam)_2$.

It is surprising that acetylacetone and dibenzoylmethane gave isolable complexes of the type $Re_2(CO)_6dik_2$ whereas benzoylacetylmethane did not. The only suggestion we can offer is based on the structures of the two types of compound. In the $Re_2(CO)_6dik_2$ compounds the two β-diketone groups were *trans* with respect to the Re—Re axis, whereas in $Re_2Cl_2(CO)_6(bamH)_2$ the two diketone groups were *cis*. It is assumed that the conversion of the intermediate $Re_2Cl_2(CO)_6(dikH)_2$ to $Re_2(CO)_6dik_2$ proceeded as shown in Fig. 2. HCl elimination was followed by the oxygen atom coming into the bridging position. To get the observed $Re_2(CO)_6dik_2$ structure the two β-ketoenol groups would have to be arranged *trans* in the $ReCl_2(CO)_6(dikH)_2$ compound.

We suggest that the reason that the *cis* complexes did not eliminate HCl, even in the presence of Na_2CO_3, was because of steric hindrance. A calculation, assuming the β-diketone–

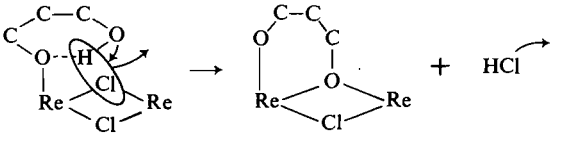

FIG. 2. A possible mechanism for conversion of *trans*-$Re_2(CO)_6Cl_2(dikH)_2$ to $Re_2(CO)_6dik_2$.

Can. J. Chem. Downloaded from www.nrcresearchpress.com by 210.87.254.42 on 09/05/12
For personal use only.

TABLE 2. Magnetic susceptibility data

Compound	χ_m(corr) ($\times 10^{-6}$) (c.g.s.u.) 77 K	296 K
$Re_2(CO)_6(bamH)_2Cl_2$	90	−70
$Re_2(CO)_6(dbm)_2$	−46	−122

β-diketone contacts were greater than twice the carbon van der Waals radius, and based on the geometries determined previously (12, 13), showed that for *cis*-$Re_2(CO)_6dik_2$ the β-diketone plane would be bent about 55° from the OReO plane (*cf.* the previous highest value of 34° (12)) and thus would make the ReOC angles about 100 and 80°, far smaller than any previously reported value for MOC angles in metal β-ketoenolate complexes.

Both series of compounds, $Re_2(CO)_6dik_2$ and $Re_2(CO)_6Cl_2(dikH)_2$, were diamagnetic, as would be expected for Re(I) complexes with roughly octahedral geometry and high field ligands. Typical results are shown in Table 2.

In retrospect, the spectroscopic data recorded for the compounds were satisfactorily explained in terms of their structures, although the data did not provide a sufficient basis for predicting the structures. The infrared spectra are reported in Table 3.[3] The compounds of the type $Re_2(CO)_6dik_2$ gave spectra in the carbonyl region which were very similar to those reported for $Repy_2(CO)_3Cl$ (14) (2041, 1934, 1891 cm^{-1}). Thus, it appears there was insignificant vibrational coupling between the C—O groups on each half of the dimer. In the $\nu_{C=C}$ and $\nu_{C=O}$ region for the β-ketoenolate group, two or three bands of varying intensity were observed for each compound. Fluorination of the ligand caused a shift to higher frequency of the highest band and a marked drop in intensity of all the bands in this region, as was observed by Nakamoto *et al.* for copper complexes (16).

The carbonyl region of the spectrum of $Re_2(CO)_6Cl_2(bamH)_2$ was expected to be similar to those of the above compounds since this molecule also contains two sets of 1,2,3-carbonyl groups. Bands were observed at similar frequencies, but there was evidence of coupling, since two of the bands are split. It is noteworthy that $Re_2(CO)_6Cl_2(bamH)_2$ contained two *neutral* ketoenol groups and yet there was no really significant difference in the spectrum in the 1500–1600 cm^{-1} region compared to those recorded for the $Re_2(CO)_6(dik)_2$ compounds. Indeed, an examination of the complete spectrum down to 250 cm^{-1} and a comparison with $Re_2(CO)_6(dbm)_2$ and $Re_2(CO)_6(acac)_2$ showed very little difference. The only differences were that for $Re_2(CO)_6Cl_2(bamH)_2$ the band caused by the Re—Cl stretch was seen at 266 cm^{-1} and no bands were observed in the 900–1000 cm^{-1} region. Most β-ketoenolate complexes show at least one band in this region, in particular a medium weak band at 930 ± 10 cm^{-1} (17–19).

Because the β-ketoenolate ligand must occupy two *cis* positions we expected the $Re(CO)_4dik$ complexes to have spectra in the carbonyl region very similar to $[Re(CO)_4Cl_2]_2$ (2114w, 2032s, 2000m, 1954m cm^{-1}). Four bands were observed for $Re(CO)_4dik$ but in general the three lowest energy bands were about 10–20 cm^{-1} lower than the corresponding bands in $[Re(CO)_4Cl]_2$. The complexes of the type $Re(CO)_3dikL$ (L = py, Ph_3P) had CO spectra very similar to $Repy_2(CO)_3I$ although in this case the upper bands were ~30 cm^{-1}, and the second bands ~15 cm^{-1}, lower than the corresponding bands in $Repy_2(CO)_3I$. The complexes of the type $Re(CO)_2dik(PPh_3)_2$ showed two strong bands in the CO region, which was consistent with a *cis* arrangement of the carbonyl ligands.

We have analyzed the carbonyl region of the spectra of the above compounds by the method of Cotton and Kraihanzel (20–22) and the results are summarized in Table 4. Comparison of the force constants for the $(Re(CO)_3dik)_2$ complexes with the results listed by Cotton (22) for *cis*-$L_3M(CO)_3$ showed that the β-ketoenolate ligand was about equivalent to phosphites or chlorophosphines; in other words it is a fair π-acceptor. The highest stretch force constants and lowest K_i (postulated by Cotton to indicate a ligand with good π-acceptor properties) were observed for the hexafluoroacetylacetone complex, which is what would be expected, since the electronegative fluorine atoms should tend to pull electron density off the metal atom. These results show the difference between the β-keto-

[3]Only the sections of the spectra discussed herein are published in Table 3. The full set of spectral data (Table 3*a*) is available at a nominal charge from the Depository of Unpublished Data, CISTI, National Research Council of Canada, Ottawa, Canada K1A 0S2.

TABLE 3. Infrared spectra of rhenium β-diketoenolate carbonyl complexes

Compound	Frequencies (cm^{-1})							
$Re_2(CO)_6(acac)_2$	2025vs	1920vs	1885vs		1580mw	1560m	1520s	
$Re_2(CO)_6(dbm)_2$	2025vs	1920vs	1885vs		1585m	1565s	1500s	
$Re_2(CO)_6(tfba)_2$	2035m	1915vs	1885vs		1600vs	1570vs		
$Re_2(CO)_6(ttfa)_2$	2035s	1915vs	1890vs		1585vs	1530w	1510w	
$Re_2(CO)_6(tfac)_2$	2030s	1940vs	1885vs		1610s	1590sh,m	1520m	
$Re_2(CO)_6(hfac)_2$	2030vs	1955vs	1935vs		1600w	1530w		
$Re_2(CO)_6(bamH)_2Cl_2$	2030s, 2025s	1940 m	1910s, 1895s		1590m	1560w	1510m	
$Re(CO)_4(acac)$	2105w	2005s	1990m	1945s	1590mw	1520mw		
$Re(CO)_4(dbm)$	2110m	2015s	1995m, 1990m	1950ms, 1945ms	1590w	1530ms		
$Re(CO)_4(tfba)$	2110w	2005s	1990m	1945s	1590mw	1560mw	1525w	
$Re(CO)_4(ttfa)$	2110w	2010s	1990m	1920s	1600m	1575s	1530w	
$Re(CO)_4(tfac)$	2110w	2015s	1995m	1955s	1605m	1530w		
$Re(CO)_4(hfac)$	2120m	2048s	2010s	1940s	1630m	1605m	1555w	1525w
$Re(CO)_3(dbm)py$	2010s	1920s	1890s		1580w	1505m		
$Re(CO)_3(dbm)PPh_3$	2015s	1915s	1890s		1580w	1515ms		
$Re(CO)_2(dbm)(PPh_3)_2$	1915s	1830s			1590mw	1540m	1515m	
$Re(CO)_2(tfac)(PPh_3)_2$	1920s	1840s			1610m	1505w		

TABLE 4. Calculation of Cotton–Kraihanzel force constants and the assignment of bands in the carbonyl region for β-diketone–carbonyl complexes of rhenium(I)

Compound	K_i	K_1	K_2	$A_1^{(2)}$	$A_1^{(1)}$	B
$Re_2(CO)_6(acac)_2$	0.62	14.78	15.51	2025	1885	1920
$Re_2(CO)_6(dbm)_2$	0.62	14.78	15.51	2025	1885	1920
$Re_2(CO)_6(tfba)_2$	0.70	14.88	15.50	2035	1885	1914
$Re_2(CO)_6(ttfa)_2$	0.56	14.67	15.76	2030	1885	1940
$Re_2(CO)_6(hfac)_2$	0.44	15.44	15.87	2030	1935	1955
$Re(CO)_3(dbm)py$	0.53	14.79	15.42	2010	1890	1920
$Re(CO)_3(dbm)PPh_3$	0.58	14.86	15.38	2015	1890	1914

Compound	K_i	K_1	A_1	B_1
$Re(CO)_2$ $dbm(PPh_3)_2$	0.64	14.17	1914	1830
$Re(CO)_2$ $tfac(PPh_3)_2$	0.61	14.28	1920	1840

Compound	K_i	K_1	K_2	$A_1^{(2)}$	$A_1^{(1)}$	B_1	B_2
$Re(CO)_4(acac)$	0.34	15.78	16.92	2103	1981	2005	1955
$Re(CO)_4(dbm)$	0.33	15.80	17.06	2109	1984	2015	1957
$Re(CO)_4(tfba)$	0.36	15.78	16.95	2109	1981	2005	1954
$Re(CO)_4(ttfa)$	0.33	15.58	17.00	2107	1971	2009	1942
$Re(CO)_4(tfac)$	0.33	15.89	17.05	2109	1989	2015	1963
$Re(CO)_4(hfac)$	0.26	15.84	17.46	2118	1964	2048	1988

enolate ion and other oxygen ligands which have essentially no π-acceptor ability (22).

The only acceptable assignment of bands for the $Re(CO)_4dik$ complexes was similar to that made by Cotton for the spectra of $[Mn(CO)_4X]_2$ complexes, rather than that proposed for *cis*-$L_2M(CO)_4$ (22). Comparison of the derived force constants with those for *cis*-$L_2M(CO)_4$ again showed that the β-ketoenolate ligand was equivalent to phosphite ligands or chlorophosphines. Again the hexafluoroacetylacetone ligand showed the smallest value of K_i, and K_2 was significantly larger than other values although K_1 was comparable. In this case however the agreement between the calculated and observed wave numbers of the bands most sensitive to K_1 was not very good.

The mass spectra of selected compounds are

Can. J. Chem. Downloaded from www.nrcresearchpress.com by 210.87.254.42 on 09/05/12
For personal use only.

TABLE 5. Mass spectra of $Re_2(CO)_6dik_2$ complexes*

	acac†		tfac‡		dbm§	
	Mass	Abundance	Mass	Abundance	Mass	Abundance
$Re_2(CO)_6(dik)_2^+$	738	3.2	846	16	—	—
$(Re_2(CO)_6(dik)_2—F)^+$	—	—	877	0.2	—	—
$(Re_2(CO)_5(dik)_2—F)^+$	—	—	799	1	—	—
$Re_2(CO)_4(dik)_2^+$	682	2.5	790	8	—	—
$Re_2(CO)_3(dik)_2^+$	654	2.3	762	7	—	—
$Re_2(CO)_2(dik)_2^+$	626	0.2	734	0.2	—	—
$Re_2(CO)(dik)_2^+$	598	0.5	706	0.4	—	—
$Re_2(dik)_2^+$	570	1.4	678	0.4	818	0.3
$Re(dik)_2^+$	385	0.3	—	—	—	—
$Re(CO)_3dik^+$	370	69.7	424	100	494	90.3
$Re(CO)_2dik^+$	342	34.6	396	54	466	5
$Re(CO)dik^+$	314	5.5	368	2	438	29
$Re(CO)(OC.CH_3CHCO)^+$	299	0.7	—	—	—	—
$Re(dikH)^+$	287	14.2	—	—	—	—
$Re\ dik^+$	286	100	340	70	410	34
ReO^+	203	7.0	203	9	—	—
Re^+	187	7.6	187	6	—	—
dikH	100	6.4	—	—	224	37
dik	—	—	—	—	223	36
CH_3CO^+	43	23.9	43	100	—	—
CO^+	28	6.7	28	38	—	—

*For the mass spectra the *m/e* listed refers to the most abundant peak in the isotopic distributions, which were correct for all peaks.
†acac: $ReO_2C_4H_4^+$, 271, 3.5%; ReO_2C_4H, 268, 1.6%; $^{187}ReO_2C_2CH_3^+$, 258, 22.1%; $^{185}ReO_2CH_3^+ + ReO_2C_3H^+$, 256, 35.8%; $ReO_2C_3H^+$, 254, 21.2%; $^{187}ReO_2C_2^+ + ReOC_3H_4^+$, 243, 10.3%; $^{185}ReO_2C_2^+ + ReOC_3H_2$, 241, 21.2%; ReO_2C^+, 231, 5.4%, $ReOC_2H_3^+$, 231, 5.4%; $O_2C_4H_5^+$, 85, 7.6%, HC_2O^+, 39, 4.6%.
‡tfac: $(Retfac—HF)^+$, 320, 8%; $(Retfac—2HF)^+$, 292, 8%; $ReOF_2^+$, 241, 19%, ReO_2F^+, 236, 8%; CF_3^+, 69, 12%; CF_2^+, 50, 2%; HF^+, 20, 3%.
§dbm: $^{187}ReOC_2HPh_2^+$, 382, 45%; $^{185}ReOC_2HPh_2^+ + {}^{187}ReO_2C_2PhC_6H_4^+$, 380, 84%; $^{185}ReO_2C_2PhC_6H_4^+ + ReO_2PhC_8H_2^+$, 378, 52% $Ph_2C_3H_2O^+$, 208, 7%; $Ph_2C_3HO^+$, 207, 7%; $Ph_2C_3H_2^+$, 192, 14%; $Ph_2C_3H^+$, 191, 6%.

shown in Tables 5 and 6. The main decomposition pathway of the $Re_2(CO)_6dik_2$ compounds appears to be the splitting of the dimer to give the five coordinate $Re(CO)_3dik^+$ fragment. Subsequent loss of carbonyl groups gave fragments of the type $Re(CO)_ndik^+$ with the most stable fragment having $n = 0$. For the more volatile complexes dimeric fragments of the type $Re_2(CO)_mdik_2^+$ were observed, corresponding to the loss of carbonyl groups, but for the dibenzoylmethane complex the highest peak observed in this series was when $m = 0$. Only for the acetylacetone complex was there any sign of fragmentation in which both diketone groups remain on one metal atom ($Redik_2^+$).

The mass spectra of complexes of the type $Re(CO)_3dikL$ showed some contrast depending on the type of ligand. When L was triphenylphosphine the fragmentation pattern could be explained entirely by the loss of CO groups in the series $Re(CO)_ndikL^+$, with $n = 0$ being the most stable fragment. When L is pyridine, however, two series were obtained. The series, $Re(CO)_ndik^+$, which involved loss of pyridine and CO groups had about four times the intensity of the $Re(CO)_ndikpy^+$ series which involved loss of CO groups only. Thus pyridine was more readily lost than carbon monoxide.

The spectrum of $Re(CO)_4hfac$, the only diketone complex of this stoichiometry which could be volatilized without decomposition to the dimer, was relatively complex. A comparison of the peaks of stoichiometry $Re(CO)_ndik^+$ for $Re_2(CO)_6tfac$ and $Re(CO)_4hfac$, showed similar intensities, suggesting the ease with which carbonyl groups were lost was similar. The spectrum of $Re(CO)_4hfac$ was much richer in fragments which involved decomposition of the diketone ligand. A comparison with the spectrum of $Re(hfac)_3$ (1) showed considerable differences in intensity for corresponding peaks. Although most of the peaks observed for $Re(CO)_4hfac$ can be explained in terms of the decomposition pathway

Can. J. Chem. Downloaded from www.nrcresearchpress.com by 210.87.254.42 on 09/05/12
For personal use only.

TABLE 6

(*a*) Mass spectra of reaction products of $Re_2(CO)_6(dik)_2$ with donor ligands

Compound ion	$Re(CO)_2dbm(P(C_6H_5)_3)_2$		$Re(CO)_2(tfac)(P(C_6H_5)_2)$		$Re(CO)_3(dbm)py$	
	m/e	Intensity	*m/e*	Intensity	*m/e*	Intensity
$Re(CO)_3dikL^+$	756	8	686	1	573	29
$Re(CO)_3dik^+$	—	—	—	—	494	100
$Re(CO)_2dikL^+$	728	31	658	37	545	19
$Re(CO)_2dik^+$	—	—	—	—	466	78
$Re(CO)dik^+$	—	—	—	—	438	34
$RedikL^+$	672	100	602	100	489	28
$Redik^+$	—	—	—	—	410	39

(*b*) Mass spectrum of $Re(CO)_4$ hfac

Ion	*m/e*	Intensity	Ion	*m/e*	Intensity	Ion	*m/e*	Intensity
$Rehfac(CO)_4^+$	506	33	$ReC_3F_3OH^+$	297	16	ReO_2F^+	238	5
$(Rehfac(CO)_4—F)^+$	487	2	$ReC_3F_3O_2$	293	3	$ReCOF^+$	234	7
$Rehfac(CO)_3^+$	478	65	$ReC_3F_2O_3^+$	290	6	$ReCO_2^+$	231	14
$(Rehfac(CO)_3—F)^+$	459	11	$ReC_2O_4^+$	275	8	ReC_2OH^+	228	7
$Rehfac(CO)_2$	450	50	$ReC_3O_3^+$	271	3	ReC_2O^+	227	3
$Rehfac(CO)^+$	422	5	$ReCF_2O_2^+$	269	20	ReF_2^+	225	10
$Rehfac^+$	394	100	$ReC_2FO_2^+$	262	6	$ReOF^+$	222	9
$(Rehfac—CH)^+$	381	3	ReC_3FOH^+	259	5	ReO_2^+	219	14
$(Rehfac—CO)^+$	366	3	$ReC_3O_2H^+$	256	3	$ReCO^+$	215	5
$(Rehfac—C_2HO)^+$	353	3	$ReOF_3^+$	250	10	ReC_2H^+	212	3
$(Rehfac—CHOF)^+$	346	3	$ReO_2F_2^+$	247	17	ReF^+	206	6
$(Rehfac—CF_2)^+$	344	11	ReF_3^+	244	5	ReO^+	203	14
$(Rehfac—CF_3)^+$	325	3	$ReOHF_2^+$	242	3	$ReCH^+$	200	15
$ReF_2C_2OH^+$	316	42	ReO_2HF^+	239	5	Re^+	187	16

we have postulated for $Re(hfac)_3$, clearly the factors influencing the distribution of products were quite different.

We thank the National Research Council of Canada for financial support of this work.

1. W. D. COURRIER, W. FORSTER, C. J. L. LOCK, and G. TURNER. Can. J. Chem. **50**, 8 (1972).
2. R. COLTON, R. LEVITUS, and G. WILKINSON. Nature, **186**, 233 (1960).
3. R. COLTON, R. LEVITUS, and G. WILKINSON. J. Chem. Soc. 4121 (1960).
4. T. G. DUNNE and F. A. COTTON. Inorg. Chem. **2**, 263 (1963).
5. M. L. LARSON and F. N. MOORE. Inorg. Chem. **1**, 856 (1962).
6. M. KILNER and A. WOJCICKI. Inorg. Chem. **4**, 591 (1964).
7. W. D. COURRIER, A. GUEST, C. J. L. LOCK, and R. H. TOMLINSON. Can. J. Chem. **46**, 2965 (1968).
8. P. W. FRAIS, A. GUEST, and C. J. L. LOCK. Can. J. Chem. **47**, 1069 (1969).
9. P. W. SELWOOD. Magnetochemistry. Interscience Publishers Inc., New York. 1956. pp. 78, 92–95.
10. G. FOEX, C-J. GORTER, and L. J. SMITS. Constantes selectionées: diamagnétisme et paramagnétisme, relaxation paramagnétique. Masson et Cie, Paris. 1957.
11. W. HIEBER and F. STANNER. Chem. Ber. **103**, 2836 (1970).
12. J. C. BARRICK, M. C. FREDETTE, and C. J. L. LOCK. Can. J. Chem. **51**, 317 (1973).
13. M. C. FREDETTE and C. J. L. LOCK. Can. J. Chem. **51**, 1116 (1973).
14. E. W. ABEL, G. B. HARGREAVES, and G. WILKINSON. J. Chem. Soc. 3149 (1958).
15. F. A. COTTON and G. WILKINSON. Advanced inorganic chemistry. 3rd ed. Wiley-Interscience, New York. 1972. p. 708.
16. K. NAKAMOTO, Y. MORIMOTO, and A. E. MARTELL. J. Phys. Chem. **66**, 346 (1962).
17. K. NAKAMOTO, P. J. MCCARTHY, A. RUBY, and A. E. MARTELL. J. Am. Chem. Soc. **83**, 1066 (1961).
18. K. NAKAMOTO, P. J. MCCARTHY, and A. E. MARTELL. J. Am. Chem. Soc. **83**, 1273 (1961).
19. K. NAKAMOTO, Y. MORIMOTO, and A. E. MARTELL. J. Am. Chem. Soc. **83**, 4533 (1961).
20. F. A. COTTON and C. S. KRAIHANZEL. J. Am. Chem. Soc. **84**, 4432 (1962).
21. C. S. KRAIHANZEL and F. A. COTTON. Inorg. Chem. **2**, 533 (1963).
22. F. A. COTTON. Inorg. Chem. **3**, 702 (1964).

Can. J. Chem. Downloaded from www.nrcresearchpress.com by 210.87.254.42 on 09/05/12
For personal use only.

Studies on Hydrogen–Oxygen Systems in the Electrical Discharge. VII. Deuterium Isotope Effects in the Chemistry of the Hydrogen Polyoxides

JOSÉ L. ARNAU[1] AND PAUL A. GIGUÈRE

Département de Chimie, Université Laval, Québec, Québec G1K 7P4

Received February 24, 1975

JOSÉ L. ARNAU and PAUL A. GIGUÈRE. Can. J. Chem. **53**, 2490 (1975).

The kinetics of oxygen evolution on warming the trapped products (at −196 °C) from water or hydrogen peroxide vapor dissociated in a glow discharge were studied by the manometric method. Under closely controlled conditions it was possible to distinguish clearly the decomposition of the two intermediates, H_2O_3 and H_2O_4. The latter begins to decompose measurably following crystallization of the glassy solid at about −115°; the trioxide decomposes readily between −50 and −35°. Typically, the yields of H_2O_3 from dissociated water vapor were of the order of 3 to 5 mol%; those of H_2O_4, only about one-tenth as much. Varying the distance between the microwave discharge and the cold trap was found to affect differently the yields of the various products. Those of water and peroxide showed a simple, direct correlation; the minor constituents H_2O_3 and H_2O_4 followed entirely different patterns. Only a small fraction of the peroxide is formed via the H_2O_4 intermediate in these systems. Less water, and more of the higher oxides, were obtained from dissociated hydrogen peroxide than from water vapor.

The deuterated systems showed some unusual isotope effects. The yields of D_2O_3 were always higher (up to twice and even more) than those of H_2O_3 under similar conditions. The other products showed little or no such effect, except for occluded oxygen and ozone which decreased by about half. Finally, the deuterium polyoxides decompose at slightly higher temperatures (10 to 15°) than their hydrogen analogs. Mechanisms are proposed for the formation and decomposition of the polyoxides.

JOSÉ L. ARNAU et PAUL A. GIGUÈRE. Can. J. Chem. **53**, 2490 (1975).

On a étudié le dégagement d'oxygène au réchauffement des produits piégés (à −196 °C) de la vapeur d'eau ou de peroxyde d'hydrogène dissociée dans une décharge électrique. On a pu ainsi distinguer nettement entre les deux intermédiaires métastables, H_2O_3 et H_2O_4. La décomposition de ce dernier commence avec la cristallisation du solide vitreux vers −115 °C; vient ensuite celle du trioxyde entre −50 et −35 °C. Les rendements en H_2O_3 à partir de la vapeur d'eau dissociée sont de l'ordre de 3 à 5% (mol), et ceux en H_2O_4, environ dix fois moindres. Par ailleurs, les rendements de tous les produits piégés varient différemment selon la distance entre la décharge microonde et le piège froid. Ainsi, le peroxyde d'hydrogène croît d'abord jusqu'à un maximum, puis décroît régulièrement; pour l'eau, c'est l'inverse. Les constituants mineurs, H_2O_3 et H_2O_4, se comportent tout autrement. On en conclut qu'une très faible fraction seulement du peroxyde formé dans ces systèmes provient du tétroxyde. Le peroxyde d'hydrogène dissocié donne moins d'eau et plus de polyoxydes que la vapeur d'eau.

Les systèmes deutériés présentent des effets isotopiques remarquables. Ainsi les rendements en D_2O_3 sont toujours plus forts (jusqu'à deux fois et même davantage) que ceux en H_2O_3 dans les mêmes conditions. Les autres produits ne montrent pas ou peu d'effet semblable, sauf l'oxygène et l'ozone occlus qui sont à moitié moins abondants. Les polyoxydes de deutérium se décomposent à des températures un peu plus élevées (de 10 à 15 °C) que ceux d'hydrogène. On propose des mécanismes pour la formation et la décomposition des polyoxydes.

Introduction

In contrast with the thermal reaction between hydrogen and oxygen the reaction mechanism in electrically dissociated water vapor is not very well understood. Our knowledge of such fundamental questions as the composition of the dissociated vapor, its evolution downstream, and the surface recombination of atoms and radicals, is rather deductive and sketchy. One valid approach to that problem is the study of the products formed on quick freezing at low enough temperature (liquid N_2). A variety of physicochemical methods have been applied to that effect, particularly over the last two decades. For an exhaustive review up to 1968, *cf.* ref. 1. Following the spectroscopic identification of the polyoxides, H_2O_3 and H_2O_4, as metastable intermediates in these systems (2–4), it seemed appropriate to reinterpret and supplement the

[1]Postdoctorate Fellow, 1972–1974. Present address: Procter & Gamble Research Laboratory, Brussels, Belgium.

Can. J. Chem. Downloaded from www.nrcresearchpress.com by 210.87.254.42 on 09/05/12
For personal use only.

existing data. Unexpectedly, this study has brought forth a remarkable deuterium isotope effect in the formation of the trioxide. It is now clear why early attempts to detect the polyoxides by infrared spectroscopy remained fruitless until deuterated systems were investigated.

Experimental

The discharge-flow system was essentially the same as before (5), except for a larger capacity vacuum system featuring a three-stage mercury diffusion pump (Leybold) with 45 l s^{-1} maximum capacity around 0.1 Torr (6). A large, spherical-shape, liquid nitrogen trap prevented back-streaming of mercury vapor. The sample of distilled water or peroxide was held in a 20 ml glass bulb fitted with a tiny O-ring joint for precise weighing. Its temperature was kept constant, *viz.* near 0 °C for water, and at room temperature for the peroxide (99% H_2O_2, ~95% D_2O_2). A Teflon-plug stopcock (Quickfit, Rotaflo) was used to control the rate of vapor flow. The pressure in the discharge tube was kept at about 0.2 Torr, which, from previous workers' (7) and our own experience, is the most suitable for a microwave discharge. It was monitored near the vapor inlet point by means of a Barocell Electronic Manometer, type 1033 (Datametrics Inc.), and a pressure sensor with three full-range scales: 1, 3, and 10 Torr. This instrument gave continuous readings, unaffected by the glow discharge nearby. It also served to follow the oxygen evolution from the condensed products on warming.

The discharge tube of Pyrex glass, 12 mm o.d., was sealed to the inlet stopcock, and connected through a taper ground joint to the cold trap. The latter, 12 cm long and 4 cm o.d. of the conventional concentric tube type, was made of thin-wall glass tubing for more precise weighing of the residue (to a few percent). The dissociated vapor stream entered through the central tube to give a uniform glassy deposit at the bottom of the trap. This arrangement was found to be preferable for a good separation of the various decomposition steps. Furthermore, it made possible a faster warming rate, (about 3 deg min^{-1}) than in previous studies (8, 9). In the reverse arrangement, condensation on the outer wall of the trap led to fractionation of the products, and an irregular deposit, even with a constant level device for liquid nitrogen. One disadvantage was that the distance from the discharge zone to the cold surface could not be reduced below a certain minimum, *viz.* 35 cm.

A typical run lasted 1 h, during which some 20 to 30 mmol of water (or half as much of peroxide) were dissociated in a microwave discharge (10) of 100 W. To minimize the effect of surface disintegration of the discharge tube, or "sputtering", a phenomenon previously described (5, 11), the discharge was always run blank for about 1 h before cooling the small trap with liquid nitrogen. Since the glassy deposit was only 0.1 mm thick on the average, the various reactions taking place therein did not affect noticeably the rate of warming. The temperature during the warming process was followed by means of a tiny copper–constantan thermocouple cemented to the bottom of the glass trap, and connected to a strip-chart recorder. The peroxide concentration in the residue was determined, to within 0.2%, from the refractive index.

Results

One major difficulty with these systems is the poor reproducibility of the data (1), due mostly to the important role of surface reactions. Although particular attention was paid this time to all possible variables, still the above mentioned "sputtering" effect, due to bombardment by the highly excited hydrogen atoms, caused some slight drift of the results for successive runs. With a different discharge tube, the results varied somewhat, but they always showed the same general trends.

Kinetics Curves

The oxygen evolution curves in Fig. 1 have been normalized to the same amount of input material, *viz.* 30 mmol of O_2 per hour, for comparison purposes. In the hydrogen systems, the two main steps reported by previous workers (9, 11) were always clearly distinguishable. A novel feature was the small maximum around −100°, following crystallization of the glassy deposit (12). Although always present, this minor feature showed poor reproducibility. In particular, it seemed very sensitive to surface conditions in the discharge tube. In spite of this, its relative intensity appeared on the average, to be at least twice as large in dissociated peroxide as in water vapor, and likewise in hydrogen as in deuterium systems. On the whole, these are the same characteristics as we observed before for the Raman bands of occluded ozone and molecular oxygen (13). Accordingly, the first minute evolution of gas is ascribed to outgassing of these two

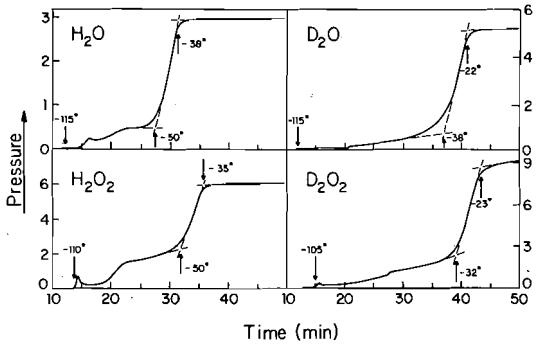

FIG. 1. Kinetics of oxygen evolution on warming the condensed products from various dissociated systems. Pressures in the same arbitrary unit throughout. (Note the different ordinate scale in each case.)

Can. J. Chem. Downloaded from www.nrcresearchpress.com by 210.87.254.42 on 09/05/12
For personal use only.

TABLE 1. Typical composition of the products condensed from various dissociated systems

System	Product	Mol%	System	Product	Mol%
H_2O	H_2O	52	D_2O	D_2O	47
	H_2O_2	42		D_2O_2	43
	H_2O_3	5		D_2O_3	8
	H_2O_4	~0.6		D_2O_4	~0.6
	$O_2 + O_3$	~0.4		$O_2 + O_3$	~0.2
	O_2 (total)*	105		O_2 (total)*	110
	H_2 (total)*	66		D_2 (total)*	70
H_2O_2	H_2O	46	D_2O_2	D_2O	41
	H_2O_2	40		D_2O_2	40
	H_2O_3	9		D_2O_3	16
	H_2O_4	~3		D_2O_4	~2.5
	$O_2 + O_3$	~1.5		$O_2 + O_3$	~0.5
	O_2 (total)*	82		O_2 (total)*	83
	H_2 (total)*	98		D_2 (total)*	97

*Percent of the O_2 and H_2 (or D_2) input accounted for in the condensed products.

species. Incidentally, ozone had previously been detected by smell in the gas given off by the condensed products of dissociated water vapor (11). The slight drop following the first pressure surge must be due to adsorption on the large (~0.15 m^2) surface of the gas measuring system, usually evacuated to 10^{-4} Torr prior to warming up. The amounts involved correspond approximately to a monolayer of adsorbed oxygen, and the time interval is of the right magnitude.

Decomposition of the Polyoxides

The two main steps in the oxygen evolution curves (Fig. 1) can now be assigned unambiguously to the decomposition of the two intermediates; first H_2O_4, then H_2O_3. This interpretation, based mainly on our spectroscopic data (2–4), is also in accordance with the predictions of thermochemistry as explained in the discussion. Of the various other hypotheses put forward over the years (1), the one closest to the truth suggested that only one species was involved, namely H_2O_4, which decomposed at different rates in the solid and the liquid phase (9, 14). It is true that the transition between the two steps, at least in the hydrogen systems, occurs in the temperature range of the two eutectics of the H_2O–H_2O_2 binary system, *viz.* −51 and −56 °C. However, this is a mere coincidence, with little or no bearing on the decomposition process, as confirmed by the following observations: (*a*) The condensed products begin to melt well below the eutectic temperatures, for instance between −73 (15) and −65° (16), depending on their composition; (*b*) The rate of gas evolution increases very little upon melting; (*c*) With the deuterated compounds (Fig. 1), the second step begins some 10 to 15° higher than with the hydrogen compounds; yet the eutectic temperatures in the two isotopic binary systems differ by less than 2° (17); (*d*) The ratio of the pressure increase in the two steps varies within wide limits depending on the composition of the systems, and other experimental conditions, as will be seen below.

Hereafter, the oxygen given off in the two main steps is taken as originating solely in the two reactions:

[1] $$H_2O_4 \rightarrow H_2O_2 + O_2$$

and

[2] $$H_2O_3 \rightarrow H_2O + O_2$$

Any possible contribution from some slight decomposition of the hydrogen peroxide present is considered negligible in view of its much greater chemical stability. In this investigation, as in the previous one (8, 9, 11, 18), the yields from the first main step were consistently smaller than those from step two, sometimes by as much as one order of magnitude (Table 1). As a result, and also because reaction 1 is obscured, at the start by the out-gassing process, and near the end by overlap of reaction 2, the present estimates for the tetroxide yields are less accurate than those for the trioxide.

Distance Effect

Previous studies of these systems (1, 5, 7, 19) have shown a marked dependence of the water

Can. J. Chem. Downloaded from www.nrcresearchpress.com by 210.87.254.42 on 09/05/12
For personal use only.

Can. J. Chem. Downloaded from www.nrcresearchpress.com by 210.87.254.42 on 09/05/12
For personal use only.

and hydrogen peroxide yields on the "time of flight" of the vapor through the discharge zone. That effect has often been described in terms of the "traversed volume". However, this is only one of the many parameters involved. For instance, the shape of that volume, the ratio of surface to volume, the rate of flow, etc. are also important in view of the dominant role of surface recombination of atoms. Under a steady flow rate, at constant pressure of the vapor, through a straight tube of constant section (to minimize turbulence in the laminar flow), as was the case here, the distance from the microwave cavity to the cold surface at the bottom of the trap is a meaningful parameter for discussing that effect.

As observed previously, upon increasing that distance the peroxide yield increased almost linearly up to a maximum for a certain "critical" distance, and then decreased. The water yield varied contrariwise (Fig. 2). Incidentally, the data in Fig. 2 (and also in Table 1) represent in fact the composition of the condensed products, *not* the yields based on the oxygen input. The latter are somewhat ambiguous because their total often exceeds 100% (by as much as 10 or 12%), due to the "sputtering" phenomenon already mentioned. In contrast, the minor constituents, H_2O_3 and H_2O_4, follow quite different patterns. With the trioxide, there is at first an increase in concentration with distance, but a maximum is reached sooner than for the peroxide. The same peculiarity had already been observed by Jones *et al.* (7) in the curve of evolved oxygen. As for the tetroxide, its low *yield* increases slightly with distance.

Isotope Effect

The first obvious consequence of deuterium substitution is a sharp increase in the trioxide yields, almost double at the minimum distance (Fig. 1). By comparison the tetroxide is hardly affected at all. As a consequence, the decomposition curve of D_2O_4 is largely overlapped by that of D_2O_3. Then, the latter is shifted some 10 to 15° higher than that of H_2O_3. Another isotope effect, minor but very real, is the reduction, by roughly one-half, in the amount of occluded O_2 and O_3. This had already been detected in the Raman spectra of the condensed products (13).

However, the most striking difference between the hydrogen and the deuterium systems of compounds is to be found in the distance effect.

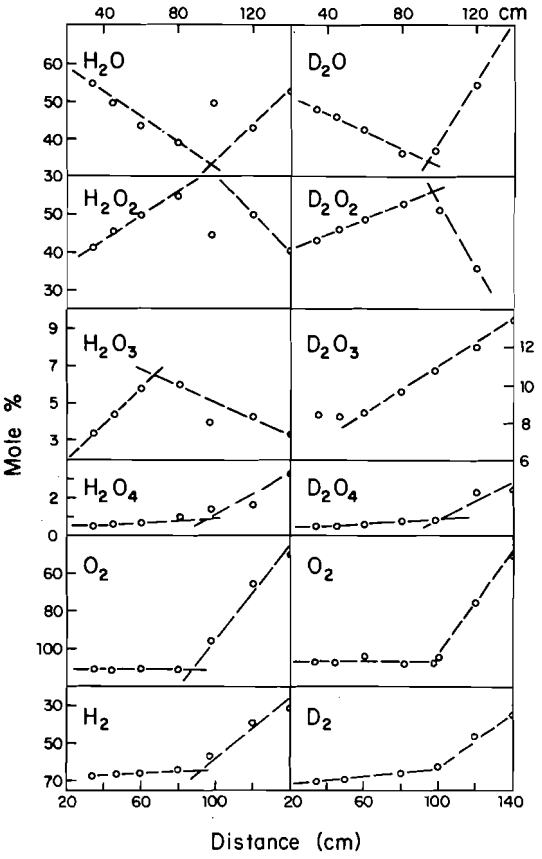

FIG. 2. Effect of distance from discharge to cold surface on the composition of condensed products from dissociated H_2O and D_2O vapor. (Note the different ordinate scales for H_2O_3 and D_2O_3.) The two bottom curves show the fraction of input oxygen and hydrogen found in the condensate.

Whereas the concentrations of water, peroxide, and tetroxide are little changed by deuteration, those of H_2O_3 and D_2O_3 show an entirely different behavior (Fig. 2). First, with H_2O_3 the linear concentration plot passes through the origin on extrapolation. On the contrary that of D_2O_3 showed a leveling off, or even an upward trend for distances shorter than 50 cm. It was not possible, unfortunately, with the present experimental arrangement to pursue this investigation to very short distances. Nevertheless, numerous runs with two different discharge tubes confirmed that peculiarity, even if the scatter of experimental points was wider than usual. Then, at longer distances, the *concentration* of D_2O_3 kept increasing linearly, without any sign of a maximum as with H_2O_3. Note however, that the

Can. J. Chem. Downloaded from www.nrcresearchpress.com by 210.87.254.42 on 09/05/12
For personal use only.

yield, based on the oxygen input, begins to decrease beyond the "critical" distance of 1 m. Because the loss of permanent gases increased rapidly beyond that point, the study of that effect became progressively more difficult and uncertain. Further investigation is planned under different experimental conditions: *i.e.* with faster flow, larger discharge tube, etc.

One last observation about the deuterium system: the "critical" distance seemed a little longer: *i.e.* 1 m *vs.* 0.9 m for the hydrogen system.

Dissociated Peroxide Vapor

Previous investigations (20–22) have shown that electrical discharges in hydrogen peroxide vapor yield less water and more evolved oxygen, *viz.* polyoxides, than discharges in water vapor. This is as expected for a more oxidizing atmosphere. Likewise, the preliminary results reported here (Fig. 1 and Table 1) show a substantial increase in the polyoxides, particularly the tetroxide, at the expense of water. Also noteworthy is an approximately threefold increase in occluded oxygen and ozone. As for the deuterium isotope effect, it follows the same pattern as in the case of dissociated H_2O and D_2O. The hydrogen recovery is nearly quantitative, while that of oxygen has dropped by nearly 20%. Whether or not the "sputtering" phenomenon is as important in the peroxide as in the water vapor discharge is not known, however. It would be instructive to study further this system as a function of pressure, distance, and power input, specially at low power level. Indeed, from mass spectrometric data (23) a mild discharge in hydrogen peroxide vapor is the best source of HO_2 radicals.

Discussion

The present results are significant mainly from four different viewpoints.

Composition of the Condensate

First, is the composition of the products from low temperature reactions in dissociated water vapor and related systems, particularly the minor constituents, H_2O_3 and H_2O_4. Previous estimates (1) had been deduced only from analysis of the final products. They rested perforce on some unconfirmed hypotheses and misleading criteria, such as the ratio of evolved oxygen to final hydrogen peroxide. The present data, although still of limited precision, are the first ones based on direct experimental evidence, namely molecular spectroscopy. Indeed, our infrared and Raman spectra (2–4) have revealed some six new O—O vibrational bands in the condensed products. From their temperature and composition behavior these bands were found to belong to two different molecular species; one, much less abundant, identified as the tetroxide, the other, as the trioxide. Furthermore, a warming up experiment (2) showed the infrared band of D_2O_4 at 820 cm^{-1} to disappear first in the crystallized solid, whereas that of D_2O_3 at 760 cm^{-1} had a half-life of some 5 h at about $-65°$, quite compatible with the present data.

From relative intensities of infrared bands we had previously estimated at 4 to 5 mol% the total concentration of the polyoxides (2). At that time, however, nothing was known of the importance of certain experimental parameters, nor of the unusual deuterium isotope effect. The failure of early attempts to detect the polyoxides by infrared absorption was then blamed on interference of the strong libration bands of water and hydrogen peroxide molecules in the glassy solid. It is now clear that this was not the only, and probably not the main obstacle, as illustrated by the spectra in Fig. 3. These two spectra,[2] taken under fairly similar conditions, show comparable intensity of the weak peroxide band at 880 cm^{-1}. In contrast, the characteristic trioxide band at 760 cm^{-1} (antisymmetric O—O stretch) is many times stronger in dissociated D_2O than that in H_2O. Indeed, in the latter it is barely visible on top of the strong, but not complete, absorption from the libration–torsion modes.

Reaction Mechanism

The second question on which this study throws some much needed light is the complex reaction mechanism in dissociated water vapor, particularly as regards the formation of hydrogen peroxide and the polyoxides. For instance, the Geib and Harteck (24) mechanism

$$[3] \qquad H + O_2 \xrightarrow[\text{wall}]{\text{cold}} HO_2$$

$$[4] \qquad H + HO_2 \xrightarrow[\text{wall}]{\text{cold}} H_2O_2$$

is further confirmed as the only important one

[2]K. Herman. Unpublished results.

Can. J. Chem. Downloaded from www.nrcresearchpress.com by 210.87.254.42 on 09/05/12
For personal use only.

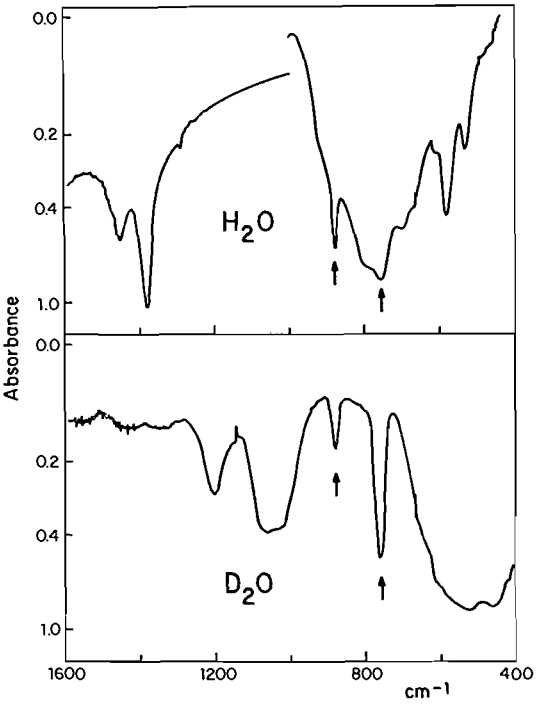

FIG. 3. Infrared absorptions of thin films of the glassy deposit condensed at liquid N_2 temperature from dissociated water and heavy water vapor in a microwave discharge.

in these systems from the distance effect. As pointed out before by Jones *et al.* (7), the peroxide increase at first can be explained by an increase in O_2 concentration from recombination (mostly on the walls) of O atoms, one of the main products of the discharge in water (25). Over that range, H atoms are in large excess, so much so that nearly one-third of the hydrogen input is lost by the system. The subsequent decrease in peroxide, beyond the "critical" distance, follows from a progressive drop in H atom concentration by recombination in the long discharge zone. Incidentally, the average linear velocity of the dissociated stream was of the order of 3 to 5 m s^{-1} in our system. Because of its high exothermicity the above mechanism becomes operative only at temperatures below $-120°$ (20). In addition to the heat of the gaseous reactions 3 and 4, respectively 46 and 89 kcal mol^{-1}, there is the heat of condensation of the products, some 18 kcal mol^{-1} (26) to be dissipated, plus any residual excitation energy of the reagent atoms and molecules.

Of the other conceivable mechanisms, the reaction first invoked by Rodebush and Wahl (27)

[5] $$OH + OH \rightarrow H_2O_2$$

makes no significant contribution here because of the low concentration of OH radicals in the dissociated stream, and the competition of other, very fast reactions (25, 28). Characteristically, no correlation whatsoever was found between OH concentration, from microwave absorption, and the amount of peroxide formed in a liquid nitrogen trap (29). As for the tetroxide mechanism proposed by Ohara (14)

[6] $$HO_2 + HO_2 \rightarrow H_2O_4,$$

our results (Table 1) indicate that it contributes only a small fraction of the *final* peroxide yield: less than 2% in dissociated water, and 6 to 8% in dissociated peroxide vapor.

Although it has little or no activation energy, reaction 6 is handicapped, requiring, as it does, simultaneous formation of two adjacent HO_2 radicals. On the other hand, the tetroxide cannot be a precursor of peroxide in the frozen products since, once stabilized, it does not decompose at a measurable rate at that low temperature, as may be gathered from our warming curves.

As for the other intermediate H_2O_3, it can only be formed by combination of OH and HO_2 radicals:

[7] $$HO_2 + OH \rightarrow H_2O_3$$

An HO_3 radical would be too unstable to exist (30), and there is no known mechanism for its formation. In dissociated water vapor the HO_2 radicals are formed at the cold surface only. In dissociated hydrogen peroxide, low concentrations of HO_2 have been detected by mass spectrometry (1), which may explain the higher yields of tetroxide in these systems (Table 1).

Lastly, regarding the occluded oxygen and ozone, the present results lend further support to our previous conclusion (13) as to the *in situ* origin of these species. Indeed, their yields show no significant increase beyond the "critical" distance; that is, when the concentration of O_2 in the dissociated vapor increases considerably. On the other hand, the deuterium isotope effect is also consistent with the proposed mechanism for oxygen atom production

[8] $$OH + OH \rightarrow H_2O + O$$

considering the rate ratio $k_H/k_D = 1.6$ found by Westenberg and Wilson (31) for that reaction.

Can. J. Chem. Downloaded from www.nrcresearchpress.com by 210.87.254.42 on 09/05/12
For personal use only.

Thermodynamic Stability

The third question to which the new results are also relevant is the chemical stability of the two intermediates, H_2O_3 and H_2O_4. From bond energy considerations Benson (30) had predicted that the latter, being endothermic, would be too unstable to exist; the trioxide might be formed at low temperature if suitable conditions were found. However, these conclusions apply to the free molecules. In condensed phase, hydrogen bond formation stabilizes both intermediates (26). Experimental confirmation of this was secured recently by the matrix isolation technique. The products of a discharge through heavy water vapor and argon trapped at 10 K showed weak infrared bands due to the polyoxides, but only at concentrations sufficient for formation of hydrogen bonded polymers (32). From the enthalpy and free energy relationships in the homologous series of the hydrogen oxides (26, 33) one might expect a greater difference between the decomposition temperature of the trioxide and the tetroxide. However, with heterogeneous reactions such as these, the kinetics do not always parallel the thermodynamics.

Preliminary measurements of the rate of decomposition of H_2O_3 at fixed temperatures between -55 and $-45°$ indicated an activation energy of the order of 15 kcal mol^{-1} in fair agreement with previous results (14, 18). From isothermal measurements at $-80°$ Jones *et al.* (18) have found a ratio of about 300 for the rates of the two oxygen evolution processes. This must be a minimum for the two corresponding decomposition reactions, because the first measured process comprised also any occluded O_2 and O_3. Again, these low activation energies bear no direct relationship to chemical stability. The latter is best considered in terms of bond dissociation energy, and by comparison with hydrogen peroxide.

Although the three molecules, H_2O_2, H_2O_3, and H_2O_4, feature the same type of O—O bond, as explained before (4), dissociation of the last two only, *viz.*

[9] $$H_2O_3 \rightarrow OH + HO_2 \rightarrow H_2O + O_2$$

and

[10] $$H_2O_4 \rightarrow 2HO_2 \rightarrow H_2O_2 + O_2$$

is accompanied by an important electron rearrangement, which makes easier a transfer of hydrogen between the two fragments. Indeed, the peroxide bond becomes a superoxide (three-electron) bond in HO_2, and the O—H bond of the latter is weakened considerably, as confirmed by spectroscopy, and the dissociation energies: $D_{HO-O} = 63$, and $D_{H-O_2} = 47$ kcal mol^{-1}, compared with $D_{HO-OH} = 50$, and $D_{H-O_2H} = 90$ kcal mol^{-1}. For an up-to-date review, *cf.* ref. 33, pp. 66, 84.

Isotope Effect

The fourth, and certainly most surprising result, is the large deuterium isotope effect in the trioxide formation. Although the present data are insufficient to arrive at a detailed explanation, a few generalizations are warranted. From the following observations, it seems that the OH radicals in the dissociated stream are responsible for this isotope effect. (*a*) Only hydrogen trioxide, and to a lesser extent, occluded oxygen and ozone, show a large deuterium isotope effect. Now, according to our proposed mechanism these species are formed from OH radicals, in contrast with hydrogen peroxide and tetroxide. (*b*) Spectroscopic studies (25, 28) have shown hydroxyls to be the only radicals present in electrically dissociated water vapor, their concentration fluctuating rapidly due to fast reactions downstream. No such investigation has been reported yet for OD radicals, but appreciable differences in the lifetime of the two isotopic species may be expected. Because these radicals are in highly excited states, population distribution among the vibrational levels will be different in OH and OD. In that connection, a spectroscopic study of the OD kinetics in these systems would certainly be useful.

As for the deuterium isotope effect in the decomposition of the two polyoxides, it must be ascribed to zero-point energy differences of the species involved. A similar effect has been detected in a few sketchy studies of deuterium peroxide kinetics (34).

Conclusions

The experimental technique used in this investigation may be regarded as an application of the "temperature jump" method. Its efficiency in freezing the system far from equilibrium is exemplified in the formation of some ozone from the strongly reducing atmosphere of dissociated water vapor.

The present results provide the first semi-quantitative data on the chemical stability of

the two polyoxides, H_2O_3 and H_2O_4. Isolation of these fragile species in measurable mounts is possible because of hydrogen bonding, which prevents diffusion of the free radicals formed at the cold surface.

The proposed reaction mechanism can account satisfactorily, if not uniquely, for the bulk of experimental observations, in particular for the variations of yields with "time of flight" in the dissociated vapor. The HO_2 radical, or hydrogen superoxide, appears as the ubiquitous intermediate in the formation and decomposition of the polyoxides as well as of hydrogen peroxide.

Finally, the remarkable isotope effect in the formation of D_2O_3 is no doubt the largest reported so far in any oxy–hydrogen system. It calls for further study, specially by spectroscopy.

The authors are grateful to the National Research Council of Canada for a continuing research grant.

1. M. VENUGOPALAN and R. A. JONES. Chemistry of dissociated water vapor and related systems, New York, Interscience Publishers. 1968.
2. P. A. GIGUÈRE and K. HERMAN. Can. J. Chem. **48**, 3473 (1970).
3. X. DEGLISE and P. A. GIGUÈRE. Can. J. Chem. **49**, 2242 (1971).
4. J. L. ARNAU and P. A. GIGUÈRE. J. Chem. Phys. **60**, 270 (1974).
5. P. E. BRUNET, X. DEGLISE, and P. A. GIGUÈRE. Can. J. Chem. **48**, 2042 (1970).
6. P. A. GIGUÈRE, E. A. SECCO, and R. S. EATON. Discuss. Faraday Soc. **14**, 104 (1953).
7. R. A. JONES, W. CHAN, and M. VENUGOPALAN. J. Phys. Chem. **73**, 3693 (1969).
8. R. A. JONES and C. A. WINKLER. Can. J. Chem. **29**, 1013 (1951).
9. I. I. SKOROKHODOV, L. I. NEKRASOV, N. I. KOBOZEV, and E. I. MAKAROVA. Russ. J. Phys. Chem. **35**, 444 (1961).
10. K. HERMAN and P. A. GIGUÈRE. Can. J. Chem. **46**, 2649 (1968).
11. N. HATA and P. A. GIGUÈRE. Can. J. Chem. **44**, 869 (1966).
12. J. A. GHORMLEY. J. Am. Chem. Soc. **79**, 1864 (1957).
13. J. L. ARNAU and P. A. GIGUÈRE. Can. J. Chem. **51**, 1525 (1973).
14. E. OHARA. J. Chem. Soc. Jap. **61**, 657 (1940).
15. J. A. GHORMLEY. J. Chem. Phys. **39**, 3539 (1963).
16. I. I. SKOROKHODOV, L. I. NEKRASOV, and N. I. KOBOZEV. Russ. J. Phys. Chem. **35**, 994 (1961).
17. P. A. GIGUÈRE and E. A. SECCO. Can. J. Chem. **32**, 550 (1954).
18. R. A. JONES, W. CHAN, and M. VENUGOPALAN. J. Chem. Phys. **51**, 1273 (1969).
19. S. S. BARTON, F. GROCH, S. E. LIPKIN, and D. BRITTAIN. J. Chem. Soc. A**689** (1968).
20. J. S. BATZOLD, C. LUNER, and C. A. WINKLER. Can. J. Chem. **31**, 264 (1953).
21. A. I. GORBANEV, A. B. TSENTSIPER, I. M. ZHITENEVA, and M. S. DANILOVA. Izv. Sib., Otd. Akad. Nauk SSSR, 43 (1958).
22. R. L. ALLMAND and F. S. STONE. Nature, **180**, 752 (1957).
23. S. N. FONER and R. L. HUDSON. Adv. Chem. Ser. **36**, 43 (1962).
24. K. H. GEIB and P. HARTECK. Ber. B**65**, 1551 (1932).
25. F. KAUFMAN. Adv. Chem. Ser. **80**, 29 (1969).
26. P. A. GIGUÈRE. Ann. N.Y. Acad. Sci. **34**, 334 (1972).
27. W. H. RODEBUSH and M. H. WAHL. J. Chem. Phys. **1**, 696 (1933).
28. F. P. DEL GRECO and F. KAUFMAN. Discuss. Faraday Soc. **33**, 128 (1962).
29. T. M. SANDERS, JR., A. L. SCHAWLOW, G. C. DOUSMANIS, and C. H. TOWNES. J. Chem. Phys. **22**, 245 (1954).
30. S. W. BENSON. J. Am. Chem. Soc. **86**, 3922 (1964).
31. A. A. WESTENBERG and W. E. WILSON. J. Chem. Phys. **45**, 338 (1966).
32. P. A. GIGUÈRE and T. K. K. SRINIVASAN. Chem. Phys. Lett. In press.
33. P. A. GIGUÈRE. Peroxyde d'hydrogène. Polyoxydes d'hydrogène. *In* Compléments au Nouveau traité de chimie minérale de P. Pascal, Vol. 4, Masson, Paris. 1975.
34. P. A. GIGUÈRE and O. MAASS. Can. J. Res. B**18**, 84 (1940).

Can. J. Chem. Downloaded from www.nrcresearchpress.com by 210.87.254.42 on 09/05/12
For personal use only.

Theory of the Spin Hamiltonian Parameters for Low Spin Cobalt(II) Complexes

B. R. McGARVEY
Department of Chemistry, University of Windsor, Windsor, Ontario N9B 3P4

Received March 11, 1975

B. R. McGARVEY. Can. J. Chem. **53**, 2498 (1975).

The theory for the spin Hamiltonian parameters of low spin cobalt(II), d^7, complexes has been developed to third order in perturbation theory for all reasonable ground states. Two extensions beyond previous treatments have been made: (*1*) the spin–orbit mixing of excited quartet states into the doublet ground state has been considered and (*2*) configuration interaction involving mixing of d_{z^2} and $d_{x^2-y^2}$ orbitals in lower symmetry has been included. In the case of axial complexes a more complete calculation has been made to assess the errors incurred in only going to third order in perturbation theory. The theory has been applied to porphyrin and phthalocyanine complexes and is shown to adequately account for the observed data on these complexes. The excited quartet states are much higher in energy than the ground state for the four coordinate porphyrin complexes but become much lower in energy when basic adducts are complexed along the z axis. Further there is mixing of the 4s orbital with the $3d_{z^2}$ orbital for the four coordinate complexes which is completely removed when basic adducts are complexed to the porphyrin system. Application of equations to lower symmetry complexes is considered and it is shown that is is difficult to make an unambiguous assignment of ground state on the basis of g and ^{59}Co hyperfine splitting values alone, although the relative values of g_y and g_z do seem to provide some clue as to the correct ground state.

B. R. McGARVEY. Can. J. Chem. **53**, 2498 (1975).

La théorie des paramètres hamiltoniens de spin pour les complexes d^7 du cobalt(II) à spin bas a été développée en théorie des perturbations du troisième ordre pour tous les états fondamentaux. Deux points ont été étudiés au-delà des traitements précédents: (*1*) on a considéré le mélange spin–orbite des états quadruplets excités en doublet de l'état fondamental et (*2*) l'interaction de configuration impliquant le mélange des orbitales d_{z^2} et $d_{x^2-y^2}$ dans une symétrie plus basse. Un calcul plus complexe a été fait dans le cas des complexes axiaux afin d'évaluer les erreurs qui résultent du passage au troisième ordre de la théorie des perturbations. Cette théorie a été appliquée aux complexes phorphyrines et phtalocyanines et elle rend bien compte des données observées avec ces complexes. Pour les complexes tétracoordonnées de la porphyrine on observe une énergie beaucoup plus élevée pour les états quadruplets excités que pour l'état fondamental. Cette énergie diminue quand des ligands basiques sont coordonnés le long de l'axe z. D'autre part, on observe le mélange des orbitales 4s et $3d_{z^2}$ du complexe tétracoordonné. Ce mélange disparait complètement quand des ligands basiques sont coordonnés au système porphyrine. L'application des équations à des complexes de symétrie plus basse a été considérée. Il n'est pas possible de faire une attribution inéquivoque de l'état fondamental en se servant seulement de g et des valeurs de la scission hyperfine du ^{59}Co, bien que les valeurs relatives de g_y et g_z semblent apporter des indices pour le choix de l'état fondamental correct. [Traduit par le journal]

Introduction

The low spin Co(II) complexes have excited considerable interest in the last few years due to the ability of some to reversibly absorb O_2. The complexes are planar four coordinate and mainly of the forms CoN_2O_2, CoN_4, or CoS_4. Many have the ability to bond to Lewis bases to form five coordinate species and it is this form that absorbs O_2.

Many e.s.r. studies have been done on these complexes and the results show a wide variation in g and A values. The phthalocyanines (1, 2) and porphyrins (3–8) which have a fourfold symmetry axis perpendicular to the plane have $g_\perp \sim 3$ and $g_\parallel$ less than 2.0 when uncomplexed. Both $A_\parallel$ and $A_\perp$ are large with $A_\parallel$ generally smaller than $A_\perp$. When complexed to nitrogen and phosphine bases, $g_\perp$ drops to 2.2–2.3 and $g_\parallel$ becomes greater than 2.0. $A_\parallel$ and $A_\perp$ decrease with the greatest change occurring for $A_\perp$. In addition, ^{14}N and ^{31}P hyperfine is often observed for the nitrogen or phosphorous atom of the complexing base.

Complexes with symmetry of D_{2h} or less always have one g value from 2.6 to 3.8 and the other two g values are near 2.0. No regular pattern is observed in the hyperfine A values. In the few single crystal studies done (9–13), the large g value is always found to be in the plane de-

Can. J. Chem. Downloaded from www.nrcresearchpress.com by 210.87.254.40 on 09/05/12
For personal use only.

Can. J. Chem. Downloaded from www.nrcresearchpress.com by 210.87.254.40 on 09/05/12
For personal use only.

fined by the coordinating ligands. This is also true for the two studies using frozen nematic solvents (14, 15). Many of the Schiff base complexes can become five coordinate by bonding to a Lewis base. In this case (14, 16–20) two g values are found in the range 2.3–2.5 and a third value is $\sim$2.0. For nitrogen Lewis bases the ^{14}N hyperfine is often observed as for the phthalocyanines and porphyrins. The assignment of spin Hamiltonian parameters to specific molecular axes is very uncertain in the case of Schiff base complexes because only one single crystal study (13) has been done and the two studies (14, 15) using frozen nematic solvents disagree as to which molecular axis is the alignment axis.

The assignment of ground states by e.s.r. has followed the method set out by Maki *et al.* (10) who derived equations for the spin Hamiltonian parameters expected for each possible ground state. The ground state is then determined as that which most closely predicts the experimental spin Hamiltonian parameters using reasonable values of $\langle r^{-3}\rangle_{av}$ and $(\lambda/\Delta E)$'s. $\langle r^{-3}\rangle_{av}$ is the average of r^{-3} for the d orbital and $(\lambda/\Delta E)_i$ is the ratio of spin–orbit coupling constant to the energy of excited doublet states which are coupled to the ground state by the spin–orbit interaction. All of the complexes studied are of the following type

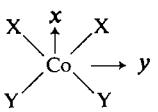

with X = Y in some instances. With one exception (9) the symmetry of the complexes requires that the principal axes x and y bisect the bond axes as shown above.

Using the above coordinate system the ground state of $(d_{x^2-y^2})^2(d_{xz})^2(d_{z^2})^2(d_{yz})$ has been reported for four cobalt complexes (10, 12, 13, 21). With one exception (13) this assignment must be considered doubtful, however, because there are errors in the equations reported for this ground state. The ground state $(d_{x^2-y^2})^2(d_{xz})^2(d_{yz})^2(d_{z^2})$ has been attributed to most other complexes (11, 14, 16, 17, 22–24). In the case of one type of CoN_4 complex, Engelhardt *et al.* (23) have proposed a $(d_{xz})^2(d_{yz})^2(d_{z^2})^2(d_{x^2-y^2})$ ground state while Urbach *et al.* (15) have proposed the more usual $(d_{x^2-y^2})^2(d_{xz})^2(d_{yz})^2(d_{z^2})$ ground state. In most instances the agreement between theory and experiment is less than satisfactory in the assignment of ground states and inconsistencies are often glossed over or ignored.

It is evident from the appearance of ^{14}N hyperfine when nitrogen bases are complexed to the porphyrins and phthalocyanines that the ground state must be $(d_{x^2-y^2})^2(d_{xz})^2(d_{yz})^2(d_{z^2})$ in these axially symmetric complexes. Walker (3) has, however, pointed out that present theories do not adequately account for the variation in hyperfine values observed when these compounds are complexed with various adducts. Present theories, also, do not account for the fact that $g_\parallel$ in these complexes becomes significantly greater than the free spin value when complexed to strong Lewis bases. Engelhardt and Green (22) and Busetto *et al.* (20) have done ligand field calculations for D_{4h} symmetry using an extended basis set and have shown that $g_\parallel$ can become greater than the free spin value for certain axial distortions. They fail to point out, however, that this could only occur when there is a significant mixing into the ground state of an excited quartet state. They also did not calculate hyperfine terms from their extended basis set.

For complexes with D_{2h} symmetry or lower no one has taken into account configuration interaction among states belonging to the same irreducible representations. Such interactions have been found to be necessary to account for **g** and **A** assymmetries observed in d^1 tetrahedral complexes (25–27) in which the ground state is predominantly d_{z^2}. Bentley *et al.* (9) did derive equations for the **g** tensor assuming a mixing of d_{z^2} and $d_{x^2-y^2}$ in C_{2v} symmetry but then assumed such mixing was negligible for the compound they were studying. Application of existing theories to the low symmetry complexes has resulted in values of $(\lambda/\Delta E)$ which required an unreasonably large difference in the energies of the d_{xz} and d_{yz} orbital to explain the large differences in g_x and g_y. Such large differences are difficult to explain, particularly when we realize that they are not found in Cu^{2+} when bound to the same ligands. It was considered likely when this work was initiated that much of the difference in g_x and g_y might result from configuration mixing rather than excessively large differences in the energy of d_{xz} and d_{yz} orbitals.

In this article the spin Hamiltonian parameters are derived for different possible ground states of strong field d^7 configurations considering the possible mixing of d_{z^2} and $d_{x^2-y^2}$ allowed by

lower symmetries. No one has previously recognized the possible importance of low lying quartet states and their related doublet states which can be coupled to the doublet ground state by the spin–orbit interaction. These states contribute to the g values only in third order or higher but contribute to the hyperfine terms in second order and hence can be as important as the excited doublet states normally included in previous calculations. These states have, therefore, been included in the following computations also.

Theory of Spin Hamiltonian

In the following discussion two ground state functions will be considered: $(ad_{x^2-y^2} - bd_{z^2})^2 (d_{xz})^2(d_{yz})^2(ad_{z^2} + bd_{x^2-y^2})$ and $(d_{x^2-y^2})^2(d_{z^2})^2(d_{xz})^2(d_{yz})$. Since $0 \leq a \leq 1$ in the first function it really represents the $(d_{x^2-y^2})^2(d_{xz})^2(d_{yz})^2(d_{z^2})$ and $(d_{z^2})^2(d_{xz})^2(d_{yz})^2(d_{x^2-y^2})$ states and all possible mixtures. The second function also represents the state $(d_{x^2-y^2})^2(d_{z^2})^2(d_{yz})^2(d_{xz})$ by a simple interchange of x and y axes. States in which one or more electrons occupy the d_{xy} orbital are not considered reasonable states for these complexes and have not been considered.

In deriving the following equations for the spin Hamiltonian parameters, the parametric approach has been used in which wave functions using only d orbitals are used and the effects of covalency appear indirectly in the altered values of the spin–orbit interaction parameter and $\langle r^{-3} \rangle_{av}$. This is the same approach used by Maki *et al.* (10). Previous studies have used the hole formalism but we shall use the wave functions themselves. This procedure is only slightly more difficult and makes it easier to assure that no important excited states are overlooked. It also results in all parameters involving the spin–orbit interaction having positive values instead of the negative values required by the hole formalism approach.

The perturbation method will be used in the calculations and where appropriate will be carried out to third order. It is possible to set up the calculations for higher orders but this becomes exceedingly complex, particularly since it may be necessary for some systems to consider up to five separate excited states to higher than second order.

$^2A_1$ *Ground State*

In designating the following states we will use the symmetry designation appropriate to C_{2v} symmetry. The ground state will be taken to be

$$[1] \qquad {}^2A_1{}^{\pm} = (d_{xz})^2(d_{yz})^2(ad_{x^2-y^2} - bd_{z^2})^2(ad^{\pm}{}_{z^2} + bd^{\pm}{}_{x^2-y^2})$$

where superscript $\pm$ refers to spin state of $\pm 1/2$. The function is taken to be a Slater's determinant and $a^2 + b^2 = 1$. This admixture of d_{z^2} and $d_{x^2-y^2}$ is allowed in C_{2v}, D_{2h}, and lower symmetries because they both belong to the same irreducible representation. The spin–orbit interaction is

$$[2] \qquad \mathcal{H}_{LS} = \sum_i \xi \boldsymbol{l}_i \cdot \boldsymbol{s}_i$$

where $\boldsymbol{l}_i$ = orbital angular momentum operator for ith electron, $\boldsymbol{s}_i$ is the spin operator for the ith electron, and ξ is the single electron spin–orbit constant (which is always positive). This interaction couples both quartet and doublet excited states with the ground state. The $l_z s_z$ term in $\mathcal{H}_{LS}$ couples the following excited states:

$$[3] \qquad {}^2A_2{}^{\pm} = (d_{xz})^2(d_{yz})^2(ad_{x^2-y^2} - bd_{z^2})^2(d_{xy}{}^{\pm})$$

$$[4] \qquad {}^4A_2\left(\pm\frac{3}{2}\right) = (d_{xz})^2(d_{yz})^2(ad^{\pm}{}_{x^2-y^2} - bd^{\pm}{}_{z^2})(ad^{\pm}{}_{z^2} + bd^{\pm}{}_{x^2-y^2})(d^{\pm}{}_{xy})$$

$$[5] \qquad {}^4A_2\left(\pm\frac{1}{2}\right) = \frac{1}{\sqrt{3}}(d_{xz})^2(d_{yz})^2\{(ad^{\pm}{}_{x^2-y^2} - bd^{\pm}{}_{z^2})(ad^{\pm}{}_{z^2} + bd^{\pm}{}_{x^2-y^2})(d^{\mp}{}_{xy}) + (ad^{\pm}{}_{x^2-y^2} - bd^{\pm}{}_{z^2})(ad^{\mp}{}_{z^2} + bd^{\mp}{}_{x^2-y^2})(d^{\pm}{}_{xy}) + (ad^{\mp}{}_{x^2-y^2} - bd^{\mp}{}_{z^2}) \times (ad^{\pm}{}_{z^2} + bd^{\pm}{}_{x^2-y^2})(d^{\pm}{}_{xy})\}$$

Can. J. Chem. Downloaded from www.nrcresearchpress.com by 210.87.254.40 on 09/05/12
For personal use only.

$$[6]\quad {}^2A_2{}^{\pm}(1,2) = (d_{xz})^2(d_{yz})^2\{d_{1,2}(ad^{\pm}_{x^2-y^2} - bd^{\pm}_{z^2})(ad^{\pm}_{z^2} + bd^{\pm}_{x^2-y^2})(d^{\mp}_{xy}) + e_{1,2}(ad^{\pm}_{x^2-y^2} - bd^{\pm}_{z^2})(ad^{\mp}_{z^2} + bd^{\mp}_{x^2-y^2})(d^{\pm}_{xy}) + f_{1,2}(ad^{\mp}_{x^2-y^2} - bd^{\mp}_{z^2})(ad^{\pm}_{z^2} + bd^{\pm}_{x^2-y^2})(d^{\pm}_{xy})\}$$

The ${}^4A_2$ and ${}^2A_2$ (1, 2) states have not previously been considered in calculations on d^7 systems. The coefficients d_i, e_i, and f_i are determined by repulsive energy terms. All we know about them is that their sum must be zero. Further on in this article we will show that to a good approximation we will not need to know their exact values.

The x and y portions of $\mathcal{H}_{LS}$ causes the ${}^2A_1$ state to couple with the following excited states:

$$[7]\quad {}^2B_1{}^{\pm} = (d_{yz})^2(d_{x^2-y^2})^2(d_{z^2})^2(d^{\pm}_{xz})$$

$$[8]\quad {}^2B_2{}^{\pm} = (d_{xz})^2(d_{x^2-y^2})^2(d_{z^2})^2(d^{\pm}_{yz})$$

$$[9]\quad {}^4B_1\left(\pm\frac{3}{2}\right) = (d_{xz})^2(ad_{x^2-y^2} - bd_{z^2})^2(d^{\pm}_{yz})(ad^{\pm}_{z^2} + bd^{\pm}_{x^2-y^2})(d^{\pm}_{xy})$$

$$[10]\quad {}^4B_1\left(\pm\frac{1}{2}\right) = \frac{1}{\sqrt{3}}(d_{xz})^2(ad_{x^2-y^2} - bd_{z^2})^2\{(d^{\pm}_{yz})(ad^{\pm}_{z^2} + bd^{\pm}_{x^2-y^2})(d^{\mp}_{xy}) + (d^{\pm}_{yz})(ad^{\mp}_{z^2} + bd^{\mp}_{x^2-y^2})(d^{\pm}_{xy}) + (d^{\mp}_{yz})(ad^{\pm}_{z^2} + bd^{\pm}_{x^2-y^2})(d^{\pm}_{xy})\}$$

$$[11]\quad {}^4B_2(M_s) = \text{same as } {}^4B_1(M_s) \text{ with } d_{xz} \text{ and } d_{yz} \text{ interchanged}$$

$$[12]\quad {}^2B_1{}^{\pm}(1,2) = (d_{xz})^2(ad_{x^2-y^2} - bd_{z^2})^2\{d_{1,2}(d^{\pm}_{yz})(ad^{\pm}_{z^2} + bd^{\pm}_{x^2-y^2})(d^{\mp}_{xy}) + e_{1,2}(d^{\pm}_{yz})(ad^{\mp}_{z^2} + bd^{\mp}_{x^2-y^2})(d^{\pm}_{xy}) + f_{1,2}(d^{\mp}_{yz})(ad^{\pm}_{z^2} + bd^{\pm}_{x^2-y^2})(d^{\pm}_{xy})\}$$

$$[13]\quad {}^2B_2{}^{\pm}(1,2) = \text{same as } {}^2B_1{}^{\pm}(1,2) \text{ with } d_{xz} \text{ and } d_{yz} \text{ interchanged}$$

The ${}^4B_1$, ${}^4B_2$, ${}^2B_1$ (1, 2,),and ${}^2B_2$(1,2) states also have not previously been considered. In writing eqs. 7 and 8 use has been made of the simplification that if both the $(ad_{x^2-y^2} - bd_{z^2})$ and $(ad_{z^2} + bd_{x^2-y^2})$ orbitals are filled the determinental function is equivalent to the simpler form given above.

The spin–orbit interaction mixes the above excited states into the ground state, producing wave functions for the ground state Kramer's doublet of the following form

$$[14]\quad \psi_{\pm} = \sum_{m=0} a_m{}^{\pm}\psi_m$$

where ψ_0 is the ground state function in the absence of a spin–orbit interaction and $\psi_{m\neq 0}$ are the excited state functions. To third order, perturbation theory gives for the coefficients a_m

$$[15]\quad a_0 = 1 - \frac{1}{2}\sum_n \frac{H_{0n}H_{n0}}{(E_0 - E_n)^2}$$

$$[16]\quad a_{m\neq 0} = \frac{H_{m0}}{E_0 - E_m} - \frac{H_{m0}H_{00}}{(E_0 - E_m)^2} + \sum_{n\neq 0}\frac{H_{mn}H_{n0}}{(E_0 - E_m)(E_0 - E_n)}$$

$$[17]\quad H_{mn} = \langle\psi_m|\mathcal{H}_{LS}|\psi_n\rangle$$

The rest of the calculation involves finding the spin Hamiltonian parameters by standard procedures (28) in terms of the a_m coefficients. We then substitute eqs. 15 and 16 keeping only terms of order $(\xi/\Delta E)^2$. It seems reasonable to expect that the ${}^2A_2$, ${}^2A_2$(1,2), ${}^2B_1$(1,2), and ${}^2B_2$(1,2) states are high in energy, so that it was assumed for these states that only terms of order $(\xi/\Delta E)$ need to be retained. Further, for the pairs of doublet states related to a quartet state such as ${}^2A_2$(1,2) it was assumed that both states in the pair had the same energy. Preliminary computations show that these states are about 15 000 cm^{-1} above the corresponding quartet state and are never separated by more

Can. J. Chem. Downloaded from www.nrcresearchpress.com by 210.87.254.40 on 09/05/12
For personal use only.

Can. J. Chem. Downloaded from www.nrcresearchpress.com by 210.87.254.40 on 09/05/12
For personal use only.

than about 1500 cm^{-1} in energy. It is this assumption that makes it unnecessary for us to know the correct values of the coefficients $e_{1,2}$, $d_{1,2}$, and $f_{1,2}$ in eqs. 6, 11, and 13.

If we define the following constants

$$\begin{aligned} c_1 &= \xi/\Delta(^2B_1) & c_6 &= \xi/\Delta(^2A_2) \\ c_2 &= \xi/\Delta(^2B_2) & c_3' &= \xi/\Delta(^2B_1(1,2)) \\ c_3 &= \xi/\Delta(^4B_1) & c_4' &= \xi/\Delta(^2B_2(1,2)) \\ c_4 &= \xi/\Delta(^4B_2) & c_5' &= \xi/\Delta(^2A_2(1,2)) \\ c_5 &= \xi/\Delta(^4A_2) \end{aligned} \quad [18]$$

where $\Delta(^2B_1)$ is the energy difference between the $^2B_1$ state and the ground state and ξ is the one electron spin–orbit constant, then the **g** tensor components are given by the equations:

$$g_z = 2.0023 + \frac{2}{3}(c_3^2 + c_4^2 + c_3c_4) + (3a^2 - b^2)c_1c_2 - (\sqrt{3}a + b)^2c_2^2 - (\sqrt{3}a - b)^2c_1^2 - 8b^2c_6 \quad [19]$$

$$g_x = 2.0023 + \frac{2}{3}c_3^2 + \frac{8}{3}a^2c_5^2 - \frac{4}{3}a(a - \sqrt{3}b)c_3c_5 + \frac{4}{3}b(\sqrt{3}a + b)c_3c_2 - (3a^2 - b^2)c_1c_2 - (\sqrt{3}a - b)^2c_1^2 + 2(\sqrt{3}a + b)^2c_2 \quad [20]$$

$$g_y = 2.0023 + \frac{2}{3}c_4^2 + \frac{8}{3}a^2c_5^2 - \frac{4}{3}a(a + \sqrt{3}b)c_4c_5 - \frac{4}{3}b(\sqrt{3}a - b)c_4c_1 - (3a^2 - b^2)c_1c_2 - (\sqrt{3}a + b)^2c_2^2 + 2(\sqrt{3}a - b)^2c_1 \quad [21]$$

The corresponding hyperfine tensor components are:

$$\begin{aligned} A_z = K + P\Big\{&\frac{4}{7}(a^2 - b^2) - \frac{2}{7}(c_3 - c_3') - \frac{2}{7}(c_4 - c_4') \\ &- \frac{1}{7}(3a^2 - 3b^2 + 2\sqrt{3}ab)c_1 - \frac{1}{7}(3a^2 - 3b^2 - 2\sqrt{3}ab)c_2 - 8b^2c_6 \\ &- \frac{8}{63}a^2(c_3^2 + c_4^2) - \frac{32}{63}a^2(2 - 3b^2)c_5^2 - \frac{3}{14}(\sqrt{3}a + b)^2c_2^2 - \frac{3}{14}(\sqrt{3}a - b)^2c_1^2 \\ &+ \frac{2}{7}c_3c_4 + \frac{4}{7}(6 - 7b^2)c_1c_2 + \frac{4\sqrt{3}}{63}a(\sqrt{3}a - b)c_5(c_3 + c_4) \\ &+ \frac{4\sqrt{3}}{21}b(\sqrt{3}b + a)c_3c_2 + \frac{4\sqrt{3}}{21}b(\sqrt{3}b - a)c_4c_1\Big\} \end{aligned} \quad [22]$$

$$\begin{aligned} A_x = K + P\Big\{&-\frac{2}{7}(a^2 - b^2) - \frac{4\sqrt{3}}{7}ab(1 + c_6) + 2(\sqrt{3}a + b)^2c_2 \\ &+ \frac{1}{7}(3a^2 - 3b^2 + 2\sqrt{3}ab)c_1 \\ &+ \frac{2}{7}(c_3 - c_3') - \frac{8\sqrt{3}}{21}ab(c_5 - c_5') - \frac{2}{63}(1 + 2b^2 - 2\sqrt{3}ab)c_3^2 \\ &+ \frac{8}{63}a(a + \sqrt{3}b)c_4^2 + \frac{8}{63}a^2(5 - 6b^2 + 6\sqrt{3}ab)c_5^2 \\ &- \frac{1}{14}(1 + 2b^2 - 2\sqrt{3}ab)(\sqrt{3}a + b)^2c_2^2 + \frac{1}{7}b(\sqrt{3}a - b)^3c_1^2 + \frac{2}{21}c_3c_4 \\ &- \frac{1}{63}(108a - 5\sqrt{3}b)(a - \sqrt{3}b)c_5c_3 + \frac{1}{21}(2 + 3b^2 + \sqrt{3}ab)c_5c_4 \\ &- \frac{1}{7}(27 - 34b^2 + 2\sqrt{3}ab)c_1c_2 + \frac{2}{21}(\sqrt{3}a + b)(\sqrt{3}a + 20b)c_3c_2 - \frac{2}{7}c_4c_1\Big\} \end{aligned} \quad [23]$$

Can. J. Chem. Downloaded from www.nrcresearchpress.com by 210.87.254.40 on 09/05/12
For personal use only.

$$[24]\quad A_y = K + P\left\{-\frac{2}{7}(a^2 - b^2) + \frac{4\sqrt{3}}{7}ab(1 + c_6) + 2(\sqrt{3}a - b)^2c_1 + \frac{1}{7}(3a^2 - 3b^2 - 2\sqrt{3}ab)c_2 + \frac{2}{7}(c_4 - c_4') + \frac{8\sqrt{3}}{21}ab(c_5 - c_5') + \frac{8}{63}a(a - \sqrt{3}b)c_3^2 - \frac{2}{63}(1 + 2b^2 + 2\sqrt{3}ab)c_4^2 + \frac{2}{21}c_3c_4 + \frac{8}{63}a^2(5 - 6b^2 - 6\sqrt{3}ab)c_5^2 - \frac{1}{7}b(\sqrt{3}a + b)^3c_2^2 - \frac{1}{14}(1 + 2b^2 + 2\sqrt{3}ab)(\sqrt{3}a - b)^2c_1^2 - \frac{1}{7}(27 - 34b^2 - 2\sqrt{3}ab)c_1c_2 + \frac{1}{21}(2 + 3b^2 - \sqrt{3}ab)c_5c_3 - \frac{1}{63}(a + \sqrt{3}b)(108a + 5\sqrt{3}b)c_5c_4 - \frac{2}{21}(6 - 3b^2 + \sqrt{3}ab)c_3c_2 + \frac{4}{21}(\sqrt{3}a - b)(\sqrt{3}a - 10b)c_4c_1\right\}$$

$$[25]\quad P = 2.0023\, g_N\beta_e\beta_N\langle r^{-3}\rangle_{av}$$

K in eqs. 22–24 is the isotropic Fermi contact interaction. An assumption has been made in just writing a constant K for the Fermi contact term in eqs. 22–24. The Fermi term for an unpaired electron in the $(ad_{z^2} + bd_{x^2-y^2})$ and $(ad_{x^2-y^2} - bd_{z^2})$ orbitals should be different than that in the d_{xy}, d_{xz}, or d_{yz} orbitals because these two orbitals are allowed to mix with the 4s orbital in C_{2v} or lower symmetries. Thus for the A_z term the Fermi term should more correctly take the form

$$[26]\quad K_0\left[1 - \frac{1}{9}(c_3^2 + c_4^2 + 8a^2c_5^2)\right] + \frac{4}{9}a^2c_5^2K_1 + K_2\left[\frac{4}{9}(c_3^2 + c_4^2) - \frac{1}{4}(\sqrt{3}a + b)^2c_2^2 - \frac{1}{4}(\sqrt{3}a - b)^2c_1^2\right]$$

where K_0 is the Fermi term for electron in $(ad_{z^2} + bd_{x^2-y^2})$ orbital, K_1 is the term in $ad_{(x^2-y^2} - bd_{z^2})$ orbital, and K_2 is the term for d_{xy}, d_{xz}, and d_{yz} orbitals. We would expect K_0 and K_1 to be positive for considerable 4s mixing and negative if not. K_2 should be negative. Since only 3rd order terms appear in this expression outside of K_0 we have assumed the Fermi term to be identical for A_x, A_y, and A_z.

In eqs. 18–25 there are twelve parameters needed to determine six experimental spin Hamiltonian parameters. Application of these equations to experiment will require a judicious choice of assumptions about the relative values of at least six of these parameters. Previous treatments have made explicit or implicit assumptions about seven of these parameters. Since the quartet states and their associated doublet states were overlooked there was the implicit assumption that c_3, c_4, c_5, c_3', c_4', and c_6' were zero. In addition it was always explicitly assumed that $a = 1$ or $b = 1$. Examination of eqs. 19–24 shows that the quartet states only contribute to the g values in third order but contribute to the hyperfine terms in second order. Since there is good reason to expect c_3, c_4, and c_5 to have magnitudes similar to c_1, c_2, and c_6 one is not justified in neglecting these quartet terms.

In the case of axial symmetry a considerable simplification occurs in the above equations since $c_1 = c_2$, $c_3 = c_4$, $c_3' = c_4'$, and $a = 1$ or $b = 1$. For $a = 1$

$$[27]\quad g_\parallel = 2.0023 + 2c_3^2 - 3c_1^2$$

$$[28]\quad g_\perp = 2.0023 + \frac{2}{3}c_3^2 + \frac{8}{3}c_5^2 - \frac{4}{3}c_3c_5 - 6c_1^2 + 6c_1$$

$$[29]\quad A_\parallel = K + P\left\{\frac{4}{7} - \frac{4}{7}(c_3 - c_3') - \frac{6}{7}c_1 + \frac{2}{63}c_3^2 - \frac{64}{63}c_5^2 + \frac{15}{7}c_1^2 + \frac{8}{21}c_5c_3\right\}$$

$$[30]\quad A_\perp = K + P\left\{-\frac{2}{7} + \frac{45}{7}c_1 + \frac{2}{7}(c_3 - c_3') + \frac{4}{21}c_3^2 + \frac{40}{63}c_5^2 - \frac{57}{14}c_1^2 - \frac{34}{21}c_5c_3\right\}$$

Can. J. Chem. Downloaded from www.nrcresearchpress.com by 210.87.254.40 on 09/05/12
For personal use only.

For $b = 1$ we obtain

[31] $$g_{\parallel} = 2.0023 + 2c_3^2 - 3c_1^2 - 8c_6$$

[32] $$g_{\perp} = 2.0023 + \frac{2}{3}c_3(c_3 + 2c_1) + 2c_1$$

[33] $$A_{\parallel} = K + P\left\{-\frac{4}{7} - \frac{4}{7}(c_3 - c_3') + \frac{6}{7}c_1 - 8c_6 + \frac{2}{7}c_3^2 - c_1^2 + \frac{8}{7}c_3c_1\right\}$$

[34] $$A_{\perp} = K + P\left\{\frac{2}{7} + \frac{11}{7}c_1 + \frac{2}{7}(c_3 - c_3') + \frac{9}{14}c_1^2 + \frac{34}{21}c_3c_1\right\}$$

$^2B_2$ Ground State

For this ground state the z portion of $\mathcal{H}_{LS}$ couples with the $^2B_1$, $^4B_1$, and $^2B_1(1,2)$ states while the x,y portion couples with $^2A_1$ and the following states which have not previously been considered in the $^2A_1$ ground state theory

[35] $$^2A_2^{\pm}(xy) = (d_{xz})^2(d_{z^2})^2(d_{x^2-y^2})^2(d^{\pm}_{xy})$$

[36] $$^2A_1^{\pm}(x^2 - y^2) = (d_{xz})^2(d_{yz})^2(ad_{z^2} + bd_{x^2-y^2})^2(ad^{\pm}_{x^2-y^2} - bd^{\pm}_{z^2})$$

[37] $$^4A_1\left(\pm\frac{3}{2}\right) = (d_{z^2})^2(d_{x^2-y^2})^2(d^{\pm}_{xy})(d^{\pm}_{xz})(d^{\pm}_{yz})$$

[38] $$^4A_1\left(\pm\frac{1}{2}\right) = \frac{1}{\sqrt{3}}(d_{z^2})^2(d_{x^2-y^2})^2\{(d^{\pm}_{xy})(d^{\pm}_{xz})(d^{\mp}_{yz}) + (d^{\pm}_{xy})(d^{\mp}_{xz})(d^{\pm}_{yz}) + (d^{\mp}_{xy})(d^{\pm}_{xz})(d^{\pm}_{yz})\}$$

[39] $$^2A_1^{\pm}(1,2) = (d_{z^2})^2(d_{x^2-y^2})^2\{e_{1,2}(d^{\pm}_{xy})(d^{\pm}_{xz})(d^{\mp}_{yz}) + d_{1,2}(d^{\pm}_{xy})(d^{\mp}_{xz})(d^{\pm}_{yz}) + f_{1,2}(d^{\mp}_{xy})(d^{\pm}_{xz})(d^{\pm}_{yz})\}$$

In this calculation a has been taken as unity because the mixing coefficients a and b appear only in a few terms and do not appreciably affect the results.

If we define the following constants

[40]
$$\eta_1 = \xi/\Delta(^2A_2(xy)) \qquad \eta_5 = \xi/\Delta(^4A_1)$$
$$\eta_2 = \xi/\Delta(^2B_1) \qquad \eta_6 = \xi/\Delta(^4B_1)$$
$$\eta_3 = \xi/\Delta(^2A_1) \qquad \eta_5' = \xi/\Delta(^2A_1(1,2))$$
$$\eta_4 = \xi/\Delta(^2A_1(x^2 - y^2))$$

the **g** tensor components will be given as

[41] $$g_z = 2.0023 + \frac{2}{3}\eta_5^2 - 3\eta_3^2 - \frac{2}{3}\eta_2\eta_5 - 3\eta_2\eta_3 + 2\eta_2$$

[42] $$g_x = 2.0023 - 2\eta_2^2 - 3\eta_2\eta_3 + 6\eta_3 + 2\eta_4$$

[43] $$g_y = 2.0023 + \frac{2}{3}\eta_5^2 - 3\eta_3^2 - 2\eta_1$$

In these calculations, third order terms only for the $^2A_1$, $^2B_1$, $^4A_1$, and $^4B_1$ states have been retained. The corresponding **A** tensor components are:

[44] $$A_z = K + P\left\{\frac{2}{7}(1 - \eta_5 + \eta_5') + \frac{3}{7}(\eta_3 - \eta_4 + \eta_1) + 2\eta_2 - \frac{2}{21}\eta_5^2 - \frac{9}{14}\eta_3^2 - \frac{8}{21}\eta_5\eta_2 - \frac{45}{14}\eta_3\eta_2\right\}$$

$$[45]\quad A_x = K + P\left\{-\frac{4}{7} + 6\eta_3 + 2\eta_4 + \frac{3}{7}(\eta_2 - \eta_1) + \frac{4}{21}\eta_5^2 + \frac{3}{14}\eta_3^2 - \frac{2}{21}\eta_5\eta_6 + \frac{4}{7}\eta_3\eta_6 - \frac{6}{7}\eta_2\eta_3 - \frac{2}{7}\eta_2\eta_5\right\}$$

$$[46]\quad A_y = K + P\left\{\frac{2}{7}(1 + \eta_5 - \eta_5') - \frac{3}{7}(\eta_2 + \eta_3 - \eta_4) - 2\eta_1 - \frac{2}{21}\eta_5^2 - \frac{8}{21}\eta_5\eta_6 + \frac{2}{7}\eta_3\eta_6 + \frac{1}{7}\eta_2\eta_5 + \frac{3}{14}\eta_2\eta_3\right\}$$

In this case there are nine adjustable parameters and judicious approximations will also be required to make use of these equations.

Applications

Co(II) Porphyrins and Phthalocyanines

These complexes are axially symmetric so that we can use frozen solution results with some confidence. Further, it is clear from previous studies (1–8) that the ground state is $^2A_1$ so that we can use eqs. 27–30 to analyze the results. An examination of eqs. 27 and 28 shows that the introduction of quartet states into the calculation has allowed us to qualitatively explain the behavior of g values as stronger bases are complexed at the fifth and sixth coordination sites. Introduction of a base along the z axis destabilizes the d_{z^2} orbital relative to the d_{xz} and d_{yz} orbitals, thus decreasing c_1. As c_1 decreases $g_\perp$ becomes smaller while $g_\parallel$ increases. When $c_3 > c_1$, $g_\parallel$ will become greater than 2.0023 as is observed experimentally. In fact, careful examination of the theory shows that for the $^2A_1$ state the only way $g_\parallel$ can become greater than 2.0023 is by mixing of higher multiplet states into the ground state. It is presumed that such a mixing is what produced $g_\parallel$ values greater than 2.0023 in the ligand field calculations of Engelhardt and Green (22) and Busetto *et al.* (20).

There are six parameters in eqs. 27–30 for only four equations. Since c_5 is certainly smaller than c_3 and appears only in third order terms we will assume it to be zero. Further, we will take c_3' as zero since it should be much smaller than c_3. With these approximations we can calculate c_1 and c_3 from $g_\parallel$ and $g_\perp$ and then find K and P from $A_\parallel$ and $A_\perp$. The results from such computations are given in Table 1 for some Co(II) porphyrin and phthalocyanine complexes reported in the literature.

The value of P for the free Co^{2+} ion (29) is 254×10^{-4} cm^{-1} and it is encouraging to note that the majority of P values in Table 1 are between 200 and 300 $\times 10^{-4}$ cm^{-1}. The variations in P in Table 1 are primarily due to errors in determining the spin Hamiltonian parameters because P is determined from the equation

$$[47]\quad P = (A_\parallel - A_\perp)\Big/\left\{\frac{6}{7}(1 - c_3) - \frac{51}{7}c_1 - \frac{10}{21}c_3^2 + \frac{87}{14}c_1^2\right\}$$

where we are computing the ratio of two differences. The errors in this calculation become appreciable when c_1 is in the range of 0.15 to 0.07 because both numerator and denominator are small. For example, P for Co(p-CH_3)TPP plus 1,3,5-trimethoxybenzene changes from 521 to 430×10^{-4} cm^{-1} when $g_\parallel$ is changed from the reported value of 2.652 to 2.660.

It should be mentioned that in obtaining the values of P and K in Table 1, $A_\parallel$ and $A_\perp$ were assumed to be positive except for those complexes for which $c_1 < 0.05$, in which it was necessary to assume $A_\perp$ negative to obtain expected values of P. Further, the effect of assuming $c_5 = 0$ was estimated by redoing the computations assuming $c_5 = c_3$. The values of the parameters obtained were only slightly changed from those in Table 1 showing, as expected, that our assumption has little effect on the final results.

The values of c_1 and c_3 are large enough in some instances to suggest that even a third order perturbation calculation may not be sufficient and therefore an exact calculation was undertaken for this system assuming $c_5 = c_3' = 0$. For the axial symmetry case of the $^2A_1$ ground state an exact calculation results in the following

Can. J. Chem. Downloaded from www.nrcresearchpress.com by 210.87.254.40 on 09/05/12
For personal use only.

Can. J. Chem. Downloaded from www.nrcresearchpress.com by 210.87.254.40 on 09/05/12
For personal use only.

TABLE 1. Computed parameters for Co(II) porphyrin and phthalocyanine complexes using perturbation and exact equations

Complex		Perturbation calculation				Exact calculation				K(ave.)*	Reference
		c_1	c_3	P^*	K^*	c_1	c_3	P^*	K^*		
Co(p-CH_3)TPP†											
Polycrystalline		0.26	0.12	229	83	0.31	0.03	258	63	58	3
In H_2(p-CH_3)TPP†		0.27	0.16	226	83	0.32	0.03	265	57	58	3
In toluene +											
1,3,5-Trinitrobenzene	(2:1)	0.26	0.11	254	61	0.30	0.03	281	43	58	3
1,3,5-Trinitrobenzene	(1:1)	0.22	0.14	288	17	0.25	0.07	314	9	46	3
Picric acid	(2:1)	0.29	0.15	231	73	0.33	0.03	279	42	56	3
Picric acid	(1:1)	0.19	0.13	254	41	0.21	0.09	265	42	43	3
2,4,5,7-Tetranitro-9-fluorenone	(2:1)	0.21	0.19	190	105	0.24	0.16	172	123	56	3
2,4,5,7-Tetranitro-9-fluorenone	(1:1)	0.19	0.11	310	−5	0.21	0.06	339	−14	36	3
1,3-Dinitrobenzene	(2:1)	0.27	0.24	232	63	0.34	0.20	212	91	45	3
1,3-Dinitrobenzene	(1:1)	0.21	0.14	281	29	0.23	0.08	301	25	51	3
(2,4,7-Trinitro-9-fluorenylidine)-malonitrile	(1:1)	0.19	0.11	253	64	0.22	0.11	248	55	45	3
2,4,5-Trinitrofluorenone	(1:1)	0.21	0.14	273	28	0.24	0.08	292	25	45	3
Nitrobenzene	(1:1)	0.18	0.14	284	21	0.20	0.12	264	42	42	3
Toluene	(2:1)	0.20	0.20	260	43	0.23	0.16	233	67	46	3
Toluene	(1:1)	0.17	0.15	261	34	0.18	0.13	216	67	40	3
1,3,5-Trichlorobenzene		0.13	0.15	462	−52	0.14	0.13	334	20	53	3
1,3,5-Trimethoxybenzene		0.12	0.13	521	−103	0.13	0.12	289	11	21	3
Pyrene		0.081	0.11	117	62	0.084	0.11	146	56	22	3
Acridine		0.079	0.13	181	17	0.082	0.12	231	8	−2	3
N,N,N',N'-tetramethyl-p-phenyline-diamine		0.074	0.13	233	−12	0.077	0.10	254	−10	−13	3
Piperidine	(2:1)	0.038	0.17	249	−49	0.040	0.16	342	−62	−50	3

Can. J. Chem. Downloaded from www.nrcresearchpress.com by 210.87.254.40 on 09/05/12
For personal use only.

TABLE 1 (*Concluded*)

Complex		Perturbation calculation				Exact calculation				K(ave.)*	Reference
		c_1	c_3	P*	K*	c_1	c_3	P*	K*		
Co(p-OCH_3)TPP†											
Polycrystalline		0.30	0.17	268	38	0.37	0.04	305	12	52	3
In Ni(p-OCH_3)TPP†		0.32	0.16	214	105	0.40	0.04	240	86	62	3
In H_2(p-OCH_3)TPP†		0.29	0.18	224	83	0.36	0.04	261	57	54	3
In toluene +											
2,4-Lutidine	(1:1)	0.068	0.12	152	21	0.070	0.12	187	16	−2	3
2,4,6-Collidine	(1:1)	0.077	0.17	204	2	0.076	0.16	389	−47	−13	3
Acridine	(1:1)	0.072	0.14	163	18	0.074	0.13	228	5	−4	3
1,1,3,3-Tetramethyl-guanidine	(1:1)	0.062	0.13	203	−7	0.064	0.13	261	−16	−17	3
Pyridine	(2:1)	0.034	0.16	248	−52	0.036	0.14	296	−53	−49	3
3-Picoline	(2:1)	0.036	0.17	260	−53	0.037	0.15	325	−58	−50	3
4-Picoline	(2:1)	0.035	0.18	250	−49	0.037	0.15	318	−55	−47	3
3,4-Lutidine	(2:1)	0.035	0.17	269	−59	0.037	0.15	334	−63	−54	3
3,5-Lutidine	(2:1)	0.035	0.18	269	−51	0.037	0.16	357	−61	−49	3
Piperidine	(2:1)	0.033	0.17	246	−49	0.035	0.15	311	−54	−48	3
CoOEP‡ in toluene +											
Trinitrobenzene		0.30	0.13	241	60	0.37	0.04	265	43	44	3
Picric acid		0.31	0.17	203	114	0.39	0.04	232	94	62	3
Toluene (1)		0.26	0.27	249	55	0.34	0.25	212	84	35	3
Toluene (2)		0.19	0.15	257	35	0.21	0.12	236	54	35	3
Pyrene		0.060	0.20	172	22	0.063	0.19	259	8	−2	3
Acridine		0.082	0.15	166	22	0.086	0.14	319	−21	−4	3
2,4-Lutidine		0.069	0.13	156	20	0.071	0.13	211	−1	−3	3
γ-Collidine		0.081	0.16	226	−2	0.086	0.16	617	−119	−11	3
Co(O—CH_3)TPP† (polycryst.)		0.17	0.17	260	38	0.19	0.15	218	69	41	3
CoPc§ in α-ZnPc§		0.074	0.10	195	27	0.077	0.10	224	24	17	1
in β-H_2Pc§		0.19	0.01	360	−12	0.21	0.02	352	−3	55	1
in β-NiPc§		0.19	0.01	390	−36	0.21	0.02	382	−27	51	1

*Units are 10^{-4} cm^{-1}.
†TPP is tetraphenylporphyrin.
‡OEP is octaethylporphyrin.
§Pc is phthalocyanine.

equations for $g_\parallel$ and $g_\perp$

[48] $$g_\parallel = 2.0023 + 6(\beta^2 - \gamma^2) - 2\delta^2$$

[49] $$g_\perp = 2.0023\,(\alpha^2 + 2\sqrt{3}\beta\gamma) - 2\sqrt{6}\alpha\delta$$

where

[50] $$\beta = \left\{c_1/\sqrt{2}\left[(c_1/c_3) - \frac{1}{2}c_1 - \varepsilon\right]\right\}\alpha$$

[51] $$\gamma = \left\{c_1/\sqrt{6}\left[(c_1/c_3) - \frac{1}{6}c_1 - \varepsilon\right]\right\}\alpha$$

[52] $$\delta = -\left\{\sqrt{3}c_1/\sqrt{2}\left(1 + \frac{1}{2}c_1 - \varepsilon\right)\right\}\alpha$$

[53] $$\alpha^2 = 1 - \beta^2 - \gamma^2 - \delta^2$$

and ε is found by solving the determinant

[54] $$\begin{vmatrix} -\varepsilon & -c_1/\sqrt{2} & -c_1/\sqrt{6} & \sqrt{3/2}c_1 \\ -c_1/\sqrt{2} & (c_1/c_3) - \frac{1}{2}c_1 - \varepsilon & 0 & 0 \\ -c_1/\sqrt{6} & 0 & (c_1/c_3) - \frac{1}{6}c_1 - \varepsilon & 0 \\ \sqrt{3/2}c_1 & 0 & 0 & 1 + \frac{1}{2}c_1 - \varepsilon \end{vmatrix} = 0$$

and taking the lowest value of the four ε's obtained. The K and P values can be obtained from the equations

[55] $$(A_\parallel - A_\perp) = P\left\{\frac{6}{7} + \frac{17}{14}(2.0023 - g_\perp) - \frac{5}{14}(2.0023 - g_\parallel) - \frac{22}{7}\beta^2 - \frac{68}{21}\gamma^2 - \frac{6\sqrt{2}}{7}\alpha\beta - \frac{32}{7}\sqrt{3}\beta\gamma\right\}$$

[56] $$(A_\parallel + 2A_\perp)/3 = K + P\left\{\frac{2}{3}(g_\perp - g_\parallel) + \frac{128}{21}\beta^2 - \frac{4}{63}\gamma^2 - \frac{6\sqrt{2}}{7}\alpha\beta + \frac{2\sqrt{6}}{7}\alpha\gamma + \frac{52}{21}\sqrt{3}\beta\gamma\right\}$$

The spin Hamiltonian parameters $g_\parallel$ and $g_\perp$ have been calculated from eqs. 48–54 for various values of c_1 and c_1/c_3. The results of such calculations are given in Fig. 1 where $g_\parallel$ is plotted against $g_\perp$. The values of c_1 and c_1/c_3 for a given complex are readily estimated from Fig. 1. Values of c_1, c_3, P, and K obtained using eqs. 48–56 are listed in Table 1 along with the corresponding values obtained from the perturbation equations.

It will be observed in Table 1 that the results from the exact calculation differ very little from the perturbation calculation. Values of c_1 determined exactly are always larger than those determined from the perturbation calculation but the difference becomes significant only for values of c_1 greater than 0.2. The only significant difference between the two sets of results is found in the values of c_3. The perturbation equations seriously overestimate the value of c_3 for complexes in which $c_1 > 0.2$. The perturbation calculation gives a nearly constant value of c_3 while the exact calculation shows c_3 to be increasing in magnitude as c_1 decreases. This latter behavior is the expected one because an increasing value of c_3 means the energy separation between the quartet state and the $^2A_1$ state is decreasing as the separation of the d_{z^2} and $d_{xz,yz}$ orbitals is increasing Since the quartet state is the ground state in an octahedral crystal field we would expect the energy separation of the quartet state and the $^2A_1$ state to diminish as the crystal field approaches an octahedral field due to basic adducts along the z axis.

The value of K fluctuates considerably due to large errors in the P term but it appears that K goes from $\sim +50 \times 10^{-4}$ cm^{-1} to $\sim -50 \times 10^{-4}$ cm^{-1} as c_1 varies from 0.3 to 0.03. The

Can. J. Chem. Downloaded from www.nrcresearchpress.com by 210.87.254.40 on 09/05/12
For personal use only.

Can. J. Chem. Downloaded from www.nrcresearchpress.com by 210.87.254.40 on 09/05/12
For personal use only.

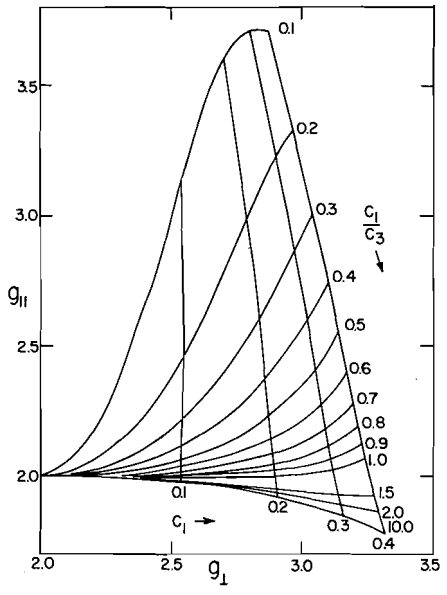

FIG. 1. Plot of $g_{\parallel}$ *vs.* $g_{\perp}$ for different values of c_1 and c_1/c_3 as obtained from the exact calculation for axial complexes with a $^2A_1$ ground state.

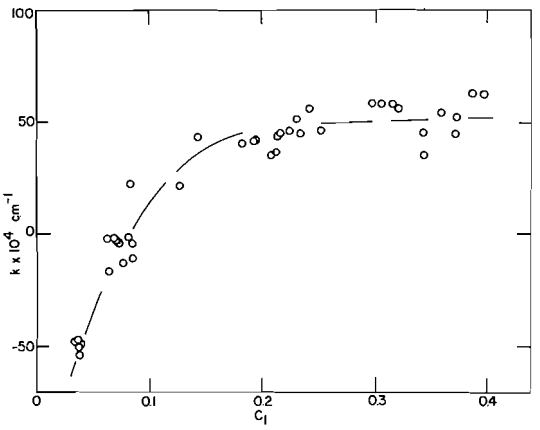

FIG. 2. K(ave.) *vs.* c_1 for porphyrin and phthalocyanine complexes.

variation in K becomes more clearly defined if we assume a constant P and use eq. 56 to determine K. This has been done using the average value ($P = 264 \times 10^{-4}$ cm^{-1}) determined from P values in Table 1. Values of K determined this way are given as K(ave.) in Table 1 and are plotted *vs.* c_1 in Fig. 2. In this plot we see that K remains nearly constant at $+50 \times 10^{-4}$ cm^{-1} above $c_1 = 0.2$ but changes rapidly to negative values when c_1 is below 0.1. A plus value of K means an admixture of the 4s orbital with the d_{z^2} orbital and therefore we must interpret Fig. 2 as showing that there is a strong admixture of the 4s orbital with the $3d_{z^2}$ orbital in the pure porphyrin or the porphyrin complexed with aromatic adducts, but this admixture is quickly reduced when bases are complexed with the porphyrin system.

Thus we see that by including the spin–orbit coupling between the doublet ground state and an excited quartet state and carrying the calculation to higher orders of perturbation, it is possible to explain the whole variation of spin Hamiltonian parameters of Co(II) porphyrins and phthalocyanines in a coherent and reasonable manner.

Nonaxial Co(II) Complexes

The problem of nonaxial complexes is difficult due to the large number of variables present in the spin Hamiltonian equations. A fair number of assumptions must be made to reduce the parameters to a manageable number and one is left with the feeling that existing data could probably be fitted to both ground states. There is one difference between the spin Hamiltonian equations for the two ground states that may be useful in distinguishing between them and this is the relative values of g_y and g_z. If one makes the reasonable assumption that the largest terms in eqs. 19, 21, 41, and 43 are those in which $(\xi/\Delta E_i)$ are raised to the first power then g_z should be less than g_y in the $^2A_1$ state while the reverse would be true for the $^2B_2$ ground state. It is possible to have values for the parameters for which this is not true but this generally requires the assumption that the d_{yz} and d_{xz} orbitals are very much different in energy. Since e.s.r. studies on copper complexes (13) of the same ligands show the d_{xz} and d_{yz} orbitals to be nearly degenerate, it seems unreasonable to accept interpretations of Co(II) e.s.r. data that require very large energy differences in these orbitals.

There are only three complexes for which g_y and g_z have been unambiguously assigned[1] in the literature. Two of them, bis(thioacetylacetanato)-cobalt(II) [Co(sacsac)$_2$] (11) and the bis(maleonitriledithiolato)cobaltate(II) ion [Co(mnt)$_2^{2-}$] (10), have $g_y > g_z$ while the third, *N,N'*-ethylenebis(salicylideneiminato)cobalt(II) [Co(salen)]

[1]The complex Co(PEt$_2$Ph)$_2$(mesityl)$_2$ (9) has the principal x and y axes directed along the bond axes and cannot therefore be treated by the present equations without modification.

TABLE 2. Values of parameters for two complexes assumed to have the $^2A_1$ ground state

Complex	c_1	c_2	c_6	b^2	K (10^{-4} cm^{-1})	P (10^{-4} cm^{-1})
Co(sacsac)$_2$	0.013	0.166	~0	0.438	−51	208
Co(mnt)$_2^{2-}$	0.031	0.101	~0	0.217	−133	341

(13), has $g_z > g_y$. The spin Hamiltonian parameters for the first two have been fitted to eqs. 19–24 for the $^2A_1$ ground state and the values obtained for the parameters are given in Table 2. In obtaining these parameters it was assumed that since the quartet terms were small for the uncomplexed porphyrins that they would be small for these complexes also so that we can take c_3, c_4, c_5, c_3', c_4', and c_5' to be zero. The sign for A_z was taken to be negative for Co(sacsac)$_2$ and Co(mnt)$_2^{2-}$ while A_x and A_y were assumed positive for Co(sacsac)$_2$ and negative for Co(mnt)$_2^{2-}$. Other assignments of sign give either smaller values of c_1 or poorer values of P.

We see from Table 2 that the e.s.r. data for both complexes can be fitted to a $^2A_1$ ground state only for a sizeable mixing of d_{z^2} and $d_{x^2-y^2}$ in the orbital containing the unpaired electron. Gregson *et al.* (11) claimed that the data for Co(sacsac)$_2$ could be fitted to a $^2A_1$ ground state with $b^2 = 0$, $c_1 = 0.04$, and $c_2 = 0.21$, but these values give $g_y = 2.17$ using eq. 21 which is in poor agreement with the experimental value of 1.904. To understand the significance of the b^2 values in Table 2, it should be noted that when $b^2 = 0.25$ the orbital containing the unpaired electron becomes the $d_{z^2-y^2}$ orbital and for $b^2 = 0.75$ it becomes the $d_{3y^2-r^2}$ orbital. The ratio of c_2 to c_1 is still large, particularly in the case of Co(sacsac)$_2$, indicating a large energy separation in the d_{xz} and d_{yz} orbitals unless the effective value of ξ is very much reduced from the free ion value.

No attempt has been made to fit the data for Co(salen) to either ground state because von Zelewsky and Fierz (13) claim to have done this for an exact calculation which implicitly ignored the quartet states. They show that the $^2B_2$ ground state is the only one which will fit the data.

Conclusion

It has been shown that to adequately explain the e.s.r. data on low spin Co(II) complexes, it is necessary to include the spin–orbit mixing of excited quartet states into the doublet ground state and that this mixing becomes important for those complexes which have formed 1:1 or 2:1 molecular complexes with basic molecules attached along the z axis. Further it has been shown that for low symmetry complexes the large anisotropy in g and A values may result from the extensive mixing of d_{z^2} and $d_{x^2-y^2}$ orbitals which is allowed in lower symmetries.

Perhaps the major conclusion to be reached is that it may be impossible to unambiguously assign ground states to low symmetry Co(II) complexes on the basis of g values and ^{59}Co hyperfine splittings alone due to the large number of variables to be adjusted in the theory. It is certainly clear that one must have g and A values clearly assigned to a particular molecular axis before one begins to interpret the data. It is not enough to take g and A from frozen glasses and to then try all combinations of assignment to molecular axes to see which gives the best fit because it will always be possible to fit the equations given here to several possible combinations. One useful piece of data which appears to be missing from systems reported upon up to the present, is the hyperfine interaction with ligand nuclei in the xy plane. Such interactions would be negligible for the $^2B_2$ ground state but should be measurable in some instances for the $^2A_1$ ground state. The d_{z^2} orbital can be written as

$$[57] \qquad d_{z^2} = (\sqrt{3})^{-1} [d_{z^2-y^2} + d_{z^2-x^2}]$$

Thus it would be reasonable to expect the hyperfine interaction from a nucleus in the xy plane to be approximately one-third that observed for a corresponding copper complex which has the unpaired electron in a $d_{x^2-y^2}$ type orbital pointed towards the nucleus. In copper complexes ^{14}N hyperfine values are typically of the order of 15×10^{-4} cm^{-1} and therefore it would seem reasonable to expect hyperfine values of $\sim 5 \times 10^{-4}$ cm^{-1} for an unpaired electron in a d_{z^2} orbital. Even if such a splitting is not resolvable it is large enough to produce a measureable broadening of the resonance in some cases and

Can. J. Chem. Downloaded from www.nrcresearchpress.com by 210.87.254.40 on 09/05/12
For personal use only.

hence should, in principle, be detectable. Unfortunately, no mention of line widths is made in the single crystal studies of complexes (12, 13) containing ^{14}N nuclei.

This work was supported by a grant from the National Research Council of Canada.

1. J. M. ASSOUR and W. A. KAHN. J. Am. Chem. Soc. **87**, 207 (1965).
2. J. M. ASSOUR. J. Am. Chem. Soc. **87**, 4701 (1965).
3. F. A. WALKER. J. Am. Chem. Soc. **92**, 4235 (1970); J. Magn. Reson. **15**, 201 (1974).
4. H. A. O. HILL, P. J. SADLER, and R. J. P. WILLIAMS. J. Chem. Soc. Dalton, 1663 (1973).
5. H. A. O. HILL, P. J. SADLER, R. J. P. WILLIAMS, and C. D. BARRY. Ann. N.Y. Acad. Sci. **206**, 247 (1973).
6. C. D. BARRY, H. A. O. HILL, P. J. SADLER, and R. J. P. WILLIAMS. Proc. R. Soc. London, A**334**, 493 (1973).
7. B. B. WAYLAND, J. V. MINKIEWIXZ, and M. E. ABD-ELMAGEED. J. Am. Chem. Soc. **96**, 2795 (1974).
8. B. B. WAYLAND and M. E. ABD-ELMAGEED. J. Am. Chem. Soc. **96**, 4809 (1974).
9. R. B. BENTLEY, E. E. MABBS, W. R. SMAIL, M. GERLOCH, and J. LEWIS. J. Chem. Soc. A, 3003 (1970).
10. A. H. MAKI, N. EDELSTEIN, A. DAVIDSON, and R. H. HOLM. J. Am. Chem. Soc. **86**, 4580 (1964).
11. A. K. GREGSON, R. L. MARTIN, and S. MITRA. Chem. Phys. Lett. **5**, 310 (1970).
12. V. P. CHACKO and P. T. MANOHARAN. J. Magn. Reson. **16**, 75 (1974).
13. A. VON ZELEWSKY and H. FIERZ. Helv. Chim. Acta, **56**, 977 (1973).
14. B. M. HOFFMAN, F. BASOLO, and D. L. DIEMENTE. J. Am. Chem. Soc. **95**, 6497 (1973).
15. F. L. URBACH, R. D. BEREMAN, J. A. TOPICH, M. HARIHARAN, and B. J. KALBACHER. J. Am. Chem. Soc. **96**, 5063 (1974).
16. E. I. OCHIAI. J. Chem. Soc. Chem. Commun. 489 (1972).
17. E. I. OCHIAI. J. Inorg. Nucl. Chem. **35**, 1727 (1973).
18. D. DIEMENTE, B. M. HOFFMAN, and F. BASOLO. Chem. Commun. 467 (1970).
19. B. M. HOFFMAN, D. DIEMENTE, and F. BASOLO. J. Am. Chem. Soc. **92**, 61 (1970).
20. C. BUSETTO, F. CARIATI, A. FUSI, M. GULLOTI, F. MORAZZONI, A. PASINI, R. UGO, and V. VALENTI. J. Chem. Soc. Dalton, 754 (1973).
21. B. J. KALBACHER and R. D. BEREMAN. Inorg. Chem. **12**, 2997 (1973).
22. L. M. ENGELHARDT and M. GREEN. J. Chem. Soc. Dalton, 724 (1972).
23. L. M. ENGELHARDT, J. D. DUNCAN, and M. GREEN. Inorg. Nucl. Chem. Lett. **8**, 725 (1972).
24. C. BUSETTO, F. CARIATI, P. C. FANTUCCI, D. GALIZZIOLI, and F. MORAZZONI. Inorg. Nucl. Chem. Lett. **9**, 313 (1973).
25. E. BANKS, M. GREENBLATT, and B. R. MCGARVEY. J. Chem. Phys. **47**, 3772 (1967); J. Solid State Chem. **3**, 308 (1971).
26. C. A. KOSKY, B. R. MCGARVEY, and S. L. HOLT. J. Chem. Phys. **56**, 5904 (1972).
27. C. EZZEH and B. R. MCGARVEY. J. Chem. Phys. **61**, 2675 (1974).
28. B. R. MCGARVEY. Transition metal chemistry, Vol. 3. *Edited by* R. L. Carlin. Marcel Dekker, New York. 1966. pp. 90–201.
29. B. R. MCGARVEY. J. Phys. Chem. **71**, 51 (1967).

Can. J. Chem. Downloaded from www.nrcresearchpress.com by 210.87.254.40 on 09/05/12
For personal use only.

Erratum: A Kinetic Electron Spin Resonance Study of the Transfer of a Hydrogen Atom from α-Tetralin Hydroperoxide to a Tertiary Alkylperoxy Radical

J. H. B. CHENIER AND J. A. HOWARD
Division of Chemistry, National Research Council of Canada, Ottawa, Canada K1A 0R9

(Ref.: Can. J. Chem. **53**, 623 (1975))
Received May 20, 1975

Throughout this paper α-$C_{10}H_{10}OOH$ should read α-$C_{10}H_{11}OOH$.

Can. J. Chem. Downloaded from www.nrcresearchpress.com by 210.87.254.5 on 09/05/12
For personal use only.

Can. J. Chem. Downloaded from www.nrcresearchpress.com by 210.87.254.5 on 09/05/12
For personal use only.

Paniculatine. A New Alkaloid from *L. paniculatum* Desvaux

M. CASTILLO, G. MORALES, AND L. A. LOYOLA
Facultad de Ciencias, Departamento de Quimica, Universidad de Chile, Santiago, Chile
AND
I. SINGH[1], C. CALVO, H. L. HOLLAND, AND D. B. MACLEAN
Department of Chemistry, McMaster University, Hamilton, Ontario L8S 4M1

Received June 19, 1975

M. CASTILLO, G. MORALES, L. A. LOYOLA, I. SINGH, C. CALVO, H. L. HOLLAND, and D. B. MACLEAN. Can. J. Chem. **53**, 2513 (1975).

The structure of paniculatine, an alkaloid of *L. paniculatum*, has been elucidated. It has a skeletal structure different from other alkaloids of the *Lycopodium* family.

M. CASTILLO, G. MORALES, L. A. LOYOLA, I. SINGH, C. CALVO, H. L. HOLLAND et D. B. MACLEAN. Can. J. Chem. **53**, 2513 (1975).

On a determiné la structure de la paniculatine, un alkaloide isolé du *L. paniculatum*. Le squelette de ce composé diffère de celui des autres alkaloides du *Lycopodium*.

[Traduit par le journal]

Examination of *Lycopodium paniculatum* Desvaux has revealed the presence of the alkaloids, lycopodine (**1**), dihydrolycopodine (**2**), acetyldihydrolycopodine (**3**), and three hitherto unreported bases. The structure of one of these new bases, to which we have assigned the trivial name, paniculatine, has been determined by spectral analysis and by an X-ray crystallographic study of the hydrobromide salt.

Paniculatine ($C_{17}H_{27}NO_2$),[2] m.p. 180–181 °C, exhibited infrared absorption ($CHCl_3$ solution) at 3620, 3600–3000, 1720, and 1040 cm^{-1}, indicating the presence of hydroxyl and carbonyl functions. The p.m.r. spectrum (100 MHz, $CDCl_3$ solution) showed the presence of *N*-methyl (δ 2.18, s) and a secondary *C*-methyl (δ 0.90, d, $J = 6.5$ Hz). A signal at δ 3.78 (broad s, $W_{1/2} = 8$ Hz) was attributed to a hydrogen geminal to hydroxyl in a secondary alcohol. Double irradiation data suggested the presence of the part structure —$CH(CH_3)$—CH_2—CH(OH)—.

The mass spectrum of paniculatine had a molecular ion at *m/e* 277 (18%, $C_{17}H_{27}NO_2$) and a series of intense ions at *m/e* 58 (100%, C_3H_8N),[3] 71 (25%, C_4H_9N), 96 (21%, $C_6H_{10}N$),

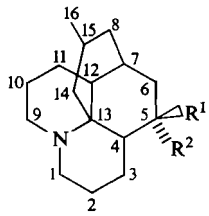

1 $R^1, R^2 = O$
2 $R^1 = OH; R^2 = H$
3 $R^1 = OAc; R^2 = H$

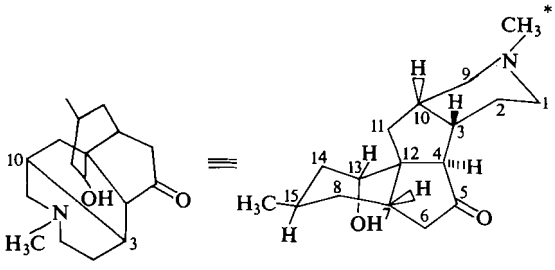

4 **4**

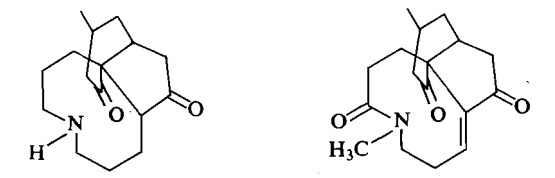

5 **6**

*The absolute configuration has not been established and may be enantiomeric to the structure shown.

[1]Present address: Department of Chemistry, Mohawk College, Hamilton, Ontario.

[2]The formula was established by high resolution mass spectrometry and by combustion analysis.

[3]Fragment ion compositions were determined by high resolution mass spectrometry.

and 110 (11%, $C_7H_{12}N$), indicative of the presence of the *N*-methyl group in a saturated heterocycle (1). The remainder of the mass spectrum, which included ions at *m/e* 262 (10%, $M - CH_3$), 248 (5%, $M - CHO$), 204 (29%, $M - C_4H_9O$), and 192 (17%, $M - C_5H_9O$), was different from the pattern established for the mass spectral fragmentation of other *Lycopodium* alkaloids of established structure (2, 3), inferring that paniculatine is a new structural type. X-ray analysis of the hydrobromide salt of paniculatine (m.p. 310–313 °C, i.r. (KBr) 3370, 2800–2400, 1725, 1040 cm^{-1}) showed that the free base has structure **4**.

A crystal of paniculatine hydrobromide, $C_{17}H_{27}NO_2 \cdot HBr$, having approximate dimensions 0.04 × 0.02 × 0.02 cm^3 was used for the X-ray measurements. The space group was uniquely determined as $P_{2_1}(C_2^2)$ from systematic absences. The monoclinic crystals had a = 11.27(2), b = 7.520(8), c = 10.58(2), β = 102.2(2), V = 876.52 $Å^3$, Z = 2, $\lambda(MoK_\alpha)$ = 0.71069. A total of 1183 unique reflections lying in the range of $0 < 2\phi < 45°$ were measured on a $P\bar{1}$ Syntex automatic diffractometer using graphite monochromatized MoK_α radiation. The data were corrected for Lorentz and polarization effects but not for absorption. The structure was solved by locating the positions of bromide ions from the Patterson function and subsequently locating the C, N, and O atoms by a combination of Fourier and difference Fourier methods. The structure was refined by a full-matrix least-squares approach to a current R = 0.089. The three dimensional structure, shown in Fig. 1, accords with the spectral data.

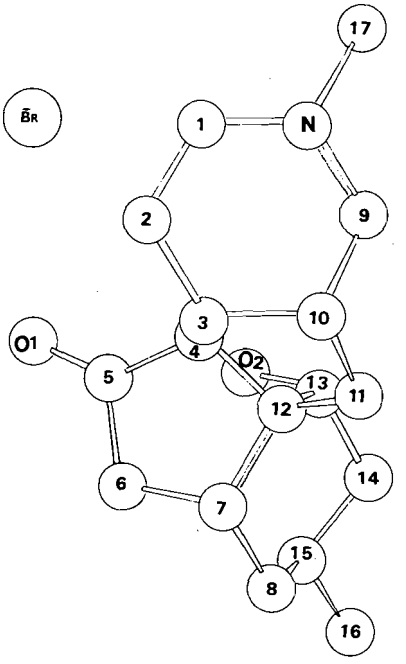

FIG. 1. The three dimensional structure of paniculatine hydrobromide.

Paniculatine bears the formal relationship to lycopodine shown in the formulas but is more closely related to fawcettimine (**5**) shown here in the open form rather than the carbinolamine (4). It differs in skeletal structure from the latter through the presence of the bond from C-3 to C-10 and by the presence of the *N*-methyl group. The C-3 to C-10 bond distinguishes paniculatine from other *Lycopodium* alkaloids of established structure (3). The formation of the C-3 to C-10 bond from a fawcettimine derivative, *e.g.* (**6**), is readily envisaged.

We thank the National Research Council of Canada for financial assistance.

1. H. J. VEITH, M. HESSE, and H. SCHMID. Helv. Chim. Acta, **53**, 1355 (1970).
2. D. B. MACLEAN. Can. J. Chem. **41**, 2654 (1963).
3. D. B. MACLEAN. *In* The alkaloids. Vol. XIV. *Edited by* R. H. F. Manske. Academic Press, New York. 1973. p. 347.
4. Y. INUBUSHI, H. ISHII, T. HARAYAMA, R. H. BURNELL, W. A. AYER, and B. ALTENKIRK. Tetrahedron Lett. 1069 (1967).

Can. J. Chem. Downloaded from www.nrcresearchpress.com by 210.87.254.5 on 09/05/12
For personal use only.

Can. J. Chem. Downloaded from www.nrcresearchpress.com by 210.87.254.105 on 09/05/12
For personal use only.

Canadian Journal of Chemistry

Published by
THE NATIONAL RESEARCH COUNCIL OF CANADA

Journal canadien de chimie

Publié par
LE CONSEIL NATIONAL DE RECHERCHES DU CANADA

Volume 53 Number 17 September 1, 1975 Volume 53 numéro 17 1 septembre 1975

Synthetic Morphinans and Hasubanans. Part IV.[1] Total Synthesis of 3,14-Dihydroxyisomorphinans, 3-Methoxy-$\Delta^{8,14}$-morphinans, and 9α-Hydroxy-3-methoxyhasubanan

IVO MONKOVIĆ,[2] HENRY WONG, BERNARD BELLEAU, IRWIN J. PACHTER,[3] AND YVON G. PERRON
Bristol Laboratories of Canada, Candiac, Quebec J5R 1J1

Received February 28, 1975

IVO MONKOVIĆ, HENRY WONG, BERNARD BELLEAU, IRWIN J. PACHTER, and YVON G. PERRON. Can. J. Chem. **53**, 2515 (1975).

The synthesis of a versatile intermediate 4a-(2-aminoethyl)-1,2,3,4,4a,9-hexahydro-6-methoxyphenanthrene (**3***a*) and its utilization in the synthesis of 9α-hydroxy-3-methoxy-17-methylhasubanan (**10**), 3,14-dimethoxy-17-methylisomorphinan (**9***l*), various 14-hydroxyisomorphinans (**9**), and 3-methoxy-$\Delta^{8,14}$-morphinan (**11***b*) is described. A number of 17-alkyl-3,14-dihydroxyisomorphinans were prepared and tested for narcotic antagonist and analgesic activities in laboratory animals. Some of these new compounds have exhibited significant activities.

IVO MONKOVIĆ, HENRY WONG, BERNARD BELLEAU, IRWIN J. PACHTER et YVON G. PERRON. Can. J. Chem. **53**, 2515 (1975).

On décrit la synthèse de l'intermédiaire versatile (aminoéthyl-2)-4a hexahydro-1,2,3,4,4a,9 méthoxy-6 phénanthrène (**3***a*) de même que son usage dans la préparation de l'hydroxy-9α méthoxy-3 méthyl-17 hasubanane (**10**), du diméthoxy-3,14 méthyl-17 isomorphinane **9***l*, de divers hydroxy-14 isomorphinanes (**9**) ainsi que du méthoxy-3 $\Delta^{8,14}$-morphinane (**11***b*). On a préparé un certain nombre d'alkyl-17 dihydroxy-3,14 isomorphinanes dont on a examiné l'activité sur des animaux de laboratoire comme antagoniste de narcotiques et comme analgésique. Quelques-uns de ces composés ont démontré des activités importantes.

[Traduit par le journal]

Introduction

At the outset of our studies on narcotic antagonists some years ago, the most exciting agent in this field was naloxone **I** (Scheme 1). Cumulative reports on its powerful antagonist activity not only against morphine but also against side effects (analgesia, psychotomimetic disorders) of other narcotic antagonists such as levalorphan (**II***a*), cyclorphan (**II***b*), cyclazocine (**III**), and others (see ref. 3 for a review) have placed naloxone in a class of its own *i.e.* a 'pure' or 'total' narcotic antagonist.

However, a more critical examination of the pharmacological properties of naloxone revealed that it suffers from a number of drawbacks: although parenterally highly potent, it is short acting, it is very poorly absorbed by the oral route, and from the chemical standpoint it is derived from thebaine which is only a minor constituent of opium. On the other hand, some totally synthetic analogs such as cyclazocine are known to be long acting and orally effective,

[1]Reference 1 is regarded as part III. For part II see ref. 2.

[2]To whom correspondence regarding this paper should be addressed.

[3]Bristol Laboratories, Syracuse, N.Y. 13201.

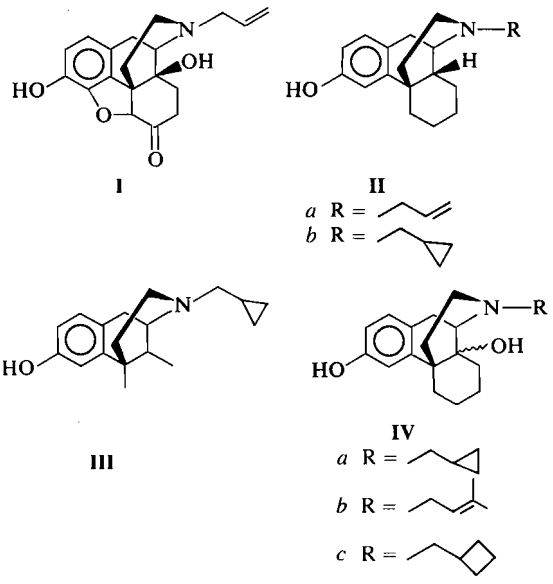

SCHEME 1

even though adverse psychomomimetic side effects have been observed with them. It seemed desirable then to prepare by total synthesis (so as to avoid opium-based starting materials) some representative 3,14-dihydroxymorphinans (**IV***a–c*) which by definition incorporate the carbon skeleton and the 14-hydroxyl substituent of naloxone as well as the nitrogen substituents of cyclazocine and pentazocine. In addition, a flexible synthetic method was desirable, which would allow for the preparation of both, 14β- and 14α-hydroxymorphinans. The latter have not been reported in the tetracyclic morphine-related structures, even though certain 14-unsubstituted isomorphinans have shown potent analgesic (4) and narcotic antagonist activities (5).

The choice of practical synthetic approaches to this end appeared to be between a classical Grewe synthesis (6, 7) which did not appear attractive to us[4] and that of a modification of thebaine, which we rejected for the already stated reasons.[5]

Consequently, we decided to utilize a synthetic approach which was initiated by one of us some years ago (10) and recently developed in our laboratories toward a successful total synthesis of D-normorphinan systems (11, 12). This approach proved to be fruitful and flexible, allowing for the preparation of various 3,14-dihydroxymorphinans (13), 3,14-dihydroxyisomorphinans (1), and a number of hasubanan derivatives (1, 2). It is the purpose of this communication to describe in full the synthesis of the common key intermediate 4a-(2-aminoethyl)-1,2,3,4,4a,9-hexahydro-6-methoxyphenanthrene **3***a* (Scheme 2), our initial studies on the intramolecular oxidative cyclization of **3***a* to morphinan and hasubanan systems, and the synthesis of a number of 3,14-dihydroxyisomorphinans, some of which exhibited moderate narcotic antagonist and analgesic activities.

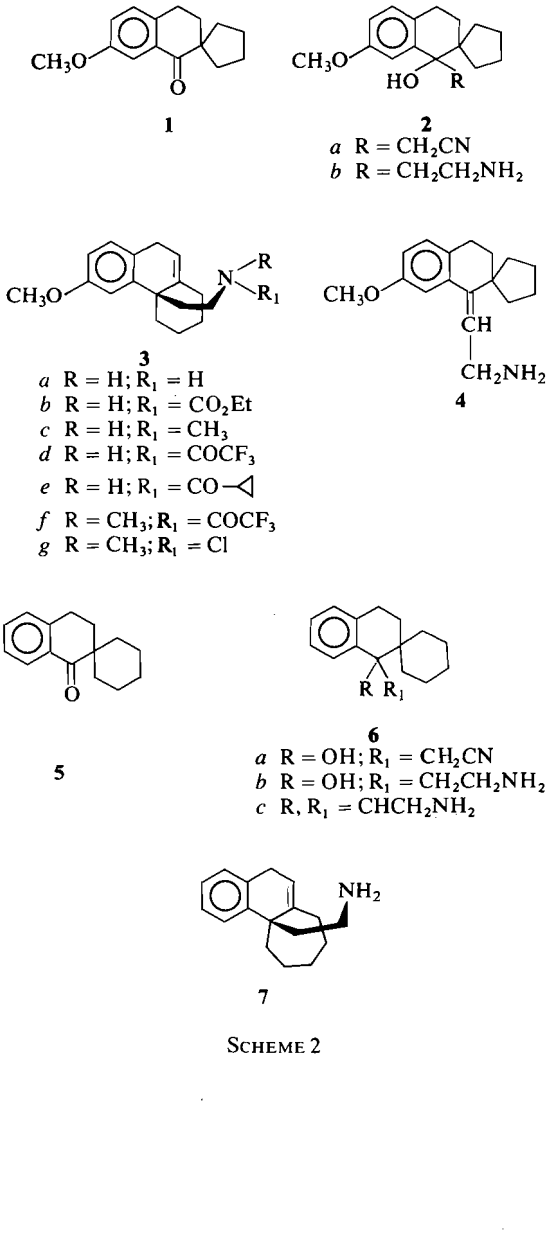

SCHEME 2

[4]Attempt along these lines has been published recently by Onda *et al.* (8).

[5]Successful conversion of thebaine to 3,14-dihydroxymorphinan derivatives was described by Sawa and Tada (9).

Can. J. Chem. Downloaded from www.nrcresearchpress.com by 210.87.254.105 on 09/05/12
For personal use only.

Can. J. Chem. Downloaded from www.nrcresearchpress.com by 210.87.254.105 on 09/05/12
For personal use only.

Results and Discussion

Our synthetic approach to various morphinan systems may be divided into two parts. The first consists in the successful practical synthesis of the unsaturated amine **3***a* a key intermediate analogous to the 3-unsubstituted analog already described (11). The starting material, 7-methoxy-1-tetralone (14) was alkylated by the method of Mousseron *et al.* (15) to give the spiro ketone **1** in high yield. Cyanomethylation of **1** (16) readily gave the hydroxy nitrile **2***a*, which was reduced *in situ* with lithium aluminum hydride to the amino alcohol **2***b*. Wagner–Meerwein rearrangement of **2***b* at 40° (in a refluxing mixture of concentrated hydrochloric acid and ether for 24 h), afforded unsaturated amine **3***a* in excellent yields. At room temperature, this reaction resulted in a 9:1 mixture of **3***a* and its positional isomer **4** which eventually rearranged to **3***a* at higher temperature. The characteristic n.m.r. absorptions of **3***a* at δ 5.71 (t, J = 3.5 Hz, olefinic proton at 10) and at δ 3.32 (broad singlet) for the benzylic protons can only be consistent with structure **3***a* (11). The isomeric olefin **4** was readily distinguished from **3***a* by the downfield shift of the olefinic proton signal (δ 5.35, J = 6 Hz) and the stronger coupling with its neighboring methylene protons (δ 3.43, J = 6 Hz). Attempted extension of the Wagner–Meerwein rearrangement to the homologous six-membered spiro intermediate **6***b* prepared from spiro ketone **5** by similar methods proved unsuccessful, the product of dehydration **6***c* as opposed to the rearranged product **7** being formed exclusively under our experimental conditions.

The second part of our synthesis consists in the oxidative cyclization of unsaturated amine **3***a* to the 14-hydroxymorphinan system **IV**. As far as we are aware, there are no direct methods for the conversion in a single step of γ,δ-unsaturated amines of general structure **V** to the corresponding 3-hydroxy piperidines **VI**. Accordingly, a stepwise approach had to be devised.

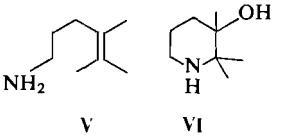

V VI

Our extensive experience in these laboratories with bromocyclizations of various β,γ- (17) and γ,δ-unsaturated systems (18, 19) proved of little use initially as regards the unsaturated amine **3***a*.[6] Attempts at the preparation of bridged aziridine systems such as **VIII** by the method of Nagata *et al.* (20) led mostly to the formation of intractable mixtures.

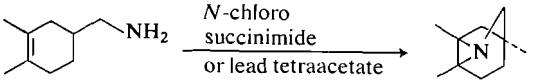

VII VIII

Our first successful formation of a morphinan functionalized at position 14 was accomplished by the method of Gassman *et al.* (21). The unsaturated amine **3***a* was first transformed into the *N*-ethoxycarbonyl derivative **3***b* followed by reduction to the *N*-methyl unsaturated amine **3***c*. This was converted to the chloramine **3***g* by reaction with *N*-chlorosuccinimide followed by methanolysis in hot methanol to give in low yield 3,14-dimethoxy-17-methylisomorphinan **9***l* (Scheme 3).

Another approach based on the intramolecular opening of an epoxide of **3***c* by the amino function was explored. In this respect it was essential to initially protect the amino function, followed by stereoselective epoxidation of the double bond in a *trans* fashion with respect to the amino ethane substituent. Next, deblocking of the nitrogen without affecting the epoxide function was desirable. Finally, it was necessary that the free amino group attack the epoxide ring regioselectively so as to give a 14-hydroxyisomorphinan rather than a 9α-hydroxyhasubanan. To this end, the unsaturated amine **3***c* was protected with a trifluoroacetyl group to give **3***f* which was then epoxidized with *m*-chloroperbenzoic acid to afford the α-epoxide **8***d* (Scheme 3). Hydrolysis of the amide function with potassium carbonate presumably gave the desired amino epoxide **8***e* which spontaneously cyclized to a 1:1 mixture of 14-hydroxyisomorphinan **9***f* and 9α-hydroxyhasubanan **10**. This approach was eventually modified so as to effect direct base-catalyzed cyclization of epoxy amides **8***a*, **8***b*, and **8***c* derived from the unsaturated amides **3***b*, **3***c*, and **3***d*. In this manner, these epoxy amides led to practical yields of the 14-hydroxy-

[6]However, subsequent experiments by Dr. T. T. Conway of these laboratories led to the successful bromocyclization of **3***a* to 9α-bromo-3-methoxyhasubanan hydrobromide, a key intermediate in our previously reported total synthesis of **11***b* (13).

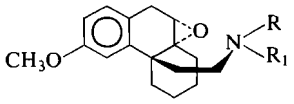

8

a R = H; R_1 = CO_2Et
b R = H; R_1 = $COCF_3$
c R = H; R_1 = CO-cyclopropyl
d R = CH_3; R_1 = $COCF_3$
e R = CH_3; R_1 = H

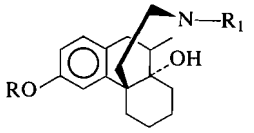

9

a R = CH_3; R_1 = CO_2Et
b R = CH_3; R_1 = $COCF_3$
c R = CH_3; R_1 = CO-cyclopropyl
d R = CH_3; R_1 = H
e R = CH_3; R_1 = CO-cyclobutyl
f R = CH_3; R_1 = CH_3
g R = CH_3; R_1 = CH_2-cyclopropyl
h R = CH_3; R_1 = CH_2-cyclobutyl
i R = H; R_1 = CH_3
j R = H; R_1 = CH_2-cyclopropyl
k R = H; R_1 = CH_2-cyclobutyl
l R = CH_3; R_1 = CH_3,14-OCH_3
m R = CH_3; R_1 = $CH_2CH{=}CH_2$
n R = H; R_1 = $CH_2CH{=}CH_2$

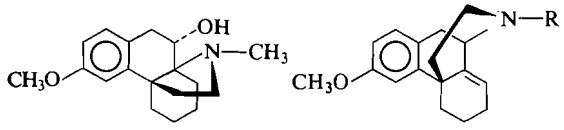

10 **11**

a R = CO_2Et
b R = H

SCHEME 3

isomorphinans **9***a*, **9***b*, and **9***c* when treated with sodium *t*-pentoxide in hot benzene (for **8***a* and **8***b*) or sodium hydride in DMSO (for **8***c*). Subsequent reduction of **9***a* and **9***c* with lithium aluminum hydride afforded the corresponding bases **9***f* and **9***g*. Alternatively, alkaline hydrolysis of **9***a* and **9***c* afforded the 14-hydroxy-3-methoxyisomorphinan **9***d* which was conveniently alkylated to **9***m* or acylated to **9***e* followed by reduction to **9***k*. Finally, cleavage of the ether function at the 3 position was accomplished with boron tribromide (22) in dichloromethane or with hot 48% hydrobromic acid. The 3,14-dihydroxyisomorphinans **9***j*, *k*, *n*, and **9***c* thus obtained, were tested for narcotic antagonist and analgesic activities in laboratory animals. Moderate activities comparable to those of pentazocine were observed with **9***j* and **9***h*.

While the general approach represented by scheme **3** → **8** → **9** provides a convenient entry into the 14-hydroxyisomorphinan system further modifications were required in order to synthesize the isomeric 14-hydroxymorphinans. This was initially accomplished by dehydrating **9***a* with phosphorus oxychloride in pyridine to give the $\Delta^{8,14}$-morphinan **11***a* which after hydrolysis to **11***b* was further transformed into various 14-hydroxymorphinans as previously described (13). Subsequently, a more elegant and practical synthesis of **11***a* was developed (see footnote 6).

Experimental

The melting points were determined on a Gallenkamp apparatus and are not corrected. The infrared (i.r.) spectra were recorded on a Unicam Sp-200G grating i.r. spectrometer. The n.m.r. spectra were recorded on a Varian A-60A spectrometer using deuteriochloroform as a solvent. The chemical shifts are expressed in δ values using tetramethylsilane as internal reference. Microanalysis were performed by Micro-Tech Laboratories Inc., Skokie, Ill.

3,4-Dihydro-7-methoxy-2,2-tetramethylene-1 (2H)-naphthalenone (1)

A suspension of sodium hydride (269 g of ≃56% washed with hexane) in benzene (3.75 l) was heated under reflux under nitrogen and to it was added dropwise *t*-amyl alcohol (220 g) followed by a solution of 7-methoxy-1-tetralone (440 g) in benzene (1.5 l). The mixture was stirred and heated under reflux for 45 min, followed by the rapid addition of a solution of 1,4-dibromobutane (650 g) in benzene (3 l). Stirring and heating were continued for 50 h, after which time the mixture was cooled and the excess of sodium hydride carefully decomposed with water. The benzene layer was washed with water, dried ($MgSO_4$), and concentrated *in vacuo*. The residual oil was fractionally distilled to give 455 g of **1**, b.p. 120–125°/0.1 Torr; i.r. (neat) 1725, 3340 cm^{-1}; n.m.r. δ 7.55 (1H, broad s), 7.05 (2H, m) 3.82 (3H, s), 2.9 (2H, t, J = 6 Hz), 2.0 (2H, t, J = 6 Hz), 1.1–2.3 (8H, m).

Anal. Calcd. for $C_{15}H_{18}O_2$: C, 78.22; H, 7.88. Found: C, 77.96; H, 7.93.

1-Hydroxy-7-methoxy-1,2,3,4-tetrahydro-2,2-tetramethylene-1-naphthaleneacetonitrile (2a) and 1-(2-Aminoethyl)-7-methoxy-1,2,3,4-tetrahydro-2,2-tetramethylene-1-naphtol (2b)

To a cooled (−80°), stirred solution of 1.6 *M* butyl lithium in hexane (1345 ml) under nitrogen was added anhydrous THF (1340 ml) followed by acetonitrile (88 g) in THF (1 l) and stirring continued for 1 h at −80°. To the resulting white suspension was added a solution of spiro ketone **1** (485 g) in THF (1.8 l). The cold bath was removed and the solution was stirred for 20 min. At this point the hydroxy nitrile *2a* can be isolated, or directly

Can. J. Chem. Downloaded from www.nrcresearchpress.com by 210.87.254.105 on 09/05/12
For personal use only.

Can. J. Chem. Downloaded from www.nrcresearchpress.com by 210.87.254.105 on 09/05/12
For personal use only.

reduced *in situ* to the amino alcohol **2***b*. Thus, the reaction mixture was poured onto cold dilute hydrochloric acid and extracted with benzene, followed by drying and evaporation of solvent to yield crude **2***a*. The pure product was obtained by recrystallization from chloroform (80% yield), m.p. 140–142°; i.r. (neat) 2260, 3420 cm^{-1}; n.m.r. δ 7.42 (1H, d, J = 2 Hz), 6.75–7.17 (2H, m), 3.85 (3H, s), 2.6–3.2 (4H, m), 1.1–2.2 (10H, m).

Anal. Calcd. for $C_{17}H_{21}NO_2$: C, 75.24; H, 7.80; N, 5.16. Found: C, 75.12; H, 7.91; N, 4.89.

Alternatively, to the above solution of **2***a* in THF was added lithium aluminum hydride (122 g) and the mixture was stirred for 2.5 h. It was then treated consecutively with water (122 ml), 5 *N* sodium hydroxide (122 ml), and again water (244 ml). The solids were removed by filtration, washed with ether, and the filtrate concentrated *in vacuo* to give 530 g of crude **2***b* as an oil which was used in the next step without further purification; i.r. (neat) 3200 cm^{-1}; n.m.r. δ 7.26 (1H, t, J = 2.5 Hz), 6.5–7.1 (2H, m), 3.83 (3H, s), 2.5–3.2 (4H, m), 1.0–2.2 (12H, m).

The oxalate salt was prepared in acetone and recrystallized from methanol, m.p. 179–180°.

Anal. Calcd. for $C_{17}H_{25}NO_2 \cdot C_2H_2O_4 \cdot CH_3OH$: C, 63.31; H, 7.70; N, 3.69. Found: C, 63.41; H, 7.43; N, 3.79.

4a-(2-Aminoethyl)-1,2,3,4,4a,9-hexahydro-6-methoxyphenanthrene (3a)

To a cooled and stirred solution of **2***b* (530 g) in ether (1 l) was added concentrated hydrochloric acid (530 ml). The cooling bath was removed and the two-phase mixture heated under reflux (steam bath) for 18 h. It was cooled, the ether layer separated, and the aqueous layer diluted with water (1 l) followed by stirring for 18 h. The deposited solid was collected by filtration, washed with acetonitrile, and dried to give 342 g of unsaturated amine hydrochloride **3***a*, m.p. 130°; i.r. (free base, neat) 3200 cm^{-1}; n.m.r. δ 6.6–7.2 (3H, m) 5.71 (1H, t, J = 3.5 Hz), 3.78 (3H, s), 3.32 (2H, broad s), 1.2–3.0 (12H).

The analytical sample was recrystallized from methanol–ether, m.p. 135°.

Anal. Calcd. for $C_{17}H_{23}NO \cdot HCl \cdot CH_3OH$: C, 66.34; H, 8.66; N, 4.29. Found: C, 66.34; H, 8.62; N, 4.26.

1-(2-Aminoethylidene)-1,2,3,4-tetrahydro-2,2-tetramethylenenaphthalene (4)

When the above rearrangement of **2***b* was carried out at room temperature for 24 h, **2***b* was all consumed but the yield of **3***a* was only 62%. However, the mother liquors contained a mixture of **3***a* and **4** in a 1:1 ratio. The unsaturated amine **4** was isolated by chromatography over alumina in 8% yield, as an oil; i.r. (neat) 3420 cm^{-1}; n.m.r. (CCl_4) δ 6.4–7.0 (3H, m), 5.35 (1H, t, J = 6 Hz), 3.67 (3H, s) 3.43 (2H, d, J = 6 Hz), 2.72 (2H, t, J = 7 Hz), 1.7 (2H, t, J = 7 Hz), 1.6 (8H, b, s).

The oxalate salt was recrystallized from methanol, m.p. 199°.

Anal. Calcd. for $C_{17}H_{23}NO \cdot C_2H_2O_4$: C, 65.69; H, 7.25; N, 4.03. Found: C, 65.81; H, 7.40; N, 4.04.

4a-[2-(Ethoxycarbonylamino)ethyl]-1,2,3,4,4a,9-hexahydro-6-methoxyphenanthrene (3b)

To a cooled (ice bath), stirred solution of unsaturated amine **3***a* (51.4 g, 0.2 mol) and triethylamine (22.2 g, 0.22 mol) in dichloromethane (200 ml) was added dropwise ethyl chloroformate (23.0 g, 0.21 mol). The mixture was stirred for 10 min and then washed with dilute hydrochloric acid (100 ml, 1 *N*) followed by water, dried, and evaporated *in vacuo*. The residual oil was dissolved in a 1:3 mixture of ether and petroleum ether (b.p. 30–60°) and the solution filtered through charcoal. The filtrate was concentrated to give 65.8 g of **3***b* as a pale yellow oil; i.r. (neat) 1725, 3340 cm^{-1}; n.m.r. δ 6.55–7.15 (3H, m), 5.7 (1H, t, J = 2.5 Hz), 4.56 (1H, m), 4.01 (2H, q, J = 7 Hz), 3.78 (3H, s), 3.25 (2H, s), 1.2–3.0 (12H, m), 1.15 (3H, t, J = 7 Hz).

Anal. Calcd. for $C_{20}H_{27}NO_3$: C, 72.9; H, 8.26; N, 4.25. Found: C, 72.71; H, 8.27; N, 4.25.

4a-[2-(Methylamino)ethyl]-1,2,3,4,4a,9-hexahydro-6-methoxyphenanthrene (3c)

To a suspension of lithium aluminum hydride (2.3 g) in dry ether (50 ml) was added dropwise under nitrogen a solution of urethane **2***b* (9.87 g) in ether (100 ml). The mixture was heated under reflux for 18 h, after which time it was worked-up in the usual manner to afford the unsaturated amine **3***c* as an oil (8.0 g); n.m.r. δ 5.60 (1H, t, J = 6 Hz, 10-H), 2.22 (3H, s, N—CH_3).

The hydrochloride salt was recrystallized from methanol–ether, m.p. 190–191°.

Anal. Calcd. for $C_{18}H_{25}NO \cdot HCl$: C, 70.22; H, 8.51; N, 4.55. Found: C, 70.39; H, 8.71; N, 4.48.

Amides 3d–3f

Amides **3***d*–**3***f* were prepared by a procedure similar to that described above for the preparation of **3***b*.

4a-[2-(Trifluoroacetylamino)ethyl]-1,2,3,4,4a,9-hexahydro-6-methoxyphenanthrene (3d)

White solid from ether – petroleum ether (89%), m.p. 99–101°.

Anal. Calcd. for $C_{19}H_{22}F_3NO_2$: C, 64.58; H, 6.28; N, 3.96. Found: C, 64.82; H, 6.25; N, 3.82.

4a-[2-(Cyclopropylcarbonylamino)ethyl]-1,2,3,4,4a,9-hexahydro-6-methoxyphenanthrene (3e)

White solid (79%) from methanol, m.p. 126–130°.

Anal. Calcd. for $C_{21}H_{27}NO_2$: C, 77.50; H, 8.36; N, 4.30. Found: C, 77.21; H, 8.40; N, 4.09.

3,4-Dihydro-2,2-pentamethylene-1(2H)-naphthalenone (5)

To a cooled stirred (ice-salt) suspension of sodium hydride (21.3 g of ≃ 56%, washed with hexane) in DMF (300 ml) was added dropwise a solution of 1-tetralone (36.55 g) and 1,5-dibromopentane (57.5 g) in DMF (150 ml) over a 2 h period. The internal temperature during the addition was maintained at 5–10°. When the addition was completed, the mixture was stirred for 30 min at 8–12° and then for 2 h at room temperature. It was then partitioned between water and petroleum ether and the organic layer washed with water, dried, and evaporated. The residual oil was distilled to give 29.5 g of spiro ketone **5**, b.p. 115–120°/0.05 Torr; i.r. (neat), 1680 cm^{-1}; n.m.r. (CCl_4), δ 7.9–8.1 (1H, m), 7.0–7.5 (3H, m), 2.93, (2H, t, J = 6 Hz), 20 (2H, t, J = 6 Hz), 1.15–2.0 (10H, m). This product was probably contaminated with some dibromopentane, as judged from the empirical analysis (carbon lower by 0.6%). It was used in the next step without further purification.

1-Hydroxy-1,2,3,4-tetrahydro-2,2-pentamethylen-1-naphthaleneacetonitrile (6a)

The hydroxynitrile **6***a* was obtained in 83% yield by a

Can. J. Chem. Downloaded from www.nrcresearchpress.com by 210.87.254.105 on 09/05/12
For personal use only.

similar procedure as given for the preparation of **2***a*, m.p. 128–131° (from benzene); i.r. 2260, 3440 cm^{-1}; n.m.r. ($CDCl_3$) δ, 7.7–7.9 (1H, m), 7.0–7.4 (3H, m), 2.6–3.1 (4H, m), 2.0–2.5 (2H, m), 1.1–1.9 (10H, m).

Anal. Calcd. for $C_{17}H_{21}NO$: C, 79.96; H, 8.29; N, 5.48. Found: C, 79.74; H, 8.28; N, 5.41.

1-(2-Aminoethyl)-1,2,3,4-tetrahydro-2,2-pentamethylene-1-naphtol (6b)

The amino alcohol **6***b* was obtained in a quantitative yield from hydroxynitrile **6***a* by the procedure described above for the preparation of **2***b*; i.r. (neat) 3220, 3470 cm^{-1}; n.m.r. ($CDCl_3$), δ 7.45–7.7 (1H, m), 6.9–7.4 (3H, m), 2.55–3.0 (4H, m), 0.8–2.5 (12H, m). The oxalate salt was prepared in ether, m.p. 167–171°.

Anal. Calcd. for $C_{17}H_{25}NO \cdot C_2H_2O_4 \cdot \frac{1}{2}H_2O$: C, 63.67; H, 7.67; N, 3.01. Found: C, 63.43; H, 7.53; N, 4.06.

1-(2-Amino-1-ethylidene)-1,2,3,4-tetrahydro-2,2-pentamethylenenaphthalene (6c)

A solution of the amino alcohol **6***b* (2.0 g) in methanol (60 ml) was added dropwise with stirring to concentrated hydrochloric acid (60 ml). The internal temperature during the addition was maintained at 30–36°. After addition was completed, stirring was continued for 15 min at the same temperature whereupon the mixture was poured onto water, basified with ammonium hydroxide, and extracted with benzene. The extract was dried and concentrated *in vacuo* to give 1.6 g of crude **6***c*; i.r. (neat) 3200 cm^{-1}; n.m.r. ($CDCl_3$) δ 7.1–7.4 (4H, m), 5.7 (1H, t, J = 7 Hz), 3.74 (2H, d, J = 7 Hz), 2.8 (2H, t, J = 6 Hz), 1.73 (2H, t, J = 6 Hz), 1.44 (10H, s).

The hydrochloride salt was prepared in ether and recrystallized from methanol–ether, m.p. 206–208°.

Anal. Calcd. for $C_{17}H_{23}N \cdot HCl$: C, 73.49; H, 8.71; N, 5.04. Found: C, 73.18; H, 8.89; N, 5.06.

10,10a-α-Epoxy-4a-[2-(ethoxycarbonylamino)ethyl]-1,2,3,4,4a,9,10,10a-octahydro-6-methoxyphenanthrene (8a)

To a cooled (5–10°) stirred solution of the urethane **3***b* (55.8 g) in dichloromethane (150 ml) was added in small portions 45 g of *m*-chloroperbenzoic acid (85% purity) and the mixture left at room temperature for 5 h. The precipitated solid was removed by filtration and the filtrate washed with aqueous sodium sulfite followed by 5% aqueous sodium bicarbonate and finally with water. Drying and evaporation of the solvent afforded an oil, which was dissolved in ether followed by the addition of petroleum ether. After filtration through Celite–charcoal and concentration of the filtrate *in vacuo*, there was obtained 65.8 g of epoxide **8***a* as an oil which solidified on standing, m.p. 75–77° (ether).

Anal. Calcd. for $C_{20}H_{27}NO_4$: C, 69.54; H, 7.77; N, 4.05. Found: C, 69.30; H, 7.95; N, 3.90.

10,10a-α-Epoxy-4a-[2-(trifluoroacetylamino)ethyl]-1,2,3,4,4a,9,10,10a-octahydro-6-methoxyphenanthrene (8b)

To a solution of amide **3***d* (7.06 g) in dichloromethane (140 ml) was added in small portions with stirring and cooling (5–10°) *m*-chloroperbenzoic acid (4.2 g, 85% purity). The mixture was left at room temperature for 18 h and then worked-up as described for the isolation of **8***a* to give 7.36 g of epoxide 7*b* as an amorphous solid. A sample was prepared for analysis by dissolving in ether followed by precipitation with excess petroleum ether; the syrup was dried under high vacuum to yield amorphous solid, m.p. 45–50°.

Anal. Calcd. for $C_{19}H_{23}F_3NO_3$: C, 61.79; H, 6.00; N, 3.79. Found: C, 62.02; H, 6.07; N, 3.74.

10,10a-α-Epoxy-4-[2-(cyclopropylcarbonylamino)ethyl]-1,2,3,4,4a,9,10,10a-octahydro-6-methoxyphenanthrene (8c)

The epoxide **8***c* was obtained in 78% yield from amide **3***c* by a procedure similar to that given for the preparation of **8***b* except that purification was accomplished by crystallization from ether, m.p. 130–132°.

Anal. Calcd. for $C_{21}H_{27}NO_3$: C, 73.87; H, 7.97; N, 4.10. Found: C, 73.71; H, 8.06; N, 4.20.

10,10a-α-Epoxy-4a-[2-(N-trifluoroacetyl-N-methylamino)ethyl]-1,2,3,4,4a,9,10,10a-octahydro-6-methoxyphenanthrene (8d)

The epoxide **8***d* was obtained as an oil in a quantitative yield by a procedure similar to that given for the preparation of **8***b*, except that the time required for completion of the reaction was 1 h.

Anal. Calcd. for $C_{20}H_{24}F_3NO_3$: C, 62.65; H, 6.31; N, 3.65. Found: C, 62.89; H, 6.48; N, 3.66.

17-Ethoxycarbonyl-14-hydroxy-3-methoxyisomorphinan (9a)

To a stirred boiling suspension of sodium hydride (3.15 g of ≃56%, washed with hexene) in dry benzene, under nitrogen atmosphere, was added a solution of anhydrous *t*-amyl alcohol (5.87 g) in benzene (50 ml). When the hydrogen evolution had subsided (*ca.* 15 min), a solution of epoxide **8***a* (23.0 g) in benzene (500 ml) was added dropwise over a 4 h period and stirring and heating were continued for 18 h. After cooling, the mixture was washed with water, dried, and concentrated *in vacuo*. The residual oil was dissolved in ether and the resulting solution was diluted with petroleum ether. The cloudy mixture was filtered through Celite–charcoal cake and the filtrate evaporated to dryness to give 20.0 g of the isomorphinan **9***a* as a yellow oil. A sample solidified after distillation at 100°/0.05 Torr, m.p. 50°; i.r. (Nujol) 1690, 3300 cm^{-1}; n.m.r. δ 6.5–7.2 (3H, m), 4.15 (2H, q, J = 7 Hz), 3.78 (3H, s), 2.3–3.8 (5H, m), 1.3–2.3 (10H, m), 1.26 (3H, t, J = 7 Hz).

Anal. Calcd. for $C_{20}H_{27}NO_4$: C, 69.54; H, 7.88; N, 4.05. Found: C, 69.21; H, 8.01; N, 3.95.

14-Hydroxy-3-methoxy-17-trifluoroacetylisomorphinan (9b)

The hydroxy amide **9***b*, an amorphous solid, was obtained from **8***b* in 68% yield together with the product of hydrolysis **8***d* (8%) by a procedure similar to that given for the preparation of **9***a* except that the reaction time was 3.5 h.

Mol. Wt. Calcd. for $C_{19}H_{23}F_3NO_3$: 369. Found (mass spectrometry): 369.

17-Cyclopropylcarbonyl-14-hydroxy-3-methoxyisomorphinan (9c)

To a stirred and cooled (5–8°) suspension of sodium hydride (1.8 g, hexane washed) in a mixture of anhydrous THF (200 ml) and DMSO (200 ml) was added epoxide **8***c* (13.08 g). The mixture was stirred at 5–8° for 3 h and

Can. J. Chem. Downloaded from www.nrcresearchpress.com by 210.87.254.105 on 09/05/12
For personal use only.

then for 1 h at room temperature. It was then poured onto water and extracted with benzene. The organic layer was washed with water several times, dried, and concentrated *in vacuo*. The residual oil was crystallized from ether to yield 6.56 g of isomorphinan **9c** (50%) as a white solid, m.p. 162–64°; i.r. (Nujol), 1640, 3410 cm^{-1}.

Anal. Calcd. for $C_{21}H_{27}NO_3$: C, 73.87; H, 7.97; N, 4.10. Found: C, 73.70, H, 8.13; N, 4.02.

14-Hydroxy-3-methoxyisomorphinan (9d)

A mixture of **9a** (10.0 g) and potassium hydroxide pellets (6.0 g) in 1-octanol (50 ml) was heated under reflux for 30 min under nitrogen. After cooling, the mixture was poured onto water and extracted with ether. The organic layer was extracted with 2 *N* hydrochloric acid (2 × 60 ml) and the extract washed with ether to remove 1-octanol. The aqueous layer was made alkaline and extracted with ether to give after drying and concentration 7.5 g of crude **9d** as an oil. The hydrochloride salt was recrystallized from isopropyl aclcohol – ether to afford 5.2 g (58%) of pure product, m.p. 261–271°; i.r. (free base), 3360 and 3460 cm^{-1}; n.m.r. ($CDCl_3$) δ 6.6–7.3 (3H, m), 3.78 (3H, s), 3.55 (1H, d, J = 7 Hz), 3.25 (1H, d, J = 7 Hz), 0.8–3.0 (13H, m).

Anal. Calcd. for $C_{17}H_{23}NO_2 \cdot HCl$: C, 65.90; H, 7.81; N, 4.52. Found: C, 65.57; H, 7.85; N, 4.27.

Alternatively, **9d** was obtained in a 53% overall yield from **8b** via **9b**, after treatment of the latter with 1.5 *N* NaOH in methanol–water (3:1) at reflux temperature for 3 h, without isolation of **9b**.

17-Cyclobutylcarbonyl-14-hydroxy-3-methoxyisomorphinan (9e)

To a stirred and cooled (ice) solution of **9d** (2.1 g) and triethylamine (1.0 g) in dichloromethane (20 ml) was added dropwise a solution of cyclobutanecarboxylic acid chloride (1.07 g) in dichloromethane (10 ml). The mixture was then washed with water, dried, and concentrated. The residual oil crystallized from ether to give **9e** (2.0 g) as a white solid, m.p. 136–138°.

Anal. Calcd. for $C_{22}H_{20}NO_3$: C, 74.33; H, 8.22; N, 3.94. Found: C, 74.53; H, 8.37; N, 3.78.

14-Hydroxy-3-methoxy-17-methylisomorphinan (9f)

To a solution of lithium aluminum hydride (3.8 g) in anhydrous ether (100 ml) was added dropwise under nitrogen atmosphere a solution of urethane **9a** (34.5 g) in ether (200 ml). The mixture was heated under reflux for 1 h and then worked-up in the usual manner. The crude product, an oil, was converted to its hydrochloride salt in methanol to give **9f** (23.0 g, 65%) as a white solid, m.p. 252–254°; i.r. (free base in $CDCl_3$) 3550 cm^{-1}; n.m.r. (free base in $CDCl_3$) δ 6.6–7.1 (3H, m), 3.76 (3H, s), 0.9–2.1 (10H, m).

Anal. Calcd. for $C_{18}H_{25}NO_2 \cdot HCl$: C, 66.76; H, 8.09; N, 4.32. Found: C, 67.03; H, 8.27; N, 4.18.

17-Cyclopropylmethyl-14-hydroxy-3-methoxyisomorphinan (9g)

A solution of **9c** (1.6 g) in THF (20 ml) was added dropwise to a solution of lithium aluminum hydride (0.47 g) in THF (10 ml) and the mixture was heated under reflux for 1 h. Work-up in the usual manner yielded **9g** as an oil which was converted to its hydrochloride salt in ether. Recrystallization from methanol afforded pure product (1.24 g, 71%) as a white solid, containing ½ mol of water of crystallization, m.p. 229–230°.

Anal. Calcd. for $C_{21}H_{29}NO_3 \cdot HCl \cdot \frac{1}{2}H_2O$: C, 67.67; H, 8.37; N, 3.72. Found: C, 67.63; H, 8.34; N, 3.65.

17-Cyclobutylmethyl-14-hydroxy-3-methoxyisomorphinan (9h)

The hydroxyisomorphinan **9h** was obtained in 74% yield from **9e** by a procedure similar to that given for the preparation of **9g**; hydrochloride salt, m.p. 239–241°.

Anal. Calcd. for $C_{22}H_{31}NO_2 \cdot HCl$: C, 69.91; H, 8.53; N, 3.71. Found: C, 69.71; H, 8.67; N, 3.48.

3,14-Dihydroxy-17-methylisomorphinan (9i)

A solution of **9f** (1.0 g) in 48% hydrobromic acid (10 ml) was heated under reflux for 10 min under nitrogen. After cooling, the mixture was diluted with water, made basic with ammonium hydroxide, and extracted with chloroform. The extract was dried, evaporated, and the residual oil crystallized from ether to afford **9i** (650 mg) as a white solid. Recrystallization from methanol–ether gave an analytical sample, m.p. 191–193°; n.m.r. ($CDCl_3$) δ 6.4–7.0 (3H, m), 2.4–3.0 (5H, m), 2.3 (3H, s), 0.8–2.2 (10H, m).

Anal. Calcd. for $C_{17}H_{23}NO_2$: C, 74.71; H, 8.48; N, 5.13. Found: C, 74.63; H, 8.52; N, 5.01.

17-Cyclopropylmethyl-3,14-dihydroxyisomorphinan (9j)

To a cooled (ice–salt) and stirred solution of boron tribromide (1.85 g) in anhydrous dichloromethane (10 ml) under nitrogen was added a solution of methoxyisomorphinan **9g** (0.80 g) in dichloromethane (10 ml) and the mixture stirred for 2 h at room temperature. It was then slowly poured onto ice–water, basified with ammonium hydroxide, and the layers separated. The organic layer was dried (Na_2SO_4), evaporated *in vacuo*, and the residual amorphous solid treated with dry hydrochloric acid in ether to give 0.59 g of hydrochloride salt of the dihydroxyisomorphinan **9j**. A sample for analysis was recrystallized from methanol, m.p. 222–224°.

Anal. Calcd. for $C_{20}H_{23}NO_2 \cdot HCl \cdot \frac{1}{4}CH_3OH$: C, 67.29; H, 8.27; N, 3.83. Found: C, 66.91; H, 8.35; N, 3.86.

17-Cyclobutylmethyl-3,14-dihydroxyisomorphinan (9k)

The dihydroxyisomorphinan **9k** was obtained in 68% yield from the methoxyisomorphinan **9h** as a white solid (free base), m.p. 162–164°, by a procedure similar to that given for the preparation of **9j**. Recrystallization from methanol gave an analytical sample, m.p. 170–171°.

Anal. Calcd. for $C_{21}H_{29}NO_2$: C, 77.02; H, 8.93; N, 4.28. Found: C, 77.17; H, 9.09; N, 4.11.

3,14-Dimethoxy-17-methylisomorphinan (9l)

A solution of chloramine **3g** (5.0 g) in methanol (150 ml) was heated under reflux for 24 h. The methanol was evaporated *in vacuo* and the residue extracted with petroleum ether. The extract was evaporated to give an oil (4.5 g), which was chromatographed on an alumina column (activity III to IV; eluent, dichloromethane) to give the dimethoxyisomorphinan **9l** (1.45 g) as an oil; n.m.r. ($CDCl_3$) δ 6.5–7.3 (3H, m), 3.84 (3H, s), 3.11 (3H, s), 2.38 (3H, s), 2.2–3.4 (5H, m), 0.8–2.2 (10H, m). The hydrochloride salt was recrystallized from isopropyl alcohol, m.p. 248–250°.

Anal. Calcd. for $C_{19}H_{27}NO_2 \cdot HCl$: C, 67.54; H, 8.35; N, 4.14. Found: C, 67.41; H, 8.35; N, 3.90.

Can. J. Chem. Downloaded from www.nrcresearchpress.com by 210.87.254.105 on 09/05/12
For personal use only.

17-Allyl-14-hydroxy-3-methoxyisomorphinan (9m)

A solution of **9d** (1.09 g), triethylamine (2.02 g), and allylbromide (0.73 g) in dry ethanol was heated under reflux and under nitrogen for 18 h. After cooling, it was partitioned between chloroform and dilute ammonium hydroxide. The organic layer was separated, dried, and evaporated to yield 1.20 g of **9m** as an oil; i.r. (neat) 3460 and 3560 cm^{-1}; n.m.r. ($CDCl_3$) δ 6.6–7.2 (3H, m), 5.0–6.4 (3H, m), 3.68 (3H, s), 0.8–3.2 (17H).

A sample for analysis was purified as the hydrochloride salt which was recrystallized from methanol–ether, m.p. 243–245°.

Anal. Calcd. for $C_{20}H_{27}NO_2 \cdot HCl$: C, 68.65; H, 8.07; N, 4.00. Found: C, 68.46; H, 8.18; N, 3.93.

17-Allyl-3,14-dihydroxyisomorphinan (9n)

To a cooled (ice–salt) solution of boron tribromide (1.75 g) in dichloromethane (10 ml) was added under nitrogen a solution of **9m** (1.1 g) in dichloromethane (10 ml) and the mixture was stirred for 1 h at room temperature. It was then treated with ice and concentrated ammonium hydroxide and the layers separated. The organic layer was dried (Na_2SO_4) and concentrated *in vacuo* to afford 1.0 g of **9n** as an oil; i.r. (neat) 3200 cm^{-1}; n.m.r. ($CDCl_3$) δ 6.1–7.1 (3H, m), 3.9–6.1 (3H, m), 0.5–3.2 (17H). The hydrochloride salt was recrystallized from 2-propanol, m.p. 248–250° (dec.).

Anal. Calcd. for $C_{19}H_{25}NO_2 \cdot HCl$: C, 67.94; H, 7.80; N, 4.17. Found: C, 67.75; H, 7.88; N, 3.96.

9α-Hydroxy-3-methoxy-17-methylhasubanan (10) and the Corresponding 14-Hydroxyisomorphinan (9f)

To a solution of *N*-trifluoroacetyl epoxide **8d** (5.4 g) in methanol (160 ml) was added a 10% aqueous solution of potassium carbonate (150 ml) and the mixture was stirred at room temperature for 2 h. It was then concentrated to a small volume, diluted with water, and extracted with ether to yield after drying and evaporation of the ether extract an oil (3.50 g). This was dissolved in methanol (50 ml) and the solution heated under reflux for 18 h under nitrogen. The solvent was then evaporated, and the residue chromatographed on an alumina column (activity III to IV; eluent, $CHCl_3$) to give at first 14-hydroxyisomorphinan **9f** (1.49 g) followed by 9α-hydroxyhasubanan **10** (1.52 g) as an oil; i.r. (neat) 3400 cm^{-1}; n.m.r. δ 6.6–7.2 (3H, m), 4.2 (1H, dd, J_1 = 6 Hz, J_2 = 9 Hz, 9-H), 3.79 (3H, s), 2.7–3.3 (4H, m), 2.62 (3H, s), 0.8–2.2 (10H, m).

The oxalate salt of **10** crystallized from methanol–acetone with ½ mol of methanol of crystallization, m.p. 109–111°.

Anal. Calcd. for $C_{18}H_{25}NO_2 \cdot C_2H_2O_4 \cdot \frac{1}{2}CH_3OH$: C, 62.58; H, 7.43; N, 3.56. Found: C, 62.69; H, 7.73; N, 3.31.

17-Ethoxycarbonyl-3-methoxy-$\Delta^{8,14}$-morphinan (11a)

To a cooled (ice–water) solution of hydroxyisomorphinan **9a** (48.0 g) in pyridine (96 ml) was added dropwise under nitrogen phosphorous oxychloride (48 ml) and the mixture was left at room temperature for 7 days. It was then diluted with benzene (200 ml) and carefully poured onto ice–water. The layers were separated and the water layer extracted with benzene (100 ml). The combined benzene extracts were washed with water, dried, and concentrated *in vacuo*. The residual brown oil was dissolved in ether followed by addition of petroleum ether. The turbid mixture was filtered through Celite–charcoal cake and evaporated to dryness to yield $\Delta^{8,14}$-morphinan **11a** (36.0 g; 79%) as a colorless oil; i.r. (neat) 1680 cm^{-1}; n.m.r. δ 6.6–7.2 (3H, m), 5.78 (1H, t, J = 4 Hz, 8-H), 4.16 (2H, q, J = 7 Hz), 3.82 (3H, s), 2.5–3.2 (5H, m), 1.28 (3H, t, J = 7 Hz), 1.2–2.4 (8H, m).

Anal. Calcd. for $C_{20}H_{25}NO_3$: C, 73.37; H, 7.70; N, 4.28. Found: C, 73.22; H, 7.33; N, 4.12.

3-Methoxy-$\Delta^{8,14}$-morphinan (11b)

A mixture of *N*-carbethoxymorphinan **11a** (32.7 g) and potassium hydroxide pellets (28.0 g) in 1-octanol (160 ml) was heated under reflux and under nitrogen for 45 min. The mixture was then worked-up as described above for the preparation of **9d** to give 20 g of a crude oily product. The oil was dissolved in acetone and treated with an acetone solution of oxalic acid. Addition of ether caused precipitation of a solid which was recrystallized from methanol–acetone to afford pure **11b** (12.0 g, 34.8%) as white crystals, m.p. 187–189°; n.m.r. (free base in CCl_4) δ 6.45–7.05 (3H, m), 5.5 (1H, t, J = 4 Hz), 3.71 (3H, s), 2.5–3.5 (5H, m), 1.2–2.5 (8H, m).

Anal. Calcd. for $C_{17}H_{21}NO \cdot C_2H_2O_4$: C, 66.07; H, 6.71; N, 4.06. Found: C, 66.28; H, 6.72; N, 4.11.

The financial support of the National Research Council of Canada through its Industrial Research Assistance Program is gratefully acknowledged. We thank Dr. V. DiTullio, Mr. J. Chapuis, and J. Lajeunesse for their technical assistance and Dr. A. Pircio of Bristol Laboratories, Syracuse, N.Y. for the pharmacological tests.

1. B. Belleau, H. Wong, I. Monković, and Y. G. Perron. Chem. Commun. 603, (1974).
2. M. Saucier and I. Monković. Can. J. Chem. **52**, 2736 (1974).
3. J. W. Lewis, K. W. Bentley, and A. Cowan. Ann. Rev. Pharmacol. **4**, 241 (1971).
4. M. Gates and W. G. Webb. J. Am. Chem. Soc. **80**, 1186 (1958).
5. M. Gates and T. Montzka. J. Med. Chem. **7**, 127 (1968).
6. R. Grewe. Naturwissenschafen, **33**, 33 (1946).
7. O. Schnider and J. Hellerbach. Helv. Chim. Acta, **33**, 1437 (1950). N. B. Eddy, J. G. Murphy, and E. L. May. J. Org. Chem. **22**, 1370 (1957).
8. M. Onda, Y. Sugama, H. Yokoyama, and F. Tada. Chem. Pharm. Bull. (Jap.), **21**, 2359 (1973).
9. Y. K. Sawa and H. Tada. Tetrahedron, **24**, 6185 (1968).
10. B. Belleau. J. Am. Chem. Soc. **75**, 1159 (1953).
11. B. Belleau, T. T. Conway, T. W. Doyle, L. Morris, Y. G. Perron, and W. Verbestel. Can. J. Chem. **53**, 237 (1975).
12. T. T. Conway, T. W. Doyle, B. Belleau, Y. G. Perron, and J. Chapuis. Can. J. Chem. **53**, 245 (1975).
13. I. Monković, T. T. Conway, H. Wong, Y. G. Perron, I. J. Pachter, and B. Belleau. J. Am. Chem. Soc. **95**, 7910 (1973).
14. F. H. Howell and D. A. H. Taylor. J. Chem. Soc. 1248 (1958).
15. M. Mousseron, R. Jacquier, and H. Christol. Bull. Soc. Chim. Fr. 346 (1957).

16. E. M. KAISER and C. R. HAUSER. J. Org. Chem. **33**, 3402 (1968).
17. T. T. CONWAY. To be published.
18. H. WONG, J. CHAPUIS, and I. MONKOVIĆ. J. Org. Chem. **39**, 1042 (1974).
19. D. E. HORNING and J. M. MUCHOWSKI. Can. J. Chem. **52**, 1321 (1974).
20. W. NAGATA, S. HIRAI, K. KAWATO and T. AOIKI. J. Am. Chem. Soc. **89**, 5045 (1967). W. NAGATA, S. HIRAI, K. KAWATO, and T. OKUMURA. J. Am. Chem. Soc. **89**, 5045 (1967). W. NAGATA, S. HIRAI, T. OKUMURA, and K. KAWATA. J. Am. Chem. Soc. **90**, 1650 (1968).
21. P. G. GASSMAN, F. HOYDA, and J. DYGOS. J. Am. Chem. Soc. **90**, 2716 (1968). P. G. GASSMAN and J. H. DYGOS. Tetrahedron Lett. 4745 (1972); 4749 (1972).
22. J. F. W. MCOMIE, M. L. WATTS, and E. E. WEST. Tetrahedron, **24**, 2289 (1968).

Can. J. Chem. Downloaded from www.nrcresearchpress.com by 210.87.254.105 on 09/05/12
For personal use only.

Total Synthesis of Monosaccharides. Synthesis of Methyl DL-Pentopyranosides with α- and β-*lyxo*, β-*ribo*, α-*xylo*, and α-*arabino* Configurations from Furfuryl Alcohol[1]

OSMAN ACHMATOWICZ, JR.[2] AND PAWEL BUKOWSKI
Institute of Organic Chemistry, Polish Academy of Sciences, 00-961, Warsaw, Poland

Received March 17, 1975

OSMAN ACHMATOWICZ, JR. and PAWEL BUKOWSKI. Can. J. Chem. **53**, 2524 (1975).

Hydroxylation and epoxidation, followed by the oxirane ring opening, of methyl 2,3-dideoxy-α and β-DL-pent-2-enopyranosides, readily available by the transformation of furfuryl alcohol, afforded the title compounds. Steric course of hydroxylation and epoxidation reactions were examined. The p.m.r. data of methyl 4-*O*-acetyl-2,3-anhydro-DL-pentopyranosides are reported.

OSMAN ACHMATOWICZ, JR. et PAWEL BUKOWSKI. Can. J. Chem. **53**, 2524 (1975).

L'hydroxylation et l'époxydation, suivie d'une ouverture du cycle oxyrannique, du didéoxy-2,3 α- et β-DL-penténo-2 pyrannosides, facilement obtenu par transformation du furanne-2 méthanol, conduit aux composés du titre. On a étudié la stéréochimie de l'hydroxylation et de l'époxydation. Les données du spectre r.p.m. du méthyl *O*-acétyl-4 anhydro-2,3 DL-pentopyrannosides sont présentées. [Traduit par le journal]

In a recent paper (1) from this laboratory we have reported on the transformation (Scheme 1) of 2-furylcarbinols of general formula **1** into methyl 2,3-dideoxy-DL-alk-2-enopyranosid-4-uloses (**2**) which are potentially useful as substrates for versatile total syntheses of sugars. In the present paper we describe the application of the above mentioned transformation to the preparation of methyl DL-pentopyranosides.

Results and Discussion

Furfuryl alcohol (**3**) was transformed in three steps (1) into methyl 2,3-dideoxy-DL-pent-2-enopyranosid-4-ulose (**4**), which on reduction with sodium borohydride gave an excellent yield of methyl 2,3-dideoxy-α-DL-*glycero*-pent-2-enopyranoside (**5**) (Scheme 2). The isomer having β configuration (**6**) was obtained from **5** by inversion of the configuration at C-4 (2). Compounds **5** and **6** served as direct substrates for the synthesis of methyl DL-pentopyranosides and methyl 2,3-anhydro-DL-pentopyranosides.

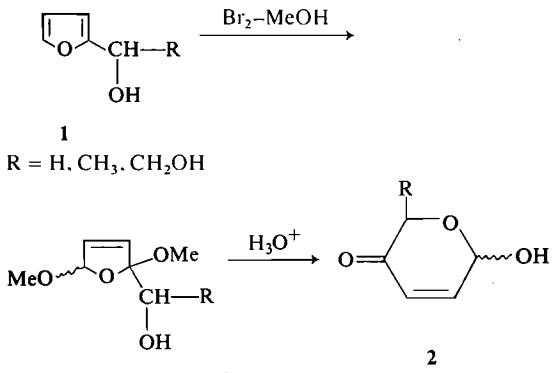

SCHEME 1

Methyl α-DL-*Lyxopyranoside (7)*

Cis hydroxylation of the double bond in **5** by means of hydrogen peroxide in the presence of catalytic amounts of osmium tetroxide (Milas' reagent) gave 45% yield of a single (t.l.c.) crystalline product. Its elemental analysis and i.r. spectrum were those required by methyl pentoside. Assuming that the hydroxylating agent was attacking from the side of the smaller steric hindrance, we assigned to the obtained product the structure of methyl α-DL-lyxopyranoside (**7**). This structure was confirmed by comparison of t.l.c. R_f values and p.m.r. spectra of the tri-*O*-acetyl derivative **7***a* with those of an authentic sample of methyl 2,3,4-tri-*O*-acetyl-α-D-lyxopyranoside.

Methyl β-DL-*Ribo- (8) and Methyl* β-DL-*Lyxopyranoside (9)*

Cis hydroxylation of methyl 2,3-dideoxy-β-DL-pent-2-enopyranoside (**6**) with Milas' reagent gave 42% yield of a mixture of two compounds

[1]This work is a part of Ph.D. thesis of P. B. at the Institute of Organic Chemistry, Polish Academy of Sciences, Warsaw, 1971.

[2]Author to whom correspondence should be addressed.

Can. J. Chem. Downloaded from www.nrcresearchpress.com by 210.87.254.6 on 09/05/12
For personal use only.

Can. J. Chem. Downloaded from www.nrcresearchpress.com by 210.87.254.6 on 09/05/12
For personal use only.

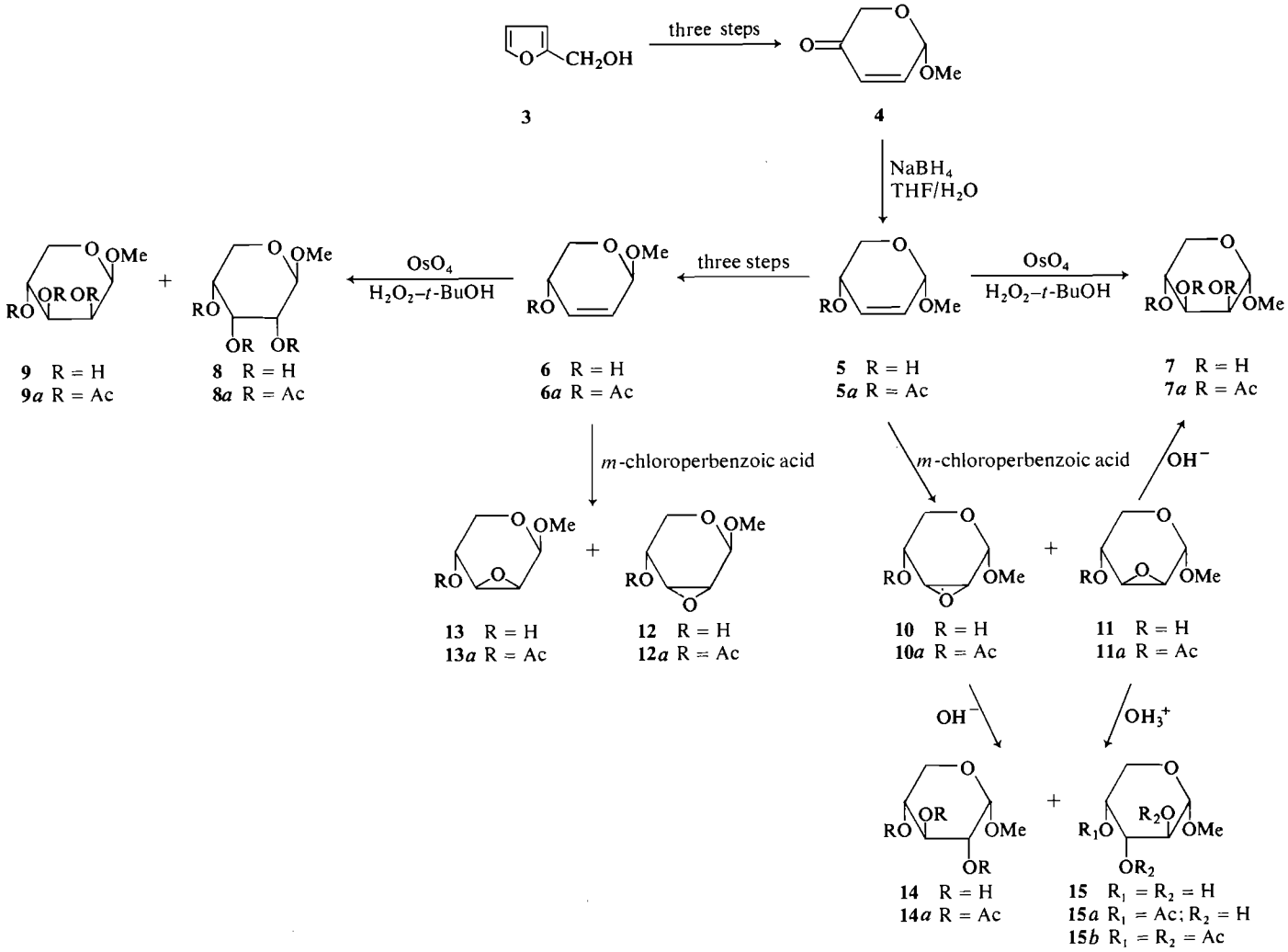

SCHEME 2[3]

[3]For the sake of simplicity all formulae relate to D-compounds, whereas they represent racemic mixtures.

Can. J. Chem. Downloaded from www.nrcresearchpress.com by 210.87.254.6 on 09/05/12
For personal use only.

TABLE 1. Epoxidation of methyl 2,3-dideoxy-DL-pent-2-enopyranosides with *m*-chloroperbenzoic acid

Substrate	Reaction time (days)	Overall yield (%)	Products: Structure	Ratios	Melting point (°C)	Boiling point/Torr (°C)	ν_{max} (cm^{-1})	Elemental analyses (%) Calculated C	Calculated H	Found C	Found H
5	2	90	**10**	9	54–58	—	3450, 1065, 910, 875, 770	49.3	6.9	49.7	7.1
			11	1	—	$70/10^{-3}$	3450, 1070, 1240, 850, 820, 755	49.3	6.9	49.4	7.3
5*a*	32	57	**10***a*	3	67–68.5	85–90/0.2	1740, 1250, 1065, 910, 870, 770	51.1	6.4	51.1	6.4
			11*a*	7	—	80–83/0.4	1740, 1235, 910, 815	51.1	6.4	51.5	6.4
6	9	91	**12***	10	50–51.5	—	3450, †	49.3	6.9	49.4	7.1
			13	1	—	$75/10^{-3}$					

*Methyl 4-*O*-acetyl-2,3-anhydro-β-DL-ribopyranoside (12*a*), m.p. 44–48°; i.r. ν_{max}; 1740, 1250, 865 cm^{-1}. Anal. Calcd. for $C_8H_{12}O_5$: C, 51.1; H, 6.4. Found: C, 51.3; H, 6.5.
†Characterized only by the p.m.r. spectrum (Table 2) of the 4-*O*-acetyl derivative 13*a*.

TABLE 2. Proton magnetic resonance data* for methyl 4-*O*-acetyl-2,3-anhydro-DL-pentopyranosides

Compound	Solvent	Chemical shifts (δ) H-1	H-2	H-3	H-4	H-5 H-5′	OMe	OAc	Coupling constants (Hz) J_{12}	J_{23}	J_{34}	J_{45}	$J_{45'}$	$J_{55'}$
10*a*	CCl_4	4.71	3.31	3.31	4.98	3.35–3.75	3.35	2.05	†	4.0	‡	9.0	6.6	‡
	C_6D_6	4.45	3.00	3.15	4.98	3.34–3.73	3.19	1.70	2.8	4.2	1.6§	9.5	5.9	10.4
11*a*	$CDCl_3$	4.76	3.07	3.25	4.93	3.87–3.50	3.46	2.10	0	3.8	0	8.0	6.4	‡
	C_6D_6	4.58	2.86	3.03	4.91	3.80–3.20	3.15	1.67	0	3.9	0	8.0	6.3	‡
12*a*	$CDCl_3$	4.82	3.12	3.52	4.92	3.82 3.40	3.43	2.14	0	4.0	4.8	4.0	2.6	12.8
	C_6D_6	4.55	2.83	3.29	4.57	3.56 3.18	3.10	1.70	0	4.0	4.7	4.1	2.6	12.8
13*a*	$CDCl_3$	4.90	3.32	‖	5.03	3.92–3.49	3.42	2.12	2.4	‡	‡	1.9	0	13.0

*Chemical shifts are in δ scale from TMS as internal standard, coupling constants were obtained by the first-order treatment.
†Apparent triplet with spacing of 1.4 Hz, due to the strong coupling of H-2 and H-3 protons.
‡Could not be obtained from the spectrum.
§J_{35} = 0.8 Hz.
‖Covered by OMe protons signal.

Can. J. Chem. Downloaded from www.nrcresearchpress.com by 210.87.254.6 on 09/05/12
For personal use only.

in the ratio 6:4 (g.l.c.). Their R_f values in t.l.c. corresponded to those of methyl β-D-ribo- and methyl β-D-lyxopyranosides. Both compounds were isolated by chromatography on silica gel columns. The preponderant component of the mixture was converted into its tri-*O*-acetyl derivative (**8***a*), having R_f values in t.l.c. and p.m.r. spectrum identical with those of methyl 2,3,4-tri-*O*-acetyl-β-D-ribopyranoside, prepared from natural D-ribose. Comparison of g.l.c. chromatograms of trimethyl silyl ethers of the second component of the mixture and methyl glycosides of natural pentoses proved that it was methyl β-DL-lyxopyranoside (**9**).

The foregoing results show the predictable (3) sensitivity of the *cis* hydroxylation with Milas' reagent towards steric hindrance. In the case of compound **5**, having both substituents on the same side of the ring, the reaction is fully stereoselective, whereas hydroxylation of compound **6**, in which the steric hindrance due to substituents at C-1 and C-4 acts in opposite directions, results in a mixture of two products.

*Methyl 2,3-Anhydro-*DL*-pentopyranosides, α- and* β*-ribo and* α*- and* β*-lyxo*

Preparation of methyl DL-pentosides having *arabino* and *xylo* configurations required an introduction of hydroxyl groups to the double bond of compound **5** or **6** in relation *trans* to each other. This was achieved by epoxidation followed by opening of the oxirane ring.

The epoxidation of compounds **5** and **6** with *m*-chloroperbenzoic acid gave mixtures of two products in the ratio 9:1 and 10:1, respectively, which were separated on silica gel column. All compounds gave elemental analysis and i.r. spectra required by methyl 2,3-anhydropentopyranosides. Their configurations were determined on the basis of p.m.r. spectra of 4-*O*-acetyl derivatives. Stereoselectivity of the epoxidation reaction was in agreement with that previously found in similar systems (4), that is, prevailing formation of the oxirane ring *cis* to the hydroxyl group. In the p.m.r. spectrum of 4-*O*-acetyl derivative (**10***a*) of the main epoxidation product obtained from **5**, the coupling constant of protons H-1 and H-2 was 2.8 Hz. Hence we ascribed[4] to it α-*ribo* configuration (**10**); α-*lyxo* configuration (**11**) was assigned to the minor product, on the basis of H-1 and H-2 coupling constants, which in this case amounted to about 0 Hz.

In the 2,3-anhydro compound, the major product from **6**, the respective coupling constants indicated a *cis* relation for protons H-3 and H-4 (J_{34} = 4.8 Hz) and *trans* for H-1 and H-2 (J_{12} = 0 Hz), hence it was assigned β-*ribo* configuration (**12**). The minor product, from the *cis* relation of H-1 and H-2 protons (J_{12} = 2.4 Hz), had β-*lyxo* (**13**) configuration.

It should be also noted that stereoselectivity of epoxidation with *m*-chloroperbenzoic acid of **5** could be reversed by carrying out reaction on its 4-*O*-acetyl derivative **5***a* (*cf.* Table 1). The results of epoxidation reactions and p.m.r. data of methyl 4-*O*-acetyl-2,3-anhydro-DL-pentopyranosides are shown in Tables 1 and 2.

Methyl α*-*DL*-Xylopyranoside (14)*

Hydrolysis of the sugar epoxides with stabilized conformation of the pyranose ring proceeds according to the Fürst–Plattner rule, *i.e.* by diaxial opening of the oxirane ring (6). For conformationally mobile[5] methyl 2,3-anhydropentopyranosides it was found that due to the inductive effect of the acetal group, the attack of the reagent at C-3 is predominant (ref. 7, p. 31 and references cited therein). In fact alkaline[6] hydrolysis of the oxirane ring in methyl 2,3-anhydro-α-DL-ribopyranoside (**10**) gave in 73% yield a mixture of two products in the ratio 8:2, which in t.l.c. had R_f values corresponding to methyl α-L-xylo- and α-D-arabinopyranosides, respectively. The main component of the mixture was isolated by chromatography on silica gel column. This crystalline material, m.p. 124–126° afforded tri-*O*-acetyl derivative **14***a* with R_f values in t.l.c. and p.m.r. spectrum identical with those of methyl tri-*O*-acetyl-α-L-xylopyranoside. In this experiment methyl α-DL-arabinopyranoside, which was present in the reaction mixture, could not be isolated in the analytically pure state.

Methyl α*-*DL*-arabinopyranoside (15)*

The major product derived from cleavage of epoxide **11** (α-*lyxo* configuration) should be methyl-α-DL-arabinopyranoside **15**, by analogy

[4]It has been shown by numerous examples (5), that in methyl 2,3-anhydropyranosides the coupling constant value of *cis* H-1 and H-2 (or H-3 and H-4) protons is between 2.5 and 4.0 Hz, whereas that of the corresponding *trans* protons is close to zero.

[5]Different factors governing regio- and stereoselectivity of oxirane ring scission were recently discussed in an excellent review (7).

[6]Hydrolysis of **10** with 80% acetic acid gave unsatisfactory results.

Can. J. Chem. Downloaded from www.nrcresearchpress.com by 210.87.254.6 on 09/05/12
For personal use only.

to the opening of epoxides possessing the α-*ribo* configuration. In the event, methyl 4-*O*-acetyl-2,3-anhydro-α-DL-lyxopyranoside **11***a*, on reaction with 80% acetic acid, afforded **15** as the only isolable product (60%) characterized by comparison to an authentic sample and its tri-*O*-acetyl derivative **15***b*. High regioselectivity of the oxirane ring opening in the anhydrosugar **11***a* is presumedly due to the neighboring acetoxy group participation. Also conformational equilibrium[7] of **11***a* favors this course of the reaction (7). In the case of the anhydro sugar **10** axial approach of the reagent to C-3 is possible for minor conformer, hence lower stereoselectivity of the oxirane ring opening.

Alkaline hydrolysis of epoxide **11***a* was accompanied by considerable 'migration' of the oxirane ring (8). As a result, the predominant product of the reaction (along with small amount of methyl α-DL-arabinopyranoside **15**) was methyl α-DL-lyxopyranoside (**7**), which was identified by direct comparison with a sample of this compound previously obtained by *cis* hydroxylation of **5**.

Conclusions

The foregoing reactions of hydroxylation and epoxidation (followed by oxirane ring opening) of racemic methyl 2,3-unsaturated glycosides **5** and **6** afforded all methyl DL-pentopyranosides. These results indicate also that the method can be used for the preparation of modified (*O*-substituted, amino-, deoxy-, *etc.*) pentoses, via 2,3-anhydro compounds **10**, **11**, and **13**, from furfuryl alcohol.

It is worth notice that furfural is the final product of the well known degradation of pentoses by acids (9). Since compounds **5** and **6** have been readily obtained from furfuryl alcohol (2) and consequently from furfural, the present report concludes the reverse process initiated in our previous paper (1), namely stereoselective transformation of furfural into methyl DL-pentopyranosides.

[7]From the coupling constants J_{45} and $J_{45'}$ (Table 2) it follows that **10***a* and **11***a* appear predominantly in the depicted conformations.

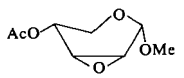

10*a*

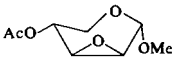

11*a*

Experimental

Melting points were determined on a Koffler block and are uncorrected. Boiling points refer to the air bath temperature. The i.r. spectra were obtained on Unicam SP-200, using KBr discs for solids and films for liquids. The p.m.r. spectra were measured on Varian HA-60-IL or Jeol JNM-4H-100 spectrometers. Gas–liquid chromatographic analyses were made with a Willy Giede gas chromatograph 18/3. Elemental analyses were carried out on micro scale. For column chromatography silica gel Schuchardt, 100–200 mesh was used. All reactions and chromatographic separations were monitored by t.l.c., which was done using silica gel G (E. Merck). Solvents were removed by rotatory evaporator under vacuum.

Acetylations were carried out with acetic anhydride – pyridine 1:1 mixture at room temperature. Epoxidations were performed according to the following general procedure. A solution of methyl 2,3-dideoxy-DL-pent-2-enopyranoside and 10% molar excess of 80% *m*-chloroperbenzoic acid in methylene chloride was left at room temperature. When reaction was complete (as indicated by t.l.c.) precipitated *m*-chlorobenzoic acid was filtered off, the solution evaporated to dryness, and pure products were isolated by column chromatography using benzene – ethyl acetate (4:1) as eluant. Epoxidation data are given in Table 1.

Methyl pentopyranosides and their tri-*O*-acetyl derivatives, which were used for comparison, were prepared from natural pentoses and had reported m.p. values and optical rotations.

Methyl α-DL-*Lyxopyranoside (7)*

A solution of 4.4 mg (0.017 mmol) of osmium tetroxide in 1 ml of *tert*-butyl alcohol was added to a solution of 260 mg (2.00 mmol) of **5** in 5 ml of 6% hydrogen peroxide in *tert*-butyl alcohol. After 6 days the reaction was completed, solvents removed and the residue chromatographed on silica gel (6 g) column. Elution with ethyl acetate and ethyl acetate – propanol (95:5) afforded 146 mg (45%) of **7**, m.p. 119–120° (methanol–ether); i.r. (KBr): 3400, 3300 (OH), 1090 cm^{-1} (C—O).

Anal. Calcd. for $C_6H_{12}O_5$: C, 43.9; H, 7.4. Found: C, 43.7; H, 7.3.

Methyl 2,3,4-tri-*O*-acetyl-α-DL-lyxopyranoside (**7***a*), m.p. 88–89° (sublimed), i.r. (KBr): 1750, 1235 cm^{-1} (—OAc).

Anal. Calcd. for $C_{12}H_{18}O_8$: C, 49.7; H, 6.3. Found: C, 49.8; H, 6.4.

Methyl β-DL-*Ribopyranoside (8)*

A solution of 19 mg (0.075 mmol) of osmium tetroxide in 1 ml of *tert*-butyl alcohol was added to a solution of 177 mg (1.36 mmol) of **6** in 6 ml of 6% hydrogen peroxide in *tert*-butyl alcohol. After 7 days the reaction mixture was evaporated to dryness and the residue chromatographed on silica gel (6 g) column. Elution with ethyl acetate gave 57 mg (26%) of **8**, colorless oil; i.r.: 3420 (OH), 1060 cm^{-1} (C—O). Compound **8**, treated with acetic anhydride – pyridine mixture gave 2,3,4-tri-*O*-acetyl derivative **8***a*, b.p. 120°/10^{-3} Torr, i.r. (film): 1745, 1240 cm^{-1} (—OAc).

Anal. Calcd. for $C_{12}H_{18}O_8$: C, 49.7; H, 6.3. Found: C, 50.0; H, 6.4.

Can. J. Chem. Downloaded from www.nrcresearchpress.com by 210.87.254.6 on 09/05/12
For personal use only.

Methyl β-DL-Lyxopyranoside (9)

Elution of the chromatographic column from the previous experiment with ethyl acetate – propanol (95:5) gave 10 mg (5%) of **8** and **9** mixture and then 37 mg (17%) of **9**; i.r. (film): 3500, 3400 (OH), 1100–1040 cm^{-1} (C—O). Compound **9** was identified by comparison of retention times of its trimethyl silyl ether with that of methyl β-D-lyxopyranoside.

Methyl α-DL-Xylopyranoside (14)

A solution of 690 mg (4.7 mmol) of **10** in 2 ml of 1 *N* aqueous sodium hydroxide was heated at 95° for 8 h, chilled, filtered through 20 ml of Amberlite IRC-50 (H^+) column, and washed with water. Combined filtrates were taken to dryness to give 811 mg of dark gum, which was chromatographed on silica gel (18 g) column. Elution with ethyl acetate and than ethyl acetate – propanol (95:5) afforded 299 mg (39%) of homogeneous (t.l.c.) **14**, m.p. 124–126° (methanol–ether), i.r. (KBr): 3400 (OH), 1100, 1050 (C—O), 940 cm^{-1} (tetrahydropyran).

Anal. Calcd. for $C_6H_{12}O_5$: C, 43.9; H, 7.4. Found: C, 44.2; H, 7.5.

Further elution of the chromatographic column with the same solvent gave 266 mg (34%) of an oil which comprised (t.l.c.) **14** and **15**.

Methyl 2,3,4-tri-*O*-acetyl-α-DL-xylopyranoside (**14***a*), m.p. 156.5–158°; i.r. (KBr): 1750, 1230 (—OAc), 1050 (C—O), 940 cm^{-1} (tetrahydropyran).

Anal. Calcd. for $C_{12}H_{18}O_8$: C, 49.7; H, 6.3. Found: C, 49.9; H, 6.3.

Rearrangement of Methyl 4-O-Acetyl-2,3-anhydro-α-DL-lyxopyranoside (11a). Methyl α-DL-Lyxopyranoside (7)

A portion (217 mg, 1.15 mmol) of **11***a*, when treated with 2 ml of 1 *N* aqueous sodium hydroxide at 95° for 4 h and worked-up as described in the previous experiment, gave 142 mg (57%) of **7**, identical in every respect (t.l.c., i.r., p.m.r.) with the sample obtained by *cis* hydroxylation of **5**.

Methyl 4-O-Acetyl-α-DL-arabinopyranoside (15a)

A solution of 735 mg (3.9 mmol) of **11***a* in 6.5 ml of 80% acetic acid was heated under reflux for 20 min, the solvent evaporated and the residue recrystallized from ethyl acetate – ether mixture to give 474 mg (59%) of **15***a*, m.p. 110.5–111.5°; i.r. (KBr): 3450 (OH), 1745, 1240 cm^{-1} (—OAc); p.m.r. (D_2O): δ 5.12 (m, 1H, H-4), 4.33 (d, J_{12} = 7.2 Hz, 1H, H-1), 3.57 (s, 3H, OCH_3), 1.89 (s, 3H, OAc).

Anal. Calcd. for $C_8H_{14}O_6$: C, 46.6; H, 6.8. Found: C, 46.7; H, 7.1.

Methyl α-DL-Arabinopyranoside (15)

To a solution of 134 mg (0.65 mmol) of **15***a* in 10 ml of methanol, about 2 mg of sodium was added. After 45 min the reaction mixture was neutralized with acetic acid, evaporated to dryness, residue dissolved in 10 ml of water, filtered through 0.5 ml Amberlite IR-120 (H^+) column, and evaporated again to give 104 mg (97%) of product, which solidified. Recrystallization from ethyl acetate afforded 80 mg of **15**, m.p. 107.5–110°; i.r. (KBr): 3450 (OH), 1090, 1070 cm^{-1} (C—O).

Anal. Calcd. for $C_6H_{12}O_5$: C, 43.9; H, 7.4. Found: C, 44.2; H, 7.4.

Methyl 2,3,4-tri-*O*-acetyl-α-DL-arabinopyranoside (**15***b*), m.p. 124–125° (recrystallization from ether – petroleum ether and sublimation), i.r. (KBr): 1750, 1230 (—OAc), 1060 cm^{-1} (C—O).

Anal. Calcd. for $C_{12}H_{18}O_8$: C, 49.7; H, 6.3. Found: C, 50.0; H, 6.5.

1. O. ACHMATOWICZ, JR., P. BUKOWSKI, B. SZECHNER, Z. ZWIERZCHOWSKA, and A. ZAMOJSKI. Tetrahedron, **27**, 1973 (1971).
2. O. ACHMATOWICZ, JR. and P. BUKOWSKI. Roczniki Chem. **47**, 99 (1973).
3. U. P. SINGH and R. K. BROWN. Can. J. Chem. **49**, 1179 (1971). R. M. SRIVASTAVA and R. K. BROWN. Can. J. Chem. **49**, 1339 (1971). T. P. MURRAY, U. P. SINGH, and R. K. BROWN. Can. J. Chem. **49**, 2132 (1971). A. KONOWAL and A. ZAMOJSKI. Roczniki Chem. **45**, 859 (1971). A. BANASZEK and A. ZAMOJSKI. Roczniki Chem. **45**, 391 (1971).
4. N. R. WILLIAMS. Advan. Carbohyd. Chem. Biochem. **25**, 119 (1970).
5. J. G. BUCHANAN, R. FLETCHER, K. PARRY, and W. A. THOMAS. J. Chem. Soc. B, 377 (1969). F. SWEET and R. K. BROWN. Can. J. Chem. **46**, 1481 (1968). H. NEWMAN. J. Org. Chem. **29**, 1461 (1964). R. J. FERRIER and N. PRASAD. J. Chem. Soc. C, 575 (1969). A. KONOWAL, A. ZAMOJSKI, M. MASOJIDKOWA, and J. KOHUTOWA. Roczniki Chem. **45**, 2089 (1971).
6. A. FÜRST and P. A. PLATTNER. Helv. Chim. Acta, **32**, 275 (1949).
7. J. G. BUCHANAN and H. Z. SABLE. *In* Selective organic transformations. Vol. 2. *Edited by* B. S. Thyagarajan. Wiley-Interscience, New York. 1972. p. 1.
8. J. G. BUCHANAN. J. Chem. Soc. 995 (1958); 2511 (1958), Chem. Ind. 1484 (1954).
9. F. H. NEWTH. Advan. Carbohydr. Chem. **6**, 83 (1951).

Diazomethane-catalyzed Transesterification of Oxalic Acid Esters[1]

J. CHRISTOPHER YOUNG

Chemistry and Biology Research Institute, Agriculture Canada, Ottawa, Canada K1A 0C6

Received April 3, 1975

J. CHRISTOPHER YOUNG. Can. J. Chem. **53**, 2530 (1975).

In the presence of an alcohol, oxalic acid esters undergo diazomethane-catalyzed transesterification. Under mild reaction conditions, esters of homologous dicarboxylic acids and other polycarboxylic acids are unaffected.

J. CHRISTOPHER YOUNG. Can. J. Chem. **53**, 2530 (1975).

En présence d'un alcool, les esters de l'acide oxalique subissent des transestérifications catalysées par le diazométhane. Dans des conditions douces de réaction, les esters des acides dicarboxiliques homologues ainsi que ceux des acides polycarboxyliques demeurent inchangées.

[Traduit par le journal]

Can. J. Chem. Downloaded from www.nrcresearchpress.com by 210.87.254.6 on 09/05/12
For personal use only.

Introduction

While developing a method for gas chromatographic (g.c.) analysis of organic acids in tobacco, three products were observed from oxalic acid when the total free acid extract was treated with an excess of ethereal diazomethane. On the basis of a comparison of infrared, nuclear magnetic resonance, and mass spectra, and gas chromatographic retention times with those of authentic samples, the products were identified as dimethyl oxalate, methylethyl oxalate, and diethyl oxalate.

The reaction of diazomethane with ketones is well known. However, there appears to be only one report (1) of this reagent attacking ester carbonyls. In that study, esters having an adjacent strong electron-withdrawing group such as $-CF_3$ or $-CCl_3$, reacted readily with diazomethane to form an ester and/or epoxide. Furthermore, diethyl oxalate was converted to methylethyl oxalate in 32% yield.

Transesterification of acetates (2, 3), benzoates (2), and lactones (3) has been observed in the presence of alcohol and diazomethane.

Results and Discussion

In the first part of this study, diazomethane was prepared from Diazald ® using the two methods given by the manufacturer. Preparation A involves use of ethanol, which partially codistills with the ether and diazomethane, and preparation B involves use of 2-(2-ethoxyethoxy)-ethanol, which does not. Aliquots of the resulting ethereal solutions containing the desired amount of diazomethane were added to ice-chilled ether solutions of oxalic acid or its esters. After standing at room temperature for about 24 h, the resulting solutions were analyzed by gas chromatography.

Normally the reaction between an acid and diazomethane is instantaneous. However, longer reaction times were required in the initial work on the tobacco acids and it was only under these conditions that the multiplicity of products was observed when diazomethane from preparation A was used.

The data in Table 1 show that when oxalic acid is treated with an alcohol-free solution of diazomethane, dimethyl oxalate is the only product. If small amounts of ethanol are present, some of the dimethyl ester is converted to the methylethyl and diethyl esters, the degree of conversion being dependent upon the amount of alcohol present. When an oxalate ester is treated with an alcohol-free solution of diazomethane there is no reaction; however, after an alcohol is added, products dependent upon the nature of the alcohol are formed. Treatment of dimethyloxalate with a blank prepared by procedure A without Diazald resulted in no change. Under these conditions no reaction was observed between diethyl oxalate and diazomethane in the absence of alcohol.

Figure 1 shows a time dependent analysis of the reaction between dimethyl oxalate and a solution containing 10 equiv. of diazomethane from preparation A and clearly indicates an equilibrium reaction.

The evidence suggests that oxalic acid esters

[1]Contribution Number 845, Chemistry and Biology Research Institute, Agriculture Canada.

TABLE 1. Product ratios of diazomethane catalyzed transesterification of oxalic acid esters

Starting compound	CH_2N_2 preparation[a]	Molar equiv. CH_2N_2	Alcohol present	Oxalic acid ester product ratios (mol%)					
				Me_2	MeEt	Et_2	MePr	EtPr	Pr_2
$(COOH)_2$	A	1	EtOH[c]	96	4				
	A	2	EtOH[c]	77	21	2			
	A	10	EtOH[c]	18	53	29			
	B	5		100					
$(COOMe)_2$[b]	A	10	EtOH[c]	23	52	25			
	A[b]	0	EtOH[c]	100					
	B	5		100					
	B	5	EtOH[d]	47	42	11			
	B	5	EtOH[e]	12	34	54			
	B	5	PrOH[d]	88			12		tr[f]
	B	5	PrOH[e]	tr			3		97
$(COOEt)_2$	A	10	EtOH[c]			100			
	B	5				100			
	B	5	MeOH[d]	50	44	6			
	B	5	PrOH[d]			91		9	tr
	B	5	PrOH[e]			1		24	75

[a]See Experimental for details of preparation, reaction procedure, and method of analysis.
[b]Blank prepared without Diazald®.
[c]EtOH present from preparation, increasing equivalent of CH_2N_2 results in proportional increase in amount of EtOH present.
[d]Small amount of alcohol added.
[e]Fivefold increase in amount of alcohol added.
[f]tr = trace.

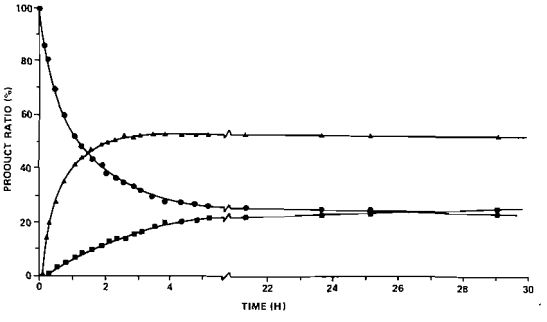

FIG. 1. Plot of product ratios for the transesterification of dimethyl oxalate in the presence of ethanol and diazomethane: ●, dimethyl oxalate; ▲, methylethyl oxalate; ■, diethyl oxalate.

undergo diazomethane-catalyzed transesterification with alcohols. This transesterification appears to be restricted to oxalic acid esters; under identical conditions using preparation A, methyl esters of homologous dicarboxylic acids (malonic, succinic, and glutaric) and other polycarboxylic acids (malic and citric) were unaffected.

Methanol has been shown (4) to form a complex with diazomethane. Bredereck *et al.* (2)

[1] $$CH_3OH + CH_2N_2 \rightleftharpoons [CH_3O]^-[H{-}CH_2N_2]^+$$

postulated that the ester carbonyl undergoes nucleophilic attack by the methoxide moiety, and the resulting transition complex dissassociates to yield a new ester and an alcohol. When R′ is aromatic, the phenol reacts irreversibly to form an ether. The majority of the acetates and benzoates studied by Bredereck *et al.* (2) had R′ aromatic and were run in methanol as solvent, both factors favoring transesterification.

[2]

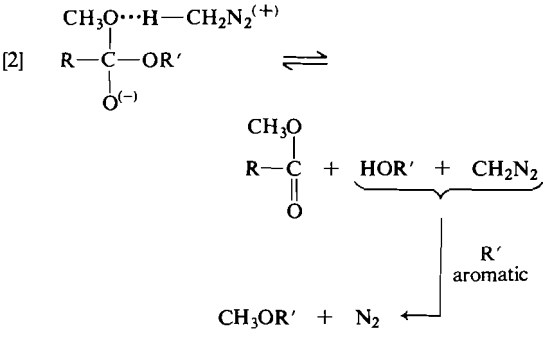

One can rationalize the apparent nonreactivity of polycarboxylic acids other than oxalic after examining the relative rates of nucleophilic alkaline hydrolysis of dicarboxylic acid esters, summarized in Table 2. It is readily apparent that nucleophilic attack by hydroxide ion proceeds at least four orders of magnitude more quickly on oxalate carbonyls than on other saturated homologs. This can be explained as due

Can. J. Chem. Downloaded from www.nrcresearchpress.com by 210.87.254.6 on 09/05/12
For personal use only.

TABLE 2. Relative rates of alkaline ester hydrolysis in water at 25 °C

Ester R	Relative rates (ref.) Me		Et	
$(COOR)_2$	12400	(5, 6)	4200	(6)
$CH_2(COOR)_2$	1.0	(5, 7, 8)	0.80	(7)
$(CH_2COOR)_2$	0.12	(7)	0.097	(7, 9)
$(CH_2CH_2COOR)_2$	0.043	(8)	0.037	(8)
ROOC/⁼\COOR	0.33	(10)	0.19	(9)
ROOC⩙COOR	5.5	(10)	2.1	(9, 10)
ROOC—C≡C—COOR			32.4	(9)

TABLE 3. Product ratios from reaction of dicarboxylic acid esters in presence of diazomethane from preparation C[a]

Ester	Molar equiv. CH_2N_2	Molar equiv. MeOH	Ester product ratios (mol%) Me_2	MeEt	Et_2
$(COOEt)_2$	0.29[b]	0		11	89
	0.33	0		4	96
	1	0		5	95
	1	5	45	43	12
	1	25	87	12	1
	0.38	30	88	11	1
	1	30	90	9	1
	1	75	94	6	
$CH_2(COOEt)_2$	1	5			100
	1	25		3	97

[a]See Experimental for details.
[b]Data from ref. 1.

to the effect of one carboxyl group inductively increasing the electrophilicity of the other. The unsaturated diesters that can be influenced by this inductive effect also show some rate enhancement over their saturated analog. An investigation of the transesterification of these unsaturated diesters would have been instructive but this reaction could not be studied since these esters readily undergo 1,3-dipolar addition of diazomethane to form pyrazoline derivatives (11).

The conditions under which diazomethane reactions are conducted can influence the results. The data in Table 3 show that when alcohol-free diazomethane is bubbled into diethyl oxalate some reaction does occur, in agreement with Green's findings (1). In the presence of methanol, transesterification of diethyl oxalate is the predominant reaction, the degree of conversion being dependent upon the amount of alcohol rather than the amount of diazomethane. Transesterification of malonate esters, not observed under the milder conditions of preparation A, does occur slightly when larger amounts of alcohol are present.

Thus, it is prudent to exercise care when alkylating carboxylic acids with diazoalkanes. Others have observed the influence of conditions on side reactions. Pike *et al.* (12) recently reported that palmitic acid and ethereal diazoethane afforded the expected ethyl ester; however, a 7% yield of the methyl ester was also observed when aqueous 1,2-dimethoxyethane was the solvent. Mlejnek (13) reported that pyrazoline formation with unsaturated diacids could be suppressed at −60 °C and higher yields of dimethyl adipate were obtained when dioxane replaced ether as solvent.

Experimental

Spectral Determinations

Infrared spectra were determined in carbon tetrachloride on a Beckman IR-20A spectrometer. Nuclear magnetic resonance spectra were determined in carbon tetrachloride on a Varian T-60 spectrometer. Mass spectra were determined on a Finnigan 9500 gas chromatograph

Can. J. Chem. Downloaded from www.nrcresearchpress.com by 210.87.254.6 on 09/05/12
For personal use only.

Can. J. Chem. Downloaded from www.nrcresearchpress.com by 210.87.254.6 on 09/05/12
For personal use only.

(1.8 m × 6.5 mm od glass column containing 3% SE-30 ultraphase on high performance Chromosorb W, 80–100 mesh) coupled to a 3100D quadrapole mass spectrometer and a 6000 computer controlled data aquisition system.

Preparation and Analysis of Diazomethane

Diazomethane was prepared from Diazald (Aldrich Chemical Company, Inc.) using the two procedures given on the reagent bottle. Preparation A involves use of ethanol as solvent and affords an alcoholic ethereal solution. Preparation B involves use of 2-(2-ethoxyethoxy)-ethanol as solvent and affords an alcohol-free ethereal solution. Preparation C, based on the method of Green (1), involves redistilling the product from preparation B and then bubbling dry nitrogen through the distillate into an ester or its solution. The resulting solutions were analyzed by adding an aliquot to an excess of benzoic acid and back titrating with a standardized sodium hydroxide solution.

Preparation of Standards

Dimethyl, diethyl, and dipropyl oxalates were prepared by refluxing a solution of oxalic acid, sulfuric acid, and the appropriate alcohol in benzene, followed by normal work-up (14). Methylethyl oxalate was prepared by treating an ethereal solution of monoethyl oxalate with ethereal diazomethane and immediately working up the reaction mixture. Methylpropyl and ethylpropyl oxalates were prepared by the method of Ivashchenko and Moshchitskii (15) by distilling a mixture of propanol and cuprous chloride and dimethyl or diethyl oxalate, respectively. Methylethyl malonate was prepared by treating an ethereal solution of monoethyl malonate (16) with ethereal diazomethane and immediately working up the reaction mixture. Other acids and esters were obtained from commercial sources. All standards showed spectral properties consistent with their structures.

Product Ratio Analysis

Product ratios were determined on a Pye 104 gas chromatograph with a flame ionization detector and 1.5 m × 6.5 mm od glass column containing 4.5% DEGS on Gas Chrom G, 80–100 mesh, or 5% Carbowax 20M on high performance Chromosorb W, 80–100 mesh. Products were isolated by gc fractionation using an effluent splitter and thermal gradient collector (17) and then identified by comparison of gc retention times and i.r. n.m.r., and mass spectra with those of standards.

Reaction of Oxalic Acid and Oxalate Esters in Presence of Diazomethane from Preparations A and B

In a typical experiment, an ice-chilled solution of 10 mg oxalic acid or its ester in 10 ml of ether was treated with a chilled ethereal solution containing the desired amount of diazomethane. After standing at room temperature for 24 h, the resulting solution was analyzed by gc. See Table 1 for relative amounts of reagents, solvent conditions, and results. The product ratios represent actual yields.

Reaction of Diethyl Oxalate and Diethyl Malonate in Presence of Diazomethane from Preparation C

Green's procedure (1) was followed. A slow stream of dry nitrogen was bubbled through an ice-chilled alcohol-free ethereal solution of diazomethane into 0.5 mmol of ester and methanol, if any, contained in a flask equipped with a Dry Ice-acetone condenser. After addition was complete, the reaction mixture was allowed to stand overnight at room temperature and then analyzed by gc. See Table 3 for relative amounts of reagents and results. The product ratios represent actual yields.

Attempted Reaction of Polycarboxylic Acid Methyl Esters in Presence of Diazomethane from Preparation A

Ethereal solutions of methyl esters of malonic, succinic, glutaric, malic, and citric acids were treated with 10 equiv. of diazomethane from preparation A and allowed to stand for 24 h at room temperature. In all cases, starting material was recovered unchanged.

The author wishes to thank Mr. J. Lapointe for technical assistance and Mr. D. Dobson, Technical Services Unit, for obtaining mass spectra.

1. C. R. Green Ph.D. Thesis. University of Virginia, Charlottesville. 1968; Chem. Abstr. **71**, 38283 (1969).
2. H. Bredereck, R. Sieber, L. Kamphenkel, and R. Bamberger. Chem. Ber. **89**, 1169 (1956).
3. T. Wieland and R. K. Rothhaupt. Chem. Ber. **89**, 1176 (1956).
4. B. Eistert, F. Arndt, L. Loewe, and A. Ayaca. Chem. Ber. **84**, 156 (1951).
5. L. P. Hammett. Physical organic chemistry. McGraw-Hill, New York. 1940. pp. 211–212.
6. A. Skrabal and A. Matievic. Monatsh. **39**, 765 (1918).
7. J. Meyer. Z. Phys. Chem. **67**, 257 (1909).
8. C. K. Ingold. J. Chem. Soc. 2170 (1930).
9. E. A. Halonen. Acta Chem. Scand. **9**, 1492 (1955).
10. R. C. Sharma and M. M. Sharma. J. Appl. Chem. **19**, 162 (1969).
11. R. Huisgen. Angew. Chem. Int. Ed. **2**, 565 (1963).
12. L. M. Pike, M. Khurshid, A. Khan, and F. Rottman. J. Org. Chem. **39**, 3674 (1974).
13. O. Mlejnek. J. Chromatogr. **70**, 59 (1972).
14. A. I. Vogel. Textbook of practical organic chemistry. 3rd ed. Longmans, London. 1956. p. 386.
15. Y. N. Ivashchenko and S. D. Moshchitskii. Ukr. Khim. Zh. **35**, 1182 (1969); Chem. Abstr. **72**, 42702 (1970).
16. D. S. Breslow, E. Baumgarten, and C. R. Hauser. J. Am. Chem. Soc. **66**, 1286 (1944).
17. R. G. Brownlee and R. M. Silverstein. Anal. Chem. **40**, 2077 (1968).

Cyclization of Some 2,3,5,6-Tetrafluorophenylhydrazine Derivatives. Use of Nuclear Overhauser Effect Measurements in Structural Assignment

ARTHUR J. ELLIOTT AND MARTIN S. GIBSON
Department of Chemistry, McMaster University, Hamilton, Ontario
Received March 18, 1975

ARTHUR J. ELLIOTT and MARTIN S. GIBSON. Can. J. Chem. **53**, 2534 (1975).

Treatment of *N*-(2,3,5,6-tetrafluorophenyl)-*N'*-thiobenzoylhydrazine and of *N*-benzoyl-*N'*-(2,3,5,6-tetrafluorophenyl)hydrazine with acetic anhydride and triethylamine proceed without rearrangement to give 4-acetyl-2-phenyl-5,6,8-trifluoro-4*H*-1,3,4-benzthiadiazine and -benzoxadiazine, respectively. Structures follow from ^{19}F n.m.r. and n.O.e. data.

ARTHUR J. ELLIOTT et MARTIN S. GIBSON. Can. J. Chem. **53**, 2534 (1975).

Le traitement de la *N*-(tétrafluoro-2,3,5,6 phényl) *N'*-thiobenzoyl hydrazine et de la *N*-benzoyl *N'*-(tétrafluoro-2,3,5,6 phényl) hydrazine par l'anhydride acétique et la triéthylamine se fait sans réarrangement; on obtient respectivement les acétyl-4 phényl-2 trifluoro-5,6,8 4*H*-benzothiadiazine-1,3,4 et la benzoxadiazine-1,3,4. On détermine les structures à partir des données de r.m.n. de ^{19}F et des données de e.O.n. [Traduit par le journal]

While cyclization of *N*-acetyl-*N*-(2,3,5,6-tetrafluorophenyl)-*N'*-thiobenzoylhydrazine (**1***b*) under basic conditions would be expected to yield 4-acetyl-2-phenyl-5,6,8-trifluoro-4*H*-1,3,4-benzothiadiazine (**2***b*) by direct nucleophilic displacement of an *ortho*-fluorine atom by the sulfur atom (path *A*) (1), an alternative (path *B*) involving a Smiles-type rearrangement (2) should also be considered. This would involve nucleophilic displacement of the acetyl-bearing nitrogen atom by the sulfur atom via a spirocyclic transition state, followed by nucleophilic displacement of an *ortho*-fluorine atom by the acetyl-bearing nitrogen atom to give compound (**3***b*). Similar considerations apply to the oxygen analog (**1***d*). These possible routes have been distinguished by recourse to ^{19}F n.m.r. and intramolecular nuclear Overhauser effect (n.O.e.) studies (3, 4).

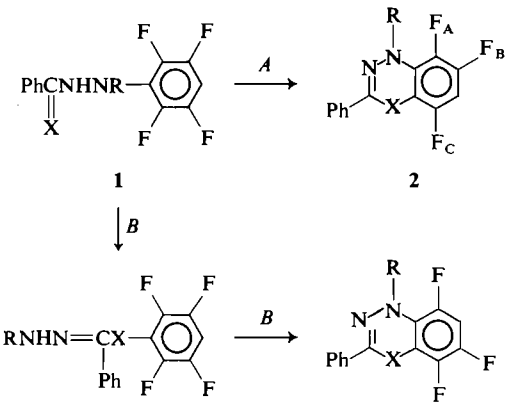

a X = S; R = H
b X = S; R = $COCH_3$
c X = O; R = H
d X = O; R = $COCH_3$

Compound **1***a* was smoothly converted by reaction with acetic anhydride (Ac_2O) and triethylamine (NEt_3) into a compound $C_{15}H_9F_3N_2OS$, subsequently identified as **2***b*; it was shown that acetylation of **1***a* preceded ring closure although the intermediate **1***b* was not isolated. Hydrolysis of **2***b* gave **2***a*. Under slightly different conditions, **1***c* was converted to **2***d*, acetylation again preceding ring closure; satisfactory conditions for hydrolysis of **2***d* to **2***c* were not realized.

The ^{19}F n.m.r. and n.O.e. data for these compounds are set out in Table 1 and are seen to substantiate formulations **2***a*, *b*, and *d* (5). The *ortho* F,F coupling constants lie in the range 20–22 Hz, distinctly larger than the corresponding *para* and (in turn) *meta* values. The *ortho* H,F coupling constants are also somewhat larger than the corresponding *meta* values. The long range couplings between the N–H and F_A and F_B in **2***a* are of special interest since a similar effect is observable for H_A in the p.m.r. spectrum of 7-bromo-2-*p*-methoxyphenyl-4*H*-1,3,4-benzothiadiazine.[1] The ^{19}F chemical shifts are consistent with these structural assignments. Notably deacetylation of **2***b* to **2***a* results in a shift upfield

[1]The p.m.r. spectrum of this compound at 100 MHz in $CDCl_3$ shows a high-field aromatic proton absorption for the C-5 proton H_A as a doublet at δ 6.56 (J_{AB} = 9.0 Hz) which is further split by coupling with the N—H proton; this collapses to a sharp doublet on exchange with D_2O.

Can. J. Chem. Downloaded from www.nrcresearchpress.com by 210.87.254.40 on 09/05/12
For personal use only.

Can. J. Chem. Downloaded from www.nrcresearchpress.com by 210.87.254.40 on 09/05/12
For personal use only.

TABLE 1. ^{19}F n.m.r. and n.O.e. data

Chemical shifts δ (p.p.m.)*		2*a*	2*b*	2*d*
F_A		82.25	54.08	52.84
F_B		54.27	50.92	55.16
F_C		36.54	36.28	57.06
Coupling constants (Hz)				
J_{AB}		21	20	22
J_{AC}		13	13	13
J_{BC}		2.5	2	0
J_{AH}		6	6	7
J_{BH}		10	9.5	10
J_{CH}		8.5	8	9
J_{AR}		3		
J_{BR}		1		
J_{CR}		0		
Nuclear Overhauser effect (%)				
Irradiate R proton(s); obsvd.	F_A	32	10	8
Irradiate C-7 proton; obsvd.	F_A	0	0	0
	F_B	22	21	23
	F_C	33	32	33

*Upfield from CF_3CCl_3.

for F_A, whereas F_B and F_C are barely affected; analogous shifts upfield for H_A occur on deacetylation of benzothiadiazines with no 5 substituent. The higher field positions of F_B and F_C in the benzoxadiazine **2***d* than in **2***b* are consistent with increased electron density in the ring, the smaller oxygen atom being capable of a greater resonance effect.

A large n.O.e. is observed for F_A when the N—H peak of **2***a* is irradiated, whereas F_B and F_C are unaffected. Saturation of the methyl protons of **2***b* produces a similar though smaller n.O.e. for F_A, while F_B and F_C are again unchanged. Large n.O.e. values are observed for F_B and F_C on saturation of the ring proton (at C-7) of **2***a* and **2***b*, while F_A is unaffected. Similar results are obtained for **2***d*.

Only structures **2***a*, *b*, and *d* are consistent with the above data and hence overall the above cyclization reactions must follow path *A* and not path *B*. Such n.O.e. measurements should continue to find use in confirming the course of substitution and cyclization reactions of polyfluoroaromatic compounds.

Experimental

^{19}F n.m.r. spectra were recorded on a Varian Associates DP-60 IL spectrometer in $CDCl_3$ solution at 56.4 MHz; results are given as p.p.m. (δ) upfield from 1,1,1-trichlorotrifluoroethane (internal standard). Proton magnetic resonance spectra were recorded on Varian Associates A-60 and T-60 spectrometers in $CDCl_3$ at 60 MHz; results are given as p.p.m. downfield from tetramethylsilane (internal standard). The presence of exchangeable protons was confirmed by use of D_2O. The procedure for n.O.e. measurements was essentially that described in ref. 4.

2,3,5,6-Tetrafluorophenylhydrazine was prepared from pentafluorobenzene and 100% hydrazine hydrate with minor modification of the published procedure and had m.p. 89–91 °C (lit. (6), m.p. 90–91.5 °C).

N-(2,3,5,6-Tetrafluorophenyl)-N′-thiobenzoylhydrazine (1a)

2,3,5,6-Tetrafluorophenylhydrazine (18.0 g, 0.1 mol) was added in portions to a stirred solution of carboxymethyl dithiobenzoate (7) (21.2 g, 0.1 mol) in aqueous 1 *M* KOH solution (100 ml) during 10 min; 1 *M* KOH was added as required to keep the p*H* at 10. The solution was then heated to 70 °C and allowed to cool to room temperature over 1 h. Dilute acetic acid was added till the p*H* reached 6. The solid was collected, washed, and dried. Crystallization from hexane gave the *thiohydrazide* **1***a* (17.1 g, 57%) as yellow needles, m.p. 90–92 °C; p.m.r. δ 9.35 (s, br 1H, exchangeable), 7.92 (s, br, 1H, exchangeable), 7.81–7.61 (m, 2H), 7.50–7.18 (m, 3H), and 7.00–6.25 (m, 1H).

Anal. Calcd. for $C_{13}H_8F_4N_2S$: C, 52.00; H, 2.67; N, 9.33. Found: C, 51.97; H, 2.68; H, 9.28.

4-Acetyl-2-phenyl-5,6,8-trifluoro-4H-1,3,4-benzothiadiazine (2b)

A mixture of **1***a* (3.0 g, 0.01 mol), NEt_3 (20 ml), and Ac_2O (20 ml) was boiled under reflux for 2 h, cooled, and poured into water. The solid was collected, washed, and dried. Crystallization from ethanol or hexane gave the *thiadiazine* **2***b* (3.1 g, 91%) as buff needles, m.p. 127–128 °C; i.r. (KBr) 1710 cm^{-1} (C=O); p.m.r. δ 8.13–7.92 (m, 2H), 7.62–7.43 (m, 3H), 7.33–6.77 (m, 1H), and 2.50 (s, 3H).

Can. J. Chem. Downloaded from www.nrcresearchpress.com by 210.87.254.40 on 09/05/12
For personal use only.

Anal. Calcd. for $C_{15}H_9F_3N_2OS$: C, 55.90; H, 2.80; F, 17.70. Found: C, 56.05; H, 2.84; F, 17.68.

In a separate experiment, a mixture of **1***a* (2.0 g), NEt_3 (15 ml), and ethanol (15 ml) was refluxed for 5 h. Evaporation *in vacuo* and crystallization from benzene–hexane gave the *1:1 adduct* or salt of **1***a* and NEt_3 as buff needles, m.p. 106–108 °C; p.m.r. δ 9.64 (s, br, 2H, exchangeable), 8.24–8.00 (m, 2H), 7.41–7.17 (m, 3H), 6.75–6.10 (m, 1H), 2.72 (q, 6H), and 1.05 (t, 9H).

Anal. Calcd. for $C_{19}H_{23}F_4N_3S$: C, 56.86; H, 5.74; N, 10.47. Found: C, 56.77; H, 5.85; N, 10.47.

Decomposition of the 1:1 adduct with boiling ethanol – concentrated HCl regenerated **1***a*, m.p. and mixture m.p. 90–91 °C; identity was confirmed by i.r. spectral correlation.

*2-Phenyl-5,6,8-trifluoro-4H-1,3,4-benzothiadiazine (**2a**)*

A mixture of **2***b* (2.0 g), ethanol (30 ml), and concentrated HCl (20 ml) was refluxed for 1 h, cooled, and the solid was collected. Crystallization from ethanol gave the *4H-thiadiazine* **2***a* (1.4 g, 80%) as yellow needles, m.p. 107–108 °C.

Anal. Calcd. for $C_{13}H_7F_3N_2S$: C, 55.71; H, 2.50. Found: C, 55.77; H, 2.53.

*N-Benzoyl-N'-(2,3,5,6-tetrafluorophenyl)hydrazine (**1c**)*

Benzoyl chloride (2.8 g, 0.02 mol) was added dropwise to a stirred solution of 2,3,5,6-tetrafluorophenylhydrazine (3.6 g, 0.02 mol) and NEt_3 (5 ml) in dry ether (50 ml) at −78 °C. Stirring was continued for 2 h at −78 °C and the mixture was then allowed to warm to room temperature. Solvent was removed *in vacuo* and the solid was washed well with ice-cold water. Crystallization from aqueous methanol gave the *hydrazide* **1***c* (4.2 g, 75%) as needles, m.p. 176 °C.

Anal. Calcd. for $C_{13}H_8F_4N_2O$: C, 54.93; H, 2.82; N, 9.86. Found: C, 54.80; H, 2.87; N, 9.83.

*4-Acetyl-2-phenyl-5,6,8-trifluoro-4H-1,3,4-benzoxadiazine (**2d**)*

A mixture of **1***c* (1.0 g), NEt_3 (5 ml), Ac_2O (5 ml), and dimethylformamide (15 ml) was boiled under reflux for 4 h, cooled, and poured into dilute acetic acid. The solid was filtered off, washed, and dried. Crystallization from hexane gave the *oxadiazine* **2***d* (0.6 g, 65%) as needles, m.p. 144–145 °C; i.r. 1700 cm^{-1} (C=O).

Anal. Calcd. for $C_{15}H_9F_3N_2O_2$: C, 58.82; H, 2.94. Found: C, 58.62; H, 2.85.

In a separate experiment, a mixture of **1***c* (1.0 g), NEt_3 (2 ml), NaOH (0.4 g), and dimethylformamide (20 ml) was refluxed for 4 h. Isolation as above gave a yellow gum which contained **1***c* and at least four other materials, none of which was fluorescent (t.l.c.).

Attempted hydrolysis of **2***d* gave dark gums.

We are indebted to Dr. J. K. Saunders for the n.O.e. measurements and the National Research Council of Canada for financial support.

1. A. J. Elliott, P. D. Callaghan, M. S. Gibson, and S. T. Nemeth. Can. J. Chem. **53**, 1484 (1975); A. J. Elliott and M. S. Gibson. J. Chem. Soc. Perkin I, 2915 (1972).
2. W. E. Truce, E. M. Kreider, and W. W. Brand. Org. React. **18**, 99 (1970); M. S. Newman. Acc. Chem. Res. **5**, 354 (1972).
3. F. A. L. Anet and A. J. R. Bourn. J. Am. Chem. Soc. **87**, 5250 (1965).
4. R. A. Bell and J. K. Saunders. Can. J. Chem. **48**, 1114 (1970).
5. J. W. Emsley, J. Feeney, and L. H. Sutcliffe. High resolution nuclear magnetic resonance spectroscopy. Vol. 2. Pergamon, Oxford. 1966. p. 897; J. W. Emsley and L. Phillips. *In* Progress in n.m.r. spectroscopy. Vol. 7. *Edited by* J. W. Emsley, J. Feeney, and L. H. Sutcliffe. Pergamon. Oxford. 1971. p. 47.
6. G. M. Brooke, J. Burdon, M. Stacey, and J. C. Tatlow. J. Chem. Soc. 1768 (1960).
7. K. A. Jensen and C. Pedersen. Acta Chem. Scand. **15**, 1087 (1961).

π-Perfluoroallyltricarbonylcobalt: Synthesis and Reaction with Triphenylphosphine

KEITH STANLEY[1] AND D. W. MCBRIDE
Department of Chemistry, University of Manitoba, Winnipeg, Manitoba R3T 2N2

Received March 17, 1975

KEITH STANLEY and D. W. MCBRIDE. Can. J. Chem. **53**, 2537 (1975).

Perfluoroallyl iodide reacts with $Zn[Co(CO)_4]_2$ to give π-$C_3F_5Co(CO)_3$ and $CF_3CF{=}CFCo(CO)_4$. The reaction of π-$C_3F_5Co(CO)_3$ with PPh_3 gives two products; *trans*-$CF_3CF{=}CFCo(CO)_3PPh_3$ and a compound tentatively identified as *cis*-$CF_2{=}CFCF_2Co(CO)_3PPh_3$; (*cis* and *trans* refer to configuration about cobalt). Infrared and n.m.r. data for the compounds are reported.

KEITH STANLEY et D. W. MCBRIDE. Can. J. Chem. **53**, 2537 (1975).

L'idodure de perfluoroallyle réagit avec $Zn[(Co(CO)_4]_2$ pour conduire à π-$C_3F_5Co(CO)_3$ et $CF_3CF{=}CFCo(CO)_4$. La réaction du π-$C_3F_5Co(CO)_3$ avec PPh_3 donne deux produits; le $CF_3CF{=}CFCo(CO)_3PPh_3$ *trans* et un autre composé identifié comme étant le $CF_2{=}CFCF_2$-$Co(CO)_3$ PPh_3 *cis* (les géométries *cis* et *trans* sont définies à partir de la configuration autour du cobalt). On rapporte les caractéristiques i.r. et r.m.n. des composés.

[Traduit par le journal]

Introduction

In view of the extensive interest in both π-allyl complexes and perfluorocarbon ligands, it seemed surprising that a π-perfluoroallyl complex had not been prepared. Attempts which may have yielded such a complex gave only σ-perfluoropropenyl or σ-perfluoroallyl (1–3) complexes. Perfluororcyclic ligands have been reported to bond to iron (4) and cobalt (5) through a π-allyl linkage. We report here the synthesis of π-perfluoroallyltricarbonylcobalt π-$C_3F_5Co(CO)_3$, and examine its reaction with triphenylphosphine.

Results

The reaction of perfluoroallyl iodide[2] with $Zn[Co(CO)_4]_2$ in pentane followed by trap-to-trap distillation *in vacuo* of the product mixture gave two products. The less volatile compound was identified as π-$C_3F_5Co(CO)_3$. The compound is an air sensitive yellow liquid at room temperature which decomposes rapidly at 35° *in vacuo*. The ^{19}F n.m.r. spectrum is properly described as an AA'BB'X pattern (Fig. 1) but analysis as an A_2M_2X pattern does not affect the coupling constants significantly. The reason for the broadening of the absorption lines of F_s cannot be determined in a first-order analysis.

The i.r. spectrum of π-$C_3F_5Co(CO)_3$ shows two sharp terminal carbonyl bands at 2115.0(m) and 2064.0(s) cm^{-1} corresponding to the A_1 and E stretching vibrations for a molecule with local C_{3v} symmetry. A medium intensity absorption at 1425 cm^{-1} is assigned to a stretching vibration of the π-allyl moiety. By comparison, the hydrocarbon analog π-$C_3H_5Co(CO)_3$ (6) shows C—O stretching bands at 2065 (A_1) and 1998 cm^{-1} (E). The $(C—C—C)_{asym}$ mode was assigned the 1388 cm^{-1} frequency.

The more volatile component was identified as $CF_3CF{=}CFCo(CO)_4$. The ^{19}F n.m.r. spectrum (see Table 1) is similar to those of other σ-perfluoropropenyl complexes studied (1–3) having a *trans* configuration[3] about the C=C bond (7) ($J_{F_A-F_B}$ = 147 Hz).

The i.r. spectrum of $CF_3CF{=}CFCo(CO)_4$ shows four carbonyl bands which is consistent with C_{3v} symmetry ($2A_1 + E$) about the cobalt

[1]Present address: Department of Chemistry, Queen's University, Kingston, Ontario K7L 3N6.

[2]In a paper by Ramsey and Brey (21) the ^{19}F n.m.r. chemical shift of the perfluoromethylene CF_2 group in $CF_2{=}CFCF_2I$ was reported to be 63.6 p.p.m. (upfield from $CFCl_3$). In our work this value was measured to be 49.7 p.p.m. All coupling constants and other δ values were found to be the same as reported. This δ value of 49.7 p.p.m. fits the trend observed by Brey and Ramsey for perfluoroallyl chloride (δ_{CF_2} = 62.0 p.p.m.) and bromide (δ_{CF_2} = 55.1 p.p.m.) derivatives.

[3]The perfluoropropenyl group in all compounds here exists in a *trans* configuration and unless specifically relating to this group the terms *cis* and *trans* will relate to the configuration about the cobalt center.

Can. J. Chem. Downloaded from www.nrcresearchpress.com by 210.87.254.105 on 09/05/12
For personal use only.

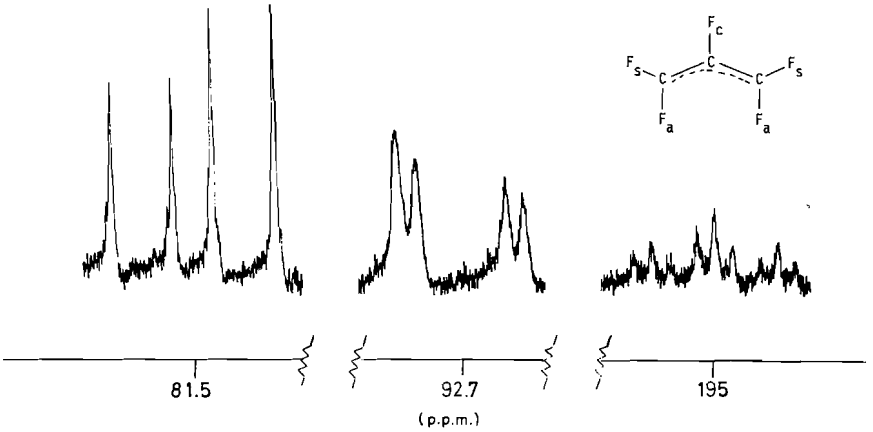

FIG. 1. ^{19}F n.m.r. spectrum of π-$C_3F_5Co(CO)_3$ in CH_2Cl_2 (5% $CFCl_3$). Chemical shifts (p.p.m. upfield from $CFCl_3$): $\delta_{F_s} = 81.5$, $\delta_{F_a} = 92.7$, $\delta_{F_c} = 195.0$. Coupling constants: $^2J_{a,s} = 118$ Hz, $J_{a,c} = 74$ Hz, $J_{c,s} = 18$ Hz, (analyzed as an A_2M_2X spectrum).

TABLE 1. ^{19}F n.m.r. and i.r. data of σ-perfluoropropenyl complexes

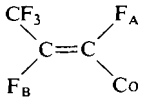

Complex*	ν(CO) (cm^{-1})	δ_{CF_3}†	δ_{F_A}	δ_{F_B}	$J_{F_A-CF_3}$	$J_{F_B-CF_3}$	$J_{F_A-F_B}$
$CF_3CF{=}CFCo(CO)_4$‡	2130.0(m)§ 2068.1(s) 2059.8(s) 2052.2(s)	66.5	155.0	89.8	24	13	147
trans-$CF_3CF{=}CFCo(CO)_3PPh_3$‖	2068.8(w) 2005.7(s) 2000.0(s)	66.5	161.0	89.9	24	13 $J_{F_A-P} = 30$ Hz	146

*Both complexes show the C=C vibration at 1640 cm^{-1} (weak).
†δ in p.p.m. upfield from $CFCl_3$, J in Hz.
‡Infrared spectrum in pentane, n.m.r. in CH_2Cl_2 (5% $CFCl_3$).
§(s) = strong, (m) = medium, (w) = weak.
‖Infrared spectrum in methylcyclohexane, n.m.r. in tetrahydrofuran (5% $CFCl_3$).

atom where the *E* mode is split due to the non-axially symmetric R_f–metal group. This splitting is seen in other $R_fCo(CO)_4$ complexes (8). The C=C stretching frequency is at 1640 cm^{-1}. The compound is a liquid above $-15°$ and is extremely thermally unstable above 0°, precluding an elemental analysis.

A ^{19}F n.m.r. spectrum of the reaction mixture after carbon monoxide evolution had essentially ceased showed, in addition to peaks due to the two products already discussed, an octet at 41.6 p.p.m. The coupling constants were almost the same as those for perfluoroallyl iodide in which the CF_2 group is at 49.7 p.p.m. (see footnote 2). It has been shown for $R_fCo(CO)_4$ compounds (9, 10) that a downfield shift of about 7 to 8 p.p.m. results when the iodine in perfluoroalkyl iodides is replaced by a $Co(CO)_4$ group. The ^{19}F n.m.r. of π-$C_5H_5Ni(CO)CF_2CF{=}CF_2$ shows that J values do not change significantly upon coordination to a metal (3). This evidence suggests that $CF_2{=}CFCF_2Co(CO)_4$ is an intermediate in the reaction. The single fluorine resonances of this complex, however, could not be observed because of the low concentration of this species in solution.

While this compound could not be isolated, its presence in low concentration in the reaction mixture indicates the initial formation of a σ-perfluoroallyl complex from which both final products originate as proposed in Scheme 1. The pathway involving the loss of carbon

Can. J. Chem. Downloaded from www.nrcresearchpress.com by 210.87.254.105 on 09/05/12
For personal use only.

Can. J. Chem. Downloaded from www.nrcresearchpress.com by 210.87.254.105 on 09/05/12
For personal use only.

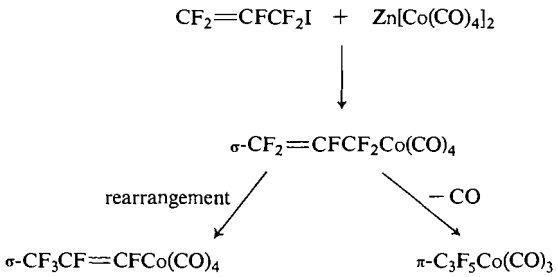

SCHEME 1

monoxide is analogous to the formation of π-$C_3H_5Co(CO)_3$ (11). The rearrangement of σ-perfluoroallyl compounds to perfluoropropenyl derivatives has been examined by Goldwhite *et al.* (12) who proposed a transition state such as **1**, in which intermolecular fluorine

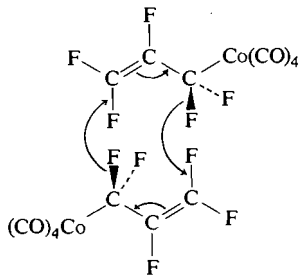

1

migration occurs to give the perfluoropropenyl group.

The reaction of π-$C_3F_5Co(CO)_3$ with triphenylphosphine proceeds without the evolution of carbon monoxide and two isomeric compounds were isolated by fractional recrystallization from methylcyclohexane. Neither complex contains the π-perfluoroallyl ligand. This result contrasts with the reaction of π-$C_3H_5Co(CO)_3$ with PPh_3 where carbon monoxide is vigorously evolved and π-$C_3H_5Co(CO)_2PPh_3$ is the only product (13).

From spectral evidence, the structures of the two isomers are concluded to be **2** and **3**.

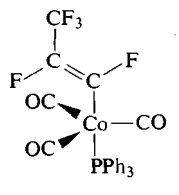

2

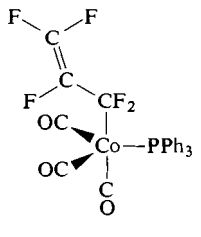

3

The ^{19}F n.m.r. spectrum of **2** (see Table 1 for spectral data on **2**) shows a perfluoropropenyl group with a *trans*-configuration (J_{FF} = 146 Hz) about the C=C bond. The coupling constant J_{P,F_A} = 30 Hz indicates a *trans* configuration about the cobalt atom as in other $R_fCo(CO)_3PPh_3$ complexes reported (8). The i.r. spectrum has three CO stretching bands which is predicted by group theory for a *trans* configuration (C_{3v} symmetry, $A_1 + E$) where the E mode is split because of the nonaxially symmetric R_f–Co group (8, 14). The C=C stretching frequency is at 1640(w) cm^{-1}. The compound is identified as *trans*-$CF_3CF{=}CFCo(CO)_3PPh_3$.

The infrared spectra for **3** suggests the structure which is drawn. A weak intensity band at 1750 cm^{-1}, assigned to the C=C stretching vibration, indicates a σ-perfluoroallyl group. The C=C stretch in perfluoroallyl iodide is at 1750 cm^{-1}. For the *cis* configuration (C_s symmetry) about the cobalt, group theory predicts (8) three equal intensity C—O absorptions. This pattern is observed for **3** (see Fig. 2).

Unfortunately, the compound is thermally unstable in solution. This instability has little effect on the i.r. spectrum (*i.e.* the spectrum does not change over a 15 min period) but the ^{19}F n.m.r. spectrum could not be recorded because of broadening by paramagnetic materials. Decomposition of the compound to paramagnetic species was rapid above 10° in any solvents in which the compound is soluble ($CHCl_3$, CH_2Cl_2, THF, $C_6H_5CH_3$); below 10° the solubility was very low.

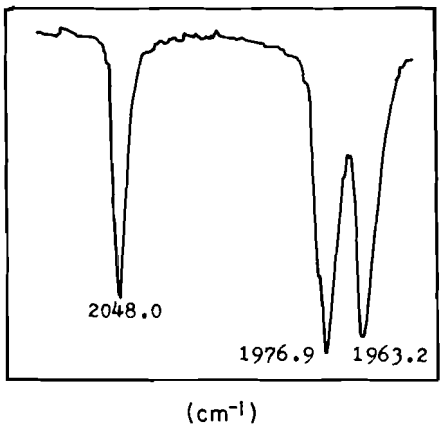

FIG. 2. Infrared carbonyl absorption bands of *cis*-σ-$CF_2{=}CFCF_2Co(CO)_3PPh_3$ in methylcyclohexane; (frequencies in cm^{-1}).

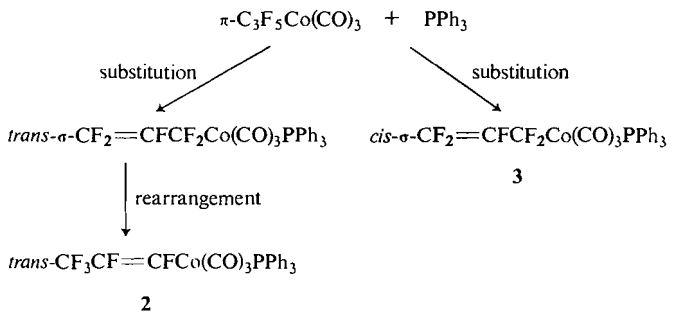

SCHEME 2

The reaction of π-$C_3F_5Co(CO)_3$ with PPh_3 can be written as shown in Scheme 2.

The reaction proceeds in two different pathways depending on whether the PPh_3 substitution results in a *cis* or *trans* configuration of the σ-perfluoroallyl and PPh_3 groups. In the *trans* route the substitution is followed by the rearrangement of the σ-perfluoroallyl ligand to the σ-perfluoropropenyl group by the mechanism of the bimolecular transition state proposed by Goldwhite *et al.* (12). This complex is similar to other *trans*-$R_fCo(CO)_3PPh_3$ complexes that have been prepared (8).

The *cis* pathway gives the complex **3** which does not undergo any further reactions for the following reasons. Cardaci *et al.* (15) in their examination of the reaction of (π-CH_2CClCH_2)-$Fe(CO)_2NO$ with PPh_3 isolated the σ-allyl intermediate *cis*-(σ-CH_2=$CClCH_2$)$Fe(CO)_2NO$-PPh_3 which decarbonylated to reform a π-allyl complex. The complex **3** does not decarbonylate but it has been shown by Cramer (16) that fluorinated olefins are poorer electron donors than hydrocarbon olefins and are therefore less likely to displace a CO group, especially in this case where the Co—CO bond has been strengthened by the presence of the coordinated PPh_3. The σ-perfluoroallyl ligand does not rearrange to a σ-perfluoropropenyl ligand as occurred in the *trans* pathway. A molecular model of complex **3** shows that because of the bulky PPh_3 in a *cis* position, a bimolecular rearrangement transition state could not be attained owing to extreme steric interactions.

Experimental

Nuclear magnetic resonance spectra were determined using a Varian A-56/60A instrument with a variable temperature unit. Infrared spectra were recorded on a Perkin-Elmer 337 instrument using double-beam techniques. Polystyrene was used to calibrate full spectra and indene used for expanded scale spectra of the carbonyl region. Melting points were taken on a Fischer-Johns melting point apparatus and are uncorrected. For compounds which were liquid at room temperature, the melting points were taken by sealing the sample inside a glass tube, cooling to −80° in Dry Ice – acetone, and allowing the bath to warm up slowly with stirring. When the frozen sample melted, the temperature of the bath was recorded as the melting point.

Perfluoroallyl chloride (17) was reacted with NaI in acetone to give perfluoroallyl iodide (18). The distilled C_3F_5I (b.p. 53–55° at 760 Torr) was stored at 0° to reduce decomposition. $Zn[Co(CO)_4]_2$ (19) was prepared from $Hg[Co(CO)_4]_2$ (20) and granulated zinc in toluene. The toluene was removed *in vacuo* and pentane added to the solid under nitrogen.

Preparation of CF_3CF=$CFCo(CO)_4$ and π-$C_3F_5Co(CO)_3$

Perfluoroallyl iodide (0.6 g, 2.4 mmol) and $Zn[Co(CO)_4]_2$ (5 g, 1.2 mmol) were reacted in pentane (40 ml) at 25° under N_2 until carbon monoxide evolution had ceased. The pentane was removed *in vacuo* (static) at −30° (bromobenzene slush bath). The products were distilled into a conventional vacuum trapping system at room temperature. The products were separated by trap-to-trap distillation techniques under dynamic vacuum (0.01 Torr). The product passing through a −30° trap was collected at −196°. It melted to a deep yellow liquid at −15° and decomposed rapidly when warmed above 0°. The compound was identified by i.r. and n.m.r. spectra as CF_3CF=$CFCo(CO)_4$ (yield 20%). An elemental analysis was not possible. The product which was trapped at −30° was stable *in vacuo* or under N_2 at room temperature. It was a yellow liquid above 5°. It was identified by i.r. and n.m.r. spectra as π-$C_3F_5Co(CO)_3$. Recrystallization from pentane (at −80°) gave the pure product, yield 25%.

Anal. Calcd. for $C_3F_5Co(CO)_3$: C, 26.3; F, 34.7. Found: C, 26.4; F, 34.7.

Nuclear magnetic resonance samples were prepared by condensing the compound, solvent, and $CFCl_3$ into the n.m.r. tube *in vacuo* and flame sealing the tube.

Infrared samples were prepared under nitrogen and transferred to a two port infrared cell (capped with 5 mm silicone rubber septa and flushed with nitrogen) by syringe.

Can. J. Chem. Downloaded from www.nrcresearchpress.com by 210.87.254.105 on 09/05/12
For personal use only.

Reaction of π-$C_3F_5Co(CO)_3$ with PPh_3

Triphenylphosphine (0.95 g, 3.6 mmol) was added to π-$C_3F_5Co(CO)_3$ (1 g, 3.6 mmol) in 50 ml pentane at 25° and stirred for 1 h *in vacuo*. No carbon monoxide was evolved as the solution went from yellow to orange. The pentane was removed under vacuum and the product mixture dissolved in a minimum amount of boiling methylcyclohexane. All purifications were carried out under N_2. The hot solution was centrifuged to remove any insoluble material and decanted. On slow cooling to 0° the product *cis*-σ-CF_2=$CFCF_2Co(CO)_3PPh_3$ **3** was obtained as a yellow powder (m.p. 110° dec.). The compound was difficult to obtain pure.

Anal. Calcd. for $C_{24}H_{15}CoF_5O_3P$: C, 53.8; H, 2.8; F, 17.7; P, 5.8. Found: C, 54.4; H, 2.9; F, 18.3; P, 5.8.

On further cooling to −80° yellow crystals of *trans*-CF_3CF=$CFCo(CO)_3PPh_3$ (**2**) were deposited (m.p. 123°.

Anal. Calcd. for $C_{24}H_{15}CoF_5O_3P$: C, 53.8; H, 2.8; F, 17.7; P, 5.8. Found: C, 53.9; H, 2.8; F, 17.8; P, 5.6.

Both products were recrystallized separately several times from methylcyclohexane.

We thank the National Research Council of Canada for financial support and Northern Electric and Alcan for fellowships to K. S.

1. H. D. KAESZ, R. B. KING, and F. G. A. STONE. Z. Naturforsch. B, **15**, 763 (1960).
2. R. B. KING, S. L. STAFFORD, P. M. TREICHEL, and F. G. A. STONE. J. Am. Chem. Soc. **83**, 3604 (1961).
3. D. W. McBRIDE, E. DUDEK, and F. G. A. STONE. J. Chem. Soc. 1752 (1964).
4. G. W. PARSHALL and G. WILKINSON. J. Chem. Soc. 1132 (1962).
5. P. B. HITCHCOCK and R. MASON. Chem. Commun. 503 (1966).
6. D. C. ANDREWS and G. DAVIDSON. J. Chem. Soc. Dalton, 1381 (1972).
7. E. PITCHER and F. G. A. STONE. Spectrochim. Acta, **17**, 1244 (1961).
8. J. B. WILFORD, A. FORSTER, and F. G. A. STONE. J. Chem. Soc. 6519 (1965).
9. E. PITCHER, A. D. BUCKINGHAM, and F. G. A. STONE. J. Chem. Phys. **36**, 124 (1962).
10. W. R. McCLELLAN. J. Am. Chem. Soc. **83**, 1598 (1961).
11. R. F. HECK and D. S. BRESLOW. J. Am. Chem. Soc. **82**, 751 (1960).
12. H. GOLDWHITE, D. G. ROWSELL, and C. VALDEZ. J. Organometal. Chem. **12**, 133 (1968).
13. R. F. HECK and D. S. BRESLOW. J. Am. Chem. Soc. **83**, 1097 (1961).
14. W. HIEBER and E. LINDNER. Chem. Ber. **95**, 2042 (1962).
15. G. CARDACI, S. M. MURGIA, and A. FOFFANI. J. Organometal. Chem. **37**, C11 (1972).
16. R. CRAMER. J. Am. Chem. Soc. **89**, 4621 (1967).
17. W. J. CUNNINGHAM, R. F. SWEENEY, and C. WOOLF. U.S. Patent No. 3,047,939; Chem. Abstr. **58**, P6693c (1963).
18. W. T. MILLER and A. H. FAINBERG. J. Am. Chem. Soc. **79**, 4164 (1957).
19. J. M. BURLITCH. J. Organometal. Chem. **9**, P9 (1967).
20. G. BRAUER (*Editor*). Handbook of preparative inorganic chemistry 2nd ed. Academic Press, New York. 1963. p. 1754.
21. K. C. RAMSEY and W. S. BREY. J. Chem. Phys. **40**, 2349 (1964).

Can. J. Chem. Downloaded from www.nrcresearchpress.com by 210.87.254.105 on 09/05/12
For personal use only.

The Role of Cobalt in Unsupported MoS_2 Hydrodesulfurization Catalysts[1]

E. FURIMSKY AND C. H. AMBERG
Department of Chemistry, Carleton University, Ottawa, Canada K1S 5B6

Received January 27, 1975

E. FURIMSKY and C. H. AMBERG. Can. J. Chem. **53**, 2542 (1975).

Crystalline MoS_2 catalysts were impregnated with cobalt over the total composition range, and their catalytic activity in the hydrodesulfurization of thiophene tested in a microreactor at 400° and near atmospheric pressure. Three principal composition regions could be distinguished in the sulfided catalysts: (*1*) Co/(Co + Mo) compositions 0–0.4. In this region intercalated Co enhances the intrinsic activity which reaches a maximum near a Co content of 0.25. The region is sulfur "deficient" with respect to $MoS_2 + Co_9S_8$ and there is no evidence for the presence of Co_9S_8. (*2*) Compositions 0.4–0.65. This region is characterized by the exact stoichiometry $MoS_2 + Co_9S_8$ and by the appearance of a Co_9S_8 phase. Surface area experiences a fivefold increase, as does percent conversion, but intrinsic activity changes very little. (*3*) Compositions > 0.65. A region of lesser interest, it is sulfur "deficient", possibly through the formation of Co_4S_3, and surface area decreases steeply with Co content.

E. FURIMSKY et C. H. AMBERG. Can. J. Chem. **53**, 2542 (1975).

On a imprégné de cobalt les catalyseurs cristallins MoS_2 dans toute l'étendue du domaine de composition. On en a vérifié l'activité catalytique par hydrodésulfurisation du thiophène dans un micro-réacteur à 400° et près de la pression atmosphérique. On peut distinguer trois régions principales de composition des catalyseurs sulfurés: (*1*) Les compositions Co/(Co + Mo) de 0 à 0.4. Dans cette région la présence de Co accroît l'activité intrinsèque qui atteint un maximum pour une teneur en Co voisine de 0.25. Cette région est "déficitaire" en soufre par rapport à $MoS_2 + Co_9S_8$ et il n'y a pas de preuve indiquant la présence de Co_9S_8. (*2*) Les compositions 0.4–0.65. Cette région est caractérisée par une stoechiométrie exacte $MoS_2 + Co_9S_8$ et par l'apparition d'une phase Co_9S_8. La surface augmente par un facteur de cinq, tout comme le pourcentage de conversion, mais l'activité intrinsèque varie très peu. (*3*) Les compositions > 0.65. C'est une région d'intérêt moindre, qui est "déficitaire" en soufre probablement à cause de la formation de Co_4S_3. La surface décroît rapidement avec la teneur en Co.

[Traduit par le journal]

Introduction

The sulfided oxides of molybdenum and cobalt, supported on alumina, are frequently used as catalysts in hydrodesulfurization. Their effective components are the metal sulfides formed during the initial conditioning (sulfiding) stage. Although a great deal of information is available regarding these "cobalt molybdate" catalysts (1–7), their structure and its impact on reaction mechanisms is so far not completely understood. For this reason the activation of unsupported MoS_2 by Co has been undertaken recently by several workers in the hope of narrowing down at least some of the complexities of the commercial catalysts. Hagenbach *et al.* (8) found that cobalt raised the activity towards both thiophene hydrodesulfurization and cyclohexene hydrogenation when added to unsupported MoS_2. A theoretical model was provided in a study by Farragher and Cossee (9), in which Ni was shown to intercalate in the edges of WS_2 crystals, thus creating a more highly faceted surface containing exposed W^{3+} ions. These latter ions were thought to be the active sites in benzene hydrogenation. The MoS_2/Co system was presumed to behave in an analogous fashion. Divalent Co ions can be accommodated in the octahedral holes between the MoS_2 layers adjacent to the exposed Mo ions, and reduce the latter to triply coordinated ions. Thus this situation can occur in the surface, even though crystal field considerations show it to be energetically unfavorable in the ideal trigonal prismatic environment of the Mo^{4+} ions in MoS_2. Catalyst particles would be particularly susceptible to intercalation, their small size leading to increased edge-to-bulk ratios, while

[1]Presented at a symposium on Catalysis in Air Pollution Control; Coal to Clean Fuels Conversion. American Institute of Chemical Engineers Meeting, Washington, D.C. December 1–5, 1974.

Can. J. Chem. Downloaded from www.nrcresearchpress.com by 210.87.254.6 on 09/05/12
For personal use only.

Can. J. Chem. Downloaded from www.nrcresearchpress.com by 210.87.254.6 on 09/05/12
For personal use only.

their method of preparation frequently introduces other crystal defects.

In the present study the promotion of MoS_2 by Co was followed by the measurement of catalytic activity in the hydrodesulfurization of thiophene. Apart from chemical analysis, catalysts were characterized by determinations of BET surface areas, X-ray spectra, and, in some instances, electron scanning micrographs.

Experimental

Materials

MoS_2, Anachemia, as received. This is the same material described previously (10); $Co(NO_3)_2$, Fisher, certified reagent; H_2, Union Carbide purified by passing through Pd catalyst, then dried over Drierite; thiophene, Eastman, purified in preparative gas chromatograph.

Catalysts

The commercial catalyst used was Girdler G35A (catalyst G), through 65 mesh, prepared from crushed pellets. This is a "cobalt molybdate" on aluminum catalyst, used in earlier work (10–12). All other catalysts investigated were made by impregnating the commercial MoS_2 with $Co(NO_3)_2$ in liquid ammonia (9). After evaporation of the ammonia the mixture was dried for 2 h at 110°. This was followed by reduction in hydrogen for 4 h at 450°. The catalyst was then placed in the microreactor and sulfided in a reaction stream under operating conditions.

The Mo and Co contents of the catalysts were determined by atomic absorption spectroscopy using a Techtron Model AA3 spectrometer. An N_2O/acetylene flame was employed for Mo and an air/acetylene flame for Co.

Sulfur content was determined gravimetrically as $BaSO_4$.

Apparatus

The microreactor and flow system were essentially the same as described in previous work by one of the authors (10). X-Ray analysis was carried out on a Siemens X-ray diffractometer using Cu(Kα) and, in some instances where higher sensitivity was desirable, Co(Kα) radiation. All BET areas were determined in a conventional volumetric apparatus, using N_2 at liquid nitrogen temperatures, after outgassing for 10 h at 200°. The low temperatures were measured by means of an oxygen vapor pressure thermometer.

Procedure

Catalysts were tested at 400°, using hydrogen flow of 30 cc min^{-1} near atmospheric pressure. The thiophene bubble saturator was kept at 0°, corresponding to a partial pressure of thiophene of 21.4 Torr. Exact pressures were, however, measured independently during each test run on a routine basis.

Thiophene conversion was analyzed by g.l.c. using a 6-ft squalane column (25% w/w) at 25°. Percent conversion was always expressed in terms of thiophene converted rather than C_4 hydrocarbons formed.

All determinations on catalysts were performed after steady-state conditions had been attained in the desulfurization reaction, except where noted otherwise.

Results and Discussion

The change in conversion during the initial stages of conditioning of the Co-promoted MoS_2 catalysts showed the customary pattern as seen in Fig. 1. The initial high value decreased and reached a steady level after about 1 h.

A typical C_4 product distribution over the promoted catalysts has been summarized in Table 1 and compared to that over the supported commercial catalyst G. Total hydrogenation as reflected by total butane yield is small over Co/MoS_2 in contrast to the significantly higher yield obtained with the supported catalyst. Apart from this the product distribution over the various catalysts showed great similarity. It should be pointed out that low yields (*e.g.* total conversion over unpromoted MoS_2) resulted in correspondingly lower accuracy of measurement with the thermal conductivity detector. The last column in Table 1 gives the ratio of thiophene converted to total C_4 yield as being close to unity. Even though there is considerable scatter owing to the combined integration errors of five chromatogram bands, the column does not indicate any loss of reactants or products through adsorption or coking.

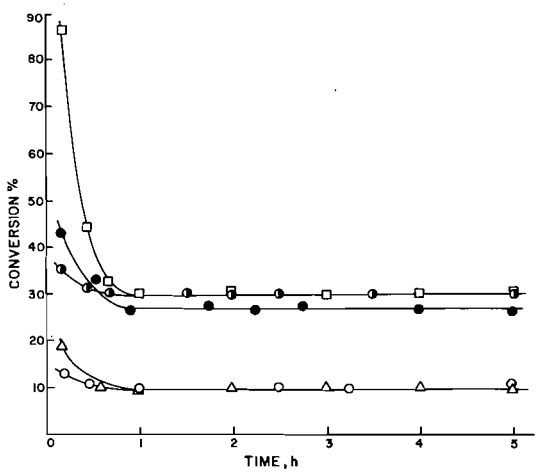

FIG. 1. Percent conversion of thiophene as a function of time in the reaction stream for catalysts of cobalt content Co/(Co + Mo), as noted. Fresh catalysts: △, 0.06; □, 0.55; ●, 0.74. Sulfided catalysts, after short exposure to atmosphere at room temperature: ○, 0.06; ◑, 0.55. Conditions: 400°; 30 ml min^{-1} H_2; partial pressure of thiophene 20 Torr; total pressure 760 Torr; 1 g catalyst.

TABLE 1. A typical products distribution, and percent conversion of thiophene, over Co-promoted MoS_2 catalysts and one commercial supported cobalt molybdate catalyst (G). Conditions: 400°; 30 ml min^{-1} H_2; partial pressure of thiophene 20 Torr; total pressure 760 Torr; 1 g catalyst

Catalyst	$\frac{Co}{(Co + Mo)}$	Product (%)				Percent conversion	$\frac{\text{Thiophene}}{C_4}$
		n-butane	1-butene	*trans*-2-butene	*cis*-2-butene		
Co/MoS_2	0.15	3.4	26.1	40.9	29.6	14.7	0.96
	0.25	4.1	26.5	42.8	26.6	19.8	1.09
	0.39	4.7	23.5	41.9	29.9	24.8	0.99
	0.46	4.5	23.4	44.0	28.1	28.5	1.09
	0.63	4.0	20.6	45.8	29.6	28.8	0.97
	0.71	3.8	22.6	43.3	30.9	27.9	0.93
	0.85	3.5	22.9	45.5	28.1	15.3	0.95
G	0.26	29.1	14.4	34.6	21.9	51.6	0.97
(Butenes only)			20.3	48.8	30.9		

Our X-ray data revealed the MoS_2 to be well crystallized material of trigonal prismatic structure. An increase in cobalt content resulted in a decrease in the intensity of the MoS_2 reflections, without affecting line width. This decrease exceeded that expected from a straight comparison with the decreasing fraction of MoS_2 present, probably because of absorption by cobalt. At Co/(Co + Mo) ratios higher than 0.40, a second phase became detectable which had lattice parameters identical with those of Co_9S_8. Hydrogen reduction equilibria determined under hydrodesulfurization conditions also confirm that Co_9S_8 is the most likely phase to be present (1). In view of the fact that other authors have expressed the opinion that Co_9S_8 exists as a separate phase at lower concentrations of Co(8) we have attempted to establish a probable lower limit for its existence. Unfortunately the only sufficiently sensitive parameter exhibiting a consistent correlation with Co concentration was the intensity of the Co_9S_8 diffraction bands, when using Co(Kα) radiation. Considerable scatter was to be expected, because the method of preparing slides from powder samples is not geared to the precise reproduction of intensity values and it must be regarded as a highly empirical procedure. Accordingly, we performed a regression analysis on the 3,1,1 and 4,0,0 lines of eight samples ranging from Co/(Co + Mo) ratios of 0.40 to 0.85; this enabled us to estimate the Co content below which the separate Co_9S_8 phase could no longer exist. The values of these zero intercepts in terms of Co/(Co + Mo) were 0.31 and 0.34 for the 3,1,1 and 4,0,0 lines respectively, with uncertainties of ±26 and ±14% at the 75% confidence level. While we do not wish to claim greater certainty for the estimate than is implied by these statistics, it is nevertheless interesting to note that the cobalt concentration at which chemical analysis coincided with the composition $MoS_2 + Co_9S_8$, was at a Co/(Co + Mo) value of 0.40.

This can be readily seen in Fig. 2, where the dashed straight line has been computed by assuming that stoichiometric MoS_2 and Co_9S_8 were the only phases present over the whole range of Co concentrations, and where the solid line represents the experimentally determined values of samples fully sulfided after impregnation, as described in the Experimental section.

In the region of fractional Co content 0.40 to

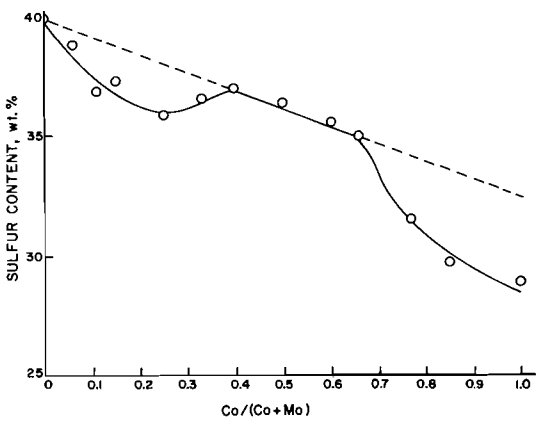

FIG. 2. Sulfur content as a function of composition: ---, calculated on the basis of $MoS_2 + Co_9S_8$; —, experimental.

Can. J. Chem. Downloaded from www.nrcresearchpress.com by 210.87.254.6 on 09/05/12
For personal use only.

Can. J. Chem. Downloaded from www.nrcresearchpress.com by 210.87.254.6 on 09/05/12
For personal use only.

0.65, the experimental values appear to conform well to those expected from the assumed nature of the two phases present. On the other hand, both below and above this range, there is a sulfur deficiency with respect to these phases. It was suggestive in the case of the higher range, that a sample of pure $Co(NO_3)_2$, which had been treated in a manner similar to that of the impregnated MoS_2 catalysts, yielded a sulfide of stoichiometry close to Co_4S_3. Unfortunately it was not of sufficient crystallinity to determine its structure. Co_9S_8 and Co_4S_3 have barely distinguishable diffraction patterns, so that the impregnated catalysts which showed that pattern may well have contained the latter form of sulfide.

The lower range of Co contents is of greater interest in terms of the catalytic reaction. As one possibility, the presumed sulfur deficiency could be associated with Co, leaving MoS_2 stoichiometrically intact. For example, at Co/(Co + Mo) = 0.25, 25% of the Co would be unsulfided, the remainder being in the form of Co_9S_8. The proportion of unsulfided Co would increase with lower overall Co content. Richardson (13) in his study of Co-promoted molybdate catalysts assumed that the true catalyst is MoS_2 promoted with "active cobalt", which must have been reduced and unsulfided. A comparison of the thermodynamic parameters of MoS_2 and Co_9S_8 shows both crystals to be stable in the temperature range under consideration, with a preference for MoS_2 under standard conditions (*e.g.*, for the reaction $4MoS_2 + 9Co \rightarrow Co_9S_8 + 4Mo$, $\Delta G_{700K}^0 \approx 43$ kcal mol^{-1}). It is unlikely, though, that these thermodynamic data could be used in support of the "active cobalt" model. Even if one could assume the exclusive existence of the compounds represented by the above equation, the initial activities at low Co concentrations are far from unity, and would certainly permit the existence of a stable Co_9S_8 phase.

However, there is now considerable evidence that such arguments do not take into account the complexity of these systems. Farragher and Cossee (9) have shown convincingly that there are several types of sulfur atoms in small MoS_2 crystals: the normal ones, which are triply bridging, each being bonded to three metal atoms; and the atypical ones, which are situated at the crystal edges and are either doubly bridging or nonbridging. The last of these are said to be most reactive in hydrogenation processes, in which they can be easily removed. Their stability can be improved by coordination to cobalt, and it is thought that at low Co concentrations all the Co can be accommodated by the available nonbridging sulfur at the crystal edges. Thus Co can be said to be dissolved in the surface regions of the MoS_2 crystal, where it contributes to its stability.

Our own results in the region of fractional Co content 0–0.4 show only a moderate increase in surface area (Fig. 3). There is no X-ray evidence for the existence of unsulfided Co in our catalysts and we regard its presence in our samples as highly unlikely. A comparison of percent thiophene conversion (Fig. 4) and reaction rate per unit surface area (Fig. 5), both as a function of fractional Co content, shows that a significant factor other than surface area increase must be operative in the initial region. In fact, the maximum rate coincides with the highest sulfur "deficiency" (Fig. 2). Under these conditions, we assume with Voorhoeve (14), and Farragher and Cossee (9) that surface anion vacancies adjacent to Mo^{3+} cations are favored, and that they are responsible for the catalytic activity. Van Sint Fiet (15) assumed that Mo^{3+} can be created from the fully reduced MoS_2 in hydrodesulfurization processes. Farragher and Cossee (9) argued that one of the necessary consequences of their model was the rounding of crystal edges of WS_2 upon impregnation with Ni. They were able to demonstrate this effect through electron microscopy. We were able to confirm a similar crystal reconstruction of MoS_2 crystals by Co with a scanning electron microscope; impregnation induced a similar rounding of edges which

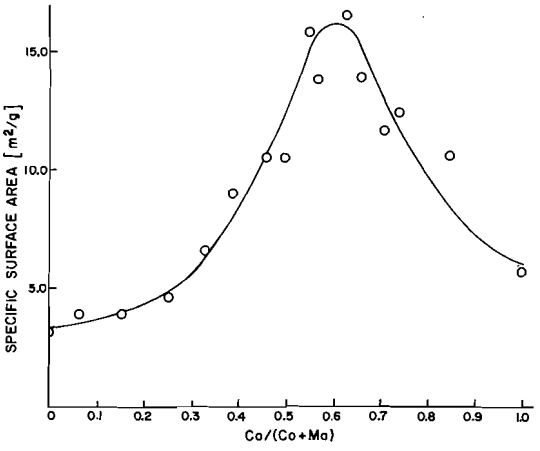

FIG. 3. Surface area as a function of catalyst composition.

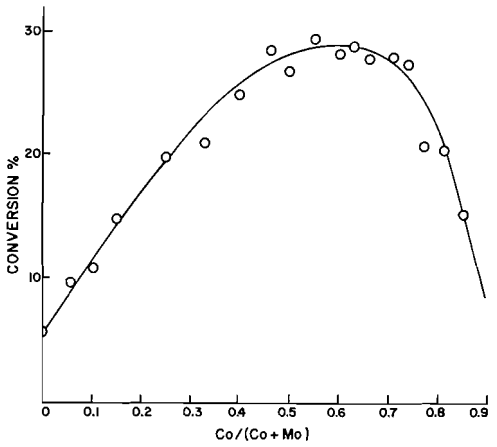

FIG. 4. Percent conversion of thiophene as a function of catalyst composition. Conditions as in Fig. 1.

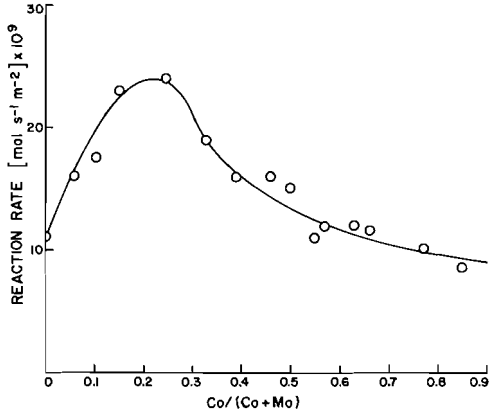

FIG. 5. Reaction rate as a function of catalyst composition. Conditions as in Fig. 1.

was identifiable even at the lower resolving power of the s.e.m.

The initial moderate rise in surface area (Fig. 3) has already been cited, but its cause is not entirely clear. It may well be connected with the increased stability in the surface region, and thus greater resistance to sintering during catalyst preparation. In the higher Co range, in which the stoichiometry coincides exactly with the composition $MoS_2 + Co_9S_8$, and in which both these crystals are clearly identifiable in the X-ray spectra, the area increases more steeply up to a maximum near a fractional Co value of 0.6. At this point it is five times that of the unpromoted MoS_2. Undoubtedly, the increased area is due to the appearance and growth of the Co_9S_8 phase. The latter could act very much like an inert catalyst support in its ability to stabilize crystal sizes. Initially it might have contributed to comminution of the MoS_2 crystallites through intercalation and subsequent growth between the weakly bonded layers of the hexagonal MoS_2 lattice, leading ultimately to cleavage. Regrettably, crystal sizes were not small enough to have enabled us to confirm the latter mechanism through X-ray line broadening; or else the appearance of such small MoS_2 crystals in the surface region was too small in extent to register in the presence of the larger sized bulk phase crystals.

The surface area increase is almost exactly mirrored by an increase in percent conversion (Fig. 4) by a similar factor, with a maximum also at Co/(Co + Mo) = 0.6. At the same time, the reaction rate (Fig. 5) experiences an only insignificant decrease in the middle region of composition. Taken together, these results can only be interpreted as meaning that the extent of the available active surface increases, but that there is little change in the intrinsic activity or surface concentration of active sites. In other words, the Co_9S_8 phase must be regarded as catalytically inactive.

The final collapse of the surface area and percent conversion sets in exactly at the composition at which the stoichiometry again begins to become sulfur "deficient", due to the possible appearance of Co_4S_3 (see above). Again, the reaction rate decreases only minimally, so that behavior in this region might be associated with sintering and crystal growth phenomena. The last point in Figs. 3 and 4 was obtained by treating a sample of pure $Co(NO_3)_2$ in the same manner as the Co-promoted MoS_2 catalysts; the surface area value was 5.6 $m^2\ g^{-1}$ as compared to 3.1 $m^2\ g^{-1}$ for unpromoted MoS_2.

Finally we wish to emphasize that the detailed structure of catalysts such as ours is very much dependent on method of preparation. Thus it is not surprising to find that Hagenbach *et al.* (8) report observations somewhat different from ours, in that their catalyst was prepared by coprecipitation rather than impregnation. This would account for the formation of a Co_9S_8 phase even at lower Co content during the initial catalyst preparation, even before the onset of a possible intercalation process. In our case Co_9S_8 appeared only after the impregnated catalyst had been subjected to sulfiding.

Can. J. Chem. Downloaded from www.nrcresearchpress.com by 210.87.254.6 on 09/05/12
For personal use only.

We are most grateful to Professor George Chao for the use of his X-ray equipment and for most helpful advice, to Mr. R. C. McAdam of the Department of Energy, Mines and Resources for sulfur analyses on two series of catalysts, and to Mr. G. Harris for laboratory assistance. We acknowledge with thanks the financial assistance provided by the National Research Council of Canada.

1. J. B. McKINLEY. *In* Catalysis, Vol. 5. *Edited by* P. H. Emmett. Reinhold, New York, 1957. p. 405.
2. P. C. H. MITCHELL. The chemistry of some hydrodesulphurisation catalysts containing molybdenum. Climax Molybdenum Co. Ltd., London. 1967.
3. S. C. SCHUMAN and H. SHALIT. Catal. Rev. **4**, 245 (1970).
4. G. C. A. SCHUIT and B. C. GATES. Am. Inst. Chem. Eng. J. **19**, 417 (1973).
5. O. WEISSER and S. LANDA. Sulphide catalysts, their properties and applications. Pergamon, Oxford/New York, 1973.
6. C. H. AMBERG. J. Less-common Met. **36**, 339 (1974).
7. P. GRANGE and B. DELMON. J. Less-common Met. **36**, 353 (1974).
8. G. HAGENBACH, P. COURTY, and B. DELMON. J. Catal. **31**, 264 (1973).
9. A. L. FARRAGHER and P. COSSEE. Proc. Vth. Int. Congr. Catal. *Edited by* J. W. Hightower. North-Holland, Amsterdam/London. 1973. p. 1301.
10. S. KOLBOE and C. H. AMBERG. Can. J. Chem. **44**, 2623 (1966).
11. P. J. OWENS and C. H. AMBERG. Adv. Chem. Ser. **33**, 182 (1961).
12. P. DESIKAN and C. H. AMBERG. Can. J. Chem. **41**, 1966 (1963).
13. J. T. RICHARDSON. Ind. Eng. Chem. Fundam. **3**, 154 (1964).
14. R. J. VOORHOEVE. J. Catal. **23**, 236 (1971).
15. T. H. M. VAN SINT FIET. Ph.D. Thesis. Eindhoven University of Technology, Eindhoven, The Netherlands. 1973.

Can. J. Chem. Downloaded from www.nrcresearchpress.com by 210.87.254.6 on 09/05/12
For personal use only.

Study of Chemically Induced Dynamic Nuclear Polarization of Aliphatic Aldehydes in D_2O and other Solvents

HOLGER E. CHEN, MICHAEL COCIVERA, AND SHIV P. VAISH
Department of Chemistry, University of Guelph, Guelph, Ontario N1G 2W1

Received April 8, 1975

HOLGER E. CHEN, MICHAEL COCIVERA, and SHIV P. VAISH. Can. J. Chem. **53**, 2548 (1975).

The chemically induced dynamic nuclear polarization arising from irradiation of aliphatic aldehydes in D_2O and various other solvents is reported. The aldehydes included acetaldehyde, propionaldehyde, isobutyraldehyde, and pivalaldehyde, and the solvents were benzene, acetonitrile, cyclohexane, methylcyclohexane, perfluoromethylcyclohexane, D_2O, and D_2O/acetonitrile. For propionaldehyde, the variation of c.i.d.n.p. with solvent can be explained by a variation of the relative importance of α-cleavage *vs.* hydrogen abstraction which occur via an excited triplet state. In addition, when D_2O is the solvent, the c.i.d.n.p. provides information about secondary radical reactions not observed in the other solvents. For the other aldehydes, the nature of the solvent does not seem to affect the relative importance of α-cleavage *vs.* hydrogen abstraction. Acetaldehyde undergoes hydrogen abstraction whereas isobutyraldehyde and pivalaldehyde undgero α-cleavage via an excited triplet state.

HOLGER E. CHEN, MICHAEL COCIVERA et SHIV P. VAISH. Can. J. Chem. **53**, 2548 (1975).

On rapporte la polarisation nucléaire dynamique induite chimiquement dérivant de l'irradiation d'aldéhydes aliphatiques en solution dans D_2O et divers autres solvants. Les aldéhydes comprennent l'acétaldéhyde, la propionaldéhyde, l'isobutyraldéhyde et le pivalaldéhyde alors que les solvants utilisés sont le benzène, l'acétonitrile, le cyclohexane, le méthylcyclohexane, le perfluorométhylcyclohexane, D_2O et D_2O/acétonitrile. Pour le propionaldéhyde, on peut expliquer la variation de la p.n.d.i.c. avec le solvant par une variation de l'importance relative du clivage α *vs.* l'enlèvement de l'hydrogène qui se produisent par l'intermédiaire d'un état triplet excité. De plus dans l'eau lourde, la p.n.d.i.c. fournit des informations concernant des réactions radicalaires secondaires qui ne sont pas observées dans d'autres solvants. Pour les autres aldéhydes, il ne semble pas que la nature du solvant affecte l'importance relative du clivage α *vs.* l'enlèvement d'hydrogène. L'acétaldéhyde subit un enlèvement d'hydrogène alors que l'isobutyraldéhyde et le pivalaldéhyde subissent un clivage α pa l'intermédiaire d'un état triplet excité. [Traduit par le journal]

The photochemistry of various aliphatic aldehydes has been studied using chemically induced dynamic nuclear polarization (c.i.d.n.p.) (1–3).

An earlier preliminary report (2*b*) briefly described the effect of solvent on the c.i.d.n.p. of propionaldehyde. In the present paper, we present the details of a c.i.d.n.p. study of solvent effects on the photochemistry of propionaldehyde as well as acetaldehyde, isobutyraldehyde, and pivalaldehyde. The solvents include perfluoromethylcyclohexane, benzene, methylcyclohexane, acetonitrile, water, and water/acetonitrile mixtures. According to previous work (1, 2), these aliphatic aldehydes in excited triplet states can react via two paths in solution.

[1] $RCHO^T \rightarrow [\dot{R}\ \dot{C}HO]^T \rightarrow$ dissociation and products

[2] $RCHO^T + RCHO \rightarrow [R\dot{C}H(OH)\ R\dot{C}O]^T \rightarrow$ dissociation and products

In these reactions, R represents the methyl, ethyl, isopropyl, or *tert*-butyl group. Reaction 1 indicates α-cleavage, and reaction 2 involves hydrogen atom abstraction. The brackets indicate a radical pair, and T signifies a triplet precursor for the radical pair. Nuclear spin polarization occurs as a result of reaction via the radical pair. The importance of each route to nuclear spin polarization depends on the R group. For the methyl group, the observed polarization can be explained by [2] (1*a*). For *tert*-butyl, [1] accounts for the polarization (2*a*). For ethyl, both [1] and [2] are needed to account for the polarization (2*b* and *c*). Furthermore the contribution of the two paths appears to depend on the solvent employed (2*b*). The results of the present study indicate that the polarization observed for acetaldehyde, isobutyraldehyde, and pivalaldehyde shows little solvent effect on the contributions of the two paths. However an interesting offshoot of this study is that the use of water as a solvent results in the observation of additional secondary reactions not detected in the other solvents.

Can. J. Chem. Downloaded from www.nrcresearchpress.com by 210.87.254.6 on 09/05/12
For personal use only.

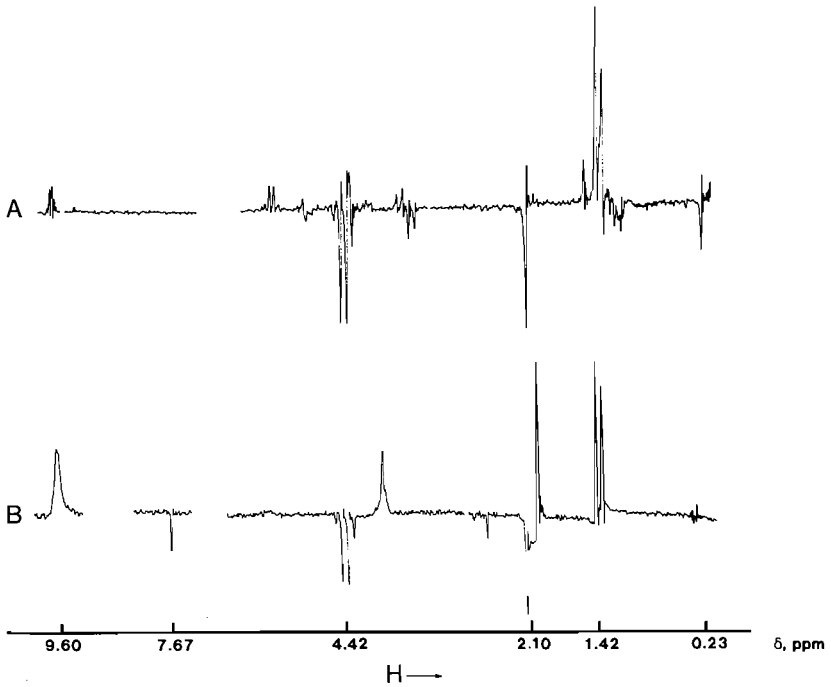

FIG. 1. Nuclear magnetic resonance spectra during irradiation of acetaldehyde in D_2O/CD_3CN (1:1 by volume). (*A*) Without CCl_4. The HDO signal position (at 4.42 p.p.m.) varies during irradiation because it is temperature sensitive. (*B*) With 0.1 *M* CCl_4.

Experimental

Chemicals

The solvents, which were usually reagent grade, were purified by fractional distillation when deemed necessary. The aldehydes were obtained from Baker or Aldrich and were purified by fractional distillation. Acetaldehyde-d_1 (Merck) was used without purification. Propionaldehyde-2,2-d_2 (Merck) was fraction distilled once at atmospheric pressure. Other compounds which were used for chemical shift determinations were not purified.

Nuclear Magnetic Resonance

The proton n.m.r. spectra at 100 MHz were obtained using a Varian HA-100-15 spectrometer which we have modified to operate on a time sharing mode. In this mode we are able to use a quartz probe which allowed direct irradiation of the sample while the n.m.r. spectrum was obtained. This probe was built in our laboratory and the details are given elsewhere (4). The probe temperature was maintained at 15 °C, although local heating due to irradiation raised the temperature of a portion of the sample. The n.m.r. spectra were obtained before, during and after irradiation. The radiation source was a 1000 W Hanovia mercury–xenon lamp. For some of the experiments, a Pyrex plate was used to filter out radiation having wavelength less than 310 nm. The detailed structure of the spectrum was the same with and without the filter. However, larger intensities were obtained without the filter.

Results

Rather than present spectra for each aldehyde in all the solvents, we present spectra for each aldehyde in acetonitrile/D_2O mixtures (50/50 by volume) without and with CCl_4 present since the largest number of products and additional reactions are observed in this solvent. The acetonitrile/D_2O mixture gives the same results as pure D_2O, although the signals are more intense in pure D_2O. This mixture was chosen to increase the solubility of CCl_4 for radical trapping experiments. Any differences between the results for this solvent and those for the other solvents are noted in the tables or in the text. Figures 1 to 4 illustrate the spectra for acetaldehyde, propionaldehyde, isobutyraldehyde, and pivalaldehyde, respectively. In each figure, spectrum *A* is obtained without CCl_4 and *B* is obtained with CCl_4 present. The dashed lines indicate signal heights after irradiation is stopped. As can be seen, a variety of enhanced absorption and emission signals are detected, indicating the occurrence of non-Boltzmann nuclear spin polariz-

Can. J. Chem. Downloaded from www.nrcresearchpress.com by 210.87.254.6 on 09/05/12
For personal use only.

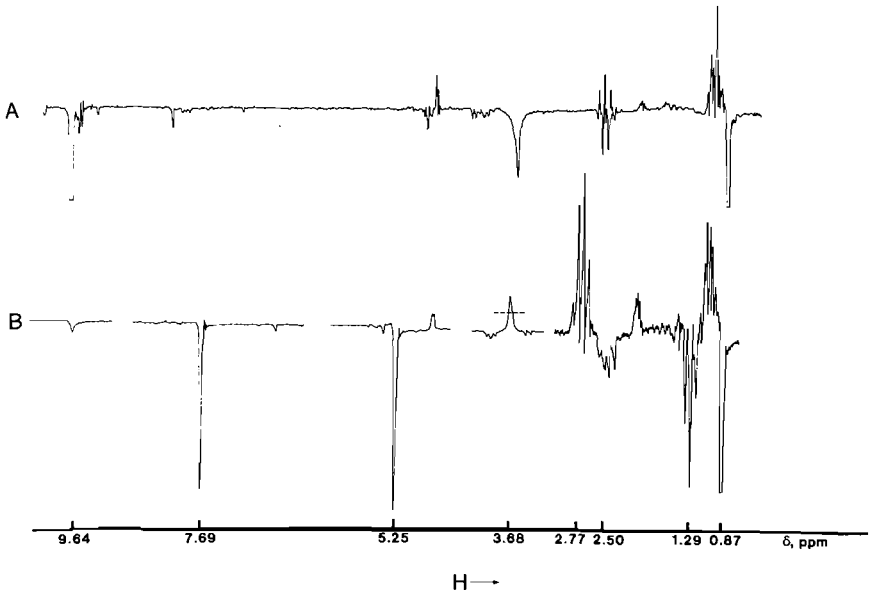

FIG. 2. Nuclear magnetic resonance spectra during irradiation of propionaldehyde in D_2O/CD_3CN (1:1 by volume). The dashed line indicates the signal height after irradiation is stopped. (*A*) Without CCl_4. (*B*) With 0.1 *M* CCl_4. As indicated by the signal to noise, part of the spectrum is recorded at higher gain. The ethane emission is off scale.

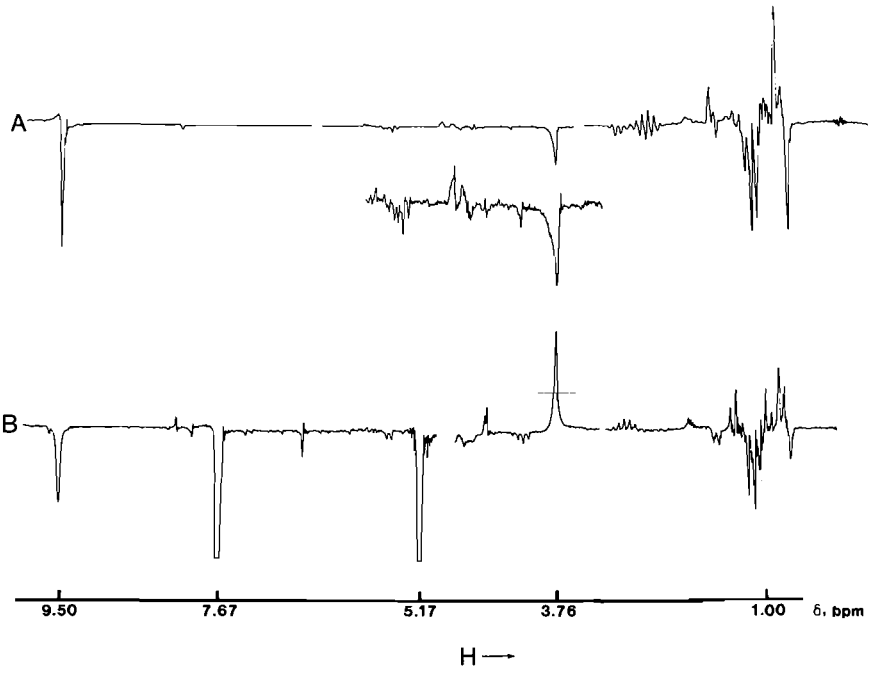

FIG. 3. Nuclear magnetic resonance spectra during irradiation of isobutyraldehyde in D_2O/CD_3CN (1:1 by volume). (*A*) Without CCl_4. The partial spectrum (between 5.3 and 3.5 p.p.m.) below the total spectrum is at higher gain. (*B*) With 0.1 CCl_4. The signals at 5.17 and 7.67 p.p.m. are off scale.

Can. J. Chem. Downloaded from www.nrcresearchpress.com by 210.87.254.6 on 09/05/12
For personal use only.

Can. J. Chem. Downloaded from www.nrcresearchpress.com by 210.87.254.6 on 09/05/12
For personal use only.

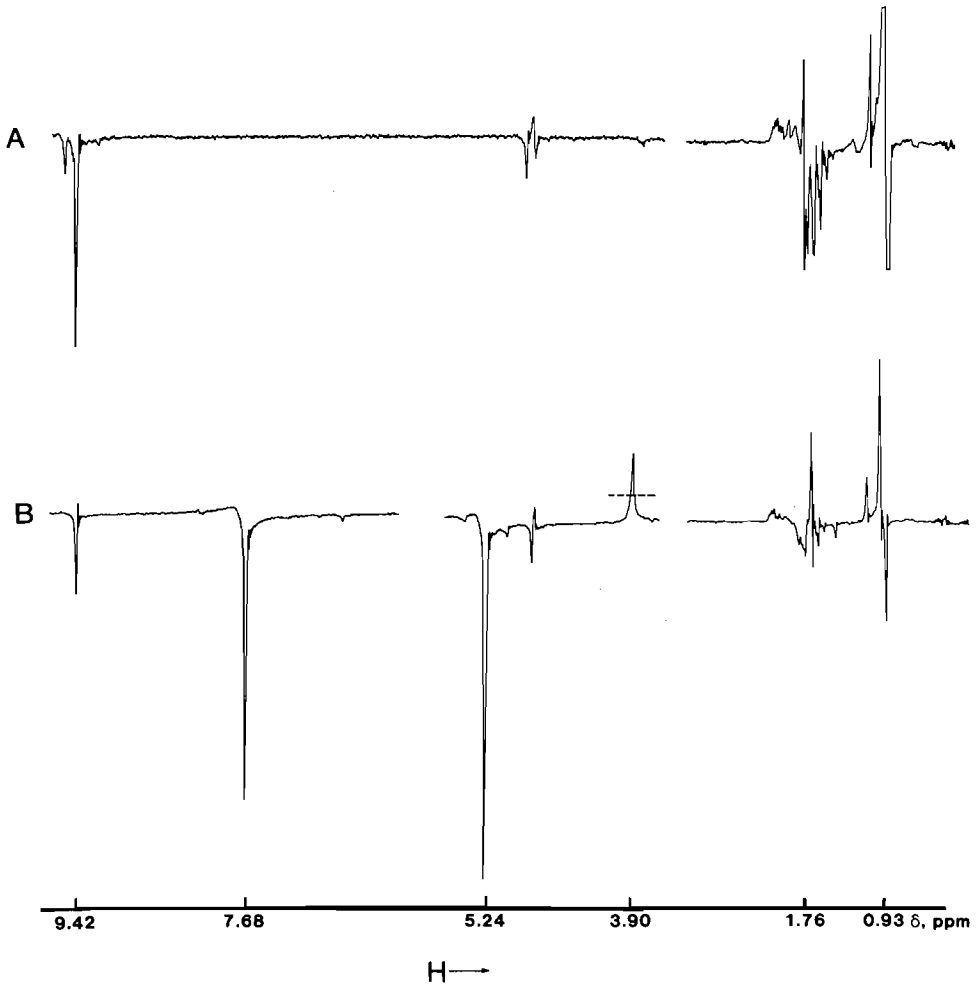

FIG. 4. Nuclear magnetic resonance spectra during irradiation of pivalaldehyde in D_2O/CD_3CN (1:1 by volume). (*A*) Without CCl_4. (*B*) With 0.1 *M* CCl_4. The isobutane resonance is off scale.

tion. The assignment of the signals at the various chemical shifts in p.p.m. relative to the methyl resonance of tetramethylsilane are given in Tables 1 to 4 for acetaldehyde, propionaldehyde, isobutyraldehyde, and pivalaldehyde, respectively. In addition, these tables also list the assignments for signals detected when perfluoromethylcyclohexane is the solvent. For other solvents (acetonitrile, benzene, methylcyclohexane, and cyclohexane), the spectra look like either the one for perfluoromethylcyclohexane or the one for the acetonitrile/D_2O mixture (except for the hydrate compounds), depending on the aliphatic aldehyde. The nature of the signal is indicated as enhanced absorption A, emission E, and multiplet with low field absorption and high field emission A/E. Two aspects which should be pointed out for the CD_3CN/D_2O solvent are the occurrence of hydrates of aldehydes and in the case of propionaldehyde, isobutyraldehyde and pivalaldehyde, the effect on the HDO signal in the absence and in the presence of 0.1 *M* CCl_4. In the absence of CCl_4 the HDO signal is in emission whereas it appears as enhanced absorption when CCl_4 is present. The same results are obtained when the sample is degassed to less than 2 μ to remove molecular oxygen. The polarization effect on HDO appears to be smaller for pivalaldehyde than for the other two aldehydes.

Discussion

The polarization results described above can be accounted for by the radical pair model (5) and the occurrence of the reactions given by [1]

TABLE 1. Assignment of n.m.r. signals and c.i.d.n.p. observed during the irradiation of acetaldehyde

	CD_3CN/D_2O			Perfluoromethylcyclohexane			
Compound	δ (p.p.m.)	c.i.d.n.p.[a]	CCl_4[b] c.i.d.n.p.	CH_3CDO c.i.d.n.p.	δ (p.p.m.)	c.i.d.n.p.	CCl_4[b] c.i.d.n.p.
CH_4	0.23	E					
CH_3CH_2OH	1.22	E + A/E		E + A/E[c]	1.14	E + A/E	
CH_3CH_2OH	3.68	A + A/E		A + A/E[c]	3.68	A + A/E	
$CH_3CHOHCOCH_3$	1.42	A + A/E	A	A[d]	1.35	A + A/E	A + A/E
$CH_3CHOHCOCH_3$	2.28	E	E	E[d]	2.09	E	E
$CH_3CHOHCOCH_3$	4.42	E + A/E	E	—	4.13	E + A/E	E + A/E
unidentified	1.60	A			1.50	A	
CH_3CHO	2.28	E	E	E	2.02	E	E
CH_3CHO	9.60	A	A	A	9.73	A	A
$CH_3CH(OD)_2$	5.25	A	—	A			
CH_2=CHOH	4.15	A	—	A[e]	3.93	A	—
CH_2=CHOH	6.50	E	—	—[e]	—	—	—
CH_3COOH	2.04	—	A	—	—	—	—
CH_3COCl	—	—	—	—	2.52	—	A
CH_3COCCl_3[f]	2.65	—	E	—	—	—	—
$CHCl_3$	7.67	—	E	—			

[a] D_2O.
[b] 0.1 *M*.
[c] CH_3CHDOD.
[d] $CH_3CDODCOCH_3$.
[e] CH_2=CDOD.
[f] Not confirmed.

and [2] and a variety of secondary radical reactions. In addition the effect on the HDO signal can be used as evidence for another reaction of the excited aldehyde. Since all of these aldehydes have been studied previously in at least one solvent (1, 2), the polarizations have been calculated already for a number of the compounds. Therefore, rather than repeat the presentation of calculated spectra, the simple Kaptein rules (6) are used to indicate the sense of the polarization for particular compounds formed by reaction via a given radical pair.

The results for propionaldehyde in Table 2 are consistent with the occurrence of [1], [2], and [3]. The importance of these routes to the polarization depends on the solvent employed. Comparison of the two solvents in Table 2 illustrates this point. In perfluoromethylcyclohexane, the carbonyl hydrogen of propionaldehyde exhibits enhanced absorption and $CH_3CH_2CH(OH)$-$COCH_2CH_3$ is formed, and their nuclear polarizations can be accounted for by [2] and [3].

$$[3] \quad [R\dot{C}H(OH)\ \dot{C}OR]^{T,F} \rightarrow R\dot{C}H(OH)^* + R\dot{C}O$$
$$R\dot{C}H(OH)^* + RCHO \rightarrow RCHO^* + R\dot{C}H(OH)$$

The asterisk indicates nuclear spin polarization. According to this scheme, the aldehyde is formed with nuclear spin polarization by a radical trapping step which involves the transfer of a hydrogen atom. Using the Kaptein rules, the carbonyl hydrogen polarization for this route agrees with the observed polarization. Thus, [3] and/or disproportionation in $[R\dot{C}H(OH)\ \dot{C}OR]^T$ to give the aldehyde plus its enol can account for the enhanced absorption observed for the carbonyl hydrogen. The fact that enhanced absorption is observed for the carbonyl hydrogen when CH_3CDO is irradiated supports the second route (see Table 1). Furthermore, as discussed below, there is also evidence in support of [3]. Thus, it appears that both mechanisms are operating.

Ethane is formed with emission which is not prevented by the presence of CCl_4. Since this polarization persists in the presence of CCl_4, it probably is not formed via F-type radical pairs. The emission of ethane is consistent with disproportionation via $[CH_3\dot{C}H_2\ \dot{C}HO]^T$ and can be taken as evidence for reaction according to [1]. However, since recombination of this radical pair would result in emission for the carbonyl hydrogen of propionaldehyde (which is not observed), reaction according to [2] and [3] is more important in perfluoromethylcyclohexane. The same conclusion appears to hold for methylcyclohexane. In contrast the mechanism given by [1] appears more important when acetonitrile/D_2O

Can. J. Chem. Downloaded from www.nrcresearchpress.com by 210.87.254.6 on 09/05/12
For personal use only.

Can. J. Chem. Downloaded from www.nrcresearchpress.com by 210.87.254.6 on 09/05/12
For personal use only.

TABLE 2. Assignment of n.m.r. signals and c.i.d.n.p. observed during irradiation of propionaldehyde

	CD_3CN/D_2O			Perfluoromethylcyclohexane			
Compound[a]	δ (p.p.m.)	c.i.d.n.p.	CCl_4[b] c.i.d.n.p.	CH_3CD_2CHO c.i.d.n.p.	δ (p.p.m.)	c.i.d.n.p.	CCl_4[b] c.i.d.n.p.
CH_3CH_3	0.87	E	E	E[c]	0.90	E	E
$\mathit{CH}_3CH_2COCH_2\mathit{CH}_3$	1.01	A + A/E	—	A[c]	1.05	A	—
$CH_3\mathit{CH}_2CO\mathit{CH}_2CH_3$	2.50	E + A/E	—	—	2.29	E	—
$\mathit{CH}_3CH_2CHOHCH_2\mathit{CH}_3$	—	—	—	—	0.97	E + A/E	—
$CH_3\mathit{CH}_2CHOH\mathit{CH}_2CH_3$	—	—	—	—	1.42	A + A/E	—
$CH_3CH_2\mathit{CH}OHCH_2CH_3$	—	—	—	—	3.55	A	—
$CH_3\mathit{CH}_2CHOHCOCH_2CH_3$	—	—	—	—	1.77	A	A
$CH_3CH_2CHOHCO\mathit{CH}_2CH_3$	—	—	—	—	2.30	E	E
$CH_3CH_2\mathit{CH}OHCOCH_2CH_2$	4.15	E	E	E[c]	4.00	E	E
CH_3CH_2CHO	1.20	—	—	—	1.10	A + A/E	A + A/E
$CH_3\mathit{CH}_2CHO$	2.52	E	E	—	2.30	E + A/E	E + A/E
$CH_3CH_2\mathit{CH}O$	9.64	E	E	E[c]	9.71	A	A
$CH_3CH_2\mathit{CH}(OD)_2$	4.90	E	E	E[c]	—	—	—
HDO	3.68[d]	E	A	E(A)[e]	—	—	—
CH_3CH_2COCl	—	—	—	—	1.21	—	N.P.[f]
$CH_3\mathit{CH}_2COCl$	—	—	—	—	2.83	—	N.P.[f]
$\mathit{CH}_3CH_2CCl_3$	1.29	—	E	E[e]	—	—	—
$CH_3\mathit{CH}_2CCl_3$	2.77	—	A	—	—	—	—
CH_3CH_2Cl	1.45	—	A	A[e]	—	—	—
CCl_3CHO	—	—	—	—	8.95	—	E
$CCl_3CH(OD)_2$	5.25	—	E	E[e]	—	—	—
$CHCl_3$	7.69	—	E	E[e]	7.21	—	E

[a]A number of other signals (many of them when CCl_4 is present) have not been identified. The chemical shifts are: 2.53, 4.28, 4.76, 4.78, 5.40, 6.66, and 8.30.
[b]0.1 *M*.
[c]CH_3CD_2H, $CH_3CD_2COCD_2CH_3$, $CH_3CD_2CHOHCD_2CH_3$, CH_3CD_2CHO, and $CH_3CD_2CH(OH)_2$.
[d]HDO moves up field during irradiation because the temperature increases.
[e]In the presence of 0.1 *M* CCl_4.
[f]Intensity the same during and after irradiation.

TABLE 3. Assignment of n.m.r. signals and c.i.d.n.p. observed during irradiation of isobutyraldehyde

Compound	CD_3CN/D_2O δ (p.p.m.)	CD_3CN/D_2O c.i.d.n.p.	CD_3CN/D_2O CCl_4[a] c.i.d.n.p.	Perfluoromethylcyclohexane δ (p.p.m.)	Perfluoromethylcyclohexane c.i.d.n.p.	Perfluoromethylcyclohexane CCl_4[a] c.i.d.n.p.
$CH_3CH_2CH_3$	0.87	A + A/E	A + A/E	0.95	A + A/E	A + A/E
$CH_3CH_2CH_3$	1.24	E + A/E	E + A/E	1.32	E + A/E	E + A/E
$(CH_3)_2CHCH(CH_3)_2$	—	—	—	0.96	A/E	—
$(CH_3)_2CHCH(CH_3)_2$	—	—	—	1.45	A/E	—
$CH_3CH{=}CH_2$	1.70	A + A/E	E	1.70	A + A/E	E
$CH_3CH{=}CH_2$	5.02	A + A/E	E	4.96	A + A/E	E
$CH_3CH{=}CH_2$	5.82	E + A/E	A	5.87	E + A/E	A
$(CH_3)_2CHCHO$	2.46	E	—	2.27	E	—
$(CH_3)_2CHCHO$	9.50	E	E	9.56	E	E
HDO	3.76[b]	E	A	—	—	—
$(CH_3)_2CHCCl_3$	1.28	—	E	1.36	—	E
$(CH_3)_2CHCCl_3$	2.78	—	A	2.70	—	A
$(CH_3)_2CHCl$	1.50	—	A	1.48	—	A
$(CH_3)_2CHCl$	4.27	—	E	4.10	—	E
$CCl_3CH(OD)_2$	5.17	—	E	—	—	—
$CHCl_3$	7.67	—	E	7.25	—	E
CCl_3CHO	—	—	—	8.95	—	E

[a]0.1 *M*.
[b]Signal position is temperature dependent.

TABLE 4. Assignment of n.m.r. signals and c.i.d.n.p. observed during irradiation of pivalaldehyde

Compound[a]	CD_3CN/D_2O δ (p.p.m.)	CD_3CN/D_2O c.i.d.n.p.	CD_3CN/D_2O CCl_4[b] c.i.d.n.p.	Perfluoromethylcyclohexane δ (p.p.m.)	Perfluoromethylcyclohexane c.i.d.n.p.	Perfluoromethylcyclohexane CCl_4[b] c.i.d.n.p.
$(CH_3)_3CH$	0.93	A + A/E	A + A/E	0.73	A + A/E	A + A/E
$(CH_3)_3CH$	1.76	E + A/E	E	1.56	E + A/E	E + A/E
$(CH_3)_3CCHO$	1.07	A	A	0.85	A	A
$(CH_3)_3CCHO$	9.42	E	E	9.22	E	E
$(CH_3)_2C{=}CH_2$	1.70	A/E	E	1.53	A/E	E
$(CH_3)_2C{=}CH_2$	4.69	A/E	E	4.48	A/E	E
HDO	3.90	E	A	—	—	—
$H_2C(OH)_2$	4.78	E	E	—	—	—
H_2CO	9.52	E	—	—	—	—
$(CH_3)_3CCl$	1.63	—	A	1.40	—	A
$CCl_3CH(OH)_2$	5.24	—	E	—	—	—
$CHCl_3$	7.68	—	E	7.24	—	E
CCl_3CHO	—	—	—	8.94	—	E

[a]Unidentified signal at 4.75 p.p.m.
[b]0.1 *M*.

is the solvent because emission is observed for the carbonyl hydrogen of propionaldehyde and the emission of ethane becomes more intense relative to the other signals. Furthermore the observation of CH_3CH_2Cl, CCl_3CHO, and $CH_3CH_2CCl_3$ when CCl_4 is present supports α-cleavage via an excited propionaldehyde. The polarization observed for $CH_3CH_2CCl_3$ is consistent with formation via the radical pair $[CH_3\dot{C}H_2\ \dot{C}Cl_3]^F$ since the *g*-factor for $\dot{C}Cl_3$ is larger than the one for $CH_3\dot{C}H_2$ (7, 8). The polarization for CH_3CH_2Cl is consistent with trapping of $CH_3\dot{C}H_2$ by CCl_4 after dissociation from this radical pair. The emission observed for CCl_3CHO is consistent with formation via the radical pair $[\dot{C}Cl_3\ \dot{C}HO]^F$. Chloroform formation can occur via both radical pairs. In addition, since the presence of CCl_4 does not prevent the emission observed for ethane and carbonyl hydrogen of propionaldehyde, these compounds must be formed in part from the initial radical pair $[CH_3\dot{C}H_2\ \dot{C}HO]^T$ because CCl_4 would pre-

Can. J. Chem. Downloaded from www.nrcresearchpress.com by 210.87.254.6 on 09/05/12
For personal use only.

Can. J. Chem. Downloaded from www.nrcresearchpress.com by 210.87.254.6 on 09/05/12
For personal use only.

vent the formation of the F-type radical pair by trapping the free radicals $CH_3\dot{C}H_2$ and $\dot{C}HO$, as mentioned above. In contrast with the acetonitrile/D_2O solvent, the use of perfluoromethyl cyclohexane does not seem to result in detectable amounts of $CH_3CH_2CCl_3$ and CH_3CH_2Cl, indicating that reaction via [1] is less important. On the other hand the fact that $CH_3CH_2CH(OH)$-$COCH_2CH_3$ is detected in acetonitrile/D_2O indicates the reaction according to [2] occurs in this solvent, also, but to a lesser extent than in the fluorocarbon. The other compounds are formed via F-type radical pairs as discussed previously for the fluorocarbon solvent (2*b* and *c*). The observation of $CCl_3CH(OH)_2$ supports the occurrence of [1] in acetonitrile/D_2O. CCl_3CH-$(OH)_2$ results from a combination of $\dot{C}Cl_3$ with $\dot{C}HO$ to form chloral which in turn hydrates in the mixed solvent. The formation of the other chloro compounds has been described previously. The polarization of the HDO signal will be discussed below.

The occurrence of [3] has been confirmed by the photolysis of propionaldehyde-2,2-d_2 in the fluorocarbon. Since disproportion of $[CH_3CD_2$-$\dot{C}H(OH)\ \dot{C}OCD_2CH_3]^T$ leads to the enol plus CH_3CD_2CDO which has no carbonyl hydrogen resonance, the detection of CH_3CD_2CHO with enhanced absorption for the carbonyl hydrogen resonance is consistent with the occurrence of [3]. A similar mechanism is used for benzaldehyde (9). To determine the sign of the polarization according to the Kaptein rules, the *g*-factors decrease in the order $CH_3CH_2\dot{C}HOH$, $CH_3\dot{C}H_2$, and $\dot{C}HO$, $\dot{C}OCH_2CH_3$ (10). Also, the value for the electron–proton hyperfine coupling constant for $\dot{C}HO$ is positive (10*a*). Thus, it appears that the reactions given by [1] and [2] occur in all of the solvents used for propionaldehyde. The relative importance of these two reactions depends on the solvent with [2] being more important when the solvent is perfluoromethylcyclohexane or methylcyclohexane and [1] more important in the other solvents. In addition in these solvents, there is evidence for the occurrence of the process given by [3].

The nature of the solvent appears to have no significant effect on the c.i.d.n.p. spectra observed during irradiation of acetaldehyde, isobutyraldehyde, or pivalaldehyde, as can be seen from the results in Tables 1, 3, and 4. The nature of the compounds and the polarization observed for isobutyraldehyde or pivalaldehyde are consistent with reaction according to [1] and subsequent reaction via F-type radical pairs. On the other hand, the nature of the compounds and polarization for irradiation of acetaldehyde are consistent with an initial reaction according to [2]. Since these mechanisms have been discussed previously for pivalaldehyde in perfluoromethylcyclohexane (2*a*), isobutyraldehyde in benzene (1*b*), and acetaldehyde in benzene (1*a*), the detailed steps will not be repeated in this paper, except for one aspect concerning acetaldehyde. The enhanced absorption observed for the carbonyl hydrogen of acetaldehyde has been explained (1*a*) by a mechanism involving disproportionation of the radical pair $[CH_3\ \dot{C}H(OH)$ $\dot{C}OCH_3]^T$ to give acetaldehyde and its enol. Since our results with propionaldehyde-d_2 indicate that the mechanism given by [3] makes an important contribution to the enhanced absorption observed for the carbonyl hydrogen of propionaldehyde, we have tested the importance of the mechanism for acetaldehyde by irradiating CH_3CDO. Under these conditions enhanced absorption is observed for the carbonyl hydrogen, as indicated in Table 1. Thus, both mechanisms may be operating for acetaldehyde and propionaldehyde.

It should be noted that polarization is observed for the hydrates of various aldehydes as well as for HDO. The polarization for each hydrate is consistent with the formation of the aldehyde according to mechanisms described above followed by hydration at a rate more rapid than the spin–lattice relaxation rate. This conclusion is consistent with the fact that no hydrate of pivalaldehyde (polarized or otherwise) is observed. An emission signal is observed for HDO during irradiation of all of the aldehydes (except acetaldehyde) in D_2O/acetonitrile mixtures. A possible mechanism might involve a reaction of radicals with molecular O_2. Degassing samples to less than 2 μ to remove molecular oxygen did not prevent the emission signal for HDO. This result does not preclude the occurrence of a path involving molecular oxygen. However, it does indicate that another reaction path is at least in part responsible for the polarization observed for HDO. A chemically reasonable route is polarization of the protons of one of the organic solutes which can exchange one of its polarized protons with D_2O. While OH protons are easily exchanged with water, it seems unlikely that any

Can. J. Chem. Downloaded from www.nrcresearchpress.com by 210.87.254.6 on 09/05/12
For personal use only.

of the OH containing compounds formed from the steps mentioned above can provide the polarization. This conclusion is based on the fact HDO is not polarized during irradiation of acetaldehyde which provides a number of OH containing compounds via the above mentioned steps. Furthermore, no OH containing compounds were detected during the irradiation of isobutyraldehyde, but HDO was polarized. Likewise the absence of HDO polarization during irradiation of acetaldehyde suggests that the formation of the formyl radical ĊHO is involved in the reaction step which provides the exchangeable proton, since α-cleavage was not detected for acetaldehyde. This conclusion is supported by the fact that HDO polarization is observed during the irradiation of propionaldehyde-2,2-d_2, thus indicating that the methylene protons do not eventually end up polarized on HDO molecules.

While the involvement of the formyl radical seems likely, a mechanism which is compatible for propionaldehyde, isobutyraldehyde, and pivalaldehyde simultaneously is difficult to conceive. The low *g*-factor of the formyl radical relative to the other radicals present and the positive hyperfine coupling constant for its proton rules out a radical trapping mechanism which would require enhanced absorption rather than the observed emission. A mechanism which could account for the HDO polarization for propionaldehyde and isobutyraldehyde but not pivalaldehyde involves the formation of the radical RR′Ċ CHO followed by disproportionation via the radical pair $[RR'\dot{C}—CHO\ \dot{C}HO]^F$ to give the enol RR′C=CH(OH) plus CO. In this case, the exchangeable OH-proton of the enol is negatively polarized. This mechanism is compatible with the HDO emission observed when propionaldehyde-2,2-d_2 is used, also.

The enhanced absorption observed for the HDO signal when CCl_4 is present is easier to explain. As indicated, the enhanced HDO signal is observed for all of the aldehydes except acetaldehyde. Since all of the aldehydes except acetaldehyde react according to [1], it seems likely that the formyl radical is involved. This conclusion is consistent with the absence of signals due to formaldehyde and its hydrate when CCl_4 is present. Thus, since the *g*-factor for each of the alkyl radicals derived from these aldehydes is larger than the one for the formyl radical, the enhanced absorption can be explained by the following mechanism.

$$[\dot{R}\ \dot{C}HO]^T \rightarrow \dot{R} + \dot{C}HO$$

$$\dot{C}HO + CCl_4 \rightarrow ClCHO + \dot{C}Cl_3$$

$$ClCHO + D_2O \rightarrow HD_2O^+ + Cl^- + CO$$

According to this mechanism, the formyl radical which results from dissociation of the radical pair $[\dot{R}\ \dot{C}HO]^T$ is trapped by CCl_4 to form ClCHO before the polarization of the proton is lost via spin–lattice relaxation. In turn, ClCHO decomposes to HCl + CO at a rate which is faster than the spin–lattice relaxation rate and provides the polarization for the HDO proton. This mechanism, which would result in enhanced absorption, is supported by the observation that ClCHO can be formed only at low temperatures and decomposes readily at room temperature (11).

In conclusion, only in the case of propionaldehyde can a solvent effect on the c.i.d.n.p. spectrum be detected conclusively. A solvent effect on the relative importance of the initial photochemical reactions given by [1] and [2] can explain the c.i.d.n.p. spectra. The nature of the solvent effect on these reactions is not clear. However, on the basis of the solvents employed it is possible to conclude that the effect cannot be based solely on solvent polarity. Furthermore, since the effect occurs with or without radiation having wavelength shorter than 310 nm, this effect is not evidence for a competition between a lower and a higher energy transition. For the other aldehydes, a solvent effect is not observed, and in all the solvents listed, the initial reaction for acetaldehyde appears to be [2] whereas [1] appears to be the initial photochemical reaction for isobutyraldehyde and pivalaldehyde. This increase in the relative importance of reaction via [1] as the branching of the alkyl group is increased is paralleled by the relative thermochemical energies of the alkyl free radicals which result from α-cleavage (12). In view of the relative energies of the alkyl free radicals and the absence of any solvent effect on the initial photochemical step for acetaldehyde and isobutyraldehyde, the solvent effect observed for propionaldehyde can involve no more than a few kilocalories. While D_2O does not take part in the photochemical or radical reactions, its reactivity with some of the

products provides information about some reactions not detected in the other solvents employed.

This work is supported in part by the National Research Council of Canada and the Petroleum Research Fund administered by the American Chemical Society.

1. (*a*) B. BLANK and H. FISCHER. Helv. Chim. Acta, **56**, 506 (1973); (*b*) B. BLANK, A. HENNE, and H. FISCHER. Helv. Chim. Acta, **57**, 920 (1974); (*c*) B. BLANK, A. HENNE, G. LAROFF, and H. FISCHER. Helv. Chim. Acta, In press.
2. (*a*) H. CHEN, A. GROEN, and M. COCIVERA. Can. J. Chem. **51**, 3032 (1973); (*b*) H. CHEN, S. VAISH, and M. COCIVERA. Chem. Phys. Lett. **22**, 576 (1973); (*c*) H. CHEN, S. VAISH, and M. COCIVERA. J. Am. Chem. Soc. **95**, 7586 (1973).
3. K. G. SEIFERT and J. BARGON. Angew Chem. **85**, 768 (1973).
4. M. COCIVERA, M. TOMKIEWICZ, and A. GROEN. J. Am. Chem. Soc. **94**, 6598 (1972).
5. A. R. LEPLEY and G. L. CLOSS (*Editors*). Chemically induced dynamic nuclear polarization. J. Wiley and Sons, New York. 1973. Chapts. 3 and 4.
6. R. KAPTEIN. Chem. Commun. 732 (1971).
7. R. FESSENDEN and R. SCHULER. J. Chem. Phys. **39**, 2147 (1963).
8. A. HUDSON and H. HUSSAIN. Mol. Phys. **16**, 199 (1969).
9. G. CLOSS and D. PAULSON. J. Am. Chem. Soc. **92**, 7229 (1970).
10. (*a*) F. ADRIAN, E. COCHRAN, and V. BOWERS. J. Chem. Phys. **36**, 1661 (1962); (*b*) H. PAUL and H. FISCHER. Helv. Chim. Acta, **56**, 1575 (1973) and references cited therein.
11. H. STAAB and A. DATTA. Angew. Chem. Int. Ed. **3**, 132 (1964).
12. S. BENSON. Thermochemical kinetics. J. Wiley and Sons, New York. 1968. p. 204.

Can. J. Chem. Downloaded from www.nrcresearchpress.com by 210.87.254.6 on 09/05/12
For personal use only.

Solution Studies of the Dynamic Stereochemistry of Palladium(II) Carboxylate Complexes

THOMAS R. JACK AND JOHN POWELL

Lash Miller Chemical Laboratories, University of Toronto, Toronto, Ontario M5S 1A1

Received March 11, 1975

THOMAS R. JACK and JOHN POWELL. Can. J. Chem. **53**, 2558 (1975).

A series of dimeric tertiary phosphine carboxylate complexes of palladium(II) of the general types $[(PR_3)Pd(O_2CR)_2]_2$ and $[(PR_3)Pd(O_2CR)(O_2CR')]_2$ have been synthesized and structurally characterized. The dynamic stereochemistry of the complexes where $PR_3 = Me_2PhP$ has been investigated using variable temperature n.m.r. techniques. Exchange of the stereochemically nonequivalent methyl groups of the coordinated Me_2PhP ligand occurs via a solvent assisted process involving ring opening of the "$Pd_2(OCO)_2$" bridged structure. For the trifluoroacetate complexes solution equilibria between monomer and dimer are readily apparent at low temperatures in the ^{19}F n.m.r. The observed equilibrium constants are a function of the solvent and the size of the PR_3 ligand. The reaction of $[(PMe_2Ph)Pd(O_2CCF_3)_2]_2$ with excess AgO_2CCF_3 gives an unusual crystalline complex of stoichiometry $Ag[(PMe_2Ph)Pd(O_2CCF_3)_3]$. A quantitative measure of the ability of a coordinated carboxylate to stabilize intermediate species via chelation has been obtained from a variable temperature n.m.r. study of [(π-2-methylallyl)Pd(O_2CR)(Me_2PhP)] (R = CH_3, CH_2Cl, $CHCl_2$, CCl_3, CF_3, CMe_3, CPh_3, CH_2Ph).

THOMAS R. JACK et JOHN POWELL. Can. J. Chem. **53**, 2558 (1975).

On a synthétisé et caractérisé au point de vue structural une série de complexes à l'état dimère de palladium(II) de formule générale $[(PR_3)Pd(O_2CR)_2]_2$ et $[(PR_3)Pd(O_2CR)(O_2CR')]_2$. On a étudié par r.m.n. à différentes températures la stéréochimie dynamique des complexes avec $PR_3 = Me_2PhP$. L'échange de groupes méthyles de Me_2PhP non équivalents du point de vue stéréochimie se fait par un procédé aidé d'un solvant qui comprend l'ouverture du noyau "$Pd_2(OCO)_2$" de la structure pontée. Pour les complexes du trifluoroacétate, l'équilibre en solution entre le momomère et le dimère est nettement apparent en r.m.n. ^{19}F à basses températures. Les constantes observées pour l'équilibre sont fonction du solvant et de la grosseur du groupe PR_3. La réaction de $[(PMe_2Ph)Pd(O_2CCF_3)_2]_2$ avec un excès de AgO_2CCF_3 donne un complexe cristallin inusité $Ag[(PMe_2Ph)Pd(O_2CCF_3)_3]$. On obtient une mesure quantitative de l'effet du groupe carboxylate coordonné sur la stabilisation des espèces intermédiaires par voie de chélation par une étude r.m.n. à différentes températures de [(π-méthylallyl-2)Pd(O_2CR)(Me_2PhP)] où (R = CH_3,CH_2Cl, $CHCl_2$, CCl_3, CF_3, CMe_3, CPh_3, CH_2Ph).

[Traduit par le journal]

Introduction

Previous studies have shown that several palladium(II) carboxylate complexes possess a dynamic stereochemistry in solution (1–4). The asymmetric solution isomer **1** (Fig. 1) of π-allylpalladium acetate undergoes an (apparently) intramolecular process which exchanges the nonequivalent π-allyl sites. A mechanism involving the inversion of the boat conformation of the $Pd_2(OCO)_2$ ring (Fig. 1) was originally postulated (1–3). The structurally related di-μ-carboxylate dimers $[(Me_2PhP)XM(O_2CR)]_2$ **2** (M = Pd or Pt; X = halide) have since been shown (4) to undergo a process in $CHCl_3$ which leads to the n.m.r. equivalence of the diastereotopic methyl groups of the Me_2PhP ligands by a mechanism involving the *dissociation* of *one* palladium–oxygen bond to give a *ring opened mono-μ-carboxylate bridged intermediate* (Fig. 2) which may re-form **2** in such a way as to effectively invert the boat conformation of the $Pd_2(OCO)_2$ ring. On the basis of solvent effects (4) it is probable that this mechanism is also the major pathway for the (apparently) intramolecular π-allyl site exchange observed for complex **1**.

We here report a further extension of our studies of the dynamic stereochemistry of the carboxylate ligand. We have synthesized and investigated the solution structures of two series of compounds of the types $[(R_3'P)Pd(O_2CR)_2]_2$ and [(π-2-methylallyl)Pd(O_2CR)($R_3'P$)]. The former are of special interest for their resemblance to the solution species which catalyze

Can. J. Chem. Downloaded from www.nrcresearchpress.com by 210.87.254.6 on 09/05/12
For personal use only.

Can. J. Chem. Downloaded from www.nrcresearchpress.com by 210.87.254.6 on 09/05/12
For personal use only.

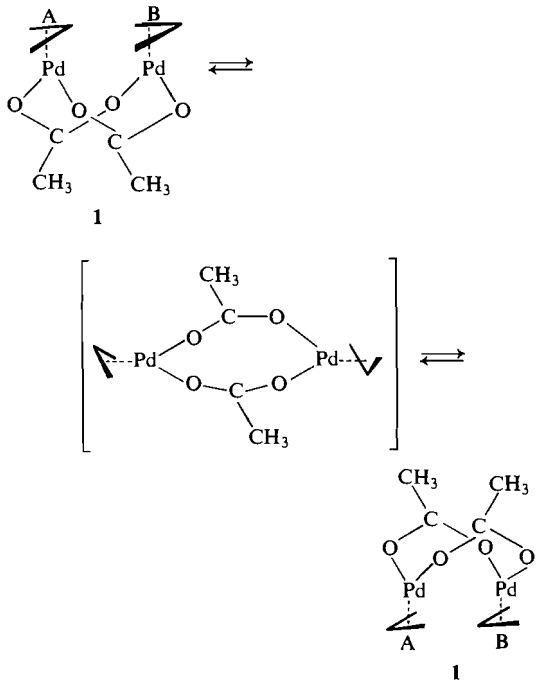

1

1

FIG. 1. The "acetate bridge inversion" mechanism originally proposed to account for the apparently intramolecular exchange of π-allyl sites (A and B) in the π-allyl palladium acetate isomer **1**.

the arylation of olefins (5, 6) and the polymerization of allenes (7, 8).

Results and Discussion

In 1967, Wilkinson and co-worker (9) prepared the complex $[(Ph_3P)Pd(OOCCH_3)_2]_2$ by the stoichiometric addition of triphenylphosphine to palladium(II) acetate. The infrared spectrum of this complex was assignable to the presence of both terminal and bridging bidentate carboxylates consistent with a structure **3**.

The complexes $[(R_3'P)Pd(OOCR)_2]_n$ described herein were prepared by the reaction of the appropriate halide bridged dimer with silver carboxylate[1]

$$[(R_3'P)PdCl_2]_2 + 4AgOOCR \rightarrow \frac{2}{n}[(R_3'P)Pd(OOCR)_2]_n + 4AgCl$$

where $n = 1$ or 2.

[1]Attempts to prepare $[(Me_2PhP)Pd(OOCCH_3)_2]_2$ in solution by the stoichiometric addition of Me_2PhP to palladium(II) acetate led to the formation of reaction mixtures which gave rise to complex ^1H n.m.r. spectra, possibly due to impurities in the reagent palladium acetate.

Attempts to prepare the analogous platinum complexes $[(R_3'P)Pt(OOCR)_2]_2$ by this route failed; only decomposition and $[(R_3'P)ClPt(OOCR)]_2$ complexes were obtained with extended reaction times.

Structural Characterization of the Compounds $[(R_3'P)Pd(O_2CR)_2]_n$

Molecular weights of the complexes $[(R_3'P)Pd(OOCR)_2]_n$ in chloroform at 37 °C depend on the nature of the phosphine and the carboxylate substituents (Table 2). The complexes $[(Me_2PhP)Pd(OOCR)_2]_n$ ($R = CH_3$, CH_2Cl, CF_3) are all dimeric (*i.e.* $n = 2$), but the triethylphosphine analogs $[(Et_3P)Pd(OOCR)_2]_n$ show evidence of partial dissociation of the dimer to monomer for the more electronegative carboxylate substituents ($R = CH_2Cl$, CF_3).

The infrared spectra are consistent with the

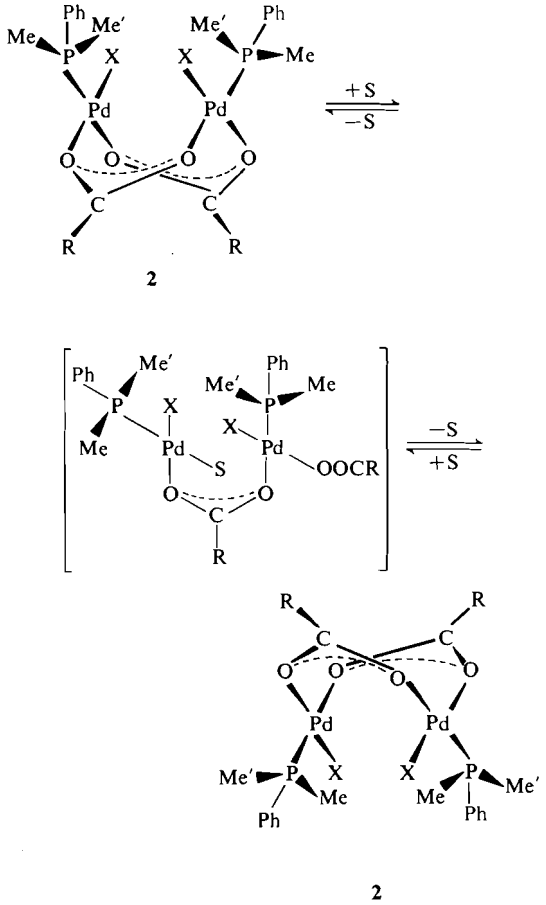

2

2

FIG. 2. The "partially dissociative" mechanism for the exchange of Me_2PhP methyl sites in the complexes $[(Me_2PhP)XPd(OOCR)]_2$.

Can. J. Chem. Downloaded from www.nrcresearchpress.com by 210.87.254.6 on 09/05/12
For personal use only.

TABLE 1. Analytical data and infrared asymmetric ν_{C-O} stretching frequencies

Compound	Melting point (°C)	% C		% H		ν_{CO} asym (cm^{-1})*	
		Calcd.	Found	Calcd.	Found	Unidentate	Bidentate
$[(PMe_2Ph)Pd(OOCCH_3)_2]_2 \cdot \frac{1}{4}C_6H_6$	144–145	41.12	40.99	4.80	4.60	1630s	1570s
$[(PMe_2Ph)Pd(OOCCH_2Cl)_2]_2 \cdot \frac{1}{4}C_6H_6$	113–117	34.69	34.61	3.60	3.56	1640s, vbr	1600vs
$[(PMe_2Ph)Pd(OOCCF_3)_2]_2$	156–159	30.63	30.60	2.36	2.22	1690m	1655vs, br (1600s)
			30.81		2.50		
$[(PEt_3)Pd(OOCCH_3)_2]_2$	164–166	35.05	35.11	6.18	6.03	1620m, br	1580w, br
$[(PEt_3)Pd(OOCCH_2Cl)_2]_2$	110–114	29.19	29.04	4.65	4.78	1680s	1605vs (1580s)
$[(PEt_3)Pd(OOCCF_3)_2]_2$	106–107	26.65	26.80	3.37	3.24	1700s, br	1660vs
$[(PPh_2Me)Pd(OOCCF_3)_2]_2$	163–167	38.33	38.25	2.46	2.50	1700s†	1655vs†
$Ag[PMe_2PhPd(OOCCF_3)_3]$	143–147	24.31	24.50	1.60	1.36		
			24.18		1.93		
$[PPh_3Pd(OOCCF_3)_2]_2$	179–182	—		—		1705s†	1680s†

*s = strong, m = medium, w = weak, br = broad, v = very.
†Nujol mull, KBr plates. All others are solution spectra in chloroform containing 0.75% EtOH as preservative. Trifluoroacetate complexes may exist as dimer ⇌ 2 monomer equilibria in solution (see text).

TABLE 2. Molecular weights, determined osmometrically in $CHCl_3$ (EtOH free) at 37 °C

Compound	Molecular weight (g/mol) Calculated	Found	Concentration (M)
$[(Me_2PhP)Pd(OOCCH_3)_2]_2$	725	697	4.8×10^{-2}
$[(Me_2PhP)Pd(OOCCH_2Cl)_2]_2$	863	853	3.7×10^{-2}
$[(Me_2PhP)Pd(OOCCF_3)_2]_2$	941	900	3.5×10^{-2}
$[(Et_3P)Pd(OOCCH_3)_2]_2$	685	638	3.1×10^{-2}
$[(Et_3P)Pd(OOCCH_2Cl)_2]_2$	823	758	3.6×10^{-2}
$[(Et_3P)Pd(OOCCF_3)_2]_2$	901	725	3.7×10^{-2}
$[(Ph_3P)Pd(OOCCF_3)_2]_2$		Insoluble	
Ag $[(Me_2PhP)Pd(OOCCF_3)_3]$	691	970	6.9×10^{-3}
		1010	1.5×10^{-2}
		1067	1.7×10^{-2}

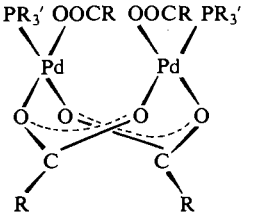

3

presence of both unidentate and bidentate carboxylate ligands in all cases as is apparent by the asymmetric C—O stretching absorptions in Table 1. Chloroform solution spectra were used to avoid solid state effects (10) which cause up to four asymmetric C—O stretching absorptions (Nujol mull).

In either solid state (Nujol mull) or chloroform solution, the trifluoroacetate complexes display at least four strong absorptions in the region 1120–1240 cm^{-1} due to C—F stretching vibrations. It has been recently pointed out (11) that a bidentate trifluoroacetate will have a minimum of two C—F stretching frequencies and a unidentate trifluoroacetate three C—F stretching frequencies in the infrared.[2] Hence the observed multiplicity is consistent with the presence of both unidentate and bidentate carboxylates as expected for structure **3**.

In the absence of exchange, the dimeric complexes $[(R_3'P)Pd(OOCR)_2]_2$ display distinct n.m.r. signals for unidentate and bidentate carboxylate ligands consistent with structure **3**. Further, where $R_3'P$ is Me_2PhP, two methyl doublet resonances are observed assignable to the nonequivalent methyl groups as expected for a dimer of structure **3**. The methyl groups are nonequivalent owing to the lack of a plane of symmetry containing the P—Pd axis. The methyl groups of the two Me_2PhP ligands are however related to each other by the twofold axis of molecular symmetry in structure **3**. For example the ^1H n.m.r. spectrum of $[(Me_2PhP)Pd(OOCH)_3)_2]_2$ in $CDCl_3$ at −30 °C (Fig. 3*A*) displays two Me_2PhP methyl doublets (J_{P-H} = 13.6 Hz) and two acetate methyl singlets, as expected for structure **3**. The low temperature n.m.r. spectra of the other dimeric complexes $[(R_3'P)Pd(OOCR)_2]_2$ are likewise consistent with structure **3**.

Variable Temperature Nuclear Magnetic Resonance Studies

On warming, a concentration independent process is observed for the dimers $[(R_3'P)Pd(OOCR)_2]_2$, which effectively exchanges the bridging and terminal carboxylate ligands. The exchange of the Me_2PhP methyl sites occurs simultaneously with the carboxylate site exchange. For $[(Me_2PhP)Pd(OOCCH_3)_2]_2$ the fast exchange ^1H n.m.r. spectrum at +35 °C is shown in Fig. 3*B*. Table 3 gives chemical shift data for all of the complexes in the region of fast carboxylate exchange.

[2]It has been observed by Orrell and co-workers (11) that for a variety of transition metal trifluoroacetate complexes, a degeneracy of two C—F stretching modes results in the appearance of two C—F stretching modes in the vibrational spectrum of a bidentate trifluoroacetate (compared to three C—F stretching modes for a monodentate trifluoroacetate). However, in light of the fact that the C_s group symmetry, to which the bidentate trifluoroacetate has been assigned, allows three nondegenerate C—F stretching modes, the observed degeneracy is accidental and may not be a generally reliable indication of the mode of trifluoroacetate coordination.

Can. J. Chem. Downloaded from www.nrcresearchpress.com by 210.87.254.6 on 09/05/12
For personal use only.

TABLE 3. Nuclear magnetic resonance data in $CDCl_3$, 37 °C*
(^1H, τ ppm relative to TMS and ^{19}F, ppm upfield of $CFCl_3$)

Compound	OOCR	R_3'P-alkyl protons
$[(Me_2PhP)Pd(OOCCH_3)_2]_2$	8.19 (s)	8.25 (d), $J_{^{31}P-^1H}$ 13.1 Hz
$[(Me_2PhP)Pd(OOCCH_2Cl)_2]_2$	6.22 (s)	8.21 (d), 13.6 Hz
$[(Me_2PhP)Pd(OOCCF_3)_2]_2$	68.3 (s)†	8.35 (d), 14.3 Hz
$[(Me_2PhP)Pd(OOCCH_3)(OOCCH_2Cl)]_2$	8.20 (s), 6.27 (s)	8.23 (d), 13.6 Hz
$[(Me_2PhP)Pd(OOCCH_3)(OOCCF_3)]_2$	8.14 (s), 67.4 (s)†	8.28 (d), 13.8 Hz
$[(Me_2PhP)Pd(OOCCH_2Cl)(OOCCF_3)]_2$	6.20 (s), 68.0 (s)†	8.29 (d), 14.0 Hz
$[(Et_3P)Pd(OOCCH_3)_2]_2$	8.09 (s)	
$[(Et_3P)Pd(OOCCH_2Cl)_2]_2$	6.02 (s)	Complex pattern
$[(Et_3P)Pd(OOCCF_3)_2]_2$	68.9 (s)†	7.9 to 9.0
$[(Ph_2MeP)Pd(OOCCF_3)_2]_2$	68.6 (s)†	8.06 (d), $J_{^{31}P-^1H}$ 13.6 Hz
$[(Ph_3P)Pd(OOCCF_3)_2]_2$	Insoluble	
Ag $[(Me_2PhP)Pd(OOCCF_3)_3]$	2 broad singlets 68.3 (overlapping)	8.30 (d), $J_{^{31}P-^1H}$ 13.7 Hz

*Aromatic proton resonances have been excluded.
†^{19}F resonances.

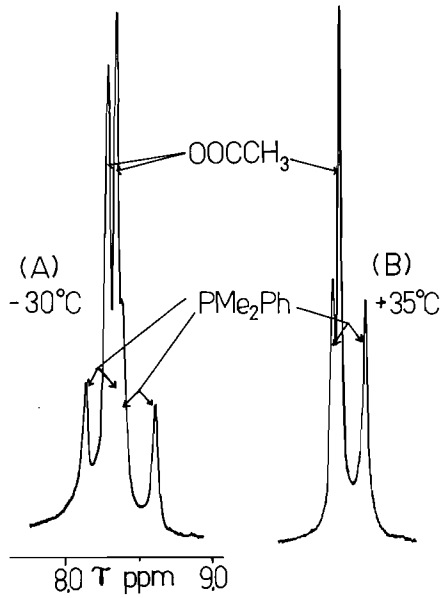

FIG. 3. The ^1H n.m.r. spectra (60 MHz) of the methyl protons in the complex $[(Me_2PhP)Pd(OOCCH_3)_2]_2$ in $CDCl_3$; (*A*) at −30 °C and (*B*) at +35 °C.

Of the two mechanisms previously postulated to account for the dynamic nature of this type of di-μ-carboxylate palladium(II) dimer (the "acetate bridge inversion" mechanism (Fig. 1) and the partially dissociative ring opening mechanism (Fig. 2)) only the latter accounts for the simultaneous exchange of both the Me_2PhP methyl sites and the terminal bridge carboxylate sites. In such a mechanism, the dissociation of one palladium–oxygen bond in $[(R_3'P)Pd(OOCR)_2]_2$ would lead to an intermediate **4** (Fig. 4) in which either of the unidentate carboxylates on the nonsolvated palladium can reform the bridge while simultaneously exchanging the Me_2PhP methyl environments. This mechanism for $[(R_3'P)Pd(OOCR)_2]_2$ complexes is identical to that found previously for the complexes $[(Me_2PhP)XPd(OOCR)]_2$ where X = halide (4).

Addition of Weak Bridge Splitting Ligands to $[(R_3'P)Pd(OOCR)_2]_2$

The addition of small aliquots of acetone or ether to a chloroform solution of $[(Me_2PhP)Pd(OOCCH_3)_2]_2$ had no effect on the ^1H n.m.r. spectra or the rate of exchange. Similar additions of methanol or acetic acid resulted in significant enhancement of the rate of exchange while, even in the fast exchange region, no exchange was observed between the added acetic acid and the acetate ligands. This behavior is identical to that observed previously for the $[(Me_2PhP)XPd(OOCR)]_2$ complexes (4) and supports the idea of a common exchange mechanism.

The addition of py, a weak bridge splitting ligand, to $[(Me_2PhP)Pd(OOCCF_3)_2]_2$ at −60 °C in a ratio of less than one py per palladium gave a new singlet resonance in the ^{19}F n.m.r. in addition to the spectrum of the reagent dimer $[(Me_2PhP)Pd(OOCCF_3)_2]_2$. The presence of

Can. J. Chem. Downloaded from www.nrcresearchpress.com by 210.87.254.6 on 09/05/12
For personal use only.

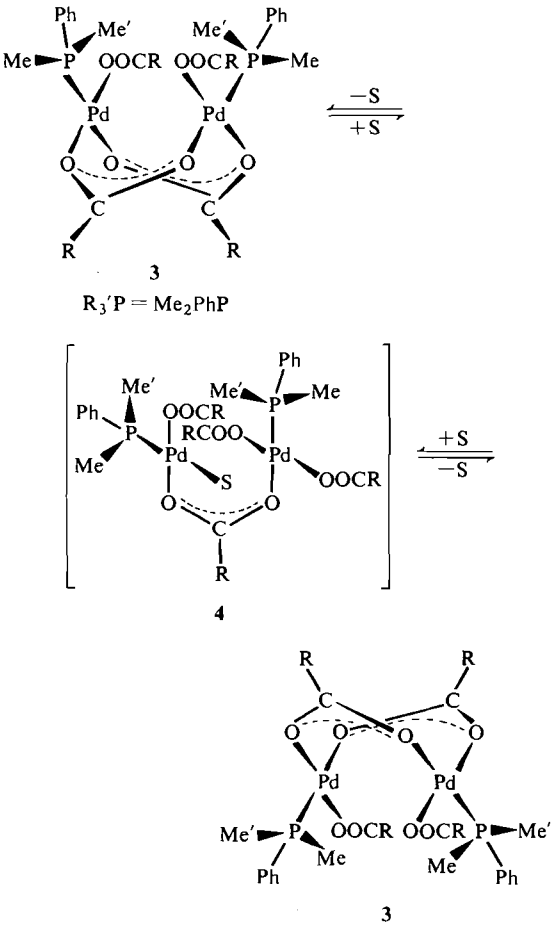

FIG. 4. The "partially dissociative" mechanism for the simultaneous exchange of the terminal and bridging acetate and Me_2PhP methyl sites in the complex $[(Me_2PhP)Pd(OOCCH_3)_2]_2$.

this species (probably *trans*-$[(Me_2PhP)Pd(OOCCF_3)_2py]$)[3] had no effect on the temperature dependent n.m.r. spectra of the residual dimer even in the region of fast exchange.

Free Energy of Activation for the Exchange Processes

The free energy of activation for both the methyl site exchange in the Me_2PhP ligand and the terminal–bridge exchange for the carboxylate ligands can be evaluated by variable temperature n.m.r. techniques.

The rate of exchange, k, at the coalescence temperature, T_c(K), is a function of the separation of the resonances in the absence of exchange, $\Delta\nu_0$ (Hz) as shown in the Gutowsky–Holm expression [1] (12).

$$[1] \qquad k = \frac{\pi}{\sqrt{2}}\Delta\nu_0$$

$$[2] \quad \Delta G_{T_c}^{\ddagger} = 4.576T_c[10.319 + \log(T_c/k)]$$

The rate of exchange k so obtained can then be substituted into the Eyring equation (eq. 2) to obtain the free energy of activation, $\Delta G_{T_c}^{\ddagger}$ (kcal/mol), for the exchange at T_c (13). The values in Table 4 for the dimers $[(R_3'P)Pd(OOCR)_2]_2$ are found to be in good agreement with those previously reported (4) for the complexes $[(Me_2PhP)XPd(OOCR)]_2$ (*e.g.* see Table 4 for data where X = I). Again this similarity in $\Delta G_{T_c}^{\ddagger}$ for the Me_2PhP methyl site exchange in the $[(Me_2PhP)XPd(OOCR)]_2$ and $[(R_3'P)Pd(OOCR)_2]_2$ systems substantiates the hypothesis of a common mechanism. $\Delta\nu_0$ increases (for either carboxylate or Me_2PhP methyl site exchange) in the order $R = CH_3 < CH_2Cl < CF_3$ and the coalescence temperatures vary in the inverse order $R = CF_3 < CH_2Cl < CH_3$. We conclude that the exchange process is facilitated by more electronegative substituents.

The Activation Energy for the Exchange Processes in $[(Me_2PhP)Pd(OOCCH_3)_2]_2$

The rates of exchange for Me_2PhP methyls and terminal–bridging acetates were determined over a range of temperatures by the method of peak separation (eq. 3) (12, 14)

$$[3] \qquad k = \frac{\pi}{\sqrt{2}}(\Delta\nu_0^2 - \Delta\nu^2)^{1/2}$$

An Arrhenius plot (Fig. 5) shows that the activation energies of the Me_2PhP methyl site exchange and the acetate terminal–bridging site exchange are approximately equal as expected if these exchanges arise from the same process. The low activation energies necessitate a large negative entropy $\Delta S^{\ddagger} \sim -30$ e.u., to account for $\Delta G_{T_c}^{\ddagger} \sim 14.5$ kcal/mol observed for the exchange processes in $[(Me_2PhP)Pd(OOCCH_3)_2]_2$.

Again the values of E_A and $\Delta S^{\ddagger}$ are essentially

[3]The singlet ^{19}F n.m.r. resonance due to the trifluoroacetates in the monomeric species is compatible with either a "*trans*" disposition of these ligands or a rapid process of site exchange which averages all the trifluoroacetate environments.

Can. J. Chem. Downloaded from www.nrcresearchpress.com by 210.87.254.6 on 09/05/12
For personal use only.

Can. J. Chem. Downloaded from www.nrcresearchpress.com by 210.87.254.6 on 09/05/12
For personal use only.

TABLE 4. The activation parameters for carboxylate and Me_2PhP site exchanges from nuclear magnetic resonance studies

Compound	Exchange of	$CDCl_3$ $\Delta\nu_0$ (Hz)	$CDCl_3$ T_c (K)	$CDCl_3$ $\Delta G_{T_c}^{\ddagger}$ (kcal/mol)	Toluene-d_8 $\Delta\nu_0$	Toluene-d_8 T_c	Toluene-d_8 $\Delta G_{T_c}^{\ddagger}$	Acetone-d_6 $\Delta\nu_0$	Acetone-d_6 T_c	Acetone-d_6 $\Delta G_{T_c}^{\ddagger}$
$[Pd(OOCCH_3)_2PMe_2Ph]_2$	Methyls	16.8	283	14.5	18.4	274	14.0	12.8	283	14.7
	$OOCCH_3$	4.2	271	14.6	11.8	282	14.6	(1.9	240	13.3)*
$[Pd(OOCCH_2Cl)_2PMe_2Ph]_2$	Methyls	17.8	264	13.5	14.3	257	13.2	12.1	268	13.9
	$OOCCH_2Cl$	—	—	—	15.2	261	13.4	5.8	265	14.1
$[Pd(OOCCF_3)_2PMe_2Ph]_2$	Methyls	22.4	238	12.0	10.5	234	12.1	Monomer ⇌ Dimer		
	$OOCCF_3$	29.7	239	11.9	6.3	219	11.6			
$[Pd(OOCCH_3)_2PEt_3]_2$	$OOCCH_3$	2.4	256	14.0	16.4	273	14.0			
$[Pd(OOCCH_2Cl)_2PEt_3]_2$	$OOCCH_2Cl$	6.0	249	13.2						
$[Pd(OOCCF_3)_2PEt_3]_n$	$OOCCF_3$	Monomer ⇌ Dimer			Monomer ⇌ Dimer			Monomer		
$[Pd(OOCCF_3)_2PPh_2Me]_n$	$OOCCF_3$	Monomer ⇌ Dimer						Monomer		
$[Pd(OOCCF_3)_2PPh_3]_n$	$OOCCF_3$	Insoluble			Insoluble			Monomer		
$[Pd(OOCCF_3)(OOCCH_2Cl)PMe_2Ph]_2$	Methyls	18.7	269	13.7						
$[Pd(OOCCF_3)(OOCCH_3)PMe_2Ph]_2$	Methyls	21.8	290	14.7						
$[Pd(OOCCH_2Cl)(OOCCH_3)PMe_2Ph]_2$	Methyls	16.0	281	14.4						
$[Pd(OOCCH_3)I(PMe_2Ph)]_2$	Methyls†	41.0	297	14.7						
$[Pd(OOCCH_2Cl)I(PMe_2Ph)]_2$	Methyls†	39.5	266	13.1						
$[Pd(OOCCF_3)I(PMe_2Ph)]_2$	Methyls†	45.9	248	12.1						

*The small $\Delta\nu_0$ makes accurate evaluation of $\Delta G_{T_c}^{\ddagger}$ using [2] impossible.
†Data taken from ref. 4.

Can. J. Chem. Downloaded from www.nrcresearchpress.com by 210.87.254.6 on 09/05/12
For personal use only.

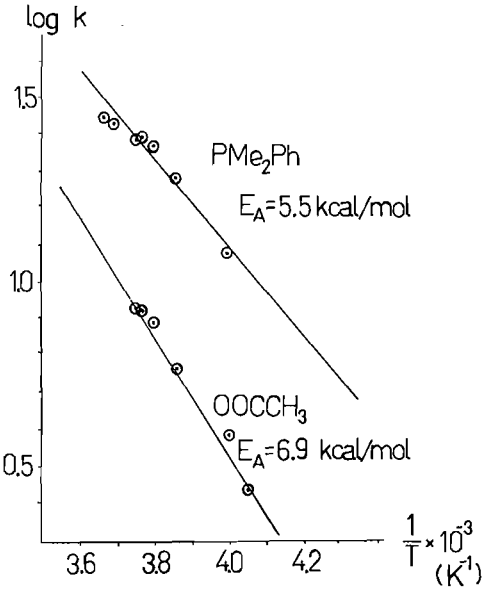

FIG. 5. The activation energies for the bridging and terminal acetate and Me_2PhP methyl site exchanges observed for the complex $[(Me_2PhP)Pd(OOCCH_3)_2]_2$ in $CDCl_3$ solution.

identical to those found for $[(Me_2PhP)XPd(OOCR)]_2$ (4).

The Importance of Chelation by Carboxylate in the Partially Dissociative Ring Opening Mechanism in the Complexes $[(Me_2PhP)Pd(OOCR)_2]_2$

We considered it possible that the ring opened intermediate might be stabilized by chelation, *i.e.* **5** in Fig. 6. To assess the relative importance of a carboxylate chelated intermediate **5** *vs.* intermediate **4** a new series of dimers $[(Me_2PhP)(OOCR')Pd(OOCR)]_2$ **6** was prepared by mixing the complexes $[(Me_2PhP)Pd(OOCR)_2]_2$ and $[(Me_2PhP)Pd(OOCR')_2]_2$ in a 1:1 ratio in $CDCl_3$ [4].

[4] $[(Me_2PhP)Pd(OOCCF_3)_2]_2 + [(Me_2PhP)Pd(OOCR)_2]_2 \rightleftharpoons 2[(Me_2PhP)(OOCCF_3)Pd(OOCR)]_2$

6

where R = CH_3 or CH_2Cl.

The low temperature n.m.r. spectrum for the reaction mixture where R = CH_3 is shown in Fig. 7. The nonequivalence of the Me_2PhP

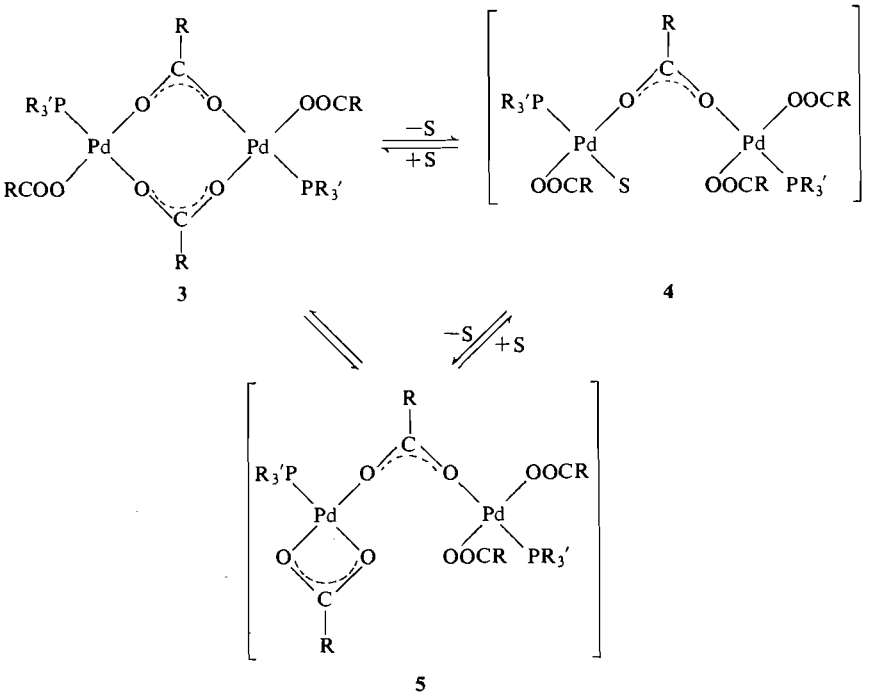

3 4

5

FIG. 6. An alternate intermediate **5** (involving carboxylate chelation) for the exchange processes observed for the complexes $[(R_3'P)Pd(OOCR)_2]_2$.

Can. J. Chem. Downloaded from www.nrcresearchpress.com by 210.87.254.6 on 09/05/12
For personal use only.

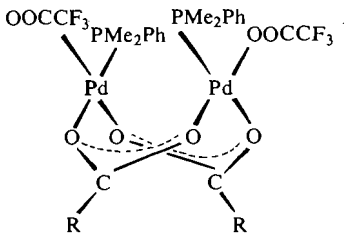

6

R = CH_3, CH_2Cl

methyl groups, typical of the dimeric structure, has been retained, but only one sharp singlet is present in the acetate protons. In the ^{19}F n.m.r. a sharp temperature invariant singlet is present for the trifluoroacetate. By the simplicity of this spectrum, it is apparent that there is only one major solution species present wherein there is one site for the acetate and one site for the trifluoroacetate in a dimeric structure. Such spectral features would be expected for the mixture in [4] if the equilibrium lay totally to the right *and* if the trifluoroacetate and acetate ligands occupied the terminal and bridging sites respectively as shown in **6** where R = CH_3. Similar spectra were obtained for R = CH_2Cl.

Since the ease of the ring opening process is related to the bidentate ability of the bridging carboxylate, the inference of the earlier variable temperature n.m.r. exchange study is that the bidentate ability of the carboxylate ligand diminishes with increasingly electronegative substitution of the carboxylate; CH_3 > CH_2Cl > CF_3. This trend has also been reported by Hammond *et al.* (15) as the controlling influence in determining the bidentate, unidentate coordination of the carboxylate in the structures of copper(I) carboxylates, $[(Ph_3P)_nCu(OOCR)]$, where $n = 2$ or 3. Consequently the preferred structure **6** having terminal trifluoroacetates and bridging acetates (or monochloroacetates) is reasonable.

Mixing the complexes $[(Me_2PhP)Pd(OOCCH_3)_2]_2$ and $[(Me_2PhP)Pd(OOCCH_2Cl)_2]_2$ in a 1:1 ratio (eq. 5) gave a system analogous to those described above in [4]. The major solution species in [5] is the mixed carboxylate species $[(Me_2PhP)Pd(OOCCH_3)(OOCCH_2Cl)]_2$ in which the *acetate functions as the bridging ligand and the monochloroacetate is a terminal ligand.*

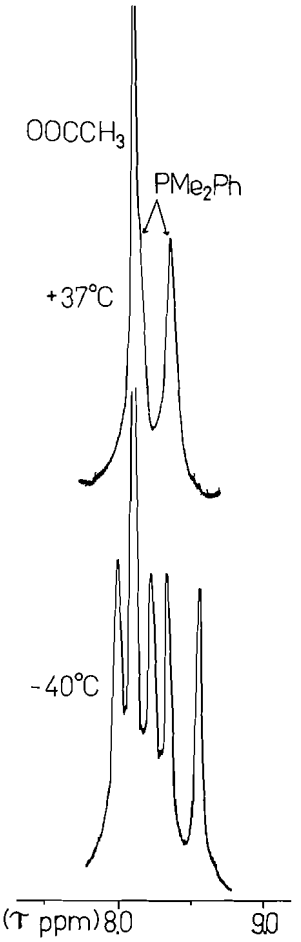

FIG. 7. The ^1H n.m.r. spectra (60 MHz) of the methyl protons in a 1:1 mixture of $[(Me_2PhP)Pd(OOCCF_3)_2]_2$ and $[(Me_2PhP)Pd(OOCCH_3)_2]_2$ in $CDCl_3$, at −40 °C and at +37 °C.

[5] $[(Me_2PhP)Pd(OOCCH_3)_2]_2 + [(Me_2PhP)Pd(OOCCH_2Cl)_2]_2 \rightleftarrows 2[(Me_2PhP)Pd(OOCCH_3)(OOCCH_2Cl)]_2$

6

In all cases warming solutions of **6** caused exchange of Me_2PhP methyl sites by the partially dissociative ring opening mechanism (Fig. 4). In each case $\Delta G_{T_c}^{\ddagger}$ for Me_2PhP methyl exchange (Table 4) is almost identical to that found for the parent complex of the least electronegatively substituted carboxylate. Thus, the exchange parameters for $[(Me_2PhP)Pd(OOCCH_3)(OOCCH_2Cl)]_2$ and $[(Me_2PhP)Pd(OOCCH_3)_2]_2$ are very similar. The implication is that the ease of exchange is a

Can. J. Chem. Downloaded from www.nrcresearchpress.com by 210.87.254.6 on 09/05/12
For personal use only.

function of the bridging carboxylate substituents but is independent of the nature of the terminal carboxylate.

In a later section, it will be established that the chelating ability of a carboxylate ligand depends on the electronegativity of its substituents. Thus, if chelation were important in the intermediate for the Me_2PhP methyl site, bridging–terminal carboxylate site exchange (*i.e.* intermediate **5**, Fig. 6) then the exchange parameters would be dependent on the nature of the terminal carboxylate and this is not observed. Therefore the chelated intermediate **5** (Fig. 6) is not important in the exchange process.

Dissociation of the Dimers $[(R_3'P)Pd(OOCR)_2]_2$ in Solution

The complex, $[(Et_3P)Pd(OOCCF_3)_2]_n$, has been observed by osmometry to exist as a monomer, dimer equilibrium (eq. 6) in chloroform at 37 °C (Table 2).

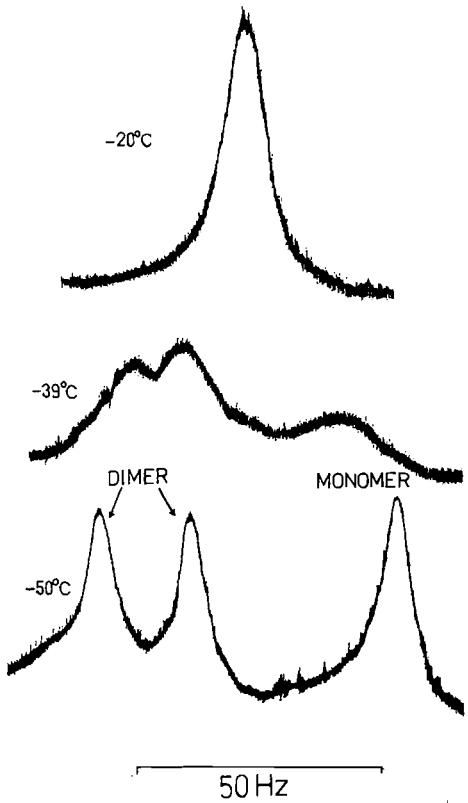

FIG. 8. The variable temperature ^{19}F n.m.r. spectra (56 MHz) of the complex $[(Et_3P)Pd(OOCCF_3)_2]_n$ in $CDCl_3$.

[6] $[(Et_3P)Pd(OOCCF_3)_2]_2 \underset{\text{monomer}}{\overset{K_6}{\rightleftharpoons}} 2[(Et_3P)Pd(OOCCF_3)_2.S]$

where S is solvent. The low temperature ^{19}F n.m.r. shown in Fig. 8 (−50 °C) exhibits two low field resonances assignable to the dimer $[(Et_3P)Pd(OOCCF_3)_2]_2$ and an upfield singlet assignable to the monomer $[(Et_3P)Pd(OOCCF_3)_2.S]$ where S is solvent.[3] Dilution of the ^{19}F n.m.r. sample increases the monomer to dimer ratio. On warming, all the ^{19}F resonances coalesce to give a singlet resonance in the fast exchange region (Fig. 8, −20 °C). From the dimer/monomer ratio obtained by integration of the ^{19}F n.m.r. spectra, the equilibrium constant, K_6 can be determined. The effect of solvent on K_6 is shown in Table 5. In toluene, dichloromethane, and chloroform containing 0.75% ethanol, the ^{19}F n.m.r. spectra are analogous to that obtained in $CDCl_3$ (Fig. 8). In ethanol and acetone only a sharp singlet is observed even at −75 °C. Since the addition of only 0.75% ethanol to a chloroform solution of $[(Et_3P)Pd(OOCCF_3)_2]_n$ at −63 °C results in substantial enhancement of the monomer concentration, we conclude that the complex exists totally as the monomer ($n = 1$) in ethanol. Similarly, only monomer ($n = 1$) is present in acetone.

The ability of acetone to promote monomer formation in the $[(Et_3P)Pd(OOCCF_3)_2]_2$ case is mimicked for the complex $[(Me_2PhP)Pd(OOCCF_3)_2]_n$, which, as noted in Table 4, is dimeric ($n = 2$) in chloroform-d_1 or toluene-d_8 but exists in a monomer ($n = 1$), dimer ($n = 2$) equilibrium in neat acetone-d_6 with a temperature dependent ^{19}F n.m.r. exactly analogous to that shown in Fig. 8. This ability of acetone to stabilize the monomer is probably related to its ability to coordinate to palladium(II) trifluoroacetate complexes, as evidenced by the isolation of complexes such as $[(acetone)Pd(OOCCF_3)_2]_2$ (9), in which the acetone functions as a ligand.

The occurrence of dimer dissociation in the complexes $[(R_3'P)Pd(OOCR)_2]_2$ (Table 4) may be rationalized in terms of electronic effects. Increasing the electronegativity of the carboxylate ligand promotes dissociation of the dimers $[(R_3'P)Pd(OOCR)_2]_2$ ($CH_3 < CH_2Cl < CF_3$), as does increasing the donor ability of the phos-

TABLE 5. The variation of the monomer, dimer equilibrium constant K_6 for $[((Et_3P)Pd(OOCCF_3)_2)]_n$ with solvent at a palladium concentration of 14.4×10^{-2} *M*

Solvent	Ratio [dimer]/[monomer]	K_6 (mol/l)	Temperature (°C)
EtOH	Monomer		−75
Acetone	Monomer		−75
Chloroform +0.75% EtOH	0.18	0.6	−63
Chloroform	1.30	0.03	−63
Toluene	1.68	0.02	−63
Dichloromethane	2.31	0.01	−63

TABLE 6. The variation in the monomer, dimer equilibrium for the solution species of $[(R_3'P)Pd(OOCCF_3)_2]_n$ in $CDCl_3$

$R_3'P$	[Pd] (mol/1)	Ratio [dimer]/[monomer]	K_6 (mol/l)	Temperature (°C)
Ph_3P		Insoluble		
Ph_2MeP	8.26×10^{-2}	3.39	0.003	−58
Me_2PhP		Dimer only		

phine ($Et_3P > Me_2PhP$) (16). A similar destabilization of the binuclear configuration of cupric carboxylates, $Cu_2(OOCR)_4.2L$, has been ascribed to the repulsive interaction between the residual charges on the adjacent copper atoms ($R = CF_3 > CH_3$) (17, 18).

The Effect of Bulky Phosphines in $[(R_3'P)Pd(OOCCF_3)_2]_n$

The introduction of bulky phosphines Ph_2MeP or Ph_3P in the complexes $[(R_3'P)Pd(OOCCF_3)_2]_n$ results in the destabilization of the dimer **3** by steric crowding. The effect of these phosphine substituents on the dimer dissociation in chloroform is summarized in Table 6. $[(Ph_3P)Pd(OOCCF_3)_2]_n$ is insoluble in $CDCl_3$ or toluene-d_8 but very soluble in alcohols or acetone. In these solvents only one sharp singlet resonance is apparent in the ^{19}F n.m.r. spectrum at −80 °C, as expected for monomer. The corresponding acetate complex, $[(Ph_3P)Pd(OOCCH_3)_2]_2$, has been formulated as a dimer by Wilkinson and co-worker (9). Such behavior is reminiscent of Lewis's cupric benzoate complexes which are polymeric for highly electron withdrawing carboxylates and dimeric for less electronegative ones (19). Thus it is possible that the steric strain imposed by the bulky Ph_3P group in $[(Ph_3P)Pd(OOCCF_3)_2]_n$ causes the loss of the binuclear structure **3** in the solid state in favor of a bridged trifluoroacetate polymeric structure.

Preparation and Characterization of $Ag(Me_2PhP)Pd(OOCCF_3)_3$

Reaction of the bridged halide dimer $[(Me_2PhP)PdCl_2]_2$ with excess $AgOOCCF_3$ yielded yellow needles which analyzed as $[Ag(Me_2PhP)Pd(OOCCF_3)_3]$ (Table 1). Three asymmetric C—O stretching frequencies are observed in the solid state infrared spectrum at 1680vs, 1660vs, and 1635vs (Nujol mull). The ^1H n.m.r. spectrum consisted of one doublet in the Me_2PhP methyl region (Table 3) which remained invariant from −60 to +35 °C in $CDCl_3$. The low temperature ^{19}F n.m.r. spectrum showed two sharp singlets in a 2:1 ratio which collapsed on warming above −30 °C to give two broad overlapping peaks at +62 °C. Molecular weight data (Table 2) showed the compound to be aggregated in solution, the degree of aggregation being concentration dependent. Even dilute solutions in chloroform (8×10^{-4} *M*) were nonconducting.

The chemical reactivity of the silver species proved consistent with the formulation

Can. J. Chem. Downloaded from www.nrcresearchpress.com by 210.87.254.6 on 09/05/12
For personal use only.

Can. J. Chem. Downloaded from www.nrcresearchpress.com by 210.87.254.6 on 09/05/12
For personal use only.

$Ag(Me_2PhP)Pd(OOCCF_3)_3$. Reaction with the bridged halide $[(Me_2PhP)PdCl_2]_2$ in a ratio of 4:1 yielded AgCl (94% yield) and the previously prepared complex, $[(Me_2PhP)Pd(OOCCF_3)_2]_2$ (eq. 7).

[7] $4Ag(Me_2PhP)Pd(OOCCF_3)_3 + [(Me_2PhP)PdCl_2]_2 \rightarrow 4AgCl\downarrow + 3[(Me_2PhP)Pd(OOCCF_3)_2]_2$

The Ag^+ could be displaced by NH_4^+ or $AsPh_4^+$ as shown in [8].

[8] $Ag(Me_2PhP)Pd(OOCCF_3)_3 + \text{cation}^+ Cl^- \xrightarrow[MeOH]{} AgCl\downarrow + \text{cation}^+ [(Me_2PhP)Pd(OOCCF_3)_3]^-$

Evaporation of the solution after removal of the AgCl precipitate gave a yellow oil for either NH_4^+ or $AsPh_4^+$. In the case of NH_4^+, dissolving this oil in CH_2Cl_2 resulted in the quantitative precipitation of NH_4OOCCF_3, leaving $[(Me_2PhP)Pd(OOCCF_3)_2]_2$ in solution. Dissolution of the $AsPh_4^+$ oil in chloroform did not precipitate $AsPh_4OOCCF_3$, and the n.m.r. spectra of the solution were very similar to those of the original silver complex: a temperature invariant methyl doublet for the Me_2PhP ligand (−59 to +35 °C) in the ^1H n.m.r. spectrum and two singlets in a 2:1 ratio in the ^{19}F n.m.r. spectrum.

In acetonitrile, a solvent of good coordinating ability and high dielectric constant $Ag(Me_2PhP)Pd(OOCCF_3)_3$ ionizes to give a conductance with a nonlinear concentration dependence which does not correspond to a simple electrolyte type.

Attempts to prepare analogous complexes of the other carboxylates (*i.e.* $Ag(Me_2PhP)Pd(OOCR)_3$, where R = CH_3 or CH_2Cl) only resulted in the formation of $[(Me_2PhP)Pd(OOCR)_2]_2$ in varying states of impurity.

The Dependence of Carboxylate Chelation Ability on the Inductive Effect of the Carboxylate Substituents

In evaluating the importance of the carboxylate chelate intermediate **5** (Fig. 6) in the exchange processes we made the hypothesis that chelation of the carboxylate ligand is a function of the electronegativity of the carboxylate substituents. This can be substantiated by studying a model system which undergoes an observable exchange process wherein the intermediate or transition state is stabilized by chelation.

It has been established that the intramolecular 3,4-allylic proton site exchange observed in the

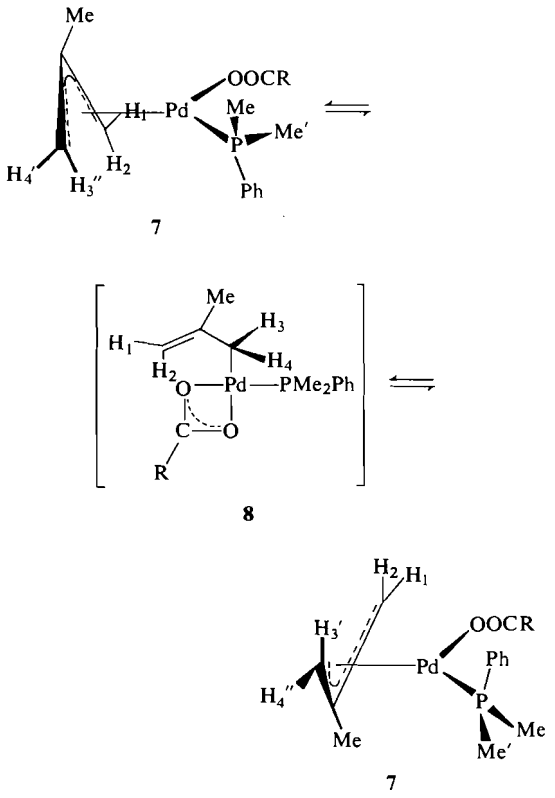

FIG. 9. The π–σ–π mechanism for the exchange of the 3,4 (syn,anti) allylic proton sites in the complex [(π-2-methylallyl) Pd(OOCR) (Me_2PhP)].

complexes, [(π-2-methylallyl)Pd(OOCR)($R_3'P$)] **7** takes place via a π–σ–π exchange mechanism (illustrated in Fig. 9) (2, 20–22). Where $R_3'P$ is Me_2PhP, a concurrent exchange of the nonequivalent Me_2PhP methyl environments is also apparent (as illustrated in Fig. 9). The ^{31}P—^1H coupling between the $R_3'P$ ligand and the 1,2-allylic protons is preserved even in the region of fast 3,4-allylic proton site exchange (2, 20–22).

To test the relative chelating ability of a series of carboxylate ligands, the complexes [(π-2-methylallyl)Pd(OOCR)($R_3'P$)] ($R_3'P$ = Me_2PhP or Ph_3P and R = CH_3, CMe_3, CPh_3, CH_2Ph, CH_2Cl, CCl_3, and CF_3) were prepared directly in an n.m.r. tube by the stoichiometric addition of $R_3'P$ to the appropriate carboxylate bridged dimer, $[(\pi\text{-2-methylallyl})Pd(OOCR)]_2$ (23) in $CDCl_3$ or C_6H_5Cl, under nitrogen, immediately prior to the n.m.r. observations.

The phosphine methyl and allylic proton chemical shift data for all the complexes in

Can. J. Chem. Downloaded from www.nrcresearchpress.com by 210.87.254.6 on 09/05/12
For personal use only.

TABLE 7. Chemical shift data (τ, p.p.m.) for allylic and methyl protons in $CDCl_3$ at +35 °C,

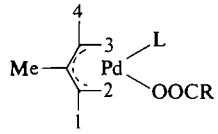

R	H_1 τ	H_1 J_{14}*	H_1 J_{PH}	H_2 τ	H_2 J_{PH}	$H_{3,4}$ τ	$H_{3,4}$ J_{14}*	Allylic methyl protons	R protons	L methyl protons τ	L methyl protons J_{PH}
L = Me_2PhP											
CH_3	5.62	2.6 ± 0.5	6.2	6.42	9.9	7.39	2	8.05	8.00	8.25	9.2
CMe_3†	5.54	2.3	6.3	6.37‡	9.9‡	7.38	2	8.02	8.00	8.31	9.3
CH_2Ph	5.59	2.8	6.2	6.42	9	7.44	2.3	8.07	6.38	8.48	9.3
CPh_3	5.60	2.1	6.2	6.39	9.5	7.43	2	8.09	—	8.55	9.5
CH_2Cl	5.54	2.2	6.0	6.40	9.5	7.38	2.2	8.02	5.98	8.30	9.2
CCl_3§	5.38	2.9	6.2	6.31	9.8	7.52(3) 7.02(4)	2.2	8.00	—	8.27	9.3
CF_3§	5.5	2.9	6.2	6.40	9.8	7.56(3) 7.06(4)	2.2	8.04	—	8.28	9.7
L = Ph_3P											
CH_3	5.43		6.0	6.24	9.6	7.33		7.98	8.20		—
CMe_3	5.41		7.0	6.28	6.3	7.38		7.99	9.00		—
CH_2Ph	5.40	2	6.6	6.26	9.3	7.34	2	7.98	6.55		—
CPh_3	5.53		6.0	6.32	9.1	7.45		8.02	—		—
CH_2Cl	5.37	2	6.1	6.26	9.7‡	7.28	2	7.97	6.22		—
CCl_3	5.25	3	6.9	6.20	10.0	7.41(3) 7.18(4)	3	7.96	—		—
CF_3	5.27	2	7.0	6.19	9.1	7.37(3) 7.06(4)	2	7.92	—		—
L = Me_2PhAs											
CH_3‖	5.52	2		6.42		7.51(3) 6.82(4)	2	7.88	7.91	8.30	
CCl_3§	5.29	2		6.29		7.43(3) 6.66(4)	2	7.92	—	8.32	
L = Ph_3As											
CH_3¶	5.38	3		6.23		7.44(3) 6.67(4)	3	7.88	8.18		—
CCl_3¶	5.09	2		6.11		7.28(3) 6.60(4)	2	7.80	—	—	

*Coupling observed in region of no exchange.
†At +25 °C.
‡Partly obscured by overlapping R proton resonances.
§At −30 °C.
‖At −60 °C.
¶At −20 °C.

TABLE 8. The free energy of activation for 3,4-allylic proton site exchange in the complexes [(π-2-methylallyl)Pd(OOCR)Ph_3P]

R	Solvent	$\Delta\nu_0$ (Hz)	$T_c \pm 2$ (K)	$\Delta G_{T_c}^{\ddagger} \pm 0.3$ (kcal/m)	Solvent	$\Delta\nu_0$ (Hz)	T_c (K)	$\Delta G_{T_c}^{\ddagger}$ (kcal/m)
CH_3	$CDCl_3$	27.9	277	13.9	CD_2Cl_2	19.8*	273*	13.9*
		28.0	276	13.9				
CMe_3	$CDCl_3$	17.9	280	14.3				
		18.4	283	14.4				
CH_2Ph	$CDCl_3$	28.8	289	14.5				
CPh_3	$CDCl_3$	4†	290†	14.4†				
CH_2Cl	$CDCl_3$	29.1	312	15.7	C_6H_5Cl	18.9	293.2	15.0
CCl_3	$CDCl_3$	17.5	344‡	17.7‡				
CF_3	$CDCl_3$	23.9	349‡	17.8‡	C_6H_5Cl	Concentration dependent syn/syn; anti/anti exchange		
		19.0	348‡	17.9‡				

*Reference 20.
†The small $\Delta\nu_0$ (Hz) makes estimation of coalescence temperature, T_c (K), inaccurate.
‡Temperature calibration by ethylene glycol standard (29).

$CDCl_3$ solution are listed in Table 7. The parameters for the intramolecular exchange of the 3,4-allylic protons by the π–σ–π mechanism (Fig. 9) are reported in Table 8, ($R_3'P = Ph_3P$) and Table 9, ($R_3'P = Me_2PhP$). $\Delta G_{T_c}^{\ddagger}$ was calculated as described above. For [(π-2-methylallyl)Pd($OOCCH_3$)(Ph_3P)] and [(π-2-methylallyl)Pd($OOCCH_2Cl$)(Ph_3P)] changing the solvent from $CDCl_3$ to CD_2Cl_2 does not appreciably alter the exchange parameters for 3,4-allylic proton exchange. However, in the trifluoroacetate complex, [(π-2-methylallyl)Pd($OOCCF_3$)(Ph_3P)], changing the solvent from $CDCl_3$ to C_6H_5Cl causes a complete change in the observed exchange process. The first process observed on warming in C_6H_5Cl is the syn,syn and anti,anti allylic proton site exchange typical of the corresponding arsine complexes [(π-allylic)Pd(OOCR)($R_3'As$)] (20). The loss of coupling between the Ph_3P (^{31}P) and the allylic protons indicates that the mechanism involves the intermolecular exchange of the Ph_3P ligand. For the series of complexes [(π-2-methylallyl)Pd(OOCR)Ph_3P] the order of increasing free energy of activation of $\Delta G_{T_c}^{\ddagger}$ ($R = CH_3 < CH_2Ph < CH_2Cl < CF_3$) for 3,4-allylic proton exchange is consistent with a decreasing ability of the carboxylate ligand to stabilize the intermediate **8** by chelation. (Although the $\Delta G_{T_c}^{\ddagger}$ values are not determined at the same temperature, the order of $\Delta G_{T_c}^{\ddagger}$ for a given series of complexes is valid where $\Delta\nu_0$ (Hz), the resonance separation in the absence of exchange, is constant or increasing in the opposite direction to $\Delta G_{T_c}^{\ddagger}$).

In the complexes [(π-2-methylallyl)Pd(OOCR)-Me_2PhP] in $CDCl_3$, the parameters for both the Me_2PhP methyl site and 3,4-allylic proton site exchange (as listed in Table 9) are consistent with the π–σ–π mechanism (Fig. 9). Again the ease of the exchange process depends on the inductive influence of the carboxylate substituents ($R = CH_3 < CH_2Ph < CH_2Cl$) and reflects the decreasing ability of the carboxylate to stabilize the σ-allylic intermediate **8** by bidentate chelation.

In the case of [(π-2-methylallyl)Pd(OOCR)-Me_2PhP] where R = CCl_3 or CF_3, the loss of ^{31}P coupling to the 1,2-allylic protons occurs before the coalescence of 3,4-allylic proton resonances (Table 9) and indicates that the Me_2PhP ligand is involved in intermolecular exchange as well as π–σ–π exchange (Fig. 9). On warming, total collapse of all the allylic proton resonances is observed as expected for simultaneous 3,4 and syn,syn and anti,anti allylic proton exchange. With two exchange processes active in the system, the values of $\Delta G_{T_c}^{\ddagger}$ obtained from Me_2PhP site exchange in the R = CF_3 and CCl_3 complexes are in effect lower limits since intermolecular exchange is already contributing to the collapse of the Me_2PhP methyl proton resonances. Thus in Fig. 10 the values of $\Delta G_{T_c}^{\ddagger}$ for R = CF_3 and CCl_3 (where $R_3'P$ is Me_2PhP) deviate markedly from the otherwise consistent trend in $\Delta G_{T_c}^{\ddagger}$

Can. J. Chem. Downloaded from www.nrcresearchpress.com by 210.87.254.6 on 09/05/12
For personal use only.

TABLE 9. The free energy of activation for the 3,4-allylic proton site exchange in the complexes [(π-2-methylallyl)Pd(OOCR)Me_2PhP]

	3,4-Allylic proton site exchange			Me_2PhP methyl site exchange		
R	$\Delta\nu_0$ (Hz)	T_c (K)	$\Delta G_{T_c}^{\ddagger}$ (kcal/m)	$\Delta\nu_0$ (Hz)	T_c (K)	$\Delta G_{T_c}^{\ddagger}$ (kcal/m)
CH_3	29.0	272	13.6	6.1	256	13.6
	28.1	271	13.6	6.0	257	13.7
CMe_3	32.4	277	13.8	4.3	260	14.0
	32.7	280	14.0	4.2	260	14.0
CH_2Ph	30.1	285	14.3	7.3	273	14.4
	30.0	287	14.4	7.0	272	14.4
CPh_3	28.2	300	15.1	11.0	288	15.0
CH_2Cl	29.2	300	15.1	3.8	278	15.1
CCl_3	Loss of ^{31}P coupling to allylic protons on warming			3.6	280	15.2
CF_3				4.0	281	15.2

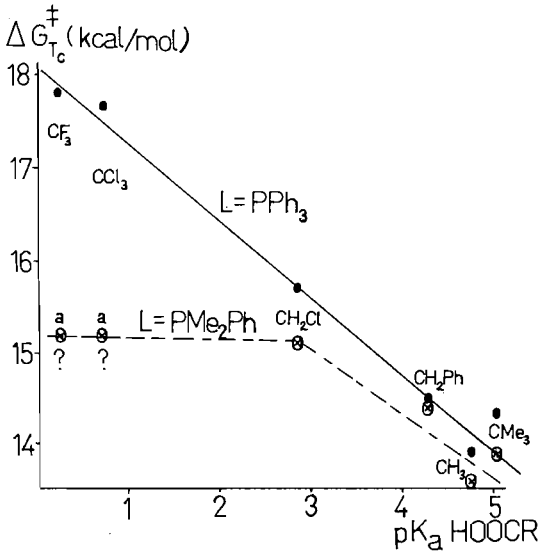

FIG. 10. The variation of the free energy of activation, $\Delta G_{T_c}^{\ddagger}$, for the 3,4-allylic proton site exchange in the complexes [(π-2-methylallyl)Pd(OOCR)(L)] with the inductive effect of the carboxylate substituents, R, expressed in terms of the pK_a of the corresponding carboxylic acid, HOOCR. a; two processes of exchange are operating (see text).

with the inductive effect of the carboxylate substituents.

From the data, summarized in Fig. 10, it may be concluded that the ability of the carboxylate ligand to stabilize a transition state by chelation diminishes with increasingly electronegative substitution.

The Influence of $AgOOCCF_3$ on 3,4-Allylic Proton Site Exchange in the Complexes [(π-2-methylallyl)Pd($OOCCF_3$)$R_3'P$]

In order to obtain reproducible results for the complexes, [(π-2-methylallyl)Pd($OOCCF_3$)$R_3'P$] where $R_3'P$ is Me_2PhP or Ph_3P, it proved necessary to completely remove all $AgOOCCF_3$ (lingering from the preparation of the reagent bridging carboxylate dimer) by passing the reagent dimer solution through activated alumina prior to the addition of $R_3'P$. The presence of even trace amounts of $AgOOCCF_3$ initiated a concentration dependent 3,4-allylic proton site exchange in $CDCl_3$ presumably due to a π–σ rearrangement (24) via a bimolecular interaction between $AgOOCCF_3$ and [(π-2-methylallyl)Pd(OOCR)$R_3'P$].

Summary and Conclusions

The facility of the intramolecular partially dissociative $Pd_2(OCO)_2$ ring opening process (Figs. 2 and 4) observed for the complexes $[(Me_2PhP)XPd(OOCR)]_2$ and $[(R_3'P)Pd(OOCR)_2]_2$ increases with the electronegativity of the carboxylate substituents, CH_3 < CH_2Cl < CF_3. Similarly, the ability of the carboxylate ligand to stabilize a transition state by chelation decreases in the same order, as noted for 3,4-allylic proton exchange in [(π-2-methylallyl)Pd(OOCR)$R_3'P$] complexes. It would appear in general then that the stability of the bidentate coordination of the carboxylate ligand (relative to unidentate coordination)

Can. J. Chem. Downloaded from www.nrcresearchpress.com by 210.87.254.6 on 09/05/12
For personal use only.

Can. J. Chem. Downloaded from www.nrcresearchpress.com by 210.87.254.6 on 09/05/12
For personal use only.

diminishes as the carboxylate substituents withdraw electron density from the oxygens of the carboxyl group.

The present work establishes the order and relative magnitude of the influence of the carboxylate substituents on various solution processes involving the chelation and bidentate bridging coordination of the carboxylate ligand. The results obtained have been used elsewhere (25) to rationalize the observed dependence of catalytic systems on the nature of carboxylate substituents such as that observed for the polymerization of butadiene by $[(\pi\text{-allylic})\text{-Ni(OOCR)}]_2$ (26, 27).

Experimental

Preparation of Compounds

The bridging halide dimers $[(R_3P)PdCl_2]_2$ were prepared by the method of Jenkins and Shaw (28). In all cases, the presence of excess silver carboxylates was avoided and special care was taken to remove extraneous silver compounds from the reaction mixtures by columning the reaction mixtures through activated alumina or Fisher Scientific Florisil.

Di-μ-acetatodiacetatobis(dimethylphenylphosphine)dipalladium(II)

A solution of di-μ-chlorodichlorobis(dimethylphenylphosphine)dipalladium(II) (0.507 g) in chloroform (15 ml) was shaken with silver acetate (0.536 g) for 3 h. The solution was columned through Florisil to remove precipitated silver chloride and unreacted silver acetate. The product was isolated by evaporation as an orange oil. Recrystallization from benzene and hexanes yielded yellow plates (0.268 g, 47%).

Di-μ-monochloroacetatodimonochloroacetatobis(dimethylphenylphosphine)dipalladium(II)

A solution of di-μ-chlorodichlorobis(dimethylphenylphosphine)dipalladium(II) (0.676 g) in dichloromethane (30 ml) was shaken with silver monochloroacetate (0.866 g) for 5 h. The solution was columned through alumina to remove silver compounds and then evaporated down to give an orange oil. Recrystallization from benzene/hexanes gave yellow solid (0.621 g, 67%).

Di-μ-trifluoroacetatoditrifluoroacetatobis(dimethylphenylphosphine)dipalladium(II)

A solution of di-μ-chlorodichlorobis(dimethylphenylphosphine)dipalladium(II) (0.509 g) in dichloromethane (20 ml) was shaken for 90 min with silver trifluoroacetate (0.711 g). The reaction mixture was columned through alumina and evaporated to yield a yellow bubbly glass. Recrystallization from benzene/hexane gave yellow needles (0.395 g, 52%).

Di-μ-acetatodiacetatobis(triethylphosphine)dipalladium(II)

A solution of di-μ-chlorodichlorobis(triethylphosphine)dipalladium(II) (0.378 g) in dichloromethane (15 ml) was shaken 3 h with silver acetate (0.430 g). The solution was columned through Florisil and evaporated to give a yellow solid. Recrystallization from dichloromethane/hexanes gave orange prisms (0.308 g, 70%).

Di-μ-monochloroacetatodimonochloroacetatobis(triethylphosphine)dipalladium(II)

A solution of di-μ-chlorodichlorobis(triethylphosphine)dipalladium(II) (0.214 g) in dichloromethane (20 ml) was shaken for 2 h with silver monochloroacetate (0.293 g). The solution was columned through Florisil and evaporated to a yellow oil. Recrystallization from dichloromethane/hexane gave yellow–orange prisms, (0.272 g, 91%).

Di-μ-trifluoroacetatoditrifluoroacetatobis(triethylphosphine)dipalladium(II)

A solution of di-μ-chlorodichlorobis(triethylphosphine)dipalladium(II) (0.138 g) in dichloromethane (10 ml) was shaken for 1 h with silver trifluoroacetate (0.207 g). The solution was columned through Florisil and evaporated to a yellow solid. Recrystallization from dichloromethane/hexanes gave yellow prisms (0.135 g, 67%).

Di-μ-trifluoroacetatoditrifluoroacetatobis(triphenylphosphine)dipalladium(II)

A solution of di-μ-chlorodichlorobis(triphenylphosphine)dipalladium(II) (0.413 g) in dichloromethane (30 ml) was shaken for 90 min with silver trifluoroacetate (0.415 g). The solution was columned through Florisil and evaporated to yellow solid. Recrystallization from dichloromethane/ether/hexanes gave yellow solid (0.436 g, 78%).

Di-μ-trifluoroacetatoditrifluoroacetatobis(methyldiphenylphosphine)dipalladium(II)

A solution of di-μ-chlorodichlorobis(methyldiphenylphosphine)dipalladium(II) (0.570 g) in dichloromethane (20 ml) was shaken for 90 min with silver trifluoroacetate (0.669 g). The solution was columned through Florisil and evaporated to orange oil. Recrystallization from chloroform/hexanes gave orange prisms (0.607 g, 76%).

Silver Tri(trifluoroacetato)dimethylphenylphosphinepalladium(II)

A solution of di-μ-chlorodichlorobis(dimethylphenylphosphine)dipalladium(II) (0.223 g) in dichloromethane (20 ml) was shaken for 2 h with silver trifluoroacetate (0.468 g). The bright yellow solution was filtered and evaporated down with continual addition of hexanes until crystallization gave bright yellow needles (0.375 g, 84%). Redissolution always left a trace of silver trifluoroacetate residue.

Physical Measurements

The variable temperature ^1H and ^{19}F n.m.r. spectra were recorded on a Varian Associates A56/60D spectrometer with temperature calibration by measurement of a methanol spectrum using the equations of Van Geet (29). The molecular weight studies were carried out osmometrically in ethanol free chloroform at 37 °C using a Mechrolab 301A Vapour Phase Osmometer. The infrared spectra were recorded using a Beckman IR-20 spectrometer; conductivity measurements were determined using a Barnstead PM70CB Conductivity Bridge; and melting points are from a Kofler hot stage apparatus and are corrected.

The authors wish to thank the National Research Council of Canada for financial support of this investigation and one of us (T.R.J.) wishes to thank the Ontario Government for an Ontario Graduate Fellowship.

1. J. POWELL. J. Am. Chem. Soc. **91**, 4311 (1969).
2. J. POWELL. J. Chem. Soc. A, 2233 (1971).
3. P. W. N. M. VAN LEEUWEN and A. P. PRAAT. Recl. Trav. Chim. Pays-Bas, **89**, 321 (1970).
4. J. POWELL and T. JACK. Inorg. Chem. **11**, 1039 (1972).
5. H-A. DIECK and R. F. HECK. J. Am. Chem. Soc. **96**, 1133 (1974).
6. K. KIKUKAWA, T. YAMANE, M. TAKAGI, and T. MATSUDA. J. Chem. Soc. D, 695 (1972).
7. G. D. SHIER. Am. Chem. Soc. Div. Pet. Chem. Prepr. **14**, B123 (1969).
8. G. D. SHIER. J. Organomet. Chem. **10**, P15 (1967).
9. T. A. STEPHENSON and G. WILKINSON. J. Inorg. Nucl. Chem. **29**, 2122 (1967).
10. K. NAKAMOTO. Infrared spectra of inorganic and coordination compounds, 2nd ed. Wiley-Interscience, New York. 1970. p. 61.
11. C. A. AGAMBAR, P. ANSTEY, and K. G. ORRELL. J. Chem. Soc. Dalton, 864 (1974).
12. H. S. GUTOWSKY and C. H. HOLM. J. Chem. Phys. **25**, 1228 (1956).
13. W. J. MOORE. Physical chemistry, 3rd ed. Prentice Hall, Englewood Cliffs, New Jersey. 1962.
14. C. S. JOHNSON, JR. Adv. Magn. Reson. **1**, 33 (1965).
15. B. HAMMOND, F. H. JARDINE, and A. G. VOHRA. J. Inorg. Nucl. Chem. **33**, 1017 (1971).
16. C. A. TOLMAN. J. Am. Chem. Soc. **92**, 2953 (1970).
17. R. C. THOMPSON and D. B. W. YAWNEY. Can. J. Chem. **43**, 1240 (1965).
18. R. L. MARTIN and H. WATERMAN. J. Chem. Soc. 1359 (1959).
19. J. LEWIS, Y. C. YIN, L. K. RAYSTON, and R. C. THOMPSON. J. Chem. Soc. 6464 (1965).
20. P. W. N. M. VAN LEEUWEN and A. P. PRAAT. J. Organomet. Chem. **21**, 501 (1970).
21. P. W. N. M. VAN LEEUWEN, A. P. PRAAT, and W. VAN DIEPEN. J. Organomet. Chem. **24**, C31 (1970).
22. P. W. N. M. VAN LEEUWEN, A. P. PRAAT, and W. VAN DIEPEN. J. Organomet. Chem. **29**, 433 (1971).
23. S. D. ROBINSON and B. L. SHAW. J. Organomet. Chem. **3**, 367 (1965).
24. T. L. TIBBETS and T. L. BROWN. J. Am. Chem. Soc. **92**, 3031 (1970).
25. R. P. HUGHES, T. JACK, and J. POWELL. J. Organomet. Chem. **63**, 451 (1973).
26. F. DAWANS, PH. TEYSIE. J. Polym. Sci. B-7, 111 (1969).
27. J. P. DURAND, F. DAWANS, and PH. TEYSIE. J. Polym. Sci. A-1, **8**, 979 (1970).
28. J. M. JENKINS and B. L. SHAW. J. Chem. Soc. A, 770 (1966).
29. A. L. VAN GEET. Anal. Chem. **42**, 679 (1970).

Can. J. Chem. Downloaded from www.nrcresearchpress.com by 210.87.254.6 on 09/05/12
For personal use only.

The Kinetics of Quinoline Hydrodenitrogenation through Reaction Intermediate Products

AHMED KADRY ABOUL-GHEIT

Petroleum Department, National Research Centre, Dokki, Cairo, Egypt

Received September 17, 1974[1]

AHMED KADRY ABOUL-GHEIT. Can. J. Chem. **53**, 2575 (1975).

Under petroleum hydrotreating conditions and in the presence of a Co–Mo–alumina catalyst, quinoline is hydrodenitrogenated through a consecutive first order reaction involving a hydrogenation step followed by two hydrocracking steps. The first step is too fast to measure whereas the second step is the slowest. The ratio of the rate constants of the second to the third step ranges between 0.33 and 0.62 at reaction temperatures between 350 and 400 °C. The second step can be considered responsible for the relatively high activation energy and enthalpy values obtained for the overall reaction. The activation entropy obtained for the overall reaction is -38.2 e.u. mol^{-1}, while the second and the third steps have values of -43.9 and -58.0 e.u. mol^{-1}, respectively. These values indicate the progressive complexity of the steps involved in the reaction sequence as it proceeds towards ammonia production.

AHMED KADRY ABOUL-GHEIT. Can. J. Chem. **53**, 2575 (1975).

Dans les conditions de traitement du pétrole et en présence d'un catalyseur Co–Mo–alumine, la quinoléine est hydrodénitrogénée en passant par une réaction du premier ordre impliquant une étape d'hydrogénation suivie de deux étapes d'hydrocraquage. La première étape est trop rapide pour être mesurée alors que la deuxième est la plus lente. Le rapport des constantes de vitesse de la deuxième à la troisième étape se situe entre 0.33 et 0.62 pour des températures de réaction de 350 à 400 °C. La seconde étape peut être considérée comme étant responsable des valeurs relativement élevées de l'énergie d'activation et de l'enthalpie obtenues pour la réaction totale. L'entropie d'activation obtenue pour la réaction globale est -38.2 u.e. mol^{-1}, alors que les deuxième et troisième étapes ont respectivement les valeurs de -43.9 et -58.0 u.e. mol^{-1}. Ces valeurs indiquent la complexité progressive des étapes impliquées dans la séquence des réactions qui conduisent à la production d'ammoniac. [Traduit par le journal]

Introduction

Hydrodenitrogenation (HDN) is a petroleum hydrotreating reaction of prime importance since nitrogen compounds cause serious problems in the processing and storage of petroleum products. Under hydrotreating conditions, HDN is much more difficult than hydrodesulfurization (1, 2). For high HDN levels, high hydrogen pressures are employed (3, 4). Temperatures above 400 °C are undesirable in hydrotreating since they enhance hydrocracking reactions that result in lower liquid yields, higher hydrogen consumption, and lower viscosity of lubricating oil stocks.

Hydrodenitrogenation is a stepwise process involving hydrogenation and hydrocracking reactions (4–9). The catalysts employed in this process possess both hydrogenation–dehydrogenation and cracking functions (dual functional catalysts). Over such catalysts, the petroleum nitrogen compounds are converted through intermediate products to ammonia. Each of these intermediates possesses different adsorptivity on the catalyst surface (9).

The subject of this paper is to study the kinetic and thermodynamic parameters for quinoline HDN involving the formation and conversion of intermediate products in order to clarify the reaction mechanism.

Experimental

Catalyst

A catalyst containing 3% cobalt oxide and 10% molybdenum oxide was prepared by impregnating $\frac{1}{8}$ in. extrudates of γ-alumina with cobalt nitrate solution, drying at 110 °C overnight, and calcinating at 550 °C for 4 h. Another impregnation with ammonium molybdate solution was then carried out followed by drying and calcination as above. The catalyst was then ground into 60–80 mesh particles because this has been shown to be the optimum size (5). The surface areas (measured by the BET method) of the alumina support and the prepared Co–Mo–alumina catalyst were 228 and 196 m^2/g, respectively.

Feedstock

Extra-pure grade Merck quinoline was redistilled under

[1]Revision received April 15, 1975.

Can. J. Chem. Downloaded from www.nrcresearchpress.com by 210.87.254.6 on 09/05/12
For personal use only.

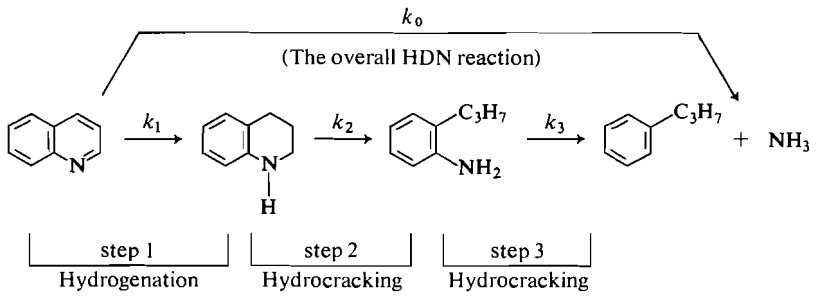

SCHEME 1

reduced pressure, then dissolved in a high purity paraffin oil. The oil exhibited no absorbance in the ultraviolet spectral region. The ebullioscopically determined average molecular weight of the oil was 185. The concentration of quinoline in the oil was 4.6 wt.%. *i.e.*, equivalent to 0.5 wt.% nitrogen. The quinoline solution was preserved in a dark container under nitrogen atmosphere and used as the feedstock.

Hydrogenation Procedure

The HDN experiments were carried out in a 2-l batch autoclave. After closing and purging twice with nitrogen and twice with hydrogen, the autoclave was filled with high purity hydrogen to a predetermined initial hydrogen pressure such that the operating pressure at the working temperature was 200 atm. The pressure dropped by only 3 atm after a reaction period of 8 h at 400 °C. The pressure drop was even less at lower temperatures and shorter reaction periods. The autoclave was heated to the reaction temperature, then a mixture of 250 g of the feedstock and 25 g of the catalyst was introduced into the reactor via a high pressure injector. At this moment, the autoclave's magnetic stirrer was switched on at a velocity of 1500 r.p.m. and the time was considered as zero. This stirring velocity has been shown to be optimum (5). Liquid samples of 2 ml volume were withdrawn from the system every hour, except for the first sample that was taken after a reaction period of $\frac{1}{2}$ h. The catalyst was removed from the sample by filtration while the dissolved ammonia was removed by bubbling a gentle current of nitrogen gas.

Analysis

The product samples were analyzed to determine the nitrogen content using a micro-Dumas technique via a Coleman Nitrogen Analyzer model 29. The individual nitrogen components were isolated from the product samples with 5% aqueous HCl solution then freed with 10% NaOH solution and extracted by ether. The ether was evaporated and the concentrate of nitrogenous components was analyzed by gas–liquid chromatography using an SE-30 column. The apparatus and conditions were described elsewhere (6, 7). Lower anilines (aniline, *o*-toluidine, and *o*-ethylaniline) in the products were always less than 2.0% and were calculated as *o*-propylaniline, whereas alkylquinolines were always less than 3.5% and were calculated as unreacted quinoline. A spectrophotometric search for pyrrolic nitrogen compounds in the product samples (10) showed the presence of negligible quantities only.

Results and Discussion

The hydrotreating process is carried out at relatively mild temperatures and high pressures, using supported or unsupported metal oxide or sulfide catalysts. Under such conditions, the hydrocarbon composition of the oil to be hydrotreated is only slightly affected, whereas the hetero compounds, including sulfur, nitrogen, and oxygen compounds, are greatly transformed. In this investigation, the paraffin-oil diluent was slightly hydrocracked, whereas the quinoline molecule was hydrodenitrogenated through a series of hydrogenation and hydrocracking reactions to yield ultimately ammonia and the "clean" hydrocarbon *n*-propylbenzene as envisaged in Scheme 1, where the subscripts 0, 1, 2, and 3 designate the overall HDN reaction, the first, second, and third step in the HDN sequence, respectively.

The overall process rate constant, k_0, has been shown (5) to be first order with respect to quinoline via both integral and differential approaches, hence, k_0 is herein graphically calculated from a plot of log $(1 - M_D)$ *vs.* t, as given in Fig. 1.

From Fig. 2, it is evident that virtually all of the quinoline reacted is converted to 1,2,3,4-

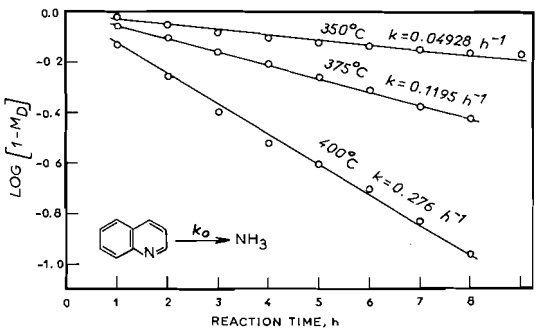

FIG. 1. First order plot for the overall hydrodenitrogenation of quinoline.

Can. J. Chem. Downloaded from www.nrcresearchpress.com by 210.87.254.6 on 09/05/12
For personal use only.

Can. J. Chem. Downloaded from www.nrcresearchpress.com by 210.87.254.6 on 09/05/12
For personal use only.

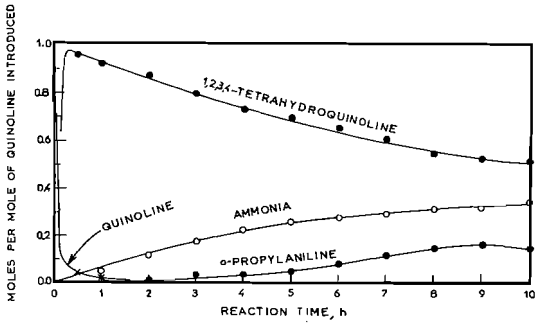

FIG. 2. Kinetic curve for quinoline hydrodenitrogenation at 350 °C.

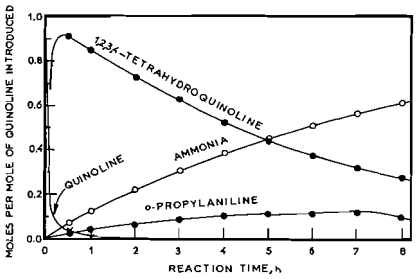

FIG. 3. Kinetic curve for quinoline hydrodenitrogenation at 375 °C.

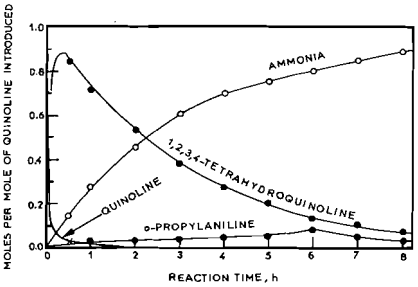

FIG. 4. Kinetic curve for quinoline hydrodenitrogenation at 400 °C.

tetrahydroquinoline at an early stage in the HDN process. The conversion is so fast that the molar concentration of the tetrahydroquinoline reaches 96% after ½ h of reaction. In this case, it appears reasonable to calculate k_2 from a plot of log $(1 - M_B)$ *vs.* t, as given in Fig. 5. The straight line relationship obtained confirms that step 2 in Scheme 1 follows first order kinetics and substantiates the feasibility of the approach used to calculate k_2.

The instantaneous rates of component concentration changes, considering first order reaction of the consecutive type are given by the following series of equations:

$$[1] \qquad dM_A/dt = -k_1 M_A$$

$$[2] \qquad dM_B/dt = k_1 M_A - k_2 M_B$$

$$[3] \qquad dM_C/dt = k_2 M_B - k_3 M_C$$

$$[4] \qquad dM_D/dt = k_3 M_D$$

where M is the component concentration, mole fraction, and the subscripts A, B, C, and D designate quinoline, 1,2,3,4-tetrahydroquinoline, *o*-propylaniline, and ammonia, respectively. The approach of quasi-stationary concentrations (steady state) is used to calculate k_3, whereby the term dM_C/dt in [3] is set equal to zero at a definite reaction time, t_{max}, where t_{max} is the reaction period at which *o*-propylaniline is of maximum concentration. From Figs. 2–4, it is evident that t_{max} is 9, 7, and 6 h at reaction temperatures of 350, 375, and 400 °C, respectively. The constants obtained for steps 2 and 3, as well as the overall HDN rate constant, at hydrotreating temperatures, are given in Table 1.

The ratio of k_2/k_3 is 0.33 at 350 °C, 0.51 at 375 °C, and 0.62 at 400 °C. The fact that step 2 is the slowest step in the HDN of quinoline is also supported by Larson (9) who has found the k_2/k_3 ratio to be 0.80. However, Larson does not indicate his method for calculating these rate constants.

TABLE 1. Reaction rate constants at hydrotreating temperatures[a]

Rate constant $\times 10^4$ (s^{-1})	Temperature (°C)		
	350	375	400
k_1[b]	Fast	Fast	Fast
k_2	0.204	0.454	0.908
k_3	0.623	0.884	1.475
k_0	0.137	0.332	0.767

[a]Rate constants refer to the use of 25 g of catalyst.
[b]k_1 is too large to be measured by the methods used in this study.

The temperature dependence of the rate constants gives linear Arrhenius plots as shown in Fig. 6. Accordingly, the rate constants can be represented by [5–7].

$$[5] \qquad k_2 = 4.416 \times 10^3 \, e^{-24700/RT} \, s^{-1}$$

$$[6] \qquad k_3 = 5.728 \, e^{-14180/RT} \, s^{-1}$$

$$[7] \qquad k_0 = 1.478 \times 10^5 \, e^{-28590/RT} \, s^{-1}$$

Since the HDN reaction is carried out in the liquid phase (11), [8] will relate the energy of

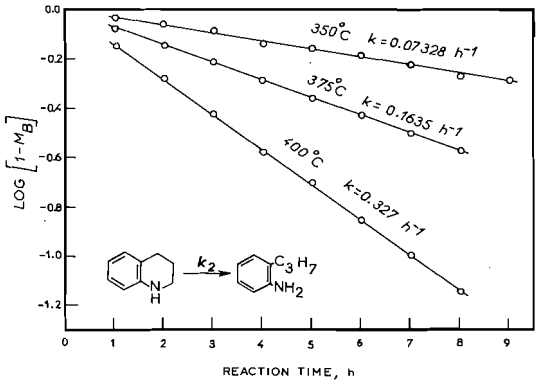

FIG. 5. First order plot for the second step in quinoline hydrodenitrogenation.

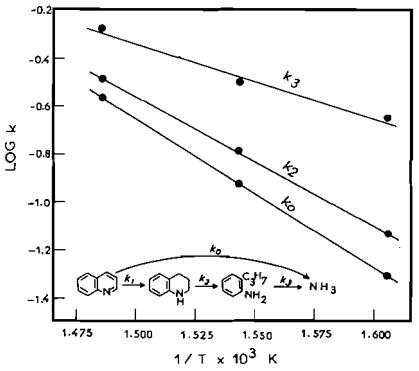

FIG. 6. Arrhenius plot for the overall reaction, the second, and third step.

activation to an enthalpy of activation

$$[8] \qquad E_a = RT + \Delta H^{\ddagger}$$

and accordingly the calculated average $\Delta H^{\ddagger}$ values, in the temperature range of 350–400 °C, are as follows: $\Delta H_2{}^{\ddagger} = 23.400$ kcal mol^{-1}; $\Delta H_3{}^{\ddagger} = 12.880$ kcal mol^{-1}; $\Delta H_0{}^{\ddagger} = 27.290$ kcal mol^{-1}.

According to the theory of absolute reaction rates (12), the rate constant is related to the entropy and enthalpy of activation by [9].

$$[9] \qquad k = \frac{k_b T}{h} \exp\left(\frac{\Delta S^{\ddagger}}{R} - \frac{\Delta H^{\ddagger}}{RT}\right)$$

where k_b = Boltzmann's constant, 1.380×10^{-16} erg/K. The following values of enthalpy and entropy of activation are calculated from plots of log k/T *vs.* $1/T$ (Fig. 7) by applying [9]:

Parameter	Value (kcal mol^{-1})	Parameter	Value (e.u. mol^{-1})
$\Delta H_2{}^{\ddagger}$	23.330	$\Delta S_2{}^{\ddagger}$	−43.9
$\Delta H_3{}^{\ddagger}$	13.265	$\Delta S_3{}^{\ddagger}$	−58.0
$\Delta H_0{}^{\ddagger}$	27.445	$\Delta S_0{}^{\ddagger}$	−38.2

The values of E_a and $\Delta H^{\ddagger}$ obtained for step 2 (the slowest step) do not significantly differ from those obtained for the overall HDN reaction; thus step 2 can be considered responsible for the relatively higher values of E_a and $\Delta H^{\ddagger}$ obtained for the overall reaction (5).

The magnitude of the entropy values obtained in this study shows that the activated complex is an immobile molecule attached to the catalyst surface and the product molecule is much like the activated complex. Since the entropy of activation for desorption is expected to be small and positive, or nil, the entropy values obtained cannot be associated with desorption as the rate controlling process. The high hydrogen pressure employed in this study should greatly influence the product desorption. The magnitude of the activation energies and enthalpies obtained also suggests that diffusion is not the rate controlling process.

Since step 1 in Scheme 1 is too fast to measure, it is not possible to calculate $\Delta S_1{}^{\ddagger}$ from the experimental data. Nevertheless, a $\Delta S_0{}^{\ddagger}$ value of −38.2 e.u. mol^{-1} compared with a value of −43.9 e.u. mol^{-1} for $\Delta S_2{}^{\ddagger}$ and −58.0 e.u. mol^{-1} for $\Delta S_3{}^{\ddagger}$, is indicative of a much smaller negative value (or even positive) for $\Delta S_1{}^{\ddagger}$.

When the quinoline molecule is first hydrogenated to the tetrahydroquinoline (which is expected to be more strongly basic than quinoline) (9), this product competes for the catalyst's

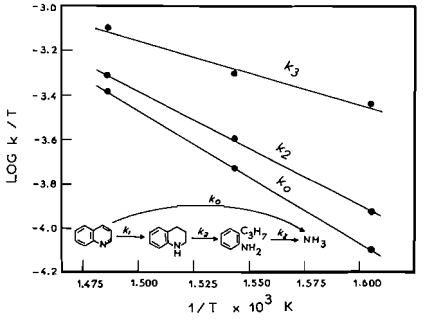

FIG. 7. Eyring plot for the overall reaction, the second step, and third step.

Can. J. Chem. Downloaded from www.nrcresearchpress.com by 210.87.254.6 on 09/05/12
For personal use only.

active sites. The complexity encountered in orienting and adsorbing on the surface of the catalyst gives rise to a loss of several degrees of freedom whereby an entropy change of -43.9 e.u. mol^{-1} is obtained.

As the tetrahydroderivative is hydrocracked to *o*-propylaniline, the latter competes to attach to the catalyst and the reaction becomes more complex due to the loss of additional degrees of freedom. Hence, a much larger negative entropy change results ($\Delta S_3^{\ddagger} = -58.0$ e.u. mol^{-1}).

The effect of basicity of the intermediates produced during the HDN reactions cannot be ignored. However, its influence is not yet clarified. For instance, Larson (9) assumes that the most adsorbed phase on the catalyst is the aniline-type compound. McIlvried (4), on the other hand, assumes that all of the intermediate basic compounds produced during the HDN of pyridine appear to be equally strongly adsorbed on the denitrogenation sites.[2] The basicity of the nitrogen compounds at the reaction temperatures should be greatly different from that measured at normal temperatures, and no decisive explanation for the behavior of the quinoline intermediates, based on their basicities, could be achieved. However, the results of this study seem to agree with Larson's assumption.

The hydrogenation function of the catalyst employed in this investigation appears high enough to achieve fast hydrogenation of the quinoline-type compounds (Figs. 2–4). On the other hand, the cracking function of the catalyst is relatively less active (step 2 is the slowest step). Therefore, if the cracking function of this catalyst is activated through some treatment, a more active HDN catalyst is obtained. For instance, when the catalyst under investigation has been treated with HCl gas, the quinoline solution employed becomes completely hydrodenitrogenated after a reaction period of 3.5 h at 400 °C.[3]

The author wishes to thank Dr. Sami A. Shama of the Lowell Technological Institute, Lowell, U.S.A., for his interest and valuable discussions.

1. A. K. Aboul-Gheit and I. K. Abdou. J. Inst. Pet. London, **58**, 305 (1972).
2. E. M. Blue and B. Spurlock. Chem. Eng. Prog. **56**, 54 (1960).
3. R. A. Flinn, O. A. Larson, and H. Beuther. Hydrocarbon Process. Pet. Refiner, **42**, 129 (1963).
4. H. G. McIlvried. Ind. Eng. Chem. Process Des. Dev. **10**, 125 (1971).
5. A. K. Aboul-Gheit and I. K. Abdou. J. Inst. Pet. London, **59**, 188 (1973).
6. A. K. Aboul-Gheit, I. K. Abdou, and A. Mustafa. 6th Arab Sci. Congr. Proc. Vol. 5. Damascus. 1969. p. 77.
7. A. K. Aboul-Gheit, I. K. Abdou, and A. Mustafa. Egypt. J. Chem. In press.
8. J. Doelman and J. C. Vlugter. 6th World Pet. Congr. Proc. Sect. III, Frankfurt. 1963. p. 247.
9. O. A. Larson. Preprints, Div. Pet. Chem., Am. Chem. Soc., **12**, B-123 (1967).
10. M. A. Muhs and F. T. Weiss. Anal. Chem. **30**, 2591 (1958).
11. J. M. Smith. Chemical engineering kinetics. McGraw-Hill, Inc., New York. 1956. p. 378.
12. S. Glasstone, K. J. Laidler, and H. Eyring. Theory of rate processes. McGraw-Hill, Inc., New York. 1941. p. 9.

[2]McIlvried differentiates the active sites of his Ni–Co–Mo–alumina catalyst into hydrogenation and denitrogenation sites.

[3]A. K. Aboul-Gheit. Unpublished results.

Can. J. Chem. Downloaded from www.nrcresearchpress.com by 210.87.254.6 on 09/05/12
For personal use only.

Recherches sur les composés éthyléniques.[1] V. Liens entre la structure des alcènes et leur fréquence de vibration $\nu_{C=C}$, influence des effets structuraux et établissement d'une relation de topo-information

J. H. Basso, S. Delattre, R. Lanteri et R. Luft[2]

Laboratoire de chimie organique, Institut Polytechique Méditerranéen, Université de Nice, 28, av. de Valrose, F 06034, Nice Cedex, France

Reçu le 1 octobre 1974[3]

J. H. Basso, S. Delattre, R. Lanteri et R. Luft. Can. J. Chem. **53**, 2580 (1975).

L'examen des données spectroscopiques de 43 alcènes montre l'influence d'un encombrement croissant au niveau du carbone positionné en α ou en β de la liaison éthylénique. Une contrainte stérique particulièrement élevée provoque l'apparition d'une seule conformation privilégiée et s'accompagne d'une forte diminution (10 cm^{-1}) de la fréquence du vibrateur $\nu_{C=C}$.

Une analyse quantitative peut être réalisée grâce à la "méthode topochimique D.A.R.C.". Des relations de topo-information ont pu être mises en évidence pour la famille des 2-alkyléthylènes et celle des 2,2-dialkyléthylènes. Elles permettent de chiffrer la contribution de chacun des sites topologiques à la valeur de la fréquence $\nu_{C=C}$. Pour la première famille, l'empreinte établie grâce à 9 composés, permet une proférence sur 30 composés; en ce qui concerne la seconde famille, la proférence est réalisée sur 159 composés, l'empreinte étant établie à partir de 13 autres alcènes.

J. H. Basso, S. Delattre, R. Lanteri, and R. Luft. Can. J. Chem. **53**, 2580 (1975).

An examination of spectroscopic data for 43 alkenes reveals the influence of increasing substitution at the carbon atoms α or β to the ethylenic bond. The presence of a particularly large steric constraint requires that there be a single preferred molecular conformation: in such a case the frequency of the $\nu_{C=C}$ vibrator is strongly decreased (10 cm^{-1}).

A quantitative analysis of the phenomenon can be achieved using the "topological-chemical method D.A.R.C.". Topologic-information relationships could be developed for the two series 2-alkylethylenes and 2,2-dialkylethylenes. These permit the calculation of the contribution of each topological site to the frequency $\nu_{C=C}$. For the first series, the relationship, based on 9 compounds, permits predictions about 30 others. For the second series, deductions are made concerning 159 compounds from a relationship established on a base of 13 compounds.

[Journal translation]

La position des bandes d'absorption infrarouge et leur intensité sont des paramètres liés aux influences des facteurs structuraux. Chaque vibrateur peut varier autour d'une fréquence moyenne et à l'intérieur des plages délimitées on peut définir des bandes plus étroites, caractérisant la taille et la nature des substituants de ces vibrateurs (2, 3). Par ailleurs, on a pu observer des relations linéaires entre différents vibrateurs d'une molécule (4).

Parallèlement aux études expérimentales il a été possible de calculer les fréquences des vibrateurs à partir des données moléculaires (5–7) et de prévoir l'intensité absolue des bandes $\nu_{C=C}$ d'alcènes-1 par la méthode CNDO (8).

Dans ce contexte, il nous a paru intéressant de mieux préciser, dans le cas des alcènes, la contribution des divers substituants aux fréquences de vibration (9).

A cet effet, nous avons examiné (tableau 1) une population d'alcènes appartenant aux trois types suivants:

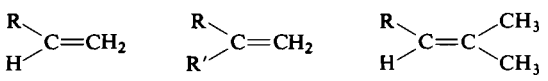

Discussion des résultats spectroscopiques

Le tableau 1 montre que la fréquence évolue avec la structure des substituants de la fonction éthylénique, selon des lois propres à chaque vibrateur.

Cette variation est très peu sensible dans le cas du vibrateur ν_{C-H}; en ce qui concerne le vibrateur $\nu_{C=C}$ on observe un effet hypsochrome, lorsqu'on passe d'un terme de la série des

[1]Articles III et IV de la série, voir réf. 1.

[2]Auteur à qui toute correspondance doit être adressée.

[3]Révision reçue le 25 avril 1975.

Can. J. Chem. Downloaded from www.nrcresearchpress.com by 210.87.254.6 on 09/05/12
For personal use only.

TABLEAU 1. Bandes d'absorption de quelques alcènes

Alcènes	ν_{C-H} (vap 25°)	$\nu_{C=C}$ (film liq 13μ)	δ_{C-H} (film liq 13μ)
Alkyl-2 éthylènes			
Propène	3086	1647	996 et 919
Butène-1	3086	1645	994 et 912
Pentène-1	3086	1643	992 et 910
Octène-1	3085	1642	992 et 909
Nonène-1	3085	1642	992 et 909
Décène-1	3085	1642	992 et 909
Undécène-1	3085	1642	992 et 909
Dodécène-1	3085	1642	992 et 909
Méthyl-3 butène-1	3086	1642	997 et 907
Méthyl-3 pentène-1	3085	1641	997 et 910
Méthyl-3 hexène-1	3085	1641	994 et 910
Méthyl-4 pentène-1	3084	1643	993 et 910
Méthyl-5 hexène-1	3087	1642	994 et 909
Diméthyl-3,3 butène-1	3090	1640	999 et 907
Diméthyl-4,4 pentène-1	3086	1641	994 et 910
Triméthyl-3,5,5 hexène-1	3084	1641	907
Dialkyl-2,2 éthylènes			
Éthyl-2 butène-1	3085	1648	886
Éthyl-2 hexène-1	3081	1646	886
t-Butyl-2 butène-1		1636	890
Isopropyl-2 méthyl-3 butène-1	3091	1638	889
Diméthyl-3,3 *t*-butyl-2 butène-1	3120	1617	900
Diméthyl-4,4 néopentyl-2 pentène-1	3079	1636	892
Méthyl-2 alcènes-2			
Méthyl-2 butène-2		1677	900
Méthyl-2 pentène-2		1675	832
Méthyl-2 hexène-2		1675	826
Diméthyl-2,4 pentène-2		1675	826
Triméthyl-2,4,4 pentène-2		1665	822
Diméthyl-2,4 hexène-2		1672	848
Diméthyl-2,5 hexène-2		1674	851
Triméthyl-2,5,5 hexène-2		1671	846
Méthyl-2 alkyl-2 éthylènes (alkyl-2 propènes)			
Méthyl-2 propène	3086	1656	887
Méthyl-2 butène-1	3085	1652	885
Méthyl-2 pentène-1	3084	1651	887
Méthyl-2 hexène-1	3083	1650	887
Méthyl-2 heptène-1	3082	1650	887
Diméthyl-2,3 butène-1	3087	1646	887
Diméthyl-2,3 pentène-1	3078	1646	887
Diméthyl-2,3 hexène-1	3080	1645	887
Diméthyl-2,4 pentène-1	3081	1649	887
Diméthyl-2,4 hexène-1		1649	888
Triméthyl-2,3,3 butène-1	3100	1639	890
Triméthyl-2,4,4 pentène-1	3081	1641	891

NOTE: Les valeurs relatives au propène et au butène-1 ont été relevées dans la littérature (7). Pour la fréquence $\nu_{C=C}$ du méthyl-2 propène nous avons opéré en solution dans le CCl_4. Les bandes $\nu_{C=C}$ et δ_{C-H} ont été déterminées avec un spectrophotomètre PE457, les bandes ν_{C-H} avec un Beckman DK 2A. L'étalonnage des appareils et le contrôle des spectres ont été réalisés en se servant des bandes de calibration de l'eau, de l'iodure de méthyle et du styrène (10, 11). Pour l'ensemble des mesures les écarts types sont de ± 1 cm^{-1} en ce qui concerne les bandes $\nu_{C=C}$ et δ_{C-H} et de ± 2 cm^{-1} en ce qui concerne les bandes ν_{C-H}. Toutes les bandes enveloppes examinées dans le présent travail sont de forme lorentzienne. Pour le pentaméthyl-2,3,3,4,4 pentène-1 Monsieur LOMAS (laboratoire du J. E. Dubois, Université de Paris VII) a mesuré $\nu_{C=C} = 1627$ cm^{-1}. Nous utiliserons cette valeur pour l'établissement des relations de topologie-information.

Can. J. Chem. Downloaded from www.nrcresearchpress.com by 210.87.254.6 on 09/05/12
For personal use only.

Can. J. Chem. Downloaded from www.nrcresearchpress.com by 210.87.254.6 on 09/05/12
For personal use only.

alkyl-2 éthylènes[4] aux termes correspondants des méthyl-2 alkyl-2 éthylènes et des diméthyl-1,1 alkyl-2 éthylènes.

Enfin, le vibrateur δ_{C-H} présente des valeurs à peu près constantes dans les séries des alkyl-2 éthylènes et des méthyl-2 alkyl-2 éthylènes. De même, les composés de cette dernière sous-population accusent, par rapport à leurs homologues déméthylés sur le carbone 2, un effet bathochrome constant.

Etude qualitative de la variation de la fréquence $\nu_{C=C}$

Examen des fréquences

Ces variations peuvent être mieux mises en évidence dans le cas du vibrateur $\nu_{C=C}$, lorsqu'on regroupe les composés du tableau 1, en tenant-compte pour chacune des trois sous-populations de la localisation des ramifications et de leur nombre.

Pour chacune des 3 sous-population nous avons retenu deux composés de base qui se différencient entre-eux par la longueur de leur chaîne alkyle (méthyle ou éthyle). Nous leur avons adjoint dans les trois cas les substances qui en dérivent grâce à la substitution progressive par des groupements méthyles du carbone terminal de leur chaîne alkyle (méthyle ou éthyle), de façon à observer l'influence d'un encombrement croissant au niveau du carbone positionné en α ou en β de la liaison éthylénique ("site α ou site β"). L'évolution de la fréquence $\nu_{C=C}$ des familles d'alcènes retenues est représentée dans la fig. 1 dont l'examen détaillé met an évidence des divergences de comportement du vibrateur $\nu_{C=C}$:

Alkyl-2 éthylènes

Chaque groupe méthyle fixé sur un site α ou un site β entraîne un abaissement de fréquence régulier.

Méthyl-2 alkyl-2 éthylènes

Au cours de la méthylation progressive du site α, chaque substitution provoque une même variation moyenne $\Delta\nu$; on observe un phénomène analogue au niveau du site β, sauf en ce qui concerne le remplacement du dernier atome d'hydrogène où la variation de fréquence est très importants (passage du groupe isobutyle au groupe néopentyle avec $\Delta\nu = -9\ cm^{-1}$).

Diméthyl-1,1 alkyl-2 éthylènes

Cette fois-ci, la méthylation du site β entraîne une variation régulière $\Delta\nu$ et on observe par contre une diminution brutale de la fréquence lors du remplacement du dernier atome d'hydrogène du site α (passage du groupe isopropyle au groupe tertiobutyle $\Delta\nu = -10\ cm^{-1}$).

S'il est évident que les variations de fréquence $\nu_{C=C}$, et en particulier les divergences que nous venons de signaler sont liées à la structure des substituants de la fonction alcène, il n'existe cependant pas, à notre connaissance, de relation simple entre la fréquence $\nu_{C=C}$ et la taille ou la position des groupements R, en dehors de celle (12) dégagée d'une étude relative à la réhybridation des atomes de la fonction alcène, sous l'action du facteur stérique.

Examen des modèles moléculaires

Seule une étude des dispositions spatiales relatives des atomes entourant la fonction alcène devrait pouvoir nous renseigner sur l'existence de contraintes éventuelles et permettre l'interprétation des divergences de comportement observées entre le méthyl-2 néopentyl-2 éthylène et le diméthyl-1,1 néopentyl-2

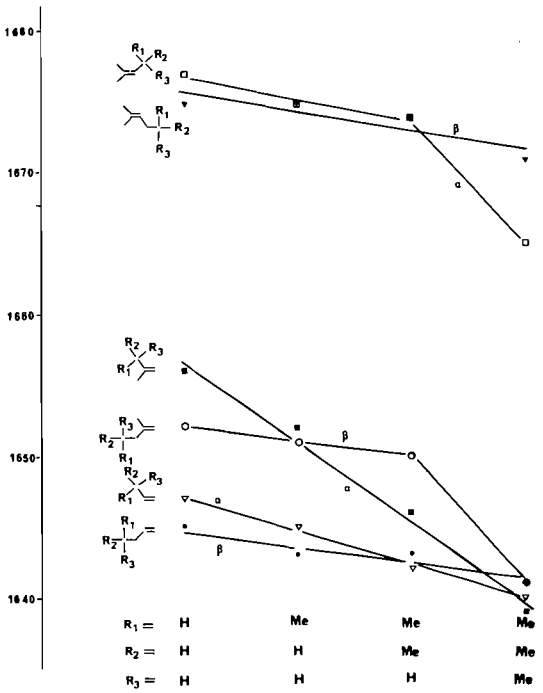

FIG. 1. Examen de l'influence, sur la fréquence $\nu_{C=C}$, de la méthylation progressive d'un atome de carbone en α ou en β du groupe fonctionnel, pour trois familles.

[4]Pour des raisons d'homogénéïté, nous avons préféré utiliser cette nomenclature de travail pour la désignation des sous-populations.

Can. J. Chem. Downloaded from www.nrcresearchpress.com by 210.87.254.6 on 09/05/12
For personal use only.

éthylène d'une part, le méthyl-2 tertiobutyl-2 éthylène et le diméthyl-1,1 tertiobutyl-2 éthylène d'autre part.

Pour cette analyse conformationnelle, nous avons utilisé les modèles moléculaires compacts Stuart–Briegleb des Ets Leybold, particulièrement adaptés à l'étude des domaines de van der Waals.

Signalons d'autre part que pour cette étude qualitative nous n'avons pas cherché à évaluer les interactions éventuelles avec les orbitales π.

Alkyl-2 éthylènes

La libre rotation n'est pas entravée, même pour les termes les plus substitués.

Méthyl-2 alkyl-2 éthylènes

Méthylation du site α — On constate une légère interaction entre les hydrogènes du substituant méthyle et ceux portés par le second atome de carbone du groupe alkyle.

Ces mêmes hydrogènes se trouvent simultanément en disposition d'interaction légère avec l'un des deux hydrogènes du carbone 1 de la fonction éthylénique; la libre rotation n'en semble pas empêchée néanmoins.

Globalement, les interactions sont plus nombreuses que dans le cas des alkyl-2 éthylènes, les écarts successifs observés, $\Delta\nu_{C=C}$, sont plus importants.

Méthylation du site β — Dans ce cas, on relève la possibilité de deux zones d'interactions qui peuvent freiner, voire empêcher, la libre rotation du groupe alkyle. On les observe à partir de deux conformations planes dans lesquelles le groupe méthyle fixé sur le site β est en interaction soit avec un hydrogène vinylique, soit avec le méthyle porté par la double liaison.

Diméthyl-1,1 alkyl-2 éthylènes

Méthylation du site α — Dans cette série l'un des deux méthyles de la fonction alcène entre en interaction avec le groupe alkyle R en disposition Z, dès que le carbone C_α de ce groupe R porte un premier substituant méthyle; il empêche ainsi la libre rotation du groupe R. Lorsque le site α porte trois groupes méthyles (R = tertioBu), la molécule atteint un contenu énergétique minimal pour une seule conformation; celle-ci correspond à la répartition symétrique des méthyles par rapport au plan moléculaire, même une faible oscillation du groupe tertiobutyle requiert une quantité d'énergie élevée.

Méthylation du site β — Lorsque les carbones C_α et C_β du groupe alkyle sont dans le plan moléculaire et dans une conformation telle que le carbone C_β soit le plus éloigné possible du méthyle Z, la libre rotation autour de la liaison C_α—C_β ne semble affectée que par un atome d'hydrogène, quel que soit le nombre de méthyles fixés sur le site β.

La libre rotation autour de l'axe C_2—C_α ne peut avoir lieu, mais dans tous les cas une oscillation de grande amplitude autour de cet axe reste possible.

Examen général des données qualitatives

En définitive, pour chacune des familles examinées il apparaît que la création d'une contrainte stérique particulièrement élevée, provoquant l'apparition d'une seule conformation privilégiée, s'accompagne d'une forte diminution de la fréquence du vibrateur $\nu_{C=C}$.

L'existence d'un lien entre cette diminution et la rigidité d'une conformation n'est pas en contradiction avec l'idée de l'intervention d'une compression stérique, que l'on envisage cette dernière sous l'aspect d'une rehybridation (12), sous celle d'une déformation des angles de liaison (7, 13) ou d'un gauchissement du plan moléculaire tel que l'envisage Rea (14) pour certains types de molécules. Seule l'étude détaillée de la géométrie rigoureuse des molécules pourrait permettre de trancher de cas à cas en faveur de l'une ou l'autre hypothèse.

Une telle étude ne nous était pas accessible, mais il nous a semblé possible d'arriver cependant à une analyse fine, quoique empirique, à l'aide de méthodes de traitement mathématique des données physicochimiques (15, 16).

Etude quantitative de l'influence des substituants sur la fréquence $\nu_{C=C}$

Pour atteindre des résultats quantitatifs, en particulier en ce qui concerne l'interaction des substituants alkyles entre eux, nous avons fait appel à l'informatique chimique et plus particulièrement au système D.A.R.C. (15). Ce dernier permet d'établir des relations quantitatives entre le comportement chimique ou physicochimique d'une population de composés et leur topologie (16–18).

Avec l'école du Dubois, nous distinguerons deux notions: le foyer "FO" qui caractérise le site privilégié commun à tous les individus de la population examinée, et les parties extérieures à ce site qui constituent l'environnement *6*

et se développent le long de "directions de développement" à partir d'origines dont le nombre est lié au choix de la structure du foyer. Pour atteindre une description correcte, il faut que cet environnement soit ordonné, pour aboutir à une "empreinte". "L'empreinte d'une population est un environnement ordonné qui rassemble les sites occupés au moins une fois dans les environnements des différents individus constitutifs de la population" (15).

L'environnement $\mathscr{E}$ est représenté par un vecteur topologie $T(\mathscr{E}) = (t_1, t_2, \ldots, t_n)$.

Si, pour un individu donné de la population, un site i est occupé, la composante t_i sera prise égale à 1, si par contre ce site n'est pas occupé, nous noterons $t_i = 0$.

De leur côté, les propriétés physicochimiques ou chimiques sont représentées par un vecteur information $I(m)$ dont les composantes, déterminées à partir des m composés qui constituent la population clef, permettent de chiffrer la contribution de chacun des sites topologiques. A partir des notions $T(\mathscr{E})$ et $I(m)$ on aboutit à une "relation de topo-information"

$$[1] \qquad I(\mathscr{E}) = \langle T(\mathscr{E}) | I(m) \rangle$$

dans laquelle l'information $I(\mathscr{E})$ est reliée à la contribution de l'environnement $\mathscr{E}$.

Cet environnement peut se caractériser par une ou plusieurs directions de développement. Dans ce dernier cas, deux situations peuvent se présenter:

il n'y a pas d'interaction, ou interaction constante entre les sites des directions de développement. L'interaction ne peut être chiffrée, la relation 1 est satisfaisante (critères statistiques basés sur le coefficient de corrélation (19) et le test d'Exner (20)).

il y a interaction, variable avec la structure, entre les arborescences issues des différentes directions de développement. Cette interaction ne se manifeste de façon sensible que sur un petit nombre de sites de l'empreinte. Pour en tenir compte, il faut introduire dans l'expression 1 un terme d'interaction; ce qui conduit à la relation

$$[2] \quad I(\mathscr{E}) = \langle T(\mathscr{E}) | I(m) \rangle + \langle T(\mathscr{E}) | M | T(\mathscr{E}) \rangle$$

où M est la matrice d'interaction.

Tentative de corrélation de la population des alkyl-2 et dialkyl-2,2 éthylènes

Nous n'avons pas réussi pour l'instant à obtenir une relation de topo-information satisfaisante pour la population globale. Cependant, le coefficient de corrélation multiple élevé ($r = 0.986$) nous a incité à étudier des populations plus restreintes, en particulier celles des alkyl-2 éthylènes et des dialkyl-2,2 éthylènes.

Cas des alkyl-2 éthylènes

La relation linéaire de topologie-information est la suivante

$$\nu_{C=C} = 1647.1 - 2.4(A_1 + A_2 + A_3) - 1.7B_{11} - 1.0(B_{12} + B_{13}) - 0.5(C_{111} + C_{112}) + 1.4C_{113}$$

$r = 0.994$, $\psi = 0.19$, écart type $= 0.15\ cm^{-1}$, structure du foyer FO: $(H_2C{=}CH{-}C)\lessgtr$. Elle a été établie à partir de 9 alkyl-2 éthylènes et nous avons contrôlé sa validité pour les trois composés suivants:

	Valeur (cm^{-1})	
	Mesurée	Estimée
Méthyl-3 pentène-1	1641	1640.5
Méthyl-4 pentène-1	1643	1642
Méthyl-3 hexène-1	1641	1640

Cas des dialkyl-2,2 éthylènes

Afin de nous limiter à un nombre minimal de paramètres, nous avons établi la relation de topo-information en nous basant sur l'hypothèse de l'apport de contributions identiques dans les deux directions de développement, complétée par celle de la possibilité d'une interaction dans les cas suivants: $A_3{}^1$ et $A_3{}^2$; $B_{13}{}^1$ et $B_{13}{}^2$; $A_3{}^1$ et $B_{13}{}^1$. Nous obtenons ainsi le graphe suivant: $r = 0.9998$, $\psi = 0.05$, écart type: $0.6\ cm^{-1}$.

Ce graphe et la relation linéaire de topo-information qui lui est associée ont été établis à partir de 13 dialkyl-2,2 éthylènes et nous avons controlé sa validité pour les composés suivants:

	Valeur (cm^{-1})	
	Mesurée	Estimée
Diméthyl-2,3 pentène-1	1646	1646
Tertiobutyl-2 butène-1	1636	1635
Triméthyl-2,4,4 pentène-1	1641	1641
Diméthyl-2,4 hexène-1	1649	1648
Diméthyl-2,3 hexène-1	1645	1645
Méthyl-2 hexène-1	1650	1650

Can. J. Chem. Downloaded from www.nrcresearchpress.com by 210.87.254.6 on 09/05/12
For personal use only.

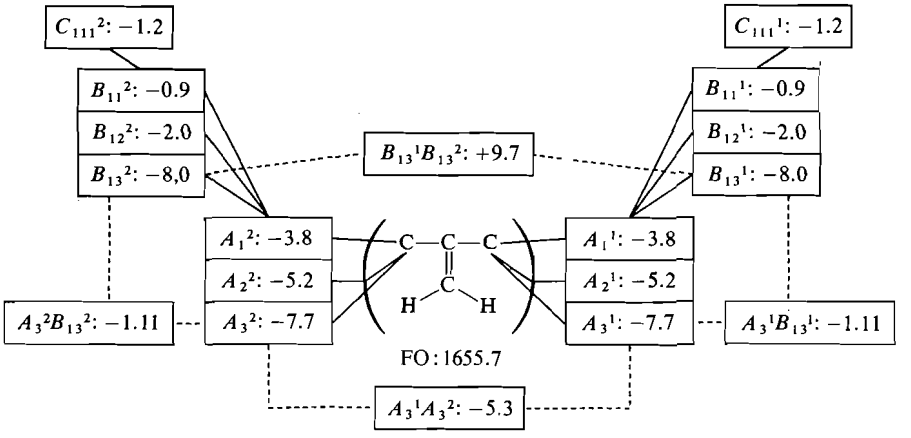

Conclusion

Pour chacune des sous-populations étudiées la relation linéaire de topo-information est très satisfaisante en fonction des critères statistiques retenus (19, 20).

La concordance entre les valeurs mesurées et estimées à l'aide des relations de topo-information justifient la proférence de ces relations sur l'ensemble des substances réunies dans les deux empreintes des sous-populations examinées. Dans le cas des alkyl-2 éthylènes cette proférence est de 30, dans le cas des dialkyl-2,2 éthylènes elle est de 159. Dans ce dernier cas notons cependant que la proférence n'est pas stricte chaque fois qu'un groupement triptyle intervient dans la molécule.

Ces résultats nous encouragent à poursuivre notre recherche en vue de l'obtention d'une relation linéaire de topo-information suffisamment générale pour englober l'ensemble de la population des alcènes examinés dans le présent travail.

Certains alcènes ont été mis à notre disposition par le laboratoire de chimie organique physique (Professeur J. E. Dubois) de l'Université de Paris VII et nous tenons à le remercier ici.

1. J. H. Basso, D. Cabrol et R. Luft. Bull. Soc. Chim. Fr. 1338, 1342 (1973).
2. M. Podzimkova, M. Prochazka et M. Palacek. Collect. Czech. Chem. Commun **34**, 2101 (1969).
3. R. E. Kitson. Anal. Chem. **25**, 1470 (1953).
4. R. L. Werner et P. D. Lark. J. Chem. Soc. 1152 (1954).
5. L. M. Sverdlov. Proc. Akad. Sci. USSR, Phys. Chem. Sect. **112**, 109 (1957).
6. L. M. Sverdlov et M. G. Borissov. Izv. Akad. Nauk. SSSR, Ser. Fiz. **22**, 1023 (1958).
7. N. Sheppard et D. M. Simpson. Q. Rev. **6**, 1 (1952).
8. R. T. C. Bownlee, J. Munday, R. D. Topson et A. R. Katrisky. J. Chem. Soc. Far. Trans. II, **69**, 349 (1973).
9. R. Lanteri. Thèse de Spécialité, Université de Nice, Nice, France. 1971.
10. Atlas of spectral and physical constants for organic compounds. C.R.C. Press, Cleveland, Ohio. 1973.
11. Tables of wave numbers for the calibration of infrared spectrometers. I.U.P.A.C. Butterworths, London. 1961.
12. F. H. A. Rummens. Rec. Trav. Chim. Pays-Bas, **85**, 5 (1965); **85**, 1003 (1965).
13. G. J. Abruscato et T. T. Tidwell. J. Am. Chem. Soc. **92**, 4125 (1970).
14. D. G. Rea. Anal. Chem. **32**, 1638 (1960).
15. J. E. Dubois, D. Laurent et A. Aranda. J. Chim. Phys. 1608, 1616 (1973).
16. J. E. Dubois, A. Massat et Ph. Guillaume. J. Mol. Struct. **4**, 403 (1969).
17. G. Lenfant, M. Chastrette et J. E. Dubois. J. Chromatogr. Sci. **9**, 220 (1971).
18. J. E. Dubois et H. Herzog. Chem. Commun. 932 (1972).
19. Y. V. Linnik. Méthode des moindres carrés. éd. Dunod, Paris. 1963.
20. O. Exner. Coll. Czech. Chem. Commun. **31**, 3222 (1966).

Can. J. Chem. Downloaded from www.nrcresearchpress.com by 210.87.254.6 on 09/05/12
For personal use only.

Synthesis and Ion-exchange Properties of Tantalum Arsenate

J. P. RAWAT AND S. QASIM MUJTABA
Department of Chemistry, Aligarh Muslim University, Aligarh, (U.P.), India

Received November 5, 1974

J. P. RAWAT and S. QASIM MUJTABA. Can. J. Chem. 53, 2586 (1975).

A new inorganic ion-exchanger, tantalum arsenate, has been prepared under varying conditions. The exchanger prepared by mixing 0.1 *M* tantalum pentoxide and 0.1 *M* sodium arsenate in the ratio of 1:4 at p*H* 0 has been studied in detail for its ion-exchange capacity, p*H* titrations, and K_d values. The material can be prepared reproducibly. Its analytical importance has been established by the following quantitative separations: Zr^{4+} from Tm^{3+}, Zr^{4+} from Eu^{3+}, Pr^{3+} from Eu^{3+}, and Pr^{3+} from Tm^{3+}.

J. P. RAWAT et S. QASIM MUJTABA. Can. J. Chem. 53, 2586 (1975).

On a préparé, utilisant diverses conditions expérimentales, un nouvel échangeur d'ions de nature inorganique. On a étudié particulièrement l'échangeur préparé en mélangeant du pentoxyde de tantale 0.1 *M* et de l'arséniate de sodium 0.1 *M* dans un rapport de 1:4 à un p*H* de 0 afin de déterminer sa capacité pour échanger des ions, pour des titrations de p*H* et pour ses valeurs K_d. On peut reproduire la préparation de ce composé. On a établi son importance analytique en suivant la séparation quantitative du Zr^{4+} de Tm^{3+}, du Zr^{4+} de Eu^{3+}, du Pr^{3+} de Eu^{3+} et du Pr^{3+} de Tm^{3+}. [Traduit par le journal]

Introduction

In recent years, there has been a revived interest in the study of synthetic inorganic ion-exchangers, since they are unaffected by ionizing radiations, are less sensitive to higher temperatures, and are selective to certain ions and hence can be used for the separation of ions in varied conditions. A wide variety of inorganic ion-exchangers has been reviewed by Amphlett (1). The emphasis has been mainly on zirconium phosphate and zirconium oxide types. Vesely and Pekarek (2, 3) have given an exhaustive literature survey on the preparation, properties, and uses of the hydrous oxides, acidic salts of multivalent metals, insoluble ferrocyanides, and various other materials as inorganic ion-exchangers. The analytical applications of inorganic ion-exchangers have been reviewed by Inczedy (4) and Walton (5). A search of the literature shows that no such studies have been reported on tantalum arsenate. The present work was, therefore, undertaken to synthesize and to investigate the ion-exchange properties of this material. Some important separations have been achieved practically.

Experimental

Reagents

Tantalum pentoxide (BARC, India) and sodium arsenate (Riedel, Germany) were used. The rest of the reagents were of AnalaR grade.

Apparatus

p*H* measurements were made with an ELICO model LI-10 p*H* meter. An electric temperature controlled SICO shaker and Stanton thermobalance type H_4 were used for equilibrium and thermogravimetric studies respectively.

Synthesis

A number of samples were prepared under a range of conditions as given in Table 1. Sodium arsenate solutions were added to tantalum pentoxide solutions slowly with constant shaking. Sodium hydroxide solution was then added dropwise with constant shaking until the p*H* was zero. The precipitate was allowed to settle for 24 h at room temperature, and was then washed several times by decantation with distilled water, filtered, and dried at 40 °C. The dried material broke down into small particles when immersed in water. The exchanger was then converted to the hydrogen form by treatment with 2 *M* HNO_3. Finally it was washed several times with demineralized water and dried at room temperature.

Ion-exchange Capacity

Ion-exchange capacities of inorganic ion-exchangers depend upon the concentration and volume of the eluent, because they are weak cation exchangers. To determine the optimum concentration and volume for the measurement of ion-exchange capacity, 0.1, 0.5, 1.0, 2.0, 3.0, and 4.0 *M* solutions of potassium nitrate were used as eluent and the capacity (per gram exchanger) was determined by the volume of NaOH consumed for 250 ml effluent collected in 5 ml fractions. It was found that the optimum results are obtained with 1 *M* KNO_3, and almost all H^+ ions are eluted in the first 100 ml solution. Ion-exchange capacity of tantalum arsenate was also determined by eluting some uni- and bivalent cations. One molar solutions of NaCl, KCl, $Mg(NO_3)_2$, $Sr(NO_3)_2$ and $BaCl_2$ were taken as eluent for this purpose. The results are given in Table 2.

Can. J. Chem. Downloaded from www.nrcresearchpress.com by 210.87.254.42 on 09/05/12
For personal use only.

TABLE 1. Synthesis and properties of tantalum arsenates

Sample number	Tantalum pentoxide		Sodium arsenate		Mixing ratio V/V Ta:As	pH of the mixture	Ion-exchange capacity in mequiv./g	Chemical composition Ta:As
	Concentration (*M*)	pH	Concentration (*M*)	pH				
T(A)	0.1	Negative	0.1	0	1:4	0	1.09	2.80:1
T(B)	0.1	Negative	0.1	0	3:7	0	1.04	3.21:1
T(C)	0.1	Negative	0.1	0	7:3	0	0.54	20:1
T(D)	0.1	Negative	0.1	0	1:1	0	0.90	6.27:1
T(E)	0.1	Negative	0.1	0	1:4	1.0	1.00	2.50:1

TABLE 2. Ion-exchange capacity of tantalum arsenate sample T(A) using some uni- and bivalent cations

Metal ion	Capacity (mequiv./g)
Na^+	0.99
K^+	1.09
Mg^{2+}	1.09
Sr^{2+}	1.00
Ba^{2+}	1.18

The change of hydrogen liberation capacity in the course of absorption was studied up to 6 cycles with 2 *M* nitric acid as regenerant and 1 *M* potassium nitrate solution as eluent. The ion-exchange capacity changes from 1.09 to 1.02 mequiv./g after six cycles.

Chemical Composition

The well powdered exchanger (TaAs, 200 mg) was dissolved in 10 ml of hot concentrated sulfuric acid. Arsenate was estimated volumetrically (6) and tantalum was determined gravimetrically as the cupferron precipitate (7) from the exchanger solution containing 5% tartaric acid and 10% H_2SO_4 (8). The results are given in Table 1.

Stability

All the samples were apparently stable in water and mineral acids. They were, however, attacked by hot concentrated sulfuric acid. All the samples were completely dissolved in concentrated sulfuric acid when heated with ammonium sulfate.

pH Titrations

pH titrations were performed on sample T(A) for LiCl–LiOH, NaCl–NaOH, KCl–KOH, and NH_4Cl–NH_4OH as described earlier (9). The curves are shown in Fig. 1.

Reproducibility Test

To check the reproducibility of the exchanger, four samples of T(A) were prepared under similar conditions and their ion-exchange capacity and chemical composition were determined. All four samples gave the same exchange capacities and the same Ta:As ratios to within 1%.

Thermal Treatment

Thermogravimetric analysis of sample T(A) in H^+ and K^+ form was performed at a heating rate of 4°/min (Fig. 2). To examine the effect of drying temperature on the ion-exchange capacity, the sample T(A) was also dried at various temperatures in a muffle furnace for 2 h. The results are given in Table 3.

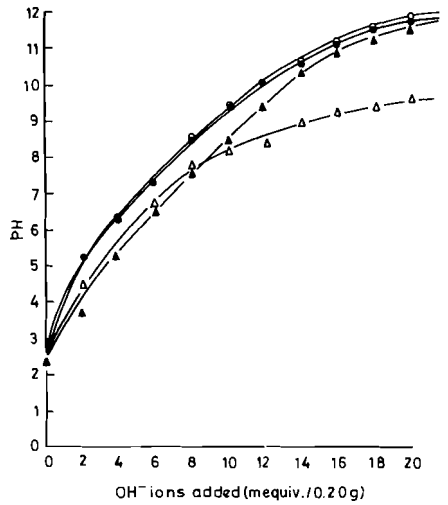

FIG. 1. pH titration curve of tantalum arsenate: ●, LiOH; ▲, NaOH; ○, KOH; △, NH_4OH.

Distribution Coefficients

In order to examine the affinity of tantalum arsenate towards various metal ions, distribution coefficients for 32 cations were determined at pH 1, pH 2, and in 1%

TABLE 3. Ion-exchange capacity of sample T(A) dried at different elevated temperatures

Temperature (°C)	Capacity (mequiv./g)
40	1.08
100	0.95
200	0.50
300	0.12
400	0.06
500	0.07
600	0.06
700	0.05

Can. J. Chem. Downloaded from www.nrcresearchpress.com by 210.87.254.42 on 09/05/12
For personal use only.

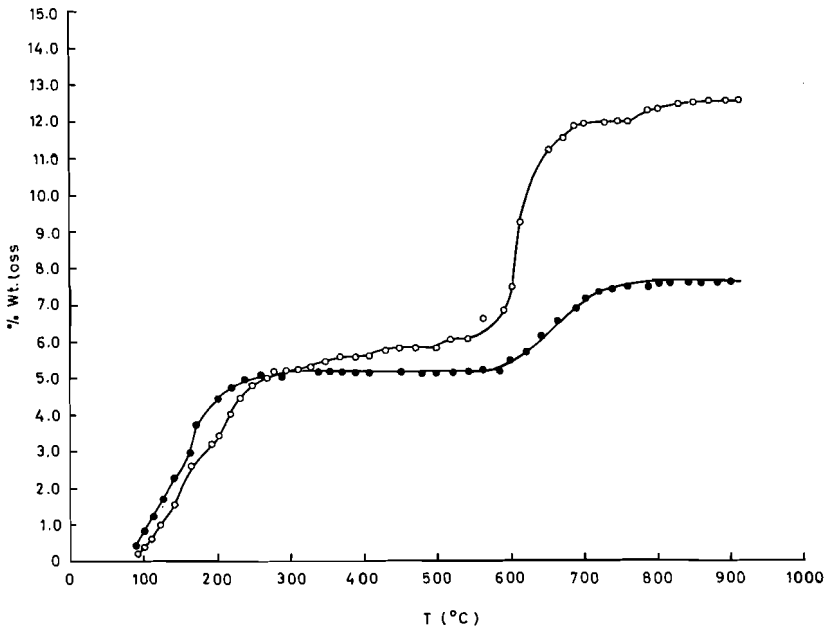

FIG. 2. Thermogravimetric analysis of sample T(A) in H^+ and K^+ form: ○, exchanger in H^+ form; ●, exchanger in K^+ form.

TABLE 4. Distribution coefficients (ml/g) of cations on tantalum arsenate (TA)

Cations	p*H* 2	p*H* 1	1% NH_4NO_3	Cations	p*H* 2	p*H* 1	1% NH_4NO_3
In^{3+}	444	426	24.0	Er^{3+}	300	91	—
Al^{3+}	348	29	175	Eu^{3+}	11.7	16.0	—
Ga^{3+}	—	190	480	Tb^{3+}	336	83	—
Fe^{3+}	350	117	160	Sm^{3+}	376	89	
Ni^{2+}	350	33.0	7.0	Y^{3+}	477	87	
Vo^{2+}	T.A.*	T.A.*	—	Gd^{3+}	330	—	
Co^{2+}	11.2	1.20	4.0	Hf^{4+}	T.A.*	T.A.*	
Pb^{2+}	540	350	44.0	Zr^{4+}	T.A.*	T.A.*	
Cu^{2+}	—	8.20	118	Ce^{3+}	1360	542	
Hg^{2+}	—	25.2	—	Pr^{3+}	1380	T.A.*	
Sr^{2+}	64	2.30	15.0	Ho^{3+}	305	105	
Ba^{2+}	122	18.2	43.0	Nd^{3+}	370	129	
Ca^{2+}	52	13.0	24.0	Tm^{3+}	73	70	
Mg^{2+}	29	4.50	24.0	Dy^{3+}	652	102	
Zn^{2+}	—	3.00	24.0	Lu^{3+}	520	63.2	
Mn^{2+}	77.0	0.00	42.0	La^{3+}	516	73.6	

*T.A. = total absorption.

NH_4NO_3 solution. The concentration of cation solutions was taken as ~3% of the total ion-exchange capacity of the exchanger. In all the cases 0.5 g of the exchanger in H^+ form was taken and the equilibrating temperatures and time were 18 ± 2 °C and 6 h respectively. The results are summarized in Table 4.

Quantitative Separations of Metal Ions on Tantalum Arsenate Sample T(A) Column

For separation studies, a glass column was filled with TaAs in the H^+ form on a glass wool support. The flow rate was 8–10 drops/min. The metal ions in 10 ml fractions of the effluent were estimated by titration with 0.002 *M* EDTA. On the basis of a large difference in K_d values (separation factor > 10), some separations were tried. Those practically achieved quantitatively are listed in Table 5.

Discussion

The results given in Table 1 show that the ion-exchange capacity of sample T(A) is highest, therefore, all the studies were made on this sample. The results given in Table 2 show that

Can. J. Chem. Downloaded from www.nrcresearchpress.com by 210.87.254.42 on 09/05/12
For personal use only.

TABLE 5. Quantitative separations of metal ions on tantalum arsenate, T(A), column

Separation	Eluents	Volume of effluent (ml)	Amount of cation loaded (μg)	Amount of cation recovered (μg)
Tm^{3+}–Zr^{4+}	Tm^{3+} – 0.05 *N* HNO_3	90	686	692
	Zr^{4+} – 0.5 *N* HNO_3 + 0.5 *N* NH_4NO_3	100	365	328
Tm^{3+}–Pr^{3+}	Tm^{3+} 0.05 *N* HNO_3	90	686	710
	Pr^{3+} 0.5 *N* HNO_3	80	394	423
Eu^{3+}–Pr^{3+}	Eu^{3+} 0.05 *N* HNO_3	110	486	425
	Pr^{3+} 0.5 *N* HNO_3	110	394	459
Eu^{3+}–Zr^{4+}	Eu^{3+} 0.05 *N* HNO_3	110	486	456
	Zr^{4+} 0.5 *N* HNO_3 + 0.5 *N* NH_4NO_3	110	365	383

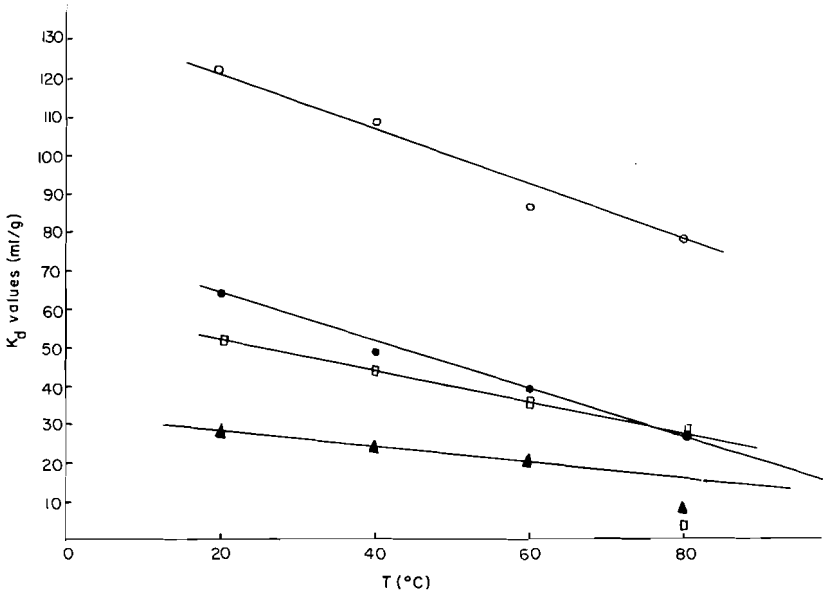

FIG. 3. Distribution coefficients as a function of temperature: ○, Ba^{2+}; ●; Sr^{2+}; □, Ca^{2+}; ▲, Mg^{2+}.

tantalum arsenate can be used as a good ion-exchanger for quantitative purposes. The ion-exchange capacity does not vary with the nature of the cation if concentration is ≥ 1 *M*. The lower value of ion-exchange capacity when the eluent taken is less than 1 *M* is observed because tantalum arsenate works as a monofunctional weak acid in H^+ form (Fig. 1), and is weakly ionized. Hence the removal of H^+ ions by salt is not complete if its concentrations are not high enough. The ion-exchange reaction is

$$RH^+ + NaNO_3 \rightleftharpoons RNa^+ + HNO_3$$

where RH^+ represents the ion-exchanger in hydrogen form and RNa^+ in sodium form. By increasing the $NaNO_3$ concentration the reaction will be favored in the forward direction and a saturation stage nearly at complete exchange of H^+ is reached at 1 *M* concentration of the salt. Tantalum arsenate shows a quantitative reversible ion-exchange behavior. The ion-exchange capacity remains nearly constant if it is measured in the regeneration cycles. A change of only 0.07 mequiv./g was observed after sixth regeneration. The exchanger can be prepared reproducibly. The chemical composition and

Can. J. Chem. Downloaded from www.nrcresearchpress.com by 210.87.254.42 on 09/05/12
For personal use only.

the ion-exchange capacity of four different samples prepared under the same conditions were nearly the same.

Heat treatment of tantalum arsenate in air on a thermobalance (Fig. 2) shows that up to 100 °C there is not much loss in weight. From 100 to 250 °C a continuous loss in weight is recorded which is due to the removal of water present in the layers of the material. At 250 °C a 5% weight loss is recorded. From 250 to 600 °C there is no appreciable weight loss and the ion-exchange capacity within this range is hardly diminished. Further heating of the material from 600 to 700 °C shows a slight weight loss (2%) in K^+ form and much more weight loss (7%) in H^+ form. This may be due to the removal of structural water after condensation which is possible in H^+ form only and not in K^+ form. The studies on composition determination show that different samples are prepared with different tantalum and arsenic ratios. The sample T(A) which has been used for most of the studies has Ta:As ratio of 2.8:1. A study of distribution coefficients of numerous metal ions in three solvent systems *viz.*, HNO_3 system (p*H* 1, p*H* 2) and 1% NH_4NO_3 solution reveals that tantalum arsenate is very selective towards certain metal ions. The relatively large K_d values for Zr^{4+}, Hf^{4+}, Pr^{3+}, Vo^{2+}, and Ce^{3+} are very useful as these metal ions can be separated from numerous other metal ions. Separations of Tm^{3+} from Zr^{4+}, Tm^{3+} from Pr^{3+}, Eu^{3+} from Pr^{3+}, and Eu^{3+} from Zr^{4+} were quantitatively achieved (Table 5). Various other separations can be tried on the basis of the difference in K_d values. This shows the application of this exchanger in separation science for particular problems. An interesting point is noted when K_d values of alkaline earth metal ions at different equilibrating temperatures are plotted as a function of temperature (Fig. 3). The K_d value decreases linearly with rise in temperature. This behavior may be applied to thermodynamic studies.

The authors are grateful to Prof. W. Rahman for research facilities.

1. C. B. AMPHLETT. Inorganic ion-exchangers. Elsevier Publishing Company, New York. 1964.
2. V. VESELY and V. PEKAREK. Talanta, **19**, 219 (1972).
3. V. PEKAREK and V. VESELY. Talanta, **19**, 1245 (1972).
4. J. INCZEDY. Analytical application of ion-exchangers. Pergamon Press, New York. 1966.
5. H. F. WALTON. Anal. Chem. **46**, 398R (1974).
6. N. H. FURMAN. Standard methods of chrmical analysis. Vol. 1. 6th ed. D. Van Nostrand Co., New York. 1963.
7. G. E. F. LUNDELL and J. I. HOFFMAN. Outlines of methods of chemical analysis. Wiley and Sons, Inc., N.Y. 1958. p. 117.
8. G. E. F. LUNDELL, H. A. BRIGHT, and J. I. HOFFMAN. Applied inorganic analysis. 2nd ed. John Wiley and Sons, Inc., New York. 1953.
9. N. E. TOPP and K. W. PEPPER. J. Chem. Soc. 3299 (1949).

Can. J. Chem. Downloaded from www.nrcresearchpress.com by 210.87.254.42 on 09/05/12
For personal use only.

Volumes and Heat Capacities of Cyclic Ethers and Amines in Water and of some Electrolytes in these Mixed Aqueous Solvents

OSAMU KIYOHARA, GÉRALD PERRON, AND JACQUES E. DESNOYERS[1]

Department of Chemistry, Université de Sherbrooke, Sherbrooke, Québec, J1K 2R1

Received April 3, 1975

OSAMU KIYOHARA, GÉRALD PERRON, and JACQUES E. DESNOYERS. Can. J. Chem. **53**, 2591 (1975).

The densities and volumetric specific heats of *p*-dioxane, tetrahydropyran, morpholine, piperidine, and piperazine were measured in water at 25 °C with a flow densimeter and a flow microcalorimeter. The same properties were also determined for LiCl, NaCl, Me_4NBr, and Bu_4NBr at 0.1 *m* in dioxane–water, morpholine–water, and piperidine–water mixtures. The derived apparent molal volumes and heat capacities of the nonelectrolytes in water and the transfer functions of the electrolytes from water to the mixed solvent suggest that all the present cyclic amines and ethers are hydrophobic; the overall structural influence is very small with dioxane and large with piperidine.

OSAMU KIYOHARA, GÉRALD PERRON et JACQUES E. DESNOYERS. Can. J. Chem. **53**, 2591 (1975).

Les masses volumiques et capacités calorifiques du *p*-dioxanne, du tétrahydropyranne, de la morpholine, de la pipéridine et de la pipérazine ont été mesurées dans l'eau à 25 °C avec un densimètre et un microcalorimètre à écoulement continu. Les mêmes propriétés ont aussi été obtenues pour LiCl, NaCl, Me_4NBr et Bu_4NBr à 0.1 *m* dans les mélanges eau–dioxanne, eau–morpholine et eau–pipéridine. Les capacités calorifiques et volumes apparents molaires des nonélectrolytes dans l'eau et les fonctions de transfert des électrolytes de l'eau aux solvants mixtes suggèrent que tous les amines et éthers cycliques présentement étudiés sont hydrophobes; l'effet structural global est très faible dans le cas du dioxanne et très marqué pour la pipéridine.

Introduction

Dioxane–water mixtures have been extensively used as a mixed solvent for the study of electrolyte solutions, primarily because of the large range of dielectric constants that can be achieved with these mixtures. Even with its low dielectric constant and dipole moment, dioxane interacts strongly with water and with ions as a result of its high quadrupole moment. Despite the numerous studies on binary and ternary systems involving *p*-dioxane and similar nonelectrolytes, much controversy still exists in the literature on the nature of the interactions between *p*-dioxane and water (1–6).

We felt that probably some progress could be made through a systematic study of the thermodynamic properties of mixed aqueous solvents, where the cosolvents would have similar geometries and molecular weights. For this purpose, the cyclic ethers and amines were examined:

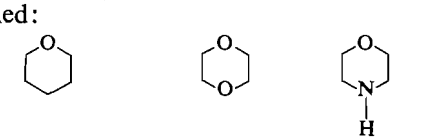

Tetrahydropyran (THP) | *p*-Dioxane (D) | Morpholine (M)

[1]To whom correspondence should be addressed.

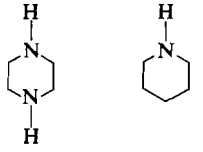

Piperazine (PZ) | Piperidine (PD)

The largest difference in molecular weight is 3. We can therefore expect that the intrinsic thermodynamic values (volume, heat capacity) of these solutes in water would be, at least as a first approximation, constant. The observed difference in properties from one solute to another should therefore reflect mostly the differences in interactions. For completeness, it would have been useful to add cyclohexane to this study, but its low solubility made this impossible.

In addition to the properties of these solutes in water, the properties of typical electrolytes in these mixed solvents were also measured whenever the solubility of the cosolvent was sufficiently large. The electrolytes chosen were LiCl, NaCl, Me_4NBr, and Bu_4NBr: NaCl is the most studied alkali halide in ternary systems, Li^+ is probably the only alkali ion with a fairly stable hydration shell, Me_4N^+ is a weak structure breaker, and Bu_4N^+ is an hydrophobic ion.

Can. J. Chem. Downloaded from www.nrcresearchpress.com by 210.87.254.40 on 09/05/12
For personal use only.

Can. J. Chem. Downloaded from www.nrcresearchpress.com by 210.87.254.40 on 09/05/12
For personal use only.

The properties we have chosen to initiate this investigation are the apparent molal volumes ϕ_V and heat capacities ϕ_C. These properties are now readily available experimentally and have been shown to be sensitive to changes in solute–solvent and solute–solute interactions. Some ϕ_V (2, 7, 8) and ϕ_C (2, 3, 9) data exist in the literature for the present binary and ternary systems, but often the concentration ranges studied were too limited or the precision too low to allow us to use the data. Also, it is not advisable to calculate transfer functions from water to a mixed solvent using properties of the mixed solvents or properties of the electrolytes which have been obtained with a different technique.

Similar studies in urea–water (10), *tert*-butyl alcohol – water (11), dimethylsulfoxide–water, and acetone–water (12) mixtures, and a comparative study of these various mixed aqueous solvents (13) are given elsewhere.

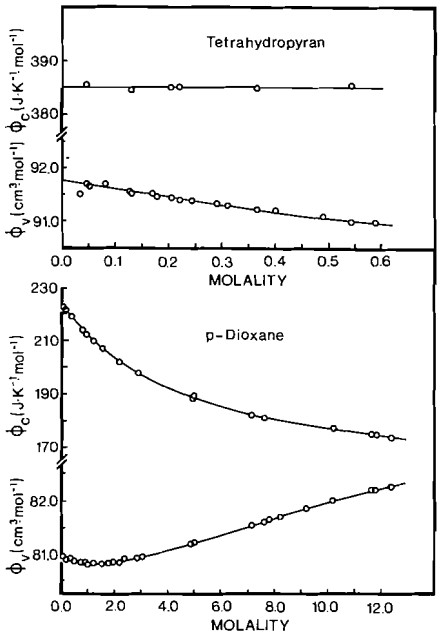

FIG. 1. Apparent molal volumes and heat capacities of *p*-dioxane and tetrahydropyran in water at 25 °C.

Experimental

The nonelectrolytes were purified as follows: PD and D (Fisher Certified Reagent) were dried with a molecular sieve (Davidson Chemical, grade 564, 3 Å), M (Practical grade, Baker Chem. Co.) was distilled (b.p. 129.5 °C) and dried with a molecular sieve, THP (98%, Aldrich Chem. Co.) was passed through M.N. Silica gel G (Macherey, Nagel and Co, D-516 Düssen, Germany), distilled (b.p. 89.0 °C) and dried with a molecular sieve, PZ (Practical grade, Eastman Kodak Co.) was recrystallized three times from benzene and dried under vacuum. Considerable care was taken to protect D and PZ from exposure to light and THP to air prior to use.

The origin and purification of the salts (LiCl, NaCl, Me_4NBr, and Bu_4NBr) were given elsewhere (14). All solutions were prepared by weight with deionized (Continental Deionized Water System) distilled water. All measurements were made at 25.00 ± 0.01 °C.

The densities d and volumetric specific heats σ were measured with a flow digital densimeter (15) and a flow microcalorimeter (16). The precision and method of calculating ϕ_V and ϕ_C of the ternary systems were discussed in the case of *tert*-butyl alcohol mixed solvents (11).

The densities and volumetric specific heats of the binary systems were measured over a wide-range of concentration[2] and the dependence on molality m of ϕ_V and ϕ_C of the nonelectrolytes are shown in Figs. 1 to 4. Significant hydrolysis occurs with the cyclic amines, and consequently the ϕ_V and ϕ_C were also measured in 0.1 N

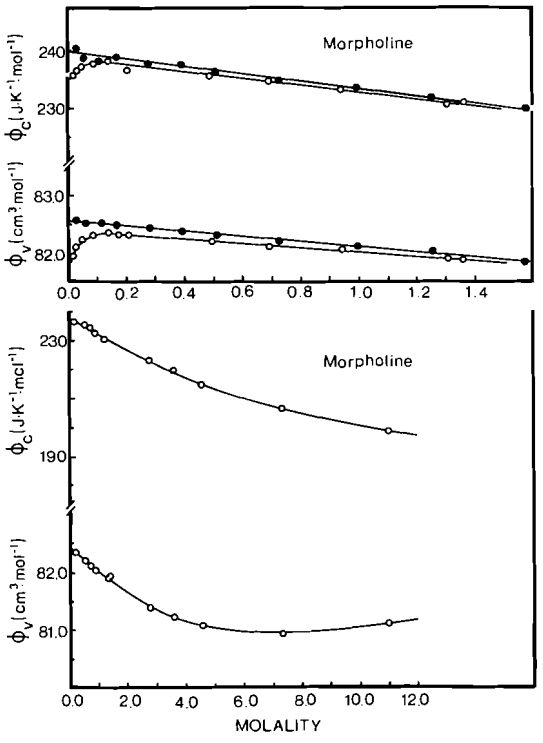

FIG. 2. Apparent molal volumes and heat capacities of morpholine in water and 0.1 N NaOH solvents at 25 °C: ○, water; ●, 0.1 N NaOH.

[2]Complete set of the actual experimental data is available, at a nominal charge, from the Depository of Unpublished Data, CISTI, National Research Council of Canada, Ottawa, Canada K1A 0S2.

Can. J. Chem. Downloaded from www.nrcresearchpress.com by 210.87.254.40 on 09/05/12
For personal use only.

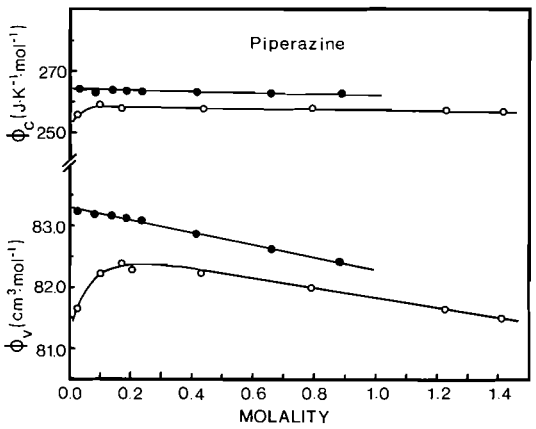

FIG. 3. Apparent molal volumes and heat capacities of piperazine in water and 0.1 *N* NaOH solvent at 25 °C: ○, water; ●, 0.1 *N* NaOH.

NaOH solution. The presence of NaOH essentially removes the sharp increase in ϕ_C and ϕ_V at low concentrations and shifts the overall ϕ_V and ϕ_C curves to higher values. As a further check, an hydrolysis correction was calculated for the PD–water system using the data and the equations given by Cabani *et al.* (7). The ϕ_V calculated for the unhydrolyzed PD are compared with those in 0.1 *N* NaOH solvent in Fig. 4. The agreement is satisfactory considering that the hydrolysis correction depends significantly on the choice of the hydrolysis constant (7). We are therefore justified in considering the data in 0.1 *N* NaOH to be close to those we would obtain for unhydrolyzed amines, and that the linear region of the ϕ_V and ϕ_C curves can be extrapolated to infinite dilution to obtain the standard $\bar{V}^0$ (= ϕ_V^0) and $\bar{C}_p^0$ (= ϕ_C^0). The ϕ_V and ϕ_C data were fitted with a parametric equation in molality

$$[1] \qquad \phi_Y = \phi_Y^0 + A_Y m + B_Y m^2 + \ldots,$$

where the symbol Y stands for V and C_p. The parameters of [1] are given in Table 1, and the standard literature values are also included for comparison. In general, the agreement between the present ϕ_V^0 data and those from the literature is excellent, but the deviations are larger with ϕ_C^0. As it will be shown in the Discussion, the group additivity gives us confidence in the reliability of the present ϕ_C data.

The standard transfer functions of the electrolyte E from water W to a water–nonelectrolyte mixture W + N are defined by

$$[2] \quad \Delta Y_E^0(W \rightarrow W + N) = \phi_Y^0(W + N) - \phi_Y^0(W)$$

It was established previously (11) that the transfer functions of an 0.1 *m* electrolyte are very close to the infinite dilution value. Therefore, ϕ_Y were measured at 0.1 *m* only.[2] The corresponding ϕ_Y data in pure water were taken from the literature: ϕ_C of LiCl and NaCl (18), of Me_4NBr and Bu_4NBr (19), ϕ_V of LiCl and NaCl (14), and of Me_4NBr and Bu_4NBr (20).

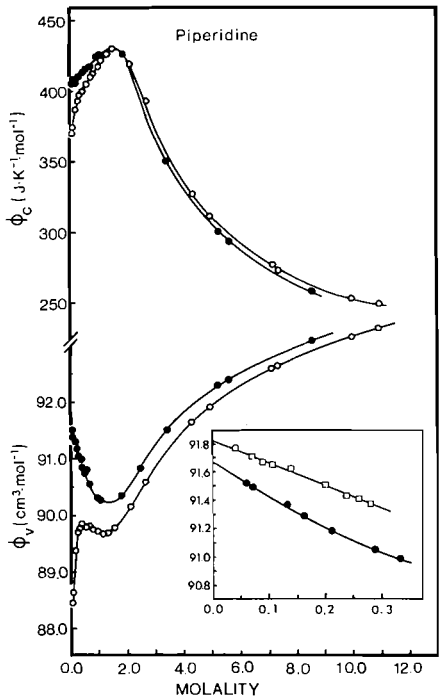

FIG. 4. Apparent molal volumes and heat capacities of piperidine in water and 0.1 *N* NaOH solvent at 25 °C: ○, water; ●, 0.1 *N* NaOH; □, corrected ϕ_V (K_a = 1.39×10^{-3}) for the hydrolysis effect at low concentration (*cf.* ref. 7).

The transfer functions of the various electrolytes from W to W–D, W–M, and W–PD are shown in Figs. 5 to 7. The solubilities in water of THP and PZ were too low to warrant measurements on the ternary systems. The effect of hydrolysis on the transfer functions was investigated in the case of NaCl and Bu_4NBr in W–PD mixtures by repeating the measurements in 0.1 *N* NaOH. These are shown in Fig. 7. As with the binary systems, a general shift in the curves is observed, but the general trends are essentially the same. Therefore, as long as only trends are examined, the effect of hydrolysis on the transfer functions can be ignored.

Discussion

Group Additivity

One of the aims of systematic studies of organic solutes is to devise methods of predicting the thermodynamic properties of large molecules from additivity rules. The present family of nonelectrolytes leads itself readily to study the additivity of various groups to the $\bar{V}^0$ and $\bar{C}_p^0$ of cyclic molecules in water. From the five compounds investigated there are various ways of calculating the group contributions. For

Can. J. Chem. Downloaded from www.nrcresearchpress.com by 210.87.254.40 on 09/05/12
For personal use only.

TABLE 1. Apparent molal volumes and heat capacities of cyclic ethers and amines in water at 25 °C. Parameters of [1] for ϕ_V and ϕ_C given in $cm^3\ mol^{-1}$ and $J\ K^{-1}\ mol^{-1}$

Solute	$\bar{V}^0$	A_V	B_V	Maximum concentration	$\bar{C}_p^0$	A_C	B_C	C_C	Maximum concentration
D	80.94	−0.172	0.061	1.5	222.4	-11.5_8	1.106	−0.0395	12
	80.96*				212§				
	81.1†								
THP‖	91.74	−1.79	0.705	0.5	384.9	0.6_1			0.5
	91.73*				373§				
	91.8†								
M(0.1 *N* NaOH)	82.54	−0.478		1.4	239.4	-6.5_0			1.4
PZ(0.1 *N* NaOH)	83.31	−1.01		0.9	263.8	-1.4_4			0.9
PD(0.1 *N* NaOH)	91.65	−2.42	1.18	0.7	405.0	16.8_7			0.7
	91.97*				424§				
	91.1‡								

*Cabani *et al.* (7).
†Franks *et al.* (2).
‡Laliberté and Conway (8).
§Cabani *et al.* (9).
‖As with all volatile solutes special precautions must be taken to prevent evaporation during the measurements (17).

Can. J. Chem. Downloaded from www.nrcresearchpress.com by 210.87.254.40 on 09/05/12
For personal use only.

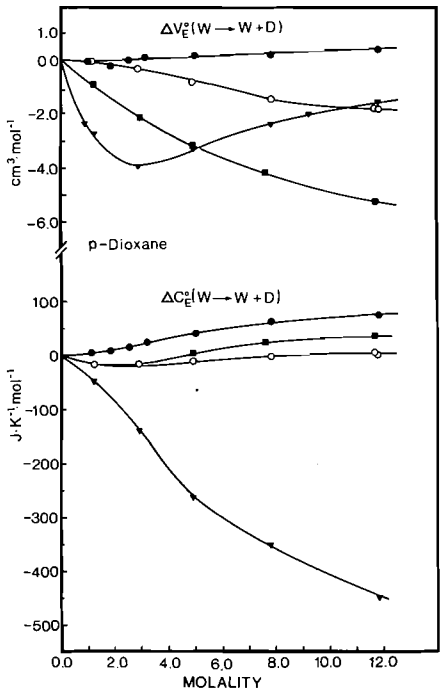

FIG. 5. Volumes and heat capacities of transfer of electrolytes at 0.100 *m* from water to water–*p*-dioxane mixtures at 25 °C: ○, LiCl; ●, NaCl; ■, Me_4NBr; ▼, Bu_4NBr.

example

$$\bar{V}^0(\text{—}CH_2\text{—}) = \tfrac{1}{6}\{2\bar{V}^0(\text{THP}) - \bar{V}^0(\text{D})\}$$
$$= \tfrac{1}{6}\{2\bar{V}^0(\text{PD}) - \bar{V}^0(\text{PZ})\}$$
$$\bar{V}^0(\text{—O—}) = \bar{V}^0(\text{D}) - \bar{V}^0(\text{THP}) + \bar{V}^0(\text{—}CH_2\text{—})$$
$$= \bar{V}^0(\text{M}) - \bar{V}^0(\text{PD}) + \bar{V}^0(\text{—}CH_2\text{—})$$

The values for each group obtained by a least-squares method are

	$\bar{V}^0$ (cm³ mol⁻¹)	$\bar{C}_p^0$ (J K⁻¹ mol⁻¹)
—CH_2—	16.9	91
—NH—	7.9	−51
—O—	7.0	−72

with a mean deviation for $\bar{V}^0$ of 0.4 cm³ mol⁻¹ and for $\bar{C}_p^0$ of 1 J K⁻¹ mol⁻¹.

The $\bar{C}_p^0$ of the five nonelectrolytes can be predicted to 1 J K⁻¹ mol⁻¹ with these values which is inside the experimental error. This test for additivity is therefore a good indication of the reliability of the present measurements. It is interesting to note that the methylene contribution is very similar to that of linear chains (*cf.* 21) which implies that cyclization has little effect on $\bar{C}_p^0$ with six-membered rings. On the other hand increasing or decreasing the ring size from six causes a significant decrease in $\bar{C}_p^0$(—CH_2—) (22). This suggests that six-membered ring molecules or ions have a geometry which is as compatible with the structure of water as a linear chain.

The additivity is not quite as good with $\bar{V}^0$ since experimentally $\bar{V}^0$ should be reliable to better than 0.1 cm³ mol⁻¹. Also $\bar{V}^0$(—CH_2—) is about 1 cm³ mol⁻¹ larger than that for linear chains (23). It could be that the addition of 0.1 *N* NaOH has a larger effect on $\bar{V}^0$ than on $\bar{C}_p^0$. Here again a change in the ring size causes a large decrease in the average $\bar{V}^0$(—CH_2—) (22). It therefore seems that $\bar{V}^0$ is more sensitive than $\bar{C}_p^0$ to geometrical and position factors. For example, the $\bar{V}^0$ of an α CH_2 group of homologous aliphatic ions is often different from those

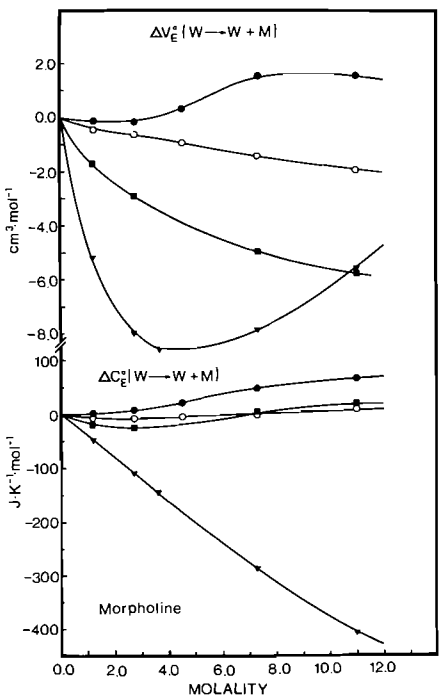

FIG. 6. Volumes and heat capacities of transfer of electrolytes at 0.100 *m* from water to water–morpholine mixtures at 25 °C: ○, LiCl; ●, NaCl, ■, Me_4NBr; ▼, Bu_4NBr.

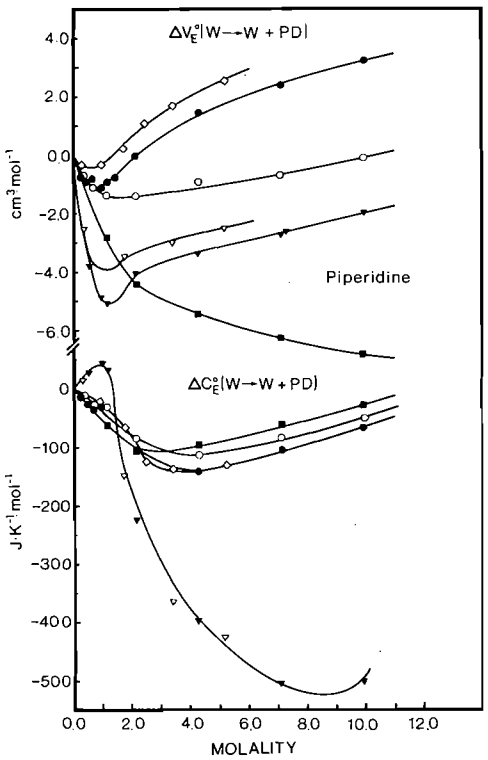

FIG. 7. Volumes and heat capacities of transfer of electrolytes at 0.100 *m* from water to water–piperidine mixtures and of NaCl and Bu_4NBr at 0.100 *m* from 0.1 *N* NaOH to 0.1 *N* NaOH–piperidine mixtures at 25 °C: ○, LiCl; ●, NaCl; ◇, NaCl (0.1 *N* NaOH); ■, Me_4NBr; ▼, Bu_4NBr; ▽, Bu_4NBr (0.1 *N* NaOH).

further away from the charge (23, 24), which is not the case with $\bar{C}_p^0$ (21).

Binary Systems

An examination of the standard functions $\bar{V}^0$ and initial slopes A_Y of the cyclic nonelectrolytes in Table 1 shows definite trends in the direction D → M → PZ → THP → PD; $\bar{V}^0$, $\bar{C}_p^0$, and A_C generally increase in value while A_V decreases. Similarly, the group contribution to $\bar{V}^0$ and $\bar{C}_p^0$ increased in the order —O—, —NH—, and $—CH_2—$.

It is not easy to interpret small changes in $\bar{V}^0$, especially when polar groups are involved (2). However, the other trends suggest that there is a large decrease in hydrophobic (or increase in hydrophilic) character when a $—CH_2—$ group is replaced by —NH— and a further small change when —NH— is replaced by an ether group. This tendency is not unexpected since, although —NH— and —O— are both polar groups, the ether group should interact more strongly with water, in view of the larger electronegativity of the oxygen atom.

The magnitude of $\bar{C}_p^0$ and concentration dependence of ϕ_V and ϕ_C of PD (Fig. 4) are typical of strong hydrophobic solutes (11); there seems to be some association similar to micellization starting at about 1.5 *m* and a characteristic maximum in ϕ_C and minimum in ϕ_V. At the other extreme, D shows a much smaller effect on water; ϕ_C^0 is still larger than the molar heat capacity of pure D (25) by about 40% suggesting that D is hydrophobic in agreement with the excess enthalpy data (26). On the other hand, little can be said about the excess functions. At high concentrations, ϕ_V and ϕ_C are tending in a very gradual way to their intrinsic values. There are some solute–solute interactions making a negative contribution to both excess functions but the effects are too small to allow an unambiguous interpretation. Therefore D is probably an hydrophobic solute but the overall structural interactions are certainly quite small. Similar conclusions can be drawn with M.

Ternary Systems

It has been shown recently (11) that the standard transfer functions $Y_E^0(W \rightarrow W + N)$ can be interpreted in terms of solute–solute interactions between E and N. At low cosolvent concentration, where only pair interactions are important, the dependence of $Y_E^0(W \rightarrow W + N)$ on the N concentration is numerically equal to the dependence of the converse standard transfer function $Y_N^0(W \rightarrow W + E)$ on E concentration (13, 27, 28).

The concentration dependence of the transfer functions $\Delta Y_E^0(W \rightarrow W + PD)$ are qualitatively the same as $\Delta Y_E^0(W \rightarrow W +$ *tert*-butyl alcohol). Again we find the maximum in heat capacities and minimum in volumes characteristic of strong hydrophobic interactions with Bu_4NBr; Bu_4N^+ probably associates with PD at high cosolvent concentrations. The trends with hydrophilic electrolytes also indicate strong hydrophilic–hydrophobic interactions at low concentration (11) and enhanced hydrophobic bonding of PD near an hydrophilic electrolyte through salting-out of the monomers.

At the other extreme, $\Delta Y_E^0(W \rightarrow W + D)$ shows very little specific interaction if we consider that at high D concentration $\Delta Y_E^0(W \rightarrow W + D)$ is tending to $\Delta Y_E^0(W \rightarrow D)$. In pure D,

Can. J. Chem. Downloaded from www.nrcresearchpress.com by 210.87.254.40 on 09/05/12
For personal use only.

Can. J. Chem. Downloaded from www.nrcresearchpress.com by 210.87.254.40 on 09/05/12
For personal use only.

$\bar{C}_p^0$ of hydrophilic solutes should be more positive (loss of structure-breaking effect) and those of hydrophobic solutes more negative. If data for $\bar{Y}^0$ were available in pure D we would be able to calculate the nonideal contribution to $\Delta Y_E^0(W, D \rightarrow W + D)$ from ref. 29

$$\bar{Y}_E^0(W + D) - X_D\bar{Y}_E^0(D) - (1 - X_D)\bar{Y}_E^0(W)$$

where X_D is the mole fraction of D. The sign of this nonideal contribution can still be seen if we assume that at high cosolvent concentration $\Delta Y_E^0(W \rightarrow W + D)$ is tending to the ideal behavior. If this is done, then the deviations in Fig. 5 are in the direction of weak hydrophobic–hydrophobic interactions with Bu_4NBr and weak hydrophobic–hydrophilic ones with the other electrolytes. The only anomaly is $\Delta V^0_{Bu_4NBr}(W \rightarrow W + D)$ which seems to suggest rather important hydrophobic–hydrophobic interactions. The $\Delta Y_E^0(W \rightarrow W + M)$ are qualitatively the same as $\Delta Y_E^0(W \rightarrow W + D)$ but as expected from the slightly more hydrophobic character of M, the trends are somewhat more pronounced.

The deductions based on the data for binary and ternary systems are consistent and suggest that probably all the presently studied cyclic ethers and amines are hydrophobic, although the net effect is very small with D. It therefore seems that the charge–dipole interactions between a simple hydrophilic ion and water are not too different from the ones between an ion and the oxygen of one-half of the D molecule (30). Even Li^+ which is usually considered highly hydrated shows little preference between the two solvents. It is only in the long-range ordering of the solvent that some differences are observed. This therefore confirms that, with properties that are not too sensitive to structural changes, the D + W system is ideal to study the effect of dielectric constant on long-range solute–solute interactions.

We are grateful to Environment Canada and to the Defence Research Board of Canada for financial assistance.

1. G. Lee and J. Jonas. J. Chem. Phys. **59**, 4845 (1973).
2. T. Franks, M. A. J. Quickenden, D. S. Reid, and B. Watson. Trans. Faraday Soc. **66**, 582 (1970).
3. R. K. Mohanty, T. S. Sarma, S. Subramanian, and J. C. Ahluwalia. Trans. Faraday Soc. **67**, 305 (1971).
4. C. J. Clemett. J. Chem. Soc. A, 455, 458, 761 (1969).
5. R. L. Kay and T. C. Broadwater. Electrochim. Acta, **16**, 667 (1971).
6. A. Ben-Naim and G. Moran. Trans. Faraday Soc. **61**, 82 (1965).
7. S. Cabani, G. Conti, and L. Lepori. J. Phys. Chem. **76**, 1338 (1972).
8. L. H. Laliberté and B. E. Conway. J. Phys. Chem. **74**, 4116 (1970).
9. S. Cabani, G. Lonti, A. Martinelli, and E. Matteoli. Proceedings of the 3rd International Conference on Thermodynamics, Vol. 3. Austria. 1973. p. 157.
10. P. R. Philip, J. E. Desnoyers, and A. Hade. Can. J. Chem. **51**, 187 (1973); N. Desrosiers, G. Perron, J. G. Mathieson, B. E. Conway, and J. E. Desnoyers. J. Solution Chem. **3**, 789 (1974).
11. L. Avédikian, G. Perron, and J. E. Desnoyers. J. Solution Chem. **4**, 331 (1975).
12. O. Kiyohara, G. Perron, and J. E. Desnoyers. Can. J. Chem. In press.
13. J. E. Desnoyers, O. Kiyohara, G. Perron, and L. Avédikian. To be published.
14. J. E. Desnoyers, M. Arel, G. Perron, and C. Jolicoeur. J. Phys. Chem. **73**, 3346 (1969); J. E. Desnoyers and G. Perron. J. Solution Chem. **1**, 199 (1972).
15. P. Picker, E. Tremblay, and C. Jolicoeur. J. Solution Chem. **3**, 377 (1974).
16. P. Picker, P. A. Leduc, P. R. Philip, and J. E. Desnoyers. J. Chem. Thermodyn. **3**, 631 (1971).
17. C. Jolicoeur, P. Picker, and G. Perron. To be published.
18. J. L. Fortier, P. A. Leduc, and J. E. Desnoyers. J. Solution Chem. **3**, 323 (1974).
19. P. R. Philip and J. E. Desnoyers. J. Solution Chem. **1**, 353 (1972).
20. G. Perron and J. E. Desnoyers. J. Chem. Eng. Data, **17**, 136 (1972).
21. P. A. Leduc, J. L. Fortier, and J. E. Desnoyers. J. Phys. Chem., **78**, 1217 (1974).
22. C. Jolicoeur, J. Boileau, S. Bazinet, and P. Picker. Can. J. Chem. **53**, 716 (1975).
23. J. E. Desnoyers and M. Arel. Can. J. Chem. **45**, 359 (1967).
24. M. Sakurai. Bull. Chem. Soc. Jpn. **46**, 1596 (1973).
25. Handbook of Chemistry and Physics, 49th ed. The Chemical Rubber Co., Cleveland, Ohio. 1968.
26. K. W. Morcom and R. W. Smith. Trans. Faraday Soc. **66**, 1093 (1970).
27. J. E. Desnoyers, G. Perron, J. P. Morel, and L. Avédikian. Chemistry and physics of aqueous gas solutions. *Edited by* W. A. Adams. The Electrochemical Society, Princeton, N.J. 1975. p. 172.
28. J. H. Stern, J. Lazartic, and D. Frost. J. Phys. Chem. **72**, 3053 (1968).
29. C. de Visser and G. Somsen. J. Solution Chem. **3**, 847 (1974).
30. E. Grunwald, G. Baughman, and G. Kohnstam. J. Am. Chem. Soc. **82**, 5801 (1960).

Thiophene Isosters of Phenylethanolamines

JEHAN F. BAGLI AND E. FERDINANDI[1]

Ayerst Research Laboratories, Montreal, Quebec H3C 3J1

Received February 21, 1975

JEHAN F. BAGLI and E. FERDINANDI. Can. J. Chem. **53**, 2598 (1975).

The reaction of a variety of substituted thiophenes, under Friedel–Craft conditions, leading to acetylthiophenes is described. Some of the by-products obtained are isolated and their mode of formation rationalized. The bromination, the reduction of the bromoketones, and their transformation to thienylethanolamines is reported. The degradation products of bromohydrin as well as isomeric amines obtained in the final substitution reaction are characterized and a possible mechanism for the formation of these compounds is proposed.

JEHAN F. BAGLI et E. FERDINANDI. Can. J. Chem. **53**, 2598 (1975).

On décrit la réaction d'une série de thiophènes substitués dans les conditions de Friedel–Craft. Cette réaction conduit aux acétyl thiophènes. Les produits secondaires de la réaction sont isolés et leurs modes de formation sont rationalisés. On décrit la bromation, la réduction des bromocétones ainsi que leur transformation en thiényléthanolamines. Les produits de dégradation de la bromhydrine ainsi que les amines isomères obtenues par la réaction de substitution finale, sont caractérisés; un mécanisme est proposé pour expliquer la formation de ces composés.

[Traduit par le journal]

Introduction

Epinephrine and norepinephrine, the two adrenergic neurotransmitters are well known for their broad biological profile. This has led to a variety of potential therapeutic utilities for them such as nasal decongestant, for pressor effects, as local anesthetics, bronchodilators, and cardiac stimulant. However, the natural sympathetic amines have a major disadvantage of having a very short half-life. Consequently, considerable effort has been spent to synthesize sympathomimetic phenylethylamines to achieve selectivity of biological activity and sustained therapeutic effect. While the isosteric nature of the thiophene ring with the phenyl nucleus is well known, only very few thiophene isosters of catacholamine analogs have been reported in the literature.

Although a number of routes to arylethanolamines (1, 2) including β-(2-thienyl)ethanolamines (3, 4) and chloro substituted thiophenethanolamines (5) have been published, the synthesis of alkoxy substituted thiophenethanolamines has not been reported. In this paper we describe the synthesis of some novel methoxy and halogen substituted thiophenethanolamines. The general sequence to the thiophenethanolamines described in this paper is shown below.

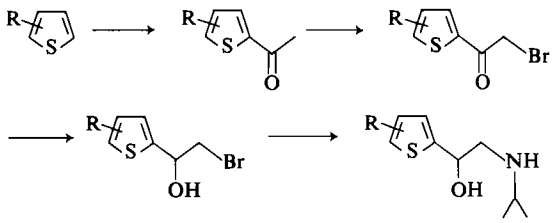

We also report some products of the side reactions encountered in the synthesis and conditions under which they can be eliminated. The formation of the by-products was rationalized as resulting from the pseudoaromatic character of the thiophene nucleus. The ethanolamines described in this paper were evaluated for their biological activity in the cardiovascular field (6).

Acetylthiophenes

Various substituted thiophenes (Table 1) required for the purpose of acylation were synthesized using known procedures or modifications thereof (7–9 and see Experimental).

The acetylthiophenes were generally prepared by the reaction of the substituted thiophene with acetyl chloride using stannic chloride as the catalyst (10). Relative to the halothiophenes, the Friedel–Crafts reaction of the methoxy- and acetoxythiophenes was much more rapid. For example, acylation of 2-acetoxy-3-bromothiophene (**1***k*) required only 30 min whereas the acylation

[1]NRCC Industrial Postdoctorate Fellow, 1970–1971.

Can. J. Chem. Downloaded from www.nrcresearchpress.com by 210.87.254.5 on 09/05/12
For personal use only.

TABLE 1. Experimental details for the reaction

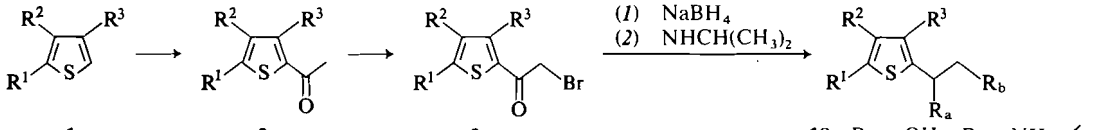

1 2 3

18 $R_a = OH$; $R_b = NH$–

19 $R_a = NH$– ; $R_b = OH$

Compound 1	R^1	R^2	R^3	Bromination method* (% yield)	Melting point (°C)	n.m.r. δ $COCH_2Br$	% yield Isomer 18	% yield Isomer 19
a	Br	H	H	A (80)	90–91	4.30	60	20
b	Br	Br	H	A (92)	68–70	4.26	54	9
c	H	Br	Br	C (55)	80–82	4.60	80	0
d	Cl	H	H	B (75)	72–73	4.30	64	21
e	Cl	Cl	H	B (80)	Oil	—	75	6
f	H	Cl	Cl	C (80)	46–47	4.53	73	7
g	OCH_3	H	H	C (16) D (15)	Oil	4.26	0	0
h	H	OCH_3	OCH_3	B (31) C (60)	94	4.41	10	80
i	OCH_3	Br	H	A (44) B (79)	95–96	4.13	8	63
j	$OC(CH_3)_3$	Br	H	—	—	—	—	—
k	$OCOCH_3$	Br	H	—	—	—	—	—
l	H	H	H	C (70)	b.p. 100°/ 0.2 Torr	4.35	45	45

*A, bromine; B, pyridinium bromide perbromide; C, copper(II) bromide; D, *n*BuLi, bromoacetyl bromide.

of 2-chlorothiophene (**1***d*) required 15 h to complete. This difference in reactivity of substituted thiophenes to the Friedel–Crafts reaction is similar to that found for substituted benzenes under analogous conditions (11).

Acylation of the *t*-butoxythiophene **1***j* with acetyl chloride – stannic chloride at 0° gave none of the desired acetylthiophene. Instead, the only isolable compound was the thiolactone **4**. When boron trifluoride etherate was used, instead of stannic chloride, the thiolactone **4** was obtained in 80% yield. Such an efficient cleavage of the *t*-butyl ethers with Lewis acids was unexpected since a similar cleavage using *p*-toluenesulfonic acid catalyst required elevated temperatures (9). The acylation of 5-methoxythiophene **1***g*, on the other hand, did give the desired acetyl derivative **2***g*, together with the compound **5** as a by-product. This by-product was eliminated by replacing the benzene by carbon disulfide in the acylation and conducting the reaction at −78° (8). In the case of 3,4-dimethoxythiophene **1***h* (12), acylation at −78° for 2 h led to acyl derivative **2***h* as the sole product.

The fact that no acylation product was obtained in the case of *t*-butoxythiophene **1***j* as against methoxythiophene **1***g* appears clearly a reflection of the difference in the rates of cleavage of the two ethers by Lewis acid catalyst. Since reaction of 3,4-dimethoxythiophene **1***h* using stannic chloride – acetyl chloride yielded exclusively the desired acetyl derivative **2***h*, the cleavage of alkyl ethers at position 2 must be regiospecific and involve a participation of unshared sulfur electrons.

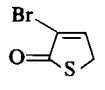

4

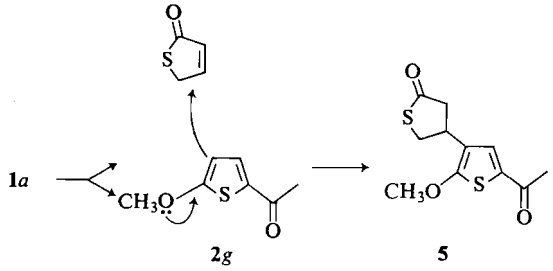

Can. J. Chem. Downloaded from www.nrcresearchpress.com by 210.87.254.5 on 09/05/12
For personal use only.

Can. J. Chem. Downloaded from www.nrcresearchpress.com by 210.87.254.5 on 09/05/12
For personal use only.

The mode of formation **5** may be rationalized by considering an attack by nucleophile **2***g* in a Michael manner on the thiolactone generated from **1***g*. The formation of **5** may be catalyzed by the Lewis acid present in the reaction mixture.

The thiolactone **4** was acetylated with acetic anhydride in pyridine to yield acetoxy thiophene (**1***k*).

The acylation of **1***k* yielded along with the desired acetylthiophene **2***k*, the thiolactone **4**. The formation of **4** in this case may be because of acid catalyzed hydrolysis of the acetate group of **1***k*. Treatment of **2***k* with base, followed by diazomethane yielded methoxy derivative **2***i*.

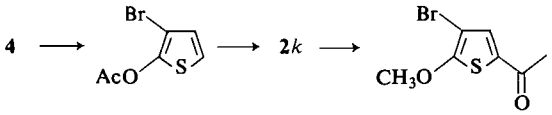

1*k* **2***i*

α-Bromoacetylthiophenes

The next step in the synthesis of the ethanolamines involved the bromination of the methyl group of the acetylthiophenes. In general, this was achieved by treating the 5-substituted 2-acetyl-thiophenes *e.g.* 5-bromo-2-acetylthiophene (**2***a*) with bromine or pyridinium bromide perbromide (PBP). The bromoacetylthiophene **3***a* was obtained in moderate yields together with the dibromoacetyl derivative **6**. The formation of the dibromoacetylthiophene was minimized when PBP was used as the brominating agent.

However, when the 5 position was unsubstituted, a significant amount of bromination oc-

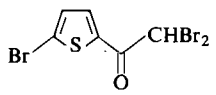

6

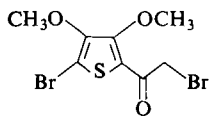

7

curred at C-5 as well as on the acetyl methyl group. For example, the reaction of 2-acetyl-3,4-dimethoxythiophene **2***h* with PBP gave the bromoacetyl derivative **3***h* and the dibromide **7** in 31 and 25% yield, respectively. This side reaction (formation of **7**) was eliminated by using copper(II) bromide as the brominating agent (14). A summary of all the bromination reactions is shown in Table 1.

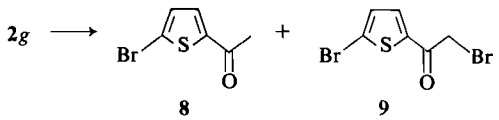

8 **9**

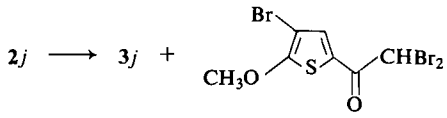

10

The bromination of 5-methoxy-2-acetylthiophene (**2***g*) took an unexpected course. The reaction with PBP gave a complicated mixture of products from which the compounds **8** and **9** were isolated. In contrast, the 2-acetyl-4-bromo-5-methoxythiophene (**2***i*) was successfully brominated either with bromine or PBP to the bromo ketone **3***j* together with small amounts of dibromide **10**. The displacement of methoxyl in **2***g* must involve a nucleophilic 1,6-addition of bromide ion at C-5 followed by elimination of the methoxide. That such a displacement does not occur in the case of **2***i* may be attributed to steric factors.

The 5-methoxyl-α-bromoacetylthiophene (**3***g*) was synthesized by two methods although the yield was low in both cases. Reacting the acetylthiophene **2***g* with copper(II) bromide or treating 2-methoxythiophene (**1***g*) with *n*-butyllithium followed by bromoacetylbromide, led to the formation of **3***g*.

Reduction of the α-Bromoketone and Reaction with Isopropylamine

The synthesis of the ethanolamine from the bromoketone required first, the reduction of the ketone, followed by reaction of the resulting bromohydrin with isopropylamine. The reduction of the ketone with sodium borohydride in methanol at 0°, gave the bromohydrin in good yield. It was found that on standing at room temperature the bromohydrins decomposed at different rates depending on the substituents on the thiophene ring. For example, the bromohydrin **11***b* was stable enough to be chromatographed and distilled while the bromohydrin **11***i* could not be isolated.

While a detailed study of the decomposition products of the various bromohydrins was not carried out, the major decomposition products

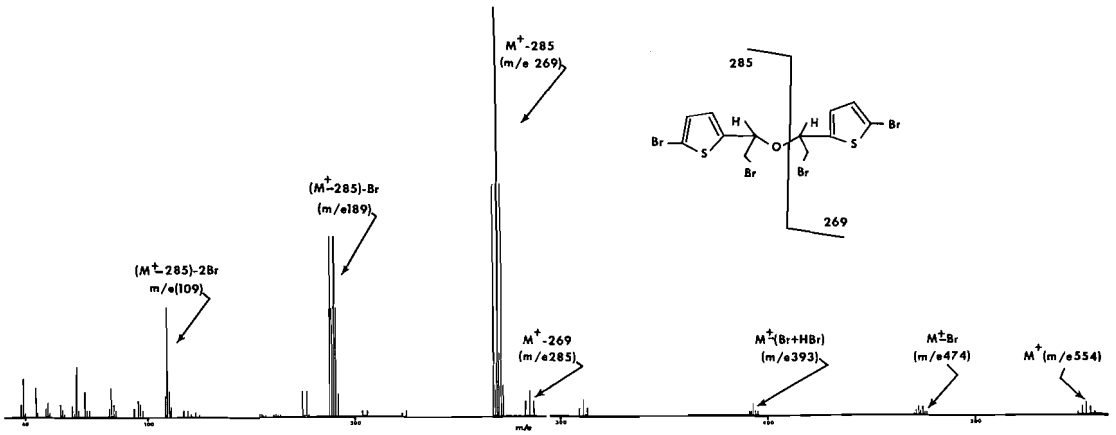

FIG. 1. Mass spectrum of tetrabromoether **12**.

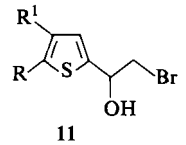

11

a R = Br; R^1 = H
b R = R^1 = Br
i R = OCH_3; R^1 = Br

of the bromohydrin **11***a* were isolated and identified. On standing (neat) at room temperature for 7 days, the bromohydrin **11***a* had decomposed to a mixture of products from which four compounds were isolated by column chromatography on silica gel and identified from their spectroscopic and analytical data. The major decomposition products were the diastereomeric tetrabromoethers **12** and **13**. The two compounds had almost identical i.r. and n.m.r. spectra. The mass spectra, which were identical for both isomers, showed a characteristic Br_4 pattern M^+ (*m/e* 554) and a fragmentation pattern consistent with the proposed structure (Fig. 1).

Not enough data were available to distinguish the two isomers. A minor component of the mixture was the vinyl bromide **14**. The n.m.r. spectrum of the olefinic protons showed two doublets, δ 6.21, 7.21, having a coupling constant of 8.0 Hz consistent for the coupling of two *cis* vinylic protons (15). The acetylthiophene **2***a*, also a minor component of the mixture, was identified by comparison of spectral data and mixture melting point with the authentic sample.

The bromohydrin **11***a* can decompose by participation of electrons of the thiophene ring (*a*, *b*) or by mesomeric effect due to C-5 bromine (*c*) to yield the intermediates **15** and **16**, respectively (Scheme 1). These intermediates upon a proton abstraction can lead to ketone **2***a*. The hydrobromic acid generated in this process can catalyze the ejection of OH^- from **11***a* leading to **17**. This intermediate can generate the olefin **14** by isomerization or can lead to the generation of **12** and **13** by nucleophilic attack of another molecule of **11***a*. This mechanism does not preclude the formation of the *trans* isomer of **14**. However, under the working conditions employed none was isolated.

The reaction of isopropylamine with the bromohydrins **11** was carried out in a pressure bottle at 90° and, in most cases, two regioisomeric ethanolamines **18** and **19** were isolated. The structural assignment of the isomers was based on the difference in the chemical shift of the α-hydroxy and α-amino protons in their n.m.r. spectra. Formation of these two isomers can conceivably involve an epoxide of the type **20** as an intermediate. Opening of the epoxide is then governed by the substituents present on the thiophene nucleus. A summary of this substitution reaction is shown in Table 1.

The nucleophilic attack occurred predominantly at the β-position. However, when the 3 or 5 position was substituted with a methoxyl group as in **11***i* and **11***h*, the α position became the predominant point of attack.

The relative stability of the halothienylbromohydrin compared with those of the methoxythienylbromohydrins and the differences in the

Can. J. Chem. Downloaded from www.nrcresearchpress.com by 210.87.254.5 on 09/05/12
For personal use only.

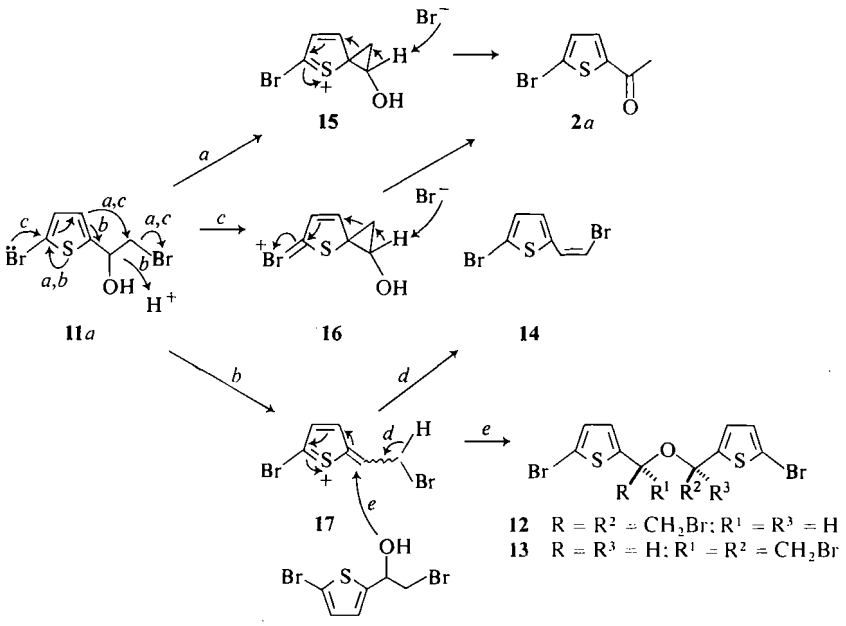

SCHEME I

regiospecificity of isopropylamine addition on to these two types of compounds appear to be a reflection of the mesomeric effect of the two substituent groups. For substituted benzene, halides have a positive while the methoxyl group has a negative value in the Hammett equation (16). The greater electron donating ability of the methoxyl group favors a resonance structure such as **21** (for the 3,4-dimethoxy analog) and the α-ethanolamine **19** is the predominant product.

To establish the intermediacy of the epoxide in the isopropylamine reaction and also to eliminate the formation of the isomer **19** in the case of **11***i* and **11***h*, the hydroxyl group of **11***i* was protected as tetrahydropyranyl ether and that of **11***h* as silyl ether. When the reaction of **11***m* and **11***n* was carried out with isopropylamine no trace of isomer **19** was detectable in either of the products. However, the yields in the case of **11***m* were very low (~10%).

Since the 5-methoxythienylbromohydrin **11***g*

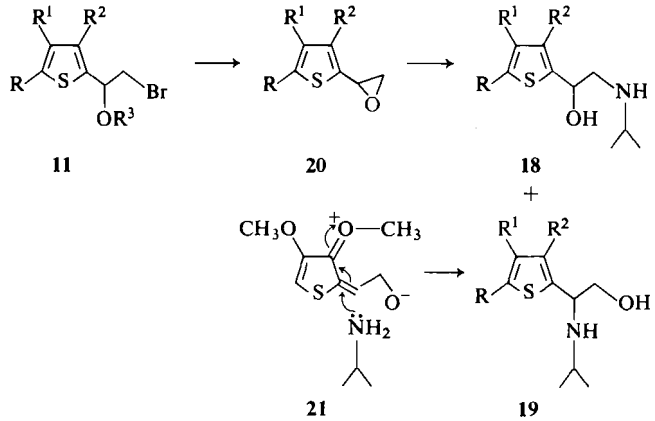

Can. J. Chem. Downloaded from www.nrcresearchpress.com by 210.87.254.5 on 09/05/12
For personal use only.

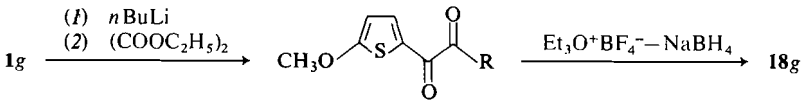

22
a R = OC_2H_5
b R = OH
c R = $NHCH(CH_3)_2$

was very unstable, no 5-methoxythiophenethanolamine was obtained by this synthetic route. An alternative approach was developed starting from 2-methoxythiophene. Treatment of the methoxythiophene **1***g* with butyllithium followed by diethyloxalate gave the α-keto ester **22***a* in good yield. Hydrolysis of the ester **22***a* gave the keto acid **22***b* which was converted to the amide **22***c* via a mixed anhydride. The overall yield in this sequence was 38%. The reduction of the keto amide **22***c* using triethyloxonium fluoroborate and sodium borohydride (17) gave the ethanolamine **18***g* in 23% yield.

The ethanolamines were converted to their hydrochloride salt for biological testing. A complete list of the compounds and their physical properties is tabulated (Table 2) in the Experimental.

Experimental

The i.r. spectra were done on a Perkin-Elmer diffraction grating instrument and u.v. spectra were recorded on a Unicam spectrophotometer. The melting points were taken on a Thomas-Hoover apparatus and are uncorrected. The n.m.r. spectra were recorded on a Varian A60A apparatus and mass spectra were performed on a Hitachi RMU-60 spectrometer. Organic extracts were dried over anhydrous magnesium sulfate and solvents were always removed under vacuum. Merck silica gel 60 (70–230 mesh) was used for column chromatography.

Substituted Thiophenes

2-Bromo- (**1***a*), 2-chlorothiophene (**1***b*), and thio-

TABLE 2. Thiophenethanolamines

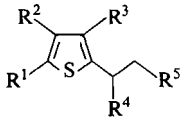

·HCl

Compound	Melting point (°C)	δ (DMSO-*d*)		Elemental analysis (%)					
				Calculated			Found		
		C*H*O	C*H*N	Cl	N	S	Cl	N	S
18*a*	122	5.30	3.3		4.67	10.69		4.82	10.64
19*a*	62–64*	3.95	4.11			12.12			12.12
18*b*	189–191	5.32	3.3		3.69	8.44		3.74	8.68
19*b*	239	3.91	4.71		3.69	8.44		3.39	8.66
18*c*	206–207	5.38	3.2		3.69	8.44		3.44	8.63
18*i*	Oil*	4.83	2.7						
19*i*	168–169	4.01	4.67		4.24	9.69		4.52	9.74
18*d*	101–102	5.26	3.2	27.73		12.50	27.51		12.49
19*d*	Oil	3.64	4.07	16.19	6.38	14.59	16.30	6.18	14.48
18*e*	194–196	5.26	3.2	36.66		11.01	36.75		11.17
19*e*	79–80*	3.63	4.02	27.95		12.59	28.02		12.66
18*f*	183–184	5.32	3.1	36.66		11.01	36.41		11.13
19*f*	Oil*	3.6	4.3	27.95		12.59	27.85		12.57
18*h*	102–103	5.65	3.35	12.59	4.69	11.32	12.60	4.84	11.35
19*h*	Oil*	3.60	4.18		5.71	13.06		5.60	13.18
18*l*	114–115	5.36	3.3		6.33	14.49		6.52	14.43
19*l*	Oil*	3.67	4.10		7.57	17.39		7.51	17.22
18*g*	100–101†				4.53	9.67		4.12	9.72

*Free amine (n.m.r. taken in $CDCl_3$).
†Maleate.

Can. J. Chem. Downloaded from www.nrcresearchpress.com by 210.87.254.5 on 09/05/12
For personal use only.

Can. J. Chem. Downloaded from www.nrcresearchpress.com by 210.87.254.5 on 09/05/12
For personal use only.

phene (**1***m*) were purchased commercially. The following compounds were prepared according to previously published procedures: 2,3-dibromothiophene (**1***b*, (19)), 3,4-dibromothiophene (**1***c*, (20)), 2-methoxythiophene (**1***g*, (8)), 3,4-dimethoxythiophene (**1***h*, (12)), and 2-*t*-butoxy-3-bromothiophene (**1***j*, (9)). 3,4-Dichlorothiophene (**1***f*, (7, 21)) was prepared (n.m.r. ($CDCl_3$) δ 7.20) from 3,4,5-trichloro-2-thiophenecarboxylic acid (**22**) using the dehalogenation and decarboxylation procedure described by Steinkopf and Köhler (7).

Acetyl Thiophenes

In general the acylation of the substituted thiophenes was carried out using acetyl chloride in benzene with stannic chloride as the catalyst (10). For example, 2-bromothiophene (**1***a*, 60 g) and acetyl chloride (28.9 g) were dissolved in 250 ml benzene and cooled to 0°. The stannic chloride (104 g) dissolved in 50 ml benzene was added dropwise. After stirring the reaction mixture for 20 h at room temperature, it was poured into ice water and extracted with ether. The ethereal extract was washed with water and saturated saline solution, dried, and concentrated. The resulting acetylthiophene **2***a* was recrystallized from hexane – ethyl acetate, m.p. 94–95° (lit. (23) m.p. 94–95°); λ_{max} ($CHCl_3$) 1675 cm^{-1}; n.m.r. ($CDCl_3$) δ 2.49 (s, 3H, CH_3).

The following acetylthiophenes, prepared in the same manner, have been previously synthesized by other acylation methods: 2-acetyl-4,5-dibromothiophene (**2***b*), m.p. 84–85° (lit. (22) m.p. 86–88°); 2-acetyl-3,4-dibromothiophene (**2***c*), m.p. 80–81° (lit. (22) m.p. 83–85°); 2-acetyl-5-chlorothiophene (**2***d*), m.p. 46° (lit. (23) m.p. 46.5–47°); 2-acetyl-3,4-dichlorothiophene (**2***f*), m.p. 51–52° (lit. (7), m.p. 56°).

2-Acetyl-4,5-dichlorothiophene (2e)

Methyl lithium (2.1 equiv.) was added to 4,5-dichloro-2-thiophenecarboxylic acid (7) (17.4 g) dissolved in 250 ml anhydrous ether and cooled to −50° under nitrogen atmosphere. The reaction mixture was slowly brought to 0° (*ca.* 1 h) and then quenched with an ice cold solution of saturated ammonium chloride. The aqueous portion was separated and extracted with ether. The combined ether phase was washed with water and saturated saline, then dried and concentrated. The title compound (10.3 g) was recrystallized from hexane, m.p. 66–67° (lit. (24) m.p. 66°).

3-Bromo-2(5H)-thiophenone (4)

Boron trifluoride etherate (42.0 g) was added dropwise over a period of 15 min to a solution of 3-bromo-2-*t*-butoxythiophene (**1***j*, 55 g) in 200 ml benzene at 0°. The solution was stirred until the reaction was complete by t.l.c. (*ca.* 1 h), then poured into ice water and extracted with ether. The ether extract was washed with water and saturated saline solution, then dried and concentrated. The crude product was chromatographed on a column of silica gel (2.2 kg) in benzene. Recrystallization from a benzene–hexane mixture gave the title compound in 80% yield, m.p. 81–82°; ν_{max} (CCl_4) 1720, 1620 cm^{-1}; n.m.r. ($CDCl_3$) δ 4.05 (d, J = 3.0 Hz, 2H, CH_2S), 7.22 (t, J = 3.0 Hz, 1H, C=C*H*); λ_{max} (95% C_2H_5OH) 239 (ε 7900), 263 nm (ε 2900).

Anal. Calcd. for C_4H_3BrOS: Br, 44.69; S, 17.87. Found: Br, 44.02; S, 17.56.

5-Methoxy-2-acetylthiophene (2g)

(*A*) The title compound was obtained in 57% yield when the acylation on 2-methoxythiophene (**1***g*) was carried out in carbon disulfide at −78° (8); ν_{max} ($CHCl_3$): 1640, 1535, 1225 cm^{-1}; n.m.r. ($CDCl_3$): δ 2.43 (s, 3H, CH_3CO), 3.96 (s, 3H, CH_3O), 6.25 (d, J = 4.5 Hz, 1H, C=C*H*).

Anal. Calcd. for $C_7H_8O_2S$: C, 53.85; H, 5.13; S, 20.51. Found: C, 53.62; H, 5.19; S, 20.42.

(*B*) 5-Methoxythiophene (**1***g*, 35 g) and acetyl chloride (24 g) were dissolved in 100 ml benzene and cooled to 0°. Stannic chloride (81 g) dissolved in 100 ml benzene was then added dropwise in over a period of 30 min. The reaction mixture was then poured into water and extracted with ether. The ether fraction was washed with water, saturated saline solution, dried and concentrated. The crude product was chromatographed on a column of silica gel (benzene – ethyl acetate 8:2) and two compounds were isolated: the title compound **2***g* (29%) and the thiolactone (10%); m.p. 117–118° (benzene–hexane); λ_{max} ($CHCl_3$) 1700, 1650, 1560, 1510, 1390, 1265 cm^{-1}; n.m.r. ($CDCl_3$) δ 2.45 (s, 3H, CH_3CO), 2.80 (m, 2H, CH_2O), 3.60 (m, 3H, CH_2S, —C=C*H*), 4.07 (s, 3H, —OCH_3), 7.11 (s, 1H, =C*H*); λ_{max} (95% C_2H_5OH) 230 (ε 12 400), 290 nm (ε 3700); mass spectrum M^+ (*m/e* 256).

Anal. Calcd. for $C_{11}H_{12}O_3S$: C, 51.55; H, 4.67; S, 25.00. Found: C, 51.61; H, 4.75; S, 24.28.

2-Acetyl-3,4-dimethoxythiophene (2h)

Stannic chloride (36 g) dissolved in 20 ml benzene, was added dropwise to a solution of 3,4-dimethoxythiophene (**1***h*, 19.7 g) and acetyl chloride (10.7 g) in 100 ml benzene at 0°. After stirring the reaction mixture at 0° for 1.5 h, it was poured onto crushed ice and extracted with ether. The ethereal extract was washed with water and saturated saline solution, dried, and concentrated. The crude product (24 g) was purified by chromatography on a column of silica gel in benzene. An analytical sample was obtained by distillation, b.p. 102°/0.5 Torr; ν_{max} (film) 1650 cm^{-1}; λ_{max} (95% C_2H_5OH) 275 (ε 12 800), 304 nm (ε 5300); n.m.r. ($CDCl_3$) δ 2.53 (s, 3H, CH_3CO), 3.83, 4.02 (two s, 3H each, CH_3O), 6.52 (s, 1H, C=C*H*).

Anal. Calcd. for $C_8H_{10}O_3S$: C, 51.61; H, 5.38; S, 17.20. Found: C, 51.82; H, 5.57; S, 17.32.

2-Acetoxy-3-bromothiophene (1k)

The bromothiolactone **4** (36 g) was added to a solution of anhydrous pyridine (70 ml) and acetic anhydride (50 ml) at 0°. The reaction mixture was stirred for 1 h then poured onto ice cold 3% hydrochloric acid and extracted with ether. The combined ether extract was washed with cold 5% sodium bicarbonate, water, and saturated saline solution. The ethereal extract was dried, concentrated, and distilled giving 25 g (75%) of the acetoxythiophene **1***k*, b.p. 75°/0.5 Torr; ν_{max} (CCl_4) 1780, 1740 cm^{-1}; n.m.r. ($CDCl_3$) δ 2.34 (s, 3H, CH_3), 6.83, 7.00 (two d, J = 6.0 Hz, 1H each, 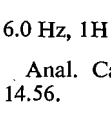).

Anal. Calcd. for $C_6H_5BrO_2S$: S, 14.48. Found: S, 14.56.

2-Acetyl-4-bromo-5-acetoxythiophene (2k)

Stannic chloride (29 g) and acetyl chloride (13 g), dissolved in 100 ml anhydrous benzene and cooled to 0°, were stirred in a nitrogen atmosphere for 2 h. The ace-

Can. J. Chem. Downloaded from www.nrcresearchpress.com by 210.87.254.5 on 09/05/12
For personal use only.

toxythiophene **1***k* (24.6 g) dissolved in 50 ml benzene was added dropwise over a period of 25 min. After stirring an additional 5 min, the solution was poured into ice water and extracted with ether. The ethereal extract was washed with water and saturated saline solution, dried, and concentrated. The resulting oil was chromatographed on a column of silica gel (1 kg, benzene elution) and two compounds were isolated: (*i*) the bromothiolactone **4** (15%) and (*ii*) the acetylthiophene **2***k*, 17.5 g (60%) was recrystallized from hexane–benzene, m.p. 66°; ν_{max} ($CHCl_3$) 1760, 1665 cm^{-1}; λ_{max} (95% C_2H_5OH) 261 (ε 6100), 310 nm (ε 7000); n.m.r. ($CDCl_3$) δ 2.41 (s, 3H, CH_3CO_2), 2.51 (s, 3H, $COCH_3$), 7.53 (s, 1H, C=C*H*).

Anal. Calcd. for $C_8H_7BrO_3S$: Br, 30.42; S, 12.17. Found: Br, 30.23; S, 12.12.

*2-Acetyl-4-bromo-5-methoxythiophene (**2***i*)*

The acetylthiophene **2***k*, (10 g), dissolved in 50 ml methanol, was rapidly added to a 1% potassium carbonate solution in aqueous methanol (200 ml) at 0°. After stirring for 5 min, the reaction mixture was poured into ice water, acidified with 10% HCl, and extracted several times with ether. The ethereal extract was washed with water and saturated saline solution and dried. An ethereal solution containing excess diazomethane was then added to the ether extract. The solution stood at room temperature for 10 min and then was concentrated. The resulting solid (9.0 g, 100%) was recrystallized from hexane–benzene, m.p. 111–112°; ν_{max} ($CHCl_3$) 1650; λ_{max} (95% C_2H_5OH) 255 (ε 4600), 324 nm (ε 9700); n.m.r. ($CDCl_3$) δ 2.47 (s, 3H, CH_3CO), 4.10 (s, 3H, CH_3O), 7.56 (s, 1H, C=C*H*).

Anal. Calcd. for $C_7H_7BrO_2S$: Br, 34.04; S, 13.62. Found: Br, 34.12; S, 13.48.

Bromination of Acetylthiophenes

An example of the bromination reactions using different reagents is described below.

(*A*) *Bromine*

Bromine (23.4 g) dissolved in 50 ml chloroform was added dropwise to a stirred solution of 2-acetyl-5-bromothiophene (**2***a*, 30 g). The reaction mixture was stirred until all the ketone had reacted (*ca.* 2 h), then diluted with ether, washed with water, 5% sodium bicarbonate, and saturated saline solution. The ethereal phase was finally dried, concentrated, and the resulting bromoketone **3***a* (33 g, 80%) was purified by crystallization from hexane – ethyl acetate, m.p. 90–91°; ν_{max} ($CHCl_3$) 1660 cm^{-1}; n.m.r. ($CDCl_3$) δ 4.30 (s, 2H, CH_2Br).

Anal. Calcd. for $C_6H_4Br_2OS$: Br, 56.34; S, 11.27. Found: Br, 57.01; S, 11.19.

A second product, the dibromomethyl ketone **6**, was isolated by column chromatography on silica gel (benzene–hexane 8:2) in 10% yield: ν_{max} ($CHCl_3$) 1680, 1655 cm^{-1}; n.m.r. ($CDCl_3$) δ 6.43 (s, 1H, $CHBr_2$), 7.20, 7.78 (two d, J = 4 Hz, 2H, C=C*H*).

(*B*) *Pyridinium Bromide Perbromide (PBP)*

2-Acetyl-5-chlorothiophene (**2***d*, 42.5 g) was dissolved in 250 ml chloroform and cooled to 0°. Pyridinium bromide perbromide (106 g) was added in four portions to the stirred solution over a period of 40 min. Upon completion of the reaction (as indicated by t.l.c.) the solution was poured into ice water and extracted with ether.The combined ether fractions were finally washed with water and saturated saline solution, dried, and concentrated. The resulting bromoketone **3***d* was recrystallized from hexane–benzene giving 46 g (75%) of the pure compound, m.p. 72–73°; ν_{max} ($CHCl_3$) 1662 cm^{-1}; n.m.r. ($CDCl_3$) δ 4.30 (s, 2H, CH_2Br).

(*C*) *Copper(II) Bromide (14)*

2-Acetyl-3,4-dimethoxythiophene (**2***h*, 16.5 g) dissolved in 125 ml chloroform was added to a suspension of copper(II) bromide (41.4 g) in refluxing ethyl acetate (12.5 ml). After 2 h refluxing the dark cupric bromide had been converted to the white cuprous bromide. The reaction mixture was then cooled, filtered, concentrated, and chromatographed on a column of silica gel (1 kg,benzene elution). The bromomethyl thienyl ketone **3***h* was isolated as an oil (14 g, 60%); ν_{max} ($CHCl_3$) 1650 cm^{-1}; n.m.r. ($CDCl_3$) δ 4.41 (s, 2H, CH_2Br).

When the bromination was carried out with PBP (procedure B), the bromomethyl ketone **3***h* was isolated in only 31% yield and α-bromomethyl 5-bromo-3,4-dimethoxy-2-thienyl ketone **7** was obtained in 25% yield; crystallized from hexane–benzene m.p. 94°; ν_{max} ($CHCl_3$) 1650 cm^{-1}; n.m.r. ($CDCl_3$) δ 3.92, 4.15 (two s, 3H each, OCH_3), 4.36 (s, 2H, CH_2Br).

Anal. Calcd. for $C_8H_8Br_2O_3S$: Br, 46.51; S, 9.30. Found: Br, 46.73; S, 9.31.

(*D*) *Bromoacetyl Bromide*

Butyllithium (1.1 equiv.) was added to an ethereal solution of 5-methoxythiophene (**1***g*). The reaction mixture was refluxed for 2 h, cooled, and transferred to a suspension of freshly prepared magnesium bromide in ether at 0°. After 30 min at room temperature, the Grignard reagent thus obtained was transferred to a dropping funnel and added dropwise to ethereal solution of bromoacetyl bromide (26.3 g) cooled to −78°. The reaction mixture was stirred for 1 h at −78° then quenched with a saturated ammonium chloride solution and extracted with ether. The ethereal extract was washed with water and saturated saline solution, dried, concentrated, and chromatographed on a column of silica gel (1 kg, benzene elution). The bromomethyl thienyl ketone **3***g* was isolated as an oil (4.4 g, 15%); ν_{max} ($CHCl_3$) 1640 cm^{-1}; n.m.r. ($CDCl_3$) δ 4.00 (s, 3H, OCH_3), 4.26 (s, 2H, CH_2Br), 6.31, 7.60 (two d, J = 4.5 Hz, 1H each C=C*H*).

Reduction of the Bromomethyl Thienyl Ketone with $NaBH_4$

Bromomethyl 5-bromothienyl ketone (**3***a*, 35 g) was suspended in 250 ml methanol and cooled to 0°. Sodium borohydride (4.68 g) in 40 ml methanol was added. The reaction was stirred at room temperature for 30 min then diluted with water and extracted with ether. The ethereal extract was washed with water and saturated saline solution, dried, and concentrated. The bromohydrin was reacted directly without further purification with isopropylamine. All the bromomethyl thienyl ketones were reacted in the same manner.

*Isolation of the Decomposition Products of α-Bromomethyl-2-(5-bromothiophene)methanol (**11***a*)*

α-Bromomethyl-2-(5-bromothiophene)methanol (**11***a*, 2 g) was left (neat) at room temperature for 1 week. The resulting mixture of compounds was chromatographed on silica gel (100 g, benzene–hexane 8:2) and four constituents of this mixture were isolated and identified.

Can. J. Chem. Downloaded from www.nrcresearchpress.com by 210.87.254.5 on 09/05/12
For personal use only.

(*i*) *cis*-2-(5-Bromothiophene)vinylbromide (**14**), (69 mg (4%)) was sublimed m.p. 45–47°; ν_{max} ($CHCl_3$) 3060, 1630 cm^{-1}; n.m.r. ($CDCl_3$) δ 6.21 (d, J = 8.0 Hz, 1H, C=C*H*Br), 7.21 (d, J = 8.0 Hz, 1H, C=C*H*), 7.01 (s, 2H, thienyl C*H*).

Anal. Calcd. for $C_6H_4Br_2S$: Br, 59.36; S, 11.91. Found: Br, 59.02; S, 12.13.

(*ii*) Di-1-[2-bromo-1-(5-bromothiophene]ethyl ether (**12**), (420 mg (22%)) was recrystallized from hexane, m.p. 85–86°; ν_{max} (CCl_4) 1085 cm^{-1}; n.m.r. ($CDCl_3$) δ 3.52 (m, 4H, CH_2Br), 4.79 (m, 2H, C*H*O), 6.43 (d, J = 4.0 Hz, 2H, C=C*H*), 7.01 (d, J = 4.0 Hz, 2H, C=C*H*); mass spectrum M^+ (*m/e* 554), $M^+ - 80$ (*m/e* 474), $M^+ - 161$ (*m/e* 393), $M^+ - 269$ (*m/e* 285), $M^+ - 285$ (*m/e* 269), $M^+ - 365$ (189), $M^+ - 445$ (*m/e* 109) (see Fig. 1 for details).

Anal. Calcd. for $C_{12}H_{10}OBr_4S_2$: Br, 57.76; S, 11.55. Found: Br, 57.94; S, 11.74.

(*iii*) Di-1-[2-bromo-1-(5-bromothiophene)]ethyl ether (**13**), (450 mg (23%)), was isolated as an oil; ν_{max} (CCl_4) 1080 cm^{-1}; n.m.r. ($CDCl_3$) δ 3.62 (m, 4H, CH_2Br), 4.95 (m, 2H, C*H*O), 6.72 (d, J = 4.0 Hz, 2H, =C*H*), 6.91 (d, J = 4.0 Hz, 2H, =C*H*); mass spectrum was identical with that described above for its isomer.

Anal. Calcd. for $C_{12}H_{10}OBr_4S_2$: Br, 57.76; S, 11.55. Found: Br, 57.33; S, 11.31.

(*iv*) 2-Acetyl-5-bromothiophene (**2***a*) was obtained as a mixture with unreacted bromohydrin **11***a*. The compound, (160 mg (11%)) was isolated by crystallization from hexane – ethyl acetate; m.p. 92–94°, mixture m.p. with authentic **2***a* 93–95°. The i.r. and n.m.r. spectra were identical with those of the authentic acetyl ketone **2***a*.

*α-Bromomethyl-2-(4-bromo-5-methoxythiophene)methyl Tetrahydropyranyl Ether (**11***m*)*

The bromohydrin **11***i* (0.65 g) was dissolved in 10 ml ether. Dihydropyran (0.21 g, 1.2 equiv.) was added followed by *p*-toluenesulfonic acid (6 mg). The reaction was followed by t.l.c. and was found to be complete after 30 min. The mixture was diluted with ether (100 ml) and washed with 5% $NaHCO_3$, water, and saturated saline solution. The ether was then dried, concentrated, and the title compound was obtained in 87% yield; ν_{max} ($CHCl_3$) 1225, 1125, 1075, 1030, 1023, 970 cm^{-1}; n.m.r. ($CDCl_3$) δ 1.70 (m, 6H, C—CH_2—C), 3.60 (m, 2H, CH_2Br), 3.70 (m, 2H, CH_2O), 3.96 (s, 3H, CH_3O), 4.98 (m, 2H, C=C—C*H*O), 6.72 (s, 1H, C=C*H*).

*α-Bromomethyl-2-(3,4-dimethoxythiophene)methyl Trimethylsilyl Ether (**11***n*)*

The bromohydrin **11***h* (1.0 g), trimethylchlorosilane (0.54 g), and hexamethyldisilazane (0.80 g) were dissolved in anhydrous tetrahydrofuran and refluxed 70 min under a nitrogen atmosphere. After cooling, the reaction mixture was poured into ether and crushed ice. This was separated and the aqueous fraction was extracted with ether. The combined ether fractions were washed with water and saturated saline solution, dried, and concentrated. The trimethylsilyl ether **11***n* was obtained in 60% yield; ν_{max} ($CHCl_3$) 3130, 845 cm^{-1}; n.m.r. ($CDCl_3$) δ 0.1 (s, 9H, Si(CH_3)$_3$), 3.46 (m, 2H, CH_2Br), 3.77, 3.84 (two s, 6H, OCH_3), 5.12 (m, 1H, C*H*O), 6.09 (s, 1H, C=C*H*).

*Reaction of the Bromohydrin **11** with Isopropylamine*

All reactions were carried out in the same manner. A typical example is described below. α-Bromomethyl-2-(5-bromothiophene)methanol (**11***a*, 30 g) was dissolved in 70 ml isopropylamine in a pressure bottle. The bottle was flushed with nitrogen, sealed, and after an initial exothermic reaction had taken place, the flask was heated to 90° for 4 h. Upon cooling, the flask was opened and the rereaction mixture was taken up in ether and water. This was separated and the ether was further extracted with cold 10% hydrochloric acid. The combined aqueous fractions were cooled with crushed ice, basified with 10% sodium hydroxide, and extracted with ether. The ethereal extract was washed with water and saturated saline solution, dried, and concentrated. The resulting mixture (26 g) of regioisomers **18***a* and **19***a* was chromatographed on a column of silica gel (chloroform–methanol 8:2). The ethanolamine **18***a*, obtained as a crystalline solid (13 g, 60%), was eluted first: crystallized from hexane, m.p. 82°; ν_{max} ($CHCl_3$) 3590, 3300 cm^{-1}; n.m.r. ($CDCl_3$) δ 1.04 (d, J = 6.5 Hz, 6H, C(CH_3)$_2$), 2.80 (m, 3H, CH_2N, C*H*N), 3.58 (m, 2H, exchangeable, O*H*, N*H*), 4.67 (m, 1H, C*H*O).

Anal. Calcd. for $C_9H_{14}BrNOS$: Br, 30.30; N, 5.30; S, 12.12. Found: Br, 30.35; N, 5.33; S, 12.13.

The regioisomer **19***a* was obtained as an amorphous solid (4 g, 20%) after further elution: m.p. 62–64°; ν_{max} ($CHCl_3$) 3605, 3430; n.m.r. ($CDCl_3$) δ 1.10 (d, J = 6.5 Hz, 6H, C(CH_3)$_2$), 2.31 (broad, 2H, exchangeable, O*H*, N*H*), 2.90 (m, 1H, C*H*N), 3.95 (m, 2H, CH_2O), 4.11 (m, 1H, C=CC*H*N), 6.74 (two d, J = 3.5 Hz, 2H, C=C*H*).

Anal. Calcd. for $C_9H_{14}BrNOS$: S, 12.12. Found: S, 12.05.

*2-(5-Methoxythiophene)-2-oxoacetic Acid (**22***b*)*

n-Butyllithium (0.135 mol) was added dropwise at room temperature to a 100 ml THF solution of 2-methoxythiophene (**1***g*, 15.4 g). The solution was stirred for 15 h at room temperature then refluxed for 1 h. The thienyllithium reagent was then transferred by means of a siphon to a dropping funnel and added to diethyl oxalate dissolved in tetrahydrofuran (150 ml) cooled to −78°. The reaction mixture was stirred at −78° for 3 h then slowly brought to −10° and quenched by the addition of a cold saturated ammonium chloride solution. The separated aqueous phase was extracted with ether and the combined ether phase was washed with water and saturated saline solution, dried, and concentrated. The resulting crude product was not purified at this point but subjected directly to basic hydrolysis.

The crude reaction mixture was stirred at room temperature for 15 h in 5% aqueous methanolic potassium hydroxide. It was then diluted with water and extracted with ether. The aqueous fraction was cooled with crushed ice, acidified with concentrated HCl, and extracted with ether. The ethereal extract was washed with water, saturated saline solution, dried and concentrated. The keto acid **22***b* was obtained as a crystalline solid in 56% yield from **1***g*; ν_{max} ($CHCl_3$) 3000, 1705 cm^{-1}.

*N-Isopropyl-2-(5-methoxythiophene)-2-oxoacetic Acid Amide (**22***c*)*

The keto acid **22***b* (14 g) and triethylamine (9 g), dissolved in THF at 0°, were treated with methyl chloro-

formate. After stirring the reaction mixture for 2 h at 0°, isopropylamine (30 ml) was added dropwise and stirring was continued for an additional 2 h at 0°. The reaction mixture was then poured into ice water and extracted with ether. The ethereal extracts were washed with water and saturated saline solution, dried, and concentrated. The crude product was chromatographed on a column of silica gel (750 g) in benzene – ethyl acetate 95:5 and the amide **22***c* was isolated in 67% yield; m.p. 72–73° (hexane–benzene); ν_{max} ($CHCl_3$) 3440, 3380, 1715, 1677, 1630 cm^{-1}.

Anal. Calcd. for $C_{10}H_{13}NO_3S$: C, 52.86; H, 5.72; N, 6.16; S, 14.09. Found: C, 52.73; H, 5.77; N, 603; S, 14.20.

*α-(Isopropylaminomethyl)-5-methoxy-2-thiophenemethanol (**18g**)*

The triethyloxonium fluoroborate was prepared according to the method described by Meerwein (18). Epichlorohydrin (3.5 ml) was added to freshly distilled boron trifluoride etherate (7.69 ml) in ether so that the solution was refluxing. After refluxing the resulting solution an additional 1.5 h with vigorous stirring, the ether was distilled off and replaced with methylene chloride (50 ml). The amide **22***c* (8 g) was then added and the solution was stirred for 56 h at room temperature. After replacing the methylene chloride with 50 ml anhydrous methanol, the solution was cooled to 0°, and sodium borohydride (4 g) was carefully added over a period of 4 h. The reaction mixture was stirred at room temperature for 24 h, then diluted with ice water and extracted with ether. The ethereal extract was washed with water and saturated saline solution, dried, and concentrated. The crude product was chromatographed on a column of silica gel (400 g) in chloroform–methanol 8:2 and the title compound was isolated in 23% yield as a crystalline solid; m.p. 81° (hexane); ν_{max} ($CHCl_3$) 3600, 3300 cm^{-1}; n.m.r. ($CDCl_3$) δ 1.04 (d, J = 6.5 Hz, 6H, —C—(CH_3)$_2$), 2.82 (m, 3H, CH_2N), 3.32 (broad, exchangeable, 2H, O*H*, N*H*), 3.84 (s, 3H, OCH_3), 4.78 (m, 1H, *CH*O), 6.02, 6.57 (two d, J = 4 Hz, 2H, C=C*H*).

Anal. Calcd. for $C_{10}H_{17}NO_2S$: C, 55.81; H, 7.91; N, 6.51; S, 14.88. Found: C, 55.75; H, 7.86; N, 6.47; S, 14.79.

Preparation of the Hydrochloride Salt

The ethanolamines **18** and **19** were converted to their hydrochloride salt by the addition of a saturated ethereal HCl solution to an ether solution of the amine. The resulting salt was filtered and recrystallized from isopropanol–methanol. The physical constants and analysis of the hydrochloride salts are listed in Table 2.

The authors wish to express their appreciation to Dr. G. Schilling and his associates for microanalytical and spectral data. Thanks are due to the National Research Council of Canada for a Fellowship (to E.F.) during the tenure of which this work was carried out.

1. R. Howe, B. S. Rao, and M. S. Chodnekar. J. Med. Chem. **13**, 169 (1970).
2. W. G. Duncan, W. T. Colwell, C. R. Scott, and D. W. Henry. J. Med. Chem. **11**, 1221 (1968).
3. C. F. Huebner, P. A. Diassi, and C. R. Scholz. J. Org. Chem. **18**, 21 (1953).
4. E. D. Bergmann and Z. Goldschmidt. J. Med. Chem. **11**, 1121 (1968).
5. C. Corral, V. Darias, M. P. Fernandez-Tome, R. Madronero, and J. del Rio. J. Med. Chem. **16**, 882 (1973).
6. J. F. Bagli, W. D. MacKay, E. Ferdinandi, I. Vavra, M. N. Cayen, and W. Lippman. In preparation.
7. W. Steinkopf and W. Köhler. Ann. **532**, 250 (1937).
8. J. Sicé. J. Am. Chem. Soc. **75**, 3697 (1953).
9. H. J. Jakobsen and S.-O. Lawesson. Tetrahedron, **21**, 3331 (1965).
10. E. D. Hartough. *In* Thiophene and derivatives, the chemistry of heterocyclic compounds. *Edited by* A. Weissberger. Interscience Publishers, Inc., N.Y. 1952. p. 325.
11. P. H. Gore. *In* Friedel–Crafts and related reactions. Vol. III, Part 1. *Edited by* G. A. Olah. Interscience Publishers, Inc., N.Y. 1965. pp. 36–51.
12. E. W. Fager. J. Am. Chem. Soc. **67**, 2217 (1945).
13. D. Taub, N. N. Girotra, R. D. Hoffsommer, C. H. Kuo, H. L. Slates, S. Weber, and N. L. Wendler. Tetrahedron, **24**, 2443 (1968). F. M. Dean, J. Goodchild, L. E. Houghton, J. A. Martin, R. B. Morton, B. Parton, A. W. Price, and N. Somvichian. Tetrahedron Lett. 4153 (1966).
14. L. C. King and G. K. Ostrum. J. Org. Chem. **29**, 3459 (1964).
15. L. M. Jackman. Nuclear magnetic resonance spectroscopy. Pergamon Press, New York. 1959. p. 85.
16. E. S. Gould. Mechanism and structure in organic chemistry. Holt, Rinehart and Winston, New York. 1959. pp. 220–227.
17. R. F. Borch. Tetrahedron Lett. 61 (1968).
18. H. Meerwein. Org. Syn. **46**, 113 (1966).
19. S. O. Lawesson. Arkiv. Kemi. **11**, 373 (1957).
20. S. Gronowitz. Acta Chem. Scand. **13**, 1045 (1959).
21. W. Mack. Angew. Chem. Int. Ed. **6**, 1083 (1967).
22. W. Steinkopf, H. Jakob, and H. Penz. Ann. **512**, 136 (1934).
23. H. D. Hartough and L. G. Conley. J. Am. Chem. Soc. **69**, 3096 (1947).
24. E. Profft and G. Solf. J. Prak. Chem. **24**, 38 (1964).

Can. J. Chem. Downloaded from www.nrcresearchpress.com by 210.87.254.5 on 09/05/12
For personal use only.

The Calculation of Effective Pair Potentials in Solution from Activity Coefficient Data: Nitrobenzene in Benzene

SAUL GOLDMAN

Department of Chemistry, University of Guelph, Guelph, Ontario N1G 2W1

Received February 18, 1975

SAUL GOLDMAN. Can. J. Chem. **53**, 2608 (1975).

The stoichiometric activity coefficients of nitrobenzene in benzene at low concentrations over the range 5.5–25 °C were represented by a temperature-dependent dimerization constant. Constant Pressure Solution Theory was used to derive a relationship between this dimerization constant and the sum of two cluster integrals. One of these integrals involves an effective nitrobenzene–nitrobenzene pair potential in benzene, and the other, an effective nitrobenzene–benzene pair potential in benzene. Two approximate mathematical models, each involving dipole–dipole and square-well potentials were used to evaluate the cluster integrals. The resultant expressions were fitted to the data. It was found that unique expressions for the pair potentials could not be obtained, and therefore ranges of solutions were reported. These solutions indicated (*i*) that the effective pair potentials in solution were of the same order of magnitude as those determined for comparable systems from gas-phase second virial coefficient data and (*ii*) that there existed a relatively short-range stabilizing effect in the nitrobenzene–benzene pair potential that was absent in the nonelectrostatic part of the nitrobenzene–nitrobenzene pair potential. This was explained in terms of a charge-transfer interaction between nitrobenzene and benzene, an explanation that is consistent with n.m.r. shift data.

SAUL GOLDMAN. Can. J. Chem. **53**, 2608 (1975).

A basses concentrations et à des températures allant de 5.5 à 25 °C, les coefficients d'activité stoichiométriques du nitrobenzène dans le benzène peuvent être représentés par une constante de dimérisation dépendante sur la température. On a utilisé la théorie de solutions à pression constante pour établir une relation entre cette constante de dimérisation et la somme des deux intégrales d'agglomérations. Un de ces intégrales implique une paire potentielle effective nitro-benzène–nitrobenzène dans le benzène, et l'autre une paire potentielle effective nitrobenzène–benzène dans le benzène. On a utilisé deux modèles mathématiques approchés pour évaluer les intégrales d'agglomération; chacun implique des potentiels dipole–dipole et point-carré. On a trouvé que l'on ne peut obtenir des expressions uniques pour les paires de potentiels; on rapporte donc des limites pour les solutions. Ces solutions indiquent (*i*) que les potentiels des paires effectives en solution sont du même ordre de grandeur que ceux déterminés en phase gazeuse pour des systèmes comparables à partir de coefficients seconds virials; (*ii*) qu'il existe un effet stabilisant agissant à courte portée dans le potentiel de la paire nitrobenzène–benzène mais qui est absent de la partie nonélectrostatique du potentiel de la paire nitrobenzène–nitrobenzène. On explique ceci en termes d'une interaction de transfert de charge entre le nitrobenzène et le benzène; cette explication est en accord avec les données des déplacements chimiques en r.m.n.

[Traduit par le journal]

Introduction

It has long been known that many dipolar nonelectrolytes behave nonideally in low dielectric constant nondissociating media (1, 2). In the past this nonideality was explained in terms of solute self-association. However, because an appropriate theoretical framework did not exist, it was not possible to interpret the association constants obtained in terms of the molecular properties of the solution under consideration. Subsequent statistical-mechanical developments have made it possible, at least for dilute solutions, to begin to interpret the thermodynamic properties of solutions in terms of the molecular properties of their constituents. A considerable amount of work has been done along these lines for aqueous electrolyte solutions (see for example refs. 3–8), and some molecular-based interpretive work has been done in the study of aqueous nonelectrolyte solutions (9–12). The object of the present work is to apply a statistical-mechanical approach to a dilute solution of a dipolar solute in a nonaqueous solvent with a view to gaining molecular-based insight into the solute–solute and solute–solvent interactions which occur in such a solution.

Can. J. Chem. Downloaded from www.nrcresearchpress.com by 210.87.254.6 on 09/05/12
For personal use only.

Can. J. Chem. Downloaded from www.nrcresearchpress.com by 210.87.254.6 on 09/05/12
For personal use only.

An important example of a nonideal system consisting of a dipolar solute dissolved in a nonaqueous solvent is the system nitrobenzene in benzene. This system has been extensively studied by a variety of methods including freezing point depression (1, 13–17), vapor pressure lowering (18), polarization measurements (1, 19), and calorimetry (20). In a previous article (20) freezing point depression and calorimetric data were combined to obtain values for the dimerization constant (or equivalently the stoichiometric activity coefficient) of nitrobenzene in benzene over the range 5.5 (freezing point of benzene) to 25 °C. In the present work, Hill's Constant Pressure Solution Theory (21–23), and the connection between this theory and McMillan–Mayer theory (23), are used to derive a relationship between the dimerization constant of nitrobenzene in benzene and the sum of two cluster integrals. One of these integrals involves the nitrobenzene–nitrobenzene pair potential in benzene, and the other, the nitrobenzene–benzene pair potential in benzene. Approximate mathematical models for this system are developed, and are used together with the experimental data to obtain a number of solutions for the pair potentials relative to the two above-mentioned interactions. The solutions are discussed in relation to both gas-phase second virial coefficient data and solution magnetic resonance data.

Derivation

Starting from the semigrand partition function for a binary system that is open with respect to the solute (component 2), closed with respect to the solvent (component 1), and maintained at fixed temperature (T) and fixed total pressure (p), Hill derived expressions for the chemical potentials of the solute and solvent as power series in the molality of the solute (21). The result that is relevant to the present purpose can be expressed in the form

$$[1]\quad \ln \gamma_2(p,T,m_2) = \sum_{k\geq 1} \left(\frac{k+1}{k}\right) C_{k+1}(p,T) \left(\frac{M_1 m_2}{1000}\right)^k$$

where $\gamma_2 \equiv$ the molal activity coefficient of the solute, $M_1 \equiv$ the molecular weight of the solvent, $m_2 \equiv$ the conventional molality of the solute, $C_n \equiv$ constant pressure coefficients. From its definition (21), γ_2 is seen to be identical with the conventional stoichiometric molal activity coefficient of a solute.

In a previous study the following relationship between the dimerization constant K, and the stoichiometric activity coefficient of nitrobenzene in benzene was derived (ref. 20, eq. 9):

$$[2]\quad \frac{1-\gamma_2(p,T,m_2)}{\gamma_2{}^2(p,T,m_2)} = 2m_2K(p,T)$$

For dilute solutions (*i.e.* $8m_2K < 1$) [2] can be written as the power series:

$$[3]\quad \ln \gamma_2(p,T,m_2) = -2K(p,T)m_2 + 6K^2(p,T)m_2{}^2 - \ldots$$

Comparing the coefficients of m_2 in [1] and [3]

$$[4]\quad K(p,T) = \frac{-C_2(p,T)M_1}{1000}$$

Next, we use Hill's result (ref. 23, eqs. 40 and 45):

$$[5]\quad 2C_2v_1 = 2B_2{}' - \bar{v}_2{}^0 + b_{11}{}'$$

where $v_1 \equiv$ the molecular volume of the pure solvent, $\bar{v}_2{}^0 \equiv$ the partial molecular volume of the solute in the solvent at infinite dilution of the solute,

$$B_2{}' \equiv -\frac{1}{2V}\int_V \int_V (e^{-W_{22}/kT} - 1)\, d\boldsymbol{r}_1 d\boldsymbol{r}_2$$

$$b_{11}{}' \equiv \frac{1}{V}\int_V \int_V (e^{-W_{12}/kT} - 1)\, d\boldsymbol{r}_1 d\boldsymbol{r}_2$$

$V \equiv$ volume of the system, $W_{22} \equiv$ the potential of mean force (see below) between two solute molecules at positions $\boldsymbol{r}_1$ and $\boldsymbol{r}_2$ in the infinitely dilute solution, $W_{12} \equiv$ the potential of mean force between one solute molecule and one solvent molecule at positions $\boldsymbol{r}_1$ and $\boldsymbol{r}_2$ in the infinitely dilute solution. It is taken as understood in [5] that all the terms are functions of pressure and temperature. The potential of mean force (introduced above) may be pictured as the effective potential energy of interaction between a selected pair of molecules in the infinitely dilute solution at fixed relative positions and orientations, statistically averaged over all possible configurations of the other (solvent) molecules in the system. For convenience these potentials of mean force will be referred to as effective pair potentials.

Can. J. Chem. Downloaded from www.nrcresearchpress.com by 210.87.254.6 on 09/05/12
For personal use only.

The final result is obtained after multiplying both sides of [5] by Avogadro's number N, and combining the result with [4]:

$$[6] \qquad 2B_2 + b_{11} = \bar{V}_2^0 - \frac{2000K}{d_1}$$

where d_1 = the density of the pure solvent; $\bar{V}_2^0 \equiv N\bar{v}_2^0$, $B_2 \equiv NB_2'$, $b_{11} \equiv Nb_{11}'$. Equation 6 provides the sought relationship between the experimental data and the sum of the two cluster integrals B_2 and b_{11}. In the subsequent sections, approximate mathematical models are developed and are fitted to the experimental data via [6] so as to obtain solutions for the functions W_{22} and W_{12}.

The electrostatic part of the interaction between two nitrobenzene molecules will be approximated by a point-dipole–point-dipole potential, and the dispersion and repulsion contributions (for both the nitrobenzene–nitrobenzene and nitrobenzene–benzene interactions) will be represented by square wells. While it is acknowledged that these potentials greatly simplify the real system, it is also pointed out that a realistic potential for this system (involving higher order multipole moments together with shape factors for both the repulsion and dispersion interactions) would introduce prohibitive complexity.

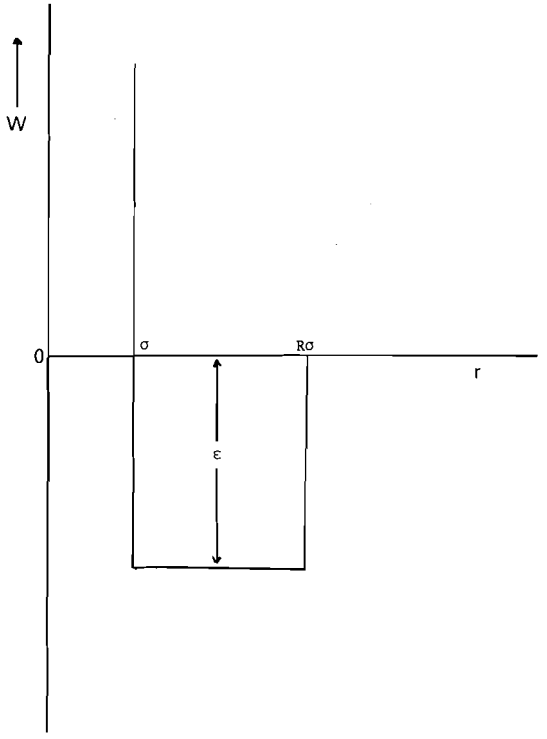

FIG. 1. A plot of potential energy *vs.* center-to-center distance for a square-well potential.

Centered Dipole Model (Model 1)

It is assumed that W_{22} can be represented by the sum:

$$[7] \qquad W_{22} = W_{22}^{ne} + W_{22}^{e}$$

where W_{22}^{ne} and W_{22}^{e} represent respectively the nonelectrostatic and electrostatic contributions to W_{22}. W_{22}^{ne} is assumed to be given by a square well (see Fig. 1), and W_{22}^{e} in model 1 is the interaction energy between two point dipoles each situated at the center of a hard sphere of diameter σ_{22}. The dipole–dipole potential is assumed to be mitigated by a factor of $1/D$ (where D is the dielectric constant of the solvent) and the dipole moment of nitrobenzene in benzene (u_2) is approximated by the equation (24):

$$[8] \qquad u_2 = u_g\left[\frac{2D+1}{2D+n_D^2}\cdot\frac{n_D^2+2}{3}\right]$$

where u_g is the gas-phase dipole moment of nitrobenzene and n_D is the refractive index of nitrobenzene for sodium light. From these considerations:

$$[9] \qquad W_{22} = \begin{cases} \infty & 0 \leqslant r < \sigma_{22} \\ -\varepsilon_{22} + \dfrac{u_2^2 g(\theta_1,\theta_2,\phi)}{Dr^3} & \sigma_{22} < r < R_{22}\sigma_{22} \\ \dfrac{u_2^2 g(\theta_1,\theta_2,\phi)}{Dr^3} & r > R_{22}\sigma_{22} \end{cases}$$

where $g \equiv 2\cos\theta_1\cos\theta_2 + \sin\theta_1\sin\theta_2\cos\phi$. In [9] r is the distance between the molecular centers, and the angles θ_1, θ_2, and ϕ are illustrated in Fig. 2, which should be read for this illustration with the quantity "a" in that figure set equal to zero. For use with angle-dependent potentials the expression for B_2 (given with [5] and [6]) is first transformed (ref. 25, p. 153)

[10] $$B_2 = -\frac{N}{4}\int_0^\infty \int_\Omega (e^{-W_{22}/kT} - 1)r^2\, dr\, d\Omega$$

where

$$\int_\Omega d\Omega = \int_0^{2\pi}\int_0^{\pi}\int_0^{\pi} \sin\theta_1 d\theta_1 \sin\theta_2 d\theta_2 d\phi = 8\pi$$

Next, [9] is inserted into [10] to give

[11] $$2B_2 = \frac{4\pi N\sigma_{22}^3}{3}\{1 - [R_{22}^3 - 1][e^{\varepsilon_{22}/kT} - 1] - e^{\varepsilon_{22}/kT}S_1 - S_2\}$$

where

$$S_1 \equiv \sum_{n=1}^{\infty} \frac{G_n}{(2n)!(2n-1)}\left(\frac{u_2^2}{DkT\sigma_{22}^3}\right)^{2n}(1 - R_{22}^{3-6n})$$

$$S_2 \equiv \sum_{n=1}^{\infty} \frac{G_n R_{22}^{3-6n}}{(2n)!(2n-1)}\left(\frac{u_2^2}{DkT\sigma_{22}^3}\right)^{2n}$$

$$G_n \equiv \frac{1}{8\pi}\int_\Omega g(\theta_1,\theta_2,\phi)^{2n}\, d\Omega = \frac{1}{2n+1}\sum_{m=0}^{n}\binom{n}{m}\frac{3^m}{2m+1}$$

$$\binom{n}{m} \equiv \text{binomial coefficients}$$

The summation given above for G_n was first given by Stockmayer (26).

The nitrobenzene–benzene pair potential is represented by the square well:

[12] $$W_{12}(r) = \begin{cases} \infty & 0 \leqslant r < \sigma_{12} \\ -\varepsilon_{12} & \sigma_{12} < r < R_{12}\sigma_{12} \\ 0 & r > R_{12}\sigma_{12} \end{cases}$$

where

$$\sigma_{12} \equiv \left(\frac{\sigma_{11} + \sigma_{22}}{2}\right)$$

ε_{12} and R_{12} are analogous to ε_{22} and R_{22} (Fig. 1). The expression for b_{11} given with [5] and [6] is first transformed (ref. 25, p. 153):

[13] $$b_{11} = 4\pi N\int_0^\infty [e^{-W_{12}/kT} - 1]r^2\, dr$$

Equation 12 is inserted into [13] to give

[14] $$b_{11} = \frac{-4\pi N\sigma_{12}^3}{3}\{1 - [R_{12}^3 - 1][e^{\varepsilon_{12}/kT} - 1]\}$$

The sought relationship for model 1 is obtained by combining [6], [11], and [14]

[15] $$\frac{4\pi N\sigma_{22}^3}{3}\{1 - [R_{22}^3 - 1][e^{\varepsilon_{22}/kT} - 1] - e^{\varepsilon_{22}/kT}S_1 - S_2\} - \frac{4\pi N\sigma_{12}^3}{3}\{1 - [R_{12}^3 - 1][e^{\varepsilon_{12}/kT} - 1]\} = \bar{V}_2^0 - \frac{2000K}{d_1}$$

Equation 15 connects the experimental stoichiometric activity coefficient data (via K) with molecular parameters that characterize the effective nitrobenzene–nitrobenzene and nitrobenzene–benzene pair potentials in benzene. This equation is now fitted to the experimental data.

Fitting Procedure

The experimental values of K, $\bar{V}_2^0$, and d_1

Can. J. Chem. Downloaded from www.nrcresearchpress.com by 210.87.254.6 on 09/05/12
For personal use only.

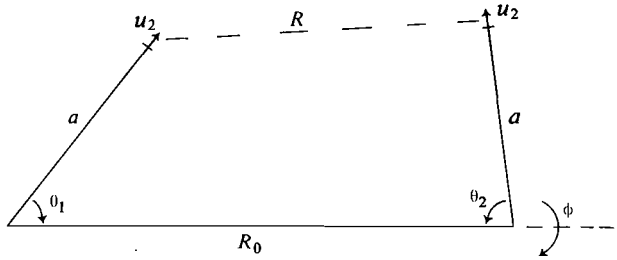

FIG. 2. Definition of parameters for centered and off-centered dipole–dipole potentials.

TABLE 1. Selected data, estimated dipole moment of nitrobenzene in benzene, and experimental function to be fitted

t (°C)	K* (m^{-1})	$\bar{V}_2^0$† (ml/mol)	D‡	d_1§ (g/ml)	$u_2 \times 10^{18}$‖ (e.s.u. cm)	$-[\bar{V}_2^0 - 2000K/d_1]$ (ml/mol)
5.5	0.335	100.6	2.313	0.8942	4.965	648.6
10	0.328	101.0	2.304	0.8894	4.962	635.9
15	0.320	101.4	2.294	0.8841	4.958	622.5
20	0.313	101.8	2.284	0.8788	4.955	610.1
25	0.306	102.3	2.274	0.8737	4.951	598.0

*Calculated by (see eq. 13 ref. 20): $\ln K = \ln(0.335) - \frac{769}{1.9872}\left[\frac{1}{278.65} - \frac{1}{T}\right]$.

†Value at 25° taken from ref. 38. Other values calculated by $\bar{V}_2^0 = \bar{V}_2^0(25) \times d_2(25)/d_2(t)$ where d_2 is the density of pure nitrobenzene (39).
‡Taken from ref. 40, pE-61.
§Taken from ref. 39.
‖Calculated by [8] using u_2 (gas) $= 4.22 \times 10^{-18}$ e.s.u. cm (ref. 40, pE-71), values of D from this table, and values of n_D from ref. 40, pC-163.

that were used are given in columns 2, 3, and 5 respectively of Table 1. The values of the experimental function $(\bar{V}_2^0 - 2000K/d_1)$ calculated from these data are given in column 7 of Table 1, and are illustrated by the solid curve in Fig. 3.

There are six unknown temperature-invariant parameters (σ_{12}, σ_{22}, R_{12}, R_{22}, ε_{12}, ε_{22}) on the left-hand side of [15]. The values sought for these parameters are those, which when substituted into the left-hand side of [15], reproduce the experimental data, *i.e.* the curve in Fig. 3. Obviously, if each of these parameters were allowed to assume any possible value, there would exist a very great number of mathematical solutions which would satisfy [15] over the experimental temperature range. It is possible, however, to greatly reduce the number of solutions by restricting the parameters to physically reasonable values. Specifically the results from scaled-particle theory will be used to obtain values for σ_{12} and σ_{22}, and gas-phase virial coefficient data will be used as a guide for establishing physically reasonable ranges for R_{12}, R_{22}, ε_{12}, and ε_{22}. In the actual fitting procedure only ε_{12} and ε_{22} will be taken as adjustable parameters.

Scaled-particle theory (27–29) has been applied to explain the surface tensions, compressibilities, and gas solubility data for a number of pure liquids including benzene and nitrobenzene (30, 31). From refs. 30 and 31 the values of σ_{22} and σ_{12} were estimated to be: $\sigma_{22} = 5.64$ Å and $\sigma_{12} = (\sigma_{11} + \sigma_{22})/2 = 5.37$ Å. These values were used for σ_{12} and σ_{22} in all the calculations described below.

Gas-phase second virial coefficient data are used as a guide in establishing possible ranges for values of R_{12}, R_{22}, ε_{12}, and ε_{22}. An examination of tabulated values of R and ε (ref. 25, p. 160), obtained by fitting a square-well potential to second virial coefficient data, reveals that for most complex polyatomic molecules R lies between ~1.2 and ~1.5, and ε is always positive but is never greater than $10kT$ ($T = 298$ K). Therefore in the present work R_{12} and R_{22} were each allowed values between 1.2 and 1.5, and ε_{12} and ε_{22} were each allowed values between 0 and $10kT$.

Equation 15 was solved for ε_{12} and ε_{22} (the adjustable parameters) as follows. With $\sigma_{12} = 5.37$ Å and $\sigma_{22} = 5.64$ Å, R_{12} and R_{22} were each allowed to vary between 1.2 and 1.5 in steps of 0.1. For every possible pair of values of R_{12} and R_{22}, a corresponding pair of values

Can. J. Chem. Downloaded from www.nrcresearchpress.com by 210.87.254.6 on 09/05/12
For personal use only.

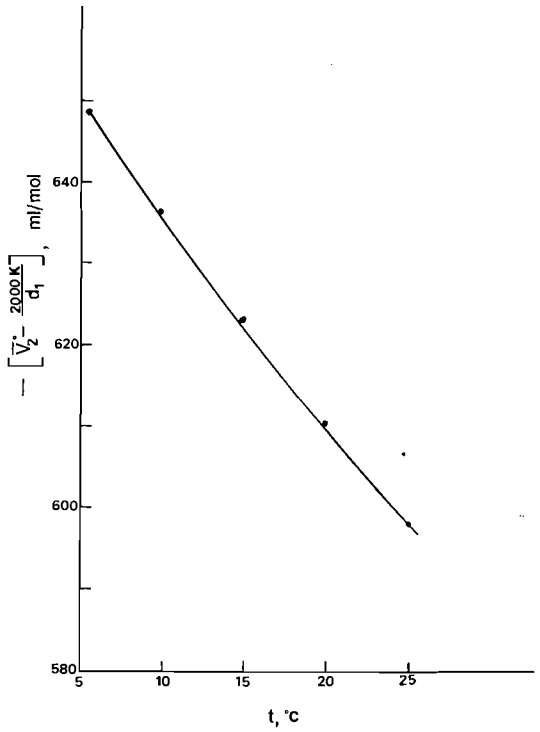

FIG. 3. Solid curve calculated from experimental data (Table 1). Points are calculated theoretically from solutions in Tables 3 and 4 used with [15] and [17] respectively.

for ε_{12} and ε_{22} that would reproduce the curve in Fig. 3 was sought by trial calculation. In seeking these solutions ε_{12} and ε_{22} were each restricted to values between 0 and $10kT$ (T = 298 K). The quantities S_1 and S_2 were obtained from the respective summations given with [11], using the values of D and u_2 entered in Table 1. These sums converged rapidly, and in practice their values were taken as the sum of the first 10 terms. The values of S_1 and S_2 used in these calculations are entered in columns 3 and 4 of Table 2.

In this way it was found that a fit to the data could only be obtained when $R_{22} > R_{12}$. That is for $R_{12} \geq R_{22}$ values of ε_{12} and ε_{22} in the range 0–$10kT$ did not satisfy [15] over the range 5.5–25 °C. However in all cases for which $R_{22} > R_{12}$ a very good fit was obtained, and each fit involved reasonable values of ε_{12} and ε_{22}. These solutions are given, each as a separate row, in Table 3. It is also seen from Table 3 that for each solution $\varepsilon_{12} > \varepsilon_{22}$. The adequacy of these solutions is illustrated by the points shown in Fig. 3. That is, the set of values entered in any single row of Table 3, when used in the left-hand side of [15] (with the appropriate values of S_1 and S_2) gives rise to the points shown in Fig. 3. Whereas the calculated value of the left-hand side of [15] at each temperature is slightly different for the different solutions, these differences are too small to be distinguished using the scale in Fig. 3.

The potential functions represented by one of these solutions (row 2, Table 3) are illustrated in Fig. 4. For comparison, the contribution of the dipole–dipole potential to W_{22} for two dipole orientations is included in Fig. 4. It is

TABLE 2. Values of functions required for calculating the contribution of the dipole–dipole potential to B_2 (σ_{22} = 5.64 Å)

t (°C)	R_{22}	Centered dipole model* S_1	S_2	Off-centered dipole model (a = 1.40 Å)† S_1'	S_2'
5.5	1.2	0.4033	0.4753	0.6298	0.7501
10	1.2	0.3907	0.4623	0.6091	0.7288
15	1.2	0.3774	0.4486	0.5876	0.7062
20	1.2	0.3650	0.4355	0.5674	0.6849
25	1.2	0.3532	0.4231	0.5484	0.6646
5.5	1.3	0.5094	0.3692	0.7755	0.5337
10	1.3	0.4937	0.3592	0.7508	0.5189
15	1.3	0.4773	0.3487	0.7250	0.5032
20	1.3	0.4618	0.3387	0.7008	0.4883
25	1.3	0.4472	0.3291	0.6779	0.4741
5.5	1.4	0.5851	0.2935	0.8759	0.3974
10	1.4	0.5674	0.2856	0.8485	0.3865
15	1.4	0.5487	0.2773	0.8199	0.3750
20	1.4	0.5311	0.2694	0.7930	0.3640
25	1.4	0.5145	0.2618	0.7675	0.3536
5.5	1.5	0.6410	0.2376	0.9482	0.3062
10	1.5	0.6217	0.2312	0.9189	0.2978
15	1.5	0.6015	0.2245	0.8883	0.2890
20	1.5	0.5824	0.2181	0.8594	0.2807
25	1.5	0.5643	0.2121	0.8322	0.2727

*Calculated by equations given with [11].
†Calculated by equations given with [16]. The values of D and u_2 (required for both sets of calculations) are taken from Table 1.

TABLE 3. Square-well parameters for centered dipole model (σ_{12} = 5.37 Å; σ_{22} = 5.64 Å)

R_{12}	ε_{12}/k (K)	R_{22}	ε_{22}/k (K)
1.2	849.0	1.3	605.7
1.2	638.1	1.4	363.9
1.2	539.7	1.5	251.6
1.3	795.5	1.4	598.3
1.3	583.8	1.5	362.3
1.4	739.3	1.5	572.9

Can. J. Chem. Downloaded from www.nrcresearchpress.com by 210.87.254.6 on 09/05/12
For personal use only.

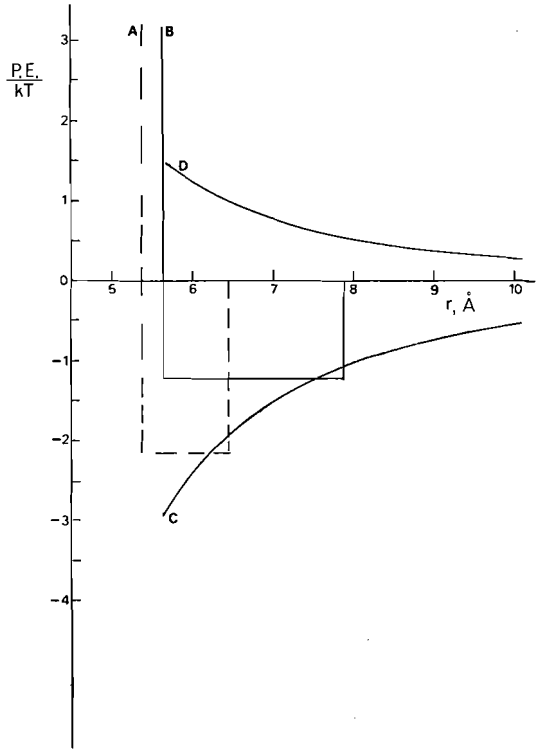

FIG. 4. The square wells A and B represent the solution given in Table 3 row 2. A is the benzene–nitrobenzene pair potential. B is the nonelectrostatic part of the nitrobenzene–nitrobenzene pair potential. C and D are the electrostatic contributions (reckoned by Model 1) for two selected dipole orientations: C, $\theta_1 = 0°$, $\theta_2 = 180°$; D, $\theta_1 = \theta_2 = 90°$, $\phi = 0°$ (value of kT is for $T = 298$ K).

seen from this figure that the contribution to W_{22} made by the dipole–dipole potential is very significant, a result which is not surprising in view of the large dipole moment of nitrobenzene (Table 1).

Off-centered Dipole Model (Model 2)

Model 1 resulted in a fit to the data only when $R_{22} > R_{12}$. This result, which may seem odd at first sight, has an interesting implication which will be discussed later (see Discussion). However Model 1 is very simple, and it is conceivable that the above result is merely an artifact of the model. Therefore it is important to determine whether or not the result $R_{22} > R_{12}$ is sustained for a model that corresponds somewhat more closely to the real system. In their studies on the second virial coefficients of polar gases Lawley and Smith (32), and Dymond and Smith (33)

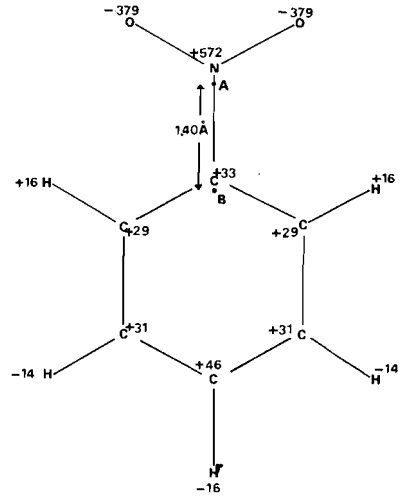

FIG. 5. The charge distribution in nitrobenzene. The charges on the atoms are given in units of 10^{-3} electrons. B is the center of mass of the molecule. A is the dipole center (electrical center of gravity).

have shown that displacement of the electrical center of a molecule from its geometric center can have a significant influence on the calculated values of the molecular parameters. Because the dipole in nitrobenzene is expected to be eccentric rather than centered, and because such a refinement is relatively simple to make, it was considered worthwhile to repeat the calculations for R_{12}, R_{22}, ε_{12}, and ε_{22} using an off-centered dipole model for the nitrobenzene molecule.

It is first necessary to obtain an estimate for the degree of eccentricity of the dipole in nitrobenzene. This was done by calculating the charge distribution in the nitrobenzene molecule, using the known geometry of the molecule (34) together with an INDO/2 molecular orbital calculation.[1] The charge distribution that resulted from this calculation is given in Fig. 5. The center of the molecule (the effective center of the dispersion and repulsion forces) is here identified with the center of mass of the molecule. Using this definition as the center, and the charge distribution given in Fig. 5, it is readily shown from simple electrostatic considerations that the center of the dipole is displaced from the center of mass by 1.40 Å (see Fig. 5).

The derivation for Model 2 parallels that

[1]The program used for the INDO/2 calculation was written by M. Zerner and J. Ridley and is similar to one described elsewhere (35).

Can. J. Chem. Downloaded from www.nrcresearchpress.com by 210.87.254.6 on 09/05/12
For personal use only.

given for Model 1, and the equations for the second virial coefficient of eccentric dipolar molecules have previously been derived (32, 33). Therefore the development given below is brief.

As with Model 1 it is assumed that the effective pair potential between two nitrobenzene molecules can be written as the sum of a square-well potential and a dipole–dipole potential

[7] $$W_{22} = W_{22}^{ne} + W_{22}^{e}$$

where

$$W_{22}^{ne} = \begin{cases} \infty & 0 \leqslant r < \sigma_{22} \\ -\varepsilon_{22} & \sigma_{22} < r < R_{22}\sigma_{22} \\ 0 & r > R_{22}\sigma_{22} \end{cases}$$

$$W_{22}^{e} = \frac{u_2^2}{DR^3}\left[3\left(\frac{R_0}{R}\right)^2 n_1 n_2 + 3\left[\left(\frac{a}{R}\right)(1 + n_1 n_2 - l_1 l_2)\right]^2 - \frac{3aR_0}{R^2}\left[(1 + n_1 n_2 - l_1 l_2)(n_1 + n_2) - n_1 n_2 + l_1 l_2\right]\right]$$

$$R \equiv (R_0^2 + 2a^2[1 + n_1 n_2 - l_1 l_2] - 2aR_0(n_1 + n_2))^{1/2}$$

$$n_i \equiv \cos\theta_i$$

$$l_1 l_2 \equiv \sin\theta_1 \sin\theta_2 \cos\phi$$

$$a \equiv \text{distance by which dipole is off-centered}$$

$$R_0 \equiv \text{hard-sphere center-to-center distance}$$

The above quantities are illustrated in Fig. 2. The equation for W_{22}^{e} gives the potential energy of interaction of two off-centered point-dipoles interacting through a medium of dielectric constant D. It was derived by combining Coulomb's law with straightforward (but lengthy) algebraic manipulations and it may be shown (apart from the factor $1/D$) to be equivalent to eq. 6 in ref. 32.[2]

Next [7] is inserted into [10]. After carrying out the simple integrations and rearranging terms, the result is

[16] $$2B_2 = \frac{4\pi N\sigma_{22}^3}{3}\{1 - [R_{22}^3 - 1][e^{\varepsilon_{22}/kT} - 1] - e^{\varepsilon_{22}/kT}S_1' - S_2'\}$$

where

$$S_1' \equiv 1 - R_{22}^3 + 3\delta^3 \int_{\sigma_{22}/a}^{R_{22}\sigma_{22}/a} \langle x\rangle r_0^2\, dr_0$$

$$S_2' \equiv -3\delta^3 \int_{R_{22}\sigma_{22}/a}^{\infty} (1 - \langle x\rangle) r_0^2\, dr_0$$

$$\delta \equiv \left(\frac{a}{\sigma_{22}}\right)$$

$$r_0 \equiv \left(\frac{R_0}{a}\right)$$

$$\langle x\rangle \equiv \frac{1}{8\pi}\int_{\Omega} e^{-W_{22}^{e}/kT}\, d\Omega$$

It is seen by comparing [11] and [16] that the quantities S_1' and S_2' of Model 2 are functionally equivalent to S_1 and S_2 respectively of Model 1.

[2]The reader should note that eq. 6 in ref. 32 gives a sign for the off-centered dipole–dipole potential that is inconsistent with Fig. 1 in that reference.

Can. J. Chem. Downloaded from www.nrcresearchpress.com by 210.87.254.6 on 09/05/12
For personal use only.

The nitrobenzene–benzene pair potential in Model 2 is assumed to be given by a square-well (*i.e.* by [12]). Hence b_{11} in Model 2 is given by [14]. Combining [6], [14], and [16], the result for Model 2 is

$$[17]\quad \frac{4\pi N\sigma_{22}^3}{3}\{1-[R_{22}^3-1][e^{\varepsilon_{22}/kT}-1]-e^{\varepsilon_{22}/kT}S_1'-S_2'\} - \frac{4\pi N\sigma_{12}^3}{3}\{1-[R_{12}^3-1][e^{\varepsilon_{12}/kT}-1]\} = \bar{V}_2^0-\frac{2000K}{d_1}$$

The integrals required for the calculation of S_1' and S_2' were obtained as follows. The integral

$$\int_{\sigma_{22}/a}^{R_{22}\sigma_{22}/a}\langle x\rangle r_0^2\,dr_0$$

was evaluated by multiple numerical integration using a 4-dimensional 16-point Gauss rule. That is, a 16-point Gauss rule was used for each of the successive integrations: $0\leqslant\theta_1\leqslant\pi$; $0\leqslant\theta_2\leqslant\pi$; $0\leqslant\phi\leqslant2\pi$; $(\sigma_{22}/a)\leqslant r_0\leqslant(R_{22}\sigma_{22}/a)$. The integral

$$\int_{R_{22}\sigma_{22}/a}^{\infty}(1-\langle x\rangle)r_0^2\,dr_0$$

was obtained analytically using the expansion for $\langle x\rangle$ given in ref. 33. By repeating one of the numerical integrations with a 4-dimensional 20-point Gauss rule it was found that the values of S_1' were known to within 0.5%. The accuracy of the programs used for these calculations was further confirmed in two other ways. They were applied, *mutatis mutandis*, to previously published work (33), and they were applied in the limit $a\rightarrow0$ whereupon it found (as expected) that $S_1'\rightarrow S_1$ and $S_2'\rightarrow S_2$. The calculated values of S_1' and S_2' are entered in columns 5 and 6 of Table 2.

Equation 17 was solved for ε_{12} and ε_{22} (the adjustable parameters) utilizing exactly the same procedure as was described for the solution of [15]. The results obtained are given in Table 4, from which it is seen that the solutions for Model 2 are qualitatively similar to those found for Model 1. That is, the experimental function $(\bar{V}_2^0-2000K/d_1)$ over the temperature range 5.5–25 °C could only be fitted when $R_{22}>R_{12}$ (when the values of R_{12} and R_{22} are restricted to the range 1.2–1.5 and the values of ε_{12} and ε_{22} are restricted to values between 0 and $10kT$). All combinations of R_{12} and R_{22} represented by $R_{12}\geq R_{22}$ did not result in a fit. For each solution it was found that $\varepsilon_{12}>\varepsilon_{22}$ (as with Model 1).

The adequacy of these solutions is demonstrated by the points in Fig. 3. Whereas each row in Table 4 (*i.e.* each solution) results, at a particular temperature, in a slightly different value for the left-hand side of [17], these values are indistinguishable from each other using the scale in Fig. 3. Likewise, using the scale in Fig. 3, these values are (at a particular temperature) indistinguishable from the corresponding values obtained with Model 1. For this reason the twelve solutions reported in this work (six in Table 3 for Model 1 and six in Table 4 for Model 2) are represented by only one set of points in Fig. 3.

Discussion

It was found with both the centered and off-centered dipole models that unique solutions for the effective pair potentials W_{12} and W_{22} could not be obtained. Therefore a range of solutions, for each model, was reported. The reason that unique solutions were unobtainable was that the experimental function $(\bar{V}_2^0-2000K/d_1)$ was equal to the sum of two cluster integrals which were similar in form but opposite in sign. However, when restrictions were placed on the possible values of the square-well parameters, and these restricted sets of values were used to seek a fit to the data, a qualitatively unique result was found. Namely, with both models: $R_{12}<R_{22}$ and $\varepsilon_{12}>\varepsilon_{22}$.

It is of interest to compare the values obtained for R_{12}, R_{22}, ε_{12}, and ε_{22} (Tables 3 and 4) with values for R and ε taken from gas-phase virial coefficient data. The second virial coefficients of

TABLE 4. Square-well parameters for off-centered dipole model ($\sigma_{12}=5.37$ Å; $\sigma_{22}=5.64$ Å; $a=1.40$ Å)

R_{12}	ε_{12}/k (K)	R_{22}	ε_{22}/k (K)
1.2	898.9	1.3	607.1
1.2	675.7	1.4	355.7
1.2	577.1	1.5	244.6
1.3	867.7	1.4	630.1
1.3	630.0	1.5	369.5
1.4	821.7	1.5	621.0

Can. J. Chem. Downloaded from www.nrcresearchpress.com by 210.87.254.6 on 09/05/12
For personal use only.

Can. J. Chem. Downloaded from www.nrcresearchpress.com by 210.87.254.6 on 09/05/12
For personal use only.

either pure nitrobenzene or benzene–nitrobenzene mixtures are unknown, so that a direct comparison is not possible. However, second virial coefficient data do exist for pure benzene and pure toluene. Since benzene was one of the constituents of the present system, and since toluene resembles nitrobenzene in size and shape (but not polarity) it is worthwhile to compare the gas-phase pair potentials for these molecules with the nonelectrostatic part of the potentials (*i.e.* the square wells) determined here. Therefore second virial coefficient data for benzene and toluene, (available for each over a range of temperatures (36)), were fitted to a square-well potential by least squares. To be consistent with the present work, the values of σ for benzene and toluene were taken from scaled-particle theory. The adjustable parameters in these fits were R and ε. The least-squares estimates for R and ε are given in Table 5. These estimates reproduce the second virial coefficient data for both benzene and toluene over the reported temperature ranges with an accuracy of about 2%. It is seen from a comparison of the values of R and ε in Table 5 with those given in Tables 3 and 4, that R and ε for both benzene and toluene fall within the range of solutions reported here. Therefore as far as it can be determined, the effective pair potentials that account for our activity coefficient data are consistent with gas-phase pair potentials for comparable molecules.

Perhaps the most significant result found in this work was the fact that for both the centered and off-centered dipole models, the square-well parameters obeyed the inequalities: $R_{12} < R_{22}$ and $\varepsilon_{12} > \varepsilon_{22}$. In other words, the data could only be fitted if the square-well that characterized the nitrobenzene–benzene pair potential was both narrower and deeper than the square-well that characterized the nonelectrostatic part of the nitrobenzene–nitrobenzene pair potential. An explanation for this is put forward below.

A narrower and deeper square-well for the benzene–nitrobenzene pair potential means that this potential, whatever its true form, has in it a relatively short-range stabilizing component that is absent in the nonelectrostatic part of the nitrobenzene–nitrobenzene pair potential. This in turn suggests that the nitrobenzene–benzene pair potential contains a stabilizing direction-dependent potential (in addition to the expected dispersion term) that is absent in the nonelectrostatic part of the nitrobenzene–nitrobenzene pair potential. The correspondence between stabilizing direction-dependent potentials, and their manifestation as narrow deep square-wells is illustrated by a simple example. When the second virial coefficients of the (isotropic) rare gases Ne, Kr, Xe are fitted to a square-well potential, R is found to be between 1.85–1.87 and (ε/k) ranges between 20–100 K (ref. 25, p. 160). However when the second virial coefficient of steam is fitted to a square-well potential, it is found that $R = 1.199$ and $(\varepsilon/k) = 1260$ K (ref. 25, p. 160). Clearly, the existence of hydrogen-bonding between two water molecules (a stabilizing direction-dependent potential that exists in addition to the dispersion potential) has the effect of making the square well of steam relatively narrow and deep. The point is that direction-dependent potentials become angle-averaged when represented by an isotropic square well and the effect of angle-averaging is to make the overall potential appear relatively short-range.

It has been found in solution n.m.r. shift measurements that benzene (an electron donor) forms a charge-transfer complex with both 1,3,5-trinitrobenzene and *para*-dinitrobenzene (electron acceptors) (37). Whereas a charge-transfer complex between benzene and nitrobenzene would be too weak to detect by n.m.r. shift measurements[3] the results with 1,3,5-trinitrobenzene and *para*-dinitrobenzene make it likely that the benzene–nitrobenzene pair potential does contain (in addition to the expected dispersion terms) some charge-transfer character. Because a charge-transfer complex between benzene and nitrobenzene would involve a stabilizing direction-dependent potential, one would expect, from the above discussion, that the use of a square well to describe such a potential would result in a relatively narrow deep square well. One would not expect the nitrobenzene–nitrobenzene pair potential to have any

TABLE 5. Square-well parameters for benzene and toluene from gas-phase second virial coefficient data

	σ^* (Å)	R	ε/k (K)
Benzene	5.10	1.28	692.4
Toluene	5.49	1.23	848.4

*Taken from refs. 30 and 31.

[3]C. A. Fyfe, private communication.

significant charge-transfer character. Thus the existence of a charge-transfer interaction between a benzene and a nitrobenzene molecule, but not between two nitrobenzene molecules, is consistent with the results found in this work.

The author is grateful to the National Research Council of Canada for financial assistance. He would also like to thank Professor M. C. Zerner for his help in calculating the charge distribution in nitrobenzene, and Professor C. A. Fyfe for pointing out the relevant charge-transfer data.

1. L. G. DAVY and N. V. SIDGWICK. J. Chem. Soc. 281 (1933).
2. B. C. BARTON, D. A. ROTHROCK, JR., and C. A. KRAUS. J. Am. Chem. Soc. **74**, 786 (1952).
3. H. L. FRIEDMAN. Ionic solution theory. Interscience Publishers, New York. 1962.
4. J. C. RASAIAH and H. L. FRIEDMAN. J. Chem. Phys. **48**, 2742 (1968).
5. J. C. RASAIAH and H. L. FRIEDMAN. J. Chem. Phys. **50**, 3965 (1969).
6. P. N. VORONTSOV-VELIAMINOV, A. M. ELIASHEVICH, J. C. RASAIAH, and H. L. FRIEDMAN. J. Chem. Phys. **52**, 1013 (1970).
7. J. C. RASAIAH. J. Chem. Phys. **52**, 704 (1970).
8. P. S. RAMANATHAN and H. L. FRIEDMAN. J. Chem. Phys. **54**, 1086 (1971).
9. D. STIGTER. J. Phys. Chem. **64**, 118 (1960).
10. D. G. HALL. Trans. Faraday Soc. **67**, 2516 (1971).
11. D. G. HALL. Trans. Faraday Soc. **68**, 25 (1972).
12. J. J. KOZAK, W. S. KNIGHT, and W. KAUZMANN. J. Chem. Phys. **48**, 675 (1968).
13. E. BECKMANN. Z. Phys. Chem. **2**, 729 (1888).
14. E. BECKMANN. Z. Phys. Chem. **2**, 734 (1888).
15. DAHMS. Ann. Phys. **54**, 496 (1895).
16. C. R. BURY and H. O. JENKINS. J. Chem. Soc. 688 (1934).
17. J. A. DAVISON. J. Am. Chem. Soc. **67**, 228 (1945).
18. J. HURWIC and J. RADZIKOWSKI. *In* Nitro compounds. Proc. Int. Symp., Warsaw. 1963. p. 419.
19. LANGE. Z. Phys. **33**, 169 (1925).
20. S. GOLDMAN and W. C. DUER. Can. J. Chem. **52**, 3918 (1974).
21. T. L. HILL. J. Am. Chem. Soc. **79**, 4885 (1957).
22. T. L. HILL. J. Am. Chem. Soc. **80**, 2923 (1958).
23. T. L. HILL. J. Chem. Phys. **30**, 93 (1959).
24. C. J. F. BÖTTCHER. Theory of electric polarization. Elsevier Publishing Co., Houston, Texas. 1952. p. 70.
25. J. O. HIRSCHFELDER, C. F. CURTISS, and W. R. BIRD. Molecular theory of gases and liquids. John Wiley and Sons, New York. 1954.
26. W. H. STOCKMAYER. J. Chem. Phys. **9**, 398 (1941).
27. H. REISS, H. L. FRISCH, and J. L. LEBOWITZ. J. Chem. Phys. **31**, 369 (1959).
28. H. REISS, H. L. FRISCH, E. HELFAND, and J. L. LEBOWITZ. J. Chem. Phys. **32**, 119 (1960).
29. J. L. LEBOWITZ, E. HELFAND, and E. PRAESTGAARD. J. Chem. Phys. **43**, 774 (1965).
30. S. W. MAYER. J. Phys. Chem. **67**, 2160 (1963).
31. E. WILHELM. J. Chem. Phys. **58**, 3558 (1973).
32. K. P. LAWLEY and E. B. SMITH. Trans. Faraday Soc. **59**, 301 (1963).
33. J. H. DYMOND and E. B. SMITH. Trans. Faraday Soc. **60**, 1378 (1964).
34. J. TROTTER. Acta Cryst. **12**, 884 (1959).
35. J. A. POPLE, D. L. BEVERIDGE, and P. A. DOBOSH. J. Chem. Phys. **47**, 2026 (1967).
36. J. D. COX and R. J. L. ANDON. Trans. Faraday Soc. **54**, 1622 (1958).
37. M. I. FOREMAN, R. FOSTER, and C. A. FYFE. J. Chem. Soc. B, 528 (1970).
38. J. TIMMERMANS. The physico-chemical constants of binary systems, Vol. 1. Interscience Publishers, Inc., New York. 1959. p. 620.
39. R. F. BRUMEL and K. V. BIBBER. *In* International critical tables. Vol. III. McGraw-Hill Book Company, Inc., New York. 1929. p. 29.
40. Handbook of Chemistry and Physics, 50th ed. The Chemical Rubber Company, Cleveland, Ohio. 1969–1970.

Can. J. Chem. Downloaded from www.nrcresearchpress.com by 210.87.254.6 on 09/05/12
For personal use only.

Chemistry of Transition Metals. V. Further Studies on the Mechanism of Reaction of *n*-Alkyl Chlorides with Metals of the First Transition Period

ROBERT W. EGAN[1] AND JOHN F. HARROD

Department of Chemistry, McGill University, P.O. Box 6070, Station A, Montreal, Quebec H3C 3G1

Received March 4, 1975

ROBERT W. EGAN and JOHN F. HARROD. Can. J. Chem. **53**, 2619 (1975).

The rate of reaction of *n*-propyl chloride on polycrystalline evaporated titanium films has been shown to follow a strictly half-order rate law in the pressure range 0.1–0.01 Torr at 220 °C. The reaction rate was not influenced by the product propene. Experiments using a mixture of 1-bromopropane and 1-chloropropane-1-d_1 gave no indication of halogen interchange on either titanium or chromium, thus excluding rapid, reversible dissociative adsorption of the carbon–halogen bond as an explanation of the half-order rate law.

ROBERT W. EGAN et JOHN F. HARROD. Can. J. Chem. **53**, 2619 (1975).

On démontre que la vitesse de réaction du chlorure de *n*-propyle sur des films polycristallins de titane évaporé suit strictement un équation de vitesse d'ordre une demie à des pressions allant de 0.1 à 0.01 Torr à 220 °C. L'équation de vitesse n'est pas modifiée par la présence du produit, le propène. Des expériences impliquant un mélange de bromo-1 propane et de chloro-1 propane d_1-1 ont été réalisées; on n'a pu détecter d'échange d'halogène soit sur le titane ou sur le chrome et on peut donc éliminer, comme explication de l'ordre une demie, la possibilité d'une adsorbtion dissociative reversible et rapide du lien carbone–halogène.

[Traduit par le journal)

Introduction

Previous investigations have shown that *n*-alkyl halides undergo dehydrohalogenation at the surfaces of metals of the first transition period (1, 2). With *n*-alkyl halides all of the halogen is deposited at the metal surface and, in most cases, leads to a rapid decrease in the rate of reaction. The main exceptions to this pattern of behavior were the metals titanium and manganese, neither of which was effectively poisoned by the surface deposited halide (1*a*, 2). In the latter two cases, the kinetic features of the reactions were investigated and were shown to have a time-order reaction of one-half over a wide range of experimental conditions. Indirect measurements of the reaction order on vanadium and chromium, both of which are poisoned by deposited halide, strongly suggested that in these cases also the order in reactant was one-half (2).

It is, to our knowledge, not possible to reconcile strict half-order kinetics over a wide range of experimental conditions with anything but a mechanism involving a dissociative pre-equilibrium. A mechanism was therefore proposed for the half-order reaction of *n*-alkyl halides on transition metals, the first step of which was a rapid, reversible, dissociative adsorption of the carbon–halogen bond at the metal surface (1*a*). Although the proposed mechanism fitted most of the observed experimental facts, it was disturbing to have to ignore an earlier conclusion of Anderson and McConkney that halogen exchange did not occur when suitably labelled methyl chlorides reacted with titanium (3). The latter observation is irreconcilable with a rapid, reversible predissociation step.

In the present paper we report some further experiments designed to test whether halogen interchange does occur with the reactants and under the conditions used by us and whether the reactions are truly half-order. A small measure of doubt remained concerning the latter point since, although a single experiment showed no influence of product on reaction rate, the concentration-order of the reactions had not in fact been rigorously tested (1*a*).

Experimental

The methods used for studying the stoichiometries and rates of reactions have been described previously (1, 2).

[1]Holder of a National Research Council of Canada Scholarship, 1969–1972.

Can. J. Chem. Downloaded from www.nrcresearchpress.com by 210.87.254.105 on 09/05/12
For personal use only.

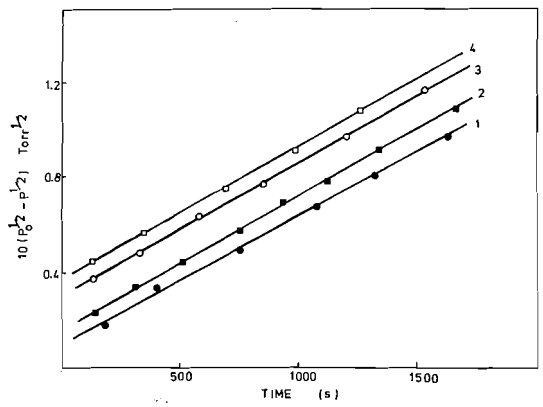

FIG. 1. Effect of added propene on the rate of dehydrochlorination of 1-chloropropane. (T = 222 °C; P_0(chloropropane) = 0.014 Torr.) Initial pressure of propene (Torr): ●, 0.0; ■, 0.013; ○, 0.045; □, 0.0. The ordinate scale refers to curve *1*; curves *2*, *3*, and *4* have been raised by 0.1, 0.2, and 0.3 units respectively to avoid congestion. Reactions carried out on a single film and reaction vessel pumped to 10^{-6} Torr between runs.

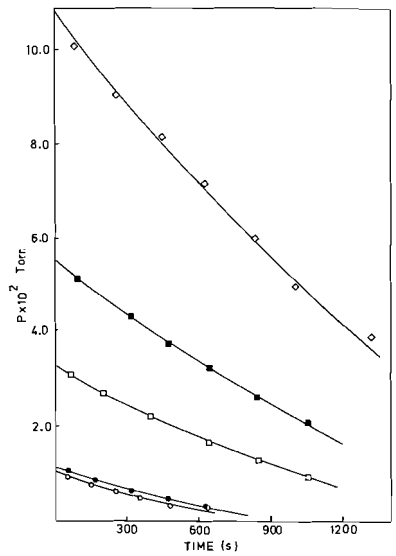

FIG. 2. Reaction of 1-chloropropane on titanium at different initial reactant pressures. Initial reactant pressures (Torr): ○, 0.012; ●, 0.013; □, 0.037; ■, 0.060; ◇, 0.110. Reaction temperature 220 °C. Reactions carried out as in Fig. 1.

The deuterated *n*-propyl halides were both prepared from 1-propanol-1-d_1 which was prepared by reaction of propanal with a 50% molar excess of lithium aluminum deuteride in ether. The bromide was prepared by reaction of the alcohol with excess phosphorus tribromide generated *in situ* by reaction of yellow phosphorus with bromine (4). The product of these reactions, after purification by preparative scale g.l.c., was found to be 1-bromopropane-1-d_1 contaminated with *ca.* 2 mol% of 2-bromopropane-1-d_1.

1-Chloropropane-1-d_1 was prepared by the zinc chloride catalyzed reaction of the alcohol with HCl (4). After distillation and purification by preparative scale g.l.c., the product was shown, by n.m.r. and analytical g.l.c., to be 1-chloropropane-1-d_1 contaminated with *ca.* 1% 2-chloropropane-1-d_1.

Results

The Effect of Added Propene on the Reaction of 1-Chloropropane with Titanium

The results of a series of reactions performed on the same metal film, in the presence and absence of added propene, are shown in Fig. 1. From these curves it is quite evident that the rate of reaction, as measured by the slope of the half-order plots, remains quite constant and that the presence of propene in the reaction mixture has no influence on the rate. The best fit slopes of the lines in Fig. 1 span the range 1.11 to 1.14×10^{-4} Torr$^{1/2}$ s^{-1}.

Determination of the Concentration Order of the Reaction of 1-Chloropropane with Titanium

The concentration order of the reaction was determined by following the decrease in reactant concentration with time for a series of reactions on the same metal film, but with differing initial reactant concentrations. The results of such a series are shown in Fig. 2. Using a standard curve-fitting program, an equation for the best line for each set of points was generated and from these equations the slope at zero time (V_0) for each curve was evaluated. A standard plot of log V_0 *vs.* log P_0, shown in Fig. 3, yielded a concentration order of 0.49 ± 0.02 and a half-order rate constant of $1.6 \pm 0.1 \times 10^{-4}$ Torr$^{1/2}$ s^{-1}. By plotting the data from each reaction separately as a half-order reaction, the rate constant for each reaction was determined. These rate constants had a median and range of $1.69 \pm 0.03 \times 10^{-4}$ Torr$^{1/2}$ s^{-1}, in excellent agreement with that determined from the effect of P_0 on V_0. There thus remains no question that this reaction proceeds by a strict half-order rate law. The differences in apparent rate constants derived from Figs. 1 and 2 arise from the nonidentical nature of different film preparations such as different geometric areas, roughness factors, and degrees of contamination.

Halogen Exchange Reactions

Design of the Experiments

It was pointed out above that a surface reaction proceeding by a strict half-order rate

Can. J. Chem. Downloaded from www.nrcresearchpress.com by 210.87.254.105 on 09/05/12
For personal use only.

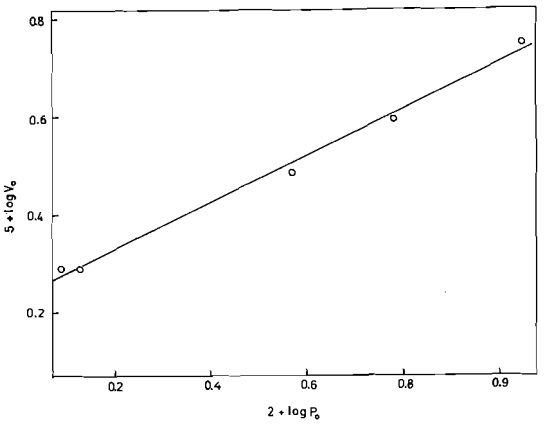

FIG. 3. Log–log plot of initial reaction rate (V_0) *vs.* initial reactant pressure (P_0) derived from curves in Fig. 2.

law is very difficult to explain by any mechanism other than one involving rapid, reversible dissociative adsorption of reactant. Further, in order that such a predissociation result in an overall half-order reaction, it must involve an equilibrium 1 which lies to the left, *i.e.* one in which $k_{-1} > k_1$.

$$[1] \qquad AB + 2^* \underset{k_{-1}}{\overset{k_1}{\rightleftharpoons}} A^* + B^*$$

where * = a univalent surface site. Thus, if an appropriately labelled mixture of reactants AB and A′B′ were reacted simultaneously, interchange of the kind shown in [2] should proceed more rapidly than any subsequent reactions.

$$[2] \qquad AB + A'B' \rightleftharpoons AB' + A'B$$

The successful experimental study of equilibrium 2, when A (or A′) = alkyl and B (or B′) = halide, for the case of dehydrohalogenation of a primary alkyl halide on titanium, required satisfaction of the following criteria. (*1*) Halogen exchange must be detectable and distinguishable from dehydrohalogenation by mass spectrometry. (*2*) Both exchanging halides must compete favorably with each other for surface sites and must undergo reaction at comparable rates. (*3*) The free energy of [2] should be close to zero. (*4*) Both reactants should react by the same mechanism.

The simplest kinds of reaction which satisfy all of the criteria outlined above are the exchanges between $R_d{}^{35}Cl$ and $R_h{}^{37}Cl$, or $R(^{12}C)^{35}Cl$ and $R(^{13}C)^{37}Cl$. The latter reaction was previously used by Anderson and McConkney (3). The limited performance of the partial pressure analyzer used in our system was insufficient to discriminate reliably between $R^{35}Cl$ and $R^{37}Cl$ under reaction conditions.

The pair of reactants 1-bromopropane and 1-chloropropane had previously been observed to react at a similar rate and according to the same rate law (1*a*). This behavior was also shown, in the course of the present study, to be true of mixtures of these reactants. The further demonstration that 1-chloropropane and 1-chloropropane-1-d_1 reacted at the same rate established the pair of reactants 1-bromopropane and 1-chloropropane-1-d_1 as apparently fulfilling all of the criteria listed above. An investigation of the possibility of halogen exchange between these reactants over titanium and chromium was therefore undertaken.

The reaction mixture used in all of the exchange experiments consisted of a mixture of 1-bromopropane (40 mol%) and 1-chloropropane-1-d_1 (60 mol%). The equilibrium product from halogen exchange in such a mixture would contain 1-bromopropane (20%), 1-bromopropane-1-d_1 (20%), 1-chloropropane (20%) and 1-chloropropane-1-d_1 (40%). By calibrating the partial pressure analyzer with each of these components, it was possible to generate a continuous series of spectra from reactants to products, assuming halogen exchange to be the only reaction. Examination of these spectra showed that two peak ratios (42/43 and 44/43) were particularly sensitive to the exchange reaction. The 42/43 peak ratio changed from 0.30 to 0.7 and the 44/43 ratio from 0.15 to 0.36 on passing from the starting mixture to exchange equilibrium.

In the absence of the full fragmentation patterns for the deuterated propenes and propanes, it was not possible to follow the detailed course of the dehydrohalogenation reaction but the overall mass spectrum was easily measured. Such measurements showed that whilst the 44/43 peak ratio only changed from 0.15 to 0.18 on proceeding to complete dehydrohalogenation, the 42/43 peak ratio changed dramatically from 0.3 in starting mixture to 2.2 at complete reaction.

Results of Exchange Experiments

Reactions were run on titanium at both 195° and 165° and at an initial reactant pressure of 0.01 Torr. At the higher temperature the dehydrohalogenation reaction proceeded to completion within the time of the experiment, but at

Can. J. Chem. Downloaded from www.nrcresearchpress.com by 210.87.254.105 on 09/05/12
For personal use only.

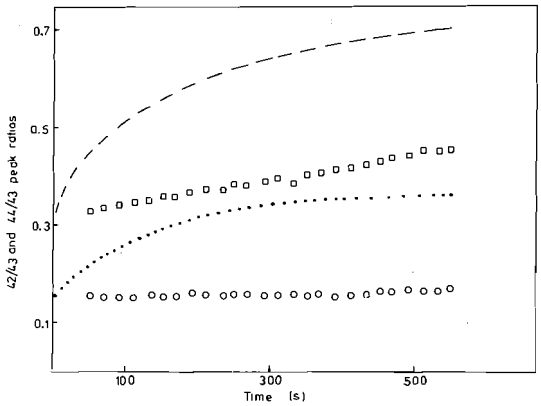

FIG. 4. Variation of 42/43 and 44/43 mass spectral peak intensity ratios for reaction of a mixture of 1-bromopropane and 1-chloropropane-1-d_1 on titanium at 165 °C. Initial pressure 0.014 Torr. Experimental points: ○, 44/43; □, 42/43. Theoretical curves, assuming equilibrium exchange after 10% dehydrohalogenation: ···, 44/43; ---, 42/43.

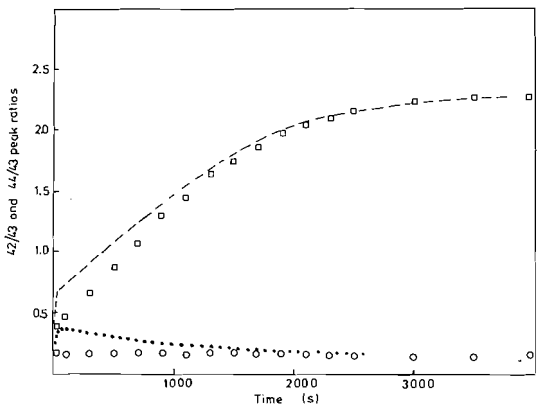

FIG. 5. Same as Fig. 4 but at 195 °C.

165° dehydrohalogenation is very slow and only proceeded to about 10% during the experiment. The results of these two experiments are shown in Figs. 4 and 5, together with curves illustrating the behavior expected for a reaction in which exchange proceeded to equilibrium by the time dehydrohalogenation was one-tenth complete. Although such a comparison is quite arbitrary, it does highlight the fact that the results give no indication of exchange occurring either before, or during, dehydrohalogenation. The rises in the 42/43 peak ratios in Figs. 4 and 5 can be entirely accounted for on the basis of the dehydrohalogenation reaction, but the failure of the 44/43 peak ratio to rise above 0.18 in either experiment cannot be reconciled with an exchange rate that is faster than dehydrohalogenation. These observations were confirmed by several repetitions of each experiment.

Although chromium metal undergoes poisoning by halide in the dehydrohalogenation of normal alkyl halides, it is possible to follow the reaction for several small doses (2). Experiments analogous to those described above gave essentially the same results on chromium, again indicating no appreciable halogen exchange.

Discussion

In the present work it has been established beyond any reasonable doubt that the high temperature dehydrochlorination of propyl chloride on titanium is a simple half-order reaction. Other studies have also shown that the reactions of ethyl and *n*-propyl chloride, bromide, and iodide (1*a*), and of 1,2-dichloroethane and 1,3-dichloropropane on titanium (1*c*) and of *n*-propyl chloride on V and Mn (2) are characterized by a reaction time-order of one-half.[2] It is now necessary to reconcile this apparently common simple kinetic pattern with the fact that halogen exchange between alkyl halides is not catalyzed by either of the metals so far studied.

The first and simplest possibility that presents itself is that the dissociative adsorption step involves not a C—Cl bond but a C—H bond. Such a dissociative adsorption at the 2-carbon atom, followed by chloride elimination would give the same overall rate behavior as the previously suggested mechanism (1*a*), in which dissociative C—Cl adsorption was followed by hydrogen elimination. The possibility that rapid reversible dissociative adsorption is occurring in these reactions has not yet been tested by, for example, looking for deuterium–hydrogen exchange between suitably labelled reactants, but the fact that 1,2-dihaloethanes and 1,3-dihalopropanes undergo clean dehalogenation without any detectable loss of hydrogen makes dissociative C—H adsorption an unlikely explanation of the half-order behavior in that case. Also, displacement of an alkyl residue from hydrogen rather than halogen as the initial step in an elimination reaction of an *n*-alkyl halide is

[2]Although the other metals of the first transition period may react similarly, the problem of surface poisoning by deposited halide precluded measurement of the kinetic rate law except for the metals cited above.

Can. J. Chem. Downloaded from www.nrcresearchpress.com by 210.87.254.105 on 09/05/12
For personal use only.

without precedent and can be argued to be unlikely on theoretical grounds (5).

A possible source of ambiguity in the present experiments is that the two alkyl halides may react selectively at different places on the reactive surface. Assuming such selective segregation of reactivity, it is possible to construct a model which accounts for lack of exchange yet still allows for the establishment of a dissociative preequilibrium between each reactant and its dissociation products at the surface. Although such a model resolves the present enigma, there is nothing in the experimental evidence to specifically support such a possibility.

Financial support for this research from the National Research Council of Canada is gratefully acknowledged.

1. J. F. HARROD and W. R. SUMMERS. (*a*) J. Am. Chem. Soc. **93**, 5051 (1971); (*b*) Can. J. Chem. **50**, 2167 (1972); (*c*) J. Oxid. Met. **6**, 117 (1973).
2. R. W. EGAN and J. F. HARROD. Can. J. Chem. **52**, 536 (1974).
3. J. R. ANDERSON and B. H. MCCONKNEY. J. Catal. **11**, 54 (1968).
4. H. GILMAN. (*Editor*). Organic synthesis, Coll. Vol. 1. John Wiley and Sons, Inc., New York. 1932. p. 36.
5. D. V. BANTHORPE. Elimination reactions. Elsevier Publishing Co., Amsterdam. 1963. p. 80.

Can. J. Chem. Downloaded from www.nrcresearchpress.com by 210.87.254.105 on 09/05/12
For personal use only.

The Infrared Spectrum Between 4000 and 200 cm^{-1} and the X-Ray Powder Diffraction Pattern of Hexamethylenetetramine Hexahydrate in Four Isotopic Forms at 100 K

JOHN E. BERTIE AND MARCO SOLINAS[1]

Department of Chemistry, University of Alberta, Edmonton, Alberta T6G 2G2

Received March 17, 1975

JOHN E. BERTIE and MARCO SOLINAS. Can. J. Chem. **53**, 2624 (1975).

The X-ray diffraction pattern of powdered hexamethylenetetramine hexahydrate (HMT-h_{12}·$6H_2O$) at 120 K has been recorded and analyzed. The thermal contraction occurs primarily along the trigonal axis. The infrared spectra of polycrystalline HMT-h_{12}·$6H_2O$, HMT-h_{12}·$6D_2O$, HMT-d_{12}·$6H_2O$, and HMT-d_{12}·$6D_2O$ at 95 K have been recorded. The most sensitive test for ice impurity is obtained from the OD stretching bands of HDO molecules in dilute solution in the hydrate, ν_{OD}(HDO), but ice impurity also affects the OH and OD stretching bands of H_2O and D_2O, $\nu_{OH}(H_2O)$ and $\nu_{OD}(D_2O)$. The absorption by HMT can be assigned to the single HMT molecule per diffraction unit cell. The symmetries of the vibrations under the C_{3v} diffraction site symmetry cannot be determined from this data, so the absorption is assigned to the parent vibration of pure HMT.

Three peaks arise from ν_{OH}(HDO) and ν_{OD}(HDO), at 2464 2369, and 2295 cm^{-1} for ν_{OD}(HDO). They can, with considerable uncertainty, be assigned to the three nonequivalent hydrogen bond lengths in the structure. An alternative assignment uses the hypothesis that the frequency of an O—D. . .O bond of given length is abnormally low when a three-coordinated oxygen atom is the base. A partial interpretation of the $\nu_{OH}(H_2O)$ and $\nu_{OD}(D_2O)$ bands is presented. It is quite clear that a large part of their breadth is due to Fermi resonance with the continuum of overtone and combination levels that lie close to the fundamental levels. Several fairly sharp features due to rotational vibrations of H_2O and D_2O, $\nu_R(H_2O)$ and $\nu_R(D_2O)$, provide the only evidence of the partial order in the positions of the hydrogen atoms. Three ν_R(HDO) frequencies have been detected, 860, 570, and 490 cm^{-1}. Their ratios agree well with the ratios of the square roots of the reciprocal moments of inertia, but not with the ratios of frequencies calculated following Blue's arguments.

JOHN E. BERTIE et MARCO SOLINAS. Can. J. Chem. **53**, 2624 (1975).

Le diagramme de poudre de l'hexaméthylènetétramine hexahydraté (HMT-h_{12}·$6H_2O$) a été pris à 120 K et a été interprété. La contraction thermique prend place principalement le long de l'axe d'ordre trois. On enregistre à 95 K les spectres infrarouges de HMT-h_{12}·$6H_2O$, HMT-h_{12}·$6D_2O$, HMT-d_{12}·$6H_2O$ et HMT-d_{12}·$6D_2O$ polycristallin. Le test le plus sensible des impuretés de glace est obtenu à partir des vibrations de valence de OD, ν_{OD}(HDO), des molécules HDO en solution diluée dans l'hydrate; mais les impuretés de glace modifient aussi les bandes de vibration de valence $\nu_{OH}(H_2O)$ et $\nu_{OD}(D_20)$ de OH et OD de H_2O et D_2O. L'absorption par HMT est attribuée à la seule molécule de HMT présente dans la maille cristalline. Il n'est pas possible de déterminer les symétries des vibrations en considérant la symétrie cristallographique ponctuelle C_{3v}; par conséquent l'absorption est attribuée à une vibration correspondante de HMT pur.

Trois pics à 2464, 2369 et 2295 cm^{-1} proviennent de ν_{OH}(HDO) et ν_{OD}(HDO) pour ν_{OD}-(HDO). On les attribue sans trop de certitude aux trois liens hydrogènes non équivalents de la structure. Une autre possibilité fait intervenir l'hypothèse que la fréquence d'une liaison O—D . . . O d'une longueur donnée est anormalement basse quand un atome d'oxygène de coordination trois en est la base. On interprète partiellement les bandes $\nu_{OH}(H_2O)$ et $\nu_{OD}(D_2O)$. Il est bien évident que la résonance de Fermi explique en grande partie la largeur des bandes avec le continuum des niveaux d'harmonique et de combinaison proche des niveaux fondamentaux. Plusieurs caractéristiques assez précises dues à des vibrations rotationnelles de H_2O et D_2O, $\nu_R(H_2O)$ et $\nu_R(D_2O)$ fournissent la seule preuve de l'ordre partiel des positions des atomes d'hydrogènes. Trois fréquences ν_R(HDO) à 860, 570 et 490 cm^{-1} ont été détectées. Leurs rapports coincident bien avec ceux des racines carrées des inverses des moments d'inertie, mais ne s'accordent pas avec les rapports des fréquences calculées d'après les arguments de Blue.

[Traduit par le journal]

[1]Present address: MacMillan-Bloedel Research, 3350 East Broadway, Vancouver, British Columbia.

Can. J. Chem. Downloaded from www.nrcresearchpress.com by 210.87.254.42 on 09/05/12
For personal use only.

Can. J. Chem. Downloaded from www.nrcresearchpress.com by 210.87.254.42 on 09/05/12
For personal use only.

Introduction

Hexamethylenetetramine hexahydrate, $C_6H_{12}N_4 \cdot 6H_2O$, (hereafter called HMT·6H$_2$O) crystallizes from saturated aqueous solutions of HMT as colorless hexagonal needles which melt at 13.05 °C (1–5). The diffraction space group at −20 °C is $R3m$ (C_{3v}^5) with one formula unit per primitive unit cell, so that the diffraction site symmetry of the HMT molecule is C_{3v} (5). Two nonequivalent types of water molecules alternate in the structure, hydrogen bonded to form slightly-puckered hexagonal rings each of which is linked to six other hexagonal rings, thus forming cavities in which the HMT molecules are located (5). The compound can, thus, be termed a clathrate hydrate (4, 5). It differs markedly from the clathrate hydrates with the common structures I and II (6) because each HMT guest molecule is hydrogen-bonded to the water lattice through three hydrogen bonds. This requires that half of the water molecules are four coordinated and half are only three coordinated. We will designate the oxygen atoms of these two types of water molecules O(IV) and O(III), respectively, to emphasize their coordination, although they are elsewhere designated O(2) and O(1), respectively (5–7).

The diffraction site symmetry of each type of water molecule is C_s, but the water molecules are partially orientationally disordered (5, 7). The X-ray results indicated that the hydrogen atoms in the three O(III)—H. . .O(IV) bonds per unit cell which join the hexagonal rings, and those in the three O(IV)—H. . .N bonds, are ordered, and the remaining six hydrogen atoms show the limited disorder which is possible within a hexagonal ring (5). However the high value of the static dielectric constant between −10 and −110 °C requires that only the hydrogen atoms in the O(IV)—H. . .N bonds are ordered and the rest are disordered (7). This means, however, that each water molecule occupies one of three possible configurations, rather than the one of six configurations possible in the disordered ices, neglecting short-range correlations in both cases. Further, each hydrogen bond between oxygen atoms is of the type O(IV). . .O(III), and the probability that the hydrogen atom is near to O(III) is 0.67, compared to 0.5 in the ices, neglecting local correlation effects in both cases. Thus the degree of order in the orientations of the water molecules in HMT·6H$_2$O is considerable. The temperature dependence of the breadth of the dielectric absorption has led to the further suggestion that long-range ordering of the hydrogen atoms may occur at low temperatures (7).

The present study forms part of an examination of the vibrational spectra of the clathrate hydrates in this laboratory, to study the absorption by water molecules in different intermolecular configurations and the spectra of the clathrated guest molecules (8–10). Of particular interest in the present study are the presence of the three-coordinated water molecules, the partial orientational order of the water molecules and the possibility of long-range order at low temperature, and the loss of degeneracy and possible activation of vibrations in HMT by the reduction in site symmetry from the T_d of pure HMT (ref. 11 and references cited therein, 12) to C_{3v} in the hydrate.

Experimental

The source and purity of the normal and perdeuterated hexamethylenetetramine (HMT-h_{12} and HMT-d_{12}) have been described (12). Laboratory distilled water and D$_2$O obtained from Atomic Energy of Canada Limited or Columbia Organic Chemicals Co. Inc. were used. The nuclear magnetic resonance spectrum of the D$_2$O, containing dimethyl sulfoxide as an internal standard, showed that it contained 0.5 ± 0.1% of hydrogen.

HMT·6H$_2$O was prepared from aqueous solutions saturated with HMT at 2 to 5 °C. The crystallization was initiated by cooling, with liquid nitrogen, the tip of the test tube which contained the solution. The tube was then warmed until only a few small crystals remained and was left for several days in a refrigerator or cold room at +3 or +5 °C, both constant to ±1 °C. When half of the solution had crystallized, the mother liquor was decanted, the crystals were dried on paper tissue, put into a glass vial, and cooled in liquid nitrogen. In most cases (see section 'Infrared Spectra') the dried crystals were further dried at 0 °C under vacuum until a white powder (HMT) was observed on their surface. HMT·6D$_2$O was prepared in the same way, after exposing the glassware to D$_2$O for at least 12 h.

The infrared samples were mulls in propane, propylene, or trifluorochloromethane (Freon-13) at 95 ± 5 K, and the spectra were recorded on a Beckman I.R. 12 spectrophotometer which was purged with dry nitrogen and calibrated to 0.5 cm^{-1} below, and 1.0 cm^{-1} above, 2000 cm^{-1}. The X-ray samples consisted of the powdered hydrate in capillary tubes at 120 ± 20 K, and a Jarrell-Ash precession camera was used as a flat-plate powder camera. Full details of the sample handling methods and the instrumentation and its calibration have been published (8–10, 13).[2]

[2]Microfiche available, at a nominal charge, from Canadian Theses Division, Cataloguing Branch, National Library of Canada, 395 Wellington Street, Ottawa, Canada K1A 0N4. For ref. 13 quote Canadian Theses on Microfiche No. 15355; for ref. 14 quote No. 15348.

TABLE 1. The powder X-ray diffraction pattern* of hexamethylenetetramine hexahydrate at 120 ± 20 K

			d (Å)	
Index†	2θ (deg)‡	Intensity§	Experiment‡	Calculated‖
101	13.57(6)	72	6.53(3)	6.52
110	15.25(5)	72	5.81(2)	5.80
021	20.49(6)	100	4.33(1)	4.33
012	22.52(3)	40	3.948(4)	3.945
211	25.68(4)	17	3.469(6)	3.471
300	26.6 (1)	21	3.35(1)	3.347
003	31.38(8)	36	2.851(7)	2.860
122				2.842
131	33.84(2)	16	2.649(1)	2.649
113	34.99(4)	2	2.564(3)	2.565
401	37.27(3)	2	2.412(2)	2.410
321	40.58(7)	14	2.223(4)	2.225
042	41.68(7)	10	2.167(4)	2.167

*Copper K_α radiation, $\lambda = 1.5418$ Å.
†Based on the triply primitive hexagonal cell of ref. 5.
‡The numbers in parentheses indicate the reproducibility of the last significant digit.
§The relative peak heights on microdensitometer traces of the photographs. The reproducibility is about 10% of the value for values greater than 10.
‖Calculated from the hexagonal axes, $a = 11.596$ Å, $c = 8.579$ Å.

TABLE 2. Lattice parameters and hydrogen bond lengths in hexamethylenetetramine hydrate at 253 and 120 K

	Value	
Parameter	253 K*	120 K
a	11.62 ± 0.01	11.60 ± 0.01
c	8.67 ± 0.01	8.58 ± 0.01
$O_1 \ldots O_2$ (between rings)	2.764 ± 0.011	2.739
$O_1 \ldots O_2$ (in ring)	2.766 ± 0.011	2.762
$O_2 \ldots N$	2.816 ± 0.009	2.807

*From ref. 5.

X-Ray Powder Diffraction Pattern

The interplanar spacings deduced from photographs of three different samples of HMT-h_{12}·6-H_2O at 120 ± 20 K are given in Table 1, with the indices, approximate intensities, and 2θ values of the reflections (CuK_α radiation, $\lambda = 1.5418$ Å). The indices are based on the triply primitive hexagonal cell of Mak (5). Except for the value 31.38° which arises from two sets of planes, the 2θ values were used to refine the lattice parameters through the Fortran IV program DREFINE (14).[2] The d-spacings calculated from the refined lattice parameters are included in Table 1 and the parameters are compared in Table 2 with those determined by Mak for HMT-h_{12}·$6H_2O$ at 253 K. Also in Table 2, the hydrogen-bond lengths determined by Mak are compared with those determined from the lattice parameters at 120 K under the assumption that the fractional coordinates of the atoms are the same at the two temperatures. It is clear that HMT·$6H_2O$ undergoes no phase change between 253 and 120 K and that the thermal contraction occurs predominantly along the threefold axis of the crystal. The mean plane of each hexagonal ring of water molecules is nearly perpendicular to c, so the O(III)...O(IV) hydrogen bonds in the ring contract very little on cooling. The O(III)...O-(IV) hydrogen bonds between the rings and the O(IV)...N bonds form angles 27 and 61°, respectively, with the c-axis, and contract by 0.025 and 0.01 Å, respectively, on cooling.

Infrared Spectra

The original spectra were of mulls in propane, propylene, and Freon 13, and contained the

Can. J. Chem. Downloaded from www.nrcresearchpress.com by 210.87.254.42 on 09/05/12
For personal use only.

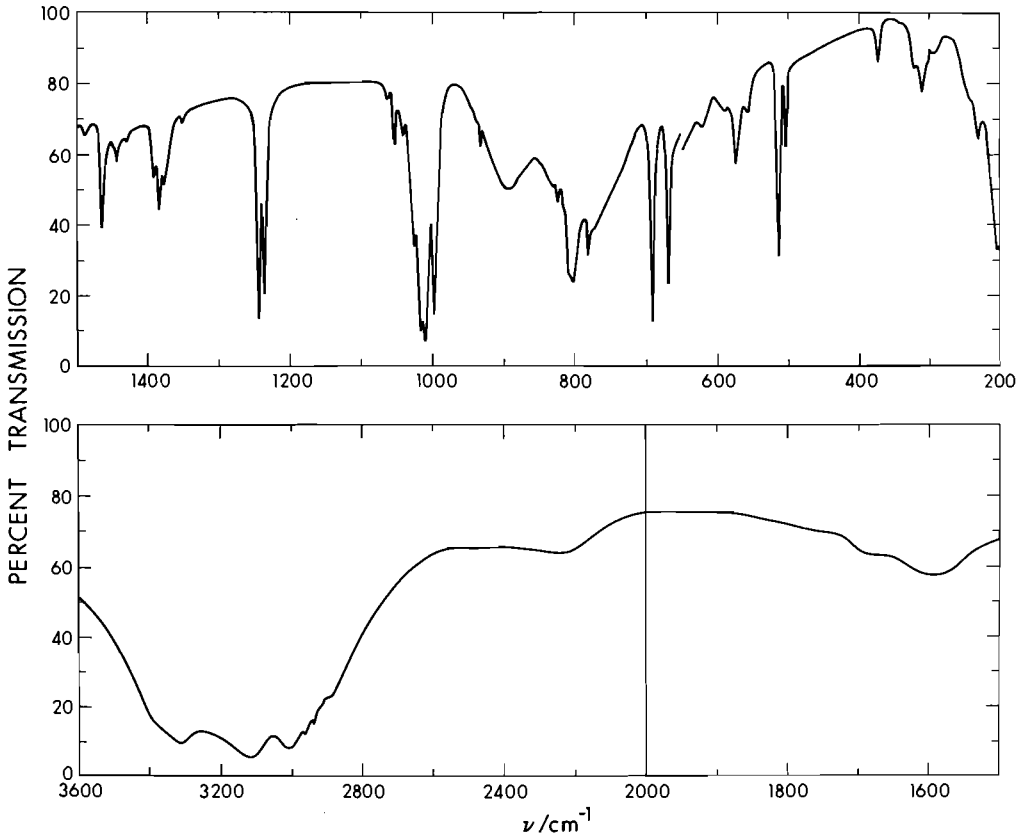

FIG. 1. The infrared spectrum of hexamethylenetetramine-h_{12} hexahydrate at 95 ± 5 K.

absorption by the mulling agents shown in Figs. 1 and 2 of ref. 9. From numerous spectra of each compound in the three mulling agents, the infrared spectra of HMT-h_{12}·6H$_2$O, HMT-d_{12}·6H$_2$O, HMT-h_{12}·6D$_2$O, and HMT-d_{12}·6D$_2$O at 95 K were deduced; these spectra are presented in Figs. 1 to 4. The resolution was better than 5 cm^{-1} below 650 cm^{-1} and better than 2 cm^{-1} above 650 cm^{-1}. The relative intensities of features taken from spectra in different mulling agents were scaled to give as accurate a description in Figs. 1 to 4 as possible. The region between 1300 and 2000 cm^{-1} has been omitted from Figs. 2 and 4 because the only observed features were the very broad features, which are due to the water, that can be seen in Figs. 1 and 3. No features were seen above 3600 cm^{-1} for HMT-h_{12}·6H$_2$O (Fig. 1) or above 3400 cm^{-1} for HMT-h_{12}·6D$_2$O (Fig. 3). The apparent drift in the absorption above 3600 cm^{-1} shown in Fig. 2 is undoubtedly due to reflection effects. The frequencies of the spectral features are listed in Table 3, with estimates of their accuracy. The only uncertainties in the spectra are: the exact shape of the high-frequency side of the strong absorption at 915 cm^{-1} by HMT-d_{12}·6H$_2$O (Fig. 2); the exact shape of the broad absorption near 1600 cm^{-1} by the deuterates (Fig. 3); the existence of the features at 1435 ± 1 cm^{-1} in the spectra of HMT-h_{12}·6H$_2$O and HMT-h_{12}·6D$_2$O (Figs. 1 and 3). All of these uncertainties are due to absorption by the mulling agents partly overlapping the features in question.

The assignment of the absorption peaks to vibrations of the water and HMT molecules follows from the isotope shifts. It is given in Table 3, where the letter subscripts to the symbol ν indicate vibrations of the water molecules and the number subscripts indicate vibrations of HMT molecules. The general assignment of the water absorption is obtained by comparison with the spectrum of ice (15).

The presence of ice impurity in the hydrate samples was carefully investigated. Initially the samples were dried on paper tissue but not under vacuum, and they all showed the very strong 00.2

Can. J. Chem. Downloaded from www.nrcresearchpress.com by 210.87.254.42 on 09/05/12
For personal use only.

Can. J. Chem. Downloaded from www.nrcresearchpress.com by 210.87.254.42 on 09/05/12
For personal use only.

TABLE 3. The mid-infrared spectral features of four isotopic modifications of hexamethylenetetramine hexahydrate at 95 ± 5 K*

HMT-h_{12}·6H_2O		HMT-d_{12}·6H_2O		HMT-h_{12}·6D_2O		HMT-d_{12}·6D_2O	
ν (cm^{-1})	Assignment	ν (cm^{-1})	Assignment	ν (cm^{-1})	Assignment	ν (cm^{-1})	Assignment
230.0 ± 0.5		229.5 ± 0.5		223.0 ± 0.5		222.3 ± 1	
240 ± 3		243 ± 2	ν_t	230 ± 3		229 ± 2	ν_t
295 ± 3 w, br	ν_t	288 ± 2 w, br		275 ± 3 w, br	ν_t	275 ± 2 w, br	
309.5 ± 0.5 m		309.7 ± 0.5 m	ν_{16}	297.4 ± 1 m		294 ± 2 m, br	
319.4 ± 0.5 m		320.4 ± 0.5 m	ν_t	306.6 ± 1 m		309.1 ± 0.5 m	ν_{16}
372.4 ± 0.5 m	ν_{16}			371.5 ± 0.5 m	ν_{16}		
						400.5 ± 0.5 s	ν_{25}
		403 ± 2 sh	ν_{25}				
		405.7 ± 0.5 m					
				415.5 ± 1 m		417.0 ± 0.5 m	
				425.0 ± 1 m			
						435 ± 2 w	
				447.0 ± 1 vw	ν_R	450.0 ± 1 vw	
				456.2 ± 1 vw		465 vw?	
				474 ± 3 sh			
		480 sh		484.2 ± 1 m		486.0 ± 1 sh	
502.6 ± 0.5 m	ν_{25}			503.3 ± 0.5 m	ν_{25}	508.0 ± 1 sh	ν_R
512.6 ± 0.5 s				510.0 ± 0.5 s		550 ± 3 sh	
556 ± 2 sh		560 ± 2 sh		550 ± 3 sh			
				560 sh			
571.2 ± 0.5 m		571.5 ± 0.5 m			ν_R		
	ν_R		ν_R	578 ± 2 s, br		576 ± 2 s, br	
589 ± 2 sh		591 ± 3 sh					
				612 ± 2 s, br		610 ± 2 s, br	
620.0 ± 1 w							
		627 ± 3 sh					
		637.0 ± 0.5 s				639.7 ± 0.5 vs	ν_{24}
			ν_{24}	645 ± 2 s, br	ν_R		
		663.2 ± 0.5 s				664.2 ± 0.5 vs	
670.9 ± 0.5 s	ν_{24}			672.2 ± 0.5 s	ν_{24}		
692.0 ± 0.5 vs				693.9 ± 0.5 vs			
						690 sh	ν_R?
		717 ± 3 sh	ν_R?				
		722.4 ± 1 s	ν_{23},				
		727.2 ± 0.5 s	$\nu_{16}+\nu_{25}$			728.5 ± 0.5 s	ν_{23}
		734 ± 3 sh				734 ± 1 sh	
750 ± 10 w	ν_R						
		751 ± 1 vw	ν_4			750 ± 1 vw	ν_4

Can. J. Chem. Downloaded from www.nrcresearchpress.com by 210.87.254.42 on 09/05/12
For personal use only.

TABLE 3 (*Continued*)

HMT-h_{12}·6H$_2$O		HMT-d_{12}·6H$_2$O		HMT-h_{12}·6D$_2$O		HMT-d_{12}·6D$_2$O	
ν (cm^{-1})	Assignment	ν (cm^{-1})	Assignment	ν (cm^{-1})	Assignment	ν (cm^{-1})	Assignment
778 ± 3 sh	ν_R						
783.9 ± 0.5 w	ν_4	784 ± 5 s, br	ν_R	783.9 ± 0.5 m	ν_4		
		801.7 ± 0.5 m	$2\nu_{25}$, ν_{15}, ν_R			800 ± 2 vw, br	$2\nu_{25}$, ν_{15}
805.2 ± 1 s 810.2 ± 1 sh 820 sh	ν_{23}, $\nu_{10}+\nu_{16}$,			812.9 ± 0.5 s	ν_{23}		
		822 ± 5 m, br		820.2 ± 0.5 m 825 ± 3 sh	$\nu_{10}+\nu_{16}$	822.5 ± 1 vw	
825.6 ± 0.5 w	ν_R						
834.0 ± 1 sh	ν_R	840 ± 5 sh	ν_9, ν_R				
						848 ± 1 vw	ν_9
		863 ± 3 w, br	ν_R				
891 ± 2 s, br	ν_R						
		905 ± 3 sh 915 ± 3 s	ν_{22}			903.3 ± 0.5 vs 911.3 ± 0.5 vs	ν_{22}
934.2 ± 0.5 w	ν_{15}?			933.4 ± 0.5 w	ν_{15}?	932.6 ± 0.5 m 936 ± 2 sh 939.1 ± 0.5 m	$\nu_{16}+\nu_{24}$
999.3 ± 0.5 vs	ν_{22}	992.0 ± 0.5 w	ν_3	998.6 ± 0.5 vs	ν_{22}	992.6 ± 0.5 w	ν_3
		997.0 ± 1 vw	ν_{13}?				
						1000 ± 1 vw	ν_{13}?
1012.3 ± 0.5 vs	ν_{22}			1012.6 ± 0.5 vs	ν_{22}		
						1019 ± 1 vw	$\nu_{16}+\nu_{23}$
1018.0 ± 0.5 vs	$2\nu_{25}$			1022 ± 3 sh	ν_9		
1027.3 ± 0.5 vs	ν_9						
1041.8 ± 0.5 m	ν_3			1040.5 ± 0.5 w	ν_3		
		1049 ± 0.5 w	ν_8			1052.0 ± 0.5 w	ν_8
1054.3 ± 0.5 m 1056.3 ± 0.5 m 1065.0 ± 0.5 w	ν_{14}, $\nu_{16}+\nu_{24}$			1054.5 ± 1 sh 1056.8 ± 0.5 s 1064.7 ± 0.5 w	ν_{14}, $\nu_{16}+\nu_{24}$		
		1078.8 ± 0.5 m 1089.0 ± 0.5 m	ν_{21}			1077.3 ± 0.5 m 1088 ± 0.5 m	ν_{21}
		1107.0 ± 0.5 m 1115.7 ± 0.5 w	ν_{20}			1105.5 ± 0.5 s 1114.7 ± 0.5 sh	ν_{20}
		1122.5 ± 0.5 w	ν_7			1120.0 ± 0.5 w	ν_7
		1139 ± 3 sh	ν_2			1133.7 ± 0.5 m	ν_2
		1142.0 ± 0.5 m 1157 sh	$\nu_{23}+\nu_{25}$			1142.0 ± 0.5 m 1156.0 ± 0.5 w	$\nu_{23}+\nu_{25}$
		1177.7 ± 0.5 vs 1190.8 ± 0.5 vs	ν_{19}			1174.2 ± 0.5 vs 1191.2 ± 0.5 vs	ν_{19}
				1200 m, br	ν_B		
		1228 ± 1 vw	$\nu_{16}+\nu_{22}$				

Can. J. Chem. Downloaded from www.nrcresearchpress.com by 210.87.254.42 on 09/05/12
For personal use only.

TABLE 3 (*Continued*)

HMT-h_{12}·6H_2O		HMT-d_{12}·6H_2O		HMT-h_{12}·6D_2O		HMT-d_{12}·6D_2O	
ν (cm^{-1})	Assignment	ν (cm^{-1})	Assignment	ν (cm^{-1})	Assignment	ν (cm^{-1})	Assignment
1232 ± 2 sh	$\nu_{10}+\nu_4$						
1237.0 ± 0.5 vs 1245.3 ± 0.5 vs	ν_{21}			1238.3 ± 0.5 s 1245.5 ± 0.5 s	ν_{21}		
				1270 sh	$\nu_{10}+\nu_{23}$		
1326.0 ± 1 vw 1335.0 ± 1 vw	ν_{13}, $2\nu_{24}$, $\nu_{23}+\nu_{25}$	1324 ± 1 vw	$\nu_{10}+\nu_{22}$	1325.4 ± 1 vw 1335 ± 1 vw	ν_{13}, $2\nu_{24}$, $\nu_{23}+\nu_{25}$		
1351.5 ± 0.5 w	ν_8			1350.0 ± 0.5 w	ν_8		
1374.6 ± 0.5 m 1382.5 ± 0.5 s	ν_{20}			1373.5 ± 0.5 m 1381.7 ± 0.5 m	ν_{20}		
1389.2 ± 0.5 m	ν_{12}?			1388.9 ± 0.5 m	ν_{12}?		
1427.0 ± 1 vw 1434.0 ± 0.5 vw	$\nu_4+\nu_{24}$			1423.3 ± 1 w 1435 ± 2 vw	$\nu_4+\nu_{24}$		
1442 ± 0.5 m	ν_2			1444.0 ± 1 m	ν_2		
1446.0 ± 1 sh	$\nu_{10}+\nu_{22}$						
1454.0 ± 1 sh	ν_7			1455 ± 2 sh	ν_7		
1461.5 ± 0.5 sh 1463.0 ± 0.5 s	ν_{19}			1461.2 ± 1 sh 1462.6 ± 0.5 s	ν_{19}		
1486.2 ± 0.5 w	$\nu_{23}+\nu_{24}$			1485.2 ± 0.5 w	$\nu_{23}+\nu_{24}$		
1610 ± 15 mbr 1690 sh 1725 ± 30 m, br 1790 ± 10 w, br 1835 ± 10 w, br	ν_B	1610 ± 20 m, br 1690 sh 1725 ± 20 sh	ν_B	1650 ± 50 m, br	$\nu_B+\nu_R$ $3\nu_R$	1675 ± 50 m, br	$\nu_B+\nu_R$ $3\nu_R$
		2086.7 ± 1 vw 2095.7 ± 1 w 2106 ± 2 vw 2114.2 ± 1 w	$\nu_3+\nu_{20}$, $\nu_{19}+\nu_{22}$, ν_1, ν_6, ν_{18}			2085 ± 1 vw 2095 ± 1 w 2112.5 ± 1 w	$\nu_3+\nu_{20}$, $\nu_{19}+\nu_{22}$, ν_1, ν_6, ν_{18}
		2122 ± 3 w	$\nu_2+\nu_3$				
		2145.2 ± 1 w 2158.5 ± 1 w	$2\nu_8$, $2\nu_{21}$			2145 ± 3 w, sh 2158 ± 3 w, sh	$2\nu_8$, $2\nu_{21}$
		2170.0 ± 1 w	$\nu_{20}+\nu_{21}$			2169.0 ± 0.5 w	$\nu_{20}+\nu_{21}$
		2200.0 vw	$\nu_2+\nu_{21}$			2200 ± 3 sh?	$\nu_2+\nu_{21}$
2250 ± 30 m, br	$\nu_B+\nu_R$, $3\nu_R$	2250 ± 30 m, br	$\nu_B+\nu_R$ $3\nu_R$	2215 ± 20 sh 2256 ± 10 vs, br 2341 ± 10 vs, br 2475 ± 20 vs, br 2530 ± 20 sh	ν_{OD}	2217 ± 5 sh 2255 ± 10 vs, br 2342 ± 10 vs, br 2475 ± 20 vs, br 2525 ± 20 sh	ν_{OD}

Can. J. Chem. Downloaded from www.nrcresearchpress.com by 210.87.254.42 on 09/05/12
For personal use only.

TABLE 3 (*Concluded*)

HMT-h_{12}·6H$_2$O				HMT-d_{12}·6H$_2$O				HMT-h_{12}·6D$_2$O				HMT-d_{12}·6D$_2$O	
ν (cm^{-1})			Assignment	ν (cm^{-1})			Assignment	ν (cm^{-1})			Assignment	ν (cm^{-1})	Assignment
2879	± 2	vw	ν_1, ν_6, ν_{18}					2885.5	± 1	m	ν_1, ν_6, ν_{18}		
2890	± 2	vw						2893.5	± 1	m			
2898	± 2	vw						2916	± 3	sh	$2\nu_2, 2\nu_{19}$		
2939	± 2	vw	$2\nu_2, 2\nu_{19}$					2937.5	± 1	m			
2965	± 2	vw	ν_{11}, ν_{17}					2961.5	± 1	m	ν_{11}, ν_{17}		
								2969	± 3	sh			
								2990.9	± 2	w	$\nu_{20}+2\nu_{23}$		
3014	± 10	vs, br	ν_{OH}	3010	± 10	vs, br	ν_{OH}						
3120	± 10	vs, br		3126	± 10	vs, br							
3215	± 10	sh		3220	± 20	sh							
3312	± 10	vs, br		3315	± 10	vs, br							
3375	± 20	sh		3380	± 10	sh							

*vw = very weak, w = weak, m = medium, s = strong, vs = very strong, sh = shoulder, br = broad. The letter subscripts to ν indicate vibrations of water; ν_B is usually called ν_2(H$_2$O) or ν_2(D$_2$O), and includes the possibility of $2\nu_R$. The numbered subscripts to ν indicate vibrations of HMT, where the vibrations are numbered as for pure HMT.

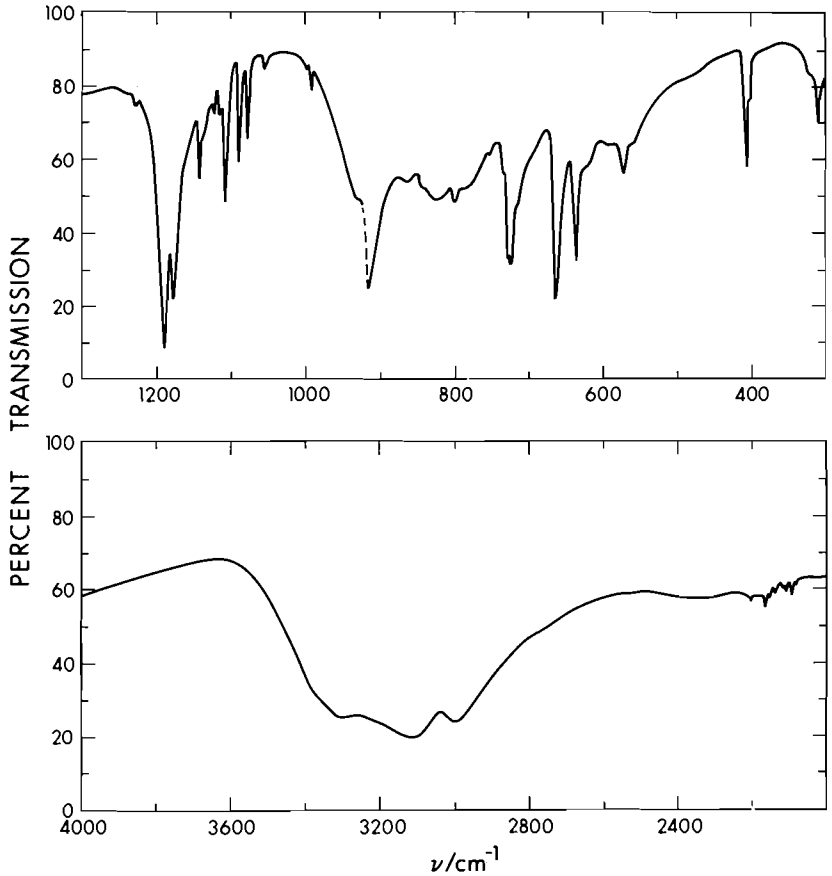

FIG. 2. The infrared spectrum of hexamethylenetetramine-d_{12} hexahydrate at 95 ± 5 K. The dashed line near 920 cm^{-1} indicates a region of slight uncertainty, due to absorption by the mulling agents. The spectrum between 1300 and 2000 cm^{-1} has been omitted for reasons given in the text.

line of ice Ih (16) as a very weak line at $2\theta \sim 24°$ in their X-ray powder pattern. The absorption by these samples is shown as curve *b* of Fig. 5. Samples that were dried under vacuum (Experimental section) showed no X-ray line at $2\theta \sim 24°$, and their absorption is shown as curve *a* of Fig. 5. Thus even a very small, as judged from the X-ray photograph, amount of ice impurity has a profound effect on the $\nu_{OH}(H_2O)$ band. The effect of ice impurity on the $\nu_{OD}(D_2O)$ band is much smaller, as shown by curves *a* (deuterate dried under vacuum) and *b* (deuterate not dried under vacuum) of Fig. 6. There was no detectable effect of ice impurity on the rest of the spectrum of either the hydrate or the deuterate.

The absorption by HDO in dilute solution in the hydrate or the deuterate provides the most sensitive test for ice impurity. The absorption by ν_{OH} and ν_{OD} of HDO in about 10 mol% solution in the deuterate and hydrate, respectively, is shown in Fig. 7. The short-dashed lines at ~3280 and 2420 cm^{-1} show where the absorption by $\nu_{OH}(HDO)$ or $\nu_{OD}(HDO)$ of ice appeared. This absorption was clearly visible even in samples whose $\nu_{OH}(H_2O)$ or $\nu_{OD}(D_2O)$ absorption was that shown as curves *a* in Figs. 5 and 6, and whose X-ray pattern gave no indication of ice impurity. The weak shoulders shown by the short-dashed lines are believed to be due to residual ice impurity. The pure HMT which was formed in small amounts when the samples were dried under vacuum did not influence the spectrum detectably, although its very strong 110 reflection (17) did contribute weakly to the X-ray powder pattern at $2\theta \sim 17°$.

The absorption by HDO molecules in the hydrate and deuterate was studied at HDO concentrations ranging from 2 to 10 mol%. The

Can. J. Chem. Downloaded from www.nrcresearchpress.com by 210.87.254.42 on 09/05/12
For personal use only.

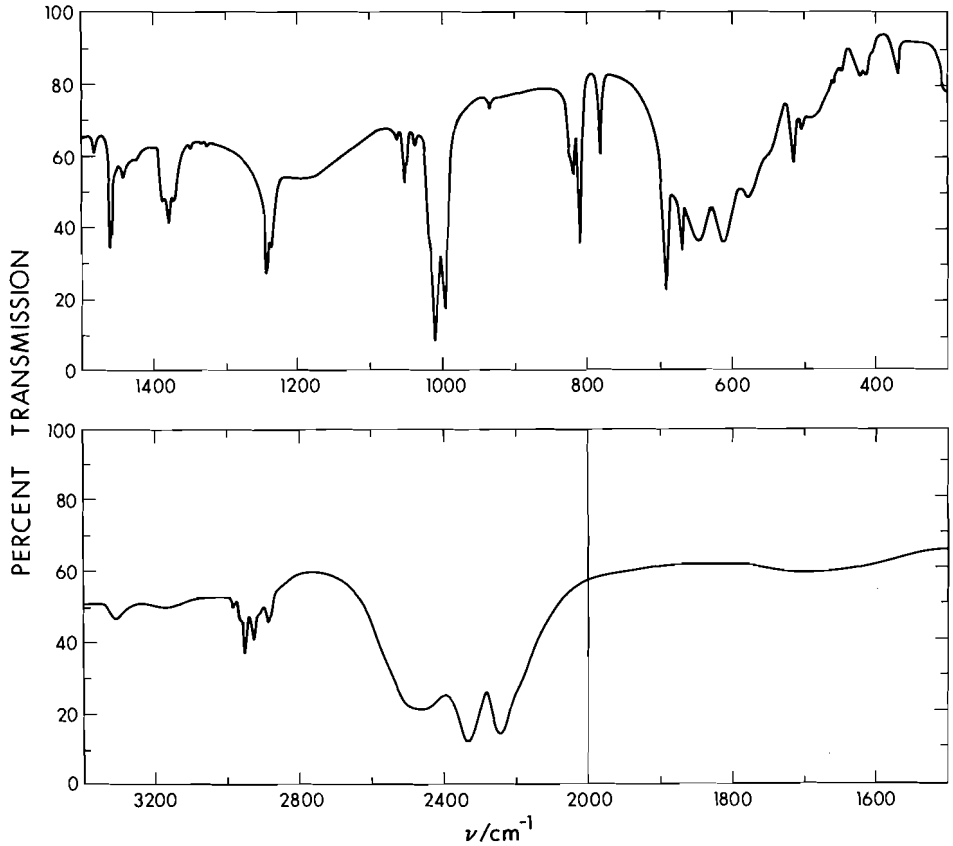

FIG. 3. The infrared spectrum of hexamethylenetetramine-h_{12} hexadeuterate at 95 ± 5 K.

frequencies, half-widths, approximate relative intensities, and isotope frequency ratios of the bands due to ν_{OH}(HDO) and ν_{OD}(HDO) are given in Table 4. Samples of hydrate and deuterate containing 10 mol% of HDO also showed HDO absorption at ~490 and 860 cm^{-1}, respectively, undoubtedly due to the rotational vibrations of HDO, ν_R(HDO). This absorption is shown in Fig. 8, which compares the absorption near the ν_R band of the host water molecules by pure hydrate and deuterate (actually 99.5% D_2O) with that by hydrate and deuterate containing 10% of HDO. These spectra show a third effect of HDO impurity, a significant broadening of the rather sharp bands due to $\nu_R(H_2O)$ at ~558, 571, and 590 cm^{-1}. These bands are expected near 420 cm^{-1} in the deuterate and probably correspond to the doublet 415.5/425 in HMT-h_{12}·6D_2O or 417.0/435 in HMT-d_{12}·6D_2O. These features in the deuterate show no effect of HDO impurity,

TABLE 4. The absorption by the O—H and O—D stretching modes of HDO in dilute solution in hexamethylenetetramine hexahydrate and hexadeuterate at 95 ± 5 K*

O—H			O—D			
ν (cm^{-1})	Relative intensity	Half-width (cm^{-1})	ν (cm^{-1})	Relative intensity	Half-width (cm^{-1})	$\frac{\nu_{OH}}{\nu_{OD}}$
3332(5)	4	45(10)	2464(5)	3.6	30(10)	1.352(5)
3184(5)	2	50(10)	2369(5)	2	35(10)	1.344(5)
3050(10)	0.7	50(10)	2295(5)	1	35(10)	1.331(9)

*The numbers in parentheses are the estimated error in the last place of the preceding value.

Can. J. Chem. Downloaded from www.nrcresearchpress.com by 210.87.254.42 on 09/05/12
For personal use only.

Can. J. Chem. Downloaded from www.nrcresearchpress.com by 210.87.254.42 on 09/05/12
For personal use only.

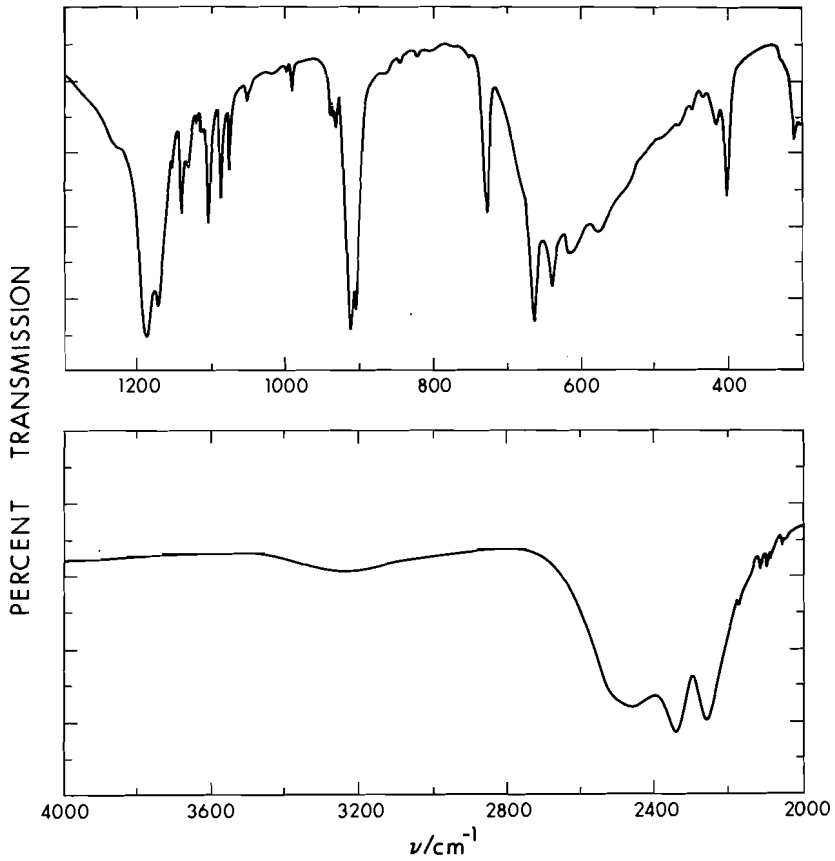

FIG. 4. The infrared spectrum of hexamethylenetetramine-d_{12} hexadeuterate at 95 ± 5 K. The spectrum between 1300 and 2000 cm^{-1} has been omitted for reasons given in the text.

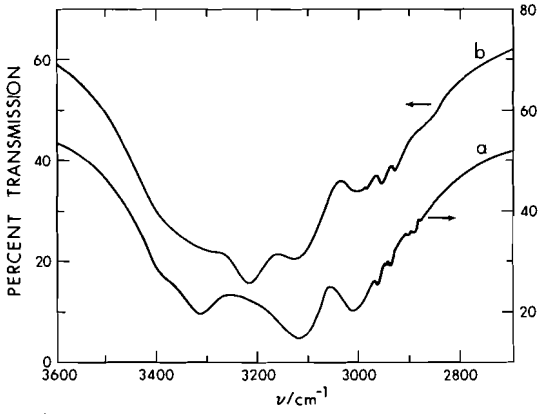

FIG. 5. The absorption by $\nu_{OH}(H_2O)$ in hexamethylenetetramine-h_{12} hexahydrate at 95 ± 5 K. The hydrate sample was dried under vacuum for curve *a* but not for curve *b*. The arrows indicate the appropriate transmission scale.

which does, however, cause an effect on the spectrum of the deuterate near 490 cm^{-1} and, as in the hydrate, near 570 cm^{-1}.

Discussion of the Absorption by the Hexamethylenetetramine Molecules

The absorption by HMT is sharp and well resolved (Figs. 1–4, 8), while that due to the water molecules is much broader. This suggests that the absorption by HMT can be interpreted by a diffraction factor group analysis of the single HMT molecule in the primitive diffraction unit cell, in spite of the known disorder of the water molecules. This may arise from the fact that neighboring HMT molecules are quite far apart (5), so that coupling of the vibrations of neighboring HMT molecules is small with the result that sharp absorption occurs even if vibrations of

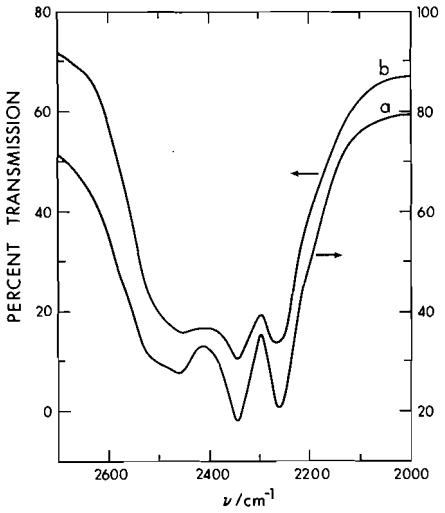

FIG. 6. The absorption by $\nu_{OD}(D_2O)$ in hexamethylenetetramine-h_{12} hexadeuterate at 95 ± 5 K. The deuterate sample was dried under vacuum for curve *a* but not for curve *b*. The arrows indicate the appropriate transmission scale.

nonzero wave vector (defined by the diffraction lattice) are active.

This interpretation also implies that no coupling occurs between the vibrations of HMT molecules and those of water molecules. This is probably not quite true, although it is a useful approximation, because there is some host dependence of the absorption by HMT. For HMT-h_{12}, the absorption at 812.9(s), 820.2(m), and 825 (sh) cm^{-1} by the deuterate (Figs. 3, 8) is sharper than, and different from, the corresponding absorption by the hydrate at 805.2(s), 810.2(sh), 820(sh), and 825.6(w) cm^{-1} (Fig. 1), even though the medium peak at 783.9 cm^{-1} is the same for both hosts. The doublet at 503.3/510.0 cm^{-1} in the spectrum of HMT-h_{12}·6D$_2$O is much weaker than the corresponding doublet at 502.6/512.6 cm^{-1} in that of HMT-h_{12}·6H$_2$O. The absorption at 999.3(vs), 1012.3(vs), 1018.0(vs), and 1027.3(vs) cm^{-1} by HMT-h_{12}·6H$_2$O changes to 998.6(vs), 1012.6(vs), and 1022(sh) cm^{-1} by HMT-h_{12}·6D$_2$O, and the doublet at 1237.0/1245.3 cm^{-1} in the spectrum of HMT-h_{12}·6H$_2$O is very well resolved while the corresponding doublet at 1238.3/1245.5 cm^{-1} in that of HMT-h_{12}·6D$_2$O is not. Similar differences can be seen in the absorption by HMT-d_{12} in the two hosts. The absorption at 728.5(s) and 734(sh) cm^{-1} by HMT-d_{12}·6D$_2$O (Fig. 4) corresponds to that at 717.3(sh), 722.4(s), 727.2(s), and 734(sh) cm^{-1} by HMT-d_{12}·6H$_2$O (Figs. 2 and 8). A shoulder and a peak appear at 403 and 405.7 cm^{-1}, respectively, in the spectrum of HMT-d_{12}·6H$_2$O, while two peaks at 400.5 and 417.0 cm^{-1} are seen in that of HMT-d_{12}·6D$_2$O, in which the 417.0 cm^{-1} peak is almost certainly due to $\nu_R(D_2O)$. Two strong, partly resolved peaks at 903.3 and 911.3 cm^{-1} in the spectrum of HMT-d_{12}·6D$_2$O correspond to a shoulder and a peak at 905 and 915 cm^{-1} in that of HMT-d_{12}·6H$_2$O, while other weaker absorptions by the deuterate at 932.6, 936, and 939.1 cm^{-1} are undetectable for the hydrate, even though they are undoubtedly due to HMT-d_{12}. Other smaller frequency and resolution differences between the spectra of the hydrate and deuterate are visible between 1100 and 1200 cm^{-1}. In particular, the very strong doublet absorption at 1177.7/1190.8 cm^{-1} by the hydrate is better resolved than that at 1174.2/1191.2 cm^{-1} by the deuterate.

Quite strong static forces exist between the water and HMT molecules, because they are joined by hydrogen bonds and because the HMT molecules are significantly distorted from the T_d symmetry of pure HMT (ref. 11 and references cited therein, 12) to the C_{3v} site symmetry in the hydrate and deuterate (5). Dynamic forces of similar origin could clearly cause the vibrations of the HMT and water molecules to interact, harmonically or anharmonically. Where the sharp HMT absorption is underlain by much broader, strong absorption by the water, such interaction is expected to broaden the sharp absorption. Transition dipole – transition dipole forces can have the same effect, and either of these forces can be used to rationalize the majority of the differences cited above, where the bands become less sharp and well-defined when they are very close to strong absorption by the water. However, it is not clear from these interpretations why the absorptions at 637.0 and 663.2 cm^{-1} by HMT-d_{12}·6H$_2$O, and those at 783.9, 670.9, and 692.0 cm^{-1} by HMT-h_{12}·6H$_2$O, are not more affected by replacement of H$_2$O by D$_2$O. Nor is it clear why the bands of HMT-h_{12} near 1000 cm^{-1} do differ so much in the spectra of the hydrates and deuterates, because neither host lattice has very strong absorption in this region, although they both probably absorb quite

Can. J. Chem. Downloaded from www.nrcresearchpress.com by 210.87.254.42 on 09/05/12
For personal use only.

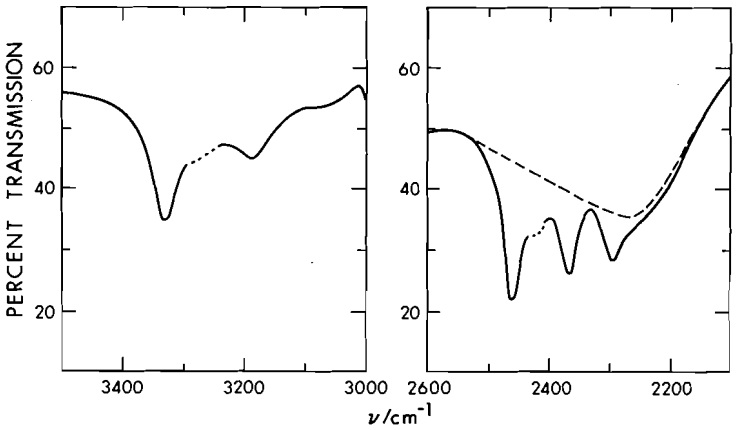

FIG. 7. The absorption by ν_{OH}(HDO) (left box) and ν_{OD}(HDO) (right box) in samples of hexamethylenetetramine hexahydrate (right box) and hexadeuterate (left box) at 95 ± 5 K which contain about 10 mol% of HDO. The long-dashed line indicates underlying H_2O absorption and the short-dashed line indicates absorption by ice impurity.

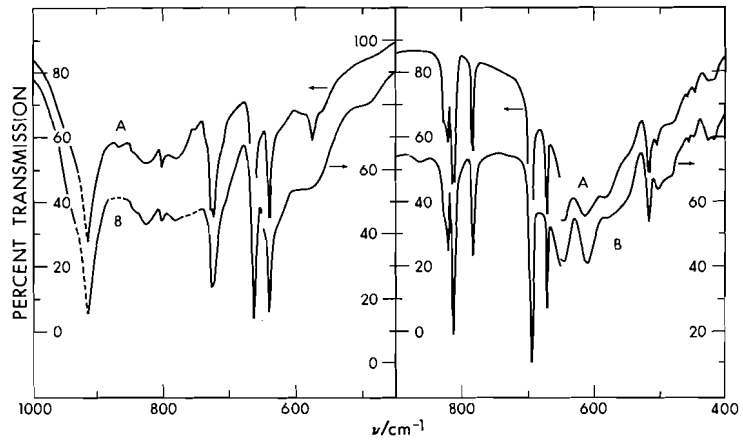

FIG. 8. Infrared absorption by HMT-d_{12}·6H_2O (left) and HMT-h_{12}·6D_2O (right) at 95 K. Curves *A* pure hydrate and deuterate (99.5% D_2O). Curves *B* samples containing 10 mol% of HDO. The breaks in the curves at 650 cm^{-1} are instrumental effects and the dashed lines indicate where the exact shape of the curve is uncertain. The arrows indicate the appropriate transmission scale.

strongly through overtone and combination transitions as is the case in ice Ih (18). Symmetry arguments cannot be used to explain these differences in behavior, because of the orientational disorder of the water molecules, and from the present evidence no further understanding seems possible. For those bands of HMT which differ in the spectra of the hydrate and the deuterate, we tentatively assume that the absorption that is sharper and better defined is characteristic of a single HMT molecule under the C_{3v} diffraction site symmetry in the hydrate or deuterate.

The correlation table between the point groups T_d and C_{3v} is given in Table 5. Lower case letters are used for the representations under C_{3v} to avoid confusion. Thus under the C_{3v} symmetry, the $9F_2$ modes of pure HMT (12) yield $9a_1 + 9e$ modes, the $6F_1$ modes become active through their *e* components, the $4A_1$ and $5E$ modes become infrared active, and only the single A_2 mode remains inactive by symmetry. The present data provide no evidence of the symmetry of the vibrations under C_{3v} that cause the various absorptions. Therefore we have assigned the HMT absorption by assuming that the frequency of a vibration in the hydrate or deuterate is very close to that of its parent vibration of pure HMT. Further, we have identified the vibrations by the number of the parent vibration (12). The

Can. J. Chem. Downloaded from www.nrcresearchpress.com by 210.87.254.42 on 09/05/12
For personal use only.

TABLE 5. Correlation table between the point groups T_d and C_{3v}

Activity*	T_d	C_{3v}	Activity*
R	A_1	a_1	i.r., R
	A_2	a_2	
R	E	e	i.r., R
	F_1	a_2	
		e	i.r., R
i.r., R	F_2	a_1	i.r., R
		e	i.r., R

*R ≡ Raman active, i.r. ≡ infrared active.

assignment of the fundamentals and a plausible, but not necessarily unique, assignment of the overtone and combination transitions is given in Table 3.

The effect of the C_{3v} site symmetry upon the vibrations of HMT is clearly seen. Nearly all of the modes derived from the A_1, E, and F_2 modes of pure HMT (12) can be readily assigned in the infrared spectra of the hydrate and deuterate, and the F_2 modes yield clear doublets ($a_1 + e$) in most cases. The only such vibrations that are not observed are those based on $\nu_{10}(E)$ of pure HMT-h_{12} and -d_{12} (~460 and ~432 cm^{-1}, respectively (12)) and the asymmetric CD_2 stretching modes, above 2200 cm^{-1} (12). However, only limited information is obtained about the F_1 modes of pure HMT. The absorptions by HMT-h_{12} and -d_{12} at 372 and 309 cm^{-1}, respectively, are undoubtedly derived from $\nu_{16}(F_1)$. The absorption by HMT-h_{12} at about 934, 1050, 1326, and 1389 cm^{-1} may be derived from $\nu_{15}(F_1)$ to $\nu_{12}(F_1)$, but may alternatively be derived from $2\nu_{10}$ or $\nu_{10} + \nu_{25}$, $\nu_{16} + \nu_{24}$, $\nu_{23} + \nu_{25}$ or $2\nu_{24}$, and $\nu_9 + \nu_{16}$ or $\nu_{10} + \nu_{15}$, respectively. Similarly, the absorption by HMT-d_{12} near 800 and 1000 cm^{-1} may be derived from $\nu_{15}(F_1)$ and $\nu_{13}(F_1)$ or from $2\nu_{25}$ and $\nu_{16} + \nu_{23}$.

Further discussion of the vibrations of HMT in its clathrate hydrate is best left until the symmetries, under C_{3v}, of the transitions causing the peaks are known from the Raman spectra of single crystals. These spectra are currently being obtained in this laboratory.

Discussion of the Absorption by the Water Molecules

OH and OD Stretching Vibrations

The frequencies, half-widths, and relative intensities of the absorption bands due to the OH and OD stretching modes of HDO (Fig. 7, Table 4) are the same for HDO concentrations between 2 and 10%. Therefore they reflect the properties of dynamically uncoupled OH or OD bonds. The half-widths are approximately the same as those for ice Ih (15, 19) and far exceed those for the ordered forms of ice, II and IX (20). Thus, they reflect the disorder in the positions of the hydrogen atoms, and give no evidence of the partial order. There are clearly three vibrationally nonequivalent types of OD (or OH) bonds in the structure, and if they were all O—D. . .O bonds, their multiplicities would be in the ratio of the absorption intensities, approximately 4, 2, and 1 in order of decreasing vibrational frequency (Table 4). One of these types of bonds must be, however, the O—D. . .N bond, whose intrinsic absorption intensity is expected to differ from that of O—D. . .O bonds.

Vibrationally nonequivalent O—D. . .O (or O—H. . .O) bonds are usually associated with different O—D. . .O lengths (9, 21). Bertie and Othen (9) have correlated the ν_{OD}(HDO) frequencies in the ice phases and ethylene oxide hydrate with the corresponding O---O distances. According to their correlations, the present frequencies correspond to the following O---O distances: 2464 cm^{-1}, 2.78 to 2.81 Å; 2369 cm^{-1}, 2.60 to 2.68 Å; 2295 cm^{-1}, 2.45 to 2.60 Å. These clearly do not agree well with the distances presented in Table 2, although the 2.78 Å may be as close to 2.76 Å as can be expected.

Falk and Knop (21) have presented two relations which correlate the frequencies reasonably well with the hydrogen bond lengths for various O—D. . .O and O—D. . .Cl bonds. To combine the two sets of data they converted the O---Cl lengths to equivalent O---O lengths, by subtracting 0.4 Å, the difference between the van der Waals radii of chlorine and oxygen (22). Their relations are: (*1*) $R = a - b(\Delta\nu)$ and (*2*) $R = C$ ($\ln d - \ln \Delta\nu$), where $a = 2.997$ Å, $b = (8.40 \pm 1.31) \times 10^{-4}$ Å cm, $\Delta\nu = (2727 - \nu)$ cm^{-1}, $C = 0.1391$ Å, and $\ln d = 25.56$.[3] These correlations gave the bond lengths associated with the frequencies 2464, 2369, and 2295 cm^{-1} as: correlation (*1*) 2.78, 2.70, 2.63 Å; correlation (*2*) 2.78, 2.74, 2.71 Å. The predicted O—D. . .N bond length can be calculated from these by the method of Falk and Knop by adding 0.1 Å, the

[3]These relations are incorrect in ref. 21. We thank M. Falk for providing the correct expressions.

Can. J. Chem. Downloaded from www.nrcresearchpress.com by 210.87.254.42 on 09/05/12
For personal use only.

Can. J. Chem. Downloaded from www.nrcresearchpress.com by 210.87.254.42 on 09/05/12
For personal use only.

difference between the van der Waals radii of nitrogen and oxygen (22). From correlation (*2*) one can, then, assign the vibrations at 2464 cm^{-1} to the six O—D. . .O bonds within the hexagonal ring (5) of the unit cell, of length 2.76 Å (Table 2) rather than the 2.78 Å calculated, the vibrations at 2369 cm^{-1} to the three O—D. . .O bonds per unit cell, of length 2.74 Å, which link the hexagonal rings, and the vibrations at 2295 cm^{-1} to the three O—D. . .N bonds per unit cell, of length 2.81 Å. Falk and Knop (21) give the standard deviation of the bond length calculated from an observed frequency using their correlations as 0.03 Å, so the difference between 2.78 and 2.76 Å is not significant. Thus both the relative intensities and the frequencies are explained in this way, if one assumes that the O—D. . .N bond absorbs less strongly than the O—D. . .O bonds by a factor of about 2.

In spite of this agreement, the reliability of this assignment is very unclear. Only one of the four possible correlations fits the frequencies and bond lengths at all well. Further, all of the correlations are based on frequencies above 2420 cm^{-1}, so large extrapolations are involved for the two lower frequencies. Finally, the separation of the frequencies associated with O—D. . .O bonds of lengths 2.76 and 2.74 Å is predicted by the correlations to be 10 or 18 cm^{-1} (9), 24 cm^{-1} ((21), correlation (*1*)) and 45 cm^{-1} ((21), correlation (*2*)), compared with the observed difference, according to this assignment, of 95 cm^{-1}. To support this point, we are aware of no crystal which is formed primarily from hydrogen-bonded water molecules in which O—D. . .O bonds which differ in length by 0.02 Å have O—D stretching frequencies which differ by more than 25 cm^{-1}; it must be admitted, however, that only a small amount of data is available on this point. In summary, it appears that, if the above assignment is correct, hexamethylenetetramine hydrate shows most unusual behavior. Two sources of such unusual behavior are evident, the hydrogen-bonded nitrogen atoms and the three-coordinated water molecules. However, the probability that these cause unusual behavior leads immediately to an alternative assignment of the bands due to ν_{OD}(HDO).

This alternative assignment is based on the hypothesis that an O(IV)—D. . .O(III) hydrogen bond, in which a three-coordinated oxygen atom acts as the base, has a much lower frequency for a given O---O distance than does a normal O(IV)—D. . .O(IV) bond or an O(III)—D. . .O-(IV) bond. There are six O(III)—D. . .O(IV) bonds, three O(IV)—D. . .O(III) bonds, and three O(IV)—D. . .N bonds per unit cell of this hydrate (5). From the intensity ratio of the bands at 2464, 2369, and 2295 cm^{-1}, the six O(III)—D. . .O(IV) bonds can be assigned to the vibrations at 2464 cm^{-1}, the three O(IV)—D. . .O(III) bonds to the vibrations at 2369 cm^{-1}, and the O(IV)—D. . .N bonds to the vibrations at 2295 cm^{-1}. In fact, since the frequencies of O(IV)—D. . .O(III) bonds are postulated to be abnormal, the intensities could also be abnormal so other permutations of the assignment are possible, but this assignment minimizes the abnormality.

There is little evidence in the literature concerning the probable frequency of an O—D. . .N bond of length 2.81 Å. Nakamoto *et al.* (23) have correlated O—H. . .N bond lengths *vs.* ν_{OH} for cyclic systems of the type

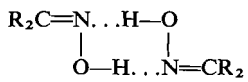

but such correlations are of little relevance to the present case, particularly as they did not result from isotopic dilution studies to eliminate the effects of intermolecular vibrational coupling. Falk (24) has studied ν_{OD}(HDO) in trimethylamine hydrate and found a single peak at 2420 cm^{-1}. This hydrate must also contain three-coordinated water molecules, since one hydrogen atom is occupied by a hydrogen bond to the nitrogen (25). However in trimethylamine hydrate the multiplicity of normal O—D. . .O hydrogen bonds with four-coordinated water molecules acting as the base is 74, while those of the O—D. . .N and the O—D. . .O bonds with a three-coordinated water molecule as the base are both 4. Thus the bands due to ν_{OD}(HDO) for the latter two types of bond may well have been too weak to observe. It must be concluded that there is no evidence to support or to refute this second assignment, and it is as likely to be correct as the assignment which is based on the bond lengths. It should be noted that the second assignment, based on the coordination of the base, implies that the frequencies due to bonds 2.74 and 2.76 Å long are close enough to be unresolved in the two higher frequency bands, which have halfwidths of 30 and 35 cm^{-1}. The correlations clearly allow

TABLE 6. The assignment of the ν_{OH}(HDO) and ν_{OD}(HDO) bands in hexamethylenetetramine hexahydrate at 95 K

ν_{OH}(HDO)*	ν_{OD}(HDO)*	Assignment† I	Assignment†‡ II
3332	2464	O—H. . .O, 2.76 Å	O(III)—H. . .O(IV) 2.76 and 2.74 Å
3184	2369	O—H. . .O, 2.74 Å	O(IV)—H. . .O(III) 2.76 and 2.74 Å
3050	2295	O—H. . .N, 2.81 Å	O(IV)—H. . .N 2.81 Å

*Frequencies in cm^{-1}.
†O—H. . .O or O—D. . .O.
‡O(III) is three-coordinated, O(IV) is four-coordinated.

this requirement as they predict the separation to be as small as 10 cm^{-1}. The two assignments of the ν_{OH}(HDO) and ν_{OD}(HDO) bands are summarized in Table 6.

The bands due to $\nu_{OH}(H_2O)$ and $\nu_{OD}(D_2O)$ in solids formed by hydrogen-bonded water molecules are not well understood (9, 15, 18, 20, 26–28). There are, however, features of these bands in the present case, and of the structure of hexamethylenetetramine hydrate, which indicate a partial interpretation. The $\nu_{OD}(D_2O)$ band has maxima at 2256, 2341, and 2475 cm^{-1} and a shoulder at 2525 cm^{-1} (Fig. 6). These frequencies are close to 2295, 2369, and 2464 cm^{-1}, those of ν_{OD}(HDO). This similarity between the frequencies of ν_{OD}(HDO) and $\nu_{OD}(D_2O)$, and the quite large differences between the three ν_{OD}(HDO) frequencies, suggest that coupling between the vibrations of different O—D bonds is much smaller in this compound than in the deuterated ices and ethylene oxide deuterate, where no similarity between the frequencies of ν_{OD}(HDO) and $\nu_{OD}(D_2O)$ exists (9, 15, 20, 26).

One can be more specific about the vibrational coupling. According to either of the assignments of the ν_{OD}(HDO) bands, intramolecular coupling between the vibrations of the two O—D bonds on the four-coordinated oxygen atoms can only shift the vibration frequencies of these bonds by $\lesssim$20 cm^{-1} ($\lesssim$10 cm^{-1} for H_2O), because their isolated frequencies are 2295 and 2369 cm^{-1}, or 2295 and 2464 cm^{-1}, too different to allow strong coupling. If the second assignment of the ν_{OD}(HDO) bands is correct, the two O—D bonds attached to the three-coordinated oxygen atoms have the isolated vibration frequency 2464 cm^{-1}, so intramolecular coupling is expected to lead to symmetric and asymmetric vibrations of D_2O, separated by about 70 cm^{-1} (40 cm^{-1} for H_2O). Further, according to this assignment, strong intermolecular coupling between O—D vibrations is only possible between the O(III)—D . . .O(IV) bonds, because the other two types of bonds are surrounded by bonds of a different type. Thus the only strong coupling expected is intramolecular coupling between the two O(III)—D. . .O(IV) bonds which are attached to the same O(III) and intermolecular coupling between the two O(III)—D. . .O(IV) bonds about the same O(IV). We thus expect the bands due to $\nu_{OD}(D_2O)$ near to 2256 and 2341 cm^{-1} to be due to essentially uncoupled vibrations of O(IV)—D. . .N and O(IV)—D. . .O(III), respectively, and the features at 2475 and 2525 cm^{-1} to be due to the vibrations of O(III)—D. . .O(IV) which are subject to intramolecular and intermolecular coupling. The intermolecular coupling is expected to be less extensive than in ice I.

Arguments based on the first assignment of ν_{OD}(HDO) lead to a similar interpretation. There can be no strong intramolecular coupling of the vibrations of the O—D bonds attached to O(IV) (see above). Further, these vibrations cannot undergo strong intermolecular coupling because the nearest neighbor bonds are all of a different type. Thus the two low frequency peaks in the $\nu_{OD}(D_2O)$ band are due to essentially uncoupled vibrations of the O—D. . .N bonds and the O—D. . .O bonds between the rings. The ν_{OD} vibrations of the O—D. . .O bonds within the hexagonal rings are subject to intramolecular or intermolecular coupling. Intramolecular coupling occurs if both of the deuterium atoms attached to a three-coordinated oxygen atom are bonded within a hexagonal ring, and there is a 33% probability that this occurs. The remaining

Can. J. Chem. Downloaded from www.nrcresearchpress.com by 210.87.254.42 on 09/05/12
For personal use only.

Can. J. Chem. Downloaded from www.nrcresearchpress.com by 210.87.254.42 on 09/05/12
For personal use only.

67% probability is that a three-coordinated oxygen atom will act as the acid in one deuterium bond in the ring and as the base in a second deuterium bond in the ring, and in this case intermolecular coupling will occur.

Thus both of these assignments of the O—D stretching vibrations of HDO lead to the same conclusion. The bands due to $\nu_{OD}(D_2O)$ at 2475 and 2525 cm^{-1} are due to the coupled vibrations of O—D bonds whose isolated frequency is 2464 cm^{-1}. The bands at 2256 and 2341 cm^{-1} are due to the essentially uncoupled vibrations whose isolated frequencies are 2295 and 2369 cm^{-1}. These latter two bands are clearly shifted by 34 ± 6 cm^{-1} to low frequency in the pure deuterate, while the two higher frequency features are centered 36 cm^{-1} to high frequency of 2464 cm^{-1}. These shifts are probably due to Fermi resonance with $2\nu_2(D_2O)$ which is expected near 2400 cm^{-1}.

The OH stretching bands can be interpreted in the same way. The $\nu_{OH}(H_2O)$ bands are broader and less well-defined than the $\nu_{OD}(D_2O)$ bands (Figs. 5 and 6), as is usually the case (9, 15, 20, 26, 28) and must be due to anharmonic effects. The extraordinary breadth and diffuseness of the $\nu_{OH}(H_2O)$ and $\nu_{OD}(D_2O)$ bands may arise from anharmonic effects, or from the combined effect of strong vibrational coupling plus the absence of selection rules in orientationally disordered crystals (15, 20, 27, 28). It has been argued above that intermolecular coupling effects must be far smaller in HMT hydrate than in the ices, yet the $\nu_{OH}(H_2O)$ and $\nu_{OD}(D_2O)$ bands of the hydrate (deuterate) are just as broad as those of the ices and the component peaks are very broad for a system with little vibrational coupling. This provides strong evidence that the breadth of these bands is largely due to anharmonic interaction (Fermi resonance) between the fundamental stretching modes and the continuum of overtone and combination levels which underlies the fundamentals. These overtone and combination levels arise from the HOH or DOD angle bending modes, the water rotational modes, and the water translational modes. An objection to this interpretation is that the $\nu_{OH}(HDO)$ and $\nu_{OD}(HDO)$ bands are superimposed on the same continuum but are much sharper than the $\nu_{OH}(H_2O)$ and $\nu_{OD}(D_2O)$ bands. An answer to this objection which is worth placing in the literature, although it needs further theoretical investigation, is that there is not a continuum of overtone and combination levels due to HDO vibrations underlying the $\nu_{OH}(HDO)$ and $\nu_{OD}(HDO)$ fundamentals. It is probable that, with the possible exception of the translational vibrations of HDO, the vibrations of HDO do not couple extensively with the continuum of vibrations due to the host H_2O or D_2O molecules. Thus they do not form a continuum of overtone and combination levels which involve HDO motion with which $\nu_{OD}(HDO)$ and $\nu_{OH}(HDO)$ can Fermi resonate strongly. This interpretation is, clearly, somewhat speculative at present, but the experimental evidence suggests strongly that an interpretation along these lines is correct.

Rotational Vibrations

The bands due to the rotational vibrations of the water molecules $\nu_R(H_2O)$ and $\nu_R(D_2O)$ contain the sharpest features that have been seen on such bands in solids which are primarily formed from hydrogen-bonded water molecules (9, 15, 20, 26), except for the very sharp features seen for the ordered forms of ice, II and IX (20). For the deuterate these features are the two main peaks of the band at 645 and 612 cm^{-1} and the subpeak at 578 cm^{-1} (Figs. 3, 4, 8). For the hydrate these features are the peak at 891 cm^{-1} (Fig. 1) and sharper features near 800 cm^{-1} (Figs. 2, 8) and, particularly, at about 590, 571, and 558 cm^{-1} (Figs. 1, 2, 8). A detailed explanation of these features cannot be given because the ν_R bands are poorly understood (27, 28), even for the ordered forms of ice for which both sharp and very broad features are seen (20). It is probable, however, that they arise from the quite different hydrogen-bond strengths which exist in HMT hydrate at 100 K, judging from the isolated OH and OD stretching frequencies and the bond lengths, and the partial order in the positions of the hydrogen atoms.

Of particular interest is the broadening effect of the presence of a few percent of HDO molecules on the sharp features near 570 cm^{-1} in the $\nu_R(H_2O)$ band (Fig. 8). The sharp $\nu_R(H_2O)$ and $\nu_R(D_2O)$ features in the spectra of the ordered forms of ice broaden in the same way, and were consequently assigned to zero-wave-vector fundamental vibrations (20). The same is probably the case here even though HMT hydrate is only partially ordered.

The presence of a few percent of HDO also affects the spectrum of the deuterate near 570 cm^{-1} (Fig. 8), so it is clear that the third $\nu_R(HDO)$

mode also absorbs in this region. This then yields the frequencies 860, 570, and 490 cm^{-1} for the three rotational vibrations of HDO. The squares of these frequencies are in the ratio 3.1:1.35:1 which agrees well with the ratio of the reciprocal moments of inertia of HDO (29), 3.6:1.4:1. Blue (30) has argued that the three rotational vibrations of an isolated H_2O or D_2O molecule in an ice-like lattice have essentially the same frequency which, from specific heat data, he places at about 700 cm^{-1} for H_2O. His argument is that the restoring force on each atom depends linearly, and only, on its displacement, and is independent of the direction of the displacement and of whether it is a hydrogen or an oxygen atom. Using this argument, the squares of the ν_R(HDO) frequencies are calculated to be in the ratio 1.5:1.1:1, and to all be lower than the isolated $\nu_R(H_2O)$ frequencies. Clearly, neither of these results agrees with the experimental ν_R(HDO) frequencies. The experimental ν_R(HDO) frequencies are comparable to those observed in the ices (15, 20), so the structure of HMT hydrate is not responsible for the disagreement. It has been suggested that the ν_R(HDO) frequencies are coupled with the ν_R vibrations of the host lattice and are pushed apart by this coupling (15). An objection to this suggestion is that they still appear as rather sharp bands, which would not be expected if they do couple extensively with the host lattice. It is probable, therefore, that the ν_R(HDO) vibrations do not couple extensively with those of the host, and that Blue's model does not describe the rotational vibrations well.

We thank the National Research Council of Canada for financial support to J.E.B. and for the award of a scholarship to M.S.

1. M. Delépine. Bull. Soc. Chim. Fr. (3) **13**, 352 (1895).
2. R. Cambier and A. Brochet. Bull. Soc. Chim. Fr. (3) **13**, 392 (1895).
3. V. Evrard. Natuurwet. Tijdshr. **11**, 99 (1929).
4. G. A. Jeffrey and T. C. W. Mak. Science, **149**, 178 (1965).
5. T. C. W. Mak. J. Chem. Phys. **43**, 2799 (1965).
6. D. W. Davidson. *In* Water a comprehensive treatise. *Edited by* F. Franks. Plenum Press, New York – London. 1973.
7. D. W. Davidson. Can. J. Chem. **46**, 1024 (1968).
8. J. E. Bertie and D. A. Othen. Can. J. Chem. **50**, 3443 (1972).
9. J. E. Bertie and D. A. Othen. Can. J. Chem. **51**, 1159 (1973).
10. J. E. Bertie, F. E. Bates, and D. K. Hendricksen. Can. J. Chem. **53**, 71 (1975).
11. J. A. K. Duckworth, B. T. M. Willis, and G. S. Pawley. Acta Cryst. **A26**, 263 (1970).
12. J. E. Bertie and M. Solinas. J. Chem. Phys. **61**, 1666 (1974).
13. M. Solinas. Ph.D. Thesis, University of Alberta, Edmonton, Alberta. 1973.
14. K. A. Simpson. Ph.D. Thesis, University of Alberta, Edmonton, Alberta. 1973.
15. J. E. Bertie and E. Whalley. J. Chem. Phys. **40**, 1637 (1964).
16. J. E. Bertie, L. D. Calvert, and E. Whalley. J. Chem. Phys. **38**, 840 (1963).
17. R. W. G. Wyckoff and R. B. Corey. Z. Kristallogr. **89**, 462 (1934).
18. J. E. Bertie, H. J. Labbé, and E. Whalley. J. Chem. Phys. **50**, 4501 (1969).
19. T. A. Ford and M. Falk. Can. J. Chem. **46**, 3579 (1968).
20. J. E. Bertie and E. Whalley. J. Chem. Phys. **40**, 1646 (1964).
21. M. Falk and O. Knop. *In* Water a comprehensive treatise. *Edited by* F. Franks. Plenum Press, New York – London. 1973. Chapt. 2.
22. L. Pauling. The nature of the chemical bond. Cornell University Press, 1945. p. 187 ff.
23. K. Nakamoto, M. Margoshes, and R. E. Rundle. J. Am. Chem. Soc. **77**, 6480 (1955).
24. M. Falk. Can. J. Chem. **49**, 1137 (1971).
25. D. Panke. J. Chem. Phys. **48**, 2990 (1968).
26. J. E. Bertie, H. J. Labbé, and E. Whalley. J. Chem. Phys. **49**, 2141 (1968).
27. E. Whalley. *In* The physics and chemistry of ice. *Edited by* E. Whalley, S. J. Jones, and L. W. Gold. Royal Society of Canada, Ottawa, Canada. 1973. p. 73.
28. E. Whalley. Dev. Appl. Spectrosc. **6**, 277 (1968).
29. W. S. Benedict, N. Gailar, and E. K. Plyler. J. Chem. Phys. **24**, 1139 (1956).
30. R. W. Blue. J. Chem. Phys. **22**, 280 (1954).

Can. J. Chem. Downloaded from www.nrcresearchpress.com by 210.87.254.42 on 09/05/12
For personal use only.

The Far Infrared Spectra of Partially Orientationally Ordered Water Molecules: Hexamethylenetetramine Hexahydrate at 95 K

JOHN E. BERTIE AND MARCO SOLINAS[1]

Department of Chemistry, University of Alberta, Edmonton, Alberta T6G 2G2

Received March 17, 1975

JOHN E. BERTIE and MARCO SOLINAS. Can. J. Chem. **53**, 2642 (1975).

The far infrared spectra of four isotopic modifications of the partially orientationally ordered clathrate hydrate hexamethylenetetramine hexahydrate at 95 K are reported. The spectra are assigned to absorption allowed under the diffraction factor group, and to disorder-allowed absorption, following the theory for absorption by translational vibrations in orientationally disordered solids. Three phases formed primarily by hydrogen-bonded water molecules are known to be significantly, but only partially, orientationally ordered, hexamethylenetetramine hexahydrate, ice V, and ice VI. Of these phases, only ice VI fails to show sharp absorption in its far infrared spectrum in addition to the broad, disorder-allowed absorption.

JOHN E. BERTIE et MARCO SOLINAS. Can. J. Chem. **53**, 2642 (1975).

On décrit les spectres infrarouge lointain à 95 K des quatre modifications isotopiques de l'hydrate-clathrate d'orientation partiellement ordonnée de l'hexaméthylènetétramine hexahydraté. On attribue les spectres à des absorptions permises dans le groupe de facteur de diffraction et à des absorptions permises de désordre, suivant la théorie d'absorption par vibrations translationnelles dans des solides d'orientation désordonnée. Trois phases, l'hexaméthylènetétramine hexahydraté et les glaces V et VI, formées principalement par des molécules d'eau liées par des hydrogènes sont essentiellement d'orientation partiellement ordonnée. Parmi ces phases, seule celle de la glace VI ne montre pas dans le spectre infrarouge lointain une bande fine d'absorption en plus de la bande large d'absorption permise de désordre. [Traduit par le journal]

Introduction

The theory for absorption by translational vibrations in orientationally disordered molecular crystals (1) has been applied to several solids which are formed primarily by orientationally disordered, hydrogen-bonded water molecules (2–6). In such solids, the dipole moment derivative with respect to the displacement, in a given crystal direction, of one of a set of diffraction-equivalent molecules depends upon which molecule of the set is displaced (1). In a fully ordered crystal there would be no such dependence. For orientationally disordered crystals, therefore, the dipole moment derivative can be considered to contain two components: the average part is invariant from molecule to molecule within the set, and the irregular part depends totally upon which molecule of the set is displaced. Two types of absorption are predicted (1) to arise from these two components of the dipole moment derivative. The average part is predicted to yield sharp absorption, which arises from those vibrations which are allowed under the diffraction factor group of the crystal. The irregular part yields broad absorption, which is subject to no selection rules and corresponds to the density of vibrational states weighted by an intensity function. This intensity function is proportional to the square of the frequency in first approximation (1).

In all of the cases, except one, that have been studied to date (2–6), only broad absorption has been seen. This was, therefore, assigned to the density of vibrational states weighted by an intensity function. The one exception is ice V (3) which showed three rather sharp features between 150 and 90 cm^{-1}. These were tentatively assigned to 3 of the 18 vibrations which are allowed under the diffraction factor group (3). The absence of diffraction factor group allowed absorption by nearly all of the disordered phases studied to date can be rationalized in the following way. The dipole moment derivative with respect to O---O distance of an O—H...O bond must oppose that of an O...H—O bond. Therefore the direction of the dipole moment derivative with respect to the displacement of a hydrogen-bonded water molecule in a crystal should be closely related to the orientation of

[1]Present Address: MacMillan-Bloedel Research, 3350 East Broadway, Vancouver, British Columbia.

Can. J. Chem. Downloaded from www.nrcresearchpress.com by 210.87.254.5 on 09/05/12
For personal use only.

Can. J. Chem. Downloaded from www.nrcresearchpress.com by 210.87.254.5 on 09/05/12
For personal use only.

that water molecule. In all of the disordered systems studied so far (2–6) the water molecules are all four-coordinated and, except in ices V and VI which are discussed later, each molecule of the sets of diffraction equivalent water molecules takes any one of the six orientations available to it with equal probability, neglecting the short-range correlation in the positions of the hydrogen atoms. Thus, the first approximation to the average part of the dipole moment derivative is zero. If the hydrogen atoms, and therefore the orientations of the water molecules, are partially ordered, the first approximation to the average part of the dipole moment derivative is not zero, and the diffraction factor-group-allowed vibrations may appear in the spectrum.

The literature concerning hexamethylenetetramine (HMT) hexahydrate has been recently reviewed (7). The diffraction factor group is isomorphous with C_{3v}. The diffraction site symmetries are C_{3v} for the one HMT molecule, and C_s for the six water molecules, per unit cell. The HMT molecules, and the three hydrogen bonds per unit cell which link them to the water molecules, are fully ordered (8). There are three four-coordinated and three three-coordinated water molecules per unit cell, and they are partially ordered to the point that they can adopt only three of the usual six orientations. The average part of the dipole moment derivative with respect to displacement of a water molecule is, therefore, expected to be quite large in the structure. Thus, sharp absorption which is allowed under the diffraction factor group is expected to be rather intense relative to the disorder-allowed absorption. In this paper we present the far infrared spectra of four isotopic modifications of HMT hexahydrate, and interpret the spectra according to the principles outlined above.

Experimental

The preparation and purification of HMT-h_{12}·6H$_2$O, HMT-h_{12}·6D$_2$O, HMT-d_{12}·6H$_2$O, and HMT-d_{12}·6D$_2$O have been reported (7). The samples were prepared as mulls in propane and held at 90 to 100 K by methods described elsewhere (5). Far infrared interferograms were recorded on a modified Beckman-R.I.I.C. model F.S. 720 interferometer, whose frequency accuracy is at least ± 0.2 cm^{-1} (5). The interferograms were recorded between $+0.65$ and -0.65 cm path differences and were Fourier transformed using triangular apodization. The intensities were obtained as the square roots of the sums of the squares of the sine and cosine transforms, and were ratioed against background spectra. The resulting spectra were then averaged in groups of four to enhance the signal-to-noise ratio. The theoretical resolution after apodization is 2.2 cm^{-1}, and spectra of gases have indicated a close similarity between the theoretical and actual resolutions.

Results and Discussion

The far infrared spectra of the four isotopic modifications of HMT hexahydrate at 95 K are shown in Fig. 1, and the frequencies of the features are listed in Table 1. The spectra clearly contain far more sharp features than those of any of the disordered phases studied previously (2–6), although a broad absorption is also present. The bands in the spectra of the HMT-d_{12} hydrate and deuterate appear rather broader than those for the HMT-h_{12} compounds. The low-temperature mulling technique is believed to be the source of this effect, because these spectra were studied

TABLE 1. Frequencies of far infrared spectral features of four isotopic forms of hexamethylenetetramine hexahydrate at 95 K*

HMT-h_{12}·6H$_2$O	HMT-h_{12}·6D$_2$O	HMT-d_{12}·6H$_2$O	HMT-d_{12}·6D$_2$O
78.2(0.5) w	78.0(0.5) w	74.2(0.5) w	74.0(0.5) w
96.3(0.5) s	95.8(0.5) s	95.7(0.5) s	94.5(0.5) s
121.5(0.5) m	120.0(0.5) m	120.8(0.5) m	119.3(0.5) m
148.8(0.5) s	143.2(0.5) s	148.0(0.5) s	141.9(0.5) s
186 (2) sh	178 (3) sh	186 (3) sh	177 (3) sh
202.4(1) s	195.6(1) s	201 (2) s	194 (2) s
229.0(1) s	222.0(1) s	229.8(1) s	223 (2) s
243 (2) sh	233 (3) sh	242 (3) sh	234 (2) sh
293 (3) w	277 (3) w	287 (3) w	276 (3) w
308.5(1) m	296.0(1) m		295.5(1) m
		309.0(1) m	308.5(0.3) m
320 (2) w	307 (2) sh	322 (3) sh	

*Frequencies are in units of cm^{-1}. w = weak; m = medium; s = strong; sh = shoulder. The uncertainty of each frequency is given in parentheses.

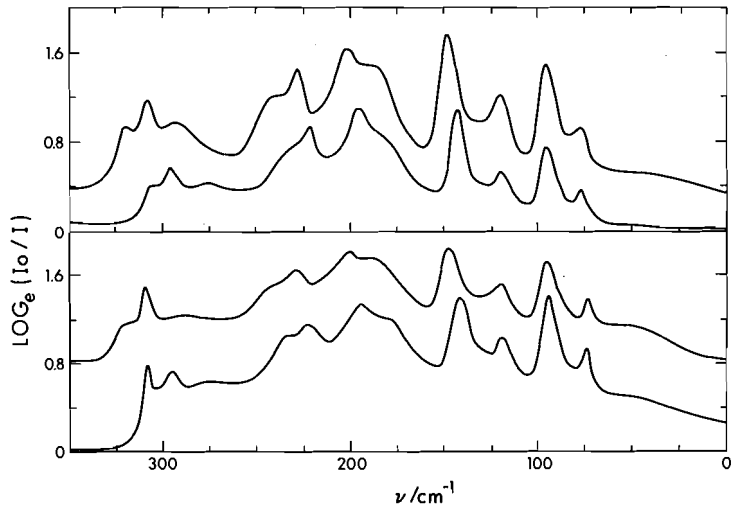

FIG. 1. Far infrared spectra of four isotopic forms of hexamethylenetetramine hexahydrate at 95 K. Upper box: upper curve is HMT-h_{12}·6H$_2$O, lower curve is HMT-h_{12}·6D$_2$O. Lower box: upper curve is HMT-d_{12}·6H$_2$O, lower curve is HMT-d_{12}·6D$_2$O.

primarily to obtain the frequencies of the features and, consequently, were not studied as extensively as those of the HMT-h_{12} compounds.

The feature at 309 cm^{-1} in the spectra of HMT-d_{12} hydrate and deuterate is due to the vibration which arises from $\nu_{16}(F_1)$ of pure HMT-d_{12} and is doubly degenerate under the C_{3v} diffraction unit cell group (7). The isotope shifts of the remaining features show that they arise from translational vibrations of water or HMT, or from rotational vibrations of HMT. The translational and rotational vibrations of HMT should be lower in HMT-d_{12} by about 4 and 9%, respectively, than in HMT-h_{12} if the HMT molecule vibrates against a body of infinite mass. In the present case, where the HMT vibrates against three water molecules, an isotope shift of about 1% is probably a closer approximation than 4% for the translational vibrations, and something less than 9% is expected for the rotational vibrations. The isotope shift on substitution of D$_2$O for H$_2$O should be 5% for relative displacements of one water molecule against another, and about 4.5% for water molecules vibrating against HMT. The exact shifts, of course, depend on the normal coordinates. The only assignments that can be made with any certainty from the observed isotope shifts are: (*1*) The rotational vibrations of HMT absorb at 78.2 cm^{-1}, shifting 5.3% on deuteration of the HMT and not significantly on deuteration of the water; (*2*) The vibration at 148.8 cm^{-1}, primarily involves translational vibrations of water molecules, with some translational motion of HMT; (*3*) The vibrations above 150 cm^{-1} are translational vibrations of water. The vibrations at 96 and 121 cm^{-1} definitely shift upon isotopic substitution, but the shifts are all very small. Apart from saying that they undoubtedly involve translational vibrations of water and HMT, no further assignment is possible until a normal coordinate calculation has rationalized these uniformly small isotope shifts.

The translational displacements of the water molecules form the representation $4A_1 + 2A_2 + 6E$ under the C_{3v} diffraction unit cell group, while the translational displacements of HMT form $A_1 + E$ and the rotational displacements form $A_2 + E$. The pure translations of the crystal form $A_1 + E$, which leaves $4A_1 + 3A_2 + 7E$ genuine vibrations with zero-wave-vector, of which $4A_1 + 7E$ are infrared active.

Eleven fairly sharp features are evident in the spectra of HMT-h_{12} hydrate and deuterate, so it is probable that these correspond to the 11 active vibrations under the diffraction factor group. Many of these features are rather broad compared with bands due to active vibrations in ordered crystals, such as ices II and IX (3), but this does not necessarily argue against this assignment. There is clearly broad, disorder-allowed absorption underlying the sharp absorption, and it is certain that diffraction factor-group-allowed vibrations can interact with the

Can. J. Chem. Downloaded from www.nrcresearchpress.com by 210.87.254.5 on 09/05/12
For personal use only.

disorder-allowed vibrations, which gain intensity through the interaction and broaden the factor-group-allowed absorption. That this is definitely the correct interpretation of these spectra cannot be fully certain until the density of states of HMT hydrate has been calculated. However, further evidence may be supplied by the Raman spectra of single crystals, in which the factor-group-allowed transitions should show clear polarization properties and should be more intense relative to the disorder-allowed transitions than in the infrared (1). These Raman spectra are being obtained in this laboratory.

It was noted earlier that the only previous evidence of factor-group-allowed transitions in the spectra of the disordered forms of ice came from the spectrum of ice V. This can be rationalized by the fact that ice V is now known to be quite significantly ordered at about 100 K (9), the temperature at which the spectra were recorded (3). Only one phase spoils the pattern that some sharp features are observed in the far infrared spectrum if the phase is significantly orientationally ordered, and none are observed if no significant ordering is present. Ice VI is now known to be significantly ordered at 110 K (10), but no sharp features were observed in its far infrared spectrum (4). No reason for different behavior by ice VI is evident, but it should be pointed out that for the partially ordered, orthorhombic ice VI at 110 K (space group *Pmmn*, D_{2h}^{13}, $Z = 10$, 2 oxygens on sites *a* of symmetry C_{2v}, 8 oxygens on sites *g* of symmetry C_1 (10, 11)) nine translational vibrations of water molecules are allowed under the diffraction unit cell group, compared with 18 allowed vibrations for ice V (3, 9). There is, thus, a greater statistical probability that some will be seen for ice V than for ice VI.

We thank the National Research Council of Canada for financial support to J.E.B. and for the award of a scholarship to M.S.

1. E. WHALLEY and J. E. BERTIE. J. Chem. Phys. **46**, 1264 (1967).
2. J. E. BERTIE and E. WHALLEY. J. Chem. Phys. **46**, 1271 (1967).
3. J. E. BERTIE, H. J. LABBÉ, and E. WHALLEY. J. Chem. Phys. **49**, 775 (1968).
4. J. E. BERTIE, H. J. LABBÉ, and E. WHALLEY. J. Chem. Phys. **49**, 2141 (1968).
5. J. E. BERTIE and D. A. OTHEN. Can. J. Chem. **50**, 3443 (1972).
6. J. E. BERTIE, F. E. BATES, and D. K. HENDRICKSEN. Can. J. Chem. **53**, 71 (1975).
7. J. E. BERTIE and M. SOLINAS. Can. J. Chem. This issue.
8. T. C. W. MAK. J. Chem. Phys. **43**, 2799 (1965).
9. W. C. HAMILTON, B. KAMB, S. J. LAPLACA, and A. PRAKASH. *In* Physics of ice. *Edited by* N. Riehl, B. Bullemer, and H. Engelhardt. Plenum Press, New York. 1969. p. 44.
10. B. KAMB. *In* Physics and chemistry of ice. *Edited by* E. Whalley, S. J. Jones, and L. W. Gold. Royal Society of Canada, Ottawa, Canada. 1973. p. 28.
11. N. F. M. HENRY and K. LONSDALE. (*Editors*). International tables for X-ray crystallography, Vol. 1. The Kynoch Press, Birmingham, England. 1965.

Can. J. Chem. Downloaded from www.nrcresearchpress.com by 210.87.254.5 on 09/05/12
For personal use only.

Infrared Spectroscopic Study of Ammonia – Sulfur Dioxide – Water Solid State System[1]

I. C. HISATSUNE AND JULIAN HEICKLEN

Department of Chemistry and Center for Air Environment Studies, The Pennsylvania State University, University Park, Pennsylvania 16802

Received March 21, 1975

I. C. HISATSUNE and JULIAN HEICKLEN. Can. J. Chem. **53**, 2646 (1975).

Products formed during the solid state reactions between ammonia and sulfur dioxide in the presence or absence of water have been investigated by infrared spectroscopy. Warming of a low-temperature matrix of SO_2 with excess NH_3 produces $(NH_3)_2 \cdot SO_2$ at -90 °C. This adduct decomposes near -50 °C into $NH_3 \cdot SO_2$ which has a yellow color. With excess SO_2 only $NH_3 \cdot SO_2$ appears at -150 °C. The 1:1 complex disappears from the low-temperature infrared window at about -20 °C. With H_2O present in the matrix, $(NH_3)_2 \cdot SO_2$ is converted at -80 °C into ammonium sulfite which is stable to room temperature where it can be pumped off readily from the infrared window. With less than the stoichiometric amount of water, the final product of the warming sequence is ammonium pyrosulfite whose infrared spectrum varies considerably with experimental conditions. The pyrosulfite reacts further with water to give ammonium bisulfite. The infrared spectra of solid ammonium bisulfite and perdeuteroammonium bisulfite show that the hydrogen in the bisulfite ion is bonded to the sulfur atom. Vibrational assignments have been made for all the compounds.

I. C. HISATSUNE et JULIAN HEICKLEN. Can. J. Chem. **53**, 2646 (1975).

On a étudié, par spectroscopie infrarouge, la nature des produits formés par réactions, à l'état solide, de l'ammoniac avec le dioxyde de soufre en présence ou en l'absence d'eau. A -90 °C, lorsqu'on réchauffe une matrice de SO_2 dans un excès de NH_3, il y a production de $(NH_3)_2 \cdot SO_2$. Cet adduit se décompose près de -50 °C pour conduire au $NH_3 \cdot SO_2$ qui a une couleur jaune. A -150 °C, lorsque le SO_2 est en excès, il n'y a production que de $NH_3 \cdot SO_2$. Le complexe 1:1 disparait des fenêtres infrarouges à basse température lorsque la température est ramenée vers -20 °C. Lorsqu'il y a de l'eau présente dans la matrice, le $(NH_3)_2 \cdot SO_2$ se transforme vers -80 °C en sulfite d'ammonium qui est stable jusqu'à la température de la pièce alors qu'il peut être facilement enlevé de fenêtres infrarouges. Lorsque les quantités d'eau utilisées sont plus faibles que les proportions stoichiométriques, le produit final résultant du réchauffement est une pyrosulfite dont le spectre infrarouge varie d'une façon considérable suivant les conditions expérimentales. Le pyrosulfite réagit avec l'eau pour donner le bisulfite d'ammonium. Les spectres infrarouges du bisulfite d'ammonium solide et du perdeutéro bisulfite d'ammonium indiquent que l'hydrogène de l'ion bisulfite est lié à l'atome de soufre. On a fait des attributions pour toutes les vibrations de tous les composés.

[Traduit par le journal]

Introduction

The formation of the solid adducts $NH_3 \cdot SO_2$ and $(NH_3)_2 \cdot SO_2$ in the gas phase reaction of NH_3 with SO_2 appears to be well established (1, 2; references to earlier studies are given in ref. 2), but the infrared spectra of these complexes have not been reported. Hata (3) had examined the infrared spectrum of the solid products formed by the reaction between anhydrous NH_3 and SO_2 but had detected only ammonium pyrosulfite containing traces of sulfite and bisulfite ions. He carried out the reaction directly in the infrared cell using reactant pressures of about 150 Torr, but he recorded the spectrum after the cell had been evacuated thoroughly. When the reaction was carried out in a 4-litre vessel with 30 to 70 Torr of reactant gases, Hata found the products of this highly exothermic reaction to be the unstable thionyl imide and a solid which was light yellow or dark yellow depending, respectively, on whether the reaction vessel was cooled or not cooled. He concluded, therefore, that the overall reaction is

$$[1] \quad 3NH_3(g) + 3SO_2(g) \rightarrow HNSO(g) + (NH_4)_2S_2O_5(s)$$

In a related study carried out subsequently, Hata reported the infrared and Raman spectra of the stable 1:1 adducts of dimethyl and

[1]CAES Report No. 388-75.

Can. J. Chem. Downloaded from www.nrcresearchpress.com by 210.87.254.105 on 09/05/12
For personal use only.

Can. J. Chem. Downloaded from www.nrcresearchpress.com by 210.87.254.105 on 09/05/12
For personal use only.

trimethyl amines with SO_2 (4). Moderately strong, polarized Raman lines observed, respectively, at 206 and 174 cm^{-1} from the melts of these complexes were assigned to the N—S bond stretching mode.

Scargill also investigated the gas phase reaction between NH_3 and SO_2 in a flow system (5). He observed no reaction on mixing the anhydrous reactant gases which were diluted with dry air by 200-fold. However with the addition of a small amount of water, he observed the formation of a white solid which was analyzed to be ammonium pyrosulfite when SO_2 was in excess. When ammonia was in excess the white solid was found to be ammonium sulfite. Scargill reported the infrared spectra of the pyrosulfite and sulfite salts but not the peak frequencies. However, more detailed spectroscopic studies of the pyrosulfite ion (6–8) and the sulfite ion (9) have been reported by other investigators. The structure of the pyrosulfite ion is also known (10).

In the present investigation, a low-temperature infrared spectroscopic technique was used to examine the reaction between NH_3 and SO_2. Solid films consisting of layers of SO_2 and NH_3 films or of mixtures of NH_3 and SO_2 with one or the other in excess were prepared. These films were allowed to warm and the progress of the resulting reactions was examined by infrared spectroscopy. By this method the infrared spectra of $NH_3 \cdot SO_2$ and $(NH_3)_2 \cdot SO_2$ have been obtained for the first time. In addition, the complete spectrum of the bisulfite ion has been identified, and it has necessitated a revision of the previous assignment of the infrared spectrum of the pyrosulfite ion.

Experimental

Ammonia and sulfur dioxide were from the Matheson Co. These gases were liquefied in a high vacuum line and distilled, the central fraction being collected in storage bulbs. The source of ND_3 was Merck, Sharp, and Dohme of Canada, Ltd., and it was used directly. Distilled water and D_2O (99.8%) from Volk Radiochemical Co. were degassed in the vacuum line before use. The infrared spectra of the reagents showed no superfluous absorption bands.

The low-temperature infrared cell made of Pyrex glass was the same cell used in an earlier study of the olefin–ozone reactions (11). The operation of the cell had been described in detail in that study. The same Perkin-Elmer Model 225 grating infrared spectrophotometer was also used in the present study.

Solid samples for spectroscopic observations were prepared in two ways. In one method a film of one reactant was condensed first on the low-temperature infrared window and then the second reactant was deposited on top. In the second method, SO_2 and NH_3 were condensed in a storage vessel, the solid allowed to warm to room temperature, and then the gas from this storage vessel was condensed on the low-temperature infrared window. Solid samples with excess NH_3, excess SO_2, or equivalent amounts of the two reactants were prepared by these methods. After the initial spectrum of the sample was recorded, the solid was allowed to warm to a given temperature and then recooled to liquid nitrogen temperature to record its spectrum again. Such warming and recooling cycles were repeated to follow the progress of the reactions taking place in the solid phase. For the study of hydrolysis reactions, a film of water was deposited on top of the $[NH_3]/[SO_2]$ matrix after it was prepared or after it was carried through one or more warming cycles.

Results

When NH_3 and SO_2 were condensed as separate layers at liquid nitrogen temperature either on the infrared window or in the storage vessel, no reaction took place. The solid had a white color and its infrared spectrum consisted of absorption bands of NH_3 solid (12) and SO_2 solid (13). The lower curve in Fig. 1 illustrates a typical spectrum from a layer sample at liquid nitrogen temperature. Here, $[NH_3]/[SO_2] = 0.86$ and SO_2 was condensed first. The prominent peaks in this spectrum are readily assigned as the degenerate N—H stretch band at 3380 (2500) cm^{-1}, the degenerate NH_3 deformation band at 1650 (1200) cm^{-1}, the antisymmetric S—O stretch band at 1320 cm^{-1}, the symmetric S—O stretch band at 1150 cm^{-1}, the symmetric NH_3 deformation band at 1060 (820) cm^{-1}, the SO_2 deformation band at 530 cm^{-1}, and the NH_3 lattice band at 360 (320) cm^{-1}. Frequencies in parentheses are for the ND_3 species at liquid nitrogen temperature.

On warming the solid sample, changes in color and spectrum occurred. In the storage vessel where color changes were more readily observable, an excess NH_3 solid sample developed a deep yellow color about 1 min after the liquid nitrogen bath was removed. The yellow coloration was lighter when the sample contained excess SO_2. Further warming of the solid containing excess NH_3 or excess SO_2 to room temperature gave a yellow residue which generally turned white on evacuation of the storage vessel. The infrared spectra of the gases from these reactions showed only bands due to NH_3 and SO_2. The middle curve in Fig. 1 is a typical infrared spectrum of a room temperature residue obtained from a layer sample with

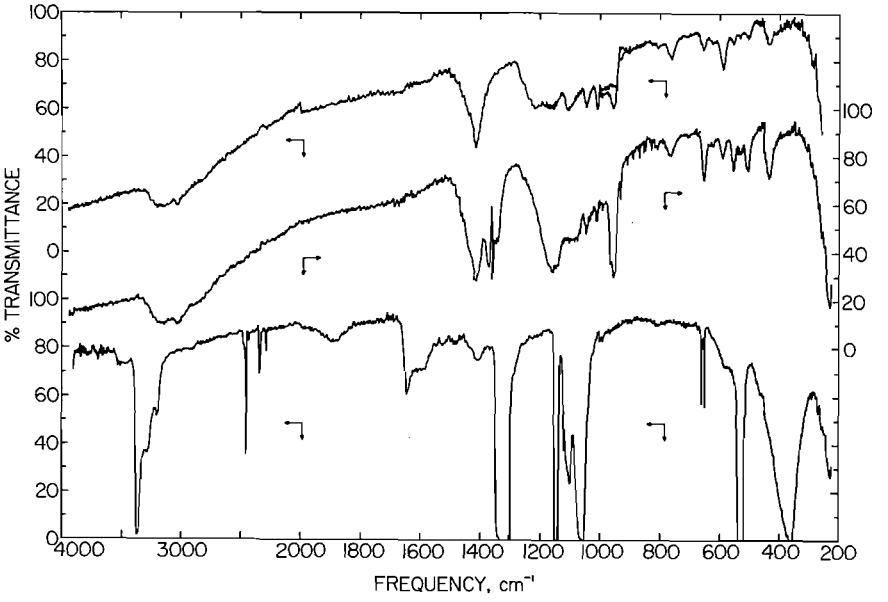

FIG. 1. Infrared spectra of residues from a solid state reaction between NH_3 and SO_2 with $[NH_3]/[SO_2] = 0.86$. Lower curve, initial solid sample at liquid nitrogen temperature; middle curve, sample after warming to room temperature; upper curve, residues after 20 min evacuation of the absorption cell.

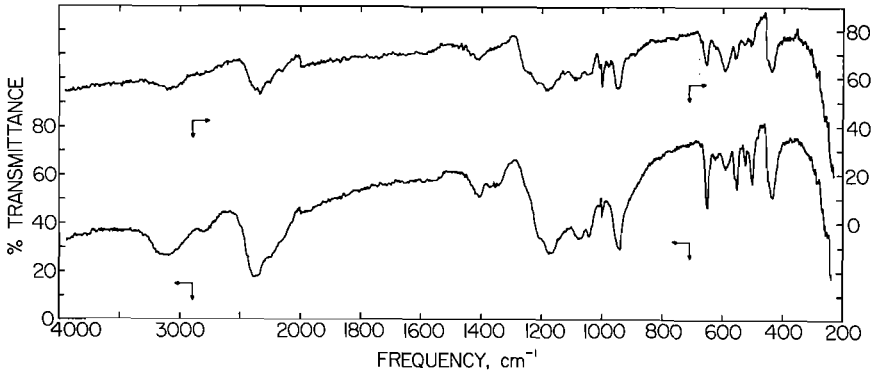

FIG. 2. Infrared spectra of residues from a solid state reaction between ND_3 and SO_2 with $[ND_3]/[SO_2] = 1.19$. Lower curve, reactant solid sample warmed to room temperature; upper curve, sample after recooling of the absorption cell to liquid nitrogen temperature.

$[NH_3]/[SO_2] = 0.86$, and the upper spectrum is from the same sample after it had been evacuated for 20 min. The room temperature residue from a layer sample with $[ND_3]/[SO_2] = 1.19$ gave the spectrum shown by the lower curve in Fig. 2. The upper curve in this figure is from the same sample after it had been recooled to liquid nitrogen temperature.

The changes in the spectra of these room temperature residues with evacuation or cooling, particularly in the S—O bond stretch mode region of 900 to 1300 cm^{-1}, indicated that these residues were somewhat volatile. However, their volatility and spectra appeared to depend on the relative concentrations of the reactants and particularly on the amount of water, added deliberately or present as an impurity, in the sample. Although the low-temperature cell and the gas transfer vacuum line were evacuated at least overnight with a three-stage oil diffusion pump, it was not possible to remove completely traces of water. Also, as our sample in the closed cell system was repeatedly warmed and recooled during an experiment which usually extended

Can. J. Chem. Downloaded from www.nrcresearchpress.com by 210.87.254.105 on 09/05/12
For personal use only.

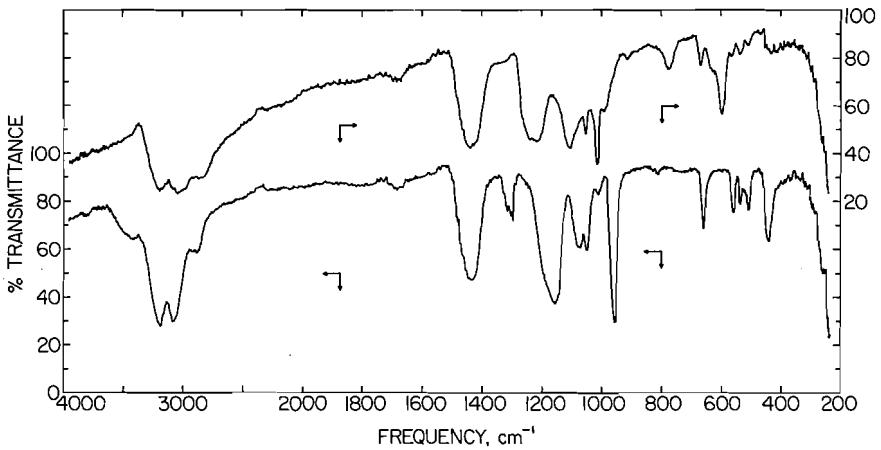

FIG. 3. Infrared spectra of residues from a solid state reaction between NH_3 and SO_2 in the presence of water. Lower curve, products from a solid sample with $[NH_3]:[SO_2]:[H_2O] = 0.68:1:0.52$ after warming to -65 °C and recooling to liquid nitrogen temperature; upper curve, residue at liquid nitrogen temperature from a sample with $[NH_3]/[SO_2] = 1.27$ after six warming and recooling cycles followed by overnight evacuation at room temperature.

over many hours, the water content appeared to increase and gave noticeable variations in the infrared spectra. Generally, the volatility of the residue appeared to decrease as the water content of the solid sample increased, and this decrease was accompanied by changes in the intensities of several infrared bands. A broad band at 1230 cm^{-1} and sharper bands near 1050, 1010, and 600 cm^{-1} increased in intensity while a prominent band at 960 cm^{-1} became weaker. At the same time the broad absorptions in the 1000 to 1200 cm^{-1} region showed changes in peak shapes and positions. The final spectrum of the residue is illustrated by the upper curve of Fig. 3. This sample was prepared by freezing the reactants with $[NH_3]/[SO_2] = 1.27$ in the storage vessel and then condensing the gas from this vessel on the low-temperature infrared window. The sample was subsequently carried through six warming and recooling cycles, warmed finally to room temperature, allowed to stand overnight while the cell was evacuated, and then recooled to obtain the spectrum shown in Fig. 3. The lower spectrum in this figure was obtained from a solid reaction mixture in which water was actually added. In this case, the gas from the storage vessel with $[NH_3]/[SO_2] = 0.68$ was condensed on the cell window and H_2O at $[NH_3]/[H_2O] = 1.30$ was condensed on top. The solid sample was warmed to -65 °C and then recooled to liquid nitrogen temperature to record the spectrum. The spectrum of this sample at room temperature was essentially the same except that it contained the *PQR*-structured 1360 cm^{-1} band of gaseous SO_2 and the doublet band of NH_4^+ near 1400 cm^{-1} had coalesced.

When more water was added to samples with $[NH_3]/[SO_2]$ of about one or less, the final residue was ammonium bisulfite. The infrared spectra of NH_4HSO_3 and ND_4DSO_3 taken at liquid nitrogen temperature are shown in Fig. 4. The frequencies of the bisulfite ion vibrational modes which involve the hydrogen atom were identified by exposing ND_4DSO_3 to H_2O vapor and NH_4HSO_3 to D_2O vapor. The hydrogen stretch and bend modes are at 2588 (1878) and 1123 (831) cm^{-1}, respectively. The values in parentheses are for the deuterium compound. Ammonium bisulfite is stable at room temperature. In the presence of pure oxygen gas, only a trace of sulfate ion was detected after overnight exposure at room temperature. Exposure of a sample to pure ozone at room temperature for about 30 min also produced no changes in its infrared spectrum. Neither did oxygen gas appear to affect the final results when it was present during the reactions to produce the residues shown by the lower spectrum of Fig. 3 and during the subsequent hydrolysis of this residue to ammonium bisulfite.

The residue from the hydrolysis of a solid reactant sample with $[NH_3]/[SO_2] > 2$ was ammonium sulfite, and its infrared spectrum is shown in

Can. J. Chem. Downloaded from www.nrcresearchpress.com by 210.87.254.105 on 09/05/12
For personal use only.

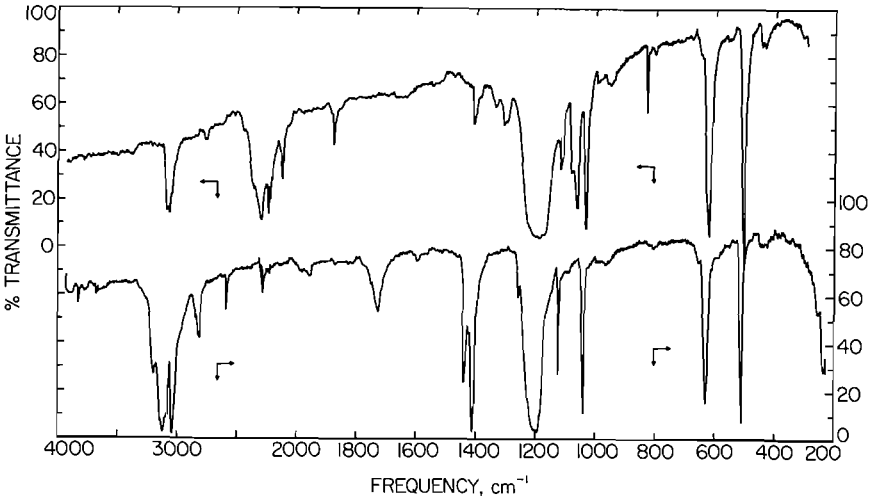

FIG. 4. Infrared spectrum of ammonium bisulfite at liquid nitrogen temperature. Lower curve, NH_4HSO_3; upper curve, ND_4DSO_3.

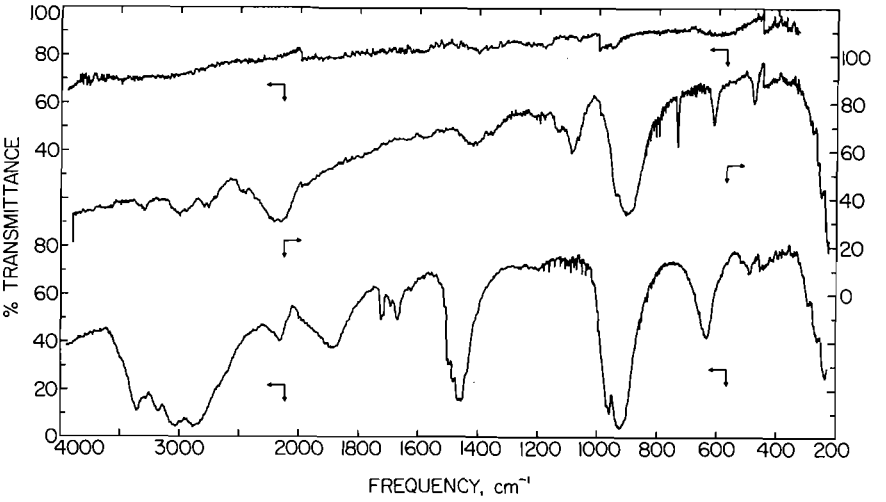

FIG. 5. Infrared spectrum of ammonium sulfite. Lower curve, $(NH_4)_2SO_3$ at room temperature; middle curve, $(ND_4)_2SO_3$ at room temperature; upper curve, $(ND_4)_2SO_3$ sample after short evacuation.

Fig. 5. This salt was very volatile at room temperature and could be pumped off the infrared window readily. The upper curve in Fig. 5 illustrates the loss of sample when the window with the $(ND_4)_2SO_3$ sample giving the middle spectrum was cooled with liquid nitrogen. During the cooling process of the cell, the infrared window is warmer than the metal window holder which comes in contact with the liquid nitrogen. Thus, samples with high vapor pressures are sublimed off the window during the recooling cycle.

When a solid sample prepared by depositing separate layers of NH_3 and SO_2 was allowed to warm slowly from liquid nitrogen temperature, NH_3 began to leave the window at about $-145\,°C$. Concomitantly, the sample started to show a light yellow coloration and a set of new absorption bands appeared in the spectrum, which did not depend on whether SO_2 was in excess or NH_3 was in excess in the original layer sample. From the rate of growth of the new peaks it was evident that a single primary product was being generated by the reaction

Can. J. Chem. Downloaded from www.nrcresearchpress.com by 210.87.254.105 on 09/05/12
For personal use only.

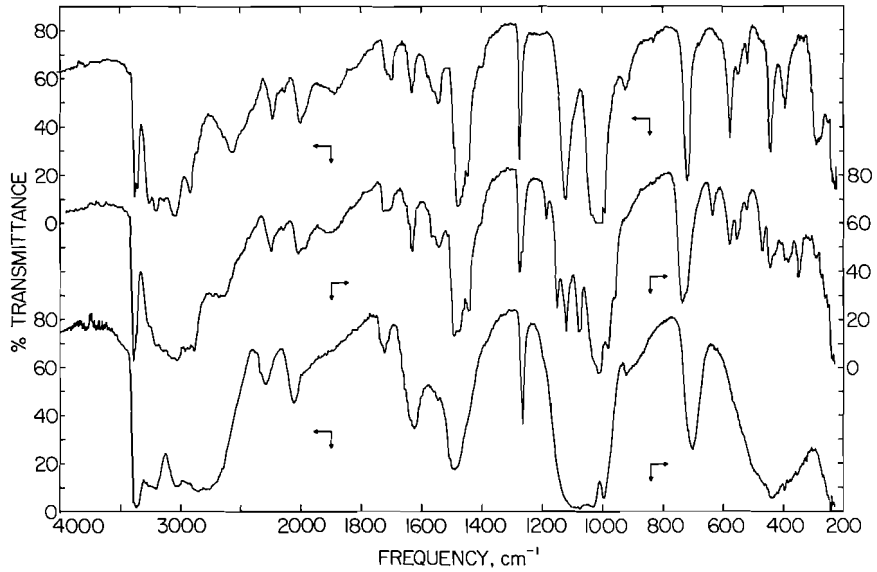

FIG. 6. Infrared spectra of NH_3–SO_2 matrix with $[NH_3]/[SO_2] = 2.67$. Lower curve, initial spectrum at liquid nitrogen temperature; middle curve, sample warmed to −90 °C and recooled; upper curve, sample warmed to −70 °C and recooled.

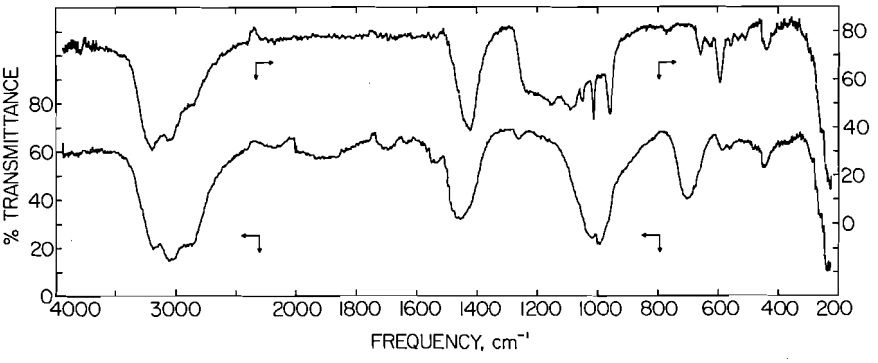

FIG. 7. Infrared spectra of NH_3–SO_2 matrix with $[NH_3]/[SO_2] = 2.67$ (continued from Fig. 6). Lower curve, sample warmed to −30 °C and recooled; upper curve, sample warmed to room temperature and evacuated for 2 h.

between SO_2 and NH_3 during the first warming sequence. The spectrum of this product consisted of broad peaks at 3190, 3050, and 2900 cm^{-1} in the N—H stretch region and at 1460 cm^{-1} in the NH_3 deformation region. Its modes associated with the SO_2 group were at 1017 cm^{-1} (stretch), 706 cm^{-1} (bend), and 446 cm^{-1} (bend). Interestingly, this spectrum was very similar to but not the same as that of ammonium sulfite. The primary product appeared to be stable to about −30 °C where its absorption bands began to weaken leaving behind a spectrum of the residues similar to those shown in Fig. 1. These changes were usually accompanied by the yellow color becoming white.

Samples prepared by condensing gaseous mixtures of NH_3 and SO_2 with $[NH_3]/[SO_2] \leq 1$ immediately showed the absorption bands of the primary product described above in the initial spectra recorded at liquid nitrogen temperature. However, with samples having $[NH_3]/[SO_2] > 2$, the initial spectra as well as many of the subsequent spectra obtained with warming were different from those described already. Figures 6 and 7 illustrate changes observed during warming of a typical sample prepared by

Can. J. Chem. Downloaded from www.nrcresearchpress.com by 210.87.254.105 on 09/05/12
For personal use only.

Can. J. Chem. Downloaded from www.nrcresearchpress.com by 210.87.254.105 on 09/05/12
For personal use only.

codepositing NH_3 and SO_2 on the low-temperature window. In this case, NH_3 and SO_2 at $[NH_3]/[SO_2] = 2.67$ were frozen separately in the storage vessel and then allowed to warm to room temperature. The gaseous mixture from this storage vessel was deposited directly in the low-temperature cell to obtain the spectra shown in Figs. 6 and 7. The lowest curve in Fig. 6 shows the initial spectrum of this white sample. There are no absorption bands which are characteristic of solid SO_2, so all SO_2 in the matrix must be coordinated to one or more ammonia molecules. Support for this interpretation also comes from the similarity of this spectrum to that obtained from the primary product of samples with $[NH_3]/[SO_2] < 1$. Warming of the matrix to $-90\,^{\circ}C$ and recooling produced the middle spectrum of Fig. 6. The sample color was still white, but the large decrease in intensity near 1070 cm^{-1} (NH_3 deformation) and 360 cm^{-1} (NH_3 lattice modes) indicated that most of the matrix NH_3 had sublimed off the sample window. The color of the sample was unchanged when the sample was warmed further to $-70\,^{\circ}C$ and recooled, but the spectrum was modified to that shown by the upper curve of Fig. 6. This spectrum and the middle spectrum in the figure each evidently represents a single compound since the major bands in each spectrum decayed together as the sample was warmed. The next warming sequence caused the sample color to become light yellow at about $-50\,^{\circ}C$, and the spectrum of this sample after recooling at $-30\,^{\circ}C$ is illustrated by the lower curve in Fig. 7. Within the limits of our experimental uncertainties, this spectrum was identical to that of the primary product obtained from reactant samples with $[NH_3]/[SO_2] \leq 1$. Finally, the compound giving rise to the lower spectrum of Fig. 7 started to decay noticeably at temperatures near $-20\,^{\circ}C$. The residue of the sample at room temperature after 2-h evacuation gave the spectrum represented by the upper curve in Fig. 7.

If water was added to the initial matrix, the compound represented by the upper spectrum of Fig. 6 still appeared as the sample was warmed to $-90\,^{\circ}C$. Further warming to $-80\,^{\circ}C$, however, caused the formation of ammonium sulfite whose spectrum is shown in Fig. 5. Changes in the spectra during the warming cycles of samples with ND_3 were more difficult to follow since the ND_3 deformation band overlapped with the S—O stretch region and there were also isotopic exchange reactions. Thus, only limited data were obtained with the ND_3 system.

Discussion

Since the chemical species which gave the lower spectrum of Fig. 7 was also the initial product in NH_3 matrices containing equimolar or excess SO_2, we conclude that this compound must be the adduct $NH_3 \cdot SO_2$. Thus, the principal reaction induced by warming a matrix with $[NH_3]/[SO_2] = 1$ is

$$[2] \qquad NH_3 + SO_2 \leftrightarrows NH_3 \cdot SO_2$$

Reaction 2 was reported to be exothermic by 9.5 kcal/mol (1), but the present work suggests in addition that its reaction activation energy must be very small. The exothermicity of this reaction presumably can cause the dehydration of $NH_3 \cdot SO_2$ in the gas phase to give HNSO which was observed by Hata (3). The initial spectra of samples prepared by the deposition of equimolar gaseous mixtures showed that $NH_3 \cdot SO_2$ was already formed at liquid nitrogen temperature, and the annealing of layers of solid NH_3 and SO_2 at $-150\,^{\circ}C$ readily generated this adduct. Under our experimental conditions, $NH_3 \cdot SO_2$ remained on the low-temperature infrared window to about $-30\,^{\circ}C$, above which temperature it decomposed evidently by the reverse of reaction 2.

Under anhydrous conditions, the decomposition of $NH_3 \cdot SO_2$ left no residue on the infrared window at room temperature. However, because of traces of water present on the walls of the low-temperature cell assembly, warming of a sample containing $NH_3 \cdot SO_2$ often led to some hydrolysis giving residues which were more difficult to remove by evacuation. The middle spectrum in Fig. 1 is due to such hydrolysis products. This spectrum is very similar to the one reported by Scargill (5) and assigned by him to the pyrosulfite salt $(NH_4)_2S_2O_5$. On the other hand, the upper spectrum of Fig. 1, which was obtained after evacuation of the same sample, is essentially the same as the spectrum of $(NH_4)_2S_2O_5$ reported by Hata (3). Although a comparison of Figs. 1 and 2 shows that, as expected for a pyrosulfite ion, the absorption bands other than those of the ammonium ion are not affected by deuterium substitution, these spectra are very different from the spectrum of $K_2S_2O_5$ reported by Buijs (14). In fact, the

Can. J. Chem. Downloaded from www.nrcresearchpress.com by 210.87.254.105 on 09/05/12
For personal use only.

latter spectrum is closer to the one obtained by Hata (3) by aging $(NH_4)_2S_2O_5$ for 12 h in the infrared cell at room temperature. These discrepancies in the observed infrared spectrum of the pyrosulfite ion are due to the strong dependence of the results on the water content of the solid sample.

The infrared spectrum of the pyrosulfite salt prepared by the reaction

[3] $$2NH_3 + 2SO_2 + H_2O \leftrightarrows (NH_4)_2S_2O_5$$

is shown by the lower curve in Fig. 3. In this case a gaseous mixture with $[NH_3]/[SO_2] = 0.68$ was deposited first, water at $[H_2O]/[SO_2] = 0.52$ was condensed on top, and then the solid was allowed to warm to -65 °C. The spectrum obtained by recooling this sample to liquid nitrogen temperature is identical with that for $K_2S_2O_4$ as observed by Buijs (14) except that we have in our spectrum bands due to the ammonium ion and one band near 1300 cm^{-1} due to solid SO_2. The three most characteristic bands in this spectrum are the intense broad peak at 1160 cm^{-1}, another strong and sharper band at 960 cm^{-1}, and a moderately intense sharp peak at 660 cm^{-1}. These peaks are absent in the spectrum of a residue at liquid nitrogen temperature shown by the upper curve of Fig. 3. This residue came from a solid mixture with $[NH_3]/[SO_2] = 1.27$ after it was subjected to six warming and recooling cycles followed by an overnight evacuation at room temperature. For convenience, we will call this residue the β-pyrosulfite to distinguish it from the α-form which gave the lower spectrum of Fig. 3. Thus, β-$S_2O_5^{2-}$ is characterized by a strong broad band at 1230 cm^{-1}, another intense band at 1100 cm^{-1}, a pair of weak but very sharp peaks at 1050 and 1010 cm^{-1}, and a moderately strong peak at 600 cm^{-1}. Most conspicuous in this spectrum is the absence of the sharp strong peak at 960 cm^{-1} which the α-form possesses.

Once the two forms of hydrolysis product of $NH_3 \cdot SO_2$ have been recognized, the spectra of various residues obtained by warming $[NH_3]/[SO_2]$ solid mixtures can be interpreted. In Fig. 1, the room temperature sample displaying the middle spectrum contains mostly α-pyrosulfite. Evacuation of this sample caused much of the α-salt to disappear presumably by the reverse of reaction 3, and the absorption bands of the β-form have now become more distinct in the upper spectrum of Fig. 1. The latter spectrum as well as the upper spectrum of Fig. 7 appears to be characteristic for a hydrolysis residue containing both α- and β-forms of the pyrosulfite ion.

According to Hata (3), the aging of a hydrolysis residue containing both α- and β-pyrosulfite caused the mixture to change into predominantly the α-salt. On the other hand, the spectra shown in Fig. 1 suggest that a reverse change had taken place on evacuation of the residue. Thus, it appears that the β-pyrosulfite is a partially dehydrated form of the α-salt and that the aging phenomenon observed by Hata is a slow conversion of the β-form to the α-form by hydration. When more water was added to the α- or the β-pyrosulfite, the final hydrolysis product was the bisulfite ion formed by the reaction

[4] $$(NH_4)_2S_2O_5 + H_2O \rightarrow 2NH_4HSO_3$$

The infrared spectrum of ammonium bisulfite is shown in Fig. 4, and the assignment of the bisulfite ion according to a C_{3v} symmetry is summarized in Table 1. Frequency values and deuterium isotope exchange studies showed clearly that the hydrogen atom in the bisulfite ion is bonded to the sulfur and not the oxygen atom. Our infrared data gave no evidence that an ion of the form $HOSO_2^-$ was present in our samples. Earlier attempts (6, 8) to assign the spectrum of HSO_3^- were severely hampered by the presence of large amounts of pyrosulfite in the samples used.

The thermal history of a solid sample containing excess NH_3 is illustrated in Figs. 6 and 7. Since the product displaying the lower spectrum of Fig. 7 has been assigned to the adduct $NH_3 \cdot SO_2$, its precursor with the upper spectrum of Fig. 6 must be the adduct $(NH_3)_2 \cdot SO_2$. The observed color changes were also consistent with this interpretation. Based on the multi-

TABLE 1. Infrared spectrum of the bisulfite ion in ammonium bisulfite at liquid nitrogen temperature

Symmetry class		Frequency (cm^{-1}) HSO_3^-	Frequency (cm^{-1}) DSO_3^-	Mode
A_1	ν_1	2588	1878	SH stretch
	ν_2	1038	1035	SO stretch
	ν_3	629	623	SO_3 deformation
E	ν_4	1200	1200	SO stretch
	ν_5	1123	831	SH bend
	ν_6	509	504	SO_3 deformation

TABLE 2. Vibrational spectrum of the sulfite ion at room temperature

Symmetry class		Infrared (solid) (NH_4^+)*	Infrared (solid) (ND_4^+)*	Infrared (solid) (Na^+)†	Raman (aqueous) (Na^+)†
A	ν_1	957 w	947 w	1010 m	967 s, pol.
	ν_2	630 m	628 m	633 s	620 w, pol.
E	ν_3	922 vs	915 vs	961 s	933 m, depol.
	ν_4	488 w	493 m	496 s	469 m, depol.

*This work.
†From Evans and Bernstein (9).

TABLE 3. Infrared spectrum of the adduct $NH_3 \cdot SO_2$ at liquid nitrogen temperature

$NH_3 \cdot SO_2$	$ND_3 \cdot SO_2$	Assignment
3190 vs	2360 m	NH stretch (A', A'')
3050 vs	2280 m	NH stretch (A')
2900 vs	2190 m	Combination
1700 w	1200 w	NH_3 deformation (A')
1540 w	1150 m	NH_3 deformation (A'')
1460 s	1100 s	NH_3 deformation (A')
1017 vs	1025 vs	SO stretch (A')
995 vs	984 vs	SO stretch (A'')
		SN stretch (A')
705 s	655 m	SO_2 deformation (A')
		SO_2 wag (A')
446 w	315 w	SO_2 rock (A'')
		NH_3 rock (A'), wag (A''), twist (A'')

plicities of the absorption bands of NH_3 at 1500, 1100, and 400 cm^{-1}, we attribute the spectrum given by the middle curve of Fig. 6 to another 2:1 adduct in which the orientation of the ammonia groups are different. In the presence of excess water, the adduct $(NH_3)_2 \cdot SO_2$ gave ammonium sulfite by

[5] $$(NH_3)_2 \cdot SO_2 + H_2O \rightarrow (NH_4)_2SO_3$$

This salt, whose infrared spectrum is shown in Fig. 5, decomposes readily into NH_3, SO_2, and H_2O. The fundamental bands of the sulfite ion are summarized in Table 2. For comparison, the data for the sodium salt due to Evans and Bernstein (9) are also given in Table 2.

Although the assignments of the spectra of the sulfite and bisulfite ions were straightforward, the spectra of the adducts $NH_3 \cdot SO_2$ and $(NH_3)_2 \cdot SO_2$ as well as that of the pyrosulfite ions were more difficult to interpret. First, the experimental data for the adducts are limited to the normal infrared region and no Raman results are available for them. Other workers have reported more extensive experimental data

TABLE 4. Infrared spectrum of the adduct $(NH_3)_2 \cdot SO_2$ at liquid nitrogen temperature

$(NH_3)_2 \cdot SO_2$	$(ND_3)_2 \cdot SO_2$	Assignment
3380 m		
3350 m	2240 m	
3260 s		
3210 s		
3140 s		$\nu_3(NH_3)$
3045 vs	2280 vs	$\nu_1(NH_3)$
2920 m		
2560 m		
2230 w		
2000 w		
1700 w	1260 w	$\nu_2(NH_3)$
1630 m		
1550 w		
1477 vs		$\nu_4(NH_3)$
1462 s	1100 s	
1128 s		SO stretch (A_1)
1010 vs	1035 vs	SO stretch (B_1), SN stretch (A_1)
993 m	985 vs	SN stretch (B_2)
718 m	704 m	SO_2 deformation (A_1)
576 m	555 w	SN_2 deformation (A_1)
447 m	445 m	SO_2 wag (B_2)
394 w	338 w	SO_2 rock (B_1)
285 w		SO_2 twist

Can. J. Chem. Downloaded from www.nrcresearchpress.com by 210.87.254.105 on 09/05/12
For personal use only.

Can. J. Chem. Downloaded from www.nrcresearchpress.com by 210.87.254.105 on 09/05/12
For personal use only.

TABLE 5. Infrared and Raman spectra of aqueous and solid potassium pyrosulfite

Raman				Infrared			
Aqueous		Solid		Aqueous	Solid		
Reference 6 (ρ)*	Reference 8†	Reference 6*	Reference 8†	Reference 6*	Reference 6*	Reference 7	$S_2O_5^{2-}$ Fundamentals
2543 m	2532 (3)						HSO_3^-
2521 w							?
2494 w							?
1196 w (0.76)	1193 (0)			1190 s	1189 s	1242 s	*A″*
1170 w (0.78)		1178 m	1177 (1)	1155 vs	1176 vs	1178 s	*A″*
1128 m (0.77)	1125 (0.5)		1122 (?)		1110 s		HSO_3^-
1085 s (0.22)	1089 (1)	1080 m	1088 (1)	1070 m	1081 vs	1086 s	*A′*
1052 vs (0.11)	1052 (8)	1059 s	1060 (5)	1050 vs	1058 s	1061 m	*A′*
1021 s (0.12)	1019 (5)			1022 s			HSO_3^-
966 w (0.14)	966 (0)	971 w		961 s	973 vs	978 s	*A′*
933 vw							SO_3^{2-}
740 vw							?
709 w	709 (0.5)						?
685 vw				690 vs			?
655 s (0.13)	655 (6)	653 s	652 (5)	648 m	668 w		*A′*
637 w (0.65)		645 w		626 m	649 s	629 s	HSO_3^-
			620 (?)		618 s	616 s	?
587 w (0.65)	586 (1)	569 w	592 (0.5)	586 w	584 w		*A″*
558 w (0.65)	552 (1)	558 m	554 (2)	551 w	558 s	562 s	*A″*
510 m (0.74)	506 (2)	517 w	514 (0.5)		509 s	512 m	*A″*
467 m (0.48)	457 (2)		471 (?)				*A′*
424 s (0.36)	423 (7)	433 s	433 (5)		439 vs	443 s	*A′*
395 w (0.75)			374 (?)	395 w			*A″*
309 s (0.48)	309 (5)	317 s	317 (2)	310 vw	313 m		*A′*
235 vs (0.40)	231 (9)	245 vs	244 (8)	250 m	236 s		*A′*
200 s (0.17)		218 s	210 (0)	225 m	210 s		*A′*
168 s (0.25)		147 s					?
			58 (3)				?

*Values in parentheses are depolarization ratios.
†Values in parentheses are relative intensities.

for the pyrosulfite, but unfortunately their samples were always contaminated with SO_3^{2-}, HSO_3^-, and possibly with other species. Thus, only a tentative assignment of the spectra of the various species will be presented here. In Table 3, we have listed the frequencies of the bands due to the adduct $NH_3 \cdot SO_2$ obtained at liquid nitrogen temperature. The strong resemblance of this spectrum (Fig. 7, lower curve) to that of ammonium sulfite (Fig. 5) suggests that the adduct $NH_3 \cdot SO_2$ must be like a sulfite ion in which one oxygen atom has been replaced with NH_3. Hence, the assignment summarized in Table 3 is based on a C_s symmetry for the adduct. The 2:1 adduct has similarly been treated as a disubstituted sulfate ion with a skeletal symmetry of C_{2v}. The assignment of $(NH_3)_2 \cdot SO_2$ is given in Table 4.

The infrared and Raman spectra of aqueous and solid potassium pyrosulfite obtained by Herlinger and Long (6), Simon and Waldmann (8), and Rocchiccioli (7) are given in Table 5. The pyrosulfite ion has a C_s symmetry (10), and its 15 fundamentals have been assigned as indicated in Table 5 from frequencies observed both by Herlinger and Long and by Simon and Waldmann. Previously, both of these research groups had assigned the medium intense polarized Raman line near 460 cm^{-1} to the bisulfite ion, but we have reassigned it to the pyrosulfite ion. Other minor differences between the present assignments and those of Herlinger and Long are: The 168 cm^{-1} Raman line was not assigned since it was not observed by Simon and Waldmann, and Herlinger and Long attributed the weak Raman line at 395 cm^{-1} to the bisulfite ion. The β-form of the pyrosulfite (Fig. 3, upper spectrum) is presumably a partially dehydrated salt, but we lack sufficient data to assign its spectrum.

This work was supported by the Division of Chemical Thermodynamics of the National Science Foundation through Grant No. G.P.-43523X and the Center for Air Environment Studies at The Pennsylvania State University. We thank N. A. Kelly and T. A. Huston for assistance in a part of the study.

1. R. LANDRETH, R. G. DE PENA, and J. HEICKLEN. J. Phys. Chem. **78**, 1378 (1974).
2. W. D. SCOTT, D. LAMB, and D. DUFFY. J. Atmos. Sci. **26**, 727 (1969).
3. T. HATA. Bull. Chem. Res. Inst. Non-Aqueous Solution, **14**, 5 (1964).
4. T. HATA, Bull. Chem. Res. Inst. Non-Aqueous Solution, **16**, 131 (1964).
5. D. SCARGILL. J. Chem. Soc. A, 2461 (1971).
6. A. W. HERLINGER and T. V. LONG II. Inorg. Chem. **8**, 2661 (1969).
7. C. ROCCHICCIOLI. Ann. Chim. **5**, 999 (1960).
8. A. SIMON and K. WALDMANN. Z. Anorg. Allg. Chem. **231**, 135 (1955).
9. J. C. EVANS and H. J. BERNSTEIN. Can. J. Chem. **33**, 1270 (1955).
10. I. LINDQVIST and M. MORTSELL. Acta Cryst. **10**, 406 (1957).
11. L. A. HULL, I. C. HISATSUNE, and J. HEICKLEN. J. Am. Chem. Soc. **94**, 4856 (1972).
12. F. P. REDING and D. F. HORNIG. J. Chem. Phys. **19**, 594 (1951).
13. R. N. WIENER and E. R. NIXON. J. Chem. Phys. **25**, 175 (1956).
14. K. BUIJS. J. Inorg. Nucl. Chem. **24**, 229 (1962).

Can. J. Chem. Downloaded from www.nrcresearchpress.com by 210.87.254.105 on 09/05/12
For personal use only.

Synthesis and Characterization of Cu(I) Complex Compounds With Methyl Isonicotinate

MOHAMED A. S. GOHER

Department of Inorganic Chemistry, Charles University, 128 40 Prague 2, Czechoslovakia[1]

Received January 31, 1975

MOHAMED A. S. GOHER. Can. J. Chem. **53**, 2657 (1975).

The preparation of Cu(I) complexes of methyl isonicotinate, MeIN, of the formula $(MeIN)_n$-CuX, in which $n = 1, 2, 3$, and 4 and X is Cl, Br, I, CN, SCN, and ClO_4, has been described. The isolated complexes are characterized by their analytical data, diamagnetism, and conductivity measurements. The $M \rightarrow L$ charge transfer bands in the visible spectra and the i.r. spectra of these complexes are discussed.

MOHAMED A. S. GOHER. Can. J. Chem. **53**, 2657 (1975).

On décrit la préparation de complexes du Cu(I), avec l'isonicotinate de méthyle (MeIN), de formule $(MeIN)_nCuX$ dans lesquels $n = 1, 2, 3$ et 4 et X = Cl, Br, I, CN, SCN et ClO_4. On a caractérisé les complexes par leurs données analytiques et des mesures de conductivité et de diamagnétisme. On discute des spectres i.r. ainsi que des bandes de transfert de charge $M \rightarrow L$ dans les spectres visibles de ces complexes. [Traduit par le journal]

Introduction

In a series of publications (1–3) we have reported the preparation and characterization of some Cu(I) complex compounds with pyridine monocarboxylic acids and their derivatives. As Cu(II) complexes of methyl isonicotinate have been studied from different points of view (4, 5), and as Cu(I) complexes of this ligand have not yet been mentioned, we tried to prepare these latter complex compounds. With methyl isonicotinate ligand we isolated Cu(I) complexes of Cu/L ratio 1:1, 1:2, 1:3, and 1:4 depending on the anion present.

Experimental

Chemicals and Apparatus

Methyl isonicotinate was g.l.c. purified. The other chemicals were analytical grade and commercially available.

Magnetic measurements were made by the Faraday method at room temperature. X-Ray powder patterns were taken on a Mikrometa 2 (Chirana, Prague) instrument, $\phi = 53.3$ mm, with λCuK_α radiation. Conductivity measurements were carried out at 25 °C on 10^{-3} *F* solutions in chloroform, nitrobenzene, and acetone under dry nitrogen with a Radiometer conductivity bridge model CDM 2e. Electronic spectra were recorded on a Unicam spectrophotometer SP 800. Reflectance spectra of the solids were measured over the 220–1000 nm range on a VSU-1 (Zeiss, Jena) instrument with MgO as a standard and diluent. Infrared spectra in the region 4000–400 cm^{-1} were measured on a UR-20 (Zeiss, Jena) spectrophotometer. The solid samples were measured as Nujol mulls or KBr pellets, and the liquid ligand as a capillary film. Far i.r. spectra have been measured on a Perkin-Elmer 325 spectrophotometer.

Analysis

Microanalysis of C, H, N were carried out on the Perkin-Elmer 240 elemental analyzer. Halogens were determined gravimetrically as AgX. Copper was determined either by titration against disodium EDTA or gravimetrically as CuSCN after degradation and oxidation of the complexes with boiling mixtures of concentrated H_2SO_4 and 30% H_2O_2.

Preparation of the Complexes

The complexes were prepared according to the procedure described previously (1, 3). Table 1 summarizes the elemental analysis and some properties of the prepared complexes.

The separation of pure Cu(I) perchlorate complexes caused some difficulties. However, the preparation of these complexes in such form was effected as follows. The 1:4 complex was prepared by mixing the ligand (six- to eightfold) with Cu(II) salt in aqueous medium, followed by addition of ascorbic acid and then sodium perchlorate pentahydrate. The final product was recrystallized from ethanol in presence of excess ligand and ascorbic acid to prevent air oxidation. The 1:3 complex was prepared from aqueous solutions of the ligand and copper in the exact molar ratio followed by slow addition of the perchlorate ion in the least amount of water. Care must be taken otherwise the complex will change immediately to one of the other two complexes. The white microcrystalline powder was prepared by mixing the ligand and copper ion in aqueous solution (Cu/L = 1:2). The faint yellow sheets were isolated by addition of an ethanolic solution of the ligand and an aqueous solution of $CuSO_4.5H_2O$ (Cu/L = 1:2) and after addition of ascorbic acid and the perchlorate ion the mixture was stirred about 15 min until faint yellow sheets isolated. This product was then recrystallized from ethanol.

[1]Permanent address: Department of Chemistry, Faculty of Science, Alexandria University, Egypt.

Can. J. Chem. Downloaded from www.nrcresearchpress.com by 210.87.254.105 on 09/05/12
For personal use only.

Can. J. Chem. Downloaded from www.nrcresearchpress.com by 210.87.254.105 on 09/05/12
For personal use only.

TABLE 1. Analytical data

Complex	Appearance	Melting point (°C)	Analysis (%) Cu Calcd.	Cu Found	X Calcd.	X Found	C Calcd.	C Found	H Calcd.	H Found	N Calcd.	N Found
(MeIN)CuCl	Yellow needles turned green		26.91	26.68	15.01	15.24	35.60	35.48	2.98	2.96	5.93	5.81
(MeIN)CuBr	Yellow needles	143	22.64	22.43	28.48	28.15	29.96	29.84	2.51	2.44	4.99	4.84
(MeIN)CuI	Yellow powder	162 dec.	19.39	19.42	38.76	38.29	25.66	26.00	2.15	2.20	4.27	4.39
(MeIN)CuCN	Pale yellow powder	178 dec.	28.03	27.98			42.38	41.98	3.11	2.97	12.35	11.92
(MeIN)CuSCN	Yellow powder	183 dec.	24.56	24.36			37.15	37.50	2.70	2.80	10.81	10.62
$(MeIN)_2CuCl$	Red-brown needles	137	17.02	17.18	9.50	9.27	44.05	44.75	3.78	3.69	7.50	7.44
$(MeIN)_2CuBr$	Brown needles	130	15.21	15.02	19.13	18.90	40.25	40.04	3.38	3.33	6.70	6.52
$(MeIN)_2CuI$	Red-orange needles	66[c]	13.67	13.39	27.32	27.05	36.18	35.72	3.03	2.89	6.02	5.90
$(MeIN)_2CuClO_4$[a]	White microcrystalline powder	145 dec.	14.53	14.31			38.45	38.01	3.23	3.11	6.40	6.20
$(MeIN)_2CuClO_4$[b]	Very faint yellow sheets		14.53	14.25			38.45	38.33	3.23	3.22	6.40	6.57
$(MeIN)_3CuClO_4$	Yellow microcrystalline powder	85	11.85	11.45			43.90	42.90	3.68	3.58	7.31	7.11
$(MeIN)_4CuClO_4$	Red-orange crystals	102	8.93	8.82			47.27	46.98	3.97	3.89	7.87	7.55

[a]Unstable form.
[b]Sufficiently stable form.
[c]At this temperature the complex changes to yellow 1:1.

TABLE 2. Reflectance spectra and conductivities[a]

Compound	π–π^*		M→L	Molar conductivities[b] (Ω^{-1} cm^2 mol^{-1}) Nitrobenzene	Acetone
MeIN	275[c]				
(MeIN)CuBr	280	350	420	Insoluble	Insoluble
(MeIN)CuI	280	320	420	Insoluble	Insoluble
(MeIN)CuCN	280		420	Insoluble	Insoluble
(MeIN)CuSCN	270		430	Insoluble	Insoluble
$(MeIN)_2CuCl$	270	[d]	490 vb	1.8	20.0
$(MeIN)_2CuBr$	280	[d]	470 vb	1.4	Yellow precipitate[e]
$(MeIN)_2CuI$	280	[d]	510 vb	Turbid	Yellow precipitate[e]
$(MeIN)_2CuClO_4$	280	[d]		29.5	132.0
$(MeIN)_3CuClO_4$	280	[d]	420	31.0	142.0
$(MeIN)_4CuClO_4$	280	[d]	470 vb	28.0	137.5

[a]λ is given in nm. vb is very broad.
[b]The conductivities given are based on the formula weights.
[c]From the electronic spectra of 10^{-4} M in chloroform.
[d]Strong absorption without definite maxima.
[e]The filtrate solutions are conducting.

Results and Discussion

The complexes were prepared simply by mixing ligand and $CuSO_4.5H_2O$ in the appropriate stoichiometric ratio in aqueous or ethanolic media followed by addition of ascorbic acid as the reducing agent and then the desired anion. By such a procedure Cu(I) nitrate complexes of MeIN have been prepared as yellow or red compounds, but they are too easily oxidized to permit their isolation and analysis. Alternatively, the halide complexes can be prepared by direct interaction between the components in suitable molar ratios. Because reactions leading to different stoichiometries are often competitive, pure samples are difficult to obtain. However, recrystallization could effect their purification.

Only in one case we isolated two isomers of the formula $(MeIN)_2CuClO_4$. One is white microcrystalline powder and not sufficiently stable and the other is faint yellow sheets and stable enough.

All the complexes isolated are colored, except the 1:2 perchlorate, diamagnetic compounds and are fairly stable in air except the 1:1 chloride and the white 1:2 perchlorate complexes. As was observed (2, 6) for Cu(I) halide complexes of other ligands, the stability with respect to air oxidation of the isolated Cu(I) complexes depends critically on the identity of the halogen and increases from chloride to iodide.

The X-ray powder patterns showed that the 1:1 bromide and iodide and the 1:2 halide complexes are isomorphous.

The Cu(I) perchlorate complexes behave in nitrobenzene (7) and acetone (8) as 1:1 electrolytes (see Table 2). The Cu(I) halide complexes, on the other hand, gave nonconducting solutions in chloroform and nitrobenzene. In acetone the measured conductivities are very small compared to those of 1:1 electrolytes (8). However, the results are reproducible for different samples and hence they are not due to impurities.

The Cu(I) halide complexes dissociate in solvents like chloroform, acetone, or alcohols to free ligand and complexes of lower ligand content or simple CuX. In general the intense red color of solutions of the 1:2 complexes obtained at higher concentrations changes very rapidly upon dilution. The faint yellow solutions obtained did not show the M → L charge transfer bands which are observed in the spectra of the solid samples.

Electronic Spectra

Table 2 summarizes the reflectance spectra data. In the u.v. region of the spectra of solutions of free ligand and complexes as well as in the spectra of the solid samples, an absorption band is observed around 275–280 nm. This band is attributed to a π–π^* transition in comparison with the assignment given for similar transition in the parent acid (9). Around 320–380 nm other absorption bands are observed in the reflectance spectra of some complexes,

Can. J. Chem. Downloaded from www.nrcresearchpress.com by 210.87.254.105 on 09/05/12
For personal use only.

Can. J. Chem. Downloaded from www.nrcresearchpress.com by 210.87.254.105 on 09/05/12
For personal use only.

TABLE 3. Infrared spectral data[a]

MeIN	1:1 bromide	1:1 iodide	1:1 cyanide	1:1 thiocyanide	1:2 chloride	1:2 bromide	1:2 iodide	1:2[a] perchlorate	1:3 perchlorate	1:4 perchlorate	Assignments
1740 vs	1740 vs,sp	1735 vs,sp	1740 vs,sp	1738 vs,sp	1735 vs,sp	1738 vs,sp	1735 vs	1738 vs,sp	1744 vs,sp	1740 vs,sp	νC=O st.
1602 m,sp	1612 vw	1612 w	1615 ms	1612 vw	1608 vw	1608 wm	1610 w	1625 w	1618 w	1618 w	ν_{8a}, ν(C—C)
1568 s,sp	1565 w	1568 w	1570 ms	1568 w	1562 w	1565 wm	1565 m,sp	1565 w,sp	1565 w	1568 wm	ν_{8b}, ν(C—C)
1497 vs,sp	1505 sh	1500 sh	1500 sh	1500 sh	1500 sh	1500 sh	1510 sh	1510 w	1510 sh	1510 sh	ν_{19a}, ν(C—C, C—N)
1440 vs	1432 s,sp	1440 vs	1440 vs,sp	1400 vs	1445 sh	1440 vs	1450 sh	1440 sh 1430 s	1445 sh	1445 sh	νR-sens.
1412 vs,sp	1418 ms	1415 s	1420 vs	1420 vs,sp	1415 s,sp	1420 s,sp	1412 vs,sp	1412 s	1420 s	1425 vs	ν_{19b}, ν(C—C, C—N), β(C—H)
1328 vs	1330 s	1325 vs	1335 vs	1330 s	1322 m,sp	1328 vs	1324 vs	1340 s,sp	1332 s,sp	1330 s,sp	ν_{14}, ν(C—C, C—N)
1220 s	1230 wm	1232 wm	1236 ms	1230 w	1230 wm	1228 ms	1225 s	1225 m	1225 wm	1228 m	ν_{9a}, β(C—H)
	1155 w	1150 sh	1150 sh	1150 sh	1150 sh	1154 wm	1160 m	1140 vs	1140 sh	1135 vs	ν_{18}, β(C—R, C—H)
1125 vs	1130 s,sp	1124 vs	1132 s,sp	1125 s	1122 s,sp	1125 vs	1128 vs	1120 vs	1130 s	1125 vs	ν_{3}, β(C—H)
1068 s,sp	1080 sh	1080 m	1085 sh	1085 sh	1082 w	1085 sh	1085 m	(++)	(++)	(++)	ν_{18b}, β(C—H)
1028 sh	1065 w	1062 ms	1068 ms,sp	1062 ms,sp	1056 w	1058 s	1058 ms	1062 s	1070 s	1060 s	ν_{12}, ring
995 ms	1020 w	1018 wm	1018 ms,sp	1020 w	1020 vw	1020 w	1016 w	1005 w	1020 w	1015 w	ν_{1}, ring, β(C—M)
	668 w	668 w	668 w	668 w	668 w	668 w	668 w	665 w	668 w	668 w	ν_{6b}, ring
485 w	490 w	492 w	498 wm	495 w	485 wm	486 w	484 w	495 w	507 vw	485 vw	ν_{6a}, ring, R—sens.
	402 vw	400 vw	408 w	400 vw	400 vw	400 vw	405 w	400 w	400 vw	400 vw	ν_{15}, R—sens.

[a]w = weak, m = medium, s = strong, v = very, b = broad, sh = shoulder, sp = sharp, st = stretching, (++) = masked by the strong absorption of ClO_4 group.

TABLE 4. Vibration frequencies (cm^{-1}) of the perchlorates, cyanide, and thiocyanate anions

Compound	ClO_4				
	ν_1	ν_3	ν_4	ν(CN)	δ(NCS)
$(MeIN)_4CuClO_4$	935 sh	1115–1080 vs	627 s		
$(MeIN)_3CuClO_4$	930 sh	1110–1090 vs	627 s		
$(MeIN)_2CuClO_4$[a]	925 w	1110 vs	627 s		
$(MeIN)_2CuClO_4$[b]	930 w	1120 vs	635 s		
		1090 vs	625 s		
		1050 s	620 m		
(MeIN)CuCN				2140 vs	
(MeIN)CuSCN				2132 vs	442 w
				2085 m	

[a]White compound.
[b]Faint yellow compound.

but not in the spectra of their solutions. These bands cannot be assigned as X → M charge transfer bands since the perchlorate compounds also showed strong absorption in this region.

Intense absorption bands are observed in the visible region of the reflectance spectra of Cu(I)—MeIN complexes, except for the 1:2 perchlorates. These bands are assigned as M → L charge transfer from the completely filled d^{10} orbitals of the Cu(I) ion to an empty π^* orbital on the ligand. Similar M → L charge transfer bands are observed in the visible spectra of Cu(I) complexes of bipyridine and phenanthroline (10, 11).

The electron attracting carbomethoxy group causes the electron density to migrate from the delocalized system on the pyridine ring to the substituent and thus lowers the electron density on the nitrogen atom. Therefore, increasing the number of ligands per Cu(I) ion increases the reducing power, that is, its tendency to accept electrons, of the acceptor part in the complex molecule, and hence M → L charge transfer band shifts to longer λ_{max} as the number of ligands increased (12), as seen from Table 2.

The cation $[(MeIN)_2Cu]^+$ is white and does not exhibit an M → L charge transfer band. Therefore the structure $[(MeIN)_2Cu]^+[CuX_2]^-$ is not probable for (MeIN)CuX (X = halide, CN, or SCN) complexes. Since these latter complexes exhibit M → L bands similar to the trigonal cation $[(MeIN)_3Cu]^+$, structures involving trigonally coordinated Cu(I) ion are, therefore, proposed for these 1:1 complexes. Similarly, the reflectance spectra of the halides of 1:2 complexes are very similar to that of the cation $[(MeIN)_4Cu]^+$ in the u.v. and visible regions. Tetrahedral geometries are, therefore, postulated for the 1:2 complexes.

Infrared Spectra

Wong and Brewer (5, 13) have carried out the coordinate analysis calculations on 1:1 complex models between Cu(II) or Zn(II) ions and MeIN among other 4-substituted pyridines. Following them, we assign the in-plane vibrations as given in Table 3. In Table 4 the vibrational frequencies of the anions are tabulated.

At 668 cm^{-1} a new band appears in the spectra of the Cu(I) complexes. It may be attributed to ν_{6b} vibration since a similar band given the same assignment was observed in the spectrum of Cu(II)—MeIN complex (5). The ν_{6a} vibration mode has been calculated to be at 516 cm^{-1} and at 488 cm^{-1} for the 1:1 complex model of Cu(II) and Zn(II) with MeIN, respectively. No bands have been observed in the spectra of both compounds to be assigned for this vibration mode. However, a band of weak to medium intensity is observed at 485–507 cm^{-1} in the spectra of all Cu(I)—MeIN complexes. It may be attributed to ν_{6a} ring vibration mode. The positions of most frequencies observed in the spectra of Cu(I) complexes are in good agreement with those observed for Cu(II) and Zn(II) complexes of MeIN (5, 13).

The position of the C=O stretching vibration frequency, as seen from Table 3, is essentially constant in free and coordinated MeIN. On the other hand, the ring C—C, C—N stretching, ring C—H in-plane, and ring breathing ν_1 and ν_{12} vibration frequencies all are blue shifted upon coordination of MeIN. These shifts are in line with those observed for coordinated

Can. J. Chem. Downloaded from www.nrcresearchpress.com by 210.87.254.105 on 09/05/12
For personal use only.

TABLE 5. Copper(I)–nitrogen stretching vibration frequencies (cm^{-1})

Complex	Cu(I)—N	Complex	Cu(I)—N
(MeIN)CuBr	226 s	$(MeIN)_2CuI$	226 s, 203 wm
(MeIN)CuI	230 s	$(MeIN)_4CuClO_4$	234 s
$(MeIN)_2CuCl$	220 m, 200	$(MeIN)_2CuClO_4$[b]	230 w
$(MeIN)_2CuBr$	235 s, 200		

pyridine (14, 15), indicating the coordination of MeIN via the nitrogen atom. Taking the shifts of the ν_{12} vibration mode as a measure of the relative π-contribution to the coordination bond (4), we observe that the π-contribution in the case of Cu(I)—MeIN complexes is slightly higher than in the case of Cu(II) or Zn(II) complexes with MeIN (5, 13).

Examination of Table 4 shows that the perchlorates of 1:4, 1:3, and the white 1:2 MeIN complexes are ionic, since the vibrations of the perchlorate groups are consistent only with noncoordinated groups (ref. 16 and references cited therein). Therefore, these complexes are formulated as $[(MeIN)_4Cu]^+ClO_4^-$, $[(MeIN)_3Cu]^+ClO_4^-$, and $[(MeIN)_2Cu]^+ClO_4^-$ with tetrahedral, trigonal, and linear geometries respectively. In the spectrum of the faint yellow 1:2 Cu(I) perchlorate complex, ν_3, the antisymmetrical stretching, and ν_4, the antisymmetrical bending, vibration modes split into three components for each. The splitting of these modes in this manner is consistent only with a bidentate perchlorate group. This compound is, therefore, formulated as $[(MeIN)_2CuClO_4]$ in which Cu(I) ion is tetrahedrally coordinated in the solid state.

For the 1:1 cyanide complex, the appearance of a single ν(CN) at 2140 cm^{-1} which is higher than those of the terminal cyanide groups in the complex $K_3Cu(CN)_4$, 2075–2095 cm^{-1} (17), strongly suggests a bridging cyanide group (18, 19). The 1:1 thiocyanate complex showed two cyanide stretching frequencies. The higher frequency indicates an S-bonded, and the lower an N-bonded, thiocyanate group (20, 21). Therefore this compound is postulated to exhibit a bridging thiocyanate group.

In an attempt to obtain further information concerning the structures of the complexes, the low frequency (200–400 cm^{-1}) i.r. spectra of some of them were measured (Table 5).

Wong and Brewer (13) have assigned the two bands observed at 230 and 203 cm^{-1} in the spectrum of Zn(II)—MeIN complex as Zn(II)—N stretching vibrations in accordance with the calculated values. Similarly we have assigned the bands in the region 220–234 cm^{-1} and around 200 cm^{-1} in the spectra of Cu(I)—MeIN complexes as Cu(I)—N stretching vibrations. As expected the 1:2 halide complexes showed two Cu(I)—N stretching frequencies. However, there are no bands attributable to Cu(I)—Cl frequencies above 200 cm^{-1} in the spectrum of the 1:2 chloride. For the 1:2 halides a structure of the type

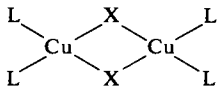

may account for these observations, with each metal atom having approximately tetrahedral geometry through halide bridges.

In the spectrum of the faint yellow Cu(I) perchlorate 1:2 compound, two bands have been observed at 251 and 264 cm^{-1}. Since these bands are absent from the spectra of all the measured complexes we attributed them to Cu(I)—O stretching vibrations. This observation confirms our conclusion that the perchlorate group acts as a bidentate ligand in this complex.

The author expresses his gratitude to Dr. M. Drátovský for valuable discussion and Dr. M. Ferles, Department of Organic Chemistry, Institute of Chemical Technology, Prague, who very kindly supplied methyl isonicotinate. His thanks are also due to Dr. Šilha and Mrs. Zemanová for their help with some measurements.

1. M. A. S. GOHER and M. DRÁTOVSKÝ, Coll. Czech. Chem. Commun. **40**, 26 (1975).
2. M. A. S. GOHER and M. DRÁTOVSKÝ. Naturwissenschaften, **62**, 96 (1975).
3. M. A. S. GOHER and M. DRÁTOVSKÝ. J. Inorg. Nucl. Chem. In press.
4. P. T. T. WONG and D. G. BREWER. Can. J. Chem. **46**, 131 (1968).
5. P. T. T. WONG and D. G. BREWER. Can. J. Chem. **46**, 139 (1968).
6. N. MARSICH, A. CAMUS, and E. CEBULEC. J. Inorg. Nucl. Chem. **34**, 933 (1972).

Can. J. Chem. Downloaded from www.nrcresearchpress.com by 210.87.254.105 on 09/05/12
For personal use only.

7. E. W. AINSCHOUGH and R. A. PLOWMAN. Austr. J. Chem. **23**, 699 (1970).
8. J. E. FERGUSSON and J. HICKFORD. Austr. J. Chem. **23**, 453 (1970).
9. H. P. STEPHENSON and H. SPONER. J. Am. Chem. Soc. **79**, 2050 (1957).
10. R. J. P. WILLIAMS. J. Chem. Soc. 137 (1955).
11. B. R. JAMES, M. PARRIES, and R. J. P. WILLIAMS. J. Chem. Soc. 4360 (1961).
12. A. B. P. LEVER. Inorganic electronic spectroscopy. Elsevier Publishing Company, Amsterdam. 1968. Chapt. 8.
13. P. T. T. WONG and D. G. BREWER. Can. J. Chem. **47**, 4590 (1969).
14. N. S. GILL, R. H. NUTTALL, D. E. SCAIFE, and R. W. A. SHARP. J. Inorg. Nucl. Chem. **18**, 79 (1961).
15. N. N. GREENWOOD and K. WADE. J. Chem. Soc. 1130 (1960).
16. K. NAKAMOTO. Infrared spectra of inorganic and coordination compounds, 2nd ed. Wiley Interscience, New York. 1970. p. 173.
17. L. H. JONES, J. Chem. Phys. **29**, 463 (1958).
18. R. D. GILLARD. J. Inorg. Nucl. Chem. **27**, 1321 (1965).
19. I. S. AHUJA and A. GARG. J. Inorg. Nucl. Chem. **34**, 2681 (1972).
20. A. TRAMER. J. Chim. Phys. **59**, 232 (1962).
21. G. CONTRERAS and R. SCHMIDTH. J. Inorg. Nucl. Chem. **32**, 127 (1970).

Can. J. Chem. Downloaded from www.nrcresearchpress.com by 210.87.254.105 on 09/05/12
For personal use only.

Chlorine-water Oxidation of Some α-Methylsulfonyl Sulfides

W. R. HARDSTAFF, R. F. LANGLER,[1] J. LEAHY, AND M. J. NEWMAN

Chemistry Department, Dalhousie University, Halifax, Nova Scotia B3H 3J5

Received February 11, 1975

W. R. HARDSTAFF, R. F. LANGLER, J. LEAHY, and M. J. NEWMAN. Can. J. Chem. **53**, 2664 (1975).

An examination of the chlorination of phenylmethyl, diphenylmethyl, and triphenylmethyl methylsulfonyl sulfides (**1**, **2**, and **3**) in aqueous acetic acid has provided indirect evidence for Pummerer rearrangement during the chlorination of an α-methylsulfonyl sulfinyl chloride. The results are discussed from both mechanistic and synthetic standpoints.

W. R. HARDSTAFF, R. F. LANGLER, J. LEAHY et M. J. NEWMAN. Can. J. Chem. **53**, 2664 (1975).

L'étude de la chloration des sulfures du phénylméthyle, du diphénylméthyle et du triphénylméthyle méthylsulfonyle (**1**, **2** et **3**) dans une solution aqueuse d'acide acétique fournit une preuve indirecte du réarrangement de Pummerer durant la chloration d'un chlorure de α-méthylsulfonyle sulfinyle. Les résultats sont discutés des points de vue du mécanisme et de la synthèse. [Traduit par le journal]

Can. J. Chem. Downloaded from www.nrcresearchpress.com by 210.87.254.40 on 09/05/12
For personal use only.

In recent years, a widespread interest in the chlorination of organosulfur compounds has become apparent. Research has been primarily directed at the chlorination of sulfides (1–6) and sulfoxides (7–19). Our own work (20, 21) has demonstrated that α-chlorodialkyl sulfides give rise to sulfonyl chlorides via sulfinyl chlorides upon chlorination in dilute aqueous acetic acid. We have proposed (21) that the sulfinyl chloride is hydrolyzed to the sulfinic acid which then reacts with chlorine to furnish the corresponding sulfonyl chloride.

The present report is the result of a desire to examine the behavior of chloro- and oxochlorosulfonium chloride salts in systems which may undergo either Pummerer rearrangement or dissociation to form carbonium ions and/or intimate ion pairs as well as sulfenyl or sulfinyl chlorides. Dissociation of this sort is not available to simple dialkyl chloro- and oxochlorosulfonium chloride salts.

The particular substrates chosen for examination (**1**, **2**, and **3**) offer two potentially useful features for such a study.

$$\overset{1}{CH_3}\cdot\overset{2}{SO_2}\cdot\overset{3}{CH_2}\cdot\overset{4}{S}\cdot\overset{5}{C}\,XYZ$$

1 X = Y = H; Z = Ph

2 X = H; Y = Z = Ph

3 X = Y = Z = Ph

[1]Enquiries should be directed to: Dr. R. F. Langler, Chemistry Department, Scarborough College, University of Toronto, West Hill, Ontario M1C 1A4.

Pummerer rearrangement of intermediate chlorosulfonium chloride salts is directed to C-3 by the α-sulfonyl group (22) thus preventing chlorination on C-5, so that the polyphenylmethyl groups retain their ability to form carbonium ions (or intimate ion pairs) as the reaction proceeds. Secondly the regular increase of the number of phenyl groups on C-5 in the series **1** → **3** increased the propensity for cleavage at progressively earlier stages during the reaction in the event that some Pummerer rearrangement preceded cleavage in the reaction of the phenylmethyl sulfide (**1**).

The sulfone-sulfides (**1**, **2**, and **3**) were prepared by refluxing the appropriate thiol anion with chloromethyl methyl sulfone in absolute ethanol (*vide* Scheme 1). Although this reaction

$$RSH + ClCH_2\cdot SO_2\cdot CH_3 \xrightarrow[EtONa]{EtOH} R\cdot S\cdot CH_2\cdot SO_2\cdot CH_3$$

SCHEME 1

is precedented (22, 23), reports that α-halosulfones are inert to nucleophilic substitution can be found in the literature (24–27). Since these reports are based on the failure of non-sulfur containing nucleophiles to displace the α-halogen atoms of α-halosulfones, we decided to examine two sulfur-containing nucleophiles in this reaction. Both sodium bisulfide and thiourea failed to react with chloromethyl methyl sulfone in refluxing ethanol. It therefore appears that the electronic nature of the nucleophilic sulfur

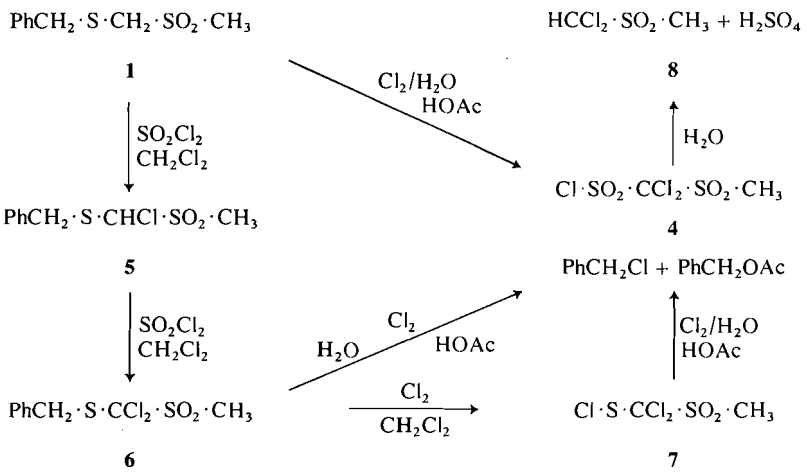

SCHEME 2

atom is quite restricted if substitution reactions are to succeed on α-halosulfones.

Chlorination of the sulfone-sulfide (**1**) in aqueous acetic acid furnished the dichlorosulfone-sulfonyl chloride (**4**) in good yield. Two approaches were undertaken in order to establish the structure of **4**. Synthetic support was obtained by the unambiguous preparation of the dichlorosulfone-sulfenyl chloride (**7**) through the known compounds **1**, **5**, and **6** (28), followed by oxidation of **7** to **4** as shown in Scheme 2. Degradative support for the structure of **4** was obtained by its hydrolysis to give the dichlorosulfone (**8**) and an equivalent of sulfuric acid. This hydrolysis reaction appears to be new and is the subject of further studies, already underway, in our laboratories.

Once the structure of **4** had been established, we directed some effort towards elucidating the pathway by which it was formed from **1**. The reaction **1** → **4** was complete after chlorination for 0.75 h. The product contained approximately 5% of the sulfone-sulfenyl chloride (**7**) and 95% of the sulfone-sulfonyl chloride (**4**). When the sulfone-sulfenyl chloride (**7**) was chlorinated under the same conditions, the reaction was only 70% completed after 14.5 h. Clearly, then, short chlorinations leave almost all intervening sulfone-sulfenyl chloride (**7**) unreacted and therefore a direct determination of **7** in crude reaction mixtures is a good measure of the amount of starting material giving rise to it.

Therefore only 5% of **1** gives rise to **7** in the reaction **1** → **4** and **4** does not form via the intermediacy of **7**. From our previous studies (20, 21) it is clear that **4** must arise from the corresponding dichlorosulfone-sulfinyl chloride (**9**). It is now evident that **9** does not arise from the dichlorosulfone-sulfenyl chloride (**7**).

Chlorination of the dichlorosulfone-sulfide (**6**) in aqueous acetic acid furnished a mixture of the dichlorosulfone-sulfonyl chloride (**4**) and the dichlorosulfone-sulfenyl chloride (**7**) in the ratio 2:3 respectively. Since little dichlorosulfone-sulfonyl chloride (**4**) could have formed from **7** in such a short time, then **4** must have arisen from **9** and **10**[2] as depicted in Scheme 3. The relatively large amount of the dichlorosulfone-sulfenyl chloride (**7**) formed from the chlorination of **6** in aqueous acetic acid essentially precludes **6** from consideration as a principal intermediate in the conversion of **1** → **4**.

The presence of the dichlorosulfone-sulfenyl chloride (**7**) in the crude product obtained from the chlorination of **6** was established in part by its detection on t.l.c. After development and drying, the plate was sprayed with ammonium hexanitratocerate(IV) solution, a new spray reagent developed in these laboratories (31). This oxidizing spray is sensitive to the nature of the substituents on sulfur and visualizes the spots more slowly as the substituents on sulfur become more electron withdrawing. When a mixture is examined on t.l.c. using an authentic sample of a component for comparison, one can compare both the R_F and the appearance time of the component in question and the authentic sample. Thus the crude product from the chlorination of **6** contained a compound

[2]The intermediacy of the β-disulfone can be ruled out on the basis of results published elsewhere (30).

Can. J. Chem. Downloaded from www.nrcresearchpress.com by 210.87.254.40 on 09/05/12
For personal use only.

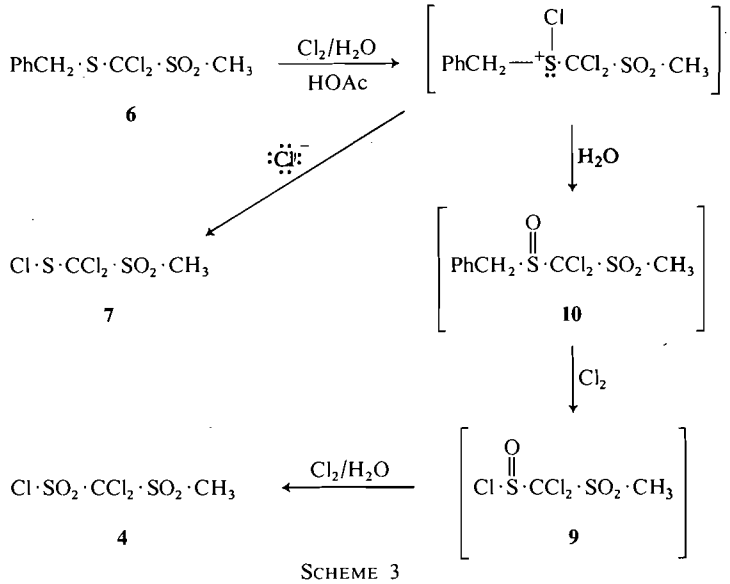

SCHEME 3

which was identical to **7** with respect to R_F and appearance time.

Two possibilities now remain for the pathway **1** → **4**. Either the benzylic sulfone-sulfide (**1**) cleaves directly after chlorosulfonium chloride formation or Pummerer rearrangement occurs leading ultimately to **4**.

If the longer pathway implicated by Pummerer rearrangement is occurring, then reaction times should be substantially shortened if the structure of the sulfone-sulfide (**1**) were modified in such a way as to facilitate direct cleavage of the chlorosulfonium chloride salt initially formed.

$$CH_3{\cdot}SO_2{\cdot}CH_2{\cdot}SO{\cdot}CH_2{\cdot}Ph$$
11

We have undertaken two approaches to facilitating immediate cleavage and suppressing Pummerer rearrangement. In our first approach, the sulfone-sulfoxide (**11**) was prepared. When **11** reacts with chlorine an oxochlorosulfonium chloride salt is formed. The sulfur atom in this case is more electron deficient than the sulfur atom in a chlorosulfonium chloride salt and should constitute a better leaving group, thereby facilitating direct cleavage without Pummerer rearrangement. Such an analysis is consistent with our previous results (20) in which we found that α-polychlorosulfoxides cleave to furnish sulfinyl chlorides upon treatment with molecular chlorine, whereas α-polychlorosulfides either react via a Pummerer rearrangement to furnish more highly chlorinated sulfides or do not react at all with molecular chlorine. Chlorination of **11** furnished **4** in the same yield with the same chlorination time as observed for **1**.

In our second approach, the diphenylsulfone-sulfide (**2**) and the triphenyl sulfone-sulfide (**3**) were prepared. The chlorosulfonium chloride salts of **2** and **3** would be expected to dissociate in an S_N1 type process more readily than the corresponding salt of **1** on the grounds that the resultant carbonium ion should be more stable as the number of phenyl rings on the central atom of the carbonium ion is increased. Again the chlorination times[3] and yields were essentially identical with those observed for **1**. These results suggest that there is no Pummerer rearrangement occurring prior to cleavage.

If, in any of these cases, cleavage is occurring prior to Pummerer rearrangement, then either or both of the intervening sulfenyl or sulfinyl chlorides must be undergoing Pummerer rearrangement in order for the dichlorosulfone-sulfonyl chloride (**4**) to be the observed product. Such a process is abnormal for sulfenyl or sulfinyl chlorides both of which are normally oxidized, under these conditions, to the corresponding sulfonyl chlorides. To examine the possibility that benzylic sulfides undergo direct cleavage upon chlorination under these reaction

[3]Exhaustive chlorinations were terminated when the reactions were no longer exothermic.

Can. J. Chem. Downloaded from www.nrcresearchpress.com by 210.87.254.40 on 09/05/12
For personal use only.

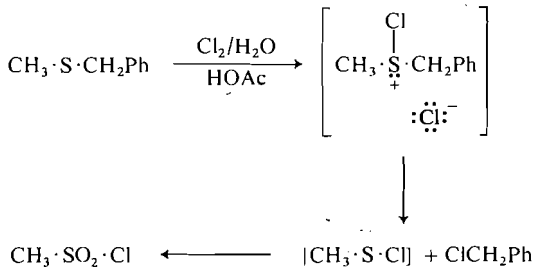

SCHEME 4

conditions, we decided to chlorinate a benzylic sulfide that would give rise to a sulfenyl and/or sulfinyl chloride which would be oxidized to the corresponding sulfonyl chloride without complicating Pummerer rearrangement. The experiment was carried out on benzyl methyl sulfide. The product obtained was an approximately equimolar mixture of methanesulfonyl chloride and benzyl chloride.[4]

Clearly the cleavage has occurred before any Pummerer rearrangement has occurred (see Scheme 4). Furthermore, it now appears likely that all three sulfone-sulfides **1**, **2**, and **3** have undergone direct cleavage upon chlorination in aqueous acetic acid.

Since the dichlorosulfone-sulfonyl chloride **4** must arise from the dichlorosulfone-sulfinyl chloride **9** and it seems very likely that chlorination of **1** leads to direct cleavage, then the precursor of **9** must be the monochlorosulfone-sulfinyl chloride **12** as shown in Scheme 5. As previously mentioned the dichlorosulfone-sulfenyl chloride (**7**) has been excluded as an intermediate.

A direct examination of the behavior of α-sulfonyl-sulfenyl and α-sulfonyl-sulfinyl chlorides cannot be undertaken until synthetic methods become available for their preparation.

Implicit in the results presented in this article is the fact that sulfonyl compounds with an α-sulfur atom are unsuitable for the preparation of simple α-sulfonyl-sulfonyl chlorides (*e.g.* methylsulfonylmethanesulfonyl chloride) because of the propensity of the intermediate species to undergo Pummerer rearrangements. The method of Opitz (32) by which sulfenes are dimerized and subsequently treated with HCl to provide α-sulfonyl-sulfonyl chlorides remains the only available method for their preparation.

[4]An immediate consequence of this result is the synthetic utility of benzylic sulfides as precursors for the preparation of sulfonyl chlorides. Further work on this method is already underway in our laboratories.

Experimental

General

The i.r. spectra were recorded on a Perkin-Elmer 237 B grating spectrophotometer. The n.m.r. spectra were obtained on a Varian T-60 instrument using TMS as the internal standard. The mass spectra were recorded on a Dupont-CEC model 21-104 mass spectrometer. The samples were directly introduced using an all glass probe and the spectra run at 30 eV with a source temperature of 150 °C. Melting points were determined on a Fisher-Johns melting point apparatus and are uncorrected. The t.l.c. was carried out on 5 × 20 cm analytical plates (0.75 mm thickness) spread with silica gel HF-254 (A.G. Merck). Spots were detected by spraying with ammonium hexanitratocerate(IV) spray (31) or by 250 nm u.v. light.

Chlorinations

Chlorine flow rates were standardized by the use of a rotameter. The rotameter was calibrated by bubbling chlorine into an aqueous solution of potassium iodide for a fixed period of time. The flow rate was calculated from the weight of chlorine trapped and the bubbling time using the ideal gas law.

Preparation of $PhCH_2{\cdot}S{\cdot}CH_2{\cdot}SO_2{\cdot}CH_3$ (1)

The preparation and properties of this compound have been described elsewhere (28).

Preparation of $Ph_2CH{\cdot}S{\cdot}CH_2{\cdot}SO_2{\cdot}CH_3$ (2)

Sodium metal (1.894 g) was dissolved in absolute ethanol (100 ml). Diphenylmethanethiol (33) (15.504 g) was added to the solution, followed by chloromethyl methyl sulfone (28) (8.028 g). The resultant reaction mixture was refluxed for 1 h. The reaction mixture was poured into ice–water (100 ml) and the resultant mixture extracted with chloroform (four 100 ml aliquots). The chloroform layers were combined, dried ($MgSO_4$), filtered, and rotary evaporated. The residue was recrystallized from benzene, furnishing **2** (14.890 g, 81.5%). The product had m.p. 118–120 °C and was homogeneous on t.l.c. (R_F, 0.29) when developed with chloroform. The i.r. bands were present ($CHCl_3$), 1325 and 1145 cm^{-1}. The n.m.r. spectrum ($CDCl_3$) showed signals at τ 2.70 (10H, m), 4.20 (1H, s), 6.40 (2H, s), and 7.03 (3H, s). The mass spectrum exhibited ions at *m/e* 215 (23%), 167 (100%), 105 (22%), 79 (9%), and 77 (14%).

Anal. Calcd. for $C_{15}H_{16}S_2O_4$: C, 61.61; H, 5.52. Found: C, 61.23; H, 5.72.

Preparation of $Ph_3C{\cdot}S{\cdot}CH_2{\cdot}SO_2{\cdot}CH_3$ (3)

Sodium metal (0.759 g) was dissolved in absolute ethanol (100 ml). Triphenylmethanethiol (9.518 g) was added to the solution, followed by chloromethyl methyl sulfone (4.030 g). The resultant reaction mixture was refluxed for 1 h. The reaction mixture was poured into ice–water (100 ml) and the resultant mixture extracted with chloroform (four 100 ml aliquots). The combined chloroform layers were dried ($MgSO_4$), filtered, and rotary evaporated. The dark brown resinous residue (12 g) was dissolved in chloroform (250 ml), boiled with norite (1 g), filtered, and the process repeated. The chloroform was evaporated furnishing a light brown resinous

Can. J. Chem. Downloaded from www.nrcresearchpress.com by 210.87.254.40 on 09/05/12
For personal use only.

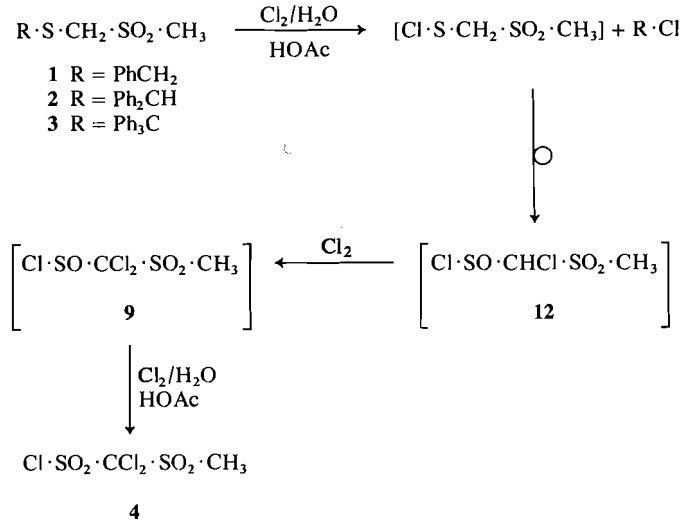

SCHEME 5

sample (10 g). This material was chromatographed on silica gel (720 g) with chloroform eluent (100 ml aliquots). Fractions 15–27 furnished the triphenylsulfone-sulfide (**3**) (5.3 g, 43.5%). After recrystallization from benzene, the product had m.p. 131.5–133.5 °C and was homogeneous on t.l.c. (R_F, 0.41) when developed with chloroform. The i.r. bands were present ($CHCl_3$), 1312 and 1130 cm^{-1}. The n.m.r. spectrum displayed signals at τ 2.80 (15H, m), 6.37 (2H, s), and 7.54 (3H, s). The mass spectrum showed ions at *m/e* 243 (100%), 166 (37%), and 79 (3%).

Anal. Calcd. for $C_{21}H_{20}S_2O_2$: C, 68.45; H, 5.55. Found: C, 68.09; H, 5.32.

Preparation of $PhCH_2{\cdot}S{\cdot}CHCl{\cdot}SO_2{\cdot}CH_3$ (5)

The sulfone-sulfide (**1**) (0.263 g) was added to methylene chloride (5 ml) and the solution brought to gentle reflux. A solution of sulfuryl chloride (0.165 g) in methylene chloride (5 ml) was added dropwise over 8 min. The reaction mixture was refluxed for 1 h. The methylene chloride was rotary evaporated and the residue spotted on two preparative t.l.c. plates. The plates were developed with chloroform and the lower band (R_F, 0.55) was scraped.

The silica gel was covered with chloroform (60 ml) and the mixture stirred for 1 h. The mixture was filtered and the chloroform rotary evaporated affording a colorless oil (0.149 g). The product had R_F 0.41 when developed with chloroform. The i.r. bands were present ($CHCl_3$), 1330 and 1135 cm^{-1}. The n.m.r. showed signals at τ 2.66 (5H, s), 4.56 (1H, s), 5.76 (2H, q, J = 13 Hz) and 6.93 (3H, s). The mass spectrum exhibited ions at *m/e* 250 (1.5%), 171 (21%), 91 (100%), and 65 (12%).

Anal. Calcd. for $C_9H_{11}ClS_2O_2$: C, 43.11; H, 4.42. Found: C, 43.31; H, 4.28.

Preparation of $PhCH_2{\cdot}S{\cdot}CCl_2{\cdot}SO_2{\cdot}CH_3$ (6)

The preparation and properties of this compound have been described elsewhere (28).

Preparation of $Cl{\cdot}S{\cdot}CCl_2{\cdot}SO_2{\cdot}CH_3$ (7)

The dichlorosulfone-sulfide (**6**) (4.941 g) was dissolved in methylene chloride (25 ml) and chlorine (232 ml/min) was bubbled through the reaction mixture for 1 h.

The methylene chloride was rotary evaporated furnishing a residue containing a 1:1 mixture of the dichlorosulfenyl chloride (**7**) and benzyl chloride. The benzyl chloride was distilled off and established as identical to authentic material by n.m.r., i.r., b.p., and t.l.c. The residue was distilled furnishing the sulfenyl chloride (**7**) (3.420 g), b.p. 128–130 °C/1.5 mm (86.1%). The sulfenyl chloride solidified and was recrystallized from carbon tetrachloride which furnished pale yellow needles. The recrystallized sulfenyl chloride had m.p. 55–57 °C and was homogeneous on t.l.c. (R_F, 0.51) when developed with chloroform. The i.r. bands were present ($CHCl_3$), 1350 and 1155 cm^{-1}. The n.m.r. spectrum displayed signals at τ 6.66 (s). The mass spectrum showed ions at *m/e* 193 (2.7%), 149 (100%), 79 (73%), 63 (21%), and 36 (30%).

Anal. Calcd. for $C_2H_3Cl_3S_2O_2$: C, 10.47; H, 1.32. Found: C, 10.62; H, 1.05.

Preparation of $PhCH_2{\cdot}SO{\cdot}CH_2{\cdot}SO_2{\cdot}CH_3$ (11)

The preparation and properties of this compound have been described elsewhere (28).

Chlorination of 1

The sulfone-sulfide (**1**) (5.003 g) was dissolved in glacial acetic acid (25 ml) and distilled water (5 ml) was added. Cl_2 (232 ml/min) was bubbled into the reaction mixture for 45 min. During the chlorination the temperature was maintained at 25–30 °C with an ice–water bath. The acetic acid was distilled off affording a residue containing benzyl chloride (1.293 g, 44%), benzyl acetate (0.845 g, 24%), and the dichlorosulfone-sulfonyl chloride (**4**) (5.659 g, 93.5%). The residue was carefully fractionated providing samples of benzyl chloride and benzyl acetate which were established as identical to authentic samples by n.m.r., i.r., b.p., and t.l.c. The dichlorosulfone-sulfonyl chloride (**4**) was distilled (b.p. 110–115 °C/1 mm). The distilled material was recrystallized from CCl_4 (5×) after which it had m.p. 72–74 °C. The i.r. bands were present ($CHCl_3$), 1390, 1355, 1180, and 1155 cm^{-1}. The n.m.r. spectrum displayed a signal at τ 6.50 (s). The mass spectrum has been discussed previously (34).

Can. J. Chem. Downloaded from www.nrcresearchpress.com by 210.87.254.40 on 09/05/12
For personal use only.

Can. J. Chem. Downloaded from www.nrcresearchpress.com by 210.87.254.40 on 09/05/12
For personal use only.

Anal. Calcd. for $C_2H_3Cl_3S_2O_4$: C, 9.19; H, 1.16. Found: C, 9.25; H, 1.16.

Chlorination of **6**

The dichlorosulfone-sulfide (**6**) (31.75 g) was dissolved in glacial acetic acid (150 ml) and distilled water (18 ml) was added. Cl_2 (448 ml/min) was bubbled through the reaction mixture for 30 min, during which the temperature was maintained at 25–30 °C. Distilled water (150 ml) was added and the resultant solution extracted with chloroform (six 100 ml aliquots). The combined chloroform layers were washed with aqueous sodium hydroxide (5%) until the aqueous layer remained basic. The chloroform was washed with distilled water (100 ml), dried ($MgSO_4$), filtered, and the chloroform rotary evaporated furnishing a residue containing benzyl chloride (4.322 g, 30.6%), benzyl acetate (2.871 g, 17%), the dichlorosulfone-sulfenyl chloride (**7**) (9.296 g, 36.4%), and the dichlorosulfone-sulfonyl chloride (**4**) (6.778 g, 23.8%). The benzyl chloride and benzyl acetate were distilled off and a sample of each shown to be identical to authentic material by i.r., n.m.r., b.p., and t.l.c.

The addition of a small portion of the dichlorosulfone-sulfenyl chloride (**7**) to a sample of the distillation residue showed the signal at 6.7 τ to have the same chemical shift as the methyl group of **7**. The distillation residue showed a compound present which was identical to **7** on t.l.c. by both R_F and appearance time ($(NH_4)_2Ce(NO_3)_6$ spray).

A portion of the distillation residue (8.004 g) was dissolved in glacial acetic acid (50 ml) and distilled water (6.6 ml) was added. Cl_2 (448 ml/min) was passed through the solution for 3 h. Water (100 ml) was added and the resultant solution extracted with chloroform (three 100 ml aliquots). The combined chloroform layers were washed with 2.5% NaOH (100 ml aliquots) until the aqueous layer was basic. The chloroform was washed with distilled water, dried ($MgSO_4$), filtered, and rotary evaporated furnishing impure **4** (6.981 g). The sample was dissolved in carbon tetrachloride, cooled, and seeded. Crystals identical to **4** (as obtained from **1**) by n.m.r., i.r., m.s., and m.p. were obtained.

Chlorination of **7**

The sulfone-sulfenyl chloride (**7**) (4.990 g) was dissolved in glacial acetic acid (25 ml) and distilled water (3.3 ml) was added. Cl_2 (232 ml/min) was bubbled through the reaction mixture for 14.5 h. The acetic acid was distilled off at reduced pressure affording a residue of the sulfone-sulfonyl chloride (**4**) (3.996 g, 70%) and unreacted sulfone-sulfenyl chloride (**7**) (1.019 g, 20%). A portion of the residue was crystallized, with seeding, from carbon tetrachloride. The first crop was shown to be identical to **4** (as obtained from **1**) by n.m.r., i.r., m.p., and mixture m.p.

Hydrolysis of **4**

The sulfone-sulfonyl chloride (**4**) (1.431 g) was added to distilled water (10 ml). The mixture was refluxed for 1 h. Shortly after reflux began the solution became homogeneous. Upon completion of the reflux, the solution was extracted with chloroform (five 15 ml aliquots) and *the aqueous phase* set aside. The combined chloroform layers were dried ($MgSO_4$), filtered, and the chloroform rotary evaporated yielding the dichlorosulfone (**8**) (0.700 g, 79%). The sulfone was recrystallized from 95% ethanol and established as identical to authentic material (29) by m.s., i.r., m.p., mixture m.p., and n.m.r.

The aqueous phase was diluted with distilled water to a volume of 200 ml. A standard gravimetric sulfate determination (35) furnished $BaSO_4$ (0.892 g, 70%). The $BaSO_4$ isolated was identical to authentic material by i.r. (KBr).

Chlorination of **11**

The sulfone-sulfoxide (**11**) (5.001 g) was dissolved in glacial acetic acid (25 ml) and distilled water (3.3 ml) was added. Cl_2 (232 ml/min) was bubbled through the reaction mixture for 45 min. The acetic acid was distilled off at reduced pressure giving a residue of crude dichlorosulfone-sulfonyl chloride (**4**) (5.259 g, 93.5%). A portion of the sample was crystallized from carbon tetrachloride furnishing **4** which was identical to previous samples by n.m.r., i.r., m.p., and mixture m.p.

Chlorination of **2**

The diphenylsulfone-sulfide (**2**) (6.006 g) was added to a solution of glacial acetic acid (25 ml) and distilled water (3.3 ml). Chlorine (232 ml/min) was bubbled through the reaction mixture for 45 min. The acetic acid was distilled off furnishing a residue containing diphenylchloromethane (2.989 g, 72%) and the dichlorosulfone-sulfonyl chloride (**4**) (4.4896 g, 84%). The crude mixture was stored in a freezer. After some time crystals of diphenylchloromethane appeared and were rapidly filtered. They were identical to authentic material by n.m.r., i.r., and b.p. The filtered solution was added to carbon tetrachloride (5 ml), stored in a freezer, and seeded with **4**. The crystals were filtered and shown to be identical to **4** by n.m.r., i.r., m.p., and mixture m.p.

Chlorination of **3**

The triphenylsulfone-sulfide (**3**) (10.7544 g) was added to a solution of glacial acetic acid (50 ml) and distilled water (6.6 ml). Cl_2 (232 ml/min) was bubbled into the reaction mixture for 45 min. During the chlorination a solid formed in the reaction mixture. At the end of the reaction the solid was filtered off and shown to be triphenylchloromethane (3.967 g). The acetic acid was distilled off affording a residue containing triphenylchloromethane (1.502 g, total 67%) and the dichlorosulfone-sulfonyl chloride (**4**) (5.497 g, 72%). The triphenylchloromethane was identical to authentic material by n.m.r., i.r., and t.l.c. The dichlorosulfone-sulfonyl chloride (**4**) was recrystallized from carbon tetrachloride (4×) and shown to be identical to previously isolated **4** by n.m.r., i.r., m.p., and mixture m.p.

Chlorination of Benzyl Methyl Sulfide

Benzyl methyl sulfide (7.706 g) was added to a solution of glacial acetic acid (25 ml) and distilled water (3.3 ml). Chlorine (232 ml/min) was bubbled into the reaction mixture for 30 min. Distilled water (35 ml) was added and the solution extracted with chloroform (three 50 ml aliquots). The combined chloroform layers were washed with 2½% w/v NaOH (two 50 ml aliquots), distilled water (75 ml), dried ($MgSO_4$), filtered, and the chloroform distilled off. The residue contained benzylsulfonyl chloride (0.368 g, 3.5%), benzyl chloride (5.958 g, 84%), and methanesulfonyl chloride (4.774 g, 75%).

After standing overnight, crystals formed, which were filtered off and shown to be identical to authentic benzylsulfonyl chloride by n.m.r., i.r., m.p., and t.l.c. Some of

the filtered residue (2.194 g) was chromatographed on silica gel (120 g) using carbon tetrachloride eluant. Elution with carbon tetrachloride (1.5 l) furnished benzyl chloride which was identical to authentic material by i.r., n.m.r., and b.p. Further elution with chloroform (500 ml) furnished methanesulfonyl chloride which was identical to authentic material by n.m.r., i.r., and b.p.

The authors are indebted to Mr. W. K. Jardine for technical assistance and to Mr. J. LeDue for running the mass spectra. We are grateful to Dalhousie University for some financial support.

1. D. L. TULEEN and V. C. MARCUM. J. Org. Chem. **32**, 204 (1967).
2. D. L. TULEEN. J. Org. Chem. **32**, 4006 (1967).
3. G. E. WILSON, JR. and M. G. HUANG. J. Org. Chem. **35**, 3002 (1970).
4. G. E. WILSON, JR. and R. ALBERT. J. Org. Chem. **38**, 2160 (1973).
5. H. KWART, R. W. BODY, and D. M. HOFFMAN. Chem. Commun. 765 (1967).
6. H. KWART and P. S. STRILKO. Chem. Commun. 767 (1967).
7. G. TSUCHIHASHI and S. IRIUCHIJIMA. Bull. Chem. Soc. Jpn. **43**, 2271 (1970).
8. R. N. LOEPPKY and D. C. K. CHANG. Tetrahedron Lett. 5415 (1968).
9. M. CINQUINI, S. COLONNA, and F. MONTANARI. Chem. Commun. 607 (1969).
10. G. TSUCHIHASHI and S. IRIUCHIJIMA. Tetrahedron Lett. 5259 (1969).
11. M. CINQUINI and S. COLONNA. J. Chem. Soc. Perkin Trans. 1, 1883 (1972).
12. M. CINQUINI, S. COLONNA, R. FORNASIER, and F. MONTANARI. J. Chem. Soc. Perkin Trans. 1, 1886 (1972).
13. M. CINQUINI, S. COLONNA, and D. LANDINI, J. Chem. Soc. Perkin Trans. 2, 297 (1972).
14. P. CALZAVARA, M. CINQUINI, S. COLONNA, R. FORNASIER, and F. MONTANARI. J. Am. Chem. Soc. **95**, 7431 (1973).
15. J. KLEIN and H. STOLLAR. J. Am. Chem. Soc. **95**, 7437 (1973).
16. G. TSUCHIHASHI and K. OGURA. Bull. Chem. Soc. Jpn. **44**, 1726 (1971).
17. K. C. TIN and T. DURST. Tetrahedron Lett. 4643 (1970).
18. T. DURST, K. C. TIN, and M. J. MARCIL. Can. J. Chem. **51**, 1704 (1973).
19. M. CINQUINI, R. ANNUNZIATA, and S. COLONNA. J. Chem. Soc. Perkin Trans. 1, 2057 (1972).
20. J. S. GROSSERT, W. R. HARDSTAFF, and R. F. LANGLER. Chem. Commun. 50 (1973).
21. J. S. GROSSERT and R. F. LANGLER. Chem. Commun. 49 (1973).
22. W. G. PHILLIPS and K. W. RATTS. J. Org. Chem. **36**, 3145 (1971).
23. P. ROBSON, P. SPEAKMAN, and D. STEWART. J. Chem. Soc. C, 2180 (1968).
24. F. G. BORDWELL and W. T. BRANNEN. J. Am. Chem. Soc. **86**, 4645 (1964).
25. L. A. PAQUETTE. J. Am. Chem. Soc. **86**, 4085 (1964).
26. F. G. BORDWELL and B. JARVIS. J. Org. Chem. **33**, 1182 (1968).
27. M. CINQUINI, D. LANDINI, and A. MAIA. Chem. Commun. 734 (1972).
28. W. R. HARDSTAFF, and R. F. LANGLER. Org. Mass Spectrom. **10**, 215 (1975).
29. W. E. TRUCE, G. H. BIRUM, and E. T. MCBEE. J. Am. Chem. Soc. **74**, 3594 (1952).
30. S. W. LEE and G. DOUGHERTY. J. Org. Chem. **5**, 81 (1940).
31. J. S. GROSSERT and R. F. LANGLER. J. Chromatogr. **97**, 83 (1974).
32. G. OPITZ. Angew. Chem. Int. Ed. Eng. **6**, 107 (1967).
33. M. KLENK, C. SUTER, and S. ARCHER. J. Am. Chem. Soc. **70**, 3846 (1948).
34. W. R. HARDSTAFF, R. F. LANGLER and M. J. NEWMAN. Org. Mass Spectrom. **9**, 1156 (1974).
35. D. A. SKOOG and D. WEST. Fundamentals of analytical chemistry. Holt, Rinehart and Winston, New York. 1963. p. 203.

Can. J. Chem. Downloaded from www.nrcresearchpress.com by 210.87.254.40 on 09/05/12
For personal use only.

Can. J. Chem. Downloaded from www.nrcresearchpress.com by 210.87.254.42 on 09/05/12
For personal use only.

New Access to Noradamantanes via Generation of Selectively Protected Bicyclic β-Diketones

D GRAVEL[1] AND S. RAHAL[2]

Department of Chemistry, University of Montreal, P.O. Box 6210, Montreal, Quebec H3C 3V1

Received May 8, 1975

D. GRAVEL and S. RAHAL. Can. J. Chem. **53**, 2671 (1975).

The synthesis of 2,9-disubstituted and 2- and 9-monosubstituted noradamantanes is described starting from 4-acetoxycyclohexanone. The key step in this approach is the generation of selectively protected 7-acetoxybicyclo[3.3.1]nonane-2,9-dione by trapping the imminium salt precursor by an acetalyzing reagent.

D. GRAVEL et S. RAHAL. Can. J. Chem. **53**, 2671 (1975).

La synthèse des noradamantanes disubstitués en 2,9 ainsi que monosubstitués en 2 et 9 est décrite à partir de l'acétoxy-4 cyclohexanone. L'étape clé dans cette voie de synthèse et l'obtention de l'acétoxy-7 bicyclo[3.3.1]nonanedione-2,9 sélectivement protégée en position-9. Ceci est rendu possible en piégeant le sel d'immonium précurseur de la dione par un agent acétalisant.

Continuing interest in the synthesis of substituted noradamantanes (1), be it for physical organic or pharmacological studies, prompts us to report our results concerning a new mode of access to the noradamantane ring system **1**.

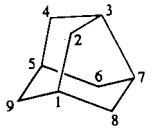

1

In 1967, Hickmott and Hargreaves (2) reported the condensation of the morpholine enamine of cyclohexanone with acryloyl chloride to yield bicyclo[3.3.1]nonane-2,9-dione after hydrolytic work up as depicted in Scheme 1. We were able to take advantage of the intermediate imminium salt in this reaction to devise a successful route to noradamantanes.

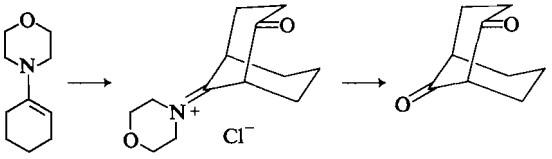

SCHEME 1

In the present communication we report the synthesis of 2,9-disubstituted and 2- and 9-monosubstituted noradamantanes starting from readily available 4-acetoxycyclohexanone (**2**)[3], as shown in Scheme 2.

The morpholine enamine of the starting ketone **2** is prepared in the usual manner and condensed *in situ* with acryloyl chloride following the procedure of Hickmott and Hargreaves (2) to yield the intermediate imminium salt **3** in the form of a dark solid. Whereas the usual (**2**) hydrolytic work up leads to β-diketone **4** which is a dead end in the projected synthesis[4], the simple filtration and washing of the precipitate with anhydrous benzene and then ether yields the white intermediate salt **3**, sufficiently pure for acetalyzation. Stirring of the imminium salt **3** in ethanedithiol or ethylene glycol for 20 h affords, after chromatography, either the monoethylenedithioacetal derivative **5**, yield[5] 15% based on **2**; b.p. 200 °C/0.1 Torr; i.r. 1705, 1730 cm^{-1}; n.m.r. singlet (3H) δ 2.07, singlet (4H) δ 3.37, multiplet (1H) δ 5.1 $W_{1/2}$ 10 Hz; or the monoethylenedioxyacetal derivative **10**, yield [5]10% based on **2**;

[1]Author to whom correspondence should be addressed.
[2]C.I.D.A. Predoctorate Fellow, 1970–1975.

[3]Compound **2** is obtained from commercial 1,4-cyclohexanediol either by monoacetylation followed by chromic oxidation (8) or by selective oxidation with silver carbonate (9) followed by acetylation.

[4]As could be anticipated, attempts to saponify the acetate or selectively acetalyze the 9-keto group in **4** were unsuccessful.

[5]Yields reported are not optimized. Reported yields (2) of 45% in the synthesis of bicyclo[3.3.1]nonane-2,9-dione (Scheme 1) could not be repeated either by ourselves or by others (3).

Can. J. Chem. Downloaded from www.nrcresearchpress.com by 210.87.254.42 on 09/05/12
For personal use only.

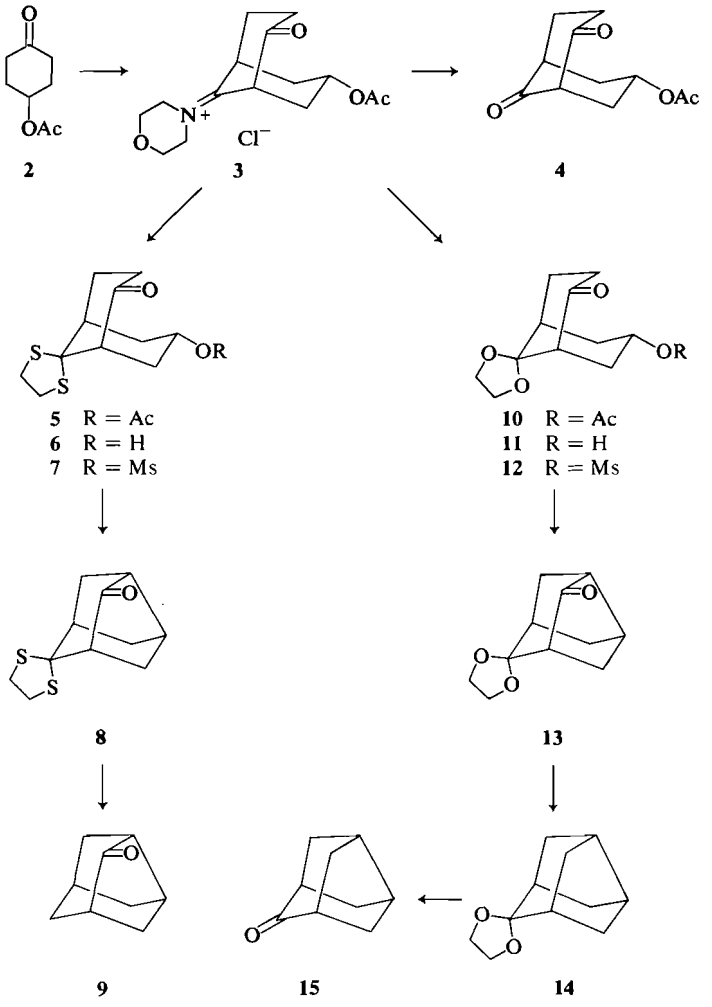

SCHEME 2

m.p. 86–87 °C; i.r. 1705, 1735 cm^{-1}; n.m.r. singlet (3H) δ 1.97, singlet (4H) δ 3.98, multiplet (1H) δ 4.97 $W_{1/2}$ 9 Hz. This procedure therefore allows the preparation from 4-acetoxycyclohexanone (**2**) of the selectively protected β-diketones **5** and **10** in essentially one step.[6]

Saponification of the ethylenedithioacetal-keto-ester **5** with aqueous sodium carbonate in refluxing methanol for 3 h gives the corresponding semisolid alcohol **6** (crude) which is mesylated under the usual conditions to give the ethylenedithioacetal-keto-mesylate **7**, yield 82% based on **5**; m.p. 104–105 °C; i.r. 1170, 1330, 1710 cm^{-1}; n.m.r. singlet (3H) δ 3.12, singlet (4H) δ 3.42, multiplet (1H) δ 5.06 $W_{1/2}$ 18 Hz. Ring closure of the precursor **7**, carried out in refluxing dioxane in presence of sodium hydride, affords 9,9-ethylenedithionoradamantane-2-one (**8**), yield 82%; m.p. 206–208 °C; i.r. 1740 cm^{-1}; n.m.r. unresolved peaks (6H) δ 2.02 and 2.17, unresolved multiplet (4H) δ 2.67, singlet (4H) δ 3.36; molecular ion, *m/e* 226.0487, calculated; 226.0485. Desulfurization of compound **8** in presence of Raney nickel under specific conditions; 35 °C, absolute ethanolic solution and vigorous stirring for 8 h gives noradamantane-2-one (**9**), yield 80%; m.p. 214–215 °C (lit. (4), 214.5–215 °C), i.r. 1748 cm^{-1}; n.m.r.: unresolved peaks δ 1.8 and 2.3; molecular ion *m/e* 136.0887, calculated 136.0888.

[6]It is important to note that this annellation method appears to be highly stereoselective yielding the desired isomer **5** or **10**. This fact is established firmly by the subsequent conversion of **7** to **8** or **12** to **13**.

In an analogous fashion the monoethylenedioxyacetal **10** may be converted into noradamantane-9-one (**15**). Saponification of **10** with methanolic sodium hydroxide at room temperature gives the corresponding alcohol **11** (crude) which is converted to the mesylate **12** in the usual manner, yield 74.5%, based on **10**; m.p. 121–122 °C; i.r. 1170, 1350, 1700 cm^{-1}; n.m.r. singlet (3H) δ 3.03, singlet (4H) δ 3.98, multiplet (1H) δ 4.95 $W_{1/2}$ 18 Hz. Cyclization of the ethylenedioxy-keto-mesylate **12** is carried out in presence of potassium *tert*-butoxide in refluxing *tert*-butanol to afford 9,9-ethylenedioxynoradamantane-2-one (**13**), yield 85%; i.r. 1745 cm^{-1}; n.m.r. three unresolved peaks (6H) δ 1.87, (2H) δ 2.30, (2H) δ 2.60, singlet (4H) δ 3.98; molecular ion *m/e* 194.0938, calculated 194.0942.

Treatment of keto-acetal **13** under the Huang-Minlon modification of the Wolff–Kishner method (5) leads to 9,9-ethylenedioxynoradamantane (**14**), yield 92%; m.p. 51–52 °C, (lit. (6, 7) 51–52 °C); i.r. 1080, 1125 cm^{-1}; n.m.r. four unresolved peaks (8H) δ 1.7 and 1.84, (2H) δ 2.05, (2H) δ 2.42, singlet (4H) δ 4.0; molecular ion *m/e* 180.1145, calculated 180.1149. Upon acid hydrolysis the acetal **14** gives noradamantane-9-one (**15**), yield 86%; m.p. 194–195 °C, (lit. (6, 7) 193–195 °C); i.r. 1715 cm^{-1}; n.m.r. two unresolved peaks (8H) δ 1.85 and (4H) δ 2.7; molecular ion *m/e* 136.0884, calculated 136.0887.

Further work is in progress to extend the use of the same starting material (**2**) to the synthesis of 1- and 3-substituted noradamantanes.

This work was supported by the National Research Council of Canada and the Ministère de l'Education du Quebec. One of us (S.R.) is grateful to the C.I.D.A. for a predoctorate fellowship.

1. J. S. WISHNOK, P. V. R. SCHLEYER, E. FUNKE, G. D. PANDIT, R. O. WILLIAMS, and A. NICKON. J. Org. Chem. **38**, 539 (1973), and references cited therein.
2. P. W. HICKMOTT and J. R. HARGREAVES. Tetrahedron, **23**, 3151 (1967).
3. R. GELIN, S. GELIN, and R. DOLMAZON. Tetrahedron Lett. 3657 (1970).
4. A. NICKON, G. D. PANDIT, and R. O. WILLIAMS. Tetrahedron Lett. 2851 (1967).
5. HUANG-MINLON. J. Am. Chem. Soc. **68**, 2487 (1946).
6. M. R. VEGAR and R. J. WELLS. Tetrahedron Lett. 2565 (1969).
7. S. RAHAL. M.Sc. Thesis, University of Montreal, Montreal, Que. 1971.
8. (*a*) E. R. H. JONES and F. SONDHEIMER. J. Chem. Soc. 615 (1949); (*b*) J. B. ALDERSLEY, G. N. BURKHARD, A. E. GILLAM, and N. C. HINDLEY. J. Chem. Soc. 10 (1940).
9. M. FETIZON and M. GOLFIER. C.R. Acad. Sci. C, **267**, 900 (1968).

Can. J. Chem. Downloaded from www.nrcresearchpress.com by 210.87.254.42 on 09/05/12
For personal use only.

Can. J. Chem. Downloaded from www.nrcresearchpress.com by 210.87.254.6 on 09/05/12
For personal use only.

Canadian Journal of Chemistry

Published by
THE NATIONAL RESEARCH COUNCIL OF CANADA

Journal canadien de chimie

Publié par
LE CONSEIL NATIONAL DE RECHERCHES DU CANADA

Volume 53 Number 18 September 15, 1975

Volume 53 numéro 18 15 septembre 1975

Infrared Spectra of the Ammonium Ion in Crystals. I. Ammonium Hexachloroplatinate(IV) and Hexachlorotellurate(IV)[1]

IAN A. OXTON AND OSVALD KNOP
Department of Chemistry, Dalhousie University, Halifax, Nova Scotia B3H 4J3
AND
MICHAEL FALK
Atlantic Regional Laboratory, National Research Council of Canada, Halifax, Nova Scotia B3H 3Z1

Received March 26, 1975

IAN A. OXTON, OSVALD KNOP, and MICHAEL FALK. Can. J. Chem. **53**, 2675 (1975).

Infrared spectra of polycrystalline $(NH_4)_2PtCl_6$ and $(NH_4)_2TeCl_6$ at various degrees of deuteration were recorded between 4000 and 1000 cm^{-1} at 30 and −165 °C. The stretching and bending vibrations of NH_4^+, NH_3D^+, $NH_2D_2^+$, NHD_3^+, and ND_4^+ ions in these two compounds were systematically examined. The observed fundamentals were unambiguously assigned by analogy with the vibrations of the partially deuterated methanes. The spectrum of isotopically dilute NH_3D^+ confirms the existence of only one crystallographically distinct type of ammonium ion in the structure, on sites of T_d symmetry. Vibrational coupling of neighboring ammonium ions was not detected.

IAN A. OXTON, OSVALD KNOP et MICHAEL FALK. Can. J. Chem. **53**, 2675 (1975).

Les spectres infrarouge de $(NH_4)_2PtCl_6$ et de $(NH_4)_2TeCl_6$ polycristallins à deutération variable ont été enregistrés entre 4000 et 1000 cm^{-1} à 30 °C et à −165 °C. Les vibrations de valence et de déformation des espèces ioniques NH_4^+, NH_3D^+, $NH_2D_2^+$, NHD_3^+ et ND_4^+ dans ces deux composés ont été systématiquement examinés. L'attribution exacte des vibrations fondamentales observées a été réalisée par analogie avec celle des méthanes partiellement deutérés. Le spectre de NH_3D^+ à dilution isotopique indique nettement l'existence d'un seul et unique type d'ion ammonium dans la structure cristalline, sur des sites de symétrie T_d. On n'a pas observé de couplage vibrationnel des ions ammonium voisins.

Infrared spectroscopy has been an important tool in the elucidation of the structural behavior of the ammonium ion in crystals (1–6) and especially useful in the detection of phase changes (7, 8). However, most of the published results are based on the spectra of undeuterated, or fully deuterated, samples and are thus limited in scope. The present study is the first in a series aimed at investigating the spectra of *all* the ionic species $NH_{4-n}D_n^+$ ($n = 0$ to 4) in various known crystalline environments, with particular attention to the spectra of the isotopically dilute NH_3D^+ and NHD_3^+ ions.

Three considerations suggest that spectra of the isotopically dilute ions may prove to be more informative than those of NH_4^+ or ND_4^+.

(*i*) Difficulty has been experienced in making the correct assignment of the stretching fundamentals ν_1 and ν_3. This basic problem may be illustrated by the assignments proposed for these modes in NH_4F by different authors:

[1]NRCC No. 14763.

	ν_1 (cm^{-1})	ν_3 (cm^{-1})
Plumb and Hornig (3)	2870	2810
Waddington (9)	—	3100
Mathieu (10)	2845	3100
Bovey (11)	3100, 3212	2725, 2830

This difficulty would not be encountered in the spectra of crystals containing a low deuterium concentration, since the N—D stretching fundamental $\nu_1(NH_3D^+)$ has a frequency far removed from the spectral region where NH_4^+ ions absorb. This should permit its unambiguous assignment. Similarly, an unambiguous assignment of the N—H stretching frequency $\nu_{3a}(NHD_3^+)$ should be possible in crystals containing a high deuterium concentration.[2]

(*ii*) The region 2700 to 3400 cm^{-1} in the i.r. spectra of undeuterated ammonium compounds is rich in absorption bands and it is likely that extensive Fermi resonance exists between many vibrational levels (3, 13). Among vibrations which may be expected to occur in this frequency range, depending upon the symmetry of the ion in each individual case, are ν_1, ν_3, $2\nu_4$, $\nu_2 + \nu_4$, $\nu_3 + \nu_6$, $\nu_1 + \nu_5$, etc. Judging by the medium-strong i.r. intensities of some of these modes, appreciable "borrowing" of intensity must take place, and the observed intensities will in general correspond to vibrational levels that are considerably perturbed (12, 13). This type of perturbation should be largely absent in the much simpler N—D (or N—H) stretching region of isotopically dilute NH_3D^+ (or NHD_3^+), so that $\nu_1(NH_3D^+)$ (or $\nu_{3a}(NHD_3^+)$) should reflect more directly the environment of the ammonium ion in the crystal.

(*iii*) Vibrational modes of neighboring ammonium ions may be coupled. In the spectra of the undeuterated or fully deuterated compounds the coupling, if present, may escape detection, but it would show up on comparing spectra of ammonium ions in crystals of suitably varied D content. Knowing whether or not vibrational coupling is present is required when ammonium frequencies in different crystal structures are to be compared. The magnitude of the frequency shifts produced by such coupling may be of structural significance, as has recently been found in the case of H_2O spectra in crystalline hydrates (14).

[2]Herzberg's nomenclature has been adopted for the vibrations of the $NH_{4-n}D_n^+$ ions (ref. 12, p. 238).

Vibrational spectra of the partially deuterated ammonium ions have not been tabulated with any completeness. Such data as exist are mainly due to the assignment of extraneous bands in the spectra of "fully" deuterated ammonium compounds (1–3, 6). Ananthakrishnan (15) tabulated some Raman frequencies of partially deuterated NH_4Cl many years ago. Recently Wiener *et al.* (16) presented some tentative assignments for the i.r. spectra of partially deuterated $NH_4H_2PO_4$ and $NH_4H_2AsO_4$. Oden and Decius (17) used an intermediate deuteration of NH_4NCS as a general illustration of the low site symmetry of the ammonium ion in this compound but made no detailed assignments.

For our first study we have selected $(NH_4)_2PtCl_6$ and $(NH_4)_2TeCl_6$. The ammonium ion in these two compounds has been shown to be located at sites of tetrahedral symmetry (see below). The various deuterated ammonium ions might thus be expected to obey the selection rules of their own molecular point groups. The expected correlation of the fundamental vibrations of these species is shown in Table 1.

The vibrational energy levels of a uniquely oriented NH_4^+ ion in a site of symmetry T_d would be expected to bear a close relationship to those of the isoelectronic ion BH_4^- (18) and molecule CH_4 (19, 20). This supposition will be examined in the light of the existing i.r. and Raman spectra of the $CH_{4-n}D_n$ (21–23) and $BH_{4-n}D_n^-$ species (18). We have also sought evidence for the vibrational coupling of neighboring, isotopically similar ammonium ions (*cf.* the coupling of the bending modes of isotopically similar water molecules in crystalline hydrates, ref. 14).

Crystallographic Features of $(NH_4)_2PtCl_6$ and $(NH_4)_2TeCl_6$

Ammonium hexachloroplatinate(IV) has the distinction of being the first reported case of coordination compound studied by X-ray diffraction (24). It is, apart from the H atoms, isostructural with the type compound K_2PtCl_6 (31) and a large number of other cubic compounds having the antifluorite-like structures $R_2[MX_6]$ of symmetry $Fm3m$ (No. 225) (Table 2). Each R atom is coordinated by 12 equivalent X atoms at the corners of a cuboctahedron of symmetry T_d (Fig. 1), $d(R\ldots X) = a_0[(x - \frac{1}{4})^2 + \frac{1}{8}]^{1/2}$. The value of x(Cl) in $(NH_4)_2PtCl_6$ is known only approximately, 0.240(5) (25). However,

Can. J. Chem. Downloaded from www.nrcresearchpress.com by 210.87.254.6 on 09/05/12
For personal use only.

Can. J. Chem. Downloaded from www.nrcresearchpress.com by 210.87.254.6 on 09/05/12
For personal use only.

$\partial d(\text{N}\ldots\text{Cl}) \sim -0.3\partial x$, so that d(N. . .Cl) is quite insensitive to uncertainties in x. An uncertainty ∂x of ± 0.01, which seems to correspond to the total range of variation of x in the cubic $R_2[MCl_6]$ (28, 30, 31), produces a change in d(N. . .Cl) of only about ± 0.003 Å. The N. . .Cl distance can thus be taken as 3.49 Å to within 0.01 Å. From the results of the neutron-diffraction study of the isostructural $(NH_4)_2SiF_6$ by Schlemper *et al.* (29) there seems little doubt that the H atoms in the hexachloroplatinate are to be looked for in the volumes defined by the N. . .3Cl trigonal pyramids shown in Fig. 1.

The isostructural (25, 30) $(NH_4)_2TeCl_6$ has been included to see what effect on the spectrum of the ammonium ion is produced by replacing the relatively small atom of a transition element, Pt, by a significantly larger atom of a non-transition element, Te. In this compound x(Cl) is 0.248(3) and d(N. . .Cl), 3.61(1) Å (30).

Experimental

$(NH_4)_2PtCl_6$ of high purity was recrystallized twice from cold water. Deuterated samples were obtained by crystallization from mixtures of H_2O and D_2O of the requisite compositions.

$(NH_4)_2TeCl_6$ was prepared by dissolving high-purity TeO_2 in concentrated HCl, adding a solution of the stoichiometric amount of NH_4Cl, and allowing the resulting solution slowly to crystallize on a hot plate. The greenish-yellow crystals were air dried. The sample of intermediate deuteration was prepared in a similar manner from 50% HCl–DCl.

Spectra were recorded at 30 and −165 °C on a Perkin-Elmer model 180 spectrophotometer in the region 4000 to 1000 cm^{-1}. Nujol mulls were supported on KBr windows. Fluorolube mulls were occasionally used to ensure that no bands were overlaid by Nujol bands. In each case the degree of deuteration was estimated from the integrated intensities of the N—H and N—D stretching absorptions at room temperature, assuming that N—D stretching bands have half the integrated intensity of the N—H stretching bands. This is known to be approximately true for D and H stretching vibrations of other systems (32).

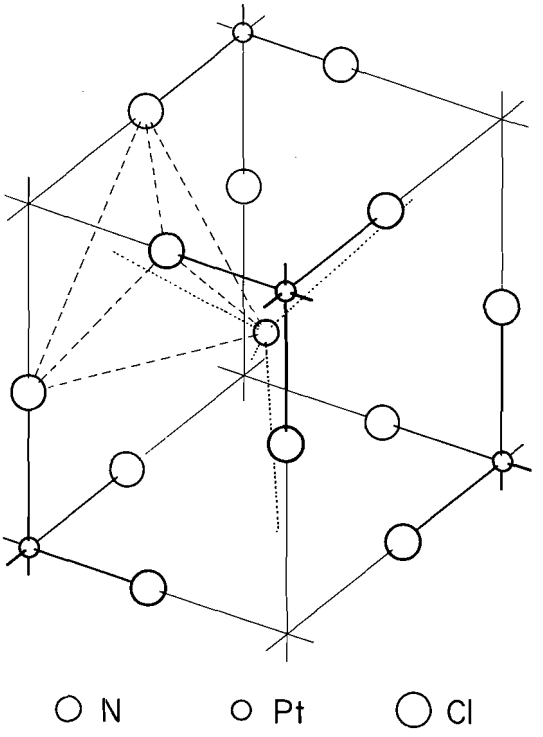

FIG. 1. One-eighth of the unit cell of $(NH_4)_2PtCl_6$. Dotted lines from the N atom indicate the averaged (equilibrium) directions of the N—H vectors.

Results and Discussion

In the room-temperature spectra the bands were broad, hence only a few absorption maxima could be located with accuracy and measurement of low-temperature spectra was essential. This was found to be especially true of the N—D stretching modes (Fig. 2). Where accurate frequency values were available for room temperature *and* liquid-nitrogen temperature, the difference due to temperature variation did not exceed 3 cm^{-1}.[3]

All frequencies quoted in the following (text and Table 3) refer to the low-temperature spectra. The accuracy of the bending frequencies is estimated to be about ± 0.5 cm^{-1} and that of the stretching frequencies, about ± 1 cm^{-1}. The hexachlorotellurate spectra were so similar to those of the hexachloroplatinate that the frequencies for the Te compound are tabulated without further comment.

Examination of the band intensities as a function of the D content of the sample allows assignment of all observed bands (Table 3). All but three of the i.r. active fundamentals predic-

[3]From his observations of the habit and optical properties of $(NH_4)_2PtCl_6$ crystals at different temperatures, Ries (33) proposed the existence of three, possibly four, polymorphs: a "probably O_h" form stable at liquid-air temperatures, a "pseudo-octahedral" form at intermediate low temperatures, and an O_h form stable from a few degrees below 0 °C to decomposition. However, he stated that a similar situation existed for K_2PtCl_6, hence his observations could not have had their cause in the temperature-dependent behavior of the NH_4^+ ion. There was no indication of polymorphism in our i.r. spectra of $(NH_4)_2PtCl_6$.

Can. J. Chem. Downloaded from www.nrcresearchpress.com by 210.87.254.6 on 09/05/12
For personal use only.

TABLE 1. Correlation of the fundamental modes of the isotopically substituted ammonium ions*

Mode	NH_4^+	NH_3D^+	$NH_2D_2^+$	NHD_3^+	ND_4^+
ν_1	a_1†	a_1	a_1	a_1	a_1†
ν_2	e†	e	$a_1 + a_2$†	e	e†
ν_3	t_2	$a_1 + e$	$a_1 + b_1 + b_2$	$a_1 + e$	t_2
ν_4	t_2	$a_1 + e$	$a_1 + b_1 + b_2$	$a_1 + e$	t_2

*The correlation is based on that of Herzberg (ref. 12, p. 238).
†Infrared-inactive modes.

TABLE 2. Crystallographic data of $(NH_4)_2PtCl_6$ and $(NH_4)_2TeCl_6$*

Atom	Equipoint	Positional parameters	Site symmetry
N	8(*c*)	$\frac{1}{4}\frac{1}{4}\frac{1}{4}$ etc.	$\bar{4}3m$–T_d
M = Pt, Te	4(*a*)	000 etc.	$m3m$–O_h
Cl	24(*e*)	*x*00 etc.	$4mm$–C_{4v}
H	[32(*f*)	*xxx* etc.]†	$3m$–C_{3v}

*Space group $Fm3m$ (No. 225); $a_0[(NH_4)_2PtCl_6] = 9.8580$ Å at 25 °C (26); $a_0[(NH_4)_2TeCl_6] = 10.203$ Å at 25 °C (27); 10.200(5) Å (30).
†This equipoint corresponds to the minimum multiplicity consistent with stoichiometry and with site symmetry T_d at the N atom. See ref. 29 for a discussion of the neutron-diffraction evidence bearing on the H atoms in the isostructural $(NH_4)_2SiF_6$.

ted by Table 1 have been located. The three remaining fundamentals, which are overlaid by more intense absorptions, have been placed by comparison with the spectra of related compounds, as outlined below. No splitting of any of the bands was observed and no fundamental frequency varied by more than 3 cm^{-1} over the whole range of deuterations.

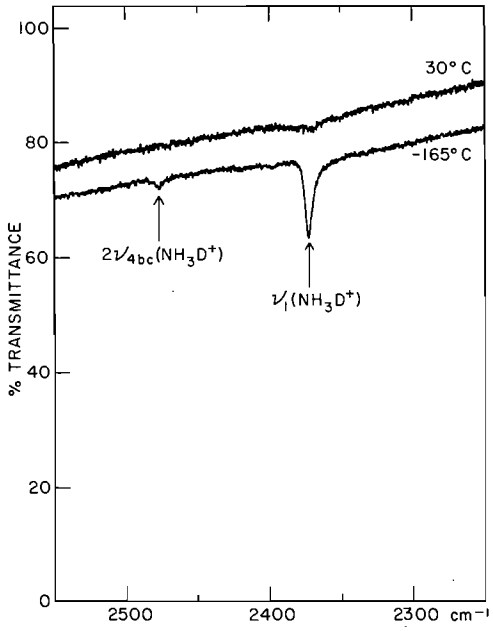

FIG. 2. The N—D stretching region of the i.r. spectrum of $(NH_4)_2PtCl_6$ (1% D) at room temperature and liquid-nitrogen temperature.

N—D Stretching Vibrations

Isotopically dilute NH_3D^+ gives rise to a sharp band at 2372 cm^{-1}, assigned unambiguously to the $\nu_1(a_1)(NH_3D^+)$ mode. The band is a singlet, which confirms the equivalence of hydrogen atom environments in the crystal structure. At intermediate D contents several bands appear in the 2500 to 2300 cm^{-1} region (Fig. 3). Inspection shows that the band assigned to $\nu_1(a_1)(NH_3D^+)$ reaches maximum intensity at a D concentration of about 25%, as would be expected from the statistical distribution of the $NH_{4-n}D_n^+$ species; the frequency of the band does not vary with the D content of the sample. The half-width of the band is 6 cm^{-1}.

At high D contents, when the predominant species is ND_4^+, a single band centered at 2430 cm^{-1} is observed, hence it is assigned to $\nu_3(t_2)(ND_4^+)$. The N—D stretching modes of the remaining species $NH_2D_2^+$ and NHD_3^+ are readily assigned to bands which reach maximum intensity at 50% D, at 2454 and 2398 cm^{-1}, and 75% D, at 2417 and 2314 cm^{-1}, respectively. The remaining bands in this region may be satisfactorily assigned to overtone and combination modes (*cf.* Table 3).

N—H Stretching Vibrations

The region 3300 to 3100 cm^{-1} (Fig. 4) is seen

TABLE 3. Vibrational frequencies of the ammonium ions in the i.r. spectra of $(NH_4)_2PtCl_6$ and $(NH_4)_2TeCl_6$

	$(NH_4)_2PtCl_6$							$(NH_4)_2TeCl_6$	
Assignment	0% D	1% D	25% D	50% D	75% D	90% D	95% D	0% D	50% D
$\nu_3(NH_4^+)$, $\nu_{3a}(NHD_3^+)$	3239	3239	3239	3238	3239 sh	3239	3240	3218	3212*
$\nu_{3b}(NH_2D_2^+)$				3218	3218	3216	3219 sh		3180*
$\nu_{3a}(NH_2D_2^+)$			3200	3202	3204 sh	3205 sh	3206 sh		
$\nu_{3a}(NH_3D^+)$			3195	3196					
$2\nu_2(NHD_3^+)$					2756				
$2\nu_{4b}(NH_2D_2^+)$				2629	2629				
$\nu_2 + \nu_{4b}(NHD_3^+)$				2495	2495	2495			
$2\nu_{4bc}(NH_3D^+)$		2472	2477	2478					2487
$\nu_2 + \nu_{4a}(NHD_3^+)$				2460		2461			2472
$\nu_{3c}(NH_2D_2^+)$			2454	2455	2455				2455
$\nu_3(ND_4^+)$			2426	2427	2427	2428	2430		2411 sh
$\nu_{3bc}(NHD_3^+)$			2417	2417	2418	2417			2404
$\nu_1(NH_2D_2^+)$			2398	2398	2400				2391
$\nu_1(NH_3D^+)$		2372	2372	2372	2373				2358
$\nu_1(NHD_3^+)$			2314	2314	2314	2314	2315		2303
$2\nu_{4b}(NH_2D_2^+)$			2296	2297	2297				
$2\nu_4(ND_4^+)$							2115		
$\nu_2(NH_3D^+)$		1586.0	1586.2	1586.3	1586.2	1587.0			1592.4
$\nu_{2a}(NH_2D_2^+)$			1546.2	1547.0	1546.6	1547.8			1548.0
								1419.4 sh*	
$\nu_4(NH_4^+)$, $\nu_4(NH_3D^+)$	1402.8	1402.0	1401.0	1401.6		1401.6	1401.2	1409.0	1405.1
$\nu_2(NHD_3^+)$			1388.0	1389.8		1390.0	1390.4		1394.2
$\nu_{4b}(NH_2D_2^+)$			1325.5	1325.5	1325.5	1326.1	1326.8		1330.4
$\nu_{4bc}(NH_3D^+)$		1240.9	1240.4	1240.8	1240.4	1241.8	1241.6		1243.9
$\nu_{4c}(NH_2D_2^+)$			1160.8	1160.0	1160.8	1161.4	1160.0		1165.1
$\nu_{4bc}(NHD_3^+)$, $\nu_{4a}(NHD_3^+)$			1105.9	1106.0	1105.9	1107.1	1106.9		1108.5
$\nu_{4a}(NHD_3^+)$			1069.9	1069.9	1069.9				1072.2
$\nu_4(ND_4^+)$			1062.8	1062.0	1062.8	1063.0	1063.9		1066.0

*Not assigned.

to contain a multiple, broad absorption in the spectra of samples of intermediate D contents. At zero, or very high, D contents this absorption consists of a single, broad band centered at 3239 and 3240 cm^{-1}, assigned to $\nu_3(NH_4^+)$ and $\nu_{3a}(NHD_3^+)$ respectively.

The absorptions arising from the N—H stretching motions of $NH_2D_2^+$ are located at 3217 and 3204 cm^{-1}. Only one band arising from NH_3D^+, at 3195 cm^{-1}, is observed; the other N—H stretching fundamental is expected at about the same frequency as the more intense $\nu_3(NH_4^+)$ fundamental.

Bending Vibrations

The bending modes of the $NH_{4-n}D_n^+$ species give rise to absorptions in the region 1600 to 1050 cm^{-1} (Fig. 5). Ten bands are observed in this region (Table 3) whilst 12 i.r. active fundamentals are predicted by Table 1.

The $\nu_{4a}(NH_2D_2^+)$ fundamental has been calculated to have the frequency of about 1120 cm^{-1} in partially deuterated ammonium thiocyanate (17). Comparison of the vibrational frequencies of Table 3 with those of the thiocyanate leads us to expect this mode between 1110 and 1100 cm^{-1}. However, this region is dominated by an intense band, assigned to $\nu_{4bc}(NHD_3^+)$, whose maximum intensity occurs at about 75% D. The calculations of Oden and Decius (17) for ammonium thiocyanate place the frequencies of $\nu_{4a}(NH_2D_2^+)$ and $\nu_{4bc}(NHD_3^+)$ within 6 cm^{-1}. The corresponding frequencies of partially deuterated methanes fall within 12 cm^{-1} of each other (ref. 12, p. 309), while those in partially deuterated BH_4^- ions coincide within 0.2 cm^{-1} (18). It is thus concluded that the absorption at 1106 cm^{-1} results from both modes and that in ammonium hexachloroplatinate the frequencies of these two modes coincide.

It is not surprising that $\nu_{4a}(NH_3D^+)$ is not observed, since we expect its frequency to coincide with that of the very intense band arising from $\nu_4(NH_4^+)$. The frequencies of the two modes

Can. J. Chem. Downloaded from www.nrcresearchpress.com by 210.87.254.6 on 09/05/12
For personal use only.

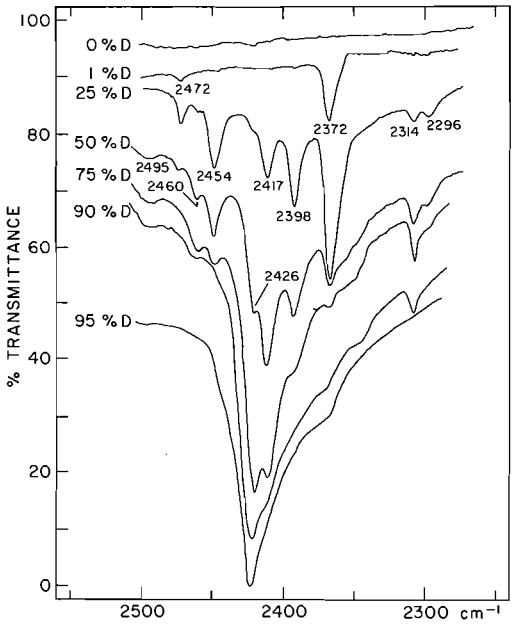

FIG. 3. The N—D stretching region of the i.r. spectrum of $(NH_4)_2PtCl_6$ at various deuterations. The D contents are approximate. The ordinate refers to 90% D; the other spectra have been displaced for clarity.

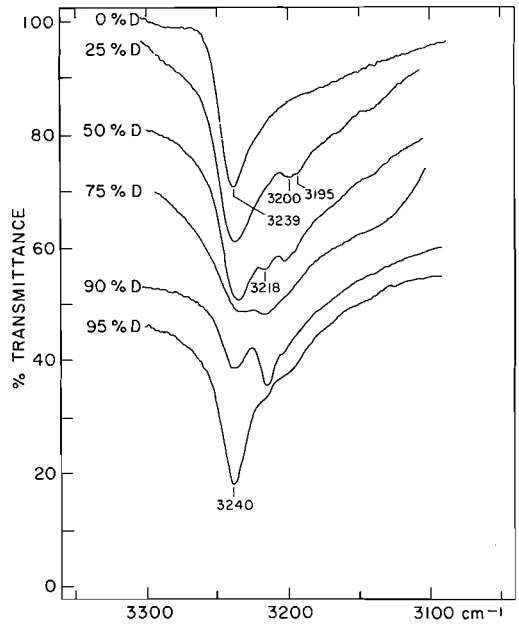

FIG. 4. The N—H stretching region of the i.r. spectrum of $(NH_4)_2PtCl_6$ at several deuterations. The ordinate refers to 90% D.

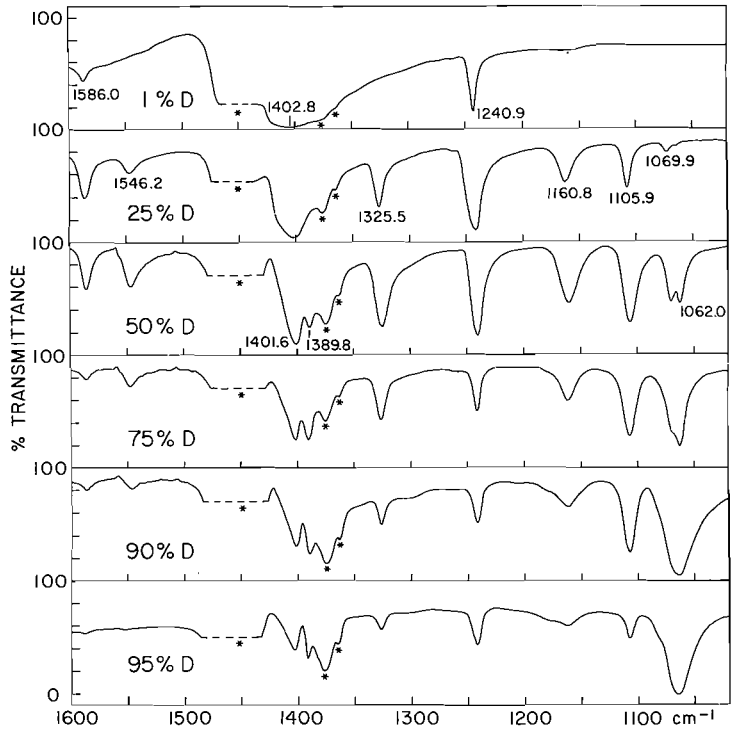

FIG. 5. The bending region of the i.r. spectrum of $(NH_4)_2PtCl_6$ at various deuterations. Nujol bands are denoted by asterisks.

Can. J. Chem. Downloaded from www.nrcresearchpress.com by 210.87.254.6 on 09/05/12
For personal use only.

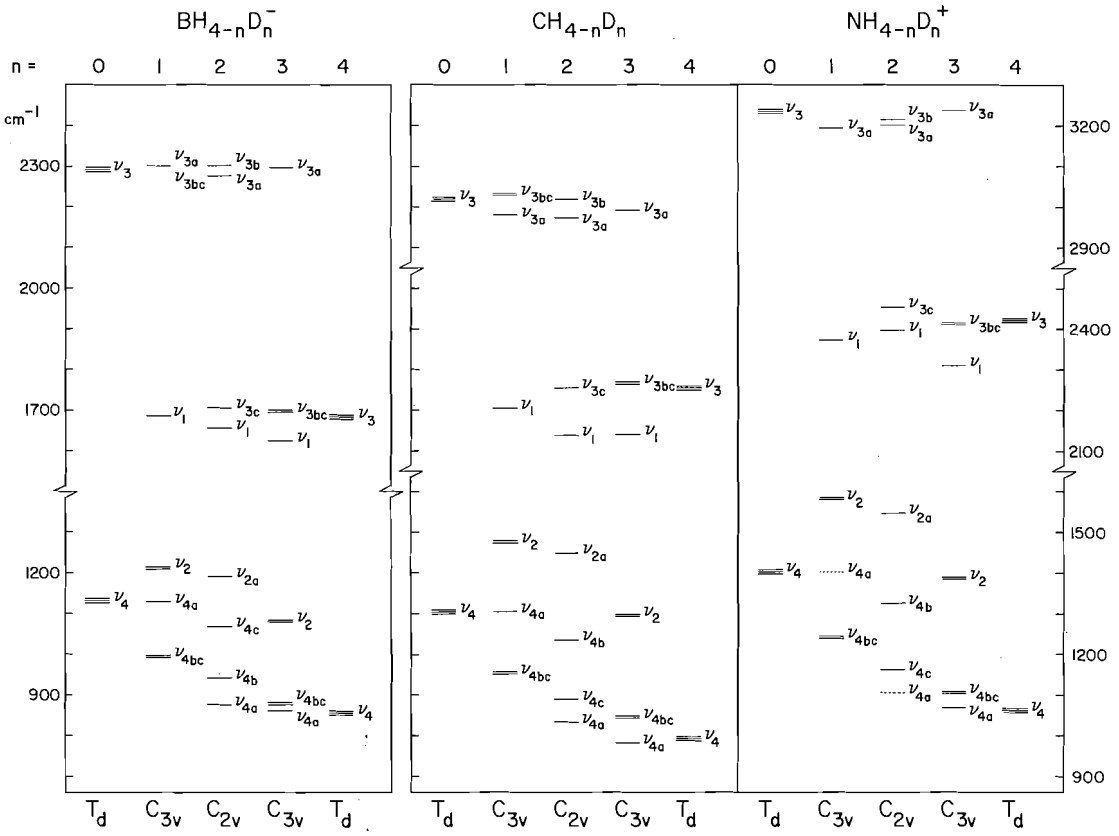

FIG. 6. Observed i.r.-active vibrational energy levels of the $BH_{4-n}D_n^-$, $CH_{4-n}D_n$, and $NH_{4-n}D_n^+$ species.

differ by only 0.4 and 1.4 cm^{-1} in the corresponding methane and borohydride species respectively.

Comparison with CH_4, CD_4, BH_4^-, and BD_4^-

The vibrational frequencies of the $NH_{4-n}D_n^+$ species are compared with those of the corresponding $CH_{4-n}D_n$ and $BH_{4-n}D_n^-$ species in Fig. 6. The overall similarity of the three sets of energy levels is striking.

For the triply degenerate modes of a tetrahedral XY_4 molecule and its isotopic counterpart $X^{(i)}Y_4^{(i)}$, the Teller–Redlich rule (ref. 12, p. 232) predicts

$$[1]\quad \omega_3^{(i)}\omega_4^{(i)}/\omega_3\omega_4 = (m_Y/m_Y^{(i)})[(m_X/m_X^{(i)})(m_X^{(i)} + 4m_Y^{(i)})/(m_X + 4m_Y)]^{1/2}$$

where ω_3 and ω_4 are the zero-order frequencies of ν_3 and ν_4 in XY_4, $\omega_3^{(i)}$ and $\omega_4^{(i)}$ are the corresponding frequencies of $X^{(i)}Y_4^{(i)}$, and m_X, m_Y, $m_X^{(i)}$, and $m_Y^{(i)}$ are the masses of the atoms X, Y, $X^{(i)}$, and $Y^{(i)}$, respectively. Hence, for the ammonium ions NH_4^+ and ND_4^+, we predict $\omega_3^{(i)}\omega_4^{(i)}/\omega_3\omega_4 = 0.553$. Setting $\nu_3 = 3239$ cm^{-1}, $\nu_4 = 1401$ cm^{-1}, $\nu_3^{(i)} = 2426$ cm^{-1}, and $\nu_4^{(i)} = 1062$ cm^{-1}, we find $\nu_3^{(i)}\nu_4^{(i)}/\nu_3\nu_4 = 0.566$. This agreement is reasonable (difference, 2.4%), since the product rule applies rigorously only for zero-order frequencies.

The corresponding values for CH_4 and CD_4 are 0.559 for the ω-product and 0.570 for the ν-product, *i.e.* in agreement to within about 2%.[4] The agreement obtained for NH_4^+ and ND_4^+ is viewed as comparable with that for CH_4 and CD_4. This suggests that no unduly large anharmonic terms are present in the vibrational potential energies of the ammonium ions as a result of their crystalline environments.

Comparison can also be made with the results

[4]Frequencies taken from ref. 12, p. 309.

Can. J. Chem. Downloaded from www.nrcresearchpress.com by 210.87.254.6 on 09/05/12
For personal use only.

of Coker and Hofer (18) for $^{11}BH_4^-$ and $^{11}BD_4^-$. Here the right-hand side of [1] yields 0.563, while the $\nu_3^{(i)}\nu_4^{(i)}/\nu_3\nu_4$ product of the observed frequencies, 0.556, has a *smaller* value, contrary to expectation. One cannot, therefore, regard as justified the assumption made by these authors, *viz.* that ν_3 as the central component of a Fermi triplet is not seriously affected by Fermi resonance.

No evidence was found in the spectra of either $(NH_4)_2PtCl_6$ or $(NH_4)_2TeCl_6$ to support the presence of vibrational coupling between neighboring ammonium ions in the crystal structure. Since the unit-cell dimensions of the two compounds encompass those of most of the cubic $R_2[MCl_6]$ compounds (28, 25), it would appear that no appreciable coupling of vibrational modes exists in any of the ammonium hexachlorometallates.

Conclusions

Unambiguous assignment of the i.r. active bending and stretching modes of the $NH_{4-n}D_n^+$ species in ammonium hexachloroplatinate(IV) and hexachlorotellurate(IV) has been made by analogy with the partially deuterated methanes. The number of observed i.r. active fundamentals is consistent with the existence of only one crystallographically distinct type of ammonium ion in a site of T_d symmetry. The bending and stretching vibrations involving the D atom of isotopically dilute NH_3D^+ ions demonstrate the equivalence of the hydrogen atoms and their positions in the crystal in a strikingly direct manner: absorptions due to the $\nu_1(a_1)$ and $\nu_{4bc}(e)$ modes appear, at liquid-nitrogen temperatures, as clear-cut singlets with half-widths of 6 and 5 cm^{-1} respectively. Vibrational coupling of the ammonium ions was not detected and must be of the order of 1 cm^{-1} or less.

A grant-in-aid-of-research from the National Research Council of Canada to one of the authors (O.K.) is hereby acknowledged.

1. E. L. Wagner and D. F. Hornig. J. Chem. Phys. **18**, 296 (1950).
2. D. F. Hornig and E. L. Wagner. J. Chem. Phys. **18**, 305 (1950).
3. R. C. Plumb and D. F. Hornig. J. Chem. Phys. **23**, 947 (1955).
4. K. B. Harvey and N. R. McQuaker. J. Chem. Phys. **55**, 4390 (1971).
5. D. A. Dows, E. Whittle, and G. C. Pimentel. J. Chem. Phys. **23**, 1475 (1955).
6. N. E. Schumaker and C. W. Garland. J. Chem. Phys. **53**, 392 (1970).
7. C. J. H. Schutte and A. M. Heyns. J. Chem. Phys. **52**, 864 (1970).
8. A. M. Heyns and C. J. H. Schutte. J. Mol. Struct. **8**, 339 (1971).
9. T. C. Waddington. J.Chem. Soc. 4340 (1958).
10. J. P. Mathieu. C.R. Acad. Sci. Ser. C. **240**, 2508 (1955).
11. L. F. H. Bovey. J. Opt. Soc. Am. **41**, 836 (1951).
12. G. Herzberg. Infrared and Raman spectra of polyatomic molecules. Van Nostrand, New York. 1945.
13. W. F. Sherman and P. P. Smulovitch. J. Chem. Phys. **52**, 5187 (1970).
14. G. H. Thomas, M. Falk, and O. Knop. Can. J. Chem. **52**, 1029 (1974).
15. R. Ananthakrishnan. Proc. Indian Acad. Sci. **5A**, 175 (1937).
16. E. Wiener (Avnear), S. Levin, and I. Pelah. J. Chem. Phys. **52**, 2891 (1970).
17. L. L. Oden and J. C. Decius. Spectrochim. Acta, **20**, 667 (1964).
18. E. H. Coker and D. E. Hofer. J. Chem. Phys. **53**, 1652 (1970).
19. A. C. Menzie and H. R. Mills. Proc. R. Soc. London, **148A**, 407 (1935).
20. W. Vedder and D. F. Hornig. J. Chem. Phys. **35**, 1560 (1960).
21. W. S. Benedict, K. Morikawa, R. Bowling Barnes, and H. S. Taylor. J. Chem. Phys. **5**, 1 (1937).
22. N. Ginsburg and E. F. Barker. J. Chem. Phys. **3**, 668 (1935).
23. G. E. MacWood and H. C. Urey. J. Chem. Phys. **4**, 402 (1936).
24. R. W. G. Wyckoff and E. W. Posnjak. J. Am. Chem. Soc. **43**, 2292 (1921).
25. G. Engel. Z. Krist. **90A**, 341 (1935).
26. H. E. Swanson, N. T. Gilfrich, and G. M. Ugrinic. Natl. Bur. Stand. Circ. 539, **5**, 3 (1955).
27. H. E. Swanson, N. T. Gilfrich, M. I. Cook, R. Stinchfield, and P. C. Parks. Natl. Bur. Stand. Circ. 539, **8**, 8 (1959).
28. R. W. G. Wyckoff. Crystal structures. 2nd ed. Vol. 3. Interscience, New York. 1965.
29. E. O. Schlemper, W. C. Hamilton, and J. J. Rush. J. Chem. Phys. **44**, 2499 (1966).
30. A. C. Hazell. Acta Chem. Scand. **20**, 165 (1966).
31. R. J. Williams, D. R. Dillin, and W. O. Milligan. Acta Cryst. B **29**, 1369 (1973).
32. H. R. Wyss and M. Falk. Can. J. Chem. **48**, 607 (1970).
33. A. Ries. Z. Krist. **49A**, 513 (1911).

Can. J. Chem. Downloaded from www.nrcresearchpress.com by 210.87.254.6 on 09/05/12
For personal use only.

Hydration of Some Acids in Sulfolane

R. L. BENOIT AND S. Y. LAM

Département de Chimie, Université de Montréal, C.P. 6210, Montréal, Québec H3C 3V1

Received March 6, 1975

R. L. BENOIT and S. Y. LAM. Can. J. Chem. **53**, 2683 (1975).

Interaction between water at low concentrations and some carboxylic acids, methanesulfonic acid and picric acid, HA, have been studied in Sulfolane at 30 °C. Vapor pressure measurements and calorimetry were used. Results are interpreted in terms of hydration constants K_1 and enthalpy changes ΔH_1, for the 1:1 complexes $H_2O\cdots HA$. The values of K_1 are low and generally increase slightly with the strength of the acid HA from ~0.4 for acetic acid to 5.7 for methanesulfonic acid.

These results in conjunction with reported data in acetonitrile suggest that the basicity of water in Sulfolane and acetonitrile is lower than that of bromide ion. The hydration enthalpies ΔH_1 do not show any definite increase with the strength of the acids HA.

R. L. BENOIT et S. Y. LAM. Can. J. Chem. **53**, 2683 (1975).

On a étudié dans le sulfolane à 30 °C, et par mesure de pressions de vapeur et calorimétrie, les interactions entre l'eau aux faibles concentrations et des acides HA, HA étant des acides carboxyliques, méthanesulfonique et picrique. On interprète les résultats sur la base des constantes d'hydration K_1 et des variations d'enthalpie ΔH_1 des complexes $H_2O\cdots HA$. Les valeurs de K_1 sont faibles et augmentent peu dans l'ensemble avec la force des acides HA depuis 0.4 pour l'acide acétique jusque 5.7 pour l'acide méthanesulfonique. Ces résultats combinés à des données sur l'acétonitrile suggèrent que la basicité de l'eau dans le sulfolane et l'acétonitrile est inférieure à celle de l'ion bromure. Les enthalpies d'hydratation ΔH_1 ne croissent pas de façon marquée avec la force des acides HA.

Can. J. Chem. Downloaded from www.nrcresearchpress.com by 210.87.254.40 on 09/05/12
For personal use only.

While protonation of water has been widely studied, complexing of water by acids has received less attention. However, the presence of water hydrogen-bonded to acids in concentrated solutions of strong acids, such as H_2SO_4 and HNO_3, has been inferred from physicochemical measurements (1). Hydrogen-bonding equilibria between water and acids in nonpolar or slightly polar solvents have also been investigated (ref. 2 and references cited therein). Kolthoff and Chantooni have reported hydration constants for some acids in acetonitrile (3). Direct spectroscopic evidence for the existence of the complex $H_2O\cdots HCl$ in a nitrogen matrix at 15 K has recently been published (4).

During the course of a study of HCl solutions in Sulfolane (5), a weakly basic dipolar solvent, it became apparent from conductivity and near-infrared measurements that the reaction $2HCl + H_2O \rightleftarrows H_3O^+ + HCl_2^-$ did not fully account for the behavior of added water in these solutions, thus suggesting the presence of the $H_2O\cdots HCl$ complex. We have therefore carried out a thermodynamic study of the hydration of a series of acids in Sulfolane using vapor pressure and calorimetric measurements with a view to determining the influence of the strength of the acid HA on the stability of the complex $H_2O\cdots HA$. It was also hoped that such an investigation combined with some results from our current work on hydration of H^+ and anions A^- in Sulfolane (6) could help to provide an understanding of the influence of residual water on the dissociation of acids HA in Sulfolane and related solvents (7).

Experimental

Chemicals

Conductivity water was used. Purification of Sulfolane was given elsewhere (8). The freshly prepared solvent had a specific conductivity of 1.00×10^{-7} cm^{-1} Ω^{-1}, and a residual water content of 4.4×10^{-3} *M* as determined by Karl Fischer titration. Acids were analyzed by titration using standardized sodium hydroxide solution and appropriate indicators. Acetic acid (99.8%) was obtained from CIL. Chloroacetic (99.6%), 3,5-dinitrobenzoic (99.4%), and methanesulfonic acids (99.9%) were from Eastman. Dichloroacetic (99.8%), trichloroacetic (99.8%), and *o*-nitrobenzoic acids (99.5%) were Baker chemicals. Trifluoroacetic acid (99.8%) was from Aldrich. *m*-Nitrobenzoic acid (99.9%) was obtained from MC and B. Picric acid (99.9%) was recrystallized from the wet product of Anachemia using ethanol.

Vapor Pressure Measurements

The apparatus and procedure for vapor pressure measurements at 30 °C were similar to that given pre-

Can. J. Chem. Downloaded from www.nrcresearchpress.com by 210.87.254.40 on 09/05/12
For personal use only.

viously (9) except that the concentrations of water after experiments were checked by Karl Fischer titration. Test solutions, 0.5 *M* in acid with variable concentrations of water, usually below 0.4 *M*, were made up in volumetric flasks by weighing. Concentrations are expressed on the molar scale.

Calorimetry

The calorimetric apparatus and procedure used have been reported previously (5). The heats of mixing known weights of water with 27 ml of 0.5 *M* acid solutions in Sulfolane at 30 °C were determined for water concentrations less than 0.12 *M*. The heats of solution in Sulfolane of acetic, dichloroacetic, and trifluoroacetic acids were also measured for concentrations less than 0.5 *M*.

Conductivity

The conductivity bridge has already been described (10). Measurements were made at 30 °C on Sulfolane solutions of 0.5 *M*, dichloro, trichloro, and trifluoroacetic, picric and methanesulfonic acids with successive additions of water from a microburette.

Results and Discussion

Vapor Pressures

The partial pressures of water for water–Sulfolane mixtures at low water concentrations were obtained by subtracting from the total pressure the very small vapor pressure of pure Sulfolane, 0.02 mm Hg determined previously (8). Measurements of partial pressures of water-free 0.5 *M* acid solutions showed that most of these had negligible pressures except in the case of acetic acid (0.33 mm Hg) and trifluoroacetic acid (0.08 mm Hg). Corrections were applied where necessary to yield the partial pressures of water plotted in Fig. 1 as a function of total water concentration.

For the binary system, water–Sulfolane, the measured vapor pressures of water are in good agreement with previous values (8). The Henry's law constant for water at infinite dilution (when only monomer is likely to be present) is calculated as 11.5 mm/*m*. If one assumes that the nonlinearity of the water vapor pressure plot is due to self-association of water, then from the water monomer concentration (given by the limiting slope of the plot of water vapor pressure *vs.* water concentration), calculated dimerization constants vary from 0.08 to 0.16 M^{-1} in passing from 0.2 to 0.7 *M* water. This water dimerization constant is close to that found in propylene carbonate (9). In order to simplify the interpretation of the vapor pressure data in the presence of water and acids, the water concentration was usually kept below 0.4 *M*, so that at least 95% of water molecules were present as monomer.

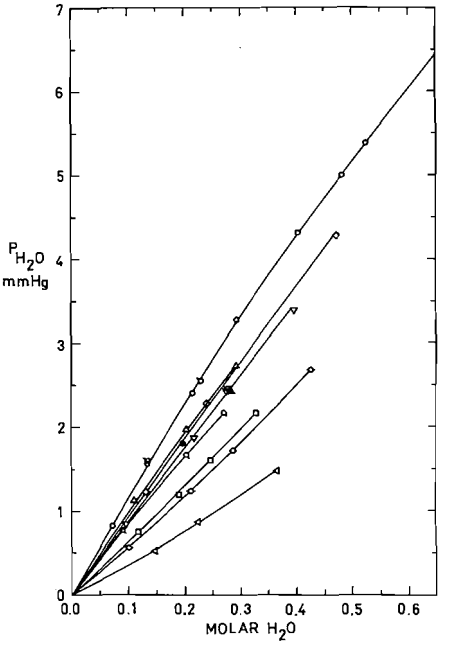

FIG. 1. Partial pressures of water for 0.5 *M* acid solutions in Sulfolane as a function of water concentration at 30 °C: ○, Sulfolane; ◔, 0.50 *M* 2,4,6-$(NO_2)_3C_6H_2OH$; △, 0.50 *M* CH_3COOH; ◇, 0.46 *M* *m*-$NO_2C_6H_4COOH$; ●, 0.48 *M* *o*-$NO_2C_6H_4COOH$; ▽, 0.50 *M* $CH_2ClCOOH$; ▲, 0.54 *M* 3,5-$(NO_2)_2C_6H_3COOH$; ◔, 0.50 *M* $CHCl_2COOH$; □, 0.50 *M* CCl_3COOH; –○–, 0.5 *M* CF_3COOH, ◁, 0.53 *M* CH_3SO_3H.

Concentration of Ionic Species

The conductivity results were used to estimate the extent to which water is protonated in side reactions such as

$$[1] \qquad HA + H_2O \rightleftarrows H_3O^+ + A^-$$

Among the acids, HA, studied here, methanesulfonic acid is the strongest acid in aqueous solution, although it is only partially dissociated in a basic dipolar aprotic solvent such as dimethylsulfoxide with a dissociation constant of 1.7×10^{-2} which is close to that of HCl (10). In Sulfolane, a much less basic solvent, the dissociation constant of methanesulfonic acid is expected to be in the order of 10^{-12} so that solutions of all the acids studied should show negligible conductivity in dry Sulfolane. However, the conductivity results plotted in Fig. 2 show that, in aqueous sulfolane, the specific conductance *L* of solutions of the acids HA, increases with the concentration of water, thus for 0.5 *M* HCH_3SO_3 it increases from 1.1×10^{-5} to 1.2×10^{-4} cm^{-1} Ω^{-1} with an increase in water concentration from 0.025 to 0.40 *M*.

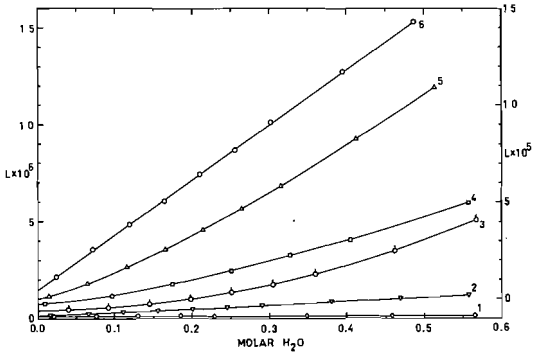

FIG. 2. Specific conductance L of 0.5 M acid solutions as a function of water concentrations at 30 °C: *1*, no acid; *2*, 0.53 M dichloroacetic acid; *3*, 0.48 M picric acid; *4*, 0.50 M trichloroacetic acid; *5*, 0.54 M trifluoroacetic acid; *6*, right-hand scale, 0.53 M methanesulfonic acid.

Calculations using an approximate limiting equivalent conductance of ~ 15 cm^2 Ω^{-1} equiv.$^{-1}$ for H_3O^+ and A^- (11) gave, for the concentrations of these ionic species, values which remain in the order of 2% of the concentration of added water. For the trifluoroacetic acid solutions, the concentrations of ionic species are reduced further by a factor of 10. It was therefore assumed that the concentration of water present as H_3O^+ in the solutions of all the acids HA could be neglected, although this leads to a small error for methanesulfonic acid.

Hydration Constants of the Acids

In order to analyze the vapor pressure data, the possibility of self association of the acids in Sulfolane has to be taken into account. Carboxylic acids are known to dimerize extensively in the vapor phase and in nonpolar or weakly polar solvents. However in solvents like Sulfolane and acetonitrile, it is expected that hydrogen-bonding of the monomer to the weakly basic solvent should favor dissociation of the dimer (12). It is generally agreed that the extent of dimerization of the carboxylic acids decreases with the introduction of electronegative substituents and there is an inverse correlation between the dimer association constant and the acid dissociation constant in water (ref. 13 and references cited therein). It was therefore thought that if CH_3CO_2H and $C_6H_5CO_2H$, the weakest acids studied, were mainly present as monomer in 0.5 M solutions in Sulfolane, then the other stronger acids would behave similarly. Precise and extensive cryoscopic determinations of molal freezing point depressions of organic solutes in Sulfolane by Della Monica *et al.* (14) revealed that the constants for benzoic acid from 0.1 to 1 M are identical to those of diphenylmethane, naphthalene, and benzene which are not expected to dimerize. We also found that the molal freezing point depression constant for 0.01 M acetic acid in Sulfolane as determined by using the LKB calorimeter was 64 $\pm$ 2° compared to normal values of 65° (14) and 64° (15) for nonassociating substances. Furthermore, the heats of mixing with Sulfolane given in Table 1 for acetic acid and the substituted acetic acids, in the range 0.02 to 0.4 M acid, are constant within $\pm$0.02 kcal per mol acid. The absence of concentration effects together with the cryoscopy results strongly suggest the presence of monomers as predominating species for the acids. We also noted that the n.m.r. chemical shift of the acidic proton of 0.1 to 0.5 M HCF_3CO_2 solutions in Sulfolane also remains constant at 11.2 $\pm$ 0.2 p.p.m., with respect to tetramethylsilane, once corrections are applied for residual water. However, it would have been difficult to draw any conclusion from this result alone since this chemical shift value is also close to that of the acid dimer (16). Having established that monomeric species predominate for both

TABLE 1. Heats of mixing of water and acids with Sulfolane, ΔH (kcal mol^{-1})

Solute	M	ΔH/mol
Water	0.040	1.61
	0.040	1.65
	0.079	1.63
	0.121	1.62
$HCHCl_2CO_2$	0.0301	−1.95
	0.0331	−1.92
	0.0493	−1.94
	0.098	−1.96
	0.222	−1.96
	0.342	−1.98
	0.430	−1.95
HCH_3CO_2	0.0178	0.90
	0.0350	0.93
	0.0396	0.93
	0.082	0.91
	0.152	0.90
	0.247	0.89
	0.363	0.87
HCF_3CO_2	0.0289	−1.47
	0.0407	−1.44
	0.0721	−1.45
	0.165	−1.46
	0.230	−1.47
	0.368	−1.46

Can. J. Chem. Downloaded from www.nrcresearchpress.com by 210.87.254.40 on 09/05/12
For personal use only.

TABLE 2. Hydration constants and hydration enthalpies at 30 °C

Acid	K_1	pK_a	ΔH_1 (kcal mol^{-1})
Acetic	0.4 ± 0.1	4.8*	−2.4 ± 0.7
Chloroacetic	0.7 ± 0.1	2.9*	−2.7 ± 0.4
Dichloroacetic	0.9 ± 0.1	1.3*	−4.0 ± 0.4
Trichloroacetic	2.0 ± 0.1	0.7*	−3.9 ± 0.1
Trifluoroacetic	2.5 ± 0.1	0†	−3.7 ± 0.1
Methanesulfonic	5.7 ± 0.6	−1.5‡	−3.7 ± 0.2
o-Nitrobenzoic	0.6 ± 0.1	2.2*	−3.6 ± 0.6
m-Nitrobenzoic	0.5 ± 0.1	3.5*	−3.1 ± 0.6
3,5-Dinitrobenzoic	0.7 ± 0.1	2.7§	−3.4 ± 0.4
Picric	~0	0.4‖	—

*Reference 25.
†Reference 26.
‡Reference 27.
§Reference 28.
‖Reference 29.

acid and water (at low water concentrations), we were able to interpret our vapor pressure results in terms of the association reaction

[2] $$H_2O + HA \rightleftarrows H_2O\cdots HA$$

The water vapor pressure curves shown in Fig. 1 for 0.5 *M* acid solutions are lower than the water–Sulfolane curve, except for picric acid. For a given water vapor pressure, unbound and bound water concentrations were calculated. Possible interactions in the gas phase between carboxylic acids and water were neglected on the basis of existing data (17). The treatment described in the text of Rossotti and Rossotti (18) was used to calculate the association constants K_1 of [2]. However, as the lowering of the vapor pressure is small, the K_1 values are only approximate for acetic acid and little meaning should be attached to the K_2 constants found for the equilibrium $H_2O + H_2OHA \rightleftarrows (H_2O)_2HA$.

The values of K_1 are given in Table 2 together with the corresponding acid dissociation constant K_a in water (corresponding values of K_a in Sulfolane are not available). The hydration constants K_1 for the acids are remarkably low and tend to increase slightly with the strength of the acids, at least within the substituted acetic acids series. It is interesting to note that a similar pattern has been found for the association constants of carboxylic acids with charged bases, such as the dichloroacetate anion in nitrobenzene (19) and Cl^- and Br^- in nitrobenzene (20), acetonitrile (21), acetone, and dimethylsulfoxide (19). Our K_1 values for the nitrobenzoic acids when compared with those of Huyskens and co-worker (20), in acetonitrile, suggest that H_2O behaves as a H-bond acceptor weaker than Cl^- and also Br^-. The low "basicity" of isolated H_2O molecules compared with the high basicity of bulk water has already been remarked upon (22, 6). Our observed low sensitivity of K_1 to the Hammett σ parameters of the substituents, in the acetic acid series, is in line with Huyskens' results on the complexation of Cl^- and Br^- in acetonitrile with substituted benzoic acids (20). Our hydration constants K_1 for methanesulfonic, picric, and 3,5-dinitrobenzoic acids in Sulfolane are not too different from, but somewhat lower than the same constants K_1 in acetonitrile, which are respectively 14, 0.5, and 1.8 (3). This difference may result from slightly weaker interactions of the acids with acetonitrile than with Sulfolane since water interactions with both solvents are similar (6). However, in a more recent study Kolthoff and Chantooni concluded from near infrared measurements that picric acid is not hydrated in acetonitrile (7). Strong intramolecular H-bonding may explain the inability of picric acid to bind a water molecule in both acetonitrile and Sulfolane.

Hydration Enthalpies

The heats of mixing of water, acetic, dichloroacetic, and trifluoroacetic acids with Sulfolane are given in Table 1. The values which are reasonably independent of concentration in the ranges studied, are respectively +1.63, +0.90, −1.95, and −1.46 ± 0.02 kcal mol^{-1}. The heats of mixing of water with 0.5 *M* acid solution in Sulfolane are listed in Table 3. In the case of

Can. J. Chem. Downloaded from www.nrcresearchpress.com by 210.87.254.40 on 09/05/12
For personal use only.

TABLE 3. Heats of mixing of water with Sulfolane solutions of acids, ΔH (kcal mol^{-1})

Acid	M_{H_2O}	ΔH/mol H_2O	Acid	M_{H_2O}	ΔH/mol H_2O
0.5 *M* CH_3COOH	0.040	1.24	0.5 *M* $CH_2ClCOOH$	0.040	0.93
	0.080	1.21		0.080	0.94
	0.080	1.22		0.081	0.95
	0.121	1.25		0.120	0.94
0.5 *M* $CHCl_2COOH$	0.039	0.42	0.5 *M* CCl_3COOH	0.040	−0.302
	0.080	0.41		0.080	−0.261
	0.081	0.42		0.119	−0.226
	0.121	0.42			
0.5 *M* CF_3COOH	0.043	−0.417	0.5 *M* CH_3SO_3H	0.040	−1.11
	0.078	−0.374		0.079	−1.08
	0.120	−0.324		0.120	−1.03
0.5 *M* *o*-$NO_2C_6H_4COOH$	0.040	0.79	0.5 *M* *m*-$NO_2C_6H_4COOH$	0.039	0.99
	0.080	0.79		0.079	1.03
	0.117	0.82		0.121	1.03
0.5 *M* 3,5-$(NO_2)_2C_6H_3COOH$	0.040	0.77	0.5 *M* 2,4,6-$(NO_2)_3C_6H_2OH$	0.040	1.64
	0.080	0.79		0.078	1.60
	0.120	0.79		0.120	1.60

0.5 *M* picric acid, the heat of mixing remains unchanged thus confirming that this acid is not appreciably hydrated. In the presence of the other acids, the heats of mixing become less endothermic or even exothermic for the stronger acids. The experimental heat change was taken as the sum of two contributions, the enthalpy of mixing of water with Sulfolane and the hydration enthalpy of the acid. By calculating the concentrations of unbound and bound water (derived from the values of the hydration constants), the enthalpy of hydration ΔH_1, of the acids were obtained and are given in Table 2. A small correction was applied to ΔH_1 in the case of methanesulfonic acid to take into account [1]. In order to calculate this correction, −9.8 kcal mol^{-1} was used for the heat of protonation of water; this value was calculated from the heat of mixing in Sulfolane, of water with an excess of $HSbCl_6$ (a strong acid in this solvent).[1] The concentration of H_3O^+ was obtained from the conductivity data. The correction was 0.2 kcal per mol of water.

The hydration enthalpies, ΔH_1, listed in Table 2, although somewhat imprecise because of weak complexing, mainly emphasize the absence of a definite increase of ΔH_1 with the strength of the acids as indicated by the pK_a values. However, it has been shown by Kebarle and co-worker (23) that the enthalpies of the related reaction for complex formation between Cl^- and acids HA in the gas phase increase with the acid strength. Thus a similar increase of the enthalpy of the hydration reaction $H_2O + HA = H_2O\cdots HA$ with the strength of the acid HA could be expected in the gas phase, at least within the substituted acetic acid series. If this increase is not observed in the solvent phase, it is partly because the interaction between the solvent and HA also increases with the strength of HA, *i.e.* both the base, H_2O, and the slightly basic solvent compete effectively for the acid HA. The results of our analysis of the solvent effect on complex formation between Cl^- and acids HA (24) support this view.

[1]J. Charbonneau, unpublished results.

The authors wish to express their gratitude to the Ministère de l'Education de la Province de Québec for their financial assistance. They also thank D. Lahaie for her technical assistance.

1. R. J. GILLESPIE. *In* Physicochemical processes in mixed aqueous solvents. *Edited by* F. Franks. American Elsevier Publishing Co. Inc., New York, N.Y. 1967.
2. S. D. CHRISTIAN, A. A. TAHA, and B. W. GASH. Q. Rev., **24**, 20 (1970).
3. I. M. KOLTHOFF and M. K. CHANTOONI, JR. Anal. Chem. **39**, 1080 (1967).
4. B. S. AULT and G. C. PIMENTEL. J. Phys. Chem. **77**, 57 (1973).
5. (*a*) R. L. BENOIT, M. RINFRET, and R. DOMAIN. Inorg. Chem. **11**, 2603 (1972); (*b*) R. DOMAIN. Ph.D. Thesis. Université de Montréal, Montréal, Québec. 1975.
6. R. L. BENOIT and S. Y. LAM. J. Am. Chem. Soc. **96**, 7385 (1974).

Can. J. Chem. Downloaded from www.nrcresearchpress.com by 210.87.254.40 on 09/05/12
For personal use only.

7. I. M. KOLTHOFF and M. K. CHANTOONI, JR. J. Am. Chem. Soc. **91**, 6907 (1969).
8. R. L. BENOIT and G. CHOUX. Can. J. Chem. **46**, 3215 (1968).
9. R. L. BENOIT and S. Y. LAM. Can. J. Chem. **52**, 718 (1974).
10. R. L. BENOIT and C. BUISSON. Electrochim. Acta, **18**, 105 (1973).
11. R. L. BENOIT, C. BUISSON, and G. CHOUX. Can. J. Chem. **48**, 2353 (1970).
12. M. KIRSZENBAUM, J. CORSET, and M. L. JOSIEN. J. Phys. Chem. **75**, 1327 (1971).
13. N. S. ZAUGG, L. E. TREJO, and E. M. WOOLLEY. Thermochim. Acta, **6**, 293 (1973).
14. M. DELLA MONICA, L. JANNELLI, and U. LAMANNA. J. Phys. Chem. **72**, 1068 (1968).
15. R. GARNSEY and J. E. PRUE. Trans. Faraday Soc. **64**, 1206 (1968).
16. H. FUJIWARA. J. Phys. Chem. **78**, 1662 (1974).
17. S. D. CHRISTIAN, H. E. AFFSPRUNG, and CHII LING. J. Chem. Soc. 2378 (1965).
18. F. J. C. ROSSOTTI and H. ROSSOTTI. The determination of stability constants. McGraw-Hill, New York, New York. 1961. pp. 108–113.
19. Z. PAWLAK. Rocz. Chem. **46**, 249 (1972).
20. D. J. PIRSON and P. L. HUYSKENS. J. Solution Chem. **3**, 503 (1974).
21. I. M. KOLTHOFF. Anal. Chem. **46**, 1992 (1974).
22. E. M. ARNETT. Acc. Chem. Res. **6**, 404 (1973).
23. R. YAMDAGNI and P. KEBARLE. J. Am. Chem. Soc. **93**, 7139 (1971).
24. S. Y. LAM, C. LOUIS, and R. L. BENOIT. To be published.
25. Stability Constants of Metal-ion Complexes. Chem. Soc. Special Publication No. 17, The Chemical Society, London, 1964, and Supplement No. 1, Special Publication No. 25, The Chemical Society, London, 1971.
26. E. GRUNWALD and J. F. HALEY. J. Phys. Chem. **72**, 1944 (1968).
27. A. K. COVINGTON and T. H. LILLY. Trans. Faraday Soc. **63**, 1749 (1967); J. H. R. CLARK and L. A. WOODWARD. Trans. Faraday Soc. **62**. 2226 (1966).
28. B. HOK. Sven. Kem. Tidskr. **65**, 182 (1953).
29. Handbook of Chemistry and Physics, 51 ed. The Chemical Rubber Co., Cleveland, Ohio. 1970.

Can. J. Chem. Downloaded from www.nrcresearchpress.com by 210.87.254.40 on 09/05/12
For personal use only.

Particle Motions in Sheared Suspensions. XXVIII. Configurations of Coiled Fibers in Shear Flow[1]

A. Okagawa and S. G. Mason

Pulp and Paper Research Institute of Canada and Department of Chemistry, McGill University, Montreal, Québec H3C 3G1

Received March 25, 1975

A. Okagawa and S. G. Mason. Can. J. Chem. **53**, 2689 (1975).

The coiling of elastomer filaments in liquids undergoing shear flow was studied experimentally. In the steady state the rotating coils were stretched along the axes of flow and vorticity, compacted along the third orthogonal axis, and became progressively more entangled as the velocity gradient increased. Although the coils did not possess spherical symmetry, the distribution of end-to-end distances and maximum projected dimensions projected on a given axis or plane corresponded closely to random coiling statistics.

A. Okagawa et S. G. Mason. Can. J. Chem. **53**, 2689 (1975).

On a étudié expérimentalement l'enroulement de filaments d'élastomère dans des liquides soumis au cisaillement d'écoulement. Dans l'état stationnaire les filaments en rotation sont allongés le long des axes d'écoulement et du rotationel comprimés le long du troisième axe orthogonal et deviennent de plus en plus enchevêtrés à mesure que le gradient de vitesse augmente. Quoique les filaments ne possèdent pas la symétrie sphérique, la distribution des distances entre les bouts de filaments et les dimensions maximales projetées sur un plan ou un axe donné correspondent de très près à une pelote statistique. [Traduit par le journal]

Introduction

Forgacs and Mason (1) have described some interesting observations of the rotational orbits of flexible threads suspended in viscous liquids subjected to simple shear flow. Three rotational orbits were observed (springy and snake, helical, and coiled) with the orbit class depending upon the amount of deformation (bending) of the thread, which in turn depended on the extended length of the thread, its bending modulus, and the deforming stresses generated by the flowing liquid.

Quantitative data was presented for the first two orbit classes, but the behavior of the entangled coils was only qualitatively described. In this brief communication we present measurements of dimensions of rotating coils and relate their statistical properties to those of random coils.

For our purposes we define several characteristic dimensions of coiled fibers as follows, using essentially the quantities as those for describing coiled linear macromolecules. Let a system of Cartesian coordinates X_i ($i = 1, 2, 3$) be fixed in space with the origin at one end of a coiled fiber as shown in Fig. 1. The end-to-end distance can be expressed by the projected lengths h_{ij} and h_i of the vector connecting the two ends of the filament on the coordinate plane X_iX_j and axis X_i respectively. The direction of h_{23} is given by the azimuthal angle ϕ_1 measured from the X_2-axis. Two of the maximum projected dimensions a_i along the coordinate axes are also defined in Fig. 1. The liquid in which the filament is suspended is subjected to a simple shear flow whose velocity components u_i are $u_1 = u_2 = 0$ and $u_3 = GX_2$ where G is the velocity gradient which together with the viscosity of the liquid determines the deforming stresses (1).

In our experiments we have measured distributions of ϕ_1, h_i, h_{ij}, and a_i at various values of G for coils which were in statistically steady states.

Experimental

The experiments were performed in a Couette apparatus described previously (2) but fitted with two counter-rotating transparent concentric cylinders. Single elastomer filaments of circular cross section (Lycra by DuPont) of diameter 40 μm cut to various lengths were suspended in a Newtonian silicone oil (Dow Corning 200; 100 stokes) and located (2) in the stationary layer ($u_3 = 0$) in the annular gap between the cylinders. The range of shear rates G was from 0.5 to 15 s^{-1}. Cinematographic records of the coil were made at 12 frames/s along the

[1]This paper is dedicated to Professor C. A. Winkler of McGill University on the occasion of his sixty-fifth birthday by a friend and colleague (S.G.M.).

Can. J. Chem. Downloaded from www.nrcresearchpress.com by 210.87.254.5 on 09/05/12
For personal use only.

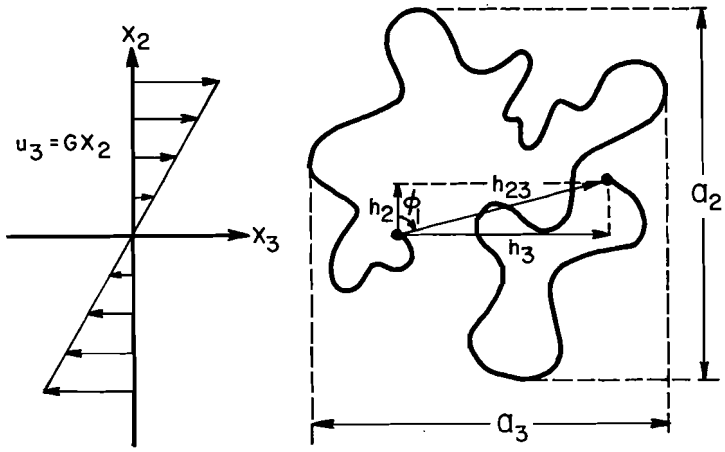

FIG. 1. Definition of end-to-end distances h_{23}, h_2, and h_3 projected on the X_2X_3-plane, X_2-axis, and X_3-axis respectively. The X_1-axis is normal to the page. The maximum projected dimensions a_2 and a_3 are also indicated. The shear field $u_3 = GX_2$ was applied as shown by the arrows. In conducting an experiment the speeds of the counter-rotating cylinders were adjusted so that the coil was located at $X_2 = 0$ and rotated (with a continuously changing configuration) in the clockwise direction about the X_1 (the vorticity) axis.

X_1-axis (viewing vertically down into the annulus) and along the X_2-axis (viewing horizontally through the transparent cylinders) and the various dimensions were measured in frame-by-frame analysis of the cine-films. The mean values obtained from more than 500 measurements at each value of G are thus the time-averaged values for a single coil rather than instantaneous number-averages for an assembly of coils.

Results and Discussion

Qualitatively, the observations were similar to those previously reported (1) with coiling and entanglement occurring over the range of G in the present experiments only with filaments longer than 20 mm. We therefore selected 25.0 mm filaments for the quantitative measurements. When the shear was applied the filament was initially aligned along the X_3-axis (*i.e.*, the initial values h_1, $h_2 = 0$, $h_3 = 25.0$ mm) after which deformation in the five successive stages previously described (1) occurred until a statistically steady state was attained in which the coiled filament rotated about the vorticity (X_1) axis with continuously changing configurations. Instantaneous photographs of typical coils in these steady states viewed along the X_1 and X_2 axes are shown in Fig. 2 for several velocity gradients. It is seen that the coils were extended along the axes of flow (X_3) and vorticity (X_1).

Projections of h_{23}, ϕ_1, a_2, and a_3 were measured from the photographic projections similar to those shown in upper part of Fig. 2, and h_2, h_3 were calculated from h_{23} and ϕ_1. In a similar way from the photographs along X_2-axis, h_1, h_3, a_1, and a_3 were obtained. As an example, $h_{23}/\bar{h}_{23}$ and ϕ_1 at $G = 3.12\ s^{-1}$ are plotted in a polar diagram in Fig. 3*A*. It is clearly seen that h_{23} exhibits a highly preferred orientation in the direction of flow. When the coil reached a statistically steady state each end of the coiled fiber appeared to behave independently of the other, with each end sometimes leading and at other times trailing. Once the coil formed, however, one end maintained an upper position along the X_1 axis with respect to the other.

In analyzing the cine-films one end of the coil was arbitrarily selected as the reference end and placed at the origin of Fig. 3*A*. Although one end or the other occasionally disappeared due to overlap with other segments of the coil, the reference end was easily identified when it reappeared several frames later. Analysis of diagrams like Fig. 3*A* showed that the distribution of ϕ_1 for h_{23} was symmetrical with respect to both the X_2 and X_3-axes. If n_{ϕ_1} is the number of configurations observed for h_{23} oriented between 0 and ϕ_1 and N is total number of observations, the cumulative distribution $P(\phi_1) = n_{\phi_1}/N$. Values of $P(\phi_1)$ for the coil at $G = 3.12\ s^{-1}$ are shown in Fig. 3*B* where for simplicity and because of symmetry mentioned above, the

Can. J. Chem. Downloaded from www.nrcresearchpress.com by 210.87.254.5 on 09/05/12
For personal use only.

Can. J. Chem. Downloaded from www.nrcresearchpress.com by 210.87.254.5 on 09/05/12
For personal use only.

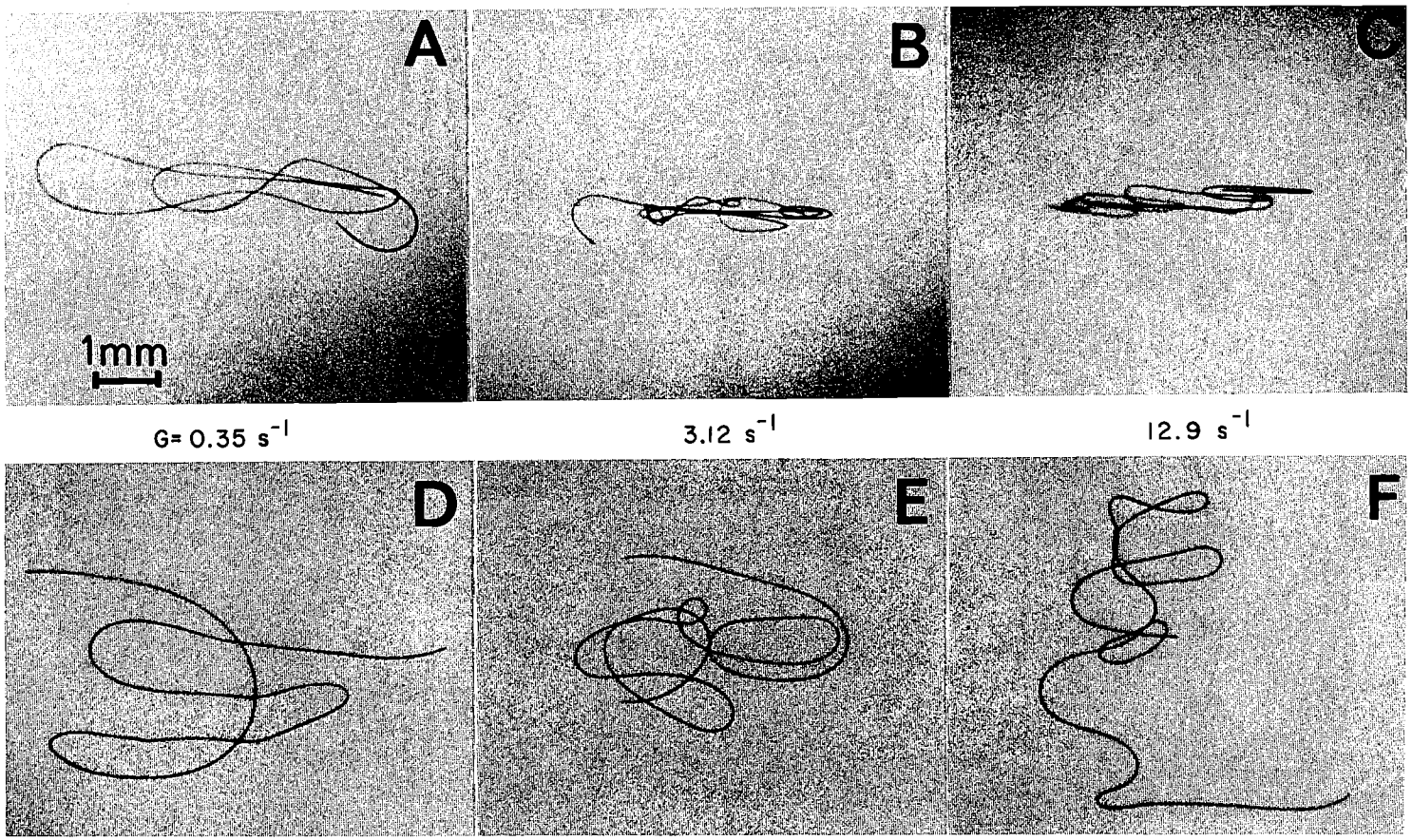

FIG. 2. Photographs of coils when viewed along the X_1-axis (*A*, *B*, and *C*) and the X_2-axis (*D*, *E*, and *F*) at various velocity gradients.

Can. J. Chem. Downloaded from www.nrcresearchpress.com by 210.87.254.5 on 09/05/12
For personal use only.

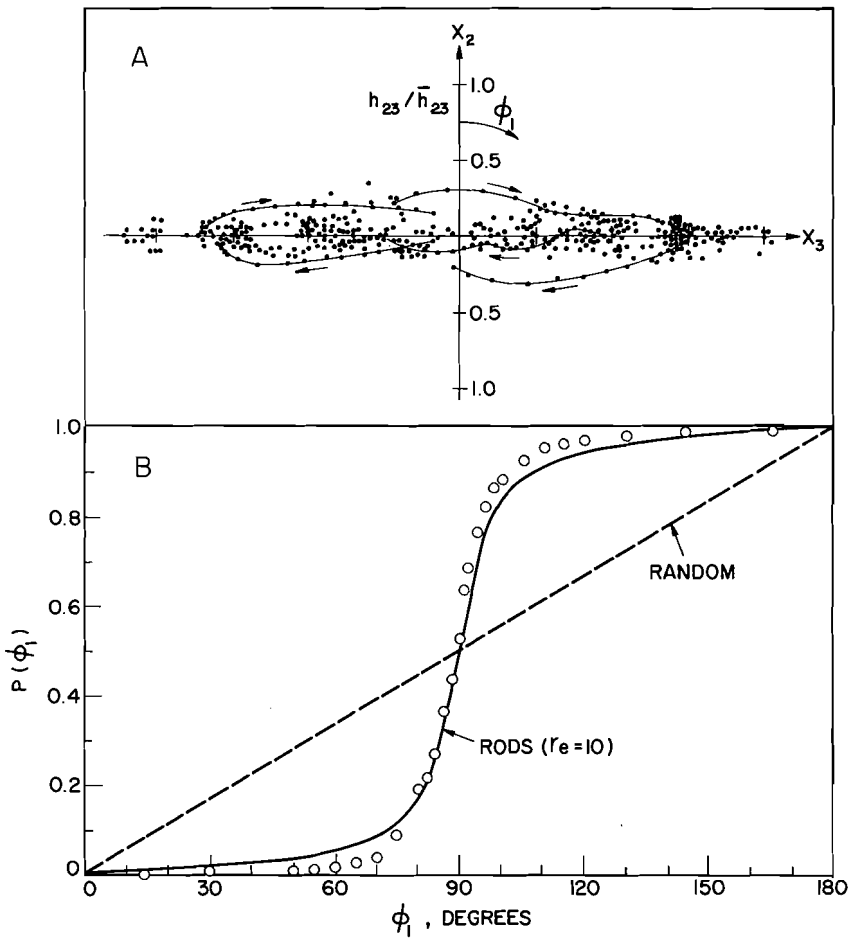

FIG. 3. (*A*) Polar plot of one end of a coil relative to the other (placed at the origin) at $G = 3.12\ s^{-1}$. Each point represents a frame of a cine film taken along the X_2-axis. (Fig. 2*B* being one such frame) when the two ends could be clearly identified. Short sections of successive points are joined and represent portions of the locus of the one end of the coil relative to the other in the directions shown by the arrows. (*B*) Integral distribution $P(\phi_1)$ of h_{23} at $G = 3.12\ s^{-1}$, plotted as points. The broken line corresponds to spherical symmetry, and the solid line is the steady state distributions for rigid prolate spheroids of $r_e = 10$ calculated from [4]. Because of symmetry about the X_2-axis in Part (A) the range of ϕ_1 for $P(\phi_1)$ has been taken to be 0 to 180°.

range of ϕ_1 was taken from 0 to 180°. $P(\phi_1)$ showed only a small increase at low ϕ_1 and increased rapidly around $\phi_1 = 90°$ indicating (as is obvious from Fig. 3*A*) that h_{23} was highly oriented in the direction of flow, and was symmetrical about $\phi_1 = 90°$ at which $P(\phi_1) = 0.5$.

Next the probability distributions $p(\alpha) = dP(\alpha)/d(\alpha/\bar{\alpha})$ of various coil dimensions were obtained graphically from the slopes of smoothed curves drawn to fit the experimental cumulative distribution functions $P(\alpha)$ when plotted against a reduced dimension $\alpha/\bar{\alpha}$, where α represents h_i, h_{ij} or a_i and $\bar{\alpha}$ is the corresponding time-averaged value.

Typical results are given in Fig. 4 where we have used $p(h_{23})$ and $p(a_3)$ at two values of G. The range of $h_{23}/\bar{h}_{23}$ varied from 0 to 2.6, and $a_3/\bar{a}_3$ from 0.4 to 2.0. The probability $p(h_{23})$ increased as h_{23} increased and reached a maximum at $h_{23}/\bar{h}_{23} = 0.8 \sim 0.9$, then decreased slowly until $p(h_{23})$ vanished at $h_{23}/\bar{h}_{23} = 2.6$. The probability $p(a_3)$ was zero up to $a_3/\bar{a}_3 = 0.4$ after which it increased sharply toward the maximum at $a_3/\bar{a}_3 = 0.8$, then decreased rapidly. Values of $p(\alpha)$ obtained in this way showed qualitatively similar distributions for the entire range of velocity gradients employed.

As a matter of interest, we have compared

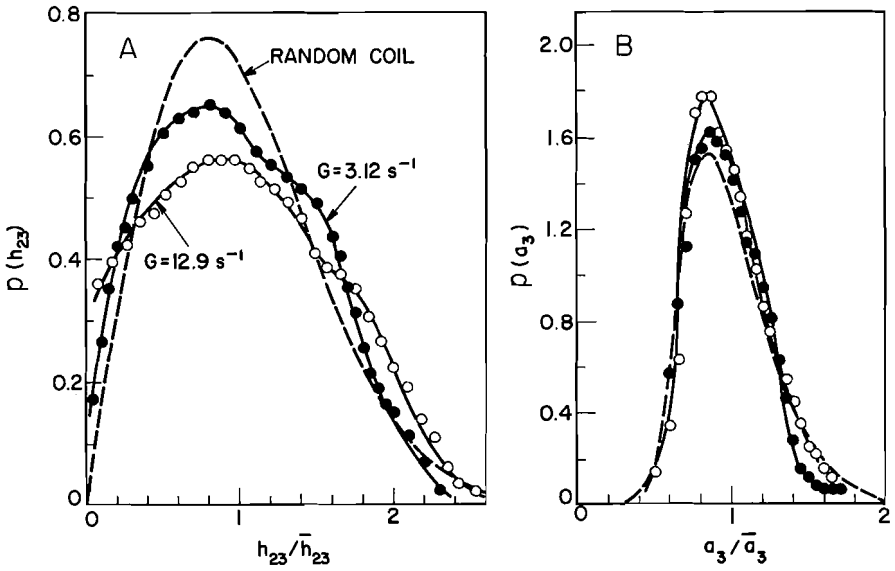

FIG. 4. Probability distributions $p(h_{23})$ and $p(a_3)$ at different values of G. The broken lines show the distributions for random coils calculated from [2] and [3].

these measured distributions with values for randomly coiled linear macromolecules in solutions at rest, when spherical symmetry should exist (3), *i.e.*, the orientation ϕ_1 is equally probable for all angles so that

$$[1] \qquad P(\phi_1) = \int_0^{\phi_1} p(\phi)\, d\phi = \phi_1/\pi$$

This is shown by the broken line in Fig. 3*B*, which of course deviates considerably from the experimental results. On the other hand, when expressed in the reduced dimensions employed above, $p(h_{23})$ corresponding to the random chain model (3) is given by

$$[2] \quad p(h_{23}) = \frac{dP(h_{23})}{d(h_{23}/\bar{h}_{23})} = \frac{\pi}{2}\left(\frac{h_{23}}{\bar{h}_{23}}\right)^2 \exp\left[-\frac{\pi}{4}\left(\frac{h_{23}}{\bar{h}_{23}}\right)^2\right]$$

As shown in Fig. 4*A*, it is striking that the measured probability distributions are qualitatively similar to those calculated from [2]. These similarities between the measured distributions for coiled fibers in shear flow and the theoretical distribution for random coils were also observed with $p(h_2)$ and $p(h_3)$. The corresponding probability $p(a_3)$ for the random chain model (3) is given by

$$[3] \quad p(a_3) = \frac{dP(a_3)}{d(a_3/\bar{a}_3)} = \pi\left(\frac{\bar{a}_3}{a_3}\right)^3 \sum_{i=1}^{\infty} \left\{\frac{\pi^3(2i+1)^2}{8}\left(\frac{\bar{a}_3}{a_3}\right) - 1\right\} \times \exp\left[\frac{-\pi^3(2i+1)^2}{16}\left(\frac{\bar{a}_3}{a_3}\right)^2\right]$$

which is plotted by the broken line in Fig. 4*B* and shows even better agreement with the experimental results.

The measured orientation distribution of ϕ_1 may be better approximated by the steady state orientation distribution of rigid prolate spheroids of axis ratio r_e subjected to a simple shear flow, which is given (4) by the theoretical equation

$$[4] \qquad P(\phi_1) = \frac{1}{\pi}\tan^{-1}\left(\frac{\tan\phi_1}{r_e}\right)$$

Although h_{23} is not constant, a value of $r_e = 10$ in [4] gave close agreement (Fig. 3*B*) with the experimental data. At this stage, we cannot assign any theoretical significance to this, but can merely regard [4] as a useful semi-empirical relation when it is applied to the coils and which indicates a highly preferred orientation of the end-to-end vector along the X_3-axis.

The effects of G on the dimensions of the coils are summarized in Table 1, where mean values of various dimensions are listed. As can

Can. J. Chem. Downloaded from www.nrcresearchpress.com by 210.87.254.5 on 09/05/12
For personal use only.

Can. J. Chem. Downloaded from www.nrcresearchpress.com by 210.87.254.5 on 09/05/12
For personal use only.

TABLE 1. Measured mean values of end-to-end distances and maximum projected dimensions of elastomer coils in shear flow*

Parameter	$G(s^{-1})$			
	0.35	0.62	3.12	12.9
$\bar{h}_{23}$	2.90	2.89	3.07	2.87
$\bar{h}_{13}$	3.21	3.78	3.38	3.35
$\bar{h}_2$	0.03	−0.05	0.02	0.04
$\bar{h}_3$	−0.03	−0.06	0.01	0.03
$\lvert\bar{h}_1\rvert$	0.76	1.28	1.09	1.95
$\lvert\bar{h}_2\rvert$	0.39	0.38	0.25	0.26
$\lvert\bar{h}_3\rvert$	3.13	3.03	2.93	2.17
$\bar{a}_1$	3.64	3.71	3.27	4.25
$\bar{a}_2$	0.73	0.68	0.75	0.52
$\bar{a}_3$	7.11	6.41	4.72	4.01
$\bar{V}(mm^3)$	14.84	12.70	9.09	6.96

*All values except G and $\bar{V}$ are in mm; the extended length of the coil is 25.0 mm.

be seen from Fig. 3*A*, h_2 and h_3 can be either positive or negative and are equally probable, so that the mean values $\bar{h}_2$ and $\bar{h}_3$ were practically zero for the entire range of velocity gradient studied. On the other hand when observed along the X_2-axis, each end of the coil maintained its relative vertical position so that h_1 remained either positive or negative depending on which end was selected as the reference so that $\pm\bar{h}_1 = |\bar{h}_1|$. On the other hand, the absolute means $|\bar{h}_2|$ and $|\bar{h}_3|$ were nonzero; and as expected from the stretching along the X_3-axis $|\bar{h}_3| \geq |\bar{h}_2|$. The variations in $|\bar{h}_1|$ with G are shown in Fig. 5. While $|\bar{h}_2|$ showed little absolute change, $|\bar{h}_3|$ decreased with G. This confirms that the coils became more compacted in the X_2X_3 plane as G increased as may be seen from the photographs in Fig. 2. Other interesting observations are that (*1*) $|\bar{h}_1|$ was always greater than $|\bar{h}_2|$ and increased with G, and (*2*) at low G $|\bar{h}_3| > |\bar{h}_1|$ but $|\bar{h}_3|$ decreased and $|\bar{h}_1|$ increased on increasing G.

Generally parallel behavior with $|\bar{h}_i|$ was observed for $\bar{a}_i$ (Table 1). This indicates that just as in dealing with coiled linear macromolecules, the end-to-end distances are useful in describing the statistical shapes of the coils. Overall changes in coil dimensions can also be expressed by the effective coil volume $\bar{V}$ which we define as an elliptic cylinder of minor and major axes of $\bar{a}_2$ and $\bar{a}_3$, and of height $\bar{a}_1$ so that $\bar{V} = (\pi/4)\bar{a}_1\bar{a}_2\bar{a}_3$. Values of $\bar{V}$ calculated from the experimental values of $\bar{a}_i$ (Table 1 and Fig. 5) were approximately halved over the range of G, showing a compaction with increasing G which started to level off at the highest gradient (Fig. 5).

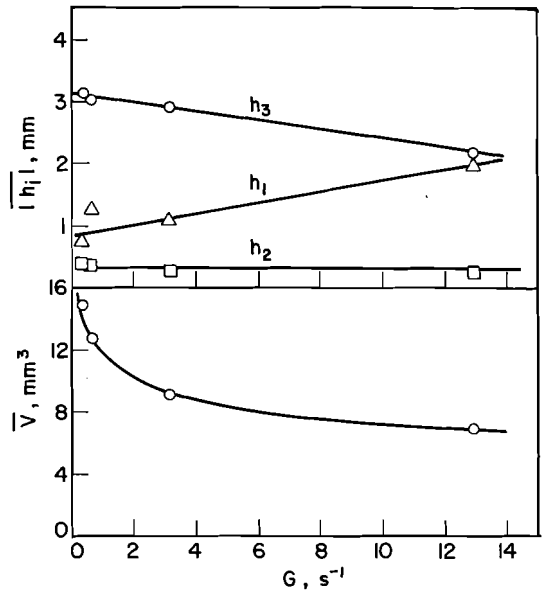

FIG. 5. Mean absolute values of end-to-end distances and the effective coil volume at various gradients.

Of all the observations, that which surprised us the most was the extension of the coil along the X_1 (vorticity) axis. Several possible explanations come to mind: firstly, in the initial stages of coiling both ends were leading (*1*) and the coil was in the X_2X_3 plane so that when the ends approached one another they deflected each other along the X_1-axis; secondly, as the coil bent it could also twist so that torques might be generated in the thread causing it to expand further along the X_1-axis.

Clearly, further experimental and theoretical investigations of these interesting phenomena are warranted, particularly on the effect of flexibility (or the bending modulus) and the torsional resistance of the thread on its configuration. However, it must be realized that theoretical studies will be complex and experimental studies very extensive, since the problem of an infinitesimally thin and infinitely flexible coil has yet to be solved.

1. O. L. FORGACS and S. G. MASON. J. Colloid Sci. **14**, 457 (1959); **14**, 473 (1959).
2. W. BARTOK and S. G. MASON. J. Colloid Sci. **12**, 243 (1957).
3. M. V. VOLKENSTEIN. Configurational statistics of polymer chains. Interscience, New York. 1963.
4. E. ANCZUROWSKI and S. G. MASON. J. Colloid Interface Sci. **23**, 522 (1967).

Semi-empirical Calculations on the Free Energy and Enthalpy of Hydration for the Trivalent Lanthanides and Actinides

SAUL GOLDMAN
Department of Chemistry, University of Guelph, Guelph, Ontario N1G 2W1
AND
LESTER R. MORSS
Department of Chemistry, Rutgers University, New Brunswick, New Jersey 08903
Received April 9, 1975

SAUL GOLDMAN and LESTER R. MORSS. Can. J. Chem. 53, 2695 (1975).

An electrostatic hydration model, that had previously been developed for ions of the noble-gas structure, was applied to the trivalent lanthanide and trivalent actinide ions. For the trivalent lanthanides it was found that a single primary hydration number resulted in a satisfactory fit of the model to the experimental free energy and enthalpy data. Subsequently, the model was applied to the trivalent actinide ions with a view to predicting values for the free energy and enthalpy of hydration for this series. A primary hydration number for the actinide series was determined by fitting the model to existing experimental enthalpy data for Pu^{3+}. The predictions for this series were found to compare favorably with the few experimental and estimated values that exist.

SAUL GOLDMAN et LESTER R. MORSS. Can. J. Chem. 53, 2695 (1975).

On a appliqué aux ions trivalents des lanthanides et des actinides un modèle d'hydratation électrostatique qui avait été développé antérieurement pour des ions de structure semblable à celle des gaz rares. Pour les lanthanides trivalents, on trouve qu'un seul nombre d'hydratation primaire conduit à une corrélation satisfaisante du modèle avec les données d'enthalpie et d'énergie libre. Par la suite, on a appliqué le modèle aux ions trivalents d'actinides en vue de prédire les valeurs d'énergie libre et d'enthalpie d'hydratation de cette série. On a déterminé un nombre d'hydratation primaire pour la série des actinides en faisant une corrélation du modèle avec les valeurs expérimentales existantes pour Pu^{3+}. On a trouvé que les prédictions pour cette série se comparent avantageusement avec les quelques valeurs expérimentales et estimées qui existent. [Traduit par le journal]

Introduction

In a previous article (1), it was found that an electrostatic model could be used to account successfully for the Gibbs free energy ($\Delta G_t°$) and enthalpy ($\Delta H_t°$) associated with the transfer of 17 closed shell ions from their standard state in the gas to their standard state in water at 25 °C. An off-centered dipole model was used to characterize the permanent electrostatic properties of water in the primary hydration shell, and a Born continuum treatment was used to calculate secondary solvation effects. This model owed its success to the fact that the interactions of closed shell ions with water are largely electrostatic. Because the unfilled f-subshells in the lanthanide and actinide ions are inner orbitals, which do not interact significantly with surrounding molecules or ions, it can be anticipated that nonelectrostatic interactions should contribute relatively little to the thermodynamic functions of hydration for these ions. Therefore an extension of the calculations in ref. 1 to the lanthanide and actinide ions seemed worthwhile.

The calculations in ref. 1 were semi-empirical in the sense that an adjustable parameter (the primary hydration number n) was required in order to fit the model to the experimental free energies and enthalpies of hydration. (Experimental hydration data refer to those calculated from available experimental processes via a thermodynamic cycle.) Accordingly, some experimental hydration data are also needed here if we are to use the approach in ref. 1. There now exist experimental values for the enthalpies and free energies of hydration for all of the trivalent lanthanides and for trivalent plutonium. In this work we have combined the model in ref. 1 with the existing hydration data for the trivalent lanthanides and actinides in order to: (*1*) confirm that the electrostatic model used in ref. 1 can be used to account for experimental

Can. J. Chem. Downloaded from www.nrcresearchpress.com by 210.87.254.5 on 09/05/12
For personal use only.

TABLE 1. Data and results for the trivalent lanthanides[a]

Ion	r_c (Å)	r_g (Å)	$-\Delta G_t°$ (kcal mol^{-1}) Calculated (n = 5.6)	$-\Delta G_t°$ (kcal mol^{-1}) Experimental	$-\Delta H_t°$ (kcal mol^{-1}) Calculated (n = 5.6)	$-\Delta H_t°$ (kcal mol^{-1}) Experimental
La^{3+}	1.045	1.590	754.8	751.2	787.1	783.6
Ce^{3+}	1.010	1.569	756.7	762.9	789.1	795.4
Pr^{3+}	0.997	1.549	764.8	772.8	797.4	805.9
Nd^{3+}	0.983	1.529	773.0	780.6	805.6	813.6
Pm^{3+}	0.97	1.509	781.6	788.0	814.3	821.0
Sm^{3+}	0.958	1.491	789.6	791.2	822.4	824.3
Eu^{3+}	0.947	1.472	798.7	803.5	831.6	836.3
Gd^{3+}	0.938	1.454	808.3	807.7	841.3	840.6
Tb^{3+}	0.923	1.437	815.1	816.0	848.1	850.6
Dy^{3+}	0.912	1.420	823.6	824.0	856.7	859.0
Ho^{3+}	0.901	1.403	832.4	829.2	866.0	864.0
Er^{3+}	0.890	1.387	840.5	833.4	873.7	869.5
Tm^{3+}	0.880	1.371	849.3	839.7	882.6	875.5
Yb^{3+}	0.868	1.355	857.5	849.7	890.0	885.0
Lu^{3+}	0.861	1.340	867.0	853.8	900.5	889.6

[a]The values of $\Delta G_t°$ and $\Delta H_t°$ are for T = 298.15 K. The standard state in the gas is the hypothetical ideal ion gas at 1 atm. The standard state in solution is the hypothetical 1 m solution.

hydration data for these ions; (*2*) predict the free energies and enthalpies of hydration of the trivalent actinides for which (with the exception of Pu^{3+}) experimental values are unavailable.

Calculations and Results

The calculations performed here for the thermodynamic transfer functions $\Delta G_t°$ and $\Delta H_t°$ are identical to those described in ref. 1 (in the section "Calculation of the Thermodynamic Transfer Functions") except for one simplification. In this work the ion – primary water Lennard–Jones term is omitted. This simplification was made necessary by the unavailability of polarization and ionization potential data for the trivalent actinides. Because n, an adjustable parameter, absorbs errors in the model, and because the Lennard–Jones ion–water term contributes relatively little to the transfer functions $\Delta G_t°$ and $\Delta H_t°$ (~1% for La^{3+}), the effect of this simplification is negligible.

In all the calculations for $\Delta G_t°$ and $\Delta H_t°$ described below, the values of the parameters used for water (size, polarizability, effective charge distribution, moments of inertia) were those given in ref. 1.

Trivalent Lanthanides

With the simplification noted above, we require values for the crystallographic radius r_c, the gas-phase radius r_g, and the primary hydration number n, in order to calculate the sought thermodynamic transfer functions $\Delta G_t°$ and $\Delta H_t°$. The values used for r_c and r_g are given in columns 2 and 3 of Table 1. The values for r_c were taken from the literature (2) and the values of r_g were estimated by a method similar to one suggested by Stokes (3). Specifically, the gas-phase radius for each of the trivalent lanthanide ions was calculated by the equation (4)

$$[1] \qquad r_g = \frac{K}{(Z - S)}$$

where K is a constant, Z is the atomic number, and S is a screening constant. The values of S for each ion were obtained by Slater's rules (4), and K for the lanthanide series was determined by applying [1] to xenon for which r_g was taken to be 2.168 Å (5). Thus it was found that the value of K for the lanthanide series was 17.9 Å.

We have also included, in columns 5 and 7 of Table 1, our selected experimental values for the quantities $\Delta G_t°$ and $\Delta H_t°$. The values of $\Delta H_t°$ (6) are based on Halliwell and Nyburg's (7) recommended value for $\Delta H_t°$ (H^+).[1] The

[1]This value (−260.7 kcal mol^{-1}) is used here in order to be consistent with previously published work on these ions (8). There are a number of other values available in the literature for this quantity (see for example refs. 9 and 10). The interested reader who may favor a different value for $\Delta H_t°$ (H^+) can correct the values of $\Delta H_t°$ and $\Delta G_t°$ reported here by adding to them the difference between the reader's selected value of $\Delta H_t°$ (H^+) and ours.

Can. J. Chem. Downloaded from www.nrcresearchpress.com by 210.87.254.5 on 09/05/12
For personal use only.

Can. J. Chem. Downloaded from www.nrcresearchpress.com by 210.87.254.5 on 09/05/12
For personal use only.

experimental values of ΔG_t° were calculated by

$$[2] \qquad \Delta G_t^\circ = \Delta H_t^\circ - T\Delta S_t^\circ$$

using the experimental values of ΔH_t° in Table 1, and values of ΔS_t° calculated by

$$[3] \qquad \Delta S_t^\circ = \bar{S}_{soln}^\circ - \bar{S}_g^\circ$$

In [3] $\bar{S}_{soln}^\circ$ is the absolute standard ionic entropy in solution and $\bar{S}_g^\circ$ is the standard ionic entropy in the gas. Values for $\bar{S}_{soln}^\circ$ were obtained from experimental conventional entropies which were converted to absolute entropies by the equation (11)

$$[4] \quad \bar{S}_{soln}^\circ = \bar{S}_{soln}^\circ(\text{conventional}) + 3\bar{S}_{soln}^\circ(H^+)$$

In [4] the values of $\bar{S}_{soln}^\circ$ (conventional) were taken from published values (12) and $\bar{S}_{soln}^\circ$ (H^+) was taken to be -5.3 cal deg^{-1} mol^{-1} (9). The values of $\bar{S}_g^\circ$ required with [3] were obtained from the Sackur–Tetrode equation written for the conditions $T = 298.15$ K and $p = 1$ atm (13). The ground-state electronic degeneracies required with the Sackur–Tetrode equation were obtained in the usual way ($g = 2J + 1$) from published ground-state term values for these ions (14).

With the values of r_g and r_c given in Table 1, and the methods described in ref. 1, values were calculated for ΔG_t° and ΔH_t° with both $n = 4$ and $n = 6$ for each of the trivalent lanthanide ions. The results of these calculations are illustrated in Figs. 1 and 2. It is readily deduced from these figures, that for each of the trivalent lanthanide ions the value of n that would result in a fit of the model to the data lies between 4 and 6.

We obtained a value of n for the trivalent lanthanides by assuming that ΔH_t° for each ion varied linearly with n for n between 4 and 6. Thus a fitted value of n was obtained for each ion and subsequently an average value of n was determined. Thus n for the trivalent lanthanides was found to be 5.6. The calculated values of ΔH_t°, obtained with $n = 5.6$, are given in column 6 of Table 1, and are illustrated in Fig. 1.

We use the same interpolative procedure to obtain values for ΔG_t°. That is, by assuming that ΔG_t° varies linearly with n (for n between 4 and 6) and by using the value $n = 5.6$, we obtained the values of ΔG_t° given in column 4 of Table 1, and illustrated in Fig. 2. A comparison of the corresponding calculated and

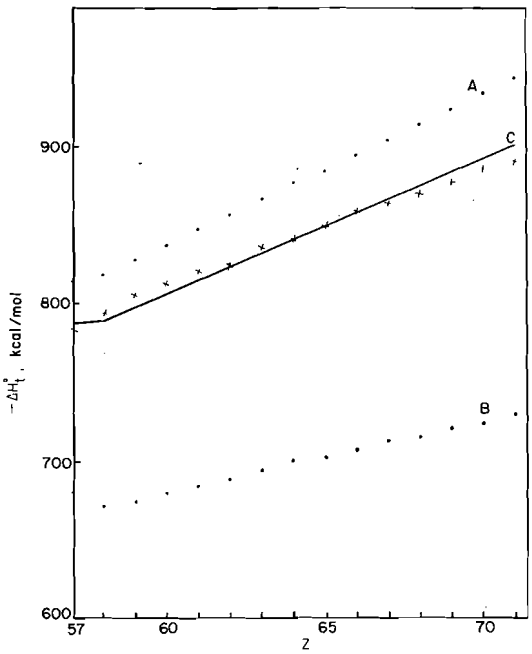

FIG. 1. Enthalpies of hydration for the trivalent lanthanides. *A*, calculated values with $n = 6$; *B*, calculated values with $n = 4$; *C* (solid line), interpolated values with $n = 5.6$; X, experimental values.

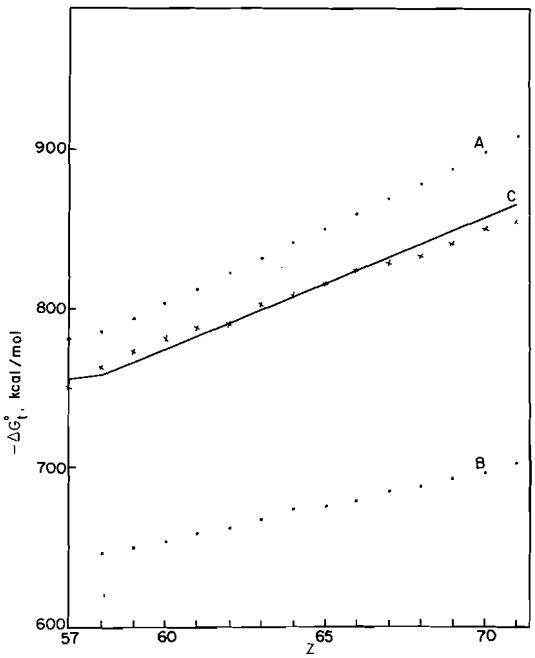

FIG. 2. Free energies of hydration for the trivalent lanthanides. *A*, calculated values with $n = 6$; *B*, calculated values with $n = 4$; *C* (solid line), interpolated values with $n = 5.6$; X, experimental values.

TABLE 2. Data and results for the trivalent actinides[a]

Ion	r_c (Å)	r_g (Å)	$-\Delta G_t°$ (kcal mol^{-1}) Calculated ($n = 6.1$)	$-\Delta G_t°$ (kcal mol^{-1}) Experimental	$-\Delta H_t°$ (kcal mol^{-1}) Calculated ($n = 6.1$)	$-\Delta H_t°$ (kcal mol^{-1}) Experimental
Ac^{3+}	1.14	1.698	747.1	—	780.7	—
Th^{3+}	1.08	1.675	747.0	—	781.0	—
Pa^{3+}	1.05	1.654	752.0	—	786.2	—
U^{3+}	1.04	1.632	762.0	—	796.4	(795)
Np^{3+}	1.02	1.612	768.9	—	803.4	(814)
Pu^{3+}	1.01	1.592	778.3	780.9	812.9	812.7
Am^{3+}	1.00	1.572	788.1	—	822.8	(822)
Cm^{3+}	0.98	1.553	795.0	—	829.9	(831)
Bk^{3+}	0.96	1.534	802.3	—	837.3	(839)
Cf^{3+}	0.94	1.516	809.0	—	844.3	—
Es^{3+}	0.925	1.498	817.4	—	852.5	—
Fm^{3+}	(0.914)[b]	1.481	826.0	—	861.3	—
Md^{3+}	(0.903)[b]	1.464	835.1	—	870.4	—
No^{3+}	(0.892)[b]	1.447	844.2	—	879.7	—
Lr^{3+}	(0.885)[b]	1.431	854.0	—	889.4	—

[a]The values of $\Delta G_t°$ and $\Delta H_t°$ are for $T = 298.15$ K. The standard state in the gas is the hypothetical ideal ion gas at 1 atm. The standard state in solution is the hypothetical 1 *m* solution.
[b]Estimated by extrapolation, using refs. 2 and 22.

experimental values for both $\Delta G_t°$ and $\Delta H_t°$ reveals that the average absolute error for all the trivalent lanthanides is about 1%, and the discrepancy for any particular ion is always within 2%. Discrepancies of this magnitude can be expected from the approximations inherent in the model, from the uncertainties in the values used for r_c and r_g, and from the uncertainties in the experimental values used for $\Delta G_t°$ and $\Delta H_t°$.

Our results for the trivalent lanthanides are noteworthy in several respects. First we point out that the value $n = 5.6$ is consistent with the value of 6 determined in ref. 1 for La^{3+} (in ref. 1 values of n were reported to the nearest integer). Second, whereas the value 5.6 is lower than other values that have previously been reported for the lanthanides (15–17), it is not necessarily inconsistent with these values. The point is that in this work n is a primary hydration number which does not include secondary hydration effects; these latter effects are accounted for separately in our calculations by a Born continuum treatment. Third, it should be pointed out that there is no agreement in the literature on whether the hydration number increases or decreases through the lanthanides. Some authors (16) consider it to decrease, while others (17) consider it to increase. Our result, a constant hydration number for the series, is therefore not at variance with what is known in this respect. Part of the problem in achieving concordant n values among various workers is that n is an operational quantity, and as such will vary somewhat from one application to another. In this work the value $n = 5.6$ is a reflection of our particular definition of n and of the approximations inherent in the model.

Despite the somewhat arbitrary character of n, our results for the trivalent lanthanides are useful. They illustrate how an electrostatic model can be used to account for the thermodynamic hydration functions for these ions, and they suggest a basis for predicting the values of $\Delta G_t°$ and $\Delta H_t°$ for the trivalent actinides, for which (except for Pu^{3+}) no experimental values exist.

Trivalent Actinides

We found that one value of n resulted in a reasonably good fit of our model to the $\Delta G_t°$ and $\Delta H_t°$ data for the trivalent lanthanides. Because of the similarity between the lanthanides and the actinides this suggests that a constant value of n should also obtain, as a good approximation, for the trivalent actinides. The assumption that n is a constant for all the trivalent actinides forms the basis of the predictions given below.

The crystallographic and gas-phase radii for the trivalent actinides that were used in

Can. J. Chem. Downloaded from www.nrcresearchpress.com by 210.87.254.5 on 09/05/12
For personal use only.

TABLE 3. Calculation of ΔH_t° for several trivalent actinide ions[a]

M	$-\Delta H_f^\circ(M^{3+}, aq)$	ΔH(subl)	$\sum I$[c]	$-\Delta H_t^\circ$[d]
U	117.2[b]	128[b]	865	795
Np	125.9[b]	110[e]	893	814
Pu	139.0[b]	83[e]	905	813
Am	147[f]	68[f]	922	822
Cm	147[g]	89[b]	910	831
Bk	138[h]	(66)[b]	950	839

[a]All entries kcal/mol.
[b]Reference 23 and references cited therein.
[c]$\sum I = I_1 + I_2 + I_3$. Calculated by extending the cycles of ref. 8 using measured ΔH°(soln,$Cs_2NaPuCl_6$) to estimate ΔH_t° and ΔH°(soln) for isostructural compounds of U, Np, Am, Cm, and Bk. See also ref. 19.
[d]$\Delta H_t^\circ = (\Delta H_f^\circ(M^{3+},aq) - \Delta H(subl) - \sum I + 314.9)$ kcal/mol.
[e]Reference 24.
[f]Reference 25.
[g]Reference 26.
[h]Reference 27.
[i]J. W. Ward. Paper to be presented at 4th International Transplutonium Element Symposium, Baden-Baden, Germany, Sept. 13–17, 1975 (unpubl.).

our calculations are given in Table 2. The crystallographic radii were taken from published values (2), and the gas-phase radii were calculated by [1]. The value of K in [1] for the actinide series was obtained by applying this equation to radon for which r_g was taken to be 2.315 Å (18). As with the lanthanides the values of S required for [1] were obtained by Slater's rules. Thus the value of K for the actinides was found to be 19.1 Å.

We determined the value of n for the actinide series by determining its value for Pu^{3+}. This was done by calculating values of ΔH_t° for Pu^{3+} with $n = 4$ and $n = 6$. Using the values of r_c and r_g for Pu^{3+} in Table 2, the results of these calculations were ΔH_t° $(n = 4) = -657.8$ kcal mol^{-1} and ΔH_t° $(n = 6) = -805.5$ kcal mol^{-1}. The experimental value for this quantity is -812.7 kcal mol^{-1} (ref. 19, corrected as follows: $\Delta H_f^\circ(Cs_2NaPuCl_6) = -546.0$ kcal/mol, using latest values for ΔH_f°(CsCl,c) and ΔH_f°(NaCl,c). The sum of the first three ionization potentials for Pu was recalculated (using most-recent auxiliary data) as 904.7 kcal/mol. Then, from eqs. 5 and 6 of ref. 8, $\Delta H_t^\circ(Pu^{3+}) = U_0(Cs_2NaPuCl_6) - 10RT + \Delta H^\circ$(soln,$Cs_2NaPuCl_6$) $- 2\Delta H_t^\circ(Cs^+) - \Delta H_t^\circ(Na^+) - 6\Delta H_t^\circ(Cl^-) = -1550 - 5.94 - 13.4 - 2(-64.6) - (-96.4) - 6(-88.5) = -812.7$ kcal/mol). Thus, using the linear interpolation described previously, $n = 6.1$. From the assumption that n is a constant for all the trivalent actinides, it follows that the value 6.1 can be used for n with the entire series.

With the values of r_g and r_c given in Table 2 and $n = 6.1$, values were calculated for ΔH_t° and ΔG_t°, by the methods described in ref. 1, for all the trivalent actinides. The results are given in columns 4 and 6 of Table 2.

Discussion

By analogy with what was found for the trivalent lanthanides, it is probable that most of the predictions given in Table 2 are correct to within 1%, and an upper limit on the error for any particular ion should be about 2%. Our predictions for the actinides are checked further below.

An experimental value is calculable for ΔG_t° for Pu^{3+}, and this value is entered in column 5 Table 2. It was obtained using the experimental value for ΔH_t° (-812.7 kcal mol^{-1}), $\bar{S}_{soln}^\circ$ (conventional) (20), the published ground-state term value (14), and eqs. 2–4. It is seen that the experimental and predicted values agree to well within 0.5%.

The values for ΔH_t° given in parentheses in column 7 of Table 2 for U^{3+}, Np^{3+}, Am^{3+}, Cf^{3+}, and Bk^{3+} were obtained as follows. The systematics of ref. 8 were extended from $Cs_2NaPuCl_6$ (for which ΔH_f° is known) to the corresponding isostructural compounds of Am and Bk (21) and to the presumed-isostructural compounds of U, Np, and Cm. The ionization potential sums ($\sum I = I_1 + I_2 + I_3$) thus calculated are given in Table 3. Using most-recent thermodynamic data, ΔH_t° for the ions was calculated by

$$[5]\quad \Delta H_t^\circ = \Delta H_f^\circ(M^{3+}, aq) - \Delta H(subl, M) - \sum I + 3\Delta H_f^\circ(H^+, aq, absolute) - 15/2RT = \Delta H_f^\circ(M^{3+}, aq) - \Delta H(subl, M) - \sum I + 314.9 \text{ kcal/mol}$$

Can. J. Chem. Downloaded from www.nrcresearchpress.com by 210.87.254.5 on 09/05/12
For personal use only.

A comparison of our predicted values for ΔH_t° with these estimated experimental quantities reveals that the average absolute error is well within 0.5%. Clearly therefore, our predictions which can be tested are quite good.

One of us (S.G.) would like to thank the National Research Council of Canada for financial support.

1. S. GOLDMAN and R. G. BATES. J. Am. Chem. Soc. **94**, 1476 (1972).
2. R. D. SHANNON and C. T. PREWITT. Acta Cryst. B**25**, 925 (1969); B**26**, 1046 (1970).
3. R. H. STOKES. J. Am. Chem. Soc. **86**, 979 (1964).
4. J. O. HIRSCHFELDER, C. F. CURTISS, and W. R. BIRD. Molecular theory of gases and liquids. John Wiley and Sons, New York. 1954. pp. 951–955.
5. A. V. GROSSE. J. Inorg. Nucl. Chem. **26**, 1801 (1964).
6. L. R. MORSS. To be published.
7. H. F. HALLIWELL and S. C. NYBURG. Trans. Faraday Soc. **59**, 1126 (1963).
8. L. R. MORSS. J. Phys. Chem. **75**, 392 (1971).
9. J. E. DESNOYERS and C. JOLICOEUR. *In* Modern aspects of electrochemistry, Vol. 5. *Edited by* J. O. M. Bockris and B. E. Conway. Plenum Press, New York, N.Y. 1969. p. 20.
10. D. F. C. MORRIS. Struct. Bonding, **4**, 63 (1968); **6**, 157 (1969).
11. D. R. ROSSEINSKY. Chem. Rev. **65**, 467 (1965).
12. R. H. SCHUMM, D. D. WAGMAN, S. BAILEY, W. H. EVANS, and V. B. PARKER. U.S. Natl. Bur. Stand. Tech. Note 270-7. 1973.
13. R. A. ROBINSON and R. H. STOKES. Electrolyte solutions. 2nd rev. ed. Butterworths, London. 1959. p. 67.
14. L. BREWER. J. Opt. Soc. Am. **61**, 1666 (1971).
15. T. MOELLER, D. F. MARTIN, L. C. THOMPSON, R. FERRUS, G. R. FEISTEL, and W. J. RANDALL. Chem. Rev. **65**, 1 (1965).
16. F. H. SPEDDING, P. F. CULLEN, and A. HABENSCHUSS. J. Phys. Chem. **78**, 1106 (1974).
17. S. L. BERTHA and G. R. CHOPPIN. Inorg. Chem. **8**, 613 (1969).
18. A. V. GROSSE. J. Inorg. Nucl. Chem. **27**, 509 (1965).
19. L. R. MORSS. J. Phys. Chem. **75**, 392 (1971).
20. R. J. HINCHEY and J. W. COBBLE. Inorg. Chem. **9**, 922 (1970).
21. L. R. MORSS, M. SIEGAL, L. STENGER, and N. EDELSTEIN. Inorg. Chem. **9**, 1771 (1970).
22. J. T. WABER and D. T. CROMER. J. Chem. Phys. **42**, 4116 (1965).
23. L. J. NUGENT, J. L. BURNETT, and L. R. MORSS. J. Chem. Thermodyn. **5**, 665 (1973).
24. R. J. ACKERMANN and E. G. RAUH. J. Chem. Thermodyn. **7**, 211 (1975).
25. J. FUGER, J. C. SPIRLET, and W. MÜLLER. Inorg. Nucl. Chem. Lett. **8**, 709 (1972).
26. J. FUGER, J. REUL, and W. MÜLLER. Inorg. Nucl. Chem. Lett. **11**, 265 (1975).
27. J. FUGER, J. R. PETERSON, J. N. STEVENSON, M. NOÉ, and R. G. HAIRE. J. Inorg. Nucl. Chem. In press.

Can. J. Chem. Downloaded from www.nrcresearchpress.com by 210.87.254.5 on 09/05/12
For personal use only.

A Total Synthesis of Dimethyl 2,3-*O*-Isopropylidene-1-*O*-oxalyl-β-DL-*ribo*-hexofuran-5-ulosuronate[1]

GEORGE JUST AND KARL GROZINGER

Department of Chemistry, McGill University, Montreal, Quebec H3C 3G1

Received March 10, 1975

GEORGE JUST and KARL GROZINGER. Can. J. Chem. **53**, 2701 (1975).

The synthesis of the title compound **5** was accomplished by a high-yield thermal rearrangement of the ozonide (**3**) of dimethyl 5,6-*O*-isopropylidene-7-oxabicyclo[2.2.1]hept-2-ene-*exo*-5,6-diol-2,3-dicarboxylate (**2***a*), which is obtained in 30% yield from the Diels–Alder adduct of furan and dimethyl acetylenedicarboxylate. Catalytic reduction of **5** gave methyl 2,3-*O*-isopropylidene-β-DL-talofuranuronate (**8**) as the major product, accompanied by a small amount of the *allo* isomer **9**.

GEORGE JUST et KARL GROZINGER. Can. J. Chem. **53**, 2701 (1975).

On a effectué la synthèse du composé mentionné dans le titre (**5**) grâce à un réarrangement thermique de l'ozonide (**3**) du *O*-isopropylidène-5,6 oxa-7 bicyclo[2.2.1] heptène-2 diol-5,6 *exo* dicarboxylate-2,3 de méthyle (**2***a*); ce réarrangement se produit avec un excellent rendement et **2***a* pu être obtenu avec un rendement de 30% par réaction de Diels-Alder entre le furanne et l'acétylènedicarboxylate de méthyle. La réduction catalytique de **5** conduit au *O*-isopropylidène-2,3 β-DL-talofuranneuronate de méthyle (**8**) comme produit majeur accompagné par une petite quantité de l'isomère *allo* **9**. [Traduit par le journal]

In connection with our investigations on *C*-nucleosides, we had occasion to study the reaction of the ozonide **3** of dimethyl 5,6-*O*-isopropylidene-7-oxabicyclo[2.2.1]hept-2-ene-*exo*-5,6-diol-2,3-dicarboxylate. This compound is obtained in good yield in the following manner: reaction of furan with dimethyl acetylenedicarboxylate gave Diels–Alder adduct **1**. Catalytic osmylation of **1** gave the *exo*-diol **2**, which was transformed to the corresponding isopropylidene derivative **2***a*, m.p. 60.5–62 °C, by treatment with acetone – dimethoxypropane – *p*-toluenesulfonic acid. Ozonolysis gave crystalline ozonide (**3**), m.p. 79–81 °C, in quantitative yield (1). Upon heating in various solvents, ozonide **3** rearranged predominantly to the stable oxalic ester **5**, m.p. 112–114 °C and to the mixed anhydride **6***a*, which was not isolated (2). Hydrolysis of the mixed anhydride led to **6**, m.p. 114–116 °C. Keto ester **6** was identified by comparison of its spectral data with those of an authentic sample described previously (1). There are many precedents for both types of rearrangements. In the furan series, oxygen insertion products of the Baeyer–Villiger type have been commonly observed (2–5).

The results of the thermal rearrangement of the ozonide **3** in various refluxing solvents are summarized in Table 1 and refer to isolated products.

The p.m.r. spectrum of **5** indicated the presence of two methoxy groups at 3.90 and 3.92 p.p.m., the anomeric proton as a singlet at 6.35 p.p.m., and an AB system corresponding to protons H_2 and H_3, centered at 5.09 p.p.m. H_3 is split into a double doublet $J_{3,2} = 6$ Hz and $J_{3,4} = 1$ Hz, H_4 appears as a doublet at 5.23 p.p.m. Mild hydrolysis of **5** gave oxalic acid monomethyl ester and further hydrolysis, followed by sublimation, gave oxalic acid. When **5** was allowed to stand in ethanol containing palladium-on-charcoal for a few hours a new product crystallized out. Spectral and analytical data indicate that the new product, m.p. 94–95 °C, is ketal-hemiketal of formula **4** or **4***a*. Although no rigorous proof is adduced, we prefer formula **4** for mechanistic reasons. A slight modification of the procedure permitted the isolation of **4** in 56% yield. Acetylation of **4** gave **7**, m.p. 147–148 °C, in 92% yield. Compound **7** is also formed by direct acetylation of **5**. Compound **7** was identified on the basis of spectroscopic evidence. The u.v. spectrum exhibited a maximum at 232 nm in ethanol and the i.r. spectrum (KBr) showed absorptions at 1782, 1769, 1748, 1725, and 1682 cm^{-1}, which is in

[1]This paper is dedicated to Professor C. A. Winkler of McGill University on the occasion of his sixty-fifth birthday by one of his colleagues (G.J.).

Can. J. Chem. Downloaded from www.nrcresearchpress.com by 210.87.254.42 on 09/05/12
For personal use only.

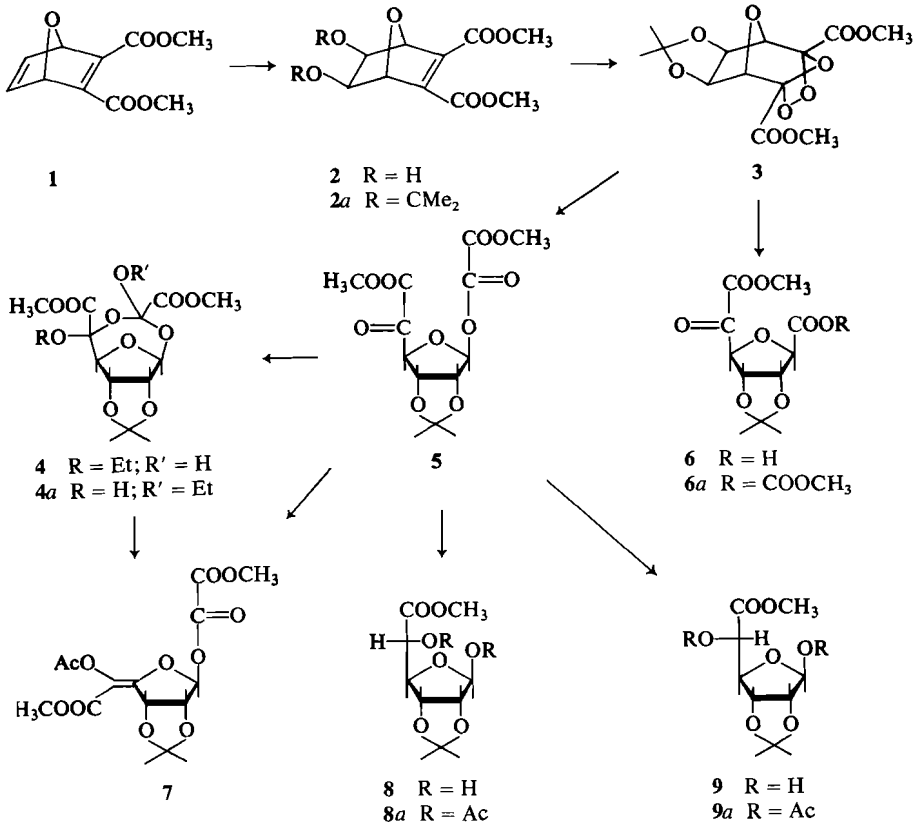

accord with the ester and C—C double bond absorption.

Catalytic hydrogenation, in the presence of a palladium catalyst, of **4** or **5** in ethanol gave two products that were isolated by column chromatography on silica with ethyl acetate – benzene (3:7). The major product was shown to be methyl 2,3-*O*-isopropylidene-β-DL-talofuranuronate **8**, m.p. 112–114 °C (67%), and gave upon acetylation a diacetate **8***a*, m.p. 77–79 °C. The minor product isolated was identified as the *allo* isomer **9**, m.p. 96–97 °C (22%). Acetylation of **9** gave the diacetate **9***a*, m.p. 133–134 °C.

These structures were established by the following reactions: **8** was heated in methanol in the presence of a catalytic amount of sulfuric acid for 2 h and the mixture separated on silica with ethyl acetate. The first product eluted was methyl (methyl 2,3-*O*-isopropylidene-β-DL-talofuranosid)uronate **10**, m.p. 63–64 °C (25%). Acetylation gave the oily monoacetate **10***a*. The next product eluted (R_f 0.5) gave the oily methyl (methyl-β-DL-talofuranosid)uronate **11** (46%). Treatment of **11** with acetone and 2,2-dimethoxypropane in the presence of *p*-toluenesulfonic acid for several hours gave a high yield of **10**, identified by p.m.r., i.r., t.l.c., m.p., and mixture m.p.

Acetylation of **11** gave the triacetate **11***a*, m.p. 105–107 °C. The p.m.r. spectrum of **11***a* proved to be slightly different from that of methyl (methyl 2,3,5-tri-*O*-acetyl-β-DL-allofuranosid)-uronate(6). A sample of this compound, m.p. 103–104 °C, obtained from Prof. Fukami, showed a m.p. depression with **11***a* and a dif-

TABLE 1. Solvent effect on product ratio

Solvent	% yield 5	6
Ethylacetate	93	0
Benzene	90	0
Acetone	90	0
Ether	10*	0
Isopropanol	60	10
Tetrahydrofuran	60	27
Water (phosphate buffer p*H* 6.0)	10†	20

*The balance consisted of recovered starting material.
†The balance consisted of unidentified products.

Can. J. Chem. Downloaded from www.nrcresearchpress.com by 210.87.254.42 on 09/05/12
For personal use only.

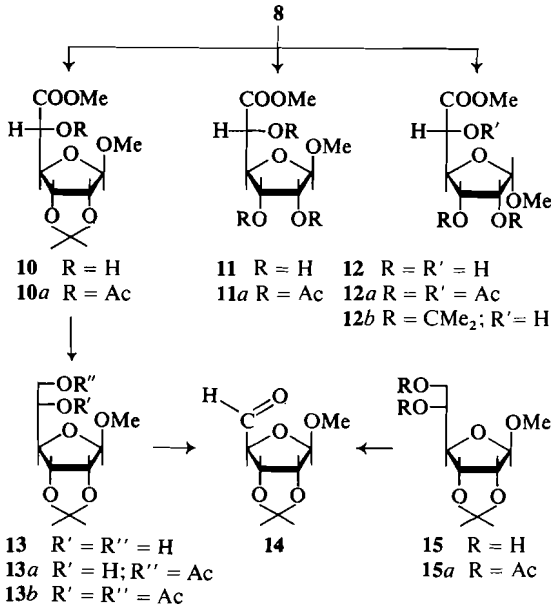

ferent pattern in the i.r. (KBr) spectrum. The α-isomer **12** was eluted last (R_f 0.2) in 29% yield. Treatment of **12** with acetone–dimethoxypropane in the presence of *p*-toluenesulfonic acid gave **12***b*, m.p. 112–113 °C. Reduction of the monoacetate **10***a* with lithium aluminum hydride in ether and direct acetylation of the reaction mixture, gave the monoacetate **13***a*, m.p. 64–65 °C, and the oily diacetate **13***b*. Compound **13** was obtained by sodium methoxide catalyzed methanolysis of **13***a* or **13***b*. Analytical data were in excellent agreement with the structures proposed.

A sample of methyl 2,3-*O*-isopropylidene-β-D-allofuranoside **15**, m.p. 94–96 °C, was not identical with **13**, nor the corresponding diacetate **15***a* with **13***b*. However when **13** was subjected to oxidative cleavage with periodate, the aldehyde **14**, m.p. 94–95 °C, showed identical i.r. (in chloroform), p.m.r., t.l.c., and retention time on g.l.c. with the aldehyde obtained from oxidative cleavage of **15**.

Experimental

Melting points were determined on an Electrothermal block and are corrected. Nuclear magnetic resonance spectra were recorded on a Varian Associates A-60 spectrometer. Infrared spectra were obtained on a Perkin-Elmer 267B spectrometer. Ultraviolet spectra were recorded on a Bausch & Lomb 505 spectrophotometer. Microanalyses were carried out by Micro-Tech. Laboratories Inc., Skokie, Illinois.

Dimethyl 7-Oxabicyclo[2.2.1]hept-2-ene-exo-5,6-diol-2,3-dicarboxylate (2)

To a solution of 42 g of crude dimethyl 7-oxabicyclo[2.2.1]hept-2,5-diene-2,3-dicarboxylate (**1**) in 80 ml of ether and 320 ml of acetone was added 40 ml of a solution made up from 1 g osmium tetroxide in 200 ml of *t*-butyl alcohol, followed by 40 ml of 30% hydrogen peroxide. After completion of the reaction as monitored by t.l.c. (chloroform–methanol 9:1) the reaction was quenched by addition of aqueous sodium bisulfite. Methylene chloride extraction gave crude **2** as an oily syrup; i.r. (film) 3425 (OH), 1710 (CO), 1620 cm^{-1} (C=C); p.m.r. ($CDCl_3$) δ 3.84 (s, OCH_3), 4.02 (s, OH), 5.00 (s, H_1, H_4).

Dimethyl 5,6-O-Isopropylidene-7-oxabicyclo[2.2.1]hept-2-ene-exo-5,6-diol-2,3-dicarboxylate (2a)

The crude diol (21 g, 0.0915 mol) was dissolved in acetone (500 ml) and dimethoxypropane (160 ml) and heated to reflux with a catalytic amount of *p*-toluenesulfonic acid for 3 h. After evaporation of the solvent, the residue was taken up in chloroform and washed with water (2 × 50 ml). The combined extracts were dried (Na_2SO_4) and concentrated. The residue was chromatographed on silicic acid using chloroform as eluent. Recrystallization of the first fraction (17.0 g, 64.5%) from isopropanol – petroleum ether gave colorless plates of **2***a*, m.p. 60.5–62 °C; i.r. (KBr) 1710 (CO), 1632 (C=C), 1360, 1370 cm^{-1} (*gem*-dimethyl); p.m.r. ($CDCl_3$) δ 1.32 (s, 3H), 2.50 (s, 3H), 3.83 (s, 3H), 4.60 (s, 2H), 5.08 (s, 2H).

Anal. Calcd. for $C_{13}H_{16}O_7$: C, 54.93; H, 5.67. Found: C, 54.82; H, 5.82.

Dimethyl 2,3-O-Isopropylidene-1-O-oxalyl-β-DL-ribo-hexofuran-5-ulosuronate (5)

An ethyl acetate (100 ml) solution of dimethyl 5,6-*O*-isopropylidene-7-oxabicyclo[2.2.1]hept-2-ene-*exo*-5,6-diol-2,3-dicarboxylate (10 g, 0.035 mol), was cooled to −60 °C and treated with ozone in oxygen at the rate of 7 mmol of ozone per hour. The reaction was continued until the blue color, characteristic of ozone, persisted. The reaction mixture was flushed with nitrogen and the solvent was evaporated at room temperature under reduced pressure to about 20 ml. The semicrystalline ozonide was heated in a water bath for 20 min until all the solvent evaporated. The product crystallized from ethyl acetate and ether, yield 10.9 g (93.2%), m.p. 114–116 °C; i.r. (KBr) 1760 (ester), 1720 (CO), 1380 cm^{-1} (*gem*-dimethyl); p.m.r. ($CDCl_3$) δ 1.39 (s, 3H), 1.56 (s, 3H), 3.90 (s, 3H), 3.92 (s, 3H), 4.83 (d, $J_{2,3}$ = 6 Hz, 1H), 5.23 (d, $J_{4,3}$ = 1 Hz, 1H), 5.36 (d, d, $J_{2,3}$ = 6 Hz, $J_{3,4}$ = 1 Hz, 1H), 6.35 (s, 1H); mass spectrum *m/e* 332 (M^+), 317 ($M^+ - CH_3$).

Anal. Calcd. for $C_{13}H_{16}O_{10}$: C, 47.22; H, 4.85. Found: C, 46.99; H, 4.85.

Alternatively, the ozonide, m.p. 79–81 °C, was isolated and the pure ozonide refluxed for 20 min and crystallized from ethyl acetate – ether to give **5**.

Treatment of Dimethyl 2,3-Di-O-isopropylidene-1-O-oxalyl-β-DL-ribo-hexofuran-5-ulosuronate (5) with Ethanol and Palladium

A solution of **5** (10.9 g, 0.033 mol) in ethanol (250 ml) was stirred with 5% palladium-on-charcoal (2 g) for 8 h.

Can. J. Chem. Downloaded from www.nrcresearchpress.com by 210.87.254.42 on 09/05/12
For personal use only.

Can. J. Chem. Downloaded from www.nrcresearchpress.com by 210.87.254.42 on 09/05/12
For personal use only.

The suspension was filtered through Celite and the catalyst washed with ethanol (5 × 25 ml). The filtrate and washings were combined and evaporated to dryness. Addition of ether afforded 7.0 g (56%) of **4**, m.p. 94–95 °C; i.r. (KBr) 3490 (OH), 1752, 1725 (ester), 1378 cm^{-1} (*gem*-dimethyl); p.m.r. ($CDCl_3$) δ 1.20 (t, J = 7 Hz, 3H), 1.35 (s, 3H), 1.45 (s, 3H), 3.82 (s, 3H), 3.97 (s, 3H), 4.60 (s, 1H), 4.85 (d, $J_{2,3}$ = 6 Hz, 1H), 5.10 (d, $J_{2,3}$ = 6 Hz, 1H), 6.21 (s, 1H); mass spectrum (70 eV) *m/e* 362 ($M^+ - CH_3$), 332 ($M^+ - C_2H_5OH$), 317, 303.

Anal. Calcd. for $C_{15}H_{22}O_{11}$: C, 47.62; H, 5.86. Found: C, 47.72; H, 5.91.

*Treatment of Dimethyl 2,3-Di-O-isopropylidene-1-O-oxalyl-β-*DL*-ribo-hexofuran-5-ulosuronate (5) with Acetic Anhydride*

A solution of **5** (166 mg, 0.5 mmol) in a mixture of acetic anhydride (1 ml) and pyridine (1 ml) was stirred for 12 h. After removal of the solvents, the oily residue was dissolved in chloroform, carefully washed with 1 *N* hydrochloric acid, and dried over sodium sulfate. Evaporation and crystallization from ether – petroleum ether gave 150 mg (80%) of **7**, m.p. 147–148 °C; i.r. (KBr) 1782, 1769, 1748, 1725 (ester), 1682 (C=C), 1437 (CH), 1389, 1370 cm^{-1} (*gem*-dimethyl); p.m.r. ($CDCl_3$) δ 1.43 (s, 3H), 1.45 (s, 3H), 2.20 (s, 3H), 3.83 (s, 3H), 3.92 (s, 3H), 4.81 (d, $J_{2,3}$ = 6 Hz, 1H), 5.90 (d, $J_{2,3}$ = 6 Hz, 1H), 6.50 (s, 1H); mass spectrum (70 eV) *m/e* 374 (M^+), 359 ($M^+ - CH_3$), 343 ($M^+ - OCH_3$), 315 ($M^+ - COOCH_3$).

Anal. Calcd. for $C_{15}H_{18}O_{11}$: C, 48.13; H, 4.85. Found: C, 48.32; H, 4.89.

Acetylation of 4

Compound **4** (500 mg, 1.34 mmol) was acetylated and purified as described above. There was obtained 465 mg (92%) of **7**, m.p. 147–148 °C; i.r. and p.m.r. spectra were identical with those of a sample obtained previously.

*Methyl 2,3-O-Isopropylidene-β-*DL*-talofuranuronate 8 and Methyl 2,3-O-Isopropylidene-β-*DL*-allofuranuronate 9, from 5*

A solution of **4** (7.0 g, 18.5 mmol) in ethanol (250 ml) containing 5% palladium-on-charcoal (2 g) was hydrogenated for 16 h at 50 p.s.i. The suspension was filtered through Celite and the catalyst washed with ethanol. The filtrate and washings were combined and evaporated to a syrup. The crude mixture showed two products on t.l.c. chromatography on a silica gel column (350 g) and elution with ethyl acetate – benzene (3:7) gave successively 3.1 g of **8** (67.5%), m.p. 112–114 °C (from acetone – petroleum ether), and 1.0 g of **9** (29%), m.p. 96–97 °C (from ether – petroleum ether).

Compound **8**: i.r. (KBr) 3400 (OH), 1745 (ester), 1442 (C—H), 1380, 1375 cm^{-1} (*gem*-dimethyl); p.m.r. (DMSO-d_6) δ 1.22 (s, 3H), 1.40 (s, 3H), 3.71 (s, 3H), 4.35 (d, $J_{2,3}$ = 6 Hz, 1H), 4.3–4.4 (m, 2H), 4.83 (d, $J_{2,3}$ = 6 Hz, 1H), 5.20 (d, $J_{1,OH}$ = 6 Hz, 1H), 5.63 (d, J = 9 Hz, OH), 7.10 (d, J = 6 Hz, OH); mass spectrum (70 eV) *m/e* 248 (M^+), 233 ($M^+ - CH_3$).

Anal. Calcd. for $C_{10}H_{16}O_7$ (248.2): C, 48.38; H, 6.50. Found: C, 48.14; H, 6.50.

Compound **9**: i.r. (KBr) 3240 (OH), 1740 (ester), 1470, 1440 (CH), 1380, 1370 cm^{-1} (*gem*-dimethyl); p.m.r. (DMSO-d_6) δ 1.30 (s, 3H), 1.40 (s, 3H), 3.70 (s, 3H), 4.10 (s, 2H), 4.47 (d, $J_{2,3}$ = 6 Hz, 1H), 4.80 (d, $J_{2,3}$ = 6 Hz, 1H), 5.20 (s, 1H), 6.23 (2 OH); mass spectrum: (70 eV) *m/e* 248 (M^+), 233 ($M^+ - CH_3$).

Anal. Calcd. for $C_{10}H_{16}O_7$ (248.2): C, 48.38; H, 6.50. Found: C, 48.49; H, 6.66.

*Methyl (2,3-O-Isopropylidene-1,5-di-O-acetyl-β-*DL*-allofuranosid)uronate (9a)*

A solution of **9** (100 mg, 0.4 mmol) in acetic anhydride (3 ml) and pyridine (3 ml) was stirred for 18 h at room temperature. After concentration to dryness, the residue was dissolved in chloroform, washed with dilute hydrochloric acid, dried (sodium sulfate), and the chloroform was evaporated. The product was crystallized from ether and petroleum ether, yield 100 mg (74%), m.p. 133–134 °C; i.r. (KBr) 1745 (ester), 1442 (C—H), 1380, 1360 cm^{-1} (*gem*-dimethyl); p.m.r. ($CDCl_3$): δ 1.35 (s, 3H), 1.46 (s, 3H), 2.08 (s, 3H), 2.19 (s, 3H), 3.79 (s, 3H), 4.59 (d, $J_{2,3}$ = 7 Hz, 1H), 4.80 (d, 2H), 5.02 (d, $J_{2,3}$ = 7Hz, 1H) 6.22 (s, 1H); mass spectrum (70 eV): *m/e* 332 (M^+), 317 ($M^+ - CH_3$), 301 ($M^+ - OCH_3$), 289 ($M^+ - CH_3CO$), 273 ($M^+ - CH_3COO$).

Anal. Calcd. for $C_{14}H_{20}O_9$ (332.3): C, 50.60; H, 6.07. Found: C, 50.51; H, 6.14.

*Methyl (2,3-O-Isopropylidene-1,5-di-O-acetyl-β-*DL*-talofuranosid)uronate (8a)*

Treatment of **8** (100 mg, 0.4 mmol) with a mixture of acetic anhydride and pyridine (1:1), under conditions identical with those described for the preparation of **9a**, gave 125 mg (93%) of **8a**, m.p. 77–79 °C; i.r. (KBr) 1770, 1755, 1742 (ester), 1433 (CH), 1378 cm^{-1} (*gem*-dimethyl); p.m.r. ($CDCl_3$) δ 1.36 (s, 3H), 1.50 (s, 3H), 2.05 (s, 3H), 2.17 (s, 3H), 3.80 (s, 3H), 4.70 (dd, $J_{2,3}$ = 6.5 Hz, $J_{3,4}$ = 1 Hz, 1H), 4.75 (d, $J_{4,5}$ = 6.5 Hz, 1H), 4.94 (dd, $J_{4,5}$ = 6.5 Hz, $J_{3,4}$ = 1 Hz, 1H), 6.20 (s, 1H); mass spectrum (70 eV) *m/e* 332 (M^+), 317 ($M^+ - CH_3$).

Anal. Calcd. for $C_{14}H_{20}O_9$ (332.3): C, 50.60; H, 6.07. Found: C, 50.61; H, 6.17.

*Methyl (Methyl 2,3-O-Isopropylidene-β-*DL*-talofuranosid)uronate (10), Methyl (Methyl β-*DL*-talofuranosid)uronate (11), and Methyl (Methyl α-*DL*-talofuranosid)uronate (12)*

A solution of 2.3 g (9.3 mmol) of **8** in methanol (100 ml) and a catalytic amount of sulfuric acid was boiled under reflux for 2 h, evaporated to dryness, and the residue chromatographed on silicic acid with ethyl acetate as eluent. Fractions (15 ml each) were collected and examined by t.l.c. Fractions 6–18 were combined and evaporated. Crystallization from hot petroleum ether yielded 610 mg (24%) of **10**, m.p. 63–64 °C; i.r. (KBr) 3435 (OH), 1743 (ester), 1455, 1442 (C—H), 1382, 1375 cm^{-1} (*gem*-dimethyl); p.m.r. ($CDCl_3$) δ 1.35 (s, 3H), 1.45 (s, 3H), 3.45 (s, 3H), 3.82 (s, 3H), 4.21 (s, 1 OH, 1H), 4.60 (d, $J_{2,3}$ = 6 Hz, 1H), 4.80 (d, $J_{4,5}$ = 2 Hz, 1H), 4.90 (d, $J_{2,3}$ = 6 Hz, 1H), 4.96 (s, 1H); mass spectrum (70 eV) *m/e* 262 (M^+), 261 ($M^+ - 1$), 247 ($M^+ - CH_3$).

Anal. Calcd. for $C_{11}H_{18}O_7$ (262.2): C, 50.37; H, 6.92. Found: C, 50.41; H, 6.97.

Fractions 22–32 were combined and evaporated to give 950 mg (46%) of **11** as a syrup; i.r. (KBr) 3400 (OH), 1735 (ester), 1437 cm^{-1} (CH); p.m.r. ($(CD_3)_2CO$) δ 2.92 (s, 1H), 3.30 (s, 3H), 3.72 (s, 4H), 3.95 (d, 1H), 4.1–4.4 (m, 4H), 4.70 (s, 1H); mass spectrum (70 eV)

Can. J. Chem. Downloaded from www.nrcresearchpress.com by 210.87.254.42 on 09/05/12
For personal use only.

222 (M^+), 190 ($M^+ - CH_3OH$), 132 ($M^+ - CH - CH_2COOCH_3$). Analytical data were obtained on the acetate **11***a*. The more polar product **12** was collected from fraction 35–43, yield 600 mg (29%); i.r. (film) 3400 (OH), 1745 (ester), 1437 (C—H); p.m.r. ($(CD_3)_2CO$) δ 2.84 (s, 1H), 3.32 (s, 3H), 3.75 (s, 3H), 3.65 (d, J = 9 Hz, 1H), 3.9–4.5 (m, 5H), 4.82 (dd, $J_{1,2}$ = 4 Hz, 1H); mass spectrum (70 eV) *m/e* 221 ($M^+ - 1$), 190 ($M^+ - CH_3OH$) 163 ($M^+ - COOCH_3$).

Anal. Calcd. for $C_8H_{14}O_7$ (222.2): C, 43.24; H, 6.35. Found: C, 42.73; H, 6.48.

*Methyl (Methyl 2,3-O-Isopropylidene-*β*-*DL*-talofuranosid)uronate (**10**) from **11***

A solution of **11** (500 mg, 2.25 mmol) in acetone (3 ml), 2,2-dimethoxypropane (5 ml), and a catalytic amount of *p*-toluenesulfonic acid was refluxed for 3 h. Chloroform extraction and crystallization from hot petroleum ether (b.p. 30–60 °C) gave 520 mg (88%) of **10**, m.p. 64–65 °C. The spectral data (i.r., p.m.r., m.s.) were identical with those of the product obtained before.

*Methyl (Methyl 2,3-O-Isopropylidene-5-O-acetyl-*β*-*DL*-talofuranosid)uronate (**10***a*)*

Compound **10** (400 mg, 1.52 mmol) was acetylated with acetic anhydride (4 ml) and pyridine (4 ml) in the usual manner. Chloroform extraction and column chromatography, using benzene–isopropanol (98:2) as eluent, gave 450 mg (97%) of **10***a*; i.r. (film) 1747 (ester), 1435 (CH), 1372 cm^{-1} (*gem*-dimethyl); p.m.r. ($CDCl_3$) δ 1.33 (s, 3H), 1.50 (s, 3H), 2.17 (s, 3H), 3.35 (s, 3H), 3.81 (s, 3H), 4.55 (dd, $J_{4,5}$ = 8 Hz, $J_{4,3}$ = 1 Hz, 1H), 4.60 (d, $J_{2,3}$ = 6 Hz, 1H), 4.90 (dd, $J_{3,4}$ = 1 Hz, $J_{3,2}$ = 6 Hz, 1H), 5.00 (s, 1H), 5.12 (d, $J_{5,4}$ = 8 Hz, 1H); mass spectrum (70 eV): *m/e* 304 (M^+), 289 ($M^+ - CH_3$), 273 ($M^+ - OCH_3$).

Anal. Calcd. for $C_{13}H_{20}O_8$ (304.3): C, 51.31; H, 6.63. Found: C, 51.67; H, 6.75.

*Methyl (Methyl 2,3,5-Tri-O-acetyl-*β*-*DL*-talofuranosid)uronate (**11***a*)*

Compound **11** (450 mg, 2 mmol) was acetylated with acetic acid (4 ml) and pyridine (4 ml) in the usual manner. Chloroform extraction and crystallization from chloroform – petroleum ether, gave 550 mg (78%), m.p. 105–107 °C; i.r. (KBr) 1763, 1740 (ester), 1440 (CH), 1375, 1368 cm^{-1} (*gem*-dimethyl); p.m.r. ($CDCl_3$) δ 2.07 (s, 3H), 2.12 (s, 3H), 2.21 (s, 3H), 3.41 (s, 3H), 3.82 (s, 3H), 4.60 (q, 1H), 4.90 (s, 1H), 5.19 (d, $J_{4,5}$ = 3.6 Hz, 1H), 5.22 (d, $J_{2,3}$ = 4.6 Hz, 1H), 5.44 (q, 1H); mass spectrum (70 eV) *m/e* 348 (M^+), 347 ($M^+ - 1$), 288 [($M^+ - 1$) – $COOCH_3$].

Anal. Calcd. for $C_{14}H_{20}O_{10}$ (348.3): C, 48.27; H, 5.79. Found: C, 48.26; H, 5.88.

*Methyl (Methyl 2,3,5-Tri-O-acetyl-*α*-*DL*-talofuranosid)uronate (**12***a*)*

A solution of **12** (100 mg, 0.45 mmol) in acetic anhydride (2 ml) and pyridine (2 ml) was stirred at room temperature for 20 h. After evaporation, the residue was purified on a silicic acid column using benzene–methanol (95:5) as eluent. The band R_f 0.5, gave triacetate **12***a*, 90 mg (57%); i.r. (film) 1750 (ester), 1435 (CH), 1370 (CH_3); p.m.r. ($CDCl_3$) δ 2.15 (s, 6H), 2.20 (s, 3H), 3.42 (s, 3H), 3.80 (s, 3H), 4.60 (m, 1H), 5.0–5.3 (m, 3H), 5.40 (d, $J_{1,2}$ = 2.5 Hz, 1H); mass spectrum (70 eV) *m/e* 317 ($M^+ - OCH_3$), 289 ($M^+ - COOCH_3$).

Anal. Calcd. for $C_{14}H_{20}O_{10}$ (348.3): C, 48.27; H, 5.79. Found: C, 48.60; H, 5.87.

*Methyl (Methyl 2,3-O-Isopropylidene-*α*-*DL*-talofuranosid)uronate (**12***b*)*

A solution of **12** (350 mg, 1.57 mmol) in acetone (5 ml) and 2,2-dimethoxypropane (10 ml), containing a catalytic amount of *p*-toluenesulfonic acid was refluxed for 2 h. Chloroform extraction and purification on a silicic acid column gave 345 mg (84%) of **12***b*, m.p. 111–112 °C as colorless needles; i.r. (KBr) 3435 (OH), 1745 (ester), 1450, 1431 (CH), 1380, 1370 cm^{-1} (*gem*-dimethyl); p.m.r. ($CDCl_3$) δ 1.38 (s, 3H), 1.58 (s, 3H), 3.05 (d, 1 OH), 3.45 (s, 3H), 3.84 (s, 3H), 4.30 (d, J = 1 Hz), 4.50 (dd, 1H), 4.6–4.8 (m, 2H), 4.93 (d, $J_{1,2}$ = 4 Hz, 1H); mass spectrum (60 eV) *m/e* 262 (M^+), 247 ($M^+ - CH_3$), 231 ($M^+ - OCH_3$), 203 ($M^+ - COOCH_3$).

Anal. Calcd. for $C_{11}H_{18}O_7$ (262.2): C, 50.37; H, 6.92. Found: C, 50.49; H, 6.97.

*Methyl 2,3-O-Isopropylidene-5,6-di-O-acetyl-*β*-*DL*-talofuranoside (**13***b*) and Monoacetate (**13***a*)*

To a slurry of lithium aluminum hydride (114 mg, 3 mmol) in anhydrous ether (50 ml) was added dropwise a solution of **10***a* (455 mg, 1.5 mmol) in ether (5 ml) at 20 °C. The mixture was refluxed for 3 h, cooled to 5 °C, and a mixture of pyridine – acetic anhydride (1:1, 10 ml) was slowly added. The reaction mixture was kept at room temperature for 20 h, poured on crushed ice, stirred for 15 min, and then extracted with three portions of chloroform. The extracts were combined, dried (sodium sulfate), and evaporated to a syrup. The residue was chromatographed on silicic acid with chloroform-methanol (98:2) for elution. Fractions (10 ml each) were collected and examined by t.l.c. The less polar oily diacetate **13***b* was eluted first. Yield of **13***b*, 180 mg (38%); i.r. (film) 1740 (ester), 1437 (CH), 1370 (CH_3) cm^{-1}; p.m.r. ($CDCl_3$) δ 1.34 (s, 3H), 1.50 (s, 3H), 2.07 (s, 3H), 2.10 (s, 3H), 3.34 (s, 3H), 4.02 (dd, 1H), 4.23 (d, 1H), 4.35 (d, 1H), 4.55 (d, J = 6 Hz, 1H), 4.75 (dd, $J_{3,2}$ = 6 Hz, $J_{3,4}$ = 2 Hz, 1H), 5.00 (s, 1H), 5.20 (m, 1H); mass spectrum (70 eV) *m/e* 318 (M^+), 317 ($M^+ - 1$), 303 ($M^+ - CH_3$), 287 ($M^+ - OCH_3$), 275 ($M^+ - COCH_3$).

Anal. Calcd. for $C_{14}H_{22}O_8$ (318.3): C, 52.82; H, 6.97. Found: C, 52.96; H, 7.03.

The more polar monoacetate **13***a* was eluted next and crystallized from hot petroleum ether (b.p. 30–60 °C). Yield 180 mg (43%), m.p. 64–65 °C; i.r. (KBr) 3380 (OH), 1742 (ester), 1462, 1437 (CH), 1375, 1365 cm^{-1} (*gem*-dimethyl); p.m.r. ($CDCl_3$) δ 1.33 (s, 3H), 1.50 (s, 3H), 2.09 (s, 3H), 3.50 (s, 3H), 3.60 (s, OH), 3.80 (m, 1H), 4.0–4.3 (m, 2H), 4.50 (s, 1H), 4.59 (d, $J_{2,3}$ = 6 Hz), 4.85 (d, $J_{2,3}$ = 6 Hz), 5.00 (s, 1H); mass spectrum (70 eV) *m/e* 276 (M^+), 261 ($M^+ - CH_3$), 245 ($M^+ - OCH_3$), 233 ($M^+ - COCH_3$).

Anal. Calcd. for $C_{12}H_{20}O_7$ (276.3): C, 52.16; H, 7.30. Found: C, 52.27; H, 7.32.

*Methyl 2,3-O-Isopropylidene-*β*-*DL*-talofuranoside (**13**)*

To a solution of **13***b* (180 mg, 0.56 mmol) in methanol (20 ml), was added a catalytic amount of sodium with stirring. After 18 h at room temperature, the mixture was neutralized with anhydrous hydrogen chloride in

ether and concentrated under reduced pressure to dryness. The residue was purified by filtration through a silica gel column using chloroform–methanol (98:2) as eluent. After combining the main fractions, **13** was obtained as a colorless syrup. Yield, 100 mg (75%); i.r. (film) 3420 (OH), 1372 cm^{-1} (*gem*-dimethyl); p.m.r. ($CDCl_3$) δ 1.32 (s, 3H), 1.50 (s, 3H), 2.90 (broad s, 2 OH), 3.48 (s, 3H), 3.65 (s, 3H), 4.50 (broad s, 1H), 4.60 (d, $J_{3,2}$ = 6 Hz, 1H), 4.85 (d, $J_{2,3}$ = 6 Hz, 1H), 5.00 (s, 1H); mass spectrum (60 eV) *m/e* 234 (M^+), 219 ($M^+ - CH_3$), 203 ($M^+ - OCH_3$), 173 ($M^+ - HO - CH_2 - CH - OH$).

Anal. Calcd. for $C_{10}H_{18}O_6$ (234.2): C, 51.27; H, 7.75. Found: C, 51.17; H, 7.81.

Treatment of **13***a* under conditions identical with those described above, gave pure **13** in 45% yield.

*Methyl 2,3-O-Isopropylidene-*β*-*DL*-ribo-pentodialdo-1,4-furanoside (**14**) from **13***

To a solution of **13** (46 mg, 0.2 mmol) in methanol (1 ml) and phosphate buffer p*H* 7.0 (0.2 ml) was added a solution of sodium metaperiodate (22 mg, 0.2 mmol) in water (1 ml). The mixture was stirred for 2 h at 20 °C. Evaporation, ether extraction, and partial evaporation of the ether gave 35 mg (89%) of **14**, m.p. 94–95 °C; i.r. ($CHCl_3$) 1730 (CO), 1372 cm^{-1} (*gem*-dimethyl; p.m.r. ($CDCl_3$) δ 1.35 (s, 3H), 1.50 (s, 3H), 3.37 (s, 3H), 4.50 (s, 1H), 4.55 (d, $J_{3,2}$ = 6 Hz, 1H), 5.05 (d, $J_{2,3}$ = 6 Hz, 1H), 5.10 (s, 1H); mass spectrum (70 eV) *m/e* 203 ($M^+ + 1$), 187 ($M^+ - CH_3$), 173 ($M^+ - CHO$).

Anal. Calcd. for $C_9H_{14}O_5$ (202.2): C, 53.46; H, 6.98. Found: C, 53.24; H, 7.12.

*Methyl (2,3-O-Isopropylidene-5,6-di-O-acetyl)-*β*-*D*-allofuranoside (**15***a*)*

Acetylation of **15** (117 mg, 0.5 mmol) in the usual manner gave 150 mg (94%), of **15***a* as a syrup; i.r. ($CHCl_3$): 1745 (CO), 1440 (CH), 1370 cm^{-1} (*gem*-dimethyl); p.m.r. ($CDCl_3$) δ 1.27 (s, 3H), 1.45 (s, 3H), 2.03 (s, 3H), 2.08 (s, 3H), 3.35 (s, 3H), 4.0–4.5 (m, 3H), 4.60 (s, 2H), 4.98 (s, OH), 5.01 (dd, 1H).

*Methyl 2,3-O-Isopropylidene-*β*-*DL*-ribo-pentodialdo-1,4-furanoside (**14**) from **15***

Compound **15**, m.p. 94–95 °C, was oxidized with sodium metaperiodate in methanol at p*H* 7 as described previously. The aldehyde **14** had identical i.r. and p.m.r. spectra, and g.l.c. and t.l.c. behavior as DL-**14**, obtained from **13**.

We thank Drs. A. S. Perlin and H. J. Koch for a sample of compound **15** and valuable discussions, and Dr. H. Fukami, Kyoto University, Kyoto, Japan, for a sample of methyl (2,3,5-tri-*O*-acetyl-β-DL-allofuranosid)uronate. We also wish to thank the National Research Council of Canada for financial support.

1. G. JUST and A. MARTEL. Tetrahedron Lett. 1517 (1973).
2. R. CRIEGEE, P. DE BRUYN, and G. LOHAUS. Ann. **583**, 19 (1953).
3. H. H. WASSERMAN and E. DRUCKEREY. J. Am. Chem. Soc. **90**, 2440 (1968).
4. H. H. WASSERMAN, F. J. VINICK, and Y. C. CHANG. J. Am. Chem. Soc. **94**, 7180 (1972).
5. H. H. WASSERMAN, A. DOUMAUX, and R. E. DAVIS. J. Am. Chem. Soc. **88**, 4517 (1966).
6. H. FUKAMI, HEN-SIK KOH, T. SAKATA, and N. NAKAJIMA. Tetrahedron Lett. 4771 (1967).

Can. J. Chem. Downloaded from www.nrcresearchpress.com by 210.87.254.42 on 09/05/12
For personal use only.

The Crystal and Molecular Structure of Pentane-2,4-dionato-(2,3,5,6-*tetrahapto*-2,3-dicarbomethoxo[2.2.1]bicycloheptadiene)rhodium(I), $Rh(C_5H_7O_2)(C_7H_6(CO_2CH_3)_2)$

DEBBIE ALLEN, COLIN JAMES LYNE LOCK,[1] AND GRAHAM TURNER
Institute for Materials Research, McMaster University, Hamilton, Ontario L8S 4M1
AND
JOHN POWELL
Lash-Miller Chemical Laboratories, University of Toronto, Toronto, Ontario M5S 1A1

Received April 23, 1975

DEBBIE ALLEN, COLIN JAMES LYNE LOCK, GRAHAM TURNER, and JOHN POWELL. Can. J. Chem. **53**, 2707 (1975).

The crystal and molecular structures of pentane-2,4-dionato-(2,3,5,6-*tetrahapto*-2,3-dicarbomethoxo[2.2.1]bicycloheptadienerhodium(I), $Rh(C_5H_7O_2)(C_7H_6(CO_2CH_3)_2)$, have been measured by single crystal X-ray diffraction. The orange crystals are monoclinic, space group $P2_1/c$, $Z = 4$, $a = 9.245(4)$, $b = 9.003(4)$, $c = 21.680(15)$ Å, $\beta = 113.41(5)°$. The calculated and observed densities are 1.645 and 1.642(5) respectively. Intensity data were collected on a Syntex $P\bar{1}$ diffractometer and a full matrix least squares refinement on 3010 observed reflections leads to a conventional $R = 0.0660$. The structure can be considered as a roughly square planar arrangement of ligands around the rhodium atom composed of two β-ketoenolate oxygen atoms (Rh—O, 2.037(5) and 2.025(5) Å) and the centers of the two ethylenic groups. The Rh—C distances for the olefin group attached to the two carbomethoxo groups, 2.117(8), 2.108(8) Å, appear to be slightly larger than those for the other olefinic group, 2.087(7), 2.082(6), and the corresponding C=C distances of 1.375(10) and 1.410(9) Å are different at the 95% confidence level.

DEBBIE ALLEN, COLIN JAMES LYNE LOCK, GRAHAM TURNER, et JOHN POWELL. Can. J. Chem. **53**, 2707 (1975).

On a mesuré, par diffraction de rayons-X d'un cristal unique, les structures cristallines et moléculaires du pentanedionato-2,4 (*tétrahapto*-2,3,5,6 dicarbométhoxo-2,3 bicyclo[2.2.1] heptadiènerhodium(I), $Rh(C_5H_7O_2)(C_7H_6(CO_2CH_3)_2)$. Les cristaux oranges sont monocliniques avec un groupe d'espace $P2_1/c$, $Z = 4$, $a = 9.245(4)$, $b = 9.003(4)$, $c = 21.680(15)$ Å, $\beta = 113.41(5)°$. Les densités calculées et observées sont respectivement de 1.645 et 1.642(5). On a recueilli les données d'intensité avec un diffractomètre Syntex $P\bar{1}$ et la structure affinée par la méthode des moindres carrés (matrice complète) pour 3010 réflexions observées a conduit à une valeur de R conventionnelle de 0.0660. On peut considérer que la structure comporte en première approximation un arrangement plan carré des ligands autour de l'atome de rhodium; cet arrangement comporte deux atomes d'oxygène du β-cétoénolate (Rh—O, 2.037(5) et 2.025(5) Å) et le centre de deux groupes éthyléniques. Il semble que les distances Rh—C (2.117(8) et 2.108(8) Å) du groupe oléfinique attaché aux deux groupes carbométhoxo sont légèrement plus larges que celles (2.087(7) et 2.082(6) Å) de l'autre groupe oléfinique. Les distances C=C correspondantes, 1.375(10) et 1.410(9) Å sont différentes au niveau de confiance de 95%.

[Traduit par le journal]

Introduction

Structural studies on the adduct of pyridine to 1,1,1,5,5,5-hexafluoropentane-2,4-dionato-(2,3,5,6-*tetrahapto*-2,3-dicarbomethoxo[2.2.1]-bicycloheptadienerhodium(I), $Rh(C_5HF_6O_2)(C_6H_7(CO_2CH_3)_2)$ (**1**), showed that the Rh—O bond lengths in the adduct, $Rh(C_5HF_6O_2)(C_6H_7(CO_2CH_3)_2)(C_5H_5N)$, were unusually long (1). It appeared that the bond-length anomaly was caused by pseudo-trigonal bipyramidal arrangement of the ligands around the rhodium atom since pentane-2,4-dionato-bis(ethylene)-rhodium(I) (2) and pentane-2,4-dionatoethylene-perfluoroethylenerhodium(I) (2) do not show abnormal Rh—O bond lengths. However, no structural studies had been made of a diene attached to rhodium in place of the two ethylene ligands. We intended to study the structure of

[1]To whom correspondence should be addressed.

Can. J. Chem. Downloaded from www.nrcresearchpress.com by 210.87.254.5 on 09/05/12
For personal use only.

Can. J. Chem. Downloaded from www.nrcresearchpress.com by 210.87.254.5 on 09/05/12
For personal use only.

the parent compound, **1**, but it has proved impossible to grow crystals suitable for X-ray diffraction studies. Instead, we have studied the structure of pentane-2,4-dionato(2,3,5,6-*tetrahapto*-2,3-dicarbomethoxo[2.2.1]bicycloheptadiene)-rhodium(I), $Rh(C_5H_7O_2)(C_6H_7(CO_2CH_3)_2)$, and we report this work here.

Experiments

The Preparation of Pentane-2,4-dionato(2,3-dicarbomethoxo[2.2.1]bicycloheptadiene)rhodium(I)

Acetylacetonatothallium(I) (0.600 g) was added to a solution of di-μ-chlorobis(2,3-dicarbomethoxo[2.2.1]bicycloheptadiene)dirhodium(I) (0.650 g) (4) in dichloromethane (30 ml) and the reaction mixture shaken for 30 min and then evaporated to dryness under reduced pressure. The residue was extracted with pentane. Evaporation of the extract under reduced pressure gave the desired product as a yellow solid which recrystallized from *n*-pentane as orange prisms (0.712 g) m.p. 100–103 °C. Crystals, suitable for X-ray work, were grown from a pentane solution.

Anal. Calcd. for $C_{16}H_{19}O_6Rh$: C, 46.8; H, 4.6. Found: C, 46.5, H, 4.4.

X-Ray Crystallography

An orange crystal, selected after microscopic examination, was approximately a cylindrical bipyramid. The crystal was 1.0 mm in length and the maximum cylinder diameter was 0.25 mm. A series of precession and Weissenberg photographs suggested the crystal was monoclinic.

The crystal was transferred to a Syntex PĪ diffractometer and accurate unit cell parameters were obtained by least squares refinement from 15 centered medium angle reflections. Examination of the intensity of reflections in the region $0 < 2\theta < 25°$ showed the systematic absences $0k0$, $k = 2n + 1$ and $h0l$, $l = 2n + 1$, showing the crystal had the space group $P2_1/c$. The density of a few crystals was measured by flotation in a degassed aqueous zinc bromide solution. Crystal data were

$C_{16}H_{19}O_6Rh$ f.w. = 410.23

Monoclinic, $a = 9.245(4)$, $b = 9.003(4)$, $c = 21.680(15)$ Å, $\beta = 113.41(5)°$, $V = 1655.0$ Å^3, $P2_1/c$ (C_{2h}^5, No. 14), $\rho_o = 1.642(5)$, $Z = 4$, $\rho_c = 1.645$ (22 °C, MoKα, $\lambda = 0.71069$ Å, $\mu = 10.34$ cm^{-1}).

Intensity data were recorded on a Syntex PĪ diffractometer using graphite monochromatized MoKα radiation for the hemidemisphere defined by h, k, $-l$ to $+l$,[2] and up to $2\theta = 55°$. Data were collected by executing a coupled θ(crystal)–2θ(counter) scan 1° on either side of the peak, scan rates varying from 8 to 24 deg/min.

The stability of the system was monitored by measuring a standard reflection after each 50 reflections. The counting e.s.d. of the standard peak was 1.1% and an analysis of the standard counts showed an overall e.s.d. of 1.3% with no systematic variation with time. The intensity of a reflection, I, and its e.s.d., σ_I, were calculated as outlined previously (1). A total of 3758 symmetry-independent reflections were measured and 297 were rejected because they were "not significantly above background" ($I < \sigma_I$).

A further 453 reflections had $I < 3\sigma_I$ and were called unobserved. Such reflections were only used in the refinement if $F_c > F_o$ for the reflection. In the final refinement 216 unobserved reflections were used with the 3008 observed reflections. Corrections were made for absorption[3] assuming the crystal had the dimensions listed above and that it was bounded by the sets of faces {6 3 1}, {0 3 1}, {6 0 1}.

Unscaled structure factor amplitudes, F, and their standard deviations, σ_F, were calculated from the expression $F = (I/Lp)^{1/2}$, $\sigma_F = (1/2)(1/\sqrt{Lp})(\sigma_I/\sqrt{I})$, where Lp, the Lorentz-polarization factor is $(1 + \cos^2 2\theta)/(2 \sin 2\theta)$.

Solution of the Structure

The coordinates of the rhodium atom were found from a three-dimensional Patterson synthesis and the six atoms nearest the rhodium atom were found from a three-dimensional difference synthesis. All remaining nonhydrogen atoms were found from successive projection Fourier and electron density difference syntheses and calculations of the likely geometry of the ligands. At this stage the rhodium and oxygen atoms were given anisotropic temperature factors; previously all temperature factors had been treated isotropically. Successive cycles of full matrix least squares refinement were terminated at $R_1 = 0.0660$, $R_2 = 0.690$.[4] For the last cycle of refinement no parameter shifted by more than 0.1σ.

A three dimensional difference map showed no significant features, the largest residual peaks being $+0.43$ e/Å^3 at 0.23, 0.43, 0.23, between the β-ketoenolate ring and C13, O3, and at 0.27, 0.93, 0.30, the closest atoms being C9 and C11. The largest valley was -0.38 e/Å^3 at 0.08, 0.50, 0.50 lying between O3 and C4.

[2]Defined with respect to the $P2_1/n$ cell. This cell was converted to the cell used here by the matrix 00—1/010/101.

[3]All calculations were carried out on a CDC6400 computer. The programs DATCO3, ABSORB, and DATRDN from the X-RAY71 package were used for preliminary treatment of data. The full matrix least square program CUDLS and Fourier program SYMFOU were written locally by J. S. Stephens and J. S. Rutherford, respectively. Least squares planes were calculated by the local program PALS by P. G. Ashmore, and diagrams were prepared by the program ORTEP by C. K. Johnson (5).

[4]
$$R_1 = \frac{||F_o| - |F_c||}{\sum |F_o|}$$

$$R_2 = \left(\frac{\sum \omega(|F_o| - |F_c|)^2}{\sum \omega F_o^2}\right)^{1/2}$$

Can. J. Chem. Downloaded from www.nrcresearchpress.com by 210.87.254.5 on 09/05/12
For personal use only.

TABLE 1. Atom parameters for $Rh(C_5H_7O_2)(C_7H_6(CO_2CH_3)_2) \times 10^4$ (estimated standard deviations are given in parentheses)

Atom	x	y	z	U (Å^2)
Rh	1694.2(6)	1787.5(5)	2803.2(2)	*
O(1)	905(6)	1552(6)	1778(2)	*
O(2)	3761(5)	2633(6)	2846(2)	*
O(3)	2441(7)	4393(6)	4558(3)	*
O(4)	3008(6)	4788(5)	3662(2)	*
O(5)	4708(7)	−367(6)	4171(3)	*
O(6)	4989(5)	2086(6)	4328(2)	*
C(1)	1653(8)	2011(8)	1435(3)	367(14)
C(2)	3076(8)	2742(8)	1662(4)	409(15)
C(3)	4045(8)	3009(8)	2343(3)	362(14)
C(4)	841(10)	1685(10)	691(4)	589(20)
C(5)	5591(10)	3810(10)	2510(4)	568(20)
C(6)	−527(8)	1552(8)	2861(3)	377(14)
C(7)	197(8)	194(8)	2954(3)	401(15)
C(8)	1709(7)	2584(7)	3710(3)	277(12)
C(9)	2452(7)	1179(7)	3809(3)	300(12)
C(10)	−40(8)	2265(8)	3566(3)	392(15)
C(11)	1153(8)	15(8)	3713(4)	415(15)
C(12)	118(9)	855(9)	4007(4)	445(16)
C(13)	2430(7)	4015(7)	4027(3)	317(13)
C(14)	3835(11)	6152(11)	3980(5)	606(22)
C(15)	4152(8)	849(8)	4118(3)	351(14)
C(16)	6658(11)	1971(11)	4515(5)	623(22)

Atom	U_{11}	U_{22}	U_{33}	U_{12}	U_{13}	U_{23}
Rh	31.7(3)	29.4(3)	26.3(2)	−3.0(2)	12.7(2)	−3.1(2)
O(1)	42(2)	51(3)	29(2)	−9(2)	14(2)	−7(2)
O(2)	37(2)	46(3)	33(2)	−4(2)	17(2)	−3(2)
O(3)	77(4)	44(3)	40(3)	−12(3)	29(3)	−14(2)
O(4)	55(3)	31(2)	41(3)	−11(2)	22(2)	−5(2)
O(5)	64(3)	39(3)	60(3)	20(3)	18(3)	1(3)
O(6)	35(2)	47(3)	40(2)	3(2)	8(2)	−1(2)

*Anisotropic temperature factors (Å$^2 \times 10^3$). The temperature factor parameters U_{ij} were obtained from $\beta_{ij} = 2\pi^2 b_i b_j U_{ij}$ where β_{ij}'s appear as a temperature effect through exp $[-(\beta_{11}h^2 + \ldots + 2\beta_{12}hk + \ldots)]$ in the structure factor expression b_i are the reciprocal lattice vectors.

Throughout the refinement, the scattering curves for C and O were those tabulated in the *International Tables for X-Ray Crystallography* (6), while that for Rh was taken from Cromer and Waber (7). Anomalous dispersion corrections were applied for Rh and were taken from Cromer (8). The final atom parameters are given in Table 1 and the values of the moduli of F_o and F_c are given in Table 2.[5]

Discussion

The molecule is illustrated in Fig. 1 and selected bond lengths and angles are given in Table 3. The rhodium atom could be considered as having rough square planar coordination,

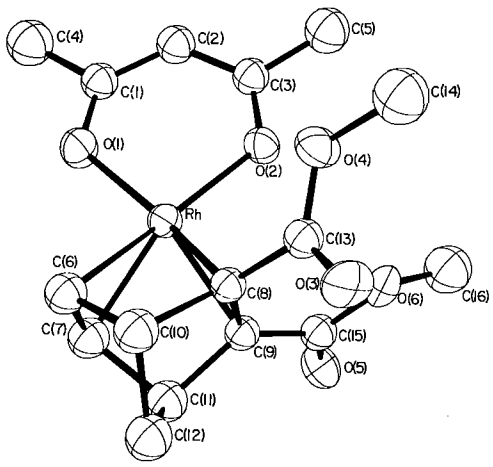

FIG. 1. The molecular structure of $Rh(C_5H_7O_2)(C_7H_6(CO_2CH_3)_2)$. The numbering of the atoms is the same as in Table 1.

[5]Table 2 is available, at a nominal charge, from the Depository of Unpublished Data, CISTI, National Research Council of Canada, Ottawa, Canada K1A 0S2.

TABLE 3. Selected interatomic distances and angles for $Rh(C_5H_7O_2)_2(C_7H_6(CO_2CH_3)_2)$ (e.s.d.'s in parentheses)

Atoms	Distance (Å)	Atoms	Distance (Å)
Bond distances			
Rh—O(1)	2.037(5)	Rh—O(2)	2.025(5)
Rh—C(6)	2.117(8)	Rh—C(7)	2.108(8)
Rh—C(8)	2.087(7)	Rh—C(9)	2.082(6)
O(1)—C(1)	1.286(10)	O(2)—C(3)	1.264(10)
C(1)—C(2)	1.375(10)	C(2)—C(3)	1.410(9)
C(1)—C(4)	1.51(1)	C(3)—C(5)	1.51(1)
C(6)—C(7)	1.370(10)	C(8)—C(9)	1.415(9)
C(7)—C(11)	1.54(1)	C(6)—C(10)	1.55(1)
C(9)—C(11)	1.54(1)	C(8)—C(10)	1.55(1)
C(11)—C(12)	1.54(1)	C(10)—C(12)	1.56(1)
C(8)—C(13)	1.49(1)	C(9)—C(15)	1.47(1)
C(13)—O(3)	1.20(1)	C(15)—O(5)	1.20(1)
C(13)—O(4)	1.32(1)	C(15)—O(6)	1.33(1)
O(4)—C(14)	1.47(1)	O(6)—C(16)	1.44(1)
Nonbonded distances			
O(1)–C(6)	3.10(1)	O(1)–C(7)	3.10(1)
O(2)–C(8)	3.15(1)	O(2)–C(9)	3.10(1)
C(6)–C(8)	2.345(8)	C(7)–C(9)	2.345(8)
O(1)–O(2)	2.893(6)		

Atoms	Angle (deg)	Atoms	Angle (deg)
O(1)—Rh—O(2)	90.8(2)	O(1)—Rh—C(6)	96.5(2)
O(1)—Rh—C(7)	97.0(2)	O(2)—Rh—C(8)	100.1(2)
O(2)—Rh—C(9)	97.6(2)	C(6)—Rh—C(8)	67.8(3)
C(7)—Rh—C(9)	68.1(3)	C(6)—Rh—C(9)	80.9(3)
C(7)—Rh—C(8)	81.2(3)	O(1)—Rh—C(8)	156.8(2)
O(1)—Rh—C(9)	158.8(2)	O(2)—Rh—C(6)	162.7(2)
O(2)—Rh—C(7)	156.2(2)	Rh—O(1)—C(1)	124.3(4)
Rh—O(2)—C(3)	125.2(4)	O(1)—C(1)—C(2)	127.2(6)
O(2)—C(3)—C(2)	126.4(7)	C(1)—C(2)—C(3)	125.2(8)
O(1)—C(1)—C(4)	114.5(6)	O(2)—C(3)—C(5)	114.9(6)
C(2)—C(1)—C(4)	118.3(8)	C(2)—C(3)—C(5)	118.7(8)
Rh—C(6)—C(7)	70.7(5)	Rh—C(7)—C(6)	71.4(5)
Rh—C(8)—C(9)	69.9(4)	Rh—C(9)—C(8)	70.4(4)
Rh—C(6)—C(10)	96.2(4)	Rh—C(7)—C(11)	95.9(4)
Rh—C(8)—C(10)	97.6(4)	Rh—C(9)—C(11)	96.8(4)
Rh—C(8)—C(13)	124.5(5)	Rh—C(9)—C(15)	112.6(5)
C(6)—C(10)—C(8)	98.4(6)	C(7)—C(11)—C(9)	99.2(6)
C(6)—C(10)—C(12)	100.8(6)	C(7)—C(11)—C(12)	101.8(6)
C(8)—C(10)—C(12)	101.1(5)	C(9)—C(11)—C(12)	100.9(6)
C(8)—C(13)—O(3)	121.4(7)	C(9)—C(15)—O(3)	124.7(6)
C(8)—C(13)—O(4)	113.3(6)	C(9)—C(15)—O(6)	111.0(6)
O(3)—C(13)—O(4)	125.3(6)	O(5)—C(15)—O(6)	124.4(6)
C(13)—O(4)—C(14)	114.9(6)	C(15)—O(6)—C(16)	116.8(6)
C(11)—C(12)—C(10)	93.9(7)		

the two β-ketoenolate oxygen atoms and the centers of the two olefinic groups occupying the corners of the square. Unlike the corresponding five coordinate pyridine adduct, Rh(hfac)py(NOR) (1),[6] the Rh—O distances were not unduly long.

Some bond lengths of interest are shown in Fig. 2*A*. Unfortunately, because of the size of the errors, one could not draw any positive conclusions about possible differences in pairs of equivalent bonds, except to say that C(1)—C(2) and C(2)—C(3) were probably of different

[6]The following abbreviations are used: acac, anion of acetylacetone, $C_5H_7O_2^-$; hfac, anion of 1,1,1,5,5,5-hexafluoroacetylacetone, $C_5F_6HO_2^-$; py, pyridine, C_5H_5N; NOR, 2,3-dicarbomethoxo[2.2.1]bicycloheptadiene, $C_7H_6(CO_2CH_3)_2$.

Can. J. Chem. Downloaded from www.nrcresearchpress.com by 210.87.254.5 on 09/05/12
For personal use only.

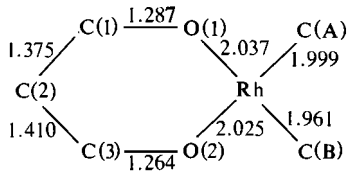

2A

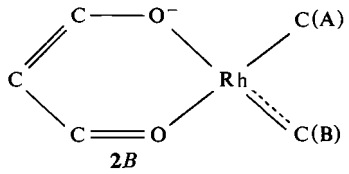

2B

FIG. 2. Part of the $Rh(C_5H_7O_2)(C_7H_6(CO_2CH_3)_2)$ molecule showing bond lengths. C(A) and C(B) represent the centers of the ethylenic bonds, the $\cdot CO\cdot OCH_3$ groups being attached to the carbon atoms represented by C(B).

lengths. The other pairs did not differ by more than about 2σ. Thus, the following comments must be regarded as speculative.

We noted that the absolute values of the bond lengths formed a set which was reasonable in terms of conventional bonding models for *trans*-influence (9) and was consistent with some localization of multiple bonding in the β-ketoenolate ring. An M—X bond, where X has some π-acceptor properties, *trans* to an olefinic group substituted with electron-withdrawing ligand, (C(B)), should be longer than a similar bond *trans* to an unsubstituted olefinic group, (C(A)), because in the competition for d–π electrons, the increased π-back bonding to the olefin would weaken the *trans* π-bond (9). We have shown previously that β-ketoenolates in low valence compounds of rhenium were π-acceptors (22), and that when β-ketoenolate oxygen atoms were *trans* to a group with good π-acceptor ability (CO) the Re—O distance was larger than normal (23). Further, Mason and Towl (10), have suggested that, for a system L—M—X, a strong L—M bond caused the M—X bond to become more ionic, and weaker, giving rise to localization of negative charge on X. If negative charge were localized on O(1), this would cause consequent localization of the bonds in the β-ketoenolate ring and we should have the situation shown in Fig. 2*B*.

O(1) appeared to have two bonds which were longer than normal (to C(1) and Rh). Brown and Shannon (11), using the concept that the bond valence of oxygen should be two, have postulated that, under that circumstance, there should be abnormally short "nonbonding" interactions to compensate for the long bond distances. The nearest atoms to O(1) were the hydrogen atoms attached to C(7) and C(11), however, and although we have not calculated the O(1)—H distances, the corresponding O(1)—C(7) and O(1)—C(11) distances were 3.55 and 3.59 Å respectively, so no significant hydrogen bonding could be taking place.

Even with bond localization, suggested above, the β-ketoenolate ring, O(1)C(1)C(2)C(3)O(2), was essentially planar and it made a dihedral angle of 6.9° with the plane RhO(1)O(2). Thus, the rhodium atom was 0.17 Å out of the plane defined by the ring. In addition, C(5) was significantly out of the plane of the ring (0.16 Å) on the opposite side to the rhodium atom.

The two sets of Rh—C distances (Rh—C(6), Rh—C(7); Rh—C(8), Rh—C(9)) were different at the 95% confidence level and the olefin with the shorter Rh—C distances (C(8)—C(9)) had the longer C—C distance, (at the 99% confidence level) as would be expected from conventional pictures of the bonding of olefins to metals (12, 13). Within the norbornadiene group, all other distances agreed well with those found in free norbornadiene (14, 15), a norbornadiene–palladium complex (16), and Rh(hfac)py(NOR) (1).[6]

Comparison of the Rh—C bond lengths in Rh(hfac)py(NOR) and Rh(acac)NOR, shows that equivalent distances were not significantly different. This was despite the fact that, within a given compound, Rh—C distances for the two types of olefin group differed, that there was a marked change in the Rh—O bond lengths, and that there was a change in geometry from pseudo-trigonal bipyramidal to pseudo-square planar. It was quite clear, after examining a number of structures (2, 3, 16–20), that Rh—C distances were almost insensitive to geometry and could be predicted entirely on the basis of whether electron-withdrawing groups (*e.g.* F or CO_2Me) were attached to the olefin or not. In the former case, Rh—C distances were most likely 2.03(2) Å and in the latter 2.13(2) Å. It should be noted that, in Rh(hfac)py(NOR), the more electronegative group was in the equatorial plane, which was contrary to what is usually found in five-coordinate trigonal bipyramidal structures (21).

The packing of the molecules in the unit cell is shown in Fig. 3. In the ***b*** direction the molecules were stacked directly above each

Can. J. Chem. Downloaded from www.nrcresearchpress.com by 210.87.254.5 on 09/05/12
For personal use only.

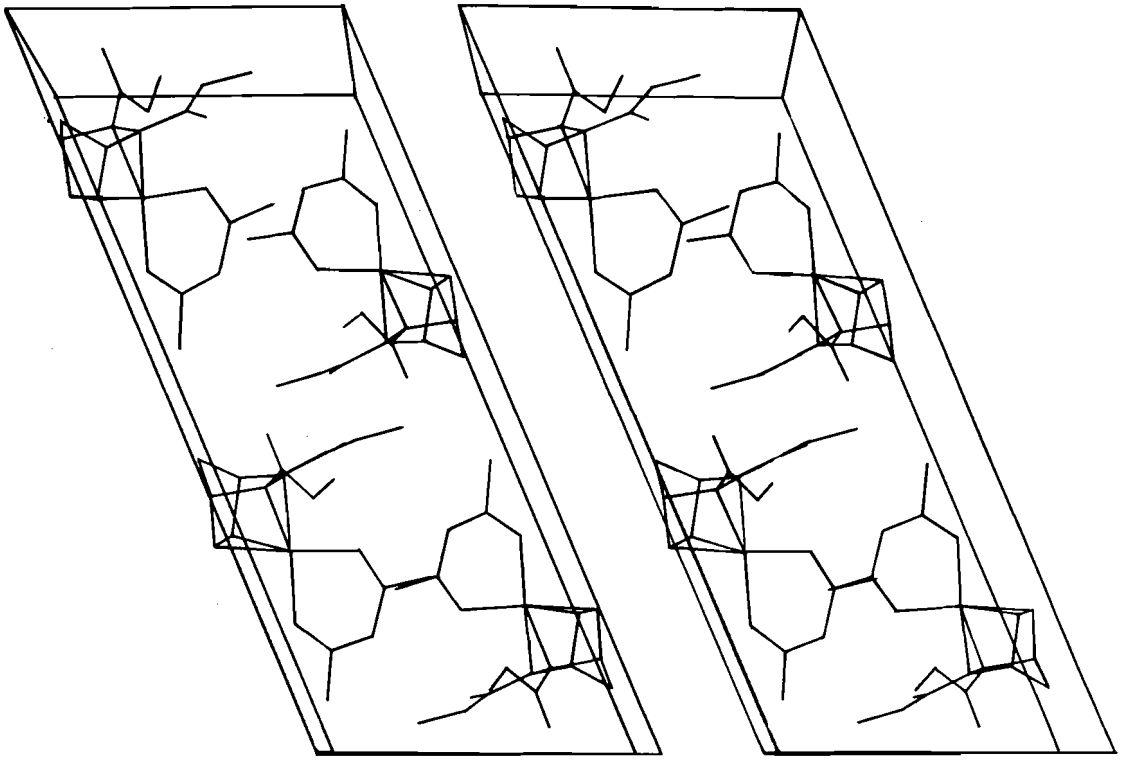

FIG. 3. Stereogram (stereoscopic pair of perspective projections) of the contents of the unit cell viewed down the ***b*** axis. The ***a*** axis is parallel to the top of the page and the c^* axis is parallel to the side of the page.

other and contact was between a carbomethoxo group on one molecule and the norbornadiene group of the next molecule. The space between the β-ketoenolate rings was occupied by the methyl group of the β-ketoenolate ring on the next molecule in the ***a*** direction. Thus, the β-ketoenolate rings of molecules related by x,y,z; $-x,\frac{1}{2}+y,\frac{1}{2}-z$, were interleaved in the ***b*** direction. For this same pair of molecules, the remaining contacts, in the ***a*** direction, were between the methyl group of a carbomethoxo unit on one molecule and a methyl group on the β-ketoenolate ring on the next molecule. The alternate set of contacts in the ***a*** direction was primarily between the norbornadiene group on one molecule and the β-ketoenolate ring in the next. In addition, there were contacts between the two norbornadiene groups. In the ***c*** direction, contact was between the methyl group on a carbomethoxo group on one molecule and the oxo unit of the carbomethoxo group on the next molecule. There was also contact between a β-ketoenolate methyl group on one molecule and the bridgehead hydrogen atoms of the norbornadiene group on the next. All contacts mentioned above were at or slightly more than the distances calculated for van der Waals contact.

We thank the National Research Council of Canada for financial support of this work.

1. R. P. HUGHES, N. KRISHNAMACHARI, C. J. L. LOCK, and J. POWELL. To be published.
2. J. A. EVANS and D. R. RUSSELL. Chem. Commun. 197 (1971).
3. L. J. GUGGENBERGER and R. CRAMER. J. Am. Chem. Soc. **94**, 3779 (1972).
4. R. CRAMER. Inorg. Chem. **1**, 722 (1962).
5. C. K. JOHNSON, U.S.A.E.C. Report ORNL-3794. Revised June 1965.
6. J. A. IBERS. International tables for X-ray crystallography. Vol. III. Kynoch Press, Birmingham. 1962.
7. D. T. CROMER and J. T. WABER. Acta Cryst. **18**, 104 (1965).
8. D. T. CROMER. Acta Cryst. **18**, 17 (1965).
9. T. G. APPLETON, H. C. CLARK, and L. E. MANZER. Coord. Chem. Rev. **10**, 335 (1973).
10. R. MASON and A. D. C. TOWL. J. Chem. Soc. A, 1601 (1970).
11. I. D. BROWN and R. D. SHANNON. Acta Cryst. A**29**, 266 (1973).
12. M. J. S. DEWAR. Bull. Soc. Chim. Fr. **18**, C71 (1951).

Can. J. Chem. Downloaded from www.nrcresearchpress.com by 210.87.254.5 on 09/05/12
For personal use only.

13. J. A. CHATT and L. A. DUNCANSON. J. Chem. Soc. 2939 (1953).
14. G. DALLINGA and L. H. TONEMAN. Rec. Trav. Chim. **87**, 205 (1968).
15. A. YOZOKEI and K. KUCHITSU. Bull. Chem. Soc. Jpn. **44**, 2356 (1971).
16. N. C. BAENZIGER, G. F. RICHARDS, and J. R. DOYLE. Acta Cryst. **18**, 924 (1965).
17. C. NAVE and M. R. TRUTER. J. Chem. Soc. Dalton, 2202 (1973).
18. P. B. HITCHCOCK, M. MCPARTLIN, and R. MASON. Chem. Commun. 1367 (1969).
19. A. IMMIRZI and G. ALLEGRA. Acta Cryst. B**25**, 120 (1969).
20. J. COETZER and G. GAFNER. Acta Cryst. B**26**, 985 (1970).
21. R. J. GILLESPIE. Molecular geometry. Van Nostrand Reinhold Co., New York. 1972. p. 68.
22. M. C. FREDETTE and C. J. L. LOCK. Can. J. Chem. In press.
23. J. C. BARRICK, M. C. FREDETTE and C. J. L. LOCK. Can. J. Chem. **51**, 317 (1973).

Can. J. Chem. Downloaded from www.nrcresearchpress.com by 210.87.254.5 on 09/05/12
For personal use only.

Electron Mobilities and Ranges in Liquid Hydrocarbons: Cyclic and Polycyclic, Saturated and Unsaturated Compounds[1]

KYOJI SHINSAKA, JEAN-POL DODELET, AND GORDON R. FREEMAN
Chemistry Department, University of Alberta, Edmonton, Alberta T6G 2G2
Received March 24, 1975

KYOJI SHINSAKA, JEAN-POL DODELET, and GORDON R. FREEMAN. Can. J. Chem. **53**, 2714 (1975).

Penetration ranges b_{GP} of secondary electrons into 21 X-irradiated liquids were estimated from measured free ion yields. The density normalized ranges $b_{GP}d$ are independent of temperature. Increasing the molecular symmetry by creating one or more cycles in the molecule causes the normalized range to increase, provided that the amount of bond distortion due to strain remains small. Ranges are smaller in compounds that contain strained rings. Energy transfer from the secondary electrons to the molecules is enhanced by the presence of distorted bonds in the molecules. The ranges in olefins are affected by the same factors as those in saturated hydrocarbons, with the addition of a contribution of transient negative ion states to the energy transfer processes. Shielding the double bond by methyl groups is not effective; the effect of the added methyl groups on the molecular symmetry is a more important factor. The magnitude of the energy transfer interaction is an inverse function of molecular symmetry.

The general correlation between b_{GP} and thermal electron mobilities u_e in liquids contains significant variations within it. For a given value of b_{GP}, u_e in different liquids increases in the order *n*-alkane < cycloalkane < cycloalkene < 1,4-cyclohexadiene or benzene. Arrhenius plots of u_e in cyclic olefins curve downwards at low temperatures, due to the formation of a deeper trapped state of the electron. The trap is deepest in 1,4-cyclohexadiene (21 kcal/mol) and is attributed to an equilibrium between solvated electrons and anions at temperatures below about 280 K.

KYOJI SHINSAKA, JEAN-POL DODELET et GORDON R. FREEMAN. Can. J. Chem. **53**, 2714 (1975).

Les parcours des électrons secondaires, b_{GP}, ont été estimés d'après les rendements en ions libres mesurés dans 21 liquides irradiés aux rayons X. Normalisés pour la densité, ces parcours, $b_{GP}d$, deviennent indépendants de la température. Une augmentation de la symétrie moléculaire par cyclisation simple ou multiple entraîne une augmentation du parcours normalisé, tant que la distorsion des liaisons demeure faible. Un important transfert d'énergie des électrons secondaires est réalisé dans le cas de molécules à cycle tendu, ce qui réduit le parcours des électrons dans de tels liquides. Les parcours électroniques dans les oléfines sont fonction des mêmes facteurs que dans les alcanes, avec en plus la possibilité d'un transfert d'énergie via la tendance à former un ion négatif éphémère. L'addition de groupes méthyles ne protège pas une double liaison, mais affecte la symétrie moléculaire. L'importance de la quantité d'énergie transférée par collision est une fonction inverse de la symétrie moléculaire. La corrélation générale entre b_{GP} et la mobilité de l'électron thermique dans les liquides présente une structure fine. Pour une valeur de b_{GP} donnée, u_e augmente selon l'ordre suivant: *n*-alcane < cycloalcane < cycloalcène < cyclohexadiène-1,4 ou benzène. La courbe obtenue en portant u_e selon l'inverse de la température présente pour les oléfines cycliques une courbure importante à basse température, prouvant l'existence d'électrons piégés dans les trappes plus profondes. Une profondeur maximum de 21 kcal/mol dans le cas du cyclohexadiène-1,4 est attribuée à un équilibre entre l'électron solvaté et l'anion qui se manifeste aux environs de 280 K et moins.

Introduction

The mobilities of thermal electrons in liquid hydrocarbons and the penetration ranges of epithermal electrons in the liquids both tend to be larger when the constituent molecules are more highly branched (1, 2). The effect of branching is not basically understood, but it seems to be associated with the fact that the more highly branched molecules are more nearly spherelike in external shape (2, 3).

The correlations of electron mobility and range with molecular shape have mainly been determined using open chain molecules, with methyl groups branching outward from a central chain or core to increase the degree of sphericity. When the liquid is made up of large molecules the effective radius of interaction of

[1]Financially assisted by the National Research Council of Canada.

Can. J. Chem. Downloaded from www.nrcresearchpress.com by 210.87.254.105 on 09/05/12
For personal use only.

Can. J. Chem. Downloaded from www.nrcresearchpress.com by 210.87.254.105 on 09/05/12
For personal use only.

the electron does not encompass the whole molecule, but seems to be limited to groups containing only two carbon–carbon bonds in series (4). This includes groups up to neopentyl in size. The average interaction of an electron with a large open chain molecule in the liquid phase is therefore the average of the interactions with its constituent groups containing two C—C bonds in series.

As an alternative to chain branching, the degree of sphericity of molecules can be increased by constructing one or more rings in them. The small amount of information available about the effect of cyclic structures cannot be explained by one model alone, because the density-normalized range of epithermal electrons in cyclopropane is smaller than that in propane (5), whereas the normalized ranges cyclopentane and cyclohexane are slightly greater than those in the corresponding *n*-alkanes (6). In the present work the effect of cyclization has been investigated further by measuring electron ranges and mobilities in several mono- and polycyclic hydrocarbons. Both saturated and unsaturated compounds were used. The molecular structure dependence of electron behavior in liquid olefins (7, 8) is peculiar and is not even qualitatively understood. The search for a key to the understanding continues.

Experimental

Materials

The purities of the hydrocarbons obtained from the suppliers were ≥99%. Cyclopentane, cyclohexane, cyclopentene, and benzene were Phillips Research Grade. Cycloheptane, cyclooctane, bicyclo[2,2,1]heptane, bicyclo[2,2,2]octane, 1,2-dimethylcyclohexene, 1,3-dimethylcyclohexene, cycloheptene, *cis*-cyclooctene, bicyclo[2,2,1]-hept-2-ene, bicyclo[2,2,1]hepta-2,5-diene, 1,3-cyclohexadiene, and 1,4-cyclohexadiene were from Chemical Samples Co. Adamantane, α(+)pinene, and α(−)pinene were from Aldrich Chemicals Co.

The compounds were purified as follows.

Cyclopentane, cyclohexane, cycloheptane, cyclooctane, and benzene were shaken with concentrated sulfuric acid, washed with distilled water, dried over CaO, then stirred under vacuum successively with KOH pellets, $LiAlH_4$, and Na–K alloy. Each purification step lasted at least 3 h.

1,3-Cyclohexadiene and 1,4-cyclohexadiene reacted with Na–K alloy. The former reacted rapidly to form a heavy, brown precipitate. The latter reacted slowly to produce benzene and hydrogen. In preparation for the measurement of the free ion yields, both liquids were stirred under vacuum with KOH pellets, then with $LiAlH_4$, then electrolyzed under vacuum before the final distillation into the measurement cell. An electron conductance transient (e.c.t.) signal could not be obtained in the 1,3-diene, due to rapid reaction of the electrons with the diene to form negative ions. A large e.c.t. signal was obtained, however, in the 1,4-diene. To increase the half-life of the e.c.t., and thereby the accuracy of the mobility measurement, the 1,4-diene was stirred for about 2 h with Na–K alloy to reduce the concentration of electron scavengers. The amount of benzene in the resulting liquid was 1.7%, measured by gas chromatography. Various concentrations of purified benzene were also added to the 1,4-diene, to permit extrapolation of the electron mobility to that in pure diene.

Bicyclo[2,2,1]heptane was stirred with Na–K alloy and distilled under vacuum.

Bicyclo[2,2,2]octane and α(+)- and α(−)pinene were distilled under vacuum and electrolyzed for 1 h at 1 kV/cm.

Adamantane was recrystallized from *n*-heptane. All attempts to purify liquid adamantane, m.p. 541 K, were unsuccessful. The background conductance of the liquid at the high temperatures involved was too large to permit measurement of the free ion yield. Measurements were therefore made on a nearly saturated solution of adamantane in *n*-heptane.

Cyclopentene, 1,2-dimethylcyclohexene, 1,3-dimethylcyclohexene, cycloheptene, and *cis*-cyclooctene were stirred under vacuum successively with KOH pellets, $LiAlH_4$, and Na–K alloy.

Bicyclo[2,2,1]heptene and bicyclo[2,2,1]heptadiene reacted with Na–K alloy to form a brown precipitate. These olefins were simply stirred under vacuum with $LiAlH_4$ and distilled.

All of the compounds were degassed by vacuum distillation or sublimation. The pressure of gas that was not condensable at 77 K was reduced to $< 5 \times 10^{-6}$ Torr before the sample cell was sealed off.

The electrolysis step in the above purification procedures has been found to be unnecessary when the sample background conductance is low, and useless when the background conductance is high. The step was therefore abandoned in the latter part of the present work.

Apparatus and Techniques

The equipment and methods of measurement were described earlier (7, 8). Briefly, a 1 μs (or 0.1 μs) pulse of 1.7 MeV X-rays delivered 3×10^{10} eV/g (or 5×10^{9} eV/g) to the sample. The free ion yield G_{fi} was measured by the charge clearing technique. The value of the product of the free ion yield and the electron mobility, $G_{fi}u_e$, was obtained from the peak magnitude of the electron conductance transient (e.c.t.), corrected for decay during the radiation pulse if necessary. The positive ion mobility u_+ was assumed to be negligible in comparison to u_e. The value of u_e was calculated from the ratio $(G_{fi}u_e/G_{fi})$.

Physical Properties of the Liquids

The densities d (9–12) and dielectric constants ε (12–14) of the liquids were obtained from the references indicated or measured during the present work. Values are recorded in Table 1. The total ionization yields in the liquids are not known. For lack of better information they were taken equal to the average gas phase value for long chain alkanes, $G_{tot} = 4.3$ (15).

Can. J. Chem. Downloaded from www.nrcresearchpress.com by 210.87.254.105 on 09/05/12
For personal use only.

TABLE 1. G_{fi}^0 and most probable electron range b_{GP} in liquid cyclic hydrocarbons

Liquid	T (K)	d (g/cm^3)[a]	ε	μ (D)	G_{fi}^0	b_{GP} (Å)[b]	$b_{GP}d$ (10^{-8} g/cm^2)	$(b_{GP}d)_{av}$ (10^{-8} g/cm^2)
			Monocyclic alkanes					
Cyclopentane	189	0.848	2.13[c]	0.0	0.068	66	56	56
	210	0.827	2.10		0.090	67	55	
	236	0.802	2.06		0.13	69	55	
	270	0.768	2.00		0.18	72	55	
	295	0.743	1.96		0.23	75	56	
	311	0.728	1.94		0.26	76	56	
	323	0.716	1.92		0.30	78	56	
Cyclohexane	295	0.777	2.02[d]	0.0	0.20	67	52	52
Cycloheptane	269	0.832	2.12[e]	0.0	0.14	62	52	52
	281	0.817	2.10		0.16	63	51	
	295	0.808	2.07		0.19	64	52	
	322	0.784	2.04		0.23	66	52	
	338	0.770	2.01		0.26	67	52	
	360	0.750	1.98		0.31	70	53	
Cyclooctane	296	0.831	2.11[e]	0.0	0.17	61	51	51
	313	0.816	2.09		0.20	62	50	
	328	0.801	2.07		0.23	63	51	
	343	0.788	2.05		0.26	64	50	
	360	0.772	2.03		0.29	66	51	
	384	0.749	1.99		0.35	69	51	
	406	0.728	1.96		0.40	71	52	
			Polycyclic alkanes					
Bicyclo[2,2,1]heptane	374	0.80[e]	2.00[f]	~0	0.59	95	76	76
Bicyclo[2,2,2]octane	450	0.762[e]	2.06[e]	0.0	1.36	153	117	117
Adamantane	396	—	—	~0	—	—	—	90[g]

Can. J. Chem. Downloaded from www.nrcresearchpress.com by 210.87.254.105 on 09/05/12
For personal use only.

TABLE 1 (*Continued*)

Liquid	T (K)	d (g/cm^3)[a]	ε	μ (D)	G_{f1}^0	b_{GP} (Å)[b]	$b_{GP}d$ (10^{-8} g/cm^2)	$(b_{GP}d)_{av}$ (10^{-8} g/cm^2
			Monocyclic alkenes					
Cyclopentene	181	0.894	2.35[e]	0.20[h]	0.038	49	44	45
	214	0.858	2.27		0.058	52	44	
	240	0.830	2.21		0.081	54	45	
	273	0.794	2.13		0.12	57	45	
	296	0.769	2.08		0.15	58	45	
	316	0.747	2.03		0.18	60	45	
Cyclohexene	293	0.813	2.23	0.55[h]	0.20	62	51	51
1,2-Dimethylcyclohexene	231	0.877	2.25[e]		0.070	52	46	46
	263	0.850	2.20		0.099	54	46	
	292	0.826	2.15		0.13	55	46	
	321	0.802	2.10		0.17	58	46	
	364	0.765	2.04		0.24	60	46	
1,3-Dimethylcyclohexene	214	0.865	2.36[e]		0.061	51	44	45
	252	0.835	2.27		0.096	54	45	
	292	0.803	2.19		0.15	56	45	
	332	0.771	2.11		0.21	60	46	
	372	0.739	2.04		0.28	64	47	
Cycloheptene	229	0.882	2.43[e]		0.067	48	42	43
	254	0.860	2.36		0.089	49	42	
	269	0.847	2.33		0.10	50	42	
	296	0.823	2.26		0.14	52	43	
	333	0.790	2.18		0.19	55	43	
	354	0.772	2.14		0.23	57	44	
cis-Cyclooctene	270	0.858	2.37[e]		0.092	47	40	41
	296	0.846	2.31		0.12	47	40	
	321	0.834	2.25		0.14	48	40	
	339	0.825	2.22		0.16	49	40	
	360	0.815	2.18		0.19	50	41	
	382	0.804	2.13		0.22	52	42	
	406	0.793	2.08		0.25	53	42	
			Polycyclic alkenes					
Bicyclo[2,2,1]heptene	336	0.837[e]	2.08[f]		0.19	57	47	48
	352	0.822	2.05		0.22	58	48	
	373	0.803	2.02		0.26	60	48	

Can. J. Chem. Downloaded from www.nrcresearchpress.com by 210.87.254.105 on 09/05/12
For personal use only.

TABLE 1 (*Concluded*)

Liquid	T (K)	d (g/cm^3)[a]	ε	μ (D)	G_{fl}^0	b_{GP} (Å)[b]	$b_{GP}d$ (10^{-8} g/cm^2)	$(b_{GP}d)_{av}$ (10^{-8} g/cm^2)
α(+)pinene	231	0.909	2.36[e]		0.068	48	44	46
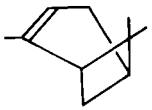	260	0.885	2.30		0.095	50	44	
	293	0.857	2.23		0.14	53	45	
	327	0.828	2.16		0.19	56	46	
	356	0.803	2.10		0.24	59	47	
	391	0.774	2.04		0.32	63	49	
	421	0.749	1.98		0.39	66	50	
α(−)pinene	229	0.911	2.36[e]		0.065	48	44	45
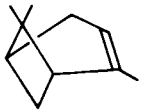	258	0.886	2.31		0.093	50	44	
	293	0.857	2.23		0.13	52	44	
	321	0.833	2.18		0.17	54	45	
	347	0.810	2.12		0.21	56	46	
	379	0.784	2.06		0.28	60	47	
	416	0.753	1.99		0.35	64	48	
			Monocyclic alkadienes					
1,3-Cyclohexadiene	233	0.908	2.50[e]	0.44[h]	0.050	40	37	34
	261	0.877	2.42		0.060	40	35	
	292	0.842	2.35		0.075	40	34	
	323	0.808	2.30		0.096	41	33	
	354	0.773	2.24		0.11	40	31	
1,4-Cyclohexadiene	233	0.924	2.33[e]	0.0	0.14	64	59	57
	266	0.888	2.27		0.18	65	57	
	295	0.855	2.21		0.23	66	56	
	313	0.835	2.18		0.26	67	56	
	342	0.814	2.14		0.30	67	55	
	351	0.793	2.10		0.34	70	56	
			Polycyclic alkadienes					
Bicyclo[2,2,1]heptadiene	293	0.909	2.16[c]		0.053	38	34	34
	328	0.874	2.10		0.071	39	34	
	352	0.851	2.06		0.087	40	34	
	387	0.817	2.00		0.12	43	35	

[a]References 9–11, except for the compounds noted.
[b]Based on the assumed value $G_{tot} = 4.3$.
[c]$\varepsilon \approx n_D^2$ when the molecular dipole moment is small. The value of n_D^2 at one temperature was obtained from ref. 9 and the Lorentz–Lorenz equation was used to calculate the values at other temperatures: molar refraction $R = (M/d)(n_D^2 - 1)/(n_D^2 + 2)$, where M is the molar weight.
[d]Reference 13.
[e]This work.
[f]Calculated from molar refraction increments from ref. 14.
[g]Extrapolated from the values for *n*-heptane and the adamantane–heptane solution, see Table 2.
[h]Reference 22. The zero values in the present table are estimates based on molecular symmetry.

Can. J. Chem. Downloaded from www.nrcresearchpress.com by 210.87.254.105 on 09/05/12
For personal use only.

Results

Free Ion Yields

Free ion yields $G_{fi}{}^{E}$ were measured at applied electric field strengths E in the range 2 to 20 kV/cm. The yields increased with field strength in the manner illustrated in Figs. 1 and 2. The curves were extrapolated to zero field strength to obtain $G_{fi}{}^{0}$, using [1] (8, 16).

$$[1] \qquad G_{fi}{}^{E} = G_{tot} \int_0^\infty F(y)\phi(y,E)\,dy$$

where G_{tot} is the total number of ion–electron pairs generated per 100 eV absorbed by the liquid, $F(y)dy$ is the fraction of thermalized electron–ion pairs that have initial intrapair separation distances between y and $y + dy$, and $\phi(y,E)$ is the probability that a pair with a given separation distance y will escape geminate neutralization (become free ions) in the presence of an applied field E (V/cm).

$$[2] \qquad \phi(y,E) = e^{-r/y}\left[1 + e^{-\beta y}\sum_{n=1}^{\infty}\frac{(\beta y)^n}{(n+1)!}\sum_{j=0}^{n-1}(n-j)\frac{(r/y)^{j+1}}{(j+1)!}\right]$$

where $r = \xi^2/\varepsilon kT$, $\xi = 4.803 \times 10^{-10}$ e.s.u., k is Boltzmann's constant, T is the absolute temperature, and $\beta = (\xi E/300kT)$.

The distribution function $F(y)$ was taken to have the form [3], which has been shown to be suitable for many liquids and has been designated YGP (8, see also footnote 3 on p. 3500 of ref. 17).

$$[3] \qquad \begin{cases} F(y) = 0.96\ \mathrm{YG} & y < 2.4b_{GP} \\ F(y) = 0.96(\mathrm{YG} + 0.5b_{GP}{}^2/y^3) & y > 2.4b_{GP} \end{cases}$$

where 0.96 is a normalization factor, YG is the three dimensional Gaussian function $(4y^2/\pi^{1/2}b_{GP}{}^3)\exp(-y^2/b_{GP}{}^2)$, and b_{GP} is the adjustable dispersion parameter. The dispersion parameter is also equal to the most probable value of y. Distribution function [3] is a Gaussian that has been extended to larger y values by the addition of a more gently decreasing power function tail.

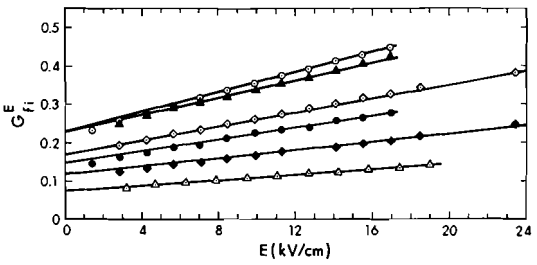

FIG. 1. Free ion yields $G_{fi}{}^{E}$ at field strength E in monocyclic hydrocarbons at 294 ± 2 K. ○, cyclopentane; ●, cyclopentene; ▲, 1,4-cyclohexadiene; △, 1,3-cyclohexadiene; ◇, cyclooctane; ◆, *cis*-cyclooctene. The lines were calculated from [1]–[3] using the parameter values in Table 1.

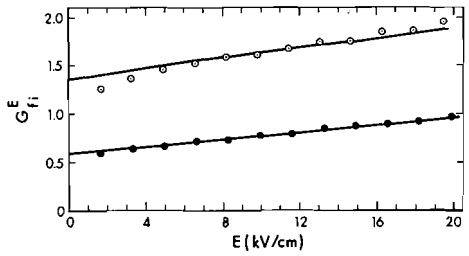

FIG. 2. Free ion yields $G_{fi}{}^{E}$ at field strength E in bicyclo[2,2,2]octane at 450 K (○), and in bicyclo[2,2,1]-heptane at 374 K (●). The lines were calculated from [1]–[3], using the parameter values in Table 1.

The terms in the infinite series in [2] display a maximum at some value of $n \geqslant 1$. The summation was terminated at $n = k$ such that the value of the kth term was $<10^{-3}$ of the maximum term value, or at $n = 55$, whichever came first. Termination at $n = 55$ was necessary because the computer saturated at (56!). The summation reached $n = 55$ when β or y was very large, in which case $\phi(y,E) = 0.999...$ and was placed equal to unity.

To fit a curve to a set of $G_{fi}{}^{E}$ *vs.* E results for a given liquid at a given temperature, a preliminary value of b_{GP} was chosen and $G_{fi}{}^{E}$ was calculated for each experimental value of E. Calculated and experimental yields were compared by calculating the average % error:

$$[4] \qquad \text{Average \% error} = 100\sum|G^E_{fi,calc} - G^E_{fi,exp}|/\sum G^E_{fi,exp}$$

The calculations were repeated with a series of b_{GP} values to find the one that gave the minimum

Can. J. Chem. Downloaded from www.nrcresearchpress.com by 210.87.254.105 on 09/05/12
For personal use only.

TABLE 2. G_{fi}^0 and most probable electron range b_{GP} in *n*-heptane–adamantane and benzene–1,4-cyclohexadiene solutions[a]

Liquid	T (K)	d (g/cm^3)[b]	ε[b]	G_{fi}^0	b_{GP} (Å)[c]	$b_{GP}d$ (10^{-8} g/cm^2)	$(b_{GP}d)_{av}$ (10^{-8} g/cm^2)
			n-Heptane–Adamantane				
n-Heptane	396	0.59[d]	1.76[f]	0.38	79	47	47
35% adamantane	396	0.74	1.96	0.40	73	54	54
			Benzene–1,4-Cyclohexadiene (1,4-CHD)				
% 1,4-CHD							
98.3	259	0.896	2.28	0.16	61	55	54
	272	0.882	2.26	0.17	62	55	
	281	0.871	2.24	0.19	62	54	
	296	0.854	2.21	0.21	64	54	
	312	0.836	2.18	0.24	65	54	
	332	0.814	2.14	0.28	66	54	
90.3	259	0.897	2.29	0.16	62	56	55
	272	0.883	2.26	0.18	63	55	
	282	0.872	2.24	0.20	63	55	
	294	0.858	2.22	0.22	64	55	
66.7	269	0.892	2.28	0.065	43	38	40
	280	0.880	2.26	0.078	45	40	
	296	0.862	2.23	0.10	46	40	
	313	0.843	2.20	0.12	48	41	
	333	0.821	2.16	0.15	49	40	
0.0							
(pure benzene)	282	0.891[e]	2.30[e]	0.070	41	37	37
	294	0.878	2.28	0.080	42	37	
	314	0.857	2.24	0.095	43	37	
	333	0.837	2.21	0.12	44	37	

[a]All % are given by weight.
[b]Calculated by assuming ideal solutions.
[c]Based on the assumed value $G_{tot} = 4.3$.
[d]This work.
[e]Reference 12.
[f]Calculated from molar refraction increments from ref. 14.

Can. J. Chem. Downloaded from www.nrcresearchpress.com by 210.87.254.105 on 09/05/12
For personal use only.

average % error. This value of b_{GP} was then used to calculate G_{fi}^0.

$$[5] \qquad G_{fi}^0 = G_{tot} \int_0^\infty F(y)\, e^{-r/y}\, dy$$

Examples of best-fit curves calculated for a number of liquids are shown in Figs. 1 and 2. Agreement between calculation and experiment became less good at high temperatures, where the calculated slope was somewhat lower than the experimental slope (*e.g.* bicyclo[2,2,2]octane curve in Fig. 2).

The values of b_{GP} and G_{fi}^0 obtained in the above manner for different compounds over a range of temperatures are listed in Table 1. To normalize the ranges b_{GP} for comparison between liquids, they were multiplied by the liquid density d. The density normalized range $b_{GP}d$ in a given liquid was essentially independent of temperature (Table 1).

In spite of extended attempts to purify adamantane and to degas it prior to melting, it always turned yellow upon melting (m.p. 541 K) and had a high background conductance. The free ion yields were therefore measured in a 35 wt.% solution of adamantane in *n*-heptane and in pure *n*-heptane, both at 396 K (Table 2). The density normalized range $b_{GP}d$ was extrapolated to pure adamantane with the aid of a plot of $(b_{GP}d)^{-2}$ against wt.% adamantane (6). The value so obtained, $b_{GP}d$(adamantane) = 90×10^{-8} g/cm^2, is included in Table 1.

Although the 99% pure 1,4-cyclohexadiene obtained from Chemical Samples Co. was adequate for the measurement of free ion yields, it had to be treated with Na–K alloy before electron mobilities could be measured in it. The alloy treatment generated benzene, so the e.c.t. measurements were actually made on benzene solutions. To extract electron mobilities from the e.c.t. measurements it was necessary to measure free ion yields in diene–benzene solutions. The results are listed in Table 2. The yields in benzene are in good agreement with those reported earlier from this laboratory (17). However, it is probably worth repeating that yields from this laboratory (4, 8, 17) are usually larger by a factor of 1.4 ± 0.2 than those reported by Schmidt and Allen (1, 6).

Electron Mobilities

Electron mobilities were measured in 13 of the present liquids and the values are listed in Table 3. The mobilities were independent of applied electric field strength over the range 2–20 kV/cm.

An e.c.t. signal could not be obtained in 1,3-cyclohexadiene, bicyclo[2,2,1]heptene, or bicyclo[2,2,1]heptadiene due to reaction of the electrons with the olefins. The lack of an e.c.t. signal in the adamantane–heptane solution was doubtless due to the presence of a trace of electron scavenging impurity, because the difficulty of transferring adamantane under vacuum prevented its purification with Na–K alloy. The pinenes were also difficult to purify and showed no e.c.t. signal.

The mobilities in pure 1,4-cyclohexadiene (Table 3) were estimated from those in the diene–benzene solutions by extrapolation of plots of log u_e against mole fraction of benzene (Fig. 3). The mobilities measured in the solutions are listed in Table 4. A given curve in Fig. 3 requires that the mobility in each solution be known at the same temperature, which was difficult to achieve experimentally. The mobilities in Fig. 3 were therefore taken at appropriate temperatures from the curves in Fig. 4.

TABLE 3. Thermal electron mobilities (u_e) in cyclic hydrocarbons

Liquid	T (K)	u_e (cm^2 V^{-1} s^{-1})
Monocyclic alkanes		
Cyclopentane	236	0.24
	252	0.43
	270	0.84
	295	1.4
	311	1.9
	323	2.2
Cyclohexane[a]	294	0.45
	315	0.62
	340	0.89
	380	1.4
	395	1.7
Cycloheptane	269	0.23
	281	0.33
	295	0.44
	307	0.56
	322	0.69
	338	0.96
Cyclooctane	296	0.17
	313	0.24
	328	0.29
Polycyclic alkanes		
Bicyclo[2,2,1]heptane	374	4.4
Bicyclo[2,2,2]octane	450	15

TABLE 3 (*Concluded*)

Liquid	T (K)	u_e (cm^2 V^{-1} s^{-1})
Monocyclic alkenes		
Cyclopentene	214	0.045
	228	0.11
	240	0.28
	254	0.44
	273	0.75
	296	1.3
	316	2.2
Cyclohexene[b]	293	1.0
	313	1.5
	324	1.8
	338	2.2
1,2-Dimethylcyclohexene	293	0.11
	313	0.24
	332	0.34
	354	0.51
1,3-Dimethylcyclohexene	293	0.068
	302	0.11
	314	0.15
Cycloheptene	254	0.040
	269	0.091
	280	0.19
	296	0.35
	312	0.56
	333	0.78
	354	1.1
cis-Cyclooctene	321	0.021
	339	0.065
	360	0.14
	382	0.19
Monocyclic alkadiene		
1,4-Cyclohexadiene[c]	259	0.3
	263	0.5
	270	1.3
	278	2.9
	286	4.6
	294	5.8
	313	7.5
	333	8.8

[a]Reference 4.
[b]Reference 7.
[c]Extrapolated from the mobilities in 1,4-cyclohexadiene–benzene solutions presented in Table 4.

The mobilities in benzene obtained in the present work were on the average 7% higher than those reported earlier from this laboratory (17). The value at 300 K is fourfold lower than that given by Minday *et al.* (18) for that temperature. The latter measurements seem to have been affected by background currents.

Discussion

Free Ion Yields and Secondary Electron Ranges

One of the long term objectives of these studies is to learn about the processes that govern energy transfer from subelectronic excitation energy electrons to liquids (19). The processes are phase dependent (20). Preliminary information about the combined effects of inelastic and

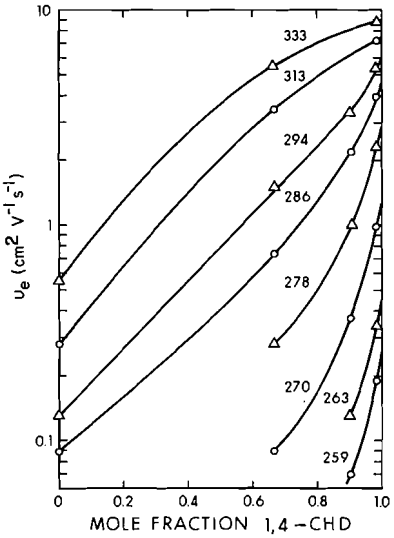

FIG. 3. Electron mobilities in 1,4-cyclohexadiene–benzene solutions plotted against the mole fraction of diene. The numbers labelling the curves indicate the absolute temperature.

TABLE 4. Thermal electron mobilities (u_e) in 1,4-cyclohexadiene–benzene solutions

Wt.% 1,4-CHD	T (K)	u_e (cm^2 V^{-1} s^{-1})
98.3	259	0.19
	272	1.2
	281	3.1
	296	5.7
	312	6.8
	332	8.7
90.3	259	0.070
	272	0.47
	282	1.7
	294	3.3
66.7	269	0.068
	280	0.40
	296	1.7
	313	3.5
	333	5.5
0.0 (pure C_6H_6)	282	0.078
	294	0.13
	304	0.19
	314	0.30
	324	0.44
	333	0.55

Can. J. Chem. Downloaded from www.nrcresearchpress.com by 210.87.254.105 on 09/05/12
For personal use only.

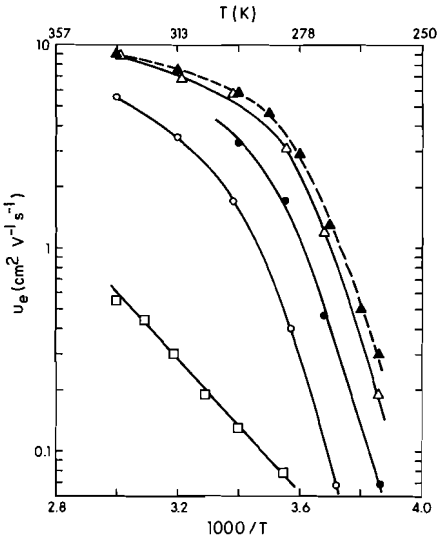

FIG. 4. Arrhenius plots of electron mobilities in 1,4-cyclohexadiene–benzene solutions and in pure benzene. Mol.% 1,4-cyclohexadiene: ▲, 100 (extrapolated u_e); △, 98.3; ● ,90.3; ○, 66.7; □, 0.0 (pure benzene). The curves were calculated using [12] and the parameter values in Table 5.

elastic scattering is obtained from the relative penetration ranges b_{GP} of secondary electrons into different liquids. The penetration ranges are inversely related to the efficiencies of the scattering processes.

The value of b_{GP} is calculated from $G_{fi}{}^{E}$ and G_{tot}. Values of G_{tot} in liquid alkanes might be about 25% greater than the corresponding gas phase values (21), but liquid phase values are in general not known. For the sake of consistency over a wide range of compounds, it is customary to take G_{tot} equal to the corresponding gas phase value (1, 4–6, 8).

To compare electron behavior in different liquids, a more convenient parameter than the range itself is the density-normalized range $b_{GP}d$. The density-normalized range in a given liquid is independent of temperature (Table 1) and compensates for the simple inverse variation of electron range with liquid density.

Monocyclic Alkanes

The density-normalized range of secondary electrons in cycloalkanes increases with increasing symmetry of the molecule, providing the strain in the C—C bonds remains small.

The normalized ranges in cyclopentane (56×10^{-8} g/cm^2) and cyclohexane (52×10^{-8} g/cm^2) are larger than those in *n*-pentane (44×10^{-8} g/cm^2) and *n*-hexane (46×10^{-8} g/cm^2) (8). The normalized ranges are essentially the same in cyclohexane, cycloheptane, and cyclooctane (Table 1), so the six-membered ring has no special properties in this regard (as it does in molecular packing, reflected in the melting points of the hydrocarbons (11)). The normalized ranges in the *n*-C_6–C_8 hydrocarbons are also equal (6) and uniformly lower than those in the cycloalkanes.

However, the range in cyclopropane (38×10^{-8} g/cm^2) is lower than that in propane (52×10^{-8} g/cm^2) (5). This is attributed to efficient energy transfer from the secondary electrons to the molecules by way of interaction with the peculiar bonds in the strained ring. Cyclopropane has a partially olefinic nature, which correlates with the fact that the normalized electron range in this liquid is intermediate between those in propane and propylene (5).

Polycyclic Alkenes

The large ranges in the polycyclic alkanes (Table 1) appear to be associated with the high degree of sphericity, relative rigidity, and lack of distorted orbitals (bond strain) in these molecules.

Bicyclo[2,2,2]octane is the most spherelike of the present molecules and the normalized range (117×10^{-8} g/cm^2) is the greatest in that liquid. It is nearly as great as that in neopentane (128×10^{-8} g/cm^2) (4). Therefore, the correlation between electron range in a liquid and the degree of sphericity of the molecules, that exists for branched chain molecules (1–4), extends to polycyclic hydrocarbons.

Monocyclic Alkenes

The density normalized ranges $b_{GP}d$ of secondary electrons in alkenes are affected by the same factors as those in alkanes, with the addition of a possible contribution of transient negative ion states to the energy transfer processes. The extra energy transfer mode tends to decrease the electron range.

The normalized ranges in all the monocyclic alkenes studied (Table 1) are larger than that in the open chain *cis*-hexene-3 (38×10^{-8} g/cm^2 (8)), but smaller than those in the corresponding monocyclic alkanes.

Either the range in cyclopentene is abnormally low by comparison with the rest of the series or that in cyclohexene is abnormally high (Fig. 5). A low range in cyclopentene might be attributed to efficient energy transfer associated with strain

Can. J. Chem. Downloaded from www.nrcresearchpress.com by 210.87.254.105 on 09/05/12
For personal use only.

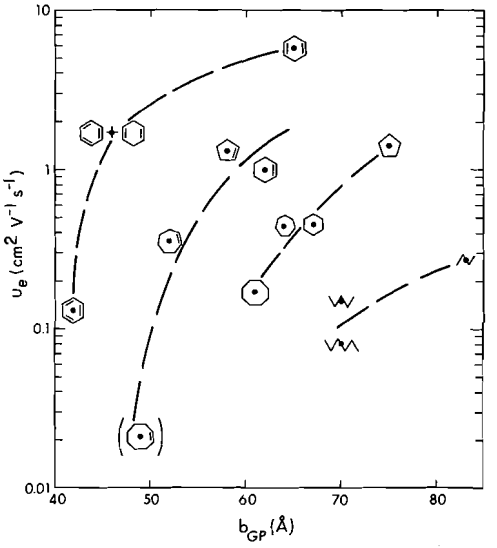

FIG. 5. Plots of u_e against b_{GP} for electrons in liquids at 295 ± 2 K, except for cyclooctene which was at 321 K. Values for the *n*-alkanes were taken from refs. 5–8 and 24. The symbols represent the carbon skeletons of the molecules. A point is included for the 66.7% cyclohexadiene solution in benzene.

in the olefinic five-membered ring, and an associated tendency of the molecule to accept an electron to form a negative ion. On the other hand, the relatively high degree of symmetry of cyclohexene might lead to a larger range in that liquid.

By analogy with behavior in *cis*-2-butene and 2,3-dimethyl-2-butene (8), it was suspected that shielding the double bond in cyclohexene might cause the electron range to increase. However, the normalized range in 1,2-dimethylcyclohexene is lower than that in cyclohexene (Table 1). Furthermore, the normalized range in 1,3-dimethylcyclohexene is essentially the same as that in the 1,2-isomer. Shielding the double bond by methyl groups is not important if it disrupts the symmetry of the molecule. Addition of methyl groups to the cyclohexene ring reduces the rotational symmetry of the molecule, which apparently increases the magnitude of the electron energy transfer interaction. It follows that the large range in 2,3-dimethyl-2-butene (72×10^{-8} g/cm^2) compared to that in *cis*-2-butene (46×10^{-8} g/cm^2) should be interpreted in terms of the greater molecular symmetry of the former, rather than in terms of shielding the double bond.

The present series of molecules have gas phase dipole moments ranging from 0.0 to 0.55 D (Table 1 and ref. 22). As noted previously (8), dipole moments were expected to influence the electron energy transfer interactions, but other effects apparently dominate that of the dipole moment in hydrocarbons. There is no detectable correlation between the electron normalized ranges $b_{GP}d$ and the gas phase molecular dipole moments (Table 1).

Polycyclic Alkenes

The ranges in the enantiomorphs α(+)- and α(−)pinene are the same, as expected. The normalized ranges in the pinenes are equal to those in the dimethylcyclohexenes (Table 1). The substituted cyclohexene character of the pinenes therefore appears to dominate in their interactions with low energy electrons in the liquid phase.

The normalized range in bicyclo[2,2,1]heptene is slightly smaller than that in cyclohexene, but is much smaller than that in bicyclo[2,2,1]heptane (Table 1). Putting a bridge methylene group between the 1- and 4-positions of cyclohexane increased $b_{GP}d$ from 52×10^{-8} g/cm^2 in cyclohexane to 76×10^{-8} g/cm^2 in bicyclo[2,2,1]heptane. The same procedure with cyclohexene decreased the normalized range from 51×10^{-8} to 48×10^{-8} g/cm^2. The effect of the bridge group on cyclohexane was in the expected direction, because adding the methylene bridge increased the degree of sphericity of the molecule. The bridge group decreased the range in the olefin in spite of the increased degree of sphericity. The fact that bicyclo[2,2,1]heptene reacts with Na–K alloy indicates that the ring strain (caused by the bridge) increases the reactivity of the molecule, somewhat analogous to the propane–cyclopropane and possibly the cyclohexene–cyclopentene case.

This supports the suggestion that one of the methods by which low energy electrons transfer energy to olefins in the liquid phase is through incipient negative ion formation. The electron and olefin coming together in collision approach the potential surface of a negative ion state. Upon separation after the collision the olefin may be left with more rotational or vibrational energy and the electron with less kinetic energy.

Monocyclic Alkadienes

The density-normalized range in 1,4-cyclohexadiene is somewhat larger than that in cyclohexene, whereas that in 1,3-cyclohexadiene is

Can. J. Chem. Downloaded from www.nrcresearchpress.com by 210.87.254.105 on 09/05/12
For personal use only.

Can. J. Chem. Downloaded from www.nrcresearchpress.com by 210.87.254.105 on 09/05/12
For personal use only.

much smaller than that in the mono-olefin (Table 1).

Introducing the second π bond in the nonconjugated 4-position increased the symmetry of the molecule, which decreased the strength of the electron–molecule energy transfer interaction. Introducing the second π bond in the conjugated 3-position increased the molecular reactivity to an extent that this effect dominated any other that the extra π bond might have had. The lower range in 1,3-cyclohexadiene is attributed to an increased electron energy loss interaction by way of negative ion states.

Polycyclic Alkadiene

The low range in bicyclo[2,2,1]heptadiene was unexpected, because the molecule is structurally related to 1,4-cyclohexadiene (Table 1). However, it turns out that bicyclo[2,2,1]heptadiene is conjugated through space (23), and the reactivity of this compound is similar to that of 1,3-cyclohexadiene. The equality of the normalized ranges in bicyclo[2,2,1]heptadiene and 1,3-cyclohexadiene is thereby explained. Negative ion states once again provide an important mode of energy transfer from the electrons to the molecules.

Benzene

The normalized range in benzene (37×10^{-8} g/cm^2) is only slightly greater than that in 1,3-cyclohexadiene (34×10^{-8} g/cm^2) and is much smaller than that in 1,4-cyclohexadiene (57×10^{-8} g/cm^2). This indicates that transient negative ion states are also important in the energy transfer mechanism for low energy electrons in liquid benzene.

Electron Mobilities

Correlation between u_e and b_{GP}

There is a general correlation between thermal electron mobilities and epithermal electron penetration ranges in liquids (4, 7). The correlation indicates that the gross properties of liquids that facilitate energy transfer from epithermal electrons also inhibit the migration of thermal electrons. However, the correlation is not perfect and it is fruitful to pick out variations within it.

The temperature dependence of u_e is much greater than that of b_{GP}, so comparisons are made between liquids at the same temperature when possible. An alternative is to compare the values obtained at the normal boiling points of the liquids. In the present work the same trends emerge from the two types of comparison, so only the former is given.

The general tendency is for u_e and b_{GP} to increase together, although the former changes much more quickly than the latter. Previously reported values of u_e in different liquids cover a range of seven orders of magnitude, while the corresponding values of b_{GP} cover a range of only two orders of magnitude. A log u_e *vs.* log b_{GP} plot was used to put all the data on a single graph (4, 7). However, to look for fine structure in the correlation it is convenient to expand the b_{GP} axis to an arithmetic scale and to use a limited range of u_e. To this end, a plot of log u_e *vs.* b_{GP} for cyclic hydrocarbons at 295 ± 2 K is shown in Fig. 5. Values for *n*-butane (5), *n*-pentane (7, 8), and *n*-hexane (6, 8, 24) are included for comparison. For a given value of b_{GP} the tendency is for u_e to increase in the order *n*-alkane < cycloalkane < cycloalkene < 1,4-cyclohexadiene or benzene.

The irregularity of shape of *n*-alkane molecules appears to have a greater effect on limiting the migration rate of thermal electrons than on de-energizing epithermal electrons. Solvent rearrangement probably makes a significant contribution to the formation of the equilibrium solvated state of electrons in hydrocarbons, as in other liquids. Solvent rearrangement increases the electron trap depth and decreases the mobility. The effect is greater in *n*-alkanes than in cycloalkanes.

By contrast, π bonds appear to have a greater effect on de-energizing epithermal electrons than on limiting the migration rate of thermal electrons. This applies only to compounds such as those in Fig. 5, which do not capture electrons to form stable negative ions. When negative ion formation is an endothermic process, epithermal electrons can interact more strongly than thermal electrons with the molecules. Interactions involving transient negative ion states thereby make a larger contribution to limiting b_{GP} than to limiting u_e in these liquids.

Temperature Dependence of u_e

Arrhenius plots of u_e in the olefins curve downwards at low temperatures (Figs. 4 and 6). The rapid change of slope indicates a change in transport mechanism.

The change of slope is particularly marked in 1,4-cyclohexadiene and the benzene–1,4-

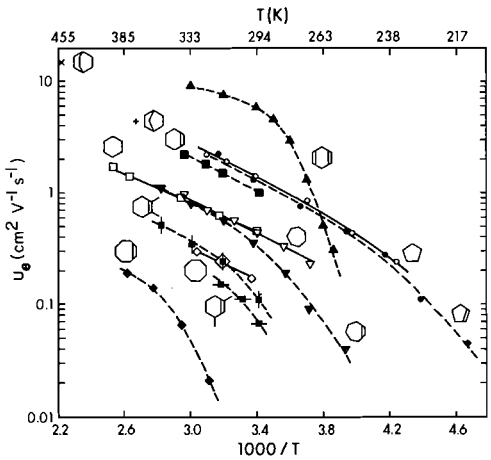

FIG. 6. Arrhenius plots of electron mobilities in cyclic hydrocarbons. The compounds are identified by their carbon skeletons on the graph. The filled points and dashed curves represent olefins. The open points and full curves represent cycloalkanes. The curves were calculated using [12] and the parameter values in Table 5.

cyclohexadiene solutions (Fig. 4). At temperatures below 280 K the Arrhenius temperature coefficient is 24–26 kcal/mol in all of the solutions. However, at about 330 K the coefficient is only 2 kcal/mol in the 98.3% diene solution and 4 kcal/mol in the 66.7% solution.

At high temperatures electron migration in hydrocarbons may occur mainly by thermal excitation from the solvated state to the conduction band.

[6] $$e^-_{solv} \rightleftharpoons e^-_{cb}$$

Optical excitation energies of solvated electrons in water and alcohols tend to decrease linearly with increasing temperature (25, 26), so the free energy and enthalpy of solvation would probably do likewise (27). By analogy, the free energy change of [6] in hydrocarbons is represented by [7].

[7] $$\Delta G_6 \approx \Delta G_6(0) - A_6T \approx \Delta H_6(0) - T\Delta S_6 - A_6T \approx \Delta H_6(0) - B_6T$$

where $\Delta H_6(0)$ is the enthalpy change extrapolated to zero Kelvin, A_6 is the temperature coefficient of the free energy change, and $B_6 = (\Delta S_6 + A_6)$. The temperature dependences of ΔS_6 and B_6 are neglected.

The large temperature coefficient of mobility at low temperatures is tentatively attributed to negative ion formation, by analogy with the reaction between solvated electrons and benzene in dimethoxyethane at low temperatures (28).

[8] $$e^-_{solv} + M \rightleftharpoons M^-_{solv}$$

Negative ion formation is negligible at high temperatures, where the slopes of the curves in Fig. 4 are small. The free energy change of [8] is assigned the same form as [7].

[9] $$\Delta G_8 \approx \Delta H_8(0) - B_8T$$

where $\Delta H_8(0)$ is the enthalpy change of [8] extrapolated to zero Kelvin and $B_8 = (\Delta S_8 + A_8)$.

$\Delta H_6(0)$ and $\Delta H_8(0)$ are opposite in sign, as are B_6 and B_8; [6] is endothermic to the right, whereas [8] is exothermic to the right.

Phenomenologically one cannot distinguish between [8] and the formation of a deeper trapped state of the electron. The present behavior is similar to that observed for electrical conduction in several liquid chalcogenides, such as As_2Te_3 (29). In those liquids the band gap is temperature dependent and has the form $E = E(0) - \gamma T$, with $E(0) \approx 20$ kcal/mol and $\gamma \approx 23$ cal deg^{-1} mol^{-1} (29).

The observed electron mobility u_e is equal to the product of the mobility u_{cb} in the conduction band and the fraction χ of the electrons that are in the conduction band. The mobilities of e^-_{solv} and M^- are considered to be negligible in the present systems.

[10] $$u_e = u_{cb}\chi$$

The fraction χ can be expressed in terms of the equilibrium constants or standard state free energy changes of [6] and [8].

[11] $$\chi = \{1 + K_6^{-1} + K_6^{-1}K_8[M]\}^{-1} = \{1 + e^{\Delta H_6^0(0)/RT}e^{-B_6^0/R} + [M]e^{(\Delta H_6^0(0) - \Delta H_8^0(0))/RT}e^{-(B_6^0 - B_8^0)/R}\}^{-1}$$

Under most conditions the first term on the right hand side of [11] is negligible and [10] may be approximated as [12].

[12] $$u_e \approx \frac{u_{cb}\, e^{B_6^0/R}\, e^{-\Delta H_6^0(0)/RT}}{1 + [M]\, e^{B_8^0/R}\, e^{-\Delta H_8^0(0)/RT}}$$

The mobility data in Figs. 4 and 6 were fitted to [12] and the values of the parameters so obtained are listed in Table 5.

Can. J. Chem. Downloaded from www.nrcresearchpress.com by 210.87.254.105 on 09/05/12
For personal use only.

TABLE 5. Electron mobility parameters for eq. 12

Liquid	$u_{cb}e^{B_6{}^0/R}$ (cm^2 V^{-1} s^{-1})[a]	$\Delta H_6{}^0(0)$ (kcal/mol)	$[M]e^{B_8{}^0/R}$	$B_8{}^{0}$[b] (cal/deg mol)	$\Delta H_8{}^0(0)$ (kcal/mol)
Cyclopentane	250	3.0	2.0×10^{-4}	−21	−4.0
Cyclohexane	74	3.0	—		—
Cycloheptane	155	3.5	—	—	—
Cyclooctane	44	3.3	—	—	—
Cyclopentene	500	3.5	6×10^{-8}	−38	−7.5
Cyclohexene	470	3.6	—	—	—
Cycloheptene	78	3.0	1.0×10^{-7}	−37	−9.0
cis-Cyclooctene	10.5	3.0	1.2×10^{-11}	−55	−17.0
1,2-Dimethylcyclohexene	36	3.0	2.3×10^{-10}	−49	−13.0
1,3-Dimethylcyclohexene	23	3.0	2.3×10^{-10}	−49	−13.0
1,4-Cyclohexadiene–benzene solutions					
100% CHD[c]	143	1.8	2.6×10^{-17}	−81	−21.3
98.3% CHD[c]	250	2.2	1.0×10^{-17}	−83	−21.8
90.3% CHD	700	3.0	7.5×10^{-17}	−79	−21.0
66.7% CHD	4100	4.4	5.5×10^{-17}	−79	−21.6
Benzene	5.4×10^4	7.6	—	—	—

[a]The value of $B_6{}^0$ is expected to be zero or positive, so these represent upper limits for u_{cb}.
[b]Estimated by taking $[M] \approx 10\,M$ for the pure solvent. 23 cal/deg mol $\equiv 1 \times 10^{-3}$ eV/deg electron.
[c]Parameters calculated using [10] and [11] instead of [12].

It is not possible to separately determine the factors u_{cb} and $e^{B_6{}^0/R}$ from mobility data alone. The value of $B_6{}^0$ is expected to be zero or positive, so $u_{cb}e^{B_6{}^0/R}$ gives an upper limit for the value of u_{cb}. In the 1,4-cyclohexadiene–benzene solutions the value of $u_{cb}e^{B_6{}^0/R}$ increases approximately exponentially with $\Delta H_6{}^0(0)$, which implies that $B_6{}^0$ increases with $\Delta H_6{}^0(0)$. Consistent with this, the values of u_{cb} in these nonspherelike hydrocarbons probably lie below that in neopentane, *i.e.* $u_{cb} \lesssim 100$ cm^2 V^{-1} s^{-1} (20).

The value of $\Delta H_8{}^0(0)$ is -21.4 ± 0.3 kcal/mol in all of the 1,4-cyclohexadiene solutions and it is attributed to an equilibrium between solvated electrons and negative ions. The temperature coefficient of $\Delta G_8{}^0$ in the diene is large, $B_8{}^0 = -81 \pm 2$ cal deg^{-1} mol^{-1} (Table 5), so the anion is relatively unstable even at the lowest temperature used: at 259 K, $\Delta G_8{}^0 = -21\,400 - (-81)259 = -400$ cal/mol.

The values of $\Delta H_8{}^0(0)$ and $B_8{}^0$ in the mono-olefins are smaller than those in the diene (Table 5). The small values in cyclopentane are attributed to the formation of a deeper trapped state of the electron in the liquid. The same may be true in the mono-olefins, without involving negative ion formation.

The authors wish to thank the personnel of the Radiation Research Center for help with the electronics.

1. W. F. SCHMIDT and A. O. ALLEN. J. Phys. Chem. **72**, 3730 (1968).
2. P. H. TEWARI and G. R. FREEMAN. J. Chem. Phys. **49**, 4394 (1968).
3. P. H. TEWARI and G. R. FREEMAN. J. Chem. Phys. **51**, 1276 (1969).
4. J.-P. DODELET and G. R. FREEMAN. Can. J. Chem. **50**, 2667 (1972).
5. M. G. ROBINSON and G. R. FREEMAN. Can. J. Chem. **52**, 440 (1974).
6. W. F. SCHMIDT and A. O. ALLEN. J. Chem. Phys. **52**, 2345 (1970).
7. J.-P. DODELET, K. SHINSAKA, and G. R. FREEMAN. J. Chem. Phys. **59**, 1293 (1973).
8. J.-P. DODELET, K. SHINSAKA, U. KORTSCH, and G. R. FREEMAN. J. Chem. Phys. **59**, 2376 (1973).
9. R. R. DREISBACH. Adv. Chem. Ser. **15** (1955).
10. F. RICHTER. (*Editor*). Beilstein's Handbuch der Organischen Chemie, 4e Auflage, 3es Ergänzungeswerk. Springer-Verlag, Berlin. 1963.
11. R. C. WEAST. (*Editor*). Handbook of chemistry and physics, 49th ed. Chemical Rubber Co., Cleveland, Ohio. 1968.
12. J. TIMMERMANS. Physicochemical constants of pure organic compounds, Vol. 1. Elsevier, New York. 1950.
13. A. A. MARYOTT and E. R. SMITH. Tables of dielectric constants of pure liquids. NBS Circular 514, Boulder, Colorado. 1951.
14. G. PANNETIER. Chimie générale, atomique et liaisons chimiques. Masson, Paris. 1962.
15. T. A. STONEHAM, D. R. ETHRIDGE, and G. G. MEISELS. J. Chem. Phys. **54**, 4054 (1971).
16. G. R. FREEMAN. J. Chem. Phys. **39**, 1580 (1963).
17. K. SHINSAKA and G. R. FREEMAN. Can. J. Chem. **52**, 3495 (1974).

Can. J. Chem. Downloaded from www.nrcresearchpress.com by 210.87.254.105 on 09/05/12
For personal use only.

18. R. M. MINDAY, L. D. SCHMIDT, and H. T. DAVIS. J. Chem. Phys. **54**, 3112 (1971).
19. G. R. FREEMAN, Quad. Area Ric. Emilia-Romagna, **2**, 55 (1972).
20. K. SHINSAKA and G. R. FREEMAN. Can. J. Chem. **52**, 3556 (1974).
21. G. R. FREEMAN and T. E. M. SAMBROOK. J. Phys. Chem. **78**, 102 (1974).
22. R. D. NELSON, JR., D. R. LIDE, JR., and A. A. MARYOTT. Selected values of electric dipole moments for molecules in the gas phase. NSRDS-NBS 10, U.S. Dept. of Commerce, Washington, D.C. 1967.
23. R. HOFFMAN. Acc. Chem. Res. **4**, 1 (1971).
24. R. M. MINDAY, L. D. SCHMIDT, and H. T. DAVIS. J. Phys. Chem. **76**, 442 (1972).
25. B. D. MICHAEL, E. J. HART, and K. H. SCHMIDT. J. Phys. Chem. **75**, 3876 (1971).
26. K. N. JHA, G. L. BOLTON, and G. R. FREEMAN. J. Phys. Chem. **76**, 3876 (1972).
27. J. JORTNER and R. M. NOYES. J. Phys. Chem. **70**, 770 (1966).
28. T. R. TUTTLE, JR. and S. I. WEISSMAN. J. Am. Chem. Soc. **80**, 5342 (1958).
29. N. F. MOTT and E. A. DAVIS. Electronic processes in noncrystalline materials. Clarendon Press, Oxford. 1971. Chapt. 7.

Can. J. Chem. Downloaded from www.nrcresearchpress.com by 210.87.254.105 on 09/05/12
For personal use only.

The Catalytic Decomposition of 2-Propanol on Magnesium Oxide

IAN M. HOODLESS AND G. DOUGLAS MARTIN
Department of Chemistry, Lakehead University, Thunder Bay, Ontario P7B 5E1
Received October 18, 1973[1]

IAN M. HOODLESS and G. DOUGLAS MARTIN. Can. J. Chem. **53,** 2729 (1975).

The catalytic decomposition of 2-propanol on powders of "pure" and lithium oxide doped magnesium oxide has been investigated in the temperature range 300–450 °C by a pulse reactor technique. With the "pure" magnesium oxide samples the selectivity for dehydrogenation decreases with increasing temperature with an abrupt change in the region of 375 °C. The effect of the lithium oxide dopant is to depress the selectivity for dehydrogenation at the lower temperatures. The dopant does not appear to affect the dehydration activity and the decrease in selectivity is ascribed to the strong chemisorption of acetone at anion vacancies.

IAN M. HOODLESS et G. DOUGLAS MARTIN. Can. J. Chem. **53,** 2729 (1975).

On a étudié la décomposition du propanol-2 sur des poudres d'oxyde de magnésium "pur" et d'autres dopées par de l'oxyde de lithium; ces études ont été effectuées à des températures de 300–450 °C par une technique de réaction à pulsation. Avec des échantillons d'oxyde de magnésium "pur" la sélectivité pour la deshydrogénation diminue à mesure que la température augmente; il y a un changement subit dans la région de 375 °C. L'effet d'un dopage par l'oxyde de lithium est de diminuer la sélectivité pour la deshydrogénation aux températures inférieures. Il ne semble pas que le dopant affecte l'activité de deshydratation; on attribue la diminution dans la sélectivité à une forte chemisorption de l'acétone au niveau des anions disponibles.
[Traduit par le journal]

Introduction

The decomposition of 2-propanol has been widely used as a model reaction for studying the principles of catalyst selectivity and reactivity of metal oxides. Below 500 °C the predominant modes of decomposition are dehydration to give propene and dehydrogenation to give acetone. Several theories have been advanced linking the catalyst selectivity with geometric factors (1, 2), with electronic factors (3, 4), and with chemical factors (5). From the extensive data available Krylov (6) has examined the various theories by correlation analysis and, although there is considerable dispersion in the data points, he finds that the catalytic activity for dehydrogenation is a function of lattice parameter, type of conductivity, work function, and width of the forbidden zone. More recently a relationship between the selectivity for dehydrogenation and mobility of surface oxygen, as measured by isotopic exchange, has been proposed (7, 8).

In view of the correlation with the conduction characteristics of the oxides, the alkaline earth oxides are surprisingly active catalysts for the dehydrogenation reaction (6, 8). In the temperature range used in the catalysis investigations, these oxides are typical insulators and it is unlikely that their activity can be associated with electronic point defects. With semiconductor oxides it is frequently difficult to differentiate between the effects of electronic defects and other lattice defects on the catalytic activity but with the insulator oxides the influence of lattice vacancies on the decomposition reaction can be investigated. It has been suggested (9) that insulator oxides depend for their dehydration activity on the presence of these vacancies at the surface. This paper reports on a study of the effects of lattice vacancies on the decomposition of 2-propanol on MgO; the temperature range covered in these measurements is one in which previous work (8) would indicate a change in the activity of MgO from a dehydrogenation to a dehydration catalyst.

Experimental

Apparatus

The decomposition of 2-propanol was investigated by a micropulse reactor technique. A sample of the "spectra-analyzed" quality alcohol (1 μl) was injected into a dry, helium carrier-gas stream and passed over a 0.4 g sample of the catalyst in an all-glass reactor. The catalyst-bed temperature was controlled to ±1° by a Thermoelectric model 400 proportional controller which was initially calibrated with a second thermocouple embedded in the catalyst sample.

The reaction products and unreacted alcohol were quantitatively analyzed at 80 °C by a Hewlett–Packard model 5750 gas chromatograph using 6 ft long stainless

[1]Revision received June 4, 1975.

Can. J. Chem. Downloaded from www.nrcresearchpress.com by 210.87.254.42 on 09/05/12
For personal use only.

TABLE 1. Catalyst selectivity for the dehydrogenation of 2-propanol over the temperature range 300–450 °C

Temperature (°C)	Catalyst				
	MgO	MgO_S*	MgO†	ML15.5‡	ML45§
300	0.92	0.91	0.91	0.83	0.54
350	0.74	0.78	0.80	0.66	0.48
375	0.73	0.75	(0.73)	0.56	0.48
400	0.71	0.72	(0.65)	0.60	0.51
425	0.70	0.70	(0.56)	0.70	0.57
450	0.66	0.66	(0.47)	0.68	0.62

*Semiconductor grade MgO.
†From ref. 8, parentheses indicates value from extrapolation of lower temperature results.
‡MgO containing 15.5×10^{-6} m.f. Li_2O.
§MgO containing 45×10^{-6} m.f. Li_2O.

steel columns, 5 ft of which was packed with "Carbowax (20M)" on "Chromosorb G" and the final 1 ft packed with "Porapak Q". In most experiments the products passed directly from the reactor to the gas chromatograph but the apparatus could be modified to include a trapping system so that the products could be trapped out at liquid nitrogen temperatures for longer times prior to admission to the analytical column; the former will be referred to as partial recovery experiments. Independent measurements in which the flow rate was varied by a factor of three showed that this did not affect the selectivity. Several injections of 2-propanol were made at each reaction temperature, the time interval between injections being approximately 30 min.

Materials

Two samples of MgO were used. One sample was semiconductor grade MgO (>99.99% purity) supplied by Research Chemical Corporation. The other was prepared from magnesium nitrate solution (Baker Analyzed Reagent) by precipitation as hydroxide followed by thermal decomposition at 900 °C for 12 h. Li^+-doped samples were prepared by the same method, the dopant being added as lithium nitrate to the original nitrate solution. The lithium content of the samples was determined by atomic absorption spectrometry. Prior to any alcohol injections the catalysts were conditioned in the reactor by annealing at 600 °C for 6 h in the carrier gas stream. Surface areas of the samples, as measured by the BET method using krypton gas, were found to be 34 ± 3, 26 ± 3, and 31 ± 3 $m^2 g^{-1}$ for the MgO prepared by decomposition of the hydroxide, the 15.5×10^{-6} m.f. Li^+-doped MgO and the 45×10^{-6} m.f. Li^+-doped MgO respectively. The latter samples will be referred to as ML15.5 and ML45 respectively.

Results

Measurements of the catalyst selectivity were made over the temperature range 300–450 °C. At higher temperatures trace amounts of decomposition products of 2-propanol were detected in the absence of the catalyst. The major products of the catalytic reaction were acetone and propene, while, at temperatures above 400 °C, small amounts of propyne and a diene were also formed. The diene has been identified by mass spectroscopy and by its retention time on the analytical column as 2-methyl-1,3-pentadiene. In the temperature range investigated there was no evidence of the formation of ethers or mesityl oxide.

One advantage of the pulse technique is that it permits investigations of changes in selectivity in the catalyst prestabilization stages. De Vleesschauwer (10), who studied the reaction in a conventional flow system, reports that considerable time was required before a uniform decomposition rate of 2-propanol was obtained, presumably due to catalyst instability. We find little evidence of this in terms of the reaction products; in general the first injection of 2-propanol on to a fresh catalyst leads to a low recovery of products and reactant but there is no evidence of this behavior with subsequent injections. The variation in selectivity at each temperature for a series of alcohol injections is less than ± 0.03 and there is no significant trend in the selectivity as a function of the number of injections. Catalyst selectivities, defined as $C_{acetone}/(C_{acetone} + C_{propene})$ are shown in Table 1 and the fractional conversion to propene and acetone, based on the products and reactants recovered, are shown in Table 2 for the partial recovery experiments.

A number of studies have also been made of the effect of catalyst pretreatment on the selectivity for dehydrogenation of the alcohol. In these experiments, the catalysts, at the reaction temperature, were subjected to pulses of hydrogen, oxygen, and water vapor followed by injection of the alcohol approximately 10 s after the pretreatment pulse. Some results of these types of experiment on the ML15.5 catalyst are given

Can. J. Chem. Downloaded from www.nrcresearchpress.com by 210.87.254.42 on 09/05/12
For personal use only.

TABLE 2. Fractional conversion of 2-propanol to propene and acetone over the temperature range 300–450 °C

Temperature (°C)	Catalyst					
	Propene			Acetone		
	MgO	ML15.5	ML45	MgO	ML15.5	ML45
300	0.017	0.025	0.035	0.20	0.12	0.04
350	0.14	0.13	0.16	0.38	0.24	0.14
375	0.19	0.20	0.23	0.47	0.25	0.21
400	0.21	0.21	0.26	0.50	0.32	0.28
425	0.23	0.22	0.29	0.53	0.49	0.37
450	0.28	0.26	0.31	0.54	0.55	0.49

TABLE 3. The effects of pretreatments on the selectivity for dehydrogenation of the ML15.5 catalyst

Temperature (°C)	Pretreatment		Fractional conversion to propene	Fractional conversion to acetone	Selectivity for dehydrogenation
	Gas	Volume (μl)			
350	H_2	300	0.09	0.19	0.67
450	H_2	300	0.26	0.57	0.69
350	O_2	300	0.15	0.24	0.62
	O_2	100	0.14	0.28	0.67
400	O_2	500	0.19	0.54	0.74
	O_2	700	0.14	0.55	0.80
425	O_2	100	0.15	0.67	0.82
375	H_2O(l)	2	0.01	0.40	0.97
	H_2O(l)	2	0.01	0.34	0.96
	H_2O(l)	2	0.02	0.40	0.96
	H_2O(l)	2	0.02	0.38	0.96

in Table 3. One significant feature regarding the pretreatment of the catalyst with water vapor is that the marked reduction in propene production is observed only with the first injection of alcohol after the pretreatment.

Discussion

The high selectivity of MgO for dehydrogenation observed at the lower temperatures, Table 1, is in good agreement with previous work (8, 10). De Vleesschauwer (10), who prepared the MgO by calcination of magnesite, reports a value of 0.92–0.96 for the selectivity at 350 °C of samples calcined at temperatures above 550 °C but found that lower calcination temperatures produce a dehydration catalyst. McCaffrey *et al.* (8) and De Vleesschauwer (10) report that the activation energy for the dehydration reaction is greater than that for the dehydrogenation reaction so that a decrease in the selectivity for dehydrogenation with increases in reaction temperature is to be expected. Selectivities at temperatures above 350 °C have been calculated by extrapolation of the results of McCaffrey *et al.* (8) for the rates of dehydration and dehydrogenation in the temperature range 270–350 °C and are shown in parentheses in Table 1. Above 400 °C the present results for MgO give a significantly higher value for the dehydrogenation selectivity than would be anticipated from the rate equations for lower temperature behavior (8).

The effect of Li^+-doping is to decrease the selectivity for dehydrogenation particularly at the lower temperatures. The level of dopant used is such that it would lead to changes in the point defect concentrations rather than new compound formation; X-ray diffraction data support this conclusion. Relatively few detailed studies have been made into the defect nature of MgO but, on the basis of theoretical estimates of defect formation energies (11) and diffusion measurements (12), it is believed that the predominant point defects are of the Schottky type. Incorporation of the dopant in the lattice would be achieved by the

Can. J. Chem. Downloaded from www.nrcresearchpress.com by 210.87.254.42 on 09/05/12
For personal use only.

following reaction

$$[1] \quad (Mg_1^{2+})(O_1^{2-}) + \tfrac{1}{2}nLi_2O \rightarrow (Mg_1^{2+}Li_n^{+})(O_{1+1/2n}^{2-}\boxed{a}_{1/2n})$$

where $\boxed{a}$ signifies an anion vacancy. The doped samples will therefore have an increased anion vacancy concentration and a decreased cation vacancy concentration relative to undoped MgO. The selectivity results for the doped samples do not support the proposal (9) that the dehydration activity of insulators is associated with cation vacancies. In Table 2 the fractional conversions to propene and acetone in partial recovery experiments on the catalysts are compared. The effect of Li^+-doping, apart from the results at 300 °C where low yields of products were obtained, is to decrease the yield of acetone particularly for reaction temperatures of 400 °C and below.

It seems unlikely that the reduction in acetone yield is directly associated with the reduced cation vacancy concentration in the doped samples. At the highest reaction temperature, 450 °C, there is good agreement in both the selectivity and the fractional conversion for all the catalysts yet, at this temperature, there should still be a depressed cation vacancy concentration in the doped samples relative to the undoped samples. It is possible that the decreased selectivity of the doped samples below 400 °C may be partially due to the strong chemisorption of acetone on the catalyst surface. Some controversy exists as to the rate-determining step in the dehydrogenation reaction on metal oxides; it has been suggested that either the reaction of the adsorbed alcohol on the surface (8, 13) or the desorption of acetone (6, 14) is rate limiting. It has been noted in the present work that in the experiments, in which the products are trapped out over a longer period of time prior to admission to the analytical column, there is an enhanced recovery of products, particularly acetone, relative to the partial recovery experiments for the lower reaction temperatures; for example with the ML45 catalyst at a reaction temperature of 350 °C the yield of acetone is approximately doubled in the trapping-out experiments while the yield of propene is essentially unchanged. Above 400 °C the selectivities obtained in the two types of experiment are the same.

Recent infrared studies of adsorption on MgO (15) have shown that acetone is strongly chemisorbed and at temperatures above 250 °C the spectra are consistent with the formation of a carboxylate ion at the surface. Since the surface of the MgO will be preferentially terminated by oxide ions (16), an anion vacancy, being a region of positive charge, is an ideal site for the chemisorption of acetone via its oxygen. It is therefore suggested that the decreased selectivity in the doped samples is, at least in part, due to the strong chemisorption of acetone at anion vacancies. In this connection it is interesting to note the effects of pretreatment of the catalyst with water vapor on the 2-propanol decomposition, Table 3. The inhibition of dehydration reaction on oxide catalysts by water vapor has been previously reported (8) but additionally we observe an enhanced recovery of acetone. Blocking of the anion vacancies by adsorption of some of the water at these sites would reduce the tendency for acetone chemisorption and hence increase the yield of acetone in the partial recovery experiments.

In the temperature range 375–400 °C there are significant changes in the dehydrogenation selectivity for all the catalysts; with MgO there is a "break" in the selectivity temperature trend in this region while for the doped samples a minimum in the selectivity is observed. Winter (17) has measured oxygen exchange on MgO and reports a marked change in the rate of exchange in the temperature region 390–410 °C; above these temperatures the activation energy for exchange is considerably lowered. The observation is interesting in light of the recent proposal (7, 8) linking high selectivity for dehydrogenation with a low activation energy for oxygen exchange on the catalyst. Winter (17) has interpreted the decrease in activation energy for exchange as indicative of the temperature of onset of significant oxide ion mobility at the surface. Following this interpretation, at temperatures above 400 °C the lifetime of individual anion vacancies will be decreased and this would lead to the observed increase in acetone desorption.

The present results do not permit identification of the active sites for the dehydration and dehydrogenation reactions. Because of the similar behavior of all the catalyst samples at 450 °C it appears that, although anion vacancies may act as trapping sites for acetone at lower temperatures, vacancies are not the active centers for catalysis. Also comparison of the yields of acetone for successive injections of 2-propanol at each temperature shows that the dehydrogenation sites are not readily poisoned. In terms of

Can. J. Chem. Downloaded from www.nrcresearchpress.com by 210.87.254.42 on 09/05/12
For personal use only.

the dehydrogenation mechanism it has been proposed (18, 19) that chemisorbed oxygen may act as a hydrogen abstractor. The effects of oxygen pretreatment of the catalyst at higher temperatures, Table 3, are consistent with this suggestion. Keier *et al.* (20) have found that lithium doping increases both the rate and amount of oxygen adsorption on magnesium oxide in the temperature region around 500 °C. The enhanced yields of acetone on the pretreated catalyst could be due to chemisorbed oxygen. However the results at lower temperatures, *i.e.* below 400 °C, are surprising. Pretreatment of the catalyst with oxygen does not significantly affect the acetone yield but it has been observed that in this temperature range treating the catalyst with oxygen some 15 min after a 2-propanol injection leads to the release of acetone from the surface. Whether this is due to the reaction of the strongly adsorbed precursor to acetone with gaseous or physisorbed oxygen or due to the displacement of chemisorbed acetone by the relatively high concentration of oxygen present is not clear.

Support of this work by the National Research Council of Canada is gratefully acknowledged.

1. A. A. BALANDIN and N. P. EGOROVA. Dokl. Akad. Nauk. SSSR, **57**, 255 (1947).
2. A. EUKEN and K. HEUER. Z. Phys. Chem. A**196**, 41 (1950).
3. K. HAUFFE. Reactions on solids and their surfaces. Russ. 1L (1962).
4. G. M. SCHWAB. Adv. Catal. **2**, 229 (1952).
5. S. Z. ROGINSKII. Dokl. Akad. Nauk. SSSR, **67**, 97 (1949).
6. O. V. KRYLOV. Catalysis by nonmetals. Academic Press, New York and London. 1970.
7. E. F. MCCAFFREY, D. G. KLISSURSKI, and R. A. Ross. Proc. 5th Int. Congr. Catal. Florida. Paper no. 3. 1972.
8. E. F. MCCAFFREY, T. A. MICKA and R. A. Ross. J. Phys. Chem. **76**, 3372 (1972).
9. D. A. DOWDEN. J. Chem. Soc. 242 (1950).
10. W. F. N. M. DE VLEESSCHAUWER. Physical and chemical aspects of adsorbents and catalysts. *Edited by* B. G. Linsen. Academic Press, London. 1970. Chapt. 6.
11. I. M. BOSWARVA and A. D. FRANKLIN. U.S. Natl. Bur. Stand. Spec. Publ. 296. 1968. p. 25.
12. R. LINDNER and G. D. PARFITT. J. Chem. Phys. **26**, 182 (1957).
13. J. E. GERMAIN, J. BIGOURD, J. P. BEAUFILS, B. GROS, and L. PONSALLE. Bull. Soc. Chim. Fr. 1777 (1961).
14. Y. DECHATRE and S. J. TEICHNER. Bull. Soc. Chim. Fr. 2804 (1967).
15. H. MIYATA, Y. TODA, and Y. KUBOKAWA. J. Catal. **32**, 155 (1974).
16. H. B. CHARMAN, R. M. DELL, and S. S. TEALE. Trans. Faraday Soc. **59**, 453 (1963).
17. E. R. S. WINTER. Adv. Catal. **10**, 196 (1958).
18. A. J. TENCH, T. LAWSON, and J. F. J. KIBBLEWHITE. Trans. Faraday Soc. **68**, 1169 (1972).
19. H. MIYATA, M. WAKAMIYA, and Y. KUBOKAWA. J. Catal. **34**, 117 (1974).
20. N. P. KEIER, L. F. RUBTSOVA, and G. F. GERASIMOVA. Kinet. Catal. **12**, 900 (1971).

Can. J. Chem. Downloaded from www.nrcresearchpress.com by 210.87.254.42 on 09/05/12
For personal use only.

The Proton–Proton and Proton–Carbon-13 Spin–Spin Coupling Constants in 1,3-Dioxole and Bis-1,3-dioxolyl. Conformational Dependence

TED SCHAEFER, KALVIN CHUM, DAVID MCKINNON, AND M. S. CHAUHAN
Department of Chemistry, University of Manitoba, Winnipeg, Manitoba R3T 2N2

Received May 12, 1975

TED SCHAEFER, KALVIN CHUM, DAVID MCKINNON, and M. S. CHAUHAN. Can. J. Chem. **53**, 2734 (1975).

The carbon-13 satellite peaks in the proton magnetic resonance spectra of 1,3-dioxole and bis-1,3-dioxolyl are analyzed under single and double resonance conditions to yield the signs and magnitudes of proton–proton coupling constants over three, four, and five bonds, and of proton–carbon-13 coupling constants over one, two, and three bonds. The conformational behavior of bis-1,3-dioxolyl contrasts sharply with that of analogous *sym*-tetrasubstituted ethane derivatives. It is indicated that the two-bond proton–carbon-13 coupling in the ethanic fragment can be used for conformational analysis in a manner similar to vicinal proton–proton couplings. The vicinal three-bond proton–carbon-13 couplings are given for dihedral angles of 180 and 120° and their relative magnitudes are as expected from a Karplus relationship. The two-bond proton–carbon-13 coupling in the olefinic fragment is, at 20.0 Hz, the largest coupling known for such a bond.

TED SCHAEFER, KALVIN CHUM, DAVID MCKINNON et M. S. CHAUHAN. Can. J. Chem. **53**, 2734 (1975).

On a analysé les pics satellites causés par le ^{13}C dans les spectres r.m.p. du dioxole et du bis-dioxolyl-1,3; utilisant des conditions de résonance simple et de résonance double, on a pu déterminer le signe et l'amplitude des constantes de couplage proton–proton sur trois, quatre et cinq liens et les constantes de couplage proton–^{13}C sur un, deux et trois liens. Le comportement conformationnel du bis-dioxolyl-1,3 est en opposition flagrante avec celui de dérivés analogues de l'éthane tétrasubstitué d'une façon symétrique. Il ressort de ces travaux que le couplage proton–^{13}C sur deux liens de la fraction éthane pourrait être utilisé pour des besoins conformationnels de la même manière que les couplages proton–proton vicinaux. On donne les couplages vicinaux proton–^{13}C sur trois liens pour des angles dièdres de 180 et 120° et leurs amplitudes relatives correspondent à ce que l'on peut attendre à partir d'une relation de Karplus. Le couplage proton–^{13}C sur deux liens du fragment oléfinique est de 20.0 Hz qui est la valeur la plus élevée connue pour un tel couplage. [Traduit par le journal]

Introduction

The observation of ^{13}C satellite peaks in the proton magnetic resonance spectra of symmetrical molecules, and their use in obtaining spin–spin coupling constants, has a long history (1, 2). More recently, ^{13}C n.m.r. spectra have been used for this purpose and, when combined with enrichment of ^{13}C, allow the unambiguous identification of $^{13}C,H$ and $^{13}C,^{13}C$ couplings. Marshall *et al.* (3) use this approach in pursuing a relationship (4) between $^{13}C,H$ and analogous H,H couplings.

In a somewhat different approach (5), a comparison between $^2J(^{13}C,H)$ and $^1J(^{13}C,H)$ gave an indication of inductive and hyperconjugative substituent effects (6) on $^2J(^{13}C,H)$. In another study (7), a relationship between $^2J(^{13}C{=}C{-}H)$ and $^3J(H{-}C{=}C{-}H)$ in some ethylenic and aromatic systems was used as a tentative measure of delocalization in a cyclic compound.[1]

The previous work (7) included compounds **1**, **2**, and **3**. In the present paper 1,3-dioxole, **4**, and bis-1,3-dioxolyl, **5**, have their ^{13}C satellite spectra analyzed. The spectra of **5** are a good example of a system in which the ^{13}C side bands in a p.m.r. spectrum yield most of the interesting $^{13}C,H$ coupling constants, as well as the signs and magnitudes of very small (0.1 Hz) H,H couplings, in a relatively inexpensive manner. The conformational dependence of $^2J(^{13}C,H)$ in the ethanic fragment appears as a potential measure of conformational preferences in ethane derivatives but such studies will be much easier to perform with pulsed ^{13}C spectrometers.

[1]Left superscripts indicate the number of bonds separating the coupled nuclei.

Can. J. Chem. Downloaded from www.nrcresearchpress.com by 210.87.254.105 on 09/05/12
For personal use only.

Can. J. Chem. Downloaded from www.nrcresearchpress.com by 210.87.254.105 on 09/05/12
For personal use only.

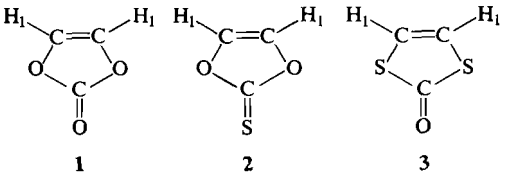

1 2 3

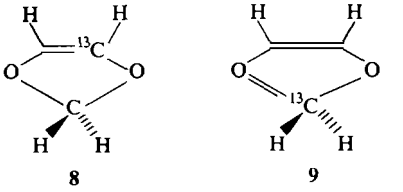

8 9

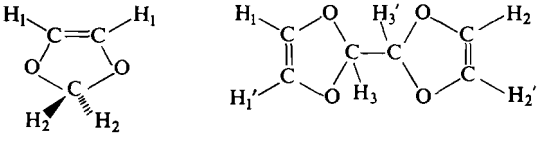

4 5

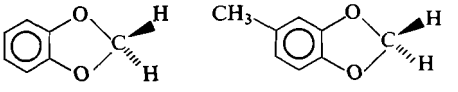

6 7

As a check on the $^{13}C,H$ parameters in **4**, the ^{13}C side bands of the methylene protons in **6** and **7** are also measured.

Experimental

Materials and Spectral Measurements

Compounds **4** and **5** were prepared by known methods (8, 9). Solutions of **4** (50 mol%) in acetone-d_6 and benzene-d_6 were degassed and their p.m.r. spectra were repeatedly calibrated at 5 Hz intervals in the frequency sweep mode of a H-100D Varian spectrometer. The scale was 1 Hz/cm and sweep times as low as 5000 s were employed. Similar statements apply to **5** as a 25 mol% solution in acetone-d_6 and as 10 mol% solutions in both acetone-d_6 and benzene-d_6. Compounds **6** and **7** were measured as 50 mol% solutions in carbon disulfide.

Molecular Orbital Calculations

The spin–spin coupling constants were calculated by approximate molecular orbital theory (10) at the INDO MO FPT and CNDO/2 MO FPT levels (11), using the original parameterization (10). Convergence to 0.01 Hz in the couplings was demanded. The geometry of **4** was based on the microwave geometry of **1** (12) and a tetrahedral H—C—H bond angle was assumed for the methylene group. A similar geometry (coordinates available from the authors) was assumed for **5**, where *trans* and *gauche* orientations of the C—H bonds about the ethanic C—C bond were taken. The relevant calculated couplings are given in Tables 1 and 2.

Results and Discussion

Spectral Analysis

The p.m.r. spectrum of **4** is a rare example of an A_2B_2 (nearly A_2X_2) spectrum, as opposed to an $[AB]_2$ spectrum (13), whereas **8** and **9** yield A_2BCX and A_2B_2X spectra, respectively. Because all but two of the transitions in **8** and **9** are observable, iteration with the computer program LAME (14, 15) combined with tickling experiments (16), gave the parameters in Table 1. It is assumed that $^1J(^{13}C,H)$ and $^3J(H,H)$ are positive. The negative sign of $^4J(H_1,H_2)$ is confirmed by experiments on bis-1,3-dioxolyl.

The spectrum of **5** containing only ^{12}C is an example of an $X_2AA'X_2'$ or $[X_2A]_2$ spectrum (17) and, assuming that $^7J(H_1,H_2)$ is zero, the presence of very weak transitions (to be seen as sharp peaks in Fig. 1*A*) yields $^3J(H_3,H_3')$ as 4.27 ± 0.03 Hz, assumed positive. The magnitudes of $^4J(H,H)$ and $^5J(H,H)$ found below reproduced the spectrum of **5** only if their signs were opposite.

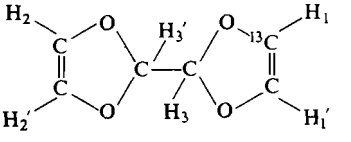

10

The spectrum of **10** was first analyzed as a first-order spectrum to give the coupling parameters in Table 2. Later its spectrum was simulated as a seven-spin system using input parameters from the analysis of **11** and good agreement with experiment was found on the basis of the isotope shifts implied by the data in Table 2.

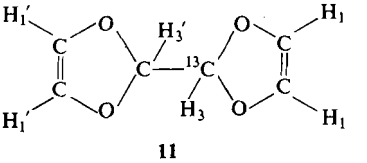

11

The spectrum of **11** was most informative. In Fig. 1*A* the spectrum of H_1 is given. Because $^7J(H_1,H_1') < 0.03$ Hz, the separation between the midpoints of the two pairs of doublets on either side of the intense resonance of the ^{12}C

Can. J. Chem. Downloaded from www.nrcresearchpress.com by 210.87.254.105 on 09/05/12
For personal use only.

TABLE 1. Proton chemical shifts* and coupling constants (in Hz) for 1,3-dioxole

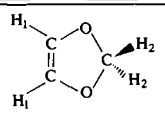

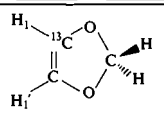

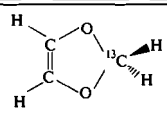

	Acetone-d_6	Benzene-d_6	INDO	CNDO/2	Acetone-d_6	Benzene-d_6	INDO	CNDO/2	Acetone-d_6	Benzene-d_6	INDO	CNDO/2
ν_1	642.74(1)†	619.52	—	—	642.34(1)‡	619.16(1)‡	—	—	642.63(1)	619.34(1)	—	—
ν_2	549.48(1)	537.63	—	—	549.40(1)	537.64(1)	—	—	549.15(1)	537.33(1)	—	—
^3J(H,H)	—	—	1.86	0.20	1.211(2)	1.203(5)	1.86	0.20	—	—	—	—
^4J(H,H)	(−)0.297(1)	(−)0.287(8)	0.16	0.39	−0.261(3)	−0.260(3)	0.16	0.39	(−)0.261(2)	−0.259(2)	—	
^1J(^{13}C,H)	—	—	—	—	205.823(7)	205.170(4)	198.3	162.8	170.161(3)	169.882(16)	148.8	116.4
^2J(^{13}C,H)	—	—	—	—	20.043(2)	19.966(6)	5.08	8.22	—	—	—	—
^3J(^{13}C,H)	—	—	—	—	2.431(14)	2.418(3)	2.35	1.74	6.706(3)	6.714(4)	6.42	4.74

*In Hz at 100 MHz to low field of internal TMS, in 50 mol% solutions.
†The numbers in brackets give the standard deviations in the last place for ν or J.
‡For ν_1' one has 642.50(1) and 619.26(1) Hz in acetone-d_6 and benzene-d_6, respectively.

TABLE 2. Proton chemical shifts* and coupling constants (in Hz) in bis-1,3-dioxolyl

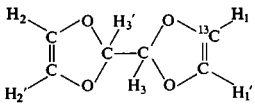

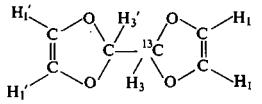

Parameter	Experimental	INDO[t]†	CBDI/2[t]	Experimental	INDO[g]	CNDO/2[g]	^{12}C molecule Experimental
ν_1	647.80(4)‡	—	—	648.06(4)	—	—	648.05(4)
ν_2	648.05(4)	—	—	—	—	—	648.05(4)
ν_3	574.26(4)	—	—	573.95(4)§	—	—	574.26(4)
$^3J(H_1,H_1)$	1.22(1)	1.84	0.21	—	1.86	0.21	—
$^3J(H_3,H_3)$	—	19.03	15.63	4.24	0.44[g]	0.64[g]	4.27(3)
$^4J(H,H)$	—	0.11	0.41	−0.28	0.03	0.39	—
$^5J(H,H)$	—	0.01	0.02	0.11(2)	0.97	0.60	—
$^1J(^{13}C,H)$	207.66(3)	197.62	162.43	175.1(1)	127.5	104.2	—
$^2J(^{13}C,H)$	19.97(2)	5.15	8.23	4.35(3)	7.70 3.42[t]	4.84 2.19[t]	—
$^3J(^{13}C,H)$ $^4J(^{13}C,H)$	Sum <2.5	1.97 −0.09	1.63 −0.05	6.75(3) —	6.33 6.30[t] −0.19	4.72 4.70[t] −0.02	— —

*In Hz at 100 MHz to low field of internal TMS, 25 mol% in acetone-d_6.
†Superscripts *t* and *g* stand for *trans* and *gauche* forms, respectively, *i.e.*, C—H_3 and C—H_3' bonds have these arrangements.
‡ν_1' = 647.97(4) Hz.
§ν_3' = 574.22(4) Hz.

molecule is $^3J(^{13}C,H_1) = 6.75 \pm 0.03$ Hz, this value agreeing with $^3J(^{13}C,H_1)$ found for the monocyclic compound, **9**. $^4J(^{13}C,H_1')$ must be less than 2.5 Hz in magnitude. The larger separation within the pairs on one side of the resonance from the ^{12}C molecule is $^4J(H_1,H_3) = \pm 0.28$ Hz and the smaller splitting is $^5J(H_1,H_3') = \pm 0.11$ Hz.

On the right hand side of Fig. 1 the spectrum of H_3' for **11** is given schematically but the long-range proton–proton splittings are omitted for reasons of clarity. It turns out that the magnitudes of $^2J(^{13}C,H_3')$ and $^3J(H_3,H_3')$ are almost equal and only the outside peaks of this multiplet are observable, the inner peaks being hidden in the intense resonance of the ^{12}C molecule. The spin states of $^{13}C,H_3$ and H_3' are indicated in the figure with the convention that a positive spin state corresponds to a high-field (low-frequency) peak for a positive coupling constant.

In Fig. 1*B*, 1*C*, and 1*D* the results of partial decoupling experiments (18) are displayed, the irradiations being indicated on the right. These experiments show that $^3J(^{13}C,H_1)/^2J(^{13}C,H_3') > 0$ and $^4J(H_1,H_3)/^3J(H_3,H_3') < 0$. In Fig. 1*E* and 1*F* the H_1 resonance is observed during irradiation of the high-field multiplet of H_3. The recorded spectra indicate $^3J(^{13}C,H_1)/^1J(^{13}C,H_3) > 0$ and $^3J(H_3,H_3')/^5J(H_1,H_3') > 0$. The results of these and other experiments are given in Table 2 on the assumption that $^1J(^{13}C,H)$ and $^3J(H_3,H_3')$ are positive. Final magnitudes of the parameters were found by successive simulations of the seven-spin spectra.

The Coupling Parameters

$^3J(H—C{=}C—H)$ and $^2J(^{13}C{=}C—H)$

The value of 1.21 Hz for **4** and **5** falls on the previous plot (7) of $^3J(H—C{=}C—H)$ *vs.* $^2J(^{13}C{=}C—H)$, characterizing **4** and **5** as ethylene derivatives and distinguishing them from delocalized species such as furan or benzene. The value of 1.21 Hz is the smallest known coupling of this nature. The value in cyclopropene is 1.3 Hz (19). $^3J(H—C{=}C—H)$ is 3 Hz in cyclopropenone (20). $^2J(^{13}C{=}C—H)$, at +20.0 Hz in **4** and **5**, is the largest known coupling in olefinic systems, its value being −2.4 Hz in ethylene (21).

$^3J(H—C—C—H)$ and the Conformation of Bis-1,3-dioxolyl

At 32 °C this coupling is $4.2_5 \pm 0.05$ Hz in 10 and 20 mol% solutions in acetone-d_6 and is 4.10 ± 0.05 Hz in a 10 mol% solution in benzene-d_6. In the 10 mol% acetone solution, $^3J(H—C—C—H)$ increases to 4.8 ± 0.1 Hz at −40 °C (precipitation occurs at lower temperatures). This behavior contrasts sharply with that observed for other *sym* tetrasubstituted ethanes.

Thus, the *gauche* conformation **12** is favored over the *trans* conformation **13** in acetone solution, the observed $^3J(H,H)$ being 4.4 Hz in *n*-hexane and 2.7 Hz in acetone (22). This

Can. J. Chem. Downloaded from www.nrcresearchpress.com by 210.87.254.105 on 09/05/12
For personal use only.

Can. J. Chem. Downloaded from www.nrcresearchpress.com by 210.87.254.105 on 09/05/12
For personal use only.

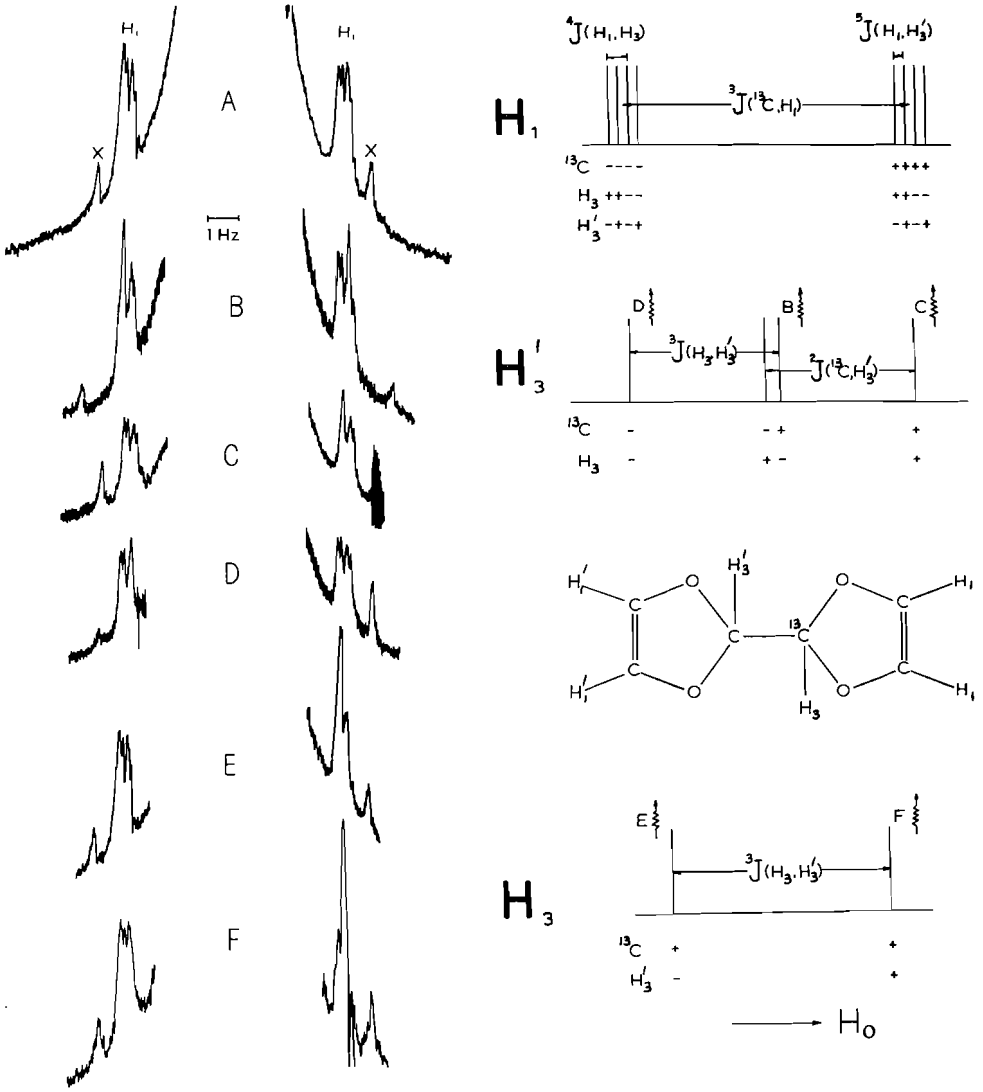

FIG. 1. On the left the H_1 proton resonance is displayed for bis-1,3-dioxolyl containing ^{13}C at one ethanic position. The intense peak from the ^{12}C molecule is flanked by two peaks marked with a cross and these peaks also arise from the ^{12}C molecule. The two pairs of doublets arise from the ^{13}C molecule. On the right the schematic resonance patterns are indicated for the protons as labelled in the formula. The vertical, curly, arrows indicate the peaks which are being irradiated while observing the lettered spectra on the left. The observed double resonance patterns are discussed in the text. The smallest splittings are 0.1 Hz in magnitude.

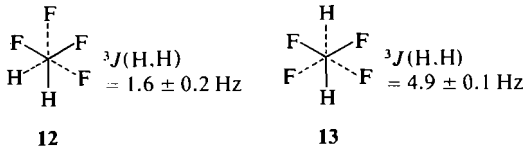

12 **13**

behavior is expected on the basis of Abraham's classical solvation theory (23), the more polar form **12** having a lower energy in the more polar medium. Similar observations are made for 1-chloro-1,2-dibromo-2-iodoethane (24), the *gauche* conformations becoming more abundant as the temperature decreases in an acetone–DME solution.

However, a less polar conformation can be stabilized by quadrupolar interactions of the solute molecule with the dielectric continuum (23), as has recently been shown for 3-pyridinealdehyde (25). The O,N-*trans* form of this molecule has a dipole moment more than 2 D

Can. J. Chem. Downloaded from www.nrcresearchpress.com by 210.87.254.105 on 09/05/12
For personal use only.

smaller than the O,N-*cis* form, yet is more stable in acetone solution by about 0.5 kcal/mol. It is clear that **5** is also behaving in this manner if ${}^3J^{H,H}_{trans} > {}^3J^{H,H}_{gauche}$.

In the absence of ${}^3J_t{}^{H,H}$ and ${}^3J_g{}^{H,H}$ values for **5** it is unreliable (25) to calculate[2] energy differences between the conformational isomers of **5** on the basis of the observed ${}^3J$(H,H). One may note, however, that the dipole moment of the *trans* form is zero while that of the *gauche* form is calculated as 1.52 D by INDO MO theory (see Experimental). As with other *sym*-tetrasubstituted ethanes (23), however, the quadrupole moment of the *trans* form is larger than that of the *gauche* form. Furthermore, INDO MO theory predicts the *gauche* form as 1.00 kcal/mol more stable than the *trans* form (see Experimental). Consequently, it may be concluded that, as the temperature decreases in the acetone solution, the quadrupolar interaction of the *trans* form with the dielectric medium outweighs both the dipolar interaction and the thermal preferences of the *gauche* form.[3] The present results emphasize that the conformational behavior of extended molecules need not follow that observed for smaller molecules of the same substitution pattern (23) about a given bond.

${}^4J(H,H)$ and ${}^5J(H,H)$

The closest useful analogy to ${}^4J$(H—C—O—C—H) in **4** is the allylic coupling in propene; particularly if the resonance structure **14** is considered, where the C=O$^+$ grouping now plays the role of the C=C double bond in propene. The relevant dihedral angle is 120°, which in propene is calculated (27) to lead to a

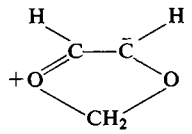

14

coupling constant of about −2 Hz, very much larger than the observed value of −0.29 Hz. However, the σ–π interaction between the C—H bond of the methylene group and the p_π orbital on oxygen presumably will be less effective than in propene (p_π orbital is contracted by the positive charge on oxygen). Furthermore, ${}^4J$(H,H) in **4** may be considered as the average of a negative allylic coupling and a positive ${}^5J$(H—C—O—C=C—H), possibly leading to the observed small, negative coupling. The INDO value, although positive (Table 1), is considerably smaller than the CNDO/2 prediction, possibly indicating the importance (10) of a π electron mechanism. ${}^4J$(H,H) in **4** is insensitive to substitution by carbon at the methylene group (*cf.* **5**).

${}^5J$(H,H) is +0.11 Hz in **5**. Comparison with the calculated values for the *trans* and *gauche* forms suggests the presence of a considerable amount of the latter in acetone solution, the calculated value for the *trans* form being 0.02 Hz at most. The coupling paths in the *gauche* form approximate more closely to an all-*trans* arrangement of bonds.

Solvent Dependence of ${}^1J({}^{13}C,H)$ in 4

The theoretical and experimental aspects of this dependence have been reviewed (28, 29). In **4** the coupling involving the olefinic carbon increases by 0.65 Hz in going from benzene to acetone solution, whereas the coupling involving the methylene carbon increases by only 0.25 Hz. In **15** the valence charge densities are given as calculated by INDO MO theory. The olefinic

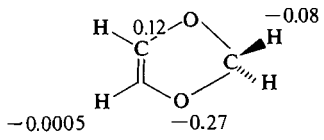

15

hydrogen atoms carry less negative charge than do the methylenic hydrogens. Therefore the specific interaction with acetone molecules, known (30) to lead to increases in ${}^1J({}^{13}C,H)$, will be larger at the olefinic site and cause the greater change in ${}^1J(=^{13}C,H)$. The change observed for ${}^1J({}^{13}C,H)$ at the methylenic carbon is about 10

[2]In *sym*-tetrachloroethane it is estimated (26) that ${}^3J_t$ and ${}^3J_g$ are 10.5 and 2.2 Hz, respectively. If the estimations (22) of 4.9 and 1.6 Hz for ${}^3J_t$ and ${}^3J_g$, respectively, in *sym*-tetrafluoroethane are combined with these and a linear dependence of ${}^3J_t$ and ${}^3J_g$ on substituent electronegativity is assumed, one predicts ${}^3J_t$ = 7.6 Hz and ${}^3J_g$ = 2.0 Hz for **5**. Then, in acetone solution at 32 °C one has n_t = 0.4 and n_g = 0.6 whereas at −40 °C, n_t = 0.5 = n_g. Assuming no entropy difference between *gauche* and *trans* forms, *i.e.*, the *gauche* form is favored by a simple statistical factor of 2, the *trans* form has a lower enthalpy of 170 cal/mol at 32 °C and of 320 cal/mol at −40 °C. Note that none of these molecules have been 'frozen out' on the n.m.r. time scale, so that ${}^3J_t$ and ${}^3J_g$ have not been measured directly. INDO MO theory (Table 2) predicts quite different values than those quoted here.

[3]A thorough study of the solvent and temperature dependence of ${}^3J$(H—C—C—H) in **5** demands FFT equipment because of the low solubility of **5** in many solvents and because of the spectral characteristics.

Can. J. Chem. Downloaded from www.nrcresearchpress.com by 210.87.254.105 on 09/05/12
For personal use only.

times smaller than for a molecule like CH_2Cl_2 (29). This can be qualitatively understood in terms of Barfield's calculations (29) in which a uniform electric field acting on the molecule causes a further transfer of charge from carbon to the substituent and to the hydrogen atom. In **15** the C—H bond is already considerably polarized, so that the reaction field due to the dielectric medium will be less effective in changing $^1J(^{13}C,H)$.

$^2J(^{13}C—C—H)$ in the Ethanic Fragment of **5**

$^2J(^{13}C—C—H)$ is +4.35 Hz in **5** while it is −4.5 Hz in ethane (21) and +1.1 Hz in *sym*-tetrabromoethane (31). The computed numbers in Table 1 demonstrate a dependence on conformation and imply that $^2J(^{13}C—C—H)$ depends on the orientation of the $^{13}C—O$ bond relative to the C—H bond, as well as on the electronegativity of the substituents attached to the $^{13}C—C—H$ fragment. Thus, in ethane the INDO value is −7.20 Hz (11), rises to +7.70 Hz in the *gauche* form of **5** where one C—O bond lies *trans* to the C—H bond in the $^{13}C—C—H$ fragment, but drops to +3.42 Hz when both C—O bonds are oriented to form dihedral angles of 60° with the C—H bond, *i.e.*, in the *trans* form.

The conclusion must be that $^2J(^{13}C,H)$ values in ethane derivatives can very likely be used in a fashion analogous to $^3J(H,H)$ in estimating conformational preferences. As with $^3J(H,H)$, the MO values are insufficiently reliable as reference points, so that ^{13}C n.m.r. measurements on compounds of known conformational preferences are necessary to establish calibration points. The intrinsic solvent dependence of $^3J(H,H)$ is apparently small (32). Such may not be true for $^2J(^{13}C,H)$.

Conformational Dependence of $^3J(^{13}C—O—C—H)$

$^3J(^{13}C—X—\overset{\|}{C}—H)$ in **1** to **4** is (5, 7) ±9.3, ±8.7, ±10.4, and +6.7 Hz, respectively. The first three numbers have been qualitatively interpreted (7) as being a consequence of the higher effective nuclear charge in the radial part of the 2s orbital on the ^{13}C atom. In this vein it is then reasonable that the coupling in **4** be smaller than in **1** to **3** because the ^{13}C atom is now formally sp^3 instead of sp^2 hybridized, thereby reducing the s electron density at the ^{13}C nucleus. The dihedral angle for this coupling path is 180° for all four compounds, expected to be a maximum for a Karplus relationship between angle and coupling. It follows that $^3J(^{13}C—X—\overset{\|}{C}—H)$ depends markedly on substituent effects and on the nature of X in addition to its dependence on dihedral angle. The INDO computations for **4** reproduce this coupling rather well.

$^3J(=^{13}C—O—C—H)$ in **4** is +2.4 Hz. The dihedral angle is 120°. It is remarkable that the ratio (0.36) of the two $^3J(^{13}C,H)$ values is nearly equal to the ratio (0.34) computed for these dihedral angles (180 and 120°) in propane (33), suggesting that $^3J(^{13}C,H)$ will follow a Karplus curve under diverse bonding conditions.

As a check on the magnitude of $^3J(=^{13}C—O—C—H)$ in **4**, the ^{13}C satellites of the methylenedioxybenzenes, **6** and **7**, were observed and gave values of ±2.05 ± 0.05 Hz for both compounds.

Isotope Shifts of the Proton Resonance

The carbon-13 isotope shifts of the proton resonance in **4** are very similar to those observed for **2** and **3** (7). They range from +0.0040 ± 0.0004 p.p.m. for directly bonded protons to 0.0008 ± 0.0004 p.p.m. for a proton separated by three bonds from ^{13}C. The measurements are not precise enough to distinguish clearly between the one-bond isotope shifts measured at olefinic or methylenic carbon centers.

Apparent Isotope Effect on $^4J(H,H)$

The data in Table 1 indicate a ^{13}C isotope effect of $+0.03 \pm 0.01_5$ Hz on $^4J(H,H)$ in **4**, this coupling being −0.30 ± 0.005 Hz in the ^{12}C molecule and −0.26 ± 0.01 Hz in the ^{13}C molecules, all in acetone-d_6. However, the spectral properties depend on solvent and concentration, to be discussed elsewhere, and suggest that the effect is an experimental artifact.

We are grateful to the National Research Council of Canada for financial assistance.

1. A. D. COHEN, N. SHEPPARD, and J. J. TURNER. Proc. Chem. Soc. 118 (1958).
2. J. H. GOLDSTEIN, V. S. WATTS, and L. S. RATTET. Prog. Nucl. Magn. Reson. Spectrosc. **8**, 103 (1972).
3. J. L. MARSHALL, D. E. MILLER, S. A. CONN, R. SEIWELL, and A. M. IHRIG. Acc. Chem. Res. **7**, 333 (1974).
4. G. J. KARABATSOS, J. D. GRAHAM, and F. M. VANE. J. Am. Chem. Soc. **84**, 37 (1962).
5. K. A. MCLAUCHLAN and T. SCHAEFER. Can. J. Chem. **44**, 321 (1966).

6. J. A. POPLE and A. A. BOTHNER-BY. J. Chem. Phys. **42**, 1339 (1965).
7. D. M. MCKINNON and T. SCHAEFER. Can. J. Chem. **49**, 89 (1971).
8. N. D. FIELD. J. Am. Chem. Soc. **83**, 3504 (1961).
9. B. FUCHS and S. HAUPTMANN. Chem. Commun. 705 (1971).
10. J. A. POPLE and D. L. BEVERIDGE. Approximate molecular orbital theory. McGraw Hill Book Co., New York. 1970.
11. J. A. POPLE, J. W. MCIVER, Jr., and N. S. OSTLUND. Chem. Phys. Lett. **1**, 465 (1967); J. Chem. Phys. **49**, 2965 (1968).
12. W. F. WHITE and J. E. BOGGS. J. Chem. Phys. **54**, 4714 (1971).
13. C. W. HAIGH. J. Chem. Soc. A, 1682 (1970).
14. S. CASTELLANO and A. A. BOTHNER-BY. J. Mol. Spectrosc. **32**, 398 (1969).
15. C. W. HAIGH and J. M. WILLIAMS. J. Mol. Spectrosc. **32**, 398 (1969).
16. R. FREEMAN and W. A. ANDERSON. J. Chem. Phys. **37**, 2053 (1962).
17. R. K. HARRIS. Can. J. Chem. **42**, 2275 (1964).
18. J. P. MAHER and D. F. EVANS. Proc. Chem. Soc. 208 (1961).
19. J. B. LAMBERT, A. P. JOVANOVICH, and W. L. OLIVER, Jr. J. Phys. Chem. **74**, 222 (1970).
20. R. BRESLOW and G. RYAN. J. Am. Chem. Soc. **89**, 3073 (1967).
21. R. M. LYNDEN-BELL and N. SHEPPARD. Proc. Roy. Soc. London, A, **269**, 385 (1962).
22. L. CAVALLI and R. J. ABRAHAM. Mol. Phys. **19**, 265 (1970).
23. R. J. ABRAHAM and E. BRETSCHNEIDER. *In* Internal rotation in molecules. *Edited by* W. J. Orville-Thomas. J. Wiley and Sons, New York. 1974. Chapt. 13.
24. G. GOVIL and H. J. BERNSTEIN. J. Chem. Phys. **49**, 911 (1968).
25. W. DANCHURA, T. SCHAEFER, J. B. ROWBOTHAM, and D. J. WOOD. Can. J. Chem. **52**, 3986 (1974).
26. R. J. ABRAHAM and M. A. COOPER. J. Chem. Soc. B, 202 (1967).
27. M. BARFIELD and B. CHAKRABARTI. Chem. Rev. **69**, 757 (1969).
28. S. L. SMITH. Top. Current Chem. **27**, 119 (1972).
29. M. BARFIELD and M. D. JOHNSTON, Jr. Chem. Rev. **73**, 53 (1973).
30. D. F. EVANS. J. Chem. Soc. 5575 (1963).
31. R. FREEMAN and W. A. ANDERSON. J. Chem. Phys. **39**, 806 (1963).
32. P. LASZLO. Prog. Nucl. Magn. Reson. Spectrosc. **3**, 231 (1967).
33. R. WASYLISHEN and T. SCHAEFER. Can. J. Chem. **50**, 2710 (1972).

Can. J. Chem. Downloaded from www.nrcresearchpress.com by 210.87.254.105 on 09/05/12
For personal use only.

The Initial Stages of the Pyrolysis of Dimethyl Ether

PHILIP D. PACEY

Department of Chemistry, Dalhousie University, Halifax, Nova Scotia B3H 4J3

Received October 15, 1974[1]

PHILIP D. PACEY. Can. J. Chem. **53**, 2742 (1975).

Dimethyl ether was pyrolized in a flow system at 782–936 K and 25–395 Torr with conversions from 0.2–10%. Product analyses were consistent with a simple Rice–Herzfeld mechanism with most chain termination by the recombination of CH_3 radicals. The rate coefficients for both the initiation and termination reactions appeared to be slightly pressure dependent. The first-order rate constant for the initiation reaction,

$$CH_3OCH_3 \rightarrow CH_3O + CH_3$$

calculated from the rate of C_2H_6 formation, was $k_1 = 10^{15.0\pm0.5} \exp(-318 \pm 8 \text{ kJ mol}^{-1}/RT)$ s^{-1}, corresponding to $\Delta H_f^0(CH_3O) = -5 \pm 8$ kJ mol^{-1}. Comparison of CH_4 and C_2H_6 yields enabled calculation of the rate constant for the reaction of CH_3 with dimethyl ether. From 373–936 K, the Arrhenius plot for this reaction is a curve.

PHILIP D. PACEY. Can. J. Chem. **53**, 2742 (1975).

On a pyrolysé l'éther méthylique dans un système à flux à des températures allant de 782 à 936 K et des pressions allant de 25 à 395 Torr; les taux de conversions étaient de 0.2 à 10%. L'analyse des produits est en accord avec le mécanisme simple de Rice–Herzfeld impliquant que la plupart des terminaisons de chaîne s'effectuent par recombinaison de radicaux méthyles. Il semble que les coefficients de vitesse des réactions d'initiation et de terminaison dépendent en faible partie de la pression. La constante de vitesse du premier ordre pour la réaction d'initiation,

$$CH_3OCH_3 \rightarrow CH_3O + CH_3$$

calculée à partir de la vitesse de formation de C_2H_6, est $k_1 = 10^{15.0\pm0.5} \exp(-318 \pm 8$ kJ mol$^{-1}/RT)$ s^{-1}, correspondant à un $\Delta H_f^0(CH_3O) = -5 \pm 8$ kJ mol^{-1}. Une comparaison des rendements en CH_4 et en C_2H_6 permet de calculer la constante de vitesse pour la réaction du CH_3 avec l'éther méthylique. De 373 à 936 K, la relation d'Arrhénius pour cette réaction est courbe. [Traduit par le journal]

Introduction

There have been several studies of the pyrolysis of dimethyl ether (1–4) but the mechanism has not been established.

The concentration of methyl radicals in this system has recently been measured spectroscopically (5). This could help provide an especially detailed knowledge of the kinetics of this pyrolysis if other mechanistic features were understood.

The simplest proposed mechanism is the following:

[1] $$CH_3OCH_3 \rightarrow CH_3O + CH_3$$

[2] $$CH_3O \rightarrow CH_2O + H$$

[3] $$H + CH_3OCH_3 \rightarrow H_2 + CH_2OCH_3$$

[4] $$CH_2OCH_3 \rightarrow CH_2O + CH_3$$

[5] $$CH_3 + CH_3OCH_3 \rightarrow CH_4 + CH_2OCH_3$$

[6] $$2CH_3 \rightarrow C_2H_6$$

According to a recent review (6), this may be the correct mechanism, although the following evidence appears to contradict it: (*i*) The observed rates, activation energies, and Arrhenius preexponential factors were greater than predicted by the mechanism using measurements of the Arrhenius parameters for reactions 5 and 6 at low temperatures and thermochemical estimates of k_1. (*ii*) Anderson and Benson (3) observed the formation of 1,2-dimethoxyethane and observed that the concentration of methyl ethyl ether impurity did not decrease as rapidly as expected. They interpreted these observations in terms of two additional termination reactions:

[7] $$CH_3 + CH_2OCH_3 \rightarrow C_2H_5OCH_3$$

[8] $$2CH_2OCH_3 \rightarrow (CH_2OCH_3)_2$$

(*iii*) McKenney and Laidler (7) found that pyrolysis of mixtures of dimethyl ether with large amounts of H_2S could be explained by a mechanism which required that reaction 1 be second order and reaction 6 be third order.

[1]Revision received June 16, 1975.

Can. J. Chem. Downloaded from www.nrcresearchpress.com by 210.87.254.42 on 09/05/12
For personal use only.

Can. J. Chem. Downloaded from www.nrcresearchpress.com by 210.87.254.42 on 09/05/12
For personal use only.

These contradictions, however, do not rule out the simple mechanism [1–6]. For example, the arguments of McKenney and Laidler did not consider the effect of heterogeneous processes, which are believed to be important in the pyrolysis of pure H_2S (7). The concentrations of dimethoxyethane ($10^{-4} \times [CH_4]$) and methyl ethyl ether ($2 \times 10^{-4} \times [CH_4]$) observed by Anderson and Benson were much less than the concentration of ethane ($10^{-2} \times [CH_4]$); this suggests that reactions 7 and 8 may be minor relative to reaction 6.

One reason for the uncertainty about the mechanism is the lack of analytical data for the early stages of the reaction. For example, C_2H_6 analyses have been reported only at conversions of 29% and greater (1).

Analysis of the simple mechanism [1–6] leads to the following relationships between the initial rates, R°, of product formation and the rate constants, k_i, for individual reactions:

$$[9] \qquad k_1 = \frac{R_{H_2}{}^0}{[C_2H_6O]} = \frac{R_{C_2H_6}{}^0}{[C_2H_6O]}$$

$$[10] \qquad \frac{k_5{}^2}{k_6} = \frac{(R_{CH_4}{}^0)^2}{R_{C_2H_6}{}^0[C_2H_6O]^2}$$

The initiation rate constant, k_1, has not previously been measured; the ratio $k_5{}^2/k_6$ has been measured at temperatures below the pyrolytic range.

The present study, using a flow reactor system, has been undertaken to obtain the required initial rates to further investigate the mechanism and to calculate k_1 and $k_5{}^2/k_6$.

Experimental

The apparatus and most details of technique have been described previously (8).

Dimethyl ether (Matheson, 99.87%) was purified by trap-to-trap distillation and by degassing at −95 °C. The major impurity remaining was methyl ethyl ether (0.02%). Concentrations of CH_4, C_2H_6, and C_2H_4 as impurities were about 1 p.p.m. For calibration purposes, methyl ethyl ether was prepared by the Williamson reaction using methanol, sodium, and ethyl iodide, followed by distillation and degassing. 1,2-Dimethoxyethane (BDH, 99.5%) was purified by fractional distillation.

Two 75-cm long quartz reactors (see ref. 8) were used: reactor i, 1.7-cm inside diameter, surface to volume ratio (S/V) = 3.1 cm^{-1}, and reactor iii, 0.2-cm inside diameter, S/V = 23 cm^{-1}. Temperatures were measured at intervals along the reactor. For a typical experiment, the computer program described in ref. 9 indicated that 91% of the reaction occurred within ±7 °C of the average reaction temperature.

The flow rate of dimethyl ether was kept below 0.2 mol/h to prevent the cooler, entering gas from distorting the temperature profile. Conversions were kept to less than 10%.

Products were analyzed by gas chromatography with thermal conductivity and flame ionization detection. Hydrogen and hydrocarbons were separated at 0 °C or 50 °C on a 0.5-m 5% NaOH on alumina column with nitrogen carrier gas. Carbon monoxide was analyzed on the same column at 0 °C using hydrogen as carrier gas. Oxygen-containing compounds were separated at 25 or 50 °C on a 3-m column containing 10% polyethylene glycol (BDH 1540) on Chromosorb P (nonacid washed) and at 65 °C on a 2-m 10% 1,2,3-tris(2-cyanoethoxy)propane on Chromosorb W column in series with a 2-m 10% DC-200 silicone oil on Chromosorb W column.

Results

Experiments have been performed at reactor temperatures from 782 to 936 K and reactant pressures of 25–395 Torr at reactor residence times from 0.06 to 106 s, with resulting conversions from 0.2 to 10%.[2]

Dependence of Rates on Reaction Time

The dependence of the rates of formation of H_2, C_2H_6, CH_4, and CO on reaction time at fixed reaction temperatures and pressures are shown in Figs. 1 and 2. The straight lines were calculated by the method of least squares. The figures show that for C_2H_6 and CH_4 the rates of formation were almost independent of time as expected for primary products, whereas for H_2 and CO, the rates increased linearly with time, as expected for predominantly secondary products.

In Fig. 1, the data for H_2 and C_2H_6, both obtained at 50 Torr and 856 K, appear to extrapolate to a common intercept. The least-squares intercepts are 1.7 (±0.7) × 10^{-3} Torr s^{-1} for H_2 and 1.48 (±0.02) × 10^{-3} for C_2H_6, consistent with a single value, within experimental uncertainty. (Unless otherwise specified, stated uncertainties are standard deviations). This agreement, predicted by the simple Rice–Herzfeld mechanism, supports reaction 6 as the main termination reaction under these conditions. The C_2H_6 data, which were easier to extrapolate to initial rates than were the H_2 data, were used in most experiments to provide an estimate of the rates of initiation and termination.

In contrast to H_2, there is no evidence of an initial rate of formation of CO. (The intercept

[2]Tables of data are available, at a nominal charge, from the Depository of Unpublished Data, CISTI, National Research Council of Canada, Ottawa, Canada K1A 0S2.

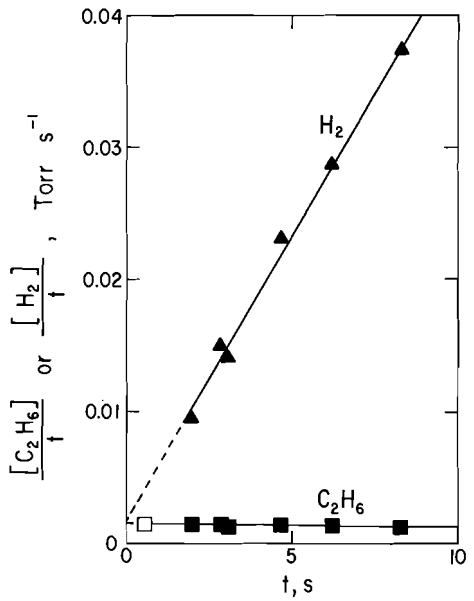

FIG. 1. Rates of formation of H_2 and C_2H_6 as a function of reactor residence time at 856 K and 50 Torr. Filled points, reactor i ($S/V = 3.1$ cm^{-1}); open point, reactor iii ($S/V = 23$ cm^{-1}). The lines were determined by the method of least squares.

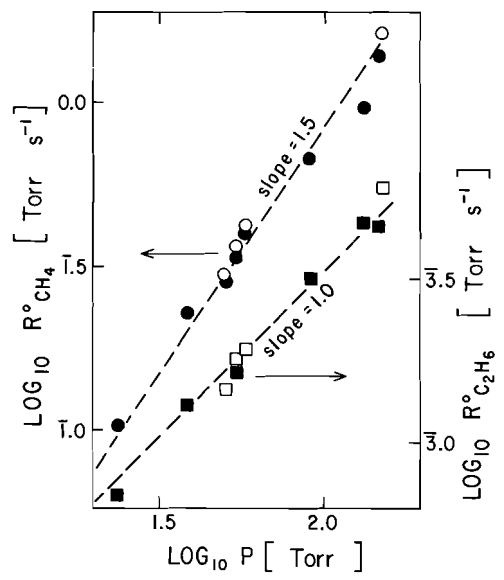

FIG. 3. Order plot for the initial rates of formation of CH_4 and C_2H_6 at 856–859 K. Filled points, reactor i; open points, reactor iii. The dashed lines have the slopes predicted by the mechanism 1–6, if reaction 1 is first order and reaction 6 is second order.

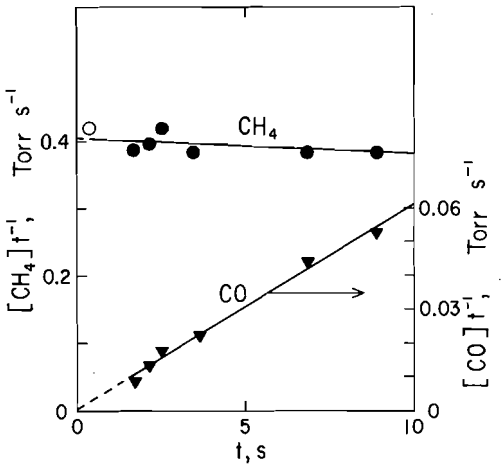

FIG. 2. Rates of formation of CH_4 and CO as a function of reactor residence time at 859 K and 58 Torr. Filled points, reactor i; open point, reactor iii. The lines were determined by the method of least squares.

in Fig. 2 is 0.5 ($\pm$1.2) $\times$ 10^{-3} Torr s^{-1}.) The secondary source of CO and H_2 is believed to be the decomposition of the product, formaldehyde (1).

Ethylene was a minor product; at 784 K and 288 Torr its initial rate of formation was 12% of that of C_2H_6 and 0.005% of the total rate of product formation; this would be expected from decomposition of methyl ethyl ether impurity.

As observed by Anderson and Benson (3), the concentration of methyl ethyl ether decreased during pyrolysis. Formation of methyl ethyl ether in amounts comparable to the C_2H_6 observed could have been masked by this impurity.

No dimethoxyethane product was observed; upper limits on the rate of formation of this substance have been established as 3% of $R_{C_2H_6}{}^0$ at 784 K and 348 Torr and 1% of $R_{C_2H_6}{}^0$ at 856 K and 50 Torr.

The major product, formaldehyde, which has been studied previously (1), was not measured in this work. No carbon deposits were observed.

Dependence of Rates on Pressure

The pressure dependences of the initial rates of formation of CH_4 and C_2H_6 at temperatures of 856–859 K are shown in the form of order plots in Fig. 3. The dashed lines have the slopes 1.5 and 1.0, respectively, predicted by the mechanism [1–6].

In view of the agreement observed thus far between the experimental results and the predictions of the simple mechanism [1–6] the rest

Can. J. Chem. Downloaded from www.nrcresearchpress.com by 210.87.254.42 on 09/05/12
For personal use only.

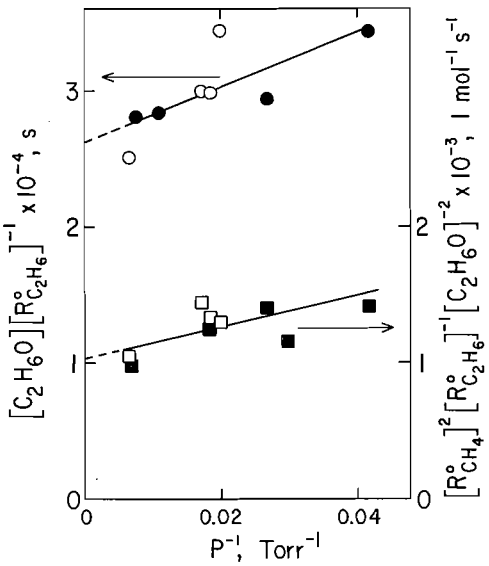

FIG. 4. Lindemann–Hinshelwood style plots for k_1^{-1} (calculated using [9]) at 858–859 K, upper line, and $k_5^2k_6^{-1}$ (calculated using [10]), at 856–859 K, lower line. The lines were obtained by the method of least squares. Solid points, reactor i; open points, reactor iii.

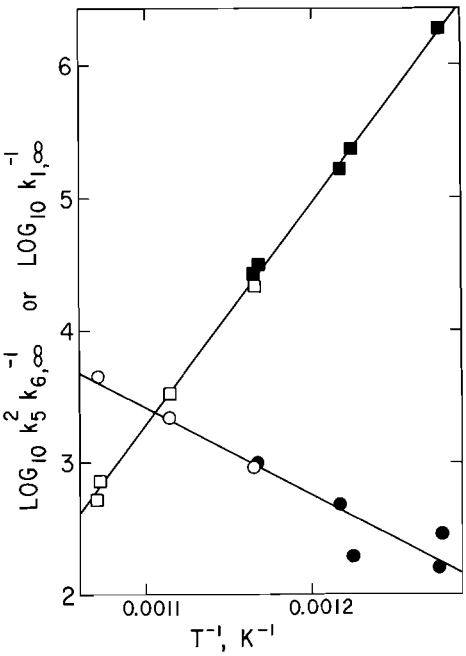

FIG. 5. Arrhenius plot of intercepts of plots like Fig. 4: ■, $\log k_1^{-1}$, reactor i; □, $\log k_1^{-1}$, reactor iii; ●, $\log k_5^2k_6^{-1}$, reactor i; ○, $\log k_5^2k_6^{-1}$, reactor iii. The lines were obtained by the method of least squares.

of the results will be interpreted in terms of this mechanism, and the possibility of errors in the mechanism will be considered in more detail in the Discussion.

There was a slight tendency for the C_2H_6 data to exhibit a slope greater than 1.0. This could be explained if k_1 is slightly pressure dependent. Values of k_1 have been calculated by means of [9] from data obtained at 858–859 K; the inverses of k_1 are plotted in the form of a Lindemann–Hinshelwood plot as the upper line in Fig. 4.

Studies with other systems (8–12) have indicated that k_6 is also pressure dependent. Values of k_5^2/k_6 have been calculated by means of [10] from the data in Fig. 3 and are plotted as the lower line in Fig. 4. Again a trend is evident.[3]

Dependence of Rates on Temperature

High pressure, extrapolated values of k_1^{-1} and k_5^2/k_6, from Fig. 4 and similar Lindemann–Hinshelwood plots, are shown in the form of Arrhenius plots in Fig. 5. Least-squares treatment of the data for k_1^{-1}, leads to an Arrhenius preexponential factor of $10^{15.2\pm0.2}$ s^{-1} and activation energy of 322 ± 4 kJ mol^{-1} for k_1 at infinite pressure.

Arrhenius parameters for reaction [5] are listed in Table 1. It can be seen that both the preexponential factor and the activation energy of the present work are substantially greater than values determined at lower temperatures.

Individual values of $k_5k_6^{-1/2}$ obtained in each of the studies in Table 1 (including square roots of the data in Fig. 5) are shown in the form of an Arrhenius plot in Fig. 6. The straight, dashed line is calculated from the Arrhenius parameters of ref. 17, which came closest to predicting the high temperature behavior. It can be seen that the overall Arrhenius plot is best described as a curve. Curved Arrhenius plots and large Arrhenius parameters at high temperatures have been observed using other techniques for several similar reactions (8, 9, 18–21); the curvature can be interpreted by means of activated complex theory (20).

Discussion

The main difficulty with the simple mechanism [1–6] has been the observation that overall Arrhenius parameters are greater than had been

[3]Half-quenching pressures obtained from Fig. 4 and similar figures at other temperatures are listed in the tables in the depository.

Can. J. Chem. Downloaded from www.nrcresearchpress.com by 210.87.254.42 on 09/05/12
For personal use only.

TABLE 1. Arrhenius parameters* for reaction 5

Experimental system (ref.)	T(K)	$\log_{10} A$ (l mol^{-1} s^{-1})	E_A (kJ mol^{-1})
$(CH_3)_2Hg$ photolysis (14)	373–473	8.3	38
$(CH_3)_2CO$ photolysis (15)	381–471	8.4	40
$(CH_3)_2CO$ photolysis (16)	407–523	8.4	40
Hg photosensitization (17)	472–565	9.0	44
Hg photosensitization (10)	473–573	8.9	44
$(CH_3)_2O$ pyrolysis (this work)	783–935	10.5 ± 0.4	63 ± 7

*All values are based on a value of 2.43×10^{10} l mol^{-1} s^{-1} for $k_{6,\infty}$ (13).

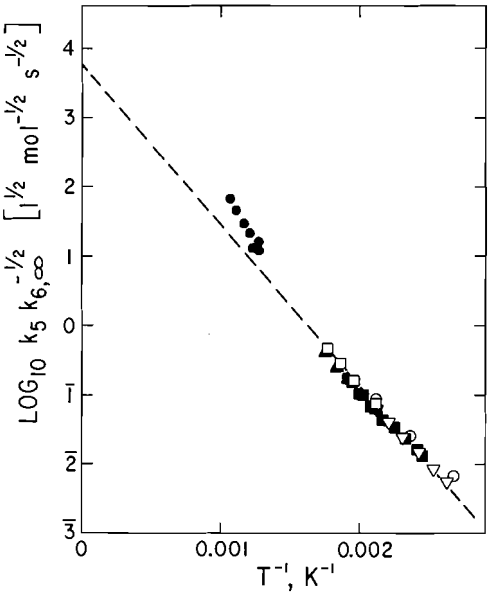

FIG. 6. Arrhenius plot for $k_5 k_6^{-1/2}$: ○, ref. 14; ▽, ref. 15; ■, ref. 16; □, ref. 17; ▲, ref. 10; ●, this work. The dashed, straight line is a least-squares fit to the data of ref. 17.

predicted. Observed overall activation energies, E_0, are 233(1), 228(2), 230(4), and 228 ± 2 (this work) kJ mol^{-1}. According to the mechanism 1–6, $E_0 = \frac{1}{2}E_1 + E_5 - \frac{1}{2}E_6$ or 224 ± 9 kJ mol^{-1}, if values of E_1 and $E_5 - \frac{1}{2}E_6$ from this work are used. In other words, the 'large' observed values of E_0 are consistent with the large E_5 of this work. Furthermore, the overall preexponential factor can be calculated from this work to be $10^{12.9 \pm 0.6}$ $l^{1/2}$ mol$^{-1/2}$ s^{-1}; this is consistent with observed values of $10^{13.6}$ (1), $10^{13.7}$ (2), $10^{13.0}$ (4), and $10^{13.2 \pm 0.2}$ (this work) $l^{1/2}$ mol$^{-1/2}$ s^{-1}.

Possible Competing Reactions

The calculation of k_5^2/k_6 assumed that reactions 5 and 6 were the only sources of CH_4 and C_2H_6 in this system. Some of the C_2H_4 formed probably results from decomposition of C_2H_5 radicals, which could also abstract hydrogen to form C_2H_6. In another system involving C_2H_5, the pyrolysis of *n*-butane (22), the rate of formation of C_2H_6 from this source was one-third the rate of formation of C_2H_4. As the rate constants for reaction of CH_3 with *n*-butane and dimethyl ether are very similar (18), it is likely that the rate constants for reaction of C_2H_5 with *n*-butane and dimethyl ether are as well. In the present system then, one can estimate that only 4% of the C_2H_6 results from this cause.

The absence of surface reactions is indicated by the insensitivity to surface-to-volume ratio illustrated in Figs. 1–5.

The calculation of k_1 assumed that reaction 6 was the only termination reaction. The similarity of $R_{C_2H_6}{}^0$ and $R_{H_2}{}^0$ and the nearly first order behavior of $R_{C_2H_6}{}^0$ were as expected if [6] were at least the major termination reaction. Nevertheless, if other radicals had concentrations comparable to CH_3, they could have been involved in minor termination reactions; the relative concentrations of these radicals can be estimated as follows: (*i*) Hydrogen atoms. If k_3 is taken from ref. 23 and k_5 from this work, the maximum initial ratio of $[H]/[CH_3]$ in these experiments can be calculated to be 2×10^{-4}, from $R_{H_2}{}^0/R_{CH_4}{}^0$ at 936 K and 51 Torr. (*ii*) Methoxy radicals. Anderson and Benson (3) found that the yield of CH_3OH (presumably from $CH_3O + C_2H_6O \rightarrow CH_3OH + CH_2OCH_3$) equalled $6 \times 10^{-4} \times [CH_4]$ at 799 K and 55 Torr. The compilation of Trotman-Dickenson and Milne (24) indicates that the abstraction reactions of CH_3O are generally faster than those of CH_3, hence 6×10^{-4} may be taken as an upper limit for $[CH_3O]/[CH_3]$. This ratio should increase at higher temperatures but should not become significant within the range of the present work. (*iii*) Methoxymethyl radicals. The upper limits es-

Can. J. Chem. Downloaded from www.nrcresearchpress.com by 210.87.254.42 on 09/05/12
For personal use only.

Can. J. Chem. Downloaded from www.nrcresearchpress.com by 210.87.254.42 on 09/05/12
For personal use only.

tablished herein for the rate of formation of dimethoxyethane by reaction 8 enable calculation of upper limits for the rate of reaction 7 with the use of the geometric mean rule, $k_7^2 = 4k_6k_8$. The greatest possible fraction of termination by reaction 7 in the present experiments is calculated to be 0.25 at 784 K and 348 Torr. Loucks and Laidler (25) have measured the rate constant ratio k_4^2/k_8 at 473–573 K. By combining their data and the data for k_5^2/k_6 from this work, it is possible to estimate that the maximum fraction of termination by reaction 7 is 0.29 at 784 K and 348 Torr.

In conclusion, reaction 6 appears to be the major termination reaction under these conditions, although reaction 7 and (to a lesser extent) reaction 8 are probably also significant. If the amount of reaction 7 predicted from Loucks and Laidler's data is taken into account, E_1 would be lowered by 8 kJ mol^{-1} and $\log_{10} A_1$ by 0.3 units. To allow for this, the Arrhenius expression could be rewritten as $k_1 = 10^{15.0\pm0.5} \exp(-318 \pm 8 \text{ kJ mol}^{-1}/RT)$ s^{-1}.

Thermochemistry of the Methoxy Radical

By assuming that k_{-1} is temperature independent, the heat of reaction for the initiation reaction, corrected to a standard state of 1 atm and 298 K, may be calculated from E_1 to be 325 ± 8 kJ mol^{-1}. With the heats of formation of CH_3 and $(CH_3)_2O$ from refs. 26 and 27, respectively, the heat of formation of CH_3O may be calculated to be -5 ± 8 kJ mol^{-1}. This may be compared with previous kinetic estimates from -3 to $+16$ kJ mol^{-1} (28, 29) and estimates from appearance potential measurements of -13 ± 13 kJ mol^{-1} (30).

With entropy data from Benson and O'Neal (29) and the value of $\log A_1$ from this work, it is possible to calculate that $\log_{10} A_{-1}$ should equal 9.1 ± 0.6.

The author wishes to thank the National Research Council of Canada for a grant in support of this research.

1. S. W. Benson and D. V. S. Jain. J. Chem. Phys. **31**, 1008 (1959).
2. N. Imai and O. Toyama. Bull. Chem. Soc. Jpn. **34**, 328 (1961).
3. K. H. Anderson and S. W. Benson. J. Chem. Phys. **36**, 2320 (1962).
4. D. J. McKenney and K. J. Laidler. Can. J. Chem. **41**, 1984 (1963).
5. P. D. Pacey. Chem. Phys. Lett. **23**, 394 (1973).
6. K. J. Laidler and D. J. McKenney. *In* The chemistry of the ether linkage. *Edited by* S. Patai. Interscience, London. 1967.
7. D. J. McKenney and K. J. Laidler. Can. J. Chem. **41**, 2009 (1963).
8. P. D. Pacey. Can. J. Chem. **51**, 2415 (1973).
9. P. D. Pacey and J. H. Purnell. J. Chem. Soc. Faraday Trans. I, **68**, 1462 (1972).
10. L. F. Loucks. Can. J. Chem. **45**, 2775 (1967).
11. A. B. Trenwith. Trans. Faraday Soc. **62**, 1538 (1966).
12. M. C. Lin and M. H. Back. Can. J. Chem. **44**, 2357 (1966).
13. H. E. Van Den Berg, A. B. Callear, and R. J. Norstrom. Chem. Phys. Lett. **4**, 101 (1969).
14. M. K. Phibbs and B. de B. Darwent. Can. J. Res. B, **28**, 395 (1950).
15. A. F. Trotman-Dickenson and E. W. R. Steacie. J. Chem. Phys. **19**, 329 (1951).
16. P. Gray and A. A. Herod. Trans. Faraday Soc. **64**, 2723 (1968).
17. R. A. Marcus, B. de B. Darwent, and E. W. R. Steacie. J. Chem. Phys. **16**, 987 (1948).
18. D. G. Hughes, R. M. Marshall, and J. H. Purnell. J. Chem. Soc. Faraday Trans. 1, **70**, 594 (1974).
19. M. B. Colket, III, D. W. Naegeli, and I. Glassman. Int. J. Chem. Kinet. **1**, 223 (1975).
20. T. C. Clark and J. E. Dove. Can. J. Chem. **51**, 2147 (1973).
21. W. T. Rawlins and W. C. Gardiner, Jr. J. Chem. Phys. **60**, 4676 (1974).
22. P. D. Pacey and J. H. Purnell. Ind. Eng. Chem. Fund. **11**, 233 (1972).
23. J. F. Meagher, P. Kim, J. H. Lee, and R. B. Timmons. J. Phys. Chem. **78**, 2650 (1974).
24. A. F. Trotman-Dickenson and G. S. Milne. Tables of bimolecular gas reactions. National Bureau of Standards, Washington. 1967.
25. L. F. Loucks and K. J. Laidler. Can. J. Chem. **45**, 2767 (1967).
26. D. R. Stull, H. Prophet *et al.* JANAF Thermochemical tables. 2nd ed. National Bureau of Standards, Washington. 1970.
27. J. D. Cox and G. Pilcher. Thermochemistry of organic and organometallic compounds. Academic Press, London, 1970.
28. P. Gray, R. Shaw, and J. C. J. Thynne. Prog. React. Kinet. **4**, 63 (1967).
29. S. W. Benson and H. E. O'Neal. Kinetic data on gas phase unimolecular reactions. National Bureau of Standards, Washington. 1970.
30. M. A. Haney and J. L. Franklin. Trans. Faraday Soc. **65**, 1794 (1969).

Carbon-13 Nuclear Magnetic Resonance Spectra of Some Dendroketose and Other Furanose Derivatives

DOLATRAI M. VYAS, HAROLD C. JARRELL, AND WALTER A. SZAREK[1]

Department of Chemistry, Queen's University, Kingston, Ontario K7L 3N6

Received April 7, 1975

D. M. VYAS, H. C. JARRELL, and W. A. SZAREK. Can. J. Chem. **53**, 2748 (1975).

The carbon-13 n.m.r. spectra of derivatives of the branched-chain sugars apiose and dendroketose, and of other furanose sugars, are reported. The study has permitted assignment of the configuration at the branching carbon atom and at the anomeric center in the dendroketose derivatives.

D. M. VYAS, H. C. JARRELL et W. A. SZAREK. Can. J. Chem. **53**, 2748 (1975).

On rapporte les spectres r.m.n. du ^{13}C de dérivés des sucres à chaîne ramifiée, apiose et dendroketose, et d'autres sucres sous forme furannose. Cette étude a permis d'attribuer, pour les dérivés du dendroketose, la configuration au niveau de l'atome de carbone portant la ramification et au centre anomérique. [Traduit par le journal]

Introduction

Until recently, the bulk of the activity in the area of carbon-13 magnetic resonance (c.m.r.) spectroscopy of carbohydrates had centered about the study of pyranose sugars and their derivatives (1), since conformational and configurational effects on ^{13}C shieldings in these compounds generally followed trends analogous to those in the well-studied cyclohexane series (for examples see refs. 1*b* and 2). In contrast, furanose sugars and their derivatives have not been subjected to an extensive investigation by c.m.r. spectroscopy, presumably because of the dearth of knowledge concerning the ^{13}C chemical shift patterns associated with conformational and configurational changes in the tetrahydrofuran ring (for examples see ref. 3). Nevertheless, the furanoid derivatives warrant a detailed c.m.r. study, since biologically important compounds such as nucleosides and nucleotides possess a furanoid moiety. Moreover, an active field of research in many laboratories is the chemical modification of nucleosides, for example, the introduction of branching into the furanoid ring. In recent years the utility of c.m.r. spectroscopy for determination of the configurations of tertiary alcoholic centers in branched-chain pyranoid derivatives has been demonstrated (4). A project in this laboratory (5) is concerned with the stereospecific synthesis of derivatives, including nucleoside analogs, of one enantiomer of the branched-chain sugar dendroketose (**1**) (6).On conversion of the acyclic structure (**1**) into its furanoid form, C-4 becomes asymmetric, giving rise to four possible isomers for the D-form and four more for the L-form. Thus, the complete structural formulation of furanoid dendroketose derivatives requires the determination of the configuration at the anomeric center and also at the branching carbon atom (C-4). The present publication describes the application of c.m.r. spectroscopy to the solution of these stereochemical problems; as part of this work the c.m.r. spectra of 1,2-*O*-isopropylidene-D-apio-β-L-furanose (**7**) and of isopropylidene derivatives of some aldohexofuranoses are also reported.

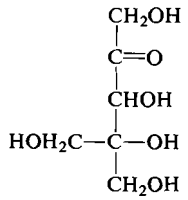

1

Results and Discussion

The ^{13}C chemical shifts of the compounds studied in this research, namely, 1,2-*O*-isopropylidene-α-D-glucofuranose (**2**), 1,2-*O*-isopropylidene-α-D-allofuranose (**3**), 1,2:5,6-di-*O*-isopropylidene-α-D-glucofuranose (**4**), 1,2:5,6-di-*O*-isopropylidene-α-D-allofuranose (**5**), 2,3:5,6-di-*O*-isopropylidene-α-D-mannofuranose (**6**), 1,2-*O*-isopropylidene-D-apio-β-L-furanose (**7**), and

[1]Author to whom inquiries should be addressed.

Can. J. Chem. Downloaded from www.nrcresearchpress.com by 210.87.254.42 on 09/05/12
For personal use only.

Can. J. Chem. Downloaded from www.nrcresearchpress.com by 210.87.254.42 on 09/05/12
For personal use only.

the ketofuranose derivatives **8–13** are documented in Table 1. The signal assignments were aided by the previous studies by Que and Gray (3*c*) on anhydro sugars and ketoses, by Usui *et al.* (3*d*) on the determination of anomeric configuration of furanoside derivatives, and by Perlin *et al.* (3*b*) on furanose sugars. In the spectra of all of the compounds listed in Table 1, the signal assignments of the anomeric carbons and of the 1,3-dioxolane-acetal carbons were readily made, since the signals appeared at low field; also, the isopropylidene-methyl signals and hydroxymethyl signals were readily identified, since they appeared at high field. The signal assignments of the remaining carbons were made as discussed below.

A comparison of the chemical-shift data reported (3*c*) for 1,4-anhydroglucitol (see footnote *b* of Table 1) with that of compound **2**[2] permitted the assignment of signals in the spectrum of the latter compound. Analogously, chemical-shift data reported (3*c*) for 1,4-anhydroallitol (see footnote *c* of Table 1) were employed for the assignment of signals in the spectrum of compound **3**. The C-2 and C-4 signals in the spectrum of compound **2** were unambiguously assigned on the expectation, based upon studies by Perlin *et al.* (3*b*) and by Que and Gray (3*c*), that the *cis* O-2,O-3 interaction in **3** should result in an upfield shift of ~5–6 p.p.m. of the C-2 signal in the spectrum of **3** relative to the corresponding signal in the spectrum of **2**. The signal assignments in the spectra of **2** and **3** were further corroborated by comparison of the chemical-shift data with that obtained for the di-*O*-isopropylidene derivatives **4** and **5**, respectively, since the shieldings of C-1, C-2, and C-3 in the mono-*O*-isopropylidene derivatives **2** and **3** should be very similar to those of the corresponding carbons in **4** and **5**. Finally, the signal assignments in the spectrum of 2,3:5,6-di-*O*-isopropylidene-α-D-mannofuranose (**6**) were made in the following manner. The C-1, C-5, and C-6 signals were readily assigned by comparison of the chemical-shift data with that of **4** and **5**. The C-2 signal was assigned on the expectation that it should occur at lower field than either the signal for C-3 or C-4, since O-2 is incorporated in a 1,3-dioxolane ring and is in a *trans* relationship with O-1. In confirmation of this reasoning is the observation of essentially identical chemical shifts for the C-2 signals in the spectra of compounds **2**, **4**, and **6**.

In a c.m.r. study of furanose sugars, Perlin *et al.* (3*b*) observed that the C-4 signal in the spectrum of methyl α-D-glucofuranoside resonated ~7 p.p.m. upfield relative to the corresponding signal in the spectrum of methyl α-D-allofuranoside. However, in the case of the spectra of 1,2-*O*-isopropylidene-α-D-glucofuranose (**2**) and 1,2-*O*-isopropylidene-α-D-allofuranose (**3**), the C-4 signals have almost identical chemical shifts, and, more surprizingly, C-4 in the allofuranose derivative **5** is shielded (2 p.p.m. upfield shift) relative to C-4 in the glucofuranose derivative **4**. The shielding of C-4 in 1,2:5,6-di-*O*-isopropylidene-α-D-allofuranose (**5**) may perhaps be partly attributed to a γ interaction between O-5 and H-4; such effects have been observed with 4,6-*O*-benzylidene derivatives of hexopyranose sugars (1*l*) and with methyl ethers of galactopyranosides (1*n*). It is possible that this γ interaction may be attenuated in 1,2:5,6-di-*O*-isopropylidene-α-D-glucofuranose (**4**) as a result of an influence of the C-3 hydroxyl group on the orientation of the 5,6-*O*-isopropylidene group.

In the case of the c.m.r. spectra of the branched-chain sugars **8–13** the signal assignments could be unequivocally made from the proton-coupled spectra; the signals for the anomeric carbon, the isopropylidene-acetal carbon, and the isopropylidene-methyl groups were readily assigned on the basis of their characteristic chemical shifts. The c.m.r. data obtained for these compounds, together with that obtained for 1,2-*O*-isopropylidene-D-apio-β-L-furanose (**7**), permitted assignment of the configuration at the branching carbon atom and at the anomeric center in compounds **8–13**.

A comparison of the chemical shifts of the C-2 signal in the spectra of 1,2-*O*-isopropylidene-D-apio-β-L-furanose (**7**), 1,2:5,6-di-*O*-isopropylidene-α-D-allofuranose (**5**), and 1,2:5,6-di-*O*-isopropylidene-α-D-glucofuranose (**4**) revealed some interesting trends which are pertinent to the assignment of the configuration at C-4 in compounds **8–13**. It was assumed that C-5 and C-6

[2]It should be noted that the spectrum of compound **2** was recorded in 1:1 (v/v) methanol–chloroform-*d*, whereas that of 1,4-anhydroglucitol (3*c*) was recorded in deuterium oxide. However, it is assumed that, in the present cases, such a solvent change does not result in an appreciable change in chemical shifts. Thus, it is found that the chemical shifts of the C-4, C-5, and C-6 signals in the spectra of the two compounds are almost identical.

Can. J. Chem. Downloaded from www.nrcresearchpress.com by 210.87.254.42 on 09/05/12
For personal use only.

TABLE 1. Carbon-13 chemical-shift data[a]

Compound	Carbon									
	1	2	3	3′	4	4′	5	6	Me_2 —OCO—	Me's
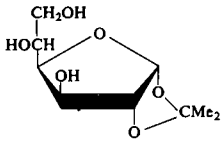 **2**[b]	105.6	85.8	75.1	—	80.7	—	70.1	65.7	112.1	26.8, 26.2
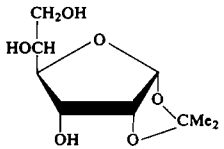 **3**[c]	104.3	80.2[d]	71.5	—	80.9[d]	—	70.9	63.6	113.2	26.7
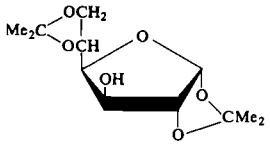 **4**	104.9	84.6	74.5	—	81.0	—	72.8	67.3	111.4 109.2	26.5, 25.9 25.0
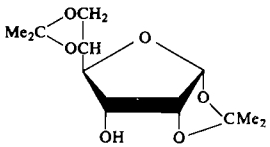 **5**	104.0	79.6	72.3	—	79.1	—	75.4	65.7	112.6 109.6	26.4, 25.3
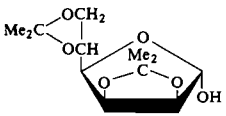 **6**	101.3	85.8	79.8[d]	—	80.2[d]	—	73.4	66.6	112.6 109.1	26.8, 26.0 25.3, 24.6

Can. J. Chem. Downloaded from www.nrcresearchpress.com by 210.87.254.42 on 09/05/12
For personal use only.

TABLE 1 (*Continued*)

Compound		Carbon									
		1	2	3	3′	4	4′	5	6	Me_2 —OCO—	Me's
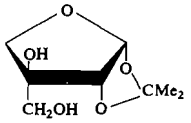	**7**	106.1	84.3	82.2	62.3	73.2	—	—	—	112.6	26.9, 26.4
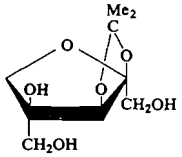	**8**	63.8	114.3[d]	79.9	—	79.4	63.4	71.7	—	112.5[d]	27.2
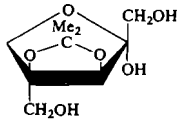	**9**[e]	64.3	105.9	86.3	—	92.5	64.0	74.3	—	114.0	27.8, 27.6
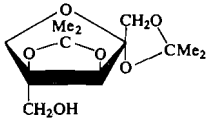	**10**[e]	69.3	113.7[d]	86.4	—	92.7	64.1	73.9	—	112.9[d] 111.9[d]	27.8, 27.6 26.6, 26.4
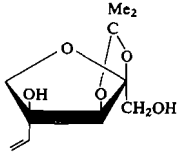	**11**[f]	63.7	113.0[d]	78.5	—	83.4	—	74.1	—	114.5[d]	27.4

Can. J. Chem. Downloaded from www.nrcresearchpress.com by 210.87.254.42 on 09/05/12
For personal use only.

TABLE 1 (*Concluded*)

Compound		Carbon									
		1	2	3	3′	4	4′	5	6	Me_2 —OCO—	Me's
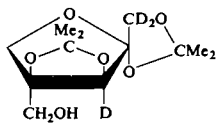	**12**[e]	—	113.7[d]	86.4[g]	—	92.7	64.1	73.9	—	112.9[d] 111.9[d]	27.8, 27.6 26.6, 26.4
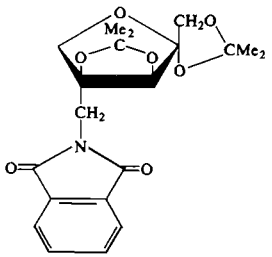	**13**[e,h]	69.1	112.7[d]	87.4	—	90.8	41.2	74.7	—	113.8[d] 111.5[d]	27.3, 26.3 26.1

[a]In p.p.m. downfield from internal tetramethylsilane (TMS). Spectra of compounds 2 and 3 were recorded in 1:1 (v/v) methanol–chloroform-*d*; those of 4–13 were recorded in chloroform-*d*.
[b]Chemical shifts for 1,4-anhydroglucitol (3*c*) carbons measured in deuterium oxide on the TMS scale are as follows: 74.4 (C-1), 77.4 (C-2), 76.9 (C-3), 80.9 (C-4), 70.0 (C-5), 64.6 (C-6).
[c]Chemical shifts for 1,4-anhydroallitol (3*c*) carbons measured in deuterium oxide on the TMS scale are as follows: 72.9 (C-1), 72.5 (C-2), 73.0 (C-3), 83.0 (C-4), 72.3 (C-5), 63.3 (C-6).
[d]Assignments for these peak positions may be reversed.
[e]Compound as DL modification.
[f]Chemical shifts for the vinyl carbons of compound **11** are as follows: 137.0 (CH=), 116.1 (CH_2=).
[g]The intensity of the C-3 signal was diminished relative to that of the C-3 signal in the spectrum of **10**, an observation indicative of only partial deuteration at this position.
[h]Chemical shifts for the carbons of the phthalimido group are as follows: 168.7 (C=O), 134.2, 132.1, and 132.4 (Ph).

Can. J. Chem. Downloaded from www.nrcresearchpress.com by 210.87.254.42 on 09/05/12
For personal use only.

have little or no effect on C-2 shieldings in compounds **4** and **5**,[3] and hence the C-2 chemical shifts in the spectra of compounds **4**, **5**, and **7** should reflect the nature and stereochemistry of the substituent at C-3. It is noteworthy that the C-2 chemical shifts are nearly identical in the spectra of 1,2:5,6-di-*O*-isopropylidene-α-D-glucofuranose (**4**) and **7**, whereas in the spectrum of 1,2:5,6-di-*O*-isopropylidene-α-D-allofuranose (**5**), the signal for C-2 is shifted upfield by ~5 p.p.m. relative to the corresponding signal in the spectrum of **7**; these observations imply that the *cis* O-2,O-3 interaction in **5** is a shielding one relative to the *cis* O-2,CH_2OH interaction in **7** (*cf.* refs. 3*b*–3*e*). In the spectrum of the dendroketose derivative **8** the C-3 and C-4 signals are shifted upfield by 4.4 and 2.8 p.p.m. relative to the corresponding signals (C-2 and C-3, respectively) in the spectrum of 1,2-*O*-isopropylidene-D-apio-β-L-furanose (**7**), an observation consistent with a *cis* O-3,O-4 arrangement in compound **8**; thus, the configuration at the branching carbon (C-4) in this dendroketose derivative is as shown in structural formula **8**. It follows also that the configuration at C-4 in the vinyl derivative **11** is as shown, since compound **8** was chemically derived from **11** by a procedure which is known not to affect the stereochemistry at C-4 (see ref. 5); in accordance with this conclusion is the observation of the upfield shift (5.8 p.p.m.) of the C-3 signal in the spectrum of compound **11** relative to the corresponding signal (C-2) in the spectrum of compound **7**.

The assignment of the configuration at the anomeric center in the dendroketose derivatives **9** and **10** was made as follows. It was observed that the C-4 signal in the spectrum of the 2,3-*O*-isopropylidene derivative **8** was shifted upfield by 13.1 p.p.m. relative to the corresponding signal in the spectrum of the 3,4-*O*-isopropylidene derivative **9**, whereas the C-2 signal in the spectrum of **9** was shifted upfield by 8.4 p.p.m. These observations are consistent with the anomeric configuration for compound **9** being as shown in the structural formula, since if **9** had possessed the opposite configuration at the anomeric center, then the C-2 signal would have been expected to have been shifted upfield by ~13 p.p.m. rather than the observed 8.4 p.p.m. shift. This conclusion is further corroborated by the chemical shift of the C-3 signal in the spectrum of **9**; this signal was shifted downfield by 6.4 p.p.m. relative to the corresponding signal in the spectrum of **8**. The structural feature responsible for the deshielding of C-3 in **9** relative to C-3 in **8** is the *cis* O-3,CH_2OH interaction as opposed to the *cis* O-3,O-4 interaction in **8**; in both of these compounds C-3 is part of a 1,3-dioxolane ring system. This reasoning is supported by the observation of Que and Gray (3*c*), in the case of the c.m.r. spectra of a series of ketohexofuranoses, that a *cis* O,CH_2OH interaction is a less shielding one relative to a *cis* O,O interaction. It is noteworthy that the chemical shift of the C-3 signal in the spectrum of **9** is almost identical to that of the corresponding signal (C-2) in the spectrum of 2,3:5,6-di-*O*-isopropylidene-α-D-mannofuranose (**6**) and differs by only 2 p.p.m. from that of the C-2 signal in the spectrum of 1,2-*O*-isopropylidene-D-apio-β-L-furanose (**7**); the similarities of these chemical shifts clearly reflect the nearly identical environments of the specified carbon atoms. In the case of the dendroketose derivative **10**, the configuration at the anomeric center was assigned as shown in the structural formula on the basis of the identity of the observed chemical shifts of the C-3 signals in the spectra of compounds **9** and **10**.

The c.m.r. spectroscopic data of the deuterated analog (**12**) of **10** are consistent with the assigned structure (see Table 1). In the spectrum of the phthalimido derivative (**13**) of **10** the only noteworthy features are the 23.9 and 1.9 p.p.m. upfield shifts of the C-4′ and C-4 signals, respectively, relative to the corresponding signals in the spectrum of **10**.

Experimental

The isopropylidenehexoses **2**, **4**, and **6** were prepared by procedures described by Schmidt (7); the isopropylideneallofuranoses **3** and **5** were prepared as described in refs. 8 and 9, respectively.[4] Procedures for the synthesis of compounds **8**–**13** are described in ref. 5.

Carbon-13 magnetic resonance spectra were recorded in chloroform-*d*, unless otherwise stated, on either a Varian CFT-20 spectrometer or a Bruker HX-60 spectrometer equipped with a FT60M Fourier transform accessory at 15.1 MHz, with tetramethylsilane (TMS) as internal standard; chemical shifts are given in parts per million downfield from TMS.

[3]This assumption was considered to be valid in the light of the c.m.r. study by Que and Gray (3*c*) on anhydro sugars; thus, it was found that the C-2 chemical shifts in the spectra of 1,4-anhydroerythritol, 1,4-anhydroribitol, and 1,4-anhydroallitol are 71.9, 72.0, and 72.5 p.p.m., respectively.

[4]An authentic sample of 1,2-O-isopropylidene-D-apio-β-L-furanose (7) was kindly provided by Dr. D. H. Ball, U.S. Army Natick Laboratories (see ref. 10).

The authors are grateful to the National Research Council of Canada for financial support in the form of a scholarship (to H.C.J.) and a grant (to W.A.S.), and to Professor J.K.N. Jones, F.R.S., for his interest and encouragement. They also thank Dr. B. K. Hunter of Queen's University and Dr. I. C. P. Smith of the National Research Council of Canada for recording the c.m.r. spectra.

1. (*a*) L. D. HALL and L. F. JOHNSON. Chem. Commun. 509 (1969); (*b*) A. S. PERLIN and B. CASU. Tetrahedron Lett. 2921 (1969); (*c*) D. E. DORMAN and J. D. ROBERTS. J. Am. Chem. Soc. **92**, 1355 (1970); (*d*) A. S. PERLIN, B. CASU, and H. J. KOCH. Can. J. Chem. **48**, 2596 (1970); (*e*) H. J. KOCH and A. S. PERLIN. Carbohydr. Res. **15**, 403 (1970); (*f*) N. NEUSS, K. F. KOCH, B. B. MOLLOY, W. DAY, L. L. HUCKSTEP, D. E. DORMAN, and J. D. ROBERTS. Helv. Chim. Acta, **53**, 2314 (1970); (*g*) D. DODDRELL and A. ALLERHAND. J. Am. Chem. Soc. **93**, 2779 (1971); (*h*) R. BURTON, L. D. HALL, and P. R. STEINER. Can. J. Chem. **49**, 588 (1971); (*i*) E. BREITMAIER, W. VOELTER, G. JUNG, and C. TÄNZER. Chem. Ber. **104**, 1147 (1971); (*j*) W. VOELTER, E. BREITMAIER, and G. JUNG. Angew. Chem. Int. Ed. Engl. **10**, 935 (1971); (*k*) E. BREITMAIER, G. JUNG, and W. VOELTER. Chimia, **25**, 362 (1971); (*l*) E. CONWAY, R. D. GUTHRIE, S. D. GERO, G. LUKACS, A. M. SEPULCHRE, E. W. HAGAMAN, and E. WENKERT. Tetrahedron Lett. 4879 (1972); (*m*) E. BREITMAIER and W. VOELTER. Tetrahedron, **29**, 227 (1973); (*n*) W. VOELTER, E. BREITMAIER, E. B. RATHBONE, and A. M. STEPHEN. Tetrahedron, **29**, 3845 (1973); (*o*) B. COXON. Ann. N.Y. Acad. Sci. **222**, 952 (1973); (*p*) D. R. BUNDLE, H. J. JENNINGS, and I. C. P. SMITH. Can. J. Chem. **51**, 3812 (1973); (*q*) K. BOCK, I. LUNDT, and C. PEDERSEN. Tetrahedron Lett. 1037 (1973); (*r*) J. HAVERKAMP, J. P. C. M. VAN DONGEN, and J. F. G. VLIEGENTHART. Carbohydr. Res. **33**, 319 (1974); (*s*) O. ACHMATOWICZ, JR., M. CHMIELEWSKI, J. JURCZAK, and L. KOZERSKI. Rocz. Chem. **48**, 481 (1974); (*t*) W. A. SZAREK, D. M. VYAS, S. D. GERO, and G. LUKACS. Can. J. Chem. **52**, 3394 (1974).
2. J. D. ROBERTS, F. J. WEIGERT, J. I. KROSCHWITZ, and H. J. REICH. J. Am. Chem. Soc. **92**, 1338 (1970).
3. (*a*) A. J. JONES, D. M. GRANT, M. W. WINKLEY, and R. K. ROBINS. J. Am. Chem. Soc. **92**, 4079 (1970); (*b*) A. S. PERLIN, N. CYR, H. J. KOCH, and B. KORSCH. Ann. N.Y. Acad. Sci. **222**, 935 (1973); (*c*) L. QUE, JR., and G. R. GRAY. Biochemistry, **13**, 146 (1974); (*d*) T. USUI, S. TSUSHIMA, N. YAMAOKA, K. MATSUDA, K. TUZIMURA, H. SUGIYAMA, S. SETO, K. FUJIEDA, and G. MIYAJIMA. Agric. Biol. Chem. (Tokyo), **38**, 1409 (1974); (*e*) P. C. M. HERVE DU PENHOAT and A. S. PERLIN. Carbohydr. Res. **36**, 111 (1974); (*f*) R. W. BINKLEY, W. W. BINKLEY, and B. WICKBERG. Carbohydr. Res. **36**, 196 (1974); (*g*) A. S. PERLIN, N. CYR, R. G. S. RITCHIE, and A. PARFONDRY. Carbohydr. Res. **37**, C1 (1974).
4. (*a*) A. M. SEPULCHRE, A. GATEAU-OLESKER, G. LUKACS, S. D. GERO, and W. VOELTER. Tetrahedron Lett. 3945 (1972); (*b*) A.M. SEPULCHRE, G. LUKACS, G. VASS, and S. D. GERO. Angew. Chem. Int. Ed. Engl. **11**, 148 (1972); (*c*) G. LUKACS, A. M. SEPULCHRE, A. GATEAU-OLESKER, G. VASS, S. D. GERO, R. D. GUTHRIE, W. VOELTER, and E. BREITMAIER. Tetrahedron Lett. 5163 (1972); (*d*) A. M. SEPULCHRE, B. SEPTE, G. LUKACS, S. D. GERO, W. VOELTER, and E. BREITMAIER. Tetrahedron, **30**, 905 (1974); (*e*) M. MILJKOVIĆ, M. GLIGORIJEVIĆ, T. SATOH, and D. MILJKOVIĆ. J. Org. Chem. **39**, 1379 (1974); (*f*) M. MILJKOVIĆ, M. GLIGORIJEVIĆ, T. SATOH, D. GLIŠIN, and R. G. PITCHER. J. Org. Chem. **39**, 3847 (1974).
5. H. C. JARRELL. M.Sc. Thesis, Queen's University, Kingston, Ontario. 1974.
6. L. M. UTKIN. Dokl. Akad. Nauk SSSR, **67**, 301 (1949).
7. O. T. SCHMIDT. Methods Carbohydr. Chem. **2**, 318 (1963).
8. P. M. COLLINS. Tetrahedron, **21**, 1809 (1965).
9. J. D. STEVENS. Methods Carbohydr. Chem. **6**, 123 (1972). See also D. C. BAKER, D. HORTON, and C. G. TINDALL, JR. Carbohydr. Res. **24**, 192 (1972).
10. D. H. BALL, F. H. BISSETT, I. L. KLUNDT, and L. LONG, JR. Carbohydr. Res. **17**, 165 (1971).

Can. J. Chem. Downloaded from www.nrcresearchpress.com by 210.87.254.42 on 09/05/12
For personal use only.

The Use of Deuterium Magnetic Resonance in the Determination of the Structure and Location of the Anilinium Ion in an Aqueous Anisotropic Surfactant Solution

PETER DIEHL AND ALAN S. TRACEY

Department of Physics, The University of Basel, Klingelbergstrasse 82, CH-4056 Basel, Switzerland

Received April 1, 1975

P. DIEHL and A. S. TRACEY. Can. J. Chem. **53**, 2755 (1975).

Anisotropic soap solutions containing the anilinium ion have been studied by n.m.r. techniques. The partially averaged proton–proton dipole couplings were used to obtain the relative positions of the hydrogen nuclei of the phenyl ring. Deuterium quadrupole splittings from the deuterium enriched ion provided information concerning the quadrupole coupling constant, Q_D, the asymmetry parameter, η, and the angles that the C—D bonds make with the coordinate systems axes. Quadrupole splittings from the deuterium enriched decylsulfate simultaneously with those from the anilinium ion established that the C_2 axis of the ion on an average lies parallel to the decylsulfate chain axis and is ordered to a similar extent. It is concluded that the aromatic ring is incorporated into the superstructure of the soap solution and that the $-NH_3^+$ group protrudes into the electrical double layer where it interacts with the oppositely charged decylsulfate and with water.

P. DIEHL et A. S. TRACEY. Can. J. Chem. **53**, 2755 (1975).

On a étudié, par r.m.n., des solutions anisotropiques de savon contenant l'ion anilinium. On a utilisé les valeurs partiellement moyennées des couplages dipolaires proton–proton pour obtenir les positions relatives de l'atome d'hydrogène du noyau phényle. Les couplages quadrupolaires du deutérium dans des ions enrichis en deutérium ont permis d'obtenir des informations relatives à la constante de couplage quadrupolaire, Q_D, au paramètre d'asymétrie, η, et aux angles que font les liens C—D avec les axes du système de coordonnées. Les couplages quadrupolaires de sulfate de décyle enrichi en deutérium observés simultanément avec ceux de l'ion anilinium ont permis d'établir que l'axe C_2 de l'ion à l'état moyen est parallèle à l'axe de la chaîne du sulfate de décyle et que l'ion est ordonné jusqu'à un degré semblable. On en conclut que le noyau aromatique est incorporé dans la superstructure de la solution de savon et que le groupe $-NH_3^+$ se trouve dans la double couche électrique où il interagit avec l'eau et avec le sulfate de décyle de charge opposée.

[Traduit par le journal]

Introduction

Recent work has established the applicability of nematic anisotropic soap solutions to the determination of ionic structures in aqueous solution (1, 2). These studies have taken advantage of the partially averaged internuclear dipole–dipole coupling in a homogeneously ordered system. Such structure determination of molecular or ionic species from n.m.r. techniques has, until the present time, utilized almost exclusively the direct dipolar coupling between proton and proton or between carbon-13 and proton. Couplings to other nuclei such as phosphorus-31 or nitrogen-15 have been used to a more limited extent.

Deuterium magnetic resonance, until the present time, has received relatively little attention as a structural tool although it has been used as a probe into the structural characteristics of macroscopically oriented smectic (3–5) and nematic (6–8) lyotropic phases. In the case of hydrocarbons, the major quadrupolar axis of deuterium deviates only slightly from the C—D bond axis and the quadrupole coupling tensor has a small asymmetry parameter. As a consequence deuterium has potentially an important role to play in structural work.

The deuterium quadrupole splitting can, in principle, provide some of the information obtained from ^{13}C substituted species. In cases where ^{13}C substitution is difficult, often the replacement of hydrogen by deuterium is a straightforward process.

The effects of many surfactants in micellar solution on the rates of reaction of various aromatic and aliphatic compounds have been extensively investigated (9, 10). These studies are important in understanding factors which influence chemical reactions and as such may provide information concerning processes in bio-

Can. J. Chem. Downloaded from www.nrcresearchpress.com by 210.87.254.40 on 09/05/12
For personal use only.

TABLE 1. Compositions of the nematic phases used in this study

Phase	Weight %				
	Sodium decylsulfate	Anilinium decylsulfate	Sodium sulfate	Decanol	Water
1	23.4	20.1	3.1	0.8	52.6*
2	23.0	20.1	2.8	0.8	53.3*
3	24.3	19.0	3.1	0.8	52.8*
4†	26.3	19.6	2.9	1.2	50.0‖
5†	26.8	19.6	2.9	1.2	49.4‖
6†‡	25.3	18.6	2.8	1.1	52.2‖
7†	27.8§	18.6	2.8	1.1	49.7‖

*Prepared with D_2O.
†Prepared with anilinium-d_5.
‡This phase was prepared with H_2O acidified to 0.1 *N* with HCl. All other phases were prepared with water acidified to 0.1 *N* with H_2SO_4.
§This sodium decylsulfate consists of 41% 2,2,3,3-tetradeuterated, 30% 2,2-dideuterated, and 29% 9,9,10,10,10-pentadeuterated sodium decylsulfate.
‖Prepared with H_2O.

logical systems. Unfortunately much of this work is hampered by a lack of definitive knowledge concerning the relative orientations of the reacting species with each other and, most particularly, with the micellar superstructure of the solution. The location of ionic species in lyotropic liquid crystals is then of interest since this information may be useful in understanding the various properties of such systems. Since dipole couplings and quadrupole splittings provide information concerning the orientation of species in anisotropic solution we have an opportunity to obtain this information quantitatively.

The anilinium ion offers a particularly good system for the demonstration of the value of quadrupole coupling constants for structure determination and simultaneously allows conclusions to be drawn about the location of this ion. In this study the anilinium ion, the pentadeuteroanilinium ion, and deuterium labelled decylsulfate, all in nematic solution, were investigated.

Experimental

Anilinium Decylsulfate

Anilinium chloride (2 gm) was added to sodium decylsulfate (4 gm), then combined with chloroform (200 ml). Water (1 ml) was added and the mixture refluxed until all sodium decylsulfate went into solution. The water was removed by codistillation with chloroform. Carbon was added to the product, then it was filtered through celite. The resultant solution was evaporated to approximately 50 ml and light petroleum (200 ml) was added. The solution was cooled to −20 °C and the product obtained by filtration, then recrystallized from chloroform – petroleum ether. The yield was quantitative.

Anilinium-d_5 Decylsulfate

Pentadeuteroaniline (1.25 gm) in methanol (20 ml) was neutralized with decylsulfuric acid prepared by passing sodium decylsulfate (3.5 gm) in water (10 ml) through a Dowex 50-H^+ column (20 ml). The product was evaporated with aliquots (100 ml) of chloroform–ethanol (99%) until the water was removed. The product was recrystallized from chloroform – petroleum ether. The yield was quantitative.

Nematic Liquid Crystals

The compositions of the nematic phases are given in Table 1. They were prepared by weighing the various components into a small test tube then alternately stirring and centrifuging until dissolution was complete. Slight warming to ~50° aided the process considerably.

Nuclear Magnetic Resonance Spectra

Proton spectra were obtained either in the FT mode at 60 MHz (samples 1 and 2, Table 1) from a Bruker spectrometer or at 100 MHz (sample 3, Table 1) from a Varian HA-100 continuous wave spectrometer. Deuterium spectra were obtained from a Bruker Hx-90 modified to pulse 50 kHz spectral widths. Operating temperatures were ~27°.

Results

It has recently been shown that nematic soap solutions are not of a single type but that at least two nematic phases occur (11, 12). The nematic Type I phase orients with its uniaxial direction parallel to the magnetic field. As a consequence when in a conventional spectrometer, this phase gives a rotation diagram according to $\frac{1}{2}(3\cos^2\phi - 1)$ where ϕ is the angle of rotation from the equilibrium angle of 0°. The nematic Type II phase orients with the hydrocarbon superstructure perpendicular to H_0. This is the usual phase which has been used as an orienting medium in lyotropic work. After prolonged spinning the uniaxial direction of this phase is parallel to the spinning axis and the spectrum is independent of rotation angle.

The nematic phases which were used in this

Can. J. Chem. Downloaded from www.nrcresearchpress.com by 210.87.254.40 on 09/05/12
For personal use only.

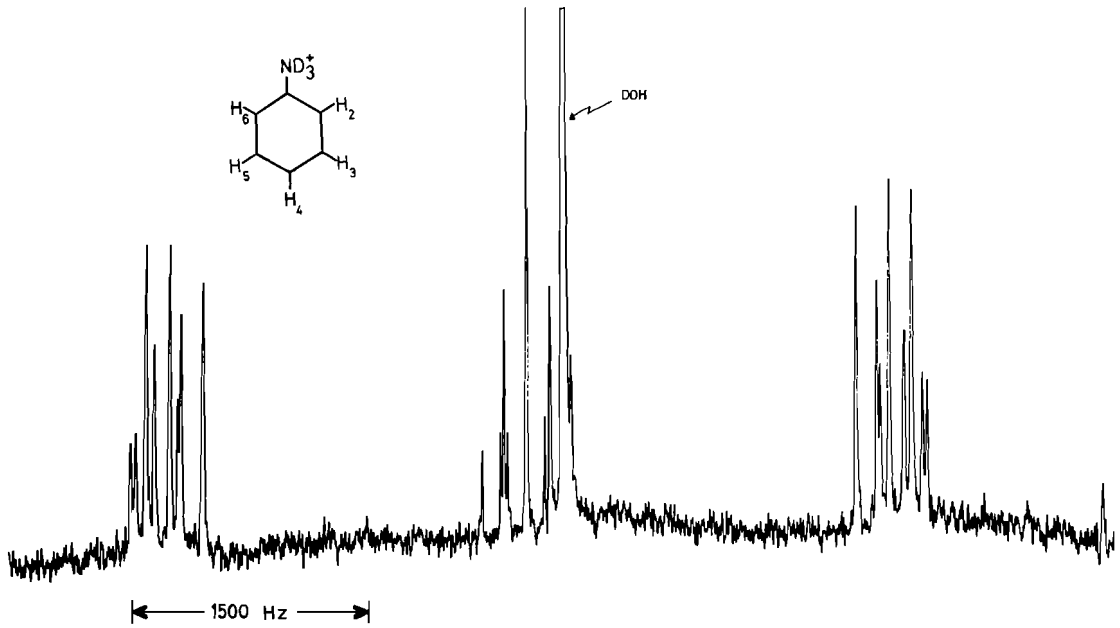

FIG. 1. A proton magnetic resonance spectrum from the anilinium ion in anisotropic solution. The resonances near the centre of the spectrum (excluding the DOH peak) arise from proton 4. The resonances at the wings arise from protons 2,6 and 3,5 (spectrum from phase 3, Table 1).

TABLE 2. Proton internuclear dipolar couplings (in Hz) from phases 1 to 3

	Phase			Isotropic†	
Parameter	1	2	3	Parameter	Value
$D_{23} = D_{56}$	−1132.8	−1154.3	−1524.5	$J_{23} = J_{56}$	8.06
$D_{24} = D_{46}$	−145.2	−145.7	−194.6	$J_{24} = J_{46}$	1.12
$D_{25} = D_{36}$	1.78	1.79	3.46	$J_{25} = J_{36}$	0.42
$D_{34} = D_{45}$	20.1	19.5	33.4	$J_{34} = J_{45}$	7.52
D_{26}	79.1	80.4	106.4	J_{26}	2.54
D_{35}	76.8	77.9	105.2	J_{35}	1.61
Root mean square*	0.207	0.244	0.323	Root mean square*	0.086
Number of transitions fitted	17	16	18	Number of transitions fitted	47

*The r.m.s. deviation between the observed and "best fit" spectra.
†Obtained from an acidified solution of anilinium chloride in D_2O.

study were of Type I. This was established by observing the n.m.r. signal from the anilinium ion on the oscilloscope of the spectrometer, then rotating the sample and observing the variation in the spectral width. The maximum width was found to occur at 0° of rotation. A typical proton spectrum is displayed in Fig. 1. The spectral analysis was straightforward and similar for all phases. The results are tabulated in Table 2. All nematic phases were prepared with water (or D_2O) acidified to approximately pH 1 with either H_2SO_4 or HCl. This pH insured that no significant quantities of free aniline were present in solution.

Figure 2 shows a deuterium spectrum obtained from the deuterated anilinium ion. The large quadrupolar doublet of 36 kHz splitting arises from D_4 and demonstrates the high degree of order along the C_4—D_4 bond (*i.e.* the C_2 axis). The next quadrupole doublet, split further by

Can. J. Chem. Downloaded from www.nrcresearchpress.com by 210.87.254.40 on 09/05/12
For personal use only.

Can. J. Chem. Downloaded from www.nrcresearchpress.com by 210.87.254.40 on 09/05/12
For personal use only.

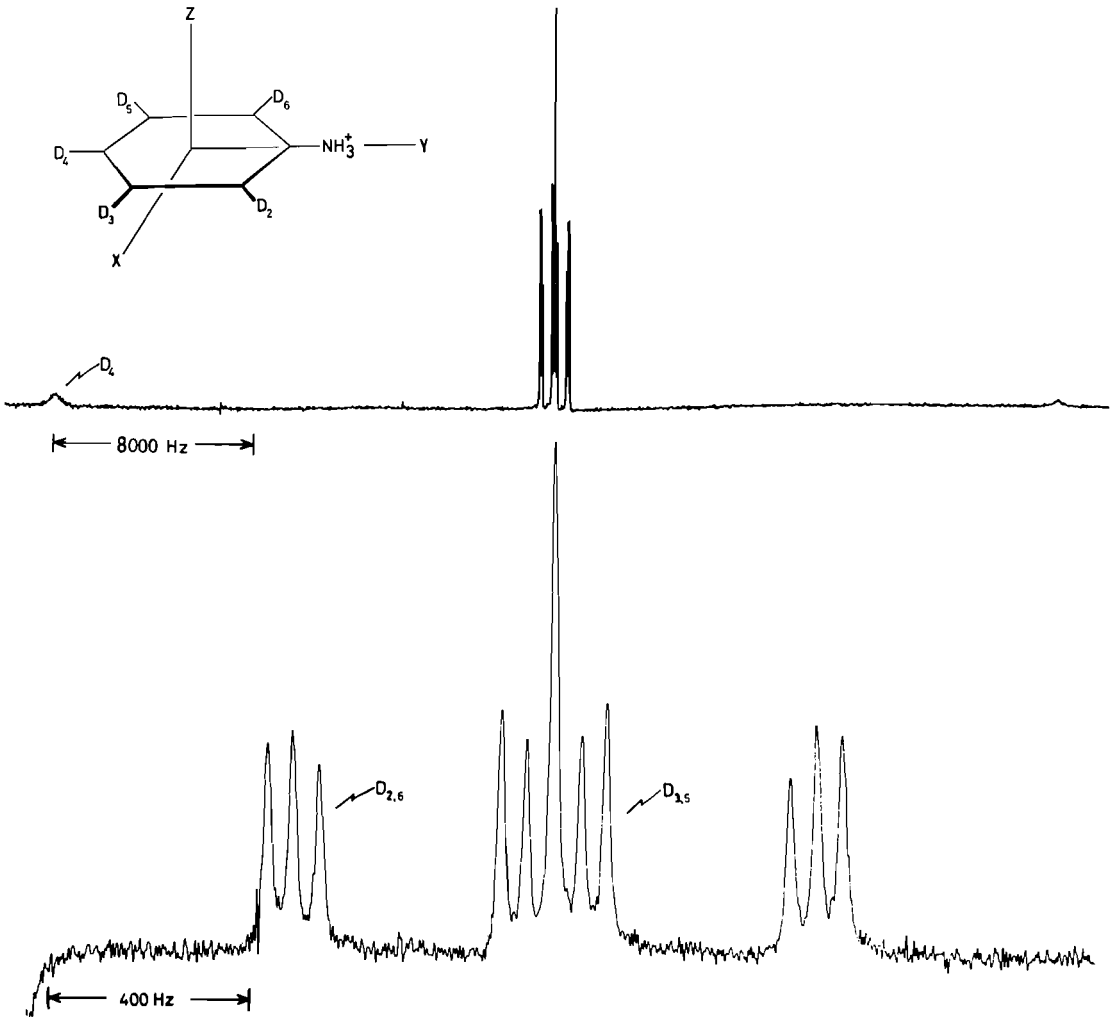

FIG. 2. A deuterium magnetic resonance spectrum from the deuterated anilinium ion in anisotropic solution. The upper trace shows the complete spectrum, the lower only the central resonances of the upper spectrum. The quadrupole doublets are labelled according to the position in the ion that they arise from (spectrum from phase 4, Table 1).

dipole couplings, arises from deuteriums 2 and 6, the overlapping triplets from deuteriums 3 and 5. The small quadrupole splittings of these two sets of deuteriums, ~ 100 and ~ 1200 Hz respectively, indicate the very small degrees of order along these C—D bonds.

Normally in nematic phases it is difficult to change the relative degrees of order along different axes significantly. In this system the quadrupolar axes of deuteriums 2,6 and 3,5 were directed along an axis so close to the zero transition angle that very small changes in S_{xx} relative to S_{yy} had a significant effect on the relative magnitudes of the quadrupolar splittings as is evident from Table 3.

The quadrupole splittings for each position are given by equations similar to [1].

$$[1]\quad \Delta\nu_D = \frac{3}{2}Q_D\left(S_{zz}' + \frac{\eta}{3}(S_{xx}' - S_{yy}')\right)$$

where $\Delta\nu_D$ is the quadrupole splitting and S_{zz}' is the degree of order along the major quadrupole axis which is assumed to be along the C—D bond. Q_D, the quadrupole coupling constant, was assumed to be equal for the three nonequivalent positions and determined from the

TABLE 3. The deuterium nuclear quadrupole splittings and dipolar couplings (both in Hz) and the orientation parameters, all obtained from phases 4 to 7

Phase	$\Delta\nu_2 = \Delta\nu_6$	$\Delta\nu_3 = \Delta\nu_5$	$\Delta\nu_4$	$D_{23} = D_{56}$	S_{xx}*	S_{yy}*
Experimental						
4	1229.8 ± 1.2	92.0 ± 1.2	48 350 ± 100	−31.68 ± 0.26	−0.0608	0.1705
5	1024.8 ± 1.5	103.8 ± 2.0	39 520 ± 100	−25.69 ± 0.41	−0.0495	0.1391
6	1028.4 ± 1.6	184.6 ± 1.5	36 140 ± 100	−23.32 ± 0.31	−0.0449	0.1273
7	1222.3 ± 1.7	209.2 ± 1.6	43 170 ± 100	−28.24 ± 0.36	−0.0537	0.1523
Normalized to the value $\Delta\nu_4$ = 36 140 Hz						
4	919.2 ± 0.9	68.8 ± 0.9	36 140 ± 75	−23.68 ± 0.19	—	—
5	937.2 ± 1.4	94.9 ± 1.8	36 140 ± 92	−23.49 ± 0.37	—	—
6	1028.4 ± 1.5	184.6 ± 1.5	36 140 ± 100	−23.32 ± 0.31	—	—
7	1023.3 ± 1.4	175.1 ± 1.3	36 140 ± 84	−23.64 ± 0.30	—	—

*Values are quoted for $\eta = 0.05$ and $r_{23} = 2.481$ Å.

TABLE 4. Geometric parameters obtained from the dipole couplings of Table 2

Parameter	Phase 1	Phase 2	Phase 3	Average	Error
r_{23}/r_{34}	1.0011	1.0004	1.0013	1.0009	±0.0005
$r_{24}/r_{34} = r_{46}/r_{34}$	1.7282	1.7282	1.7305	1.7290	±0.0013
$r_{25}/r_{34} = r_{36}/r_{34}$	1.9962	1.9963	2.0001	1.9975	±0.0022
r_{26}/r_{34}	1.7196	1.7210	1.7286	1.7231	±0.0048
r_{35}/r_{34}	1.7344	1.7340	1.7344	1.7343	±0.0002
r_{35}/r_{26}	1.0086	1.0075	1.0033	1.0065	±0.0028
S_{xx}*	−0.0511	−0.0518	−0.0698	—	—
S_{yy}*	0.1446	0.1470	0.1946	—	—
Root mean square†	0.138	0.295	0.081	—	—

*The orientation parameters are based on the assumed distance r_{34} = 2.481 Å.
†The r.m.s. deviation of the calculated dipolar couplings from those observed.

quadrupole splittings and the dipole coupling D_{23}. D_{23}, within a very small error is directed along the y axis. The assumption that the three Q's are equal has a negligibly small effect on any parameters obtained. The deuterium and proton spectral parameters were obtained with the aid of a modified UEA (13) n.m.r. computer program. The modified program iterates on all parameters, chemical shifts, indirect couplings, direct couplings, and quadrupole splittings.

Discussion

The Structural Information Provided by the Internuclear Proton–Proton Dipole Couplings

No structural information concerning the $-NH_3^+$ was obtainable since the NH exchange could not be slowed enough for observation of the NH_3 protons. Information concerning the positions of the aromatic protons was obtainable.

The phenyl ring has C_{2v} symmetry, so two orientation parameters are necessary to define its order while three distance ratios are required for a description of its structure. As a consequence five dipole couplings are needed for a complete analysis of the system. Since the spectrum provides six dipole couplings the system is overdetermined by one D value. The iterative least squares computer program SHAPE (14) was used to obtain the optimal structure parameters. Three independent structure determinations were made. The coordinate system was chosen so that the y axis was along the C_2 symmetry axis, the x axis in the plane of the ring, and the z axis perpendicular to the plane.

The results are summarized in Table 4. The benzene proton–proton distance of 2.481 Å was used as a reference distance to obtain the orientation constants. It is evident that the proton structure deviates only slightly from a regular hexagonal geometry. The distance r_{26} is increased by the factor 1.0065 ± 0.0028 from the

Can. J. Chem. Downloaded from www.nrcresearchpress.com by 210.87.254.40 on 09/05/12
For personal use only.

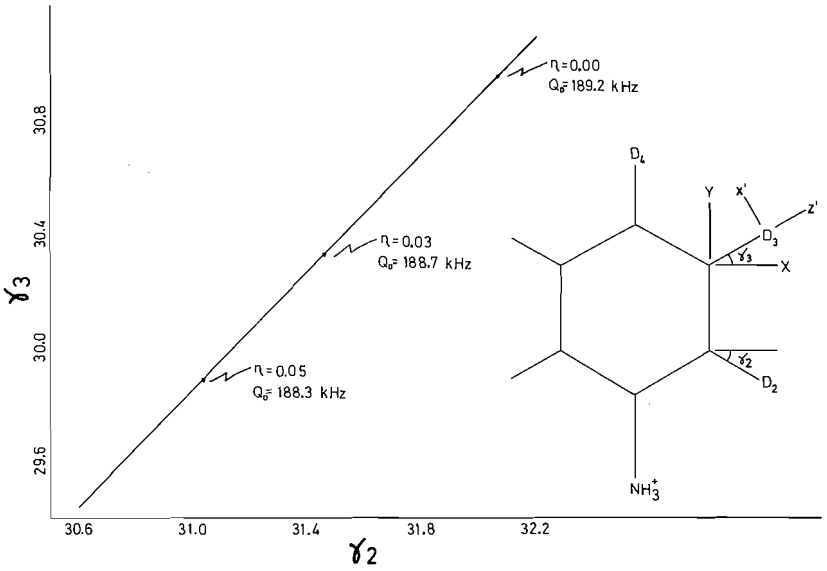

FIG. 3. This diagram shows the coordinate system employed to describe the quadrupole splittings. The angles γ_2 and γ_3 are used so that the quadrupole coordinates x', y', and z' can be easily related to the coordinate system of the ion, x, y, and z. The relationship between γ_2 and γ_3 is shown on the graph for the region of interest. Values which correspond to specific angles are also shown.

distance r_{35}. The ratio $r_{35}/r_{34} = 1.7343 \pm 0.0002$ is slightly larger than that of a true hexagon where this value is $\sqrt{3} = 1.7320$ while the value $r_{26}/r_{34} = 1.7231 \pm 0.0048$ is smaller. The values of the distances r_{23} and r_{34} are nearly equal ($r_{23}/r_{34} = 1.0009 \pm 0.0005$) as required for hexagonal geometry.

The proton evidence thus indicates that the aromatic hydrogens are arranged in a nearly hexagonal geometry but with a slight displacement of the hydrogens 2 and 6 towards the nitrogen.

The Information Provided by the Deuterium Quadrupole Splittings

With the assumptions that the quadrupole coupling constants Q_D and the asymmetry parameters η vary insignificantly with position within the aromatic ring and that a principal axis of the quadrupole coupling tensor is directed along the C—D bond axis it is possible to derive eqs. 2 to 4 from [1] where the $\Delta\nu_i$ are the observed quadrupole splittings for positions i.

$$[2]\quad \Delta\nu_2 = \frac{3}{2}Q_D\Big[S_{yy} - \cos^2\gamma_2(S_{yy} - S_{xx}) + \frac{\eta}{3}(2S_{xx} + S_{yy} + \cos^2\gamma_2(S_{yy} - S_{xx}))\Big]$$

$$[3]\quad \Delta\nu_3 = \frac{3}{2}Q_D\Big[S_{yy} - \cos^2\gamma_3(S_{yy} - S_{xx}) + \frac{\eta}{3}(2S_{xx} + S_{yy} + \cos^2\gamma_3(S_{yy} - S_{xx}))\Big]$$

$$[4]\quad \Delta\nu_4 = \frac{3}{2}Q_D\Big[S_{yy} + \frac{\eta}{3}(2S_{xx} + S_{yy})\Big]$$

The angles γ_2 and γ_3 are shown in Fig. 3 as is the axis system for deuterium 3. The transformation from the quadrupolar coordinate system to the ionic coordinate system is straightforward and utilizes equations of the type [5]

$$[5]\quad S_{zz}' = \cos^2\phi_{xx}S_{xx} + \cos^2\phi_{yy}S_{yy}$$

where ϕ_{xx} and ϕ_{yy} are the angles that the quadrupolar axes make with the coordinate axes of the ion and are given by the angles γ_i.

If we substitute eq. 4 into [2] and [3] and let $k_0 = S_{yy} - S_{xx}$, $p = \cos^2\gamma_2$, and $p' = \cos^2\gamma_3$ we obtain the expressions [6] and [7].

$$[6]\quad 2(\Delta\nu_2 - \Delta\nu_4) = Q_D p k_0(\eta - 3)$$

$$[7]\quad 2(\Delta\nu_3 - \Delta\nu_4) = Q_D p' k_0(\eta - 3)$$

Q_D, p, p', k_0, and η are the unknowns of interest. Unfortunately, as may be seen from the equations, the unknowns always arise as products so

Can. J. Chem. Downloaded from www.nrcresearchpress.com by 210.87.254.40 on 09/05/12
For personal use only.

Can. J. Chem. Downloaded from www.nrcresearchpress.com by 210.87.254.40 on 09/05/12
For personal use only.

that individual determination is not possible. Furthermore additional spectra from ions with different relative orientations will not help the analysis since for each new equation there is also a new unknown. This situation is quite similar to that encountered when attempting to obtain internuclear distances from dipolar couplings. Only the ratios of S_{ij} to r_{ij}^3 can be obtained and consequently only relative distances within a system of interacting nuclei. It occurs similarly in the problem of obtaining relative populations in an equilibrating system. Here only the product of relative population and degree of order is obtainable even though the geometry of the individual components may be known.

In the present problem only the ratio (p/p') can be determined from [6] and [7], that is, the ratio of the angles γ_2 to γ_3 is defined very accurately. The value $\cos\gamma_2/\cos\gamma_3 = 0.98817 \pm 0.00004$ was found. A plot of γ_3 *vs.* γ_2 is shown in Fig. 3.

The η and Q_D values corresponding to the individual points on this plot can be obtained by the following procedure. S_{yy} is given by the observed direct deuterium–deuterium dipolar coupling (Table 3), the geometric relationships of Table 4, and an assumed r_{34} of 2.481 Å. S_{xx} can then be obtained on the basis of the argument that the S_{yy}/S_{xx} ratio is the same for the deuterium spectra as from the proton spectra. As can be seen from Table 4 the variation of the ratio is small between different phases. From S_{xx} and S_{yy} as well as a chosen value of η the corresponding Q_D was provided by [4]. Finally substitution of S_{xx}, S_{yy}, η, and Q_D into [6] and [7] gives the angles γ_2 and γ_3 which match the η and Q_D values. In practice the four deuterium spectra were fitted simultaneously and the less stringent requirement, that the average value S_{yy}/S_{xx} for the deuterium spectra was the same as the average from the proton spectra, was imposed. The errors quoted for γ_2 were obtained mainly from the extreme deviation of the ratio S_{yy}/S_{xx} from its average value *i.e.* $S_{yy}/S_{xx} = -2.818 \pm 0.030$ from Table 4.

As shown in Fig. 3 a value of $\eta = 0$ (often assumed) leads to the angles $\gamma_2 = 32.0 \pm 0.13°$ and $\gamma_3 = 30.96°$. These angles when combined with the relevant proton data lead to a highly distorted carbon skeleton for the ring. As a consequence $\eta = 0$ is highly improbable. The asymmetry parameter has been obtained experimentally for several aromatic systems and found to be approximately 0.04 to 0.06 (15). Using the value $\eta = 0.05$ the angles $\gamma_2 = 31.05 \pm 0.13°$ and $\gamma_3 = 29.89°$ as well as $Q_D = 188.3 \pm 1.3$ kHz were obtained. This gives a reasonable carbon skeleton and also agrees well with the values for similar compounds in the literature (16, 17). An estimation of the vibrational corrections to γ_2 and γ_3 indicate that they are negligible.

The Orientation and Location of the Anilinium Ion

It has been established that the nematic phases in this study give rotationally dependent spectra from a conventional spectrometer. The angular dependence of quadrupole splittings from various monatomic ions (11) and of methanol (11) in various similar phases has been found to be identical. That is, all species behave similarly with respect to their orientation. Such a result would be anticipated if the hydrocarbon superstructure is not significantly different on going from one Type I phase to another and if the phases are composed of hydrocarbon layers separated by interstitial water and oriented so that the plane of hydrocarbon superstructure is perpendicular to H_0. The axis of an extended decyl chain then is parallel to H_0. Information about the degree of order of this axis was obtained by observing the deuterium spectrum from specifically labelled decylsulfate. Simultaneously the spectrum from the deuterated anilinium ion was obtained. The order of the chain axis (S_{Ch}) is given by

$$[8] \qquad \Delta\nu_D = \tfrac{3}{2}Q_D\tfrac{1}{2}(3\cos^2 90° - 1)S_{Ch}$$

where it is assumed that one S value is sufficient to describe the orientation of the chain as has been established for lamellar phases prepared from sodium decanoate (5). The term $\frac{1}{2}(3\cos^2 90° - 1) = -0.5$ transfers the order from the C—D bond to the chain axis to which it is perpendicular. Q_D is ~170 kHz for methylene groups.

Deuterium quadrupole splittings of 20.42, 18.82, and 9.70 kHz were obtained for positions 2, 3, and 9 of the decyl chain respectively, corresponding to order parameters S_{Ch}, of 0.1613, 0.1489, and 0.0761. The degree of order of the long axis (S_{yy}) of the anilinium ion in the same phase was 0.1528. This large degree of order is

Can. J. Chem. Downloaded from www.nrcresearchpress.com by 210.87.254.40 on 09/05/12
For personal use only.

almost identical to that of the hydrocarbon chains at the 2 and 3 positions and twice as large as that at the 9 position.

Several ionic species have been investigated in Type II phases. One characteristic in common with all oriented species was their rather low degrees of order [$(-1$ to $-10) \times 10^{-3}$] along a C_3 axis (12). The degree of order of the major axis of the anilinium ion ranges between $+0.13$ and $+0.19$ dependent on the particular phase. This is much larger than has been observed for other ions and similar to that of the degree of order of the hydrocarbon chains in the superstructure.

It has been found that substitution of other ions for sodium generally converts Type I phases into Type II (11). A survey of the literature shows that sodium sulfate (or occasionally another inorganic salt) has almost invariably been used as an additive in the preparation of nematic phases since this insures the formation of Type II phases. For this anilinium case it was found that addition of sodium sulfate did not convert the Type I into a Type II phase. When attempts were made to use more anilinium decylsulfate and less sodium decylsulfate (see Table 1 for the proportions used for the nematic phases), nematic phases would no longer be prepared but only smectic phases. These results indicate that the anilinium ion is a strong structure building component of the phase which stabilizes the lamellar structure.

It is clear from the results that the anilinium ion has become an integral part of the phase superstructure with its C_2 (or long axis) directed preferentially perpendicular to the surface of the lamellae. A positive or negative direction of the order axis cannot be assigned. However, since the aromatic ring is quite hydrophobic it can be expected that the phenyl ring penetrates into the superstructure and the charged $—NH_3^+$ group sits in the electrical double layer where it interacts efficiently with water and negatively charged decylsulfate headgroups. The opposite sense to the order, that is with the $—NH_3^+$ penetrating into the superstructure is not reasonable. That the degree of order of the C_2 axis of the ion is so much larger than that obtained from position 9 of the decyl chain shows that the ion does not spend a significant amount of its time in the interior of the superstructure.

The relative magnitudes of S_{xx} and S_{zz} indicate that the C_2 axis of the ion oscillates about H_0 more freely in the xy than in the zy plane. This result might be anticipated since oscillation in the xy plane would require substantially less free volume than that in the yz plane.

We would like to thank Dr. S. Sýkora of Bruker for obtaining the 60 MHz proton spectra for us and Bruker for providing the facility. We would also like to thank M. Reinhold for obtaining the deuterium spectra and the Swiss National Foundation for the Advancement of Science for the financial support.

1. L. W. Reeves, J. Sanchez de Cara, M. Suzuki, and A. S. Tracey. Mol. Phys. **25**, 1481 (1973).
2. L. W. Reeves, A. S. Tracey, and M. M. Tracey. J. Am. Chem. Soc. **95**, 3799 (1973).
3. J. Charvolin, P. Manneville, and B. Deloche. Chem. Phys. Lett. **23**, 345 (1973).
4. J. Seelig and W. Niederberger. J. Am. Chem. Soc. **96**, 2069 (1974).
5. P. Diehl and W. Niederberger. J. Magn. Reson. **15**, 391 (1974).
6. F. Fujiwara, L. W. Reeves, A. S. Tracey, and L. A. Wilson. J. Am. Chem. Soc. **96**, 5249 (1974).
7. D. M. Chen, L. W. Reeves, A. S. Tracey, and M. M. Tracey. J. Am. Chem. Soc. **96**, 5349 (1974).
8. L. W. Reeves and A. S. Tracey. J. Am. Chem. Soc. In press.
9. J. H. Fendler and E. Fendler. Adv. Phys. Org. Chem. **8**, 271 (1970).
10. E. H. Cordes. (*Editor*). Reaction kinetics in micelles. Plenum Press, New York, New York. 1973.
11. K. Radley, L. W. Reeves, and A. S. Tracey. J. Phys. Chem. In press.
12. C. L. Khetrapal, A. C. Kunwar, A. S. Tracey, and P. Diehl. NMR basic principles and progress, Vol. 9. *Edited by* P. Diehl, E. Fluck, and R. Kosfeld. Springer-Verlag, Berlin. 1975.
13. J. A. Ferritti, R. K. Harris, and R. B. Johannesen. J. Magn. Reson. **3**, 84 (1970).
14. P. Diehl, P. M. Henrichs, and W. Niederberger. Mol. Phys. **20**, 139 (1971).
15. R. G. Barnes and J. W. Bloom. J. Chem. Phys. **57**, 3082 (1972).
16. D. G. Lister, J. K. Tyler, J. H. Høg, and N. W. Larsen. J. Mol. Struct. **23**, 253 (1974).
17. I. Nitta, T. Watanabe, and I. Taguchi. Bull. Chem. Soc. Jpn. **34**, 1405 (1961).

Mechanisms of Acylal Hydrolysis in Sulfuric Acid Solutions

ROBERT ALLAN MCCLELLAND
Department of Chemistry, University of Toronto, Toronto, Ontario M5S 1A1
Received March 3, 1975

ROBERT ALLAN MCCLELLAND. Can. J. Chem. **53**, 2763 (1975).

The acid-catalyzed hydrolysis (in aqueous H_2SO_4) of acylals $ArOCH_2OAc$ is reported, and compared with that of normal acetate esters. On the basis of *r* plot behavior and the effects of the aromatic substituents, an A_{Ac}-2 ester hydrolysis mechanism is shown to occur in dilute acids, with a changeover to a mechanism analogous to A_{A1}-1 ester hydrolysis (intermediate cation $ArOCH_2^+$) in more concentrated acids, the position of the changeover being dependent on the substituent. Methylene diacetate is also investigated and shown to display the same behavior, with an A-1 mechanism involving an intermediate $CH_3COOCH_2^+$ becoming important at about 75% H_2SO_4. The relative A_{A1}-1 reactivities for acetates ROAc, R = CH_3OCH_2, *tert*-butyl, $C_6H_5OCH_2$, $C_6H_5CH_2$, 4-$NO_2C_6H_4OCH_2$, CH_3COOCH_2, isopropyl, are 6×10^3, 5×10^2, 1, 7×10^{-2}, 4×10^{-2}, 1.1×10^{-2}, 1.3×10^{-4} respectively.

ROBERT ALLAN MCCLELLAND. Can. J. Chem. **53**, 2763 (1975).

On rapporte l'hydrolyse acido-catalysé (dans l'acide sulfurique aqueux) d'acylals du type $ArOCH_2OAc$ et on compare ces hydrolyses à celles d'esters acétiques normaux. En se basant sur le comportement des courbes *r* et les effets des substituants aromatiques, on démontre qu'un mécanisme A_{Ac}-2 d'hydrolyse d'ester se produit en milieux acides dilués; en milieux acides plus concentrés, un mécanisme similaire à un mécanisme A_{A1}-1 d'hydrolyse d'ester (cation $ArOCH_2^+$ intermédiaire) devient prépondérant. La position du changement de mécanisme dépend du substituant. On a aussi examiné le diacétate de méthylène et on a démontré qu'il réagit de la même manière; le mécanisme A-1 impliquant un intermédiaire $CH_3COOCH_2^+$ devient important dans l'acide sulfurique 75%. Les réactivités A_{A1}-1 relatives des acétates ROAc où R = CH_3OCH_2, *tert*-butyle, $C_6H_5OCH_2$, $C_6H_5CH_2$, 4-$NO_2C_6H_4OCH_2$, CH_3COOCH_2, *iso*-propyle sont respectivement de 6×10^3, 5×10^2, 1, 7×10^{-2}, 4×10^{-2}, 1.1×10^{-2}, 1.3×10^{-4}.

[Traduit par le journal]

The class of organic molecules known as acylals (*e.g.* $ROCH_2OOCR'$) has received attention recently as suspected intermediates in enzymatic processes (1). These are somewhat unusual species in that they can be regarded both as carboxylate esters and as acetals. Thus, three reasonable mechanistic possibilities for their acid-catalyzed hydrolysis can be proposed (Scheme 1); as esters, an A_{Ac}-2 hydrolysis, and as acetals two A-1 reactions (2).[1]

In previous investigations, all three have been found or proposed, particularly when the acylal is incorporated in a cyclic system (4). Acyclic acylals seem however to prefer the A-1(b) pathway (2, 5–7) whose ease can be attributed to the resonance stabilization in the incipient oxycarbonium ion **1***b*. A mixture of A-1(b) and A_{Ac}-2 reactions has been suggested with formic acid acylals (5, 6) (more efficient bimolecular attack) and with 2-chloroethoxy acylals (8) (destabilized oxycarbonium ion). Methylene diacetate and ethylidene diacetate follow only the bimolecular route (9), presumably in order to avoid the formation of an acyloxycarbonium ion. No A-1(a) process has been observed with acyclic acylals; this also involves an intermediate acyloxycarbonium ion **1***a*.

Our interest in this system stems from the fact that the A-1(b) pathway can also be looked upon as an A_{A1}-1 ester hydrolysis,[2] so that the hydrolysis of the acyclic acylals can in a sense be regarded as a competition between unimolecular and bimolecular ester hydrolysis. This is the same type of competition that has been investigated in some detail for normal esters (11, 12),

[1]Recently a number of acetals have been encountered which show general acid-catalyzed hydrolysis (2, 3). For our purposes, we will not distinguish this from the above specific acid-catalyzed reactions, since the same intermediate carbonium ion is formed in both cases. In any event the acylals considered here do not possess the structural features that are likely to lead to the general catalysis.

[2]This hydrolysis can proceed with protonation at either oxygen of the carboxylate group. At present, no distinction can be made, although the carbonyl oxygen is the more basic site (10).

Can. J. Chem. Downloaded from www.nrcresearchpress.com by 210.87.254.42 on 09/05/12
For personal use only.

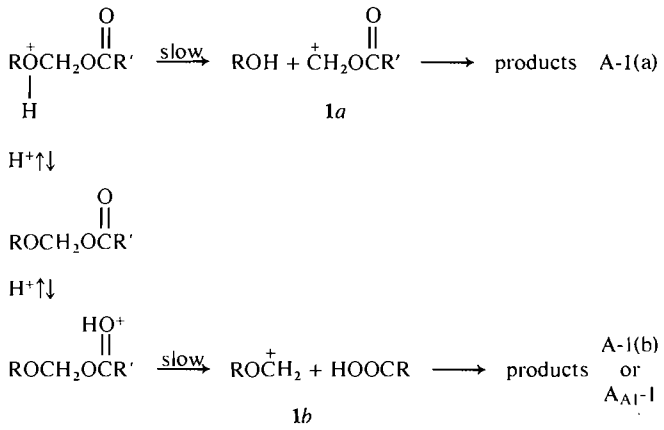

SCHEME 1

and we decided therefore to see if similar considerations apply in the acylal system. In particular this paper centers mainly on acylals of the type $ArOCH_2OAc$, in which the effects of the phenyl and its substituents are evaluated. We have also extended the study of methylene diacetate to more concentrated acid solutions.

The aryl acylals have seen little prior investigation. Fife and De have recently reported on the hydrolyses of a pair of *p*-nitrophenyl acylals (1). In acidic solutions the cyclic acylal 3-(*p*-nitrophenoxy)phthalide seemed to hydrolyze via a bimolecular mechanism, while its acyclic analog **2** was suggested to follow a unimolecular route; there were however certain ambiguities in both cases.

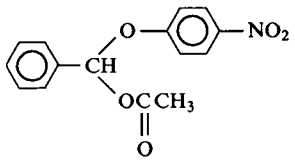

2

Results

In Table 1, first-order rate constants at 25 °C for the hydrolysis of a series of aryloxymethyl acetates are reported as a function of sulfuric acid concentration. Also included are data for methylene diacetate and methoxymethyl acetate. For the latter compound the literature values (determined by analysis of liberated formaldehyde (5)) show excellent agreement with those measured in this work (by following the u.v. absorbance change at 205 nm).

For the two activated aromatics, and to some extent the unsubstituted and 4-chloro compounds, considerable decomposition was observed above a certain acidity. This is probably caused by condensation reactions between the phenol and formaldehyde products since in the absence of formaldehyde the phenol is stable under the same conditions. This prevented extension of the study for the 4-methoxy and 4-methyl compounds to any higher acidity than that reported in Table 1. With the other two where the decomposition was less severe, rate constants in the more concentrated acids were calculated by the Guggenheim method.

In Table 2, second-order rate constants obtained on hydrolysis in aqueous sodium hydroxide at 25 °C are reported for the aryl acylals. These were obtained by following the hydrolysis under pseudo-first-order conditions in excess base (10^{-2} *M* NaOH, 10^{-4} *M* substrate). In the case of the unsubstituted compound, a number of sodium hydroxide concentrations were employed, and the rate was shown to be first order in base as well.

Discussion

In sulfuric acid solutions acetate esters have generally been found (11) to hydrolyze via the $A_{Ac}2$ mechanism in the dilute acid region, followed at some acidity by a changeover to one of two A-1 mechanisms, the type of A-1 and the position of changeover being dependent on the ester structure. With the exception of simple primary alkyl acetates and phenyl acetates, an $A_{Al}1$ reaction is involved, and a considerable variety of behavior can be observed, depending essentially on the stability of the carbonium ion

Can. J. Chem. Downloaded from www.nrcresearchpress.com by 210.87.254.42 on 09/05/12
For personal use only.

Can. J. Chem. Downloaded from www.nrcresearchpress.com by 210.87.254.42 on 09/05/12
For personal use only.

TABLE 1. Rates of acylal hydrolysis in aqueous sulfuric acid solutions at 25 °C

CH_3OCH_2OAc		4-$MeOC_6H_4OCH_2OAc$		4-$MeC_6H_4OCH_2OAc$		$C_6H_5OCH_2OAc$		4-$ClC_6H_4OCH_2OAc$	
%H_2SO_4	10^4k_ψ[a]	%H_2SO_4	10^4k_ψ	%H_2SO_4	10^4k_ψ	%H_2SO_4	10^4k_ψ	%H_2SO_4	10^4k_ψ
2.71	7.43	9.96	1.36	9.96	1.35	9.96	1.35	9.96	1.32
6.95	31.1[b]	15.6	2.19	15.6	2.20	15.6	2.21	15.6	2.24
8.08	35.8	19.5	3.52	19.5	3.40	19.5	3.43	19.5	3.33
10.7	61.6[b]	24.9	5.97	24.9	5.25	24.9	5.17	24.9	4.87
13.1	88.4	31.0	10.10	31.0	8.40	31.0	8.05	31.0	7.33
17.5	182[b]			35.5	12.3	35.5	10.9	35.5	9.57
18.5	204			40.2	19.3	40.2	14.1	40.2	12.6
20.7	287[b]					45.0	25.2	45.0	15.7
27.0	1040[b]					49.3	48.3	49.3	20.8
						51.9	76.7	54.5	40.0
						54.5	127	56.9	65.0
						56.9	230	59.2	115
						59.2	426	61.2	180
						62.7	930	63.1	308
								66.0	660

3-$ClC_6H_4OCH_2OAc$		4-$CNC_6H_4OCH_2OAc$		3-$NO_2C_6H_4OCH_2OAc$		4-$NO_2C_6H_4OCH_2OAc$		$CH_2(OAc)_2$	
%H_2SO_4	10^4k_ψ	%H_2SO_4	10^4k_ψ	%H_2SO_4	10^4k_ψ	%H_2SO_4	10^4k_ψ	%H_2SO_4	10^4k_ψ
9.96	1.30	9.96	1.30	9.96	1.30	9.96	1.25	9.96	2.14
19.5	3.36	15.6	3.21	15.6	2.10	15.6	2.03	19.5	5.30
31.0	7.30	31.0	7.13	24.9	5.02	19.5	3.22	31.0	12.1
40.1	12.2	35.5	9.33	35.5	9.46	24.9	4.79	35.5	15.8
49.3	19.1	49.3	18.9	40.2	12.0	31.0	7.29	40.2	20.4
59.2	61.2	54.5	22.8	45.0	16.0	35.5	9.37	45.0	26.4
63.9	132	59.2	27.2	49.3	19.5	40.2	12.2	49.3	33.3
65.7	194	62.7	31.4	54.5	24.8	45.0	15.8	54.5	42.8
67.5	316	65.7	41.1	59.2	30.2	49.3	19.2	59.2	52.5
69.9	670	68.6	57.4	66.0	50.6	54.5	24.0	66.0	65.2
71.3	950	70.4	79.9	70.9	110	59.2	27.0	70.9	70.8
		72.8	158	72.8	166	65.0	29.4	73.1	69.0
		74.5	257	74.5	288	68.9	36.7	78.9	126
		76.0	400	76.0	437	73.1	71.1	80.2	187
		77.7	700	77.7	750	74.5	115	81.7	315
						76.2	180	83.1	517
						77.0	230	84.2	750
						78.9	387		
						80.2	585		

[a]Pseudo-first-order rate constants, in s^{-1}.
[b]Reference 5.

Can. J. Chem. Downloaded from www.nrcresearchpress.com by 210.87.254.42 on 09/05/12
For personal use only.

TABLE 2. Hydrolysis of $ArOCH_2OAc$ in aqueous sodium hydroxide at 25 °C

Ar	k_{OH}-(M^{-1} s^{-1})
4-$MeOC_6H_4$	0.93
4-MeC_6H_4	0.96
C_6H_5	1.10
4-ClC_6H_4	1.44
3-ClC_6H_4	1.60
3-$NO_2C_6H_4$	2.25
4-$NO_2C_6H_4$	2.41

so formed. For example, in the series 4-methoxybenzyl acetate, benzyl acetate, 4-nitrobenzyl acetate, the acid concentration at which the A_{Al}-1 reaction becomes important (20%, 60%, 80% H_2SO_4 respectively (11)) is a direct reflection of the stabilization in the benzylic carbonium ions. In the case of strongly stabilized carbonium ions, the unimolecular process can predominate even in dilute acids and no bimolecular hydrolysis is observed, as for example with *tert*-butyl acetate (13).

In this sense then, an acylal like methoxymethyl acetate can be seen to fit this latter category, the methoxymethyl carbonium ion is stabilized sufficiently that only the unimolecular hydrolysis is observed (5, 6). With the aryloxymethyl acetates however, the intermediate oxycarbonium ion should be considerably less stabilized due to the competition for the oxygen electron pairs between the phenyl ring and the cationic center. In consequence the bimolecular hydrolysis becomes a very real possibility, particularly in the more dilute acids, and by analogy with normal esters, the A_{Al}-1 mechanism might be expected to occur only in more concentrated acids, the acidity being dependent on the actual stability of this cation.

In Fig. 1 the rate–acidity profiles obtained with the aryloxymethyl acetates are shown and compared with that of methoxymethyl acetate. Although all the curves exhibit a monotonic increase in rate with increasing acidity, there are considerable differences. Methoxymethyl acetate, like *tert*-butyl acetate (13), shows an immediate rapid increase in rate even in dilute acids. With the phenyl acylals, however, the rise in rate in the dilute acids is quite moderate; this is followed at some intermediate acid concentration by a much more pronounced increase, similar to that of the methoxymethyl compound. We will show that these profiles are reflecting precisely the con-

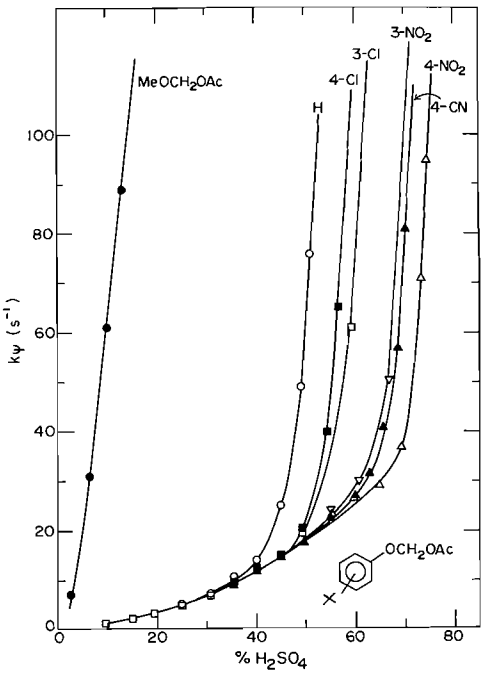

FIG. 1. Rate variation as a function of acidity for aryloxymethyl acetates at 25 °C.

siderations of the previous discussion, *i.e.* an A_{Ac}-2 hydrolysis in dilute acids giving way to an A_{Al}-1 hydrolysis at intermediate acidity, this mechanistic changeover being characterized by the change in the rate of increase of k_ψ.

The first piece of evidence for this behavior comes upon application of the *r* hydration treatment (11) to the rate–acidity data. Although the significance of the *r* values obtained from this approach is open to question (14), it has proven successful in suggesting mechanisms and mechanistic changes, in particular when applied to the hydrolysis of esters (11, 12). The *r* plots obtained with the acylals are depicted in Fig. 2. These take the form $\log k_\psi - \log (h_0^m/h_0^m + K_{SH^+})$ *vs.* $\log a_{H_2O}$ (11), where *m* and K_{SH^+} are parameters pertaining to the protonation step ($\log [BH^+]/[B] = m(-H_0) + pK_{SH^+}$). These terms could not be obtained with the acylals, since hydrolysis in the concentrated acids is too rapid. Consequently these plots are based on protonation data previously obtained with other acetate esters (11, 15), $m = 0.60$, $pK_{SH^+} = -4$.[3] Small devia-

[3]In acids below 65% H_2SO_4 the ordinate of the *r* plot then is equivalent to $\log k_\psi + mH_0 +$ constant.

TABLE 3. Mechanisms of acylal hydrolysis in sulfuric acid solutions based on r plots

Acylal	Initial r value[a] (A_{Ac}-2 hydrolysis)	Final r value[a] (A_{Al}-1 hydrolysis)	Region of changeover (%)
$MeOCH_2OAc$	—	−7.5	—
$C_6H_5OCH_2OAc$	+1.37	−0.91	45–50
$4\text{-}ClC_6H_4OCH_2OAc$	+1.68	−0.80	50–55
$3\text{-}ClC_6H_4OCH_2OAc$	+1.76	−0.61	55–60
$4\text{-}CNC_6H_4OCH_2OAc$	+1.71	−0.71	65–70
$3\text{-}NO_2C_6H_4OCH_2OAc$	+1.65	−0.70	65–70
$4\text{-}NO_2C_6H_4OCH_2OAc$	+1.61	−0.64	65–72
$CH_2(OAc)_2$	+1.53	−0.88	70–75

[a]Correlation coefficients greater than 0.995.

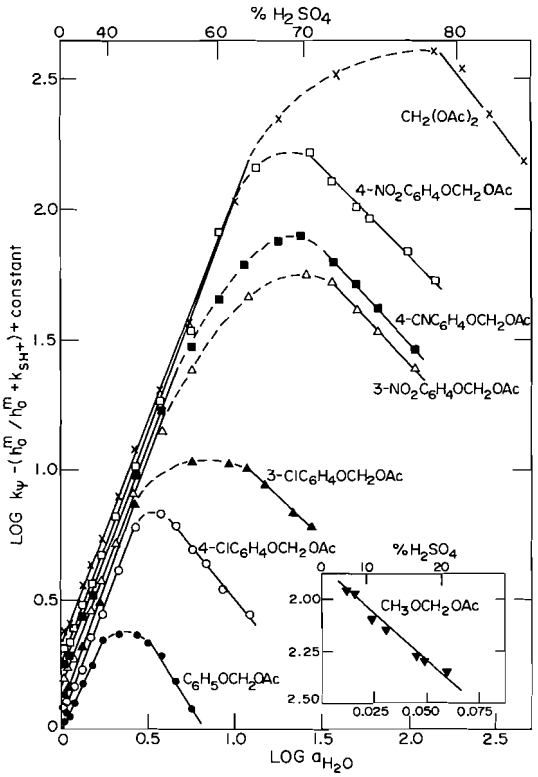

FIG. 2. r Plots for acylal hydrolysis. Plots for each substrate have been shifted by a different constant to avoid overlap in dilute acid region. Note different scales of insert.

tions from this behavior will not affect the following qualitative interpretations in any way.

The plots can be seen to be of the form that has been generally observed for simple acetates (11). The aryl acylals exhibit initially a linear region of positive log a_{H_2O} dependence; this is characteristic of the A_{Ac}-2 hydrolysis. At some acidity there is a pronounced break to another linear region which shows a negative log a_{H_2O} dependence; this is characteristic of a mechanistic changeover to an A-1 reaction. The magnitudes of the slopes (*i.e.* r values) in this latter region ($r = -0.6$ to -0.9) are furthermore those found for A_{Al}-1 hydrolysis rather than A_{Ac}-1 hydrolysis (r values normally around -0.2 (11)). Methoxymethyl acetate produces a plot with a strongly negative log a_{H_2O} dependence beginning in dilute acids, consistent with its unimolecular character throughout. The r values calculated for the linear regions of these plots and the mechanistic conclusions are summarized in Table 3. Significantly the acidities where the mechanistic changeovers are predicted to occur are those where the rate profiles also show their changes in behavior.

With the aryl acylals, further evidence for these mechanistic assignments can be seen in the effect of the substituents. In Fig. 3 are plotted log k_ψ values at various acidities as a function of the Hammett σ constant. In dilute acids (up to *ca.* 25% H_2SO_4), there is very little difference in the rates across the entire range of substituents; the ρ value for the hydrolysis at these acidities is -0.03 (± 0.01). This is what is normally found for A_{Ac}-2 ester hydrolysis (*e.g.* phenyl acetates, $\rho = -0.17$ (16); benzyl acetates, $\rho = -0.05$ (16)) and can be attributed to the near cancellation of the substituent effects on the two steps in the hydrolysis (12). With these acylals a further factor contributing to the very small ρ value lies simply in the remoteness of the substituent from the reaction center. This consideration is borne out by the base hydrolysis, which follows a normal ester B_{Ac}-2 mechanism (1, 17). For the acylals of this study a ρ value of $+0.41$ is obtained (Fig. 4). This can be compared to values obtained in systems in which the substituent change is occurring closer to the reaction center: benzyl acetates $\rho_{base} = +0.8$ (12); phenyl ace-

Can. J. Chem. Downloaded from www.nrcresearchpress.com by 210.87.254.42 on 09/05/12
For personal use only.

Can. J. Chem. Downloaded from www.nrcresearchpress.com by 210.87.254.42 on 09/05/12
For personal use only.

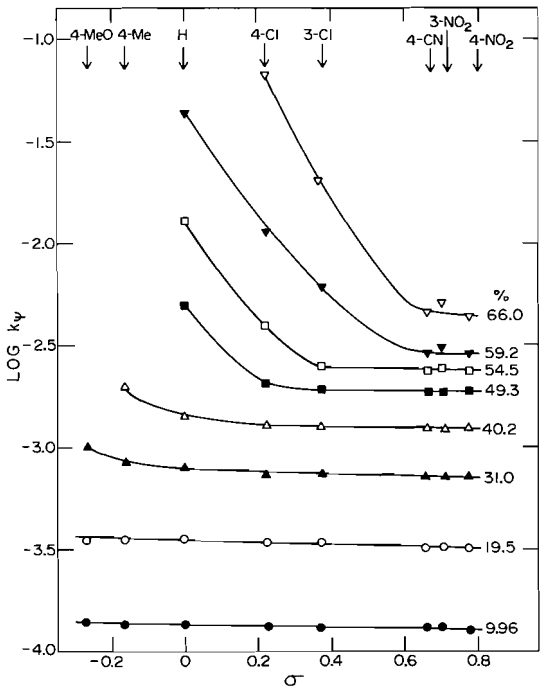

FIG. 3. Log k_ψ versus σ for hydrolysis of $ArOCH_2OAc$ at varying concentrations of H_2SO_4.

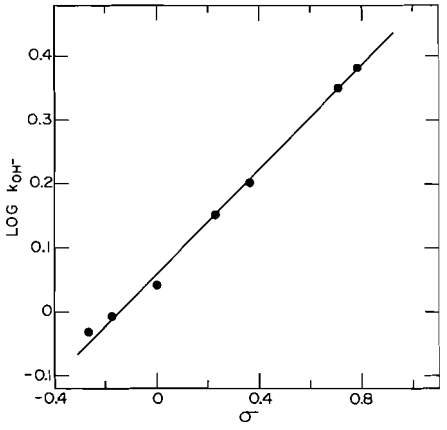

FIG. 4. Hammett σ plot for base hydrolysis of $ArOCH_2OAc$.

tates, $\rho_{base} = +1.5$ (12). In fact, for these series in which the substituent change is occurring in the alkyl portion of the ester, the ratio ρ_{base}/ρ_{acid} is quite similar.

In more concentrated acids, the plots for the acylals no longer show a linear behavior. As the A-1 reaction becomes important for each compound, its point on the σ plot shows a positive deviation from the line of the A_{Ac}-2 hydrolysis. Again, the acidities where these deviations first occur correspond to the acidities where the *r* plots and rate profiles show the mechanistic changeover.

A direct estimate of the ρ value for the unimolecular reaction is difficult with the competing bimolecular hydrolysis. In principle this could be determined at an acidity where only the former is occurring (*i.e.* very concentrated acids), but this is impossible in the present case since at such an acidity the rates for most of the acylals would be far too rapid to measure.

An alternative approach involves measuring the relative rates for pairs of compounds of overlapping A_{Al}-1 reactivity, and by a stepwise technique similar to that used to determine relative basicities in acidity function studies (18), extending this over the entire range of substituents. This is illustrated in Fig. 5, in which values of log k_ψ are plotted as a function of acidity for those regions where the *r* plots predict that only the A-1 hydrolysis is occurring. Parallel lines are obtained, and the reactivities relative to the unsubstituted acylal can be estimated by proceeding in a stepwise manner from this compound. (A slight extrapolation is required at the 3-chloro : 3-nitro pair). These relative rates are listed in Table 4, and plotted as a function of σ in Fig. 6. A reasonably linear plot (correlation coefficient = 0.996) results with a slope $\rho = -3.02$, showing a relatively strong retardation by electron-withdrawing substituents. Qualitatively the same effect is seen in the considerably later acidities at which the A-1 reaction first occurs for the acylals with electron-withdrawing substituents.

This substantial dependence on the aryl substituent is completely consistent with the unimolecular hydrolysis proceeding via the A_{Al}-1

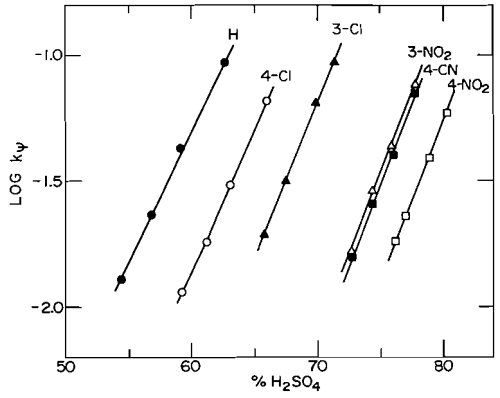

FIG. 5. A_{Al}-1 reactivities for $ArOCH_2OAc$ as a function of acidity.

Can. J. Chem. Downloaded from www.nrcresearchpress.com by 210.87.254.42 on 09/05/12
For personal use only.

TABLE 4. Relative A_{Al}-1 reactivities of aryloxymethyl acetates

Substituent	$\log (k_{-X}/k_{-H})$
H	0.0
4-Cl	−0.57
3-Cl	−1.06
3-NO_2	−1.96
4-CN	−2.01
4-NO_2	−2.39

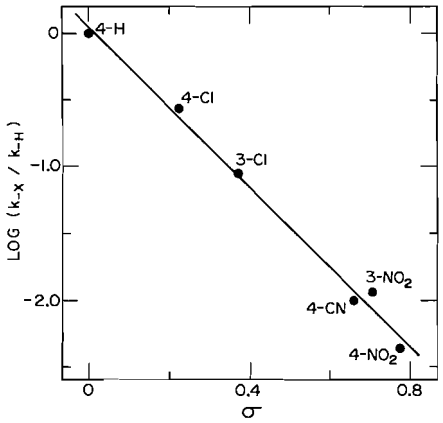

FIG. 6. Hammett σ plot for A_{Al}-1 hydrolysis of $ArOCH_2OAc$.

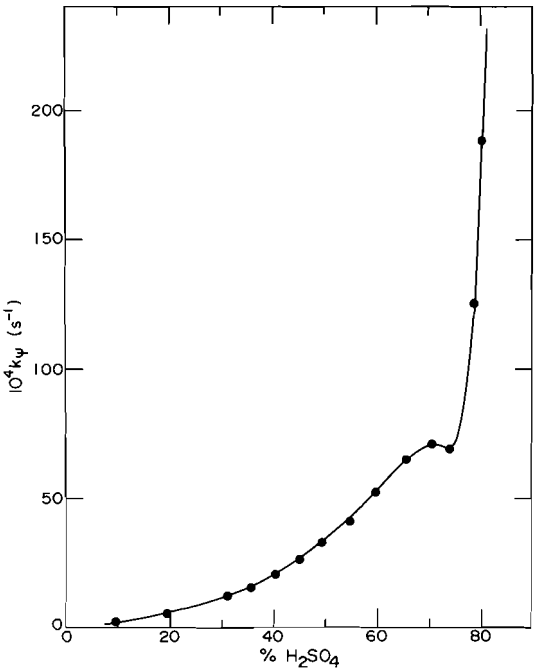

FIG. 7. Rates of hydrolysis of methylene diacetate in sulfuric acid solutions at 25 °C.

pathway, in which an $ArOCH_2^+$ carbonium ion would be formed in the rate-determining step. A comparison can be made with the hydrolysis of a series of alkoxymethyl acetates ($ROCH_2OAc$), which like methoxymethyl acetate hydrolyze by this route even in dilute acids, forming $ROCH_2^+$ (7). Based on σ* substituent constants for the varying R groups, this series is found to have a ρ* value of −3.42 (2), *i.e.* very similar to that of the aromatic compounds. Furthermore, the effect is inconsistent with the alternate A-1(a) pathway, in which a neutral phenol (plus a carbonium ion) would be formed in the slow step. A number of acetal hydrolyses proceed in this fashion (*e.g.* $ArOCH_2OMe$) and exhibit considerably smaller ρ values, although in the same direction (ρ values in the range 0 to −1 (see section C of Table II, ref. 2.)). Finally an A_{Ac}-1 ester hydrolysis reaction can be ruled out again, since this has been shown to be favored by electron-withdrawing groups in the neutral departing molecule (11).

The observation that these phenyl acylals hydrolyze via the A_{Al}-1 mechanism in moderately concentrated sulfuric acid leads to methylene diacetate, from which an acyloxycarbonium ion must be produced by this reaction. The previous study (9) on this compound was carried out in aqueous hydrochloric acid, and was therefore not extended to media of high acidity. Accordingly we have measured the rates of hydrolysis in sulfuric acid over a considerably wider range of acid concentration, and so obtained the rate profile of Fig. 7. Behavior similar to the aryloxymethyl acetates is observed, in this case with a hint perhaps of the rate maximum often found with A_{Ac}-2 ester hydrolysis (11, 12, 19).[4] The *r* plot (Fig. 2) and derived parameters (Table 3) confirm this similarity, and show that although the A_{Ac}-2 hydrolysis is preferred in dilute acids as noted before (9), by increasing the acidity sufficiently the reaction involving the acyloxycarbonium ion does occur.

Thus, in summary, the hydrolysis of these acetate acylals does follow the same trends observed with simple acetates; a conventional A_{Ac}-2 ester hydrolysis in dilute acids with a changeover at some acidity to an A-1 reaction. It is interesting in this respect to compare reactivities in the two types of compound. In

[4]Such maxima are not observed with the aryloxymethyl acetates because of the earlier changeover to the unimolecular hydrolysis.

Can. J. Chem. Downloaded from www.nrcresearchpress.com by 210.87.254.42 on 09/05/12
For personal use only.

TABLE 5. Rates of A_{Ac}-2 hydrolysis of acetates in 15% H_2SO_4 at 25 °C

Ester	$10^4 k_\psi$[a](s^{-1})	Reference
Ethyl acetate	2.5	19
Isopropyl acetate	1.5	11
Phenyl acetate	1.8	11
Benzyl acetate	2.0	11
Phenoxymethyl acetate	2.1	This work
Methylene diacetate	2.1[b]	This work

[a]Interpolated from plots of k_4 *vs.* $\%H_2SO_4$.
[b]$k_4/2$, since there are two acetate groups in the molecule.

Table 5, a number of A_{Ac}-2 hydrolysis rates (in 15% H_2SO_4) are listed. As is expected from the great deal of study which has been devoted to this reaction (12), the effect of these structural variations is very small, and is probably mainly steric in origin. Certainly the additional oxygen in the acylals has introduced no new effect.

On the other hand a wide variety of behavior is observed for the A_{Al}-1 reactions, being due to the considerable differences in the stabilities of the intermediate carbonium ions. Relative A_{Al}-1 reactivities for a number of acetates are summarized in Table 6. As with the aryloxymethyl acetates (Table 4) these data are not based on direct comparison, but on an extension of the stepwise technique. The measurable A_{Al}-1 rates for benzyl acetate, methylene diacetate, and isopropyl acetate overlap with one (or more) of the aryloxymethyl acetates. In the following paper (20) is reported the hydrolysis of a series of thioacylals with A_{Al}-1 reactivities which cover the dilute acid region (0–60% H_2SO_4), allowing the relative rates for the more reactive acetates of Table 6 to be estimated.[5] Unfortunately a simple primary alkyl group cannot be included in Table 6, since such acetates hydrolyze by an A_{Ac}-1 mechanism in concentrated acids (11).

A number of points arise from these comparisons. The first is the variation within the acylals themselves. The phenyl ring does show its predicted effect when compared with methyl, a considerable rate decrease due to the lesser availability of the oxygen lone pairs for stabilization of the adjacent cationic center. In this respect it can be seen that the acetoxymethyl carbonium ion derived from methylene diacetate is the least stable of the oxycarbonium ions, although there is not a great deal of difference with that derived from the 4-nitrophenoxy compound.

[5]See Fig. 6 and Table 8 of ref. 20.

Significantly however this study reveals that these "destabilized" oxycarbonium ions are still comparable to what are normally regarded as moderately stable carbonium ions, for example isopropyl and benzyl. This illustrates the very large conjugative stabilizing effect of oxygen lone pairs adjacent to a positive carbon, even in cases in which there is a considerable competition for these electrons with another π system.

In the light of such comparisons, the behavior of the acetate acylal **2** is interesting.[6] This compound would give a carbonium ion bearing two moderately stabilizing groups, phenyl and 4-nitrophenoxy. In consequence the combined effects of the two results apparently in sufficient stabilization to make this compound the most reactive acetate in Table 6, even when compared with $MeOCH_2OAc$.

Finally, we can comment on the behavior of cyclic acylals (1, 4). On the basis of our results, all such compounds to date investigated would be expected to hydrolyze as simple A_{Al}-1 esters, particularly since there is usually some additional substituent such as phenyl present to stabilize the intermediate carbonium ion of that reaction. The occurrence then of other pathways[7] must be due to some factor or factors associated with the cyclic nature of these compounds, as have been discussed in previous studies (1, 4).

Experimental

Materials

Sulfuric acid solutions were prepared and standardized as previously described (21). The preparation of the aryloxymethyl acetates has been reported elsewhere (22). Standard procedures were used for the preparation of methylene diacetate (9) and methoxymethyl acetate (5).

Kinetics

Rates were obtained on a Cary 16 spectrophotometer equipped with an external recorder and a thermostatted cell compartment. With the aryloxymethyl acetates, stock solutions were prepared in methanol, and reactions initiated by addition of 3 μl of these solutions to pre-equilibrated cuvettes containing 3 ml of aqueous solution. Final concentrations of substrates were $1–5 \times 10^{-4}$ *M*. Reactions were monitored by following the absorbance increase at the wavelengths given in Table 7. For methoxymethyl acetate and methylene diacetate, the substrate was added directly to the solution in the cuvette (concen-

[6]Based on the data of Table 5 and accompanying discussion, the conclusion of an A_{Al}-1 hydrolysis for this compound appears valid, since its rate is far too rapid for an A_{Ac}-2 acetate hydrolysis.

[7]As has been recognized in the reports on these hydrolyses (1, 4) there are definite uncertainties in the mechanistic assignments.

TABLE 6. Relative A_{Al}-1 reactivities for acetate esters (ROAc)

R	k_{rel}[a]	Reference
4-NO_2PhOCHPh (2)	2×10^{5}[b]	1
$MeOCH_2$	6×10^{3}[c]	5, this work
tert-Butyl	5×10^{2}[c]	13
$PhOCH_2$	1.0	This work
3-$ClPhOCH_2$	9×10^{-2}[c]	This work
$PhCH_2$	7×10^{-2}[c]	11
4-NO_2PhOCH_2	4×10^{-2}[c]	This work
CH_3COOCH_2	1.1×10^{-2}[c]	This work
Isopropyl	1.3×10^{-4}[c]	11

[a]Rate relative to phenoxymethyl acetate.
[b]Based on comparison with rates of methoxymethyl acetate in dilute HCl.
[c]Based on stepwise comparison of overlapping rates in H_2SO_4 (see text).

TABLE 7. Wavelengths employed to follow hydrolysis of aryloxymethyl acetates

	λ (nm)	
Substituent	Acid	Base
4-MeO	295	310
4-Me	280	305
H	275	290
4-Cl	285	300
3-Cl	280	300
4-CN	255	—
3-NO_2	340	380
4-NO_2	340	395

tration 2×10^{-2} *M*), and the absorbance decrease at 205 nm was followed (11).

First-order rate constants were calculated from plots of ln $(A_\infty - A_t)$ (or ln $(A_t - A_\infty)$) *vs.* time. With the exceptions noted below, these plots are linear to several half-lives.

Above a certain acidity, stable infinity values could not be obtained with some of the aryloxymethyl acetates. In fact, these solutions can be observed to go cloudy during hydrolysis. This problem is most severe with the activated compounds, and the rates can not be measured above the acidities for which data are reported in Table 1. With the unsubstituted and 4-chloro compounds, decomposition is less serious, and the hydrolysis could be followed for 3–4 half-lives, and the rates were calculated by the Guggenheim method. This applies to the data above 45% H_2SO_4 for the unsubstituted compound, and above 55% H_2SO_4 for 4-chloro.

Products of Hydrolysis

Hydrolysis of the aryloxymethyl acetates produces the phenol. The u.v. spectrum of the product is quantitatively superimposable (within ±2%) on the u.v. spectrum of the phenol in the same solution. With methylene diacetate and methoxymethyl acetate, the u.v. spectrum of the hydrolysis product is identical to that of acetic acid under the same conditions.

1. T. H. FIFE and N. C. DE. J. Am. Chem. Soc. **96**, 6158 (1974.)
2. E. H. CORDES and H. G. BULL. Chem. Rev. **74**, 581 (1974).
3. T. H. FIFE. Acc. Chem. Res. **8**, 264 (1972).
4. P. SALOMAA and S. LAIHO. Acta. Chem. Scand. **17**, 103 (1963); T. H. FIFE. J. Am. Chem. Soc. **87**, 271 (1965); D. P. WEEKS and G. W. ZUORICK. J. Am. Chem. Soc. **91**, 477 (1969); D. P. WEEKS, A. GRADSKI, and R. FANUCCI. J. Am. Chem. Soc. **90**, 4958 (1968); D. P. WEEKS and J. P. CRANE. J. Org. Chem. **38**, 3375 (1973); D. P. WEEKS, J. CELLA, and L. T. CHEN. J. Org. Chem. **38**, 3383 (1973).
5. P. SALOMAA. Acta. Chem. Scand. **11**, 132 (1957).
6. P. SALOMAA. Acta. Chem. Scand. **11**, 141, 235, 239 (1957); **14**, 586 (1960); E. K. EURANTO and R. H. ISOTALO. Suom. Kemistil B, **43**, 271 (1970).
7. P. SALOMAA. Suom. Kemistil. B, **33**, 11 (1960).
8. P. SALOMAA and R. L. LINNANTIE. Acta. Chem. Scand. **14**, 586 (1960).
9. P. SALOMAA. Acta. Chem. Scand. **11**, 247 (1957).
10. T. BIRCHALL and R. J. GILLESPIE. Can. J. Chem. **43**, 1045 (1965); G. A. OLAH, D. H. O'BRIEN, and A. M. WHITE. J. Am. Chem. Soc. **89**, 5694 (1967).
11. K. YATES. Acc. Chem. Res. **4**, 136 (1971); K. YATES and R. A. MCCLELLAND. J. Am. Chem. Soc. **89**, 2686 (1967).
12. A. J. KIRBY. *In* Comprehensive chemical kinetics, Vol. 11. *Edited by* C. H. Bamford and C. F. H. Tipper. Elsevier Publishing Co. Amsterdam. 1972. pp. 57–142.
13. P. SALOMAA. Suom. Kemistil. B, **32**, 145 (1959); C. A. BUNTON, J. H. CRABTREE, and L. ROBINSON, J. Am. Chem. Soc. **90**, 1258, (1968).
14. C. R. SMITH and K. YATES. J. Am. Chem. Soc. **93**, 6578 (1971); **94**, 8811 (1972).
15. D. G. LEE and M. H. SADAR. J. Am. Chem. Soc. **96**, 2862 (1974).
16. E. TOMMILA and C. N. HINSHELWOOD. J. Chem. Soc. 1801 (1938).
17. M. L. BENDER, J. A. REINSTEIN, M. S. SILVER, and R. MIKULAK. J. Am. Chem. Soc. **87**, 4545 (1965); K. BOWDEN and M. A. LAST. J. Chem. Soc. Perkin Trans. 2, 358 (1973).
18. C. H. ROCHESTER. Acidity functions. Academic Press, London. 1970 pp. 9–20.
19. C. A. LANE, M. F. CHEUNG, and G. F. DORSEY. J. Am. Chem. Soc. **89**, 2686 (1967).
20. R. A. MCCLELLAND. Can. J. Chem. This issue.
21. K. YATES and R. A. MCCLELLAND. Can. J. Chem. **52**, 1098 (1974).
22. R. A. MCCLELLAND. J. Org. Chem. In press.

Can. J. Chem. Downloaded from www.nrcresearchpress.com by 210.87.254.42 on 09/05/12
For personal use only.

Mechanisms of Thioacylal Hydrolysis in Sulfuric Acid Solutions

ROBERT ALLAN MCCLELLAND
Department of Chemistry, University of Toronto, Toronto, Ontario M5S 1A1
Received March 3, 1975

ROBERT ALLAN MCCLELLAND. Can. J. Chem. **53**, 2772 (1975).

The acid-catalyzed hydrolysis (aqueous H_2SO_4) of thioacylals CH_3SCH_2OAc and $ArSCH_2OAc$ is reported. The former is shown to react solely by an A-1 mechanism proceeding via an intermediate $CH_3SCH_2^+$ cation. In the latter series hydrolysis in dilute acids involves both this A-1 mechanism and a normal A_{Ac}-2 ester hydrolysis mechanism occurring simultaneously; as the acidity is increased the proportion of A-1 reaction increases until it completely dominates. The A-1 reaction shows lesser importance with electron-withdrawing substituents. The 4-nitro compound in fact shows no A-1 mechanism until about 40% H_2SO_4. These hydrolyses are compared with those of the corresponding acylals, which show a similar mechanistic behavior. Relative A-1 reactivities for $RXCH_2OAc$, RX = CH_3O, CH_3S, C_6H_5S, C_6H_5O are 81, 49, 1, 0.022, relative to $C_6H_5SCH_2OAc$. Discussions pertaining to the effects of the oxygen and the sulfur in these systems are presented.

ROBERT ALLAN MCCLELLAND. Can. J. Chem. **53**, 2772 (1975).

On rapporte l'hydrolyse acido-catalysée (H_2SO_4 en milieu aqueux) de thioacylals du type CH_3SCH_2OAc et $ArSCH_2OAc$. On démontre que le premier réagit uniquement par un mécanisme A-1 se produisant par l'intermédiaire d'un cation $CH_3SCH_2^+$. Dans la deuxième série, l'hydrolyse par des acides dilués implique à la fois ce mécanisme A-1 et un mécanisme d'hydrolyse A_{Ac}-2 normal pour les esters et se produisant d'une façon simultanée; à mesure que l'acidité du milieu augmente, la proportion de réaction se produisant par un mécanisme A-1 augmente jusqu'à ce qu'elle devienne prédominante. Lorsque les groupes portent des substituants électro-attracteurs, l'importance de la réaction A-1 diminue. En fait dans le cas du composé portant un groupe nitro en position 4, le mécanisme A-1 ne commence à intervenir que dans l'acide sulfurique à 40%. On compare ces hydrolyses avec celles des acylals correspondants qui, du point de vue mécanistique, réagissent d'une façon similaire. Les réactivités A-1 relatives (au $C_6H_5SCH_2OAc$) pour $RXCH_2OAc$ où RX = CH_3O, CH_3S, C_6H_5S, C_6H_5O sont respectivement 81, 49, 1, 0.022. On présente une discussion relative aux effets de l'oxygène et du soufre dans ces systèmes. [Traduit par le journal]

In the previous paper (1) an investigation into the sulfuric acid catalyzed hydrolysis of acylals of the type CH_3OCH_2OAc and $ArOCH_2OAc$ was reported. In this paper the study is extended to the sulfur analogs of these compounds, CH_3SCH_2OAc and $ArSCH_2OAc$. No prior investigation into the acid hydrolysis of any such thioacylal appears to have been carried out. Fife and De (2) have recently looked into the hydrolysis in buffered and basic solutions, and concluded that their behavior is similar to that of the corresponding acylals.

Results

The rates of hydrolysis of five thioacylals are reported in a number of sulfuric acid solutions in Table 1. No aromatic with an electron-releasing substituent is included because extensive decomposition occurred during the kinetic runs, even in dilute acids. Kinetics were followed by u.v. spectroscopy for the four aromatic compounds: a hydroxamic acid – ferric chloride assay (3) was used with methylthiomethyl acetate. With the aromatics the appropriate benzenethiols were shown to be formed on hydrolysis by comparison of the u.v. spectra of the products with those of authentic samples. This was confirmed in the case of the unsubstituted compound where a quantitative yield of benzenethiol was found by g.c. analysis.

In Fig. 1, these rates are plotted as a function of the sulfuric acid concentration; also included are the profiles previously obtained for methoxymethyl acetate and phenoxymethyl acetate (1). All compounds exhibit a similar behavior in the sense of a monotonic rate increase with increasing acidity. The aromatic compounds, however, are characterized by a more moderate rate increase in the dilute acids followed by a change at some acidity to a more pronounced increase.

Rates of hydrolysis as a function of temperature are listed for selected thioacylals (and one

Can. J. Chem. Downloaded from www.nrcresearchpress.com by 210.87.254.40 on 09/05/12
For personal use only.

Can. J. Chem. Downloaded from www.nrcresearchpress.com by 210.87.254.40 on 09/05/12
For personal use only.

TABLE 1. Rates of thioacylal hydrolysis in aqueous sulfuric acid solutions at 25 °C[a]

CH_3SCH_2OAc		$C_6H_5SCH_2OAc$		4-$ClC_6H_4SCH_2OAc$		3-$ClC_6H_4SCH_2OAc$		4-$NO_2C_6H_4SCH_2OAC$	
$\%H_2SO_4$	10^4k_ψ	$\%H_2SO_4$	10^4k_ψ	$\%H_2SO_4$	10^4k_ψ	$\%H_2SO_4$	10^4k_ψ	$\%H_2SO_4$	10^4k_ψ
2.71	4.50	9.96	1.26	9.96	1.03	9.96	0.905	9.96	0.700
5.24	11.0	15.6	2.82	15.6	1.83	15.6	1.57	15.6	1.153
8.08	21.0	19.5	5.20	19.5	3.18	19.5	2.63	19.5	1.77
10.50	32.8	24.9	10.9	24.9	5.25	24.9	3.96	24.9	2.70
13.1	53.2	31.0	31.7	31.0	12.4	31.0	7.51	31.0	4.08
15.1	72.4	35.5	76.7	35.5	26.5	35.5	13.81	35.5	5.10
18.5	114	37.9	128.3	37.9	41.0	40.2	29.0	40.2	6.63
		40.2	218	40.2	75.0	45.0	74.7	45.0	10.53
		42.6	389	42.6	118	47.1	105	49.3	18.50
				45.0	207	49.3	174	51.9	30.2
				47.1	317	50.8	245	54.5	50.0
				49.3	603	51.9	339	56.9	96.7
						53.3	447	58.2	129
						54.5	591	59.2	168
								60.6	250
								62.7	427
								63.9	575

[a]First-order rate constant in units of s^{-1}.

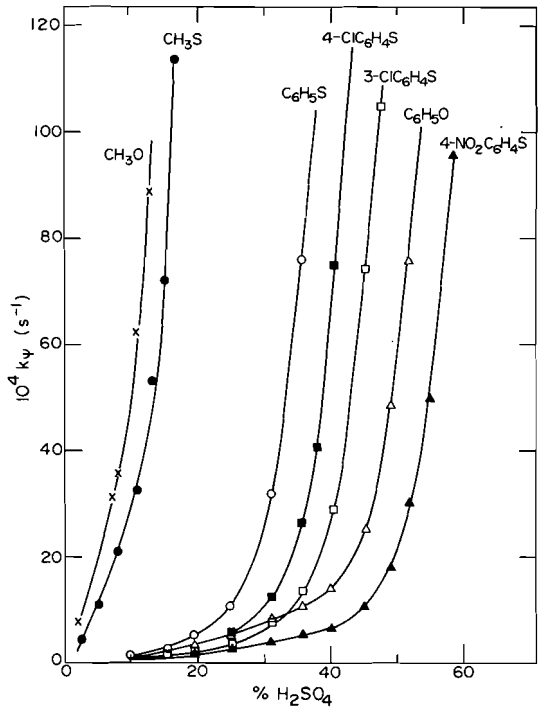

FIG. 1. Rates of hydrolysis of thioacylals and acylals ($RXCH_2OAc$) as a function of sulfuric acid concentration. Rate data for acylals were taken from ref. 1.

acylal) in Table 2. Plots of log (k_ψ/T) *vs.* $1/T$ are depicted in Fig. 2, and the derived activation parameters given in Table 3. Of particular significance is the observation that the two plots for phenylthiomethyl acetate show curvature, particularly the one in the more dilute acid (the deviation from linearity in 24.9% H_2SO_4 is probably not outside the limit of experimental error).

In Table 4, second-order rate constants for the basic hydrolysis of the aromatic thioacylals are given. These were obtained under pseudo-first-order conditions in 0.01 *N* aqueous sodium hydroxide. In Fig. 3, a plot of log k_{OH^-} *vs.* the Hammett substituent constant is shown; from this a ρ value of +0.44 is obtained. This is very similar to values observed for the base hydrolysis of 3-(*para*-substituted thiophenyl) phthalides (2), as well as the aryloxymethyl acetates (1) (+0.42 and +0.41 respectively). The base hydrolysis of these thioacylals and acylals has been shown to proceed by a normal B_{Ac}-2 ester hydrolysis mechanism (2, 4).

In addition the products of solvolysis of two of the thioacylals in acidic (0.02 $M[H^+]$) methanol

TABLE 2. Rates of thioacylal hydrolysis in sulfuric acid solutions as a function of temperature[a]

Compound	$\%H_2SO_4$	T (°C)	$10^4 k_\psi$
CH_3SCH_2OAc	2.71	15.1	1.17
		25.0	4.50
		36.1	18.2
		48.2	75.7
$C_6H_5SCH_2OAc$	9.96	25.0	1.26
		35.5	3.73
		47.1	15.03
		56.9	49.42
	24.9	25.0	10.9
		35.5	31.8
		47.1	119
		56.9	332
$4\text{-}NO_2C_6H_4SCH_2OAc$	9.96	25.0	0.700
		34.9	1.84
		43.6	3.74
		53.8	9.05
$C_6H_5OCH_2OAc$	9.95	25.0	1.35
		36.6	3.83
		46.5	9.08
		57.0	20.3

[a]First-order rate constants in units of s^{-1}.

were determined. Methylthiomethyl acetate was found to give a quantitative yield of the thioacetal **1**.

$$CH_3SCH_2OAc \xrightarrow[CH_3OH]{H^+} CH_3SCH_2OCH_3 \quad (1)$$

No methanethiol could be detected; acetic acid is also formed but is rapidly esterified to methyl acetate. In the same solution phenylthiomethyl acetate gives benzenethiol (95%) and thioacetal **2** (5%).

$$C_6H_5SCH_2OAc \xrightarrow[CH_3OH]{H^+} C_6H_5SH(95\%) + C_6H_5SCH_2OCH_3(5\%) \quad (2)$$

Control experiments demonstrated that both products are stable under the reaction conditions. Methyl acetate and a trace of acetic acid are also formed; again the latter is converted to the former during the solvolysis.

In order to determine the effect of a change from water to methanol on the solvolysis rate for an acetate whose hydrolysis proceeds by the A_{Ac}-2 mechanism, the rate of *trans*-esterification of *p*-nitrophenyl acetate was determined in acidic methanol. First-order rate constants were measured at three acid concentrations from 0.01 to 0.06 $M[H^+]$; these give a value for the second-

Can. J. Chem. Downloaded from www.nrcresearchpress.com by 210.87.254.40 on 09/05/12
For personal use only.

TABLE 3. Activation parameters for acid-catalyzed thioacylal hydrolysis

Substrate	Acid solution	$\Delta H^{\ddagger}$ (kcal/mol)	$\Delta S^{\ddagger}$ (e.u.)
CH_3OCH_2OAc[a]	Dilute HCl	22.0	+3.4
CH_3SCH_2OAc	2.71% H_2SO_4	22.6	+1.8
$C_6H_5SCH_2OAc$	9.96% H_2SO_4	—[b]	—[b]
$C_6H_5SCH_2OAc$	24.9% H_2SO_4	20.5	−3.6
$4\text{-}NO_2C_6H_4SCH_2OAc$	9.96% H_2SO_4	16.5	−22.3
$C_6H_5OCH_2OAc$	9.96% H_2SO_4	16.0	−22.7

[a]Calculated from the data of Salomaa (22) and based on second-order rate constants ($k_\psi/[H^+]$). In all other cases k_ψ has been used in the calculations.
[b]Noticeable curvature.

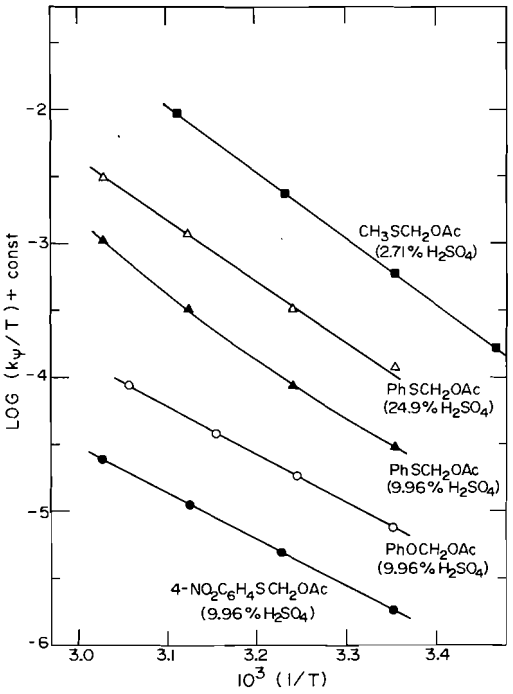

FIG. 2. Activation plots for the hydrolysis of thioacylals and acylals in sulfuric acid.

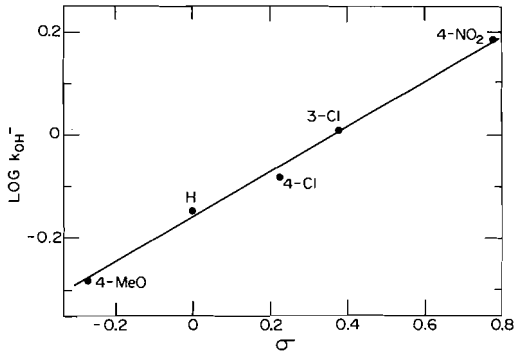

FIG. 3. Hammett σ plot for the hydrolysis in aqueous sodium hydroxide of arylthiomethyl acetates ($ArSCH_2OAc$).

TABLE 4. Hydrolysis of arylthiomethyl acetates ($ArSCH_2OAc$) in aqueous NaOH at 25 °C

Ar	$k_2(M^{-1}\,s^{-1})$
$4\text{-}MeOC_6H_4$	0.521
C_6H_5	0.712
$4\text{-}ClC_6H_4$	0.827
$3\text{-}ClC_6H_4$	1.021
$4\text{-}NO_2C_6H_4$	1.531

order rate constant ($k_2 = k_\psi/[H^+]$) of 0.0015 $M^{-1}\,s^{-1}$. Coupled with data for the hydrolysis reaction (3), the ratio $k_2(CH_3OH)/k_2(H_2O)$ is 25. For an acetate whose hydrolysis proceeds via the A_{Al}-1 route this rate ratio is 6, based on literature data for the methanolysis (5) and hydrolysis (6) of methoxymethyl acetate. Thus although both types are faster in methanol, the effect is greater for the bimolecular reaction.

Discussion

From the previous study of the acylals (1) the mechanistic behavior of the thioacylals is expected to revolve around a competition between a normal A_{Ac}-2 ester hydrolysis and a unimolecular process analogous to an A_{Al}-1 ester hydrolysis, involving in this case a carbonium ion center adjacent to sulfur. We will show in the following discussion that this is the case, permitting in consequence a comparison to be made of the ability of oxygen and sulfur to form such stabilized cationic species.

[1] $CH_3\overset{\overset{O}{\|}}{C}OCH_2SR \overset{H^+}{\rightleftarrows} CH_3\overset{\overset{{}^+OH}{|}}{C}OCH_2SR \rightarrow CH_3COOH + {}^+CH_2SR \rightarrow$ product

Can. J. Chem. Downloaded from www.nrcresearchpress.com by 210.87.254.40 on 09/05/12
For personal use only.

Can. J. Chem. Downloaded from www.nrcresearchpress.com by 210.87.254.40 on 09/05/12
For personal use only.

Methylthiomethyl Acetate

The oxygen analog of this compound is well known to hydrolyze solely via a unimolecular pathway similar to [1] (1, 6) and the results for the thioacylal suggest an identical behavior. Thus, there is a striking similarity in the rate–acidity profiles of the two compounds (Fig. 1), as well as their entropies of activation (Table 3). The latter values are small and slightly positive as is characteristic of A-1 hydrolysis reactions (7). Particularly conclusive evidence is afforded by the methanolysis experiment, where the thioacetal $CH_3SCH_2OCH_3$ arises from methanol attack on the intermediate carbonium ion $CH_3SCH_2^+$. A bimolecular solvolysis (*trans*-esterification) would be expected to yield (eventually) methanethiol.[1] (A similar experiment has been carried out with methoxymethyl acetate; $CH_3OCH_2OCH_3$ is formed in quantitative amounts (5).)

4-Nitrophenylthiomethyl Acetate

In the oxygen series replacement of the methyl group of CH_3OCH_2OAc by aryl results in sufficient destabilization of the oxycarbonium ion intermediate of the A-1 hydrolysis that in dilute acids the reaction proceeds by an A_{Ac}-2 ester hydrolysis mechanism, while the unimolecular process only becomes important in some more concentrated acid. The 4-nitrophenyl thioacylal appears to behave similarly, with the mechanistic changeover at *ca.* 40–50% H_2SO_4. Thus, when the relative rates of hydrolysis of this compound and its oxygen analog (A-2 until 65% H_2SO_4) are compared (Table 5) the ratio of reactivities is found to be essentially constant up to 40% H_2SO_4, implying a common mechanistic behavior. At this point as the A-1 process takes over with the thioacylal the rate ratio increases dramatically. In addition, the *r* hydration plot (8) exhibits the form characteristic of such a mechanistic behavior, a linear region of positive slope (+1.37) up to 40% H_2SO_4 (A_{Ac}-2 reaction), followed by a changeover to another linear region of negative slope (−1.01) (A-1 reaction). Finally the entropy of activation (Table 3) for the hydrolysis in 10% H_2SO_4 is large and negative, as is consistent with A-2 hydrolysis (7). The $\Delta S^{\neq}$ value is in fact very similar to that of phenoxymethyl acetate in the same acid.

TABLE 5. A comparison of the rates of hydrolysis of $4\text{-}NO_2C_6H_4OCH_2OAc$ and $4\text{-}NO_2C_6H_4SCH_2OAc$ in sulfuric acid solutions at 25 °C

% H_2SO_4	k_ψ(—S—)/k_ψ(—O—)[a]
9.96	0.56
15.6	0.57
19.5	0.55
24.9	0.56
31.0	0.56
35.5	0.54
40.2	0.54
45.0	0.67
49.3	0.96
54.5	2.08
59.2	6.25

[a]Taken from ref. 1.

Other Arylthiomethyl Acetates

For the other three aromatic thioacylals, it appears as if the decrease in A-1 reactivity due to the aromatic ring is not sufficient to completely inhibit this reaction even in the dilute acids. However, the decrease is enough to allow the A_{Ac}-2 reaction to compete, and what is occurring is a mixture of the two, up until some intermediate acidity (40–50% H_2SO_4) where the A-1 reaction finally dominates.

This behavior is seen particularly in the effect of the aromatic substituents. In the previous paper it was shown that the A_{Ac}-2 hydrolysis rates for $ArOCH_2OAc$ depend very little on the nature of Ar ($\rho = -0.03$), while the A-1 hydrolysis demonstrates a strong dependence ($\rho = -3$). A similar behavior should occur here, as for example in their base hydrolyses, where the two series $ArXCH_2OAc$ give very similar ρ values. In Fig. 5 are depicted plots at four acidities of $\log k_\psi$ for the thioacylals as a function of σ. Two features are apparent, the substantial and changing slopes, and the curvature. A hydrolysis proceeding solely via the A_{Ac}-2 mechanism would have resulted in lines of very small slope passing through the 4-nitro points (for example the dotted line in 9.96% H_2SO_4). The deviations from such lines are caused by the A-1 reaction. These deviations fall in the order H > 4-Cl > 3-Cl as is consistent with the substituent dependence for that reaction, and

[1]The comparison of unimolecular and bimolecular reactivities in methanol and water rules out the possibility of a mechanistic difference between the two solvents, since the bimolecular reaction would be favored in methanol. That is, if the solvolysis in methanol is unimolecular, hydrolysis likely follows the same route.

Can. J. Chem. Downloaded from www.nrcresearchpress.com by 210.87.254.40 on 09/05/12
For personal use only.

TABLE 6. Amount of A-1 hydrolysis of $ArSCH_2OAc$ in sulfuric acid solutions

	%(A-1)[a]		
$\%H_2SO_4$	C_6H_5	4-ClC_6H_4	3-ClC_6H_4
9.96	41	29	21
19.45	64	42	31
31.0	86	66	44
40.2	95	90	77

[a]Log $k_\psi(A_{Ac}\text{-}2) = \log k_\psi(4\text{-}NO_2) + 0.03(0.78 - \sigma)$; $k_\psi(A\text{-}1) = k_\psi(obs.) - k_\psi(A_{Ac}\text{-}2)$.

become more serious as the acidity is increased and the A-1 reaction assumes a greater importance. The amount of hydrolysis proceeding through each of the two pathways can in fact be approximated on the basis of such considerations, evaluating the A_{Ac}-2 rates from the rates of the 4-nitro compound with small corrections for the substituent dependence of that reaction. This is illustrated in Table 6, using the ρ value of −0.03 observed in the oxygen series.

The substituent effects not only point to the occurrence of an A-1 process, but also provide

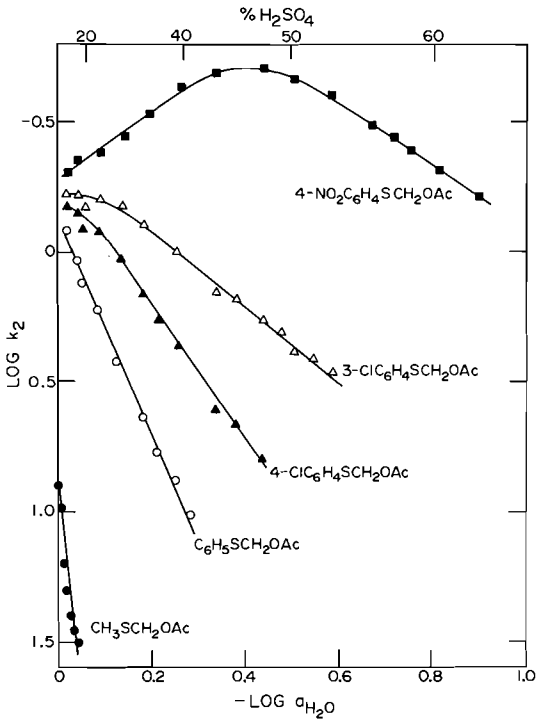

FIG. 4. r Hydration plots for the hydrolysis of thioacylals in aqueous sulfuric acid. Log k_2 = log k_ψ + mH_0, m = 0.60 (1). (No correction for protonation is necessary (8).)

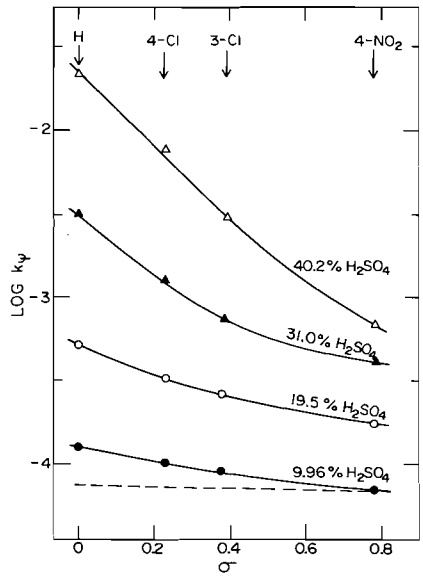

FIG. 5. Plots of log k_ψ for the acid hydrolysis of $ArSCH_2OAc$ as a function of σ. The dotted line is drawn with a slope of −0.03, and represents approximately the behavior that is expected if hydrolysis in 9.96% H_2SO_4 is occurring solely by the bimolecular pathway.

evidence that this is proceeding via the pathway of [1], with an intermediate of the form $ArSCH_2^+$. As will be described later a ρ value of −2.6 can be calculated for this reaction, *i.e.* of the same order as that of the acylals. This value is also similar (in fact, identical) to that obtained in the hydrolysis of $ArSCH_2Cl$ in 50% aqueous dioxane, a reaction which produces the same cationic intermediate (9). Moreover such a value makes unlikely a route involving protonation on sulfur followed by C—S cleavage to give ArSH and CH_2OAc^+. Such reactions occur with certain thioacetals and give ρ values of the order −0.9 (10), *i.e.* considerably less negative.

Further evidence is obtained in the methanolysis of $C_6H_5SCH_2OAc$. The benzenethiol product arises from a bimolecular process (via an intermediate $C_6H_5SCH_2OH$) while the thioacetal is the result of A-1 solvolysis. In addition the relative proportion of the two is in fairly good agreement with the situation in water. Assuming that the effect of changing solvent is that described previously, then the 5:95 proportion of A-1:A-2 in methanol implies a ratio of 18:82 in water. This applies to hydrolysis in very dilute acid and will increase as the acidity is increased. The ratio in the most dilute aqueous acid studied,

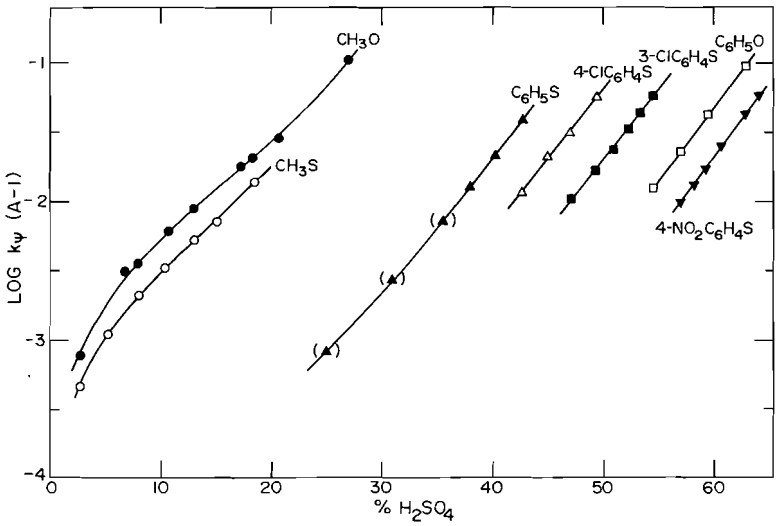

FIG. 6. A-1 hydrolysis rates for thioacylals and acylals ($RXCH_2OAc$). The points in parentheses for C_6H_5S— have been corrected for the A_{Ac}-2 contribution (Table 6).

9.96% H_2SO_4, is 41 : 59 (Table 6). In addition the actual observation of the thioacetal is significant, since this provides further strong evidence for the intermediacy of the thiocarbonium ion $C_6H_5SCH_2^+$ in the A-1 solvolysis reactions of this thioacylal.

Finally, with the considerable difference in the entropies of activation for A-1 and A-2 reactions, if a compound is undergoing hydrolysis by both routes simultaneously, it should exhibit some curvature in its activation plot. This is the case for $C_6H_5SCH_2OAc$ hydrolysis (Fig. 2). The curvature is particularly serious in 9.96% H_2SO_4 where at 25 °C there is a very close balance between the two reactions; it is less serious in 24.9% H_2SO_4 where the A-1 route predominates at 25 °C (and will become even more favored as the temperature is increased).

In concluding this section, a word should be said about the r plots for these compounds (Fig. 4). At first glance their behavior appears to be that of typical A-1 acetates, *i.e.* negative slopes. However, what is occurring here is that the substantial water activity dependence for the A-1 reaction in dilute acids (*e.g.* $r = -14$ for CH_3SCH_2OAc) has the dominating influence on the r plot behavior, even where the reaction itself is only a minor component. A similar situation arises with 4-methoxybenzyl acetate, where again there are competing hydrolyses in dilute acids (8, 11). These cases represent a serious breakdown of this mechanistic criterion for acid-catalyzed reactions, although such failures are probably restricted to the more dilute acid region where log a_{H_2O} does not change very greatly.

Relative A-1 Reactivities for Acylals and Thioacylals

In summary the thioacylals are exhibiting the same mechanistic behavior as the acylals (1), namely a competition between what are essentially A_{Ac}-2 and A_{A1}-1 ester hydrolysis reactions. The differences lie only in the acidities at which the latter reaction becomes important.[2] In previous investigations it has been established (1, 8, 11) that the determining factor in this is the stability of the intermediate carbonium ion, and in consequence the A-1 behavior of the thioacylals and acylals is a reflection of the relative stabilities of thiocarbonium ions and oxycarbonium ions, *i.e.* the relative stabilizing effect of sulfur and oxygen adjacent to a cationic center. These relative A-1 reactivities can be estimated quantitatively using the stepwise procedure outlined previously (1), employing Fig. 6 where the rates of hydrolysis are plotted in acids where the reaction is substantially unimolecular. The rates relative to $C_6H_5SCH_2OAc$ are listed in Table 7. (From this table, a ρ value of −2.6 for A-1 hydrolysis of $ArSCH_2OAc$ is obtained (Fig. 7).)

The most surprising result is the very close

[2]There is only a small difference in $A_{Ac} = 2$ hydrolysis rates (see for example Table 5 and the discussion in the previous paper (1)).

Can. J. Chem. Downloaded from www.nrcresearchpress.com by 210.87.254.40 on 09/05/12
For personal use only.

Can. J. Chem. Downloaded from www.nrcresearchpress.com by 210.87.254.40 on 09/05/12
For personal use only.

TABLE 7. Relative A_{Al}-1 reactivities of thioacylals and acylals

Substrate	k_{rel}[a]
CH_3OCH_2OAc	81
CH_3SCH_2OAc	49
$C_6H_5SCH_2OAc$	1.000
$4\text{-}ClC_6H_4SCH_2OAc$	0.32
$3\text{-}ClC_6H_4SCH_2OAc$	0.099
$C_6H_5OCH_2OAc$	0.022
$4\text{-}NO_2C_6H_4SCH_2OAc$	0.010

[a]Rate relative to $C_6H_5SCH_2OAc$.

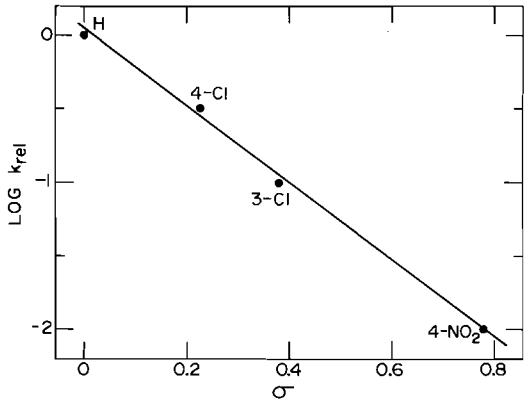

FIG. 7. Hammett σ plot for the A-1 hydrolysis of $ArSCH_2OAc$.

reactivity of the two aliphatic compounds. Previous solution studies would suggest a considerably greater stabilizing effect of oxygen, as for example in the S_N1 solvolysis of CH_3XCH_2Cl where $k_{-O-}/k_{-S-} \approx 1500$ (12), or in comparing σ^+ substituent constants, CH_3O, −0.78; CH_3S, −0.60 (13). On the other hand gas phase investigations (14, 15) (as well as a recent theoretical study (16)) imply an opposite behavior. Thus our result actually lies somewhat intermediate between these two extremes. No simple explanation is apparent; a number of factors are important in determining the solution reactivity (*e.g.* solvation and extent of charge development), and it is probable that these are responsible for the various behaviors. Certainly in our system there is an inherent difference in that the heterolysis starts with a cationic (protonated) species[3] and furthermore involves an excellent leaving group in the neutral acetic acid molecule.

The second intriguing observation of this work involves the results obtained on replacing methyl by phenyl. As is expected the rate is decreased in both cases. However, the decrease is far greater with oxygen than with sulfur. With the similarity in the two aliphatic compounds this means that for the aromatic pair $C_6H_5SCH_2OAc$ and $C_6H_5OCH_2OAc$ the sulfur compound is considerably more reactive. In this comparison, the situation is complicated by the adjacent aromatic ring which is also conjugated with the heteroatom and the difference in behavior undoubtedly involves this consideration in some way. However, again, no simple explanation offers itself, and we will refrain from further speculation until more experimental and theoretical results become available.

[3]It is highly unlikely that there is much difference in the protonation step (11, 17).

Experimental

Materials

Sulfuric acid solutions were prepared and standardized as previously described (18). The preparation of the arylthiomethyl acetates has been reported elsewhere (19). Standard procedures were used for the preparation of CH_3SCH_2OAc (14) and $CH_3SCH_2OCH_3$ (20).

$C_6H_5SCH_2OCH_3$ (2) was prepared using the method of Dunn and Bruice (21) and had b.p. 110 (11 mm); n.m.r. (CCl_4, TMS): δ 7.5–7.1 (5H, m, ArH); 4.85 (2H, s, CH_2); 3.32 (3H, s, CH_3).

Kinetics

Rate data for the aromatic thioacylals were obtained from the u.v. spectral change, as described in the previous paper (1). Wavelengths used are listed in Table 8. With methylthiomethyl acetate, the hydroxamic acid – ferric chloride method for the analysis of esters (3) was employed. Control experiments demonstrated that there were no problems associated with the measurements because of the fact that this substrate is not a simple ester.

Products of Hydrolysis

For the arylthiomethyl acetates the u.v. spectra of the products were found to be identical to those of the appropriate benzenethiols in the same acid. In the case of the unsubstituted compound, the quantitative formation of this product was confirmed by g.c. analysis. Solutions of the thioacylal in various acids were allowed to react for

TABLE 8. Wavelengths employed to follow hydrolysis of arylthiomethyl acetates

	λ (nm)	
Substituent	Acid	Base
4-MeO	—	280
H	230	280
4-Cl	240	285
3-Cl	235	285
$4\text{-}NO_2$	330	385

7–10 half-lives, and then extracted with methylene chloride. A known amount of naphthalene was added and the methylene chloride layer was analyzed by g.c. This was performed on a Carlo-Erba model 61 chromatograph, with a column (2 m × 6 mm) of 30% Carbowax 20M on Chromosorb P operating at 130 °C. The amount of benzenethiol present was determined from its peak area relative to that of naphthalene. The relative response of the two was determined from synthetic mixtures. In all acids, a 95–105% yield based on thioacylal was obtained, *i.e.* quantitative within experimental error.

Methanolysis

In a methanol solution containing 0.02 *M* benzenesulfonic acid (monohydrate) were placed the thioacylal (0.02 *M*) and g.c. standard (for the CH_3SCH_2OAc experiment, chlorobenzene; for $C_6H_5SCH_2OAc$, naphthalene). At appropriate intervals this solution was injected directly into the gas chromatograph (conditions as above, the temperature for CH_3SCH_2OAc was 60 °C). The products were identified by comparison of retention times with those of authentic samples. Their yields were calculated from peak areas relative to that of the standard, again referenced to a relative response determined from synthetic mixtures. Control experiments were carried out in the same fashion starting with authentic samples of the products.

The kinetics for the methanolysis of *p*-nitrophenyl acetate were studied in solutions which were 0.01 *M*, 0.03 *M*, and 0.05 *M* in benzenesulfonic acid, by following the increase in u.v. absorbance at 305 nm. The concentration of ester was 2×10^{-4} *M*. Excellent first-order plots of ln $(A_\infty - A_t)$ *vs.* *t* were obtained.

1. R. A. McClelland. Can. J. Chem. This issue.
2. T. H. Fife and N. C. De. J. Am. Chem. Soc. **96**, 6158 (1974).
3. K. Yates and R. A. McClelland. J. Am. Chem. Soc. **89**, 2686 (1967).
4. M. L. Bender, J. A. Reinstein, M. S. Silver, and R. Mikulak. J. Am. Chem. Soc. **87**, 4545 (1965); K. Bowden and M. M. Last. J. Chem. Soc. Perkin Trans. 2, 358 (1973).
5. E. K. Euranto and R. H. Isotalo. Suom. Kemistil. B, **43**, 271 (1970).
6. P. Salomaa. Acta Chem. Scand. **11**, 132 (1957).
7. L. L. Schaleger and F. A. Long. Adv. Phys. Org. Chem. **1**, 1 (1963).
8. K. Yates. Acc. Chem. Res. **4**, 136 (1971).
9. F. G. Bordwell, G. D. Cooper, and H. Morita. J. Am. Chem. Soc. **79**, 376 (1957).
10. L. R. Fedor and B. S. R. Murty. J. Am. Chem. Soc. **95**, 8407 (1973).
11. R. A. McClelland, T. A. Modro, and K. Yates. J. Am. Chem. Soc. In press.
12. F. J. Bordwell and P. J. Bouton. J. Am. Chem. Soc. **78**, 854 (1956); H. Böhme. Ber. **74**, 248 (1949); H. Böhme, H. Fisher, and R. Frank. Ann. **563**, 54 (1949); T. C. Jones and E. R. Thornton. J. Am. Chem. Soc. **89**, 4863 (1967).
13. L. H. Stock and H. C. Brown. Adv. Phys. Org. Chem. **1**, 35 (1963).
14. F. H. Field and D. P. Weeks. J. Am. Chem. Soc. **92**, 6521 (1970).
15. R. W. Taft, Jr., R. H. Martin, and F. W. Lampe. J. Am. Chem. Soc. **87**, 2490 (1965); B. G. Keyes and A. G. Harrison. J. Am. Chem. Soc. **90**, 5671 (1968); A. G. Harrison, A. Ioko, and D. van Raalte. Can. J. Chem. **44**, 1625 (1966); B. G. Hobrock and R. W. Kiser. J. Phys. Chem. **67**, 1283 (1963).
16. F. Bernardi, I. G. Csizmadia, H. B. Schlegel, and S. Wolfe. Can. J. Chem. **53**, 1144 (1975).
17. D. G. Lee and M. H. Sadar. J. Am. Chem. Soc. **96**, 2862 (1974).
18. K. Yates and R. A. McClelland. Can. J. Chem. **52**, 1098 (1974).
19. R. A. McClelland. J. Org. Chem. To be published.
20. D. Martin and H. J. Niclas. Ber. **102**, 31 (1969).
21. B. M. Dunn and T. C. Bruice. J. Am. Chem. Soc. **92**, 2411 (1970).
22. P. Salomaa. Acta Chem. Scand. **14**, 239 (1957).

Can. J. Chem. Downloaded from www.nrcresearchpress.com by 210.87.254.40 on 09/05/12
For personal use only.

Proton Magnetic Resonance Studies of Dinucleotide Conformation in Aqueous Solution. 2′-Deoxythymidylyl-(3′,5′)-2′-deoxy-3′-thymidylate, d(TpTp)

DONALD J. WOOD,[1] KELVIN K. OGILVIE,[2] AND FRANK E. HRUSKA
Department of Chemistry, University of Manitoba, Winnipeg, Manitoba R3T 2N2

Received January 31, 1975

DONALD J. WOOD, KELVIN K. OGILVIE, and FRANK E. HRUSKA. Can. J. Chem. **53**, 2781 (1975).

Proton magnetic resonance studies of 2′-deoxythymidine, its 3′- and 5′-monophosphate, its 3′,5′-diphosphate, and the dimer molecules d(TpT) and d(TpTp) in aqueous solution are described. Spectral analysis yields ^1H–^1H and ^1H–^{31}P coupling constants and ^1H chemical shifts which can be discussed in terms of the conformational properties of the nucleoside fragments. An important observation is the apparent phosphate–phosphate interaction in a 3′,5′-diphosphate fragment which stabilizes the *gauche-gauche* conformation about the $C_{4'}$—$C_{5'}$ bond.

DONALD J. WOOD, KELVIN K. OGILVIE et FRANK E. HRUSKA. Can. J. Chem. **53**, 2781 (1975).

On décrit des études r.m.p. sur des solutions aqueuses de déoxy-2′ thymidine, de ses monophosphates-3′ et -5′, de son diphosphate-3′,5′ et des molécules dimères d(TpT) et d(TpTp). L'analyse des spectres fournit les constantes de couplage ^1H–^1H et ^1H–^{31}P et les déplacements chimiques du ^1H qui peuvent être discutés en termes de propriétés conformationnelles de fragments nucléosides. Une observation importante est l'interaction apparente phosphate–phosphate dans le fragment diphosphate-3′,5′ qui stabilise la conformation *gauche-gauche* autour du lien $C_{4'}$—$C_{5'}$. [Traduit par le journal]

Introduction

The study by spectroscopic and theoretical methods of the physicochemical properties of nucleosides and their monophosphate derivatives is one approach towards the understanding of the properties of polynucleotides (1–7). These monomer studies do not, however, allow for the evaluation of factors such as internucleoside interactions, phosphate–phosphate interactions etc., which might influence polymer stereochemistry. Studies on 3′,5′-diphosphates (7), however, do provide information on the interactions between adjacent phosphates. Dinucleoside mono-, di-, and triphosphates possessing a 3′,5′-phosphodiester linkage are better model systems. Recent X-ray studies (8–13) have revealed features of dimer stereochemistry in the solid state. Solution studies at the dimer level have been concerned primarily with the problems of base-stacking forces and geometry. Several groups (14–20) have attempted complete analysis of the complex ^1H and ^{13}C spectra of the sugar-phosphate moiety of several dinucleoside monophosphates and discussed the effect of formation of the 3′,5′-phosphodiester linkage upon sugar-phosphate conformation. As a sequel to our study on 2′-deoxythymidylyl-(3′,5′)-2′-deoxythymidine, d(TpT) (17–19), and its u.v. damaged derivative (18, 19), we present here the p.m.r. data of its phosphorylated derivative, d(TpTp) (Fig. 1). Data for 2′-deoxythymidine (dT), its 3′- and 5′-monophosphates (3′dTMP, 5′dTMP), and its 3′,5′-diphosphate (pdTp) (Fig. 2) are also presented. Comparison of all the data

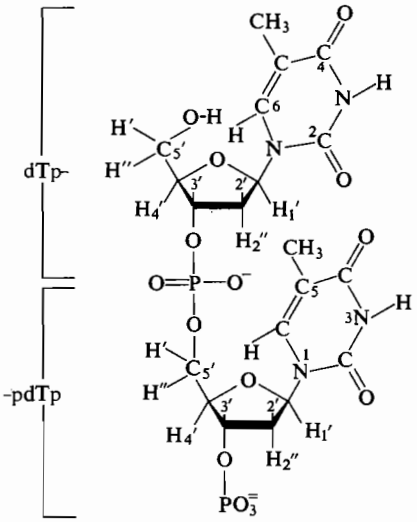

FIG. 1. Structural formula of 2′-deoxythymidylyl-(3′,5′)-2′-deoxy-3′-thymidylate, d(TpTp). dTp- and -pdTp refer to the free 5′- and 3′-terminal fragments of d(TpTp), respectively.

[1]Postdoctoral fellow.

[2]Present address: Chemistry Department, McGill University, Montreal, Quebec.

Can. J. Chem. Downloaded from www.nrcresearchpress.com by 210.87.254.6 on 09/05/12
For personal use only.

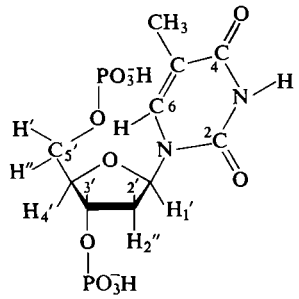

FIG. 2. Structural formula of thymidine-3′,5′-diphosphate, pdTp.

allows us to assess the effect of 3′- and 5′-phosphorylation and incorporation into the nucleoside mono- and diphosphates upon the conformation of dT. An observation of particular interest is the *concerted* enhancement of the *gauche-gauche* conformer population by the 3′- and 5′-phosphates in a nucleoside-3′,5′-diphosphate fragment.

Experimental

The compounds d(TpTp) and pdTp were prepared and purified by the method of Letsinger *et al.* (21). dT was obtained from the Sigma Chemical Co., and used without further purification. The p.m.r. samples were lyophilized three times from D_2O and then were dissolved in 100% D_2O to a concentration of 0.10 *M*. The p*D* of the samples (dT, d(TpTp): 7.0; pdTp: 5.8) was adjusted with NaOD or DCl. Sodium 3-trimethylsilylpropionate-2,2,3,3-d_4 (TSP) was used as an internal reference.

The p.m.r. spectrum of dT was recorded on a Varian HD 100 MHz spectrometer; the spectra of pdTp and d(TpTp) (Fig. 3) were recorded at the Canadian 220 MHz Centre, Sheridan Park, Ontario, on a Varian HR 220 MHz spectrometer. All spectra were analyzed using the computer program LAME (22) and computer simulations (Fig. 3) were used as a final test of the derived chemical shift (δ) and coupling constant (*J*) data. The *J* (H–H and H–P) and δ values (along with data for 3′dTMP, 5′dTMP and d(TpT) from ref. 17) are given in Table 1; the δ data also appear in Fig. 4.

Spectra for pdTp and d(TpTp) were recorded at 65 °C, whereas for dT a slightly higher temperature (70 °C) was required to expose the $H_{3'}$ resonances obscured at 65 °C by the HDO resonance. The relatively high temperature was needed owing to the broadness of the resonances[3] for pdTp and d(TpTp) at ambient (and lower) temperatures. However, except for this line broadening, the general features of the spectra are very similar in the temperature interval examined (30–70 °C). Thus, our main conclusions regarding molecular conformation should apply at the lower temperatures.

In the discussion section dTp- and -pdTp will be used to designate the 5′- and 3′-*terminal* fragments of d(TpTp), respectively. For the corresponding fragments of d(TpT), dTp- and -pdT will be used. Wherever confusion from the use of dTp- might occur, the appropriate dimer, d(TpT) or d(TpTp), will be indicated.

We must also point out here that at our experimental temperatures the dimers are unstacked. Our conformational conclusions apply, therefore, strictly to the extended molecules. In the transition to the folded forms the conformational distributions about the P—O bonds, in particular, and about the $C_{4'}$—$C_{5'}$ and $O_{5'}$—$C_{5'}$ bonds to a lesser extent, will change.

Results and Discussion

Spectral Assignment

The spectral assignments for dT, 3′dTMP, 5′dTMP, and d(TpT) have been presented (17). The assignment of the spectra of pdTp was facilitated by comparison with those of the other monomers (dT, etc.) and confirmed by decoupling experiments. In the 2′,2″ region of the pdTp spectrum, $H_{2''}$ was assigned to the low-field portion on the basis of arguments by Fang *et al.* (23) concerning the deshielding influence of a 3′-phosphate on the *cis* ($H_{2''}$) hydrogens. In the 5′,5″ region of all molecules examined here, $H_{5'}$ was assumed to be to low field of $H_{5''}$ (following Remin and Shugar (24)).[4]

The assignment of the various bands in the spectrum of d(TpTp) was initiated with the assumption that the quartets at 6.37 and 6.25 p.p.m. were attributable to the 1′-hydrogens of the -pdTp and dTp- fragments, respectively. This assumption is made reasonable by the appearance of $H_{1'}$ (pdTp) at 6.37 p.p.m. and $H_{1'}$ (3′dTMP) at 6.28 p.p.m. Spin decoupling experiments facilitated the location of bands attributable to other hydrogens on the two fragments. Differentiation between the 2′- and 2″-hydrogens on the dTp- fragment and between the 2′- and 2″-hydrogens on -pdTp was first made with the assumption that the deshielding effect on 3′-phosphorylation at the monomer level (dT → 3′dTMP; 5′dTMP → pdTp) was similar to its effect at the dimer level (d(TpT) → d(TpTp)). The assignment made on this basis is

[3]Extensive hydration may contribute to the line broadening; the dinucleotide d(pTpT) is extensively hydrated in the solid state (13).

[4]We cannot be certain that the Remin and Shugar assignment applies to each of the molecules examined here. However, because we are concerned, in the $C_{4'}$—$C_{5'}$ conformational problem, primarily with the *gg* population, any misassignment is not serious since the calculated P_{gg} values are invariant with change in 5′,5″ assignment. See footnote 1 in ref. 25 for comments on 5′,5″ assignment in 2′-deoxyriboses.

Can. J. Chem. Downloaded from www.nrcresearchpress.com by 210.87.254.6 on 09/05/12
For personal use only.

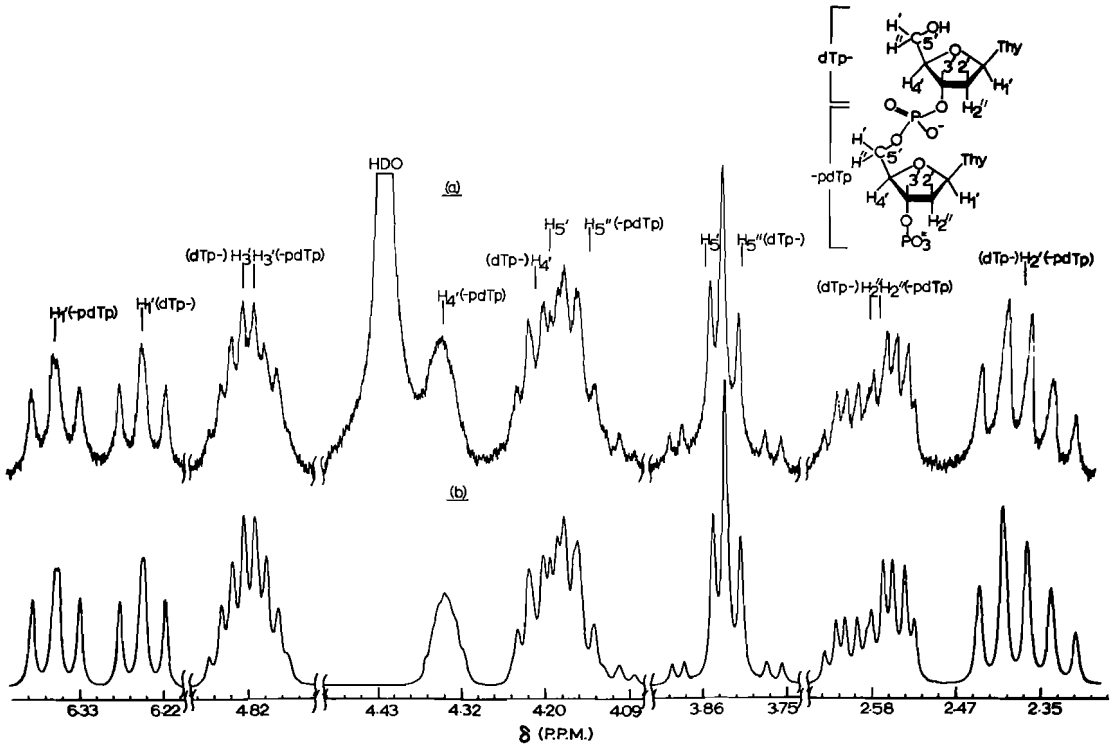

FIG. 3. (*a*) Single scan, continuous-wave, 220 MHz spectrum of d(TpTp) (p*D* 7.0, 65 °C, 0.1 *M* in D_2O). Sweep width 250 Hz. (*b*) Computer simulated spectrum. Included for simulation were $J_{2',P_3'} = 0.7$ Hz and $J_{4',P_3'} = 0.5$ Hz for both 3′-nucleotide fragments and $J_{3',5''} = 0.9$ Hz for -pdTp. Similar magnitudes are indicated for these coupling constants in the spectrum of pdTp.

consistent with a 2′,2″ assignment based on the assumptions that $J_{2'',3'} \simeq J_{3',4'}$ and $J_{1',2''} \simeq J_{2',3'}$ for 'normal' (26, 27) 2′-deoxyriboses (17).

The 2′,2″ assignments for all entries (except those for 5′dTMP and the -pdT fragment of d(TpT)) in Table 1 adhere to the proposal that $J_{2'',3'} \simeq J_{3',4'}$ and $J_{1',2''} \simeq J_{2',3'}$. In the exceptional cases $H_{2'}$ and $H_{2''}$ are too strongly coupled for meaningful assignment and only the sums $J_{1',2'} + J_{1',2''}$ and $J_{2',3'} + J_{2'',3'}$ can be obtained; in Table 1 one-half of the appropriate sum has been arbitrarily entered for these four coupling constants.

The Sugar-Base Torsion Angle (χ)

Accurate χ values (2, 13, 28, 29) for crystalline 2′-deoxythymidine residues (dT, 39.3 °C; 5′dTMP, 43.5 °C; pdTp- of d(pTpT), 27 °C; -pdT of d(pTpT), 34 °C) reveal a remarkable degree of conformational similarity in dT fragments and the absence of drastic changes in χ(*anti*) upon 3′- or 5′-phosphorylation of dT or upon its incorporation into a dimer molecule. In *solution* the chemical shift of the 6-hydrogen should be sensitive to changes in χ (30). The striking similarity in the δ_6 values for the series dT, 3′dTMP, dTp- of d(TpT) and dTp- of d(TpTp) argues, therefore, that extension of the dT molecule in the 5′ → 3′ direction by sequential addition of a 3′-phosphate, a dT fragment, etc., has little effect on the χ-value distribution under our experimental conditions. This suggestion is supported by the relative invariance, for this same series, of the $\delta_{1'}$ values which fall in the narrow range from 6.24 to 6.28 p.p.m. Similarly, the relative invariance of the δ_6 data on the one hand and the $\delta_{1'}$ data on the other for the 5′-phosphorylated fragments (5′dTMP, -pdT of d(TpT)) and for the 3′,5′-phosphorylated fragments (pdTp and -pdTp of d(TpTp)) indicates that extension in the 3′ → 5′ direction has little influence on χ(dT). The remarkable

Can. J. Chem. Downloaded from www.nrcresearchpress.com by 210.87.254.6 on 09/05/12
For personal use only.

Can. J. Chem. Downloaded from www.nrcresearchpress.com by 210.87.254.6 on 09/05/12
For personal use only.

TABLE 1. Proton magnetic resonance parameters[a] for D_2O solutions of thymine derivatives[b] at +65 °C[c]

Parameter	dT	5′dTMP[d]	-pdT[d]	pdTp	-pdTp	3′dTMP[d]	dTp-[d] of d(TpT)	dTp- of d(TpTp)
$\delta_{1'}$	6.26	6.31	6.32	6.37	6.37	6.28	6.24	6.25
$\delta_{2'}$	2.36	<2.37[i]	<2.38	2.42	2.38	2.41	2.36	2.38
$\delta_{2''}$	2.40	<2.38	<2.39	2.55	2.58	2.56	2.57	2.59
$\delta_{3'}$	4.47	4.57	4.57	4.87	4.81	4.76	4.80	4.82
$\delta_{4'}$	4.03	4.16	4.14[l]	4.34	4.34	4.17	4.19	4.21
$\delta_{5'}$	3.84	<4.05	4.16[l]	<4.10	4.20	3.87	3.84	3.86
$\delta_{5''}$	3.77	<4.04	4.09[l]	<4.09	4.14	3.81	3.79	3.81
δ_5	1.91	1.93	1.92	1.94	1.93	1.91	1.90	1.91
δ_6	7.62	7.72	7.68	7.78	7.74	7.64	7.63	7.64
$J_{1'2'}$	6.7	[7.0[j]	[6.8	8.0	7.7	7.1	7.8	7.4
$J_{1'2''}$	6.8	[7.0	[6.8	6.2	6.4	6.6	6.3	6.3
$J_{2'2''}$	−14.1	−14.4[k]	−14.2[k]	−14.0	−14.1	−14.3	−14.2	−14.1
$J_{2'3'}$	6.3	[4.9	[5.4	6.7	6.9	6.9	6.6	7.0
$J_{2''3'}$	4.6	[4.9	[5.4	2.3	2.7	3.8	3.5	3.5
$J_{3'4'}$	4.0	3.3	3.7[l]	3.0	3.3	3.7	3.6	3.6
$J_{4'5'}$	3.9	[3.9	2.5[l]	[3.3	2.1	3.7	3.4	3.5
$J_{4'5''}$	5.0	[3.9	5.0[l]	[3.3	4.4	5.0	5.5	4.7
$J_{5'5''}$	−12.4	−12.1[k]	−12.1[l]	−12.0[k]	−11.8	−12.5	−12.3	−12.3
$J_{P3'}$[e]	—[h]	—	—	6.4	6.6	7.6	7.1	6.4
$J_{P4'}$	—	1.5	1.6[l]	1.5	1.8	—	—	—
$J_{P5'}$	—	[5.4	4.0[l]	[4.8	4.5	—	—	—
$J_{P5''}$	—	[5.4	5.0[l]	[4.8	4.9	—	—	—
J_{56}	1.3	1.2	1.2	1.1	0.9	1.2	1.2	1.0
Σ[f]	8.9	7.8	7.5[l]	6.6	6.5	8.7	8.9	8.2
Σ'[g]	—	10.8	9.0	9.6	9.4	—	—	—

[a]Chemical shifts reported in p.p.m. from TSP. Coupling constants reported in Hz. Estimated errors: J, ±0.3 Hz; δ, ±0.01 p.p.m.
[b]See experimental for abbreviations.
[c]dT at 70 °C.
[d]Data from ref. 17.
[e]All J_{Pi} are ^3J except $J_{P4'}$ ($=^4J$) which involves the P atom and $H_{4'}$ displaced in the 5′ → 3′ sense.
[f]$\Sigma = J_{4'5'} + J_{4'5''}$.
[g]$\Sigma' = J_{P5'} + J_{P5''}$.
[h]Not observed or not applicable.
[i]The 0.01 p.p.m. shift is arbitrary *i.e.* $\delta_i \simeq \delta_j$.
[j]Owing to near equivalence of chemical shifts, only the sum of connected ([) coupling constants is significant.
[k]Arbitrary. When $\delta_i \simeq \delta_j$, the spectrum is independent of J_{ij}.
[l]Owing to overlap of resonances, these values are less certain.

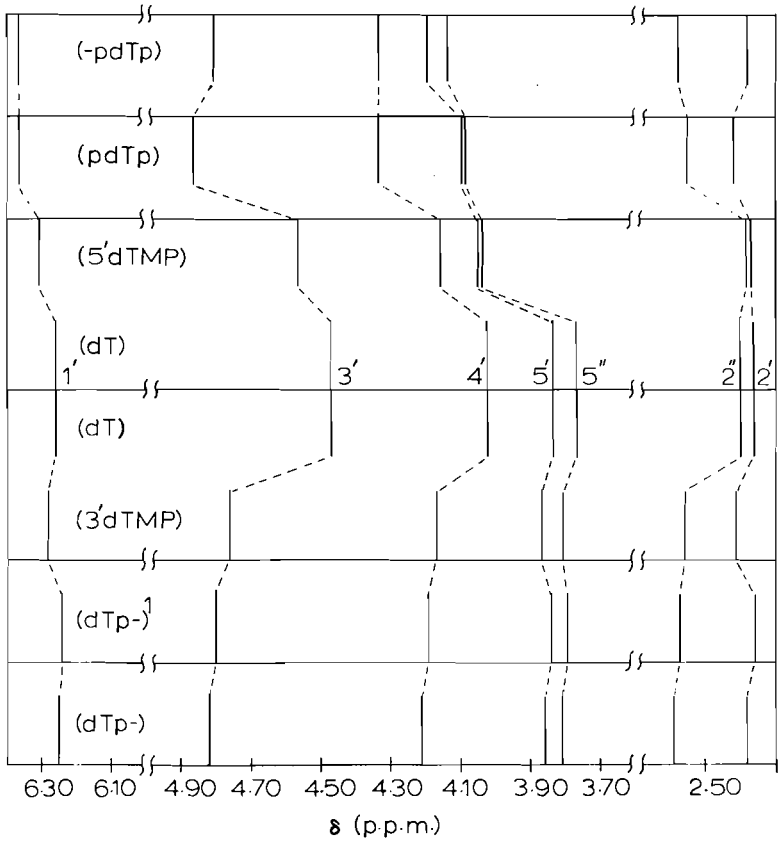

FIG. 4. Chemical shifts of the deoxyribo hydrogens of dT, 3′dTMP, 5′dTMP, pdTp, d(TpT), and d(TpTp) in p.p.m. relative to internal TSP. Plotted data from Table 1. $(dTp-)^1$ and (dTp-) refer, respectively, to the dTp- fragment of d(TpT) and d(TpTp). In comparing $\delta_{3'}$ for -pdTp and pdTp, bear in mind that the acidity conditions (experimental section) were such that the 3′-phosphate in the former is diionized and monoionized in the latter. At $pD < 5.5$, $H_{3'}$(-pdTp) is located 0.09 p.p.m. to lower field.

conservation of χ(dT) values in the solid state is apparently achieved in aqueous solution as well.

Puckering of the 2′-Deoxyribose

The magnitudes of the *trans* coupling constants ($J_{1'2'}$, $J_{2''3'}$, $J_{3'4'}$) and the *cis* coupling constants ($J_{1'2''}$, $J_{2'3'}$) are related to the mode and extent of puckering of the 2′-deoxyribose ring (26, 27). A striking feature of these data in Table 1 is the similarity in corresponding values for all entries. Thus we must conclude that the puckering of a dT fragment is little affected by 3′- or 5′-phosphorylation or by incorporation into the dimer molecules. What little variation there is in the *J* values conforms, however, with our expectations based on a 2′-*endo* (S) ↔ 3′-*endo* (N) model. Firstly, we note that the overall range for the *trans* coupling constants is consistently larger ($J_{1'2'}$ = 1.3 Hz; $J_{2''3'}$ = 2.3 Hz; $J_{3'4'}$ = 1.0 Hz) than that for the *cis* coupling constants ($J_{1'2''}$ = 0.6 Hz; $J_{2'3'}$ = 0.7 Hz). This is expected since, whereas the *cis* pairs of hydrogens (1′2″, 2′3′) assume a quasi-axial-equatorial (*ae*) disposition in both the 2′- and 3′-*endo* modes, the disposition of the *trans* pairs (1′2′, 2″3′, 3′4′) alters from *aa* (or *ee*) to *ee* (or *aa*) in the 2′-*endo* to 3′-*endo* change. Thus any shift in the 2′-*endo* ↔ 3′-*endo* balance should be manifest in proportionate changes in the *trans* coupling constants and (somewhat) attenuated changes in the *cis* values (26, 27). Secondly, there is a prevailing tendency for $J_{2''3'}$ and $J_{3'4'}$ to increase concomitantly with decreases in $J_{1'2'}$. These inverse relations are best revealed by the relative constancy of the sums $J_{1'2'} + J_{3'4'}$ which lie in the range 11.0 ± 0.3 Hz for our molecules and by the sums $J_{1'2'} + J_{2''3'}$ which, with pdTp excepted, lie in the range 11.1 ±

Can. J. Chem. Downloaded from www.nrcresearchpress.com by 210.87.254.6 on 09/05/12
For personal use only.

Can. J. Chem. Downloaded from www.nrcresearchpress.com by 210.87.254.6 on 09/05/12
For personal use only.

0.2 Hz. The larger deviation from the norm for $J_{1'2'} + J_{2''3'}$ for pdTp (10.3 Hz) might be a consequence of a somewhat less accurate value for $J_{2''3'}$ owing to obscured fine structure in the 3′ region of its proton spectrum, though a conformational interpretation cannot be discounted (see below).

An approximation of the relative contributions to the 2′-*endo* ↔ 3′-*endo* blend can be obtained from [1].

$$[1] \qquad \% \text{ 3′-}endo = 10J_{3'4'}$$

In Table 2 we have entered the % populations of the predominant (2′-*endo*) form. A bias of 60–70% for 2′-*endo* is evident in each instance. At the monomer level phosphorylation appears to enhance the 2′-*endo* bias within the small overall range. Incorporation into the dinucleoside mono- or diphosphate does not produce significant further change in this bias. This conservation of structure is also apparent in the crystal state; with only two exceptions (2, 31, 32) 2′-deoxyribo rings favor the 2′-*endo* pucker in the solid state.

One further trend appears in the data in Table 1. For dT we find that $J_{2''3'}$ is *larger* than $J_{3'4'}$ by 0.6 Hz; for the 3′-phosphorylated species (3′dTMP, dTp- of d(TpT) and of d(TpTp)), $J_{2''3'}$ and $J_{3'4'}$ differ by only 0.1 Hz whereas in the 3′,5′-phosphorylated species (pdTp and -pdTp of d(TpTp)) $J_{2''3'}$ is *smaller* than $J_{3'4'}$ by 0.6–0.7 Hz. Thus there appears to be a significant (1.3 Hz) spread in the difference $J_{2''3'} - J_{3'4'}$ in this series of molecules. This trend is understood (26, 27) if, in the sequence from dT to 3′-phosphorylated fragments to 3′,5′-phosphorylated fragments, the characteristic P_N values increase and/or the P_S values decrease.[5] If this is the appropriate interpretation of the trend in the value of $J_{2''3'} - J_{3'4'}$, then we must further predict, following Altona and Sundaralingam (27), that for 2′-*endo* decreases in $J_{2''3'} - J_{3'4'}$ should be coupled to decreases in $J_{1'2''}$ and to increases in $J_{2'3'}$ values. Trends in the *cis* couplings are less clear because of their small overall variation but it is interesting nevertheless to observe (Table 1) that, as $J_{2''3'} - J_{3'4'}$ *decreases* by 1.3 Hz as we pass from dT to pdTp, $J_{1'2''}$ *decreases* by 0.6 Hz while $J_{2'3'}$ *increases* by 0.4 Hz. In fact for the entries in Table 1 there is the prevailing tendency for $J_{1'2''} - J_{2'3'}$ to decrease with $J_{2''3'} - J_{3'4'}$. These correlated decreases are expected for a decrease in phase angle of pseudorotation P in 2′-*endo*, the favored pucker of 2′-deoxyriboses (26, 27). To summarize in conformational terms, we state that our data are consistent with shifts towards lower P_S values upon phosphorylation of a dT fragment. Granted, this statement follows from interpretation of small changes in coupling. Nevertheless it will be interesting to see whether similar trends can be observed in the more accurately-determinable crystal conformations. This comparison awaits evaluation of the effects of phosphorylation (and incorporation into dimer molecules) on the phase angle of pseudorotation in crystalline 2′-deoxyribosides.

[5] P_N and P_S are the so-called 'phase angles of pseudorotation' for the N and S ranges (26, 27).

Conformation about the Exocyclic $C_{4'}$—$C_{5'}$ Bond

The $J_{4'5'}$ and $J_{4'5''}$ data can be translated into approximate values of the *gauche-gauche* (*gg*), *gauche-trans* (*gt*), and *trans-gauche* (*tg*) populations (Fig. 5) according to ref. 17. The main trends in the calculated populations (P_{gg}, P_{gt}, P_{tg} in Table 2) are as follows. (*i*) In the series dT, 3′dTMP, dTp- of d(TpT) and dTp- of d(TpTp) which progresses by extension in the 5′ → 3′ direction, we find little change in the $C_{4'}$—$C_{5'}$ rotamer population for the free 5′-terminal hydroxymethyl group. The *gg* conformation in this series is slightly favored but remains in the nar-

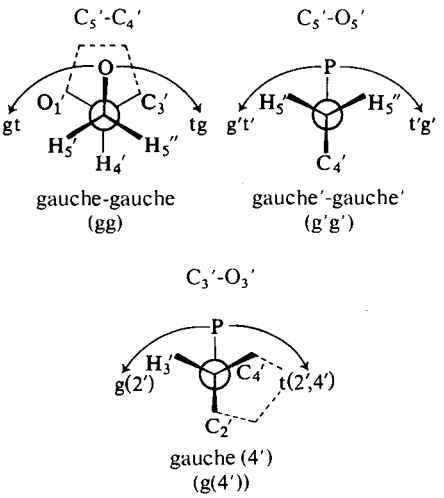

FIG. 5. Dominant conformations viewed along the $C_{5'}$–$O_{5'}$ bond (*gauche'-gauche'* (*g'g'*), *gauche'-trans'* (*g't'*), *trans'-gauche'* (*t'g'*)), the $C_{4'}$—$C_{5'}$ bond (*gauche-gauche* (*gg*), *gauche-trans* (*gt*), *trans-gauche* (*tg*)), and the $C_{3'}$—$O_{3'}$ bond (*gauche* (2′) (*g*(2′)), *gauche* (4′) (*g*(4′)), *trans* (2′,4′) (*t*(2′,4′))).

TABLE 2. Calculated conformer[a] populations[b] of thymine derivatives[c] at +65 °C[d] in D_2O solution

	$C_{5'}—O_{5'}$	$C_{4'}—C_{5'}$			2′-Deoxyribose pucker
	$P_{g'g'}$	P_{gg}	P_{gt}	P_{tg}	$P_{2'\text{-}endo}$
dT	—[e]	41	35	24	60
5′dTMP	73	52	—	—	67
(-pdT) of d(TpT)	83[f]	55[f]	35[f]	10[f]	63
pdTp	80	64	—	—	70
(-pdTp) of d(TpTp)	81	65	29	6	67
3′dTMP	—	43	35	22	63
(dTp-) of d(TpT)	—	41	40	19	64
(dTp-) of d(TpTp)	—	48	32	20	64

[a]See Fig. 1 for a designation of the abbreviations.
[b]Calculated values given as percentages. Estimated error is ± 5%.
[c]See text for thymine derivative abbreviations.
[d]dT at +70 °C.
[e]Not applicable or not attainable.
[f]These values are less certain than the others reported (Table 1). Estimated error ± 10%.

row range from 41–48%. (*ii*) 5′-Phosphorylation of dT enhances the *gg* bias (5′dTMP: 55%) and (*iii*) this bias is further enhanced by subsequent phosphorylation at the 3′-position (pdTp: 64%). (*iv*) Incorporation of 5′dTMP into the dimer d(TpT) has little effect on P_{gg} (-pdT: 55%). However, 3′-phosphorylation of d(TpT) enhances noticeably the P_{gg} value for this fragment (-pdTp of d(TpTp): 64%) in line with observations at the monomer level (point *iii*). We should point out here that both dimer molecules are probably predominantly in the extended form at our experimental (65 °C) temperature. For dimer molecules in a stacked conformation, larger calculated P_{gg} values (100%?) are expected. (*v*) The extension of a 5′-thymidylyl fragment in the 3′ → 5′ direction has little effect upon P_{gg} for this fragment. (Compare data for 5′dTMP and -pdT of d(TpT) and for pdTp and -pdTp of d(TpTp).)

The observed trends (points *i–v*) are, for the most part, in agreement with X-ray data. Thus, *gg* appears most often in 2′-deoxyriboses at the monomer level (2) and at the dimer level (13). The increase in P_{gg} with 5′-phosphorylation (point *ii*) and the absence of significant variation in P_{gg} for dT, 3′dTMP, dTp- of d(TpT) and of d(TpTp) (point *i*) are consistent with the "rigid nucleotide" concept (2, 33) which proposes that 5′- (but not 3′-phosphorylation *by itself*) will enhance the *gg* conformer population.

The effect of 3′-phosphorylation upon P_{gg} of a 5′-nucleotide (points *iii* and *v*) is interesting since it must (in view of the absence of a similar effect at the nucleoside level (point *i*)) be a manifestation of an interaction between the phosphates on a 3′,5′-diphosphate. Estimations of the magnitude of this interaction can be made using the P_{gg} etc., values for -pdT of d(TpT) and for -pdTp of d(TpTp); they reveal a destabilizing effect of the 3′-phosphate of 250 and 500 cal/mol, respectively, upon the *gt* and *tg* conformers *relative* to the energy of *gg*. That the destabilization is larger for *tg* is reasonable since the negatively charged phosphates can be at minimum separation when the 3′,5′ diphosphate is *tg*. However, the destabilization of *gt* relative to *gg* can not be related simply to separation of charges since it is in *gt* rather than in *gg* that the maximum phosphate–phosphate separation is obtained. It should be of interest to compare the 3′-phosphate effect noted here with the calculations by Yathindra and Sundaralingam (7) on 5′dTMP and pdTp. These authors have estimated for the $C_{2'}$-*endo* situation that the *gg* conformation is slightly destabilized (0.3–0.4 kcal) by 3′-phosphorylation; this translates into a reduction from 94 to 90% in their estimated *gg* population. For $C_{3'}$-*endo* sugars the calculations reveal a larger decrease from 90 to 62% in the *gg* population resulting from 3′-phosphorylation.

Conformation about the $O_{5'}—C_{5'}$ Bond

The $J_{5'P}$ and $J_{5''P}$ values can be translated (17) into values of the *gauche'-gauche'* (*g'g'*), *gauche'-trans'* (*g't'*), and *trans'-gauche'* (*t'g'*) conformer populations ($P_{g'g'}$, $P_{g't'}$, $P_{t'g'}$) of a 5′-nucleotidyl fragment (Fig. 5). In 5′dTMP and pdTp the 5′- and 5′′-hydrogens are strongly coupled; thus

Can. J. Chem. Downloaded from www.nrcresearchpress.com by 210.87.254.6 on 09/05/12
For personal use only.

Can. J. Chem. Downloaded from www.nrcresearchpress.com by 210.87.254.6 on 09/05/12
For personal use only.

only the sum, $\sum'$ ($= J_{5'P} + J_{5''P}$) can be determined and translated into $P_{g'g'}$ and $P_{g't'} + P_{t'g'}$ values (17). The important conclusions which may be drawn from the calculated rotamer populations (Table 2) are as follows. Firstly, all 5′-nucleotide fragments (5′dTMP, pdTp, -pdT of d(TpT), -pdTp of d(TpTp)) show a pronounced preference for $g'g'$. This is consistent with previous work (34) that revealed in 5′-nucleotides a bias for $g'g'$ that surpassed their bias for gg. The $g'g'$ conformation is found in all crystalline 5′-nucleotides studied.

Second, in ref. 34 a linear correlation between $\sum(P_{gg})$ and $\sum'(P_{g'g'})$ values for the 5′-monophosphates was revealed; it is consistent with the view that a $g'g'$ conformation is a required feature of a gg oriented molecule, whereas for gt (or tg), $g'g'$ is no longer required but is nevertheless still preferred. Interestingly the $\sum,\sum'$ data for the 5′-nucleotide fragments studied here fall near to the correlation line. Through a consideration of space-filling models, this correlation between the conformer distribution about $C_{4'}$—$C_{5'}$ and $O_{5'}$—$C_{5'}$ may be rationalized. When any β-5′-nucleotide is rotated into its gg form, unfavorable close-contact interactions between the phosphoryl oxygens and the furanose and base substituents preclude rotation into the $g't'$ and $t'g'$ conformations. However, if we rotate the molecule into either the gt or tg forms, the hindrance from the base to rotation about $O_{5'}$—$C_{5'}$ is removed and that from the sugar ring substituents becomes less severe. On this basis the $g't'$ and $t'g'$ modes are expected to become more accessible in a gt or tg orientation. Furthermore, it is reasonable to postulate *similar* conformational distributions about $O_{5'}$—$C_{5'}$ for all gt (tg) oriented β-5′-nucleotides since the important distinguishing feature (the base) now lies distant from the 5′-phosphate. In other words, it appears that the conformational state of the $C_{4'}$—$C_{5'}$ bond is of foremost importance insofar as the conformational preferences about $O_{5'}$—$C_{5'}$ are concerned. The location of $\sum,\sum'$ data for -pdT of d(TpT) and -pdTp of d(TpTp) near to the $\sum,\sum'$ correlation plot defined originally by a collection of 5′-monophosphates must mean, therefore, that addition of a dT fragment onto the 5′-phosphate of 5′dTMP or of pdTp does not lead to any *new steric* interactions which might influence the $O_{5'}$—$C_{5'}$ conformational distribution. This is again clear from space-filling models of a dimer. When the 5′-nucleotide fragment of d(TpT) or d(TpTp) is oriented gg (and necessarily $g'g'$) or when it is oriented $gt(tg)$ (and preferentially but not necessarily $g'g'$), the dT fragment on the 5′-phosphate is distant from the sugar and thus can introduce no new steric interactions.

Third, we note that 3′-phosphorylation enhances $P_{g'g'}$ at the monomer level. (Compare $P_{g'g'}$ for 5′dTMP and pdTp.) This is expected in view of the influence that 3′-phosphorylation has on P_{gg} of 5′dTMP and the demonstration that $g'g'$ is excluded in gg oriented 5′-nucleotides. However, though we expect an increase of $P_{g'g'}$ for -pdTp of d(TpTp) relative to -pdT of d(TpT) this is not observed.

The four-bond $^4J_{P4'}$ couplings provide information about the $C_{4'}$—$C_{5'}$ and $O_{5'}$—$C_{5'}$ bond conformations (35) although they are expected to be less reliable than $\sum$ and $\sum'$ as conformational (P_{gg} and $P_{g'g'}$) probes owing to their small magnitudes. Using the correlation plots of P_{gg} and $P_{g'g'}$ *vs.* $^4J_{P4'}$ (35) and the values of $^4J_{P4'}$ (Table 1), we estimate the P_{gg} ($P_{g'g'}$) values: 5′dTMP, 63% (81%); -pdT, 68% (83%); pdTp, 63% (81%); -pdTp, 72% (84%). Considering the uncertainty in translating coupling constants into populations, we feel the agreement is good between these estimates and those made from the magnitudes of the vicinal coupling constants (Table 2). Thus our data support the contention that 5′-monophosphates and 5′-nucleotidyl fragments of oligonucleotides possessing the thymine base show a bias for the gg conformation and a stronger bias for the $g'g'$ conformation. One should bear in mind that under the experimental conditions employed ($T \simeq 70$ °C) the dimers are largely destacked. Helical polynucleotides are expected to assume in solution the gg, $g'g'$ combination with the virtual exclusion of any of the *trans* conformers about the $O_{5'}$—$C_{5'}$ and $C_{5'}$—$C_{4'}$ bonds. Our findings for the dimers should be useful in any discussion of the conformational consequences of the denaturation of an ordered oligonucleotide. Further, our data reveal a prevailing tendency towards the gg, $g'g'$ combination as the chain is elongated with phosphate and nucleoside fragments. Recent n.m.r. studies (36) have revealed that base stacking in dinucleoside monophosphates enhances the gg, $g'g'$ bias.

Conformation about the $C_{3'}$—$O_{3'}$ Bond

The magnitude of the vicinal $J_{P3'}$ is related to the conformation about $C_{3'}$—$O_{3'}$ of a 3′-nucleotide fragment (Fig. 5). All values lie in the nar-

Can. J. Chem. Downloaded from www.nrcresearchpress.com by 210.87.254.6 on 09/05/12
For personal use only.

row range from 6.4 to 7.6 Hz. However, these values cannot be interpreted in an unambiguous way if one expects a 3–5 Hz value for a *gauche* $J_{P3'}$ and 23–25 Hz value for a *trans* $J_{P3'}$. Previously (5, 15–17) 6.0–9.0 Hz values have been interpreted as evidence for the $g(2')$ and/or $g(4')$ conformational ranges. However, one cannot rule out contributions from $t(2',4')$ on the basis of $J_{P3'}$ coupling constants of this magnitude.

Chemical Shifts

The trends in the δ values for the hydrogens of the deoxyribo moieties are consistent with our spectral assignment and conformational conclusions. The 'stick' representation (Fig. 4) facilitates discussion. Centered in the diagram is the data for dT. Upon 3′-phosphorylation (3′dTMP) downfield shifts are observed for the 3′-hydrogen and the *exo* hydrogens near to the 3′-position ($3' > 4' \simeq 2''$) whereas the *endo* hydrogens (2′, 5′, and 5″) are considerably less influenced by 3′-phosphorylation. The *exo*-$H_{1'}$ is also little affected as might be predicted from the 1′–3′ separation. Extension in the 5′ → 3′ direction to dTp- of d(TpT) and of d(TpTp) produces little further change in δ for any hydrogen. This is to be expected since this extension does not result in major conformational changes in the original dT fragment. Furthermore, in the *unfolded* dimer conformation no significant shielding effects from the 3′-terminal base is expected. The similarity in the δ values for 3′dTMP and dTp- of the dimers, coupled with the similarity in their $J_{P3'}$ values suggests that 5′ → 3′ extension has not drastically altered their $C_{3'}$—$O_{3'}$ conformational distribution.

5′-Phosphorylation of dT produces large changes in δ(5′,5″) and smaller changes in δ(3′,4′), as expected from distance considerations. Considerably smaller effects (<0.05 p.p.m.) are noted for δ(1′,2′,2″). It is interesting to point to the absence of any influence of 5′-phosphorylation on $\delta_{2'}$ since rotation of 5′-dTMP in the *gg*, *t′g′* conformation places $H_{2'}$ near to the negative charge. However, earlier solution studies (35, 36) revealed that the *trans* conformations (*t′g′* and *g′t′*) are not likely in *gg* oriented 5′-monophosphates; they have never been observed in the crystal state under any circumstances (2, 3, 37). 3′-Phosphorylation of 5′dTMP (pdTp) parallels in a striking manner its influence on the δ values of dT. This is best seen from comparison of δ(dT-3′dTMP) and δ(5′dTMP-pdTp) values for each hydrogen (in p.p.m.): 1′(0.02, 0.06); 2′(0.05, 0.05); 2″(0.16, 0.17); 3′(0.29, 0.30); 4′(0.14, 0.18); 5′(0.03, 0.05); 5″(0.04, 0.05), respectively. Extension of pdTp to -pdTp has little effect on the shifts except for the 0.1 p.p.m. downfield shift of $H_{5'}$.

Conclusions

The p.m.r. data of dT, 3′dTMP, 5′dTMP, -pdTp, d(TpT), and d(TpTp) in aqueous solution are discussed. They reveal that the conformation of the dT nucleoside fragment is similar in this series of molecules. However, 5′-phosphorylation, but not 3′-phosphorylation, of dT enhances the population of the *gg* conformer. This observation is consistent with the rigid nucleotide concept. 3′-Phosphorylation of a 5′-nucleotidyl fragment (5′dTMP → pdTp; d(TpT) → d(TpTp)) enhances the population of the *gg* conformation. This enhancement suggests the presence of a through-space interaction between a 3′-phosphate and a 5′-phosphate which stabilizes the *gg* conformer relative to the *gt* and *tg* conformers. During the course of this study several n.m.r. papers on nucleotide stereochemistry have appeared (38–40). Their results are in good agreement with our discussion of mononucleotides.

This research was supported by grants from the National Research Council of Canada, The North Atlantic Treaty Organization, and The Faculty of Graduate Studies. We thank Dr. A. A. Grey and Mrs. Valerie Robinson of the Canadian 220 MHz Centre for obtaining the 220 MHz spectra and the members of the n.m.r. group in Manitoba for valuable discussions.

1. M. SUNDARALINGAM. Biopolymers, **7**, 821 (1969).
2. M. SUNDARALINGAM. *In* Proceedings international symposium on the conformation of biological molecules and polymers, symposia on quantum chemistry and biochemistry. Vol. 5. *Edited by* B. Pullman and E. D. Bergmann. Academic Press, Jerusalem. 1973. p. 417.
3. W. SAENGER. Angew. Chem. Int. Ed. **12**, 591 (1973).
4. F. E. HRUSKA. *In* Proceedings international symposium on the conformation of biological molecules and polymers, symposia on quantum chemistry and biochemistry. Vol. 5. *Edited by* B. Pullman and E. D. Bergmann. Academic Press, Jerusalem. 1973. p. 345.
5. I. C. P. SMITH, H. H. MANTSCH, R. D. LAPPER, R. DESLAURIERS, and T. SCHLEICH. *In* Proceedings international symposium on the conformation of biological molecules and polymers, symposia on quantum chemistry and biochemistry. Vol. 5. *Edited by* B. Pullman and E. D. Bergmann. Academic Press, Jerusalem. 1973. p. 381.
6. C. GIESSNER-PRETTRE and B. PULLMAN. J. Theor. Biol. **40**, 441 (1973).
7. A. YATHINDRA and M. SUNDARALINGAM. Biopolymers, **12**, 2261 (1973).

8. E. SHEFTER, M. BARLOW, R. SPARKS, and K. TRUEBLOOD. J. Am. Chem. Soc. **86**, 1872 (1964).
9. N. C. SEEMAN, J. L. SUSSMAN, H. M. BERMAN, and S. H. KIM. J. Mol. Biol. **66**, 403 (1972).
10. J. RUBIN, T. BRENNAN, and M. SUNDARALINGAM. Biochemistry, **11**, 3112 (1972).
11. R. O. DAY, N. C. SEEMAN, J. M. ROSENBERG, and A. RICH. Proc. Natl. Acad. Sci. U.S.A. **70**, 849 (1973).
12. J. M. ROSENBERG, N. C. SEEMAN, J. P. KIM, F. L. SUDDATH, H. B. NICHOLAS, and A. RICH. Nature, **243**, 150 (1973).
13. N. C. CAMERMAN, J. K. FAWCETT, and A. CAMERMAN. Science **182**, 1142 (1973).
14. N. S. KONDO and S. S. DANYLUK. J. Am. Chem. Soc. **94**, 5121 (1972).
15. C. ALTONA, J. H. VAN BOOM, J. DE JAGER, H. J. KOENER, and G. VAN BENST. Nature, **247**, 560 (1974).
16. C. ALTONA. *In* Proceedings 4th Harry Steenbock symposium on structure and conformation of nucleic acids and protein-nucleic acid interactions, 1974. *Edited by* M. Sundaralingam and S. Rao. University Press, College Park, Md. In press.
17. D. J. WOOD, F. E. HRUSKA, and K. K. OGILVIE. Can. J. Chem. **52**, 3353 (1974).
18. F. E. HRUSKA, D. J. WOOD, and K. K. OGILVIE. *In* Proceedings 4th Harry Steenbock symposium on structure and conformation of nucleic acids and protein-nucleic acid interactions, 1974. *Edited by* M. Sundaralingam and S. Rao. University Press, College Park, Md. In press.
19. F. E. HRUSKA, D. J. WOOD, K. K. OGILVIE, and J. L. CHARLTON. Can. J. Chem. **53**, 1193 (1975).
20. T. SCHLEICH, B. P. CROSS, B. J. BLACKBURN, and I. C. P. SMITH. Proceedings, 4th Harry Steenbock symposium on structure and conformation of nucleic acids and protein-nucleic acid interactions, 1974. *Edited by* M. Sundaralingam and S. Rao. University Press, College Park, Md. In press.
21. R. L. LETSINGER, K. K. OGILVIE, and P. S. MILLER. J. Am. Chem. Soc. **91**, 3360 (1969).
22. C. W. HAIGH and J. M. WILLIAMS. J. Mol. Spectrosc. **32**, 398 (1969).
23. K. N. FANG, M. S. KONDO, P. S. MILLER, and P. O. P. TS'O. J. Am. Chem. Soc. **93**, 6647 (1971).
24. M. REMIN and D. SHUGAR. Biochem. Biophys. Res. Commun. **48**, 636 (1972).
25. F. E. HRUSKA, D. J. WOOD, T. N. MCCAIG, A. A. SMITH, and A. HOLY. Can. J. Chem. **52**, 497 (1974).
26. C. ALTONA and M. SUNDARALINGAM. J. Am. Chem. Soc. **94**, 8205 (1972).
27. C. ALTONA and M. SUNDARALINGAM. J. Am. Chem. Soc. **95**, 2333 (1973).
28. D. W. YOUNG, P. TOLLIN, and H. R. WILSON. Acta Crystallogr. B, **25**, 1423 (1969).
29. K. N. TRUEBLOOD, P. HORN, and V. LUSSATI. Acta Crystallogr. **14**, 965 (1961).
30. S. I. CHAN and J. H. NELSON. J. Am. Chem. Soc. **91**, 168 (1969).
31. S. C. JAIN and H. M. SOBELL. J. Mol. Biol. **68**, 1 (1972).
32. E. SUBRAMANIAN and D. J. HUNT. Acta Crystallogr. B, **26**, 303 (1970).
33. J. RUBIN, T. BRENNAN, and M. SUNDARALINGAM. Biochemistry, **11**, 3112 (1972).
34. D. J. WOOD, R. J. MYNOTT, F. E. HRUSKA, and R. H. SARMA. FEBS Lett. **34**, 323 (1973).
35. R. H. SARMA, R. J. MYNOTT, D. J. WOOD, and F. E. HRUSKA. J. Am. Chem. Soc. **95**, 6457 (1973).
36. F. E. EVANS, C. H. LEE, and R. H. SARMA. Biochem. Biophys. Res. Commun. In press.
37. W. SAENGER and D. SUCK. Nature, **242**, 610 (1973).
38. D. B. DAVIES and S. S. DANYLUK. Biochemistry, **13**, 4417 (1974).
39. R. H. SARMA, C. H. LEE, F. EVANS, and M. SUNDARALINGAM. J. Am. Chem. Soc. **96**, 7337 (1974).
40. D. B. DAVIES and S. S. DANYLUK. Biochemistry, **14**, 543 (1975).

Can. J. Chem. Downloaded from www.nrcresearchpress.com by 210.87.254.6 on 09/05/12
For personal use only.

The Hydrolysis of Imidate Salts. Stereoelectronic Control in the Cleavage of the Hemiorthoamide Tetrahedral Intermediate

PIERRE DESLONGCHAMPS,[1] SERGE DUBÉ, CLAUDE LEBREUX, DENNIS R. PATTERSON, AND ROLAND J. TAILLEFER

Laboratoire de synthèse organique, Université de Sherbrooke, Sherbrooke, Québec J1K 2R1

Received April 7, 1975

PIERRE DESLONGCHAMPS, SERGE DUBÉ, CLAUDE LEBREUX, DENNIS R. PATTERSON, and ROLAND J. TAILLEFER. Can. J. Chem. **53**, 2791 (1975).

A new stereoelectronic theory for the cleavage of the tetrahedral intermediate (hemiorthoamide) in the hydrolysis of amides is presented. In this new theory, the precise conformation of the tetrahedral intermediate controls the nature of the hydrolysis products. It is postulated that the breakdown of the tetrahedral intermediate depends upon the orientation of the lone pair orbitals of the heteroatoms. Specific cleavage of a carbon–oxygen or a carbon–nitrogen bond in any conformer is allowed only if the other heteroatoms (oxygen and nitrogen) each have an orbital oriented antiperiplanar to the leaving *O*-alkyl or *N*-alkyl group. Experimentally, a study of the basic hydrolysis of a variety of *N,N*-dialkylated imidate salts having either a *syn* or an *anti* conformation demonstrates clearly that there is a stereoelectronic control in the cleavage of the hemiorthoamide.

PIERRE DESLONGCHAMPS, SERGE DUBÉ, CLAUDE LEBREUX, DENNIS R. PATTERSON et ROLAND J. TAILLEFER. Can. J. Chem. **53**, 2791 (1975).

Une nouvelle théorie stéréoélectronique sur la décomposition de l'intermédiaire tétrahédrique (hémi-orthoamide) au cours de l'hydrolyse des amides est présentée. Dans cette nouvelle théorie, il y a une relation directe entre la conformation précise de l'intermédiaire tétrahédrique et la nature des produits d'hydrolyse. Il est aussi postulé que c'est l'orientation des paires d'électrons libres sur les hétéroatomes qui contrôle la décomposition de l'intermédiaire. La coupure d'un lien carbon–oxygène ou d'un lien carbone–azote d'un intermédiaire est permise lorsque les deux autres hétéroatomes possèdent chacun une orbitale d'électrons libres orientée d'une manière antipériplanaire au groupe partant (*O*-alkyl ou *N*-alkyl). On démontre expérimentalement par l'hydrolyse en milieu basique sur des sels imidates ayant une conformation *syn* ou *anti* qu'il y a effectivement un contrôle stéréoélectronique lors de la décomposition d'un hémiorthoamide.

Introduction

We have recently reported a new stereoelectronic theory for the hydrolysis of esters (1, 2) and amides (2, 3). In this new theory, the nature of the products formed from the hydrolysis of an ester or amide depends upon the conformation of the tetrahedral hemiorthoester or hemiorthoamide intermediate formed in the reaction. It is further postulated that the breakdown of a tetrahedral conformer depends upon the orientation of the lone pair orbitals of the heteroatoms; specific cleavage of a carbon–oxygen or a carbon–nitrogen bond being allowed only if the other two heteroatoms (oxygen or nitrogen) of the tetrahedral intermediate each have an orbital oriented antiperiplanar to the leaving *O*-alkyl or *N*-alkyl group.

We have reported in detail our experiments which show that there is indeed a stereoelectronic control in the cleavage of hemiorthoesters (1). We have also obtained experimental evidence that there is a stereoelectronic control in the cleavage of hemiorthoamides (3), based on a study of the basic hydrolysis of some *N,N*-dialkylated imidate salts. These results were published in a preliminary form (3). We have now completed this work with a variety of imidate salts and wish to detail our results.[2]

When we started this investigation, it was clear to us that we could obtain experimental evidence for the new stereoelectronic theory by observing the products formed from the cleavage of a hemiorthoamide such as **2**. Consequently, it was first important to find a method for the generation of a hemiorthoamide which would then break down to products (ester or amide) in an irreversible manner. It is not possible to produce

[1]To whom all correspondence should be addressed.

[2]For recent experimental and theoretical studies related to this subject, see refs. 4–6.

Can. J. Chem. Downloaded from www.nrcresearchpress.com by 210.87.254.105 on 09/05/12
For personal use only.

Can. J. Chem. Downloaded from www.nrcresearchpress.com by 210.87.254.105 on 09/05/12
For personal use only.

such a hemiorthoamide in a mild and irreversible fashion by treating an amide with an alkoxide (hydroxide) ion. Similarly, it cannot be obtained by treating an ester with an amide anion. It was therefore desirable to find an alternative precursor to the hemiorthoamide. An ideal precursor appeared to be an *N,N*-dialkylated imidate salt, which can be considered to be an activated amide. Indeed, it is known that imidate salts are rapidly hydrolyzed under basic conditions, at room temperature, to give ester and amine or amide and alcohol as products (7).

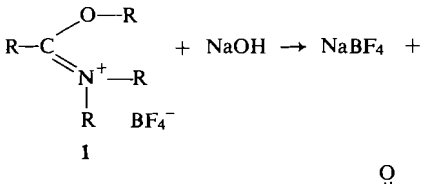

1

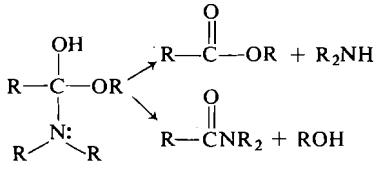

2

When a fluoroborate imidate salt such as **1** reacts with sodium hydroxide, it forms sodium fluoroborate and the intermediate **2** which rapidly breaks down to the products of the reaction. The amide and alcohol products will always completely predominate over the ester and amine products under equilibrating conditions. The amide and alcohol products are therefore the thermodynamic products resulting from the cleavage of the intermediate **2**. If ester and amine are obtained as products, it is clear that it is the result of kinetically controlled cleavage of **2** and will indicate that the transition state leading to those products is of lower energy than the one leading to the more stable amide and alcohol products. However, it is possible that in some cases, the amide and alcohol are also the kinetic products of the cleavage of the intermediate **2**. In such a circumstance, it is in principle possible to use the result as evidence for the new stereoelectronic theory, if it can be clearly established that the reaction is kinetically controlled. If the corresponding ester and amine are not converted into the thermodynamic products under the experimental conditions, it demonstrates that the formation of amide and alcohol is the result of a kinetically controlled cleavage of the intermediate **2**.

It is experimentally very difficult to know the precise conformation of a hemiorthoamide such as **2**. However, the conformation of **2** can be obtained indirectly by the utilization of the new stereoelectronic theory and the knowledge of the precise conformation of the starting imidate salt **1**. If a good correlation between the proposed conformation of **2** and its cleavage is obtained, it constitutes experimental evidence in favor of the new stereoelectronic theory. Thus, the conformation of the imidate salts must first be taken into consideration.

Stereoelectronic Control in the Cleavage of Hemiorthoamide

We believe that imidate salts are planar and thus can exist in two different conformations, the *anti* (**1***a*) or the *syn* (**1***b*) form. In the *anti* conformation **1***a*, the O—R bond is antiperiplanar to the C—R bond. In the *syn* conformation **1***b*, the O—R bond is *cis* to the C—R bond. Application of the new stereoelectronic theory on each type of imidate salt leads to the following predictions concerning the precise conformation of the intermediate **2** and to the manner by which each conformer of **2** should then break down.

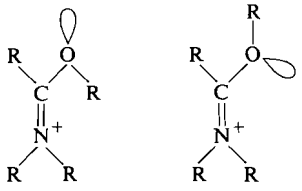

1*a* **1***b*

According to this theory, the reaction of hydroxide ion with the *anti* form **1***a* of an imidate salt should give the tetrahedral conformer **2***a* specifically (Scheme 1). Conformer **2***a* is the

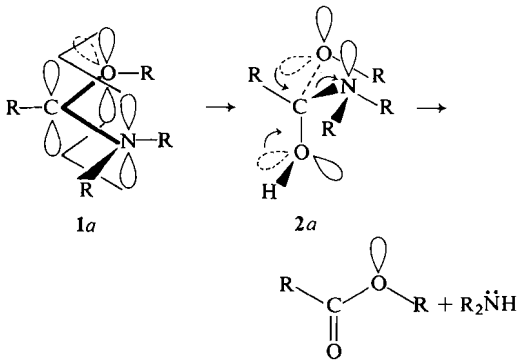

1*a* **2***a*

SCHEME 1

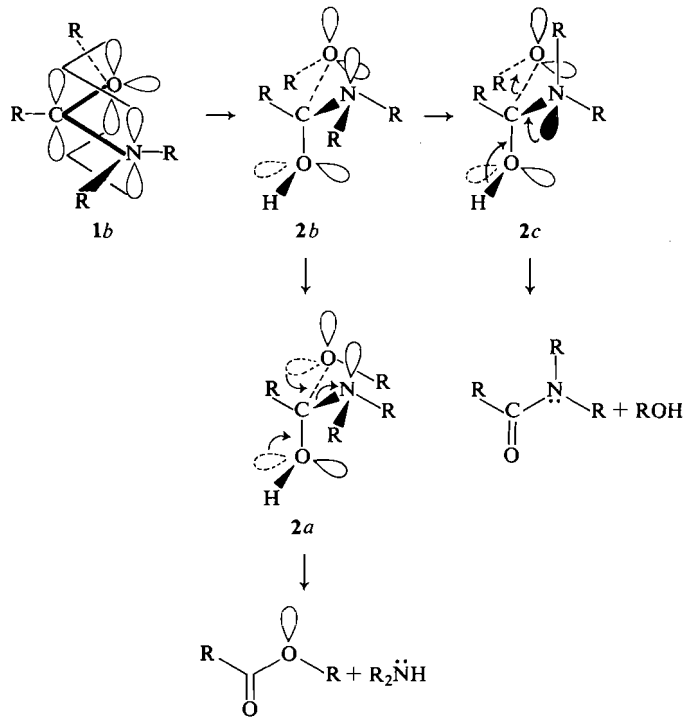

SCHEME 2

result of hydroxide ion attack perpendicular to the plane of the salt **1***a*. The conformation of the starting imidate salt **1***a* is thus transposed to the intermediate **2***a*; the R—C bond in **2***a* is antiperiplanar to the O—R bond and to one of the N—R bonds as in the *anti* imidate **1***a*.[3] As a consequence of the stereoelectronic theory, one of the lone pair orbitals of the oxygen of the OR group and the lone pair orbital of the nitrogen must be oriented antiperiplanar to the new carbon–oxygen bond. Thus, the reverse reaction, the ejection of the hydroxyl group can be achieved by an orbital assisted mechanism because there are two heteroatoms each having a lone pair orbital properly oriented antiperiplanar to the leaving group. The principle of microscopic reversibility is thus adhered to.

One more assumption has to be made to render the preceding theory valid. Whenever a tetrahedral intermediate possesses proper orbital orientation, its half-life is very short and it breaks down to products immediately. This implies that the energy barrier for conformational changes by rotation of C—N and C—O bonds in **2***a* is higher than the energy barrier for its breakdown. With such a condition, no tetrahedral conformer other than **2***a* must be taken into consideration.

Examination of the orientation of the lone pair orbitals in **2***a* indicates that this conformer should break down to yield the ester and the amine only. The nitrogen orbital is not properly oriented to assist in expelling the OR group. At the same time, both oxygens have a lone pair orbital oriented antiperiplanar to the C—N bond to permit a facile ejection of the amino group. Consequently, it is predicted that the basic hydrolysis of the *anti* form **1***a* of an imidate salt should lead to the exclusive formation of ester and amine as a result of the cleavage of conformer **2***a*.

If the preceding stereoelectronic theory is valid, the reaction of hydroxide ion on the *syn* form **1***b* will give specifically the conformer **2***b* (Scheme 2). Again, **2***b* is the result of an attack perpendicular to the plane of the salt **1***b* by hydroxide ion. The conformation of **1***b* has also been retained in the intermediate **2***b*. There are lone pair orbitals on

[3]In principle, hydroxide ion attack on the imidate can either lead to conformer **2***a* or two other conformers which differ in the orientation of the O—H bond. These three conformers can be interconverted by proton transfer. This interconversion occurs at a diffusion controlled rate (8). Since we assume that the breakdown of the tetrahedral intermediate is a slower process than proton transfer, the three conformers are therefore equivalent as far as the theory is concerned.

Can. J. Chem. Downloaded from www.nrcresearchpress.com by 210.87.254.105 on 09/05/12
For personal use only.

Can. J. Chem. Downloaded from www.nrcresearchpress.com by 210.87.254.105 on 09/05/12
For personal use only.

the nitrogen and on the oxygen of the OR group which are each oriented antiperiplanar to the C—OH bond.

It is interesting to note that conformer **2***b* cannot break down to products by an orbital assisted mechanism; the nitrogen nonbonded orbital is not antiperiplanar to the C—OR bond. Similarly, the oxygen atom of the OR group does not have a nonbonded orbital properly oriented antiperiplanar to the C—N bond. In this case, we postulate that rotation of C—N and C—O bonds in conformer **2***b* becomes more facile than its breakdown to products and new conformers must be considered. If these new conformers have their orbitals properly oriented, they will break down immediately to give products. The energy barrier for carbon–nitrogen rotation should be of the same order of magnitude as the one for carbon–oxygen rotation. Both types of rotation must therefore be taken into consideration.

For example, by rotation of the carbon–nitrogen bond, conformer **2***b* can give a new conformer such as **2***c*. In conformer **2***c*, the hydroxyl oxygen and the nitrogen each have a lone pair orbital oriented antiperiplanar to the C—OR bond. Intermediate **2***c* should thus immediately produce the amide and alcohol products. By rotation of the C—OR bond in **2***b*, a new conformer such as **2***a* can also be obtained. We have already described that **2***a* should give the ester and amine products. Other conformers can be obtained by other rotations in **2***b*. The relative proportions of ester and amine products *vs.* amide and alcohol products will thus depend on the new conformers that will be formed by bond rotation in conformer **2***b*. Consequently, it is predicted that the basic[4] hydrolysis of the *syn* form **1***b* of an imidate salt will give in principle mixtures of products.

Hydrolysis of *Anti* Imidate Salts

We will first describe the results obtained from the basic hydrolysis of imidate salts having an *anti* conformation. The first substrate selected was the five-membered ring imidate salt **3** in which the *anti* conformation is assured by the cyclic structure. Hydrolysis of **3** with 3 equiv. of sodium carbonate in a mixture of acetonitrile and water gave the benzoate amine **4** exclusively. The reaction was followed by proton n.m.r. spectroscopy and was complete after 10 min at room temperature. Compound **4** was isolated as the acetamide derivative **5** by treating the reaction mixture with an excess of pyridine and acetic anhydride. If the reaction mixture was left at room temperature for a period of 24 h, the aminobenzoate **4** was completely converted into the more stable benzamide alcohol **6**. This product was isolated also as its acetate derivative **7**.

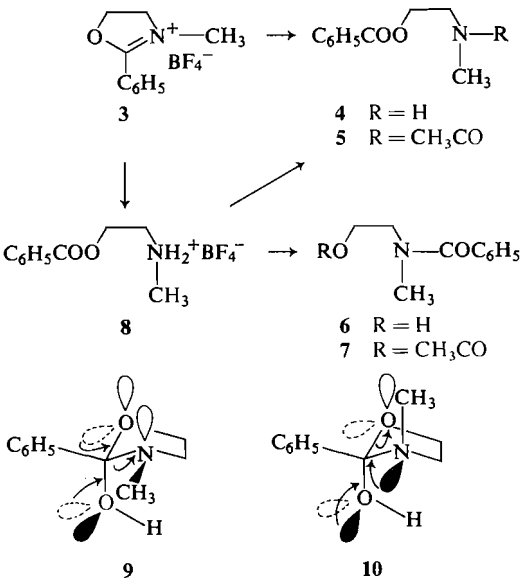

These experimental results can be easily explained by the stereoelectronic theory. The salt **3** forms the hemiorthoamide intermediate **9** in which the energy barrier for fragmentation is lowered by the alignment of the orbitals on both oxygen atoms. Indeed, under kinetically controlled conditions, the ester amine product **4** is the only product formed.[5] It is possible that the ex-

[4]It should be emphasized that this prediction is valid in basic medium only. This condition is important because the protonation of the basic nitrogen of the tetrahedral intermediate effectively ties up its lone pair orbital (7). Thus the nitrogen atom cannot participate in an orbital assisted decomposition of the tetrahedral intermediate under acidic conditions.

[5]The basic hydrolysis of **3** was also carried out with sodium hydroxide. Under these conditions, the imidate salt **3** gave directly the benzamide alcohol **6**, while the benzoate amine **4** was not detected. This unexpected result can be explained if the transformation of the benzoate amine **4** into the more stable benzamide alcohol **6** is very rapid in the presence of sodium hydroxide. This assertion was shown to be true in the following way. The benzoate ammonium salt **8** was prepared by the hydrolysis of **3** in neutral water. When the ammonium salt **8** was treated with sodium hydroxide under the conditions described for the hydrolysis of **3**, it gave directly the benzamide alcohol **6**. Treatment of **8** with sodium carbonate gave the benzoate amine **4**.

Can. J. Chem. Downloaded from www.nrcresearchpress.com by 210.87.254.105 on 09/05/12
For personal use only.

perimental conditions used favor the reformation of tetrahedral intermediates by an attack of the amino group on the ester function of **4**. Compound **4** can either reform **9** or form a new intermediate such as **10**, which has its orbitals properly aligned to yield the more stable product, the amide alcohol **6**. Consequently, the final result will be the exclusive formation of the thermodynamic product under those equilibrating conditions. These conditions were obtained after a period of 24 h with sodium carbonate; they were immediately obtained when sodium hydroxide was utilized.[5]

The hydrolysis of imidate salt **11** was also carried out with sodium carbonate. After 10 min, it gave mainly the acetate amine **12** which was then slowly converted into the acetamide alcohol **13** after standing for 1.5 h at room temperature. It is interesting to note that the conversion of **12** into **13** in the presence of sodium carbonate occurs at a much faster rate than the conversion of **4** into **6** under similar conditions. This result, however, can be easily explained by the fact that **12** is an acetate ester, thus more reactive than **4** which is a benzoate ester.

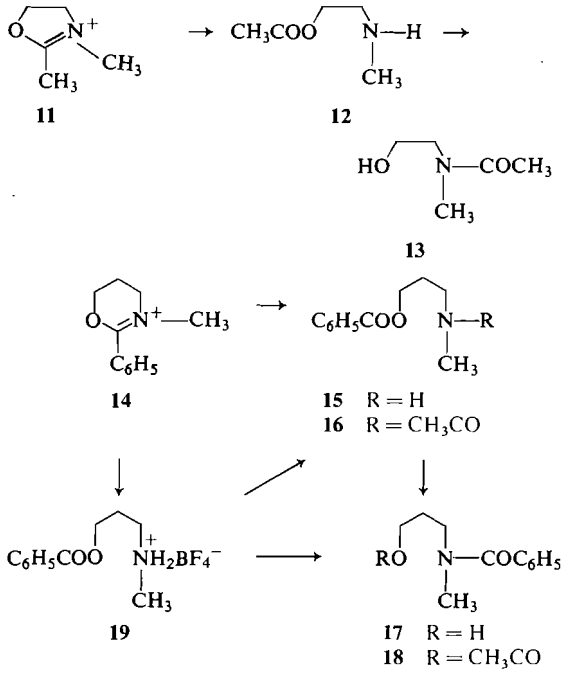

The basic hydrolysis of a six-membered ring imidate salt was also performed. After 15 min at room temperature, the hydrolysis of **14** with sodium carbonate gave the benzoate amine **15** exclusively. The presence of benzamide alcohol **17** was not detected in the reaction mixture even after a period of 5 h. Compound **15** was isolated and characterized as its corresponding acetamide derivative **16**.

The hydrolysis of **14** was also carried out with sodium hydroxide. The imidate salt was completely hydrolyzed after a few minutes and it yielded mainly the benzoate amine **15** (≃95%) with a small quantity of the benzamide alcohol **17** (≃5%). After standing for a period of 30 min at room temperature, the reaction mixture consisted of the benzamide alcohol **17** only, which was isolated as its acetate derivative **18**. This result indicates again that the ester **15** is first formed and then converted into the more stable amide product **17**. This assumption was verified by treating the ammonium salt **19** under identical basic conditions. Like the imidate **14**, **19** also gave the benzoate amine **15** first, which was then completely converted into the benzamide alcohol **17** within a period of 30 min. The ammonium salt **19** had been obtained by the hydrolysis of **14** in neutral water.

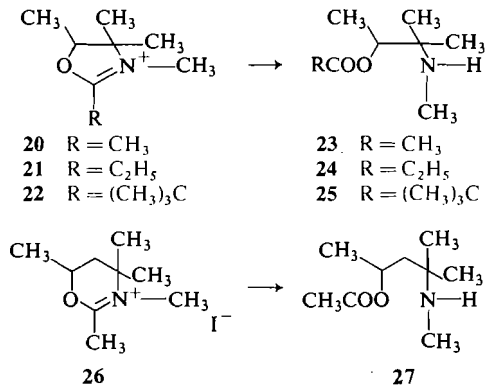

The basic hydrolysis of the imidate salts **20**, **21**, and **22** has been previously reported by Allen and Ginos (9). These salts gave the corresponding ester amine products **23**, **24**, and **25** in basic conditions. We have also carried out the basic hydrolysis of imidate salt **26** (10) and it gave the ester amine **27**. There are two factors which help the cleavage of the C—N bond in the hydrolysis of **20**, **21**, **22**, and **26**. According to the theory, **20**, **21**, and **22** should form the intermediate **28** which has proper orbital alignment to yield the corresponding ester amine products. In **28**, there is also a pseudo 1,3-diaxial type of interaction between the OH group and one of the methyl groups which promotes the cleavage of the carbon–nitrogen bond. Compound **26** should give the intermediate **29** in which there is again a

Can. J. Chem. Downloaded from www.nrcresearchpress.com by 210.87.254.105 on 09/05/12
For personal use only.

similar steric compression factor. This, combined with the orbital orientation factor, favors the carbon–nitrogen bond cleavage.

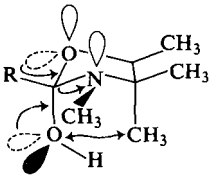

28

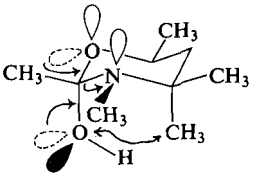

29

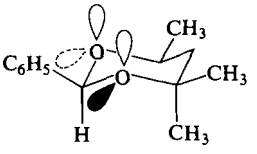

30

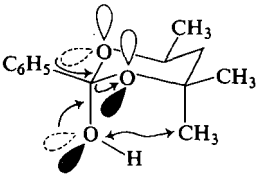

31

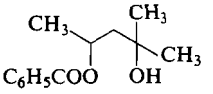

32

It was of interest to find out if this steric compression factor was important enough to direct the cleavage of the intermediate exclusively in one direction. We have verified experimentally that this factor is indeed important by carrying out the ozonolysis of the acetal **30** (11). Oxidation of **30** by ozone gave the ester **32** exclusively. During this reaction, it is postulated that the intermediate **31** is formed. In **31** the orientation of the nonbonded orbitals favors the opening in both directions equally well. Consequently, the experimental results demonstrate that the interaction between the OH group and the axial methyl group in **31** is strong enough to allow a specific cleavage in one direction. This result is in agreement with the minimum value of 2.4 kcal/mol which has been estimated for 1,3-diaxial interaction between a hydroxyl and a methyl group.[6]

Having a good estimate for the importance of the steric decompression factor, it is in principle possible to obtain some idea about the magnitude of the orbital orientation effect by opposing these two factors in the same system. The salt **33** was therefore prepared for that purpose. Its reaction with hydroxide ion should give the intermediate **34**, in which the orbital orientation promotes the cleavage of the C—N bond, while the 1,3-diaxial methyl–hydroxyl steric interaction favors the cleavage of the C—O bond. Hydrolysis of **33** with sodium carbonate gave exclusively the ester amine product **35** which was characterized as its acetamide derivative **36**. Additionally, salt **37** was also prepared. Its hydrolysis yielded first the ester amine **38** which was rapidly transformed under the experimental conditions into the benzamide alcohol **39**. In the above examples, the reaction was still specific despite an opposing steric factor (estimated to be $\geq$2.4 kcal/mol) which had first to be surmounted. It is considered that a reaction path is specific when it is favored by at least 2.4 kcal/mol. The minimum value for the orbital orientation effect can therefore be estimated to be at least 5 kcal/mol.

So far, we have described the hydrolysis of rigid *anti* imidate salts. These compounds were predicted to give the ester amine products exclusively. The preceding experimental results

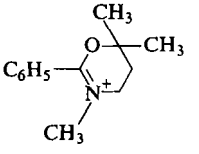

33

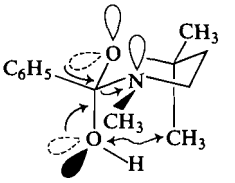

34

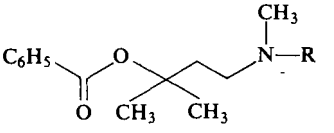

35 R = H
36 R = CH_3CO

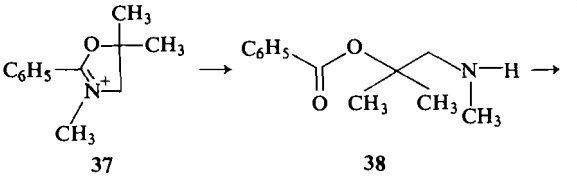

37 38

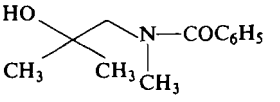

39

[6]The energy difference between the two conformers of *cis*-3-methylcyclohexanol can be estimated at about 3.8 kcal/mol and an experimental value of 2.4 kcal/mol (12) is taken as the basis for the 1,3-diaxial methyl–hydroxyl interaction (13).

Can. J. Chem. Downloaded from www.nrcresearchpress.com by 210.87.254.105 on 09/05/12
For personal use only.

clearly demonstrate that, indeed, the ester amine products are the only products observed under kinetically controlled conditions. We must conclude that orbital orientation is an important factor in lowering the energy barrier for the breakdown of a tetrahedral intermediate. In fact, we believe that it is the determining factor.

Hydrolysis of *Syn* Imidate Salts

We have also undertaken the basic hydrolysis of the imidate salts **40** and **41** which have a *syn* conformation owing to their cyclic structure. The hydrolysis of **40** should give the intermediate **42** which is equivalent to **2***b*. Thus, **42** cannot break

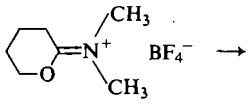

40

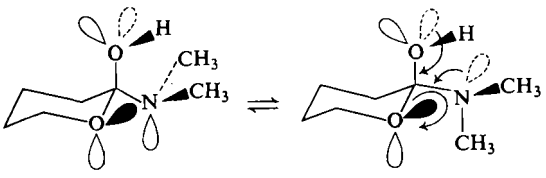

42 **43**

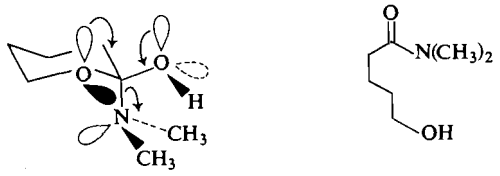

44 **46**

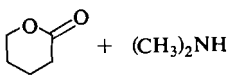

45

down easily if the stereoelectronic theory is valid. However, intermediate **42** can undergo conformational changes to yield either **43** by carbon–nitrogen rotation or **44** by chair inversion. Conformer **43** has its orbitals properly oriented to give the hydroxy amide **46** whereas conformer **44** should yield the lactone **45** and dimethylamine. Thus, the stereoelectronic theory predicts a mixture of products **45** and **46** from the basic hydrolysis of **40**. The hydrolysis of **40** was carried out with sodium hydroxide in aqueous acetonitrile. Indeed, the imidate salt **40** gave a mixture of hydroxy amide **46** (66%) and δ-valerolactone (**45**, 33%) and dimethylamine (33%). The relative proportion of products was determined directly in the reaction mixture by measuring (n.m.r.) the relative proportion of dimethylamine and *N*,*N*-dimethylamide produced. Likewise, the hydrolysis of the imidate salt **41** gave a one to one mixture of the corresponding hydroxy amide **47** and γ-butyrolactone (**48**).

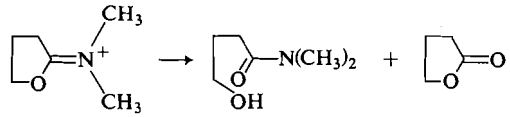

41 **47** **48**

We have also studied the basic hydrolysis of a series of imidate salts **49**, in which the R group was varied (R = hydrogen, methyl, isopropyl, cyclohexyl, *t*-butyl, and phenyl). Such salts can exist in principle in the *anti* (**49***a*) or the *syn* (**49***b*) form. The extent of the electronic interaction which stabilizes or destabilizes either of these two forms is as yet unknown. There is, however, a steric repulsion between the R group and the ethyl group in the *syn* form *b*. There is also a 1,3-synperiplanar interaction between the ethyl and the methyl groups in the *anti* form *a*. When R is a small group, one can postulate that the *syn* form *b* might be favored since it avoids the rather strong interaction which exists in the *anti* form *a*. However, when R is a large group such as

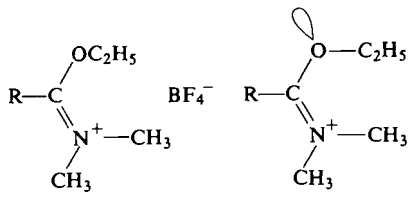

49 **49***a*

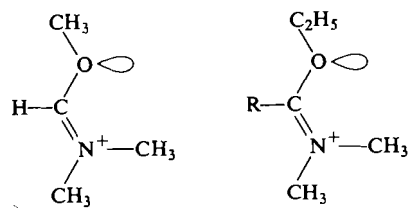

50 **49***b*

Can. J. Chem. Downloaded from www.nrcresearchpress.com by 210.87.254.105 on 09/05/12
For personal use only.

TABLE 1. Basic hydrolysis of imidate salts **49***†

R	%ester	%amide
H	50	50
CH_3	81	19
C_6H_{11}‡	50	50
$(CH_3)_3C$	100	0
C_6H_5	100	0

*Hydrolysis was carried out with NaOH (1–2 *N*) in a mixture (≃ 1:1) CD_3CN–H_2O in an n.m.r. tube.
†Yields were estimated by n.m.r. spectroscopic analysis.
‡Yields were estimated by v.p.c. analysis.

the *t*-butyl or the planar phenyl group, the *anti* form *a* might predominate so that the rather severe interaction between the ethyl group and the large group R is now avoided. If this assumption is valid, it would indicate that **49** (R = H) exists mainly as the *syn* form. A nuclear Overhauser effect study on the salt **50** indicates that it exists mainly in the *syn* conformation.[7] When R is a methyl, an isopropyl, or a cyclohexyl group, **49** would exist either as the pure *syn* form or as an equilibrium mixture of the *syn* and the *anti* forms. Finally, when R is a *t*-butyl or a phenyl group, **49** would exist in the pure *anti* form.

The above reasoning, in conjunction with stereoelectronic theory predicts that mixtures of ester amine and amide alcohol products should be observed in the hydrolysis of **49** when R is a hydrogen, a methyl, an isopropyl, and a cyclohexyl group. It also predicts that the basic hydrolysis of **49** when R is a *t*-butyl or a phenyl group should give the ester and amine products exclusively. The result of the hydrolysis of those salts (carried out with sodium hydroxide) is described in Table 1. This data is in striking accord with the preceding discussion.

We have also studied the bicyclic imidate salt **51**; imidate **51** can exist either in the *syn* (**51***a*) or the *anti* (**51***b*) form. Steric interactions in **51** are similar to those of salt **49** (R = CH_3). Application of the stereoelectronic theory to this system leads to the following conclusions. We assume that the *syn* conformation **51***a* must be predominant. Reaction of **51***a* with hydroxide ion should yield the conformer **52***a* specifically. Since conformer **52***a* cannot break down by an orbital assisted mechanism, conformational changes should take place. Nitrogen inversion is possible in **52***a* to give the new conformer **52***c*. However, this new conformer, like **52***a*, does not have proper orbital orientation to break down. Since **52***c* is equivalent to a *cis*-decalin system, it can undergo a chair inversion to give conformer **52***d*. Conformer **52***d* should break down to give the lactam product **53** in a stereoelectronically controlled fashion. However, in conformer **52***d*, there are two severe 1,3-diaxial steric interactions between two methylene groups of ring A and the oxygen of the OCH_3 group. The energy barrier for the conversion of **52***a* into **52***d* will be increased accordingly. Thus, if **52***a* can undergo other conformational changes having a lower energy barrier and leading to a new conformer which can break down via stereoelectronic control, the pathway through **52***d* can be eliminated from consideration.

Conformer **52***a* can also change its conformation by rotation of the O—CH_3 bond. In this fashion, it can give either **52***b* or **52***e*. (In principle, **52***b* could also be obtained directly from the *anti* form **51***b*.) These two conformers have proper orbital orientation to break down to yield the ester amine product **54**. The magnitude of the anomeric effect (15), which occurs whenever two lone pair orbitals are in a 1,3-synperiplanar arrangement is approximately the same in **52***b* and **52***e*. However, on steric grounds, **52***e* should be more stable than **52***b* since there is a 1,3-synperiplanar interaction[8] between the OCH_3 group and the methylene group adjacent to the nitrogen atom in **52***b*. Conformer **52***b* should give the ester amine in its thermodynamically more stable *E* form (**54***a*), whereas **52***e* should yield the same product in its less stable *Z* form **54***b* (14). If the route **52***a* → **52***e* → **54***b* were operative, **54***b* would be converted by bond rotation into the more stable *E* form **54***a*. If the instability of the *Z* ester relative to the *E* ester (11) is transposed to the energy barrier for the cleavage of the more stable conformer **52***e*, one must conclude that the hydrolysis of **51** could very well occur via both intermediates **52***b* and **52***e*. These two intermediates lead to the ester

[7]Saturation of the OCH_3 absorption (δ = 4.8) causes an area enhancement of 15% of the methine proton (δ = 8.8). Irradiation of the N—CH_3 group *cis* to the methine proton (doublet, J = 2 Hz, δ = 3.6) resulted in a 16% area increase of this absorption, whereas saturation of the *trans* N—CH_3 group (singlet, δ = 3.8) had no effect. We are grateful to professor J. K. Saunders for this experiment.

[8]A 1,3-synperiplanar interaction is identical to a 1,3-diaxial interaction in a cyclohexane ring.

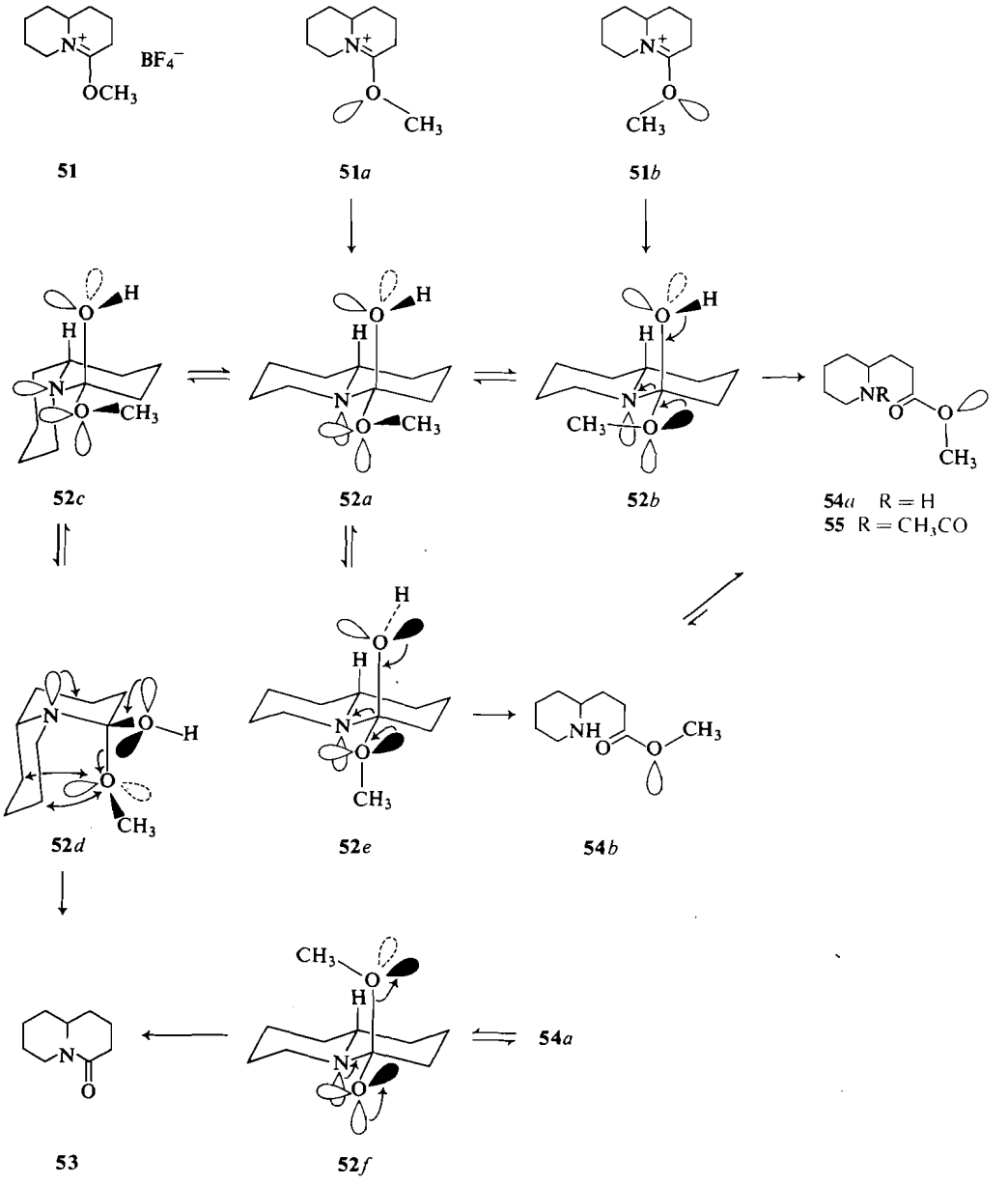

amine **54***a*. Formation of **54***a* via **52***b* and **52***e* is an easier process than formation of the lactam **53** via the sterically unfavored **52***d*. The kinetic product of the hydrolysis reaction of **51** must therefore be the ester amine **54***a*.

In the experiment, the imidate salt **51** was hydrolyzed with sodium carbonate and gave the ester amine **54***a* exclusively after 15 min of reaction. The ester amine **54***a* was then slowly converted into the lactam **53** in the reaction mixture (66% of conversion after 76 h). In another experiment, the hydrolysis of **51** was allowed to proceed for 15 min, then the reaction mixture was treated with a large excess of acetic anhydride and pyridine. The ester amine **54***a* was trapped as the acetamide ester **55** in good yield. Thus, it appears that the formation of lactam **53** via stereoelectronic control must occur by the new tetrahedral conformer **52***f* which can be easily formed from the ester amine **54***a*.

Can. J. Chem. Downloaded from www.nrcresearchpress.com by 210.87.254.105 on 09/05/12
For personal use only.

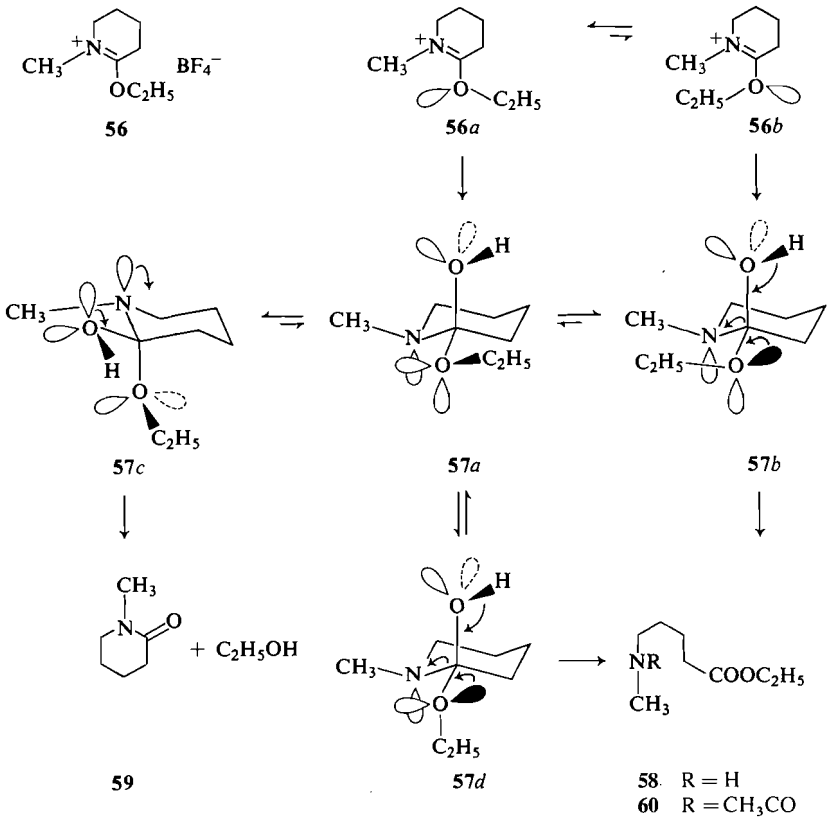

The hydrolysis of the imidate salt **56** was also carried out. It gave a mixture of ester amine **58** (83%) and lactam **59** (17%). The ester amine **58** was isolated as its acetamide derivative **60**. The salt **56** can be considered as the monocyclic version of the bicyclic salt **51** that gives tetrahedral intermediates (**52**) which cannot undergo a proper nitrogen inversion without creating severe steric interactions. The salt **56** can form tetrahedral intermediates (**57***a*, *b*, *c*, and *d*) in which proper nitrogen inversion can occur as well as rotation of the C—OCH_3 bond. Thus, we should expect some lactam product from **56**. This prediction is in agreement with the experimental result. A similar result was obtained from the hydrolysis of the salt **61** which also gave a mixture of ester amine **63** (65%) and lactam **62** (35%). The ester amine **63** was isolated and characterized as its acetamide derivative **64**.

The hydrolysis of the bicyclic imidate salt **65** was also investigated. Its hydrolysis with aqueous sodium carbonate gave directly the lactam **66**, while none of the expected amine ester **67** was detected. However, hydrolysis of **65** in aqueous acid gave the ester ammonium salt **68**. On treatment of **68** with aqueous sodium carbonate only the lactam **66** was obtained. The amine ester **67** was not observed. Consequently, the above result cannot be used against the stereoelectronic theory, because the basic hydrolysis of **65** gives directly the thermodynamic product (**66**) under

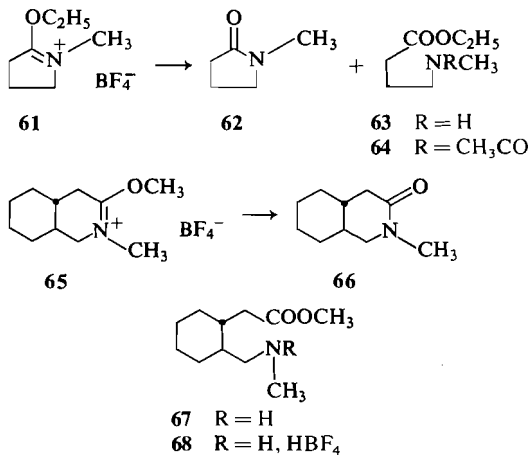

Can. J. Chem. Downloaded from www.nrcresearchpress.com by 210.87.254.105 on 09/05/12
For personal use only.

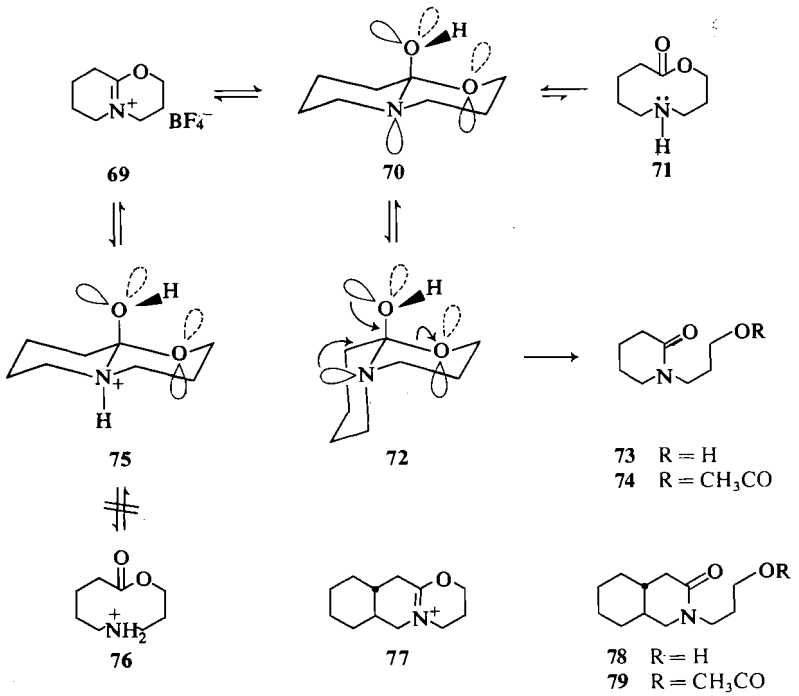

conditions where the kinetic product (**67**) cannot long survive.

Hydrolysis of Bicyclic Imidate Salts 69 and 77

The hydrolysis of the *anti* bicyclic imidate salt **69** was also examined. If the stereoelectronic rule is followed, the salt **69** should give the intermediate **70** which has its orbitals properly aligned to yield the amino lactone **71**. The presence of the large ring in **71** keeps the nitrogen in close proximity to the carbonyl of the ester function. It is therefore logical to expect that the reformation of intermediate **70** from **71** should be especially facile. If **70** has a sufficient lifetime because it is in mobile equilibrium with **71**, it can undergo a conformational change to **72** by nitrogen inversion. Stereoelectronically controlled cleavage of **72** yields the hydroxy lactam **73** which is the thermodynamic product of the reaction. So, even if the conversion of **70** into **72** is a much slower process than its breakdown into **71**, once **72** is obtained, it represents a means by which the reaction can become thermodynamically controlled. Consequently, kinetically controlled conditions should be difficult to obtain in this case. Accordingly, the basic hydrolysis of salt **69** was carried out and it led to the exclusive formation of hydroxy lactam **73** which was characterized by its acetate derivative **74**.

On the other hand, the reaction of **69** in acidic medium should give the intermediate **75** which can break down into the lactonium ammonium salt **76** by an orbital assisted mechanism. The intermediate **75** cannot undergo a conformational change to give the protonated form of **72**; the nitrogen in **75** cannot be inverted because its lone pair orbital is now protonated. The formation of hydroxy lactam **73** should therefore not be observed in acidic medium. The hydrolysis of **69** was attempted in aqueous hydrochloric acid (0.1 *N*) and this compound was found to be completely stable under those conditions for a period of 8 months. Thus, not only the hydroxy lactam product **73** was not formed but the ammonium salt **76** was not even produced. The stability of **69** in aqueous acid can be explained in two ways: (*a*) the salt **69** does not react with water to form a tetrahedral intermediate and it is therefore stable; (*b*) it does react with water to form the intermediate **75** but it prefers to give back the starting salt **69**, for the reason that **69** is more stable than the ammonium salt **76**. We think that the first explanation is not valid. It is difficult to find one good reason to explain the resistance of **69** to form a tetrahedral inter-

Can. J. Chem. Downloaded from www.nrcresearchpress.com by 210.87.254.105 on 09/05/12
For personal use only.

Can. J. Chem. Downloaded from www.nrcresearchpress.com by 210.87.254.105 on 09/05/12
For personal use only.

mediate in acidic medium. All other imidate salts that we have reported in this article do form an intermediate since they are all hydrolyzed in aqueous acid. We have prepared the tricyclic imidate salt **77** which has a structure similar to **69** and we should thus expect the same kind of reactivity. In aqueous base, **77** gave the expected hydroxy lactam **78** which was characterized by its acetate derivative **79**. In aqueous acid, it was found to be completely stable.

Hydrolysis of Imidate Salts 80 and 86

The basic hydrolysis of the bicyclic imidate salt **80** was undertaken next. Reaction of **80** with hydroxide ion should give the intermediate **81**

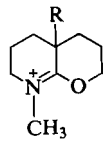

80 R = CH_3
86 R = H

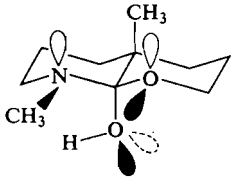

81

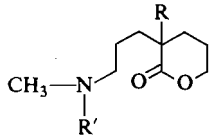

83 R = CH_3, R′ = H, HBF_4
84 R = CH_3, R′ = CH_3CO
89 R = H, R′ = H, HBF_4
90 R = H, R′ = CH_3CO

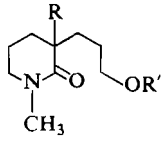

82 R = CH_3, R′ = H
85 R = CH_3, R′ = CH_3CO
87 R = H, R′ = H
88 R = H, R′ = CH_3CO

which cannot break down in a stereoelectronically controlled fashion unless considerable twisting of the molecule can occur. It was therefore of interest to find out if the tetrahedral intermediate **81** could be detected in the reaction mixture since the energy barrier for its breakdown must be abnormally high. The hydrolysis of **80** was carried out in aqueous sodium carbonate. This imidate gave the hydroxy lactam **82** which was also isolated as its acetate derivative **85**. We have found that **80** is hydrolyzed in aqueous acid to the lactone ammonium salt **83** which was further transformed into its acetamide derivative **84**. When **83** was treated with aqueous base, it gave directly the hydroxy lactam **82**. This result shows that the products of the basic hydrolysis of **80** were those of thermodynamic control. (The fact that **80** is hydrolyzed in aqueous acid brings additional support that **69** is in equilibrium with the intermediate **75** under the same conditions.) The specific formation of the lactone ammonium salt **83** shows that the nitrogen lone pair in the tetrahedral intermediate is always protonated under acidic conditions; the lone pair is, therefore, never available to expel an OR group. The successful hydrolysis of **80** under basic conditions indicates that the breakdown of a tetrahedral intermediate can be accomplished without the help of two lone pair orbitals acting synergistically. The tetrahedral intermediate can be cleaved through a higher energy barrier. If the cleavage of **81** had become the slow step of the reaction, its presence could have been detected.

We have also prepared the closely related imidate salt **86** and have obtained a similar result. Under basic conditions, **86** gave the hydroxy lactam **87** which was also characterized as its acetate derivative **88**. Under acidic conditions, **86** gave the lactone ammonium salt **89** which was transformed into the hydroxy lactam **87** by treatment with aqueous sodium carbonate. Treatment of the salt **89** with pyridine and acetic anhydride gave the lactone acetamide **90**.

Conclusion

The products of hydrolysis of the imidate salts examined were accurately predicted by application of the straightforward argument presented here. The application of the postulate of conformational changes combined with the principle of stereoelectronic control provide a very attractive mechanism to explain the products formed in the hydrolysis of imidate salts under basic conditions. We believe that the preceding results combined with our work on the oxidation of acetals (11) and the hydrolysis of orthoesters (1) constitute strong experimental evidence which support this new stereoelectronic theory.[9]

Experimental

The i.r. spectra were taken on a Perkin-Elmer 257 spectrophotometer. Proton n.m.r. spectra (δ value) were

[9]In this work, we have not taken account of the p*H* of the reaction medium, except that we have tried to use the most basic conditions which allow a kinetically controlled reaction. So, whenever possible, sodium hydroxide was used. In other cases, the less suitable sodium carbonate had to be used. We also used mixed aqueous–organic solvents so that the products of the reaction could be conveniently analyzed by n.m.r. spectroscopy. We have also undertaken the hydrolysis of some *N,N*-dialkylated imidate salts in aqueous solution over a range of p*H* values. The results obtained confirm the conclusion of this work and will be reported in the near future.

Can. J. Chem. Downloaded from www.nrcresearchpress.com by 210.87.254.105 on 09/05/12
For personal use only.

recorded on a Varian A-60 spectrometer in solvent indicated. All chemical shifts are recorded relative to internal TMS as standard. The vapor phase chromatographic analyses were done on Varian chromatographs models 600-D and 2800. Mass spectra were run on a Hitachi-Perkin-Elmer RMU-6 spectrometer. Microanalyses were performed by Dr. C. Daesslé, Organic Microanalyses, Montreal and by Mr. J. Tamas, Laboratoire de Microanalyse, Université de Sherbrooke.

The imidate salts **3**, **11**, **14**, **33**, and **37** were obtained by alkylation with trimethyloxonium tetrafluoroborate (16) of compounds **91**, **92**, **93**, **94**, and **95**, respectively. Compound **94** was prepared from the chloroamide **97** which was obtained from the olefinic amide **96**. The imidate salt **40** was prepared from δ-valerolactone via intermediates **46** and **98**. Similarly, the salt **41** was obtained from γ-butyrolactone via compounds **47** and **99**. The imidate salts **49**, **50**, **51**, **56**, **61**, and **65** were prepared by alkylation with the appropriate trialkyloxonium tetrafluoroborate of the corresponding amides or lactams. The lactam **66** was prepared from lactam **100**. The salt **69** was prepared by cyclization of **102** which was obtained by *N*-alkylation of **101** with 1-bromo-3-chloropropane. An authentic sample of **73** was prepared by alkylation of **101** with 3-chloro-1-propanol tetrahydropyranyl ether (**103**) followed by acid hydrolysis. The salt **77** was obtained by a similar route using **100** and **104** as intermediates. The salts **80** and **86** were prepared by cyclization of **106** and **107**. *C*-Alkylation of **105** and **59** gave the chloroamides **106** and **107** respectively. Finally, alkylation of **59** gave **105** (17).

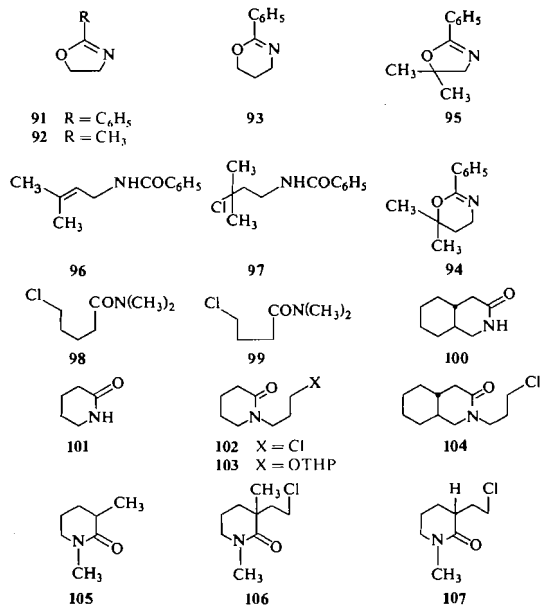

General Method of Preparation of Imidate Salts

The imino ether, amide, or lactam (1 equiv.) was treated with trialkyloxonium tetrafluoroborate (1 equiv.) in anhydrous dichloromethane. The solution was kept at room temperature for 12 h. The solvent was removed *in vacuo*. The reactions are essentially quantitative. When the imidate salt could not be obtained crystalline, it was used directly without further purification. The structure and purity of such salts can be easily verified by n.m.r. and i.r. spectroscopic analysis.[10]

A Typical Procedure for the Basic Hydrolysis of Cyclic Imidate Salts

Imidate Salt 3

Procedure A—Imidate salt **3** (50 mg, 0.20 mmol) was dissolved in deuterated acetonitrile (0.3 ml). Sodium carbonate (0.66 mmol) in deuterated water (0.3 ml) was added. After 10 min, analysis by n.m.r. spectroscopy indicated the presence only of benzoate amine **4** (n.m.r. (CD_3CN—D_2O): δ 7.55–8.05 (5H, multiplet, aromatic protons), 4.45 (2H, triplet, J = 5.5 Hz, CH_2O), 3.02 (2H, triplet, J = 5.5 Hz, CH_2N), and 2.48 (3H, singlet, CH_3N). The reaction mixture was left at room temperature for 24 h. Nuclear magnetic resonance analysis indicated the presence of benzamide alcohol **6** as the sole product. The solvent was removed *in vacuo*, brine was added, and the mixture was extracted with chloroform. The organic phase was dried over magnesium sulfate, filtered, and evaporated to dryness to yield crude benzamide alcohol **6**; i.r. ($CHCl_3$): 3520–3200 and 1615 cm^{-1}; n.m.r. ($CDCl_3$): δ 7.45 (5H, singlet, aromatic hydrogens), 3.76 (5H, multiplet, OCH_2CH_2N and OH), 3.21 (3H, singlet, CH_3N), and 3.09 (3H, singlet, CH_3N). Acetylation of benzamide alcohol **6** with pyridine and acetic anhydride gave benzamide acetate **7**; i.r. ($CHCl_3$): 1625 and 1740 cm^{-1}; n.m.r. ($CDCl_3$): δ 7.44 (5H, aromatic hydrogens), 4.33 (2H, unresolved triplet, CH_2O), 3.72 (2H, unresolved triplet, CH_2N), 3.08 (3H, singlet, CH_3N), and 2.09 (3H, singlet, CH_3CO).

Procedure B—Imidate salt **3** (200 mg, 0.8 mmol) was dissolved in acetonitrile (5 ml) and sodium carbonate (44 mmol) in water (2 ml) was added. After 10 min at room temperature, acetic anhydride (50 ml) and pyridine (10 ml) were added. The reaction was left for 12 h at room temperature. It was cooled to 0 °C and methanol (50 ml) was added. Water was then added and the mixture was extracted with dichloromethane. The organic phase was washed with water, dried, and evaporated to dryness to yield pure benzoate acetamide **5** (180 mg, 100%); i.r. ($CHCl_3$): 1635 and 1715 cm^{-1}; n.m.r. ($CDCl_3$): δ 7.55–8.10 (5H, multiplets, aromatic hydrogens), 4.50 (2H, triplet, J = 6 Hz, CH_2O), 3.70–3.80 (2H, two triplets, J = 6 Hz, CH_2N), 3.06–3.12 (3H, two singlets, CH_3N), and 2.11–2.18 (3H, two singlets, CH_3CO).

Procedure C—Imidate salt **3** (50 mg, 0.20 mmol) was dissolved in deuterated acetonitrile (0.3 ml). Sodium carbonate (0.66 mmol) in deuterated water (0.3 ml) was added. After 10 min, n.m.r. analysis indicated the presence of only benzoate amine **4**. Sodium hydroxide in deuterated water (1 *N*, 0.3 ml) was added. Nuclear magnetic resonance analysis of this solution showed only benzamide alcohol **6**.

Procedure D—Imidate salt **3** (30 mg, 0.20 mmol) was dissolved in acetonitrile (0.3 ml) and deuterated water (0.1 ml). The reaction is complete after 10 h at room temperature and gives the ammonium salt **8** n.m.r.

[10]The experimental procedures and spectroscopic data for the imidate salts and the various compounds described in this work are available, at a nominal charge, from the Depository for Unpublished Data, CISTI, National Research Council of Canada, Ottawa, Canada KIA 0S2.

Can. J. Chem. Downloaded from www.nrcresearchpress.com by 210.87.254.105 on 09/05/12
For personal use only.

(CD_3CN—D_2O): δ 7.65–8.10 (5H, multiplet, aromatic hydrogens), 4.53 (2H, multiplet, CH_2O), 3.48 (2H, multiplet, CH_2N), and 2.83 (3H, singlet, CH_3N). A solution of sodium hydroxide (0.25 ml, 1 *N*) is added. Nuclear magnetic resonance analysis indicated the presence of benzamide alcohol **6** only.

Procedure E—Imidate salt **3** (30 mg, 0.12 mmol) was dissolved in acetonitrile (0.3 ml) and deuterated water (0.1 ml). After 18 h at room temperature, sodium carbonate (0.66 mmol) in deuterated water (0.3 ml) was added. Nuclear magnetic resonance analysis indicated the presence of benzoate amine **4**. After standing for 100 h, n.m.r. analysis indicated the presence of benzamide alcohol **6**.

Hydrolysis of Imidate Salt ***11***

Acetate amine ***12***—n.m.r. (CD_3CN–D_2O): δ 4.15 (2H, triplet, J = 6 Hz, CH_2O), 2.77 (2H, triplet, J = 6 Hz, CH_2N), and 2.32 (3H, singlet, CH_3N).

Acetamide alcohol ***13***—i.r. ($CHCl_3$): 3200–3550 and 1630 cm^{-1}; n.m.r. ($CDCl_3$): δ 4.70 (1H, broad singlet, OH), 3.60 (4H, multiplet, NCH_2CH_2O), 2.95–3.10 (3H, two singlets, CH_3N), and 2.08–2.14 (3H, two singlets, CH_3CO).

Hydrolysis of Imidate Salt ***14***

Benzoate amine ***15***—n.m.r. (CD_3CN–D_2O): δ 7.55–7.90 (5H, two multiplets, aromatic hydrogens), 4.35 (2H, triplet, J = 6 Hz, CH_2O), 2.88 (2H, triplet, J = 7 Hz, CH_2N), 2.42 (3H, singlet, CH_3N), and 2.02 (2H, multiplet, CH_2).

Benzoate acetamide ***16***—i.r. ($CHCl_3$): 1630 and 1715 cm^{-1}; n.m.r. ($CDCl_3$): δ 7.57–8.10 (5H, two multiplets, aromatic hydrogens), 4.40 (2H, triplet, J = 6 Hz, CH_2O), 3.52–3.58 (2H, two triplets, J = 6 Hz, CH_2N), 2.98–3.06 (3H, two singlets, CH_3N), 2.10–2.11 (3H, two singlets, CH_3CO), and 2.11 (2H, multiplet, CH_2).

Acetate benzamide ***18***—i.r. ($CHCl_3$): 1620 and 1730 cm^{-1}; n.m.r. ($CDCl_3$): δ 7.45 (5H, singlet, aromatic hydrogens), 4.11 (2H, multiplet, CH_2O), 3.55 (2H, multiplet, CH_2N), 3.05 (3H, singlet, CH_3N), and 2.02 (5H, multiplet, CH_2 and CH_3CO).

Benzoate ammonium salt ***19***—n.m.r. (CD_3CN): δ 7.65–8.10 (5H, two multiplets, aromatic hydrogens), 4.41 (2H, triplet, J = 6 Hz, CH_2O), 3.20 (2H, triplet, J = 7 Hz, CH_2N), 2.70 (3H, singlet, CH_3N), and 2.11 (2H, multiplet, CH_2).

Hydrolysis of Imidate Salt ***26***

Acetate amine ***27***—i.r. ($CHCl_3$): 1725 cm^{-1}; n.m.r. ($CDCl_3$): δ 5.15 (1H, multiplet, CHO), 2.30 (3H, singlet, CH_3N), 2.02 (3H, singlet, CH_3CO), 1.24 (3H, doublet, J = 7 Hz, CH_3CH), and 1.05 (6H, singlet, $(CH_3)_2C$).

Hydrolysis of Imidate Salt ***33***

Benzoate amine ***35***—n.m.r. (CD_3CN–D_2O): δ 7.6–7.90 (5H, two multiplets, aromatic hydrogens), 2.32 (3H, singlet, CH_3N), and 1.60 (6H, singlet, $(CH_3)_2C$).

Acetamide benzoate ***36***—i.r. ($CHCl_3$): 1750 and 1630 cm^{-1}; n.m.r. (CD_3CN): δ 7.6–8.10 (5H, two multiplets, aromatic hydrogens), 3.52 (2H, multiplet, CH_2N), 2.86–2.98 (3H, two singlets, CH_3N), 1.95–2.04 (3H, two singlets, CH_3CO), and 1.62 (6H, singlet, $(CH_3)_2C$).

Hydrolysis of Imidate Salt ***37***

Benzoate amine ***38***—n.m.r. (CD_3CN–D_2O): δ 7.80 (5H, multiplet, aromatic hydrogens), 3.06 (2H, singlet, CH_2N), 2.52 (3H, singlet, CH_3N), and 1.62 (6H, singlet, $(CH_3)_2C$).

Benzamide alcohol ***39***—i.r. ($CHCl_3$): 3200–3600, and 1615 cm^{-1}; n.m.r. ($CDCl_3$): δ 7.45 (5H, singlet, aromatic hydrogens), 3.96 (1H, broad singlet, OH), 3.60 (2H, singlet, CH_2N), 3.10 (3H, singlet, CH_3N), and 1.28 (6H, singlet, $(CH_3)_2C$).

Hydrolysis of Imidate Salt ***40***

The n.m.r. spectrum indicated a mixture of dimethylamine (31%), the hydroxy carboxylic acid sodium salt of δ-valerolactone (**45**) and hydroxy amide **46**; n.m.r. (CD_3CN–H_2O): δ 3.57 (2H, unresolved triplet, CH_2O), 3.04–2.88 (6H, two singlets, $(CH_3)_2NCO$), and 2.27 (6H, singlet, $(CH_3)_2ND$).

Hydrolysis of Imidate Salt ***41***

The n.m.r. spectrum indicated a mixture of dimethylamine (50%), the hydroxy carboxylic acid sodium salt of γ-butyrolactone (**48**), and hydroxy amide **47**; n.m.r. (CD_3CN–D_2O): δ 3.56 (2H, triplet, CH_2O), 3.04–2.88 (6H, two singlets, $(CH_3)_2NCO$), and 2.25 (6H, singlet, $(CH_3)_2ND$).

Hydrolysis of Imidate Salt ***51***

Ester amine ***54***—n.m.r. (CD_3CN–H_2O): δ 3.68 (3H, singlet, CH_3O).

Acetamide ester ***55***—i.r. ($CHCl_3$): 1730 and 1620 cm^{-1}; n.m.r. ($CDCl_3$): δ 3.67 (3H, singlet, CH_3O), 2.36 (2H, multiplet, CH_2CO), 2.08 (3H, singlet, CH_3CO), and 1.62 (10H, broad multiplet).

Hydrolysis of Imidate Salt ***56***

Ester amine ***58*** *(observed in a mixture with* ***57****)*—i.r. (CH_2Cl_2): 1725 cm^{-1}; n.m.r. (90 MHz, CD_2Cl_2): δ 4.22 (2H, quadruplet, J = 7 Hz, OCH_2), 2.53 (2H, triplet, J = 7 Hz, CH_2N), 2.35 (3H, singlet, CH_3N), 2.28 (2H, triplet, J = 7 Hz, CH_2CO), 1.52 (2H, multiplet), and 1.21 (3H, triplet, J = 7 Hz, OCH_2CH_3).

Lactam ***59***—i.r. ($CHCl_3$): 1625 cm^{-1}; n.m.r. ($CDCl_3$): δ 3.30 (2H, unresolved multiplet, CH_2N), 2.96 (3H, singlet, CH_3N), 2.40 (2H, multiplet, CH_2CO), and 1.85 (4H, multiplet).

Acetamide ester ***60***—i.r. ($CHCl_3$): 1725 and 1630 cm^{-1}; n.m.r. ($CHCl_3$): δ 4.28 (2H, quartet, J = 7 Hz, OCH_2), 3.40 (2H, multiplet, CH_2N), 2.98–3.06 (3H, two singlets, CH_3CO), 2.35 (2H, multiplet, CH_2CO), 2.12–2.14 (3H, two singlets, CH_3N), 1.60 (4H, multiplet), and 1.26 (3H, triplet, J = 7 Hz, OCH_2CH_3).

Hydrolysis of Imidate Salt ***61***

Ester amine ***63*** *(observed in a mixture with* ***62****)*—i.r. (CH_2Cl_2): 1735 cm^{-1}; n.m.r. (90 MHz, CH_2Cl_2): δ 4.11 (2H, quartet, J = 7 Hz, OCH_2CH_3), 2.54 (2H, triplet, J = 7 Hz, CH_2N), 2.34 (3H, singlet, CH_3N), 2.30 (2H, triplet, J = 7 Hz, CH_2CO), 1.21 (3H, triplet, J = 7 Hz, OCH_2CH_3).

Lactam ***62***—i.r. (neat): 1670 cm^{-1}; n.m.r. ($CDCl_3$): δ 3.41 (2H, triplet, J = 7 Hz, CH_2N), 2.85 (3H, singlet, CH_3N), 2.30 (4H, multiplet).

Acetamide ester ***64***—n.m.r. ($CDCl_3$): δ 4.18 (2H, quartet, J = 7 Hz, OCH_2CH_3), 3.40 (2H, multiplet, CH_2N), 2.94–3.02 (3H, two singlets, CH_3N), 2.08–2.10 (3H, two singlets, CH_3CO), 2.10 (4H, multiplet), and 1.28 (3H, triplet, J = 7 Hz, OCH_2CH_3).

Hydrolysis of Imidate Salt ***65***

Basic conditions—Imidate salt ***65*** (93 mg, 0.345 mmol) was dissolved in acetonitrile-d_3 (300 μl) in an n.m.r. tube. Dry sodium carbonate (79 mg, 0.744 mmol) was added, along with deuterium oxide (700 μl). The heterogeneous

Can. J. Chem. Downloaded from www.nrcresearchpress.com by 210.87.254.105 on 09/05/12
For personal use only.

mixture was shaken for 10 min at room temperature. The n.m.r. spectrum at this time showed no resonances due to starting material. Solvent was removed *in vacuo* and the residue was triturated with chloroform. The triturant was concentrated *in vacuo* to leave a clear oil which was the lactam **66** (60 mg, 100%). This material was homogeneous by t.l.c. and identical to the lactam prepared via methylation of lactam **100** by n.m.r., i.r., and t.l.c. comparison.

Acidic Conditions—Imidate salt **65** (43 mg, 0.16 mmol) was dissolved in aqueous hydrochloric acid (1 *N*, 300 μl) in an n.m.r. tube. The sample was allowed to stand at room temperature for 5 days. At the end of this time no resonances due to starting material remained. New resonances characteristic of the ester ammonium salt **68** at δ 3.80 (singlet) and 2.80 p.p.m. (triplet, $J = 3$ Hz) had appeared. Solvent was removed *in vacuo*. The i.r. of the semisolid thus obtained in chloroform showed absorptions at 3500–3000 (NH), 1720, and 1625 cm^{-1}.

Ammonium ester **68** (25 mg, 0.067 mmol) was placed in an n.m.r. tube along with deuteriochloroform (300 μl). Aqueous sodium carbonate (1 *N*, 300 μl) was added and the tube was shaken vigorously. Within 3 min the n.m.r. spectrum was essentially that of lactam **66**. Solvent was removed *in vacuo*. The oily solid which remained was triturated with methylene chloride and the triturant was dried over sodium sulfate. Solvent was removed *in vacuo* to give the lactam **66** (10 mg, 90%) as a clear oil. The t.l.c., i.r., and n.m.r. characteristics of this sample were identical to an authentic sample.

Hydrolysis of Imidate Salt 69

Basic Conditions—Imidate salt **69** ($X = ClO_4^-$) (59 mg, 0.247 mmol) was dissolved in acetonitrile-d_3 (300 μl) in an n.m.r. tube. Aqueous sodium carbonate (4 *N* in D_2O, 250 μl, 1 mmol) was added. The heterogeneous mixture thus obtained was stirred vigorously and the progress of the reaction was followed by n.m.r. The hydrolysis was judged complete after 15 h at room temperature. The contents of the n.m.r. tube were extracted with chloroform and the extract dried over sodium sulfate. Removal of solvent *in vacuo* gave hydroxy lactam **73** in good yield. The hydroxy lactam **73** obtained from this experiment was identical to hydroxy lactam prepared from the tetrahydropyranyl ether **103**.

Imidate salt **69** ($X = ClO_4^-$) (62 mg, 0.260 mmol) was dissolved in acetonitrile-d_3 (30 μl) in an n.m.r. tube. Aqueous sodium hydroxide (4 *N*, 65 μl, 0.26 mmol) was added, and the resulting heterogeneous mixture was shaken vigorously. The progress of the reaction was followed by n.m.r. After 19 min at room temperature the salt **69** was completely hydrolyzed to hydroxy lactam **73**. As in the previous experiment, **73** was isolated in good yield. The basic hydrolysis of **69** ($X = BF_4^-$) also gives the hydroxy lactam **73**.

Acidic Conditions—Imidate salt **69** ($X = BF_4^-$) (21 mg, 0.09 mmol) was dissolved in aqueous hydrochloric acid (300 μl, 0.1 *N* in D_2O) in an n.m.r. tube. During 8 months at room temperature, there was no change in the n.m.r. spectrum of this sample. At the end of this time solvent was removed *in vacuo*. The residue (31 mg) was triturated with dichloromethane. The triturant was concentrated *in vacuo* to give the imidate salt **69** (13 mg, 62%). Crystallization from dichloromethane – ethyl ether gave pure **69** (11 mg); m.p. 161–163 °C. A 50:50 w/w mixture of authentic **69** and **69** recovered from the aqueous acidic reaction gave m.p. 162–163 °C.

Hydrolysis of Imidate Salt 77

Basic Conditions—Imidate salt **77** (57 mg, 0.196 mmol) was dissolved in acetonitrile-d_3 (300 μl). Aqueous sodium carbonate (4 *N* in deuterium oxide, 200 μl) was added. At this point some sodium carbonate precipitated and the solution was filtered into an n.m.r. tube. After 19 h at room temperature the salt **77** had been completely hydrolyzed, as shown by n.m.r. The resulting solution was extracted with chloroform and the extract was dried over potassium carbonate. Removal of solvent *in vacuo* left an oil (40 mg). Preparative t.l.c. (silica gel, $CHCl_3$ – 6% (v/v) CH_3OH, R_f 0.2) gave the hydroxy lactam **78** (30 mg, 70%) as a clear oil; i.r. (CCl_4): 3400 and 1630 cm^{-1}; n.m.r. ($CDCl_3$): δ 4.20 (1H, singlet, OH), 3.9–2.6 (6H, multiplet), 2.5–0.6 (14 H, multiplet); m.s.: *m/e* 211 (M^+), 193 ($M^+ - H_2O$).

Hydroxy lactam **78** (255 mg, 1.21 mmol) was dissolved in acetic anhydride (2 ml) and dry pyridine (2 ml). This mixture was stirred overnight at room temperature, under nitrogen. Solvent was removed *in vacuo* to leave a yellow oil (280 mg). Preparative t.l.c. (silica gel, $CHCl_3$ – 6% (v/v) CH_3OH, R_f 0.5) gave the acetoxy lactam **79** (240 mg, 78%). Low temperature crystallization from hexane gave **79** as a white solid; m.p. 27 °C; i.r. (CCl_4): 1745 and 1650 cm^{-1}; n.m.r. ($CDCl_3$): δ 4.15 (2H, triplet, $J = 7$ Hz, CH_2O), 3.7–2.5 (4H, multiplet), 2.4–0.8 (14 H, multiplet), and 2.05 (3H, singlet, CH_3CO); m.s.: *m/e* 253 (M^+), 210 ($M^+ - CH_3CO$), 193 ($M^+ - CH_3COOH$).

Anal. Calcd. for $C_{14}H_{23}NO_3$: C, 66.37; H, 9.15. Found: C, 66.29; H, 9.17.

Acidic Conditions—Tricyclic salt **77** (25 mg, 0.089 mmol) was dissolved in hydrochloric acid (0.1 *N* in deuterium oxide, 300 μl) in an n.m.r. tube. There was no appreciable change in the n.m.r. spectrum of this sample during 8 months at room temperature. At the end of this time solvent was removed *in vacuo* and the residue was triturated with dichloromethane. The triturant was concentrated *in vacuo* to give the imidate **77** (16 mg, 65%) as an oil. This material crystallized from cold absolute ethanol to give pure **77** (12 mg); m.p. 78–80 °C. A 1:1 (w/w) mixture of authentic **77** and **77** isolated from aqueous acid showed m.p. 78–79.5 °C.

Hydrolysis of Imidate Salt 80

Basic Conditions—Imidate salt **80** (60 mg, 0.236 mmol) was dissolved in deuteriochloroform (400 μl), in an n.m.r. tube. Aqueous sodium carbonate (300 μl, 0.270 mmol, 0.9 *N* in D_2O) was added and the reaction was followed by n.m.r. After 2.5 h approximately 10% of the imidate remained; after standing 12 h at room temperature, no starting material was detectable by n.m.r. Solvent was removed *in vacuo*. The residue obtained was triturated with chloroform. The triturant was concentrated *in vacuo* to leave a yellow oil (50 mg). Trituration with diethyl ether gave pure lactam alcohol **82** (33 mg, 75%) as a clear, ether soluble, oil; t.l.c.: R_f 0.5 on silica gel using $CHCl_3$ – 7% (v/v) CH_3OH eluent; i.r. (CCl_4): 3450 and 1640 cm^{-1}; n.m.r. ($CDCl_3$): δ 3.8–3.5 (2H, multiplet), 3.5–3.15 (2H, multiplet), 2.90 (3H, singlet), 2.2–1.25 (9H, multiplet), and 1.20 (3H, singlet); m.s.: *m/e* 186 (M^+).

In another experiment the hydrolysis of imidate salt **80** was carried out in aqueous sodium carbonate with no cosolvent. Work-up as described above gave the hydroxy lactam **82** in quantitative yield. The hydrolysis was complete within 5 min after mixing the reagents.

Hydroxy lactam **82** (115 mg, 0.62 mmol) was dissolved

Can. J. Chem. Downloaded from www.nrcresearchpress.com by 210.87.254.105 on 09/05/12
For personal use only.

in a mixture of acetic anhydride (1 ml) and dry pyridine (1 ml), under argon. This was allowed to stand overnight at room temperature. Solvent was removed *in vacuo* to leave a slightly yellow oil (137 mg). Short path distillation gave pure acetoxy lactam **85** (95 mg, 68%) as a clear oil; b.p. 80 °C/0.1 Torr; i.r. (CCl_4): 1740 and 1640 cm^{-1}; n.m.r. ($CDCl_3$): δ 4.2–3.9 (2H, multiplet), 3.5–3.1 (2H, multiplet), 2.90 (3H, singlet, CH_3N), 2.05 (3H, singlet, CH_3CO), 2.0–1.3 (8H, multiplet), and 1.20 (3H, singlet, CH_3C); m.s.: *m/e* 227 (M^+).

Anal. Calcd. for $C_{12}H_{21}NO_3$: C, 63.41; H, 9.31. Found: C, 63.18; H, 9.38.

Acidic Conditions—Imidate salt **90** (106 mg, 0.416 mmol) was dissolved in aqueous fluoroboric acid (86 mg, 48% HBF_4–H_2O, 0.50 mmol) in an n.m.r. tube. Deuterium oxide (300 μl) was added and the solution was allowed to stand at room temperature for 3 months. No resonances owing to starting material could be detected in the n.m.r. spectrum of the sample at this time. Solvent was removed *in vacuo* and the residue was triturated with chloroform. The triturant gave an oil (110 mg) whose i.r. spectrum in acetonitrile showed an absorption due to the presence of the lactone function at 1720 cm^{-1} corresponding to compound **83**. The oil was stirred at room temperature in a mixture of acetic anhydride (1 ml) and dry pyridine (1 ml), under argon, overnight. Solvent was removed *in vacuo* to leave a brown oil. Preparative t.l.c. (silica gel, $CHCl_3$ – 6% (v/v) CH_3OH, R_f 0.2) gave pure lactone **84** (40 mg, 43%), as a clear oil; i.r. (CCl_4): 1730 and 1640 cm^{-1}; n.m.r. ($CDCl_3$): δ 4.5–4.2 (2H, multiplet), 3.5–3.1 (2H, multiplet), 3.1–2.8 (3H, two lines due to CH_3NCO), 2.7–1.0 (11H, multiplet), and 2.10 (3H, singlet, CH_3CO); m.s.: *m/e* 227 (M^+).

Hydrolysis of Imidate Salt 86

Basic Conditions—Imidate salt **86** (21 mg, 0.091 mmol) was dissolved in acetonitrile-d_3 in an n.m.r. tube. Aqueous sodium hydroxide (4 *N* in deuterium oxide, 50 μl) was added and the n.m.r. spectrum was run immediately. Resonances due to the imidate **86** had completely disappeared. One new resonance, at 2.9 p.p.m., was particularly diagnostic of the methyl group of a 1-methyl-2-piperidone. No further changes occurred in the n.m.r. spectrum of this sample during 1 h of intermittent observation. In another experiment, imidate **86** (21 mg, 0.091 mmol) was dissolved in aqueous sodium carbonate (1 g Na_2CO_3 – 10 ml D_2O, 0.94 *N*, 300 μl) in an n.m.r. tube. The n.m.r. spectrum of this sample was run within 5 min after mixing. No resonances from **86** remained and the spectrum obtained was identical to the one obtained in the previous experiment.

To fully characterize the product of the basic hydrolysis of imidate **86**, the reaction was scaled up. Imidate salt **86** (91 mg, 0.395 mmol) was dissolved in aqueous sodium hydroxide (1 *N*, 5 ml). The mixture was stirred at room temperature for 30 min. The resulting solution was saturated with sodium chloride, then extracted with chloroform. The extract was dried over sodium sulfate, then solvent was removed *in vacuo* to leave a clear oil (75 mg). Preparative t.l.c. (silica gel, $CHCl_3$ – 5% (v/v) CH_3OH, R_f 0.2 gave the hydroxy lactam **87** ((18), 60 mg, 87%) as an oil which crystallized from cold diethyl ether; m.p. 56–56.5 °C; i.r. (CCl_4): 3400 and 1630 cm^{-1}; n.m.r. ($CDCl_3$): δ 3.85–3.55 (3H, multiplet), 2.95 (3H, singlet, CH_3N), and 2.6–1.2 (11H, multiplet); m.s.: *m/e* 153 ($M^+ - H_2O$).

Anal. Calcd. for $C_9H_{17}NO_2$: C, 63.13; H, 10.01. Found: C, 63.07; H, 10.48.

Hydroxy lactam **87** (12 mg, 0.07 mmol) was dissolved in a mixture of acetic anhydride (2 ml) and dry pyridine (1 ml). This solution was stirred at room temperature, under nitrogen, for 3 h. Solvent was removed *in vacuo* to leave a clear oil (13 mg). After preparative t.l.c. (silica gel, $CHCl_3$ – 6% (v/v) CH_3OH, R_f 0.8) this oil gave pure lactam acetate **88** (6 mg, 40%) as a clear oil; i.r. (CCl_4): 1740 and 1640 cm^{-1}; n.m.r. ($CDCl_3$): δ 4.18 (2H, triplet, J = 6 Hz, CH_2O), 3.6–3.2 (2H, multiplet), 3.00 (3H, singlet, CH_3N), 2.5–1.4 (9H, multiplet), and 2.10 (3H, singlet, CH_3CO); m.s.: *m/e* 213 (M^+).

Acidic Conditions—Imidate tetrafluoroborate salt **86** (100 mg, 0.434 mmol) was dissolved in deuterium oxide (300 μl) along with aqueous tetrafluoroboric acid (86 mg of 48% HBF_4–H_2O, 0.5 mmol HBF_4). The progress of the reaction was followed by n.m.r. After 1 month at room temperature, solvent was removed *in vacuo* to leave a clear oil (148 mg). This oil was dissolved in acetonitrile and the solution dried over sodium sulfate. Solvent was removed *in vacuo* to leave a waxy semisolid (142 mg). This was triturated extensively first with dichloromethane, then with acetonitrile. The dichloromethane was evaporated *in vacuo* to leave a clear oil (29 mg) which consisted for the most part of unreacted imidate **86**. The acetonitrile solution was diluted with diethyl ether. Upon cooling in the refrigerator, the desired lactone ammonium salt **89** (79 mg, 100%) precipitated as a waxy semisolid; i.r. (CH_3CN): 1730 cm^{-1}; n.m.r. (CD_3CN): δ 7.3–6.3 (1H, multiplet), 4.5–4.25 (2H, multiplet), 3.8–3.4 (1H, multiplet), 3.3–2.9 (2H, multiplet), 2.72 (3H, triplet, J = 5 Hz), and 2.2–1.3 (partially obscured by solvent).

Ammonium lactone salt **89** (113 mg, 0.455 mmol) was dissolved in acetic anhydride (5 ml) under nitrogen. Dry pyridine (1 ml) was added with vigorous stirring. This was stirred for 3 h at room temperature, then solvent was removed *in vacuo*. The residue was triturated with dichloromethane. Evaporation of the dichloromethane *in vacuo* left crude **90** (54 mg) as an oil. Preparative t.l.c. (silica gel, $CHCl_3$ – 6% (v/v) CH_3OH, R_f 0.6) gave pure **90** (10 mg, 10%) as a clear oil (the crude yield is reasonable but the recovery off the t.l.c. plate is inexplicably poor); i.r. (CCl_4): 1740 and 1650 cm^{-1}; n.m.r. ($CDCl_3$): δ 4.40 (1H, triplet, J = 5 Hz), 4.3–4.00 (1H, multiplet), 3.8–3.20 (2H, multiplet), 3.2–2.95 (3H, singlet, CH_3NCO), 2.7–1.10 (9H, multiplet), and 2.18 (3H, singlet, CH_3CO); m.s.: *m/e* 213 (M^+), 170 ($M^+ - CH_3CO$).

Basic Hydrolysis of Lactone Ammonium Salt 89

Lactone ammonium salt **89** (10 mg) was dissolved in deuterium oxide in an n.m.r. tube. One drop of sodium hydroxide in deuterium oxide (4 *N*) was added, then the n.m.r. spectrum of this solution was run immediately. The spectrum showed no resonance due to starting material, and the spectrum did not change during 30 min. Solvent was removed *in vacuo* to leave a clear oil whose t.l.c. retention time and spectral characteristics (i.r. and n.m.r.) were identical to those of a sample of hydroxy lactam **87**.

Support for this work by the National Research Council of Canada, and by The Ministère de l'Education, Québec, is gratefully acknowledged.

1. P. DESLONGCHAMPS, P. ATLANI, D. FRÉHEL, and A. MALAVAL. Can. J. Chem. **50**, 3405 (1972); P. DESLONGCHAMPS, R. CHÊNEVERT, R. J. TAILLEFER, C. MOREAU, and J. K. SAUNDERS. Can. J. Chem. **53**, 1601 (1975); P. DESLONGCHAMPS, R. J. TAILLEFER, C. MOREAU, and R. CHÊNEVERT. In preparation.
2. P. DESLONGCHAMPS. Pure Appl. Chem. In press.
3. P. DESLONGCHAMPS, C. LEBREUX, and R. J. TAILLEFER. Can. J. Chem. **51**, 1665 (1973).
4. J. F. KING and A. D. ALLBUTT. Tetrahedron Lett. 49, (1967); Can. J. Chem. **48**, 1754 (1970).
5. E. L. ELIEL and F. W. NADER. J. Am. Chem. Soc. **91**, 536 (1969); **92**, 584 (1970).
6. H. B. BÜRGI, J. D. DUNITZ, and E. SHEFTER. J. Am. Chem. Soc. **95**, 5065 (1973); H. B. BÜRGI, J. D. DUNITZ, and E. SHEFTER. Acta Crystallogr. B, **30**, 1517 (1974); J. M. LEHN, G. WIPFF, and H. B. BÜRGI. Helv. Chim. Acta, **57**, 493 (1974); H. B. BÜRGI, J. M. LEHN, and G. WIPFF. J. Am. Chem. Soc. **96**, 1956 (1974); H. B. BÜRGI, J. D. DUNITZ, J. M. LEHN, and G. WIPFF. Tetrahedron, **30**, 1563 (1974); J. M. LEHN and G. WIPFF. J. Am. Chem. Soc. **96**, 4048 (1974).
7. G. L. SCHMIR and B. A. CUNNINGHAM. J. Am. Chem. Soc. **87**, 5692 (1965); B. A. CUNNINGHAM and G. L. SCHMIR. J. Am. Chem. Soc. **88**, 551 (1966); B. A. CUNNINGHAM and G. L. SCHMIR. J. Am. Chem. Soc. **89**, 917 (1967); W. P. JENCKS and M. GILCHRIST. J. Am. Chem. Soc. **90**, 2622 (1968); G. M. BLACKBURN and W. P. JENCKS. J. Am. Chem. Soc. **90**, 2638 (1968); G. L. SCHMIR. J. Am. Chem. Soc. **90**, 3478 (1968); R. K. CHATURVEDI and G. L. SCHMIR. J. Am. Chem. Soc. **90**, 4413 (1968); T. C. PLETCHER, S. KOEHLER, and E. H. CORDES. J. Am. Chem. Soc. **90**, 7072 (1968); T. OKUYAMA and G. L. SCHMIR. J. Am. Chem. Soc. **94**, 8805 (1972); T. OKUYAMA, T. C. PLETCHER, D. J. SAHN, and G. L. SCHMIR. J. Am. Chem. Soc. **95**, 1253 (1973); T. OKUYAMA, D. J. SAHN, and G. L. SCHMIR. J. Am. Chem. Soc. **95**, 2345 (1973).
8. M. EIGEN. Angew. Chem. Int. Ed. Engl. **3**, 1 (1964).
9. P. ALLEN and J. GINOS. J. Org. Chem. **28**, 2759 (1963).
10. A. I. MEYERS and N. NAZARENKO. J. Am. Chem. Soc. **94**, 3243 (1972).
11. P. DESLONGCHAMPS and C. MOREAU. Can. J. Chem. **49**, 2465 (1971); P. DESLONGCHAMPS, C. MOREAU, D. FRÉHEL, and P. ATLANI. Can. J. Chem. **50**, 3402 (1972); P. DESLONGCHAMPS, P. ATLANI, D. FRÉHEL, A. MALAVAL, and C. MOREAU. Can. J. Chem. **52**, 3651 (1974); P. DESLONGCHAMPS, C. MOREAU, D. FRÉHEL, and R. CHÊNEVERT. Can. J. Chem. **53**, 1204 (1975).
12. H. HANACK. *In* Conformation theory Vol. 3. *Edited by* A. T. Blomquist. Academic Press, New York and London. 1965. p. 116.
13. E. L. ELIEL and H. HAUBENSTOCK. J. Org. Chem. **26**, 3504 (1961).
14. R. HUISGEN and H. OTT. Tetrahedron, **6**, 253 (1959).
15. R. U. LEMIEUX. Pure Appl. Chem. **25**, 527 (1971); H. BOOTH and R. U. LEMIEUX. Can. J. Chem. **49**, 777 (1971); E. L. ELIEL. Angew. Chem. **84**, 779 (1972) and Angew. Chem. Int. Ed. Engl. **11**, 739 (1972).
16. H. MEERWEIN. Org. Synth. **46**, 113, 120 (1966).
17. P. DESLONGCHAMPS, U. O. CHERIYAN, and D. R. PATTERSON. Can. J. Chem. **53**, 1682 (1975).
18. W. SCHNEIDER, H. MOEHRLE, V. WEDE, and E. KAEMERER. Arch. Pharm. (Weinheim), **300**, 540 (1967).

Can. J. Chem. Downloaded from www.nrcresearchpress.com by 210.87.254.105 on 09/05/12
For personal use only.

Erratum: Bicyclooctanone Rearrangement, [3.2.1] → [3.3.0], via β-Enolization. Evidence for γ-Enolization in Bicyclo[3.3.0]octan-2-one

A. L. JOHNSON, N. O. PETERSEN, M. B. RAMPERSAD, AND J. B. STOTHERS
Department of Chemistry, University of Western Ontario, London, Ontario N6A 3K7
Received June 19, 1975
(Ref.: Can. J. Chem. **52**, 4143 (1974))

The second author should be N. O. Petersen and not as given immediately following the title of this communication. In the Author Index to the volume, this author appears incorrectly as an author entry under the spelling N. O. Peterson.

Erratum: Substituted 5-Allyl-9-oxobenzomorphans. Versatile Intermediates for Investigations in the Field of Analgesics and Narcotic Antagonists. Part 1

IVO MONKOVIĆ
Bristol Laboratories of Canada, 100 Industrial Boulevard, Candiac, P.Q. J5R 1J1
Received June 19, 1975
(Ref.: Can. J. Chem. **53**, 1189 (1975))

The structures **III** and **V** appeared erroneous inadvertently. The correct structures are:

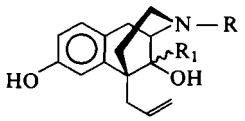

III

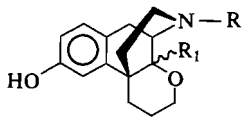

V

Reference 6 should be added to the end of the first paragraph.

Erratum: ^{13}C Nuclear Magnetic Resonance Studies. Part 48. ^{13}C Spectra of a Variety of Bicyclic Ketones

S. H. GROVER, D. H. MARR, J. B. STOTHERS, AND C. T. TAN
Department of Chemistry, University of Western Ontario, London, Ontario N6A 3K7
Received June 19, 1975
(Ref.: Can. J. Chem. **53**, 1351 (1975))

In the second page of Table 1 (p. 1355) the blank space in the column headed C-3 should contain the number 216.3.

Can. J. Chem. Downloaded from www.nrcresearchpress.com by 210.87.254.42 on 09/05/12
For personal use only.

Can. J. Chem. Downloaded from www.nrcresearchpress.com by 210.87.254.5 on 09/05/12
For personal use only.

Canadian Journal of Chemistry

Published by
THE NATIONAL RESEARCH COUNCIL OF CANADA

Journal canadien de chimie

Publié par
LE CONSEIL NATIONAL DE RECHERCHES DU CANADA

Volume 53 Number 19 October 1, 1975

Volume 53 numéro 19 1 octobre 1975

The Equilibrium Constant for the Formation of $Al_2(OH)_2^{4+}$ in Aqueous Solutions[1,2]

R. C. TURNER[3]

Soil Research Institute, Agriculture Canada, Ottawa, Canada K1A 0C6

Received April 16, 1975

R. C. TURNER. Can. J. Chem. **53**, 2811 (1975).

The equilibrium constant for the formation of the aluminum hydroxy dimer, $Al_2(OH)_2^{4+}$, was calculated from measured values of p*H* and the concentrations of the dimer and trivalent aluminum in aqueous solutions at 25 °C. The concentrations of $Al_2(OH)_2^{4+}$ was determined by a method based on its rate of reaction with an 8-hydroxyquinoline – sodium acetate solution. Experiments were made with various concentrations of aluminum and different ionic strengths. With an ionic strength of 0.06, the equilibrium constant was $10^{-7.42}$ and increased with decreasing ionic strength. The negative log of the equilibrium constant when the ionic strength approaches zero was estimated to be 6.95 ± 0.05.

R. C. TURNER. Can. J. Chem. **53**, 2811 (1975).

On a calculé la constante d'équilibre pour la formation du dimère alumino-hydroxy, $Al_2(OH)_2^{4+}$ à partir des valeurs mesurées du p*H* et des concentrations de dimère et d'aluminium trivalent dans des solutions aqueuses à 25 °C. On a déterminé les concentrations de $Al_2(OH)_2^{4+}$ par une méthode basée sur son taux de réaction avec une solution d'hydroxy-8 quinoléine et d'acétate de sodium. On a fait des expériences à différentes concentrations d'aluminium et différentes forces ioniques. A une force ionique de 0.06, la constante d'équilibre est de $10^{-7.42}$ et cette valeur augmente au fur et à mesure que la force ionique diminue. On estime à 6.95 ± 0.05 la valeur du logarithme négatif de la constante d'équilibre quand la force ionique approche zéro.

[Traduit par le journal]

There is considerable variation in the published values for the equilibrium constant for the formation of the aluminum hydroxy dimer, $Al_2(OH)_2^{4+}$. The largest value, $10^{-6.27}$ with ionic strength μ approaching zero, found by Kubota (1) was calculated from p*H* values after making the NaOH/Al mole ratio 0.25. Faucherre (2), using the slope of p*H* *vs.* dilution, calculated values of $10^{-8.06}$ and $10^{-8.24}$ for μ equal to 0.12 and 0.06 respectively. Greenwald and Fong (3) reported a value of $10^{-7.45}$ as μ approaches zero at 30 °C, derived from the slope of p*H* *vs.* amount of acid added at the p*H* of a pure $AlCl_3$ solution. Kenttamaa (4) using the slope of p*H* *vs.* amount of base added arrived at a value of $10^{-7.55}$ with μ between 0.048 and 0.03. Aveston (5) used ultracentrifugation and acidity measurements to calculate a value of $10^{-7.07}$ (μ = 1). Mesmer and Baes (6) reported $10^{-7.45}$ at 25 °C in 1 *M* KCl. None of these values were calculated from direct measurements of the concentration of $Al_2(OH)_2^{4+}$ in solution. In the work reported here an attempt was made to measure the concentration of the dimer in solution and from this to calculate the equilibrium constant for its formation.

It has been shown (7) that it is possible to differentiate between mononuclear and poly-

[1]Contribution No. 541.

[2]This paper is dedicated to Professor C. A. Winkler of McGill University on the occasion of his sixty-fifth birthday by one of his former students.

[3]Retired.

Can. J. Chem. Downloaded from www.nrcresearchpress.com by 210.87.254.5 on 09/05/12
For personal use only.

nuclear hydroxyaluminum cations by using an 8-quinolinolate extraction technique. Turner and Sulaiman (8) showed that the polynuclears reacted with a standard 8-quinolinol – sodium acetate solution via a pseudo first order process with a specific rate constant of 0.16 min^{-1} at 26 °C. It was observed in subsequent work, however, that with very low mole ratios of NaOH to total aluminum in the solution the reaction was first order with the usual rate constant after the first 2 min but during the first 2 min it was much faster. An investigation of this anomaly led to a method for determining the concentration of $Al_2(OH)_2^{4+}$ by a kinetic technique.

Experimental

The concentrations used were approximately 10^{-2}, 10^{-3}, 5×10^{-4}, and 10^{-4} *M* $AlCl_3$ all adjusted to an ionic strength of 0.06 with NaCl. The latter three concentrations were also used with μ equal to that imposed by the aluminum salt, and $Al(ClO_4)_3$ as well as $AlCl_3$ was used at 10^{-2} *M*. Reagent grade sodium hydroxide, at concentrations 10 times that of the Al salt solution, was added dropwise slowly, while the solutions were stirred vigorously with a magnetic stirrer. The NaOH/Al mole ratio was 0.116 in all cases. After the addition of the base, the solutions were aged at 25 °C with gentle agitation for one month before the measurements were made. The p*H* of the solutions were then measured with an expanded scale p*H* meter and the rate of reaction studies were done.

Rate of reaction studies were made by placing 10 ml of chloroform in a dry separatory funnel to which was then added the appropriate volume of the test solution. Two and one-half millilitres of 8-quinolinol stock solution (10 gm 8-quinolinol dissolved in 25 ml of glacial acetic acid and diluted to 1000 ml) was mixed with H_2O and 2.5 ml of *N* NaOAc added; the amount of H_2O used was such that the total volume was 25 ml less the volume of the test solution added to the chloroform. The 8-quinolinol–NaOAc solution was then added to the chloroform plus test solution in the separatory funnel and shaken vigorously by hand for 10 s. The two liquids were allowed to separate and the chloroform layer drained off through the drainage tube which contained a dry cotton plug to remove H_2O. The concentration of Al in the chloroform was determined by the depth of color of the Al–quinolinolate complex. Because the reactions are essentially stopped immediately shaking in the separatory funnel begins, the Al in the chloroform layer was considered to be that which reacted immediately. The chloroform extraction was repeated except that this time the test solution was placed in a dry separatory funnel. The 8-quinolinol–NaOAc solution was added and the combined solutions were allowed to react with gentle agitation for the desired length of time. Chloroform (10 ml) was then added followed by vigorous shaking and the chloroform layer was drawn off as before. The lengths of time of reaction were ½, 1, 2, 15, and 30 min. The above was replicated 10 times for each concentration and ionic strength.

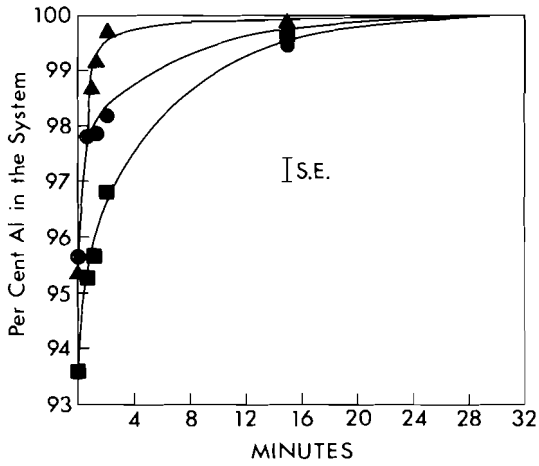

FIG. 1. Percent of the total aluminum in the system measured after increasing lengths of time of reaction. Each point is the mean of 10 replicates. The smooth curves were calculated from [2]. S.E.: standard error of the means, ▲, 10^{-2} *M*; ●, 10^{-3} *M*; ■, 10^{-4} *M*; ionic strength 0.06.

Results and Discussion

Figure 1 shows the mean of 10 determinations for each of three concentrations, 10^{-2}, 10^{-3}, and 10^{-4} *M* with $\mu = 0.06$, as the percent of the aluminum in the solutions measured after the different lengths of time of reaction. The smooth curves were calculated from [2]. When the concentration was 10^{-2} *M* practically all of the Al in the solution, 99.5%, was measured after only 2 min reaction, whereas with the 10^{-3} and 10^{-4} *M* solutions 98.3 and 96.4%, respectively, were measured. It should also be noted that, because the NaOH/Al mole ratio was very small, most of the Al was measured at zero time of reaction, causing the large standard error of the means shown in the figure. The standard error was the same on a percent basis for the three concentrations. This also indicates why it was necessary to use ten replicates rather than the usual two or three and to apply statistics in the interpretation of the data.

Assuming a first order process, a first approximation to the specific rate constant, k_1, for the very fast reaction was estimated from the results at ½ min reaction time with 10^{-2} *M* $AlCl_3$; *i.e.*, as near zero time as possible with the Al concentration at which the very fast one represented most of the reaction (Fig. 1). The mean of k_1's found for the 10 replicates was 3.1 min^{-1}. From this result and published data (8), the least

TABLE 1. Means of fraction represented by the fast reaction calculated from different lengths of time of reaction

No.*	Total [Al] M	Ionic strength	a at time = ½ min	a at time = 1 min	a at time = 2 min	Mean of means
1	0.91×10^{-4}	0.0006	0.280 ± 0.032†	0.258 ± 0.029†	0.229 ± 0.029†	0.225 ± 0.023†
2	4.7×10^{-4}	0.003	0.553 ± 0.058	0.543 ± 0.044	0.606 ± 0.042	0.562 ± 0.042
3	0.94×10^{-3}	0.006	0.713 ± 0.025	0.669 ± 0.025	0.683 ± 0.037	0.689 ± 0.026
4	0.92×10^{-4}	0.06	0.227 ± 0.030	0.196 ± 0.042	0.239 ± 0.030	0.221 ± 0.029
5	4.7×10^{-4}	0.06	0.482 ± 0.038	0.463 ± 0.055	0.448 ± 0.056	0.464 ± 0.046
6	0.94×10^{-3}	0.06	0.511 ± 0.049	0.430 ± 0.066	0.413 ± 0.048	0.451 ± 0.046
7	0.95×10^{-2}	0.06	0.929 ± 0.141	0.884 ± 0.064	1.056 ± 0.210	0.956 ± 0.102
8‡	1.01×10^{-2}	0.06	0.832 ± 0.075	0.798 ± 0.100	0.955 ± 0.121	0.859 ± 0.073

*Number of experiment. For comparison with other tables.
†Standard errors.
‡$Al(ClO_4)_3$. The others are $AlCl_3$.

number of reactions possible is two, with specific rate constants of 3.1 and 0.16 min^{-1}.

The slower reaction represents reaction with the polynuclear cations (8) which have an OH/Al mole ratio of approximately 2.5 (5, 9, 10).[4] Assuming these two reactions, the fraction of Al remaining to react, R, at any time t is

$$[1] \qquad R = ae^{-3.1t} + (1 - a)e^{-0.16t}$$

where a is the fraction of aluminum in the reacting material represented by the fast reaction and $(1 - a)$ that represented by the slower one. The values of a were calculated by means of [1] at $t = \frac{1}{2}$, 1, and 2 min for 10 replicates for each of 10^{-2} M $AlCl_3$ and $Al(ClO_4)$ and 20 replicates for 10^{-3} M $AlCl_3$ ($\mu = 0.06$). The means of a for the three reaction times for each replicate were then used to recalculate k_1 at ½ min reaction for the 40 replicates. The mean of these 40 gave a second approximation for k_1 equal to 3.6 min^{-1}. A third approximation was not different from the second.

Equation 1 was changed to

$$[2] \qquad R = ae^{-3.6t} + (1 - a)e^{-0.16t}$$

and a was calculated at $t = \frac{1}{2}$, 1, and 2 min for each of the replicates for all concentrations and ionic strengths. The means for a and their standard errors from these calculations are presented in Table 1. An analysis of variance showed that there was no difference even at $P_{0.50}$ in the values due to the length of time of reaction used in the calculations. The results strongly support the hypothesis that [2] represents the reactions occurring. Furthermore, the fraction represented by the fast reaction was greatest for the highest concentrations and least for the lowest concentration when the ionic strength was 0.06 and was generally higher for the lower ionic strengths at the same concentration. Although this does not prove that the fast reaction represented reaction with the dimer $Al_2(OH)_2^{4+}$, the results are at least in accordance with the hypothesis.

Assuming that the fast reaction was in fact reaction with $Al_2(OH)_2^{4+}$ and the slower one the reaction with the polynuclear cations (8), it was possible to calculate the concentrations of the dimer for each replicate of each experiment at reaction times of ½, 1, and 2 min. The means of the replicates and their standard errors calculated from the results for the three reaction times are presented in Table 2. The differences between the means for the different lengths of time of reaction were not significant at $P_{0.20}$ level, except in one case out of the 24 possible comparisons. Consequently, the means of the values calculated for the three lengths of time of reaction were used to calculate a value for K_{2c} for each replicate in each experiment, where

$$[3] \qquad K_{2c} = \frac{[Al_2(OH)_2^{4+}](H^+)^2}{[Al^{3+}]^2}$$

and the square brackets and parenthesis denote concentrations and activities respectively.

It was necessary to know the concentration of Al^{3+} before K_{2c} could be calculated. The values from zero time of reaction with 8-quinolinol are not represented entirely by Al^{3+}. As a first approximation, it was assumed that

$$[4] \qquad [Al_0] = [Al^{3+}] + [AlOH^{2+}]$$

[4]Also, L. B. Sillen, "Hydrolytic Aqueous Species," lecture, Houston, Texas, November, 1962.

Can. J. Chem. Downloaded from www.nrcresearchpress.com by 210.87.254.5 on 09/05/12
For personal use only.

TABLE 2. Means of 10 replicates for $Al_2(OH)_2^{4+}$ concentrations calculated from different lengths of time of reaction

	Concentration (M) at time =		
No.*	½ min	1 min	2 min
1	$9.85 \pm 1.08\dagger \times 10^{-7}$	$9.26 \pm 1.20\dagger \times 10^{-7}$	$8.19 \pm 1.15\dagger \times 10^{-7}$
2	$6.48 \pm 0.91 \times 10^{-6}$	$6.66 \pm 0.76 \times 10^{-6}$	$7.25 \pm 0.71 \times 10^{-6}$
3	$1.68 \pm 0.12 \times 10^{-5}$	$1.64 \pm 0.15 \times 10^{-5}$	$1.50 \pm 0.14 \times 10^{-5}$
4	$6.78 \pm 1.00 \times 10^{-7}$	$5.92 \pm 1.34 \times 10^{-7}$	$7.16 \pm 1.09 \times 10^{-7}$
5	$4.69 \pm 0.59 \times 10^{-6}$	$4.26 \pm 0.35 \times 10^{-6}$	$4.05 \pm 0.41 \times 10^{-6}$
6	$1.05 \pm 0.18 \times 10^{-5}$	$0.86 \pm 0.13 \times 10^{-5}$	$0.70 \pm 0.14 \times 10^{-5}$
7	$1.91 \pm 0.30 \times 10^{-4}$	$1.96 \pm 0.29 \times 10^{-4}$	$2.06 \pm 0.32 \times 10^{-4}$
8‡	$1.64 \pm 0.16 \times 10^{-4}$	$1.62 \pm 0.22 \times 10^{-4}$	$1.87 \pm 0.21 \times 10^{-4}$

*Number of experiment. For comparison with other tables.
†Standard errors.
‡$Al(ClO_4)_3$. The others are $AlCl_3$.

TABLE 3. Means of 10 replicates for pK_{1c}, pK_{3c}, and pK_{4c} for four concentrations and three ionic strengths

No.*	Total [Al] (M)	Ionic strength	pK_{1c} per f.w. $AlOH^{2+}$	pK_{3c} per f.w. Al_2OH^{5+}	pK_{4c} per f.w. $Al_{13}(OH)_{32}^{7+}$
1	0.91×10^{-4}	0.0006	$5.17 \pm 0.02\dagger$	—	$100.7 \pm 0.1\dagger$
2	4.7×10^{-4}	0.003	5.13 ± 0.02	—	100.9 ± 0.1
3	0.94×10^{-3}	0.006	5.16 ± 0.02	—	101.2 ± 0.1
4	0.92×10^{-4}	0.06	5.26 ± 0.02	—	103.8 ± 0.2
5	4.7×10^{-4}	0.06	5.21 ± 0.05	—	103.1 ± 0.1
6	0.94×10^{-3}	0.06	5.28 ± 0.02	—	103.4 ± 0.1
7	0.95×10^{-2}	0.06	—	$2.96 \pm 0.36\dagger$	—
8‡	1.01×10^{-2}	0.06	—	3.30 ± 0.16	—

*Number of experiment. For comparison with other tables.
†Standard errors.
‡$Al(ClO_4)_3$. The others are $AlCl_3$.

where $[Al_0]$ is the total concentration of Al measured at zero time of reaction. Using $10^{-5.00}$ as the thermodynamic hydrolysis constant for $AlOH^{2+}$ (11, 12), it was possible to calculate the concentration of $AlOH^{2+}$ and therefore the concentration of Al^{3+} from the measured $[Al_0]$. The Al^{3+} concentrations calculated in this way were used to calculate the pK_{2c}'s and the results were essentially the same as those reported in Table 3. It was observed, however, that only about 65% of the base added could be accounted for with the 10^{-2} M Al concentrations.

According to the assumptions used so far, the total OH in the system is represented by the equation

$$[5] \quad [B] + [H^+] = [AlOH^{2+}] + 2[Al_2(OH)_2^{4+}] + 2.5[Al_p]$$

where B represents base added and $[Al_p]$ is the concentration of Al in the polynuclear cations. As stated above, only about 65% of the base added could be accounted for when [5] was used for the 10^{-2} M Al concentrations with either $AlCl_3$ or $Al(ClO_4)_3$. As the concentration of Al was decreased with μ maintained at 0.06, this discrepancy decreased and essentially disappeared with the 10^{-4} M concentration. It appeared, therefore, that there was some other aluminum hydroxy species that became appreciable in amount, and was measured at zero time of reaction, at the higher Al concentrations only. The only conceivable product was Al_2OH^{5+}. It was decided, therefore, to calculate K_{1c} for $AlOH^{2+}$ from the results for the lowest Al concentration, 10^{-4} M, with μ equal to 0.06, where

$$[6] \quad K_{1c} = \frac{[AlOH^{2+}](H^+)}{[Al^{3+}]}$$

assuming at this low Al concentration that Al_2OH^{5+} could be ignored. The concentration of $AlOH^{2+}$ was calculated by means of [5] and then [4] was used to calculate the concentration of Al^{3+}. The mean value for pK_{1c} from the ten replicates with 10^{-4} M $AlCl_3$ and μ equal to 0.06 was 5.26 with a standard error of 0.02.

Can. J. Chem. Downloaded from www.nrcresearchpress.com by 210.87.254.5 on 09/05/12
For personal use only.

TABLE 4. Means of 10 replicates for Al^{3+} and $Al_2(OH)_2^{4+}$ concentrations and pK_{2c}

No.*	pH	Ionic strength	$[Al^{3+}]$ (M)	$[Al_2(OH)_2^{4+}]$ (M)	pK_{2c} per f.w. $Al_2(OH)_2^{4+}$	
1	4.65	0.0006	$6.45 \pm 0.06\dagger \times 10^{-5}$	$9.09 \pm 0.94\dagger \times 10^{-7}$	$6.98 \pm 0.05\dagger$	6.96§
2	4.35	0.003	$3.82 \pm 0.03 \times 10^{-4}$	$6.81 \pm 0.74 \times 10^{-6}$	7.05 ± 0.06	7.03
3	4.24	0.006	$7.87 \pm 0.04 \times 10^{-4}$	$1.61 \pm 0.13 \times 10^{-5}$	7.06 ± 0.05	7.07
4	4.76	0.06	$6.55 \pm 0.05 \times 10^{-5}$	$6.63 \pm 1.00 \times 10^{-7}$	7.32 ± 0.06	7.34
5	4.42	0.06	$3.83 \pm 0.04 \times 10^{-4}$	$4.33 \pm 0.29 \times 10^{-6}$	7.38 ± 0.04	7.36
6	4.31	0.06	$7.90 \pm 0.04 \times 10^{-4}$	$0.93 \pm 0.13 \times 10^{-5}$	7.49 ± 0.07	7.45
7	3.95	0.06	$7.91 \pm 0.08 \times 10^{-3}$	$1.98 \pm 0.25 \times 10^{-4}$	7.45 ± 0.06	7.40
8‡	3.92	0.06	$8.51 \pm 0.16 \times 10^{-3}$	$1.71 \pm 0.15 \times 10^{-4}$	7.48 ± 0.05	7.45

*Number of experiment. For comparison with other tables.
†Standard errors.
‡$Al(ClO_4)_3$. The others are $AlCl_3$.
§Calculated from the means.

The concentrations of Al^{3+}, $AlOH^{2+}$, and Al_2OH^{5+} for each of the replicates of the 10^{-2} M $AlCl_3$ and $Al(ClO_4)_3$ experiments were calculated, using [6] with K_{1c} equal to $10^{-5.26}$ and [7] and [8], shown below.

$$[7] \quad [Al_0] = [Al^{3+}] + [AlOH^{2+}] + 2[Al_2OH^{5+}]$$

$$[8] \quad [B] + [H^+] = [AlOH^{2+}] + [Al_2OH^{5+}] + 2[Al_2(OH)_2^{4+}] + 2.5[Al_p]$$

The value of K_{3c} was then calculated for each replicate, where

$$[9] \qquad K_{3c} = \frac{[Al_2OH^{5+}](H^+)}{[Al^{3+}]^2}$$

The difference between the means of pK_{3c} for the two salts, $AlCl_3$ and $Al(ClO_4)_3$, was not significant at the $P_{0.20}$ level, the overall mean being 3.1 (Table 3).

The value of pK_{1c} was then calculated, using pK_{3c} equal to 3.1, for the 10^{-3} and 5×10^{-4} M solutions with μ equal to 0.06. The difference between the means for the two Al concentrations was not significant at the $P_{0.20}$ level, the overall mean for pK_{1c} being 5.25 (Table 3). Introducing K_{3c} into the calculations for the 10^{-4} M solutions had no effect on the calculated value for K_{1c}. Thus the mean value for pK_{1c} for all concentrations of Al with μ equal to 0.06 was 5.25 with a standard error of 0.02. The mean values for pK_{1c} for all the Al concentrations and ionic strengths are shown in Table 3. The values for K_{1c} for the different ionic strengths are in general agreement with published results (1, 11, 12) arrived at by different techniques. This is rather convincing evidence that the assumptions concerning the various products used in the above are correct. As a further test of the assumptions, the equilibrium constant for one of the formulaes proposed for the polynuclears, and for which an equilibrium constant was reported, was calculated for all of the replicates where this was possible.

It was suggested by Aveston (5) that the most probable formula for the polynuclear cations is $Al_{13}(OH)_{32}^{7+}$ with pK_{4c} equal to 104.5 at an ionic strength of 1.0, where

$$[10] \qquad K_{4c} = \frac{[Al_{13}(OH)_{32}^{7+}](H^+)^{32}}{[Al^{3+}]^{13}}$$

Using this formula the mean value for K_{4c} with μ equal to 0.06 was $10^{-103.4}$, with higher values for the lower ionic strengths, the highest value being $10^{-100.7}$ for the lowest ionic strength (Table 3). These values are in general agreement with that found by Aveston, which was arrived at by entirely different methods. Thus all of the experimental evidence supports the interpretation regarding the three hydroxyaluminum species, $AlOH^{2+}$, Al_2OH^{5+}, and the polynuclear cations in addition to the dimer, $Al_2(OH)_2^{4+}$, which will be dealt with now.

The concentration of Al^{3+} for each replicate was calculated with pK_{1c} equal to 5.26 and pK_{3c} equal to 3.1 for the 10^{-2} M Al concentrations and for 10^{-3} and 5×10^{-4} M Al concentrations with μ equal to 0.06, *i.e.* using [6], [7], and [9]. Introducing K_{3c} into the calculations for the 10^{-4} M solutions at μ equal to 0.06 had no effect whatever. At the lower ionic strengths, [4], [5], and [6] were used, *i.e.*, K_{3c} was ignored because no value for it could be obtained and the values for K_{1c} and K_{4c} were not out of line, indicating that K_{3c} had little effect. The mean values of Al^{3+} and $Al_2(OH)_2^{4+}$ concentrations are presented in Table 4. The value of K_{2c} was calculated for each replicate. The mean values for

Can. J. Chem. Downloaded from www.nrcresearchpress.com by 210.87.254.5 on 09/05/12
For personal use only.

TABLE 5. Summary of calculated values for the equilibrium constant for $Al_2(OH)_2^{4+}$ as μ approaches zero

A_1	A_2	pK_0	Slope*	Standard deviation of slope
3.0	4.0	6.92	1.79	0.11
2.47	4.0	6.94	1.27	0.13
2.0	4.0	6.95	0.97	0.10
3.0	5.9	6.94	1.03	0.12
2.47	5.0	6.94	0.97	0.10
2.0	3.9	6.95	0.99	0.11
2.0	3.9	6.96†	0.96†	0.10†

*Linear regression coefficient of pK_{2c} on $pf(\mu)$.
†Calculated from the results of each individual replicate. All others calculated from the means of the 10 replicates for each concentration and ionic strength.

pK_{2c} (Table 4) were relatively independent of Al concentration providing the ionic strength was kept constant at 0.06; none of the differences between the different concentrations were significant at the $P_{0.05}$ level. The mean of all the replicates for μ equals 0.06 was 7.42 with a standard error of 0.04. With the lower ionic strengths, pK_{2c} was significantly lower. Thus the assumption that the fast reaction involved the dimer and not some other hydrolysis product is in fact consistent with the experimental results. Further support for the assumption was that no other single species would give a K_{2c} value that was independent of concentration at constant ionic strength and show higher values when the ionic strength was decreased at a given concentration.

The pK_{2c}'s can be calculated from the mean values for the concentrations of Al^{3+} and $Al_2(OH)_2^{4+}$ shown in Table 4 for each concentration and ionic strength rather than for the individual replicates. The values calculated in this way, shown in the last column of Table 4, are essentially the same as the means of the individual replicates shown in next to the last column.

An approximation of the value for pK_{2c} as μ approaches zero can be made using the Debye-Hückel equation

$$[11] \qquad -\log f_1 = \frac{0.5 z_i^2 \mu^{1/2}}{1 + A_i \mu^{1/2}}$$

where z_i is the charge on the ith ion, f_i its activity coefficient, and A_i is a constant for a given ion species, the magnitude of which depends on the distance of closest approach between the ions. Using [11] and K_0 for K_{2c} as μ approaches zero, A_1 for Al^{3+}, and A_2 for $Al_2(OH)_2^{4+}$, it follows that

$$[12] \qquad pK_0 = pK_{2c} - pf(\mu)$$

where

$$[13] \quad pf(\mu) = \frac{\mu^{1/2} + (9A_2 - 8A_1)\mu}{1 + (A_1 + A_2)\mu^{1/2} + A_1 A_2 \mu}$$

The problem is to assign values to A_1 and A_2. An approximation to [11], suggested by Kielland (13), is to replace A_i with z_i. This gives A_1 a value of 3 and A_2 a value of 4. Kubota (1) however, used 2.47 for A_1 and Greenwald and Fong (3) claimed that it should be assigned the value 2. It is possible to estimate the value of A_2 for any given value of A_1 from the pK_{2c}'s in Table 4. Thus there are a number of possibilities which are summarized, along with the results obtained for each possibility, in Table 5.

From the results in Table 5, it is obvious that Kielland's approximation (14), A_1 and A_2 equal to 3 and 4 respectively, gave the regression coefficient of pK_{2c} on $pf(\mu)$ too much greater than unity to be in accordance with [12]. All of the other combinations of A_1 and A_2, with the possible exception of 2.47 and 4.0, gave regression coefficients very near unity, and pK_2 calculated for $pf(\mu)$ equals zero for these combinations varied from 6.94 and 6.96. The results in Table 5, except those designated †, were calculated using the means of the 10 replicates in each case. The values designated † were obtained by using each individual pK_{2c} for all replicates in order to get a fair estimate of the standard deviation of the calculated regression coefficients. From the last four pK_0's in Table 5 and the standard deviation designated † the value for pK_0 was estimated to be 6.95 ± 0.05.

Can. J. Chem. Downloaded from www.nrcresearchpress.com by 210.87.254.5 on 09/05/12
For personal use only.

1. J. KUBOTA. Ph.D. Thesis. University of Wisconsin, Madison, Wisconsin. 1956. University Microfilms, Ann Arbor, Michigan. No. 16 183.
2. J. FAUCHERRE. C.R. **227**, 1367 (1948).
3. E. GREENWALD and DODD-WIND FONG. J. Phys. Chem. **73**, 650 (1969).
4. J. KENTTAMAA. Ann. Acad. Sci. Fenn. Ser. A2. **67**, 39 (1955).
5. J. AVESTON. J. Chem. Soc. 4438 (1965).
6. R. E. MESMER and C. F. BAES. Inorg. Chem. **10**, 2290 (1971).
7. T. OKURA, K. GOTO, and T. YOTUYANAGI. Anal. Chem. **34**, 581 (1962).
8. R. C. TURNER and W. SULAIMAN. Can. J. Chem. **49**, 1683 (1971).
9. C. BROSSET, B. BIEDERMANN, and L. G. SILLEN. Acta Chem. Scand. **8**, 1917, (1959).
10. E. MATIJEVIĆ, K. G. MATHOI, R. H. OTTEWILL, and M. KERKER. J. Phys. Chem. **65**, 826 (1961).
11. R. K. SCHOFIELD and A. W. TAYLOR. J. Chem. Soc. 4445 (1954).
12. C. R. FRINK and M. PEECH. Inorg. Chem. **2**, 473 (1963).
13. J. KIELLAND. J. Am. Chem. Soc. **59**, 1675 (1937).

Can. J. Chem. Downloaded from www.nrcresearchpress.com by 210.87.254.5 on 09/05/12
For personal use only.

Reductive Cleavage of Acetals and Ketals by Borane. Part II. The Kinetics of the Reaction[1,2]

HENRY I. BOLKER AND BRUCE I. FLEMING

Pulp and Paper Research Institute of Canada, and Department of Chemistry, McGill University, Montreal, Quebec H3C 3GI

Received March 21, 1975

HENRY I. BOLKER and BRUCE I. FLEMING. Can. J. Chem. **53**, 2818 (1975).

The reductive cleavage of acetals with borane in tetrahydrofuran was found to be first order in acetal and close to third order in borane. The high order in borane may be due to the participation of three BH_3 units in the transition state with subsequent formation of a $B_2H_7^-$ ion. All the hydrogen atoms of borane are available for the reduction of excess acetal at 30 °C.

HENRY I. BOLKER et BRUCE I. FLEMING. Can. J. Chem. **53**, 2818 (1975).

On a trouvé que la scission réductrice des acétals par le borane dans le tétrahydrofuranne est du premier ordre en acétal et près d'ordre trois en borane. L'ordre élevé en borane pourrait être dû à la participation de trois unités de BH_3 dans l'état de transition avec une formation subséquente d'un ion $B_2H_7^-$. A 30 °C, tous les atomes d'hydrogène du borane sont disponibles pour la réduction d'un excès d'acétal.

[Traduit par le journal]

In a previous publication (1) we discussed the possibility of complex borohydride formation during the cleavage of acetals by borane in tetrahydrofuran (THF). We now present evidence to support this hypothesis.

Two acetals, one simple (benzaldehyde dimethylacetal) and one cyclic (2-phenyl-1,3-dioxolane), were chosen to exemplify the kinetics of the reaction between acetals and borane in THF. In the procedure used for benzaldehyde dimethylacetal, standard dilutions of borane taken from a stock solution (1.15 *M*) were made with dry THF. When the solution had equilibrated in a constant temperature bath for a few minutes, sufficient acetal was added to bring the concentration to 0.025 *M*. The ratio of borane to acetal was made as high as possible to achieve pseudo first-order conditions, for which rate equation [1] is simplified to [2].

$$[1] \qquad \frac{d[\text{Product}]}{dt} = k[\text{Acetal}]^m[BH_3]^n$$

$$[2] \qquad \frac{d[\text{Product}]}{dt} = k_{obsvd}[\text{Acetal}]^m$$

$$[3] \qquad k_{obsvd} = \frac{1}{t}\log_e \frac{A}{A - x}$$

$$[4] \qquad k_{obsvd} = k[BH_3]^n$$

After fixed time intervals samples of the reaction mixture were removed, quenched by addition of aqueous sodium carbonate, and the organic material was analyzed by gas liquid chromatography (g.l.c.). Figure 1 shows the results obtained, plotted according to the integrated first-order equation [3] where A is the initial concentration of acetal and x is the product concentration at time t.

The majority of the experimental points lie very close to straight lines of zero intercept and we may conclude that the reduction is first order in acetal. Towards the end of the reaction the plots exhibit a slight tendency to zero order.

The slopes of the pseudo first-order graphs yielded the rate constants k_{obsvd}. The dramatic effect of reducing the borane concentration can be seen from the values of k_{obsvd} and the half-life periods shown in Table 1. A log–log plot of k_{obsvd} *vs.* borane concentration yielded a straight line graph of slope 2.9.[3] This is the value of n (eq. 4). The intercept of the graph yielded a k value of 5.4×10^{-2} min^{-1} mol$^{-2.9}$.

[1]Taken from the Ph.D. Thesis of B. I. Fleming, McGill University, Montreal, Quebec, 1974.

[2]This paper is dedicated to Professor C. A. Winkler of McGill University on the occasion of his sixty-fifth birthday by one of his colleagues (H.I.B.).

[3]A slope of 2.91 was calculated by the least-squares method; standard error around the fitted line = 0.058.

Can. J. Chem. Downloaded from www.nrcresearchpress.com by 210.87.254.105 on 09/05/12
For personal use only.

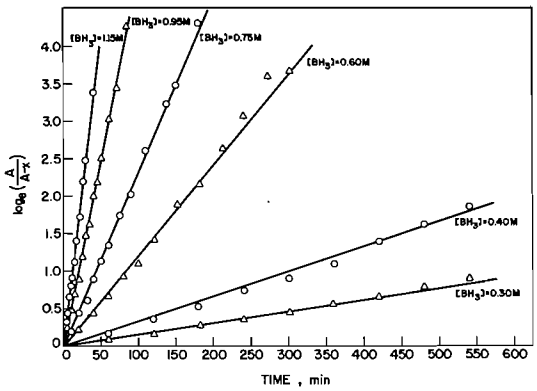

FIG. 1. Pseudo first-order plot for the reaction of benzaldehyde dimethylacetal with borane in THF at 17 °C.

TABLE 1. Rates of reduction of 0.025 *M* benzaldehyde dimethylacetal by borane in THF at 17 °C

[Borane] (*M*)	Half-life (min)	k_{obsvd} (min^{-1})	k (min^{-1} $mol^{-2.9}$)
1.15	9	0.079	5.7×10^{-2}
0.95	14	0.049	5.7×10^{-2}
0.75	30	0.023	5.3×10^{-2}
0.60	57	0.012	5.3×10^{-2}
0.40	200	0.0035	5.0×10^{-2}
0.30	400	0.0017	5.7×10^{-2}

The values for the rate constant k given in Table 1 were calculated from [4] using $n = 2.9$.

Thus, within error limits, the reductive cleavage of benzaldehyde dimethylacetal appeared to be third order in borane. Such a high order in borane was unexpected and further experiments were therefore initiated to check the observation. This time a fresh batch of borane in THF and a different acetal, 2-phenyl-1,3-dioxolane, were employed. After cleavage and hydrolysis, this acetal yields an alcohol which shows a slightly tailing peak in the gas chromatogram and thus causes some difficulty in analyzing very small amounts of product. It was therefore necessary to work with higher (0.208 *M*) concentrations of acetal. Since the borane was no longer in large excess, pseudo first-order conditions did not obtain; therefore, the initial reaction rate was used to determine the order of reaction. Table 2 shows the initial rates over the region zero to 0.5 mmol of product formed (5% of the total reaction). A plot of $\log_e$ (initial rate) *vs.* $\log_e$ [BH_3] yielded a straight line of slope 2.8.[4] The slope agrees well with that found for benzaldehyde dimethylacetal.

TABLE 2. Rates of reduction of 0.208 *M* 2-phenyl-1,3-dioxolane by borane in THF at 0 °C

[Borane] (*M*)	Time taken to form 0.5 mmol product, Δt (min)	Initial rate, dx/dt* (mmol/min)
1.15†	6	0.085
0.95	10	0.052
0.75	19	0.026
0.60	33	0.015
0.40	117	0.0043
0.30	243	0.0020

*Over the range 0–0.5 mmol, $\Delta x/\Delta t$ is assumed equal to dx/dt.
†The nominal concentration of the stock solution from which accurate dilutions were made.

Some of these experiments were repeated with redistilled cyclic acetal and a third batch of borane in THF. The results gave, within error limits, the same slope (2.73, with standard error of 0.12).

One possible interpretation of the high observed order in borane is that in some way three BH_3 units participate in the transition state (eq. 5). Such a situation would certainly lead

[5] 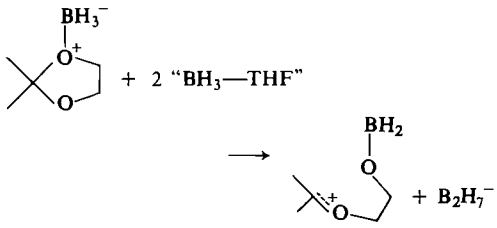

to borane species of high stability: the alkoxyborane being stabilized by pπ–pπ double bonding, and $B_2H_7^-$ being more stable than BH_4^- when an excess of borane is present (2–4). Since BH_4^- reduces borane to $B_2H_7^-$ in ether solvents (5*a*), it would not be surprising if the more powerful hydride donor $ROBH_3^-$,[5] which tends to form as the C—O acetal bond cleaves (eq. 6), is likewise capable of reducing borane species.

Transition states involving the concatenation of several borane units are probably not uncom-

[4]Calculated slope; 2.80, standard error; 0.045.
[5]Alkoxyboranes have resonance contributions which reduce their Lewis acidities compared to BH_3 (see ref. 5*b*). Consequently alkoxyborohydride should be a better hydride donor than BH_4^-.

Can. J. Chem. Downloaded from www.nrcresearchpress.com by 210.87.254.105 on 09/05/12
For personal use only.

TABLE 3. The reaction of borane* with excess acetal† at 30 °C

Time (min)	2 ml-aliquots: H_2 evolved (mmol)	2 ml-aliquots: H_3BO_3 found (mmol)	Borane, empirical formula	Hydride available for reduction (mmol)	Reduction product found‡ (mmol)
Prior to addition of acetal	3.7	1.4	$BH_{2.7}$	33	0
0§	—	—	$BH_{2.5}$	30	0
20	2.3	1.4	$BH_{1.6}$	20	12
40	1.1	1.4	$BH_{0.8}$	10	17
80	0.62	1.3	$BH_{0.5}$	6	22
160	0.22	1.4	$BH_{0.16}$	2	26
1115	0	1.4	BH_0	0	30

*12.2 mmol of "$BH_{2.7}$" in 10 ml of THF.
†53 mmol of benzaldehyde dimethylacetal.
‡$PhCH_2OMe$ as analyzed by gas chromatography.
§When the reagents were mixed, 3.1 mmol of H_2 was evolved, possibly because of moisture in the system, thus diminishing the hydride available for reduction.

[6] 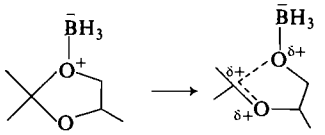

mon. For example, the hydride exchange between $B_2H_7^-$ and B_2H_6, known from n.m.r. observations to be rapid in ether solvents at room temperature (6), presumably passes through such a transition state. Also analogous is the proposed mechanism for the formation of certain polyhedral borane anions (7), which involves sequential addition of borane units to an adduct formed from a base and borane.

The nature of the reacting species shown as "BH_3—THF" in [5] is open to speculation. Three possible candidates are B_2H_6, H_3B—H—BH_2·THF and BH_3·THF; these species are all likely to be in equilibrium in THF solvent. The first two could be directly attacked by $ROBH_3^-$ to yield $ROBH_2$ and $B_2H_7^-$, whereas BH_3·THF could give the same products after two sequential additions to $ROBH_3^-$.

An unexpectedly high order was found once before for a borane reduction: Klein and Dunkelblum (8) observed that the reduction of carbonyl groups was $\frac{3}{2}$ order in "B_2H_6" (THF solution), showing this reduction to be much more complex than the originally proposed hydride transfer by a single borane unit (*5b*).

The Reaction of Borane with Excess Acetal

In this experiment the tables were turned: an excess of acetal, not borane, was employed. Thus, from the yield of reduced product it is possible to determine whether all three hydrogens of borane are available for acetal reduction.[6] The results (Table 3) revealed that for every available hydrogen atom initially present in the borane solution, one molecule of acetal was reduced to ether after 18 h at 30 °C. Consequently, under these conditions, all three hydrogens of borane are available for acetal reduction.

Selectivity in Borane Reductions

In ref. 5, page 250, Brown states: "....carboxylic acid and aldehyde groups possess reactivities that would be competitive with the hydroboration reaction. Fortunately....aldehyde groups can be protected as the acetals." It is clear from the work presented here and in the previous article (1) that this protection will not be complete under all experimental conditions. However, it should generally be easy to effect selective hydroborations on molecules possessing both olefinic double bonds and acetal groups provided that low temperatures are employed and an excess of borane is avoided. The rate of hydroboration is immeasurably fast even at temperatures below zero, whereas cyclic acetal cleavage requires hours at 30–50 °C for completion. Selectivity could be further improved by using dilute THF solutions, since acetal reduction is close to third order in borane and hydroboration of olefins is first order in diborane (8).

Descriptions of such selective reductions are to be found in the literature. For example, Lehmann (10) has been successful in the hydro-

[6]Brown and Korytnyk (9) have shown that the third hydrogen of borane reacts very slowly with ketones and nitriles.

Can. J. Chem. Downloaded from www.nrcresearchpress.com by 210.87.254.105 on 09/05/12
For personal use only.

Can. J. Chem. Downloaded from www.nrcresearchpress.com by 210.87.254.105 on 09/05/12
For personal use only.

boration of carbohydrate derivatives having a double bond and isopropylidene groups. He employed a slight excess of borane for 2 h at room temperature. Likewise hydroboration of unsaturated steroids has been accomplished when ketal groups were present in the molecule (11). Complications may arise however, if the acetal group is a substituent on the double bond, see, for example, ref. 13.

Carboxylic acid groups are also extremely reactive to borane (5, 9) and selective reduction in presence of acetals should present no problem. However, no generalizations can be made for more slowly reacting groups such as nitriles, epoxides and esters. For these compounds, selective reduction in the presence of acetals will depend on the particular structures concerned.

Experimental

Kinetic Studies of the Reaction between Excess Borane and Acetals

A solution of borane was diluted to the required concentration with dry tetrahydrofuran[7] (THF) and placed in a constant temperature bath, and the acetal (10 mmol) was added. The solution in the reaction flask was stirred with a magnetic stirrer and was protected by a calcium chloride tube. Aliquots (0.2 ml) removed after fixed times were dropped into saturated aqueous sodium carbonate (0.2 ml) to quench the reaction.

Gas–liquid chromatographic analysis of the samples so obtained was effected on a 120-cm SE-30 column at 110 °C (see ref. 1 for details). The g.l.c. system gave a slightly greater molar response for the acetal than for its cleavage product. From injections of equimolar amounts of acetal and its reduction product, response factors of 0.94 for benzyl methyl ether and 0.98 for 2-(benzyloxy)ethanol (relative to the corresponding acetal) were obtained.

As the mole percentage of product formed, calculated from the ratio of the product peak area to the total area, was independent of the size of the injected sample, the results were highly replicable. Four injections of the same sample (Fig. 1, $[BH_3] = 0.6\ M$ curve, 60 min sample) indicated the following amounts of benzyl methyl ether: 4.93, 4.81, 4.69, and 4.93 (mmol), a relative standard deviation of $\pm 2.4\%$.

The Reaction of Borane with Excess Benzaldehyde Dimethylacetal

Borane (12.2 mmol) in THF (10 ml) was added to an excess of the acetal (53 mmol) in a flask attached to a gas burette. There was an exothermic reaction and some hydrogen (3.1 mmol) was evolved. As the reaction proceeded, aliquots (2 ml) were withdrawn by syringe through a septum for (*i*) analysis of boron and hydrogen content[8] and (*ii*) g.l.c. analysis of the organic fraction. The results are shown in Table 3. Analysis of the standard borane solution prior to reaction showed it to have the empirical formula $BH_{2.7}$. Therefore the borane taken initially contained 33.0 mmol of hydride. Discounting the initial hydrogen evolution, 30 mmol of hydride are theoretically available for reduction. After 18 h at 30 °C, a sample of reaction mixture evolved no hydrogen gas upon addition of water and the yield of benzyl methyl ether was found to be 30 mmol. Therefore all the hydrogens of borane were consumed in the reduction of excess acetal at 30 °C.

The source of the acetals and of their reduction products was given in ref. 1.

The authors are indebted to Dr. I. S. Butler for help and advice during preparation of the manuscript and to the National Research Council of Canada for financial support.

1. B. Fleming and H. I. Bolker. Can. J. Chem. **52**, 888 (1974).
2. H. C. Brown, P. F. Stehle, and P. A. Tierney. J. Am. Chem. Soc. **79**, 2020 (1957).
3. H. C. Brown and P. A. Tierney. J. Am. Chem. Soc. **80**, 1552 (1958).
4. H. Beall and C. H. Bushweller. Chem. Rev. **73**, 465 (1973).
5. H. C. Brown. Hydroboration. W. A. Benjamin, New York. 1962. (*a*) p. 87; (*b*) p. 246.
6. D. F. Gaines. Inorg. Chem. **2**, 523 (1963).
7. H. C. Miller, N. E. Miller, and E. L. Muetterties. Inorg. Chem. **3**, 1456 (1964).
8. J. Klein and E. Dunkelblum. Tetrahedron, **23**, 205 (1967).
9. H. C. Brown and W. Korytnyk. J. Am. Chem. Soc. **82**, 3866 (1960).
10. J. Lehmann. Carbohydr. Res. **2**, 1 (1966).
11. M. Nussim and F. Sondheimer. Chem. Ind. (London), 400 (1960).
12. P. Kohn, L. M. Lerner, A. Chan, S. D. Ginocchio, and C. A. Zitrin. Carbohydr. Res. **7**, 21 (1968).
13. G. Zweifel, A. Horng, and J. E. Plamondon. J. Am. Chem. Soc. **96**, 316 (1974).

[7]Fisher reagent grade, dried over sodium, distilled, and stored in the dark over clean sodium wire.

[8]Hydrogen was estimated as H_2 by adding water to the borane solution in a flask attached to a gas burette. Mannitol in excess was then added to the boric acid residue in the flask and the mixture was titrated with potassium hydroxide to phenolphthalein end point (12).

Free Ion Yields and Electron Ranges in X Irradiated Simple Liquids: Unusual Behavior in Carbon Dioxide and Carbon Disulfide[1]

TERANCE E. M. SAMBROOK AND GORDON R. FREEMAN

Chemistry Department, University of Alberta, Edmonton, Alberta T6G 2G2

Received April 22, 1975

TERANCE E. M. SAMBROOK and GORDON R. FREEMAN. Can. J. Chem. **53**, 2822 (1975).

The radiolysis free ion yields G_{fi}^0 and electron penetration ranges b_{GP} in the liquids carbon dioxide and carbon disulfide are much larger than would be predicted by extrapolation from earlier studies of unsaturated hydrocarbons. In the isoelectronic, nonpolar compounds carbon dioxide and propadiene at 212 ± 4 K $G_{fi}^0 = 0.19$ and 0.022, respectively, with $b_{GP} = 116$ and 37 Å. In carbon disulfide $G_{fi}^0 = 0.44 \pm 0.02$, independent of temperature over the range 169 to 354 K; the electron penetration range appears to increase with decreasing temperature in this liquid. In the unsymmetrical, polar compound carbonyl sulfide, $G_{fi}^0 = 0.089$ and $b_{GP} =$ 37 Å at 214 K; the behavior is similar to that in ethers.

TERANCE E. M. SAMBROOK et GORDON R. FREEMAN. Can. J. Chem. **53**, 2822 (1975).

Les rendements en ions libres, G_{fi}^0, et les parcours des électrons, b_{GP}, dans le dioxyde et le disulfure de carbone liquides sont beaucoup plus importants qu'on aurait pu le prévoir en extrapolant les études antérieures sur les hydrocarbures non saturés. Pour le dioxyde de carbone et le propadiène qui sont non polaires et isoélectroniques, on trouve à 212 ± 4 K: $G_{fi}^0 = 0.19$ et 0.022, respectivement, avec un parcours b_{GP} de 116 et 37 Å. Pour le disulfure de carbone, $G_{fi}^0 = 0.44 \pm 0.02$ est indépendant de la température depuis 169 jusqu'à 354 K; le parcours électronique dans ce liquide semble augmenter lorsque la température diminue. Pour l'oxysulfure de carbone, composé non symétrique et polaire, $G_{fi}^0 = 0.089$ et $b_{GP} = 37$ Å à 214 K. Son comportement est semblable à celui des éthers.

Introduction

In studies of the behavior of electrons in liquids, one of the subjects of major interest is processes that govern energy transfer from low energy ($\lesssim 1$ eV) electrons to the molecules of the liquid. Preliminary information about the processes is obtained from the relative penetration ranges of secondary electrons into X irradiated liquids (1, 2). The ranges are inversely related to the rates of energy loss of the electrons.

Penetration ranges in liquid hydrocarbons depend on the molecular structure. In saturated compounds the ranges increase with increasing degree of sphericity of the molecules (1, 2). If the molecules are large, the range correlates with the average sphericity of groups containing two carbon–carbon bonds in series (3). In unsaturated hydrocarbons the correlation between molecular structure and electron penetration is obscure (4). For example, the presence of dipole moments up to 0.6 D seem to have negligible influence, whereas an electron–dipole interaction might have been expected to reduce the electron penetration range.

Most organic molecules have relatively complex structures. In the present work a series of three simple triatomic compounds containing π bonds were studied. They are carbon dioxide (O=C=O), carbonyl sulfide (O=C=S), and carbon disulfide (S=C=S), all comprised of linear molecules.

Penetration ranges are estimated from the radiolysis free ion yields in the liquids (1–4).

Experimental

Materials

The three compounds were obtained from Matheson Co.

Spectral grade carbon disulfide was dried over either anhydrous magnesium carbonate or anhydrous calcium chloride, fractionally distilled (retaining the central portion), then thoroughly degassed by distillation under vacuum.

Carbonyl sulfide was purified by bubbling the gas through two concentrated potassium hydroxide solutions, then two solutions of lead acetate. The gas was then passed through a 30 cm column of potassium hydroxide pellets and eight 40 cm columns of Drierite, then condensed in a cold trap. The compound was thoroughly degassed by successive distillations into cold traps from which gases noncondensable at 77 K were continuously removed by the vacuum system.

Carbon dioxide gas was passed through a 50 cm column of Drierite. Gases noncondensable at 77 K were

[1]Assisted financially by the National Research Council of Canada.

Can. J. Chem. Downloaded from www.nrcresearchpress.com by 210.87.254.5 on 09/05/12
For personal use only.

Can. J. Chem. Downloaded from www.nrcresearchpress.com by 210.87.254.5 on 09/05/12
For personal use only.

removed by successive sublimations of the carbon dioxide into traps that were continuously pumped on.

Apparatus and Techniques

The equipment and methods of measurement were the same as those described elsewhere (4). Briefly, a 1 μs pulse of 1.7 MeV X-rays delivered 3×10^{10} eV/g to the sample. The free ion yield $G_{fi}{}^{E}$ was measured by the charge clearing technique, normally using applied electric field strengths E in the range 1–60 kV/cm.

The measured yields were extrapolated to zero applied field strength by using [1] (4, 5).

$$[1] \qquad G_{fi}{}^{E} = G_{tot} \int_0^\infty F(y)\phi(y,E)\,dy$$

where G_{tot} is the total number of ion–electron pairs generated per 100 eV absorbed by the liquid, $F(y)dy$ is the fraction of thermalized electron–ion pairs that have initial intrapair separation distances between y and $y + dy$, and $\phi(y,E)$ is the probability that a pair with a given separation distance y will escape geminate neutralization (become free ions) in the presence of an applied field E.

$$[2] \quad \phi(y,E) = e^{-r/y}\left(1 + e^{-\beta y}\sum_{n=1}^{\infty}\frac{(\beta y)^n}{(n+1)!} \times \sum_{j=0}^{n-1}(n-j)\frac{(r/y)^{j+1}}{(j+1)!}\right)$$

where $r = \xi^2/\varepsilon kT$, $\xi = 4.803 \times 10^{-10}$ e.s.u., ε is the dielectric constant of the liquid, k is Boltzmann's constant, T is the absolute temperature, and $\beta = (\xi E/300kT)$.

The distribution function $F(y)$ was taken to have the form [3], which has been designated YGP (4).

$$[3] \quad F(y) = 0.96(4y^2/\pi^{1/2}b_{GP}{}^3)\exp(-y^2/b_{GP}{}^2) \qquad y < 2.4b_{GP}$$

$$F(y) = 0.96[(4y^2/\pi^{1/2}b_{GP}{}^3)\exp(-y^2/b_{GP}{}^2) + 0.5b_{GP}{}^2/y^3] \qquad y > 2.4b_{GP}$$

where 0.96 is a normalization factor and b_{GP} is the adjustable dispersion parameter. The latter is also the most probable value of y. At $E = 0$, [1] reduces to

$$[4] \quad G_{fi}{}^{0} = G_{tot} \int_0^\infty \exp(-\xi^2/\varepsilon kTy)F(y)\,dy$$

Physical Properties of the Liquids

The densities d (6–8) were obtained by interpolation or extrapolation of data in the references quoted. The dielectric constant of carbon disulfide was similarly obtained from ref. 6*b*. That for carbon dioxide was calculated from the Clausius–Mosotti equation and the molar polarization listed for the liquid in ref. 9. The dielectric constant of carbonyl sulfide was measured at 0.4 and 4 kHz, using a capacitance bridge (Electroscientific Inc.) and a standard capacitor (General Radio 1422 CD). Values are recorded in Table 1.

The total ionization yields G_{tot} in the liquid are not known. As a first approximation they were taken equal to the gas phase yields, which are 3.0 ion pairs/100 eV in carbon dioxide (10–12), 3.8 in carbon disulfide[2] (13), and ~3.5 in carbonyl sulfide. The last value was interpolated with the aid of the ionization potentials of the three gases, which are respectively 13.8, 10.1, and 11.2 eV (14).

Results and Discussion

Free Ion Yields

The yields in the different liquids at the same temperature increase in the order OCS < OCO < SCS. Yields at 210 ± 6 K are included in Fig. 1. The difference between the yields in carbon dioxide and carbon disulfide is due mainly to the greater dielectric constant of the latter ([4] and Table 1). The yield in carbonyl sulfide is smaller than those in the other liquids in spite of the larger dielectric constant of the former. The small yield must be attributed to a small electron range y, to be discussed later.

There is relatively little effect of temperature on the yields in carbonyl sulfide over the region measured (Fig. 1). This is similar to the behavior in ethers (15). It has been attributed to the magnitude of the increase of the dielectric constant of the polar liquid with decreasing temperature; the product εT is nearly independent of temperature.

In carbon disulfide the free ion yields $G_{fi}{}^{E}$ *increase* with *decreasing* temperature (Fig. 2). This is opposite to the direction of change expected for a nonpolar liquid. The influence of temperature is relatively small at $T > 295$ K, but is marked at $T < 295$ K. The effect is attributed to unusual electron penetration ranges, discussed in the next section. Earlier estimates of $G_{fi}{}^{0}$ at 296 K (1, 16) were 30–40% smaller than the present value of 0.44 (Table 1). The discrepancy is a general one that exists between free ion yield measurements in the Brookhaven and Edmonton laboratories and is not understood (4, 5).

Electron Ranges

The values of the most probable electron ranges b_{GP} were obtained by fitting eqs. 1–3 to the experimental yields $G_{fi}{}^{E}$, and are listed in Table 1.

The range in carbon dioxide ($b_{GP} = 116$ Å) is much greater than that in the isoelectronic hydrocarbon propadiene ($b_{GP} = 37$ Å (17)), and is greater even than that in the analogous saturated hydrocarbon (propane, $b_{GP} = 84$ Å (17)). Carbon dioxide in dilute solution in either a polar (18) or nonpolar (19) solvent is an efficient

[2]Gas phase ion yield estimated from the results of J. J. Thomson.

TABLE 1. Liquid parameters, ion yields, and electron ranges

Liquid	T (K)	ε	d (g/cm^3)	G_{tot}[h]	G_{fi}[o]	b_{GP} (Å)	$b_{GP}d$ (10^{-8} g/cm^2)
O=C=O	216	1.81[c]	1.20[f]	3.0	0.19	116	139
O=C=S	185	4.5[d]	1.25[g]	3.5[i]	0.084	36	45
	214	3.9	1.21		0.089	37	44
S=C=S	169	2.95[e]	1.45[e]	3.8(2)[j]	0.44	125(191)[k]	181
	183	2.91	1.43		0.44	117(177)	168
	205	2.86	1.39		0.43	105(159)	146
	236	2.78	1.35		0.44	95(145)	128
	295	2.63	1.26		0.44	80(123)	101
	318	2.57	1.23		0.45	77(119)	95
	354	2.48	1.17		0.46	73(114)	85
$CH_3—CH_2—CH_3$[a]	205	1.85	0.612	4.1	0.102	84	52
$CH_3—CH=CH_2$[a]	214	2.07	0.625	4.0	0.031	45	28
$CH_2=C=CH_2$[b]	208	2.24	0.700	4.0	0.022	37	26
$CH_3—C\equiv CH$[b]	210	3.60	0.725	4.1	0.12	44	32

[a]Reference 17.
[b]Reference 4.
[c]Calculated from the Clausius–Mosotti equation and the liquid phase molar polarization reported in ref. 9.
[d]Present work.
[e]Reference 6.
[f]Reference 7.
[g]Reference 8.
[h]Taken equal to the gas phase value.
[i]Interpolated value.
[j]Best compromise value obtained by fitting eqs. 1–3 to the experimental results over the temperature range was $G_{tot} = 2$. The low value probably indicates that the distribution function YGP decreases too rapidly at large y.
[k]Ranges in parentheses were calculated by taking $G_{tot} = 2$.

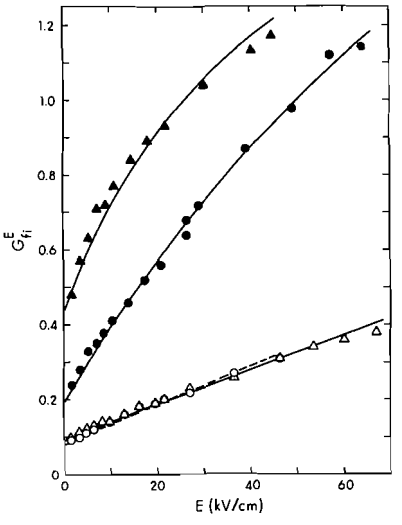

FIG. 1. Free ion yields G_{fi}^E as a function of applied electric field strength E in liquids. Carbon disulfide, ▲, 205 K. Carbon dioxide, ●, 216 K. Carbonyl sulfide: ○, 185 K; △, 214 K. The lines were calculated from eqs. 1–3, using the parameter values listed in Table 1 and $G_{tot} = 2$ in carbon disulfide. The dashed line refers to carbonyl sulfide at 185 K.

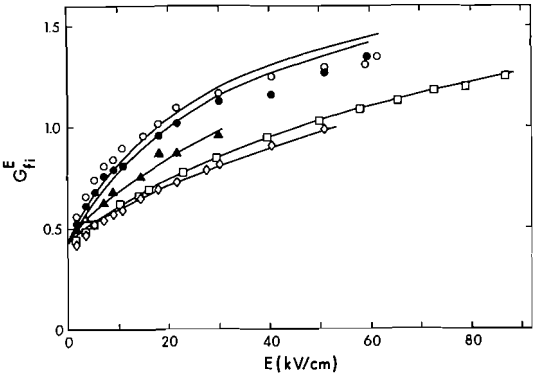

FIG. 2. Free ion yields in carbon disulfide at different temperatures: ○, 169 K; ●, 183 K; ▲, 263 K; □, 295 K; ◇, 354 K. The lines were calculated from eqs. 1–3, using the parameter values listed in Table 1 and $G_{tot} = 2$.

scavenger of electrons. One might have expected that the electron capturing property of carbon dioxide would enhance the electron energy transfer cross section of the molecule via negative ion states. The penetration range of low energy electrons into liquid carbon dioxide might therefore have been expected to be smaller than that in propane. However, the reverse is true, so the contribution of negative ion states to the electron energy transfer cross section of carbon dioxide in the liquid phase appears to be negligible.

The symmetry and degree of sphericity of carbon dioxide are greater than those of propadiene which partly rationalizes the larger electron range in the former liquid (3). However, the apparent lack of influence of the double bonds in carbon dioxide, evidenced by the ranges

Can. J. Chem. Downloaded from www.nrcresearchpress.com by 210.87.254.5 on 09/05/12
For personal use only.

Can. J. Chem. Downloaded from www.nrcresearchpress.com by 210.87.254.5 on 09/05/12
For personal use only.

falling in the order carbon dioxide > propane > propadiene (Table 1), is surprising.

Electron behavior in carbon disulfide is similar to that in carbon dioxide. Both compounds are efficient electron scavengers when present as a dilute solute in water (18), yet electron ranges in both pure liquids are large (Table 1). The high vapor pressure of liquid carbon dioxide prevented the temperature dependence of $G_{fi}{}^{E}$ being measured in that liquid. However, peculiar temperature effects were found in carbon disulfide. The *increasing* free ion yield with *decreasing* temperature displayed in Fig. 2 can only be explained by an increasing electron range with decreasing temperature (Table 1). The yield extrapolated to zero field strength, $G_{fi}{}^{0}$, is nearly independent of temperature (Table 1 and Fig. 2), which is different from the behavior in hydrocarbons (1, 3–5, 20).

The yields $G_{fi}{}^{E}$ calculated as a function of E, using eqs. 1–3 and $G_{tot} = 3.8$, agreed with the experimental results only at the highest temperature. At lower temperatures the calculated field dependence of $G_{fi}{}^{E}$ was too large. To obtain agreement at the lower temperatures, either the range distribution function $F(y)$ had to be altered to decrease less rapidly at large y, or the assumed value of G_{tot} had to be reduced. It is improbable that G_{tot} in the liquid is temperature dependent. However, it is impractical to develop a new distribution function $F(y)$ on the basis of a single compound, so the assumed value of G_{tot} was decreased to determine the magnitude of the problem. The "best fit" value of G_{tot} obtained using the distribution function [3] was ~4 at 354 K and it reduced gradually to 1.6 at 169 K. The sensitivity of the curve fitting to the assumed value of G_{tot} increased with decreasing temperature.

Yields calculated using $G_{tot} = 2.0$ are shown in Fig. 2 to demonstrate the variation of agreement or disagreement with temperature. The curves were selected by adjusting the value of b_{GP} in [3] to give the minimum average deviation from the experimental points, with the restriction that G_{tot} be held at 2.0. If the calculated curves had been fitted to the experimental yields at high field strengths, the calculated yields at low field strengths would have been too large at high temperatures and too small at low temperatures.

The simple exponential distribution function[3] (21, 22) and the exponential function with the power tail (designated YEP, 22) are also inappropriate. All decrease too rapidly at large y. Other compounds will have to be studied before distribution functions for nonhydrocarbons can be devised with confidence.

Mohler and Taylor measured the steady state X radiation induced electrical conductance of liquid carbon disulfide at field strengths up to 70 kV/cm, presumably at room temperature (13). The shape of their curve at $E > 20$ kV/cm was the same as that of the 295 K curve in Fig. 2. At lower fields the Mohler and Taylor curve fell more rapidly than the present one, due to greater ion loss by second order neutralization in the steady state system. The early authors (13) used Jaffe's theory of columnar ionization (23) to extrapolate the ion current to infinite field strength. Then using a comparison of the ionization produced in the liquid with that produced in air they estimated $W(CS_2$ liquid) = 24 eV/ion pair, or G_{tot} (liquid) = 4.2 ionizations/100 eV. This yield seems reasonable by comparison with the gas phase value G_{tot} (gas) = 3.8 (13), but the treatment was inaccurate on two counts: (*a*) the columnar ionization model does not apply to X or γ irradiated systems; (*b*) extrapolation of the high field current-voltage curve to zero field strength and comparison of that value with the Jaffe extrapolation to infinite field strength gives $G_{fi}{}^{0}/G_{tot} = 0.3$, which would indicate $G_{fi}{}^{0} = 1.2$ from their treatment. That value of $G_{fi}{}^{0}$ is 3–5 times greater than the present and the Brookhaven (1, 16) determinations.

It must be concluded that electrons behave differently in carbon disulfide than in liquids previously studied. Other similar systems should be sought.

The range in carbonyl sulfide is much smaller than those in carbon dioxide and carbon disulfide (Table 1). The smaller range ties in with more efficient electron de-energization by molecules that lack symmetry and have a large dipole moment (Table 2). However, it should be noted that there is no detailed correlation between electron ranges in different liquids and the molecular dipole moments or anisotropies of polarizability (Table 2). The inverse correlation between range and anisotropy of polarizability that was noted for simple alkanes (3) is not a general property.

Dipole moment and polarizability relate to long range electrostatic interactions, so these do not govern low energy electron energy loss pro-

[3]R. L. Platzman, 4th International Congress on Radiation Research, Evian, France, 1970, unpublished results.

TABLE 2. Density normalized ranges of electrons in liquids, and gas phase molecular dipole moments μ and anisotropies of polarizability α^a

Liquid	T (K)	$b_{GP}d^a$ (10^{-8} g/cm^2)	μ (D)[b]	α^a (Å^3)
O=C=O	216	139	0.00	2.2[c]
O=C=S	214	44	0.712	5.4[d]
S=C=S	205	146	0.00	8.6[e]
CH_3—CH_2—CH_3	205	52	0.084	0.9[f]
CH_3—CH=CH_2	214	28	0.366	2.1[f]
CH_2=C=CH_2	208	26	0.00	4.1[f]
CH_3—C≡CH	210	32	0.781	3.2[f]

[a]Table 1.
[b]Reference 24.
[c]Reference 25.
[d]Average of values for CO_2 and CS_2.
[e]Average of values from refs. 25 and 26.
[f]Estimated from bond polarizabilities in ref. 27.

cesses in liquids. The nature of the controlling short range interactions remains obscure. The peculiar temperature effect in carbon disulfide seems to be a clue. It should be sought in other liquids.

We would like to thank the personnel of the Radiation Research Center for aid with the electronics.

1. W. F. SCHMIDT and A. O. ALLEN. J. Phys. Chem. **72**, 3730 (1968).
2. P. H. TEWARI and G. R. FREEMAN. J. Chem. Phys. **49**, 4394 (1968).
3. J.-P. DODELET and G. R. FREEMAN. Can. J. Chem. **50**, 2667 (1972).
4. J.-P. DODELET, K. SHINSAKA, U. KORTSCH, and G. R. FREEMAN. J. Chem. Phys. **59**, 2376 (1973).
5. K. SHINSAKA and G. R. FREEMAN. Can. J. Chem. **52**, 3495 (1974).
6. E. W. WASHBURN. (*a*) International critical tables, Vol. 3. McGraw-Hill, New York. 1928. p. 23; (*b*) International critical tables, Vol. 6. McGraw-Hill, New York. 1929. p. 76.
7. R. R. DREISBACH. Adv. Chem. Ser. **29**, 459 (1961).
8. J. TIMMERMANS. Physico-chemical constants of pure organic compounds, Vol. 2. Elsevier, Amsterdam. 1965. p. 388.
9. H. H. UHLIG, J. G. KIRKWOOD, and F. G. KEYES. J. Chem. Phys. **1**, 155 (1933).
10. G. G. MEISELS. J. Chem. Phys. **41**, 51 (1964).
11. P. ALDER and H. K. BOTHE. Z. Naturforsch. **20**a, 1700 (1965).
12. R. COOPER and R. M. MOORING. Aust. J. Chem. **21**, 2417 (1968).
13. F. L. MOHLER and L. S. TAYLOR. J. Res. Natl. Bur. Stand. **13**, 659 (1934).
14. R. W. KISER. Introduction to mass spectrometry and its applications. Prentice-Hall, Englewood Cliffs, N.J. 1965. Appendix IV.
15. J.-P. DODELET and G. R. FREEMAN. Can. J. Chem. **53**, 1263 (1975).
16. C. CAPELLOS and A. O. ALLEN. J. Phys. Chem. **73**, 3264 (1969).
17. M. G. ROBINSON and G. R. FREEMAN. Can. J. Chem. **52**, 440 (1974).
18. S. GORDON, E. J. HART, M. S. MATHESON, J. RABANI, and J. K. THOMAS. Discuss. Faraday Soc. **36**, 193 (1963).
19. G. R. FREEMAN and E. D. STOVER. Can. J. Chem. **46**, 3235 (1968).
20. G. R. FREEMAN. J. Chem. Phys. **39**, 988 (1963).
21. G. C. ABELL and K. FUNABASHI. J. Chem. Phys. **58**, 1079 (1973).
22. J.-P. DODELET and G. R. FREEMAN. J. Chem. Phys. **60**, 4657 (1974).
23. G. JAFFÉ. Ann. Phys. **42**, 303 (1913).
24. R. D. NELSON, JR., D. R. LIDE, JR., and A. A. MARYOTT. NSRDS-NBS 10, Selected values of electric dipole moments for molecules in the gas phase. U.S. Government Printing Office, Washington, D.C. 1967.
25. LANDOLT-BÖRNSTEIN. Zahlenwerte und Funktionen, 6 Auflage, I Bd., 3 Teil. Springer-Verlag, Berlin. 1951.
26. R. J. W. LE FÈVRE. Adv. Phys. Org. Chem. **3**, 1 (1965).
27. R. J. W. LE FÈVRE. Rev. Pure Appl. Chem. **20**, 67 (1970).

Can. J. Chem. Downloaded from www.nrcresearchpress.com by 210.87.254.5 on 09/05/12
For personal use only.

Stereoselective Total Synthesis of Copa and Ylango Sesquiterpenoids: Preparation of (−)-(1*S*,4*S*,5*R*,7*R*)-1,7-Dimethyl-4-isopropylbicyclo[3.2.1]octa-6,8-dione and (+)-(1*R*,4*S*,5*S*,7*S*)-1,7-Dimethyl-4-isopropylbicyclo[3.2.1]octa-6,8-dione

EDWARD PIERS, RONALD W. BRITTON, M. BERT GERAGHTY, ROBERT J. KEZIERE, AND R. DEAN SMILLIE

Department of Chemistry, University of British Columbia, 2075 Wesbrook Place, Vancouver, British Columbia V6T 1W5

Received May 15, 1975

EDWARD PIERS, RONALD W. BRITTON, M. BERT GERAGHTY, ROBERT J. KEZIERE, and R. DEAN SMILLIE. Can. J. Chem. **53**, 2827 (1975).

The efficient, stereoselective syntheses of two diastereomeric bicyclo[3.2.1]octadiones (**23** and **24**) are described and the potential use of these materials for the synthesis of the copa (**1–5**) and the ylango (**7–11**) sesquiterpenoids, respectively, is outlined. Conversion of (+)-carvomenthone (**26**) into the corresponding *n*-butylthiomethylene derivative **28**, followed by alkylation of the latter with ethyl 2-iodopropionate, gave compound **29**. Removal of the blocking group from the latter was accompanied by ester hydrolysis and afforded keto acid **30**. An efficient intramolecular Claisen condensation of the corresponding ester **31** yielded (−)-(1*S*,4*S*,5*R*,7*R*)-1,7-dimethyl-4-isopropylbicyclo[3.2.1]octa-6,8-dione (**23**). Conversion of the known octalone **39** into the cross-conjugated keto aldehyde **41** was accomplished by standard reactions. Treatment of the latter with lithium dimethylcuprate, followed by trapping of the resultant enolate anion with acetyl chloride gave compound **42**. Oxidative ozonolysis of this material yielded the keto acid **43**. Esterification of the latter, followed by intramolecular Claisen condensation of the resulting keto ester **45**, afforded (+)-(1*R*,4*S*,5*S*,7*S*)-1,7-dimethyl-4-isopropylbicyclo[3.2.1]octa-6,8-dione (**24**).

EDWARD PIERS, RONALD W. BRITTON, M. BERT GERAGHTY, ROBERT J. KEZIERE et R. DEAN SMILLIE. Can. J. Chem. **53**, 2827 (1975).

On a décrit les synthèses efficaces et stéréosélectives des deux bicyclo[3.2.1]octanediones (**23** et **24**) et leurs usages potentiels pour la synthèse de sesquiterpenoides copa (**1–5**) et ylango (**7–11**). La conversion de la (+) carvomenthone (**26**) en dérivé butylthiométhylène correspondant (**28**) suivie d'une alkylation de ce dernier par l'iodo-2 propionate d'éthyle conduit au composé **29** qui après élimination du groupe protecteur et hydrolyse de l'ester fournit le céto-acide **30**. Une condensation de Claisen intramoléculaire et efficace effectuée sur l'ester correspondant **31** conduit à la (−) (1*S*,4*S*,5*R*,7*R*) diméthyl-1,7 isopropyl-4 bicyclo[3.2.1]octanedione-6,8 (**23**). On a transformé l'octalone connue **39** en céto-aldéhyde **41** par des techniques standards. Le traitement de **41** par du diméthylcuprate de lithium suivi par le piégeage de l'anion énolate qui en résulte par du chlorure d'acétyle conduit au composé **42** qui par ozonolyse oxydante fournit le céto-acide **43**. L'estérification de ce dernier suivie par une conduisation de Claisen intramoléculaire du céto-ester **45** conduit à la (+) (1*R*,4*S*,5*S*,7*S*) diméthyl-1,7 isopropyl-4 bicyclo[3.2.1]-octanedione-6,8 (**24**).

[Traduit par le journal]

The structurally related series of compounds (+)-copacamphor (**1**), (+)-copaborneol (**2**), (+)-copaisoborneol (**3**), (−)-copacamphene (**4**), and (−)-cyclocopacamphene (**5**) together make up part of the copa[1] group of sesquiterpenoids. In similar fashion, the structurally related substances (−)-ylangocamphor (**7**), (−)-ylangoborneol (**8**), (−)-ylangoisoborneol (**9**), (+)-sativene (**10**), and (+)-cyclosativene (**11**) together constitute part of the ylango[1] group of sesquiterpenoids. These two series of compounds can be considered as 'isoprenologs' of the well-known series of monoterpenoids camphor (**13**), borneol (**14**), isoborneol (**15**), camphene (**16**), and tricyclene (**17**) (see Chart 1).

Of the copa and ylango sesquiterpenoids listed in Chart 1, only four have as yet been isolated from naturally occurring sources. Thus, (+)-

[1]The terms 'copa' and 'ylango' have by convention been derived from the sesquiterpenoids (−)-α-copaene (**6**) (1, 2) (structurally related to **1–5**), and (+)-α-ylangene (**12**) (3) (structurally related to **7–11**). On the basis of this structural analysis and system of nomenclature, the more consistent names for sativene (**10**) and cyclosativene (**11**) would be ylangocamphene and cycloylangocamphene, respectively.

Can. J. Chem. Downloaded from www.nrcresearchpress.com by 210.87.254.105 on 09/05/12
For personal use only.

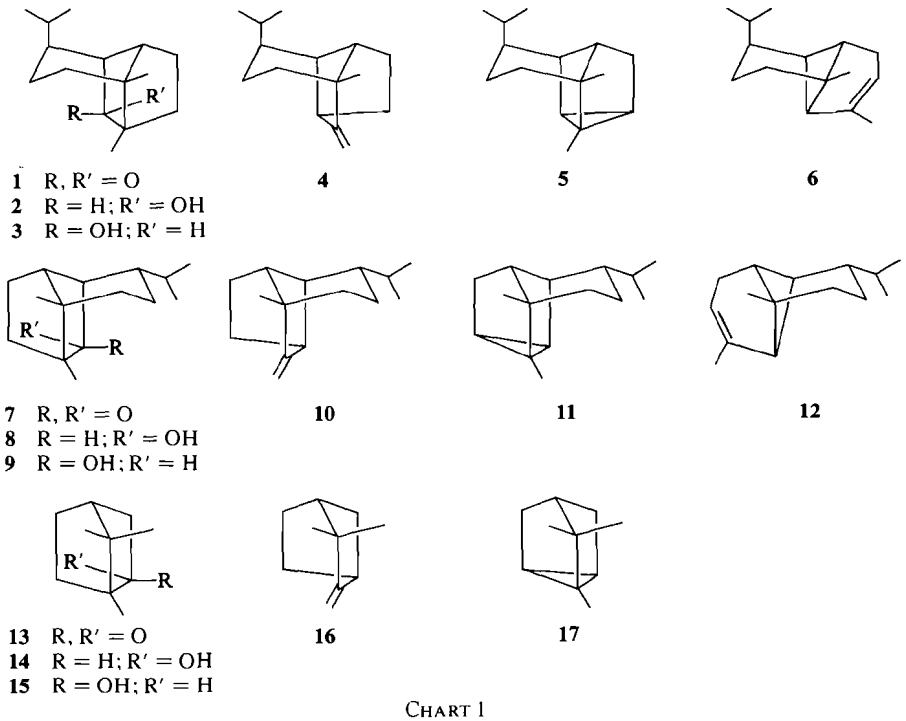

CHART 1

copaborneol (**2**) was found to be the major sesquiterpenoid alcohol occurring in the wood of *Pinus silvestris* L. and in Swedish sulfate turpentine (4–6), while several vetiver oils have been shown to contain (+)-cyclocopacamphene (enantiomer of **5**) (7). The latter has also been obtained by chemical conversion from cyclocopacamphenic acids (8). Although (+)-copacamphor (**1**), (+)-copaisoborneol (**3**), and (−)-copacamphene (**4**) have not as yet been obtained from living systems, they have been acquired by chemical transformation from (+)-copaborneol (6).

(−)-Sativene (enantiomer of **10**) has been isolated from *Helminthosporium sativum*, a fungus responsible for widespread destruction and loss of cereal crops (9). The enantiomer, (+)-sativene (**10**), as well as the structurally and configurationally related tetracyclic compound (+)-cyclosativene (**11**), have been acquired from the cortical turpentine of a number of different *Abies* species (10–12). The remaining three ylango sesquiterpenoids (**7**, **8**, and **9**) have yet to be isolated as natural products and were, in fact, unknown compounds until the completion of our synthetic work.

A careful analysis of the structure of the various copa and ylango sesquiterpenoids listed in Chart 1 reveals a number of different approaches which might be employed to carry out the stereoselective synthesis of these compounds.[2] Our own work was based upon the observation that all of these substances can, from a structural point of view, be considered as derivatives of two diastereomeric substituted bicyclo[3.2.1]octanes. For example, the copa compounds would have as the parent structure the bicyclooctane **18** and each of the specific sesquiterpenoids (+)-copacamphor, (−)-copacamphene, and (−)-cyclocopacamphene would have the two additional

[2]At the time that our work was initiated, relatively little synthetic work had been done in this area. In this connection, the very elegant synthesis of racemic sativene by McMurry (13) deserves special mention. During the time that our studies were underway, and after their completion, several reports concerning the synthesis of one or more of the copa and/or ylango sesquiterpenoids appeared. These reports involved, in each case, synthetic routes very different from those employed in our work. In summary, the following syntheses have been reported: partial synthesis of (+)-copacamphor, (+)-copaborneol, (+)-copaisoborneol (6), and (+)-sativene (9); total synthesis of (±)-sativene (13,14), (±)-cyclosativene (15,16), (±)-copacamphene (17,15*b*), (±)-copacamphor (18,14), (±)-ylangocamphor (18,14), (−)-sativene, (−)-copacamphene, (+)-ylangocamphor, and (+)-copacamphor (19).

Can. J. Chem. Downloaded from www.nrcresearchpress.com by 210.87.254.105 on 09/05/12
For personal use only.

Can. J. Chem. Downloaded from www.nrcresearchpress.com by 210.87.254.105 on 09/05/12
For personal use only.

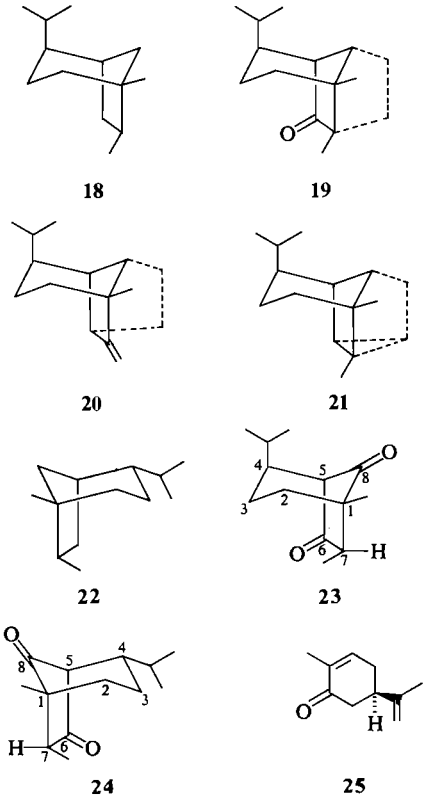

18 19 20 21 22 23 24 25

required carbon atoms attached in a different way from the one-carbon bridge to the two-carbon bridge (*cf.* **19**, **20**, and **21**). A similar analysis can be made for the ylango sesquiterpenoids, with the parent bicyclo[3.2.1]octane being **22**. Therefore, more explicitly, our synthetic plan was to attempt the stereoselective synthesis of two substituted bicyclo[3.2.1]octadiones, one (**23**) to serve as the synthetic precursor to the copa sesquiterpenoids and the other (**24**) to be employed as the starting point for the preparation of the ylango sesquiterpenoids. In each case, the carbonyl group contained in the one-carbon bridge (C-8) was to serve as a 'handle' for the introduction of the additional two carbon atoms necessary to complete the various 15-carbon skeletons. Similarly, the carbonyl group present in the two-carbon bridge (at C-6) was to be employed to effect directly a necessary mode of cyclization or to introduce appropriate functionality to allow for the necessary mode(s) of ring closure.

In this paper we report the stereoselective total synthesis of (−)-(1*S*,4*S*,5*R*,7*R*)-1,7-dimethyl-4-isopropylbicyclo[3.2.1]octa-6,8-dione (**23**) and of (+)-(1*R*,4*S*,5*S*,7*S*)-1,7-dimethyl-4-isopropylbicyclo[3.2.1]octa-6,8-dione (**24**).[3] Interestingly, the readily available monoterpenoid (−)-carvone (**25**), a substance of known absolute configuration, served as the starting material for the synthesis of both **23** and **24**. In subsequent papers (22,23) we describe the conversion of the bicyclic ketones **23** and **24** into the copa and ylango sesquiterpenoids, respectively.

Synthesis of (−)-(1S,4S,5R,7R)-1,7-Dimethyl-4-isopropylbicyclo[3.2.1]octa-6,8-dione (23) (see Scheme 1)

Conversion of (+)-carvomenthone (**26**)[4] into the corresponding *n*-butylthiomethylene derivative **28**, via the hydroxymethylene compound **27**, was accomplished in 69% overall yield by standard procedures (25). Alkylation of the blocked ketone **28**[5] with ethyl 2-iodopropionate in the presence of potassium *t*-butoxide in *t*-butyl alcohol was highly regioselective[6] and stereoselective, producing in 73% yield the alkylated product **29**.[7] Treatment of the latter with potassium hydroxide in refluxing aqueous diethylene glycol (25) concomitantly resulted in removal of the *n*-butylthiomethylene blocking group and hydrolysis of the ester functionality. Esterification (ethereal diazomethane) of the resulting crude keto acid **30** afforded in 85% overall yield (from **29**) the keto ester **31**. As might be expected, spectral and gas–liquid chromatographic analysis of this material revealed that it consisted of a mixture of two diastereomers (with respect to the chiral center in the ester-bearing side chain) in a ratio

[3]For preliminary reports regarding part of this work, see refs. 20 and 21.

[4]This compound can readily be obtained by hydrogenation of (−)-carvone (**25**); see ref. 24.

[5]Extensive experimentation on the direct alkylation of (+)-carvomenthone (**26**) with ethyl 2-halopropionates under a variety of conditions did not produce synthetically useful yields of desired product.

[6]Interestingly, alkylation of **28** with ethyl 2-bromopropionate under a variety of conditions (including potassium *t*-butoxide in *t*-butyl alcohol) consistently afforded mixtures of *O*- and *C*-alkylation products, in a ratio of approximately 1:1. It is known, however, that changing the leaving group of the alkylating agent from bromide to iodide favors, relatively speaking, *C*-alkylation. For an excellent discussion regarding the various structural and experimental factors which influence *O*- *vs.* *C*-alkylation of ambident anions, see ref. 26.

[7]A discussion of the stereochemistry of **29** and the subsequent synthetic intermediates is deferred until a later section of the paper (*vide infra*).

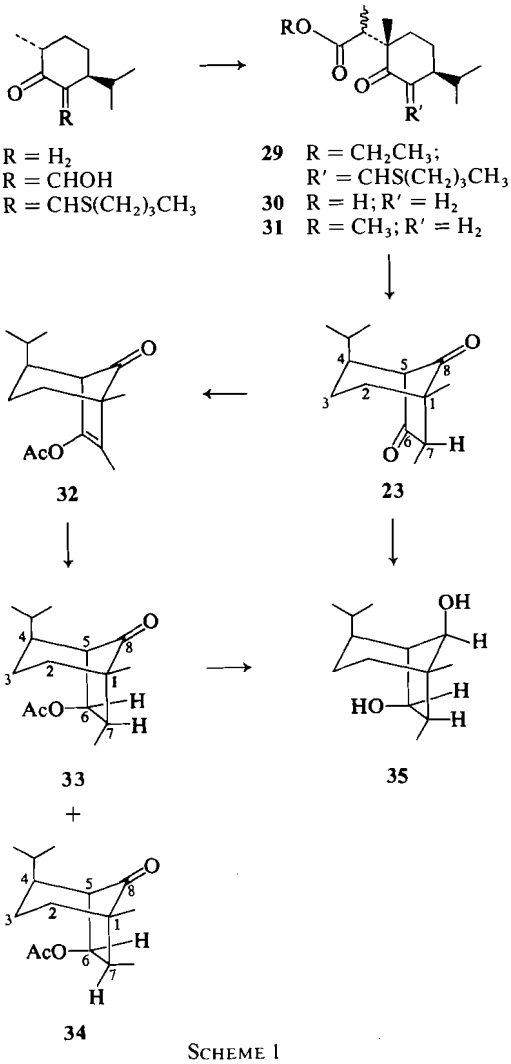

SCHEME 1

of approximately 1 : 1. However, no attempt was made to separate these epimers, since it was anticipated that this stereochemical ambiguity would disappear upon successful completion of the next synthetic step.

Conversion of the keto ester **31** into the desired bicyclic diketone **23** required an intramolecular Claisen condensation reaction. To this end, keto ester **31** was treated with sodium hydride in dimethoxyethane[8] under a variety of experimental conditions. However, only very poor yields of the desired diketone were obtained. Therefore, the use of alternative bases was investigated and it was eventually found that the desired condensation could be accomplished conveniently and efficiently by treatment of the keto ester **31** with slightly more than 2 equiv. of sodium bis(trimethylsilyl)amide (28) in refluxing dimethoxyethane for 1 h, followed by quenching the reaction mixture with aqueous acetic acid. In this manner, the desired levorotatory bicyclic diketone **23** was obtained in 90% yield as a crystalline, sharp-melting solid.

Although the success of the intramolecular Claisen condensation was very gratifying, there were at this stage of the planned synthetic sequence two stereochemical features of the condensation product (**23**) which required further investigation. Firstly, the stereochemical orientation of the secondary methyl group at C-7 was not known. Although this point was not crucial to any of the subsequent proposed syntheses, it was nevertheless of interest to us to determine whether the methyl group at C-7 was *endo* or *exo* to the bicyclooctane ring system. Secondly, and much more importantly, the stereochemistry at C-1 of compound **23** was also uncertain. This point was directly related, of course, to the question of whether or not one could predict with certainty the stereochemical outcome of the alkylation of the blocked ketone **28**, since it was at this stage of the synthetic sequence that the chiral center under discussion (C-1 of **23**) was formed. In this connection, a perusal of the chemical literature dealing with many different ketone alkylations, along with our own experiences in this area, clearly indicated that, in fact, very little certainty could be ascribed to any predictions which might be made concerning the stereochemistry of the conversion of **28** into **29**. Therefore, it was felt that independent unambiguous evidence concerning this point would have to be obtained.

The stereochemistry at C-7 in the bicyclic diketone **23** was shown as follows. First of all, this material was recovered unchanged from treatment with potassium carbonate in aqueous dioxan. However, an identical treatment with deuterium oxide in the place of water effected the incorporation of one deuterium atom (at C-7). Therefore, it was clear that we were dealing with the thermodynamically more stable epimer.

Conversion of the diketone **23** into the corresponding enol acetate **32** was accomplished in high yield by heating the former with isopropenyl

[8]For a similar type of intramolecular condensation leading to a substituted bicyclo[4.2.1]nonadione, see ref. 27.

Can. J. Chem. Downloaded from www.nrcresearchpress.com by 210.87.254.105 on 09/05/12
For personal use only.

Can. J. Chem. Downloaded from www.nrcresearchpress.com by 210.87.254.105 on 09/05/12
For personal use only.

acetate in the presence of a catalytic amount of sulfuric acid.[9] Hydrogenation of the carbon–carbon double bond of **32** would be expected to take place primarily with *cis* stereochemistry from the less hindered *exo* face of the bicyclic system, to afford predominantly the keto acetate **33**. In the event, hydrogenation of **32** over 5% palladium-on-barium sulfate in ethanol gave a very high yield (97%) of two products, in a ratio of approximately 9:1. These compounds were separated by preparative g.l.c. The spectral properties of the major product were found to be in complete accord with those expected for the keto acetate **33**. Of particular importance was the p.m.r. spectrum in which the C-6 proton adjacent to the acetoxy functionality appeared as a pair of doublets at τ 4.61. The observed coupling constants ($J_{5,6}$ = 7.0 Hz, $J_{6,7}$ = 10.0 Hz)[10] were in full agreement with structure **33**. Explicitly, molecular models clearly indicated that if the proton at C-6 had been *endo* to the bicyclic system, the coupling constant between the C-5 and C-6 protons would have been very small (dihedral angle ~ 80–90°). However, the coupling constant between the C-5 proton and a C-6 *exo* proton (as in structure **33**) was expected to be in the 6–8 Hz region (dihedral angle ~ 20–30°).[11] Similarly, the coupling constant between the C-6 and C-7 protons in **33** was expected to be quite large (dihedral angle ~ 0°), whereas $J_{6,7}$ of the epimeric compound (at C-7) would presumably be significantly smaller (dihedral angle ~ 120°).

A similar analysis of the p.m.r. spectrum of the minor hydrogenation product led to the conclusion that this material possessed structure **34**. Thus, the C-6 proton adjacent to the acetoxy group in this compound appeared as a pair of doublets at τ 5.30, with coupling constants $J_{5,6}$ = 7.0 Hz and $J_{6,7}$ = 4.0 Hz.[10] On the basis of an argument similar to that used above in the case of keto acetate **33**, these observed coupling constants were consistent only with structure **34**. Although the formation of this compound in the hydrogenation reaction was initially unexpected, its appearance as a minor product is not inconsistent with mechanistic proposals for hydrogenations (29).

Reduction of the major hydrogenation product, keto acetate **33**, with lithium aluminum hydride in refluxing ether afforded, in 92% yield, the crystalline diol **35**. The *same* diol could also be obtained by a similar reduction of the original bicyclic diketone **23**. In each of these reductions, one would expect that the ketone carbonyl group at C-8 would be reduced from the less hindered side, away from the axially oriented isopropyl group at C-4. Thus, the stereochemistry of the chiral center at C-8 in the product could be confidently assigned as shown in structure **35**. Furthermore, the p.m.r. spectrum (C-6 proton as a pair of doublets at τ 5.71, with $J_{5,6}$ = 7.0 Hz and $J_{6,7}$ = 10.5 Hz) of the latter was again in full accord with the assigned structure. Therefore, assuming that our conclusions regarding the structure of the keto acetate **33** were correct, the fact that the same diol **35** was obtained by reduction of either **33** or the diketone **23** led automatically to the conclusion that the methyl group at C-7 in the dione **23** was *endo* to the bicyclic system.

The stereochemistry at C-1 of the dione **23** was shown indirectly by an independent, unambiguous synthesis of the diastereomeric dione **24**. Not only did this synthesis supply the required information regarding the stereochemistry of **23** but it also produced the precursor (**24**) necessary for the projected syntheses of the ylango sesquiterpenoids **7–11**.

Synthesis of (+)-(1R,4S,5S,7S)-1,7-Dimethyl-4-isopropylbicyclo[3.2.1]octa-6,8-dione (24) (see Scheme 2)

It is well known that Robinson annelation of (+)-dihydrocarvone (**36**)[12] with 1-diethylamino-3-pentanone methiodide affords a mixture of products, of which the crystalline, easily isolable ketol **37** predominates (an average of ~65% isolated yield in our experiments) (31,32). For our synthetic purposes, the established *trans* configurational relationship between the isopropenyl group and the angular methyl group was of crucial importance. Hydrogenation of the ketol

[9]This transformation could also be conveniently carried out by treatment of the dione **23** with sodium bis(trimethylsilyl)amide in benzene, followed by trapping of the resultant enolate with acetyl chloride or acetic anhydride.

[10]These coupling constants were confirmed by appropriate decoupling experiments. See Experimental for details.

[11]In this connection, it should be noted that the proton adjacent to the hydroxyl group in (+)-copaisoborneol (**3**) appeared in the p.m.r. spectrum as a doublet with J = 8.0 Hz, while the corresponding proton in (+)-copaborneol (**2**) produced a broad singlet (6).

[12]This compound can readily be obtained by appropriate reduction of (−)-carvone (**25**) (30).

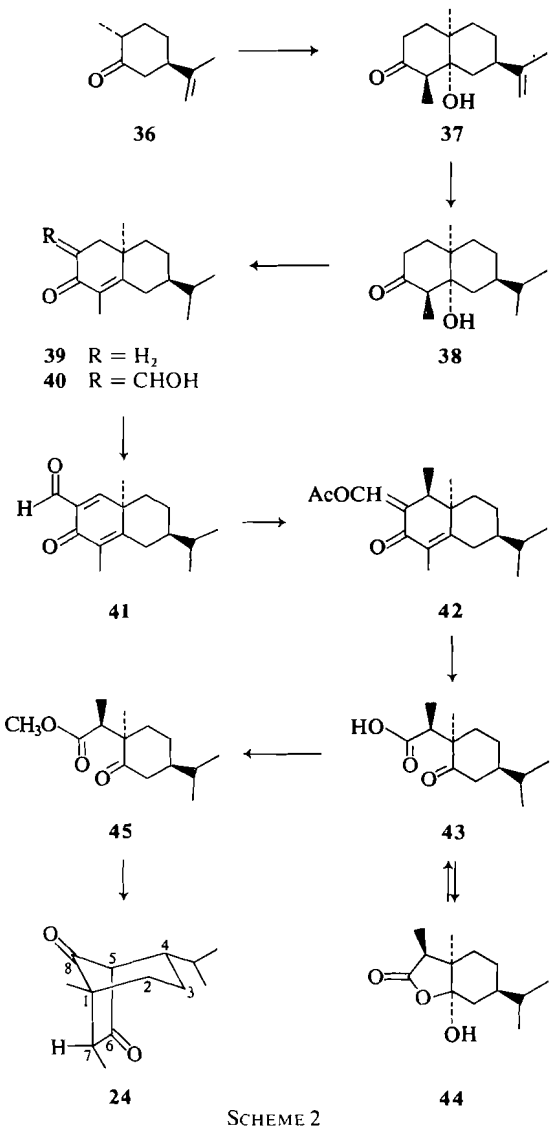

SCHEME 2

37 over palladium-on-charcoal, followed by base-promoted dehydration of the resultant product **38**, afforded in greater than 95% yield the known levorotatory octalone **39** (33).

It can readily be seen that introduction of a methyl group at C-1[13] of compound **39**, followed by oxidative cleavage of the C-2—C-3 and the C-4—C-5 bonds would result in the formation of a keto acid of known absolute configuration. In order to accomplish the first transformation (introduction of a methyl group at C-1), it was necessary to convert **39** into a compound in which the C-1 center became electrophilic. To this end, compound **39** was transformed into the hydroxymethylene derivative **40** and the latter was subjected to dehydrogenation with 2,3-dichloro-5,6-dicyanobenzoquinone (DDQ) (34) in dioxan. The resultant product, the crystalline cross-conjugated keto aldehyde **41**, was formed in 91% overall yield from **39**.[14] Treatment of compound **41** with excess lithium dimethylcuprate (37) in ether at 0 °C, followed by quenching of the resultant enolate with acetyl chloride, gave the somewhat unstable enol acetate **42**[15] in good yield. Ozonolysis of the crude material in methylene chloride at −78 to −25 °C, followed by oxidative decomposition of the resulting ozonide with hydrogen peroxide and base, afforded the crude keto acid **43**. Although the bulk of this material was used directly for the next synthetic step, a small sample crystallized on standing and could readily be recrystallized from hexane – ethyl acetate. The resulting crystalline material exhibited interesting spectral properties. The i.r. spectrum in Nujol showed strong absorption bands at 3415 (OH stretch) and at 1750 cm^{-1} (C=O stretch). On the other hand, the i.r. spectrum in chloroform exhibited a hydroxyl absorption at 3590, a broad band at 3560–2500 characteristic of a carboxylic acid, and two carbonyl absorptions at 1760 and 1705 cm^{-1}. These data clearly indicated that the keto acid **43** crystallized in the lactol form **44**, while in chloroform solution there existed an equilibrium between **43** and **44**. A careful analysis of the p.m.r. spectrum of this material in deuteriochloroform at 40 °C indicated that the ratio of the two compounds in solution was approximately 1:1.

Esterification of the crude keto acid **43** with ethereal diazomethane gave the keto ester **45** in

[13]The numbering system used here is that normally employed for eudesmane-type sesquiterpenoids.

[14]Direct dehydrogenation of **39** with DDQ produced only low yields of the corresponding cross-conjugated dienone (see ref. 35). The described sequence (octalone → hydroxymethylene derivative → cross-conjugated keto aldehyde) had been employed previously in our laboratory (36) in a related case.

[15]The stereochemistry of the newly introduced chiral center (at C-1) of this compound was not rigorously established. However, considerable literature precedent (38, 39) for this type of reaction clearly indicated that the product should have the stereochemistry as shown in **42**. In any event, this point was not crucial to the subsequent syntheses, since the stereochemical integrity of this center would be lost at a later stage of the projected synthetic sequence.

Can. J. Chem. Downloaded from www.nrcresearchpress.com by 210.87.254.105 on 09/05/12
For personal use only.

Can. J. Chem. Downloaded from www.nrcresearchpress.com by 210.87.254.105 on 09/05/12
For personal use only.

60% overall yield from the dienone aldehyde **41**. It is important to note that spectral and g.l.c. properties of the keto ester **45** clearly showed that this material was different from *both* of the epimeric keto esters **31** obtained by alkylation of blocked (+)-carvomethone (**28**). Since the stereochemistry of **45** was on firm ground, this comparison clearly established the stereochemistry of **31** and, by implication, the configuration at C-1 of the bicyclic diketone **23**. The latter point was further verified by the successful cyclization of **45** into the dione **24** (*vide infra*), which was clearly diastereomeric with the previously prepared dione **33**.

The intramolecular Claisen condensation of the keto ester **45** proved to be much more troublesome and capricious than expected on the basis of our earlier experience with keto ester **31**. Thus, subjection of the former compound **45** to condensation conditions similar to those used previously for **31** resulted in the formation of only poor yields of the desired bicyclic ketone **24**. The crude product of the reaction consisted largely of unidentified high-boiling material. At this stage, considerable effort was expended to find conditions which would provide increased yields of the dione **24**. A number of different bases (sodium hydride, sodium and lithium bis(trimethylsilyl)amide, trityllithium, tritylsodium) and/or different solvents (benzene, dimethoxyethane, tetrahydrofuran) were employed under a variety of conditions. In general, although the degree of success varied somewhat from experiment to experiment, most of the attempted reactions proved unsatisfactory. Eventually, it was found that the conditions which afforded by far the highest yield (75%) and which gave reproducible results, were the following. A benzene solution of the keto ester **45** was added over a period of 65 min to a solution of sodium bis(trimethylsilyl)amide (2.6 equiv.) in benzene kept at 79–80 °C (internal temperature). This temperature was maintained for a further 75 min and the reaction mixture was then poured into aqueous acetic acid. It was found that the choice of reaction temperature was crucial. At lower temperatures, some starting material was recovered, whereas at higher temperatures the crude product contained considerable amounts of high-boiling material. Similarly, longer reaction times also gave appreciable quantities of undistillable products.

The crystalline, dextrorotatory diketone **24** obtained from the above-described condensation reaction was, as previously mentioned, clearly diastereomeric with the dione **23** obtained earlier. Although the stereochemistry at C-7 of **24** was not rigorously demonstrated[16], it could be assigned as shown by analogy with **23**. In this connection, it should be pointed out that the p.m.r. spectra of both **23** and **24** showed that there existed, in each case, a small coupling (J = 1.5 Hz) between the protons at C-5 and C-7.[17] This similarity strongly indicated that the stereochemical relationship between the two protons was the same for both compounds.

Experimental

General[18]

Melting points, which were determined on a Kofler block, and boiling points are uncorrected. The u.v. spectra were, unless otherwise noted, measured in methanol solution on either a Cary, model 14, or a Unicam, model SP 800, spectrophotometer. Optical rotations were obtained at the sodium D line, using a Rudolph polarimeter, model 219, a Bendix ETL-NPL automatic polarimeter, type 143A, or a Perkin-Elmer model 141 automatic polarimeter. Routine i.r. spectra were recorded on a Perkin-Elmer model 710 spectrophotometer, while comparison spectra were recorded on a Perkin-Elmer model 457 spectrophotometer. Proton magnetic resonance spectra were, unless otherwise noted, taken in deuteriochloroform solution on Varian Associates spectrometers, models A-60, T-60, and/or HA-100 or XL-100. Signal positions are given in the Tiers scale, with tetramethylsilane as an internal standard; the multiplicity, integrated peak areas, and proton assignments are indicated in parentheses. High resolution mass spectrometric measurements were carried out on an AEI type MS-9 mass spectrometer. Gas–liquid chromatographic analyses were carried out on Varian Aerograph g.l.c. units, models 700 or 90-P. The following columns were employed, with the inert supporting material being, in each case, 60–80 mesh Chromosorb W (unless otherwise noted): column A (10 ft × ¼ in.), 20% SE 30; column B (10 ft × ¼ in.), 15% Ionox 330; column C (10 ft × ⅜ in.), 30% SE 30; column D (5 ft × ¼ in.), 20% SE 30; column E (10 ft × ¼ in.), 20% Carbowax 20M; column F (10 ft × ¼ in.), 10% OV-210; column G (10 ft × ¼ in.), 8% FFAP on 60–80 mesh Chromosorb G; column H (5 ft × ¼ in.), 3% SE 30; column I (10 ft × ¼ in.), 20% Apiezon J; column J (20 ft × ⅜ in.), 30% SE 30; column K (10 ft × ⅜ in.), 30% Apiezon J; column L (10 ft × ⅜ in.), 8% FFAP on 60–80

[16]Complete recovery of **24** from epimerizing reaction conditions (potassium carbonate in aqueous dioxan) clearly demonstrated that we were again dealing with the thermodynamically more stable C-7 epimer.

[17]In the case of compound **24** this was confirmed by an appropriate decoupling experiment. See Experimental for details.

[18]This general section is applicable to the two succeeding, accompanying papers (22, 23) as well as to the present paper.

Can. J. Chem. Downloaded from www.nrcresearchpress.com by 210.87.254.105 on 09/05/12
For personal use only.

mesh Chromosorb G; column M (10 ft × ¼ in.), 20% FFAP. The specific column used, along with the column temperature and carrier gas (helium) flow rate (in ml/min), are indicated in parentheses. Microanalyses were performed by Mr. P. Borda, Microanalytical Laboratory, University of British Columbia, Vancouver, B.C.

Preparation of the Hydroxymethylene Derivative ***27***

To an ice-cooled, stirred suspension of powdered sodium methoxide (81.5 g, 1.51 mol) in 300 ml of dry benzene, kept under an atmosphere of dry nitrogen, was added a solution of 77.2 g (0.502 mol) of (+)-carvomethone **26** in 300 ml of dry benzene. The resulting mixture was stirred for 10 min and then a solution of 112 g (1.51 mol) of ethyl formate in 60 ml of dry benzene was added. The mixture was warmed to room temperature and allowed to stir overnight. Water was added, the mixture was thoroughly shaken, and the layers were separated. The organic layer was extracted with two portions of 10% aqueous sodium hydroxide. The combined aqueous layer and alkaline extracts were cooled, acidified with concentrated hydrochloric acid, and thoroughly extracted with ether. The combined ethereal extracts were washed with water and brine, and dried over anhydrous magnesium sulfate. Removal of solvent, followed by distillation of the residual oil under reduced pressure, gave 75.3 g (83%) of the hydroxymethylene derivative **27** as a pale yellow oil, b.p. 89–93 °C at 1.0 Torr; n_D^{21} 1.4936; u.v. λ_{max} 291 nm (ε 6570), λ_{max} (NaOH added) 317 nm (ε 17 000); i.r. (film) ν_{max} 1730, 1701, 1629, 1582, 1453, 1360 cm^{-1}.

Preparation of the n-Butylthiomethylene Derivative ***28***

A solution of the hydroxymethylene derivative **27** (62.0 g, 0.341 mol), *n*-butanethiol (36.8 g 0.408 mol), and *p*-toluenesulfonic acid (40 mg) in 400 ml of dry benzene was refluxed in a nitrogen atmosphere under a Dean–Stark water separator overnight, at which time 6 ml of water had been collected. The cooled solution was washed with saturated aqueous sodium bicarbonate, then with water, and finally dried over anhydrous magnesium sulfate. Removal of the solvent gave an oil, which, upon distillation under reduced pressure, afforded 72.1 g (83%) of the *n*-butylthiomethylene derivative **28**, b.p. 120–126 °C at 0.2 Torr; n_D^{21} 1.5252; u.v. λ_{max} 302 nm (ε 11 700); i.r. (film) ν_{max} 1667, 1536, 1450, 1165, 799 cm^{-1}.

Anal. Calcd. for $C_{15}H_{26}OS$: C, 70.82, H, 10.30; S, 12.58. Found: C, 70.57; H, 10.42, S, 12.40.

Alkylation of the n-Butylthiomethylene Derivative ***28*** *with Ethyl 2-Iodopropionate*

The *n*-butylthiomethylene derivative **28** (101.6 g, 0.40 mol) was added to 1 l of dry *t*-butyl alcohol containing 46.0 g (0.46 mol) of potassium *t*-butoxide and the resulting solution was stirred at room temperature for 10 min and then cooled to 0 °C. Ethyl 2-iodopropionate (228 g, 1.0 mol) was added slowly and the reaction mixture was stirred at room temperature under an atmosphere of dry nitrogen overnight. Most of the solvent was removed under reduced pressure and the residue was diluted with water. The resulting mixture was extracted with ether and the organic layer was washed with water and brine, and dried over anhydrous magnesium sulfate. Removal of the solvent gave an oil, which upon distillation under reduced pressure, afforded 103.2 g (73%) of the desired alkylated product **29**, b.p. 172–180 °C at 0.8 Torr; n_D^{24} 1.5181; u.v. λ_{max} 301 nm (ε 10 300); i.r. (film) ν_{max} 1727, 1667, 1536, 1453, 1176 cm^{-1}.

Anal. Calcd. for $C_{20}H_{34}O_3S$: C, 67.76; H, 9.67; S, 9.03. Found: C, 67.74; H, 9.49; S, 9.00.

Preparation of Keto Ester ***31***

To a solution of the alkylated *n*-butylthiomethylene derivative **29** (103 g) in 450 ml of diethylene glycol was added 450 ml of 25% aqueous potassium hydroxide and the resulting solution was refluxed under nitrogen for 22 h. The reaction mixture was cooled, acidified with concentrated hydrochloric acid, and then thoroughly extracted with ether. The ethereal layer was dried over anhydrous magnesium sulfate and then concentrated. The crude acid **30** thus obtained was reacted with excess ethereal diazomethane and the excess diazomethane was destroyed by the addition of acetic acid. The ethereal layer was washed with water, a 10% sodium carbonate solution, brine, and then dried over anhydrous magnesium sulfate. Removal of the solvent followed by distillation of the residual oil gave 61.2 g (85%) of the desired keto ester **31** (epimeric mixture of diastereomers), b.p. 120–126 °C at 0.2 Torr; n_D^{21} 1.4722; i.r. (film) ν_{max} 1733, 1701, 1456, 1193 cm^{-1}; p.m.r. τ 6.34, 6.36 (s, s, 3H, methyl ester protons), 7.00, 7.13 (q, q, 1H, protons adjacent to the ester carbonyls, J = 7.5, 7.0 Hz, respectively), 8.76, 8.87 (s, s, 3H, tertiary methyls), 8.84, 8.89 (d, d, 3H, secondary methyls, J = 7.5, 7.0 Hz, respectively), 9.09 (d, 6H, isopropyl methyls, J = 6.0 Hz).

Anal. Calcd. for $C_{14}H_{24}O_3$: C, 69.96; H, 10.07. Found: C, 69.84; H, 9.90.

*(−)-(1S,4S,5R,7R)-1,7-Dimethyl-4-isopropylbicyclo-[3.2.1]octa-6,8-dione (****23****)*

To a solution of 80.6 g (0.44 mol) of sodium bis(trimethylsilyl)amide in 900 ml of dry dimethoxyethane was added a solution of 48.0 g (0.20 mol) of the keto ester **31** in 100 ml of dry dimethoxyethane, and the resulting mixture was refluxed under an atmosphere of dry nitrogen for 1.0 h. The reaction mixture was cooled and poured into a rapidly stirred solution of 27.0 g (0.45 mol) of glacial acetic acid in 300 ml of ice water. The resultant mixture was concentrated and the residue was thoroughly extracted with ether. The ethereal extracts were combined and washed with water, a 10% sodium bicarbonate solution, brine, and then dried over anhydrous magnesium sulfate. Removal of the solvent afforded a crystalline material which was recrystallized from petroleum ether (b.p. 60–110 °C) to yield 37.4 g (90%) of the desired diketone **23**, m.p. 76–77 °C; $[\alpha]_D^{20}$ −56° (*c*, 4.0 in $CHCl_3$); i.r. ($CHCl_3$) ν_{max} 1767, 1727, 1453, 1182 cm^{-1}; p.m.r. τ 7.08 (broadened d, 1H, bridgehead proton, J = 4.8 Hz), 7.66 (q of d, C-7 H, $J_{5,7}$ = 1.5 Hz, $J_{7\text{-}CH_3}$ = 7.0 Hz), 8.75 (d, 3H, secondary methyl, J = 7.0 Hz), 8.90 (s, 3H, tertiary methyl), 9.00, 9.10 (d, d, 6H, isopropyl methyls, J = 6.3 Hz).

Anal. Calcd. for $C_{13}H_{20}O_2$: C, 74.96; H, 9.68. Found: C, 74.80; H, 9.75.

Mol. Wt. Calcd. for $C_{13}H_{20}O_2$: 208.146. Found (high resolution mass spectrometry): 208.143.

Preparation of the Keto Acetate ***32***

A stirred mixture of the bicyclic diketone **23** (2.94 g, 15 mmol), isopropenyl acetate (25 ml), and concentrated sulfuric acid (0.06 ml) was placed under an atmosphere of

Can. J. Chem. Downloaded from www.nrcresearchpress.com by 210.87.254.105 on 09/05/12
For personal use only.

nitrogen and then heated gently. An acetone enriched distillate was collected in a Dean–Stark water separator. After 4 h, an additional 0.06 ml of concentrated sulfuric acid was added and heating was continued for a further 2 h. The reaction mixture was cooled and poured into ice water. The resulting mixture was extracted thoroughly with ether. The combined extracts were washed successively with cold dilute aqueous sodium bicarbonate, cold water, and brine, and then dried over anhydrous magnesium sulfate. Removal of the solvent, followed by distillation (air-bath temperature 110–112 °C at 0.2 Torr) of the residual oil afforded 3.3 g (87%) of a pale yellow oil. Analysis of this material by g.l.c. (column A, 200 °C, 100) indicated that the enol acetate **32** and the diketone **23** were present in a ratio of 97:3. An analytical sample of the enol acetate **32**, collected by preparative g.l.c. (column A, 200 °C, 100), exhibited n_D^{20} 1.4830; $[\alpha]_D^{22}$ −10.4° (*c*, 0.55 in $CHCl_3$); i.r. (film) ν_{max} 2940, 1755, 1675, 1450, 1365, 1205, 1175, 1090, 876 cm^{-1}; p.m.r. τ 6.97 (unresolved m, 1H, C-5 H), 7.85 (s, 3H, $COCH_3$), 8.42 (d, 3H, vinyl methyl, J = 0.8 Hz), 8.99 (s, 3H, tertiary methyl), 9.05, 9.11 (d, d, 6H, isopropyl methyls, J = 6.0 Hz). In a decoupling experiment, irradiation of the multiplet signal at τ 6.97 (C-5 H) effected collapse of the doublet at τ 8.42 to a sharp singlet, thus demonstrating the presence of homoallylic coupling between the vinyl methyl group at C-7 and the bridgehead proton at C-5.

Anal. Calcd. for $C_{15}H_{22}O_3$: C, 71.97; H, 8.86. Found: C, 72.16; H, 8.67.

Hydrogenation of the Keto Acetate 32

To a solution of the enol acetate **32** (5.63 g, 22.6 mmol) in 340 ml of 100% ethanol was added 2.26 g of 5% palladium-on-barium sulfate. The reaction mixture was stirred vigorously under hydrogen for 5 h. At this time, an additional amount of hydrogenation catalyst was added and hydrogenation was continued for a further 4 h. After filtration through Celite, the reaction mixture was concentrated under reduced pressure and the residue was distilled (air-bath temperature 120–124 °C, 0.15 Torr) to afford 5.5 g (97%) of a colorless oil. Gas–liquid chromatographic analysis (column B, 220 °C, 90) of this material indicated the presence of the two keto acetates **33** and **34**, in a ratio of 9:1, respectively. Analytical samples of the two isomers were obtained by preparative g.l.c. (column B, 220 °C, 90).

The major product **33** exhibited n_D^{20} 1.4793; $[\alpha]_D^{22}$ +43.8° (*c*, 0.40 in $CHCl_3$); i.r. (film) ν_{max} 2975, 1735, 1465, 1385, 1368, 1235, 1038 cm^{-1}; p.m.r. τ 4.61 (d of d, 1H, C-6 H, $J_{5,6}$ = 7.0 Hz, $J_{6,7}$ = 10.0 Hz), 7.15 (d of d, 1H, C-5 H, $J_{4,5}$ = 3.0 Hz, $J_{5,6}$ = 7.0 Hz), 7.91 (s, 3H, $COCH_3$), 8.94 (d, 3H, secondary methyl, J = 7.4 Hz), 9.05, 9.15 (d, d, 6H, isopropyl methyls, J = 6.3 Hz), 9.15 (s, 3H, tertiary methyl). In decoupling experiments, irradiation of the C-5 proton signal (τ 7.15) effected collapse of the C-6 proton signal (τ 4.61) to a doublet ($J_{6,7}$ = 10.0 Hz). Similarly, irradiation at τ 4.61 caused collapse of the C-5 proton signal to a doublet ($J_{4,5}$ = 3.0 Hz). Finally, irradiation of the somewhat masked C-7 proton multiplet at τ 7.87 produced collapse of the C-7 methyl doublet (τ 8.94) to a sharp singlet, as well as the collapse of the C-6 proton signal to a doublet ($J_{5,6}$ = 7.0 Hz).

Anal. Calcd. for $C_{15}H_{24}O_3$: C, 71.39; H, 9.59. Found: C, 71.10; H, 9.38.

The minor keto acetate **34** exhibited $[\alpha]_D^{22}$ +55.8° (*c*, 0.50 in $CHCl_3$); i.r. (film) ν_{max} 2975, 1735, 1470, 1450, 1383, 1368, 1245, 1142, 1087, 1038 cm^{-1}; p.m.r. τ 5.30 (d of d, 1H, C-6 H, $J_{5,6}$ = 7.0 Hz, $J_{6,7}$ = 4.0 Hz), 7.12 (d of d, 1H, C-5 H, $J_{4,5}$ = 3.0 Hz, $J_{5,6}$ = 7.0 Hz), 7.90 (s, 3H, $COCH_3$), 9.00 (d, 3H, secondary methyl, J = 7.4 Hz), 9.03, 9.09 (d, d, 6H, isopropyl methyls, J = 7.0 Hz), 9.13 (s, 3H, tertiary methyl). A series of decoupling experiments similar to those carried out on the keto acetate **33** (see above) fully corroborated the p.m.r. assignments.

Anal. Calcd. for $C_{15}H_{24}O_3$: C, 71.39; H, 9.59. Found: C, 71.23; H, 9.41.

Preparation of the Diol 35

(a) By Lithium Aluminum Hydride Reduction of Diketone 23

To a solution of lithium aluminum hydride (50 mg) in anhydrous ether (5 ml) was added 208 mg (1.0 mmol) of the bicyclic diketone **23**. The resulting solution was refluxed for 4.5 h and then cooled to 0 °C. Excess hydride was quenched by careful addition of water and the resulting mixture was filtered. The aqueous layer of the filtrate was washed thoroughly with ether, the combined extracts were washed with water and brine, and then dried over anhydrous magnesium sulfate. Removal of the solvent afforded 192 mg (91%) of a colorless crystalline material. Recrystallization of a small sample gave an analytical sample of the diol **35**, m.p. 175–176 °C; $[\alpha]_D^{22}$ −9.8° (*c*, 0.60 in $CHCl_3$); i.r. ($CHCl_3$) ν_{max} 3640, 1460, 1025 cm^{-1}; p.m.r. τ 5.71 (d of d, 1H, C-6 H, $J_{5,6}$ = 7.0 Hz, $J_{6,7}$ = 10.5 Hz), 6.58 (d, 1H, C-8 H, $J_{5,8}$ = 5.0 Hz), 7.48 (broad m, 1H, C-5 H), 9.03, 9.09 (d, d, 6H, isopropyl methyls, J = 6.5 Hz), 9.06 (d, 3H, secondary methyl, J = 7.5 Hz), 9.19 (s, 3H, tertiary methyl).

Anal. Calcd. for $C_{13}H_{24}O_2$: C, 73.54; H, 11.39. Found: C, 73.39; H, 11.48.

(b) By Lithium Aluminum Hydride Reduction of Keto Acetate 33

The reduction of the keto acetate **33** was carried out under conditions identical with those described for the reduction of **23** (see above). From 26 mg of **33** there was obtained 20 mg (92%) of the crystalline diol **35**. This material was identical (m.p., mixture m.p., i.r., p.m.r.) with the diol obtained by hydride reduction of the diketone **23**.

Preparation of the Hydroxymethylene Derivative 40

To a stirred suspension of powdered sodium methoxide (102.5 g, 1.9 mol) in 1400 ml of dry benzene containing 153 ml (2.25 mol) of ethyl formate was added, at 0 °C, a solution of 140 g (0.635 mol) of the (−)-octalone **39** in 1400 ml of dry benzene. The cooling bath was removed and the reaction mixture was stirred at room temperature in an atmosphere of nitrogen for 4 days. The cooled mixture was acidified with 6 *N* hydrochloric acid, the layers were separated, and the aqueous layer was extracted with ether. The combined organic extracts were washed twice with brine and dried over anhydrous magnesium sulfate. Removal of the solvent gave 157 g (98%) of the hydroxymethylene derivative **40** as yellow crystals. An analytical sample of this material, obtained by recrystallization of a small amount of the crude product from hexanes, exhibited m.p. 64.5–65 °C; $[\alpha]_D^{27}$ −8.5° (*c*, 2.5 in $CHCl_3$); i.r. ($CHCl_3$) ν_{max} 1638, 1563 cm^{-1};

Can. J. Chem. Downloaded from www.nrcresearchpress.com by 210.87.254.105 on 09/05/12
For personal use only.

p.m.r. (CCl_4) τ −3.73 (broad signal, 1H, exchangeable, =CHO*H*), 2.68 (d, 1H, =*CH*OH, J = 1.6 Hz), 8.17 (d, 3H, vinyl methyl, J = 1.2 Hz), 8.90 (s, 3H, tertiary methyl), 9.01, 9.07 (d, d, 6H, isopropyl methyls, J = 6.0 Hz).

Anal. Calcd. for $C_{16}H_{24}O_2$: C, 77.38; H, 9.74. Found: C, 77.31; H, 9.86.

Preparation of the Dienone Aldehyde 41

A solution of 2,3-dichloro-5,6-dicyanobenzoquinone (5.0 g, 22.0 mmol) in 75 ml of dry dioxan was added to a solution of the hydroxymethylene derivative **40** (5.0 g, 20.1 mmol) in 75 ml of dry dioxan. The resulting mixture was stirred at room temperature in an atmosphere of nitrogen for 10 min and then 300 ml of methylene chloride was added. The precipitate was removed by filtration and the filtrate was passed quickly through a short column of neutral alumina (activity III). The column was thoroughly eluted with methylene chloride. Removal of the solvents gave 4.6 g (93%) of the desired dienone aldehyde **41** as pale yellow crystals. An analytical sample, obtained by recrystallization of a small amount of the crude material from hexanes, exhibited m.p. 78.5–79 °C; $[\alpha]_D^{27}$ +161° (*c*, 2.5 in $CHCl_3$); u.v. λ_{max} 228 (ε 10 200), 239 (ε 9800) (shoulder), 266 nm (ε 6800) (shoulder); i.r. ($CHCl_3$) ν_{max} 1700, 1648, 1623, 1600, 855, 824 cm^{-1}; p.m.r. τ −0.31 (s, 1H, aldehydic H), 2.51 (s, 1H, vinyl H), 8.03 (d, 3H, vinyl methyl, J = 1.2 Hz), 8.67 (s, 3H, tertiary methyl), 9.04, 9.17 (d, d, 6H, isopropyl methyls, J = 6.0 Hz).

Anal. Calcd. for $C_{16}H_{22}O_2$: C, 78.01; H, 9.00. Found: C, 78.18; H, 9.09.

Preparation of the Keto Ester 45

To a stirred suspension of anhydrous cuprous iodide (15.6 g, 82.0 mmol) in 300 ml of anhydrous ether at −25 °C was added, over a period of 5 min, 73.7 ml of 2.2 *M* ethereal methyllithium. The resulting solution was stirred in an atmosphere of nitrogen for 10 min and then the temperature was raised to 0 °C. A solution of the dienone aldehyde **41** (11.6 g, 47.0 mmol) in 300 ml of anhydrous ether was added over a period of 40 min and the resulting mixture was stirred at 0 °C for 2 h. A solution of acetyl chloride (12 ml) in 240 ml of anhydrous ether was then added over a period of 5 min and stirring was continued at 0 °C for a further 10 min, by which time the reaction mixture was composed of a clear supernatant and a sticky precipitate. The clear solution was poured into a rapidly stirred mixture (1200 ml) of concentrated ammonium hydroxide and crushed ice (1:2) and the ether layer was quickly separated. The aqueous layer was rapidly extracted twice with cold ether and the combined ether extracts were washed with cold brine until neutral, dried over anhydrous magnesium sulfate, and concentrated to give 11.1 g of the enol acetate **42** as a viscous oil. This material was somewhat unstable and was used without further purification in the next reaction (ozonolysis). It exhibited i.r. (film) ν_{max} 3110, 1768, 1672, 1612 cm^{-1}; p.m.r. τ 1.85 (s, 1H, vinyl H), 7.12 (q, 1H, CH_3CH—, J = 7.0 Hz), 7.76 (s, 3H, CH_3COO—), 8.13 (s, 3H, vinyl methyl), 8.82 (s, 3H, tertiary methyl), 8.96 (d, 3H, secondary methyl, J = 7.0 Hz), 9.06 (poorly resolved multiplet, 6H, isopropyl methyls).

The solid residue remaining in the reaction flask was treated with 500 ml of concentrated ammonium hydroxide and crushed ice (1:1) and 500 ml of ether. This mixture was stirred vigorously for 15 min, sodium chloride was added, and the layers were separated. The aqueous layer was extracted twice with cold ether and the combined ether extracts were washed with cold brine until neutral. Drying over anhydrous magnesium sulfate and removal of the solvent gave 3.0 g of a gum-like material. Infrared and p.m.r. spectra indicated that about one-half of this material was the desired enol acetate **42** so it was combined without further purification with the material obtained above.

A solution of the combined crude enol acetate product (14.1 g) in 200 ml of methylene chloride was treated with ozone at −78 °C until the solution turned blue and then for a further 30 min at −25 °C. The cooling bath was removed and 300 ml of a 5% solution of sodium hydroxide in methanol–water (7:1) was added, followed by the careful addition of 120 ml of 30% hydrogen peroxide. The resulting mixture was gradually heated, effecting distillation of the methylene chloride. The temperature of the remaining mixture was raised to reflux and refluxing was continued until foaming ceased. The solution was cooled to 40 °C and 60 ml of 30% hydrogen peroxide was added, followed by refluxing as before. This process was repeated once more with a further 60 ml of hydrogen peroxide. The methanol was removed at aspirator pressure, the residue was diluted with water and acidified with 6 *N* hydrochloric acid. The resulting mixture was thoroughly extracted with ether and the combined ether extracts were washed twice with brine and then dried over anhydrous magnesium sulfate. Removal of the solvent gave 10.9 g of a viscous oil which solidified overnight. A small sample of this solid was recrystallized from hexanes and then from hexanes – ethyl acetate to give an analytical sample of the lactol **44** which exhibited m.p. 83.5–84 °C; i.r. ($CHCl_3$) 3590, 3560–2500, 1760, 1705 cm^{-1}; i.r. (Nujol) 3415, 1750 cm^{-1}; p.m.r. τ 6.88, 7.13 (q, q, 1H, CH_3CHCO_2H and $CH_3CHCO_2C(OH)$— (lactol), J = 7.2, 7.2 Hz).

Anal. Calcd. for $C_{13}H_{22}O_3$: C, 68.99; H, 9.80. Found: C, 69.03; H, 9.83.

The total crude keto acid **43** – lactol **44** product was esterified by treatment with excess ethereal diazomethane. The excess diazomethane was then destroyed with acetic acid, the mixture was washed with sodium bicarbonate solution, with brine, and dried over anhydrous magnesium sulfate. Removal of the solvent and distillation (air-bath temperature 98–106 °C/0.15 Torr) of the residual oil gave 6.75 g (60% overall from the dienone aldehyde **41**) of the desired keto ester **45**. An analytical sample, obtained by preparative g.l.c. (column C, 205 °C, 180), exhibited n_D^{20} 1.4699; $[\alpha]_D^{25}$ +151° (*c*, 2.0 in $CHCl_3$); i.r. (film) ν_{max} 1732, 1705 cm^{-1}; p.m.r. τ 6.30 (s, 3H, $-OCH_3$), 6.91 (q, 1H, $CH_3CHCO_2CH_3$, J = 7.1 Hz), 9.00 (s, 3H, tertiary methyl), 9.03 (d, 3H, secondary methyl, J = 7.1 Hz), 9.07, 9.08 (d, d, 6H, isopropyl methyls, J = 6.3 Hz).

Anal. Calcd. for $C_{14}H_{24}O_3$: C, 69.96; H, 10.07. Found: C, 69.93; H, 9.93.

(+)-(1R,4S,5S,7S)-1,7-Dimethyl-4-isopropylbicyclo-[3.2.1]octa-6,8-dione (24)

To a solution of sodium bis(trimethylsilyl)amide (30g,

164 mmol) in 400 ml of dry benzene, kept at 79–80 °C (internal temperature) under an atmosphere of nitrogen, was added over a period of 65 min a solution of the keto ester **45** (15.0 g, 62.5 mmol) in 650 ml of dry benzene. This temperature was maintained for a further 75 min, then the reaction mixture was cooled and poured into 1000 ml of cold water containing 30 ml of acetic acid. The layers were separated and the aqueous layer was extracted once with ether. The combined organic layers were washed twice with sodium bicarbonate solution, with brine, and dried over anhydrous magnesium sulfate. Removal of the solvent and distillation (air-bath temperature 90–105 °C/0.2 Torr) of the resulting crystalline residue gave 10.9 g of the crystalline diketone **24**. Analysis of this material by g.l.c. (column A, 165 °C, 110) showed that it consisted of 91% diketone and two unidentified minor components. Recrystallization of this material from hexane yielded 9.8 g (75%) of pure diketone. This compound exhibited m.p. 77.5–78 °C; $[\alpha]_D^{27}$ +102° (*c*, 1.6 in $CHCl_3$); i.r. ($CHCl_3$) ν_{max} 1765, 1725 cm^{-1}; p.m.r. τ 7.07 (broad s, 1H, C-5 H, width at half-height 3.5 Hz), 7.68 (q of d, 1H, C-7 H, J = 7.1, 1.5 Hz), 8.80 (d, 3H, secondary methyl, J = 7.1 Hz), 8.88 (s, 3H, tertiary methyl), 8.99, 9.12 (d, d, 6H, isopropyl methyls, J = 6.0 Hz). A frequency-swept decoupling experiment in which the proton at τ 7.07 was irradiated, thus causing the quartet of doublets at τ 7.68 to collapse to a quartet (J = 7.1 Hz), showed that the C-7 proton was coupled with the bridgehead C-5 proton (J = 1.5 Hz).

Anal. Calcd. for $C_{13}H_{20}O_2$: C, 74.96; H, 9.68. Found: C, 74.98; H, 9.80.

Financial support from the National Research Council of Canada and the University of British Columbia Committee on Research is gratefully acknowledged.

1. V. H. KAPADIA, B. A. NAGASAMPAGI, V. G. NAIK, and S. DEV. Tetrahedron, **21**, 607 (1965).
2. P. DE MAYO, R. E. WILLIAMS, G. BÜCHI, and S. H. FEAIRHELLER. Tetrahedron, **21**, 619 (1965).
3. Y. OHTA and Y. HIROSE. Tetrahedron Lett. 1601 (1969).
4. L. WESTFELT. Acta Chem. Scand. **20**, 2829 (1966).
5. L. WESTFELT. Acta Chem. Scand. **20**, 2841 (1966).
6. M. KOLBE-HAUGWITZ and L. WESTFELT. Acta Chem. Scand. **24**, 1623 (1970).
7. N. H. ANDERSEN. Tetrahedron Lett. 4651 (1970).
8. F. KIDO, R. SAKUMA, H. UDA, and A. YOSHIKOSHI. Tetrahedron Lett. 3169 (1969).
9. P. DE MAYO and R. E. WILLIAMS. J. Am. Chem. Soc. **87**, 3275 (1965).
10. L. SMEDMAN and E. ZAVARIN. Tetrahedron Lett. 3833 (1968).
11. L. A. SMEDMAN, E. ZAVARIN, and R. TERANISHI. Phytochemistry, **8**, 1457 (1969).
12. L. A. SMEDMAN, K. SNAJBERK, E. ZAVARIN, and T. R. MON. Phytochemistry, **8**, 1471 (1969).
13. J. E. MCMURRY. J. Am. Chem. Soc. **90**, 6821 (1968).
14. G. L. HODGSON, D. F. MACSWEENEY, and T. MONEY. J. Chem. Soc. Perkin Trans. 1, 2113 (1973).
15. J. E. MCMURRY. (*a*) Tetrahedron Lett. 55 (1969); (*b*) J. Org. Chem. **36**, 2826 (1971).
16. S. W. BALDWIN and J. C. TOMESCH. Tetrahedron Lett. 1055 (1975).
17. J. E. MCMURRY. Tetrahedron Lett. 3731 (1970).
18. G. L. HODGSON, D. F. MACSWEENEY, and T. MONEY. Tetrahedron Lett. 3683 (1972).
19. C. R. ECK, G. L. HODGSON, D. F. MACSWEENEY, R. W. MILLS, and T. MONEY. J. Chem. Soc. Perkin Trans. 1, 1938 (1974).
20. E. PIERS, R. W. BRITTON, R. J. KEZIERE, and R. D. SMILLIE. Can. J. Chem. **49**, 2620 (1971).
21. E. PIERS, M. B. GERAGHTY, F. KIDO, and M. SOUCY. Synth. Commun. **3**, 39 (1973).
22. E. PIERS, R. W. BRITTON, M. B. GERAGHTY, R. J. KEZIERE, and F. KIDO. Can. J. Chem. This issue.
23. E. PIERS, M. B. GERAGHTY, R. D. SMILLIE, and M. SOUCY. Can. J. Chem. This issue.
24. E. J. COREY and S. NOZOE. J. Am. Chem. Soc. **87**, 5728 (1965), and references cited therein.
25. R. E. IRELAND and J. A. MARSHALL. J. Org. Chem. **27**, 1615 (1962), and references cited therein.
26. W. J. LE NOBLE. Synthesis, 1 (1970).
27. B. W. ROBERTS, M. S. POONIAN, and S. C. WELCH. J. Am. Chem. Soc. **91**, 3400 (1969).
28. M. TANABE and D. F. CROW. Chem. Commun. 1498 (1969), and references cited therein.
29. H. O. HOUSE. Modern synthetic reactions. 2nd ed. W. A. Benjamin, Inc., Menlo Park, California. 1972. pp. 19–23.
30. W. COCKER, D. P. HANNA, and P. V. R. SHANNON. J. Chem. Soc. C, 489 (1966).
31. F. J. MCQUILLIN. J. Chem. Soc. 528 (1955); R. HOWE and F. J. MCQUILLIN. J. Chem. Soc. 2423 (1955); R. HOWE and F. J. MCQUILLIN. J. Chem. Soc. 2670 (1956).
32. T. G. HALSALL, D. W. THEOBALD, and K. B. WALSHAW. J. Chem. Soc. 1029 (1964).
33. H. HIKINO, T. KOHAMA, and T. TAKEMOTO. Tetrahedron, **25**, 1037 (1969).
34. D. WALKER and J. D. HIEBERT. Chem. Rev. **67**, 153 (1967).
35. E. PIERS and K. F. CHENG. Can. J. Chem. **45**, 1591 (1967).
36. E. PIERS and K. F. CHENG. Can. J. Chem. **48**, 2234 (1970).
37. H. O. HOUSE, W. L. RESPESS, and G. M. WHITESIDES. J. Org. Chem. **33**, 949 (1968).
38. R. M. COATES and J. E. SHAW. J. Am. Chem. Soc. **92**, 5657 (1970).
39. E. PIERS, W. M. PHILLIPS-JOHNSON, and C. BERGER. Can. J. Chem. **53**, 1291 (1975), and references cited therein.

Can. J. Chem. Downloaded from www.nrcresearchpress.com by 210.87.254.105 on 09/05/12
For personal use only.

Stereoselective Total Synthesis of Copa and Ylango Sesquiterpenoids: (+)-Copacamphor, (+)-Copaborneol, (+)-Copaisoborneol, (−)-Ylangocamphor, (−)-Ylangoborneol, (−)-Ylangoisoborneol

EDWARD PIERS, RONALD W. BRITTON, M. BERT GERAGHTY, ROBERT J. KEZIERE, AND FUSAO KIDO

Department of Chemistry, University of British Columbia, 2075 Wesbrook Place, Vancouver, British Columbia V6T 1W5

Received May 15, 1975

EDWARD PIERS, RONALD W. BRITTON, M. BERT GERAGHTY, ROBERT J. KEZIERE, and FUSAO KIDO. Can. J. Chem. **53**, 2838 (1975).

Efficient, stereoselective syntheses of the tricyclic sesquiterpenoids (+)-copacamphor (**3**), (+)-copaborneol (**4**), (+)-copaisoborneol (**5**), (−)-ylangocamphor (**6**), (−)-ylangoborneol (**7**), and (−)-ylangoisoborneol (**8**) are described. Conversion of the keto acetate **9** (previously synthesized from the dione **1**) into the keto tosylate **17** was accomplished via an eight-step sequence. Intramolecular alkylation of **17** afforded, in high yield, (+)-copacamphor (**3**), which had previously been converted into the corresponding alcohols **4** and **5** by Kolbe-Haugwitz and Westfelt. Alkylation of the enolate anion of the bicyclic dione **2** with 2-bromopropane in hexamethylphosphoramide gave mainly the *O*-alkylation product **19**. Conversion of **19** into the keto mesylate **29** was carried out in 5 synthetic steps. Intramolecular alkylation of **29** afforded (−)-ylangocamphor (**6**). Reduction of the latter with calcium in liquid ammonia gave (−)-ylangoborneol (**7**), while reduction with lithium aluminum hydride yielded (−)-ylangoisoborneol (**8**).

EDWARD PIERS, RONALD W. BRITTON, M. BERT GERAGHTY, ROBERT J. KEZIERE et FUSAO KIDO. Can. J. Chem. **53**, 2838 (1975).

On décrit des synthèses efficaces et stéréosélectives des sesquiterpenoides tricycliques (+) copacamphre (**3**), (+) copabornéol (**4**), (+) copaisobornéol (**5**), (−) ylangocamphre (**6**), (−) ylangobornéol (**7**) et (−) ylangoisobornéol (**8**). Huit étapes sont nécessaires pour effectuer la conversion du céto-acétate (**9**) (synthétisé antérieurement à partir de la dione **1**) en céto-tosylate **17**. Une alkylation intramoléculaire de **17** fournit, avec un bon rendement le (+) copacamphre (**3**) qui avait été transformé antérieurement en alcools **4** et **5** correspondants par Kolbe-Haugwitz et Westfelt. L'alkylation de l'anion énolate de la dione bicyclique (**2**) par le bromo-2 propane dans l'hexaméthylphosphoramide conduit principalement au produit de *O*-alkylation **19**. On a effectué la transformation de **19** en céto-mésylate **29** en cinq étapes. L'alkylation intramoléculaire de **29** fournit le (−) ylangocamphre (**6**) qui par réduction avec du calcium dans l'ammoniac liquide conduit au (−) ylangobornéol (**7**) alors que la réduction de **6** par $LiAlH_4$ fournit le (−) ylangoisobornéol (**8**).

[Traduit par le journal]

In the preceding paper (1) we described the stereoselective total synthesis of both (−)-(1*S*,4*S*,5*R*,7*R*)- and (+)-(1*R*,4*S*,5*S*,7*S*)-1,7-dimethyl-4-isopropylbicyclo[3.2.1]octa-6,8-dione (**1** and **2**, respectively), and indicated in general terms how these two diastereomeric compounds could potentially serve as excellent precursors for the total synthesis of a number of copa and ylango sesquiterpenoids, respectively. In this paper we report the successful completion of a portion of this overall goal. Specifically, we describe here: (*a*) the conversion of the diketone **1** into the sesquiterpenoids (+)-copacamphor (**3**), (+)-copaborneol (**4**), and (+)-copaisoborneol (**5**), and (*b*) the conversion of diketone **2** into (−)-ylangocamphor (**6**) and the two corresponding epimeric alcohols (−)-ylangoborneol (**7**) and (−)-ylangoisoborneol (**8**).[1] As noted in the preceding paper (1), only one ((+)-copaborneol (**4**)) of these six sesquiterpenoids has, up to the present time, been isolated from naturally occurring sources (4–6). However, at the time we began our synthetic work, (+)-copacamphor (**3**) and (+)-copaisoborneol (**5**) were also known compounds, having been obtained, by appropriate chemical transformations, from the natural product **4** (6). The three remaining sesquiterpenoids (**6**–**8**) were, until completion of our synthetic work, unknown compounds.

[1]For preliminary communications regarding portions of this work, see refs. 2 and 3. For a summary of other synthetic work done in this general area, see ref. 1, footnote 2.

Can. J. Chem. Downloaded from www.nrcresearchpress.com by 210.87.254.105 on 09/05/12
For personal use only.

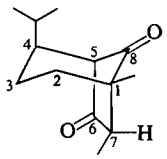

1

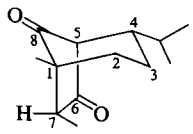

2

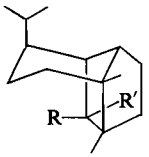

3 R, R′ = O
4 R = H; R′ = OH
5 R = OH; R′ = H

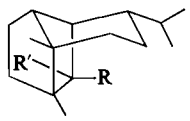

6 R, R′ = O
7 R = H; R′ = OH
8 R = OH; R′ = H

Conversion of Diketone 1 into (+)-Copacamphor (3), (+)-Copaborneol (4), and (+)-Copaisoborneol (5) (see Scheme 1)

Comparison of the structure of the synthetic intermediate **1** with that of (+)-copacamphor (**3**) clearly showed that in any planned overall conversion of **1** into **3**, the carbonyl group at C-6 (in **1**) should be retained. At the same time, the ketone functionality at C-8 would have to serve as a 'handle' for the introduction of the two additional carbon atoms necessary to complete the required 15-carbon skeleton. Clearly, then, it was necessary at the outset to distinguish chemically between the two carbonyl groups present in **1**. Although, theoretically, there were potentially a number of alternative routes open to us via which this could be accomplished, we had already carried out, in a fairly efficient manner, the conversion of **1** into the keto acetate **9**, (1). Therefore, in the portion of our synthetic work presently being discussed, compound **9** served as the starting material.

Treatment of the keto acetate **9** with methoxymethylenetriphenylphosphorane in ether afforded the enol ether acetate **10** (mixture of geometric isomers), accompanied by some of the corresponding alcohols **11**.[2] Direct subjection of this mixture to reduction by lithium aluminum hydride effected the transformation of the remaining **10** into the enol ether alcohol **11**. As shown by the p.m.r. spectrum, the latter material consisted of a mixture of geometric isomers, in a ratio of approximately 3:1. Hydrolysis of **11** with aqueous perchloric acid in ether at room temperature produced an epimeric mixture of the two hydroxy aldehydes **12** and **13**. On the basis of conformational analysis and on the fact that the relative proportion of these two epimers in the product varied appreciably from experiment to experiment, it was clear that we were not dealing with a fully equilibrated mixture. Presumably, the double bond of the enol ether moiety in **11** was, at least to some extent, kinetically protonated from the less hindered

[2]The ratio of **10** to **11** in the product varied somewhat from experiment to experiment. However, since the next synthetic step involved reduction of the acetate functionality, no attempt was made to experimentally control the reaction in the sense of avoiding the formation of the alcohols **11**.

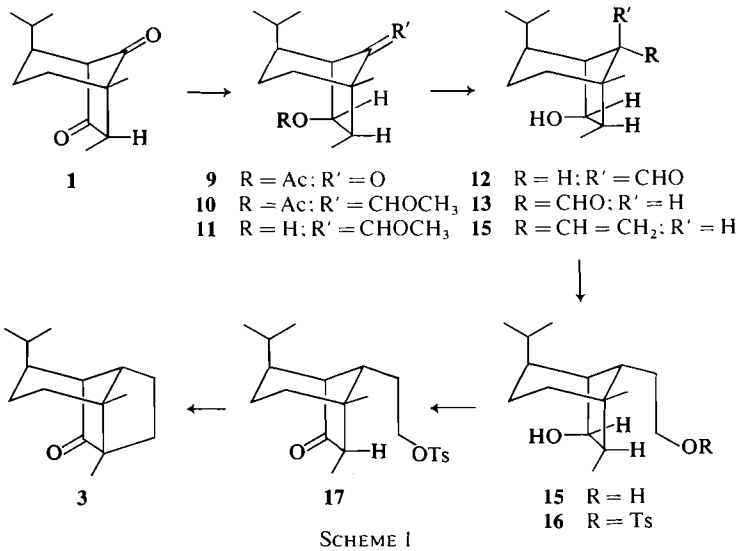

1

9 R = Ac; R′ = O
10 R = Ac; R′ = $CHOCH_3$
11 R = H; R′ = $CHOCH_3$

12 R = H; R′ = CHO
13 R = CHO; R′ = H
15 R = $CH=CH_2$; R′ = H

3

17

15 R = H
16 R = Ts

SCHEME I

Can. J. Chem. Downloaded from www.nrcresearchpress.com by 210.87.254.105 on 09/05/12
For personal use only.

Can. J. Chem. Downloaded from www.nrcresearchpress.com by 210.87.254.105 on 09/05/12
For personal use only.

side (equatorial to the six-membered ring, away from the axially oriented isopropyl group) to afford initially the hydroxy aldehyde **12**. Obviously, compound **12** would, owing to the 1,3-diaxial interaction between the isopropyl group and the aldehyde moiety, be considerably less stable than the epimeric aldehyde **13** and one would thus expect complete equilibration to largely favor the latter isomer. Therefore, the mixture of hydrolysis products (**12** and **13**) was subjected to treatment with potassium carbonate in aqueous methanol. The product, formed in 91% overall yield from **11**, was shown by g.l.c. and spectral analysis to be homogeneous and, on the basis of the conformational analysis argument mentioned above, was assigned structure **13**. When the latter was allowed to react with methylenetriphenylphosphorane in dry dimethyl sulfoxide (7), the crystalline olefinic alcohol **14** was produced in 92% yield.

It should be noted that a number of possible synthetic pathways can be envisaged whereby the two carbon atoms (vinyl group in **14**) would be introduced into the keto acetate **9** in one step, rather than in two separate synthetic transformations as outlined above. However, we chose the latter route for stereochemical reasons. That is, use of the hydroxy aldehydes **12** and/or **13** as synthetic intermediates ensured, in either case, the possibility of epimerizing the center adjacent to the carbonyl group, thus allowing for stereochemical control at this center. This was particularly advantageous in the present synthesis, since the desired hydroxy aldehyde **13** was, as mentioned above, obviously more stable than the epimeric compound **12**. Therefore, it was not at all difficult to predict that subjection of a mixture of the two epimers **12** and **13** to epimerizing conditions would afford, irregardless of the initial ratio of the two compounds, a product consisting largely or entirely of the desired intermediate **13**.

Hydroboration of the olefinic alcohol **14** with borane in tetrahydrofuran, followed by oxidation of the resulting organoborane intermediate with alkaline hydrogen peroxide (8), afforded the diol **15**. Treatment of this material with slightly more than 1 equiv. of *p*-toluenesulfonyl chloride in pyridine at room temperature effected selective tosylation of the primary alcohol functionality, thus producing the hydroxy tosylate **16**. Oxidation of this material with chromium trioxide – pyridine complex in dichloromethane (9, 10) gave, in 72% overall yield from the olefinic alcohol **14**, the crystalline keto tosylate **17**.

The final synthetic transformation necessary to complete the total synthesis of (+)-copacamphor (**3**) involved the intramolecular alkylation of the keto tosylate **17**. This proved to be a very facile process. Thus, when a solution of compound **17** in dimethyl sulfoxide containing sodium methylsulfinylmethide (11) was allowed to stand at room temperature for 35 min, (+)-copacamphor (**3**) (6) was produced in 87% yield. This material exhibited the expected physical and spectral properties and was shown to be identical in every respect with an authentic sample of (+)-copacamphor.[3] Since Kolbe-Haugwitz and Westfelt (6) had already described the conversion of (+)-copacamphor (**3**) into both (+)-copaborneol (**4**) and (+)-copaisoborneol (**5**), the total synthesis of **3** described above also constitutes a formal total synthesis of the other two sesquiterpenoids (**4** and **5**).

Conversion of Diketone 2 into (−)-Ylangocamphor (6), (−)-Ylangoborneol (7), and (−)-Ylangoisoborneol (8) (see Scheme 2)

The conversion of the second totally synthetic bicyclic diketone **2** (1) into the three ylango sesquiterpenoids **6**, **7**, and **8** was accomplished via a route which was in some of the individual synthetic steps quite similar to that described above for the overall transformation of **1** into **3**. However, there were also aspects in which the two synthetic sequences significantly differed and these features will be stressed in the following discussion.

The two carbonyl groups of the bicyclic dione **2** were chemically differentiated in a manner different from and more efficient than that used in the case of the dione **1**. Obviously, in both of these compounds, only the C-6 carbonyl group was capable of enolate anion formation and there existed, therefore, the possibility of directly protecting this keto group via a corresponding enol ether. The latter functionality appeared to be an ideal protecting group, since it would be stable to the conditions of the next proposed synthetic step (Wittig reaction) and would also, presumably, be easily reconverted by simple acid hydrolysis into the ketone. To this end, the diketone **2** was allowed to react with excess sodium bis(trimethylsilyl)amide (12) in hexamethylphosphoramide and the resulting solution

[3]We are very grateful to Dr. L. Westfelt for a generous sample of (+)-copacamphor.

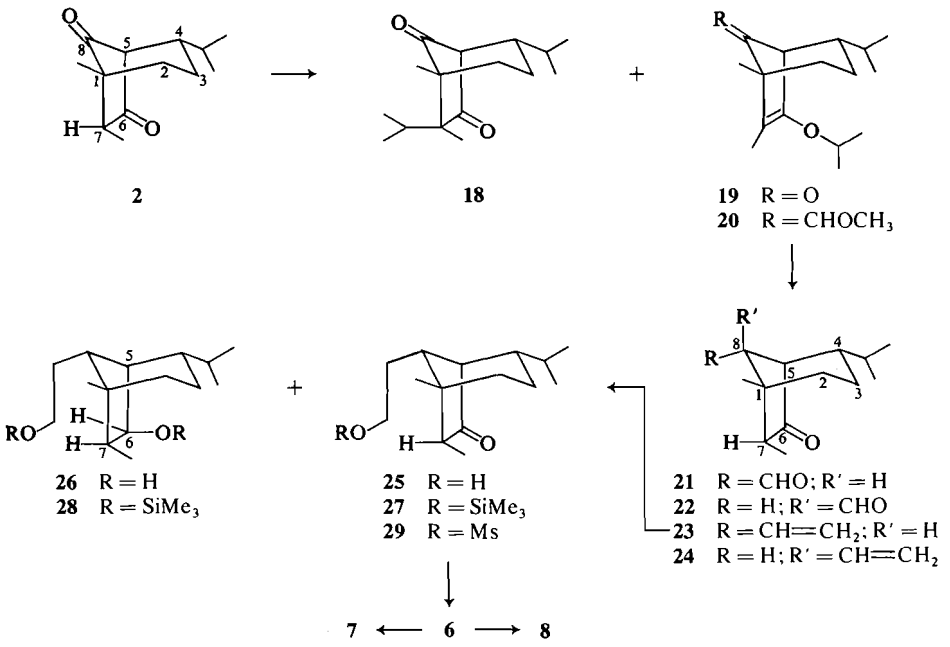

SCHEME 2

of enolate anion was treated with excess 2-bromopropane. After a reaction time of 45 min at room temperature, there was obtained, in addition to some starting material (approximately 10%), a near quantitative yield of a mixture of two products in a ratio of approximately 8:1. Separation of the three components was efficiently accomplished by a combination of distillation and column chromatography. Spectral analysis of the resulting pure compounds clearly showed that the major product was the desired *O*-alkylated material **19**, while the minor product **18**, was the result of *C*-alkylation. Although the configuration at C-7 of the latter compound was not unequivocally established, it was assigned as shown on the basis of the prediction that the alkylating agent (2-bromopropane) would approach the enolate anion from the less hindered *exo* side of the molecule.

It should be noted that it was important to use hexamethylphosphoramide as the solvent in the alkylation described above. It is known that this polar, aprotic solvent, along with others such as dimethyl sulfoxide and sulfolane, promotes *O*-alkylation of enolate anions.[4] However, in the present instance, it was found that dimethyl sulfoxide and sulfolane were considerably inferior to hexamethylphosphoramide. Thus, although the alkylation reaction proceeded smoothly in the two former solvents, in each case the proportion of the desired *O*-alkylated material in the product was significantly less than when the reaction was carried out in hexamethylphosphoramide.

Treatment of the keto enol ether **19** with excess methoxymethylenetriphenylphosphorane in refluxing ether for 30 min afforded, in essentially quantitative yield, compound **20** as a mixture of two geometric isomers. Since both of these diastereomers gave rise to the same products in the next synthetic step, no attempt was made to effect their separation. Hydrolysis of both of the enol ether functionalities in **20** was accomplished by exposure of this material to aqueous perchloric acid in ether. The resultant mixture of keto aldehydes **21** and **22** (ratio approximately 1:1) was equilibrated (potassium carbonate in aqueous methanol), thus affording in 80% yield from **20** a mixture of **21** and **22** in a ratio of 84:16, respectively. Since attempted separation of these epimers by column chromatography led to considerable loss of both compounds, the next reaction was performed on the equilibrium mixture of the two materials. Accordingly, treatment of the mixture with methylenetri-

[4]For an excellent discussion regarding the various structural and experimental factors which influence *C- vs. O*-alkylation of ambident anions, see ref. 13.

Can. J. Chem. Downloaded from www.nrcresearchpress.com by 210.87.254.105 on 09/05/12
For personal use only.

Can. J. Chem. Downloaded from www.nrcresearchpress.com by 210.87.254.105 on 09/05/12
For personal use only.

phenylphosphorane in dimethyl sulfoxide (7) produced in very high yield[5] a mixture of the epimeric keto olefins **23** and **24**, in the expected ratio of approximately 84:16, respectively. These two materials were cleanly separated by column chromatography. The major product **23** was an oil at room temperature, while the minor component was a low-melting, crystalline solid.

The stereochemical assignment made with respect to the two keto olefins **23** and **24** merits comment. It had been assumed, on the basis of conformational analysis, that in the mixture of keto aldehydes **21** and **22**, the major component at equilibrium would be the desired compound **21**, with the formyl group in an equatorial orientation with respect to the six-membered ring. Consequently, the major product in the corresponding mixture of keto olefins **23** and **24** was assumed to be **23**. The first indication that this assumption was indeed correct was provided by a comparison of the p.m.r. spectra of the two epimers. The C-5 proton of the major, oily compound **23** appeared as a broad singlet (width at half-height = 4.5 Hz) at τ 7.41. Obviously, therefore, there was very little coupling between the protons on C-5 and C-8.[6] On the other hand, the C-5 proton of the minor, crystalline epimer **24** produced a broadened doublet (τ 7.42) and was thus clearly coupled with the C-8 proton ($J_{5,8}$ = 5.6 Hz).[6] These observations were fully in line with what would be expected on the basis of the dihedral angles involved. That is, a molecular model of the keto olefin **23** showed that the dihedral angle between the protons on C-5 and C-8 was approximately 75–80° and, on the basis of the Karplus equation (14), only a very small coupling constant would be expected. On the other hand, the dihedral angle between the C-5 and C-8 protons of the keto olefin **24** was, on the basis of a molecular model, approximately 40–45° and the Karplus equation (14) predicts a coupling constant of magnitude similar to that observed (5.6 Hz). That these initial conclusions regarding the stereochemistry of **23** and **24** were indeed correct was shown unambiguously by the subsequent successful conversion of the former compound into (−)-ylangocamphor (**6**) (*vide infra*).

Subjection of the major keto olefin **23** to hydroboration with disiamylborane (15) in tetrahydrofuran at 0 °C afforded, in 81% yield, a mixture of the desired keto alcohol **25** and the diol **26**, in a ratio of approximately 85:15. Since direct separation of these two compounds proved troublesome, they were eventually separated by preparative g.l.c. on the corresponding trimethylsilyl ether derivatives **27** and **28**. The spectral data obtained from pure samples of the keto alcohol **25** (regenerated from **27**) and the diol **26** (regenerated from **28**) were in complete accord with the assigned structures. In particular, it is pertinent to note that the p.m.r. spectrum of the diol **26** fully corroborated the proposed stereochemistry.[7] Thus, the C-6 proton appeared as a pair of doublets at τ 5.60, with $J_{5,6}$ = 6.9 Hz and $J_{6,7}$ = 10.6 Hz. The former coupling constant was in agreement with that expected on the basis of the Karplus equation (14), since molecular models indicated that the dihedral angle between the C-5 proton and a C-6 *exo*-proton (as in **26**) was approximately 15–25°. If the configuration at C-6 of the diol had been epimeric with that shown in **26**, the dihedral angle between the C-5 and C-6 protons would have been approximately 90° and a very small coupling constant would have been expected.[8] Furthermore, molecular models indicated that the dihedral angle between the C-6 and C-7 protons in **26** was near 0° and the observed coupling constant (10.6 Hz) was therefore also in good agreement with that expected (14).

Treatment of the pure keto alcohol **25** with methanesulfonyl chloride in pyridine at room

---

[5]When the Wittig reaction was carried out in ethyl ether or other ether solvents, only poor yields of product were formed.

[6]It is important to note that the p.m.r. spectra of a number of compounds in this series (**2**, **18**, **19**, **23**, **24**) consistently showed that the coupling between the C-4 and C-5 protons was very weak. For example, in compounds **2**, **18**, and **19**, the bridgehead proton at C-5 appeared, in each case, as a broad singlet, with half-height width in the range of 3.5–4.5 Hz.

[7]This stereochemical assignment was initially made on the basis of steric approach control. That is, it seemed highly likely that the reducing agent (disiamylborane) would approach the carbonyl group (of **23**) from the less hindered *exo* side of the bicyclic system, thus producing the *endo* alcohol.

[8]In this connection, it had already been noted in the chemical literature (6) that the carbinol proton in copaborneol (**4**) appeared as a broad singlet, while that in copaisoborneol (**5**) appeared as a doublet with J = 8.0 Hz.

Can. J. Chem. Downloaded from www.nrcresearchpress.com by 210.87.254.105 on 09/05/12
For personal use only.

temperature gave the keto mesylate **29**, which was subjected to intramolecular alkylation without extensive purification. Thus, exposure of **29** to sodium bis(trimethylsilyl)amide (12) in dimethoxyethane at room temperature smoothly afforded, in 84% yield from the keto alcohol **25**, pure (−)-ylangocamphor (**6**). This material, which crystallized on cooling, exhibited m.p. 25–25.5 °C, $[\alpha]_D^{26}$ −58°, and produced spectra data which were very similar to, but clearly different from, those obtained from (+)-copacamphor (**3**).

It is pertinent to note that (−)-ylangocamphor (**6**) could also be conveniently obtained from the 85:15 mixture of the keto alcohol **25** and the diol **26**, and the rather tedious (although efficient) separation of these two materials could, therefore, be avoided. Thus, treatment of the mixture of **25** and **26** with excess methanesulfonyl chloride in pyridine, followed by exposure of the resultant mixture of mesylate derivatives to sodium bis(trimethylsilyl)amide in dimethoxyethane, gave a crude product which upon simple distillation afforded pure (−)-ylangocamphor (**6**) in 50% overall yield from the keto olefin **23**.

Two highly stereoselective reductions effected the conversion of (−)-ylangocamphor (**6**) into the two corresponding alcohols **7** and **8**. Thus, treatment of **6** with calcium in anhydrous liquid ammonia (16, 17) afforded, in 95% yield, (−)-ylangoborneol (**7**) as the only detectable product. This crystalline material exhibited spectral data in full accord with the assigned structure. Of particular note was the p.m.r. spectrum in which the proton on the hydroxyl-bearing carbon appeared as a broad singlet at τ 6.26 (see footnote 8). Reduction of **6** with lithium aluminum hydride in refluxing ether gave, in 91% yield, (−)-ylangoisoborneol (**8**). This compound produced spectra very similar to, although clearly different from, those obtained from the epimeric material **7**. In the p.m.r. spectrum of **8**, the carbinol proton produced, as expected (see footnote 8), a doublet (τ 6.27) with a coupling constant of 7.7 Hz.

The synthetic work described in this paper not only provides unambiguous evidence for the structure and absolute stereochemistry of the six sesquiterpenoids **3**–**8**, inclusive, but may also be an example of the total synthesis of one or more natural products before actual isolation from natural sources.

Experimental[9]

Preparation of the Hydroxy Enol Ether 11

To a stirred slurry of methoxymethyltriphenylphosphonium chloride (54.5 g, 159 mmol) in 350 ml of anhydrous ether at room temperature under a nitrogen atmosphere was added 69.2 ml of 2.3 *M* *n*-butyllithium (159 mmol) in hexane. The resulting dark red solution was cooled to −25 °C and 8.0 g (31.8 mmol) of keto acetate **9** was added dropwise over a period of 10 min. The reaction mixture was stirred at −20 to −30 °C for 1 h, at room temperature for 2 h, and then filtered through Celite. The filtrate was washed with cold water, with brine, and then concentrated. The residual material was diluted with water and the resulting mixture was thoroughly extracted with hexane. The combined extracts were washed with brine and dried over anhydrous magnesium sulfate. Removal of the solvent afforded an orange oil which, on the basis of spectral data, was shown to contain a mixture of the enol ether acetates **10** and the enol ether alcohols **11**. This material was dissolved in anhydrous ether (175 ml), lithium aluminum hydride (1.5 g) was added, and the resulting solution was refluxed under nitrogen for 4 h. The reaction mixture was cooled to 0 °C, the excess hydride was destroyed by careful addition of water, and the mixture was filtered through Celite. The filtrate was diluted with additional water and was then thoroughly extracted with ether. The combined extracts were washed with brine and dried over anhydrous magnesium sulfate. Removal of the solvent, followed by distillation (air-bath temperature 130–135 °C; 0.5 Torr) of the residual oil afforded 4.2 g (55%) of the hydroxy enol ether **11** (mixture of geometric isomers) as a colorless oil, n_D^{20} 1.5048; i.r. (film) ν_{max} 3450, 2940, 1695, 1460, 1383, 1370, 1235, 1215, 1110, 1035 cm^{-1}; p.m.r. τ 4.30, 4.34 (s, s, 1H, $=CHOCH_3$ of isomers, ratio 1:3), 5.66 (d of d, 1H, C-6 H, $J_{5,6}$ = 7.0 Hz, $J_{6,7}$ = 11.0 Hz), 6.54, 6.57 (s, s, 3H, $=CHOCH_3$ of isomers, ratio 1:3), 7.45 (m, 1H, C-5 H).

Anal. Calcd. for $C_{15}H_{26}O_2$: C, 75.58; H, 10.99. Found: C, 75.44; H, 11.01.

Preparation of Hydroxy Aldehyde 13

To a mixture of 35% aqueous perchloric acid (135 ml) and ether (675 ml) was added 5.06 g (21.3 mmol) of the hydroxy enol ethers **11**. The reaction mixture was stirred at room temperature for 2.5 h and was then neutralized by careful addition of solid potassium carbonate. The aqueous layer was thoroughly extracted with ether; the combined ether extracts were washed with brine and dried over anhydrous magnesium sulfate. Removal of the solvent afforded an oil which, as shown by spectral analysis, consisted of a mixture of the two epimeric aldehydes **12** and **13**. This material was dissolved in 550 ml of 1:10 water–methanol containing 5.4 g of potassium carbonate and the resulting solution was stirred at room temperature for 2.5 h. Most of the methanol was removed under reduced pressure, the residue was diluted with water, and the resulting mixture was thoroughly extracted with ether. The combined extracts were washed with water and brine and then dried over anhydrous magnesium sulfate.

[9]For pertinent general information, see the preceding paper (ref. 1).

Can. J. Chem. Downloaded from www.nrcresearchpress.com by 210.87.254.105 on 09/05/12
For personal use only.

Removal of the solvent, followed by distillation (air-bath temperature 158–176 °C; 0.1 Torr) of the residual oil afforded 4.35 g (91%) of the hydroxy aldehyde **13** as a pale yellow oil, n_D^{20} 1.5060; i.r. (film) ν_{max} 3470, 2740, 1712, 1460, 1380, 1120, 1038, 1025 cm^{-1}; p.m.r. τ 0.17 (d, 1H, —CHO, J = 2.5 Hz), 5.40 (d of d, 1H, C-6 H, $J_{5,6}$ = 7.0 Hz, $J_{6,7}$ = 10.5 Hz), 7.30 (broad d, 1H, C-5 H, $J_{5,6}$ = 7.0 Hz), 7.62 (d, 1H, C-8 H, J = 2.5 Hz), 8.93 (s, 3H, tertiary methyl), 9.04, 9.15 (d, d, 6H, isopropyl methyls, J = 5.5 Hz), 9.09 (d, 3H, secondary methyl, J = 7.5 Hz).

Anal. Calcd. for $C_{13}H_{24}O_2$: C, 73.54; H, 11.39. Found: C, 73.57; H, 11.21.

Preparation of the Olefinic Alcohol ***14***

A solution of methyltriphenylphosphonium bromide (25.8 g, 72.2 mmol) in anhydrous dimethyl sulfoxide (70 ml) was added to a solution of sodium methylsulfinylmethide (7.14 g, 71.4 mmol) in anhydrous dimethyl sulfoxide (70 ml). The solution was stirred for 15 min and then a solution of 4.15 g (18.5 mmol) of the hydroxy aldehyde **13** in 90 ml of dry dimethyl sulfoxide was added. The reaction mixture was maintained at 40–50 °C for 1 h, cooled, and diluted with water. The resulting mixture was extracted thoroughly with hexane. The combined extracts were washed with brine and dried over anhydrous magnesium sulfate. Removal of the solvent, followed by distillation (air-bath temperature 100–102 °C; 0.3 Torr) of the residual oil gave 3.78 g (92%) of the olefinic alcohol **14** as a colorless oil. This material crystallized on standing. An analytical sample, obtained by sublimation (40–50 °C/0.35 Torr) of a small sample of this material exhibited m.p. 56.5–57 °C; $[\alpha]_D^{20}$ +43.2° (*c*, 4.0 in $CHCl_3$); i.r. ($CHCl_3$) ν_{max} 3525, 2940, 1637, 1462, 1385, 1115, 1040, 985, 908 cm^{-1}; p.m.r. τ 4.04–4.42 (m, 1H, C*H*=CH_2), 4.86–5.12 (m, 2H, CH=C*H*$_2$), 5.42 (d of d, 1H, C-6 H, $J_{5,6}$ = 7.0 Hz, $J_{6,7}$ = 11.0 Hz), 9.04, 9.12 (d, d, 6H, isopropyl methyls, J = 6.2 Hz), 9.08 (d, 3H, secondary methyl, J = 7.5 Hz), 9.20 (s, 3H, tertiary methyl).

Anal. Calcd. for $C_{15}H_{26}O$: C, 81.02; H, 11.79. Found: C, 80.92; H, 11.75.

Conversion of the Olefinic Alcohol ***14*** *into the Keto Tosylate* ***17***

To a cold (0 °C), stirred solution of the olefinic alcohol **14** (1.0 g, 4.5 mmol) in dry tetrahydrofuran (90 ml), under an atmosphere of nitrogen, was added 7.2 ml of 1.25 *M* borane (9.0 mmol) in tetrahydrofuran. The resulting solution was stirred at room temperature for 1.5 h and then cooled to 0 °C. After successive careful additions of 3 *N* aqueous sodium hydroxide (13.5 ml) and 30% hydrogen peroxide (13.5 ml), the reaction mixture was stirred at room temperature for 1 h, diluted with water, and then thoroughly extracted with ether. The combined extracts were washed with brine and dried over anhydrous magnesium sulfate. Removal of the solvent afforded 1.2 g of the diol **15** as a colorless, viscous oil (i.r. (film) ν_{max} 3390, 1465, 1385, 1145, 1120, 1040 cm^{-1}) which was used directly for the next step.

To a solution of the crude diol **15** in 45 ml of dry pyridine was added 2.25 g of *p*-toluenesulfonyl chloride and the resulting solution was stirred at room temperature, under nitrogen, for 3 h. The reaction mixture was diluted with ether and the resultant solution was successively washed with dilute aqueous sodium bicarbonate, water, and brine, and then dried over anhydrous magnesium sulfate. Removal of the solvent afforded a viscous yellow oil which was subjected to chromatography on neutral silica gel (125 g). Elution of the column with 1:1 chloroform–ether gave 1.4 g (79%) of the hydroxy tosylate **16**, as a viscous oil, i.r. (film) ν_{max} 3510, 1605, 1465, 1365, 1190, 1183, 943 cm^{-1}; p.m.r. τ 2.19, 2.67 (d, d, 4H, aromatic protons, J = 8.5 Hz), 5.44–6.02 (complex m, 3H, C-6 H, and —C*H*$_2$OTs), 7.56 (s, 3H, aromatic methyl), 9.09, 9.22 (d, d, 6H, isopropyl methyls, J = 6.0 Hz), 9.13 (d, 3H, secondary methyl, J = 7.5 Hz), 9.25 (s, 3H, tertiary methyl).

To a stirred solution of dry pyridine (3.42 ml) in anhydrous methylene chloride (95 ml) at room temperature was added 2.14 g of anhydrous chromium trioxide. The solution was stirred at room temperature for 15 min and then a solution of 1.4 g of the hydroxy tosylate **16** in 5 ml of methylene chloride was added. The reaction mixture was stirred for 15 min and then decanted. The black residue was washed thoroughly with ether and the combined organic solutions were successively washed with 5% aqueous sodium hydroxide, 5% hydrochloric acid, dilute aqueous sodium bicarbonate, and brine, and then dried over anhydrous magnesium sulfate. Removal of the solvent afforded 1.25 g (72%, based on olefinic alcohol **14**) of the crude keto tosylate **17** as a semicrystalline material. An analytical sample of the keto tosylate **17**, obtained by recrystallization of a small sample of this material from pentane–ether, exhibited m.p. 117–119 °C; $[\alpha]_D^{25}$ −13.1° (*c*, 1.1 in $CHCl_3$); i.r. ($CHCl_3$) ν_{max} 1733, 1608, 1473, 1368, 1175, 1100 cm^{-1}; p.m.r. τ 2.19, 2.66 (d, d, 4H, aromatic protons, J = 8.5 Hz), 5.80–6.04 (complex m, 2H, —C*H*$_2$OTs), 7.55 (s, 3H, aromatic methyl), 7.70 (m, 1H, C-5 H), 9.00 (d, 3H, secondary methyl, J = 7.2 Hz), 9.02 (s, 3H, tertiary methyl), 9.10, 9.21 (d, d, 6H, isopropyl methyls, J = 6.3 Hz).

Anal. Calcd. for $C_{22}H_{32}O_4S$: C, 67.30; H, 8.22; S, 8.18. Found: C, 67.05; H, 8.05; S, 8.01.

(+)-Copacamphor (3)

To a stirred solution of sodium methylsulfinylmethide (0.21 g, 2.1 mmol) in dry dimethyl sulfoxide (21 ml) at room temperature under nitrogen, was added a solution of the keto tosylate **17** (0.41 g, 1.1 mmol) in 4 ml of dimethyl sulfoxide. The solution was stirred at room temperature for 35 min and then poured into cold water. The resulting mixture was thoroughly extracted with hexane. The combined extracts were washed with brine and dried over anhydrous magnesium sulfate. Removal of the solvent, followed by distillation (air-bath temperature 95–100 °C; 0.5 Torr) of the residual oil afforded 0.20 g (87%) of (+)-copacamphor (**3**) as a colorless oil, $[\alpha]_D^{25}$ +106° (*c*, 1.05 in $CHCl_3$) (lit. (6) $[\alpha]_D$ +98.7° (*c*, 1.7 in $CHCl_3$)); i.r. (film) ν_{max} 1739, 1473, 1450, 1390, 1326, 1300, 1272, 1042, 1013 cm^{-1}; p.m.r. τ 9.06, 9.10 (s, s, 6H, tertiary methyls), 9.09, 9.11 (d, d, 6H, isopropyl methyls, J = 6.4 Hz).

Anal. Calcd. for $C_{15}H_{24}O$: C, 81.76; H, 10.98. Found: C, 81.70; H, 10.95.

Preparation of the Keto Enol Ether ***19***

A solution of the bicyclic diketone **2** (10.4 g, 50 mmol) in 100 ml of dry hexamethylphosphoramide was added to a solution of sodium bis(trimethylsilyl)amide (25 g,

Can. J. Chem. Downloaded from www.nrcresearchpress.com by 210.87.254.105 on 09/05/12
For personal use only.

136 mmol) in 150 ml of dry hexamethylphosphoramide. This mixture was stirred at room temperature in an atmosphere of nitrogen for 15 min, then cooled to 0 °C, and 25 ml of 2-bromopropane was added over a period of 3 min. The cooling bath was removed and stirring was continued at room temperature for 45 min. The reaction mixture was poured into cold brine and the resulting mixture was thoroughly extracted with ether. The combined ether extracts were washed three times with brine and dried over anhydrous magnesium sulfate. Removal of the solvent gave 12.3 g of a mobile oil. A g.l.c. analysis of this material (column D, 168 °C, 100) showed the presence of three components. These were shown to be starting material (diketone **2**), the desired *O*-alkylated product **19**, and the *C*-alkylated product **18** in the ratio of approximately 1:8:1, respectively. Distillation of this crude product through a 2-in. Vigreux column gave 11.0 g of material (b.p. 73–81 °C at 0.025 Torr), which consisted of the starting material, the desired *O*-alkylated product, and a trace of the *C*-alkylated product. The keto enol ether **19** was readily separated from this mixture by chromatography of the latter on activity III neutral alumina. Elution of the column with 2–15% benzene in petroleum ether (b.p. 65–110 °C) afforded 9.55 g (88% based on unrecovered starting material) of pure keto enol ether **19**. This material exhibited n_D^{20} 1.4747; $[\alpha]_D^{25}$ + 145° (*c*, 2.0 in $CHCl_3$); i.r. (film) ν_{max} 1760, 1660 cm^{-1}; p.m.r. τ 5.95 (septet, 1H, $-OCH(CH_3)_2$, J = 6.1 Hz), 6.99 (broad s, 1H, C-5 H, $w_{\frac{1}{2}}$ = 3.3 Hz), 8.32 (d, 3H, vinyl methyl, J = 0.9 Hz), 8.74, 8.89 (d, d, 6H, $-OCH(CH_3)_2$, J = 6.1 Hz), 8.98 (s, 3H, tertiary methyl), 9.04, 9.13 (d, d, 6H, isopropyl methyls, J = 6.4 Hz).

Anal. Calcd. for $C_{16}H_{26}O_2$: C, 76.75; H, 10.47. Found: C, 76.55; H, 10.46.

Further elution of the column with 15–50% benzene in petroleum ether (b.p. 65–110 °C) gave 1.37 g of the crystalline starting material (diketone **2**), containing a very small amount of *C*-alkylated material. A pure sample of the latter compound was obtained as follows. Hot box distillation (air-bath temperature 115 °C; 0.3 Torr) of the still-pot residue of the original distillation (see above) yielded 1.2 g of crystalline material. Recrystallization of this material from hexanes gave an analytical sample of **18**, which exhibited m.p. 60.5 °C; i.r. ($CHCl_3$) ν_{max} 1758, 1722 cm^{-1}; p.m.r. τ 7.15 (broad s, 1H, C-5 H, $w_{\frac{1}{2}}$ = 4.3 Hz), 8.85, 8.90 (s, s, 6H, tertiary methyls), 8.97, 9.12 (d, d, 6H, isopropyl methyls, J = 6.9 Hz).

Anal. Calcd. for $C_{16}H_{26}O_2$: C, 76.75; H, 10.47. Found: C, 76.60; H, 10.55.

Preparation of the Diethers ***20***

A slurry of methoxymethyltriphenylphosphonium chloride (71.5 g, 208 mmol) in 615 ml of anhydrous ether was cooled to 0 °C under an atmosphere of nitrogen. To this stirred mixture was added, via a syringe, 73.5 ml of a 2.34 *M* hexane solution of *n*-butyllithium over a period of 2 min. The resulting phosphorane solution was stirred for a further 10 min. A solution of the keto enol ether **19** (11.65 g, 46.5 mmol) in 170 ml of anhydrous ether was then added over a period of 4 min, the cooling bath was removed, and the reaction mixture was refluxed for 30 min. The cooled solution was poured into cold water, the layers were separated, and the aqueous layer was extracted once with ether. The combined ether layers were washed twice with brine and dried over anhydrous magnesium sulfate. Removal of the solvent and distillation of the resultant crude material (55.0 g) gave 14.2 g of colorless oil with b.p. 94–103 °C at 0.2 Torr. Analysis by g.l.c. (column D, 155 °C, 110) showed that this material contained three unidentified minor components to the extent of approximately 10%, thus indicating that the desired diethers **20** were formed in quantitative yield. The ratio of the component diastereomers **20** as determined by g.l.c. (same column and conditions) varied somewhat from experiment to experiment but the average ratio was approximately 65:35, with the same isomer always predominating. Attempts to remove the impurities from this distilled material by column chromatography (neutral alumina, activity I or III, or Florisil) were unsuccessful because of poor recovery of the diethers from the columns and/or owing to poor separation. Consequently, this mixture was used in the next reaction without further purification. An analytical sample of the diastereomeric diether mixture **20**, was obtained, however, by preparative g.l.c. (column E, 185 °C, 105) and it exhibited i.r. (film) ν_{max} 1707, 1664 cm^{-1}; p.m.r., τ 4.43, 4.52 (s, s, 1H, vinyl protons), 5.92, 5.97 (septets, 1H, J = 6.1, 6.1 Hz), 6.49, 6.56 (s, s, 3H, methoxy methyls).

Anal. Calcd. for $C_{18}H_{30}O_2$: C, 77.65; H, 10.86. Found: C, 77.52; H, 11.11.

Preparation of the Keto Aldehydes ***21*** *and* ***22***

A solution of the impure diethers **20** (10.8 g) in 180 ml of ether was added to a solution of 70% perchloric acid (120 ml) in 700 ml of ether. The resulting mixture was stirred at room temperature under a nitrogen atmosphere for 1.5 h. It was then washed successively with ice water, with dilute sodium bicarbonate solution, and with brine, and dried over anhydrous magnesium sulfate. Removal of the solvent and distillation of the residual oil gave 7.7 g of material with b.p. 108–110 °C at 0.07 Torr. A g.l.c. analysis (column F, 168 °C, 110) of this material showed that the ratio of the keto aldehydes **21** and **22** was approximately 1:1.

This material (7.7 g) was dissolved in 325 ml of methanol and the resulting solution was added to a solution of anhydrous potassium carbonate (9.5 g) in 800 ml of water. The resultant mixture was stirred at room temperature under a nitrogen atmosphere for 1.5 h. It was then diluted with water and extracted three times with petroleum ether (b.p. 68 °C) – ether (4:1). The combined extracts were washed with water, with brine, and dried over anhydrous magnesium sulfate. Removal of the solvent and distillation of the residue gave 7.05 g of a colorless oil, b.p. 106–109 °C at 0.05 Torr. A g.l.c. analysis (column F, 168 °C, 110) of this material showed that it was composed of the desired products (88%), keto aldehydes **21** and **22** in a ratio of 84:16, respectively, and impurities (12%) which were not identified but were presumably related to those in the starting material. Thus the effective overall yield for the hydrolysis and epimerization reactions was 80%. Owing to the unstable nature of the epimeric keto aldehydes **21** and **22**, it was not possible to separate these epimers from each other or from the other contaminants by column chromatography (silica gel or activity III neutral alumina). Consequently, this material was used in the next reaction without further

Can. J. Chem. Downloaded from www.nrcresearchpress.com by 210.87.254.105 on 09/05/12
For personal use only.

purification. The impure keto aldehyde product mixture exhibited i.r. (film) ν_{max} 2745, 1735, 1715 (shoulder) cm^{-1}; p.m.r. τ −0.10, −0.03 (d, d, 1H, aldehydic protons, J = 1.0, 2.0 Hz, respectively).

Preparation of Keto Olefins ***23*** *and* ***24***

To a stirred solution of sodium methylsulfinylmethide (2.25 g, 22.5 mmol) in dry dimethyl sulfoxide (52 ml) at 20 °C, under an atmosphere of nitrogen, was added 9.64 g (27.0 mmol) of methyltriphenylphosphonium bromide and the resulting solution was stirred at room temperature for 10 min. To this solution was added, over a period of 3 min, a solution of 1.046 g (approximately 4.15 mmol) of the impure keto aldehyde mixture (**21** and **22**) in 26 ml of dry dimethyl sulfoxide. Stirring was continued for a further 1 h at room temperature. The solution was poured into ice water and the resulting mixture was extracted three times with petroleum ether (b.p. 68 °C). The combined extracts were washed with brine and dried over anhydrous magnesium sulfate. Removal of the solvent and distillation (air-bath temperature 82–95 °C; 0.07 Torr) of the residue gave 991 mg of a colorless oil. A g.l.c. analysis (column G, 175 °C, 110) showed that this material was composed of a mixture of the keto olefins (92%), **23** and **24** in a ratio of 84:16, respectively, and unidentified minor components (8%). This represents a quantitative yield of keto olefins based on pure starting material. The two epimers were only partially separated by column chromatography on silica gel. However, total separation was achieved by column chromatography using Camag Kieselgel for t.l.c. (without binder) and 98:2 petroleum ether (b.p. 68 °C) – ether as eluting solvent. A positive pressure (nitrogen) was required to maintain a reasonable flow rate. The ratio of compound to silica gel was 1:100. The recovery of both keto olefins from the column was quantitative. However, while the minor epimer **24**, a colorless crystalline compound, was obtained in pure form, the major epimer **23** contained minor impurities (approximately 4% as determined by g.l.c.). Therefore, an analytical sample of the keto olefin **23** was obtained by preparative g.l.c. (column C, 198 °C, 170) of the material obtained from chromatography on silica gel. This analytical sample, a colorless oil, exhibited $[\alpha]_D^{25}$ +51.5° (*c*, 2.0 in $CHCl_3$); i.r. (film) ν_{max} 3080, 1730, 1634, 910 cm^{-1}; p.m.r. τ 3.99–4.37 (m, 1H, $-CH{=}CH_2$), 4.86–5.10 (m, 2H, $-CH{=}CH_2$), 7.41 (broad s, 1H, C-5 H, $w_{\frac{1}{2}}$ = 4.5 Hz), 7.79 (d, 1H, C-8 H, J = 7.9 Hz), 7.97 (q, 1H, C-7 H, J = 7.2 Hz), 8.99 (s, 3H, tertiary methyl), 8.99, 9.20 (d, d, 6H, isopropyl methyls, J = 6.2 Hz), 9.06 (d, 3H, secondary methyl, J = 7.2 Hz).

Anal. Calcd. for $C_{15}H_{24}O$: C, 81.76; H, 10.98. Found: C, 81.64; H, 11.07.

The crystalline keto olefin **24** (the minor component) was recrystallized from pentane and exhibited m.p. 28.5–29 °C; $[\alpha]_D^{25}$ +130° (*c*, 2.5 in $CHCl_3$); i.r. ($CHCl_3$) ν_{max} 3080, 1724, 1633, 916 cm^{-1}; p.m.r. τ 3.71–4.08 (m, 1H, $-CH{=}CH_2$), 4.68–4.92 (m, 2H, $-CH{=}CH_2$), 7.42 (broadened d, 1H, C-5 H, $J_{5,8}$ = 5.6 Hz), 7.64 (d of d, 1H, C-8 H, J = 8.3, 5.6 Hz), 8.17 (q, 1H, C-7 H, J = 7.0 Hz), 9.01 (d, 3H, secondary methyl, J = 7.0 Hz), 9.05 (s, 3H, tertiary methyl), 9.05, 9.18 (d, d, 6H, isopropyl methyls, J = 5.9 Hz).

Anal. Calcd. for $C_{15}H_{24}O$: C, 81.76; H, 10.98. Found: C, 81.52; H, 11.10.

Preparation of the Keto Alcohol ***25***

To a stirred solution of disiamylborane (1.8 g, 12.7 mmol) in dry tetrahydrofuran (16 ml) at 0 °C under a nitrogen atmosphere was added a solution of the keto olefin **23** (0.66 g, 3 mmol) in 7 ml of dry tetrahydrofuran and the resulting reaction mixture was stirred for 45 min at 0 °C. The reaction was quenched by the careful addition at 0 °C of 6 ml of 3 *N* aqueous sodium hydroxide followed by 6 ml of 30% hydrogen peroxide. The cooling bath was removed and stirring was continued at room temperature for 1 h. The tetrahydrofuran was removed at aspirator pressure, water was added to the residue, and the resulting mixture was thoroughly extracted with ether. The combined organic extracts were washed with brine and dried over anhydrous magnesium sulfate. Removal of the solvent and distillation (air-bath temperature 135–145 °C; 0.2 Torr) of the residue gave 579 mg (81%) of a viscous oil. A g.l.c. analysis (column H, 175 °C, 100) of this material indicated the presence of two components in the approximate ratio of 85:15. Chromatography of this mixture on silica gel or activity III neutral alumina afforded no useful separation of the two products.

Pure samples of the desired keto alcohol **25** and of the contaminating diol **26** were obtained for analytical purposes via their silyl ether derivatives. Thus, a solution of 239 mg (1.0 mmol) of the product mixture in 2 ml of dry pyridine containing 0.4 ml of hexamethyldisilazane and 0.2 ml of trimethylchlorosilane was stirred in an atmosphere of nitrogen at room temperature for 15 min. This mixture was filtered, the solvent was evaporated, and the residue was distilled (air-bath temperature 125–130 °C; 0.25 Torr) to give 323 mg of a mobile oil. This material was shown by g.l.c. analysis (column D, 190 °C, 100) to consist of a mixture of two components in a ratio of 85:15. An attempt to separate the components on a silica gel column resulted in the partial hydrolysis of the silyl ether blocking groups but an efficient separation was effected by preparative g.l.c. (column C, 220 °C, 200). Thus, 300 mg of the mixture yielded, after collection and distillation, 204 mg of the pure keto trimethylsilyl ether **27** and 44 mg of the bistrimethylsilyl ether derivative **28**. The keto trimethylsilyl ether **27** exhibited i.r. (film) ν_{max} 1727, 1250, 1090, 840, 745 cm^{-1}; p.m.r. τ 6.39 (complex m, 2H, $-CH_2OTMS$), 7.45 (broad s, 1H, C-5 H, $w_{\frac{1}{2}}$ = 4.6 Hz), 8.97 (s, 3H, tertiary methyl), 9.00, 9.18 (d, d, 6H, isopropyl methyls, J = 6.1 Hz), 9.04 (d, 3H, secondary methyl, J = 7.0 Hz), 9.88 (s, 9H, $-OSi(CH_3)_3$).

Hydrolysis of the keto trimethylsilyl ether **27** gave the desired keto alcohol **25**. Thus, a solution of the silyl ether (220 mg, 0.71 mmol) in 3 ml of ethanol and 0.1 ml of water was refluxed in an atmosphere of nitrogen for 4 h. The solvent was removed at aspirator pressure and the residue was distilled (air-bath temperature 127–130 °C; 0.04 Torr) to give 150 mg (89%) of a viscous oil. Analysis of this material by g.l.c. (column H, 175 °C, 100) showed that it was one component. It exhibited $[\alpha]_D^{25}$ +30.5° (*c*, 0.7 in $CHCl_3$); i.r. (film) ν_{max} 3400, 1724 cm^{-1}; p.m.r. τ 6.34 (complex m, 2H, $-CH_2OH$), 7.46 (broad s, 1H, C-5 H, $w_{\frac{1}{2}}$ = 4.8 Hz), 7.87 (s, 1H, exchangeable, —OH), 8.96 (s, 3H, tertiary methyl), 8.99, 9.18 (d, d, 6H, isopropyl methyls, J = 6.1 Hz), 9.03 (d, 3H, secondary methyl, J = 7.1 Hz).

Anal. Calcd. for $C_{15}H_{26}O_2$: C, 75.58; H, 10.99. Found: C, 75.32; H, 11.19.

Can. J. Chem. Downloaded from www.nrcresearchpress.com by 210.87.254.105 on 09/05/12
For personal use only.

The minor component **28** in the silyl ether mixture was also collected by preparative g.l.c., as mentioned above. It exhibited i.r. (film) ν_{max} 1250, 1060, 840, 750 cm^{-1}; p.m.r. τ 5.53 (d of d, 1H, —C*H*OTMS, J = 6.8, 10.5 Hz), 6.40 (complex m, 2H, —CH_2OTMS), 7.73 (broadened d, 1H, C-5 H, J = 6.8 Hz), 9.10, 9.20 (d, d, 6H, isopropyl methyls, J = 6.5 Hz), 9.15 (s, 3H, tertiary methyl), 9.23 (d, 3H, secondary methyl, J = 7.0 Hz), 9.89, 9.95 (s, s, 18H, —OTMS groups). This material was hydrolyzed to the diol **26** in a manner similar to that used for the hydrolysis of the keto silyl ether **27**. From 44 mg of **28** there was obtained 25 mg of the viscous diol **26** which exhibited i.r. (film) ν_{max} 3350 cm^{-1}; p.m.r. τ 5.60 (d of d, 1H, —C*H*OH, J = 6.9, 10.6 Hz), 6.41 (complex m, 2H, —CH_2OH), 7.83 (broadened d, 1H, C-5 H, J = 6.9 Hz), 9.18, 9.28 (d, d, 6H, isopropyl methyls, J = 6.6 Hz), 9.25 (s, 3H, tertiary methyl), 9.29 (d, 3H, secondary methyl, J = 7.1 Hz). This diol decomposed slowly on standing in deuteriochloroform solution at room temperature.

(−)-Ylangocamphor (6)

(a) From the Pure Keto Alcohol 25

A solution of the keto alcohol **25** (109 mg, 0.458 mmol) in 3.5 ml of dry pyridine containing 229 mg (1.0 mmol) of methanesulfonyl chloride was stirred in an atmosphere of nitrogen at room temperature for 2.25 h. The reaction mixture was then poured into 25 ml of cold water and the aqueous layer was extracted three times with ether. The combined ether extracts were washed with cold 10% hydrochloric acid, with water, and with brine, and dried over anhydrous magnesium sulfate. Removal of the solvent gave 173 mg of a viscous oil which exhibited i.r. (film) ν_{max} 1728 cm^{-1}. A solution of this crude keto mesylate in 2 ml of dry dimethoxyethane was added to a solution of sodium bis(trimethylsilyl)amide (450 mg, 2.46 mmol) in 5 ml of dry dimethoxyethane at 0 °C. The cooling bath was immediately removed, the reaction mixture was stirred at room temperature in an atmosphere of nitrogen for 40 min, and was then poured into 25 ml of cold water. The resulting mixture was thoroughly extracted with hexane. The combined extracts were washed with water and brine and dried over anhydrous magnesium sulfate. Removal of the solvent and distillation (air-bath temperature 72–74 °C; 0.04 Torr) of the residue gave 85 mg (84% from the keto alcohol **25**) of (−)-ylangocamphor (**6**). This material was pure by gas–liquid chromatographic analysis (columns: A, 170 °C, 115; E, 190 °C, 110; I, 201 °C, 118) and it crystallized on refrigeration. A sample was recrystallized from hexanes at −35 to −40 °C yielding colorless crystals with m.p. 25–25.5 °C; $[\alpha]_D^{26}$ −58° (*c*, 1.0 in $CHCl_3$); i.r. (film) ν_{max} 1733 cm^{-1}; p.m.r. τ 7.76 (broad s, 1H, bridgehead H adjacent to —C=O, $w_{\frac{1}{2}}$ = 3.0 Hz), 9.02, 9.19 (d, d, 6H, isopropyl methyls, J = 6.5 Hz), 9.10, 9.11, (s, s, 6H, tertiary methyls).

Anal. Calcd. for $C_{15}H_{24}O$: C, 81.76; H, 10.98. Found: C, 81.91; H, 11.18.

(b) From the Mixture of Keto Alcohol 25 and Diol 26

The keto alcohol – diol mixture (239 mg) obtained from hydroboration of the keto olefin **23** (*vide supra*) was converted into the mesylate derivative mixture by a procedure identical with that used in the case of the pure keto alcohol. Similarly, the crude mixture of mesylate derivatives thus obtained was cyclized (without purification) as above, using 915 mg (5 mmol) of sodium bis(trimethylsilyl)amide and 14 ml of dry dimethoxyethane. Simple distillation of the product (hot box) yielded 135 mg (50% overall from the keto olefin **23**) of pure (−)-ylangocamphor (**6**). This material exhibited physical and spectral properties identical with those recorded above.

(−)-Ylangoborneol (7)

To a reaction vessel containing 12.5 ml of refluxing anhydrous ammonia was added 50 mg (1.25 mmol) of calcium metal followed, 5 min later, by a solution of (−)-ylangocamphor (**6**) (57 mg, 0.259 mmol) in 1.1 ml of anhydrous ether. The resulting mixture was stirred at reflux temperature for 30 min and 150 µl of anhydrous ethanol was then added. Care was taken at all times to exclude water from the system. When the blue color was discharged, ether was added and the mixture was poured into water. The water layer was thoroughly extracted with ether and the combined extracts were washed with brine until neutral and then dried over anhydrous magnesium sulfate. Filtration through Celite and removal of the solvent from the filtrate gave a residue which was distilled (air-bath temperature 108 °C; 0.04 Torr) to yield 55 mg (96%) of crystalline (−)-ylangoborneol (**7**). This material consisted of only one component by gas–liquid chromatographic analysis (columns: E, 188 °C, 110; D, 168 °C, 100; I, 195 °C, 105. Note: columns E and I resolve a mixture of ylangoborneol and ylangoisoborneol). Recrystallization from hexanes gave a sample exhibiting m.p. 60.5–61 °C; $[\alpha]_D^{25}$ −23° (*c*, 0.4 in $CHCl_3$); i.r. ($CHCl_3$), ν_{max} 3610, 3460 cm^{-1}; p.m.r. (*i*) ($CDCl_3$) τ 6.17 (broad s, 1H, —C*H*OH, $w_{\frac{1}{2}}$ = 3.2 Hz), 8.60 (s, 1H, exchangeable, —OH), 9.05, 9.15 (d, d, 6H, isopropyl methyls, J = 6.4 Hz), 9.13, 9.19 (s, s, 6H, tertiary methyls); (*ii*) (CCl_4) 6.26 (broad s, 1H, —C*H*OH, $w_{\frac{1}{2}}$ = 3.2 Hz), 8.90 (s, 1H, exchangeable, —OH), 9.06, 9.14 (d, d, 6H, isopropyl methyls, J = 6.5 Hz), 9.15, 9.19 (s, s, 6H, tertiary methyls).

Anal. Calcd. for $C_{15}H_{26}O$: C, 81.02; H, 11.79. Found: C, 80.75; H, 11.69.

(−)-Ylangoisoborneol (8)

An anhydrous ether solution (5 ml) of (−)-ylangocamphor (**6**) (110 mg, 0.5 mmol) containing 25 mg of lithium aluminum hydride was refluxed under an atmosphere of nitrogen for 1 h. The reaction mixture was cooled to 0 °C, 1 ml of saturated aqueous ammonium chloride solution was added, and stirring was continued for 45 min at room temperature. The mixture was filtered through Celite and the Celite was thoroughly washed with ether. The filtrate was washed with brine and dried over anhydrous magnesium sulfate. Removal of the solvent followed by distillation (air-bath temperature 100–102 °C; 0.12 Torr) of the residue gave 101 mg (91%) of (−)-ylangoisoborneol (**8**). This material consisted of only one component on analysis by g.l.c. (columns and conditions: same as for (−)-ylangoborneol) and it crystallized on refrigeration. Recrystallization from hexanes at −10 °C gave colorless crystals which were somewhat soft at room temperature (22 °C) and exhibited m.p. 31.5–32.5 °C; $[\alpha]_D^{26}$ −28° (*c*, 1.0 in $CHCl_3$); i.r. (film) ν_{max} 3630, 3495 cm^{-1}; p.m.r. (*i*)

($CDCl_3$) τ 6.22 (d, 1H, —C*H*OH, J = 7.6 Hz), 7.88 (broadened d, 1H, bridgehead H adjacent to —CHOH, J = 7.6 Hz), 8.68 (s, 1H, exchangeable, —OH), 9.04, 9.17 (d, d, 6H, isopropyl methyls, J = 6.5 Hz), 9.15, 9.21 (s, s, 6H, tertiary methyls); (*ii*) (CCl_4) τ 6.27 (d, 1H, —C*H*OH, J = 7.6 Hz), 7.91 (broadened d, 1H, bridgehead H adjacent to —CHOH, J = 7.6 Hz), 8.87 (s, 1H, exchangeable, —OH), 9.08, 9.20 (d, d, 6H, isopropyl methyls, J = 6.5 Hz), 9.18, 9.22 (s, s, 6H, tertiary methyls). The chemical shift assigned to the bridgehead proton adjacent to the —CHOH was confirmed by a frequency-swept decoupling experiment in which the proton at τ 6.27 was irradiated, thus causing the doublet at τ 7.91 to collapse to a broadened singlet.

Anal. Calcd. for $C_{15}H_{26}O$: C, 81.02; H, 11.79. Found: C, 80.99; H, 11.86.

Financial support from the National Research Council of Canada and the University of British Columbia Committee on Research is gratefully acknowledged.

1. E. PIERS, R. W. BRITTON, M. B. GERAGHTY, R. J. KEZIERE, and R. D. SMILLIE. Can. J. Chem. This issue.
2. E. PIERS, R. W. BRITTON, R. J. KEZIERE, and R. D. SMILLIE. Can. J. Chem. **49**, 2620 (1971).
3. E. PIERS, M. B. GERAGHTY, F. KIDO, and M. SOUCY. Synth. Commun. **3**, 39 (1973).
4. L. WESTFELT. Acta Chem. Scand. **20**, 2829 (1966).
5. L. WESTFELT. Acta Chem. Scand. **20**, 2841 (1966).
6. M. KOLBE-HAUGWITZ and L. WESTFELT. Acta Chem. Scand. **24**, 1623 (1970).
7. R. GREENWALD, M. CHAYKOVSKY, and E. J. COREY. J. Org. Chem. **28**, 1128 (1963).
8. G. ZWEIFEL and H. C. BROWN. Org. React. **13**, 1 (1963).
9. J. C. COLLINS, W. W. HESS, and F. J. FRANK. Tetrahedron Lett. 3363 (1968).
10. R. RATCLIFFE and R. RODEHORST. J. Org. Chem. **35**, 4000 (1970).
11. E. J. COREY and M. CHAYKOVSKY. J. Am. Chem. Soc. **87**, 1345 (1965).
12. M. TANABE and D. F. CROW. Chem. Commun. 1498 (1969), and references cited therein.
13. W. J. LENOBLE. Synthesis, 1 (1970).
14. M. KARPLUS. J. Am. Chem. Soc. **85**, 2870 (1963).
15. H. C. BROWN and G. ZWEIFEL. J. Am. Chem. Soc. **83**, 1241 (1961).
16. W. S. MURPHY and D. F. SULLIVAN. Tetrahedron Lett. 3707 (1971).
17. A. COULOMBEAU and A. RASSAT. Chem. Commun. 1587 (1968).

Can. J. Chem. Downloaded from www.nrcresearchpress.com by 210.87.254.105 on 09/05/12
For personal use only.

Stereoselective Total Synthesis of Copa and Ylango Sesquiterpenoids: (−)-Copacamphene, (−)-Cyclocopacamphene, (+)-Sativene, (+)-Cyclosativene

EDWARD PIERS, M. BERT GERAGHTY, R. DEAN SMILLIE, AND MARCEL SOUCY

Department of Chemistry, University of British Columbia, 2075 Wesbrook Place, Vancouver, British Columbia V6T 1W5

Received May 15, 1975

EDWARD PIERS, M. BERT GERAGHTY, R. DEAN SMILLIE, and MARCEL SOUCY. Can. J. Chem. **53**, 2849 (1975).

Stereoselective total syntheses of the tricyclic sesquiterpenoids (−)-copacamphene (**1**) and (+)-sativene (**3**) and of the related tetracyclic compounds (−)-cyclocopacamphene (**2**) and (+)-cyclosativene (**4**) are described. An efficient four-step synthetic sequence was employed to convert the bicyclic dione **5** into the olefinic ketone **8**. The latter compound was converted in four steps into the olefinic alcohol **23**. Eliminative cyclization of the corresponding tosylate **25** gave (−)-copacamphene (**1**) in high yield. In similar fashion, (+)-sativene (**3**) was obtained by cyclization of the olefinic tosylate **42**, which in turn was derived via a four-step synthetic sequence from the olefinic ketone **9**. Oxidation of the olefinic alcohol **23** afforded the aldehyde **34**. Conversion of the latter compound into the *p*-tosylhydrazone **35**, followed by pyrolysis of the corresponding lithium salt **36**, gave the pyrazoline **37**. Photolysis of **37** afforded, in high yield, (−)-cyclocopacamphene (**2**). Similarly, (+)-cyclosativene (**4**) was obtained from the olefinic alcohol **41** via the pyrazoline **46**.

EDWARD PIERS, M. BERT GERAGHTY, R. DEAN SMILLIE et MARCEL SOUCY. Can. J. Chem. **53**, 2849 (1975).

On décrit des synthèses totales et stéréosélectives des sesquiterpénoides tricycliques (−) copacamphène (**1**) et (+) sativène (**3**) et des composés tétracycliques (−) cyclocopacamphène (**2**) et (+) cyclosativène (**4**) qui leur sont reliés. On a utilisé une séquence de synthèse efficace impliquant 4 étapes pour transformer la dione **5** en cétone non-saturée **8**. On a converti ce dernier composé en alcool oléfinique **23** en quatre étapes. L'élimination cyclisante du tosylate correspondant **25** donne le (−) copacamphène (**1**) avec un bon rendement. De la même manière, on obtient le (+) sativène (**3**) par cyclisation du tosylate non-saturé **42**, qui dérive de la cétone non-saturée **9** par l'intermédiaire d'une séquence de synthèse en 4 étapes. L'oxydation de l'alcool insaturé **23** fournit l'aldéhyde **34** qui est transformé en *p*-tosylhydrazone **35**. La pyrolyse du sel de lithium de cette dernière (**36**) donne la pyrazoline **37** qui par photolyse conduit, avec un bon rendement, au (−) cyclocopacamphène (**2**). On obtient le (+) cyclosativène (**4**) de la même manière à partir de l'alcool **41** par l'intermédiaire de la pyrazoline **46**.

[Traduit par le journal]

The tricyclic olefinic sesquiterpenoid (−)-copacamphene (**1**) has not as yet been directly isolated from a naturally occurring source, although it has been obtained by rearrangement of a derivative of (+)-copaborneol (1).[1] The structurally related tetracyclic compound (+)-cyclocopacamphene (enantiomer of **2**) has been obtained by chemical conversion from cyclocopacamphenic acids (2) and has been shown to occur in a number of vetiver oils (3). The corresponding ylango sesquiterpenoids are known natural products. (−)-Sativene (enantiomer of **3**) is a well-known compound first isolated in 1965 from the fungus *Helminthosporium sativum* (4), while (+)-sativene (**3**), as well as the structurally and configurationally related tetracyclic compound (+)-cyclosativene (**4**), have been acquired from the cortical turpentine of a number of different *Abies* species (5–7).

In a previous paper (8) we described the stereoselective total synthesis of the diastereomeric bicyclic diketones **5** and **6**. Both of the compounds were prepared from the well-known monoterpenoid (−)-carvone (**7**) and were thus of known absolute stereochemistry. We report herein the

[1]Although Kolbe-Haugwitz and Westfelt (1) were correct in their assignments regarding absolute stereochemistry, it is now clear that copacamphene of absolute configuration as shown in **1** is levorotatory ($[\alpha]_D^{21}$ −159°, *vide infra*) and not dextrorotatory ($[\alpha]_D$ +28.9°) as reported (1). It has not been possible to trace the reason for this discrepancy (private communication from Dr. Westfelt).

Can. J. Chem. Downloaded from www.nrcresearchpress.com by 210.87.254.6 on 09/05/12
For personal use only.

Can. J. Chem. Downloaded from www.nrcresearchpress.com by 210.87.254.6 on 09/05/12
For personal use only.

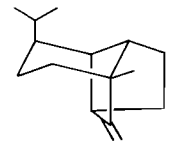

1

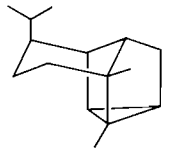

2

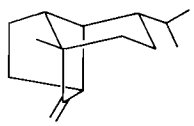

3

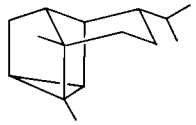

4

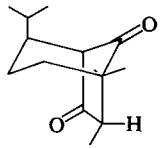

5

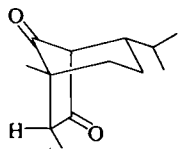

6

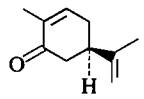

7

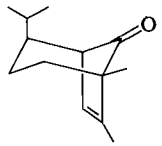

8

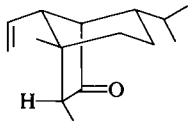

9

total synthesis of (−)-copacamphene (**1**), (−)-cyclocopacamphene (**2**), (+)-sativene (**3**), and (+)-cyclosativene (**4**) via synthetic routes which unambiguously establish the structure and absolute configuration of all four sesquiterpenoids.[2] More explicitly, we describe in this paper (*a*) the conversion of the bicyclic diketone **5** into the olefinic ketone **8**, (*b*) the transformation of compound **8** into the sesquiterpenoids **1** and **2**, and (*c*) the conversion of the olefinic ketone **9** (obtained, as described previously (11), from the bicyclic dione **6**) into the natural products **3** and **4**.

[2]For preliminary communications regarding portions of this work, see refs. 9 and 10. For a summary of other synthetic work done in this general area, see ref. 8, footnote 2.

Conversion of Diketone 5 into Olefinic Ketone 8 (see Scheme 1)

The synthetic plan for the overall synthesis of (−)-copacamphene (**1**) and (−)-cyclocopacamphene (**2**) from the bicyclic diketone **5** involved in the early stages the conversion of the latter compound into the olefinic ketone **8**. The carbonyl group of this material was to be employed for the subsequent introduction of the two necessary additional carbon atoms, suitably functionalized to allow for the completion of the carbon skeletons of **1** and **2**.

A number of different routes for the overall conversion of **5** into **8** were investigated. The first of these was based on the known reduction of enol phosphate derivatives to the corresponding olefin (12–14). Thus, treatment of the dione **5** with sodium bis(trimethylsilyl)amide (15) in tetrahydrofuran, followed by quenching of the resultant enolate anion by addition of a solution of diethyl phosphorochloridate in pyridine, afforded in 94% yield the enol phosphate derivative **10**. Reduction of this material with lithium in ethylamine containing *t*-butyl alcohol (12) gave, in mediocre yield, a mixture of products consisting of the desired olefinic ketone **8**, the olefinic alcohol **11**, the saturated ketone **12**, and a number of minor unidentified components. This reduction reaction was studied in considerable detail and the effect of varying a number of reaction parameters (reactant concentration, reaction temperature, proton source, reaction time) was investigated. However, the reaction proved to be capricious and the maximum yield of desired product **8** obtained was about 25%. Furthermore, although subjection of the crude product to oxidation effected conversion of the olefinic alcohol **11** into the desired ketone **8** and thus reduced the number of individual components in the mixture, a rather tedious preparative g.l.c. procedure was necessary to effect final isolation of the desired product. In view of these difficulties, an alternative synthetic route to **8** was sought.

It is known that pyrolysis of salts of *p*-toluenesulfonylhydrazone derivatives of aldehydes and ketones produces the corresponding diazo compounds, which, depending mainly upon the character of the solvent employed, can decompose *in situ* by carbenic or cationic processes (16). In many cases, this process, known as the Bamford–Stevens reaction, results in the formation of the

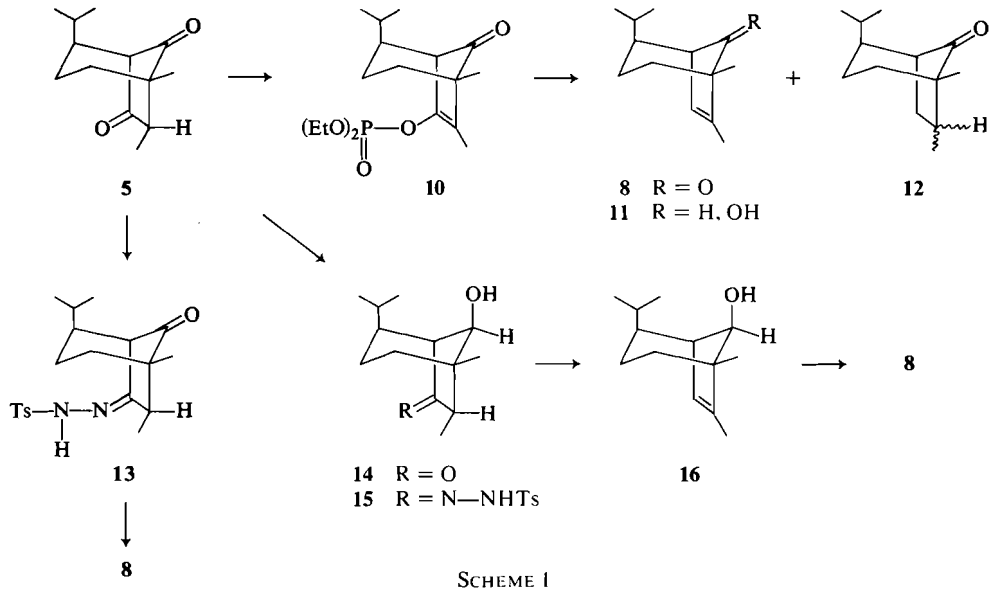

SCHEME 1

corresponding alkene as the major product. When the bicyclic dione **5** was allowed to react with *p*-toluenesulfonylhydrazide in methanol in the presence of an acid catalyst, the required mono *p*-tosylhydrazone **13** was produced in good yield. Although the crude material was used directly for the next synthetic step, an analytical sample of **13** was obtained by column chromatography of a small sample of the crude product and exhibited spectral data in full accord with the assigned structure. Subjection of the crude *p*-tosylhydrazone **13** to the Bamford–Stevens reaction under protic conditions (sodium ethylene glycolate in ethylene glycol) produced in low yield a crude product consisting of many components. However, use of aprotic conditions proved to be more successful. Thus, when the sodium salt of **13** (formed by reaction of **13** with sodium bis(trimethylsilyl)amide in tetrahydrofuran) was mixed with a small amount of Nujol and the resulting mixture was heated under reduced pressure to 125 °C with direct distillation of product, a clear oil was obtained in reasonably good yield. Analysis of this material by g.l.c. indicated that although the major product was the desired olefinic ketone **8**, a number of minor unidentified components were also present. Again, purification of this material by a combination of column chromatography and g.l.c. proved to be quite tedious and the isolated yield of pure **8** was only ~40%. Although this was a definite improvement over the enol phosphate reduction route, it remained synthetically unsatisfying.

Another, more recently developed method for the conversion of a *p*-tosylhydrazone into an alkene involves treatment of the former with an excess of an alkyllithium reagent (17–21). Obviously, however, this method would not be directly applicable to the *p*-tosylhydrazone **13**, since the alkyllithium reagent would presumably add to the carbonyl group in addition to effecting decomposition of the hydrazone moiety. This undesirable possibility was avoided by employing a somewhat circuitous, albeit very efficient, route.

It was found that the two carbonyl groups of the bicyclic dione **5** could be differentiated by selective reduction. Thus, when **5** was allowed to react with one equivalent of sodium borohydride in ethanol at 0 °C, the C-8 carbonyl group was preferentially reduced. The reaction appeared to be completely stereoselective as well as siteselective and the keto alcohol **14** could be isolated in 89% yield. The p.m.r. spectrum of the product was in full accord with structure **14**. In particular, the carbinol proton at C-8 appeared as a doublet (J = 5.5 Hz) at τ 6.12. Clearly, had preferential reduction of the C-6 carbonyl group of **5** taken place, the carbinol proton of the product would have appeared as a pair of doublets. Furthermore, the stereochemistry of the reduction

Can. J. Chem. Downloaded from www.nrcresearchpress.com by 210.87.254.6 on 09/05/12
For personal use only.

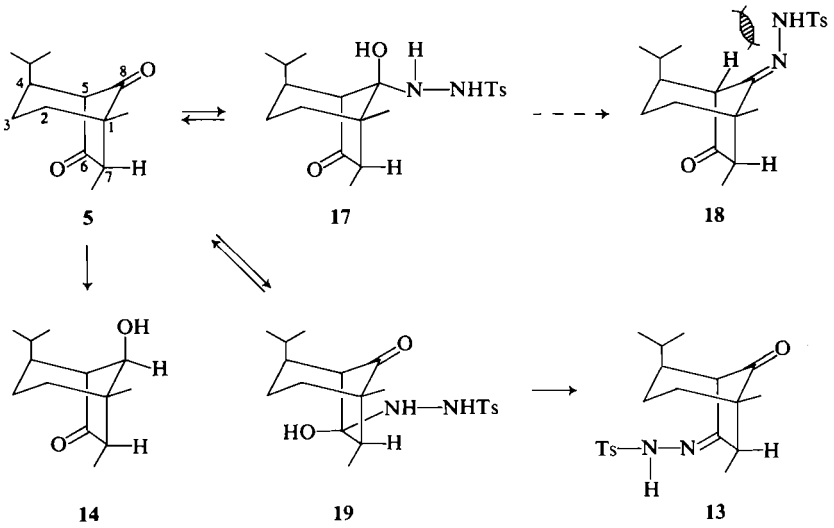

5 17 18

14 19 13

product, expected to be as shown in **14** on the basis of approach of the reducing agent from the less hindered side of the carbonyl group, was also confirmed by the p.m.r. spectrum. Explicitly, the observed coupling constant (5.5 Hz) between the protons on C-5 and C-8 was in good agreement with that predicted by the Karplus equation (22) for a dihedral angle of about 40–45°. Had the reduction reaction produced the epimeric alcohol, the dihedral angle between these two protons would have been approximately 75–80° and a very small coupling constant would have been expected.

Conversion of the keto alcohol **14** into the corresponding *p*-tosylhydrazone **15**, followed by treatment of the latter with 8 equiv. of methyllithium in tetrahydrofuran–ether at 0 °C (21), afforded, in 86% overall yield, the levorotatory olefinic alcohol **16**. Oxidation of this material with either Collins' reagent (23, 24) or with Jones' reagent (25) produced good yields (about 90% in each case) of the desired keto olefin **8**. Even though this overall conversion of **5** into **8** involved more synthetic steps than either of the two previously described methods, it was considerably more efficient on two counts. Firstly, the overall yield was 69%, a notable improvement over previous yields. Secondly, a simple distillation of the crude product obtained from oxidation of **16** produced pure **8**, and tedious separation procedures could therefore be avoided.

At this point a brief diversion is in order. It is interesting to note that whereas borohydride reduction of the bicyclic dione **5** selectively produced the keto alcohol **14** (reaction at C-8), reaction of **5** with *p*-toluenesulfonylhydrazide regioselectively afforded the *p*-tosylhydrazone **13** (reaction at C-6). Although it is perhaps difficult to delineate all of the reasons underlying this interesting difference, it is nevertheless tempting to propose that the major cause is to be found in the obvious angle strain associated with an sp^2 center at C-8. Molecular models of **5** clearly show that the angle traced in going from C-1 to C-8 to C-5 is constrained to a value significantly less than 120°. The resulting strain, which would obviously be relieved by conversion of the C-8 carbon from an sp^2 center into an sp^3 center, could largely account for the fact that with respect to (irreversible) borohydride reduction, the C-8 carbonyl group of **5** was considerably more reactive than the C-6 carbonyl group. If one accepts this argumentation, then it appears likely that *p*-toluenesulfonylhydrazide should also preferentially attack the C-8 carbonyl group. However, conversion of the resultant intermediate **17** into the corresponding *p*-tosylhydrazone **18** would not only reintroduce the above-mentioned angle strain but would also result in $A^{1,3}$ steric strain (26) between the C-5 proton and the NH—Ts moiety. Therefore, this step would be energetically unfavorable with respect to the reverse reaction (**17** → **5**). The alternative mode of reaction, involving (slower) attack at C-6, followed by loss of water from the resultant intermediate **19**, would not be subject to the same difficulties. Therefore, the observation that the *p*-tosylhydrazone **13** was the only observed prod-

Can. J. Chem. Downloaded from www.nrcresearchpress.com by 210.87.254.6 on 09/05/12
For personal use only.

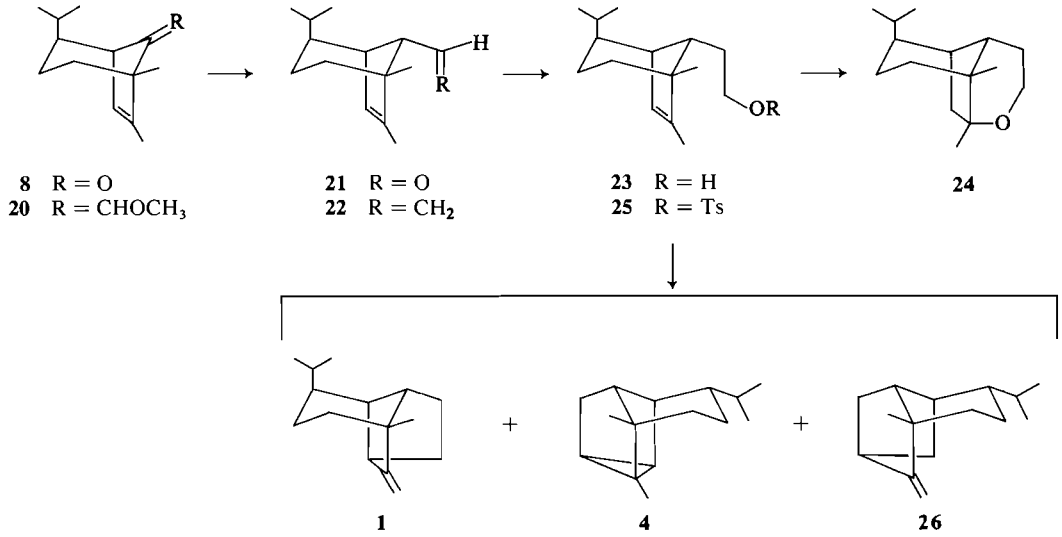

SCHEME 2

uct presumably reflected the fact that, overall, the reaction was thermodynamically controlled and that compound **13** was significantly more stable than the isomeric material **18**.

Synthesis of (−)-Copacamphene (1) (see Scheme 2)

The keto olefin **8** already contained 13 of the 15 carbons necessary for the synthesis of (−)-copacamphene (**1**). The two additional carbons necessary to complete the carbon skeleton were added via a synthetic route very similar to that already employed in a related case (11). Thus, reaction of **8** with methoxymethylenetriphenylphosphorane in dimethyl sulfoxide (27) gave, in 71% yield, a diastereomeric mixture of the corresponding enol ethers **20**. Hydrolysis of this material with aqueous perchloric acid in ether at room temperature, followed by equilibration (potassium carbonate in aqueous methanol) of the initially formed product (see ref. 11), afforded the olefinic aldehyde **21** in 86% yield. Treatment of the latter compound with methylenetriphenylphosphorane in dimethyl sulfoxide (27) gave the diene **22** (83% yield).

Conversion of the diene **22** into an intermediate suitable for eliminative cyclization to (−)-copacamphene (**1**) required initially the selective functionalization of the vinyl group at the terminal carbon atom. This was efficiently accomplished by hydroboration of the diene **22** with disiamylborane in tetrahydrofuran (28), followed by the usual oxidative work-up. The resulting olefinic alcohol **23**, formed in 91% yield, was somewhat unstable and, even in the presence of only a trace of acid, readily cyclized to the corresponding cyclic ether **24**. However, when the freshly isolated olefinic alcohol **23** was immediately treated with *p*-toluenesulfonyl chloride in pyridine, the corresponding olefinic *p*-tosylate **25** could be isolated in high yield. This material, presumably largely owing to the proximity of the *p*-tosylate functionality and the olefinic double bond, exhibited a high propensity towards eliminative cyclization. Indeed, it was found that when the freshly prepared compound was transferred to the top of a silica gel column and the column was eluted with pentane, a clear oil could be isolated (89% yield) from the eluant. Analysis of this material by g.l.c. showed that it consisted of a mixture of three compounds, in a ratio of approximately 98:1:1. The major component, isolated in pure form by column chromatography of the mixture on silver nitrate impregnated silica gel, was shown to be (−)-copacamphene (**1**), $[\alpha]_D^{21}$ −159°. This compound exhibited spectral data which were in excellent agreement with those published for copacamphene (1) and showed g.l.c. retention times and spectral data identical with those of racemic copacamphene (29, 30).[3] The two minor compounds formed during the eliminative cycliza-

[3]We are very grateful to Professor J. E. McMurry for a sample of (±)-copacamphene.

Can. J. Chem. Downloaded from www.nrcresearchpress.com by 210.87.254.6 on 09/05/12
For personal use only.

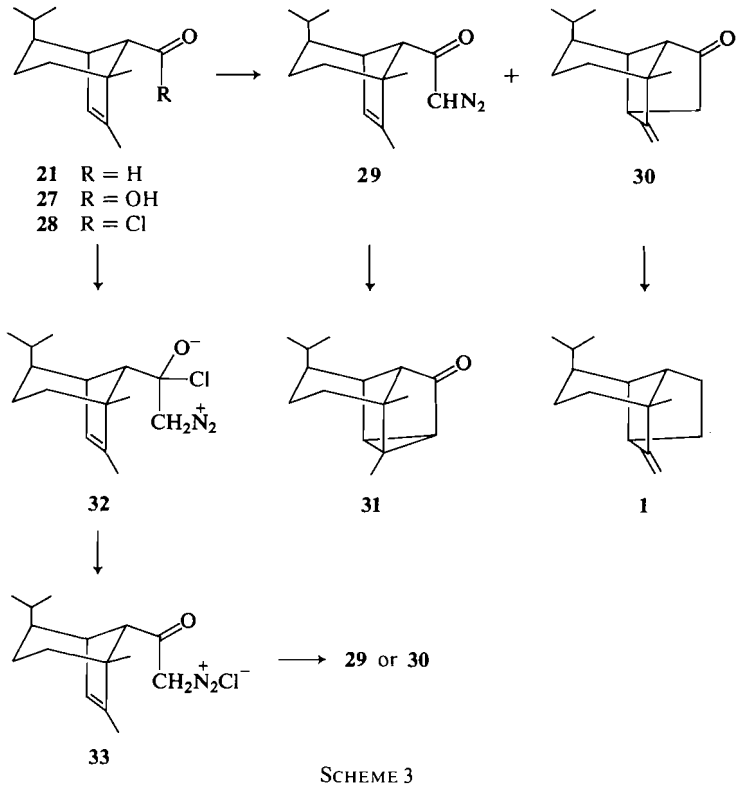

SCHEME 3

tion of the olefinic tosylate **25** were isolated by subjection of the appropriate fractions from the above-mentioned column chromatography to preparative g.l.c. and were identified (g.l.c. retention times and i.r. spectra) as (+)-cyclosativene (**4**) and (−)-isosativene (**26**) (31, 30). The formation of these two compounds was explicable on the basis of the known acid-catalyzed rearrangement of copacamphene to a mixture of sativene, cyclosativene, and isosativene (31, 30).

Synthesis of (−)-Cyclocopacamphene (2)

The synthetic route which was initially chosen for the preparation of (−)-cyclocopacamphene (**2**) involved in the early stages the projected conversion of the olefinic aldehyde **21** into the diazoketone **29** (see Scheme 3). Appropriate carbenoid cyclization of **29**, followed by removal of the carbonyl group from the resulting tetracyclic ketone **31**, would then afford the sesquiterpenoid.

Oxidation of the olefinic aldehyde **21** with chromium trioxide in pyridine containing a small amount of water (32) gave, in 80% yield, the crystalline acid **27**. A suspension of the dry sodium salt of this material in anhydrous ether at 0 °C was treated with oxalyl chloride. The crude acid chloride **28** (ν_{max} 1812 cm^{-1}) thus obtained was dissolved in dry ether and the resulting solution was added slowly to excess alcohol-free ethereal diazomethane. However, an i.r. spectrum of the resulting crude product revealed that the desired diazoketone **29** was present in only minor amounts, since the appropriate absorptions (ν_{max} 2130, 1656 cm^{-1}) were very weak. The most notable absorptions in the i.r. spectrum were at 1745, 1665, and 879 cm^{-1}, indicating that the major product contained a cyclopentanone carbonyl group and an exocyclic methylene double bond. The most likely structure for this material was **30** and this was subsequently shown to be correct (*vide infra*).

When a cyclohexane solution of the crude product obtained from the attempted diazoketone formation was heated in the presence of cupric sulfate (33), a colorless oil was produced (60% yield from the olefinic acid **27**). Analysis of this material by g.l.c. showed that it contained about 84% of the keto olefin **30**, 8% of the tetra-

Can. J. Chem. Downloaded from www.nrcresearchpress.com by 210.87.254.6 on 09/05/12
For personal use only.

Can. J. Chem. Downloaded from www.nrcresearchpress.com by 210.87.254.6 on 09/05/12
For personal use only.

cyclic ketone **31**, and a number of minor unidentified components. Analytical samples of compounds **30** and **31**, obtained by preparative g.l.c., exhibited spectral properties in full accord with the assigned structures. The structure of the major product was further confirmed by its conversion, via Huang-Minlon reduction (34), into (−)-copacamphene (**1**).

It is appropriate to comment briefly regarding the possible pathway involved in the formation of the keto olefin **30**. Attack of diazomethane on the carbonyl group of the acid chloride **28**, followed by expulsion of chloride ion from the resultant intermediate **32**, would afford the charged species **33**. Abstraction of a proton from the nitrogen-bearing carbon of the latter would produce, in addition to hydrogen chloride (presumably rapidly destroyed by the excess diazomethane), the diazoketone **29**. However, because of the possibility of close proximity between the olefinic double bond and the electrophilic carbon adjacent to the carbonyl group, intermediate **33** could also undergo rapid eliminative cyclization to produce compound **30**. Apparently, this intramolecular cyclization was energetically favored over intermolecular proton abstraction. Some support for this proposal was obtained as follows. When the crude product obtained by a repetition of the acid chloride – diazomethane reaction was subjected to treatment with *p*-toluenesulfonic acid in benzene, the initially present i.r. absorptions due to the diazoketone moiety disappeared almost immediately. Analysis (g.l.c.) of the product showed that it consisted mainly (~90%) of the keto olefin **30** and contained none of the tetracyclic ketone **31**. Presumably, the small amount of diazoketone **29** originally present was protonated and the resulting intermediate (like **33**) cyclized to compound **30**. In this connection, it should be noted that, recently, the noncarbenoid, acid-catalyzed intramolecular cyclization of olefinic diazoketones has been demonstrated by a number of other research groups (35–38).

Although the work just described resulted in an interesting alternative preparation of (−)-copacamphene (**1**), the sequence was clearly unsatisfactory for the synthesis of (−)-cyclocopacamphene (**2**). Therefore, an alternative route was considered, based upon the possibility of achieving an intramolecular carbenoid-type cyclization of an olefinic diazoalkane, rather than a diazoketone. For this purpose, the previously

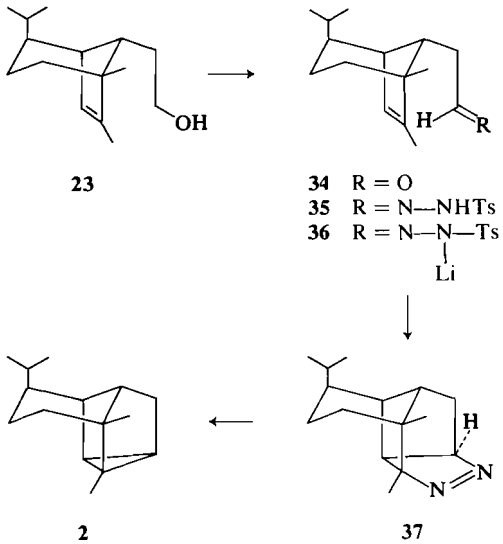

23 **34** R = O; **35** R = N—NHTs; **36** R = N—N(Li)—Ts; **2** **37**

SCHEME 4

synthesized olefinic alcohol **23** served as the starting material (see Scheme 4).

Oxidation of compound **23** with chromium trioxide-pyridine in dichloromethane (23, 24) gave the olefinic aldehyde **34** in 91% yield. The latter compound was, particularly in the presence of traces of acid, quite susceptible to intramolecular cyclization (internal Prins reaction (39)) and was therefore not amenable to storage. However, when the freshly prepared material was allowed to react with *p*-toluenesulfonylhydrazide in refluxing benzene for 5 min, the *p*-tosylhydrazone **35** was smoothly formed. Since compound **35** was also somewhat unstable, it was immediately converted (*n*-butyllithium in tetrahydrofuran) into the corresponding lithium salt **36**. Pyrolysis of this material at 120–140 °C under reduced pressure (0.25 Torr) with direct distillation of the product (40) afforded, in 81% yield, a clear colorless oil. This material, not unexpectedly, proved to be the pyrazoline **37**, obviously formed by intramolecular 1,3-dipolar cycloaddition of the initially formed (40) olefinic diazoalkane. The facility with which this reaction took place was presumably a function of the potential proximity of the two reacting functional groups and of the fairly strained nature of the carbon–carbon double bond (see ref. 41). The regioselectivity of the cycloaddition reaction was clearly shown by the p.m.r. spectrum of the product **37**, which showed that there was only one proton (multiplet at τ 5.11) adjacent to the —N=N— moiety (42).

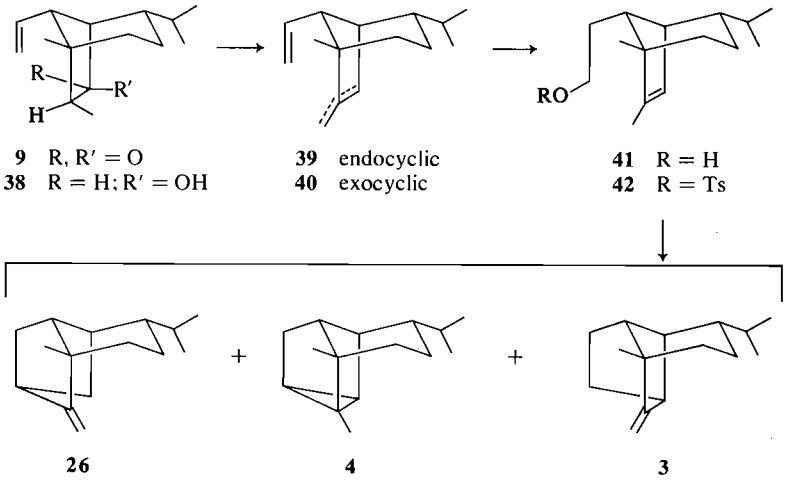

SCHEME 5

An ether solution of the pyrazoline **37** was irradiated at room temperature for approximately 1 h, using a Rayonet reactor equipped with 3500 Å lamps and a Pyrex filter. The product, formed in 92% yield, was (−)-cyclocopacamphene (**2**). The i.r. and p.m.r. spectra of this material were identical with those of authentic (+)-cyclocopacamphene (47).[4]

Synthesis of (+)-Sativene (3) (see Scheme 5)

The synthesis of (+)-sativene (**3**) was achieved via a sequence which was in the later steps very similar to the preparation of (−)-copacamphene (**1**). However, the required bicyclic diene **39** was prepared via a route quite different from that employed for the corresponding compound **22** in the copa series. Thus, for the synthesis of (+)-sativene (**3**) the immediate starting material was the keto olefin **9**, a compound which had previously been prepared from the dione **6** (11) and which already contained the 15 carbon atoms necessary to complete the carbon skeleton of the natural product.

Initial investigations showed that a number of potentially suitable routes for the conversion of **9** into **39** were unsatisfactory. For example, we were unable to effect the transformation of **9** into the corresponding *p*-tosylhydrazone, even under quite drastic reaction conditions (43). Furthermore, conversion of **9** into a corresponding enol phosphate derivative, followed by reduction (12–14) of the latter with lithium in ethylamine – *t*-butyl alcohol under a variety of conditions, failed to produce synthetically acceptable yields of the desired diene **39**. In view of our previous difficulties in a related case (*vide supra*), this difficulty was perhaps not entirely unexpected.

The desired transformation (**9** → **39**) was finally accomplished as follows. Lithium aluminum hydride reduction of the olefinic ketone **9** afforded in nearly quantitative yield, the corresponding alcohol **38**. The stereochemistry of the latter compound was expected to be as shown (steric approach control) and this was fully corroborated by the p.m.r. spectrum of the reduction product. Dehydration of compound **38** with 6 equiv. of thionyl chloride[5] in pyridine at 40–45 °C for 3 h gave, in 75% yield, a mixture of the two isomeric dienes **39** and **40**, in a ratio of about 2:1, respectively. Attempts to avoid the formation of the unwanted diene **40** by employing alternative conditions and/or methods for the dehydration of **38** proved unsuccessful. In short, whenever dehydration did occur, both of the dienes **39** and **40** were produced. However, the two isomeric compounds could readily be separated by subjection of the mixture to column chromatography over silver nitrate impregnated silica gel. Furthermore, the overall efficiency of the process was improved by the discovery that the undesired diene **40**, upon treatment with a

[4]We are very grateful to Dr. Kido for his help in carrying out this comparison.

[5]Use of 1 equiv. of thionyl chloride produced mainly the corresponding sulfite ester (see ref. 44). Dehydration occurred most efficiently when a fairly large excess of reagent was employed.

Can. J. Chem. Downloaded from www.nrcresearchpress.com by 210.87.254.6 on 09/05/12
For personal use only.

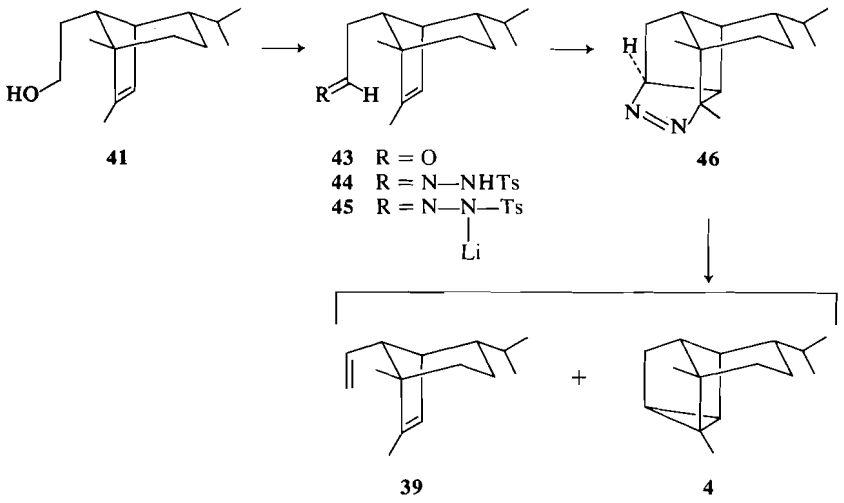

SCHEME 6

catalytic amount of *p*-toluenesulfonic acid in refluxing benzene for 30 min produced, in 94% yield, a mixture of **39** and **40** in a ratio of 7:3, respectively.

The synthetic route employed for the conversion of the diene **39** into (+)-sativene (**3**) paralleled that described previously (*vide supra*) for the transformation of diene **22** into (−)-copacamphene (**1**). Briefly, successive subjection of **39** to hydroboration–oxidation (disiamylborane in tetrahydrofuran; alkaline hydrogen peroxide), *p*-tosylation (*p*-toluenesulfonyl chloride in pyridine), and eliminative cyclization (silica gel column) afforded, in order, the primary alcohol **41**, the corresponding *p*-tosylate **42**, and a clear, colorless oil (58% overall yield). Analysis of the latter material by g.l.c. showed that it consisted of a mixture of three compounds, in a ratio of approximately 75:22:3. The minor component (3%) was identified (g.l.c. retention times on three different columns) as cyclosativene (**4**). Pure samples of the other two components were obtained by preparative g.l.c. The major compound (75%) was (+)-sativene (**3**), identified by direct comparison (i.r., p.m.r.) with an authentic sample.[6] The remaining component (22%), again identified by direct comparison with an independently synthesized sample, was (−)-isosativene (**26**) (31, 30). The formation of compounds **26** and **4** during the eliminative cyclization of olefinic tosylate **42** is explicable on the basis of the known acid-catalyzed interconversion of sativene, isosativene and cyclosativene (45), the mechanism of which has been discussed in detail by McMurry (30).

Synthesis of (+)-Cyclosativene (4) (see Scheme 6)

The conversion of the olefinic alcohol **41** into (+)-cyclosativene (**4**) was accomplished via a synthetic route which was fully analogous to that previously employed for the synthesis of (−)-cyclocopacamphene (**2**) from the bicyclic alcohol **23** (*vide supra*). Oxidation (23, 24) of **41** afforded the aldehyde **43**, which in turn was converted into the *p*-tosylhydrazone **44**. Pyrolysis (105–130 °C) of the corresponding lithium salt **45** under reduced pressure (0.1 Torr) with direct distillation of the product gave the pyrazoline **46** (50% overall yield from **41**). Photolysis of **46** in dry ether afforded in high yield an oil which was shown by g.l.c. analysis to consist of two compounds in a ratio of 11:1. This mixture was separated by preparative g.l.c. and the major product was identified (i.r., p.m.r.) as (+)-cyclosativene (**4**).[6] The minor product was shown (i.r.) to be identical with the diene **39**, presumably formed from the pyrazoline **46** by retro-1,3-dipolar addition, followed by carbene formation and insertion into an adjacent C—H bond (see ref. 46).

[6]We are very grateful to Professor J. E. McMurry for samples of sativene and cyclosativene.

Can. J. Chem. Downloaded from www.nrcresearchpress.com by 210.87.254.6 on 09/05/12
For personal use only.

Can. J. Chem. Downloaded from www.nrcresearchpress.com by 210.87.254.6 on 09/05/12
For personal use only.

Experimental[7]

Preparation of the Keto Enol Phosphate ***10***

To a solution of 6.6 g (36 mmol) of sodium bis(trimethylsilyl)amide in 90 ml of dry tetrahydrofuran was added a solution of 5.0 g (24 mmol) of the bicyclic diketone **5** in 10 ml of dry tetrahydrofuran. The reaction mixture was stirred at room temperature under an atmosphere of dry nitrogen for 20 min and then a solution of 10.7 g (62 mmol) of diethyl phosphorochloridate in 30 ml of dry pyridine was added. After the resulting mixture had been stirred at room temperature for 30 min it was concentrated under reduced pressure. The residual material was diluted with water and the resulting mixture was thoroughly extracted with ether. The combined ethereal extracts were washed with water and saturated brine, and dried over anhydrous magnesium sulfate. Removal of the solvent, followed by distillation (air-bath temperature 135–145 °C; 0.25 Torr) of the residual oil under reduced pressure afforded 7.8 g (94%) of the desired keto enol phosphate **10**, n_D^{21} 1.4722; $[\alpha]_D^{25}$ −5.8° (*c*, 1.4 in $CHCl_3$); i.r. (film) ν_{max} 1755, 1678, 1270, 1094, 1025, 960, 876, 833 cm^{-1}; p.m.r. τ 4.82 (d of q, 4H, $-OCH_2CH_3$, J = 7.0 Hz, $J_{H\text{-}P}$ = 1.0 Hz), 8.30 (d of d, 3H vinyl methyl, $J_{5\text{-}CH_3}$ = 1.0 Hz, $J_{H\text{-}P}$ = 2.2 Hz), 8.63 (d of t, 6H, $-O-CH_2CH_3$, J = 7.0 Hz, $J_{H\text{-}P}$ = 1.0 Hz), 8.98 (s, 3H, tertiary methyl), 9.08 (d, 6H, isopropyl methyls, J = 6.3 Hz).

Anal. Calcd. for $C_{17}H_{29}O_5P$: C, 59.29; H, 8.49. Found: C, 59.18; H, 8.45.

Preparation of the Keto Alcohol ***14***

A solution of the bicyclic diketone **5** (14.0 g, 67.3 mmol) in 170 ml of ethanol was cooled to 0 °C and a solution of 825 mg (21.8 mmol) of sodium borohydride in 30 ml of ethanol was added. The resulting solution was stirred at 0 °C for 15 min and then 4.4 g (74.0 mmol) of acetic acid was added. The reaction mixture was concentrated under reduced pressure, the residue was diluted with water, and the resulting mixture was thoroughly extracted with ether. The combined ethereal extracts were washed with a saturated sodium carbonate solution and brine, and then dried over anhydrous magnesium sulfate. Removal of the solvent followed by distillation of the residual oil under reduced pressure afforded 12.5 g (89%) of the desired keto alcohol **14**, b.p. 125–130 °C at 0.4 Torr; n_D^{25} 1.4916; $[\alpha]_D^{25}$ −69° (*c*, 1.0 in $CHCl_3$); i.r. (film) ν_{max} 3475, 1725, 1460, 1110, 1100 cm^{-1}; p.m.r. τ 6.12 (d, 1H, C-8 H, J = 5.5 Hz), 7.30 (m, 1H, C-5 H), 8.92 (d, 3H, secondary methyl, J = 7.0 Hz), 8.97 (s, 3H, tertiary methyl), 9.02, 9.13 (d, d, 6H, isopropyl methyls, J = 6.5 Hz).

Anal. Calcd. for $C_{13}H_{22}O_2$: C, 74.24; H, 10.54. Found: C, 74.12; H, 10.50.

Preparation of the Olefinic Alcohol ***16***

To a hot (90 °C) solution of the keto alcohol **14** (12.0 g, 57.2 mmol) and *p*-toluenesulfonylhydrazide (11.7 g, 62.8 mmol) in 9.0 ml of methanol was added 300 μl of acetyl chloride. The reaction mixture was stirred under an atmosphere of dry nitrogen at 90–100 °C for 3 h, cooled, and diluted with water. The resulting mixture was thoroughly extracted with ether. The combined ethereal extracts were washed with 10% aqueous sodium bicarbonate, then with brine, and finally dried over anhydrous magnesium sulfate. Removal of the solvent under reduced pressure yielded 21.2 g (98%) of the *p*-toluenesulfonylhydrazone **15** as a viscous yellow oil (i.r. (film) ν_{max} 3620, 3355, 3320, 1655, 1600, 1170 cm^{-1}). This material was used without further purification.

To an ice-cooled solution of the *p*-toluenesulfonylhydrazone **15** (21.2 g, 56.2 mmol) in 1100 ml of dry tetrahydrofuran was added 214 ml of 2.1 *M* ethereal methyllithium over a period of 30 min. The reaction mixture was allowed to warm to room temperature and was stirred under an atmosphere of dry nitrogen for an additional 3 h. The solution was then cooled to 0 °C and the excess methyllithium was destroyed by the careful addition of water. The reaction mixture was concentrated, the residue was diluted with water, and the resulting mixture was thoroughly extracted with ether. The combined ethereal extracts were washed with brine and dried over anhydrous magnesium sulfate. Removal of the solvent followed by distillation of the residual oil under reduced pressure afforded 9.57 g (88%) of the desired olefinic alcohol **16** as a colorless oil, b.p. 80 °C at 0.25 Torr; n_D^{25} 1.4898; $[\alpha]_D^{25}$ −61° (*c*, 0.7 in $CHCl_3$); i.r. (film) ν_{max} 3400, 3050, 1620, 1450, 1090, 1066, 805 cm^{-1}; p.m.r. τ 4.60 (unresolved m, 1H, vinyl proton), 5.57 (s, 1H, hydroxyl proton), 6.36 (d, 1H, C-8H, J = 5.5 Hz), 7.34 (m, 1H, C-5H), 8.38 (d of d, 3H, vinyl methyl, $J_{6\text{-}CH_3}$ = 1.6 Hz, $J_{5\text{-}CH_3}$ = 1.0 Hz), 9.10 (s, 3H, tertiary methyl), 9.03, 9.13 (d, d, 6H, isopropyl methyls, J = 6.5 Hz).

Anal. Calcd. for $C_{13}H_{22}O$: C, 80.35; H, 11.41. Found: C, 80.16; H, 11.27.

Preparation of the Keto Olefin ***8***

(a) By Lithium–Ethylamine Reduction of the Keto Enol Phosphate ***10***

A solution of 1.38 g (200 mmol) of lithium metal in approximately 70 ml of dry ethylamine was stirred at room temperature for 20 min. To this solution was added dropwise, over a period of 10 min, a solution of the keto enol phosphate **10** (3.43 g, 10.0 mmol) and *t*-butyl alcohol (1.48 g, 20.0 mmol) in 10 ml of dry ether. The reaction mixture was stirred for an additional 5 min and was then filtered through a small glass wool plug into a rapidly stirred ether–water mixture. The resulting mixture was extracted twice with ether, the combined ethereal extracts were washed with water and brine, and dried over anhydrous magnesium sulfate. The ether was removed at aspirator pressure and the crude product was distilled (air bath temperature 65–75 °C; 0.5 Torr) under reduced pressure to afford 900 mg of a yellow oil. Gas–liquid chromatographic analysis (column A, 170 °C, 95) of the distilled product indicated that it consisted of a mixture of approximately 50% of the keto olefin **8**, 20% of the corresponding alcoholic olefin **11**, 10% of the saturated ketone **12**, and several minor, unidentified components.

Standard chromic acid solution (25) was added to a solution of the distilled reduction product (900 mg) in acetone (25 ml) at 0 °C until the orange color persisted. Isopropyl alcohol was added to destroy the excess oxidizing reagent, and the solution was evaporated under reduced pressure. The residual material was diluted with water and thoroughly extracted with ether. The combined ethereal extracts were dried over anhydrous magnesium

[7]For pertinent general information, see ref. 8.

Can. J. Chem. Downloaded from www.nrcresearchpress.com by 210.87.254.6 on 09/05/12
For personal use only.

sulfate and the ether was removed at aspirator pressure. The desired keto olefin **8** was obtained from the resulting mixture by means of preparative g.l.c. (column J, 230 °C, 200). The keto olefin **8** thus obtained (500 mg, 26%) was a colorless oil and exhibited n_D^{23} 1.4789; $[\alpha]_D^{23}$ −29° (*c*, 1.3 in $CHCl_3$); i.r. (film) ν_{max} 3040, 1750, 1630, 1060, 818 cm^{-1}; p.m.r. τ 4.13 (unresolved m, 1H, vinyl proton), 7.17 (unresolved m, 1H, C-5 H), 8.25 (d of d, 3H, vinyl methyl, $J_{6\text{-}CH_3}$ = 1.6 Hz, $J_{5\text{-}CH_3}$ = 1.0 Hz), 9.00 (s, 3H, tertiary methyl), 9.00, 9.09 (d, d, 6H, isopropyl methyls, J = 6.0 Hz).

Anal. Calcd. for $C_{13}H_{20}O$: C, 81.20; H, 10.48. Found: C, 81.30; H, 10.59.

(b) By Bamford–Stevens Reaction of the p-Toluenesulfonylhydrazone 13

To a solution of the bicyclic diketone **5** (11.6 g, 56.0 mmol) in 10 ml of methanol was added *p*-toluenesulfonylhydrazide (13.0 g, 70.0 mmol) and the resulting mixture was heated and stirred under an atmosphere of dry nitrogen until a homogeneous solution was obtained. Acetyl chloride (100 µl) was added to the solution and the reaction mixture was stirred at room temperature for 3 h. The methanol was removed under reduced pressure, the residue was diluted with water, and the resulting mixture was thoroughly extracted with ether. The ethereal extracts were washed with a 10% solution of sodium bicarbonate and brine, and dried over anhydrous magnesium sulfate. Removal of the solvent under reduced pressure yielded 21.1 g (100%) of the crude *p*-toluenesulfonylhydrazone **13**. In general, this material was used for the next reaction without further purification. However an analytical sample of compound **13**, obtained by recrystallization of a small amount of this material from methanol exhibited m.p. 77–80 °C; i.r. ($CHCl_3$) ν_{max} 3520, 3205, 1745, 1653, 1600, 1165 cm^{-1}; p.m.r. τ 2.18, 2.72 (d, d, 4H, aromatic protons, J = 9.0 Hz), 7.50 (s, 3H, aromatic methyl), 8.82 (d, 3H, secondary methyl, J = 7.0 Hz), 9.05 (s, 3H, tertiary methyl), 9.02, 9.19 (d, d, 6H, isopropyl methyls, J = 6.0 Hz).

To a solution of the crude *p*-toluenesulfonylhydrazone **13** (21.1 g, 56.0 mmol) in 150 ml of dry tetrahydrofuran was added a solution of 10.7 g (58.7 mmol) of sodium bis(trimethylsilyl)amide and 2.2 ml of high boiling Nujol (> 210 °C at 0.2 Torr) in 50 ml of dry tetrahydrofuran, and the resulting reaction mixture was stirred under an atmosphere of dry nitrogen for 1 h. The reaction mixture was then concentrated under reduced pressure. The remaining mixture of Nujol and the sodium salt of the *p*-toluenesulfonylhydrazone was heated slowly to 125 °C under reduced pressure (water aspirator, 10–20 Torr) at which temperature decomposition of the salt was observed to take place. At this temperature, direct distillation of the product was accomplished by application of a vacuum pump (0.3 Torr) to the reaction system. The product thus obtained was redistilled (air-bath temperature 75–80 °C; 0.5 Torr) and those distillation fractions containing significant amounts of keto olefin (g.l.c. analysis, column A, 170 °C, 95) were chromatographed on silica gel. Elution with 10:1 petroleum ether (b.p. 30–60 °C) – ether afforded fractions containing significant amounts of keto olefin (g.l.c. analysis, column A, 170 °C, 95). These fractions were then subjected to preparative g.l.c. (column J, 230 °C, 150) and 4.0 g (38%) of the pure keto olefin **8** was obtained in this manner. This material was identical (g.l.c. retention time, i.r., and p.m.r. spectra) with the keto olefin **8** prepared previously.

(c) By Jones Oxidation of the Olefinic Alcohol 16

Standard chromic acid solution (25) was added to a solution of the olefinic alcohol **16** (1.94 g, 10 mmol) in acetone (50 ml) at 0 °C, until the orange color persisted. Isopropyl alcohol was added to destroy the excess oxidizing agent and the solution was evaporated under reduced pressure. The residual material was diluted with water and the resulting mixture was thoroughly extracted with ether. The combined ethereal extracts were washed with brine and dried over anhydrous magnesium sulfate. Removal of the solvent, followed by distillation (air bath temperature 70–75 °C; 0.5 Torr) of the residual oil under reduced pressure afforded 1.71 g (89%) of the keto olefin **8**. This material was identical (g.l.c. retention time, i.r., and p.m.r. spectra) with the keto olefin **8** prepared previously.

Preparation of the Olefinic Enol Ethers 20

To a stirred solution of sodium methylsulfinylmethide (0.84 g, 8.4 mmol) in 9 ml of dry dimethyl sulfoxide at room temperature, under an atmosphere of dry nitrogen, was added a solution of methoxymethyltriphenylphosphonium chloride (3.07 g, 10 mmol) in 12 ml of dry dimethyl sulfoxide. The resulting solution was stirred for 10 min and then a solution of the keto olefin **8** (320 mg, 1.67 mmol) in 9 ml of dimethyl sulfoxide was added. The reaction mixture was heated at 40–50 °C for 1.5 h, then cooled, diluted with water, and the resulting mixture was thoroughly extracted with petroleum ether (b.p. 30–60 °C). The combined extracts were washed twice with water, once with saturated brine, and then dried over anhydrous magnesium sulfate. Removal of the solvent, followed by distillation (air-bath temperature 75–80 °C; 0.5 Torr) of the residual oil under reduced pressure yielded 262 mg (71%) of the olefinic enol ethers **20** as a colorless oil, n_D^{21} 1.4927; u.v. λ_{max} 208 nm (ε 8030); i.r. (film) ν_{max} 3030, 1700, 1450, 1236, 1215, 1112 cm^{-1}; p.m.r. τ 4.43 (broad signal, 2H, vinyl protons), 6.51, 6.54 (s, s, 3H, —OCH_3), 7.23 (broad s, 1H, C-5H).

Anal. Calcd. for $C_{15}H_{24}O$: C, 81.76; H, 10.98. Found: C, 82.00; H, 11.11.

Mol. Wt. Calcd. for $C_{15}H_{24}O$: 220.183. Found (high resolution mass spectrometry): 220.183.

Preparation of the Olefinic Aldehyde 21

To a solution of 10 ml of 35% perchloric acid dissolved in 45 ml of ether was added a solution of 250 mg of the olefinic enol ethers **20** in 5 ml of ether. The reaction mixture was stirred for 1 h at room temperature and was then neutralized by the slow addition of solid sodium carbonate. The resulting mixture was thoroughly extracted with ether and the combined extracts were washed with brine and concentrated. The residue was dissolved in 5 ml of methanol and added to a stirred solution of 0.5 g potassium carbonate in 2.5 ml water and 25 ml of methanol. The resulting solution was stirred for 2 h and then concentrated. The residue was diluted with water and the resulting mixture was thoroughly extracted with ether. The combined ethereal extracts were washed with brine and dried over anhydrous magnesium sulfate. Removal of the solvent, followed by distillation (air-bath temperature 100–105 °C; 0.3 Torr) of the residual oil

Can. J. Chem. Downloaded from www.nrcresearchpress.com by 210.87.254.6 on 09/05/12
For personal use only.

under reduced pressure yielded 202 mg (86%) of the olefinic aldehyde **21** as a colorless oil, n_D^{21} 1.4931; $[\alpha]_D^{22}$ −20° (*c*, 1.7 in $CHCl_3$); i.r. (film) ν_{max} 3030, 2725, 1715, 1645, 1450, 1380, 808 cm^{-1}; p.m.r. τ 0.40 (d, 1H, aldehydic proton, J = 4.2 Hz), 4.56 (unresolved m, 1H, vinyl proton, $w_{\frac{1}{2}}$ = 6.0 Hz), 7.53 (unresolved m, 1H, C-5 H), 7.80 (d, 1H, C-8 H, J = 4.2 Hz), 8.38 (d of d, 3H, vinyl methyl, $J_{6\text{-}CH_3}$ = 1.6 Hz, $J_{5\text{-}CH_3}$ = 1.0 Hz), 8.97 (s, 3H, tertiary methyl), 9.08, 9.16 (d, d, 6H, isopropyl methyls, J = 6.2 Hz).

Mol. Wt. Calcd. for $C_{14}H_{22}O$: 206.167. Found (high resolution mass spectrometry): 206.166.

Preparation of the Diene 22

To a stirred solution of sodium methylsulfinylmethide (2.25 g, 22.5 mmol) in dry dimethyl sulfoxide (27 ml) at room temperature, under an atmosphere of nitrogen, was added a solution of methyltriphenylphosphonium bromide (9.65 g, 27.0 mmol) in 36 ml of dimethyl sulfoxide. The solution was stirred for 10 min and then a solution of the olefinic aldehyde **21** (900 mg, 4.5 mmol) in 27 ml of dimethyl sulfoxide was added. The reaction mixture was heated at 40–50 °C for 1 h, cooled, and diluted with water and the resulting mixture was thoroughly extracted with petroleum ether (b.p. 30–60 °C). The combined petroleum ether extracts were washed twice with water, once with saturated brine, and then dried over anhydrous magnesium sulfate. Removal of the solvent, followed by distillation (air-bath temperature 90–95 °C; 0.3 Torr) of the residual oil under reduced pressure afforded 740 mg (83%) of the desired diene **22**, n_D^{26} 1.4820; $[\alpha]_D^{21}$ +4.3° (*c*, 1.5 in $CHCl_3$); i.r. (film) ν_{max} 3030, 1640, 1450, 997, 906, 842, 806 cm^{-1}; p.m.r. τ 4.00–4.42 (m, 1H, —C*H*=CH_2), 4.67 (unresolved m, 1H, C-6H, $w_{\frac{1}{2}}$ = 6.0 Hz), 4.84–5.24 (m, 2H, —CH=CH_2), 7.67 (unresolved m, 1H, C-5 H, $w_{\frac{1}{2}}$ = 8 Hz) 7.83 (d, 1H, C-8 H, J = 9.0 Hz), 8.42 (d of d, 3H, vinyl methyl, $J_{6\text{-}CH_3}$ = 1.6 Hz, $J_{5\text{-}CH_3}$ = 1.0 Hz), 9.07, 9.15 (d, d, 6H, isopropyl methyls, J = 6.5 Hz), 9.16 (s, 3H, tertiary methyl).

Anal. Calcd. for $C_{15}H_{24}$: C, 88.16; H, 11.84. Found: C, 88.08; H, 12.00.

Mol. Wt. Calcd. for $C_{15}H_{24}$: 204.188. Found (high resolution mass spectrometry): 204.188.

Preparation of the Olefinic Alcohol 23

To a stirred solution of 0.51 g (3.3 mmol) of disiamylborane in 8 ml of dry tetrahydrofuran at 0 °C, under an atmosphere of dry nitrogen, was added a solution of the diene **22** (306 mg, 1.5 mmol) in 6 ml of tetrahydrofuran. The reaction mixture was stirred at room temperature for 1.5 h. The reaction mixture was cooled to 0 °C and 2 ml of 3 *N* NaOH was added slowly, followed by addition of 2 ml of 30% hydrogen peroxide. The resulting mixture was warmed to room temperature, stirred for 1 h, and then concentrated. The residual material was diluted with water and thoroughly extracted with ether. The combined ether extracts were washed with a saturated brine solution and dried over anhydrous magnesium sulfate. Removal of the solvent, followed by distillation (air-bath temperature 115–120 °C; 0.2 Torr) of the residual material under reduced pressure afforded 300 mg (91%) of the desired olefinic alcohol **23** as a colorless oil. An analytical sample was obtained by preparative g.l.c. (column A, 210 °C, 100) and exhibited n_D^{24} 1.4936; $[\alpha]_D^{20}$ +8.5° (*c*, 5.6 in $CHCl_3$); i.r. (film) ν_{max} 3300, 3020, 1642, 1450, 1375, 1055 cm^{-1}; p.m.r. τ 4.68 (unresolved m, 1H, vinyl proton, $w_{\frac{1}{2}}$ = 4.2 Hz), 6.38 (m, 2H, —CH_2OH), 7.63 (unresolved m, 1H, C-5H), 8.44 (d of d, 3H, vinyl methyl, $J_{6\text{-}CH_3}$ = 1.6 Hz, $J_{5\text{-}CH_3}$ = 1.0 Hz), 9.08, 9.14 (d, d, 6H, isopropyl methyls, J = 6.0 Hz), 9.10 (s, 3H, tertiary methyl).

Anal. Calcd. for $C_{15}H_{26}O$: C, 81.02; H, 11.79. Found: C, 80.78; H, 11.78.

Mol. Wt. Calcd. for $C_{15}H_{26}O$: 222.198. Found (high resolution mass spectrometry): 222.198.

Preparation of the Olefinic Acid 27

A solution of 206 mg (10.0 mmol) of the olefinic aldehyde **21** in 1.5 ml of pyridine was added to a solution of 1.2 g of chromium trioxide in 12 ml of pyridine. Five drops of water were added and the resulting dark mixture was stirred for 18 h at room temperature. The reaction mixture was diluted with water and extracted with ether. The combined ethereal extracts were washed with water, with a dilute hydrochloric acid, and then extracted with 10% aqueous sodium hydroxide. The alkaline extracts were cooled, acidified with 6 *N* hydrochloric acid, and the resulting mixture was thoroughly extracted with ether. The combined ethereal extracts were washed with water and dried over anhydrous magnesium sulfate. Removal of the solvent afforded 174 mg (82%) of the crystalline olefinic acid **27**, m.p. 138–139.5 °C; $[\alpha]_D^{26}$ −16.7° (*c*, 1.2 in $CHCl_3$); i.r. ($CHCl_3$) ν_{max} 1704 cm^{-1}; p.m.r. τ 0.18 (very broad signal, 1H, acid proton), 4.55 (unresolved m, 1H, vinyl proton, $w_{\frac{1}{2}}$ = 6.0 Hz), 7.19 (unresolved m, 1H, C-5 H), 7.50 (s, 1H, C-8 H), 8.40 (d of d, 3H, vinyl methyl, $J_{6\text{-}CH_3}$ = 1.6 Hz, $J_{5\text{-}CH_3}$ = 1.0 Hz), 8.89 (s, 3H, tertiary methyl), 9.07, 9.11 (d, d, 6H, isopropyl methyls, J = 6.0 Hz)..

Anal. Calcd. for $C_{14}H_{22}O_2$: C, 75.63; H, 9.97. Found: C, 75.33; H, 9.98.

Preparation of the Tricyclic Keto Olefin 30

The olefinic carboxylic acid **27** (111 mg, 0.5 mmol) was dissolved in aqueous sodium hydroxide (0.55 mmol), the water was evaporated under reduced pressure, and the residue was dried in a vacuum oven at 70 °C. A stirred suspension of the resulting dry sodium salt in 10 ml of anhydrous ether containing 20 μl of dry pyridine was cooled to 0 °C and 640 mg (5.0 mmol) of oxalyl chloride was added. The reaction mixture was stirred at 0 °C for 15 min under an atmosphere of dry nitrogen, then filtered, and concentrated under reduced pressure (vacuum pump). The solution was kept at 0 °C during this process. The crude acid chloride **28** (i.r. (film) ν_{max} 1812 cm^{-1}) thus obtained was dissolved in 15 ml of anhydrous ether and the resulting solution was added to excess alcohol-free ethereal diazomethane which had been dried over potassium hydroxide. The resulting reaction mixture was stirred at 0 °C for 2.5 h, then the excess diazomethane and solvent was removed under reduced pressure. The crude reaction product (i.r. (film) ν_{max} 1745 cm^{-1} (strong), 2130, 1656 cm^{-1} (weak)) was dissolved in 15 ml of dry cyclohexane and cupric sulfate (400 mg) was added. The resulting suspension was refluxed, with stirring, for 3 h. The cooled reaction mixture was filtered, the filtrate was washed with saturated aqueous sodium bicarbonate, water, and brine, and then dried over anhydrous magnesium sulfate. Removal of the solvent, followed by distillation (air-bath temperature 110–115 °C; 0.25 Torr) of

Can. J. Chem. Downloaded from www.nrcresearchpress.com by 210.87.254.6 on 09/05/12
For personal use only.

the residual material under reduced pressure, yielded 66 mg (60%) of a colorless oil. This material was shown by g.l.c. analysis (column I, 200 °C, 95) to consist mainly (~84%) of the keto olefin **30**. In addition, the tetracyclic ketone **31** (~8%) and a number of minor unidentified compounds were also present. Compounds **30** and **31** were isolated by preparative g.l.c. (column K, 240 °C, 200). The tetracyclic ketone **31** thus obtained exhibited i.r. (film) ν_{max} 3058, 1745, 876, 831 cm^{-1}; p.m.r. τ 8.82, 9.08 (s, s, 6H, tertiary methyls), 9.12, 9.15 (d, d, 6H, isopropyl methyls, J = 6.0 Hz).

The keto olefin **30** exhibited n_D^{24} 1.5036; $[\alpha]_D^{26}$ −100° (*c*, 1.0 in $CHCl_3$); i.r. (film) ν_{max} 3065, 1745, 1665, 1462, 1170, 879 cm^{-1}; p.m.r. τ 5.03, 5.27 (s, s, 2H, vinyl protons), 7.13 (unresolved m, 1H, allylic proton), 8.99 (s, 3H, tertiary methyl), 9.12 (d, 6H, isopropyl methyls, J = 6.0 Hz).

Mol. Wt. Calcd. for $C_{15}H_{22}O$: 218.167. Found (high resolution mass spectrometry); 218.165.

The attempted formation of the diazoketone **29** was repeated employing a reaction procedure identical with that just described. The crude product (i.r. (film) ν_{max} 1745 (strong), 2130, 1656 (weak) cm^{-1}) obtained by reaction of the acid chloride **28** with diazomethane was dissolved in approximately 1 ml of dry benzene, and the resulting solution was added to 25 ml of a 5.0 m*M* solution of *p*-toluenesulfonic acid in benzene. The reaction mixture was stirred for 30 min at room temperature under an atmosphere of dry nitrogen. Appropriate analysis of an aliquot showed that the i.r. absorptions due to the diazoketone moiety had disappeared after a period of a few minutes. The solution was washed with saturated aqueous sodium bicarbonate, water and brine, and then dried over anhydrous magnesium sulfate. Removal of the solvent, followed by distillation of the residual material under reduced pressure yielded 65 mg (60%) of a colorless oil. Analysis of this material by g.l.c. (column I, 200 °C, 95) indicated the presence of the keto olefin **30** (~90%), along with a number of minor components (unidentified). The keto olefin **30** was obtained by preparative g.l.c. (column K, 240 °C, 200) and was shown (g.l.c. retention time, i.r., and p.m.r. spectra) to be identical with the material prepared previously.

(−)-Copacamphene (1)

(a) From the Olefinic Alcohol 23

To a solution of 200 mg (0.9 mmol) of the olefinic alcohol **23** in 4 ml of dry pyridine was added a solution of 342 mg (1.8 mmol) of *p*-toluenesulfonyl chloride in 1 ml of dry pyridine. The reaction mixture was stirred under an atmosphere of dry nitrogen for 2.5 h. The solution was diluted with hexane and the resulting mixture was washed with aqueous sodium bicarbonate, water and brine, and dried over anhydrous magnesium sulfate. The solvent was removed first at water aspirator pressure and finally the last traces of pyridine were removed by application of a vacuum pump. The residual oil (the crude *p*-tosylate **25**) was transferred to the top of a silica gel column (5.0 g) and the column was eluted with approximately 50 ml of pentane. Removal of the solvent from the eluant, followed by distillation (air-bath temperature 75–80 °C; 0.25 Torr) of the residual oil afforded 164 mg (89%) of a colorless oil. Gas–liquid chromatographic analysis (column G, 135 °C, 85) of this material indicated that it consisted of a major component (98%) accompanied by two minor components (in a ratio of approximately 1:1) that comprised 1–2% of the total mixture. Final purification was effected by column chromatography of the mixture on 10% silver nitrate impregnated silica gel. Elution with 25:1 pentane–ether afforded pure (−)-copacamphene (**1**) $[\alpha]_D^{21}$ −159° (*c*, 2.2 in $CHCl_3$); i.r. (film) ν_{max} 3065, 1658, 1389, 1370, 876 cm^{-1}; p.m.r. τ 5.21, 5.49 (s, s, 2H, vinyl protons), 7.54 (broad signal, 1H, allylic proton), 9.00 (s, 3H, tertiary methyl), 9.10 (d, 6H, isopropyl methyls, J = 6.0 Hz). This material was found to be identical (g.l.c. retention time, i.r.) with authentic (±)-copacamphene.

Mol. Wt. Calcd. for $C_{15}H_{24}$: 204.188. Found (high resolution mass spectrometry): 204.188.

The minor components from the reaction described above were collected by preparative g.l.c. (column L, 145 °C, 120) and were identified as (+)-cyclosativene (**4**) and (−)-isosativene (**26**) by direct comparison (g.l.c. retention time, i.r. spectra), in each case, with an authentic sample.

(b) By Reduction of the Keto Olefin 30

A solution of 50 mg of the keto olefin **30** in 2.0 ml of ethylene glycol containing 0.1 ml of 85% hydrazine hydrate and 100 mg of potassium hydroxide was refluxed for 2 h. The reflux condensor was removed and replaced by a distillation head and the temperature of the reaction mixture was slowly raised to 200 °C and maintained at this temperature for 3 h. The distillate was collected in a Dry Ice – acetone cooled receiver and combined with the cooled reaction mixture. This solution was diluted with water and the resulting mixture was thoroughly extracted with petroleum ether (b.p. 30–60 °C). The combined petroleum ether extracts were washed with water and brine and dried over anhydrous magnesium sulfate. The dried petroleum ether extracts were filtered through 2 g of silica gel and the column was further eluted with petroleum ether. Removal of the solvent from the eluant followed by distillation of the residual oil produced 27 mg (58%) of (−)-copacamphene (**1**). This material was identical (g.l.c. retention time, specific rotation, i.r., and p.m.r. spectra) with the (−)-copacamphene prepared as described above.

Preparation of the Olefinic Aldehyde 34

To a solution of 286 mg (3.6 mmol) of dry pyridine in 4.0 ml of dry methylene chloride was added 180 mg (1.8 mmol) of dry chromium trioxide. The solution was stirred under an atmosphere of dry nitrogen at room temperature for 15 min. To this mixture was added a solution of 64 mg (0.3 mmol) of the olefinic alcohol **23** in 0.5 ml of methylene chloride. The reaction was allowed to proceed for 15 min, then approximately 10 ml of ether was added and the resulting solution was washed with saturated aqueous sodium carbonate, with water, and then dried over anhydrous magnesium sulfate. Removal of the solvent followed by distillation (air-bath temperature 80–85 °C; 0.25 Torr) of the residual oil yielded 58 mg (91%) of the desired olefinic aldehyde **34**, as a colorless oil, n_D^{24} 1.4906; $[\alpha]_D^{21}$ −39° (*c*, 1.6 in $CHCl_3$); i.r. (film) ν_{max} 3040, 2715, 1724, 1675, 1458, 1385 cm^{-1}; p.m.r. τ 0.20 (t, 1H, aldehydic proton, J = 2.5 Hz), 4.60 (unresolved m, 1H, vinyl proton), 8.42 (d of d, 3H, vinyl methyl, $J_{6\text{-}CH_3}$ = 1.6 Hz, $J_{5\text{-}CH_3}$ = 1.0 Hz), 9.07, 9.13

Can. J. Chem. Downloaded from www.nrcresearchpress.com by 210.87.254.6 on 09/05/12
For personal use only.

(d, d, 6H, isopropyl methyls, J = 6.5 Hz), 9.10 (s, 3H, tertiary methyl).

Anal. Calcd. for $C_{15}H_{24}O$: C, 81.76; H, 10.98. Found: C, 81.45; H, 10.98.

Preparation of the Pyrazoline 37

In a 5-ml flask equipped with a Dean–Stark water separator there was placed 58 mg (0.26 mmol) of the olefinic aldehyde **34** and 49 mg (0.263 mmol) of *p*-toluenesulfonylhydrazide in 2.5 ml of dry benzene. The reaction mixture was refluxed in an atmosphere of dry nitrogen for 5 min. The solvent was then removed, and replaced with 2.5 ml of dry tetrahydrofuran. To the resulting stirred solution was added 0.13 ml of 2 *M* *n*-butyllithium in hexane. After 30 min, the solvent was removed and the residual lithium salt of the *p*-toluenesulfonylhydrazone (**36**) was heated slowly under reduced pressure (0.25 Torr). Between the temperatures of 120 and 140 °C, 50 mg (81% yield from the aldehyde **34**) of the pyrazoline **37** was collected as a colorless oil, n_D^{24} 1.5042; $[\alpha]_D^{22}$ +95° (*c*, 1.0 in $CHCl_3$); u.v. λ_{max} 334 nm (ε 232); i.r. (film) ν_{max} 1550, 1456, 1377, 1122 cm^{-1}; p.m.r. τ 5.11 (m, 1H, proton adjacent to the —N=N— moiety), 8.42, 9.18 (s, s, 6H, tertiary methyls), 9.14 (d, 6H, isopropyl methyls, J = 6.0 Hz).

The instability of this material precluded the acquisition of satisfactory analytical data.

(−)-Cyclocopacamphene (2)

A solution of 35 mg of the pyrazoline **37** in 35 ml of dry ether was irradiated in a Rayonet Reactor, using 3500 Å lamps and a Pyrex filter, for 1 h. Removal of the solvent, followed by distillation (air-bath temperature 80 °C) of the residual oil under reduced pressure (0.3 Torr) afforded 30 mg (93%) of pure (−)-cyclocopacamphene (**2**), $[\alpha]_D^{21}$ −42° (*c*, 1.1 in $CHCl_3$); i.r. (film) ν_{max} 3039, 1460, 1387, 862, 847, 826 cm^{-1}; p.m.r. τ 8.99, 9.26 (s, s, 6H, tertiary methyls), 9.10, 9.13 (d, d, 6H, isopropyl methyls, J = 6.5 Hz), 9.32, 9.37 (broad signals, 2H, cyclopropyl protons). The i.r. and p.m.r. spectra of this material were identical with those of authentic (+)-cyclocopacamphene.

Anal. Calcd. for $C_{15}H_{24}$: C, 88.14; H, 11.84. Found: C, 88.35; H, 11.90.

Preparation of the Olefinic Alcohol 38

To a solution of lithium aluminum hydride (75 mg) in dry ether (5 ml) was added 330 mg of the keto olefin **9** and the resulting solution was refluxed gently for 1 h. The reaction mixture was cooled in an ice water bath and 3 ml of saturated aqueous ammonium chloride was added. The mixture was stirred at room temperature for 30 min and filtered through Celite. The filtrate was washed with brine and dried over anhydrous magnesium sulfate. Removal of the solvent, followed by distillation (air-bath temperature 86–89 °C; 0.08 Torr) of the residual oil, gave 325 mg (98%) of the olefinic alcohol **38** as a clear colorless oil, $[\alpha]_D^{25}$ −30° (*c*, 0.63 in $CHCl_3$); i.r. (film) ν_{max} 3510, 3105, 1640, 1460, 1383, 1132, 1110, 1016, 910 cm^{-1}; p.m.r. τ 3.92–4.50 (m, 1H, —C*H*=CH_2), 4.83–5.17 (m, 2H, —CH=C*H*$_2$), 5.37 (d of d, 1H, C-6 H, $J_{5,6}$ = 7.0 Hz, $J_{6,7}$ = 10.7 Hz), 9.04, 9.16 (d, d, 6H, isopropyl methyls, J = 6.7 Hz), 9.12 (d, 3H, secondary methyl, J = 7.5 Hz), 9.18 (s, 3H, tertiary methyl).

Anal. Calcd. for $C_{15}H_{26}O$: C, 81.02; H, 11.79. Found: C, 80.80; H, 11.61.

Dehydration of the Olefinic Alcohol 38

To a solution of the olefinic alcohol **38** (3.0 g, 13.5 mmol) in 125 ml of dry pyridine was added 9.6 g of redistilled thionyl chloride. The resulting mixture, under an atmosphere of nitrogen, was heated to 40 °C and then kept at this temperature for 3 h. The solution was cooled and poured into rapidly stirred ice-cold dilute hydrochloric acid. The resulting mixture was extracted thoroughly with 1:1 ether – petroleum ether (b.p. 65–110 °C). The combined extracts were successively washed with cold dilute hydrochloric acid, aqueous sodium bicarbonate, and brine, and then dried over anhydrous magnesium sulfate. Removal of the solvents afforded 2.7 g of a crude yellow oil which was subjected to column chromatography on 210 g of 15% silver nitrate impregnated silica gel. The column was eluted with petroleum ether (b.p. 65–110 °C) containing increasing amounts of ether. From the earlier fractions there was obtained 0.75 g (27%) of the pure diene **40**, which was distilled under reduced pressure (0.25 Torr) at an air-bath temperature of 69–71 °C, and exhibited $[\alpha]_D^{26}$ −6.3° (*c*, 0.8 in $CHCl_3$); i.r. (film) ν_{max} 3085, 1650, 1640, 990, 910, 870 cm^{-1}; p.m.r. τ 4.03–4.63 (m, 1H, —C*H*=CH_2), 4.90, 5.01 (d, d, 2H, $\diagdown$C=C*H*$_2$, J = 2.5 Hz), 5.08–5.37 (m, 2H, —CH=C*H*$_2$), 9.03 (s, 3H, tertiary methyl), 9.09, 9.12 (d, d, 6H, isopropyl methyls, J = 6.0 Hz).

Anal. Calcd. for $C_{15}H_{24}$: C, 88.16; H, 11.84. Found: C, 88.37; H, 11.91.

From the later petroleum ether – ether fractions in the above-mentioned chromatography 1.32 g (48%) of the pure diene **39** was obtained, which was distilled under reduced pressure (0.3 Torr) at an air-bath temperature of 70–72 °C, and exhibited $[\alpha]_D^{26}$ +37° (*c*, 0.64 in $CHCl_3$); i.r. (film) ν_{max} 3095, 3060, 1640, 1450, 1380, 1365, 995, 910 cm^{-1}; p.m.r. τ 3.98–4.35 (m, 1H, —C*H*=CH_2), 4.72 (unresolved m, 1H, C-6 H, $w_{\frac{1}{2}}$ = 6.0 Hz), 4.96–5.21 (m, 2H, —CH=C*H*$_2$), 7.64 (unresolved m, 1H, C-5H, $w_{\frac{1}{2}}$ = 5.0 Hz), 8.09 (d, 1H, C-8 H, J = 9.0 Hz), 8.42 (unresolved m, 3H, vinyl methyl, $w_{\frac{1}{2}}$ = 3.5 Hz), 9.12, 9.21 (d, d, 6H, isopropyl methyls, J = 6.5 Hz), 9.16 (s, 3H, tertiary methyl).

Anal. Calcd. for $C_{15}H_{24}$: C, 88.16; H, 11.84. Found: C, 87.96; H, 12.00

Acid-catalyzed Isomerization of the Diene 40

To a solution of the diene **40** (170 mg) in 3 ml of dry benzene was added a few crystals of *p*-toluenesulfonic acid and the resulting solution was refluxed for 30 min. The solution was cooled, washed successively with aqueous sodium bicarbonate and brine, and dried over anhydrous magnesium sulfate. Removal of the solvent yielded 160 mg (94%) of an oil which was shown by g.l.c. analysis (column A, 160 °C, 100) to consist of a mixture of the two dienes **39** and **40**, in a ratio of 7:3, respectively. These two materials could be separated by column chromatography as described above.

Preparation of the Olefinic Alcohol 41

To a stirred solution of disiamylborane (0.32 g, 2.1 mmol) in dry tetrahydrofuran (6 ml) at 0°, under an atmosphere of nitrogen, was added a solution of 204 mg (1.0 mmol) of the diene **39** in 4 ml of tetrahydrofuran. The solution was stirred at room temperature for 2.5 h and then cooled to 0 °C. There was successively added

Can. J. Chem. Downloaded from www.nrcresearchpress.com by 210.87.254.6 on 09/05/12
For personal use only.

2 ml of 3 *N* aqueous sodium hydroxide and 2 ml of 30% hydrogen peroxide, and the resulting mixture was stirred at room temperature for 60 min. After being diluted with water, the reaction mixture was thoroughly extracted with a 2:1 petroleum ether (b.p. 65–75 °C) – ether mixture. The combined extracts were washed with brine and dried over anhydrous magnesium sulfate. Removal of the solvents afforded an oil (340 mg) which was subjected to column chromatography on Florisil (48 g). Elution of the column with petroleum ether (b.p. 65–75 °C) containing increasing amounts of ether afforded 158 mg (71%) of the pure olefinic alcohol **41**, which was distilled under reduced pressure (0.1 Torr) at an air-bath temperature of 105–107 °C. Compound **41** exhibited $[\alpha]_D^{23}$ +45° (*c*, 0.31 in $CHCl_3$); i.r. (film) ν_{max} 3355, 3075, 1460, 1380, 1040, 1015 cm^{-1}; p.m.r. τ 4.73 (unresolved m, 1H, C-6 H, $w_{\frac{1}{2}}$ = 6.0 Hz), 6.20–6.73 (m, 2H, —C*H*$_2$OH), 7.58 (unresolved m, 1H, C-5 H, $w_{\frac{1}{2}}$ = 5.5 Hz), 8.41 (unresolved m, 3H, vinyl methyl, $w_{\frac{1}{2}}$ = 4.0 Hz), 9.08 (s, 3H, tertiary methyl), 9.09, 9.18 (d, d, 6H, isopropyl methyls, *J* = 6.0 Hz).

Anal. Calcd. for $C_{15}H_{26}O$: C, 81.02; H, 11.79. Found: C, 80.79, H, 11.85.

(+)-Sativene (3)

To a solution of the olefinic alcohol **41** (45 mg) in 1 ml of dry pyridine was added 90 mg of *p*-toluenesulfonyl chloride. The solution was stirred at room temperature for 2.5 h and then diluted with petroleum ether. The resulting solution was extracted with aqueous sodium bicarbonate and brine, and dried over anhydrous magnesium sulfate. Removal of the solvent afforded 56 mg of the crude olefinic tosylate **42**. The latter was transferred to the top of a small column of silica gel (4 g) and the column was eluted with petroleum ether. Evaporation of the eluant gave an oil which, upon distillation (air-bath temperature 50–52 °C; 0.08 Torr) afforded 34 mg (82%) of a clear colorless oil. Analysis of the latter by g.l.c. (column M, 120 °C, 90) indicated that it consisted of a mixture of three components in a ratio of approximately 3:75:22. Coinjection with an authentic sample indicated that the minor component was (+)-cyclosativene (**4**). The major component was collected by preparative g.l.c. and was identified as (+)-sativene (**3**): $[\alpha]_D^{24}$ +185°; i.r. (film) ν_{max} 3110, 1660, 1470, 1450, 1380, 1365, 870 cm^{-1}; p.m.r. τ 5.27, 5.60 (s, s, 2H, =CH_2), 7.41 (unresolved m, 1H, $w_{\frac{1}{2}}$ = 6 Hz), 8.98 (s, 3H, tertiary methyl), 9.11, 9.15 (d, d, 6H, isopropyl methyls, *J* = 6.0 Hz).

Anal. Calcd. for $C_{15}H_{24}$: C, 88.16; H, 11.84. Found: C, 88.31; H, 12.00.

The third component was isolated by preparative g.l.c. and was identified as isosativene (**26**): i.r. (film) ν_{max} 3090, 1650, 1455, 1377, 1359, 860 cm^{-1}; p.m.r. τ 5.25, 5.53 (s, s, 2H, =CH_2), 7.39 (unresolved m, 1H, $w_{\frac{1}{2}}$ = 9.0 Hz), 9.08 (s, 3H, tertiary methyl), 9.17 (d, 6H, isopropyl methyls, *J* = 6.0 Hz).

Preparation of the Olefinic Aldehyde 43

To a solution of 474 mg (6.0 mmol) of dry pyridine in 8 ml of dichloromethane was added 300 mg (3.0 mmol) of dry chromium trioxide. The mixture was stirred under an atmosphere of nitrogen at room temperature for 15 min and then a solution of the olefinic alcohol **41** (111 mg, 0.5 mmol) in 0.4 ml of dichloromethane was added. The reaction mixture was stirred at room temperature for 15 min and then diluted with ether. The organic solution was washed with saturated aqueous potassium carbonate and brine, and then dried over anhydrous magnesium sulfate. Removal of the solvent, followed by distillation (air-bath temperature 85–88 °C; 0.1 Torr) of the residual material under reduced pressure, afforded 84 mg (76%) of a clear oil. The latter was shown by g.l.c. analysis (column F, 130 °C, 100) to consist of the olefinic aldehyde **43** and an unidentified component in a ratio of 92:8. An analytical sample of compound **43**, collected by preparative g.l.c., exhibited $[\alpha]_D^{24}$ +71 (*c*, 0.64 in $CHCl_3$); i.r. (film) ν_{max} 3060, 2740, 1726, 1455, 1440, 1380, 1365 cm^{-1}; p.m.r. τ 0.23 (t, 1H, —C*H*O, *J* = 2.0 Hz), 4.70 (unresolved m, 1H, C-6 H, $w_{\frac{1}{2}}$ = 12 Hz), 7.53–7.67 (m, 2H, —C*H*$_2$CHO), 8.06 (d, 1H, C-5 H, *J* = 6.5 Hz), 8.42 (unresolved m, 3H, vinyl methyl, $w_{\frac{1}{2}}$ = 3.0 Hz), 9.09 (s, 3H, tertiary methyl), 9.12, 9.17 (d, d, 6H, isopropyl methyls, *J* = 6.0 Hz).

Mol. Wt. Calcd. for $C_{15}H_{24}O$: 220.183. Found (high resolution mass spectrometry): 220.184.

Preparation of the Pyrazoline 46

A solution of the olefinic aldehyde **43** (80 mg, 0.36 mmol) and *p*-toluenesulfonylhydrazide (67 mg, 0.36 mmol) in 6 ml of dry benzene was refluxed under a Dean–Stark water separator for 15 min. The solution was cooled and the solvent was evaporated under reduced pressure. The residual crude *p*-toluenesulfonylhydrazone **44** was dissolved in 4 ml of dry tetrahydrofuran and the resulting solution was treated with a solution of *n*-butyllithium (1 equiv.) in hexane. The solution was stirred at room temperature under nitrogen for 90 min and then the solvents were removed under reduced pressure. The residual lithium salt **45** was heated slowly under reduced pressure (0.1 Torr), with direct distillation of the product. Between 105 and 130 °C, 88 mg of a colorless oil was collected. The latter was redistilled (air-bath temperature 110–115 °C; 0.1 Torr) to afford 64 mg (72%) of the pure pyrazoline **46**, which exhibited u.v. λ_{max} 334 nm (ε 235); i.r. (film) ν_{max} 1550, 1460, 1370 cm^{-1}; p.m.r. τ 4.98 (m, 1H, proton adjacent to the —N=N— group), 8.33, 9.20 (s, s, 6H, tertiary methyls), 9.16 (d, 6H, isopropyl methyls, *J* = 6.0 Hz).

The instability of this compound precluded the acquisition of satisfactory analytical data.

(+)-Cyclosativene (4)

A solution of the pyrazoline **46** (50 mg) in 50 ml of dry ether was irradiated in a Rayonet Reactor (3500 Å lamps, Pyrex filter) for 90 min. Removal of the solvent, followed by distillation (air-bath temperature 70–75 °C; 0.1 Torr) of the residual oil gave 36 mg of a clear oil. Gas–liquid chromatographic analysis of the latter (column M, 120 °C, 100) showed that it consisted of a mixture of two components, in a ratio of approximately 11:1. The two compounds were collected by preparative g.l.c. The minor product was identified (i.r.) as the bicyclic diene **39**. The major product (30 mg, 68%) was identified as (+)-cyclosativene (**4**): $[\alpha]_D^{24}$ +84° (*c*, 0.36 in $CHCl_3$); i.r. (film) ν_{max} 3075, 1450, 1380, 1362, 845, 826 cm^{-1}; p.m.r. τ 9.03, 9.26 (s, s, 6H, tertiary methyls), 9.11, 9.14 (d, d, 6H, isopropyl methyls, *J* = 6.0 Hz).

Mol. Wt. Calcd. for $C_{15}H_{24}$: 204.188. Found (high resolution mass spectrometry): 204.189.

Financial support from the National Research Council of Canada and the University of British Columbia Com-

mittee on Research, and a NRCC Postdoctorate Fellowship (to M.S.) are gratefully acknowledged.

1. M. KOLBE-HAUGWITZ and L. WESTFELT. Acta Chem. Scand. **24**, 1623 (1970).
2. F. KIDO, R. SAKUMA, H. UDA, and A. YOSHIKOSHI. Tetrahedron Lett. 3169 (1969).
3. N. H. ANDERSEN. Tetrahedron Lett. 4651 (1970).
4. P. DE MAYO and R. E. WILLIAMS. J. Am. Chem. Soc. **87**, 3275 (1965).
5. L. SMEDMAN and E. ZAVARIN. Tetrahedron Lett. 3833 (1968).
6. L. A. SMEDMAN, E. ZAVARIN, and R. TERANISHI. Phytochemistry, **8**, 1457 (1969).
7. L. A. SMEDMAN, K. SNAJBERK, E. ZAVARIN, and T. R. MON. Phytochemistry, **8**, 1471 (1969).
8. E. PIERS, R. W. BRITTON, M. B. GERAGHTY, R. J. KEZIERE, and R. D. SMILLIE. Can. J. Chem. This issue.
9. E. PIERS, R. W. BRITTON, R. J. KEZIERE, and R. D. SMILLIE. Can. J. Chem. **49**, 2623 (1971).
10. E. PIERS, M. B. GERAGHTY, and M. SOUCY. Synth. Commun. **3**, 401 (1973).
11. E. PIERS, R. W. BRITTON, M. B. GERAGHTY, R. J. KEZIERE, and F. KIDO. Can. J. Chem. This issue.
12. R. E. IRELAND and G. PFISTER. Tetrahedron Lett. 2145 (1969).
13. M. FETIZON, M. JURION, and N. T. ANH. Chem. Commun. 112 (1969).
14. R. E. IRELAND, D. C. MUCHMORE, and U. HENGARTNER. J. Am. Chem. Soc. **94**, 5098 (1972).
15. M. TANABE and D. F. CROW. Chem. Commun. 1498 (1969), and references cited therein.
16. W. KIRMSE. Carbene chemistry. 2nd ed. Academic Press, Inc., New York. 1971. pp. 29–34.
17. R. H. SHAPIRO and M. J. HEATH. J. Am. Chem. Soc. **89**, 5734 (1967).
18. G. KAUFMAN, F. COOK, H. SHECHTER, J. BAYLESS, and L. FRIEDMAN. J. Am. Chem. Soc. **89**, 5736 (1967).
19. J. MEINWALD and F. UNO. J. Am. Chem. Soc. **90**, 800 (1968).
20. W. G. DAUBEN, M. E. LORBER, N. D. VIETMEYER, R. H. SHAPIRO, J. H. DUNCAN, and K. TOMER. J. Am. Chem. Soc. **90**, 4762 (1968).
21. A. K. BOSE and N. G. STEINBERG. Synthesis, 595 (1970).
22. M. KARPLUS. J. Am. Chem. Soc. **85**, 2870 (1963).
23. J. C. COLLINS, W. W. HESS, and F. J. FRANK. Tetrahedron Lett. 3363 (1968).
24. R. RATCLIFFE and R. RODEHORST. J. Org. Chem. **35**, 4000 (1970).
25. K. BOWDEN, I. M. HEILBRON, E. R. H. JONES, and B. C. L. WEEDON. J. Chem. Soc. 39 (1946).
26. F. JOHNSON. Chem. Rev. **68**, 375 (1968).
27. R. GREENWALD, M. CHAYKOVSKY, and E. J. COREY. J. Org. Chem. **28**, 1128 (1963).
28. H. C. BROWN and G. ZWEIFEL. J. Am. Chem. Soc. **83**, 1241 (1961).
29. J. E. MCMURRY. Tetrahedron Lett. 3731 (1970).
30. J. E. MCMURRY. J. Org. Chem. **36**, 2826 (1971).
31. J. E. MCMURRY. Tetrahedron Lett. 3735 (1970).
32. W. S. JOHNSON, J. C. COLLINS, R. PAPPO, M. B. RUBIN, P. J. KROPP, W. F. JOHNS, J. E. PIKE, and W. BARTMANN. J. Am. Chem. Soc. **85**, 1409 (1963).
33. M. M. FAWZI and C. D. GUTSCHE. J. Org. Chem. **31**, 1390 (1966), and references cited therein.
34. HUANG-MINLON. J. Am. Chem. Soc. **68**, 2487 (1946).
35. W. F. ERMAN and L. C. STONE. J. Am. Chem. Soc. **93**, 2821 (1971).
36. R. MALHERBE, N. T. T. TAM, and H. DAHN. Helv. Chim. Acta, **55**, 245 (1972).
37. P. N. CHAKRABORTTY, R. DASGUPTA, S. K. DASGUPTA, S. R. GHOSH, and U. R. GHATAK. Tetrahedron, **28**, 4653 (1972).
38. D. J. BEAMES, L. N. MANDER, and J. V. TURNER. Aust. J. Chem. **27**, 1977 (1974), and previous papers in the series.
39. C. W. ROBERTS. *In* Friedel–Crafts and related reactions. Vol. II, Pt. 2. *Edited by* G. A. Olah. Interscience Publishers, Inc., New York. 1963. pp. 1175–1210.
40. G. M. KAUFMAN, J. A. SMITH, G. G. VANDER STOUW, and H. SHECHTER. J. Am. Chem. Soc. **87**, 935 (1965).
41. G. W. COWELL and A. LEDWITH. Qt. Rev. **24**, 119 (1970).
42. R. J. CRAWFORD, A. MISHRA, and R. J. DUMMEL. J. Am. Chem. Soc. **88**, 3959 (1966).
43. R. O. HUTCHINS, C. A. MILEWSKI, and B. E. MARYANOFF. J. Am. Chem. Soc. **95**, 3662 (1973).
44. M. J. FRAZER, W. GERRARD, G. MACHELL, and B. D. SHEPHERD. Chem. Ind. 931 (1954).
45. J. E. MCMURRY. Tetrahedron Lett. 55 (1969).
46. D. F. EATON, R. G. BERGMAN and G. S. HAMMOND. J. Am. Chem. Soc. **94**, 1351 (1972).
47. F. KIDO. Ph.D. Thesis. Tohoku University, Sendai, Japan. 1970.

Can. J. Chem. Downloaded from www.nrcresearchpress.com by 210.87.254.6 on 09/05/12
For personal use only.

Oxidation of Hydrocarbons. VII. Kinetics of the Oxidation of Naphthalenes by Ruthenium Tetroxide[1]

UDO A. SPITZER AND DONALD G. LEE
Department of Chemistry, The University of Regina, Regina, Saskatchewan S4S 0A2

Received May 12, 1975

UDO A. SPITZER and DONALD G. LEE. Can. J. Chem. 53, 2865 (1975).

The kinetics of the oxidation of naphthalene by ruthenium tetroxide have been investigated. When the reaction was monitored using an absorption band at 385 nm it was possible to detect two processes; the first, a rapid second-order reaction which yielded a ruthenium(VI) moiety, was followed by a much slower first-order decomposition of this intermediate. The initial reaction exhibited an inverse isotope effect when naphthalene-d_8 was used as a substrate and was accelerated by the introduction of electron donating substituents. The decomposition of the intermediate was not sensitive to the presence of substituents, but involved carbon–hydrogen bond cleavage as indicated by the occurrence of a primary deuterium isotope effect.

UDO A. SPITZER et DONALD G. LEE. Can. J. Chem. 53, 2865 (1975).

On a étudié la cinétique de l'oxydation du naphtalène par le tétroxyde de ruthénium. Quand on suit l'évolution de la réaction en examinant la bande d'absorbtion à 385 nm, on peut détecter deux processus; le premier, une réaction rapide du deuxième ordre, conduit à une portion contenant du ruthénium (VI) et le deuxième, beaucoup plus lent et du premier ordre, correspond à la décomposition de l'intermédiaire. La première réaction montre un effet isotopique inverse lorsque du naphtalène-d_8 est utilisé comme substrat et est accélérée par l'introduction de substituants électro-donneurs. La décomposition de l'intermédiaire n'est pas sensible à la présence de substituants mais elle implique un bris du lien carbone–hydrogène tel qu'on peut le mettre en évidence par la présence d'un effet isotopique primaire du deutérium.

[Traduit par le journal]

Can. J. Chem. Downloaded from www.nrcresearchpress.com by 210.87.254.40 on 09/05/12
For personal use only.

Introduction

Although a variety of oxidants are capable of converting substituted naphthalenes into the corresponding phthalic acids (1) or phthalic anhydrides (2), the use of ruthenium tetroxide for these purposes is attractive because it does not result in the destruction of alkyl side chains and because it can be used in conjunction with other, less expensive co-oxidants (3). Previous publications (4, 5) have shown that ruthenium tetroxide can be used catalytically (along with sodium hypochlorite) for the oxidation of substituted naphthalenes. Phthalic acid is the sole product obtained from naphthalene and its derivatives bearing electron donating substituents (4, 5). However, mixtures of substituted and unsubstituted phthalic acids are obtained if the substituents are electron withdrawing (4). Hence the reaction is of practical importance because of the commercial value of the products and theoretically interesting because of the large changes in oxidation number which occur in both the oxidant and the reductant.

In this paper we wish to describe the kinetics which are observed when a limited amount of ruthenium tetroxide is allowed to react with naphthalene and naphthalene derivatives in carbon tetrachloride solutions.

Experimental

All kinetic determinations were made by following changes in absorbance at 385 nm. A Perkin-Elmer 356 double wavelength spectrophotometer equipped with a thermostated cell compartment and a rapid mixing device was used. With this instrument spectrophotometric measurements can be made despite the presence of precipitates because the sample may be placed close to a large collimating lens which directs scattered energy to the photomultiplier. Consequently, the precipitation of ruthenium dioxide from these solutions did not interfere seriously with the kinetic determinations.

Spectral grade carbon tetrachloride reacts slowly with ruthenium tetroxide; however, it can be purified by repeated treatment with ruthenium tetroxide until no ruthenium dioxide is observed to precipitate, followed by distillation.

As indicated in Fig. 1 the reactions were all characterized by a rapid initial increase in absorbance, followed by a much slower decrease. Attempts to fit these curves

[1]For parts V and VI see refs. 4 and 23, respectively.

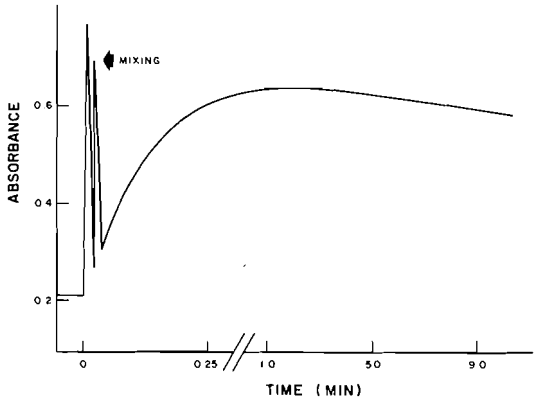

FIG. 1. Time *vs.* absorbance for a typical kinetic determination.

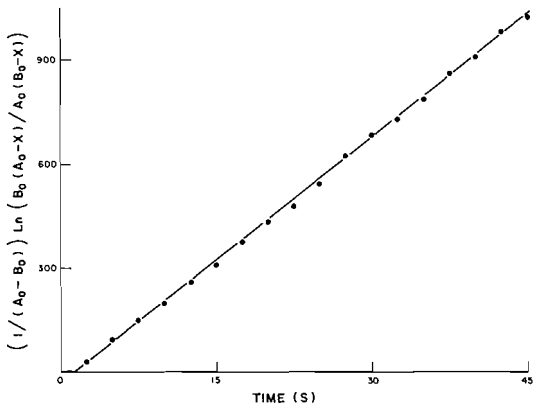

FIG. 2. Typical second-order plot: A_0 = [Naphthalene]$_0$ = 2.15×10^{-3} M; B_0 = [Ruthenium tetroxide]$_0$ = 1.8×10^{-4} M; X = [Intermediate]; temperature = 25.0 °C; correlation coefficient = 0.999.

quantitatively to integral rate laws indicated that the initial reaction was first order in both oxidant and reductant. As indicated by the following equations, the resulting second-order rate law can be expressed in terms of the extinction coefficient of ruthenium tetroxide (ε_R), the extinction coefficient of the intermediate (ε_I), the initial absorbance (A_0) and the absorbance at time t, (A_t).

$$[1] \qquad A_t = [RuO_4]_t\varepsilon_R + [I]_t\varepsilon_I$$

$$[2] \qquad A_t = [RuO_4]_0\varepsilon_R - [I]_t\varepsilon_R + [I]_t\varepsilon_I$$

$$[3] \qquad [I]_t = \frac{A_t - [RuO_4]_0\varepsilon_R}{\varepsilon_I - \varepsilon_R} = \frac{A_t - A_0}{\varepsilon_I - \varepsilon_R}$$

$$[4] \qquad \frac{-d[RuO_4]}{dt} = k_2[RuO_4][C_{10}H_8]$$

$$[5] \qquad \frac{1}{[RuO_4]_0 - [C_{10}H_8]_0} \times \ln \frac{[C_{10}H_8]_0([RuO_4]_0 - [I]_t)}{[RuO_4]_0([C_{10}H_8]_0 - [I]_t)} = k_2t$$

Plots of the left hand side of [5] against time consistently gave good straight lines. A typical example has been reproduced in Fig. 2.

The spectrum of ruthenium tetroxide was similar to that previously reported (6) and the spectrum of the intermediate could be easily obtained because the second reaction is comparatively slow (Fig. 1). The absorbance of the intermediate at 385 nm was observed to obey Beer's law if it was assumed that 1 mol of intermediate formed from each mole of oxidant present: apparently the intermediate is generated irreversibly from ruthenium tetroxide and naphthalene and its concentration is limited by the oxidant which was always present in lower molar amounts.

Decomposition of the intermediate was found to be a first-order process, but because of complications owing to precipitate formation in latter stages of the decomposition, it was most convenient to obtain these rate constants from initial reaction rates.

An attempt was made to detect the presence of free radicals in these solutions by use of a Varian 100 kHz electron paramagnetic resonance spectrophotometer. Solutions were prepared and placed immediately in the instrument but no free radical signals were ever obtained.

Results and Discussion

The excellent correlation of experimental data with a second-order equation for the formation of the intermediate and with a first-order relationship for its decomposition is consistent with a reaction sequence such as that given in [6] and [7].

$$[6] \qquad RuO_4 + \text{Naphthalene} \xrightarrow{k_2} \text{Intermediate}$$

$$[7] \qquad \text{Intermediate} \xrightarrow{k_1} \text{Products}$$

The lack of a primary deuterium isotope effect (Table 1) on the initial reaction indicates that no carbon–hydrogen bonds are appreciably cleaved in the transition state and the effect of substituents suggests that the organic moiety has acquired some positive charge. It is likely that the intermediate is formed in a two- rather than a one-electron transfer step. If only one electron had been transferred the products would have been ruthenium(VII) and the naphthyl radical cation. However, no e.s.r. signals could be obtained under conditions where ruthenium(VII) and the naphthalene radical cation had previously been detected. Furthermore the characteristic color associated with the naphthyl radical cation was not observed (7) nor is the spectrum of the intermediate characteristic of perruthenate (Fig. 3).

Can. J. Chem. Downloaded from www.nrcresearchpress.com by 210.87.254.40 on 09/05/12
For personal use only.

Can. J. Chem. Downloaded from www.nrcresearchpress.com by 210.87.254.40 on 09/05/12
For personal use only.

TABLE 1. Summary of kinetic data[a]

Compound	$k_2(s^{-1}\,M^{-1})$	$k_1(s^{-1}) \times 10^4$
Naphthalene	24.1	3.2
Naphthalene-d_8	27.7	1.3
2-Chloronaphthalene	6.54	1.9
1-Chloronaphthalene	7.57	1.7
1-Fluoronaphthalene	10.1	2.1
1-Methylnaphthalene	71.5	3.2
2-Methylnaphthalene	79.8	2.5
1,4-Dimethylnaphthalene	147	1.4
2,3-Dimethylnaphthalene	139	1.5
2-Methoxynaphthalene	168[b]	2.9
1-Methoxynaphthalene	652[b]	3.2

[a]Temperature = 25.0 ± 0.1 °C; $[RuO_4] = 2.40 \times 10^{-4}$ *M*; [Naphthalene] = 2–50 × 10^{-4} *M*.
[b]For these very fast reactions the number of experimental points was rather small (4–6); in all other cases at least 15 points were obtained in each determination.

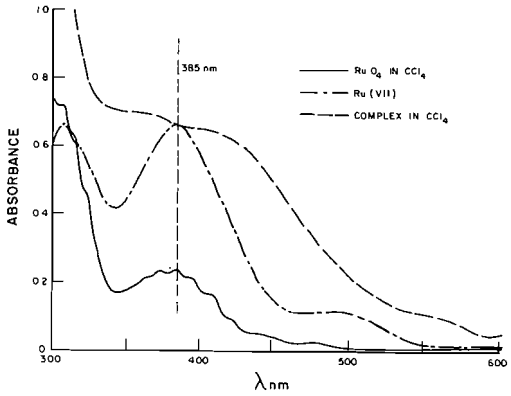

FIG. 3. Spectra of RuO_4 in CCl_4 before and after addition of naphthalene. RuO_4^- spectrum as reported in ref. 6.

The observation of an inverse isotope effect for the initial step of the reaction indicates that one or more carbon atoms are undergoing a change in hybridization from sp^2 to sp^3 (8, 9). This in turn suggests that the reaction sequence may be initiated by an electrophilic aromatic substitution reaction as indicated in Scheme 1. (Other electrophilic aromatic substitutions are also known to exhibit inverse isotope effects (10).) The dipole structure formed would then very likely condense to give a cyclic ruthenate diester (**1**), which must subsequently decompose by a slower first-order reaction in which C—H bond cleavage occurs. One possibility (involving the internal transfer of a hydride ion) is shown in Scheme 1.

It is not possible to apply an exact linear free energy correlation to the effect of substituents because the oxidant does not attack the substituted ring exclusively when it bears electron withdrawing substituents (4). However, if it is assumed that reaction will take place most readily at the 1-position of naphthalene and at the 4-position of 1-methyl- and 1-methoxynaphthalene (11), an approximate Hammett ρ value can be calculated (12). If σ_R^0 substituent parameters (13) are used a ρ value of about −3.5 is obtained. This result is also consistent with an electrophilic aromatic substitution reaction in which a partial positive charge is developed in the transition state (14).

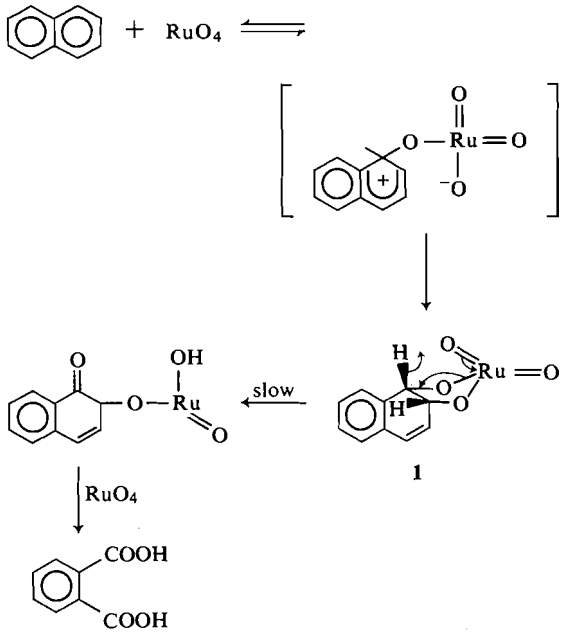

SCHEME 1

The electrophilic aromatic substitution reaction which would be most directly comparable with the mechanism depicted in Scheme 1 is sulfonation by sulfur trioxide in a nonaqueous medium. A neutral electrophile (SO_3) is believed to attack the aromatic ring and in so doing undergoes reduction (15). Consequently one method of testing the proposed mechanism would be to compare the activation parameters of reaction 6 with those observed during sulfonation reactions. When the effect of temperature on the rate of the reaction between ruthenium tetroxide and naphthalene was investigated the activation parameters were found to be $\Delta H^{\ddagger} = 11.3 \pm 0.4$ kcal/mol and $\Delta S^{\ddagger} = -15 \pm 5$ e.u. (or $E^* = 12$ kcal/mol and $\log A =$

Can. J. Chem. Downloaded from www.nrcresearchpress.com by 210.87.254.40 on 09/05/12
For personal use only.

9.9). These values are similar to those which have been reported for the sulfonation of a variety of aromatic compounds in oleum (16) and identical, within the limits of experimental error, with those obtained for the sulfonation of *p*-dichlorobenzene in trichlorofluoromethane (17).

When considering possible mechanisms for the second step of the process it should be noted that this reaction is quite insensitive to the effects of substituents (Table 1) and that it exhibits a substantial deuterium isotope effect. The latter observation indicates that a carbon–hydrogen bond is likely broken in this step. Such a cleavage can take place coincidentally with reduction of the ruthenium(VI) moiety by either hydrogen atom or hydride ion transfer. Although it is difficult to distinguish between these two processes the observed activation parameters ($\Delta H^{\ddagger} = 15.9 \pm 0.4$ and $\Delta S^{\ddagger} = -20 \pm 5$ e.u.) are more similar to those obtained for a number of other oxidation reactions which are presumed to proceed by way of hydride transfers (18). Such reactions are usually characterized by a negative entropy of activation of about −20 e.u., whereas oxidations by cobaltic (19), manganic (20), and ceric (21) salts as well as by halogen atoms (22) which are considered to be reacting by free radical steps usually exhibit much larger (positive) entropies of activation.

If the second step is taken to be a hydride transfer the product would be a keto derivative which would be subject to second stage oxidation, eventually leading to formation of phthalic acid if sufficient oxidant is available.

The authors gratefully acknowledge the financial assistance of the National Research Council of Canada. We also thank Dr. J. A. Weil and Mr. B. D. Perlson for assistance in obtaining the e.s.r. spectra.

1. R. STEWART. *In* Oxidation in organic chemistry. Vol. 5A. *Edited by* K. B. Wiberg. Academic Press, New York. 1965. p. 47. D. G. LEE. *In* Oxidation: techniques and applications in organic synthesis. Vol. 1. *Edited by* R. L. Augustine. Marcel Dekker, Inc., New York. 1969. pp. 30–46.
2. J. K. DIXON and J. E. LONGFIELD. *In* Catalysis. Vol. VIII. *Edited by* P. H. Emmett. Reinhold, New York. 1960. pp.183–280.P. W. SHERWOOD. Petrol. Refiner, **32**, 113 (1953). R. LANDAU and R. W. SIMON. Chem. Ind. (London), 70 (1962).
3. D. G. LEE and M. VAN DEN ENGH. *In* Oxidation in organic chemistry, Vol. 5B. *Edited by* W. S. Trahanovsky. Academic Press, New York. 1973. pp. 177–227.
4. U. A. SPITZER and D. G. LEE. J. Org. Chem. **39**, 2468 (1974).
5. D. C. AYRES and A. M. M. HOSSAIN. Chem. Commun. 428 (1972).
6. R. E. CONNICK and C. R. HURLEY. J. Am. Chem. Soc. **74**, 5012 (1952).
7. I. C. LEWIS and L. S. SINGER. J. Chem. Phys. **43**, 2712 (1965).
8. A. W. KAANDORP, H. CERFONTAIN, and F. L. J. SIXMA. Rec. Trav. Chim. **81**, 969 (1962).
9. E. A. HALEVI. Progr. Phys. Org. Chem. **1**, 169 (1963).
10. G. A. OLAH, S. J. KUHN, and S. H. FLOOD. J. Am. Chem. Soc. **83**, 4571 (1961); **83**, 4581 (1961). G. A. OLAH, S. J. KUHN, and B. A. HARDIE. J. Am. Chem. Soc. **86**, 1055 (1964).
11. H. N. SCHMEISING and R. L. MILLER. J. Chem. Phys. **40**, 926 (1964). H. CERFONTAIN and A. TELDER. Rec. Trav. Chim. **86**, 527 (1967).
12. L. P. HAMMETT. Physical organic chemistry. 2nd. ed. McGraw-Hill, Toronto. 1970. Chapt. 11.
13. P. R. WELLS, S. EHRENSON, and R. W. TAFT. Progr. Phys. Org. Chem. **6**, 147 (1968).
14. E. BERLINER. Progr. Phys. Org. Chem. **2**, 253 (1964).
15. K. L. NELSON. *In* Friedel–Crafts and related reactions. Vol. III, Pt. 2. *Edited by* G. A. Olah. Interscience. 1964. pp. 1355–1392.
16. J. C. D. BRAND. J. Chem. Soc. 1004 (1950). W. A. COWDREY and D. S. DAVIS. J. Chem. Soc. 1871 (1949).
17. J. K. BOSSCHER and H. CERFONTAIN. Tetrahedron, **24**, 6543 (1968).
18. P. D. BARTLETT and J. D. MCCOLLUM. J. Am. Chem. Soc. **78**, 1441 (1956). E. J. STROJNY, R. T. IWAMASA, and L. K. FREVEL. J. Am. Chem. Soc. **93**, 1171 (1971). R. M. BARTER and J. S. LITTLER. J. Chem. Soc. B, 205 (1967). D. G. LEE and M. VAN DEN ENGH. Can. J. Chem. **50**, 2000 (1972); **50**, 3129 (1972).
19. A. A. CLIFFORD and W. A. WATERS. J. Chem. Soc. 2796 (1965). D. G. HOARE and W. A. WATERS. J. Chem. Soc. 2560 (1964). C. E. H. BAWN and J. A. SHARP. J. Chem. Soc. 1854 (1957).
20. T. J. KEMP and W. A. WATERS. J. Chem. Soc. 339 (1964); 1192 (1964).
21. R. RAMASWAMY, M. S. VENKATACHALAPATHY, and H. V. K. UDUPA. Bull. Chem. Soc. Jpn. **35**, 1751 (1962).
22. A. F. TROTMAN-DICKENSON. Adv. Free-Radical Chem. **1**, 1 (1965).
23. U. A. SPITZER and D. G. LEE. J. Org. Chem. In press.

Synthesis of Methyl 12*S*- and 12*R*-Hydroxylabd-8(17)-en-19-oates

RUSSELL A. BELL, MICHAEL B. GRAVESTOCK, AND VINCENT Y. TAGUCHI

Department of Chemistry, McMaster University, Hamilton, Ontario L8S 4M1

Received September 5, 1974[1]

RUSSELL A. BELL, MICHAEL B. GRAVESTOCK, and VINCENT Y. TAGUCHI. Can. J. Chem. **53**, 2869 (1975).

A formal total synthesis using podocarpic acid as the relay of methyl 12*S*- and 12*R*-hydroxylabd-8(17)-en-19-oates, **7** and **8** respectively, has been achieved. Carbons 13 → 16 of the labdane side chain were formed by the nucleophilic addition of *s*-butyllithium to the bicyclic acid **5***a* or the aldehyde **4**, and the configuration of the alcohols assigned from a consideration of product distributions and physical and spectroscopic properties. The spectroscopic properties of the synthetic alcohols were in agreement with those reported for two alcohols isolated from *Juniperus phoenicea* L. and assigned structures **7** and **8**.

RUSSELL A. BELL, MICHAEL B. GRAVESTOCK et VINCENT Y. TAGUCHI. Can. J. Chem. **53**, 2869 (1975).

On a réussi une synthese totale formelle des hydroxy-12*R* (et 12*S*) labdène-8(17) oates-19 de méthyle **7** (et **8**) en utilisant l'acide podocarpique comme relais. On a introduit les carbones 13 → 16 de la chaîne latérale du labdane par addition nucléophile du *s*-butyllithium sur l'acide bicyclique **5***a* ou sur l'aldéhyde correspondant **4**; on a attribué la configuration des alcools en se basant sur la distribution des produits et aussi sur leurs propriétés physiques et spectroscopiques. Les propriétés spectroscopiques des alcools de synthèse sont en accord avec celles rapportées pour deux alcools isolés du *Juniperus phoenicea* L. et auxquels les structures **7** et **8** avaient été attribuées. [Traduit par le journal]

The reported isolation in 1968 of two isomeric 12-hydroxylabd-8(17)-en-19-oic acids by Tabacik-Wlotzka and Laporthe (1) from *Juniperus phoenicea* L. led us to undertake a partial synthesis of these two compounds from podocarpic acid **1***a*. The interest in these two diterpenes lies in the positioning of the hydroxyl group at carbon 12 which is an unusual site of oxidation for simple labdane diterpenoids.[2] The synthesis of such 12-hydroxylabdenes appeared attractive because of the ready availability of the bicyclic acid **5***a* and the aldehyde **4**, both of which possessed electrophilic centers at C-12.

Podocarpic acid as its methyl ester **1***b* had previously been transformed (3) by ozonolysis into the hydroperoxide **2** and this material on catalytic reduction to the keto acid **3**. A standard Reformatsky reaction and decarboxylation sequence converted **3** into the olefin acid **5***a* in overall yields of 43% (4). The aldehyde **4** was available from the diester **5***b* by a simple oxidation reduction sequence (4). The remaining step to

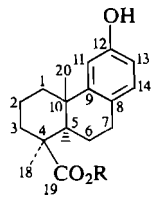

I

a R = H
b R = Me

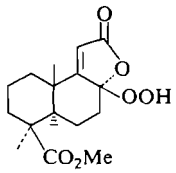

2

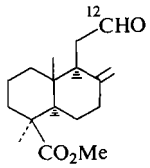

4

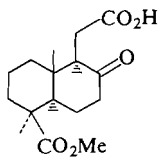

3

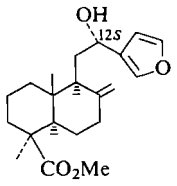

9

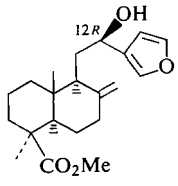

10

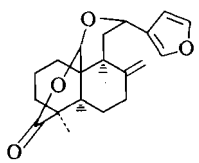

i

[1]Revision received June 13, 1975.

[2]More highly oxygenated labdanes such as sciadin (i) do have oxygen attached to C-12 (2).

Can. J. Chem. Downloaded from www.nrcresearchpress.com by 210.87.254.5 on 09/05/12
For personal use only.

Can. J. Chem. Downloaded from www.nrcresearchpress.com by 210.87.254.5 on 09/05/12
For personal use only.

generate the labdene skeleton was then the straightforward addition of a *s*-butyl group and this was carried out in two ways using *s*-butyllithium as the nucleophile.

Firstly, the *s*-butyl group was introduced by the action of *s*-butyllithium (*s*-BuLi) on the free acid **5***a* at room temperature to give the keto acid **6***a*, but the purification of this acid proved difficult and conversion to the ester with diazomethane gave, after chromatography, a 50% yield of the keto ester **6***b*. It is interesting to note here that *s*-BuLi has behaved in a manner analogous to other strong bases in aprotic solvents (5) in completely demethylating the hindered C-19 methyl ester of **5***a*. The purified keto ester **6***b* obtained was expected to be a mixture of two diastereomers that are epimeric at C-13, since the nucleophilic reagent was racemic *s*-BuLi, but in our hands the diastereomers proved inseparable and **6***b* always behaved as a single species. The $NaBH_4$ reduction of **6***b* gave rise to two easily separable 12-alcohols, **7** and **8**, in a ratio of 70:30. The same two alcohols were obtained more directly in a second experiment in 60% yield in a ratio of 75:25 by the selective addition of *s*-BuLi to the aldehyde **4** at −70 °C (see Scheme 1).

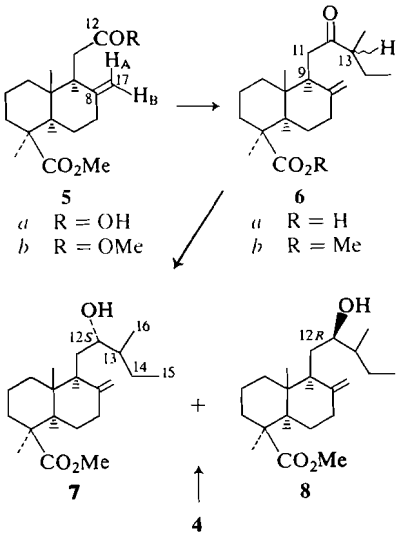

SCHEME 1

This latter low temperature addition showed no hydrolysis of the C-19 methyl noted in the room temperature reactions and more importantly it showed clearly that although two C-12 alcohols could be readily separated, each alcohol remained a mixture of two diastereomers which were epimeric at C-13 since again racemic *s*-BuLi was the reagent. In a number of thin-layer chromatographic (t.l.c.) experiments no physical differences could be observed between these 13-epimers, a fact which suggests that the configuration at C-13 has a very small influence on the properties of either of the alcohols **7** or **8**, or the ketone **6***b*.

Before commenting in more detail on the assignment of the configuration at C-12 in **7** and **8**, it should be noted that neither of the synthetic alcohols possessed spectroscopic properties exactly identical with the *erythro* and *threo* stereoisomers isolated by Tabacik-Wlotzka and Laporthe[3] and proposed to have structures **7** and **8**. The differences particularly in the proton magnetic resonance (p.m.r.) spectra of the naturally occurring and synthetic alcohols initially led us to suppose that the proposed structures for the natural alcohols were incorrect, despite the fact that we had been unable to separate the 13*S* and 13*R* stereoisomers of **7** and **8**. While the natural alcohols are most likely to possess a single configuration at C-13, our experience noted above suggests that any p.m.r. or i.r. spectroscopic differences should not be apparent if the synthetic alcohols differ from the natural compounds merely in their configurations at C-13. However, the natural alcohols were reported to be isolated in a ratio of 65:35, virtually identical with that obtained in our reduction experiments on the synthetic ketone **6**. We now consider that the isolated alcohols do in fact have structures **7** and **8** and that the spectroscopic differences arose from the presence of impurities (benzene) in the synthetic samples used for p.m.r. spectra. The most disturbing feature was the occurrence of a doublet at 4.14 p.p.m. in the p.m.r. spectrum of natural **8** which was not present in synthetic **8**. The absorption was assigned (1) to H-12, but in our view, the lines are better assigned to the proton of the OH group which would then allow the movement of its lines underneath the methylene envelope in the synthetic **8** by exchange with any traces of acids or bases present in the sample. The H-12 in the

[3]We thank Mme Tabacik-Wlotzka for copies of the i.r. and p.m.r. spectra in addition to the reported physical data. Samples of either alcohol were unfortunately not available.

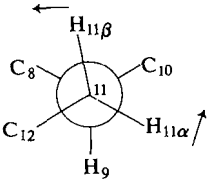

FIG. 1. Conformational torsion about the 9,11-bond of labd-8(17)-enes.

natural material should then be assigned to a broad absorption between 3.27 and 3.77 p.p.m. which is partly masked by the ester methyl group at 3.6 p.p.m.[4]

To place the position of the hydroxyl group in synthetic **7** and **8** on even firmer ground, the high resolution mass spectra of both alcohols were recorded. The expected fragmentation α to the hydroxyl occurred and strong ions were observed at *m/e* 279 showing the loss of carbons 13 → 16 and at *m/e* 87 showing the OH group was contained in the fragment of carbons 12 → 16.

The assignment of the configuration of C-12 in **7** and **8** was based largely on standard conformational analysis coupled with close scrutiny of Dreiding molecular models. X-Ray structural studies on 8α-hydroxylabdanes (6) indicated that there was torsion about the 9,11-bond which moved H-11β away from the 20-methyl and H-11α away from H-1β. While such torsion need not be so pronounced in the present molecules with their 8(17)-double bonds, the presence of some twisting about the 9,11-bond as shown in Fig. 1 does relieve the serious H-11α, H-1β interaction and places C-12 at more acceptable distances from C-17. Taking a rotation of 15–30° about the 9,11-bond as reasonable, the conformers about the 11,12-bond of ketone **6** can be represented as in Fig. 2. Even if it is assumed that the carbonyl group can move away somewhat from an eclipsing orientation when steric forces demand it, it is clear from molecular models that conformer **c** is prohibited because of the *s*-butyl group being thrust into the vinylic hydrogen H-17A. The two remaining conformers **a** and **b** have their topsides or β faces completely shielded by H-17A and thus undergo attack by

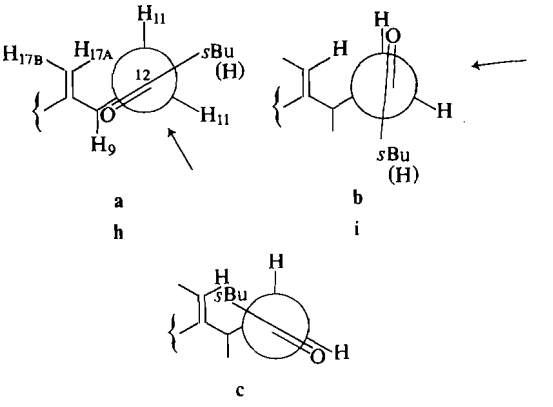

FIG. 2. Conformers of ketone **6** about 11,12-bond, **a**, **b**, and **c**; and conformers about 11,12-bond of aldehyde **4**, **h** and **i**, where *s*-Bu is replaced by H.

hydride from the α face as illustrated in Fig. 2. Both transition states from **a** and **b** result in the development of O,H-17A interactions, but in conformer **b** the O atom of the carbonyl is always closer to H-17A by some 0.3–0.4 Å than is the O atom in conformer **a** no matter how much rotation occurs about the 9,11-bond. Thus the transition state resulting from conformer **b** will be of higher energy than the transition state from conformer **a** and, therefore, the major product will be that derived from hydride ion attack on the α face of conformer **a**; that is, the major product has the 12*S* configuration and is assigned structure **7**.[5] Further support for **7** possessing the 12*S* configuration was found in the chromatographic and spectroscopic properties of this isomer. Thus it was more polar than the 12*R* isomer **8** and was eluted last on column chromatography; it showed the vinylic proton H-17A at low field, 4.72 p.p.m., in its p.m.r. spectrum, whereas the 12*R* isomer showed H-17A at 4.40 p.p.m., the same shift as observed for H-17A in aldehyde **4**; and it showed the presence of strong intermolecular hydrogen bonding in its i.r. spectrum, while the 12*R* isomer showed very weak intermolecular hydrogen bonding at normal concentrations. These differences in properties are

[4]That the 12-hydrogens in both the 12*S* and 12*R* isomers should have similar chemical shifts was further supported by the shifts of the two 12-alcohols **9** and **10** prepared during a synthesis of lambertianic acid (4), where H-12 of **9** and **10** absorbed at 4.48–4.85 p.p.m.

[5]Crams rule (7) as applied to conformer **a** does in fact predict the 12*S* stereoisomer as the major product but in the present case the rule is a simplification of the reasons for the observed product distribution. Hydrogen-17A so effectively shields the β face of the carbonyl group in **a** that the rule would predict the formation of no 12*R* stereoisomer at all.

Can. J. Chem. Downloaded from www.nrcresearchpress.com by 210.87.254.5 on 09/05/12
For personal use only.

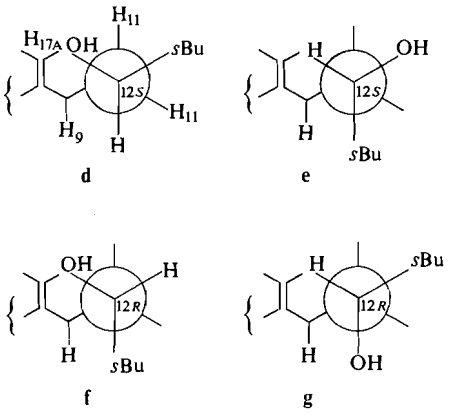

FIG. 3. Stable conformers of 12*S*-alcohol **7**, **d** and **e**; and stable conformers of 12*R*-alcohol **8**, **e** and **f**.

readily rationalized upon inspection of the conformers about the 11,12-bond for **7** and **8** (see Fig. 3). For simplicity the conformers where the *s*-butyl group is juxtaposed to H-17A are omitted since the liklihood of these conformers being significantly populated is negligible. The two 12*S* conformers **d** and **e** are probably fairly evenly populated as the O,H-17A interaction in **d** is roughly counterbalanced by the H-9,*s*-Bu *gauche* interaction in **e** but the populations of the 12*R* isomer should show a strong preference for conformer **g** since there are OH,H-17A and H-9,*s*-Bu interactions present in **f** and only a *gauche* H-9,OH interaction present in **g**. Conformer **d** of the 12*S* isomer is well populated and therefore the OH can be expected to deshield H-17A as is observed, whereas conformer **e** leaves the OH group relatively exposed on the outskirts of the molecule and thus readily able to bind to chromatographic absorbents and to undergo intermolecular hydrogen bonding. The main populated conformer **g** of the 12*R* isomer on the other hand has the OH removed from H-17A and therefore having no deshielding effect on it. In addition this OH is effectively buried within the molecule, firstly by H-9 and secondly by the *s*-butyl group. Thus the 12*R* isomer **8** should show less polar behavior on chromatographic adsorbents and less intermolecular hydrogen bonding in its i.r. spectrum than **7**.

The product-distribution argument used above to assign the configurations of **7** and **8** received further support from the addition of *s*-butyllithium to the aldehyde **4** where a similar product ratio of **7**:**8** was obtained. This experiment confirmed the view that it is the O,H-17A interaction in the transition states derived from conformers **h** and **i** (see Fig. 2) that determine the product distribution rather than any interactions of the *s*-butyl group, for it would be unlikely that the aldehyde hydrogen of **4** and the *s*-butyl group of **6** would experience transition state interactions so identical that they would lead to the same product distribution. Furthermore, the same product ratio of 12*S*:12*R* alcohols was observed when 3-furyllithium was employed as the nucleophile (4) which again suggests that the nucleophile is unimportant and the O,H-17A interaction is the controlling influence over the products. It is pertinent to note here that the two stereoisomers **9** and **10** obtained from **4** and 3-furyllithium (4) exhibited the same chromatographic and spectroscopic behavior as the isomers **7** and **8**, and their assignments were based on the arguments presented here.

In summary, methyl 12*S*-hydroxylabd-8(17)-en-19-oate (**7**) and methyl 12*R*-hydroxylabd-8(17)-en-19-oate (**8**) have been synthesized from the acid **5***a* by *s*-butyllithium addition to the acid **5***a* and reduction of the resulting ketone with $NaBH_4$. The addition of *s*-butyllithium to the aldehyde **4** furnished the alcohols **7** and **8** in the same ratio as the $NaBH_4$ reduction and this fact is used in a stereochemical argument to assign the configurations of **7** as 12*S* and **8** as 12*R*. The observed spectroscopic properties of **7** and **8** are closely similar to those recorded for two alcohols isolated from *Juniperus phoenicea* L. and it is concluded that the natural products possess the proposed structures **7** and **8**.

Experimental

Spectra were recorded in the following solvents and instruments: i.r. ($CHCl_3$) Perkin-Elmer 337; p.m.r. ($CDCl_3$) Varian Associates T-60 and A-60, tetramethylsilane as internal standard; mass spectra, Hitachi Perkin-Elmer RMU-6A (at 80 eV) and C.E.C. 21-110. In the experimental descriptions to follow, the organic substrates were isolated by extraction with the appropriate solvent (2×) followed by washing of the combined solvent layer with water, saturated brine, and finally drying with anhydrous Na_2SO_4. The solvents were removed by evaporation at reduced pressure on a Buchi Rotavapor.

Methyl 12-Oxolabd-8(17)-en-19-oate (6b)

The olefin acid **5***a*, 0.114 g (0.39 mmol; m.p. 153–155 °C (4)) was dissolved in 5 ml of anhydrous ether in a flask under nitrogen sealed with a septum inlet. Two millilitres of *s*-butyllithium (2.4 mmol) in hexane were added to the stirred solution cooled to 0 °C in an ice bath and after stirring for 6 h at 0 °C, a further 1 ml of reagent was added and the stirred solution allowed to warm to room temperature overnight. The reaction mixture was quenched

Can. J. Chem. Downloaded from www.nrcresearchpress.com by 210.87.254.5 on 09/05/12
For personal use only.

Can. J. Chem. Downloaded from www.nrcresearchpress.com by 210.87.254.5 on 09/05/12
For personal use only.

with 5% NaH_2PO_4 solution, extracted with benzene, and worked up in the usual way to give 130 mg of colorless oil. The p.m.r. spectrum of the crude reaction mixture showed the presence of 60% of keto acid **6***a* and 40% of starting material accompanied by some quantity of butyl telomeric material. Separation of **6***a* from starting material proved troublesome even after extensive sodium bicarbonate extraction and the oil was esterified with diazomethane in ether and chromatographed on Florisil. Elution with 50% petroleum ether (30–60 °C) – benzene gave unwanted telomer and benzene elution yielded 65 mg (50%) of keto ester **6***b* (mixture of epimers at C-13) as a colorless oil; i.r. ν_{max} 3015, 2940, 2885, 2880, 1720, 1650, 1470, 1220, 1165, 878 cm^{-1}; u.v. λ_{max} 265 (40) nm; p.m.r. δ 0.54 (s, 3H, C-20 CH_3), 1.20 (s, 3H, C-18 CH_3), 3.60 (s, 3H, C-19 CO_2CH_3) 4.30 (s, 1H, $W_{h/2}$ = 3 Hz, H-17A), 4.73 (s, 1H, $W_{h/2}$ = 3 Hz, H-17B) p.p.m.; mass spectrum, *m/e* 334 (M^+), 319 (M − 15), 302 (M − 32), 275 and 277 (M − 59/57) ($COOCH_3$ and *s*-C_4H_9), 235 (M − 57 − 42), 176 (M − 57 − 42 − 59). Thin-layer chromatography on alumina and SiO_2 supports in various solvents always showed **6***b* as one spot.

Methyl 12S-Hydroxylabd-8(17)-en-19-oate (7) and Methyl 12R-Hydroxylabd-8(17)-en-19-oate (8)

By reduction of 6 with $NaBH_4$

A sample of 0.03 g (0.09 mmol) of the keto ester **6***b* was dissolved in 2 ml of absolute ethanol, 0.150 g $NaBH_4$ added, and the whole heated at reflux for 30 min. The reaction mixture was quenched with 5% NaH_2PO_4 solution and the organic material extracted with benzene to yield 31 mg of the alcohols as a colorless oil. The p.m.r. spectrum of the crude reaction product showed the presence of only two alcohols and triangulation of the absorptions in the vinylic region (4.2–5.0 p.p.m.) showed them to be present in a ratio of 70±5:30±5. The alcohols were separated by chromatography on Florisil and identified as given below.

By Addition of s-BuLi to Aldehyde 4

To a solution of 0.183 g (0.66 mmol) of the aldehyde **4** (4) in 15 ml of dry ether under a nitrogen atmosphere at −70 °C were added 2.2 ml (2.65 mmol, 4.0 equiv.) of a 1.2 *M* solution of *s*-butyllithium in hexane. After 5 min the reaction was quenched with 25 ml of a 5% solution of NaH_2PO_4 and the whole allowed to warm to room temperature. The products were isolated via benzene extraction in the usual way to give 191 mg of a yellow oil. The p.m.r. spectrum of the crude product showed the presence of 81% alcohols and 19% unreacted aldehyde **4**, and the products from two experiments were combined (280 mg) and chromatographed on 28 g Florisil. Elution with benzene gave initially aldehyde and then the less polar 12*R*-alcohol, **8**, contaminated with aldehyde. Final purification of the 12*R*-alcohol was achieved by gas–liquid chromatography (Varian Aerograph A90-P) when only one peak was observed for the alcohol. The 12*R*-alcohol, **8**, was obtained as a colorless oil, 34 mg (15% based on recovered aldehyde) and showed: i.r. ν_{max} 3600 (non-bonded OH), 2965, 2930, 2875, 2850, 1715 (C=O), 1640 (C=C), 1460, 1380, 1206, 1154, 1134, 1092, 1031, 986, 971, 891 cm^{-1}; p.m.r. δ 0.50 (s, 3H, C-20 CH_3), 1.17 (s, 3H, C-18 CH_3), 3.58 (s, 3H, C-19 CO_2CH_3), 3.52 (br, 1H, H-12 α to OH), 4.40 (s, 1H, $W_{h/2}$ = 4 Hz, H-17A), 4.83 p.p.m. (s, 1H, $W_{h/2}$ = 3.5 Hz, H-17B); u.v. featureless; mass spectrum, *m/e* 336 (M^+, calcd. for $C_{21}H_{36}O_3$: 336.2658; found: 336.2652), 318 (M − H_2O), 279 (M − C_4H_9, calcd. for $C_{17}H_{27}O_3$: 279.1998; found: 279.2036), 277 (M − CO_2CH_3); 261 (M − H_2O − C_4H_9), 259 (M − H_2O − CO_2CH_3), 235 (M − H_2O − C_6H_{11}; allylic 9(11)-bond cleavage), 87 (M − $C_{16}H_{25}O_2$, calcd. for $C_5H_{11}O$: 87.0831; found: 87.0853). Further elution of the chromatographic column with benzene gave the pure 12*S*-alcohol (7), 104 mg (45% based on recovered aldehyde) as a colorless oil which showed i.r. ν_{max} 3680 (non-bonded OH), 3540 (bonded OH), 2960, 2940, 2875, 2850, 1715 (C=O), 1635 (C=C), 1465, 1380, 1206, 1154, 1135, 1093, 1031, 984, 894 cm^{-1}; p.m.r. δ 0.50 (s, 3H, C-20 CH_3), 1.17 (s, 3H, C-18 CH_3), 3.58 (s, 3H, C-19 CO_2CH_3), 3.52 (br, 1H, H-12 α to OH), 4.72 (s, 1H, $W_{h/2}$ = 4 Hz, H-17A), 4.88 p.p.m. (s, 1H, $W_{h/2}$ = 3.5 Hz H-17B); mass spectrum, *m/e* 336 (M^+, calcd. for $C_{21}H_{36}O_3$: 336.2664; found: 336.2664), 318 (M − H_2O, calcd. for $C_{21}H_{34}O_2$: 318.2516; found: 318.2472), 279 (M − C_4H_9, calcd. for $C_{17}H_{27}O_3$: 279.1973; found: 279.1986), 277 (M − CO_2CH_3), 261 (M − H_2O − C_4H_9), 259 (M − H_2O − CO_2CH_3), 249 (M − $C_5H_{11}O$, calcd. for $C_{16}H_{25}O_2$: 249.1853; found 249.1851), 235 (M − H_2O − C_6H_{11}, allylic 9(11)-bond cleavage), 87 (M − $C_{16}H_{25}O_2$, calcd. for $C_5H_{11}O$: 87.0763; found: 87.0716). Thin-layer chromatography on alumina and SiO_2 supports in a variety of solvents always showed **7** and **8** to behave as single species.

12-Hydroxylabd-8(17)-en-19-oic Acid

The mixed 12 and 13 *S* and *R* stereoisomers of the acids corresponding to **7** and **8** were prepared by treating a 20 mg sample of **7** and **8** (ratio 7:3) dissolved in anhydrous ether with 2 ml of *s*-BuLi (1.2 *M* in hexane) at 0 °C for 2 h. The reaction mixture was quenched with 5% NaH_2PO_4 solution and worked up via benzene to give 18 mg of the mixed acids (C-19 CO_2H) as a colorless oil. The acids showed i.r. ν_{max} 3600–2800, 1720 (COOH), 1640 (C=C), 1460, 1230, 1160, 900 cm^{-1}; u.v., featureless; p.m.r. δ 0.565 (s, 3H, C-20 CH_3), 1.18 (s, 3H, C-18 CH_3), 3.56 (m, 1H, $W_{h/2}$ = 30 Hz, H-12's α to OH), 4.40 (s, 0.15 H, $W_{h/2}$ = 4 Hz, H-17A of 12*R*-epimer), 4.70 (s, 0.35 H, $W_{h/2}$ = 4 Hz, H-17A of 12*S*-epimer), 4.80 (s, 0.15 H, $W_{h/2}$ = 3.5 Hz, H-17B of 12*R*-epimer), 4.87 p.p.m. (s, 0.35 H, $W_{h/2}$ = 3.5 Hz, H-17B of 12*S*-epimer). The COOH/OH peak was located by D_2O exchange at 1.5–1.7 p.p.m. beneath the methylene envelope.

We wish to thank the National Research Council of Canada for financial support of this work and for a Fellowship to M.B.G. and an NRCC Bursary to V.Y.T. (1970–1971).

1. C. Tabacik-Wlotzka and Y. Laporthe. Tetrahedron Lett. 3141 (1968).
2. M. Sumimoto. Tetrahedron, **19**, 643 (1963); C. Kaneko, T. Tsuchiya, and M. Ishikawa. Chem. Pharm. Bull. (Japan), **11**, 271 (1963).
3. R. A. Bell and M. B. Gravestock. Can. J. Chem. **48**, 1105 (1970).
4. R. A. Bell, M. B. Gravestock, and V. Y. Taguchi. Can. J. Chem. **50**, 3749 (1972).
5. F. C. Chang and N. F. Wood. Tetrahedron Lett. 2969 (1964).
6. K. Bjamer, G. Ferguson, and R. D. Melville. Acta Cryst. B, **24**, 855 (1968).
7. E. L. Eliel. Stereochemistry of carbon compounds. McGraw-Hill, New York, N.Y. 1962.

Acylsilane Photolyses: 1,1-Diphenyl-1-Silacyclohexanone-2 in Cyclohexane

A. G. BROOK, J. B. PIERCE, AND J. M. DUFF[1]

Department of Chemistry, University of Toronto, Toronto, Ontario M5S 1A1

Received March 11, 1975

A. G. BROOK, J. B. PIERCE, and J. M. DUFF. Can. J. Chem. **53**, 2874 (1975).

Photolysis of the cyclic acylsilane 1,1-diphenyl-1-silacyclohexanone-2 yields 1,1-diphenyl-1-silacyclopentane and two dimeric products whose structures were established by chemical and spectroscopic methods. A mechanism involving a siloxycarbene intermediate which is trapped by a second acylsilane molecule, is proposed for the formation of the dimers.

A. G. BROOK, J. B. PIERCE et J. M. DUFF. Can. J. Chem. **53**, 2874 (1975).

La photolyse de l'acylsilane cyclique, diphényl-1,1 sila-1 cyclohexanone-2, conduit au diphényl-1,1 sila-1 cyclopentane et à deux produits dimères dont les structures ont été établies par des méthodes chimiques et spectroscopiques. Pour la formation des dimères, on propose un mécanisme impliquant un intermédiaire siloxycarbène qui est piégé par une seconde molécule d'acylsilane. [Traduit par le journal]

Over the past few years we have been engaged in elaborating the photochemical behavior of acylsilanes (R_3SiCOR'). It has been shown that depending on the structure of the acylsilane and particularly on the solvent employed, two types of reaction can occur. These are (*i*) the photoisomerization of the acylsilane to a siloxycarbene which may revert back to acylsilane in a dark reaction if not trapped by a suitable reagent, and (*ii*) a radical type process which generally occurs less readily than reactions involving the siloxycarbene. Our findings are summarized in Scheme 1.

Most acylsilanes studied to date show this dual photochemical behavior. The photochemically formed siloxycarbenes insert into the polar bonds of protic solvents to give adducts (1), form cyclopropanes with suitably reactive alkenes (2), or form oxiranes (or their hydrolysis products) on reaction with certain carbonyl compounds (3). When photolyzed in halogenated solvents, acylsilanes yield radical type products (which may arise through exciplex formation (4)), including R_3SiCl and R'COCl (5). More recently it was found that when acyclic acylsilanes such as acetyl- or phenylacetyltriphenylsilane were photolyzed in cyclohexane, a solvent unreactive towards silyl radicals or siloxycarbenes, a variety of products was obtained whose mode of formation was best explained as arising from the initial addition of silyl radicals to the carbonyl oxygen of a second molecule of acylsilane followed by normal radical behavior (6).

We now wish to report a new photochemical behavior of acylsilanes, namely photodimerization, which was observed when the cyclic acylsilane 1,1-diphenyl-1-silacyclohexanone-2 was photolyzed in cyclohexane. This investigation was actually one of the earliest studies in our laboratory of the photochemical behavior of acylsilanes (7), but because the structures of the two main products could not be assigned unambiguously from the available chemical and physical data, we deferred publication until the structures of the photodimers were confirmed recently by X-ray structure analysis by Nyburg *et al.* (8) of our department.

Irradiation of diphenylsilacyclohexanone **1** in

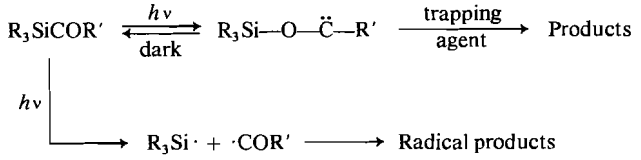

SCHEME 1

[1]Dow Corning Postdoctoral Fellow 1973–1975.

Can. J. Chem. Downloaded from www.nrcresearchpress.com by 210.87.254.42 on 09/05/12
For personal use only.

Can. J. Chem. Downloaded from www.nrcresearchpress.com by 210.87.254.42 on 09/05/12
For personal use only.

dry, oxygen-free, cyclohexane with a mercury spot lamp ($\lambda_{max} \simeq 360$ nm) gave three main products, 1,1-diphenyl-1-silacyclopentane, **2** (18–22%), and two dimers, **3** (20–53%) and **4** (9–12%), whose structures are given below.

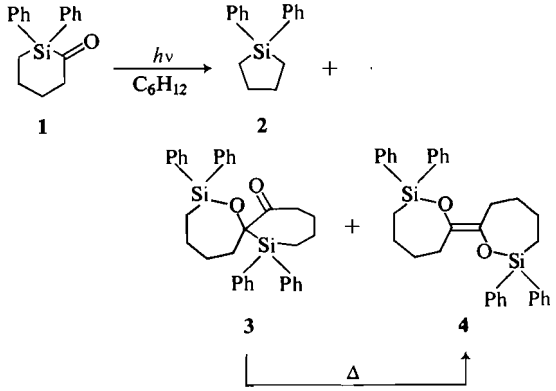

The photolysis appeared to be quite clean and the low yield of isolated products in some cases was due more to the difficulty in isolating pure compounds than to the presence of significant amounts of unidentified products.

It was noted that **3** was thermally labile, the β-ketosilane functionality being quantitatively converted into the siloxyalkene functionality in **4** in less than 20 h at reflux in cyclohexane.[2] In accord with this observation, if the photolysis was carried out with cooling, higher yields of **3** (55%) were obtained, compared to the 20% isolated from photolysis at ambient temperature (35–40 °C). However, even at low temperatures, significant amounts of **4** were obtained and hence **4** is believed to arise, at least in part, directly as a result of the photolysis.

The diphenylsilacyclopentane may result from a Norrish type I cleavage to a diradical, followed by loss of carbon monoxide and ring closure. However, since none of the other types of products usually obtained from the photolysis of cycloalkanones were obtained (aldehydes, alkenes) and since none of the usual products resulting from silyl radicals were obtained (6), it is possible that the diphenylsilacyclopentane arose from a concerted extrusion of carbon monoxide.

It seems unlikely that **3** (and **4**) arise from a radical process, since, by analogy with previous studies (6), the silyl radical resulting from cleavage of the acylsilane (Scheme 2) would be expected to attack the carbonyl oxygen of a second acylsilane molecule and the resulting diradical would then presumably close to the 8,6-spiro compound **3***b*, shown in Scheme 2; in fact the 7,7-spiro compound **3** (Scheme 1) is the observed product.

The formation of the dimeric products can be explained logically as arising from attack of a cyclic siloxycarbene, which is nucleophilic in character, on the carbonyl group of a second molecule of the silacyclohexanone, analogous to the observed addition reactions of siloxycarbenes with other carbonyl compounds such as acetaldehyde, acetone, and cyclohexanone (3). The resulting intermediate, **5**, could then react by any of the three routes shown in Scheme 3.

Unlike the reaction with acetaldehyde (3), there was no evidence obtained for the closure of the intermediate **5** to give the oxirane **6**. However a 1,2-migration of silicon to the electron deficient center in **5**, accompanied by reformation of the carbonyl group accounts for the formation of **3** (route *b*). Alternatively, the attack of the oxyanion center on the neighboring silicon atom, with displacement of electrons toward the electron deficient center, forming a carbon–carbon double bond, accounts for the formation of **4** directly from the intermediate (route *c*).

This behavior attributed to **5**, reacting by routes *b* and *c*, follows closely the behavior of the intermediate formed between acylsilanes and diazomethane, where β-ketosilanes and siloxyalkenes are likewise formed competitively (10, 11).

Other routes to **3** and **4** can be envisioned but

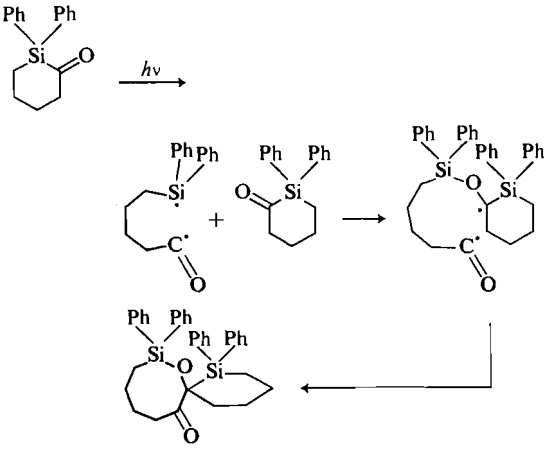

3*b*

SCHEME 2

[2]This was the first observed case of a β-ketosilane to siloxyalkene thermal rearrangement (9, 10).

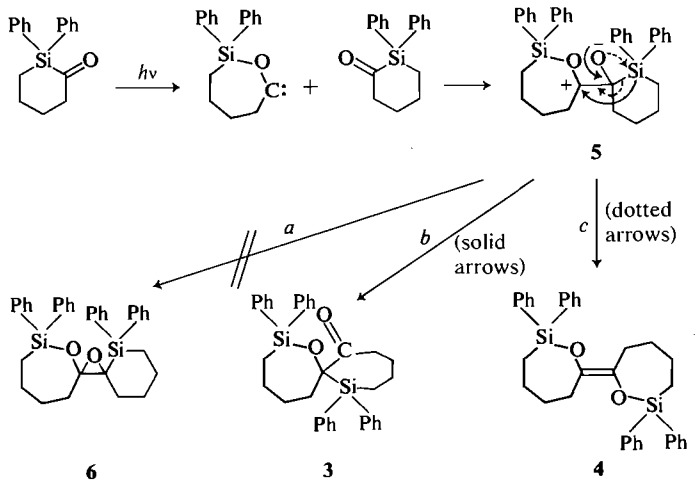

SCHEME 3

appear less likely. Thus **3** could arise by direct insertion of the siloxycarbene into the silicon–acyl bond of the second acylsilane molecule but this is unprecedented. Compound **4** could arise by direct coupling of two siloxycarbenes but the probable concentration of siloxycarbene in the system makes the formation of **4** in significant amounts by this route unlikely.

Therefore it appears that the photodimers formed in the photolysis of diphenylsilacyclohexanone in cyclohexane arise from siloxycarbenes, in contrast to the behavior of acyclic acylsilanes whose photolysis in cyclohexane led to radical-derived products (6). A similar tendency for cyclic acylsilanes to react via siloxycarbenes under conditions where acyclic acylsilanes are either unreactive or react by radical pathways has been observed previously (in reactions with C=C and C=O) but it is not yet clear whether this difference arises because the cyclic siloxycarbenes are more reactive, are more readily formed, or are longer-lived than their acyclic counterparts.

The structures of products **3** and **4** were originally assigned partly on the preceding mechanistic arguments and also on the basis of chemical and spectroscopic data. Thus **3** was believed to be a β-ketosilane by virtue of the relatively long wavelength carbonyl absorption at 5.90 μm (11). No other functional groups appeared to be present. Hydrolysis of **3** gave a compound formulated as **7** (Scheme 4), containing silanol and α-hydroxyketone groups. Isolation of such a product fails to distinguish between **3** and **3***b*, whose possible modes of formation were described earlier in Schemes 2 and 3. The identity of **7** was confirmed by its reduction to the diol and cleavage with lead tetraacetate to give the known 5-(diphenylhydroxysilyl)pentanal, **8**, and the related acid, **9** (12).

Compound **4** (or its possible alternative **4***b*) derived either directly from the photolysis or indirectly by the thermolysis of **3** (or **3***b*) showed no OH, C=O, or C=C i.r. absorption although its Raman spectrum showed a band at 5.93 μm (symmetrical 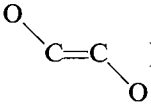). Mild acid hydrolysis of this dimer similarly gave **7** but this fact again failed to distinguish unambiguously between the possible structures **4** and **4***b*.

In an attempt to distinguish **4** from **4***b* the compound was treated with ozone, followed by careful anhydrous work-up using triphenylphosphine to destroy the ozonide. The product isolated, contaminated with some triphenylphosphine oxide, was the silalactone **10**, expected from **4**. However, the possibility that the macrocyclic bis-lactone derivable from **4***b* might have broken down to give **10** during work-up could not be ruled out.

Numerous other attempted structure-proving reactions, including reduction, and reaction with methylmagnesium iodide, failed to distinguish between the possible pairs of isomers and hence it was necessary to confirm the proposed structures for **3** and **4** by X-ray diffraction techniques.

Can. J. Chem. Downloaded from www.nrcresearchpress.com by 210.87.254.42 on 09/05/12
For personal use only.

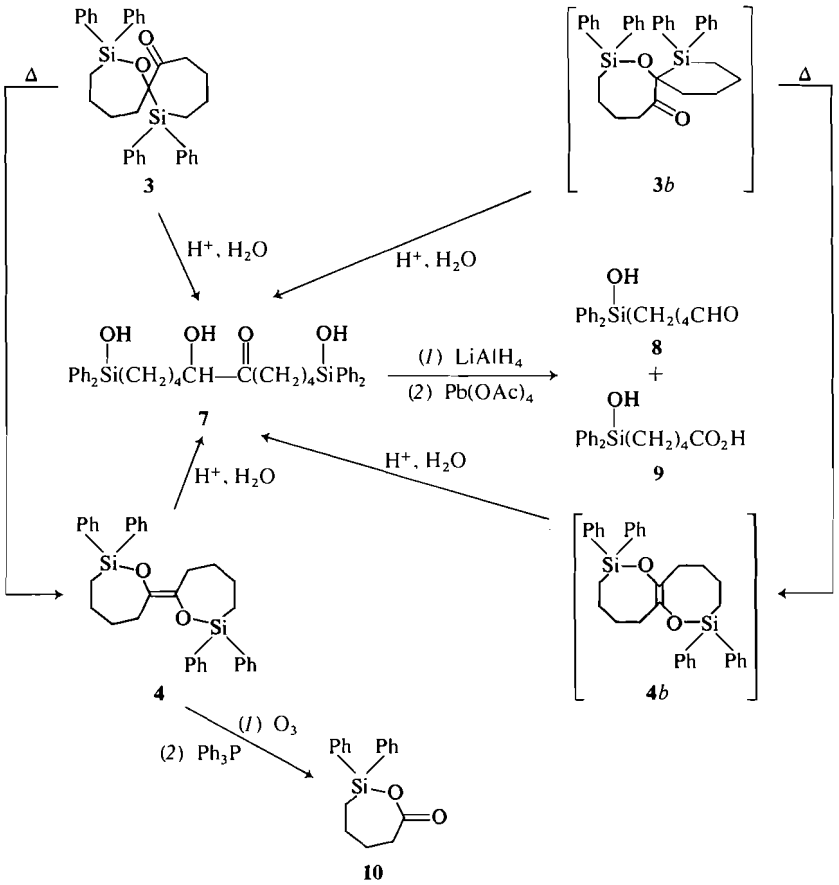

SCHEME 4

The silalactone **10** was also formed in significant yield along with silacyclopentane **2** when the cyclic acylsilane **1** was photolyzed in cyclohexane saturated with oxygen. When **1** was photolyzed in methanol, the cyclic acetal **11**, expected from trapping of the siloxycarbene (1), was obtained.

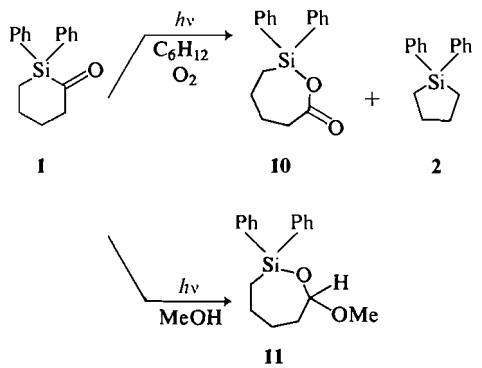

One major question remaining is the apparent ease (80 °C, <20 h) with which the β-ketosilane **3** rearranges to siloxyalkene **4**. Other than this case, the most facile β-ketosilane–siloxyalkene rearrangement known is that of triphenylsilylacetophenone, which required about 18 h at 100 °C for complete rearrangement; only 10% rearrangement occurred in 18 h at 80 °C (13). It is known that incorporation of a β-ketosilane functionality into a seven-membered ring considerably reduces the ease of thermal rearrangement compared to acyclic systems. For example, 1,1-dimethyl-1-silacycloheptanone-3 rearranged about 5 times more slowly than trimethylsilylacetone and 170 times more slowly than triphenylsilylacetophenone (13). This appears to be reasonable since models suggest that approach of the carbonyl oxygen to the β-silicon atom is more difficult in the cyclic system. The difficulty of such an approach in the spiro compound **3** appears to be even more pronounced. Therefore,

Can. J. Chem. Downloaded from www.nrcresearchpress.com by 210.87.254.42 on 09/05/12
For personal use only.

the observed ease of rearrangement of **3** suggests that the α-siloxy functionality is playing an important role, not yet understood, in facilitating the β-ketosilane to siloxyalkene rearrangement; the fact that the siloxy-silicon atom of **3** is somewhat closer (3.02 Å) to the carbonyl oxygen than is the β-silicon atom with which bonding ultimately occurs (3.77 Å) is probably of some relevance.

Experimental

The synthesis of 1,1-diphenyl-1-silacyclohexanone-2 has been described previously (12).

Photolyses were carried out in Pyrex flasks using a Westinghouse PAR 38 100 W mercury spot lamp. Solvents were carefully dried by standard methods and photolysis solutions were deoxygenated by bubbling dry nitrogen through them. The extent of photolyses was determined by withdrawing small samples and following the disappearance of the carbonyl absorption of the acylsilane at 6.08 μm.

Nuclear magnetic resonance spectra were recorded on a Varian A60 instrument, i.r. spectra on a Beckman IR8. Column chromatography used Grace activated silica gel, grade 923, 100–200 mesh. Melting points are uncorrected.

*Photolysis of **1** in Cyclohexane*

This reaction was carried out many times and variations in the conditions and work-up procedure significantly affected the results. The isolations of the three photolysis products are described separately.

*Photolysis at 0 °C. Isolation of Dimer **3**, 2,2,8,8-Tetraphenyl-1-oxa-2,8-disilaspiro[7.7]tridecanone-13*

A solution of 4.4 g of **1** in 80 ml of cyclohexane, cooled to 0 °C in an ice bath, was irradiated for 8 h. The solution was evaporated to dryness at reduced pressure without heating and the residue was dissolved in 30 ml of dry hexane. The solution was stored at room temperature for 20 h to give 2.41 g (54.8%) of dimer **3** as white crystals. The product was recrystallized by dissolving it in a minimum of cold dichloromethane and reprecipitating it with hexane; m.p. 152–154 °C; i.r. (CCl_4) 5.90 (Si—C—C=O) 7.0, 9.0 μm (Si—Ph); n.m.r. ($CDCl_3$) δ 7.0–7.85 (m, 20H, Ph), 2.15–2.96 (broad, 2H, CH_2CO), 0.85–2.1 p.p.m. (m, 14H, ring protons).

Mol. Wt. Calcd. for $C_{34}H_{36}O_2Si_2$: 532. Found (osmometry): 544.

Anal. Calcd. for $C_{34}H_{36}O_2Si_2$: C, 76.65; H, 6.76. Found: C, 76.93; H, 6.83.

*Photolysis at 15 °C; Isolation of Dimer **4**, trans-7,7′-Bicyclo(2,2-diphenyl-1-oxa-2-silacycloheptylidene)*

Photolysis of 2.0 g of **1** in cyclohexane cooled by a cold finger condenser (solution temperature *ca.* 15 °C) followed by crystallization from hexane, as above, gave a total of 1.06 g (53%) of dimer **3**. The mother liquor was then evaporated to dryness and the oily residue was taken up in a small amount of diethyl ether. This solution was stored at −20 °C to yield 0.17 g (9%) of dimer **4**. This compound, which was more readily obtained from thermolysis of **3** (see below), had the following properties: m.p. 149–151 °C; i.r. (CCl_4) 7.0, 9.0 μm (Si—Ph); Raman (powder) 5.93 μm (O—C=C—O); n.m.r. ($CDCl_3$) δ 7.2–7.75 (m, 20H, Ph), 2.3–2.6 (m, 4H, CH_2—C=C—CH_2), 1.1–2.0 p.p.m. (m, 12H, ring protons).

Mol. Wt. Calcd. for $C_{34}H_{36}O_2Si_2$: 532. Found (osmometry): 527.

Anal. Calcd. for $C_{34}H_{36}O_2Si_2$: C, 76.65; H, 6.76. Found: C, 76.78; H, 6.93.

*Photolysis at Ambient Temperature; Isolation of **2**, 1,1-Diphenyl-1-silacyclopentane*

Following the photolysis of 4.3 g (0.016 mol) of **1** in cyclohexane at ambient temperature (solution temperature *ca.* 40 °C) and crystallization of dimer **3** (1.06 g, 25%) from petroleum ether (b.p. 60–70 °C) the residual product was distilled. This afforded 0.70 g (18%) of 1,1-diphenyl-1-silacyclopentane, b.p. 115–120 °C/0.2 Torr, which was identified by comparison with the authentic material (14).

*Thermal Rearrangement of **3** to **4***

A solution of 1.06 g of **3** in 50 ml of cyclohexane was refluxed for 20 h by which time the i.r. carbonyl absorption of **3** (5.90 μm) had disappeared. Removal of solvent gave a solid which was washed twice with cold ether to give 0.92 g (90%) of **4**, m.p. 150–150.5 °C, identical to the material obtained from the photolysis. An additional 0.06 g (total yield 93%) was crystallized from the ether washings.

*Hydrolysis of **3** with Aqueous Acid; Isolation of **7***

A solution of 0.5 g (0.96 mmol) of **3** in 25 ml of acetone containing 10 drops of 5% aqueous hydrochloric acid was stirred at room temperature for 2 days. The acetone was evaporated and the residue was extracted with ether and water. The organic product was chromatographed on silica gel. Elution with ether gave an oil which was identified as pure **7** (0.53 g, 97%) on the basis of the following data: i.r. (CCl_4) 2.70 (Si—OH), 2.90 (broad, C—OH), 5.85 (C=O), 7.0, 9.0 μm (Si—Ph); n.m.r. (DMSO) δ 6.48 (s, 2H, SiO*H*), 5.10 p.p.m. (d, 1H, CHO*H*).

Anal. Calcd. for $C_{34}H_{40}O_4Si_2$: C, 71.80; H, 7.09. Found: C, 72.02; H, 7.01.

*Reduction and Cleavage of **7** to **8**, 5-(Diphenylhydroxysilyl)pentanal*

To 0.25 g (0.44 mmol) of **7**, obtained as above, in ether solution was added 0.20 g (5.3 mmol) of lithium aluminum hydride. After 18 h at reflux, normal aqueous work-up yielded material having both Si—H (i.r. 4.7 μm) and Si—OH groups present. The Si—H function was hydrolyzed to SiOH by brief treatment of the product in aqueous alkaline ethanol. Work-up gave an oil (0.26 g, 96%) presumed to be the expected bis(diphenylhydroxysilyl)-diol; i.r. (CCl_4) 2.70 (Si—OH) 2.98 μm (broad, strong, C—OH).

To 0.14 g (0.25 mmol) of the above in 25 ml of benzene was added 0.13 g (0.29 mmol) of freshly recrystallized lead tetraacetate. After 18 h at room temperature saturated aqueous sodium bicarbonate was added and the solution was extracted with ether to give a mixture of 5-(diphenylhydroxysilyl)pentanal, **8**, and the corresponding acid, **9**. The acid was removed by extraction with sodium bicarbonate to give 0.066 g (39%) of the pure aldehyde, the spectra of which were identical to those of the authentic material (12).

Acidification of the sodium bicarbonate solution and extraction with ether afforded 0.053 g (31%) of 5-(diphenylhydroxysilyl)pentanoic acid, **9**, m.p. 102–104 °C,

Can. J. Chem. Downloaded from www.nrcresearchpress.com by 210.87.254.42 on 09/05/12
For personal use only.

Can. J. Chem. Downloaded from www.nrcresearchpress.com by 210.87.254.42 on 09/05/12
For personal use only.

which was identified by mixture m.p. with the authentic material (12).

A control experiment showed that the aldehyde, **8**, was partly converted by lead tetraacetate into the acid, **9**, under the conditions of the reaction.

Hydrolysis of Dimer 4

Hydrolysis of dimer **4** in dilute aqueous acidic acetone for 4 days at room temperature gave the hydroxyketone, **7** (identical to the above), in almost quantitative yield.

Ozonolysis of Dimer 4; Isolation of Silalactone 10

A solution of 1.12 g (2.11 mmol) of **4** in cyclohexane was treated with ozone under anhydrous conditions. Following completion of the reaction 0.53 g (2.11 mmole) of pure dry triphenylphosphine was added and the solution was concentrated and then distilled under vacuum (175–187 °C/0.05 Torr) to give a mixture of 5-(diphenylhydroxysilyl)pentanoic acid lactone, **10**, and triphenylphosphine oxide which were identified spectroscopically.

The mixture was hydrolyzed with dilute acid and the resultant product was chromatographed. Elution with chloroform yielded 0.23 g (37%) of triphenylphosphine oxide, m.p. 155–157 °C, and 0.29 g (21%) of 5-(diphenylhydroxysilyl)pentanoic acid, **9**, m.p. 102–102.5 °C.

Photolysis of 1 in the Presence of Oxygen

The acylsilane **1** (2.55 g, 9.58 mmol) was irradiated in 40 ml of cyclohexane through which oxygen was bubbled. After completion of the photolysis (6 h) the solvent was removed and the residue (i.r. 5.76 μm) was distilled to give 0.40 g (18%) of 1,1-diphenyl-1-silacyclopentane, **2**, (102–112 °C/0.03 Torr), and 0.72 g (27%) of lactone **10** (180–185 °C/0.25 Torr).

The above lactone was hydrolyzed in wet ether to give crystalline 5-(diphenylhydroxysilyl)pentanoic acid (73% yield) which was identified by mixture m.p. with authentic material.

Preparation of 5-(Diphenylhydroxysilyl)pentanoic Acid Lactone, 10

A solution of 0.75 g of the acid, **9**, in 25 ml of acetic anhydride was slowly distilled at atmospheric pressure until the acetic acid and anhydride were largely removed. The residue was distilled to give 0.33 g (47%) of the expected lactone, **10**; b.p. 150–152 °C/0.005 Torr; n_D^{25} 1.5814; i.r. (CCl_4) 5.76 μm (C=O); n.m.r. (CCl_4) δ 7.2–7.7 (m, 10H, Ph), 1.21–2.24 p.p.m. (m, 8H, ring protons).

Anal. Calcd. for $C_{17}H_{18}O_2Si$: C, 72.3; H, 6.38. Found: C, 71.9; H, 6.30.

This lactone slowly hydrolyzed to the acid, **9**, in moist air.

Photolysis of 1 in Methanol; Formation of 11

The photolysis of a solution of 1.0 g of **1** in 25 ml of methanol was complete in 0.5 h. Removal of the solvent gave an oil, the spectra of which indicated it to consist of over 95% of the cyclic acetal, **11**, contaminated with the corresponding open-chain aldehyde. Distillation gave a sample of pure acetal (0.40 g, 36%); b.p. 130–132 °C/0.04 Torr; i.r. (CCl_4) 3.51 (OCH_3), 7.0, 9.0 μm (SiPh); n.m.r. (CCl_4) δ 7.1–7.75 (m, 10H, Ph), 4.9 (broad, t, 1H, O—CH—O), 3.23 (s, 3H, OCH_3), 0.91–2.15 p.p.m. (m, 8H, ring protons).

Anal. Calcd. for $C_{18}H_{22}O_2Si$: C, 72.43; H, 7.43. Found: C, 72.70; H, 7.48.

This acetal was readily converted to the aldehyde, **8**, in aqueous alkaline tetrahydrofuran.

The authors wish to acknowledge the financial support of the National Research Council of Canada, and the support of Dow Corning Corporation for a postdoctoral fellowship to J.M.D.

1. A. G. Brook and J. M. Duff. Can. J. Chem. **51**, 2869 (1973).
2. A. G. Brook, H. Kucera, and R. Pearce. Can. J. Chem. **49**, 1618 (1971).
3. A. G. Brook, R. Pearce, and J. B. Pierce. Can. J. Chem. **49**, 1622 (1971).
4. N. A. Porter and P. M. Iloff, Jr. J. Am. Chem. Soc. **96**, 6200. (1974).
5. A. G. Brook, P. J. Dillon, and R. Pearce. Can. J. Chem. **49**, 133 (1971).
6. A. G. Brook and J. M. Duff. Can. J. Chem. **51**, 352 (1973).
7. J. B. Pierce. Ph.D. Thesis. University of Toronto, Toronto, Ontario. 1966.
8. P.-T. Cheng, W. K. Wong-Ng, S. C. Nyburg, and S. Van der Heijden. Acta Crystallogr. In press; P.-T. Cheng and S. C. Nyburg. Acta Crystallogr. In press.
9. A. G. Brook, D. M. MacRae, and W. W. Limburg. J. Am. Chem. Soc. **89**, 5493 (1967).
10. A. G. Brook, W. W. Limburg, D. M. MacRae, and S. A. Fieldhouse. J. Am. Chem. Soc. **89**, 704 (1967).
11. A. G. Brook. Adv. Organometal. Chem. 7, 95 (1968).
12. A. G. Brook and J. B. Pierce. J. Org. Chem. **30**, 2566 (1965).
13. A. G. Brook, D. M. MacRae, and A. R. Bassindale. J. Organometal. Chem. **86**, 185 (1975).
14. R. A. Benkeser, Y. Nagai, J. L. Noe, R. F. Cunico, and P. H. Gund. J. Am. Chem. Soc. **86**, 2446 (1964).

^{13}C Nuclear Magnetic Resonance Spectra of Organic Sulfur Compounds: Cyclic Sulfides, Sulfoxides, Sulfones, and Thiones

M. S. CHAUHAN AND I. W. J. STILL

Department of Chemistry, University of Toronto, Toronto, Ontario M5S 1A1

Received April 21, 1975

M. S. CHAUHAN and I. W. J. STILL. Can. J. Chem. **53**, 2880 (1975).

^{13}C Chemical shift data have been obtained for more than 50 thiochromanone and related sulfoxide and sulfone derivatives. The assignments of the various resonances in the most important of these have been made using the limited data already available and also by comparison with certain model compounds, such as thioanisole, diphenyl sulfide, and the corresponding sulfoxides and sulfones.

Within each of these three series and in a fourth which comprises derivatives of thiochromone, including three α,β-unsaturated thiones, we have examined the effects on ^{13}C chemical shift of substitution at various positions in the thiochromanone skeleton. Among the substituents examined in this context are methyl, phenyl, methoxyl, bromine, and carbomethoxyl. Attempts to compare the ^{13}C chemical shifts for the thiochromanone series with those in a few oxygen containing analogs and in a small number of structurally similar analogs are also discussed.

M. S. CHAUHAN et I. W. J. STILL. Can. J. Chem. **53**, 2880 (1975).

On a déterminé les déplacements chimiques du ^{13}C de plus de 50 thiochromanones ainsi que des sulfoxydes et sulfones correspondantes. On a attribué les positions principales de résonance en faisant appel aux quelques données disponibles et aussi par comparaison avec divers composés modèles comme le thioanisole et le sulfure de diphényle ainsi que les sulfoxydes et les sulfones correspondantes.

Dans chacune de ces trois séries et dans une quatrième comprenant des dérivés de la thiochromone incluant trois thiones α,β non-saturées, on a examiné les effets, sur le déplacement chimique du ^{13}C, de substitutions à diverses positions sur le noyau thiochromanone. Dans ce contexte, on a examiné l'influence des substituants méthyle, phényle, méthoxyle, bromure et carbométhoxyle. On discute des essais que nous avons faits afin de comparer les déplacements chimiques du ^{13}C dans la série de la thiochromanone avec ceux de quelques analogues contenant de l'oxygène et d'un petit nombre d'analogues de structures similaires.

[Traduit par le journal]

Our recent application of ^{13}C n.m.r. chemical shifts to the elucidation of the structure of an unusual rearrangement product from the base-catalyzed methylation of 3-methylthiochroman-4-one (1) demonstrated to us the scarcity of ^{13}C n.m.r. data for even the most common types of sulfur-containing functionality. By way of an example, one (3) of several excellent introductory texts on ^{13}C n.m.r. to appear recently (2–4) contains 500 spectra but reports data for only one sulfone, one thione, and not one sulfoxide. The availability in our laboratory of a considerable number of sulfides, sulfoxides, and sulfones which had been synthesized as part of a continuing investigation of the photochemical behavior of such compounds (5–7) prompted us to undertake an extensive compilation of ^{13}C n.m.r. data for these compounds, and a few related thiones, under identical experimental conditions, the results of which we now wish to discuss.

Experimental

The i.r. spectra were recorded as neat films or Nujol mulls on a Perkin-Elmer 337 grating spectrophotometer and the u.v. spectra on a Unicam SP8000 instrument. ^1H Nuclear magnetic resonance spectra were recorded on Varian T-60 or HA-100 spectrometers with tetramethylsilane (TMS) as internal reference. Mass spectra were recorded on a Bell and Howell 21-490 spectrometer and accurate mass measurements on the A.E.I. MS-902 machine. Elemental analyses were performed by the Scandinavian Microanalytical Laboratory, Box 25, Herlev, Denmark or by A. B. Gygli, 329 St. George St., Toronto. All melting and boiling points are uncorrected. Satisfactory spectral and analytical data were obtained for all new compounds.

The ^{13}C n.m.r. spectra were obtained in 12–15% $CDCl_3$ solution for natural abundance compounds on a Varian Associates XL-100-15 instrument at 25.16 MHz, with approximately 5% TMS added as internal reference. The deuterium of the solvent was used as lock and primary reference and the chemical shifts were obtained from listings supplied by the 16K-620i computer, with an accuracy of ±0.1 p.p.m. Normal operating conditions included an acquisition time of 0.9 s/transient with a delay of 0.3 s and a routine spectral width of 6000 Hz, at an r.f. pulse width of 35 μs and a probe temperature of

Can. J. Chem. Downloaded from www.nrcresearchpress.com by 210.87.254.40 on 09/05/12
For personal use only.

Can. J. Chem. Downloaded from www.nrcresearchpress.com by 210.87.254.40 on 09/05/12
For personal use only.

32 ± 3 °C. Off-resonance proton decoupled spectra were obtained for all compounds. Of the model compounds for which data are recorded in Table 1, the diphenyl sulfide, sulfoxide, and sulfone were used as commercially supplied. Thiobenzophenone was prepared from benzophenone by refluxing with P_2S_5 in toluene.

Thiochroman-4-one (now commercially available) and its 5-, 6-, 7-, and 8-methyl analogs, as well as the 6-methoxy derivative were all prepared by the base-catalyzed reaction of the appropriate benzenethiol with β-propiolactone, followed by ring closure of the resulting acid with concentrated sulfuric acid (5). The preparation of the 2- and 3-methyl and the 2- and 3-methoxycarbonyl analogs of **1**, and of isothiochromanone **4** also followed our previously outlined procedures (5). The preparation of 3-bromothiochroman-4-one (8), thiochroman-3-one (9), and 2-phenylthiochroman-4-one (10) closely followed the literature methods, although a modified procedure for 6-methyl-2-phenylthiochroman-4-one is described below. 3,3-Dimethylthiochroman-4-one was prepared by methylation of **1** with sodium hydride – methyl iodide, and similar methylation of isothiochroman-4-one and of 2,2-dimethylthiochroman-4-one produced 3,3-dimethylisothiochromanone and 2,2,3,3-tetramethylthiochroman-4-one respectively.

2,2-Dimethylthiochroman-4-one

A mixture of thiophenol (30 g), β,β-dimethylacrylic acid (20 g) and hydrobromic acid in acetic acid (30%, 100 ml) was heated under reflux for 12 h after which it was diluted with water and extracted with ether. The ether extract was washed, dried, and evaporated. The oil obtained was distilled under reduced pressure. Distillate collected up to 120 °C (2 Torr) was discarded. This was found to be a mixture of thiophenol and some products arising from reactions of the unsaturated acid. The temperature was maintained at 120 °C until no more distillate collected. The residue in the flask was cooled, extracted with ether and the ether solution was then extracted four times with saturated sodium bicarbonate solution. The bicarbonate extracts were combined, acidified with concentrated hydrochloric acid, and the precipitated acid was extracted with ether, washed, and dried. The product (17.6 g, 42%) obtained on evaporation of the solvent was recrystallized from petroleum ether, m.p. 60–61 °C. Infrared 3300–2500, 1705 cm^{-1}; n.m.r. δ 1.4 (s, 6H), 2.55 (s, 2H), 7.15–7.65 (m, 5H), 12.9 (s, 1H) p.p.m. This acid, 3-methyl-3-phenylthiobutanoic acid, was cyclized to 2,2-dimethylthiochroman-4-one by the following procedure.

The acid (15.5 g) was dissolved in dry benzene (60 ml). A paste of phosphorus pentoxide (25 g) and Hyflo Super Cel (15 g) was prepared with dry benzene (80 ml) and the paste was added in small amounts to the solution of the acid with stirring. The mixture was then heated under reflux at 100 °C for 5 h, stirring all the time. The solution was filtered and the residue was extracted with boiling benzene three times. The benzene solutions were combined, washed with water, sodium hydroxide solution, and again water, dried and evaporated. The oil so obtained crystallized (8.0 g, 56%) and was recrystallized from petroleum ether, m.p. 44–45 °C Infrared, 1680, 1590, and 1315 cm^{-1}; n.m.r. δ 1.45 (s, 6H), 2.85 (s, 2H), 7.25 (m, 3H), 8.15 (br d, 1H) p.p.m.

Anal. Calcd. for $C_{11}H_{12}OS$: C, 68.73; H, 6.29; S, 16.64. Found: C, 68.49; H, 6.29; S, 16.65.

6-Methyl-2-phenylthiochroman-4-one

A mixture of *p*-thiocresol (30 g), methyl cinnamate (33 g), absolute ethanol (100 ml), and piperidine (4.0 g) was heated under reflux at 100 °C for 72 h. The unreacted thiocresol was removed from the mixture by steam distillation. Hydrochloric acid (6 *N*) (350 ml) and acetone (20 ml) were then added and the mixture was heated under reflux for 12 h; on cooling, crystals of the acid, 3-[*p*-methylphenylthio]hydrocinnamic acid, were formed. The product was filtered off and purified by dissolving it in saturated sodium bicarbonate solution and reprecipitating with concentrated hydrochloric acid. Recrystallization from petroleum ether – benzene gave the pure product (28 g, 52%), m.p. 106–107 °C, lit. (8) m.p. 106 °C.

The acid (13 g) was mixed with phosphorus oxychloride (60 g) and heated on a steam bath for 25 min after which the mixture was cooled and then poured over ice. Extraction with ether gave an impure product (8 g, 66%) which was recrystallized from ethanol, m.p. 95–96 °C, lit. (8) m.p. 96 °C. Infrared 1670, 1600, 1465, 1400, 1300, 1280 cm^{-1}; n.m.r. δ 2.30 (s, 3H), 3.2 (m, 2H), 4.65 (m, 1H) 7.15–7.45 (m, 7H), 8.0 (m, 1H) p.p.m.

2,3-Dimethylthiochroman-4-one

A mixture of tiglic acid (2-methyl-*cis*-2-butenoic acid) (15.0 g), thiophenol (12.0 g), and piperidine (6 drops) was heated at 170–180 °C for 12 h and then distilled under vacuum to remove unreacted thiophenol and tiglic acid. The fraction collected at b.p. 170–172 °C/0.5 Torr was the required acid (23.0 g, 85%). Infrared 3600–2500, 1700 cm^{-1}; n.m.r. δ 1.17–1.40 (m, 6H), 2.62 (m, 1H), 3.51 (m, 1H), 7.10–7.57 (m, 5H), 11.65 (br s, 1H) p.p.m.

The thioacid (5.0 g) and concentrated sulfuric acid (40 g) were kept at room temperature for 4 h. The viscous reddish brown mixture was poured over ice and the solution extracted with ether. The combined ether extracts were dried ($MgSO_4$) and then evaporated. The residue was chromatographed on silica, elution with benzene affording 2,3-dimethylthiochromanone (3.0 g, 64%). Infrared 1670 cm^{-1}; n.m.r. δ 1.14–1.47 (m, 6H), 2.33–3.74 (m, 2H), 6.84–7.42 (m, 3H), 7.99 (br d, 1H) p.p.m.

1-Thiaindan-3-one (6)

This was prepared essentially by the route described in the literature (11, 12) via cyclization of the acid chloride of *S*-phenylthioglycolic acid (prepared from thiophenol and bromoacetic acid in alkali) using aluminum chloride as the catalyst. Yields of the acid chloride (attempted with various chlorinating agents) and of the final product were invariably poor. The product was recrystallized from *n*-hexane – petroleum ether as a pink solid, m.p. 67–69 °C (lit. (13) m.p. 71 °C), which rapidly turned purple if allowed to stand at room temperature. Infrared 1665 cm^{-1}; n.m.r. δ 3.7 (s, 2H), 6.95–7.55 (m, 3H), 7.6–7.85 (m, 1H) p.p.m.

The preparations of thiochromone **7***a* and of 4*H*-thiochromene-4-thione **9** described below illustrate the general methods also used to prepare the 2- and 3-methyl and the 2,3-dimethyl analogs of **7***a*, and the other thiones listed in Table 3, respectively.

Thiochromone (7a) (14)

The crude red triphenylmethyl perchlorate (prepared just before use by dissolving triphenylmethanol (13.0 g) in 60% perchloric acid (50 ml), warming briefly, cooling, and filtering) was added to thiochroman-4-one (6.0 g) in

Can. J. Chem. Downloaded from www.nrcresearchpress.com by 210.87.254.40 on 09/05/12
For personal use only.

TABLE 1. Carbon-13 chemical shifts[a] and aromatic shielding parameters[b] of model compounds

Compound[c]	C-1	C-2, 6(*o*)	C-3, 5(*m*)	C-4(*p*)
Thioanisole (3)	138.6[d]	126.6	128.7	124.9
(—S—)	(+10.0)	(−2.0)	(+0.1)	(−3.7)
Diphenyl sulfide	135.8	131.0	129.1	127.0
(—S—)	(+7.2)	(+2.4)	(+0.5)	(−1.6)
Methyl phenyl sulfoxide	145.9[e]	123.4	129.7	130.8
(—SO—)	(+17.3)	(−5.2)	(+0.6)	(+2.2)
Diphenyl sulfoxide	145.7	124.7	129.2	131.0
(—SO—)	(+17.1)	(−3.9)	(+0.6)	(+2.4)
Methyl phenyl sulfone	140.6[f]	127.1	129.3	133.6
($—SO_2—$)	(+12.0)	(−1.5)	(+0.7)	(+5.0)
Diphenyl sulfone	141.6	127.6	129.3	133.2
($—SO_2—$)	(+13.0)	(−1.0)	(+0.7)	(+4.6)
Thiobenzophenone	147.2	129.5	127.9	131.9
(—CS—)	(+18.6)	(+0.9)	(−0.7)	(+3.3)

[a]In p.p.m. downfield from TMS. [b]In p.p.m. from benzene (128.6). Positive value indicates a downfield shift, relative to TMS. [c]In $CDCl_3$ solution. [d]Methyl, 15.6q. [e]Methyl, 43.7q. [f]Methyl, 44.2q.

glacial acetic acid (60 ml). After addition of acetic anhydride (9 ml) an exothermic reaction occurred and the mixture was then boiled for 10 min before cooling in ice and filtering off the yellow 4-hydroxy-1-thiobenzo[*b*]pyrylium perchlorate. This salt, after being washed with anhydrous ether, was stirred briefly with saturated sodium bicarbonate solution and the liberated thiochromone filtered off in almost quantitative yield. Recrystallization from petroleum ether – benzene (4:1) gave white prisms, m.p. 78–80 °C, lit. (8) m.p. 78 °C. Infrared 1635, 1590 cm^{-1}; u.v. $\lambda_{max}^{CH_3OH}$ 248 (ε, 11 100), 256sh (ε, 10 900), 280 (ε, 4300), 333 (ε, 9500) nm; n.m.r. δ 6.9 (d, J = 10 Hz, 1H), 7.8 (d, J = 10 Hz, 1H) 7.5–7.6 (m, 3H), 8.4–8.6 (m, 1H) p.p.m.

4H-Thiochromene-4-thione (9)

Thiochromone (3.24 g) was refluxed in dry benzene for 4 h with phosphorus pentasulfide (4.45 g). The red solution was cooled, filtered, and the solvent evaporated. The crude residue was extracted with boiling petroleum ether (60–80 °C). Filtration of the hot solution and concentration gave red crystals of the thione (2.89 g, 81%), m.p. 90–91 °C, lit. (15) m.p. 91 °C. Infrared 1150 cm^{-1} (C=S); u.v. $\lambda_{max}^{CH_3OH}$ 236 (ε, 16 000), 289 (ε, 6450), 405 (ε, 15 400) nm; n.m.r. δ 7.3 (d, J = 9 Hz, 1H), 8.1 (d, J = 9 Hz, 1H), 7.5–7.7 (m, 3H), 8.9–9.1 (m, 1H) p.p.m.

Using the general procedure illustrated below for the case of 3-methylthiochroman-4-one we have experienced no difficulty in converting the thiochromanones into the corresponding sulfoxides in yields (isolated) ranging from 43–90% with virtually no contamination by the corresponding sulfones. Similarly, the general procedure previously described (5) converted the sulfides into the corresponding sulfones in isolated yields of 42–91%.

3-Methylthiochroman-4-one 1-oxide

A solution of 3-methylthiochroman-4-one (9.0 g) in acetic acid (35 ml) was cooled in an ice bath and 30% hydrogen peroxide (6.4 g) was added slowly with stirring. The mixture was allowed to remain for 12 to 16 h at 25 °C before dilution with water and extraction with ether to remove unreacted sulfide. Extraction with methylene chloride, followed by washing ($NaHCO_3$, water) and drying gave the sulfoxide (6.0 g, 66%). Final purification was achieved by chromatography on silica (eluting with 30% acetone – methylene chloride) and recrystallization from *n*-hexane–benzene, m.p. 116–117 °C. Infrared 1689, 1031 cm^{-1}.

Anal. Calcd. for $C_{10}H_{10}O_2S$: C, 61.86; H, 5.15; S, 16.49. Found: C, 61.64; H, 5.17; S, 16.62.

Results and Discussion

Carbon-13 chemical shift data for a series of cyclic keto-sulfides derived mainly from thiochroman-4-one (**1**) and including also the isomeric isothiochromanone (**4**) and thiochroman-3-one (**5**), as well as 1-thiaindan-3-one (**6**) and the oxime derived from **1**, are collected in Table 2. A number of other oximes were also available but their insolubility in $CDCl_3$ rendered them unsuitable for the present study. The simple oxygen analogs of **1** and of thioflavanone (**3***a*) (chromanone (**2**) and flavanone (**3***b*)) are also included to provide some comparisons between S- and O-series of compounds.

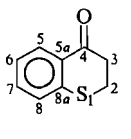

1

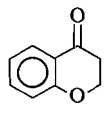

2

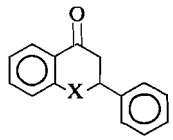

3*a* X = S
3*b* X = O

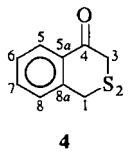

4

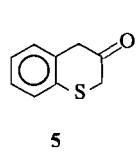

5

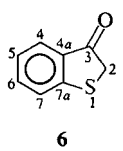

6

The assignments of the six aromatic chemical shifts in thiochroman-4-one were made using the

Can. J. Chem. Downloaded from www.nrcresearchpress.com by 210.87.254.40 on 09/05/12
For personal use only.

aromatic shielding parameters of the $COCH_3$ group (2) and by subtracting from the various chemical shifts of thioanisole (3) (Table 1) the chemical shift of benzene, which was 128.6 p.p.m. under the present conditions. This rather simplifying assumption gave remarkably good agreement between theory and prediction for the four unsubstituted carbons, C-5 to C-8, none of the deviations exceeding 1.0 p.p.m. Not unexpectedly, as other authors have noted (16), the agreement between prediction and observation for C-5*a* and C-8*a* was much poorer, the deviations being 4.8 and 3.4 p.p.m., respectively. The relative lack of data for the shielding parameters of sulfur-containing substituents as compared to the carbonyl substituent and the presence of the second (heterocyclic) ring may account for this result. Results from the 6-methyl and 6-methoxy analogs, however, reveal *para*-substituent effects of −3.3 and −8.7 p.p.m. respectively and give excellent corroboration of the correctness of the C-5*a* and C-8*a* assignments in **1**. A similar procedure was carried out for chromanone using the well documented aromatic shift parameters for $COCH_3$ and OCH_3 (2) groups. The maximum deviation observed was 3.6 p.p.m. (for C-8), while the agreement for the ring fusion carbons C-5*a* and C-8*a* was very good in this case, neither of the deviations exceeding 2.0 p.p.m. The assignment of the resonance at 26.2 to C-2 and that at 39.5 p.p.m. to C-3 in thiochromanone was obvious from an examination of the chemical shifts in tetrahydrothiophene, cyclopentanone and cyclopentane, as well as being in accord with the substituent effects produced in the C-2 and C-3 methylated analogs.

The 2-methyl, 3-methyl, 2,2-dimethyl, and 3,3-dimethyl analogs of **1** were also examined in the analogous sulfoxide (Table 5) and sulfone (Table 6) series and the substituent effects have been compared in Table 7 for all three series. Generally speaking, methyl substitution at C-2 produces a more pronounced downfield shift at that carbon than does methyl substitution at C-3, α to the carbonyl group. Roberts and Weigert (17) observed this effect in simple methylcyclohexanones. As Table 7 reveals, however, there are a number of curious variations in the methyl substituent effect pattern and the likelihood that the heterocyclic ring may exist in both the half-chair and the sofa conformations, as well as the widely different electronic effects of S, SO, and SO_2 and the existence of diastereomeric sulfoxides (in some cases) make rationalization difficult. As expected, substitution of methyl (or phenyl) groups on C-2 or C-3 has in general no significant influence on the chemical shifts of C-5*a*, C-8*a* or the carbonyl carbon (C-4). The one exception to this is in the downfield shift of the carbonyl carbon in the 3-methyl compound (+2.4 p.p.m.) and in the 3,3-dimethyl compound (+4.5 p.p.m.). The shift of the carbonyl carbon on going from cyclohexanone to 2-methylcyclohexanone is +1.5 p.p.m. Significant shifts in the position of the carbonyl carbon were noted in thiochroman-3-one (**5**), where the downfield shift is attributable to the loss of conjugation with the aromatic ring, and in 1-thiaindan-3-one (**6**), where the downfield shift is due to the five-membered ring. In thiochroman-4-one oxime the C-2 and C-3 signals had almost identical chemical shifts and the C-4 carbon appeared in the normal range for oximes (2) at 153.6 p.p.m.

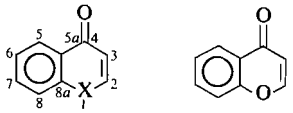

7*a* X = S
7*b* X = SO_2

8

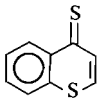

9

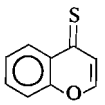

10

The 10 compounds appearing in Table 3 under the generic heading 'thiochromones' strictly include only four members of that class of compound. However, the three thiones **9**, **10**, and the 2-phenyl analog of **10**, the thiochromone sulfone (**7***b*), and the oxygen analogs chromone (**8**) and flavone all possess as a common structural feature a double bond between C-2 and C-3 and furthermore all contain an α,β-unsaturated ketone (or thione) moiety in a six-membered ring, with an electron-withdrawing group (O, S, SO_2) attached to the β-carbon, and we have thus felt justified in treating them for the present purpose as a related group of compounds. Finding suitable model compounds is more difficult for this series, but at least for the ketone members of the series we have utilized the well-documented effects of α- and β-methyl substitution in 2-cyclohexen-1-one (2) and the generally much lower field position observed for the β-carbon in assigning the C-2 and C-3 resonances. In assigning the aromatic carbon reson-

Can. J. Chem. Downloaded from www.nrcresearchpress.com by 210.87.254.40 on 09/05/12
For personal use only.

TABLE 2. Carbon-13 chemical shifts[a] of cyclic sulfides (thiochromanones)

Compound[b]	C-2	C-3	C-4 (C=O)	C-5a	C-8a	C-5, 6, 7, 8
Thiochroman-4-one, **1**	26.6t	39.5t	193.8s	130.9s	142.1s	124.9d (C-6); 127.5d (C-8); 129.1d (C-5); 133.1d (C-7)
Chromanone, **2**	66.9t	37.7t	191.4s	121.4s	161.8s	117.8d (C-8); 121.2d (C-6); 127.0d (C-5); 135.8d (C-7)
2-Methyl-**1**[c]	36.2d	47.6t	193.9s	130.2s	141.6s	124.6d (C-6); 127.3d (C-8); 128.8d (C-5); 133.1d (C-7)
2,2-Dimethyl-**1**[d]	44.5s	53.8t	194.5s	129.7s	141.2s	124.6d (C-6); 127.5d (C-8); 128.6d (C-5); 133.5d (C-7)
3-Methyl-**1**[e]	33.0t	42.1d	196.2s	130.4s	141.8s	124.7d (C-6); 127.2d (C-8); 129.4d (C-5); 133.3d (C-7)
3,3-Dimethyl-**1**[f]	39.1t	40.9s	198.3s	129.5s	141.4s	124.8d (C-6); 127.1d (C-8); 130.0d (C-5); 132.7d (C-7)
2,3-Dimethyl-**1**[g] (cis- + trans-)	40.6, 41.7 d	46.9, 48.7 d	196.3, 196.7 s	129.7, 129.9 s	140.4, 140.8 s	124.6d (C-6); 127.0, 127.3d (C-8); 129.0, 129.3d (C-5); 133.0d (C-7)
6-Methyl-**1**[h]	26.7t	39.8t	194.3s	130.8s	138.8s	127.5d (C-8); 129.3d (C-5); 134.4d (C-7); 134.9s (C-6)
8-Methyl-**1**[i]	26.0t	39.1t	194.3s	131.1s	141.7s	124.1d (C-6); 126.9d (C-5); 134.3d (C-7); 135.4s (C-8)
6-Methoxy-**1**[j]	26.8t	39.6t	193.6s	131.5s	133.4s	111.3d (C-5); 121.9d (C-7); 128.7d (C-8); 157.3s (C-6)
2-Phenyl-**1** (thioflavanone, **3***a*)	45.4d	46.6t	194.0s	130.4s	142.0s	125.1–133.5d[k]; 138.4s (C-1′)
Flavanone, **3***b*	79.5d	44.6t	191.6s	120.9s	161.5s	118.0d (C-8); 121.5d (C-6); 126.1–128.7d[l]; 136.0d (C-7); 138.8s (C-1′)
1, oxime	26.3t[r]	26.0t[r]	153.6[m]	129.5s	136.3s	125.6–129.3d[r]
Isothiochromanone, **4**	30.5t[n]	37.0t	190.8s	131.8s	141.8s	127.7–128.9d[r]; 132.9d (C-7)
Thiochroman-3-one, **5**	46.5t	204.7s[o]	37.3t	132.8s	134.0s	127.0–129.0d[r]
1-Thiaindan-3-one, **6**	39.1t	199.8s[o]	—	130.9s[p]	155.2s[q]	124.6–126.5d[r]; 135.5s (C-6)

[a]In p.p.m. downfield from TMS; numbering of carbons as in **1**. [b]In $CDCl_3$ solution. [c]Methyl, 20.3q. [d]Methyls, 28.5q. [e]Methyl, 14.9q. [f]Methyls, 23.5q. [g]Methyls, 15.9, 19.9q(C-2); 11.1, 13.4q(C-3) [h]Methyl, 20.8q. [i]Methyl, 20.0q. [j]Methoxyl, 55.4q. [k]C-5, C-6, C-7, C-8, C-2′, C-3′, C-4′. [l]C-5, C-2′, C-3′, C-4′. [m]C=NOH. [n]C-1. [o]C=O. [p]C-4*a*. [q]C-7*a*.
[r]Individual assignments uncertain.

TABLE 3. Carbon-13 chemical shifts[a] of unsaturated cyclic sulfides (thiochromones)

Compound[b]	C-2	C-3	C-4 (C=O)	C-5*a*	C-8*a*	C-5, 6, 7, 8
Thiochromone, **7***a*	137.9d	126.6d	179.4s	132.2s	137.5s	125.7d (C-6); 127.7d (C-8); 128.5d (C-5); 131.4d (C-7)
Chromone, **8**	145.5d	113.0d	177.6s	125.0s	156.6s	118.3d (C-8); 125.3, 125.8d (C-5, C-6)[j]; 133.8d (C-7)
2-Methyl-**7***a*[c]	151.0s	124.6d	179.9s	130.5s	137.4s	125.9d (C-6); 127.3d (C-8); 128.2d (C-5); 131.2d (C-7)
3-Methyl-**7***a*[d]	132.7d	133.0s	179.3s	130.6s	137.4s	126.3d (C-6); 127.0d (C-8); 128.5d (C-5); 131.0d (C-7)
2,3-Dimethyl-**7***a*[e]	144.3s	129.8s	179.3s	130.7s	136.8s	125.3d (C-6); 126.9d (C-8); 128.9d (C-5); 130.5d (C-7)
2-Phenyl-**8** (flavone)	163.3s	107.6d	178.3s	124.0s	156.3s	118.1d (C-8); 125.2–131.6[f]d; 131.8s (C-1′); 133.7d (C-7)
Thiochromone1,1-dioxide, **7***b*	140.6d	132.2d	177.8s	128.2s	141.1s	123.1d (C-8); 128.5d (C-5); 133.0d (C-7); 135.0d (C-6).
4*H*-Thiochromene-4-thione, **9**	137.6d	131.4d	204.4s[g]	132.5s	138.4s	127.3–129.0[h]d; 132.0d (C-7)
4*H*-Chromene-4-thione, **10**	146.0d	126.2d	202.8s[g]	130.9s	151.4s	118.6d (C-8); 124.8d (C-6); 128.6d (C-5); 134.2d (C-7)
2-Phenyl-**10**	153.8s	120.1d	201.4s[g]	130.8s	151.3s	118.3d (C-8); 125.9-131.7[i]d; 129.7s (C-1′); 133.9d (C-7)

[a]In p.p.m. downfield from TMS; numbering of carbons as in **7***a*. [b]In $CDCl_3$ solution. [c]Methyl, 23.0q. [d]Methyl, 18.9q. [e]Methyls, 21.6q (C-2), 13.0q (C-3). [f]C-5, C-6, C-2′, C-3′, C-4′. [g]C=S. [h]C-5 C-6, C-8. [i]C-5, C-6, C-2′, C-3′, C-4′.
[j]Individual assignments uncertain.

TABLE 4. Shielding parameters[a] in α,β-unsaturated cyclic ketones

Substituent	Effect on β-carbon[b]	Effect on α-carbon[b]
β-Methyl(2-methyl-7*a*)	+13.1 (+11.5)	−2.0 (−2.8)
α-Methyl(3-methyl-7*a*)	−5.2 (−5.2)	+6.4 (+6.5)
α,β-Dimethyl(2,3-dimethyl-7*a*)	+6.4 (+3.9)	+3.2 (+1.6)

[a]In $CDCl_3$ solution. [b]In p.p.m. from corresponding values in thiochromone (7*a*) and cyclohexenone (in parentheses), respectively. Positive value indicates a downfield shift, relative to TMS.

ances, for example in the parent thiochromone and chromone systems, (7*a* and **8**), we have adopted the guideline that those carbon atoms whose resonances are significantly shifted (upfield or downfield) from the 128.6 p.p.m. value for benzene in $CDCl_3$ will experience much the same electronic effects as those in the saturated analogs, **1** and **2**, and have assigned them accordingly. The carbonyl carbon atoms (C-4) in the first seven members of the series all appear within the narrow range 177.6–179.9 p.p.m., thus indicating that not only methyl substitution (α- or β-), but also β-phenyl substitution or even the replacement of the cyclic β-sulfur substituent with oxygen or sulfone groups, produces little effect at C-4. The same situation occurs for the thiones **9**, **10**, and 2-phenyl-**10**, where the carbon of the C=S group appears within the range 201.4–204.4 p.p.m. Comparison of the chemical shifts in chromone and thiochromone with those in the corresponding thiones, **10** and **9** respectively, reveals a general similarity in the α,β-unsaturated ketone and thione systems. Indeed, in the thiochromone ketone and thione pair the only significant change is a downfield shift of +4.8 p.p.m. in the C-3 resonance on going from the ketone to the thione. A similar downfield shift was observed for C-3 of the alicyclic thione, thiocamphor, compared to C-3 in camphor itself, in an earlier study by Demarco *et al.* (18). In the ketone and thione of the chromone series, where the electronic influence of the ring oxygen is much greater, the corresponding downfield shift of the C-3 signal is +13.2 p.p.m. in going from C=O to C=S. Attempts to prepare thiones corresponding to the thiochromanone series of compounds in Table 2 unfortunately met with no success.

Some justification for comparing the thiochromone ring system with the simple cyclohexenone system is obtained by examining the effects of α- and β-(C-3 and C-2)methyl-substitution. Table 4 shows the remarkably good agreement between the shielding parameters for the thiochromones and the corresponding cyclohexenones. As expected, methyl substitution at C-2 and C-3 exerted little effect on the aromatic carbon atoms. The methyl resonance in 3-methylthiochromone appeared at 4.1 p.p.m. upfield relative to that in the 2-methyl analog. Once again this follows the pattern observed for the 2- and 3-methylthiochromanones in Table 2 and is attributable to the alignment of the 3-methyl substituent in the plane of the carbonyl group (17).

Comparison of the two 2-phenyl substituted compounds in Table 3 with their unsubstituted analogs **8** and **10** reveals that substitution at C-2 (or C-3), as already observed for the methyl derivatives, produces no significant alteration in the chemical shift of any of the aromatic carbon atoms, including C-5*a* and C-8*a*; indeed this consistency was of some assistance in making the given assignments. The (downfield) shift of the C-2 carbon differs considerably, however, being +17.8 for 2-phenyl substitution in the chromone and only +7.8 for the analogous thione. The upfield shift observed at C-3 is almost the same on the other hand, −5.4 and −6.1 respectively. The larger deshielding effect observed for phenyl substitution at C-2 in the ketone may reflect the greater electronegativity of the (carbonyl) oxygen or a greater degree of conjugation in the ketones than in the thiones.

The difference in chemical shift between C-2 and C-3 is, as expected, greater for the chromenethione (**10**) than the thiochromene-thione (**9**) (19.8 *vs.* 6.2 p.p.m.)just as the presumably greater

Can. J. Chem. Downloaded from www.nrcresearchpress.com by 210.87.254.40 on 09/05/12
For personal use only.

Can. J. Chem. Downloaded from www.nrcresearchpress.com by 210.87.254.40 on 09/05/12
For personal use only.

TABLE 5. Carbon-13 chemical shifts[a] of cyclic sulfoxides

Compound[b]	C-2	C-3	C-4 (C=O)	C-5*a*	C-8*a*	C-5, 6, 7, 8
Thiochromanone 1-oxide, **11**	47.1t	30.7t	191.9s	129.1s	145.6s	128.3d (C-8); 129.7d (C-5); 132.0d (C-6); 134.4d (C-7)
2-Methyl-**11**[c,d]	50.5, 55.8 d	37.1, 40.3 t	191.6, 192.5 s	129.1, 129.3 s	143.3, 146.9 s	127.0, 128.4d (C-8); 129.9, 131.1d (C-5); 132.3d (C-6); 134.6d (C-7)
2,2-Dimethyl-**11**[e]	56.5s	45.7t	192.1s	129.1s	144.0s	128.2d (C-8); 129.1d (C-5); 131.4d (C-6); 134.9d (C-7)
3-Methyl-**11**[f,g]	51.8t	32.1d	195.3s	129.4s	142.5s	129.4d (C-8); 130.4d (C-5); 132.8d (C-6); 134.4d (C-7)
3,3-Dimethyl-**11**[h]	60.7t	43.0s	196.7s	127.9s	147.2s	126.7d (C-8); 129.6d (C-5); 131.1d (C-6); 134.2d (C-7)
2,2,3,3-Tetramethyl-**11**[i]	63.4s	51.2s	197.3s	128.4s	143.3s	127.8d (C-8); 128.8d (C-5); 130.8d (C-6); 134.5d (C-7)
6-Methyl-**11**[j]	46.6t	30.1t	192.4s	129.1s	142.4s	128.9d (C-8); 129.4d (C-5); 135.3d (C-7); 143.1s (C-6)
8-Methyl-**11**[k]	43.5t	27.0t	193.1s	130.2s	141.0s	126.7d (C-5); 132.3d (C-6); 136.5d (C-7); 139.3s (C-8)
6-Methoxy-**11**[l]	46.2t	29.3t	192.4s	131.1s	136.6s	112.6d (C-5); 120.9d (C-7); 131.2d (C-8); 162.7s (C-6)
2-Phenyl-**11**[c] (thioflavanone 1-oxide)	60.1, 66.0 d	34.1, 39.3 t	191.8, 193.5 s	—[p]	143.5, 147.4 s	127.1–133.3[p]; 134.6, 134.8d (C-7)
2-Phenyl-6-methyl-**11**[c,m]	60.4, 66.0 d	34.2, 39.1 t	192.3, 193.9 s	—[p]	140.7, 142.0 s	127.2–135.7[p]; 144.1s (C-6)
3-Bromo-**11**	54.9t	42.1d	186.1s	130.3s	144.2s	129.5d (C-8); 130.5d (C-5); 132.8d (C-6); 135.3d (C-7)
Isothiochromanone 2-oxide, **12**	52.2t[n]	58.8t	188.0s	—[p]	—[p]	128.2–131.6[p]; 135.4d (C-7)

[a]In p.p.m. downfield from TMS; numbering of carbons as in Table 2. [b]In $CDCl_3$ solution. [c]Mixture of diastereoisomers. [d]Methyl, 13.5, 15.4q. [e]Methyls, 19.3, 24.3q. [f]Very small differences in chemical shift indicated a mixture of isomers, with one predominating. [g]Methyl, 14.9q. [h]Methyls, 24.5, 26.9q. [i]Methyls, 15.0, 19.2, 20.0, 20.4q. [j]Methyl, 21.4q. [k]Methyl, 18.9q. [l]Methoxyl, 55.8q. [m]Methyl, 21.3, 21.4q. [n]C-1.
[p]Individual assignments uncertain.

TABLE 6. Carbon-13 chemical shifts[a] of cyclic sulfones

Compound[b]	C-2	C-3	C-4 (C=O)	C-5*a*	C-8*a*	C-5, 6, 7, 8
Thiochromanone 1,1-dioxide, **13**	49.3t	36.8t	190.1s	130.3s	141.5s	123.7d (C-8); 128.8d (C-5); 133.3d (C-7); 134.9d (C-6)
2-Methyl-**13**[c]	54.5d	44.2t	190.4s	130.6s	136.8s	124.2d (C-8); 128.5d (C-5); 133.2d (C-7); 134.9d (C-6)
2,2-Dimethyl-**13**[d]	58.6s	50.5t	190.5s	130.5s	139.1s	124.8d (C-8); 128.1d (C-5); 133.1d (C-7); 135.2d (C-6)
3-Methyl-**13**[e]	55.6t	41.4d	193.2s	129.9s	141.9s	123.4d (C-8); 128.7d (C-5); 133.2d (C-7); 134.7d (C-6)
3,3-Dimethyl-**13**[f]	59.7t	45.1s	196.1s	129.3s	141.9s	123.2d (C-8); 129.3d (C-5); 133.2d (C-7); 134.6d (C-6)
5-Methyl-**13**[g]	48.4t	37.4t	192.0s	129.2s	142.4s	121.9d (C-8); 133.3d (C-7); 137.3d (C-6); 142.6s (C-5)
6-Methyl-**13**[h]	49.4t	36.8t	190.5s	130.2s	138.8s	123.8d (C-8); 129.1d (C-5); 135.5d (C-7); 144.5s (C-6)
7-Methyl-**13**[i]	49.4t	36.7t	189.9s	128.0s	141.3s	121.7d (C-8); 128.9d (C-5); 134.1d (C-6); 146.7s (C-7)
2-Methoxycarbonyl-**13**[j]	64.1d	39.8t	188.1s[k]	130.9s	139.3s	124.1d (C-8); 128.4d (C-5); 133.7d (C-7); 134.7d (C-6)
3-Methoxycarbonyl-**13**[l]	47.5t	93.2s[m]	171.0s[n]	129.8s	138.1s	123.2d (C-8); 127.2d (C-5); 132.3d (C-7); 133.3d (C-6)
2-Phenyl-**13** (thioflavanone 1,1-dioxide)	64.0d	43.1t	190.8s	130.5s	141.5s	124.4–135.0[r]
Isothiochromanone 2,2-dioxide, **14**	55.5t[o]	62.4t	186.5s	130.9s[r]	132.7s[r]	129.9–130.6[r]; 135.6d (C-7)
3,3-Dimethyl-**14**[p]	50.1t[o]	68.2s	192.5s	129.5s[r]	131.1s[r]	129.2–130.4[r]; 134.6d (C-7)

[a]In p.p.m. downfield from TMS; numbering of carbons as in Table 2. [b]In $CDCl_3$ solution. [c]Methyl, 11.6q. [d]Methyls, 21.1q. [e]Methyl, 15.2q. [f]Methyls, 26.4q. [g]Methyl, 22.7q. [h]Methyl, 21.6q. [i]Methyl, 21.9q. [j]Methoxyl, 53.9q. [k]Ester C=O, 164.9s. [l]Methoxyl, 52.8q. [m]Enol carbon (see Discussion). [n]Ester C=O, 162.9. [o]C-1. [p]Methyls, 17.7q.
[r]Individual assignments uncertain.

Can. J. Chem. Downloaded from www.nrcresearchpress.com by 210.87.254.40 on 09/05/12
For personal use only.

degree of conjugation in chromone (**8**) accounts for a C_β–C_α chemical shift difference of 32.5 p.p.m., compared with 11.3 p.p.m. for thiochromone (*7a*). Chemical shifts of the aromatic carbon atoms in the pair of compounds **8** and **10** and also in *7a* and **9** are generally very similar. The chemical shift difference between the ring fusion positions (C-8*a* – C-5*a*) is, however, much greater in chromone (31.6 p.p.m.) than in the corresponding thione (20.5 p.p.m.), reflecting once more perhaps the greater degree of conjugation in the unsaturated ketones referred to above.

Chemical shift data for the cyclic sulfoxides and sulfones in our study are collected in Tables 5 and 6, respectively. The electron-withdrawing character of the sulfoxide and sulfone functionalities is reflected in the downfield shifts at C-2, relative to thiochromanone itself, of +20.5 p.p.m. in thiochroman-4-one 1-oxide (**11**) and of +22.7 p.p.m. in thiochroman-4-one 1,1-dioxide (**13**). Interestingly, the replacement of the cyclic sulfur atom in thiochroman-4-one by the sulfoxide functionality produces an *upfield* shift at C-3 of −8.8 p.p.m., whereas in the corresponding sulfone the upfield shift at C-3 is only −2.7 p.p.m. The C-4 (carbonyl) carbon is not greatly affected by these changes, showing upfield shifts of −1.9 p.p.m. in the sulfoxide and a further −1.8 p.p.m. in the sulfone. The assignment of the aromatic carbon resonances, including the ring junctions, C-5*a* and C-8*a*, in **11** and **13** was carried out using information obtained from the model compounds in Table 1 and the shielding parameters of aromatic $COCH_3$ substituents (2), as well as by comparison with thiochroman-4-one itself. Our assignments are further supported by the generally good agreement between the observed aromatic resonances in the 6- and 8-methyl- and 6-methoxythiochroman-4-one 1-oxides and in the 5-, 6-, and 7-methylthiochroman-4-one 1,1-dioxides with the values calculated using the known aromatic substituent effects of CH_3 and OCH_3 (2).

In the series diphenyl sulfone, diphenyl sulfoxide, thiobenzophenone (Table 1), and benzophenone (19) the *p*-substituent (deshielding) effects are in the order $SO_2 > C{=}O > C{=}S > S{=}O$, being (+) 4.6, 3.7, 3.3, and 2.4 p.p.m. respectively. In diphenyl sulfide, of course, the *p*-effect is in the opposite sense, although the shift of −1.6 p.p.m. is considerably less than the −3.7 p.p.m. observed in thioanisole (3). A similar reduction in the upfield shift at the *p*-position

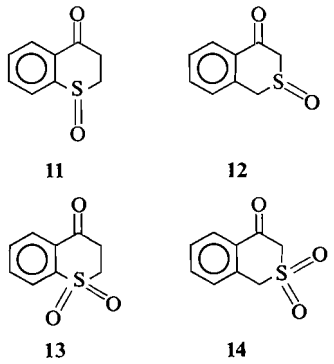

11 **12** **13** **14**

is observed in diphenyl ether as compared to anisole. The *o*-effects in the above series (*cf.* Table 1) show much less consistency, being small and in the downfield direction in thiobenzophenone and benzophenone (+0.9 and +1.3 p.p.m., respectively), whereas in diphenyl sulfoxide and diphenyl sulfone they are in the upfield direction, being −3.9 and −1.0 p.p.m., respectively. In diphenyl sulfide, the *o*-effect is +2.4 p.p.m.

The effects of methyl-substitution at C-2 and C-3 in the sulfide, sulfoxide, and sulfone series (Tables 2, 5, 6) show interesting variations and the data for the three series has been collected in Table 7. Although general trends are difficult to discern, it does appear that substitution of a methyl group at C-2 produces more 'normal' shifts at both C-2 and C-3 than is the case for the corresponding 3-methyl and 3,3-dimethyl series. In fact, downfield shifts at C-3 are generally small, the single exception being in going from the 3-methyl to the 3,3-dimethyl sulfoxide where a change of +10.9 p.p.m. is observed. Once again, in both the sulfoxide and sulfone series, the tendency of α-methyl (C-3) substitution to produce downfield shifts of the C-4 (carbonyl) resonance is just as pronounced as it was for the sulfides in Table 2. The differences in chemical shifts for the methyl resonances themselves at C-2 and C-3, referred to in the discussion of Table 2, are no longer so evident in Tables 5 and 6, not only because of the non-equivalence of methyl groups in 2,2- and (to a lesser extent) 3,3-dimethylthiochroman-4-one 1-oxides, but also no doubt because of the shielding influence, not present in the thiochromanones, of the S=O bond(s) on the C-2 methyls. In general, as was the case for the corresponding sulfides, the effect of C-2 or C-3 methyl substitution on even the closest aromatic (ring-junction) carbon atoms is

Can. J. Chem. Downloaded from www.nrcresearchpress.com by 210.87.254.40 on 09/05/12
For personal use only.

not very great, as expected, and is probably attributable to steric crowding of one or both of the polar functionalities at C-1 and C-4, which reaches its maximum expression in 2,2,3,3-tetramethylthiochroman-4-one 1-oxide.

In thioflavanone 1-oxide and thioflavanone 1,1-dioxide, the effect of phenyl substitution at C-2 is to produce downfield shifts of +15.9 (taking the mean value for the two diastereoisomers) and +14.7 p.p.m. respectively. The corresponding shifts so produced at C-3 amount to +6.0 and +6.3 p.p.m., respectively, much the same behavior as was observed in thioflavanone itself. In all three 2-phenyl substituted compounds, the increased complexity of the aromatic region of the ^{13}C n.m.r. spectra prevented the individual assignment of all signals. This problem becomes particularly acute in the case of 2-phenylthiochroman-4-one 1-oxide and 2-phenyl-6-methylthiochroman-4-one 1-oxide owing to the existence of diastereoisomers, since the separation of lines (due to configurational isomerism) becomes quite small for the aromatic carbons which are relatively remote from the chiral centers, leading to much overlapping of neighboring peaks in the relatively narrow region of the spectrum involved. The spectrum of 3-bromothiochroman-4-one 1-oxide reveals that the α-effect produced by replacing hydrogen by bromine is +11.4 and the β-effect +7.8 p.p.m. which, at least as far as the α-effect is concerned, seems to agree well with results quoted by Levy and Nelson (2). The effect of introducing a bromine α to the carbonyl group produces an upfield shift of −5.8 p.p.m. in the resonance due to the C-4 carbon. This compares favorably with the value of −5.3 p.p.m. reported for 3-*endo*-bromocamphor (20). As usual, the signals due to the aromatic carbons were not greatly affected by introduction of the bromine although a general drift downfield of approximately 1 p.p.m. was noted.

The two sulfones which bear an ester functionality in the heterocyclic ring (Table 6) deserve comment. In 2-methoxycarbonylthiochroman-4-one 1,1-dioxide, the α-effect of the ester group is +14.8 p.p.m. and the β-effect +3.0. Very recently, Gordon *et al.* (21) have reported their results from a ^{13}C n.m.r. study of a series of methyl esters in which the α-effect was +15.4 p.p.m. and the β-effect +1.3 p.p.m. for the cyclohexyl system. In our 2-methoxycarbonyl substituted case, the only other significant effect was to produce an upfield shift of −2.0 p.p.m. in the carbonyl carbon (Gordon *et al.* (21) report a γ-effect for simple cyclohexanes of −2.3 p.p.m.). In distinct contrast to the rather routine effects observed in the 2-substituted case, the 3-methoxycarbonylthiochroman-4-one 1,1-dioxide produced a quite unexpected result. It will be noted that this is in fact a β-keto ester and the ^{13}C n.m.r. spectrum indicates quite clearly that in $CDCl_3$ solution at the concentration used (12–15% w/v) enolization is complete. Thus, the C-3 signal appears as a singlet rather than a doublet, as a value of 93.2 p.p.m., far removed from the 36.8 p.p.m. observed in the unsubstituted sulfone, whereas the position of the C-2 signal is altered only slightly. The electron-releasing effect of the enolic OH group, enhanced by the electron-withdrawing effect of the COOMe group, accounts for the unusually high field location for the sp^2 carbon at C-3. As expected, the C-4 carbon shows a chemical shift closer to what one would expect for an sp^2 carbon bonded to oxygen, appearing at 171.0 p.p.m. The methyl and ester carbonyl signals, as well as the signals for the aromatic carbons in the two ester derivatives, are virtually identical.

The remaining compounds for which data are included in Tables 5 and 6 are isothiochromanone 2-oxide (**12**) and isothiochromanone 2,2-dioxide (**14**) and its 3,3-dimethyl derivative. The assignment of the C-1 and C-3 signals in **12** and in **14** as well as in isothiochromanone (**4**) itself was made initially in the expectation that the signal due to C-3, α to the carbonyl, would be downfield from that due to C-1, which is a benzylic methylene, and the assumption that the C-3 signal in particular would not be greatly changed in position from C-3 of thiochroman-4-one. In the sulfoxide (**12**) the C-1 and C-3 signals are shifted downfield by +21.7 and +21.8 p.p.m., respectively, while in the sulfone (**14**) the corresponding shifts are +25.0 and +25.4 p.p.m. These values are very similar to the effects observed at C-2 in the analogous thiochromanones, in proceeding through the series sulfide, sulfoxide, sulfone. Further evidence in support of these assignments comes from a consideration of 3,3-dimethylisothiochromanone 2,2-dioxide (Table 6), where the change in chemical shift at C-3 between this compound and the unsubstituted analog is +5.8 p.p.m., while the corresponding change in chemi-

TABLE 7. Methyl substituent effects[a] at C-2 and C-3

Series	Substituent	Effect at C-2[b]	Effect at C-3[b]
Thiochromanones	2-Methyl	+9.6	+8.1
	2,2-Dimethyl	+17.9	+14.3
	3-Methyl	+6.4	+2.6
	3,3-Dimethyl	+12.5	+1.4
	2,3-Dimethyl[c]	+14.6	+8.3
Thiochromanone sulfoxides	2-Methyl[c]	+6.1	+8.0
	2,2-Dimethyl	+9.4	+15.0
	3-Methyl	+4.7	+1.4
	3,3-Dimethyl	+13.6	+12.3
	2,2,3,3-Tetramethyl	+16.3	+20.5
Thiochromanone sulfones	2-Methyl	+5.2	+7.4
	2,2-Dimethyl	+9.3	+13.7
	3-Methyl	+6.3	+4.6
	3,3-Dimethyl	+10.4	+8.3

[a]In p.p.m.; positive values indicate downfield shifts.
[b]All shifts are related to values for C-2 and C-3 in the parent compounds (**1**, **11**, or **13**), including those for the dimethyl substituted derivatives.
[c]Mean value taken for diastereoisomers.

cal shift at C-3 between thiochroman-4-one 1,1-dioxide and its 3,3-dimethyl analog is +8.3 p.p.m. In general the C-4 (carbonyl) carbon appears at higher field in isothiochromanone and its sulfoxide and sulfone, the differences ranging between 3–4 p.p.m. Once again, however, in the case of 3,3-dimethylisothiochromanone 2,2-dioxide, the characteristic downfield shift in the C-4 (carbonyl) frequency produced by α-methylation is observed. The numerical value of this shift, 6.0 p.p.m., is exactly the same as that observed in 3,3-dimethylthiochroman-4-one 1,1-dioxide. The removal of the electron-withdrawing sulfur group at C-1 in isothiochromanone sulfoxide and sulfone to the C-2 position produces a very marked closing of the gap in chemical shifts between C-5*a* and C-8*a* observed in the analogous thiochromanone sulfoxide and sulfone to about 2 p.p.m. and furthermore greatly reduces the spread in chemical shifts arising from the carbons 5, 6, and 8 to the point at which attempts to make individual assignments become somewhat nebulous.

In Table 7 are gathered data on the effects of methylation at C-2 and C-3 in the thiochromanone and related sulfoxide and sulfone series, calculated from the chemical shifts in Tables 2, 5, and 6. It may be noted that for 2,3-dimethylthiochroman-4-one the total downfield shift observed at C-2 and C-3 approximates quite closely that obtained by simply adding the contributions from the 2-methyl and 3-methyl derivatives. This additivity is not so apparent in 2,2,3,3-tetramethylthiochroman-4-one 1-oxide, where the steric crowding must cause considerable distortion of the heterocyclic ring. Even in this case, however, the relative magnitude of the shifts at C-2 and C-3 is correctly predicted by summing the values from the 2,2-dimethyl and 3,3-dimethyl sulfoxides.

We thank Mr. N. Plavac of this department for his help and cooperation in recording the ^{13}C n.m.r. spectra. We wish to acknowledge also the experimental contributions of Dr. M. T. Thomas, Miss M. H. Kwan, and Mr. Peter Lau in making available some of the compounds included in this study.

1. I. W. J. STILL, M. S. CHAUHAN, and M. T. THOMAS. Can. J. Chem. **51**, 839 (1973).
2. G. C. LEVY and G. L. NELSON, Carbon-13 nuclear magnetic resonance for organic chemists. Wiley-Interscience, New York. 1972.
3. L. F. JOHNSON and W. C. JANKOWSKI. Carbon-13 n.m.r. spectra. John Wiley and Sons, Inc., New York. 1972.
4. J. B. STOTHERS. Carbon-13 n.m.r. spectroscopy. Academic Press, New York. 1972.
5. I. W. J. STILL and M. T. THOMAS. J. Org. Chem. **33**, 2730 (1968).
6. I. W. J. STILL and M. T. THOMAS. Tetrahedron Lett. 4225 (1970).
7. I. W. J. STILL, M. S. CHAUHAN, and M. T. THOMAS. Tetrahedron Lett. 1311 (1973).
8. F. ARNDT. Chem. Ber. **58**, 1612 (1925).
9. W. C. LUMMA and G. A. BERCHTOLD. J. Org. Chem. **34**, 1566 (1969).

Can. J. Chem. Downloaded from www.nrcresearchpress.com by 210.87.254.40 on 09/05/12
For personal use only.

10. F. ARNDT. Chem. Ber. **56**, 1269 (1923).
11. J. P. CLAËSSON. Bull. Soc. Chim. Fr. **23**, 441 (1875).
12. Chem. Zentralbl. (I) 1811 (1908).
13. P. FRIEDLÄNDER. Chem. Ber. **39**, 1060 (1906).
14. W. BONTHRONE and D. H. REID. J. Chem. Soc. 2773 (1959).
15. L. LEGRAND. Bull. Soc. Chim. Fr. 1599 (1959).
16. K. N. SCOTT. J. Am. Chem. Soc. **94**, 8564 (1972).
17. F. J. WEIGERT and J. D. ROBERTS. J. Am. Chem. Soc. **92**, 1347 (1970).
18. P. V. DEMARCO, D. DODDRELL, and E. WENKERT. Chem. Commun. 1418 (1969).
19. I. W. J. STILL and M. S. CHAUHAN, unpublished results.
20. E. LIPPMAA, T. PEHK, J. PAASIVIRTA, N. BELIKOVA, and A. PLATÉ. Org. Magn. Reson. **2**, 581 (1970).
21. M. GORDON, S. H. GROVER, and J. B. STOTHERS. Can. J. Chem. **51**, 2092 (1973).

Can. J. Chem. Downloaded from www.nrcresearchpress.com by 210.87.254.40 on 09/05/12
For personal use only.

Studies Related to Antitumor Antibiotics. Part VI. Correlation of Covalent Cross-linking of DNA by Bifunctional Aziridinoquinones with their Antineoplastic Activity

M. HUMAYOUN AKHTAR,[1] ASHER BEGLEITER,[2] DOUGLAS JOHNSON,[3] J. WILLIAM LOWN, LARRY MCLAUGHLIN,[4] AND SOO-KHOON SIM[5]

Departments of Chemistry and Biochemistry, University of Alberta, Edmonton, Alberta T6G 2G2

Received April 14, 1975

M. HUMAYOUN AKHTAR, ASHER BEGLEITER, DOUGLAS JOHNSON, J. WILLIAM LOWN, LARRY MCLAUGHLIN, and SOO-KHOON SIM. Can. J. Chem. **53**, 2891 (1975).

Certain bisaziridinopyrrolidinoquinone analogs, which contain the structural moieties essential for physiological activity in the parent antitumor agent mitomycin C, have been synthesized. These compounds efficiently induce covalent cross-links in DNA as shown by the ethidium fluorescence assay which was confirmed by an independent S_1-endonuclease assay. The interaction of clinically active and structurally related antitumor aziridinoquinones with DNA have been examined similarly. The aziridinoquinones cross-link DNA efficiently with a marked p*H* dependence. Parallel dependence is observed on p*H* and concentration of alkylating species in the concomitant alkylation which does not result in cross-linking as measured by the suppression of the before heat fluorescence. The latter phenomenon was shown by the application of radiolabelled polynucleates not to be accompanied by depurination. A direct correlation exists between the extent of covalent cross-linking and (G + C) content of various DNA's of comparable molecular weight as in the case of mitomycin C. Estimates of the average number of cross-links per DNA molecule range from 0.61 to 1.71 depending on (G + C) content. The rate of acid assisted opening of a model aziridinoquinone measured spectrophotometrically at different p*H* values parallels the observed rate of covalent cross-linking and alkylation. It was shown independently that the intermediate 2,5 bis(2-acetoxyethylamino)-3,6-dimethoxy-1,4-benzoquinone does not cross-link DNA. A correlation is made of antineoplastic activity against a variety of tumors with covalent cross-linking ability using λ-DNA.

M. HUMAYOUN AKHTAR, ASHER BEGLEITER, DOUGLAS JOHNSON, J. WILLIAM LOWN, LARRY MCLAUGHLIN et SOO-KHOON SIM. Can. J. Chem. **53**, 2891 (1975).

On a synthétisé certains analogues de la bis-aziridinopyrrolidinoquinone qui contiennent la fraction structurale essentielle pour l'activité physiologique de la mitomycine C, agent actif contre les tumeurs. Ces composés induisent d'une façon efficace des liaisons transversales covalentes dans l'ADN; on a pu démontrer cette propriété par les tests de fluorescence à l'éthidium et la confirmer par un test indépendant avec la S_1-endonuclease. On a examiné, de la même manière, l'interaction entre l'ADN et les aziridinoquinones de structures semblables, actives du point de vue clinique contre les tumeurs. Les aziridinoquinones provoquent d'une façon efficace des liaisons transversales dans l'ADN; ce processus varie d'une façon importante avec le p*H* et la concentration des espèces alkylantes dans l'alkylation concomitante qui ne conduit pas à une liaison transversale telle que mesurée par la suppression de la fluorescence d'avant chauffage. On a démontré ce dernier phénomène par l'application de polynucléates marqués qui n'est pas accompagnée d'une dépurination. Une corrélation directe existe entre la quantité de liaisons transversales covalentes et le contenu (G + C) de divers ADN de poids moléculaires comparables à ceux utilisés dans le cas de la mitomycine C. On évalue que le nombre moyen de liaisons transversales par molécule d'ADN varie de 0.61 à 1.71 suivant le contenu (G + C). Le taux d'ouverture, aidée par les acides, de l'aziridinoquinone modèle, tel que mesuré spectrophotométriquement à divers p*H*, est parallèle au taux observé pour la formation de liaisons transversales covalentes et l'alkylation. On a démontré d'une façon indépendante que l'intermédiaire bis(acétoxy-2 éthylamino)-2,5 diméthoxy-3,6 benzoquinone-1,4 ne cause pas de liaisons transversales dans l'ADN. On présente une corrélation entre l'activité antinéoplastique contre une variété de tumeurs avec l'habilité de causer des liaisons transversales covalentes dans la λ-ADN.

[Traduit par le journal]

[1]National Cancer Institute of Canada Postdoctoral Fellow 1973–1975.

[2]NRCC Studentship holder 1971–1974. Province of Alberta Graduate Fellowship holder 1974–present.

[3]MRC Scholarship holder 1972–present.

[4]NRCC Studentship holder 1975–present.

[5]NRCC Postdoctorate Fellow 1974–present.

Can. J. Chem. Downloaded from www.nrcresearchpress.com by 210.87.254.40 on 09/05/12
For personal use only.

Can. J. Chem. Downloaded from www.nrcresearchpress.com by 210.87.254.40 on 09/05/12
For personal use only.

Introduction

In the alkylating class of antitumor antibiotics the most effective are bifunctional including many chemically important agents such as mitomycin C and synthetic agents *e.g.* Trenimon (1*a*). There is much evidence to indicate that DNA is the cell component most sensitive to the attack of such agents (2). As we described in Part V of this series the method of fluorescence enhancement employing the intercalative trypanocidal dye ethidium bromide which specifically detects double stranded DNA is a convenient procedure for investigating many aspects of the interaction of alkylating agents with the cell's genetic material (3). We describe the application of this technique to a study of the rate, extent, geometrical, substituent, and purine base specificity requirements for the covalent cross-linking of polynucleates, and attempt to correlate such factors with their antineoplastic properties.

Results and Discussion

Synthesis of Analogs of Mitomycin C which Covalently Cross-link DNA

In their studies on the mode of action of mitomycin C, **1**, Szybalski and Iyer (4) showed that the rate of cell death correlated well with the degree of DNA cross-linking and have calculated that one cross-link per genome is sufficient to cause cell death. An examination of the literature of cancer chemotherapy reveals that many effective bifunctional agents have quite widely different geometries (1*a*). To examine further the characteristics of cross-linking of DNA with a view ultimately of establishing a rapid and convenient screen for potential antitumor agents, we sought initially a group of analogs of mitomycin C. Despite intensive and ongoing efforts by several groups of workers, mitomycin C has not as yet yielded to a total synthesis (5). There is also interest in chemically modified forms of mitomycin C

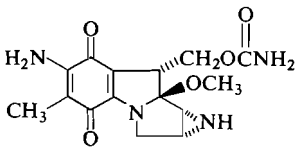

1

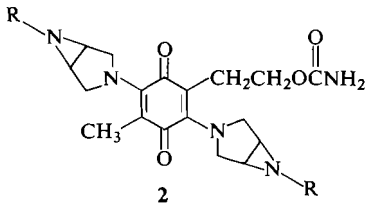

2

(5*h*). We have prepared a group of analogs which possess what are regarded as the essential structural moieties for physiological activity, *i.e.* the bisaziridinopyrrolidinoquinones, **2**.

The rationale is that compounds **2** retain the reactive aziridine and carbamate functions which separately have been shown to alkylate DNA (1*b*, 6). The distance between the two potential aziridine alkylating centers in **2** is comparable with that of the clinically useful 2,5-diaziridinoquinones (1). In addition, the greater conformational flexibility between the alkylating centers of **2** with the concomitant increase in the number of possible alkylating sites on DNA may compensate for the reduction in reactivity resulting from the loss of conjugative enhancement afforded by the indole nucleus in **1**. It has not been demonstrated that the rate of alkylation is significant in determining antitumor activity. The quinone function is retained for two reasons (*i*) so that the structure of analogs **2** should resemble **1** for possible intercalative properties (7) and (*ii*) we have established that mitomycin (3) in common with the structurally related antibiotic streptonigrin (8) degrades DNA employing its oxidative capacity which contributes significantly to their cytotoxic properties. In this connection there is much accumulated evidence that quinone containing substances display marked antibacterial and antitumor activity (5*h*, 9). In the event, analogs of type **2** proved to be quite efficient cross-linking agents which are useful in delineating the geometrical and conformational constraints in cross-linking of DNA.

Functionalized quinones bearing the required carbamate side chain were prepared by the route illustrated in Scheme 1. The required bicyclic aziridines were prepared via 1,3-dipolar azide addition to 3-pyrroline and subsequent photolysis of the triazolines (10) (Scheme 2). The bicyclic aziridines were then coupled to the functionalized quinones using copper acetate as catalyst (11) (Scheme 3).

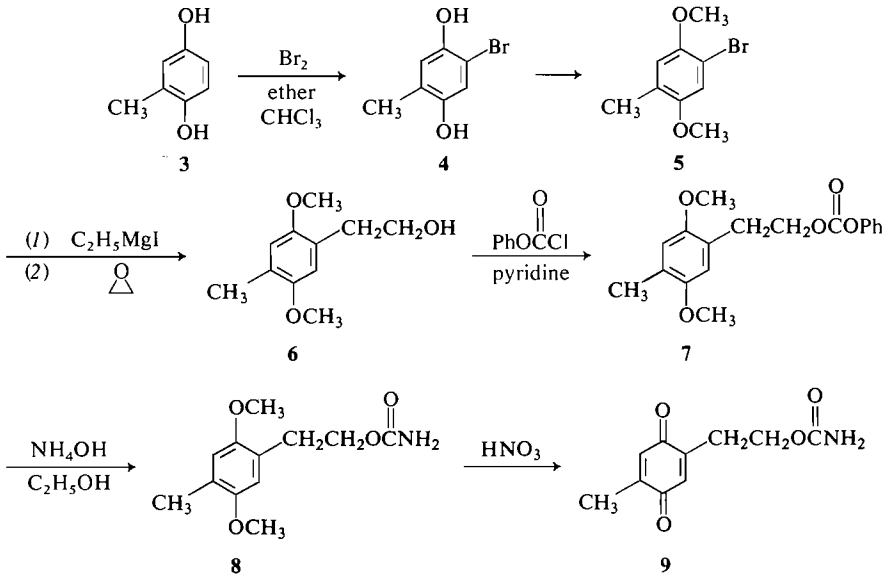

SCHEME 1

Detection of Covalent Cross-linking of DNA by Bicycloaziridinoquinones and Confirmation by S_1-Endonuclease

When the synthetic analogs **13** were incubated in 20% aqueous pyridine with λ-phage DNA (mol. wt. = 31 × 10^6) in an acetate buffer the induction of covalent cross-links was detected as summarized in Table 1. It is evident from the results that covalent cross-linking to the DNA is occurring quite efficiently across the two aziridine positions (compare **13***d* with **13***b*). The span between C_1 and C_{10} of the activated form of mitomycin is *ca.* 4.3 Å compared with the span between the alkylating centers of **13***d* of 10.1–10.8 Å indicating bifunctional agents of quite different dimensions may be accommodated by cross-linked DNA. Secondly, an electron-withdrawing group in R_1 enhances the efficiency of covalent cross-linking.

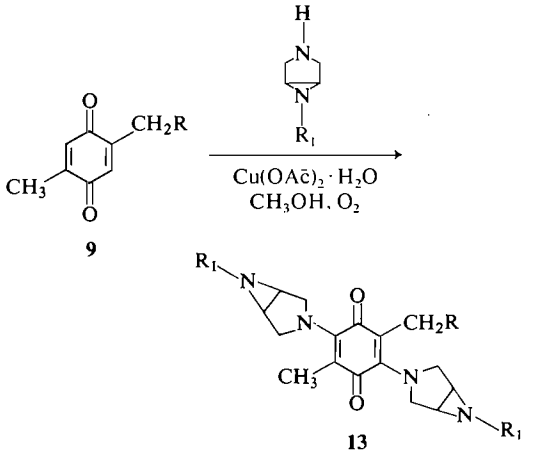

a R = CH_2OCONH_2; R_1 = C_6H_5
b R = CH_2OCONH_2; R_1 = $pBrC_6H_5$
c R = CH_2OCONH_2; R_1 = $pCH_3OC_6H_4$
d R = H; R_1 = $pBrC_6H_4$

SCHEME 3

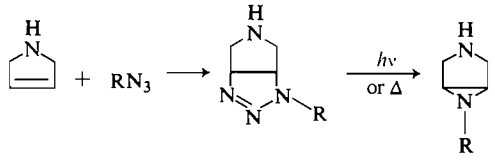

a R = $pBrC_6H_4$
b R = C_6H_5
c R = $pCH_3OC_6H_4$

SCHEME 2

The induction of CLC sequences with compounds **13***d* received independent confirmation by the use of the S_1-endonuclease assay described previously employing *Escherichia coli* DNA (3) (see Table 2).

The substantially lower values for the induction of covalent cross-linking reflects the use of *E. coli* DNA of much lower molecular weight (14.8 × 10^6) than that of λ-DNA (31 × 10^6). Since only one cross-link is re-

Can. J. Chem. Downloaded from www.nrcresearchpress.com by 210.87.254.40 on 09/05/12
For personal use only.

TABLE 1. Induction of covalent cross-links in λ-DNA by mitomycin C analogs

Compound	Concentration (μg/μl)	Max in cross-linking (%)	Time to max in cross-linking (min)
13*d*	2.5	78	240
13*b*	2.5	61	180
13*a*	2.5	38	90
13*c*	2.5	34	240

TABLE 2. Confirmation of covalent cross linking of DNA by mitomycin analogs with S_1-endonuclease assay

	Time (min)			
	10	90	195	270
% cross-linking by CLC assay	16	20	27	25
% cross-linking by S_1-endonuclease assay	9	15	19	16

quired per molecule to be detected by the CLC assay, a given concentration of alkylating agent will induce proportionately fewer cross-links in the *E. coli* DNA. The S_1-endonuclease assay gives lower values because the time required for digestion permits a small amount of spontaneous renaturation of the *E. coli* DNA especially at the neutral p*H* used to be compatible with the enzyme. In addition the ambient temperature used in the enzyme digestion probably permits some slow degradation of double stranded DNA presumably via the natural 'breathing' mechanism which produces transient single strand regions (12). There was no evidence of radical induced single strand cleavage of PM2 circular DNA by **13***d* as has been found for mitomycin C and streptonigrin (3).

Mode of Cytotoxic Action of Structurally Related Aziridinoquinones

Many aziridine containing compounds of quite different structures have useful antitumor properties (1*b*). Thus TEM (**14**, 2,4,6-tris(1-aziridinyl)-*s*-triazine) was the first alkylating agent found suitable for oral administration and is still in clinical use (13). Also included are tetramin (**15**) active against leukemia L1210 (14), TEPA (**16***a*), phosphoramides like tris(1-aziridinyl)phosphine oxide triethylene phosphoramide and thio-TEPA the sulfur analog **16***b* which effect complete regression of Flexner-Jobling rat carcinoma (15), and *N,N'*-octamethylenebis-1-aziridineacetamide (**17**) which is active against Ehrlich ascites carcinoma in mammals (16). Interest in the antitumor properties of the above compounds led to the synthesis and evaluation of many aziridinoquinones from which many effective agents were found including the clinically active benzoquinones 2,5-bis(1-aziridinyl)-3,6-dipropoxy-*p*-benzoquinone (**18***a*), 2,5-bis(1-aziridinyl)-3,6-bis(2-methoxyethoxy)-*p*-benzoquinone (**18***b*) (17), and tris(1-aziridinyl)-*p*-benzoquinone, Trenimon (**19**) (18). In common with other alkylating agents, they exhibit greatest effectiveness against leukemias and other lymphomas such as Hodgkin's disease. The mechanisms by which aziridine containing agents exert their antitumor activity cannot as yet be stated with confidence. Among the suggestions that have been made include (*i*) their alkylating ability (2*a*), (*ii*) their covalent cross-linking of DNA (1, 2), and (*iii*) that hydrogen peroxide or other oxidizing species formed by intracellular redox reactions of quinones are the real cytostatic agent (19). Efforts have been made, without notable success, to correlate antitumor activity with magnetic susceptibility and electron delocalization

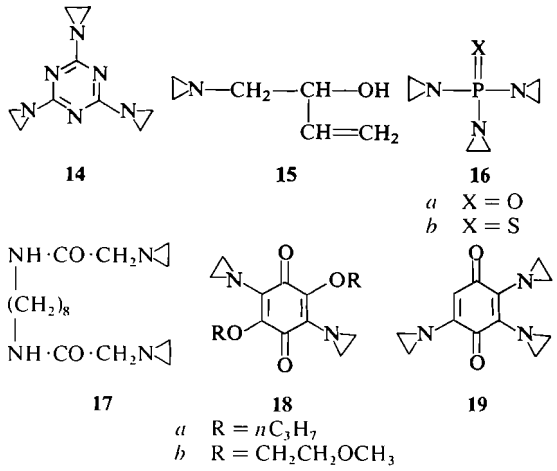

Can. J. Chem. Downloaded from www.nrcresearchpress.com by 210.87.254.40 on 09/05/12
For personal use only.

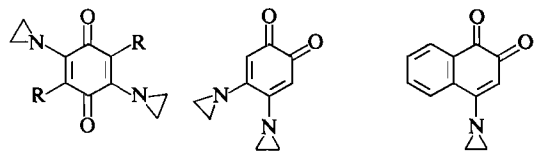

20 21 22

(20), and with partition coefficients between benzene and aqueous phosphate buffer solutions (21).

The convenience of the ethidium fluorescence assay described above offers a means for investigating many of the suggestions that have been made with respect to the modes of action. Three general types of aziridinoquinones were synthesized **20**, **21**, and **22**. The induction of CLC sequences in λ-DNA was established for compounds of the type **20** and **21** in the concentration range 0.05–1.00 μg/μl using the ethidium assay (3, 22) as illustrated in Fig. 2 and Tables 6 and 7 where agents are listed in order of cross-linking ability. Independent confirmation that this assay detects CLC sequenced DNA for this group of bifunctional alkylating agents was obtained by the S_1-endonuclease assay (3) as summarized in Table 3.

A correspondence is again noted for these independent assays bearing in mind the remarks about the S_1 assay made earlier. It may be seen that for 1,4-benzoquinones alkoxy substituents enhance both antineoplastic activity and cross-linking efficiency whereas chloro substituents suppress both these phenomena. A carbamate side chain, unless activated as in the mitomycin C structure does not contribute to increased DNA cross-linking. *Ortho* substituted bifunctional agents are particularly effective in cross-linking and *in vivo* antitumor data are awaited with interest. The monofunctional aziridine *ortho* and *para* substituted naphthoquinones are included as controls and, as expected, do not exhibit cross-linking.

pH Dependence of Covalent Cross-Linking and Alkylation without Depurination of DNA by Aziridinoquinones

As has been observed with the antitumor antibiotic mitomycin C (3), the detection of CLC sequenced DNA is accompanied by a suppression of the before heat denaturation fluorescence reading. A synthetic polynucleotide containing selective radioactive labels in the purine and pyrimidine bases was treated with an aziridinoquinone to the stage where in a control experiment an appreciable decrease in before-heat fluorescence value was observed. The alkylated DNA's were washed with trichloroacetic acid and counted. The results summarized in Table 4 show that no depurination accompanies alkylation or covalent cross-linking as

TABLE 3. Confirmation of covalent cross-linking of DNA by aziridinoquinone (**20**) with S_1-endonuclease assay

	Time (min)		**20** R = CH_3	
	0	45	135	270
% cross-linking by CLC assay	3.4	42.5	65.3	36.8
% cross-linking by S_1-endonuclease*	9.7	26.7	42.0	30.6

*Corrected for double strand digestion and the fact that FU/A260 for single stranded DNA ≈ 1/2 FU/A260 for double stranded DNA.

TABLE 4. Radioactivity assay for monoalkylation of polynucleates with aziridinoquinones with no depurination

Time (h)	^{3}H(FP/TCA channel) counts × 10^{-3}	^{14}C(FP/TCA channel) counts × 10^{-3}	^{3}H/^{14}C
0	11.4	16.0	0.713
2	11.3	17.5	0.646
18	12.6	20.4	0.618
46	14.3	22.4	0.638
65	16.7	23.6	0.708

Can. J. Chem. Downloaded from www.nrcresearchpress.com by 210.87.254.40 on 09/05/12
For personal use only.

Can. J. Chem. Downloaded from www.nrcresearchpress.com by 210.87.254.40 on 09/05/12
For personal use only.

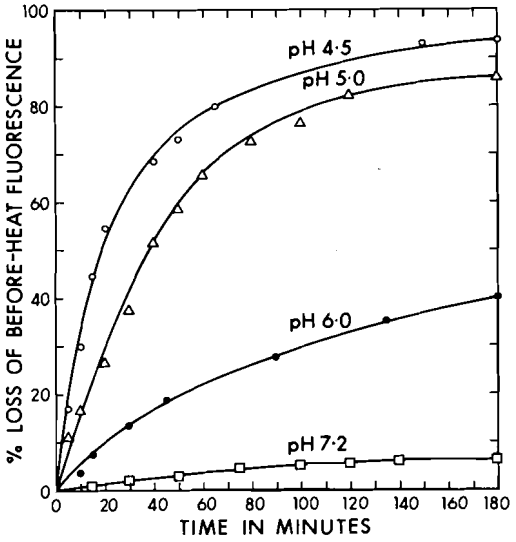

FIG. 1. The p*H* dependence of alkylation of λ-DNA by 2,5-bis(aziridinyl)-3,6-dimethoxy-1,4-benzoquinone at a final concentration of 0.8 μg/μl. Reactions were performed in 1.0 *M* buffered aqueous solutions at 37 °C with a final DNA concentration of 1.40 O.D.$_{260}$ units.

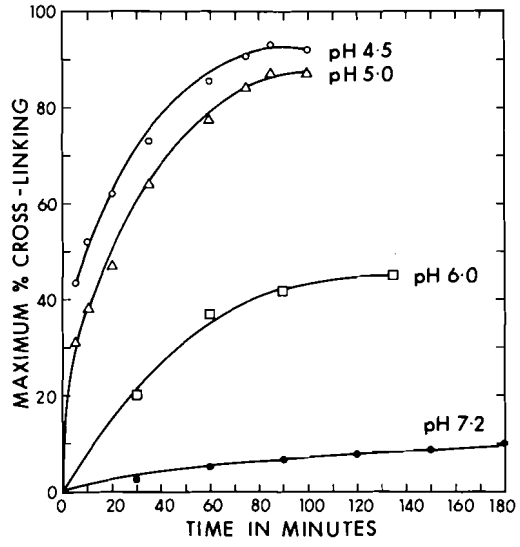

FIG. 2. The p*H* dependence of covalent cross-linking of λ-DNA by 2,5-bis(aziridinyl)-3,6-dimethoxy-1,4-benzoquinone at a final concentration of 0.05 μg/μl. Reactions were carried out in *ca.* 1.0 *M* buffered aqueous solutions at 37 °C with a final DNA concentration of 1.40 O.D.$_{260}$ units.

was found for the antibiotic mitomycin C. This evidence together with the close parallel between cross-linking and suppression of before-heat fluorescence (see Figs. 1 and 2) strongly suggest that the latter phenomenon is due to alkylation of DNA which does not lead to cross-links and is manifest by a destruction of potential ethidium intercalation sites. Several physical explanations are possible for the latter phenomenon, for example steric hindrance to approach of the ethidium or a referee has suggested quenching of the ethidium fluorescence by nearby bound drug or by drug modified bases. We are currently examining the physical cause by employing a range of ethidium analogs but meanwhile the decrease in before-heat fluorescence is used as a measure of single covalent attachment of drugs to DNA.

Freese and Cashel (23) have reported a small amount of induced cross-links in DNA by low p*H* alone. For example at p*H* 4.2 and at 25 °C their sample was cross-linked to the extent of 11% over a 2 h period. In our studies of p*H* dependence (Figs. 1 and 2) strict controls were run with λ-DNA at the corresponding p*H* but in the absence of the substrate. Over the time scale of our experiments no acid induced cross-linking was detected by the CLC assay.

The extent of alkylation as measured by the decrease in before-heat fluorescence showed a much more pronounced p*H* dependence than was found with mitomycin C (see Fig. 1). Similarly the concomitant covalent cross-linking of DNA by the aziridinoquinones shows a much more marked p*H* dependence than reduced mitomycin C (see Fig. 2). This reflects the structural differences; while the aziridine moiety of the activated mitosene **23** receives assistance to opening by conjugative interaction of the indole nitrogen lone pair at any p*H* value (4), the aziridine groups in **24** require protonation to assist alkylation.

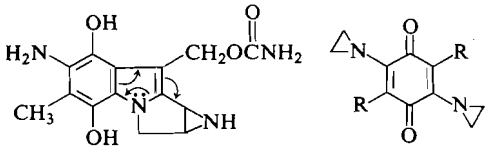

23 **24**

Dependence of Extent of Covalent Cross-linking of DNA's by Aziridinoquinones on (G + C) Content of DNA

No evidence has as yet been presented for any base preference in the alkylation of DNA by aziridinoquinones. Therefore we examined

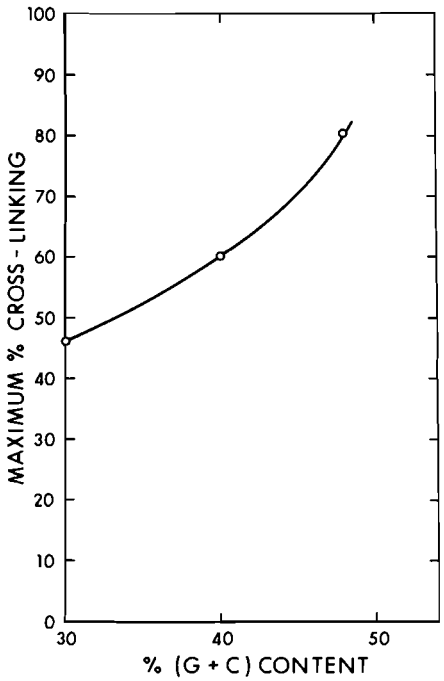

FIG. 3. The dependence of maximum percentage covalent cross-linking of DNA's by 2,5-bis(aziridinyl)-3,6-dimethoxy-1,4-benzoquinone (0.05 μg/μl) on the percentage (G + C) content of the DNA. The DNA's used were, *Clostridium perfringens* (30% G + C), mol. wt. 11.4×10^6; calf thymus (40% G + C), mol. wt. 10.8×10^6; *E. coli* (50% G + C), mol. wt. 14.8×10^6, with final concentrations respectively of 1.40, 1.145, and 1.03 $O.D._{260}$ units.

the interaction of **20** ($R = OCH_3$) with three different natural DNA's of different (G + C) content: *Clostridium perfringens*, 30%; calf thymus, 40%; and *E. coli* 50%. These three DNA's had comparable molecular weights as determined by sedimentation velocity studies and therefore their reactivity towards the aziridinoquinone could be compared directly. It may be seen from Fig. 3 that a direct correlation obtains between maximum extent of covalent cross-linking with higher (G + C) content for a given concentration of the cross-linking agents. Assuming a Poisson's distribution of the links and further that one link is sufficient to permit the spontaneous renaturation of the molecule an estimate of the average number of cross-links per molecule was made, $m = \ln(1/P_0)$ where P_0 is the proportion of the molecules unlinked as 0.62, 0.93, and 1.71 for the three DNA's. These are closely comparable with similar estimates made by Iyer and Szybalski (24) for mitomycin cross-linking. Recent work by Tomasz (25) rules out direct alkylation of the N-7 position of guanine by mitomycin C but does not exclude reaction at O-6 as originally suggested by Szybalski and Iyer (4). This may then apply to the aziridinoquinones.

Kinetics of Acid Assisted Ring Opening of Aziridinoquinones

The rate of acid assisted opening of **20** in 1 *M* sodium acetate buffers in the range p*H* 4.0 to 6.0 in 25% tetrahydrofuran – 75% water was determined spectrophotometrically employing concentrations comparable with those used for DNA cross linking by measuring the rate of appearance of the ring opened species **26** at 380 nm. Since attempts at product isolation at intermediate stages afforded only **20** or **26** it was concluded that the lifetime of **25** was very short under the solvolysis conditions and therefore its equilibrium contribution to the absorbance at 380 nm could be neglected to a first approximation (Scheme 4).

The pseudo unimolecular rate constants at different p*H* values are listed in Table 5. It may be seen that the p*H* dependence of the aziridine opening parallels the rate of covalent cross-linking (Table 5 and Fig. 2) and of alkylation of DNA (Fig. 1). It was shown in an independent experiment that the diacetate **26** in which the aziridine rings were opened did not cross-link DNA. Therefore the strong p*H* dependence of the cross-linking suggests, as expected, that the active species involved directly in covalent bonding to DNA is the intermediate aziridinium ion.

Correlation of Covalent Cross-Linking with Antineoplastic Activity

Having established a convenient procedure for detecting alkylation and covalent cross-linking of various DNA's by aziridinoquinones and other alkylating agents it is encouraging to observe that a fairly good correlation exists between the extent and rate of covalent cross-linking of DNA and antineoplastic activity against leukemia L1210 and several solid tumors (see Table 6). This parameter may prove useful for prescreening antitumor agents for clinical trials. It is recognized that other biological and pharmacological parameters, in addition to DNA covalent cross-linking (*i.e.* drug uptake,

Can. J. Chem. Downloaded from www.nrcresearchpress.com by 210.87.254.40 on 09/05/12
For personal use only.

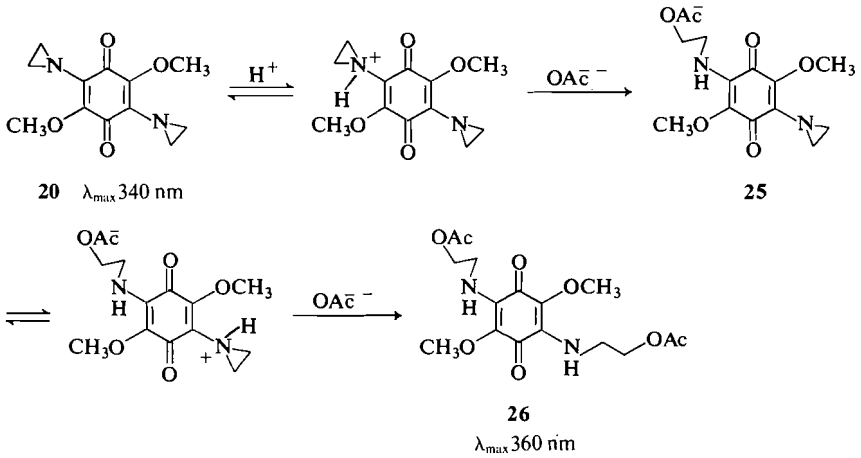

SCHEME 4

TABLE 5. Pseudo unimolecular rate constants for the acid catalyzed ring opening of 2,5-diaziridino-3,6-benzoquinone

p*H*	Rate constant $k \times 10^{-5}$ (s^{-1})
4.5	9.04
5.0	8.35
6.0	2.14
7.2	Too slow to measure
8.7	Too slow to measure

partition, metabolism, and toxicity) contributes to the ultimate effectiveness of cancer inhibitory properties. Table 7 lists covalent cross-linking results for additional aziridinoquinones for which, as yet, no *in vivo* antitumor data is available.

Experimental

Melting points were determined on a Fisher-Johns apparatus and are uncorrected. The i.r. spectra were recorded on a Perkin-Elmer model 421 spectrophotometer and only the principal, sharply defined peaks are reported. The n.m.r. spectra were recorded on Varian A-60 and A-100 analytical spectrometers. The spectra were measured on approximately 10–15% (w/v) solutions usually in $CDCl_3$, with tetramethylsilane as a standard. Line positions are reported in p.p.m. from the reference. Mass spectra were determined on an Associated Electrical Industries MS-9 double focusing high resolution mass spectrometer. The ionization energy, in general, was 70 eV. Peak measurements were made by comparison with perfluorotributylamine at a resolving power of 15000. Kieselgel DF-5 (Camag, Switzerland) and Eastman Kodak precoated sheets were used for thin-layer chromatography. Microanalyses were carried out by Mrs. D. Mahlow of this department. First derivative e.p.r. spectra were measured on a Varian V-2503 spectrometer fitted with a V-4532 dual cavity operating at a nominal frequency of 9.5 GHz. The microwave power incident on the cavity was attenuated to 10 dB below maximum. Hyperfine couplings were measured by comparison with a peroxylamine disulfonate solution in the audio cavity. The triplet spacing of the standard was taken to be 13.0 Oe.

Materials

Ethidium bromide, calf thymus DNA, and α-amylose powder were purchased from Sigma Chemical Co., Sephadex G-100 superfine was from Pharmacia and DEAE cellulose was obtained from Whatman and washed before use.

4-Phenyl-2,3,4,7-tetraazobicyclo[3.3.0]oct-1-ene

A mixture of 6.14 g (60 mmol) of phenylazide and 5.60 g (60 mmol) of 3-pyrroline (75% pure) was set aside in the dark at ambient temperature for 3 weeks. The resulting precipitate was collected, washed with light petroleum, and recrystallized from ethyl acetate – petroleum ether to give **11***b* 6.75 g (57% yield) as a tan solid m.p. 111–112 °C.

Anal. Calcd. for $C_{10}H_{12}N_4$ (mol. wt. 188.1062): C, 63.81; H, 6.43; N, 29.76. Found 188.1072 (mass spectrum): C, 63.80; H, 6.19; N, 29.45.

The i.r. spectrum $\nu_{max}(CHCl_3)$: 3323 (NH); 1590 cm^{-1} (N=N). The n.m.r. spectrum $\delta_{TMS}(CDCl_3)$: 1.43 (s, 1H, NH); 2.68–3.60 (m, 4H, CH_2); 4.32 (dd, 1H, H_1, $J_{15} = 10$ Hz, $J_{18'} = 4$ Hz), 5.15 (dd, 1H, H_5, $J_{56'} = 6$ Hz); 6.80–7.60 (m, 5H, ArH).

*4-(p-Methoxyphenyl)-2,3,4,7-tetraazabicyclo[3.3.0]-oct-1-ene (**11***c*)

This compound was prepared in a similar fashion from 2.2 g (15 mmol) of *p*-methoxyphenylazide and 1.4 g (15 mmol) of 3-pyrroline (75% pure) in 30% yield as a white crystalline solid m.p. 108.5–109 °C.

Anal. Calcd. for $C_{11}H_{14}N_4O$ ($M - N_2$ 190.1106): C, 60.53; H, 6.47; N, 25.67. Found 190.1107 (mass spectrum): C, 60.52; H, 6.42; N, 25.19.

The i.r. spectrum $\nu_{max}(CHCl_3)$: 3305 (NH), 1580 cm^{-1} (N=N). The n.m.r. spectrum $\delta_{TMS}(CDCl_3)$: 1.46 (broad 1H, NH); 2.69–3.62 (m, 4H, CH_2); 3.79 (s, 3H,

Can. J. Chem. Downloaded from www.nrcresearchpress.com by 210.87.254.40 on 09/05/12
For personal use only.

Can. J. Chem. Downloaded from www.nrcresearchpress.com by 210.87.254.40 on 09/05/12
For personal use only.

TABLE 6. Correlation of covalent cross-linking of λ-DNA by bifunctional alkylating agents with antitumor activity against various tumors*

Structure	L1210†		W-256		CA-755		S-180		KB	λ-DNA cross-linking		
	OD	ILS	OD	ILS	OD	TWI	OD	TWI	ED_{50}	Concentration (μg/μl)	Maximum (%)	Time to reach maximum (min)
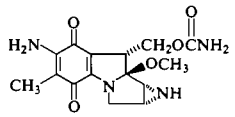 1	1.5	60	1.0	95	1.0	90	3.0	75	0.04	0.04 0.02	100 93	5 5
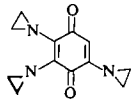	0.1	47	0.1	96	0.04	70	0.13	49	<0.01	0.4 0.04	100 100	2 10
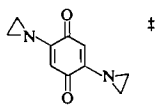 ‡	0.5	26	—	—	0.25	60	1.25	39	<1.0	0.01	92	10
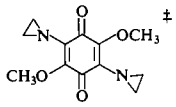 ‡	2.0	36	2.0	95	—	—	—	—	—	0.4 0.04	92 82	60 120
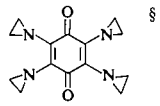 §	0.01	39	—	—	0.05	80	0.13	65	4.9	0.4 0.04	90 85	25 100

Can. J. Chem. Downloaded from www.nrcresearchpress.com by 210.87.254.40 on 09/05/12
For personal use only.

TABLE 6 (*Concluded*)

Structure	L1210† OD	L1210† ILS	W-256 OD	W-256 ILS	CA-755 OD	CA-755 TWI	S-180 OD	S-180 TWI	KB ED_{50}	λ-DNA cross-linking Concentration (μg/μl)	λ-DNA cross-linking Maximum (%)	λ-DNA cross-linking Time to reach maximum (min)
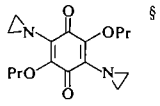 §	4	50	1.0	95	3.0	78	5.0	5.0	0.07	0.4 0.04	85.5 79	30 60
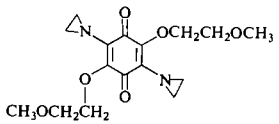	2.0	7.0	0.98	84	2.0	80	3.0	63	—	0.4	55	255
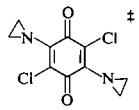 ‡	11, 22	0	—	—	11	50	25	35	—	0.4	18	120
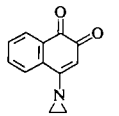	100	Toxic	—	—	—	—	—	—	—	0.4	0	—

*Abbreviations used: OD optimal dose, ILS increased life span of test animals; TWI percentage tumor weight inhibition; ED_{50} effective dose for 50% survival.
†L1210, leukemia 1210; W-256, Walker carcinoma 256; CA-755, carcinoma 755; S-180, Erlich ascites (9).
‡Shows antibacterial activity against *Staphylococcus aureus*, *E. coli*, and *Streptococcus faecalis*.
§Shows marked carcinostatic activity against Jensen sarcoma.

TABLE 7. Covalent cross-linking of λ-DNA by aziridinoquinones

Structure	Concentration	λ-DNA cross-linking	
		Maximum (%)	Time to reach maximum
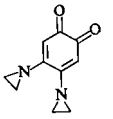	0.4	85.5	30
	0.04	80	105
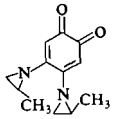	0.4	78.4	120
	0.04	32.3	45
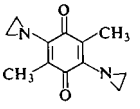	0.4	59	60
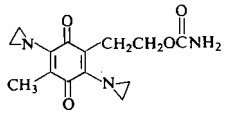	0.4	38	30
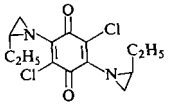	0.24	24	270
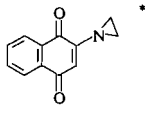	0.4	0	—

*Shows substantial monoalkylation.

OCH_3); 4.35 (dd, 1H, H_1, $J_{15} = 10$ Hz, $J_{18'} = 4$ Hz); 5.15 (dd, 1H, H_5, $J_{56'} = 6.5$ Hz); 6.80–7.33 (m, 4H, ArH).

6-Phenyl-3,6-diazabicyclo[3.1.0]hexane

A solution of 2.60 g (14 mmol) of 4-phenyl-2,3,4,7-tetraazabicyclo[3.3.0]oct-1-ene in 280 ml of tetrahydrofuran under nitrogen was irradiated with a Hanovia high pressure mercury lamp (200 W) fitted with a Pyrex filter with stirring and cooling for 6 h. The solvent was removed *in vacuo* and the residue extracted with hot ether (6 × 100 ml). The ether extracts were concentrated giving **12***b* as a red brown oil, 1.95 g (87% yield).

Mol. Wt. Calcd. for $C_{10}H_{12}N_2$: 160.1001. Found (mass spectrum): 160.1007.

The n.m.r. spectrum $\delta_{TMS}(CDCl_3)$: 1.65–2.07 (broad 1H, NH), 2.66 (s, 2H, methine); 2.75 (AB quartet, 4H, CH_2, $J = 12.5$ Hz); 6.65–7.34 (m, 5H, ArH). The absorption spectrum: 239 (log ε 4.75), 277 nm (log ε 3.90).

6-(p-Methoxyphenyl)-3,6-diazabicyclo[3.1.0]hexane

A solution of 0.906 g (4 mmol) of 4-(*p*-methoxyphenyl)-2,3,4,7-tetraazabicyclo[3.3.0]oct-1-ene in 120 ml of tetrahydrofuran under nitrogen was irradiated as described in the above procedure. The solvent was evaporated and the residue treated with 100 ml of ether. The resulting precipitate was filtered. The filtrate was evaporated and the residue crystallized from benzene – light petroleum affording **12***c* 0.742 g (98% yield) as an off-white solid, m.p. 36–38 °C.

Anal. Calcd. for $C_{11}H_{14}N_2O$ (mol. wt. 190.1106); C, 69.45; H, 7.42; N, 14.72. Found 190.1105 (mass spectrum): C, 68.90; H, 7.57; N, 14.67.

The n.m.r. spectrum $\delta_{TMS}((CD_3)_2CO)$: 2.79 (s, 2H, methine); 3.70 (s, 3H, OCH_3) 2.82 (AB quartet, 4H, methylenes, $J = 12.5$ Hz, 6.41–7.08 (m, 4H, ArH). The absorption spectrum (CH_3CN): 238 (log ε 4.21), 295 nm (log ε 3.30).

2,5-Bis-3'[-6'-p-bromophenyl-3',6'-diazabicyclo[3.1.0]-hexane]3-(β-carbamoyloxyethyl)-6-methyl-1,4-benzoquinone

A solution of 0.400 g (2.0 mmol) of freshly crushed cupric acetate monohydrate and 1.800 g (7.5 mmol) of 6-(*p*-bromophenyl)-3,6-diazabicyclo[3.1.0]hexane (23)

Can. J. Chem. Downloaded from www.nrcresearchpress.com by 210.87.254.40 on 09/05/12
For personal use only.

Can. J. Chem. Downloaded from www.nrcresearchpress.com by 210.87.254.40 on 09/05/12
For personal use only.

in 40 ml of methanol was purged with oxygen. While bubbling oxygen through the stirred solution, a solution of 0.313 g (1.5 mmol) of 2-(β-carbamoyloxyethyl)-5-methyl-1,4-benzoquinone (24) in 75 ml of methanol was added. The reaction mixture was stirred at room temperature for 2 days, then was concentrated to *ca.* 5 ml and subjected to chromatography on a neutral alumina (Woelm) column eluting with methanol. The dark red band was collected and concentrated and the residue was crystallized from ethyl acetate – light petroleum to afford **13***b* as a purple solid, m.p. 111–113 °C, which slowly turned brown on exposure to light and air.

Anal. Calcd. for $C_{30}H_{29}Br_2N_5O_4$ (mol. wt. 683): N, 10.25; Br, 23.39. Found (683, ebullioscopic): N, 9.89; Br, 23.05.

The i.r. spectrum ν_{max}($CHCl_3$): 3544, 3434 (NH_2), 1720 (carbamate C=O), 1585 cm^{-1} (quinone C=O). The absorption spectrum (CH_3CN): 248 (log ε 4.26), 282 (log ε 3.67), 396 (log ε 3.09), 503 nm (log ε 2.57). The e.p.r. spectrum (generated by treating a 1.2×10^{-2} *M* methanolic solution of **13***b* with sodium methoxide in air), developed a signal of maximum intensity in 30 min which persisted for 2½ h consisting of 10 lines h.f.s. 1.4–1.8 Oe of spectrum width 12.3 Oe.

2,5-Bis-3′-[6′-p-bromophenyl-3′,6′-diazabicyclo[3.1.0]-hexane]-3,6′dimethyl-1,4-benzoquinone

A similar reaction between 0.300 g (1.5 mmol) of freshly crushed cupric acetate monohydrate and 1.800 g (7.5 mmol) of 6-(*p*-bromophenyl)-3,6-diazabicyclo[3.1.0]-hexane (26) with 0.204 g (1.5 mmol) of 2,5-dimethyl-1,4-benzoquinone in methanol afforded **13***d* 0.511 g (56% yield) as a brownish purple solid, m.p. 107–110 °C, which slowly changed to a brown solid on exposure to light and air.

Anal. Calcd. for $C_{28}H_{24}Br_2N_4O_2$: N, 9.18, Br, 26.18. Found: N, 9.06; Br, 27.89.

The i.r. spectrum ν_{max}($CHCl_3$): 1588 cm^{-1} (C=O). The absorption spectrum (CH_3CN): 250 (log ε 4.70), 285 (log ε 3.88), 328 (log ε 3.63), 395 (log ε 3.33), 501 nm (log ε 2.76). The e.p.r. spectrum (generated by treating a 1.2×10^{-2} *M* methanolic solution of **13***d* with sodium methoxide in air), developed a signal of maximum intensity within 30 min which persisted for 2½ h and consisted of 11 lines, h.f.s. 1.4–1.7 Oe of total spectrum width 14.2 Oe.

2,5-Bis-3′-[6′-phenyl-3′,6′-diazabicyclo[3.2.0]hexane]-3-(β-carbamoyloxyethyl)-6-methyl-1,4-benzoquinone

A similar reaction between 0.400 g (2.0 mmol) of cupric acetate and 1.60 g (10.0 mmol) of 6-phenyl-3,6-diazabicyclo[3.1.0]hexane with 0.418 g (2.0 mmol) of 2-(β-carbamoyloxyethyl)-5-methyl-1,4-benzoquinone(24) in methanol afforded **13***a* as a red-brown solid from ethyl acetate – light petroleum, 0.892 g (85% yield), m.p. 80–83 °C, which slowly turned brown on exposure to air and owing to its instability was characterized spectroscopically.

The i.r. spectrum ν_{max}($CHCl_3$): 3546, 3426 (NH_2); 1725 (carbamate C=O); 1595 cm^{-1} (quinone C=O). The absorption spectrum (CH_3CN): 241 (log ε 4.58), 282 (log ε 3.92), 394 (log ε 3.22), 503 nm (log ε 2.72). The e.p.r. spectrum (generated from **13***a* as described above) developed a signal due to the semiquinone of maximum intensity in 30 min which persisted for 2½ h and consisted of 10 lines h.f.s. 1.5–1.8 Oe of total spectrum width 12.5 Oe.

2,5-Bis-3′-[6′-p-methoxyphenyl-3′,6′-diazabicyclo[3.1.0]-hexane]-3-(β-carbamoyloxyethyl)-6-methyl-1,4-benzoquinone

A similar reaction of 0.400 (2.0 mmol) of cupric acetate and 1.900 g (10 mmol) of 6-*p*-methoxyphenyl-3,6-diazabicyclo[3.1.0]hexane in 50 ml of methanol with 0.418 g (2.0 mmol) of 2-(β-carbamoyloxyethyl)-5-methyl-1,4-benzoquinone (27) afforded **13***c* 0.199 g (17% yield) as a purple solid from ethyl acetate, m.p. 98–103 °C which slowly turned brown on exposure to light and air.

Anal. Calcd. for $C_{32}H_{35}N_5O_6$: C, 65.63; H, 6.02; N, 11.96. Found: C, 65.11; H, 6.41; N, 9.99.

The i.r. spectrum ν_{max}($CHCl_3$): 3520 and 3418 (NH_2); 2826 (OCH_3), 1723 (carbamate C=O), 1568 cm^{-1} (quinone C=O). The absorption spectrum (CH_3CN): 242 (log ε 4.52), 290 (log ε 3.97), 397 (log ε 3.47), 506 nm (log ε 2.94). The e.p.r. spectrum (generated from **13***c* as described above) developed a signal of the semiquinone within 30 min which persisted for over 2 h and consisted of an unresolved singlet of spectrum width 5.8 Oe.

Synthesis of Aziridinoquinones

Most of the aziridinoquinones studied were prepared by published procedures (17). The general method is illustrated by the following example.

Preparation of Tetramethoxy-1,4-benzoquinone

A slurry of 24.5 g (0.1 mol) of chloranil in 75 ml of methanol was added to a solution of 9.8 g (0.42 mol) of sodium in 250 ml of methanol. During addition the temperature of the reaction mixture was kept at 15–25 °C by means of external cooling. The reaction mixture was then heated on a steam bath for 6 h. The cooled reaction mixture deposited bright orange crystals which were collected, washed with cold water, and taken up in dichloromethane. The solution was decolorized with charcoal, filtered and the solvent removed *in vacuo* to give bright orange crystals of the product, 16.7 g (73.2% yield), m.p. 133–134 °C (lit. (28) m.p. 135–136 °C).

Reaction of Tetramethoxy-1,4-benzoquinone with Aziridine

To a suspension of 1.05 g (5 mmol) of tetramethoxy-1,4-benzoquinone in 30 ml of methanol was added a solution of 0.280 g (65 mmol) of aziridine in 10 ml of methanol. The reaction mixture was stirred at room temperature for 2 days. The resulting reddish-brown 2,5-bis(aziridinyl)-3,6-dimethoxy-1,4-benzoquinone was collected by filtration, 0.875 g (79% yield), m.p. 189–190 °C (lit. (17*a*) m.p. 193–194.5 °C). The n.m.r. spectrum: δ_{TMS}($CDCl_3$): 2.28 (s, 8H, aziridinyl protons) and 3.92 (s, 6H, OCH_3).

New compounds prepared using these procedures include:—

(i) 2,5-Bis(2-methylaziridinyl)-3,6-dimethyl-1,4-benzoquinone in 63% yield, m.p. 147–150 °C.

Anal. Calcd. for $C_{14}H_{18}N_2O_2$: C, 68.29, H, 7.31, N, 11.38. Found: C, 68.21, H, 7.61; N, 11.72.

(ii) 2,5-Bis(2-ethylaziridinyl)-3,6-dimethyl-1,4-benzoquinone in 50% yield, m.p. 125–126 °C.

Anal. Calcd. for $C_{16}H_{22}N_2O_2$: C, 70.44; H, 8.03; N, 10.08. Found: C, 70.04; H, 8.54; N, 10.38.

Can. J. Chem. Downloaded from www.nrcresearchpress.com by 210.87.254.40 on 09/05/12
For personal use only.

(iii) 4,5-Bis(2-methylaziridinyl)-1,2-benzoquinone in 47% yield, m.p. 135–138 °C.

Anal. Calcd. for $C_{12}H_{14}N_2O_2$: C, 66.05; H, 6.42; N, 12.85. Found: C, 65.85; H, 6.51; N, 13.01.

Fluorescence Assay for Detecting CLC Sequences and Monoalkylation

The general procedure employing a G. K. Turner and associates model 430 spectrofluorometer has been described previously. The assay mixture was prepared by mixing 2 ml of a 1 *M* K_2HPO_4–KOH buffer (at p*H* 12.0) with 0.2 ml of a 0.2 *M* solution of EDTA disodium salt (buffered at p*H* 8 with 2 *M* K_3PO_4) and with 0.05 ml of a 1 mg/ml solution of ethidium bromide in water. The resulting mixture was made up to 100 ml with distilled water and was covered with aluminum foil to protect it from the light. The instrument was blanked using 2 ml of the above solution. The cross-linking assays were carried out as follows.

Bicycloaziridinobenzoquinones

The cross-linking agents were added as 5 μg/μl solutions in 40% pyridine – 60% water. DNA was added as an aqueous solution. Reactions were buffered to p*H* 4.5 with 1 *M* sodium acetate – acetic acid buffer. Cross-linking reactions were carried out on a 60 μl scale. The reaction solutions were incubated at 37 °C and had concentrations of 1.06 $O.D._{260}$ units of λ-DNA, 0.05 *M* of buffer, 2.5 μg/μl of cross-linking agent and 20% pyridine; 10 μl aliquots were removed at timed intervals and analyzed for the extent of cross-linking by CLC assay described previously (3). A control reaction mixture prepared exactly as above but containing no cross-linking agent was run with each experiment. In no case was there evidence for acid induced covalent cross-linking.

Bisaziridinoquinones

A 10 μl aliquot of the cross-linking reaction mixture (*ca.* 5 μg/μl of alkylating agent in 25% tetrahydrofuran – 75% water, 1 *M* sodium acetate buffer and DNA) was diluted in 2 ml of the solution. Similarly a 10 μl aliquot was withdrawn from a reaction mixture containing no alkylating agent (control) and was diluted in 2 ml of the assay solution. The solutions were analyzed by the CLC assay described previously (3). A typical run is given in complete form for 2,5-bis(aziridino)-3,6-dimethoxy-1,4-benzoquinone at p*H* 5.0 with a concentration of 0.8 μg/μl.

Time (min)	Before-heat fluorescence*	After-heat fluorescence	% Cross-linking
0	70	3.5	0
5	64	12.5	19.5
10	60	17	28.3
20	52	23	44.2
30	45	24	53
40	35	20	57
50	30	18	63
60	25	17	67
80	20	15	75
100	15	12	80
120	13	11	82
150	10	8	80
180	9	6	67

*Control fluorescence = 70 constant throughout experiment.

Covalent Cross-Linking of DNA's with Different (G + C) Content with 2,5-Bis(aziridino)-3,6-dimethoxy-1,4-benzoquinone

The CLC assays were performed at p*H* 4.5 and 37 °C as described above using the following solutions of natural DNA's.

Clostridium perfringens DNA (30% G + C)

The assay mixture was prepared using 7 μl of the DNA stock solution ($O.D._{260}$ = 20), 5 μl of 1 *M* sodium acetate buffer p*H* 4.5, 8 μl of water, and 80 μl of a solution of **20** (R = OCH_3) in 25% aqueous tetrahydrofuran (final concentration of agent 0.05 μg/μl and final concentration of DNA was 1.40 $O.D._{260}$). The control was similar but lacked **20** (R = OCH_3).

Calf Thymus DNA (40% G + C)

The assay mixture was prepared using 30 μl of the DNA stock solution ($O.D._{260}$ = 4.58), 5 μl of 1 *M* sodium acetate buffer p*H* 4.5, 5 μl of water, and 80 μl of the solution of agent **20** (R = OCH_3) (final concentration of agent was 0.05 μg/μl and of DNA 1.145 $O.D._{260}$). Control as above.

E. coli DNA (50% G + C)

The assay mixture was prepared using 25 μl of the DNA stock solution ($O.D._{260}$, 1.03), 5 μl of 1 *M* sodium acetate p*H* 4.5, 5 μl of water, and 40 μl of a 25% aqueous solution of **20** (R = OCH_3) (final concentration of agent 0.05 μg/μl, and final concentration of DNA was 1.03 $O.D._{260}$). Control as above.

Assay for Covalent Cross-Linking of E. coli DNA using S_1-Endonuclease

E. coli DNA which had been covalently cross-linked with the bifunctional alkylating agent was dialyzed overnight at 40 °C *vs.* 10 m*M* potassium phosphate at p*H* 11.5, 0.1 m*M* EDTA, neutralized with 0.5 *M* tris hydrochloride p*H* 7.5 (~25 m*M*), and heat denatured (5 min at 95 °C then ice treatment). To 80 μl were added 20 μl 5 × S_1 buffer p*H* 4.5 (final p*H* about 4.6). After removal of the first aliquot, 2 μl of purified S_1-endonuclease (610 U/mg, 1.28 mg/ml) was added and the mixture incubated at 45 °C. Aliquots were removed and examined with ethidium bromide solution p*H* 8.0 and read as described previously. Heat denatured and native *E. coli* DNA's were incubated as controls.

Assay for Depurination of Radioactively Labelled Polynucleates Treated with 2,5-Bis(aziridino)-3,6-dimethoxy-1,4-benzoquinone

Poly dG.dC(^{14}CG).d(^{3}HC) 0.339 A_{260}/ml was incubated at 37 °C in 50 m*M* sodium buffer p*H* 5.0 with 360 μg/ml of 2,5-bis(aziridino)-3,6-dimethoxy-1,4-benzoquinone in 18% aqueous tetrahydrofuran. At intervals duplicate samples were removed, placed on Whatman filter discs, washed with 5% trichloroacetic acid, then twice with ethanol, dried, and counted. The results summarized in Table 4 show no loss of purine or pyrimidine bases accompany treatment of the DNA by the aziridinoquinone.

Kinetic Studies of the Rate of Acid Catalyzed Ring Opening of Aziridinoquinones

A 1.04 × 10^{-3} *M* solution of the 2,5-bis(aziridinyl)-3,6-dimethoxy-1,4-benzoquinone was prepared in 25% THF – 75% H_2O at room temperature and transferred in 160 μl aliquots to reaction tubes and then 10 μl of water, 20 μl of λ-DNA, and 10 μl of 1 *M* sodium acetate

Can. J. Chem. Downloaded from www.nrcresearchpress.com by 210.87.254.40 on 09/05/12
For personal use only.

TABLE 8. Absorption spectra

Wavelength (nm)	Absorbance **20**	Absorbance **26**
330	0.29	0.20
340	0.31	0.29
350	0.275	0.375
360	0.20	0.43
370	0.135	0.39
380	0.08	0.270
400	0.03	0.055

TABLE 9. Rate of acid assisted ring opening of 2,5-bis(1-aziridinyl)-3,6-dimethoxy-1,4-benzoquinone

Time (min)	Optical density	$k \times 10^5$ (s^{-1})
0	0.08	—
30	0.11	9.15
60	0.135	9.04
90	0.154	8.97
120	0.169	9.08
150	0.185	9.03
210	0.211	8.75
270	0.225	9.04
330	0.240	9.14
420	0.251	9.13

buffer (of the appropriate p*H*) were added. The tubes were sealed with Parafilm and placed in a constant temperature bath. Several reaction tubes were withdrawn at convenient intervals, diluted with 25% THF – 75% H_2O to 5 ml and the concentration of 2,5-bis(2-acetoxyethylamino)-3,6-dimethoxy-1,4-benzoquinone was established by its absorbance at 380 nm. It was demonstrated that both the aziridinoquinone and the 2-acetoxyethylaminoquinone obeyed the Beer–Lambert Law in the optical density range of 0.02–0.4. Allowance was made for residual absorption at 380 nm due to the aziridine (see Table 8).

The reaction followed good first-order (pseudo unimolecular) kinetics for the formation of the diacetate the time dependence of which is shown in full for the run at p*H* 4.5 (see Table 9).

This research was supported by grants to J. W. L. from the National Cancer Institute of Canada, the National Research Council of Canada, and by the Department of Chemistry, University of Alberta. We thank Dr. A. Hogg and Mr. R. Swindlehurst for the mass and n.m.r. spectra, and Mrs. Talat Akhtar for the preparation of many intermediates.

1. J. A. MONTGOMERY, T. P. JOHNSTON, and Y. F. SHEALY. *In* Drugs for neoplastic diseases. *In* Medicinal Chemistry. Pt. 1. *Edited by* A. Burger. Wiley-Interscience, New York. 1970. (*a*) p. 680; (*b*) p. 695.
2. (*a*) W. C. J. Ross. Biological alkylating agents. Butterworths, London. 1962; (*b*) G. P. WHEELER. Cancer Res. **22**, 651 (1962).
3. J. W. LOWN, A. BEGLEITER, A. R. MORGAN, and D. JOHNSON. Can. J. Biochem. In press.
4. (*a*) W. SZYBALSKI and V. N. IYER. Fed. Proc. **23**, 946 (1964). (*b*) W. SZYBALSKI and V. N. IYER. *In* Antibiotics I – mechanism of action. *Edited by* D. Gottlieb and P. D. Shaw. Springer-Verlag, New York. 1967. p. 211.
5. (*a*) W. A. REMERS and M. J. WEISS. J. Med. Chem. **11**, 737 (1968) and papers cited therein. (*b*) R. W. FRANCK *et al.* J. Org. Chem. **38**, 3487 (1973); **39**, 3739 (1974) and references therein. (*c*) T. HIRATA, Y. YAMADA, and M. MATSUI. Tetrahedron Lett. 4107 (1969). (*d*) T. TAKADA and S. OHKI. Chem. Pharm. Bull. (Jpn.), **19**, 977 (1971). (*e*) T. TAKADA, S. KUNUGI, and S. OHKI. Chem. Pharm. Bull (Jpn.), **19**, 982 (1971). (*f*) P. GERMERAAD and H. W. MOORE. J. Org. Chem. **39**, 774 (1974). (*g*) T. TAKADA and M. AKIBA. Chem. Pharm. Bull (Jpn.), **20**, 1785 (1972). (*h*) S. KINOSHITA, K. UZU, K. NAKANO, M. SHIMIZU, T. TAKAHASHI, and M. MATSUI. J. Med. Chem. **14**, 103 (1971); **14**, 109 (1971).
6. (*a*) S. V. BHIDE. Chem. Biol. Interactions, **8**, 19 (1974). (*b*) G. PRODI, P. ROCCHI, and S. GRILLI. Cancer. Res. **30**, 2887 (1970). (*c*) T. A. LAWSON and A. W. POUND. Pathology, **3**, 223 (1971). (*d*) T. A. LAWSON and A. W. POUND. Chem. Biol. Interactions, **4**, 329 (1970).
7. (*a*) E. F. GALE, E. CUNDLIFFE, P. E. REYNOLDS, M. H. RICHMOND, and M. J. WARING. The molecular basis of antibiotic action. J. Wiley, New York. 1972. p. 214. (*b*) L. S. LERMAN. J. Mol. Biol. **3**, 18 (1961).
8. (*a*) P. HOCHSTEIN, J. LASZLO, and D. MILLER. Biochem. Biophys. Res. Commun. **19**, 289 (1965). (*b*) J. R. WHITE and H. L. WHITE. Mol. Pharm. **4**, 579 (1968). (*c*) R. CONE, S. K. HASAN, J. W. LOWN, and A. R. MORGAN. In press.
9. (*a*) Proc. Symp. Quinones as Anticancer Agents. Cancer. Chemother. Rep. **4**, (1974). (*b*) E. F. ELSLAGER. *In* Medicinal Chemistry. 2nd ed. *Edited by* A. Burger. Interscience Publishers, New York. 1960. pp. 851–876. (*c*) P. TRUITT, F. MAHON, O. PLATAS, R. L. HALL, and T. EL ERIS. J. Org. Chem. **25**, 962 (1960).
10. (*a*) S. OIDA, H. KUWANO, Y. OHASHI, and E. OHKI. Chem. Pharm. Bull (Jpn.), **18**, 2478 (1970). (*b*) P. SCHIENER. Tetrahedron, **24**, 2757 (1968).
11. A. H. CROSBY and R. E. LUTZ. J. Am. Chem. Soc. **78**, 1233 (1956).
12. B. MCCONNELL and P. H. VON HIPPEL. J. Mol. Biol. **50**, 297 (1970).
13. (*a*) S. M. BUCKLEY, C. C. STOCK, M. L. CROSSLEY, and C. P. RHOADS. Cancer Res. **10**, 207 (1950). (*b*) J. H. BURCHENAL, M. L. CROSSLEY, C. C. STOCK, and C. P. RHOADS. Arch. Biochem. Biophys. **26**, 321 (1950).
14. (*a*) H. OETTEL. Angew. Chem. **71**, 222 (1959). (*b*) J. M. VENDETTI, A. GOLDIN, and I. KLINE. Cancer Chemother. Rep. **4**, 73 (1961). (*c*) W. SCHULZE. Deut. Med. Wochschr. **82**, 1465 (1957); (*d*) F. R. WHITE. Cancer Chemother. Rep. **4**, 52 (1959).
15. C. HEIDELBURGER and M. E. BAUMANN. Cancer Res. **17**, 277 (1957).
16. W. A. SKINNER and J. SCHOLLER. Cancer Chemother. Rep. **51**, 205 (1967).
17. (*a*) S. PEDERSEN, W. GAUSS, and E. URBSCHAT. Angew. Chem. **67**, 217 (1955). (*b*) W. GAUSS and S.

PEDERSEN. Angew. Chem. **69**, 252 (1957). (*c*) G. DOMAGK. Ann. N.Y. Acad. Sci. **68**, 1197 (1958).
18. W. GAUSS and G. DOMAGK. German Patent 1,044,816 (1958). Chem. Abstr. **55**, 11435f (1961).
19. (*a*) H. BERG and G. HORN. Naturwissenschaften, **50**, 356 (1963). (*b*) G. HORN. Chem. Zvesti, **18**, 363 (1964); Chem. Abstr. **61**, 15947.
20. (*a*) G. MAYR and G. C. RABOTTI. Experientia, **13**, 252 (1957). (*b*) E. M. MCCRAY and H. F. SCHOOF. J. Econ. Entomol. **60**, 60 (1967).
21. A. H. SOLOWAY *et al.* J. Med. Pharm. Chem. **5**, 1371 (1962).
22. (*a*) A. R. MORGAN and V. PAETKAU. Can. J. Biochem. **50**, 210 (1972). (*b*) A. R. MORGAN and D. E. PULLEYBANK. Biochim. Biophys. Res. Commun. **61**, 346 (1974). (*c*) M. COULTER, W. FLINTOFF, V. PAETKAU, D. PULLEYBANK, and A. R. MORGAN. Biochemistry, **13**, 1603 (1974).
23. E. FREESE and M. CASHEL. Biochim. Biophys. Acta, **91**, 67 (1964).
24. V. N. IYER and W. SZYBALSKI. Proc. Natl. Acad. Sci. **50**, 355 (1963).
25. M. TOMASZ. Biochim. Biophys. Acta, **213**, 288 (1970).
26. J. W. LOWN and A. BEGLEITER. Can. J. Chem. **52**, 2331 (1974).
27. H. NAKAO, M. ARAKAWA, T. NAKAMURA, and M. FUKASHIMA. Chem. Pharm. Bull. (Jpn.), **20**, 1962, 1968 (1972).
28. B. EISTERT and G. BOCK. Ber. **92**, 1239 (1959).

Can. J. Chem. Downloaded from www.nrcresearchpress.com by 210.87.254.40 on 09/05/12
For personal use only.

General-base-catalyzed Proton Exchange in Glycocyamidiniom Ions: A Comparison of Activation by Protonation and by Alkylation

ROSS STEWART AND R. SRINIVASAN

Department of Chemistry, University of British Columbia, Vancouver, British Columbia V6T 1W5

Received April 28, 1975

ROSS STEWART and R. SRINIVASAN. Can. J. Chem. **53**, 2906 (1975).

The rates of exchange of methylene protons in seven glycocyamidinium ions in formate and chloroacetate buffers were measured in D_2O by means of proton magnetic resonance spectroscopy. When protonation and methylation of glycocyamidines occur at the same site the methylated products react faster than the protonated products by factors of 1.8–1.9. Replacing ring protons in glycocyamidinium ions by methyl groups causes small increases in the methylene exchange rate whereas corresponding substitution at the exocyclic nitrogen causes small rate decreases. It is concluded that in this reaction a quaternary ion ZR^+ can serve as a satisfactory model for the analogous conjugate acid ZH^+.

ROSS STEWART et R. SRINIVASAN. Can. J. Chem. **53**, 2906 (1975).

Faisant appel à la résonance magnétique nucléaire du proton, on a mesuré, dans des tampons de formiate et de chloracétate dans D_2O, les vitesses d'échange des deux protons du méthylène de sept ions glycocyamidinium. Lorsque la protonation et la méthylation des glycocyamidines se produisent au même niveau, les produits méthylés réagissent environ 1.8–1.9 fois plus rapidement que les produits protonés. Lorsqu'on remplace les protons du cycle d'ions glycocyamidinium par des groupes méthyles, il y a une légère augmentation dans la vitesse d'échange au niveau du méthylène; par ailleurs une substitution correspondante au niveau de l'azote exocyclique conduit à une faible diminution. On en conclut que dans cette réaction, un ion quaternaire ZR^+ peut servir comme modèle satisfaisant pour l'acide conjugué analogue ZH^+.

[Traduit par le journal]

The rate-controlling step in general-acid-catalyzed hydrogen exchange reactions can be either protonation of the substrate by general acids or abstraction of a proton from the conjugate acid of the substrate by general bases (1). Many heterocyclic compounds undergo exchange by the latter route and the reasonable assumption has sometimes been made that a quaternary salt ZR^+ can serve as a model for the corresponding conjugate acid ZH^+, and that the rate of proton abstraction from ZR^+ by a base will be equal to that for the conjugate acid. Thus, Coburn *et al.* (2) used the agreement between the directly measured rate of hydrogen exchange at the 2-position of 3-ethylthiazolium iodide, **1**, and the value calculated for protonated thiazole, **2**, in aqueous buffers, to support the idea that the exchange in thiazole occurs through **2** and not through the tautomeric *C*-protonated form **3**.

Other examples in heterocyclic chemistry of the use of quaternary salts as surrogates for conjugate acids are to be found in the work of Olofson and co-workers (3) on isothiazole exchange, Cox (4) on iodination of acetylpyridines, and Katritzky and co-workers (5) on exchange and substitution reactions of several heteroaromatic systems.

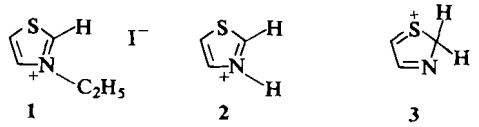

1 **2** **3**

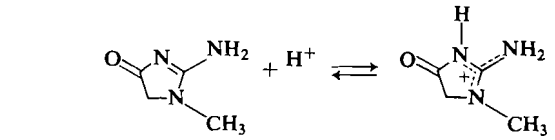

[1] **4** **5**

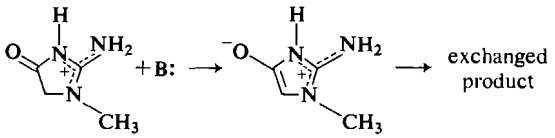

We have previously studied the exchange of the methylene protons in creatinine, **4**, catalyzed by general acids and general bases. The general-acid route was rationalized in terms of eq. 1 and rates were obtained for the rate-controlling step, abstraction of a proton from position 5 of **5** by various bases (6). (The ring is numbered starting with the alkylated nitrogen atom.)

Can. J. Chem. Downloaded from www.nrcresearchpress.com by 210.87.254.5 on 09/05/12
For personal use only.

Can. J. Chem. Downloaded from www.nrcresearchpress.com by 210.87.254.5 on 09/05/12
For personal use only.

We now compare these rates with those for proton abstraction from the corresponding *N*-methylated quaternary salt **6**.

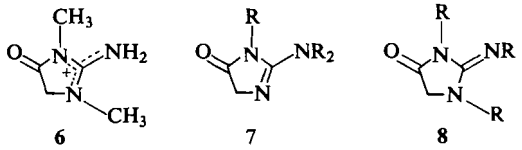

6 **7** **8**

The glycocyamidine system (7, 8), to which creatinine belongs, also includes compounds of type **7** and **8** and since these can give rise to cations having the same charge distribution as **5** and **6** we have also examined the reactivity of several of the protonated and alkylated derivatives of these compounds. The bases used in this work were formate ion and chloroacetate ion and the rates of proton abstraction from the methylene group of the various glycocyamidinium ions were determined in buffered D_2O by means of n.m.r. spectroscopy, as before (6).

Experimental

Acidity measurements were made on buffer solutions containing the dissolved substrate using a Radiometer model 26 p*H* instrument with an aqueous glass–calomel assembly. The electrode was calibrated with standard aqueous buffers; the p*D* values were obtained from the relationship p*D* = 'p*H* reading' + 0.40 (9).

Solvents and Reagents

The deuterated solvents, D_2O (99.7 atom% D) and aqueous solutions of NaOD were obtained from Merck, Sharp and Dohme of Canada Limited. Prior to use D_2O was heated to boiling and allowed to cool with a slow stream of nitrogen bubbling through it.

Chloroacetic acid and formic acid were purified by crystallization from benzene – petroleum ether and by distillation, respectively.

1-Methyl-2-amino-2-imidazolin-4-one (creatinine) (**4**) was purchased from Matheson, Coleman and Bell and purified by crystallization from aqueous ethanol.

2-Amino-2-imidazolin-4-one (9) hydrochloride was prepared as described previously (10), m.p. 208–210 °C dec. (lit. (7) m.p. 211–212 °C dec.).

1-Methyl-2-amino-2-imidazolin-5-one (**10**) was obtained by methylation of 2-amino-2-imidazolin-4-one (**9**) with iodomethane followed by neutralization of the resulting hydriodide salt, m.p. 228–231 °C dec. (lit. (8) 233–235 °C dec.).

1,3-Dimethyl-2-iminoimidazolidin-4-one (**11**) hydriodide was obtained by methylating creatinine (**4**) with iodomethane (8), m.p. 213–215 °C dec. (lit. (8) m.p. 213–215.5 °C dec.).

1,3-Dimethyl-2-methyliminoimidazolidin-4-one (**13**) hydriodide was obtained as described previously (8) and identified by conversion to its conjugate base (**13**), m.p. 72–74 °C (lit. (8) m.p. 71–73 °C).

1-Methyl-2-methylamino-2-imidazolin-4-one (**12**) was synthesized by isomerization of **11** (8), m.p. 197–199 °C (lit. (8) m.p. 196.5–198.5 °C).

2-Dimethylamino-2-imidazolin-4-one (**14**) hydriodide was prepared as described previously (8) and converted to its conjugate base (**14**) for purposes of identification, m.p. 228–232 °C dec. (lit. (8) m.p. 230–232 °C dec.).

Rate Measurements

The exchange of methylene protons was followed to about 70% completion at 34.5 °C (the probe temperature) with a Varian T-60 MHz spectrometer at a sweep width of 100 Hz, using the procedure outlined previously (6). The ionic strength was kept constant at 1.2 by addition of sodium chloride. The exchange rate measurements were made by dissolving the substrate in the conjugate acid form (**9′**, **10′**, **11′**, and **13′**) or in the free base form (**4**, **12**, and **14**). The concentration of the substrate was kept at about 0.32 *M*.

The exchange of methylene protons was followed by integrating the methylene proton signal periodically, the signal of non-exchanging *N*-Me protons serving as reference. If the n.m.r. tube was kept in the probe during the reaction with all the conditions held constant the intensity of the reference signal was found to be practically invariant. Consequently, the exchange of **9′** was followed by integrating only the methylene signal. The acidity of the medium did not change during the course of the reaction.

The exchange followed first-order kinetics. The observed first-order exchange constant, k_{obs}, was obtained by plotting the data according to equation 2.

$$[2] \qquad \ln \frac{R_t}{S_t} = k_{obs}t$$

R_t = average area of *N*-methyl peak(s) and S_t = average area of methylene peak both at time t. With **9′**, R_t was arbitrarily assigned a constant value. The reproducibility was better than ±10%.

Results and Discussion

On protonation or alkylation all three kinds of glycocyamidines represented by **4**, **7**, and **8** would be expected to give resonance-stabilized guanidinium cations, of which **6** is an example. Kenyon and Rowley (8) and others (6) have shown this to be so in several instances and, for protonation at least, is probably always the case.

The second-order exchange constant, k_2, for abstraction of proton from glycocyamidinium ion by carboxylate is obtained from k_{obs} (Equation 3) (6).

$$[3] \qquad k_{obs} = k_2\left(\frac{[D^+]}{[D^+] + K'_{SD^+}}\right)[A^-]$$

K'_{SD^+} = the equilibrium constant for dissociation of glycocyamidinium ion at 34.5 °C in D_2O, ionic strength 1.2 and $[A^-]$ = the concentration of carboxylate anion. Since the required pK'_{SD^+} values are available for creatininium ion (**4′**) only (pK'_{SD^+} = 5.41) (6) the difference between the pK'_{SD^+} and thermodynamic pK_{SD^+} value (water, 25 °C) (8) for cations **9′**, **12′**, and **14′** is assumed to be the same as that for creatininium ion (**4′**).

Can. J. Chem. Downloaded from www.nrcresearchpress.com by 210.87.254.5 on 09/05/12
For personal use only.

Rate measurements in formate and chloroacetate buffers were made at pD 4.3 and 3.8 respectively and at these pD values K'_{SD^+} is sufficiently smaller than $[D^+]$ that significant errors in k_2 are not introduced by the use of this assumption. The ratio, $[D^+]/[D^+] + K'_{SD^+}$, is taken to be unity for compounds **10′**, **11′**, and **13′**. For each of these $[D^+] \gg K'_{SD^+}$ (8). The pK_{DA} values for formate and chloroacetate were calculated from the general relation $pK_{DA} = 1.02\ pK_{HA} + 0.41$ (11).

It is found that under experimental conditions the exchange is almost completely accounted for by the loss of proton by glycocyamidinium ion to the carboxylate and self-catalysis is negligible as shown by studies of exchange rates at different concentrations of carboxylate (Table 1).

Scheme 1 shows the structures of the seven cations whose exchange rates in formate and chloroacetate buffers are given in Table 2 together with the structures of the neutral compounds that can give rise to them through protonation or methylation. Also listed are the average relative rates, based on the cation **9′**, calculated by averaging the relative rates found with formate and chloroacetate ions.

A number of interesting comparisons can be made using the results shown in Scheme 1.

1. When protonation and methylation occur at the same site, as they do for compounds **9**, **4**, and **12**, the alkylated products react faster than the protonated products by factors of 1.81, 1.73, and 1.89. (Compare cations **9′** and **10′**, **4′** and **11′**, and **12′** and **13′**.)

2. The effect of replacing the proton at position 1 in **9′** by a methyl group is to increase the rate by a factor of 1.68 (compare **9′** and **4′**) and the effect of a similar substitution at position 3 is 1.81 (compare **9′** and **10′**). The similarity in these two quantities suggests that any steric effects that might have been expected to be present because of the proximity of the N-1 alkyl group and the reactive methylene at C-5 are small.

3. The effects of alkyl substitution at the ring nitrogens is cumulative. The 1,3-dimethyl cation **11′** reacts 2.91 times as fast as the unsubstituted cation **9′**, which is close to the expected value of 3.04 (the product of the rates of the two monomethyl cations, **4′** and **10′**). Similarly the rate of 2.00 for the trimethyl cation **13′** is close to the expected value of 1.92 (the product of the rates of the monomethyl cation **10′** and the dimethyl cation **12′**).

4. Methyl substitution at the exocyclic nitrogen lowers the reactivity of the cation. The effects are smaller and less regular than those found

TABLE 1. Exchange kinetics for creatininium ion in formate buffer; pD = 4.27; T = 34.5 °C; μ = 1.2; [creatininium ion] = 0.32 M

[Buffer] (M)	$[HCO_2^-]$ (M)	$k_{obs} \times 10^3$ (min^{-1})	$k_2 \times 10^{2*}$ ($M^{-1}\ min^{-1}$)
0.3	0.162	2.28	1.52
0.6	0.324	3.99	1.32
0.9	0.486	6.22	1.38
1.2	0.648	8.42	1.40

*Calculated using equation 3.

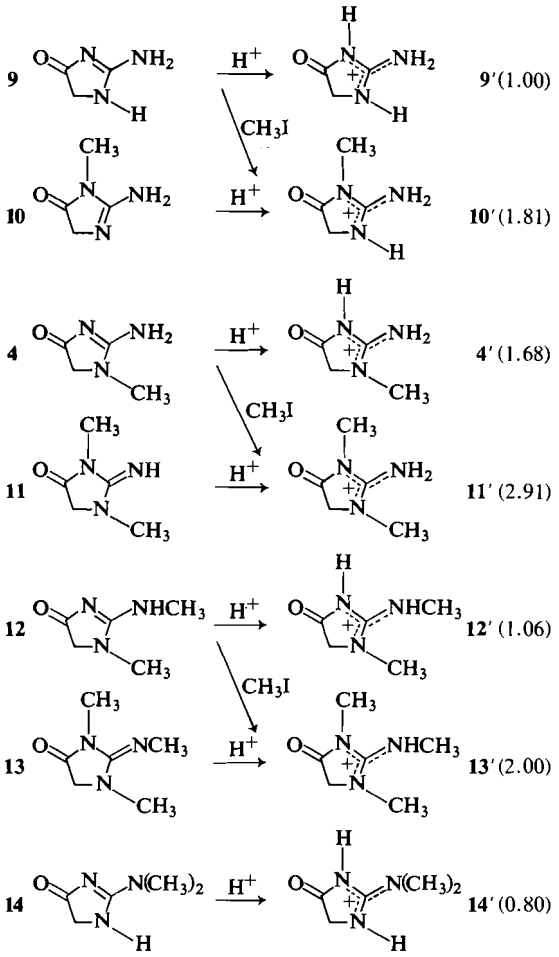

SCHEME 1. The relationship between various glycocyamidines and their protonated or methylated derivatives. The relative rates shown in parentheses are averages of the values shown in Table 2 for the reactivities of the cations with formate ion and chloroacetate ion.

TABLE 2. Specific catalytic constants for exchange of glycocyamidinium ions in D_2O catalyzed by formate and chloroacetate ions. $T = 34.5$ °C; $\mu = 1.2$

	Formate ion		Chloroacetate ion	
Cation*	$k_2 \times 10^3$ (M^{-1} min^{-1})	Relative rate	$k_2 \times 10^3$ (M^{-1} min^{-1})	Relative rate
9′	8.42	1.00	2.28	1.00
4′	14.0	1.66	3.88	1.70
10′	15.3	1.82	4.11	1.80
11′	23.9	2.84	6.80	2.98
12′	9.00	1.07	2.40	1.05
13′	16.1	1.91	4.74	2.08
14′	6.53	0.78	1.89	0.83

*Numbers correspond to structures in Scheme 1.

for substitution at the ring nitrogens but in all cases they are negative. (Compare cations **4′** and **12′**, **11′** and **13′**, and **9′** and **14′**.)

The modest deactivating effect on the rate of proton abstraction from the ring methylene group that results from substituting methyl for hydrogen in the exocyclic amino group of glycocyamidinium ions is not unreasonable. The cations would be expected to be stabilized by the inductive effect of methyl and, since the intermediate that is formed by proton loss is formally neutral, methylation should decrease the rate, as is observed. The intermediate, and the transition state leading thereto, is highly polar (see below) and the fact that a large amount of positive charge remains in the guanidinium portion of the system is doubtless the cause of the modest effects referred to in point 4, above .Two other systems that undergo analogous reactions, 4-acetylpyridinium ions (4) and 1,4,6-trimethylpyrimidonium ions[1] also show rate decreases when methyl replaces hydrogen.

In terms of the discussion above, the uniform rate increases that accompany methyl substitution at *ring* nitrogens are anomalous. A possible explanation for this effect follows. The formally neutral intermediate formed by proton loss from the methylene group of glycocyamidinium ions is, in fact, mesoionic, as shown in **15**.

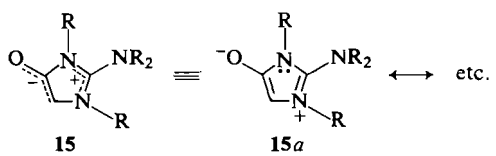

[1]R. Srinivasan and R. Stewart. Unpublished results.

The aromatic character of the intermediate is apparent from a scrutiny of the canonical form **15*a***, which is a substituted imidazolium ion. The aromaticity of such species depends on the availability of an unshared pair of electrons on nitrogen and it is interesting to speculate that the inductive effect of methyl groups attached to the ring nitrogen atoms stabilizes the intermediate by this means. Though the effects are small they are regular and, regardless of the validity or otherwise of the above rationalization, the system provides an interesting example of alkyl substitution stabilizing neutral compounds to a greater degree than cations.

The results presented herein are in agreement with the generally held notion that quaternization activates a substrate towards proton loss elsewhere in the system to roughly the same degree as does protonation. The span of reactivities among the seven cations studied is a factor of less than four, with substitution of methyl for hydrogen increasing the reactivity of the ion in some cases and decreasing it in others.

The financial support of the National Research Council of Canada is gratefully acknowledged.

1. (a) M. L. BENDER. Mechanisms of homogeneous catalysis from protons to proteins. Wiley-Interscience, New York. 1971. Chapt. 4; (b) R. P. BELL. The proton in chemistry. 2nd ed. Cornell University Press, Ithaca, New York 1973. Chapt. 9; (c) R. STEWART and J. M. MCANDLESS. J. Chem. Soc. Perkin Trans.2, 376 (1972); (d) J. TOULLEC and J. E. DUBOIS. J. Am. Chem. Soc. **96**, 3524 (1974).
2. R. A. COBURN, J. M. LANDESBERG, D. S. KEMP, and R. A. OLOFSON. Tetrahedron. **26**, 685 (1970).
3. (a) R. A. OLOFSON and J. M. LANDESBERG. J. Am. Chem. Soc. **88**, 4263 (1966); (b) R. A. OLOFSON, J. M.

Can. J. Chem. Downloaded from www.nrcresearchpress.com by 210.87.254.5 on 09/05/12
For personal use only.

LANDESBERG, K. N. HOUK, and J. S. MICHELMAN. J. Am. Chem. Soc. **88**, 4265 (1966).
4. B. G. COX. J. Am. Chem. Soc. **96**, 6823 (1974).
5. (a) A. R. KATRITZKY and C. D. JOHNSON. Angew. Chem. Int. Ed. Engl. **6**, 608 (1967); (b) C. D. JOHNSON, A. R. KATRITZKY, B. J. RIDGEWELL, and M. VINEY. J. Chem. Soc. B, 1204 (1967); (c) U. BRESSEL, A. R. KATRITZKY, and J. R. LEA. J. Chem. Soc. B, 4 (1971); (d) A. G. BURTON, P. P. FORSYTHE, C. D. JOHNSON, and A. R. KATRITZKY. J. Chem. Soc. B, 2365 (1971); (e) A. R. KATRITZKY, M. KINGSLAND, and O. S. TEE. J. Chem. Soc. B, 1484 (1968).
6. R. SRINIVASAN and R. STEWART. Can. J. Chem. **53**, 224 (1975).
7. K. MATSUMOTO and H. RAPOPORT. J. Org. Chem. **33**, 552 (1968).
8. G. L. KENYON and G. L. ROWLEY. J. Am. Chem. Soc. **93**, 5552 (1971).
9. (a) P. K. GLASOE and F. A. LONG. J. Phys. Chem. **64**, 188 (1960); (b) E. MIKKELSEN and S. O. NIELSEN. J. Phys. Chem. **64**, 632 (1960); (c) P. SALOMAA, L. SCHALEGER, and F. A. LONG. J. Am. Chem. Soc. **86**, 1 (1964).
10. I. S. BENGELSDORF. J. Am. Chem. Soc. **75**, 3138 (1953).
11. A. C. MCDOUGALL and F. A. LONG. J. Phys. Chem. **66**, 429 (1962).

Can. J. Chem. Downloaded from www.nrcresearchpress.com by 210.87.254.5 on 09/05/12
For personal use only.

Analyse en résonance magnétique nucléaire du ^1H et du ^{13}C de dérivés azuléniques extraits de l'*Eriocephalae punctulactus*

J.-R. LLINAS, D. ROARD ET M. DERBESY

Ecole Supérieure de Chimie de Marseille, Centre de Saint-Jérôme, Rue Henri Poincaré - 13397 Marseille Cedex 4

ET

E.-J. VINCENT

Laboratoire de Chimie Organique Physique, Université de Droit, d'Economie et des Sciences, Rue Henri Poincaré - 13397 Marseille Cedex 4

Reçu le 1 Avril 1975

J.-R. LLINAS, D. ROARD, M. DERBESY et E.-J. VINCENT. Can. J. Chem. **53**, 2911 (1975).

L'analyse de l'essence d'*Eriocephalae punctulactus* a permis d'isoler deux composés azuléniques. Leur structure a été déterminée sans ambiguité par spectroscopie r.m.n. comme étant celle du diméthyl-1,4 azulène et du diméthyl-1,4 éthyl-7 azulène. La r.m.n. du carbone-13 a confirmé ces structures et nous a permis de mettre en évidence sur ces composés ainsi que sur le guaiazulène (diméthyl-1,4 isopropyl-7 azulène) des effets de substitution du noyau azulénique.

J.-R. LLINAS, D. ROARD, M. DERBESY, and E.-J. VINCENT. Can. J. Chem. **53**, 2911 (1975).

Two azulene compounds were isolated from the extract of *Eriocephalae punctulactus*; their structures were determined unambiguously by n.m.r. as those of 1,4-dimethylazulene and 1,4-dimethyl-7-ethylazulene. These structures were confirmed by ^{13}C n.m.r. The effects of substitution in the azulene ring on the ^{13}C n.m.r. spectra were demonstrated using these compounds as well as guaiazulene (1,4-dimethyl-7-isopropylazulene).

[Journal translation]

Dans le cadre de l'analyse effectuée sur l'essence d'*Eriocephalae punctulactus* (encore appelée "plante bleue") en vue de déterminer ses principaux constituants (11), nous avons isolé et étudié deux composés présentant les charactéristiques principales des dérivés azuléniques (coloration bleue, absorption à 596–603 nm). La séparation de ces produits nécessite un fractionnement par distillation sur colonne bande tournante suivi d'une chromatographie sur colonne complété enfin par chromatographie préparative sur couche mince (11). Par spectroscopie d'absorption dans le visible, les concentrations dans l'essence ont été évaluées à 0.07% pour le dérivé **1** et 0.32% pour le dérivé **2**. L'analyse en résonance magnétique nucléaire du proton et du carbone-13 que nous allons décrire, nous a permis d'identifier ces deux produits comme étant le diméthyl-1,4 éthyl-7 azulène (dérivé **1**) et le diméthyl-1,4 azulène (dérivé **2**).

Partie expérimentale

Les spectres de résonance ^1H ont été enregistrés sur spectromètre R 32 opérant en mode locké à la fréquence de 90 MHz, en solution dans CCl_4 (15% v/v) et en présence de TMS pris comme référence interne. La température de la sonde est de 30 °C. Les déplacements chimiques ont été évalués avec une précision de ± 0.01 p.p.m. et les constantes de couplage à 0.1 Hz près, par simulation de spectre sur ordinateur HP 2100 à l'aide d'une version adaptée du programme LAOCOON III (9). Dans certains cas, la précision des mesures a été limitée par la présence de nombreux couplages à longue distance inférieurs à 0.2 Hz. Les mises en évidence d'effet Overhauser nucléaire ont été réalisées sur des solutions identiques préalablement dégazées. Les exaltations d'intensités observées ont été rapportées aux intensités maximales des signaux obtenus soit en l'absence d'irradiation, soit en présence d'une irradiation de même puissance à une fréquence nettement décalée par rapport à la résonance du pic irradié. Les valeurs obtenues ont été évaluées sur une dizaine d'intégrations.

Les déplacements chimiques du carbone-13 ont été obtenus à partir des spectres totalement découplés par bruit. Nous avons opéré sur un spectromètre NV-14 équipé d'une unité à transformée de FOURIER (8192 points) opérant à la fréquence de 15.087 MHz. Les composés ont été étudiés en solution dans $CDCl_3$, en présence de TMS choisi comme référence interne. Le spectre ^{13}C du dérivé **2** est rapporté dans la figure 4.

Analyse des spectres de resonance du ^1H

Les résultats sont consignés dans le tableau 1. L'analyse des spectres des dérivés **1** et **2** a été réalisée à partir des attributions relatives aux spectres de l'azulène (1, 5, 13) et de certains de ses dérivés (1, 2, 12, 13) et les dernières am-

Can. J. Chem. Downloaded from www.nrcresearchpress.com by 210.87.254.6 on 09/05/12
For personal use only.

Can. J. Chem. Downloaded from www.nrcresearchpress.com by 210.87.254.6 on 09/05/12
For personal use only.

TABLEAU 1. Spectres ^1H*

Composé	R	R′	R″	ν_1	ν_2	ν_3	ν_4	ν_5	ν_6	ν_7	ν_8	ν_R	$\nu_{R'}$	$\nu_{R''}$	J_{23}	J_{56}	J_{67}	J_{78}	J_{68}	J_{58}
Azulène†	H	H	H	7.24	7.75	7.24	8.12	6.89	7.34	6.89	8.12	—	—	—	3.9	—	—	—	—	—
Di-Me-1,4 azulène (dérivé 2)	Me	Me	H	—	7.59	7.19	—	6.89	7.30	6.89	8.08	2.63	2.81	—	3.7	10.0	10.0	9.7	1.1	0.6
Di-Me-1,4 Et-7 azulène (dérivé 1)	Me	Me	Et	—	7.61	7.21	—	6.94	7.36	—	8.14	2.64	2.80	1.33 et 2.82	3.6	10.5	—	—	1.9	0.2
Di-Me-1,4 *i*Pr-7 azulène‡	Me	Me	*i*Pr	—	7.61	7.20	—	6.94	7.36	—	8.19	2.65	2.80	1.34 et 3.06	3.8	10.7	—	—	1.9	0.3

*Les déplacements chimiques sont obtenus à ±0.01 p.p.m. et les couplages à ±0.1 Hz.
†Réference 1.
‡Valeurs obtenues selon l'attribution réalisée dans réf. 1.

Can. J. Chem. Downloaded from www.nrcresearchpress.com by 210.87.254.6 on 09/05/12
For personal use only.

biguités ont été levées à l'aide de manipulations de double irradiation.

Dérivé 1

Le spectre obtenu est très voisin de celui du guaiazulène (diméthyl-1,4 éthyl-7 azulène):

Région aromatique

On observe le même type de superposition de deux figures de type AB et ABX. Dans le système AB, le couplage J_{AB} (3.6 Hz) est caractéristique des couplages $^3J_{HH}$ mesurés sur les cycles à cinq chainons du noyau azulénique alors que dans le système ABX, le couplage J_{AB} obtenu (10.5 Hz), est lui caractéristique du cycle à sept chainons (1, 3).

Région aliphatique

Deux groupements méthyles résonnent aux mêmes fréquences que les homologues du guaiazulène, un groupement éthyle se substituant dans le spectre au groupement isopropyle. Le spectre ayant été totalement analysé, l'attribution de chacun des signaux a été faite en plusieurs étapes.

(*i*) L'irradiation du méthyle résonnant à 2.64 p.p.m. provoque, par suppression du couplage à distance, un affinement important du doublet à champ fort du système AB. Le méthyle irradié étant fixé en position 1, le proton observé est en position 2 sur le cycle à cinq chainons.

(*ii*) Le déplacement chimique très important du proton X du système ABX est caractéristique des positions 4 ou 8 (1). D'autre part, le couplage J_{AX} observé (1.9 Hz) est comparable au couplage $^4J_{H_6H_8}$ du guaiazulène (2.0 Hz). Il permet d'attribuer au proton A la position 6 et par conséquent, au proton B la position 5 si X est en 8, ou la position 7 si X est en 4.

(*iii*) L'ambiguité précédente a pu être levée en mettant en évidence la proximité du proton X et du groupement méthyle en position 1, à l'aide de l'effet Overhauser nucléaire. Une irradiation de faible puissance appliquée à 2.64 p.p.m. se traduit par une augmentation moyenne d'intensité de 12% au niveau du proton X. Cette valeur, bien qu'éloignée de l'effet n.O.e. maximum, est toutefois suffisante pour conclure à la proximité de ces groupements ce qui permet d'affecter la position 8 au proton X et donc aux protons A et B les positions respectives 6 et 5 (*cf.* Fig. 1).

(*iv*) L'attribution de la position 4 au second groupement méthyle repose sur la valeur très

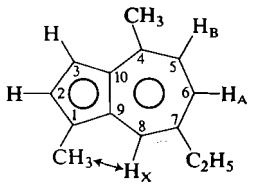

FIG. 1. Diméthyl-1,4 ethyl-7 azulène (dérivé **1**).

élevée de son déplacement chimique (2.80 p.p.m.), valeur comparable à celle observée pour le guaiazulène (2.73 p.p.m.) et pour le triméthyl-4,6,8 azulène (2.98 p.p.m.) (4). Cet effet de déblindage s'explique essentiellement par une densité électronique réduite en position 4 et 8 (4, 1, 5).

Il en résulte que le groupement éthyle restant est fixé en position 7. Ces dernières attributions seront confirmées par l'analyse des effets de substitution observés en r.m.n. du ^{13}C. La structure ainsi déterminée est celle du chamazulène (diméthyl-1,4 éthyl-7 azulène).

Dérivé 2

La partie aliphatique du spectre du dérivé **2** fait uniquement apparaître deux groupements méthyles résonant aux mêmes fréquences que ceux du chamazulène et guaiazulène. Les six protons aromatiques constituent un massif complexe qui peut être analysé en deux figures superposées (*cf.* Fig. 2): (*a*) un sous-spectre de type AB: le couplage J_{AB} observé (3.8 Hz) permet de caractériser deux protons vicinaux du cycle à cinq chainons, un groupement méthyle étant donc substitué en position 1 sur

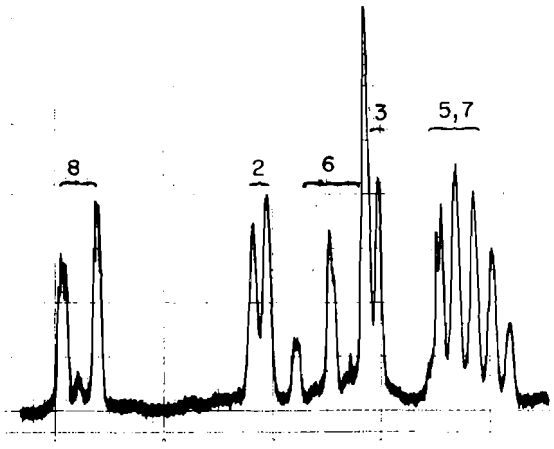

FIG. 2. Etalement de la partie aromatique du spectre ^1H du dérivé **2**.

Can. J. Chem. Downloaded from www.nrcresearchpress.com by 210.87.254.6 on 09/05/12
For personal use only.

TABLEAU 2. Déplacement chimique du ^{13}C*

Composé	R	R′	R″	C_1	C_2	C_3	C_4	C_5	C_6	C_7	C_8	C_9	C_{10}	R	R′	R″	R″
Azulène†	H	H	H	118.1	137.1	118.1	136.5	122.7	137.1	122.7	136.5	140.3	140.3	—	—	—	—
Di-Me-1,4 azulène (dérivé 2)	CH_3	CH_3	H	126.5	136.3	114.3	146.1	125.7	136.3	120.3	133.8	136.0 ou 136.8		12.8	14.3	—	—
Di-Me-1,4 Et-7 azulène (dérivé 1)	CH_3	CH_3	C_2H_5	125.3	136.5	113.1	144.4	125.2	136.5	135.9	134.9	137.7 ou 139.1		12.8	24.1	34.0	17.4
Di-Me-1,4 *i*Pr-7 azulène	CH_3	CH_3	iC_3H_7	125.2	136.3	113.0	144.2	125.2	134.9	139.9	133.2	137.5 ou 136.5		12.9	23.9	38.3	24.8

*Erreur sur les déplacements chimiques: ±0.1 p.p.m.
†Attribution réalisée par Lauterbur (4).

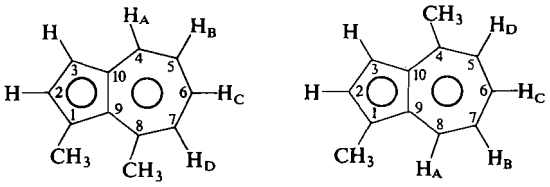

FIG. 3. Diméthyl-1,4 azulène (dérivé **2**).

le cycle. L'irradiation du groupement méthyle à 2.63 p.p.m. permet de mettre en évidence un couplage à distance entre ce méthyle et le proton à champ fort du système AB; ce groupement méthyle a été ainsi attribué à la position 1, et les positions 2 et 3, aux protons A et B. (*b*) Un sous-spectre ABCD pour lequel une analyse au second ordre nous a donné les couplages suivants:

$$J_{AB} = J_{BC} = 10.0 \text{ Hz}$$

$$J_{CD} = 9.7 \text{ Hz}$$

Ces couplages ne peuvent être que des couplages vicinaux $^3J_{HH}$ entre protons fixés sur le cycle à sept chainons. Deux structures restent alors possibles **2***a* et **2***b* (Fig. 3).

Cette dernière ambiguité a été levée par la mise en évidence d'un effet Overhauser nucléaire significatif entre le méthyle en position 1 et le proton A, le plus déblindé du système ABCD. Lorsqu'on irradie faiblement le groupement méthyle à 2.63 p.p.m., l'augmentation moyenne d'intensité du signal du proton A est de 15%, mesurée sur plusieurs intégrations. Cet effet n.O.e. traduit la proximité des deux espèces en présence; nous avons donc affecté la position 8 au proton A et les positions 7, 6 et 5 aux protons B, C et D.

Le dérivé **2** est donc identifié comme étant le diméthyl-1,4 azulène. L'analyse de certaines bandes d'absorption caractéristiques en spectroscopie u.v. est en accord avec les observations déjà réalisées sur le diméthyl-1,4 azulène et le diméthyl-1,4 éthyl-7 azulène (10). Toutefois, afin de confirmer la position des divers substituants fixés sur le noyau azulènique, nous avons étudié les mêmes molécules en r.m.n. du carbone-13.

Analyse des spectres de resonance du ^{13}C

Les résultats de l'analyse des spectres ^{13}C de l'azulène, du guaiazulène et des dérivés A et B sont consignés dans le tableau 2. L'identification des positions des substituants (sites 1, 4 et 7) a été réalisée à partir du spectre de l'azulène (4, 5,

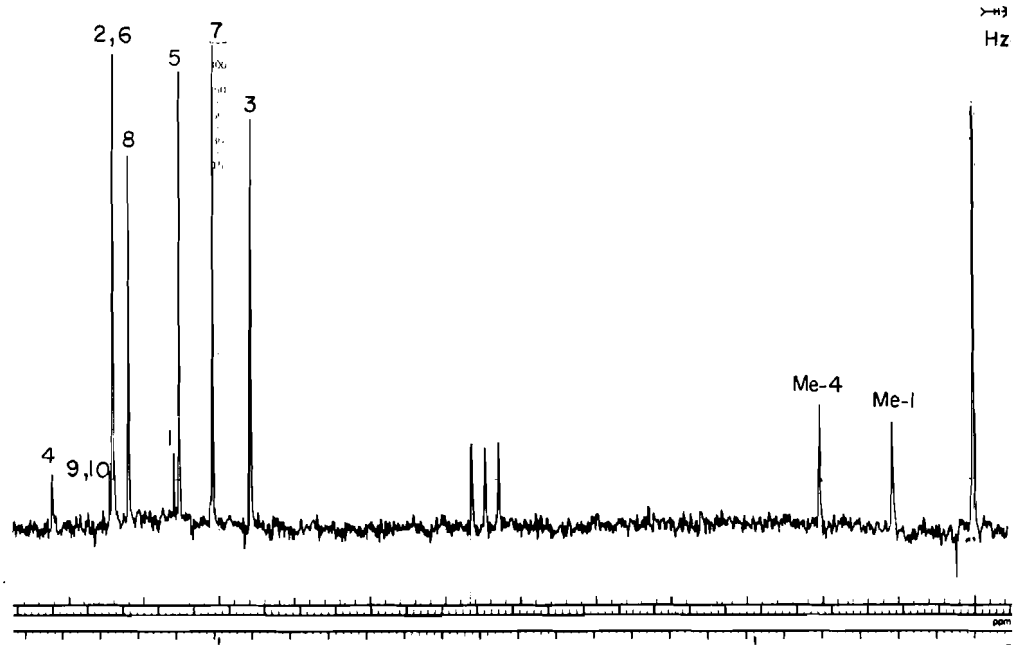

FIG. 4. Spectre ^{13}C du dérivé **2** totalement découplé en proton.

Can. J. Chem. Downloaded from www.nrcresearchpress.com by 210.87.254.6 on 09/05/12
For personal use only.

TABLEAU 3. Effets de substitution sur les déplacements chimiques des carbones 1, 4 et 7 rapportés aux carbones homologues de l'azulène

Composés	C_1	C_4	C_7
Azulène (δ ^{13}C)	118.1	136.5	122.7
Di-Me-1,4 azulène	+8.4	+9.5	−2.4
Di-Me-1,4 Et-7 azulène	+7.2	+7.8	+13.2
Di-Me-1,4 *i*Pr-7 azulène	+7.0	+7.7	+17.2

8) en tenant compte des observations suivantes. (*i*) La substitution d'un groupement méthyle sur le noyau azulénique se traduit par un déblindage d'environ 8 p.p.m. du carbone porteur, comme cela a été observé pour le triméthyl-4,6,8 azulène (4). (*ii*) Le déblindage est amplifié dans le cas de substitution par des radicaux éthyle ou isopropyle (14). (*iii*) L'intensité des signaux des carbones substitués est nettement plus faible que celle des carbones non substitués. Cette différence s'expliquant par la diminution du processus de relaxation de type dipole–dipole.

Les effets de substitution sur les carbones 1, 4 et 7 rapportés dans le tableau 3 sont très proches de ceux qui ont déjà été évalués sur les noyaux aromatiques (14). La valeur négative observée pour le carbone 7 du diméthyl-1,4 azulène traduit un effet de blindage en position δ des groupements méthyles. Pour chaque composé, les signaux intenses correspondants aux carbones 2, 6, 8, 3, 5 ont été attribués par des découplages sélectifs des différents protons liés à ces carbones. Les carbones 9 et 10 n'ont pu être définitivement attribués. L'étude en r.m.n. du carbone-13 vient donc compléter et confirmer sans aucune ambiguité les résultats acquis en r.m.n. du proton pour établir la structure des composés azuléniques extraits de la plante bleue.

1. S. S. DANYLUK et W. G. SCHNEIDER. Can. J. Chem. **40**, 1777 (1962). D. MEUCHE et E. HEILBRONNER. Helv. Chim. Acta, **45**, 1965 (1962). D. MEUCHE, B. MOLLOY, D. REID et E. HEILBRONNER. Helv. Chim. Acta, **46**, 2483 (1963). T. SCHAEFER et W. G. SCHNEIDER. Can. J. Chem. **41**, 966 (1963).
2. H. J. BERNSTEIN, J. A. POPLE et W. G. SCHNEIDER. Can. J. Chem. **35**, 65 (1957).
3. V. E. MUHLE. Ann. Phys. **18**, 130 (1966).
4. P. C. LAUTERBUR. J. Am. Chem. Soc. **83**, 1838 (1961).
5. A. J. JONES, T. D. ALGER, D. M. GRANT et W. M. LICHTMAN. J. Am. Chem. Soc. **92**, 2386 (1970).
6. W. R. WOOLFENDEN et D. M. GRANT. J. Am. Chem. Soc. **88**, 1496 (1966).
7. D. M. GRANT et B. V. CHENEY. J. Am. Chem. Soc. **89**, 5315 (1967).
8. L. F. JOHNSON et W. C. JANKOWSKI. Carbon-13 NMR spectra. Wiley Interscience, New York. 1972.
9. A. A. BOTHNER-BY et S. M. CASTELLANO. J. Chem. Phys. **41**, 3863 (1964). J. R. LLINAS. D. E. A. (Marseille), 1970.
10. G. GIANOTTI. C.R. **256**, 2416 (1963).
11. D. ROARD et M. DERBESY. A paraître.
12. V. EVDOMIKOFF, B. TOCCI-BUCCI et G. CAVAZZUTI. Farmaco, **27**, 163 (1972).
13. A. J. FRY, B. W. BOWEN et P. A. LEERMAKERS. J. Org. Chem. **32**, 1970 (1967).
14. J. B. STOTHERS. Carbon-13 NMR spectroscopy. Academic Press, New York. 1972. G. C. LEVY et G. L. NELSON. Carbon-13 nuclear magnetic resonance for organic chemists. Wiley-Interscience, New York. 1972.

Can. J. Chem. Downloaded from www.nrcresearchpress.com by 210.87.254.6 on 09/05/12
For personal use only.

Thermal Decomposition of Ammonium Metavanadate

K. C. KHULBE AND R. S. MANN

Chemical Engineering Department, University of Ottawa, Ottawa, Canada K1N 6N5

Received February 4, 1975

K. C. KHULBE and R. S. MANN. Can. J. Chem. **53**, 2917 (1975).

X-Ray, infrared, and electron spin resonance (e.s.r.) studies were made on the samples prepared by the thermal decomposition of ammonium metavanadate at various temperatures between 100 and 700 °C. A new intermediate compound has been identified to be formed between 100 and 150 °C. This new compound is stable up to 200 °C, and is a complex ammonium–vanadyl compound, since while the infrared studies showed the presence of an NH_4 group, and V—N bond, the e.s.r. gave the signal of VO^{2+} ions ($V^{4+} + O^{2-} = VO^{2+}$). A mechanism of the decomposition of ammonium metavanadate has been given.

K. C. KHULBE et R. S. MANN. Can. J. Chem. **53**, 2917 (1975).

On a étudié par rayons-X, infra-rouge et résonance paramagnétique électronique (r.p.e.) des échantillons préparés par décomposition thermique, à diverses températures entre 100 et 700 °C, de métavanadate d'ammonium. On a identifié qu'un nouveau composé intermédiaire se forme entre 100 et 150 °C. Ce nouveau composé est stable jusqu'à 200 °C et il s'agit d'un composé complexe de vanadyl–ammonium; cette conclusion découle des études i.r. qui montrent la présence d'un groupe NH_4 et d'un lien V—N et des études r.p.e. qui présentent un signal dû aux ions VO^{2+} ($V^{4+} + O^{2-} = VO^{2+}$). On donne un mécanisme de décomposition du métavanadate d'ammonium.

[Traduit par le journal]

Introduction

Ammonium metavanadate is generally the starting material in the preparation of vanadium compounds. The manufacture of vanadium pentoxide from ammonium metavanadate involves a series of chemical reactions (1–5). Although the thermal decomposition of ammonium metavanadate has been studied by several investigators, yet there is no general agreement on the course of the reaction. It has been established that a stable intermediate is formed, but it has not been positively identified and its physical characteristics are not reported. No electron spin resonance (e.s.r.) or infrared studies have been reported on the products formed by the thermal decomposition of ammonia metavanadate at various temperatures. In the present paper, we report the results obtained by e.s.r., X-ray, and infrared techniques on the vanadium compounds prepared by the thermal decomposition of ammonium metavanadate between 100 and 700 °C.

Experimental

Vanadium pentoxide was prepared by the thermal decomposition of ammonium metavanadate (Sample A). Ammonium metavanadate (Baker Analyzed Reagent) was dissolved in a minimum quantity of warm distilled water, and the solution evaporated over a hot plate with a magnetic stirrer, at low heat. The residue was dried for 12 h at 60 °C. The temperature was increased in stages to 100, 150, 200, 250, 300, 400, 500, 600, and 700 °C and maintained at each of the temperatures for 24 h. The samples were taken from the bulk at these temperatures before the temperature was raised to the next level, Samples B, C, D, E, F, G, H, I, and J refer to the samples obtained by the decomposition of ammonium metavanadate at 100, 150, 200, 250, 300, 400, 500, 600 and 700 °C respectively. The e.s.r. measurements were carried out using a Bruker 416 spectrometer in which the microwave frequency was in the X-band, g value was calculated by comparison with the g value of the free radical DPPH (2.003). The Phillips defractometer was used for the X-ray analysis of the samples. Measurements were carried out by the Debye–Sherrer method at room temperature using a Cobalt target and an iron filter. Infrared absorption spectra were observed on a Perkin-Elmer model 421 spectrophotometer. The samples were formed into discs with KBr (0.5% sample in KBr).

Results and Discussion

X-Ray Analysis

Table 1 gives the results of the X-ray analysis of the samples prepared by the thermal decomposition of ammonium metavanadate at various temperatures. At 250 °C, all ammonium metavanadate was decomposed and pure V_2O_5 was formed. No other phases (that is other oxides of vanadium) appeared to be present at or above 250 °C. The color of the mass changed from light yellow to dark yellow as the temperature

Can. J. Chem. Downloaded from www.nrcresearchpress.com by 210.87.254.40 on 09/05/12
For personal use only.

TABLE 1. X-Ray analysis of the products obtained by thermal decomposition of ammonium metavanadate at different temperatures and g value of different samples

Samples	Temperature (°C)	Identified phases	g
A (ammonium metavanadate)	Room temperature	Ammonium metavanadate	
B	100	Ammonium metavanadate	
C	150	Unidentified (X)	1.968
D	200	Unidentified (same as C)	1.965
E	250	Vanadium pentoxide	1.965
F	300	V_2O_5	1.965
G	400	V_2O_5	1.964
H	500	V_2O_5	1.965
I	600	V_2O_5	1.965
J	700	V_2O_5	1.968

was raised. The products obtained by the decomposition of ammonium metavanadate at 150 and 200 °C could not be identified specifically by X-ray analysis, though they appeared to be the same as indicated by their similar X-ray diffraction pattern. Table 2 shows the d-values and intensity of lines of the unidentifiable product. Thus X-ray analysis showed beyond doubt that a new compound really formed between 100 and 200 °C, though it could not be specifically identified. Lamure and Colin (5) studied the pyrolysis of ammonium metavanadate and reported the formation of bivanadate ($2V_2O_5 \cdot O(NH_4)_2$) and trivanadate ($3V_2O_5 \cdot O(NH_4)_2$) preceding the formation of V_2O_5. Taniguchi and Ingraham (1) studied the thermal decomposition of ammonium metavanadate at 225 °C and reported the compound's formula as $(NH_4)_2 \cdot O \cdot V_2O_5$. But the X-ray analysis data obtained for $(NH_4)_2 \cdot O \cdot V_2O_5$ was not the same as that obtained in the present investigation. It

TABLE 2. Powder diffraction data for samples C and D

d*	I†	d*	I†
7.591	100	2.405	5
6.619	10	2.202	40
5.707	80	2.115	10
4.947	30	2.018	40
4.193	10	1.941	5
3.869	30	1.891	10
3.521	50	1.829	5
3.203	100	1.743	5
3.056	5	1.588	10
2.892	60	1.541	20
2.722	5	1.482	10
2.592	5	1.433	20
2.460	20	Plus other faint lines	

*Interplanar spacing.
†Relative peak intensity.

is possible that the compound obtained by the decomposition of ammonium metavanadate in the temperature range of 150 to 200 °C was not the same as identified by Lamure and Colin (5) and Taniguchi and Ingraham (1).

Infrared Absorption Measurements

Figure 1 *a* and *b* show the infrared absorption spectra obtained for various samples. The spectra for sample A were very similar to that observed for sample B, which indicated that there was no structural change, when the temperature of pure ammonium metavanadate was raised to 100 °C and maintained at that temperature for 24 h. However when the temperature of ammonium metavanadate was raised to 150 °C and its (sample C) spectra observed, a definite change in its structure was noticed. The spectra for sample C was different from that observed for sample B. The spectra for samples C and D were identical, indicating that when the decomposition temperature was raised from 150 to 200 °C no noticeable structural change took place. When the decomposition temperature was raised from 200 to 250 °C a change in the structure and formation of a new compound was indicated by the spectra for sample E, which was different from the one observed for sample D. The spectra of all samples prepared by the decomposition of ammonium metavanadate at temperatures greater than 250 °C were identical to the one observed for sample E. This indicated that no structural change took place when the decomposition temperature was increased from 250 to 700 °C. The infrared spectra for samples B, C, and D show that as the temperature of decomposition was raised from 100 to 200, two new bands appeared. This band is entirely different from the one observed for ammonium

Can. J. Chem. Downloaded from www.nrcresearchpress.com by 210.87.254.40 on 09/05/12
For personal use only.

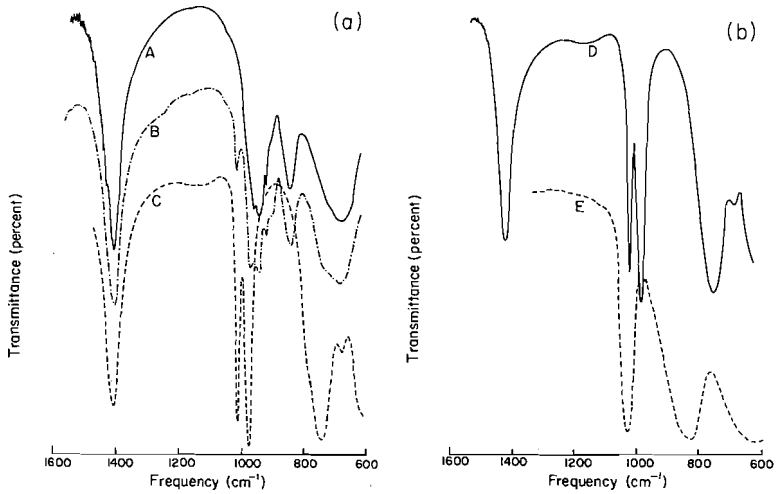

FIG. 1. (*a*) Infrared absorption spectra for samples A (—), B (-·-·-), and C (---). (*b*) Infrared absorption spectra for samples D (—) and E (---).

Can. J. Chem. Downloaded from www.nrcresearchpress.com by 210.87.254.40 on 09/05/12
For personal use only.

[1] $O_2V{-}O^-NH_4^+ \rightleftharpoons OV^+{-}O^- + NH_3 \rightleftharpoons$

1 **2**

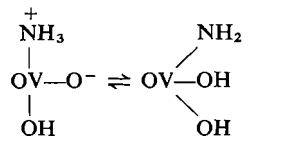

3 **4**

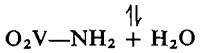

5

[2] $O_2V{-}NH_2 + OV^+{-}O^- \rightleftharpoons$

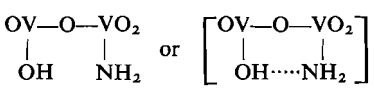

6

[3] **6** → $O_2V{-}O{-}VO_2 + NH_3$ (1); → $VO^{2+} + VO_3^{2-} + NH_3$ (2); → $OV{-}O^+ + VO_2^-$ (3)

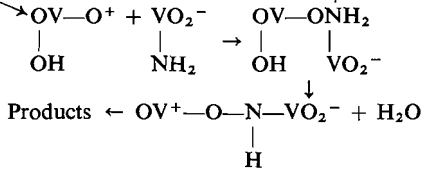

metavanadate in the region 600 to 1000 cm^{-1}. The peak observed at about 1010 cm^{-1} for samples B, C, and D is possibly due to V=O (6). This peak shifts towards higher frequency on raising the decomposition temperature on the formation of V_2O_5 (characteristic peak of V=O in V_2O_5 is 1020 cm^{-1}) (6–9) which indicates that the band strength of V=O strengthens with the increase of the decomposition temperatures. The characteristic peak of ammonia (NH_4), 1397 to 1400 cm^{-1} (10), disappeared totally at 250 °C. A comparison of the intensity and shape of the peak at 1010–1020 cm^{-1} for the samples B, C, D, and E indicates that the product obtained by the decomposition of ammonium metavanadate in the temperature range of 100–200 °C cannot be a mixture of the compound and V_2O_5. The peak observed for samples C and D at about 980 cm^{-1} may be attributed to V—O band with slightly weaker bonding strength (characteristic peak of V^+:O is 990 cm^{-1}) (6). The observed 825 cm^{-1} band in Figs. 1 and 2 is apparently due to the vibrations of the V—O—V bond (8, 9). The band in the region of absorption at 640–400 cm^{-1} is assigned to lattice vibrations. The band observed at around 750 cm^{-1} in samples C and D may be due to the V—N bond (11–13) but it is not possible to postulate at present as to what exactly is bonded to N, *i.e.* V—NO, V—NH_2, etc. (10, 11). Usually covalent nitrite gives a peak in this region (R—O—NO) (14). Taniguchi and Ingraham (1) observed that the

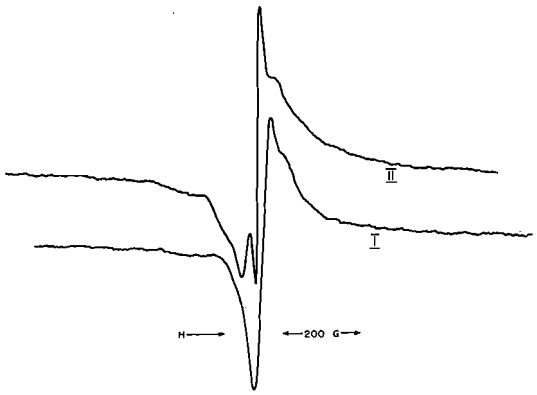

FIG. 2. Electron spin resonance spectra for samples C (I) and D (II).

amount of ammonia fell short of the theoretical value, *i.e.* some part of ammonia changed into nitrogen through either its oxidation or decomposition (15). The loss in weight of ammonium metavanadate to vanadium pentoxide was very small in the temperature range between 100 and 200 °C. Thus it can be concluded from infrared measurements that the compound formed during the thermal decomposition of ammonium metavanadate at temperatures greater than 100 °C and less than 200 °C should be a new compound of ammonia–vanadium–nitrogen–oxygen or a mixture of ammonia–vanadium–oxygen and vanadium–oxygen–nitrite.

Electron Spin Resonance Measurements

All samples gave e.s.r. signals except samples A and B. The thermal decomposition of ammonium metavanadate started at temperatures higher than 100 °C. Representative spectra for the samples C, D, H, and J are shown in Figs. 2 and 3. In studying the sequence of the spectra of the samples prepared by the thermal decomposition of the ammonium metavanadate at temperatures between 100 and 700 °C, it was observed that the two lines (a–a′) observed for samples D broadened to form a large broad line near the center of the spectral pattern (Fig. 2). The spectra observed for samples E, F, G, and H contained some broad lines (h.f.s.) (Fig. 3). These also disappeared as the samples were heated over 500 °C (samples H, I, and J). The spectra obtained for samples I and J were essentially similar.

Vanadium contains 99.8% of an isotope with a spin of 7/2 and should either give a spectrum consisting of eight components or one broad line of about 80 G observed in the absence of exchange interaction. The e.s.r. spectra in V_2O_5 is due to VO^{2+} ion in the unit structure VO^{2+}-$5O^{2-}$ (16). The VO^{2+} ion (3d′ electron configuration) is formed when a V^{4+} ion is bound to an oxygen ion by a strong, double covalent bond. The nature of this bond has been described in terms of molecular orbitals of the vanadyl pentahydrate complex ($VO^{2+}\cdot 5H_2O$) by Ballhausen and Gray (17). Table 2 gives the *g* values calculated (16) for all the samples. It appears that in all cases the spectra is due to VO^{2+} ions ($V^{4+} + O^{2-} = VO^{2+}$). The two lines observed at low temperature (*i.e.* 200 °C) are due to VO^{2+} ions. The sharp line (a) corresponds to perpendicular orientation of the internal magnetic field (*H*) and the electric field (*E*) of the VO^{2+} ions, whereas the broad, (a′), line corresponds to parallel orientation of (*H*) and (*E*). The lines are due to V^{4+} ions in the compound surrounded by six distorted O atoms. It seems from the i.r. and e.s.r. study that the new compound should be an ammonium vanadyl compound.

The line width increased for the samples C, D, E, and F; for samples G, H, I, and J, the line width remained constant. There are various factors affecting the line width. The magnetic dipole interaction is assumed to be the major factor (16). In other words the local fields produced by the nearest V^{4+} ions contribute mainly to the line width. The concentration of V^{4+} ions increases with the increase of temperature up to 300 °C and then remains constant.

Conclusion

During the thermal decomposition of ammonium metavanadate between 100 and 200 °C, a new intermediate compound has been identified

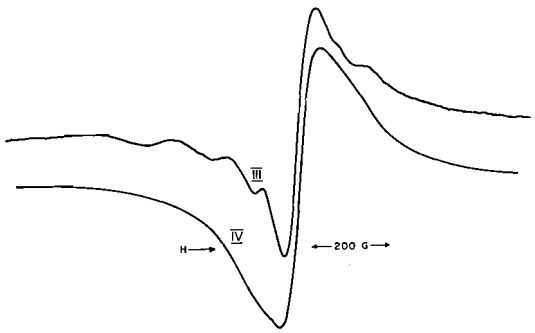

FIG. 3. Electron spin resonance spectra for samples H (III) and J (IV).

Can. J. Chem. Downloaded from www.nrcresearchpress.com by 210.87.254.40 on 09/05/12
For personal use only.

from e.s.r., infrared, and X-ray studies. This new compound is stable up to 200 °C. While the infrared studies showed the presence of an NH_4 group and N—V bond, the e.s.r. gave the signal of VO^{2+} ions. It can thus be concluded that the new intermediate identified in the present study is a complex of vanadyl compound.

The following mechanism is possible for the decomposition of ammonium metavanadate.

The authors are grateful to the National Research Council of Canada for financial assistance for the project (A-1125). The authors wish to express their gratitude to Dr. A. Manoogian, Physics Department and Dr. J. L. Argo, Chemical Engineering Department, Ottawa University for useful discussions. The authors are also indebted to Mr. E. J. Murray of the Mineral Science Division of Mines Branch, Department of Energy, Mines and Resources for the X-ray analysis.

1. M. TANIGUCHI and T. R. INGRAHAM. Can. J. Chem. **42**, 2467 (1964).
2. J. TRAU. Rocz. Chem. **36**, 1365 (1962).
3. K. TARAMA and S. TAERANISHI. J. Chem. Soc. Jpn. **55**, 68 (1952).
4. P. DUBOIS and P. BRETON. C. R. **206**, 1969 (1938).
5. J. LAMURE and COLIN. C. R. **258**, 6433 (1964).
6. S. YOSHIDA. Shokubai **10**, 90 (1968).
7. B. E. ZAITSEU, Z. I. EZHKOVA, and I. I. IOFFE. Kinet. Katal. **7**, 755 (1966).
8. K. YOSHIYA and K. HIROTA. J. Phys. Chem. **73**, 3973 (1969).
9. Y. KERA, S. TERATANI, and K. HIROTA. Bull. Chem. Soc. Jpn. **40**, 2458 (1967).
10. H. W. MORGAN, P. A. STAATS, and J. H. GOLDSTIEN. J. Chem. Phys. **27**, 1212 (1957).
11. C ADDISON, D. W. ANOS, D. SUTTON, and W. H. H. HOYLE. J. Chem. Soc. A, 808 (1967).
12. S. D. Ross. Inorganic infrared and Raman spectra. McGraw Hill Book Co. Ltd., New York. 1972. p. 157. Table 613b.
13. R. J. H. CLARK and C. S. WILLIAMS. J. Chem. Soc. A, 1425 (1966).
14. N. B. COLTHUP. J. Opt. Soc. Am. **40**, 397 (1950).
15. M. ONCHI and E. MA. J. Phys. Chem. **67**, 2241 (1963).
16. K. C. KHULBE, R. S. MANN, and A. MANOOGIAN. J. Chem. Phys. **66**, 4810 (1974).
17. G. J. BALLHAUSEN and H. B. GRAY. Inorg. Chem. **1**, 111 (1962).

Can. J. Chem. Downloaded from www.nrcresearchpress.com by 210.87.254.40 on 09/05/12
For personal use only.

Electrochemistry of Ruthenium Ammine Complexes

C. M. ELSON,[1] I. J. ITZKOVITCH,[2] J. MCKENNEY,[3] AND JOHN A. PAGE
Department of Chemistry, Queen's University, Kingston, Ontario K7L 3N6

Received April 24, 1975

C. M. ELSON, I. J. ITZKOVITCH, J. MCKENNEY, and JOHN A. PAGE. Can. J. Chem. **53**, 2922 (1975).

The electrochemistry of ruthenium(III) penta- and tetraammine chloro complexes has been investigated. In each case, the ruthenium(III) species was found to undergo an initial one electron reduction step, followed by hydrolysis of the chloride(s) in the ruthenium(II) product. The rate constants for the substitution steps were evaluated by cyclic voltammetry. An aqueous 0.30 *M* methane sulfonate electrolyte of p*H* 2.0 was used at 25 °C.

Values for the reversible "$E_{1/2}$" (V *vs.* SCE) and first order rate constants for the (stepwise) replacement of the Cl^- are: $Ru(NH_3)_5Cl^+$, −0.282 V and 17 s^{-1}; *cis*-$Ru(NH_3)_4Cl_2^+$, −0.328 V, 80 s^{-1}, and 5 s^{-1}; *trans*-$Ru(NH_3)_4Cl_2^+$, −0.412 V, 2 s^{-1}, and 0.4 s^{-1}.

The electrochemistry of $Ru(NH_3)_5SO_2^{2+}$ was also investigated. In a 0.10 *M* CH_3SO_3H – 0.20 *M* CH_3SO_3Na electrolyte the ruthenium(II) species was found to undergo an initial one electron oxidation step with "$E_{1/2}$" = +0.50 V, followed by a slow hydrolysis of the SO_2 in the ruthenium(III) product with $k = 2.4 \times 10^{-2}$ s^{-1} at 25 °C.

C. M. ELSON, I. J. ITZKOVITCH, J. MCKENNEY et JOHN A. PAGE. Can. J. Chem. **53**, 2922 (1975).

On a étudié l'électrochimie des complexes penta- et tétraammine chloro du ruthénium(III). On a trouvé, dans chaque cas, que les espèces ruthénium(III) subissent en premier lieu une réduction impliquant un électron et que celle-ci est suivie par une hydrolyse des chlorures dans le produit ruthénium(II). On a évalué les constantes de vitesse des étapes de substitution par voltamètrie cyclique. On a utilisé une solution aqueuse 0.30 *M* d'électrolyte de méthane sulfonate à un p*H* de 2.0 et une température de 25 °C.

Les valeurs pour le réversible "$E_{1/2}$" (V *vs.* SCE) et les constantes de vitesse du premier ordre pour les remplacements successifs de Cl^- sont: $Ru(NH_3)_5Cl^+$, −0.282 V et 17 s^{-1}; *cis*-$Ru(NH_3)_4Cl_2^+$, −0.328 V, 80 s^{-1} et 5 s^{-1}; *trans*-$Ru(NH_3)_4Cl_2^+$, −0.412 V, 2 s^{-1} et 0.4 s^{-1}.

On a aussi étudié l'électrochimie du $Ru(NH_3)_5SO_2^{2+}$. On a trouvé que, dans un électrolyte 0.10 *M* CH_3SO_3H – 0.20 *M* CH_3SO_3Na, les espèces ruthénium(II) subissent en premier lieu une oxydation impliquant un électron avec un "$E_{1/2}$" = +0.50 V, et que celle-ci est suivie par une hydrolyse lente du SO_2 dans le produit ruthénium(III) avec $k = 2.4 \times 10^{-2}$ s^{-1} à 25 °C.

[Traduit par le journal]

Introduction

The solution chemistry of ruthenium ammine complexes has had considerable recent attention (1) and a number of recent papers have been concerned with the electrochemistry of these species (2–6). This paper extends the previous work and reports new electrochemical and kinetic results for $Ru(NH_3)_6^{3+}$, $Ru(NH_3)_5Cl^{2+}$, *cis*- and *trans*-$Ru(NH_3)_4Cl_2^+$, and $Ru(NH_3)_5SO_2^{2+}$.

Experimental

The electrochemistry experiments were carried out using a PAR Model 170 unit. The cell had an internal Pt counter electrode and a Luggin probe to a saturated calomel reference electrode. All potentials are relative to this reference. The cell was thermostatted at 25 °C and purified Ar (4) was used for deaeration.

The voltammetry with the hexaammine and Cl substituted species was carried out at a hanging mercury drop electrode (h.m.d.e.) formed at a Metrohm E410 Kemula type electrode assembly. The area of the electrode, calculated from the weight of the mercury and assuming a simple sphere, was 0.0355 cm^2. The voltammetry of the SO_2 substituted species involved more positive potentials and was carried out at a Pt disk electrode of area 0.0557 cm^2.

The voltammograms were recorded without filtering over a range of scan rates (v) and switching potentials (E_λ), with i.r. compensation at the faster scan rates. At high scan rates (0.1 V s^{-1} < v < 200 V s^{-1}) the output of the PAR 170 instrument was recorded using a Biomation Model 1015 Waveform Recorder (4096 words × 10 bits/word; 0.01 to 100 kHz sample rates). The compensation of the resistance between the reference electrode probe and the working electrode was achieved with the positive feedback network of the 170 instrument using

[1]Present address: Department of Chemistry, St. Mary's University, Halifax.
[2]Present address: Ontario Research Foundation, Sheridan Park, Ontario.
[3]Present address: International Nickel Company Research Laboratories, Sheridan Park, Ontario.

TABLE 1. Polarographic data for ruthenium ammines

	$E_{1/2}$*† (V)	Slope‡ (mV)	D ($cm^2\ s^{-1}$)
$Ru(NH_3)_6^{3+}$	−0.178	−63.5	5.7×10^{-6}
$Ru(NH_3)_6^{2+}$	$(-0.174)^{ox}$	−61.0	
$Ru(NH_3)_5Cl^{2+}$	−0.185	−64.2	6.6×10^{-6}
$Ru(NH_3)_5H_2O^{3+}$	−0.169	−63.1	
$Ru(NH_3)_5H_2O^{2+}$	$(-0.171)^{ox}$	−72	
cis-$Ru(NH_3)_4Cl_2^{+}$	−0.274	−63.8	6.3×10^{-6}
cis-$Ru(NH_3)_4(H_2O)_2^{3+}$	−0.155	−63.1	
cis-$Ru(NH_3)_4(H_2O)_2^{2+}$	$(-0.144)^{ox}$	−62.3	
trans-$Ru(NH_3)_4Cl_2^{+}$	−0.380	−61.9	5.8×10^{-6}

*Intercept of plot of log $(i/(i_d - i))$ *vs.* E.
†ox is oxidation wave.
‡Slope of plot of log $(i/(i_d - i))$ *vs.* E.

an oscilloscope to monitor the summing amplifier output. For a particular current range the compensation was adjusted to the maximum value consistent with amplifier stability under conditions of "zero" faradaic current through the cell. The voltammograms obtained were corrected for residual and charging current contributions by running the blank electrolyte at the same scan rate, then subtracting the observed currents from those obtained with the ruthenium ammines present in the electrolyte. The polarography at the dropping mercury electrode was done in the sampled mode without filtering. The drop time was controlled (t = 2 s) and a slow scan rate was used (v = 0.002 V s^{-1}). The apparatus and cell used for the controlled potential coulometric analysis have been described together with the specific ion electrode and cell used to monitor displaced Cl^- (7).

The starting material for the preparation of the various species was pure $Ru(NH_3)_6 \cdot Cl_3$ obtained from Johnson Matthey Chemicals Limited (Lot B/8). The preparation and characterization of the $Ru(NH_3)_5Cl \cdot Cl_2$ and the *cis*-$Ru(NH_3)_4Cl_2 \cdot Cl$ has been described (7) while the *trans*-$Ru(NH_3)_4Cl_2 \cdot Cl$ was prepared by the method of Gleu and Breuel (8) using an ICl oxidation of the *trans*-$Ru(NH_3)_4(SO_2)Cl \cdot Cl$. The absorption spectra of the chlorotetraammines was in agreement with the literature values (9). The *cis* isomer gave twin peaks at 312 and 352 nm (ε 1500 and 1300) and the *trans* isomer a peak at 330 nm (ε 4700).

The $Ru(NH_3)_5SO_2 \cdot Cl_2$ was prepared from the *trans*-$Ru(NH_3)_4(SO_2)Cl \cdot Cl$ again using a method of Gleu and Breuel (10). The procedure involved preparation of $Ru(NH_3)_5SO_3 \cdot 2H_2O$ by reaction of the starting material with dilute aqueous ammonia and precipitation from a cold solution with ethanol. The freshly prepared pentaammine derivative was then reacted with aqueous 3 *M* HCl at the boiling point, and the dark red $Ru(NH_3)_5SO_2 \cdot Cl_2$ precipitated from cold solution with ethanol.

The electrochemistry was studied in a noncomplexing methane sulfonate electrolyte prepared from reagent CH_3SO_3H and reagent NaOH. The work with the SO_2 complex was carried out in an acid 0.10 *M* CH_3SO_3H – 0.20 *M* CH_3SO_3Na electrolyte, while all the other complexes were studied in a 0.30 *M* CH_3SO_3Na electrolyte adjusted to p*H* 2.0 ± 0.1.

The solutions were prepared using weighed amounts of the salts and were 1–1.5 m*M* in ruthenium. The purity of the ruthenium(III) salts was verified by coulometric assay. In each case, electrolysis at a Hg cathode controlled at −0.50 V was clean and rapid with a negligible background. Results, expressed as apparent n values, for triplicate analyses with ~10 C amounts of the ruthenium(III) species were: $Ru(NH_3)_6Cl_3$ (1.03 ± 0.02), $Ru(NH_3)_5Cl \cdot Cl_2$ (1.02 ± 0.02), *cis*-$Ru(NH_3)_4Cl_2 \cdot Cl$ (0.98 ± 0.04) and *trans*-$Ru(NH_3)_4Cl_2 \cdot Cl$ (0.92 ± 0.05). Some water of hydration is indicated in the *trans* isomer.

The composition of the $Ru(NH_3)_5SO_2 \cdot Cl_2$ was verified by chemical analysis of the prepared salt. The results (N 21.6%, Cl 21.8%, S 10.0%) indicated a high degree of purity.

Results

The polarographic data are given in Table 1 while Figs. 1 and 2 show data obtained at various scan rates by cyclic voltammetry. The polarographic $E_{1/2}$ were determined from the intercept of a plot of log $(i/(i_d - i))$ *vs.* E_{dme}. The slopes of the plot are given for comparison with the expected −59.2 mV for a reversible one electron reduction process. The diffusion coefficients given were calculated from the observed i_d and the simple Ilkovic relation. In each case they agreed closely (±5%) with values calculated from the observed voltammetric $(i_p)_c$ and the Randles–Sevcik relation (11).

Ru(NH₃)₆³⁺

The behavior was consistent with a one electron charge transfer and a stable product

$$Ru(NH_3)_6^{3+} + e \rightleftarrows Ru(NH_3)_6^{2+}$$

Polarography of the ruthenium(III) species gave a well defined reduction wave, while cyclic voltammetry gave one cathodic peak on the forward scan with one anodic peak on the reverse scan. Over the range of scan rates studied $(i_p)_c$ varied directly as $v^{1/2}$, and both the peak current ratio $((i_p)_c/(i_p)_a)$ and the peak potential separation $(\Delta E_p = (E_p)_c - (E_p)_a)$ were just equal

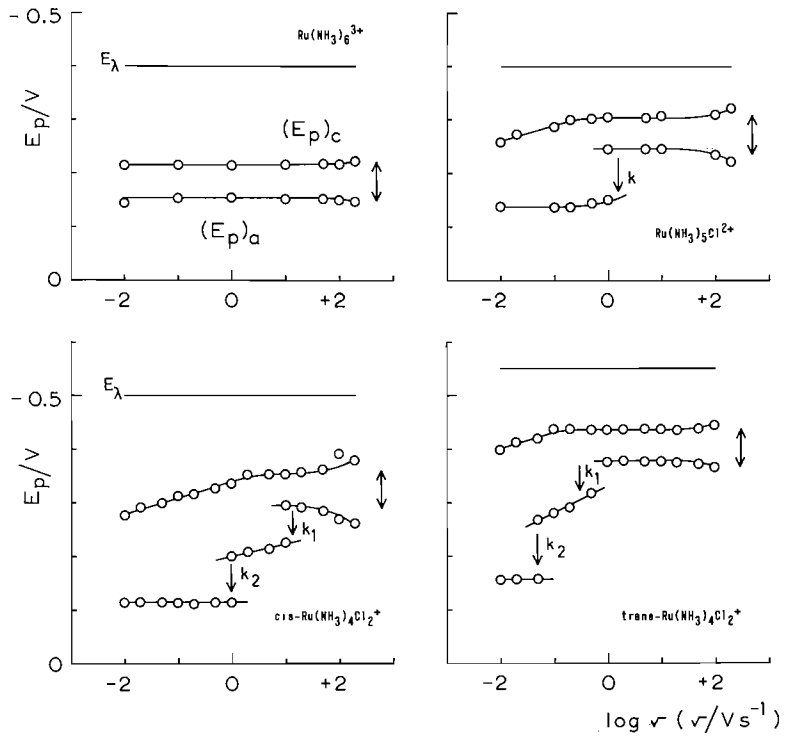

FIG. 1. Cyclic voltammetry of ruthenium(III) ammines: upper curve gives $(E_p)_c$ on forward scan, upper line indicates E_λ and lower curve(s) give $(E_p)_a$ on reverse scan, $\xrightarrow{k}$ indicates v leading to half reaction of ruthenium(II) products.

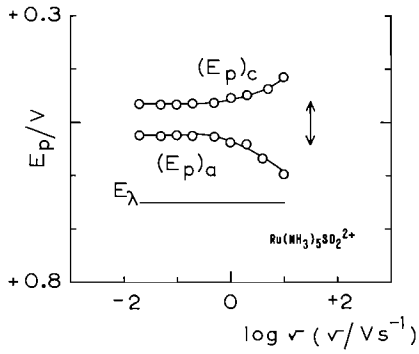

FIG. 2. Cyclic voltammetry of $Ru(NH_3)_5SO_2^{2+}$: lower curve gives $(E_p)_a$ on forward scan, lower line gives E_λ, and upper curve gives $(E_p)_c$ on reverse scan.

to those expected for a reversible cyclic process. There was some increase in ΔE_p at the highest scan rates, but this is probably an instrument response artifact. Controlled potential electrolysis at a Hg cathode at -0.50 V was found to produce $Ru(NH_3)_6^{2+}$ quantitatively. The quantity of electricity required was reproducible and in close agreement with the amount of $Ru(NH_3)_6Cl_3$ taken, while polarography of the resultant solution gave a well defined oxidation wave for the ruthenium(II) species.

$Ru(NH_3)_5Cl^{2+}$

The behavior was consistent with the steps:

$$Ru(NH_3)_5Cl^{2+} + e \rightleftarrows Ru(NH_3)_5Cl^+$$

$$Ru(NH_3)_5Cl^+ + H_2O \xrightarrow{k_1} Ru(NH_3)_5H_2O^{2+} + Cl^-$$

Polarography of the ruthenium(III) species gave a well defined reduction wave while cyclic voltammetry gave just one cathodic peak on the forward scan. With increasing scan rate $(E_p)_c$ shifted to more negative potentials although $(i_p)_c$ remained proportional to $v^{1/2}$. At the higher scan rates one anodic peak, assigned to the oxidation of the $Ru(NH_3)_5Cl^+$, was apparent on the reverse scan. Here the peak current ratio and the separation of the peak potentials were near the reversible value. As the scan rate was decreased the cathodic peak moved to less negative potentials and on the reverse scan an anodic peak

assigned to the oxidation of $Ru(NH_3)_5H_2O^{2+}$ appeared. This second anodic peak grew at the expense of the first so that at the slower scan rates only one anodic process was apparent on the reverse scan with a peak current equivalent to that of the cathodic peak on the forward scan.

Multicycle experiments on the $Ru(NH_3)_5Cl^{2+}$ at 0.1 V s^{-1} resulted in a limiting situation characterized by a major cathodic peak at −0.19 V, a minor cathodic peak at −0.29 V, and one major anodic peak at −0.13 V. This is in keeping with a reaction involving the oxidation and reduction of aquo species present in the layer of solution adjacent to the electrode. The reduction peak at −0.29 V persists as fresh $Ru(NH_3)_5Cl^{2+}$ is continually supplied by diffusion from the bulk solution.

Controlled potential coulometric electrolysis of the $Ru(NH_3)_5Cl^{2+}$ at −0.50 V was found to result in the displacement of the Cl^- and the quantitative formation of $Ru(NH_3)_5H_2O^{2+}$ (4). Polarography of the resultant solution gave one well defined oxidation wave while cyclic voltammetry at 0.1 V s^{-1} gave two peaks with $(E_p)_a = -0.132$ V, $(E_p)_c = -0.194$ V, and $(i_p)_a/(i_p)_c$ equal to the reversible value. Reoxidation of the solution by controlled potential coulometric electrolysis at −0.05 V was found to result in the quantitative formation of $Ru(NH_3)_5H_2O^{3+}$. Polarography of the oxidized solution gave one well defined reduction wave while cyclic voltammetry at 0.1 V s^{-1} gave two peaks with $(E_p)_c = -0.192$ V, $(E_p)_a = -0.120$ V, and $(i_p)_c/(i_p)_a$ equal to the reversible value.

cis and trans-$Ru(NH_3)_4Cl_2^+$

The behavior was consistent with the steps:

$$Ru(NH_3)_4Cl_2^+ + e \rightleftarrows Ru(NH_3)_4Cl_2$$

$$Ru(NH_3)_4Cl_2 + H_2O \xrightarrow{k_1} Ru(NH_3)_4(H_2O)Cl^+ + Cl^-$$

$$Ru(NH_3)_4(H_2O)Cl^+ + H_2O \xrightarrow{k_2} Ru(NH_3)_4(H_2O)_2^{2+} + Cl^-$$

For each isomer, polarography of the ruthenium(III) species gave a well defined reduction wave while cyclic voltammetry always gave one cathodic peak on the forward scan with $(i_p)_c$ proportional to $v^{1/2}$. At the higher scan rates only one current peak assigned to the reoxidation of the $Ru(NH_3)_4Cl_2$ was apparent on the reverse scan. Under these conditions the separation of the peak potentials were close to the reversible value. As the scan rate was continually decreased from the higher values a more positive anodic second peak assigned to the oxidation of $Ru(NH_3)_4(H_2O)Cl^+$ grew at the expense of the first peak and, in turn, this peak was eventually replaced by a still more positive third peak assigned to the oxidation of $Ru(NH_3)_4(H_2O)_2^{2+}$. At the lower scan rates only this third anodic peak was present with height equivalent to that of the cathodic peak on the forward scan.

Multicycle experiments were also carried out at 0.1 V s^{-1}. In the case of the *cis* isomer these gave, in the limit, a major cathodic peak at −0.18 V, a minor cathodic peak at −0.32 V, and one (major) anodic peak at −0.11 V. The behavior of the *trans* isomer was similar with the major cathodic peak at −0.23 V, the minor cathodic peak at −0.42 V, and the one (major) anodic peak at −0.16 V. These results are again in keeping with a situation where the cyclic processes giving the major peaks involve aquo species within the layer next to the electrode surface and the minor cathodic peaks result from the continual diffusion of fresh $Ru(NH_3)_4Cl_2^+$ to the electrode surface. The potentials associated with the various *cis* and *trans* isomers are sufficiently distinct that isomerization during the voltammetric experiment should be detectable. However experiments involving 20 consecutive cyclic scans at 0.02 V s^{-1} showed no current peaks other than those for the isomer taken.

Controlled potential coulometric electrolysis of the *cis*-$Ru(NH_3)_4Cl_2^+$ at −0.50 V was found to result in the quantitative formation of *cis*-$Ru(NH_3)_4(H_2O)_2^{2+}$. The substitution of the Cl^- groups evidently involves a ruthenium(II) catalyzed substitution in the ruthenium(III) species (7). Polarography of the reduced solution gave a well defined oxidation wave, while cyclic voltammetry at 0.1 V s^{-1} gave $(E_p)_a = -0.11$ V and $(E_p)_c = -0.18$ V with $(i_p)_a/(i_p)_c$ equal to the reversible cyclic value. A further electrolysis of the solution at −0.05 V resulted in quantitative oxidation to *cis*-$Ru(NH_3)_4(H_2O)_2^{3+}$.

Attempts to prepare *trans*-$Ru(NH_3)_4(H_2O)_2^{2+}$ by electrolysis of *trans*-$Ru(NH_3)_4Cl_2^+$ resulted in a displacement of the Cl^- and quantitative formation of ruthenium(II), but the cyclic voltammetric experiment on the reduced solution at 0.1 V s^{-1} gave two pairs of major peaks with $(E_p)_a = -0.11$ and −0.16 V and $(E_p)_c = -0.18$ and −0.24 V. If the peaks at −0.16 and −0.24 V are assigned to the *trans*

species, the peaks at −0.11 and −0.18 V would indicate some isomerization has taken place over the relatively long time required for the controlled potential reduction. Polarography of the reduced solution gave a well defined but drawn out oxidation wave with $E_{1/2} = -0.20$ V.

$Ru(NH_3)_5SO_2^{2+}$

The behavior was consistent with the steps:

$$Ru(NH_3)_5SO_2^{2+} - e \rightleftarrows Ru(NH_3)_5SO_2^{3+}$$

$$Ru(NH_3)_5SO_2^{3+} + H_2O \xrightarrow{k_1} Ru(NH_3)_5H_2O^{3+} + SO_2$$

The aquation of the ruthenium(III) species was found to be slow, and the aquo substituted product was not observed over the range of voltammetric experiments. At low scan rates the charge transfer step (on Pt) appeared reversible but irreversibility was indicated as the separation of the anodic and cathodic potentials increased with scan rate. However $(i_p)_a$ varied directly as $v^{1/2}$ over the range of scan rates, and the ratio $(i_p)_a/(i_p)_c$ remained near that for a reversible process.

The slow aquation step could be observed after a controlled potential electrolysis of the $Ru(NH_3)_5SO_2^{2+}$. Oxidation at a Pt anode at +0.64 V proceeded smoothly with a rapid exponential decay in i_a (Fig. 3). The solution color turned from brick red to purple, and coulometry indicated just *over* 1*F* of electricity per mol of ruthenium(II) taken. The solution, maintained with Ar bubbling through the electrolyte and the Pt electrode at +0.64 V, then slowly decolorized and the formation of the $Ru(NH_3)_5H_2O^{3+}$ was followed by analytical voltammetry at a h.m.d.e. Small portions of the electrolyte were withdrawn at intervals, and scanned from 0 to −1.0 V using a scan rate of 0.1 V s^{-1} after an initial hold at 0 V.

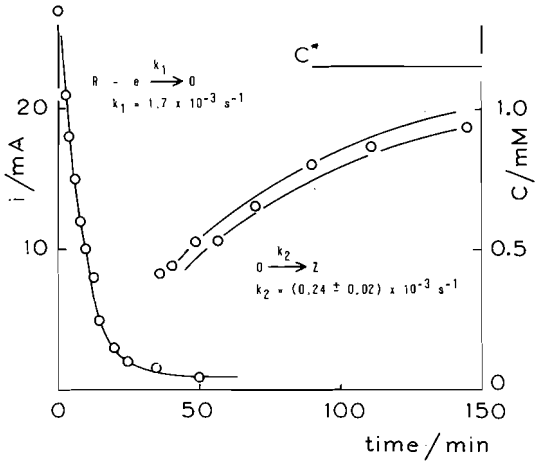

FIG. 3. Controlled potential oxidation of $Ru(NH_3)_5SO_2^{2+}$: Pt anode at +0.64 V; 1.15 m*M* $Ru(NH_3)_5SO_2^{2+}$. Left hand curve gives i_a as function of time. Right hand points give $Ru(NH_3)_5H_2O^{3+}$ concentration as function of time.

A well defined peak for the reduction of the ruthenium(III) aquo species was obtained and $(i_p)_c$ was related to the concentration through a calibration curve. Quantitative substitution without side reactions was indicated, and the nature of the product was confirmed both by the peak potentials on cyclic voltammetry and the u.v. absorption spectra of the solution. The substitution process was accompanied by small anodic electrolysis currents and this could be accounted for by the direct oxidation of the displaced SO_2 at the Pt anode. Most of the SO_2 would be removed from the system by the Ar gas flow, but some would be expected to react directly at the electrode. This possibility was indicated by voltammetry on SO_2 dissolved in the methane sulfonic acid electrolyte. On a Pt electrode the SO_2 gave an anodic peak with $(E_p)_a = +0.56$ V at a scan rate of 0.1 V s^{-1}. Integration of the electrolysis current over the whole experiment gave (in duplicate) 1.4 *F* of electricity per mol of ruthenium(II) taken.

It was found that the stepwise process occurring on electrolysis could be chemically reversed. A solution of $Ru(NH_3)_5(H_2O)^{3+}$ was prepared in the methane sulfonic acid electrolyte and SO_2 was passed through the solution. It immediately turned purple indicating the formation of $Ru(NH_3)_5SO_2^{3+}$, and then as bubbling continued it slowly turned to the brick red of $Ru(NH_3)_5SO_2^{2+}$.

Rate Constants

The first order rate constants for the substitution steps can be calculated from the voltammetric data and the values are given in Table 2.

For a reversible charge transfer step, followed by an irreversible chemical reaction (Nicholson and Shain, Case VI (12)):

$$O + e \rightleftarrows R \quad R \xrightarrow{k} Z$$

it can be shown that at 25 °C

$$(E_p)_c = \left\{E_{1/2} - 0.06708 \text{ V} + \frac{0.05916}{2} \text{V} \log k_1\right\} - \frac{0.05916}{2} \text{V} \log v$$

TABLE 2. Rate constants for substitution in ruthenium(II) ammines

	$E_{1/2}$* (V)	k_1 (s^{-1})	k_2 (s^{-1})
$Ru(NH_3)_5Cl^+$	−0.282	17 ± 2†	
		10 ± 4‡	
cis-$Ru(NH_3)_4Cl_2$	−0.328	81 ± 8†	6.0–4.5§
		73 ± 24‡	
trans-$Ru(NH_3)_4Cl_2$	−0.412	2.2 ± 0.2†	0.36–0.27§
		4.4 ± 2.1‡	

*$E_{1/2}$ estimated from rev $(E_p)_c$; $E_{1/2} = (E_p)_c + 0.028$ V.
†k_1 from [1]; limits correspond to ±0.005 V in $((E_p)_c - E_{1/2})$.
‡k_1 from v giving $(i_p)_a/(i_p)_c = 0.5$; limits correspond to ±0.1 v.
§k_2 from v giving $(i_p)_a' = (i_p)_a''$; limits correspond to $(\tau/1\text{–}\tau/0.75)$.

The relation assumes that there is no significant contribution from reoxidation of the substituted ruthenium(II) product at $(E_p)_c$. For each of the ruthenium(III) chloro species $(E_p)_c$ was plotted as a function of log v and a best straight line of slope −0.05916/2 V fitted to the data at low scan rates. Values of k_1 were calculated from the intercept of these plots and the estimated $E_{1/2}$.

The rate constant for the first substitution step can also be calculated from the peak current ratios observed on cyclic voltammetry. There is some difficulty in estimating $(i_p)_a$ since the reoxidation of the immediate product overlaps that of the substituted ruthenium(II) species but the scan rate that gave $(i_p)_a/(i_p)_c = 0.5$ was estimated. This corresponds to a value of $k_1\tau = 1.00$, where τ is the time in seconds required to scan forward from $E_{1/2}$ to E_λ on the cyclic voltammogram.

For the second substitution step in the ruthenium(II) tetraammines the same relations were used. In this case the scan rate that produced nearly equal peak heights for the oxidation of $Ru(NH_3)_4(H_2O)Cl^+$ and $Ru(NH_3)_4(H_2O)_2^{2+}$ was estimated from the cyclic voltammograms. A first estimate of the rate constant was then made on the assumption that this corresponded to a value of $k_2\tau = 1.00$. This assumes that the first substitution step is fast relative to the second; the assumption will give an estimate of the rate constant that is too large since ~25% more time is consumed in scanning from $E_{1/2}$ to the anodic peaks than is allowed for in the Nicholson and Shain relations. The rate constant was assumed to lie within the limits $1/\tau$ and $0.75/\tau$.

The rate constant for the aquation of the $Ru(NH_3)_5SO_2^{3+}$ was estimated from the voltammetric data obtained after controlled potential electrolysis of the $Ru(NH_3)_5SO_2^{2+}$. The results were fitted to the case:

$$R - e \xrightarrow{k_1} O \quad O \xrightarrow{k_2} Z$$

according to Frost and Pearson (13). A value of the electrolytic rate constant $k_1 = 1.7 \times 10^{-3}$ s^{-1} was first estimated from the slope of the linear ln i_a *vs.* t plot, and k_2 was then estimated by generating Z *vs.* t plots corresponding to various values of k_2. A value of $k_2 = (2.4 \pm 0.2) \times 10^{-4}$ s^{-1} was found to match the duplicate experimental results as shown in Fig. 3. The calculation ignored any back reaction involving the Z, it being assumed that the free SO_2 concentration was negligible as a result of displacement and electrolytic oxidation.

Discussion

The ruthenium(III) complexes were all found to undergo an initial one electron reduction process and formal reduction potentials derived from the observed peak potentials are listed in Table 3. The reduction process has been discussed by Movius and Linck (9) and involves a change in the metal from a t_{2g}^5 to a t_{2g}^6 electron configuration. The values reported are close to those reported by Lim *et al.* in a previous tabulation (5).

In these complexes it is seen that the presence of one or two Cl^- groups stabilizes the ruthenium(III) relative to the ruthenium(II) and this can be related to the σ donating ability of the Cl^-. The replacement of the Cl^- with neutral non-π-bonding species gives ruthenium(III) species that are more easily reduced with the H_2O more effective than the NH_3. This can be related to an inductive effect since H_2O is more capable of withholding electron density from the metal center. A comparison of the $Ru(NH_3)_4Cl_2^+$ species shows that the *trans* ruthenium(III) is more difficult to reduce than the *cis* isomer; here in the *trans* case there would be competition for the same metal electrons in σ bonding to the two Cl^-, but in the *cis* isomer this competition

TABLE 3. Formal reduction potentials of ruthenium complexes

	E (V *vs.* NHE)§	
cis-$Ru(NH_3)_4(H_2O)_2^{3+}$	+0.10†	(+0.100)
$Ru(NH_3)_5(H_2O)^{3+}$	+0.07†	(+0.066)
$Ru(NH_3)_6^{3+}$	+0.057*	(+0.051)
trans-$Ru(NH_3)_4(H_2O)_2^{3+}$	+0.04†	(+0.020)
cis-$Ru(NH_3)_4(H_2O)Cl^{2+}$	+0.03‡	—
$Ru(NH_3)_5Cl^{2+}$	−0.034*	(−0.042)
trans-$Ru(NH_3)_4(H_2O)Cl^{2+}$	−0.05‡	—
cis-$Ru(NH_3)_4Cl_2^{+}$	−0.082*	(−0.100)
trans-$Ru(NH_3)_4Cl_2^{+}$	−0.166*	(−0.180)
$Ru(NH_3)_5(SO_2)^{3+}$	+0.250*	—

*Value is average of $(E_p)_c$ and $(E_p)_a$ at scan rates where reversible behavior indicated (Fig. 1, 2).
†Value is average of $(E_p)_c$ and $(E_p)_a$ obtained at 0.1 V s^{-1} (see text).
‡$(E_p)_c$ not observed, value is $(E_p)_a$ −0.03 V (Fig. 1).
§Values in parentheses are previously reported values in noncomplexing electrolytes (5). All values will differ from actual E by 0.030 log $\{D_{ox}/D_{red}\}$ V (12).

would be minimized and the metal center would be more highly charged.

With the SO_2 ligand the ruthenium(II) pentaammine is highly stabilized relative to the ruthenium(III) species. The SO_2 group is sulfur bonded to the metal center (14) and the ruthenium(II) is stabilized by π back bonding from the metal to the ligand.

The rate constants for the hydrolysis reactions are given in Table 2 and are consistent with previous reports. For $Ru(NH_3)_5Cl^{+}$ Coleman *et al.* (2) have estimated $k = 6.3 \pm 0.3\ s^{-1}$ (25°) by voltammetry in a 0.171 *M* *p*-toluene sulfonic acid electrolyte. They found the rate constant to increase with decreasing acidity but interpreted the change as an ionic strength effect. Baxendale *et al.* (15) had previously estimated $k = 4.7 \pm 0.4\ s^{-1}$ (20°) using a pulse radiolysis technique and an aqueous 0.1 *M* methanol electrolyte. Our results were correspondingly reproducible and precise, but the larger spread reported results from the introduction of an estimate of the uncertainty in determining the peak potentials or the critical scan rate.

As far as the tetraammines are concerned previous estimates are uncertain. Movius and Linck (9) have estimated values from the slow absorptivity changes that followed the vanadium(II) reduction of the ruthenium(III) species. For the *cis*-ruthenium(II) species values of $k_1 = 16 \pm 8$ and $k_2 = 4 \pm 2\ s^{-1}$ were obtained. For the *trans* species estimates of $k_1 < 0.1$ and $k_2 < 0.1\ s^{-1}$ were made. These results were obtained in a 0.1 *M* *p*-toluene sulfonic acid electrolyte at 25°.

The present study gives significantly higher rates for the hydrolysis of the *trans* species although these remain significantly less than the rates for the corresponding *cis* species. Using the peak potentials observed in the cyclic voltammetry as a criteria, the reactions are stereospecific as observed by Ford and Sutton (16) in other ruthenium(II) substitution reactions. The hydrolysis rate observed with the *cis*-$Ru(NH_3)_4(H_2O)Cl^{+}$ is greater than that observed with the *trans*-$Ru(NH_3)_4(H_2O)Cl^{+}$ but comparable to that observed with $Ru(NH_3)_5Cl^{+}$. Thus the substitution of an NH_3 for an H_2O in a position *trans* to the Cl^{-} significantly increases the hydrolysis rate but substitution in the *cis* position has little effect. This is contrary to the behavior noted with $Co^{III}(en)_2XCl$ species (17, 18) but interpretation will require data for the hydrolysis of other $Ru^{II}(NH_3)_4XCl$ species.

The ruthenium(II) SO_2 species is stable to hydrolysis, but the ruthenium (III) complex undergoes a slow substitution in the acid solution in contrast to the inert ruthenium(III) chloro species.

Financial support in the form of a grant from the National Research Council of Canada and a graduate scholarship (C.M.E.) from the Province of Ontario are gratefully acknowledged.

J. McKenny was the holder of a National Research Council of Canada 1967 Graduate scholarship.

1. P. C. FORD. Coord. Chem. Rev. **5**, 75 (1970).
2. G. N. COLEMAN, J. W. GESLER, F. A. SHIRLEY, and J. R. KUEMPEL. Inorg. Chem. **12**, 1036 (1973).
3. C. M. ELSON, J. GULENS, I. J. ITZKOVITCH, and J. A. PAGE. Chem. Commun. 875 (1970).

4. I. J. ITZKOVITCH and J. A. PAGE. Can. J. Chem. **46**, 2743 (1968).
5. H. S. LIM, D. J. BARCLAY, and F. C. ANSON. Inorg. Chem. **11**, 1460 (1972).
6. T. J. MEYER and H. TAUBE. Inorg. Chem. **7**, 2369 (1968).
7. C. M. ELSON, I. J. ITZKOVITCH, and J. A. PAGE. Can. J. Chem. **48**, 1639 (1970).
8. K. GLEU and W. BREUEL. Z. Anorg. Allg. Chem. **237**, 197 (1938).
9. W. G. MOVIUS and R. G. LINCK. J. Am. Chem. Soc. **92**, 2677 (1970).
10. K. GLEU and W. BREUEL. Z. Anorg. Allg. Chem. **235**, 211 (1937).
11. P. DELAHAY. New instrumental methods in electrochemistry. Interscience Publishers Inc., New York. 1954. p. 119.
12. R. S. NICHOLSON and I. SHAIN. Anal. Chem. **36**, 706 (1964).
13. A. A. FROST and R. G. PEARSON. Kinetics and mechanism, 2nd ed. John Wiley and Sons, Inc., New York. 1961. p. 166.
14. L. H. VOGT, J. L. KATZ, and S. E. WIBERLY. Inorg. Chem. **4**, 1157 (1965).
15. J. H. BAXENDALE, M. A. J. RODGERS, and M. D. WARD. J. Chem. Soc. A, 1246 (1970).
16. P. C. FORD and C. SUTTON. Inorg. Chem. **7**, 1544 (1969).
17. F. BASOLO and R. G. PEARSON. Mechanisms of inorganic reactions, 2nd ed. John Wiley and Sons, Inc., New York. 1967. p. 172.
18. J. M. PRATT and R. G. THORP. Cis and trans effects in cobalt(III) complexes. Advances in inorganic chemistry and radiochemistry, Vol. 12. Academic Press, New York. 1969.

The Crystal and Molecular Structures of Pyrazolyl-, 3-Methylpyrazolyl-, and Indazolylgallium Dimethyl Dimers

DAVID F. RENDLE, ALAN STORR, AND JAMES TROTTER

Department of Chemistry, University of British Columbia, 2075 Wesbrook Place, Vancouver, British Columbia V6T 1W5

Received April 7, 1975

DAVID F. RENDLE, ALAN STORR, and JAMES TROTTER. Can. J. Chem. **53**, 2930 (1975).

Crystals of the pyrazolylgallium dimethyl dimer (**1***a*) are monoclinic, $a = 16.914(3)$, $b = 21.747(6)$, $c = 8.117(2)$ Å, $\beta = 92.09(3)°$, $Z = 8$, space group $P2_1/c$, those of the 3-methylpyrazolylgallium dimethyl dimer (**1***b*) are also monoclinic, $a = 13.473(6)$, $b = 7.162(2)$, $c = 18.468(4)$ Å, $\beta = 113.78(2)°$, $Z = 4$, space group $P2_1/c$, and those of the indazolylgallium dimethyl dimer (**1***c*) are orthorhombic, $a = 8.909(2)$, $b = 27.463(3)$, $c = 15.738(2)$ Å, $Z = 8$, space group *Pbca*. All three structures were solved by Patterson and Fourier methods and were refined by full-matrix least-squares methods to final R values of 0.065, 0.061, and 0.036 for 2542, 2011, and 1986 reflections with $I \geq 3\sigma(I)$ respectively. The three crystal structure analyses emphasize the critical role of steric interaction in determining the molecular geometry for these molecules. The results clearly demonstrate that changing deuterium for methyl groups on the gallium atoms and introducing substituents on the bridging 'pyrazolyl' ligands in the $[D_2Ga{\cdot}N_2C_3H_3]_2$ dimer cause a pronounced flattening of the central Ga—(N—N)$_2$—Ga boat conformation and a noticeable lengthening of the Ga—N bonds. Average Ga—N distances are 1.996, 1.986, 1.996 Å, and V-angles (the angle between the $Ga_2N_2C_3$ moieties) are 131.5, 139.5, and 147.8° in **1***a*, **1***b*, and **1***c* respectively.

DAVID F. RENDLE, ALAN STORR et JAMES TROTTER. Can. J. Chem. **53**, 2930 (1975).

Les cristaux du dimère du complexe (**1***a*) du pyrazolyle avec le diméthyl gallium sont monocliniques, $a = 16.914(3)$, $b = 21.747(6)$, $c = 8.117(2)$ Å, $\beta = 92.09(3)°$, $Z = 8$, groupe d'espace $P2_1/c$ alors que ceux du dimère du complexe (**1***b*) du méthyl-3 pyrazolyle avec le diméthyl gallium sont aussi monocliniques, $a = 13.473(6)$, $b = 7.162(2)$, $c = 18.468(4)$ Å, $\beta = 113.78(2)°$, $Z = 4$, groupe d'espace $P2_1/c$ et ceux du dimère du complexe (**1***c*) de l'indazolyle avec le diméthyl gallium sont orthorhombiques $a = 8.909(2)$, $b = 27.463(3)$, $c = 15.738(2)$ Å, $Z = 8$, groupe d'espace *Pbca*. On a résolu ces trois structures par les méthodes de Patterson et de Fourier et on les a affinées par la méthode des moindres carrés (matrice complète) jusqu'aux valeurs finales respectives de R de 0.065, 0.061 et 0.036 pour 2542, 2011 et 1986 réflexions avec $I \geq 3\sigma(I)$. L'analyse de ces trois structures cristallines met en relief que les interactions stériques jouent un rôle critique pour déterminer la géométrie moléculaire de ces molécules. Les résultats permettent aussi de démontrer sans ambiguité que le remplacement, au niveau des atomes de gallium, de deutérium par des groupes méthyles et que l'introduction de substituants sur les ligands pyrazolyles dans le dimère $[D_2Ga{\cdot}N_2C_3H_3]_2$ produit premièrement un applatissement notable de la conformation bateau du Ga—(N—N)$_2$—Ga central et deuxièmement un allongement important des liens Ga—N. Pour les composés **1***a*, **1***b* et **1***c* respectivement, les distances Ga—N moyennes sont 1.996, 1.986 et 1.996 Å et les angles V (l'angle entre les deux portions de $Ga_2N_2C_3$) sont de 131.5, 139.5 et 147.8°.

[Traduit par le journal]

Introduction

A previous report (1) presented the first structural characterization of a member of the class of symmetrical dimeric compounds, *viz.* $[D_2Ga{\cdot}N_2C_3H_3]_2$, involving pyrazole ligands and Group III moieties, and containing as the central feature a six-membered M—(N—N)$_2$—M ring (where M = B, Al, or Ga). Crystal structures of numerous related pyrazolyl–borate and –gallate transition metal complexes have been published (refs. 2 and 3 and references therein) but these differ from the title compounds in having unsymmetrical six-membered M—(N—N)$_2$—M′ rings (where M = B, or Ga; M′ = transition metal) incorporating the Group III atom. The present investigation probes the steric effects of substituents, on both the gallium atoms and on the 'pyrazolyl' bridging moieties, on the geometry of the central symmetrical Ga—(N—N)$_2$—Ga rings in this class of compound. Three crystal structure determinations are described, pyrazolylgallium dimethyl dimer, $(Me_2Ga{\cdot}N_2C_3H_3]_2$, **1***a*; 3-methyl pyrazolylgallium dimethyl dimer, $[Me_2Ga{\cdot}N_2C_4H_5]_2$, **1***b*; and indazolylgallium dimethyl

Can. J. Chem. Downloaded from www.nrcresearchpress.com by 210.87.254.40 on 09/05/12
For personal use only.

Can. J. Chem. Downloaded from www.nrcresearchpress.com by 210.87.254.40 on 09/05/12
For personal use only.

dimer, $[Me_2Ga{\cdot}N_2C_7H_5]_2$, **1***c*. The results clearly demonstrate that changing deuterium for methyl groups on the gallium atoms and introducing substituents on the bridging ligands cause a pronounced flattening of the Ga—(N—N)$_2$—Ga boat conformation found in the original $[D_2Ga{\cdot}N_2C_2H_3]_2$ dimer (1).

Experimental

The three compounds studied were prepared[1] by reacting stoichiometric ratios of trimethylgallium and the "active-hydrogen" containing ligand in refluxing benzene solvent under an atmosphere of dry nitrogen. On cessation of methane evolution the benzene solvent was removed and the products recrystallized from toluene. The three compounds were air-stable and no precautions were necessary in mounting crystal samples for X-ray study.

*Crystallographic Studies of the Pyrazolylgallium Dimethyl Dimer (**1a**)*

The crystal chosen for study was mounted with c^* parallel to the goniostat axis and had dimensions of *ca.* 0.25 × 0.29 × 0.42 mm^3. Unit cell and space group data were obtained from film and diffractometer measurements. The unit cell parameters were refined by a least-squares treatment of $\sin^2\theta$ values for 16 reflections measured on a diffractometer with CuK$_\alpha$ radiation. Crystal data are: $C_{10}H_{18}Ga_2N_4$ f.w. = 333.7 Monoclinic, a = 16.914(3), b = 21.747(6), c = 8.117(2) Å, β = 92.09(3)°, V = 2983.5 Å^3, Z = 8 (2 molecules per asymmetric unit), ρ_c = 1.485 g cm^{-3}, $F(000)$ = 1344 (20 °C, CuK$_\alpha$, λ = 1.5418 Å, μ = 46.5 cm^{-1}.) Absent reflections: $0k0$, $k \neq 2n$ and $h0l$, $l \neq 2n$ define uniquely the space group $P2_1/c$ (C_{2h}^5, No. 14).

Intensities were measured on a Datex-automated General Electric XRD 6 diffractometer equipped with a scintillation counter, nickel filter, and pulse height analyzer. The θ–2θ scan technique was employed at a rate of 2° min^{-1} in 2θ. Data were measured to 2θ = 115° and a standard reflection was monitored every 40 reflections. The data were accordingly scaled, Lorentz and polarization corrections were applied, and the structure amplitudes derived. No absorption correction was applied because of the irregular crystal surface. Of the 4091 independent reflections measured, 1536 had intensities less than $3\sigma(I)$ above background where $\sigma^2(I) = S + B + (0.05S)^2$ with S = scan count and B = time averaged background count. These reflections were given zero weight in the refinement.

The structure was solved via the Patterson function and successive difference-Fourier syntheses. Two cycles of full-matrix least-squares refinement in which all nonhydrogen atoms were permitted anisotropic thermal motion reduced R to 0.070. A difference-Fourier synthesis at this point failed to reveal the majority of the hydrogen atom positions and so positions for the hydrogens were calculated assuming C—H 1.0 Å and ideal sp^2 and sp^3 geometry about the appropriate carbon atoms. Hydrogen atoms were placed in these positions, included in structure factor calculations (B = 6 Å^2), but not refined. Refinement converged with R 0.065 and R_w 0.085 [$R_w = (\Sigma w(|F_o| - |F_c|)^2/\Sigma w|F_o|^2)^{1/2}$] for 2542 reflections with $I \geq 3\sigma(I)$. Thirteen reflections (−1 0 2, −1 −1 1, −5 −1 1, 2 0 0, 4 0 0, 6 0 0, 2 1 0, 4 1 0, 6 3 0, 0 4 0, 4 1 1, 5 1 1, and 4 0 2) were given zero weight in the last cycle of refinement because of suspected extinction effects. The function minimized in the refinement was $\Sigma w(|F_o| - |F_c|)^2$ with weights w derived from counting statistics. The scattering factors for the nonhydrogen atoms were taken from ref. 4 and those for H from ref. 5. Those for Ga were corrected for the real and imaginary parts of anomalous dispersion (6). The maximum shift to error ratio in the refined parameters at convergence was 0.95 (the U_{13} term of atom C(17)) while the average value was 0.21. The error in an observation of unit weight was 1.48.

*Crystallographic Studies of the 3-Methylpyrazolylgallium Dimethyl Dimer (**1b**)*

Experimental details for **1***b* are the same as for compound **1***a* except where noted. The crystal was mounted with b parallel to the goniostat axis and had dimensions of *ca.* 0.32 × 0.61 × 0.30 mm^3. Seventeen reflections measured with CuK$_\alpha$ radiation were employed in the refinement of the unit cell parameters. Crystal data are: $C_{12}H_{22}Ga_2N_4$ f.w. = 361.8 Monoclinic, a = 13.473(6), b = 7.162(2), c = 18.468(4) Å, β = 113.78(2)°, V = 1630.9Å^3, Z = 4, ρ_c = 1.473 g cm^{-3}, $F(000)$ = 736 (20 °C, CuK$_\alpha$, λ = 1.5418 Å, μ = 43.0 cm^{-1}). Absent reflections: $0k0$, $k \neq 2n$ and $h0l$, $l \neq 2n$ define uniquely the space group $P2_1/c$ (C_{2h}^5, No. 14).

Of the 2416 independent reflections measured with $2\theta \leq 120°$, 398 had intensities less than $3\sigma(I)$ above background.

The coordinates of the gallium atoms were deduced from a three-dimensional Patterson function, and the remainder of the atomic positions from successive difference-Fourier syntheses. The nonhydrogen atoms were refined with anisotropic temperature factors and R fell to 0.072. A difference-Fourier synthesis revealed the positions of the hydrogen atoms and these were included in the refinement with isotropic thermal parameters. Convergence was reached with R 0.061 and R_w 0.078 for 2011 reflections with $I \geq 3\sigma(I)$. Seven reflections (2 0 −6, 1 1 −5, 2 0 −4, 2 0 −2, 4 0 −2, 0 0 2, and 0 0 4) were given zero weight in the final cycle because of suspected extinction errors. The error in an observation of unit weight was 2.29. The mean shift to error ratio in the refined parameters was 0.48 and the largest was 1.98 (the temperature factor of H(9*c*)).

*Crystallographic Studies of the Indazolylgallium Dimethyl Dimer (**1c**)*

Experimental details for **1***c* are the same as for **1***a* again, except where noted. The crystal was mounted with a parallel to the goniostat axis and had dimensions of *ca.* 0.40 × 0.21 × 0.25 mm^3. Twelve reflections measured with CuK$_\alpha$ radiation were employed in the refinement of the unit cell parameters. Crystal data are: $C_{18}H_{22}Ga_2N_4$ f.w. = 433.8 Orthorhombic, a = 8.909(2), b = 27.463(3), c = 15.738(2) Å, V = 3850.7 Å^3, Z = 8, ρ_c = 1.496 g cm^{-3}, $F(000)$ = 1760 (20 °C, CuK$_\alpha$, λ = 1.5418 Å, μ = 37.5 cm^{-1}). Absent reflections: $0kl$, $k \neq 2n$, $h0l$, $l \neq 2n$, $hk0$, $h \neq 2n$ define uniquely the space group $Pbca$ (D_{2h}^{15}, No. 61).

Of the 2635 independent reflections measured with $2\theta \leq 115°$, 643 had intensities less than $3\sigma(I)$ above background.

[1] T. Baker and A. Storr. Unpublished results.

Can. J. Chem. Downloaded from www.nrcresearchpress.com by 210.87.254.40 on 09/05/12
For personal use only.

TABLE 1. Final positional parameters (fractional × 10^4, Ga × 10^5) with estimated standard deviations in parentheses

Atom	x	y	z
	$[Me_2Ga{\cdot}N_2C_3H_3]_2$		
Ga(1)	94616(7)	42633(7)	26844(16)
Ga(2)	46053(8)	11236(6)	37745(17)
Ga(3)	25074(8)	15575(7)	36431(18)
Ga(4)	74800(8)	36408(7)	19561(18)
N(1)	3001(5)	980(4)	2046(10)
N(2)	3771(5)	797(4)	2195(10)
N(3)	9206(5)	3549(4)	1238(11)
N(4)	7962(5)	3842(4)	4188(10)
N(5)	3414(5)	2132(4)	3837(11)
N(6)	8471(5)	3292(4)	1060(10)
N(7)	8698(6)	4054(4)	4413(10)
N(8)	4179(5)	1976(4)	3927(11)
C(1)	2664(7)	720(6)	732(15)
C(2)	3212(10)	338(6)	41(15)
C(3)	3897(8)	402(6)	932(16)
C(4)	3396(9)	2762(7)	4094(15)
C(5)	4127(9)	2992(6)	4242(16)
C(6)	4598(7)	2497(7)	4131(17)
C(7)	5573(7)	1190(7)	2515(17)
C(8)	4572(8)	742(5)	5953(14)
C(9)	2396(8)	1121(7)	5800(16)
C(10)	1665(7)	1995(8)	2467(17)
C(11)	9704(8)	3208(7)	368(18)
C(12)	9326(9)	2719(7)	−387(19)
C(13)	8564(9)	2780(6)	61(16)
C(14)	7626(8)	3778(6)	5651(17)
C(15)	8194(11)	3945(8)	6870(16)
C(16)	8839(9)	4123(7)	6055(16)
C(17)	10514(8)	4115(7)	3634(19)
C(18)	9193(8)	5027(6)	1623(14)
C(19)	6741(8)	2941(7)	2175(20)
C(20)	7155(7)	4402(6)	869(14)
H(1)	2109	709	345
H(2)	2959	4992	4373
H(3)	4547	258	741
H(4)	2756	2912	4309
H(5)	4535	3406	4698
H(6)	5236	2519	4294
H(7*a*)	5893	849	2405
H(7*b*)	5523	1481	1584
H(7*c*)	6144	1304	2962
H(8*a*)	4617	243	5848
H(8*b*)	5046	353	7117
H(8*c*)	4211	264	6275
H(9*a*)	1822	967	5830
H(9*b*)	3044	972	6224
H(9*c*)	2083	1384	6610
H(10*a*)	1249	1936	2058
H(10*b*)	1363	2312	3620
H(10*c*)	1793	2170	1524
H(11)	10342	3268	468
H(12)	9830	2476	−1191
H(13)	8018	2540	−76
H(14)	6997	3661	5585

TABLE 1 (*Continued*)

Atom	*x*	*y*	*z*
H(15)	8064	4076	8255
H(16)	9485	4331	6696
H(17*a*)	10955	4201	3077
H(17*b*)	10698	4502	4315
H(17*c*)	10545	3760	4336
H(18*a*)	9063	5073	370
H(18*b*)	8659	5143	1239
H(18*c*)	9328	5408	2282
H(19*a*)	6461	2969	3318
H(19*b*)	6364	2767	225
H(19*c*)	7304	2443	2783
H(20*a*)	6520	4458	813
H(20*b*)	7593	4701	606
H(20*c*)	7231	4483	−227
	$[Me_2Ga{\cdot}N_2C_4H_5]_2$ (H × 10^3)		
Ga(1)	19996(6)	5176(13)	13740(4)
Ga(2)	33334(7)	10502(12)	35264(4)
N(1)	4105(4)	816(7)	2808(3)
N(2)	3574(4)	825(7)	1999(3)
N(3)	1472(4)	2203(8)	1991(3)
N(4)	2024(4)	2416(8)	2796(3)
C(1)	5171(5)	701(9)	2998(4)
C(2)	5343(6)	654(11)	2322(5)
C(3)	4345(6)	731(11)	1718(5)
C(4)	578(7)	3277(12)	1786(5)
C(5)	522(7)	4136(11)	2413(5)
C(6)	1432(7)	3545(12)	3037(5)
C(7)	5986(8)	652(15)	3850(6)
C(8)	−228(9)	3370(18)	898(6)
C(9)	1538(9)	−1972(17)	1469(9)
C(10)	1743(10)	1517(20)	328(5)
C(11)	2947(12)	−1377(20)	3742(10)
C(12)	4053(9)	2873(17)	4362(6)
H(2)	589(6)	50(9)	223(4)
H(3)	418(5)	45(8)	123(4)
H(5)	−2(7)	502(13)	235(5)
H(6)	167(6)	397(10)	348(4)
H(7*a*)	599(9)	227(17)	417(6)
H(7*b*)	662(7)	40(11)	386(4)
H(7*c*)	557(6)	2(11)	424(4)
H(8*a*)	1(10)	253(15)	58(7)
H(8*b*)	−97(8)	300(15)	86(8)
H(8*c*)	−26(10)	469(15)	71(6)
H(9*a*)	210(10)	−321(17)	153(6)
H(9*b*)	101(11)	−245(19)	95(8)
H(9*c*)	120(17)	−196(34)	161(13)
H(10*a*)	168(6)	279(12)	38(5)
H(10*b*)	232(11)	158(21)	22(7)
H(10*c*)	85(14)	130(20)	0(8)
H(11*a*)	262(12)	−203(20)	342(8)
H(11*b*)	326(10)	−185(19)	400(7)
H(11*c*)	252(14)	−126(24)	406(10)
H(12*a*)	424(12)	345(22)	411(8)
H(12*b*)	370(7)	325(13)	469(5)
H(12*c*)	468(10)	248(15)	470(7)

Can. J. Chem. Downloaded from www.nrcresearchpress.com by 210.87.254.40 on 09/05/12
For personal use only.

TABLE 1 (*Concluded*)

Atom	*x*	*y*	*z*
	$[Me_2Ga{\cdot}N_2C_7H_5]_2$ (H × 10^3)		
Ga(1)	13669(8)	16137(2)	13889(4)
Ga(2)	42037(7)	10219(2)	−221(4)
N(1)	989(5)	1144(2)	440(3)
N(2)	1979(5)	951(1)	−106(3)
N(3)	3213(5)	1925(2)	947(3)
N(4)	4300(5)	1689(1)	496(3)
C(1)	−385(7)	971(2)	252(4)
C(2)	−311(6)	651(2)	−405(4)
C(3)	1226(6)	646(2)	−634(3)
C(4)	1757(8)	357(2)	−1308(4)
C(5)	681(10)	89(3)	−1738(5)
C(6)	−818(9)	93(3)	−1532(5)
C(7)	−1336(8)	367(2)	−886(5)
C(8)	3792(6)	2362(2)	1189(3)
C(9)	5268(6)	2410(2)	887(3)
C(10)	5530(7)	1975(2)	443(4)
C(11)	3129(8)	2741(2)	1653(4)
C(12)	3978(10)	3146(2)	1809(4)
C(13)	5436(9)	3191(3)	1507(5)
C(14)	6102(8)	2833(3)	1075(5)
C(15)	1904(13)	1239(4)	2391(5)
C(16)	−301(10)	2084(4)	1330(8)
C(17)	4925(10)	558(3)	807(5)
C(18)	5039(11)	1128(4)	−1163(5)
H(1)	−116(7)	108(2)	55(4)
H(4)	291(7)	37(2)	−148(3)
H(5)	103(7)	−10(3)	−211(5)
H(6)	−160(7)	−9(2)	−188(4)
H(7)	−227(6)	36(2)	−75(3)
H(10)	647(7)	188(2)	18(3)
H(11)	227(6)	271(2)	188(3)
H(12)	349(6)	337(2)	209(3)
H(13)	576(7)	345(2)	163(4)
H(14)	697(6)	282(2)	77(3)
H(15*a*)	276(8)	106(3)	233(5)
H(15*b*)	209(8)	139(3)	279(4)
H(15*c*)	113(10)	104(3)	251(5)
H(16*a*)	−67(9)	221(3)	97(5)
H(16*b*)	−121(11)	187(4)	137(6)
H(16*c*)	−9(9)	232(3)	186(5)
H(17*a*)	467(8)	54(2)	130(4)
H(17*b*)	480(7)	25(3)	64(4)
H(17*c*)	580(8)	57(3)	82(5)
H(18*a*)	456(8)	143(2)	−143(4)
H(18*b*)	596(9)	121(3)	−112(5)
H(18*c*)	516(9)	90(3)	−144(5)

The coordinates of the gallium atoms were again deduced from the Patterson function, difference-Fourier syntheses revealing the remainder of the molecule. The nonhydrogen atoms were refined with anisotropic temperature factors and R fell to 0.055. A difference-Fourier synthesis at this point revealed all the hydrogen atoms and they were included in the refinement with isotropic thermal parameters. At convergence R was 0.036 and R_w 0.052 for 1986 reflections with $I \geq 3\sigma(I)$. Six reflections (2 0 0, 0 4 0, 1 2 1, 0 0 2, 0 6 2, and 0 6 4) were given zero weight in the final cycle because of suspected extinction errors. The error in an observation of unit weight was 1.47 and the mean shift to error ratio in the refined parameters was 0.419. The largest ratio was 2.22 (the temperature factor of H(16*b*)). Measured and calculated structure factors have been placed in the Depository of

Can. J. Chem. Downloaded from www.nrcresearchpress.com by 210.87.254.40 on 09/05/12
For personal use only.

Can. J. Chem. Downloaded from www.nrcresearchpress.com by 210.87.254.40 on 09/05/12
For personal use only.

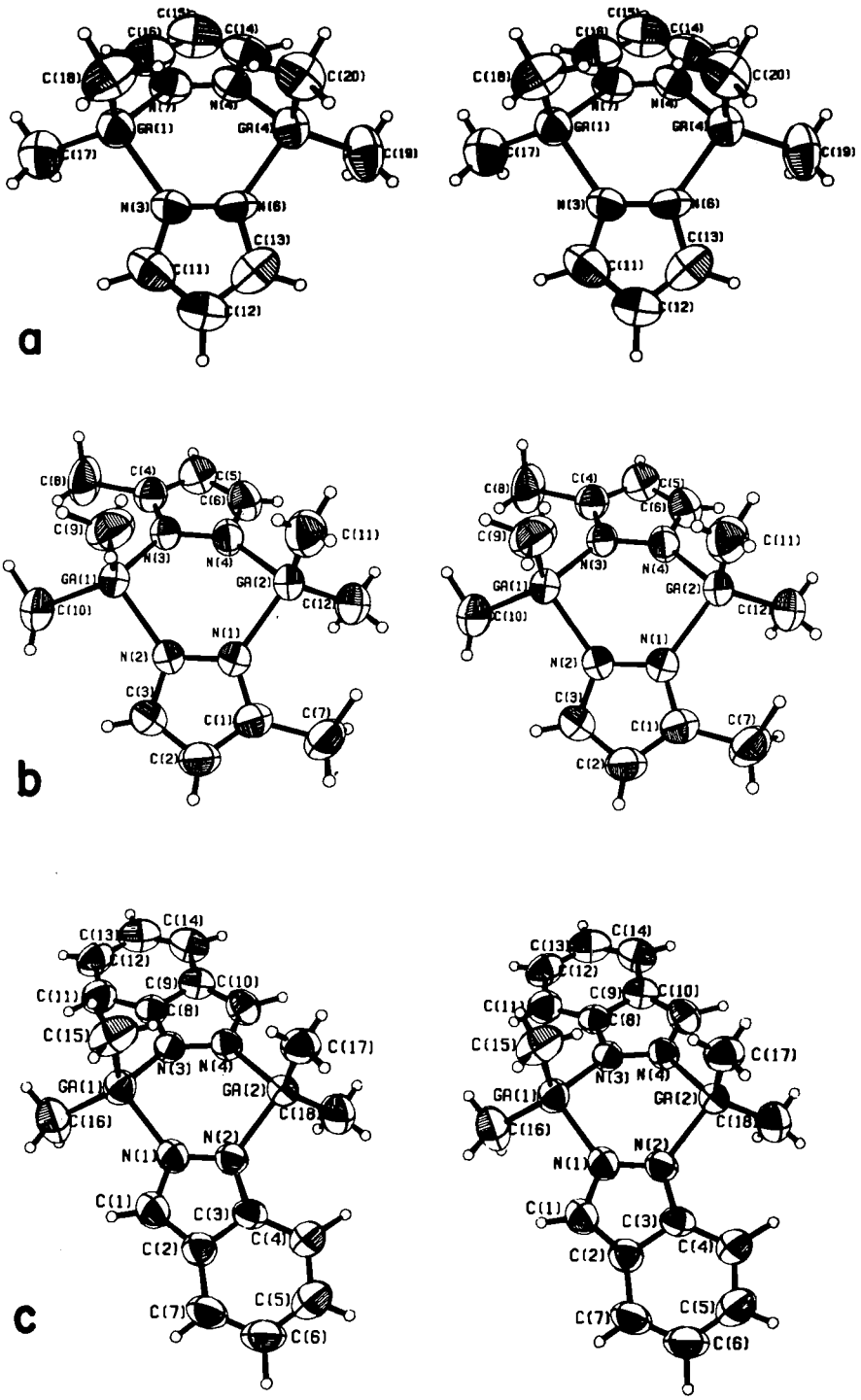

FIG. 1. Stereoscopic views of the molecules **1***a*, **1***b*, and **1***c*.

Can. J. Chem. Downloaded from www.nrcresearchpress.com by 210.87.254.40 on 09/05/12
For personal use only.

TABLE 2. Final thermal parameters and their estimated standard deviations
(*a*) Anisotropic thermal parameters[a] ($U_{ij} \times 10^3$ Å^2)

Atom	U_{11}	U_{22}	U_{33}	U_{12}	U_{13}	U_{23}
			$[Me_2Ga{\cdot}N_2C_3H_3]_2$			
Ga(1)	64(1)	81(1)	66(1)	−5(1)	7(1)	−7(1)
Ga(2)	70(1)	68(1)	73(1)	6(1)	10(1)	5(1)
Ga(3)	65(1)	84(1)	78(1)	−3(1)	18(1)	−6(1)
Ga(4)	64(1)	76(1)	78(1)	−6(1)	5(1)	2(1)
N(1)	68(6)	69(6)	60(5)	−8(5)	10(5)	−2(5)
N(2)	78(6)	58(6)	59(5)	−7(5)	16(4)	−3(5)
N(3)	64(6)	76(6)	63(6)	6(5)	12(5)	−14(5)
N(4)	67(6)	72(6)	59(5)	7(5)	14(4)	7(5)
N(5)	67(6)	67(7)	75(6)	−1(5)	11(5)	−3(5)
N(6)	79(7)	62(6)	57(5)	14(5)	1(4)	−16(5)
N(7)	83(7)	82(7)	44(5)	4(5)	7(5)	−3(4)
N(8)	62(6)	62(6)	84(7)	−4(5)	12(5)	−6(5)
C(1)	74(8)	78(9)	82(8)	−19(7)	−3(7)	−6(7)
C(2)	138(13)	70(9)	78(9)	−29(9)	19(9)	−1(7)
C(3)	94(9)	71(8)	82(8)	−5(7)	32(7)	−9(7)
C(4)	123(12)	74(10)	76(8)	16(8)	10(8)	−4(7)
C(5)	109(11)	76(10)	83(9)	−18(9)	6(8)	−13(7)
C(6)	77(9)	88(10)	108(10)	−14(8)	−6(7)	12(8)
C(7)	69(8)	126(12)	115(10)	15(8)	29(7)	28(9)
C(8)	136(11)	64(8)	76(8)	8(7)	10(7)	22(6)
C(9)	95(9)	119(11)	87(9)	−23(8)	42(7)	−1(8)
C(10)	61(8)	180(15)	105(10)	20(9)	11(7)	16(11)
C(11)	79(9)	111(12)	104(10)	12(9)	29(8)	−1(9)
C(12)	99(11)	104(12)	127(12)	15(9)	22(9)	−34(10)
C(13)	122(12)	81(10)	84(9)	−15(8)	−9(8)	−9(8)
C(14)	102(10)	93(10)	82(9)	23(8)	43(8)	14(8)
C(15)	150(14)	131(13)	56(8)	14(11)	30(9)	11(8)
C(16)	132(12)	109(11)	60(8)	10(9)	4(8)	−8(7)
C(17)	92(10)	132(13)	124(12)	−10(9)	1(8)	−21(10)
C(18)	130(11)	79(9)	65(8)	−1(8)	−13(7)	1(7)
C(19)	81(9)	127(12)	151(14)	−38(9)	11(9)	18(11)
C(20)	91(9)	92(9)	74(8)	14(7)	−1(6)	19(7)
			$[Me_2Ga{\cdot}N_2C_4H_5]_2$ (Ga $\times 10^4$)			
Ga(1)	537(5)	767(6)	437(5)	−58(4)	159(4)	−69(4)
Ga(2)	560(5)	740(6)	423(5)	−16(4)	163(4)	30(4)
N(1)	52(3)	63(3)	49(3)	−2(2)	18(3)	0(2)
N(2)	54(3)	71(3)	44(3)	−5(3)	21(3)	−1(2)
N(3)	53(3)	65(3)	45(3)	1(3)	17(2)	8(2)
N(4)	63(3)	75(4)	47(3)	7(3)	20(3)	0(3)
C(1)	51(4)	63(4)	68(5)	1(3)	23(3)	5(3)
C(2)	52(4)	78(5)	78(5)	1(4)	30(4)	3(4)
C(3)	63(5)	86(5)	61(5)	−6(4)	32(4)	−7(4)
C(4)	60(5)	72(5)	59(6)	2(4)	19(4)	10(4)
C(5)	76(5)	71(5)	78(6)	11(4)	31(5)	4(4)
C(6)	86(6)	78(5)	60(5)	9(4)	34(5)	−3(4)
C(7)	55(5)	106(7)	76(6)	3(5)	10(4)	16(5)
C(8)	84(6)	129(9)	55(6)	37(6)	0(5)	9(6)
C(9)	69(5)	91(7)	100(8)	−18(5)	28(5)	−16(5)
C(10)	80(7)	137(10)	51(5)	−9(6)	15(5)	3(5)
C(11)	88(7)	91(8)	72(7)	−9(6)	24(6)	10(7)
C(12)	83(6)	108(7)	59(5)	−13(6)	22(5)	−19(5)

TABLE 2 (*Concluded*)

Atom	U_{11}	U_{22}	U_{33}	U_{12}	U_{13}	U_{23}
			$[Me_2Ga{\cdot}N_2C_7H_5]_2$ (Ga × 10^4)			
Ga(1)	616(5)	696(5)	631(4)	−112(4)	110(3)	−56(3)
Ga(2)	498(4)	596(4)	594(4)	19(3)	−16(3)	−24(3)
N(1)	50(3)	67(3)	69(3)	−3(2)	7(2)	−5(2)
N(2)	51(3)	56(3)	69(3)	0(2)	−2(2)	−4(2)
N(3)	53(3)	56(3)	60(2)	−8(2)	5(2)	−6(2)
N(4)	52(3)	53(2)	67(3)	−4(2)	3(2)	0(2)
C(1)	59(4)	77(4)	87(4)	−6(3)	10(3)	−12(4)
C(2)	58(3)	58(3)	74(3)	0(3)	−1(3)	−2(3)
C(3)	52(3)	52(3)	67(3)	0(3)	−13(3)	0(3)
C(4)	74(4)	80(4)	85(4)	5(3)	−8(4)	−21(4)
C(5)	104(6)	92(5)	92(5)	3(5)	−11(5)	−30(4)
C(6)	79(5)	85(5)	111(6)	−6(4)	−31(5)	−23(4)
C(7)	56(4)	79(4)	114(5)	−12(3)	−13(4)	−12(4)
C(8)	57(3)	58(3)	53(3)	−2(2)	−3(3)	4(3)
C(9)	68(4)	47(3)	70(3)	−8(3)	−8(3)	9(3)
C(10)	58(4)	69(4)	85(4)	−5(3)	8(3)	7(3)
C(11)	77(4)	76(4)	72(4)	−7(4)	2(4)	−6(3)
C(12)	106(6)	58(4)	81(4)	2(4)	−15(4)	−16(3)
C(13)	104(6)	50(4)	94(5)	−16(4)	−19(4)	7(4)
C(14)	76(5)	70(4)	90(5)	−20(4)	−2(4)	14(4)
C(15)	123(8)	98(6)	67(5)	−28(6)	−4(5)	0(4)
C(16)	70(5)	105(6)	128(8)	7(5)	23(5)	−13(6)
C(17)	83(5)	71(5)	74(5)	6(4)	−14(4)	1(4)
C(18)	82(6)	105(6)	82(5)	2(5)	16(4)	−2(5)

(*b*) Isotropic thermal parameters (U × 100)

Atom	U (Å²)	Atom	U (Å²)
	$[Me_2Ga{\cdot}N_2C_4H_5]_2$		
H(2)	7(2)	H(9*b*)	16(5)
H(3)	5(2)	H(9*c*)	9(4)
H(5)	10(3)	H(10*a*)	8(3)
H(6)	6(2)	H(10*b*)	22(6)
H(7*a*)	17(4)	H(10*c*)	24(6)
H(7*b*)	10(3)	H(11*a*)	8(7)
H(7*c*)	8(2)	H(11*b*)	11(6)
H(8*a*)	15(5)	H(11*c*)	27(9)
H(8*b*)	14(4)	H(12*a*)	16(7)
H(8*c*)	15(4)	H(12*b*)	11(3)
H(9*a*)	14(4)	H(12*c*)	14(4)
	$[Me_2Ga{\cdot}N_2C_7H_5]_2$		
H(1)	11(2)	H(15*b*)	14(3)
H(4)	9(2)	H(15*c*)	20(4)
H(5)	13(3)	H(16*a*)	21(4)
H(6)	11(2)	H(16*b*)	26(4)
H(7)	8(2)	H(16*c*)	23(3)
H(10)	10(2)	H(17*a*)	9(3)
H(11)	5(2)	H(17*b*)	12(2)
H(12)	7(2)	H(17*c*)	11(3)
H(13)	6(2)	H(18*a*)	9(2)
H(14)	6(2)	H(18*b*)	13(3)
H(15*a*)	14(3)	H(18*c*)	13(3)

[a]The anisotropic temperature factor expression is of the form: $\exp[-2\pi^2(U_{11}h^2a^{*2} + U_{22}k^2b^{*2} + U_{33}l^2c^{*2} + 2U_{12}hka^*b^* + 2U_{13}hla^*c^* + 2U_{23}klb^*c^*)]$.

Can. J. Chem. Downloaded from www.nrcresearchpress.com by 210.87.254.40 on 09/05/12
For personal use only.

Can. J. Chem. Downloaded from www.nrcresearchpress.com by 210.87.254.40 on 09/05/12
For personal use only.

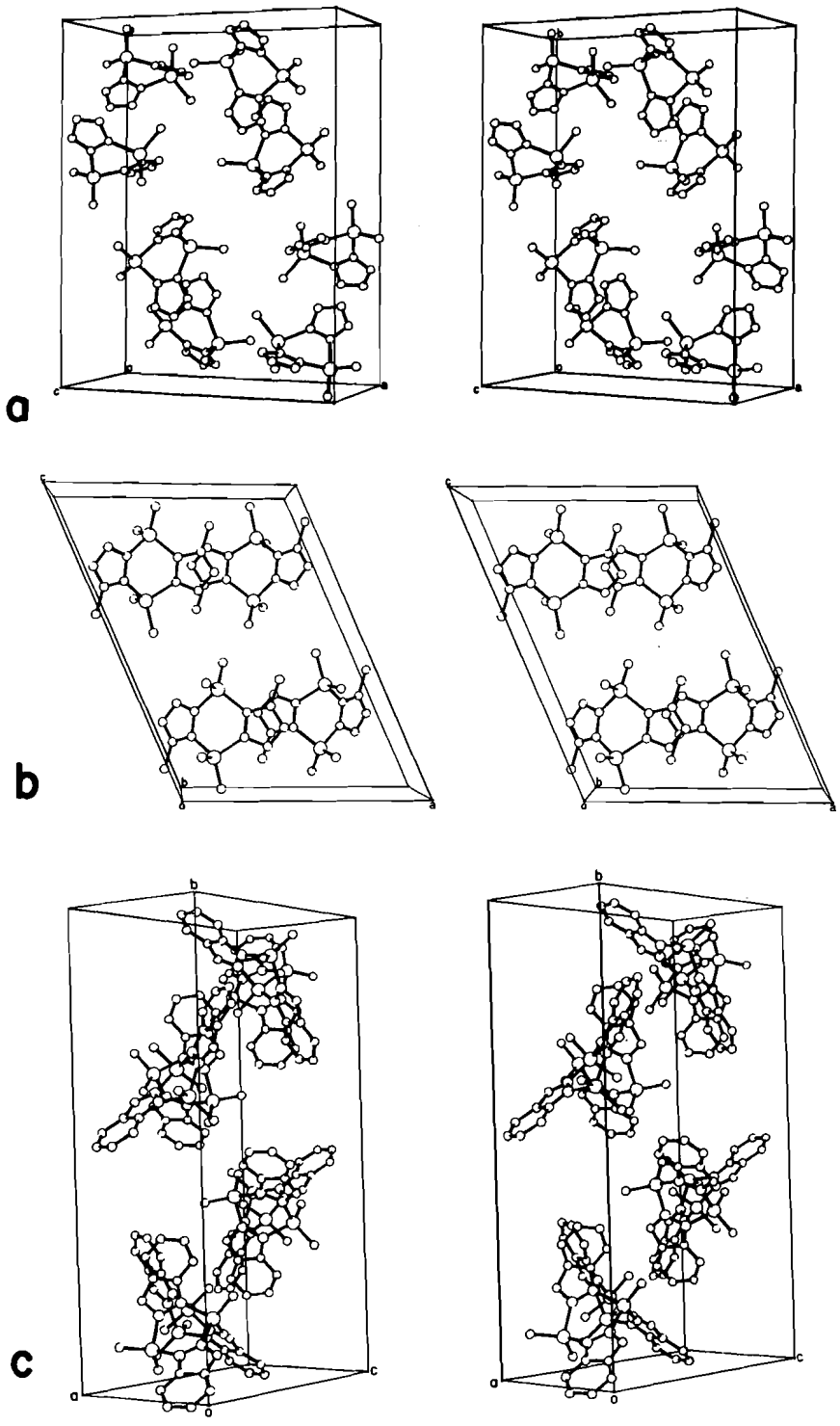

FIG. 2. Stereoscopic views of the unit cells for **1***a*, **1***b*, and **1***c*.

TABLE 3. Bond lengths (Å) with estimated standard deviations in parentheses

Bond	Distance (Å)	Bond	Distance (Å)
	$[Me_2Ga{\cdot}N_2C_3H_3]_2$		
Ga(1)—N(3)	1.985(9)	Ga(4)—C(19)	1.981(15)
Ga(1)—N(7)	1.995(9)	Ga(4)—C(20)	1.947(13)
Ga(1)—C(17)	1.941(14)	Ga(4)—N(4)	2.006(8)
Ga(1)—C(18)	1.919(12)	Ga(4)—N(6)	2.002(9)
N(3)—N(6)	1.37(1)	N(4)—N(7)	1.33(1)
N(3)—C(11)	1.34(2)	N(4)—C(14)	1.34(2)
N(6)—C(13)	1.39(2)	N(7)—C(16)	1.35(2)
C(11)—C(12)	1.37(2)	C(12)—C(13)	1.36(2)
C(14)—C(15)	1.40(2)	C(15)—C(16)	1.35(2)
	$[Me_2Ga{\cdot}N_2C_4H_5]_2$		
Ga(1)—N(2)	1.977(6)	N(1)—C(1)	1.336(10)
Ga(1)—N(3)	1.978(6)	N(2)—C(3)	1.336(11)
Ga(1)—C(9)	1.920(12)	N(3)—C(4)	1.348(11)
Ga(1)—C(10)	1.956(10)	N(4)—C(6)	1.332(11)
Ga(2)—N(1)	1.995(6)	C(1)—C(2)	1.359(11)
Ga(2)—N(4)	1.993(6)	C(2)—C(3)	1.359(12)
Ga(2)—C(11)	1.903(15)	C(4)—C(5)	1.340(13)
Ga(2)—C(12)	1.955(11)	C(5)—C(6)	1.368(13)
N(1)—N(2)	1.372(7)	C(1)—C(7)	1.513(12)
N(3)—N(4)	1.376(7)	C(4)—C(8)	1.560(15)
	$[Me_2Ga{\cdot}N_2C_7H_5]_2$		
Ga(1)—N(1)	2.001(5)	N(4)—C(10)	1.350(7)
Ga(1)—N(3)	1.980(4)	C(1)—C(2)	1.359(9)
Ga(1)—C(15)	1.943(9)	C(2)—C(3)	1.417(7)
Ga(1)—C(16)	1.972(9)	C(3)—C(4)	1.406(8)
Ga(2)—N(2)	1.996(4)	C(4)—C(5)	1.384(11)
Ga(2)—N(4)	2.006(4)	C(5)—C(6)	1.375(12)
Ga(2)—C(17)	1.934(8)	C(6)—C(7)	1.348(11)
Ga(2)—C(18)	1.967(9)	C(7)—C(2)	1.420(9)
N(1)—N(2)	1.343(6)	C(8)—C(9)	1.404(8)
N(3)—N(4)	1.366(6)	C(9)—C(10)	1.404(8)
N(1)—C(1)	1.347(8)	C(8)—C(11)	1.400(8)
N(2)—C(3)	1.357(7)	C(11)—C(12)	1.368(10)
N(3)—C(8)	1.361(7)	C(12)—C(13)	1.389(12)
C(13)—C(14)	1.335(10)	C(14)—C(9)	1.410(9)

Unpublished Data.[2] Final atomic coordinates and thermal parameters for all three compounds are listed in Tables 1 and 2 respectively.

Results and Discussion

The three compounds contain as the central feature a six-membered Ga—(N—N)$_2$—Ga ring in the boat conformation. A previous study (1) reported the first example of this class of compound and the present investigation emphasizes the critical role of steric interactions, between the gallium methyl groups and substituents on the pyrazolyl rings, in determining the molecular geometry for these molecules. Stereoscopic views of the three molecules are shown in Fig. 1. Figure 2 shows stereoscopic views of the three unit cells. Bond lengths and valency angles are given in Tables 3 and 4 respectively and Table 5 gives selected mean planes and dihedral angles. Table 6 compares a number of parameters with similar data obtained for $[D_2Ga{\cdot}N_2C_3H_3]_2$ (1) and $[Me_2Ga{\cdot}N_2C_5H_7]_2$ (7), and Table 7 lists some important intramolecular nonbonded distances. As there are no significant differences of real importance between the two independent molecules in **1***a*, only one is shown in Fig. 1 and referred to in the tables of bond distances and valency angles.

[2]The structure factor table is available, at a nominal charge, from the Depository of Unpublished Data, CISTI, National Research Council of Canada, Ottawa, Canada K1A 0S2.

Can. J. Chem. Downloaded from www.nrcresearchpress.com by 210.87.254.40 on 09/05/12
For personal use only.

Can. J. Chem. Downloaded from www.nrcresearchpress.com by 210.87.254.40 on 09/05/12
For personal use only.

TABLE 4. Valency angles (deg) with estimated standard deviations in parentheses

Bonds	Angle (deg)	Bonds	Angle (deg)
	$[Me_2Ga{\cdot}N_2C_3H_3]_2$		
N(3)—Ga(1)—N(7)	96.0(4)	N(3)—Ga(1)—C(17)	106.3(5)
N(3)—Ga(1)—C(18)	111.7(4)	N(7)—Ga(1)—C(17)	106.9(5)
N(7)—Ga(1)—C(18)	111.4(5)	C(17)—Ga(1)—C(18)	121.5(6)
N(4)—Ga(4)—N(6)	95.3(4)	N(4)—Ga(4)—C(19)	108.9(5)
N(4)—Ga(4)—C(20)	108.9(4)	N(6)—Ga(4)—C(19)	106.3(5)
N(6)—Ga(4)—C(20)	112.6(4)	C(19)—Ga(4)—C(20)	121.7(6)
Ga(1)—N(3)—N(6)	124.1(7)	Ga(1)—N(3)—C(11)	128.1(8)
N(6)—N(3)—C(11)	107.7(9)	Ga(4)—N(4)—N(7)	123.0(6)
Ga(4)—N(4)—C(14)	127.2(8)	N(7)—N(4)—C(14)	109.7(9)
Ga(4)—N(6)—N(3)	125.3(7)	Ga(4)—N(6)—C(13)	129.1(9)
N(3)—N(6)—C(13)	105.5(9)	Ga(1)—N(7)—N(4)	127.4(6)
Ga(1)—N(7)—C(16)	124.9(9)	N(4)—N(7)—C(16)	108(1)
N(3)—C(11)—C(12)	112(1)	C(11)—C(12)—C(13)	104(1)
C(12)—C(13)—N(6)	111(1)	N(4)—C(14)—C(15)	107(1)
C(14)—C(15)—C(16)	106(1)	C(15)—C(16)—N(7)	109(1)
	$[Me_2Ga{\cdot}N_2C_4H_5]_2$		
N(2)—Ga(1)—N(3)	98.4(2)	N(1)—N(2)—C(3)	106.1(6)
N(2)—Ga(1)—C(9)	111.2(4)	Ga(1)—N(3)—N(4)	121.8(4)
N(2)—Ga(1)—C(10)	104.9(4)	Ga(1)—N(3)—C(4)	132.3(5)
N(3)—Ga(1)—C(9)	108.1(4)	N(4)—N(3)—C(4)	105.8(6)
N(3)—Ga(1)—C(10)	112.6(4)	Ga(2)—N(4)—N(3)	128.5(4)
C(9)—Ga(1)—C(10)	119.7(6)	Ga(2)—N(4)—C(6)	123.9(5)
N(1)—Ga(2)—N(4)	98.5(2)	N(3)—N(4)—C(6)	107.1(6)
N(1)—Ga(2)—C(11)	108.8(5)	N(1)—C(1)—C(2)	108.9(7)
N(1)—Ga(2)—C(12)	110.8(4)	N(1)—C(1)—C(7)	121.8(7)
N(4)—Ga(2)—C(11)	110.4(6)	C(2)—C(1)—C(7)	129.3(8)
N(4)—Ga(2)—C(12)	103.2(4)	C(1)—C(2)—C(3)	105.9(8)
C(11)—Ga(2)—C(12)	122.4(6)	N(2)—C(3)—C(2)	110.5(7)
Ga(2)—N(1)—N(2)	122.8(5)	N(3)—C(4)—C(5)	112.0(8)
Ga(2)—N(1)—C(1)	128.6(4)	N(3)—C(4)—C(8)	119.0(8)
N(2)—N(1)—C(1)	108.6(6)	C(5)—C(4)—C(8)	129.0(9)
Ga(1)—N(2)—N(1)	126.9(5)	C(4)—C(5)—C(6)	104.0(8)
Ga(1)—N(2)—C(3)	125.9(5)	N(4)—C(6)—C(5)	111.1(7)
	$[Me_2Ga{\cdot}N_2C_7H_5]_2$		
N(1)—Ga(1)—N(3)	99.0(2)	Ga(1)—N(1)—C(1)	123.0(4)
N(1)—Ga(1)—C(15)	107.9(3)	C(1)—N(1)—N(2)	108.4(5)
N(1)—Ga(1)—C(16)	105.0(4)	Ga(2)—N(2)—N(1)	124.8(3)
N(3)—Ga(1)—C(15)	108.0(4)	Ga(2)—N(2)—C(3)	126.3(3)
N(3)—Ga(1)—C(16)	109.1(3)	N(1)—N(2)—C(3)	108.2(4)
C(15)—Ga(1)—C(16)	124.8(5)	Ga(1)—N(3)—N(4)	124.5(3)
N(2)—Ga(2)—N(4)	99.2(2)	Ga(1)—N(3)—C(8)	126.7(3)
N(2)—Ga(2)—C(17)	108.1(3)	N(4)—N(3)—C(8)	107.2(4)
N(2)—Ga(2)—C(18)	109.2(3)	Ga(2)—N(4)—N(3)	127.9(3)
N(4)—Ga(2)—C(17)	108.2(3)	Ga(2)—N(4)—C(10)	122.8(4)
N(4)—Ga(2)—C(18)	102.7(3)	N(3)—N(4)—C(10)	109.3(4)
C(17)—Ga(2)—C(18)	126.1(4)	N(1)—C(1)—C(2)	110.6(5)
Ga(1)—N(1)—N(2)	128.6(3)	C(1)—C(2)—C(3)	104.4(5)
C(2)—C(3)—N(2)	108.4(4)	N(3)—C(8)—C(11)	129.8(5)
C(2)—C(3)—C(4)	121.6(5)	C(9)—C(8)—C(11)	120.2(5)
N(2)—C(3)—C(4)	130.1(5)	C(8)—C(9)—C(10)	104.2(5)
C(3)—C(4)—C(5)	115.8(6)	C(8)—C(9)—C(14)	120.0(5)
C(4)—C(5)—C(6)	123.7(7)	C(10)—C(9)—C(14)	135.9(6)
C(5)—C(6)—C(7)	120.9(7)	N(4)—C(10)—C(9)	109.3(5)
C(6)—C(7)—C(2)	119.3(6)	C(8)—C(11)—C(12)	117.7(6)
C(7)—C(2)—C(3)	118.7(5)	C(11)—C(12)—C(13)	121.9(7)
C(1)—C(2)—C(7)	136.9(6)	C(12)—C(13)—C(14)	121.6(7)
N(3)—C(8)—C(9)	110.0(4)	C(13)—C(14)—C(9)	118.6(6)

Can. J. Chem. Downloaded from www.nrcresearchpress.com by 210.87.254.40 on 09/05/12
For personal use only.

TABLE 5

(*a*) Equations of weighted least-squares planes in the form $lX + mY + nZ = p$ where X, Y, Z are orthogonal coordinates in Å. Deviations (Å) of atoms from the planes are given in square brackets

Crystal	Plane	Atoms in plane	Equation[a]
$[Me_2Ga{\cdot}N_2C_3H_3]_2$	1	Ga(1), Ga(4), N(3), N(6), C(11), C(12), C(13)	$-0.1014X + 0.5954Y - 0.7970Z = 2.1705$
	2	Ga(1), Ga(4), N(4), N(7), C(14), C(15), C(16)	$-0.3662X + 0.9285Y - 0.0615Z = 2.6428$
	3	N(3), N(4), N(6), N(7) [Ga(1) 0.647(1), Ga(4) 0.737(1)]	$-0.2805X + 0.8322Y - 0.4782Z = 1.5617$
$[Me_2Ga{\cdot}N_2C_4H_5]_2$	4	Ga(1), Ga(2), N(3), N(4), C(4), C(5), C(6)	$0.6535X + 0.7484Y - 0.1135Z = 1.1060$
	5	Ga(1), Ga(2), N(1), N(2), C(1), C(2), C(3)	$0.0083X + 0.9946Y - 0.1039Z = 0.1436$
	6	N(1), N(2), N(3), N(4) [Ga(1) −0.633(1), Ga(2) −0.542(1)]	$0.3537X + 0.9317Y - 0.0833Z = 1.4055$
$[Me_2Ga{\cdot}N_2C_7H_5]_2$	7	Ga(1), Ga(2), N(1), N(2), C(1), C(2), C(3)	$-0.0775X + 0.7608Y - 0.6444Z = 1.8685$
	8	Ga(1), Ga(2), N(3), N(4), C(8), C(9), C(10)	$-0.4548X + 0.3871Y - 0.8021Z = -0.5893$
	9	N(1), N(2), N(3), N(4) [Ga(1) −0.538(1), Ga(2) −0.474(1)]	$-0.2707X + 0.5847Y - 0.7647Z = 1.1284$

[a] X, Y, and Z are derived as follows:

$$\begin{bmatrix} X \\ Y \\ Z \end{bmatrix} = \begin{bmatrix} a & 0 & c\cos\beta \\ 0 & b & 0 \\ 0 & 0 & c\sin\beta \end{bmatrix} \begin{bmatrix} x \\ y \\ z \end{bmatrix}$$

(*b*) Dihedral angles (deg) between planes

Planes	Angle (deg)
(1)–(2)	129.7
(4)–(5)	139.5
(7)–(8)	147.8

TABLE 6. Selected intramolecular distances (Å) and angles (deg)[a]

Compound	Ga—N	Ga...Ga	N—Ga—N	Ga—N—N	V-angle[e]
$[D_2Ga{\cdot}N_2C_3H_3]_2$[b]	1.974	3.529	96.6	123.6	128.4
$[Me_2Ga{\cdot}N_2C_3H_3]_2$[c]	1.996	3.652	96.1	125.2	131.5
$[Me_2Ga{\cdot}N_2C_4H_5]_2$[c]	1.986	3.663	98.5	125.0	139.5
$[Me_2Ga{\cdot}N_2C_7H_5]_2$[c]	1.996	3.736	99.1	126.5	147.8
$[Me_2Ga{\cdot}N_2C_5H_7]_2$[d]	1.993	3.840	102.9	128.3	180.0

[a]Where possible, weighted means are shown. In the case of $[Me_2Ga{\cdot}N_2C_3H_3]_2$, distances and angles have been averaged over the two independent molecules present.
[b]Reference 1.
[c]This work.
[d]Reference 7.
[e]V-angle = angle between $Ga_2N_2C_3$ moieties.

TABLE 7. Selected intramolecular nonbonded contacts (Å)

Contact	Distance (Å)	Contact	Distance (Å)
	$[Me_2Ga{\cdot}N_2C_3H_3]_2$[a]		
C(17)...C(16)	3.51	C(19)...C(13)	3.60
C(17)...C(11)	3.54	C(19)...C(14)	3.63
	$[Me_2Ga{\cdot}N_2C_4H_5]_2$		
C(6)...C(12)	3.42	C(1)...C(12)	3.76
C(3)...C(10)	3.46	C(4)...C(10)	3.84
	$[Me_2Ga{\cdot}N_2C_7H_5]_2$		
C(1)...C(16)	3.50	C(8)...C(16)	3.73
C(10)...C(18)	3.46	C(3)...C(18)	3.74

[a]Distances quoted for one independent molecule only.

The three molecules exhibit structures predicted on the basis of the previous study on the dimer, $[D_2Ga{\cdot}N_2C_3H_3]_2$ (1). They all contain a central boat conformation for the Ga—(N—N)$_2$—Ga ring with a planar arrangement of bonds about the four nitrogen atoms and planar 'pyrazolyl' or 'indazolyl' groupings. This molecular arrangement allows delocalization of π-electrons in each of the bridging ligand moieties with consequent gain in stabilization energy. The deviation from a totally planar configuration for the molecules, an arrangement which would also allow delocalization of the π-electrons but one which is somewhat more strained, is indicated by the V-angles listed in Table 6. The larger the V-angle observed for a particular compound the flatter the boat conformation for the Ga—(N—N)$_2$—Ga ring, until at a V-angle of 180° a planar arrangement is attained. This trend to flatter boats and eventual planarity is thought to be the result of increasing steric demands within the molecules. The increasing steric requirements are reflected also in trends to larger values for the N—Ga—N angles and to longer Ga...Ga nonbonded distances. It may be noteworthy that generally in the molecules having the larger V-angles, the Ga—N distances are longer than the distance of 1.97 Å found normally in four-coordinate gallium compounds (8, 9). This may reflect a tendency in these systems to reduce steric interactions by *both* a flattening of the boat conformation *and* a lengthening and weakening of the Ga—N bond. Supportive evidence for this hypothesis is forthcoming in the observation that the most strained molecule, the planar $[Me_2Ga{\cdot}N_2C_5H_7]_2$ (7), having long Ga—N bonds, is slowly attacked by water to remove one of the bridging 'pyrazolyl' groups and thereby relieve steric tension. In contrast the three complexes of the present report are moisture stable.

Another aspect of this qualitative argument concerns the proximity of the equatorial gallium methyl groups to the carbon atoms in the ligands. These nonbonded distances in **1***a*, *b*, *c* are compared in Table 7 (the distances listed are not necessarily the shortest in each molecule, but involve equivalent atoms in all three molecules). In **1***a*, one might expect all distances quoted to be the same. They are slightly different, and the reason is probably that Ga(1) is not as far above the plane through N(3), N(4), N(6), N(7) as is Ga(4) (Table 5). In **1***b* and **1***c* marked differences in C...C distances appear. Instead of the distances associated with one gallium methyl group being approximately the same (as in **1***a*) they occur as one long and one short distance. In both cases the longer distance is the one associated with the substituted carbon in the 'pyrazolyl' ring, and the shorter distance with the unsubstituted carbon atom. The equatorial methyl groups on the gallium atoms are effectively crowded toward

Can. J. Chem. Downloaded from www.nrcresearchpress.com by 210.87.254.40 on 09/05/12
For personal use only.

the unsubstituted part of a bridging ligand. This effect is stronger in the case of **1***b* presumably because of the larger substituent (methyl group) on the 'pyrazolyl' ring. There are no intermolecular nonbonded contacts ≤ 3.5 Å in any of the structures. The failure to locate the hydrogen atoms in **1***a* may probably be attributed to, amongst other things, a lack of short inter- and intramolecular nonbonded contacts with consequent high thermal motion in the methyl groups. It is interesting to note that the calculated density of **1***c* is the highest of the three compounds, an unexpected occurrence, since the light atom/heavy atom ratio is higher than in **1***a* or **1***b*. This seemingly more efficient molecular packing in **1***c* would account for the ease with which all the hydrogen atoms in **1***c* were located and their superior refinement.

We thank the National Research Council of Canada for financial support and the University of British Columbia Computing Centre for assistance.

1. D. F. RENDLE, A. STORR, and J. TROTTER. J. Chem. Soc. Dalton, 2252 (1973).
2. L. J. GUGGENBERGER, C. T. PREWITT, P. MEAKIN, S. TROFIMENKO, and J. P. JESSON. Inorg. Chem. **12**, 508 (1973).
3. D. J. PATMORE, D. F. RENDLE, A. STORR, and J. TROTTER. J. Chem. Soc. Dalton, 718 (1975).
4. D. T. CROMER and J. B. MANN. Acta Cryst. A**24**, 321 (1968).
5. R. F. STEWART, E. R. DAVIDSON, and W. T. SIMPSON. J. Chem. Phys. **42**, 3175 (1965).
6. D. T. CROMER and D. LIBERMAN. J. Chem. Phys. **53**, 1891 (1970).
7. D. F. RENDLE, A. STORR, and J. TROTTER. Can. J. Chem. This issue.
8. D. F. SHRIVER and C. E. NORDMAN. Inorg. Chem. **2**, 1298 (1963).
9. W. HARRISON, A. STORR, and J. TROTTER. J. Chem. Soc. Dalton, 1554 (1972).

Can. J. Chem. Downloaded from www.nrcresearchpress.com by 210.87.254.40 on 09/05/12
For personal use only.

The Crystal and Molecular Structures of the 3,5-Dimethylpyrazolylgallium dimethyl dimer, $[Me_2Ga \cdot N_2C_5H_7]_2$, and the Hydroxy-bridged Species, $[Me_2Ga(OH)(N_2C_5H_7)GaMe_2 \cdot 2N_2C_5H_8]$

DAVID F. RENDLE, ALAN STORR, AND JAMES TROTTER

Department of Chemistry, University of British Columbia, 2075 Wesbrook Place, Vancouver, British Columbia V6T 1W5

Received April 7, 1975

DAVID F. RENDLE, ALAN STORR, and JAMES TROTTER. Can. J. Chem. **53**, 2944 (1975).

Crystals of the 3,5-dimethylpyrazolylgallium dimethyl dimer $[Me_2Ga \cdot N_2C_5H_7]_2$ (**1***a*) are monoclinic, $a = 8.660(3)$, $b = 13.776(1)$, $c = 8.443(2)$ Å, $\beta = 112.45(2)°$, $Z = 2$, space group $P2_1/c$, and crystals of the hydroxy-bridged species $[Me_2Ga(OH)(N_2C_5H_7)GaMe_2 \cdot 2N_2C_5H_8]$ (**1***b*) are monoclinic, $a = 28.778(3)$, $b = 9.098(3)$, $c = 20.222(2)$ Å, $\beta = 100.72(1)°$, $Z = 8$, space group $C2/c$. Both structures were solved by Patterson and Fourier methods and were refined by full-matrix least-squares methods to final R values of 0.071 and 0.045 for 1443 and 2746 reflections with $I \geq 3\sigma(I)$ respectively. Molecules of **1***a* lie on crystallographic centers of symmetry, the central Ga—(N—N)$_2$—Ga ring being almost planar as a result of steric interactions between gallium-methyl groups and those on the 'pyrazolyl' rings. The mean Ga—N and Ga—C distances are 1.993 Å and 1.962 Å respectively. Compound **1***b* was formed by the attack of moisture on the strained dimer **1***a*. The central feature is a five-membered Ga_2N_2O ring, with two 3,5-dimethylpyrazole molecules hydrogen-bonded to it (N—H...O, O—H...N, 2.851 and 2.892 Å) and to each other (N—H...N, 2.907 Å). The five-membered ring adopts a slightly distorted envelope conformation, the angle between the Ga_2N_2 and N_2O moieties being 13.9°. The mean Ga—N and Ga—O distances are 1.989 and 1.934 Å respectively.

DAVID F. RENDLE, ALAN STORR et JAMES TROTTER. Can. J. Chem. **53**, 2944 (1975).

Les cristaux du dimère du complexe (**1***a*) du diméthyl-3,5 pyrazolyle avec le diméthyl gallium $[Me_2Ga \cdot N_2C_5H_7]_2$ sont monocliniques, $a = 8.660(3)$, $b = 13.776(1)$, $c = 8.443(2)$ Å, $\beta = 112.45(2)°$, $Z = 2$, groupe d'espace $P2_1/c$ et les cristaux des espèces (**1***b*) comportant des ponts hydroxyles $[Me_2Ga(OH)(N_2C_5H_7)GaMe_2 \cdot 2N_2C_5H_8]$ sont monocliniques, $a = 28.778(3)$, $b = 9.098(3)$, $c = 20.222(2)$ Å, $\beta = 100.72(1)°$, $Z = 8$, groupe d'espace $C2/c$. Chaque structure a été résolue par les méthodes de Patterson et de Fourier et on les a affinées par la méthode des moindres carrés (matrice complète) jusqu'à des valeurs finales de R respectives de 0.071 et 0.045 pour 1443 et 2746 réflexions avec $I \geq 3\sigma(I)$. Les molécules de **1***a* reposent au centre cristallographique de symétrie; le noyau Ga(N—N)$_2$Ga central est presque plan à cause des interactions stériques entre les groupes méthyles du gallium et ceux des cycles pyrazolyles. Les distances moyennes Ga—N et Ga—C sont respectivement de 1.993 et 1.962 Å. Le composé **1***b* se forme par attaque de l'humidité sur le composé **1***a* qui est très tendu. La caractéristique centrale de **1***b* est un cycle à cinq chaînons formé par Ga_2N_2O; deux molécules de diméthyl-3,5 pyrazole y sont liées par des ponts hydrogènes (N—H...O, O—H...N de 2.851 et 2.892 Å) qui les lient aussi entre elles (N—H...N, 2.907 Å). Le cycle à cinq chaînons existe sous forme d'enveloppe déformée; l'angle entre la position Ga_2N_2 et N_2O est de 13.9°. Les valeurs moyennes des distances Ga—N et Ga—O sont respectivement de 1.989 et 1.934 Å.

[Traduit par le journal]

Introduction

The preceding paper (1) describes the structural effects of substituting bulkier groups on both the gallium atoms and the pyrazolyl fragments in the dimer, $[D_2Ga \cdot N_2C_3H_3]_2$. In the three structures described, a pronounced flattening of the boat conformation of the central six-membered Ga—(N—N)$_2$—Ga rings was noted when compared to the arrangement observed in the deuterio complex (2). The present report describes, firstly, the structure of the 3,5-dimethylpyrazolylgallium dimethyl dimer, $[Me_2Ga \cdot N_2C_5H_7]_2$, **1***a*, in which the boat conformation of the central Ga—(N—N)$_2$—Ga ring is lost and, instead, an almost planar arrangement is adopted by the two gallium and four nitrogen atoms. Secondly, the report describes the structure of a novel compound $[Me_2Ga(OH)(N_2C_5H_7)GaMe_2 \cdot 2N_2C_5H_8]$, **1***b*, formed by the attack of moisture on the above strained dimer, $[Me_2Ga \cdot N_2C_5H_7]_2$. Steric interactions in this dimer are reduced by replacement of one of the bridging 3,5-dimethylpyrazolyl moieties with a bridging hydroxy group. The

Can. J. Chem. Downloaded from www.nrcresearchpress.com by 210.87.254.105 on 09/05/12
For personal use only.

Can. J. Chem. Downloaded from www.nrcresearchpress.com by 210.87.254.105 on 09/05/12
For personal use only.

novel structure which results has, as the central feature, a nonplanar, five-membered Ga_2N_2O ring. The molecular unit is completed by two hydrogen-bonded 3,5-dimethylpyrazole molecules which form a large heterocyclic ring incorporating the bridging hydroxy group and positioned approximately at right angles to the bridging 3,5-dimethylpyrazolyl moiety.

Experimental

Preparative and analytical data for the two compounds of this study, together with similar data for the three compounds of the preceding report, will be published in a forthcoming article.[1] Briefly, the 3,5-dimethylpyrazolylgallium dimethyl dimer was prepared by refluxing a benzene solution containing 1:1 stoichiometric amounts of gallium trimethyl and 3,5-dimethylpyrazole, the reaction being performed under a nitrogen atmosphere. The white solid product was recrystallized from toluene and a crystal, suitable for X-ray study, was mounted in a capillary tube under nitrogen. The tube was flame sealed to prevent reaction of the sample with atmospheric moisture.

The hydroxy species was first isolated when a sample of the dimer $[Me_2Ga{\cdot}N_2C_5H_7]_2$ which had been air-exposed for several months, was recrystallized from toluene solution. The crystals which were deposited were the hydroxy-bridged species, $[Me_2Ga(OH)(N_2C_5H_7)GaMe_2{\cdot}2N_2C_5H_8]$ rather than the expected dimer. This hydroxy-bridged species has since been prepared less serendipitously by reacting the original dimer with water and 3,5-dimethylpyrazole in toluene. Fractional crystallization of the resultant solution yields, firstly, unreacted 3,5-dimethylpyrazole (m.p. 107–108 °C), secondly, the hydroxy-bridged compound (m.p. ~87 °C), and, finally, unreacted dimer (m.p. 110–111 °C). A crystal of the hydroxy-bridged compound was mounted in a capillary tube for X-ray study.

Crystallographic Studies of the 3,5-Dimethylpyrazolylgallium Dimethyl Dimer (1a)

The crystal chosen for study was mounted with a^* parallel to the goniostat axis and had dimensions of *ca.* 0.51 × 0.23 × 0.45 mm³. Unit cell and space group data were obtained from film and diffractometer measurements. The unit cell parameters were refined by a least-squares treatment of $\sin^2\theta$ values for 16 reflections measured on a diffractometer with CuK_α radiation. Crystal data are:

$C_{14}H_{26}Ga_2N_4$ f.w. = 389.8

Monoclinic, $a = 8.660(3)$, $b = 13.776(1)$, $c = 8.443(2)$ Å, $\beta = 112.45(2)°$, $V = 930.9$ Å³, $Z = 2$, $\rho_c = 1.391$ g cm^{-3}, $F(000) = 400$ (20 °C, CuK_α, $\lambda = 1.5418$ Å, $\mu = 38.1$ cm^{-1}). Absent reflections: $0k0$, $k \neq 2n$ and $h0l$, $l \neq 2n$ define uniquely the space group $P2_1/c$ (C_{2h}^5, No. 14).

Intensities were measured on a Datex-automated General Electric XRD 6 diffractometer equipped with a scintillation counter, nickel filter, and pulse height analyzer. The θ–2θ scan technique was employed at a rate of 2 deg min^{-1} in 2θ. Data were measured to $2\theta = 145°$ and a standard reflection was monitored every 40 reflections. The data were accordingly scaled, Lorentz and polarization corrections were applied, and the structure amplitudes derived. No absorption correction was applied because of the irregular crystal surface. Of the 1841 independent reflections measured, 392 had intensities less than $3\sigma(I)$ above background where $\sigma^2(I) = S + B + (0.05S)^2$ with S = scan count and B = time averaged background count. These reflections were given zero weight in the refinement.

The structure was solved via the Patterson function and successive difference-Fourier syntheses. Two cycles of full-matrix least-squares refinement in which all non-hydrogen atoms were permitted anisotropic thermal motion reduced R to 0.086. A difference-Fourier synthesis at this point revealed the hydrogen atom positions and they were included in the refinement with isotropic thermal parameters. Refinement converged with R 0.071 and R_w 0.086 [$R_w = \Sigma w(|F_o| - |F_c|)^2 / \Sigma w|F_o|^2$] for 1443 reflections with $I \geq 3\sigma(I)$. Six reflections (1 0 0, 2 0 0, 4 0 0, 6 0 0, 8 0 0, and 0 2 0) were given zero weight in the final cycle because of suspected extinction errors. The function minimized in the refinement was $\Sigma w(|F_o| - |F_c|)^2$ with weights w derived from counting statistics. The scattering factors for the nonhydrogen atoms were taken from ref. 3 and those for H from ref. 4. Those for Ga were corrected for the real and imaginary parts of anomalous dispersion (5). The maximum shift to error ratio in the refined parameters at convergence was 1.45 (the x coordinate of H(3*a*)) while the average value was 0.16. The error in an observation of unit weight was 2.41.

Crystallographic Studies of the Hydroxy-bridged Species $[Me_2Ga(OH)(N_2C_5H_7)GaMe_2{\cdot}2N_2C_5H_8]$ (1b)

Experimental details for **1b** are the same as for compound **1a** except where noted. The crystal was mounted with b parallel to the goniostat axis and had dimensions of *ca.* 0.20 × 0.51 × 0.18 mm³. Twenty reflections measured with CuK_α radiation were employed in the refinement of the unit cell parameters. Crystal data are:

$C_{19}H_{36}Ga_2N_6O$ f.w. = 504.0

Monoclinic, $a = 28.778(3)$, $b = 9.098(3)$, $c = 20.222(2)$ Å, $\beta = 100.72(1)°$, $V = 5202$ Å³, $Z = 8$, $\rho_c = 1.287$ g cm^{-3}, $F(000) = 2096$ (20 °C, CuK_α, $\lambda = 1.5418$ Å, $\mu = 29.0$ cm^{-1}). Absent reflections: hkl, $h + k \neq 2n$ and $h0l$, $l \neq 2n$ define the space groups $C2/c$ (C_{2h}^6, No. 15) and Cc (C_s^4, No. 9).

Of the 3564 independent reflections measured with $2\theta \leq 115°$, 818 had intensities less than $3\sigma(I)$ above background. Intensity statistics (6) were calculated and they heavily favored the centrosymmetric space group $C2/c$. The vector distribution in the Patterson function was concurrent with this choice, providing the coordinates of both gallium atoms. All nonhydrogen atoms were refined with anisotropic thermal parameters and R fell to 0.065. A difference-Fourier synthesis revealed all the hydrogen atoms associated with carbon atoms and they were refined with isotropic temperature factors. The highest peaks in a subsequent difference-Fourier synthesis were close to O, N(3), and N(5) suggesting that hydrogen atoms were localized on these atoms. However, smaller peaks (approximately half the height of those mentioned above) were also found, close to O, N(4), and N(6) suggesting that throughout the crystal some asymmetric units may have hydrogen atoms localized on O, N(3), and N(5), and others may have them localized on O, N(4), and N(6). An attempt to include six hydrogen atoms in the refinement

[1] T. Baker and A. Storr. Unpublished data.

Can. J. Chem. Downloaded from www.nrcresearchpress.com by 210.87.254.105 on 09/05/12
For personal use only.

TABLE 1. Final positional parameters (fractional × 10^4, Ga × 10^5, H × 10^3) with estimated standard deviations in parentheses

Atom	*x*	*y*	*z*
	$[Me_2Ga{\cdot}N_2C_5H_7]_2$		
Ga	17504(9)	3894(5)	21048(10)
N(1)	1853(6)	−554(4)	368(7)
N(2)	−592(6)	884(4)	1064(6)
C(1)	3249(8)	−1051(5)	506(11)
C(2)	2869(10)	−1693(5)	−823(12)
C(3)	4906(11)	−865(10)	1936(22)
C(4)	−1210(9)	1575(5)	1793(9)
C(5)	−128(16)	2104(8)	3381(13)
C(6)	3192(12)	1492(8)	2162(19)
C(7)	1886(23)	−391(9)	4106(14)
H(2)	353(9)	−212(6)	−103(9)
H(3*a*)	490(19)	−66(11)	309(22)
H(3*b*)	549(16)	−144(9)	248(16)
H(3*c*)	556(30)	−43(13)	170(29)
H(5*a*)	70(15)	167(8)	429(15)
H(5*b*)	25(18)	285(13)	333(21)
H(5*c*)	−42(25)	214(15)	378(28)
H(6*a*)	302(16)	173(8)	111(18)
H(6*b*)	295(15)	218(11)	272(15)
H(6*c*)	379(19)	142(10)	226(20)
H(7*a*)	134(16)	−101(10)	360(16)
H(7*b*)	257(18)	−74(10)	416(18)
H(7*c*)	159(20)	−18(10)	487(19)
	$[Me_2Ga(OH)(N_2C_5H_7)GaMe_2{\cdot}2N_2C_5H_8]$		
Ga(1)	13053(2)	10368(7)	7900(3)
Ga(2)	9224(2)	−11642(6)	18811(3)
O	1277(1)	−910(4)	1166(2)
N(1)	896(1)	995(4)	2009(2)
N(2)	1021(1)	1896(4)	1529(2)
N(3)	2215(2)	−2053(6)	1460(2)
N(4)	2291(1)	−3053(5)	995(2)
N(5)	1462(2)	−3669(5)	−26(2)
N(6)	1064(1)	−2973(4)	62(2)
C(1)	750(2)	1854(6)	2476(2)
C(2)	782(2)	3305(6)	2288(3)
C(3)	953(2)	3308(5)	1695(2)
C(4)	2609(2)	−1806(6)	1891(3)
C(5)	2954(2)	−2666(8)	1707(4)
C(6)	2747(2)	−3426(6)	1145(3)
C(7)	1354(2)	−4675(6)	−508(2)
C(9)	702(2)	−3552(6)	−373(3)
C(10)	598(4)	1199(12)	3079(4)
C(11)	1064(4)	4546(8)	1269(4)
C(12)	2941(4)	−4522(12)	714(5)
C(13)	2638(5)	−724(15)	2450(6)
C(14)	209(3)	−3014(14)	−413(5)
C(15)	1732(4)	−5592(13)	−723(5)
C(16)	860(3)	1123(9)	−60(3)
C(17)	1962(3)	1711(11)	909(5)
C(18)	290(3)	−1862(13)	1515(6)
C(19)	1321(4)	−2077(12)	2654(4)
H(O1)	128(2)	−137(7)	96(3)
H(N3)	196(2)	−157(6)	141(3)
H(N5)	167(2)	−353(7)	23(3)
H(2)	68(3)	425(8)	250(4)
H(5)	324(2)	−273(6)	192(3)
H(8)	72(2)	−514(7)	−103(3)

TABLE 1 (*Concluded*)

Atom	*x*	*y*	*z*
H(10*a*)	62(3)	28(11)	312(5)
H(10*b*)	76(3)	161(9)	349(5)
H(10*c*)	35(3)	159(9)	312(4)
H(11*a*)	97(3)	436(9)	78(5)
H(11*b*)	82(3)	522(11)	129(5)
H(11*c*)	133(3)	500(9)	143(4)
H(12*a*)	269(3)	−540(11)	51(5)
H(12*b*)	325(3)	−419(10)	64(5)
H(12*c*)	313(3)	−518(10)	96(4)
H(13*a*)	235(3)	−28(8)	249(4)
H(13*b*)	265(4)	−98(13)	279(6)
H(13*c*)	290(3)	−9(10)	248(4)
H(14*a*)	24(3)	−208(10)	−17(5)
H(14*b*)	8(2)	−329(8)	−11(4)
H(14*c*)	3(3)	−253(11)	−80(5)
H(15*a*)	201(3)	−576(9)	−37(4)
H(15*b*)	179(3)	−567(10)	−110(5)
H(15*c*)	170(3)	−640(10)	−65(4)
H(16*a*)	58(3)	77(7)	6(3)
H(16*b*)	79(3)	223(9)	−17(4)
H(16*c*)	93(2)	38(8)	−32(3)
H(17*a*)	206(3)	143(8)	130(4)
H(17*b*)	214(3)	111(9)	82(5)
H(17*c*)	194(3)	304(11)	78(4)
H(18*a*)	19(3)	−118(8)	119(4)
H(18*b*)	31(3)	−255(10)	134(5)
H(18*c*)	9(3)	−162(8)	174(4)
H(19*a*)	154(4)	−161(13)	279(6)
H(19*b*)	112(3)	−225(9)	296(4)
H(19*c*)	146(3)	−298(12)	256(5)

with half-occupancies failed. With all other atoms fixed, a further attempt was made to obtain meaningful parameters for the six 'half-hydrogen' atoms by refining their coordinates, temperature factors, and occupancy factors. This resulted in occupancy factors of 0.75, 0.33, 0.75, 0.39, 0.57, and 0.30 for H(O1), H(O2), H(N3), H(N4), H(N5), and H(N6) respectively. The corresponding isotropic temperature factors were: 6.2, 0.1, 5.8, 2.6, 5.2, and 12.7 Å^2. This result certainly agrees with our assumption that the three hydrogen atoms assumed to be present are associated with atoms O, N(3), and N(5), and O, N(4), and N(6) throughout the crystal in the approximate ratio 2:1. This would appear to be a more feasible explanation than, say, rapid hydrogen exchange between O and N(3), O and N(6), and N(4) and N(5), a situation which would require elongated peaks of electron density between the three sets of atoms concerned, or at least a 1:1 correspondence in the peak heights of the two 'half-hydrogen' atoms localized on O and the single 'half-hydrogen' atoms localized on N(3), N(4), N(5), and N(6).

Since no real advantage was to be gained by refining six hydrogen atoms with partial occupancies, refinement was continued with three localized hydrogens on O, N(3), and N(5). Several low angle, high intensity reflections appeared to suffer extinction effects and, unlike compound **1***a*, the introduction and refinement of an extinction coefficient proved successful. The function now minimized was: $\Sigma w(|F_o| - \{|F_c|/(1 + gI)\})^2$ where g is the extinction coefficient and I is the uncorrected intensity of reflection. Two cycles of refinement brought convergence at R 0.045 and R_w 0.058. The average shift/error ratio in the refined parameters was 0.38 and the largest was 2.57 (the z coordinate of H(N5)). The final value for the extinction coefficient was $0.72(3) \times 10^{-6}$ and the error in an observation of unit weight was 1.66. Measured and calculated structure factors have been placed in the Depository of Unpublished Data.[2] Final atomic coordinates and thermal parameters for the two compounds are listed in Tables 1 and 2 respectively.

Results and Discussion

Numerous crystal structures of compounds incorporating pyrazolyl–borate (7) and pyrazolyl–gallate (8, 9) ligands in transition metal complexes have been reported recently. In addition, several crystallographic studies have been concerned with the related class of symmetrical dimer molecules incorporating a central Ga—(N—N)$_2$—Ga ring (1, 2). The present study is concerned with a member of this latter class of

[2]The structure factor table is available, at a nominal charge, from the Depository of Unpublished Data, CISTI, National Research Council of Canada, Ottawa, Canada K1A 0S2.

Can. J. Chem. Downloaded from www.nrcresearchpress.com by 210.87.254.105 on 09/05/12
For personal use only.

TABLE 2. Final thermal parameters and their estimated standard deviations

(*a*) Anisotropic thermal parameters[a] ($U_{ij} \times 10^4$ Å^2 for Ga, $\times 10^3$ Å^2 for others)

Atom	U_{11}	U_{22}	U_{33}	U_{12}	U_{13}	U_{23}
			$[Me_2Ga{\cdot}N_2C_5H_7]_2$			
Ga	479(5)	512(5)	530(5)	−28(3)	106(3)	−36(3)
N(1)	45(3)	52(3)	62(3)	3(2)	17(2)	−5(2)
N(2)	52(3)	50(3)	51(3)	1(2)	19(2)	−4(2)
C(1)	42(3)	63(4)	96(5)	8(3)	22(3)	0(4)
C(2)	65(4)	57(4)	119(7)	6(3)	53(5)	−10(4)
C(3)	49(4)	94(8)	135(10)	13(5)	2(5)	−15(7)
C(4)	68(4)	53(4)	70(4)	0(3)	38(3)	−3(3)
C(5)	110(8)	72(6)	69(5)	4(5)	35(5)	−20(4)
C(6)	51(4)	69(5)	134(9)	−15(4)	23(5)	−12(6)
C(7)	158(12)	76(7)	60(5)	13(8)	26(6)	14(5)
			$[Me_2Ga(OH)(N_2C_5H_7)GaMe_2{\cdot}2N_2C_5H_8]$			
Ga(1)	612(4)	685(4)	508(4)	118(3)	162(3)	−16(3)
Ga(2)	706(4)	596(4)	551(4)	71(3)	123(3)	8(3)
O	66(2)	60(2)	57(2)	13(2)	15(2)	−9(2)
N(1)	61(2)	61(2)	48(2)	3(2)	15(2)	−4(2)
N(2)	67(3)	57(3)	52(2)	11(2)	17(2)	0(2)
N(3)	59(3)	85(3)	76(3)	20(3)	0(2)	−6(2)
N(4)	62(3)	75(3)	73(3)	17(2)	12(2)	−7(2)
N(5)	68(3)	75(3)	61(3)	−2(3)	9(3)	−8(2)
N(6)	61(3)	67(3)	68(3)	6(2)	14(2)	3(2)
C(1)	59(3)	75(4)	56(3)	0(3)	17(2)	−12(3)
C(2)	80(4)	65(3)	67(3)	8(3)	22(3)	−18(3)
C(3)	65(3)	59(3)	58(3)	10(2)	8(2)	−7(2)
C(4)	72(4)	75(4)	74(4)	9(3)	1(3)	4(3)
C(5)	56(4)	103(5)	98(5)	9(3)	−4(3)	9(4)
C(6)	61(3)	76(3)	82(4)	16(3)	16(3)	6(3)
C(7)	83(4)	67(3)	52(3)	2(3)	17(3)	−6(3)
C(8)	90(4)	79(4)	53(3)	−10(3)	5(3)	−5(3)
C(9)	65(3)	75(4)	63(3)	2(3)	12(3)	15(3)
C(10)	110(6)	111(6)	71(4)	−10(5)	46(4)	−12(4)
C(11)	128(7)	64(4)	86(5)	3(4)	24(5)	6(4)
C(12)	97(6)	117(6)	133(7)	36(6)	43(5)	−10(6)
C(13)	126(9)	124(8)	96(7)	19(7)	−11(6)	−30(6)
C(14)	78(5)	142(9)	89(6)	13(5)	22(4)	23(6)
C(15)	118(7)	102(7)	92(6)	33(5)	33(5)	−18(5)
C(16)	87(5)	100(5)	62(4)	22(4)	6(3)	−5(4)
C(17)	76(4)	115(6)	89(5)	2(4)	18(4)	−10(5)
C(18)	73(4)	109(6)	117(7)	2(5)	28(4)	−27(6)
C(19)	128(7)	105(6)	75(5)	31(6)	3(5)	16(4)

compound, $[Me_2Ga{\cdot}N_2C_5H_7]_2$, and a novel hydroxy species derived from it, $[Me_2Ga(OH)(N_2C_5H_7)GaMe_2{\cdot}2N_2C_5H_8]$. The two molecules are shown in stereo in Fig. 1 and stereoscopic views of the unit cells for the two compounds are shown in Fig. 2. Bond lengths and valency angles are collected in Tables 3 and 4 respectively. Table 5 lists selected mean planes and dihedral angles whilst Table 6 collects important non-bonded distances for the molecules.

$[Me_2Ga{\cdot}N_2C_5H_7]_2$

Most 'pyrazolyl'-based structures determined to date display a central six-membered M—(N—N)$_2$—M′ ring in a boat conformation (where M = B or Ga; M′ = transition metal or Ga) (1, 2, 7–9). This arrangement allows planarity to be maintained about the nitrogen atoms with consequent gain in stabilization energy stemming from an ability to delocalize π-electrons in the bridging 'pyrazolyl' units. A planar central ring would also allow such π-electron delocalization but the environment of the Group III atoms is somewhat more strained. Two previous examples have shown nonboat conformations for the central six-membered

Can. J. Chem. Downloaded from www.nrcresearchpress.com by 210.87.254.105 on 09/05/12
For personal use only.

TABLE 2 (*Concluded*)

(*b*) Isotropic thermal parameters ($U \times 100$)

Atom	U(Å^2)	Atom	U(Å^2)	Atom	U(Å^2)
		$[Me_2Ga{\cdot}N_2C_5H_7]_2$			
H(2)	7(2)	H(5*b*)	23(6)	H(6*c*)	13(6)
H(3*a*)	18(6)	H(5*c*)	27(10)	H(7*a*)	16(4)
H(3*b*)	13(4)	H(6*a*)	14(5)	H(7*b*)	11(5)
H(3*c*)	31(8)	H(6*b*)	19(5)	H(7*c*)	17(6)
H(5*a*)	8(4)				
		$[Me_2Ga(OH)(N_2C_5H_7)GaMe_2{\cdot}2N_2C_5H_8]$			
H(O1)	9(3)	H(12*a*)	15(4)	H(16*a*)	11(3)
H(N3)	7(2)	H(12*b*)	12(4)	H(16*b*)	14(3)
H(N5)	12(3)	H(12*c*)	16(4)	H(16*c*)	12(2)
H(2)	12(3)	H(13*a*)	11(3)	H(17*a*)	11(3)
H(5)	8(2)	H(13*b*)	21(6)	H(17*b*)	20(4)
H(8)	9(2)	H(13*c*)	22(4)	H(17*c*)	19(3)
H(10*a*)	16(5)	H(14*a*)	20(4)	H(18*a*)	12(3)
H(10*b*)	14(4)	H(14*b*)	10(3)	H(18*b*)	14(4)
H(10*c*)	16(4)	H(14*c*)	18(4)	H(18*c*)	9(3)
H(11*a*)	19(4)	H(15*a*)	22(3)	H(19*a*)	20(6)
H(11*b*)	19(4)	H(15*b*)	22(4)	H(19*b*)	15(3)
H(11*c*)	15(4)	H(15*c*)	12(4)	H(19*c*)	20(5)

[a]The anisotropic temperature factor expression is of the form: $\exp[-2\pi^2(U_{11}h^2a^{*2} + U_{22}k^2b^{*2} + U_{33}l^2c^{*2} + 2U_{12}hka^*b^* + 2U_{13}hla^*c^* + 2U_{23}klb^*c^*)]$.

TABLE 3. Bond lengths (Å) with estimated standard deviations in parentheses

Bond	Distance (Å)	Bond	Distance (Å)
	$[Me_2Ga{\cdot}N_2C_5H_7]_2$		
Ga—N(1)	1.988(5)	N(2)—C(4)	1.351(8)
Ga—N(2)	1.998(5)	C(1)—C(2)	1.367(11)
Ga—C(6)	1.955(9)	C(1)—C(3)	1.503(12)
Ga—C(7)	1.969(10)	C(4)—C(2′)	1.364(11)
N(1)—N(2′)	1.360(7)	C(4)—C(5)	1.499(12)
N(1)—C(1)	1.355(8)		
	$[Me_2Ga(OH)(N_2C_5H_7)GaMe_2{\cdot}2N_2C_5H_8]$		
Ga(1)—O	1.936(4)	Ga(1)—C(16)	1.946(7)
Ga(2)—O	1.932(4)	Ga(1)—C(17)	1.959(8)
Ga(1)—N(2)	1.993(4)	Ga(2)—C(18)	1.940(8)
Ga(2)—N(1)	1.985(4)	Ga(2)—C(19)	1.945(8)
N(1)—N(2)	1.369(5)	C(2)—C(3)	1.378(7)
N(3)—N(4)	1.356(7)	C(3)—C(11)	1.488(10)
N(5)—N(6)	1.350(7)	C(4)—C(5)	1.370(9)
N(1)—C(1)	1.350(6)	C(4)—C(13)	1.489(14)
N(2)—C(3)	1.351(6)	C(5)—C(6)	1.370(9)
N(3)—C(4)	1.314(8)	C(6)—C(12)	1.498(12)
N(4)—C(6)	1.335(7)	C(7)—C(8)	1.356(9)
N(5)—C(7)	1.330(7)	C(7)—C(15)	1.498(12)
N(6)—C(9)	1.343(7)	C(8)—C(9)	1.378(8)
C(1)—C(2)	1.381(8)	C(9)—C(14)	1.489(11)
C(1)—C(10)	1.495(10)		

M—(N—N)$_2$—M′ ring. The first example was reported by Cotton *et al.* (10) *viz.* $[Et_2B(N_2C_3H_3)_2](h^3\text{-}C_3H_5)(N_2C_3H_4)(CO)_2Mo$, and the shallow chair conformation adopted by the B—(N—N)$_2$—Mo ring was argued to result from severe steric interactions. The second example (9) involves the bis[dimethylbis(3,5-dimethyl-1-pyrazolyl)gallato]copper(II) complex,

Can. J. Chem. Downloaded from www.nrcresearchpress.com by 210.87.254.105 on 09/05/12
For personal use only.

Can. J. Chem. Downloaded from www.nrcresearchpress.com by 210.87.254.105 on 09/05/12
For personal use only.

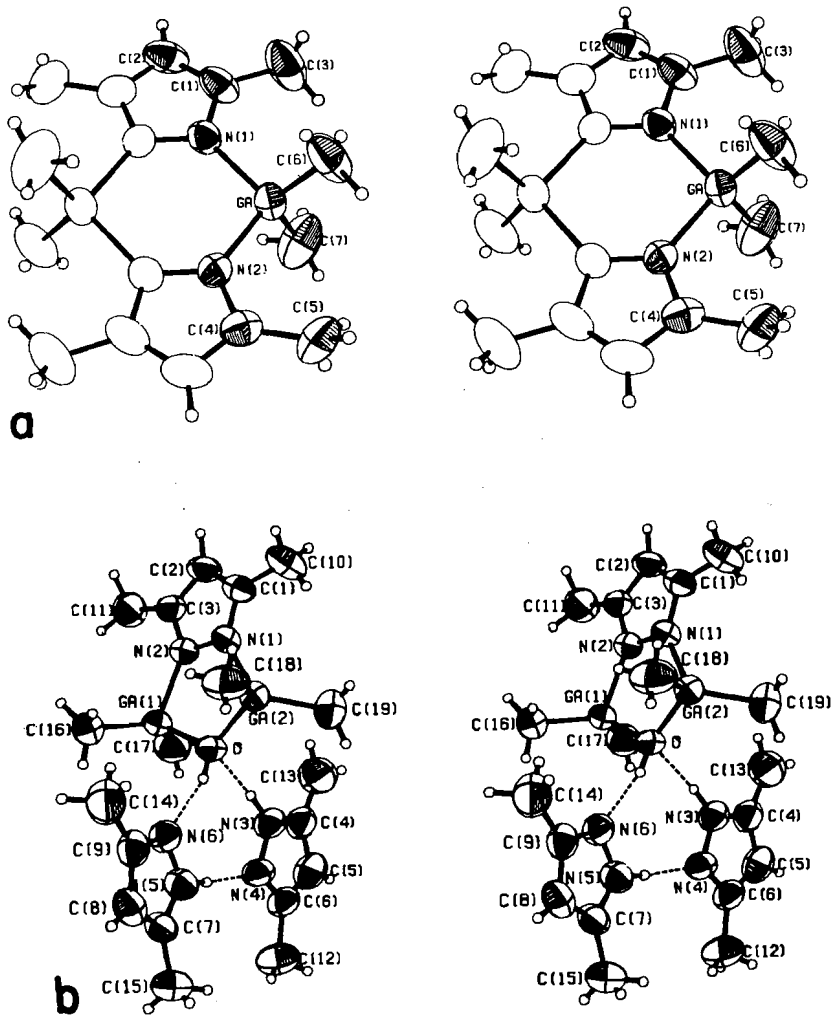

FIG. 1. Stereoscopic views of the molecules **1***a* and **1***b*.

$[Me_2Ga(N_2C_5H_7)_2]_2Cu$, in which steric requirements necessitate an almost planar arrangement for the two Ga—(N—N)$_2$—Cu six-membered rings. The present dimer structure represents the third example where steric requirements dictate a nonboat conformation for the central six-membered ring; the first example in the case of a symmetrical six-membered Ga—(N—N)$_2$—Ga ring. In the present example a shallow chair conformation is adopted but the deviation from planarity is small, the two gallium atoms being 0.131 Å above and below the mean plane through the four nitrogen atoms in the molecule. The almost planar arrangement for the tricyclic system incorporating the two bridging 3,5-dimethylpyrazolyl ligands and the two gallium atoms (see Table 5), and the positioning of the two GaC units at right angles to this plane, minimizes the steric interactions between adjacent methyl groups on the gallium atoms and on the bridging 'pyrazolyl' moieties. The relevant nonbonded C...C distances are collected in Table 6 and range from 3.51 to 3.80 Å. In addition to the planarity adopted by the Ga—(N—N)$_2$—Ga ring the Ga—N distances in the molecule (1.988, 1.998 Å) are longer than the distance of 1.97 Å normally observed in four-coordinate gallium compounds (11, 12). Both

Can. J. Chem. Downloaded from www.nrcresearchpress.com by 210.87.254.105 on 09/05/12
For personal use only.

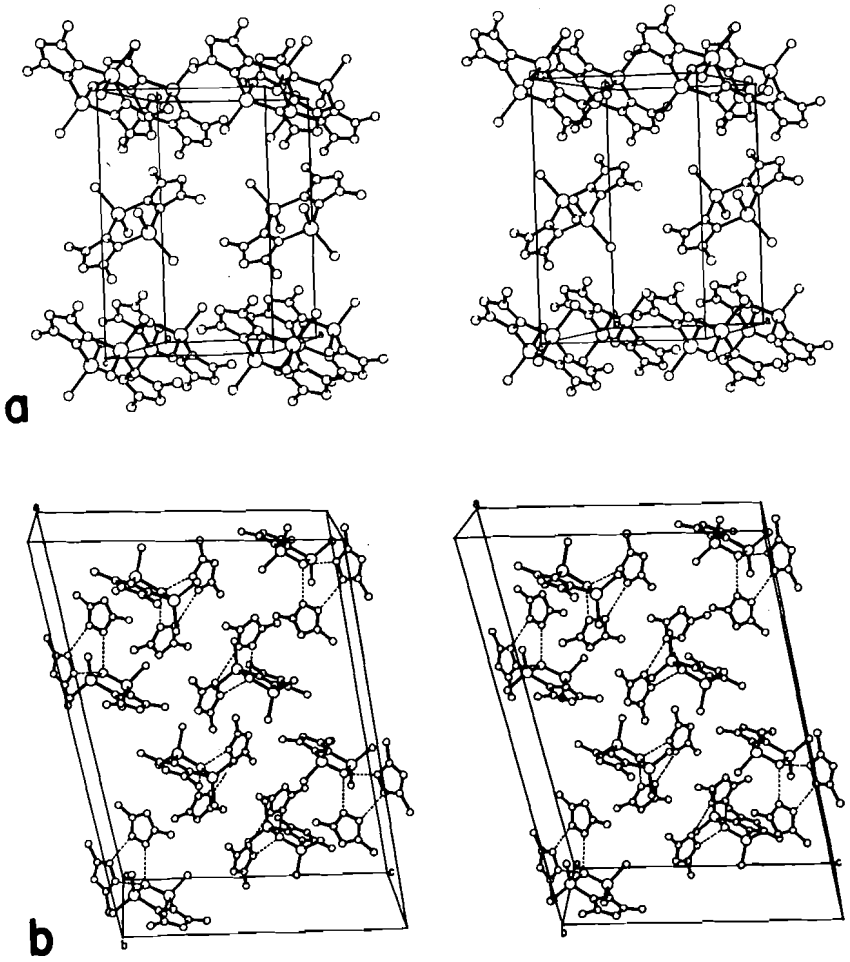

FIG. 2. Stereoscopic views of the unit cells for **1***a* and **1***b*.

these factors, the imposed planarity with consequent strain about the gallium atoms, and the long and probably weak Ga—N bonds, may contribute to the willingness of this particular dimer to react with water and thereby allow replacement of a bridging 3,5-dimethylpyrazolyl group with a bridging hydroxy group. Such a transformation relieves the steric interactions, still inherent in the planar dimer, between the methyl groups on the gallium atoms and on the bridging 'pyrazolyl' units. The planar dimer molecules occur as discrete entities in the unit cell with no intermolecular nonbonded contacts of less than 3.5 Å.

$[Me_2Ga(OH)(N_2C_5H_7)GaMe_2 \cdot 2N_2C_5H_8]$

The formation of this compound from the above dimer is probably encouraged by the reduction of steric strain which occurs as a result of the transformation. Thus nonbonded C...C distances in the hydroxy species between the Ga—Me and the 3-methyl and 5-methyl groups on the bridging 'pyrazolyl' moiety are increased over those found in the dimer molecule and now have the range 3.82–4.18 Å (*cf.* 3.51–3.80 Å) (Table 6). The molecule incorporates a bridging hydroxy function between the two gallium dimethyl units and this part of the structure may be compared with the $[Me_2GaOH]_4$

TABLE 4. Valency angles (deg) with estimated standard deviations in parentheses

Bonds	Angle (deg)	Bonds	Angle (deg)
	$[Me_2Ga{\cdot}N_2C_5H_7]_2$		
N(1)—Ga—N(2)	102.9(2)	Ga—N(2)—C(4)	123.5(5)
N(1)—Ga—C(6)	108.6(4)	N(1′)—N(2)—C(4)	108.5(6)
N(1)—Ga—C(7)	105.7(4)	N(1)—C(1)—C(2)	109.2(7)
N(2)—Ga—C(6)	106.1(4)	N(1)—C(1)—C(3)	122.0(8)
N(2)—Ga—C(7)	106.3(6)	C(2)—C(1)—C(3)	128.8(8)
C(6)—Ga—C(7)	125.1(6)	C(1)—C(2)—C(4′)	106.4(7)
Ga—N(1)—N(2′)	128.8(4)	N(2)—C(4)—C(2′)	108.7(6)
Ga—N(1)—C(1)	123.8(5)	N(2)—C(4)—C(5)	122.0(8)
N(2′)—N(1)—C(1)	107.2(6)	C(2′)—C(4)—C(5)	129.3(8)
Ga—N(2)—N(1′)	127.8(4)		
	$[Me_2Ga(OH)(N_2C_5H_7)GaMe_2{\cdot}2N_2C_5H_8]$		
N(2)—Ga(1)—O	90.7(2)	Ga(2)—N(1)—C(1)	133.5(3)
N(2)—Ga(1)—C(16)	110.7(3)	N(2)—N(1)—C(1)	107.8(4)
N(2)—Ga(1)—C(17)	107.9(3)	Ga(1)—N(2)—N(1)	119.7(3)
O—Ga(1)—C(16)	108.3(3)	Ga(1)—N(2)—C(3)	131.2(3)
O—Ga(1)—C(17)	110.4(3)	N(1)—N(2)—C(3)	108.9(4)
C(16)—Ga(1)—C(17)	123.0(4)	C(4)—N(3)—N(4)	110.1(5)
N(1)—Ga(2)—O	91.0(2)	N(3)—N(4)—C(6)	107.0(4)
N(1)—Ga(2)—C(18)	108.5(4)	C(7)—N(5)—N(6)	109.5(5)
N(1)—Ga(2)—C(19)	110.5(4)	N(5)—N(6)—C(9)	107.6(4)
O—Ga(2)—C(18)	110.0(3)	N(1)—C(1)—C(2)	108.4(4)
O—Ga(2)—C(19)	109.7(4)	N(1)—C(1)—C(10)	121.1(6)
C(18)—Ga(2)—C(19)	122.5(6)	C(1)—C(2)—C(3)	107.0(5)
Ga(1)—O—Ga(2)	118.0(2)	N(2)—C(3)—C(2)	107.8(4)
Ga(2)—N(1)—N(2)	118.6(3)	N(2)—C(3)—C(11)	121.2(5)
C(2)—C(3)—C(11)	130.9(5)	N(5)—C(7)—C(8)	107.9(5)
N(3)—C(4)—C(5)	107.6(5)	N(5)—C(7)—C(15)	120.9(6)
N(3)—C(4)—C(13)	122.4(7)	C(15)—C(7)—C(8)	131.1(6)
C(13)—C(4)—C(5)	129.9(8)	C(7)—C(8)—C(9)	107.1(5)
C(4)—C(5)—C(6)	106.7(6)	N(6)—C(9)—C(8)	107.8(5)
N(4)—C(6)—C(5)	108.6(5)	N(6)—C(9)—C(14)	121.5(6)
N(4)—C(6)—C(12)	119.6(6)	C(8)—C(9)—C(14)	130.6(6)
C(5)—C(6)—C(12)	131.8(6)		

tetramer (13). The Ga—O distances of 1.932 and 1.936 Å of the present structure are shorter, though probably not significantly so, than the 1.94 and 1.98 Å Ga—O distances found in the tetramer, and somewhat longer than the tetrahedral Ga—O distances of 1.879 and 1.869 Å reported recently in the structure of a Ga,O,N cage compound (14). The latter structure, however, displays triply bridging oxygen atoms rather than doubly bridging hydroxy groups found in the present structure and in the tetramer, $[Me_2GaOH]_4$. The novel five-membered Ga_2N_2O ring is nonplanar with a dihedral angle of 13.9° between the mean planes through the atoms Ga(1), O, Ga(2) and Ga(1), N(1), N(2), Ga(2) respectively (Table 5). This folding about the gallium atoms results in the GaC_2 planes deviating from a 90° angle to the mean plane through the bridging 'pyrazolyl' unit, with consequent nonequivalent C...C nonbonded distances between the Ga—Me and the 3-Me and 5-Me groups (Table 6). The structure is completed by two hydrogen-bonded 3,5-dimethylpyrazole molecules which form a large heterocyclic ring incorporating the bridging hydroxy group, and which is approximately at right angles to the bridging 3,5-dimethylpyrazolyl moiety (see mean planes, Table 5). This arrangement 'staggers' the Ga—Me and the adjacent Me groups on the hydrogen-bonded 'pyrazoles' and thereby minimizes steric interactions between them. The relevant C...C nonbonded distances are listed in Table 6 and range from 4.01 to 4.21 Å, significantly longer than the nonbonded distances in the dimer molecule between neighboring Me groups.

Can. J. Chem. Downloaded from www.nrcresearchpress.com by 210.87.254.105 on 09/05/12
For personal use only.

Can. J. Chem. Downloaded from www.nrcresearchpress.com by 210.87.254.105 on 09/05/12
For personal use only.

TABLE 5

(*a*) Equations of weighted least-squares planes in the form $lX + mY + nZ = p$ where X, Y, Z are orthogonal coordinates in Å. Deviations (Å) of atoms from the planes are given in square brackets

Crystal	Plane	Atoms in plane	Equation[a]
$[Me_2Ga{\cdot}N_2C_5H_7]_2$	1	N(1), N(2), N(1′), N(2′) [Ga −0.131(1), Ga′ 0.131(1)]	$0.4646X + 0.6984Y - 0.5444Z = 0$
	2	N(1), C(1), C(2), N(2′), C(4′)	$0.4641X + 0.6985Y - 0.5447Z = -0.0002$
	3	Ga, C(6), C(7)	$0.7689X - 0.6175Y - 0.1658Z = 0.0401$
$[Me_2Ga(OH)(N_2C_5H_7)GaMe_2{\cdot}2N_2C_5H_8]$	4	Ga(1), Ga(2), O	$-0.7110X - 0.1946Y - 0.6758Z = -3.7037$
	5	Ga(1), Ga(2), N(1), N(2) [O −0.239(4)]	$-0.8190X - 0.0032Y - 0.5738Z = -3.7363$
	6	N(1), N(2), C(1), C(2), C(3)	$-0.8549X - 0.0395Y - 0.5173Z = -3.6597$
	7	N(3), N(4), C(4), C(5), C(6)	$0.3407X + 0.7397Y - 0.5803Z = -1.0823$
	8	N(5), N(6), C(7), C(8), C(9)	$0.2667X + 0.6827Y - 0.6803Z = -1.1214$
	9	Ga(1), C(16), C(17)	$0.3333X - 0.9139Y - 0.2319Z = -0.0727$
	10	Ga(2), C(18), C(19)	$0.4969X - 0.6161Y - 0.6112Z = -0.6645$
	11	O, N(3), N(6)	$0.4098X + 0.6745Y - 0.6141Z = -0.6555$

[a] X, Y, and Z are derived as follows:

$$\begin{bmatrix} X \\ Y \\ Z \end{bmatrix} = \begin{bmatrix} a & 0 & c\cos\beta \\ 0 & b & 0 \\ 0 & 0 & c\sin\beta \end{bmatrix} \begin{bmatrix} x \\ y \\ z \end{bmatrix}$$

(*b*) Dihedral angles (deg) between planes

Planes	Angle (deg)	Planes	Angle (deg)	Planes	Angle (deg)
(1)–(2)	0.1	(7)–(8)	7.9	(6)–(8)	84.4
(4)–(5)	13.9	(5)–(7)	87.0	(6)–(9)	97.4
(5)–(9)	97.9	(1)–(3)	89.1	(6)–(10)	94.8
(5)–(10)	93.1	(4)–(11)	90.4	(5)–(8)	80.2
(5)–(11)	89.2	(6)–(7)	91.2		

TABLE 6. Selected intramolecular nonbonded contacts (Å)

Contact	Distance (Å)	Contact	Distance (Å)
	$[Me_2Ga{\cdot}N_2C_5H_7]_2$		
C(3)...C(6)	3.61	C(5)...C(6)	3.51
C(3)...C(7)	3.78	C(5)...C(7)	3.80
	$[Me_2Ga(OH)(N_2C_5H_7)GaMe_2{\cdot}2N_2C_5H_8]$		
C(10)...C(18)	4.18	C(11)...C(16)	4.09
C(10)...C(19)	3.83	C(11)...C(17)	3.82
C(13)...C(17)	4.02	C(14)...C(16)	4.21
C(13)...C(19)	4.08	C(14)...C(18)	4.01
Ga(1)...Ga(2)	3.316		

The hydrogen-bonding system alone provides an interesting topic for discussion. Pyrazole itself has been the subject of a number of crystallographic studies (15–17) and it has been concluded that the tautomeric NH proton is localized on one of the nitrogen atoms in the solid state, and shows no tendency to migrate to the other nitrogen atom. In contrast, a crystal structure determination of 3-methyl-5-phenylpyrazole (18) failed to locate the NH hydrogen atoms and it was concluded that they exist as a loose association within molecular groupings. Our findings in this study appear to fall midway between the results of the pyrazole and 3-methyl-5-phenylpyrazole studies. Figure 1 shows only the hydrogen atoms associated with the major component of the two systems discussed in the Experimental section. There is one N—H...O hydrogen bond (N(3)...O 2.851(6), N(3)—H(N3) 0.84(6), O...H(N3) 2.03(6) Å, and N(3)—H(N3)...O 165(6)°), one O—H...N hydrogen bond (O...N(6) 2.892(6), O—H(O1) 0.60(6), N(6)...H(O1) 2.31(6) Å, and O—H(O1)...N(6) 164(8)°), and one N—H...N hydrogen bond (N(4)...N(5) 2.907(7), N(5)—H(N5) 0.72(7), N(4)...H(N5) 2.19(7) Å, N(5)—H(N5)...N(4) 178(7)°). Of these bonds the N—H...N bond is the strongest and the O—H...N bond the weakest when compared with documented distances for such bonds (19). Indeed, the N(4)...N(5) contact is quite short at 2.907 when one considers the sum of the van der Waals radii is 3.0 Å (20). Corresponding N...N contacts in 3-methyl-5-phenylpyrazole are even shorter still and lie in the range 2.824–2.913 Å.

The multicyclic molecules are quite well separated in the unit cell, there being only two intermolecular nonbonded contacts less than 3.5 Å: N(5)...C(11)[$x,y-1,z$] 3.46(1) Å, and N(6)...C(11)[$x,y-1,z$] 3.33(1) Å.

We thank the National Research Council of Canada for financial support and the University of British Columbia Computing Centre for assistance.

1. D. F. RENDLE, A. STORR, and J. TROTTER. Can. J. Chem. This issue.
2. D. F. RENDLE, A. STORR, and J. TROTTER. J. Chem. Soc. Dalton, 2252 (1973).
3. D. T. CROMER and J. B. MANN. Acta Cryst. A **24**, 321 (1968).
4. R. F. STEWART, E. R. DAVIDSON, and W. T. SIMPSON. J. Chem. Phys. **42**, 3175 (1965).
5. D. T. CROMER and D. LIBERMAN. J. Chem. Phys. **53**, 1891 (1970).
6. I. L. KARLE, K. S. DRAGONETTE, and S. A. BRENNER. Acta Cryst. **19**, 713 (1965).
7. L. J. GUGGENBERGER, C. T. PREWITT, P. MEAKIN, S. TROFIMENKO, and J. P. JESSON. Inorg. Chem. **12**, 508 (1973).
8. D. F. RENDLE, A. STORR, and J. TROTTER. J. Chem. Soc. Dalton, 176 (1975).
9. D. J. PATMORE, D. F. RENDLE, A. STORR, and J. TROTTER. J. Chem. Soc. Dalton. 718 (1975).
10. F. A. COTTON, B. A. FRENZ, and A. G. STANISLOWSKI. Inorg. Chim. Acta, 7, 503 (1973).
11. D. F. SHRIVER and C. E. NORDMAN. Inorg. Chem. **2**, 1298 (1963).
12. W. HARRISON, A. STORR, and J. TROTTER. J. Chem. Soc. Dalton, 1554 (1972).
13. G. S. SMITH and J. L. HOARD. J. Am. Chem. Soc. **81**, 3907 (1959).
14. S. J. RETTIG, A. STORR, and J. TROTTER. Can. J. Chem. **53**, 753 (1975).
15. F. K. LARSEN, M. S. LEHMANN, I. SOTOFTE, and S. E. RASMUSSEN. Acta Chem. Scand. **24**, 3244 (1970).
16. J. BERTHOU, J. ELGUERO, and C. KERAT. Acta Cryst. B**26**, 1880 (1970).
17. H. W. W. EHRLICH. Acta Cryst. **13**, 946 (1960).
18. E. N. MASLEN, J. R. CANNON, A. H. WHITE, and A. C. WILLIS. J. Chem. Soc. Perkin 2, 1298 (1974).
19. W. C. HAMILTON and J. A. IBERS. Hydrogen bonding in solids. Benjamin, New York. 1968. pp. 260–265.
20. L. PAULING. The nature of the chemical bond. Cornell University Press, Ithaca, New York. 1960. p. 260.

Can. J. Chem. Downloaded from www.nrcresearchpress.com by 210.87.254.105 on 09/05/12
For personal use only.

Synthèse et réactions d'une bis(α-dicétone) carboranique. Explication par la méthode CNDO/2

GUY RABILLOUD ET BERNARD SILLION

Etablissement de Recherche de l'Institut Français du Pétrole, Centre d'Etudes Nucléaires de Grenoble, B.P. 85, Centre de Tri, 38041 Grenoble Cédex, France

ET

JEAN ROSSARIE,[1] MONIQUE BLAIN ET SIMONE ODIOT

Laboratoire de Recherches Physiques – Service Infrarouge – Laboratoire Associé au C.N.R.S. Université de Paris VI, 4 place Jussieu, 75230 Paris Cédex 05, France

Reçu le 16 juillet 1974[2]

GUY RABILLOUD, BERNARD SILLION, JEAN ROSSARIE, MONIQUE BLAIN et SIMONE ODIOT. Can. J. Chem. **53**, 2955 (1975).

On a préparé le bis(phénylglyoxyloyl)-1,7 *m*-carborane par différentes méthodes, le meilleur rendement étant obtenu en faisant réagir le dilithio-1,7 *m*-carborane et le diméthoxy-2,2 phénylglyoxal. Opposé à l'*o*-phénylènediamine, ce nouveau composé ne donne pas la quinoxaline attendue mais un mélange de *m*-carborane, de phényl-3 quinoxalinone-2 et de benzoyl-2 benzimidazole. Il réagit également avec les bases pour donner du *m*-carborane et de l'acide phénylglyoxylique. L'étude théorique de la molécule par la méthode CNDO/2 indique une grande différence de réactivité entre les carbonyles situés en α et β du noyau carborane.

GUY RABILLOUD, BERNARD SILLION, JEAN ROSSARIE, MONIQUE BLAIN, and SIMONE ODIOT. Can. J. Chem. **53**, 2955 (1975).

1,7-Bis(phenylglyoxyloyl)-*m*-carborane has been prepared by different methods but the best yield was obtained with 1,7-dilithio-*m*-carborane and 2,2-dimethoxyphenylglyoxal. Mixed with *o*-phenylenediamine this new compound failed to yield the expected quinoxaline but afforded *m*-carborane, 3-phenyl-2-quinoxalinone, and 2-benzoylbenzimidazole. Moreover, under the action of bases, we observed a cleavage of the carbon–carbon bond giving *m*-carborane and phenylglyoxylic acid. A theoretical study of the molecule by CNDO/2 indicated a significant difference between chemical reactivities of the α and β carbonyl groups.

Can. J. Chem. Downloaded from www.nrcresearchpress.com by 210.87.254.6 on 09/05/12
For personal use only.

Introduction

La chimie des composés organiques contenant un noyau carborane s'est considérablement développée au cours de ces dix dernières années, soit à partir du dicarba-1,2-closo-dodécaborane-12 (*ortho*-carborane), soit avec le dicarba-1,7-closo-dodécaborane-12 (*méta*-carborane). En particulier, la synthèse des alkyl et aryl carboranylcétones a été réalisée par condensation des métallocarboranes sur les chlorures d'acides carboxyliques (1), sur les esters et les anhydrides d'acides aliphatiques et aromatiques (2) ou encore par oxydation des alcools secondaires obtenus dans la réaction d'un aldéhyde sur un lithiocarborane (3).

Ces méthodes générales semblent, à priori, utilisables pour fixer sur le noyau carborane le radical phénylglyoxyloyle (C_6H_5—CO—CO—) mais, dans la plupart des cas, nous avons observé la formation de produits secondaires ou de substances résineuses en quantités très importantes qui limitent considérablement les voies d'accès au bis(phénylglyoxyloyl)-1,7 *m*-carborane (**1**).

$$C_6H_5—CO—CO—CB_{10}H_{10}C—CO—CO—C_6H_5$$
1

Synthèse du bis(phénylglyoxyloyl)-1,7 *m*-carborane

L'introduction des substituants organiques sur les deux atomes de carbone du noyau carborane est effectuée à partir du dilithio-1,7 *m*-carborane (**2**) obtenu par transmétallation du *m*-carborane avec le butyllithium.

$$HCB_{10}H_{10}CH + 2C_4H_9Li \rightarrow 2C_4H_{10} + LiCB_{10}H_{10}CLi$$
2

A l'aide du dilithien **2** ainsi formé, quatre voies de synthèse ont été étudiées. L'ensemble de ces réactions est représenté dans la fig. 1.

[1]Nouvelle adresse: Centre de Recherches de la Compagnie Française de Raffinage, Gonfreville l'Orcher 76700, France.

[2]Revision reçue le 16 juin 1975.

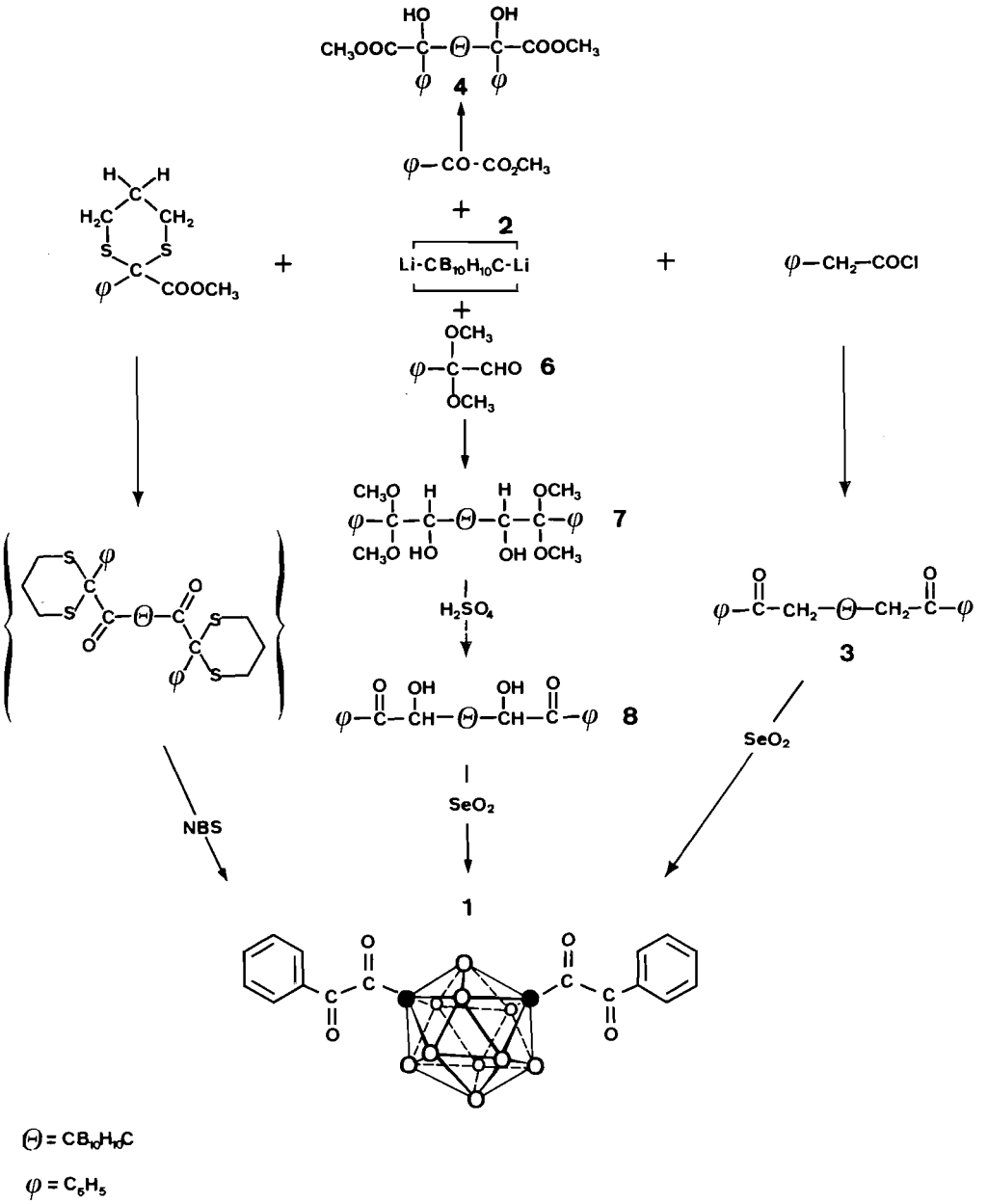

FIG. 1. Synthèse du bis(phénylglyoxyloyl)-1,7 *m*-carborane; θ = —$CB_{10}H_{10}C$—; φ = C_6H_5—.

(*i*) La condensation du composé **2** sur le chlorure de phénacétyle donne 12% seulement de bis(phénacétyl)-1,7 *m*-carborane (**3**) accompagné de *m*-carborane, d'acide mandélique, d'acide phénylacétique et de résidus lourds non identifiés. L'oxydation ultérieure de la cétone **3** par l'oxyde de sélénium permet de préparer le composé **1** avec un rendement global d'environ 4–5%.

(*ii*) En remplaçant le chlorure de phénacétyle par le phénylglyoxylate de méthyle on n'observe pas la formation de la tétracétone **1** mais il est possible d'isoler une petite quantité de l'ester alcool **4** qui proviendrait d'une attaque du composé métallique au niveau du carbonyle cétonique.

(*iii*) Pour éviter ce genre de réaction, la fonc-

Can. J. Chem. Downloaded from www.nrcresearchpress.com by 210.87.254.6 on 09/05/12
For personal use only.

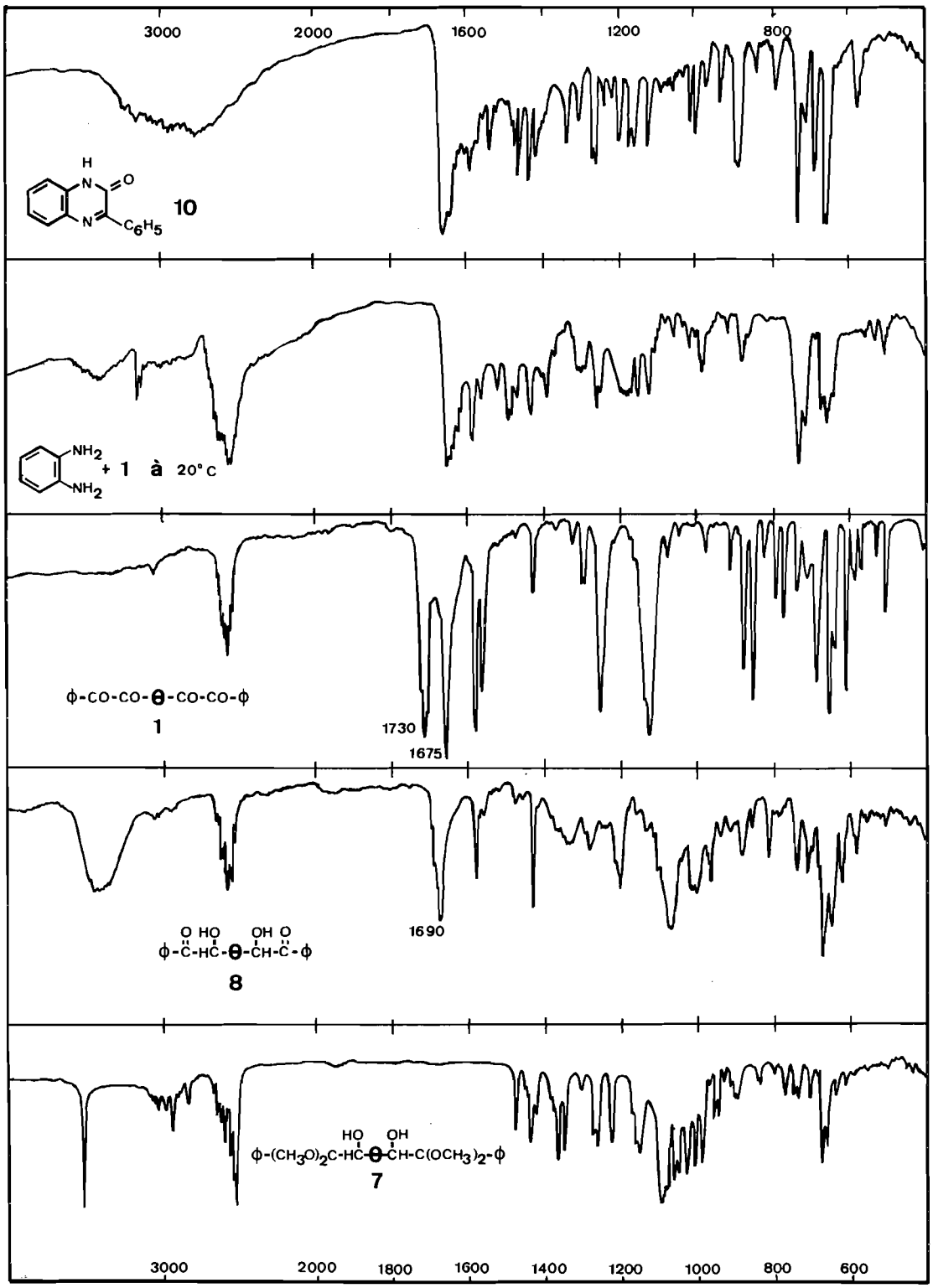

FIG. 2. Spectres i.r. des intermédiaires de réaction.

Can. J. Chem. Downloaded from www.nrcresearchpress.com by 210.87.254.6 on 09/05/12
For personal use only.

tion cétone du phénylglyoxylate de méthyle est protégée par le propanedithiol-1,3. Le méthoxy-

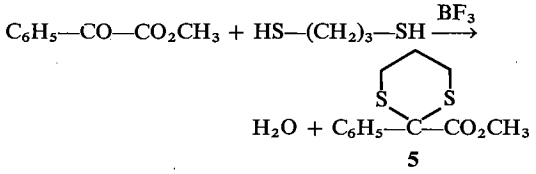

carbonyl-2 phényl-2 dithiane-1,3 (**5**) est alors opposé au dilithio-1,7 *m*-carborane (**2**) dans un mélange éther–hexane à 40 °C. Le traitement final permet de récupérer 90% des réactifs de départ inchangés et 10% d'un composé impur qui est directement oxydé par la méthode de Corey et Erickson (4) en tétracétone **1**.

(*iv*) L'absence de sélectivité de ces différentes synthèses nous a conduit à étudier une nouvelle séquence réactionnelle basée sur le diméthoxy-2,2 phénylglyoxal (**6**) préparé lui-même à partir de la dichloro-1,1 acétophénone (5). La fonction aldéhyde du dérivé **6** réagit de façon normale sur le lithien **2** pour donner le bis(hydroxy-1 diméthoxy-2,2 phénéthyl)-1,7 *m*-carborane (**7**). L'hydrolyse des fonctions acétals par l'acide sulfurique dans le dioxanne régénère les groupes carbonyles avec un rendement de 90% en bis(benzoylhydroxyméthyl)-1,7 *m*-carborane (**8**). L'oxydation de ce composé par l'oxyde de sélénium en suspension dans le toluène à reflux, en présence d'une faible quantité d'acide acétique, conduit au bis(phénylglyoxyloyl-)1,7 *m*-carborane (**1**) avec un rendement de 75%.

Les spectres i.r. des composés **1**, **7** et **8**, réunis sur la fig. 2, permettent de suivre les étapes de la réaction. Les transitions vibrationnelles de valence ν_{BH} (2650–2500 cm^{-1}) subissent d'importantes modifications selon la nature des substituants fixés sur les atomes de carbone de la cage carboranique. La structure fine des bandes d'absorption correspondantes a été récemment étudiée par cryospectrophotométrie i.r. et Raman (6).

La vibration de valence ν_{OH}, sensible à l'encombrement stérique autour de la liaison C—OH, est une bande fine très intense à 3525 cm^{-1} dans le dialcool **7** et une bande d'association large mal résolue (3530–3150 cm^{-1}) pour le céto alcool **8**. Le phénomène marquant est la valeur élevée de la fréquence de vibration de valence $\nu_{C=O}$ des carbonyles en α de la tétracétone **1** (1730 cm^{-1}) qui est à rapprocher de celle des carbonyles du diacétyl-1,7 *m*-carborane (1730 cm^{-1}) (3). Pour les carbonyles en β, la position de la bande à 1675 cm^{-1} est comparable à celle des composés aromatiques comme le benzile (1670 cm^{-1}).

Réaction du bis(phénylglyoxyloyl-1,7 *m*-carborane avec l'orthophénylène-diamine

La réaction de condensation des α-dicétones sur l'*o*-phénylènediamine est une voie assez générale de synthèse des quinoxalines et nous attendions de la tétracétone **1** qu'elle conduise dans ces conditions au bis(phényl-3 quinoxalinyl-2)-1,7 *m*-carborane (**9**). Or, quelles que soient les méthodes expérimentales, nous n'avons jamais pu mettre en évidence la présence d'une quinoxaline fixée au noyau carborane.

Dans les solvants neutres (benzène, chloroforme, dioxanne, éthanol) ou modérément acides (*m*-crésol, acide acétique) chauffés au reflux, on isole, à la fin de la réaction, du *m*-carborane et deux hétérocycles isomères: la phényl-3 1*H*-quinoxalinone-2 (**10**) accompagné d'une faible quantité de benzoyl-2 benzimidazole (**11**). Ces deux derniers composés ont été identifiés par comparaison avec les produits préparés séparément par des méthodes connues: oxydation du benzyl-2 benzimidazole avec l'anhydride chromique (7) et condensation de l'acide phénylglyoxylique sur l'*o*-phénylènediamine (8).

A température ambiante, dans ces mêmes solvants, il se forme progressivement un précipité très coloré qu'il n'est pas possible de purifier car les essais de cristallisation ou de sublimation induisent, au chauffage, une transformation en *m*-carborane et en composés hétérocycliques **10** et **11**. Les spectres i.r. (fig. 2) et r.m.n. sont loin d'être une superposition des spectres individuels des corps **10** et **11**. Cependant les données spectroscopiques ne permettent pas d'établir la structure de cet intermédiaire instable.

Enfin, si la réaction entre la tétracétone **1** et l'*o*-phénylènediamine est conduite dans un solvant basique comme la diméthylaniline, connue pour favoriser la formation des quinoxalines (9), les seuls produits isolés avec un rendement de 90% sont le *m*-carborane et la phényl-3 quinoxalinone-2 **10**.

Acétalisation et clivage par les bases

Les réactions du composé **1** *vis à vis* de l'*o*-phénylènediamine sont nettement différentes de celles des α-dicétones aromatiques et afin de poursuivre cette comparaison, nous avons étudié

Can. J. Chem. Downloaded from www.nrcresearchpress.com by 210.87.254.6 on 09/05/12
For personal use only.

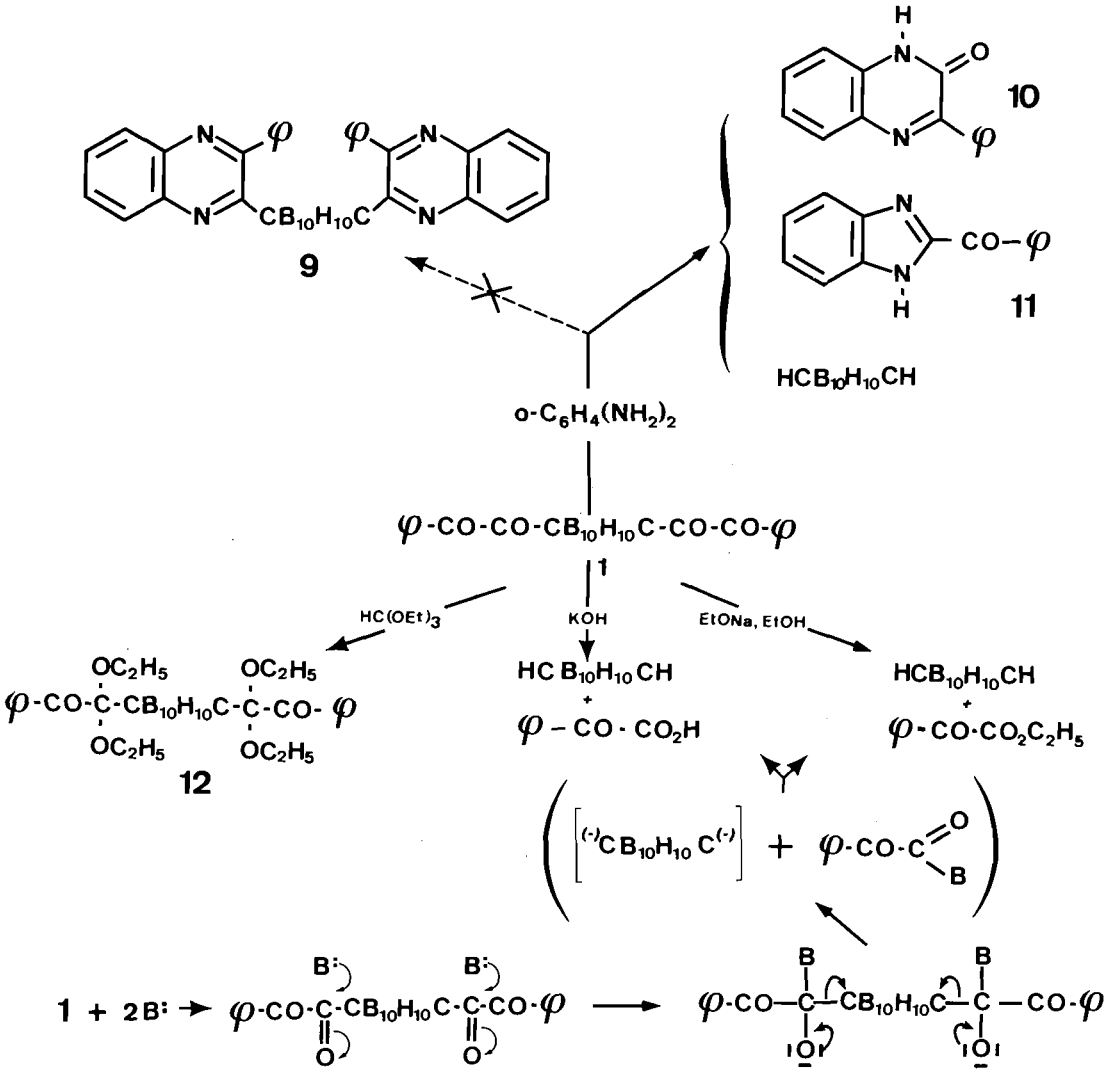

FIG. 3. Réactions du bis(phénylglyoxyloyl)-1,7 *m*-carborane.

son comportement avec les bases et les réactifs d'acétalisation.

L'acétalisation de la tétracétone **1** par l'orthoformiate d'éthyle se fait uniquement sur la fonction carbonyle située en α du carborane. En effet, on observe sur le spectre i.r. une disparition progressive de la bande d'absorption à 1730 cm^{-1} alors que le pic du carbonyle en β à 1680 cm^{-1} ne subit pas de modification sensible. La réaction est pratiquement achevée au bout de 2 h et les spectres i.r. et r.m.n. du produit brut correspondent bien à la structure **12** du bis(diéthoxy-1,1 phénylglyoxyloyl)-1,7 *m*-carborane (fig. 3).

On sait que, *vis à vis* des bases les α-dicétones aromatiques comme le benzile peuvent subir deux réactions principales: la coupure entre les deux carbonyles conduisant au benzaldéhyde et à l'acide benzoïque et le réarrangement benzilique. Dans le cas de la tétracétone **1** on n'observe aucune de ces réactions.

Dans les conditions du réarrangement benzilique dans la potasse éthanolique, il y a formation de *m*-carborane et d'acide phénylglyoxylique. De la même manière, l'action de traces d'éthylate de sodium dans l'éthanol absolu conduit au *m*-carborane et au phénylglyoxylate de méthyle (fig. 3).

Can. J. Chem. Downloaded from www.nrcresearchpress.com by 210.87.254.6 on 09/05/12
For personal use only.

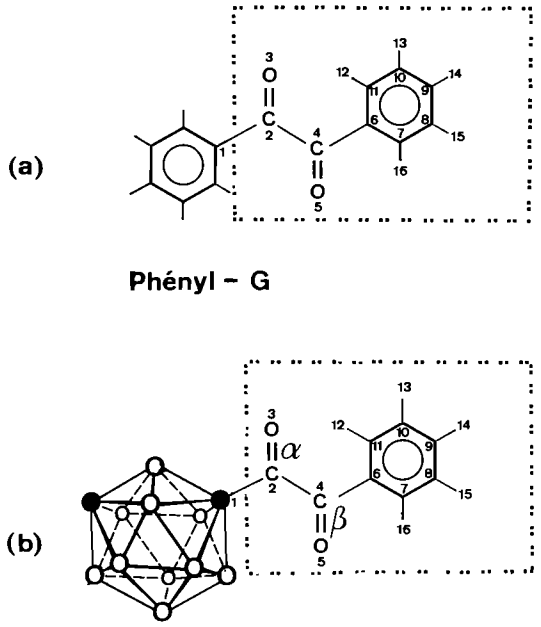

FIG. 4. Numérotation des centres pour le calcul des charges.

Conclusion

L'ensemble de ces résultats met en évidence la sensibilité de cette tétracétone carboranique à l'action des agents basiques organiques et minéraux. Il semble que l'attaque nucléophile se situe toujours sur les carbonyles en α du noyau carborane avec, ultérieurement, un clivage des liaisons C—C entre les atomes de carbone de ces carbonyles et ceux de la cage carborane qui stabiliserait le dianion $CB_{10}H_{10}C$ (fig. 3).

Ces résultats peuvent être rapprochés de ceux qui ont été observés dans la coupure alcaline de certains composés fonctionnels carbonylés des *o*- et *m*-carboranes (10, 11).

Interprétation théorique dans l'approximation des orbitales moléculaires

Les structures géométriques et électroniques d'une série de carboranes, isomères et dérivés substitués, ont été particulièrement bien analysées (12), à l'aide de la méthode CNDO/2 (13).

Néanmoins, dans cette approximation, la validité que l'on attache aux nombres, éléments de la matrice densité, reste relative. Ils doivent être considérés comme compléments d'information aux données expérimentales pour exprimer une tendance phénoménologique.

TABLEAU 1. Indices de liaison π* des deux liaisons C—C de la chaîne cétonique et des deux groupements C=O en position α et β

Indices de liaison π	a	b
$P_{C_2—C_4}$	0.2538	0.2548
$P_{C_4—C_6}$	0.2972	0.2998
$P_{C=O(\alpha)}$	0.9026	0.9174
$P_{C=O(\beta)}$	0.9026	0.9036

$P_{AB\pi_l} = 2\,\Sigma_{l\,occ} C^l_{2pz_A} C^l_{2pz_B}$ où $C^l_{2pz_{A\text{ ou }B}}$ est le coefficient affecté à l'orbitale atomique $2pz_{A\text{ ou }B}$ dans le développement de la *l*ème orbitale moléculaire occupée.

Le choix de cette méthode semi-empirique à l'égard des méthodes *ab initio* est économiquement imposé ici par la taille des composés, dans le cadre d'une étude de la restructuration électronique des dérivés fonctionnels par l'introduction du noyau *m*-carborane-1,7 $C_2B_{10}H_{12}$.

Les composés étudiés et la numérotation des centres sont représentés sur la fig. 4. La géométrie adoptée pour les calculs est la géométrie standard. Les résultats des calculs sont rassemblés dans les tableaux 1, 2 et 3. Dans le tableau 1 sont mentionnés les indices de liaison (*i*) entre les deux carbones qui assurent la conjugaison du groupe phényle d'une part et de la liaison entre les deux carbonyles d'autre part, avec le système moléculaire **a** ou **b**, et (*ii*) entre le carbone et l'oxygène des deux C=O. Le tableau 2 donne la distribution des charges nettes électroniques, sur chaque centre numéroté selon la fig. 4, ainsi que les charges nettes globales portées par les groupements G (*cf.* fig. 4), phényle de G et *m*-carboranyle. Dans le tableau 3 figurent les polarités des deux liaisons C=O en absence ou en présence de *m*-carborane. La polarité de la liaison C=O est mesurée par la différence entre les charges nettes du carbone et de l'oxygène.

Si l'on examine les tableaux 1 et 3, on constate que lors du remplacement d'un phényle par un noyau *m*-carboranique: (*i*) Les deux groupements carbonyles se différencient l'un de l'autre. Les indices de liaison ($P_{C=O}$) sont différents tout comme leur polarité. Le C=O en α du carborane devient plus réactif que celui en β (indice de liaison et polarité plus élevés). L'attaque nucléophile par un groupement basique doit toucher

Can. J. Chem. Downloaded from www.nrcresearchpress.com by 210.87.254.6 on 09/05/12
For personal use only.

Can. J. Chem. Downloaded from www.nrcresearchpress.com by 210.87.254.6 on 09/05/12
For personal use only.

TABLEAU 2. Distribution des charges électroniques

	Charges nettes	
Centres	a	b
2	0.1882	0.2034
3	−0.2407	−0.2172
4	0.1882	0.1914
5	−0.2407	−0.2237
6	−0.0077	−0.0060
7	0.0222	0.0254
8	−0.0006	0.0012
9	0.0209	0.0251
10	0.0021	0.0044
11	−0.0001	0.0023
12	0.0306	0.03
13	−0.0049	0.0003
14	−0.0050	−0.0003
15	−0.0042	0.0005
16	0.0031	0.006
G	−0.0486	0.0428
ϕ	+0.048	0.0889
m-Carborane		−0.0416

TABLEAU 3. Polarité des liaisons carbonyles

	Polarité	
Liaisons	a	b
C=O (α)	0.4289	0.4206
C=O (β)	0.4289	0.4151

en tout premier lieu le C=O en α. (*ii*) L'indice de liaison de C=O en β augmente de façon peu significative, mais par contre, sa polarité diminue. Une réaction d'addition sur ce carbonyle est alors défavorisée par rapport à l'addition sur le composé phénylé (**a**), en accord avec les observations expérimentales.

L'analyse des résultats du tableau 2 souligne une fois de plus le caractère attracteur d'électrons du *m*-carborane qui prend une charge égale à −0.04 *e*. Lorsque l'on passe du composé **a** au composé **b** on constate sur le tableau 2 que le groupement G primitivement chargé négativement (−0.0486) devient positif (+0.0428) et que le groupe phényle cède des électrons puisque sa charge passe de +0.048 à +0.0889 et ceci d'autant plus aisément que l'indice de liaison $\pi,P_{C_4-C_6}$ augmente (0.2972–0.2998 (tableau 1)), assurant une meilleure conjugaison.

Conditions expérimentales de synthèse

Les spectres i.r. ont été réalisés sur pastilles de KBr avec un appareil Perkin-Elmer 257. Les spectres r.m.n. ont été effectués à l'aide d'un Perkin-Elmer R-24 de 60 MHz et sont donnés en unités δ par rapport au TMS utilisé comme étalon interne. Les températures de fusion instantanées ont été mesurées avec un banc Kofler. Le *m*-carborane utilisé dans les synthèses de composés fonctionnels est commercialisé par Research in Inorganic and Organic Chemicals et par Ventron Chemical Corp.—Alfa Products Division. Ce produit est utilisé sans purification supplémentaire quand sa pureté, contrôlée par chromatographie en phase gazeuse est de 99.7%. Les lots de *m*-carborane contenant de l'*o*-carborane sont isomérisés à 600 °C dans un appareil en quartz identique à celui qui est décrit dans la littérature (14).

Synthèse du bis(phénacétyl)-1,7 m-carborane (3)

Le *m*-carboranyldilithium **2** est préparé dans un ballon de 500 ml équipé d'un agitateur, d'un thermomètre, d'une ampoule d'addition à robinet et d'une arrivée d'argon. On introduit dans le ballon 137 ml d'une solution 1.61 *M* de butyllithium dans l'hexane et 100 ml d'éther anhydre. L'ampoule d'addition est chargée avec une solution de *m*-carborane (14.4 g, 0.1 mol) dans 100 ml d'éther. Le *m*-carborane est ajouté goutte à goutte, avec une forte agitation, au butyllithium refroidi à 0 °C en 1 h environ puis le mélange est agité une nuit à température ambiante pour compléter la réaction de transmétallation.

A cette suspension de dilithiocarborane refroidie à −50 °C on ajoute peu à peu une solution de chlorure de phénacétyle (31 g, 0.2 mol) dans 80 ml d'éther. Le mélange réactionnel est ensuite laissé 5 h à 20 °C puis hydrolysé avec de la glace et de l'acide chlorhydrique dilué. La phase organique est lavée à l'eau, séchée sur Na_2SO_4 et les solvants sont évaporés sous pression réduite. Le résidu est une huile jaune très visqueuse constituée de plusieurs produits parmi lesquels on identifie par chromatographie en couche mince du *m*-carborane, de l'acide mandélique, de l'acide phénylacétique, des alcools carboraniques tertiaires non identifiés et 4.56 g (12%) de bis(phénacétyl)-1,7 *m*-carborane. Ce composé recristallisé de l'hexane a les caractéristiques suivantes: p.f. 95 °C; i.r. (cm^{-1}): 2670–2550 (ν_{B-H}), 1740 ($\nu_{C=O}$).

Masse moléculaire calc.: 380.6. Trouvé (tonométrie): 378.

Anal. calc. pour $C_{18}H_{24}B_{10}O_2$: C, 56.80; H, 6.35; B, 28.43. Trouvé: C, 56.96; H, 6.51; B, 28.22.

Oxydation du composé 3

Le composé **3** (3.8 g, 0.01 mol) est chauffé à reflux pendant 5 h dans 40 ml d'anhydride acétique avec un excès d'oxyde de sélénium (3.5 g). A la fin de la réaction, le sélénium est éliminé par filtration et le solvant est distillé sous pression réduite. Le résidu est repris au chloroforme et chromatographié sur une colonne d'alumine acide de 20 × 100 mm (éluant $CHCl_3$). Les fractions contenant la tétracétone **1** sont réunies et donnent après évaporation du solvant 1.84 g de produit qui est purifié par cristallisation de l'heptane, p.f. 100–101 °C.

Condensation du phénylglyoxylate de méthyle sur le m-carboranyldilithium

Une solution de 8.2 g de phénylglyoxylate de méthyle dans 50 ml d'éther est ajoutée peu à peu à une suspension

Can. J. Chem. Downloaded from www.nrcresearchpress.com by 210.87.254.6 on 09/05/12
For personal use only.

de *m*-carboranyldilithium (0.01 mol) dans l'éther–hexane refroidie à −80 °C. A la fin de la réaction exothermique on laisse revenir à température ambiante en une heure et on hydrolyse sur un mélange glace–HCl. Les produits de réaction sont principalement des oligomères infusibles contenant le noyau carborane. Par chromatographie sur colonne d'alumine d'activité III, on sépare 200 mg d'un ester alcool carboranique dont les caractéristiques analytiques et spectroscopiques sont en accord avec la formule **4** du bis(méthoxycarbonyl-α hydroxy-α benzyl)-1,7 *m*-carborane, p.f. 85 °C; i.r. (cm^{-1}): 3450 (ν_{OH}), 3030 (ν_{CH} aromatique), 2970 et 2870 (ν_{CH_3}), 2550 (ν_{BH}), 1720 ($\nu_{C=O}$).

Masse moleculaire calc.: 472.6. Trouvé (tonométrie): 484.

Anal. calc. pour $C_{20}H_{28}B_{10}O_6$: C, 50.82; H, 5.97; B, 22.89. Trouvé: C, 50.68; H, 5.78; B, 22.96.

Méthoxycarbonyl-2 phényl-2 dithiane-1,3 (5)

Un mélange de phénylglyoxylate de méthyle (2 ml), de propanedithiol-1,3 (2 ml), d'acide acétique (5 ml), et de BF_3 éthérate dans l'éther éthylique (3 ml) est chauffé 3 h à 100 °C. En diluant à l'eau, il se forme un précipité blanc cristallin qui est filtré et lavé plusieurs fois avec du méthanol aqueux; i.r. (cm^{-1}): 3100 et 3030 (ν_{CH} aromatique), 2950, 2900 et 2830 (ν_{CH} aliphatique), 1730 ($\nu_{C=O}$); r.m.n. ($CDCl_3$): 3.67 (s, 3H, CH_3O), 1.7–2.2 (m, 2H, dithiane), 2.5–2.4 (m, 4H, dithiane), 7.2–7.9 (m, 5H, aromatique).

Anal. calc. pour $C_{12}H_{14}O_2S_2$: C, 56.65; H, 5.54; S, 25.21. Trouvé: C, 56.69; H, 5.70; S. 25.58.

Condensation du composé 5 sur le m-carboranyldilithium

Une solution du composé **5** (2.54 g) dans 40 ml de benzène est ajoutée peu à peu à une suspension de *m*-carboranyldilithium (5 mmol) dans 20 ml d'éther–hexane. Après 1 h de réaction à température ambiante, le mélange est chauffé à 40 °C (30 min) puis hydrolysé avec 150 ml d'acide chlorhydrique dilué. Le produit brut obtenu par le traitement habituel est chromatographié sur une colonne de silice (éluant, benzène–hexane 30:70). Les trois fractions principales correspondent au *m*-carborane et au composé **5** (90% des quantités de départ) et à un composé brut qui est dissous dans 4 ml d'acétone et oxydé par une solution de *N*-bromosuccinimide (2.85 g) dans 30 ml d'acétone contenant 3% d'eau. A la fin de la réaction, on isole par chromatographie 282 mg de tétracétone **1**, p.f. 99–101 °C.

Diméthoxy-2,2 phénylglyoxal (6)

Ce composé est préparé par la méthode de Henery-Logan et Fridinger (5) modifiée de la façon suivante. Une solution de méthylate de sodium est préparée en ajoutant à 1.5 l de méthanol anhydre refroidi à 0 °C 120 g de suspension d'hydrure de sodium à 50% dans l'huile lourde. Quand le dégagement d'hydrogène cesse, on additionne peu à peu 209.5 g de dichloro-1,1 acétophénone en refroidissant pour maintenir le mélange à 35–40 °C. Après une nuit à température ambiante, le chlorure de sodium est filtré et la plus grande partie du méthanol distillée sous vide. Le résidu est repris à l'éther et traité avec de l'acide chlorhydrique dilué jusqu'à neutralité. La phase éthérée est lavée à l'eau, séchée sur Na_2SO_4 et le solvant est évaporé sous pression réduite.

Le produit de réaction est distillé à 60–62 °C sous 0.15 Torr; rendement, 164.8 g (83%). Les spectres i.r. et r.m.n. sont identiques à ceux qui ont été publiés (5).

Bis(diméthoxy-2,2 hydroxy-1 phénéthyl)-1,7 m-carborane (7)

Dans un réacteur de 500 ml tenu sous atmosphère inerte, on prépare du *m*-carboranyldilithium en ajoutant une solution de 14.4 g (0.1 mol) de *m*-carborane dans 200 ml d'éther à 165 ml de butyllithium 1.52 *N* dans l'hexane. On ajoute ensuite peu à peu 43 g de diméthoxy-2,2 phénylglyoxal à 20 °C et la réaction est poursuivie pendant 1 h après la fin de l'addition.

Le mélange est hydrolysé sur de la glace, extrait à l'éther et lavé à l'eau jusqu'à neutralité. Une partie des sous-produits de la réaction est éliminée par distillation sous vide ($p.é._{0.1}$ 80–100 °C). Le résidu, repris par le pentane, donne un solide blanc qui est cristallisé d'un mélange benzène (100 ml) – hexane (150 ml). On isole 25 g (50%) de diol **7** qui n'a pas de température de fusion franche; spectre de masse, pic moléculaire *M* 506 (^{11}B); i.r. (cm^{-1}): 3520 (ν_{OH}), 3090, 3065, 3050, 3030 et 3018 (ν_{CH} aromatique), 2960, 2940, 2900 et 2830 (ν_{CH} de CH_3O), 2692, 2662, 2658, 2643, 2638, 2624, 2610, 2600, 2578 et 2558 (ν_{BH} 10 bandes fines bien résolues), 1448 et 1380 (δ_{CH_3}).

Masse moleculaire calc.: 504.7. Trouvé (tonométrie): 502.

Anal. calc. pour $C_{22}H_{36}B_{10}O_6$: C, 52.35; H, 7.19; B, 21.43. Trouvé: C, 52.48; H, 7.31; B, 21.12.

Bis(benzoylhydroxyméthyl)-1,7 m-carborane (8)

A une solution de 13 g de composé **7** dans 300 ml de tétrahydrofuranne on ajoute 300 ml d'une solution aqueuse à 48% d'acide sulfurique. Le mélange est agité pendant une nuit à 20 °C. Le précipité qui s'est formé est isolé par filtration, lavé à l'eau jusqu'à neutralité et séché, rendement 10.6 g (100%). Une cristallisation du benzène donne 9 g de produit pur, p.f. 192–195 °C; spectre de masse, pic moléculaire *M* 414 (^{11}B); i.r. (cm^{-1}): 3500 à 3300 (bande large ν_{OH} associé), 3080, 3060, 3020 (ν_{CH} aromatique), 2644, 2630, 2620, 2612, 2584, 2575, 2565, 2548 et 2538 (ν_{BH}), 1688 (ν_{CO}); r.m.n. ($CDCl_3$–DMSO-d_6 60:40) δ: 5.16 (s, —CH—), 6.57 (s large, —OH), 7.20–7.70 (m, 3H, aromatique), 7.80–8.05 (m, 2H, aromatique en *ortho* du carbonyle).

Anal. calc. pour $C_{18}H_{24}B_{10}O_4$: C, 52.40; H, 5.86; B, 26.22. Trouvé: C, 52.36; H, 5.80; B, 26.28.

Bis(phénylglyoxyloyl)-1,7 m-carborane (1)

On chauffe à reflux pendant 24 h un mélange de 10 g de composé **8**, 60 ml de toluène anhydre, 6.2 g d'oxyde de sélénium et 10 gouttes d'acide acétique glacial. A la fin de la réaction, le sélénium métallique est isolé par filtration et lavé avec deux fois 20 ml de toluène. Les phases organiques sont réunies, lavées à l'eau et séchées sur sulfate de sodium. L'évaporation du toluène laisse un résidu marron qui est purifié par cristallisation de 50 ml d'heptane en présence de charbon décolorant. Le rendement en composé **1** est de 7.4 g (74%); p.f. 101 °C; spectre de masse, pic moléculaire *M* 410 (^{11}B); i.r. (cm^{-1}): 3066 et 3012 (ν_{CH} aromatique); 2650, 2638, 2629, 2618, 2609, 2589, 2580, 2578 et 2562 (ν_{BH}), 1723, 1732, 1736 (ν_{CO} en α du carborane), 1675, 1677, 1687 (ν_{CO} en β du carborane); r.m.n. ($CDCl_3$) δ: 7.2–7.7 (m, 3H), 7.8–8.05 (m, 2H en *ortho* du carbonyle).

Anal. calc. pour $C_{18}H_{20}B_{10}O_4$: C, 52.92; H, 4.93; B, 26.48. Trouvé: C, 53.08; H, 5.11; B, 26.57.

Can. J. Chem. Downloaded from www.nrcresearchpress.com by 210.87.254.6 on 09/05/12
For personal use only.

*Condensation de la tétracétone **1** avec l'o-phénylènediamine*

Dans 50 ml de *m*-crésol désaéré on ajoute successivement 2.16 g (20 mmol) d'*o*-phénylènediamine et 4.08 g (10 mmol) de tétracétone **1**. Après 1 h de réaction à température ambiante, le mélange est porté à 200 °C en 2 h et laissé 1 h à cette température. Le solvant est ensuite évaporé sous pression réduite et le résidu est repris avec 100 ml de pentane–éther (80:20). La fraction soluble, purifiée par chromatographie sur colonne d'alumine donne 1.3 g de *m*-carborane identifié par spectrométrie de masse et i.r. Le résidu insoluble dans le pentane est extrait à l'éther. La fraction qui se dissout dans ce solvant est ensuite isolée et cristallisée du benzène. On obtient ainsi environ 0.3 g d'un composé hétérocyclique dont la température de fusion et les caractéristiques spectroscopiques (i.r., r.m.n.) sont identiques à celles du benzoyl-2 benzimidazole (**11**) synthétisé séparément ci-dessous. Le résidu insoluble dans l'éther est cristallisé de l'alcool, puis sublimé à 230 °C sous vide. On isole ainsi 3.7 g d'un second composé hétérocyclique isomère du précédent qui est identifié par comparaison avec un échantillon authentique de phényl-3 1*H*-quinoxalinone-2 (**10**).

Par rapport aux quantités de réactifs utilisées, le bilan de la réaction s'établit ainsi: 90% de **1** est transformé en *m*-carborane, l'*o*-phénylènediamine donnant 83.5% de quinoxalinone **10** et 6.7% de benzimidazole **11**.

*Phényl-3 quinoxalinone-2 **10***

Le produit est obtenu en faisant réagir l'acide phénylglyoxylique et l'*o*-phénylènediamine (8), p.f. 251 °C; u.v. (éthanol) λ_{max} en nm (ε_{max}): 207 (32 400), 222–228 (23 900), 307.5 (12 360), 365 (12 100); i.r. (cm^{-1}): 3150–2715 (11 bandes ν_{N-H}), 1670 et 1660 ($\nu_{C=O}$), 1610 ($\nu_{C=N}$), 1598, 1535, 1480, 1448, 1432; r.m.n. (DMSO) δ: 7.15 (dd, H8), 7.25–7.45 (m, 5H), 7.3 (dd, H5), 8.1–8.45 (m, H2′ et 6′), 12.55 (s, NH).

*Benzoyl-2 benzimidazole **11***

Ce composé est préparé par oxydation du benzyl-2 benzimidazole par CrO_3 dans l'acide acétique (7); p.f. 214–215 °C; i.r. (cm^{-1}): 3220–2200 (ν_{NH}), 1660 ($\nu_{C=O}$), 1600, 1590, 1515, 1485, 1430; r.m.n. (DMSO) δ: 7.2–7.8 (m, 7H), 8.4–8.65 (m, H2′ et 6′), 13.45 (s large, NH).

Le processus réactionnel de condensation entre la tétracétone **1** et l'*o*-phénylènediamine est identique à celui que nous venons de décrire lorsque la réaction est effectuée au reflux dans d'autres solvants tels que le dioxanne, le tétrahydrofuranne, l'éthanol, le chloroforme ou l'acide acétique pendant plusieurs heures. Par contre, si la réaction est conduite dans les mêmes solvants entre 0–20 °C, on isole au bout d'une dizaine d'heure 90% d'un composé intermédiaire instable qui ne peut être purifié ni par cristallisation, ni par sublimation. Le produit brut a les caractéristiques suivantes: p.f. ≃190 °C; analyse élémentaire: $C_{30}H_{32}B_{10}N_4O_2$; masse moléculaire par tonométrie dans le THF, *M* 590; i.r. (cm^{-1}): 3500–3300 (ν_{NH} ou ν_{OH}), 3100, 3060 (ν_{CH}), 3000–2700 (ν_{NH} ou ν_{OH} associé), 2665, 2620, 2605, 2580, 2570, 2560 (ν_{BH}), 1670 large ($\nu_{C=O}$); r.m.n. ($CDCl_3$) δ: 5.08 (s large, 2H, NH et/ou OH), 7.1–7.6 (m, 6H), 7.6–8.15 (m, 3H).

En chauffant 250 mg de ce produit dans 4 ml de *m*-crésol pendant 1 h à 200 °C, on isole 50–60 mg de *m*-carborane et 150 mg d'un mélange des hétérocycles **10** et **11** qui sont séparés par cristallisation fractionnée en benzoyl-2 benzimidazole (10 mg) et phényl-3 quinoxalinone-2 (140 mg).

Dans la diméthylaniline

En faisant réagir 4 h à 20 °C les mêmes proportions de réactifs dans 4 ml de diméthylaniline, on obtient quantitativement un précipité de phényl-3 quinoxalinone-2 **10**. La solution traitée à l'acide chlorhydrique dilué et extraite à l'éther donne la quantité correspondante de *m*-carborane.

*Bis(diéthoxy-1,1 phénylglyoxyloyl)-1,7 m-carborane (**12**)*

Un mélange de tétracétone **1** (204 mg), d'orthoformiate d'éthyle (500 mg), d'alcool éthylique absolu (3 ml) et d'acide chlorhydrique concentré (1 goutte) est agité à température ambiante. L'avancement de la réaction est suivi en i.r. sur la bande à 1730 cm^{-1}. L'intensité de celle-ci diminue rapidement pour devenir nulle après 2 heures environ. L'évaporation des solvants à 100 °C sous vide laisse un résidu vitreux transparent qui n'a pas été purifié en raison des difficultés de recristallisation. Les caractéristiques spectroscopiques de ce composé sont les suivantes: i.r. (cm^{-1}): 2990, 2960, 2940, 2835 (ν_{C-H}), 2690, 2660, 2640, 2625, 2600, 2580, 2559 (ν_{B-H}), 1675 ($\nu_{C=O}$), 1477 (δ CH_2), 1440, 1400 (δ CH_3), 1110 (ν_{C-O-C}); r.m.n. ($CDCl_3$) δ: 1.22 (t, CH_3), 3.62 (m, CH_2), 7.2–7.7 (m, H3′, 4′, 5′ aromatique), 7.92 (dd, H2′, 6′).

*Réaction de la tétracétone **1** avec la potasse éthanolique*

Une solution de potasse (30 mg) dans 0.5 ml d'éthanol est ajoutée à 204 mg de tétracétone **1** dans 8 ml d'éthanol absolu chauffé à 80 °C. Après 30 min de réaction, le solvant est évaporé sous pression réduite et le résidu est extrait avec de l'hexane chaud. La fraction soluble dans l'hexane, purifiée par chromatographie sur colonne d'alumine, donne 62 mg de *m*-carborane. Le résidu insoluble dans l'hexane est acidifié avec de l'acide chlorhydrique dilué, extrait à l'éther et, après évaporation de l'éther, cristallisé du tétrachlorure de carbone. On isole ainsi 120 mg environ d'acide phénylglyoxylique qui est identifié par comparaison avec un échantillon commercial.

*Réaction de la tétracétone **1** avec l'éthylate de sodium*

A une solution de **1** (408 mg) dans 13 ml d'éthanol absolu on ajoute une solution d'éthylate de sodium préparée en faisant réagir 4 mg de sodium dans 2 ml d'éthanol. Le mélange est agité 6 h à 20 °C et le solvant évaporé sous pression réduite. Par chromatographie en couche mince on identifie deux constituants: le *m*-carborane et le phénylglyoxylate d'éthyle. Ces composés sont ensuite séparés par chromatographie préparative en phase gazeuse qui donne en une seule injection 100 mg de *m*-carborane et 250 mg d'ester.

Ce travail a été effectué dans le cadre d'un contrat avec la Direction des Recherches et Moyens d'Essais que nous tenons à remercier ici.

1. L. I. Zakharkin et A. I. L'Vov. Izvest. Akad. Nauk SSSR, Ser. Khim. 151 (1966).
2. L. I. Zakharkin et A. V. Kazantsev. Zh. Obshch. Khim. **37**, 554 (1967).
3. L. I. Zakharkin et A. V. Kazantsev. Zh. Obshch. Khim. **37**, 1211 (1967).
4. E. J. Corey et B. W. Erickson. J. Org. Chem. **36**, 3553 (1971).

5. K. R. HENERY-LOGAN et T. L. FRIDINGER. J. Chem. Soc. Chem. Commun. 130 (1968).
6. B. BARTET, R. FREYMANN, D. GANDOLFO, F. MATHEY, G. RABILLOUD, J. ROSSARIE et B. SILLION. C. R. Acad. Sci. Paris, B, **279**, 283 (1974).
7. S. C. AGARWAL et T. R. SESHADRI. Tetrahedron, **20**, 17 (1964).
8. G. RABILLOUD et B. SILLION. Bull. Soc. Chim. Fr. 4052 (1970).
9. J. C. E. SIMPSON. *Dans* The chemistry of heterocyclic compounds. *Redigé par* A. Weissberger. Interscience Publishers Inc., New York. 1953.
10. V. I. STANKO, A. I. KLIMOVA, YU. A. CHAPOVSKII et T. P. KLIMOVA, Zh. Obshch. Khim. **36**, 1779 (1966).
11. L. I. ZAKHARKIN. Dokl. Akad. Nauk Uzb. SSR, **162**, 817 (1965).
12. C. C. S. CHEUNG, R. A. BEAUDET et G. A. SEGAL. J. Am. Chem. Soc. **92**, 4158 (1970).
13. J. A. POPLE, D. P. SANTRY et G. A. SEGAL. J. Chem. Phys. **43**, 5129 (1965); J. A. POPLE et G. A. SEGAL. J. Chem. Phys. **43**, 5136 (1965) et **44**, 3289 (1966).
14. S. PAPETTI, C. OBENLAND et T. L. HEYING. Ind. Eng. Chem. Prod. Res. Develop. **5**, 334 (1966).

Can. J. Chem. Downloaded from www.nrcresearchpress.com by 210.87.254.6 on 09/05/12
For personal use only.

Relation between van der Waals and Partial Molal Volumes of Organic Molecules in Water[1]

JOHN T. EDWARD AND PATRICK G. FARRELL

Department of Chemistry, McGill University, P.O. Box 6070, Station A, Montreal, Quebec H3C 3G1

Received April 3, 1975

JOHN T. EDWARD and PATRICK G. FARRELL. Can. J. Chem. **53**, 2965 (1975).

The partial molal volumes $\bar{v}$ of nonpolar organic molecules (*i.e.* those having more than three aliphatic carbon atoms per polar hydroxyl, ether, amine, amide, or urea group) in water at 25 °C are given by their van der Waals volumes v_w plus the additional empty volume provided by an enclosing shell 0.53 Å thick. An equation relates $\bar{v}$ to v_w. More polar compounds (*i.e.* those having fewer than two or three aliphatic carbon atoms per polar group) have $\bar{v}$ smaller than calculated by the equation; the shrinkage in $\bar{v}$ from that computed is linearly related to the fraction of the total surface area of the molecule occupied by the polar group.

JOHN T. EDWARD et PATRICK G. FARRELL. Can. J. Chem. **53**, 2965 (1975).

Les volumes molaires partiels $\bar{v}$ de composés organiques non-polaires (*i.e.* ceux contenant plus que trois atomes de carbone aliphatique pour chaque groupement hydroxyle, éther, amine, amide ou urée) dans l'eau à 25 °C sont égaux à leurs volumes van der Waals v_w avec l'incrément du volume vide donné par une enveloppe d'une épaisseur de 0.53 Å. La relation entre $\bar{v}$ et v_w est contenue dans une équation. Les composés plus polaires (ayant moins d'atomes de carbone aliphatique) ont $\bar{v}$ plus petit; la diminution fractionnelle en $\bar{v}$ est liée à la proportion de la surface moléculaire occupée par le groupement polaire.

In connection with other work, we needed to know the densities of aqueous solutions of various organic compounds. In principle, such values could be derived from the apparent molal volumes of the compounds, which were shown many years ago by Traube (1) to be given by the summation of atomic or group increments plus a covolume of about 13 ml/mol. In this paper we devise a simple model for calculating partial molal volumes $\overline{V}$ of organic molecules in water from their van der Waals volumes; we defer for a later paper a comparison of our results with those of Traube.

Stillinger (2) has pointed out that $\overline{V}$ "represents three distinct contributions:

1. The first is the volume increase that would result even for a point particle (not interacting with solvent molecules) on account of its kinetic contribution to the pressure . . . . .

2. The second is just the geometric volume occupied by the solute particle. In the general case, there may be some ambiguity about the precise magnitude of this volume . . . . .

3. Finally, one expects that solvent molecule rearrangement to accommodate the solute particle will normally result in a change in packing efficiency for those solvent molecules . . . . ."

Stillinger's first contribution represents the empty volume (3) required to accommodate any kinetic particle in a liquid, and is akin to Traube's covolume. In our model we identify the second contribution with the van der Waals' volume of the molecule, as defined by various authors (4–6). We discuss below the varying extents to which the volumes of solids, liquids, and solutions are made up in part of the van der Waals volumes of their constituent molecules, and in part of empty volume.

The Varying Proportion of the Volume of Solids and Liquids Made Up of Empty Volume

In a crystalline solid made up of spherical molecules at 0 K the centers of the molecules are separated by a distance which we may define as $2r_w$, r_w being the van der Waals radius of the molecule. This radius in turn defines a spherical van der Waals surface of area A_w, enclosing the van der Waals volume v_w of the molecule. The molar volume V of the solid may be considered to be made up of a molar van der Waals volume $V_w = Nv_w$ of Avogadro's number N of touching spheres, packed in a regular lattice arrangement, and of the void or "empty volume" (3) between the spheres.

[1]Dedicated to Professor C. A. Winkler of McGill University on the occasion of his sixty-fifth birthday by two of his colleagues, one of whom is also a former student (J.T.E.).

Can. J. Chem. Downloaded from www.nrcresearchpress.com by 210.87.254.5 on 09/05/12
For personal use only.

Can. J. Chem. Downloaded from www.nrcresearchpress.com by 210.87.254.5 on 09/05/12
For personal use only.

The van der Waals surface areas A_w and volumes v_w of most organic molecules can be computed by addition of the van der Waals increments of their constituent atoms or groups listed in the literature (4, 5). From the v_w thus computed we can obtain $r_w \equiv (3v_w/4\pi)^{1/3}$. Even though all molecules (with the exception only of noble gas atoms) are not perfect spheres, this parameter, which treats the molecule as a sphere of equivalent volume, proves useful in calculations of various molecular properties such as diffusion coefficients (4) and ion conductances (7) when the molecules or ions are roughly spherical.

The proportion of the volume of a crystalline solid made up of empty volume depends on how the molecules are packed in the crystal. The closest possible packing of spheres or ellipsoids, when each particle is in contact with 12 nearest neighbors, gives a packing density ρ^* ($\equiv Nv_w/V$) of 0.74, and in spite of their nonspherical shapes, most complex organic molecules pack into crystals with 12 nearest neighbors so that at 0 K they have $\rho^* = 0.74 \pm 0.4$ (6).

The expansion of a solid when it warms up from 0 K involves an increase in empty volume, because of the increasing amplitude of molecular vibrations; when the solid melts, there is usually a further increase of 10–15%. At the boiling point the molal volume of most liquids made up of small molecules is about half empty volume.

The Volume of the Solvent Cavity Containing the Solute Molecule

The volume of a solution obtained by dissolving a solid or liquid solute in a solvent is usually (although not always) greater than the original volume of the solvent; however, the increase is not necessarily equal to volume of the added solute, because of variations in the empty volume associated with each molecule of solute in its old and its new environment. If the apparent molal volume at different concentrations is extrapolated to zero concentration we obtain the partial molal volume $\bar{V}$ of the solute at infinite dilution;[2] this is the product of N times the partial molal volumes $\bar{v}$ for a single molecule.

[2]Some of the data from the literature which we have used are for very dilute solutions rather than for infinite dilution; however, the differences are within the accuracy to be expected for our model. Similarly, in a few cases experimental values are recorded for 20° or 30° rather than 25°; again the difference will usually be negligible for our purposes.

Now consider the volume changes $\bar{v}$ accompanying the dissolution of the molecules of two solids, B and C, in a liquid (Fig. 1). For simplicity we postulate spherical molecules and, more importantly, molecules of *the same chemical character*, so that the attraction of molecules of both B and C for solvent molecules will be similar. In such a case, the *average separation of the solvent from solute molecules B and C should be the same* (Stillinger's first contribution). This is represented in Fig. 1 by having molecules of B and of C in cavities having the same separation Δ of the solute molecule from the solvent (represented in Fig. 1, for convenience only, as a continuum); *i.e.*, having $\bar{r} = r_w + \Delta$, where $\bar{r} \equiv (3\bar{v}/4\pi)^{1/3}$. Since $\bar{r}/r_w = 1 + \Delta/r_w$, we come to the important relationship

$$[1] \qquad \left(\frac{\bar{v}}{v_w}\right)^{1/3} = 1 + \frac{\Delta}{r_w}$$

A test of this relation is shown in Fig. 2 in which $(\bar{v}/v_w)^{1/3}$ is plotted against $1/r_w$ for five aliphatic and aromatic hydrocarbons. As required by [1], the points lie close to a straight line having an intercept = 1 and a slope $\Delta = 0.53$ Å. This last can be considered a measure of the separation of solute hydrocarbon molecules from solvent water molecules, the latter perhaps being organized into a quasi-clathrate "cage." We shall accordingly use [2] with $\Delta = 0.53$ Å to

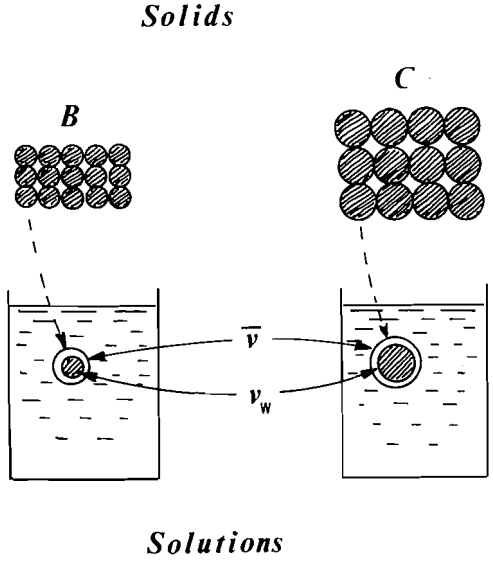

FIG. 1. Schematic representation of volume changes accompanying the dissolution of one molecule of B or of C in a solvent.

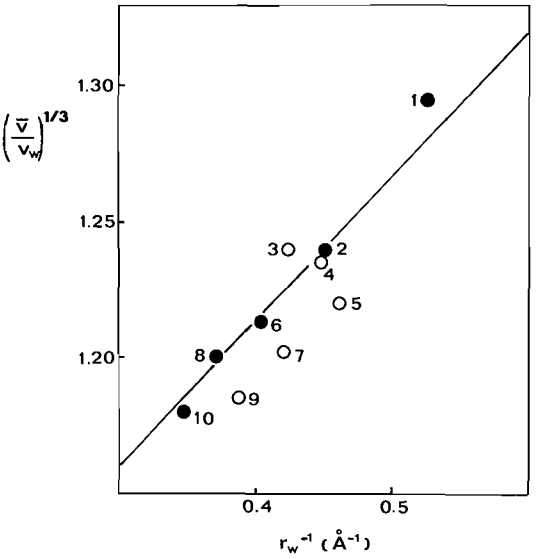

FIG. 2. Dependence of $(\bar{v}/v_w)^{1/3}$ on $1/r_w$ for hydrocarbons (●) and haloalkanes (○) in water at 25°. Curve: theoretical for eq. 1 with $\Delta = 0.53$ Å. Points: experimental data for: 1, methane (refs. 8, 9); 2, ethane (ref. 8); 3, methyl iodide (ref. 10); 4, methyl bromide (ref. 10); 5, methyl chloride (ref. 10); 6, propane (ref. 8); 7, methylene chloride (ref. 11); 8, benzene (ref. 8); 9, chloroform (ref. 12); 10, toluene (ref. 13).

calculate $\bar{v}$ (and thence $\overline{V}$) of hydrophobic molecules from r_w

$$[2] \qquad \bar{v} = \tfrac{4}{3}\pi(r_w + \Delta)^3$$

This equation shows that even for a point molecule $\bar{v}$ would be finite ($=\frac{4}{3}\pi\Delta^3$), corresponding to Stillinger's first contribution. While for small molecules the difference between $\bar{v}$ and v_w is considerable, for large molecules the difference disappears as $\Delta/r_w \to 0$. It may be noted that the cavities associated with hydrocarbon molecules in other solvents can be much greater than those in water. Thus the apparent molal volume of methane in hexane (8) indicates $\Delta = 0.88$ Å. The closer wrapping of the water molecules about hydrocarbons has been attributed to the greater internal pressure of water (8), or to a volume loss due to the partial fit of hydrocarbon molecules into the cavities of an icelike component of water (19).

Shrinkage of the Solvent Cavity When It Contains Hydrophilic Molecules

Stillinger (2) has pointed out that for the majority of water molecules in a clathrate cage surrounding a hard-sphere solute molecule the dipole moment direction cannot point either towards or directly away from the center of the solute molecule. Consequently, such a cage should be partially disrupted when the solute particle is an ion or a strong dipole (Stillinger's third "contribution" to volume). This may account for the alkyl chlorides in Fig. 2 having values of $\bar{v}/v_w$ slightly less than expected; *i.e.* Δ is slightly less than 0.53 Å, so that water molecules are packed more closely in the immediate environment of the solute molecule. This accords with other indications (*e.g.* from Hansch's π values (15)) that chloroalkanes are less hydrophobic than alkanes.

We may, then, expect [2] to hold only for preponderantly hydrophobic molecules. In fact, we find that for molecules containing three or more alkyl carbon atoms for each hydrophilic group (hydroxyl, ether, amine, amide, or urea) [2] with $\Delta = 0.53$ Å works reasonably well. This is illustrated for eight apolar molecules in Table 1; other molecules having $\overline{V}$ agreeing to within 4% of that predicted by [2] are: 1-propanol (11, 14, 21), 2-propanol (14, 21), 1-butanol (11, 12, 14, 21), 2-butanol (14, 21), 2-methyl-1-propanol (14), 1-pentanol (11, 14), 2,2-dimethyl-1-propanol (12), cyclohexanol (12, 16), cycloheptanol (16), benzyl alcohol (14), tetrahydropyran (12, 18, 24), dioxane (18, 24), *n*-propylamine (16), *n*-butylamine (16), *t*-butylamine (12), *n*-pentylamine (16), *n*-hexylamine (16), *n*-heptylamine (16), diethylamine (16), di-*n*-propylamine (16), diethylmethylamine (16), piperidine (16), heptamethyleneimine (16), *N*-methylpyrrolidine (16), *N*-methylpiperidine (16), isopropyl urea (21), *n*-butylurea (21), 1,1-diethylurea (21), 1,3-diethylurea (21), and tetramethylurea (21, 23).

With hydrophilic molecules having less than two alkyl carbon atoms per polar group, on the other hand, [2] fails badly. This is illustrated for eight polar molecules in Table 1; in all cases $\overline{V}$ is 10–20% smaller than calculated from [2], the solvent cavity shrinking for reasons discussed above.

The extent of shrinkage might be expected to vary, depending on (*a*) the differing abilities of different polar groups to form hydrogen bonds to water, and (*b*) the differing extent to which the surface area of the molecule is occupied by these polar groups. These surface areas can be computed by addition of the van der Waals surface increments given for different atoms and groups

Can. J. Chem. Downloaded from www.nrcresearchpress.com by 210.87.254.5 on 09/05/12
For personal use only.

Can. J. Chem. Downloaded from www.nrcresearchpress.com by 210.87.254.5 on 09/05/12
For personal use only.

TABLE 1. Partial molal volumes $\overline{V}$ of polar and apolar molecules in water

Compound	$\overline{V}$ (ml mol^{-1}) Calculated	Experimental	Shrinkage (%)
Apolar molecules			
tert-Butyl alcohol	89.0	87.4 (12)	1.8
3-Pentanol	102.2	101.3 (16)	0.9
Cyclopentanol	91.1	89.1 (16)	2.2
Tetrahydrofuran	77.8	76.5 (17)	1.8
Tetrahydrofuran	77.8	76.9 (18)	1.2
Trimethylamine	78.6	78.8 (16)	—
Trimethylamine	78.6	78.4 (19)	0.3
Trimethylamine	78.6	77.9 (20)	0.9
Triethylamine	121.5	120.9 (16)	0.5
Triethylamine	121.5	119.7 (20)	1.5
n-Pentylamine	106.7	105.7 (16)	0.9
n-Butylurea	118.8	116.0 (21)	1.9
Polar molecules			
Methanol	43.2	38.1 (21)	11.8
Methanol	43.2	38.05[a] (14)	12.0
Ethylene glycol	65.9	55.4[a] (22)	15.9
Ethylene glycol	65.9	55.9 (21)	15.2
Glycerol	87.6	71.44[a] (11)	18.9
Glycerol	87.6	73.5 (21)	16.1
1,3-Dioxolane	72.6	65.4 (18)	9.9
Ammonia	32.2	24.85 (16)	22.8
Ammonia	32.2	24.6 (19)	23.6
Methylamine	47.2	41.68 (16)	11.7
Methylamine	47.2	41.6 (19)	11.9
Formamide	49.5	39.2 (21)	20.8
Formamide	49.5	38.6 (12)	22.0
Urea	60.2	45.0 (21)	25.2
Urea	60.2	44.24 (23)	26.6

[a]At 20 °C.

by Bondi (5). An example of their use is given in Fig. 3; it is assumed that the polar surface area (p.s.a.) of methanol and of 1-propanol is made up of the hydroxyl group, and the nonpolar surface area (n.p.s.a.) of the methyl or *n*-propyl group. The shrinkage of $\overline{V}$ of various alcohols in water is found to be a linear function of the percentage of the molecular surface area occupied by the hydroxyl group, as shown in Fig. 4*A*.

Similar relations are found to hold for amines, amides, and ureas (Fig. 4*B–E*). While the example of 1,3-dioxolane (Table 1) indicates that the ether oxygen atom can be effective in hydrogen-bonding to water and thus shrinking the solvent cavity, the example of trimethylamine (Table 1) indicates that hydrogen-bonding by the amine nitrogen is comparatively ineffective. Consequently, in calculating the polar surface area (% p.s.a.) for primary and secondary amines in Fig. 4*B* and *C* we have taken account only of the surface area of the hydrogen atoms attached to

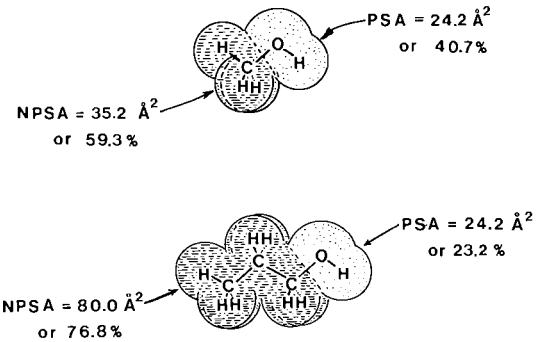

FIG. 3. Comparison of the polar surface area (p.s.a.) and nonpolar surface area (n.p.s.a.) of methanol and of 1-propanol as a percentage of the total surface of the molecule.

nitrogen groups. This is the reason for the apparently small % p.s.a. of these compounds; if the p.s.a. were taken as the total areas of the $-NH_2$ or —NH— groups, the % p.s.a. of the primary amines (*e.g.*, methylamine, compound 2

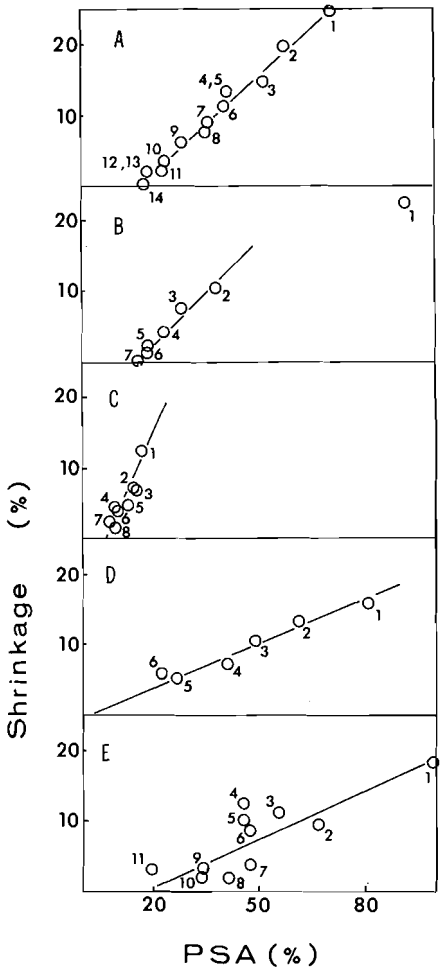

FIG. 4. Effect of percentage of polar surface area (p.s.a.) of a molecule on the shrinkage of $\bar{v}$ in water: (*A*) (Alcohols): 1, erythritol (ref. 25); 2, glycerol (ref. 12); 3, ethylene glycol (ref. 22); 4, 1,2-propanediol (ref. 22); 5, 1,3-propanediol (ref. 22); 6, methanol (refs. 11, 14); 7, 1,4-butanediol (ref. 22); 8, 1,3-butanediol (ref. 22); 9, ethanol (refs. 11, 14); 10, 2-propanol (ref. 14); 11, 1-propanol (refs. 11, 14); 12, 1-butanol (refs. 11, 12, 14); 13, 2-butanol (ref. 14); 14, *tert*-butyl alcohol (refs. 12, 17). (*B*) (Ammonia and primary amines); 1, ammonia (ref. 16); 2, methylamine (ref. 16); 3, ethylamine (ref. 16); 4, *n*-propylamine (ref. 16); 5, *t*-butylamine (ref. 12); 6, *n*-butylamine (ref. 16); 7, *n*-pentylamine (ref. 16). (*C*) (Secondary amines): 1, aziridine (ref. 18); 2, dimethylamine (ref. 16); 3, azetidine (ref. 18); 4, hexamethyleneimine (ref. 18); 5, pyrrolidine (ref. 18); 6, piperidine (ref. 18); 7, heptamethyleneimine (ref. 18); 8, diethylamine (ref. 16). (*D*) (Amides): 1, formamide (refs. 12, 21); 2, acetamide (ref. 21); 3, propionamide (ref. 21); 4, *n*-butyramide (ref. 21); 5, *N*,*N*-dimethylformamide (ref. 21); 6, *N*,*N*-dimethylacetamide (ref. 21). (*E*) (Ureas): 1, urea (refs. 12, 21, 23); 2, methylurea (ref. 21); 3, ethylurea (ref. 21); 4, 1,1-dimethylurea (refs. 21, 23); 5, 1,3-dimethylurea (refs. 21, 23); 6, *n*-propylurea (ref. 21); 7, isopropylurea (ref. 21); 8, *n*-butylurea (ref. 21); 9, 1,1-diethylurea (ref. 21); 10, 1,3-diethylurea (ref. 21); 11, tetramethylurea (refs. 21, 23).

of Fig. 4*B*) would be greater than those of the corresponding alcohols (*e.g.*, methanol, compound 6 of Fig. 4*A*). Obviously, our definition of polar surface is somewhat arbitrary, but at least it has the virtue of affording very simply a quantitative measure of polar character which is consistent as long as it is restricted to a single class of compounds.[3]

The limited data in the literature indicate that the % n.p.s.a. correlates roughly with Hansch's π values (15), with the *h* values of Cabani *et al.* (16, 18), and with Neal and Goring's $d\phi_2/dT$ values (12), all of which have been proposed as quantitative measures of hydrophobic character; however, further work will be required to discover how generally useful it is.

Limitations of the Model

The foregoing model has been tested only with fairly small molecules, none of which departs too far from a spherical shape. Thus, if *n*-pentane is considered to be a prolate ellipsoid having a volume equal to that of its spherical isomer, neopentane, but an axial ratio of 2.3, its surface is only 11% greater than that of neopentane, and consequently the empty volume surrounding the molecule should be only about 11% greater. However, for more extended molecules [1] and [2] become increasingly inadequate; the problem of such molecules will be dealt with in a later paper. For relatively simple and compact water-soluble molecules (ketones, ethers, esters, amino acids, carbohydrates [2] has proved moderately successful, as will be shown in subsequent papers of this series.

We are indebted to two referees for most helpful criticism, which has led to substantial modification of this paper, to Dr. D.A.I. Goring for encouragement and discussion, and to the National Research Council of Canada for financial support of our experimental work.

[3]We have chosen to consider the entire surface of urea as polar, so that % p.s.a. = 100% in Fig. 4*E*. Roseman and Jencks (26) argue that the flat upper and lower surfaces of the urea molecule, covered by the π-orbitals, are apolar, the polar character residing only in the hydrogen-bonding capabilities of the hydrogen and oxygen atoms in an equatorial plane of the molecule. Such an approach would shift the points of Fig. 4*E* to the left and increase the slope of the line.

Can. J. Chem. Downloaded from www.nrcresearchpress.com by 210.87.254.5 on 09/05/12
For personal use only.

1. J. TRAUBE. Samml. Chem. Vortr. **4**, 255 (1899).
2. F. H. STILLINGER. J. Solution Chem. **2**, 141 (1973).
3. A. BONDI. J. Phys. Chem. **58**, 929 (1954).
4. J. T. EDWARD. Chem. Ind. London, 774 (1956); J. Chem. Educ. **47**, 261 (1970).
5. A. BONDI. J. Phys. Chem. **68**, 441 (1964); Physical properties of molecular crystals, liquids, and glasses. John Wiley, New York. 1968. Chapt. 14.
6. A. I. KITAIGORODSKII. Organic chemical crystallography. Consultants Bureau. New York. 1961. pp. 65–67.
7. J. T. EDWARD. Sci. Proc. R. Dublin Soc. **27**, 287 (1957); *In* Advances in chromatography, Vol. 2. *Edited by* J. C. Giddings and R. A. Keller. M. Dekker, New York. 1966. p. 63.
8. W. L. MASTERTON. J. Chem. Phys. **22**, 1830 (1954).
9. E. W. TIEPEL and K. E. GUBBINS. J. Phys. Chem. **76**, 3044 (1972).
10. H. G. HOLLAND and E. A. MOELWYN-HUGHES. Trans. Faraday Soc. **52**, 297 (1956).
11. D. M. ALEXANDER. J. Chem. Eng. Data, **4**, 252 (1959).
12. J. L. NEAL and D. A. I. GORING. J. Phys. Chem. **74**, 658 (1970).
13. J. E. DESNOYERS and F. M. ICHAPORIA. Can. J. Chem. **47**, 4639 (1969).
14. M. E. FRIEDMAN and H. A. SCHERAGA. J. Phys. Chem. **69**, 3795 (1965).
15. C. HANSCH. Acc. Chem. Res. **2**, 232 (1969).
16. S. CABANI, G. CONTI, and L. LEPORI. J. Phys. Chem. **78**, 1030 (1974).
17. F. FRANKS and H. T. SMITH. J. Chem. Eng. Data, **13**, 538 (1968); Trans. Faraday Soc. **64**, 2962 (1968).
18. S. CABANI, G. CONTI, and L. LEPORI. J. Phys. Chem. **76**, 1338 (1972).
19. S. D. HAMANN and S. C. LIM. Aust. J. Chem. **7**, 329 (1959).
20. B. E. CONWAY and R. E. VERRALL. J. Phys. Chem. **70**, 3952 (1966); R. E. VERRALL and B. E. CONWAY. J. Phys. Chem. **70**, 3961 (1966).
21. T. T. HERSKOVITZ and T. M. KELLY. J. Phys. Chem. **77**, 381 (1973).
22. K. NAKANISHI, N. KATO, and M. MASUYAMA. J. Phys. Chem. **71**, 814 (1967).
23. P. R. PHILIP, G. PERRON, and J. E. DESNOYERS. Can. J. Chem. **52**, 1709 (1974).
24. F. FRANKS, M. A. S. QUICKENDEN, D. S. REID, and B. WATSON. Trans. Faraday Soc. **66**, 582 (1970).
25. L. G. LONGSWORTH. J. Phys. Chem. **67**, 689 (1963).
26. M. ROSEMAN and W. P. JENCKS. J. Am. Chem. Soc. **97**, 631 (1975).

Can. J. Chem. Downloaded from www.nrcresearchpress.com by 210.87.254.5 on 09/05/12
For personal use only.

Regioselective *O*-Alkylation of Sterically Hindered Steroidal Ethynyl Carbinols

Z. G. HAJOS AND G. R. DUNCAN

Faculty of Pharmacy, University of Toronto, Toronto, Ontario M5S 1A1

Received March 3, 1975

Z. G. HAJOS and G. R. DUNCAN. Can. J. Chem. **53**, 2971 (1975).

A synthetic method is described for the direct regioselective *O*-alkylation of sterically hindered acetylenic carbinols in the presence of other alcoholic functional groups. The method is not sensitive to the configuration of the latter or to the stereochemistry of ring fusion; the preparation of 5β- and 5α- 20α-ethynyl-20β-methoxy-pregnan-3β-ol **1***b* and **2***b* from the corresponding 20-ols is exemplary. In addition, a straightforward high yield four-step procedure is described for the preparation of the regio-isomer, 20α-ethynyl-3β-methoxy-5β-pregnan-20β-ol **1***c* from 5β-pregnan-3β-ol-20-one **3***a* via **3***b*, **3***c* and **3***d*.

Z. G. HAJOS et G. R. DUNCAN. Can. J. Chem. **53**, 2971 (1975).

On décrit une méthode de synthèse pour la *O*-alkylation directe et régiosélective de carbinols acétyléniques stériquement empêchés en présence d'autres groupes fonctionnels hydroxylés. La méthode n'est pas sensible à la configuration de ces derniers ou à la stéréochimie de la fusion des cycles; on propose à titre d'exemple la préparation des éthynyl-20α méthoxy-20β 5β- (et 5α-)pregnanols-3β (**1***b* et **2***b*) à partir des composés hydroxy-20 correspondants. De plus on décrit une méthode simple en quatre étapes permettant d'obtenir avec un bon rendement le régioisomère éthynyl-20α méthoxy-3β 5β-pregnanol-20β (**1***c*) à partir de la 5β-pregnanol-3β one-20 (**3***a*) par l'intermédiaire de **3***b*, **3***c* et **3***d*.

[Traduit par le journal]

During the course of the investigation of the physiological activity of norcholane analogs of cucurbitacins the problem of regioselective *O*-alkylation of the previously reported (1) diol (**1***a*) arose. Based on electronic considerations we expected the acetylenic carbinol to be the more reactive alcoholic group in **1***a*. Dreiding model studies, however, of the steric arrangment (2) of the molecule indicated a rather hindered C-20 hydroxyl group. Thus one could not predict with certainty which of the two factors would prevail. Rotation around the C_{17}–C_{20} axis would result in even more serious interactions between the C_{13}-methyl and the C_{20}-methyl or ethynyl groups, respectively. Alkylation of a sterically less hindered 17α-ethynyl, 17β-steroidal alcohol using an equimolecular amount of sodamide in liquid ammonia has been previously reported in the patent literature (3), however, no yields were given.

We formed the anion of **1***a* with 2 molecular equiv. of sodium hydride in dry *N*,*N*-dimethyl formamide at 20 °C, and monoalkylated it with an excess of methyl iodide to give exclusively 20α-ethynyl-20β-methoxy-5β-pregnan-3β-ol (**1***b*), m.p. 126–136 °C (91%). A comparison of its n.m.r. spectrum with that of the starting material (**1***a*) revealed that no methylation of the 3β-axial hydroxyl group occurred under the aforementioned reaction conditions. In agreement with the indicated stereochemistry the signal of the C-3 equatorial proton appeared as a relatively narrow multiplet at about 4.1 p.p.m. in both compounds (4).

Since it has been known that equatorial alcohols are more reactive in esterification reactions than their axial counterparts (5), it was of interest to find out if the observed selectivity of ethynyl ether formation could be maintained in the presence of the more reactive equatorial hydroxyl group. Alkylation of the previously reported (1) diol **2***a* with methyl iodide under the above described reaction conditions (**1***a* → **1***b*) gave exclusively 20α-ethynyl-20β-methoxy-5α-pregnan-3β-ol (**2***b*), m.p. 166–178 °C (92.5%).

In comparison with the n.m.r. spectra of **1***a* and **1***b* the signal of the C-3 axial proton of **2***b* appeared at higher field, δ 3.57 (m, 3*a*-H), essentially at the same position as in the starting material (**2***a*) as a broad multiplet due to large diaxial coupling constants. This showed that the 3β-equatorial alcohol had not been alkylated under the above reaction conditions.

These results provide a new and simple procedure for the regioselective *O*-alkylation of

Can. J. Chem. Downloaded from www.nrcresearchpress.com by 210.87.254.5 on 09/05/12
For personal use only.

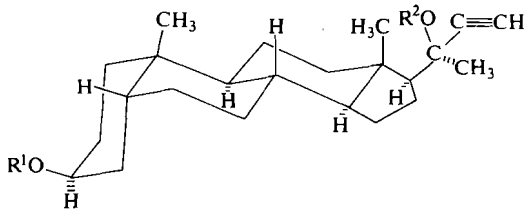

1*a* $R^1 = R^2 = H$
1*b* $R^1 = H; R^2 = CH_3$
1*c* $R^1 = CH_3; R^2 = H$

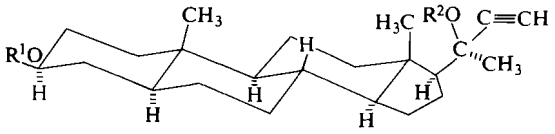

2*a* $R^1 = R^2 = H$
2*b* $R^1 = H; R^2 = CH_3$

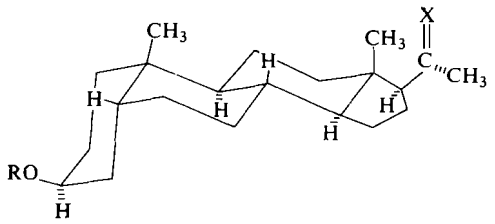

3*a* $R = H; X = O$
3*b* $R = H; X = N{-}OCH_3$
3*c* $R = CH_3; X = N{-}OCH_3$
3*d* $R = CH_3; X = O$

gem-substituted sterically hindered ethynyl carbinols. It avoids the alkylation of the non-acetylenic alcoholic function regardless of its axial or equatorial orientation. No elimination of water was observed, which would have led to undesired enyne formation. The reaction proceeded in good yield and high regioselectivity with both A/B-*cis* (**1***a*) and A/B-*trans* (**2***a*) steroids.

It became evident that in order to achieve the regioselective *O*-alkylation of the cyclohexanol-type oxygen function at the steroidal C-3 position, the C-20 position would have to be protected. Therefore, the keto alcohol **3***a* (1) was converted to its C-20 oxime ether **3***b*. The signal of the C-3 equatorial proton appeared as a relatively narrow multiplet at about 4.1 p.p.m., similar to the signal found in compounds **1***a* and **1***b*.

Methylation under the aforementioned reaction conditions (**1***a* → **1***b*) gave the methyl ether **3***c* in excellent yield (94%). The relatively narrow multiplet of the C-3 equatorial proton appeared at higher field in agreement with the literature (4).

Hydrolysis of the oxime ether group of **3***c* under mild reaction conditions to avoid isomerization at the steroidal C-17 position (6) gave 3β-methoxy-5β-pregnan-20-one (**3***d*) in 97% yield. The compound appeared to be a waxy solid, which resisted all attempts at purification by crystallization or by preparative thin layer chromatography. It has been identified by infrared and by n.m.r. spectroscopy. The 21-H signal of **3***d* was shifted downfield to 2.10 p.p.m. as expected from data obtained with **3***a* (1) and showed no trace of the oxime-ether methyl signal at 3.80 p.p.m.

The addition of acetylene to the 20-keto group of **3***d* gave **1***c*, the 3-methyl ether derivative of the acetylenic carbinol **1***a*. The synthesis of the regio-isomer of **1***b* has thus been accomplished. The high yield (94%) and the good quality of the crude product (**1***c*) is due to the reaction conditions, *i.e.* the introduction of acetylene gas during the reaction of **3***d* with the lithium acetylide – ethylene diamine complex (7). This optimized the yield of conversion and minimized undesired dimer formation as shown by thin layer chromatography.

The observed n.m.r. data are in good agreement with the structural differences between the regio-isomers **1***b* and **1***c*, as shown by the shift in the positions of the 21 and of the 3*e*-H signals. The assignment of the 18- and 19-H signals, on the other hand, has been derived from the n.m.r. spectrum of a mixture containing **1***c* and the 17α-isomer of **1***c*. This fraction, a very minor side product of the acetylene reaction (4.6%), has been obtained by preparative thin layer chromatography of the combined mother liquors of crystallization. It showed the three C-19 protons at 0.95 p.p.m., while the signal of the three C-18 protons appeared at 0.83 as well as at 0.81 p.p.m. respectively, indicating an approximately 1:1 mixture of **1***c* and its 17α-epimer in this particular fraction. The 17β → 17α isomerization is well known from the literature (6), and it has been maintained at a minimum by the introduction of acetylene gas (*C*-acidic compound) during the execution of the reaction.

Can. J. Chem. Downloaded from www.nrcresearchpress.com by 210.87.254.5 on 09/05/12
For personal use only.

Can. J. Chem. Downloaded from www.nrcresearchpress.com by 210.87.254.5 on 09/05/12
For personal use only.

Experimental

Melting points were determined on a Kofler block and are corrected. Absorption spectra were determined in absolute $CHCl_3$ using a Beckman IR-8 i.r. spectrophotometer, and in $CDCl_3$ with TMS as internal standard using a Varian HA-100 or a T-60 n.m.r. spectrophotometer, as indicated in the discussion part of this paper. Elemental analyses were performed by A. B. Gygli, Microanalysis Laboratory, Toronto, Ontario. "Worked up as usual" will mean a solution of the reaction mixture in a water immiscible organic solvent was washed with saturated NaCl in water (two or three times), dried over anhydrous Na_2SO_4, filtered through Celite, and evaporated *in vacuo*.

*20α-Ethynyl-20β-methoxy-5β-pregnan-3β-ol (**1b**)*

To a 50% dispersion of sodium hydride in mineral oil (11.0 mg, 0.23 mmol) was added 35.0 mg (0.1 mmol) of the acetylenic diol **1***a* dissolved in 0.4 ml of dry *N,N*-dimethyl formamide (DMF). It was stirred under nitrogen for approximately 2 min. Methyl iodide (0.2 ml, treated with CaH_2 at 20 °C for 24 h) was added to 1.0 ml anhydrous DMF, and 0.2 ml of this solution ($\simeq$0.5 mmol of CH_3I) was added to the anion of **1***a* in dry DMF. The system was stirred under nitrogen at 20 °C for 24 h. It was then poured into 0.5 ml of water, and worked up as usual with $CHCl_3$ to give 33.1 mg (92%) of crude, crystalline methyl ether **1***b*; ν_{max} 3700, 3650 (OH), 3333 (—C≡CH), 1060 cm^{-1} (—OCH_3). Recrystallization from ether–hexane gave analytically pure **1***b*; m.p. 126–136 °C. The ^1H n.m.r. spectrum of **1***b* (100 MHz) showed δ 0.90 (s, 3, 18-H), 0.98 (s, 3, 19-H), 1.40 (s, 3, 21-H), 2.45 (s, 1, —C≡C—H), 3.36 (s, 3, —OCH_3), and 4.14 (m, 1, 3*e*-H).

Anal. Calcd. for $C_{24}H_{38}O_2$: C, 80.39; H, 10.68. Found: C, 80.89; H, 10.81.

*20α-Ethynyl-20β-methoxy-5α-pregnan-3β-ol (**2b**)*

To a 50% dispersion of sodium hydride in mineral oil (22.7 mg, 0.47 mmol) was added 61.0 mg (0.18 mmol) of the acetylenic diol **2***a* dissolved in 1.0 ml dry DMF. It was stirred under nitrogen for 5 min. Methyl iodide (0.2 ml, treated with CaH_2 at 20 °C for 24 h) was added to 1.0 ml anhydrous DMF and 0.4 ml of this solution (approximately 1.0 mmol CH_3I) was added to the anion of **2***a* in dry DMF. The system was stirred under nitrogen at 20 °C for 1 h. It was then poured into 1.0 ml of ice water, and worked up as usual with benzene. The solid residue (65.0 mg) was placed under high vacuum to remove traces of DMF and gave 58.0 mg of the methyl ether **2***b* (92.5%), identified by n.m.r. spectroscopy (*vide supra*). Recrystallization from ether gave analytically pure **2***b*; m.p. 166–178 °C. The ^1H n.m.r. spectrum of **2***b* (60 MHz) showed δ 0.90 (s, 3, 18-H), 0.81 (s, 3, 19-H), 1.45 (s, 3, 21-H), 2.45 (s, 1, C≡CH), 3.36 (s, 3, —OCH_3), and 3.57 (m, 1, 3*a*-H).

Anal. Calcd. for $C_{24}H_{38}O_2$: C, 80.39; H, 10.68. Found: C, 80.21; H, 10.67.

*3β-Methoxy-20-methoxyimino-5β-pregnane (**3c**)*

A 50% dispersion of sodium hydride in mineral oil (542 mg, 11.3 mmol) was washed free of oil with dry petroleum ether. To this was added while stirring under nitrogen at 20 °C, 622.0 mg (1.8 mmol) of the oxime ether alcohol **3***b* dissolved in 12.0 ml of dry DMF. The addition took approximately 3 min and it was then stirred under nitrogen at 20 °C for 50 min. Methyl iodide (1.25 ml, treated with CaH_2 at 20 °C for 24 h) was added to 1.0 ml dry DMF. This solution (approx. 18.7 mmol of CH_3I) was added within 5 min while stirring under nitrogen to the anion of **3***b* in dry DMF. Stirring was continued for 16 h with the exclusion of moisture. A few drops of methanol were then added, and it was poured into 50 ml of ice water and worked up as usual with $CHCl_3$. The resulting oil was placed under high vacuum to remove traces of DMF. The oily residue crystallized upon the addition of 1.0 ml of methanol to give 612.1 mg (94%) of the methyl ether **3***c*, identified by n.m.r. spectroscopy. Recrystallization from methanol gave analytically pure **3***c*; m.p. 84–86 °C. The ^1H n.m.r. spectrum of **3***c* (60 MHz) showed δ 0.60 (s, 3, 18-H), 0.93 (s, 3, 19-H), 1.78 (s, 3, 21-H), 3.26 (s, 3, 3β-OCH_3), 3.50 (m, 1, 3*e*-H), and 3.80 (s, 3, =N—OCH_3).

Anal. Calcd. for $C_{23}H_{39}NO_2$: C, 76.40; H, 10.87. Found: C, 76.36; H. 10.43.

*20-Methoxyimino-5β-pregnan-3β-ol (**3b**)*

The 20-keto steroid **3***a* (193 mg, 0.61 mmol) was dispersed in 2.0 ml of methanol. Methoxylamine hydrochloride (73.0 mg, 0.87 mmol) was added in 3.0 ml of methanol, followed by 92.0 mg (1.06 mmol) of anhydrous sodium acetate and 3.0 ml of methanol. The reaction mixture was stirred for 16 h, water (15.0 ml) was then added, and the crystalline precipitate was filtered off. It was then dissolved in $CHCl_3$, and worked up as usual to give 257.7 mg of a solid. This was broken up in methanol and filtered to give 199.4 mg (94%) of the oxime ether **3***b*. Recrystallization from methanol gave analytically pure **3***b*; m.p. 136–139.5 °C; ν_{max} 3750, 3500–3650 (OH), 1660, 1600 (weak C=N bands), 1060 cm^{-1} (—OCH_3). The ^1H n.m.r. spectrum of **3***b* (60 MHz) showed δ 0.62 (s, 3, 18-H), 0.97 (s, 3, 19-H), 1.83 (s, 3, 21-H), 3.85 (s, 3, =N—OCH_3), and 4.12 (m, 1, 3*e*-H).

Anal. Calcd. for $C_{22}H_{37}NO_2$: C, 76.03; H, 10.73; N, 4.03. Found: C, 76.24; H, 10.61; N, 4.00.

*20α-Ethynyl-20β-hydroxy-3β-methoxy-5β-pregnane (**1c**)*

a. Hydrolysis of the 20-methoxyimino compound 3c to the 20-keto compound 3d

The oxime ether **3***c* (612 mg, 1.69 mmol) in 45.0 ml of 0.066 *N* HCl in acetone–water (40.4 ml of acetone and 4.5 ml of 0.66 *N* aqueous HCl) was refluxed for 4 h. It was then allowed to stand at 20 °C for 18 h. Thin layer chromatography showed the presence of some residual starting material (benzene/ethyl acetate, 9:1 on Silica Gel; R_f of **3***c* 0.4; of **3***d* 0.29). Therefore, 1.0 ml of 2.0 *N* aqueous HCl was added, and refluxing continued for 4 h; it was then allowed to stand at 20 °C for 18 h. No starting material (**3***c*) was indicated by t.l.c. The clear solution was evaporated *in vacuo* at 20 °C to remove the acetone. The usual work up with $CHCl_3$ gave 549.0 mg (97%) of the desired 20-keto compound **3***d* in the form of a waxy solid; ν_{max} 1705 (20-CO) and 1088 cm^{-1} (—OCH_3); n.m.r. spectrum (*vide supra*). It was rather insoluble in methanol, slightly more soluble in ethyl alcohol, soluble in acetone, in ether, and in *n*-hexane. It resisted all attempts at crystallization. A 63.0 mg sample of **3***d* was dissolved in $CHCl_3$, and applied to two 20 × 20 cm,

1.0 mm thick SiO_2-gel plates with fluorescence indicator; it was developed with anhydrous ether. A 1.0 cm wide strip of each plate was cut away and sprayed with phosphomolybdic acid. Based on this 4 zones have been marked and separated into fronts 1–4. Fraction 2 gave 31.0 mg of clean (by t.l.c. developed with ether or benzene/ethyl acetate, 1:1 and 9:1 respectively) 20-keto compound **3***d*, which could be broken up with methanol into a waxy solid, but still resisted all attempts at crystallization. The ^1H n.m.r. spectrum of **3***d* (60 MHz) showed δ 0.60 (s, 3, 18-H), 0.90 (s, 3, 19-H), 2.10 (s, 3, 21-H), 3.30 (s, 3, 3β-OCH_3), and 3.50 (m, 1, 3*e*-H).

b. Acetylene addition to 5β-pregnan-3β-ol-20-one-3-methyl ether (3d) to give 1c

Into a 50.0 ml 3-necked flask equipped with magnetic stirring bar, serum cap, gas inlet tube, and reflux condenser with $CaCl_2$ filled tube at the top was placed 5.0 ml of anhydrous DMSO (dimethylsulfoxide). Acetylene gas (cooled to −75 °C and purified with two H_2SO_4, one $CaO/CaCl_2$ and one fritted-glass filter tower) was introduced over the DMSO level while stirring for 40 min at 20 °C. Lithium-acetylide – ethylenediamine complex (stored under Argon, freshly opened bottle; 460 mg, 4.8 mmol) was added at once; it dissolved to give a light brown solution. To this was added 526.7 mg (1.59 mmol) of crude, unpurified 20-keto compound **3***d* dissolved in 6.0 ml of anhydrous DMSO with the help of a syringe through the serum cap within 10 min while stirring under a continuous flow of acetylene gas for an additional 4 h. The dark brown solution was sealed under acetylene, and it was stirred at 20 °C for 16 h. It was then cooled with ice water, and 600 mg of ammonium chloride in 4 ml of water was added to it dropwise. Approximately 300 mls of benzene and 100 ml of water was added, and the mixture was carefully acidified with 2 *N* HCl. The benzene solution was then worked up as usual to give 650.5 mg of crude **1***c*, a dark brown solid. This was dissolved in 60.0 ml of $CHCl_3$ and treated with Darco G-60 at 20 °C for 30 min. It was filtered through Celite, and evaporated *in vacuo* to give 535.0 mg (94%) of light yellow, crystalline ethynyl carbinol **1***c*; t.l.c. on 0.25 mm thick SiO_2-gel developed with benzene/ethyl acetate, 9:1 showed R_f 0.18; spraying with vanillin–H_3PO_4 and heating to 80 °C gave a cherry red colour; it showed some slower moving impurities, n.m.r. spectrum (*vide infra*).

Due to the slower moving impurity the compound (**1***c*) was dissolved in 25 ml of benzene, 7.0 g of Silicagel III (Woelm, for dry column chromatography) was added, and the solvent evaporated *in vacuo*. The dry SiO_2 powder and **1***c* were placed on top of an 87 cm long column of the same absorbent of 2.5 cm diameter. It was developed with 300 ml of anhydrous ether in 3.0 ml fractions. The first ten fractions contained the desired material as shown by t.l.c., and gave 496.6 mg of almost colorless **1***c* (87%). Thin layer chromatography indicated no slower moving impurities. Recrystallization from ethyl acetate and petroleum ether (b.p. 30–60 °C) gave analytically pure ethynyl carbinol **1***c* 305.9 mg m.p. 150–156 °C; t.l.c. (*vide supra*); ν_{max} 3400–3550, 3330 (OH), 3270 (—C≡CH), 1100 and 1075 cm^{-1} (—C—O-stretching). The ^1H n.m.r. spectrum of **1***c* (60 MHz) showed δ 0.83 (s, 3, 18-H), 0.95 (s, 3, 19-H), 1.50 (s, 3, 21-H), 2.48 (s, 1, —C≡CH), 3.30 (s, 3, 3β-OCH_3), and 3.50 (m, 1, 3*e*-H).

Anal. Calcd. for $C_{24}H_{38}O_2$: C, 80.39; H, 10.68. Found: C, 80.19; H, 10.65.

The mother liquors of crystallization were combined and evaporated *in vacuo* to give 140 mg of crude **1***c*. This was dissolved in 1.0 ml CH_2Cl_2 and applied to two 20 × 20 cm, 1.0 mm thick SiO_2-gel plates with fluorescence indicator. They were developed with anhydrous ether. A 1.0 cm wide strip of each plate was cut away and sprayed with vanillin–H_3PO_4 (desired band turned pink). Work up of the desired band gave 90.0 mg of a crystalline fraction, which was indistinguishable from **1***c* by t.l.c. in different solvent systems (one spot in benzene/ethyl acetate, 1:1, in ether, and in ethyl acetate). It showed, however, m.p. 100–110 °C. It was extracted with refluxing petroleum ether (b.p. 30–60 °C) to give 34.6 mg of **1***c* (insoluble in petroleum ether) m.p. 150–156 °C; n.m.r. spectrum superimposable to that of authentic **1***c*. Total yield of pure, crystalline acetylenic carbinol **1***c* was thus 340.5 mg (59.5%). The anomalous n.m.r. spectrum of the petroleum ether soluble fraction (55.0 mg) has been described in the discussion part of this paper.

The authors wish to express their thanks to the Medical Research Council of Canada (MA 2996) for supporting this investigation.

1. B. M. KAPUR, A. MANNAN, and G. R. DUNCAN. J. Chem. Soc. Chem. Commun. 775 (1975).
2. F. SONDHEIMER, N. DANIELLI, and Y. MAZUR. J. Org. Chem. **24**, 1278 (1959).
3. O. ENGELFRIED and M. SCHENK. Ger. Patent No. 1,062,698 (August, 1959).
4. J. E. BRIDGEMAN, P. C. CHERRY, A. S. CLEGG, J. M. EVANS, E. R. H. JONES, A. KASAI, V. KUMAR, G. D. MEAKINS, Y. MORISAWA, E. E. RICHARDS, and P. D. WOODGATE. J. Chem. Soc. C, 250 (1970).
5. E. L. ELIEL and C. A. LUKACH. J. Am. Chem. Soc. **79**, 5986 (1957).
6. A. SERINI, W. LOGEMANN, and W. HILDEBRAND. Ber. **72**, 391 (1939).
7. O. F. BEUMEL, JR. and R. F. HARRIS. J. Org. Chem. **29**, 1872 (1964).

Can. J. Chem. Downloaded from www.nrcresearchpress.com by 210.87.254.5 on 09/05/12
For personal use only.

Can. J. Chem. Downloaded from www.nrcresearchpress.com by 210.87.254.42 on 09/05/12
For personal use only.

The Preparation and Synthetic Utility of *tert*-Butyldiphenylsilyl Ethers[1]

STEPHEN HANESSIAN AND PIERRE LAVALLEE[2]
Department of Chemistry, University of Montreal, Montreal, Quebec H3C 3V1
Received June 27, 1975

STEPHEN HANESSIAN and PIERRE LAVALLEE. Can. J. Chem. **53**, 2975 (1975).

The utility of *tert*-butyldiphenylsilyl chloride as a reagent for the protection of hydroxyl groups was explored. The corresponding *tert*-BDPSi ethers have much greater stability to acids, and under conditions of hydrogenolysis, than related silyl and trityl ethers. Preferential removal of trityl, tetrahydropyranyl, benzyl, and other silyl ethers and acetals can be effected in presence of *tert*-BDPSi ethers. Treatment with fluoride ion causes smooth cleavage of the latter.

STEPHEN HANESSIAN et PIERRE LAVALLEE. Can. J. Chem. **53**, 2975 (1975).

L'utilité synthétique du chlorure de *tert*-butyldiphenylsilyle pour la protection temporaire des fonctions hydroxyles a été explorée. Les éthers *tert*-BDPSi démontrent une stabilité supérieure dans des conditions acides et d'hydrogénolyse, par rapport à d'autres éthers silylés analogues, et aux éthers de triphenylméthyle, tétrahydropyrannyle, et benzyle. Plusieurs fonctions y inclus des acétals, peuvent être préférentiellement hydrolysés en présence de la fonction *O-tert*-BDPSi.

The availability of appropriate protecting groups for hydroxyl, and related functions (1, 2) is oftentimes a crucial problem in the planning and execution of a synthetic stratagem involving polyfunctional molecules. Silyl ethers, and in particular, *tert*-butyldimethylsilyl ethers, have been extensively used in recent synthetic work related to the prostaglandins (3), and also in the deoxynucleoside series (4).

We wish to report on the protection of hydroxyl groups as *tert*-butyldiphenylsilyl ethers (*tert*-BDPSi). In addition to retaining all the known features that are associated with silyl ethers, such as their ease and selectivity of formation, their adaptability to various analytical techniques, and their compatibility with a variety of conditions or synthetic transformations in organic chemistry (3), the *tert*-BDPSi group offers some unique and novel features that constitute a significant improvement over the existing related groups, and warrants their communication at this time.

Selectivity—Primary hydroxyl groups are silylated preferentially to secondary, as indicated by the following examples. Treatment of methyl α-D-glucopyranoside with 1.1 equiv. of *tert*-butyldiphenylsilyl chloride[3] in DMF containing 2.2 equiv. of imidazole (3) (25 °C, 4 h[4]), afforded the corresponding 6-*O*-*tert*-DBPSi derivative as an amorphous solid, (75–80%); m.p. 119–121 °C; $[\alpha]_D^{23}$ +61.6° (*c* 1.15, $CHCl_3$).[5] Similar silylation of methyl 2-benzyloxycarbonylamino-2-deoxy-α-D-glucopyranoside (25 °C, 4 h) gave the corresponding crystalline 6-*O*-*tert*-DBPSi derivative (84%); m.p. 90.5–91.5 °C (ether–hexane); $[\alpha]_D^{23}$ +34.4° (*c* 1.16, $CHCl_3$).[6]

Silylation was equally effective in the case of secondary hydroxyl groups, including axially

[1]Presented in part at the 169th National Meeting of the American Chemical Society, April 1975, Philadelphia Pa., CARB 5, and at the 58th Canadian Chemical Conference, May 1975, Toronto.

[2]NRCC and Quebec Ministry of Education predoctoral fellow.

[3]Prepared from dichlorodiphenylsilane and *tert*-butyl lithium in refluxing pentane; b.p. 90 °C/0.015 Torr; 95%.

[4]Silylation could also be accomplished in pyridine, in the absence of imidazole, but the reaction times were longer.

[5]The presence of the phenyl chromophore in the *tert*-BDPSi group greatly facilitates the detection of products on chromatograms by spectrophotometric methods, a feature which is not shared by the related *O-tert*-butyldimethylsilyl group. Also in many instances there was no need for chromatographic separations.

[6]Satisfactory spectroscopic (i.r., n.m.r., mass) data were obtained for the compounds described herein. Crystalline compounds gave correct microanalyses.

Can. J. Chem. Downloaded from www.nrcresearchpress.com by 210.87.254.42 on 09/05/12
For personal use only.

disposed groups, utilizing the same combination of reagents and at temperatures ranging from 25–60 °C.

Stability and Compatibility—The *O-tert*-BDPSi group offers unique acid stability properties relative to related analogs. Thus, it is virtually unaffected under conditions that cause complete cleavage of *O*-trityl, *O-tert*-butyldimethylsilyl, and *O*-tetrahydropyranyl groups. In such a study, 2,3:4,5-di-*O*-methylene-D-mannitol was monosilylated as usual, and the resulting syrupy *O-tert*-BDPSi ether, $[\alpha]_D^{23}$ +32.3° (*c* 1.34, $CHCl_3$), was converted into the corresponding 6-*O*-trityl, 6-*O*-tetrahydropyranyl, and 6-*O-tert*-butyldimethylsilyl ethers. Treatment of these derivatives individually with 80% acetic acid caused selective cleavage of the 6-ether groups, and the 6-*O-tert*-BDPSi derivative was recovered in each case in over 96% yield.

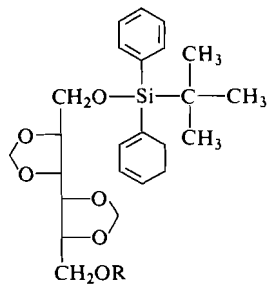

R = H, Tr, THP, $Si(CH_3)_2C(CH_3)_3$

A distinctive feature of the *O-tert*-BDPSi group is its compatibility under conditions required for the acid-catalyzed formation, and cleavage of acetals. The following synthetic transformation will illustrate this point. Silylation of cytidine (1.1 equiv. *tert*-BDPSiCl, 2.2 equiv. imidazole, 25 °C, 3 h) gave the 5′-*O-tert*-BDPSi derivative (87%); m.p. 223–226 °C ($CHCl_3$); $[\alpha]_D^{23}$ +56.5° (*c* 1.14, MeOH). Treatment of the former with 2,2-dimethoxypropane and concentrated hydrochloric acid (25 °C, 24 h), followed by conventional workup, gave the corresponding 5′-*O-tert*-BDPSi-2′,3′-*O*-isopropylidene derivative (95.5%); m.p. 138–143 °C ($CHCl_3$–ether–hexane); $[\alpha]_D^{23}$ +30.3° (*c* 1.08, $CHCl_3$); M^+ 521; 506 (*M* − 15); 464 (*M* − 57), etc. Treatment with 50% aqueous trifluoroacetic acid – dioxane (25 °C, 15 min) gave the starting crystalline silyl ether derivative (64%). Benzylidene acetals of the 2-phenyl-1,3-dioxane type could also be preferentially hydrolyzed in the presence of secondary *O-tert*-BDPSi groups.[7]

The *tert*-BDPSi group is unaffected under conditions of hydrogenolysis.[8] Thus, benzylation of methyl 6-*O-tert*-butyldiphenylsilyl-α-D-glucopyranoside ($PhCH_2Br$, NaH, DMF) gave the corresponding crystalline tribenzyl ether; m.p. 115.5–116 °C; $[\alpha]_D^{23}$ +18.7° (*c* 1.04, $CHCl_3$). Catalytic hydrogenolysis in the presence of 20% palladium hydroxide-on-charcoal (6) gave the starting silyl ether, m.p. 117–118 °C, in 93% yield. The *O-tert*-BDPSi group was also found to be stable under the following conditions: 25–75% aqueous formic acid – dioxane, 25 °C, 2–6 h (90% recovery); 50% aqueous trifluoroacetic acid – dioxane, 25 °C, 15 min; hydrogen bromide in glacial acetic acid (2 equiv.), 12 °C, 2 min; catalytic amounts of sodium methoxide in methanol, 25 °C, 24 h (95% recovery); 9 *M* ammonium hydroxide – dioxane, 60 °C 2 h (96% recovery).

Upon treatment with a *M* solution of tetra-*n*-butyl-ammonium fluoride in THF (2 equiv.) (3), smooth cleavage occurred within 1–5 h at 25 °C to regenerate the parent alcohol in over 90% yield in all cases studied.[9] Hydrolysis could also be brought about in 3% methanolic hydrogen chloride (25 °C, 3 h, 71%), and in 2 *N* sodium hydroxide containing 50% ethanol (25 °C, 7 h, 93%).

Thus, the novel *tert*-BDPSi group becomes an important complement to the trityl and other silyl groups, for the selective protection of primary hydroxyl groups, with the added advantage of much greater stability under acidic and hydrogenolytic conditions. It is also a convenient and versatile protecting group for secondary hydroxyl groups, and as

[7]Little, if any migration of silyl groups was observed under these conditions. When kept in solution (CH_2Cl_2, etc.) for prolonged periods of time, some change (t.l.c.) was observed presumably due to a migration to suitably disposed primary hydroxyl groups. This possibility is presently under study.

[8]Some silyl ethers are susceptible to hydrogenolysis (3); see also ref. 5.

[9]Partial migration of ester (acetate, benzoate) groups occurs during the desilylation reaction in compounds where the esters functions are suitably disposed. This observation has been recently recorded by others also (5).

such, complements the tetrahydropyranyl and benzyl groups in a variety of synthetic transformations. Other applications are presently under study.

Financial assistance from the National Research Council of Canada is gratefully acknowledged.

1. J. F. W. McOMIE. Protective groups in organic chemistry. Plenum Press. 1973.
2. S. COFFEY. (*Editor*). Rodd's chemistry of carbon compounds. Vol. 1F. 2nd ed. Elsevier Publishing Co., New York. 1967.
3. E. J. COREY and A. VENKATESWARLU. J. Am. Chem. Soc. **94**, 6190 (1972).
4. K. K. OGILVIE. Can. J. Chem. **51**, 3799 (1973); K. K. OGILVIE, E. A. THOMPSON, M. A. QUILLIAM, and J. B. WESTMORE. Tetrahedron Lett. 2865 (1974).
5. G. M. DODD, B. T. GOLDING, and P. V. IOANNOU. Chem. Commun. 249 (1975).
6. W. M. PEARLMAN. Tetrahedron Lett. 1663 (1967).

Can. J. Chem. Downloaded from www.nrcresearchpress.com by 210.87.254.42 on 09/05/12
For personal use only.

Can. J. Chem. Downloaded from www.nrcresearchpress.com by 210.87.254.6 on 09/05/12
For personal use only.

Canadian Journal of Chemistry

Published by
THE NATIONAL RESEARCH COUNCIL OF CANADA

Volume 53 Number 20 October 15, 1975

Journal canadien de chimie

Publié par
LE CONSEIL NATIONAL DE RECHERCHES DU CANADA

Volume 53 numéro 20 15 octobre 1975

Kinetics and Equilibrium of Binding of Fe^{3+} by a Fulvic Acid: A Study by Stopped Flow Methods[1]

COOPER H. LANGFORD[2] AND TAHIR R. KHAN
Department of Chemistry, Carleton University, Ottawa, Canada K1S 5B6

Received June 3, 1974[3]

COOPER H. LANGFORD and TAHIR R. KHAN. Can. J. Chem. **53**, 2979 (1975).

The first report of a rate of binding of a metal ion (Fe^{3+}) by a soluble fulvic acid is derived from stopped flow measurements. The rate of complex formation is normal in Wilkins' sense and similar to that for sulfosalicylic acid. Dissociation is slow ($t_{1/2} > 10$ s). The binding of Fe^{3+} by the fulvic acid in acid solution, pH = 1–2.5, was investigated by kinetic analysis in which the reaction of free Fe^{3+} with sulfosalicylic acid was followed by stopped flow spectrophotometry on a time scale short compared to release of Fe^{3+} by fulvic acid. Conditional equilibrium constants found were $1.5 \pm 0.3 \times 10^4$ at pH = 1.5 and 2.5, and $2.8 \pm 0.3 \times 10^3$ at pH = 1.0 at 25 °C (ionic strength 0.1).

COOPER H. LANGFORD et TAHIR R. KHAN. Can. J. Chem. **53**, 2979 (1975).

On dérive de mesures à flux stoppé le premier rapport d'une vitesse de fixation d'un ion métallique (Fe^{3+}) par l'acide fulvique soluble. La vitesse de formation du complexe est normale dans le sens de Wilkins et semblable à celle rapportée pour l'acide sulfosalicylique. La dissociation est lente ($t_{1/2} > 10$ s). On a étudié la fixation du Fe^{3+} par l'acide fulvique en milieu acide, pH = 1–2.5, par une analyse cinétique dans laquelle la réaction du Fe^{3+} libre avec l'acide sulfosalicylique est déterminée par spectrophotométrie à flux stoppé sur une échelle de temps faible comparée à la vitesse de libération du Fe^{3+} par l'acide fulvique. On a trouvé que les constantes d'equilibre conditionnel sont de $1.5 \pm 0.3 \times 10^4$ à pH = 1.5 et 2.5 et $2.8 \pm 0.3 \times 10^3$ à pH = 1.0 à 25 °C (force ionique = 0.1).

[Traduit par le journal]

Introduction

Eigen (1) introduced the concept of 'kinetic spectrometry' which refers to the description of a complex chemical system in terms of a set of rate constants characteristic of its components. These rate constants are, of course, reciprocals of a set of frequencies which may be said to form a spectrum. The metaphor is especially appealing when relaxation techniques such as ultrasonic absorption are used to study kinetics because the kinetic spectrum is seen directly in the instrumental output.

For purposes of analysis of mixtures, the kinetic spectrum supplies an interesting set of frequencies by which different components may be recognized and estimated. The idea has been successfully exploited recently by groups in the United States (2, 3) and the Soviet Union (4). The most promising experimental approach is stopped flow spectrometry where a concentration pulse is applied and the system is followed during the time course of the relaxation of the components of interest to a common product by

[1]Supported by the National Research Council of Canada and the Research Incentives Office, Inland Waters Directorate. We thank Dr. D. S. Gamble, Soil Research Institute, Agriculture Canada, for the fulvic acid sample and valuable discussion.

[2]To whom correspondence should be addressed.

[3]Revision received June 26, 1975.

Can. J. Chem. Downloaded from www.nrcresearchpress.com by 210.87.254.6 on 09/05/12
For personal use only.

following changes in the visible–ultraviolet spectrum.

So far, such studies have usually prepared a set of components (*e.g.* metal ions, M^{2+}) as some favorable molecular species (*e.g.* EDTA complexes) and reacted them with a common reagent (*e.g.* Cu^{2+}) to produce a common product (*e.g.* CuEDTA) which is monitored at a characteristic wavelength. Our interest is similar with one exception. We are interested in reagents which react with the analyte *without* prior treatment of the analyte. In this way, we seek to develop analysis for the *molecular species* originally in the *analyte*, as they are characterized by their rate constants for reaction with a given reagent.

This paper reports a *primitive* example of the above program. We analyze equilibrium mixtures of aquoiron(III) (aquo Fe(III)) species and a soluble fulvic acid to determine conditional average binding constants. In this case, the unbound aquo Fe(III) species react rapidly with the reagent (excess sulfosalicylic acid) such that the free iron can be determined prior to significant perturbation of the iron – fulvic acid complex. We have only one kinetically important species. To establish this point, some investigations were made of the kinetics of interaction of Fe(III) with fulvic acid using the (small!) absorbance changes in the spectrum of the fulvic acid. Also, one run used an excess of fulvic acid.

The system under study is difficult for alternative methodologies and some significant interest attaches to the results. The binding of iron by fulvic acids is thought to be quite important to iron dissolution and transport in fresh water. Moreover, metal – fulvic acid complexes have sometimes been referred to as 'non-labile' without detailed evidence. The present study contains, to our knowledge, the first direct examination of the kinetics of such an interaction.

Experimental

Materials

The fulvic acid sample was generously supplied by D. S. Gamble, Soil Research Institute, Agriculture Canada (5). It is a sample extracted from the Bh horizon of an imperfectly drained podzol soil in Prince Edward Island. The number average molecular weight is approximately 900. It contains 3.3 mequiv./dry g of phenolic sites *ortho* to carboxylic acid sites (salicylic acid type sites) and an additional 4.4 mequiv./dry g of carboxylic acid sites. Alcoholic, ketonic, and quinoid functionality is also present (5). Stock solutions were prepared and stored in the dark. They were found to be stable (no spectral change) for periods much longer than the storage time allowed prior to any of the experiments reported.

Iron(III) solutions were prepared from A.R. Grade metal by dissolution in nitric acid. The p*H* of the stock solutions was checked with a Fisher 'accumet' p*H* meter. Dilute Fe(III) solutions of specified p*H* were prepared by diluting the Fe(III) stock with water and precisely calculated (comparatively large) amounts of standardized $HClO_4$ solution.[4] The ionic strength was maintained at 0.10 using $NaClO_4$ solutions.

Recrystallized Baker 'analyzed' sulfosalicylic acid (SSA) was used to prepare stock solutions. These were found to be stable (no change in spectrum) for periods of over three months.

Kinetics

There were three types of kinetic measurements: (*1*) reaction between fulvic acid and Fe(III); (*2*) reaction between SSA and Fe(III); (*3*) reaction between SSA and the equilibrated Fe(III) – fulvic acid mixtures. All were made on a Durrum-Gibson stopped flow spectrometer thermostatted by circulating water at 25.0 °C. Two modes of data recording were employed. In most runs, the data were recorded conventionally on photographs of the record displayed on the Durrum-Gibson device's storage oscilloscope. In later runs, data were stored in six-bit digital form by a Biomation 610B Transient Recorder and read out on a teletype. There is no substantial difference in resolution between the two cases when only one rate constant is involved.

The data treatment for experiments of type (*1*) was necessarily simple. Good data for these experiments are very difficult to obtain, mainly due to two factors. One is that fulvic acid gives an almost flat absorption band starting from 900 nm and rising into the ultraviolet. The other is that the total change in absorbance due to binding with iron is very small (maximally 0.05 absorbance units). Kinetic runs under the most favorable conditions (540 nm) do not produce enough well resolved points for a fully meaningful pseudo first order (in fulvic acid) plot, although such plots were 'satisfactorily' linear. Thus, rate constants were calculated from half lives which in turn were estimated assuming absorbance proportional to transmittance. This implies that results are of low precision. The implication is valid! In type (*2*) experiments, conventional first order plots were constructed on the absorbance data at 500 nm (the product absorbs) over more than four half lives. Rate constants were obtained from least-squares fits. Type (*3*) experiments were similar except that the fulvic acid (free and complexed) added a constant absorbance. The data were analyzed using the multicomponent program suggested by Willis *et al.* (6) with the fulvic acid plus fulvic acid complex functioning as the constant concentration and considering only free Fe(III) as the time varying component.

The data are processed by fitting under a least-square criterion (6) the following equation for the observed absorbance, *P*.

$$P = A_0(1 - e^{-kt}) + X$$

[4]Note that p*H* is precisely determined by this procedure.

Can. J. Chem. Downloaded from www.nrcresearchpress.com by 210.87.254.6 on 09/05/12
For personal use only.

where A_0 is the absorbance proportional to the initial concentration of free Fe(III) and X is all time invariant contributions (especially that due to fulvic acid and its Fe complex). k is the known rate constant for reaction between sulfosalicylic acid and aquo Fe(III) calibrated directly in conjunction with the run on the mixture. The use of the methodology of ref. 6 allows for maximal use of the information in the early time part of the runs before there can be any complication due to a slight reaction of the fulvic acid complex with SSA. At the same time, this analysis does not overweight early points.

Results

First order rate constants for reaction of fulvic acid with excess Fe(III) at pH = 1.65 are shown in Fig. 1. Fe^{3+} is in excess and the plot gives pseudo first order rate constants for rate of approach to equilibrium. Under these circumstances $k_{obs} = k_d + k_f[Fe^{3+}]$ where $[Fe^{3+}]$ is a constant in any run (k_d is the rate constant for dissociation, k_f is for complex formation). The first order rate constant for reaction of Fe(III) with 1.00×10^{-2} M sulfosalicylic acid (a large excess) was estimated at the three pH values, 1.00, 1.50, and 2.50. The rate constants found were 0.89 ± 0.04, 3.81 ± 0.13, and 10.60 ± 0.35 s^{-1}, respectively. These values are in satisfactory agreement with higher ionic strength studies (7). The values are averaged over runs at concentrations from 1.0×10^{-4} to 1.0×10^{-5} M Fe(III). The error specified is the standard deviation of eight runs. It is also possible to calculate an extinction coefficient for the sulfosalicylic acid complex essentially from infinity time absorbance which will be useful for comparison with non-kinetic data to indicate accuracy in Fe(III) concentration determination. Values at pH 1.0, 1.5, and 2.5 are 159_1, 185_0, and 170_8 respectively.

In experiments on the equilibrium mixture, free Fe(III) is the directly evaluated quantity. In order to ensure that SSA is not attacking fulvic acid bound Fe and what we are measuring is free Fe only, the rate of Fe–SSA formation was observed over a time scale five to ten times longer than the time scale used in actual measurements and T_∞'s were closely observed. In each case, (Fe – fulvic acid solutions at pH 1.0, 1.5, and 2.5) simple exponential decays were observed with a constant T_∞. The kinetics of a typical run, for 1:1 Fe – fulvic acid concentration higher than used in the present work (2.5×10^{-4}), is shown in Fig. 2. In addition, an experiment with fulvic acid increased ten times in concentration compared to other runs at pH = 1.5 was carried out. The free Fe^{3+} concentration found was 7.7×10^{-5} M which yields a calculated equilibrium constant of 1.7×10^4. *If any iron bound to fulvic acid were contributing to reaction with SSA, the value calculated should be low.* It is not (*vide infra*). These experiments were not elaborated because of difficulties associated with high absorbance when fulvic acid is large. The main results are presented in terms of free (unbound) Fe(III) con-

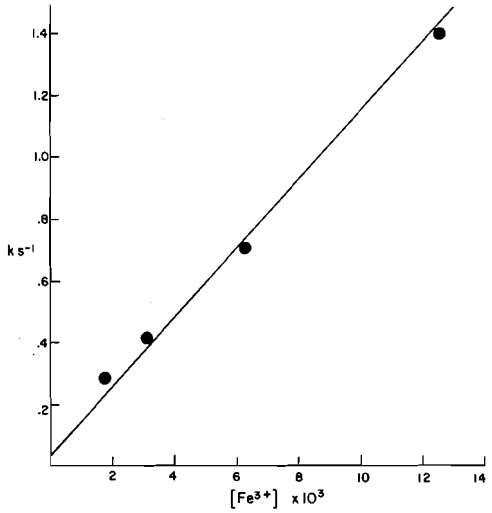

FIG. 1. Dependence of observed rate constants on Fe(III) concentration for the reaction of Fe(III) and fulvic acid. The effective fulvic acid concentration is approximately 3×10^{-4} M; pH = 1.65.

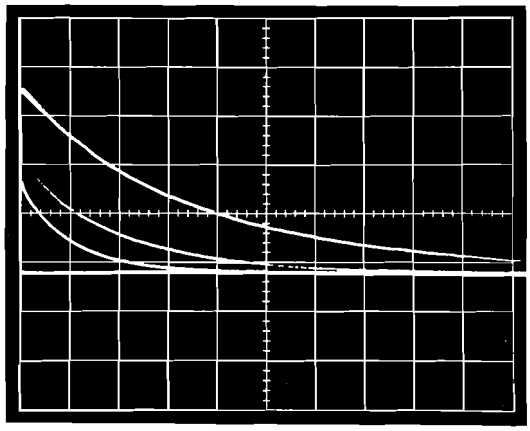

FIG. 2. A stopped flow photograph showing a 1:1 mixture of Fe^{3+} (2.5×10^{-4} M) with fulvic acid reacting at pH = 1.5 with 1.0×10^{-2} M SSA. Runs are at 50, 100, and 200 ms per division. Note the stability of the infinity. Wavelength is 500 nm and T = 25 °C (0.1 M $NaClO_4$).

Can. J. Chem. Downloaded from www.nrcresearchpress.com by 210.87.254.6 on 09/05/12
For personal use only.

centration as a function of total Fe(III) introduced. Such free Fe(III) concentration values are plotted against total Fe(III) in Fig. 3. It is clear that differences between free Fe(III) and total Fe(III) are not large in the range of these experiments. Lower total Fe(III) would not be advantageous because the extinction coefficient of the analytical product is not large enough. We have chosen to fit data in the figures by a straight line because a more than one parameter representation of the function does not seem justified experimentally.

Assuming a linear relationship, corrected values for free Fe(III) are read from these plots and are used to calculate conditional formation constant K defined as usual as [Fe – fulvic acid]/-[Fe(III)-free][fulvic acid] at the pH specified and an overall ionic strength of 0.1 where brackets represent concentration. Initial fulvic acid concentration is calculated on the basis of a molecular weight 900 offering 3 mequiv./g of binding sites.

The results in Fig. 3 have been converted in Fig. 4 into plots of the binding function which is *commonly* presented for discussion of binding of fulvic acid (5). This is a plot of moles of

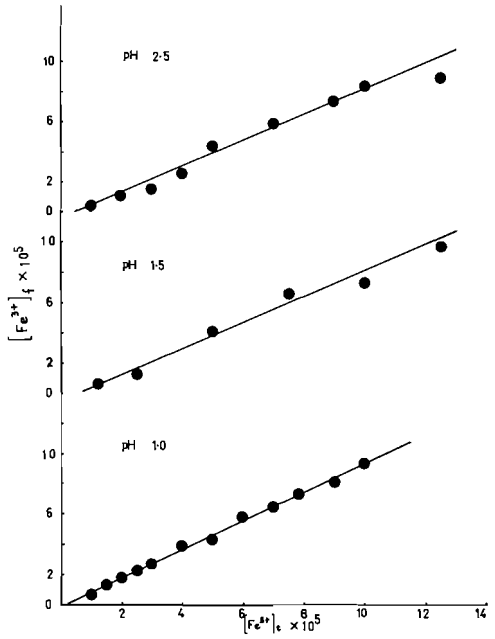

FIG. 3. Measured free Fe(III) concentration plotted *vs.* total Fe(III) concentration in equilibrium mixtures of Fe(III) and a fixed fulvic acid concentration 3.0×10^{-5} M.

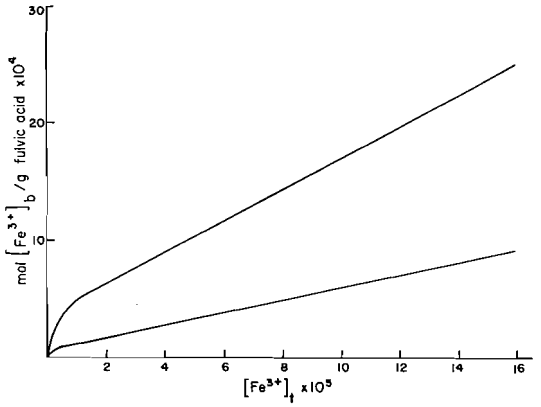

FIG. 4. Plot of the conventional binding function *vs.* total Fe(III) concentration in various mixtures of Fe(III) and fulvic acid. Top curve represents binding at pH 2.50 and 1.50 and bottom curve represents binding at pH 1.00.

bound metal ion per gram of fulvic acid plotted against total Fe(III) concentration. The ordinate in the plot also provides a scale for the measure of binding sites of fulvic acid available to Fe(III). The highest ordinate value on the figure represents 3 mequiv./g fulvic acid which approached the limit of available type I functional groups. Below this limit, as the plot shows, binding continues to increase.

The conditional formation constants at 25 °C, ionic strength 0.1, are:

K	pH
$2.8 \pm 0.3 \times 10^4$	1.0
$1.5 \pm 0.3 \times 10^4$	1.5
$1.5 \pm 0.3 \times 10^4$	2.5

Discussion

Analytical Aspects

The accuracy with which A_0 can be estimated depends heavily but not uniquely upon the measurement of infinity transmittance in kinetic runs. The value for the spectrophotometrically least sensitive kinetic curve is reproducible within 1%. Averaged T_∞ (converted to A_∞) when plotted against respective Fe(III) concentrations to obtain the extinction coefficient at pH 1.5 gave 185_0, which is to be compared with 187_0 obtained on a Cary 14, a difference of 1.2%. The rate constant values themselves exhibited a maximum standard deviation of 3.6% at pH 2.5. Our situation is analytically favorable in that there is only one kinetically important

Can. J. Chem. Downloaded from www.nrcresearchpress.com by 210.87.254.6 on 09/05/12
For personal use only.

component. We are intending to proceed to two and three components. For two or three component mixtures, precision similar to that of Pausch and Margerum (8) (~3%) can be anticipated in concentration if other rate constants can be determined as accurately as that for free aquo iron.

It is not easy to check precision in the equilibrium fulvic acid system, since concentration of any reference solution is determined by the fulvic acid equilibria. Inferred precision is similar to that for Fe(III) only solutions. One confirmation arises from looking at estimated values of bound Fe(III) in solutions of highest total Fe(III) concentration (10^{-4} *M*) where most Fe(III) is (and should be) free. The difference of the two large numbers is small and allows for only a few percent deviation in free iron.

Binding "Constant"

It should be made clear at the outset that *K* values are not true thermodynamic constants for the reaction of Fe(III) and fulvic acid. They represent ratio of bound Fe(III) to free over the range of binding sites available at the experimental ligand concentration (3×10^{-5} *M*). For a polyelectrolyte with more than one functional group the experimentally measured constant is a function of extent of participation by functional groups and charge accumulated on the polymeric molecule. These constants are thus regarded as weighted average values for the range investigated.

Results show that the binding constant at p*H* 1.0 is slightly larger than at p*H* 1.5 and 2.5. This pattern may be explained *qualitatively* by considering the nature of Fe(III) and fulvic acid species present. Solutions of Fe(III) would contain predominantly a mixture of Fe_{aq}^{3+} and $Fe(OH)^{2+}$. In the most strongly acidic solutions Fe_{aq}^{3+} is predominant and decreases towards higher p*H* values. Hydrolysis equilibria from data of Bray and Hershey (9) and Lamb and Jacques (10) were corrected to our ionic strength (11) and used to estimate the ratio of $FeOH^{2+}$ to Fe_{aq}^{3+}. The ratio is plotted against p*H* in Fig. 5. The degree of ionization of fulvic acid (α_1), presumably deprotonation of type I carboxyl groups as defined by Gamble and Schnitzer (5), in 0.1 *M* KCl close to ionic strength of present solutions is also plotted in the figure. The ratios of free to total Fe(III) (results from present study) are shown at the top left in the figure. The p*H* 1.0 value of the ratio of $FeOH^{2+}$ to Fe^{3+} (9×10^{-3}) increases four times at p*H* 1.5 and about 30 times at p*H* 2.5. Extrapolation of the fulvic acid plot shows that ionization of fulvic acid is negligible at p*H* 1.0 but significant at higher p*H*. At higher p*H* overall charge on Fe species decreases steadily due to larger proportions of $FeOH^{2+}$ but cumulative charge on fulvic acid increases. These two opposing factors (see Fig. 5) approximately compensate and qualitatively explain why the binding of Fe(III) by fulvic acid remains relatively insensitive to p*H* in these acidic media.

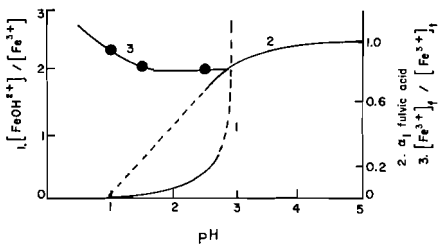

FIG. 5. The hydrolysis of Fe_{aq}^{3+} to $FeOH^{2+}$ is shown in curve *1* as the ratio $[FeOH^{2+}]/[Fe^{3+}]$. The first acid ionization of our fulvic acid is shown in curve *2* as α_1 fulvic acid, the fraction of strong acid sites ionized. These two factors contribute to an understanding of the small p*H* dependence of the ratio of free to total Fe(III) in the equilibrium system of Fe(III) with fulvic acid illustrated by curve *3*.

Kinetic Aspects

First, it must be observed that the small absorbance changes available limit precision. Especially, the intercept of Fig. 1 is of *no great significance*. (It could be zero!) The dissociation rate is less than 0.1 s^{-1}. A more meaningful estimate will be derived below from a combination of k_f with the conditional stability constant. It is worth observing next that the rate of formation of the fulvic acid complex is similar to that for sulfosalicylic acid and 'normal' (12) in the sense that it is comparable to rate of complex formation with monodentate ligands.[5] This suggests strongly that substitution of a first iron site by a binding site on fulvic acid is rate determining and that completion of the chelate ring is relatively rapid (12). We do not observe the slower complex formation commonly associated with rate limiting ring closure (12).

With respect to dissociation of the complex, the intercept in Fig. 1 showed that it was small

[5]See for a review ref. 13.

compared to the formation rate. Using the conditional stability constant to try to obtain a more precise value, we estimate 7×10^{-3} s^{-1}. This rate is slow but certainly faster than dissociation of small molecule chelates of high stability such as $FeEDTA^-$. It has sometimes been suggested that humic ligands play a role in rendering metal ions 'nonlabile in aqueous systems.' If this is the case in the sense of making them slowly available on time scales of hours to days, it does not seem that the effect arises from simple complex formation–dissociation reactions. Such a statement does not exclude nonlability due to mass transport rates in heterogeneous systems where humic ligands are suspended.

1. M. EIGEN. Z. Elektrochem. **64**, 115 (1960).
2. L. C. COOMBS, J. VASILIADES, and D. W. MARGERUM. Anal. Chem. **44**, 2325 (1972).
3. A. C. JAVIER, S. R. CROUCH, and H. V. MALMSTADT. Anal. Chem. **41**, 239 (1969).
4. L. I. BUDARIN, K. B. YATSIMIRSKY, and A. G. KHACHATRYAN. Zh. Anal. Khim. **24**, 1499 (1971).
5. D. S. GAMBLE and M. SCHNITZER. Trace metals and metal-organic interactions in natural water. Ann Arbor Science Publishers, Ann Arbor, Michigan. 1973. Chapt. 9.
6. B. G. WILLIS, W. H. WOODRUFF, J. R. FRYSINGER, D. W. MARGERUM, and H. L. PARDUE. Anal. Chem. **42**, 1350 (1970).
7. G. SAINI and E. MENTASTI. Inorg. Chim. Acta, **4**, 210 (1970).
8. J. B. PAUSCH and D. W. MARGERUM. Anal. Chem. **41**, 226 (1969).
9. W. C. BRAY and A. V. HERSHEY. J. Am. Chem. Soc. **56**, 1889 (1934).
10. A. B. LAMB and A. G. JACQUES. J. Am. Chem. Soc. **60**, 1215 (1938).
11. E. RABINOWITCH and W. H. STOCKMAYER. J. Am. Chem. Soc. **64**, 335 (1942).
12. R. G. WILKINS. Acc. Chem. Res. **3**, 408 (1970).
13. V. S. SASTRI and C. H. LANGFORD. MTP International Revs of Sci., Inorganic Chemistry, Series One **9**, 203 (1972).

Can. J. Chem. Downloaded from www.nrcresearchpress.com by 210.87.254.6 on 09/05/12
For personal use only.

Arene Derivatives of Bis(trichlorogermanium)tetracarbonylruthenium(II)[1]

ROLAND K. POMEROY AND WILLIAM A. G. GRAHAM
Department of Chemistry, University of Alberta, Edmonton, Alberta T6G 2E1

Received June 4, 1975

ROLAND K. POMEROY and WILLIAM A. G. GRAHAM. Can. J. Chem. **53**, 2985 (1975).

Arenes react with *trans*-$Ru(CO)_4(GeCl_3)_2$ at 150 °C or higher to form the very stable complexes (η-arene)$Ru(CO)(GeCl_3)_2$ (arene = benzene, toluene, *o*-, *m*-, and *p*-xylene, mesitylene). The reactions may proceed via the more reactive *cis*-isomer, as suggested by a study of the reaction of benzene with *trans*-$Ru(CO)_4(SiCl_3)_2$ at 80 °C to form (η-C_6H_6)$Ru(CO)(SiCl_3)_2$. Benzene is displaced from (η-C_6H_6)$Ru(CO)(GeCl_3)_2$ by CO or mesitylene forming *trans*-$Ru(CO)_4(GeCl_3)_2$ and (η-mesitylene)$Ru(CO)(GeCl_3)_2$, respectively.

ROLAND K. POMEROY et WILLIAM A. G. GRAHAM. Can. J. Chem. **53**, 2985 (1975).

A des températures de 150 °C ou plus, les arènes réagissent avec le *trans*-$Ru(CO)_4(GeCl_3)_2$ pour conduire à des complexes très stables de formule (η-arène)$Ru(CO)(GeCl_3)_2$ (arène = benzène, toluène, *o*-, *m*-, ou *p*-xylène et mésitylène). Les réactions se produisent par l'intermédiaire de la forme *cis* qui est plus réactive; cette conclusion est basée sur une étude de la réaction, à 80 °C, du benzène avec le *trans*-$Ru(CO)_4(SiCl_3)_2$ conduisant au (η-C_6H_6)$Ru(CO)(SiCl_3)_2$. Le benzène du complexe (η-C_6H_6)$Ru(CO)(GeCl_3)_2$. est déplacé par le CO ou par le mésitylène pour conduire suivant le cas au *trans*-$Ru(CO)_4(GeCl_3)_2$ ou au (η-mésitylène)-$Ru(CO)(GeCl_3)_2$.

[Traduit par le journal]

Introduction

Energy-factored carbonyl stretching force constants for *cis*-$Ru(CO)_4(GeCl_3)_2$ are high and very nearly equal for the axial and equatorial sets of carbonyls.[2] The *trans influence* of a trichlorogermanium group, as inferred from this parameter, is very similar to that of the carbonyl group.[3] The molecule might accordingly be expected to resemble $Mo(CO)_6$ in some respects, and the reactions reported here with various benzene derivatives were undertaken to develop this analogy.

Results and Discussion

We have found that *trans*-$Ru(CO)_4(GeCl_3)_2$ (more readily available than this *cis* form, but *vide infra*) reacts with many arenes to form compounds of the type (η-arene)$Ru(CO)(GeCl_3)_2$. This is entirely analogous to the well-known reaction of molybdenum hexacarbonyl with arenes to form (arene)$Mo(CO)_3$ derivatives (4). Reactions were carried out in evacuated sealed tubes for the low boiling arenes, but simple refluxing in the appropriate ligand was sufficient for the xylene and mesitylene derivatives.

Although *trans*-$Ru(CO)_4(GeCl_3)_2$ was used in the reactions, it is known to isomerize at reaction temperatures (5), and we consider it likely, in analogy to $Ru(CO)_4(SiCl_3)_2$,[3] that the *cis* form would more readily dissociate carbon monoxide. The reaction between benzene and *trans*-$Ru(CO)_4(SiCl_3)_2$ was better suited for the elucidation of this point.[4] At 80 °C, *trans*-$Ru(CO)_4(SiCl_3)_2$ isomerizes at a moderate rate (6), and (η-C_6H_6)$Ru(CO)(SiCl_3)_2$ was formed at this temperature. The reaction was monitored by infrared, and only carbonyl stretching bands of starting material and product were observed; no bands due to *cis*-$Ru(CO)_4(SiCl_3)_2$ were observed, indicating its preferential reaction with benzene.

All of the (η-arene)$Ru(CO)(GeCl_3)_2$ complexes prepared in this work are colorless or

[1]Organometallic Compounds Having Metal–Metal Bonds, Part XX. For part XIX, see ref. 1.

[2]The values are k_{eq} = 18.1, k_{ax} = 18.2 mdyn Å^{-1} (2). The two force constants are also nearly equal to one another in the case of *cis*-$Ru(CO)_4(SiCl_3)_2$ (3).

[3]The *trans effect* (from ^{13}CO exchange rates) is in contrast much greater for $GeCl_3$ than for CO in this molecule, which has been ascribed to different relative stabilities of possible five-coordinate transition state isomers (3).

[4]*trans*-$Ru(CO)_4(GeCl_3)_2$ was not suitable because the equilibrium *trans:cis* ratio was *ca.* 98:3, so that the *cis*-isomer would have been difficult to detect even if it did not react preferentially. The equilibrium *trans:cis* ratio for $Ru(CO)_4(SiCl_3)_2$ is 65:35 (decalin, 84.6 °C) (6).

Can. J. Chem. Downloaded from www.nrcresearchpress.com by 210.87.254.40 on 09/05/12
For personal use only.

TABLE 1. Melting points and carbonyl stretching bands

Compound	Melting point (°C)	ν(CO) (cm^{-1})	
		CH_2Cl_2	Nujol
$(C_6H_6)Ru(CO)(GeCl_3)_2$	>300	2040	2048
$(CH_3C_6H_5)Ru(CO)(GeCl_3)_2$	236	2037	2030, 2020*
$[o\text{-}(CH_3)_2C_6H_4]Ru(CO)(GeCl_3)_2$	221–222	2031	2026
$[m\text{-}(CH_3)_2C_6H_4]Ru(CO)(GeCl_3)_2$	246–248	2032	2018
$[p\text{-}(CH_3)_2C_6H_4]Ru(CO)(GeCl_3)_2$	240–242	2034	2037, 2024
$[(CH_3)_3C_6H_3]Ru(CO)(GeCl_3)_2$	>300	2029	2027, 2020
$(C_6H_6)Ru(CO)(SiCl_3)_2$	203 (dec)	2016	—
$[(CH_3)_3C_6H_3]Ru(CO)(GeBr_3)_2$	—	2027	—

*A very weak band also observed at 2035 cm^{-1}.

pale yellow solids of remarkable thermal stability; they exhibit no decomposition before their melting points, which range from 200 °C to over 300 °C. The solids are stable in air, although $(\eta\text{-}C_6H_6)Ru(CO)(GeCl_3)_2$ showed some surface darkening. They are insoluble in nonpolar solvents, and sufficiently insoluble in polar solvents that n.m.r. spectra could not be obtained in all cases. The low solubility, high melting point, and lack of volatility of these complexes are perhaps due to dipole–dipole interactions; $(arene)Cr(CO)_3$ complexes have large dipole moments directed from arene towards the metal (7), and these would be expected to be larger in the present compounds due to the electronegative groups on germanium.

Molecular ions are observed in the mass spectra of the compounds, although at low intensity; the peak due to $[P—Cl]^+$ is much more intense (in $(\eta\text{-}C_6H_6)Ru(CO)(GeCl_3)_2$, the intensities of P and P—Cl are 2.3:87). This is reminiscent of $(\eta\text{-}C_5H_5)Fe(CO)H(SiCl_3)_2$ (8), in which the heaviest ion observed was $[P—Cl]^+$. Nuclear magnetic resonance spectra were obtained only for the benzene and mesitylene complexes; ring proton resonances were shifted to higher field than in the free ligands, while the methyl resonance of the latter complex occurred at higher field than in the free ligand.

Infrared carbonyl stretching frequencies (Table 1) shift to lower frequencies with increasing methyl substitution, consistent with greater electron release by methyl groups. Solubility requirements necessitated the use of a polar solvent (CH_2Cl_2) for infrared studies, and the broad bands encountered under these conditions were not useful in determining the possible existence in solution of isomers. We refer here to different orientations of the arene ring about an axis from its midpoint to the ruthenium atom. Although two bands were observed in the mull spectra of several of the compounds, the splitting could result from nonequivalent molecular environments in the crystal lattice so the results are ambiguous.

Two reactions involving displacement of arene were carried out, which further illustrate the analogy with arenetricarbonylmolybdenum compounds. Thus, $(\eta\text{-}C_6H_6)Ru(CO)(GeCl_3)_2$ with carbon monoxide (50 atm, 150 °C) was converted to *trans*-$Ru(CO)_4(GeCl_3)_2$ (the immediate displacement product may have been *cis*, which isomerized to the equilibrium mixture),[4] while refluxing in mesitylene afforded $[\eta\text{-}(CH_3)_3C_6H_3]Ru(CO)(GeCl_3)_2$. The latter reacted with benzene (150 °C, sealed tube) to reform the benzene complex.

The compounds reported here belong to the class of arene complexes of ruthenium(II), of which few examples were known until recently. Two investigations have now been reported of complexes of the type $(arene)RuX_2L$ (X = halogen, L = phosphine) (9–11); the route by which they were obtained was quite different, involving the dehydrogenation of cyclic 1,3-dienes by ethanolic ruthenium trichloride. It is of interest that Zelonka and Baird (10) found evidence for a very unstable compound, presumed to be $(\eta\text{-}C_6H_6)Ru(CO)Cl_2$, when carbon monoxide was bubbled into a solution of $(C_6H_6)RuCl_2$ in acetonitrile.

There seemed little doubt that the complexes reported here would have a half-sandwich structure similar to that of the benzenechromium tricarbonyl. This has now been confirmed by an X-ray study of $(\eta\text{-}C_6H_6)Ru(CO)(GeCl_3)_2$ (12).

Can. J. Chem. Downloaded from www.nrcresearchpress.com by 210.87.254.40 on 09/05/12
For personal use only.

Can. J. Chem. Downloaded from www.nrcresearchpress.com by 210.87.254.40 on 09/05/12
For personal use only.

TABLE 2. Analytical data for arene derivatives

Compound	C		H		O		X	
	Calculated	Experimental	Calculated	Experimental	Calculated	Experimental	Calculated	Experimental
$(C_6H_6)Ru(CO)(GeCl_3)_2$	14.88	15.01	1.07	1.05	2.83	2.98	37.64	37.58
$(CH_3C_6H_5)Ru(CO)(GeCl_3)_2$	16.59	16.93	1.39	1.38	2.76	3.16	36.73	35.66
$[o\text{-}(CH_3)_2C_6H_4]Ru(CO)(GeCl_3)_2$	18.22	18.53	1.70	1.70	2.70	—	35.86	—
$[m\text{-}(CH_3)_2C_6H_4]Ru(CO)(GeCl_3)_2$	18.22	18.75	1.70	1.84	2.70	—	35.86	—
$[p\text{-}(CH_3)_2C_6H_4]Ru(CO)(GeCl_3)_2$	18.22	18.54	1.70	1.91	2.70	—	35.86	—
$[(CH_3)_3C_6H_3]Ru(CO)(GeCl_3)_2$	19.78	20.32	1.99	2.19	2.64	2.81	35.03	35.21
$(C_6H_6)Ru(CO)(SiCl_3)_2$	17.66	18.06	1.27	1.37	3.36	3.47	44.68	45.00
$[(CH_3)_3C_6H_3]Ru(CO)(GeBr_3)_2$	13.74	14.04	1.38	1.30	1.83	2.14	54.86	55.98

Can. J. Chem. Downloaded from www.nrcresearchpress.com by 210.87.254.40 on 09/05/12
For personal use only.

Details of the structure, and a comparison with reported (11) structures of two (arene)-$Ru[P(CH_3)_2C_6H_3]Cl_2$ complexes will be presented elsewhere (12).

Experimental Section

Reactions were carried out under a nitrogen atmosphere or in evacuated sealed tubes. Melting points were measured using a microscope with Kofler hot stage. Infrared carbonyl stretching frequencies were recorded and calibrated as previously described (8). Analyses (Table 2) were carried out by the Microanalytical Laboratory of this department and by Pascher Mikroanalytisches Laboratorium, Bonn, West Germany. The synthesis of *trans*-$Ru(CO)_4(GeCl_3)_2$ and *trans*-$Ru(CO)_4(SiCl_3)_2$ will be described elsewhere (5).

Preparation of $(\eta\text{-}C_6H_6)Ru(CO)(GeCl_3)_2$

Benzene (25 ml) and *trans*-$Ru(CO)_4(GeCl_3)_2$ (0.57 g, 1.0 mmol) were heated in an evacuated sealed tube at 150 °C for 6 days. Approximately every 12 h during this period the tube was cooled (care!) and reevacuated. After this time the tube was allowed to stand at *ca.* 6 °C for 24 h. The benzene was then removed from the large, pale yellow needles of the product, $(\eta\text{-}C_6H_6)$-$Ru(CO)(GeCl_3)_2$ (0.41 g, 72%). The mother liquor contained $Ru_2(CO)_5GeCl_6$ (5) as well as this product. The crystals were washed with two 10-ml portions of *n*-hexane, and appeared from infrared examination to be pure at this stage. Analytical samples were recrystallized from benzene or *n*-hexane – dichloromethane; n.m.r. (dichloromethane): singlet, τ 3.38.

The corresponding toluene derivative, $(\eta\text{-}CH_3C_6H_6)$-$Ru(CO)(GeCl_3)_2$ was prepared in the same manner. An attempt to prepare $(\eta\text{-}C_6H_6)Ru(CO)(GeBr_3)_2$ by the same method led to isolation of 25 mg of greenish-yellow crystals which had the expected i.r. spectrum (2037 cm^{-1}, CH_2Cl_2 solution), but which did not give a satisfactory analysis. An infrared spectrum of the benzene solution showed mainly $Ru_2(CO)_5GeBr_6$ (5). A similar experiment using *trans*-$Ru(CO)_4(SnCl_3)_2$ gave only $Ru_2(CO)_5SnCl_6$ (13).

Preparation of $(\eta\text{-}C_6H_6)Ru(CO)(SiCl_3)_2$

Benzene (10 ml) and *trans*-$Ru(CO)_4(SiCl_3)_2$ (0.241 g, 0.5 mmol) were refluxed under a nitrogen atmosphere for 48 h. Infrared spectra taken during this time showed only starting material and product *i.e.*, no *cis*-$Ru(CO)_4$-$(SiCl_3)_2$ was present. After 2 days the solution was filtered and evaporated to dryness to give an almost quantitative yield of crude product. The analytical sample, in the form of white crystals, was obtained by two recrystallizations from CH_2Cl_2 – *n*-heptane; n.m.r. ($CDCl_3$): singlet, τ 3.42.

Preparation of $[\eta\text{-}(CH_3)_3C_6H_3]Ru(CO)(GeCl_3)_2$

A solution of *trans*-$Ru(CO_4)(GeCl_3)_2$ (0.57 g, 1.0 mmol) in mesitylene was refluxed for 11 h. The solution was then filtered and placed in the refrigerator overnight. The product (0.45 g, 75%) was separated from mesitylene, washed with hexane, and dried under vacuum. Recrystallization from benzene or CH_2Cl_2–*n*-hexane gave the analytical sample; n.m.r. ($CDCl_3$): τ 3.68 (s, 1), 7.36 (s, 3). Reaction times much longer than 11 h led to extensive decomposition and reduced yields.

Xylene Derivatives

The xylene derivatives were prepared in a similar manner only with reflux times of 70 to 90 h; n.m.r. spectra of these compounds could not be obtained due to their insolubility.

$[\eta\text{-}(CH_3)_3C_6H_3]Ru(CO)(GeBr_3)_2$

The bromo derivative $[\eta\text{-}(CH_3)_3C_6H_3]Ru(CO)(Ge$-$Br_3)_2$ was prepared in the same way as the chloro analog; the yield, however, was low (12%).

Reaction of $(\eta\text{-}C_6H_6)Ru(CO)(GeCl_3)_2$ *with Carbon Monoxide*

An autoclave containing $(\eta\text{-}C_6H_6)Ru(CO)(GeCl_3)_2$ (0.057 g) in *n*-heptane was pressurized with carbon monoxide (50 atm) and heated at 150 °C for 24 h. The autoclave was cooled and the gas vented. An infrared spectrum of the *n*-heptane solution showed only *trans*-$Ru(CO)_4(GeCl_3)_2$.

Reaction of $(\eta\text{-}C_6H_6)Ru(CO)(GeCl_3)_2$ *with Mesitylene*

A solution of $(C_6H_6)Ru(CO)(GeCl_3)_2$ (0.057 g, 0.1 mmol) in mesitylene (10 ml) was refluxed for 20 min, filtered, and allowed to cool. Crystals of $[\eta\text{-}(CH_3)_3$-$C_6H_3]Ru(CO)(GeCl_3)_2$ (0.040 g, 66%) were washed with *n*-hexane and dried under vacuum. The product was identified by its infrared spectrum.

In a similar reaction $[\eta\text{-}(CH_3)_3C_6H_3]Ru(CO)(GeCl_3)_2$ was heated in benzene at 150 °C in an evacuated sealed tube for 12 h. The product was found to be $(\eta\text{-}C_6H_6)$-$Ru(CO)(GeCl_3)_2$.

We thank the National Research Council of Canada for financial support and for a scholarship to R.K.P.

1. W. K. Dean and W. A. G. Graham. J. Organometal. Chem. In press.
2. R. S. Gay. Ph.D. Thesis, University of Alberta, Edmonton, Alberta. 1970.
3. R. K. Pomeroy, R. S. Gay, G. O. Evans, and W. A. G. Graham. J. Am. Chem. Soc. **94**, 272 (1972).
4. E. O. Fischer and K. Ofele. Chem. Ber. **90**, 2532 (1957).
5. R. K. Pomeroy and W. A. G. Graham. To be published.
6. R. K. Pomeroy and W. A. G. Graham. J. Am. Chem. Soc. **94**, 274 (1972).
7. E. O. Fischer and S. Schreiner. Chem. Ber. **92**, 938 (1959).
8. W. Jetz and W. A. G. Graham. Inorg. Chem. **10**, 1159 (1971); W. Jetz. Ph.D. Thesis, University of Alberta, Edmonton, Alberta. 1971.
9. R. A. Zelonka and M. C. Baird. J. Organometal. Chem. **35**, C43 (1972).
10. R. A. Zelonka and M. C. Baird. Can. J. Chem. **50**, 3063 (1972).
11. M. A. Bennett, G. B. Robertson, and A. K. Smith. J. Organometal. Chem. **43**, C41 (1972).
12. L. Y. Y. Chan and W. A. G. Graham. Inorg. Chem. In press.
13. R. K. Pomeroy, M. Elder, D. Hall, and W. A. G. Graham. Chem. Commun. 381 (1969).

Détermination du pouvoir sulfonant des acides disulfurique et chlorosulfurique dans le sulfolane

PATRICK PIERENS, YVES AUGER, JEAN CLAUDE FISCHER ET MICHEL WARTEL
Université de Lille I, Laboratoire de Chimie Minérale I, Bâtiment C8, BP. 36, 59650 Villeneuve d'Ascq, France
Reçu le 10 mars 1975

PATRICK PIERENS, YVES AUGER, JEAN CLAUDE FISCHER et MICHEL WARTEL. Can. J. Chem. **53**, 2989 (1975).

L'étude du système électrochimique dans le sulfolane

$$AgCl + SO_3 + e^- \rightleftarrows Ag + SO_3Cl^-$$

a permis de calculer la constante de dissociation de l'ion chlorosulfate suivant: $SO_3Cl^- \rightleftarrows SO_3 + Cl^-$ ($K_{SO_3Cl^-} = 10^{-14.3}$) le chlorodisulfate $S_2O_6Cl^-$ étant entièrement dissocié en SO_3Cl^- et SO_3. Les constantes des équilibres

$$H_2S_2O_7 \rightleftarrows H_2SO_4 + SO_3 \ (K_{H_2S_2O_7} = 10^{-1.45})$$

$$HSO_3Cl \rightleftarrows HCl + SO_3 \ (K_{HSO_3Cl} = 10^{-4.2})$$

ont été déterminées, l'une par complexation de SO_3 par H_2SO_4, l'autre à partir de la différence d'acidité entre HCl et HSO_3Cl. Le pouvoir sulfonant des composés étudiés varie selon $S_2O_6Cl^- > H_2S_2O_7 > HSO_3Cl \gg SO_3Cl^-$. La constante d'acidité de l'acide chlorosulfurique est $k = 10^{-4.4}$, supérieure à celle de $H_2S_2O_7$ ($k = 10^{-5}$).

PATRICK PIERENS, YVES AUGER, JEAN CLAUDE FISCHER, and MICHEL WARTEL. Can. J. Chem. **53**, 2989 (1975).

On the basis of potentiometric study of the system

$$AgCl + SO_3 + e^- \rightleftarrows Ag + SO_3Cl^-$$

in sulfolane, the dissociation constant of the reaction $SO_3Cl^- \rightleftarrows SO_3 + Cl^-$ has been found to be $K_{SO_3Cl^-} = 10^{-14.3}$ assuming that the chlorodisulfate ion is completely dissociated to SO_3Cl^- and SO_3. The equilibrium constants of the reactions

$$H_2S_2O_7 \rightleftarrows H_2SO_4 + SO_3 \ (K_{H_2S_2O_7} = 10^{-1.45})$$

$$HSO_3Cl \rightleftarrows HCl + SO_3 \ (K_{HSO_3Cl} = 10^{-4.2})$$

have been determined on the one hand by complexation of SO_3 with H_2SO_4, and on the other by the difference of acidity between HCl and HSO_3Cl. The acidity constant of HSO_3Cl ($k = 10^{-4.4}$) is slightly higher than that of $H_2S_2O_7$ ($k = 10^{-5}$). The sulfonating power of some compounds have been found to follow the order $S_2O_6Cl^- > H_2S_2O_7 > HSO_3Cl \gg SO_3Cl^-$.

Introduction

Dans la préparation des dérivés sulfonés, utilisés comme colorants et détergents, on emploie l'acide sulfurique, l'acide chlorosulfurique ou plus souvent les oléums sulfuriques à des concentrations variables. Parmi ces oléums, il existe des composés définis $H_2SO_4 \cdot nSO_3$, le plus connu étant l'acide disulfurique ($H_2SO_4 \cdot SO_3$ ou $H_2S_2O_7$). Il était intéressant de déterminer le pouvoir sulfonant d'un tel composé, et de le comparer à celui de HSO_3Cl. La mesure de ce pouvoir ne peut être effectuée que si l'on connaît un composé SO_3X très stable et une méthode permettant de suivre la dissociation en SO_3 et X. S'il semble difficile de suivre la variation de concentration en SO_3, la détermination de X peut être facilement réalisée si $X = Cl^-$. En effet, nous avons montré que dans le nitrométhane, les chlorosulfates SO_3Cl^- sont peu dissociés (1) (la constante de l'équilibre

[1] $$SO_3Cl^- \rightleftarrows SO_3 + Cl^-$$

y est égale à $10^{-14.1}$). Les solutions concentrées de SO_3 dans ce solvant étant peu stables (2), nous avons choisi un autre solvant de constante diélectrique très voisine, le sulfolane. Les caractéristiques sont: $t_f^0 = 28$ °C, $t_e^0 = 285$ °C, $\varepsilon = 43.3$ à 30 °C, viscosité = 0.1029 poise (3). En raison de la valeur élevée de la viscosité les constantes de diffusion sont faibles (4). Nous avons donc, pour l'étude voltampérométrique, utilisé des solutions plus concentrées que dans le nitro-

Can. J. Chem. Downloaded from www.nrcresearchpress.com by 210.87.254.6 on 09/05/12
For personal use only.

méthane (supérieures à 10^{-3} mol/l) ce qui diminue l'effet parasite de l'eau.

Partie expérimentale

Reactifs

Le sulfolane est un produit Merck. Nous avons repris, pour la purification les méthodes préconisées par Coetzee *et al.* (3) et Benoit et Choux (5) en y apportant quelques modifications. Le mode opératoire adopté est le suivant: le solvant mis à reflux pendant 18 h environ, puis distillé sous pression réduite est placé sur carbone actif à 40 °C, pendant une journée. Après filtration, le sulfolane incolore est distillé une seconde fois sous pression réduite. Sa teneur en eau est alors de 15 à 30 p.p.m. Les dernières traces d'eau sont éliminées par passage sur une colonne remplie d'alumine neutre d'activité 1 (séchée à 350° sous pression réduite), adaptée directement sur la cellule de mesure. Le solvant ainsi obtenu a une conductivité inférieure à 10^{-8} Ω^{-1} cm^{-1} (limite de l'appareillage dont nous disposons) et sa teneur en eau est inférieure à 10 p.p.m. (méthode de Karl Fischer).

L'acide chlorosulfurique Carlo Erba est utilisé sans purification.

L'acide sulfurique 100% est préparé par addition d'oléum (suivie par conductimétrie) à de l'acide sulfurique R.P. prolabo.

L'acide disulfurique est synthétisé par addition de SO_3 pur à de l'acide sulfurique 100%. Les solutions de cet acide ou d'oléums dans le sulfolane sont stables, contrairement aux observations de Benoit *et al.* (15).

Les solutions d'acide chlorhydrique anhydres sont obtenues par passage dans le solvant de HCl gaz (libéré par chauffage d'un mélange de H_3PO_4 anhydre et NaCl). La solution est titrée dans l'eau.

Le chlorosulfate de tétraéthylammonium est préparé par neutralisation d'un solution de HSO_3Cl dans le nitrométhane avec le chlorure de tétraéthylammonium. Le solide est extrait par évaporation du solvant sous pression réduite (6).

Le chlorure de tétraéthylammonium, le perchlorate de tétraéthylammonium sont des produits Eastman Kodak, ils sont séchés à 80° sous pression réduite.

Le perchlorate d'argent Flucka est deshydraté à 60° sous pression réduite.

Le chlorodisulfate d'ammonium est préparé par action de SO_3 sur NH_4Cl en proportions stoechiométriques dans SO_2 liquide (7).

Mesures: toutes les mesures sont effectuées à 30 ± 0.1 °C

Les courbes voltampérométriques sont réalisées à l'aide d'un ensemble Tacussel comprenant un potentiostat PRT 20.2.X, un correcteur de chute ohmique C.D.C.O., un pilote $GSTP_3$, un millivoltmétre et un enregistreur XY LUXY TRACE.

Potentiométrie: les mesures potentiométriques ont été faites avec un millivoltmétre Tacussel ISIS 4000, suivi d'un enregistreur permettant d'apprécier la stabilité des potentiels.

L'électrode de réf. 8 est constituée par la demi-pile $Ag/AgClO_4$ $N/10$. Un pont rempli d'une solution de perchlorate de tétraéthylammonium $N/10$ la relie à la cellule de mesure. Le potentiel de cette électrode très stable, est néanmoins contrôlé après chaque expérience en mesurant le potentiel de demi vague d'une solution de ferrocène, pris comme origine des potentiels.

Les solutions étudiées ont généralement une concentration voisine de 10^{-2} *M*. Le réactif est ajouté à l'aide d'une micro burette Gilmont (2 cm^3).

Résultats et discussion

Détermination de la constante de dissociation de l'ion SO_3Cl^- dans le sulfolane

L'ion SO_3Cl^- se dissocie selon

$$[1] \qquad SO_3Cl^- \rightleftarrows SO_3 + Cl^-$$

La mesure de l'activité de Cl^- conduit à la détermination de la constante d'équilibre

$$K_{SO_3Cl^-} = \frac{[SO_3][Cl^-]}{[SO_3Cl^-]}$$

Si l'électrode d'argent est bien indicatrice de Cl^- dans ce solvant (9), il fallait montrer qu'elle l'était encore pour le complexe SO_3Cl^- c'est à dire étudier le système oxydoréducteur

$$[2] \qquad SO_3 + AgCl\downarrow + e^- \rightleftarrows Ag\downarrow + SO_3Cl^-$$

dans l'hypothèse ou les chloropolysulfates sont totalement dissociés en SO_3Cl^- et SO_3 en solution. Le potentiel normal E_2^0 de ce système défini pour $[SO_3] = [SO_3Cl^-]$ dépend de P, produit de solubilité du chlorure d'argent, de K la constante de dissociation de l'ion chlorosulfate suivant

$$E_2^0 = E_{Ag/Ag^+}^0 + 0.06 \log \frac{P}{K}$$

où E_{Ag/Ag^+}^0 est le potentiel normal du système $Ag^+ + e^- \rightleftarrows Ag$.

En vue d'étudier la réversibilité du système, nous avons tracé les courbes voltampérométriques à l'électrode d'argent des solutions de chlorosulfate de tétraéthylammonium en présence de perchlorate de tétraéthylammonium comme électrolyte indifférent. Les vagues d'oxydation obtenues sont reproductibles et bien définies si la teneur en eau du solvant est très faible, mais la proximité du mur d'oxydation rend difficile l'évaluation du courant limite de diffusion. En traçant cependant la transformée logarithmique de la courbe intensité potentiel, correspondant au couple oxydo réducteur [2], on obtient une droite de pente 65 mV. En présence de SO_3 et SO_3Cl^-, la détermination du courant limite d'oxydation est encore plus difficile et ne peut plus être évaluée avec précision.

Cependant, en réduction on constate que le courant limite de diffusion i_{SO_3} est proportionnel à la concentration de l'anhydride sulfurique. Pour confirmer l'hypothèse initiale de dissocia-

Can. J. Chem. Downloaded from www.nrcresearchpress.com by 210.87.254.6 on 09/05/12
For personal use only.

Can. J. Chem. Downloaded from www.nrcresearchpress.com by 210.87.254.6 on 09/05/12
For personal use only.

tion élevée des chloropolysulfates selon:

$$(SO_3)_nCl^- \rightleftarrows (n-1)SO_3 + SO_3Cl^-$$

nous avons tracé les courbes intensité potentiel sur platine d'une solution de chlorodisulfate d'ammonium. Nous observons une vague d'oxydation avec passivation. Ce phénomène a déjà été observé par Marchon et Badoz (10) lors de l'oxydation du chlorure sur électrode de platine dans le nitrométhane. Cette vague correspondrait soit à

[3] $$SO_3 + \tfrac{1}{2}Cl_2 + e^- \rightleftarrows SO_3Cl^-$$

soit à

[4] $$2SO_3 + \tfrac{1}{2}Cl_2 + e^- \rightleftarrows (SO_3)_2Cl^-$$

En réduction, nous notons une vague identique à la réduction des solutions de SO_3 seul, ce qui élimine la complexation de SO_3 par SO_3Cl^- (les potentiels de demi vague sont identiques pour des solutions de même concentration). L'addition de $N(C_2H_5)_4{}^+SO_3Cl^-$ modifie uniquement la hauteur du palier correspondant au courant limite d'oxydation. Ces résultats montrent donc qu'en solution seul le couple oxydo réducteur [3] intervient et que le chlorodisulfate est donc dissocié totalement en SO_3Cl^- et SO_3. L'écriture du couple [2] est donc justifiée.

Pour déterminer le potentiel normal du couple [1], nous avons suivi par potentiométrie le dosage d'une solution de chlorosulfate de tétraéthylammonium par une solution de perchlorate d'argent (fig. 1). L'étude mathématique de la courbe obtenue montre que

$$E = f\left(\log \frac{|[SO_3]|}{|[SO_3Cl^-]|}\right)$$

est une droite de pente 62 mV (fig. 2), confirmant ainsi la dissociation du chlorodisulfate, et que le potentiel normal du couple [2] est de 123 ± 5 mV par rapport au potentiel normal du couple ferrocène ferricinium pour une température de 30 °C (en assimilant concentration et activité pour des molécules neutres. L'activité des ions est calculée à partir de la formule de Debye–Hückel avec $a = 4$ Å (9)).

Nous avons redéterminé le produit de solubilité de AgCl et le potentiel normal du couple Ag^+/Ag; les valeurs trouvées sont $P_{AgCl} = 3.7 \times 10^{-19}$ et $E_{Ag^+/Ag}{}^0 = 0.373$ V. Ces valeurs sont comparables à celles trouvées par Benoit *et al.* (9) $P_{AgCl} = 8 \times 10^{-19}$ et $E_{Ag/Ag^+}{}^0 = 0.380$ V. La constante de l'équilibre $SO_3Cl^- \rightleftarrows SO_3 +$

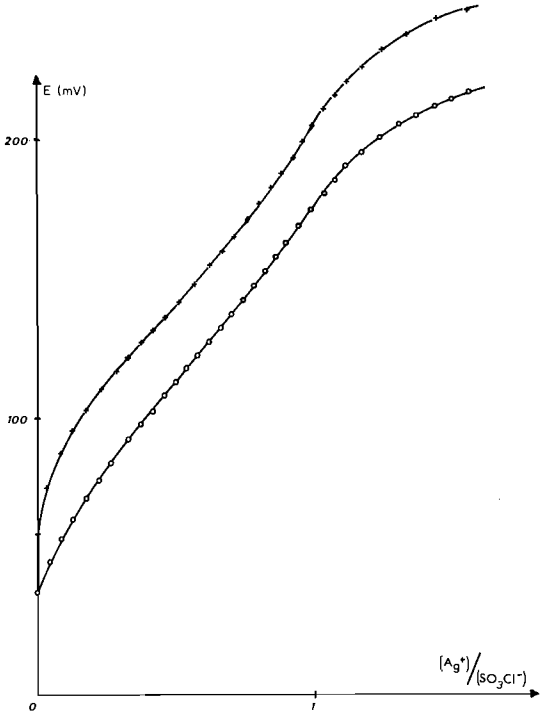

FIG. 1. Courbe potentiométrique de titrage d'une solution de $(C_2H_5)_4N\,SO_3Cl$ par une solution de $AgClO_4$ en milieu $(C_2H_5)_4ClO_4$ $N/10$, courbe (+); courbe (○), en présence de H_2SO_4.

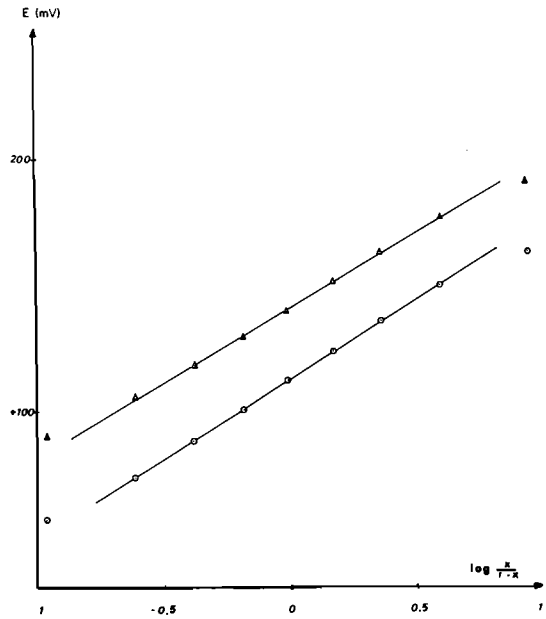

FIG. 2. Analyse mathématique des courbes représentées sur la fig. 1. $x = (Ag^+)/(SO_3Cl^-)$ initial; Δ, $(C_2H_5)_4NSO_3Cl + AgClO_4$; ○, $(C_2H_5)_4NSO_3Cl + H_2SO_{4(excès)} + AgClO_4$.

Cl^- est donc égale à $10^{-14.3\pm0.2}$ mol/l avec $E_2{}^0 = 123 \pm 5$ mV.

Cette valeur est très proche de celle trouvée dans le nitrométhane. Dans ce dernier solvant, en utilisant le potentiel de demi vague déduit des courbes $i = f(E)$ du couple [2] nous trouvons $pK = 14.1$. Ces résultats confirment les propriétés très voisines de ces deux solvants. Le chlorosulfate est donc un donneur très faible de SO_3, et la réaction

$$SO_3A + Cl^- \rightleftarrows SO_3Cl^- + A$$

devrait permettre de déterminer le pouvoir donneur de SO_3 des composés SO_3A à condition que les propriétés basiques de Cl^- n'interfèrent pas.

Détermination des constantes de dissociation des acides $H_2S_2O_7$ et HSO_3Cl dans le sulfolane

Il est connu depuis très longtemps (11) que l'acide chlorosulfurique peut être préparé en faisant passer du gaz chlorhydrique dans les oléums et en particulier dans l'acide disulfurique selon

$$H_2S_2O_7 + HCl \rightarrow HSO_3Cl + H_2SO_4$$

L'acide disulfurique est un meilleur donneur de SO_3 que l'acide chlorosulfurique. Cette réaction ne permet pas une détermination directe de la constante de dissociation de $H_2S_2O_7$ suivant

[5] $$H_2S_2O_7 \rightleftarrows H_2SO_4 + SO_3$$

elle nécessite en outre la connaissance du pouvoir sulfonant de HSO_3Cl. Pour atteindre cette constante nous avons étudié le système électrochimique

[6] $$AgCl\downarrow + H_2S_2O_7 + e^- \rightleftarrows H_2SO_4 + SO_3Cl^- + Ag\downarrow$$

en réalisant en présence d'un excès connu de H_2SO_4($C = 0.1$ mol/l) (fig. 1) la réaction

$$(C_2H_5)_4N^+SO_3Cl^- + Ag^+ClO_4^- + H_2SO_4 \rightleftarrows AgCl + H_2S_2O_7 + (C_2H_5)_4N^+ClO_4^-$$

L'analyse mathématique de la courbe potentiométrique obtenue (fig. 2) permet par comparaison avec le potentiel normal du système (2) d'atteindre la constante de dissociation de $H_2S_2O_7$ selon l'équilibre (5)

$$K_{H_2S_2O_7} = \frac{[H_2SO_4][SO_3]}{[H_2S_2O_7]} = 10^{-1.45\pm0.30} \text{ mol/l}$$

avec $E_6{}^0 = 36 \pm 5$ mV déterminé pour $[SO_3Cl^-] = [H_2S_2O_7]$ et $[H_2SO_4] = 0.1 f_\pm$ ($f_\pm$ étant le coefficient d'activité moyen).

Cerfontain (12) a montré par des mesures spectrométriques que cette constante dans l'acide sulfurique est inférieure ou égale à $10^{-0.7}$, valeur proche de celle trouvée dans le sulfolane. Les réactions de sulfonation réalisées dans l'acide sulfurique en utilisant l'acide disulfurique ou les oléums plus concentrés (que l'on peut considérer comme donneurs de SO_3 plus forts que $H_2S_2O_7$) peuvent être effectuées dans le sulfolane, solvant dont l'étendue des domaines d'électroactivité et de pH utilisables est beaucoup plus importante que celle dont on peut disposer dans l'acide sulfurique. Le sulfolane devrait donc permettre de différencier plus facilement les différents donneurs de SO_3, afin de les classer sur une échelle pSO_3.

L'acide chlorosulfurique étant également très souvent utilisé comme agent sulfonant il était intéressant de le comparer à l'acide disulfurique dans le sulfolane. La constante de dissociation de HSO_3Cl selon

[7] $$HSO_3Cl \rightleftarrows SO_3 + HCl$$

c'est à dire

$$K_{HSO_3Cl} = \frac{[SO_3][HCl]}{[HSO_3Cl]}$$

dépend de la constante de dissociation de l'ion SO_3Cl^- et du rapport des constantes d'acidité de HCl et de HSO_3Cl.

$$K_{HSO_3Cl} = (K_{SO_3Cl^-})\frac{k_{HSO_3Cl}}{k_{HCl}}$$

k_{HSO_3Cl} et k_{HCl} étant les constantes d'acidité des acides HSO_3Cl et HCl.

L'acide chlorhydrique étant associé dans le sulfolane (13) nous avons, pour déterminer la différence de pK de ces deux acides, étudié le couple électrochimique

[8] $$AgCl\downarrow + HSO_3Cl + e^- \rightleftarrows Ag\downarrow + SO_3Cl^- + HCl$$

en titrant une solution de HCl par une solution de perchlorate d'argent, l'électrolyte étant le chlorosulfate de tétraéthylammonium (fig. 3). (Une étude conductimétrique en cours montre que les constantes de dissociation de $N(C_2H_5)_4ClO_4$ et $N(C_2H_5)_4SO_3Cl$ sont très voisines.)

En comparant les potentiels normaux $E_{Ag/Ag^+}{}^0 = 373$ mV et $E_8{}^0 = 125 \pm 5$ mV (calculé en tenant compte de la concentration de $N(C_2H_5)_4SO_3Cl$,: $c = 0.08$ mol/l) et un utilisant le produit de solubilité de AgCl ($P = 3.7 \times 10^{-19}$) nous

Can. J. Chem. Downloaded from www.nrcresearchpress.com by 210.87.254.6 on 09/05/12
For personal use only.

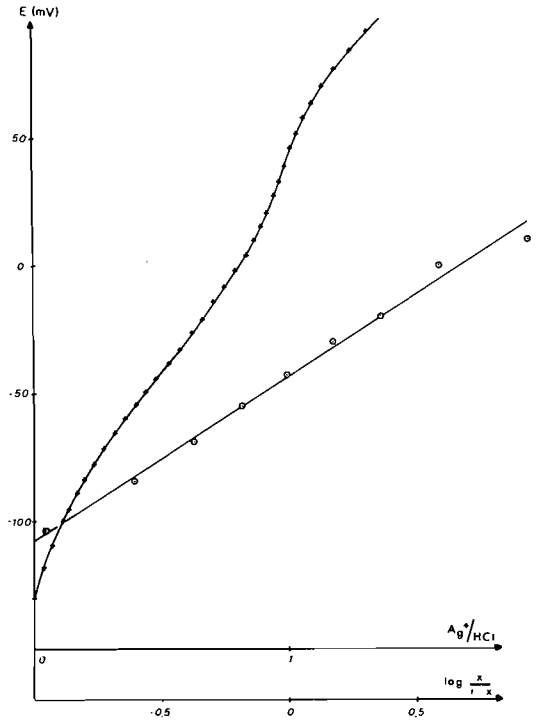

FIG. 3. Courbe potentiométrique de titrage d'une solution de HCl par une solution de $AgClO_4$ en milieu $(C_2H_5)_4NSO_3Cl$ $N/10$. ○, analyse mathématique de la courbe potentiométrique. $x = (Ag^+)/(HCl)$ initial.

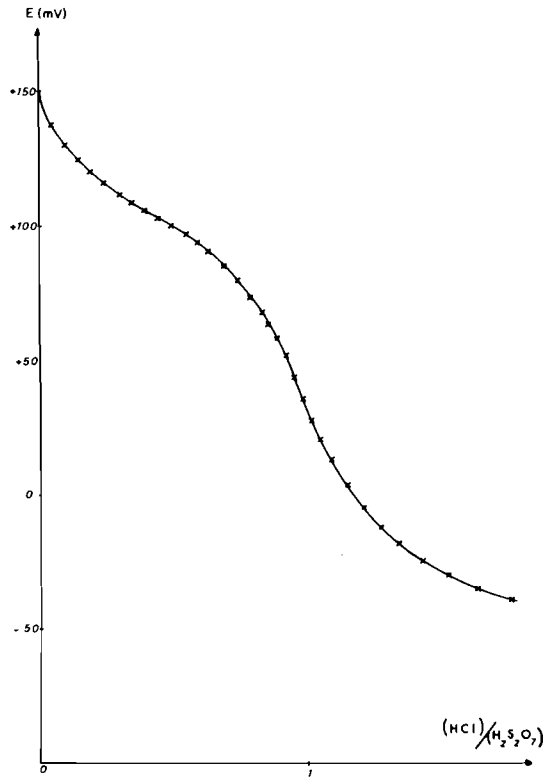

FIG. 4. Courbe potentiométrique de titrage d'une solution de $H_2S_2O_7$ par une solution de HCl en milieu $(C_2H_5)_4ClO_4$ $N/10$.

obtenons $pk_{HCl} - pk_{HSO_3Cl} = 10.1 \pm 0.2$. Dans l'hypothèse où les acides ne donnent pas d'hétéroconjugaison entre HCl et SO_3Cl^-, la constante de dissociation de HSO_3Cl est donc:

$$K_{HSO_3Cl} = \frac{[SO_3][HCl]}{[HSO_3Cl]} = 10^{-4.2\pm0.5} \text{ mol/l}$$

Richards et Woolf (14) ont déterminé cette constante dans HSO_3Cl par des mesures calorimétriques et trouvé $10^{-5.3}$. Le chlorure de sulfuryle étant moins donneur de Cl^- que SO_3Cl^- l'équilibre $2HSO_3Cl \rightleftarrows H_2SO_4 + SO_2Cl_2$ n'intervient pas ici. Cette valeur plus faible que celle de l'acide disulfurique, justifie l'obtention de HSO_3Cl à partir de $H_2S_2O_7$ et la possibilité de doser des solutions de $H_2S_2O_7$ ou d'oléums par des solutions d'acide chlorhydrique, en suivant cette réaction à l'aide d'une électrode d'argent comme indicatrice (fig. 4). Un travail doit être publié prochainement sur ce sujet.

En conclusion, les composés étudiés dans ce travail peuvent être classés d'une part suivant leur pouvoir sulfonant croissant selon $SO_3Cl^- \ll HSO_3Cl < H_2S_2O_7 < (SO_3)_2Cl^-$ et d'autre part, en utilisant les résultats de Coetzee *et al.* (4) et ceux de Benoit *et al.* (15) suivant leur caractère acide $pk_{HClO_4} = 3$ (4) ou 2.7 (15), $pk_{HSO_3F} = 3.3$ (15), $pk_{HSO_3Cl} = 4.4$, $pk_{H_2S_2O_7} = 5$ (15), $pk_{HCl} = 14.5$ (4).

Les acides chlorosulfurique et fluorosulfurique sont plus forts que l'acide disulfurique, contrairement à ce que l'on observe dans d'autres solvants de constantes diélectriques voisines comme le nitrométhane (16) ou le nitrobenzène (17, 18), les ions SO_3Cl^- et SO_3F^- devant être moins solvatés, dans ces deux derniers solvants que $HS_2O_7^-$ plus volumineux.

Nous nous proposons de compléter ces échelles d'acidité et de pSO_3 dans le but de permettre un choix plus judicieux de l'agent de sulfonation.

Nous remercions la Délégation Générale à la Recherche Scientifique et Technique, pour l'aide financière apportée à ces travaux. Contrat D.G.R.S.T CN 73-7-1827. Laboratoire de Chimie Minérale I-C8-59650, Villeneuve D'Ascq.

Can. J. Chem. Downloaded from www.nrcresearchpress.com by 210.87.254.6 on 09/05/12
For personal use only.

1. JC. FISCHER, Y. AUGER et M. WARTEL. C.R. Acad. Sci., **276**c, 1579 (1973).
2. H. A. LEHMANN, G. KEMPE et M. RUPPERT. Z. Anorg. Allg. Chem. **293**, 311 (1958).
3. J. F. COETZEE, JM. SIMON et R. J. BERTOZZI. Anal. Chem. **41**, 766 (1969).
4. J. F. COETZEE et R. J. BERTOZZI. Anal. Chem. **45**, 1064 (1973).
5. R. L. BENOIT et G. CHOUX. Can. J. Chem. **46**, 3215 (1968).
6. JC. FISCHER. Thèse de 3èmecycle. Lille, France 1972.
7. G. H. WEINREICH. Bull. Soc. Chim. Fr. 2820 (1963).
8. J. DESBARRES, P. PICHET et R. L. BENOIT. Electrochem. Acta, **13**, 1899 (1968).
9. R. L. BENOIT, A. L. BEAUCHAMP et M. DENEUX. J. Phys. Chem. **73**, 3268 (1969).
10. J. C. MARCHON et J. BADOZ LAMBLING. Bull. Soc. Chim. Fr. 4660 (1967).
11. L. GMELIN. Handbuch der Anorganischen Chemie, "Schwefel B". Verlag Chemie, Weinheim. 1963. p. 1835.
12. H. CERFONTAIN. Recl. Trav. Chim. Pays-Bas, **80**, 257 (1961).
13. R. N. ALDER, G. R. CHALKLEY et M. C. WHITING. Chem. Commun. **13**, 405 (1966).
14. G. W. RICHARDS et A. A. WOOLF. J. Chem. Soc. A, 1118 (1967).
15. R. L. BENOIT, C. BUISSON et G. CHOUX. Can. J. Chem. **48**, 2353 (1970).
16. JC. FISCHER et M. WARTEL. Bull. Soc. Chim. Fr. 3302 (1972).
17. R. C. PAUL, S. C. AHLUWALIA, C. SUBHASH et R. PARKASH. Indian J. Chem. **7**(8), 815 (1969).
18. W. REED, D. W. SECRET, R. C. THOMPSON et P. A. YEATS. Can. J. Chem. **47**, 4275 (1969).

Can. J. Chem. Downloaded from www.nrcresearchpress.com by 210.87.254.6 on 09/05/12
For personal use only.

The Systems Indium Trichloride – Pyridine and Indium Trichloride – Pyridine – Water: Equilibrium Diagrams and Heat of Formation of $InCl_3.3C_5H_5N$

ELINOR M. KARTZMARK

Department of Chemistry, University of Manitoba, Winnipeg, Manitoba R3T 2N2

Received May 8, 1975

ELINOR M. KARTZMARK. Can. J. Chem. **53**, 2995 (1975).

The equilibrium diagram of the system indium trichloride – pyridine – water, at 25 °C, shows the existence of two compounds, $InCl_3.C_5H_5N.2H_2O$ and $InCl_3.3C_5H_5N$. The melting point diagram shows that the compound $InCl_3.3C_5H_5N$ melts incongruently at 242 °C. The heat of the reaction

$$InCl_3 + 3C_5H_5N \rightarrow InCl_3.3C_5H_5N$$

is $\Delta H = -34.6$ kcal/mol and the heat of formation of $InCl_3.3C_5H_5N$ is -137.0 kcal/mol.

ELINOR M. KARTZMARK. Can. J. Chem. **53**, 2995 (1975).

Le diagramme d'équilibre du système trichlorure d'indium – pyridine – eau à 25 °C montre l'existence de deux composés: $InCl_3.C_5H_5N.2H_2O$ et $InCl_3.3C_5H_5N$. Le diagramme de point de fusion montre que le composé $InCl_3.3C_5H_5N$ fond d'une façon non congruente à 242 °C. La chaleur de la réaction

$$InCl_3 + 3C_5H_5N \rightarrow InCl_3.3C_5H_5N$$

est $\Delta H = -34.6$ kcal/mol et la chaleur de formation de $InCl_3.3C_5H_5N$ est de -137.0 kcal/mol.

[Traduit par le journal]

Introduction

It is well known that indium trichloride has an appreciable solubility in many organic solvents, *e.g.* 51% in methanol, 38% in acetone (1). In an earlier paper (2) this author reported the formation of compounds between indium trichloride and *p*-dioxane, which have an appreciable solubility in water. In 1903 Renz (3) and subsequently in 1904 Dennis and Geer (4) reported the formation of a white crystalline compound when indium trichloride dissolved in absolute alcohol, was treated with pyridine. Renz gave a formula $InCl_3.3C_5H_5N$ and reported a melting point of 253 °C. The present paper deals with the phase diagram for the system indium trichloride – pyridine – water at 25 °C and the freezing point diagram of the binary system indium trichloride – pyridine. The heat of formation of the anhydrous compound from its constituents was also determined.

Experimental

Materials

For much of the solubility work, a concentrated acid-free solution (58 wt.%) of indium trichloride in water, provided without charge by Cominco, was used. Indium trichloride trihydrate was also prepared by refluxing pure indium metal with excess concentrated hydrochloric acid until solution was complete. The product was evaporated on a steam bath until on cooling it solidified. The salt was dissolved in water and crystallization repeated. The resulting salt gave a solution neutral to litmus. Analysis showed it to be pure indium trichloride. The anhydrous trichloride cannot be obtained pure by heating above 100 °C, because hydrolysis occurs. When the anhydrous salt was required for the measurements of heat of formation and the melting point diagram, BDH laboratory reagent indium trichloride was used. The pyridine was obtained from the Fisher Scientific Company, Certified ACS, and used without further purification. Conductance water was used throughout.

Analysis of the System Indium Trichloride – Pyridine – Water

The chloride was estimated gravimetrically as silver chloride, and pyridine by distillation from a strong sodium hydroxide solution, followed by titration with standard hydrochloric acid, using a conductimetric technique. The method for pyridine was tested by analysis of a known sample and gave an accuracy of $\pm 0.5\%$. This error is magnified in the drawing of tie-lines, as a means of determining composition of compounds, especially if the "wet residue" is appreciably damp. Because of the difference in molecular weights, there is no doubt of the indium trichloride to pyridine ratio in the compound, but the degree of hydration, if any, presents some difficulty. All solutions, except those high in pyridine, were very viscous and slow to filter. While the "wet residue"

Can. J. Chem. Downloaded from www.nrcresearchpress.com by 210.87.254.42 on 09/05/12
For personal use only.

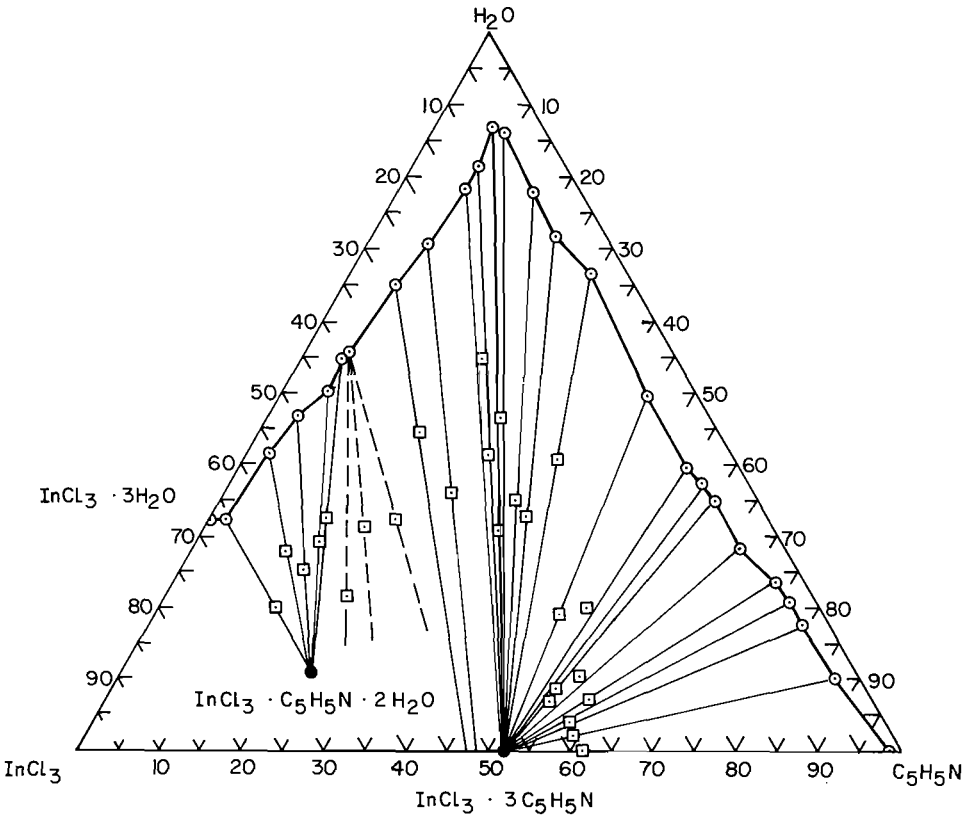

FIG. 1. Equilibrium diagram for the system indium trichloride – pyridine – water at 25 °C.

appeared to be sufficiently free from mother liquor, it was found necessary to separate them further by placing the filtered residue between thick layers of filter paper and subjecting it to a hydraulic pressure (2000 psi). Despite this treatment, the lever rule indicated that about 50% mother liquor was still present.

Calorimetry

The heat of reaction between indium trichloride (anhydrous) and pyridine was determined in a stoppered Dewar flask, fitted with thermistor, stirrer, and heating coil. Weighed amounts of indium trichloride were added intantaneously to about 300 g of well stirred pyridine. Anhydrous indium trichloride is very hygroscopic so all transfers were done in a dry-box before weighing. Reaction is rapid and therefore no attempt was made to exclude the atmosphere during measurements. The average was taken over ten measurements with a reproducibility of ±3%.

Freezing Point Diagram

Because pyridine is volatile, it was necessary to make the measurements in a closed system. A thermal analysis technique was tried unsuccessfully, because of extreme supercooling, which could not be overcome in a sealed vessel. Thick-walled glass tubes were charged with weighed quantities of the components and sealed off. Owing to the possibility of explosion on heating above 100 °C, the tubes were heated in an apparatus used previously to determine critical temperature (5). The temperatures of initial thawing and final disappearance of solid were measured using a copper–constantan thermocouple, calibrated with the freezing points of pure pyridine (−42 °C), water, and tin (231.9 °C). The tubes were removed from time to time during the heating and shaken vigorously.

Experimental Results

The solubility data are given in Table 1,[1] and are plotted in Fig. 1. The freezing point diagram, Fig. 2, is based on the measurements shown in Table 2.

Discussion

The existence of two compounds of indium trichloride and pyridine is shown in the ternary phase diagram; $InCl_3.C_5H_5N.2H_2O$, incongruently saturating, decomposes on addition of water to give a solution of composition 39.5%

[1]Table 1 is available, at a nominal charge, from the Depository of Unpublished Data, CISTI, National Research Council of Canada, Ottawa, Canada K1A 0S2.

Can. J. Chem. Downloaded from www.nrcresearchpress.com by 210.87.254.42 on 09/05/12
For personal use only.

Can. J. Chem. Downloaded from www.nrcresearchpress.com by 210.87.254.42 on 09/05/12
For personal use only.

TABLE 2. Melting points in the system indium trichloride – pyridine

Wt.% pyridine	Peritectic temperature (°C)	Temperature of liquidus (°C)
40	240	330
45	245	315
52	242	295
60	242	242
70	—	178
80	—	132
85	—	124
90	—	100
95	−42 (eutectic)*	74
100	−42	−42

*The temperature and composition of the eutectic are very nearly those of pure pyridine.

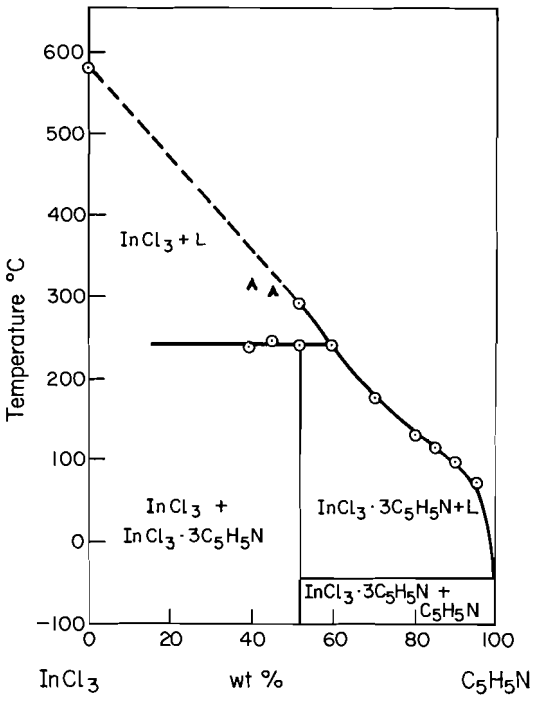

FIG. 2. Melting point diagram for the system indium trichloride – pyridine.

$InCl_3$, 5.3% C_5H_5N, and a second, anhydrous, compound, $InCl_3.3C_5H_5N$. The latter compound has very limited solubility in pyridine (1.0%) and is congruently saturating in water, with a solubility of 13 g per 100 g solution. The phase diagram indicates some slight solubility of indium chloride in the compound, to a maximum of about 6%.

The compound $InCl_3.3C_5H_5N$ forms with marked evolution of heat. A calorimetric study gave a value of -34.6 ± 1.0 kcal, for the reaction

$$InCl_3(s) + 3C_5H_5N(l) \rightarrow InCl_3.3C_5H_5N(s)$$

Using the value of −154.2 kcal given by Campbell *et al.* (6) for the heat of formation of $InCl_3(s)$ and a value of +17.2 kcal for pyridine, one obtains a value of −137.0 kcal per mol for the heat of formation of $InCl_3.3C_5H_5N(s)$.

Renz (3) reported a congruent melting of $InCl_3.3C_5H_5N$ at a temperature of 253 °C. The phase diagram, Fig. 2, indicates a peritectic temperature at 242 °C, at which decomposition occurs to anhydrous indium chloride and a liquid of 60 wt.% pyridine.

From a simple interpretation of the formulae of the compounds in the ternary system, it appears that pyridine replaces water in the solvation of $InCl_3.3H_2O$, resulting in the compounds $InCl_3.C_5H_5N.2H_2O$ and $InCl_3.3C_5H_5N$. There is no evidence for the existence of the third possible compound, *viz.* $InCl_3.2C_5H_5N.H_2O$. Systems in this region were stirred for several days to rule out the possibility of metastability. In the corresponding system, indium trichloride – dioxane – water, the trihydrate retains its water of crystallization and adds three molecules of dioxane (2, 7).

1. W. F. LINKE and A. SEIDEL. Solubilities of inorganic and metal organic compounds, Vol. 1. 4th ed. American Chemical Society, Washington. 1958.
2. E. M. KARTZMARK. Can. J. Chem. **52**, 3459 (1974).
3. C. RENZ. Z. Anorg. Chem. **36**, 101 (1903).
4. L. M. DENNIS and W. C. GEER. J. Am. Chem. Soc. **26**, 437 (1904).
5. A. N. CAMPBELL and E. M. KARTZMARK. Can. J. Chem. **41**, 1088 (1962).
6. A. N. CAMPBELL, E. M. KARTZMARK, and O. M. BHATNAGAR. Can. J. Chem. **52**, 1954 (1974).
7. E. M. KARTZMARK. Can. J. Chem. **53**, 1854 (1975).

Studies of Ternary Nematic Phases by Nuclear Magnetic Resonance. Alkali Metal Decyl Sulfates/Decanol/D_2O[1]

KEITH RADLEY[2] AND LEONARD WALLACE REEVES

Chemistry Department, University of Waterloo, Waterloo, Ontario N2L 3G1

Received February 26, 1975

KEITH RADLEY and LEONARD WALLACE REEVES. Can. J. Chem. **53**, 2998 (1975).

The nematic regions of the ternary phase diagram for alkali metal decyl sulfates/decanol/D_2O have been investigated. The lithium detergent system has a very restricted region of type I nematic phase which orients parallel to the magnetic field with a long time constant. The sodium detergent also forms a rather restricted nematic region which may be type II, oriented perpendicular to the magnetic field or type I oriented parallel to the magnetic field, depending on the decanol content. The rubidium and potassium detergents were insufficiently soluble to form phases while the cesium detergent forms a very extensive type II nematic phase region with wide variations in water contents and with decanol between 2 and 7 wt.%. It is clear that the cesium decyl sulfate system has considerable advantage over the sodium detergent in forming nematic phases for use as orienting media for small molecules and ions in n.m.r. studies.

The partially averaged nuclear quadrupole coupling constants of Li-7, Na-23, and Cs-133 in ions and D-2 in the D_2O have been used as the primary tool in investigating the phase behavior. Quadrupole couplings have been reduced to unit quadrupole moment for the nucleus. The resultant quantity "E_s" in Hz b^{-1} reflects the strongly increasing electric field gradient induced in the monatomic ions by the nematic medium in going from Li^+ to Cs^+. The partially averaged quadrupole splittings which appear for the alkali metal ions in these uniaxial media are the result of distortion of the spherical symmetry of the ion and should not be interpreted in terms of degrees of orientation of the ion.

KEITH RADLEY et LEONARD WALLACE REEVES. Can. J. Chem. **53**, 2998 (1975).

On a étudié les régions nématiques du diagramme de phase ternaire: sulfates de décyle de métaux alcalins/décanol/D_2O. Le système comprenant un sel de lithium du détergent possède pour une région très restreinte, une phase nématique de type I qui s'oriente parallèlement au champ magnétique et qui possède une longue constante de temps. Le détergent sous forme de sel de sodium possède aussi, sur une région relativement restreinte, une phase nématique de type II orientée perpendiculairement au champ magnétique ou de type I orientée parallèlement au champ magnétique; les variations dépendent du contenu en décanol. Les sels de rubidium et de potassium du détergent ne sont pas suffisamment solubles pour former des phases; les sels de césium du détergent possèdent une phase nèmatique de type II sur une région très large impliquant de grandes variations dans le contenu en eau et à des concentrations de décanol allant de 2 à 7% en poids. Il est donc évident que le système contenant des sels de césium du sulfate de décyle possède des avantages marqués sur les sels de sodium lorsqu'il s'agit de former des phases nématiques destinées à orienter des petites molécules et des ions pour étude r.m.n.

Le principal outil utilisé pour étudier le comportement des phases a été les constantes de couplage quadrupolaires nucléaires partiellement moyennées des ions ^7Li, ^{43}Na et ^{133}Cs et de ^2D dans D_2O. Pour le noyau on a réduit les couplages quadrupolaires au moment quadrupolaire unitaire. La quantité "E_s" qui en résulte et qui s'exprime en Hz b^{-1} montre qu'il y a une augmentation importante de gradient de champ électrique induit dans les ions monoatomiques par le milieu nématique lorsque l'on passe di Li^+ à Cs^+. Les couplages quadrupolaires partiellement moyennés qui apparaissent pour les ions des métaux alcalins dans ces milieux uniaxiaux résultent d'une distorsion de la symétrie sphérique de l'ion et ne devraient pas être interprétés en termes de degrés d'orientation de l'ion.

[Traduit par le journal]

Introduction

A communication by Flautt and Lawson (1) reported the use of a lyotropic liquid crystal solvent to orient small solute molecules for nuclear magnetic resonance (n.m.r.) studies. The nematic phase was prepared from sodium octyl or decyl sulfate, octyl or decyl alcohol, water,

[1]This research was generously supported by the National Research Council of Canada and the Defense Research Board of Canada.

[2]In partial fulfillment for the Ph.D. degree, University of Waterloo, 1974.

Can. J. Chem. Downloaded from www.nrcresearchpress.com by 210.87.254.40 on 09/05/12
For personal use only.

Can. J. Chem. Downloaded from www.nrcresearchpress.com by 210.87.254.40 on 09/05/12
For personal use only.

and sodium sulfate. This phase (2–14) or small variations of it (12, 15) has proved to be a useful orienting medium for small molecules but to a much more restricted extent than the thermotropic liquid crystal solvents (16, 17). Most solute molecules in greater than 1 wt.% concentration in the lyotropic phase destroy the nematic properties, but this becomes less and less a limitation as the Fourier transform technique with rapid signal enhancement becomes a standard accessory to n.m.r. spectrometers (18) and dilute solutes can be reliably observed.

The lyotropic liquid crystal systems used in n.m.r. studies have been further generalized by Reeves *et al.* (19, 20) by substituting the simple counter ion for complex ions in both anionic detergent and cationic detergent phases. In this event the concentration of the complex ion can be high enough to allow study with the most elementary n.m.r. teaching instrument. The flexibility of these nematic phases with respect to counter ion exchange, variation of temperature, variation of detergent used, the use of mixed detergents, variation of p*H* in the water component etc., has prompted a series of studies from this and the São Paulo laboratory (21–30). The present study is a systematic investigation of the alkali metal decyl sulfates as components of ternary phases with decyl alcohol and water to probe the extent of nematic phase formation and type of nematic phase formed. The n.m.r. tool is applied to measure partially averaged nuclear quadrupole coupling constants and their variation with composition. The results should be a good guideline for those contemplating use of these mixtures as media for orienting solute molecules.

Experimental Section

The general methods developed for the preparation of alkali metal decyl sulfates have been previously described (19, 28, 30) and were followed in this study. The Varian VF16 variable frequency 2–16 MHz broad line spectrometer used to observe spectra was driven by a Schomandl ND30M frequency synthesizer to eliminate frequency drift of the variable frequency oscillator (v.f.o.) and to provide easy calibration by changing frequency after completing a sweep of the spectrum. The observation of one nucleus after another on the same oriented sample was facilitated by choosing a magnetic field where the nuclei observed had n.m.r. frequencies in the range 4–8.5 MHz. In this manner the optimum field was not used, but minor adjustments of the probe, v.f.o., and frequency synthesizer sufficed to observe one nucleus after the other. Li-7 fell outside this frequency range at all fields which were suitable for D-2, Na-23, and Cs-133. A probe change to 8–16 MHz was necessary in this case. The standard observation frequencies were Li-7 10.214 MHz, Na-23 8.300 MHz, Cs-133 4.120 MHz, and D-2 4.822 MHz. The H_1 field and modulation widths were adjusted optimally for each nucleus and sample (30) as before. Modulation frequencies were 40 Hz.

Nematic phases were prepared by the usual techniques described before (19, 21, 30). The cesium decyl sulfate (CsDS) formed by far the most extensive birefringent phases in the nematic region of the phase diagram. The compositions of these phases are described in Fig. 1. All phases contained 50 parts by weight of CsDS and $a \rightarrow f$ in the diagram describes increasing decanol content. Figure 1*a* is 2 parts by weight decanol, (*b*) 3 parts, (*c*) 4 parts, (*d*) 5 parts, (*e*) 6 parts, and (*f*) 7 parts. The horizontal lines indicate the extent of variation of water content in the nematic phases. The first line (*f*) indicates mesophases formed between 120 and 88 parts water (D_2O), 7 parts decanol, and 50 parts CsDS. As the decanol content decreases at constant weight of CsDS the extent of mesophase existence with variation of water content decreases and the amount of water required to form the mesophase decreases. To the lower left of the diagram an isotropic phase forms, to the bottom right a solid is formed, to the top right a birefringent phase occurs which is not oriented by a magnetic field and yields a powder pattern spectrum (30), and to the top left two phases separate, the upper one yielding a powder pattern spectrum (30) and the lower phase isotropic. Some of the above solid samples near the phase change, changed to nematic phases when stored in sealed tubes over a three month period thermostated at 27 °C.

Lithium decyl sulfate/decanol/water systems have an extremely limited range of nematic behavior with composition changes. A deuterium doublet for D_2O was obtained for birefringent phases with 32.5 parts by weight LiDS, 76–84 parts D_2O, and between 9.5 and 10.5 parts by weight decanol. The phases were never clear but had a very light milky appearance even after orienting in the magnet and this is unusual in our experience. The range of existence of nematic phases in the sodium decyl sulfate NaDS/decanol/D_2O was also very limited but more extensive than the LiDS system. Samples were prepared in a region with decanol 2.5 to 8.5 parts by weight, D_2O 44 to 62 parts, and NaDS 35 parts. In all cases where the magnetic field failed to orient the samples to give single crystal spectra and powder pattern spectra persisted indefinitely, it was assumed that lamellar type phases had formed. The samples were thermostated in a water bath at 27 °C the temperature of the n.m.r. measurements. Marked deterioration of the LiDS samples occurred over a four month period. All but a few of the samples initially nematic and birefringent phases became isotropic. Being an ion which generates the hydronium ion in water, it is probable that some hydrolysis of the decyl sulfate ion occurs with loss of weighed compositions. The solid samples formed, remained solid and birefringent when stored in sealed tubes over the same period of time. Similar aging was observed with NaDS sample although not as extensive.

The rubidium and potassium decyl sulfates prepared were insufficiently soluble in water to form mesophases. The most extensive work reported here therefore will describe the behavior of CsDS/decanol/water systems.

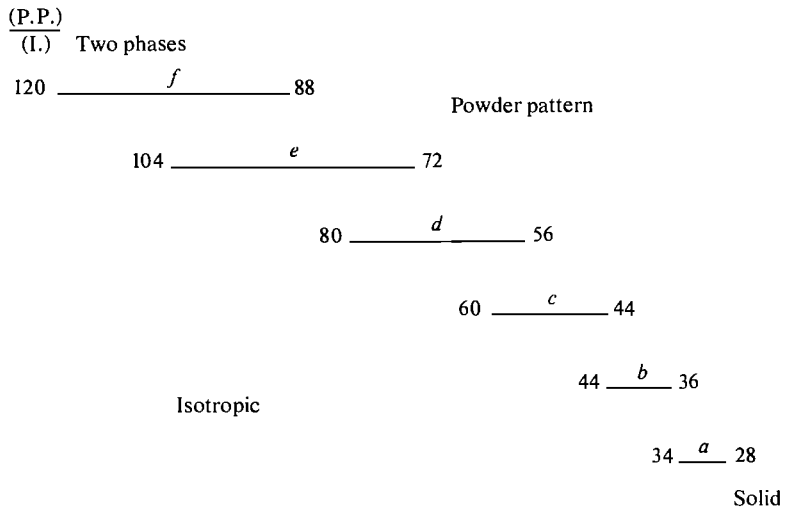

FIG. 1. Compositions of nematic mixtures in the cesium decyl sulfate/decanol/D_2O system. All phases were prepared by weighing 50 parts of cesium decyl sulfate. The decanol weighings were (*a*) 2 parts, (*b*) 3 parts, (*c*) 4 parts, (*d*) 5 parts, (*e*) 6 parts, and (*f*) 7 parts. Horizontal bars indicate the variation in heavy water content within the nematic region, *e.g.* nematic phases are staple for 80 to 56 parts by weight D_2O, 5 parts by weight decanol, and 50 parts by weight cesium decyl sulfate (horizontal bar *d*). To the top right powder pattern spectra were observed at the bottom extreme solid samples, to the left isotropic phases and upper left two phases. The upper phase gave a powder pattern spectrum, the lower one was isotropic.

Results

Mixtures containing Lithium and Sodium Decyl Sulfate

The Na-23 and D-2 n.m.r. spectra of the ternary nematic phases NaDS/decanol/D_2O were observed with nonspinning samples and after some time in the magnet became homogeneously oriented along the direction of the magnetic field (20). Single crystal spectra which were 1:1 doublets for deuterium and 3:4:3 triplets for the Na-23 n.m.r. were recorded. For low decanol contents the quadrupole splittings were in the range 700–1000 Hz for D-2 and 20–24 kHz for Na-23 while at higher decanol content the separations of transitions were 150–400 Hz for D-2 and 7–12 kHz for Na-23. These two types of phases formed have been identified with those previously reported (30) with mixed detergents as (*a*) type I orienting parallel to the magnetic field (*b*) type II orienting perpendicular to the field respectively. It is interesting that partial substitution of counter ions previously studied (30), and variation of the decanol content reported here, can induce phase changes from type I to type II. Low angle X-ray diffraction on magnetically oriented samples is required to fully interpret the changes in superstructure array. This change in phase has been explained (30) in terms of small alterations in the micro degrees of order of phase components but with a perpendicular change in the nematic direction. The quadrupole couplings in the two types of phases are thus related by a factor $\frac{1}{2}$ and a sign change in the degree of order at the coexistence point. In the solid samples formed with low water and low decanol, which were transparent and birefringent, the D-2 n.m.r. spectra were "powder pattern" type. The doublet separation was in the range 400–600 Hz for these samples.

After storing for four months, only six of the samples in the LiDS ternary system were homogeneous, transparent, and birefringent, while a large number were isotropic and a lesser number were solids. The Li-7 and D-2 n.m.r. spectra were investigated on these samples and the Li-7 signal was the expected 3:4:3 triplet with splittings between the outer peaks in the range 250 to 350 Hz and a 1:1 doublet with a separation of 450–650 Hz respectively. The D-2 n.m.r. of some of the birefringent and transparent solid phases formed in a region with low decanol and low water content was a powder pattern with a doublet spitting between 430–500 Hz. If the ratio of the Li-7 to D-2 splitting is compared to the ratio in our previous investigation (and identification of two types of phases) these six

Can. J. Chem. Downloaded from www.nrcresearchpress.com by 210.87.254.40 on 09/05/12
For personal use only.

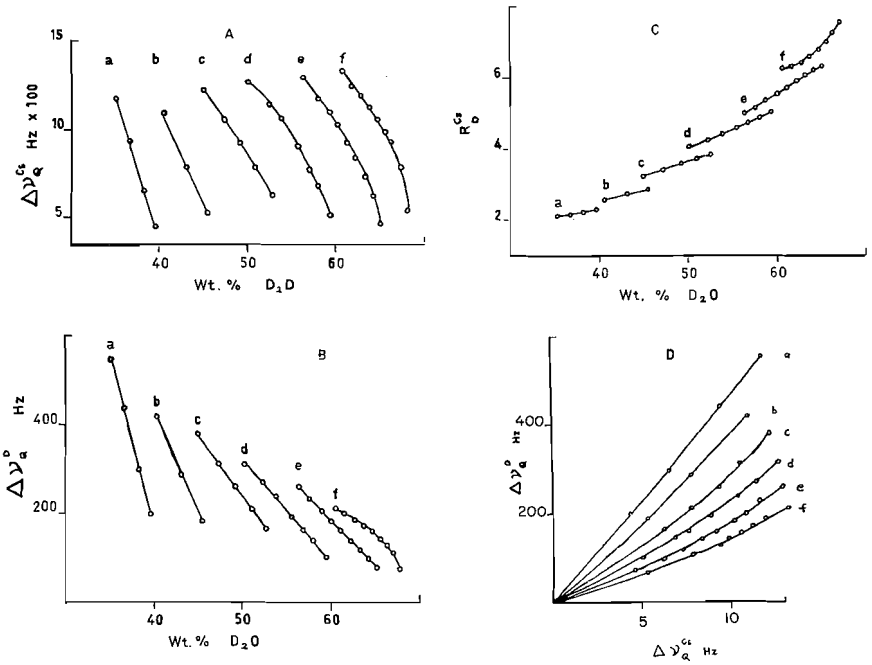

FIG. 2. The results of cesium and deuterium magnetic resonance spectra of CsDS/decanol/D_2O phases described in Fig. 1. (*A*) Cesium quadrupole splitting *vs.* water content. (*B*) Deuterium quadrupole splitting *vs.* water content. (*C*) Ratio of cesium to deuterium quadrupole splitting *vs.* water content. (*D*) Deuterium quadrupole splitting *vs.* cesium quadrupole splitting. The letters *a* to *f* denote decanol content of the phases as in Fig. 1.

nematic phases can be considered to be of type I (30).

The nematic ternary component mesophases of LiDS and NaDS were not investigated in great detail but results are cited here to serve as guidelines to those interested in using these phases as orienting media.

Cesium Decyl Sulfate/Decanol/D_2O System

The range of nematic mesophase formation in this system is so extensive that it is now the preferred solvent medium in our laboratory for orienting small molecules and ions. These CsDS phases are always of type II and no phase change is induced when small quantities of electrolyte or solute are added. After an initial orientation time which is very short the sample may be rotated in both cryogenic and convention magnet spectrometers to improve resolution (30).

The Cs-133 spectrum in single crystal nematic samples appears as a septet with intensity ratios 7:12:15:16:15:12:7 for first order quadrupolar perturbation on the Zeeman spectrum with spin $I = 7/2$ (30). The quadrupole splittings were measured as separations of adjacent peaks for both deuterium and cesium spectra and are reported in Fig. 2 for the phase compositions summarized in Fig. 1.

The Cs-133 splittings in Fig. 2*A* follow quite closely the form of the D-2 splittings in Fig. 2*B* as a function of composition. Figure 2 (*a*) to (*f*) in each subfigure indicates increasing decanol content as in Fig. 1 while the horizontally displaced curves go from low water contents with large Cs-133 and D-2 splittings to low Cs-133 and D-2 splittings with higher water content. The decanol and water content of the phases has large effects on the local degrees of order. The characteristic dependence of these splittings is further illustrated in Fig. 2*C* where the ratio of cesium to deuterium quadrupole splittings is set out as a function of decanol and water content of the nematic phases. In Fig. 2*D* the deuterium quadrupole splittings are shown to be related in a linear fashion with zero intercept at low decanol contents to the cesium quadrupole couplings but this relationship becomes increasingly nonlinear as the decanol content of the phase increases. This nonlinearity at high decanol contents as the water composition is

Can. J. Chem. Downloaded from www.nrcresearchpress.com by 210.87.254.40 on 09/05/12
For personal use only.

changed may be associated with the influence of chemical exchange between the water deuterium and the decanol-OD deuterium, which is much more highly ordered in the head groups of the hydrophobic/hydrophillic interface. All the nematic phases of CsDS are of type II with orientation of the uniaxial direction perpendicular to the magnetic field.

The phase transitions in the CsDS/decanol/D_2O system can be described as

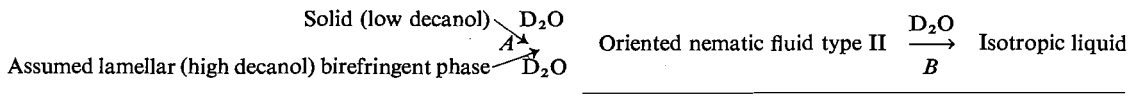

At low decanol contents with little D_2O the system is solid and with water addition passes directly to the type II nematic phases whose behavior was described above. At high decanol contents a lamellar phase is probably formed which also passes on addition of further D_2O into the type II nematic phase. On further addition of D_2O the nematic phase undergoes a transition to an isotropic micellular solution.

Both the solid phase at low decanol content and the lamellar phase exhibit n.m.r. spectra, which are powder pattern type. The quadrupole splitting of the powder doublet (30) varied from 1000 to 500 Hz at the phase change *A* for 27 °C. In the isotropic micellular phase the quadrupole splitting was zero and typical single line spectra were observed for deuterium and sodium resonances.

Discussion

Nuclear Quadrupole Couplings

The nuclear quadrupole couplings in spherical or cubic symmetries are known to be zero (31). The appearance of a quadrupole coupling energy which has a nonzero average on the time scales of the n.m.r. experiment (the inverse of the quadrupole coupling energy in radians in the present case), must indicate a distortion of the spherical symmetry of the alkali metal ions in the nematic phase (23). In a nematic medium, it is most reasonable to assume a statistically uniaxial distortion into an ellipsoidal shape with two equal axis leading to a quadrupole coupling tensor with no asymmetry parameter. This is consistent with previous experiments (27, 30).

The effective Hamiltonian, which leads to the nuclear quadrupole splitting, in the n.m.r. spectra of a uniaxially distorted spherical ion is (27)

$$[1] \quad H_Q = \sum_i \left[\frac{e^2Q^{(i)}\langle q_{zz}{}^{(i)}\rangle}{4I^{(i)}(2I^{(i)}-1)}\right] \times [3I_z{}^{(i)2} - I^{(i)}(I^{(i)}+1)]$$

where the superscript (i) refers to nucleus i and $-e\langle q_{zz}{}^{(i)}\rangle$ is the nonzero averaged value of the principal electric field gradient (e.f.g.) which we have shown to be along the nematic axis (27, 30). $eQ^{(i)}$ is the nuclear quadrupole moment of nucleus i, $I^{(i)}$ its spin quantum number, and $I_z(i)$ the z component of the spin angular momentum. The spacing of the quadrupolar split lines in the spectrum is

$$\nu_Q{}^{(i)} = \left|\frac{3e^2Q^{(i)}\langle q_{zz}{}^{(i)}\rangle}{2I^{(i)}(2I^{(i)}-1)h}\right| \text{ Hz}$$

The evaluation of $-e\langle q_{zz}{}^{(i)}\rangle$ requires a knowledge of the contribution of p states, which must necessarily become mixed with the s ground states in order to accommodate the distortion of the ion, as well as further antishielding effects (31). As was recently pointed out (27) there is no degree of orientation involved but merely a distortion of cubic or spherical symmetry around the nuclear site over a sufficiently long period of time to lead to secular perturbation of the Zeeman energies by a quadrupole coupling energy. The relaxation of Na-23 nuclei in the simple ion in a aqueous solution is dominated by the fluctuating electric quadrupole coupling (32–34).

$$[2] \quad \frac{1}{T_1} = \frac{2\pi^2}{5}\left(\frac{e^2q_{zz}}{h}\right)^2 T_c$$

T_c is a local correlation time for the appropriate fluctuating motion which is of the order 10^{-11} to 10^{-12} s though the value cannot actually be determined. The quadrupole coupling term which occurs in [2] has been the subject of estimates only. The quadrupole coupling constants measured for sodium in solid materials are highly temperature dependent and vary a great deal with the crystal (31). These couplings in solids are characteristic of the local forces at the crystalline site which distort the ion from spherical symmetry. There has been a tendency

Can. J. Chem. Downloaded from www.nrcresearchpress.com by 210.87.254.40 on 09/05/12
For personal use only.

Can. J. Chem. Downloaded from www.nrcresearchpress.com by 210.87.254.40 on 09/05/12
For personal use only.

to assign degrees of orientation of the sodium ion e.f.g. vector (26, 35, 36) by relating the quadrupole couplings in lyotropic phases to those in solids by the equation

$$[3] \qquad \Delta\nu = 2\nu_Q S_{zz}$$

where $\Delta\nu$ is the quadrupole splitting between outer transitions in the lyotropic phase and ν_Q is a value typical for solids. S_{zz} has been interpreted (26, 35, 36) as an approximate degree of orientation of the e.f.g. for the sodium ion but it is much better interpreted as some measure of the distortion of the spherical electron distribution in the ion (27). The relaxation time T_1 of sodium in aqueous isotropic solution is approximately 50 ms and decreases to about 5 ms in the electrical double layer (e.d.l.) of lamellar phases (32, 37).[3] This decrease may of course be derived from larger fluctuating quadrupole coupling energies in the e.d.l. as well as longer T_c values.

The distortion of the spherical ions as manifested in the quadrupole splitting in these nematic phases does follow quite closely the variation of the degree of orientation of the deuterium in the water of the phase (26, 31). The relationship between the two quantities is in principle a complex one. It is the purpose of this experimental study to use the quadrupole couplings as a tool in the investigation of the e.d.l. and the nematic phases, so that apart from the above clarifying discussion on those couplings no attempt will be made to quantify them in a theoretical manner.

The quadrupole couplings of the alkali metal ions can be reduced by taking into account the quadrupole moments on the respective nuclei, which are now more precisely known (38). In units of barns (10^{-24} cm^2) the values of Q are: Li-7 3×10^{-2}, Na-23 0.14 to 0.15, Cs-133 -3×10^{-3}, and D-2 2.73×10^{-3}. The D_2O is the immediate neighbor of the alkali metal ions and thus the degree of order associated with the local nematic axis at the ion is represented in the deuterium quadrupole coupling. The results section and previous studies (30) indicate that the quadrupole couplings of the alkali metal nuclei are approximately proportional to that of deuterium in the immediate water environment. A proper measure to compare e.f.g.'s in different alkali metal ions would be to reduce the measured quadrupole couplings from the nuclear quadrupole moments. A quantity defined as E_s indicating a value in Hz b^{-1} can be defined.

$$[4] \qquad E_s = \left[\frac{\nu_Q(i)}{Q^{(i)}}\right] \text{Hz b}^{-1}$$

where (i) refers to the alkali metal nucleus, $eQ^{(i)}$ is the nuclear quadrupole moment of the alkali metal nucleus, and $\nu_Q{}^{(i)}$ is the quadrupole coupling splitting observed in Hz.

In Table 1 the values of E_s are given for each alkali metal nucleus in typical nematic phases encountered. Middle of range values are selected in each case and the third column lists the nuclear quadrupole coupling constant for deuterium in the D_2O of the same phases. Multiplying the magnitude of the deuterium quadrupole coupling of type II phases by two to correct for perpendicular alignment of the nematic axis, it is evident that the middle of the range values do not differ a great deal from phase to phase. The degree of orientation of the water surrounding the alkali metal ions varies by less than $\pm 35\%$ from 800 Hz with respect to a corrected common parallel axis direction. The reduced quadrupole coupling E_s for the alkali metal nuclei represents a quantity proportional to the electric field gradient $\langle eq_{zz} \rangle$ and this increases by a factor more than 10^2 in going from lithium to cesium. This increase is understandable qualitatively in terms of the binding energy of the hydration sphere and its increasing tendency to distort easily from cubic symmetries in the uniaxial medium as the alkali metal ion becomes larger.

The e.d.l. has been treated by macroscopic theories and divided between the adsorbed or Stern counter ion layer and a more diffuse Gouy layer which extends into the aqueous division of the interface (39). In all cases the D_2O and monatomic ions in the n.m.r. experiment are observed in average environments, since exchange processes between different portions of the aqueous electrical double half layer are rapid compared to the inverse frequency differences of quadrupole coupling constants and chemical shift changes. The monatomic ions have in principle a strongly decreasing concentration gradient from the negative interface outward. In recent work we have shown to a good degree of

[3]More recent preliminary measurements by L. A. Wilson and L. W. Reeves indicate a $T_1 \sim 38$–40 ms in nematic media for Na-23. (Unpublished work.)

TABLE 1. Computation of induced electric field gradient E_s in Hz b^{-1} for alkali metal ions in lyotropic nematic phases

Phase		$Q^{(J)}$ (b)*	$\nu_Q{}^D$ (Hz)†	$\nu_Q{}^{(J)}$ (kHz)‡	E_s (Hz b^{-1})
LiDS	Type I	-3×10^{-2}	650	0.175	−5.83
NaDS	Type I	+0.145	1000	12.0	+82.76
	Type II		400	−6.0	−41.38 (82.8)§
CsDS	Type II	-3×10^{-3}	300	−1.3	+433.33 (−866.7)§

*Nuclear quadrupole moment of the nucleus measured.
†Nuclear quadrupole splitting for deuterium in the D_2O of typical phases.
‡Nuclear quadrupole splitting of the alkali metal nucleus (Li-7, Na-23, or Cs-133) in the same phases. Negative signs appropriate for perpendicular alignment of the type II phase.
§Figures in parentheses include a factor of two to correct for the direction of alignment.

approximation that the distribution of ions within the alkali metal series for mixed counter ion double layers is essentially independent of the ion (30). The quadrupole coupling ratios for phases of type I and II with varying contents of Li^+, Na^+, and Cs^+ change less than 8% in the whole nematic range. This is considerable evidence that the ion charges alone are the major determining effect in a distribution function of concentration from the surface outward.

1. T. J. FLAUTT and K. D. LAWSON. J. Am. Chem. Soc. **89**, 5489 (1967).
2. P. J. BLACK, K. D. LAWSON, and T. G. FLAUTT. J. Chem. Phys. **50**, 542 (1969); Mol. Cryst. Liq. Cryst. **7**, 201 (1969).
3. R. C. LONG, K. R. LONG, and J. H. GOLDSTEIN. Mol. Cryst. Liq. Cryst. **21**, 299 (1973).
4. R. C. LONG and J. H. GOLDSTEIN. Mol. Cryst. Liq. Cryst. **23**, 137 (1973).
5. L. W. REEVES, J. M. RIVEROS, R. A. SPRAGG, and J. R. VANIN. Mol. Phys. **25**, 9 (1973).
6. S. A. BARTON, M. A. RAZA, and L. W. REEVES. J. Magn. Reson. **9**, 45 (1973).
7. K. HAYAMIZU and O. YAMAMOTO. J. Magn. Reson. **2**, 377 (1970); **5**, 94 (1971).
8. R. C. LONG, S. L. BAUGHCUM, and T. H. GOLDSTEIN. J. Magn. Reson. **7**, 253 (1972).
9. R. C. LONG and J. H. GOLDSTEIN. J. Chem. Phys. **54**, 1563 (1971); J. Mol. Spectrosc. **40**, 632 (1971).
10. J. LINDON and B. P. DAILEY. Mol. Phys. **20**, 937 (1971).
11. J. MARTIN ANDERSON and A. C. F. LEE. J. Magn. Reson. **4**, 160 (1971).
12. R. C. LONG. J. Magn. Reson. **12**, 216 (1973).
13. G. J. DEN OTTER, W. HEIJSER, and C. MACLEAN. J. Magn. Reson. **13**, 11 (1974).
14. H. WENNERSTRÖM, N. O. PERSSON, and B. LINDMAN. J. Magn. Reson. **13**, 348 (1974).
15. C. L. KHETRAPAL, A. C. KUNWAR, and A. V. PATANKAR. J. Magn. Reson. **15**, 219 (1974).
16. S. MEIBOOM and L. C. SNYDER. Acc. Chem. Res. **4**, 81 (1971).
17. P. DEIHL and C. L. KHETRAPAL. NMR basic principles and progress. Vol. 1. Springer-Verlag, New York, Heidelberg, Berlin. 1969. p. 1.
18. E. D. BECKER and T. C. FARRAR. Pulse and Fourier transform NMR. Academic Press, New York. 1971.
19. L. W. REEVES, J. SANCHES DE CARA, M. SUZUKI, and A. S. TRACEY. Mol. Phys. **25**, 1481 (1973).
20. L. W. REEVES, A. S. TRACEY, and M. M. TRACEY. J. Am. Chem. Soc. **95**, 3799 (1973).
21. L. W. REEVES and A. S. TRACEY. J. Am. Chem. Soc. **96**, 365 (1974).
22. L. W. REEVES, M. SUZUKI, A. S. TRACEY, and J. A. VANIN. Inorg. Chem. **13**, 999 (1974).
23. F. FUJIWARA, L. W. REEVES, A. S. TRACEY, and L. A. WILSON. J. Am. Chem. Soc. **96**, 5249 (1974).
24. D. M. CHEN, L. W. REEVES, A. S. TRACEY, and M. M. TRACEY. J. Am. Chem. Soc. **96**, 5349 (1974).
25. F. FUJIWARA, L. W. REEVES, and A. S. TRACEY. J. Am. Chem. Soc. **96**, 5250 (1974).
26. D. M. CHEN, K. RADLEY, and L. W. REEVES. J. Am. Chem. Soc. **96**, 5251 (1974).
27. D. BAILEY, A. D. BUCKINGHAM, F. FUJIWARA, and L. W. REEVES, J. Magn. Reson. **18**, 344 (1975).
28. L. W. REEVES and A. S. TRACEY. J. Am. Chem. Soc. In press.
29. Y. LEE and L. W. REEVES. Can. J. Chem. **53**, 161 (1975).
30. K. RADLEY, L. W. REEVES, and A. S. TRACEY. J. Phys. Chem. In press.
31. M. H. COHEN and F. REIF. Solid State Phys. Suppl. **5**, 321 (1962).
32. M. EISENSTADT and H. L. FREIDMAN. J. Chem. Phys. **44**, 1407 (1966); **46**, 2182 (1967).
33. C. DEVERELL. Progress in nuclear magnetic resonance spectroscopy, Vol. 4. *Edited by* J. W. Emsley, J. Feeney, and L. M. Sutcliffe. Pergamon Press, Oxford. 1969. Chapt. 4.
34. T. L. JAMES and J. M. NOGGLE. J. Am. Chem. Soc. **91**, 3424 (1969).
35. G. LINDBLOM and B. LINDMAN. Mol. Cryst. Liq. Cryst. **22**, 45 (1973).
36. G. LINDBLOM, N. O. PERSSON, B. LINDMAN, and G. ARVIDSON. Ber. Bunsenges. Phys. Chem. **78**, 955 (1974).
37. F. W. COPE. Biophys. J. **10b**, 843 (1970).
38. Handbook of chemistry and physics. 53rd ed. C.R.C. Press, Cleveland, Ohio. 1972–1973. p. E57 and E58.
39. M. J. SPARNAAY. The electrical double layer. Pergamon Press, Oxford, New York, Toronto, Sydney, Braunsdreig. 1972.

Can. J. Chem. Downloaded from www.nrcresearchpress.com by 210.87.254.40 on 09/05/12
For personal use only.

Stéréochimie de l'addition homolytique de l'acide thioacétique à des dérivés méthylènes cyclohexaniques[1]

JEAN-CLAUDE RICHER ET CLAUDE LAMARRE[2]

Département de Chimie, Université de Montréal, B.P. 6210, Montréal, Québec, H3C 3V1

Reçu le 15 avril 1975

JEAN-CLAUDE RICHER et CLAUDE LAMARRE. Can. J. Chem. **53**, 3005 (1975).

On a examiné la stéréochimie de l'addition homolytique de l'acide thioacétique au *tert*-butyl-4 diméthyl-2,2 méthylène-1 cyclohexane, au triméthyl-3,3,5 méthylène-1 cyclohexane, au β-pinène et, pour fins de comparaison, au *tert*-butyl-4 méthylène-1 cyclohexane. Les résultats obtenus au cours de cette étude sont comparés à ceux obtenus lors de la réduction des cétones correspondantes par $LiAlH_4$.

JEAN-CLAUDE RICHER and CLAUDE LAMARRE. Can. J. Chem. **53**. 3005 (1975).

The stereochemistry of the homolytic addition of thioacetic acid to 4-*tert*-butyl-2,2-dimethyl-1-methylenecyclohexane, to 3,3,5-trimethyl-1-methylenecyclohexane, to β-pinene and, for comparison purposes, to 4-*tert*-butyl-1-methylenecyclohexane has been examined. The results obtained during this study are compared to those obtained from the reduction of the corresponding ketones by $LiAlH_4$.

[Journal translation]

Introduction

Dans le cadre de nos travaux sur la stéréochimie des réactions d'addition sur des cétones cycliques (1), sur des carbocations contenus dans des systèmes cycliques (2) et sur des doubles liaisons endo- et exocycliques (3, 4*a* et *b*, 5), nous avons été amenés à examiner la stéréochimie des réactions d'addition homolytique d'acide thioacétique aux dérivés méthylènes cyclohexaniques (**1***a*, **2***a*, **3***a*). Ce sont les résultats obtenus au cours

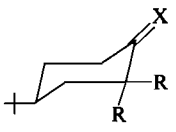

1

a R = CH_3; X = CH_2
b R = H; X = CH_2
c R = CH_3; X = O
d R = H; X = O

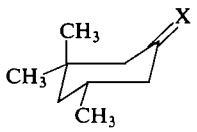

2

a X = CH_2
b X = O

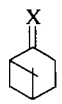

3

a X = CH_2
b X = O

de cette étude qui font l'objet de la présente communication. Pour fins de comparaison nous avons repris les travaux de Bordwell *et al.* (6) impliquant une telle addition sur le *tert*-butyl-4 méthylène-1 cyclohexane (**1***b*). Alors que le présent travail était terminé, Claise *et al.* (7) ont rapporté l'étude de l'addition homolytique de l'acide thioacétique au β-pinène (**3***a*) en utilisant le peroxyde comme initiateur. Ces auteurs ont analysé le mélange réactionnel par c.p.g.; la distribution des produits est dans un rapport de 3:1 mais la stéréochimie des thioacétates obtenus n'a pas été déterminée. Les résultats rapportés dans le présent travail confirment ces données et les complètent.

Partie expérimentale

Les instruments utilisés pour déterminer les propriétés physiques des produits obtenus au cours de cette étude ont été décrits dans une publication précédente (4*a*). Les poids moléculaires ont été déterminés au moyen d'un osmomètre à pression de vapeur de la compagnie Perkin-Elmer modèle 115 en utilisant le chloroforme comme solvant. La précision est de ±2%. Les spectres u.v. ont été mesurés dans l'éthanol 95% à l'aide d'un appareil Bausch and Lomb Spectronic 505. Les indices de rotation ont été déterminés à l'aide d'un spectropolarimètre photoélectrique Rudolph modèle 80.

Synthèse des méthylènes exocycliques ***1a, 1b et 2a***

Les méthylènes exocycliques sont préparés par l'action du méthylène de la triphénylphosphine sur la cétone correspondante selon la méthode de Wittig et Schöllkopf (8). Les propriétés physiques de chaque oléfine sont semblables à celles rapportées dans la littérature: **1***a* (3), **1***b* (9, 10) et **2***a* (4*b*, 10). Le β-pinène (**3***a*) est obtenu commercialement et purifié par distillation.

Synthèse des alcools primaires ***4a–11a***

Les alcools primaires **4***a*–**7***a* ainsi que **10***a* et **11***a* ont déjà été synthétisés par l'addition du diborane, préparé *in situ*, dans le diglyme à 0 °C, sur le méthylène correspon-

[1]Les résultats rapportés dans cette communication sont tirés en partie dans la thèse de doctorat présentée par Claude Lamarre, Université de Montréal, Montréal, Québec 1971.

[2]Adresse actuelle: Institut de Recherche de l'Hydro-Québec à Varennes.

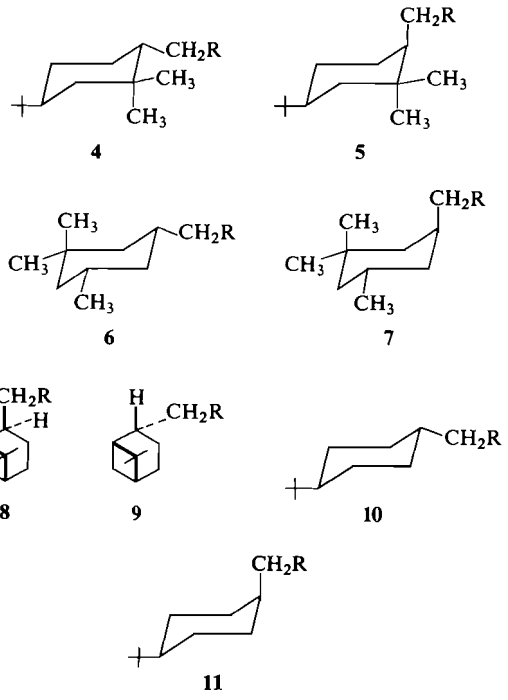

4 5 6 7 8 9 10 11

a R = OH; *b* R = OTs; *c* R = S—C(=O)—CH$_3$

dant selon la méthode de Brown et Zweifel (11). Les propriétés physiques des alcools primaires **4***a*–**7***a* ainsi que celles du **10***a* et **11***a* sont connues (4*b*, 12).

Le *cis*-myrtanol (**8***a*) est obtenu par hydroboration du β-pinène (**3***a*) dans le tétrahydrofuranne selon la technique de Brown et Zweifel (13). Le *trans*-myrtanol (**9***a*) est obtenu par une isomérisation du *cis*-myrtanylborane à 135–140 °C suivie par une hydrolyse alcaline et d'une oxydation par l'eau oxygénée à 30%. Les propriétés physiques des alcools primaires **8***a* et **9***a* ont déjà été décrites (14, 15).

Synthèse des tosylates **4***b*–**11***b*

De façon générale, 5 mmol d'alcool primaire et 6 mmol de chlorure de tosyle sont dissous dans 4 ml de pyridine anhydre et abandonnés 3 jours au réfrigérateur. Le mélange est versé sur une solution glacée d'acide chlorhydrique à 25% et extrait à l'éther. La phase éthérée est lavée par de l'eau jusqu'à neutralité, séchée sur Na_2SO_4 anhydre et évaporée. Le résidu est cristallisé jusqu'à un point de fusion constant. Les propriétés physiques des tosylates **4***b*–**9***b* sont consignées dans le tableau 1; celles des tosylates **10***b* et **11***b* ont déjà été rapportées dans la littérature (12).

Synthèse des thioacétates **4***c*–**11***c*

De façon générale, 3 mmol de tosylate et 10 mmol du sel de potassium de l'acide thioacétique sont dissous dans 9 ml d'éthanol absolu et chauffés à reflux pendant 6 h sous une atmosphère d'azote. Le sel de potassium de l'acide *para*-toluènesulfonique se dépose durant la réaction. Après refroidissement, le thioacétate est extrait par le pentane. Les propriétés physiques des thioacétates **4***c*–**9***c* sont consignées dans le tableau 2; celles des thioacétates **10***c* et **11***c* sont déjà connues.

Addition homolytique de l'acide thioacétique aux méthylènes exocycliques **1***a*, **1***b*, **2***a* *et* **3***a*

Dans une expérience type, l'acide thioacétique est ajouté au dérivé méthylène cyclohexanique dans un tube de quartz et la solution est refroidie sous l'eau du robinet avec agitation pendant 15 min avant irradiation. Une lampe u.v. Hanovia 450 W, sans filtre, est utilisée pour irradier la solution et sa durée est de 30 min. Après ce temps, les produits de la réaction sont isolés par l'éther; la phase éthérée est lavée par une solution sursaturée de bicarbonate de sodium, lavée à l'eau jusqu'à neutralité, séchée sur Na_2SO_4 anhydre et évaporée. Le résidu est analysé par c.p.g. ou par r.m.n. Les résultats des additions homolytiques sont résumés dans les tableaux 3, 4, 5 et 6. Les pourcentages relatifs des thioacétates consignés dans les tableaux 3, 4 et 5 ont été déterminés par c.p.g. Dans le but de vérifier si tous les pourcentages relatifs sont exacts, des mélanges connus d'épimères ont été préparés par pesée et analysés par c.p.g. Dans chaque cas, le pourcentage obtenu par c.p.g. s'est avéré exact. Les pourcentages relatifs des thioacétates **8***c* et **9***c* consignés dans le tableau 6 ont été déterminés par r.m.n. de la façon suivante: le glissement chimique des groupements *gem*-diméthyles en position 7 sont respectivement de 1.20 et 1.05 p.p.m. et 1.20 et 0.80 p.p.m. pour les épimères **8***c* et **9***c*. Chaque groupement *gem*-diméthyle possède donc un méthyle dont le glissement chimique (1.20) est identique pour les deux épimères. Le rapport des intégrations des glissements chimiques situés à 1.20 p.p.m. et à 1.05 p.p.m. permet d'effectuer un dosage du pourcentage du thioacetate-*cis* **8***c* (moyenne de 10 déterminations du rapport des intégrations). Un mélange étalon, préparé par pesée, des thioacétates **8***c* et **9***c*, a démontré que le dosage par r.m.n. permet une détermination précise de la composition du mélange réactionnel.

Stabilité des thioacétates

Chaque thioacétate pur (45 mg) a été irradié pendant 30 min en présence de 60 mg d'acide thioacétique. Les analyses par c.p.g. ou par r.m.n. indiquent que le thioacétate de départ est récupéré intact; aucune transformation n'est observée.

Résultats et discussions

La stéréochimie de l'addition homolytique de l'acide thioacétique aux alcènes **1***a*, **1***b*, **2***a* et **3***a* est résumée dans le tableau 7; l'attribution des configurations relatives des divers produits d'addition se fait par leur comparaison, en chromatographie en phase gazeuse ou par r.m.n., avec des produits authentiques obtenus à partir d'alcools primaires (**4***a*–**11***a*) dont la configuration a été démontrée précédemment. Les résultats rapportés dans ce tableau correspondent à un contrôle cinétique de la réaction puisque les produits n'évoluent pas lorsque remis dans les conditions de la réaction. Les résultats obtenus pour l'addition sur le *tert*-butyl-4 méthylène-1

TABLEAU 1. Propriétés physiques des tosylates 4*b*–9*b*

Produit	Point de fusion (°C)	Infrarouge (CCl_4)	$[\alpha]_D^{25}$	Résonance magnétique nucléaire*					Poids moléculaire	
				tert-Butyle	CH_3	p-C_6H_4—CH_3	CH_2OTs	Protons aromatiques A_2B_2	Calculé	Trouvé
4*b*	78–79 (MeOH)	1600–1182 1170		0.80	0.75 et 0.83	2.45	3.57 (q, J_{vic} 6.50 J_{gem} 9.37) 4.05 (q, J_{vic} 3.37 J_{gem} 9.37)	7.10 et 7.65 (J = 8.25)	352.5	345
5*b*	91 (MeOH)	1600–1185 1170		0.76	0.85 et 0.97	2.45	3.96 (q, J_{vic} 6.00 J_{gem} 9.81) 4.03 (q, J_{vic} 9.51 J_{gem} 9.81)	7.35 et 7.60 (J = 8.25)	352.5	360
6*b*	58 ($EtOH$–H_2O)	1600–1185 1175			0.87	2.45	3.66 (d, J = 6.00)	7.30 et 7.70 (J = 8.25)	310.4‡	304
7*b*	†	1600–1192 1175			0.80 ($CDCl_3$)	2.40	3.93 (multiplet)	7.32 et 7.74 (J = 7.5)	—	—
8*b*	74–75 ($EtOH$–H_2O)	1600–1190 1175	−11.5° (c = 5.1%, benzène)		0.82 et 1.11	2.45	3.85 (d, J = 7.50)	7.30 et 7.70 (J = 8.25)	308.4	297
9*b*	44–46 ($EtOH$–H_2O)	1600–1190 1175	−11.0° (c = 5.5%, benzène)		0.77 et 1.16	2.42	3.70 (d, J = 6.00)	7.27 et 7.70 (J = 8.25)	308.4	304

*A moins d'indications contraires, les spectres r.m.n. ont été déterminés dans le CCl_4. La partie AB du système ABX du CH_2OTs est obtenue par calcul du premier ordre. Les constantes de couplage des spins, J, sont exprimées en Hz. Le centre de symétrie est rapporté pour le signal d'un multiplet.
†Liquide visqueux qui n'a pu être cristallisé. Il se décompose sous l'influence de la chaleur.
‡En spectrométrie de masse seul 6*b*, présente un pic correspondant à l'ion moléculaire.

TABLEAU 2. Propriétés physiques des thioacétates 4*c*–9*c*

Produit	Point d'ébullition (°C/Torr)	n_D(°C)	Infrarouge	Ultraviolet		Chromatographie en phase gazeuse*	$[\alpha]_D^{25}$	Résonance magnétique nucléaire†			
				λ_{max}	ε			*tert*-Butyle	CH_3	$SCOCH_3$	CH_2—$SCOCH_3$
4*c*	104/1.0	1.4920(24)	1685–1125 1100–945	233	4041	Colonne A T_r 32 min		0.80 (C_6D_6)	0.71 1.00	1.96	2.43 (q, J_{vic} 6.00 J_{gem} 15.0) 3.35 (q, J_{vic} 2.00 J_{gem} 15.0)
5*c*	100/1.0	1.4934(24)	1685–1130 1115–945	233	4010	Colonne A T_r 29.5 min		0.82	0.98	2.30	2.74 (q, J_{vic} 10.69 J_{gem} 13.12) 3.18 (q, J_{vic} 4.69 J_{gem} 13.12)
6*c*	86/1.3	1.4838(27.5)	1690–1130 1100–950	233	3618	Colonne B T_r 6.5 min			0.90	2.33	2.76 (d, J = 6.00)
7*c*‡	90/1.2	1.4913(20)	1690–1135 1100–950	232	3760	Colonne B T_r 6.75 min			0.92	2.30	2.90 (multiplet)
8*c*	84/0.3	1.5102(27)	1685–1125 1095–945	233	3845		−25.7° (c = 4.7%, EtOH 95%)		1.05 1.20	2.29	2.96 (d, J = 7.5)
9*c*	84/0.3	1.5095(27)	1690–1135 1105–955	232	3879		−24.9° (c = 5%, EtOH 95%)		0.80 1.20	2.28	2.79 (multiplet)

*Les analyse par c.p.g. ont été effectuées à l'aide d'un appareil F et M (modèle 700) muni d'un détecteur à ionisation de flamme. Colonne A: SE-30 à 10% sur Chromport XXX 80–90 mesh; longueur 12 pieds; diamètre ¼ po; T, 200 °C; gaz porteur He 30 ml/min. Colonne B: UCW 98 à 10% sur Diatoport-S 80–100 mesh; longueur 6 pieds; diamètre ¼ de po; T, 190 °C et gaz porteur He à 10 ml/min.
†A moins d'indications contraires les spectres r.m.n. ont été déterminés dans le $CDCl_3$.
‡Lors de la spectrométrie de masse, le thioacétate 7*c* est le seul à ne pas présenté de pic correspondant à l'ion moléculaire.

TABLEAU 3. Addition homolytique de l'acide thioacétique au *tert*-butyl-4 diméthyl-2,2 méthylène-1 cyclohexane **1***a*

Essais*	Alcène:AcSH	*cis*-**5***c* (%)	*trans*-**4***c* (%)
1	1:0.52	8.6	91.4
2	1:1.00	8.7	91.3
3	1:1.09	8.8	91.2
4	1:1.20	9.2	90.8
5	1:1.27	9.8	90.2
6	1:1.44	9.2	90.8
7	1:1.53	9.3	90.7
8	1:1.70	9.2	90.8
9	1:2.10	10.0	90.0
10	1:3.07	9.0	91.0
11	1:4.00	9.4	90.6
12	1:5.00	8.9	91.1
13	1:4.00	10.0	90.0
		9.3	90.7 moyenne

*Les essais sont effectués à la température ambiante; sauf, le dernier essai qui a été effectué à une température inférieure à −40 °C (MeOH–CO_2).

TABLEAU 4. Addition homolytique de l'acide thioacétique au *tert*-butyl-4 méthylène-1 cyclohexane **1***b*

Essais*	Alcène:AcSH	*cis*-**11***c* (%)	*trans*-**10***c* (%)
1	1:0.90	9.9	90.1
2	1:1.00	10.2	89.8
3	1:1.20	10.1	89.9
4	1:1.42	9.7	90.3
5	1:1.56	9.9	90.1
6	1:1.76	9.3	90.7
7	1:2.00	9.7	90.3
8	1:3.10	10.0	90.0
9	1:3.92	10.8	89.2
10	1:5.00	10.6	89.6
11	1:2.00	10.3	89.7
		10.0	90.0 moyenne

*Les essais sont effectués à la température ambiante; sauf, le dernier essai qui a été effectué à une température inférieure à −40 °C (MeOH–CO_2).

cyclohexane (**1***b*) sont en parfait accord avec ceux rapportés par Bordwell *et al.* (6).

Les quantités relatives d'esters **8***c* et **9***c* formées lors de l'addition homolytique, induite photochimiquement, de l'acide thioacétique sur le β-pinène (**3***a*) sont en accord avec les valeurs obtenues par Claise *et al.* (7) pour l'addition homolytique de l'acide thioacétique au β-pinène (**3***a*) utilisant le peroxyde de benzoyle comme initiateur; dans le présent travail, nous pouvons attribuer les configurations relatives aux deux esters formés (**8***c* et **9***c*) et confirmer que, contrairement à ce qui est généralement observé (16–19), cette addition homolytique de l'acide thioacétique ne provoque pas une ouverture du β-pinène (**3***a*) pour conduire à des produits de structure *p*-menthénique du type **12**.

D'une manière générale, le mécanisme de l'addition homolytique d'un thiol sur une double liaison peut être représenté par la série d'équations du schéma 1 proposée par Kharash *et al.* (20).

L'addition du radical $CH_3COS\cdot$ (éq. 2) sur la double liaison s'effectue de façon inverse à celle prédite par la règle de Markonikoff et elle peut être reversible. L'abstraction d'un radical H· (éq. 3) de la molécule de thiol par le radical intermédiaire conduit au produit de la réaction; on considère généralement que cette étape détermine la vitesse de la réaction et qu'elle est irréversible (21).

Walling et Helmreich (22) et Huyser et ses collaborateurs (23, 24) ont démontré que si la réversibilité de la réaction est une étape importante, la distribution des produits de la réaction varie

TABLEAU 5. Addition homolytique de l'acide thioacétique au triméthyl-3,3,5 méthylène-1 cyclohexane **2***a*

Essais*	Alcène:AcSH	*cis*-**6***c* (%)	*trans*-**7***c* (%)
1	1:0.50	75.2	24.8
2	1:1.11	74.9	25.1
3	1:1.38	74.3	25.7
4	1:1.40	73.4	26.6
5	1:1.58	73.5	26.5
6	1:1.76	73.3	26.7
7	1:1.97	73.6	26.4
8	1:2.90	71.8	28.2
9	1:3.81	71.7	28.3
10	1:5.10	74.0	26.0
11	1:1.40	73.6	26.4
		73.6	26.4 moyenne

*Les essais sont effectués à la température ambiante; sauf, le dernier essai qui a été effectué à une température inférieure à −40 °C (MeOH–CO_2).

TABLEAU 6. Addition homolytique de l'acide thioacétique au β-pinène **3***a*

Essais*	Alcène:AcSH	*cis*-**8***c* (%)	*trans*-**9***c* (%)
1	1:1.50	73.2	26.8
2	1:2.00	74.9	25.1
3	1:2.40	75.0	25.0
4	1:3.00	74.5	25.5
5	1:4.00	74.6	25.4
6	1:2.00	75.0	25.0
		74.6	25.4 moyenne

*Les essais sont effectués à la température ambiante; sauf, le dernier essai qui a été effectué à une température inférieure à −40 °C (MeOH–CO_2).

TABLEAU 7. Pourcentage d'approche axiale

Réactif	Abstraction de H· par radicaux intermédiaires	Réactif	Réduction par $LiAlH_4$
1*a*	90.7	**1***c*	95 (ref. 31)
1*b*	90.0	**1***d*	91 (ref .32)
2*a*	73.6	**2***b*	45 (ref. 33)
3*a*	25.4	**3***b*	10*

*Résultat inédit.

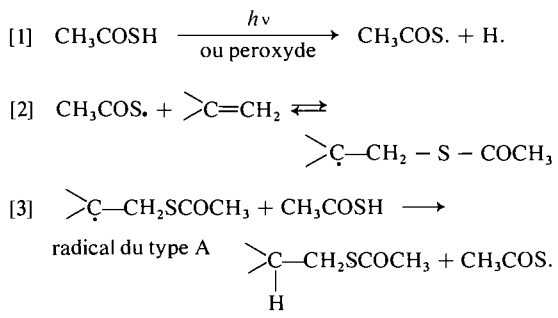

SCHÉMA I

avec la concentration du thiol. Les résultats consignés dans les tableaux 3, 4, 5 et 6 indiquent que la distribution des produits n'est pas influencée par la variation de la concentration de l'acide thioacétique. Cette observation suggère que la vitesse d'élimination du radical CH_3COS· des radicaux intermédiaires (type A) représentés par une hybridisation planaire (voir réf. 25–28), est plus lente que la vitesse de la réaction des radicaux du type A avec l'acide thioacétique qui cède un H· pour donner les produits de la réaction. La distribution des thioacétates isomères est donc déterminée par l'approche de la molécule de l'acide thioacétique qui cède H· aux radicaux du type A au cours de l'étape représentée par [3]. Si l'on admet que l'acide thioacétique se comporte, au cours de ce transfert de H·, comme un réactif peu volumineux, l'approche axiale ou équatoriale de la molécule d'acide thioacétique à chaque centre radicalaire pourrait donc être comparée à l'approche d'un ion hydrure à la cétone correspondante. La stéréochimie des additions homolytiques de l'acide thioacétique serait donc déterminée par des facteurs stériques (1) et torsionnels (29) similaires à ceux proposée pour expliquer la stéréochimie des réductions des cétones par les hydrures complexes. Le tableau 7 résume les résultats stéréochimiques observés au cours du présent travail et permet la comparaison avec les résultats stéréochimiques obtenus lors de la réduction des cétones **1***c*, **1***d*, **2***b* et **3***b* par $LiAlH_4$ dans l'éther. Le parrallélisme entre ces deux séries de résultats stéréochimiques ressort d'une manière évidente. La proportion plus grande d'attaque axiale lors de l'addition homolytique de l'acide thioacétique sur l'alcène **2***a* par opposition à la stéréochimie de la réduction de la cétone **2***b* par $LiAlH_4$ pourrait être rationalisée en faisant appel aux conclusions de Kawamura *et al.* (30) qui suggèrent que la conformation privilégiée du radical intermédiaire, lors de l'addition de thiols sur des oléfines, est celle où la liaison C_β—S est parallèle à l'orbitale p du centre radicalaire. Dans de tels cas, il peut y avoir participation de l'électron célibataire avec l'atome de soufre pour former un pont dans les intermédiaires (**13***a* et **13***b*) issus de l'alcène **2***a*. Le conformère A, impliquant une interaction 1:3 diaxiale avec le groupe méthyle en position 3, serait défavorisé par rapport au conformère B qui conduirait ainsi, par rapport à la réduction de la cétone **2***b*

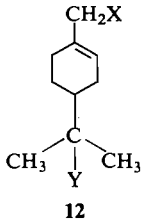

12

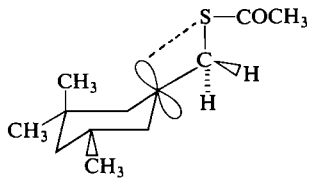

13*a*
Conformère A

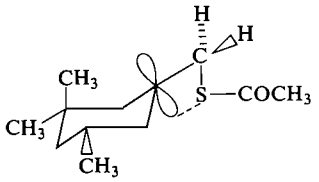

13*b*
Conformère B

par $LiAlH_4$, à une attaque en proportions plus élevées par la face axiale.

Les résultats présentés dans le travail actuel suggèrent donc que l'addition homolytique de l'acide thioacétique sur des doubles liaisons exocycliques se fait par l'intermédiaire de radicaux du type A, que cette addition n'est pas reversible et que la stéréochimie des produits formés par le transfert du H· de l'acide thioacétique, peut être expliquée en faisant appel à des facteurs stériques et torsionnels.

Les auteurs remercient vivement le Conseil national de recherches du Canada et le Ministère de l'Education de la Province de Québec pour l'aide financière apportée sous forme d'octroi de recherches (CNR A-1295) et de bourses de perfectionnement (C.L. 1966–1969).

1. J. C. Richer. J. Org. Chem. **30**, 324 (1965).
2. J. C. Richer et R. Bisson. Can. J. Chem. **47**, 2488 (1969).
3. J. C. Richer et C. Lamarre. Can. J. Chem. **47**, 2349 (1969).
4. (*a*) J. C. Richer et C. Lamarre. Can. J. Chem. **53**, 556 (1975); (*b*) **53**, 2033 (1975).
5. C. Freppel et J. C. Richer. Tetrahedron Lett. 2321 (1972).
6. F. G. Bordwell, P. S. Landis et G. S. Whitney. J. Org. Chem. **30**, 3764 (1965).
7. J. A. Claise, D. I. Davies et L. T. Parfitt. J. Chem. Soc. C, 258 (1970).
8. G. Wittig et U. Schöllkopf. Chem. Ber. **87**, 1318 (1954).
9. B. Cross et G. H. Whitman. J. Chem. Soc. 3892 (1960).
10. A. Sevin et J. M. Cense. Bull. Soc. Chim. Fr. 963 (1974).
11. H. C. Brown et G. Zweifel. J. Am. Chem. Soc. **83**, 1241 (1961).
12. Nobuo Mori. Bull. Soc. Chim. Jpn. **34**, 1567 (1961).
13. H. C. Brown et G. Zweifel. J. Am. Chem. Soc. **83**, 2554 (1961).
14. J. C. Braun et G. S. Fisher. Tetrahedron Lett. 9 (1960).
15. R. Dulou et J. Chrétien-Bessière. Bull. Soc. Chim. Fr. 1362 (1959).
16. M. Vilkas, G. Dupond et R. Dulou. Bull. Soc. Chim. Fr. 1056 (1970).
17. G. Dupond, R. Dulou et G. Clement. C. R. **236**, 2512, (1953).
18. B. Paskoff, M. Cazaux et R. Lalande. Bull. Soc. Chim. Fr. 2946 (1968).
19. R. Lalande et M. Cazaux. C. R. **258**, 4567 (1974).
20. M. S. Kharash, A. T. Read et F. R. Mayo. Chem. Ind. (London), 759 (1938).
21. C. Severtz, W. Andrews, W. Elsdon et K. Graham. J. Polym. Sci. **19**, 587 (1956).
22. C. Walling et W. Helmreich. J. Am. Chem. Soc. **81**, 1144 (1959).
23. E. S. Huyser et J. R. Jeffrey. Tetrahedron, **21**, 3083 (1965).
24. E. S. Huyser, H. Benson et H. J. Sennege. J. Org. Chem. **32**, 622 (1967).
25. R. J. Gritter et R. J. Albers. J. Org. Chem. **29**, 728 (1964).
26. M. Gruselle, J. Fossey et D. Lefort. Tetrahedron Lett. 2069 (1970).
27. S. Ogawa et R. W. Fessenden. J. Chem. Phys. **41**, 994 (1964).
28. M. C. R. Symons. Nature, **198**, 1196 (1963).
29. M. Chérest et H. Felkin. Tetrahedron Lett. 2205 (1968).
30. T. Kawamura, M. Ushio, T. Fujimoto et T. Yonezawa. J. Am. Chem. Soc. **93**, 908 (1971).
31. J. C. Richer et G. Perrault. Can. J. Chem. **43**, 18 (1965).
32. E. L. Eliel et Y. Senda. Tetrahedron, **26**, 2411 (1970).
33. H. Haubenstock et E. L. Eliel. J. Am. Chem. Soc. **84**, 2363 (1962).

Reduction of Some Alkylisoxazoles with Lithium Aluminum Hydride

A. L. KHURANA AND A. M. UNRAU

Department of Chemistry, Simon Fraser University, Burnaby, British Columbia V5A 1S6

Received February 17, 1975

A. L. KHURANA and A. M. UNRAU. Can. J. Chem. **53**, 3011 (1975).

Lithium aluminum hydride reduction of alkyl substituted isoxazoles gave a variety of products. The major constituent was identified (i.r., n.m.r., m.s.) as hydroxyethylaziridine. Specifically, reduction of 3,4,5-trimethylisoxazole gave as the major product 2,3-dimethyl-3-β-hydroxyethylaziridine. Two of the more prominent minor products were identified as 2,3-dimethyl-3-ethylaziridine and 4-amino-3-methyl-2-pentanol. The corresponding products were identified when 3,5-dimethylisoxazole was reduced with LAH.

A. L. KHURANA et A. M. UNRAU. Can. J. Chem. **53**, 3011 (1975).

La réduction, par $LiAlH_4$, d'isoxazoles substitués par des groupes alkyles conduit à une variété de produits. Le constituant principal, identifié par i.r., r.m.n. et s.m., est l'hydroxyéthylaziridine. D'une façon spécifique, la réduction de la triméthyl-3,4,5 isoxazole conduit, comme produit majeur, à la diméthyl-2,3 β-hydroxyéthyl-3 aziridine. On a identifié deux des produits mineurs les plus importants comme étant la diméthyl-2,3 éthyl-3 aziridine et l'amino-4 méthyl-3 pentanol-2. On a identifié les produits correspondants lorsque la diméthyl-3,5 isoxazole a été réduite par LAH.

[Traduit par le journal]

The reduction of isoxazolines with lithium aluminum hydride (LAH) has been described by Kotera *et al.* (1, 2). Whereas previous reports (3–6) described the formation of only the 1,3-amino alcohol, Kotera *et al.* (1) obtained significant yields (20–80%) of aziridine as well as the corresponding amino alcohol. The relative proportion of aziridine to amino alcohol was found to be solvent dependant (1). The stereochemistry of the substituted aziridines obtained was deduced from n.m.r. data for the proteo and corresponding deuterio compounds (1).

We have previously described the mechanism of 3,4,5-trimethylisoxazole (**1**) formation from nitroethane as well as that for 3,4-dimethylisoxazole (**2**) using ^{14}C- and ^{2}H-labelled precursors (7). Among alternate methods considered for the location of label in the isoxazoles thus formed, lithium aluminum hydride reduction appeared as a viable procedure for the conversion of the heterocyclic compounds to the corresponding alicyclic 1,3-amino alcohols.

Treatment of 3,4,5-trimethylisoxazole (**1**) and 3,5-dimethylisoxazole (**2**) with LAH in tetrahydrofuran for 48 h resulted in greater than 80% conversion of isoxazole to products. Analysis of the reaction mixtures by g.l.p.c. employing low inlet (120–130 °C) and detector (t.c.) (130–140 °C) temperatures together with column temperature programming (55–145 °C) gave in the case of trimethylisoxazole, a spectrum of more than eight peaks with one component constituting about 50% of the total peak area. The major as well as some of the more prominent minor constituents were collected in sufficient quantity to facilitate spectral analysis and consequent structure assignment. In some instances, the major component was collected and converted directly to the corresponding ester by trapping in a pyridine solution of *p*-nitrobenzoylchloride.

Using the general procedure indicated, 3,4,5-trimethylisoxazole gave as the major product 2,3-dimethyl-3-β-hydroxyethylaziridine (**3**). Two minor products were identified by spectroscopic means as 2,3-dimethyl-3-ethylaziridine (**4**) and 4-amino-3-methyl-2-pentanol (**5**). Similarly, 3,5-dimethylisoxazole (**2**) was converted to 2-methyl-3-β-hydroxyethylaziridine (**6**). Two minor products were identified as 2-methyl-3-ethylaziridine (**7**) and 4-amino-2-pentanol (**8**). It has been reported that 3,4-diphenylisoxazole will not undergo LAH reduction (1). This apparent difference in reactivity is probably due to inductive effects of the differing ring substituents.

The stereochemistry of the products resulting from the LAH reduction of the isoxazoles was deduced from a comparison of our n.m.r. data with those of Kotera *et al.* (1) and a consideration of the likely mechanisms involved. In the case of hydroxyaziridine formation, hydride attack apparently occurs at C_5 followed by $C_4 \rightarrow N$ cyclization and N–O bond fission. The

Can. J. Chem. Downloaded from www.nrcresearchpress.com by 210.87.254.6 on 09/05/12
For personal use only.

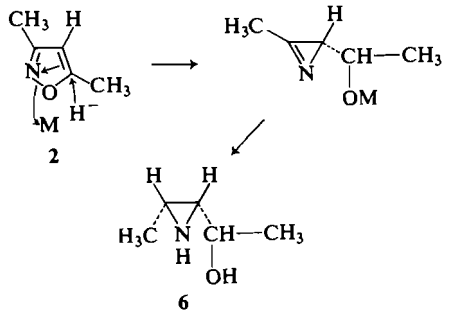

SCHEME 1

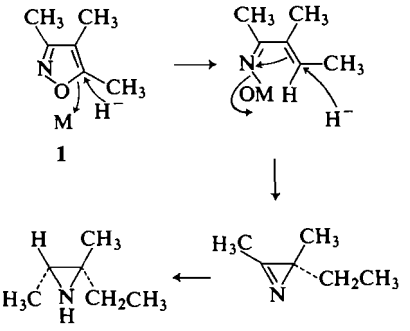

SCHEME 2

intermediate hydroxyazirine is then reduced by hydride attack on the least hindered side to the corresponding hydroxyaziridine (Scheme 1). The formation of the norhydroxyaziridine may be visualized to proceed by hydride attack at C_5 followed by C_5—O bond fission. Hydride attack at C_5 of the noncyclic oximino intermediate followed by $C_4 \rightarrow N$ cyclization and N—O bond fission would again generate the intermediate azirine. Preferential hydride attack would be expected on the less hindered side of the intermediate azirine although in this case, selectivity should be somewhat reduced (Scheme 2).

Experimental

Melting points were determined on a Fisher-Johns apparatus and are uncorrected. The n.m.r. spectra were obtained on a Varian A56-60 instrument with tetramethylsilane as internal standard (chemical shifts expressed on the δ scale and J values in Hz). Peak multiplicity is indicated as s, singlet; d, doublet; t, triplet; q, quartet; and m, multiplet. Infrared spectra were obtained using a Perkin-Elmer 427 and Beckman IR-12 grating instruments. Mass spectra were obtained from a Perkin-Elmer-Hitachi double focusing RMU-D6 instrument (electron ionization voltage 75 eV).

LAH Reduction Products of 2,3,5-Trimethylisoxazole (1). General Procedure

To a solution (200 ml) of lithium aluminum hydride (20 g) in THF was slowly added with stirring a solution (50 ml) of the isoxazole (5 g) in THF. The mixture, which became hot during addition of the solution of isoxazole, was cooled (ice water) for 1 h followed by refluxing for 40 h. Excess LAH was decomposed by addition of sodium sulfate and ethyl acetate. After filtration, solvent was removed by column distillation and the residual liquid distilled under reduced pressure yielding a pale yellow oil (2–3 g). The product was examined by vapor phase chromatography using two different columns: (*a*) A1 column, 1/4 in. × 5 ft, 15% SE550 on HMDS-Chromosorb W, He carrier gas, inlet and detector (t.c.) temperature 135 °C. column temperature programmed from 50 to 140 °C at 10 °C/min; (*b*) A1 column 1/4 in. × 5 ft, 20% Versamid on HMDS-Chromosorb W, otherwise conditions as in *a*. The latter column was utilized in preparative separation of components for spectral analysis. Analysis of the LAH reduction products from 3,4,5-trimethylisoxazole (**1**) on column *a* indicated six components, one of major (50%) proportion. Analysis on column *b* showed 11 components with retention indices (R_I, THF as reference) of 1.76 (2.1%); 2.50, 2.63 (4.4%); 3.03 (0.6%); 3.33, 3.50 (5.8%); 4.20 (7.7%, starting compound); 5.00 (14.5%, aziridine); 5.18 (5.8%); 5.83 (48.2%, hydroxyaziridine); and 6.36 (3.5%, amino alcohol). Repeated injection and collection of components gave sufficient quantities for characterization of four components (R_I 5.00, 4.20, 5.83, and 6.36).

2,3-Dimethyl-3-β-hydroxyethylaziridine (3) (R_I, 5.83)

The spectral data (i.r., n.m.r., m.s.) were consistent with the proposed structure; i.r. ν_{max} (liquid film), 3260–3300 (broad OH and NH), 1460, 1290, 1085, 1030, 970, 940, 890, and 840 cm^{-1}; n.m.r., C_2-*H*, 1.98, q, J = 5.5 (1H); C_2-C*H*$_3$, 1.05, d, J = 5.5 (3H); C_3-C*H*$_3$, 1.1, s (3H); C_4-*H*, 3.49, q, J = 7.2 (1H); C_5-*H*$_3$, 1.18, d, J = 7.2 (3H); N*H*–O*H*, broad region at 3.49 (2H), D_2O exchangeable; mass spectrum M^+ 115; $C_6H_{13}ON$ requires 115.

Anal. Calcd. for $C_6H_{13}ON$: C, 62.61; H, 11.30; N, 12.17. Found: C, 62.82; H, 11.25; N, 11.95.

N,O-Di-p-nitrobenzoyl-2,3-dimethyl-3-β-hydroxyethylaziridine (3a)

The v.p.c. effluent, R_I 5.83, was directly passed through a solution of *p*-nitrobenzoyl chloride in pyridine. The mixture was poured into a saturated aqueous solution of $NaHCO_3$ and the precipitated ester recrystallized from ethyl acetate, m.p. 163–165 °C. Infrared spectrum showed absence of OH and NH; n.m.r., OH and NH region absent, low-field aromatic protons, 7.6–7.7 (8H), except for slight shifts, spectrum otherwise similar to that of the parent compound; mass spectrum M^+ = 413; $C_{20}H_{19}O_7N_3$ requires 413.

Anal. Calcd. for $C_{20}H_{19}O_7N_3$: C, 58.11; H, 4.60; N, 10.17. Found: C, 58.06; H, 4.67; N, 10.05.

2,3-Dimethyl-3-ethylaziridine (4) (R_I 5.00)

The spectral characteristics were consistent with the proposed structure; i.r., ν_{max} (liquid film), 3260 cm^{-1} (relatively sharp NH), similar in other respects to the

Can. J. Chem. Downloaded from www.nrcresearchpress.com by 210.87.254.6 on 09/05/12
For personal use only.

spectrum of the hydroxy analog (**3**); n.m.r., C_2-*H*, 1.95, q, J = 5.5 (1H); C_2-CH_3, 0.95, d, J = 5.5 (3H); C_3-CH_3, 1.05, s (3H); C_4-H_2, 2.05, J = 7.1 (2H); C_5-H_3, 0.98, t, J = 7.1 (3H); mass spectrum M^+ = 99; $C_6H_{13}N$ requires 99.

Anal. Calcd. for $C_6H_{13}N$: C, 72.73; H, 13.13; N, 14.14. Found: C, 72.65; H, 13.19; N, 13.89.

The aziridine (**4**) was converted to the corresponding *N-p*-nitrobenzoyl ester (**4***a*) which after recrystallization (ether) had m.p. 108–110 °C; i.r. spectrum, NH absorption absent; n.m.r., the D_2O exchangeable NH proton absent, low-field aromatic protons, 7.6–7.7 (4H), rest of the spectrum was basically similar to that of the parent compound; mass spectrum M^+ = 248; $C_{13}H_{16}O_3N_2$ requires 248.

Anal. Calcd. for $C_6H_{15}ON$: C, 61.53; H, 12.82, N, 11.96. Found: C, 61.66; H, 12.65; N, 11.80.

LAH Reduction Products of 2,5-Dimethylisoxazole (2)

2-Methyl-3-β-hydroxyethylaziridine (6) (R_I 5.12)

The spectral characteristics were consistent with the proposed structure; i.r., broad band for NH and OH at 3260–3400 cm^{-1}; n.m.r., C_2-*H*, 2.05, m, J = 5.5, 6.5 (1H); C_2-CH_3, 1.02, d, J = 5.5 (3H); C_3-*H*, 1.72, q, (AXY), J = 6.5, 7.8 (1H); C_4-*H*, 3.44, m, J = 7.8, 7.2 (1H); C_5-H_3, 1.15, d, J = 7.2 (3H); D_2O exchangeable N*H* and O*H*, (2H); mass spectrum M^+ = 101; $C_5H_{11}ON$ requires 101.

Anal. Calcd. for $C_5H_{11}ON$: C, 59.40; H, 10.89; N, 13.86. Found: C, 59.22; H, 10.95; N, 13.70.

2-Methyl-3-ethylaziridine (7) (R_I 4.10)

Spectral characteristics were consistent with the proposed structure; i.r. (liquid film, NaCl plate) relatively sharp NH absorption 3280 cm^{-1}; n.m.r., C_2-*H*, 2.05, m, J = 5.5, 6.5 (1H); C_2-CH_3, 0.93, d, J = 5.5 (3H); C_3-*H*, 2.32, q, (AXY), J = 6.5, 7.3 (1H); C_3-ethyl-(CH_2), 2.15, m, J = 7.3, 7.1 (2H); C_3-ethyl-(CH_3), 0.96, t, J = 7.1 (3H); mass spectrum M^+ = 85; $C_5H_{11}N$ requires 85.

Anal. Calcd. for $C_5H_{11}N$: C, 70.58; H, 12.94; N, 16.47. Found: C, 70.72; H, 12.81, N, 16.66.

4-Amino-2-pentanol (8) (R_I 6.28)

The tentative identity of this compound was established from the following spectroscopic characteristics: i.r. broad absorption band 3260–3400 cm^{-1}; n.m.r., overlapping CH_3 doublets, 0.96–1.2 (6H); CH_2, 2.3, m, (2H); C-*H*, broad, overlapping at 3.3 (2H); mass spectrum M^+ = 103; $C_5H_{13}ON$ requires 103.

Financial support from the National Research Council of Canada is gratefully acknowledged.

1. K. KOTERA, Y. TAKANO, A. MATSUURA, and K. KITAHONOKI. Tetrahedron, **26**, 539 (1970).
2. K. KOTERA, Y. TAKANO, A. MATSUURA, and K. KITAHONOKI. Tetrahedron Lett. 5759 (1968).
3. G. W. PERHOLD and F. V. K. VON REICHE. J. Am. Chem. Soc. **79**, 465 (1957).
4. P. GRUNANGER and M. R. LANGELLA. Gazz. Chim. Ital. **91**, 1112 (1961).
5. N. BARBULESCU and A. QUILICO. Gazz. Chim. Ital. **91**, 326 (1961).
6. G. BIANCHI, A. COGOLI, and R. GANDOLFI. Gazz. Chim. Ital. **91**, 74 (1968).
7. R. A. LOCKHART, K. W. NG, P. E. NOTT, and A. M. UNRAU. Can. J. Chem. **47**, 3197 (1969).

Can. J. Chem. Downloaded from www.nrcresearchpress.com by 210.87.254.6 on 09/05/12
For personal use only.

Photoreaction of Nitroso Compounds in Solution. Part XXXI. Mechanisms of Intramolecular Acid Catalyzed Cleavage Reactions and a Hydride Initiated Rearrangement of *C*-Nitroso Alkanes[1]

K. Somosekharen Pillay, Shi C. Chen, Thomas Mojelsky, and Yuan L. Chow

Department of Chemistry, Simon Fraser University, Burnaby, British Columbia V5A 1S6

Received February 4, 1975

K. Somosekharen Pillay, Shi C. Chen, Thomas Mojelsky, and Yuan L. Chow. Can. J. Chem. **53**, 3014 (1975).

Two novel rearrangements of nitroso alkanes, one intramolecular acid catalyzed cleavage reaction and the other ring enlargement during hydride reduction, are described. Aminium radical initiated addition to norbornene under nitrogen gave *cis-exo-* and *trans*-2-nitroso-3-ammonium norbornanes in a good yield. Whereas the *trans* isomer underwent the usual nitroso group reactions, *i.e.*, tautomerization, dimerization, and HNO addition, the *cis-exo* isomer and its hydroxy analog cleaved extremely readily to give 1,3-bisformylcyclopentane derivatives. The stereoelectronic driving force in this cleavage is interpreted as the intramolecular proton transfer and the electron reorganization via a cyclic transition state. Metal hydride reduction of the *trans* isomer was accompanied by ejection of the neighboring amino group and an expansion of the ring to form an azabicyclic compound. A sequence involving an intramolecular displacement to form aziridine followed by the reductive cleavage is proposed.

K. Somosekharen Pillay, Shi C. Chen, Thomas Mojelsky et Yuan L. Chow. Can. J. Chem. **53**, 3014 (1975).

On décrit deux nouveaux réarrangements des nitroso alkanes: une réaction de coupure intramoléculaire catalysée par les acides et une autre impliquant une expansion de cycle au cours d'une réduction par les hydrures. L'addition au norbornène initiée par le radical amminium, se fait sous atmosphère d'azote et conduit, avec de bons rendements, aux *cis-exo-* et *trans*-nitroso-2 ammonium-3 norbornanes. Alors que le groupe nitroso de l'isomère *trans* réagit normalement, à savoir tautomérisation, dimérisation et addition de HNO, l'isomère *cis-exo* et son analogue hydroxylé se coupent extrêmement facilement pour conduire aux dérivés bisformyl-1,3 cyclopentanes. On suggère que la force stéréoélectronique aidant cette rupture est le transfert intramoléculaire d'un proton et la réorganisation électronique par l'intermédiaire d'un état de transition cyclique. La réduction de l'isomère *trans* par les hydrures complexes est accompagnée par une expulsion du groupe amino voisin et par une expansion de cycle conduisant à un composé azabicyclique. On propose un mécanisme impliquant un déplacement intramoléculaire conduisant à une aziridine qui serait ensuite coupée lors de la réduction.

[Traduit par le journal]

Introduction

Radical additions to norbornene are complicated by nonbonded interaction, steric strain, and torsional effects and their stereochemistry have been the subject of considerable studies (1–4). For relatively larger addends, the radical attack occurs without exception from the less hindered *exo* side (1); however, small addends, such as HBr, involve some initial *endo* attack (5, 6). The direction of the radical combination step (or chain transfer process) is controlled by two factors, namely those of nonbonded interaction from 5- and 6-hydrogens and torsional effects from the bridgehead 4-hydrogen to give 2-*exo*-3-*exo*(*cis-exo*) and 2-*exo*-3-*endo* (*trans*) orientations (1–4). Inspection of the literature shows that the distribution of this stereochemistry varies widely, ranging from a 100% *trans* product on the addition of *p*-tosyl chloride (7) to a 100% *cis-exo* product in the addition of ethyl α-bromoacetate (8). It is noteworthy that the additions of nitrosyl halides (9) and formate (10) to norbornene give the *cis* adducts in good yields and have been suggested to follow a four-centered addition mechanism. The further striking features of these additions are (*i*) that no skeletal rearrangement occurs despite the fact that these addends can undergo ionic reaction (9) and (*ii*) that the *trans* adducts are absent (9, 10). These reports intensified our interest in the stereochemical aspects of the study of nitrosamine

[1]For Part XXX, see ref. 23.

Can. J. Chem. Downloaded from www.nrcresearchpress.com by 210.87.254.5 on 09/05/12
For personal use only.

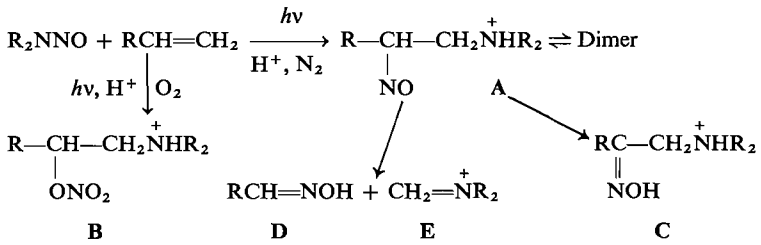

SCHEME 1

addition to norbornene that was then in progress.

Photoaddition of *N*-nitrosopiperidine (NNP) or *N*-nitrosodimethylamine (NND) in an acidic solution to an olefin (for example $RCH{=}CH_2$) gives a 1-nitroso-2-ammonium alkane, **A** (Scheme 1). It has been shown that the primary photoprocess is the dissociation of the nitrosamines to give the aminium and nitric oxide radicals and that the former initiates the addition to the olefin (11). In the presence of oxygen, the photoreaction is not quenched but nitric oxide is efficiently oxidized to the $\cdot NO_3$ radical; this leads to the clean formation of 1-nitrato-2-ammonium alkanes, **B** (12). The *C*-nitroso compound **A** is generally not stable under the experimental conditions and undergoes various competing secondary reactions; the common ones are tautomerization (**A** → **C**) and dimerization (13).

Our initial objective was to determine the stereochemical distribution of the nitrosamine photoaddition to norbornene in order to elucidate the nature of the radical pair generated in nitrosamine photolysis (12) and to compare the results with those obtained in the nitrosyl derivative additions (9, 10). While these aims were only partially fulfilled, we have gained some insight into the relatively obscure chemistry of *C*-nitroso compounds. These investigations also enable us to propose a mechanism for the novel cleavage reaction of 1-nitroso-2-ammonium alkanes (**A** → **D** + **E**).

Results

Photoaddition of NND to norbornene under nitrogen in the presence of hydrochloric acid exhibited the emergence of the u.v. absorption typical of a *C*-nitroso dimer at 290 nm similar to those observed in some previous cases (12–14). The photolysate, after the usual work up, gave an unusually large amount of the neutral fraction. The basic fraction contained the *anti* dimer of *endo*-2-nitroso-*exo*-3-dimethylaminobicyclo[2.2.1]norbornane (**1**) and *syn-exo*-3-dimethylaminobicyclo[2.2.1]norbornanone oxime (**2**) and its *anti* isomer (**3**).

The neutral fraction consisted of at least five compounds as shown by v.p.c. examinations and appeared to change composition on attempted chromatographic separations. With some difficulties as described in the Experimental, the examinations of the i.r. and n.m.r. spectra of semipure fractions obtained from chromatography allowed us to identify the following compounds, 1,3-bisdimethoxymethylcyclopentane (**5**), 1-formyl-3-dimethoxymethylcyclopentane (**6**) and its oxime (**7**), 1,3-bisformylcyclopentane (**8**) and its monooxime (**9**). These compounds[2] were identified by the typical spectral data of the functional groups. An aldoxime group exhibited i.r. peaks at 1630 and 900 ~ 1000 cm^{-1} and a n.m.r. doublet at *ca.* τ 2.5, a formyl group at 2700 and 1715 cm^{-1} and a weakly split doublet at *ca.* τ 0.0, and a dimethyl acetal group 1060 cm^{-1} and a doublet at *ca.* τ 6.0 and a singlet at *ca.* τ 6.5 in the ratio of 1:6. Both **6** and **7** showed a very strong mass peak at 75 corresponding to the $(CH_3O)_2CH^+$ species. All of these semipure fractions or the crude neutral fraction gave good yields of the bis-2,4-DNPH of **8** (15) on treatment with Brady's reagent.

A similar photolysis with three fold excess of NND was carried out until most of NND was consumed. The reaction gave 2-*endo*-(*N*-nitrosohydroxylamino)-3-*exo*-dimethylaminobicyclo-[2.2.1]heptane (**10**, 17%) in addition to oximes **2** and **3** and the 'neutral fraction.' In spite of some

[2]While these cyclopentane derivatives should have the *cis* configuration, acid catalyzed isomerization might have occurred changing the configuration of the isolated products. In some v.p.c. of such fractions, isomeric compounds were detected (see Experimental).

Can. J. Chem. Downloaded from www.nrcresearchpress.com by 210.87.254.5 on 09/05/12
For personal use only.

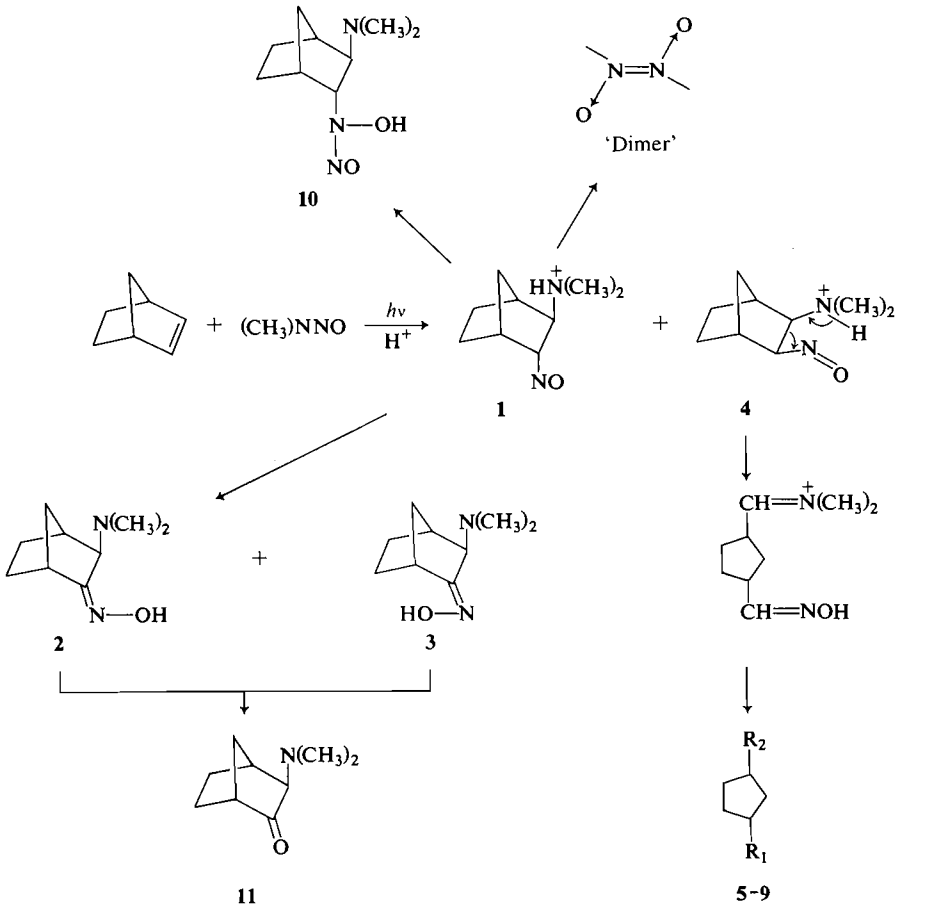

5 $R_1, R_2 = CH(OCH_3)_2$
6 $R_1 = CHO; R_2 = CH(OCH_3)_2$
7 $R_1 = CH(OCH_3)_2; R_2 = CH{=}NOH$
8 $R_1, R_2 = CHO$
9 $R_1 = CHO; R_2 = CH{=}NOH$

searching, the 2-*exo*-isomer corresponding to **10** could not be found in the photolysate.

The structure and stereochemistry of the basic products **2**, **3**, **10** and the dimer of **1** were determined primarily by spectral data particularly by the n.m.r. parameters that were elicited, in some cases, from decoupling experiments at 100 MHz. The common feature for all these compounds was the *exo* configuration of the dimethylamino group at the C-3. The 3-proton, which must have the *endo*-configuration, was shown to couple with the *anti*-7-proton through a W-plan and to have insignificant spin interaction with the 4-proton (16). The *exo* configuration of the 2-proton in **10** and the dimer of **1** was indicated by the coupling constants of $J_{1,2}$ and $J_{2,3}$ of *ca.* 4 Hz.

The *syn* and *anti* isomeric relation of oximes **2** and **3** was indicated by the following: (*i*) the dimer of *C*-nitroso compound **1** was converted quantitatively to **2** and **3** and a small amount of 3-*exo*-dimethylaminobicyclo[2.2.1]heptan-2-one (**11**); (*ii*) ketone **11** was oximated to give **2** and **3** in a ratio of 5:1; (*iii*) either isomeric oxime could be isomerized by a dilute acid to the other isomer; (*iv*) the mass spectra of oximes **2** and **3** were indistinguishable. Comparisons of the proton chemical shifts at the C-1 (τ 7.53 and 7.12) in oximes **2** and **3** and those at the C-3 for the same oximes (τ 6.58 and 6.67) indicated that **2** must have the *syn* and **3** the *anti* configuration because of the inverse chemical shift relation which had ample precedent from our publication (17). Further the chemical shift difference at

Can. J. Chem. Downloaded from www.nrcresearchpress.com by 210.87.254.5 on 09/05/12
For personal use only.

Can. J. Chem. Downloaded from www.nrcresearchpress.com by 210.87.254.5 on 09/05/12
For personal use only.

the C-1 (0.41 p.p.m.) of this oxime pair (**2** and **3**) compared favorably with that of the oxime pair derived from norcamphor (0.52 p.p.m.). However, both oximes exhibited a green color on dissolution in cupric sulfate solution; this was the only case so far in which the cupric ion test failed to distinguish the *syn* and *anti* oximes (17).

A crude hydrochloride salt of the dimer of **1** was readily precipitated on evaporation of a photolysate. The free base of the dimer liberated from this salt fraction was virtually pure and exhibited a clean n.m.r. spectrum. This implied that the crude product contained the single dimer, namely that of **1**, out of three possible diastereoisomeric dimers that could be generated from the adducts. The unique stereochemical purity of the 2-*endo*-3-*exo*- configuration was also observed in **10**. It was noteworthy that hydroxylamine **10** exhibited the 3-proton at the unusually low τ value of 6.00 for a proton geminal to an amine. This suggested that **10** might be a zwitterion in which the amine group was protonated by the weakly acidic *N*-nitroso-hydroxylamine group. The high solubility of **10** in water is suggested by the difficulty of its recovery from aqueous mother liquors.

The dimer of **1** possessed the expected i.r. absorption at 1210 cm^{-1} and the u.v. band at 295 nm. Whereas catalytic hydrogenation of the dimer in the presence of PtO_2 was unsuccessful, LAH reduction in ether gave a complex mixture

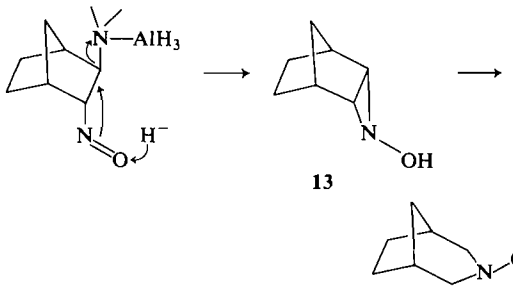

from which a small amount of *N*-hydroxy-3-azabicyclo[3.2.1]octane (**12**) was obtained. However, when a THF solution of the dimer was added to an ether solution of LAH, hydroxylamine **12** was obtained as the major product. The n.m.r. spectrum exhibited the signals at τ 6.82, 7.45, and 7.75 in 1:1:1 ratio. The lowest field signal was assigned to the equatorial protons at C-2 and C-4 which were coupled geminally to the axial protons (J = 10 Hz) and vicinally to the bridgehead proton (C-1 and C-5, τ 7.75). The doublet (J = 10 Hz) of the axial protons at τ 7.45 was only slightly coupled to the C-1 and C-4 bridgehead protons.

In the next phase of the study, the *anti* dimer of 2-*exo*-nitroso-3-*exo*-formyloxybicyclo[2.2.1]-heptane (**14**) was synthesized by addition of nitrosylformate to norbornene (10) and was purified by recrystallization without decomposition. Treatment of the dimer in 0.02% KOH solution at room temperature gave a mixture which showed the presence of aldehyde and aldoxime groups as judged by its n.m.r. and i.r. spectra. This mixture gave an essentially quantitative yield of bis-2,4-DNPH of **8** on treatment with Brady's reagent (15). In addition, the formate group of the dimer of **14** was hydrolyzed with a HCN—CN^- solution in methanol to give the sparingly soluble *anti* dimer of 2-*exo*-nitroso-3-*exo*-hydroxybicyclo[2.2.1]heptane (**15**). Prolonged heating of the dimer of **15**

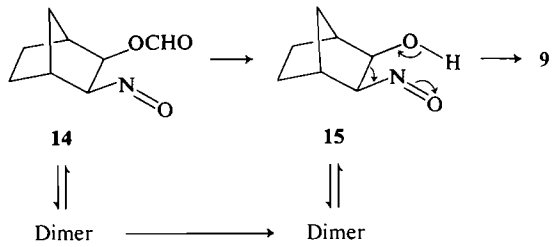

in methanol slowly gave an oily mixture of **8** and **9**. However, the dimer dissolved in trifluoroacetic acid from which the bis-2,4-DNPH of **8** was obtained quantitatively on addition of the hydrazine. The results demonstrated that, whatever the conditions were, the formation of hydroxy nitroso compound **15** was immediately followed by an extremely facile cleavage pathway to give **9**.

Discussion

That *trans* addition has occurred in the photoaddition is proven by isolation of the dimer of **1** and *N*-nitrosohydroxylamine **10**, both of which have the 2-*endo*-3-*exo*-configuration. The latter compound is stable and derived from the addition of HNO generated *in situ* to **1** (13). Under the photolysis conditions, **1** tautomerizes concurrently to oximes **2** and **3** as demonstrated. From the reported patterns of radical additions to norbornene (1–4), it should be expected that

Can. J. Chem. Downloaded from www.nrcresearchpress.com by 210.87.254.5 on 09/05/12
For personal use only.

not only *trans* **1** but *cis-exo*-**4** also can be formed though *a priori* the ratio is unknown. Significantly, the dimer and the *N*-nitrosohydroxylamine derived from *cis-exo* isomer **4** are not isolated indicating **4** may react very efficiently by other pathways. The observations that the yields of the 'basic fraction' are always low and that **1** exclusively tautomerizes to *syn* and *anti* oximes **2** and **3** strongly suggest that the neutral products **5**–**9** are derived from the second photoadducts, *cis-exo* isomer **4**. Precedents for such a cleavage reaction in acyclic 1-nitroso-2-ammonium alkanes have been reported (18, 19) and they have been assumed to occur by the intramolecular proton transfer and electron shifts as indicated in **4** (18). In the present case it is unusual that the cleavage reaction appears to occur exclusively over the tautomerization and dimerization pathways.

While it is desirable to prove that *cis*-*C*-nitroso compound **4** exclusively undergoes the cleavage reaction, the dimer of **4** is not available. Hydroxy nitroso compound **15** is an ideal model compound since it can be obtained from its stable *anti* dimer which is prepared from the hydrolysis of the dimer of formate **14**. The extreme facility of **15** to cleave cleanly to **9** is in sharp contrast to the stability of its dimer and formate **14** and to the exclusive tautomerization of **1**. Undoubtedly it is the ready proton transfer from the hydroxyl group to the nitroso group in the *cis-exo* configuration (see **15**) that makes the remarkable cleavage pathway possible. The propensity to undergo this pathway is also shown by the absence of competing tautomerization under neutral, acidic, or basic conditions.

Judging from the extent of dissociation, a protonated amino group is expected to donate a proton more readily than a hydroxyl group. Extension of the above argument leads us to conclude that the *cis*-*C*-nitroso compound **4** has been formed during photoaddition and undergoes the cleavage reaction so rapidly that neither the dimer nor the *N*-nitrosohydroxylamine corresponding to **10** can be isolated. Although there is no direct proof that **4** does not tautomerize to give oximes **2** and **3**, it can be safely assumed to be so in view of its facile cleavage reaction.

This cleavage reaction is a new type broadly classified as 'heterolytic fragmentation' (20). Generally, stereochemical requirements are critical for this type of reaction. The evidence presented above indicates that in this cleavage reaction a *cis*-coplanar configuration of the functional group, such as in **4** and **15**, is a precondition which allows the intramolecular proton transfer to occur through a cyclic transition state though the process may not necessarily be a concerted one as represented in **16**. The *trans* orientation, as in **1**, and in *trans*-2-dimethylamino-1-nitrosocyclohexane (12), does not meet the stereochemical requirements and fails to undergo the cleavage reaction but preferentially tautomerizes to give the corresponding oximes.

After the first suggestion of the cyclic cleavage mechanism had been made, Pritzkow and Thieme (19) stated that such a mechanism was not necessarily operating on the basis of an undocumented acidity effect on the cleavage of three acyclic 2-piperidinonitrosoalkanes. For the flexible acyclic nitrosoalkanes, a *cis*-coplanar orientation of the functional groups results in an eclipsing conformation of the substituents R^1, R^2, R^3, R^4, and the *N*-alkyl groups as shown in **16**. The cleavage of such compounds is expected to require an additional activation energy to overcome the steric requirements. This explains why cleavage of acyclic 1-ammonium-2-nitrosoalkanes scarcely competes successfully with tautomerization as observed previously (12, 18). The amino groups in these compounds ($pK_a \cong 10$) are completely protonated under the

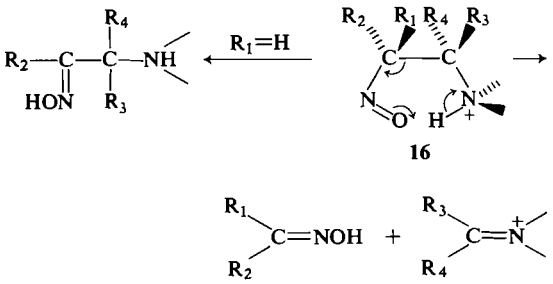

16

conditions of Pritzkow's experiments as well as our photoaddition. An increased acidity may strengthen the polarity of the solvent and increase solvation of the functional groups; this may conceivably reduce the rate of the cleavage pathway by disfavoring the required conformation. However such effects are expected to be small.

The ring enlargement observed in the LAH reduction of the dimer of **1** is a new rearrangement involving a nitroso group. It is assumed that aziridine derivative **13** serves as a probable intermediate as such derivatives are known in LAH reduction of nitroso and nitro compounds

Can. J. Chem. Downloaded from www.nrcresearchpress.com by 210.87.254.5 on 09/05/12
For personal use only.

(21) and oximes (22). While it is uncertain whether the dimer or monomer is involved in the reduction, it is likely that the *trans* configuration in **1** facilitates the displacement of the coordinated amino group.

Experimental

General

Microanalyses were performed by Dr. A. Bernhardt, Engelskirschen, West Germany, and Mr. M. K. Yang, Department of Biological Science, Simon Fraser University. The n.m.r. spectra were taken with a Varian A56/60 spectrometer using TMS as the internal standard in $CDCl_3$ solution or the solvent specified. The n.m.r. data are expressed in τ values and coupling patterns (s = singlet, d = doublet, t = triplet, m = multiplet, b = broad), coupling constants and the protons are given in the brackets. Unless specified, the i.r. spectra were measured in a Perkin-Elmer Model 457 in Nujol mulls or liquid film, the u.v. spectra with an Unicam SP-800 spectrophotometer, and the mass spectra with a Hitachi RMU-6E at 80 eV using a heated inlet. The melting points were determined in a Fischer-Johns hot stage and are uncorrected. Nitrosamines (Eastman Kodak Co.) and norbornene (Aldrich Chemical Co.) were redistilled and stored in a refrigerator.

Addition of NND to Norbornene

A solution of norbornene (7.2 g, 76 mmol), NND (5.2 g, 70 mmol), and concentrated hydrochloric acid (6 ml, 72 mmol) in methanol (120 ml) was externally cooled with an acetone–CO_2 bath and was irradiated with a 450-W Hanovia u.v. lamp for 1 h. The photolysate was evaporated (*ca.* 40 ml) and cooled to give the dimeric hydrochloride of *endo*-2-nitroso-*exo*-3-dimethylaminonorbornane dimer (**1**) (1.2 g, 8.2%) as crystals: m.p. 122–123 °C (dec.); i.r. 2650, 1425, 1310, 1230, and 1175 cm^{-1}; n.m.r. (D_2O) τ 4.50 (t, J = 4 Hz, 1H), 6.00 (m, 1H), and 7.60 (s, 6H). Attempts to recrystallize this compound resulted in decomposition. Upon treatment with saturated $NaHCO_3$ solution, the hydrochloride gave the free basic dimer of **1** which was recrystallized at room temperature by dissolving the crystals in one portion of CH_2Cl_2 and subsequently pouring in five portions of ether. Repetition of the recrystallization afforded fine needles: m.p. 112–113 °C; i.r. 2765, 1470, 1300, 1270, 1210, and 1150 cm^{-1}; n.m.r., τ 4.90 (t, J = 4 Hz, H_2), 7.10 (dd, J = 4 and 1 Hz, H_3), 7.15 (m, H_1), 7.55 (d, J = 4 Hz, H_4), 8.15 (d, J = 10.5 Hz, H_{7s}), 8.74 (md, J = 10.5 Hz, H_{7a}), 7.85 (s, 6H); *m/e* (%) 168(15), 151(18), 96(50), 84(100); u.v. (MeOH) 295 nm (ε 9 × 10^3).

Anal. Calcd. for $C_{18}H_{32}N_4O_2$: C, 64.25; H, 9.59; N, 16.65. Found: C, 64.47; H, 9.65; N, 16.83.

After removal of the hydrochloride of the dimer the filtrates were worked-up in the usual manner (18) to give a neutral fraction and a basic fraction.

The 'neutral' ether extract gave a clear liquid (3.9 g), which was a mixture containing more than five compounds as indicated by t.l.c. This mixture was roughly separated into two fractions by passing through a neutral alumina column (120 g). The first fraction eluted with 50% CH_2Cl_2 in benzene (500 ml) gave a colorless liquid (*ca.* 600 mg), which showed a single spot on silicic acid t.l.c. However, it exhibited two major peaks of ratio *ca.* 1:6 in v.p.c. This mixture contained exclusively 1,3-bis-dimethoxymethylcyclopentane (**5**) as indicated by the n.m.r. signals at τ 6.12 (d, J = 7 Hz, 2H), 6.87 (s, 12H), and 7.90–9.10 (m, 8H) and i.r. absorptions at 2940, 2830, 1450, 1060, and 930 cm^{-1}. This substance was hydrolyzed in 0.5 *N* methanolic hydrochloric acid solution (5 ml) at room temperature overnight. The resultant solution was diluted with water (5 ml) and extracted with ether. The ether was dried ($MgSO_4$) and evaporated to give a colorless liquid (280 mg), which was identified as 1,3-bisformylcyclopentane (**8**): i.r. 2708, 1720, 1105, and 1060 cm^{-1}; n.m.r. 0.44 (d, J = 2 Hz, 2H), 7.17 (t, unresolved, 2H), 7.70–9.20 (m, 6H); *m/e* (%) 126(8), 124(8), 98(30), 68(40), and 58(100). The 2,4-DNPH derivative was recrystallized from tetrahydrofuran–ethanol, m.p. 224–225 °C (dec.) (lit. (15) m.p. 225–226 °C). The second fraction (*ca.* 1.5 g) was rechromatographed on silicic acid repeatedly furnishing three pure compounds in small amounts. The least polar compound was found to be 1-formyl-3-dimethoxymethylcyclopentane (**6**): i.r. 2710, 1720, 1450, 1060 cm^{-1}; n.m.r. τ 0.1 (d, J = 2 Hz, 1H), 5.72 (d, J = 7 Hz, 1H), 6.55 (s, 6H); *m/e* (%) 172(7), 140(10), and 75(100). The more polar compound was identified as 1-formyl-3-dimethoxymethylcyclopentane oxime (**7**): i.r. 3350, 1640, 1050, and 930 cm^{-1}; n.m.r. τ 2.36 (d, J = 7 Hz, 1H), 5.67 (d, J = 7 Hz, 1H), 6.54 (s, 6H); *m/e* (%) 187(2), 141(6), 81(26), and 75(100).

Anal. Calcd. for $C_9H_{17}NO_3$: C, 57.73; H, 9.15; N, 7.48. Found: C, 57.59; H, 8.95; N, not analyzed.

The most polar eluate was found to be impure 1,3-diformylcyclopentane monoxime (**9**): i.r. 2700, 1715, 1630, and 950 cm^{-1}; n.m.r. τ 0.36 (s, 1H, D_2O exchangeable), 2.68 (d, J = 7 Hz, 1H), 5.85 (d, J = 7 Hz, 1H); *m/e* (%) 141.

The basic extract (2.1 g) was dissolved in ether and chromatographed on a basic alumina column (59 g). The first fraction eluted with ether (100 ml) gave a mixture (300 mg) which contained *ca.* 70% of the dimer of **1** and 30% of the decomposition products as indicated by n.m.r. and t.l.c. Subsequent eluates from ether and CH_2Cl_2 were mixtures, which were combined (1.4 g) and further purified by chromatography on a silicic acid column (70 g). Elution with 2% methanol in CH_2Cl_2 (699 ml) gave *anti-exo*-3-dimethylamino-2-norbornanone oxime (**3**) (250 mg, 2%). Sublimation afforded an analytically pure sample: m.p. 72–73 °C; i.r. 1665, 950, 935, and 855 cm^{-1}; n.m.r. τ 0.8 (s, OH), 6.67 (d, J = 2 Hz, H_3), 7.1 (m, H_1), 7.36 (m, H_4), and 7.57 (s, 6H); *m/e* (%) 168(4), 151(100), 123(8), 95(12), and 82(16).

Anal. Calcd. for $C_9H_{16}N_2O$: C, 64.24; H, 9.55; N, 16.65. Found: C, 64.13; H, 9.40; N, 16.54.

Further elution with 1% methanol in CH_2Cl_2 (100 ml) gave *syn-exo*-3-dimethylamino-2-norbornanone oxime (**2**) (1.1 g, 9%): n.m.r. τ 6.58 (bs, H_3), 7.48 (d, J = 1 Hz, H_4), 7.53 (d, J = 2 Hz, H_1), 8.05 (md, J = 10.5 Hz, H_{7s}), 8.71 (md, J = 10.5 Hz, H_{7a}), 7.7 (S, 6H); m.p. 142–143 °C; i.r. 1660, 1003, 964, 950, and 936 cm^{-1}; *m/e* (%) 168(4), 151(100), 123(8), 95(12), and 82(16).

Anal. Calcd. for $C_9H_{16}N_2O$: C, 64.24; H, 9.55; N, 16.65. Found: C, 64.47; H, 9.67; N, 16.70.

A solution of an excess of NND (3.71 g, 50 mmol) and norbornene (1.89 g, 20 mmol) in methanolic hydrochloric acid (0.43 *N*, 135 ml, 58 mmol) was irradiated using a 200-W Hanovia lamp with a uranium glass filter. The

Can. J. Chem. Downloaded from www.nrcresearchpress.com by 210.87.254.5 on 09/05/12
For personal use only.

photocell was cooled externally in an acetone–CO_2 bath. The u.v. absorption at 295 nm increased to a maximum at 3 h irradiation, and then slowly decreased. At 11 h, the 295 nm absorption still persisted. Therefore, an additional portion of the nitrosamine (742 mg, 10 mmol) and enough acid was added and the acetone–CO_2 bath replaced by an ice bath. The absorption at 295 nm disappeared after further irradiation for 8 h without the filter. The photolysate was made strongly basic ($pH \sim 10$) and extracted with CH_2Cl_2 (30 ml × 3) to give a viscous liquid, which contained mostly oximes **2** and **3** as indicated by t.l.c. and n.m.r. analysis. The aqueous solution was neutralized with 4 *N* hydrochloric acid and stirred overnight. The solution was readjusted to pH 7 next day and treated with charcoal, filtered, and the filtrate extracted with CH_2Cl_2 (40 ml × 3). The extract was worked-up in the usual manner to afford a brownish viscous liquid, which on standing overnight partially crystallized to give *endo*-2-*N*-nitrosohydroxylamino-*exo*-3-dimethylaminonorbornane (**10**) (483 mg, 16.6%). Sublimation gave a white solid which recrystallized from isopropanol to furnish an analytical sample: m.p. 212–213 °C (dec.); i.r. 3400, 1500, 1320, and 930 cm^{-1}; *m/e* (%) 182, 169(72), 151(7), 84(100), and 58(20); n.m.r. (D_2O) τ 5.45 (dd, J = 4 and 4.5 Hz, H_2), 6.00 (dd, J = 4.5 and 1.5 Hz, H_3), 7.10 (m, H_1), 7.24 (m, H_4), 7.15 (s, 6H).

Anal. Calcd. for $C_9H_{17}N_3O_2$: C, 54.25; H, 8.60; N, 21.09. Found: C, 54.13; H, 8.72; N, 20.90.

Acid Treatment of the Dimer of 1

A 2 *N* HCl solution (20 ml) of the dimer (780 mg, 2.3 mmol) in an Erlenmeyer flask was stirred at room temperature for 60 h. The resultant solution was extracted with ether (30 ml × 3). Nothing was obtained in the ether extract. The aqueous layer was then made basic with saturated Na_2CO_3 solution to give a crystalline precipitate, which was filtered and shown to be recovered dimer (70 mg, 9%). The aqueous filtrate was extracted with CH_2Cl_2 (30 ml × 3) to give a viscous substance (595 mg) which partially crystallized on standing overnight. The t.l.c. of this substance showed three spots, of which two in the lower R_f region corresponded to oximes **2** and **3**. This mixture was chromatographed on a silicic acid column (37 g). The first fraction eluted with $CHCl_3$ (500 ml) was shown to be *exo*-3-dimethylamino-2-norbornanone (290 mg, 45%) (**11**): i.r. 2815, 2770, 1742, and 1045 cm^{-1}; n.m.r. τ 7.25 (m, 2H), 7.55 (s, 6H), 7.80 (m, 2H). The 2,4-DNPH derivative was recrystallized from ethanol: m.p. 240 °C (dec.); *m/e* (%) 333(17), 316(9), 290(5), 151(100). The second fraction eluted with 5% methanol in $CHCl_3$ (550 ml) afforded the oxime **3** (90 mg, 13%). Subsequent elution with 10% methanol in $CHCl_3$ (600 ml) gave the isomeric oxime **2** (140 mg, 20%).

Oximation of Ketone 11

Ketone **11** (114 mg, 0.75 mmol) and a large excess of hydroxylamine hydrochloride (400 mg, 57.5 mmol) in ethanol (5 ml) and 2 *N* NaOH solution (10 ml) was refluxed for 4 h. The resultant solution was concentrated *in vacuo* to remove ethanol and made basic with Na_2CO_3 solution to give a crystalline precipitate. The crystals were removed by filtration to give the oxime **2** (70 mg). The filtrate was extracted and worked-up to give a solid (41 mg), which exhibited two spots of approximately the same size on a t.l.c. plate, corresponding to isomeric oximes **2** and **3**.

Isomerization of Oxime 2

A solution of **2** in 2 *N* HCl solution (5 ml) was stirred at room temperature for 10 h. A drop of the solution was pipetted out and made basic, spotted on a silica gel t.l.c. plate, and eluted with 10% methanol in $CHCl_3$. In addition to a large spot of starting material, two spots corresponding to **11** and **3** appeared in higher R_f regions. After stirring for 45 h, the acidic solution was worked-up to recover a liquid (41 mg). Thin-layer chromatographic analysis indicated that the mixture contained **2**, **3**, and **11** in much the same ratio as that from the hydrolysis of the dimer.

Isomerization of 3

In a procedure similar to that described above, oxime **3** (21 mg) was treated with 2 *N* hydrochloric acid (0.5 ml) and stirred at room temperature. Thin-layer chromatographic analysis was carried out at 7 h intervals. Estimation of the composition of the products was made by comparison of t.l.c. spot areas with those from the mixtures obtained from the acid hydrolysis of dimer. Within 7 h, nearly equal amounts of **2** and **3** were obtained and after 14 h the spot corresponding to **11** appeared and grew bigger as the reaction proceeded.

LAH Reduction of the Dimer of 1

A solution of the dimer (300 mg) in THF (20 ml) was added to a LAH (170 mg) suspension in boiling ether (20 ml) and the mixture was refluxed for 2 h. The mixture was decomposed with water (0.6 ml) and the precipitate was washed with ether. The combined organic layer was worked-up in the usual manner to give a liquid (258 mg) which was chromatographed on silicic acid. The oil recovered from 1% MeOH in CH_2Cl_2 eluent was sublimed at 60 °C to give hydroxylamine **12** (41 mg): m.p. 86–87 °C; i.r. 3180, 1450, 1212, 1205, and 877 cm^{-1}; n.m.r. τ 2.40 (OH), 6.82 (dd, J = 10 and 4 Hz, 2H), 7.45 (d, J = 10 Hz, 2H), and 7.75 (m, 2H); *m/e* (%) 127(4), 110(14), 81(15), 79(14), 67(29), 60(71), 44(74), and 41(100).

Preparation and Decomposition of the Dimer of 14

The *anti* dimer of nitroso formate **14** was prepared by the known method (10). The crude product was recrystallized from ethyl acetate to afford white crystals of the dimer: m.p. 161–162 °C; i.r. 1725, 1385, 1240, and 1165 cm^{-1}; n.m.r. τ 4.71 (md, J = 7 and 1 Hz, H_2), 5.18 (md, J = 7 and 0.5 Hz, H_3), 7.14 (m, H_1), 7.59 (m, H_4), 7.95 (md, J = 11 Hz, H_{7a}). Decoupling at 100 MHz showed that the 2- and 3-protons formed a AB quartet each of which was further coupled to the *anti*-7-proton slightly. Further, these two protons were not coupled with the bridgehead protons at τ 7.14 and 7.59.

A suspension of the dimer of **14** (400 mg) was stirred in methanol (100 ml) containing potassium hydroxide (0.05 g) overnight. The homogeneous reaction mixture was diluted with water and extracted with CH_2Cl_2 to afford a crude oil (308 mg); n.m.r. τ 0.5, 2.5 and 3.0; i.r. 3300, 1725, 1630, 780, 760, and 700 cm^{-1}. The bis-2,4-DNPH of 1,3-diformylcyclopentane **8** (340 mg) was prepared from the oil (150 mg) and was recrystallized from an ethyl acetate – ethanol mixture, m.p. 226–228 °C.

Mild Hydrolysis of the Dimer of 14

The dimer (200 mg) was stirred in a solution consisting of concentrated hydrochloric acid (0.19 ml), potassium cyanide (230 mg), and methanol for 18 h. The precipi-

tate (70 mg) was filtered and was recrystallized from ethyl acetate to give the *anti* dimer of **15**; m.p. 170–171 °C; i.r. 3390, 1235, 1085, 875, and 795 cm^{-1}; *m/e*(%) 282 (M^+), 264(1), 142(41), 124(14), 111(32), 93(55), 72(73), 67(100). The methanol solution was evaporated and was worked-up in the usual manner to afford an oil which gave the 2,4-DNPH of **8** on treatment with Brady's reagent.

The dimer of **15** (30 mg) dissolved in trifluoroacetic acid (1 ml) exhibited an n.m.r. spectrum very similar to that of **8** and **9** in the same solvent. This solution was stirred into an ethanol solution of 2,4-dinitrophenylhydrazine to give a yellow precipitate of the 2,4-DNPH of **8** (115 mg).

The dimer of **15** (70 mg) was refluxed in ethanol. The solid gradually dissolved. At the end of 24 h, the remaining solid (22 mg) was filtered and the ethanol solution was treated with Brady's reagent to afford the *bis*-2,4-DNPH of **8** (220 mg).

The authors are grateful to the National Research Council of Canada, for the financial support.

1. D. I. Davies and S. J. Cristol. Adv. Free-Radical Chem. **1**, 155 (1965).
2. P. von R. Schleyer. J. Am. Chem. Soc. **89**, 701 (1967).
3. F. R. Jensen, L. H. Gail, and J. E. Rodgers. J. Am. Chem. Soc. **90**, 5793 (1968).
4. C. L. Osborn, T. V. Van Auken, and D. J. Trecker. J. Am. Chem. Soc. **90**, 5806 (1968).
5. N. A. LeBel. J. Am. Chem. Soc. **82**, 623 (1960); N.A. LeBel, J. E. Huber, and L. H. Zalkow. J. Am. Chem. Soc. **84**, 2226 (1962); N. A. LeBel, P. D. Beirne, E. R. Karger, J. C. Powers, and P. M. Subramanian. J. Am. Chem. Soc. **85**, 3199 (1963).
6. H. Kwart and J. L. Nyce. J. Am. Chem. Soc. **86**, 2601 (1964).
7. S. J. Cristol and J. A. Reeder. J. Org. Chem. **26**, 2182 (1961).
8. K. Schrage. Tetrahedron, **23**, 3033 (1967).
9. J. Meinwald, Y. C. Meinwald, and T. N. Baker, III. J. Am. Chem. Soc. **86**, 4074 (1964).
10. H. C. Hamann and D. Swern. J. Am. Chem. Soc. **90**, 6481 (1968).
11. Y. L. Chow. Acc. Chem. Res. **6**, 354 (1973).
12. Y. L. Chow, J. N. S. Tam, C. J. Colon, and K. S. Pillay. Can. J. Chem. **51**, 2469 (1973).
13. Y. L. Chow, S. C. Chen, and D. W. L. Chang. Can. J. Chem. **48**, 157 (1970).
14. Y. L. Chow. Can. J. Chem. **43**, 2711 (1965).
15. R. H. Perry, Jr. J. Org. Chem. **24**, 829 (1959).
16. J. C. Davis, Jr. and T. V. Van Auken. J. Am. Chem. Soc. **87**, 3900 (1965); F. A. L. Anet. Can. J. Chem. **39**, 789 (1961).
17. Y. L. Chow and C. J. Colon. J. Org. Chem. **33**, 2598 (1968).
18. Y. L. Chow, C. J. Colon, and S. C. Chen. J. Org. Chem. **32**, 2109 (1967); Y. L. Chow J. Am. Chem. Soc. **87**, 4642 (1965).
19. W. Pritzkow and H. Thieme. J. Prakt. Chem. **36**, 180 (1967).
20. C. A. Grob and P. W. Schiess. Angew. Chem. **79**, 1 (1967).
21. S. J. Dominianni and P. V. Demarco. J. Org. Chem. **36**, 2534 (1971); G. E. Lee, W. R. Wragg, S. J. Corne, N. D. Edge, and H. W. Reading. Nature, **181**, 1717 (1958).
22. J. L. M. A. Schlatmann, J. G. Korstoot, and J. Schut. Tetrahedron, **26**, 949 (1970).
23. H. H. Quon and Y. L. Chow. Tetrahedron, In press.

Can. J. Chem. Downloaded from www.nrcresearchpress.com by 210.87.254.5 on 09/05/12
For personal use only.

Photoreaction of Nitroso Compounds in Solution. Part XXXII. Synthesis and Reaction of 2-Nitrato-3-Aminonorbornanes[1]

K. Somosekharen Pillay, Kaoru Hanaya,[2] and Yuan L. Chow
Department of Chemistry, Simon Fraser University, Burnaby, British Columbia V5A 1S6

Received February 4, 1975

K. Somosekharen Pillay, Kaoru Hanaya, and Yuan L. Chow. Can. J. Chem. **53**, 3022 (1975).

Oxidative photoaddition of nitrosamines to norbornene gave both *cis-exo-* and *trans*-2-nitrato-3-aminonorbornanes that were stable in their protonated form under photolysis conditions. The free bases underwent a novel cleavage reaction assisted by the lone pair of the amino group to give 1,3-bis(formyl)cyclopentane. In addition these nitrates also underwent solvolysis to give *cis-exo*-2-hydroxy-3-aminonorbornane. The mechanisms of these basic decompositions are discussed.

K. Somosekharen Pillay, Kaoru Hanaya et Yuan L. Chow. Can. J. Chem. **53**, 3022 (1975).

La photoaddition oxydative des nitrosamines au norbornène conduit aux *cis-exo-* et *trans*-nitrato-2 amino-3 norbornanes; dans les conditions de la photolyse, ces deux isomères sont stables sous leur forme protonée. Les bases libres subissent une nouvelle réaction de fission aidée par le doublet libre du groupe amino et fournissent le bis(formyl)1,3 cyclopentane. De plus ces nitrates subissent une solvolyse pour conduire aux *cis-exo*-hydroxy-2 amino-3 norbornane. On discute des mécanismes de ces décompositions en milieu basique.
[Traduit par le journal]

Can. J. Chem. Downloaded from www.nrcresearchpress.com by 210.87.254.6 on 09/05/12
For personal use only.

Previously we discovered that oxygen does not quench nitrosamine photoaddition to cyclohexene but instead diverts the reaction cleanly to form 1-nitrato-2-aminoalkanes (3). It is suggested that oxygen intercepts photolytically generated nitric oxide to form a nitrogen trioxide radical which is scavenged by a *C*-radical intermediate. This remarkably efficient process, which is termed an oxidative photoaddition, is by far the mildest and simplest method of synthesizing nitrate esters and has been investigated in our laboratory. While such addition to simple olefins generally proceeds readily to give the expected amino nitrates which can be reduced by LAH to amino alcohols, the addition to norbornene gives amino nitrates that exhibit an interesting new cleavage reaction. This novel cleavage pathway and an application of the oxidative photoaddition are described in this paper.

Results

Photolysis of a methanolic solution of NND, norbornene, and hydrochloric acid under oxygen exhibited clean zero-order decreases of the nitrosamine n–π^* band at 335 nm in contrast to the emergence of the 290 nm band due to the *anti* dimer of *C*-nitroso alkanes in the non-oxidative photoaddition (3). The colorless photolysate, however, turned to a dark brown solution rapidly on addition of base and gave a complex mixture with the usual work up.

In the initial phase of the experiments, it was hoped to isolate stable salts of the photoadduct by running the photoaddition of NNP to norbornene under oxygen in the presence of perchloric acid. This oxidative photoaddition gave a mixture of the perchlorate (19%) of *exo*-2-nitrato-*exo*-3-piperidinobicyclo[2.2.1]heptane (**2**) and *endo*-2-nitrato-*exo*-3-piperidinobicyclo[2.2.1]heptane (**1**) in a 1:1 ratio. Attempts to recrystallize this mixture resulted in darkening of the solutions. Basification of the above photolysate at 0 °C followed by a quick extraction and work up gave a crude mixture showing strong i.r. absorption at 1620, 1275, and 865 cm^{-1} for a nitrate and 1720 cm^{-1} for an aldehyde group. Immediate reduction with LAH gave a complex mixture of products from which a small amount of 3-*exo*-piperidino-*endo*-bicyclo[2.2.1]heptan-2-ol (**7**, $R_2 = -(CH_2)_5-$) was isolated as the hydrochloride salt. To avoid the decomposition

[1]For Part XXXI, see ref. 1. Part of the report was published in the preliminary communication (see ref. 2).
[2]On sabbatical leave from Yamagata University, Yamagata, Japan, 1973–1974.

Can. J. Chem. Downloaded from www.nrcresearchpress.com by 210.87.254.6 on 09/05/12
For personal use only.

on basification, hydrogenation of the acidic photolysate in the presence of various catalysts was examined but failed to give clean reduction. For the convenience of n.m.r. analysis the major work was carried out using NND as the addend.

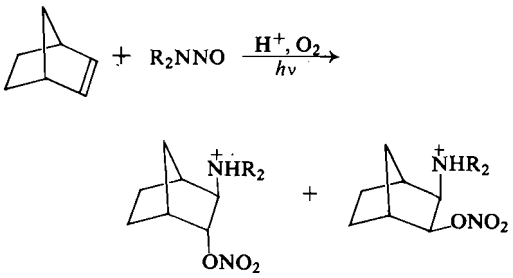

$R_2 = -(CH_2)_5-$ **1** **2**

$R = CH_3$ **3** **4**

A similar oxidative photoaddition of NND gave the hydrochloride (the acid used in the reaction) of *endo*-2-nitrato-*exo*-3-dimethylaminobicyclo[2.2.1]heptane (**3**). Efforts to isolate the corresponding *exo*-nitrato isomer **4** were not successful. However when the photolysate was worked-up immediately under mild conditions, the 'first basic fraction' contained *endo*-nitrate **5** ($R = CH_3$), *exo*-2-dimethylamino-*exo*-bicyclo-[2.2.1]heptan-2-ol (**8**, $R = CH_3$), and *exo*-nitrate **6** ($R = CH_3$) as shown by the n.m.r. singlets at τ 7.78, 7.69, and 7.52 in nearly equal intensities. The n.m.r. and i.r. spectra also showed the presence of 1,3-bisformylcyclopentane (**9**, τ 0.22 and 0.35, and 1720 and 2720 cm^{-1}) and a small amount of *exo*-3-dimethylaminobicyclo[2.2.1]hepta-2-one (**10**, 1740 cm^{-1}).

Immediate reduction of the 'basic fraction' with LAH gave a 'second basic fraction' which accounted for only 50% of the 'first basic fraction' and contained *endo*-alcohol **7** and *exo*-alcohol **8** in a ratio of 3:7 as indicated by the intensity ratio of the N–CH_3 singlets at τ 7.80 and 7.71. Extensive chromatography of this mixture afforded *exo*-alcohol **8**, but the *endo*-alcohol **7** was isolated only as a mixture with **8**.

Subsequently the 'first basic fraction' was allowed to decompose in an aqueous solution at p*H* 10 and the recovered oil was reduced with LAH as above. The basic portion from this reduction was only 5% of the theoretical yield and contained only *exo*-alcohol **8**; *endo*-alcohol **7** was not found from chromatography and n.m.r. examinations. The major product after decomposition and reduction was recovered as the 'neutral fraction' and was shown to be 1,3-bis-dihydroxymethylcyclopentane which was isolated as the *p*-nitrobenzoyl derivative. This indicated that dialdehyde **9** was obtained in the decomposed mixture which indeed afforded a good yield of the bis-2,4-DNPH on treatment with Brady's reagent.

Summarizing these observations, it could be concluded that both *trans*-nitrates (**1** and **3**) and *cis*-nitrates (**2** and **4**) were formed in the oxidative photoaddition and that the nitrates were decomposed by bases to give mainly *exo*-alcohol **8** and dialdehyde **9** in addition to a small amount of ketone **10**. To clarify the stereochemical requirements of the basic decomposition, the pure hydrochloride of *endo*-nitrate **3** was neutralized in an aqueous solution and the total recovered oil was allowed to decompose in neat liquid. Immediately after the recovery the oil exhibited strong i.r. and n.m.r. absorptions for *endo*-nitrate **5** (1625, 1285, and 870 cm^{-1}, and τ 5.03 and 7.78) and for dialdehyde **9** (1720 cm^{-1} and τ 0.37); a small amount of *exo*-alcohol **8** (τ 6.41 and 7.60) and ketone **10** (1745 cm^{-1}) were also noted. As the nitrate absorptions gradually diminished, those absorptions due to dialdehyde **9** and *exo*-alcohol **8** built up considerably; the ketone absorption at 1745 cm^{-1} however remained static and finally showed as a faint shoulder. Gas chromatographic – mass spectral analysis of this final product showed that it contained dialdehyde **9** (61%), *exo*-alcohol **8** (31%), and other products (8%).

The structures of the products were determined by combinations of spectroscopic data. In particular the stereochemistry of the bicyclic derivatives was decided by the n.m.r. coupling patterns of the 2- and 3-protons and was, in many cases, clarified by decoupling experiments. From considerations of steric hindrance (4–6), an aminium radical would be expected to attack from the *exo* face of norbornene. In the case of **3** and **8**, the *endo*-3-proton was shown to couple with the 7-*anti*-proton through the long range W-plan and was not (or very weakly) coupled to the 4-proton (7). Since the 2-protons were generally shifted more downfield, analysis of their coupling patterns was much easier than were those of the 3-proton. The *trans* configuration such as in **1**, **3**, and **7** exhibited the 2-*exo*-proton as a triplet ($J = 4$ Hz) indicating the expected spin interaction with 1- and 3-*endo*-

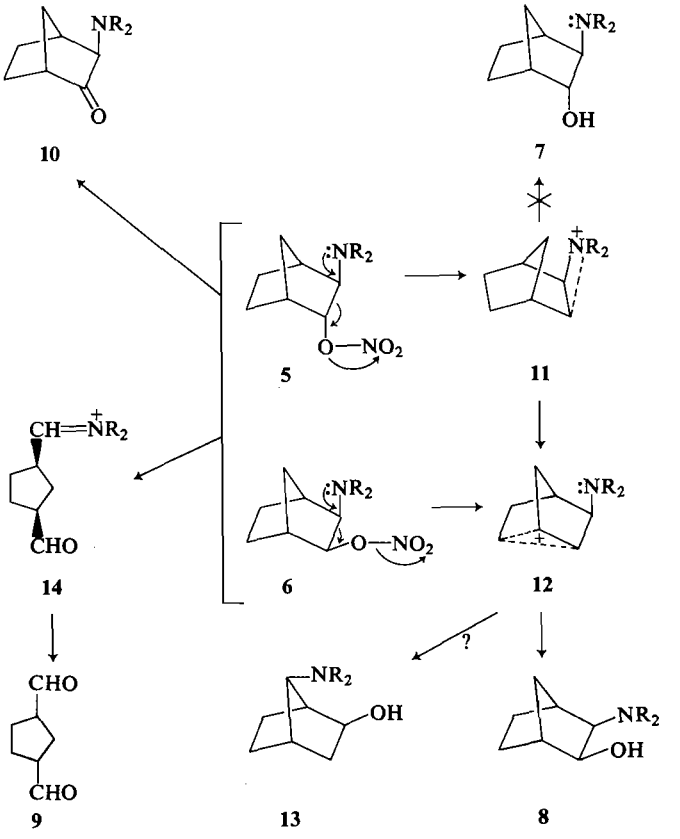

$R_2 = -(CH_2)_5-$ or $(CH_3)_2$

SCHEME I

protons. The *exo-cis* configuration in **2**, **4**, and **8** showed that the 2-*endo*-proton coupled with the 3-*endo*-proton ($J \cong 6$ Hz) and the 7-*anti*-proton ($J = 1$–2 Hz) but not with the 1-proton.

The mass spectral fragmentation also showed a common pattern typical for the bicyclic systems; for example both alcohols **7** ($R_2 = -(CH_2)_5-$) and **8** ($R = CH_3$) gave strong peaks for the following fragments.

	7 (%)	8 (%)
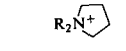	138(100)	98(54)
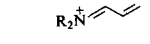	124(55)	84(44)
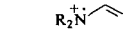	111(87)	71(48)
$R_2\overset{+}{N}=CH_2$	98(93)	58(100)

Discussion

From our observations it is concluded that the oxidative photoaddition of NND or NNP to norbornene clearly gave both *trans* and *cis* isomeric salts of the nitrate esters **1**–**4** and that, whereas these nitrate esters **5** and **6** are stable under acidic conditions in the protonated forms, they decompose rapidly under basic conditions. The formation of *exo*- and *endo*-nitrates is in agreement with the reported patterns of radical addition to norbornene (4–6); however, our efforts to determine the ratio of the isomers have been unsuccessful. Nitrate esters have been shown to undergo various basic decompositions (8, 9); among them are hydrolysis (10) or bimolecular nucleophilic substitution (11) by hydroxide to give alcohols and α-elimination of nitrite to give ketones (12). The presence of the neighboring amino group and the bicyclic

Can. J. Chem. Downloaded from www.nrcresearchpress.com by 210.87.254.6 on 09/05/12
For personal use only.

Can. J. Chem. Downloaded from www.nrcresearchpress.com by 210.87.254.6 on 09/05/12
For personal use only.

structure are expected to influence strongly the decomposition pathways.

The probable decomposition pathways of the nitrate isomers **5** and **6** are summarized in Scheme 1. While some pathways are established, *e.g.*, those of **5** → **8** and **5** → **9**, others are rationalized on the basis of the well-investigated solvolytic chemistry of norbornyl systems (13) and neighboring-group participation (14). Solvolysis of *endo*-nitrate **5**, which occurs only with the free base, is no doubt facilitated by participation of the neighboring amino group and the intermediate aziridinium ion **11** may be postulated. The aziridinium ion **11** may convert rapidly to the nonclassical carbonium ion **12** and eventually to **8** instead of directly reacting with hydroxide ion to give *endo*-alcohol **7** as this compound was not isolated from a prolonged basic decomposition. The ionization of *exo*-nitrate **6** to **12** is believed to be facile owing to the well established σ-bond participation in a norbornyl system (13). The cationic charge may be stabilized by the nitrogen lone pair but only to a slight extent, since subsequently hydroxide ion should be able to approach stereospecifically from the *exo* face at the 2-position to give **8**. The merit of the pathway **12** → **8** may be questioned in regard to the absence of the rearrangement products such as **13** which may have been formed as a very minor product but has escaped isolation. Alternatively, it may be suggested that the 3-amino group affects the position of entry of hydroxide ion.

endo-Alcohol **7** is derived solely from the immediate LAH reduction of *endo*-nitrate **5** before its exclusive solvolysis by the route of **5** → **11** → **12** → **8**. It is known that LAH reduction of nitrate esters gives alcohols without isomerization at the carbon center (3). In theory, *endo*-alcohol **7** can also be obtained from LAH reduction of ketone **10**. As demonstrated, the very low yield of ketone **10** during basic decomposition may be the reason why the *endo*-alcohol has not been obtained.

The α-elimination of HNO_2 from a nitrate ester is generally a minor side reaction under basic conditions (15). Such an elimination in nitrates **5** and **6** obviously requires the assistance of hydroxide ion since it occurs only in aqueous basic solution, but not in the neat liquid, to give a small yield of ketone **10**. Alternatively, nitrates **5** and **6** can eliminate nitrite ion by the electron shifts shown to give the immonium salt **14** (the precursor of **9**); this process obviously requires assistance from the lone pair of the amino group since it occurs only with the free bases. In view of the high yield of **9**, this cleavage pathway apparently requires a much lower activation energy than other decomposition processes mentioned.

The cleavage pathway of amino nitrates described above is also a novel reaction among heterolytic fragmentation reactions (16). In contrast to the facile cleavage of 2-ammoniumnitrosoalkanes (1), 2-amino nitrates are stable in their protonated forms but undergo cleavage reaction from the free bases. This strongly hints that the stereoelectronic requirements for 2-amino nitrate cleavage are an *anti*-periplanar arrangement of the functional groups (17, 18) as opposed to a *cis*-coplanar arrangement in 2-ammoniumnitrosoalkane cleavage (1). This has support from the result that *trans*-amino nitrate **5** readily cleaves to give dialdehyde **9**. While there is no positive proof, it is believed 2-amino nitrate **6** with the *cis-exo*-arrangement also cleaves in the same way in view of the copious yield of **9**, though this cleavage may not be as extensive as that of **5**.

The strained bicyclic structural features no doubt greatly facilitate the cleavage of amino nitrates **5** and **6**. It is also found now that in an aqueous basic solution, 1-piperidino-2-nitratocyclohexane (**15**) also undergoes the same type of cleavage to the extent of 10% in addition to the major pathways reported previously (3). Careful examination of the decomposition products shows the presence of 1,6-hexanedial (**16**) and 1-cyclopentenecarboxaldehyde (**17**) in addition to the products identified in our previous report. Oxidative photoaddition of NND to *trans*-2-octalin gave a mixture of various possible stereoisomeric amino nitrates. Decomposition of this mixture under basic conditions, however, gave no corresponding dialdehyde as shown by the i.r. and n.m.r. examinations. The major products[3] are cyclohexanol and cyclohexanone derivatives that resist attempts at purification.

[3]The details of the synthesis of *trans*-2-octalin, the photoaddition and isolation are described in the Ph.D. thesis of K. S. Pillay, Simon Fraser University, presented to the Faculty of Graduate Studies, September, 1975.

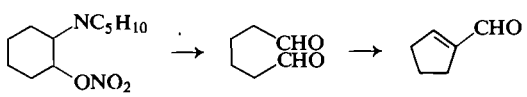

15 16 17

Experimental

The general experimental conditions are the same as those described in the preceding paper (1).

Oxidative Addition of NNP to Norbornene

A methanol solution (300 ml) of NNP (6.84 g, 0.06 mol), norbornene (3.76 g, 0.04 mol), and perchloric acid (60%, 10 ml) was irradiated (200-W Hanovia lamp) through a Nonex filter under an oxygen atmosphere at 0 °C for 4.5 h. At the end of the photolysis, the absorption at 345 nm had disappeared completely and a colorless solution was obtained. The solvent was distilled under reduced pressure at 10 °C. The residue was crystallized from ethyl alcohol – petroleum ether to give a white solid (2.61 g, 19%). This solid was recrystallized from methanol to give a mixture of the perchlorates of *endo*-2-nitrato-*exo*-3-piperidinobicyclo[2.2.1]heptane (**1**) and *exo*-2-nitrato-*exo*-3-piperidinobicyclo[2.2.1]heptane (**2**): m.p. 130–162 °C (decomposition with evolution of gas); i.r. 1645(s), 1275(s), 1110(s), 1080(s), 1065(s), and 840(s) cm^{-1}; n.m.r. (DMSO-d_6) τ 1.0 (D_2O exchangeable), 4.58 (t, J = 4 Hz), 4.73 (d, J = 7 Hz). The intensity ratio of the last two signals was 1:1.

After separating the salts, the filtrate was evaporated under vacuum. The residue was washed with ether and neutralized with saturated K_2CO_3 solution to p*H* 7.5. This was extracted with methylene chloride to give a reddish oil (4.81 g): i.r. 1740, 1720, 1620, 1275, and 865 cm^{-1}. This oil was not investigated further.

A methanol solution (300 ml) of NNP (5.47 g, 0.048 mol), norbornene (3.76 g, 0.04 mol), and concentrated hydrochloric acid (4.8 ml) was irradiated as described above. After the completion of the photolysis (2 h), the photolysate was immediately worked-up in the usual manner (3) to give a basic fraction.

A crude basic fraction (7 g) dissolved in anhydrous THF (50 ml) was added to a suspension of LAH (3.04 g, 0.08 mol) in THF (50 ml). The grey suspension was stirred for 24 h. The resultant reaction mixture was decomposed with water and filtered. The solid was washed thoroughly with THF. The filtrate and washings were combined and dried over anhydrous magnesium sulfate. The solvent was evaporated to give a thick colorless oil (6.25 g): i.r. 3360(s), 1105(m), 1050(s), and 1010(m) cm^{-1}; n.m.r. τ 5.93(m), 6.35 (m, partially D_2O exchangeable), 7.63(m), and 8.5(m).

The crude mixture was treated with ether containing a small amount of HCl to give a crystalline solid (500 mg, 5%). This solid was recrystallized from methanol to give the hydrochloride of *exo*-3-piperidino-*endo*-bicyclo[2.2.1]-heptan-2-ol (**7**): sublimes at 165 °C; i.r. 3345(s), 3295(s), 2660(s), 2550(m), 1090(s), 1080(s), and 1070(s) cm^{-1}; n.m.r. (D_2O) τ 5.76 (t, J = 4 Hz, H_2), 6.70 (m, 4H), 7.36 (d, J = 4 Hz, H_3), 7.38 (m, H_1), 7.58 (m, H_4), and 8.30 (m, 12H); *m/e*(%) 195(24), 194(6), 178(8), 138(88), 124(42), 111(73), 98(100), and 84(30). Decoupling experiments confirmed that the signal at τ 5.76 was coupled to the signals at τ 7.36 and 7.38 (J = 4 Hz).

M^+ Calcd. for $C_{12}H_{21}NO$: 195.1623. Found (high resolution mass spectrum): 195.1633.

Anal. Calcd. for $C_{12}H_{22}NOCl$: C, 62.19; H, 9.57; N, 6.05. Found: C, 61.91; H, 9.67; N, 6.16.

The hydrochloride (30 mg) was dissolved in saturated Na_2CO_3 solution and extracted with methylene chloride to give the free base of alcohol **7** (20 mg): m.p. 95–97 °C; i.r. 3200(sb), 2830(s), 1060(s), and 1045(s) cm^{-1}; *m/e*(%) (M^+, 41), 194(10), 178(11), 152(22), 138(100), 124(55), 111(87), 110(27), 98(93), and 84(33).

Oxidative Addition of NND to Norbornene

A solution of NND (3.552 g, 0.048 mol), norbornene (3.76 g, 0.04 mol), and concentrated hydrochloric acid (4.8 ml) in methanol (320 ml) was photolysed in a similar manner as described above. After irradiation (2 h), the methanol was removed at 10 °C. The residual solution was diluted with water and extracted with ether to give an oil (480 mg). This oil showed several spots on a t.l.c. plate and a complex n.m.r. spectrum containing no absorptions due to the N—CH_3 group. The aqueous solution was made basic with saturated Na_2CO_3 solution (p*H* 8.5) and extracted with methylene chloride to give a yellow oil (4.51 g): i.r. 2830(m), 2780(m), 2720(m), 1745(m), 1720(s), 1625(s), 1280(s), and 870(m) cm^{-1}; n.m.r. τ 0.22 (d, J = 2 Hz), 0.35 (d, J = 2 Hz), 7.52(s), 7.69(s), and 7.78(s). The g.c. analysis (20% SE-30, 150 °C) gave more than 10 peaks.

The crude basic fraction was reduced with LAH (3.42 g, 0.09 mol) in THF (100 ml) for 24 h. The reduced product was isolated in the usual manner to give an oil (3.5 g) which exhibited i.r. absorptions at 3400, 1050, and 1035 cm^{-1} due to a hydroxyl function. This oil was separated by extraction to the neutral (350 mg) and the basic fraction (1.76 g, 19%). The basic fraction contained *exo*-3-dimethylamino-*endo*-bicyclo[2.2.1]-heptan-2-ol (**7**) and *exo*-2-dimethylamino-*exo*-bicyclo[2.2.1]heptan-2-ol (**8**) in a ratio of 3:7 as shown by the intensities of the N—CH_3 singlets at τ 7.80 and 7.71: i.r. 3400(s), 2830(s), 2780(s), 1140(m), 1050(s), and 1035(s) cm^{-1}. The t.l.c. of this mixture showed two strong spots.

A portion of this mixture (500 mg) was chromatographed on neutral alumina (45 g). Elution with 0–10% chloroform in benzene gave an oil (92 mg) which showed one spot on a t.l.c. plate and a single peak on g.c. analysis (20% SE-30, 150 °C). This oil was distilled at 25 °C/0.03 Torr to give *exo*-alcohol **8** as a colorless oil: i.r. 3300(m), 2830(m), 2785(m), 1050(s), and 1035(s) cm^{-1}; n.m.r. τ 6.40 (dd, J = 1.3 and 6.3 Hz, H_2), 7.62 (s, 6H), 7.73 (m, H_3), 7.80 (m, 1H), 8.23–8.79 (m, 4H), 8.88 (m, 2H), 8.95 (m, H_{7s}), and 5.18 (D_2O, exchangeable); *m/e*(%) at 90 °C, 155(M^+, 15), 154(21), 126(38), 124(15), 98(54), 84(44), 71(48), and 58(100). Decoupling experiments showed that the signals at τ 6.40 and 7.73 were coupled mutually (J = 6.3 Hz) and also to the signal at τ 8.95 (J = 1.3 Hz).

Anal. Calcd. for $C_9H_{17}NO$: C, 69.63; H, 11.04; N, 9.02. Found: C, 69.30; H, 11.01; N, 9.20.

Subsequent fractions (392 mg) eluted with 20–50% chloroform in benzene gave mixtures of *endo*-alcohol **7** and *exo*-alcohol **8**: i.r. 3400(s), 1050(s), and 1035(s)

Can. J. Chem. Downloaded from www.nrcresearchpress.com by 210.87.254.6 on 09/05/12
For personal use only.

Can. J. Chem. Downloaded from www.nrcresearchpress.com by 210.87.254.6 on 09/05/12
For personal use only.

cm^{-1}; n.m.r. τ 7.73(s) and 7.79(s). The g.c. analysis (20% SE-30, 150 °C) showed two peaks at 5.3 and 5.7 min.

In a separate experiment, a solution of NND (3.55 g, 0.048 mol), norbornene (3.76 g, 0.04 mol) and concentrated hydrochloric acid (4.8 ml) in methanol (320 ml) was irradiated as described above. The methanol was distilled under reduced pressure, and the residue was washed with ether and made basic to p*H* 10 with saturated Na_2CO_3 solution. The aqueous solution was left for 24 h and extracted with methylene chloride to give a reddish oil (2.3 g) which was reduced with LAH (1.52 g, 0.04 mol) in ether for 24 h. The reduced product was isolated in the usual manner to give a basic fraction (310 mg, 5%): i.r. 3350(s), 1050(s), and 1030(s) cm^{-1}; n.m.r. τ 6.55 (dd, J = 1.5 and 6.5 Hz) and 7.67(s). This oil was purified on a neutral alumina column to give *exo*-alcohol **8**. No *endo*-alcohol **7** was detected in the n.m.r. spectrum.

The neutral fraction from LAH reduction was isolated in the usual manner. A part (233 mg) of this oil was heated with *p*-nitrobenzoyl chloride (555 mg, 0.003 mol) in pyridine (10 ml) on a steam bath for 1 h. The reaction mixture was poured into ice water. A solid was separated which was washed thoroughly with Na_2CO_3 solution followed by water. The solid was recrystallized from methanol to give the bis-*p*-nitrobenzoate of 1,3-bis(hydroxymethyl)cyclopentane (356 mg, 46%): m.p. 117–118 °C; i.r. 1720(s), 1605(m), 1530(s), 1520(s), 1345(s), 1285(s), 1275(s), 1120(s), 1100(s), and 720(s) cm^{-1}; n.m.r. τ 1.74 (m, 8H), 5.65 (m, 4H), 7.48 (m, 2H), and 7.25–9.11 (m, 6H); *m/e*(%) at 240 °C 428 (M^+, <0.1), 261(4), 150(63), 104(22), 94(100), and 79(56).

Exact Mass Calcd. for $C_7H_4NO_3$: 150.0191. Found (high resolution mass spectrum at *m/e* 150): 150.0228.

Exact Mass Calcd. for C_7H_{10}: 94.0782. Found (high resolution mass spectrum at *m/e* 94): 94.0762.

Anal. Calcd. for $C_{21}H_{26}N_2O_8$: C, 58.88; H, 4.71; N, 6.54; Found: C, 58.86; H, 4.64; N, 6.70.

A portion of the crude basic oil (300 mg) from the photolysate was treated with 2,4-dinitrophenylhydrazine solution in ethanol. The yellow solid (821 mg, 71%) was recrystallized from acetone to give the 2,4-DNPH of 1,3-bisformylcyclopentane **9**: m.p. 224–225 °C (lit. (19) m.p. 225–226 °C).

Decomposition of endo-2-Nitrato-exo-3-dimethylamino-bicyclo[2.2.1]heptane (5)

A methanol solution (320 ml) of NND (3.55 g, 0.048 mol), norbornene (3.76 g, 0.04 mol) and concentrated hydrochloric acid (4.8 ml) was photolyzed under an oxygen atmosphere as described earlier. The methanol was evaporated to a small volume at 10 °C. This solution was then diluted with ether and left at −5 °C for several months to give a small amount of a solid (600 mg) which was recrystallized from 2-propanol to give the hydrochloride of *endo*-2-nitrato-*exo*-3-dimethylaminobicyclo-[2.2.1]heptane (**3**) as a white crystalline compound: m.p. 161–162 °C (dec.); i.r. 3100(w), 1645(s), 1310(s), 1285(s), 1100(sb), and 850(s) cm^{-1}; n.m.r. (methanol-d_4) τ 4.65 (t, J = 4.0 Hz, H_2), 6.82 (dd, J = 4.0 and 2.5 Hz, H_3), 7.03 (S, 6H), 7.24 (m, 2H), and 7.95–8.74 (m, 6H). Decoupling experiments showed that the signals at τ 6.82 and 7.24 were not coupled to each other but coupled to the signals at τ 4.65 (J = 4.0 Hz) and at τ 7.95–8.74 (J = 2.5 Hz).

The HCl salt **3** (300 mg) dissolved in water was made basic with saturated Na_2CO_3 solution to p*H* 10 at 0 °C. The solution was immediately extracted with methylene chloride and the extract was washed with cold water and dried over anhydrous magnesium sulfate and was evaporated to give an oil (238 mg): i.r. 3350(w), 2830(s), 2780(s), 1745(w), 1720(m), 1625(s), 1285(s), 870(s), and 855(s) cm^{-1}; n.m.r. τ 0.37(m), 5.03 (t, J = 3.5 Hz), and 6.41 (d, J = 6.0 Hz) in the ratio 3.5:4.5:2. This oil was left at room temperature (color darkened) from which samples were withdrawn at different intervals (17, 24, and 44 h) and analyzed by i.r., n.m.r., and g.c.–m.s. (20% SE-30).

After 17 h, the sample showed strong i.r. absorptions at 1720 cm^{-1} for dialdehyde **9**, at 1625, 1285, 870, and 855 cm^{-1} for *endo*-nitrate **5**, and a weak peak at 3350 cm^{-1} for *exo*-alcohol **8**. The ratio of **9**:**5**:**8** was estimated to be 3.5:4:2 from the n.m.r. signals at τ 0.37, 5.02, and 6.35.

After 24 h, the intensity of absorption at 3350 cm^{-1} remained weak and that at 1720 cm^{-1} increased considerably compared to that of the nitrate peaks. The corresponding n.m.r. peak ratio was 5:4:4.

After 44 h, the absorption at 3350 cm^{-1} remained weak; the intensity at 1720 cm^{-1} increased enormously while that of the nitrate group decreased. The weak carbonyl absorption of **10** (1745 cm^{-1}) present at the zero-hour sample was now a barely visible shoulder merging with the 1720 cm^{-1} band. This sample was analyzed by g.c.–m.s. (100–200 °C, programmed at 10°/min) and was found to be a mixture of four compounds: 1.03 min (30.5%, *cis*-**9**), *m/e*(%) 126 (M^+, 47), 108(11), 98(26), 97(27), 80(23), 79(100), 70(48), 69(30), 67(88), and 57(52); 1.07 min (30.5%, *trans*-**9**) *m/e*(%) 126 (M^+, 6), 98(48), 80(22), 79(30), 67(43), and 57(100); 1.27 min (8.4%, unknown) *m/e*(%) 125(21), 85(10), and 84(100); 1.33 min (30.5%; **8**) *m/e*(%) 155 (M^+, 35), 140(26), 126(49), 98(100), 84(74), 71(81), 58(86), 45(27), 44(42), and 42(37).

The authors are grateful to the National Research Council of Canada for the financial support.

1. K. S. PILLAY, S. C. CHEN, T. MOJELSKY, and Y. L. CHOW. Can. J. Chem. This issue.
2. K. S. PILLAY, R. N. LOCKHART, T. TEZUKA, and Y. L. CHOW. J. Chem. Soc. Chem. Commun. 80 (1974).
3. Y. L. CHOW, J. N. S. TAM, C. J. COLÓN, and K. S. PILLAY. Can. J. Chem. **51**, 2469 (1973).
4. P. VON R. SCHLEYER. J. Am. Chem. Soc. **89**, 701 (1967).
5. F. R. JENSEN, L. H. GAIL, and J. E. RODGERS. J. Am. Chem. Soc. **90**, 5793 (1968).
6. C. L. OSBORN, T. V. VAN AUKEN, and D. J. TRECKER. J. Am. Chem. Soc. **90**, 5806 (1968).
7. J. C. DAVIS, JR. and T. V. VAN AUKEN. J. Am. Chem. Soc. **87**, 3900 (1965); F.A.L. ANET. Can. J. Chem. **39**, 789 (1961).
8. R. BOSCHAN, R. T. MERROW, and R. W. VAN DOLAH. Chem. Rev. **55**, 485 (1955).
9. N. W. CANNON, Ph.D. Thesis, Purdue University, Lafayette, Illinois, 1967.

10. R. SHRINER and E. PARKER. J. Am. Chem. Soc. **55**, 766 (1933).
11. F. HODOSAN, I. JUDE, N. SERBAN, and A. BOLOGH. Chem. Ber., **95**, 1094 (1962).
12. E. KAUFMAN, H. COOK, and S. DAVIS. J. Am. Chem. Soc. **74**, 4997 (1952).
13. J. A. BERSON. *In* Molecular rearrangements. *Edited by* P. de Mayo. Interscience Publishers, New York. 1963. p. 112.
14. B. CAPON. Q. Rev. **18**, 45 (1964).
15. J. W. BAKER and D. M. EASTY. J. Chem. Soc. 1193 (1952); 1208 (1952). J. W. BAKER and T. G. HEGGS, J. Chem. Soc. 616 (1955).
16. C. A. GROB and P. W. SCHIESS. Angew. Chem. **79**, 1 (1967).
17. C. A. GROB, H. R. KIEFER, H. J. LUTZ, and H. WILKENS. Helv. Chim. Acta, **50**, 416 (1967).
18. P. S. WHARTON and G. A. HIEGEL. J. Org. Chem. **30**, 3254 (1965).
19. R. H. PERRY, JR. J. Org. Chem. **24**, 829 (1959).

Can. J. Chem. Downloaded from www.nrcresearchpress.com by 210.87.254.6 on 09/05/12
For personal use only.

The Mechanism of Hydrolysis of Imidate Salts. The Importance of Stereoelectronic Control and p*H* of the Reaction Medium on the Cleavage of Tetrahedral Intermediates

PIERRE DESLONGCHAMPS AND ROLAND J. TAILLEFER

Laboratoire de synthèse organique, Université de Sherbrooke, Sherbrooke, Québec J1K 2R1

Received April 22, 1975

PIERRE DESLONGCHAMPS and ROLAND J. TAILLEFER. Can. J. Chem. **53**, 3029 (1975).

Hydrolysis of *anti* imidate salts give the ester amine products exclusively over the entire range of p*H*. Hydrolysis of *syn* imidate salts in acidic and neutral conditions give the ester amine products only; in basic conditions, mixtures of ester amine and amide alcohol products are observed. These results are explained by the application of the new theory of stereoelectronic control on the various ionic forms T^+, $T^\pm$, and T^- of the tetrahedral intermediate. For *syn* imidate salts, conformational changes of the tetrahedral intermediate must occur in order to have cleavage with stereoelectronic control.

PIERRE DESLONGCHAMPS et ROLAND J. TAILLEFER. Can. J. Chem. **53**, 3029 (1975).

L'hydrolyse des sels imidates *anti* conduit toujours aux produits ester amine quelque soit le p*H* du milieu réactionnel. En milieu acide ou légèrement basique, les sels imidates *syn* donnent uniquement les produits ester amine. En milieu basique, ils donnent des mélanges des produits ester amine et amide alcool. Ces résultats sont expliqués par la nouvelle théorie de contrôle stéréoélectronique au niveau de l'intermédiaire tétrahédrique et par les diverses formes ioniques T^+, $T^\pm$ et T^- que peut prendre cet intermédiaire. De plus, dans le cas des imidates *syn*, il faut aussi postuler des changements conformationnels de l'intermédiaire tétrahédrique pour qu'il puisse se briser avec contrôle stéréoélectronique.

We have described recently a new theory of stereoelectronic control for the cleavage of tetrahedral intermediates which are formed during the hydrolysis of esters (1), and amides (2–4). In this new theory, the precise conformation of the tetrahedral intermediate (hemiorthoester or hemiorthoamide) plays a major role in determining the products formed. It is postulated that the precise conformation of the tetrahedral intermediate is transmitted into the products of the reaction and that the specific decomposition of such an intermediate is controlled by the orientation of the lone pair orbitals of the heteroatoms. Stereoelectronic cleavage of a tetrahedral intermediate is defined in the following way: specific cleavage of a carbon–oxygen or a carbon–nitrogen bond which occurs when two heteroatoms (oxygen or nitrogen) of the tetrahedral intermediate each have an orbital oriented antiperiplanar to the departing *O*-alkyl or *N*-alkyl leaving group.[1]

We have reported a study of the basic hydrolysis of several imidate salts having either a *syn* or an *anti* conformation (2, 3). The stereoelectronic theory predicts that an imidate salt having an *anti* conformation such as **1***A* (Scheme 1) will react with hydroxide ion to give the tetrahedral conformer **2***A*. Conformer **2***A* has a lone pair orbital on each oxygen properly oriented so that it can be cleaved with stereoelectronic control to yield the ester amine products. The theory also implies that when a tetrahedral intermediate can break down in a stereoelectronically controlled fashion, the energy barrier for its cleavage is much lower than that for rotation to give other conformers. So, there is no need to consider conformers other than **2***A* with an *anti* imidate salt. Such salts should therefore yield the ester amine products exclusively. We have obtained experimental results which support this prediction completely.

The theory also predicts that an imidate salt having a *syn* conformation such as **1***B* will react with hydroxide ion to give the tetrahedral conformer **2***B*. Conformer **2***B* does not have its orbitals properly aligned to allow a breakdown via an orbital-assisted mechanism. We have therefore postulated that the barriers of rotation of the C—O and the C—N bonds will be lower than the barrier for the cleavage of **2***B*. Thus, **2***B* will undergo conformational changes

[1]Theoretical calculations have been carried out and support this theory (5).

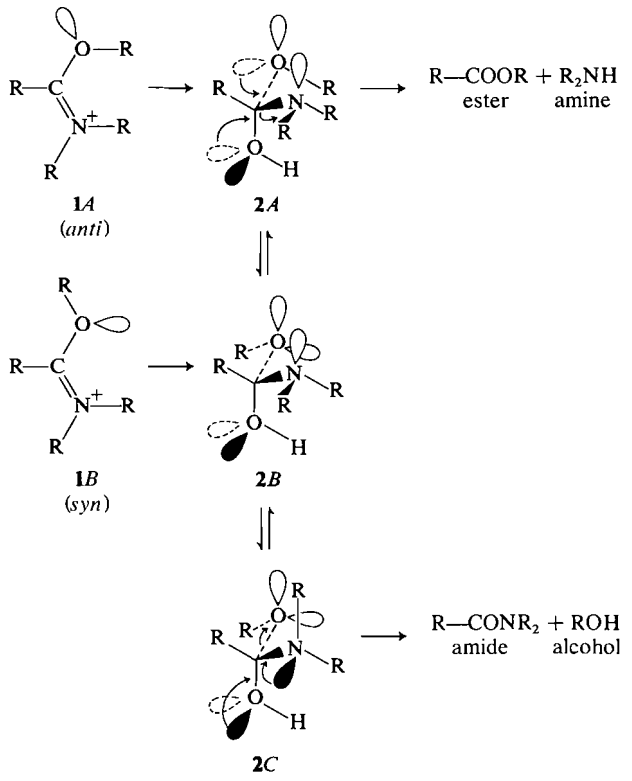

SCHEME I

by rotation to give new conformers such as **2***A* and **2***C* which can break down with stereoelectronic control yielding the ester amine and amide alcohol products, respectively. Conformer **2***C* has a lone pair orbital on one oxygen (the OH group) and on the nitrogen which are both properly oriented to eject the OR group with stereoelectronic control yielding the amide alcohol products. Since the barrier to rotation of the C—O and the C—N bonds must be of the same order of magnitude, **2***A* and **2***C* will be formed competitively from **2***B*. Mixtures of ester amine and amide alcohol products should therefore be observed in the basic hydrolysis of *syn* imidate salts. We have obtained experimental results which support this conclusion.

During our previous study on the basic hydrolysis of imidate salts, we have not taken account of the exact p*H* of the reaction medium. We have however used such basic conditions as to allow a kinetically controlled reaction and to suppress the protonation of the nitrogen in the tetrahedral intermediate. We had also to use a mixed aqueous–organic solvent so that the products of the reaction could be directly analyzed by n.m.r. spectroscopy. It was important to follow the reaction directly in the reaction mixture in order to ensure that the observed results were produced by a kinetically controlled reaction. To complete this investigation, we have undertaken a study of the products formed in the hydrolysis of some *N,N*-dialkylated imidate salts in aqueous solvent over a range of p*H* values. We wish to describe this work and to discuss the new stereoelectronic theory with respect to the generally accepted mechanism for the hydrolysis of imidate salts in acidic and basic media.

We have selected for this study, the imidate salts **3**, **4**, **5**, and **6**. The results of their hydrolyses as a function of p*H* are shown in Fig. 1. At p*H*

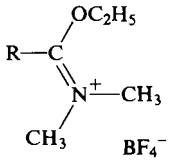

3 R = CH_3
4 R = C_6H_{11}(cyclohexyl)
5 R = C_6H_5
6 R = $(CH_3)_3C$

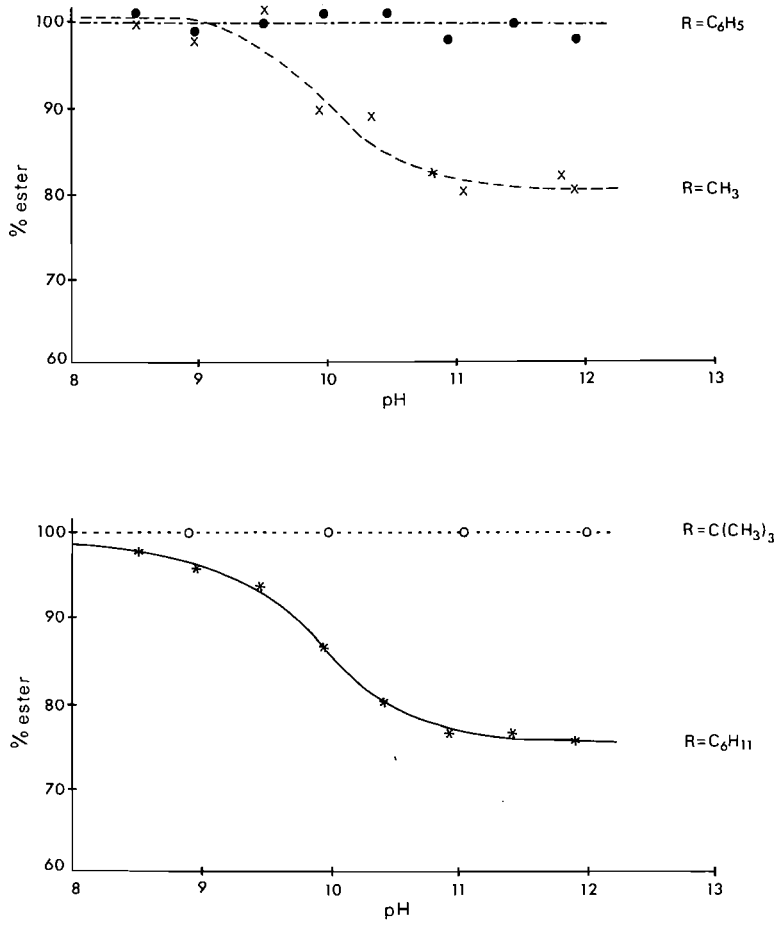

FIG. 1. Products of the hydrolysis of salts **3** (×), **4** (*), **5**(●), and **6** (○) as a function of p*H*. Buffer concentrations were 0.05 *M* (except for NaOH buffers) and the ionic strength was 1.0 *M* (maintained with KCl). In the case of **4**, the amide was assayed and the percentage ester was obtained by subtraction from 100.

8.5 or lower, the four imidate salts yield the ester amine products exclusively. The imidate salts **5** and **6** yield the ester amine products over the entire range of p*H* values. At p*H* greater than 8.5, imidate salts **3** and **4** start to produce the amide alcohol products which reach a maximum yield at p*H* 11 (20% for **3** and 25% for **4**) and that value remains unchanged at higher p*H*. These results are essentially identical with those obtained in our previous study using mixed aqueous–organic solvents.

Several previous studies on the hydrolysis of imidate salts have resulted in the following proposed mechanism (6, 7). Hydroxide ion reacts with an imidate salt such as **1** (Scheme 2) to give the tetrahedral intermediate T^0. It is assumed that proton transfer on the tetrahedral intermediate is faster than its breakdown, thus, T^0 is kinetically equivalent to $T^{\pm}$. Consequently, T^0 will also exist as $T^{\pm}$ at the p*H* corresponding to the pK_a of the tetrahedral intermediate (p$H \simeq 10$). At low p*H*, T^0 will exist as T^+ and at high p*H* as T^-. The variation in product formation with p*H* was thus explained by the various charged forms of T^0.[2] It was proposed that T^+ and $T^{\pm}$ expel amine to form the ester[3] while T^- could

[2]The breakdown of $T^{\pm}$ should be much easier than that of T^0. The R_2NH^+ group in $T^{\pm}$ is a much better leaving group than the R_2N group in T^0. Also, the negatively charged oxygen in $T^{\pm}$ must be an extra driving force to facilitate the cleavage of the intermediate. Since $T^{\pm}$ and T^0 are kinetically equivalent, T^0 can therefore be neglected.

[3]The R_2NH^+ group is a better leaving group than the OR group, so the cleavage of the C—N bond in T^+ and $T^{\pm}$ should be a more facile process than that of the C—OR bond.

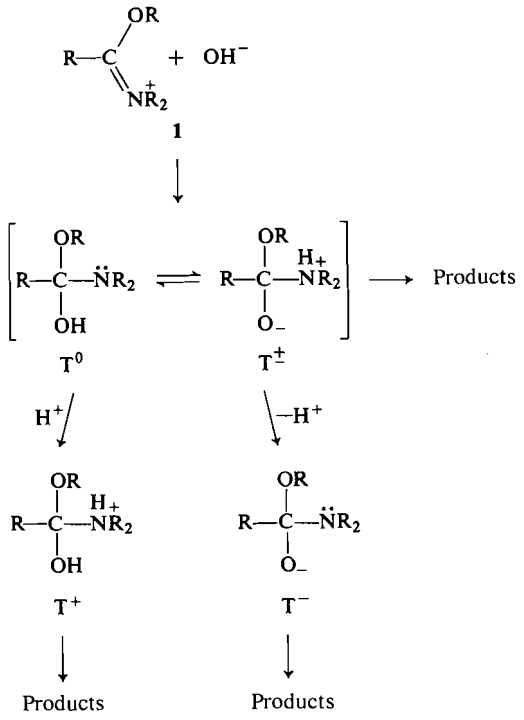

SCHEME 2

expel the alkoxide ion only with the consequent formation of amide.[4]

The results that we have obtained in the hydrolysis of imidate salts **2**, **4**, **5**, and **6** in acidic and slightly basic media can be explained by the preceding mechanism. However, the observed results in strongly basic medium cannot be rationalized by the same mechanism. The exclusive formation of the ester amine products from imidate salts **5** and **6** cannot be explained. Similarly, this mechanism does not offer an explanation for the partial formation of the ester amine products in the basic hydrolysis of imidate salts **3** and **4**. New parameters must be considered in order to explain the observed apparent anomalies. Clearly, the conformation of the tetrahedral intermediate must be one of the key points. Indeed, the application of the new stereoelectronic theory which we have developed appears to offer a complete explanation of the observed results.

We will first consider an imidate salt having an *anti* conformation such as **1***A*. According to the theory, **1***A* will form the intermediate **2***A*. In acidic medium, **2***A* will exist as the protonated form T^+, in slightly basic medium (near the pK_a of T^0, $pH \simeq 10$), it will exist as $T^{\pm}$ and in basic medium ($pH > 11$), it will exist as T^-. Again, $T^{\pm}$ is considered to be equivalent to T^0, thus T^0 can be neglected. Conformer **2***A* in the ionic form T^+, $T^{\pm}$, and T^- has proper orbital orientation to break down via stereoelectronic control to yield the ester amine products only.[5] *Anti* imidate salts should therefore yield ester amine products only, regardless of the pH of the reaction media.

The imidate salts **5** and **6** are considered to exist in the *anti* conformation[6] and indeed they give ester and amine as products of their hydrolysis over the complete range of pH values. We have also studied the hydrolysis in mixed aqueous–organic solvents of several cyclic imidate salts which can only exist in the *anti* conformation and these salts gave the ester amine products exclusively.[7]

When an imidate salt is in the *syn* conformation, it will first form the tetrahedral conformer **2***B* which will exist either as the T^+, $T^{\pm}$, or T^- form depending on the pH of the reaction medium. Since conformer **2***B* cannot break down via stereoelectronic control, we propose that conformational changes by rotation to give **2***A* (C—O bond rotation) or **2***C* (C—N bond rotation) will occur prior to cleavage.

When conformer **2***C* is in the T^+ or $T^{\pm}$ ionic form, it cannot be cleaved with stereoelectronic control because the nitrogen of the hemiorthoamide is sufficiently basic to be always protonated and its lone pair orbital is therefore not available to expel the OR group. Consequently, in media which favor T^+ or $T^{\pm}$, conformer **2***B* can be converted to either **2***A* or **2***C* but cleavage with stereoelectronic control can occur with con-

[4]The OR group is a better leaving group than the R_2N group, so the cleavage of the C—OR bond in T^- should be easier than that of the C—N bond.

[5]This implies that complete proton transfer can occur before cleavage even with tetrahedral intermediates which have two antiperiplanar lone pairs. It has also been suggested that the cleavage of some intermediates could occur prior to the proton transfer equilibrium giving different results (8).

[6]For a discussion concerning the conformation of these salts, see refs. 2 and 3.

[7]A study of the pH–product profile in an aqueous solution cannot be conveniently carried out with these cyclic salts. Under basic conditions, the ester amine products which are formed from these salts are very rapidly transformed into their corresponding amide alcohol products directly in the reaction mixture. It is, therefore, difficult to analyze the products resulting from the reaction under kinetically controlled conditions.

former **2***A* only. Thus, under those conditions, *syn* imidate salts should yield the ester amine products only.

When intermediate **2***C* exists in the T^- ionic form, it can be cleaved with stereoelectronic control. Consequently, in media which favor T^-, conformer **2***B* can be either converted to **2***A* or **2***C*; **2***A* yielding the ester amine products and **2***C* the amide alcohol products. Thus, in strong basic medium, *syn* imidate salts can give the amide alcohol as well as the ester amine products.

Thus, in acidic or neutral media which favor the formation of T^+ and $T^\pm$, *syn* imidate salts should only give the ester amine products. When the reaction medium becomes basic enough to allow the existence of T^-, the amide alcohol products should start to be formed. When the medium becomes strongly basic, T^- is then the only ionic species which should yield both the ester amine and amide alcohol products at a constant ratio for a given substrate. The ratio of products will depend on the relative energy barriers of rotation of the C—O and C—N bonds. One should therefore expect that the value of the ratio will vary with different *syn* imidate salts.

The imidate salts **3** and **4** are considered to exist in the *syn* conformation[6,8] and they do indeed exhibit the following behavior. They give the ester amine products in acidic and neutral conditions, and, starting at p*H* 8.5, the amide alcohol products which reach a constant maximum yield at p*H* 11 and above. In our previous investigation with mixed aqueous–organic solvents, we studied the basic hydrolysis of some cyclic imidate salts which can only exist in the *syn* conformation and a mixture of ester amine and amide alcohol products was also obtained (2, 3).

We would like to emphasize that the stereoelectronic theory permits the understanding of why a tetrahedral intermediate would prefer to eject the R_2N group in presence of the OR group, a normally better leaving group under basic conditions. Thus, the application of the postulate of conformational changes in tetrahedral intermediates combined with the theory of stereoelectronic control on the various ionic forms T^+, $T^\pm$, and T^- of such intermediates provide a very attractive mechanism to explain the products formed in the hydrolysis of imidate salts at various p*H* values.

In the course of the presentation of this new theory, we had to make several postulates concerning conformational changes during reactions and also about the relative energy barriers of bond rotation and cleavage of the intermediate (9).[9] These postulates remain to be supported by direct experimental evidence.

We have postulated that the energy barrier for the stereoelectronic cleavage of a tetrahedral intermediate such as **2***A* and **2***C* in the T^- ionic form, is much lower than that for rotation to give other conformers. The fact that *anti* imidate salts (which generate **2***A*) give the ester amine products, can be considered as experimental evidence for that postulate. However, it would be desirable to find an experiment which can show that conformational changes do not take place in the hydrolysis of *anti* imidate salts. Also, we have not yet obtained any experimental support that conformer **2***C* in the ionic form T^- behaves in a similar way. Good arguments can be brought to show that the energy barrier for the cleavage of **2***C* should be lower than that for **2***A*, thus indicating that if **2***A* does not undergo conformational changes, **2***C* will certainly not. The cleavage of the C—OR bond in **2***C* ought to be easier than that for the C—NR_2 bond in **2***A*.[4] It is also reasonable to assume that the lone pair orbital of the nitrogen in **2***C* must be a more powerful one to eject a leaving group than that of the oxygen of the OR group in **2***A*.

We have also postulated that the energy barrier for a nonstereoelectronically controlled cleavage of a tetrahedral intermediate is higher than that for rotation to give new tetrahedral conformers. Experimental evidence for the conformational change of **2***B* in the T^+ or $T^\pm$ forms

[8]It is possible that the salts **3** and **4** exist to some extent in the *anti* form which would be in equilibrium with the *syn* form (2, 3). This new situation does not change the above conclusion. The *syn* form would still produce the amide alcohol products and a certain percentage of the ester amine products. The remaining portion of ester amine products observed would come from the *anti* form.

[9]This implies that the energy barrier for conformational changes in tetrahedral intermediates must be relatively high. The energy barrier for rotation and inversion in benzyl-*t*-butylmethylamine have been found to be 6.4 and 6.3 kcal/mol, respectively (10). In tetrahedral intermediates, the anomeric effect (11) must also play an important role which could very well increase the energy barrier for conformational changes. For instance, dimethoxymethane is known to exist preferentially in the *gauche-gauche* conformation (12), thus its energy barrier for rotation must be high (it has been estimated to be $\simeq 3.0$ kcal/mol (13)).

has not yet been obtained. If the stereoelectronic theory is neglected, one can still predict on the basis of the ability of the two leaving groups[3] that an intermediate such as **2***B* should yield the ester amine products exclusively under acidic or slightly basic conditions. So, the fact that *syn* imidate salts yield only the ester amine products under those conditions does not constitute evidence for a conformational change of the tetrahedral intermediate prior to cleavage.

Similarly, we have not yet described an experiment to show that when conformer **2***B* exists in the ionic form T^-, it prefers to undergo conformational changes to **2***A* and **2***C* before cleavage.[10] The fact that *syn* imidate salts yield a mixture of products under basic conditions is very well explained by this postulate and the present level of knowledge does not present any alternative explanation. The hydrolysis of imidate salt **7** that we have recently reported (3) provides additional evidence for conformational changes. This *syn* salt produces a tetrahedral intermediate which is equivalent to **2***B*. However, only the C—O bond rotation is allowed in this intermediate, as the C—N bond rotation is a much more difficult process. Therefore, the intermediate can change only to new conformers which can produce the ester amine products. Indeed, the basic hydrolysis of this salt gave the ester amine **8** only, despite its *syn* conformation (Scheme 3).

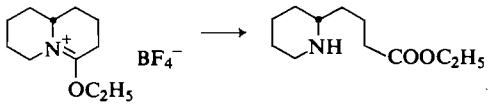

7 8

SCHEME 3

The bicyclic *syn* imidate salt **9** must form the intermediate **10** which is equivalent to **2***B* but **10** cannot undergo rotation of either the C—O or the C—N bond unless considerable twisting of the molecule could take place. This salt is thus an ideal model to find out if cleavage can occur without stereoelectronic control. In the absence of cleavage, the intermediate **10** would be isolated. We have found (3) that compound **9** is hydrolyzed under basic conditions to give the lactam alcohol product **11**; under acidic conditions, it gave the lactone ammonium salt **12** (Scheme 4). These results indicate that cleavage without stereoelectronic control can occur. The energy barrier of such a cleavage is simply higher than that for a cleavage with stereoelectronic control. However, when conformational changes to new conformers are possible, such high energy processes are of course avoided.

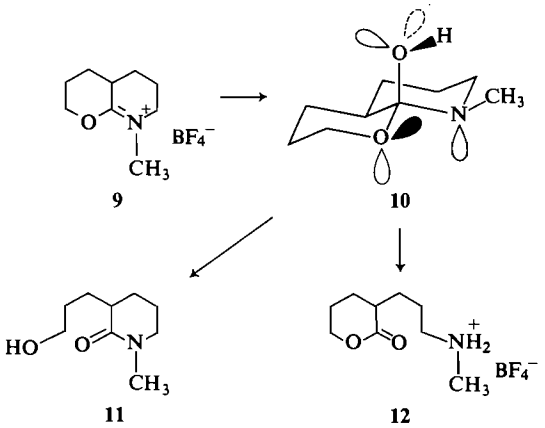

9 10 11 12

SCHEME 4

All the imidate salts described gave the ester amine products in acidic or neutral media. This result shows that when an intermediate exists in the T^+ or $T^\pm$ form, it prefers to eject the R_2NH^+ group instead of the OR group. The bicyclic *anti* imidate salt **13** was shown to be stable under acidic conditions (3). This salt must form the intermediate **14** in which the expected cleavage of the C—N bond would produce the large ring amino lactone **15** (Scheme 5). The formation of **15** is apparently not favored and **16** is not observed. Therefore, the intermediate **14** can only revert to starting material **13**. This result shows that a tetrahedral intermediate in the ionic form T^+ or $T^\pm$ cannot eject the OR group even when the normally competing ejection of the R_2NH^+ group is forbidden.

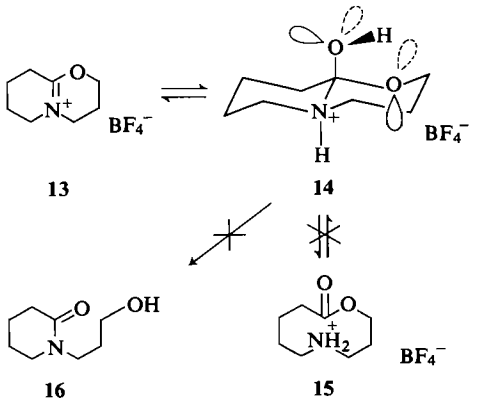

13 14 16 15

SCHEME 5

[10]When **2***B* exists as T^-, the energy barrier for its cleavage must be higher than when it exists as $T^\pm$ (and possibly as T^+). The R_2N group in T^- is a poorer leaving group than the R_2NH^+ group in $T^\pm$. Thus, conformational change is more likely to occur when **2***B* exists as T^-.

TABLE 1. Ester formed during the hydrolysis of **3**[a]

pH	Buffer	Reaction time (min)	% ester	Deviation[b]
8.6	Borate	45	101	2[c]
9.0	Borate	20	98	4
9.5	Borate	10	104	2
10.0	Borate	8–15	89	5[d]
10.4	DMG[e]	1	88	3
10.9	DMG	1	82	3
11.2	DMG	0.5	80	2
11.9	DMG–TEA[f]	1	82[g]	3[c]
12.1	NaOH	0.5	80[h]	2

[a]Hydrolysis performed at room temperature, at buffer concentration of 0.05 *M* (except sodium hydroxide buffers) and at ionic strength of 1.0 *M*, maintained with potassium chloride.
[b]Deviation from average of two sets of duplicate results.
[c]Deviation from average of two results.
[d]Average deviation of three sets of duplicate results.
[e]Dimethyl glycine.
[f]Dimethyl glycine buffer at pH 10.9 and containing 0.1 *M* triethylamine.
[g]The yield in ester in the standard was 92%.
[h]The yield in ester in the standard was 95%.

We would like to emphasize that when a tetrahedral intermediate such as **2***A* exists in the T^- ionic form, it does not first eject the amide ion to be protonated by the solvent to give the secondary amine. Both, the protonation and the ejection processes must be synchronized (14). In aqueous solution, the nitrogen lone pair orbital of **2***A* must first be hydrogen bonded with the solvent. When the cleavage starts to occur, the C—N bond becomes longer and weaker, the nitrogen atom becomes more basic, the nitrogen–hydrogen bond must become shorter and stronger. When the cleavage is almost complete, the nitrogen–hydrogen bond must be near the length of a full bond, so that the group can leave as a secondary amine.

We have stressed the fact that conformational changes of the tetrahedral intermediate have not yet been rigorously established experimentally. We think that this should be done because it is a fundamental principle of the stereoelectronic theory. Furthermore, this principle of conformational change can become a crucial point when the stereoelectronic theory is applied to the mechanism of hydrolysis by enzymes. For instance, it could lead to the prediction that conformational changes are necessary for the stereoelectronic assistance of hydrolysis by enzymes.

Work is now in progress to demonstrate that conformational changes do indeed take place in such reactions.

Experimental

The imidate salts have been obtained as described elsewhere (3). Buffers were commercial products and were used without purification. Their concentrations were normally 0.05 *M* and the ionic strength was 1.0 *M*, maintained with potassium chloride.

Calorimetric determinations were done with a Zeiss PMQ II spectrophotometer or a Varian Techtron spectrophotometer model 634. Vapor phase chromatographic analyses were done on a Varian model 2800 instrument, with thermal conductivity detection and temperature programming when necessary. Columns used were 10% SE-30 on Chromosorb W or 10% Apiezon L on Chromosorb W. Proton n.m.r. spectra were recorded on a Varian A-60 spectrometer using TMS as the internal standard.

*Hydrolysis of Salts **3** and **5** and Product Analysis*

The ester produced during the hydrolysis of salts **3** and **5** was assayed using the hydroxamic acid method (8, 15). In a typical experiment, 100 μl of the imidate solution (0.15–0.25 *M* in acetone) were introduced using a rapid-injection syringe (Hamilton push-button syringe) into 10 ml of buffer solution. After an appropriate time, a 2.0 ml aliquot was withdrawn and added to 1.0 ml of alkaline hydroxylamine (prepared hourly by adding 1 volume of NH_3OH–HCl, 8 *M*, and 1.2 volumes of sodium hydroxide, 7 *N*). After 20 min, 4.0 ml of a ferric chloride solution ($FeCl_3$ $6H_2O$, 10% in hydrochloric acid, 0.7 *N*) were added. The optical density was determined after 10 min at 520 (**5**) or 540 nm (**3**) and compared against a standard curve.

Each hydrolysis was done in duplicate and was accompanied by a duplicate sample of pure ester of similar concentration treated under the same conditions of hydrolysis and analysis. Corrections for ester hydrolysis were made when necessary. Optical densities were measured against a blank consisting of 100 μl of acetone treated in the same manner as the imidate sample. The results are shown in Tables 1 and 2.

*Hydrolysis of Salt **4** and Product Analysis*

In a typical experiment, 100 μl of the imidate solution (0.185 *M* in acetonitrile) were introduced using a rapid-injection syringe (Hamilton push-button syringe) into 10 ml of buffer solution. A few seconds before the hydrolysis ended, 100 μl of a solution of a standard (*n*-propyl benzoate, 0.168 *M* in acetonitrile) were added and the reaction solution was extracted with methylene chloride

TABLE 2. Ester formed during the hydrolysis of **5**[a]

pH	Buffer	Reaction time (min)	% ester	Deviation[b]
8.6	Borate	180	101	1
9.0	Borate	180	99	2
9.5	Borate	30	100	1
10.0	Borate	10	101	2
10.5	DMG[c]	3	101	2
11.0	DMG[c]	2	98	1
11.5	NaOH	2	100	1
12.0	NaOH	1	98	3

[a]Hydrolysis performed at room temperature, at buffer concentration of 0.05 *M* (except sodium hydroxide buffers) and at ionic strength of 1.0 *M*, maintained with potassium chloride.
[b]Deviation from average of two results.
[c]Dimethyl glycine.

TABLE 3. Amide formed during the hydrolysis of **4**[a]

pH	Buffer	Reaction time	% amide	Deviation[b]
8.6	Borate	5 h	2	1
9.0	Borate	4.6 h	4	0
9.5	Borate	1 h	6	1
10.0	Borate	30 min	13	1
10.5	DMG[c]	10 min	20	2
11.0	DMG	1 min	24	1
11.5	NaOH	1 min	24	0
11.9	NaOH	1 min	25	1

[a]Hydrolysis performed at room temperature, at buffer concentration of 0.05 *M* (except sodium hydroxide buffers) and at ionic strength 1.0 *M*, maintained with potassium chloride.
[b]Deviation from average of two results.
[c]Dimethyl glycine.

(3 × 3–4 ml). The extracts were dried over Na_2SO_4, filtered, concentrated, and assayed by vapor phase chromatography. The percentage amide produced was obtained by comparison of the weight (in mg) of the amide peak with that of the standard peak. The method (extraction and chromatographic analysis) was calibrated using pure amide treated in the same conditions as the hydrolysis[11] (a 1:1 molar correspondence was obtained between amide and standard).

Each hydrolysis was done in duplicate and was accompanied by a duplicate sample of pure amide of similar concentration and treated with the same conditions of hydrolysis. The results are shown in Table 3.

Hydrolysis of Salt 6 and Product Analysis

The product of the hydrolysis of salt **6**, pivalic acid ethyl ester, is very volatile (b.p. 118 °C (16)) such that a normal concentration procedure would involve some loss of the compound. Accordingly, in a typical experiment, the solid salt (150–200 mg) was added to the buffer solution (30 ml) and was stirred vigorously for an appropriate amount of time. The solution was then extracted with methylenechloride (5 ml). After drying (Na_2SO_4), a sample was removed and analyzed directly by n.m.r. spectroscopy using added TMS as an internal standard and by vapor phase chromatography. The results are shown in Table 4.

The extraction procedure was checked as follows: in a separate experiment, when 4.1 mol% of amide was present with the starting imidate, there was 3.6 mol% of amide present with ester after hydrolysis at pH 12, as detected by n.m.r. spectroscopy.

Mixing Experiments

Since imidate salts are very reactive in alkaline solutions (7), mixing problems could have arisen when the salt, dissolved in an organic solvent, is introduced into the buffer solution. The salt could react before complete mixing of the organic solvent and the buffer has occurred.

TABLE 4. Ester formed during the hydrolysis of **6**[a]

pH	Buffer	Reaction time	% ester
1	HCl	12.5 h	100
7	KCl	18 h	100
9	Borate	4 h	100[b]
10	Borate	0.5 h	100
11	DMG[c]	3 min	100
12	NaOH	0.5 min	100

[a]Hydrolysis performed at room temperature, at buffer concentration of 0.05 *M* (except for hydrochloric acid and sodium hydroxide buffers) and at ionic strength 1.0 *M*, maintained with potassium chloride.
[b]A trace of amide (< 1%) was consistently obtained at this pH.
[c]Dimethyl glycine.

[11]The ester could not be assayed at the same time because some of it was lost during the sample concentration procedure.

TABLE 5. Influence of the mode of addition of the imidate **3** solution into the buffer solution on the product composition[a]

Mode of addition[b]	% ester
1	76
2	82
3	85
4	84
5	79
6	82

[a]Hydrolysis performed at room temperature, at buffer concentration of 0.05 *M* at p*H* 10.9 (dimethyl glycine buffer) and at 1.0 *M* ionic strength maintained with potassium chloride.
[b]*1*, graduated pipette; *2*, Hamilton syringe; *3*, rapid injection syringe (Hamilton push-button syringe); *4*, rapid injection syringe with vortex stirring, *5*, rapid injection syringe with vortex stirring; 5 ml of reacting solution; *6*, rapid injection syringe in a buffer solution containing 0.1 *M* triethylamine (p*H* 11.9); the ester yield was 92%.

TABLE 6. Effect of buffer concentration on the hydrolysis of salt **3**[a]

[Buffer] (*M*)[b]	% ester	Deviation[c]
0.01	80	4
0.05	80	2
0.10	82	4

[a]Hydrolysis performed at room temperature and at ionic strength of 1.0 *M*, maintained with potassium chloride.
[b]Dimethyl glycine buffer at p*H* 11.0.
[c]Deviation from average of two results.

The net result of such a situation would be that the salt initially is hydrolyzed at a given p*H*, but as base is removed locally, the p*H* falls and hydrolysis would continue. Thus, some of the ester product could come from neutral or even acid hydrolysis of the salt. To check this possibility, a number of methods for adding the salt into the buffer solution were tried in which the rapidity of the mixing process varies considerably. Salt **3** was used and the procedure for the hydrolysis and product analysis was carried out as described above for this salt. The results are shown in Table 5.

Entry 6 of Table 5 is quite significant. If penetration of the base into the droplets of organic solvent during the initial mixing process would have caused local initial changes in p*H*, triethylamine should have been more efficient than hydroxide ion. Thus, these experiments show that no problems occur with mixing in these reactions.

Effect of Buffer Concentration

The effect of buffer concentration was investigated for the hydrolysis of salt **3**. Hydrolysis and product analysis was carried out in the same way as described above for this salt. The results are shown in Table 6. A variation by a factor of 10 in the buffer concentration does not influence the product composition.

Support for this work by the National Research Council of Canada, and by the Ministère de l'Education, Quebec, is gratefully acknowledged.

We also thank professor W. P. Jencks (Brandeis University) who kindly accepted one of us (R.J.T.) in his laboratory for a period of one month to learn various experimental techniques. We also deeply appreciate his help and encouragement through several discussions.

1. P. DESLONGCHAMPS, P. ATLANI, D. FRÉHEL, and A. MALAVAL. Can. J. Chem. **50**, 3405 (1972); P. DESLONGCHAMPS, R. CHÊNEVERT, R. J. TAILLEFER, C. MOREAU, and J. K. SAUNDERS. Can. J. Chem. **53**, 1601 (1975); P. DESLONGCHAMPS, R. J. TAILLEFER, C. MOREAU, and R. CHÊNEVERT. To be published.
2. P. DESLONGCHAMPS, C. LEBREUX, and R. J. TAILLEFER. Can. J. Chem. **51**, 1665 (1973).
3. P. DESLONGCHAMPS, S. DUBÉ, C. LEBREUX, D. R. PATTERSON, and R. J. TAILLEFER. Can. J. Chem. **53**, 2791 (1975).
4. P. DESLONGCHAMPS. Pure and Applied Chemistry. In press.
5. J. M. LEHN and G. WIPFF. J. Am. Chem. Soc. **96**, 4048 (1974).
6. G. L. SCHMIR and B. A. CUNNINGHAM. J. Am. Chem. Soc. **87**, 5692 (1965); B. A. CUNNINGHAM and G. L. SCHMIR. J. Am. Chem. Soc. **88**, 551 (1966); B. A. CUNNINGHAM and G. L. SCHMIR. J. Am. Chem. Soc. **89**, 917 (1967); W. P. JENCKS and M. GILCHRIST. J. Am. Chem. Soc. **90**, 2622 (1968); G. L. SCHMIR. J. Am. Chem. Soc. **90**, 3478 (1968); R. K. CHATURVEDI and G. L. SCHMIR. J. Am. Chem. Soc. **90**, 4413 (1968); T. C. PLETCHER, S. KOEHLER, and E. H. CORDES. J. Am. Chem. Soc. **90**, 7072 (1968); T. OKUYAMA and G. L. SCHMIR. J. Am. Chem. Soc. **94**, 8805 (1972); T. OKUYAMA, T. C. PLETCHER, D. J. SAHN, and G. L. SCHMIR. J. Am. Chem. Soc. **95**, 1253 (1973); T. OKUYAMA, D. J. SAHN, and G. L. SCHMIR. J. Am. Chem. Soc. **95**, 2345 (1973).
7. G. M. BLACKBURN and W. P. JENCKS. J. Am. Chem. Soc. **90**, 2638 (1968).
8. A. C. SATTERTHWAIT and W. P. JENCKS. J. Am. Chem. Soc. **96**, 7018 (1974).
9. J. P. GUTHRIE. J. Am. Chem. Soc. **96**, 3608 (1974).
10. C. H. BUSHWELLER, W. G. ANDERSON, P. E. STEVENSON, D. L. BARKEG, and J. W. O'NEIL. J. Am. Chem. Soc. **96**, 3892 (1974).
11. R. U. LEMIEUX. *In* Molecular rearrangements. Pt 2. *Edited by* P. de Mayo. Interscience, New York. 1964; R. U. LEMIEUX. Abstract of Papers, Am. Chem. Soc. **135**, 5E (1959); R. U. LEMIEUX. Pure Appl. Chem. **25**, 527 (1971); H. BOOTH and R. U. LEMIEUX. Can. J. Chem. **49**, 777 (1971); E. L. ELIEL. Angew. Chem. Int. Ed., **11**, 739 (1972).
12. E. E. ASTRUP. Acta Chem. Scand. **25**, 1494 (1971).
13. I. TVAROŠKA and T. BLEHA. J. Mol. Struct. **24**, 249 (1975).
14. W. P. JENCKS. Chem. Rev. **72**, 705 (1972).
15. F. LIPMANN and L. C. TUTTLE. J. Biol. Chem. **159**, 21 (1945).
16. P. G. STECHER. (*Editor*). The Merck index. 8th ed. Merck & Co., Inc., Rahway, New Jersey. 1968. p. 841.

The Preparation of Hexamethylcyclotriphosphazene

RICHARD T. OAKLEY AND NORMAN L. PADDOCK[1]

Department of Chemistry, University of British Columbia, 2075 Wesbrook Place, Vancouver, British Columbia V6T 1W5

Received April 10, 1975

RICHARD T. OAKLEY and NORMAN L. PADDOCK. Can. J. Chem. **53**, 3038 (1975).

Dimethyltrichlorophosphorane reacts with methylamine hydrochloride to give an oil which decomposes on heating, yielding the quaternary chloride $N_3P_3Me_6 \cdot MeCl$ as the principal product. The controlled pyrolysis of this salt gives $N_3P_3Me_6$ in high yield. A simple method for the separation of $N_3P_3Me_6$ and $N_4P_4Me_8$ is described, based on the different solubilities of their salts in acetonitrile.

RICHARD T. OAKLEY et NORMAN L. PADDOCK. Can. J. Chem. **53**, 3038 (1975).

Le diméthyltrichlorophosphorane réagit avec le chlorhydrate de méthylamine pour conduire à une huile qui se décompose, sous l'influence de la chaleur, pour donner, comme produit principal, le chlorure quaternaire $N_3P_3Me_6 \cdot MeCl$. La pyrolyse controlée de ce sel fournit le $N_3P_3Me_6$ avec un bon rendement. On décrit une méthode simple permettant de séparer $N_3P_3Me_6$ et $N_4P_4Me_8$; cette méthode fait appel à la différence de solubilité de leurs sels dans l'acétonitrile.

[Traduit par le journal]

Although the methylphosphazenes $(NPMe_2)_{3,4}$ have been known for many years (1), studies of their chemistry have been based mainly on the tetramer. Both compounds are produced as hydrochlorides (2, 3) in the reaction between dimethyltrichlorophosphorane and ammonium chloride in tetrachloroethane, according to eq. 1

[1] $$Me_2PCl_3 + NH_4Cl \rightarrow 1/n(NPMe_2)_n + 4HCl \quad (n = 3, 4)$$

the molar ratio (trimer:tetramer) being about 1:4 (3); if the solvent is omitted, the dihydrochloride of the tetramer is the sole product (4). The neutral compounds can be released either by a tertiary amine (3, 4) or aqueous alkali (2). Mixtures of $N_3P_3Me_6$ and $N_4P_4Me_8$ are also formed by heating $Me_2P(NH_2)_2Cl$ (4, 5) but, however the mixture is produced, the separation of the individual components is tedious. The tetramer is the more easily obtained, because it is the major product of such reactions and forms good crystals. It can also be prepared in high yield by the methylation of the corresponding fluoride (6), a method which fails for the trimer (7). The present paper is intended to help in two ways. It describes in the Experimental (*a*) a convenient preparation of $N_3P_3Me_6$ in high yield and (*b*) a method for separating the trimer and tetramer, which can be usefully applied to mixtures produced in other ways.

The preparative method described below is a modification of that first used (1), with the substitution of methylamine hydrochloride for ammonium chloride. An oily intermediate is formed, which has not been characterized but, by analogy with the comparable reactions of PCl_5 (8) and $PhPCl_4$ (9) probably contains the dimeric phosphazane $(Me_2PCl \cdot NMe)_2$. Pyrolysis of the oil *in vacuo* gives a mixture of the quaternary chloride $N_3P_3Me_6 \cdot MeCl$ and a small amount of the diquaternary salt $N_4P_4Me_8 \cdot 2MeCl$, which can be separated by taking advantage of the solubility of the former compound in acetonitrile. The neutral $N_3P_3Me_6$ is obtained from $N_3P_3Me_6 \cdot MeCl$ by heating it *in vacuo*. There appears to be a similarity, in principle, to the formation of $N_3P_3Ph_6$ by the dehydrohalogenation of $(Ph_2PF \cdot NH)_2$ (10).

We add three comments: (*i*) The oily product should not be heated for too long in the presence of the solvent. If it is, increasing quantities of the tetramer are eventually formed, possibly as a result of the polymerization of the dimeric phosphazane, known to occur (11) on prolonged heating of the analogous $(F_3P \cdot NMe)_2$. (*ii*) The insolubility of the diquaternary salt $N_4P_4Me_8 \cdot 2MeCl$ in acetonitrile is a result of the double positive charge on the cation. Since $N_3P_3Me_6$ forms a monohydrochloride (2, 3), mixtures of the hydrochlorides can similarly be separated more easily than the neutral compounds prepared from them by the addition of a

[1]To whom all correspondence should be addressed.

Can. J. Chem. Downloaded from www.nrcresearchpress.com by 210.87.254.42 on 09/05/12
For personal use only.

Can. J. Chem. Downloaded from www.nrcresearchpress.com by 210.87.254.42 on 09/05/12
For personal use only.

base. (*iii*) There is an interesting difference from the behavior of $(Cl_3P{\cdot}NMe)_2$, prepared from methylamine hydrochloride and PCl_5 (8). On pyrolysis, this compound does not give a quaternary salt, presumably because the chlorophosphazenes are too weakly basic; a high polymer of composition $NPCl_2$ is formed instead (12). The positive charge on the quaternized methylphosphazenes would tend to prevent such polymerization.

Experimental

Reaction of Dimethyltrichlorophosphorane with Methylamine Hydrochloride

Dimethyltrichlorophosphorane was prepared by the chlorination of tetramethyldiphosphine disulfide (13) in carbon tetrachloride and was dried *in vacuo* for 24 h. The methylamine hydrochloride, a commercial product, was dried at 120 °C for 24 h.

Dimethyltrichlorophosphorane (32.0 g, 191 mmol) was added to a slurry of methylamine hydrochloride (12.0 g, 191 mmol) in 125 ml chlorobenzene and the mixture heated to reflux. When this temperature was reached, evolution of hydrogen chloride commenced and the reactants rapidly fused into a pale yellow oil which was immiscible with the solvent. After heating for 1 h under reflux, the solvent was distilled off, leaving a viscous oil. (As stated above, prolonged heating under reflux reduces the relative yield of trimer; it also lowers the overall yield of phosphazenes.) The oil was then heated at 165 °C/0.05 Torr for 4 h. During this time the oil solidified to an off-white powdery solid. After cooling, the solid was extracted with 3 × 200 ml hot acetonitrile. The extracts were combined and concentrated, whereupon a white slightly hygroscopic solid (11.94 g) crystallized out. A further 0.84 g of the same solid was obtained by evaporation of the mother liquor under N_2. The whole was recrystallized from acetonitrile and identified by its analysis and ^1H n.m.r. spectrum as the quaternary salt $N_3P_3Me_6{\cdot}MeCl$; m.p. 195–200 °C (dec.) (12.8 g, 73%); ^1H n.m.r., 100 MHz (δ, CD_3CN, internal TMS) 2.94 (3H, triplet, J_{PH} = 10.5 Hz), 1.87 (12H, doublet, J_{PH} = 13.5 Hz), 1.57 (6H, doublet, 14.5 Hz, long range J_{PH} = 1.5 Hz); i.r. ν(P=N) 1190, 1245 cm^{-1} (Nujol mulls for all compounds; assignments provisional).

Anal. Calcd. for $C_7H_{21}ClN_3P_3$: C, 30.5; H, 7.7; Cl, 12.9; N, 15.2. Found: C, 30.9; H, 7.75; Cl, 13.0; N, 14.8.

Slow pyrolysis of $N_3P_3Me_6{\cdot}MeCl$ at 200 °C/0.1 Torr decomposed the salt and $N_3P_3Me_6$ was collected, in nearly quantitative yield, by sublimation on to a water-cooled cold finger; m.p. 187–188 °C, (lit. (1) 195–195 °C, (5) 187–190 °C (dec.)); i.r. ν(P=N) 1180 cm^{-1} (lit. (1) 1180 cm^{-1}).

Anal. Calcd. for $C_6H_{18}N_3P_3$: C, 32.0; H, 8.0; N, 18.7. Found: C, 32.1; H, 8.0; N, 18.8.

The residue from the acetonitrile extraction (2.76 g) was dried *in vacuo* and recrystallized from hot methanol–chloroform. The hygroscopic solid was identified by its analysis and ^1H n.m.r. spectrum as the diquaternary salt $N_4P_4Me_8{\cdot}2MeCl$ (6.9 mmol, 15%); m.p. >275°; ^1H n.m.r., 60 MHz, (δ, D_2O, internal DSS) 2.93 (6H, triplet, J_{PH} = 11.5 Hz), 2.03 (24H, doublet, J_{PH} = 13.5 Hz); i.r.: ν(P=N), 1350 cm^{-1}.

Anal. Calcd. for $C_{10}H_{30}Cl_2N_4P_4$: C, 29.9; H, 7.5; Cl, 17.7; N, 14.0. Found: C, 29.7; H, 7.7; Cl, 18.0; N, 13.8.

Separation of Hexamethylcyclophosphazene and Octamethylcyclotetraphosphazene

A mixture of $N_3P_3Me_6$ (1.34 g, 5.94 mmol) and $N_4P_4Me_8$ (1.41 g, 4.71 mmol) was dissolved in 200 ml diethyl ether. Hydrogen chloride gas was bubbled through the solution until precipitation of the methylphosphazene hydrochlorides was complete. The resulting white precipitate was filtered off and dried *in vacuo* (3.36 g). The solid was shaken with 100 ml of hot acetonitrile and the mixture filtered. The residual $N_4P_4Me_8{\cdot}2HCl$ (1.78 g, quantitative) was identified by its i.r. spectrum: ν(P=N) 1282, 1322 cm^{-1} (lit. (2) 1286 cm^{-1}, (4) 1278, 1320 cm^{-1}).

Anal. Calcd. for $C_8H_{26}Cl_2N_4P_4$: C, 25.8; H, 7.0; Cl, 19.0; N, 15.0. Found: C, 25.6; H, 6.8; Cl, 18.9; N, 15.1.

Evaporation of the acetonitrile from the filtrate gave $N_3P_3Me_6{\cdot}HCl$ (1.51 g, 97%) m.p. 247–249 °C: i.r. ν(P=N) 1170, 1230 cm^{-1}.

Anal. Calcd. for $C_6H_{19}ClN_3P_3$: C, 27.5; H, 7.3; Cl, 13.6; N, 16.1. Found: C, 27.3, H, 7.4; Cl, 13.3; N, 16.2.

The neutral methylphosphazenes can be regenerated from their hydrochlorides by treatment with a base; triethylamine (3, 4) and aqueous alkali (2) have both been used.

We are grateful to the National Research Council of Canada for financial support, and for an NRCC Scholarship (to R.T.O.).

1. H. T. Searle. Proc. Chem. Soc. 7 (1959).
2. J. Dyson. Ph.D. Thesis. University of Manchester, Manchester, England. 1964.
3. H. T. Searle, J. Dyson, T. N. Ranganathan, and N. L. Paddock. J. Chem. Soc. Dalton, 203 (1975).
4. F. A. Cotton and A. Shaver. Inorg. Chem. **10**, 2362 (1971).
5. H. H. Sisler and S. E. Frazier. Inorg. Chem. **4**, 1204 (1965).
6. T. N. Ranganathan, S. M. Todd, and N. L. Paddock. Inorg. Chem. **12**, 316 (1973).
7. N. L. Paddock, T. N. Ranganathan, and S. M. Todd. Can. J. Chem. **49**, 164 (1971).
8. A. C. Chapman, W. S. Holmes, N. L. Paddock, and H. T. Searle. J. Chem. Soc. 1825 (1961).
9. I. N. Zhmurova, U. I. Dolgushina, and A. V. Kirsanov. Zhur. Obshch. Khim. **37**, 1797 (1967).
10. R. Schmutzler. Z. Naturforsch. **19b**, 1101 (1964).
11. K. Utvary and W. Czysch. Monatsh. **103**, 1048 (1972).
12. H.-G. Horn. Z. Anorg. Allg. Chem. **406**, 199 (1974).
13. G. W. Parshall. Org. Synth. **45**, 102 (1965).

A Correlation between Bond Length and Ionic Bond Order. Application to the Ylide–Ylene Problem

MYUNG-HWAN WHANGBO AND SAUL WOLFE
Department of Chemistry, Queen's University, Kingston, Ontario K7L 3N6
AND
FERNANDO BERNARDI
Instituto di Chimica Organica, Universita di Bologna, 40136-Bologna, Italy
Received May 27, 1975

MYUNG-HWAN WHANGBO, SAUL WOLFE, and FERNANDO BERNARDI. Can. J. Chem. **53**, 3040 (1975).

The C—O and C—S bond lengths of the cations, radicals, and anions CH_3O, CH_3S, CH_2OH, and CH_2SH have been found not to correlate with the overlap populations of the C—X bonds. On the other hand, very satisfactory linear relations are observed with the *ionic* bond orders of the C—X bonds. It is suggested that, in certain molecular systems, it may be more meaningful to associate shortening of a bond A—B with greater coulombic attraction (or smaller coulombic repulsion) between the two point charges represented by the net atomic charges on the atoms A and B than with an increase in the overlap population between these atoms. It is noted that such an interpretation can account for the short C—P bond in a phosphonium ylide without resort to $(p \rightarrow d)_\pi$ conjugation.

MYUNG-HWAN WHANGBO, SAUL WOLFE et FERNANDO BERNARDI. Can. J. Chem. **53**, 3040 (1975).

On a trouvé qu'il n'y a pas de corrélation entre les longueurs des liaisons C—O et C—S des cations, radicaux et anions CH_3O, CH_3S, CH_2OH et CH_2SH et les populations de recouvrement des liens C—X. Par ailleurs on a trouvé qu'il existe des relations linéaires très satisfaisantes avec les ordres de liaison *ionique* des liens C—X. On suggère que, dans certains systèmes moléculaires, il pourrait s'avérer plus significatif d'associer le racourcissement d'un lien A—B avec une attraction coulombique plus grande (ou une répulsion coulombique plus petite) entre les deux charges ponctuelles représentées par les charges atomiques nettes sur les atomes A et B que par une augmentation dans la population de recouvrement entre ces atomes. On note qu'une telle interprétation peut rendre compte de la longueur plus courte de la liaison C—P de l'ylure de phosphonium sans avoir recours à la conjugaison $(p \rightarrow d)_\pi$.
[Traduit par le journal]

One of the important objectives of bonding theory is to relate the length of a chemical bond to some property of the atoms that form this bond. For the most part, theoretical (1) and empirical (2) approaches to this problem have assumed that the length of the bond A—B can be correlated with some property related to the electron distribution *between* the nuclei A and B. In π-electron theories, this property of the charge distribution has been taken to be the covalent bond order (3) of the bond population (4), and very good linear relations are observed between covalent bond orders and bond lengths (2*a*, 5). In LCAO–MO theories, which take overlap into account explicitly, the overlap population (6) has commonly been employed as a measure of the covalent bond order. However, the precise relationship between these two quantities is not clear, as can be seen from the number of definitions of bond order that exist (3, 4, 6, 7).

Ideally, any property of the atoms A and B that is to rationalize the length of the bond A—B should be permitted to vary as the molecular environments of A and B are varied. However, although r_{AB} is known to depend upon whether A and B are neutral, positive, or negative (8, 9), systematic studies of such bond length alterations, and the properties of A and B to which these alterations might be related, appear to be lacking.

In connection with other work, we have recently performed *ab initio* SCF–MO computations on the anion (10), radical (11), and cation (12) species CH_3X and CH_2XH, as well as

Can. J. Chem. Downloaded from www.nrcresearchpress.com by 210.87.254.40 on 09/05/12
For personal use only.

TABLE 1. Net atomic charges (q_i), overlap populations (p_{ij}), ionic bond orders ($-p'_{ij}$), and C—X bond lengths in CH_3X and CH_2XH

Molecule A—B—C—D	q_A	q_B	q_C	q_D	p_{BC}	$-p'_{BC}$	r_{BC}
$H_3{\equiv}C{-}O{-}H$	0.472	−0.120	−0.751	0.399	0.156	0.063	1.433 (1.434)*
$H_3{\equiv}C{-}O^+$	1.161	−0.361	0.200		0.046	−0.053	1.362
$H_3{\equiv}C{-}O^{\cdot}$	0.546	−0.180	−0.365		0.116	0.046	1.428 (1.44)†
$H_3{\equiv}C{-}O^-$	−0.038	0.011	−0.973		0.260	−0.007	1.401 (1.39)†
$H_2{=}C^+{-}O{-}H$	0.684	0.291	−0.514	0.539	0.257	−0.119	1.252
$H_2{=}C^{\cdot}{-}O{-}H$	0.310	0.009	−0.735	0.415	0.138	−0.005	1.382
$H_2{=}C^-{-}O{-}H$	−0.101	−0.362	−0.855	0.318	0.118	0.199	1.559
$H_3{\equiv}C{-}S{-}H$	0.605	−0.639	−0.050	0.084	0.234	0.017	1.883
$H_3{\equiv}C{-}S^+$	0.999	−0.787	0.788		0.205	−0.335	1.852
$H_3{\equiv}C{-}S^{\cdot}$	0.620	−0.679	0.059		0.200	−0.021	1.881
$H_3{\equiv}C{-}S^-$	0.262	−0.578	−0.684		0.191	0.207	1.910
$H_2{=}C^+{-}S{-}H$	0.711	−0.392	0.450	0.231	0.300	−0.107	1.653
$H_2{=}C^{\cdot}{-}S{-}H$	0.406	−0.501	−0.001	0.097	0.210	−0.000	1.812
$H_2{=}C^-{-}S{-}H$	0.019	−0.620	−0.328	−0.071	0.244	0.104	1.957

*Experimental value from Ivash and Dennison (21).
†Values in parentheses are taken from Yarkony *et al.* (20).

the neutral molecules CH_3XH, in which X is sulfur and oxygen. Restricted and unrestricted Hartree–Fock formalisms (13) were employed to calculate the total energies of closed shell and open shell species, respectively. In each case, the geometry was optimized by minimization of the total energy with respect to all bond lengths, valence angles, and dihedral angles. Table 1 summarizes the optimized C—O and C—S bond lengths of these systems (r_{BC}) and, in addition, lists q_i, the net atomic charge on the ith atom (or group of atoms) and p'_{BC}, the ionic bond order.[1]

The data of Table 1 permit the relationship between lengths and overlap populations of C—O and C—S bonds in different environments to be examined. In the two series CH_2OH (cation, radical, and anion) and CH_3S (cation, radical, and anion), the C—X bond length decreases as its overlap population increases. In these cases, therefore, overlap population seems to be a reliable measure of the bond order. However, in the series CH_3O and CH_2SH, no correlation between these quantities is evident.

The ionic bond order of the bond A—B is defined (14) as $p'_{AB} = -q_A q_B / r_{AB}$. This quantity represents the interaction energy of the net charges on atoms A and B and is attractive when $p'_{AB} > 0$, and repulsive when $p'_{AB} < 0$. Figure 1 shows plots of C—X bond length *vs.* ionic bond order for each of the series CH_3X and CH_2XH. In contrast to the absence of a uniform correlation with overlap population, there is in all cases a fairly good linear relation between r_{CX} and p'_{CX}. These findings indicate that, in each series, it may be physically more meaningful to associate a shorter C—X bond length with greater coulombic attraction (or smaller coulombic repulsion) between the two point charges represented by the net atomic charges on the atoms C and X than with an

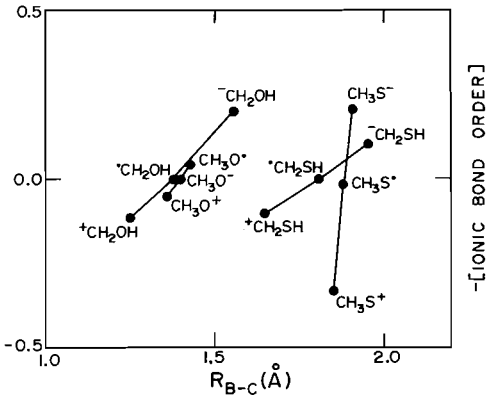

FIG. 1. The relationship between ionic bond order and C—X bond length in the various species CH_3X and CH_2XH (X = O, S). Data taken from Table 1.

[1]In the present work, the C—O bond length of CH_3O is computed to be 0.005 Å shorter than that of methanol. A recent study by D. R. Yarkony *et al.* (20) finds the C—O bond of CH_3O to be longer than that of methanol by 0.006 Å.

Can. J. Chem. Downloaded from www.nrcresearchpress.com by 210.87.254.40 on 09/05/12
For personal use only.

Can. J. Chem. Downloaded from www.nrcresearchpress.com by 210.87.254.40 on 09/05/12
For personal use only.

TABLE 2. Overlap population and ionic bond order of the C—P bond in $H_3\overset{+}{P}—CH_2^-$ and $H_2P—CH_3$ as a function of basis set (19)

Molecule	r_{PC} (Å)	p'_{PC}*	p_{PC}
H_3PCH_2†	1.66	0.29	0.88
H_2PCH_3†	1.863	0.08	0.59
H_3PCH_2‡	1.66	0.05	1.08
H_2PCH_3‡	1.863	−0.01	0.67

*Bond lengths are expressed in Å in the calculation of p'.
†Without d-type functions on phosphorus.
‡With d-type functions on phosphorus.

increase in the overlap population between these atoms.[2]

Although it has been a common practice to associate a decrease in the bond length with an increase in the covalent bond order (overlap population), an interpretation in terms of ionic bond order may sometimes be more suitable. A particular example is the carbon–phosphorus bond length of a phosphonium ylide. There has been much discussion (16) concerning the relative importance of the ylide (**1**) and ylene (**2**) representations of these species. The ylene formulation, which usually invokes $(p \rightarrow d)_\pi$ conjugation, has been favored by some workers because of the 0.09–0.17 Å shortening of the C—P bond that accompanies the deprotonation of a phosphonium salt (**3**) (see ref. 17 for a discussion of this point). However, n.m.r. and e.s.r. studies (18) seem more compatible with the ylide structure.

$\overset{+}{R_3P}—\overset{-}{C}HR$ (**1**) $\quad R_3P{=}CHR$ (**2**) $\quad \overset{+}{R_3P}—CH_2R\ X^-$ (**3**)

Absar and Van Wazer (19) have performed *ab initio* computations on $H_3\overset{+}{P}—CH_2^-$ and $H_2P—CH_3$ using fixed C—P bond lengths in each case. Inspection of their wave functions (Table 2) reveals that, in the ylide, which has the shorter bond length, both the ionic bond order and the overlap population of the C—P bond are greater, whether d-type functions are present on phosphorus or not. In addition, π-like interactions are present in the C—P bonds, even when d character is not allowed (19). Therefore, it seems unnecessary to rationalize the shorter C—P bond of the ylide in terms of $(p \rightarrow d)_\pi$ conjugation. One should, rather, emphasize the correlation with the ionic bond order. We believe that the significance of the present work is to demonstrate that, since the length of a chemical bond is the result of both ionic and covalent effects, the ionic interaction should not be ignored in the explanation of bond length variations of charged and zwitterionic systems.

[2]Because the Mulliken population employed in the present work is not basis set invariant (15), conclusions based upon this analysis are subject to the usual criticisms of the Mulliken population analysis. However, it should be noted that our arguments are based upon trends observed from computations with the same quality basis set for each series of closely related compounds. For a modified population analysis see ref. 15*c*.

We thank the National Research Council of Canada for financial support of this work, and Prof. S. Fliszár and a second, anonymous, referee for their constructive criticism of the manuscript.

1. L. SALEM. The molecular orbital theory of conjugated systems. W. A. Benjamin, Inc., New York. 1966; G. VAN HOOYDONK. Z. Naturforsch. **29***a*, 971 (1974).
2. (*a*) L. PAULING. The nature of the chemical bond. 2nd ed. Cornell University Press, Ithaca, N.Y. 1940; (*b*) V. SCHOMAKER and D. P. STEVENSON. J. Am. Chem. Soc. **75**, 4126 (1941).
3. C. A. COULSON. Proc. R. Soc. London Ser. A, **169**, 419 (1939).
4. N. S. HAM and K. RUEDENBERG. J. Chem. Phys. **29**, 1215 (1958).
5. W. C. HERNDON. J. Am. Chem. Soc. **96**, 7605 (1974) and refs. cited therein.
6. R. S. MULLIKEN. J. Chem. Phys. **23**, 1833 (1955); **23**, 2338 (1955); **23**, 2343 (1955).
7. B. H. CHIRGWIN and C. A. COULSON. Proc. R. Soc. London Ser. A, **201**, 196 (1950); K. B. WIBERG. Tetrahedron, **24**, 1083 (1968); I. COHEN. J. Chem. Phys. **57**, 5076 (1972).
8. C. A. COULSON. Valence. 2nd ed. Oxford University Press, Oxford. 1961. p. 188.
9. W. J. ORVILLE-THOMAS. The structure of small molecules. Elsevier, London. 1966.
10. F. BERNARDI, I. G. CSIZMADIA, A. MANGINI, H. B. SCHLEGEL, M. H. WHANGBO, and S. WOLFE. J. Am. Chem. Soc. **97**, 2209 (1975).
11. F. BERNARDI, N. D. EPIOTIS, W. CHERRY, H. B. SCHLEGEL, M. H. WHANGBO, and S. WOLFE. J. Am. Chem. Soc. In press.
12. F. BERNARDI, I. G. CSIZMADIA, H. B. SCHLEGEL, and S. WOLFE. Can. J. Chem. **53**, 1144 (1975).
13. W. J. HEHRE, W. A. LATHAN, R. DITCHFIELD, M. D. NEWTON, and J. A. POPLE. Gaussian 70. Quantum Chemistry Program Exchange, Indiana University, Bloomington, Indiana.
14. R. S. MULLIKEN. J. Chem. Phys. **23**, 1841 (1955).
15. (*a*) R. S. MULLIKEN. J. Chem. Phys. **36**, 3428 (1962); (*b*) P. POLITZER and R. S. MULLIKEN. J. Chem. Phys. **55**, 5135 (1971) and refs. cited therein; (*c*) S. FLISZAR, A. GOURSOT, and H. DUGAS. J. Am. Chem. Soc. **96**, 4358 (1974).

16. A. W. JOHNSON. Ylid chemistry. Academic Press, New York. 1966; J. C. J. BART. J. Chem. Soc. B, 350 (1969); Z. YOSHIDA, K. IWATA, and S. YONEDA. Tetrahedron Lett. 1519 (1971); H. L. AMMON, G. L. WHEELER, and P. H. WATTS. J. Am. Chem. Soc. **95**, 6158 (1973).
17. H. SCHMIDBAUR. Adv. Organomet. Chem. **9**, 259 (1970).
18. G. A. GRAY. J. Am. Chem. Soc. **95**, 5094 (1973); **95**, 7736 (1973); H. SCHMIDBAUR. Chem. Ber. **100**, 1032 (1967); **101**, 595 (1968); **101**, 604 (1968); E. A. C. LUCKEN and C. J. MAZELINE. J. Chem. Soc. A, 439 (1967).
19. I. ABSAR and J. R. VAN WAZER. J. Chem. Phys. **56**, 1284 (1972); I. ABSAR and J. R. VAN WAZER. J. Am. Chem. Soc. **94**, 2382 (1972).
20. D. R. YARKONY, H. F. SCHAEFER, and S. ROTHENBERG. J. Am. Chem. Soc. **96**, 656 (1974).
21. E. V. IVASH and D. M. DENNISON. J. Chem. Phys. **21**, 1804 (1953).

Can. J. Chem. Downloaded from www.nrcresearchpress.com by 210.87.254.40 on 09/05/12
For personal use only.

Can. J. Chem. Downloaded from www.nrcresearchpress.com by 210.87.254.42 on 09/05/12
For personal use only.

Reaction of Xenon Difluoride. Part II. Oxidative-fluorination of Phosphorus and Iodine Compounds and Cleavage of Silicon–Sulfur and Silicon–Nitrogen Bonds[1]

JAMES ANDREW GIBSON, RONALD KIRK MARAT, AND ALEXANDER F. JANZEN
Department of Chemistry, University of Manitoba, Winnipeg, Manitoba R3T 2N2

Received March 10, 1975

JAMES ANDREW GIBSON, RONALD KIRK MARAT, and ALEXANDER F. JANZEN. Can. J. Chem. **53**, 3044 (1975).

Reaction of alkyl(aryl)phosphines with xenon difluoride gives alkyl(aryl)hydridofluorophosphoranes which were characterized by proton and fluorine n.m.r. spectroscopy. With phenylchlorophosphines, substitution of chlorine by fluorine accompanied oxidative-fluorination to give phenylfluorophosphoranes, $(C_6H_5)_nPF_{5-n}$. With *tert*-butylchlorophosphines, chlorination of the *tert*-butyl group accompanied oxidative-fluorination, and a mixture of products was obtained. Reaction of xenon difluoride with methyl iodide gives methyliodine(III) difluoride, characterized by proton and fluorine n.m.r. spectroscopy.

Silicon–sulfur and silicon–nitrogen bonds are cleaved by xenon difluoride and an intermediate containing a xenon–nitrogen bond is postulated.

Reaction of xenon difluoride with hexafluoroacetone, perfluoropinacol, or disodium perfluoropinacolate failed to give stable xenon esters.

JAMES ANDREW GIBSON, RONALD KIRK MARAT et ALEXANDER F. JANZEN. Can. J. Chem. **53**, 3044 (1975).

La réaction des alkyl(aryl)phosphines avec le difluorure de xénon conduit aux alkyl(aryl)-hydridofluorophosphoranes que l'on a caractérisé par spectroscopie r.m.n. du proton et du fluor. Avec les phénylchlorophosphines, une substitution du chlore par du fluor accompagne la fluoration oxydative pour fournir des phénylfluorophosphoranes, $(C_6H_5)_nPF_{5-n}$. Avec les *tert*-butylchlorophosphines, une chloration du groupement *tert*-butyle accompagne la fluoration oxydative et on obtient un mélange de produits. La réaction du difluorure de xénon avec l'iodure de méthyle fournit le méthyl difluorure d'iode(III) que l'on a caractérisé par spectroscopie r.m.n. du fluor et du proton.

Les liens Si—S et Si—N sont coupés par le difluorure de xénon et on fait l'hypothèse qu'il y a formation d'un intermédiaire contenant un lien Xe—N.

La réaction du difluorure de xénon avec l'hexafluoroacétone, le perfluoropinacol ou le perfluoropinacolate de sodium ne donne pas d'esters stables du xenon.

[Traduit par le journal]

The reactions of xenon difluoride with a variety of main group compounds were investigated with the aim of comparing the reactivity and fluorinating ability of XeF_2 to the more common fluorinating agents of groups VA to VIIA. Previously we described some reactions of XeF_2 with organosilicon compounds (1) and with $(C_6H_5)_2PC(OH)(CF_3)_2$ (2), while other workers have reported the reactions with organic compounds, including aromatics (3), olefins (4), acetylenes (5), and acids (6). XeF_2 is known to react with chlorides of various metals (7), and the oxidation of zinc tetraphenylporphyrin has been reported (8). Adducts of XeF_2 with metal fluorides have been studied in some detail and recent review articles are available (9).

Results and Discussion

XeF_2 and Phosphines

The previous finding that XeF_2 did not attack silicon–hydrogen bonds (1) suggested that oxidative-fluorination of phosphines might occur without destruction of the P—H bond. This was confirmed for reactions of XeF_2 with dialkyl(aryl)phosphines and monoalkylphosphines (eqs. 1 and 2).

[1] $$R_2PH + XeF_2 \longrightarrow \underset{\mathbf{1}}{\begin{array}{c} R \\ R \end{array}\!\!>\!\!\begin{array}{c} F \\ | \\ P \\ | \\ F \end{array}\!\!-H} + Xe$$

a $R = C_6H_5$
b $R = CH_2CH_2CN$

[1]Taken in part from the doctoral dissertation of J. A. Gibson, University of Manitoba, 1973. Presented in part at the 6th International Symposium on Fluorine Chemistry, Durham, England, July 18–23, 1971, and at the 55th Canadian Chemical Conference, Quebec City, June 4–7, 1972.

TABLE 1. Proton and fluorine n.m.r. chemical shifts and coupling constants of some alkyl(aryl)hydridofluorophosphoranes

Compound	Chemical shifts (p.p.m.)*		Coupling constants, J (Hz)				
	H_e	F_a	H_eP	H_ePF_a	H_ePCH	F_aP	F_aPCH
1*a* $(C_6H_5)_2PHF_2$	−6.45	+51.7	773.4	110	—	612	—
1*b* $(NCCH_2CH_2)_2PHF_2$	−6.92	+61.2	757.7	100.5	3.5	595	6.5
2*a* $NCCH_2CH_2PH_2F_2$	−6.94	+60.5	743.0	89	3.8	556	6.0
2*b* $C_6H_{11}PH_2F_2$	−6.75	+65.2	714	92	br	567	br

*Proton and fluorine chemical shifts relative to internal TMS and external $CFCl_3$. Compounds were dissolved in 1:2 (v/v) mixture of $CDCl_3$ and CD_3CN and spectra recorded at ambient probe temperatures.

[2] $RPH_2 + XeF_2 \longrightarrow R{-}P(F)(H)(H)(F) + Xe$ (**2**)

a R = CH_2CH_2CN
b R = C_6H_{11}

Reactions were carried out in acetonitrile solution in standard n.m.r. tubes under anhydrous conditions at −35 to −15 °C and the products were formed in yields of at least 90%. Xenon gas was removed and identified by mass spectrometry and the products were characterized by proton and fluorine n.m.r. The n.m.r. data are consistent with trigonal bipyramidal geometry in which fluorines occupy axial positions and alkyl(aryl) and hydrogen substituents occupy equatorial positions.

The chemical shifts and coupling constants of products **1** and **2** are summarized in Table 1 and typical proton n.m.r. spectra of **1***b* and **2***a* are shown in Figs. 1 and 2. The n.m.r. spectra are well resolved at room temperature thus indicating that intermolecular fluorine or hydrogen exchange is extremely slow on the n.m.r. time scale. Only the cyclohexyldihydridofluorophosphorane **2***b* showed somewhat broadened lines in the n.m.r. spectrum, hence J_{F_aPCH} and J_{H_ePCH} could not be estimated, but this broadening could be due to conformational equilibrium of the cyclohexyl ring.

The n.m.r. spectra were recorded in acetonitrile solution and, since it is known that acetonitrile forms a 1:1 complex with phosphorus pentafluoride (10), it is possible that products **1** and **2** interact with solvent CH_3CN in a typical Lewis acid–base manner (eq. 3) involving five and six

[3] $RPH_2F_2 + CH_3CN \rightleftharpoons RPH_2F_2{:}NCCH_3$

coordinate structures. In order to examine this possibility the preparation of $NCCH_2CH_2PH_2F_2$ **2***a* was carried out in CH_2Cl_2 solution. The

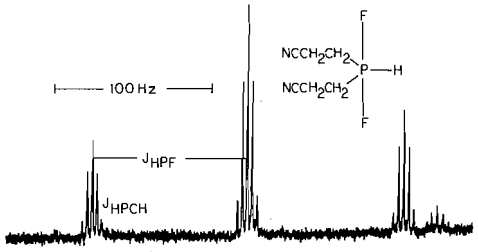

FIG. 1. Proton n.m.r. spectrum of $(NCCH_2CH_2)_2PHF_2$ showing low field half of symmetrical doublet (P—H coupling). Chemical shifts and coupling constants are found in Table 1.

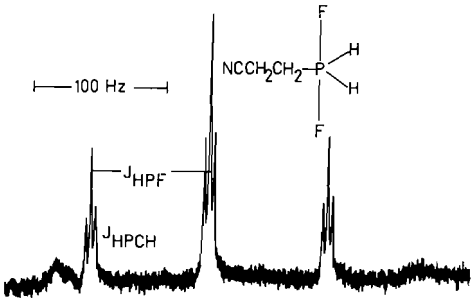

FIG. 2. Proton n.m.r. spectrum of $NCCH_2CH_2PH_2F_2$ showing low field half of symmetrical doublet (P—H coupling). Chemical shifts and coupling constants are found in Table 1.

n.m.r. spectrum in CH_2Cl_2 gave a chemical shift of F_a = 58.7 p.p.m. and $J_{H_ePF_a}$ = 89 Hz, J_{H_ePCH} = 3.8 Hz, and J_{F_aP} = 566 Hz. These values are reasonably close to those observed in acetonitrile solution and therefore the equilibrium of [3], if it is rapid, must be essentially to the left and the data of Table 1 refer to five coordinate molecules.

Rapid intramolecular Lewis acid–base reaction is also possible, but the equilibrium of [4] must lie essentially to the left, since the chemical shifts and coupling constants of **1***a* and **2***b*, where no cyano substituent is present, are very similar to those of **1***b* and **2***a*.

Can. J. Chem. Downloaded from www.nrcresearchpress.com by 210.87.254.42 on 09/05/12
For personal use only.

[4] 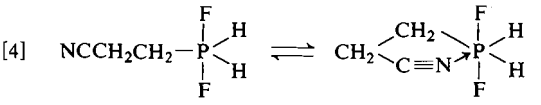

The reaction of XeF_2 with phosphines represents a convenient synthesis of mono- and dihydridofluorophosphoranes, although other synthetic routes are known, such as addition of alcohols, thiols, or amines to fluorophosphines (11), reaction of fluorophosphoranes with trimethylstannane or trimethylsilane (12), and reaction of KHF_2 with chlorophosphines or HF with alkylphosphines and phosphorous acids (13).

Reaction of chlorophosphines with XeF_2 was studied since it was of interest to establish whether oxidative-fluorination would occur without affecting the P—Cl bond. In the case of organosilicon chlorides, XeF_2 invariably converted Si—Cl to Si—F bonds (1).

The reaction of chlorophenylphosphines with XeF_2 gave fluorophenylphosphoranes, as well

[5] $$C_6H_5PCl_2 \xrightarrow{XeF_2} C_6H_5PF_4$$

[6] $$(C_6H_5)_2PCl \xrightarrow{XeF_2} (C_6H_5)_2PF_3$$

as Xe and Cl_2. Intermediate chlorofluorophenylphosphoranes were not identified and the relative ease of oxidative-fluorination *vs.* chlorine substitution could not be studied. Since one of the end products of reactions 5 and 6 is Cl_2, there is the further possibility that fluorophenylphosphoranes are formed as a result of oxidative-chlorination followed by fluorination. The reaction with triphenylphosphine was therefore carried out, as Cl_2 is not produced in this re-

[7] $$(C_6H_5)_3P \xrightarrow{XeF_2} (C_6H_5)_3PF_2$$

action, and oxidative-fluorination occurred under conditions very similar to those of $C_6H_5PCl_2$ and $(C_6H_5)_2PCl$; hence it is reasonable to assume that XeF_2 is the effective oxidizing reagent in reactions 5–7.

When the reaction was extended to *tert*-butylchlorophosphines, oxidative-fluorination was again observed but, at the same time, extensive chlorination of the *tert*-butyl group occurred and the products were not characterized. Chlorination of alkyl groups was observed previously during reactions of $(CH_3)_2SiCl_2$ and $C_6H_5(CH_3)_2SiCl$ where $CH_3(CH_2Cl)SiF_2$ and $C_6H_5(CH_3)(CH_2Cl)SiF$ were formed in about 25% yield (1).

XeF_2 and Iodine Compounds[2]

The syntheses of perfluoroalkyliodine(III and V) fluorides involve the use of powerful fluorinating agents such as F_2, BrF_3, and ClF_3 (14–19) and these would not be applicable to the syntheses of alkyliodine fluorides owing to destructive fluorination of alkyl groups. Since XeF_2 oxidizes phosphorus(III) compounds without attacking alkyl or aryl groups (unless a P—Cl bond is present), it seemed reasonable that oxidation of iodine compounds might also be accomplished under mild conditions.

The reaction of XeF_2 with an excess of methyl iodide proceeded smoothly for 20 min, in the absence of solvent at room temperature, in essentially quantitative yield; no reaction was observed below −40 °C.

$$XeF_2 + CH_3I \rightarrow CH_3IF_2 + Xe$$

The proton and fluorine n.m.r. spectra of CH_3IF_2, dissolved in excess methyl iodide, gave a triplet at −4.23 p.p.m. (external TMS) and a quartet at +176.4 p.p.m. (external $CFCl_3$) with J_{HCIF} = 7 Hz (Fig. 3). The fluorine chemical shift is close to that of CF_3IF_2 (+172.7 p.p.m. (15)) and other iodine(III) fluorides, such as CF_3IF_2·pyridine (+174.6 (17), $SF_5(CF_2)_2IF_2$ (+175.6 (16)), and IF_3 (+165 (18)).

CH_3IF_2 was found to be surprisingly stable in solution, 50% remaining after 4 h at 20 °C, suggesting that the product is at least as stable as CF_3IF_2 (14, 15). Excess of methyl iodide may be removed *in vacuo* from the involatile product. The product reacts slowly with glass and rapidly with mercury, while decomposition at room temperature gives iodine and oily material.

The reaction of XeF_2 with isopropyl iodide was also carried out; however, the reaction was extremely rapid at 0 °C and iodine was one of the end products. Fluorine n.m.r. confirmed the disappearance of XeF_2 but failed to detect the desired isopropyliodine(III) difluoride.

Reaction of XeF_2 with excess phenyl iodide proceeded at 0 °C to give a product with a fluorine chemical shift of +170.4 p.p.m. (half-height width 4 Hz). The chemical shift is characteristic of iodine(III) fluorides and is assigned to $C_6H_5IF_2$. The product is fairly stable, 80% remaining after standing at 5 °C for 12 h. During this time another peak appeared at +173.8 p.p.m., half-height width 18 Hz, which may be

[2]The synthesis of methyliodine(III) difluoride has been reported in a preliminary account (40).

Can. J. Chem. Downloaded from www.nrcresearchpress.com by 210.87.254.42 on 09/05/12
For personal use only.

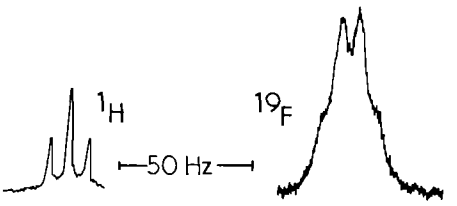

FIG. 3. Proton and fluorine n.m.r. spectra of CH_3IF_2. See text for chemical shifts and coupling constants.

assigned to partially fluorinated phenyliodide(III) difluoride, $C_6H_xF_yIF_2$, since the chemical shift is that of an iodine(III) fluoride while the half-height width is consistent with coupling to *ortho* fluorines (J_{FICF} = 26 Hz for $C_6F_5IF_4$ (19)).

The stability of $C_6H_5IF_2$ may be compared with $C_6F_5IF_2$ which decomposes rapidly above −5 °C (20). It is interesting that both CH_3IF_2 and $C_6H_5IF_2$ are found to be at least as stable as their perfluoro analogs, however, this 'stability' probably reflects the influence of impurities, since any synthesis involving XeF_2 probably introduces fewer impurities than reagents such as F_2 or ClF_3 and catalyzed decompositions are less likely.

Reaction of XeF_2 with I_2 in acetonitrile solution occurred very slowly and the iodine color was discharged over a period of 24 h at 20 °C. This slow reaction is probably due to the introduction of HF, as a result of decomposition of XeF_2/CH_3CN solution (1, 39), since it has been shown that I_2 is rapidly oxidized by XeF_2 in CH_3CN if an acid such as HF is introduced (21). It was also observed that reaction with I_2 could be speeded up by adding $(CH_3)_3SiF$ to the solution, and the iodine color was now discharged within 5 min. In separate experiments it was shown that $(CH_3)_3SiF$ does not react with XeF_2 or with I_2, therefore, $(CH_3)_3SiF$ must be a sufficiently strong Lewis acid to catalyze oxidation of I_2 in the manner of HF, BrF_3, and SO_2 (21, 22).

XeF_2 and Organosilicon Compounds

Reactions of Si—S, Si—N, and Si—O compounds with, for example, fluorides of phosphorus (23), sulfur (24), or iodine (25) have been widely used to prepare substituted derivatives of these elements. We therefore studied the reactions of Si—S and Si—N compounds (Si—O bonds are unreactive towards XeF_2 (1)) with the aim of preparing Xe—S or Xe—N compounds or, failing that, to gain evidence of their formation as intermediates.

The reaction of XeF_2 with *tert*-butylthiotrimethylsilane in acetonitrile solution proceeded smoothly to give di-*tert*-butyldisulfide in high

$$XeF_2 + (CH_3)_3SiSC(CH_3)_3 \rightarrow (CH_3)_3CSSC(CH_3)_3 + (CH_3)_3SiF + Xe$$

yield, along with minor amounts of $(CH_3)_3CSSSC(CH_3)_3$ and $(CH_3)_3CSH$. Xenon and $(CH_3)_3SiF$ were recovered quantitatively.

In the absence of solvent, the reaction was more complex, most probably due to the rapidity of the reaction and inadequate cooling, and the products were S_8, $(CH_3)_3CS_nC(CH_3)_3$ where n = 2–7, and $(CH_3)_3CF$, as well as the expected Xe and $(CH_3)_3SiF$.

The reactions of XeF_2 with silicon–nitrogen compounds such as $[(CH_3)_3Si]_2NH$ and $(CH_3)_3SiNR_2$ where R = CH_3, C_2H_5, $(CH_3)_2CH$ were studied extensively but few firm conclusions can be made at this time, partly because of the hazardous nature of these reactions (see Experimental section).

Despite difficulties, it was possible to show that reaction

$$XeF_2 + 2(CH_3)_3SiNR_2 \rightarrow 2(CH_3)_3SiF + Xe + R_2N(?)$$

gave quantitative yield of xenon and always more than 90% $(CH_3)_3SiF$. The fate of the dialkylamino fragment was investigated as described in greater detail in the Experimental section. All reactions produced dialkylamines with yields in the order $(CH_3)_2NH < (C_2H_5)_2NH < [(CH_3)_2CH]_2NH$. Presumably, $R_2N\cdot$ radicals are formed in solution, followed by hydrogen abstraction from solvent acetonitrile or reagents. Nitrogen-containing radicals are known to react with CH_3CN (26) and a g.c./m.s. study of products from reaction of $(CH_3)_3SiN(CH_3)_2$ showed a g.c. peak with ions *m/e* 84, 83, 58, 44, 42 assigned to $(CH_3)_2NCH_2CN$.

Oily, polymeric material was formed in all reactions with Si—N compounds, in some cases molecular weights greater than 750 were confirmed by mass spectrometry. Polymerization via dialkylamino, *e.g.*

$$(CH_3)_2N\cdot \rightarrow CH_3N{=}CH_2 \rightarrow \text{polymer}$$

radicals has been suggested in the literature (27).

The original goal of preparing Xe—N or Xe—S compounds was not realized, however, the production of $R_2N\cdot$ and $RS\cdot$ radicals is consistent with homolytic bond fission of intermediates such as F—Xe—NR_2 or F—Xe—SR. The

Can. J. Chem. Downloaded from www.nrcresearchpress.com by 210.87.254.42 on 09/05/12
For personal use only.

Can. J. Chem. Downloaded from www.nrcresearchpress.com by 210.87.254.42 on 09/05/12
For personal use only.

reaction of $(CH_3)_3SiN(CH_3)_2$ with XeF_2 gave further evidence of an intermediate, since it was observed that reaction at -25 to -30 °C produced a white solid, before the onset of violent reaction, and it is tentatively suggested that the solid is $FXeN(CH_3)_2$. LeBlond and DesMarteau have reported very recently the synthesis of a stable Xe—N compound $FXeN(SO_2F)_2$ which decomposes at 70 °C to give $[N(SO_2F)_2]_2$, Xe, and XeF_2 (28).

Attempts to prepare xenon–nitrogen compounds[3] by reaction of XeF_2 and $(CH_3)_3SiN{=}C(CF_3)_2$ gave only Xe, $(CH_3)_3SiF$, and $(CF_3)_2C{=}NH$, while reaction with $(CF_3)_2C{=}NLi$ gave Xe, $(CF_3)_2C{=}NH$, and LiF.

Impurities and Fluorine Exchange

Previously we showed that H_2O and HF impurities are invariably present in solutions containing reactive fluorides and that n.m.r. spectroscopy may conveniently monitor the presence of these impurities (29). In the case of the less reactive $(CH_3)_3SiF$, hydrolysis and fluorine exchange are catalyzed by dialkylamines (30).

The elimination of trace amounts of impurities was also one of the recurring experimental problems encountered in this work. Since reactions were carried out with XeF_2/CH_3CN solutions, which decompose at room temperature in Pyrex glassware (1, 39), it appears likely that HF and H_2O, along with other impurities, were present in reaction mixtures. Decomposition of hydridofluorophosphoranes and methyliodine(III) difluoride was catalyzed by impurities and it is not known to what extent the isolation of new xenon derivatives may have been prevented by impurities.

In some reactions, n.m.r. spectroscopy confirmed the presence of H_2O and HF impurities. For example, $(CH_3)_3SiF$ and dialkylamines were produced in reactions of XeF_2 and silicon–nitrogen compounds (*vide supra*) and the proton n.m.r. spectrum of $(CH_3)_3SiF$ in some samples showed a single peak rather than the expected doublet. This collapse of the doublet is due to the dialkylamine catalyzed hydrolysis of $(CH_3)_3SiF$

$$(CH_3)_3SiF + H_2O \rightleftharpoons (CH_3)_3SiOH + HF$$

as reported previously (30). No evidence was found of fluorine exchange between XeF_2 and $(CH_3)_3SiF$, as the chemical shift and coupling constant of unreacted XeF_2 showed no change in these solutions.

XeF_2 and Hexafluoroacetone, Perfluoropinacol, and Disodium Perfluoropinacolate

No reaction was detected between hexafluoroacetone and XeF_2, either in acetonitrile as solvent, without solvent, or in the presence of CsF. Some $(CF_3)_2CFOH$ was produced slowly when reaction was carried out in acetonitrile, but this may be explained as the product of HF addition to $(CF_3)_2CO$. Perfluoropinacol was also resistant to attack by XeF_2.

Reaction of XeF_2 with $OC(CF_3)_2C(CF_3)_2O^{2-}2Na^+$ failed to give a stable xenon heterocyclic derivative, the products being NaF, Xe, $(CF_3)_2CO$, and $HOC(CF_3)_2C(CF_3)_2OH$. Perhaps the desired intermediate was formed, which then oxidized to $(CF_3)_2CO$ or reacted with trace amounts of HF or H_2O to liberate perfluoropinacol, but this could not be established.

Experimental

CAUTION: Reaction of XeF_2 with silicon–nitrogen compounds may lead to explosions. Furthermore, the production of Cl_2 or Cl from reaction of XeF_2 with chlorides of P, Si, Ge, etc., may lead to potentially hazardous chlorinations. All reactions involving XeF_2 were carried out behind $\frac{3}{8}$ in. acrylic plastic safety shields within a fume cupboard.

General

XeF_2 was prepared photochemically (31) or obtained commercially (PCR, Gainesville) and dissolved in dried (P_2O_5) and distilled CH_3CN to give approximately 0.5 *M* solutions. These solutions were standardized by reacting aliquots with mercury and weighing xenon gas produced. $(CH_3)_3SiN(CH_3)_2$ was prepared by treating $(CH_3)_3SiCl$ with a 2:1 excess of dimethylamine in xylene (32) and distilling the product. $(CH_3)_3SiN[CH(CH_3)_2]_2$ was prepared in a similar manner. $(CH_3)_3SiN(C_2H_5)_2$ (PCR) and methyl iodide (Eastman) were redistilled prior to use. $(CH_3)_3SiSC(CH_3)_3$ was kindly supplied by O. C. Vaidya and checked to be free of *tert*-butylthiol. Hexamethyldisilazane (Alfa), organochlorosilanes (PCR), $(CH_3)_3GeBr$ (Alfa), organophosphines (Aldrich), chloro-*tert*-butylphosphines (Strem), and di-*tert*-butyldisulfide (PCR) were used without further purification.

Fluorine and proton nuclear magnetic resonance spectra were recorded on Varian A-56/60A and HA100D spectrometers. Chemical shifts are relative to TMS and $CFCl_3$, positive shifts indicating high field shifts. Mass spectra were obtained on a Finnigan 1015 quadrupole mass spectrometer coupled to a Varian 1700 gas chromatograph. Electron spin resonance experiments were carried out on a Varian E-3 e.p.r. instrument. Elemental analyses were performed by Alfred Bernhardt, West Germany.

[3]A. F. Janzen and S. N. Kay. Unpublished results.

Can. J. Chem. Downloaded from www.nrcresearchpress.com by 210.87.254.42 on 09/05/12
For personal use only.

XeF_2 and Triphenylphosphine

$(C_6H_5)_3P$ (0.052 g, 0.20 mmol) in CH_3CN (0.3 ml) was added to XeF_2 (0.12 mmol) in CH_3CN (0.3 ml) at −10 °C. Reaction occurred on warming to room temperature, complete within 4 min, to give $(C_6H_5)_3PF_2$ (94%), identified by fluorine n.m.r. (33).

XeF_2 and Diphenylphosphine

$(C_6H_5)_2PH$ (0.14 g, 0.75 mmol) was syringed onto XeF_2 (0.64 mmol) in CH_3CN (0.2 ml) at −196 °C. Reaction occurred at −25 °C to give $(C_6H_5)_2PHF_2$, identified by proton and fluorine n.m.r. (Table 1).

A violent reaction occurred when a chloroform solution of $(C_6H_5)_2PH$ was added to solid XeF_2 at room temperature.

XeF_2 and Bis(2-cyanoethyl)phosphine

$(NCCH_2CH_2)_2PH$ (0.12 g, 0.85 mmol) in CD_3CN was syringed onto XeF_2 (0.82 mmol) in CD_3CN (0.4 ml) at −196 °C. All operations were carried out in a dry box. Reaction occurred at −20 °C and was complete within 5 min to give $(NCCH_2CH_2)_2PHF_2$, identified by proton and fluorine n.m.r. (Table 1 and Fig. 1). The clear solution turned yellow and a solid formed after several days at room temperature.

XeF_2 and (2-Cyanoethyl)phosphine

$NCCH_2CH_2PH_2$ (0.1 g, 1.2 mmol) was syringed onto XeF_2 (0.87 mmol) in CD_3CN (0.4 ml) at −196 °C. All operations were carried out in a dry box. Reaction occurred at −35 °C and was complete within 5 min to give $NCCH_2CH_2PH_2F_2$, identified by proton and fluorine n.m.r. (Table 1 and Fig. 2). The clear solution turned yellow and a solid formed after several days at room temperature.

The reaction was repeated on the same scale in CH_2Cl_2 solvent. Reaction occurred at −15 °C and required 30 min for completion to give $NCCH_2CH_2PH_2F_2$. Decomposition to a white solid occurred within 1 day.

XeF_2 and Cyclohexylphosphine

$C_6H_{11}PH_2$ (0.10 g, 0.86 mmol) was syringed onto XeF_2 (0.83 mmol) in CD_3CN (0.4 ml) at −196 °C in a dry box. Reaction occurred at −20 °C to give $C_6H_{11}PH_2F_2$, identified by proton and fluorine n.m.r. (Table 1). The product decomposed after several days at room temperature to give a yellow solid.

XeF_2 and Diphenylchlorophosphine

$(C_6H_5)_2PCl$ (0.022 g, 0.10 mmol) was added to XeF_2 (0.15 mmol) in CH_3CN (0.3 ml) at −10 °C. Reaction occurred on warming to room temperature, complete within 4 min, to give $(C_6H_5)_2PF_3$, identified by fluorine n.m.r. (33).

XeF_2 and Phenyldichlorophosphine

$C_6H_5PCl_2$ (0.012 g, 0.07 mmol) was condensed into a solution of XeF_2 (0.15 mmol) in CH_3CN (0.3 ml) at −196 °C. On warming to 0 °C, a vigorous reaction occurred, complete within 1 min, to give $C_6H_5PF_4$, identified by fluorine n.m.r. (33).

XeF_2 and Di-tert-butylchlorophosphine and tert-Butyldichlorophosphine

$[(CH_3)_3C]_2PCl$ (0.11 g, 0.61 mmol) was added in aliquots of 10 μl to XeF_2 (0.59 mmol) in CH_3CN (0.2 ml) at −20 °C. Reaction occurred immediately on addition of $[(CH_3)_3C]_2PCl$ to give a pale yellow–green solution and a mixture of products which were not fully characterized but assumed to be partially chlorinated alkylfluorophosphoranes, since the mass spectrum revealed fragments containing three chlorine atoms (isotopic ratio) and the proton n.m.r. showed complex peaks in the *tert*-butyl region, while the fluorine n.m.r. showed a sharp doublet (J_{FP} = 726 Hz) at +71.6 p.p.m. (external $CFCl_3$) and a broad doublet (J_{FP} = 1030 Hz) at +56.8 p.p.m.

When the reaction was repeated in cyclohexene solution, the products again showed complex peaks in the *tert*-butyl region, but a fluorine signal was not observed.

Similar results were obtained for the reaction of XeF_2 with $(CH_3)_3CPCl_2$.

XeF_2 and Methyl Iodide

Solid XeF_2 (0.6 mmol) was added to excess methyl iodide (1.5 g) at −196 °C and the solution slowly warmed to room temperature. No reaction was observed below −40 °C; however, at room temperature the reaction proceeds smoothly for 20 min to give an essentially quantitative yield of CH_3IF_2, as monitored by fluorine n.m.r. Excess of methyl iodide may be removed *in vacuo* from the involatile product; however, attempts to purify the product were unsuccessful.

CH_3IF_2 could also be prepared by reaction of XeF_2 (0.20 mmol) in CH_3CN (0.4 ml) with excess methyl iodide at +20 °C. The reaction was slower, requiring 100 min for 75% reaction, while decomposition appeared to be faster and was complete after several hours.

XeF_2 and Phenyl Iodide and Isopropyl Iodide

Reaction of XeF_2 (0.1 g, 0.6 mmol) with excess phenyl iodide (1.9 g) was carried out at 0 °C. The fluorine n.m.r. spectrum of the product showed a single peak (half-height width 4 Hz) at +170.4 p.p.m. assigned to $C_6H_5IF_2$. After 12 h at 5 °C a second peak appeared at +173.8 p.p.m. (half-height width 18 Hz) of relative intensity 18%, which may be assigned to *ortho*-fluorinated $C_6H_4FIF_2$ or $C_6H_3F_2IF_2$.

The reaction of XeF_2 with excess isopropyl iodide at 0 °C was extremely rapid and appeared to give iodine as the major product. Fluorine n.m.r. examination failed to detect any iodine(III) difluoride product.

XeF_2 and Iodine

A few crystals of iodine were dissolved in a solution of XeF_2 (0.12 mmol) in CH_3CN (0.4 ml). The color of the iodine was discharged slowly over a period of 24 h at 20 °C.

In a similar experiment, a few crystals of iodine were dissolved in a solution of XeF_2 (0.11 mmol) in CH_3CN (0.4 ml) but this time dried $(CH_3)_3SiF$ was slowly bubbled into the solution. The iodine color was now replaced by a milky brown coloration which in turn faded to give a colorless solution. The reaction took 3–5 min for completion.

Reaction of XeF_2 with tert-Butylthiotrimethylsilane

In Solvent Acetonitrile

$(CH_3)_3SiSC(CH_3)_3$ (0.28 g, 1.73 mmol) was added to XeF_2 (0.83 mmol) in CH_3CN (0.3 ml) at −196 °C. The reaction mixture was allowed to warm to −7 °C in an ice–salt bath and reaction was complete within 7–9 min, resulting in a pale solution. Products were separated by

Can. J. Chem. Downloaded from www.nrcresearchpress.com by 210.87.254.42 on 09/05/12
For personal use only.

trap-to-trap distillation and identified by n.m.r. and mass spectrometry by comparison with authentic samples. Products (and yields) were Xe (100%), $(CH_3)_3SiF$ (100%), $(CH_3)_3CSSC(CH_3)_3$ (85%), $(CH_3)_3CSSSC(CH_3)_3$ (7%), and $(CH_3)_3CSH$ (7%).

Without Solvent

XeF_2 (0.83 mmol) was weighed into a U-tube, cooled to −196 °C, and $(CH_3)_3SiSC(CH_3)_3$ (0.25 g, 1.54 mmol) was added. On warming to about −30 °C, a rapid exothermic reaction occurred, complete within 1 min, and the final temperature of the mixture was +60 °C. Volatile products were removed and identified as Xe (100%), $(CH_3)_3SiF$ (86%), and $(CH_3)_3CF$ (12%). The residue consisted of a solid identified as S_8 (0.12 g), and a yellow oil which was soluble in $CHCl_3$. The oil showed no fluorine peaks in the n.m.r. but the proton n.m.r. showed at least six singlet peaks in the *tert*-butyl region. By comparison with authentic samples, it was possible to identify $(CH_3)_3CSSC(CH_3)_3$ (12%) and $(CH_3)_3CSSSC(CH_3)_3$ (3%). The remaining *tert*-butyl peaks in the n.m.r. spectrum are assigned to $(CH_3)_3CS_nC(CH_3)_3$ where $n = 4$–7, since mass spectral examination of the oil confirmed the presence of compounds with $n = 2$–7. After three weeks at room temperature, S_8 precipitated from the oil and the yield of $(CH_3)_3CSSC(CH_3)_3$ and $(CH_3)_3CSSSC(CH_3)_3$ increased.

Reaction of XeF_2 with Dimethylaminotrimethylsilane

Without Solvent

Reactions of XeF_2 and $(CH_3)_3SiN(CH_3)_2$ in the absence of solvent were found to be explosive and the following behavior was typical: a mixture of XeF_2 and $(CH_3)_3SiN(CH_3)_2$ appeared stable from −196 to −35 °C. No reaction was apparent on standing at −35 °C for 10 h. At −30 to −25 °C, XeF_2 was observed to react and a white solid formed, followed shortly by a loud detonation which completely destroyed the glass reaction tube. Explosions occurred on two other occasions. When the reaction was attempted in $CFCl_3$, in which XeF_2 is insoluble, a detonation occurred on warming the mixture to approximately −15 °C, shortly after the formation of a white solid had been observed. A similar detonation occurred when a saturated solution of XeF_2 in CH_3CN was used.

Using adequate safety precautions, $(CH_3)_3SiN(CH_3)_2$ (0.35 g, 3.0 mmol) was condensed onto solid XeF_2 (1.65 mmol) at −196 °C and the reaction monitored by changes in pressure. By alternately warming the reaction mixture to −22 °C to initiate reaction, and rapidly cooling to −196 °C, the reaction could be moderated. When pressure build-up ceased, the reaction was assumed complete and all volatile products were removed and identified as Xe (100%), $(CH_3)_3SiF$ (86%), and $(CH_3)_2NH$ (17%). A liquid residue showed a variety of peaks in the dimethylamino region. One of these peaks, at −2.21 p.p.m., is tentatively assigned to $(CH_3)_2NN(CH_3)_2$ (20%) on the basis of the n.m.r. of an authentic sample (kindly supplied by H. D. Gesser) and the m.p. of its methyl iodide derivative 207–211 °C (lit. (34) 222–223 °C). Removal of liquid products under reduced pressure left behind an oil (0.04 g) which analyzed as C, 33.07%; H, 9.17%; N, 19.17%; F, 38.91%. The high fluorine content of the oil and the carbon to nitrogen to hydrogen ratio of 2.01:1.00:6.65 suggests that the oil consists of a mixture of ionic $(CH_3)_2NH_2F$, $(CH_3)_2NH_2HF_2$, and polymeric $(C_2H_6N)_n$.

In Solvent Acetonitrile

Reactions in CH_3CN solution were carried out many times. Typically, $(CH_3)_3SiN(CH_3)_2$ (0.049 g, 0.42 mmol) was condensed onto a solution of XeF_2 (0.20 mmol) in CH_3CN (0.3 ml) at −196 °C. As reactants warmed to above −20 °C a brisk exothermic reaction occurred, complete within 1–2 min. The color of the resulting solution depended on the effectiveness of the cooling of the mixture during reaction. Pale brown solutions could be obtained by maintaining the temperature between −20 and −15 °C, while over-heating resulted in very dark solutions and larger quantities of oily, intractable material. Separation of volatile products gave Xe and $(CH_3)_3SiF$ in quantitative yield and $(CH_3)_2NH$ in 20–30% yield.

Attempts to identify products remaining in CH_3CN solution were unsuccessful, partly because the reactions were carried out on a small scale for safety reasons. Nuclear magnetic resonance showed at least 12 singlet peaks in the dimethylamino region −1.25 to −3.25 p.p.m., their relative intensities varying from reaction to reaction and some products appeared unstable with time. Combined gas chromatography – mass spectrometry using columns Chromasorb 103 and 8% FFAP on Chromasorb 45 showed at least 20 compounds, most of their fragmentation patterns suggesting products containing some or more of the groupings $(CH_3)_2N$, CH_2CN, and CH_3NCH_2. One g.c. peak showed ions *m/e* 84, 83, 58, 44, 42 which may be assigned to $(CH_3)_2NCH_2CN$ and its fragments. Other products could not be assigned with certainty.

Removal of all volatile components from reaction mixture left behind an oily material.

An electron spin resonance study was undertaken to see if free radicals could be detected. $(CH_3)_3SiN(CH_3)_2$ (0.025 g, 0.21 mmol) was allowed to react with XeF_2 (0.10 mmol) in CH_3CN (0.3 ml) at −10 °C in a silica tube. At the onset of a vigorous reaction, the solution was rapidly cooled to −196 °C and the e.s.r. spectrum recorded. A very poorly resolved but nevertheless reproducible spectrum was obtained, with splitting of 28 G, in agreement with that reported for the $(CH_3)_2N$ radical (35). If the reaction was allowed to go to completion, no e.s.r. signal was observed. Starting materials were checked to be free of e.s.r. signals.

Reaction of XeF_2 with Diethylaminotrimethylsilane

In a typical reaction, $(CH_3)_3SiN(C_2H_5)_2$ (0.049 g, 0.34 mmol) was added to a solution of XeF_2 (0.16 mmol) in CH_3CN (0.5 ml) at −10 °C. A brisk reaction occurred, complete within 1–2 min, to give a brown solution. Products were Xe (100%), $(CH_3)_3SiF$ (90%), diethylamine, and an oily residue. The yield of diethylamine was variable, but generally accounted for 70–80% of available diethylamino groups. In an e.s.r. experiment similar to that above, no free radicals could be detected.

The reaction was repeated many times in baked out glassware, silylated glassware, Teflon tubes, monel reactor, and polypropylene container, all giving essentially similar results.

Reaction of XeF_2 with Diisopropylaminotrimethylsilane

In a typical reaction, $(CH_3)_3SiN[CH(CH_3)_2]_2$ (0.074 g,

Can. J. Chem. Downloaded from www.nrcresearchpress.com by 210.87.254.42 on 09/05/12
For personal use only.

0.42 mmol) was added to XeF_2 (0.20 mmol) in CH_3CN (0.4 ml) at −10 °C. On warming to room temperature the solution turned brown and reaction was complete within 5 min to give Xe (100%), $(CH_3)_3SiF$ (90%), $[(CH_3)_2CH]_2NH$ (80–90%), and an oily residue.

Electron spin resonance experiments proved misleading, since a well resolved signal was observed at room temperature, but this signal was also observed in a sample of unreacted $(CH_3)_3SiN[CH(CH_3)_2]_2$ and may be attributed to a trace of $[(CH_3)_2CH]_2NO$ (36), present in the starting material.

Reaction of XeF_2 with Hexamethyldisilazane

$[(CH_3)_3Si]_2NH$ (0.52 g, 3.3 mmol) was condensed onto XeF_2 (3.2 mmol) in CH_3CN (8 ml) at −196 °C and reaction monitored by changes in pressure. Reaction occurred slowly at room temperature and was complete after 30 min to give Xe (100%), $(CH_3)_3SiF$ (95%), a small amount of noncondensable gas (at −196 °C) assumed to be nitrogen, and an oily residue.

The oil contained organic polymeric material since the mass spectrum showed peaks up to *m/e* 750, with a complex fragmentation pattern dominated by loss of 14 mass units (loss of CH_2 or N). Washing the oily residue with CH_3CN and drying under vacuum gave a pale brown solid (0.03 g) which analyzed as C, 7.55%, H, 5.55%; N, 22.56%; F, 30.30%. The ratio H:N:F of 3.42:1.00:0.99 suggests the solid is mainly NH_4F. Its i.r. spectrum showed broad N—H bands and the solid was soluble in water and partly soluble in acetone.

Monitoring the Reaction of XeF_2 with Organosilicon Chlorides

The production of Cl_2 from reaction of XeF_2 with organosilicon chlorides (1) was confirmed in this study as follows: a u.v. cell with two chambers, each of 4.375 mm path length, was stoppered with a drilled (to permit escape of Xe) Teflon stopper. One chamber contained XeF_2 (0.33 mmol) in CH_3CN, the other $(CH_3)_3SiCl$ (0.074 g, 0.68 mmol) in CH_3CN. The cell was cooled to 0 °C and reaction initiated by quickly inverting cells. The u.v. spectrum was scanned every 20–30 s and an increase in absorption at 315–320 nm (37) confirmed the production of Cl_2. Repeating the experiment with a 20:1 molar ratio of $(CH_3)_3SiCl$ to XeF_2 suppressed the build-up of Cl_2. Evidently, chlorination of excess $(CH_3)_3SiCl$ gave $(CH_2Cl)(CH_3)_2SiCl$. Chloromethyl derivatives gave characteristic downfield shifts of the CH_2Cl protons, −3.06 p.p.m. for $CH_2Cl(CH_3)_2SiCl$ and −2.98 p.p.m. for $CH_2Cl(CH_3)_2SiF$.

To verify the n.m.r. spectra of chloromethyl derivatives, $CH_2Cl(CH_3)SiF_2$ was prepared from a commercial sample of $(CH_3)_2SiF_2$ (1.97 g, 20.5 mmol) and Cl_2 (1.12 g, 15.8 mmol) in a sealed Pyrex tube exposed to sunlight for 3 days. Fluorine n.m.r. of the product gave a quartet of triplets at +138.2 p.p.m. $J_{F-CH_3} = 6$ Hz, $J_{F-CH_2Cl} = 4$ Hz. Proton n.m.r. showed a triplet (CH_3) at −0.56 p.p.m. and a triplet (CH_2Cl) at −2.91 p.p.m., with intensity ratio 3:2, consistent with the product $CH_2Cl(CH_3)SiF_2$.

Reaction of organochlorosilanes could also be monitored by fluorine n.m.r., for example reaction of XeF_2 with $(CH_3)_3SiCl$ in CH_3CN occurred at a moderate rate at 0 °C, and the decrease of XeF_2 and increase of $(CH_3)_3SiF$ concentration could be followed conveniently. However, accurate rate studies were not carried out.

Reaction of XeF_2 and Trimethylgermanium Bromide

$(CH_3)_3GeBr$ (0.079 g, 0.40 mmol) was added to XeF_2 (0.25 mmol) in CH_3CN (0.4 ml). Reaction occurred at 25 °C and was complete within 10 min to give Xe and $(CH_3)_3GeF$ in quantitative yield, and bromine. The color of the solution was reddish brown and the presence of Br_2 was confirmed by adding olefins which discharged the color. $(CH_3)_3GeF$ was identified by mass spectrometry and fluorine n.m.r., dectet at +186.5 p.p.m., $J_{FH} = 7$ Hz, and proton n.m.r., doublet at −0.6 p.p.m.

XeF_2 and Hexafluoroacetone

Hexafluoroacetone (0.10 g, 0.60 mmol) was condensed onto XeF_2 (0.15 mmol) in CH_3CN (0.3 ml) at −196 °C and contents sealed in an n.m.r. tube. Fluorine n.m.r. showed no initial reaction, however, after 3 weeks at room temperature, all XeF_2 was consumed and the solution now contained $(CF_3)_2CFOH$, identified by fluorine n.m.r., doublet ($J_{FF} = 2$ Hz) at +82.8 p.p.m. and septet at +125.8 p.p.m.

In attempts to prepare a fluoroxy derivative, $(CF_3)_2CFOF$, hexafluoroacetone and XeF_2 without solvent were kept at room temperature for 5 days; in another experiment CsF was added as a catalyst, but no evidence of the desired product was found.

XeF_2 and Disodium Perfluoropinacolate

Disodium perfluoropinacolate, $OC(CF_3)_2C(CF_3)_2O^{2-}$ $2Na^+$ was prepared in THF (38). In separate experiments it was found that solutions of XeF_2 in THF were unstable, hence it was necessary to replace THF by CH_3CN by removing THF under vacuum and adding CH_3CN and repeating procedure several times.

In a typical experiment XeF_2 (0.35 mmol) was added to a solution of $OC(CF_3)_2C(CF_3)_2O^{2-}$ $2Na^+$ (0.32 mmol) in CH_3CN (0.5 ml), prepared as described above, at −196 °C and the reaction monitored by pressure changes. At −20 °C, the original pale brown solution turned yellow to greenish-yellow and finally colorless, and a white solid formed. Volatile products were identified as $(CF_3)_2CO$ and $HOC(CF_3)_2C(CF_3)_2OH$. The solid was identified as sodium fluoride by X-ray powder pattern; very faint lines indicated that the powder contained some Na_2SiF_6.

Perfluoropinacol was found to be resistant to attack by XeF_2.

The financial assistance of the National Research Council of Canada and the Petroleum Research Fund, administered by the American Chemical Society, is gratefully acknowledged. We also thank NRCC for a postgraduate scholarship (to J.A.G.).

1. J. A. GIBSON and A. F. JANZEN. Can. J. Chem. **49**, 2168 (1971).
2. A. F. JANZEN and O. C. VAIDYA. Can. J. Chem. **51**, 1136 (1973).
3. M. J. SHAW, H. H. HYMAN, and R. FILLER. J. Org. Chem. **36**, 2917 (1971); D. R. MACKENZIE and J. FAJER. J. Am. Chem. Soc. **92**, 4994 (1970); L. D. SHUSTOV, T. N. BOCHAROVA, T. I. YURASOVA, N. G. MARCHENKOVA, V. A. LEGASOV, and L. N.

Can. J. Chem. Downloaded from www.nrcresearchpress.com by 210.87.254.42 on 09/05/12
For personal use only.

NIKOLENKO. Zh. Obshch. Khim. **43**, 841 (1973); Chem. Abstr. **79**, 52490k (1973).
4. T. C. SHIEH, N. C. YANG, and C. L. CHERNICK. J. Am. Chem. Soc. **86**, 5021 (1964); M. ZUPAN and A. POLLAK. J. Chem. Soc. Chem. Commun. 845 (1973); Tetrahedron Lett. 1015 (1974).
5. M. ZUPAN and A. POLAK. J. Org. Chem. **39**, 2646 (1974).
6. M. EISENBERG and D. D. DESMARTEAU. Inorg. Nucl. Chem. Lett. **6**, 29 (1970); F. SLADKY. Monatsh. Chem. **101**, 1559, 1571, 1578 (1970); N. BARTLETT, M. WECHSBERG, G. R. JONES, and R. D. BURBANK. Inorg. Chem. **11**, 1124 (1972).
7. N. BARTLETT. Endeavour, **23**, 3 (1964); V. A. LEGASOV and A. S. MARININ. Zh. Neorgan. Khim. **17**, 2408 (1972).
8. J. FAJER, D. C. BORG, A. FORMAN, D. DOLPHIN, and R. H. FELTON. J. Am. Chem. Soc. **92**, 3451 (1970).
9. H. SELIG. *In* Halogen chemistry, Vol. 1. *Edited by* V. Gutmann. Academic Press, New York. 1967. p. 403; N. BARTLETT and M. WECHSBERG. Z. Anorg. Allg. Chem. **385**, 5 (1971).
10. E. L. MUETTERTIES, T. A. BITHER, M. W. FARLOW, and D. D. COFFMAN. J. Inorg. Nucl. Chem. **16**, 52 (1960); F. N. TEBBE and E. L. MUETTERTIES. Inorg. Chem. **6**, 129 (1967); L. KOLDITZ and W. REHAK. Z. Anorg. Allg. Chem. **342**, 32 (1966).
11. L. F. CENTOFANTI and R. W. PARRY. Inorg. Chem. **12**, 1456 (1973); G. I. DROZD, S. Z. IVIN, V. V. SHELUCHENKO, and M. A. LANDAU. Zh. Obshch. Khim. **38**, 1653 (1968); G. I. DROZD, S. Z. IVIN, and V. V. SHELUCHENKO. Zh. Obshch. Khim. **38**, 1655 (1968).
12. R. A. GOODRICH and P. M. TREICHEL. Inorg. Chem. **7**, 694 (1968); P. M. TREICHEL, R. A. GOODRICH, and S. B. PIERCE. J. Am. Chem. Soc. **89**, 2017 (1967); A. H. COWLEY and R. W. BRAUN. Inorg. Chem. **12**, 491 (1973); J. W. GILJE, R. W. BRAUN, and A. H. COWLEY. J. Chem. Soc. Chem. Commun. 813 (1973).
13. B. BLASER and K. H. WORMS. Angew. Chem. **73**, 76 (1961); Z. M. IVANOVA and A. V. KIRSANOV. Zh. Obshch. Khim. **31**, 3991 (1961); F. SEEL and K. RUDOLPH. Z. Anorg. Allg. Chem. **363**, 233 (1968).
14. M. SCHMEISSER and E. SCHARF. Angew. Chem. **71**, 524 (1959); C. S. RONDESTVEDT, JR. J. Am. Chem. Soc. **91**, 3054 (1969); V. V. LYALIN, V. V. ORDA, L. A. ALEKSEEVA, and L. M. YAGULPOL'SKII. Zh. Org. Khim. **6**, 329 (1970); L. M. YAGULPOL'SKII, V. V. LYALIN, V. V. ORDA, and L. A. ALEKSEEVA. Zh. Obshch. Khim. **38**, 2813 (1968).
15. O. R. CHAMBERS, G. OATES, and J. M. WINFIELD. J. Chem. Soc. Chem. Commun. 839 (1972).
16. G. OATES and J. M. WINFIELD. J. Fluorine Chem. **4**, 235 (1974).
17. J. BAUMANNS, L. DENEKEN, D. NAUMANN, and M. SCHMEISSER. J. Fluorine Chem. **3**, 323 (1973).
18. G. OATES and J. M. WINFIELD. J. Chem. Soc. Dalton. 119 (1974).
19. J. A. BERRY, G. OATES, and J. M. WINFIELD. J. Chem. Soc. Dalton. 509 (1974).
20. M. SCHMEISSER, K. DAHMEN, and P. SARTORI. Chem. Ber. **103**, 307 (1970).
21. N. BARTLETT and F. O. SLADKY. Chem. Commun. 1046 (1968).
22. I. L. WILSON. J. FLUORINE Chem. **5**, 13 (1975).
23. R. SCHMUTZLER. *In* Halogen chemistry, Vol. 2. *Edited by* V. Gutmann. Academic Press, New York. 1967. p. 31.
24. O. GLEMSER and R. MEWS. Adv. Inorg. Chem. Radiochem. **14**, 333 (1972).
25. G. OATES, J. M. WINFIELD, and O. R. CHAMBERS. J. Chem. Soc. Dalton, 1380 (1974).
26. J. R. ROBERTS and K. U. INGOLD. J. Am. Chem. Soc. **93**, 6686 (1971).
27. H. GESSER, J. T. MULLHAUPT, and J. E. GRIFFITHS. J. Am. Chem. Soc. **79**, 4834 (1957).
28. R. D. LEBLOND and D. D. DESMARTEAU. J. Chem. Soc. Chem. Commun. 555 (1974).
29. J. A. GIBSON, D. G. IBBOTT, and A. F. JANZEN. Can. J. Chem. **51**, 3203 (1973).
30. J. A. GIBSON and A. F. JANZEN. Can. J. Chem. **50**, 3087 (1972).
31. J. H. HOLLOWAY. J. Chem. Educ. **43**, 202 (1966).
32. O. MJÖRNE. Sven. Kem. Tidskr. **62**, 120 (1950); Chem. Abstr. **44**, 9342e (1950).
33. E. L. MUETTERTIES, W. MAHLER, and R. SCHMUTZLER. Inorg. Chem. **2**, 613 (1963).
34. R. L. BELTRAMI and E. R. BISSELL. J. Am. Chem. Soc. **78**, 2467 (1956).
35. P. W. JONES and H. D. GESSER. Chem. Ind. 566 (1970).
36. P. B. AYSCOUGH. Electron spin resonance in chemistry. Methuen, 1967. p. 283.
37. R. E. BUCKLES and J. F. MILLS. J. Am. Chem. Soc. **76**, 3716 (1954).
38. M. ALLAN, A. F. JANZEN, and C. J. WILLIS. Can. J. Chem. **46**, 3671 (1968).
39. H. MEINERT and S. RÜDIGER. Z. Chem. **7**, 239 (1967); H. MEINERT and G. KAUSCHKA. Z. Chem. **9**, 70 (1969).
40. J. A. GIBSON and A. F. JANZEN. J. Chem. Soc. Chem. Commun. 739 (1973).

Reagents for High Temperature Aqueous Chemistry: Trifluoromethanesulfonic Acid and its Salts

LEONARD FABES AND THOMAS WILSON SWADDLE[1]

Department of Chemistry, The University of Calgary, Calgary, Alberta T2N 1N4

Received June 13, 1975

LEONARD FABES and THOMAS WILSON SWADDLE. Can. J. Chem. **53**, 3053 (1975).

The rate of decomposition of trifluoromethanesulfonic acid (HTFMS) in water is first order with respect to each of H^+ and $TFMS^-$. The bimolecular rate coefficient k_H can be represented by

$$k_H = 1.7 \times 10^{14} \exp(2.15 \times 10^5/8.314T) \text{ kg mol}^{-1} \text{ s}^{-1}$$

at ionic strength 1.0 mol kg^{-1} over the temperature range $571 < T < 593$ K, although the decomposition occurs by two pathways of comparable importance, one leading to C(II) and S(VI) and the other to C(IV) and S(IV). In alkaline solution, the rate of decomposition of $TFMS^-$ is first order in each of $TFMS^-$ and OH^-, and the bimolecular rate coefficients k_{OH} at ionic strength 2.3 are given by

$$k_{OH} = 4.1 \times 10^8 \exp(1.46 \times 10^5/8.314T) \text{ kg mol}^{-1} \text{ s}^{-1}$$

This represents a single reaction pathway leading initially to C(II) and S(VI) and ultimately to CO_3^{2-}, SO_4^{2-}, F^-, and H_2, since C(II) (as formate) reduces aqueous alkali to H_2 under the reaction conditions. No decomposition of NaTFMS could be detected after 24 h at 620 K in neutral aqueous solution. HTFMS reduces certain aqueous species at significant rates at moderate temperatures (*e.g.*, Fe(III) to Fe(II) at 470 K), and metals which depend on oxide films for their corrosion resistance are attacked by HTFMS even at 294 K (*e.g.*, Ti dissolves giving $Ti(H_2O)_6^{3+}$). Otherwise, HTFMS and its salts have good potentialities as inert electrolytes for aqueous studies at high temperatures.

LEONARD FABES et THOMAS WILSON SWADDLE. Can. J. Chem. **53**, 3053 (1975).

La vitesse de décomposition de l'acide trifluorométhane sulfonique (HTFMS) dans l'eau est du premier ordre par rapport à H^+ et par rapport à $TFMS^-$. Le coefficient de vitesse bimoléculaire, k_H, peut être représenté par l'équation

$$k_H = 1.7 \times 10^{14} \exp(2.15 \times 10^5/8.314T) \text{ kg mol}^{-1} \text{ s}^{-1}$$

à une force ionique de 1.0 mol kg^{-1}, à des températures allant de 571 à 593 K même si la décomposition se produit suivant deux voies d'égale importance, une conduisant à C(II) et S(VI) et l'autre à C(IV) et S(IV). En solution alcaline, la vitesse de décomposition du $TFMS^-$ est du premier ordre en $TFMS^-$ et du premier ordre en OH^- et le coefficient de vitesse bimoléculaire, k_{OH}, à force ionique 2.3, est donné par l'équation

$$k_{OH} = 4.1 \times 10^8 \exp(1.46 \times 10^5/8.314T) \text{ kg mol}^{-1} \text{ s}^{-1}$$

Ceci represente une seule voie pour la réaction qui conduit originalement à C(II) et S(VI) et ultérieurement à CO_3^{2-}, SO_4^{2-}, F^- et H_2 puisque C(II) (sous forme de formate) réduit, dans les conditions de la réaction, une solution aqueuse d'alkali en H_2. A 620 K, en solution aqueuse neutre, on ne peut pas noter de décomposition du NaTFMS après 24 h. A des températures modérées, l'acide HTFMS réduit à des vitesses significatives certaines espèces en solutions aqueuses (par exemple Fe(III) en Fe(II) à 470 K); les métaux qui dépendent sur la formation de films d'oxyde pour devenir résistants à la corrosion sont aussi attaqués par l'acide HTFMS même à 294 K (par exemple le Ti se dissout pour donner du $Ti(H_2O)_6^{3+}$). Autrement il semble que l'acide HTFMS et ses sels présentent de bonnes potentialités comme électrolytes inertes pour des études aqueuses à hautes températures.

[Traduit par le journal]

Introduction

Measurements of the parameters (acid dissociation constants, stability constants, rate coefficients, etc.) which govern the chemistry of aqueous electrolytes can, in principle, be made on pressurized solutions far above the normal boiling point of water, much as at room temperature, if a thermally stable, strongly ionized,

[1]Author to whom correspondence should be addressed.

Can. J. Chem. Downloaded from www.nrcresearchpress.com by 210.87.254.40 on 09/05/12
For personal use only.

Can. J. Chem. Downloaded from www.nrcresearchpress.com by 210.87.254.40 on 09/05/12
For personal use only.

poorly complexing, 'inert' electrolyte is available. The traditional electrolyte, perchloric acid, is remarkably stable kinetically towards spontaneous thermal decomposition in dilute aqueous solution, largely as a result of a high activation energy combined with a high reaction order (1), but recent work by T. C. T. Wong in our laboratories has shown that this decomposition can be catalyzed by aqueous metal ions. Thus, aqueous $HClO_4$ (1.0 *m*, *i.e.* 1.0 mol kg^{-1}) containing 0.01 *m* Fe(III) yields 0.01 *m* chloride ion after 28 h at 473 K in Teflon lined autoclaves, whereas in the absence of Fe(III) the acid would decompose only to the extent of 3×10^{-8} *m* (1). Furthermore, perchloric acid solutions can oxidize many species of interest directly as one goes toward high temperatures and kinetic barriers are removed (2, 3).

A nonoxidizing alternative to perchloric acid is trifluoromethanesulfonic acid, HTFMS ('trimsylate' (4) or 'triflic acid'). The discoverers of this acid (5) recognized its remarkable resistance to thermal decomposition and hydrolysis, and also that it is one of the strongest protonic acids known, as has subsequently been amply verified (6–13). No universal series of relative acid strength exists, since the protonating powers of various acidic solutes vary from solvent to solvent (13), but it seems safe to conclude that HTFMS will be at least as fully ionized in water at high temperatures as is $HClO_4$, which cannot be more than slightly associated in water up to 600 K (1). The $TFMS^-$ ion is also a very weak complexing agent, being only slightly more effective in complexing aqueous Cr(III) than is perchlorate ion (14), although $TFMS^-$ complexes with UO_2^{2+} (15) and Mo_2^{4+} (16) have been isolated. Thus, $TFMS^-$ offers an excellent alternative to ClO_4^-, BF_4^-, PF_6^-, etc., especially when reagents which are potential oxidants or are solvolytically unstable must be avoided (17–19).

The aqueous $TFMS^-$ ion has been reported to be stable in acidic solution up to at least 550 K (20) and in neutral or alkaline solution up to 620 K (21). This stability, however, is kinetic rather than thermodynamic, and we have therefore sought to define it in terms of the appropriate rate equations and parameters for the various hydrolysis pathways as functions of p*H* and temperature, thereby permitting upper limits to be set to the extent of spontaneous decomposition of the reagent in typical experimental situations, as well as gaining information on the reaction mechanisms.

Experimental

Anhydrous HTFMS, as purchased from the 3M Company, was black, presumably with organic char (20), but a simple distillation under anhydrous conditions at reduced pressure was sufficient to give a product which analyzed correctly for H^+, contained no detectable HF, and gave the same kinetic results from batch to batch. A further careful fractional distillation of this colorless liquid led to no detectable change.

Kinetic Measurements

The pressure vessels, previously described (1), were of titanium – 0.2% palladium alloy or (with basic samples only) of Type 316 stainless steel, and were protected from corrosion by the samples with silica liners (acidic solutions only) or Teflon liners; the silica liners were slightly attacked, presumably by the HF produced in the decomposition of HTFMS, but the Teflon vessels appeared to be completely inert to both acidic and alkaline solutions. The free volume in the autoclaves was 47 cm^3. The $TFMS^-$ solutions were made up on a volume basis, but concentrations were expressed on the molal (mol/kg) scale using the measured densities and corrected for the evaporative loss entailed in generating the saturated vapor pressure of the solution (taken to be that for pure water) at the reaction temperatures. The derived kinetic results were the same whether a 10 or a 25 cm^3 aliquot of the $TFMS^-$ solution was placed in the autoclave.

The solution samples were sealed into the autoclaves under an air or a nitrogen atmosphere at 0.1 MPa (the results were shown to be independent of the presence or absence of oxygen) and brought to the desired temperature in a preheated Blue M Conwate CW-160HF-1 forced-convection oven (constancy ± 0.3 K during a run). It was established, by extrapolating reactant concentrations back to their original values as functions of time, that the effective zero time of the reactions was the same at which the oven temperature (measured as described previously (1)) was seen to be stabilized, which was 40 min after placing the vessels in the oven. In general, conditions were chosen to give slow reaction rates, so as to minimize any errors associated with sample warm-up. Autoclaves were removed as required and quenched rapidly to room temperature with water.

The $TFMS^-$ content of the solutions could not easily be determined directly with good precision, but it was found that an Orion 92-81 perchlorate ion selective electrode, used in conjunction with an Orion 801 p*H* meter and 90-02 double-junction reference electrode, gave a linear response to $TFMS^-$ when the p*H* was adjusted to about 5 with sodium acetate, and could be used to measure $[TFMS^-]$ in the range 0.002–0.05 *m* without significant interference from the decomposition products F^-, HCO_3^-, HSO_3^-, or SO_4^{2-}. The Gran method (22) enabled $TFMS^-$ concentrations to be measured with a standard deviation of 7%, which, though poor, was acceptable for measurement of the rate of disappearance of $TFMS^-$ in acidic solutions, since the usual alternative of following the formation of the reaction products was not feasible; the S and C products were distributed amongst various oxidation states, while the F product,

Can. J. Chem. Downloaded from www.nrcresearchpress.com by 210.87.254.40 on 09/05/12
For personal use only.

present as volatile HF, was partially depleted by reaction with the autoclave walls or possibly by vapor loss on opening the pressure vessels.

The fluoride contents of the solutions were measured with about 1% precision using an Orion 94-09 ion selective electrode, as previously described (23). This method was effective in measuring the rate of hydrolysis of $TFMS^-$ in alkaline solution.

Reaction Products

Dissolved fluoride was measured with the Orion 94-09 electrode. Sulfate was measured gravimetrically as $BaSO_4$. Sulfite was estimated by redox titration. Carbonate was measured by a p*H* titration procedure, which also gave rough indications of the F^- and SO_3^{2-} contents through inflexions in the titration curves at lower p*H* than for CO_3^{2-}.

The gaseous decomposition products of aqueous HTFMS were determined by mass spectroscopy, the samples of the aqueous acid having been sealed into quartz ampoules which were heated in autoclaves, partially filled with water to pressurize the tubes externally. This procedure was not followed with alkaline $TFMS^-$ solutions, as these would have attacked any available material other than Teflon, which would have been too soft to form a gastight ampoule at high temperatures. Nevertheless, when NaTFMS was decomposed in 9 *m* NaOH for 19 h in a Teflon lined autoclave at 572 K, a sample drawn from the gas space of the cooled autoclave immediately on opening was found by mass spectrometry to contain much hydrogen gas; in the same way, sodium formate was shown to yield H_2 under these conditions.

Results

Reaction Products

The gaseous products of the partial thermal decomposition of aqueous HTFMS were primarily CO_2, CO, and SO_2, with traces of H_2S, F_2CO, CS_2, and some trivial components with unassignable mass numbers. The recorded 44:28 (CO_2:CO) mass ratio rose from 1.6 for samples decomposed at 563 K to 2.9 for 593 K, as compared with 5.7 for pure CO_2 (CO_2^+ undergoes partial fragmentation to CO^+); these data indicate that two parallel paths of comparable importance were operating in the decomposition of HTFMS in acidic solution, one of relatively low activation energy E_a leading to CO and one of higher E_a leading to CO_2. Some elemental sulfur was recovered, especially at the higher temperatures, so that this product may be associated with the CO_2 producing reaction. The aqueous phase contained HF, HCO_3^-, SO_4^{2-}, and HSO_3^-. It was shown in separate experiments that S(IV) disproportionates to S(0) and S(VI) in aqueous acid at high temperatures (*e.g.*, in 3 *m* HCl or H_2SO_4 at 584 K over 19 h), thus accounting for the presence of elemental sulfur in the decomposition products of HTFMS. The disproportionation of S(IV) is thermodynamically possible in aqueous systems at all p*H* values even at 298 K (24), but mechanistic limitations evidently prevent its occurrence except at high temperatures (~570 K) and high acidities, on the usual experimental time scale. The disproportionation reaction was insufficient to account for all the S(VI) produced in the acidic decomposition of HTFMS, and in any event the decomposition path leading to C(II) (carbon monoxide) must produce S(VI) directly. The main reactions in the decomposition of $TFMS^-$ in acidic solutions are therefore 1, 2*a*, and 2*b*.

[1] $CF_3SO_3^- + 2H_2O = 3HF + HSO_4^- + CO$

[2*a*] $CF_3SO_3^- + 2H_2O + H^+ = 3HF + H_2SO_3 + CO_2$

[2*b*] $3H_2SO_3 = 2HSO_4^- + S + H_2O + 2H^+$

In alkaline solutions at about 570 K, $TFMS^-$ was hydrolyzed *quantitatively* to $3F^-$, SO_4^{2-}, and CO_3^{2-}, and it was shown qualitatively that H_2 was a major product. It was also established that SO_3^{2-} quantitatively survives heating at about 580 K in 1 *m* NaOH for several days, so that no pathway analogous to reaction 2 could have been operative in the alkaline decomposition of $TFMS^-$. In alkaline solution, a S(VI) producing reaction analogous to reaction 1 would yield formate rather than CO (ref. 24, p. 278), and formate ion is thermodynamically capable of reducing alkaline water to H_2 even at 298 K (25):

[3] $HCO_2^- + OH^- = H_2 + CO_3^{2-}$ $\Delta G^0 = -35$ kJ mol^{-1}

Thus, the final products of an alkaline hydrolysis of $TFMS^-$ producing initially S(VI) and C(II) should be F^-, SO_4^{2-}, CO_3^{2-}, and H_2, if reaction 3 is sufficiently rapid at the reaction temperature, and this is indeed what is observed.

[4] $CF_3SO_3^- + 6OH^- = 3F^- + SO_4^{2-} + CO_3^{2-} + H_2 + 2H_2O$

Exploratory measurements showed that the rate of decomposition of formate ion in 1.9 *m* NaOH at 586 K, as followed by $KMnO_4$ titration, was very close to that calculated by Arrhenius extrapolation (see below) for the disappearance of $TFMS^-$ under the same conditions, so that a substantial buildup of formate ion during the alkaline hydrolysis of $TFMS^-$ was neither expected nor observed.

Can. J. Chem. Downloaded from www.nrcresearchpress.com by 210.87.254.40 on 09/05/12
For personal use only.

TABLE 1. Initial rates of decomposition of trifluoromethane sulfonate ion in acidic aqueous solution

Nominal temperature (K)	Actual temperature (K)	Initial $[CF_3SO_3^-]$ (mol kg^{-1})	Mean $[CF_3SO_3^-]$ (mol kg^{-1})	Initial $[H^+]$ (mol kg^{-1})	Ionic strength (mol kg^{-1})	$-\frac{d}{dt}[CF_3SO_3^-] \times 10^6$ (mol kg^{-1} s^{-1})	$k_H \times 10^6$ (kg mol^{-1} s^{-1})
571.6±1.1	571.2	1.856	1.731	1.856	1.856	11.9	3.7
	570.7	1.750	1.584	1.750	1.750	12.6	4.5
	572.2	1.145	1.068	1.145	1.145	5.9	4.8
	570.8	0.991	0.947	0.991	0.991	3.4	3.6
	572.7	0.397	0.388	0.397	0.397	0.73	4.7
582.6±0.7	582.4	2.757	2.543	2.757	2.757	32	4.6
	583.6	2.223	2.040	2.223	2.223	32	7.1
	582.2	1.308	1.214	1.308	1.308	14.1	8.9
	582.8	1.236	1.148	1.236	1.236	11.4	8.0
	583.7	1.198	1.095	1.198	1.198	9.1	6.9
	582.7	1.019	0.945	1.019	1.019	8.3	8.6
	581.6	0.625	0.598	0.625	0.625	3.5	9.4
	583.0	2.617	2.536	0.692	2.617*	11.7	6.7
	582.8	2.610	2.497	1.406	2.610*	19.4	5.5
	582.4	1.941	1.836	1.327	1.941	15.1	6.2
592.9±0.4	592.8	2.165	1.885	2.165	2.165	69	17
	592.9	1.661	1.479	1.661	1.661	40	16
	592.4	1.334	1.195	1.334	1.334	30	19
	593.2	0.661	0.614	0.661	0.661	10.1	25
	593.3	0.318	0.307	0.318	0.318	2.1	22

*HTFMS + NaTFMS.

TABLE 2. Initial rates of decomposition of trifluoromethane sulfonate ion in alkaline aqueous solution

Nominal temperature (K)	Actual temperature (K)	Initial $[CF_3SO_3^-]$ (mol kg^{-1})	Initial $[OH^-]$ (mol kg^{-1})	Ionic strength (mol kg^{-1})	$-\frac{d[CF_3SO_3^-]}{dt} \times 10^6$ (mol kg^{-1} s^{-1})	$k_{OH} \times 10^6$ (kg mol^{-1} s^{-1})
552	551.1	0.0152	2.115	2.13	0.181	5.6
	552.3	0.0293	2.115	2.14	0.404	6.5
	551.9	0.0942	2.175	2.27	1.29	6.3
	551.5	0.0942	1.094	2.28*	0.624	6.1
	551.6	0.0957	0.664	2.28*	0.390	6.1
	551.3	0.0938	1.094	1.19	0.346	3.4
523	522.9	0.0943	1.094	2.28*	0.119	1.15
538	538.2	0.0943	1.094	2.28*	0.271	2.6
563	563.3	0.0943	1.094	2.28*	1.25	12.1

*Ionic strength maintained with NaCl.

Can. J. Chem. Downloaded from www.nrcresearchpress.com by 210.87.254.40 on 09/05/12
For personal use only.

Kinetics

Because the formal reaction 2*a* (at least) consumes H^+ whereas reaction 1 does not, the time dependence of the HTFMS concentration could not be expected to follow a simple integrated rate expression over a substantial fraction of the decomposition reaction. Instead, the concentration of $TFMS^-$ was monitored over the first 20% of the reaction in acidic solution, and the slope of the crudely linear plot of $[TFMS^-]$ against time t was taken to be $-d[TFMS^-]/dt$ at the mean $[TFMS^-]$. These data are collected in Table 1. The reproducibility of these rates was as poor as $\pm 14\%$, but this is as good as could be expected in view of the 7% uncertainty in the $[TFMS^-]$ analyses and the difficulty of presetting the nominal reaction temperatures accurately.

Log–log plots of the rate data of Table 1 at a given nominal reaction temperature against stoichiometric [HTFMS] when $[H^+] = [TFMS^-]$ were linear, within the experimental uncertainty, with a slope of about 1.8, which suggests a second-order reaction with a retarding ionic strength effect (*cf.* the decomposition of aqueous $HClO_4$, which is actually 4th order with an apparent reaction order of 3.5). A plot of log(rate) *vs.* log $[H^+]$ for 583 K and nearly constant ionic strength (2.6–2.7 *m*) had slope ~0.9, showing the reaction to be essentially first order with respect to each of H^+ and $TFMS^-$, and accordingly bimolecular rate coefficients k_H are given in Table 1. At the nominal temperatures 582.6 and 592.9 K, k_H values generally decreased as the ionic strength I increased, and can be represented to within the rather large experimental error by equations 5 and 6.

$$[5] \quad k_H^{582.6} = (10.3 - 1.8I) \times 10^{-6}\ m^{-1}\ s^{-1}$$

$$[6] \quad k_H^{592.9} = (2.6 - 0.5I) \times 10^{-5}\ m^{-1}\ s^{-1}$$

For $I = 1.0\ m$, we have $k_H \sim 4.3 \times 10^{-6}$, 8.5×10^{-6}, and $2.1 \times 10^{-5}\ m^{-1}\ s^{-1}$ at 571.6, 582.6, and 592.9 K respectively. These data give a somewhat curved Arrhenius plot (concave upwards, as expected for two parallel reactions having the same rate law) but can be reproduced satisfactorily by an activation energy of 215 kJ mol^{-1} and a preexponential factor of 1.7×10^{14} $m^{-1}\ s^{-1}$, the uncertainty in these parameters being about 20%.

The rate of disappearance of $TFMS^-$ in alkaline solution is much more readily measured as one-third of the rate of formation of F^-, low concentrations of which were determined with 1% precision. This permitted rate measurements to be made with OH^- in large excess over $TFMS^-$, and the initial rates of $TFMS^-$ collected in Table 2 were reproducible to 5%, most of this margin representing the difficulty of reproducing the reaction temperature from one run to another. Examination of the data of Table 2 shows that the reaction is accurately first order in each of OH^- and $TFMS^-$ at a given ionic strength, and the corresponding bimolecular rate coefficients k_{OH} listed for 552 K, $I = 2.2 \pm 0.1\ m$ are obviously constant within 5% standard deviation. The data for $I = 2.28\ m$ as a function of temperature gave a good Arrhenius plot with $E_a = 146$ kJ mol^{-1} and a preexponential factor of $4.1 \times 10^8\ m^{-1}\ s^{-1}$. The alkaline hydrolysis rate is evidently accelerated by increasing the ionic strength; this is opposite to the ionic strength effect on the acidic hydrolysis reaction, as expected for reactions of opposite charge types.

Neutral solutions of NaTFMS (1 *m*) underwent no detectable decomposition, even at 620 K over 24 h.

Reaction of HTFMS with Metals and Metal Ions

At 294 K, type 316 stainless steel tubing was visibly etched within one day by deaerated HTFMS (1.0 *m*), and commercial titanium dissolved in it to give a purple solution of $Ti(H_2O)_6^{3+}$ over a few hours; Ti – 0.2% Pd alloy was more resistant, but nevertheless gave an appreciably yellow-orange solution over 24 h. By contrast, these metals were not detectably attacked by 1 *m* $HClO_4$ or H_2SO_4 over several days.

The divalent metal ions Mn, Fe, Co, Ni, and Cu were unchanged after 24 h in 1.0 *m* HTFMS at 570–580 K. Further studies in our laboratories by T. C. T. Wong, however, have shown that HTFMS reduces aqueous iron(III) to iron(II) under relatively mild conditions (*e.g.*, 0.05 *m* Fe(III) in 1.5 *m* HTFMS is reduced to the extent of at least 7% in 24 h at 473 K, with the concomitant formation of HF).

Discussion

The rate determining step in the alkaline hydrolysis of $TFMS^-$ evidently involves nucleophilic attack of OH^- on the S atom of $TFMS^-$

$$[7] \quad HO^- + SO_3CF_3^- \rightarrow HOSO_3^- + CF_3^-$$

Can. J. Chem. Downloaded from www.nrcresearchpress.com by 210.87.254.40 on 09/05/12
For personal use only.

The actual initial products of this step may be SO_4^{2-} and HCF_3, or SO_4^{2-}, CF_2, and F^-, but in any event the fluorocarbon moiety will hydrolyze to HCO_2^- in alkali (26). We have demonstrated that formate ion is oxidized to carbonate with H_2 evolution at a rate sufficiently rapid at the temperatures involved here to to account for the observed reaction products, sulfate, carbonate, fluoride, and hydrogen.

In acidic solution, the reactions 1 and 2*a* occur simultaneously, with reaction 1 accounting for some 33% of the decomposition rate at 563 K and about 16% at 593 K, on the basis of the mass spectroscopic yields of CO and CO_2, corrected for the difference in the ionization cross-sections of these molecules (27). Both acidic decomposition pathways are evidently first order in each of $TFMS^-$ and H^+, if ionic strength effects are allowed for, and accordingly, neutral solutions of $TFMS^-$ were found not to hydrolyze significantly even at temperatures approaching the critical point of water. The decomposition mechanisms presumably involve the undissociated HTFMS molecule (in which case HTFMS must still be a fairly strong acid in water at 600 K, in order to give the observed reaction orders).

[8] $$H^+ + CF_3SO_3^- \rightleftharpoons CF_3SO_3H$$

Assuming, for argument's sake, a bimolecular mechanism for the hydrolysis of HTFMS, nucleophilic attack of water on the S atom of HTFMS will be seen to give S(VI) and C(II), much as in equation 7, whereas attack of the water molecule on the C atom will yield C(IV) and S(IV),

[9] $$H_2O + CF_3SO_3H \rightarrow HOCF_3 + H_2SO_3$$

the postulated trifluoromethanol intermediate hydrolyzing rapidly to carbonic acid and HF.

Whether the decomposition of $TFMS^-$ proceeds via reaction 1, 2*a*, or 4, the potential reducing power of this anion is clearly seen, since a familiar reducing agent (CO, SO_2, H_2) is produced in each case. This reducing power can be exercised directly at relatively low temperatures. Thus, Fe(III) is reduced to Fe(II) in acidic aqueous solution around 470 K, and metals (*e.g.*, titanium) or alloys (*e.g.*, stainless steels) which are corrosion resistant by virtue of having a tenacious oxide film are attacked quite rapidly by aqueous HTFMS even at 290 K, presumably because of reduction of the oxide coat. The latter property has been utilized to activate passive metals prior to chromium plating (28). These considerations limit the usefulness of HTFMS as a high-temperature aqueous reagent, but nevertheless it can be of great value in situations where a strong electrolyte of good thermal stability is required and reducing conditions can be tolerated.

Finally, this study serves to illustrate the fact that much familiar 'room temperature chemistry' exists only by virtue of high kinetic barriers to the realization of thermodynamic exigency. The resistance of $TFMS^-$ to hydrolysis is due in part to the high activation energies of the various hydrolysis pathways, and in part to the need to involve either H^+ or OH^- in the decomposition mechanisms. Similarly, SO_2 should disproportionate in water, and formate ion (*i.e.*, CO) should reduce aqueous alkali to hydrogen, at 298 K; these reactions do occur on a relatively short time-scale at 500–600 K, where many kinetic barriers are overcome.

We thank J. W. Cobble for first drawing our attention to the potential uses of HTFMS, and Atomic Energy of Canada, Ltd., for financial support of this work.

1. M. P. Henderson, V. I. Miasek, and T. W. Swaddle. Can. J. Chem. **49**, 317 (1971).
2. T. W. Swaddle, J. H. Lipton, G. Guastalla, and P. Bayliss. Can. J. Chem. **49**, 2433 (1971).
3. P.-C. Kong, T. W. Swaddle, and P. Bayliss. Can. J. Chem. **49**, 2442 (1971).
4. Anonymous. Chem. Eng. News, **49**(3), 33 (1971).
5. R. N. Haszeldine and J. M. Kidd. J. Chem. Soc. 4228 (1954).
6. T. Gramstad. Tidsskr. Kjemi, Bergvesen, Metall. **19**, 62 (1959).
7. E. S. Lane. Talanta, **8**, 849 (1961).
8. Yu. Ya. Fialkov and V. I. Ligus. Dokl. Akad. Nauk SSSR, **197**, 1353 (1971).
9. A. Engelbrecht and B. M. Rode. Monatsh. Chem. **103**, 1315 (1972).
10. B. M. Rode and A. Engelbrecht. Z. Phys. Chem. (Leipzig), **253**, 17 (1973).
11. M. Bos and E. A. M. F. Dahmen. Anal. Chim. Acta, **63**, 185 (1973).
12. R. L. Benoit and C. Buisson. Electrochim. Acta, **18**, 105 (1973).
13. D. G. Russell and J. B. Senior. Can. J. Chem. **52**, 2975 (1974).
14. A. Scott and H. Taube. Inorg. Chem. **10**, 62 (1971).
15. A. I. Skoblo and D. N. Suglobov. Radiokhimiya, **16**, 518 (1974).
16. E. H. Abbott, F. Schoenewolf, Jr., and T. Backstrom. J. Coord. Chem. **3**, 255 (1974).
17. A. R. Bowen and H. Taube. Inorg. Chem. **13**, 2245 (1974).

18. D. K. LAVALLEE, C. LAVALLEE, J. C. SULLIVAN, and E. DEUTSCH. Inorg. Chem. **12**, 570 (1973).
19. D. STROUPE and D. F. SHRIVER. Inorg. Chem. **13**, 2652 (1974).
20. T. GRAMSTAD and R. N. HASZELDINE. J. Chem. Soc. 4069 (1957).
21. T. J. BRICE and P. W. TROTT. U.S. Patent No. 2,732,398 (January, 1956).
22. G. GRAN. Analyst, **77**, 661 (1952).
23. T. W. SWADDLE and W. E. JONES. Can. J. Chem. **48**, 1054 (1970).
24. W. M. LATIMER and J. H. HILDEBRAND. Reference book of inorganic chemistry. 3rd ed. The Macmillan Co., New York, N.Y. 1951. p. 252.
25. W. M. LATIMER. Oxidation potentials. 2nd ed. Prentice Hall, Inc., Englewood Cliffs, N.J. 1952. pp. 32, 130.
26. S. K. MALIK, W. SCHMIDT, and L. O. SPREER. Inorg. Chem. **13**, 2986 (1974).
27. J. W. OTVOS and D. P. STEVENSON. J. Am. Chem. Soc. **78**, 546 (1956).
28. H. BROWN. Fr. Patent No. 1,407,483 (July 30, 1965); U.S. Patent No. 3,310,480 (March 21, 1967).

Can. J. Chem. Downloaded from www.nrcresearchpress.com by 210.87.254.40 on 09/05/12
For personal use only.

The Electroreduction of some *N*-Haloamides[1]

DENIS BÉRUBÉ, JEAN CAZA, FRANK M. KIMMERLE, AND JEAN LESSARD
Département de chimie, Université de Sherbrooke, Sherbrooke, Québec J1K 2R1

Received January 9, 1975

DENIS BÉRUBÉ, JEAN CAZA, FRANK M. KIMMERLE, and JEAN LESSARD. Can. J. Chem. **53**, 3060 (1975).

The electroreduction of nine *N*-haloamides (ZCONRX) at a dropping mercury electrode has been investigated in protic and aprotic media. Preparative electrolysis indicated the possibility of capturing the intermediate amide radical by intermolecular addition to olefins or by intramolecular hydrogen abstraction.

DENIS BÉRUBÉ, JEAN CAZA, FRANK M. KIMMERLE et JEAN LESSARD. Can. J. Chem. **53**, 3060 (1975).

On a étudié la réduction électrochimique de neuf *N*-haloamides (ZCONRX) à l'électrode à goutte de mercure tombante en milieu protique et aprotique. Les électrolyses préparatives laissent croire que le radical amide intermédiaire peut être capté par addition intermoléculaire à des oléfines et par abstraction intramoléculaire d'hydrogène.

Can. J. Chem. Downloaded from www.nrcresearchpress.com by 210.87.254.5 on 09/05/12
For personal use only.

Our interest in *N*-haloamides and amide radicals (1–4), and in particular in the chromous chloride promoted addition of *N*-haloamides to olefins (1, 2), led us to study the electrochemical reduction of some *N*-haloamides. It is obvious that if by an electrochemical route the reduction of the nitrogen–halogen bond leads to an amide radical Z—CO—$\dot{N}$—R then a facile means of the production of a promising synthetic intermediate has been attained. Furthermore, it was hoped that the study of the electron transfer at a solid electrode would give additional insight regarding the mechanism of the transition metal catalyzed reaction. As a first step in this direction we have investigated the reduction of the nine compounds in Table 1 by classical d.c. polarography, cyclic voltammetry and preparative electrolysis.

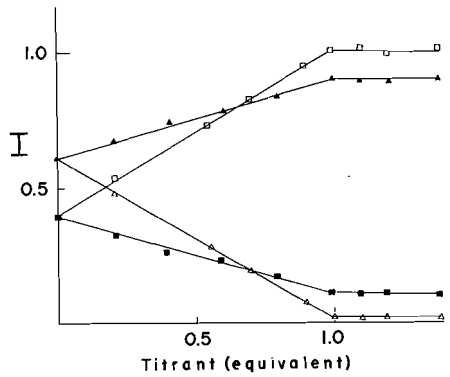

FIG. 1. Amperometric titration of NCU (**1**) (20 m*M*) in 0.2 *M* methanolic solution of $LiClO_4$. (*a*) Titrant is acetic acid: □ I_1, △ ($I_2 - I_1$). (*b*) Titrant is sodium methoxyde: ■ I_1, ▲ ($I_2 - I_1$). I_1 (at −1.0 V *vs.* s.c.e.) and I_2 (at −1.6 V *vs.* s.c.e.) are given in arbitrary units.

Polarographic Studies

In methanolic solutions *N*-chlorourethane (NCU) (**1**), and *N*-chloroacetamide (NCA) (**2**), show two diffusion controlled reduction waves. NCU: $(E_{1/2})_1 = -0.60$ V, $(E_{1/2})_2 = -0.96$ V *vs.* a saturated calomel electrode (s.c.e.); NCA: $(E_{1/2})_1 = -0.43$ V, $(E_{1/2})_2 = -1.12$ V *vs.* s.c.e. $(E_{1/2})_1$ is p*H* independent, $(E_{1/2})_2$ is displaced cathodically only at operational p*H* values in excess of p*H* 11, but the respective currents I_1 and I_2 are p*H* dependent. The dependence is so exact that it can serve as the basis of an amperometric titration analysis illustrated in Fig. 1 for NCU (**1**).

Indeed, the waves correspond to highly irreversible two electron reduction steps involving the neutral molecule (acid) and the anion (base) respectively:

[1] $SH^+ + ZCONHCl + 2e^- \rightarrow ZCONH_2 + Cl^- + S$

and

[2] $2SH^+ + ZCO\bar{N}Cl + 2e^- \rightarrow ZCONH_2 + Cl^- + 2S$

where SH^+ is a proton donor (*e.g.* ZCONHCl or CH_3OH). The overall reactions are in perfect accord with the results of mass electrolysis (100 ± 2% coulombic efficiency) and chemical

[1]Taken in part from the M.Sc. thesis of J. Caza, Université de Sherbrooke, 1973.

TABLE 1. Reduction of *N*-haloamides at a mercury electrode in acetonitrile (0.2 *M* $LiClO_4$)

N-Haloamide	$(E_{1/2})_1$ V *vs.* s.c.e.	$(E_{1/2})_2$ V *vs.* s.c.e.	*n*	Electrolysis products	Yield (%)[a]
$CH_3CH_2OCONHCl$ (**1**)	−0.22	−1.22	2	$CH_3CH_2OCONH_2$	94
	−0.40(Pt)	[b]	2	$CH_3CH_2OCONH_2$	94[c]
$CH_3CONHCl$ (**2**)	−0.35	−1.21	2	CH_3CONH_2	[d]
$ClCH_2CONHCl$ (**3**)	−0.11	[b]	2	$ClCH_2CONH_2$	[d]
$Cl_2CHCONHCl$ (**4**)	−0.09	[b]	2	$Cl_2CHCONH_2$	[d]
$Cl_3CCONHCl$ (**5**)	+0.05	[b]	2	Cl_3CCONH_2	70
				$Cl_2CHCONH_2$	19
$CH_3CONHBr$ (**6**)	−0.15	−0.82	[b]	[e]	
	−0.10(Pt)	[b]	[b]	[e]	
CH_2—CO | | CH_2CONCl (**7**)	−0.04		2	CH_2—CO | | CH_2CONH	[d]
C_2H_5 | CH_3CONCl (**8**)	−0.10		[b]	[e]	
t-C_4H_9 | $CH_3(CH_2)_3CONCl$ (**9**)	−0.13		1	Cl t-C_4H_9 | | $CH_3CH(CH_2)_2CONH$	37
				t-C_4H_9 | $CH_3CH_2(CH_2)_2CONH$	55

[a]Of isolated products.
[b]Not determined.
[c]By v.p.c. The electrolysis in the presence of an equivalent of acetic acid gave a quantitative yield of urethane.
[d]The exact yield was not determined because of the high solubility of the amides in water.
[e]No preparative electrolysis was carried out.

analysis of the products (see Preparative Electrolyses).

For electroanalytical purposes it may be noted that the polarographic diffusion currents are linear functions of the concentration from 10^{-4} to 5×10^{-3} *M* and vary with the square root of the mercury column height for all compounds listed in Table 1. The half wave potentials do not vary with concentration although for compounds **3** to **6** they are somewhat ill defined (±0.05 V) due to incipient polarographic maxima.

In an aprotic medium such as acetonitrile, NCU (**1**), NCA (**2**), and *N*-bromoacetamide (NBA) (**6**) show the two reduction waves due to the neutral molecule [1] and the anion [2] respectively (Table 1). Indeed the corresponding lithium salts show the second wave only; upon addition of acetic acid, the first wave appears and when two or more equivalents of acid are added, only the first wave can be seen. The polarographic reduction of NCU (**1**) and NCA (**2**) remains truly irreversible (αn values of the order of 0.3 and 0.4 for the first wave) and the reduction products (urethane, acetamide) are not reoxidized even at a platinum anode before the anodic decomposition of the electrolyte. The polarographic reduction of the *N*-chloro-α-chloroacetamides **3** to **5** is also irreversible ($\alpha n \sim 0.9$, $n = 2$). At potentials more cathodic than −0.8 V *vs.* s.c.e., two or more waves appear, one being most probably due to the reduction of the N—Cl bond of the anions, and the other(s) to the reduction of the C—Cl bonds; this region was not further investigated.

Since the mechanism proposed by Lessard *et al.*[2] for the chromous chloride promoted addition of *N*-haloamides to olefins implied an amide radical species, we had hoped to be able to discern two consecutive one electron transfer steps (*e.g.* [3] and [4]) constituting [1] or [2]:

$$[3] \qquad ZCONHCl + e^- \rightarrow ZC\dot{O}NH$$

$$[4] \qquad ZC\dot{O}NH + e^- + SH^+ \rightarrow ZCONH_2 + S$$

In retrospect it may not be surprising that the insertion of the second electron [4] should be faster than or as fast as the insertion of the

[2]H. Driguez, J. M. Paton, and J. Lessard, presented at the 55th Chemical Conference of the Chemical Institute of Canada, Quebec, June 1972.

Can. J. Chem. Downloaded from www.nrcresearchpress.com by 210.87.254.5 on 09/05/12
For personal use only.

Can. J. Chem. Downloaded from www.nrcresearchpress.com by 210.87.254.5 on 09/05/12
For personal use only.

first and hence indiscernable by normal electroanalytical techniques. We also searched for chemical evidences of the formation of the amide radical [3], by coupling, trapping by hydrogen abstraction from methanol, and by addition to olefins, in preparative electrolyses at a mercury and a platinum cathode but without any success.[3] However addition products have been isolated when preparative electrolyses of NCU (**1**) were carried out at a graphite electrode in the presence of an olefin under special conditions.

Although standard electrode potentials could not be established (anodic region inaccessible), the $E_{1/2}$ values show useful trends with the chemical structures of the depolarizers (Table 1). Since we can assume that the same functional group (—C(=O)—NH—X) is involved, we expect the $E_{1/2}$ values to reflect the activation energy of the first electron transfer step and also the stability of the intermediate species (7).

The two possible mechanisms for the addition of the first electron are: (*1*) addition to the N—X bond whose fission leads to the amide radical and the halide anion [5];

$$[5] \quad ZCONHX + e^- \rightarrow [ZCONH \cdots X]^{\cdot -} \rightarrow ZCO\dot{N}H + X^-$$

(*2*) addition to the π system with the subsequent cleavage of the N–X bond (which might be concerted with the electron transfer) leading to the amide radical and the halide anion [6].[4]

$$[6] \quad ZCONHX + e^- \rightarrow [Z\overset{O^{\cdot}}{\overset{|}{C}}-NH-X]^- \rightarrow ZCO\dot{N}H + X^-$$

For both mechanisms, one would expect that an electron withdrawing group Z should facilitate electron acceptance and render the reduction potential more anodic, but probably more so for the second mechanism. For the reduction of the *N*-chlorocarboxamides, $E_{1/2}$ becomes more anodic in the sequence **2** ($Z = CH_3$) < **3** ($Z = CH_2Cl$) < **4** ($Z = CHCl_2$) < **5** ($Z = CCl_3$), the effect being the largest for the introduction of the first chlorine. The reduction potential of NCU (**1**, $Z = OC_2H_5$) is more anodic than that of NCA (**2**, $Z = CH_3$) but more cathodic than that of *N*-chloro-α-chloroacetamide (**3**, $Z = CH_2Cl$). Although an ethoxy group should have a stronger inductive effect than a chloromethyl group, this effect should be partly compensated in the former by its ability to share its electrons with the carbonyl group of the amide. The more anodic reduction potential of *N*-chlorosuccinimide (**7**) as compared to that of *N*-chloroacetamide (**2**) can be accounted for also by either mechanism. *N*-chloro-*N*-ethylacetamide (**8**) and *N*-chloro-*N*-tertiobutylpentanamide (**9**) are more easily reduced than *N*-chloroacetamide (**2**) in agreement with the stabilizing influence of an alkyl group, as compared to an hydrogen atom, in the intermediate amide radical. Finally NBA (**6**) is more readily reduced than NCA (**2**) as expected on the basis of bond strength, polarizabilities and ease of reduction of organic (alkyl, aryl, vinyl) halides (10).

Preparative Electrolyses

In methanol, using $LiClO_4$ electrolyte, the reduction of NCU (**1**) at a mercury electrode in

[3]The experimental results for the reduction at a mercury electrode do not allow us to distinguish between the direct reduction of the amide radical [4] and the reduction of an intermediate species resulting from the trapping of the amide radical by mercury. Mann *et al.* (5) suggested an analogous interaction of the organo radical with mercury in the reduction of a cyclopropyl bromide.

Two reduction waves have been observed for the alkylmercuric halides (6). In order to eliminate the possibility of the two reduction waves of NCU (**1**), NCA (**2**), and NBA (**6**) being due to the rapid formation of organomercuric halides upon contact with mercury, the reaction of NCU (**1**) and NBA (**6**) with mercury was investigated. The original polarographic waves disappeared slowly, a new wave appeared, and a grey precipitate, consisting primarily of colloïdal mercury and calomel, was formed. These reactions could be prevented by imposing a slightly cathodic potential on the mercury metal and were not investigated extensively (see Experimental).

[4]For the electroreduction of the vinyl halides, Miller and Riekena (8) have suggested that the first electron may add to the π system to give an anion radical which loses a halide anion to form the vinyl radical. For the reductive hydrogenolysis of *p*-carbomethoxy- and *p*-cyano-substituted benzyl methyl ether, benzyl acetate and benzylidyne trifluoride in protic medium, electron transfer to the substituent followed by the cleavage of the C—O and C—F bonds has been proposed as the first step (9).

Can. J. Chem. Downloaded from www.nrcresearchpress.com by 210.87.254.5 on 09/05/12
For personal use only.

the presence of an equimolar amount of acetic acid (reduction of the neutral molecule)[5] yielded 92% (isolated) urethane. The reduction carried out in the presence of an equimolar quantity of sodium methoxyde (reduction of the anion)[5] gave a quantitative yield (by v.p.c.) of urethane. In either reduction, no *N,N'*-dicarboethoxyhydrazine (coupling of two urethane radicals) could be detected by vapor phase chromatography (v.p.c.). Also attempts to detect formaldehyde prove inconclusive.[6]

In acetonitrile ($LiClO_4$ electrolyte), the reduction of NCU (**1**) and the *N*-chloroacetamides **2** to **5** at the mercury electrode gave the corresponding amides in the yields indicated in Table 1. No traces of dimerization products (coupling of amide radicals) could be detected. The results were identical for the reduction of NCU (**1**) at a platinum electrode.

Electroreduction of NCU (**1**) in the presence of electron-poor olefins such as acrylonitrile (**10**, Y = CN) and methyl acrylate (**10**, Y = $COOCH_3$) in a methanol–chloroform (2:3) mixture readily led to the addition product $C_2H_5OCONHCH_2CH_2Y$ (**11**). The mechanism does not involve radicals but involves the addition of anions. The product may be formed directly from the urethane anion, the path followed being similar to that proposed by Baizer and Chruma (11) in their study of the reduction of organic *gem*-halides in the presence of electrophilic double bonds:

$$[7]\quad C_2H_5OCO\bar{N}H + \underset{\mathbf{10}}{CH_2{=}CHY} \rightarrow C_2H_5OCONHCH_2\bar{C}HY \xrightarrow{SH^+} \underset{\mathbf{11}}{C_2H_5OCONHCH_2CH_2Y}$$

where SH^+ is a proton donor, predominantly $C_2H_5OCONHCl$ (**1**). A ready source of protons will favor the formation of urethane (reaction 1, Z = OC_2H_5) while extremely low concentrations of SH^+ would favor polymerization reactions (11). Alternatively, the product may be formed indirectly from the NCU anion:

$$[8]\quad C_2H_5OCO\bar{N}Cl + \underset{\mathbf{10}}{CH_2{=}CHY} \rightarrow C_2H_5OCO\overset{\overset{Cl}{|}}{N}CH_2\bar{C}HY \xrightarrow{SH^+} \underset{\mathbf{12}}{C_2H_5OCO\overset{\overset{Cl}{|}}{N}CH_2CH_2Y}$$

followed by:

$$[9]\quad C_2H_5OCO\overset{\overset{Cl}{|}}{N}CH_2CH_2Y + 2e^- \xrightarrow{SH^+} \underset{\mathbf{11}}{C_2H_5OCONHCH_2CH_2Y} + Cl^-$$

It was shown that the homogeneous reaction 8 followed by bisulfite reduction yielded **11** (*e.g.* 46% yield for Y = CN). As has been demonstrated above, the *N*-chloro-*N*-alkyl carboxamides are more readily reduced than the ZCONHCl species itself so that [9] competes favorably with [1]. In mass electrolysis **12** is thus readily reduced and **11** constitutes the major product (50% yield for Y = CN, 61% yield for Y = $COOCH_3$).[7] No trace of α-chlorinated products ($C_2H_5OCONHCH_2\overset{\overset{Cl}{|}}{C}HY$) expected from a radical chain mechanism could be detected.

Reduction of NCU (**1**) at a mercury cathode in acetonitrile in the presence of norbornene (10 fold excess) gave urethane only according to v.p.c. analysis. No traces of addition products could be detected. Thus, if a radical is indeed formed upon addition of the first electron [3], it would seem that in the competition between the insertion of a second electron and the chemical reaction, the former usually wins out. This is in direct contrast to the chromous chloride catalysed addition of *N*-chlorourethane to olefins where each Cr(II) ion can contribute but one electron. There, the competition depends on the chance encounter with a second chromous ion or the olefin. In that case addition was favored by maintaining the concentration of the discrete electron source, the Cr(II)

[5]NCU (**1**) is a weaker acid than acetic acid ($\Delta pK_a = 3.3$ in methanol–water 1:1) but much stronger than methanol.

[6]Formaldehyde was formed in the chromous chloride reduction of NCU (**1**) in methanol as the result of hydrogen abstraction from methanol by the urethane radical (see footnote 2).

[7]No attempt was made to identify the nature of the remaining products.

Can. J. Chem. Downloaded from www.nrcresearchpress.com by 210.87.254.5 on 09/05/12
For personal use only.

species, as low as practical. At the electrode however, a virtually unlimited supply of electrons is available and it becomes necessary to enhance the chances of chemical reaction.

In order to increase the concentration of olefin near the electrode we employed a cathode consisting of a graphite paste constituted by mixing NCU (**1**) with a five fold excess of cyclohexene or norbornene. After electrolysis for nine hours at room temperature the *cis* and *trans* addition products were obtained, analyzed, and isolated. With cyclohexene, a 18% yield of 1,2-adducts **13** and **14** (*cis–trans* 0.5:1) was obtained, and with norbornene the yield was 14% of **16** and **17** (*cis–trans* 1:1). Urethane still constituted the major product. In a control experiment in which the graphite paste (NCU (**1**) and cyclohexene) was kept at room temperature for ten hours, there was an 8% loss of active chlorine (iodometric titration) and formation of *ca.* 0.9% (by v.p.c.) of 1,2-adducts **13** and **14** (*cis–trans* 0.5:1).

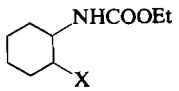

13 X = Cl (*cis*)
14 X = Cl (*trans*)
15 X = H

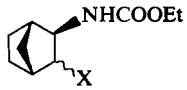

16 X = Cl (*exo*)
17 X = Cl (*endo*)
18 X = H

Thus it seems probable that, in the above electrolyses, most of the addition products were formed via the electrochemically generated urethane radical [3] by a chain mechanism:

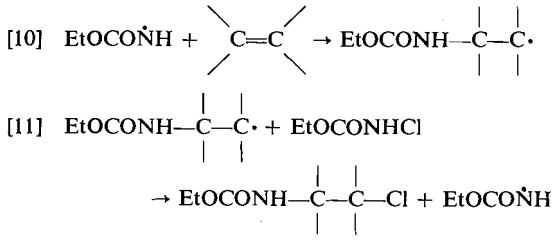

Chain termination by a second electron transfer step to the radical according to [4] is in fair accord with the number of coulombs passed and p*H* changes. No traces of the reduced products, *N*-cyclohexylurethane (**15**) or *N*-(2-*exo*-norbornyl)urethane (**18**), could be detected. Compound **18** is the major product (54%) in the chromous ion reduction of NCU in the presence of norbornene (1).

The addition products **13** to **18** were shown to be much more difficult to reduce than NCU and thus, once formed, unlikely to disappear during electrolysis. We therefore conclude that the reduction of the intermediate β-amidoalkyl radical must be slower than its reaction with NCU [11].

In order to confirm the intervention of an amide radical in the electrolytic reduction of the *N*-chloro-*N*-alkyl carboxamides we employed another approach since the addition of *N*-alkylamido radicals to olefins is more difficult than the addition of the corresponding *N*-hydroamido radicals (3, 4). Neale *et al.* (12) have shown that aliphatic (C_4 to C_6) *N*-chloro-*N*-alkyl carboxamides can be rearranged photolytically to the 4-chloro derivative, the preferred *N*-substituent being the *t*-butyl group. For instance, photolysis of *N*-chloro-*N*-*t*-butyl pentanamide (**9**) in benzene gave the 4-chloro derivative **19** and *N*-*t*-butyl pentanamide (**20**) in a 43% and 42% yield respectively (12). The radical chain reaction involved include a selective intramolecular hydrogen abstraction at C_4 by the amide radical through a six atom transition state.

Electrolysis of *N*-chloro-*N*-*t*-butyl pentanamide (**9**) at the mercury cathode yielded 37% of the 4-chloro derivative **19** and 55% of the carboxamide **20** for a total product yield of 92% (the proportion of **19** and **20** was calculated from the n.m.r. spectrum of the crude product. The chemical proof of the presence of **19** was obtained by the synthesis of the iminolactone **21**).

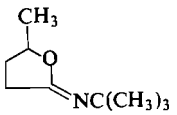

21

Here the product yield is competitive with the photolysis results. The coulombic efficiency was close to 200%, clearly indicating a radical-chain mechanism:

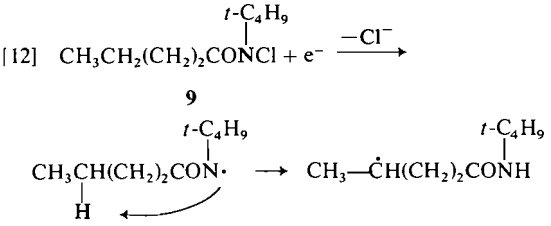

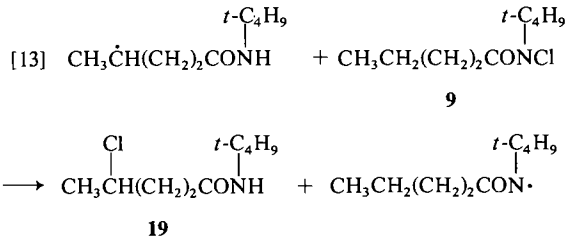

The main chain termination step most likely involves the reaction 14 giving rise to **20**:

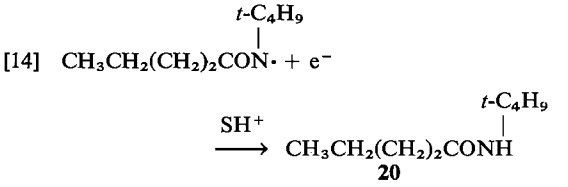

Under conditions identical to those of the electrolysis but without applying any potential, the *N*-chloroamide **9** reacted with mercury (31% loss of active chlorine) with the formation of a black precipitate. No 4-chloro-*N*-*t*-butyl-pentanamide (**19**) could be detected, the sole organic product formed being the pentanamide **20**. Therefore the formation of the 4-chloro derivative **19** during the electrolysis most probably involves the electrochemically generated amide radical [12].

Conclusions

The electroreduction of *N*-halocarboxamides and *N*-chlorourethane (**1**) in aprotic and protic media proceeds at the mercury electrode at $E_{1/2}$ potentials depending on the chemical nature of the depolarizer, the p*H* and to a lesser degree the nature of the solvent. The reduction involves two consecutive one electron steps. The very irreversible first electron transfer and formation of a radical species is followed by a considerably faster uptake of the second electron to form the anion. We believe that the intermediate radical in the reduction of NCU (**1**) has been trapped under special conditions by intermolecular addition to olefins. In the case of *N*-chloro-*N*-*t*-butyl pentamide (**9**) the radical has been captured by intramolecular hydrogen abstraction to a degree offering possible applications in synthesis. The addition of NCU (**1**) to acrylonitrile and methylacrylate has been shown to proceed readily and to involve the addition of anions.

Experimental

Solvents and Electrolyte

Acetonitrile (Fischer ACS reagent) was purified by distillation from phosphorous pentoxide. Chloroform (anhydrous reagent, Fischer) was used without further purification and absolute methanol was obtained by standard procedure. Lithium perchlorate (anhydrous reagent, Alfa Inorganics Co.) was used after drying in a vacuum oven for 24 h at 100 °C.

Electrochemical Instrumentation

A three electrode potentiostat (Tacussel type ASA 100) with an automatic drop dislodger (Tacussel type MPO3) or a rotating platinum electrode (Tacussel type Controvit) was used to record respectively the polarograms and voltammograms. Potentials were measured with respect to an aqueous saturated calomel electrode with a KCl saturated agar salt bridge separated from the electrolysis vessel by a compartment containing supporting electrolyte between two fritted glass discs in order to prevent water contamination.

A glass cell of concentric construction containing the anode in a central compartment separated by a fritted glass disc from the exterior catholyte compartment (50 or 200 ml volume) was employed for mass electrolysis. A three electrode system controlled by a Tacussel type ASA 100 potentiostat was employed for all but the electrolysis involving a graphite paste electrode. In the latter case the high resistance of the porcelaine cup (see below) rendered potentiostatic control impossible unless the reference electrode was buried in the carbon paste, but the conditions employed (both electrolysis at fixed current and constant applied potential) correspond to about 1/5 of the limiting current and entail little danger of provoking alternate reactions. For coulometric determination the progress of the electrolysis was followed by recording polarograms after a fixed number of coulombs had passed and by iodometric titration of the remaining halogen derivatives. The charge passed was obtained by graphically integrating the current time curves and by using an electrochemical coulometer.

All voltammetric analyses as well as mass electrolyses were carried out in a nitrogen atmosphere. For the polarographic reduction of *N*-bromoacetamide (**6**), Nujol was added at the bottom of the cell to isolate the solution from mercury and the cell was cooled in an ice bath. In mass electrolyses, a slight negative potential was applied at the mercury electrode before adding the *N*-haloamide in order to prevent the formation of a precipitate (see reaction of *N*-haloamides with mercury).

Analysis of Products and Starting Materials

Melting points were determined on a Büchi apparatus and are uncorrected. The i.r. spectra were determined on a Perkin-Elmer 257 spectrometer. The n.m.r. spectra were recorded on a Varian A-60 instrument and chemical shifts are reported in δ. The mass spectra were taken on a Hitachi RMU-6E spectrometer. The v.p.c. analyses were performed on a Hewlett Packard chromatograph model 5750 equipped with both thermal conductivity and flame-ionization detectors. A 6 ft × 0.25 in. OS-138 on Chromosorb W column was used. Merck silica gel GF_{254} was used for thin and preparative layer chromatography. Organic phases from extractions were dried over anhydrous sodium sulfate.

Can. J. Chem. Downloaded from www.nrcresearchpress.com by 210.87.254.5 on 09/05/12
For personal use only.

Can. J. Chem. Downloaded from www.nrcresearchpress.com by 210.87.254.5 on 09/05/12
For personal use only.

N-Haloamides

N-Chlorourethane (**1**) (88% active chlorine), *N*-chloro-2-chloroacetamide (**3**) and *N*-chloro-2,2-dichloroacetamide (**4**) (100% active chlorine) were prepared from the corresponding amides by the sodium hypohalite method (13). *N*-Chloroacetamide (**2**) was prepared according to the method described by Orton and Bradfield (14), m.p. 109–110 °C (100% active chlorine). *N*-Chloro-2,2,2-trichloroacetamide (**5**) was prepared according to the method of Park *et al.* (15), m.p. 124–125 °C (100% active chlorine). *N*-Chloro-*N*-ethylacetamide (**8**) was prepared by treatment of an aqueous solution of the corresponding amide containing sodium bicarbonate with chlorine followed by extraction with methylene chloride and distillation under reduced pressure; b.p. 46–47 °C (15 Torr) (96% active chlorine, 75% yield). *N*-Chloro-*N*-tertiobutylpentanamide (**9**) was prepared by the method described by Neale *et al.* (12) in a 65% yield (85% active chlorine). The *N*-bromoacetamide (**6**) and *N*-chlorosuccinimide (**7**) were obtained commercially (Aldrich Chemical Co.) and were recrystallized from methylene chloride (> 99% active chlorine).

The lithium salts of NCU (**1**) and NBA (**6**) were obtained as a foam by treating the *N*-haloamide with an equimolar amount of lithium methoxyde in anhydrous methanol and evaporating to dryness under vacuum.

Reaction of N-Haloamides with Mercury

N-Chlorourethane (1)

A solution of 626 mg (99% active chlorine, 5.07 mmol) of NCU (**1**) in 10 ml of a 0.2 *M* $LiClO_4$ solution in acetonitrile was stirred at room temperature with 11 g of mercury under a nitrogen atmosphere. A grey precipitate began to appear after a few minutes. The reaction was followed by polarography. A new wave appeared at +0.10 V *vs.* s.c.e., the waves due to NCU and its anion disappearing gradually. The current of the new wave reached a maximum after 5.5 h corresponding to 48% of $I_1 + I_2$ of the starting solution and then decreased slightly. After 20 h the reaction mixture was filtered and the precipitate washed with acetonitrile then methylene chloride. The resulting solution was concentrated under reduced pressure (~ 10 ml) and water (40 ml) was added. There was no NCU left according to iodometric assay. Continuous extraction with methylene chloride afforded 253 mg of urethane (56% yield). The grey precipitate (3.9 g) was treated with dilute nitric acid and the resulting solution continuously extracted with methylene chloride to yield an additional 82 mg of urethane (total yield of 74%).

The reaction was repeated and the precipitate was isolated after 3 h, dried, and analyzed for mercury and chloride ion: Hg, 92.6 ± 1.1%; Cl^-, 4.1 ± 0.4%; the remaining 3% was probably organic in nature.

The reaction was carried out in CD_3CN and followed by n.m.r., each aliquot being carefully freed from the solid suspension. After a few hours, the spectrum showed only unresolved broad absorptions for possibly NH protons and protons of an ethoxycarbonyl group. After 24 h, the spectrum was well resolved and identical to that of urethane.

N-Bromoacetamide (6)

The reaction was carried out on 0.98 mmol of NBA in the polarographic cell. A white precipitate was formed immediately upon the addition of mercury and became grey after a few minutes. The wave at *ca.* −0.1 V *vs.* s.c.e. disappeared while a new wave at −0.29 V was appearing. After 4 h the polarogram showed only this new wave. No attempt was made to isolate and characterize the products.

N-Chloro-N-tertiobutylpentanamide (9)

A solution of 1.13 g (85% active chlorine, 4.95 mmol) of *N*-chloro-*N*-tertiobutylpentanamide (**9**) in 10 ml of a 0.2 *M* $LiClO_4$ solution in acetonitrile was stirred at room temperature with 4 g mercury under a nitrogen atmosphere. A black precipitate began to appear almost as soon as mercury was added. After 24 h, the reaction mixture was filtered, worked up in the usual way, analyzed for active chlorine (3.40 mmol, 69% of unreacted **9**), then treated with a saturated solution of sodium bisulfite until the reduction of active chlorine was completed. Extraction with methylene chloride gave 0.825 g of *N*-tertiobutylpentanamide (**20**), m.p. 44–47 °C (89% by taking into account the 15% present in the starting material). The presence of the 4-chloro-derivative **19** could not be detected in the n.m.r. spectrum. The precipitate (2.24 g) was analyzed for mercury and chloride ion: Hg, 97.2 ± 0.3%; Cl^- (as Hg_2Cl_2), 2.6 ± 0.1% (total of 99.8 ± 0.3%). An X-ray powder diffraction analysis confirmed the presence of the crystalline Hg_2Cl_2 phase.

An identical solution of the *N*-chloroamide **9** kept at room temperature for 24 h but without adding mercury gave the following results: 4.75 mmol (92%) of unreacted **9**; 0.850 g of *N*-tertiobutylpentanamide (**20**), m.p. 43–47 °C (91%) after reduction with sodium bisulfite.

Electrolyses

Some typical electrolyses are summarized below.

Electroreduction of N-Chlorourethane (1)

In Methanol—A solution of 1.22 g (88% active chlorine, 10 mmol) of *N*-chlorourethane (**1**) and 0.6 g (10 mmol) of acetic acid in 50 ml of a 0.2 *M* methanolic solution of $LiClO_4$ was electrolyzed at a cathode potential of −0.7 V. The anode compartment (auxiliary electrode, Mg) contained 5 to 7 ml of the 0.2 *M* electrolyte solution. The electrolysis was discontinued when no more active chlorine was present (negative potassium iodide – starch paper test). The catholyte was poured into water (*ca.* 50 ml) then extracted with methylene chloride (3 × 100 ml). The organic layers were washed with water then combined and dried. The solution was concentrated to a volume of *ca.* 50 ml by distilling the solvent and then analyzed by v.p.c. (170 °C). Urethane was the main component. No traces of the dimer *N,N'*-dicarboethoxyhydrazine could be detected. Small amounts of products with lower retention times than that of urethane were present and were not investigated. Removal of the solvent in the rotatory evaporator left 0.81 g (92%) of urethane, m.p. 43–45 °C, identified further by comparison of the i.r. and n.m.r. spectra with those of an authentic sample (Aldrich Chemical Co.).

The electrolysis carried out in the presence of an equimolar (10 mmol) amount of sodium methoxyde (instead of acetic acid) and at a cathode potential of −1.2 V, the other conditions being exactly the same as

Can. J. Chem. Downloaded from www.nrcresearchpress.com by 210.87.254.5 on 09/05/12
For personal use only.

above, gave urethane only according to the v.p.c. analysis (100% yield).

In Acetonitrile—The electrolysis was carried out on 10 mmol as described above except that acetonitrile was used as solvent and no base or acid was added. The cathode potential was −0.3 V (auxiliary electrode, Mg). The usual work-up gave, after complete evaporation of the solvent, 0.84 g (94%) of urethane, m.p. 44–45 °C. The dimer *N,N'*-dicarboethoxyhydrazine could not be detected by v.p.c. analysis.

The electrolysis was repeated in the presence of an excess of norbornene (100 mmol). Urethane was the only product formed according to the v.p.c. analysis. No traces of the adducts **16**, **17** or **18** could be detected.

Electrochemical Reduction of N-Chloro-2,2,2-trichloroacetamide (5)

A solution of 315 mg (1.50 mmol) of *N*-chloro-2,2,2-trichloroacetamide (**5**) in 50 ml of a 0.2 *M* solution of $LiClO_4$ in acetonitrile was electrolyzed at a cathode potential of −1.0 V (auxiliary electrode, Mg) until the test for active chlorine was negative. The usual work-up followed by evaporation of the solvent left 155 mg of a crystalline residue. The v.p.c. analysis showed that it consisted of trichloroacetamide and dichloroacetamide in a 9:1 ratio (authentic samples were used as standards). Crystallization from methylene chloride gave practically pure trichloroacetamide, m.p. 138–140 °C. Continuous extraction with methylene chloride for several days gave an additional 16 mg of 2,2-dichloroacetamide. Thus the yield of trichloroacetamide was 70% and that of dichloroacetamide 19%. Both amides were further identified by the comparison of their i.r. spectra with those of authentic samples.

Electroreduction of N-Chlorourethane (1) in the Presence of Methyl Acrylate and Acrylonitrile

Methyl Acrylate—The cathode compartment was filled with 50 ml of a 0.2 *M* $LiClO_4$ solution in a 2:3 mixture of absolute methanol and chloroform and 42 ml (40 g, 465 mmol) of methylacrylate were added. The anode compartment (auxiliary electrode, Pt) contained 10 to 15 ml of the electrolyte solution. A potential of −0.3 V was applied and 8 ml of a 2.25 *M* *N*-chlorourethane (**1**) solution (18 mmol) in methanol–chloroform 2:3 were added dropwise in order to maintain a current of 50 mA. The addition took 3 h and, after the current had reached 10 mA, 20 ml of a saturated $NaHSO_3$ solution were added to reduce the active chlorine left. The mixture was extracted with methylene chloride (3 × 100 ml). The organic layers were combined and dried. The resulting solution was concentrated in the rotatory evaporator then transferred into a 50 ml volumetric flask with methylene chloride. Analysis by v.p.c. (180 °C) showed that methyl 3-carboethoxyaminopropionate (**11**, Y = $COOCH_3$) was formed in a 61% yield. An authentic sample prepared from β-alanine[8] was used as standard. Evaporation of the solvent followed by distillation of the residue under reduced pressure gave 1.51 g (48%) of adduct **11** (Y = $COOCH_3$), b.p. 134 °C (5 Torr), identified with the authentic material by comparison of the i.r. and n.m.r. spectra.

Acrylonitrile—The reduction was carried out exactly as described above except that methylacrylate was replaced by acrylonitrile (500 mmol). Microdistillation of the residue at 115 °C (1 Torr) afforded 0.53 g of a mixture of urethane and compound **11** (Y = CN). Separation of an aliquot by preparative v.p.c. (OS-138, 175 °C, 6 ft × 3/8 in. column) gave the pure 3-carboethoxyaminopropionitrile (**11**, Y = CN) but with low recovery due to decomposition on the column; υ_{max} ($CHCl_3$) 3420 (>NH), 2240 (—C≡N), 1720 (amide I), 1515 (amide II), 1250 and 1200 cm^{-1} (—CO—O—Et); δ ($CHCl_3$), 1.25 (t, J = 7 Hz, CH_3—CH_2—O—), 2.62 (t, J = 7 Hz, —CH_2—CH_2—CN), 3.50 (q, J = 7 Hz, —NH—CH_2—CH_2—), 4.20 (q, J = 7 Hz, CH_3—CH_2—O—), and 5.22 (m, —NH—); *m/e* 142 (M^+).

The reaction was repeated and the yield of **11** (Y = CN) was determined by v.p.c. using the pure sample obtained above as standard: 50%.

Addition of the Lithium salt of N-Chlorourethane (1) to Acrylonitrile

The solution of 18 mmol of *N*-chlorourethane in 150 ml of a 2:3 mixture of absolute methanol and chloroform was treated with an equimolar amount of lithium methoxyde (prepared from lithium metal and absolute methanol). Excess acrylonitrile (33 ml) was added and the mixture was kept at room temperature overnight under a nitrogen atmosphere. Sodium bisulfite (20 ml of a saturated aqueous solution) was added to reduce the active chlorine and the mixture was extracted with methylene chloride (3 × 100 ml). The organic layers were combined and dried, and the solvent was removed at the rotatory evaporator. Analysis by v.p.c. (175 °C) showed that 3-carboethyoxyaminopropionitrile (**11**, Y = CN) was formed in a 46% yield using the authentic sample obtained above as standard.

Electroreduction of N-Chlorourethane (1) at Graphite Cathode in the Presence of Olefins

In the Presence of Cyclohexene—In a cylindrical (20 × 175 mm) porous porcelain crucible were placed 6 g of graphite powder, 3.50 g (88% active chlorine, 25 mmol) of *N*-chlorourethane (**1**) and 10 ml (8.1 g, 99 mmol) of cyclohexene. The mixture was stirred with a glass rod until an homogeneous paste was obtained. The electrical contact was ensured by a graphite rod immersed in the paste. A cylindrical platinum anode surrounded the cathode compartment and the anolyte consisted of 50 ml of a 0.2 *M* solution of $LiClO_4$ in acetonitrile. A potential of −10 V was applied between the two electrodes and the electrolysis was discontinued when the active chlorine test (potassium iodide – starch paper) was negative; 2789 coulombs (29×10^{-3} F) were passed in 9 h. The anolyte was extracted with methylene chloride in the usual manner after the addition of water (*ca.* 20 ml). The two solutions were combined, concentrated, then transferred into a 50 ml volumetric flask. The v.p.c. analysis gave the following results: urethane, 66%; ethyl *cis*-*N*-(2-chlorocyclohexyl)carbamate (**13**), 6%; and ethyl *trans*-*N*-(2-chlorocyclohexyl)carbamate (**14**), 12%. Authentic samples of **13** and **14** (1) were used as standards. No trace of *N*-cyclohexylurethane (**15**) could be detected. The isolation of compounds **13** and **14** for complete identification is described below.

The solution above was further concentrated and ether was added. A crystalline product was collected

[8]H. Driguez, Ph.D. Thesis, Université de Sherbrooke, 1971.

Can. J. Chem. Downloaded from www.nrcresearchpress.com by 210.87.254.5 on 09/05/12
For personal use only.

(580 mg, m.p. 134–135 °C) and was identified as *trans-N*-(2-chlorocyclohexyl)acetamide by comparison of the i.r. and n.m.r. spectra with those of an authentic sample.[8] The formation of this product can be explained by the diffusion of cyclohexene from the catholyte to the anolyte since Faita *et al.* (16) have shown that the oxidation of chloride ions in the presence of cyclohexene in acetonitrile gave *trans-N*-(2-chlorocyclohexyl)acetamide, the chloride ions being provided in the present case by the reduction of *N*-chlorourethane (**1**).

Separation of the mother liquors by preparative layer chromatography on silica gel afforded 1.22 g of urethane (48% taking into account the presence of 12% in the starting material), 0.27 g (5%) of the *cis* adduct **13** m.p. 53–56 °C, and 0.59 g (12%) of the *trans* adduct **14** m.p. 90–92 °C. Both adducts were fully identified by comparison of their i.r. and n.m.r. spectra with those of authentic samples (1).

In a control experiment the graphite paste was kept at room temperature for 10 h under a nitrogen atmosphere without applying any potential. After work up as above, the solution was analyzed for active chlorine: 4.6 mmol, 92% of unreacted NCU (**1**). The active chlorine was reduced with a saturated sodium bisulfite solution. The organic phase was washed with water then dried. The v.p.c. analysis gave the following results: urethane, 96%; *cis* 1,2-adduct **13**, ~0.3%; *trans* 1,2-adduct **14**, ~0.6%.

In the Presence of Norbornene—The reaction was carried out as described above for cyclohexene with 9.0 g (95 mmol of norbornene and 3.20 g (88% active chlorine, 22.8 mmol) of *N*-chlorourethane (**1**). No active chlorine was present after 962 coulombs (9.96×10^{-3} F) were passed. The methylene chloride washings of the catholyte and the methylene chloride phases from the extraction of the anolyte were combined and the solvent removed in the rotatory evaporator. The residue was separated by preparative layer chromatography on silica gel to yield 0.80 g (35%, taking into account the presence of 12% in the starting material) of urethane, 0.36 g (7%) of ethyl *N*-[2-*exo*-(3-*exo*-chloronorbornyl)]-carbamate (**16**), m.p. 45–58 °C, and 0.33 g (7%) of ethyl *N*-[2-*exo*-(3-*endo*-chloronorbornyl)]carbamate (**17**), m.p. 85–88 °C. Both 1,2-adducts **16** and **17** were fully identified by comparison of their i.r. and n.m.r. spectra with those of authentic samples (1). The v.p.c. analysis of the other fractions showed no trace of *N-exo*-norbornylurethane (**18**), and they were not examined further.

Electroreduction of N-Chloro-N-tertiobutylpentamide (9)

A solution of 4.18 g (85% active chlorine, 18.5 mmol) of *N*-chloro-*N*-tertiobutylpentanamide (**9**) in 25 ml of 0.2 *M* $LiClO_4$ in acetonitrile was electrolyzed at a cathode potential of −0.3 V. The anode compartment (Pt auxiliary electrode) contained 10 ml of the 0.2 *M* electrolyte solution. The electrolysis was discontinued when no more active chlorine was present (23 h at a current of *ca.* 10 mA). The usual working-up (addition of water, methylene chloride extractions, etc.,) gave 2.93 g of crude product. The n.m.r. spectrum was compared with that of the crude product obtained from the photolysis of the same *N*-chlorocarboxamide **9** carried out as described by Neale *et al.* (12). The weight ratio of *N*-tertiobutylpentanamide (**20**) to *N*-tertiobutyl-4-chloropentanamide (**19**) was calculated to be approximately 1:2 from the relative integration of the protons of the terminal methyl group which appears at 0.9 δ (ill-defined triplet) in the carboxamide **20** and at 1.51 δ (d, J = 6 Hz) in the 4-chloroderivative **19**. Thus assuming that the carboxamide **20** and the 4-chloro derivative **19** were the sole components of the crude product (in fact some impurities were present in small amount, <5% according to the n.m.r. spectra), the yield of the 4-chlorocarboxamide **19** is 37% and that of the carboxamide **20**, 55%.

A chemical proof of the presence of the 4-chlorocarboxamide **19** in the crude product was obtained in the following manner. An aliquot of 1.46 g of the crude product from the electroreduction was treated with an excess of silver perchlorate (10 mmol) in 50 ml of 50% aqueous acetonitrile at 60 °C for 1 h. The mixture was poured onto crushed ice, treated with 5% NaOH, then extracted with ether (3 × 50 ml). The ether layers were combined and dried. Removal of the ether by distillation was followed by microdistillation of the residue at 69 °C (10 Torr) to give 0.26 g of the iminolactone **21**. The i.r. and n.m.r. spectra were identical to those of the sample obtained by the same procedure from the photolysis crude product. The hydrochloride had m.p. 120–121 °C (lit. (12), m.p. 123 °C).

Support for this work by the Ministère de l'Education, Québec, and the National Research Council of Canada is gratefully acknowledged.

1. J. Lessard and J. M. Paton. Tetrahedron Lett. 4883 (1970).
2. J. Lessard, H. Driguez, and J. P. Vermes. Tetrahedron Lett. 4887 (1970).
3. D. Touchard and J. Lessard. Tetrahedron Lett. 4425 (1971).
4. D. Touchard and J. Lessard. Tetrahedron Lett. 3827 (1973).
5. C. K. Mann, J. L. Webb, and H. M. Walborsky. Tetrahedron Lett. 2249 (1966).
6. N. S. Hush and K. B. Oldam. J. Electroanal. Chem. **6**, 34 (1962).
7. P. Zuman. Substituent effects in organic polarography. Plenum Press, New York 1967. p. 23 ff.
8. L. L. Miller and E. Riekena. J. Org. Chem. **34**, 3359 (1969).
9. J. P. Coleman, H. G. Gilde, J. H. P. Utley, and B. C. L. Weedon. Chem. Commun. 738 (1970).
10. M. R. Rifi. *In* Organic electrochemistry, *edited by* M. M. Baizer. Marcel Dekker, Inc., New York, N.Y. 1972. p. 279.
11. M. M. Baizer and J. L. Chruma. J. Org. Chem. **37**, 1951 (1972).
12. R. S. Neale, N. L. Marcus, and R. Schepers. J. Am. Chem. Soc. **88**, 3056 (1966).
13. C. Bachand, H. Driguez, J. M. Paton, D. Touchard, and J. Lessard. J. Org. Chem. **39**, 3136 (1974).
14. K. J. P. Orton and A. E. Bradfield. J. Chem. Soc. 986 (1927).
15. J. D. Park, H. J. Gerjovich, W. R. Lycan, and J. R. Lacher. J. Am. Chem. Soc. **74**, 2189 (1952).
16. G. Faita, M. Fleischmann, and D. Pletcher. J. Electroanal. Chem. **25**, 455 (1970).

The Importance of Anharmonicity of the Vibrational Excited States in Chemical Kinetics

JAN BRON

Department of Chemistry, University of Natal, Durban, South Africa

Received March 26, 1975

JAN BRON. Can. J. Chem. **53**, 3069 (1975).

The corrections to rate constants for anharmonicity of vibrational excited states have been evaluated over the temperature range of 200–1100 K. The reaction $O_2 + X$, where X is H or D, has been chosen as the model system. Only the influence of vibrational anharmonicity of the triatomic transition state has been determined. Two geometric shapes for the transition state, bent and isosceles configurations, have been investigated in detail by the bond order method.

It is found that the correction can be large, depending upon the geometry and force field of the transition state and the temperature. The magnitude of the correction for anharmonicity of the vibrational excited states depends mainly, at a particular temperature, on the strength of the O—X bond in the transition state. In the case of a large correction, anharmonicity may lead to a nonlinear Arrhenius plot.

Because of cancellation effects, the correction for anharmonicity of the excited vibrational states in kinetic isotope effects can be ignored in the lower temperature region. It has also been found that anharmonicity of the vibrational *ground state* can explain unexpected large isotope effects.

JAN BRON. Can. J. Chem. **53**, 3069 (1975).

On a évalué, pour des températures allant de 200 à 1100 K, les corrections qu'il faut apporter aux constantes de vitesse à cause de l'anharmonicité des états vibrationnels excités. On a choisi la réaction $O_2 + X$, où X = H ou D, comme système modèle. On a déterminé uniquement l'influence de l'anharmonicité de l'état de transition triatomique. On a étudié en détail, par la méthode des ordres de liaison, deux formes goémétriques de l'état de transition soit les configurations isocèle et penchée.

On a trouvé que suivant la température, la géométrie et le champ de force de l'état de transition, la correction peut être grande. L'amplitute de la correction pour l'anharmonicité des états excités vibrationnels dépend principalement, à une température donnée, de la force de la liaison O—X dans l'état de transition. Dans le cas d'une correction importante, l'anharmonicité peut conduire à une relation d'Arrhénius qui ne soit pas linéaire.

Dû à des effets d'annulation, on peut omettre, à basse température, la correction pour l'anharmonicité des états vibrationnels excités dans les effets isotopiques cinétiques. On a aussi trouvé que l'anharmonicité de l'état vibrationnel *fondamental* peut expliquer des effets isotopiques plus grands que prévus autrement.

[Traduit par le journal]

Introduction

Rate constants of chemical reactions are usually calculated by making the simplifying assumption that the molecule vibrates harmonically (1–4). The correction for anharmonicity of the vibrational ground state for kinetic isotope effects has been discussed recently (5, 6). Anharmonicity of the vibrational excited states was ignored since it was argued that, at reasonably low temperatures, excited states were not sufficiently important and hence could be ignored.

Rate constant calculations involve, within the framework of the transition state theory, the evaluation of the partition functions of reactants and transition state (1). In order to calculate the partition function of any molecular species, the complete potential energy surface should be known. For only a few small stable molecules, the potential energy surface has been evaluated by spectroscopic methods. The potential energy surfaces of transition states can only be evaluated by theoretical means which, at the moment, are inferior to the experimental methods used for stable molecules.

In stable molecules, anharmonicity is usually a small perturbation and perturbation theory can be used to evaluate the expressions for the anharmonicity constants. It can be argued that anharmonicity in transition states is much more important than in stable molecules (2) and, since anharmonicity may then be a large pertur-

Can. J. Chem. Downloaded from www.nrcresearchpress.com by 210.87.254.5 on 09/05/12
For personal use only.

Can. J. Chem. Downloaded from www.nrcresearchpress.com by 210.87.254.5 on 09/05/12
For personal use only.

bation, the usual perturbation methods cannot be applied. No quantitative evidence supplied by detailed calculations have been given so far as to the importance of anharmonicity in transition states. However, judging solely by the success of the harmonic approximation, in rate constant and rate constant ratio (kinetic isotope effect) calculations, in explaining the detailed behavior of chemical reactions, anharmonicity *may be*, at least for normal modes with real frequencies, of similar magnitude in both transition states and stable molecules.

The purpose of the present investigation is to determine the validity of the assumption that anharmonicity of the excited states can be ignored in rate constant and kinetic isotope effect calculations and to determine under which conditions this assumption becomes invalid. As before (5, 6), it will be postulated that the reaction coordinate, which corresponds to the normal mode with the zero or imaginary frequency, is completely separate from the other normal modes with real frequencies of vibration.

General Considerations

The reactions that serve as a model system are

[1] $$H + O_2 \rightleftharpoons HO_2^* \rightarrow OH + O \ (k_H)$$
$$D + O_2 \rightleftharpoons DO_2^* \rightarrow OD + O \ (k_D)$$

The molecules HO_2^* and DO_2^* are the transition states. The rate constants, which have been measured in the temperature region of 800 to 1000 K by Kurzius and Boudart (7), may be written for present purposes as

[2] $$k_X = k_X' \cdot \alpha(X) \cdot \beta(X) \quad (X = H, D)$$

The quantities $\alpha(X)$ and $\beta(X)$ are the corrections for anharmonicity of the vibrational ground and excited states respectively and apply only to the transition states XO_2^*. The rate constant k_X' is a calculated quantity in which the assumption that the transition state vibrates harmonically is the only approximation.

No attempt will be made to reproduce the magnitude of the experimental rate constants for the $O_2 + X$ reaction theoretically, since this has already been done (7) by Kurzius and Boudard (K.B.). Strictly speaking, the experimental value for k_X should put constraints on the range of transition state parameters that determine $\alpha(X)$ and $\beta(X)$. However, since the theoretical quantity k_X' involves in itself many adjustable parameters, any change in the parameters that determine $\alpha(X)$ and $\beta(X)$ can be compensated for by a corresponding adjustment of the parameters that determine k_X'. These adjustments should, of course, be reasonable.

As mentioned above, transition state parameters cannot be evaluated by experimental means directly. Transition state parameters are usually assigned values by analogy to stable, real molecules. However, some quantities are typical for transition states, such as a zero or imaginary frequency of vibration. K.B. assumed the complex to be "entirely loose with the reactants of masses m_1 and m_2 preserving their identity", which is, again, only possible for a transition state. The "looseness" of the bonds between the fragments or atoms making up the transition state can be defined in terms of bond order.

The bond order approach will be used in the present study; a low bond order will mean a loose bond. Bond order and transition state parameters, such as bond distances and force constants, will be related by equations to be given in the next section. These relationships have been postulated to be valid also for transition states, since they hold approximately for stable molecules. However, no direct theoretical evidence exists that these relationships are valid for transition states. Therefore, the implications of deviations from these relationships for $\alpha(X)$ and $\beta(X)$ will be investigated. It will be implied that some of the conclusions drawn below can be extrapolated to other reactions involving the isotopes of hydrogen. Larger transition states cannot be investigated in the same detail, since the addition of one extra atom to the transition state increases the computer time required for the calculation of $\alpha(X)$ and $\beta(X)$ by a factor of about 50.

The correction for anharmonicity of the ground vibrational state of the transition state, XO_2^*, has the form (5, 6)

[3] $$\alpha(X) = \exp\left[\left(\tfrac{1}{2}\textstyle\sum\omega_i - \mathrm{ZPE}\right)hc/kT\right]$$

The quantity ZPE, for which the explicit expression has been given before (8), is the ground state vibrational energy. The quantity $\frac{1}{2}\sum\omega_i$ is the harmonic zero-point energy and ω_i is the harmonic frequency of vibration. The correction to a partition function due to anharmonicity of the excited states in the absence of vibrational degeneracy has been given by Pennington and Kobe (9)

$$[4]\quad \beta(X) = \prod_i \left(\frac{1 - \exp(-u_i)}{1 - \exp(-u_1')}\right) \times \left(1 - \sum_{i \leqslant j} \sum f_{ij}\right)$$

Here $u_i = \omega_i hc/kT$ and ω_i is the harmonic frequency; $u_i' = \nu_i hc/kT$ and ν_i is the fundamental frequency; $\nu_i = \omega_i + 2x_{ii} + \frac{1}{2}\sum_{k \neq i} x_{ik}$; $f_{ij} = x_{ij}(hc/kT)[\exp(u_i') - 1]^{-1}[\exp(u_j') - 1]^{-1}$; $f_{ii} = 2x_{ii}(hc/kT)[\exp(u_i') - 1]^{-2}$, and x_{ij} is the anharmonicity constant.

Geometry, Internal Coordinates, and Force Field for XO_2* Species

The isosceles **1** and bent **2** shapes of the XO_2* activated complex will be investigated.

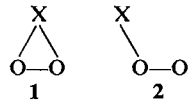

1 **2**

The bond lengths and force constants follow the relationships given by Johnston (1) and Pauling (10): $R = R^{(s)} - 0.26 \ln(n)$ and $F(r) = F(r)^{(s)}n$. The maximum values of the bond order for the O—H and O—O bonds in the activated complexes are unity. The force constants and bond lengths of the O—H and O—O bonds in the HO_2* species are based on those of the O_2 and OH molecules. From the frequencies of vibration of the diatomic molecules given by Herzberg (11), it follows that $F(r)_{OH}^{(s)} = 8.6697$ mdyn/Å and $F(r)_{O_2}^{(s)} = 11.7676$ mdyn/Å. The bond distances $R_{OH}^{(s)} = 0.9706$ Å and $R_{O_2}^{(s)} = 1.2074$ Å are also given in the same reference.

Only diagonal cubic and quartic stretching force constants have been considered (5, 6). They follow the relationships which are approximately followed by stable molecules (5), $F_{rrr} = -12F_{rr}$ and $F_{rrrr} = 48F_{rr}$. The bending quadratic force constants are 0.1 of the arithmetic mean of the two O—H and O—O diagonal quadratic force constants, which in turn are calculated from the bond order relationships. The bent species has the two bond stretches (S_1, S_2) and valence angle bending (S_3) as internal coordinates. For the triangular species (isosceles) the three bond stretches (S_1, S_2, and S_3) have been chosen as coordinates. The harmonic frequencies of vibration of the transition state have been calculated by means of the **FG** matrix method. The above relationships only reflect the magnitudes of the cubic and quartic force constants, whose units are (mdyn/Å^2) and (mdyn/Å^3) respectively. The input parameters for [4] have been calculated by methods used previously (5) and by making use of standard definitions (11).

In the bent transition state a zero frequency has been obtained by taking the geometric mean of the two diagonal quadratic stretching force constants as the interaction force constant, *i.e.* $F_{12} = (F_{11}F_{22})^{1/2}$. Similarly, in the triangular species the interaction force constant between the two diagonal quadratic force constants, that correspond to the two OH stretches, has been taken as the geometric mean of these two force constants. As before (5, 6), once the reaction coordinate has been identified by its zero frequency, *all* spectroscopic quantities related to this frequency and the normal coordinate were either set equal to zero or left out in the calculation of the anharmonicity correction.

Results and Discussion

The expression for $\beta(X)$, [4], shows that part of the correction for anharmonicity of the excited states for the partition function of XO_2* consists of replacing the harmonic by the fundamental frequency. The second part of the correction, which involves $\sum\sum f_{ij}$, is usually smaller (12). The temperature dependence of $\beta(X)$ is complex and a plot of $\ln \beta(X)$ *vs.* T^{-1} may not be linear if $\beta(X)$ varies considerably over a certain temperature range.

In order to determine the value of the correction for anharmonicity of the excited states of the transition state, $\beta(X)$, the bent species has been studied first. The bond orders n_1(O—O bond) and n_2 (O—H bond) have been varied from 0.1 to 0.9, while keeping their sum equal to unity. In all these cases $\beta(H)$ and $\beta(D)$ varied at the most from 1.001 at 200 K to 1.05 at 1100 K, values which for most purposes are negligible. The correction factor $\alpha(X)$ is, especially at lower temperatures, always larger than $\beta(X)$. For example, if the bond order of the O—H bond is equal to 0.9, $\alpha(H)$ and $\beta(H)$ are 3.08 and 1.00 respectively at 200 K. The correction terms $\alpha(D)$ and $\beta(D)$ are, under these circumstances, 1.80 and unity respectively. The latter result is not unexpected since anharmonicity is less important for heavier particles.

The corrections $\alpha(X)$ and $\beta(X)$ are largest when the bond order of the O—X bond is almost unity. The bond orders of the bonds determine,

Can. J. Chem. Downloaded from www.nrcresearchpress.com by 210.87.254.5 on 09/05/12
For personal use only.

Can. J. Chem. Downloaded from www.nrcresearchpress.com by 210.87.254.5 on 09/05/12
For personal use only.

via the relationships stated above, the quadratic, cubic, and quartic force constants. It has been found that anharmonicity is due mainly to the anharmonicity of the O—X stretching vibration. Figure 1 shows the dependency of β(X) on F_{11}, which is the quadratic stretching force constant of the O—X bond ($n_2 = 0.9$), at 1100 K. All other parameters of the XO_2* species are unchanged. It can be seen that β(H) is quite insensitive towards changes in F_{11} up to the point $F_{11} = 5.0$, after which it increases sharply. The quantity β(D) seems to be quite insensitive over the whole range.

Figure 2 shows the variation of β(H) with F_{111} ($n_2 = 0.9$, O—H bond) and is compared with α(H). The results are similar to the one shown in Fig. 1. Again the temperature is 1100 K and all other transition state parameters have been kept constant. The decrease of F_{111} and F_{11} have the effect, if the other force constants are kept the same, of increasing the anharmonicity (6). The exact shapes of the curves of β(X) in Figs. 1 and 2 are difficult to explain, since β(X) is at a given temperature a complex function of the harmonic and fundamental frequencies and the anharmonicity constants.

The isosceles transition state XO_2* has also been investigated by varying the bond orders of the O—O and O—H bonds. In this species the bond orders n_1 and n_2 of the two O—X bonds are always equal. The O—O bond has been assigned a bond order of n_3. The sum of n_1, n_2, and n_3 is kept equal to unity. This triangular transition state is similar to the one used previously (6) to investigate the effect of anharmonicity of the vibrational ground state on the kinetic isotope effect in a 1,2-hydride shift. The bond order n_3 has been varied from 0.9 to 0.1. Between these limits β(X) increased from a few percent to a factor of two ($n_3 = 0.1$) at 1100 K. It seems that anharmonicity of the excited states is much more important for the isosceles transition state. As before, β(X) is largest at high temperatures and maximum O—H bond order. The results for the variation of α(H) and β(H), with n_3 (O—O bond) equal to 0.1, with temperature can be found in Fig. 3. It should be noted that, from the bond order of the O—O bond (0.1) and the above definitions, all parameters for the transition state can be deduced.

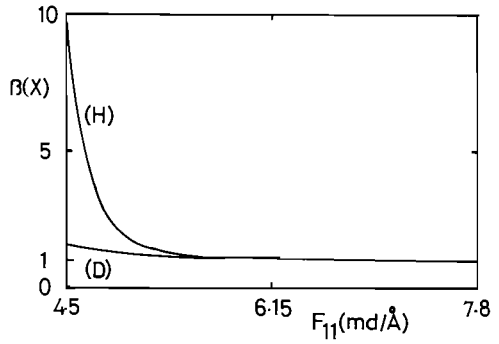

FIG. 1. The correction for anharmonicity of the excited states, β(X), as a function of the *quadratic* stretching force constant F_{11} (bent species); bond order of the O—X bond determines all transition state parameters via the relationships given in text, except F_{11} (and F_{12}, to obtain a zero frequency), which has been varied.

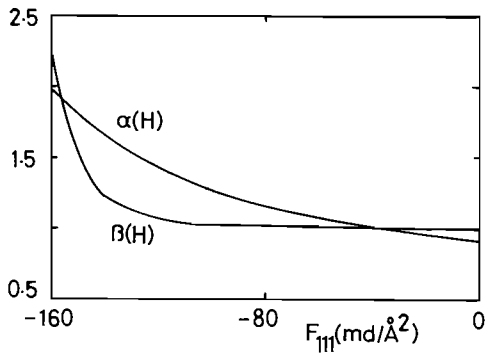

FIG. 2. The correction for anharmonicity of the excited states, β(H), as a function of the *cubic* stretching force constant F_{111} (bent species; bond order of the O—X bond is 0.9, 1100 K). The bond order of the O—X bond determines all transition state parameters, via the relationships given in text, except F_{111}, which has been varied. β(H) is compared with α(H).

Also plotted in Fig. 3 is the function EXC(H). This quantity can be defined by the equation:

$$[5] \quad \mathrm{EXC(H)} = \left[\frac{(1 - e^{-u})_{O_2}}{(1 - e^{-u_1^*})(1 - e^{-u_2^*})}\right]$$

The quantities u_1* and u_2* refer to the two real nonzero harmonic frequencies of vibration of the transition state, while $u(O_2)$ is determined by the frequency of vibration of the O_2 (reactant) molecule. EXC(H) is the excitation term in k_H'. It takes into account the contribution of the vibrational (harmonic) excited states to the partition functions of reactant molecules and transition state.

The shapes of the curves in Fig. 3 deserve some comments. It follows from the definition, [3], that the relationship between ln α(H) and T^{-1} is linear. It can be seen in Fig. 3 that the

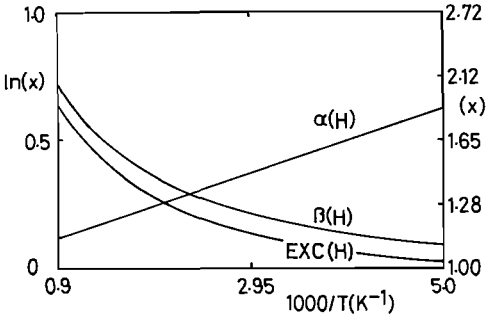

FIG. 3. Arrhenius type of plot of α(H), β(H), and EXC(H) for isosceles transition state HO_2^*. The bond order of the O—O bond is 0.1 and all other transition state parameters can be deduced from the relationships given in text.

plots of ln β(H) and ln EXC(H) *vs.* T^{-1} show considerable curvature, which is not unexpected considering the forms of [4] and [5]. Furthermore, the magnitudes of EXC(H) and β(H) are similar. The curvature of ln EXC(H) is mainly caused by the smallest harmonic frequency of vibration (489 cm^{-1}) of the transition state. The curvature of ln β(H) mainly arises from differences between the two harmonic frequencies of vibration (489 and 3418 cm^{-1}) and the fundamental frequencies (320 and 3180 cm^{-1}) of the transition state. Hence the sources of curvature in plots of ln EXC(H) and ln β(H) *vs.* T^{-1} are basically different.

Curvature in Arrhenius plots of reactions involving H or D can also be associated with tunnelling through the energy barrier (13). Tunnelling is usually important at lower temperatures. However, β(X) and EXC(X) assume considerable values only at higher temperatures. For intermediate temperatures curvature may then be caused by tunnelling, anharmonicity of vibration, and EXC(X). Tunnelling is most important for reactions involving protons, which is similar to the behavior of α(X) and β(X). It follows that, under certain conditions, it may be ambiguous to explain curvature of an Arrhenius plot in terms of tunnelling only. The results as summarized in Fig. 3 were obtained for a force field for which the frequency associated with the reaction coordinate is zero, and hence, the tunnelling correction as given by (14)

$$[6] \qquad \tau = \tfrac{1}{2}|u^*|/\sin(\tfrac{1}{2}|u^*|)$$

is unity. Curvature in Arrhenius plots due to quantum-mechanical tunnelling has been discussed recently by Stern and Weston (15).

From the above results it appears that the correction β(X) may be considerable, depending upon the temperature, geometry, and force field. At temperatures around 300 K β(X) is usually close to unity and may be ignored. However, at high temperatures β(X) is not necessarily negligible and it is worthwhile to take it into account. The importance of anharmonicity decreases as the atomic weight of X increases, so α(H) > α(D) and β(H) > β(D). The anharmonicity corrections are determined mainly by the anharmonicity of vibration of the O—X bond which contains the light atom.

The kinetic isotope effect, k_H/k_D, can be written by means of [1] as (1)

$$[7] \qquad \frac{k_H}{k_D} = \frac{q(D)}{q(H)} \cdot \frac{q(HO_2^*)}{q(DO_2^*)} = 2.8250 \frac{q(HO_2^*)}{q(DO_2^*)}$$

The quantities q in [7] are the partition functions of the species indicated in parentheses. For k_H/k_D the corrections β(X) largely cancel. Therefore, the present calculations seem to indicate that the assumption that anharmonicity of the excited states is not important for kinetic isotope effects is a reasonable one, especially at lower temperatures.

In addition to explaining curvature of an Arrhenius plot, quantum-mechanical tunnelling is also used to rationalize unexpected high isotope effects (16). An upper limit for kinetic isotope effects is calculated by means of the harmonic approximation (16). Considerable deviations from this upper limit, especially for hydrogen isotope effects, are then explained in terms of tunnelling. However, the correction for anharmonicity of the vibrational–rotational ground state, which, like the tunnelling correction, increases with decreasing temperature (*cf.* [3]), can also explain deviations from the estimated upper limit for k_H/k_D, since for a given geometry and force field of the initial and transition states in a particular reaction, a correction factor of two at 200 K can be obtained readily. It is interesting to note that α(H)/α(D) = 2 at 200 K gives a correction factor of 1.0×10^6 at 10 K and 1.6 at 300 K.

Similarly to tunnelling, the anharmonicity corrections α and β are largest for reactions involving the isotopes of hydrogen. At low temperatures the correction for anharmonicity of

Can. J. Chem. Downloaded from www.nrcresearchpress.com by 210.87.254.5 on 09/05/12
For personal use only.

excited states, β, can be safely taken as unity. The correction factor α may be considerable however, but, as mentioned above, the temperature dependence of α does not account for curvature in an Arrhenius plot. As has been reported earlier (6), the correction α can also be smaller than unity for kinetic isotope effects and, therefore, α can also account for smaller effects than expected. From the above discussion a situation can be created in which the tunnelling correction is large (always greater than unity for k_H/k_D), but results in a "normal" isotope effect because of anharmonicity.

As mentioned earlier, the study of reactions involving a larger transition state (more than three atoms) is prohibitive because of computation time. However, it is anticipated that the anharmonicity corrections, α(X) and β(X), will increase if the number of bonds which vibrate anharmonically is increased. This is especially important for bonds containing light isotopes. Therefore, the estimates for α(X) and β(X) for the triatomic transition states may be *lower* limits. In these calculations anharmonicity of vibration in the initial state (O_2) has been ignored. This is reasonable since the anharmonicity correction for molecules containing only heavy atoms is small (5).

In fact, it is more general to allow the correction factors α and β to include anharmonicity for both reactants and transition state. If anharmonicity is important in both reactants and transition state, the correction factors α and β may still be small because of cancellation. Hence, α and β for the model reaction chosen, [1], for this discussion may be greater than the corresponding correction factors for other systems.

The anharmonicity correction α for a system for which the anharmonic force field of the transition state is closely related to that of a stable molecule, has been discussed recently (6). In transition states, atomic movements are much greater than in stable molecules and anharmonicity effects may be larger for these unstable species. Hence, the postulate, that anharmonic force fields of transition states are closely related to the force fields of stable molecules, may be an oversimplification, but this final point can be settled by a detailed theoretical study.

1. H. S. JOHNSTON. Gas phase reaction rate theory. Ronald Press Company, New York. 1966.
2. W. FORST. Theory of unimolecular reactions. Academic Press, New York. 1973.
3. C. J. COLLINS and N. S. BOWMAN. (*Editors*). ACS monograph. Isotope effects in chemical reactions. Van Nostrand Reinhold Company, Toronto. 1971.
4. R. E. WESTON, JR. and H. A. SCHWARZ. Chemical kinetics. Prentice-Hall, Englewood Cliffs, New Jersey. 1972.
5. J. BRON and S. O. HACKER. Can. J. Chem. **51**, 2765 (1973).
6. J. BRON. J. Chem. Soc. Faraday Trans. II, **70**, 240 (1974).
7. S. C. KURZIUS and M. BOUDART. Combust. Flame, **12**, 477 (1968).
8. J. BRON and M. WOLFSBERG. J. Chem. Phys. **57**, 2862 (1972).
9. R. E. PENNINGTON and K. A. KOBE. J. Chem. Phys. **22**, 1442 (1954).
10. L. PAULING. J. Am. Chem. Soc. **69**, 542 (1947).
11. G. HERZBERG. Molecular spectra and molecular structure. I. Spectra of diatomic molecules. Van Nostrand Reinhold Company, New York. 1950.
12. K. S. PITZER. Quantum chemistry. Prentice Hall, Englewood Cliffs, N. J. 1961.
13. M. D. HARMONY. Chem. Soc. Rev. **1**, 211 (1972).
14. R. P. BELL. The proton in chemistry. Methuen, London. 1959.
15. M. J. STERN and R. E. WESTON, JR. J. Chem. Phys. **60**, 2803 (1974).
16. R. P. BELL. Chem. Soc. Rev. **3**, 513 (1974).

Can. J. Chem. Downloaded from www.nrcresearchpress.com by 210.87.254.5 on 09/05/12
For personal use only.

Geminate Recombination of Ion Pairs in the Radiolysis of Dense Hydrocarbon Gases[1]

MASARU NISHIKAWA

Department of Pure and Applied Sciences, University of Tokyo, 3-8-1 Komaba, Meguro-ku, Tokyo, Japan 153

Received March 17, 1975

MASARU NISHIKAWA. Can. J. Chem. **53**, 3075 (1975).

The distribution functions of ion–electron pair separation distances in irradiated hydrocarbon gases are transformed into those of neutralization times by means of the r^3 rule of time–distance obtained under the approximation that Coulomb field predominates in their mutual diffusion. In this approximation lifetime distribution is a function of $(3Dr_c)^{1/3}/b$, where D is the total diffusion constant, $D_+ + D_e$, r_c is the Onsager distance, and b is the characteristic distance of the respective spatial distribution function. Using the values of parameters previously estimated for supercritical hydrocarbons, it was found that for butanes the lifetime in the gas phase at density $\simeq$0.4 g/ml is shorter than that in the liquid phase at room temperature.

MASARU NISHIKAWA. Can. J. Chem. **53**, 3075 (1975).

On transforme les fonctions de distribution des distances de séparation ion–paire d'électron dans des hydrocarbures gaseux irradiés en fonction de temps de neutralisation à l'aide de la règle en r^3 du temps *vs.* distance lorsque l'on fait l'approximation que le champ de Coulomb prédomine lors de leur diffusion mutuelle. Dans cette approximation, la distribution des durées de vie est une fonction de $(3Dr_c)^{1/3}/b$ où D est la constante totale de diffusion, $D_+ + D_e$, r_c est la distance de Onsager et b la distance caractéristique des fonctions respectives de distribution spaciale. Utilisant les valeurs de paramètres obtenues antérieurement pour des hydrocarbures supercritiques, on a trouvé pour les butanes que la durée de vie en phase gaseuse à densité d'environ 0.4 g/ml est plus courte que celle en phase liquide à température de la pièce.

[Traduit par le journal]

The lifetime distribution of the electron produced in a medium by irradiation with respect to neutralization has been the subject of numerous theoretical studies, in which several different approaches have been used (1–6, 12). In one approach the evolution of neutralization is described by the Smoluchowski equation, which is then solved either under 'the prescribed diffusion' approximation (1), numerically (2), with analog computer (3), or by Laplace transform method (4). In another approach the motion of electrons is approximated by their drift motion in the Coulomb field of ions (forced diffusion approximation), where the distribution of neutralization times is generated by the distribution of ion–electron separation distances (5, 6). The results obtained along with these and other approaches give rise to different forms of the distribution, but the experimental data to compare with them are rather limited at the present time. However, the comparison of both approximations made by Dodelet and Freeman (5), and a recent success of the latter approximation in describing the observed neutralization in liquid propane (6) seem to indicate the usefulness of the forced diffusion approximation.

The objective of the present calculation is to find out semiquantitatively how the lifetime of electrons is related to the density of gases, utilizing the fact that a spatial distribution function can easily be transformed into that of lifetime under the forced diffusion approximation.

Lifetime Distribution Functions

Under the assumption that the process of geminate neutralization is dominated by the ion–electron Coulomb force, Williams obtained a simple time–distance relationship

$$[1] \qquad t = \varepsilon kTr^3/(3De^2) = r^3/(3Dr_c)$$

$$r_c = e^2/(\varepsilon kT)$$

where t is the return time for neutralization starting from the separation distance r, D is the mutual diffusion coefficient, and ε is the di-

[1]Partially supported by the Grant in Aid from the Ministry of Education.

Can. J. Chem. Downloaded from www.nrcresearchpress.com by 210.87.254.40 on 09/05/12
For personal use only.

Can. J. Chem. Downloaded from www.nrcresearchpress.com by 210.87.254.40 on 09/05/12
For personal use only.

electric constant of the medium (7). Admittedly this approximation is an oversimplification which tends to underestimate the neutralization time (1, 8), but in view of the usefulness of this approach it should be sufficient for the present purpose.

Using this relationship in a spatial distribution, $f(r)$, one obtains the corresponding distribution function $f(t)$. $f(t)\mathrm{d}t$ represents the fraction that undergoes neutralization between t and $t + \mathrm{d}t$. The fraction of ion pairs, $F(t)$, which exists at any time t after an instantaneous pulse irradiation can be determined simply by integrating $f(t)$ over all values greater than t

$$[2] \qquad F(t) = \int_t^\infty f(t)\,\mathrm{d}t$$

Although hitherto numerous forms of $f(r)$ have been compared and tested against experimentally observed behaviors of electrons in liquid hydrocarbons (5, 9, 10, 17), no single form has yet been established as the universally satisfactory $f(r)$ (10). Since no such test has been performed in dense gases, we choose a single parameter Gaussian, [3], and a simple exponential function, [6], in the calculation mainly on grounds of their simple forms and of the fact that both forms have been shown to give an adequate description of experimental results under some restriction in the range of applicability (9, 10), which appears to fit the present case (11).

For a Gaussian spatial distribution function [3], $f(t)$ and $F(t)$ are

$$[3] \quad f(r) = (4r^2/\pi^{1/2}b^3)\exp(-r^2/b^2)$$

$$[4] \quad f(t) = (4a^2t^{2/3}/\pi^{1/2}b)\exp(-a^2t^{2/3})$$

$$a = (3Dr_c)^{1/3}/b$$

$$[5] \quad F(t) = (2at^{1/3}/\pi^{1/2})\exp(-a^2t^{2/3}) + \mathrm{erfc}(at^{1/3})$$

$$\mathrm{erfc}\,x = \frac{2}{\sqrt{\pi}}\int_x^\infty \mathrm{e}^{-s^2}\,\mathrm{d}s$$

For a simple exponential distribution function [6], they are,

$$[6] \qquad f(r) = (1/b)\exp(-r/b)$$

$$[7] \qquad f(t) = (1/b)\exp(-at^{1/3})$$

$$[8] \qquad F(t) = \exp(-at^{1/3})$$

Lifetime Distribution in Dense Gases

The values of b and D for dense gases have been estimated previously (11).[2] *n*-Butane and isobutane are chosen, both in liquid and gaseous states, as the model for the calculation of lifetime distribution. The values of parameters to be used in the calculation are summarized in Table 1. $F(t)$ calculated by [5] are shown in Fig. 1. For liquid *n*-butane, $F(t)$ by [8] together with the one obtained by Rzad *et al.* ([9]) on the basis of an empirical dependence of electron scavenging on scavenger concentration (12) are included in Fig. 1 for comparison.

$$[9] \qquad F(t) = \exp(\lambda t)\,\mathrm{erfc}\,(\lambda t)^{1/2}$$

where $\lambda = 3Dr_c/b^3$ (13).

All the curves start at unity and decrease to the respective fractions of free ion. It is interesting to note that the lifetime distributions according to [8] and [9] are quite similar to each other and they are both characterized by a faster initial decay and a longer tail. A much shorter tail for [5] is simply a reflection of the Gaussian form of spatial distribution pointed out previously (9, 14). The general trend in the lifetimes that in a medium with faster decay the free ion fraction is larger is in agreement with the result obtained under the prescribed diffusion approximation (1).

In the density range from 0.36 to about 0.6 g/cm^3 (in the liquids), lifetimes are seen to decrease with the decrease in the density. It is more clearly demonstrated by the magnitude of $t_{1/2}^{gn}$, time required for the fraction not neutralized to reach $1.0 - 0.5F_{gn}$ where F_{gn} is the fraction of electrons that undergo geminate neutralization (Table 1). Evidently the lifetimes are much longer in dilute gases at an ordinary irradiation dose rate where ions and electrons recombine homogeneously (15). Thus, the present calculation suggests that in the intermediate regions where neutralization is still largely geminate, electrons may be more short-lived than in the liquid phase. The behavior is common to all three equations of $F(t)$, [5], [8], and [9], which are expressed by the same set of parameters, D, r_c, and b.

[2]Extrapolation of recently determined electron mobilities in dense ethane gas (18) to higher densities indicates that the estimated values (11) are in the right order of magnitude.

TABLE 1. Parameter values and ion–electron neutralization time*

Density (g/cm^3)	b(Å) (*i*)	b(Å) (*ii*)	D(cm^2/s) (*i*)	D(cm^2/s) (*iii*)	r_c (Å)	$t_{1/2}^{gn}$(ps) [5]	$t_{1/2}^{gn}$(ps) [8]
n-Butane (443 K)							
0.583	86	80	0.0068†	0.0068†	320	11.6	2.1
(liq. 293 K)							
0.41	150	182	0.46	2.3	256	0.85	0.043
0.36	174	225	1.03	7.7	263	0.53	0.019
Isobutane (443 K)							
0.552	113	112	0.13†	0.13†	326	1.3	0.26
(liq. 294 K)							
0.42	145	173	0.38	1.2	246	0.95	0.075
0.36	187	252	0.76	5.0	260	0.85	0.037

*(*i*) From ref. 11. (*ii*) b for [6] estimated from G_{fi} in ref. 11. (*iii*) Estimated from b by the method described in ref. 11.
†Calculated from $D = \mu_e kT/e$ from μ_e given in ref. 19.

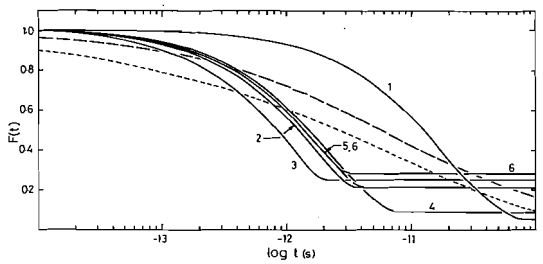

FIG. 1. Ion–electron neutralization time distributions calculated according to [5] for *n*-butane and isobutane. *n*-Butane: *1*, liquid; $d = 0.583$ g/ml, 293 K; *2*, $d = 0.41$ g/ml, 443 K; *3*, $d = 0.36$ g/ml, 443 K. Isobutane: *4*, liquid, $d = 0.552$ g/ml, 294 K; *5*, $d = 0.42$ g/ml, 443 K; *6*, $d = 0.36$ g/ml, 443 K. The --- and – – – curves were calculated for liquid *n*-butane (293 K) using [8] with a properly chosen set of parameter values for the exponential distribution and [9] with those for the Gaussian distribution, respectively.

Obviously, this density dependence is determined by a rather rapid increase in the estimated values of D with the decrease in density. Lifetime curves relatively insensitive to density change for isobutane are due to a more gradual change in D with density compared to that in *n*-butane, which is further moderated by the increase in b upon determining the magnitude of a. A similar tendency has been experimentally observed for the electron mobilities in butanes at the phase change from liquid to gas (16). It is highly desirable to establish the values of electron mobilities and other parameters directly in dense gases, as the conclusion of this calculation is strongly dependent on their reliability.

The author appreciates valuable discussions with Dr. Kenji Fueki of Nagoya University.

1. A. MOZUMDER. J. Chem. Phys. **48**, 1659 (1968).
2. A. HUMMEL and P. P. INFELTA. Chem. Phys. Lett. **24**, 559 (1974).
3. P. K. LUDWIG. J. Chem. Phys. **50**, 1787 (1969).
4. (*a*) G. C. ABELL, A. MOZUMDER, and J. L. MAGEE. J. Chem. Phys. **56**, 5422 (1972); (*b*) P. P. INFELTA. J. Chim. Phys. **69**, 1526 (1972).
5. J.-P. DODELET and G. R. FREEMAN. Can. J. Chem. **50**, 2729 (1972).
6. K. FUEKI. J. Chem. Phys. In press.
7. FF. WILLIAMS. J. Am. Chem. Soc. **86**, 3954 (1964).
8. FF. WILLIAMS. J. Chem. Phys. **48**, 4077 (1968).
9. J.-P. DODELET, P. G. FUOCHI, and G. R. FREEMAN. Can. J. Chem. **50**, 1617 (1972).
10. J.-P. DODELET and G. R. FREEMAN. J. Chem. Phys. **60**, 4657 (1974).
11. M. NISHIKAWA, Y. YAMAGUCHI, and K. FUJITA. J. Chem. Phys. **61**, 2356 (1974).
12. S. J. RZAD, P. P. INFELTA, J. M. WARMAN, and R. H. SCHULER. J. Chem. Phys. **52**, 3971 (1970).
13. S. J. RZAD and K. M. BANSAL. J. Phys. Chem. **76**, 2374 (1972).
14. J.-P. DODELET, K. SHINSAKA, U. KORTSCH, and G. R. FREEMAN. J. Chem. Phys. **59**, 2376 (1973).
15. M. C. SAUER, JR. and W. A. MULAC. J. Chem. Phys. **56**, 4995 (1972).
16. L. G. CHRISTOPHOROU, R. P. BLAUNSTEIN, and D. PITTMAN. Chem. Phys. Lett. **18**, 509 (1973).
17. G. C. ABELL and K. FUNABASHI. J. Chem. Phys. **58**, 1079 (1973).
18. L. G. CHRISTOPHOROU. Int. J. Radiat. Phys. Chem. **7**, 205 (1975).
19. M. G. ROBINSON and G. R. FREEMAN. Can. J. Chem. **52**, 440 (1974); P. G. FUOCHI and G. R. FREEMAN. J. Chem. Phys. **56**, 2333 (1972).

Can. J. Chem. Downloaded from www.nrcresearchpress.com by 210.87.254.40 on 09/05/12
For personal use only.

Stereospecific Synthesis and Acetolysis of *anti*-Tricyclo[4.4.1.1^{2,5}]dodecan-11-yl and Related Derivatives

J. HAYWOOD-FARMER,[1] B. T. FRIEDLANDER, A. CRAWFORD, L. M. THOMPSON, AND W. WETZER

Department of Chemistry, Bishop's University, Lennoxville, Quebec J1M IZ7

Received April 25, 1975

J. HAYWOOD-FARMER, B. T. FRIEDLANDER, A. CRAWFORD, L. M. THOMPSON, and W. WETZER. Can. J. Chem. **53**, 3078 (1975).

Stereospecific conversion of tricyclo[4.4.1.1^{2,5}]dodecan-11-one and of several related unsaturated and cyclopropanated ketones into *syn* or *anti* alcohols is described. Acetolysis of *anti*-tricyclo[4.4.1.1^{2,5}]dodecan-11-yl *p*-bromobenzenesulfonate, *anti*-tricyclo[4.4.1.1^{2,5}]dodec-3-en-11-yl *p*-bromobenzenesulfonate, and *anti*-tetracyclo[5.4.1.1^{2,6}.0^{3,5}]tridecan-12-yl *p*-bromobenzenesulfonate each proceeds at about the same rate as other equatorial cyclohexyl *p*-bromobenzenesulfonates to give complex mixtures of rearranged acetates and hydrocarbons. No evidence for neighboring group participation by the remote double bond or cyclopropane ring in these esters was found. The stereochemically interesting ketone reductions, the unambiguous structural proofs of the reduction products, and possible explanations of the solvolysis rates are discussed.

J. HAYWOOD-FARMER, B. T. FRIEDLANDER, A. CRAWFORD, L. M. THOMPSON et W. WETZER. Can. J. Chem. **53**, 3078 (1975).

On décrit la conversion stéréospécifique de la tricyclo[4.4.1.1^{2,5}]dodécanone-11 et de plusieurs cétones non-saturées et cyclopropaniques apparentées en alcools *syn* ou *anti*. Les vitesses d'acétolyse des *p*-bromobenzènesulfonates des tricyclo[4.4.1.1^{2,5}]dodécanol-11 *anti*, tricyclo[4.4.1.1^{2,5}]dodécène-3 ol-11 et tétracyclo[5.4.1.1^{2,6}.0^{3,5}]tridécanol-12 sont toutes semblables et d'un ordre de grandeur similaire à d'autres *p*-bromobenzènesulfonates de cyclohexanols équatoriaux et les produits sont toujours formés d'un mélange complexe d'hydrocarbures et d'acétates réarrangés. Les résultats n'indiquent pas qu'il y a participation de la double liaison ou du noyau cyclopropanique dans ces réactions. On discute des réductions stéréochimiquement intéressantes des cétones, des preuves non ambigues des structures des produits de réduction et des explications plausibles des vitesses de solvolyse.

[Traduit par le journal]

Introduction

The use of rigid polycyclic molecules with reasonably well-known geometries has been instrumental to a better understanding of many aspects of organic chemistry including the study of neighboring group participation in carbonium ion and related reactions (1, 2). In an attempt to define better the geometrical requirements for interactions of double bonds and cyclopropane rings with remote electron deficient centers we have undertaken the synthesis and solvolytic study of several rigid polycyclic derivatives. It is our hope that the relative importance of the several geometrical factors of importance to neighboring group participation (2) can be understood once the behavior of a number of molecules with different geometries is known.

Towards this end we have developed stereospecific syntheses of alcohols with the tricyclo[4.4.1.1^{2,5}]dodecan-11-yl skeleton and have studied the acetolysis of suitable derivatives which we would like to report at this time.

Results and Discussion

It has been known for some time that reduction of trienone **1** with $LiAlH_4$ in ether gives only **2**-OH (3, 4), the structure of which was based on the very small value observed for $J_{1,11}$ and on the acetolysis behavior of **2**-OTs. We expected that a similar steric course would be followed in the reduction of closely related ketones and were surprised, therefore, when **5** (5) was reduced under the same conditions to yield predominantly **6**-OH (Table 1) with C-11 inverted with respect to **2**-OH.[2] This stereochem-

[1]To whom correspondence should be addressed.

[2]This reduction has been reported in preliminary form by other workers (6) with no comment regarding its stereochemistry and, although different physical constants for **5** and **6**-OH were reported than those obtained by us, Dr. Itô has kindly informed us that the i.r. spectra of the independently prepared samples are virtually identical.

Can. J. Chem. Downloaded from www.nrcresearchpress.com by 210.87.254.42 on 09/05/12
For personal use only.

Can. J. Chem. Downloaded from www.nrcresearchpress.com by 210.87.254.42 on 09/05/12
For personal use only.

TABLE 1. Stereochemistry of reduction of several ketones

Ketone	*syn*-Alcohol[a] (%)	Method of analysis
1	100	n.m.r., g.l.c.
9	100	n.m.r., g.l.c.
4	88	n.m.r.
5	12	n.m.r., g.l.c.
11	0	n.m.r., g.l.c.

[a]Values considered accurate to ±4%; the remaining fraction is *anti* epimer.

ical assignment was tentatively made on the basis of the larger observed value (*ca.* 5 Hz) for $J_{1,11}$ compared to that for **2**-OH but we felt that this conclusion was ambiguous. Although the unsaturated C-7–C-10 bridge of **2**-OH is rigid giving relatively fixed dihedral angles at C-11 of *ca.* 85 and 35°,[3] the saturated bridge of **6**-OH is flexible with at least three different conformations. In the two eclipsed conformers, **12** and **13**, both dihedral angles at C-11 are *ca.* 60° but in the staggered conformer, **14**, angles of *ca.* 85 and 35° are found once more. Because we could not unequivocally determine which conformer is preferred or, whether or not **6**-OH is conformationally mobile at the temperature and time scale of our n.m.r. instrument, we were uncertain of the C-11 configuration of **6**-OH. Because it was obviously crucial for our solvolytic studies to correctly assign this structure, we sought a more rigorous structural proof.

Addition of small amounts of the n.m.r. shift reagent Eu(fod)$_3$ to a solution of **2**-OH in $CDCl_3$ caused a marked downfield shift of the H-3 (H-4) signal and a much smaller downfield shift for H-7–H-10 (Fig. 1). Similar treatment of **6**-OH did not shift the olefinic proton appreciably although the behavior of H-11 was similar to that in **2**-OH (Fig. 1). These differences are in full accord with the assigned structures of **2**-OH and **6**-OH.

Catalytic hydrogenation of **2**-OH and **6**-OH gave the two saturated alcohols **3**-OH and **7**-OH, respectively, which were shown to be epimeric by their oxidation to the single known ketone **4** (5, 7). These two compounds have almost identical melting points which are not depressed on mutual mixing and, in our hands proved to be inseparable by g.l.c., but they had distinctly different i.r. and n.m.r. spectra. In particular, the H-11 signal is a relatively sharp singlet in

[3]These are the dihedral angles between H-1 (H-6) and the *syn* and *anti* positions at C-11, respectively, as measured from Dreiding models.

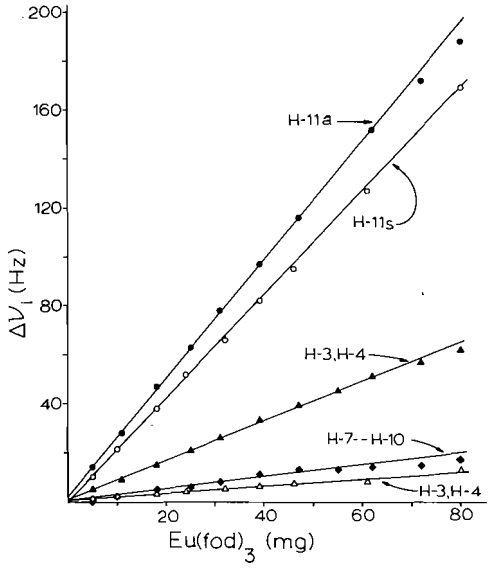

FIG. 1. A plot of chemical shift induced by shift reagent, $\Delta\nu_i$, *vs.* amount of added shift reagent for some protons of **2**-OH (solid points) and **6**-OH (open points).

3-OH ($w_{1/2}$ = 3.5 Hz) at slightly higher field (0.2 p.p.m.) than the broad singlet ($w_{1/2}$ = 11 Hz) of **7**-OH. These data are in accord with a predominance of conformer **14** for the tricyclo-[4.4.1.1^{2,5}]dodecane ring system. Unlike the distinct triplets observed for H-11 of the unsaturated **6**-OH and cyclopropanated **10**-OH (*vide infra*), no fine structure was observed in the broad peak of **7**-OH. The reason for this behavior is unclear.

Prolonged reduction of **1** with $LiAlH_4$ in refluxing tetrahydrofuran gave the dienol **8**-OH whose u.v. spectrum is typical of the conjugated diene chromophore (5). This reaction is similar to the well-known stereospecific reduction of the *syn* double bond of 7-oxygenated norbornadienes (8) and provides interesting support for the structure of **2**-OH. Oxidation gave the known ketone **9** (7); the sequence of reduction of **1** followed by oxidation to **9** provides an alternative route to the previously reported (7) selective hydrogenation of the isolated double bond of **1**.

The spectroscopic and chemical evidence outlined above provides overwhelming proof of the structures of **2**-OH and **6**-OH and for the other alcohols prepared in this study.

Treatment of either **6**-OH or **5** with CH_2N_2 in the presence of Cu_2Cl_2 (9) led cleanly to **10**-OH and **11** respectively. The cyclopropane

Can. J. Chem. Downloaded from www.nrcresearchpress.com by 210.87.254.42 on 09/05/12
For personal use only.

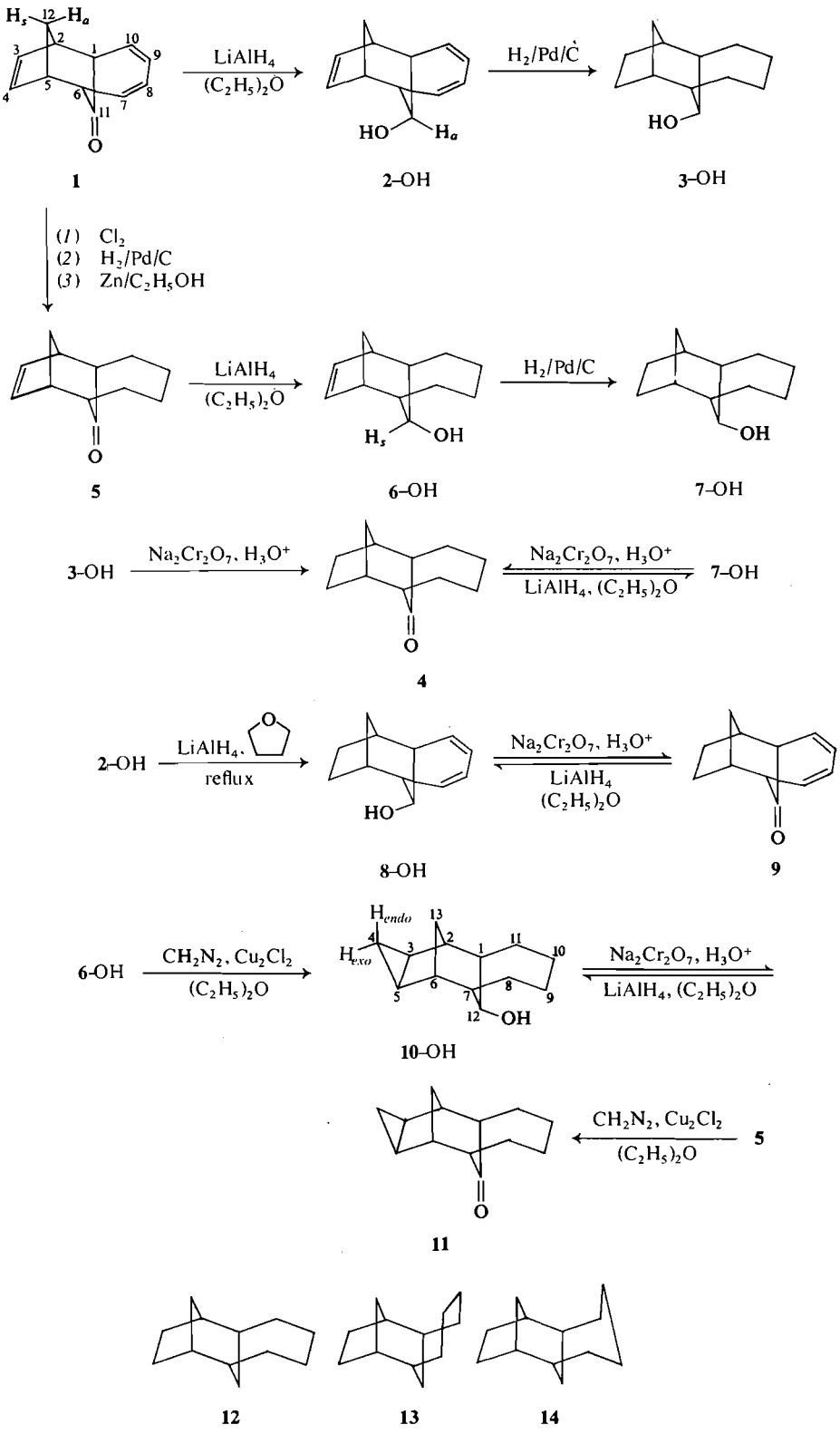

1 2-OH 3-OH 5 6-OH 7-OH 4 8-OH 9 10-OH 11 12 13 14

Can. J. Chem. Downloaded from www.nrcresearchpress.com by 210.87.254.42 on 09/05/12
For personal use only.

ring was assigned the *exo* structure found in the related epoxide (5). The n.m.r. spectrum showed H-3 and H-5 to be coupled only very weakly to H-2 and H-6 as anticipated (5). H-4_{exo} is found at relatively high field (*ca.* τ 9.8); this value is typical of *exo*-tricyclo[3.2.1.$0^{2,4}$]octanes (10) and demonstrates the previously noted (5) similarity of the tricyclo[4.4.1.$1^{2,5}$]dodecanyl and norbornyl ring systems.

The stereochemistry of reduction of **1**, **4**, **5**, **9**, and **11** has proven to be most interesting. Both **1** and **9**, in which the C-7–C-10 diene unit is present, reduce to give *syn* alcohols **2**-OH and **8**-OH exclusively (Table 1). In **4**, **5**, and **11**, however, the steric preference is reversed, *anti* alcohols **7**-OH, **6**-OH, and **10**-OH now being the predominant products. We are unaware of another example in which partial or total hydrogenation of remote unsaturation so dramatically changes the preferred direction of approach of reducing agents to a carbonyl group. In a related study (11) **15** was shown to reduce to only the *syn* alcohol **16**-OH. Partial or complete saturation of the diene unit (*i.e.* **17**, **18**, and **19**) resulted in an increase in attack from the *syn* side but the predominant products still had the *syn* stereochemistry. Despite a recent explanation of the stereochemistry of cyclohexanone reductions based on the induction of anisotropy in the electron density of the carbonyl group by the σ bonds in the six-membered ring (12), and other possible electronic explanations, we prefer to interpret our results in simple steric terms. Examination of a Dreiding model of **1** and calculations of congestion (13) based on this model[4] reveal that the *anti* side of the molecule is much more open to attack than is the *syn* side. In **9** attack from the *syn* side is even more hindered. These two ketones thus give exclusively *syn* alcohol. In **4**, **5**, and **11** the situation is reversed. The two most likely conformers, **12** and **14**, have severe congestion on the *anti* side of the carbonyl group making the *syn* side much more

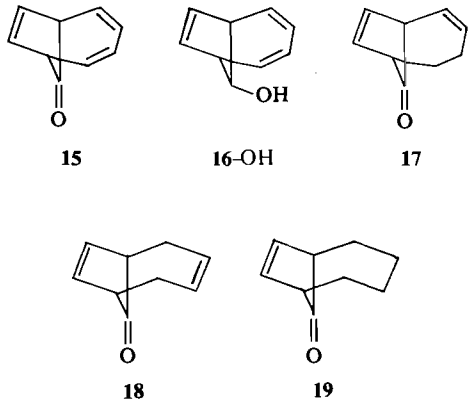

15 **16**-OH **17**

18 **19**

open to attack by nucleophiles and explaining the observed steric preference. The third conformer, **13**, does not have the *anti* side congestion of **12** and **14** but is probably not a major component because of a severe interaction between H-12*a* and the C-8—C-9 bond. We are not yet able to explain why reduction of **11** is more stereospecific than that of **4** or **5**.

The acetolysis of each ester (**6**-OBs, **7**-OBs, and **10**-OBs) is a clean first order process (Table 2) with no evidence in either the kinetic or product studies to indicate ion pair return. The three brosylates acetolyze at about the same rates as suitable model compounds (Table 3). Particularly striking is the similarity to molecules which also incorporate an equatorially substituted cyclohexane chair despite the improbability (Bredt's rule (*cf.* 14)) of direct hydrogen elimination leading to olefinic products. This is a major pathway in the acetolysis of cyclohexyl sulfonates (*cf.* 15). We conclude that neighboring group participation is a relatively inefficient process in the acetolysis of **6**-OBs and **10**-OBs. This conclusion is in accord with the assumed geometrical similarity of ketones **4**, **5**, and **11**, in ν_{CO} (**4**: 1707; **5**: 1710; **11**: 1706; cyclohexanone: 1716 (16)) and in λ_{max} n $\rightarrow \pi^*$ (**4**: 297 (ε 22); **5**: 294 (ε 35); **11**: 294 (ε 31); cyclohexanone: 283 (ε 17)) both of which have been correlated with anchimeric assistance in other systems (16–18). Recent ^{13}C n.m.r. data (19), however, do indicate a possible interaction between the double bond and carbonyl group of **5**.

The acetolyses of **6**-OBs, **7**-OBs, and **10**-OBs all result in the formation of very complex mixtures of as yet unidentified products (Table 2) which are >95% rearranged. The principal products in all cases are those of elimination. The

[4]Although we believe that these calculations are qualitatively meaningful, the angles in the C-7–C-10 bridge of the model are somewhat larger than 120° so that the six atoms C-1, C-6–C-10 may be incorporated in a coplanar arrangement. In the molecule itself it is possible that the conjugated diene unit is puckered to relieve the strain of angle distortion. The present lack of accurate structural data on **1** or any other member of this ring system makes quantitative discussion impossible. Such a puckering would alter the magnitude of the congestion factors but probably not their relative order. Models of **4**, **5**, and **11** appear to be relatively unstrained.

TABLE 2. Kinetic and product data for the acetolysis of *anti*-tricyclo[4.4.1.1^{2,5}]-dodecan-11-yl and related *p*-bromobenzenesulfonates[a]

Compound	Temperature (°C)	$k \times 10^5$ (s^{-1})	No. of hydrocarbon products	No. of acetate products	Hydrocarbon: acetate ratio
7-OBs[b]	65.2	4.79			
	85.6	52.5	8	4	9:1
	(75.0)[c]	15.6			
6-OBs[d]	65.2	5.75			
	85.6	63.3	9	7	2:1
	(75.0)[c]	18.8			
10-OBs[e]	75.5	3.65			
	95.9	40.7	6	9	2:1
	(75.0)[c]	3.45			

[a]See Experimental for conditions.
[b]$\Delta H^* = 27.6$ kcal/mol, $\Delta S^* = 3.0$ e.u. (75 °C).
[c]Interpolated or extrapolated.
[d]$\Delta H^* = 27.7$ kcal/mol, $\Delta S^* = 3.7$ e.u. (75 °C).
[e]$\Delta H^* = 29.4$ kcal/mol, $\Delta S^* = 9.8$ e.u. (75 °C).

TABLE 3. Relative buffered acetolysis rates of several brosylates at 75 °C

Brosylate	k_{rel}	k/k_{sat}	Notes
Cyclopentyl	13		*a,b*
Cyclohexyl	1		*a,b*
Cycloheptyl	23	1	*a,b*
4-Cyclohepten-1-yl	0.9	0.04	*c*
cis,cis-Bicyclo[5.1.0]oct-4-yl	3.2	0.14	*c*
exo-Bicyclo[3.2.1]oct-3-yl	3.9	1	*b,d,e*
exo-Bicyclo[3.2.1]oct-6-en-3-yl	2.7	0.7	*e,f*
7-OBs	1.1	1	
6-OBs	1.3	1.2	
10-OBs	0.25	0.22	

[a]Extrapolated or interpolated from data given in ref. 28.
[b]Unbuffered acetic acid.
[c]Interpolated from data given in ref. 29.
[d]Interpolated from data given in ref. 30.
[e]Calculated from data reported for the corresponding tosylate.
[f]Interpolated from data given in ref. 21.

presence of major peaks at $\tau > 9.5$ in the n.m.r. spectrum of the crude product from **10**-OBs indicates retention of the cyclopropane ring. The complex nature of the product mixtures, although not unprecedented in systems exhibiting large anchimeric assistance (20), is corroborative evidence for the absence of neighboring group participation.

Our failure to observe even a portion of the tremendous anchimeric acceleration found in other systems, notably in those related to 7-norbornyl (1*a*, 2), is at first surprising in view of the apparent similarity in geometry between **6**-OBs, **10**-OBs, and the more reactive molecules. Closer examination reveals a number of rationalizations based on geometrical and electronic factors that could be advanced to explain the apparent discrepancy; we are not yet in a position to choose between them. The distance between the potential neighboring group and the reaction center in **6**-OBs and **10**-OBs is 2.6–2.8 Å (Dreiding models), somewhat longer than that in *anti*-7-norbornenyl and related esters (2.3–2.4 Å). This distance was cited previously (21) to explain the absence of participation by the double bond in the acetolysis of *exo*-bicyclo[3.2.1]oct-6-en-3-yl tosylate. Molecular models also predict that the developing p orbitals of **6**-OBs and **10**-OBs lie almost parallel to, but displaced from, the planes of the potential neighboring groups. The effective overlap predicted (18*b*, 22) for the transition states for the ionization of *anti*-7-norbornenyl and related esters is therefore much less likely for the ionization of **6**-OBs and **10**-OBs. Also

Can. J. Chem. Downloaded from www.nrcresearchpress.com by 210.87.254.42 on 09/05/12
For personal use only.

Can. J. Chem. Downloaded from www.nrcresearchpress.com by 210.87.254.42 on 09/05/12
For personal use only.

pertinent is the expectation that a molecular distortion analogous to that predicted (18*b*) to increase overlap, and hence stability, in the delocalized 7-norbornenyl cation, should decrease overlap in **20** and **21**. The differences in *I* strain (*cf.* 23) between the tricyclo[4.4.1.$1^{2,5}$]dodecan-11-yl and 7-norbornyl systems might also be used to explain our kinetic results.

Finally, it has been predicted recently by Goldman (24) that the homoaromatic stabilization expected for ions such as **20** and **21** (*cf.* 25) should be overcome by the antisymmetric alignment of the flanking σ bonds, *i.e.* C-1—C-2 and C-5—C-6, possibly resulting in a rate retardation by the potential neighboring group. Experimental verification of this proposal is not yet available in compounds without geometrical ambiguities so that its applicability to the present study is uncertain.

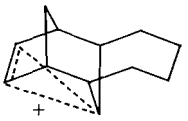

20

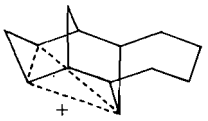

21

We are continuing our efforts to analyze the complex products from **6**-OBs, **7**-OBs, and **10**-OBs and also to synthesize and study the ionization of other geometrically interesting molecules.

Experimental

Melting points were determined on a Thomas–Hoover apparatus and are uncorrected. The n.m.r. spectra were obtained on a Varian A60 A spectrometer in $CDCl_3$ solution. Peak positions are given in units of τ relative to internal tetramethylsilane at τ 10.00 or $CHCl_3$ at τ 2.75; in all cases the relative peak areas are consistent with the assigned structure. Infrared spectra were recorded on Nujol mulls, neat liquids, and solutions in CCl_4 using a Unicam SP 200, a Beckman IR 10, or a Perkin-Elmer 710 spectrophotometer; the peak positions are given in wave numbers. Ultraviolet spectra were recorded in 95% ethanol solution on a Unicam SP 800 recording spectrophotometer; peak positions are given in nm. Gas–liquid chromatographic analyses were carried out on Varian Aerograph A90 P3 or an F and M 700 chromatograph employing copper or stainless steel columns packed with Carbowax 20M unless otherwise stated. Combustion microanalyses were obtained from Galbraith Laboratories, Inc., Knoxville, Tenn. 37921.

General Procedure for $LiAlH_4$ Reductions

About 50 mg of pure ketone was added to a stirred slurry of *ca.* 100 mg of $LiAlH_4$ in 15 ml $(C_2H_5)_2O$ at room temperature under an atmosphere of N_2. The mixture was refluxed for *ca.* 0.5 h, cooled to 0 °C and the excess $LiAlH_4$ destroyed by the cautious addition of H_2O. The precipitated aluminum salts were dissolved by adding 10% aqueous H_2SO_4 and the aqueous solution extracted with 3 × 50 ml $(C_2H_5)_2O$. The ether was washed with 10% aqueous Na_2CO_3 solution and dried ($MgSO_4$), and the solvent removed to give crude product which was analyzed directly by g.l.c. or n.m.r.

syn-Tricyclo[4.4.1.$1^{2,5}$]dodeca-3,7,9-trien-11-ol, 2-OH

Treatment of **1** as described above gave a yellow oil which crystallized on standing. A pure sample of **2**-OH was prepared by g.l.c., m.p. 29.5–31.5 °C (lit. (3) m.p. 32.5–34.5 °C); n.m.r.: 3.62 (singlet, H-3, H-4), 4.03 (multiplet, H-1, H-2, H-5, H-6, OH), 7.73 (doublet, J = 10.5 Hz, H-12*a*), 8.3–8.8 (multiplet, H-12*s*); n.m.r. and g.l.c. revealed that only one alcohol was present.

syn-Tricyclo[4.4.1.$1^{2,5}$]dodecan-11-ol, 3-OH

Crude **2**-OH (50 mg) was dissolved in 5 ml of 95% C_2H_5OH and stirred under H_2 at *ca.* 1.1 atm at room temperature in the presence of 35 mg of 10% Pd-on-charcoal. After the H_2 uptake had ceased, the mixture was filtered and the solvent removed to give 50 mg (95% yield overall from **1**) of white crystals of **3**-OH which could be purified by g.l.c. or by vacuum sublimation (105 °C, 15 Torr), m.p. 75–76.5 °C. A mixed sample with **7**-OH had m.p. 74–76 °C; i.r.: 3375, 1075, 1040, 1035, 1025; n.m.r.: 6.12 (singlet, $w_{1/2}$ = 3 Hz, H-11*a*), 7.8–9.2 (multiplet, all other protons).

Anal. Calcd. for $C_{12}H_{20}O$: C, 79.94; H, 11.18. Found: C, 80.02; H, 11.29.

Oxidation of 3-OH

The oxidation was carried out according to the published procedure (26). A solution of 30 mg **3**-OH in *ca.* 110 μl of $(C_2H_5)_2O$ was treated at 0 °C for 10 min with 220 μl of a solution containing 100 g $Na_2Cr_2O_7$ and 136 g 97% H_2SO_4 and diluted with H_2O to a total volume of 500 ml. The reaction mixture was diluted with *ca.* 50 ml $(C_2H_5)_2O$ and 20 ml H_2O, the layers separated, and the aqueous one extracted with 50 ml $(C_2H_5)_2O$. The combined $(C_2H_5)_2O$ solutions were washed with 10% aqueous Na_2CO_3 solution, dried ($MgSO_4$), filtered, and the solvent evaporated to give 19 mg (64%) of a colorless oil; g.l.c. showed that only one component was present; i.r. showed it to be identical to a previously prepared sample of **4** (5); i.r.: 1707; u.v.: λ_{max} 297, ε 22.

anti-Tricyclo[4.4.1.$1^{2,5}$]dodec-3-en-11-ol, 6-OH

Treatment of 60 mg of the previously prepared **5** (5) (i.r.: 1710; u.v.: λ_{max} 294, ε 35) with $LiAlH_4$ as described in the general procedure above gave 60 mg (99%) of yellowish crystals. The g.l.c. and n.m.r. analyses of the crude product showed the presence of two alcohols in the ratio of 88:12. The major component was identified as **6**-OH, the minor one was assumed to be its C-11 epimer on the basis of the shape of the H-11 n.m.r. signal (see text) but this product was not further characterized. A sample of **6**-OH was purified by g.l.c., m.p. 82–83.5 °C (lit. (6) volatile liquid[2]); i.r.: 3400, 3075, 1580; n.m.r.: 3.78 (singlet, H-3, H-4), 5.69 (triplet, J = 5.5 Hz, H-11*a*), 7.2–9.2 (complex multiplet, all other protons).

Nuclear Magnetic Resonance Shift Experiments

Solutions of **2**-OH and **6**-OH of *ca.* 1.2 *M* were prepared in a total volume of *ca.* 450 μl $CDCl_3$ and a total

Can. J. Chem. Downloaded from www.nrcresearchpress.com by 210.87.254.42 on 09/05/12
For personal use only.

of 80 mg of the shift reagent europium(III)-tris-1,1,-1,2,2,3,3-heptafluoro-7,7-dimethyl-4,5-octanedione (Eu-(fod)$_3$) (Norell Chemical Co., Landisville, New Jersey 08326) added to each sample in increments of *ca.* 8 mg. The n.m.r. spectrum was recorded after each addition, the chemical shift change of each peak measured (assuming no change in internal tetramethylsilane) and the results plotted. Each peak in the spectrum of **2**-OH could be analyzed but only the olefinic peaks and H-11*s* could be analyzed for **6**-OH because of unresolved peak overlap. The plots for the most pertinent signals are shown in Fig. 1 and clearly show that the assigned configurations of **2**-OH and **6**-OH are correct.

anti-Tricyclo[4.4.1.1^{2,5}]dodecan-11-ol, 7-OH

A 50 mg sample of purified **6**-OH was dissolved in 5 ml of 95% C_2H_5OH, 40 mg of 10% Pd-on-charcoal added and the mixture stirred under H_2 at *ca.* 1.1 atm at room temperature. After the gas uptake had ceased, the mixture was filtered and the solvent evaporated to give 48 mg (95%) of white crystalline **7**-OH, a sample of which was purified by g.l.c., m.p. 72–73.5 °C. A mixed sample with **3**-OH had m.p. 74–76 °C; i.r.: 3350, 1070, 1020; n.m.r.: 5.93 (broad singlet, $w_{1/2}$ = 11 Hz, H-11*s*), 7.7–9.3 (complex multiplet, all other protons).

Anal. Calcd. for $C_{12}H_{20}O$: C, 79.94; H, 11.18. Found: C, 79.76; H, 11.00.

Similar hydrogenation of a crude sample of **6**-OH gave a solid whose n.m.r. spectrum clearly showed the presence of both **7**-OH and **3**-OH in the ratio of 88:12.

Oxidation of 7-OH

A sample of **7**-OH (35 mg) was oxidized as described above for **3**-OH to give 32 mg (92%) of a single ketone shown by i.r. to be **4** (5).

Reduction of 4

A freshly prepared sample of **4** (from hydrogenation of **1** (5)) was reduced with $LiAlH_4$ according to the general procedure described above giving a quantitative yield of crystalline alcohol. The n.m.r. analysis showed that it contained **7**-OH and **3**-OH in the ratio 92:8. These two alcohols proved to be unseparable by g.l.c. on columns of Carbowax 20M, LAC 728, SE 30, UCW 98, Apiezon L, and TCEP.[5]

syn-Tricyclo[4.4.1.1^{2,5}]dodeca-7,9-dien-11-ol, 8-OH

Solid **1** (310 mg) was added to a stirred slurry of *ca.* 1 g $LiAlH_4$ in 35 ml of freshly distilled tetrahydrofuran and the mixture refluxed for 50 h. The solution was cooled to 0 °C and H_2O slowly added to destroy the excess $LiAlH_4$. The precipitated aluminum salts were dissolved by adding 10% aqueous H_2SO_4 and the solution extracted with 3 × 100 ml of $(C_2H_5)_2O$. The combined $(C_2H_5)_2O$ layers were washed with 100 ml H_2O, 10% aqueous Na_2CO_3 solution, dried ($MgSO_4$), and filtered. Evaporation of the solvent gave 285 mg of a yellowish oil which was shown by g.l.c. to contain at least five components. The major one (*ca.* 70%) was purified by g.l.c. and vacuum sublimation (115 °C, 12 Torr) and shown to be **8**-OH, m.p. 75–76 °C; i.r.: 3320, 3020, 1595; u.v.: λ_{max} 275, ε 2990; 264, ε 5400; 254, ε 5240; 249, sh; 245, sh; n.m.r.: 4.41 (multiplet, H-7–H-10), 5.62 (singlet, $w_{1/2}$ = 4 Hz, H-11*a*), 7.1–9.2 (complex multiplet, all other protons).

Anal. Calcd. for $C_{12}H_{16}O$: C, 81.77; H, 9.15. Found: C, 81.47; H, 9.22.

Tricyclo[4.4.1.1^{2,5}]dodeca-7,9-dien-11-one, 9

Crude **8**-OH (155 mg) was oxidized as described above for **3**-OH to give 110 mg of a yellowish oil from which 40 mg of pure **9**, m.p. 96.5–98.5 °C (lit. (7) m.p. 92 °C) was obtained by g.l.c.; n.m.r.: 3.8–4.5 (complex multiplet H-1, H-6), 7.1–9.2 (complex multiplet, all other protons).

Reduction of 9

A sample of **9** was treated with $LiAlH_4$ according to the general procedure described above. Both n.m.r. and g.l.c. analyses of the crude product showed the presence of only one alcohol confirmed by i.r. to be **8**-OH. Other unidentified products were formed in this reaction but they contained neither carbonyl nor hydroxyl groups.

anti-Tetracyclo[5.4.1.1^{2,6}.0^{3,5}]tridecan-12-ol, 10-OH

Diazomethane was prepared by treatment of *N*-methyl-*N*-nitrosourea with 50% aqueous KOH solution and carried in a stream of N_2 into a stirred solution of 917 mg **6**-OH in 25 ml anhydrous $(C_2H_5)_2O$ containing 500 mg suspended Cu_2Cl_2 according to the convenient procedure of Pincock and Wells (9). The cyclopropanation was monitored by g.l.c. After several hours when the reaction was near completion it was terminated, the solution filtered, and the solvent removed to give 1.04 g of a green oil which was eluted with $(C_2H_5)_2O$ through a short column of alumina to remove the residual copper compounds. A small sample of the resulting colorless crystals (1.0 g, 100%) was purified by g.l.c., m.p. 67–68 °C; i.r.: 3380, 3070, 3010; n.m.r.: 5.38 (triplet, J = 5.5 Hz, H-12*s*), 7.2–8.9 (complex multiplet, H-1, H-2, H-6–H-11, H-13, OH), 9.08 (doublet of doublets, J = 3.6, 8 Hz, H-3, H-5), 9.34–9.95 (multiplet, H-4).

Anal. Calcd. for $C_{13}H_{20}0$: C, 81.20; H, 10.48. Found: C, 81.01; H, 10.54.

Tetracyclo[5.4.1.1^{2,6}.0^{3,5}]tridecan-12-one, 11

A 50 mg sample of **10**-OH was treated as described above for the oxidation of **3**-OH to give 32 mg (65%) of liquid **11** which was purified by g.l.c.; i.r.: 3100, 3050, 1706; u.v.: λ_{max} 294, ε 31; n.m.r.: 7.35 (multiplet, H-1, H-7), 7.78–8.67 (complex multiplet, H-2, H-6, H-8–H-13), 8.92 (doublet of doublets, H-3, H-5), 9.3–9.85 (multiplet, H-4).

Anal. Calcd. for $C_{13}H_{18}O$: C, 82.06; H, 9.53. Found: C, 81.83; H, 9.48.

This ketone could also be formed by direct cyclopropanation of **5** as described for the synthesis of **10**-OH in which attack by diazomethane at the carbonyl group with subsequent ring expansion did not effectively compete.

Reduction of 11

Treatment of 50 mg of **11** with $LiAlH_4$ by the general procedure described above gave 50 mg (99%) of an alcohol which was shown by g.l.c. and n.m.r. to be sterically homogeneous and by i.r. to be **10**-OH.

General Procedure for the Preparation of p-Bromobenzenesulfonates (Brosylates)

Equimolar amounts of alcohol and *p*-bromobenzene-

[5]The analyses on the TCEP capillary column were carried out by D. C. Wigfield, Carleton University, Ottawa, Canada to whom we express our thanks.

Can. J. Chem. Downloaded from www.nrcresearchpress.com by 210.87.254.42 on 09/05/12
For personal use only.

sulfonyl chloride were dissolved in dry pyridine (*ca.* 2 ml per g acid chloride) and the solution allowed to stand in a refrigerator at 0 °C until the deposition of pyridine hydrochloride appeared to be complete. This usually took several days. Water was then added to the mixture and the resulting crystalline mass of crude brosylate collected by filtration. The crystals were washed well with H_2O and 10% aqueous Na_2CO_3, dried, and recrystallized from hexane.

anti-Tricyclo[4.4.1.1^{2,5}]dodecan-11-yl p-Bromobenzenesulfonate, 7-OBs

The brosylate isolated in 60% yield by the above procedure had m.p. 79.5–80 °C (dec.); n.m.r.: 2.33 (multiplet, aromatic ring protons); 5.13 (broad singlet, $w_{1/2}$ = 11 Hz, H-11*s*), 7.4–9.3 (multiplet, all other protons).

Anal. Calcd. for $C_{18}H_{23}SO_3Br$: C, 54.14; H, 5.80; S, 8.03; Br, 20.01. Found: C, 54.35; H, 5.76; S, 9.13; Br, 20.21.

anti-Tricyclo[4.4.1.1^{2,5}]dodec-3-en-11-yl p-Bromobenzenesulfonate, 6-OBs

The brosylate isolated in 60% yield by the above procedure had m.p. 87–88 °C (dec.); n.m.r.: 2.33 (multiplet, aromatic protons), 4.05 (singlet, $w_{1/2}$ = 4 Hz, H-3, H-4), 5.05 (triplet, J = 5.5 Hz H-11*s*), 7.4–9.0 (multiplet, all other protons).

Anal. Calcd. for $C_{18}H_{21}SO_3Br$: C, 54.41; H, 5.33; S, 8.07; Br, 20.11. Found: C, 54.54; H, 5.40; S, 8.15; Br, 20.27.

anti-Tetracyclo[5.4.1.1^{2,6}.0^{3,5}]tridecan-12-yl p-Bromobenzenesulfonate, 10-OBs

The brosylate isolated in 65% yield by the above procedure had m.p. 120.5–121 °C (dec.); n.m.r.: 2.25 (multiplet, aromatic protons), 4.53 (triplet, J = 6.2 Hz, H-12*s*), 7.5–8.8 (multiplet, H-1, H-2, H-6–H-11, H-13), 9.04 (doublet of doublets, J = 3.6, 8 Hz, H-3, H-5), 9.3–9.9 (multiplet, H-4).

Anal. Calcd. for $C_{19}H_{23}SO_3Br$: C, 55.48; H, 5.63; S, 7.79; Br, 19.43. Found: C, 55.60; H, 5.70; S, 7.77; Br, 19.44.

Kinetic Studies

Acetolysis rates of the three brosylates **7**-OBs, **6**-OBs, and **10**-OBs were measured by the usual procedure (*cf.* 27). Solutions *ca.* 0.01 *M* in brosylate were prepared in glacial acetic acid buffered with *ca.* 0.025 *M* NaOAc and divided equally among 12 sample tubes which were then sealed. The tubes were placed simultaneously in an oil bath at the appropriate temperature. After a short thermal equilibration period (*ca.* 10 min), the zero sample was removed and cooled quickly to room temperature. Other samples were similarly removed at appropriate times. After all samples had been taken, 1-ml aliquots of each were added to 5 ml of *ca.* 0.005 *M* $HClO_4$ in glacial acetic acid and the excess $HClO_4$ titrated with *ca.* 0.005 *M* NaOAc in glacial acetic acid to the bromophenol blue end point. Each run was followed for at least 2.5 half-lives, infinity samples being taken after at least 8 half-lives. No color developed in runs on **7**-OBs and **10**-OBs but **6**-OBs samples turned yellow particularly at long reaction times. All runs gave good first-order plots. One run on each compound was carried out at a concentration of *ca.* 0.005 *M* in brosylate. This did not affect the obtained rate constants. The data are given in Table 2.

Product Studies

Samples of the brosylates, *ca.* 0.01 *M*, were prepared in glacial acetic acid containing 0.02 *M* NaOAc and heated at an appropriate temperature for more than 10 half-lives. The solutions were cooled to room temperature, diluted with pentane, and the pentane solution extracted with H_2O. The H_2O washes were back-extracted with pentane and the combined pentane solutions washed with H_2O and 10% aqueous $NaHCO_3$ and dried ($MgSO_4$). The mixture was filtered and the solvent removed to leave an oily product which was analyzed spectroscopically and by g.l.c. on several columns. The mixtures were reduced with $LiAlH_4$ and hydrogenated over Pd-on-charcoal by the general procedures described above. None of the large number of products was identified. Our preliminary data is collected in Table 2 and discussed briefly in the text.

The authors are indebted to the National Research Council of Canada for their gracious financial support.

1. (*a*) G. A. Olah and P. v. R. Schleyer (*Editors*). Carbonium ions. Vols. 1–4. Wiley–Interscience, New York. 1968, 1970, 1972, 1973. Chapts. 22–26; (*b*) L. N. Ferguson. Highlights of alicyclic chemistry. Vol. 1. Franklin Publishing Co., Palisade, New Jersey. 1973. pp. 114–123.
2. J. Haywood-Farmer. Chem. Rev. **74**, 315 (1974).
3. S. Itô, Y. Fujise, T. Okuda, and Y. Inoue. Bull. Chem. Soc. Jpn. **39**, 1351 (1966).
4. S. Itô, T. Otomo, Y. Fujise, and K. Sakan. Chem. Commun. 782 (1968).
5. J. Haywood-Farmer, B. T. Friedlander, and L. M. Hammond. J. Org. Chem. **38**, 3145 (1973).
6. S. Itô, H. Ohtani, and S. Amiya. Tetrahedron Lett. 1737 (1973).
7. R. C. Cookson, B. V. Drake, J. Hudec, and A. Morrison. Chem. Commun. 15 (1966).
8. B. Franzus and E. I. Snyder. J. Am. Chem. Soc. **85**, 3902 (1963); **87**, 3423 (1965).
9. R. E. Pincock and J. I. Wells. J. Org. Chem. **29**, 965 (1964).
10. J. Haywood-Farmer and R. E. Pincock. J. Am. Chem. Soc. **91**, 3020 (1969); J. Haywood-Farmer, H. Malkus, and M. A. Battiste. J. Am. Chem. Soc. **94**, 2209 (1972).
11. M. Sakai. Tetrahedron Lett. 2297 (1973).
12. J. Klein. Tetrahedron Lett. 4307 (1973); C. L. Liotta. Tetrahedron Lett. 519 (1975).
13. W. T. Wipke and P. Gund. J. Am. Chem. Soc. **96**, 299 (1974).
14. G. Köbrich. Angew. Chem. Int. Ed. Engl. **12**, 464 (1973); G. L. Buchanan. Chem. Soc. Rev. **3**, 41 (1974).
15. J. B. Lambert and G. J. Putz. J. Am. Chem. Soc. **95**, 6313 (1973).
16. C. S. Foote. J. Am. Chem. Soc. **86**, 1853 (1964).
17. P. v. R. Schleyer. J. Am. Chem. Soc. **86**, 1854 (1964); **86**, 1856 (1964).
18. (*a*) R. E. Pincock and J. Haywood-Farmer. Tetrahedron Lett. 4759 (1967); E. I. Snyder and B. Franzus. J. Am. Chem. Soc. **86**, 1166 (1964); (*b*) R. Hoffmann. Tetrahedron Lett. 3819 (1965).
19. J. B. Stothers, J. R. Swenson, and C. T. Tan. Can. J. Chem. **53**, 581 (1975).

20. M. A. BATTISTE, J. HAYWOOD-FARMER, H. MALKUS, P. SEIDL, and S. WINSTEIN. J. Am. Chem. Soc. **92**, 2144 (1970); M. A. BATTISTE and J. W. NEBZYDOSKI. J. Am. Chem. Soc. **92**, 4450 (1970).
21. N. A. LEBEL and R. J. MAXWELL. J. Am. Chem. Soc. **91**, 2307 (1969).
22. R. J. PICCOLINI and S. WINSTEIN. Tetrahedron, **19**, Suppl. 2, 423 (1963).
23. H. C. BROWN. J. Chem. Soc. 1248 (1956); YA. L. GOL'DFARB and L. I. BELEN'KII. Russ. Chem. Rev. **29**, 214 (1960).
24. T. D. GOLDMAN. Tetrahedron, **28**, 3175 (1972).
25. S. WINSTEIN. Q. Rev. **23**, 141 (1969); R. C. HADDON. Tetrahedron Lett. 2797 (1974).
26. H. C. BROWN, C. P. GARG, and K.-T. LIU. J. Org. Chem. **36**, 387 (1971).
27. P. D. BARTLETT and W. P. GIDDINGS. J. Am. Chem. Soc. **82**, 1240 (1960).
28. H. C. BROWN and G. HAM. J. Am. Chem. Soc. **78**, 2735 (1956).
29. P. G. GASSMAN, J. SETER, and F. J. WILLIAMS. J. Am. Chem. Soc. **93**, 1673 (1971).
30. C. W. JEFFORD, D. T. HILL, and J. GUNSHER. J. Am. Chem. Soc. **89**, 6881 (1967).

Can. J. Chem. Downloaded from www.nrcresearchpress.com by 210.87.254.42 on 09/05/12
For personal use only.

Esters chromiques dérivés d'alcools tertiaires[1]

JEAN-CLAUDE RICHER ET JEAN-MARIE HACHEY[2]
Département de chimie, Université de Montréal, Montréal, Québec H3C 3V1
Reçu le 2 mai 1975

JEAN-CLAUDE RICHER et JEAN-MARIE HACHEY. Can. J. Chem. 53, 3087 (1975).
Des esters chromiques dérivés d'alcools tertiaires ont été synthétisés et caractérisés par spectroscopie infrarouge, ultraviolette et résonance magnétique nucléaire.

JEAN-CLAUDE RICHER and JEAN-MARIE HACHEY. Can. J. Chem. 53, 3087 (1975).
Chromic acid esters derived from tertiary alcohols have been synthesized and characterized via infrared, ultraviolet, and proton magnetic resonance spectroscopy.

Introduction

Les esters chromiques dérivés d'alcools tertiaires ont été décrits sommairement par un grand nombre de chercheurs; dans un article de revue, Treibs (1) rappelle les principaux travaux publiés dans ce domaine depuis les origines jusqu'à 1967. Des esters chromiques dérivés d'amines (2–4), des esters di- et trichromiques dérivés du tertiobutanol (5), des esters chromiques polymérisés dérivés de diols (6, 7) de même que des esters chromiques dérivés de thiols (8) sont décrits dans la littérature. En 1956, Zeiss et Matthews (9) proposent un mécanisme pour la formation des esters chromiques dérivés d'alcools tertiaires. Plus récemment, des chercheurs ont élucidé la structure d'esters chromiques dérivés d'alcools tertiaires à l'aide du spectre de diffraction des rayons-X (10).

Dans ce travail, nous décrivons des méthodes de synthèse et caractérisons des esters chromiques dérivés d'alcools tertiaires par i.r., u.v. et r.m.n. Plusieurs de ces esters chromiques ont été utilisés comme agents oxydants (11).

Résultats et discussion

Synthèse d'esters chromiques dérivés d'alcools tertiaires

Des descriptions typiques de la synthèse d'esters chromiques solides ou liquides sont données dans la partie expérimentale.

Les remarques suivantes pourraient être faites concernant la synthèse des esters chromiques décrites ici: (*a*) Les rendements sont pratiquement quantitatifs (90% et plus en général). (*b*) Lorsqu'ils ne sont pas en solution dans un solvant neutre, les esters chromiques liquides se décomposent assez rapidement au contact de l'air, de la lumière, de la chaleur pour donner un résidu visqueux brun-noir. (*c*) Une autre méthode de synthèse décrite par Zeiss et Pease (12) consistant à utiliser le chlorure de chromyle en solution dans le CCl_4 présente au départ certains inconvénients à cause de la grande réactivité du CrO_2Cl_2. Après l'essai infructueux des divers procédés expérimentaux décrits dans la littérature (7, 13) pour la synthèse d'esters chromiques polymérisés, la synthèse faisant intervenir CrO_2Cl_2 fut tentée pour les diols suivants: le bicyclo[2.2.2]octanediol-1,4 et le benzopinacol. Ces réactions donnèrent après évaporation du solvant un résidu gommeux brun-noir qui ne fut pas étudié davantage. (*d*) Lorsqu'ils ne sont plus en solution dans un solvant neutre (benzène, CCl_4, pentane. . .) les esters chromiques liquides sont relativement instables. La détermination de leurs propriétés physiques (n_D, analyse du chrome, i.r., u.v., r.m.n.) s'est donc avérée particulièrement délicate. (*e*) Les résultats obtenus ont permis de constater que l'utilisation de solution aqueuse de CrO_3 donnait des rendements inférieurs ou nuls en esters chromiques.

Propriétés d'esters chromiques dérivés d'alcools tertiaires

Analyse du chrome

Dans le cas des esters chromiques liquides, la teneur en chrome est déterminée par une méthode volumétrique (14): il s'agit de trans-

[1]Les résultats rapportés dans ce travail sont extraits en partie de la thèse présentée par M. Jean-Marie Hachey en vue de l'obtention du grade de Ph.D., Faculté des Sciences, Université de Montréal, Janvier 1972.

[2]Adresse actuelle: Département des sciences pures, Université du Québec à Chicoutimi, Chicoutimi, Québec G7H 2B1.

Can. J. Chem. Downloaded from www.nrcresearchpress.com by 210.87.254.6 on 09/05/12
For personal use only.

Can. J. Chem. Downloaded from www.nrcresearchpress.com by 210.87.254.6 on 09/05/12
For personal use only.

FOR ERRATA SEE
Vol 54(6) 1976 p. 840

TABLEAU 1. Propriétés physiques d'esters chromiques dérivés d'alcools tertiaires

Esters chromiques RO—CrO_2—OR		Chrome (%)		Indice de refraction ou p.f.	Ultraviolet		Infrarouge	
		Observé	Calculé		λ (nm)	log ε	ν(cm^{-1})	
(*tert*-BuO)$_2CrO_2$ (chromate de ditertiobutyle) 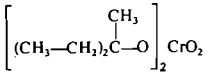	$C_8H_{18}O_4Cr$	*		*	288†	3.5	988	988
					368	3.4	962	964
							922	925
							903	905
							800	(5)
	$C_{12}H_{26}O_4Cr$	18.01	18.16	n_D^{26} 1.5363	284	3.65	985	
					376	3.47	962	
							785	
(chromate de di(méthyl-3 pentyl-3)) 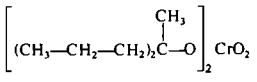	$C_{14}H_{30}O_4Cr$	16.46	16.54	n_D^{27} 1.5345	287	3.60	986	
					376	3.45	962	
							788	
(chromate de di(méthyl-3 hexyl-3)) 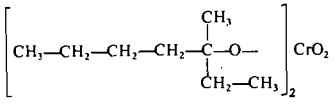	$C_{16}H_{34}O_4Cr$	15.23	15.19	n_D^{24} 1.5274	285	3.55	985	
					376	3.46	960	
							786	
(chromate de di(méthyl-3 heptyl-3)) 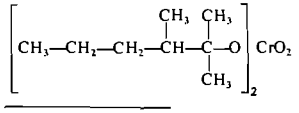	$C_{16}H_{34}O_4Cr$	15.31	15.19	n_D^{25} 1.5352	280	3.50	990	
					374	3.35	965	
							790	

Can. J. Chem. Downloaded from www.nrcresearchpress.com by 210.87.254.6 on 09/05/12
For personal use only.

TABLEAU 1 (*suite et fin*)

Esters chromiques RO—CrO_2—OR		Chrome (%)		Indice de refraction ou p.f.	Ultraviolet		Infrarouge
		Observé	Calculé		λ (nm)	log ε	ν(cm^{-1})
(chromate de di(diméthyl-2,3 hexyl-2))							
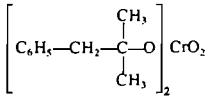	$C_{20}H_{26}O_4Cr$	13.49	13.60	n_D^{26} 1.5759	282 388	3.50 3.27	990 966 818
(chromate de di(benzyl-2 propyl-2))							
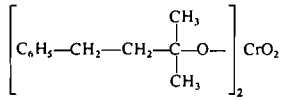	$C_{22}H_{30}O_4Cr$	12.23	12.67	n_D^{26} 1.5717	280 374	3.52 3.34	983 961
(chromate de di[(méthyl-2 phényl-4)-butyl-2])							
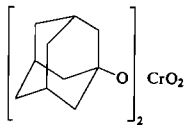	$C_{20}H_{30}O_4Cr$	13.27	13.46	p.f.161–164 °C(déc.)	298 395	3.60 3.53	993 965 800
(chromate de diadamantyl-1)							
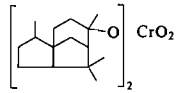	$C_{30}H_{50}O_4Cr$	9.87 9.88 (7)	9.87	p.f.118–120 °C(déc.) 110–122 °C(déc.)(7)	296 382	3.66 3.58	975 958
(chromate de dicédryle)							

*Propriété non déterminée à cause de l'instabilité de l'ester si non en solution (explosion observée).
†Propriété déterminée d'après la quantité d'alcool mise en solution.

TABLEAU 2. Spectres r.m.n. d'alcools tertiaires et des esters chromiques correspondants. Solutions 50% (v/v) dans CCl_4 à 25 °C; TMS standard interne

Alcools (ROH) (Y = H)				Esters Chromiques ($ROCrO_2OR$) (Y = CrO_2—OR)			
Protons	p.p.m.	Multiplicité*	Intensité relative	Protons	p.p.m.	Multiplicité*	Intensité relative
			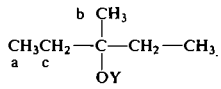				
a	0.85	t	6H	a	0.90	t	6H
b	1.07	s	3H	b	1.37	s	3H
c	1.42	q	4H	c	1.70	q	4H
Y (—OH)	2.98 (J = 7.5 Hz)	s	1H	Y (—OH disparu)	(J = 7.5 Hz)		
			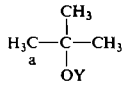				
a	1.20	s	9H	a	1.47	s	9H
Y (—OH)	4.32	s	1H	Y (—OH disparu)			
			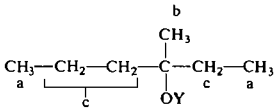				
a	0.90	t	6H	a	0.9	t	6H
b	1.07	s	3H	b	1.37	s	3H
c	1.35	m	6H	c	1.6	m	6H
Y (—OH)	3.10 (J = 7 Hz)	s	1H	Y (—OH disparu)	(J = 7 Hz)		
			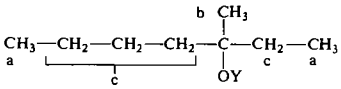				
a	0.90	t	6H	a	0.9	t	6H
b	1.07	s	3H	b	1.37	s	3H
c	1.33	m	8H	c	1.6	m	8H
Y (—OH)	2.78 (J = 7 Hz)	s	1H	Y (—OH disparu)	(J = 7 Hz)		

former tout le chrome sous forme de bichromate puis de réduire le bichromate en Cr(III) au moyen du sulfate ferreux ammoniacal. Les esters chromiques solides sont analysés selon une méthode gravimétrique (9), la combustion d'un ester chromique laissant un résidu de Cr_2O_3. Les résultats des analyses du chrome sont donnés au tableau 1.

Spectre infrarouge

Les bandes d'absorption en infrarouge pour quelques esters chromiques ont été rapportées dans la littérature (1, 5, 9). Les esters chromiques synthétisés au cours de ce travail présentent des bandes d'absorption Cr—O dans l'infrarouge entre 785 et 993 cm^{-1}. Des bandes i.r. caractéristiques sont résumées au tableau 1.

Spectre ultraviolet

Les esters chromiques examinés dans ce travail présentent deux bandes d'absorption dans l'ultraviolet (solvant: *n*-pentane), une première

Can. J. Chem. Downloaded from www.nrcresearchpress.com by 210.87.254.6 on 09/05/12
For personal use only.

TABLEAU 2 (*suite et fin*)

Alcools (ROH) (Y = H)				Esters Chromiques ($ROCrO_2OR$) (Y = CrO_2—OR)			
Protons	p.p.m.	Multiplicité*	Intensité relative	Protons	p.p.m.	Multiplicité*	Intensité relative
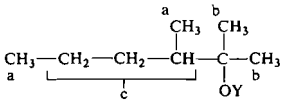							
a	~0.9	m	6H	a	~0.9	m	6H
b	1.10	s	6H	b	1.37	s	6H
c	~1.5	m	5H	c	~1.5	m	5H
Y (—OH)	2.62	s	1H	Y (—OH disparu)			
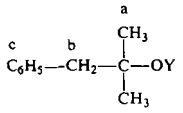							
a	1.18	s	6H	a	1.39	s	6H
b	2.65	s	2H	b	2.88	s	2H
c	7.12	s	5H	c	7.14	s	5H
Y (—OH)	2.78	s	1H	Y (—OH disparu)			
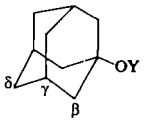							
—OH	1.02	s	1H	1.3 à 2.0†	Y (—OH disparu)		
β	1.60	d	6H	1.64†			
γ	1.93	m	3H	2.12†	1.93(β+γ)	s‡	9H
δ	1.45 (J = 3 Hz)	t	6H	1.64†	1.37(δ)	s‡	6H

*s, singulet; d, doublet; t, triplet; q, quadruplet; m, multiplet.
†Réf. 26.
‡Large.

se situant entre 280 et 298 nm et une seconde entre 368 et 395 nm. Il est à noter que Wiberg et Schafer (15) indique un log ε 3.47 et 3.46 pour le chromate de ditertiobutyle alors que dans ce travail, des valeurs de 3.4 et 3.5 sont rapportées. Le détail des spectres u.v. se trouve au tableau 1.

Spectre résonance magnétique nucléaire

Une comparaison entre les spectres r.m.n. des alcools tertiaires étudiés et de leurs esters chromiques permet de souligner les caractéristiques suivantes pour ces esters. (*i*) Disparition complète du groupement hydroxyle (confirmée également par i.r.). (*ii*) Selon la structure de la molécule, l'effet de déblindage du groupement chromate varie de ~12 à ~20 Hz pour les protons aliphatiques liés à des carbones directement fixés sur le carbone carbinolique et s'atténue progressivement avec l'éloignement. (*iii*) De façon générale et, compte tenu des limites de précision de l'appareil (±0.5 Hz), la valeur de la constante de couplage J de l'alcool n'est pas sensiblement affectée dans l'ester chromique correspondant. Toutefois, le spectre r.m.n. du chromate de diadamantyl-1 laisse voir une coalescence de signaux; dans ce cas, deux singulets larges sont observés. Le signal à 1.37 p.p.m. et celui à 1.93 p.p.m. sont attribués respectivement aux six protons en position δ d'une part et aux neuf protons en position β et γ d'autre part. Ces attributions sont basées sur la remarque faite au paragraphe précédent. Ainsi, un déblindage de 19.8 Hz est observé pour les protons en β dans l'ester chromique dérivé de l'adamantanol-1.

Les caractéristiques des spectres r.m.n. de quelques alcools tertiaires et de leurs esters chromiques sont résumées au tableau 2.

Can. J. Chem. Downloaded from www.nrcresearchpress.com by 210.87.254.6 on 09/05/12
For personal use only.

Can. J. Chem. Downloaded from www.nrcresearchpress.com by 210.87.254.6 on 09/05/12
For personal use only.

Partie expérimentale

Les points de fusion sont déterminés sur un microscope chauffant de la compagnie Reichert (Autriche) à l'aide d'un thermomètre calibré. Les spectres i.r. sont pris sur un spectrophotomètre modèle IR-8 de la compagnie Beckman. Les produits liquides sont examinés sans solvant et sous forme de film; les solides sont mis en suspension sous forme d'émulsion dans le Nujol. Les indices de réfraction sont mesurés sur un réfractomètre de type Abbe de la compagnie Karl Zeiss. Les analyses par chromatographie en phase gazeuse sont effectuées de la façon suivante. Alcools tertiaires: Appareil de la compagnie F & M à détection par ionisation de flamme; colonne en cuivre (14 pied × ¼ po) contenant 10% d'Hyprose sur Chromosorb P 60/80; gaz vecteur: 60 ml He/min^{-1}; température de la colonne: 140 °C. Alcools secondaires: Appareil de la compagnie Microtek à détection par conductivité thermique; colonne en cuivre (12 pied × ¼ po) contenant 10% de silicone SE-30 sur Chromoport XXX; gaz vecteur: 60 ml He/min; température de la colonne: 180–200 °C.

Les spectres u.v. sont déterminés sur un spectrophotomètre de la compagnie Bausch & Lomb, modèle Spectronic 505, solvant: pentane.

Les spectres r.m.n. sont déterminés sur un spectrophotomètre Varian, modèle A-60 et Hitachi-Perkin-Elmer, modèle R-24, solvant: CCl_4. Les déplacements chimiques se réfèrent au TMS utilisé d'une façon interne.

Propriétés des alcools tertiaires

Les alcools tertiaires utilisés dans la synthèse des esters chromiques provenaient de la compagnie Aldrich. Ils ont d'abord été soumis à une distillation (ou à une recristallisation dans le pentane) puis à une détermination du point d'ébullition (ou du point de fusion).

La chromatographie en phase gazeuse sur une colonne d'Hyprose 10% à 140 °C telle que décrite au début de la partie expérimentale révéla la présence d'un seul pic dans chaque cas. Le spectre i.r. confirma également la pureté de ces alcools. Les propriétés physiques (points d'ébullition ou points de fusion et indices de réfraction) des alcools tertiaires purifiés se comparent bien à celles décrites dans la littérature (16–24).

Synthèse et propriétés d'esters chromiques dérivés d'alcools tertiaires

L'expérience a permis de constater que deux modes de synthèse peuvent être employés pour l'obtention d'esters chromiques dérivés d'alcools tertiaires suivant que l'alcool soit solide et peu soluble dans les solvants peu polaires ou apolaires (pentane, benzène, CCl_4, . . .) ou liquides. De plus, il a été observé que les alcools liquides étudiés donnaient des esters chromiques liquides et que les alcools solides donnaient des esters chromiques solides.

Préparation d'un ester chromique dérivé d'un alcool tertiaire solide insoluble dans les solvants peu polaires

Selon la méthode générale de Wienhaus (25) en utilisant AcOH glacial au lieu du pentane

La réaction se fait à la température ambiante. Il suffit de dissoudre le CrO_3 solide dans une solution d'acide acétique[3] contenant déjà une quantité équimolaire d'alcool. Le mélange réactionnel se colore immédiatement rouge-orange. La recristallisation de l'ester chromique est réalisée dans l'acide acétique[3] après avoir chassé l'excès de solvant s'il y a lieu *i.e.* si la recristallisation de l'ester n'est pas amorcée après *ca.* 30 min.

Selon la méthode décrite par Fieser et Ourisson (7)

Dans cette méthode, $Na_2Cr_2O_7{\cdot}2H_2O$ est utilisé au lieu du CrO_3 solide. Le solvant pour la réaction et la recristallisation est l'acide acétique glacial purifié par reflux et distillation sur CrO_3. Les proportions de réactifs sont toutefois de 1 mol de $Na_2Cr_2O_7{\cdot}2H_2O$ pour 2 mol d'alcool.

Préparation d'un ester chromique dérivé d'un alcool tertiaire liquide

La méthode suivante qui constitue une adaptation de la méthode générale décrite par Wienhaus (25) s'est avérée la plus efficace (sauf pour le *tert*-BuOH où on doit faire réagir le CrO_3 et l'alcool selon le rapport molaire 1.1 et 2 respectivement).

L'alcool tertiaire (0.3–1 g) à estérifier est dissous dans 25 ml de pentane pur contenu dans un ballon de 50 ml; la réaction se fait à la température de la pièce. Tout en maintenant l'agitation (au moyen d'un agitateur magnétique) une quantité équimoléculaire de CrO_3 anhydre (conservé dans un dessicateur) est ajoutée. Il y a coloration immédiate de la solution en rouge-orange et apparition de gouttelettes d'eau au fond du ballon. L'agitation est poursuivie durant 3–5 min à la température ambiante. Le mélange réactionnel est ensuite décanté, transféré dans une fiole conique puis séché sur du Na_2SO_4 anhydre. L'ester chromique anhydre ainsi obtenu est finalement débarrassé de son solvant par évaporation sous pression réduite à la température de la pièce. Il est préférable de toujours protéger le mélange réactionnel de l'action de la lumière durant toute la durée de la synthèse. Un produit liquide plus ou moins visqueux, rouge foncé est ainsi obtenu.

La procédure expérimentale suivante fut adoptée pour la détermination des caractéristiques physiques et spectroscopiques: sur l'échantillon d'ester chromique fraîchement préparé (0.3–0.5 g) la pureté était d'abord contrôlée par i.r. (disparition totale de la bande —OH et apparition de bandes Cr—O). Une propriété était alors déterminée. La synthèse était répétée jusqu'à ce que l'on obtienne au moins deux ou trois valeurs subséquentes identiques.

Détermination de la teneur en chrome des esters chromiques préparés

Détermination volumétrique (14)

C'est une réaction d'oxydo-réduction. La méthode consiste à transformer tout le chrome sous forme de bichromate par l'intermédiaire du nitrate d'argent et du persulfate d'ammonium puis à réduire le bichromate sous forme de Cr(III) au moyen du sulfate ferreux ammoniacal; la diphényl amine fut utilisée comme indicateur.

Détermination gravimétrique (9)

Elle repose sur le fait que la combustion d'un ester chromique laisse un résidu solide vert (Cr_2O_3). Quelques 100–300 mg de l'ester chromique à analyser sont placés

[3]AcOH purifié par reflux et distillation sur CrO_3.

dans un creuset en porcelaine recouvert partiellement d'un couvercle. L'intensité du chauffage est accrue lentement afin d'éviter toute projection. Après quelques minutes, le chauffage est poussé au maximum avec un brûleur Fisher durant 20–30 min. Le creuset est ensuite refroidi à l'air libre pendant quelques minutes puis transféré dans un dessicateur. Le résidu vert de Cr_2O_3 est finalement pesé. Cette méthode est apparue difficilement applicable dans le cas des esters chromiques liquides (à cause des projections difficiles à éviter) mais elle s'est avérée très efficace pour les esters chromiques solides.

Les auteurs remercient vivement le Conseil national de recherches du Canada, la compagnie C.I.L. et le Conseil de recherches pour la défense pour leur aide financière.

1. W. TREIBS. Chem. Ztg. Chem. Appar. **91**, 953 (1967).
2. C. A. VESSEY et A. S. HARRIS. Congr. F.A.T.I.P.E.C. **8**, 289 (1966); Chem. Abstr. **66**, 19914k (1967).
3. I. L. ROZENFELD, F. I. RUBINSTEIN, V. P. PERSIANTSEVA et S. V. YAKUBOVITCH. Ann. Univ. Ferrara Sez 5, Suppl. 4 (2), 751 (1966).
4. H. BRUNEL. U.S. Patent No. 3,320,164 (May, 1967); Chem. Abstr. **67**, 55956e (1967).
5. W. J. BEHR et J. FUCHS. Z. Naturforscher, **28**b, 597 (1973).
6. F. TIEMANN et R. SCHMIDT. Ber. **28**, 1782 (1895).
7. L. F. FIESER et G. OURISSON. Bull. Soc. Chim. Fr. **20**, 1152 (1953).
8. I. BALDEA et S. SCHÖN. Cluj. Rumania. Univ. Babes-Bolyai. Studia Univ. Babes-Bolyai. Series Chem. **18**, 47 (1973).
9. H. H. ZEISS et C. N. MATTHEWS. J. Am. Chem. Soc. **78**, 1694 (1956).
10. M. DOBLER, J. D. DUNITZ, B. GUBLER, H. P. WEBER, G. BÜCHI et J. PADILLA. Proc. Chem. Soc. 383 (1963); V. AMIRTHALINGAM, D. F. GRANT et A. SENOL. Acta Crystallogr. B, **28**, 1340 (1972).
11. J. C. RICHER et J. M. HACHEY. Can. J. Chem. **52**, 2475 (1974).
12. H. H. ZEISS et D. W. PEASE, JR. J. Am. Chem. Soc. **78**, 3182 (1956).
13. R. LOMBARD et G. AMBROISE. Bull. Soc. Chim. Fr. 230 (1961).
14. A. I. VOGEL. A textbook of quantitative inorganic analysis, theory and practice, Longmans, London. 1951. p. 297.
15. K. B. WIBERG et H. SCHAFER. J. Am. Chem. Soc. **91**, 927 (1969).
16. BEIL. 1 (2), 413.
17. BEIL. 1 (2), 411.
18. P. M. GINNINGS et M. HAUSER. J. Am. Chem. Soc. **60**, 2581 (1938).
19. R. C. HUSTON, R. L. GUILE, J. J. SCULATI et W. N. WASSON. J. Org. Chem. **6**, 252 (1941).
20. BEIL. 1 (3), 1729.
21. R. HECK et S. WINSTEIN. J. Am. Chem. Soc. **79**, 3432 (1957).
22. BEIL, **6**, 548.
23. H. STETTER, M. SCHWARZ et A. HIRSCHORN. Ber. **92**, 1629 (1959).
24. H. ERDTMAN et B. R. THOMAS. Acta Chim. Scand. **12**, 267 (1958).
25. H. WIENHAUS. Ber. **47**, 322 (1914).
26. R. C. FORT, JR. et P. R. SCHLEYER. J. Org. Chem. **30**, 789 (1965).

Can. J. Chem. Downloaded from www.nrcresearchpress.com by 210.87.254.6 on 09/05/12
For personal use only.

Oxilorphan and Butorphanol.[1] Potent Narcotic Antagonists and Nonaddicting Analgesics in the 3,14-Dihydroxymorphinan Series. Part V[2]

IVO MONKOVIĆ,[3] HENRY WONG, ANTHONY W. PIRCIO,[4] YVON G. PERRON, IRWIN J. PACHTER,[4] AND BERNARD BELLEAU

Bristol Laboratories of Canada, Candiac, Quebec J5R 1J1

Received May 26, 1975

IVO MONKOVIĆ, HENRY WONG, ANTHONY W. PIRCIO, YVON G. PERRON, IRWIN J. PACHTER, and BERNARD BELLEAU. Can. J. Chem. **53**, 3094 (1975).

A series of 3,14-dihydroxymorphinans **8** was synthesized via a method of (*a*) acylation of 3-methoxy-$\Delta^{8,14}$-morphinan **4***a* (*b*) stereospecific epoxidation of the resultant amides to β-epoxides **5** (*c*) simultaneous reduction of amide and epoxide functions and (*d*) demethylation of the resultant 3-methoxy-14-hydroxymorphinans **7**. Alternatively deblocking of the amine function in **5***b* by hydrolysis followed by reduction of the resultant amino epoxide **5***e* afforded 14-hydroxy-3-methoxymorphinan **7***e*, which is readily alklyated and demethylated to give various **8**. On a basis of interesting pharmacological profiles compounds *l*-**8***c* (oxilorphan) and *l*-**8***d* (butorphanol) were selected for clinical studies.

IVO MONKOVIĆ, HENRY WONG, ANTHONY J. PIRCIO, YVON J. PERRON, IRWIN J. PACHTER et BERNARD BELLEAU. Can. J. Chem. **53**, 3094 (1975).

On a synthétisé une série de dihydroxy-3,14 morphinanes **8** par l'intermédiaire des réactions suivantes: (*a*) acylation du méthoxy-3 $\Delta^{8,14}$ morphinane **4***a*, (*b*) époxydation stéréospécifique en β des amides obtenues, (*c*) réduction simultanée des fonctions amide et époxyde et (*d*) déméthylation du méthoxy-3 hydroxy-14 morphinane **7** qui en résulte. On peut aussi (*a*) débloquer la fonction amine de **5***b* par hydrolyse et (*b*) réduire l'amino époxyde **5***e* qui en découle pour obtenir l'hydroxy-14 méthoxy-3 morphinane, **7***e*, qui peut être alkylé facilement puis déméthylé pour fournir une variété de composés **8**. En se basant sur des profils pharmacologiques intéressants, on a choisi les *l*-**8***c* (oxilorphane) et *l*-**8***d* (butorphanol) pour des études cliniques.

[Traduit par le journal]

Introduction

The rapid increase in drug abuse in recent years has stimulated the renewal of research efforts in order that this serious medical and socioeconomic problem may be effectively controlled. To this end we have reported earlier as part of our efforts to synthesize potent, long acting, orally effective, pure narcotic antagonists and non-abusable analgesics via the versatile intermediate 4a-(2-aminoethyl)-1,2,3,4,4a,9-hexahydro-6-methoxyphenanthrene **1** (Chart 1) (1, 2). The experimental work which led to butorphanol, oxilorphan and their congeners, as well as preliminary and more advanced pharmacological studies, form the subject of this communication.

Results and Discussion

Two different routes led to 3-methoxy-$\Delta^{8,14}$-morphinan **4***a*, a crucial intermediate in the synthesis of 3,14-dihydroxymorphinans. The first involves the dehydration of the 17-carboethoxy-14-hydroxyisomorphinan (**3**) to **4***b* followed by hydrolysis to **4***a* (1). A shorter and more practical route involves the bromocyclization of unsaturated amine **1** to bromohasubanan **2** followed by rearrangement to **4***a* (2).[5]

Further transformations of the unsaturated system of **4** to the 14-hydroxymorphinan system **7** appears straight forward provided that the double bond can yield the corresponding β-epoxide stereoselectively. Our initial studies on the epoxidation of **4***b* by treatment with *m*-chloroperbenzoic acid indicated the formation of a 1:1 mixture of epoxides **5***a* and **6**, which was difficult to separate. The desired 14-hydroxymorphinan **7***b* was prepared in low yield by

[1]Approved generic names for *l*-17-cyclopropylmethyl-3,14-dihydroxymorphinan and *l*-17-cyclobutylmethyl-3,14-dihydroxymorphinan.

[2]For part IV see ref 1.

[3]Author to whom correspondence should be addressed.

[4]Bristol Laboratories, Syracuse, New York, 13201.

[5]Experimental details will be published by T. T. Conway of these laboratories.

Can. J. Chem. Downloaded from www.nrcresearchpress.com by 210.87.254.6 on 09/05/12
For personal use only.

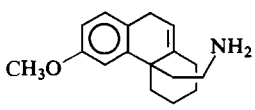

1

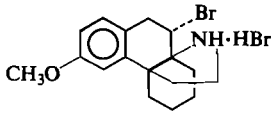

2

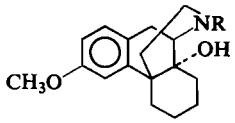

3

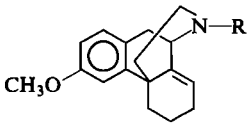

4

R
- *a* H
- *b* CO_2Et
- *c* $COCF_3$
- *d* CO-cyclopropyl
- *e* CO-cyclobutyl

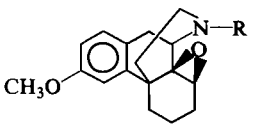

5

R
- *a* CO_2Et
- *b* $COCF_3$
- *c* CO-cyclopropyl
- *d* CO-cyclobutyl
- *e* H

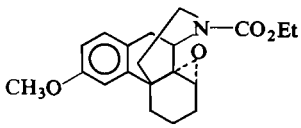

6

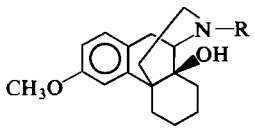

7

R
- *a* CO_2Et
- *b* CH_3
- *c* CH_2-cyclopropyl
- *d* CH_2-cyclobutyl
- *e* H
- *f* $COCH_2CH_3$
- *g* $CH_2CH_2CH_3$
- *h* $CH_2CH{=}CH_2$
- *i* $CH_2C{=}C(CH_3)_2$
- *j* $CH_2C{\equiv}CH$
- *k* $CH_2CH_2CH{-}CH_2$

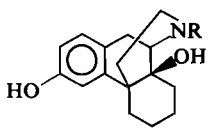

8

R
- *a* H
- *b* CH_3
- *c* CH_2-cyclopropyl
- *d* CH_2-cyclobutyl
- *e* $CH_2CH_2CH_3$
- *f* $CH_2CH{=}CH_2$
- *g* $CH_2C{\equiv}CH$
- *h* $CH_2C{=}C(CH_3)_2$
- *i* $CH_2CH_2COH(CH_3)_2$
- *j* $CH_2CH_2CH{=}CH_2$
- *k* CH_2CH_3

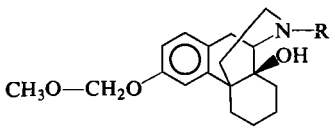

9

R
- *a* CH_2-cyclopropyl
- *b* CH_2-cyclobutyl

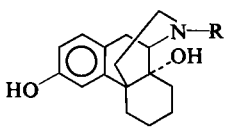

10

R
- *a* CH_3
- *b* CH_2-cyclopropyl
- *c* CH_2-cyclobutyl
- *d* $CH_2CH{=}CH_2$

CHART 1

Can. J. Chem. Downloaded from www.nrcresearchpress.com by 210.87.254.6 on 09/05/12
For personal use only.

Can. J. Chem. Downloaded from www.nrcresearchpress.com by 210.87.254.6 on 09/05/12
For personal use only.

treatment of this mixture with sodium borohydride followed by isolation of **7***a* (column chromatography), and reduction with lithium aluminum hydride. Fortunately, amides **4***c*, **4***d*, and **4***e*, which were prepared by standard procedures from **4***a*, underwent stereoselective epoxidation to give predominantly β-epoxides **5***c*, **5***d*, and **5***e*. The corresponding α-isomers were detected by t.l.c. and these minor constituents were removed as such (**5***b* and **5***e*), or after the next step (**5***d*) simply by recrystallization.

Evidently, the ratio of α- to β-epoxides is affected by the nature of the substituent on the nitrogen. The directional effect could be rationalized in terms of an amide–percid complex (or lack of it) prior to the epoxidation step. A similar *cis*-directing effect in the epoxidation of an allylic amide in cyclohexene series has been observed previously by Goodman, Winstein, and Boschan (4).

The amide and epoxide functions in **5***c* and **5***d* were reduced simultaneously by treatment with lithium aluminum hydride. As expected, reduction of the epoxide ring led exclusively to the formation of the tertiary rather than secondary alcohols.

Alternatively hydrolysis of epoxyamide **5***b* followed by reduction of the resultant epoxyamine **5***e* with lithium aluminum hydride afforded the versatile intermediate 14-hydroxy-3-methoxymorphinan **7***e* which could be easily converted to various *N*-substituted derivatives either via direct alkylation (**7***h–k*) or via acylation followed by reduction (**7***f*, *g*).

Resolution of **7***e* with *d*- and *l*-tartaric acids gave the optical isomers (*l*-**7***e* and *d*-**7***e*). Reductive *N*-methylation of *l*-**7***e* (formaldehyde, Raney Ni/H_2) afforded *l*-14-hydroxy-3-methoxy-17-methylmorphinan (*l*-**7***b*), which was identical in every respect with an authentic specimen derived from thebaine (3).

Demethylation of the methyl ethers **7** was effected in most cases (**7***b*, *c*, *g–j*) with boron tribromide in dichloromethane (5). Alternatively **7***e* was demethylated with pyridine hydrochloride, and **7***k* with sodium ethylthiolate (6). Demethylation of **7***i* with boron tribromide led to partial hydration of the double bond, and in addition to the expected unsaturated base **8***h*, we also obtained some triol **8***i*.

Resolution of the biologically most interesting products **8***c* and **8***d* was effected by recrystallization of the respective *d*- and *l*-tartaric acid salts. Methoxy methylation of the resultant *l*-isomers (*l*-**8***c* and *l*-**8***d*) to **9***a* and **9***b* was accomplished by treatment with sodium hydride and chloromethyl methyl ether in benzene.

Biological Results

The methods of biological evaluation are outlined in the experimental part. Compounds **8**, **9** and several previously reported 3,14-dihydroxyisomorphinans **10** (1) were screened for narcotic antagonist and analgesic activities and the results are shown in Table 1. It is evident that the *l*-3,14-dihydroxymorphinans **8** are the most active compounds of the series, while the corresponding *d*-isomers are inactive and isomorphinans **10** are only moderately active. The most interesting compounds *l*-**8***c*, a strong narcotic antagonist with weak analgesic activity and *l*-**8***d*, a powerful analgesic with moderate antagonist activity, were further biologically evaluated, and

TABLE 1. Pharmacological activity of some dihydroxymorphinans **8**, hydroxymorphinans **9**, and dihydroxyisomorphinans **10**

Compound	ED_{50} (mg/kg)[e]	
	Antagonist activity (oxymorphone-induced Straub tail)	Analgesic activity (mouse writhing)
8*a*[a]	>40	40
l-**8***a*[a]	30	20
8*b*[a]	>40	0.15
l-**8***b*[a]	>40	0.1
8*c*[b]	0.3	9
l-**8***c*[c]	0.2	13
d-**8***c*[d]	>40	38
8*d*[a]	3	0.06
l-**8***d*[c]	0.1	0.05
d-**8***d*[d]	42	26
8*e*[b]	1.2	40
8*f*[b]	0.5	46
l-**8***g*[a]	0.7	>40
l-**8***h*[b]	>20	0.1
l-**8***i*[b]	>20	8
8*j*[b]	0.5	4.5
l-**8***k*[d]	3	0.6
l-**9***a*[a]	1.4	11
d-**9***a*[d]	>40	40
l-**9***b*[a]	20	0.3
10*a*[a]	>40	5
10*b*[b]	6	10
10*c*[a]	9	7
10*d*[b]	5	>40

[a]Free base.
[b]HCl salt.
[c]*l*-tartarate.
[d]*d*-tartarate.
[e]Subcutaneous injection.

TABLE 2. A comparison of the pharmacological activity of oxilorphan and butorphanol with standard analgesics and narcotic antagonists

	ED_{50} (mg/kg)[a]				
	Analgesic activity		Antagonist activity		
Test compound	Phenylquinone writhing in mice	Phenylquinone writhing in rats	Oxymorphone induced Straub tail	Oxymorphone induced narcosis	Antagonism of morphine analgesia (rat tail flick)
l-**8***c*	12.8	8.0	0.19	0.03	0.012
l-**8***d*	0.051	0.040	0.98	0.27	0.430
dl-Cyclazocine	0.047	0.029	0.81	0.12	0.040
dl-Pentazocine	3.7	0.95	12.0	10.1	12.2
Naloxone.HCl	>80	>80	0.09	0.02	0.010
Morphine.H_2SO_4	0.56	0.16	—	—	—

[a]Subcutaneous injection.

comparative data with reference agents are given in Table 2. In these studies, *l*-**8***c* was four times more potent than *dl*-cyclazocine as an antagonist; *l*-**8***d* was 30 times more potent than *dl*-pentazocine both as an antagonist and as an analgesic. Furthermore, acute and chronic toxicity and addiction potential evaluations in laboratory animals, including monkeys, showed that these drugs possess high therapeutic ratios with low abuse potential. Consequently, these agents were selected for clinical investigations. In initial studies with non-dependent humans, the duration of the agonist action of *l*-**8***c* was equivalent to that of *dl*-cyclazocine (7). However, the side effect potential of *l*-**8***c* was estimated to be only one quarter of *dl*-cyclazocine. These findings indicate, therefore, that the duration of antagonist activity of *l*-**8***c* should be comparable to that of *dl*-cyclazocine.

In the course of initial studies in man, *l*-**8***c* was also found to increase urinary output (8). The potential clinical significance of this effect is under study.

In postoperative patients, double blind studies showed that *l*-**8***d* is a potent analgesic surpassing morphine and *dl*-pentazocine, in potency by factors of 10 and 30 respectively (9). Thus the effective parenteral dose appears to be in the range of 1 to 2 mg, a level at which the drug is well tolerated.

In addition, *l*-**8***d* was found to be a powerful antitussive agent in animals. By the subcutaneous route of administration, it was up to 140 times as active as codeine (10), which is a surprising novel feature of a narcotic antagonist.

Because of current shortages of opium-derived products and the need for their replacement with safer, nonabusable synthetic drugs *l*-**8***d* may find a number of useful clinical applications.

Experimental

The melting points were determined on a Gallenkamp apparatus, and are uncorrected. The infrared (i.r.) spectra were recorded on a Unicam Sp-200G grating i.r. spectrometer. The n.m.r. spectra were recorded on a Varian A-60A spectrometer using deuteriochloroform. The chemical shifts are expressed in δ values using tetramethylsilane as internal reference. Microanalyses were performed by Micro-Tech Laboratories Inc., Skokie, Ill.

Assays for Analgesic and Antagonist Activities

The method used for evaluation of analgesic activity was essentially that described by Siegmund *et al.* (11). Compounds were administered subcutaneously (15 min) before the intraperitoneal injection of phenylquinone (2 mg/kg). Beginning 5 min after the phenylquinone injection, the animals were observed for writhing and the number of writhes was counted over a period of 10 min. The dose which produced a 50% reduction in the number of writhes, as compared to the control group, was called the ED_{50}.

The antagonist assays were as follows: Mice were injected with oxymorphone (2 mg/kg s.c.), and the potential antagonist was administered subcutaneously 10 min after oxymorphone. The antagonist ED_{50} was defined as the dose which antagonized the Straub tail response (elevation greater than 45°) in 50% of the mice.

The ability to reverse oxymorphone narcosis in the rat was used as a measure of narcotic antagonist activity (12). The antagonist ED_{50} was defined as the dose which reversed the loss of righting reflex in 50% of the rats.

The percent antagonism and the ED_{50} of morphine induced analgesia were calculated as described by Harris and Pierson (13).

Racemic 3-Methoxy-17-trifluoroacetyl-$\Delta^{8,14}$-morphinan, **4***c*

To a cooled (ice), stirred solution of **4***a* (71.4 g) and triethylamine (31.3 g) in dichloromethane (300 ml) was added dropwise a solution of trifluoroacetic anhydride

Can. J. Chem. Downloaded from www.nrcresearchpress.com by 210.87.254.6 on 09/05/12
For personal use only.

Can. J. Chem. Downloaded from www.nrcresearchpress.com by 210.87.254.6 on 09/05/12
For personal use only.

(65.1 g) in dichloromethane (150 ml). After addition, the mixture was stirred for 15 min, and then washed with ice-cold water (500 ml), followed by dilute hydrochloric acid and again with water. The organic layer was dried (Na_2SO_4), filtered over charcoal and evaporated *in vacuo* to give 98 g (theoretical yield) of amide **4***c* as a thick oil; i.r. neat 1700 cm^{-1}; n.m.r. δ 6.6–7.2 (3H, m), 5.85 (1H, t, J = 4 Hz), 4.2–5.4 (2H, m), 3.82 (3H, s), 2.5–4.1 (3H, m), 1.2–2.3 (8H, m). The oil crystallized from ether to give white solid, m.p. 94–96 °C.

Anal. Calcd. for $C_{19}H_{20}NO_2$: C, 64.95; H, 5.74; N, 3.99. Found: C, 65.34; H, 5.75; N, 4.03.

Racemic 3-Methoxy-17-cyclopropylcarbonyl-$\Delta^{8,14}$-morphinan, 4d

The amide **4***d* was similarly prepared in 95% yield by treatment of **4***a* with cyclopropane carboxylic acid chloride. A sample recrystallized from ether showed m.p. 133–135 °C; i.r. (Nujol) 1645 cm^{-1}; n.m.r. δ 6.6–7.1 (3H, m), 5.78 (1H, t, J = 4 Hz), 3.8–5.5 (2H, m), 3.8 (3H, s), 0.5–3.5 (16H, m).

Anal. Calcd. for $C_{21}H_{25}NO_2$: C, 77.98; H, 7.79; N, 4.33. Found: C, 77.86; H, 7.87; N, 4.30.

Racemic 3-Methoxy-17-cyclobutylcarbonyl-$\Delta^{8,14}$-morphinan, 4e

The amide **4***e* was similarly prepared in 88.5% yield by treatment of **4***a* with cyclobutanecarboxylic acid chloride. Recrystallization from cyclohexane gave an analytical sample, m.p. 95–97 °C; i.r. (Nujol), 1650 cm^{-1}; n.m.r. δ 6.7–7.2 (3H, m), 5.8 (1H, d, J = 4 Hz), 4.2–5.6 (2H, m), 3.83 (3H, m), 1.2–3.6 (18H, m).

Anal. Calcd. for $C_{22}H_{27}NO_2$: C, 78.30; H, 8.06; N, 4.15. Found: C, 78.35; H, 8.15; N, 4.24.

Racemic 17-Ethoxycarbonyl-8,14-epoxy-3-methoxymorphinan, 5a and Corresponding Isomorphinan, 6

To a cooled (ice), stirred solution of urethane **1***b* (7.0 g) in dichloromethane (25 ml) was added in small portions *m*-chloroperbenzoic acid (5.63 g, 85% purity) and the mixture was left at room temperature for 6 h. Then the solid was removed by filtration, and the filtrate washed with aqueous sodium sulfite followed by 5% aqueous sodium bicarbonate and finally with water. Drying, filtration over celite-charcoal mixture, and concentration *in vacuo* gave 5.64 g of a mixture of **5***a* and **6**; i.r. (neat) 1700 cm^{-1}; n.m.r. δ 6.6–7.2 (3H, m), 4.16 (2H, q, J = 7 Hz), 3.8 (3H, s), 1.25 (3H, t, J = 7 Hz), 1.0–4.5 (14H, m). A sample for analysis distilled at 145 °C/0.05 Torr.

Anal. Calcd. for $C_{20}H_{25}NO_4$: C, 69.25; H, 7.34; N, 4.08. Found: C, 69.39; H, 7.35; N, 4.05.

Racemic 8,14-Epoxy-3-methoxy-17-trifluoroacetylmorphinan, 5b

The epoxide **5***b* was obtained as a white solid in 83% yield by oxidation of **4***c* with *m*-chloroperbenzoic acid by the procedure given for the preparation of **5***a*; m.p. 102–105 °C from ether; i.r. (Nujol) 1705 cm^{-1}; n.m.r. δ 6.7–7.3 (3H, m), 4.2–4.6 (1H, m), 3.85 (3H, s), 0.8–4.2 (14H, m).

Anal. Calcd. for $C_{19}H_{20}F_3NO_3$: C, 62.12; H, 5.49; N, 3.82. Found: C, 62.07; H, 5.38; N, 3.73.

Racemic 17-Cyclopropylcarbonyl-8,14-epoxy-3-methoxymorphinan, 5c

The epoxide **5***c* was obtained in 71% yield as a white solid by oxidation of **4***d* by the above given procedure; m.p. 140–142 °C from ether; i.r. (Nujol), 1650 cm^{-1}; n.m.r. δ 6.7–7.2 (3H, m), 3.9–4.6 (2H, m), 3.83 (3H, s), 0.6–3.4 (17H, m).

Anal. Calcd. for $C_{21}H_{25}NO_3$: C, 74.31; H, 7.42; N, 4.13. Found: C, 74.13; H, 7.39; N, 4.13.

Racemic 17-Cyclobutylcarbonyl-8,14-epoxy-3-methoxymorphinan, 5d

The epoxide **5***d*, an oil, containing some α-epoxide, was obtained in quantitative yield by oxidation of **4***e* as described above; i.r. (neat) 1650 cm^{-1}; n.m.r. δ 6.6–7.2 (3H, m), 3.8–4.7 (2H, m), 3.85 (3H, s), 1.1–3.7 (19H, m). Mol. Wt. Calcd. for $C_{31}H_{48}O_3$: 353. Found (mass spectrum): 353. In the course of the preparation of this manuscript, an ether solution of **5***d* was crystallized to give a white solid, m.p. 110–111 °C.

Racemic 8,14-epoxy-3-methoxymorphinan, 5e

A mixture of the epoxide **5***b* (18.35 g) and sodium borohydride (1.9 g) in dry ethanol (100 ml) was heated under reflux for 5 min. After cooling, the reaction mixture was acidified with dilute hydrochloric acid and extracted with ether. The ether extract was discarded and the aqueous layer was made basic with ammonium hydroxide and extracted with dichloromethane. The resulting extract was dried (Na_2SO_4) and concentrated *in vacuo* to yield 12.9 g of epoxide **5***e* as an oil; i.r. (neat) 3300 cm^{-1}; n.m.r. δ 6.6–7.3 (3H, m), 3.8 (3H, s), 0.8–3.7 (14H, m). Mol. Wt. Calcd. for $C_{17}H_{21}NO_2$: 271. Found (mass spectrum): 271.

Racemic 17-Ethoxycarbonyl-14-hydroxy-3-methoxymorphinan, 7a

To a mixture of epoxides **5***a* and **6** (2.5 g) in dry ethanol (100 ml) was added sodium borohydride (0.76 g), and the resultant mixture was heated under reflux for 3 h, after which time additional portions of sodium borohydride (0.38 g) were added every hour during 7 h. Then the mixture was cooled, acidified with dilute hydrochloric acid, and extracted with dichloromethane. The extract was dried and concentrated *in vacuo* and the residual oil was chromatographed over alumina. Elution with chloroform gave at first some 14-hydroxyisomorphinan analog, which was described earlier (1) followed by 1.27 g of **7***a*, as a white solid from ether-petroleum ether; m.p. 139–140 °C; i.r. (Nujol) 1690, 3434 cm^{-1}; n.m.r. δ 6.4–7.1 (3H, m), 4.1 (2H, q, J = 7 Hz), 3.8–4.3 (2H, m), 3.7 (3H, s), 1.2. (3H, t, J = 7 Hz), 0.9–3.4 (13H, m).

Anal. Calcd. for $C_{20}H_{27}NO_4$: C, 69.54; H, 7.88; N, 4.05. Found: C, 69.09; H, 7.99; N, 4.02.

Racemic 14-Hydroxy-3-methoxy-17-methylmorphinan, 7b

To a stirred solution of lithium aluminum hydride (0.17 g) in anhydrous tetrahydrofuran (10 ml) was added, under nitrogen, a solution of urethane **7***a* (0.518 g) in tetrahydrofuran (10 ml) and the mixture heated under reflux for 18 h. After cooling and the usual isolation procedure, the product, an oil, crystallized from petroleum ether to give 280 mg of **7***b*. Recrystallization from methanol gave an analytical sample: m.p. 113–115 °C; i.r. (Nujol) 3360 cm^{-1}; n.m.r. 6.5–7.2 (3H, m), 3.8 (3H, s), 2.38 (3H, s), 1.1–3.7 (14H, m), 1.0 (1H, dt, J_1 = 7 Hz, $J_2 \simeq$ 1.5 Hz).

Anal. Calcd. for $C_{18}H_{25}NO_2$: C, 75.23; H, 8.77; N, 4.87. Found: C, 75.26; H, 8.76; N, 4.68.

Can. J. Chem. Downloaded from www.nrcresearchpress.com by 210.87.254.6 on 09/05/12
For personal use only.

Racemic 17-Cyclopropylmethyl-14-hydroxy-3-methoxymorphinan, 7c

A solution of epoxide **5c** (60 g) in anhydrous tetrahydrofuran (100 ml) was added dropwise during 30 min to a stirred suspension of lithium aluminum hydride (18 g) in tetrahydrofuran (500 ml) and the mixture heated under reflux for 1 h. After cooling and the usual work-up, the product, an oil, was dissolved in acetone and treated with dry hydrogen chloride followed by an addition of a few ml of ether. The deposited crystals were collected by filtration to give after drying 61.5 g of **7c** hydrochloride; m.p. 223–225 °C. An analytical sample crystallized with $\frac{1}{2}H_2O$ from methanol–ether; m.p. 259–260 °C. Free base, i.r. (neat) 3420 cm^{-1}; n.m.r. δ 6.6–7.2 (3H, m), 3.8 (3H, s), 1.08 (1H, d, J = 9 Hz), 0.0–3.3 (21H, m).

Anal. Calcd. for $C_{21}H_{29}NO_2 \cdot HCl \cdot \frac{1}{2}H_2O$: C, 67.67; H, 8.37; N, 3.76. Found: C, 67.70; H, 8.02; N, 3.72.

Racemic 17-Cyclobutylmethyl-14-hydroxy-3-methoxymorphinan, 7d

The hydroxymorphinan **7d** was obtained in 69% yield by reduction of epoxide **5d** as described for the preparation of **4c**; i.r. (neat) 3440 cm^{-1}; n.m.r. δ 66.72 (3H, m), 3.8 (3H, s), 1.2–3.3 (23H, m), 1.0 (1H, d, J = 9 Hz). The hydrochloride salt was recrystallized from methanol; m.p. 248–250 °C.

Anal. Calcd. for $C_{22}H_{31}NO_2 \cdot HCl \cdot \frac{1}{2}H_2O$: C, 68.28; H, 8.60; N, 3.62. Found: C, 68.25; H, 8.40; N, 3.75.

From mother liquors it was possible to isolate by fractional crystallization or chromatography on alumina 10–15% of the corresponding isomorphinan (1).

Racemic 14-Hydroxy-3-methoxymorphinan, 7e

A solution of amino-epoxide **5e** (8 g) in tetrahydrofuran (50 ml) was added dropwise to a solution of lithium aluminum hydride (5 g) in tetrahydrofuran (50 ml) and the mixture was heated under reflux for 15 min. After cooling and the usual work-up, the product, an oil, was dissolved in ether, filtered over a celite–charcoal mixture and the filtrate treated with a solution of hydrogen chloride in ether to give 7.2 g of **7e** as its hydrochloride salt. A sample recrystallized from methanol contained $\frac{1}{2}$ mol of methanol of crystallization; m.p. 243–244 °C; free base: i.r. (neat), 3340, 3440 cm^{-1}; n.m.r. δ 6.7–7.2 (3H, m), 3.8 (3H, s), 1.2–3.6 (15H, m), 0.97 (1H, d, t, J = 13 Hz, J_2 = 2 Hz).

Anal. Calcd. for $C_{17}H_{23}NO_2 \cdot HCl \cdot \frac{1}{2}CH_3OH$: C, 64.50; H, 8.04; N, 4.30. Found: C, 64.18; H, 7.81; N, 4.25.

Resolution of 14-Hydroxy-3-methoxymorphinan, 7e

To a hot solution of racemic amino-alcohol **7e** (27.3 g) in methanol (60 ml) was carefully added a hot solution of *l*-tartaric acid (15. 0 g) in methanol (40 ml), and the mixture left at room temperature for five days. The separated solid (32.0 g) was removed by filtration and recrystallized from methanol (1.1 l) to give after drying at 80 °C/0.05 Torr, 12 g of acidic *l*-**7e** *l*-tartrate; m.p. 214–217; $[\alpha]_D^{25}$ −32.5° (*c* 0.1, CH_3OH).

Anal. Calcd. for $C_{17}H_{23}NO_2 \cdot C_4H_4O_6$: C, 59.56; H, 6.90; N, 3.31. Found: C, 59.90; H, 7.04; N, 3.26.

The free base showed m.p. 106–108 °C and $[\alpha]_D^{25}$ −44.97° (*c* 0.53, $CHCl_3$).

Anal. Calcd. for $C_{17}H_{23}NO_2$: C, 74.69; H, 8.48; N, 5.12. Found: C, 74.56; H, 8.46; N, 5.08.

The mother liquors were combined, evaporated to dryness and the residue partitioned between aqueous ammonium hydroxide and chloroform to afford after drying and evaporation of chloroform 18.0 g of the free base **7e**, which was similarly treated with *d*-tartaric acid to give 6.6 g of *d*-**7e** *d*-tartarate; m.p. 215–217 °C; $[\alpha]_D^{25}$ +33.4° (*c*, 0.39, CH_3OH).

Anal. Calcd. for $C_{17}H_{23}NO_2 \cdot C_4H_4O_6$: C, 59.56; H, 6.90; N, 3.31. Found: C, 60.00; H, 6.97; N, 3.31.

The free base had m.p. 107–109 °C and $[\alpha]_D^{25}$ +45.0° (*c* 1.2, $CHCl_3$).

l-14-Hydroxy-3-methoxy-17-methylmorphinan, 7b

The *l*-amino alcohol **7e** (2.70 g) in methanol (5 ml) was added to a suspension of Raney nickel catalyst in methanol (100 ml) and formaldehyde (1 ml of 36% aqueous solution), and the mixture was hydrogenated for 30 min at 40 p.s.i. The catalyst was removed by filtration and filtrate was concentrated to dryness to afford 2.7 g of *l*-**7b** as a white solid. A sample for analysis was recrystallized from methanol; $[\alpha]_D^{25}$ −77° (*c* 0.1, $CHCl_3$); m.p. 142–144 °C; lit. (3) $[\alpha]_D$ −76.6°; m.p. 143–144.5 °C

Anal. Calcd. for $C_{18}H_{25}NO_2$: C, 75.23; H, 8.77; N, 4.87. Found: C, 75.20; H, 8.89; N, 4.68.

d-14-Hydroxy-3-methoxy-17-methylmorphinan, 7b

The *d*-hydroxymorphinan **7b** was similarly prepared from the corresponding *d*-amino alcohol **7e**; $[\alpha]_D$ +77.1° (*c* 0.35, $CHCl_3$); m.p. 142–144 °C.

Anal. Calcd. for $C_{18}H_{25}NO_2$: C, 75.23; H, 8.77; N, 4.87. Found: C, 75.38; H, 8.72; N, 4.85.

Racemic 14-Hydroxy-3-methoxy-17-propionylmorphinan, 7h

To a cooled (ice) stirred solution of racemic amino alcohol **7e** (1.14 g) and triethylamine (0.50 g) in dichloromethane (15 ml) was added dropwise a solution of propionylchloride (0.42 g) in dichloromethane (5 ml). After the usual work-up, there was obtained 1.13 g of **7f** as a white solid; m.p. 149–150 °C from methanol; i.r. (Nujol) 3320, 1620 cm^{-1}; n.m.r. δ 6.7–7.3 (3H, m), 4.2–5.0 (2H, m), 3.9 (3H, s), 1.18 (3H, t, J = 7 Hz), 0.8–3.7 (17H, m).

Anal. Calcd. for $C_{20}H_{27}NO_3$: C, 72.92; H, 8.26; N, 4.25. Found: C, 72.98; H, 8.39; N, 4.08.

Racemic 14-Hydroxy-3-methoxy-17-propylmorphinan, 7g

The reduction of amide **7f** to the amine **7g** was accomplished by a procedure similar to the one given above for the reduction of amido epoxides. The product was obtained in 92% yield as an oil. Infrared (neat) 3340 cm^{-1}; n.m.r. δ 6.6–7.2 (3H, m), 3.8 (3H, s), 0.8–3.2 (19H, m), 0.92 (3H, t, J = 7 Hz). The hydrochloride salt was recrystallized from ethanol–ether; m.p. 259–261 °C.

Anal. Calcd. for $C_{20}H_{29}NO_2 \cdot HCl$: C, 68.26; H, 8.59; N, 3.98. Found: C, 68.06; H, 8.60; N, 3.88.

Racemic 17-Allyl-14-hydroxy-3-methoxymorphinan, 7h

Allylbromide (6.05 g) was added to a solution of racemic amino alcohol **7e** (0.90 g) and triethylamine (1.7 g) in absolute ethanol (12 ml), and the mixture was heated under reflux under nitrogen for 18 h. Then it was evaporated to dryness, and the residue partitioned between ether and 20% aqueous sodium carbonate. The ether layer was washed with water, dried and filtered through a celite–charcoal mixture. The filtrate was evaporated to dryness to give 620 mg of **7h** as an oil; i.r. (neat) 3430 cm^{-1}; n.m.r. δ 6.6–7.2 (3H, m), 5.0–6.2

Can. J. Chem. Downloaded from www.nrcresearchpress.com by 210.87.254.6 on 09/05/12
For personal use only.

(3H, m), 3.78 (3H, s), 1.1–3.5 (16H, m), 1.0 (1H, d, $J = 8$ Hz). Mol. Wt. Calcd. for $C_{20}H_{27}NO_2$: 313. Found (mass spectrum): 313.

The hydrochloride salt was recrystallized from methanol–ether; m.p. 244–246 °C.

Anal. Calcd. for $C_{20}H_{27}NO_2 \cdot HCl$: C, 68.65; H, 8.07; N, 4.00. Found: C, 68.01; H, 7.97; N, 3.90.

l-17-(3,3-Dimethylallyl)-14-hydroxy-3-methoxymorphinan, 7i

A mixture of *l-7e* (1.85 g), triethylamine (3.33 g) and dimethylallyl bromide (1.49 g) in dry ethanol (25 ml) was heated under reflux for 3 days. Work-up as above afforded an oil which was chromatographed on alumina (elution with chloroform) to yield 1.50 g of *l-7i* as an oil; i.r. (neat) 3430 cm^{-1}; n.m.r. δ 6.5–7.0 (3H, m), 5.09 (1H, t, $J = 7$ Hz), 3.7 (3H, s), 1.7 (3H, s), 1.63 (3H, s), 1.1–3.2 (16H, m), 1.0 (1H, d, $J = 8$ Hz). The hydrochloride salt was recrystallized from methanol–ether; m.p. 224–226 °C.

Anal. Calcd. for $C_{22}H_{31}NO_2 \cdot HCl$: C, 69.91; H, 8.53; N, 3.71. Found: C, 69.88; H, 8.42; N, 3.54.

l-14-Hydroxy-3-methoxy-17-propargylmorphinan, 7j

To a cooled mixture of *l-7e* (1.65 g) and triethylamine (0.61 g) in dichloromethane (10 ml) was added a solution of propargyl bromide (0.72 g) in dichloromethane (5 ml) and the mixture stirred at room temperature for 3 days. Then it was evaporated *in vacuo*, and the residual oil partitioned between aqueous sodium carbonate and ether. Drying and evaporation of solvent gave an oil which was chromatographed on an alumina column. Elution with chloroform yielded 0.50 g of solid *l-7j* which was recrystallized from methanol; m.p. 132–134 °C; $[\alpha]_D$ −62.02° (*c* 0.466, $CHCl_3$); i.r. ($CHCl_3$) 3450 cm^{-1}; n.m.r. δ 6.4–7.0 (3H, m), 3.68 (3H, s), 3.25 (2H, d, $J = 2$ Hz, CH_2—C≡CH), 2.17 (1H, t, $J = 2$ Hz, —C≡CH), 0.8–3.1 (15H, m).

Anal. Calcd. for $C_{20}H_{25}NO_2$: C, 77.14; H, 8.09; N, 4.52. Found: C, 77.05; H, 8.22; N, 4.28.

Racemic 17-(3-Butenyl)-14-hydroxy-3-methoxymorphinan, 7k

The *N*-homoallyl-morphinan **7***k*, an oil, was prepared by the procedure given for the preparation of **7***h*; i.r. (neat) 3430 cm^{-1}; n.m.r. δ 6.7–7.2 (3H, m), 4.8–6.1 (3H, m), 3.78 (3H, s), 1.1–3.1 (18H, m), 1.0 (1H, d, $J = 9$ Hz; outer signal split into t, $J = 3$ Hz). The hydrochloride salt was recrystallized from methanol–ether; m.p. 223–225 °C.

Anal. Calcd. for $C_{21}H_{29}NO_2 \cdot HCl$: C, 69.31; H, 8.31; N, 3.85. Found: C, 69.36; H, 8.19; N, 3.78.

Racemic 3,14-Dihydroxymorphinan, 8a

A mixture of amino alcohol **7***e* (2.0 g) and pyridine hydrochloride (8.0 g) was heated at 185–200 °C under nitrogen for 1 h. After cooling, the mixture was treated with concentrated aqueous ammonium hydroxide (4 ml) and water (4 ml) and extracted with a mixture of chloroform–ethanol (9:1). The extract was dried and evaporated *in vacuo* to give 1.5 g of a solid **8***a*. A sample for analysis was recrystallized from 90% ethanol; m.p. 259–261 °C; i.r. (Nujol), 3360, 3440 cm^{-1}; n.m.r. (DMSO-d_6) δ 6.6–7.2 (3H, m), 3.1–3.3 (2H, m), 2.5–3.0 (3H, m), 1.8–2.3 (4H, m), 1.3–1.8 (5H, m), 1.0 (1H, dt, $J_1 = 11$ Hz, $J_2 \simeq 1.5$ Hz).

Anal. Calcd. for $C_{16}H_{21}NO_2$: C, 74.10; H, 8.16; N, 5.40. Found: C, 73.84; H, 8.35; N, 5.33.

l-3,14-Dihydroxymorphinan, 8a

The *l*-isomer was similarly prepared from *l-7e*; $[\alpha]_D$ −30.0° (*c* 0.14, CH_3OH); m.p. 242–244 °C.

3,14-Dihydroxymorphinans, 8b–8g

The phenolic compounds **8***b*–**8***g* were prepared by demethylation of the corresponding methyl ethers by the method of McOmie *et al.* (5).

To a stirred solution of boron tribromide (3.53 g, 0.14 mol) in dichloromethane (50 ml) under nitrogen was added dropwise during 1 h a solution of the methyl ether (80 mmol) in dichloromethane (100 ml). The stirring was continued for 3 h and then the mixture was carefully treated with water (50 ml) and concentrated aqueous ammonia (*ca.* 50 ml) and extracted with dichloromethane.

Drying and concentration yielded dihydroxymorphinans **8***b*–**8***g* which were purified as free bases or as hydrochloride salts. In the latter case, most salts crystallized with ½ mol of solvent of crystallization.

Racemic 3,14-Dihydroxy-17-methylmorphinan, 8b

The yield of **8***b* was 94%; m.p. 206–208 °C from methanol; i.r. (Nujol) 3300 cm^{-1}; n.m.r. δ 6.6–7.2 (3H, m), 3.37 (3H, s), 1.2–3.36 (14H, m), 1.05 (1H, d, $J = 8$ Hz).

Anal. Calcd. for $C_{17}H_{23}NO_2$: C, 74.69; H, 8.48; N, 5.12. Found: C, 74.82; H, 8.58; N, 4.97.

l-3,14-Dihydroxy-17-methylmorphinan, 8b

The yield of *l-8b* was 93%; m.p. 244–246 °C from methanol; $[\alpha]_D$ −79.2° (*c* 1.048, $CHCl_3$); lit. (3) m.p. 246–248 °C, $[\alpha]_D$ −80.3° (*c* 1.048, $CHCl_3$).

Anal. Calcd. for $C_{17}H_{23}NO_2$: C, 74.69; H, 8.48; N, 5.12. Found: C, 74.82; H, 8.57; N, 5.00.

Racemic 17-Cyclopropylmethyl-3,14-dihydroxymorphinan, 8c

The yield of **8***c* was 87%; m.p. 157–159 °C from methanol; i.r. (Nujol) 3250 cm^{-1}; n.m.r. δ 6.6–7.2 (3H, m), 0.0–3.0 (21H, m), 1.03 (1H, d, $J = 9$ Hz). The hydrochloride salt was recrystallized from methanol; m.p. 179–181 °C.

Anal. Calcd. for $C_{20}H_{27}NO_2 \cdot HCl \cdot \frac{1}{2}CH_3OH$: C, 67.32; H, 8.37; N, 3.83. Found: C, 67.56; H, 8.20; N, 3.90.

Racemic Cyclobutylmethyl-3,14-dihydroxymorphinan, 8d

The yield of **8***d* was 86%; m.p. 186–188 °C from benzene; i.r. (Nujol) 3240 cm^{-1}; n.m.r. 6.6–7.1 (3H, m), 1.2–3.1 (23H, m), 1.0 (1H, d, $J = 10$ Hz).

Anal. Calcd. for $C_{21}H_{29}NO_2$: C, 67.96; H, 8.49; N, 3.69. Found: C, 67.59; H, 8.26; N, 3.71.

Racemic 3,14-Dihydroxy-17-propylmorphinan, 8e

The yield of amine **8***e* (white solid) was 92%; i.r. (Nujol) 3240 cm^{-1}; n.m.r. δ 6.6–7.1 (3H, m), 0.95 (3H, m), 0.95 (3H, t, $J = 7$ Hz), 0.8–3.1 (19H, m). The hydrochloride salt was recrystallized from ethanol–ether; m.p. 170–172 °C.

Anal. Calcd. for $C_{19}H_{27}NO_2 \cdot HCl \cdot \frac{1}{2}C_2H_5OH$: C, 66.56; H, 8.66; N, 3.88. Found: C, 66.42; H, 8.34; N, 4.07.

Can. J. Chem. Downloaded from www.nrcresearchpress.com by 210.87.254.6 on 09/05/12
For personal use only.

Racemic 17-Allyl-3,14-dihydroxymorphinan, 8f

The yield of **8***f* was 47%, isolated as its hydrochloride salt, after crude product was chromatographed on alumina column (grade IV, eluent:chloroform). It was recrystallized from methanol–acetone; m.p. 190–192 °C. Free base: i.r. (Nujol) 3250 cm^{-1}; n.m.r. δ 6.6–7.1 (3H, m), 5.0–6.3 (3H, m), 3.1 (2H, d, J = 6 Hz), 1.1–3.0 (14H, m), 1.0 (1H, d, J = 10 Hz).

Anal. Calcd. for $C_{10}H_{25}NO_2 \cdot HCl \cdot \frac{1}{2}CH_3OH$: C, 66.56; H, 8.02; N, 3.98. Found: C, 66.65; H, 7.76; N, 3.88.

l-3,14-Dihydroxy-17-propargylmorphinan, 8g

The yield of **8***g* was 88%; m.p. 173–175 °C from methanol; $[\alpha]_D$ −67.2° (*c* 0.44, $CHCl_3$); i.r. (Nujol) 3240 cm^{-1}; n.m.r. δ 6.4–7.1 (3H, m), 3.28 (2H, d, J = 2 Hz, $CH_2C{\equiv}CH$), 1.7–3.1 (5H, m), 0.8–1.7 (10H, m).

Anal. Calcd. for $C_{19}H_{23}NO_2$: C, 76.73; H, 7.80; N, 4.71. Found: C, 76.63; H, 7.86; N, 4.52.

l-3,14-Dihydroxy-17-(2,2-dimethylallyl)-morphinan, 8h and l-3,14-Dihydroxy-17-(3-hydroxy-3-methylbutyl)-morphinan, 8i

The dimethylallyl intermediate **7***i* (3.012 g) was treated with borontribromide as above to yield 2.4 g of an oil. This was stirred with 1 *N* hydrochloric acid in methanol (20 ml) for 1 h and then partitioned between water and ether. The water layer was made alkaline with ammonium hydroxide and extracted with dichloromethane. The extract was dried and evaporated *in vacuo* to give 1.8 g of a mixture of **8***h* and **8***i*. This was chromatographed over alumina to afford at first (elution with chloroform containing 2% methanol) **8***h* as an oil, which was recrystallized as its hydrochloride salt from methanol–ether to give 450 mg of solid; m.p. 243–245 °C; $[\alpha]_D^{22}$ −69.1° (*c* 0.36, CH_3OH). Free base, i.r. (neat) 3300 cm^{-1}; n.m.r. δ 6.4–7.0 (3H, m), 4.7 (1H, t, J = 7 Hz), 2.4–3.1 (7H, m), 1.76 (6H, s) 1.1–2.4 (9H, m), 1.02 (1H, d, J = 9 Hz).

Anal. Calcd. for $C_{21}H_{29}NO_2 \cdot HCl \cdot \frac{1}{2}CH_3OH$: C, 67.96; H, 8.49; N, 3.69. Found: C, 67.57; H, 8.51; N, 3.81.

Further elution of the column with chloroform–methanol yielded an oil, which was purified as its hydrochloride salt by recrystallization from methanol–ether–acetone to give 600 mg of **8***i*; m.p. 188–190 °C, $[\alpha]_D^{22}$ −42.8° (*c* 0.37, CH_3OH); n.m.r. (free base) δ 6.5–7.0 (3H, m), 2.4–3.0 (7H, m), 1.27 (6H, s), 1.2–2.3 (12H, m), 1.0 (1H, d, J = 9 Hz).

Anal. Calcd. for $C_{21}H_{31}NO_3 \cdot HCl \cdot \frac{1}{2}CH_3OH$: C, 64.89; H, 8.61; N, 3.52. Found: C, 65.04; H, 8.42; N, 3.26.

Racemic 17-(3-Butenyl)-3,14-dihydroxymorphinan, 8j

To a stirred suspension of sodium hydride (1.3 g of 56%, washed with hexane) in DMF (10 ml) under nitrogen was added a solution of ethanethiol (1.86 g) in DMF (15 ml). This was stirred for 30 min and then to it was added a solution of methoxymorphinan **7***k* (1.1 g) in DMF (20 ml) and the mixture heated under gentle reflux for 18 h. After cooling, it was partitioned between water and benzene–ether mixture. Drying and evaporation of the organic layer gave 0.60 g of crude **8***j* as an oil. It was purified as its hydrochloride salt by recrystallization from methanol–ether; m.p. 244–246 °C; n.m.r. (free base) δ 6.6–7.1 (3H, m), 4.9–5.8 (3H, m), 1.2–3.2 (18H, m), 1.0 (1H, d, J = 9 Hz).

Anal. Calcd. for $C_{20}H_{27}NO_2 \cdot HCl$: C, 68.65; H, 8.07; N, 4.00. Found: C, 68.36; H, 8.34; N, 3.90.

l-17-Ethyl-3,14-dihydroxymorphinan, 8k

A solution of *l*-**8***a* (300 mg), acetic anhydride (2 ml) and triethylamine (2 ml) in benzene (5 ml) was heated under reflux for 30 min. Then, to it was added methanol (3 ml) and heating continued for another 5 min. After cooling, the mixture was partitioned between water and benzene, and the organic layer was dried and evaporated *in vacuo*. The residual oil (360 mg) was dissolved in THF (5 ml) and this solution was added to a boiling solution of lithium aluminum hydride (300 mg) in THF (10 ml). After heating under reflux for 4 h and usual work-up procedure, there was obtained 180 mg of a crude **8***k* as a thick oil. It was dissolved in acetone, and the solution filtered to remove solid impurities. The filtrate was treated with a solution of equimolar amount of *d*-tartaric acid in acetone. A solid precipitate was recrystallized from methanol–acetone to give 220 mg of acidic *l*-**8***k* *d*-tartarate; m.p. 207–209 °C; $[\alpha]_D^{22}$ −33.0° (*c* 0.10, CH_3OH); n.m.r. (free base), δ 6.5–7.1 (3H, m), 1.07 (3H, t, J = 7 Hz), 1.0–3.1 (17H, m).

Anal. Calcd. for $C_{18}H_{25}NO_2 \cdot C_4H_6O_6$: C, 60.39; H, 7.14; N, 3.20. Found: C, 60.01; H, 7.23; N, 3.18.

Resolution of 17-Cyclopropylmethyl-3,14-dihydroxymorphinan, 8c

To a solution of the racemic **8***c* (52.0 g) in hot methanol (100 ml) was added a solution of *d*-tartaric acid (25.9 g) in methanol (50 ml), followed by acetone (300 ml) and the mixture let stand at 5 °C for 3 days. The deposited solid was removed by filtration and recrystallized twice from methanol–acetone (2:1) to give 18.0 g of the salt. This was dissolved in minimum amount of hot water (8 ml) and left at room temperature for 24 h, to give 13.5 g of optically pure *d*-**8***c* as its *d*-tartarate with $\frac{1}{2}H_2O$ of crystallization; m.p. 184–187 °C; $[\alpha]_D^{22}$ +86.4° (*c* 0.103, H_2O).

Anal. Calcd. for $C_{20}H_{27}NO_2 \cdot \frac{1}{2}C_4H_6O_6 \cdot \frac{1}{2}H_2O$: C, 66.48; H, 7.86; N, 3.52. Found: C, 66.76; H, 7.87; N, 3.46.

The mother liquors were combined and concentrated. The residual oil was dissolved in hot water, and this solution was made basic with ammonium hydroxide. After cooling, the solid was collected by filtration and dried in the air to afford 40 g of the free base. This was dissolved in hot methanol (80 ml) and treated with a solution of *l*-tartaric acid (19.2 g) in methanol (40 ml) followed by acetone (240 ml). The above procedure was then followed to afford 22.0 g of a salt which was recrystallized from water (10 ml) to yield 16.5 g of optically pure *l*-**8***c* as its acidic *l*-tartarate with $\frac{1}{2}H_2O$ of crystallization; m.p. 184–187 °C, $[\alpha]_D^{22}$ −86.1° (*c* 0.1, H_2O).

Anal. Calcd. for $C_{20}H_{27}NO_2 \cdot \frac{1}{2}C_4H_6O_6 \cdot \frac{1}{2}H_2O$: C, 66.48; H, 7.86; N, 3.52. Found: C, 66.62; H, 7.78; N, 3.56.

The free base showed m.p. 173–175 °C (methanol), and $[\alpha]_D$ −102.5° (*c* 0.44, $CHCl_3$).

Resolution of 17-Cyclobutylmethyl-3,14-dihydroxymorphinan, 8d

To a hot suspension of racemic **8***d* (262 g) in methanol

(1 l) was added carefully a hot solution of *l*-tartaric acid (120 g) in methanol (250 ml). The solution was filtered to remove insoluble material, and let stand at room temperature for 5 days to give 126 g of solid. This was dissolved in hot water – methanol (9:1 1.1 l) mixture. After standing at room temperature for 5 days, the solid was removed by filtration and dried for 2 days under high vacuum in a dessicator. There was obtained 108 g of *l*-**8***d* as its *l*-tartaric acid salt; m.p. 217–219 °C;, $[\alpha]_D^{22}$ −64.0° (*c* 0.4; MeOH).

Anal. Calcd. for $C_{21}H_{29}NO_2 \cdot C_4H_6O_6$: C, 62.87; H, 7.39; N, 2.93. Found: C, 62.55; H, 7.40; N, 2.92.

The free base showed m.p. 215–217 °C (methanol), and $[\alpha]_D$ −70.0° (*c* 0.1, CH_3OH).

The mother liquors were combined and concentrated to a small volume. This was made basic with ammonium hydroxide and the solid removed by filtration to afford 200 g of the free base **8***d* enriched in the *d*-isomer. This was treated with *d*-tartaric acid by the procedure given above to give 136 g of *d*-**8***d* as its acidic *d*-tartarate; m.p. 217–219 °C; $[\alpha]_D$ +63.0° (*c* 0,4. MeOH).

Anal. Calcd. for $C_{21}H_{29}NO_2 \cdot C_4H_6O_6$: C, 62.87; H 7.39; N, 2.93. Found: C, 62.56; H, 7.46; N, 3.00.

The mother liquors were kept for isolation of additional amounts of the *l*-**8***d*.

l-17-Cyclopropylmethyl-14-hydroxy-3-methoxymethyl-morphinan, 9a and Corresponding d-Isomer

A solution of *l*-dihydroxymorphinan **8***c* (3.14 g) in dry benzene (60 ml) was added dropwise to a suspension of sodium hydride (870 mg of 55%, washed with hexene) in benzene (10 ml) and the mixture stirred for 1 h. Then, to it was added a solution of chloromethylmethyl ether (1.61 g) in benzene (10 ml) and the mixture stirred for 18 h. Work-up afforded 3.6 g of crude product, which was chromatographed on alumina. Elution with chloroform gave 2.6 g of *l*-**9***a* as an oil. A sample for analysis was distilled at 170 °C/0.02 Torr; $[\alpha]_D$ −82.5° (*c* 0.412, $CHCl_3$); i.r. (neat) 3420 cm^{-1}; n.m.r. δ 6.7–7.1 (3H, m), 5.15 (2H, s), 3.5 (3H, s), 0.0–3.1 (21H, m), 1.02 (1H, d, J = 9 Hz).

Anal. Calcd. for $C_{22}H_{31}NO_3$: C, 73.91; H, 8.74; N, 3.91. Found: C, 73.51; ,H 8.50; N, 3.65.

Similarly prepared was *d*-**9***a*; $[\alpha]_D$ +82.0° (*c* 0.410, $CHCl_3$).

l-17-Cyclobutylmethyl-14-hydroxy-3-methoxymethyl-morphinan, 9b

The *l*-methoxymethyl ether **9***b*, an oil, was similarly prepared. The analytical sample was obtained by drying at 80 °C/0.05 Torr; $[\alpha]_D^{22}$ −70.87° (*c* 0.388, $CHCl_3$); i.r. (neat) 3420 cm^{-1}; n.m.r. δ 6.8–7.2 (3H, m), 5.18 (2H, s), 3.52 (3H, s), 1.2–3.1 (23H, m), 1.0 (1H, d, J = 4 Hz).

Anal. Calcd. for $C_{23}H_{33}NO_3$: C, 74.36; H, 8.95; N, 3.77. Found: C, 74.14; H, 9.08; N, 3.47.

The financial support of The National Research Council of Canada through its Industrial Research Assistance Program is gratefully acknowledged. We thank Drs. M. Gordon[4] and M. Menard for their suggestions and discussions and Dr. V. DiTullio, Mr. J. Chapuis and J. Lajeunesse for their technical assistance.

1. I. Monković, H. Wong, B. Belleau, I. J. Pachter, and Y. G. Perron. Can. J. Chem. **53**, 2515 (1975).
2. I. Monković, T. T. Conway, H. Wong, Y. G. Perron, I. J. Pachter, and B. Belleau. J. Am. Chem. Soc. **95**, 7910 (1973).
3. Y. K. Sawa and H. Tada. Tetrahedron. **24**, 6185 (1968).
4. L. Goodman, S. Winstein, and R. Boschan. J. Am. Chem. Soc. **80**, 4312 (1958).
5. J. F. W. McOmie, M. L. Watts, and E. E. West. Tetrahedron, **24**, 2289 (1968).
6. G. I. Feutrill and R. N. Mirrington. Aust. J. Chem. **25**, 1719 (1972).
7. A. W. Pircio and J. A. Gylys. J. Pharmacol. Expt. Ther. **193**, 23 (1975).
8. J. G. Nutt and D. R. Jasinski. Clin. Pharmacol. and Ther. **15**, 361 (1974).
9. A. B. Dobkin, S. Eamkaow, S. Zak, and F. S. Caruso. Can. Anaesth. Soc. J. **21**, 600 (1974).
10. R. L. Cavanagh, J. A. Gylys, and M. E. Bierwagen. Pharmacologist, **16**, 248 (1974).
11. E. Siegmund, R. Cadmus, and F. Lu. Proc. Soc. Exp. Biol. Med. **95**, 729 (1957).
12. H. Blumberg, P. S. Wolf, and H. B. Dayton. Prod. Soc. Exp. Biol. Med. **118**, 763 (1965).
13. L. S. Harris and A. K. Pierson. J. Pharmacol. Exp. Ther. **143**, 141 (1964).

Can. J. Chem. Downloaded from www.nrcresearchpress.com by 210.87.254.6 on 09/05/12
For personal use only.

The Selective Lithiation and *In Situ* Trimethylsilylation of Benzyldiphenylchlorosilane and its Methoxy Analog. Compounds Which Could Conceivably Lead to Stable Si=C Species on Pyrolysis

K. G. RUTHERFORD[1] AND R. J. SEIDEWAND[2]

Department of Chemistry, University of Windsor, Windsor, Ontario N9B 3P4

Received April 8, 1975

K. G. RUTHERFORD and R. J. SEIDEWAND. Can. J. Chem. **53**, 3103 (1975).

The selective lithiation and *in situ* trimethylsilylation of benzyldiphenylchlorosilane and its methoxy analog to give (α-trimethylsilylbenzyl)diphenylchlorosilane and (α-trimethylsilylbenzyl)diphenylmethoxysilane in excellent yields is reported. These compounds exhibit much greater stability on pyrolysis than β-halocarbosilanes. A stable Si=C species was not obtained on pyrolysis of the compounds synthesized.

K. G. RUTHERFORD et R. J. SEIDEWAND. Can. J. Chem. **53**, 3103 (1975).

On rapporte la lithiation sélective et la triméthylsilylation *in situ* du benzyldiphénylchlorosilane et de son analogue méthoxylé; ces réactions qui se produisent avec d'excellents rendements conduisent au (α-triméthylsilylbenzyl)diphénylchlorosilane et au (α-triméthylsilylbenzyl)diphénylméthoxysilane. Ces composés, comparés aux β-halocarbosilanes, sont beaucoup plus stables vis-à-vis de la pyrolyse. On n'a pu obtenir d'espèces Si=C par pyrolyse des composés synthétisés.

[Traduit par le journal]

Introduction

The exceptional thermal instability of β-haloalkylsilanes (1, 2) has been known for some time. A few representative compounds shown in Fig. 1 decomposed (3, 4) upon attempted distillation to produce a silyl halide and an olefin.

$$Et_3SiCH_2CH_2Cl \xrightarrow{80\,^\circ C} Et_3SiCl + CH_2{=}CH_2$$

$$Me_3SiCH_2CHBrCH_3 \xrightarrow{40\,^\circ C} Me_3SiBr + CH_2{=}CHCH_3$$

$$Me_3SiCH_2CHClCH_3 \xrightarrow{90\,^\circ C} Me_3SiCl + CH_2{=}CHCH_3$$

FIG. 1. Thermal cleavage of β-haloalkylsilanes.

These elimination reactions have been postulated to proceed through a four-centered activated complex (Fig. 2), promoted by overlap of the lone pair of electrons on the β-heteroatom with the vacant d orbitals of silicon (2).

In addition to halogen substituents, the cleavage reaction also occurs when there is a β-oxygen atom capable of being transferred, presumably in a *cis*-like manner, to silicon via a similar four-centered transition state.

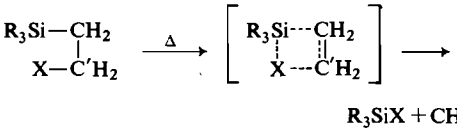

FIG. 2. Proposed mechanism for β-haloalkylsilane cleavage.

The intriguing ramifications of this mechanism involve the carbon atom C′. If C′ were to be replaced by a silicon atom and if appropriate groups were to be attached to the Si and C atoms which could allow for resonance and/or steric stabilization, the possibility of generating a stable silico-olefin may be realized on pyrolysis. Incorporation of a sufficient molecular weight may also add to the stability of the resultant Si=C species. The transient existence of molecules containing (p–p)π bonded silicon and germanium has been well documented in the literature over the past few years (5), however, stable systems have not as yet been synthesized. Model compounds[3] aimed at providing stable systems were thus synthesized for pyrolytic studies.

Results and Discussion

Benzyldiphenylchlorosilane (**1**) was readily

[1]To whom all inquiries should be directed.

[2]Present address: Dwight P. Joyce Research Center, Glidden-Durkee, Division of SCM Corporation, Strongsville, Ohio 44136.

[3]Previous compounds synthesized and pyrolyzed are reported in ref. 6.

Can. J. Chem. Downloaded from www.nrcresearchpress.com by 210.87.254.40 on 09/05/12
For personal use only.

Can. J. Chem. Downloaded from www.nrcresearchpress.com by 210.87.254.40 on 09/05/12
For personal use only.

obtained from the reaction of benzylmagnesium chloride and diphenyldichlorosilane. Benzyldiphenylmethoxysilane (**2**) was obtained from the methanolysis of **1**.

In 1971, West (7) reported that the methyl group of trimethylsilyl derivatives can be metalated by the strongly hindered base, *tert*-butyllithium. Trimethylchlorosilane (**3**), for example, can be metalated and then trapped by excess chlorosilane. We found that the addition of *tert*-butyllithium to a *mixture* of **1** and **3** proved to be an excellent procedure for the synthesis of (α-trimethylsilylbenzyl)diphenylchlorosilane (**4**). An analogous selective lithiation reaction with a mixture of **2** and **3** conveniently afforded (α-trimethylsilylbenzyl)diphenylmethoxysilane (**5**). The above reactions (crude yields ≥75%) are summarized in Fig. 3. Both compounds **4** and **5** now provided us with the desired 1,4-juxtaposition of silicon and a heteroatom substituent (Fig. 2).

Attempted pyrolytic elimination (6) of **3** from **4** at temperatures up to 470 °C resulted essentially only in recovery of starting material. The pyrolysis of **5** in the temperature range 300–470 °C did result in decomposition but led to a complex mixture, as shown by i.r. and n.m.r. analysis, as well as furnishing trimethylmethoxysilane **6**, $(CH_3)_3SiOCH_3$, in a 50% yield. None of the desired Si=C compound was obtained.

The nature of the route leading to **6** can only be speculated, but if it does involve the formation of $Ph_2Si{=}CHPh$, the high temperatures employed probably favor intermolecular processes leading to a complex high molecular weight residue.

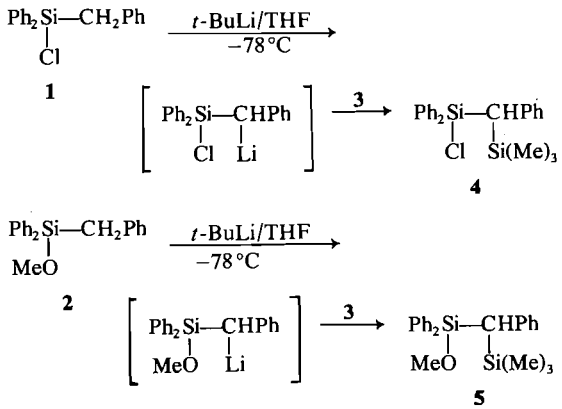

FIG. 3. Selective lithiation by *tert*-butyllithium and *in situ* trapping by trimethylchlorosilane.

The reason for the stability of **4**, when under the same conditions **5** completely decomposes, remains rather obscure at this point.

Experimental

Infrared spectra were recorded on a Beckman IR-12 spectrometer in chloroform. Nuclear magnetic resonance spectra were obtained with a Jeolco C-60 HL spectrometer in deuteriochloroform with methylene chloride as an internal standard (τ 4.70). Gas–liquid chromatography (g.l.c.) was performed on Hewlett Packard 720 and 5750 instruments. Columns utilized were as follows: 6 ft × ¼ in. 10% SE 30 on 60–80 Chromosorb W, 8 ft × ¼ in. 20% SE 30 on 60–80 Chromosorb W and 6 ft × ¼ in. 10% Dexsil 300 on 60-80 Chromosorb W. All reactions were run in dried apparatus under an atmosphere of nitrogen and the silyl chlorides were purified prior to use. Microanalyses were performed by Schwarzkopf Microanalytical Laboratory, Woodside, N.Y.

Benzyldiphenylchlorosilane (1)

Benzylmagnesium chloride (200 mmol) in 150 ml of ether and diphenyldichlorosilane (53.2 g, 210 mmol) in 125 ml of ether were stirred for 15 min at 0 °C and then refluxed 2 h. Upon cooling, the solution was filtered through Super Cel under an atmosphere of N_2 with the aid of an additional 150 ml of ether and the filtrate was concentrated. Methylene chloride (50 ml) was added and the solution was refiltered and concentrated to a pale yellow liquid. Short path distillation gave 40.9 g (66%) of **1**: b.p. 147–150 °C (0.003 Torr); m.p. 52–57 °C; n_D^{25} 1.6085; i.r. 7.0, 8.97, and 19.0 (SiCl) μ; n.m.r. τ 2.7 (m, 15) and 7.2 (s, 2).

Anal. Calcd. for $C_{19}H_{17}ClSi$: C, 73.87; H, 5.54;, Cl, 11.47. Found: C, 73.76; H, 5.58; Cl, 11.38.

(α-Trimethylsilylbenzyl)diphenylchlorosilane (4)

To 4 g (13 mmol) of **1** and 1.65 ml (13 mmol) of **3** in 25 ml of THF at −78 °C was added dropwise 6.2 ml (14 mmol) of 2.26 *M* *tert*-butyllithium in pentane in 25 ml of pentane. The resulting clear orange solution was stirred at −78 °C for 2 h. After addition of 0.3 ml (2 mmol) of **3** the solution was allowed to warm to room temperature and then stirred for an additional 2 h. Lithium chloride was removed by filtration under nitrogen using Super Cel and the colorless filtrate was concentrated. Methylene chloride (20 ml) was added and the solution was refiltered, concentrated, and distilled (short path) to give 3.0 g of a colorless viscous oil: b.p. 154–155.5 °C (0.003 Torr); n_D^{25} 1.5877. Gas–liquid chromatography and subsequent i.r. and n.m.r. analyses revealed **4** (94%), **1** plus a lower retention component (1%), and an unidentified high retention time component (5%). Preparative g.l.c. afforded pure **4**: i.r. 7.0, 9.03, 11.7, and 19.4 μ; n.m.r. τ 2.6 (m, 15), 7.52 (s, 1, CH), and 10.1 (CH_3Si).

Anal. Calcd. for $C_{22}H_{25}ClSi_2$: C, 69.34; H, 6.61; Cl, 9.30. Found: C, 69.23; H, 6.89; Cl, 9.35.

Benzyldiphenylmethoxysilane (2)

Benzyldiphenylchlorosilane (**1**) (5.17 g) was converted by the method of Sauer (9) into **2** (3.9 g, 76%); b.p. 142–144 °C (0.005 Torr); n_D^{25} 1.5923; i.r. 3.52, 7.0, 8.93, and 9.17 μ; n.m.r. τ 2.7 (m, 15), 6.42 (s, 3), and 7.24 (s, 2).

Anal. Calcd. for $C_{20}H_{20}OSi$: C, 78.89; H, 6.62; Si, 9.22. Found: C, 78.55; H, 6.78; Si, 8.90.

(α-Trimethylsilylbenzyl)diphenylmethoxysilane (5)

To 3.96 g (13 mmol) of **2** and 1.65 ml (13 mmol) of **3** in 25 ml of THF at −78 °C was added dropwise 6.2 ml (14 mmol) of 2.26 *M tert*-butyllithium in pentane in 20 ml of pentane. The resulting yellow solution was stirred at −78 °C for 2 h. After addition of 0.3 ml (2 mmol) of **3** the solution was allowed to warm to room temperature and then stirred for an additional 2 h. Lithium chloride was removed by filtration under nitrogen using Super Cel and the colorless filtrate was concentrated. Methylene chloride (20 ml) was added and the solution was refiltered, concentrated, and distilled (short path) to give 3.8 g of a colorless viscous oil; b.p. 151–153 °C (0.005 Torr); n_D^{25} 1.5757. Gas–liquid chromatography and subsequent i.r. and n.m.r. analysis revealed **5** (88%) and an unresolved peak (12%) at the same retention time as **2**. Preparative g.l.c. gave pure **5**: i.r. 3.53, 7.0, 8.98, 9.18, 11.7, and 19.2 μ; n.m.r. τ 2.6 (m, 15), 6.45 (s, 3, OCH_3), 7.75 (s, 1, CH), and 10.05 (s, 9, CH_3Si).

Anal. Calcd. for $C_{23}H_{28}OSi_2$: C, 73.34; H, 7.49; Si, 14.91. Found: C, 73.39; H, 7.51; Si, 14.61.

The authors wish to thank A. G. Brook of the University of Toronto, Toronto, Ontario and M. Rabin of Wayne State University, Detroit, Michigan for many helpful discussions during the course of this work. Financial support by the National Research Council of Canada is gratefully acknowledged.

1. C. Eaborn and R. W. Bott. *In* Organometallic compounds of group IV elements, Vol. 1. *Edited by* A. G. MacDiarmid. Marcel Dekker, New York, N.Y. 1968. Pt. 2, pp. 378–389.
2. A. W. P. Jarvie. Organomet. Chem. Rev. Sect. A, **6**, 153 (1970).
3. L. H. Sommer, D. L. Bailey, and F. C. Whitmore. J. Am. Chem. Soc. **70**, 2869 (1948).
4. L. H. Sommer, L. J. Tyler, and F. C. Whitmore. J. Am. Chem. Soc. **70**, 2872 (1948).
5. T. J. Barton and J. A. Kilgour, J. Am. Chem. Soc. **96**, 2278 (1974) and references contained therein.
6. K. G. Rutherford and R. J. Seidewand. Can. J. Chem. **53**, 67 (1975).
7. R. West and G. A. Gornowicz. J. Organomet. Chem. **28**, 25 (1971).
8. H. Gilman and W. E. Catlin. Organic syntheses, Vol. 1. Wiley, New York, N.Y. 1941. p. 471.
9. R. O. Sauer. J. Am. Chem. Soc. **66**, 1707 (1944).

Can. J. Chem. Downloaded from www.nrcresearchpress.com by 210.87.254.40 on 09/05/12
For personal use only.

Studies in Solvolysis. Part VII. The Neutral Hydrolysis of Methyl Perchlorate

ROSS ELMORE ROBERTSON AND ADRIANNA ANNESA
Chemistry Department, University of Calgary, Calgary, Alberta
AND
JOHN MARSHALL WILLIAM SCOTT
Chemistry Department, Memorial University of Newfoundland, St. John's, Newfoundland A1C 5S7

Received January 20, 1975

ROSS ELMORE ROBERTSON, ADRIANNA ANNESA, and JOHN MARSHALL WILLIAM SCOTT. Can. J. Chem. **53**, 3106 (1975).

The temperature dependence of the rate of hydrolysis of methyl perchlorate has been measured and the entropy ($\Delta S^{\neq}$), enthalpy ($\Delta H^{\neq}$), and heat capacity ($\Delta C_p^{\neq}$) of activation calculated. The measurements confirm that the perchlorate ion is superior to all other leaving groups in water. The isotope effect related to the hydrolysis of methyl-d_3 perchlorate has been measured at three temperatures and shown to be inverse. The thermodynamic parameters and the isotope effect were examined with respect to the mechanism of substitution at a primary carbon atom.

ROSS ELMORE ROBERTSON, ADRIANNA ANNESA et JOHN MARSHALL WILLIAM SCOTT. Can. J. Chem. **53**, 3106 (1975).

On a mesuré l'influence de la température sur les vitesses d'hydrolyse de perchlorate de méthyle et on a calculé l'entropie ($\Delta S^{\neq}$), l'enthalpie ($\Delta H^{\neq}$) et la capacité calorifique ($\Delta C_p^{\neq}$) d'activation. Ces mesures confirment que, dans l'eau, l'ion perchlorate est le meilleur nucléofuge. On a mesuré, à trois températures, l'effet isotopique relié à l'hydrolyse du perchlorate de méthyle-d_3 et on a montré qu'il est inverse. On a examiné les paramètres thermodynamique et l'effet isotopique en fonction du mécanisme de substitution au niveau d'un carbone primaire.
[Traduit par le journal]

Introduction

On the basis of a series of kinetic studies Koskikallio (1–3) has suggested that the reaction between methyl perchlorate and water

[1] $CH_3ClO_4 + 2H_2O \rightarrow CH_3OH + H_3O^+ + ClO_4^-$

takes place via an S_N1 mechanism. This conclusion follows from the fact that the entropy of activation for reaction 1 is positive[1] (0.92 e.u.) in contrast to negative values found for the hydrolyses of methyl chloride (−4.77 e.u.), methyl bromide (−2.97 e.u.), methyl nitrate (−1.88 e.u.), and methyl benzenesulfonate (−9.27 e.u.). On the other hand, the mechanism for the methanolysis of methyl perchlorate was considered to be S_N2 because of a much lower enthalpy of activation [$\delta_M\Delta H^{\neq}(H_2O \rightarrow MeOH) = -7$ kcal/mol] and a negative entropy of activation in the alcoholic solvent ($\Delta S^{\neq} = -20.9$ cal mol^{-1} deg^{-1}). The solvent change from water to acetone–water was also considered to alter the mechanism in the S_N2 direction.

Entropies of activation are often useful in detecting mechanistic changes but only in cases where $\delta_R\Delta S^{\neq}$ is large (5, 6) can mechanistic distinctions be drawn with confidence.[2] Thus the change in mechanism $B_{Ac}2 \rightarrow S_N1$ for simple alkyl trifluoroacetates is characterized by a very large change in the entropy of activation ($\delta_R\Delta S^{\neq} \simeq 50$ e.u.), whereas the difference between $\Delta S^{\neq}$ for methyl chloride and methyl perchlorate is relatively small ($\delta_X\Delta S^{\neq} \simeq 6$ e.u.). There are, however, other ways of explaining the

[1]The original value reported (5.62 e.u. (2)) is not in agreement with the value reported in the more extensive study reported here, but both studies concur in that $\Delta S^{\neq}$ is positive at 25 °C (see Table 2 in this paper). The entropy values are compared at 25 °C and were calculated from the reported B and C coefficients (4) of the temperature dependence equation

[2] $$\log k = A/T + B \log T + C$$

from which the expression

[3] $$\Delta S^{\neq}(25\,^{\circ}C) = 13.3098(B-1) + 4.57573C - 47.2128$$

can be derived via the absolute rate theory at $T = 25$ °C. A comparison between our value and that reported by Koskikallio is best made at 12.5 °C (see Table 2).

[2]δ_R and δ_X are chemical operators denoting changes in the structure of the alkyl group (R) and leaving group (X), respectively.

Can. J. Chem. Downloaded from www.nrcresearchpress.com by 210.87.254.105 on 09/05/12
For personal use only.

TABLE 1. Rate data for the hydrolysis of methyl perchlorate and methyl-d_3 perchlorate in water

T	$k_{(obs)} \times 10^4$	a	$k_{(calc)} \times 10^4$	$k(H)/k(D)$
5.007	1.119 ± 0.001	4	1.083	—
8.609	1.912 ± 0.001	1	1.892	—
10.269	2.409 ± 0.009	3	2.404	—
12.181	3.149 ± 0.010	3	3.155	—
15.000	4.628 ± 0.083	4	4.667	—
15.707	5.163 ± 0.005	4	5.140	—
17.833	6.812 ± 0.02	4	6.847	—
20.447	9.651 ± 0.01	3	9.668	—
24.055	15.33 ± 0.12	4	15.35	—
27.297	22.99 ± 0.05	4	22.97	—
30.190	32.46 ± 0.14	3	32.58	—
11.907[a]	3.243 ± 0.03	6	3.035	0.93_6
23.115[a]	14.74 ± 0.03	3	13.63	0.92_5
23.14[b]	14.79 ± 0.02	3	13.67	0.92_4

[a]The $k_{(obs)}$ values are those for the CD_3ClO_4 ester and the $k_{(calc)}$ values refer to the CH_3ClO_4 ester.
[b]Refers to the second batch of CD_3ClO_4.

small positive shift between the chloride and perchlorate without invoking mechanistic differences.

The acceleration of a given displacement at a saturated carbon atom by added lyate ion (OH^-) is one of the classical tests for an S_N2 process (7) and acceleration of the rate of displacement by this reagent signals the importance of nucleophilic driving forces. Koskikallio (2) observed such an acceleration for methyl perchlorate reacting with hydroxide ion, but the mechanistic conclusions related to this observation were ignored. Since the solvolytic rate in water for methyl perchlorate, when divided by the molar concentration of water is correlated by the Swain–Scott (8) linear free energy relationship (l.f.e.r.) the bimolecular nature of the rate-determining step appears well established. Finally, the displacement rates of methyl perchlorate in water and methanol give a value of the Grunwald–Winstein "m" parameter (9) for methyl perchlorate ($m = 0.13$) which is a "typical S_N2" value. Clearly, the evidence presented by Koskikallio conflicts with his own mechanistic proposals since the experimental data are all consistent with a simple S_N2 interpretation.[3]

In the present paper we report a study of the temperature dependence of the enthalpy of activation ($\Delta C_p^{\ddagger}$) for methyl perchlorate as well as the secondary isotope effect involving methyl-d_3 perchlorate. These results combined with other data provide a useful basis for certain theoretical considerations.

Experimental

Methyl perchlorate was synthesized by the reaction of dry silver perchlorate (12) with methyl iodide in carbon tetrachloride at room temperature. The resulting ester was purified by distillation, b.p. 50 °C/670 mm Hg.[4] The deuterated ester was prepared in the same way using methyl-d_3 iodide which was nominally 99% deuterium content (Merck, Sharp and Dohme; lot E 223). Mass spectra showed that both isotopic samples of the perchlorate ester contained trace amounts of carbon tetrachloride and the appropriate methyl iodide. In both cases the contaminants were considered to be kinetically insignificant ($t_{1/2}$ at 25 °C for methyl iodide is estimated from available data (13) to be *ca.* 104 days). A second sample of methyl-d_3 perchlorate gave an isotope effect identical to that observed for the first specimen.

Rate Measurements

The rates of hydrolysis of the normal and deuterated esters were determined conductimetrically, and the details of the method have been described elsewhere (14). Rate constants measured at various temperatures are reported in Table 1. Assuming all the significant errors to be in the rate rather than in the temperature, a least squares treatment of the temperature dependence of the nonaveraged rates for methyl perchlorate gives

$$[4] \quad \log k = 92.3541 - 27.1347 \log T - 8340.40/T$$

Rate constants calculated from [4] at 0, 15, and 25 °C are respectively, 5.12×10^{-5}, 4.66×10^{-4}, and 1.74×10^{-3} s^{-1}. Koskikallio (2) reports 5.04×10^{-5}, 4.66×10^{-4}, and 1.79×10^{-3} s^{-1} at the same temperatures.

[3]The S_N1 description has also been rejected by Kevill and Shen (10) on the basis of $k(MeX)/k(EtX)$ ratios.

[4]NOTE: Methyl perchlorate is usually considered to be a very dangerous substance (11).

Can. J. Chem. Downloaded from www.nrcresearchpress.com by 210.87.254.105 on 09/05/12
For personal use only.

Can. J. Chem. Downloaded from www.nrcresearchpress.com by 210.87.254.105 on 09/05/12
For personal use only.

TABLE 2. Derived pseudothermodynamic parameters for the hydrolysis of methyl perchlorate in water

T(°C)	$\Delta H^{\ddagger}$ (kcal mol^{-1})	$\Delta S^{\ddagger}$ (cal mol^{-1} deg^{-1})
5	22.59	4.82
15	22.30	2.84
25	21.49	0.93
35	20.91	−0.91
50	20.70	−3.56
75	18.67	−7.73
100	17.27	−11.61
12.5	22.17	3.32
12.5[a]	22.53	5.62

[a]Taken from ref. 2.

The agreement between the two sets of data is generally satisfactory, but the differences show a slight trend. The pseudothermodynamic parameters reported in Table 2 were obtained by invoking the usual premises of the absolute rate theory along with the further assumption that the experimental errors do not justify any further terms in T to adequately reproduce the experimental rates. Since our rates differ from those of Koskikallio the observation that values of $\Delta H^{\ddagger}$ and $\Delta S^{\ddagger}$ calculated from our data differ from the same parameters derived from the earlier work is not surprising. A comparison of the two sets is best made at 12.5 °C, the midpoint of the temperature range employed in the previous study (see Table 2).

The rate data for the two samples of methyl-d_3 perchlorate are reported in Table 2 and the isotope effect is inverse and similar in magnitude (0.931) to that observed for the Menschutkin reaction involving the perchlorate and *N,N*-dimethylaniline (15).

Discussion

Relative Rates, Free Energies of Activation

In Table 3 we have collected rate data for a series of primary halides and esters. The range of reactivity of the substances listed in Table 3 exceeds six powers of ten, methyl perchlorate being the most reactive compound.

There is an unjustified but general tendency in chemical literature to regard "fast" S_N displacements as tending towards the S_N1 type (21). This may partly explain Koskikallio's predilection for the S_N1 description for the solvolysis of methyl perchlorate. However, knowledge of the relative rates of a single nucleophile attacking a series of methyl compounds (see Table 3) does not establish the mechanism of displacement for any particular methyl compound in the series. Since all the methyl compounds in Table 3 react with hydroxide ion faster than they react with water the mechanisms are anticipated to be uniformly S_N2 or "S_N2-like" with both water and hydroxide. This proposal is further supported by the observation that several of these methyl compounds when reacting with a series of nucleophiles yield second order rate constants which are adequately correlated by the Swain–Scott (8) l.f.e.r. (see however (22)). Thus, the high reactivity of methyl perchlorate with water is not a compelling reason for invoking an S_N1 mechanism.

The Entropy of Activation

Although substances which are considered to react by S_N1 displacement often have positive entropies of activation in water,[5] the sign of the entropy of activation for any particular substance is not a reliable mechanistic criterion. Indeed, as a consequence of the large heat capacity of activation associated with displacement, the entropy of activation for methyl perchlorate changes sign at *ca.* 30 °C. This observation further emphasizes the inadequacy of using isolated thermodynamic quantities as a basis for mechanistic diagnosis. On the other hand the entropy of the transition state $S^{\ddagger}$ appears to be a useful quantity in assessing the significance of the entropies of activation from a series of closely related reactions (23). The quantity $S^{\ddagger}$ is calculated from

$$[5] \qquad S^{\ddagger} = S_g^0 + \delta_s S + \Delta S^{\ddagger}$$

where the quantities on the right hand side are in the order given; the gas phase entropy of the substrate, the entropy of solution of the substrate, and the entropy of activation. The approach adopted is to compare the quantity $S^{\ddagger}$ with the entropies of thermodynamically stable species which might reasonably be expected to resemble the transition state. For a series of methyl compounds, CH_3X, the following linear relationsip was proposed (23)

$$[6] \qquad S^{\ddagger}(CH_3X) = \alpha S(X^-) + \text{constant}$$

where $S(X^-)$ is the standard entropy of the aqueous ionic leaving group. In cases where experimental values of S_g^0 and $\delta_s S$ are not available, satisfactory estimates of these quantities can be calculated from

$$[7] \qquad S_g^0(CH_3X) = S_g^0(HX) + 11.3$$

and

[5]See for instance Table VIB in ref. 4.

TABLE 3. Rate constants and related data for the attack of hydroxide (k_1^0)ion and water (k_e^0) on primary compounds RX $T = 25$ °C

R	X	$-\log k_{0w}$[a]	$-\log k_{01}$[a]	$-\log K_e$
CH_3	F	10.847[b]	7.479[d]	15.12
CH_3	Cl	9.364[b]	5.185[e]	9.98
CH_3	Br	8.135[b]	3.480[e]	8.23
CH_3	I	8.874[b]	4.196[e]	7.24
CH_3	SO_3CH_3	7.039[b]	3.398[f]	10.08
CH_3	OSO_2OCH_3	5.525[b]	2.032[f]	9.23
CH_3	ClO_4	4.504[c]	1.141[g]	8.80
CH_3	NO_3	10.343[b]	6.223[h]	11.22
CH_3CH_2	Tosylate	6.909[b]	4.399[i]	15.05

[a]Rate constants are second order rate constants in the usual units (see also ref. 16).
[b]Calculated from data collected in ref. 4.
[c]This work.
[d]For details see ref. 16.
[e]Calculated from data in ref. 17, p. 234, Table X.
[f]Calculated from data given in ref. 18.
[g]Calculated from data in ref. 2.
[h]Calculated from data in ref. 19, $\Delta H^{\ddagger} = 25.91$ kcal mol^{-1}, $\Delta S^{\ddagger} = -0.1$ e.u.
[i]Calculated from data in ref. 20 via a Swain–Scott (8) l.f.e.r. The observed rate is not well correlated and deviates positively from a correlation which is satisfactory for the other nucleophiles. This may be a consequence of concurrent elimination and substitution. A smoothed rate constant from the l.f.e.r. is reported here.

TABLE 4. Entropy[a] data for a series of methyl substrates reacting in water $T = 25$ °C

X	$S_g(CH_3X)$	$V(CH_3X)$[d]	$-\delta_s S(CH_3X)$	$\Delta S^{\ddagger}$[g]	$S^{\ddagger}$[h]	$S(X^-)$[i]
F	46.95	32.6	14.1[e]	−9.52	23.33	−2.3
Cl	49.62	42.5	17.3[e]	−4.77	27.55	13.16
Br	52.39	47.2	18.3[e]	−2.97	31.12	19.29
I	54.50	55.5	18.3[e]	0.58	36.76	26.14
NO_3	68.57[b]	58.2	19.6[d,f]	−1.90	47.06	35.00
ClO_4	73.10[c]	82.6	24.2[d,f]	0.91	49.78	43.20

[a]Entropy data in cal mol^{-1} deg^{-1}, standard state = 1 mol/l in both solution and gaseous phases, see ref. 23 for further details.
[b]Calculated from $S_g(HNO_3)$ (see ref. 25) and [7].
[c]Calculated from $S_g(HClO_4)$ (see ref. 26) and [7].
[d]Calculated from data in ref. 24.
[e]See ref. 23.
[f]Calculated from [8].
[g]Calculated from [3] and data in ref. 4 and this paper.
[h]Calculated from [5] and data in this paper.
[i]Data from ref. 27.

$$[8]\quad \delta_s S(CH_3X) = (-0.19 \pm 0.04)V(CH_3X) - (8.58 \pm 1.88)$$

where the quantity $V(CH_3X)$ is the "molecular volume" of the methyl compound. The quantity $V(CH_3X)$ can be readily calculated from data reported by Edward (24) and ourselves (23). The meanings of the other symbols in [7] and [8] require no further comment.

The general background to these calculations together with a collection of related data are given in ref. 23 and the numerical quantities relevant to the present study are reported in Table 4. For X = —F, —Cl, —Br, —I, —NO_3, and —ClO_4 the correlation between $S^{\ddagger}(CH_3X)$ and $S(X^-)$ is

$$[9]\quad S^{\ddagger}(CH_3X) = (0.64 \pm 0.06)S(X^-) + (21.71 \pm 1.50)$$

and a graphical representation of the relationship is given in Fig. 1. The correlation is considered satisfactory since the errors in $S^{\ddagger}(CH_3X)$ may be *ca.* ±3 e.u. These arise in part because the calculation of the entropies of activation for methyl fluoride and methyl nitrate require extrapolations remote from the temperature range of the experimental measurements (see ref. 4 and references therein). The slope of the correlation between $S^{\ddagger}$(MeX) and $S(X^-)$ may be related reasonably to the charge development ($Z^{\ddagger}$) in the transition state (23). If $S(X^-)$ is proportional to Z^2 then $Z^{\ddagger} = 0.80$,

Can. J. Chem. Downloaded from www.nrcresearchpress.com by 210.87.254.105 on 09/05/12
For personal use only.

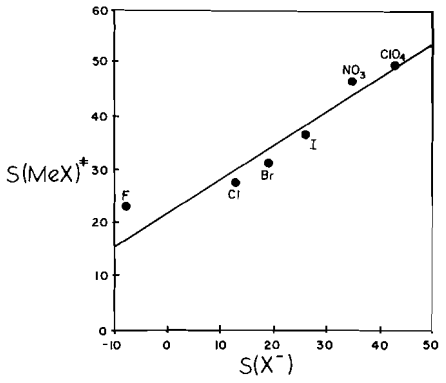

FIG. 1. A correlation between the entropy of the transition state with the entropy of the related anion.

or if $S(X^-)$ varies directly as Z then $Z^{\ddagger} = 0.64$. Further aspects of the interpretation of the slope of the $S^{\ddagger}(MeX)$ *vs.* $S(X^-)$ correlation have been discussed elsewhere (23, 28). Irrespective of how $S(X^-)$ depends on Z, the slope of the correlation will give a lower limit to $Z^{\ddagger}$. This is a consequence of the fact that the structure $CH_3^+(nH_2O)$ is associated with the anion in the transition state. Such a structure will exert a "ponderal effect" (29) on the entropy of the transition state. The ponderal increase to $S^{\ddagger}$-(MeX) will be most significant for the least massive anion. This may account in part for the positive deviation in the case of the fluoride ion – methyl fluoride point in Fig. 1, but the other reasons mentioned above are probably of equal importance. The previous conclusions with respect to $Z^{\ddagger}$ are now modified only to the extent that the range of $Z^{\ddagger}$ is either $0.64 < Z^{\ddagger} < 1$ or $0.80 < Z^{\ddagger} < 1$. Hence the entropies of activation lend support to an ion-pair mechanism for displacement reactions of the methyl halides, previously advanced (16) by one of us. For such a mechanism the quantity $S^{\ddagger}(CH_3X)$ will refer to the second transition state of the scheme.

$$[10] \qquad CH_3X \underset{k_2}{\overset{k_1}{\rightleftharpoons}} CH_3^+ X^- \xrightarrow{k_{2n}} \text{products}$$

Since the second step is relatively rapid (see ref. 16) the transition state for this step will, according to the Hammond postulate (30), resemble the intermediate. The Hammond postulate requires both the intermediate and the second transition state to have ionic character if the above interpretation of the relationship between $S^{\ddagger}(CH_3X)$ and $S(X^-)$ is acceptable.

The Heat Capacity of Activation

Since methyl perchlorate is the first perchlorate ester for which the heat capacity of activation has been measured, comparison is not possible. However, the value of the heat capacity of activation of methyl perchlorate derived from the temperature dependence of the rates is similar to that found for methyl iodide (13).

The perchlorate ion combines large size with the presence of oxygen atoms, and, like the nitrate ion, when fully charged, should be a "structure breaker". On the basis of arguments advanced by Robertson (4) this might lead to a more negative heat capacity of activation for perchlorate in comparison with iodide. That a more negative heat capacity of activation is not found might be interpreted as a reflection of less charge development in the case of the perchlorate. Such a notion would be consistent with the Hammond postulate (30) in the sense that methyl perchlorate, being the most reactive of the methyl esters, should have a transition state which most resembles the reactant molecule. However, the correlation between $S^{\ddagger}(CH_3X)$ and $S(X^-)$ discussed above strongly suggests activation leads to fairly uniform charge development[6] in the methyl compounds and the charge on the anion and cationic moieties in the transition state are close to unity.

Isotope Effects

Secondary hydrogen–deuterium isotope effects related to methyl and methyl-d_3 esters and halides have been reported frequently for both solvolytic (32) and definite bimolecular displacements (33–37). According to Shiner (38) these effects are related to the net change between initial and transition states of the force constants between the α C—H (or C—D) bond and the incoming and leaving groups. These effects can be usefully grouped in two ways. Firstly there are those effects in which the nucleophile (N) is fixed and the leaving group (X) is altered and secondly there are effects for which the nucleophile is varied in relation to a constant leaving

[6]Streitwieser (31) states that the Hammond postulate refers primarily to geometry, not charge distribution, and argues that for a given geometrical change a delocalized system will have a correspondingly greater charge separation. This may be true but the logic of the proposal is not obvious. Delocalization will be absent in the case of the halogens but may be important in the nitrate and perchlorate ions.

Can. J. Chem. Downloaded from www.nrcresearchpress.com by 210.87.254.105 on 09/05/12
For personal use only.

TABLE 5. Isotope effect and related data[a] for a series of primary compounds RX, $T = 25$ °C

	R	X	N	$-\log k_{0n}$	$\Delta G_{0n}^{\ddagger}$	$\log k_{2n}$	$\delta_1\Delta G^{\ddagger}$	$\Delta G_{2n}^{\ddagger}$	Reference
1	CH_3	F	H_2O	10.847	32.25	4.27	—	11.63	16, 4
2	CH_3	Cl	H_2O	9.364	30.22	0.61	19.9	16.61	32, 4
3	CH_3	Br	H_2O	8.135	28.55	0.09	23.8	17.33	32, 4
4	CH_3	I	H_2O	8.874	29.56	1.64	32.4	19.68	32, 4
5	CH_3	SO_3CH_3	H_2O	7.039	27.05	3.09	12.6	13.31	32, 4
6	CH_3	OSO_2OCH_3	H_2O	5.525	24.99	3.71	4.8	12.39	32, 4
7	CH_3	ClO_4	H_2O	4.504	23.60	4.29	16.5	11.60	This work
8	CH_3	NO_3	H_2O	10.343	31.56	0.88	21.6	16.25	32, 4
9	CH_3CH_2	Tosylate	H_2O	6.909	27.88	8.14	−12.00	6.35	39
10	CH_3	I	N_3^-	4.227	23.22	3.01	18.9	13.34	33
11	CH_3	I	I^-	3.308	21.96	3.93	8.94	12.09	34, 40
12	CH_3	I	CN^-	3.224	21.85	4.01	15.2	11.98	17, 35
13	CH_3	I	$S_2O_3^{2-}$	1.498	19.50	5.74	5.9	9.62	16, 36, 40
14	CH_3	I	CH_3COO^-	3.083	25.64	—	24.9	~15.76	33 (T=313.2 K)
15	CH_3	Br	$S_2O_3^{2-}$	1.483	19.47	6.75	6.0	8.25	37[b]
16	CH_3	SO_3CH_3	$S_2O_3^{2-}$	1.400	19.36	8.68	−11.5	5.61	37[b]

[a]Rate constants are all second order constants in the usual units. (See ref. 16.) $\Delta G_{0n}^{\ddagger}$, $\Delta G_{2n}^{\ddagger}$ are in kcal mol^{-1} and $\delta_1\Delta G^{\ddagger}$ is in cal mol^{-1}.
[b]Isotope effects in 50% v/v ethanol–water are more inverse by *ca.* 6% on the basis of a comparison of reaction 12 in water and the mixed aqueous solvent.

group. A collection of all the available data relevant to the present discussion is assembled in Table 5. The isotope effects are reported in terms of the quantity $\delta_1\Delta G^{\ddagger}$ which is related to the observed rate ratio $k(H)/k(D)$ and the temperature (T) by

$$[11] \quad \delta_1\Delta G^{\ddagger} = -\{2.3026\, RT/n\} \log \{k(H)/k(D)\}$$

The quantity n is the number of α-deuterium atoms in the deuterated substrate, three in the case of the methyl compounds and two in the case of the ethyl compounds. The range of reactivity displayed by the methyl compounds in Table 5 precludes the preferred situation in which all the isotope effects are measured and compared at a common temperature. Hopefully, the use of [11] to quantify the isotope effects will normalize any differences which are a consequence of temperature. The secondary isotope effects when combined with the correlation between $S^{\ddagger}$(MeX) and $S(X^-)$ and the kinetic solvent isotope effect (k.s.i.e.), $k(H_2O)/k(D_2O)$, provide considerable insight into the structure of the transition state for the displacement process.

The Hammond postulate[7] is a useful tool for relating the magnitude of the isotope effect to the structural characteristics of the transition state. Prior to the application of the Hammond postulate the statistical treatment used by Shiner must be translated into less formal chemical language. This necessity is accomplished readily by relating the isotope effect to the extent of bond making and bond breaking in the transition state.

When the nucleophile (N) is varied and the leaving group (X) is fixed the Hammond postulate requires that the extent of bond making will be the greatest for the weakest nucleophile (H_2O). Since the isotope effect for the attack of thiosulfate ion on methyl and methyl-d_3 iodide is inverse, and since thiosulfate ion is the most reactive nucleophile known towards the methyl halides (see Table 3), then nucleophiles weaker than thiosulfate are anticipated to give isotope effects which are more inverse than that observed for thiosulfate. The experimental results are in almost complete accordance with this simple prediction. Indeed, there is a smooth relationship (Fig. 2) between $\delta_1\Delta G^{\ddagger}$ and $\Delta G^{\ddagger}$ for methyl iodide and methyl-d_3 iodide reacting with water, azide, cyanide, acetate, and thiosulfate. However the symmetrical displacement

$$[12] \quad CL_3I + I^{*-} \rightarrow CL_3I^* + I^-$$

where L = H or D gives an isotope effect which is poorly correlated with the free energy of activation for the L = H process. The reasons for the deviant behavior of [12] are not clear. Since Seltzer and Zavitsas's (34) rate for the reaction (L = H, $T = 20$ °C) does not agree

[7]For a pithy version of the Hammond postulate see Schowen (ref. 42, p. 307).

Can. J. Chem. Downloaded from www.nrcresearchpress.com by 210.87.254.105 on 09/05/12
For personal use only.

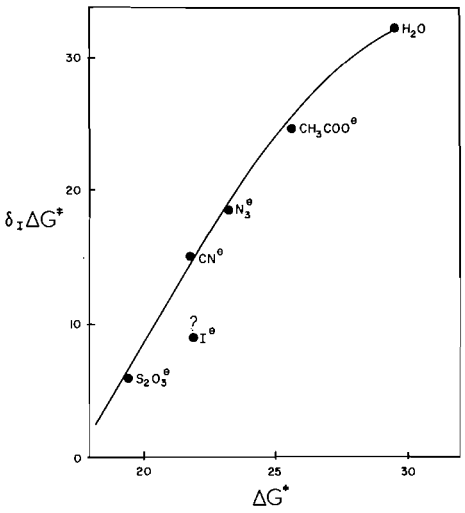

FIG. 2. A correlation of $\delta_I\Delta G^\ddagger$ *vs.* $\Delta G^\ddagger$ for a fixed leaving group.

with that calculated from the older measurements reported by Swart and le Roux (40) the more recent measurements may be in error. Combining Seltzer's rate for L = D with the L = H rate constant calculated from the Arrhenius parameters reported by Swart and le Roux gives an inverse effect, whereas Seltzer's own measurements give a normal effect which deviates from the correlation in Fig. 2 so much that it cannot be represented on the graph. Without new experimentation further discussion of the deviant behavior of [12] is unwarranted.

Whilst the relative degree of bond making in the reaction of a series of nucleophiles with a fixed methyl compound can be deduced from the Hammond postulate the extent of bond making for any particular nucleophile remains obscure. This question is usefully considered via the entropy correlation presented above. Displacement reactions at primary carbon centers are standard examples of S_N2 reactions. Such a reaction takes place by the Heitler–London mechanism with a parallelism (7) between the bond-making and bond-breaking processes, *i.e.*, bond making and bond breaking are concerted. The correlation between $S^\ddagger$(MeX) and $S(X^-)$, when water is the nucleophile, signifies substantial bond breaking for the weakest nucleophile which is presumably accompanied by considerable bond making, *i.e.*, the reaction of the methyl compounds with water is characterized by a product-like transition state.

The k.s.i.e., when examined for the substrates for which the solvolytic displacement rates and secondary isotope effects are known, suggest that the product-like description is inadequate when water is the nucleophile. Schowen (42), in a recent review of the $k(H_2O)/k(D_2O)$ ratios (43) considers the k.s.i.e. is consistent with S_N2 transition states which are only 20–30% "towards products". The conclusions from the k.s.i.e. are evidently in conflict with the entropy correlation. This disagreement can be resolved if the water molecule is postulated to attack a highly reactive ionic intermediate which can be described as a tight or intimate or contact ion pair. Since the intermediate is reactive the transition state related to its destruction will resemble the intermediate. This suggests that the transition state has little oxonium ion character, *i.e.*, resembles **1** rather than **2**

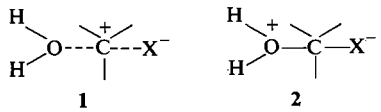

1 **2**

We now turn our attention once more to the secondary rather than the solvent isotope effects. For such the pre-equilibrium mechanism [10],

$$[13] \qquad \log k_0 = \log K_e + \log k_{2n}$$

If δ_I is an operator which denotes changes in the isotopic content of the substrate then

$$[14] \qquad \delta_I \log k_0 = \delta_I \log K_e + \delta_I \log k_{2n}$$

The variation of the isotope effect with the nature of the nucleophile N is established using the operator δ_N

$$[15] \qquad \delta_N\delta_I \log k_0 = \delta_N\delta_I \log K_e + \delta_N\delta_I \log k_{2n}$$

Since $\delta_N\delta_I \log K_e = 0$ then changes in the magnitude of the isotope effect for the fixed substrate variable N case are dominated by changes in the k_{2n} step. Thus, the ion-pair mechanism requires minor modification of our previous discussion of the fixed X variable N case in terms of a classical S_N2 displacement. The main difference between the descriptions is related to the bond-making step which now involves an ion pair rather than a neutral substrate.

In cases where the nucleophile is fixed and the substrate is altered the ion-pair mechanism provides a more convincing analysis of the

Can. J. Chem. Downloaded from www.nrcresearchpress.com by 210.87.254.105 on 09/05/12
For personal use only.

Can. J. Chem. Downloaded from www.nrcresearchpress.com by 210.87.254.105 on 09/05/12
For personal use only.

secondary isotope effect than the S_N2 unitary mechanism. For the fixed N variable X case the Hammond postulate becomes less reliable. This statement is particularly true for methyl perchlorate. According to the Hammond postulate methyl perchlorate involves the least amount of nucleophilic assistance since it is the most reactive methyl ester.[8] However only the halides have isotope effects which are more inverse, and, if Shiner's normalized isotope effects for methyl substrates are correct (38) then methyl perchlorate has the most inverse effect of all the methyl compounds so far investigated. The failure of the Hammond postulate in the case of methyl perchlorate provides an important mechanistic clue which can be understood in terms of the ion-pair mechanism.

When the leaving group is fixed and the nucleophile is altered the overall reactivity change depends only on the k_{2n} step since for a fixed substrate the quantity K_e is independent of the attacking nucleophile. However, alteration of the leaving group gives rise to simultaneous alteration of K_e and k_{2n}, and the overall rate consequently reflects both of these quantities, not just the k_{2n} step. If the k_{2n} step is the paramount factor in determining the isotope effect then a relationship between $\delta_I\Delta G^{\ddagger}$ and $\Delta G_{2n}{}^{\ddagger}$ is anticipated with the isotope effect becoming more inverse as the height of the k_{2n} barrier increases. The calculation of k_{2n} proceeds via the calculation of K_e using the expression

$$[16]\quad \log K_e = \frac{\rho_{nw}}{\rho_{nw} - \rho_{nI}} \log k_{0w} - \frac{\rho_{nI}}{\rho_{nw} - \rho_{nI}} \log k_{0I} + C$$

The quantities k_{0w} and k_{0I} are respectively the second order rate constants of the substrate with water and hydroxide ion, and C is a constant. The selectivity of the hydroxide ion ρ_{nI} is taken as unity and the best numerical value[9] for ρ_{nw} is $\rho_{nw} = (1.285 \pm 0.058)\rho_{nI}$.[10] These values differ from those reported previously. Because the newer values are based on a more extensive series of measurements,[11] they are to be preferred to those reported earlier (16). A more extensive discussion of the new quantities associated with [16] will appear elsewhere. The alteration of the numerical values appropriate to [16] requires no major revision with respect to the conclusions in an earlier presentation (13) although the k_{2n} values reported in that paper are increased and the K_e values decreased. The quantities required for these calculations are assembled in Table 3.

In Fig. 3 we present a correlation between $\delta_I\Delta G^{\ddagger}$ and $\Delta G_{2n}{}^{\ddagger}$ for all the primary centers for which data are available. The correlation is satisfactory and in the sense anticipated. The scatter observed may arise as a consequence of the diversity of temperatures at which the isotope effects were established. In contrast, the correlation (Fig. 4) between $\delta_I\Delta G^{\ddagger}$ and $\Delta G^{\ddagger}$, the free energy of activation for the overall rate of the hydrogen compound, is random apart from the series considered specifically in Fig. 2.

Kinetic isotope effects for a particular series of chemical reactions are manifestations of the degree of curvature of potential energy hypersurfaces in regions of the surface which define the reactants and transition states. In the present context, the Hammond postulate represents a very restrictive condition requiring that changes in the curvature between the appropriate turning points parallel the differences in free energies between the two equilibrium states defined by the turning points. Such intricate requirements suggest the correlation in Fig. 3 to be remarkable rather than merely satisfactory.

The above considerations also cast some light on a correlation between $k_0(H_2O)/k_0(OH^-)$ for a series of CH_3X compounds and the related isotope effect $k(CH_3X)/k(CD_3X)$ measured in water originally established by Hartman and Robertson (18). Although this correlation differs from that presented in Fig. 3 in several respects the differences are less important than the similarities. When water is the nucleophile [13] gives

[8]There are indications in the literature that methyl trifluoromethanesulfonate may be more reactive than methyl perchlorate but the appropriate measurements in water have not yet been reported.

[9]The former empirical relationship was (16)

$$[17]\quad \log k_{nw} = (1.51 \pm 0.13) \log k_{nI} - 5.97 \pm 0.22$$

whereas more extensive data (41) give

$$[18]\quad \log k_{nw} = (1.285 \pm 0.058) \log k_{nI} - 5.545 \pm 0.09$$

[10]Equation 16 is derived from [18] by eliminating k_{nw} and k_{nI} using the relationship between log K_e and k_{0w} and k_{0I} which is specified in [13] for n = l and n = w.

[11]J. M. W. Scott, unpublished results.

$$\log k_{0w} = \log K_e + \log k_{2nw}$$

or

[19] $$\log k_{2nw} = \log k_{0w} - \log K_e$$

Eliminating $\log K_e$ between [19] and [16] gives

[20] $$\log k_{2nw} = -\frac{\rho_{nw}}{\rho_{nl} - \rho_{nw}} \log \frac{k_{0l}}{k_{0w}} + C$$

Hence the rates of destruction of the ion-pairs in water (k_{2nw}) are related to the k_{0l}/k_{0w} rates and thus the correlation between the isotope effect and k_{0l}/k_{0w} is formally equivalent to the correlation in Fig. 3. The fact that log (k_{0l}/k_{0w}) = log k_{2nl}/k_{2nw} is obvious enough but the relationship represented by [20] is less so.

The above discussion indicates that α deuterium isotope effects associated with attack at primary centers are mainly influenced by the endothermicity of the k_{2n} step and in harmony with the Hammond postulate, become more inverse as the endothermicity of this step increases. Since the observed isotope effect contains $\delta_I \log K_e$ term, the empirical observations presented suggest that $\delta_X \delta_I \log K_e \simeq 0$, *i.e.*, the isotope effect on K_e is relatively insensitive to the nature of the leaving group. This conclusion appears to be in agreement with some theoretical calculations reported by Stern and Wolfsberg (44, 45) in which the $K_e(H)/K_e(D)$ ratio for the stretching of the C—X bond in CD_3X and CH_3X to what might be termed a contact ion pair, seems relatively insensitive to the nature of X and also gives a normal effect. In contrast, the extension of the theoretical calculations to S_N2-like transition states gives inverse effects which are much larger (more inverse) than those observed experimentally. Stern and Wolfsberg (44, 45) point out that adjustments of the force constants can be made to accommodate the model to experiment. If the ion-pair description for these reactions is valid and if the isotope on the ratio $K_e(H)/K_e(D)$ is the same as the theoretical value then the small (less inverse) $k_{2n}(H)/k_{2n}(D)$ must relate to the force constants of the second transition state of the ion-pair displacement mechanism (eq. 13). If binding between the nucleophile and the leaving group is weak the transition state will be "looser" with respect to the methyl out-of-plane bending vibration. This will produce an isotope effect which is either less inverse or possibly normal.

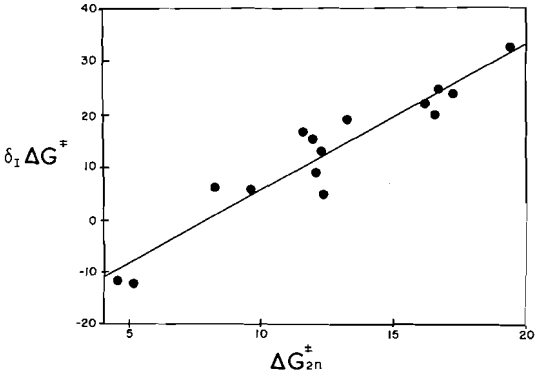

FIG. 3. A correlation of $\delta_I \Delta G^{\neq}$ and $\Delta G_{2n}{}^{\neq}$ for a series of displacement reactions.

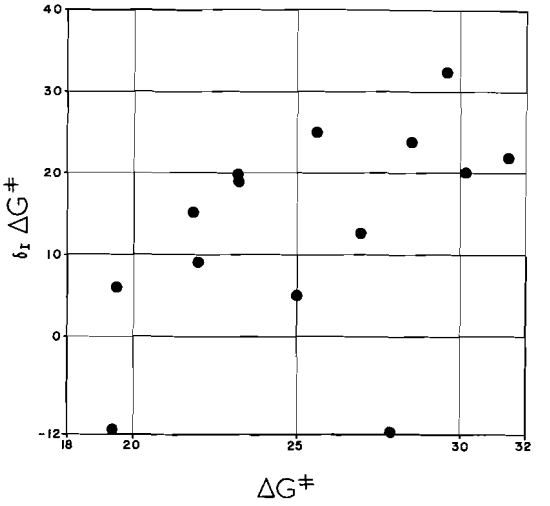

FIG. 4. An attempted correlation between $\delta_I \Delta G^{\neq}$ and $\Delta G^{\neq}$ for a series of substitution reactions.

The contact ion-pair mechanism thus offers a satisfactory account of the entropy correlation, the k.s.i.e. and the secondary isotope effects whereas the classical S_N2 description provides fewer insights. The above evidence also repudiates some recent criticisms by Abraham (46, 47) which are based on a crude thermochemical calculation and which make no attempt to explain the complexities of these reactions (see ref. 16). We believe that the results presented in this paper cannot be understood in terms of a unitary S_N2 displacement.

The authors wish to thank the National Research Council of Canada for partly defraying the cost of this work.

Can. J. Chem. Downloaded from www.nrcresearchpress.com by 210.87.254.105 on 09/05/12
For personal use only.

1. J. KOSKIKALLIO. Suom. Kemistil. B, **40**, 199 (1967).
2. J. KOSKIKALLIO. Acta Chem. Scand. **23**, 1477 (1969).
3. J. KOSKIKALLIO. Suom. Kemistil. B, **34**, 92 (1969).
4. R. E. ROBERTSON. *In* Progress in physical organic chemistry, Vol 4. *Edited by* A. Streitwieser, Jr. and R. Taft. Interscience, John Wiley, 1967. p. 213.
5. L. SCHALEGER and F. A. LONG. Advances in physical organic chemistry, Vol. 1. *Edited by* V. Gold. 1963. p. 1.
6. J. M. W. SCOTT and J. G. WINTER. Can. J. Chem. **46**, 2887 (1968).
7. C. K. INGOLD. Structure and mechanism in organic chemistry, 2nd ed. Cornell University Press. Ithaca, New York. 1969. Chapt. 7.
8. C. G. SWAIN and C. B. SCOTT. J. Am. Chem. Soc. **75**, 141 (1953).
9. E. GRUNWALD and S. WINSTEIN. J. Am. Chem. Soc. **70**, 846 (1948).
10. D. N. KEVILL and B. SHEN. Chem. Ind. London, 1466 (1971).
11. N. V. SIDGWICK. Chemical elements and their compounds. Oxford University Press, London. 1950. pp. 1235, 1236.
12. J. MEYER and W. SPORMANN. Z. Anorg. Chem. **228**, 341 (1936).
13. R. C. HEPPOLETTE and R. E. ROBERTSON. Proc. R. Soc. London, A**252**, 273 (1959).
14. R. E. ROBERTSON and S. SUGAMORI. J. Am. Chem. Soc. **91**, 7254 (1969).
15. D. N. KEVILL. Petroleum research fund, abstracts of research, Vol. 15, 1970. p. 139.
16. J. M. W. SCOTT. Can. J. Chem. **48**, 3807 (1970).
17. E. A. MOELWYN HUGHES. Chemical statics and kinetics of solutions. Academic Press, London and New York. 1971. Chapt. 8.
18. S. HARTMAN and R. E. ROBERTSON. Can. J. Chem. **38**, 2033 (1960).
19. S. JOKINEN, E. LUKKONEN, J. RUOSTESUO, J. VIRTANEN, and J. KOSKIKALLIO. Acta Chem. Scand. **25**, 3367 (1971).
20. R. E. DAVIS, R. NEHRING, W. J. BLUME, and C. R. CHUANG. J. Am. Chem. Soc. **91**, 91 (1969).
21. H. M. R. HOFFMANN. J. Chem. Soc. 6762 (1965).
22. J. KOSKIKALLIO. Acta Chem. Scand. **26**, 2101 (1972).
23. R. L. HEPPOLETTE, R. E. ROBERTSON, and J. M. W. SCOTT. Can. J. Chem. **37**, 803 (1959).
24. J. T. EDWARD. J. Chem. Ed. **47**, 261 (1970).
25. Selected values of thermodynamic properties. Circ. 500. National Bureau of Standards. 1952.
26. J. G. TROWBRIDGE and E. F. WESTRUM. J. Phys. Chem. **68**, 42 (1964).
27. V. P. VASIL'EV, E. K. ZOLOTAREV, A. F. KAPUSTINSKII, K. P. MISHCHENKO, E. A. PODGORNAYA, and K. B. YATSIMIRSKI. Russ. J. Phys. Chem. **34**, 840 (1960).
28. R. E. ROBERTSON and J. M. W. SCOTT. J. Chem. Soc. 1596 (1961).
29. C. K. INGOLD. Q. Rev. **11**, 1 (1957).
30. G. HAMMOND. J. Am. Chem. Soc. **77**, 334 (1955).
31. A. STREITWIESER, JR. Solvolytic displacement reactions. McGraw-Hill Book Co., New York, N.Y. 1962.
32. J. A. LLEWELLYN, R. E. ROBERTSON, and J. M. W. SCOTT. Can. J. Chem. **38**, 222 (1960).
33. A. V. WILLI and C. M. WON. J. Phys. Chem. **76**, 427 (1972).
34. S. SELTZER and A. A. ZAVITSAS. Can. J. Chem. **45**, 2023 (1967).
35. A. V. WILLI and C. M. WON. J. Am. Chem. Soc. **90**, 5999 (1968).
36. A. V. WILLI and C. M. WON. Can. J. Chem. **48**, 1452 (1970).
37. K. T. LEFFEK and G. E. JACKSON. Can. J. Chem. **47**, 1537 (1969).
38. V. J. SHINER. *In* Isotope effects in chemical reactions. *Edited by* C. J. Collins and W. S. Bowman. Van Nostrand-Rheinhold Co., New York. 1970.
39. K. T. LEFFEK, J. A. LLEWELLYN, and R. E. ROBERTSON. Can. J. Chem. **38**, 1505 (1960).
40. E. R. SWART and L. J. LE ROUX. J. Chem. Soc. 406 (1957).
41. R. A. HASTY and S. SUTTER. Can. J. Chem. **47**, 4537 (1969).
42. R. SCHOWEN. *In* Progress in physical organic chemistry, Vol. 9. *Edited by* A. J. Streitwieser, Jr. 1972. p. 275.
43. R. E. ROBERTSON and P. M. LAUGHTON. Solvent solute interactions. *Edited by* C. D. Ritchie and J. F. Coetzee. Marcel Dekker, New York and London. 1969.
44. M. J. STERN and M. WOLFSBERG. Pure Appl. Chem. **8**, 225 (1964).
45. M. J. STERN and M. WOLFSBERG. Pure Appl. Chem. **8**, 325 (1964).
46. M. H. ABRAHAM. J. Chem. Soc. 1893 (1973).
47. M. H. ABRAHAM. Chem. Commun. 51 (1973).

Can. J. Chem. Downloaded from www.nrcresearchpress.com by 210.87.254.105 on 09/05/12
For personal use only.

Formation Cross Sections of Iodine and Tellurium Isomers Produced in the Fission of ^{238}U by Protons of Energies 30–85 MeV[1,2]

M. DIKŠIĆ AND L. YAFFE

Department of Chemistry, McGill University, Montreal, Quebec H3C 3G1

Received February 26, 1975

M. DIKŠIĆ and L. YAFFE. Can. J. Chem. **53**, 3116 (1975).

Formation cross sections of isomers of ^{130}I, ^{132}I, ^{134}I, ^{131}Te, and ^{133}Te have been obtained from the fission of natural uranium by protons of energies 30–85 MeV. The high-spin isomer is favored in the production and increase in bombarding energy favors the production of the high-spin isomer. From the isomer ratios values of $(\overline{J^2})^{1/2}$, the root-mean-square angular momentum, were obtained. These increase with increasing bombarding energy.

M. DIKŠIĆ et L. YAFFE. Can. J. Chem. **53**, 3116 (1975).

On a obtenu la section efficace de formation des isomères de ^{130}I, ^{132}I, ^{134}I, ^{131}Te et ^{133}Te à partir de la fission de l'uranium naturel par des protons d'énergie 30–85 MeV. L'isomère à spin élevé est favorisé lors de la production et une augmentation de l'énergie de bombardement favorise la formation de l'isomère de haut spin. On a obtenu les moments angulaires quadratiques moyens $(\overline{J^2})^{1/2}$ à partir des rapports des valeurs. Ceux-ci augmentent lorsque l'on augmente l'énergie de bombardement.

[Traduit par le journal]

Introduction

A knowledge of formation cross sections of isomers and their ratios is intrinsically important. In addition, however, light may be cast upon the mechanism of the fission process itself by using the ratios to obtain information about the distribution of the angular momentum of the fragments after scission. At this point in the fission process the nucleus is greatly deformed and finally divides into the two fragments. A knowledge of the dynamics of these nascent fragments is very important, particularly since recent theoretical calculations (1) have used such data to derive information about the fission process using a two-dimensional deformed harmonic oscillator for the description of the nuclear fission process. Several theoretical studies (2, 3) do attempt to predict the angular momentum of the fragments but, unfortunately at the present time, insufficient experimental data have been derived in order to test the validity of the models. Theoretical attempts to derive ratios of production cross sections of the metastable and ground state isomers, σ_m and σ_g respectively, suffer from too many adjustable parameters.

Some experimental isomer ratios for various nuclei and various fissioning systems have been measured (4–6) in our laboratory, and an energy-dependent calculation was developed for the calculation of isomer ratios formed in fission in the proton bombarding-energy range of 30–85 MeV. The calculation was based on the formalism of Huizenga and Vandenbosch (7). A calculation based on the same formalism has been made for ^{115}Cd and ^{134}Cs isomers in several fissioning systems by Loveland and Shum (8). In all of these calculations the root-mean-square angular momentum, $(\overline{J^2})^{1/2}$, was adjusted until the calculated ratio agreed with that determined experimentally.

In this paper are reported isomer ratios for ^{130}I, ^{132}I, and ^{134}I, as well as the independent cross sections for both isomers in the fission of ^{238}U with protons in the energy range 30–85 MeV. Isomeric ratios for ^{131}Te and ^{133}Te isomers are reported, based on earlier data by Dikšić *et al.* (9).

Experimental

Experimental procedures have been reported in detail elsewhere (9, 10) and only a very brief description is given here.

Uranium metal foil or uranyl nitrate was irradiated for periods ranging from 1–5 min in the internal circulating beam of the McGill proton synchrocyclotron. Different energies of irradiation were obtained by placing the targets at various radii.

[1]This paper is dedicated to Professor C. A. Winkler of McGill University on the occasion of his sixty-fifth birthday by one of his colleagues (L.Y.).

[2]With financial assistance from the National Research Council of Canada.

Can. J. Chem. Downloaded from www.nrcresearchpress.com by 210.87.254.105 on 09/05/12
For personal use only.

Can. J. Chem. Downloaded from www.nrcresearchpress.com by 210.87.254.105 on 09/05/12
For personal use only.

The fission-produced iodine was chemically separated and converted to silver iodide for the activity measurements. These were done with a 30 cc Ge(Li) detector coupled to a 4096-channel pulse-height analyzer. The resolution of the system was 2.8 keV at 1.33 MeV. The net peak areas were computed using a computer code which subtracted a straight-line background. The resultant decay curves were resolved into their various components by use of the CLSQ least squares computer program (11).

The isomer ratios, σ_m/σ_g, were calculated by using the count rates under several full-energy peaks, except for ^{134}I where the independent cross-section for ^{134m}I was calculated. In addition, values of $\sigma_m + \sigma_g$ were obtained, thus enabling one to obtain values of σ_m and σ_g.

Errors in isomeric ratios for the iodine isomers then arise only from small uncertainties in the measured activities. No errors due to uncertainties in the half-lives were included in the case of the iodine isotopes. These would be of the order of 2–3%. Total errors, however, in the determination of the Te isomers are reported.

Results

In Table 1 are given the cross sections for the metastable and ground states. From these the isomeric ratios, σ_H/σ_T, have been calculated where H refers to the high-spin isomer and T the total. Because of the repeated determinations and the relatively high production yields at these bombarding energies it was possible to determine the half-lives very accurately: ^{130m}I = 8.9 ± 0.2 min, ^{132m}I = 83.6 ± 0.1 min, ^{134m}I = 3.8 ± 0.1 min.

Values for ^{130m}I and ^{134m}I agree well with presently-accepted values of 9.2 min (12) and 3.56 min (13) respectively, while as yet there has only been published (10) the above value for ^{132m}I.

Treatment of Results

The theoretical cross section ratios were calculated using the Huizenga–Vandenbosch formalism (7) adapted for fission by Saha and Yaffe (4).

In the present calculations it was assumed that each fragment has an initial spin distribution of form (14)

$$[1] \quad N(J_i) = (2J_i + 1) \exp [-J_i(J_i + 1)/2b^2]$$

where $(\overline{J^2})^{1/2}$, the root-mean-square angular momentum of the primary fragment, is given by

$$[2] \quad (\overline{J^2})^{1/2} = 2^{1/2}b$$

The parameter b is adjustable and was varied until the best fit, between experimental and theoretical results, was obtained. The energy of the emitted neutrons was taken as $2T$ (4), where T is the nuclear temperature of the residual nucleus. The average excitation energy removed by each emitted neutron is $B_n + 2T + \delta$, where B_n is the neutron binding energy (21) and δ is the pairing energy (15). The relationship (16) between nuclear temperature and excitation energy, U, is given by

$$[3] \quad E = aT^2 - 4T$$

where a is the level-density parameter, taken (17) equal to $A/10$ MeV^{-1}, A being the fragment mass number.

The excitation of a nucleus undergoing fission was calculated as previously described (9) using the VEGAS calculation (18, 19) and a Monte Carlo evaporation code (20). The excitation energy of the two primary fragments was estimated using eq. 5 in the Saha–Yaffe calculation (4). Mass excesses and the average total kinetic energy of the complementary primary fragments have been taken from refs. 21 and 22 respectively. The simple assumption was made that the excitation energy of the fissioning nucleus would divide itself in proportion to the masses of the complementary primary fragments (4).

The average γ energy (16), $\bar{E}_\gamma$, and the number of γ-rays (23), N_γ, emitted in the last stage of de-excitation were estimated by

$$[4] \quad \bar{E}_\gamma = 4[(E/a) - (5/a^2)] \text{ MeV}$$

and

$$[5] \quad N_\gamma = (aE)^{1/2}/(L + 1)$$

where E is the excitation energy and L is the multipolarity of the γ-rays. All γ-rays were assumed to be dipolar (7). The transmission coefficients, $T_l(E_n)$, for neutrons used in this calculation were computed for a diffuse-edge, surface-absorption potential according to Bjorklund and Fernback (24), using Auerbach's ABACUS-2 code (25).

The formalism of Huizenga and Vandenbosch (7) and code of Hafner *et al.* (26) were used to calculate the spin distribution after the emission of neutrons and γ-rays. New values of the spin cut-off parameters, σ_n and σ_γ, were entered into the calculation after the emission of each neutron and γ-ray, from the relationships (26, 27) $\sigma_n^2 = I_R t/\hbar^2$ and $\sigma_\gamma^2 = I_{eff} t/\hbar^2$, where I_R and I_{eff} are the rigid body and effective moments of inertia, respectively, and t is the thermodynamic

Can. J. Chem. Downloaded from www.nrcresearchpress.com by 210.87.254.105 on 09/05/12
For personal use only.

TABLE 1. Independent formation cross section (mb) of some iodine and tellurium isotopes and their isomeric ratios*

Proton energy (MeV)	^{130}I			^{132}I			^{134}I			^{131}Te	^{133}Te
	σ_m	σ_g	σ_H/σ_T*	σ_m	σ_g	σ_H/σ_T	σ_m	σ_g	σ_H/σ_T	σ_H/σ_T	σ_H/σ_T
30	0.74±0.10	3.2 ±0.3	0.81±0.03	6.3±1.2	3.1±0.6	0.67±0.03	13.9±0.9	7.5±0.7	0.65±0.07	0.82±0.06	0.69±0.07
40	0.97±0.10	8.0 ±1.0	0.89±0.04	12.8±2.5	5.2±1.0	0.71±0.04	15.8±1.1	7.8±0.8	0.67±0.07	0.83±0.08	0.84±0.07
50	1.55±0.2	17.0 ±1.3	0.92±0.04	23.0±4.4	5.0±1.0	0.82±0.05	13.2±0.8	5.9±1.1	0.69±0.06	0.86±0.06	0.88±0.06
60	0.95±0.06	18.0 ±1.6	0.95±0.03	21.6±4.1	6.8±1.2	0.76±0.04	13.8±1.1	10.4±1.1	0.57±0.07	0.84±0.07	0.96+0.02 −0.08
70	0.81±0.06	19.06±2.0	0.96±0.04	18.4±3.7	9.0±1.8	0.67±0.05	13.7±1.1	8.4±0.8	0.62±0.07	0.83±0.07	0.97+0.02 −0.07
85	0.98±0.1	17.08±1.6	0.95±0.04	18.0±3.0	5.0±0.9	0.78±0.04	11.3±0.9	8.2±0.8	0.58±0.07	0.84±0.07	0.98+0.01 −0.07

*$\sigma_T = \sigma_m + \sigma_g$, σ_H = high-spin isomer.

Can. J. Chem. Downloaded from www.nrcresearchpress.com by 210.87.254.105 on 09/05/12
For personal use only.

temperature (27), related to the excitation energy E, by $E = at^2 - t$. Dudey and Sugihara (28) have pointed out that, for $E < 10$ MeV, $I_{eff} < I_R$. Ericson (27) and Lang (33) have shown that the moment of inertia increases with increasing excitation energy and approaches the rigid body value as an upper limit. Since neutron emission takes place in the high excitation region, $E > 10$ MeV, we used the above relation for the determination of σ_n. The rigid body moment of inertia of the fragment was computed from $I_R = \frac{2}{5}(MAR^2)$, where M is the nuclear mass, and the nuclear radius $R = r_0A^{1/3}$ where r_0, the radius parameter, was taken to be 1.2×10^{-13} cm. The ratio (for excitation energies less than 10 MeV) of I_{eff}/I_R used was 0.6 to calculate σ_γ. This was not varied, since b was used as an adjustable parameter.

The assumptions were made that the final fragment spin distribution was divided between the isomeric states, and that the transition to any state involves the lowest spin change. In the event of a transition which involved equal spin change to either state, equal population of both states has been assumed. Values of $(\overline{J^2})^{1/2}$ are given in Table 2.

Discussion

It is very difficult to investigate the effects of the various parameters on the final cross-section ratios, since these represent averages resulting from many different primary fragments, which depend on the excitation energy and its division between the fragments, the kinetic energies of the fragments, the nature of the fissioning system, etc.

Various investigators have analyzed isomer ratios in different fissioning systems to obtain values of $(\overline{J^2})^{1/2}$ and some examples are given below. Sarantites *et al.* (29), for thermal fission of ^{235}U obtained a value of 6 $\hbar$ for isomers of ^{131}Te and ^{133}Te. Saha and Yaffe (4) reported values of 11–16 $\hbar$ for ^{134}Cs isomers in the fission of ^{239}Pu with protons of energies 30–85 MeV. Hoffman (30) calculated an average angular momentum of the fragments for thermal neutron fission of ^{233}U, ^{235}U, and ^{239}Pu, using a torque on uniformly charged bodies to simulate fragments in the latter stages of the fission process and obtained values of 5–6 $\hbar$ for each fragment. Using γ-ray anisotropies as an indicator for quadrupole transitions he found an average angular momentum of $7 \pm 2\hbar$. The fragment angular momentum deduced from γ-ray angular momentum correlation measurements is an average over all fragment masses. He proposed, as did Strutinski (31) earlier, that angular momentum is generated in the fission process.

Loveland and Shum (8) who, as discussed earlier, had investigated fission fragment angular momenta for ^{134}Cs and ^{115}Cd from several fissioning systems had concluded that the fragment angular momentum did not correlate with the compound nucleus angular momentum. They suggested that an increase of fragment angular momentum occurred with decreasing values of Z and A of the fissioning system.

An increase of fragment angular momentum with increasing bombarding energy has been found by several workers (4–6, 8, 32).

From Table 1 in this paper it is clear that, with the possible exception of ^{134}I, the isomers with high spin are favored, and the fraction of total cross section appearing in the high-spin portion increases with increasing bombarding energy. Isomers of ^{134}I may be being influenced by neighboring shells. Theoretical values for $(\overline{J^2})^{1/2}$ vary from 10–11 $\hbar$ at 30 MeV to 16–17 $\hbar$ at 85 MeV, except for ^{131}Te and ^{134}I which do not show as great an increase with increasing bombarding energy. In general these values agree with those found previously (4–6) in the same energy range for fission of ^{233}U and ^{239}Pu, using the same assumptions. However, it should once again be emphasized that the absolute values of the angular momenta of the fragments are still uncertain because of the lack of detailed knowledge about the de-excitation cascade, energy division between fragments, etc.

Nevertheless, it can be concluded that the fragment angular momenta in medium-energy

TABLE 2. Values of root-mean-square angular momentum

Fragment*	$(\overline{J^2})^{1/2}$† (units of $\hbar$)
^{130}I(5^-,2^+)	10–16
^{132}I(5^+,8^-)	11–17
^{134}I(5^+,8^-)	11–13
^{131}Te($3/2^+$,$11/2^-$)	10–11
^{133}Te($3/2^+$,$11/2^-$)	8.5–17

*The numbers in parentheses are the spins used for theoretical calculation of the isomeric cross-section ratios.

†The initial primary-fragment angular momentum which gave agreement between the theoretical and experimental results in the proton energy region 30–85 MeV; the first gave the best fit at 30 and the second one at 85 MeV protons.

fission are higher than those observed in low-energy fission. As the bombarding energy increases, the higher-spin isomer is preferentially populated. On the basis of the ^{134}Cs data, no difference can be seen if one compares these data with the fission of ^{233}U (6), ^{235}U (6), and ^{239}Pu (4), showing very little influence of these fissioning systems on the fragment angular momenta.

The authors acknowledge with thanks the ready co-operation of Dr. S. K. T. Mark, Director of the Foster Radiation Laboratory, with regard to the irradiations performed in connection with this work.

1. P. Holzer, U. Mosel, and W. Greiner. Nucl. Phys. A**138**, 241 (1969).
2. J. R. Nix and W. J. Swiatecki. Nucl. Phys. **71**, 1 (1964).
3. J. O. Rasmussen, W. Nörenberg, and H. J. Mang. Nucl. Phys. A**136**, 465 (1969).
4. G. B. Saha and L. Yaffe. J. Inorg. Nucl. Chem. **31**, 1891 (1969).
5. J. H. Forster and L. Yaffe. Can. J. Chem. **46**, 1763 (1968).
6. G. B. Saha, I. Tomita, and L. Yaffe. J. Inorg. Nucl. Chem. **31**, 3731 (1969).
7. J. R. Huizenga and R. Vandenbosch. Phys. Rev. **120**, 1305 (1960).
8. W. D. Loveland and Y. S. Shum. Phys. Rev. C**4**, 2282 (1971).
9. M. Dikšić, D. K. McMillan, and L. Yaffe. J. Inorg. Nucl. Chem. **36**, 7 (1974).
10. M. Dikšić, L. Yaffe, and D. G. Sarantites. Phys. Rev. **10**C, 1172 (1974).
11. J. B. Cumming. Application of computers to nuclear and radiochemistry, National Academy of Science – National Research Council Nucl. Sci. Series No. NAS-NS-3107, 1962. p. 25.
12. D. D. Wilkey and J. E. Willard. J. Chem. Phys. **44**, 970 (1966).
13. C. D. Coryell, H. N. Erten, P. K. Hopke, W. B. Walters, R. Dams, and H. C. Griffin. Nucl. Phys. A**179**, 689 (1972).
14. H. Warhanek, and R. Vandenbosch. J. Inorg. Nucl. Chem. **26**, 669 (1964).
15. A. G. W. Cameron. Can. J. Phys. **36**, 1040 (1958).
16. H. K. Vonach, R. Vandenbosch, and J. R. Huizenga. Nucl. Phys. **60**, 70 (1964).
17. C. T. Bishop. Argonne National Laboratory Report ANL-6405. 1961.
18. N. Metropolis, R. Bivins, M. Storm, A. Turkevich, J. M. Miller, and G. Friedlander. Phys. Rev. **110**, 185 (1958).
19. K. Chen, Z. Fraenkel, G. Friedlander, J. R. Grover, J. M. Miller, and Y. Shimamoto. Phys. Rev. **166**, 949 (1968).
20. I. Dostrovsky, Z. Fraenkel, and P. Rabinowitz. Proceedings of the 2nd International Conference on the Peaceful Uses of Atomic Energy, Vol. 15, UN, Geneva. 1958. p. 301.
21. W. D. Myers and W. J. Swiatecki. University of California Radiation Laboratory, Report UCRL-11980. 1965.
22. J. C. D. Milton and J. S. Fraser. Can. J. Phys. **40**, 1626 (1962).
23. V. M. Strutinsky, L. V. Groshev, and M. K. Akimova. Nucl. Phys. **16**, 657 (1960).
24. F. Bjorklund and S. Fernbach. Phys. Rev. **109**, 1295 (1958).
25. E. H. Auerbach. ABACUS-2, Brookhaven National Laboratory, BNL-6562. 1962.
26. W. L. Hafner, J. R. Huizenga, and R. Vandenbosch. Argonne National Laboratory Report ANL-6662, 1962.
27. T. Ericson. Adv. Phys. **9**, 425 (1960).
28. N. D. Dudey and T. T. Sugihara. Phys. Rev. **139**, B896 (1965).
29. D. G. Sarantites, G. E. Gordon, and C. D. Coryell. Phys. Rev. **138**, B353 (1965).
30. M. M. Hoffman. Phys. Rev. **133**B, 714 (1964).
31. V. M. Strutinski. J. Exp. Theor. Phys. **10**, 613 (1960).
32. C. Rudy, R. Vandenbosch, and C. T. Ratcliffe. J. Inorg. Nucl. Chem. **30**, 365 (1968).
33. L. W. Lang. Nucl. Phys. **42**, 353 (1963).

Can. J. Chem. Downloaded from www.nrcresearchpress.com by 210.87.254.105 on 09/05/12
For personal use only.

Ligand Field Photochemistry of Cobalt(III) Phenanthroline and Bipyridyl Complexes

CAROL P. J. VUIK, NOEL A. P. KANE-MAGUIRE, AND COOPER H. LANGFORD[1]

Chemistry Department, Carleton University, Ottawa, Canada K1S 5B6

Received April 3, 1975

CAROL P. J. VUIK, NOEL A. P. KANE-MAGUIRE, and COOPER H. LANGFORD. Can. J. Chem. **53**, 3121 (1975).

The ligand field photochemistry of $Cophen_2C_2O_4^+$, $Cobipy_2C_2O_4^+$, and of $Cophen_3^{3+}$ in the presence of added oxalate has been investigated. In all cases reduction to cobalt(II) complexes occurs with moderate quantum yields (>0.01). The nature of the reactive excited states is discussed, as is the mechanism of the $Cophen_3^{3+}$–oxalate photoreaction.

CAROL P. J. VUIK, NOEL A. P. KANE-MAGUIRE et COOPER H. LANGFORD. Can. J. Chem. **53**, 3121 (1975).

On a examiné la photochimie de ligand de champ des $Cophen_2C_2O_4^+$, $Cobipy_2C_2O_4^+$ et $Cophen_3^{3+}$ en présence d'oxalate additionné. Dans tous les cas, il y a une réduction aux complexes du Co(II) qui se produit avec des rendements quantiques modérés (>0.01). On discute de la nature des états excités réactifs de même que du mécanisme de la photoréaction entre du $Cophen_3^{3+}$ et l'oxalate.

[Traduit par le journal]

Introduction

The ligand field (l.f.) photochemistry of cobalt(III) complexes, so far as it is known, exhibits two major types of behavior. The very strong field $Co(CN)_6^{3-}$ and $Co(CN)_5OH_2^{2-}$ complexes undergo cyanide aquation with high quantum yields (1) while the weaker field amine complexes undergo photosubstitution with very low quantum yields (2). (A puzzling exception to this generalization is the report (3) that on irradiation at 520 nm $Co(NH_3)_5N_3^{2+}$ loses ammonia with a quantum yield of 0.2.) The low quantum yields found for simple amines have been ascribed by several authors (4) to high rates of relaxation to the $^1A_{1g}$ ground state from the $^1T_{1g}$ or $^3T_{1g}$ excited states considered responsible for photoreaction. However, there is some evidence against this hypothesis. In the presence of $Fe(CN)_6^{4-}$, l.f. irradiation of $Coen_3^{3+}$ gives a red product, apparently via intermediate formation of $Coen_3^{2+}$ and $Fe(CN)_6^{3-}$; the quantum yield for this reaction is 0.2 (5). This suggests that not only can the primary quantum yield for a cobalt(III) complex be relatively high, but also that if a suitable reducing agent is present, the predominant photoreaction following this Co(III) l.f. excitation is reduction, not substitution.

It has been reported (6) that on irradiation with sunlight, neutral solutions of both $Cophen_2C_2O_4^+$ and $Cobipy_2C_2O_4^+$ (phen = 1,10-phenanthroline and bipy = 2,2′-dipyridyl) deposit pink–orange, paramagnetic materials, presumably containing Co(II). The possibility of observing photoreduction on irradiation of l.f. bands, without adding an external reducing agent, prompted an investigation of these complexes using precisely defined wavelengths from laser sources to populate l.f. states.

Experimental

Synthesis of Complexes and Spectra

$[Cophen_3](ClO_4)_3.3H_2O$ was prepared by the method of Gorton and co-workers (7) and characterized by elemental analysis.

Anal. Calcd. for $C_{36}H_{30}N_6O_{15}Cl_3Co$: C, 45.42; H, 3.18; N, 8.83. Found: C, 45.74; H, 3.31; N, 8.91.

$[Co(bipy)_2C_2O_4]I.H_2O$ and $Cophen_2C_2O_4I.H_2O$ were prepared by the method of Broomhead and Kane-Maguire (6), and converted to solutions of the chloride salts by metathesis with silver chloride. $[Cophen_2C_2O_4]Cl.4H_2O$ was isolated from such a solution by adding saturated sodium chloride and keeping at 0 °C for 24 h. It was characterized by elemental analysis.

Anal. Calcd. for $C_{26}H_{24}N_4O_8ClCo$: C, 50.79; H, 3.93; N, 9.11. Found: C, 50.58; H, 4.23; N, 9.27.

An attempt to isolate the chloride salt of $Cobipy_2C_2O_4^+$ in the same way failed due to the greater solubility of this salt. All experiments involving this complex were accordingly carried out using the $Cobipy_2C_2O_4^+$ solution which contained excess sodium chloride.

The pink precipitate formed on photolyzing $Cophen_2C_2O_4^+$ in neutral solution was identified as the stoichiometric composition $[CophenC_2O_4]^0$.

[1]To whom correspondence should be addressed.

Can. J. Chem. Downloaded from www.nrcresearchpress.com by 210.87.254.105 on 09/05/12
For personal use only.

Can. J. Chem. Downloaded from www.nrcresearchpress.com by 210.87.254.105 on 09/05/12
For personal use only.

Anal. Calcd. for $C_{14}H_8N_2O_4Co$: C, 51.4; H, 2.45; N, 8.56; Co, 17.9. Found: C, 51.75; H, 2.40; N, 8.53; Co (as Co(II)), 15.30.

Spectra of the phenanthroline and bipyridyl complexes used in this study were either recorded on a Cary 14 spectrophotometer, or plotted manually using a Gilford 240 spectrophotometer. Resolution of the visible spectra into Gaussian components was performed with a DuPont curve analyzer on spectra of absorbance plotted against frequency.

Photochemistry

The stoichiometry of the photolysis of $Cophen_2C_2O_4^+$ was determined by photolyzing a degassed aliquot of $Cophen_2C_2O_4^+$ solution with a 150 W tungsten reflector spot lamp. The carbon dioxide produced was determined manometrically using an apparatus which had been calibrated using carbon dioxide produced by photolyzing $Fe(C_2O_4)_3^{3-}$. For neutral solutions, the pink precipitate which formed was filtered off, washed with water, and dissolved in 7 *M* sulfuric acid (1 ml). The resulting solution was analyzed for Co(II) by the method of Kitson (8). An aliquot of the filtrate was similarly acidified and analyzed for Co(II). (Throughout this study solutions containing phenanthroline or dipyridyl complexes were acidified before being analyzed for Co(II), to prevent interferences by Co(II) complexes of these ligands.)

Quantum yields were determined using monochromatic light from a Coherent Radiation 1 W argon ion laser (457.9, 488, and 514.5 nm) or a Rayonet photoreactor (350 nm). In the experiments using the laser, the beam was passed through an appropriate interference filter, a lens to defocus the beam, and into a thermostatted 10 cm quartz cell containing the photolyte. Except for the experiments at 457.9 nm, where only *ca.* 90% of the incident light was absorbed by the solution, photolyte concentrations were such that > 99% of the incident light was absorbed. Light intensities at 457.9, 488, and 514.5 nm were measured by Reinecke's salt actinometry (9), absorbance-matched solutions being used at 457.9 nm. Light intensities at 350 nm were measured by ferrioxalate actinometry (10). Cobalt(II) was measured as outlined above, and photolyses were carried out to less than 10% conversion. Although neutral or basic solutions of $Cophen_3^{3+}$ containing oxalate ion initially remain clear on photolysis, on standing they slowly deposit yellow crystals which give a strong positive test for Co(II). Immediately after photolysis, the clear photolyte (*ca.* 30 ml) was therefore quantitatively diluted to 50 ml with concentrated sulfuric acid, which prevented the precipitation of the Co(II) product. The solution was then analyzed for Co(II) in the usual manner. Analyses for NH_3 were carried out using the indophenol method (11).

For interpretation purposes, it was important to resolve visible spectra into components corresponding to l.f. and c.t. bands. For analysis of spectra of the phenanthroline and bipyridyl complexes it was not possible to exactly reproduce the spectra with Gaussian components. Since knowledge of the maximum amount of reaction occurring by direct irradiation of c.t. bands is crucial to the interpretation of the l.f. bands, the component curves in the visible region were chosen to *maximize* the contribution of the higher frequency (c.t.) component. For the discussion, this is a worst case choice.

Results

The stoichiometries of the l.f. irradiation of $Cophen_2C_2O_4^+$ in acid and neutral solutions are given in Table 1. Under neutral conditions a yellow solution is produced as well as the pink precipitate noted by Broomhead *et al.* (6). If a neutral solution is irradiated for a short period of time (< 10 min), the pink precipitate does not appear immediately, but only on standing. It analyzes for the formula $CophenC_2O_4$. The pink material can also be slowly precipitated by mixing Co^{2+} and phenanthroline (1:2) with $Cophen_2C_2O_4^+$; Co^{2+} in the absence of phenanthroline has no detectable effect on $Cophen_2C_2O_4^+$. The yellow solution produced on photolysis initially gave a negative test for Co(II); on prolonged heating a positive test is obtained. Thus at room temperature and in neutral solution the overall reaction is

$$[1]\quad 4Cophen_2C_2O_4^+ \xrightarrow{h\nu} 2[CophenC_2O_4]^0(s) + 2Co(III) + 6phen + C_2O_4^{2-} + 2CO_2$$

The exact disposition of the phenanthroline ligands in the yellow solution is undetermined, but speculatively we suggest $Cophen_3^{3+}$. The spectrum is consistent with this assignment and the neutral solution gives a negative test for free phenanthroline after passage through cation exchange paper.

In view of the complicated nature of the reactions in neutral solution, all further experiments

TABLE 1. Stoichiometry for the photolysis of $Cophen_2C_2O_4^+$

Co(III) reacted ($\times 10^5$) (mol)	Co(II) formed ($\times 10^5$) (mol)	CO_2 formed ($\times 10^5$) (mol)
In 1 *M* H_2SO_4		
0.62	0.68	
0.56	0.49	
1.2	1.2	
	0.56	0.56
	1.1	1.2
	0.90	0.94
	0.64	0.69
In neutral solution		
2.1	1.1*	
1.5	0.84*	
1.6	0.88*	
1.5	0.80*	
0.89	0.42*	
1.7	0.82*	0.72

*Co(II) in the pink precipitate; the yellow solution gave a negative test for Co(II).

TABLE 2. Quantum yields for photolysis of cobalt(III) complexes

Complex	Conditions	λ (nm)	$\phi_{Co(II)}$
$Cophen_2C_2O_4^+$	1 *M* H_2SO_4, 24.9 °C	514.5	0.095 ± 0.004
		457.9	0.097 ± 0.006
	1 *M* H_2SO_4, 46.5 °C	514.5	0.140 ± 0.012
$Cobipy_2C_2O_4^+$	1 *M* H_2SO_4 + 1.5 *M* NaCl, 24.9 °C	514.5	0.062±0.002
$Cophen_3^{3+}$	0.1 *M* Na_2CO_4 + 1 *M* H_2SO_4	488	$< 3 \times 10^{-4}$
	0.1 *M* $Na_2C_2O_4$	488	0.022, 0.021, 0.019
	0.2 *M* Na_2CO_4 + 1 × 10^{-3} *M* NaOH	488	0.027, 0.028
	0.5 *M* $K_2C_2O_4$ + 4 × 10^{-3} *M* NaOH	488	0.032
	0.8 *M* $K_2C_2O_4$ + 4 × 10^{-3} *M* NaOH	488	0.036
	0.2 *M* Na_2CO_4 + 1 × 10^{-3} *M* NaOH	350	0.056±0.001
$Coen_3^{3+}$	0.2 *M* Na_2CO_4 + 1 × 10^{-3} *M* NaOH	488	$< 5 \times 10^{-4}$
$Co(NH_3)_5Cl^{2+}$	1 × 10^{-2} *M* $HClO_4$	488	5.26×10^{-3}*
			5.07×10^{-3}*†
	1 × 10^{-2} *M* $HClO_4$ + 2.6 *M* isopropanol	488	5.21×10^{-3}*

*Quantum yield is ϕ_{NH_3}.
†Reference 2*a*.

were carried out in acidified solutions where the simpler stoichiometry of [2] obtains

$$[2]\quad 2Cophen_2C_2O_4^+ \xrightarrow{h\nu} 2Co^{2+} + 4phen + C_2O_4^{2-} + 2CO_2$$

By analogy with [2] the photolyses of $Cobipy_2C_2O_4^+$ in acid solution and of the $Cophen_3^{3+}/C_2O_4^{2-}$ mixtures were assumed to obey [3] and [4] respectively.

$$[3]\quad 2Cobipy_2C_2O_4^+ \xrightarrow{h\nu} 2Co^{2+} + 4bipy + C_2O_4^{2-} + 2CO_2$$

$$[4]\quad 2Cophen_3^{3+} + C_2O_4^{2-} \xrightarrow{h\nu} 2Co^{2+} + 6phen + 2CO_2$$

Quantum yields for photolysis at 25 °C of $Cophen_2C_2O_4^+$, $Cobipy_2C_2O_4^+$, and of $Cophen_3^{3+}$ and $Coen_3^{3+}$ in the presence of oxalate are given in Table 2. Table 2 also gives the temperature-dependence of $\phi_{Co(II)}$ for the irradiation of $Cophen_2C_2O_4^+$ at 514.5 nm; from these values the apparent activation energy over the temperature range 25–45 °C can be calculated to be 1000–1400 cm^{-1}. Table 2 also gives the result of an experiment to determine the effect on the quantum yield, ϕ_{NH_3}, for loss of ammonia from $Co(NH_3)_5Cl^{2+}$ of adding isopropanol as a chlorine radical scavenger. The reason for this experiment will be mentioned below.

Discussion

Analysis of the Spectra and the Nature of the Electronic States Populated by the Incident Radiation

In the case of $Cophen_2C_2O_4^+$, laser lines were available for irradiation on both the high and low energy sides of the maximum in the l.f. band of the spectrum. This allowed for irradiation at points where the intensity of any tail from the u.v. band (of either metal to ligand charge transfer or intraligand character) would vary considerably. The invariance of quantum yield between the two wavelengths shows that reaction originates *from population of the l.f. state* not from the weak tail of the u.v. band. This is, *a priori*, the most reasonable assignment because (*a*) the c.t. tail must be weak and (*b*) the c.t. state being metal to ligand is not of the sort associated with metal reduction. We assume that this conclusion can be extended to the $Cobipy_2C_2O_4^+$ and $Cophen_3^{3+}$ reactions, but the assumption can be supported by reasonable approximate arguments.

Gaussian curve analysis of the spectra of $Cophen_2C_2O_4^+$ and $Cobipy_2C_2O_4^+$ indicated that irradiation of either complex at 514.5 nm initially populates only the $^1T_{1g}$ l.f. state centered at 507 and 495 nm respectively. Similarly, less than 1% of the radiation absorbed by $Cophen_2C_2O_4^+$ at 457.9 nm populates the c.t. state centered at *ca.* 350 nm; the rest of the light at this wavelength populates the $^1T_{1g}$ l.f. state. These figures differ somewhat from those given in an

Can. J. Chem. Downloaded from www.nrcresearchpress.com by 210.87.254.105 on 09/05/12
For personal use only.

Can. J. Chem. Downloaded from www.nrcresearchpress.com by 210.87.254.105 on 09/05/12
For personal use only.

earlier publication (12), which were calculated by a less rigorous method, but the conclusions are invariant under the change of approximation. There may be slight reaction at 457.9 nm via direct population of the c.t. state, but if so, reaction via this pathway is not much more efficient than reaction via the l.f. state.

Analysis of the $Cophen_3^{3+}$ spectrum is more difficult, and the results are less clear-cut. The tail of the intense c.t. transition centered at *ca.* 290 nm is not well separated from the peak of the weak l.f. band at *ca.* 465 nm. However, even allowing a maximum contribution from the c.t. state, the Gaussian curve analysis showed that at 488 nm less than 5% of the light absorbed could be ascribed to the c.t. component, the other 95% corresponding to the $^1A_{1g} \rightarrow {}^1T_{1g}$ l.f. transition. At 350 nm, however, 100% of the light absorbed populates a c.t. state.[2] These figures disagree somewhat with those calculated using Gorton and co-workers' analysis (7) of the spectrum of $Cophen_3^{3+}$. However, the method of Gorton and co-workers (13) was used only to define the position of the l.f. maximum; it was not intended to measure the relative importances of l.f. and c.t. transitions in the region where the latter decrease very rapidly. Furthermore, an attempt was made to analyze the spectrum by assuming Gorton's values of ε_{max} and λ_{max} for the l.f. band and a Gaussian shape for the c.t. band, but it was not possible to reproduce the observed spectrum with these conditions. The Gaussian analysis of the spectrum given above, and the values of $\phi_{Co(II)}$ found in 0.2 *M* oxalate indicate that both the l.f. and c.t. states are photoactive, but to a different degree. Assuming a maximum of 5% c.t. character at 488 nm, the wavelength dependence of $\phi_{Co(II)}$ for $Cophen_3^{3+}$ in 0.2 *M* oxalate gives $\phi_{Co(II)}$ for the c.t. state as 0.056 and for the l.f. state as $\geqslant 0.026$ and $\leqslant 0.028$ under the conditions obtaining.

Stoichiometry and Nature of the Reactive State in the $Cophen_2C_2O_4^+$ and $Cobipy_2C_2O_4^+$ Irradiations

The stoichiometry of the photoreactions of $CoL_2C_2O_4^+$ (L = phen, bipy) in acidic solutions can be explained by the mechanism

$$[5] \quad CoL_2C_2O_4^+ \xrightarrow{h\nu} [CoL_2C_2O_4^+]^*$$

$$[6] \quad [CoL_2C_2O_4^+]^* \rightarrow [Co^{II}L_2(C_2O_4^-)]^+$$

$$[7] \quad [Co^{II}L_2(C_2O_4^-)]^+ \rightarrow CoL_2^{2+} + C_2O_4^-$$

$$[8] \quad CoL_2C_2O_4^+ + C_2O_4^- \rightarrow CoL_2C_2O_4^0 + 2CO_2$$

Without a flash photolysis experiment, no information can be deduced as to the exact nature of the radical intermediates in [6] to [8]; as written, these equations are in accord with recent results (14, 15) on the flash photolysis of $Co(C_2O_4)_3^{3-}$. But regardless of the nature of the oxalato-radicals, at some stage the reactive state (not necessarily $^1T_{1g}$) must relax onto the potential surface corresponding to a Co(II) complex and an organic radical ([6]). In addition, the observed quantum yield is that for the sum of processes 5 to 8, so that the values of $\phi_{Co(II)}$ given in Table 2 are twice the quantum yield for the primary photochemical act ([5] to [7]), as the Co(II):CO_2 ratio requires.

The complicated stoichiometry seen in neutral solutions is due to subsequent thermal reactions of the Co(II) complexes produced in steps 7 and 8, *viz*:

$$[9] \quad CoL_2C_2O_4^0 \rightleftharpoons CoL_2^{2+} + C_2O_4^{2-}$$

$$[10] \quad CoL_2C_2O_4^+ + CoL_2^{2+} \rightarrow [CoLC_2O_4]^0(s) + CoL_3^{3+}$$

In acidic solutions the equilibrium

$$[11] \quad CoL_2^{2+} + 2H^+ \rightleftharpoons Co^{2+} + 2LH^+$$

lies far to the right; since Co^{2+} itself does not react with $Cophen_2C_2O_4^+$ (*vide supra*) [9] and [10] do not occur.

Both the mode of reaction and the relatively high quantum yields found for $Cophen_2C_2O_4^+$ and $Cobipy_2C_2O_4^+$ are unusual in the photochemistry of cobalt(III) amine complexes. Thus the presence of heterocyclic aromatic amines confers special physical or chemical properties on the complexes. Balzani *et al.* (16) suggested that the observation of wavelength-dependent photoreduction on irradiating l.f. bands of $Co(NH_3)_5NO_2^{2+}$ could be explained by assuming reaction occurred via a c.t. state which is substantially distorted from the ground state geometry. Its potential minimum thus lies lower than that of the l.f. state, even though Franck–Condon restrictions means the absorption $^1A_{1g} \rightarrow$ c.t. appears at higher energies than the $^1A_{1g} \rightarrow {}^1T_{1g}$ l.f. tran-

[2]Although there are inherent limitations to Gaussian analysis, we remind the reader that c.t. contribution was maximized (see experimental) so that we present our conclusions for the conditions least favorable to our argument. This should compensate for deviation from Gaussian behavior.

Can. J. Chem. Downloaded from www.nrcresearchpress.com by 210.87.254.105 on 09/05/12
For personal use only.

sition. A similar situation is possible for the $Cophen_2C_2O_4^+$ and $Cobipy_2C_2O_4^+$ complexes where even in vertical excitation the absorptions corresponding to c.t. transitions lie fairly close ($\sim$370 nm for $Cophen_2C_2O_4^+$ and $\sim$350 nm for $Cobipy_2C_2O_4^+$) to those for the octahedral $^1A_{1g} \rightarrow {}^1T_{1g}$ transition. Since the lowest c.t. bands in $Coen_2C_2O_4^+$ occur at $\sim$225 nm, the low-lying bands in $Cophen_2C_2O_4^+$ and $Cobipy_2C_2O_4^+$ no doubt involve Co–phen and Co–bipy charge transfer, quite probably in the metal to ligand direction. If this is so, it is hard to see why populating these states leads to oxidation of oxalate, even though a few cases of 'wrong ligand' oxidation have been documented (17). It is noteworthy that the low apparent activation energy for the $Cophen_2C_2O_4^+$ irradiation at 514.5 nm is normal for transition metal complexes (4*b*, p. 12); it is also low enough to exclude reaction via a reactive c.t. state for which the potential minimum is much more than 1 kK above that of the $^1T_{1g}$ state.

It is more interesting to consider the possibility that reaction occurs from one of the ligand field states. Either the $^1T_{1g}$ state directly populated on irradiation or the $^3T_{1g}$ state which can be reached by intersystem crossing could be the reactive state. Both these states have the electronic configuration $t_{2g}^5 e_g^1$ and one-electron transfer from the oxalate ligand to the t_{2g} shell would produce an unstable low-spin Co(II) phenanthroline or bipyridyl complex. Rapid reaction of this species to the corresponding high-spin complex would provide a pathway for relaxation to the observed products. The high ligand field strengths of phenanthroline and bipyridyl should stabilize the low-spin Co(II) species, where a lower field ligand like ethylenediamine would not. This could explain why $Cophen_2C_2O_4^+$ and $Cobipy_2C_2O_4^+$ are photoactive but simple amine oxalato-complexes are not. Alternatively, Kane-Maguire and Langford (5) have suggested that provided a suitable reducing agent is available, photoreduction is a normal consequence of ligand field irradiation, and that the reaction might occur via the $^5T_{2g}$ state. The Tanabe–Sugano diagram for Co(III) shows that at the average ligand field strength for amino-oxalato-complexes the lowest-lying l.f. state is $^3T_{1g}$. But if the excited states are distorted from the ground state geometry, the average ligand field experienced by the Co(III) will decrease, and the lowest l.f. state may become $^5T_{2g}$. The electronic configuration of this state is $t_{2g}^4 e_g^2$. Therefore it only requires a one-electron transfer from the oxalate ion to the t_{2g} shell to give the stable high-spin Co(II) product.

Although the nature of the reactive excited state is in doubt among three candidates, a phenomenological explanation of the unusual reactivity of the phenanthroline and bipyridyl complexes is possible. It appears that the thermodynamic ease of reduction of the substrate to the stable, high-spin Co(II) product is a major factor in determining photosensitivity. The $E_{1/2}{}^0$ values are not available for $Cophen_2C_2O_4^+$ and $Cobipy_2C_2O_4^+$, but Ohashi (18) has demonstrated a linear correlation between $E_{1/2}{}^0$ for the process

[12] $$CoL_2C_2O_4^{n+} + e^- \rightarrow CoL_2C_2O_4^{(n-1)+}$$

and the second order rate constant for the reaction

[13] $$CoL_2C_2O_4^{n+} + Fe^{2+} \rightarrow CoL_2C_2O_4^{(n-1)+} + Fe^{3+}$$

Extrapolation of this correlation gives $E_{1/2}{}^0$ as 0.095 for $Cophen_2C_2O_4^+$ and 0.060 for $Cobipy_2C_2O_4^+$. Not only are these values substantially more favorable than that for reduction of $Coen_2C_2O_4^+$, but their ratio is within experimental error equal to the ratio of quantum yields for the two complexes. It is possible to explain this behavior qualitatively by remembering that the excited state must relax onto the potential surface corresponding to a Co(II) complex and the oxalate radical. The smaller the energy gap between the excited state and product surfaces, the more efficient this relaxation will be. For simple amineoxalates like $Coen_2C_2O_4^+$ the Co(II) product is relatively unstable and the energy gap is too large for photoreduction to occur. A similar explanation rationalizes photoreduction by oxalate of $Cophen_3^{3+}$ and not $Coen_3^{3+}$, and also the insensitivity of ϕ_{NH_3} for $Co(NH_3)_5Cl^{2+}$ to the presence of isopropanol (see Table 2). For $Co(NH_3)_5Cl^{2+}$ and similar complexes it is possible to consider the reaction mechanism

[14] $$Co(NH_3)_5Cl^{2+} \xrightarrow{h\nu} [Co(NH_3)_5Cl^{2+}]^*$$

[15] $$[Co(NH_3)_5Cl^{2+}]^* \rightarrow Co^{II}(NH_3)_5(Cl^{\cdot})^{2+}$$

[16] $$Co^{II}(NH_3)_5(Cl^{\cdot})^{2+} + H_2O \rightarrow Co^{II}(NH_3)_4(H_2O)(Cl^{\cdot})^{2+} + NH_3$$

[17] $$Co^{II}(NH_3)_4(H_2O)(Cl^{\cdot})^{2+} \rightarrow Co^{III}(NH_3)_4(H_2O)(Cl^-)^{2+}$$

Although isopropanol would scavenge any $Cl^{\cdot}$ radicals that were formed (19), the potential sur-

face for $Co(NH_3)_5^{2+}$ and the chlorine radical lies too far above that of the excited state for the redox reaction to occur.

The Photoreduction of Cophen$_3^{3+}$ by Oxalate

In line with [5] to [8], the overall reaction occurring on irradiation of $Cophen_3^{3+}$ in the presence of oxalate is assigned as

$$[18]\quad Cophen_3^{3+} + C_2O_4^{2-} \xrightarrow{h\nu} Cophen_3^{2+} + C_2O_4^{-}$$

$$[19]\quad Cophen_3^{3+} + C_2O_4^{-} \rightarrow Cophen_3^{2+} + 2CO_2$$

Again the observed quantum yields given in Table 2 are twice the quantum yields for the primary photochemical act ([18]).

The dependence of the quantum yields on the concentration of oxalate is shown in Fig. 1. A weighted least squares fit to the function

$$[20]\qquad \phi_{Co(II)} = \frac{a[C_2O_4^{2-}]}{1 + b[C_2O_4^{2-}]}$$

assuming that there is a constant percentage error in $\phi_{Co(II)}$ gives $a = 0.44 \pm 0.04$, $b = 11.4 \pm 1.4$ M^{-1}, and the percentage error in $\phi_{Co(II)}$ as 5%. The observed dependence on $[C_2O_4^{2-}]$ can be explained by considering two simple schemes (although some more complex ones might also work).

In the first scheme, two absorbers with similar extinction coefficients at 488 nm are postulated, namely $Cophen_3^{3+}$ and *its ion pair with oxalate*. Only the ion pair is considered to be reactive. In this model, the parameter b is the ion pairing equilibrium constant. The success of the model turns on the reasonableness of a value of 11.4 ± 1.4 M^{-1} for this ion pairing constant. No convenient approach for an independent experimental determination of the constant in these media is available. However, many studies of thermal kinetics in similar media show that the Fuoss–Eigen equation is a successful method of approximating such ion association constants. Extrapolating the value of 11.4 M^{-1} at ionic strength 0.3 (our lowest experimental ionic strength) to zero ionic strength with the Davies equation (20) gives a value of 320 M^{-1}. A calculation following Fuoss (21), assuming a distance of closest approach of 7.5 Å, gives 270 M^{-1}. The model must be regarded as satisfactory in qualitatively accounting for the results.

In the second simple scheme, the reaction is assumed to proceed via a *dynamic competition* between deactivation of the reactive excited state and its reaction with oxalate. This will lead to an equation of the form of [20] if the rate constant for deactivation is much less than the product of the rate constant for diffusional encounter between $Cophen_3^{3+}$ and oxalate multiplied by the oxalate concentration. In particular, the value of b requires that the deactivation rate constant is smaller than the diffusion rate constant by a factor of at least 11.4. This is also qualitatively reasonable although it requires a longer lifetime for a Co(III) excited state than earlier workers have preferred (4).

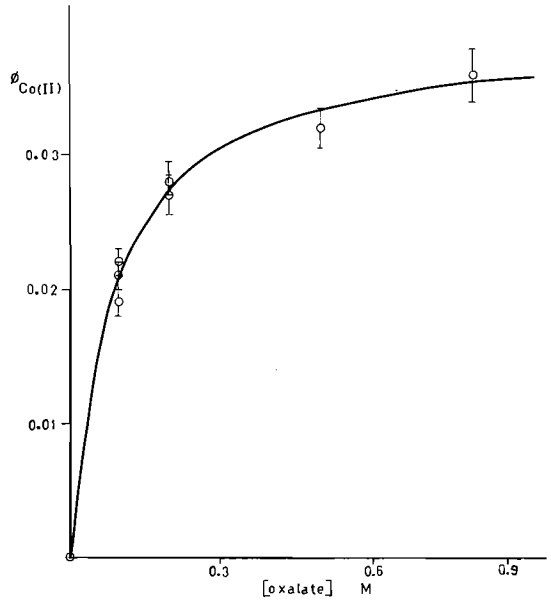

FIG. 1. The quantum yield for reduction of $Cophen_3^{3+}$ as a function of oxalate concentration.

As to the intimate mechanism of the outer sphere reduction, electron transfer from the oxalate ion into the t_{2g} shell would generate a low spin $Cophen_3^{2+}$ complex, which would be relatively stabilized by the phen ligands. Hoffman and Simic (22) showed low spin $Cobipy_3^{2+}$ was not generated during the thermal reaction of $Cobipy_3^{3+}$ with a solvated electron, but this process requires electron transfer to the high energy e_g level, so it does not *a priori* exclude low spin $Cophen_3^{2+}$ as an intermediate in reactions of a $^3T_{1g}$ or $^1T_{1g}$ excited state with a vacancy in the t_{2g} shell. Consequently, the present results taken in conjunction with those of Hoffman and Simic cannot be used to favor reaction from a ^5T excited state, however reasonable such a mechanism may seem.

Can. J. Chem. Downloaded from www.nrcresearchpress.com by 210.87.254.105 on 09/05/12
For personal use only.

We thank the National Research Council of Canada for financial support, and Dr. J. H. Carey for helpful discussions.

1. (*a*) L. Moggi, F. Bolletta, V. Balzani, and F. Scandola. J. Inorg. Nucl. Chem. **28**, 2589 (1966); (*b*) M. Wrighton, G. S. Hammond, and H. B. Gray. J. Am. Chem. Soc. **93**, 5254 (1971).
2. (*a*) R. A. Pribush, C. K. Poon, C. M. Bruce, and A. W. Adamson. J. Am. Chem. Soc. **96**, 3027 (1974); (*b*) P. S. Sheridan and A. W. Adamson. J. Am. Chem. Soc. **96**, 3032 (1974).
3. G. Ferraudi and J. F. Endicott. J. Chem. Soc. Chem. Commun. 674 (1973).
4. (*a*) C. Furlani. Coord. Chem. Rev. **1**, 51 (1966); (*b*) V. Balzani and V. Carassiti. Photochemistry of co-ordination compounds. Academic Press, London. 1970. p. 239.
5. N. A. P. Kane-Maguire and C. H. Langford. J. Chem. Soc. Chem. Commun. 351 (1973).
6. J. A. Broomhead, M. Dwyer, and N. Kane-Maguire. Inorg. Chem. **7**, 1388 (1968).
7. C. S. Lee, E. M. Gorton, H. M. Neumann, and H. R. Hunt. Inorg. Chem. **5**, 1397 (1966).
8. R. E. Kitson. Anal. Chem. **22**, 664 (1950).
9. E. E. Wegner and A. W. Adamson. J. Am. Chem. Soc. **88**, 394 (1966).
10. C. G. Hatchard and C. A. Parker. Proc. R. Soc. London, Ser. A, **235**, 518 (1956).
11. W. T. Bolleter, C. J. Bushman, and P. W. Tidwell. Anal. Chem. **33**, 592 (1961).
12. C. H. Langford, C. P. J. Vuik, and N. A. P. Kane-Maguire. Inorg. Nucl. Chem. Lett. **11**, 377 (1975).
13. H. M. Neumann and N. C. Cook. J. Am. Chem. Soc. **79**, 3026 (1957).
14. L. Cordemans, J. D'Olieslager, J. Hendrix, and S. De Jaegere. J. Phys. Chem. **78**, 1361 (1974).
15. N. S. Rowan, M. Z. Hoffman, and R. M. Milburn. J. Am. Chem. Soc. **96**, 6060 (1974).
16. V. Balzani, R. Ballardini, N. Sabbatini, and L. Moggi. Inorg. Chem. **7**, 1398 (1968).
17. (*a*) G. Caspari, R. G. Hughes, J. F. Endicott, and M. Z. Hoffman. J. Am. Chem. Soc. **92**, 6801 (1970); (*b*) S. Sundararajan and E. L. Wehry. J. Phys. Chem. **76**, 1528 (1972); (*c*) S. Sundararajan and E. L. Wehry. J. Inorg. Nucl. Chem. **34**, 3699 (1972).
18. K. Ohashi. Bull. Chem. Soc. Jpn. **45**, 3093 (1972).
19. (*a*) P. Natarajan and J. F. Endicott. J. Phys. Chem. **77**, 1823 (1973); (*b*) A. Caspari, R. G. Hughes, J. F. Endicott, and M. Z. Hoffman. J. Am. Chem. Soc. **92**, 6801 (1970); (*c*) M. S. Matheson, W. A. Mulac, and J. Rabani. J. Phys. Chem. **67**, 2613 (1963); (*d*) M. E. Langmuir and E. Hayon. J. Phys. Chem. **71**, 3808 (1967).
20. C. W. Davies. Ion association. Butterworths, London. 1962. p. 41.
21. R. M. Fuoss. J. Am. Chem. Soc. **80**, 5059 (1958).
22. M. Z. Hoffman and M. Simic. J. Chem. Soc. Chem. Commun. 640 (1973).

Can. J. Chem. Downloaded from www.nrcresearchpress.com by 210.87.254.105 on 09/05/12
For personal use only.

Direct Observation of the Radicals Formed in the Radiolysis of Liquid Benzyl Alcohol. An Electron Spin Resonance and Spin Trapping Method[1]

FREDERICK PETER SARGENT AND EDWARD MICHAEL GARDY

Research Chemistry Branch, Atomic Energy of Canada Limited, Whiteshell Nuclear Research Establishment, Pinawa, Manitoba R0E 1L0

Received June 5, 1975

FREDERICK PETER SARGENT and EDWARD MICHAEL GARDY. Can. J. Chem. **53**, 3128 (1975).

Intermediates formed during radioylsis of benzyl alcohol have been identified by an e.s.r. and spin trapping method. Solutions of *tert*-BuNO in benzyl alcohol were irradiated *in situ* with 3 MeV electrons and the e.s.r. spectra of the resulting nitroxides directly recorded.

$$\textit{tert}\text{-BuNO} + R\cdot \rightarrow \textit{tert}\text{-BuN}(O\cdot)\text{—}R$$

These demonstrated that benzyl, $PhCH_2\cdot$, and hydroxybenzyl, $Ph\dot{C}HOH$, radicals are formed in the radiolysis. By an examination of the effects of the addition of electron scavengers, it was shown that the benzyl radicals are probably directly formed from the reaction of electrons with benzyl alcohol. Since these scavengers had no effect on the yield of $Ph\dot{C}HOH$ trapped, this radical is not derived from the reactions of electrons. It is suggested that it is partly produced by reaction of the alkoxy radical, $PhCH_2O\cdot$, with the solvent benzyl alcohol.

$$PhCH_2O\cdot + PhCH_2OH \rightarrow Ph\dot{C}HOH + PhCH_2OH$$

FREDERICK PETER SARGENT et EDWARD MICHAEL GARDY. Can. J. Chem. **53**, 3128 (1975).

On a identifié, par r.p.e. et par la méthode de piégeage de spin, les intermédiaires qui se forment au cours de la radiolyse de l'alcool benzylique. On a irradié, *in situ* avec des électrons à 3 MeV, des solutions de *tert*-BuNO dans l'alcool benzylique et on a enregistré directement les spectres r.p.e. des nitroxydes qui se forment.

$$\textit{tert}\text{-BuNO} + R\cdot \rightarrow \textit{tert}\text{-BuN}(O\cdot)\text{—}R$$

Ces spectres ont permis de démontrer que des radicaux benzyles, $PhCH_2\cdot$, et hydroxybenzyles, $Ph\dot{C}HOH$, se forment lors de la radiolyse. En examinant les effets produits par addition de pièges à électrons, on a pu montrer que les radicaux benzyles se forment probablement directement par réaction des électrons avec l'alcool benzylique. Puisque l'addition de ces pièges n'a aucune influence sur le rendement en radicaux $Ph\dot{C}HOH$ on peut en déduire que ce radical n'est pas formé par réactions des électrons. On croit qu'il se forme, en partie, par réaction du radical alkoxy, $PhCH_2O\cdot$, avec l'alcool benzylique.

$$PhCH_2O\cdot + PhCH_2OH \rightarrow Ph\dot{C}HOH + PhCH_2OH$$

[Traduit par le journal]

Introduction

We have recently used the technique of spin trapping (1) to detect the intermediates formed in the radiolysis of simple alcohols (2, 3). In this paper we describe its application to a study of the radiation chemistry of benzyl alcohol. The method involves conversion of the reactive intermediates, R·, formed in the radiolysis, and which have lifetimes in the range of micro- to milliseconds, to comparatively stable nitroxides. This is achieved by their addition to a nitrone or a nitroso compound as in [1] and [2].

[1] $$\textit{tert}\text{-BuNO} + R\cdot \rightarrow \textit{tert}\text{-BuN}(O\cdot)\text{—}R$$

[2] $$PhCH{=}NO\text{—}\textit{tert}\text{-Bu} + R\cdot \rightarrow PhCH(R)\text{—}N(O\cdot)\text{—}\textit{tert}\text{-Bu}$$

The resulting nitroxide has an e.s.r. spectrum characteristic of R·. The most commonly used trapping agents are nitroso-*tert*-butane, *tert*-BuNO, and phenyl-*tert*-butyl nitrone. Although

[1]AECL No. 5198.

Can. J. Chem. Downloaded from www.nrcresearchpress.com by 210.87.254.105 on 09/05/12
For personal use only.

Can. J. Chem. Downloaded from www.nrcresearchpress.com by 210.87.254.105 on 09/05/12
For personal use only.

each has its merits, we prefer to use *tert*-BuNO because the resulting nitroxide spectra are distinctive and vary considerably with R·. However, one of the disadvantages of this compound is that although the nitroxides are much longer lived than their precursors, R·, they are not completely stable and some of them decay in a few seconds (2). We have overcome this problem by coupling the e.s.r. spectrometer to a high energy electron accelerator, which permits the direct observation of e.s.r. spectra while the sample is being irradiated.

The transient optical absorption detected in pulse irradiated neat benzyl alcohol (4) and its solution in cyclohexane (5) has been assigned to benzyl radicals. It was suggested that these were formed by the dissociative electron capture reaction

[3] $$PhCH_2OH + e \rightarrow PhCH_2\cdot + OH^-$$

Our spin trapping results support this but also show the presence of another radical not detected in the pulse radiolysis studies. The e.s.r. coupling constants show this to be the PhĊHOH radical.

Experimental

The e.s.r. spectrometer was coupled to a nominally 4 MeV electron accelerator by extending the flight tube axially into the magnet. The pole caps were fitted with a field compensating device to give a field homogeneity of 5 μT (50 mG) over the sample volume. The conventional T102 rectangular microwave cavity was modified to permit irradiation of the samples.

Solutions to be irradiated were deoxygenated by bubbling with 99.999% argon and continuously flowed through the e.s.r. sample cavity where they were irradiated with 3 MeV electrons at beam currents in the range of 1 to 7 μA at temperatures a few degrees above ambient. The sample tubes were made of cerium doped glass which does not give an appreciable e.s.r. signal on irradiation (6, 7). The magnetic field sweep ranges were calibrated with an n.m.r. magnetometer and were found to be reproducible to at least 1%.

Nitroso-*tert*-butane, *tert*-BuNO, was prepared by oxidation of *tert*-butylamine using the method of Stowell (8), recrystallized from *n*-pentane and stored in a refrigerator. Benzyl alcohol was Fisher Certified grade which contains less than 0.20% chloride. Reagent grade methyl iodide and carbon tetrachloride were used as received.

Results and Discussion

The e.s.r. spectrum observed during the radiolysis of benzyl alcohol containing 10 mol/m^3 (0.01 *M*) *tert*-BuNO is shown in Fig. 1. This is a composite of the spectra from three different nitroxides, referred to as **1**, **2**, and **3**, which are formed by the trapping of three different intermediates. The spectrum is interpreted in terms of nitroxide **1** with a nitrogen coupling of 1.4 mT (14.0 G) and a proton coupling of 1.27 mT (12.7 G), nitroxide **2** with a nitrogen coupling of 1.52 mT (15.2 G) and a proton coupling of 0.3 mT (3.0 G), and nitroxide **3** with a nitrogen coupling of 1.60 mT (16.0 G) and a pair of protons with a coupling of 0.84 mT (8.4 G). The simulated composite spectrum shown in Fig. 1*b* was computed with these values and the ratios of concentrations were adjusted to give close agreement with the observed spectrum. Nitroxide **1** is identified as *tert*-BuNHO·, and the coupling constants are in close agreement with those previously observed in other alcohols (2, 3) and water (9). Nitroxide **3** is formed by the trapping of benzyl radicals, [4],

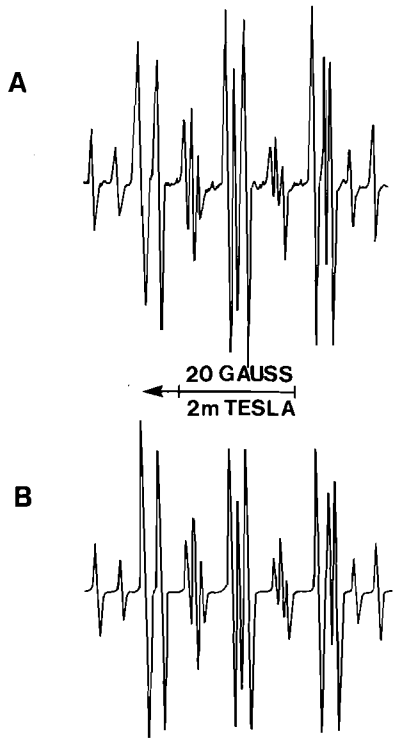

FIG. 1. (*a*) Electron spin resonance spectrum observed during irradiation of benzyl alcohol containing 10 mol/m^3 (0.01 *M*) *tert*-BuNO. (*b*) Computer simulated spectrum.

[4] $$PhCH_2\cdot + \textit{tert}\text{-BuNO} \rightarrow \textit{tert}\text{-BuN}(O\cdot)\text{—}CH_2\text{—Ph}$$

and the coupling constants are in reasonable agreement with those reported (10) after allowing for the well known solvent effect. Nitroxide **2**

Can. J. Chem. Downloaded from www.nrcresearchpress.com by 210.87.254.105 on 09/05/12
For personal use only.

comes from the trapping of a radical with only one α-proton. This, together with the magnitude of the coupling constants, strongly suggests PhĊHOH, as in [5]

[5] $$\mathrm{Ph\dot{C}HOH} + \textit{tert}\text{-BuNO} \rightarrow \textit{tert}\text{-BuN}(\mathrm{O\cdot})\text{—}\mathrm{C}(\mathrm{H})(\mathrm{OH})\text{—Ph}$$

Saturating the solution with nitrous oxide prior to radiolysis had no effect on the observed e.s.r. spectrum suggesting that [6] does not occur to any appreciable extent.

[6] $$e + N_2O \rightarrow N_2 + O^-$$

This could mean that solvated electrons are not formed in benzyl alcohol; certainly, none were detected in the pulse radiolysis study (4). However, since the solubility of nitrous oxide in benzyl alcohol is unknown, we decided to examine the effects of high concentrations of other electron scavengers such as methyl iodide, carbon tetrachloride, and benzophenone. These had a most marked effect on the relative intensity of nitroxide **3**. This is best illustrated by the addition of benzophenone as in Fig. 2 where the solution contained 10 mol/m^3 (0.01 *M*) *tert*-BuNO and 50 mol/m^3 (0.05 *M*) benzophenone. This had little effect on nitroxides **1** and **2** but **3** was considerably diminished, indicating a lower yield of benzyl radicals. When methyl iodide was used, not only was **3** decreased but methyl radicals were also trapped due to [7] and [8].

[7] $$e + CH_3I \rightarrow CH_3\cdot + I^-$$

[8] $$CH_3\cdot + \textit{tert}\text{-BuNO} \rightarrow \textit{tert}\text{-Bu—N}(\mathrm{O\cdot})\text{—}CH_3$$

These results show that the benzyl radicals are indeed derived from electrons and provide supporting evidence for [3].

Since electron scavengers had very little effect on the yield of *tert*-BuNHO· it is clearly not derived from electrons. We propose that it originates from the reaction of PhĊHOH with *tert*-BuNO as in [9].

[9] $$\textit{tert}\text{-BuNO} + \mathrm{Ph\dot{C}HOH} \rightarrow \textit{tert}\text{-BuNHO}\cdot + \mathrm{PhCHO}$$

This reaction, which is in competition with [5], might involve electron or hydrogen atom transfer. Analogous reactions of the α radicals of simple alcohols, such as $\cdot CH_2OH$ or $(CH_3)_2\cdot COH$, are well established (11). It has also been shown

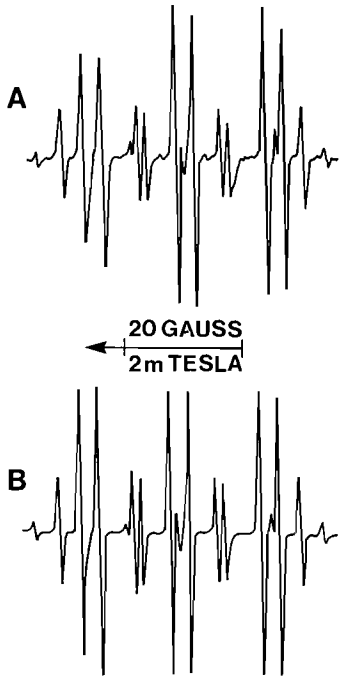

FIG. 2. (*a*) Electron spin resonance spectrum observed during irradiation of benzyl alcohol containing 10 mol/m^3 (0.01 *M*) *tert*-BuNO and 50 mol/m^3 (0.05 *M*) benzophenone. (*b*) Computer simulated spectrum.

that the rate of such reactions is much higher in alkaline solutions where the donor would be the radical anion (12). Therefore, we examined the effects of base on the spectra from solutions of *tert*-BuNO in benzyl alcohol. The e.s.r. spectrum in Fig. 3 was taken during radiolysis of a solution of *tert*-BuNO containing 10 mol/m^3 (0.01 *M*) potassium hydroxide. This shows the presence of **1** and **3** but **2** is absent and in addition the yield of **1** is considerably enhanced.[2] This means that all the α-radicals, PhĊHOH, have reacted by the electron transfer reaction 10 and none have been trapped. If benzophenone is also added to suppress the formation and trapping of benzyl radicals, the spectra (see Fig. 4), consists principally of *tert*-BuNHO from [10] and [11].

[10] $$\mathrm{Ph\dot{C}HOH} + OH^- \rightarrow \mathrm{PhCHO^-} + H_2O$$

[2]The *tert*-BuNHO· is not converted to *tert*-BuNO$^-$ by the KOH in benzyl alcohol. This seems to be generally true for alcohols since *tert*-BuNHO· is observed in alkaline methanol and ethanol (F. P. Sargent and E. M. Gardy, unpublished results). This is in marked contrast to aqueous solutions where the transition to *tert*-BuNO$^-$ occurs in quite weakly alkaline solutions at p*H* 7–9 (16).

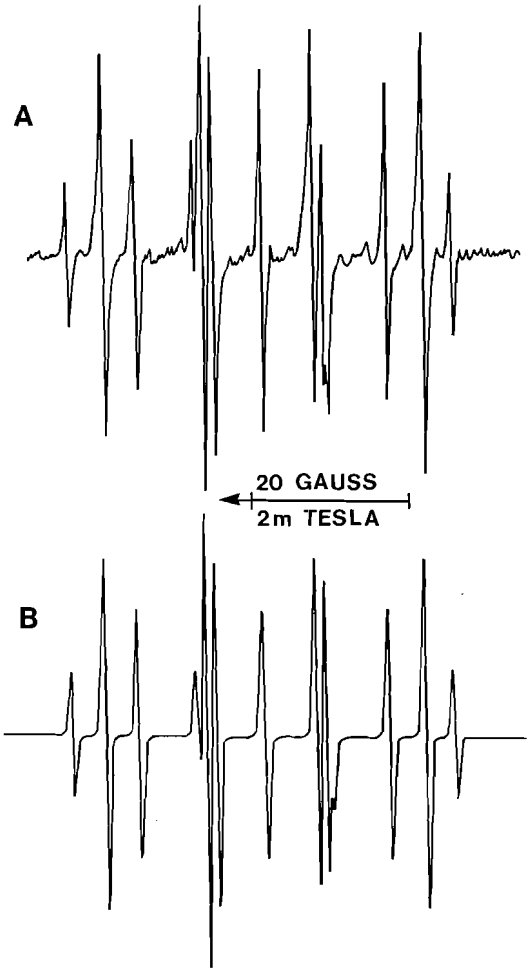

FIG. 3. (*a*) Electron spin resonance spectrum observed during irradiation of benzyl alcohol containing 10 mol/m^3 (0.01 *M*) *tert*-BuNO and 10 mol/m^3 (0.01 *M* potassium hydroxide. (*b*) Computer simulated spectrum.

[11] $PhCHO^- + \textit{tert}\text{-BuNO} + PhCH_2OH \rightarrow$
$\textit{tert}\text{-BuNHO}\cdot + PhCHO + PhCH_2O^-$

These results show that the radiolysis of benzyl alcohol does indeed produce benzyl radicals and that these are derived from electrons. They do not provide concrete proof for [3] since there are other reactions of the electrons which might conceivably produce benzyl radicals but [3] is the most probable.

Using the spin trapping technique, we have been able to show the presence of PhĊHOH radicals which were not detected by pulse radiolysis (4). However, we were unable to detect any nitroxides which would show the presence of the alkoxy radical $PhCH_2O\cdot$. This failure could be due to several factors. The *tert*-BuNO might not be a very efficient trapper of these radicals. It is certainly known that the nitroxides formed by the trapping of simple alkoxy radicals are unstable. In addition, Perkins and Roberts (13) have recently shown that the trapping efficiency for *tert*-butoxy radicals decreases with increasing temperatures because the reverse reaction becomes more dominant. These factors together with the possibility of [12], which undoubtedly is very rapid, make it most unlikely that $PhCH_2O\cdot$ would be trapped. Therefore failure to detect this radical cannot be taken as evidence that it is not formed in the radiolysis.

[12] $PhCH_2O\cdot + PhCH_2OH \rightarrow$
$PhĊHOH + PhCH_2OH$

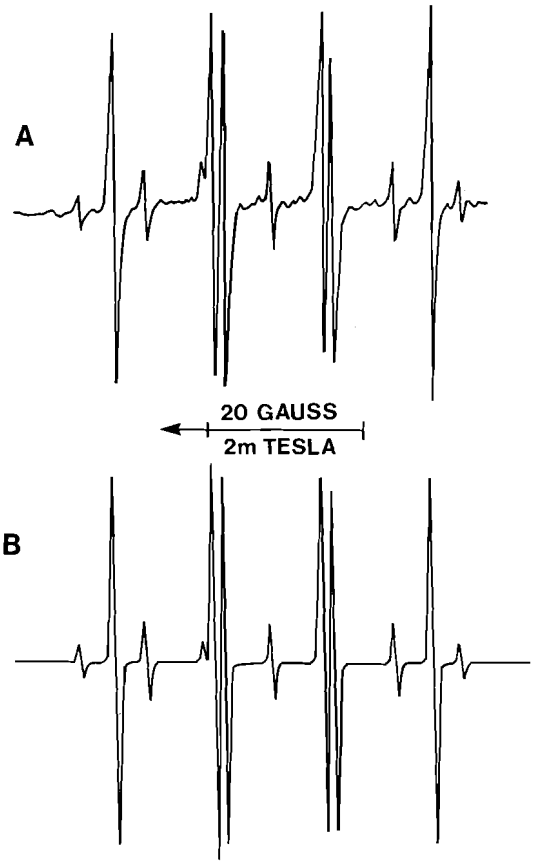

FIG. 4. (*a*) Electron spin resonance spectrum observed during irradiation of benzyl alcohol containing 10 mol/m^3 (0.01 *M*) *tert*-BuNO, 50 mol/m^3 (0.05 *M*) benzophenone, and 10 mol/m^3 (0.01 *M*) potassium hydroxide. (*b*) Computer simulated spectrum.

Can. J. Chem. Downloaded from www.nrcresearchpress.com by 210.87.254.105 on 09/05/12
For personal use only.

In view of this uncertainty, we cannot establish whether PhĊHOH is a primary product of the radiolysis or whether it all comes from [12]. However, by analogy with the known radiation chemical yields in simple alcohols such as methanol and ethanol (14, 15), it is probable that the primary yields of $PhCH_2O\cdot$ and PhĊHOH are of the same order of magnitude.

1. E. G. JANZEN. Acc. Chem. Res. **4**, 31 (1971).
2. F. P. SARGENT, E. M. GARDY, and H. R. FALLE. Chem. Phys. Lett. **24**, 120 (1974).
3. F. P. SARGENT and E. M. GARDY. Can. J. Chem. **52**, 3645 (1974).
4. A. KIRA and J. K. THOMAS. J. Chem. Phys. **60**, 766 (1974).
5. R. L. MCCARTHY and A. MACLACHLAN. Trans. Faraday Soc. **56**, 1187 (1960).
6. B. SMALLER, J. R. REMKO, and E. C. AVERY. J. Chem. Phys. **48**, 5174 (1968).
7. B. SMALLER, E. C. AVERY, and J. R. REMKO. J. Chem. Phys. **55**, 2414 (1971).
8. J. C. STOWELL. J. Org. Chem. **36**, 3055 (1971).
9. F. P. SARGENT and E. M. GARDY. In press.
10. M. J. PERKINS, P. WARD, and A. HORSFIELD. J. Chem. Soc. B, 395 (1970).
11. K. D. ASMUS, H. MOCKEL, and A. HENGLEIN. J. Phys. Chem. **77**, 1218 (1973).
12. G. E. ADAMS and R. L. WILLSON. J. Chem. Soc. Faraday Trans. I, **69**, 719 (1973).
13. M. J. PERKINS and B. P. ROBERTS. J. Chem. Soc. Perkins Trans. II, 297 (1974).
14. F. S. DAINTON, I. JANOVSKY, and G. A. SALMON. Proc. R. Soc. London, Ser. A, **327**, 305 (1972).
15. D. H. ELLISON, G. A. SALMON, and F. WILKINSON. Proc. R. Soc. London, Ser. A, **328**, 23 (1972).
16. W. A. WATERS. J. Chem. Soc. Chem. Commun. 1087 (1972).

Can. J. Chem. Downloaded from www.nrcresearchpress.com by 210.87.254.105 on 09/05/12
For personal use only.

The Water-activity of Supersaturated Aqueous Solutions of NaCl, KCl, and K_2SO_4 at 25 °C

FABIO LENZI, TUONG-TU TRAN, AND TJOON-TOW TENG

Département de Génie Chimique, Ecole Polytechnique, Campus de l'Université de Montréal, Case Postale 6079, Succursale "A", Montréal, Québec H3C 3A7

Received May 23, 1975

FABIO LENZI, TUONG-TU TRAN, TJOON-TOW TENG. Can. J. Chem. **53**, 3133 (1975).

Reverse application of the Reilly–Wood–Robinson and Zdanovskii–Stokes–Robinson equations to the water-activity data of various ternary aqueous systems containing NaCl, KCl, K_2SO_4 as one of the components yields self-consistent estimates of the water-activity of binary aqueous supersaturated solutions of the individual salts; these can be further extended by curvilinear extrapolation to give: $a_{w(NaCl)} = 1 + \Sigma_1^{10} A_i m^i$ with $A_1 = -3.28806 \times 10^{-2}$, $A_2 = 1.12512 \times 10^{-4}$, $A_3 = -4.30034 \times 10^{-4}$, $A_4 = 2.70506 \times 10^{-5}$, $A_5 = 1.43435 \times 10^{-6}$, $A_6 = 1.30209 \times 10^{-7}$, $A_7 = -1.51941 \times 10^{-8}$, $A_8 = 1.00520 \times 10^{-9}$, $A_9 = -4.21593 \times 10^{-10}$, $A_{10} = 2.62532 \times 10^{-11}$, valid to $a_{w(NaCl)} = 0.5422$, $m_{NaCl} = 11.0 \approx 1.8 \times m^{sat}_{NaCl}$; $a_{w(KCl)} = 1 + \Sigma_1^7 B_i m^i$ with $B_1 = -3.21884 \times 10^{-2}$, $B_2 = 9.77773 \times 10^{-4}$, $B_3 = -6.05349 \times 10^{-4}$, $B_4 = 1.18422 \times 10^{-4}$, $B_5 = -7.91572 \times 10^{-6}$, $B_6 = -3.88125 \times 10^{-8}$, $B_7 = 1.55125 \times 10^{-8}$, valid to $a_{w(KCl)} = 0.7115$, $m_{KCl} = 9.00 \approx 2.0 \times m^{sat}_{KCl}$; $a_{w(K_2SO_4)} = 1 + \Sigma_1^4 C_i m^i$ with $C_1 = -4.16810 \times 10^{-2}$, $C_2 = 1.16033 \times 10^{-2}$, $C_3 = -4.80543 \times 10^{-3}$, $C_4 = 7.15536 \times 10^{-4}$, valid to $a_{w(K_2SO_4)} = 0.9301$, $m_{K_2SO_4} = 2.20 \approx 3.0 \times m^{sat}_{K_2SO_4}$.

FABIO LENZI, TUONG-TU TRAN et TJOON-TOW TENG. Can. J. Chem. **53**, 3133 (1975).

L'application à rebours des équations de Reilly–Wood–Robinson et de Zdanovskii–Stokes–Robinson aux données de l'activité de l'eau de plusieurs systèmes ternaires contenant du NaCl ou du KCl ou du K_2SO_4 a été effectuée. Des valeurs de l'activité de l'eau de solutions aqueuses binaires sursaturées de chacun de ces sels ont été obtenues avec, dans chaque cas, bonne concordance. Les plages d'estimation ont été prolongées par extrapolation curvilineaire.

Introduction

A knowledge of the water-activity, a_w, is important in the correlation and prediction of both equilibria and kinetics in moderate to concentrated mixed aqueous solutions of electrolytes and nonelectrolytes. Areas of application include, for example, crystallization and reverse osmosis. In particular a knowledge of the a_w of mixed aqueous solutions near, at, or beyond saturation is required for the prediction of ternary solubility diagrams from binary data.

It has been noted (1, 2) that supersaturated binary data are often necessary for the computation of a_w of mixed concentrated ternary or more complex solutions from binary data. In the case of electrolytes the computation of the ternary a_w from binary data can, in principle, be made accurately via the full Reilly–Wood–Robinson (3), RWR, equation; this requires binary and extensive ternary common-ion a_w values at the ionic strength of the mixed concentrated solution. In the absence of such ternary data, coarser but still useful estimates can be made using only binary a_w data and either the first approximation to the RWR equation or its other approximate forms (4). In either situation it is necessary to estimate the a_w or φ (osmotic coefficient) values of binary aqueous solutions at the ionic strength of the mixed solution. This latter value may itself be higher than that of the binary at saturation, thus leading to a need for binary supersaturated a_w values.

The prediction of the a_w of mixed concentrated aqueous solutions containing nonelectrolytes or electrolytes and nonelectrolytes can be done in general by the Zdanovskii–Stokes–Robinson (5), ZSR, equation. In this case it is necessary to know the molality m of a binary aqueous solution at the a_w of the mixed solution, which is often less than the a_w of the binary at saturation. Again this calls for binary supersaturated a_w values.

Empirical and semiempirical methods of estimating supersaturated binary a_w values have been recently reviewed (2); the authors concluded that

Can. J. Chem. Downloaded from www.nrcresearchpress.com by 210.87.254.40 on 09/05/12
For personal use only.

the safest way of obtaining such values was to use the ZSR equation in reverse on ternary data. In this paper we shall show that reverse RWR is equally applicable, and we shall use both methods on various ternary data to obtain self-consistent estimates of supersaturated a_w values for binary aqueous solutions of NaCl, KCl, and K_2SO_4 up to twice their molality at saturation.

Reverse Application of the Reilly–Wood–Robinson Equation to Ternary Data

This will be illustrated by the calculation of supersaturated a_w values for aqueous NaCl by the reverse application of the RWR[1] equation to the ternary data for $LaCl_3$–NaCl in water (6).

Consider the three aqueous solutions shown in Fig. 1. Then, in the RWR nomenclature (3), for the common-ion mixture:

$$1 - \varphi_{mix} = -\frac{1}{mE}\left[\frac{(Z_{Na}m_{Na})(-Z_{Cl}m_{Cl})(Z_{Na} - Z_{Cl})(1 - \varphi^0_{NaCl})}{Z_{Na}Z_{Cl}} + \frac{(Z_{La}m_{La})(-Z_{Cl}m_{Cl})(Z_{La} - Z_{Cl})(1 - \varphi^0_{LaCl_3})}{Z_{La}Z_{Cl}}\right]$$

where $$E = \sum_{\text{cations}} (Zm) = Z_{Na}m_{Na} + Z_{La}m_{La} = m_{Na} + 3m_{La}$$

and $$m = \sum_{\text{anions+cations}} m_i = m_{Cl} + m_{Na} + m_{La}$$

thus

[1] $$1 - \varphi_{mix} = \frac{1}{m(m_{Na} + 3m_{La})}[2m_{Na}m_{Cl}(1 - \varphi^0_{NaCl}) + 4m_{La}m_{Cl}(1 - \varphi^0_{LaCl_3})]$$

and

$$1 - \varphi^0_{NaCl} = \frac{1}{2m_{Na}m_{Cl}}[m(m_{Na} + 3m_{La})(1 - \varphi_{mix}) - 4m_{La}m_{Cl}(1 - \varphi^0_{LaCl_3})]$$

but

$$m_{Na} = m_1, \quad m_{La} = m_2, \quad m_{Cl} = m_1 + 3m_2, \quad \text{and} \quad m = 2m_1 + 4m_2$$

also

$$\varphi^0_{NaCl} = -\frac{\ln a^0_{w(NaCl)}}{2(m_{NaCl})_I \times 0.018}$$

$$\varphi^0_{LaCl_3} = -\frac{\ln a^0_{w(LaCl_3)}}{4(m_{LaCl_3})_I \times 0.018}$$

$$\varphi_{mix} = -\frac{\ln a_{w(mix)}}{(2m_1 + 4m_2) \times 0.018}$$

If $$A \equiv \frac{1}{2m_1(m_1 + 3m_2)}\left[m(m_1 + 3m_2)\left\{1 + \frac{\ln a_{w(mix)}}{0.018(2m_1 + 4m_2)}\right\} - 4m_2(m_1 + 3m_2)\left\{1 + \frac{\ln a^0_{w(LaCl_3)}}{4(m_{LaCl_3})_I 0.018}\right\}\right]$$

then

[2] $$a^0_{w(NaCl)} = e^{\{(A-1)2(m_{NaCl})_I 0.018\}}$$

which constitutes the reverse RWR equation.

[1]The relation used here is the first approximation (3) to the full RWR expression; it is not possible to use the full expression to compute a_w or φ for a common-ion system unless a full set of ternary data is available. In this case the following aqueous ternary systems: NaCl–LaX_3 or NaX–$LaCl_3$, NaCl–NaX, NaX–LaX_3, $LaCl_3$–LaX_3 (where X is a suitable anion), as well as all the individual binary aqueous data, would be necessary to compute NaCl–$LaCl_3$.

Can. J. Chem. Downloaded from www.nrcresearchpress.com by 210.87.254.40 on 09/05/12
For personal use only.

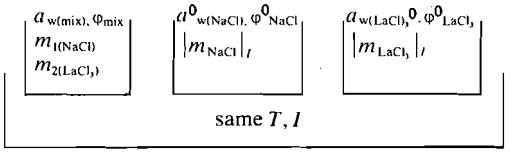

FIG. 1. Binary solutions of aqueous NaCl and $LaCl_3$ at the same temperature and ionic strength as a ternary aqueous system containing both NaCl and $LaCl_3$.

At 25 °C the saturation molality of aqueous NaCl is 6.0 m = ionic strength, I; the ternary data of Kirgintsev and Luk'yanov (6) at $I < 6.0$ for aqueous NaCl–$LaCl_3$ are shown in Table 1 together with values calculated by the RWR first approximation, [1]. Comparison of the a_w values in Table 1 shows that the RWR first approximation gives very good predictive results in this case, and that there is consequently no need to make an empirical correction analogous to the Kirgintsev–Luk'yanov (7) b for ZSR deviations. Indeed $LaCl_3$–NaCl (aqueous) is a type 'A' system (5) with a very small value of b.

It would thus appear reasonable to assume that there is no sudden departure in applicability of [1], and hence of [2], as the ionic strength passes from below to above 6 m, the saturation value for aqueous NaCl. (Tran and Lenzi (2) have shown that there is no essential change in character of the a_w *vs.* molality plots as saturation is reached and passed.) The ternary data (6) at $I > 6$ have been collected in Table 2, together with binary supersaturated values of $a_{w(NaCl)}$ calculated by [2]. These values are plotted in Fig. 2. It can be observed that all the values of $a^{obs}_{w(mix)}$ lie above the value of $a^{sat}_{w(NaCl)} = 0.76$, thus making the reverse application of ZSR impossible in this case.

Other Ternary Data Involving NaCl

For aqueous NaCl at 25 °C, $a^{sat}_{w(NaCl)} = 0.76$, $m^{sat}_{(NaCl)} = 6.0$; thus reverse RWR will only apply to ternary data whose $I_{mix} > 6.0$ m, while

TABLE 1. Ternary data for aqueous NaCl–$LaCl_3$ (6) at 25 °C for $I_{mix} < 6.0$ m

m_1 (NaCl in mix)	m_2 ($LaCl_3$ in mix)	$a^{obs}_{w(mix)}$	$a^{cal}_{w(mix)}$ ([1])
2.2931	0.1899	0.9030	0.9033
1.5088	0.5162	0.9030	0.9033
2.3170	0.3220	0.8886	0.8886
1.3795	0.7005	0.8886	0.8887
2.6463	0.3677	0.8690	0.8688

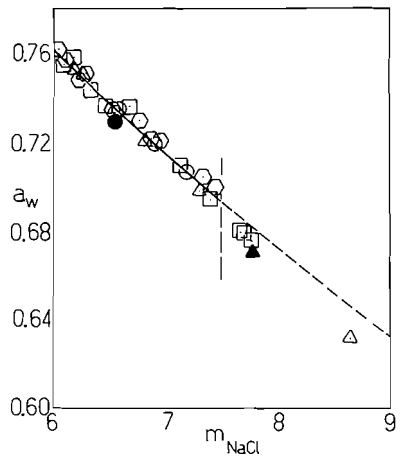

FIG. 2. Supersaturated binary aqueous values of a_w for NaCl: △, data from $LaCl_3$/NaCl; ○, data from LiCl/NaCl; ●, data from Na_2SO_4/NaCl; ▲, data from $MgSO_4$/NaCl; □, data from $MgCl_2$/NaCl; ◇, data from $MnCl_2$/NaCl; —, polynomial from [4]; ---, curvilinear extrapolation ([4*a*]).

reverse ZSR will only be of interest when $a_{w(mix)} < 0.76$. In each case the procedure followed is similar to that shown above for NaCl–$LaCl_3$ for reverse RWR or to that already given (1) for reverse ZSR. Ternary data below $I_{mix} = 6.0$ m or above $a_{w(mix)} = 0.76$ are examined and compared with a_w values calculated either by the RWR first approximation or the uncorrected form of the ZSR equation. Should there be good agreement, as is shown in Table 1 in the case of NaCl–$LaCl_3$, then the uncorrected RWR first approximation (or the uncorrected ZSR equation) is used to compute supersaturated a_w values. Otherwise an empirical correction term of the 'b' (7) type is fitted to the unsaturated $a_{w(mix)}$ data either as a constant 'b' independent of a_w, or, if necessary, as a simple function of a_w, such as $b = b_0 + b_1 a_w$, as previously suggested (1).

In case of appreciable deviations of the ternary data from the RWR first approximation at $I_{mix} < I^{sat}$ of the solute of interest, it has been found[2] that at roughly constant ionic fraction of one solute, the departures from the RWR first approximation can be expressed by

$$[3] \quad \frac{1}{0.018 \sum_j \nu_j m_j} \ln \frac{a_w^{obs}}{a_w^{cal}} = c_0 + c_1 a_w^{obs}$$

[2]T. T. Tran and F. Lenzi, unpublished data.

Can. J. Chem. Downloaded from www.nrcresearchpress.com by 210.87.254.40 on 09/05/12
For personal use only.

TABLE 2. Ternary data for aqueous NaCl–$LaCl_3$ (6) at 25 °C for $I_{mix} > 6.0\,m$ and supersaturated values of a_w for NaCl calculated via [2]

m_1 (NaCl in mix)	m_2 ($LaCl_3$ in mix)	$m_{NaCl}^{supersat}$ ($=I=m_1+6m_2$)	$a_{w(mix)}^{obs}$	$a_{w(NaCl)}^{supersat}$ ([2])
2.6812	0.5858	6.196	0.8409	0.7520
4.1890	0.3470	6.271	0.7997	0.7488
1.1831	0.9399	6.8225	0.8690	0.7198
1.8046	0.9164	7.303	0.8409	0.6977
2.1382	1.0858	8.653	0.7997	0.6315

TABLE 3. Supersaturated a_w and m values for NaCl at 25 °C

Aqueous system	m_1	m_2	$a_{w(mix)}$	ZSR or RWR corrections*	$m_{NaCl}^{supersat}$	$a_{w(NaCl)}^{supersat}$	Reference
LiCl–NaCl	2.0352	3.9468	0.7336	$b_0 = -0.0082$	6.5931	0.7336	14
	3.1002	2.8998	0.7194	$b_1 = -0.0187$	6.9153	0.7194	
	4.0194	1.9806	0.7065		7.1800	0.7065	
Na_2SO_4–NaCl	3.5694	0.9962	0.8229	$c_0 = -0.3207$	6.5580	0.7292	15
				$c_1 = 0.3188$			
$MgSO_4$–NaCl	1.4518	1.9647	0.8768	$c_0 = -0.5115$	7.7719	0.6703	16
				$c_1 = 0.5172$			
$MgCl_2$–NaCl	0.4248	5.1952	0.7530		6.4696	0.7352	15, 17
	0.2393	5.6188	0.7530		6.3367	0.7431	
	1.3009	3.2306	0.7530	$c_0 = 0.1634$	7.1333	0.7086	
				$c_1 = -0.1592$			
	2.0188	1.6186	0.7530	$c_0 = -0.1528$	7.6750	0.6795	
	2.0578	1.5356	0.7530	$c_1 = 0.1574$	7.7090	0.6789	
	2.1387	1.3516	0.7530		7.7677	0.6754	
	1.6584	2.4251	0.7530	$c_0 = -0.1584$	7.4003	0.6941	
				$c_1 = 0.1631$			
	1.8427	0.6534	0.8289	$c_0 = -0.1577$	6.1815	0.7583	
	2.0168	0.6285	0.8098	$c_1 = 0.1626$	6.6789	0.7360	
	1.3688	1.9980	0.8139		6.1044	0.7549	
$MnCl_2$–NaCl	1.3687	2.0062	0.8339	$c_0 = 0.3091$	6.1123	0.7573	18
	1.2456	2.3091	0.8307	$c_1 = -0.2813$	6.0459	0.7614	
	1.5834	2.2049	0.8087		6.9551	0.7207	
	1.4293	2.4840	0.8087		6.7719	0.7290	
	1.4469	1.9517	0.8307		6.2924	0.7508	
	1.2500	3.7015	0.7705	$c_0 = 0.3341$	7.4515	0.6997	
	1.9601	1.0247	0.8307	$c_1 = -0.3005$	6.9050	0.7216	
	1.0688	3.1255	0.8087		6.3319	0.7481	
	1.2212	3.6707	0.7736		7.3343	0.7040	
	0.6212	4.6764	0.7736		6.5400	0.7336	
	0.5573	4.8646	0.7705		6.5365	0.7337	

*ZSR corrections obtained by using a Kirgintsev–Luk'yanov b correction of the form (1) $b = b_0 + b_1 a_w$ while RWR corrections obtained via [3].

where a_w^{cal} = water-activity calculated by the RWR first approximation. Provided suitable $I_{mix} < I^{sat}$ ternary data are available to determine c_0 and c_1, the values of $a_w^{supersat}$ can be obtained by the use of [2] and [3]. Examples of the results of such a procedure are given in Table 3 for NaCl (as well as in Tables 4 and 5 for KCl and K_2SO_4).

The supersaturated points for $a_{w(NaCl)}$ from Tables 2 and 3 are plotted in Fig. 2. In general the results for six different ternaries using both reverse methods show fair agreement. The agreement is satisfactory up to 7.5 m, beyond which there is some spread in the results. A polynomial (8) to give a minimum standard deviation has been fitted to the unsaturated a_w–molality data (9, 10) and the 26 supersaturated points obtained

Can. J. Chem. Downloaded from www.nrcresearchpress.com by 210.87.254.40 on 09/05/12
For personal use only.

TABLE 4. Supersaturated a_w and m values for KCl at 25 °C

Aqueous system	m_1	m_2	$a_{w(mix)}$	ZSR or RWR corrections*	$m_{KCl}^{supersat}$	$a_{w(KCl)}^{supersat}$	Reference
LiCl–KCl	2.1555	2.3445	0.8273	$b_0 = 0.0887$	5.3500	0.8273	14
	1.4905	3.5095	0.8182	$b_1 = -0.1219$	5.5797	0.8182	
	2.3950	2.6050	0.8044		6.0331	0.8044	
	3.2370	1.7630	0.7888		6.6018	0.7888	
NaCl–KCl	4.6690	1.2871	0.7744	$b_0' = 0.0129$	7.4400	0.7744	11
	5.5509	0.5624	0.7602	$b_1' = -0.0075$	8.0546	0.7602	
$SrCl_2$–KCl	1.3286	0.9799	0.8889	$c_0 = 0.2704$	4.9657	0.8372	19
	1.5544	1.1465	0.8650	$c_1 = -0.2639$	5.8097	0.8085	
	1.4516	1.0707	0.8760		5.4255	0.8213	
	1.3386	1.6128	0.8650	$c_0 = 0.3048$	5.6286	0.8149	
	1.2472	1.5026	0.8760	$c_1 = -0.2965$	5.2442	0.8279	
	1.4363	1.7305	0.8527		6.0394	0.8001	
	0.7780	2.7345	0.8650	$c_0 = 0.0793$	5.0685	0.8341	
	0.8400	2.9523	0.8527	$c_1 = -0.0762$	5.4723	0.8201	
	0.3031	3.9718	0.8527		4.8811	0.8405	
$MgCl_2$–KCl	0.9661	2.0559	0.8671	$c_0 = 0.4295$	4.9542	0.8356	20
	1.0627	2.2613	0.8511	$c_1 = -0.3903$	5.4494	0.8185	
	0.4456	3.6274	0.8511	$c_0 = 0.1403$	4.9642	0.8377	
				$c_1 = -0.1271$			
$NaNO_3$–KCl	3.4819	2.1295	0.8478	$c_0 = 0.2426$	5.6114	0.8108	21
				$c_1 = -0.2379$			
	2.1910	2.7029	0.8615	$c_0 = 0.4295$	4.8939	0.8426	
	2.4127	2.9764	0.8478	$c_1 = -0.3903$	5.3891	0.8267	

*System LiCl–KCl corrected by $b = b_0 + b_1 a_w$; but NaCl–KCl corrected by $b = b_0' + b_1' I$.

here to 7.5 m:

$$[4] \qquad a_{w(NaCl)} = 1 + \sum_1^5 A_i' m^i$$

with $A_1' = -3.13449 \times 10^{-2}$, $A_2' = -2.22625 \times 10^{-3}$, $A_3' = 6.28750 \times 10^{-4}$, $A_4' = -1.52868 \times 10^{-4}$, $A_5' = 1.16207 \times 10^{-5}$, and $\sigma = 0.00134$ where σ is the standard deviation of the fit. The range for supersaturated values can be further extended by means of the curvilinear extrapolation (2) recently proposed to $m = 11.0$ $m \approx 1.5 \times 7.5$ m. The final polynomial thus obtained to $a_w = 0.5422$, $m_{NaCl} = 11.0$ is given by

$$[4a] \qquad a_{w(NaCl)} = 1 + \sum_1^{10} A_i m^i$$

with $A_1 = -3.28806 \times 10^{-2}$, $A_2 = 1.12512 \times 10^{-4}$, $A_3 = -4.30034 \times 10^{-4}$, $A_4 = 2.70506 \times 10^{-5}$, $A_5 = 1.43435 \times 10^{-6}$, $A_6 = 1.30209 \times 10^{-7}$, $A_7 = -1.51941 \times 10^{-8}$, $A_8 = 1.00520 \times 10^{-9}$, $A_9 = -4.21593 \times 10^{-10}$, $A_{10} = 2.62532 \times 10^{-11}$, $\sigma = 0.00012$, and is shown in Fig. 2.

Ternary Data Involving KCl

For aqueous KCl at 25 °C, $a_{w(KCl)}^{sat} = 0.8426$, $m_{KCl}^{sat} = 4.8$. Table 4 lists the ternary systems used to obtain supersaturated data by both reverse methods. It was found[3] that differences between the ZSR equation and the observed (11) NaCl–KCl data were corrected better by a Kirgintsev–Luk'yanov (7) correction $b' = b_0' + b_1' I$ rather than by the more usual (1) $b = b_0 + b_1 a_w$ correction term. The supersaturated a_w values for KCl from Table 4, together with directly-obtained (12) supersaturated values are plotted in Fig. 3. Except for two of the four RWR $NaNO_3$–KCl points and the two NaCl–KCl points, there is good overall agreement between the nineteen calculated and the two experimental supersaturated values. The $NaKCl_2$ complex formation noted by Stearn (13) may account for the $NaNO_3$–KCl and NaCl–KCl deviations.

A polynomial (8) has been fitted to the unsaturated a_w–molality data and to the 19 corroborated points to $m_{KCl} = 6.0$ m:

$$[5] \qquad a_{w(KCl)} = 1 + \sum_1^4 B_i' m^i$$

with $B_1' = -3.22956 \times 10^{-2}$, $B_2' = 8.25683 \times 10^{-4}$, $B_3' = -3.67164 \times 10^{-4}$, $B_4' = 3.83407 \times$

[3] T. T. Teng and F. Lenzi, unpublished data.

Can. J. Chem. Downloaded from www.nrcresearchpress.com by 210.87.254.40 on 09/05/12
For personal use only.

TABLE 5. Supersaturated a_w and m values for K_2SO_4 at 25 °C

Aqueous system	m_1	m_2	$a_{w(mix)}$	ZSR or RWR corrections	$m^{supersat}_{K_2SO_4}$	$a^{supersat}_{w(K_2SO_4)}$	Reference
$KCl-K_2SO_4$	0.6770	0.1242	0.9739	$b_{avg} = 0.061$*	0.7465	0.9739	22
	0.6317	0.1616	0.9739		0.7336	0.9739	
	0.5406	0.2442	0.9739		0.7418	0.9739	
	0.4925	0.2862	0.9739		0.7392	0.9739	
	0.6036	0.2008	0.9735		0.7892	0.9735	
	0.6862	0.2290	0.9700		0.8766	0.9700	
	0.6902	0.2301	0.9698		0.8937	0.9698	
	0.7907	0.2630	0.9654		1.0053	0.9654	
	0.8614	0.2203	0.9647		1.0330	0.9647	
	0.7396	0.3341	0.9647		1.0452	0.9647	
	0.6740	0.3917	0.9647		1.0371	0.9647	
	1.0547	0.3516	0.9544		1.4052	0.9544	
	1.1418	0.3798	0.9505		1.5170	0.9505	
	1.0548	0.3516	0.9544	$c_0 = 0.2428$	0.7032	0.9750	
	1.1418	0.3798	0.9505	$c_1 = -0.2441$	0.7604	0.9727	
$Na_2SO_4-K_2SO_4$	0.3816	0.3816	0.9735	$b_{avg} = -0.077$	0.7526	0.9735	22
	0.5331	0.2379	0.9730		0.7496	0.9730	
	0.4327	0.3446	0.9730		0.7651	0.9730	
	0.2724	0.5127	0.9730		0.7787	0.9730	
	0.4412	0.4415	0.9698		0.8650	0.9698	
	0.8027	0.3846	0.9608		1.1506	0.9608	
	0.4987	0.6886	0.9608		1.1550	0.9608	
	0.3816	0.3816	0.9735	$c_0 = 0.0677$	0.7632	0.9733	
	0.5331	0.2379	0.9730	$c_1 = -0.0736$	0.7710	0.9724	
	0.4327	0.3446	0.9730		0.7773	0.9727	
	0.2724	0.5127	0.9730		0.7851	0.9728	
	0.4412	0.4415	0.9698		0.8827	0.9695	
	0.8027	0.3846	0.9608		1.1873	0.9602	
	0.4987	0.6886	0.9608		1.1873	0.9602	
$NaCl-K_2SO_4$	0.6761	0.2252	0.9700	$b_{avg} = -0.027$	0.8657	0.9700	22
	0.6789	0.2262	0.9698		0.8689	0.9698	
	0.6659	0.2401	0.9696		0.8553	0.9696	
	0.5923	0.3228	0.9696		0.8926	0.9696	
	0.7786	0.2590	0.9654		1.0424	0.9654	
	1.0211	0.3397	0.9551		1.3742	0.9551	
	1.0340	0.3444	0.9544		1.3827	0.9544	
	1.1195	0.3724	0.9505		1.4973	0.9505	
	1.2687	0.4226	0.9439		1.7293	0.9439	
	1.8084	0.3781	0.9266		2.3435	0.9266	
	1.6389	0.5585	0.9266		2.2933	0.9266	
	1.5084	0.7000	0.9266		2.2851	0.9266	
	1.1195	0.3724	0.9505	$c_0 = 0.3821$	0.7456	0.9736	
	1.2687	0.4226	0.9439	$c_1 = -0.3877$	0.8455	0.9714	
	1.6389	0.5585	0.9266		1.1048	0.9632	
	1.8084	0.3781	0.9266		0.9809	0.9656	
	1.5084	0.7000	0.9266		1.2028	0.9605	

*Average values of b are used (1) for the ZSR method.

10^{-5}, and $\sigma = 0.00064$. The range for supersaturated values can be further extended by curvilinear extrapolation to $m_{KCl} = 9.0$ $m = 1.5 \times 6.0\,m$. The final polynomial thus obtained to $a_w = 0.7115$ is given by

$$[5a] \qquad a_{w(KCl)} = 1 + \sum_{1}^{7} B_i m^i$$

with $B_1 = -3.21884 \times 10^{-2}$, $B_2 = 9.77773 \times 10^{-4}$, $B_3 = -6.05349 \times 10^{-4}$, $B_4 = 1.18422 \times 10^{-4}$, $B_5 = -7.91572 \times 10^{-6}$, $B_6 = -3.88125 \times 10^{-8}$, $B_7 = 1.55125 \times 10^{-8}$, $\sigma = 0.00015$, and is shown in Fig. 3.

Ternary Data Involving K_2SO_4

Three ternary systems involving K_2SO_4 and calculated results using both reverse methods are

Can. J. Chem. Downloaded from www.nrcresearchpress.com by 210.87.254.40 on 09/05/12
For personal use only.

Can. J. Chem. Downloaded from www.nrcresearchpress.com by 210.87.254.40 on 09/05/12
For personal use only.

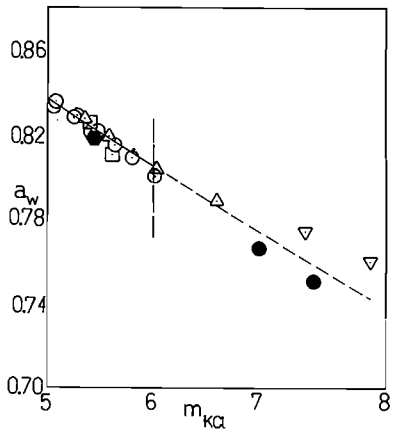

FIG. 3. Supersaturated binary aqueous values of a_w for KCl: ●, supersaturated values from ref. 12; △, data from LiCl/KCl; ▽, data from NaCl/KCl; □, data from $NaNO_3$/KCl; ⬣, data from $MgCl_2$/KCl; ○, data from $SrCl_2$/KCl; —, polynomial from [5]; ---, curvilinear extrapolation ([5*a*]).

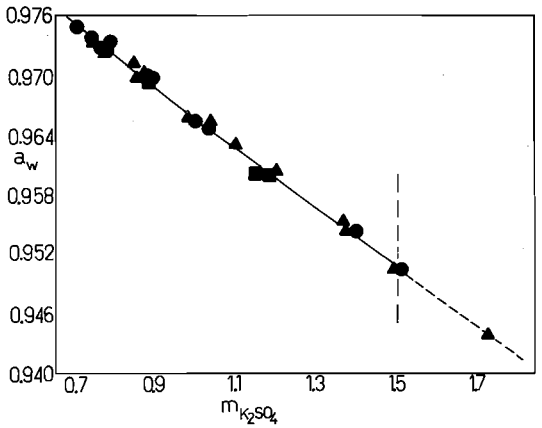

FIG. 4. Supersaturated binary aqueous a_w values for K_2SO_4: ●, data from KCl/K_2SO_4; ■, data from Na_2SO_4/K_2SO_4; ▲, data from NaCl/K_2SO_4; —, polynomial from [6]; ---, curvilinear extrapolation ([6*a*]).

given in Table 5, and the supersaturated $a_{w(K_2SO_4)}$ are plotted in Fig. 4. There is good agreement in general; an initial polynomial comprising both unsaturated values (9) and the 30 supersaturated values to $m_{K_2SO_4} = 1.507$ is given by

$$[6] \qquad a_{w(K_2SO_4)} = 1 + \sum_1^3 C_i' m^i$$

with $C_1' = -4.12827 \times 10^{-2}$, $C_2' = 9.94478 \times 10^{-3}$, $C_3' = -2.81312 \times 10^{-3}$, and $\sigma = 0.00036$. The range for supersaturated values can again be extended further to give $a_{w(K_2SO_4)}$ estimates to $m_{K_2SO_4} = 2.20\,m \approx 1.5 \times 1.5\,m$; the final polynomial thus obtained to $a_{w(K_2SO_4)} = 0.9301$ is given by

$$[6a] \qquad a_{w(K_2SO_4)} = 1 + \sum_1^4 C_i m^i$$

with $C_1 = -4.16810 \times 10^{-2}$, $C_2 = 1.16033 \times 10^{-2}$, $C_3 = -4.80543 \times 10^{-3}$, $C_4 = 7.15536 \times 10^{-4}$, and $\sigma = 0.00002$.

TABLE 6. Supersaturated water activities of NaCl and KCl solutions at 25 °C (from [5*a*] and [4*a*])

Molality	$a_{w(KCl)}$	$a_{w(NaCl)}$
5.0	0.8372*	
5.2	0.8308*	
5.4	0.8245*	
5.6	0.8183*	
5.8	0.8122*	
6.0	0.8063*	
6.2	0.7995	0.7505*
6.4	0.7932	0.7413*
6.6	0.7869	0.7324*
6.8	0.7807	0.7237*
7.0	0.7745	0.7154*
7.2	0.7682	0.7076*
7.4	0.7620	0.7004*
7.6	0.7557	0.6938
7.8	0.7495	0.6811
8.0	0.7432	0.6725
8.2	0.7368	0.6640
8.4	0.7305	0.6555
8.6	0.7241	0.6470
8.8	0.7177	0.6384
9.0	0.7115	0.6299
10.0		0.5861
11.0		0.5422

*Calculated from [5] and [4].

TABLE 7. Supersaturated water activities of K_2SO_4 solutions at 25 °C (from [6])

Molality	$a_{w(K_2SO_4)}$
0.74	0.9737
0.76	0.9730
0.80	0.9719
0.85	0.9705
0.88	0.9694
1.00	0.9657
1.10	0.9627
1.20	9.9599
1.40	0.9540
1.50	0.9509
1.60	0.9479*
1.80	0.9421*
2.00	0.9361*
2.20	0.9031*

*Calculated from [6*a*].

The results for all three salts are summarized in Tables 6 and 7 which list supersaturated a_w values at rounded values of the molality for the three salts calculated via [4], [4*a*], [5], [5*a*], and [6], [6*a*].

The generally good agreement obtained for different ternaries by both reverse methods confirms the validity of the approach. The errant points obtained for KCl from $NaNO_3$–KCl and NaCl–KCl show the need for using as many different ternary systems as possible.

We thank the National Research Council of Canada and la Direction Generale de l'Enseignement Supérieur, Quebec, for financial aid.

1. J. SANGSTER, T. T. TENG, and F. LENZI. Can. J. Chem. **51**, 2626 (1973).
2. T. T. TRAN and F. LENZI. Can. J. Chem. Eng. **52**, 798 (1974).
3. P. J. REILLY, R. H. WOOD, and R. A. ROBINSON. J. Phys. Chem. **75**, 1305 (1971).
4. J. SANGSTER and F. LENZI. Can. J. Chem. Eng. **52**, 392 (1974).
5. H. CHEN, J. SANGSTER, T. T. TENG, and F. LENZI. Can. J. Chem. Eng. **51**, 234 (1973).
6. A. N. KIRGINTSEV and A. V. LUK'YANOV. Russ. J. Phys. Chem. **39**, 389 (1965).
7. A. N. KIRGINTSEV and A. V. LUK'YANOV. Russ. J. Phys. Chem. **40**, 953 (1966).
8. T. T. TENG and F. LENZI. Can. J. Chem. Eng. **52**, 387 (1974).
9. R. A. ROBINSON and R. H. STOKES. Electrolyte solutions, 2nd ed. rev. Butterworths, London. 1970.
10. G. SCATCHARD, W. J. HAMER, and S. E. WOOD. J. Am. Chem. Soc. **60**, 3061 (1938).
11. R. A. ROBINSON. J. Phys. Chem. **65**, 662 (1961).
12. International Critical Tables, Vol. III. McGraw-Hill, New York. 1928. p. 297.
13. A. E. STEARN. J. Am. Chem. Soc. **44**, 670 (1922).
14. R. A. ROBINSON and C. K. LIM. Trans. Faraday Soc. **49**, 1144 (1953).
15. Y. C. WU, R. M. RUSH, and G. SCATCHARD. J. Phys. Chem. **72**, 4048 (1968).
16. Y. C. WU, R. M. RUSH, and G. SCATCHARD. J. Phys. Chem. **73**, 2047 (1969).
17. R. F. PLATFORD. J. Phys. Chem. **72**, 4053 (1968).
18. C. J. DOWNES. J. Chem. Eng. Data, **18**, 412 (1973).
19. C. J. DOWNES. J. Chem. Thermodyn. **6**, 317 (1974).
20. A. N. KIRGINTSEV and A. V. LUK'YANOV. Russ. J. Phys. Chem. **40**, 686 (1966).
21. C. P. BEZBORUAH, A. K. COVINGTON, and R. A. ROBINSON. J. Chem. Thermodyn. **2**, 431 (1970).
22. R. A. ROBINSON, R. F. PLATFORD, and C. W. CHILDS. J. Solution Chem. **1**, 167 (1972).

Can. J. Chem. Downloaded from www.nrcresearchpress.com by 210.87.254.40 on 09/05/12
For personal use only.

Can. J. Chem. Downloaded from www.nrcresearchpress.com by 210.87.254.5 on 09/05/12
For personal use only.

The Bioorganic Chemistry of *N*-Allyl and *N*-Propargyl Substituents in Drug Interactions with Flavin-linked Oxidases

J.-L. KRAUS[1] AND B. BELLEAU

Department of Chemistry, McGill University, Montreal, Quebec H3C 3G1

Received May 12, 1975

J.-L. KRAUS and B. BELLEAU. Can. J. Chem. **53**, 3141 (1975).

Attention is focused on recent mechanistic proposals concerning the unique inhibitory properties of *N*-propargyl substituents toward flavin-linked oxidases. Model studies with sarcosine oxidase have revealed that the enzyme displays absolute substrate specificity. Unexpectedly however, substitution of the *N*-methyl group of the substrate by the *N*-allyl or *N*-propargyl functions led to a time-dependent irreversible inactivation of the enzyme. The rate of inactivation by these substrate analogs was markedly retarded by deuterium substitution in the methylene group of the allyl and propargyl functions. It is concluded, mainly on that basis, that *N*-allyl and *N*-propargyl glycine are inhibitory substrates for the enzyme, alkylating species being generated at the active site level of the enzyme. The implications of these findings in the mechanism of action of medicinally important drugs are briefly mentioned.

J.-L. KRAUS et B. BELLEAU. Can. J. Chem. **53**, 3141 (1975).

Le mécanisme de l'action inhibitrice unique du substituent *N*-propargyle au niveau des oxydases du type flavine est soumis à l'étude. A l'aide du système modèle sarcosine oxydase, il a été établie que l'enzyme possède une spécificité absolue pour son substrat. Cependant, la substitution du *N*-méthyle de la glycine par un *N*-allyle ou *N*-propargyle conduit à une inhibition irreversible qui apparait graduellement. La vitesse d'inactivation par ces deux analogues est fortement retardée par la substitution des hydrogènes du groupement méthylène de l'allyle et du propargyle par le deutérium. Ceci conduit à la conclusion que ces deux analogues du substrat se comportent comme des substrats 'inhibiteurs' de l'enzyme, des intermédiaires à propriétés alkylantes étant générés au niveau du centre actif. Les implications de ces résultats dans le mécanisme d'action de drogues d'une importance thérapeutique sont brièvement discutées.

Recently much interest has been focused on the rational chemical development of specific active site-directed irreversible inhibitors of enzymes using as a basis the latter's potential ability to generate catalytically from suitable substrate analogs highly reactive intermediate species capable of covalent bond formation with an active site nucleophile (1, 2). Of fundamental relevance to medicinal chemistry is the recent discovery that various drugs incorporating a favorably disposed acetylenic function can behave as specific 'irreversible inhibiting substrates' (or k_{cat} inhibitors (2)) for certain flavin-linked oxidases such as monoamine-oxidase (MAO) (2) and bacterial lactate oxidase and dehydrogenase (3). Other interesting examples of inhibitory substrates for pyridoxal and nicotinamide adenine dinucleotide-linked enzymes have been reviewed and discussed by Rando (2). For the medicinally important case of acetylenic amines of the Parglyine class of drugs, the enzymatically catalyzed formation of a reactive allene intermediate is thought to be involved in the inactivation reaction of the MAO active site (2). However, no evidence is available for this mechanism. Very recently, bioorganic model studies with 3-methyl lumiflavin led to the elucidation of the structure of an adduct with 3-dimethylamino-1-propyne. It was shown that covalent bond formation between N-5 of the cofactor and C-1 of the inhibitor (4) is involved. The relevance of these observations to MAO inactivation by Pargyline remains to be determined. The fact that oxidative *N*-dealkylations and especially *N*-demethylations play an important role in drug activation and inactivation *in vivo* led us to ask the following questions. (*a*) Is the concept of inhibitory sub-

[1]Holder of a France–Quebec Exchange Programme Fellowship. Present address: Department of Chemistry, Université de Bretagne Occidentale, Brest, France.

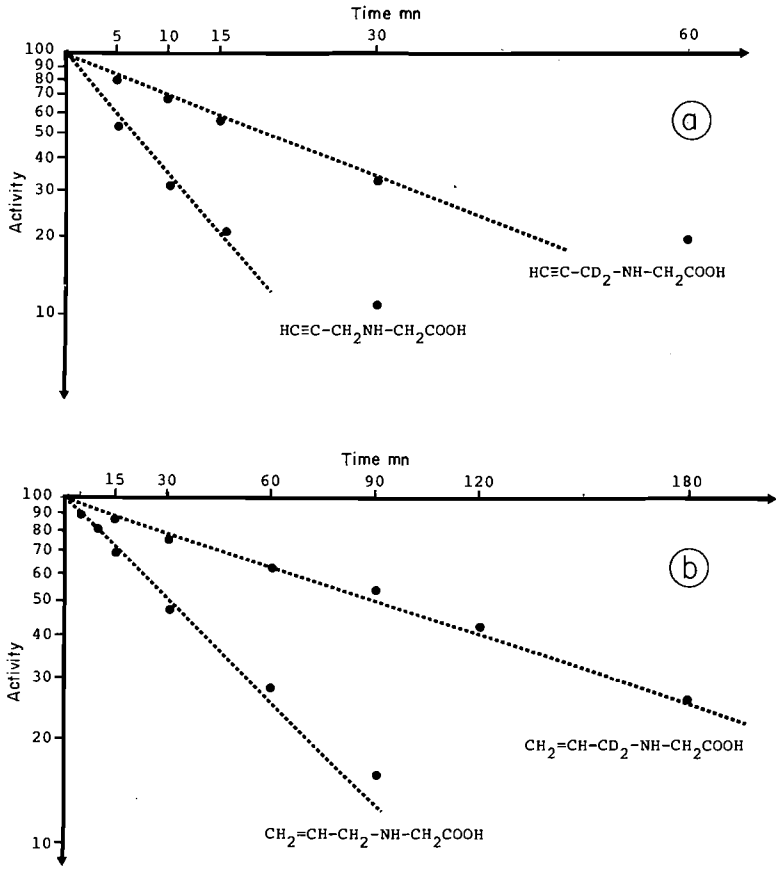

FIG. 1. Percentage inhibition of rat liver sarcosine oxidase *vs.* pre-incubation time with 10 μmoles of irreversible inhibitors in a total volume of 2.4 ml of suspension containing mitochondria from 0.5 g of rat liver (5, 6) in 0.075 *M* phosphate buffer (0.1 m*M* in Mg^{+2}), p*H* 7.8 at 37 °C. Residual enzyme activity was evaluated by measuring formaldehyde production from sarcosine according to the literature (5, 6). (*a*) Pseudo first-order kinetics of inhibition by the *N*-propargyl glycines ($r = 0.998$ and 0.973); rate ratio $k_H/k_D = 2.0$. (*b*) Pseudo first-order kinetics of inhibitors by the *N*-allyl glycines ($r = 0.985$ and 0.998); rate ratio $k_H/k_D = 2.3$. The fall-off in rates after 80–90% inhibition by the propargyl glycines (Fig. 1*a*) indicates that secondary reactions may occur in the late stages. This is not the case with the *N*-allyl analogs.

strates applicable to other flavin-linked oxidases including substrate specific *N*-demethylases? (*b*) Is the proposed mechanism of enzyme inactivation by acetylenic amines generally correct and of predictive value in drug design? The present communication is to offer preliminary answers to these questions. For our purposes, we selected the well-known flavin-linked enzyme sarcosine oxidase which demethylates the specific substrate sarcosine to glycine (5, 6) and submitted it to the action of candidate inhibitory substrates.

Rat liver sarcosine oxidase was isolated and assayed as described in the literature (5, 6). Using conventional literature methods (7), the following *N*-substituted glycines were prepared: ethyl (8), m.p. 175 °C; *n*-propyl (9), m.p. 195 °C; *n*-butyl (10), m.p. 192 °C; allyl (11, 12), m.p. 121 °C; propargyl, m.p. 162 °C; cyclopropylmethyl, m.p. 185 °C; benzyl, m.p. 182 °C. The synthesis of *N*-(α,α-dideuterioallyl)glycine and *N*-(α,α-dideuteriopropargyl)glycine (**1** and **2** respectively) was accomplished by the same

$CH_2{=}CH{-}CD_2NHCH_2CO_2H$

1

$HC{\equiv}C{-}CD_2NHCH_2CO_2H$

2

method using the appropriately deuterated

Can. J. Chem. Downloaded from www.nrcresearchpress.com by 210.87.254.5 on 09/05/12
For personal use only.

Can. J. Chem. Downloaded from www.nrcresearchpress.com by 210.87.254.5 on 09/05/12
For personal use only.

amines which in turn were prepared as follows: the anthracene adduct with acrylonitrile (13) was reduced to the amine with excess $LiAlD_4$ followed by retro-Diels–Alder to α,α-dideuterioallyl amine (14) (>98% labelled). Reduction of propiolonitrile (15) with $LiAlD_4$ in the presence of magnesium bromide (16) gave α,α-dideuteriopropargyl amine (>98% labelled) in 20–25% yield. The rate of enzyme inactivation was followed by assaying for residual sarcosine oxidase activity as a function of time. All incubations were carried out at 37 °C at p*H* 7.8 in phosphate buffer as previously described (5, 6). The results were as follows: none of the simple alkyl analogs of sarcosine acted as substrates or inhibitors (up to 10^{-2} *M*) of the enzyme. However, both the *N*-allyl and *N*-propargyl analogs at 10^{-4} to 10^{-3} *M* caused gradual irreversible inhibition of the enzyme (no activity recovered after dialysis at 0 °C for 24 h against 0.075 *M* phosphate buffer, p*H* 7.8). The time-course of these inhibitory reactions is shown in Figs. 1*a* and *b* where it can be seen that α,α-dideuteration of the allyl and propargyl group decreased the rate of inhibition by factors of 2.3 and 2.0 respectively. Clearly then, a rate-limiting abstraction of an α-hydrogen from the allyl or propargyl group conditions the appearance of irreversible inhibition, thus establishing that the enzyme generates reactive alkylating species leading to covalent bond formation with the active site. An attractive mechanism for these reactions is illustrated in **3** and **4**. Alternatively, intermediates **3** and **4** may generate acrolein and propargyl-

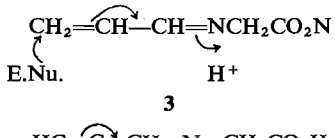

3

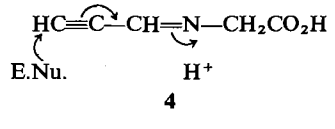

4

aldehyde at the active site followed by alkylation of a proximal nucleophile. Experiments are under way which should allow a choice between these two possibilities. The mechanistic significance of similar primary deuterium isotope effects on the rates of inhibition was discussed previously (17, 18). As expected, the competitive inhibitor methoxyacetate (6) was markedly effective in retarding the inactivation reaction. On that basis, we conclude that *N*-allyl and *N*-propargyl glycine behave as inhibitory substrates for the substrate binding site of sarcosine oxidase. While the results are not inconsistent with the formation of an intermediate allene in the inhibitory action of the *N*-propargyl derivative (2), the fact that the *N-allyl analog can hardly give rise to such an intermediate* strongly favors the alternative mechanism illustrated in **3** and **4**. Interestingly, the *N*-cyclopropylmethyl glycine analog behaved only as a weak reversible inhibitor ($K_1 \simeq 10^{-2}$ *M*) of the enzyme. One may recall that this *N*-substituent confers highly effective antagonistic properties to a variety of opiate-like structures (19). These observations bring to light a previously unsuspected specific equivalence of a substrate *N*-methyl group and *N*-allyl or *N*-propargyl functions as regards *productive* binding on a flavin-linked enzyme. The implications of these findings in medicinal chemistry and especially drug design deserve further investigation.[2]

We are grateful to the National Research Council of Canada for the financial support of this work.

1. K. Bloch. Acc. Chem. Res. **2**, 193 (1969).
2. R. R. Rando. Science, **185**, 320 (1974).
3. C. T. Walsh, A. Schonbrunn, O. Lockbridge, V. Massey, and R. H. Abeles. J. Biol. Chem. **247**, 6004 (1972); C. H. Walsh, R. H. Abeles, and H. R. Kaback. J. Biol. Chem. **247**, 7858 (1972).
4. A. L. Maycock. J. Am. Chem. Soc. **97**, 2270 (1975).
5. C. G. Mackenzie and J. Harris. J. Biol. Chem. **227**, 393 (1957).
6. R. H. Abeles, W. R. Frisell, and C. G. Mackenzie. J. Biol. Chem. **235**, 853 (1959).
7. A. J. Spesiale and E. G. Jaworski. J. Org. Chem. **25**, 728 (1960).
8. V. G. Yashunskii, V. F. Vasil'eva, and Y. N. Sheinker. Zh. Obshch. Khim. **29**, 2718 (1959).
9. C. M. Paine and C. Heinz. J. Biol. Chem. **235**, 1080 (1960).
10. L. B. Kier and D. Dhawan. J. Pharm. Sci. **51**, 1058 (1962).
11. E. A. Adelberg. J. Bacteriol. **76**, 326 (1958).
12. L. I. Tsegel'nyuk and E. A. Shilov. Zh. Vses. Khim. Ova. **13**, 463 (1968).
13. P. D. Barlett and F. A. Tate. J. Am. Chem. Soc. **75**, 91 (1953).
14. J. J. Kurland and R. P. Lutz. Chem. Somm. 1097 (1968).
15. S. Murahashi, T. Takizawa, S. Kurioka, and S. Maekawa. Nippon Kagaku Zasshi, **77**, 1689 (1956).

[2]Deuteration of the Pargyline methylene group ($C_6H_5CH_2N(CH_3)CD_2C{\equiv}CH$) reduced the rate of MAO inactivation by a factor of 2, thus indicating that mechanism **4** may also be applicable to this well-known drug (J.-L. Kraus and J. J. Yaouanc, manuscript in preparation).

16. E. WIBERG and R. BAUER. Z. Naturforsch. Teil B, **7**, 131 (1952).
17. B. BELLEAU and J. MORAN. Ann. N.Y. Acad. Sci. **107**, 822 (1963).
18. B. BELLEAU. Stud. Biophys. **4**, 95 (1967).
19. B. BELLEAU, I. MONKOVIC, T. T. CONWAY, H. WONG, Y. G. PERRON, and I. J. PACHTER. J. Am. Chem. Soc. **95**, 7910 (1973).

Stereospecific Synthesis of *dl*-Triacetyldaunosamine

CHIU MING WONG, TSE-LOK HO, AND WALTER P. NIEMCZURA
Department of Chemistry, University of Manitoba, Winnipeg, Manitoba R3T 2N2

Received July 21, 1975

CHIU MING WONG, TSE-LOK HO, and WALTER P. NIEMCZURA. Can. J. Chem. **53**, 3144 (1975).

Daunosamine triacetate was synthesized via a stereospecific non-carbohydrate approach. The *N*-benzoyl-β-amino lactone (**9**) could be an interesting intermediate for the very important and highly deoxygenated amino sugar, 4-deoxydaunosamine.

CHIU MING WONG, TSE-LOK HO et WALTER P. NIEMCZURA. Can. J. Chem. **53**, 3144 (1975).

On a synthétisé le triacétate de la daunosamine par une approche stéréospécifique n'impliquant pas de carbohydrates. La *N*-benzoyl β-amino lactone (**9**) pourrait s'avérer être un intermédiare interessant pour la synthèse du sucre aminé très important et très désoxygené qu'est la désoxy-4 daunosamine.

[Traduit par le journal]

The antileukemic drug daunomycin (daunorubicin), **1**, is split into daunomycinone and the amino sugar daunosamine, **2**, on mild acid hydrolysis (1). In a previous communication, an approach to the aglycone daunomycinone (2) was described; we now wish to disclose the total synthesis of triacetyldaunosamine.

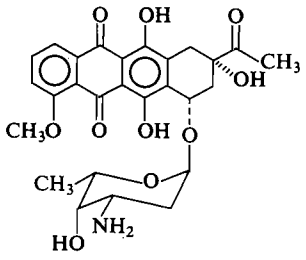

1

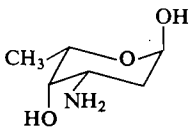

2

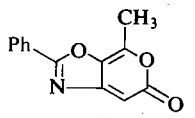

3

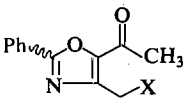

4 X = H
5 X = Br
6 X = CN
7 X = $COOCH_3$
8 X = COOH

L-Daunosamine has been synthesized by Goodman and co-workers (3) and the *N*-acyl derivatives of the unnatural D-isomer were also prepared by Baer *et al.* (4) and by Richardson (5), all starting from natural sugars. In our route, a substituted oxazolo-α-pyrone **3** served as the key intermediate. It was envisaged that catalytic hydrogenation of **3** would furnish the lactone corresponding to daunosamine provided that all *cis*-addition of hydrogen to the unsaturated system is operative.

The synthesis of **3** was initiated by the preparation of the oxazole **4** (ν_{CO} 1680 cm^{-1}; δ 2.48 (3H, s), 2.52 (3H, s), 7.3–7.6 (3H, m), and 7.9–8.2 (2H, m); *m/e* 201 (M^+)) by benzoyloxylation of 2,4-pentanedione morpholine enamine (6). Compound **4** was selectively brominated at the 'benzylic' position with NBS to give **5** (m.p. 108–110 °C; ν_{CO} 1680 cm^{-1}; δ 2.57 (3H, s), 4.75 (2H, s), 7.3–7.6 (3H, m), and 7.9–8.2 (2H, m); *m/e* 279, 281 (M^+)). Conversion of the bromide **5** into the nitrile **6** could not be achieved by conventional procedure, presumably owing to the high acidity of the 'benzylic' hydrogens of **6** which reacted further, uncontrollably. However, nitrile **6** (ν 2270 and 1680 cm^{-1}; δ 2.67 (3H, s), 412 (2H, s) 7.3–7.6 (2H, m), and 7.9–8.2 (2H,

Can. J. Chem. Downloaded from www.nrcresearchpress.com by 210.87.254.5 on 09/05/12
For personal use only.

16. E. WIBERG and R. BAUER. Z. Naturforsch. Teil B, **7**, 131 (1952).
17. B. BELLEAU and J. MORAN. Ann. N.Y. Acad. Sci. **107**, 822 (1963).
18. B. BELLEAU. Stud. Biophys. **4**, 95 (1967).
19. B. BELLEAU, I. MONKOVIC, T. T. CONWAY, H. WONG, Y. G. PERRON, and I. J. PACHTER. J. Am. Chem. Soc. **95**, 7910 (1973).

Stereospecific Synthesis of *dl*-Triacetyldaunosamine

CHIU MING WONG, TSE-LOK HO, AND WALTER P. NIEMCZURA
Department of Chemistry, University of Manitoba, Winnipeg, Manitoba R3T 2N2

Received July 21, 1975

CHIU MING WONG, TSE-LOK HO, and WALTER P. NIEMCZURA. Can. J. Chem. **53**, 3144 (1975).

Daunosamine triacetate was synthesized via a stereospecific non-carbohydrate approach. The *N*-benzoyl-β-amino lactone (**9**) could be an interesting intermediate for the very important and highly deoxygenated amino sugar, 4-deoxydaunosamine.

CHIU MING WONG, TSE-LOK HO et WALTER P. NIEMCZURA. Can. J. Chem. **53**, 3144 (1975).

On a synthétisé le triacétate de la daunosamine par une approche stéréospécifique n'impliquant pas de carbohydrates. La *N*-benzoyl β-amino lactone (**9**) pourrait s'avérer être un intermédiare interessant pour la synthèse du sucre aminé très important et très désoxygené qu'est la désoxy-4 daunosamine.

[Traduit par le journal]

The antileukemic drug daunomycin (daunorubicin), **1**, is split into daunomycinone and the amino sugar daunosamine, **2**, on mild acid hydrolysis (1). In a previous communication, an approach to the aglycone daunomycinone (2) was described; we now wish to disclose the total synthesis of triacetyldaunosamine.

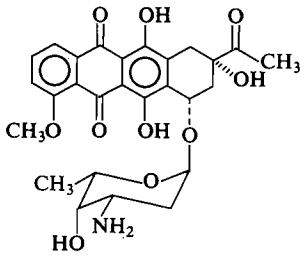

1

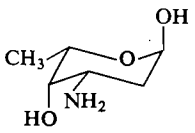

2

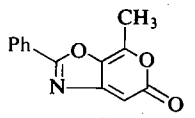

3

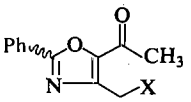

4 X = H
5 X = Br
6 X = CN
7 X = $COOCH_3$
8 X = COOH

L-Daunosamine has been synthesized by Goodman and co-workers (3) and the *N*-acyl derivatives of the unnatural D-isomer were also prepared by Baer *et al.* (4) and by Richardson (5), all starting from natural sugars. In our route, a substituted oxazolo-α-pyrone **3** served as the key intermediate. It was envisaged that catalytic hydrogenation of **3** would furnish the lactone corresponding to daunosamine provided that all *cis*-addition of hydrogen to the unsaturated system is operative.

The synthesis of **3** was initiated by the preparation of the oxazole **4** (ν_{CO} 1680 cm^{-1}; δ 2.48 (3H, s), 2.52 (3H, s), 7.3–7.6 (3H, m), and 7.9–8.2 (2H, m); *m/e* 201 (M^+)) by benzoyloxylation of 2,4-pentanedione morpholine enamine (6). Compound **4** was selectively brominated at the 'benzylic' position with NBS to give **5** (m.p. 108–110 °C; ν_{CO} 1680 cm^{-1}; δ 2.57 (3H, s), 4.75 (2H, s), 7.3–7.6 (3H, m), and 7.9–8.2 (2H, m); *m/e* 279, 281 (M^+)). Conversion of the bromide **5** into the nitrile **6** could not be achieved by conventional procedure, presumably owing to the high acidity of the 'benzylic' hydrogens of **6** which reacted further, uncontrollably. However, nitrile **6** (ν 2270 and 1680 cm^{-1}; δ 2.67 (3H, s), 412 (2H, s) 7.3–7.6 (2H, m), and 7.9–8.2 (2H,

Can. J. Chem. Downloaded from www.nrcresearchpress.com by 210.87.254.42 on 09/05/12
For personal use only.

Can. J. Chem. Downloaded from www.nrcresearchpress.com by 210.87.254.42 on 09/05/12
For personal use only.

m); *m/e* 226 (M^+)) was obtained by cyanide displacement in a sealed tube employing liquid hydrogen cyanide as a cosolvent (KCN:HCN–Et_2O, 75 °C, 36 h). Reaction of **6** with hydrogen chloride-saturated methanol gave the methyl ester **7** (ν_{CO} 1740 and 1680 cm^{-1}; δ 2.57 (3H, s) 3.75 (3H, s), 4.5 (2H, s), 7.3–7.6 (3H, m), and 7.9–8.2 (2H, m); *m/e* 259 (M^+)) which was hydrolyzed to the carboxylic acid **8** (m.p. 194 °C dec.; ν_{CO} 1725 and 1683 cm^{-1}) by HCl in aqueous HOAc at ambient temperature. This acid underwent decarboxylation readily on heating to regenerate the oxazole **4**, therefore it must be handled with care. Treatment of **8** with thionyl chloride in anhydrous chloroform afforded the desired oxazolo-α-pyrone (m.p. 185–187 °C dec.; ν 1740 and 1690 cm^{-1}; δ 2.517 (3H, d, J = 0.8 Hz) and 6.158 (1H, q, J = 0.8 Hz); *m/e* 227 (M^+)).

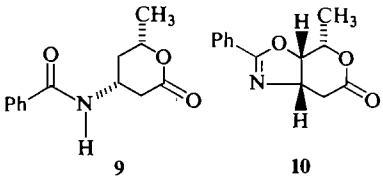

9 **10**

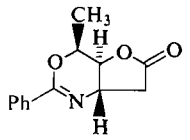

11

Attempts at hydrogenating **3** using Adams catalyst in ethyl acetate resulted in the generation of the benzamide **9** (ν_{CO} 1730 and 1670 cm^{-1}) and its hexahydro derivative. Hydrogenolysis could be avoided when the reduction was carried out with 5% Rh/Al_2O_3 as catalyst. The product retained a C=N bond and its structure **10** was supported by spectral data, especially its mass spectrum. It was thermodynamically unstable, and was converted upon heating into a γ-lactone **11** (ν_{CO} 1760 cm^{-1}). This facile transformation suggested that **10** indeed possesses an all *cis* stereochemistry whose preferred conformation is **10***a* with the oxygen atom of the oxazoline ring assuming an axial orientation, whereas both the nitrogen and the methyl group are equatorial. In view of the occurrence of this rearrangement,

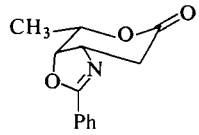

10*a*

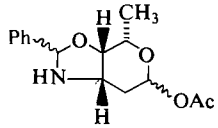

12

the lactone carbonyl was reduced by sodium di(2-methoxyethoxy) aluminum hydride to the lactol and then acetylated [Ac_2O-pyr]. Further hydrogenation (5% Rh/Al_2O_3 in EtOAc) of this lactol acetate gave compound **12**. The benzylidene group was removed by acid treatment and the crude product was reacetylated to yield the triacetyl derivatives. Preparative t.l.c. on silica gel permitted the isolation of triacetyldaunosamine. Identification of this final product was by spectral comparison (i.r., m.s.) with a sample derived from natural sources.

Borohydride reduction of the ketoester **8** afforded lactone **13** which could be a useful synthetic intermediate of ristosamine **14** (7). All new compounds gave satisfactory analysis or exact mass molecular ions.

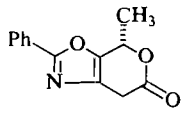

13

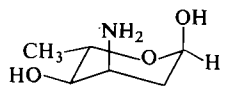

14

Support of this investigation by the National Research Council of Canada is gratefully acknowledged. We thank Dr. D. Henry (Stanford Research Institute) for a generous gift of daunosamine hydrochloride, and C.M.W. thanks Professor Woodward (Harvard) for his hospitality.

1. F. Arcamone, G. Cassinelli, P. Orezzi, G. Franceschi, and R. Mondelli. J. Am. Chem. Soc. **86**, 5335 (1964).
2. C. M. Wong, R. Schwenk, D. Popien, and T.-L. Ho. Can. J. Chem. **51**, 466 (1973).
3. J. Marsh, Jr., C. W. Mosher, E. M. Acton, and L. Goodman. Chem. Commun. 973 (1967).
4. H. H. Baer, K. Čapek, and M. C. Cook. Can. J. Chem. **47**, 89 (1969).
5. A. C. Richardson. Carbohydr. Res. **4**, 422 (1967).
6. H. J. Jakobsen, E. H. Larsen, P. Madsen, and S.-O. Lawesson. Ark. Kemi, **24**, 519 (1965).
7. N. N. Lomakina, L. A. Szpiridonova, R. Bognar, M. Puskás, and F. Sztaricskai. Antibiotiki, **13**, 975 (1968); R. Bognar, F. Sztaricskai, M. E. Munk, and J. Tamas. J. Org. Chem. **39**, 2971 (1974).

Can. J. Chem. Downloaded from www.nrcresearchpress.com by 210.87.254.42 on 09/05/12
For personal use only.

Canadian Journal of Chemistry

Published by
THE NATIONAL RESEARCH COUNCIL OF CANADA

Journal canadien de chimie

Publié par
LE CONSEIL NATIONAL DE RECHERCHES DU CANADA

Volume 53 Number 21 November 1, 1975

Volume 53 numéro 21 1 novembre 1975

The Radical Ion $S_3N_2^+$. Preparation, Electron Spin Resonance Spectrum, and Crystal Structure of Thiodithiazyl Hexafluoroarsenate $S_3N_2^+AsF_6^-$

R. J. GILLESPIE, P. R. IRELAND, AND J. E. VEKRIS

Department of Chemistry, McMaster University, Hamilton, Ontario, L8S 4M1

Received April 29, 1975

R. J. GILLESPIE, P. R. IRELAND, and J. E. VEKRIS. Can. J. Chem. **53**, 3147 (1975).

The compound $S_3N_2^+AsF_6^-$ has been prepared by the reaction of S_4N_4 with AsF_5. The crystal structure has been determined from three-dimensional X-ray counter data. Crystals are monoclinic, space group $P2_1/c$ with $a = 8.499(4)$, $b = 8.298(4)$, $c = 11.069(8)$, $\beta = 94.59(5)$, $V = 778.1$ Å^3, $Z = 4$, and $D_c = 2.67$ g cm^{-3}. The structure was solved by Patterson methods and refined to a conventional R factor of 0.028 for 798 independent reflections with $I \geqslant 3\sigma(I)$. The structure consists of discrete AsF_6^- ions and planar cyclic $S_3N_2^+$ ions. Solutions of $S_3N_2^+AsF_6^-$ in methylene chloride gave a five-line electron spin resonance spectrum with an intensity ratio of 1:2:3:2:1 showing that the unpaired electron in $S_3N_2^+$ is coupled to two equivalent nitrogen atoms in full accord with the results of the crystal structure determination.

R. J. GILLESPIE, P. R. IRELAND et J. E. VEKRIS. Can. J. Chem. **53**, 3147 (1975).

Le composé $S_3N_2^+AsF_6^-$ a été préparé par la réaction de S_4N_4 avec AsF_5. La structure du cristal de ce composé a été déterminée par un compteur de données de rayons-X à trois dimensions. Les cristaux sont monocliniques, groupe d'espace $P2_1/c$ avec $a = 8.499(4)$, $b = 8.298(4)$, $c = 11.069(8)$, $\beta = 94.59(5)$, $V = 778.1$ Å^3, $Z = 4$ et $D_c = 2.67$ g cm^{-3}. La structure a été résolue par la méthode de Patterson et raffinée jusqu'à un facteur conventionnel final R de 0.028 pour 798 réflexions indépendantes avec $I \geqslant 3\sigma(I)$. La structure consiste en cations planaires cycliques $S_3N_2^+$ et en anions AsF_6^- discrets. Des solutions dans du chlorure de méthylène ont donné un spectre de résonance paramagnétique électronique montrant cinq bandes avec un rapport d'intensités de 1:2:3:2:1 ce qui indique que l'électron apparié de $S_3N_2^+$ est couplé avec deux atomes d'azote qui sont équivalents comme le montrent les résultats de la détermination de la structure cristalline.

[Traduit par le journal]

Introduction

Although tetrasulfur tetranitride was first prepared in 1835 (1) many aspects of its chemistry are still far from well understood. Several investigators have reported the formation of a sulfur–nitrogen radical in freshly prepared solutions of S_4N_4 in concentrated sulfuric acid but this radical has never been identified with certainty. Chapman and Massey (2) observed a five-line e.s.r. spectrum from a solution of S_4N_4 in concentrated sulfuric acid which they attributed to a radical containing two equivalent nitrogen atoms and which they supposed to be SN_2^+. Later Symons and his co-workers (3) observed the same e.s.r. spectrum from solutions of S_4N_4 in both SbF_5 and sulfuric acid and on the basis of spin density calculations concluded that the radical could not be SN_2^+ but was more probably $S_2N_2^+$ with a square planar structure analogous to that of the neutral molecule S_2N_2 (4). Further studies of the e.s.r. spectrum of solutions of S_4N_4 in 100% H_2SO_4 were made by Jolly and co-workers (5) who found in agreement with the earlier workers that the radical had $g =$

Can. J. Chem. Downloaded from www.nrcresearchpress.com by 210.87.254.42 on 09/05/12
For personal use only.

2.011 and a hyperfine coupling constant of 3.21 G. In order to establish the number of sulfur atoms in the radical they also made measurements using S_4N_4 enriched in ^{33}S. They found that they could simulate the complicated spectrum that they obtained by assuming that the radical contained two equivalent sulfur atoms, but they could not exclude the possibility that the radical might also contain other nonequivalent sulfur atoms or even oxygen.

We have shown recently (6) that elemental sulfur is oxidized by various oxidizing agents including sulfuric acid, oleum, AsF_5, and SbF_5 to the polyatomic cations S_{16}^{2+}, S_8^{2+}, and S_4^{2+} and it seemed reasonable to suppose that the oxidation of S_4N_4 by sulfuric acid or by SbF_5 might be a similar process and that we might be able to establish the nature of the products by the same methods as we had used previously. We have also found that similar cationic species can be made from selenium and tellurium (6) and that a useful general reaction for the preparation of such species is reaction of the neutral molecule with a solution of AsF_5 in SO_2. We show in this paper that the reaction of AsF_5 with S_4N_4 in solution in SO_2 leads to the formation of $S_3N_2^+AsF_6^-$ and we describe the determination of the structure by X-ray crystallography and also some e.s.r. studies.

Experimental Section

Preparation of $S_3N_2^+AsF_6^-$

In a typical preparation AsF_5 (3.62 mmol) was condensed onto a frozen solution of S_4N_4 (1.206 mmol) in sulfur dioxide at −196 °C. The mixture was allowed to warm slowly to room temperature and stirred for 24 h. A clear red solution was obtained as the reaction mixture warmed up to room temperature and no further changes were observed during the next 24 h. On slow evaporation of the volatile materials, *i.e.*, the solvent sulfur dioxide, excess arsenic pentafluoride and arsenic trifluoride produced in the reaction, deep red-brown, almost black, crystals were obtained together with a light brown microcrystalline powder, which was not identified. Suitable crystals for X-ray crystallographic work were selected in a dry box equipped with a microscope and were then sealed in thin-walled quartz capillaries.

Crystal Data

$S_3N_2^+AsF_6^-$ f.w. = 313.10

Monoclinic, $a = 8.499(4)$, $b = 8.298(4)$, $c = 11.069(8)$ Å, $\beta = 94.59(5)°$, $V = 778.1$ Å^3, $Z = 4$, $D_c = 2.67$ g cm^{-3}. No experimental density was obtained because of the sensitivity of the compound to moisture. Single crystal precession photographs revealed the systematic absences: $h0l$, $l = 2n + 1$; $0k0$, $k = 2n + 1$. These unambiguously indicated the space group $P2_1/c$, No. 14 in the *International Tables for X-ray Crystallography* (7).

X-Ray Measurements

A small, poorly formed, but approximately spherical crystal (radius 0.1 mm) was mounted on a Syntex P$\bar{1}$ diffractometer. Intensities were measured with graphite monochromated MoK_α radiation ($\lambda = 0.71069$ Å). Accurate cell parameters were obtained from a least squares refinement using 12 high angle reflections in the region $20 < 2\theta < 30°$. Intensity data were collected at room temperature (20 °C) by the θ–2θ scan technique, with scan rates varying from 2.0 to 24.0 deg min^{-1} (in 2θ) so that the weaker reflections were examined more slowly to minimize counting errors. Stationary background counts with a time equal to half the scan time for each reflection were made at each end of the scan range. The scan width varied from 2° at low 2θ to 2.5° for the higher angle data. Two standards were regularly checked to monitor the stability of the crystal and its alignment, but no significant time dependent trends were observed. Reflections with a unique quadrant with $2\theta < 55°$ were measured resulting in 798 reflections with intensities greater than three times their standard deviation based on counting statistics. The linear absorption coefficient for the material is 54.4 cm^{-1} for the MoK_α radiation used, with $\mu R = 0.5$. Absorption effects were therefore negligible, and no absorption corrections were applied. Lorentz and polarization corrections were applied to the observed data.

Solution and Refinement of the Structure

The positions of the heavy As atoms were readily located from inspection of the three dimensional Patterson function. Least squares refinement of positional and isotropic temperature parameters for this atom gave a conventional agreement index R_1, ($R_1 = \Sigma\Delta/\Sigma|F_o|$ where $\Delta = ||F_o| - |F_c||$), of 0.39. A difference Fourier synthesis revealed the positions of the 11 remaining atoms. Full matrix refinement of positional and anisotropic temperature factors for all atoms converged at $R_1 = 0.028$, while the weighted agreement index R_2, ($R_2 = (\Sigma w\Delta^2/\Sigma wF_o)^{1/2}$) was 0.031 with unit weights. An examination of the data showed that $\Sigma w\Delta^2$ was approximately independent of $|F_o|$ and $(\sin\theta)/\lambda$ with unit weights, so no weighting scheme was considered necessary. The largest shift of any parameter divided by its estimated standard deviation was 0.2 in the final refinement cycle. The top three peaks in a final difference Fourier, (0.3–0.5 e/Å^3) were all within 1.0 Å of the AsF_6^- ion which had been refined with highly anisotropic thermal parameters. No systematic trends indicating the need for an extinction correction were evident in the data.

Atomic scattering factors for arsenic, sulfur, fluorine, and nitrogen atoms with anomalous dispersion corrections for the arsenic atom were taken from ref. 8. All calculations were performed on a CDC 6400 computer using the series programs in the X-ray 71 system (9) and our own programs. The final atomic positional coordinates and temperature factors are presented in Table 1. A tabulation of observed and calculated structure factors is available.[1]

Electron Spin Resonance Measurements

Spectra were obtained with a JEOLCO Model JES

[1]Complete set of tabular data is available, at a nominal charge, from the Depository of Unpublished Data, CISTI, National Research Council of Canada, Ottawa, Canada K1A 0S2.

Can. J. Chem. Downloaded from www.nrcresearchpress.com by 210.87.254.42 on 09/05/12
For personal use only.

TABLE 1. Atomic coordinates and anisotropic thermal parameters* ($U_{ij} \times 10^2$) for $S_3N_2^+AsF_6^-$

Atom	x	y	z	U_{11}	U_{22}	U_{33}	U_{12}	U_{13}	U_{23}
S(1)	0.6441(2)	0.0712(2)	0.3587(2)	3.9(1)	4.9(1)	8.6(2)	0.1(1)	−1.8(1	1.0(1)
S(2)	0.9568(2)	0.1579(2)	0.3862(2)	3.8(1)	3.6(1)	4.6(1)	−0.1(1)	0.4(1)	0.9(1)
S(3)	0.8498(2)	0.1375(2)	0.5548(2)	4.4(1)	4.0(1)	4.7(1)	0.4(1)	0.8(1)	−0.9(1)
N(1)	0.8021(7)	0.1141(8)	0.3007(5)	5.9(4)	5.6(4)	4.4(4)	1.2(4)	−1.4(3)	0.9(3)
N(2)	0.6767(6)	0.0871(7)	0.4976(6)	3.2(3)	4.4(4)	8.5(5)	0.7(3)	1.2(3)	0.3(4)
As(1)	0.26963(8)	0.10706(9)	0.12376(7)	3.44(4)	2.92(3)	5.19(4)	−0.01(4)	−0.51(3)	0.16(4)
F(1)	0.2347(8)	0.0251(8)	−0.0124(5)	14.2(6)	11.0(5)	6.7(4)	−0.3(4)	−0.1(4)	−3.4(4)
F(2)	0.1644(6)	0.2785(5)	0.0798(5)	6.7(3)	4.1(3)	12.6(5)	1.4(2)	−3.0(3)	1.1(3)
F(3)	0.2925(7)	0.1871(8)	0.2655(5)	11.8(5)	11.5(5)	7.0(4)	0.2(4)	−1.2(3)	−2.9(4)
F(4)	0.3680(7)	−0.0621(6)	0.1711(7)	9.2(4)	4.9(3)	18.4(7)	2.3(3)	−4.3(4)	1.8(4)
F(5)	0.4384(6)	0.1966(6)	0.0976(7)	5.6(3)	6.7(4)	20.9(7)	−2.1(3)	4.6(4)	0.8(4)
F(6)	0.0948(6)	0.0238(7)	0.1611(6)	7.2(4)	7.3(4)	13.9(5)	−2.5(3)	3.7(4)	−0.2(4)

*x, y, and z are atomic coordinates expressed as fractions of the cell edges. The form of the anisotropic thermal ellipsoid is: $[\exp -2\pi^2(h^2a^{*2}U_{11} + \ldots + 2hka^*b^*U_{12} + \ldots)]$. Least-squares-estimated standard errors in the least significant digits are given in parentheses.

3B5-X spectrometer and g values were obtained by comparison with the third and fourth lines of the spectrum of a trace manganous ion contained in solid SrO.

Materials

A sample of tetrasulfur tetranitride[2] had been prepared and purified by the method described by Becke-Goehring (10). Arsenic pentafluoride (Ozark-Mahoning) was used without purification, its purity having been checked by gas-phase infrared spectroscopy. Sulfur dioxide (Matheson) and methylene chloride (Fisher) were repeatedly distilled from, and kept over, phosphoric oxide before they were used.

Discussion

Figure 1 shows the atom labelling, thermal ellipsoids, and the important bond lengths in the $S_3N_2^+$ cation, while Table 2 gives a more complete list of intermolecular and intramolecular distances and angles. The packing of the ions in the unit cell is shown in Fig. 2. It is clear that the compound $S_3N_2^+AsF_6^+$ consists of discrete $S_3N_2^+$ and AsF_6^- ions, the former being a planar five-membered ring and the AsF_6^- ion being octahedral. The average As—F distance in AsF_6^- is 1.69 Å. The $S_3N_2^+$ cation is unusual in that it is a stable radical ion and is the only known sulfur–nitrogen radical that has been obtained as a stable crystalline salt. It is the second example of a five-membered S–N ring, the other being the closely related $S_3N_2Cl^+$ ion (11).

The average S—N bond length in the $S_3N_2^+$ ion is 1.58 Å. This is comparable to the average S—N distance in other S–N ring compounds, *e.g.*, $S_4N_3^+$ 1.55 Å (12), $S_3N_2Cl^+$ 1.59 Å (11), $S_3N_3Cl_3$ 1.61 Å (13), and S_4N_4 1.62 Å (14) and is much shorter than the value of 1.74 Å calculated for an S—N single bond from Paulings covalent radii. Two compounds in which the S—N bonds seem very likely to be single bonds are $S_4N_4H_4$ (15) and $NH_3SO_3^-$ (16) where the bond distances are respectively 1.67 and 1.73 Å. Thus it may be concluded that the S—N bonds in $S_3N_2^+$ have considerable double-bond character. The S—S bond has a length of 2.15 Å which is very similar to that found for the unique S—S bond in $S_3N_2Cl^+$ (2.14 Å) (11) and slightly longer than that in $S_4N_3^+$ (2.06 Å) (12) and in the S_8 molecule (2.04 Å) (16). It seems reasonable to suppose, therefore, that the S—S bond in $S_3N_2^+$ may be regarded as a single bond. As an isolated $S_3N_2^+$ ion would be expected to have C_{2v} symmetry the different lengths of the S(3)N(2) and S(2)N(1) and of the S(1)N(2) and S(1)N(1) bonds may be due to experimental error or to distortion of the ion in the crystal. However, the average S(1)N(1), S(1)N(2) and S(2)N(1), S(3)-N(2) bond lengths of 1.56 and 1.60 Å respectively would appear to be significantly different. Indeed this difference can be predicted on the basis of simple valence-bond structures. If it is assumed that structures in which there is more than one charged atom and/or an S—S double bond are relatively unimportant and may be ignored, there is a total of nine possible structures, *a* to *e* in Fig. 3 where *a*, *b*, *c*, and *d* each represent two structures as a consequence of the presumed C_2 axis. Assuming that each of these structures has equal weight leads to a bond order of 1.66 for the S(1)N(1) bond and of 1.44 for the S(2)N(1) bond. These bond orders are consistent with our

[2]This sample was kindly donated by the late Dr. F. P. Olsen of this department.

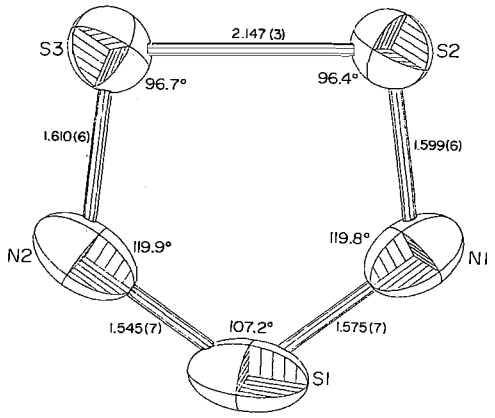

FIG. 1. Bond angles, bond lengths, and thermal ellipsoids for the $S_3N_2^+$ ion.

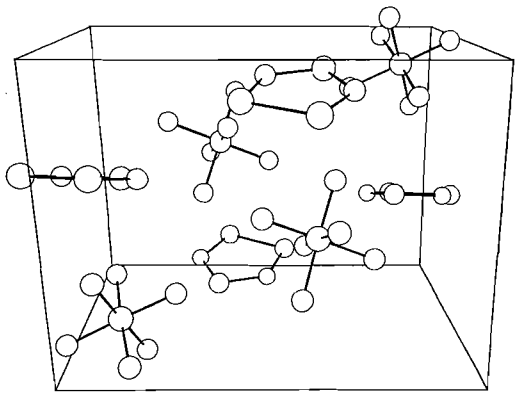

FIG. 2. Unit cell of $S_3N_2^+AsF_6^-$.

Can. J. Chem. Downloaded from www.nrcresearchpress.com by 210.87.254.42 on 09/05/12
For personal use only.

TABLE 2. (*a*) Selected bond distances and angles for $S_3N_2^+AsF_6^-$

Intramolecular		Intermolecular			
Bond	Distance (Å)	Bond	Distance (Å)	Bonds	Angle (deg)
S(1)—N(1)	1.575(7)	S(2)—F(2)	2.717(6)	N(1)—S(1)—N(2)	107.2(3)
—N(2)	1.545(7)	S(3)—F(2)	2.755(5)	N(1)—S(2)—S(3)	96.4(3)
S(2)—N(1)	1.599(6)			N(2)—S(3)—S(2)	96.7(3)
S(3)—N(2)	1.610(6)			S(1)—N(1)—S(2)	119.8(4)
S(2)—S(3)	2.147(3)			S(1)—N(2)—S(3)	119.9(4)
As—F(1)	1.658(6)			F(1)—As—F(2)	91.8(3)
—F(2)	1.730(5)			—F(3)	176.0(3)
—F(3)	1.701(6)			—F(4)	89.4(3)
—F(4)	1.695(5)			—F(5)	96.9(3)
—F(5)	1.661(6)			—F(6)	87.6(3)
—F(6)	1.719(6)			F(2)—As—F(3)	87.5(3)
				—F(4)	177.8(3)
				—F(5)	91.0(3)
				—F(6)	87.7(3)
				F(3)—As—F(4)	91.2(3)
				—F(5)	87.1(3)
				—F(6)	88.4(3)
				F(4)—As—F(5)	90.8(3)
				—F(6)	90.4(3)
				F(5)—As—F(6)	175.4(3)

(*b*) Equation of plane through $S_3N_2^+$

Equation	Atom	Distance from plane (Å)*
$-2.19x + 8.01y - 0.35z = -0.96$	S(1)	−0.007
	S(2)	−0.008
	S(3)	0.004
	N(1)	0.011
	N(2)	0.0002

*The r.m.s. standard deviation of the atoms from the plane is 0.008 Å.

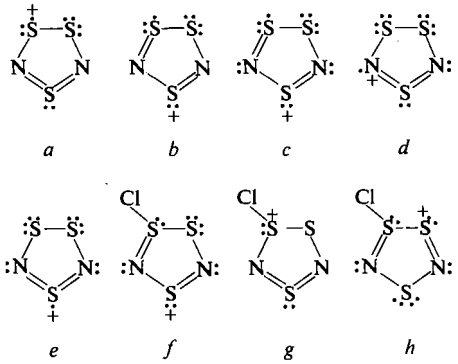

FIG. 3. Valence bond structures for $S_3N_2^+$ and $S_3N_2Cl^+$.

conclusion that the S(1)N(1) bonds are shorter than the S(2)N(1) bonds.

It is interesting to compare the geometry of $S_3N_2^+$ with that of $S_3N_2Cl^+$. The latter is slightly puckered but nevertheless the bond angles in the two rings are very similar as are the bond distances. Using the same criteria as above only three reasonable valence-bond structures can be written for $S_3N_2Cl^+$ (*f*, *g*, and *h*, Fig. 3). These simple structures predict bond orders of 1.66 for the S(3)N(2) and S(1)N(1) bonds and 1.33 for the S(1)N(2) and S(2)N(1) bonds. As may be seen from Table 3 these bond orders are quite consistent with the observed bond lengths for $S_3N_2Cl^+$ and they are also consistent with the bond orders and bond lengths for $S_3N_2^+$ and with a bond order of 1.5 for $S_3N_3Cl_3$ which has six equal S—N bond lengths (13).

A solution of $S_3N_2^+AsF_6^-$ in methylene chloride gave a five-line e.s.r. spectrum with intensity ratios of 1:2:3:2:1, $g = 2.01$, and a hyperfine coupling constant of 3.15 G. This is clearly the same spectrum obtained by Jolly and co-workers (5) and other workers (2, 3) from

Can. J. Chem. Downloaded from www.nrcresearchpress.com by 210.87.254.42 on 09/05/12
For personal use only.

TABLE 3. Bond lengths and bond orders for some SN bonds*

Bond	Order	Length (Å)
$\overset{+}{N}H_3SO_3^-$	1.0	1.73
$S_4N_4H_4$	1.0	1.67
$S_3N_2Cl^+$	1.33	1.62
$S_3N_2^+$	1.44	1.61
$S_3N_3Cl_3$	1.5	1.605
$S_3N_2Cl^+$	1.66	1.56†
$S_3N_2^+$	1.66	1.56‡
SN	2.5	1.49§
NSF	3.0	1.45‖
NSF_3	3.0	1.42¶

*The bond orders quoted here have been obtained as indicated in the text. SN is assumed to have a bond order of 2.5 and N≡S—F and N≡SF_3 are assumed to have bond orders of 3.0. These bond order values are somewhat lower than those given recently by Nyburg (18), as he takes the bond order in SN^+ (1.25 Å) to be 3.0. In the present authors' opinion this bond length is anomalously short; perhaps because of the positive charge and we believe that the bond lengths in NSF and NSF_3 correspond more closely to a bond order of 3.0.

†Mean of the observed distances of 1.54 and 1.58 Å.

‡Mean of the observed distances of 1.545 and 1.575 Å.

§Reference 19.

‖Reference 20.

¶Reference 21.

solutions of S_4N_4 in sulfuric acid and by Symons and co-workers (3) from a solution of S_4N_4 in SbF_5. It would appear that $S_3N_2^+$ is an important initial product of the reaction of S_4N_4 with sulfuric acid but it is unstable in this medium and appears to undergo oxidation to other as yet unidentified species.

The five-line e.s.r. spectrum is due to coupling of the odd electron with the two equivalent nitrogen atoms and this is consistent with the structures in Fig. 3, particularly with the two structures *c* in which the unpaired electron is on the two equivalent nitrogen atoms. These structures predict spin densities of 0.33 on each of the equivalent sulfur atoms, of 0.11 on each of the nitrogen atoms, and of 0.11 on the nonequivalent sulfur atom.

The mechanism of the reaction by which S_4N_4 is oxidized to $S_3N_2^+$ by AsF_5 is not entirely clear at the present time as the other products of the reaction were not identified. However, as S_8 is oxidized initially by AsF_5 to S_8^+ (6) it seems reasonable to suppose that the first step of the oxidation is the loss of one electron to give $S_4N_4^+$ with the consequent rupturing of one of the weak S—S bonds followed by fission of the molecule, as follows

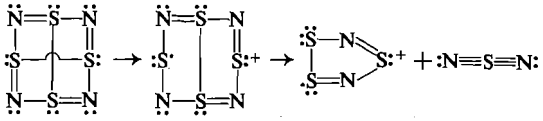

NOTE ADDED IN PROOF:

Since submitting this paper for publication we have become aware of a recent determination of the crystal structure of the closely related compound $S_6N_4^{2+}(S_2O_6Cl^-)_2$ (22). The cation consists of two symmetry related planar S_3N_2 rings held together by two long SS bonds (3.027 Å). The dimensions of the rings S(1)N(1) 1.57 Å, S(2)N(1) 1.60 Å, ∠NSS 97°, ∠SNS 119°, ∠NSN 108°, are almost identical with those listed in Table 2.

We thank the National Research Council of Canada for financial support of this work.

1. M. GREGORY. J. Pharm. **21**, 315 (1835).
2. D. CHAPMAN and A. G. MASSEY. Trans. Faraday Soc. **58**, 1291 (1962).
3. D. A. C. MCNEIL, M. MURRAY, and M. C. R. SYMONS. J. Chem. Soc. A, 1019 (1967).
4. J. R. W. WARN and D. CHAPMAN. Spectrochim. Acta, **22**, 1371 (1966).
5. S. A. LIPP, J. J. CHANG, and W. L. JOLLY. Inorg. Chem. **9**, 1970 (1970).
6. R. J. GILLESPIE and J. PASSMORE. Acc. Chem. Res., **12**, 413 (1971).
7. International Tables for X-ray Crystallography, Vol. I. Kynoch Press, Birmingham, England. 1962.
8. International Tables for X-ray Crystallography, Vol. III. Kynoch Press, Birmingham, England. 1962. pp. 215–216.
9. J. M. STEWART, F. A. KUNDELL, and J. C. BALDWIN. X-ray 71 System of Crystallographic Programs, University of Maryland Technical Report. 1971.
10. M. BECKE-GOEHRING. Inorg. Synth. **6**, 124 (1962).
11. A. ZALKIN, T. E. HOPKINS, and D. H. TEMPLETON. Inorg. Chem. **5**, 1767 (1966).
12. J. WEISS. Z. Anorg. Allg. Chem. **333**, 314 (1964).
13. G. A. WIEGERS and A. VOS. Acta Cryst. **20**, 192 (1966).
14. G. A. WIEGERS and A. VOS. Acta Cryst. **16**, 152 (1963).
15. R. L. SASS and J. DONOHUE. Acta Cryst. **11**, 497 (1958).
16. L. PAULING. The nature of the chemical bond, 3rd ed. Cornell University Press, 1960.
17. S. C. ABRAHAMS. Acta Cryst. **8**, 661 (1955).
18. S. C. NYBERG. J. Cryst. Struct. **3**, 331 (1973).
19. BARROW, DRUMMOND, and ZEEMAN. Proc. Phys. Soc. **67**, 365 (1954).
20. W. H. KIRCHOFF and E. B. WILSON. J. Am. Chem. Soc. **85**, 1726 (1963).
21. W. H. KIRCHOFF and E. B. WILSON. J. Am. Chem. Soc. **84**, 334 (1962).
22. A. I. BANNISTER, H. G. CLARKE, I. RAYMOND, and H. M. M. SHEARER. Inorg. Nucl. Chem. Lett. **10**, 647 (1974).

Can. J. Chem. Downloaded from www.nrcresearchpress.com by 210.87.254.42 on 09/05/12
For personal use only.

The Formation and Reactions of Disulfide Radical Anions in Aqueous Solution

TZU-LIN TUNG[1] AND JOHN A. STONE
Chemistry Department, Queen's University, Kingston, Ontario K7L 3N6
Received May 28, 1975

TZU-LIN TUNG and JOHN A. STONE. Can. J. Chem. **53**, 3153 (1975).

Transient disulfide radical anions have been produced by flash photolysis. Cyclic anions decay only by second order reaction as opposed to the first order decay found for linear ones at low concentration. Linear disulfides, except oxidized penicillamine, increase the rate of decay of the cystine radical anion. The p*H* dependence of the reaction with cystine suggests that the disulfide radical anion is an electrophile.

TZU-LIN TUNG et JOHN A. STONE. Can. J. Chem. **53**, 3153 (1975).

Faisant appel à la photolyse flash, on a produit, à l'état transitoire, les radicaux anions du disulfure. Les anions cycliques ne se décomposent que par une réaction du deuxième ordre alors que les anions linéaires se décomposent, à basse concentration, par une réaction du premier ordre. Les disulfures linéaires, à l'exception de la penicillamine oxydée, augmentent le taux de décomposition du radical anion de la cystine. Le fait que la réaction avec la cystine dépend du p*H* indique que le radical anion du disulfure est un électrophile.

[Traduit par le journal]

Can. J. Chem. Downloaded from www.nrcresearchpress.com by 210.87.254.42 on 09/05/12
For personal use only.

Introduction

The lifetimes of disulfide radical anions ($RSSR^-$) are increased in the presence of sulfhydryl compounds (1, 2). By studying the flash photolysis and pulse radiolysis of aqueous solutions of cysteine we showed that this increased lifetime was due to a complex mode of decay (3). Our postulated reaction scheme is shown by [1] to [6] in which CyS· represents the cysteinyl group and Cy· the alanyl radical.

[1] $$CyS^- + h\nu \rightarrow CyS\cdot + e_{aq}^-$$

[2] $$e_{aq}^- + CySH \rightarrow Cy\cdot + SH^-$$

[3] $$Cy\cdot + CySH \rightarrow CyH + CyS\cdot$$

[4] $$CyS\cdot + CyS^- \rightleftharpoons CySSCy^-$$

[5] $$CyS\cdot + CySSCy^- \rightarrow \text{Products}$$

[6] $$H_2O + CySSCy^- \rightarrow CyH + CySS\cdot + OH^-$$

In the presence of excess cysteine the equilibrium 4 supercedes the usual fast, first order decay observed following electron capture by a disulfide (2).

[7] $$CySSCy^- \rightarrow CyS\cdot + CyS^-$$

The mode of decay then depends on concentration. At disulfide radical anion concentrations greater than $\sim 10^{-6}$ *M* a second order p*H* dependent decay occurs (reaction 5) while at concentrations less than 6×10^{-7} *M* there is a p*H* independent, first order decay (reaction 6). Similar first order decays have also been observed in the pulse radiolysis of penicillamine (4) and in the flash photolysis of 2-mercaptoethanol and benzenethiol (5).

Since the participation of disulfides in reactions leading to radiation protection of biological materials has been suggested (6) a knowledge of the properties of these radical anions is required. We here report studies of their decay in the presence and absence of disulfides of differing structure and also studies of the decay of cyclic disulfide radical anions which may be representative of bridge disulfide linkages which are important in biological systems.

Experimental

The flash photolysis and pulse radiolysis procedures have been described (3). The optical absorptions due to disulfide radical anions were usually followed at 410 nm. All solutions were deoxygenated by bubbling with oxygen free nitrogen.

Results and Discussion

The Decay of Cyclic Disulfide Radical Anions

Flash photolysis of aqueous solutions of lipoic acid ($\overline{CH_2CH_2S—SCH(CH_2)_4COOH}$) or of any of the other disulfides studied did not yield observable transients in the region 370–500 nm. A

[1]Present address: University of California, Berkeley, California 94720.

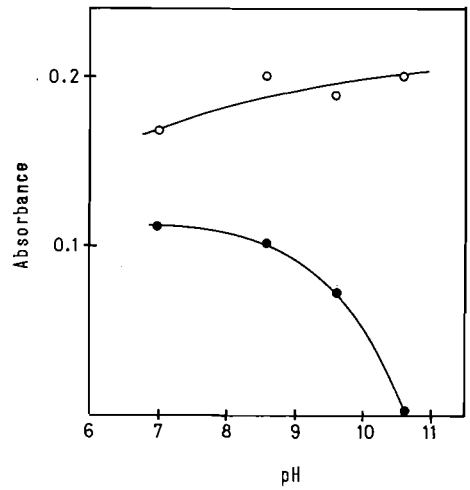

FIG. 1. Initial absorbance at 410 nm for a solution 1.0×10^{-3} *M* in cysteine; ●, no lipoic acid; ○, 5×10^{-4} *M* lipoic acid.

transient absorption was observed for solutions 5×10^{-4} *M* in lipoic acid and 1×10^{-3} *M* in cysteine at p*H* values in the range 7–10.6. At p*H* 7 the decay of the absorbance at 410 nm showed two components (*a*) at times below 1 ms an approximately first order decay ($k \sim 1.6 \times 10^3$ s^{-1}) attributable to the decay of $CySSCy^-$ while above 1 ms the decay became second order ($k \sim 2 \times 10^8$ M^{-1} s^{-1}) which is consistent with the second order decay of the disulfide radical anion formed from lipoic acid ($k = 1.4 \times 10^8$ M^{-1} s^{-1} (2)). With increasing p*H* the first order decay became less marked, consistent with the reported decreasing yield of $CySSCy^-$ (3). At p*H* 10.6 an almost pure second order decay was observed ($k = 2.5 \times 10^8$ M^{-1} s^{-1}). Figure 1 shows the initial yield of the transient at 410 nm together with the absorbance at this same wavelength obtained for the same flash intensity but in the absence of lipoic acid. This result is consistent with flash photolysis producing solvated electrons from CyS^- (reaction 1) which are then scavenged by lipoic acid. Electron transfer from $CySSCy^-$ to lipoic acid might also account for these results. However production of $CySSCy^-$ by pulse radiolysis of an N_2O saturated solution 1×10^{-3} *M* in cysteine and 1×10^{-5} *M* in lipoic acid at p*H* 9.6 when $CySSCy^-$ alone is formed initially showed only the first order decay of $CySSCy^-$ with no evidence of a longer lived transient that could have been formed by electron transfer from $CySSCy^-$ to lipoic acid.

In summary the above results show that the disulfide radical anion formed at low concentration from lipoic acid does not exhibit the slow first order decay found for linear disulfide radical anions and electron transfer from $CySSCy^-$ to lipoic acid does not occur to any measurable extent ($k < 10^7$ M^{-1} s^{-1}).

The absorption spectrum of the cyclic transient obtained by flash photolysis of dithiothreitol ($HSCH_2CH(OH)CH(OH)CH_2SH$) at p*H* 7 is identical in the region above 350 nm with that obtained by pulse radiolysis (7). The transient decays by a pure second order process independent of dithiothreitol concentration with a rate constant of $2k = 4.1 \times 10^8$ and 3×10^8 M^{-1} s^{-1} at p*H* 8.7 and 10 respectively (literature values 6.0×10^8 M^{-1} s^{-1} at p*H* 7 (7) and $\sim 1.7 \times 10^8$ M^{-1} s^{-1} at p*H* 7–10 (8)). There is no evidence for a change to first order decay at radical ion concentrations as low as 8×10^{-8} *M*.

Small cyclic disulfide radical anions are therefore different in their decay behavior than the linear ones. The reaction equivalent to [5] is not readily available to these species since the close proximity of the RS· and RS^- groups ensures an extremely low concentration of RS· radicals. The nonoccurrence of the first order reaction, thought to involve the solvent (reaction 6), must be due to steric limitations imposed by the small size ring. Such effects may also play a part in the radiation chemistry of biological molecules containing disulfide bridges especially those shielded from the aqueous environment. If neither the second order nor the first order decay is open to the relatively immobile disulfide radical anion formed by the addition of an electron then they will be very long lived. Klassen *et al.* (9) have observed a very slow first order decay ($k \sim 600$ s^{-1}) of the disulfide radical anions formed in the pulse radiolysis of the large ring disulfides oxytocin and lysine vasopressin. These may be examples of behavior intermediate between those of linear and small ring disulfide radical anions.

The Reaction of the Cystine Radical Anion with Disulfides

Flash photolysis of aqueous cysteine solutions in the presence of cystine under conditions where only the first order decay of the radical anion occurs produced $CySSCy^-$ in exactly the same yield as in the absence of disulfide. This is as expected since the electron formed in reaction 1 can also be scavenged by cystine ($k \sim 10^{10}$ M^{-1}

Can. J. Chem. Downloaded from www.nrcresearchpress.com by 210.87.254.42 on 09/05/12
For personal use only.

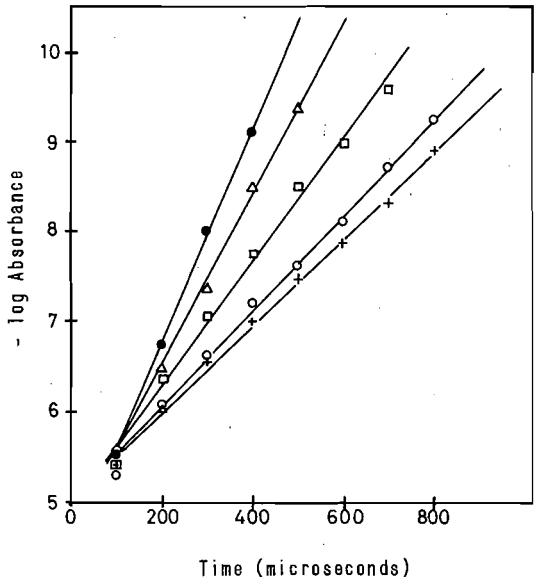

FIG. 2. The decay of $CySSCy^-$ in the presence of cystine at pH 7. Cystine concentrations: +, 0; ○, 2×10^{-4} M; □, 4×10^{-4} M; △, 6×10^{-4} M; ●, 10×10^{-4} M. Cysteine 1.0×10^{-3} M.

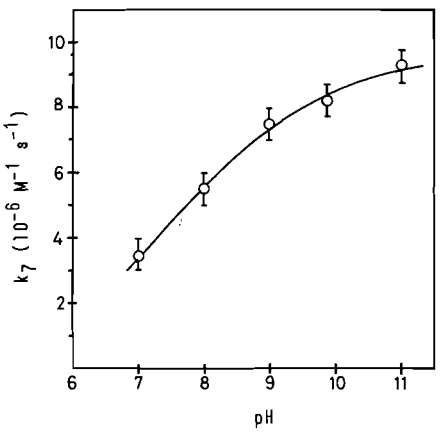

FIG. 3. The rate constant for the reaction of $CySSCy^-$ and cystine as a function of pH.

s^{-1} (2)). The fast first order decay of the resulting $CySSCy^-$ ($k \sim 3 \times 10^5$ M^{-1} s^{-1} (2)) will bring $CySSCy^-$, CyS·, and CyS^- into equilibrium within the time of first measurement (~50 μs from the commencement of the 30 μs flash). Afterwards the decay of $CySSCy^-$ still remains first order but the rate constant k_{obs} now depends on the cystine concentration

$$k_{obs} = k_7[CySSCy] + k_6$$

where k_6, the rate constant for reaction 6, is practically independent of pH (3). The value for k_{obs} obtained from the first order plots shown in Fig. 2 yields $k_7 = 3.4 \times 10^6$ M^{-1} s^{-1} at pH 7. The pH dependence of k_7 is shown in Fig. 3. Direct involvement of $CySSCy^-$ and not the CyS· radical is indicated since an increase in cysteine concentration from 1 to 3×10^{-3} M has no effect on k_7 whereas if the radical were a reactant k_7 would be proportional to $1/[CyS^-]$. Electron transfer from disulfide radical anion to disulfide cannot be a factor since such a reaction would leave the system unchanged.

Since the observed reaction apparently does not involve electron transfer from the anion the increase in k_7 with pH (Fig. 3) can be associated with the increasing ionization of cystine (pK_a = 7.85 (10)). The disulfide radical anion shows behavior similar to other radical anions *e.g.* $(CNS)_2^-$, Br_2^-, Cl_2^-, and I_2^- which are electrophilic, reacting at a greater rate as the degree of ionization of the added solute increases (11). By analogy a suggested mechanism for the reaction is electron transfer from the disulfide to the radical anion followed by hydrolysis of the resulting disulfide cation.

[8] $CySSCy^- + RSSR \rightarrow 2CyS^- + RSSR^+$

[9] $RSSR^+ + H_2O \rightarrow$ Products

An attempt was made to study the effects of other disulfides on the decay of $CySSCy^-$. Solutions containing 1.0×10^{-3} M cysteine together with one of the disulfides oxidized glutathione, oxidized penicillamine, dithiodipropionic acid, and cystamine were flash photolyzed. In all cases there was a decrease in the yield of the transient absorbing at 410 nm which was roughly linear with disulfide concentration. The decrease was greatest for dithiodipropionic acid and least for cystamine as shown in Fig. 4. It was ascertained that there was no decrease in total thiol concentration in these systems. The time between initial mixing of thiol and disulfide in the aqueous solution and photolysis was at least 15 min and in this time there will probably have been almost complete randomization of RS groups between thiol and disulfide (12, 13). The maximum absorbance of the transient remained at or near 410 nm in all cases as might be expected even for mixed disulfide radical anions since the absorbances of most disulfide radical anions maximize close to this wavelength (2). The decreases

Can. J. Chem. Downloaded from www.nrcresearchpress.com by 210.87.254.42 on 09/05/12
For personal use only.

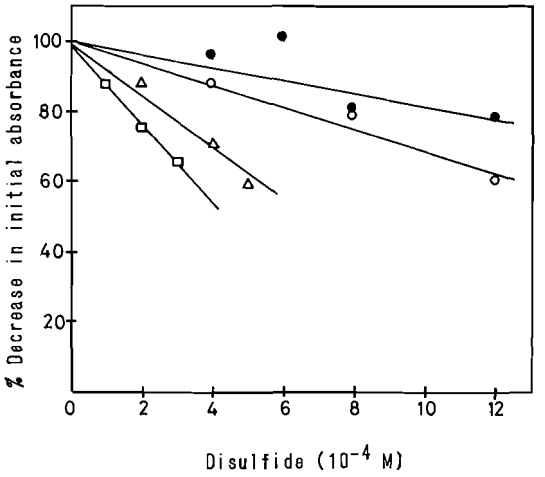

FIG. 4. The decreases in the initial absorbances at 410 nm for 1.0×10^{-3} *M* cysteine solutions containing: ●, cystamine; ○, oxidized penicillamine; △, 3,3′-dithiodipropionic acid; □, oxidized glutathione.

in yields of transients can be attributed to one or both of two factors: (*a*) A difference in the number of thiyl radicals formed by the flash. For example at p*H* 8.7 there is more cysteine in the form of the anion CyS^- than there is glutathione in the form of the anion GS^- (14). (*b*) The equilibrium analogous to 4 for the mixture will probably be different than that for cysteine alone. For example the equilibrium constant for penicillamine (4) is an order of magnitude less than that for cysteine (2).

Just as with the cysteine/cystine system the decay rate of the 410 nm transient is increased with increasing disulfide concentration (Table 1). Because of exchange the form of the disulfides is not known but at low concentrations of added disulfide the mixed disulfide or cystine should predominate. The increased decay rate bears no relation to the decrease in maximum absorbance at 410 nm and the enhanced decay must be attributed to a reaction of disulfide radical anion with disulfide. The only linear disulfide for which enhanced decay is not observed is penicillamine which is consistent with the suggested electron transfer reaction (8) since the methyl groups of penicillamine in either the disulfide or the disulfide radical anion would sterically hinder electron transfer.

TABLE 1. Rate constants (k_7) for the reactions of disulfides with $CySSCy^-$

Disulfide	p*H*	k_7 (M^{-1} s^{-1})
Oxidized glutathione	7	4.3×10^6
	8.7	13.4×10^6
Cystamine	8.7	5.7×10^5
3,3′-Dithiodipropionic acid	8.7	3.1×10^6
Oxidized penicillamine	8.7	$< 10^5$
Cystine	7	3.4×10^6
	8.7	7.5×10^6

Flash Photolysis in the Presence of Alcohols

It has been shown on numerous occasions that sulfhydryl compounds are able to 'repair' the radicals formed by H abstraction from alcohols by OH radicals (4, 14). For example with methanol the following sequence is suggested to occur

$$OH\cdot + CH_3OH \rightarrow H_2O + \cdot CH_2OH$$

$$\cdot CH_2OH + RSH \rightarrow CH_3OH + RS\cdot$$

Dixon and Grant (15) studied the photolysis of aqueous alcoholic solutions of cystine in quartz cells and attributed the increasing yields of cysteine with increasing alcohol concentration to scavenging of CyS· radicals by the alcohol which would "otherwise undergo pair wise combination in the solvent cage". If such scavenging can occur then flash photolysis of alcoholic cysteine solutions should lead to no increase in the absorbance of the transient at 410 nm but might indeed lead to a decrease together with an increased rate of decay. For 1 *M* isopropanol there is actually an increase of ~10% in transient yield. We suggest that the explanation is that flash photolysis of alcoholic solutions of thiols and disulfides produces radicals in addition to thiyl radicals, in particular H atoms (16, 17) which will lead to cysteine production when scavenged by cystine.

In alcoholic solution the first order decay rate of the $CySSCy^-$ transient decreases, being 1.5×10^3 and 1.3×10^3 s^{-1} in 1 and 9 *M* *tert*-butyl alcohol respectively compared with 2.0×10^3 in nonalcoholic solution. The decay is not pure first order above a concentration of 3×10^{-7} *M*, *i.e.* about one-half that in aqueous solution. Both these observations are in line with decay via reactions 4 and 6.

The authors thank the Defence Research Board of Canada and the National Research Council of Canada for financial assistance.

1. G. E. ADAMS, G. S. MCNAUGHTON, and B. D. MICHAEL. *In* The chemistry of ionization and excitation. *Edited by* G. R. A. Johnson and G. Scholes. Taylor and Francis, London. 1967. p. 281.

Can. J. Chem. Downloaded from www.nrcresearchpress.com by 210.87.254.42 on 09/05/12
For personal use only.

2. M. Z. HOFFMAN and E. HAYON. J. Am. Chem. Soc. **94**, 7950 (1972).
3. T.-L. TUNG and J. A. STONE. J. Phys. Chem. **78**, 1130 (1974).
4. J. W. PURDIE, H. A. GILLIS, and N. V. KLASSEN. Can. J. Chem. **51**, 3132 (1973).
5. G. CASPARI and A. GRANZOW. J. Phys. Chem. **74**, 836 (1970).
6. A. PIHL and T. SANNER. *In* Radiation protection and sensitization. *Edited by* H. L. Moroson and M. Quintilani. Taylor and Francis, London. 1970. p. 43.
7. J. L. REDPATH. Radiat. Res. **54**, 364 (1973).
8. P. C. CHAN and B. H. J. BIELSKI. J. Am. Chem. Soc. **95**, 5504 (1973).
9. N. V. KLASSEN, J. W. PURDIE, K. R. LYNN, and M. D'IORIO. Int. J. Radiat. Biol. **26**, 127 (1974).
10. Handbook of Biochemistry. Chemical Rubber Co., Cleveland, Ohio. 1968. p. J-161.
11. G. E. ADAMS, J. E. ALDRICH, R. H. BISBY, R. B. CUNDALL, J. H. REDPATH, and R. L. WILSON. Radiat. Res. **49**, 278 (1972).
12. L. ELDJARN and A. PIHL. J. Am. Chem. Soc. **79**, 4589 (1957).
13. H. A. SMITH, G. DOUGHTY, and G. GORIN. J. Org. Chem. **29**, 1484 (1964).
14. R. E. BENESCH and R. BENESCH. J. Am. Chem. Soc. **77**, 5877 (1955).
15. C. J. DIXON and D. W. GRANT. Photochem. Photobiol. **18**, 387 (1973).
16. P. J. SULLIVAN and W. S. KOSKI. J. Am. Chem. Soc. **84**, 1 (1962); **85**, 384 (1963).
17. M. C. R. SYMONS. J. Chem. Soc. 263 (1959).

Can. J. Chem. Downloaded from www.nrcresearchpress.com by 210.87.254.42 on 09/05/12
For personal use only.

Can. J. Chem. Downloaded from www.nrcresearchpress.com by 210.87.254.40 on 09/05/12
For personal use only.

Réactivité de la combinaison anthracène–lithium vis-à-vis des nitriles[1]

JEAN-PAUL MAZALEYRAT
Groupe de Recherche n° 12, C.N.R.S., 2 à 8 rue Henri Dunant, 94320 Thiais, France

Reçu le 28 février 1975

JEAN-PAUL MAZALEYRAT. Can. J. Chem. **53**, 3158 (1975).

L'anthracène–lithium en solution éthérée se comporte comme un réactif basique vis à vis des nitriles possédant un hydrogène acide. Mais dans le cas des nitriles à C_α tertiaire, deux réactions compétitives peuvent avoir lieu: l'addition nucléophile et le transfert d'électron. L'addition nucléophile est la réaction la plus rapide, mais à cause de sa réversibilité, le mélange réactionnel évolue par le processus de transfert d'électron, suivi de la coupure irréversible de la liaison C—CN, vers la formation d'un alcoyl-9 dihydro-9,10 anthracène.

JEAN-PAUL MAZALEYRAT. Can. J. Chem. **53**, 3158 (1975).

Lithium anthracenylide in ethereal solution behaves as a basic reagent towards nitriles with acidic hydrogens. However, in the case of nitriles with a tertiary α-carbon atom, two competitive reactions may occur: nucleophilic attack and electron transfer. The nucleophilic addition is faster, but because of its reversibility, the reaction proceeds, through the electron transfer process which is followed by the irreversible breaking of the C—CN bond, towards the formation of 9-alkyl-9,10-dihydroanthracene.

Introduction

Il est connu que la coupure C—CN des nitriles peut être réalisée par les métaux alcalins au sein de différents solvants. C'est le cas, par exemple, pour le sodium dans l'éthanol, qui donne deux réactions compétitives; la réduction du groupement CN, conduisant à une amine, et l'élimination réductrice du CN, conduisant à un hydrocarbure (1).

$$\text{R—CN} \xrightarrow[\text{(éthanol)}]{\text{Na}} \begin{matrix} \text{RH + NaCN} \\ \text{RCH}_2\text{NH}_2 \end{matrix}$$

L'utilisation de l'hexamethylphosphorotriamide (HMPT) comme solvant, a permis récemment d'orienter ces réductions vers la formation sélective de l'hydrocarbure RH (2).

La liaison C—CN des nitriles (3, 4), de même que celle des α-aminonitriles (5, 6), est également coupée par les métaux dissous dans l'ammoniac liquide. Dans les deux cas, un mécanisme en plusieurs étapes impliquant un transfert d'électron, a été proposé (3, 6) (schéma 1).

[1] $\text{R—CN} + \text{NH}_3{}^{\cdot-}\text{M}^+ \rightarrow \text{R—CN}^{\cdot-}\text{M}^+ + \text{NH}_3$

[2] $\text{R—CN}^{\cdot-}\text{M}^+ \rightarrow \text{R}^\cdot + \text{CN}^-\text{M}^+$

[3] $\text{R}^\cdot + \text{NH}_3{}^{\cdot-}\text{M}^+ \rightarrow \text{R}^-\text{M}^+ + \text{NH}_3$

[4] $\text{R}^-\text{M}^+ + \text{NH}_3 \rightarrow \text{RH} + \text{NH}_2{}^-\text{M}^+$

[1]Ce travail fait partie de la Thèse de Doctorat d'Etat de J. P. Mazaleyrat, enregistrée au C.N.R.S. sous le N° AO 7747.

a R = —C(|)— *b* R = —C(|)—N(<)

SCHÉMA 1

Lorsque les électrons sont fournis, non plus par un métal alcalin, mais par voie électrochimique, les nitriles subissent également la coupure C—CN (7).

Ainsi, dans deux types de réactions où le milieu est susceptible de fournir des électrons solvatés, le groupement CN se comporte comme un pseudo-halogène, et les nitriles subissent une hydrogenolyse de la même façon que les halogénures.

Or, il est connu que les combinaisons métaux alcalins – hydrocarbures aromatiques constituent également une source d'électrons, et en particulier, qu'elles sont susceptibles de substituer l'halogène des halogénures d'alcoyle, par un mécanisme tout à fait comparable au précédent (8) (schéma 2*a*).

[5] $\text{A}^{\cdot-}\text{M}^+ + \text{RX} \rightarrow \text{R}^\cdot + \text{MX} + \text{A}$

[6] $\text{R}^\cdot + \text{A}^{\cdot-}\text{M}^+ \rightarrow \text{AR}^-\text{M}^+$

[7] $\text{AR}^-\text{M}^+ \xrightarrow[\text{(ou H}_2\text{O)}]{\text{SH}} \text{ARH + MS (ou MOH)}$

a R = Alcoyle; X = Halogène

b R = —C(|)—N(<); X = CN

A = Aromatique

SCHÉMA 2

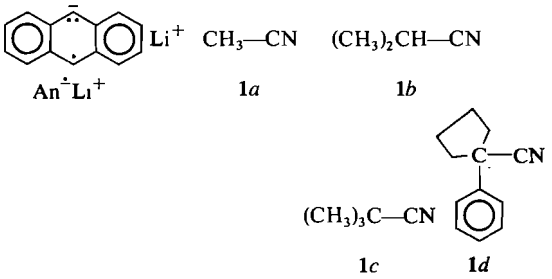

FIG. 1. Les composés **1***a*, **1***b*, **1***c* et **1***d*.

Par conséquent, puisque le groupement nitrile peut, au même titre qu'un halogène, être éliminé par coupure hydrogénolytique au moyen des métaux alcalins ou par voie électrochimique, il y a lieu de supposer qu'il puisse l'être également par les combinaisons métaux alcalins – hydrocarbures aromatiques.

Dans le cas des α-aminonitriles, il se produit effectivement une réaction d'aminoalcoylation de l'hydrocarbure aromatique (9), dont le mécanisme est comparable à celui qui a lieu avec les halogénures[2] (schéma 2*b*). Mais on peut penser toutefois que les α-aminonitriles constituent un cas particulier dans lequel la possibilité de coupure C—CN peut être due à la stabilité du radical aminoalcoyle $-\dot{C}-N\diagup\diagdown$ formé au cours de l'étape 5.

Pour savoir ce qu'il en était dans le cas des nitriles ordinaires, nous avons recherché les produits formés dans la réaction de la combinaison anthracène–lithium $An^{\cdot-}Li^+$, avec les composés **1***a*, **1***b*, **1***c* et **1***d* (fig. 1).

Résultats

Les réactions ont été effectuées en additionnant les différents nitriles à une solution de radicaux anions anthracène–lithium préparée dans l'éther par action directe du lithium sur l'anthracène. Les rendements en chacun des composés obtenus après hydrolyse, ont été déterminés soit directement par pesée, soit par chromatographie en phase gazeuse, au moyen d'étalons internes.

[2]Une différence entre le cas des halogénures et celui des α-aminonitriles est que pour ces derniers, il y a formation intermédiaire d'un radical anion aminonitrile $RCN^{\cdot-}M^+$ (9), qui se coupe dans une étape ultérieure, alors que pour les halogénures, le radical anion $RX^{\cdot-}M^+$ n'étant certainement pas suffisamment stable pour constituer un intermédiaire (10), le transfert d'électron doit être accompagné de la coupure R—X.

Les résultats montrent que lorsque le nitrile est énolisable (composés **1***a* et **1***b*), il se produit seulement une réaction d'arrachement de l'hydrogène acide (conduisant à la formation ultérieure de dihydro-9,10 anthracène), ce qui n'est pas étonnant car il est connu que les combinaisons métaux alcalins – hydrocarbures aromatiques sont des entités basiques qui réagissent sur l'eau (11), mais qui sont également susceptibles d'arracher tout proton suffisamment mobile situé en α d'un groupement attracteur CO (12) ou CN (13).

Avec le pivalonitrile **1***c* (tableau 1), nous obtenons, au bout de 20 h d'agitation, et après hydrolyse acide prolongée, le *tert*-butyl-9 dihydro-9,10 anthracène **2***c* résultant de la coupure, avec un très faible rendement, l'essentiel du nitrile de départ étant récupéré. A côté de cet hydrocarbure, nous obtenons une cétone **4***c* qui provient de l'imine **3***c*. La proportion hydrocarbure **2***c* – cétone **4***c* est d'environ 1:2 (14).

Avec le phényl-1 cyclopentane nitrile **1***d*, nous constatons qu'après un temps de réaction voisin, le rendement en hydrocarbure **2** est très nettement supérieur à celui obtenu avec le pivalonitrile et qu'il ne se forme pas d'imine **3***d*. Par contre, si nous hydrolysons le mélange réactionnel dès la fin de l'addition du nitrile, les proportions sont complètement changées: l'imine **3***d* est obtenue avec un bon rendement, tandis que l'hydrocarbure **2***d* n'est présent qu'à l'état de traces. Une étude approximative par c.p.g. de l'évolution des produits confirme que l'imine **3***d*, formée quasi immédiatement, voit sa concentration diminuer au cours du temps, tandis que la concentration en **2***d* augmente parallèlement.

Enfin, lorsque l'imine **3***d* est mise dans les conditions réactionnelles, en présence d'un gros excès de combinaison anthracène–lithium, elle disparait totalement après 17 h d'agitation, pour donner naissance à l'hydrocarbure **2***d*, accompagné d'une faible proportion de nitrile **1***d*.

Identification. Données de résonance magnétique nucléaire

Les structures des composés ont été établies de la manière habituelle (voir Partie Expérimentale), et, dans ce qui suit, nous discuterons seulement le spectre de r.m.n. du composé **2***d*, lequel est très différent des spectres habituels des dihydro-9,10 anthracènes monosubstitués en position 9. En effet, ces derniers présentent généralement aux alentours de δ 4 p.p.m., un

Can. J. Chem. Downloaded from www.nrcresearchpress.com by 210.87.254.40 on 09/05/12
For personal use only.

TABLEAU 1. Rendements par rapport aux nitriles **1** des différents composés formés dans la réaction. Dans tous les cas, le dihydro-9,10 anthracène et l'anthracène sont présents en quantités importantes

Réactif	R	Temps de réaction	R—CN **1**	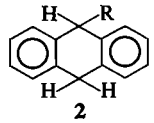 **2**	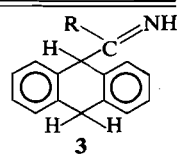 **3**
1*c*	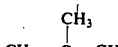	20 h	77	5	10*
1*d*	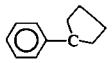	17 h	9	78	0
	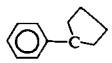	3 min	21	3	66
3*d*	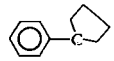	17 h	6	67	0

*Isolé après hydrolyse sous forme de cétone **4***c*.

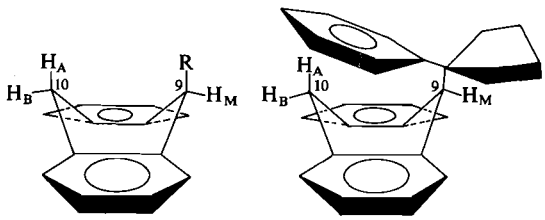

2*d*

FIG. 2. La conformation proposée pour le composé **2***d*.

TABLEAU 2. Déplacements chimiques (en p.p.m. par rapport au TMS) des protons H_A, H_B et H_M (fig. 2)

Composés	δ H_M	δ H_A	δ H_B	J_{AB} (Hz)
4*c*	5.47	4.74	3.74	18
3*d*	4.82	4.35	3.68	18
2*c*	3.55	4.15	3.58	19
2*d*	4.08	1.85	3.12	19

quadruplet caractéristique du système AB constitué par les deux protons en position 10, dont la constante de couplage se situe toujours aux environs de 18–20 Hz (15), et dont les signaux relatifs au proton le plus déblindé sont élargis (16). En outre, le groupement substituant R adoptant préférentiellement la position quasi-axiale ou *perp* (fig. 2), il est connu que le doublet 'élargi' apparaissant au champ le plus faible, correspond au proton H_A *perp*, et que le doublet 'fin' apparaissant au champ le plus fort, correspond au proton H_B *lin* (15, 16).

Les valeurs de déplacement chimique relatives aux protons H_A et H_B, des composés **4***c*, **3***d*, et **2***c* (tableau 2), reflètent bien la situation attendue. Cependant, dans le cas du composé **2***d*, nous constatons que l'un des deux doublets relatifs aux hydrogènes en position 10 apparait à un champ très élevé tout à fait inhabituel (1.85 p.p.m.), à tel point qu'il se trouve noyé dans le massif correspondant aux protons du groupement cyclopentyle. Le second doublet apparait également à un champ relativement élevé (3.12 p.p.m.).

Ce résultat peut s'interpréter en envisageant, pour le composé **2***d*, l'existence d'une conformation privilégiée dans laquelle le groupement phényle est axé vers l'intérieur du cycle central dihydroanthracénique (fig. 2). Dans cette géométrie en effet, nous constatons que les protons H_A et H_B se trouvent tous deux dans la partie blindante du cône d'anisotropie du phényle, ce qui explique que leurs signaux soient déplacés vers les champs forts. Cependant, le proton H_A *perp* se trouvant très proche du phényle, doit subir un effet de blindage beaucoup plus intense que le proton H_B *lin*: nous pensons donc que le doublet à 3.12 p.p.m. correspond au proton H_B, la règle générale "proton *perp* à champ plus faible que proton *lin*" se trouvant ici mise en

Can. J. Chem. Downloaded from www.nrcresearchpress.com by 210.87.254.40 on 09/05/12
For personal use only.

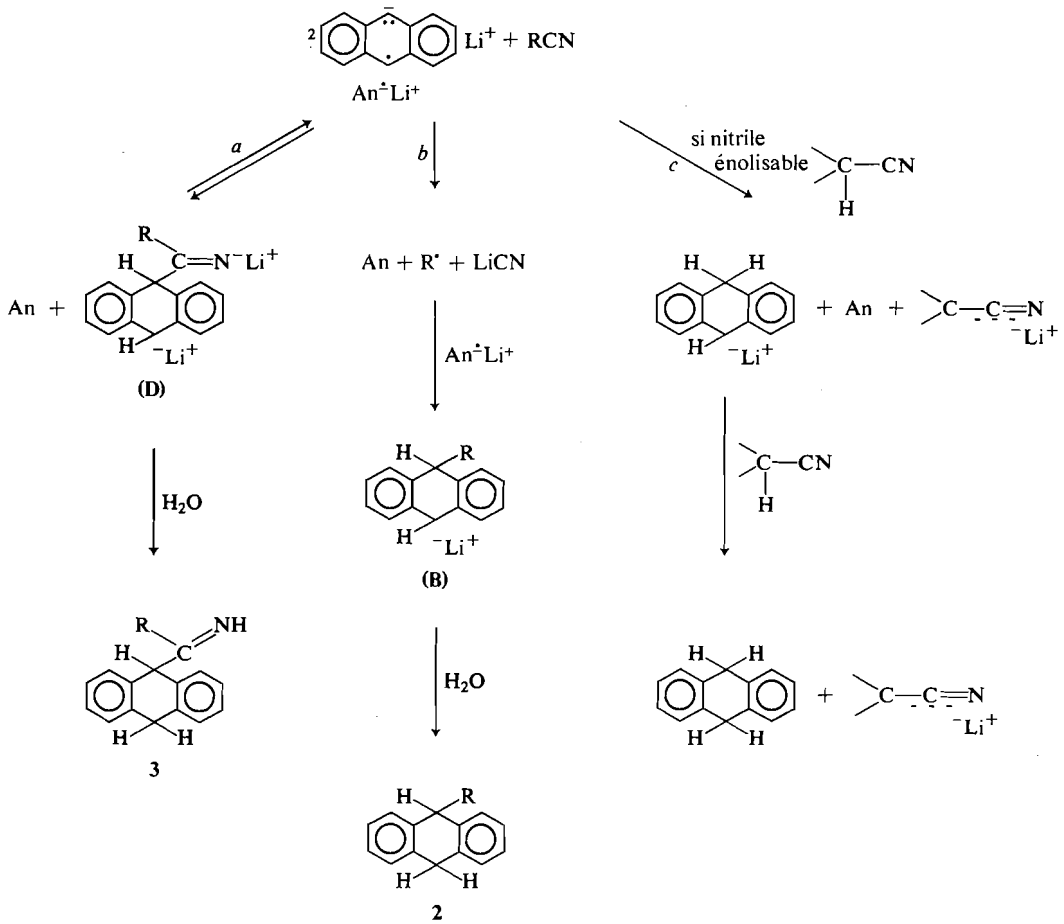

SCHÉMA 3

défaut pour la première fois à notre connaissance.[3]

Discussion

Il est connu que les combinaisons métaux alcalins – hydrocarbures aromatiques peuvent se comporter de différentes manières: ce sont comme nous l'avons vu des réactifs basiques, mais aussi à la fois des agents de transfert d'électron et des agents nucléophiles (8, 17). Les produits obtenus lors de l'action du radical anion anthracène–lithium sur les nitriles représentent une illustration de ces trois modes de réactivité; il se forme en effet trois types de composés: le dihydro-9,10 anthracène, un hydrocarbure **2** et une imine **3** (ou la cétone correspondante).

Mécanisme de formation de l'hydrocarbure 2

La formation de l'hydrocarbure **2** implique une rupture de liaison C—CN. Par analogie avec le cas des halogénures (8), ou des α-aminonitriles (9), il est permis de penser que cette rupture ne devient possible qu'après apport préalable d'un électron, fourni par le radical anion anthracène–lithium $An^{\cdot-}Li^+$, et conduisant à un radical anion nitrile. Ce dernier peut alors conduire, par

[3]Ainsi que le suggère l'un des rapporteurs, que nous remercions, l'effet Overhauser observé lors de l'irradiation des protons des noyaux phényle du groupement dihydro-9,10-anthryle, doit être plus important pour le signal relatif au proton H_B que pour le signal relatif au proton H_A (15). Cependant, cette étude comparative n'est possible que si les signaux en question sont bien isolés dans le spectre, et ce n'est malheureusement pas le cas pour le doublet attribué au proton H_A, qui se trouve noyé dans un massif. Pour le moment donc, notre attribution du signal à champ fort pour le proton H_A, et du signal à champ faible pour le proton H_B, résulte d'une interprétation qui nous parait raisonnable, mais souffre de l'absence de preuve ferme.

Can. J. Chem. Downloaded from www.nrcresearchpress.com by 210.87.254.40 on 09/05/12
For personal use only.

Can. J. Chem. Downloaded from www.nrcresearchpress.com by 210.87.254.40 on 09/05/12
For personal use only.

départ de LiCN, à un radical R$^{\bullet}$, lequel se recombine avec un second radical anion $An^{\dot{-}}Li^{+}$, pour donner un organométallique **B** précurseur de l'hydrocarbure **2** (schéma 3; voie *b*).

Ainsi que nous l'avons souligné précédemment, ce mécanisme est tout à fait comparable au mécanisme de la réduction de ces mêmes nitriles par les métaux dissous ou par électrolyse, le radical anion $An^{\dot{-}}Li^{+}$ jouant le rôle d'une cathode. La seule différence est que, après formation du radical R$^{\bullet}$, la réaction évolue vers un organométallique **B**, au lieu d'évoluer vers un anion R^{-} comme dans le cas de la réduction (schéma 1). Cela est certainement dû au fait que l'hydrocarbure aromatique utilisé est l'anthracène, lequel possède une grande affinité électronique (10), ce qui explique que le radical anion $An^{\dot{-}}Li^{+}$ préfère capter le radical R$^{\cdot}$ et son électron, plutôt que de lui céder un deuxième électron.

Mécanisme de formation de l'imine 3

La formation de l'imine **3** est une illustration du comportement nucléophile du radical anion anthracène–lithium, lequel s'additionne sur le carbone électrophile du groupement —C≡N de la même façon qu'il s'additionne sur les cétones (18) ou sur le CO_2 (19). Le mécanisme généralement admis de ces réactions d'addition nucléophile (17, 20), implique la formation d'un dianion **D** qui se protonne lors de l'hydrolyse du mélange réactionnel pour conduire au composé **3** (schéma 3; voie *a*).

Signification des résultats

La nature des produits formés dans les différents cas étudiés permet d'avoir une idée de la façon dont le radical anion anthracène–lithium fait son choix parmi les possibilités de réaction énumérées précédemment.

Dans le cas d'un nitrile tertiaire, où la réaction d'énolisation (schéma 3; voie *c*) ne peut avoir lieu, les résultats montrent qu'il n'y a pas réellement compétition entre la réaction de coupure conduisant, par l'intermédiaire d'un radical R$^{\bullet}$, à l'organométallique **B** (schéma 3; voie *b*), et la réaction d'addition nucléophile conduisant au dianion **D** (voie *a*).

Cette dernière est en effet beaucoup plus rapide puisque lorsque nous hydrolysons le mélange réactionnel seulement 3 min après l'addition du nitrile **1***d*, nous obtenons l'imine **3***d* avec un bon rendement (66%), alors que l'hydrocarbure **2***d* n'est présent qu'à l'état de traces (3%). La formation ultérieure de l'hydrocarbure, au détriment de l'imine, ne peut alors s'expliquer que par une réversibilité de la voie *a*, alimentant le milieu en radicaux anions $An^{\dot{-}}Li^{+}$ et en nitrile, et permettant ainsi à la réaction irréversible de coupure C—CN (voie *b*) de se produire. Cette réversibilité de la voie *a* peut être attribuée à la formation d'un intermédiaire dianionique **D**, dont l'énergie doit être relativement élevée.

Quant à la vitesse de formation, de l'hydrocarbure **2**, elle dépend de la vitesse de coupure C—CN, laquelle est liée à la stabilité du radical R$^{\bullet}$. Lorsque R$^{\bullet}$ est un radical *tert*-butyle, le composé **2***c* est formé en 20 h avec un rendement de 5%, alors que dans le cas du nitrile **1***d*, où le radical R$^{\bullet}$ doit être particulièrement stable, l'électron célibataire se trouvant en α d'un groupement phényle et sur un cyclopentane (9), le composé **2***d* est formé en 17 h avec un rendement de 78%.

Le fait que l'imine **3***d* placée dans un excès de combinaison anthracène–lithium, conduise à la formation de **2***d*, peut constituer une preuve de la réversibilité de la voie *a*, bien qu'il soit possible d'envisager aussi la formation intermédiaire d'un organométallique **E** (au lieu du dianion **D**), suivie d'un départ de nitrile R—CN (schéma 4).

Par conséquent, l'ensemble des résultats relatifs à l'action du radical anion $An^{\dot{-}}Li^{+}$ sur le nitrile **1***d* ou sur l'imine **3***d*, permet de conclure à l'existence d'une réaction d'addition nucléophile rapide du radical anion sur le groupement nitrile, la formation lente de l'hydrocarbure **2** n'ayant lieu que grâce à la réversibilité de cette réaction d'addition.

Il reste encore à comprendre pourquoi le rendement global (**2** + **3**) est si différent pour les nitriles **1***c* (15%) et **1***d* (78%), ou en d'autres termes, pourquoi la fraction de nitrile **1** qui ne s'est pas transformée en hydrocarbure **2** en fin de réaction, n'est-elle pas toujours récupérée totalement sous forme d'imine **3** après hydrolyse. Les deux explications possibles tiennent compte des vitesses de protonation du radical anion $An^{\dot{-}}Li^{+}$ et du dianion **D**, entités en équilibre dans le milieu au moment de l'hydrolyse (schéma 5).

Si l'interconversion entre le radical anion $An^{\dot{-}}Li^{+}$ et le dianion **D** est lente par rapport à

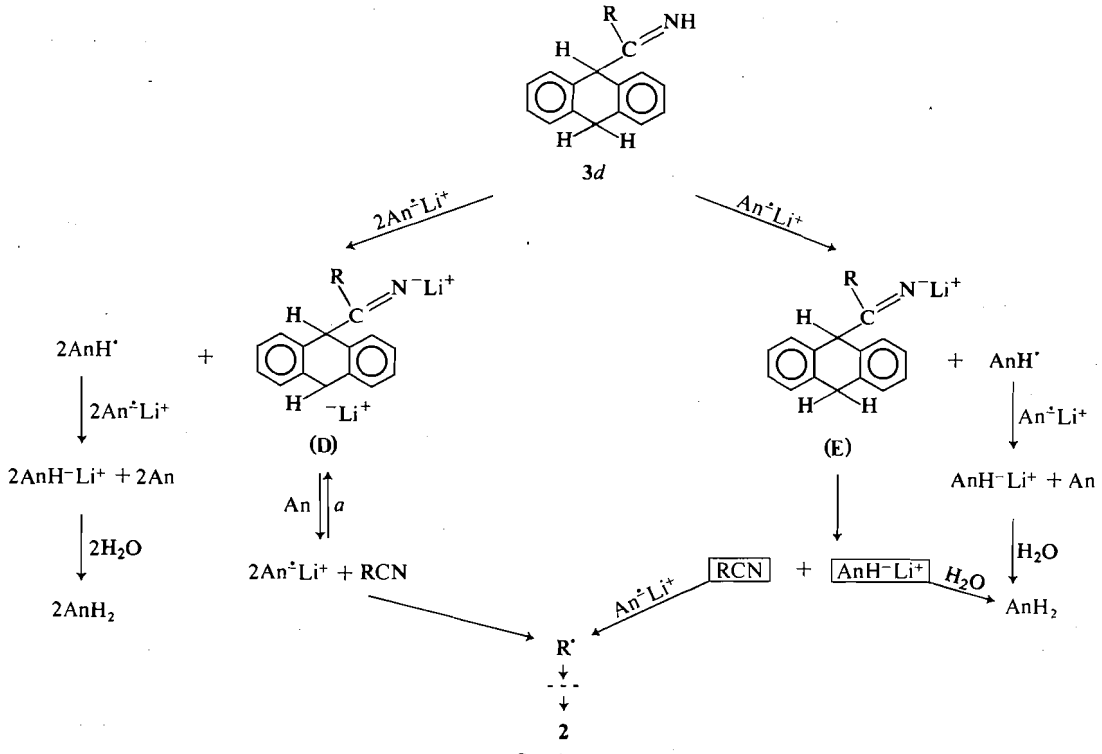

SCHÉMA 4

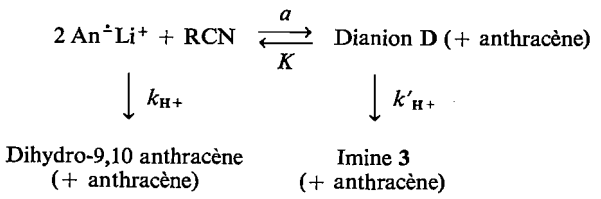

SCHÉMA 5

leurs vitesses de protonation par l'eau, k_{H^+} et k'_{H^+}, la composition du mélange obtenu après hydrolyse doit refléter uniquement la proportion de ces deux espèces. Dans cette optique, si l'equilibre est très déplacé vers le dianion **D**, nous devons obtenir une majorité d'imine **3** (ce serait le cas pour le nitrile **1***d*), et si l'équilibre est très déplacé vers le radical anion $An^{\cdot-}Li^+$, nous devons obtenir très peu d'imine et une majorité de dihydro-9,10 anthracène (ce serait le cas pour le nitrile **1***c*).

Si l'interconversion entre $An^{\cdot-}Li^+$ et **D** est rapide par rapport aux vitesses de protonation par l'eau k_{H^+} et k'_{H^+} de ces deux espèces, la composition du mélange doit refléter surtout le rapport k_{H^+}/k'_{H^+}. Dans cette optique, étant donné que k_{H^+} doit être constant quelle que soit la nature du nitrile, les résultats obtenus signifieraient que k'_{H^+} (**1***c*) est inférieur à k'_{H^+} (**1***d*).

Le même raisonnement peut être tenu dans le cas des nitriles énolisables **1***a* et **1***b*. En effet, comme il est connu que les radicaux anions métaux alcalins–anthracène ne sont que des entités faiblement basiques (11), il peut sembler étonnant de ne pas obtenir d'imine en fin de réaction, mais seulement du dihydro-9,10 anthracène. Ce résultat peut signifier que la vitesse d'établissement de l'équilibre *a* est lente devant la vitesse k_{H^+} de protonation du radical anion $An^{\cdot-}Li^+$ par un hydrogène énolisable du nitrile

Can. J. Chem. Downloaded from www.nrcresearchpress.com by 210.87.254.40 on 09/05/12
For personal use only.

Can. J. Chem. Downloaded from www.nrcresearchpress.com by 210.87.254.40 on 09/05/12
For personal use only.

(c'est à dire que la basicité de l'anthracène–lithium l'emporte sur sa nucléophilie); cependant même si la vitesse d'interconversion entre $An^{\cdot-}$-Li^+ et **D** est grande par rapport à k_{H^+}, il est possible d'obtenir uniquement du dihydro-9,10 anthracène si k'_{H^+} est beaucoup plus petit que k_{H^+}.

Conclusions

En résumé, malgré la complexité liée à la réactivité des radicaux anions anthracène–lithium, qui peuvent se comporter soit comme agents de transfert d'électron, soit comme réactifs basiques, soit comme réactifs nucléophiles, les présents résultats permettent d'apporter les précisions suivantes concernant le mécanisme et la généralité de leur action sur les nitriles: (*i*) Lorsque le nitrile est énolisable, l'anthracène–lithium en solution éthérée se comporte uniquement comme un agent basique; (*ii*) dans la compétition entre l'addition nucléophile sur le nitrile, conduisant à une imine, et le mécanisme de rupture de la liaison C—CN, conduisant à un hydrocarbure, c'est l'addition nucléophile qui est la réaction la plus rapide; (*iii*) cette addition nucléophile est réversible, ce qui est sans doute dû à l'instabilité de l'intermédiaire dianionique formé; (*iv*) l'existence d'une telle réversibilité rend possible la réaction de coupure de la liaison C—CN, plus lente, mais irréversible; (*v*) par analogie avec les réactions de réduction des nitriles, effectuées au moyen des métaux dissous, ou par électrolyse, il est permis de penser que cette coupure se produit après transfert préalable d'un électron fourni par le radical anion anthracène–lithium, ce qui augmente le niveau d'énergie de la molécule de nitrile et active ainsi le départ de l'ion cyanure, habituellement mauvais groupe partant dans les réactions hétérolytiques.

Partie expérimentale

Les points de fusion ont été déterminés sur un appareil Tottoli. Les analyses élémentaires ont été effectuées par le Centre de Microanalyse de Thiais. Les spectres infrarouge ont été enregistrés sur un spectromètre Infracord Perkin-Elmer et sur un appareil EPI G 2 Hitachi. Les spectres de r.m.n. ont été enregistrés sur des spectromètres Varian A 60 et T 60, le tétraméthylsilane étant pris comme référence interne. La chromatographie en phase gazeuse analytique a été effectuée sur un appareil Girdel 75 FS à ionisation de flamme.

Les nitriles **1***a*, **1***b*; **1***c* et **1***d* sont commerciaux. La combinaison anthracène–lithium est préparée dans l'éther, par action du lithium sur l'anthracène. Le lithium est préalablement décapé dans l'alcool absolu, séché, et découpé en fins morceaux. La solution de coloration violette est agitée pendant 4 h à température ambiante, sous atmosphère d'argon sec. On y additionne alors un défaut de nitrile. Après un temps d'agitation variable, le mélange réactionnel est hydrolysé.

*Action des nitriles **1a** et **1b***

Réactifs: anthracène, 0.04 mol; lithium, 0.04 mol; éther, 200 cm^3; **1***a* ou **1***b*, 0.02 mol. Après hydrolyse, la phase éthérée est lavée à l'eau et séchée. Dans les deux cas, le spectre de r.m.n. du produit brut, ainsi que la c.p.g. analytique, indiquent l'absence de composés de substitution du type **2** et d'addition du type **3**. Les seuls produits 'lourds' présents dans le mélange sont l'anthracène et le dihydro-9,10-anthracène.

*Action du pivalonitrile (**1c**)*

Réactifs: anthracène, 3.9 g (0.022 mol); lithium, 0.25 g (0.035 mol); éther, 150 cm^3; **1***c* 0.83 g (0.01 mol). Après hydrolyse au bout de 20 h d'agitation, la phase éthérée est agitée pendant 3 h en présence d'une solution aqueuse de HCl 20%. La phase aqueuse acide est ensuite lavée à l'éther, puis alcalinisée par la soude; l'extraction à l'éther ne fournit aucun produit. La phase éthérée acide est reprise, lavée à l'eau, et séchée; l'éther est chassé. Cette partie neutre est constituée d'un mélange des composés suivants: dihydro-9,10 anthracène et anthracène; nitrile de départ **1***c* (rendement, 77%); composés **2***c* (rendement, 5%) et **4***c* (rendement, 10%).

Le dihydro-9,10 anthracène en excès, et l'anthracène, sont partiellement éliminés par cristallisation dans l'éthanol. Les composés **2***c* et **4***c* sont ensuite séparés par c.p.g. préparative (appareil Aerograph 700; colonne SE 52 5%, *T* 200 °C; débit d'hydrogène, 250 cm^3/min).

*tert-Butyl-9 dihydro-9,10 anthracène (**2c**)*—p.f. (EtOH) 123 °C (litt. (15) p.f. 125–126 °C); spectre r.m.n. (CS_2) identique à celui décrit dans la littérature (15).

Anal. calc. pour $C_{18}H_{20}$: C, 91.47; H, 8.53. Trouvé: C, 91.35; H, 8.56.

*Pivaloyl-9 dihydro-9,10 anthracene (**4c**)*—p.f. (éther de pétrole) 129–132 °C; spectre i.r.: bande C=O à 1700 cm^{-1}; spectre r.m.n. ($CDCl_3$): massif à 7.16 p.p.m., correspondant à 8 protons aromatiques; singulet à 5.47 p.p.m., correspondant au proton H_M; quadruplet AB (J = 18 Hz), correspondant aux protons H_A et H_B, constitué d'un doublet 'élargi' centré à 4.74 p.p.m. pour le proton H_A, et d'un doublet 'fin' centré à 3.74 p.p.m. pour le proton H_B; singulet à 1.23 p.p.m., correspondant à 9 protons du groupement *tert*-butyle.

Anal. calc. pour $C_{19}H_{20}O$: C, 86.32; H, 7.63; O, 6.05. Trouvé: C, 86.45; H, 7.71; O, 6.07.

*Action du phenyl-1 cyclopentane nitrile (**1d**)*

1ère expérience

Réactifs: anthracène, 1.78 g (0.01 mol); lithium, 0.07 g (0.01 mol); éther, 100 cm^3; **1***d*, 0.428 g (0.0025 mol). Dès le début de l'addition du nitrile à la solution violette d'anthracène–lithium, la coloration vire au marron-rouge. Après 17 h d'agitation, la solution est de couleur marron-noir. L'hydrolyse est alors effectuée et la phase éthérée est lavée à l'eau. Une extraction acide-base fournit deux parties: (*a*) partie basique: 0.008 g; (*b*) partie neutre: 2.033 g, constituée du mélange suivant: dihydro-9,10 anthracène et anthracène; nitrile de départ **1***d* (rendement, 9%); composé **2***d* (rendement, 78%).

Can. J. Chem. Downloaded from www.nrcresearchpress.com by 210.87.254.40 on 09/05/12
For personal use only.

TABLEAU 3. Le rapport des surfaces des pics correspondant aux composés **2***d* et **3***d*

t	$\frac{S(3d)}{S(2d + 3d)} \cdot 100$
3 min	93.3
30 min	79.0
45 min	71.6
1 h	63.5
1 h 15 min	65.6
1 h 30 min	59.9
1 h 45 min	55.2
2 h	53.7
2 h 30 min	44.4
3 h	48.6
4 h	38.6
5 h	31.2
19 h	15.7
21 h	15.0

2ème expérience

Réactifs: anthracène, 7.12 g (0.04 mol); lithium 0.28 g (0.04 mol); éther, 350 cm^3; **1***d*, 1.76 g (0.0103 mol). Le nitrile **1***d* est ajouté rapidement à la solution violette d'anthracène–lithium. L'hydrolyse est effectuée après 3 min d'agitation, alors que la coloration de la solution est marron-rouge. Une extraction acide-base fournit deux parties: (*a*) partie basique: 2.382 g d'imine **3***d*, soit rendement, 66%; (*b*) partie neutre, constituée du mélange suivant: dihydro-9,10 anthracène et anthracène; nitrile de départ **1***d* (rendement, 21%); composé **2***d* (rendement 3%).

3ème expérience

Les proportions des réactifs sont identiques aux précédentes. Des prélèvements du mélange réactionnel sont effectués au cours du temps, à l'aide d'une seringue. Après hydrolyse de chaque prélèvement, le produit brut est piqué en c.p.g. (colonne SE 52 5%; 0.50 mètre; T = 190 °C; t_R **2***d*, 1 min 36 s; t_R **3***d*, 4 min 48 s). On détermine le rapport des surfaces des pics correspondant aux composés **2***d* et **3***d* (tableau 3).

(Phényl-1′ cyclopentyl)-9 dihydro-9,10 anthracène (2d)

Le dihydro-9,10 anthracène et l'anthracène sont éliminés partiellement de la partie neutre de la **1**ère expérience par cristallisation dans l'éthanol. L'hydrocarbure **2***d* est ensuite séparé par chromatographie sur plaques (Kieselgel 60 F 254 PSC Fertigplatten–Merck; éluant, pentane): p.f. (pentane), 109–110 °C; spectre r.m.n. ($CDCl_3$): massif entre 6.3 et 7.7 p.p.m., correspondant à 13 protons aromatiques; singulet à 4.08 p.p.m. correspondant au proton H_M; doublet 'fin' centré à 3.12 p.p.m. (J = 19 Hz), correspondant au proton H_B; doublet centré à 1.85 p.p.m. (J = 19 Hz), correspondant au proton H_A; massif entre 1.3 et 2.7 p.p.m. correspondant à 8 protons du cycle cyclopentanique.

Anal. calc. pour $C_{25}H_{24}$: C, 92.54; H, 7.46. Trouvé: C, 92.51; H, 7.29.

L'irradiation du proton H_A à 1.85 p.p.m. a pour conséquence la disparition du couplage et l'apparition d'un pic à 3.12 p.p.m., au centre du doublet correspondant au proton H_B.

De même, l'irradiation du proton H_B à 3.12 p.p.m. a pour conséquence l'apparition d'un pic à 1.85 p.p.m., au centre du doublet correspondant au proton H_A. Spectre de masse: pic moléculaire à *m/e* 324; pic (M − 2) à *m/e* 322, correspondant à une aromatisation par départ de H_2.

(Dihydro-9,10 anthryl)-9 (phényl-1′ cyclopentyl) cétimine (3d)

L'imine **3***d* obtenue à l'état brut (partie basique de la 2ème expérience), est cristallisée dans l'éthanol. On obtient des cristaux blancs: p.f. 139–140 °C; spectre i.r.: bande C═NH à 1620 cm^{-1}; spectre r.m.n. ($CDCl_3$): massif entre 6.3 et 7.5 p.p.m., correspondant à 13 protons aromatiques; singulet à 4.82 p.p.m., correspondant au proton H_M; quadruplet AB (J = 18 Hz), correspondant aux protons H_A et H_B, constitué d'un doublet 'élargi' centré à 4.35 p.p.m. pour le proton H_A, et d'un doublet 'fin' centré à 3.68 p.p.m. pour le proton H_B; massif entre 1.5 et 2.5 p.p.m., correspondant à 8 protons du cycle cyclopentanique.

Anal. calc. pour $C_{26}H_{25}N$: C, 88.84; H, 7.17; N, 3.98. Trouvé: C, 88.91; H, 7.13; N, 3.97.

Action de l'imine 3d

Réactifs: anthracène, 0.9 g (0.005 mol); lithium, 0.035 g (0.005 mol); éther, 160 cm^3; **3***d*, 0.350 g (0.001 mol). Après addition de l'imine à la solution violette d'anthracène–lithium, la coloration vire au marron rouge (comme lors de l'addition du nitrile correspondant **1***d*). Au bout de 17 h d'agitation, la solution possède une coloration marron-noir. Après hydrolyse et extraction acide–base, nous constatons l'absence de partie basique. La partie neutre est constituée d'un mélange des composés suivants: dihydro-9,10 anthracène et anthracène; nitrile **1***d* (rendement, 6%); composé **2***d* (rendement, 67%).

Détermination des rendements

Les rendements indiqués entre parenthèses dans tout

TABLEAU 4. Les résultats des analyses par chromatographie en phase gazeuse

Composé	Produit étalon	Colonne	T (°C)	t_R Composé	t_R Etalon
1*c*	Toluène C_7H_8	UKON 20% 1.7 m	80	1 min 55 s	3 min 53 s
2*c*	*n*-Tetracosane $C_{24}H_{50}$	Apiezon L 15%	180	3 min 12 s	8 min 24 s
4*c*	*n*-Tetracosane $C_{24}H_{50}$	Apiezon L 15%	180	5 min 36 s	8 min 24 s
1*d*	Dicyclohexylamine $C_{12}H_{23}N$	SE 52, 2.5%, 0.5 m	110	0 min 50 s	0 min 28 s
2*d*	*n*-Tetracosane $C_{24}H_{50}$	SE 52, 2.5%, 0.5 m	160	8 min 45 s	4 min 30 s

ce qui précède ont été établis par c.p.g. du produit réactionnel brut, après adjonction d'étalons internes. Des courbes d'étalonnage ont été déterminées pour les nitriles **1***c* et **1***d*, ainsi que pour les composés **2***c*, **4***c* et **2***d*. Les conditions de sortie en c.p.g. de ces différents composés, ainsi que des produits étalons, sont indiquées ci-dessous (tableau 4).

Ce travail a été réalisé sous la direction de Mr. Z. Welvart, que nous tenons à remercier particulièrement. Nous remercions également MM. A. Tchapla et J. P. Bégué pour leur contribution à la discussion des spectres de r.m.n.

1. L. A. WALTER et S. M. MCELVAIN. J. Am. Chem. Soc. **56**, 1614 (1934).
2. T. CUVIGNY, M. LARCHEVEQUE et H. NORMANT. C.R. C, **274**, 797 (1972); T. CUVIGNY, M. LARCHEVEQUE et H. NORMANT. Bull. Soc. Chim. Fr. 1174 (1973).
3. P. G. ARAPAKOS. J. Am. Chem. Soc. **89**, 6794 (1967).
4. L. H. BALDINGER et J. A. NIEWLAND. J. Am. Chem. Soc. **55**, 2851 (1933); L. I. SMITH et L. J. SPILLANE. J. Am. Chem. Soc. **65**, 206 (1943); *cités par* H. SMITH. *Dans* Organic reactions in liquid ammonia. Vol. 1, pt. 2. *Edité par* G. Hander, H. Spandau et C. C. Addison. Interscience Publishers, New York, N.Y. 1964. p. 157.
5. H. THIES, H. SCHONENBERGER et P. QASBA. Arch. Pharm., **302**, 610 et 897 (1969).
6. C. FABRE, M. HADJ ALI SALEM et Z. WELVART. Bull. Soc. Chim. Fr. 178 (1975).
7. P. G. ARAPAKOS et M. K. SCOTT. Tetrahedron Lett. 1975 (1968).
8. J. F. GARST. Acc. Chem. Res. 400 (1971).
9. C. FABRE, M. HADJ ALI SALEM, Z. WELVART, P. ACKERMANN, J. P. GERMAIN et H. ROBERT. Bull. Soc. Chim. Fr. 3814 (1972).
10. M. SZWARC. *Dans* Progress in physical organic chemistry. Vol. 6. *Edité par* A. Streitweiser Jr. et R. W. Taft. Interscience. 1968. p. 323.
11. S. BANK et B. BOCKRATH. J. Am. Chem. Soc. **93**, 430 (1971); M. SZWARC. Acc. Chem. Res. 169 (1972); A. RAINIS, R. TUNG et M. SZWARC. J. Am. Chem. Soc. **95**, 659 (1973); E. R. MINNICH, L. D. LONG, J. M. CERASO et J. L. DYE. J. Am. Chem. Soc. **95**, 1061 (1973).
12. H. NORMANT et B. ANGELO. Bull. Soc. Chim. Fr. 354 (1960).
13. L. HORNER et H. GUSTEN. Ann. Chem. **652**, 99 (1962).
14. J. P. MAZALEYRAT et Z. WELVART. C.R. C, **274**, 800 (1972).
15. A. W. BRINCKMANN, M. GORDON, R. G. HARVEY, P. W. RABIDEAU, J. B. STOTHERS et A. L. TERNAY JR. J. Am. Chem. Soc. **92**, 5912 (1970).
16. R. LAPOUYADE et P. LABANDIBAR. Tetrahedron Lett. 1589 (1970).
17. J. VIDAL et Y. CHAUVIN. Rev. Inst. Fr. Pet. **19**, 1219 (1964).
18. P. BERCOT. Ann. Chim. Fr. **6**, 193 (1961); P. WALKER. J. Org. Chem. **26**, 2994 (1961).
19. J. MATHIEU. Ann. Chim. Fr. **20**, 215 (1945); C. S. RONDESVEST JR. et I. NICHOLSON. J. Org. Chem. **20**, 346 (1955).
20. D. E. PAUL, D. LIPKIN et S. I. WEISSMAN. J. Am. Chem. Soc. **78**, 116 (1956), *cité par* P. REMPP. Bull. Soc. Chim. Fr. 1605 (1968).

Can. J. Chem. Downloaded from www.nrcresearchpress.com by 210.87.254.40 on 09/05/12
For personal use only.

Etude Magnétique des sels alcalins de quelques amino acides

MAURICE A. BERNARD, NICOLE BOIS ET MICHELLE DAIREAUX
Laboratoire de Chimie Minérale B – Groupe de Cristallographie et Chimie du Solide, E.R.A. 305 – U.E.R. de Sciences – Université de Caen – 14032 Caen Cedex – France

Reçu le 9 juin 1975

MAURICE A. BERNARD, NICOLE BOIS et MICHELLE DAIREAUX. Can. J. Chem. **53**, 3167 (1975).

Nous avons déterminé par la méthode de Faraday les susceptibilités magnétiques molaires des sels alcalins M(NH_2—R—COO) de quelques amino acides. (R = —CH_2—, >CH—CH_3, >CH—CH(—CH_3)(—CH_3), >CH—$(CH_2)_2$—CH_3, >CH—CH(—CH_3)—CH_2—CH_3, >CH—$(CH_2)_3$—CH_3).

Nous en déduisons par la méthode de Veiel les susceptibilités magnétiques des anions (NH_2—R—COO^-).

MAURICE A. BERNARD, NICOLE BOIS, and MICHELLE DAIREAUX. Can. J. Chem. **53**, 3167 (1975).

Using the Faraday method molar magnetic susceptibilities of the alkali metal salts M(NH_2—R—COO) of several amino acids (R = —CH_2—, >CH—CH_3, >CH—CH(—CH_3)(—CH_3), >CH—$(CH_2)_2$—CH_3, >CH—CH(—CH_3)—CH_2—CH_3, >CH—$(CH_2)_3$—CH_3) have been determined.

Using the Veiel method, the magnetic susceptibilities of the anions (NH_2—R—COO^-) were deduced.

Introduction

Dans le cadre d'une étude générale sur les glycinates métalliques, nous avions déterminé les susceptibilités magnétiques des glycinates alcalins (1). Nous avons étendu ce travail aux sels alcalins des amino acides suivants:

les α-alaninates (amino-2 propanoates) M(NH_2—CH(—COO)—CH_3); les valinates (amino-2 méthyl-3 butanoates) M(NH_2—CH(—COO)—CH(—CH_3)—CH_3); les norvalinates (amino-2 pentanoates) M(NH_2—CH(—COO)—CH_2—CH_2—CH_3); les isoleucinates (amino-2 méthyl-3 pentanoates) M(NH_2—CH(—COO)—CH(—CH_3)—CH_2—CH_3); les norleucinates (amino-2 hexanoates) M(NH_2—CH(—COO)—CH_2—CH_2—CH_2—CH_3); M = Li, Na et K.

Nous nous sommes limités aux amino acides de commercialisation courante (c'est pourquoi nous n'avons pas envisagé l'étude de sels d'amino acides dont la chaîne carbonée serait formée de quatre carbones) et nous avons essayé de regrouper un amino acide simple avec ses homologues supérieurs. Par exemple, l'α-alanine, la norvaline et la norleucine, sont les homologues supérieurs de la glycine.

Partie expérimentale

Préparation des produits

L'action de la glycine sur les nitrates alcalins dissous dans l'ammoniac liquide permet d'isoler les glycinates alcalins (2). Ce mode opératoire n'est pas généralisable aux sels alcalins des autres amino acides.

Nous les avons isolé par la réaction de Voss et Guttman (3), c'est à dire par action de l'amino acide sur une solution diluée du métal dans l'ammoniac. Ces réactions sont particulièrement violentes, la coloration caractéristique du métal dans l'ammoniac liquide disparaît rapidement et un précipité très fin, blanc, difficile à filtrer, apparaît progressivement.

Nous avons ainsi préparé les sels de lithium, sodium et potassium de l'α-alanine, la valine, la norvaline, l'isoleucine et la norleucine. Ces produits blancs, pulvérulents et très hygroscopiques, n'ont pas été, à notre connais-

Can. J. Chem. Downloaded from www.nrcresearchpress.com by 210.87.254.5 on 09/05/12
For personal use only.

TABLEAU 1. Susceptibilités magnétiques molaires des amino acides

	$\chi_M \times 10^6$ (en c.g.s.)	$(\Sigma n_A \chi_A) \times 10^6$	$\lambda \times 10^6$ (en c.g.s.)
NH_2-CH_2-COOH	−40.3	−41.5	+1.2
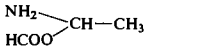	−50.5	−53.3	+2.8
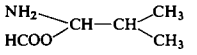	−74.3	−77.0	+2.7
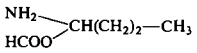	−75.6	−77.0	+1.4
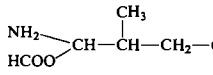	−84.9	−88.9	+4.0
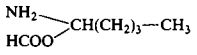	−86.7	−88.9	+2.2

sance, signalés dans la littérature, à l'exception de l'α-alaninate de sodium mentionné sans précision sur sa préparation (3). Les pourcentages expérimentaux en carbone, hydrogène, azote et métal des composés préparés sont en bon accord avec les pourcentages théoriques correspondants.

Dispositif expérimental

Les susceptibilités magnétiques de ces composés ont été déterminées par la méthode de Faraday avec une balance de Cahn. Les mesures ont été effectuées avec un champ de 3000 G sur un échantillon de poudre. La référence utilisée a été le mercurithiocyanate de cobalt dont la susceptibilité magnétique est de $+16.23 \times 10^{-6}$ (en c.g.s.) à 298 K par gramme de substance.

Résultats et discussion

Détermination des susceptibilités magnétiques molaires des amino acides étudiés

Nous n'avons trouvé dans la littérature que les susceptibilités magnétiques molaires de l'α-alanine, de l'isoleucine et de la valine (4). Pour combler cette lacune, nous avons déterminé les susceptibilités magnétiques molaires de la norvaline et de la norleucine. Tous ces composés sont diamagnétiques.

Nous avons ensuite essayé de calculer théoriquement ces susceptibilités magnétiques. En effet, pour les composés d'après Pascal *et al.* (5):

$$\chi_M = \Sigma n_A \chi_A + \lambda$$

n_A = nombre d'atomes de susceptibilité χ_A dans la molécule; λ est un terme correctif dépendant de la nature des liaisons. Les susceptibilités magnétiques des éléments ont été empruntées à la systématique de Pascal *et al.* (6, 7). L'increment de structure λ a été calculé pour les amino acides considérés.

Nous avons rassemblé dans le tableau 1 les valeurs des susceptibilités magnétiques molaires, les calculs théoriques de $\Sigma n_A \chi_A$ et les valeurs de λ. Dans le cas de la glycine, les résultats sont empruntés à un travail antérieur (8). Une étude critique des résultats nous permet d'estimer que l'erreur commise sur les valeurs déterminées est toujours inférieure à 1%.

Détermination des susceptibilités magnétiques molaires des sels alcalins

Nous avons déterminé à 298 K les susceptibilités magnétiques molaires des sels alcalins des amino acides étudiés. Tous ces sels sont diamagnétiques.

Les valeurs des susceptibilités magnétiques molaires sont données dans le tableau 2. Elles résultent chacune de la moyenne d'au moins 10 mesures. Ces valeurs sont d'ailleurs en assez bon accord avec les valeurs théoriques que nous avons pu calculer en adoptant les increments déterminés précédemment.

Can. J. Chem. Downloaded from www.nrcresearchpress.com by 210.87.254.5 on 09/05/12
For personal use only.

TABLEAU 2. Susceptibilités magnétiques molaires des sels alcalins des amino acides

R	M	$\chi_M \times 10^6$ (en c.g.s.) Expérimentales	Théoriques
$-CH_2-$	Li	−41.4	−42.5
	Na	−46.3	−47.5
	K	−53.5	−56.8
	Rb	−66.8	−65.5
$>CH-CH_3$	Li	−50.3	−51.8
	Na	−56.8	−56.8
	K	−63.6	−66.1
$>CH-CH<^{CH_3}_{CH_3}$	Li	−73.7	−75.6
	Na	−80.7	−80.6
	K	−87.6	−89.9
$>CH-(CH_2)_2-CH_3$	Li	−75.4	−76.9
	Na	−82.5	−81.9
	K	−88.7	−91.2
$>CH-\underset{CH_3}{CH}-CH_2-CH_3$	Li	−85.4	−86.2
	Na	−90.6	−91.2
	K	−97.8	−100.5
$>CH-(CH_2)_3-CH_3$	Li	−87.4	−88.0
	Na	−92.4	−93.0
	K	−99.6	−102.3

La principale cause d'erreur est due au fait que les sels alcalins avec lesquels nous opérons sont particulièrement hygroscopiques. Nous devons effectuer rapidement les pesées pour limiter au maximum l'incertitude sur nos mesures qui ont été effectuées sous une atmosphère inerte. Dans ces conditions opératoires, nous estimons la précision à 1% environ.

Détermination des susceptibilités magnétiques des anions (NH_2—R—COO^-)

Afin de déterminer la susceptibilité magnétique de l'anion (NH_2—R—COO^-), nous avons employé la méthode de Veiel (9). D'après Veiel, en effet lorsque la susceptibilité molaire est portée sur un graphique en fonction du numéro atomique du métal pour un groupe d'éléments donné du tableau périodique, on obtient une droite. Nous avons constaté en portant les valeurs trouvées pour les sels de lithium, sodium et potassium des amino acides que celles-ci étaient pratiquement alignées. Dans le cas de la glycine, nous avons également le sel de rubidium qui est le seul sel de rubidium que nous avons pu isoler (8). L'ordonnée à l'origine pour chacune des droites donne la valeur de la susceptibilité de l'anion (NH_2—R—COO^-). Les résultats obtenus sont consignés dans le tableau 3.

TABLEAU 3. Susceptibilités magnétiques des anions (NH_2—R—COO^-)

R	$\chi_M \times 10^6$ (NH_2—R—COO^-) (en c.g.s.)
$-CH_2-$	−38.4
$>CH-CH_3$	−48.5
$>CH-CH<^{CH_3}_{CH_3}$	−72.2
$>CH-(CH_2)_2-CH_3$	−73.6
$>CH-\underset{CH_3}{CH}-CH_2-CH_3$	−82.5
$>CH-(CH_2)_3-CH_3$	−84.4

De plus, nous constatons que ces droites sont parallèles elles ont une pente de −0.77. Nous pouvons établir une relation permettant d'estimer

Can. J. Chem. Downloaded from www.nrcresearchpress.com by 210.87.254.5 on 09/05/12
For personal use only.

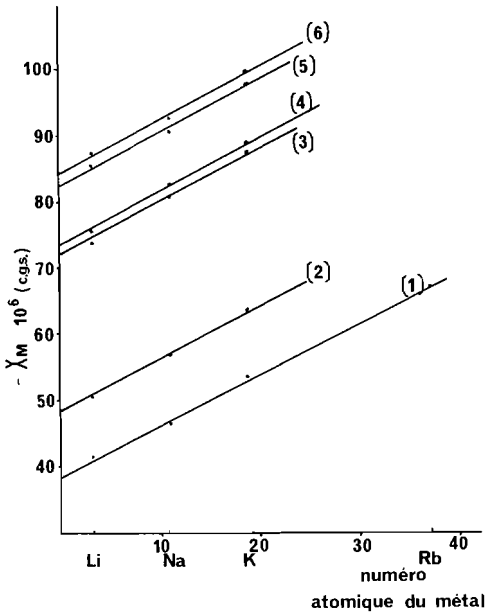

FIG. 1. Susceptibilités magnétiques molaires des sels alcalins des amino acides en fonction du numéro atomique du métal correspondant:

(1) $-CH_2-$; *(2)* $>CH-CH_3$;

(3) $>CH-CH<^{CH_3}_{CH_3}$; *(4)* $>CH-(CH_2)_2-CH_3$;

(5) $>CH-\underset{CH_3}{CH}-CH_2-CH_3$; *(6)* $>CH-(CH_2)_3-CH_3$

les susceptibilités magnétiques molaires des sels alcalins des amino acides (NH_2—R—COOH).

$$\chi_{M(NH_2RCOO)} = \chi_{(NH_2RCOO^-)} - 0.77Z$$

Z = numéro atomique du métal.

Nous avons de cette façon déterminé les susceptibilités magnétiques molaires des sels de rubidium et de césium. En effet, ces composés, très difficiles à isoler sont tellement hygroscopiques qu'ils ne peuvent donner lieu à des mesures magnétiques. Les valeurs sont rassemblées dans le tableau 4. Notons que cette méthode pourrait également permettre d'estimer les susceptibilités magnétiques molaires d'autres amino acides (par exemple des amino acides dont la chaîne carbonée serait formée de quatre carbones).

TABLEAU 4. Estimation des susceptibilités magnétiques molaires des sels de rubidium et de césium des amino acides étudiés

R	M	$\chi_M \times 10^6$ (en c.g.s.) estimées
$>HC-CH_3$	Rb	− 77.0
	Cs	− 90.9
$>CH-CH<^{CH_3}_{CH_3}$	Rb	−100.7
	Cs	−114.5
$>CH-(CH_2)_2-CH_3$	Rb	−102.1
	Cs	−115.9
$>CH-\underset{CH_3}{CH}-CH_2-CH_3$	Rb	−111.0
	Cs	−124.8
$>CH-(CH_2)_3-CH_3$	Rb	−112.9
	Cs	−126.7

1. N. BOIS. Thèse Doctorat ès-Sciences Physiques, Caen. 1972.
2. M. A. BERNARD, A. BUSNOT et N. DECKER. Bull. Soc. Chim. Fr. **7**, 2475 (1970).
3. W. Voss et R. GUTTMANN. Ber. **63**, 1726 (1930).
4. Handbook of chemistry and physics. Chemical Rubber Publishing Company, USA. 1973–1974.
5. P. PASCAL, A. PACAULT et J. HOARAU. C.R. **233**, 1078 (1951).
6. P. PASCAL. C.R. **158**, 1895 (1914).
7. A. PACAULT. Rev. Sci. **86**, 52 (1948).
8. M. A. BERNARD, A. BUSNOT et N. DECKER. Bull. Soc. Chim. Fr. **12**, 4271 (1970).
9. P. N. SELWOOD. Magnetochemistry. Interscience Publishers, N.Y. 1956. p. 74.

Can. J. Chem. Downloaded from www.nrcresearchpress.com by 210.87.254.5 on 09/05/12
For personal use only.

Sterically Hindered Aromatic Compounds. VI. A Remote ε-Deuterium Kinetic Isotope Effect in the Solvolysis of Perdeutero-2,4,6-tri-*tert*-butylbenzyl Chloride

L. Ross C. Barclay, John R. Mercer, and Peter J. MacAulay

Department of Chemistry, Mount Allison University, Sackville, New Brunswick E0A 3C0

Received May 21, 1975

L. Ross C. Barclay, John R. Mercer, and Peter J. MacAulay. Can. J. Chem. **53**, 3171 (1975).

2,4,6-Tri-*tert*-butylbenzyl chloride deuterated at the three *tert*-butyl groups was synthesized. Conductimetric solvolysis studies of the normal and perdeutero-2,4,6-tri-*tert*-butylbenzyl chloride at 30.06 °C in 80% ethanol–water provides evidence for an inverse remote ε-deuterium isotope effect, $k_H/k_D = 0.873$–0.874. Under the same conditions the α-deuterium isotope effect was $k_H/k_{\alpha D} = 1.166$ per deuterium, indicative of limiting solvolytic behavior. The remote ε-deuterium isotope effect for the perdeutero compound is discussed in terms of the inductive effect of deuterium and steric effects on the transition state conformation.

L. Ross C. Barclay, John R. Mercer et Peter J. MacAulay. Can. J. Chem. **53**, 3171 (1975).

On a synthétisé du chlorure de tri-*tert*-butyl-2,4,6 benzyle deutéré dans les trois groupements *tert*-butyles. Des études de solvolyse conductimétriques effectuées sur des chlorures de tri-*tert*-butyl-2,4,6 benzyles normal et perdeutéré, à 30.06 °C et dans un mélange à 80% d'éthanol–eau, indiquent qu'il existe un effet isotopique inverse dû au deutérium-ε éloigné, $k_H/k_D = 0.873$–0.874. Dans les mêmes conditions, l'effet isotopique du deutérium α est $k_H/k_{\alpha D} = 1.166$ par deutérium indiquant un comportement solvolytique liminant. On discute de l'effet isotopique du deutérium-ε éloigné en termes d'effet inductif du deutérium et d'effets stériques sur la conformation de l'état de transition.

[Traduit par le journal]

Introduction

There has been a continuing interest in the role of steric contributions to secondary deuterium isotope effects since Bartell (1) estimated that a major part of such α and β effects could be attributed to differences in nonbonded repulsions between hydrogen and deuterium. The expectation for a steric contribution to isotope effects is based on the fact that the amplitudes of vibration of hydrogen atoms are greater than those of deuterium atoms. In effect this means that deuterium occupies less space than hydrogen. In a recent review of steric isotope effects, Carter and Melander (2) suggested certain specific requirements for experimental tests of such effects; namely, (*1*) the reaction should cause a minimum of change in the reaction medium; (*2*) it is desirable that steric effects play as important a role in the reaction as possible; (*3*) a transition state of well-known conformation is a necessary prerequisite for the quantitative application of the theory. These requirements are met during configurational inversion of suitably substituted biaryls and considerable experimental results on steric deuterium isotope effects have been observed for isotopically substituted biaryl derivatives (2). Recently Boekelheide and coworkers (3) reported an interesting large ($k_D/k_H = 1.20 \pm 0.04$) isotope effect for conformational flipping of a monodeuterated (2,2)-metaparacyclophane.

As Carter and Melander pointed out (2), solvolytic reactions do not generally fulfill the 'requirements' for experimental tests of steric isotope effects. Such reactions involve changes in structure of both the medium and the substrate; the role of the steric effect is not necessarily dominant, and the transition state geometry is difficult to define precisely.

For this investigation we selected perdeutero-2,4,6-tri-*tert*-butylbenzyl chloride (**1**) as a model to probe the relative importance of steric effects in remote deuterium isotope effects.

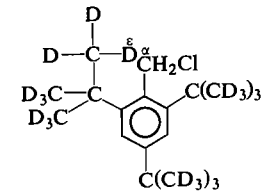

1

Can. J. Chem. Downloaded from www.nrcresearchpress.com by 210.87.254.105 on 09/05/12
For personal use only.

Can. J. Chem. Downloaded from www.nrcresearchpress.com by 210.87.254.105 on 09/05/12
For personal use only.

There are certain properties of this system which make it useful in this study of the question of steric deuterium isotope effects in solvolysis. (*1*) There is ample evidence for severe steric interactions between the functional group and the *o-tert*-butyl groups from both chemical and physical properties (4, 5). (*2*) The mechanism of solvolysis of 2,4,6-tri-*tert*-butylbenzyl chloride has been established to be limiting by previous studies (4, 5). The deuterium isotope effects from the *o-tert*-butyls would be expected to be magnified 18 times and any effects would be readily detected by the available precision conductimetric method. (*3*) Electronic effects from the ε-C—D(H) bonds are expected to be slight at the reaction site and the controversial question of hyperconjugation effects should not concern us. (*4*) Finally solvolysis of **1** might give further insight into the unusual high reactivity of 2,4,6-tri-*tert*-butylbenzyl chloride.

Karabatsos and coworkers (6) earlier studied remote (ε) deuterium isotope effects in such systems as **2** as a test of the relative importance of hyperconjugation and nonbonded interactions to secondary isotope effects.

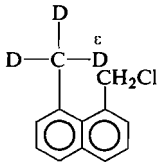

2

However the overall isotope effect here was relatively slight (k_H/k_D = 1.013). Furthermore the pronounced steric effects present in 2,4,6-tri-*tert*-butylbenzyl chloride are not so evident in **2**, for neither kinetic acceleration nor n.m.r. compression shifts (7).

Experimental[1]

Syntheses of Deuterium Labelled Compounds

Perdeutero-1,3,5-tri-tert-butylbenzene (1)

It was desirable to modify the procedure involving direct alkylation of benzene with a large excess of *tert*-butyl chloride (8) because of the prohibitive expense involved with the labelled chloride. Benzene (0.391 g, 5 mmol) and *tert*-butyl-d_9 chloride (Merck Sharp & Dohme, minimum isotopic purity 99 atom % D, 3.08 ml, 25 mmol) were added to a small three-necked flask and the system purged with dry nitrogen. The mixture was cooled below −40 °C and anhydrous aluminum chloride (0.335 g) was added over 15 min to the mixture which was maintained at −40 °C for 35 min. The temperature was slowly raised to −13 °C in 30 min; between −30 and −20 °C reaction was rapid with copious evolution of hydrogen chloride. The progress of the reaction was followed by g.l.c. analysis on small aliquots using an 8 ft. × ¼ in. 20% carbowax column at 165 °C and 60 ml/min flow rate of helium. Under these conditions the 1,3,5-tri-*tert*-butylbenzene has a shorter retention time than 1,4-di-*tert*-butylbenzene.

The results were as follows:

Reaction time (h)	1,3,5-$(C_4D_9)_3C_6H_3$ (%)	1,4-$(C_4D_9)_2C_6H_4$ (%)
2	88	12
3	92	8
4	90	3.4

The reaction mixture was terminated after four hours by which time it contained 90% 1,3,5-tri-*tert*-butylbenzene and approximately equal amounts (3%) of *tert*-butylbenzene, 1,3-di-*tert*-butylbenzene and 1,4-di-*tert*-butylbenzene. The 1,3,5-*tert*-$(C_4D_9)_3C_6H_3$ was identified by separation and analysis on a Varian MAT 111 GC-MS. It showed the expected parent mass at 273.

An estimate of the deuterium content of the 1,3,5-*tert*-$(C_4D_9)_3C_6H_3$ was made by n.m.r. integrations of the small peak in the region for ordinary *tert*-C_4H_9- in this hydrocarbon (1.34 δ) relative to the resonance for the aryl-H^s (7.37 δ). The *tert*-butyl groups contained slightly more than 99% deuterium.

Perdeutero-2,4,6-tri-tert-butylbromobenzene, 2,4,6-tert-$(C_4D_9)_3C_6H_2Br$

The crude perdeutero-1,3,5-tri-*tert*-butylbenzene was brominated using the 'neutral' conditions of Myhre and coworkers (9). The required bromo compound (79% of the crude product) was separated by a g.l.c. method on a Wilkens Autoprep using repeated injections of a benzene solution on an 8 ft × ¼ in. 20% Carbowax column at 215 °C and 60 ml/min He. Recrystallization of the collected material from methanol yielded colorless crystals, m.p. 171.5–172.5 °C (lit. (10) m.p. 177–177.5 °C).

The mass spectrum[2] of this perdeutero compound was compared with that of ordinary 2,4,6-tri-*tert*-butylbromobenzene. The latter showed molecular ions at *m/e* 324 and 326 of equal intensity corresponding to the bromine isotopes in $C_{18}H_{29}Br$. The base peaks were at *m/e* 309 and 311 for $M^+ - CH_3$. Peaks for $M^+ - C_4H_9$ at *m/e* 267 and 269 were approximately 3% of the base peaks. The perdeutero compound showed the expected mass spectral pattern with the molecular ions at *m/e* 351 and 353 of equal intensity corresponding to $C_{18}D_{27}H_2Br$. The base peaks now were at *m/e* 333 and 335 corresponding to $M^+ - CD_3$. Peaks for $M^+ - C_4D_9$ appeared at 285 and 287 as expected.

Perdeutero-2,4,6-tri-tert-butylbenzyl Chloride (1), 2,4,6-tert-$(C_4D_9)_3C_6H_2CH_2Cl$

The required substituted benzyl chloride (**1**) was synthesized by reaction of the aryl lithium derivative with

[1]The general procedures were as outlined previously (4).

[2]The comparative mass spectra reported herein were obtained on a Dupont 21-110B instrument.

TABLE 1. Solvolysis of 2,4,6-tri-*tert*-butylbenzyl chloride and -α-d_2 chloride in 80% ethanol–water at 30.06 °C

Compound	Rate constants ($k_1 \times 10^4$ s^{-1})	Average	% deviation
2,4,6-Tri-*tert*-butylbenzyl chloride	4.128 4.128 4.103 4.163	4.130	0.60
2,4,6-Tri-*tert*-butylbenzyl-α-d_2 chloride	3.046 3.037 3.022 3.034	3.034	0.32
		$k_H/k_D = \frac{4.130}{3.034} = 1.361$	
		k_H/k_D per D = 1.166	

TABLE 2. Solvolysis of perdeutero-2,4,6-tri-*tert*-butylbenzyl chloride in 80% ethanol–water at 30.06 °C

Run*	Rates ($k_1 \times 10^4$ s^{-1})	Average	% deviation	k_H/k_D
1	4.742 4.711 4.712 4.726	4.723	0.31	$\frac{4.130}{4.723} = 0.874$
2	4.761 4.716 4.709 4.733	4.729	0.49	$\frac{4.130}{4.729} = 0.873$

*The two runs were carried out by different investigators, J. R. Mercer and P. J. MacAulay.

chloromethyl methyl ether, followed by low temperature cleavage of the resulting substituted methyl benzyl ether with boron trichloride according to the reaction sequences used earlier (11). The chloride (**1**) obtained was purified by fractional vacuum sublimation to give colorless crystals, m.p. 141–142 °C (lit. (11) m.p. 141–144 °C).

The mass spectrum of this deuterated chloride (**1**) was compared with that of ordinary 2,4,6-tri-*tert*-butylbenzyl chloride. The latter showed the molecular ion as expected at *m/e* 294. The base peak was at *m/e* 259 for $M^+ - Cl$. A peak at *m/e* 279 for $M^+ - CH_3$ was 50% of the base peak. The perdeutero chloride (**1**) showed the expected mass spectral pattern with the molecular ion at *m/e* 321 corresponding to $(C_4D_9)_3C_6H_2CH_2Cl$. The base peak was at *m/e* 286 corresponding to $M^+ - Cl$. The peak at *m/e* 303 for $M^+ - CD_3$ was 50% of the base peak.

Kinetic Measurements

Kinetic measurements were made using the solvent 80% ethanol–water in stirred cells by the precision conductance method. Four determinations of each rate constant were made. Details on the procedure and the treatment of the data were published earlier (4, 5). The results are outlined in Tables 1 and 2 (Results and Discussion).

Results and Discussion

The α-Deuterium Isotope Effect

It was desirable to first determine the α-deuterium isotope effect for the system chosen and under the conditions used in this investigation (80% ethanol–water, 30.06 °C). The results of this study are given in Table 1.

The high value (approximately 1.17 per D) for the α-deuterium isotope effect confirms the limiting nature of the solvolysis under these conditions and is consistent with our earlier results (5).

The Remote ε-Deuterium Isotope Effect

Results for the solvolysis of perdeutero-2,4,6-tri-*tert*-butylbenzyl chloride are summarized in Table 2.

A significant *inverse* overall kinetic isotope effect was observed (k_H/k_D = 0.873–0.874) for the perdeutero compound with very good reproducibility of the results. A qualitative evaluation of these results is in order in terms of the main contributing electronic and steric effects that might be expected and the anticipated effect that these remote ε-deuteriums should have at least in the direction, *acceleration* or *retardation*, on the solvolysis rate.

Can. J. Chem. Downloaded from www.nrcresearchpress.com by 210.87.254.105 on 09/05/12
For personal use only.

Can. J. Chem. Downloaded from www.nrcresearchpress.com by 210.87.254.105 on 09/05/12
For personal use only.

Inductive Effect of Deuterium

It has long been recognized that deuterium is electron releasing relative to hydrogen (12) and the inductive contribution on secondary deuterium isotope effects is inverse and relatively slight. For example the δ-nonadeuterated derivative of dimethylneopentylcarbinyl chloride $(CD_3)_3CCH_2C(CH_3)_2Cl$ showed $k_H/k_D = 0.983$ in 80% ethanol–water and the result was attributed to the inductive effect of deuterium (13). The inductive isotope effect of an alkyl, such as a *meta*-trideuteromethyl (14), on the limiting solvolysis reaction of a substituted benzylic chloride is similarly small and inverse. It is very probable that the multiple inductive isotope effect of the *three* nonadeutero *tert*-butyl groups accounts for a significant portion (at least a half) of the observed inverse isotope effect in **1**.

Steric Acceleration Effects

If a reaction proceeds with relief of strain from a sterically congested initial state (*e.g.* steric acceleration) involving congestion of hydrogen atoms, the hydrogen derivative is expected to be more strained than the deuterium derivative in the initial state and the former would react at a faster rate. This kind of argument has been used before (1, 12, 15) but there is relatively meager convincing evidence of this 'normal' isotope effect, at least in systems where the possibility of hyperconjugation effects do not obscure this steric factor. It has been estimated (6) that, in ordinary systems where hyperconjugation is possible, only a small portion (2–5%) of the observed effect is due to nonbonded interactions. Despite the severe crowding in 2,4,6-tri-*tert*-butylbenzyl chloride, we find little (if any) evidence for this kind of steric contribution to the isotope effect although other effects could mask such effects (see below).

The Question of Long Range Vertical Stabilization of the Cation

It was suggested earlier (4) that the solvolytic reactivity of 2,4,6-tri-*tert*-butylbenzyl chloride might be accounted for by through space vertical stabilization of the cation by interaction (σ–π) between the cationic center and the C—H bonds of the *o-tert*-butyls which are very close in space. Such an effect would weaken these C—H bonds in the transition state and therefore result in a significant 'normal' isotope effect ($k_H/k_D > 1$) for the perdeutero chloride (**1**). This is obviously not at all the case so we now discount this as a possible explanation for the high reactivity of this chloride.

Steric Effect on the Transition State Conformation

Steric inhibition of coplanarity could affect the geometry of the 2,4,6-tri-*tert*-butylbenzyl cation by twisting the carbonium ion away from the plane of the benzene ring (4).

The resulting steric inhibition of resonance could be somewhat less when all hydrogens of the *o-tert*-butyls are replaced by deuterium. The result would be a somewhat more stable cation for the perdeutero compound and a more favorable transition state leading to it. This isotope effect would tend to accelerate the rate but we have no way as yet to estimate the magnitude of this effect.

We conclude that the inductive effect of deuterium combined with a possible steric effect on the transition state geometry account for the inverse kinetic isotope effect observed in the solvolysis of **1**. On the other hand, relief of steric strain does not appear to be a significant factor in such remote deuterium isotope effects.

Financial support of this research provided by the National Research Council of Canada is gratefully acknowledged. We thank Dr. W. D. Jamieson of the National Research Council, Atlantic Regional Laboratory for the mass spectral analyses.

1. L. S. BARTELL. J. Am. Chem. Soc. **83**, 3567 (1961).
2. R. E. CARTER and L. MELANDER. Adv. Phys. Org. Chem. **10**, 1 (1973).
3. S. A. SHERROD, R. L. DACOSTA, R. A. BARNES, and V. BOEKELHEIDE. J. Am. Chem. Soc. **96**, 1565 (1974).
4. L. R. C. BARCLAY, H. R. SONAWANE, and J. C. HUDSON. Can. J. Chem. **50**, 2318 (1972).
5. L. R. C. BARCLAY, J. R. MERCER, and J. C. HUDSON. Can. J. Chem. **50**, 3965 (1972).
6. G. J. KARABATSOS, G. C. SONNICHSEN, C. G. PAPAIOANNOU, S. E. SCHEPPELE, and R. L. SHONE. J. Am. Chem. Soc. **89**, 463 (1967).
7. D. C. KLEINFELTER and P. H. CHEN. J. Org. Chem. **34**, 1741 (1969).
8. J. M. A. BAAS, H. VAN BEKKUM, M. A. HOEFNAGEL, and B. M. WEPSTER. Rec. Trav. Chim. **88**, 1110 (1969).
9. P. C. MYHRE, G. S. OWEN, and L. L. JAMES. J. Am. Chem. Soc. **90**, 2115 (1968).
10. E. E. BETTS and L. R. C. BARCLAY. Can. J. Chem. **33**, 1768 (1955).
11. L. R. C. BARCLAY, H. R. SONAWANE, and M. C. MACDONALD. Can. J. Chem. **50**, 281 (1972).
12. E. A. HALEVI. Prog. Phys. Org. Chem. **1**, 109 (1963).
13. J. G. JEWETT and R. P. DUNLAP. J. Am. Chem. Soc. **90**, 809 (1968).
14. R. H. GRIFFIN and J. G. JEWETT. J. Am. Chem. Soc. **92**, 1104 (1970).
15. H. C. BROWN, M. E. AZZARO, J. C. KOELLING, and G. J. MCDONALD. J. Am. Chem. Soc. **88**, 2520 (1966).

Mass Spectrometry of *N*-Benzoyl-2-hydroxyalkylamines. Role of the Hydroxylic Hydrogen in the Fragmentation Pattern

DON C. DEJONGH,[1] DENIS C. K. LIN, PIERRE LECLAIR-LANTEIGNE, AND DENIS GRAVEL[1]

Département de Chimie, Université de Montréal, C.P. 6210, Succ. A, Montréal, Québec H3C 3V1

Received May 2, 1975

DON C. DEJONGH, DENIS C. K. LIN, PIERRE LECLAIR-LANTEIGNE, and DENIS GRAVEL. Can. J. Chem. **53**, 3175 (1975).

An interesting rearrangement has been observed in the mass spectra of a series of *N*-benzoyl-2-hydroxyalkylamines. The hydrogen atom of the hydroxyl group is transferred to the *N*-benzoyl portion of the molecular ion and the bond between positions 1 and 2 in the *N*-alkyl group is cleaved. A rearrangement ion, observed at *m/e* 135, is formed along with a neutral aldehyde or ketone. When the hydroxylic hydrogen is replaced by a trimethylsilyl substituent, the latter group is transferred with comparable efficiency. Differences in the relative importance of this rearrangement in the mass spectra of a series of related compounds with decreasing substitution at position 2, have been explained by differences in the stabilities of the neutral molecules formed along with *m/e* 135 and by the occurrence of a double hydrogen rearrangement which competes if hydrogen atoms are present in a relationship *gamma* and *delta* to the carbonyl group.

DON C. DEJONGH, DENIS C. K. LIN, PIERRE LECLAIR-LANTEIGNE et DENIS GRAVEL. Can. J. Chem. **53**, 3175 (1975).

Un réarrangement intéressant a été observé dans les spectres de masse d'une série de *N*-benzoyl hydroxy-2-alkylamines. Dans ce réarrangement, l'atome d'hydrogène du groupe hydroxyle est transposé à la partie *N*-benzoyle de l'ion moléculaire et le lien entre les positions 1 et 2 dans le groupe *N*-alkyle est scindé. Ceci donne lieu à la formation d'un ion, observé à *m/e* 135, ainsi qu'à un fragment neutre aldéhyde ou cétone. Lorsque l'hydrogène hydroxylique est remplacé par un groupe triméthylsilyle, ce dernier est aussi transposé avec une facilité comparable. Les différences observées dans l'importance relative de ce réarrangement dans les spectres de masse d'une série de composés reliés ont été expliquées par des différences dans les stabilités relatives des molécules neutres produites à côté de l'ion *m/e* 135 ainsi que par l'apparition d'un réarrangement à deux hydrogènes qui entre en compétition avec le processus décrit plus haut, lorsque la molécule possède des hydrogènes en position *gamma* et *delta* par rapport au carbonyle.

Introduction

Much attention has been focused on intramolecular hydrogen rearrangements observed upon electron impact. A recent review has covered those undergone by aliphatic hydrocarbons and aromatic compounds (1), whereas another has treated exclusively the so-called McLafferty rearrangement (2). The fact that the latter review contains 651 references attests to the importance of this reaction in mass spectrometry. Similarities between the McLafferty rearrangement, produced upon electron impact, and the Norrish Type II photochemical reaction also have been observed and discussed (3–6).

[1]To whom correspondence should be addressed. Presented in part at the 22nd Annual Conference, American Society for Mass Spectrometry, Philadelphia, May 1974.

The McLafferty rearrangement is defined as the transfer of a hydrogen in a relationship *gamma* to a double-bonded atom through a six-membered transition state, with *beta* bond cleavage (2). For example, an abundant ion is found in the mass spectrum of *N*-*p*-tolyl-3-phenyl-3-oxopropionamide, corresponding to the McLafferty rearrangement, Eq. 1 (4). At 15 eV, the molecular ion is the base peak in the

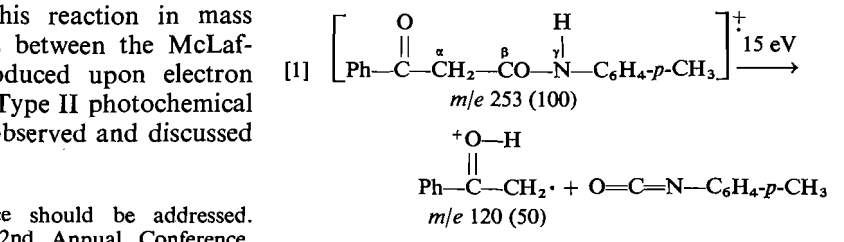

mass spectrum, and the relative intensity of the rearrangement ion at *m/e* 120 is 50%. Upon

Can. J. Chem. Downloaded from www.nrcresearchpress.com by 210.87.254.6 on 09/05/12
For personal use only.

Can. J. Chem. Downloaded from www.nrcresearchpress.com by 210.87.254.6 on 09/05/12
For personal use only.

photolysis, the same compound decomposes to acetophenone and *p*-tolylisocyanate, via the Norrish Type II reaction, Eq. 2.

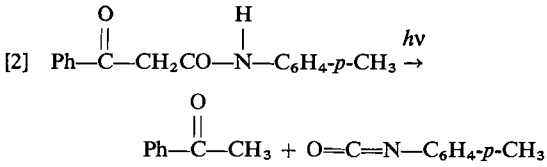

The McLafferty rearrangement has been observed in all classes of carbonyl compounds and also in noncarbonyl systems, such as unsaturated systems, sulfur-containing systems, nitrogen-containing systems, etc. If a hydrogen *gamma* to the double-bonded atom is not available or if the normal process is less favorable for structural or energetic reasons, an alternative or competing process may be preferred. For example, in the mass spectra of some esters containing the tetrahydrofuranyl system, a hydrogen remote from the carbonyl group is abstracted, Eq. 3 (7).

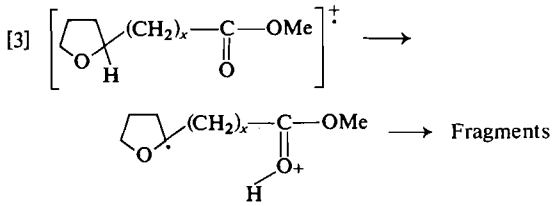

x = 2, 4, 7, and 13

In conjunction with a study of the photochemistry of *N*-substituted unsaturated amides, we have observed a rearrangement in the mass spectra of a series of *N*-benzoyl-2-hydroxyalkylamines of general structure **1**. During the course of the rearrangement, the hydrogen atom of the hydroxyl group is transferred to the *N*-benzoyl

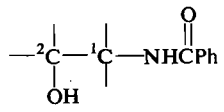

1

portion of the molecular ion and the single bond between carbons 1 and 2 cleaves.

Mass spectra of amides have been previously reported (8–10). If a γ-hydrogen atom is present in the acyl group of an amide, the McLafferty rearrangement predominates in its mass spectrum. McLafferty rearrangements can also occur between the carbonyl oxygen and a hydrogen in the *N*-alkyl group of the amide. Furthermore, the cleavage of the bond between positions 1 and 2 in the *N*-alkyl group is characteristic of the fragmentation of secondary amides.

In this article, we will present the mass spectra of a series of compounds of general structure **1** in order to define the rearrangement. Then, we will show the effects of substitution in the 2-position of the *N*-alkyl group and compare the hydrogen-donating aptitudes of various groups. Mass-spectral data are presented in Schemes; however, structures given in the Schemes for ions are speculative. Relative intensities are also given in the Schemes, in parentheses.

Results

In the 15 eV mass spectrum of *N*-benzoyl-2-hydroxy-2,2-diphenylethylamine (**2**), the molecular ion is weak and the base peak is found at *m/e* 135, Scheme 1. Minor peaks are present corresponding to fragmentations expected from alcohols: cleavage adjacent to the hydroxyl group (*m/e* 183) and elimination of H_2O (*m/e* 299). In the present case, we will focus our

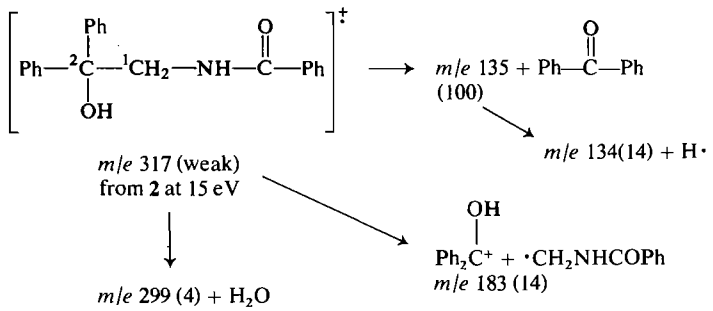

SCHEME 1

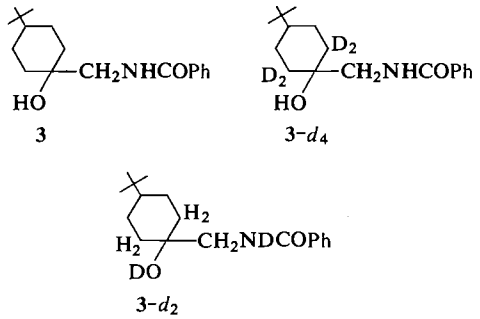

attention on the formation of the ion found at *m/e* 135.

In the low-voltage mass spectrum of *N*-benzoyl-1-aminomethyl-4-*tert*-butylcyclohexanol (**3**), essentially the only peak present is the one at *m/e* 135. At 70 eV, there are weak peaks corresponding to the molecular ion and loss of $CH_3\cdot$, H_2O, and $CH_3\cdot + H_2O$, and intense peaks at *m/e* 135, 134 ($135 \xrightarrow{m^*} 134 + H\cdot$), 105 (PhCO), and 77 ($C_6H_5$).

Two deuterated analogs of **3**, **3**-d_4, and **3**-d_2, were also studied and provide some insight into the formation of this ion found at *m/e* 135. In the 15 eV mass spectrum of **3**-d_4, the rearrangement ion remains exclusively at *m/e* 135; however, in the 15 eV mass spectrum of **3**-d_2, the ion is found at *m/e* 137:

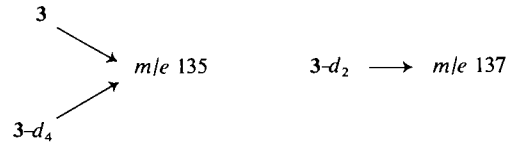

After correcting for the percentage of monodeuteration (there was ~16.5% d_1), the ratio of *m/e* 136 to *m/e* 137 was found to be 6:94 in the mass spectrum of **3**-d_2. Thus, there is no less than 94% transfer of deuterium from —OD and no more than 6% of transfer of hydrogen from C—H.

In terms of mass spectra taken at various voltages, deuterium labeling, exact-mass measurements, and metastable peaks, the rearrangement and subsequent fragmentations are consistent with the pathway presented in Scheme 2. The hydroxyl hydrogen is transferred to the *N*-benzoyl group and the bond between carbons 1 and 2 in the *N*-alkyl group cleaves, resulting in the elimination of a stable molecule containing a carbonyl group. We have placed the transferred hydrogen on the carbonyl group of the amide in Scheme 2, in analogy with the McLafferty rearrangement, although we have no information on the exact structures of the ions.

In order to have a point of reference, we have compared the mass spectra of **2** and **3** with the fragmentations observed in the 15 eV mass

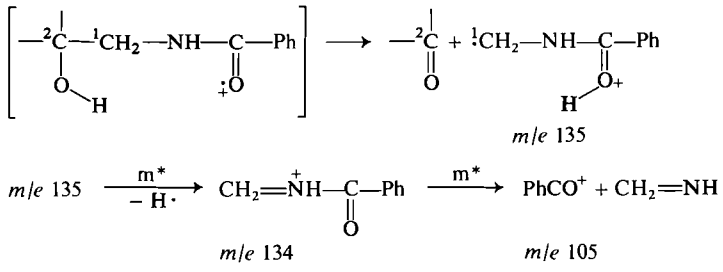

SCHEME 2

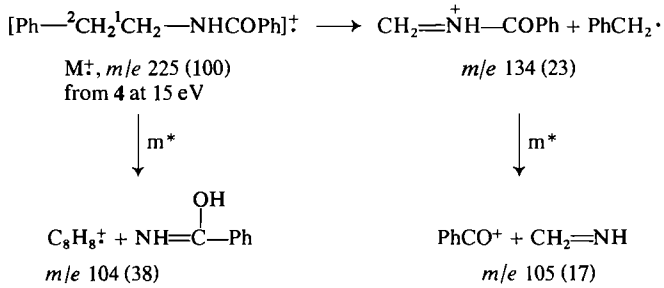

SCHEME 3[2]

[2]The structures and formulas are in agreement with the results of exact-mass measurements.

Can. J. Chem. Downloaded from www.nrcresearchpress.com by 210.87.254.6 on 09/05/12
For personal use only.

Can. J. Chem. Downloaded from www.nrcresearchpress.com by 210.87.254.6 on 09/05/12
For personal use only.

spectrum of *N*-benzoyl-2-phenylethylamine (**4**), Scheme 3. Compound **4** lacks a hydrogen in the *N*-alkyl group which could be involved in a transfer analogous to the one shown in Scheme 2. However, it does contain hydrogens *gamma* to the carbonyl, making the McLafferty rearrangement possible in the *N*-2-phenylethyl group. Two major fragmentation pathways are observed: (*1*) the cleavage of the benzylic bond, yielding the ion at *m/e* 134, and (*2*) a McLafferty rearrangement, with the charge remaining on the C_8H_8 portion. These are precisely the fragmentations expected from secondary amides (8–10).

In order to examine the effect of substitution on the carbon atom bearing the hydroxyl group in **1**, we have studied a series of *N*-benzoyl-2-hydroxyalkylamines, **5–7**. Compound **5** is similar to compounds **2** and **3** in the sense

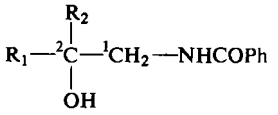

	R_1	R_2
5	CH_3	CH_3
6	CH_3	H
7	H	H

that it contains no hydrogen atoms *gamma* to the carbonyl group, thus the McLafferty rearrangement is blocked. However, compounds **6** and **7** do have hydrogen atoms *gamma* to the carbonyl group, as does **4**, as well as the hydrogen atom on the hydroxyl group, making possible a competition between the two rearrangements.

The 70 eV mass spectra of **5–7** are given in Table 1. Even though no molecular ions are observed in the spectra of **5** and **6**, peaks are found for MH^+ and $MH^+ - H_2O$ at high sample pressures, from a small amount of chemical ionization. Peaks are present for a fragmentation giving an ion corresponding to $M^{\cdot+} - CH_3\cdot$. All three compounds eliminate H_2O for which a metastable peak is present in the mass spectrum of **7**. From the consistent behavior of these compounds in different mass spectrometers at different ion-source temperatures, we feel confident that the elimination of H_2O from **5** and **6**, also, is induced by electron impact rather than by thermal excitation.

In the 15 eV mass spectrum of **5**, Scheme 4 (70 eV mass spectrum is given in Table 1), there is only one prominent fragmentation pathway, the elimination of acetone. This is essentially the same result observed in the mass spectra of compounds **2** and **3**. No peak is found for the molecular ion; however, peaks are present for MH^+, arising from a small amount of chemical ionization, and for the loss of a methyl group.

In the mass spectra of **6** (15 eV, Scheme 5; 70 eV, Table 1), there are indeed two competing hydrogen rearrangements. However, the McLafferty rearrangement, Eq. 4, is not observed.

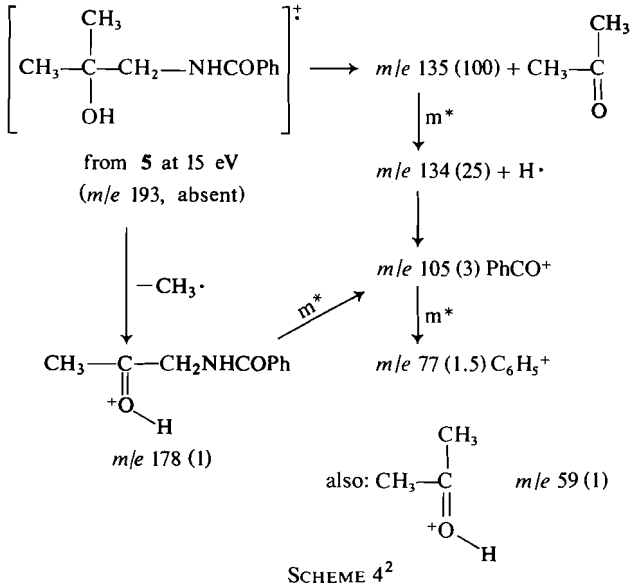

SCHEME 4[2]

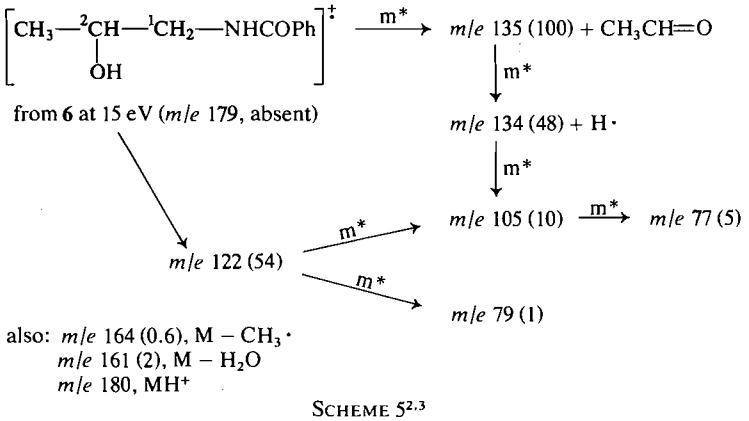

SCHEME 5[2,3]

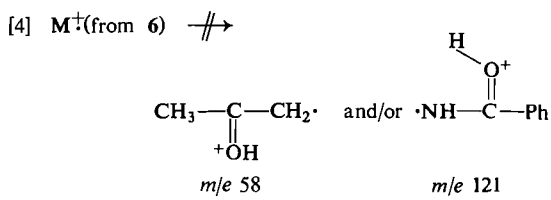

The rearrangements observed are those leading to the fragment at *m/e* 135, already observed in the spectra of **2**, **3**, and **5**, and a double hydrogen rearrangement leading to the ion found at *m/e* 122, Eq. 5. The double hydrogen transfer is a reaction typical of esters (11).

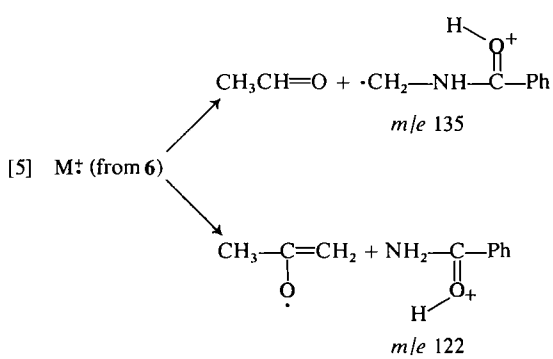

The presence of metastable peaks indicates that there are at least two further fragmentations of the ion found at *m/e* 122, Eq. 6. It is possible that the structure of the ion at *m/e* 122 is better represented by protonation on nitrogen, or by a mixture of protonated, tautomeric forms.[4] We have obtained the chemical ionization (isobutane) mass spectrum of benzamide. The MH^+ ion at *m/e* 122 is the base peak. The only important fragmentation is the elimination of NH_3

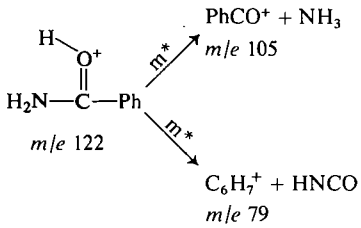

giving *m/e* 105, along with a metastable peak for the process.

In the mass spectrum of **7** (15 eV, Scheme 6; 70 eV, Table 1), the situation has shifted largely in favor of the double hydrogen transfer: the base peak is the ion at *m/e* 122. The molecular ion is relatively abundant, as is the loss of H_2O. Thus, as substitution decreases on the 2-carbon atom (in **1**), the relative importance of cleavage of the bond between positions 1 and 2 decreases and the intensity of the molecular ion increases. Also, the double hydrogen transfer becomes more abundant with increasing hydrogen atom availability on the 2-carbon.

In contrast to what is observed in the spectra of previous compounds, *m/e* 134 is more intense than *m/e* 135, in the spectrum of **7**. This can be rationalized by a competing formation of *m/e* 134 by cleavage of the 1,2-bond, as was observed in the mass spectrum of **4**, Scheme 3, and as is observed in the mass spectra of secondary amides in general (8–10).

It now becomes important to look more closely at the competition between hydrogen

[3]Also see Eqs. 5 and 6.

[4]The u.v. spectra of benzamide in concentrated sulfuric acid show a tautomeric change from the *N*-protonated form in 60% sulfuric acid to the *O*-protonated form in 100% sulfuric acid (12).

Can. J. Chem. Downloaded from www.nrcresearchpress.com by 210.87.254.6 on 09/05/12
For personal use only.

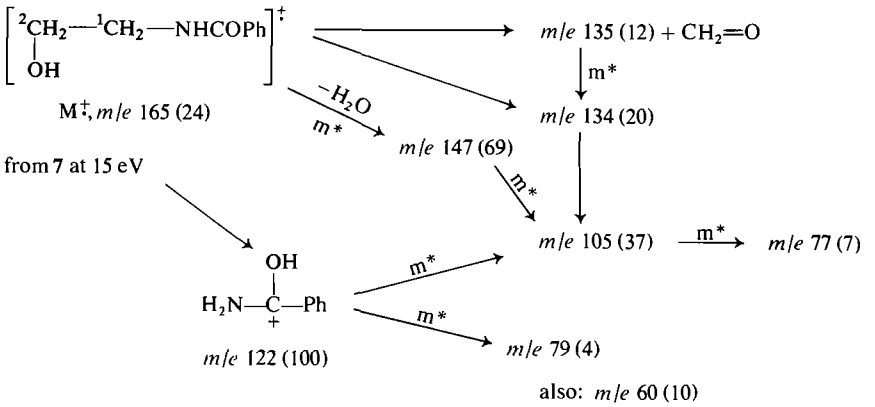

SCHEME 6[2,5]

TABLE 1. The 70 eV mass spectra of compounds **5**–**7**[a]

m/e	**5**	**6**	**7**
178	3		
175	0.5		
165			4
164		1	
148			2
147			13
136	8	5	
135	86	53	4
134	100	59	10
123		2	1
122		22	18
117	2	2	1
116	4	1	
106	9	9	7
105	90	100	100
79		3	
78	6	4	7
77	55	44	76
59	16		
51	20	13	34
45		4	
43	12		

[a]Relative intensities from *m/e* 200–40 are given in percentage of the most intense peak. Ions less abundant than 1% are not included except for M^+, $(M - CH_3)^+$, and $(M - H_2O)^+$.

transfers from OH and from CH, giving ketonic *vs.* enolic neutral products (see structure **8**). We have already shown (*vide supra*) that the ion at *m/e* 135 in the mass spectrum of **3** shifts overwhelmingly to *m/e* 137 in the mass spectrum of **3**-d_2. This preference is all the more impressive in light of the statistical factor of 4 in favor of C—H transfer over O—D transfer, and the

[5]The abundance of *m/e* 135 has been corrected for the isotopic contribution of *m/e* 134.

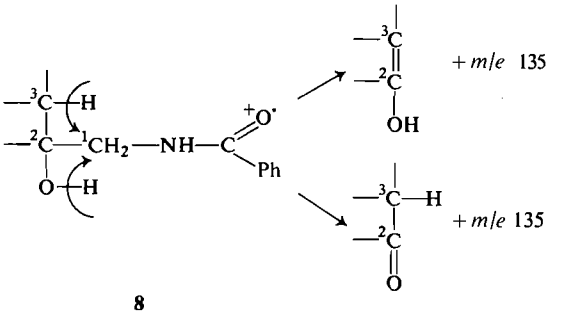

8

isotope effect which would run in favor of transfer of H over D.

We were also interested in observing the course which fragmentation would take if there were no 2-hydroxyl group and if the McLafferty and double hydrogen rearrangements were rendered impossible. To that effect, the *N*-benzoyl derivative (**9**) of 2,2-dimethylpropylamine was prepared, and its mass spectrum (Scheme 7) was compared with that of 2-

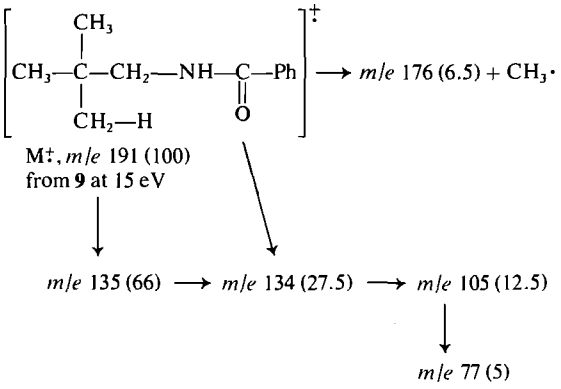

SCHEME 7[2,5]

Can. J. Chem. Downloaded from www.nrcresearchpress.com by 210.87.254.6 on 09/05/12
For personal use only.

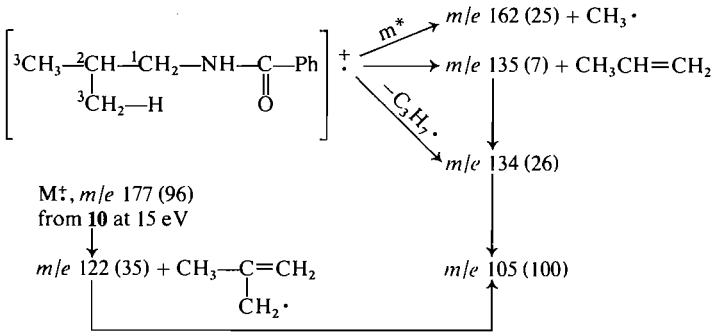

SCHEME 8[2,5]

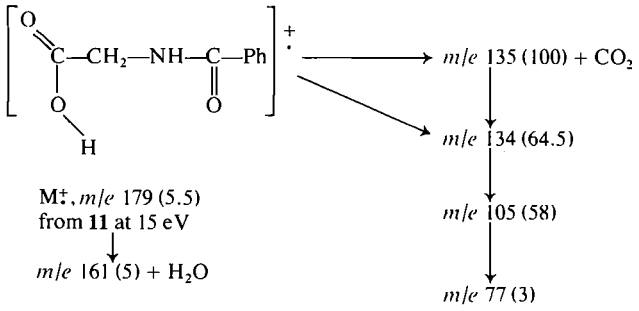

SCHEME 9[2]

hydroxy-2-methylpropylamine (**5**, Scheme 4). The fragmentations are essentially the same. However, the molecular ion from **5** is absent, whereas the molecular ion from **9** is the base peak; the rearrangement ion found at *m/e* 135 is the base peak in the mass spectrum of **5**. The presence of the rearrangement ion at *m/e* 135 in the mass spectrum of **9** shows that hydrogen is transferred from carbon if the other rearrangements are blocked by lack of appropriate hydrogens to transfer. However, transfer of hydrogen from a methyl group on the 2-position is obviously much less favorable than transfer of hydrogen from a hydroxyl group on the 2-position.

Likewise, **6** was compared with its counterpart having a methyl group in place of hydroxyl. In the 15 eV mass spectrum (Scheme 8) of the *N*-benzoyl derivative of isobutylamine (**10**), the double hydrogen rearrangement, giving *m/e* 122, is more prominent than the formation of *m/e* 135. Once again, hydrogen transfer from OH is shown to be more favorable than transfer from CH_3.

In order to test the generality of the observed rearrangement of hydroxylic hydrogen atoms, we have taken the mass spectrum of the *N*-benzoyl derivative of glycine (**11**; 15 eV spectrum, Scheme 9). Now there is only one abundant fragmentation path, the formation of *m/e* 135. In the mass spectrum of the ethyl ester of **11**, on the other hand, the formation of ion 135 is blocked. The base peak corresponds to the molecular ion, and there are two fragmentation pathways: (*1*) loss of EtOH, and (*2*) loss of EtO· followed by CO, or of EtOCO·, giving *m/e* 134.

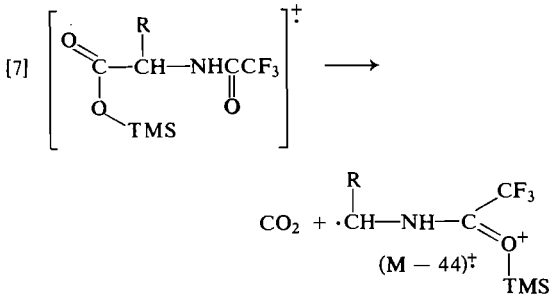

Can. J. Chem. Downloaded from www.nrcresearchpress.com by 210.87.254.6 on 09/05/12
For personal use only.

[8]

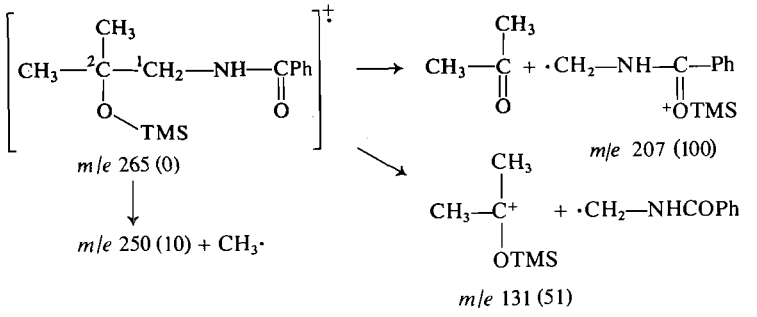

The result obtained from the ethyl ester shows that, even though the hydrogen transfer is highly favored, transfer of an alkyl group does not occur. However, trimethylsilyl (TMS) groups have been found to be transferred in the mass spectra of *N*-trifluoroacetyl α-amino acid trimethylsilyl esters, Eq. 7 (13). For this reason, we prepared the TMS esters of compounds **5** and **7**. The base peak in the mass spectrum of the *O*-TMS derivative of **5** is found at *m/e* 207, Eq. 8. The only other abundant ion present in the 15 eV spectrum of this derivative is found at *m/e* 131, due to cleavage of the bond between positions 1 and 2.

In contrast, the 15 eV mass spectrum of the *O*-TMS derivative of **7** is dominated by the elimination of HOTMS, Eq. 9, and the intensity of *m/e* 207 is only 4%. These are fragmentations characteristic of the mass spectra of *O*-TMS derivatives of alcohols (14).

[9]

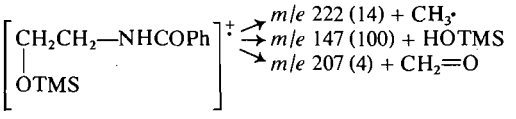

m/e 237 (4)

Discussion

It is interesting to compare our results with those obtained from *N*-*n*-propylsuccinimide (**12**) (15). Even though the McLafferty rearrangement is not important in the mass spectrum of **12**, a competition between single hydrogen transfer and double hydrogen transfer occurs, Scheme 10. The authors were not willing to decide upon a most-favored structure for the ion at *m/e* 113; however, deuterium labeling showed that the two hydrogens on the 1-carbon were retained and that 90% of the hydrogen transferred originated from the 3-carbon atom of the alkyl chain. The base peak occurs at *m/e* 100; in this case the source of the transferred hydrogens was principally the 2- and 3-carbon atoms of the *N*-alkyl chain.

In the case of the compounds of general structure **1**, the one hydrogen transfer is, for all practical purposes, the only fragmentation if there are no hydrogens on the 2-carbon atom of the *N*-alkyl chain. Hydrogen from a hydroxyl group on C-2 is much more readily transferred than hydrogen from a methyl group on C-2. If hydrogen is present on the 2-position, two transfers compete, just as they do in the mass spectrum of **12** (compare Schemes 10 and 11).

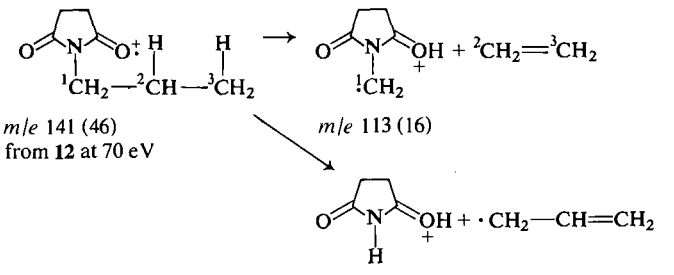

SCHEME 10

Can. J. Chem. Downloaded from www.nrcresearchpress.com by 210.87.254.6 on 09/05/12
For personal use only.

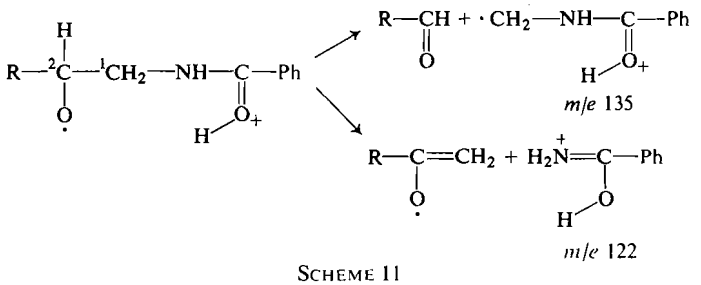

SCHEME 11

In fact, we can use the deuterium-labeling studies (Scheme 10) reported earlier (15) to support our suggestion in Scheme 11 that the peak at *m/e* 122 forms via transfer of hydrogens from the 2-carbon atom and from the hydroxyl group. We have shown the rearrangements in two steps rather than concerted. This is in agreement with evidence, recently reviewed (2), that indicates that the McLafferty rearrangement proceeds via a stepwise pathway: initial hydrogen transfer followed by carbon–carbon bond cleavage.

It is interesting to note that the base peak in the mass spectrum of *N*-*n*-propyl-2-pyrrolidone is *m/e* 98, resulting from α-cleavage of the alkyl chain (15). The abundance of the ion due to double hydrogen rearrangement (*m/e* 86) is only 7% and that due to single hydrogen rearrangement (*m/e* 99, similar to formation of *m/e* 113 in Scheme 10) is 6.5%. The authors speculated that the difference in the modes of fragmentation of the molecular ions of the *N*-alkylsuccinimides and the *N*-alkyl-2-pyrrolidones studied might be attributed to the larger number of atoms involved in resonance forms of the molecular ions in the former compounds. In regard to our compounds, the ions formed from these two rearrangements are always *m/e* 122 and *m/e* 135, so we must attribute differences in fragmentation to differences in the *N*-alkyl groups and the neutral species formed.

It has been generally observed that a large proportion of skeletal rearrangements induced by electron impact are accompanied by expulsion of neutral entities which have favorably negative heats of formation (16). This is also true of the neutral molecules ejected from the *N*-benzoyl-2-hydroxyalkylamines (**5–7**) and from the *N*-benzoyl derivative (**11**) of glycine upon formation of *m/e* 135, as shown in Table 2. The percentage of the total ion current carried by *m/e* 135 is included in Table 2 for comparison.

TABLE 2. Heats of formation (17) of neutral molecules accompanying the formation of *m/e* 135

From compound	Neutral molecule	(g kcal/mol at 25 °C) ΔH_f	*m/e* 135[a]
5	$(CH_3)_2C{=}O$	−51.8	76
6	$CH_3CH{=}O$	−39.8	45
7	$CH_2{=}O$	−27.7	4
9	$(CH_3)_2C{=}CH_2$	−3.3	30
10	$CH_3CH{=}CH_2$	+4.9	2.5
11	CO_2	−94.1	42

[a]Percent of total ion current.

It can be seen from Table 2 that the importance of *m/e* 135 decreases in the series **5–7** and **9–10**. This can be rationalized by two factors: (*1*) the stabilities of the neutral molecules formed decrease,[6] and (*2*) as the substitution decreases on position 2, competing rearrangements occur. The differences in the stabilities of the neutral molecules formed can also be involved to explain the greater importance of *m/e* 135 in the mass spectra of **5** compared to **9** and of **6** compared to **10**.

The relative intensities of the molecular ions and of the rearrangement ions *m/e* 135 and 122 are compared in Table 3. Two main observations can be made from these data. First, the presence

[6]The assumption implied here is that the compounds compared are sufficiently similar to allow the following approximations: since compound A: AP (*m/e* 135) = ΔH_f (*m/e* 135) + ΔH_f (neutral fragment) − ΔH_f (compound A) + E_A, and compound B: AP (*m/e* 135) = ΔH_f (*m/e* 135) + ΔH_f (neutral fragment) − ΔH_f (compound B) + E_B. Then, ΔAP (*m/e* 135) = $\Delta\Delta H_f$ (neutral fragments) − $\Delta\Delta H_f$ (compounds), where (*1*) $\Delta\Delta H_f$ (neutral fragments) > $\Delta\Delta H_f$ (compounds), (*2*) $E_A \cong E_B$, and (*3*) the ion at *m/e* 135 is the same from compounds A and B.

Can. J. Chem. Downloaded from www.nrcresearchpress.com by 210.87.254.6 on 09/05/12
For personal use only.

TABLE 3. Relative intensities of M^+, *m/e* 135, and *m/e* 122

Compound	M^+	*m/e* 135	*m/e* 122	Preferred fragment expelled
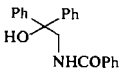	**2**	~0	100	—	
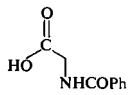	**11**	5.5	100	—	CO_2
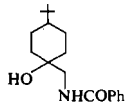	**3**	0	100	—	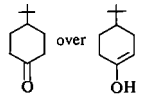
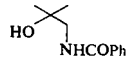	**5**	0	100	—	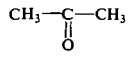
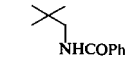	**9**	100	66	—	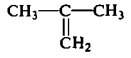
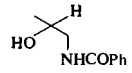	**6**	0	100	54	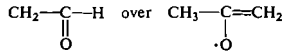
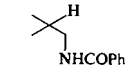	**10**	~100	7	35	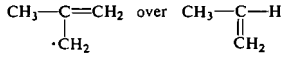
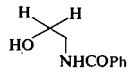	**7**	24	12	100	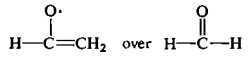

of a hydroxyl group at position 2 of the *N*-alkyl group renders the molecular ions very labile. It can be seen from Eqs. 8 and 9 that this is also true of the presence of an *O*-TMS group. This is related to the fact that the transfer of hydrogen from a hydroxyl group on C-2 is preferred over the transfer of hydrogen from a methyl group at C-2, as was shown in the spectra of **3** and its deuterated analogs. This conclusion is supported by the fact that the molecular ions are the base peaks in the spectra of **9** and **10** which contain no hydroxyl groups. This behavior is in agreement with the weaker bond strength of the O—H bond with respect to the C—H bond and also in agreement with the greater stability of keto forms over corresponding enol forms (18).

The second main observation drawn from Table 3 is that the formation of *m/e* 122, the ion formed by double hydrogen rearrangement competes increasingly successfully with formation of *m/e* 135 as substitution decreases at position 2 and in the absence of a hydroxyl group at position 2. From the comparison of the spectra of **6** and **10**, it can be seen that the hydroxylic hydrogen still plays a predominant role in giving fragmentation patterns which should reflect to a certain extent the relative stabilities of the neutral fragments formed. However, a more rigorous analysis cannot be

Can. J. Chem. Downloaded from www.nrcresearchpress.com by 210.87.254.6 on 09/05/12
For personal use only.

made at this stage due to the large number of variables at play.

Experimental

Mass spectra were obtained from AEI MS902 and Hitachi Perkin-Elmer RMU6D mass spectrometers, via the direct-probe introduction system. The low-voltage data reported are values read directly from the dials. In each case, spectra were taken at various dial readings, and small variations of the voltage did not change the results qualitatively. Exact-mass data were obtained from the MS 902, in conjunction with a PDP-8 computer.

The i.r. spectra were recorded in $CHCl_3$ solution, unless otherwise stated, on a Beckman model IR-8 double beam spectrometer. The n.m.r. spectra were recorded in $CDCl_3$ solution, unless otherwise specified, using a Varian A-60 spectrometer; peak positions are recorded in δ units and the internal standard used was TMS. Melting points were taken on a Büchi apparatus and are uncorrected.

N-Benzoyl-1-aminomethyl-4-tert-butylcyclohexanol-cis (3)

Product **3** is prepared under Schotten–Baumann conditions (19) by adding over a period of 3 h a solution of 3.44 g (24 mmol) of benzoyl chloride in 200 ml of benzene to a dispersion of 4.51 g (24 mmol) of 1-aminomethyl-4-*tert*-butylcyclohexanol (20), 3.26 g (24 mmol) of potassium carbonate, 50 ml of ether, and 50 ml of water. The mixture is left standing overnight and after the usual work-up and crystallization from chloroform–hexane yields 5.65 g (80%) of the pure *N*-benzoyl derivative (**3**); m.p. 192–193 °C; i.r. (Nujol) 3330, 1640, and 1545 cm^{-1}; n.m.r. (CF_3COOH) 0.95 (9H, s), 1.70 (10H, m), 4.00 (2H, d, J = 6 Hz), 7.80 (5H, m), and 9.10 p.p.m. (1H, t, J = 6 Hz).

N-Benzoyl-1-aminomethyl-4-tert-butyl-2,2,6,6-tetradeuterocyclohexanol-cis (3-d_4)

The tetradeuterated analog of **3** is prepared in the same manner as described above with the exception that 4-*tert*-butyl-2,2,6,6-tetradeuterocyclohexanone instead of the undeuterated ketone is used as starting material. The deuteration is carried out according to the procedure of Cope and Gale (21), *i.e.* by heating to reflux a mixture of 4-*tert*-butylcyclohexanone and heavy water. Yield 88%; mass spectrum *m/e* 158, 157, and 156 in respective ratios of 93%, 6%, and 1% which indicates 98% deuteration; i.r. (Nujol) 3350, 1640, and 1545 cm^{-1}; n.m.r. 0.95 (9H, s), 1.42 (5H, m), 2.45 (1H, m), 3.43 (1H, d, J = 6 Hz), 3.60 (1H, d, J = 6 Hz), 6.80 (1H, m), and 7.70 p.p.m. (5H, m).

N-Deutero-O-deutero-N-benzoyl-1-aminomethyl-4-tert-butylcyclohexanol-cis (3-d_2)

The dideutero analog **3**-d_2 is prepared by stirring 0.110 g (0.4 mmol) of the *N*-benzoyl derivative **3** in 1 ml of methanol O—D (purity 99%). After exchange is complete, aliquots of the solution are introduced into the mass spectrometer by means of a direct probe. Methanol O—D was introduced simultaneously via a reservoir inlet system.

N-Benzoyl-β-phenethylamine (4)

The title compound is prepared by treating 6.05 g (50 mmol) of β-phenethylamine with benzoyl chloride under Schotten–Baumann conditions (*vide supra*). Yield 10.46 g (93%); m.p. (chloroform–hexane) 116–117 °C; i.r. 3470, 1655, and 1515 cm^{-1}; n.m.r. 2.85 (2H, t, J = 7.2 Hz), 3.63 (2H, m), 6.64 (1H, broad), and 7.41 p.p.m. (10H, complex system).

N-Benzoyl-2-hydroxyisobutylamine (5)

2-Hydroxyisobutylamine

The title compound is prepared according to the procedure of Nace and Smith (22) by adding 13.60 g (150 mmol) of acetone cyanohydrin (23), dissolved in 200 ml of anhydrous ether, to a stirred suspension of 6.1 g (160 mmol) of lithium aluminum hydride in 300 ml of anhydrous ether. The mixture is heated to reflux for 3 h and the intermediate salts hydrolyzed with 7 ml of water and 7 ml of 5% aqueous potassium carbonate. The mixture is decanted and the residue triturated and digested with 200 ml of ether. The mixture is cooled and decanted after which both ethereal fractions are joined, dried, and evaporated to yield 4.81 g (34%) of the amino alcohol which is purified by distillation; b.p. 49 °C/2.5 Torr (lit. (24) 81 °C/20 Torr).

N-Benzoyl-2-hydroxyisobutylamine (5)

The title compound is prepared by treating 7.53 g (60 mmol) of 2-hydroxyisobutylamine hydrochloride with benzoyl chloride under Schotten–Baumann conditions (*vide supra*). Yield 11.03 g (95%); m.p. (chloroform–hexane) 104–105 °C; i.r. 3500–3300, 1650, and 1525 cm^{-1}; n.m.r. 1.25 (6H, s), 3.43 (2H, d, J = 6 Hz), 4.18 (1H, s), and 7.72 p.p.m. (6H, m).

N-Benzoyl-2-hydroxy-n-propylamine (6)

The title compound is prepared by treating 7.50 g (100 mmol) of 2-hydroxy-*n*-propylamine with benzoyl chloride under Schotten–Baumann conditions (*vide supra*). Yield 17.23 g (96%); m.p. (chloroform–hexane) 93–94 °C; i.r. 3500–3300, 1645, and 1525 cm^{-1}; n.m.r. 1.15 (3H, d, J = 6 Hz), 3.30 (2H, m), 3.80 (1H, m), 3.90 (1H, s), and 7.50 p.p.m. (6H, m).

N-Benzoyl-2-hydroxyethylamine (7)

The title compound is prepared by treating 4.88 g (80 mmol) of ethanolamine with benzoyl chloride under Schotten–Baumann conditions (*vide supra*). Yield 11.52 g (87%); m.p. (chloroform–hexane) 64–65 °C; i.r. (Nujol) 3500–3300, 1630, and 1550 cm^{-1}; n.m.r. 3.57 (4H, m), 4.77 (1H, s), and 7.48 p.p.m. (6H, m).

N-Benzoylneopentylamine (9)

Pivalaldoxime

The title compound is prepared (25) by adding 60 ml of an aqueous solution of sodium carbonate (10.6 g, 100 mmol) to a stirred suspension of 12.92 g (150 mmol) of pivalaldehyde in a solution of 14.02 g (200 mmol) of hydroxylamine hydrochloride in 25 ml of cold water. The mixture is stirred for one additional hour and extracted three times with 15 ml of chloroform. The organic layer is then washed with a saturated solution of sodium chloride, dried, and evaporated *in vacuo*. The residue is recrystallized from hexane to yield 10.45 g (69%) of pivalaldoxime, m.p. 38–39 °C (lit. (26) 41 °C).

Can. J. Chem. Downloaded from www.nrcresearchpress.com by 210.87.254.6 on 09/05/12
For personal use only.

Can. J. Chem. Downloaded from www.nrcresearchpress.com by 210.87.254.6 on 09/05/12
For personal use only.

Neopentylamine Hydrochloride

Pivalaldoxime is reduced according to the procedure of Cristol and Stermitz (27) by adding a solution of 10.10 g (100 mmol) of the oxime in 200 ml of anhydrous ether to a stirred suspension of 7.6 g (200 mmol) of lithium aluminium hydride in 100 ml of anhydrous ether, at such a rate as to cause a slight reflux. The mixture is then heated to reflux for 18 h and the intermediate hydrolyzed, first with humid ether, then with 5–10 ml of water. The ethereal layer is decanted and the white residual mass digested with 200 ml of chloroform for 1 h. The chloroformic phase is decanted, combined with the ethereal fraction, dried, and evaporated *in vacuo*. The residue is dissolved in 100 ml of anhydrous ether and treated with gaseous hydrogen chloride to yield 6.34 g (52%) of neopentylamine hydrochloride; m.p. (absolute ethanol – ether) 266–267 °C (lit. (28*a*) 274 °C; lit. (28*b*) 275 °C; lit. (28*c*): 273 °C).

N-Benzoylneopentylamine (9)

The title compound is prepared by treating 6.20 g (44 mmol) of neopentylamine hydrochloride under Schotten–Baumann conditions (*vide supra*). Yield 8.03 g (84%); m.p. (chloroform–hexane) 112–113 °C; i.r. 3480, 1660, and 1520 cm^{-1}; n.m.r. 0.98 (9H, s), 3.24 (2H, d, $J = 6.8$ Hz), 6.27 (1H, broad), and 7.59 p.p.m. (5H, complex system).

N-Benzoylisobutylamine (10)

The title compound is prepared by treating 7.3 g (100 mmol) of isobutylamine with benzoyl chloride under Schotten–Baumann conditions (*vide supra*). Yield 16.65 g (94%); m.p. (chloroform–hexane) 57–58 °C; i.r. 3480, 3380, 1660, and 1520 cm^{-1}; n.m.r. 0.93 (6H, d, $J = 6.6$ Hz), 1.85 (1H, n, $J = 6.6$ Hz), 3.17 (2H, t, $J = 6.6$ Hz), and 7.50 p.p.m. (6H, complex system).

Ethyl-N-benzoylglycinate

The title compound is obtained by treating 27.92 g (200 mmol) of ethylglycinate hydrochloride with benzoyl chloride under Schotten–Baumann conditions (*vide supra*). Yield 33.48 g (80%); m.p. (chloroform–hexane) 59–60 °C; i.r. 3450, 3370, 1740, 1660, and 1520 cm^{-1}; n.m.r. 1.23 (3H, t, $J = 6.8$ Hz), 4.05 (2H, d, $J = 5.3$ Hz), 4.09 (2H, quad., $J = 6.8$ Hz), and 7.53 p.p.m. (6H, complex system).

N-Benzoylglycine (11)

A solution of 8.90 g (43 mmol) of ethyl-*N*-benzoylglycinate in 50 ml of methanol is treated with 50 ml of a 10% aqueous solution of potassium hydroxide and the mixture heated to reflux for 6 h. The methanol is evaporated *in vacuo* and the remaining aqueous solution is washed with chloroform, acidified with dilute hydrochloric acid, and cooled in the refrigerator to complete crystallization, filtered *in vacuo*, and dried. Yield 6.36 g (83%); m.p. (chloroform–hexane) 186–187 °C (lit. (29) 186–187 °C); i.r. (Nujol) 3355, 3500–2500, 1740, 1600, and 1550 cm^{-1}; n.m.r. 4.05 (2H, d, $J = 5.7$ Hz), 6.70 (5H, complex system), 8.87 (1H, t, $J = 5.7$ Hz), and 11.68 p.p.m. (1H, broad).

N-Benzoyl-2-hydroxy-2,2-diphenylethylamine (2)

A solution of 20.70 g (100 mmol) of ethyl-*N*-benzoylglycinate in 50 ml of ether is added dropwise to a solution of phenylmagnesium bromide in ether at such a rate as to cause a slight reflux. The Grignard reagent is prepared by adding slowly, at room temperature, a solution of 31.4 g (200 mmol) of phenyl bromide in 400 ml of ether to 5.28 g (220 mmol) of magnesium turnings covered with a little ether. The reaction mixture is stirred at room temperature for an additional 15 min. The resulting magnesium salt is hydrolyzed with an ice-cold saturated solution of ammonium chloride in water until two layers are formed. The layers are decanted and the aqueous solution extracted with chloroform. The ethereal and chloroformic fractions are joined and the resulting mixture dried and evaporated *in vacuo*. Yield 25.42 g (82%); m.p. (absolute ethanol) 181–182 °C; i.r. (Nujol) 3435, 3360, 1630, and 1530 cm^{-1}; n.m.r. (DMSO-d_6) 4.12 (2H, d, $J = 5.3$ Hz), 6.25 (1H, s), 7.43 (15H, complex system), and 8.00 p.p.m. (1H, t, $J = 5.3$ Hz).

We wish to acknowledge financial support from the National Research Council of Canada. The exact-mass data were obtained by Dr. A. S. Blair.

1. J. T. Bursey, M. M. Bursey, and D. G. I. Kingston. Chem. Rev. **73**, 191 (1973).
2. D. G. I. Kingston, J. T. Bursey, and M. M. Bursey. Chem. Rev. **74**, 215 (1974).
3. R. C. Dougherty. *In* Topics in current chemistry. Vol. 45. Springer-Verlag, New York. 1974. p. 93.
4. J. Reisch and D. H. Niemeyer. Tetrahedron, **27**, 4637 (1971).
5. M. M. Bursey, D. G. Whitten, M. T. McCall, W. E. Punch, M. K. Hoffman, and S. A. Benezra. Org. Mass Spectrom. **4**, 157 (1970).
6. F. P. Boer, T. W. Shannon, and F. W. McLafferty. J. Am. Chem. Soc. **90**, 7239 (1968).
7. R. Brandt and C. Djerassi. Helv. Chim. Acta, **51**, 1750 (1968).
8. J. A. Gilpin. Anal. Chem. **31**, 935 (1959).
9. Z. Pelah, M. A. Kielczewski, J. M. Wilson, M. Ohashi, H. Budzikiewicz, and C. Djerassi. J. Am. Chem. Soc. **85**, 2470 (1963).
10. H. Budzikiewicz, C. Djerassi, and D. H. Williams. Mass spectrometry of organic compounds. Holden-Day, San Francisco. 1967. p. 336.
11. J. H. Beynon, R. A. Saunders, and A. E. Williams. Anal. Chem. **33**, 221 (1961).
12. M. Liler. J. Chem. Soc. Perkin Trans. 2, 71 (1974).
13. L. Birkofer and G. Schmidtberg. Org. Mass Spectrom. **7**, 1387 (1973).
14. A. G. Sharkey, R. A. Friedel, and S. H. Langer. Anal. Chem. **29**, 770 (1957).
15. A. M. Duffield, H. Budzikiewicz, and C. Djerassi. J. Am. Chem. Soc. **87**, 2913 (1965).
16. P. Brown and C. Djerassi. Angew. Chem. Int. Ed. Engl. **6**, 477 (1967).
17. R. A. Keller. Basic tables in chemistry. McGraw-Hill, Toronto. 1967.
18. A. Gero. J. Org. Chem. **19**, 1960 (1954).
19. E. M. Hancock and A. C. Cope. J. Am. Chem. Soc. **66**, 1738 (1944).
20. D. Gravel. Ph.D. Thesis. University of Montreal, Montreal, Quebec. (1962).

21. A. C. COPE and D. M. GALE. J. Am. Chem. Soc. **85**, 3747 (1963).
22. H. R. NACE and B. B. SMITH. J. Am. Chem. Soc. **74**, 1861 (1952).
23. R. F. B. COX and R. T. STORMONT. Org. Syn. Coll. **2**, 7 (1943).
24. W. PFLEIDERER and H. ZONDLER. Chem. Ber. **99**, 3008 (1966).
25. E. W. BOUSQUET. Org. Syn. Coll. **2**, 313 (1943).
26. BEILSTEIN. Band I, Vol. 1, Supl. 1. p. 354.
27. S. J. CRISTOL and F. R. STERMITZ. J. Am. Chem. Soc. **82**, 4692 (1960).
28. (*a*) C. K. INGOLD and C. S. PATEL. J. Chem. Soc. 67 (1933); (*b*) M. FREUND and F. LENZE. Ber. **24**, 2156 (1891); (*c*) F. C. WHITMORE and A. H. HOMEYER. J. Am. Chem. Soc. **54**, 3435 (1932).
29. A. W. INGERSOLL and S. H. BABCOCK. Org. Syn. **12**, 40 (1932).

Can. J. Chem. Downloaded from www.nrcresearchpress.com by 210.87.254.6 on 09/05/12
For personal use only.

Rate Constants for the Reaction of Fluorine Atoms with Nitric Oxide in the Presence of Various Third Bodies[1,2]

EDWARD G. SKOLNIK, STEPHEN W. VEYSEY, MAHMOODA G. AHMED, AND WILLIAM E. JONES

Department of Chemistry, Dalhousie University, Halifax, Nova Scotia B3H 4J3

Received October 1, 1974[3]

EDWARD G. SKOLNIK, STEPHEN W. VEYSEY, MAHMOODA G. AHMED, and WILLIAM E. JONES. Can. J. Chem. **53**, 3188 (1975).

Absolute rate constants are reported for the reaction of fluorine atoms with nitric oxide in the presence of the third bodies Ar, He, Ne, N_2, NO, CO_2, CF_4, SF_6, and C_2F_6. The values determined in the present study are compared to those found for reactions of Cl, H, and O with NO.

EDWARD G. SKOLNIK, STEPHEN W. VEYSEY, MAHMOODA G. AHMED et WILLIAM E. JONES. Can. J. Chem. **53**, 3188 (1975).

On rapporte les constantes absolues des vitesses de réaction des atomes de fluor avec l'oxyde d'azote en présence de Ar, He, Ne, N_2, NO, CO_2, CF_4, SF_6 et C_2F_6. On compare les valeurs obtenues au cours de ce travail avec celles rapportées pour les réactions du Cl, H et O avec NO.

[Traduit par le journal]

Introduction

Until recent years, very few studies of the reaction kinetics of fluorine atoms were attempted. This was mainly due to the difficulty of producing fluorine atoms while at the same time minimizing competitive reactions involving fluorine molecules. Recently, fluorine atoms have been produced from a radio-frequency discharge through F_2 (1), by reaction of active nitrogen with NF_2 (2), by photolysis of heavy metal fluorides (3–5), and by microwave discharge through F_2 (6) or CF_4 (7).

In this paper we describe measurements of the kinetics of the reaction of fluorine atoms with nitric oxide in the presence of various third bodies. In the present study, fluorine atoms have been produced by microwave decomposition of CF_4. Kolb and Kaufman (7) found that microwave decomposition of CF_4 produced fluorine atoms essentially free of contamination by molecular fluorine.

Johnston and co-workers (8, 9) found that the reaction of fluorine atoms with nitric oxide produced a continuous visible emission between 640 and 510 nm, with a maximum intensity at 609.5 ± 1 nm. The reaction of fluorine atoms with nitric oxide in the presence of a third body produces nitrosyl fluoride in both ground and excited electronic states. The electronically excited FNO* molecules decay to ground state FNO by both radiative and nonradiative processes. In addition to reaction with NO, fluorine atoms may be lost by a wall reaction. The process may be represented as follows:

$$\text{[1]} \qquad \mathrm{F + NO + M} \xrightarrow{k_{1a}} \mathrm{FNO + M}$$

$$\mathrm{F + NO + M} \xrightarrow{k_{1b}} \mathrm{FNO^* + M}$$

$$\text{[2]} \qquad \mathrm{FNO^*} \xrightarrow{k_2} \mathrm{FNO} + h\nu$$

$$\text{[3]} \qquad \mathrm{FNO^* + M} \xrightarrow{k_3} \mathrm{FNO + M}$$

$$\text{[4]} \qquad \mathrm{F + (wall)} \xrightarrow{k_w} \text{Products}$$

The intensity of the observed emission is directly proportional to the concentration of FNO*. By assuming steady state conditions for [FNO*], it may be shown that for any given concentration of nitric oxide and third body M, the intensity is directly proportional to the concentration of fluorine atoms

$$\text{[5]} \qquad I \propto \frac{k_{1b}k_2[\mathrm{NO}][\mathrm{M}]}{k_2 + k_3[\mathrm{M}]}[\mathrm{F}]$$

[1]This paper is dedicated to Professor C. A. Winkler of McGill University on the occasion of his sixty-fifth birthday by one of his former students (W.E.J.).

[2]The work described in this paper was supported by a Defence Research Board Grant, No. 9530-115.

[3]Revision received July 8, 1975.

Can. J. Chem. Downloaded from www.nrcresearchpress.com by 210.87.254.40 on 09/05/12
For personal use only.

Can. J. Chem. Downloaded from www.nrcresearchpress.com by 210.87.254.40 on 09/05/12
For personal use only.

By measuring the emission I at various reaction times, the variation in fluorine atom concentration with time may be determined and the absolute rate of the reaction of fluorine atoms with nitric oxide, $k_1 = k_{1a} + k_{1b}$, may be calculated.

Experimental

The fast flow apparatus (Fig. 1) consisted of a rectangular Pyrex reaction cell, 35 cm in length and 2.8 cm on a side. CF_4 (flow rate 0.2 μmol s^{-1}) and either Ar or He were passed through a 2450 MHz microwave discharge produced by a Burdick MW/200 Microwave Diathermy unit. The fluorine atoms produced were introduced through a 0.5 mm nozzle fitted concentrically into the reaction cell by means of a Soveril screw joint. Nitric oxide and various third bodies entered the reaction cell through a 10 mm tube 3 cm upstream from the nozzle. The fluorine atoms and carrier gas thus entered an atmosphere of nitric oxide and third body. Flow rates were calibrated and controlled by standard methods. The pressure in the reaction cell was monitored by a manometer filled with Dow Corning #702 Silicone Oil. The Welch Vacuum Pump Model 1397 had a pumping speed of 500 l min^{-1}. Flow rates varied from 50–700 μmol s^{-1} depending upon the nature of the third body and object of the experiment.

The emission was monitored by a photomultiplier tube (EMI 9592 B) operating at e.h.t. 1050 V, equipped with an Oriel interference filter allowing transmission from 615 to 625 nm. The photomultiplier was mounted on a movable base which allowed tracking along the length of the reaction cell. The photomultiplier output was recorded on a Texas Instrument Recorder. By moving the photomultiplier along the reaction zone at a constant speed, a reaction profile (emission intensity *vs.* time) was obtained.

Argon and helium were obtained from Linde, and were passed through a trap containing 80–100 mesh molecular sieve #5A at −196 °C (He) or −78 °C (Ar). Nitric oxide (Matheson) was degassed and purified by passing it through ascarite. Neon, carbon tetrafluoride, sulfur hexafluoride, and perfluoroethane (Matheson) were degassed and used without further purification. Nitrogen (Linde) was passed through a silica gel trap immersed in Dry Ice and then through a liquid nitrogen trap. Carbon dioxide (Liquid Carbonic) was stated to have a purity of 99.99% and was used after degassing without further purification.

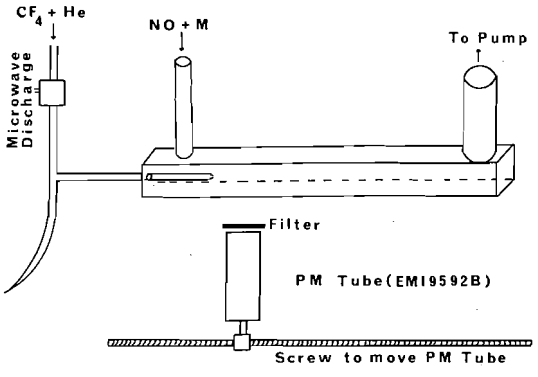

FIG. 1. Schematic of reaction vessel.

Results

Any of the substances present in the reaction zone may act as third bodies. For the very simplest case this means that at least NO and the inert carrier gas will act in this way. Additional third bodies are present during other experiments. For the general case, the steps resulting in the removal of fluorine atoms are:

$$[1NO] \quad F + NO + NO \xrightarrow{k_{1NO}} FNO + NO$$

$$[1M] \quad F + NO + M \xrightarrow{k_{1M}} FNO + M$$

$$[1M'] \quad F + NO + M' \xrightarrow{k_{1M'}} FNO + M$$

and other third bodies as necessary.

$$[4] \quad F\,(+\text{ wall}) \xrightarrow{k_w} \text{Products}$$

The disappearance of fluorine atoms may be expressed as

$$[6] \quad -\frac{d[F]}{dt} = k_{1NO}[F][NO]^2 + k_{1M}[F][NO][M] + k_{1M'}[F][NO][M'] + \ldots + k_w[F]$$

Under pseudo-first order conditions ([F] ≪ [NO] and [M]),

$$[7] \quad -\frac{d[F]}{dt} = k'[F]$$

where $k' = k_{1NO}[NO]^2 + k_{1M}[NO][M] + k_{1M'}[NO][M'] + \ldots + k_w$

Since [F] ∝ I, a plot of ln I *vs.* time, gives a slope k'. Sample plots showing this pseudo-first order behavior are presented in Fig. 2, where fluorine atoms are allowed to react with excess NO in the presence of He.

A series of values of k' were determined by the above method at various concentrations of helium while maintaining a constant concentration of nitric oxide. A plot of k'/[NO] *vs.* [He] as shown in Fig. 3 gives a straight line, the slope of which is $k_{1He} = (4.2 \pm 0.1) \times 10^{16}$ cm^6 mol^{-1} s^{-1}.

In order to calculate a value for k_{1NO}, values of k' were determined for various concentrations of NO, at a constant concentration of car-

Can. J. Chem. Downloaded from www.nrcresearchpress.com by 210.87.254.40 on 09/05/12
For personal use only.

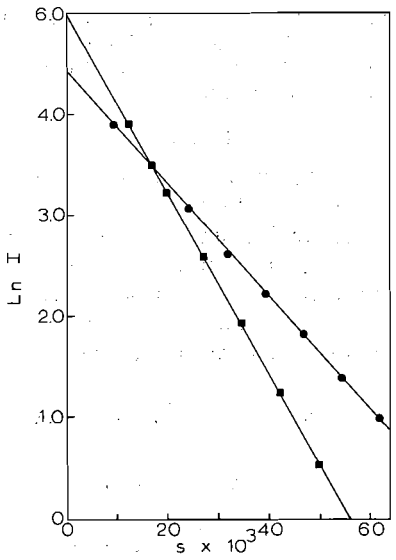

FIG. 2. Sample plots showing pseudo-first order behavior for reaction of nitric oxide with fluorine atoms in helium. [He] = 80.2×10^{-9} mol cm^{-3}; ■, [NO] = 22.1×10^{-9} mol cm^{-3}; ●, [NO] = 12.8×10^{-9} mol cm^{-3}.

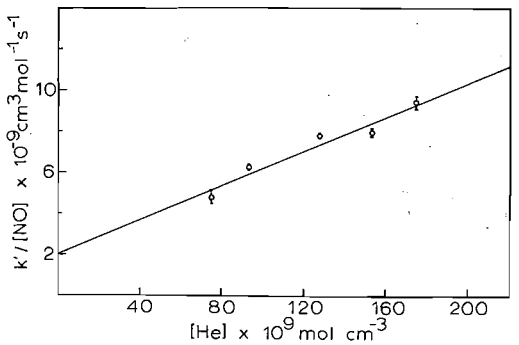

FIG. 3. Dependence of k'/[NO] on the concentration of helium for the reaction of fluorine atoms with nitric oxide in the presence of helium. [NO] = 8.0×10^{-9} mol cm^{-3}.

rier gas (He). The set of equations $k' = k_{1NO}[NO]^2 + k_{1He}[He][NO] + k_w$ was solved using linear regression techniques to give the best values of k_{1NO}, k_{1He}, and k_w. The value determined for k_w was 12 ± 19 s^{-1}, in reasonable agreement with Pollock and Jones (10). k_{1NO} was found to be $(4.8 \pm 6.4) \times 10^{16}$ cm^6 mol^{-2} s^{-1}, which may be compared with a value of 11×10^{16} cm^6 mol^{-2} s^{-1} obtained by MacLean and co-workers from e.s.r. studies (11), and k_{1He} was calculated to be $(3.2 \pm 2.8) \times$

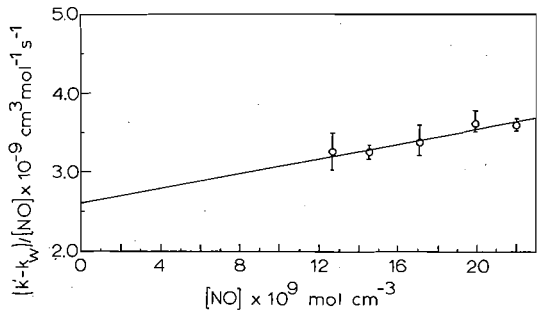

FIG. 4. Dependence of $(k' - k_w)$/[NO] on the concentration of nitric oxide for the reaction of fluorine atoms with nitric oxide in the presence of helium. [He] = 80.2×10^{-9} mol cm^{-3}.

10^{16} cm^6 mol^{-2} s^{-1}, which compares favorably with the value of $4.2 \pm 0.4 \times 10^{16}$ cm^6 mol^{-2} s^{-1} determined by variation of [He]. This value may also be compared to the value of 2.8×10^{16} cm^6 mol^{-2} s^{-1} found by MacLean and co-workers (11). In order to give an indication of the variation of the data in these calculations a plot of $(k' - k_w)$/[NO] *vs.* [NO] is given in Fig. 4. As is subsequently shown in the discussion, the effect of CF_4 as a third body may be ignored in these calculations.

The values of k_{1M} were determined for M = Ar, Ne, N_2, CO_2, CF_4, SF_6, and C_2F_6, from plots of k'/[NO] *vs.* [M] as shown in Figs. 5 and 6. In each case at least six determinations of k' were made from plots of ln I *vs.* time at each concentration of M. All values determined for k' have been collected in several tables and placed in the Depository of Unpublished Data.[4]

For M = Ar, two different sets of measurements were made. The first in which argon was used both as the gas to support the microwave discharge with additional argon mixed with the nitric oxide, and the second in which helium was used as the carrier gas and argon was added only to the nitric oxide stream. A plot of k'/[NO] *vs.* [Ar] for each set of measurements is given in Fig. 5. The values of k_{1Ar} obtained in the absence and presence of helium are $(3.2 \pm 0.3) \times 10^{16}$ and $(2.5 \pm 0.1) \times 10^{16}$ cm^6 mol^{-2} s^{-1}. These values may be compared with the

[4]Complete set of tables is available, at a nominal charge, from the Depository of Unpublished Data, CISTI, National Research Council of Canada, Ottawa, Canada K1A 0S2, or directly from Dr. W. E. Jones, Department of Chemistry, Dalhousie University, Halifax, Nova Scotia B3H 4J3.

TABLE 1. Third order rate constants for various third bodies

M	$k_{1M} \times 10^{-16}$ (cm^6 mol^{-2} s^{-1})	Method	Reference
NO	4.8 ± 6.4	Variation of [NO] (see text)	This work
	11	Electron spin resonance	11
	4.5 ± 4 exp [−(0.2 ± 0.1)/*RT*]	Electron spin resonance	12
He	4.2 ± 0.4	Slope k'/[NO] *vs.* [He]	This work
	3.2 ± 2.8	Variation of [NO] (see text)	This work
	2.8	Electron spin resonance	11
	2.99 ± 0.18	Electron spin resonance	12
Ar	2.5 ± 0.1	Slope k'/[NO] *vs.* [Ar] (He carrier)	This work
	3.2 ± 0.3	Slope k'/[NO] *vs.* [Ar] (Ar carrier)	This work
	2.8	Electron spin resonance	11
Ne	2.1 ± 0.2	Slope k'/[NO] *vs.* [Ne]	This work
N_2	3.9 ± 0.6	Slope k'/[NO] *vs.* [N_2]	This work
CO_2	13 ± 1	Slope k'/[NO] *vs.* [CO_2]	This work
CF_4	16 ± 1	Slope k'/[NO] *vs.* [CF_4]	This work
SF_6	14 ± 1	Slope k'/[NO] *vs.* [SF_6]	This work
C_2F_6	11 ± 1	Slope k'/[NO] *vs.* [C_2F_6]	This work

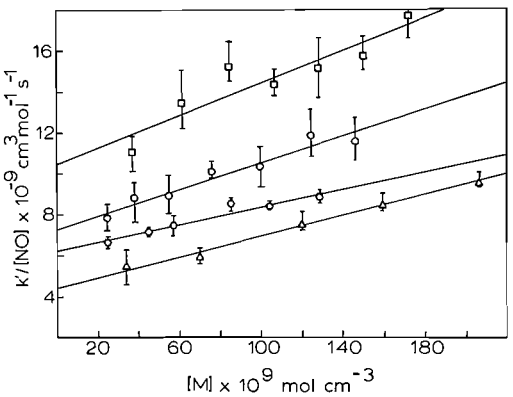

FIG. 5. Dependence of k'/[NO] on the concentration of third bodies N_2, Ne, Ar (Ar carrier), and Ar (He carrier), for the reaction of fluorine atoms with nitric oxide. □, M = N_2, [NO] = 10.4 × 10^{-9} mol cm^{-3}, [He] = 23 × 10^{-9} mol cm^{-3}; ⬡, M = Ne, [NO] = 14.4 × 10^{-9} mol cm^{-3}, [He] = 23 × 10^{-9} mol cm^{-3}; ○, M = Ar, [NO] = 11.3 × 10^{-9} mol cm^{-3}, [He] = 0 mol cm^{-3}; △, M = Ar, [NO] = 11.6 × 10^{-9} mol cm^{-3}, [He] = 23 × 10^{-9} mol cm^{-3}.

value $k_{1Ar} = 2.8 \times 10^{16}$ cm^6 mol^{-2} s^{-1} determined by MacLean and co-workers (11).

N_2, while Fig. 6 gives these plots for CO_2, CF_4, CF_4, SF_6, and C_2F_6), helium was used as the carrier gas to sustain the discharge. Figure 5 presents the plots of k'/[NO] *vs.* [M] for Ne and N_2, while Fig. 6 gives these plots for CO_2, CF_4, SF_6, and C_2F_6. In Fig. 6 several different scales for the vertical axis have been used to allow placing the plots on one graph, the scale which should be used for each symbol is indicated by the symbols at the top of the figure. In each of Figs. 5 and 6 the average value of k'/[NO] is signified by the symbols, while the error bars represent the largest positive and negative deviation from the average value.

Table 1 summarizes the values obtained for the third order rate constants, k_{1M}, for the reaction of fluorine atoms with nitric oxide. The error limits on the rate constants determined in this work are standard deviations calculated from the plot of k'/[NO] *vs.* [M]. Where avail-

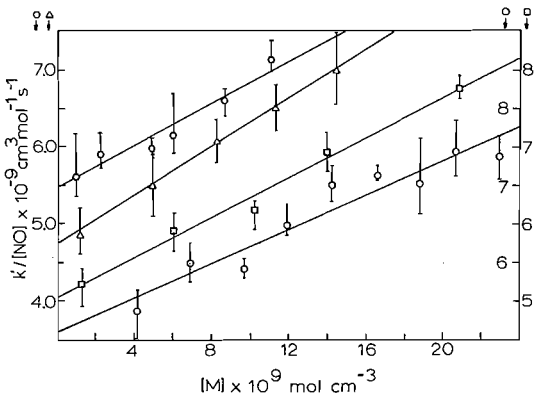

FIG. 6. Dependence of k'/[NO] on the concentration of third bodies SF_6, CF_4, CO_2, C_2F_6, for the reaction of fluorine atoms with nitric oxide in the presence of helium. ⬡, M = SF_6, [NO] = 13.8 × 10^{-9} mol cm^{-3}, [He] = 23 × 10^{-9} mol cm^{-3}; △, M = CF_4, [NO] = 14.2 × 10^{-9} mol cm^{-3}, [He] = 23 × 10^{-9} mol cm^{-3}; □, M = CO_2, [NO] = 14.0 × 10^{-9} mol cm^{-3}, [He] = 23 × 10^{-9} mol cm^{-3}; ○, M = C_2F_6, [NO] = 13.2 × 10^{-9} mol cm^{-3}, [He] = 23 × 10^{-9} mol cm^{-3}. Note that the vertical axes vary for different lines, the symbols at the top of the figure indicate which scale is to be used with each line.

Can. J. Chem. Downloaded from www.nrcresearchpress.com by 210.87.254.40 on 09/05/12
For personal use only.

Can. J. Chem. Downloaded from www.nrcresearchpress.com by 210.87.254.40 on 09/05/12
For personal use only.

TABLE 2. Three body recombination rate constant ratios

Reaction + M	$k_{Ar} \times 10^{-16}$ ($cm^6\ mol^{-2}\ s^{-1}$)	M									Reference
		Ar	He	Ne	N_2	NO	CO_2	CF_4	SF_6	C_2F_6	
F + NO	2.8*	1	1.5	0.75	1.4	6.4	4.6	5.7	5.0	3.9	This work
F + NO	2.8	1	1			3.9					11
Cl + NO	2.9	1	1.2		1.2				1.2		13
H + NO	1.4	1	1.1	0.54							14
H + NO	1.1	1					2.0		3.6		15
H + NO	0.87	1	0.76	0.83							16
H + NO	1.02	1	1.03								17
O + NO	2.7	1	0.67		1.1						18
O + NO	2.2	1	0.77		1.5		2.1	2.2	2.6		19
$O + O_2$	0.015	1	1		1.4		3.7	4.0	8.5		20

*This value is an average of that obtained in the presence and absence of helium.

able, values from other determinations are included for comparison purposes.

Discussion

In the calculations of all the rate constants, an assumption is made that the concentration of CF_4 used as the source of fluorine atoms is too small to be an effective third body. The rate constant k_{1CF_4} is 1.6×10^{17} cm^6 mol^{-1} s^{-1}. The CF_4 concentration in those experiments where CF_4 is used only as a fluorine atom source is of the order of 0.1×10^{-9} mol cm^{-3}. The NO concentration is of the order of 12×10^{-9} mol cm^{-3}. The importance of CF_4 as a third body is represented by the term $k_{1CF_4}[CF_4][NO]$ in the expression for k'. Under the above conditions the value of this term is about 0.2 s^{-1} which is insignificant when compared with the overall value of k'.

In Table 2 we have compared the rate constants obtained for the reaction of F + NO in the presence of various third bodies with the atom – diatomic molecule reactions Cl + NO, H + NO, O + NO, and O + O_2.

The only previous measurement for the rate constant of the reaction of F + NO + M is also included in Table 2. The results by MacLean and co-workers were presented in two different reports (11, 12). Although there is some disagreement among their values as presented in the two reports (see Table 1), especially for M = NO, the value for M = Ar agrees favorably with the value found in the present work. The values presented in ref. 11 for M = Ar, He, and NO, show a similar trend to those found in the present study when the ratios k_{1M}/k_{1Ar} are compared.

When the reactions of F + NO are compared with other combination reactions of an atom with a diatomic molecule, very similar results are observed for the rate constant ratios k_{1He}/k_{1Ar}, k_{1Ne}/k_{1Ar}, and k_{1N_2}/k_{1Ar}. However, minor variations are observed when the ratios for larger third bodies are compared.

We thank Dr. J. A. Coxon of the Department of Chemistry, Dalhousie University, for helpful comments.

1. R. J. McIntyre and F. K. McTaggart. Aust. J. Chem. **24**, 2683 (1971).
2. K. H. Homann, W. C. Solomon, J. Warnatz, H. Gg. Wagner, and C. Zetzsch. Ber. Bunsenges. Phys. Chem. **74**, 585 (1970).
3. K. L. Kompa and J. Wanner. Chem. Phys. Lett. **12**, 560 (1972).
4. J. H. Parker and G. C. Pimentel. J. Chem. Phys. **51**, 91 (1969).
5. M. J. Berry. Chem. Phys. Lett. **15**, 269 (1972).
6. H. Gg. Wagner, J. Warnatz, and C. Zetzsch. Angew. Chem. Int. Ed. Eng. **10**, 564 (1971).
7. C. E. Kolb and M. Kaufman. J. Phys. Chem. **76**, 947 (1972).
8. H. S. Johnston and H. J. Bertin. J. Mol. Spectrosc. **3**, 683 (1959).
9. D. Rapp and H. S. Johnson. J. Chem. Phys. **33**, 695 (1960).
10. T. L. Pollock and W. E. Jones. Can. J. Chem. **51**, 2041 (1973).
11. P. Kim, D. I. MacLean, and W. G. Valance. Abstr. 164th National Meeting Am. Chem. Soc. N.Y. 1972.
12. P. Kim, D. I. MacLean, and W. G. Valance. Office of Naval Research Technical Report FRK-122. 1972.
13. T. C. Clark. M. A. A. Clyne, and D. H. Stedman. Trans. Faraday Soc. **62**, 3354 (1966).
14. J. J. Ahumada, J. V. Michael, and D. T. Osborne. J. Chem. Phys. **57**, 3736 (1972).
15. D. B. Hartley and B. A. Thrush. Proc. R. Soc. London, Ser. A, **297**, 520 (1967).
16. M. A. A. Clyne and B. A. Thrush. Discuss. Faraday Soc. **33**, 139 (1962).
17. S. Miyakazi and S. Takahashi. Mem. Def. Acad. Math. Phys. Chem. Eng. Yokosuka Jpn. **9**, 643 (1969).
18. M. A. A. Clyne and B. A. Thrush. Proc. R. Soc. London, Ser. A, **269**, 404 (1962).
19. F. Kaufman. Ann. Rev. Phys. Chem. **20**, 45 (1967).
20. F. Kaufman and J. R. Kelso. J. Chem. Phys. **46**, 4541 (1967).

Can. J. Chem. Downloaded from www.nrcresearchpress.com by 210.87.254.40 on 09/05/12
For personal use only.

CNDO/2 Studies on Ion Solvation by Methanol

MARK SALOMON
335 Fair Haven Road, Fair Haven, New Jersey 07701
Received April 3, 1975

MARK SALOMON. Can. J. Chem. **53**, 3194 (1975).

CNDO/2 calculations are presented for the solvation of the ions H^+, Li^+, Na^+, F^-, and Cl^- by methanol. The results are compared with previous calculations for solvation by water and with the experimental data of Kebarle. Predicted stabilization energies are grossly overestimated but differences in stabilization energies agree well with the experimental data.

MARK SALOMON. Can. J. Chem. **53**, 3194 (1975).

On présente des calculs CNDO/2 pour la solvatation des ions H^+, Li^+, Na^+, F^- et Cl^- dans le méthanol. On compare les résultats avec des calculs antérieures de solvatation par l'eau et aussi avec des données expérimentales de Kebarle. Les énergies de stabilisation prédites sont de beaucoup surestimées mais les différences entre les énergies de stabilisation s'accordent bien avec les données expérimentales.

[Traduit par le journal]

Can. J. Chem. Downloaded from www.nrcresearchpress.com by 210.87.254.5 on 09/05/12
For personal use only.

Introduction

Semiempirical and *ab initio* SCF–MO calculations have been reported for a variety of hydrogen bonded systems (1). These calculations have led to several important structural features concerning the hydrogen bond. In pure water (2) and methanol (2*a*, 2*b*, 3) the trend is of increasing H-bond energies as the size of the solvent cluster increases. CNDO studies on $(H_2O)_n$ polymers indicate that chain structures are favored for small values of n ($n = 2, 3$) (2*a*, 2*b*) and cyclic structures are favored for large values of n ($n \geq 4$) (3*a*). *Ab initio* studies on $(H_2O)_n$ favor cyclic over chain structures for $n \geq 3$ (2*c*). For methanol polymers, $(MeOH)_n$, CNDO studies show that open chain structures are more stable than cyclic ones for values of n from 2–6 (2*a*, 2*b*, 3*b*). CNDO and *ab initio* studies on protonated water (4), $H^+(H_2O)_n$, show similar behavior; the former calculations (4*a*) weakly favor open chain structures whereas the latter ones (4*b*) favor cyclic structures for $n > 4$. Both methods show that protons serve as a bridge for charge delocalization and that charge transfer along the chain is significant. The present paper is mainly concerned with the analogous system $H^+(MeOH)_n$.

Alkali metal and halide ion solvation by water have been studied by the CNDO (5–8) and *ab initio* (7, 9) methods and CNDO calculations are presented below for the solvation of these ions by methanol. The reactions studied are

[1] $$n\text{MeOH} + M^+ = M^+(\text{MeOH})_n$$

and

[2] $$\text{MeOH} + X^- = X^-(\text{MeOH})$$

where M = H, Li, and Na, and X = F and Cl. For proton solvation, clusters of up to five molecules are considered and for all other cases, only the monomer ($n = 1$) is considered.

Calculations and Results

The CNDO/2 method of Pople *et al.* (10) was used in its original form. Complete evaluation of the potential energy surfaces was not attempted. Carbon was assumed always to be tetrahedral and the C—O and C—H bond distances were fixed at 1.43 and 1.09 Å, respectively. The C—O—H and H. . .O—H angles and O—H and O. . .O distances were optimized.

$MeOH_2^+$ Monomer

Figure 1 shows the geometrical model of $CH_3OH_2^+$. Both β and θ were optimized starting with a planar configuration where $\beta = 120°$ and $\theta = 0°$. Selected results for total energies, E_t, stabilization energies, ΔE_s, and the stabilization energy per O. . .H interaction, $\Delta E_s/n$, are given

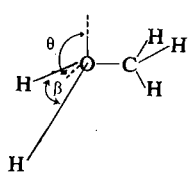

FIG. 1. $CH_3OH_2^+$ monomer geometry.

TABLE 1. CNDO results for selected protonated methanol species

Structure type	Species	$-E_t$ (a.u.)	$-\Delta E_s$ (kcal)	$-\Delta E_s/n$
Planar chains (Fig. 2*c*)	$H^+(MeOH)$	28.9788	265.0	265.0
proton between	$H^+(MeOH)_2$	57.6022	318.2	159.1
molecules 1 and 2	$H^+(MeOH)_3$	86.2206	345.8	115.3
	$H^+(MeOH)_4$	114.8054	363.5	90.9
	$H^+(MeOH)_5$	143.3862	378.7	75.7
proton between	$H^+(MeOH)_4$	114.8182	371.5	92.9
molecules 2 and 3	$H^+(MeOH)_5$	143.4008	387.9	77.6
Eigen	$H^+(MeOH)_3$	86.2308	340.3	113.4
	$H^+(MeOH)_4$	114.8076	349.1	87.3

in Table 1.[1] The stabilization energy is defined by

$$[3]\quad \Delta E_s = E_t\{H^+(MeOH)_n\} - nE_t(MeOH)$$

For the methanol monomer, E_t(MeOH) values were obtained from previous work (3*b*). For planar $H^+(MeOH)_n$, E_t(MeOH) for the staggered configuration and a C—O—H angle of 120° equals −28.5565 a.u. For the optimized $H^+(MeOH)_n$ structures, E_t(MeOH) is −28.5628 a.u. (staggered structure where the C—O—H angle is 109.5°). Although the planar structure is not the most stable one, it is of interest since X-ray data indicate its predominance in liquid MeOH (see discussion, ref. 3*b*). The rotational energy, ΔE_R, for planar $MeOH_2^+$ is negligible (0.02 kcal/mol). The calculation of ΔE_R for the optimized $MeOH_2^+$ was not performed.

$H^+(MeOH)_n$ Polymers

In Fig. 2, models of planar $(MeOH)_n$ and $H^+(MeOH)_n$ are shown. Calculations for cyclic structures were not carried out. Several chain type structures were considered. Figure 2*b* is the structure where $MeOH_2^+$ exists as a separate entity in the chain. The most stable configuration turned out to be that for a symmetrically located proton as shown in Fig. 2*c*. In Fig. 2*c*, the proton is shown between MeOH molecules 1 and 2 and moving the proton between molecules 2 and 3 resulted in an increase in stability (see Table 1).

The geometric quantities optimized for the planar chains were the O—H and O. . .H distances. The O—H distance in O—H. . .O is 1.05 Å compared to 1.03 Å for a free hydroxyl group. For these planar structures, both the C—O—H and H—O. . .H angles were fixed at 120° and the O. . .H—O angles at 180°. Optimization of these bond angles was carried out and resulted in C—O—H, H—O. . .H, and O. . .H—O angles of 109.5, 109.5, and 180°, respectively. These optimized structures are referred to as bent chains.[1]

Several other $H^+(MeOH)_n$ structures were investigated. Figure 3 shows an Eigen type structure for $H^+(MeOH)_4$ which is modeled after the structures for $H_9O_4^+$ and $H_{11}O_5$ (11). Removing the MeOH molecule marked with an asterisk in Fig. 3 results in an Eigen type structure for $H^+(MeOH)_3$ which differs from the bent chain structure in that $MeOH_2^+$ exists as a separate entity whereas in the latter, the proton is symmetrically located between molecules 1 and 2 of Fig. 2*c*. Another structure was considered in which a proton is coordinated to the oxygens of MeOH for n values of 3 and 4. For these central proton models, both planar and trigonal pyramidal configurations (O. . .H. . .O angle = 109.5°) were investigated for $n = 3$, and a tetrahedral configuration for $n = 4$.[1]

Alkali Metal and Halide Monosolvates

The geometric models for monomer solvates are shown in Figs. 4 and 5 for cations and anions, respectively. Also shown in these figures are the models for the water solvates. The results for the monomer solvates are given in Table 2. The stabilization energies in Table 2 were calculated from [4].

$$[4]\quad \Delta E_s = E_t\{\text{ion} - (MeOH)_n\} - (n-1)E_t(MeOH) - E_t(MeOH + \text{ion})$$

The last term in this equation, E_t(MeOH +

[1]Complete set of tabular data is available, at a nominal charge, from the Depository of Unpublished Data, CISTI, National Research Council of Canada, Ottawa, Canada K1A 0S2.

Can. J. Chem. Downloaded from www.nrcresearchpress.com by 210.87.254.5 on 09/05/12
For personal use only.

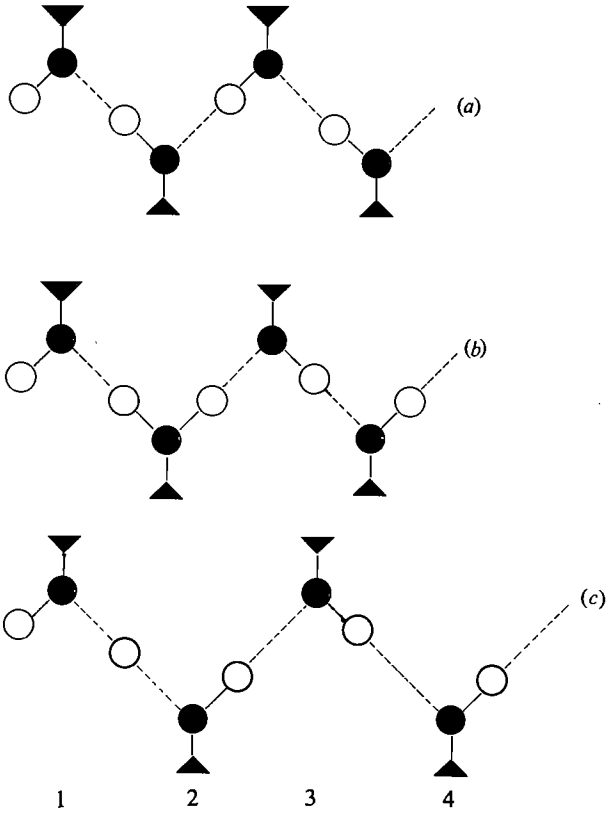

FIG. 2. Chain structures: ● = O, ▲ = CH_3; ○ = H. (*a*) Methanol chain; (*b*) and (*c*) protonated methanol chains.

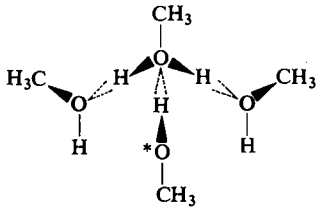

FIG. 3. Eigen structure for $H^+(MeOH)_4$.

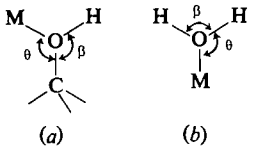

FIG. 4. Models for cation solvation by (*a*) methanol and (*b*) water.

ion), refers to the reactants at infinite separation, r_∞. For calculation purposes, r_∞ was taken as 15–20 Å. Included in Table 2 are the aqueous CNDO/2 results which were obtained from refs. 4–8.

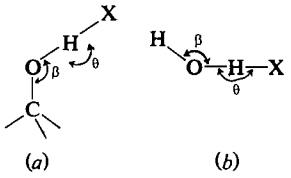

FIG. 5. Models for anion solvation by (*a*) methanol and (*b*) water.

Discussion

$H^+(MeOH)_n$ Systems

In calculating ΔE_s from [3], the important structures appear to be the open chain planar and bent models. The Eigen type and central proton structures are not considered to contribute significantly to the structure of $H^+(MeOH)_n$ clusters. The stabilization energies for the reactions

[1] $$H^+ + n\text{MeOH} = H^+(MeOH)_n$$

are grossly overestimated, *e.g.* the experimental proton affinity of methanol is −182 kcal/mol

Can. J. Chem. Downloaded from www.nrcresearchpress.com by 210.87.254.5 on 09/05/12
For personal use only.

TABLE 2. Geometries and energies of monomeric solvates

Solvent	Ion	r(O—ion) (Å)	r(O—H)* (Å)	β (deg)	θ (deg)	E_t (a.u.)	ΔE_s (kcal/mol)
H_2O	H^+	1.05		110.0	110.0	−20.2934	−252.57†
	H^+	20.0		110.0	110.0	−18.3415	
	Li^+	2.30		107.1	126.5	−19.9632	−45.18
	Li^+	20.0		107.1	126.5	−19.8912	
	Na^+	3.00		107.1	126.5	−19.9482	−32.40
	Na^+	20.0		107.1	126.5	−19.8912	
	F^-	2.22	1.12	107.1	180.0	−47.5021	−79.62
	F^-	15.0	1.03	107.1	180.0	−47.3752	
	Cl^-	2.75	1.03	107.1	180.0	−36.0329	−23.32
	Cl^-	20.0	1.03	107.1	180.0	−35.9957	
MeOH	H^+	1.05		109.5	109.5	−28.9898	−267.90†
	H^+	20.0		109.5	109.5	−27.0393	
	Li^+	2.25		109.5	80.0	−28.7251	−101.76
	Li^+	20.0		109.5	80.0	−28.5629	
	Na^+	2.75		109.5	90.0	−28.6727	−68.86
	Na^+	20.0		109.5	90.0	−28.5629	
	F^-	2.20	1.13	109.5	114.5	−56.1937	−92.04
	F^-	15.0	1.03	109.5	114.5	−56.0471	
	Cl^-	2.74	1.03	109.5	109.5	−44.7086	−25.64
	Cl^-	20.0	1.03	109.5	109.5	−44.6677	

*Distance on the O–anion axis.
†Calculated from [3]. All other ΔE_s are from [4].

TABLE 3. CNDO/2 and experimental energies for reaction 5

	ΔE_5 (kcal)		Experimental*	
$n, n-1$	Planar chains	Bent chains	ΔH_5 (kcal)	ΔS_5^0 (cal/deg)†
2,1	−53.2	−50.5	−33.1	−30.5
3,2	−27.6	−28.2	−21.3	−28.2
4,3	−25.7‡	−15.7	−16.1	−28.9
5,4	−16.4‡	−11.9	−13.5	−28.7

*From ref. 12.
†ΔS^0 values are referred to 300 K, standard state of 1 atm.
‡Proton between molecules 2 and 3 (Fig. 2*c*).

(12) whereas the CNDO result is −265 kcal/mol. Similarly, the proton affinity of water is, experimentally, −165 kcal/mol (13) and the CNDO result (4*a*) is −250 kcal/mol. The overestimation of stabilization energies is a recognized weakness of the CNDO method (10, 14, 15), but trends in stabilities and geometries do appear to be well reproduced (14, 15). ΔE_s for [1] is, correctly, given by [4]. Taking $r_\infty = 20$ Å for the MeOH. . .H^+ separation, $E_t(\text{MeOH} + H^+) = -27.0393$ a.u.[2] Using this value for the last term in [4] leads to abnormally large ($\simeq 10^3$ kcal) values for ΔE_s. If one considers the reactions

[5] $\quad H^+(\text{MeOH})_{n-1} + \text{MeOH} = H^+(\text{MeOH})_n$

where $n \geq 2$, for which

[6] $\quad \Delta E_5 = E_t\{H^+(\text{MeOH})_n\} - E_t\{H^+(\text{MeOH})_{n-1}\} - E_t(\text{MeOH})$

it is found that considerable accuracy in the CNDO results is achieved. Table 3 compares the calculated ΔE_5 values with the experimental (12) enthalpies, ΔH_5, for the gas phase reactions. It should be noted that E_t values neglect kinetic, zero-point, and correlation energies, but a considerable portion of these factors probably cancel when differences in E_t values are considered.

The addition of a proton to MeOH results in a large delocalization of the positive charge to every atom except carbon.[1] Successive solvation of $MeOH_2^+$ results in progressive delocaliza-

[2]The closed shell CNDO calculation for this state is actually that for $MeOH^{2+} + H^-$ and is not therefore the state of interest. A proper occupation of orbitals would permit [4] to be used. (The author is grateful to one of the reviewers for pointing out this fact.)

Can. J. Chem. Downloaded from www.nrcresearchpress.com by 210.87.254.5 on 09/05/12
For personal use only.

Can. J. Chem. Downloaded from www.nrcresearchpress.com by 210.87.254.5 on 09/05/12
For personal use only.

tion of positive charge over the chain. For $n \geq 3$, a significant donation of electrons to the chain oxygens occurs mainly from the methyl hydrogens. Similar results were reported for $H^+(H_2O)_n$ chains (4). This is due to the shielding of the oxygens in the chain due to the increasing positive charges on the H-bonded hydrogens. The stabilization energy per O. . .H interaction, $\Delta E_s/n$ (Table 1) is seen to decrease as n increases. This result suggests that the O. . .H. . .O bonds weaken as the chain length increases. In $(MeOH)_n$ clusters, charge transfer was observed to increase to the terminal molecules of the chain and the stabilization energy per O. . .H interaction thereby increased (3).

The nature of proton solvation by methanol thus appears to be similar to that by water with the exception that Eigen type and, probably, cyclic type clusters do not contribute significantly to the overall properties. If the planar and bent structures can be identified with the condensed and gas phases respectively, then the average strength of a hydrogen bond appears to be greater in the condensed system. In Frank and Wen's flickering cluster model of solvent structure (16), the increase or decrease in chain length (see also discussion in refs. 3 and 4) can be thought of as being followed by rapid charge delocalization amongst the hydroxyl hydrogens thus affording the anomalous Grothuss type conductivity properties. In water–methanol mixtures containing 15–20 mol% methanol, the protonic conductivity reaches a minimum value which is attributed to classical transport of H_3O^+ and/or $MeOH_2^+$ (17). It would be of interest to extend the CNDO calculations to mixed H_2O–MeOH clusters.

Alkali Metal and Halide Monosolvates

Experimental data for ion solvation by methanol are scarce. For the solvation of Cl^- by MeOH, the enthalpy for the gas phase reaction 2 is 14.1 kcal/mol (18). For the gas phase reactions with water

$$[7] \qquad H_2O + Y = Y(H_2O)$$

the following enthalpies were measured: for Y = F^- and Cl^-, $\Delta H_7^0 = 23.3$ and 13.1 kcal/mol, respectively (18); for Y = Li^+ and Na^+, $\Delta H_7^0 = 34.0$ and 24.0 kcal/mol, respectively (19). *Ab initio* results (9) for [7] give the following: for Y = Li^+ and Na^+, $\Delta H_7^0 = 34.1$ and 23.3 kcal/mol, respectively. There is no doubt that the CNDO results overestimate the stabilization energies to an extent which cannot be corrected for by the kinetic, zero-point, and correlation energies which amount, at most, to ~3 kcal/mol (9). A similar effect was seen above to exist for the $H^+(MeOH)_n$ systems and which is typical of the CNDO method. However differences in stabilization energies were seen to give acceptable results. For the alkali metal cations and halide anions, stabilization energy differences (ΔE_8) for the gaseous reactions are defined for

$$[8] \qquad MeOH + Y(H_2O) = H_2O + Y(MeOH)$$

where Y is Li^+, Na^+, F^-, or Cl^-. Table 4 compares the CNDO/2 values of ΔE_8 with the experimental (12, 18) enthalpies, ΔH_8. For the two cases where experimental data exist, the agreement is quite good despite the neglect of kinetic, zero-point, and correlation energies from ΔE_8. The fact that ΔE_8 for Li^+ and Na^+ are 2–4 times larger than that for H^+ is similar to the behavior of these ions in solution (20).

TABLE 4. CNDO/2 and experimental energies for reaction 8

Ion	ΔE_8 (kcal/mol)	ΔH_8*
H^+	−15.3	−15.2
Li^+	−56.6	
Na^+	−36.5	
F^-	−12.4	
Cl^-	−2.3	−1.0

*From refs. 12 and 18.

1. (*a*) P. A. KOLLMAN and L. C. ALLEN. Chem. Rev. **72**, 283 (1972); (*b*) C. N. R. RAO. Water, a comprehensive treatise, Vol. 1. *Edited by* F. Franks. Plenum, New York. 1972. Chapt. 3.
2. (*a*) A. S. N. MURPHY, R. E. DAVIS, and C. N. R. RAO. Theor. Chim. Acta, **13**, 81 (1968); (*b*) J. R. HOYLAND and L. B. KIER. Theor. Chim. Acta, **15**, 1 (1969); (*c*) J. DEL BENE and J. A. POPLE. Chem. Phys. Lett. **4**, 426 (1969); J. Chem. Phys. **52**, 4858 (1970); (*d*) D. HANKINS, J. MOSKOWITZ, and F. STILLINGER. J. Chem. Phys. **53**, 4544 (1970).
3. (*a*) L. C. ALLEN and P. A. KOLLMAN. Science, **167**, 1443 (1970); (*b*) M. SALOMON. J. Chem. Soc. Faraday Trans. In press.
4. (*a*) M. DE PAZ, S. EHRENSON, and L. FRIEDMAN. J. Chem. Phys. **52**, 3362 (1970); (*b*) M. D. Newton and S. Ehrenson. J. Am. Chem. Soc. **93**, 4971 (1971).
5. H. LISCHKA. TH. PLESSER, and P. SCHUSTER. Chem. Phys. Lett. **6**, 263 (1970).
6. R. E. BURTON and J. DALY. Trans. Faraday Soc. **66**, 1282 (1970).
7. K. G. BREITSCHWERDT and H. KISTENMACHER. Chem. Phys. Lett. **14**, 288 (1972).

8. A. GUPTA and C. N. R. RAO. J. Phys. Chem. **77**, 2888 (1973).
9. (*a*) E. CLEMENTI and H. POPKIE. J. Chem. Phys. **57**, 1077 (1972); (*b*) H. KISTENMACHER, H. POPKIE, and E. CLEMENTI. J. Chem. Phys. **59**, 5842 (1973); **58**, 1689 (1973); (*c*) P. A. KOLLMAN and I. D. KUNTZ. J. Am. Chem. Soc. **96**, 4766 (1974).
10. (*a*) J. A. POPLE, D. P. SANTRY, and G. A. SEGAL. J. Chem. Phys. **43**, S129 (1965); (*b*) J. A. POPLE and G. A. SEGAL. J. Chem. Phys. **43**, S136 (1965); **44**, 3289 (1966).
11. E. WICKE, M. EIGEN, and TH. ACKERMANN. Z. Phys. Chem. Frankfurt, **1**, 340 (1954).
12. (*a*) K. HIRAOKA, E. P. GRIMSRUD, and P. KEBARLE. J. Am. Chem. Soc. **96**, 4971 (1974); (*b*) E. P. GRIMSRUD and P. KEBARLE. J. Am. Chem. Soc. **95**, 7939 (1973).
13. J. LONG and B. MUNSON. J. Am. Chem. Soc. **95**, 2427 (1973).
14. J. A. POPLE and M. S. GORDON. J. Am. Chem. Soc. **89**, 4253 (1967).
15. J. A. POPLE and D. L. BEVERIDGE. Approximate molecular orbital theory. McGraw-Hill, New York. 1970.
16. H. S. FRANK and W. Y. WEN. Discuss. Faraday Soc. **24**, 133 (1957).
17. B. E. CONWAY, J. O'M. BOCKRIS, and H. LINTON. J. Chem. Phys. **24**, 834 (1956).
18. (*a*) M. ARSHADI, R. YAMDAGNI, and P. KEBARLE. J. Phys. Chem. **74**, 1475 (1970); (*b*) R. YAMDAGNI and P. KEBARLE. J. Am. Chem. Soc. **93**, 7139 (1971).
19. I. DZIDIC and P. KEBARLE. J. Phys. Chem. **74**, 1466 (1970).
20. C. M. CRISS and M. SALOMON. Physical chemistry of organic solvent systems. *Edited by* A. K. Covington and T. Dickinson. Plenum, New York. 1973. Chapt. 2.4.

Can. J. Chem. Downloaded from www.nrcresearchpress.com by 210.87.254.5 on 09/05/12
For personal use only.

Mössbauer and Related Studies of Complexes of $R_2Sn(NCS)_2$ with Neutral Ligands Containing Oxygen Donor Atoms

F. PATRICIA MULLINS

Department of Chemistry, Mount St. Vincent University, Halifax, Nova Scotia B3M 2J6

AND

COLUMBA CURRAN

Department of Chemistry and Radiation Laboratory, University of Notre Dame, Notre Dame, Indiana 46556

Received May 22, 1975

F. PATRICIA MULLINS and COLUMBA CURRAN. Can. J. Chem. **53**, 3200 (1975).

Mössbauer, infrared, and electric dipole moment data are reported for several complexes of the type (*i*) $R_2Sn(NCS)_2L_2$ and (*ii*) R_2SnX_2B (where R = C_4H_9, C_2H_3, C_6H_5; X = Cl, NCS; L = monodentate ligands with O, S donor atoms; B = bidentate ligands with O, P, As donor atoms). Quadrupole splittings indicate *trans* C—Sn—C bonds in octahedral complexes of divinyl- and diphenyltin diisothiocyanate with bidentate oxygen-donor ligands, in contrast to a *cis* configuration for complexes with bidentate nitrogen-donor ligands. Data indicate that the 1:2 complex of 2,2-bipyridyl-*N*,*N*′-dioxide with $Bu_2Sn(NCS)_2$ is polymeric, with octahedral monomer units having one bridging and one terminal NCS group, a bridging $bipyO_2$ ligand and *trans* butyl groups. $[Ph_2Sn(NCS)_2]_2 \cdot bipyO_2$ appears to be a dimer with a bridging $bipyO_2$ ligand and five-coordinate tin atoms. Mössbauer parameters for $R_2SnX_2L_2$ and R_2SnX_2B complexes having oxygen donors are similar.

F. PATRICIA MULLINS et COLUMBA CURRAN. Can. J. Chem. **53**, 3200 (1975).

On rapporte, pour plusieurs complexes de type (*i*) $R_2Sn(NCS)_2L_2$ et de type (*ii*) R_2SnX_2B (où R = C_4H_9, C_2H_3, C_6H_5; X = Cl, NCS; L = ligands monodentates avec des atomes d'oxygène et de soufre comme donneurs; B = ligands bidentates avec des atomes d'oxygène, de phosphore et d'arsenic comme donneurs), des données de Mössbauer, d'infrarouge et de moment dipolaire. Les couplages quadripolaires indiquent que les liens C—Sn—C sont *trans* dans les complexes octaédriques des diisothiocyanates de divinyl- et diphényl étain avec des ligands bidentates contenant des atomes d'oxygène comme donneurs alors qu'ils ont une configuration *cis* pour les complexes avec des ligands bidentates contenant des atomes d'azote comme donneurs. Les données indiquent que le complexe 1:2 du bipyridyl-2,2 *N*,*N*′-dioxyde avec le $Bu_2Sn(NCS)_2$ existe à l'état de polymère avec des unités octaédriques possédant un groupe NCS terminal et un autre servant de pont, un ligand $bipyO_2$ agissant comme pont et des groupements butyles en position *trans*. Il semble que le $[Ph_2Sn(NCS)]_2 \cdot bipyO_2$ existe sous forme de dimère avec un ligand $bipyO_2$ agissant comme pont et des atomes d'étain pentacoordonnés. Les paramètres de Mössbauer pour les complexes $R_2SnX_2L_2$ et R_2SnX_2B possédant des oxygènes comme donneurs sont semblables.

[Traduit par le journal]

Introduction

Previous studies of Mössbauer spectra and electric dipole moments of complexes of $R_2Sn(NCS)_2$ with *o*-phenanthroline and with 2,2-dipyridyl reveal a change from *trans* C—Sn—C bonds in dibutyl compounds to *cis* C—Sn—C bonds in divinyl and diphenyl compounds; the corresponding R_2SnCl_2 complexes are all *trans* (1–3). $R_2Sn(tropolonate)_2$ compounds also have *trans* butyl and *cis* vinyl and phenyl groups (3, 4). It is of interest to determine the configuration of complexes of $R_2Sn(NCS)_2$ with neutral bidentate ligands having oxygen donor atoms. The work of Bancroft *et al.* (5) on complexes of R_2SnCl_2 with the dioxides of 1,2-bis(diphenylphosphino)ethane, bis(diphenylarsino)methane, and 2,2′-bipyridyl suggested the complexing of these oxygen-donor ligands, along with 1,2-bis(diphenylarsino)ethane dioxide, with $R_2Sn(NCS)_2$. Attempts to prepare complexes of the diisothiocyanates with bidentate ligands having P, As, and S as donor atoms were unsuccessful.

Complexes with R_3PO and R_3AsO afford a comparison with those of the above bidentate ligands. Holloway *et al.* (6) report only 1:1 complexes of these monodentate ligands with $Ph_2Sn(NCS)_2$; only 2:1 complexes were isolated in the present investigation.

Previous studies have shown an excellent correlation between configurations of octahedral diorganotin(IV) complexes as revealed by Mössbauer spectra of solids and electric dipole moments in solution (1–3, 7). In the present study only the Bu_3PO and Ph_3AsO complexes of $R_2Sn(NCS)_2$ were sufficiently soluble and undissociated in benzene for meaningful dielectric constant measurements.

Experimental

Preparation of Compounds

Hexamethylphosphoric triamide (HMPA) was a Baker Analyzed reagent, and tetramethylthiourea (TMTU) was purchased from Aldrich Chemical Co. Inc. 1,2-Bis(diphenylphosphino)ethane, 1,2-bis(diphenylarsino)ethane, bis(diphenylarsino)methane, and *o*-phenylenebis(dimethylarsine) (DIARS) were obtained from Strem Chemicals Inc. Absolute ethanol was purchased from Consolidated Alcohols Ltd; all other solvents were Baker or Fisher Scientific Analyzed Reagents. The sources of other reagents have been indicated previously (3, 7). Thiophene-free benzene was refluxed over phosphorus pentoxide for several hours before being distilled.

Di-*n*-butyl-, diphenyl-, and divinyltin diisothiocyanate were prepared as described previously (2, 3). Complexes of these compounds with monodentate ligands were formed by mixing their absolute ethanol solutions with the ligands in diethyl ether and/or benzene solutions in a 1:2 ratio; diphenyltin diisothiocyanate was also mixed with these ligands in a 1:1 ratio. In all cases chemical analyses showed that 1:2 complexes were formed with the monodentate ligands. The complexes of Ph_3PO, Ph_3AsO, and HMPA formed as white precipitates on mixing; that of $Ph_2Sn(NCS)_2$ with TMTU precipitated as a cream–yellow powder. The complexes of Bu_3PO were obtained on evaporation of ethanol–benzene–ether solutions as cream (dibutyl) and peach (diphenyl) colored crystals.

The dioxides of the bidentate ligands, 2,2′-bipyridyl, 1,2-bis(diphenylphosphino)ethane, 1,2-bis(diphenylarsino)ethane, and bis(diphenylarsino)methane (hereafter referred to as $bipyO_2$, B(DPO)E, B(DAO)E, and B(DAO)M respectively) were prepared by their oxidation with 30% hydrogen peroxide as described previously (8–12). They were obtained as white powders: $bipyO_2$, decomposed above 270 °C (lit. (8) 297 °C, (9) 310 °C (dec.)); B(DPO)E, m.p. 262–264 °C (lit. (10) 256–258 °C, (11) 275–276 °C, (12) 266 °C); B(DAO)E, 160 °C (dec.) (lit. (10) 178–179 °C); B(DAO)M, 130 °C (dec.). Complexes of these ligands were obtained as white or pale cream precipitates on mixing absolute ethanol solutions of R_2SnX_2 with the ligands in ethanol and/or benzene solutions. Data for complexes of $bipyO_2$ with $R_2Sn(NCS)_2$ indicated bridging, but the other complexes were obtained as 1:1 monomers. R_2SnX_2 complexes with B(DP)E and DIARS were obtained as white and cream powders upon evaporation or cooling of their ethanol–benzene–ether solutions.

All precipitates were filtered under vacuum, washed with the solvent used and light petroleum ether (b.p. 30–60 °C) and all complexes were dried under vacuum for several hours.

Attempts to isolate complexes of dimethylsulfoxide, 8-aminoquinoline, triphenylphosphine, triphenylarsine, tetramethylenediamine, tetramethylurea, dimethoxyethane, triphenylphosphine sulfide, tripiperidinephosphine sulfide, tripyrrolidinophosphine sulfide with $R_2Sn(NCS)_2$ were not successful. Attempts to purify $R_2Sn(NCS)_2$ complexes of B(DP)E, B(DA)E, and DIARS resulted in dissociation.

Analytical data and melting points for the complexes are given in Table 1.

Mössbauer and Infrared Spectra

The instrumentation and data processing were described previously (1, 3, 7), except that an LTV LING AITEC LTD (England) Type 106 constant acceleration transducer was used instead of an Austin Science Associates Mössbauer Spectrometer Drive Model S3 Model K3 constant acceleration linear motor. In measurements with the AM-1 spectrometer, dibutyltin(kojate)$_2$ was used as a secondary standard (δ = 1.38 mm s^{-1}, ΔE_Q = 3.70 mm s^{-1} (5)). Isomer shifts, δ, relative to barium stannate and quadrupole splittings, ΔE_Q, listed in Table 3 are considered to be accurate to $\pm$0.05 mm s^{-1} with a relative precision of $\pm$0.03 mm s^{-1}. Γ_1 and Γ_2 are absorption half-widths. The spectrum of $Ph_2Sn(NCS)_2(TMTU)_2$ is illustrated in Fig. 1. Asymmetries are present in the doublet spectra for compounds **5**, **6**, **7**, **18**, **20**, and **22**.

Infrared spectra in potassium bromide disks were obtained with Perkin-Elmer 521 and 457 and Beckman IR-33 spectrometers.

Dielectric Constants of Benzene Solutions

These were obtained as in previous investigations (13) using an oscillator similar to that described by Estok (14). The $\Delta\varepsilon/wf_2$ ratios listed in Table 2 are extrapolated values, except for $Ph_2Sn(NCS)_2(Ph_3AsO)_2$ where an average value was used. Electric moments were calculated from the Higasi equation, using a value of 0.8481 for B (15–17).

Discussion of Results

Complexes with Monodentate Ligands

The quadrupole splittings obtained for compounds **1–9** indicate that they have octahedral configurations with the R groups *trans* in the solid state. As in *trans* complexes investigated previously (2, 3), the isomer shifts are smaller and the quadrupole splittings larger for the diisothiocyanates than for the corresponding dichlorides, consistent with a greater polarity for the Sn—NCS than for the Sn—Cl bond.

Ph_3AsO has a greater dipole moment than Ph_3PO (18) and is expected to effect a slightly greater electron release to tin on complex formation. In line with this expectation, the quadrupole splittings for the Ph_3AsO complexes, **1**, **5**, are smaller than for the corresponding Ph_3PO complexes, **3**, **7**. The electric dipole moments of R_3PO and R_3AsO complexes, Table 2, are complicated by rotation about the O—Sn bond.

TABLE 1. Analysis and melting points of $R_2SnX_2L_2$ and R_2SnX_2B complexes

Complex	C (%) Calculated	C (%) Found	H (%) Calculated	H (%) Found	Melting point (°C)
1 $Bu_2Sn(NCS)_2(Ph_3AsO)_2$	55.61	54.87	4.87	4.95	170–171
2 $Bu_2Sn(NCS)_2(Bu_3PO)_2$	51.97	51.79	9.24	9.24	48–50
3 $Bu_2Sn(NCS)_2(Ph_3PO)_2$	61.01	60.75	5.34	5.08	129–131
4 $Bu_2Sn(NCS)_2(HMPA)_2$	37.35	37.26	7.69	7.35	72 (dec.)
5 $Ph_2Sn(NCS)_2(Ph_3AsO)_2$	58.11	57.94	3.90	4.22	190–192
6 $Ph_2Sn(NCS)_2(Bu_3PO)_2$	55.28	55.38	7.81	7.91	98 (dec.)
7 $Ph_2Sn(NCS)_2(Ph_3PO)_2$	63.51	63.26	4.26	4.49	188–189
8 $Ph_2Sn(NCS)_2(HMPA)_2$	41.78	41.23	6.20	6.38	204–206
9 $Ph_2Sn(NCS)_2(TMTU)_2$	44.11	43.55	5.24	5.29	151–153
10 $Ph_2SnCl_2 \cdot TMTU$	42.89	42.31	4.66	4.82	111–113
11 $Ph_2SnCl_2 \cdot bipyO_2$	49.67	49.59	3.41	3.68	224–225
12 $[Ph_2Sn(NCS)_2]_2 \cdot bipyO_2$	47.23	46.37	2.92	2.92	190 (dec.)
		46.84		3.14	
		47.15		3.25	
13 $[Bu_2Sn(NCS)_2]_2 \cdot bipyO_2$	40.65	39.74	5.00	5.17	60 (dec.)
		41.81		4.61	
14 $Bu_2Sn(NCS)_2 \cdot B(DPO)E$	55.47	55.99	5.43	5.53	191–193
15 $Bu_2SnCl_2 \cdot B(DPO)E$	55.61	56.31	5.77	6.13	170 (dec.)
16 $Ph_2SnCl_2 \cdot B(DPO)E$	58.95	58.14	4.43	4.41	258–260
17 $Ph_2Sn(NCS)_2 \cdot B(DPO)E$	58.62	57.70	4.18	4.28	232–234
18 $Vin_2Sn(NCS)_2 \cdot B(DPO)E$	53.47	53.26	4.18	3.28	206–208
19 $Bu_2Sn(NCS)_2 \cdot B(DAO)E$	49.85	49.51	4.88	4.88	174–176
20 $Bu_2SnCl_2 \cdot B(DAO)E$	49.67	49.88	5.15	5.16	193–195
21 $Ph_2SnCl_2 \cdot B(DAO)E$	52.94	52.07	3.98	3.90	199–201
22 $Vin_2Sn(NCS)_2 \cdot B(DAO)E$	47.60	46.29	3.71	3.37	158–159
23 $Bu_2Sn(NCS)_2 \cdot B(DAO)M$	49.26	48.74	4.72	4.63	130 (dec.)
24 $Ph_2SnCl_2 \cdot B(DAO)M$	52.40	51.62	3.80	3.73	231–233
25 $Ph_2SnCl_2 \cdot DIARS$	41.95	41.39	4.16	3.18	140 (dec.)
26 $Ph_2SnCl_2 \cdot B(DP)E$	61.49	61.08	4.62	4.88	102–103

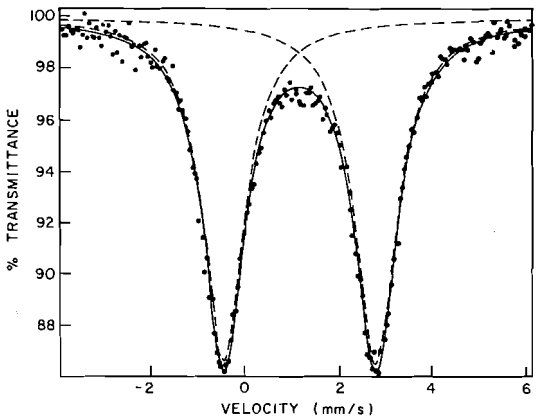

FIG. 1. ^{119m}Sn Mössbauer spectrum of $Ph_2Sn(NCS)_2(TMTU)_2$ *vs.* a $Ba^{119m}SnO_3$ source.

Values calculated for an all-*trans* configuration are 5 and 6 D, respectively, for the Bu_3PO and Ph_3AsO complexes (7), and for a *cis* arrangement of oxide ligands, 13.5 and 15 D (7, 2). The experimental values indicate a *trans* arrangement of all ligands. The values of $\Delta\varepsilon/wf_2$ for the dibutyltin(IV) complexes increase with decreasing solute concentration; the values listed in Table 2 are extrapolated. For complete dissociation of the complexes, the calculated values of $\Delta\varepsilon/wf_2$ are 10.6 and 10.5. The data suggest a partial dissociation of these all-*trans* complexes, increasing with decreasing concentration.

TABLE 2. Electric moment data in benzene solutions at 25 °C

Compound	$1000wf_2$	$\Delta\varepsilon/wf_2$	μ_H (D)
$Bu_2Sn(NCS)_2(Ph_3AsO)_2$	1.1–18.4	5.9	7.4
$Bu_2Sn(NCS)_2(Bu_3PO)_2$	14.7–38.3	7.6	7.4
$Ph_2Sn(NCS)_2(Ph_3AsO)_2$	5.4–10.1	3.5	5.8
$Ph_2Sn(NCS)_2(Bu_3PO)_2$	13.6–44.4	4.8	6.0

A comparison of the quadrupole splittings for $Ph_2Sn(NCS)_2(HMPA)_2$, 3.73 mm s^{-1}, and $Vin_2Sn(NCS)_2(HMPA)_2$, 4.20 mm s^{-1} (3), indicates a significant deviation from 180° for the C—Sn—C bond angle in the former compound. The Mössbauer parameters for both

TABLE 3. Mössbauer parameters (mm s^{-1}) at 80 K and infrared frequencies (cm^{-1})

Compound	δ	ΔE_Q	Γ_1	Γ_2	ν_{C-N}	$\nu_{As-O/P-O/N-O}$
1 $Bu_2Sn(NCS)_2(Ph_3AsO)_2$	1.47	4.16	1.11	1.14	2038	888
						868
2 $Bu_2Sn(NCS)_2(Bu_3PO)_2$	1.47	4.48	0.94	0.94	2060	1108
3 $Bu_2Sn(NCS)_2(Ph_3PO)_2$	1.53	4.41	0.98	0.93	2045	1137
4 $Bu_2Sn(NCS)_2(HMPA)_2$	1.44	4.27	0.97	1.08	2045	1192
						1130
5 $Ph_2Sn(NCS)_2(Ph_3AsO)_2$	1.18	3.71	0.98	1.25	2042	883
6 $Ph_2Sn(NCS)_2(Bu_3PO)_2$	1.10	3.60	0.97	1.09	2060	1110
7 $Ph_2Sn(NCS)_2(Ph_3PO)_2$	1.13	3.79	0.93	0.80	2052	1140
8 $Ph_2Sn(NCS)_2(HMPA)_2$	1.07	3.73	1.10	1.12	2065	1188
						1155
9 $Ph_2Sn(NCS)_2(TMTU)_2$	1.20	3.39	1.14	1.12	2040	
10 $Ph_2SnCl_2 \cdot TMTU$	1.29	2.60	1.12	1.19		
11 $Ph_2SnCl_2 \cdot bipyO_2$	1.31	3.67	1.17	1.13		1224
						1208
12 $[Ph_2Sn(NCS)_2]_2 \cdot bipyO_2$	0.77	2.10	1.26	1.36	2040	1220
						1205
13 $[Bu_2Sn(NCS)_2]_2 \cdot bipyO_2$	1.52	4.02	1.21	1.30	2040	1220
					2070	1202
14 $Bu_2Sn(NCS)_2 \cdot B(DPO)E$	1.52	4.38	1.21	1.21	2045	1150
						1090
15 $Bu_2SnCl_2 \cdot B(DPO)E$	1.65	4.19	1.08	1.08		1160
						1085
16 $Ph_2SnCl_2 \cdot B(DPO)E$	1.29	4.00	1.17	1.20		1145
						1085
17 $Ph_2Sn(NCS)_2 \cdot B(DPO)E$	1.21	4.12	1.19	1.09	2038	1142
						1087
18 $Vin_2Sn(NCS)_2 \cdot B(DPO)E$	1.19	4.01	1.30	1.14	2040	1150, 1142
						1090
19 $Bu_2Sn(NCS)_2 \cdot B(DAO)E$	1.42	4.23	0.97	1.00	2050	890
						863
20 $Bu_2SnCl_2 \cdot B(DAO)E$	1.49	4.22	1.01	1.14		858
21 $Ph_2SnCl_2 \cdot B(DAO)E$	1.17	3.67	1.09	1.05		877
22 $Vin_2Sn(NCS)_2B(DAO)E$	1.10	3.83	1.24	1.09	2050	860
23 $Bu_2Sn(NCS)_2B(DAO)M$	1.40	4.31	1.03	1.03	2050	875
						860sh
24 $Ph_2SnCl_2 \cdot B(DAO)M$	1.20	3.63	1.13	1.12		870
						855sh
25 $Ph_2SnCl_2 \cdot DIARS$	1.30	3.07	1.24	1.17		
26 $Ph_2SnCl_2 \cdot B(DP)E$	1.31	3.27	1.07	1.11		

$Ph_2SnCl_2 \cdot TMTU$, **10**, and $Vin_2SnCl_2 \cdot TMTU$ (3) are expected values for five-coordinate tin complexes. The relatively small quadrupole splitting for $Ph_2Sn(NCS)_2(TMTU)_2$, **9**, is a reflection of the greater electron release by sulfur than by oxygen on complex formation. The larger isomer shift for this compound than for compounds **5** to **8** indicates that the tin s character of the Sn—S bond is more important than the shielding effect of the electrons of the Sn—S bond in determining the relative isomer shift.

A single infrared absorption associated with the O → Sn stretching vibration is expected for compounds **1** to **8** in an all-*trans* configuration. The complexity of the spectra makes it difficult to assign a definite absorption to this or to the N—Sn vibration. However, in the majority of spectra, a single peak, not assigned to the ligands, is present in each of the 407–367 and in the 336–288 cm^{-1} regions, lending support to an all-*trans* configuration. The absorptions assigned to ν_{P-O} in Table 3 represent the expected decreases in frequency on complex formation. The absorption associated with the N—C—N antisymmetric stretching vibration at 1504 cm^{-1} in tetramethylthiourea (19) is shifted to 1555 and 1578 cm^{-1} in the spectra of **9** and **10** respectively; these frequencies compare with 1550 and 1579 cm^{-1} for the corresponding divinyl compounds (3).

Complexes with Bidentate Ligands

The large quadrupole splittings obtained for the 1:1 complexes of diphenyl- and divinyltin diisothiocyanate with B(DPO)E and B(DAO)E reveal *trans* C—Sn—C bonds in these complexes, in contrast to *cis* C—Sn—C bonds in complexes with *o*-phenanthroline and 2,2-bipyridyl (2, 3). These two sets of complexes differ not only in the nature of the donor atoms, but in having seven-membered and five-membered chelate rings, respectively. It is of interest to study complexes of $R_2Sn(NCS)_2$ with bidentate ligands having one oxygen and one nitrogen donor atom; attempts at synthesis of such complexes are underway in these laboratories. The absorptions associated with the PO stretching vibrations in the B(DPO)E complexes listed in Table 3 compare with 1185 cm^{-1} for pure B(DPO)E (12).

The similarity in the Mössbauer parameters of compounds **19** and **23**, and of **21** and **24**, indicate a negligible difference between the effects of the seven-membered ring in the B(DAO)E complexes and the six-membered ring in the B(DAO)M complexes. The relative quadrupole splittings for **14** and **19**, and for **18** and **22**, indicate a greater electron release by the AsO than by the PO donor groups, as in the complexes of the monodentate ligands.

The relative values of the quadrupole splittings for Ph_2SnCl_2·DIARS, 3.07 cm^{-1} and Ph_2SnCl_2·B(DP)E, 3.27 cm^{-1}, indicate the expected greater electron release by the arsenic than by the phosphorus donor atoms, and signficantly greater electron release than by the AsO and PO groups. The similar isomer shifts for the DIARS and B(DP)E complexes may indicate a greater tin s-character for the Sn—As bond, resulting in a decreased tin s-character for the Sn—C bond in the DIARS complex.

$BipyO_2$ forms a 1:2 complex with $Bu_2Sn(NCS)_2$, **13**. The shift in the absorptions associated with the NO stretching vibrations from 1262 and 1255 cm^{-1} in $bipyO_2$ (20) to 1218 and 1200 cm^{-1} in the spectrum of the complex indicates the formation of O → Sn dative bonds. The composition requires a bridging $bipyO_2$ ligand. The presence of two approximately equal absorptions in the antisymmetric NCS stretching region, at 2070 and 2040 cm^{-1}, indicate that half the NCS groups are bridging and half terminal. This implies polymerization with six-coordination for each tin atom. The 2070 cm^{-1} absorption compares to about 2100 cm^{-1} for Sn—NCS—Sn bridging in solid $R_2Sn(NCS)_2$ compounds and suggests a weaker S—Sn bond in **13**, likely associated with steric effects. The large quadrupole splitting, 4.02 cm^{-1} (which compares with 4.07 for $Me_2Sn(NCS)_2$·$bipyO_2$ (5)), indicates *trans* C—Sn—C bonds. The values of δ and ΔE_Q for **13** are intermediate between those for bridged $Bu_2Sn(NCS)_2$ and unbridged $Bu_2Sn(NCS)_2$·bipy (2). We have obtained a 1:1 complex of $Vin_2Sn(NCS)_2$ with $bipyO_2$ for which the infrared spectrum in the C—Sn stretching region (3) indicates *trans* C—Sn—C bonds. The composition, the NO frequencies at 1205 and 1220 cm^{-1}, and the single NCS absorption at 2040 cm^{-1} indicate a bridged dimer for $[Ph_2Sn(NCS)_2]_2$·$bipyO_2$, **12**, with five-coordination for each tin atom.

The financial assistance of the National Research Council of Canada and the generous cooperation of Dr. M. Falk of the Atlantic Regional Laboratory in Halifax are gratefully acknowledged. Special thanks are due to Dr. W. Lieper and his research assistants of the Physics Department, to Dr. O. Knop of the Chemistry Department of Dalhousie for the use of their Mössbauer facilities and computer programs, and to E. Nelson of Mount St. Vincent University for technical assistance with the monodentate ligand work. We are also grateful to the Radiation Laboratory for the use of their Mössbauer and computer facilities for the bidentate ligand portion of the study. The Radiation Laboratory is operated by the University of Notre Dame under contract with the U.S. Energy Research and Development Administration; this is ERDA Document No. C00-38-1003.

1. M. A. Mullins and C. Curran. Inorg. Chem. **6**, 2017 (1967).
2. M. A. Mullins and C. Curran. Inorg. Chem. **7**, 2584 (1968).
3. D. V. Naik and C. Curran. J. Organomet. Chem. **81**, 177 (1974).
4. D. V. Naik, J. C. May, and C. Curran. J. Coord. Chem. **2**, 309 (1973).
5. G. M. Bancroft, V. G. K. Das, and K. D. Butler. J. Chem. Soc. Dalton, 2355 (1974).
6. J. H. Holloway, G. P. McQuillan, and D. S. Ross. J. Chem. Soc. A, 1935 (1971).
7. F. P. Mullins. Can. J. Chem. **49**, 2719 (1971).
8. P. G. Simpson, A. Vinciguerra, and J. V. Quagliano. Inorg. Chem. **2**, 282 (1963).
9. R. S. Nyholm and A. Turco. J. Chem. Soc. 1121 (1962).
10. S. S. Sandhu and S. S. Sandhu. J. Inorg. Nucl. Chem. **31**, 1363 (1969).
11. P. Gans and B. C. Smith. J. Chem. Soc. 4172 (1964).
12. B. J. Brisdon. J. Chem. Soc. Dalton, 2247 (1972).

13. C. CURRAN, P. A. MCCUSKER, and H. S. MAKOWSKI. J. Am. Chem. Soc. **79**, 5188 (1957).
14. G. K. ESTOK. J. Chem. Educ. **39**, 478 (1962).
15. K. HIGASHI, H. TAKAHASHI, and M. NAKAMURA. Mem. School Sci. Eng. Waseda Univ. **37**, 91 (1973).
16. K. HIGASI. Bull. Inst. Phys. Chem. Res. Tokyo, **22**, 805 (1943).
17. E. CLAEYS, G. VAN DER KELEN, and Z. EECKHAUT. Bull. Soc. Chim. Belg. **70**, 462 (1961).
18. A. L. MCCLELLAN. Tables of experimental dipole moments, Vol. 2. Rahara Enterprises, El Cerrito, Cal. 1974. pp. 663, 665.
19. M. SCHAFER and C. CURRAN. Inorg. Chem. **5**, 265 (1966).
20. A. VINCIGUERRA, P. G. SIMPSON, Y. KAKIUTI, and J. V. QUAGLIANO. Inorg. Chem. **2**, 286 (1963).

Apparent Molal Volumes and Heat Capacities of Tetrabutylammonium Bromide in Aqueous Electrolyte Solutions

NICOLE DESROSIERS AND JACQUES E. DESNOYERS[1]

Department of Chemistry, Université de Sherbrooke, Sherbrooke, Quebec J1K 2R1

Received April 30, 1975

NICOLE DESROSIERS and JACQUES E. DESNOYERS. Can. J. Chem. **53**, 3206 (1975).

The apparent molal volumes and heat capacities of Bu_4NBr were measured in aqueous solutions of NaF, NaCl, NaBr, KBr, NaAc, and NH_4Ac at 25 °C with a flow densimeter and a flow microcalorimeter. The derived transfer functions of Bu_4NBr from water to the electrolyte solutions, after correction for the long-range coulombic forces, are all negative. This suggests that the noncoulombic interactions between hydrophobic and hydrophilic ions result in negative contributions to volumes and heat capacities.

NICOLE DESROSIERS et JACQUES E. DESNOYERS. Can. J. Chem. **53**, 3206 (1975).

Les capacités calorifiques et les volumes apparents molaires de Bu_4NBr ont été mesurés dans les solutions aqueuses de NaF, NaCl, NaBr, KBr, NaAc et NH_4Ac à 25 °C au moyen d'un microcalorimètre et d'un densimètre digital à écoulement continu. Les capacités calorifiques et les volumes de transfert de Bu_4NBr de l'eau aux solutions électrolytiques, dérivés à partir de ces données et corrigés pour les forces coulombiennes à longue portée, sont tous négatifs. Ceci suggère que les interactions non-coulombiennes entre un ion hydrophobe et un ion hydrophile contribuent négativement aux volumes et aux capacités calorifiques.

Introduction

The studies of aqueous mixed electrolyte solutions are usually aimed at a better understanding of the specific ion interactions in solutions (1). As seen from the recent review of Anderson and Wood (2), most of the thermodynamic functions of mixing of the electrolytes were measured on common ion mixtures at constant ionic strength. Using Friedman's nomenclature (3), the maximum free energy of mixing of the electrolytes MX and NX is characterized by the parameter

$$[1]\quad g_0 = (B_{MN} - B_{MM} - B_{NN}) + I(B_{MNX} - B_{MMX} - B_{NNX})$$

where the B's are the cluster integrals representing the various pair and triplet interactions between ions and I is the ionic strength. Similar equations can be written for the other thermodynamic functions of mixing.

The mixing functions involving tetraalkylammonium halides are of particular interest since the larger members of this family of electrolytes are hydrophobic. The free energies (4), enthalpies (5), and volumes (6) of mixing are vastly different in magnitude and sign from the mixing of inorganic electrolytes. For example, Wood and Anderson (5) find that the heats of mixing of two structure breakers are usually endothermic while those of structure breakers with hydrophobic electrolytes are large and exothermic. These functions of mixing are reflecting primarily the decrease in the hydrophobic–hydrophobic interactions due to a dilution effect and do not give us much information on the interactions between hydrophobic and hydrophilic ions. To overcome this difficulty, it is often preferable to measure the standard functions of transfer of hydrophobic electrolytes from water to aqueous electrolyte solutions. Keeping the hydrophobic electrolyte near infinite dilution and varying the concentration of the hydrophilic electrolyte, it should be possible to see the importance of increasing hydrophobic–hydrophilic interactions. Such measurements were made by Cassel and Wen (7) for the transfer free energies, enthalpies, and entropies of tetraalkylammonium bromides from water to aqueous urea solutions and by Ahluwalia and co-workers for the enthalpies of transfer of the larger tetraalkylammonium bromides from water to aqueous electrolyte solutions (8). From the temperature dependence of these enthalpies of transfer it is possible to derive the corresponding heat capacities of transfer (8), but this method is not always sufficiently precise to determine unambiguously the dependence of the heat capacities of transfer on the electrolyte concen-

[1]To whom correspondence should be addressed.

Can. J. Chem. Downloaded from www.nrcresearchpress.com by 210.87.254.40 on 09/05/12
For personal use only.

Can. J. Chem. Downloaded from www.nrcresearchpress.com by 210.87.254.40 on 09/05/12
For personal use only.

tration and its specificity with various electrolytes.

We therefore felt it would be useful to measure the heat capacities and volumes of transfer of Bu_4NBr from water to aqueous electrolyte solutions from specific heat and density data.

Experimental

The origin of and the purification procedure for alkali halides (9) and Bu_4NBr (10) have been given elsewhere. The ammonium and sodium acetates (NH_4Ac and NaAc) (Fisher Certified) were dried under vacuum for about 36 h at 50 °C. The NH_4Ac solutions were prepared under nitrogen atmosphere, and the densities of the solutions were found to be identical, within experimental uncertainty, to those obtained with solutions prepared from the freeze-dried salt (11). All solutions were prepared by weight with deionized distilled water (Continental Deionized Water System) and the concentrations expressed in molalities, *i.e.*, number of moles of solute per kg of solvent (or mixed solvent). The general technique and instrumentation used for density (12) and heat capacity (13) measurements have been described elsewhere.

Results

The apparent molal volumes ϕ_V and heat capacities ϕ_C of Bu_4NBr in the electrolyte solutions were calculated in the usual manner (14) from the experimental densities and volumetric specific heats considering the mixture (water + electrolyte) as the solvent. Combining these results (15) with the corresponding ones in pure water (16, 17), the standard functions Y of transfer from water (W) to an electrolyte solution (W + E) can be derived:

$$[2]\quad \Delta\overline{Y}^0_{Bu_4NBr}(W \rightarrow W + E) = \overline{Y}^0(W + E) - \overline{Y}^0(W)$$

These standard partial molal functions would normally be obtained by extrapolation of the ϕ_Y data to infinite dilution. However, we have found that even the transfer functions of Bu_4NBr from water to 11.4 m ammonium acetate were the same, within experimental uncertainty, for Bu_4NBr concentrations of 0.05 and 0.1 m. Therefore all measurements were made at 0.1 m Bu_4NBr, and the transfer functions were assumed to be equal to those at infinite dilution.

Contrary to the mixing functions at constant ionic strength, the transfer functions are influenced by the long-range coulombic forces; Bu_4NBr is dilute but not the added electrolyte. Since we are primarily interested in the more specific noncoulombic interactions, it would be preferable, if possible, to correct the data for the long-range coulombic forces. This can be achieved by subtracting from each ϕ_V or ϕ_C the contribution from the limiting Debye–Hückel law at 25 °C; for ϕ_V in $cm^3\ mol^{-1}$ and ϕ_C in $J\ K^{-1}\ mol^{-1}$ these terms are respectively 1.868 $(d_0I)^{1/2}$ (18) and 28.99 $(d_0I)^{1/2}$ (16) where d_0 is the density of the pure solvent. These corrections are of course exact only at very low concentrations, but they are still useful in showing the correct initial trends in the transfer functions.

The corrected standard transfer volumes $\Delta\overline{V}^*_{Bu_4NBr}(W \rightarrow W + E)$ and heat capacities $\Delta\overline{C}^*_{Bu_4NBr}(W \rightarrow W + E)$ are shown in Figs. 1 and 2 for the systems where the cosolvents are NaF, NaCl, NaBr, KBr, NaAc, and NH_4Ac. The corresponding apparent molal quantities of the binary system can be represented as a function of the molality by

$$[3]\quad \phi_Y = \phi_Y^0 + A_Y(d_0m)^{1/2} + B_Ym + \ldots$$

where A_Y is the slope of the limiting Debye–Hückel theory. The functions $\phi_Y - \phi_Y^0 - A_Y(d_0m)^{1/2}$ are plotted against m in Fig. 3. At low concentrations, these results agree well with those previously published for alkali halides (9, 19), sodium and ammonium acetates (11).

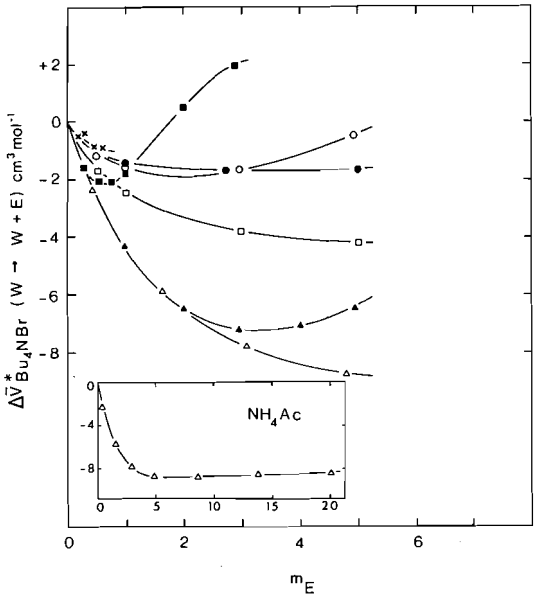

FIG. 1. Volumes of transfer of Bu_4NBr from water to aqueous electrolyte solutions at 25 °C, corrected for the long-range Debye–Hückel forces. ×, NaF; ○, NaBr; ●, KBr; □, NaCl; ▲, NaAc; △, NH_4Ac; ■, $\Delta\overline{V}^*_{NaAc}$ (W → W + Bu_4NBr).

Can. J. Chem. Downloaded from www.nrcresearchpress.com by 210.87.254.40 on 09/05/12
For personal use only.

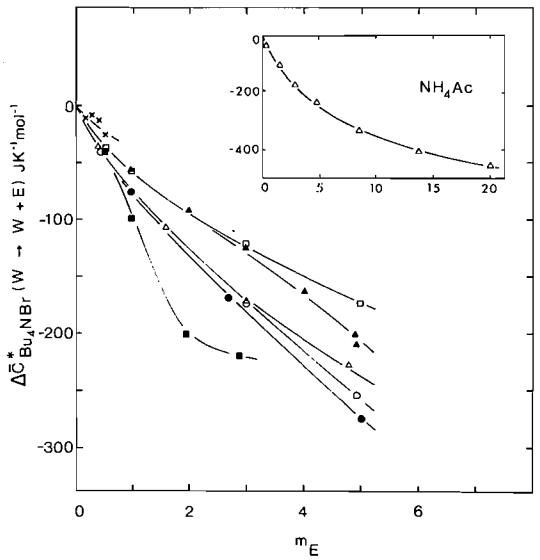

FIG. 2. Heat capacities of transfer of Bu_4NBr from water to aqueous electrolyte solutions at 25 °C, corrected for the long-range Debye–Hückel forces. ×, NaF; □, NaCl; ▲, NaAc; △, NH_4Ac; ○, NaBr; ●, KBr; ■, △ $\bar{C}^*_{NaAc}$ (W → W + Bu_4NBr).

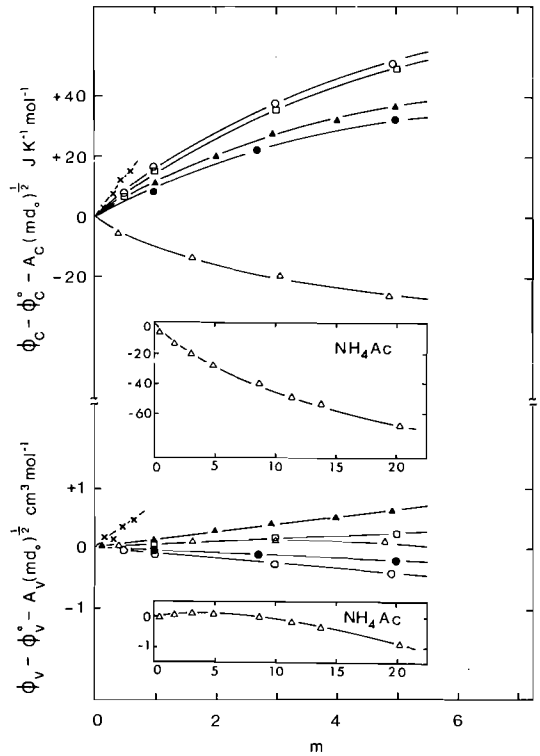

FIG. 3. Apparent molal volumes and heat capacities of the electrolytes in water at 25 °C. ×, NaF; ○, NaBr; □, NaCl; ▲, NaAc; ●, KBr; △, NH_4Ac.

In order to distinguish between pair and triplet interactions in the ternary systems, the complementary transfer functions $\Delta \bar{Y}^*_{NaAc}$(W → W + Bu_4NBr) were also measured and are shown in Figs. 1 and 2.

Discussion

The observed $\Delta \bar{Y}^*_{Bu_4NBr}$(W → W + E), corrected for the Debye–Hückel interactions, are all negative at low concentrations. There have been two main approaches to the interpretation of the transfer functions of electrolytes from water to binary systems: the binary system may be considered a uniform medium less structured or more structured than water or the ternary system can be interpreted in terms of solute–solute interactions.

The first approach can be exemplified with urea as a cosolvent. The transfer functions to urea solutions, $\Delta \bar{Y}^0_{Bu_4NBr}$(W → W + urea) all tend to level off at high concentration and their signs are opposite those we would expect for the hydration function of Bu_4NBr (20). If most of the hydration of Bu_4NBr is assumed to be structural in origin, *i.e.* if it depends on the long-range structure of water, then we can interpret the data in terms of the urea–water mixture being a less-structured medium than pure water (21, 22).

The uniform solvent approach fails if the cosolvent is hydrophobic or if it is an hydrophilic electrolyte. The enthalpy of transfer $\Delta \bar{H}^0_{Bu_4NBr}$(W → W + *tert*-butyl alcohol) is positive (23), while a negative value is predicted if a *tert*-butyl alcohol solution is assumed to be more structured than pure water at low concentration. Also $\Delta \bar{V}^0_{Bu_4NBr}$(W → W + alkali halide) are negative in contradiction with $\Delta \bar{V}_{Bu_4NBr}$(W → W + urea) (22) if both alkali halides and urea are assumed structure breakers. Finally, the lack of correlation between the ternary (Figs. 1 and 2) and binary systems (Fig. 3) seems to exclude this model as being generally applicable.

The solute–solute approach seems more promising. The present transfer functions can be interpreted in a way similar to the ternary system electrolyte–nonelectrolyte–water (24, 25). The cosolvent concentration dependence of the general transfer functions, corrected for the long-range coulombic forces, is given by

$$[4]\quad \frac{d}{dm_E}\{\Delta \bar{Y}^*_{Bu_4NBr}(W \rightarrow W + E)\} = \sum B_{ij} + m_E \sum B_{ijj} + \ldots$$

Can. J. Chem. Downloaded from www.nrcresearchpress.com by 210.87.254.40 on 09/05/12
For personal use only.

where the B's are interaction parameters between pairs, triplets, etc. At low cosolvent concentrations where only pair interactions are important $\sum B_{ij}$ should be equal to $\sum B_{ji}$ (24). It therefore follows that if the reference electrolyte is at infinite dilution

$$[5]\quad \frac{d}{dm_E}\{\Delta \bar{Y}^*_{Bu_4NBr}(W \rightarrow W + E)\} = \frac{d}{dm_{Bu_4NBr}}\{\Delta \bar{Y}_E^*(W \rightarrow W + Bu_4NBr)\}$$

This is in fact observed in the case of NaAc; it therefore seems that the transfer functions of electrolytes at 0.1 m are not too different from the standard values.

Neglecting the self interactions of Bu_4NBr in comparison with the mixed interactions, there is a total of four pair interactions responsible for the observed initial slopes: Bu_4N^+–X^-, Bu_4N^+–M^+, Br^-–M^+, and Br^-–X^-. The magnitude of the interactions between hydrophilic ions can be predicted from the excess functions of alkali halides (9, 19). Up to 1 m, ϕ_V and ϕ_C can be represented by [3] where B_Y is a measure of all the interactions in excess to the Debye–Hückel ones. With alkali halides, these B_Y parameters are in general an order of magnitude smaller than $\sum B_{ij}$ of the ternary system. Therefore, the pair interactions Br^-–M^+ and Br^-–X^- cannot be too important in comparison with the ones involving Bu_4N^+. An examination of Fig. 1 also shows that, in general, changing the anion of the electrolyte MX has a larger effect than changing the cation. This is expected from the Brønsted principle (1, 26), which states that specific interactions between like charged particles are less probable than between unlike charged ones. Therefore, it seems that the observed transfer functions of Bu_4NBr from water to an electrolyte solution are primarily reflecting interactions between hydrophobic and hydrophilic ions of opposite signs, and these interactions are negative for both volumes and heat capacities.

The signs of the specific hydrophobic–hydrophilic pair interactions between ions are the same as those observed between nonelectrolytes and hydrophilic ions. Ben-Naïm and Egel-Thal (27) and Tiepel and Gubbins (28) have measured the transfer functions of argon from water to aqueous electrolyte solutions and their results suggest that the hydrophobic–hydrophilic parameters are positive for free energies, enthalpies, and entropies and negative for volumes. Desnoyers *et al.* (24) also measured similar transfer enthalpies, volumes, and heat capacities of *tert*-butyl alcohol from water to electrolyte solutions and found endothermic interactions for enthalpies and negative volumes and heat capacities for the transfer to hydrophilic electrolyte solutions. They have also measured transfer volumes of *tert*-butyl alcohol from water to water + Bu_4NBr mixtures. They have observed a minimum, the values being initially negative and becoming positive around 2 m Bu_4NBr. Tiepel and Gubbins (28) have measured a positive transfer volume of argon from water to an aqueous solution of Bu_4NBr at approximately 2 m. As they do not have results at lower concentrations, it is impossible to know if the transfer of argon also shows a minimum at low concentration of Bu_4NBr. It is important to note that while hydrophobic–hydrophilic and hydrophobic–hydrophobic interactions seem to have the same sign for volumes and enthalpies, they seem to have opposite ones for heat capacities; the interactions between two strongly hydrophobic solutes lead to a positive contribution to the concentration dependence of the heat capacity (14, 20, 24). While the signs of these interactions are now fairly well established, there is not, to our knowledge, any simple model that can account for all these trends.

The volumes of transfer seem to be much more specific to the nature of the anion than the heat capacities of transfer. In some cases the origin of the specificity is obvious. For example, in the transfer functions $\Delta\bar{Y}^*_{NaAc}(W \rightarrow W + Bu_4NBr)$, the deviations from linearity are in the direction of hydrophobic bonding. In the vicinity of hydrophobic ions, Bu_4N^+ will have a stronger tendency to associate, and this association results in an increase in volume and decrease in heat capacity (14). No such association is possible with NaAc and the transfer functions $\Delta\bar{Y}^*_{Bu_4NBr}$ $(W \rightarrow W + NaAc)$ are linear to much higher concentrations.

At very high concentration, $\Delta\bar{Y}^*_{Bu_4NBr}(W \rightarrow W + E)$ must be tending to $\Delta\bar{Y}^*_{Bu_4NBr}(W \rightarrow E)$, where E represents the hypothetical molten electrolyte at 25 °C. It therefore seems that in a molten salt ϕ_C^0 of Bu_4NBr would be much less positive than in pure water. This is not unexpected if we consider that the three-dimensional structure of water, which is responsible for the high heat capacity of Bu_4NBr, is no longer present. The sign of $\Delta\bar{V}^*_{Bu_4NBr}(W \rightarrow E)$ is less

obvious since this function is also sensitive to geometrical factors and coulombic interactions in addition to structural effects. It does not seem possible at present to draw any unambigous relation between the order of the transfer functions at high cosolvent concentration and the properties of the cosolvent electrolyte.

We are grateful to the Defence Research Board of Canada for financial assistance. N.D. would also like to thank the National Research Council of Canada for the award of a scholarship.

1. H. S. HARNED and R. A. ROBINSON. Multicomponent electrolyte solutions. Pergamon Press, New York. 1968.
2. H. L. ANDERSON and R. H. WOOD. *In* Water, a comprehensive treatise, Vol. 3. *Edited by* F. Franks. Plenum Press, New York. 1973.
3. H. L. FRIEDMAN. J. Chem. Phys. **32**, 1134 (1960); H. L. FRIEDMAN, Ionic solution theory, Interscience, New York. 1962.
4. W.-Y. WEN, K. MIYAJIMA, and A. OTSUKA. J. Phys. Chem. **75**, 2148 (1971).
5. R. H. WOOD and H. L. ANDERSON. J. Phys. Chem. **71**, 1871 (1967); J. S. FALCONE, JR., A. S. LEVINE, and R. H. WOOD. J. Phys. Chem. **77**, 2137 (1973).
6. W.-Y. WEN and K. NARA. J. Phys. Chem. **71**, 3907 (1967); **72**, 1137 (1968); W.-Y. WEN, K. NARA, and R. H. WOOD. J. Phys. Chem. **72**, 3048 (1968).
7. R. B. CASSEL and W.-Y. WEN. J. Phys. Chem. **76**, 1369 (1972).
8. T. S. SARMA and J. C. AHLUWALIA. J. Phys. Chem. **76**, 1366 (1972); B. CHAWLA and J. C. AHLUWALIA. J. Phys. Chem. **76**, 2582 (1972); B. CHAWLA, S. SUNDER, and J. C. AHLUWALIA. J. Phys. Chem. **77**, 2335 (1973); J. C. AHLUWALIA and B. CHAWLA. J. Chem. Soc. Faraday Trans. I, **69**, 434 (1973).
9. J. E. DESNOYERS, M. AREL, G. PERRON, and C. JOLICOEUR. J. Phys. Chem. **73**, 3346 (1969).
10. B. E. CONWAY, R. E. VERRALL, and J. E. DESNOYERS. Trans. Faraday Soc. **62**, 2738 (1966).
11. P. A. LEDUC and J. E. DESNOYERS. Can. J. Chem. **51**, 2993 (1973).
12. P. PICKER, E. TREMBLAY, and C. JOLICOEUR. J. Solution Chem. **3**, 377 (1974).
13. P. PICKER, P. A. LEDUC, P. R. PHILIP, and J. E. DESNOYERS. J. Chem. Thermodyn. **3**, 631 (1971).
14. L. AVÉDIKIAN. G. PERRON, and J. E. DESNOYERS. J. Solution Chem. **4**, 331 (1975).
15. N. DESROSIERS. Ph.D. Thesis, Université de Sherbrooke, Sherbrooke, Québec. In preparation.
16. P. R. PHILIP and J. E. DESNOYERS. J. Solution Chem. **1**, 353 (1972).
17. G. PERRON and J. E. DESNOYERS. J. Chem. Eng. Data, **17**, 136 (1972).
18. O. REDLICH and D. M. MEYER. Chem. Rev. **64**, 221 (1964).
19. J. L. FORTIER, P. A. LEDUC, and J. E. DESNOYERS. J. Solution Chem. **3**, 323 (1974).
20. G. PERRON, N. DESROSIERS, and J. E. DESNOYERS. In preparation.
21. N. DESROSIERS, G. PERRON, J. G. MATHIESON, B. E. CONWAY, and J. E. DESNOYERS. J. Solution Chem. **3**, 789 (1974).
22. P. R. PHILIP, J. E. DESNOYERS, and A. HADE. Can. J. Chem. **51**, 187 (1973).
23. R. K. MOHANTY, T. S. SARMA, S. SUBRAMANIAN, and J. C. AHLUWALIA. Trans. Faraday Soc. **67**, 305 (1971).
24. J. E. DESNOYERS, G. PERRON, J. P. MOREL, and L. AVÉDIKIAN. *In* Chemistry and physics of aqueous gas solutions. *Edited by* W. A. Adams, Electrochemical Society, Princeton. 1975.
25. F. L. WILCOX and E. E. SCHRIER. J. Phys. Chem. **75**, 3757 (1971).
26. J. N. BRØNSTED. J. Am. Chem. Soc. **44**, 877, 938 (1922); **45**, 2898 (1923).
27. A. BEN-NAÏM and M. EGEL-THAL. J. Phys. Chem. **69**, 3250 (1965).
28. E. W. TIEPEL and K. E. GUBBINS. J. Phys. Chem. **76**, 3044 (1972).

Can. J. Chem. Downloaded from www.nrcresearchpress.com by 210.87.254.40 on 09/05/12
For personal use only.

Reaction of Hydrazonyl Halides with Derivatives of Thiourea and Thiosemicarbazide; A New Source of *C*-Amino- and *C*-Hydrazino-1,2,4-triazoles

PEDER WOLKOFF

Department of General and Organic Chemistry, University of Copenhagen, H. C. Ørsted Institute, Universitetsparken 5, DK-2100 Copenhagen, Denmark[1]

AND

STEVEN T. NEMETH AND MARTIN S. GIBSON[2]

Department of Chemistry, Brock University, St. Catharines, Ontario L2S 3A1

Received April 23, 1975

PEDER WOLKOFF, STEVEN T. NEMETH, and MARTIN S. GIBSON. Can. J. Chem. **53**, 3211 (1975).

Reaction of hydrazonyl halides with (substituted) thioureas and thiosemicarbazides gives mainly 1,3,4-thiadiazolines, the stronger base being preferentially eliminated in the process. Similar reactions in presence of triethylamine give *C*-amino- and *C*-hydrazino-1,2,4-triazoles, respectively, together with the hydrazonyl sulfide.

Potassium cyanide cleavage of a hydrazonyl disulfide gives the corresponding 1,3,4-thiadiazoline and thiohydrazide.

PEDER WOLKOFF, STEVEN T. NEMETH et MARTIN S. GIBSON. Can. J. Chem. **53**, 3211 (1975).

La réaction des halogénures d'hydrazonyle avec des thiourées et des thiosemicarbazides (substituées) conduit principalement au thiadiazolines-1,3,4; au cours de ce processus, la base la plus forte est éliminée. Des réactions semblables effectuées en présence de triéthylamine donnent respectivement des *C*-amino et des *C*-hydrazinotriazoles-1,2,4 aux côtés de sulfure d'hydrazonyle.

La rupture d'un disulfure d'hydrazonyle par le cyanure de potassium conduit à la thiohydrazide et à la thiadiazoline-1,3,4 correspondante.

[Traduit par le journal]

Reaction of hydrazonyl halide **1***a* with phenylthiourea in ethanol in presence of excess triethylamine (molar ratio 2:1:4) was found to give the hydrazonyl sulfide **4***a* in high (88%) yield, contrasting markedly with the formation of 5-phenylimino-2,4-diphenyl-1,3,4-thiadiazoline (**6***a*), when **1***a* and phenylthiourea (molar ratio 1:1) were refluxed together in ethanol (1); see eq. 1. The significant difference in reaction course led us to reexamine and extend the previous work by Fusco on the reaction of hydrazonyl halides (**1**) with various derivatives of thiourea and thiosemicarbazide (1, 2).

[1] $PhCCl{=}NNHPh + PhNHCSNH_2$

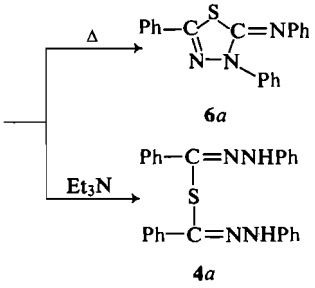

The two hydrazonyl halides **1***a* and *b* used in this study together with products isolated are depicted in Scheme 1 and the results of the reactions examined are summarized in Table 1.

The reactions performed in refluxing ethanol reveal two general trends: (*i*) the products isolated are all 1,3,4-thiadiazolines, (*ii*) the least basic part of the sulfur nucleophile (Base–C(S)–Base′) remains in the cyclic product (*cf.* Table 1). These results may be rationalized in terms of a sulfur attack at the α carbon atom in **1** with displacement of the halogen, exemplified in eq. 2 with **1***a* and 4-phenyl-3-thiosemicarbazide, to give a hydrazonylated adduct, which undergoes ring closure; elimination of hydrazine, followed by deprotonation then affords **6***a*. The base elimination step follows principally the sequence $NH_3 > NH_2NH_2 > PhNHNH_2 > PhNH_2$ according to the decreasing order of base strength; in reaction 2, hydrazine is preferred over aniline as the leaving base. Normally the eliminated base

[1]Address for correspondence.

[2]Sabbatical leave 1974–1975; University of California, Berkeley, California, U.S.A.

Can. J. Chem. Downloaded from www.nrcresearchpress.com by 210.87.254.40 on 09/05/12
For personal use only.

Can. J. Chem. Downloaded from www.nrcresearchpress.com by 210.87.254.40 on 09/05/12
For personal use only.

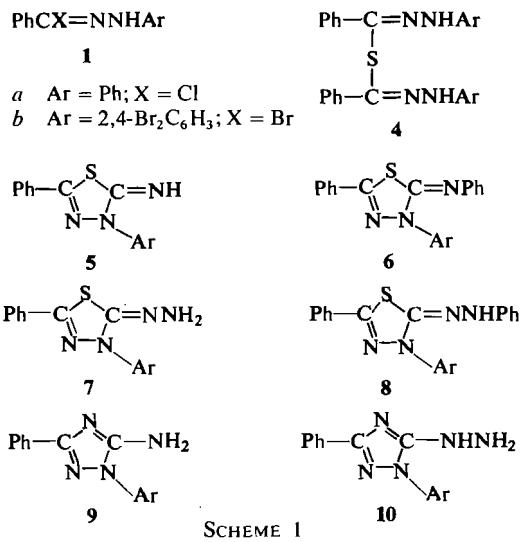

SCHEME 1

[2] $PhCCl{=}NNHPh + PhNHCSNHNH_2 \xrightarrow{-Cl^-}$ (1a)

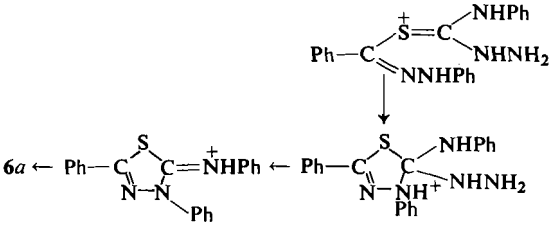

functions as the deprotonating agent but in the reaction of **1***a* with 1,4-diphenylthiosemicarbazide, the eliminated phenylhydrazine is apparently not sufficiently strong for this purpose as **6***a* was isolated as the hydrochloride from this reaction.

Similar experiments (see Table 1) were conducted in the presence of excess triethylamine (4 equiv.) and the general products were found to be the hydrazonyl sulfide (**4**) and a 1,2,4-triazole (**9** and **10**). Thus reacting **1***a* with thiourea in ethanol in presence of triethylamine (molar ratio 2:1:4) gave **4***a* (21%) and 5-amino-1,3-diphenyl-1,2,4-triazole (**9***a*) (59%); see eq. 3. These results

[3] $PhCCl{=}NNHPh + NH_2CSNH_2 \xrightarrow{Et_3N}$ (1a)

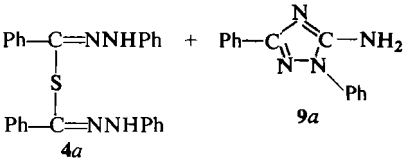

may be interpreted in terms of two competitive reactions, one leading to **4** and one to **9** (or **10**, in the case of thiosemicarbazide), via a common intermediate. Hydrogen sulfide abstraction from thiourea by the reactive nitrilimine (**2***a*), formed *in situ* by dehydrochlorination of **1***a* with triethylamine (3), produces a thiohydrazide (**3***a*) and cyanamide (eqs. 4 and 5); **3***a* then becomes the source of **4***a* (eqs. 6–9) by processes already discussed (4).

[4] $PhCCl{=}NNHPh \xrightarrow[-HCl]{Et_3N} PhC{\equiv}\overset{+}{N}\bar{N}Ph$ (1a) (2a)

[5] $PhC{\equiv}\overset{+}{N}\bar{N}Ph + NH_2CSNH_2 \longrightarrow PhCSNHNHPh + NH_2C{\equiv}N$ (2a) (3a)

TABLE 1. Reactions examined

Reactant	Hydrazonyl halide	Products (yield %) By refluxing in EtOH	Products (yield %) In presence of Et_3N
NH_2CSNH_2	**1***a*		**4***a* (21) + **9***a* (59)
NH_2CSNH_2	**1***b*	**5***b* (70)*	**4***b* (10) + **9***b* (64)
$PhNHCSNH_2$	**1***a*	**6***a* (24)	**4***a* (88) + $PhNHC{\equiv}N$ (18)*
$PhNHCSNH_2$	**1***b*	**6***b* (46)	**4***b* (66) + **5***b* (21)*
$NH_2CSNHNH_2$	**1***a*	†, 7‡	**4***a* (44) + **10***a* (36)§
$NH_2CSNHNH_2$	**1***b*		**4***b* (14) + **10***b* (31)§
$NH_2CSNHNHPh$	**1***a*	**8***a* (31)	
$PhNHCSNHNH_2$	**1***a*	**6***a* (22)	
$PhNHCSNHNHPh$	**1***a*	**6***a*§	
KSCN	**1***a*	**5***a* (48)	**5***a* (66)
KSCN	**1***b*	**5***b* (98)	**5***b* (66)

*Isolated as benzoyl derivative.
†Six spots on t.l.c.
‡Reference 1.
§Isolated as hydrochloride(bromide).

Can. J. Chem. Downloaded from www.nrcresearchpress.com by 210.87.254.40 on 09/05/12
For personal use only.

[6] $PhC\equiv\overset{+}{N}NPh + PhCSNHNHPh \longrightarrow$ **4***a*

[7] $PhCSNHNHPh + Et_3N \longrightarrow [PhCSNNHPh]^- + Et_3NH^+$

[8] $PhCCl{=}NNHPh + [PhCSNNHPh]^- \longrightarrow$ **4***a*

[9] $PhC\equiv\overset{+}{N}\overset{-}{N}Ph + [PhCSNNHPh]^- \rightarrow$ Ph—C(S—C(Ph)=NN̄Ph)=NNHPh

[10] $PhC\equiv\overset{+}{N}\overset{-}{N}Ph + NH_2C\equiv N \longrightarrow$

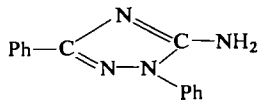

9*a*

A cycloaddition reaction between **2***a* and the cyanamide formed may give **9***a* (eq. 10) in a similar way to the nitrilimine–nitrile reaction to give 1,2,4-triazoles (5). The initial formation of thiohydrazides and cyanamides is supported in some experiments by examination of reaction mother liquors (t.l.c. and mass spectrum); in the reaction between **1***a*, phenylthiourea, and triethylamine, phenylcyanamide was actually recovered after benzoylation as the benzoyl derivative Ph(PhCO)NC≡N.

The competition between these reactions is very favorable to triazole formation with thiourea, but less so with thiosemicarbazide, and so unfavorable with phenylthiourea that no triazole was obtained in the cases examined. In the last cases, hydrazonyl sulfides are the major products and a new process becomes evident which leads (by loss of aniline) to a 1,3,4-thiadiazoline (**5***b*). The former reactions constitute reasonable sources of the triazole derivatives.

Finally the reactions of **1** with KSCN and the hydrazonyl disulfide **11** with KCN were examined. The reaction with KSCN afforded **5**, independently of reaction conditions and with no detection of a hydrazonyl thiocyanate (**1**; X = SCN) (i.r.).[3] Indirect evidence for an intermediate hydrazonyl thiocyanate was found when **4***b* was isolated as a by-product from treatment of **11** with KCN at room temperature in chloroform, the major products being **5***b* and **3***b*. The isolation of **4***b* may be rationalized in terms of heterolytic cleavage of the hydrazonyl S—S bond by action of the cyanide ion, in a similar way to that known for ordinary disulfides (6), to give the thiohydrazide anion and **1** (X = SCN); see eq. 11. Nucleophilic displacement of thiocyanate ion from **1** (X = SCN), before cyclization to **5***b*, by the thiohydrazide anion would then give the sulfide **4***b*. Compound **11** is very easily cleaved by KCN in refluxing acetonitrile to give approximately equal amounts of **3***b* and **5***b*.

[11] Ph—C(S—S—C(Ph)=NNH-2,4-$Br_2C_6H_3$)=NNH-2,4-$Br_2C_6H_3$ + CN^- ⟶ PhC(S⁻)=NNH-2,4-$Br_2C_6H_3$

PhC(SCN)=NNH-2,4-$Br_2C_6H_3$ ⟶ **5***b*

11

This work provides a convenient alternative method for the preparation of *C*-amino- and *C*-hydrazino-1,2,4-triazoles (7).

Experimental

Melting points were determined using a Reichert microscope. Ethanol (EtOH) used was absolute grade. All experiments performed under basic conditions were stirred at least 2 h before the addition of triethylamine (Et_3N).

Reactions with Thiourea

Et_3N (5 ml) was added to a stirred solution of **1***a* (8, 9) (2.30 g, 10.0 mmol) and thiourea (0.38 g, 5.0 mmol) in EtOH (250 ml). After 7 h the solution was concentrated *in vacuo* to *ca.* 50 ml, filtered, and the solid washed carefully with water to give **4***a* (0.41 g, 21%), m.p. 161–162 °C (lit. (4) 158–160 °C) (0.24 g after crystallization from benzene; identified by i.r. spectrum (4)). The ethanolic filtrate was evaporated and the residue was dissolved in benzene (20 ml). Addition of aqueous HCl (20 ml; 4 *M*) afforded a precipitate which was collected and washed with ether to give a white solid (1.32 g). This was stirred in concentrated ammonia (15 ml) for 30 min, filtered, and dried. Crystallization from benzene–hexane (1:1) gave **9***a* (0.70 g, 59%), m.p. 149–151 °C (after recrystallization, m.p. 149–151 °C); mass spectrum *m/e* 236 (M^+).

Anal. Calcd. for $C_{14}H_{12}N_4$: C, 71.17; H, 5.12; N, 23.71. Found: C, 70.93; H, 5.05; N, 24.15.

[3]Recently the synthesis of 5-imino-2-benzoyl-4-aryl-1,3,4-thiadiazolines by reacting aroylhydrazonyl halides with KSCN has been reported (13).

Can. J. Chem. Downloaded from www.nrcresearchpress.com by 210.87.254.40 on 09/05/12
For personal use only.

The benzene – aqueous HCl filtrate was separated and the benzene layer washed with water, dried, and evaporated; t.l.c. showed one main spot corresponding to **3***a* (4).

Compound **1***b* (10) (4.33 g, 10.0 mmol) and thiourea (1.52 g, 20.0 mmol) were refluxed together in EtOH (25 ml) for 1 h. The solution was filtered and evaporated; dissolution in $CHCl_3$, washing (aqueous NaOH, water), drying and evaporation gave an oil. A mass spectrum showed *m/e* 413, 411, 409 consistent with the formation of **5***b*. The oil was treated with benzoyl chloride (2 ml) in pyridine (20 ml) for 30 min and the mixture was then poured into EtOH (50 ml), stirred, and filtered to give 5-(*N*-benzoylimino)-2-phenyl-4-(2,4-dibromophenyl)-1,3-4-thiadiazoline (3.58 g, 70%), m.p. 201–202 °C (lit. (2) 198 °C).

Compound **1***b* (10.0 mmol), thiourea (0.38 g, 5.0 mmol), and Et_3N (5 ml) were stirred together in EtOH (300 ml) for 3 days. Filtration afforded **4***b* (0.27 g, 7%), m.p. 193–196 °C. Addition of water precipitated a further quantity (0.14 g) of **4***b* contaminated with **9***b* (mass spectrum). The ethanol–water filtrate was extracted with $CHCl_3$ and the chloroform phase was worked-up. Crystallization from benzene afforded **9***b* (1.26 g, 64%), m.p. 221–222 °C; mass spectrum *m/e* 396, 394, 392 (M^+).

Anal. Calcd. for $C_{14}H_{10}Br_2N_4$: C, 42.67; H, 2.56; N, 14.21. Found: C, 42.82; H, 2.73; N, 13.76.

Reactions with Phenylthiourea

Compound **1***a* (1.15 g, 5.0 mmol) and phenylthiourea (0.76 g, 5.0 mmol) were refluxed together in EtOH (25 ml) for 1 h. The solution was chilled overnight (refrigerator) and filtered. Two crystallizations from ether gave **6***a* (0.40 g, 24%), m.p. 113–116 °C (lit. (1) 122 °C); mass spectrum *m/e* 329 (M^+).

Compound **1***a* (4.60 g, 20.0 mmol), phenylthiourea (1.52 g, 10.0 mmol), and Et_3N (10 ml) were stirred together in EtOH (200 ml) for 6 h. Filtration and careful washing with water gave **4***a* (3.70 g, 88%), m.p. 162–164 °C (after crystallization from benzene 3.13 g (75%), m.p. 162–164 °C (corr.); identified by i.r. spectrum). The ethanolic filtrate was evaporated, the residue was dissolved in benzene, and the solution washed with water, dried (Na_2SO_4), and evaporated. The residual oil was treated with benzoyl chloride (1 ml) in pyridine (10 ml) for 30 min and the mixture was poured into water whereupon an oil deposited. The aqueous phase discarded. Addition of EtOH afforded a white solid which crystallized from EtOH to give *N*-benzoyl-*N*-phenylcyanamide (0.40 g, 18%), m.p. 122–125 °C; ν_{max} 2240 (C≡N) and 1730 cm^{-1} (C=O); mass spectrum *m/e* 222 (M^+).

Anal. Calcd. for $C_{14}H_{10}N_2O$: C, 75.65; H, 4.54; N, 12.61. Found: C, 75.68; H, 4.06; N, 12.44.

Compound **1***b* (2.16 g, 5.0 mmol) and phenylthiourea (0.76 g, 5.0 mmol) were refluxed together in EtOH (25 ml) for 1 h. An oil separated on cooling; the ethanol phase was discarded and the oil dissolved in ether, filtered, and left at room temperature for evaporation. Crystallization from ethanol–chloroform (2:1) afforded **6***b* (1.12 g, 46%), m.p. 111–117 °C (lit. (1) 116 °C); mass spectrum *m/e* 487, 485, 483 (M^+).

Compound **1***b* (4.32 g, 10.0 mmol), phenylthiourea (0.76 g, 5.0 mmol) and Et_3N (5 ml) were stirred together in EtOH (300 ml) for 20 h. Filtration give **4***b* (2.41 g, 66%), m.p. 193–195° C (after crystallization from benzene, 2.15 g (58%); m.p. 202–204° C; identified by i.r. spectrum (4)). The ethanolic filtrate was evaporated, the residue was dissolved in benzene, and the solution washed with aqueous acetic acid and water, dried, and evaporated. The residual oil was treated with benzoyl chloride (1 ml) in pyridine (10 ml) for 30 min. Addition of EtOH (25 ml), stirring (30 min), and filtration gave 5-(*N*-benzoylimino)-2-phenyl-4-(2,4-dibromophenyl)-1,3,4-thiadiazoline (0.54 g, 21%), m.p. 198–201 °C; mass spectrum *m/e* 517, 515, 513 (M^+).

Reactions with Thiosemicarbazide

Compound **1***a* (2.30 g, 10.0 mmol), thiosemicarbazide (0.46 g, 5.0 mmol), and Et_3N (5 ml) were stirred together in EtOH (100 ml) for 4 h. Filtration followed by careful washing with water gave **4***a* (0.93 g, 44%), m.p. 166–167 °C (after crystallization from benzene, 0.67 g (32%), m.p. 162–164 °C; identified by i.r. spectrum). The ethanolic filtrate was evaporated. The residue, which appeared to consist of **10***a* contaminated with **7***a* and possibly **3***a* and **5***a* (mass spectrum), was suspended in $CHCl_3$ (20 ml) and filtered. Crystallization from acetonitrile gave the hydrochloride of **10***a* (0.51 g, 36%), m.p. 251–253 °C (dec.) (second crystallization).

Anal. Calcd. for $C_{14}H_{13}N_5 \cdot HCl$: C, 58.43; H, 4.90; N, 24.34. Found: C, 58.45; H, 4.91; N, 24.28.

Compound **1***b* (2.16 g, 5.0 mmol) and thiosemicarbazide (0.46 g, 5.0 mmol) were refluxed together in EtOH (50 ml) for 1 h. Thin-layer chromatography of the reaction mixture showed six spots, one corresponding to thiohydrazide **3***b* (4). The solution was left for one week at room temperature and filtered. Crystallization of the crude product (0.65 g) from benzene–ethanol (4:1) gave a solid (0.10 g), m.p. 286–289 °C (lit. (1) 285–286 °C). Attempts to isolate **7***b* were not pursued, but it was confirmed that **1***b* and acetone thiosemicarbazone gave the acetone derivative of **7***b* (1).

Compound **1***b* (10.0 mmol), thiosemicarbazide (0.46 g, 5.0 mmol), and Et_3N (5 ml) were stirred together in EtOH (300 ml) for 4 h. Filtration gave **4***b* (0.51 g, 14%), m.p. 195–197 °C (after crystallization, m.p. 202–204 °C; identified by i.r. spectrum). From the ethanolic filtrate was isolated the hydrobromide of **10***b* (0.77 g, 31%) (after crystallization from acetonitrile), m.p. 252–254 °C (dec.).

Anal. Calcd. for $C_{14}H_{11}Br_2N_5 \cdot HBr$: C, 34.31; H, 2.47; N, 14.29. Found: C, 34.20; H, 2.54; N, 14.46.

Reactions with Substituted Thiosemicarbazides

Compound **1***a* (1.15 g, 5.0 mmol) and 1-phenyl-3-thiosemicarbazide (0.84 g, 5.0 mmol) were refluxed together in EtOH (25 ml) for 2 h. Thin-layer chromatography of the dark green reaction mixture showed one main spot together with four minor ones, one of these corresponding to the thiohydrazide **3***a* (4). The solution was cooled for 5 h and filtered. Crystallization of the crude product (1.12 g) from ethanol–water (5:1) gave **8***a* (0.53 g, 31%) as brown prisms, m.p. 121–125 °C; ν_{max} 3280 cm^{-1} (N—H); mass spectrum *m/e* 344 (M^+).

Anal. Calcd. for $C_{20}H_{16}N_4S$: C, 69.74; H, 4.68; N, 16.27; S, 9.31. Found: C, 69.60; H, 4.88; N, 16.29; S, 9.32.

Compound **1***a* (1.15 g, 5.0 mmol) and 4-phenyl-3-thiosemicarbazide (0.84 g, 5.0 mmol) were refluxed together in EtOH (25 ml) for 45 min. The solution was chilled overnight (refrigerator) and filtered. The crude product

Can. J. Chem. Downloaded from www.nrcresearchpress.com by 210.87.254.40 on 09/05/12
For personal use only.

was **6***a* apparently contaminated with **7***a* (mass spectrum). Crystallization from EtOH gave **6***a* (0.37 g, 22%), m.p. 111–113 °C; identified by i.r. and mass spectrum.

Compound **1***a* (2.30 g, 10.0 mmol) and 1,4-diphenylthiosemicarbazide (2.44 g, 10.0 mmol) were refluxed together in EtOH (25 ml) for 90 min. The solution was evaporated to dryness and the residue suspended in benzene. Water was added and the solid was filtered off and washed with water. Crystallization of the crude product (2.08 g) from acetonitrile gave the hydrochloride of **6***a*, m.p. *ca.* 260 °C (dec.); ν_{max} 2730 (broad) (N^+—H) and 1575 cm^{-1} (strong) (C=N) (lit. (11) 1575 cm^{-1}).

Anal. Calcd. for $C_{20}H_{15}N_3S \cdot HCl$: C, 65.65; H, 4.41; N, 11.49; Cl, 9.69. Found: C, 65.50; H, 4.00; N, 11.70; Cl, 9.58.

Reactions with KSCN

Compound **1***a* (1.15 g, 5.0 mmol) and KSCN (0.50 g, 5.0 mmol) were refluxed together in EtOH (25 ml) for 30 min and filtered. Evaporation and treatment of the residue with benzene followed by filtration and evaporation afforded an oil with properties consistent with **5***a* (1.25 g, 99%); mass spectrum *m/e* 253 (M^+). Benzoyl chloride (1 ml) in pyridine (5 ml) for 1 h in the normal way afforded 5-(*N*-benzoylimino)-2,4-diphenyl-1,3,4-thiadiazoline (0.85 g, 48%), m.p. 164–165 °C (lit (2) 166 °C).

Compound **1***a* (1.15 g, 5.0 mmol) KSCN (0.50 g, 5.0 mmol), and Et_3N (2.5 ml) in EtOH (150 ml) gave **5***a* (1.23 g, 98%); mass spectrum *m/e* 253 (M^+). Treatment with benzoyl chloride gave 5-(*N*-benzoylimino)-2,4-diphenyl-1,3,4-thiadiazoline (1.17 g, 66%), m.p. 163–164 °C; mass spectrum *m/e* 357 (M^+).

Compound **1***b* (2.16 g, 5.0 mmol) and KSCN (1.00 g, 10.0 mmol) gave a semicrystalline mass (2.15 g). The mass spectrum was consistent with formation of **5***b* (*m/e* 413, 411, 409 (M^+)); i.r. spectrum showed no SC≡N. Benzoylation afforded 5-(*N*-benzoylimino)-2-phenyl-4-(2,4-dibromophenyl)-1,3,4-thiadiazoline (98%), m.p. 202–203 °C.

Compound **1***b* (2.16 g, 5.0 mmol), KSCN (0.50 g, 5.0 mmol), and Et_3N (2.5 ml) gave after benzoylation 5-(*N*-benzoylimino)-2-phenyl-4-(2,4-dibromophenyl)-1,3,4-thiadiazoline (1.70 g, 66%), m.p. 200–201 °C (after crystallization from ethyl acetate); mass spectrum *m/e* 517, 515, 513 (M^+); i.r. spectrum showed no SC≡N.

Cleavage of Hydrazonyl Disulfide ***11***

(*i*) Compound **11** (12) (3.08 g, 4.0 mmol) and KCN (0.52 g, 8.0 mmol) were stirred together in $CHCl_3$ (50 ml) for 2 days. The solution was filtered and the solvent removed *in vacuo*; the residue was suspended in EtOH (25 ml) and filtered. Crystallization from benzene gave **4***b* (0.15 g, 5%), m.p. 198–201 °C; identified by i.r. spectrum. The ethanolic filtrate was evaporated and the residue was dissolved in benzene and extracted twice with aqueous NaOH. The benzene layer was washed with water, dried, evaporated, and benzoylated (in pyridine) to give 5-(*N*-benzoylimino)-2-phenyl-4-(2,4-dibromophenyl)-1,3,4-thiadiazoline (1.62 g, 79%), m.p. 201–203 °C; identified by i.r. spectrum. The aqueous NaOH phase was neutralized and extracted with benzene; the benzene phase was washed with water, dried, and evaporated. Crystallization of the crude product (1.60 g) from benzene–hexane (1:1) gave **3***b* as small pale yellow needles (0.70 g, 46%), m.p. 107–109° C (lower melting polymorph); identified by i.r. spectrum ($CHCl_3$) (4); mass spectrum *m/e* 388, 386, 384 (M^+).

Anal. Calcd. for $C_{13}H_{10}Br_2N_2S$: C, 40.44; H, 2.61; N, 7.26. Found: C, 40.55; H, 2.76; N, 7.34.

(*ii*) Compound **11** (1.54 g, 2.0 mmol) and KCN (0.52 g, 8.0 mmol) were refluxed together in CH_3CN for 30 min. The i.r. spectrum of the filtered and evaporated reaction mixture showed no presence of SC≡N. Work-up (as above) gave 5-(*N*-benzoylimino)-2-phenyl-4-(2,4-dibromophenyl)-1,3,4-thiadiazoline (0.75 g, 73%), m.p. 202–204° C and **3***b* (0.71 g, 92%); crystallization from benzene–hexane (1:1) gave **3***b* (45%), m.p. 106–108 °C.

We thank the National Research Council of Canada and the Danish Statens naturvidenskabelige Forskningsraad (to P. W.) for financial support.

1. R. Fusco. Rend. Ist. Lomb. Sci. Lett. A, **71**, 425 (1938).
2. R. Fusco and C. Musante. Gazz. Chim. Ital. **68**, 147 (1938).
3. R. Huisgen. Angew. Chem. Int. Ed. Engl. **2**, 565 (1963); A. F. Hegarty, M. P. Cashman, and F. L. Scott. J. Chem. Soc. Perkin Trans. 2, 44 (1972).
4. P. Wolkoff, S. Hammerum, P. D. Callaghan, and M. S. Gibson. Can. J. Chem. **52**, 879 (1974).
5. R. Huisgen, R. Grashey, M. Seidel, G. Wallbillich, H. Knupfer, and R. Schmidt. Liebigs Ann. Chem. **653**, 105 (1962).
6. W. A. Pryor. Mechanisms of sulfur reactions. McGraw-Hill, New York. 1962.
7. B. T. Heitke and C. C. McCarty. J. Org. Chem. **39**, 1522 (1974); H. Gehlen and H. Segeletz. J. Prakt. Chem. **313**, 294 (1971).
8. P. Wolkoff. Can. J. Chem. **53**, 1333 (1975).
9. R. Huisgen, M. Seidel, G. Wallbillich, and H. Knupfer. Tetrahedron, **17**, 3 (1962).
10. F. D. Chattaway and A. J. Walker. J. Chem. Soc. 975 (1925).
11. R. Huisgen, R. Grashey, M. Seidel, H. Knupfer, and R. Schmidt. Liebigs Ann. Chem. **658**, 169 (1962).
12. P. Wolkoff and M. S. Gibson. J. Chem. Soc. Perkin Trans. 1, 1173 (1974).
13. A. S. Shawali and A. O. Abdelhamid. Tetrahedron Lett. 163 (1975).

Isotope Effects in Nucleophilic Substitution Reactions. I. The Mechanism of the Reaction of Phenylbenzyldimethylammonium Ion with Thiophenoxide Ion

KENNETH CHARLES WESTAWAY AND RAYMOND ALCIDE POIRIER

Department of Chemistry, Laurentian University, Sudbury, Ontario P3E 2C6

Received March 3, 1975

KENNETH CHARLES WESTAWAY and RAYMOND ALCIDE POIRIER. Can. J. Chem. **53**, 3216 (1975).

A kinetic study of the nucleophilic substitution reactions of a series of *para*-substituted phenylbenzyldimethylammonium nitrates with sodium thiophenoxide at 0 °C in *N,N*-dimethylformamide containing a large excess of sodium nitrate, has shown the reaction to be a second-order process which is first-order in both the substrate and the nucleophile. A Hammett ρ value of +2.04 for different *para*-substitutents on the *N*-phenyl group of the quaternary ammonium salt and a large nitrogen kinetic isotope effect of 1.0200 ± 0.0007 have excluded any mechanism involving a carbonium ion intermediate but are in accord with an S_N2 mechanism with a substantial amount of carbon–nitrogen bond rupture in the transition state.

KENNETH CHARLES WESTAWAY et RAYMOND ALCIDE POIRIER. Can. J. Chem. **53**, 3216 (1975).

Une étude cinétique des réactions de substitution nucléophile d'une série de nitrates de *p*-X-phénylbenzyldiméthylammonium par le thiophénolate de sodium, à 0 °C dans la *N,N*-diméthylformamide contenant un grand excès de nitrate de sodium, a permis de démontrer que la réaction est du deuxième ordre soit du premier ordre dans chacun des réactifs. Sur la base (*a*) d'une valeur ρ de Hammett de +2.04 pour différents substituants en *para* du groupement phényle du sel d'ammonium quaternaire et (*b*) d'un grand (1.0200 ± 0.0007) effet isotopique cinétique de l'azote, on peut exclure tout mécanisme impliquant un intermédiaire carbocationique; toutefois les résultats sont en accord avec un mécanisme S_N2 impliquant une portion importante de rupture du lien carbone–azote dans l'état de transition.

[Traduit par le journal]

Introduction

Several authors (1–7) have studied the nucleophilic substitution reactions of quaternary ammonium ions

[1] $$Nu^- + R'\overset{+}{N}R_3 \rightarrow NuR' + \ddot{N}R_3$$

Nu^- = Nucleophile

and the reverse of this reaction (the Menschutkin reaction) in both protic (1–4) and dipolar aprotic solvents (4–7). The earliest reports, based on extensive kinetic studies using alcohols or water as a solvent, indicated that these reactions proceed by a simple S_N2 mechanism, eq. 2.

[2] $$Nu^- + R'\overset{+}{N}R_3 \rightarrow [\overset{\delta-}{Nu}\text{---}R'\text{---}\overset{\delta+}{N}R_3] \rightarrow NuR' + \ddot{N}R_3$$

More recently, Leffek and co-workers (5–7) have studied these reactions in the dipolar aprotic solvents chloroform and acetone and have concluded on the basis of an extensive kinetic study (5) and large alpha secondary hydrogen–deuterium isotope effects (1.20 in acetone and 1.25 in chloroform (6)) that these reactions proceed by an "ionic internal nucleophilic substitution mechanism" (6, 7) involving triple ions of the type $[(R'\overset{+}{N}R_3)_2Nu^-]^+$.[1] The rate-determining step of the reaction involves ionization of the carbon–nitrogen bond to give a carbonium ion intermediate (R'^+) which reacts in a fast step with the nucleophile in the triple ion complex to give the products, eq. 3.

[3] $$3\ R'\overset{+}{N}R_3\overset{-}{X} \underset{k_{-1}}{\overset{k_1}{\rightleftharpoons}} [(R'\overset{+}{N}R_3)_2\overset{-}{X}]^+ + [R'\overset{+}{N}R_3\overset{-}{X}_2]^-$$

$$[(R'\overset{+}{N}R_3)_2\overset{-}{X}]^+ \xrightarrow{\text{slow}} [R'\ddot{N}R_3\ R'\overset{+}{N}R_3\ \overset{-}{X}]^+ \xrightarrow{\text{fast}} R'X + \ddot{N}R_3 + R'\overset{+}{N}R_3$$

Leffek's work which suggested that quaternary ammonium salts reacted by an S_N1 mechanism fits very nicely with a proposal by Sneen and Larsen (8, 9) which suggested that all nucleophilic substitution reactions proceed by the ionizing or carbonium ion mechanism illustrated in eq. 4. A quaternary ammonium ion has been

[1] K. T. Leffek, private communication.

Can. J. Chem. Downloaded from www.nrcresearchpress.com by 210.87.254.42 on 09/05/12
For personal use only.

used to illustrate how Sneen's proposal would apply to the reactions under investigation.

$$\overset{+}{R'}\ddot{N}R_3 \underset{k_{-1}}{\overset{k_1}{\rightleftarrows}} R'^{+} + \ddot{N}R_3 \qquad [4]$$

$$R'^{+} + Nu^- \xrightarrow{k_2} R'—Nu$$

If the k_1 step in eq. 4 is rate determining ($k_2 \gg k_{-1}$ [$\ddot{N}R_3$]) then first-order kinetics would be observed. This corresponds to the normal S_N1 mechanism. If, on the other hand, the k_2 step is rate-determining (k_{-1} [$\ddot{N}R_3$] $\gg$ k_2) then there is a pre-equilibrium followed by a slow bimolecular reaction and second-order kinetics would be observed. This mechanism, which has been referred to as an 'ion-pair S_N2' (10) or an S_N2C^+ (11) mechanism, often cannot be distinguished from the normal S_N2 mechanism even by a detailed kinetic analysis (10). Thus both Sneen's proposal which suggests that reactions involving a carbonium ion intermediate can be kinetically identical to normal S_N2 reactions, and Leffek's work imply that quaternary ammonium ions react only by a carbonium ion mechanism rather than by the S_N2 mechanism proposed by earlier workers. This investigation, which was started with the object of establishing whether the nucleophilic substitution reactions of quaternary ammonium ions occur by an S_N1–S_N2C^+ or by an S_N2 mechanism, was undertaken because it was not obvious why a reaction thought to proceed by an S_N2 mechanism in protic solvents should react by an S_N1 mechanism in dipolar aprotic solvents and because several workers (12) had cast doubt on Sneen's proposal that all nucleophilic substitution reactions proceed by a carbonium ion mechanism.

Results

Product Analysis

The reactions of several *para*-substituted phenylbenzyldimethylammonium nitrates with sodium thiophenoxide were studied at 0 °C in *N*,*N*-dimethylformamide containing a large excess of an inert salt (sodium nitrate) to eliminate the salt effects which were observed at lower ionic strengths. The products of the reaction were identified from their spectra and from a comparison of their gas chromatographic retention times with those of authentic samples. A quantitative gas chromatographic analysis using

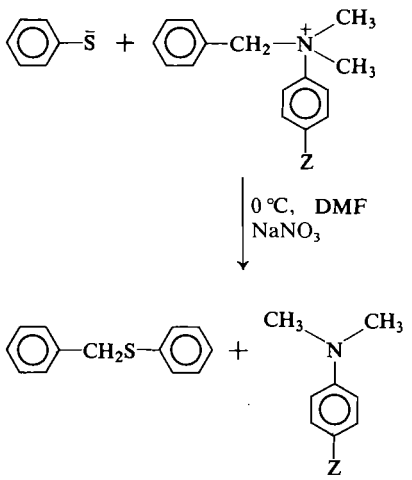

[5]

the internal standard technique (13), showed that the benzylphenyl sulfide was formed quantitatively. This result was confirmed when it was found that a theoretical yield of *N*,*N*-dimethylaniline could be recovered from a reaction taken to completion. This analysis was done using the micro-kjeldahl method (14) on the *N*,*N*-dimethylaniline recovered from a reaction taken to completion. Finally, the only possible side products (methylphenyl sulfide and benzylmethylphenyl amine produced by attack at an *N*-methyl carbon) were found in a gas chromatographic analysis to account for only 0.4% of the product. Thus there is, in essence, only one reaction occurring and the isotope effects and other constants are clearly those associated with the reaction shown in eq. 5.

Kinetics and Hammett ρ Value

The reactions of the different *para*-substituted phenylbenzyldimethylammonium salts were monitored by titrating the unreacted thiophenoxide ion with mercury(II) ion (15). The individual rate constants were obtained when the data was treated using the usual method for a second-order reaction that is first-order in each reactant. Good straight line plots (correlation coefficients of > 0.99) up to more than 90% of completion were obtained for each run. The rate constants given in Table 1 are the average of the values obtained from at least three separate kinetic runs where the concentration of the quaternary ammonium salt was approximately 0.025 *M* and where the concentration of the thiophenoxide ion ranged from 0.025 to 0.080 *M*.

The rate constants in Table 1 were used to

Can. J. Chem. Downloaded from www.nrcresearchpress.com by 210.87.254.42 on 09/05/12
For personal use only.

Can. J. Chem. Downloaded from www.nrcresearchpress.com by 210.87.254.42 on 09/05/12
For personal use only.

TABLE 1. Rate constants for the nucleophilic substitution reaction of *para*-substituted phenylbenzyldimethylammonium nitrates with thiophenoxide ions at 0 °C

Substituent (Z) on the *N*-phenyl group	$k \times 10^2$ (l mol^{-1} s^{-1})
—Cl	5.55
—H	1.73
—CH_3	0.917
—OCH_3	0.493

construct the Hammett plot shown in Fig. 1. The ρ value for substitution in the leaving group was found to be +2.04 with a correlation coefficient of 0.998. This ρ value indicates that there is a substantial reduction of the positive charge on the nitrogen atom bonded to the phenyl group in the transition state of the rate-determining step of the reaction.

Nitrogen Kinetic Isotope Effect

The nitrogen kinetic isotope effect for the reaction of phenylbenzyldimethylammonium nitrate and sodium thiophenoxide at 0 °C was calculated using eq. 6 (16).

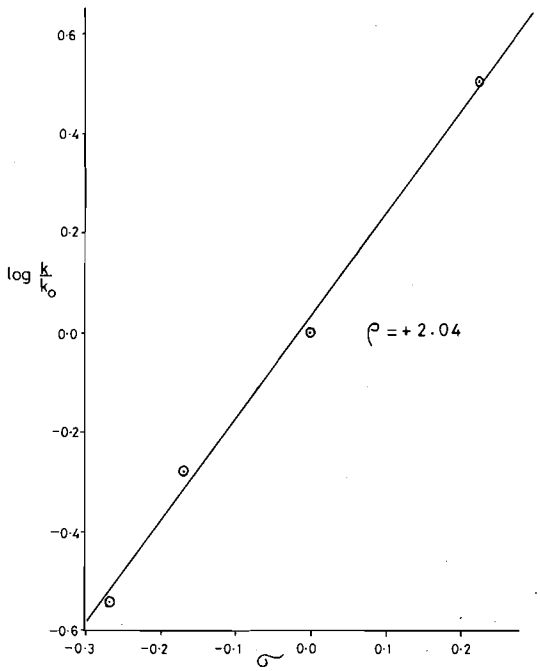

FIG. 1. Correlation of log k/k_0 and the Hammett ρ constants for the reaction of a series of *para*-substituted phenylbenzyldimethylammonium nitrates with sodium thiophenoxide in DMF.

$$[6] \qquad k^{14}/k^{15} = \frac{\ln (1 - f)}{\ln \left(1 - \left(\frac{R_0}{R_f}\right) f\right)}$$

where f is the mole fraction of quaternary ammonium salt that has reacted, R_0 is the ratio of the $^{14}N/^{15}N$ in the ammonium nitrogen of the starting material and R_f is the ratio of the $^{14}N/^{15}N$ in the nitrogen of the *N,N*-dimethylaniline produced when the reaction was taken to small extents of completion. Since there were two nitrogen atoms in the starting material, the $^{14}N/^{15}N$ ratio of the ammonium nitrogen atom had to be determined by analyzing the nitrogen gas obtained from the degradation of the *N,N*-dimethylaniline (17) that was produced in a reaction taken 100% to completion. The $^{14}N/^{15}N$ ratio in the product was obtained by analyzing the nitrogen gas from the *N,N*-dimethylaniline produced when the reaction was taken to various extents of reaction between 17 and 38% of completion. The results of these experiments are given in Table 2. The large nitrogen kinetic isotope effect, $k^{14}/k^{15} = 1.0200$ indicates that there is substantial carbon–nitrogen bond rupture in the transition state of the rate-determining step of this reaction.

Discussion

Product Analysis and Kinetic Studies

The product analysis study has shown that the nucleophilic substitution reaction of each of the *para*-substituted phenylbenzyldimethylammonium ions with thiophenoxide ion occurs only at the benzyl carbon to give a quantitative yield of benzylphenyl sulfide and the corresponding *para*-substituted *N,N*-dimethylaniline. This ensures that all the parameters reported in this paper are those for the nucleophilic substitution reaction shown in eq. 5.

This reaction can occur by way of either an S_N2 mechanism, eq. 7, or by one of the several possible variations of the carbonium ion mechanism shown in Scheme 1.

The kinetic study showed that each of these reactions were second-order processes which were first-order in both the nucleophile and the substrate. While these results do not establish the mechanism they can be used to eliminate some of the mechanisms depicted in eq. 7 and Scheme 1.

Second-order kinetics are obviously consistent with the simple, one-step S_N2 mechanism.

TABLE 2. Nitrogen kinetic isotope effect in the nucleophilic substitution reaction of phenylbenzyldimethylammonium nitrate with sodium thiophenoxide at 0 °C

Experiment number	Initial concentration of quaternary ammonium salt (M)	Initial concentration of thiophenoxide ion (M)	Extent of reaction* (%)	$\frac{k^{14}}{k^{15}}$
1	0.03835	0.06492	16.6	1.0200
2	0.02751	0.02953	16.6	1.0197
3	0.02501	0.07869	21.3	1.0191
4	0.02637	0.07021	21.7	1.0203
5	0.02464	0.05439	22.0	1.0200
6	0.01653	0.06618	37.8	1.0212
				1.0200 ±0.0007†

*Based on the yield of benzylphenyl sulfide and *N,N*-dimethylaniline.
†The error limits are the standard deviation.

[7]

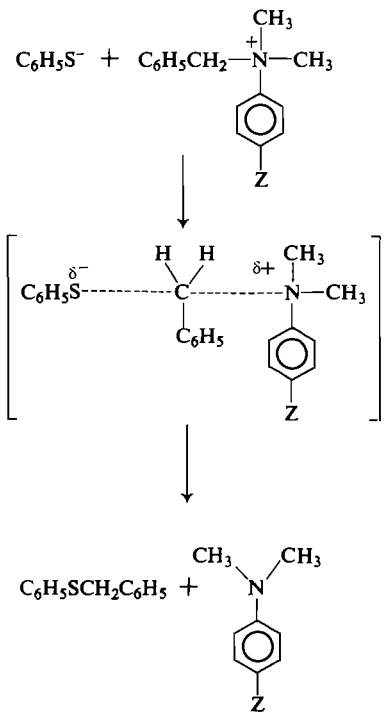

They are not, however, consistent with several of the mechanisms described in Scheme 1. If the slow or rate-determining step of the reaction is any of the k_1, the k_2 or the k_3 steps of Scheme 1, the rate will only depend on the concentration of the quaternary ammonium ion and first-order kinetics will be observed. The rate expressions for these three possible mechanisms are shown as No. 2, 3 and 4 of Table 3. It is perhaps worth noting that this conclusion holds true no matter how the products are formed *i.e.* by reaction 4, 5 or 6 or even by some combination of these three reactions. These mechanisms are examples of the S_N1 mechanism.

The second group of mechanisms that are described in Scheme 1 are the S_N2C^+ mechanisms where the reaction between one of the carbonium ion intermediates and the thiophenoxide ion is the slow or rate-determining step of the reaction. Two possibilities exist within this framework. The first mechanism involves the formation of a free carbonium ion ($C_6H_5CH_2^+$) which reacts in the slow k_6 step with the thiophenoxide ion. Since the k_6 step is slow and since the $C_6H_5CH_2^+$ does not accumulate during the reaction, the free carbonium ion is formed reversibly and

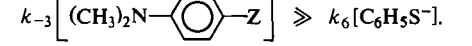

This requires the rate expression to have a term

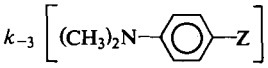

in the denominator (mechanism 5, Table 3) and means that the observed rate constant should decrease during the reaction in the same way, and for the same reason that the mass law effect is observed.

Since the second-order rate constants do not decrease during the reaction even though the concentration of the *para*-substituted *N,N*-dimethylaniline increases markedly, the nucleophilic substitution reaction cannot proceed to any substantial degree by way of the free carbonium ion.

Can. J. Chem. Downloaded from www.nrcresearchpress.com by 210.87.254.42 on 09/05/12
For personal use only.

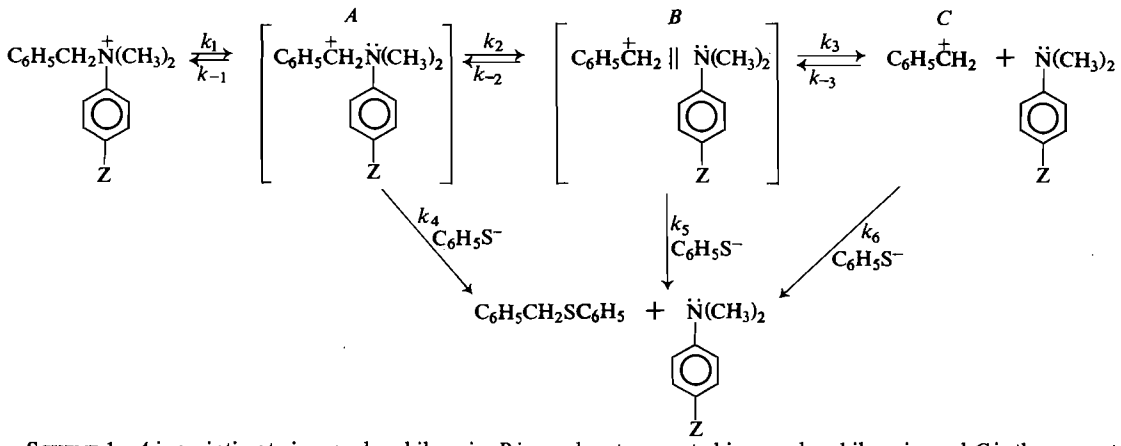

SCHEME 1. *A* is an intimate ion-nucleophile pair, *B* is a solvent separated ion-nucleophile pair, and *C* is the separate carbonium ion intermediate. The product may be formed via one or more of the k_4, k_5 or k_6 steps. The counter ions have been omitted to simplify the diagram.

TABLE 3. Rate expressions for different mechanisms based on Scheme 1*

Type of mechanism	Rate-determining step	Rate expression†
1. S_N2	the only step	$k[R_4\overset{+}{N}NO_3^-][\overset{+}{Na}\overset{-}{S}C_6H_5]$
2. S_N1	k_1	$k_1[R_4\overset{+}{N}NO_3^-]$
3. S_N1	k_2‡	$\dfrac{k_1k_2[R_4\overset{+}{N}NO_3^-]}{k_{-1}}$
4. S_N1	k_3§	$\dfrac{k_1k_2k_3[R_4\overset{+}{N}NO_3^-]}{k_{-1}\,k_{-2}}$
5. S_N2C^+	k_6§	$\dfrac{k_1k_2k_3k_6[R_4\overset{+}{N}NO_3^-][\overset{+}{Na}\overset{-}{S}C_6H_5]}{k_{-1}\,k_{-2}\,k_{-3}\,[(CH_3)_2N-C_6H_4-Z]}$
6. S_N2C^+	k_4	$\dfrac{k_1k_4[R_4\overset{+}{N}NO_3^-][\overset{+}{Na}\overset{-}{S}C_6H_5]}{k_{-1}}$
7. S_N2C^+	k_5‡	$\dfrac{k_1k_2k_5[R_4\overset{+}{N}NO_3^-][\overset{+}{Na}\overset{-}{S}C_6H_5]}{k_{-1}\,k_{-2}}$
8. S_N2C^+	$k_4 + k_5$	$\left[k_4 + \dfrac{k_5k_2}{k_{-2}}\right]\dfrac{k_1[R_4\overset{+}{N}NO_3^-][\overset{+}{Na}\overset{-}{S}C_6H_5]}{k_{-1}}$

*$R_4\overset{+}{N}NO_3^-$ represents the phenylbenzyldimethylammonium nitrate and $\overset{+}{Na}\overset{-}{S}C_6H_5$ represents sodium thiophenoxide.
†The rate expression does not imply that the reactants are ion pairs.
‡Assumes that no product is formed via the k_4 step.
§Assumes that no products are formed by either the k_4 or k_5 steps.

The second set of mechanisms where the final step is rate-determining involve the formation of either the intimate or solvent separated carbonium ion complexes in pre-equilibrium steps which are followed by a slow reaction (k_4 for the intimate ion complex and k_5 for the solvent separated complex respectively) with the thiophenoxide ion. Both these mechanisms would lead to second-order kinetics (No. 6 and 7, Table 3) and are, therefore, consistent with the observed results. This would also be true for a process where both the intimate and solvent

Can. J. Chem. Downloaded from www.nrcresearchpress.com by 210.87.254.42 on 09/05/12
For personal use only.

TABLE 4. Hammett ρ values for reactions producing or destroying quaternary ammonium salts

Number	Reaction	Solvent	ρ	Reference
1	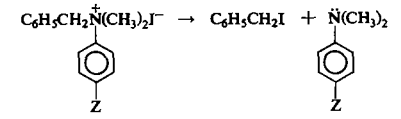	$CHCl_3$	+1.4	18
2	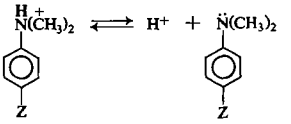	70% water 30% ethanol	+3.43	19*a*
3	Reaction 2	50% water 50% ethanol	+4.19	19*a*
4	Reaction 2	70% DMSO 30% water	+3.87	20
5	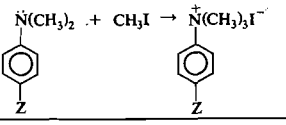	90% acetone 10% water	−3.30	19*b*

separated ion complexes exist and react with the nucleophile in a slow step (mechanism 8, Table 3).

Thus, the kinetic investigation has eliminated several mechanisms and has indicated that these reactions are either S_N2 or S_N2C^+ processes involving an intimate and/or a solvent separated carbonium ion complex.

Hammett ρ Value

The Hammett plot shown in Fig. 1 indicated that the ρ value found by changing the *para*-substituent on the phenyl ring of the leaving group (eq. 5) was +2.04. The sign of the ρ value indicates that the positive charge on the quaternary ammonium nitrogen has decreased in the transition state of this reaction (18). An estimate of the extent to which the positive charge has been reduced and thus the amount of carbon–nitrogen bond rupture that has occurred in the transition state, can be obtained by comparing the observed ρ value with those found in similar reactions of other quaternary ammonium salts. Some relevant reactions and their ρ values are given in Table 4.

Burns and Leffek (18) found a ρ value of +1.4 for the reactions of *para*-substituted phenylbenzyldimethylammonium ions with iodide ion in chloroform and suggested that there was only a small degree of carbon–nitrogen bond rupture in the transition state. Other workers (19, 20) who have studied equilibrium reactions where the positive charge is completely destroyed (mechanisms 2–4, Table 4) have found large ρ values ranging from +3.4 – +4.2.[2] Since the observed ρ value of +2.04 is approximately half way between the value reported by Burns and Leffek and the extreme values observed for the equilibrium reactions, it would seem that there is quite a substantial reduction in the positive charge on nitrogen and thus considerable (but not nearly complete) carbon–nitrogen bond rupture in the transition state of this reaction.

The magnitude of the ρ value can also be used to give some indication of the mechanism of the reaction. The S_N2C^+ mechanism requires that the carbon–nitrogen bond is broken in a rapid pre-equilibrium step and that the product is formed in a rate-determining reaction between one of the carbonium ion complexes and the nucleophile. If the reaction proceeds by this mechanism then the ρ value should be that observed for an equilibrium reaction of the type shown in Table 4 *i.e.* a ρ value of greater than +3.4.[2] The much smaller value of +2.04 is obviously not consistent with the S_N2C^+ mechanism.

The smaller ρ value is however, in the range

[2]The ρ value should be at least as large for an equilibrium involving quaternary ammonium salts since hydrogens on the ammonium nitrogen hydrogen bond to solvent and lower the ρ value. Equilibrium ρ values range from +2.8 – +3.5 for anilinium ions (19, 20) and from +3.4 – +4.2 for *N,N*-dimethylanilinium ions where hydrogen bonding to solvent is greatly reduced (20).

Can. J. Chem. Downloaded from www.nrcresearchpress.com by 210.87.254.42 on 09/05/12
For personal use only.

Can. J. Chem. Downloaded from www.nrcresearchpress.com by 210.87.254.42 on 09/05/12
For personal use only.

expected for an S_N2 mechanism. The ρ value for the formation of a quaternary ammonium salt from methyl iodide and *para*-substituted *N,N*-dimethylanilines (reaction 5, Table 4) is large and negative ($\rho = -3.30$) indicating that the nitrogen atom has attained almost a full positive charge and that the carbon–nitrogen bond formation is almost complete in the transition state of this S_N2 reaction. The principle of microscopic reversibility requires that the transition state for the reverse reaction, the decomposition of the quaternary ammonium salt in an S_N2 reaction, have an early transition state with a fairly small amount of carbon–nitrogen bond rupture. As a result, a reasonably small positive ρ value should be observed. The observed ρ value of +2.04 is obviously consistent with an S_N2 mechanism.

Thus the ρ value suggests that the nucleophilic substitution reactions of *para*-substituted phenylbenzyldimethylammonium ions with thiophenoxide ion proceed by way of an S_N2 mechanism with considerable, but not nearly complete carbon–nitrogen bond rupture in the transition state.

Nitrogen Kinetic Isotope Effect

The above conclusions have been confirmed by the large nitrogen kinetic isotope effect ($k^{14}/k^{15} = 1.0200 \pm 0.0007$) observed for this reaction. In an S_N2C^+ reaction the carbon–nitrogen bond is broken in a pre-equilibrium step and the nitrogen isotope effect should be very small, probably only a few tenths of one percent.[3] For an S_N2 process on the other hand, the carbon–nitrogen bond is broken in the transition state of the rate-determining step and a normal nitrogen kinetic isotope effect of 1–3% ($k^{14}/k^{15} = 1.01$–1.03) should be observed.

The nitrogen kinetic isotope effect of 1.0200 observed for this reaction is approximately half of the theoretical maximum nitrogen isotope effect of 1.03–1.04 at 0 °C (21) and clearly illustrates that the carbon–nitrogen bond is broken in the rate-determining step of the reaction. Since the kinetics have established that the carbon–sulfur bond is formed in the rate-determining step, both the bond changes must occur in the same step and thus the nucleophilic substitution reactions of quaternary ammonium ions in dipolar aprotic solvents do, indeed, proceed by way of an S_N2 mechanism.

It is worth noting that a test for an S_N2C^+ mechanism, based on the leaving group isotope effect (22), fails in this case. Graczyk and Taylor have shown that the value of a leaving group heavy atom isotope effect will vary in an S_N2C^+ process when the concentration of the attacking nucleophile is changed. This occurs because the ionization (k_1) step (eq. 4) becomes more rate-determining as the concentration of the attacking nucleophile is increased and k_2 [Nu^-] becomes greater than k_{-1} [$\dot{N}R_3$]. This shift in the rate-determining step requires that the observed heavy atom isotope effect (significant only when the carbon-leaving group bond is broken in the rate-determining step) increase with increasing concentration of the attacking nucleophile.[4] This trend is not even suggested by the individual results shown in Table 2, even though the relative concentrations of thiophenoxide ion (attacking nucleophile) have been varied over a larger range than those of Graczyk and Taylor, *i.e.* from very small values (reaction 2 where $[C_6H_5S^-]/R_4\overset{+}{N}NO_3^-] = 1.18$) to large values (reaction 3 where $[C_6H_5S^-]/[R_4\overset{+}{N}NO_3^-] = 3.15$).

The magnitude of the nitrogen kinetic isotope effect has been used to give an accurate measure of the relative amount of carbon–nitrogen bond rupture in the transition states of a series of closely related compounds (23). This comparison cannot be made with any certainty in this case because the isotope effect measured in this study is the first value that has been determined for a nucleophilic substitution reaction of a quaternary ammonium salt. Some estimate of the degree of carbon–nitrogen bond rupture can be obtained however, from a comparison with the nitrogen isotope effects for concerted 1,2-elimination reactions of quaternary ammonium salts where a C—N^+ bond is broken in the transition state. Typical values for these reactions range from $k^{14}/k^{15} = 1.009$–1.0186 at 60 °C (23) and the reactions with an isotope effect of $\gtrsim 1.014$ are thought to have substantial carbon–nitrogen bond rupture in the transition state.

[3]A simple calculation (19c) of the isotope effect expected for a pre-equilibrium C—N bond rupture has shown that the isotope effect, based on the observed frequencies of the stretching vibrations of the quaternary ammonium salt and the *N,N*-dimethylaniline, is very small or inverse. The bending modes do not appear to modify the value of the isotope effect to any significant degree.

[4]This effect would be observed only if k_{-1} [$\dot{N}R_3$] and k_{-2} [Nu^-] are the same order of magnitude.

Can. J. Chem. Downloaded from www.nrcresearchpress.com by 210.87.254.42 on 09/05/12
For personal use only.

The nitrogen isotope effect in the substitution reaction under investigation would be roughly equivalent to an isotope effect of 1.016–1.017 at 60 °C (14). Since this value is near the largest values observed for elimination reactions and in fact, is approximately half of the theoretical maximum isotope effect, it would appear that there must be substantial weakening of the carbon–nitrogen bond in the transition state of this reaction. Finally, it is worth noting that the magnitude of the Hammett ρ value and the nitrogen isotope effect both indicate that this reaction is one where there is substantial carbon–nitrogen bond rupture in the transition state.

Selectivity of the Reaction

The mechanism of these reactions has been confirmed in yet another way. The benzhydryldimethylphenylammonium ion was prepared and treated under the normal reaction conditions. If a carbonium ion intermediate were produced during the reaction, then this compound would form a very stable carbonium ion and react very much faster than the benzyl compounds reported in this paper. In fact, the benzhydryl compound did not react and it is safe to conclude that the benzhydryl carbonium ion did not form. It is then obvious that the less stable benzyl carbonium ion would not form and one must again conclude that the phenylbenzyldimethylammonium ions react by an S_N2 mechanism. The benzhydryl compound probably fails to react because the benzhydryl carbon is too sterically crowded to allow the nucleophile to attack in an S_N2 reaction.

Finally, one unusual feature of the reactions of the phenylbenzyldimethylammonium ions is the high selectivity, *i.e.* the benzyl carbon is approximately 500 times more reactive than the methyl carbon. This difference in reactivity, which is more characteristic of carbonium ion processes (benzyl:methyl greater than 400:1) than of S_N2 reactions (benzyl:methyl $\simeq$ 4:1) (24), is thought to be caused by the poor leaving groups in these reactions. This large difference in reactivity has been observed in reactions of other quaternary ammonium salts (1–3, 25) and thus would seem to be normal for S_N2 reactions with poor leaving groups. This suggests that a large selectivity cannot be used as an indication of a carbonium ion mechanism.

In conclusion, these results clearly illustrate (*1*) that Sneen's proposals concerning nucleophilic substitution reactions are incorrect and that while many reactions do proceed by the S_N1–S_N2C^+ mechanism (22, 26) that some reactions do, indeed, react by way of an S_N2 mechanism, and (*2*) that the nucleophilic substitution reactions of quaternary ammonium salts in dipolar aprotic solvents and probably also in protic solvents as the early results indicated (1–3), react by an S_N2 mechanism. Finally the reasonably large Hammett ρ value and nitrogen kinetic isotope effect both suggest there is substantial carbon–nitrogen bond rupture in the transition state of these reactions.

Experimental

Materials

The quaternary ammonium bromides were prepared by stirring benzyl bromide with a 10% excess of the appropriate *para*-substituted *N,N*-dimethylaniline in benzene at room temperature for 24 h. The solid bromides were recovered by filtration, dissolved in water, and treated with silver oxide for 3 h (14). The solution was filtered and the filtrate neutralized with nitric acid (1). The water was then removed under reduced pressure to give the quaternary ammonium nitrates which were purified by recrystallization. All the products except the *p*-methoxyphenylbenzyldimethylammonium nitrate which was recrystallized from acetone and ether, were recrystallized from isopropanol–ether mixtures. The yields of the purified products based on the benzyl bromide and the melting points of each product are: *p*-methoxyphenylbenzyldimethylammonium nitrate (40%, 95.5–96.0 °C), *p*-methylphenylbenzyldimethylammonium nitrate (59%, 138–139 °C), *p*-chlorophenylbenzyldimethylammonium nitrate (55%, 127–128 °C), and phenylbenzyldimethylammonium nitrate (70%, 157–158 °C). All of the reactants with the exception of the *p*-methoxy- and *p*-chloro-*N,N*-dimethylanilines were commercially available.

The *p*-methoxy-*N,N*-dimethylaniline was prepared from *p*-anisidine using the method described by Leffek (18). The *p*-chloro-*N,N*-dimethylaniline was prepared from *p*-chloroaniline using the method described by Chambers (27). Freshly distilled *p*-chloroaniline (63 g, 0.49 mol) were mixed with 230 g (0.68 mol) of polyphosphoric acid and 48 g (1.5 mol) of methanol at room temperature. After the mixture had been heated at 190–200 °C for 24 h, it was cooled and made basic by adding a 40% NaOH solution. The product was then extracted with ether. The remaining alkaline solution was mixed with 128 g NaOH and steam distilled. The additional product in the distillate was extracted with ether. The combined ether layers were dried, the ether removed under reduced pressure, and the product distilled under reduced pressure to give 48 g (63%) of *p*-chloro-*N,N*-dimethylaniline. The melting point of the product was 33–34 °C; lit. (18) m.p. 32–33 °C.

The benzhydryldimethylphenylammonium bromide was prepared by refluxing 9.45 g (0.038 mol) of benzhydryl bromide with 6.90 g (0.057 mol) of *N,N*-dimethylaniline in 20 ml of anhydrous benzene for 24 h. The benzene was removed under reduced pressure and the solid

recrystallized from acetone and water to give 5.5 g (39%) of benzhydryldimethylphenylammonium bromide of m.p. 134.5–135.0 °C. The benzhydryl bromide required for this synthesis was obtained by bubbling HBr through a solution of 10.0 g (0.054 mol) of benzhydrol in 25 ml of anhydrous benzene for 2 h, removing the benzene under reduced pressure, and recrystallizing the solid from ligroin (b.p. 30–60 °C) (28). The yield of benzhydryl bromide was 9.45 g (71%) and the m.p. was 39–39.5 °C; lit. (28) m.p. 42–44 °C.

The solvent, Fisher reagent grade *N,N*-dimethylformamide, was further purified before use. After the solvent had been dried for at least 24 h over solid NaOH, several grams of sodium thiophenoxide were added and the solvent was distilled at a reduced pressure under a nitrogen atmosphere.

The sodium thiophenoxide was prepared by mixing a 10% excess of freshly distilled benzene thiol with a sodium ethoxide solution prepared from anhydrous ethanol. The ethanol was removed under reduced pressure and the solid was quickly transferred to a glove bag filled with nitrogen. The product was washed several times with ether and then transferred to a vacuum desiccator where it was stored under vacuum until it was required.

Product Identification and Analysis

All the *para*-substituted *N,N*-dimethylanilines were available or had been prepared during the synthesis of the quaternary ammonium salts. The other products were prepared as follows. The benzylphenyl sulfide was formed when 9.3 g (0.05 mol) of benzyl bromide were refluxed for 2 h with a sodium thiophenoxide solution prepared from 5.7 g (0.04 mol) of benzene thiol and 30 ml of a 2.25 *N* solution of sodium ethoxide in ethanol (29). The product was recovered by filtration of the solid that formed when the reaction mixture was poured into a large excess of water. Recrystallization from ethanol gave 6.2 g (72%) of benzylphenyl sulfide, m.p. 42 °C; lit. (29) m.p. 40–41 °C. Methylphenyl sulfide was produced in the same way by refluxing 30 g (0.21 mol) of methyl iodide with 100 ml of a 2.25 *N* solution of sodium thiophenoxide in ethanol. The product, a liquid, was separated from the aqueous layer, dried and distilled under reduced pressure (b.p. 60–62 °C at 8 Torr; lit. (30) b.p. 58–60 °C at 6 Torr). The yield was 22.5 g (86%).

The amine impurity, benzylmethylphenyl amine was prepared using the procedure described by Grillot and co-workers (31, 32). Equimolar amounts (0.1 mol) of benzene thiol (10 g) *N*-methylaniline (10.7 g) and a 35–40% solution of formaldehyde (8 ml) were dissolved in 20 ml ethanol and refluxed for 9 h. After the mixture had cooled, the bottom layer was removed and extracted with ether. The combined ether layers were dried and then the ether was removed under reduced pressure and the product distilled (b.p. 159 °C at 1 Torr, lit. (31) m.p. 36–38 °C) to give 32 g (70%) of *N*-methyl-*N*-phenylaminomethyl sulfide. This product was mixed with THF and added slowly to the Grignard reagent prepared by reacting 25.2 g (0.16 mol) bromobenzene with 4 g (0.17 mol) magnesium in THF. The mixture was refluxed for 1 h after the addition was complete, and then poured onto a mixture of 350 g crushed ice, 20 g NH_4Cl and 200 ml of water. The product was extracted with ether. The ether layers were washed with a 10% solution of NaOH and then the amine was extracted with 2 *N* HCl.

The aqueous extracts were made basic and the amine was extracted into ether. After drying over KOH the ether was removed under reduced pressure and the product distilled to give 27.6 g (70%) of benzylmethylaniline with a b.p. 120 °C at 1 Torr, lit. (32) b.p. 162–3 °C at 8 Torr.

The products of the reaction were recovered quantitatively from reaction mixtures in the following manner. The reaction mixture was poured into 1400 ml of p*H* 12 water (the p*H* was adjusted using NaOH) and the products were extracted with 100, 75, 70 and 70 ml of ether. The last traces of DMF were removed by extracting the combined ether layers three times with 50 ml of p*H* 12 water.

The products were identified in two ways. One method involved concentrating the ether layer to a volume of a few ml on a rotary evaporator and examining the concentrate by gas chromatography. The analysis was done using a flow rate of 50 ml/min and a 15 ft, ¼ in. column of 10% Carbowax 20 M on Chromosorb P at 168 °C until the dimethylaniline and methylphenyl sulfide had been eluted, and then at 235 °C where the benzylphenyl sulfide and benzylmethylphenyl amine were eluted. The products had retention times identical to those of authentic samples. An analysis based on the area under each peak indicated that at least 99.6% of the product was formed by reaction at the benzyl carbon.

The major products were also identified by comparing their infrared and n.m.r. spectra with those of authentic samples. The products were first separated by extracting the ether solution once with 70 ml and three times with 40 ml of 2.5% H_2SO_4. Evaporation of the ether gave the sulfide product which was dissolved in a few ml of spectrograde CCl_4. The acid layers were combined, made basic by adding solid NaOH and extracted with three 50 ml portions of ether. Evaporation of the ether gave the amine product which was dissolved in a few ml of spectrograde CCl_4. These solutions were examined by n.m.r. and i.r. spectroscopy. The spectra were identical to those of authentic samples of benzylphenyl sulfide and the *para*-substituted *N,N*-dimethylanilines.

The extent of reaction and yield of each product were obtained from the quantitative analysis of both the benzylphenyl sulfide and the *N,N*-dimethylaniline. The analyses were carried out on the ether solution containing the sulfide and the sulfuric acid solution containing the dimethylaniline. The analysis of the benzylphenyl sulfide involved concentrating the ether solution to approximately 5 ml on the rotary evaporator and adding it to approximately 45 mg (accurately weighed) of the internal standard, diphenyl ether. The solution was diluted to 10 ml and analyzed using the internal standard technique (13) on a 15 ft, ¼ in. column of 10% SE-30 on Chromosorb P at 150 °C and a flow rate of 110 ml/min.

The first step in the analysis of the *N,N*-dimethylaniline was removing the water in the sulfuric acid solution under reduced pressure. The concentrate was then mixed with 100 mg of red mercuric oxide, 2.5 g of potassium sulfate and 2 ml of concentrated H_2SO_4 and heated for approximately 6 h (2 h after the solution had become clear and colorless) in a kjeldahl digestion apparatus.

The ammonium sulfate solution from the kjeldahl

Can. J. Chem. Downloaded from www.nrcresearchpress.com by 210.87.254.42 on 09/05/12
For personal use only.

digestion was placed in a kjeldahl-type distillation apparatus, made basic with an excess of 40% aqueous sodium hydroxide solution, and the ammonia distilled into 50 ml of 0.01 *N* sulphuric acid. Back titration with 0.01 *N* NaOH gave the amount of ammonia and thus the amount of the *N,N*-dimethylaniline that had been produced in the reaction.

Quantitative yields of benzylphenyl sulfide and the *N,N*-dimethylanilines were obtained for reactions taken 100% to completion. The extent of reaction in runs stopped part way to completion was obtained by averaging the results of the benzylphenyl sulfide and the *N,N*-dimethylaniline analyses.

Kinetic Measurements

The rates of the reactions were measured at 0 °C in an ice-distilled water bath. The following preparations for a kinetic run were performed in a glove bag under a nitrogen atmosphere. Thirty ml of DMF cooled to 0 °C, were pipetted into a 50 ml volumetric flask containing 2.40 g of $NaNO_3$ and sufficient quaternary ammonium salt to prepare 50 ml of a 0.025 *M* solution of the quaternary ammonium salt. An amount of sodium thiophenoxide such that 20 ml of the solution would contain sufficient thiophenoxide ion to prepare 50 ml of a solution between 0.030 and 0.075 *M* in thiophenoxide ion, was weighed into a tared 25 ml volumetric flask. Finally, approximately 30 ml of cold DMF were placed in a ground-glass stoppered flask.

After all the containers had been temperature equilibrated, 25 ml of DMF were added under a stream of nitrogen, to the 25 ml volumetric containing the sodium thiophenoxide. When the salt had dissolved, 20 ml of this solution was poured under a stream of nitrogen into the 50 ml volumetric flask containing the quaternary ammonium salt. This flask was fitted with a serum cap and the reaction was followed by titrating the unreacted thiophenoxide ion contained in a 2.5 ml sample with a standard solution of Hg^{2+} ion (15).

Nitrogen Kinetic Isotope Effect

The nitrogen isotope effect was determined by comparing the $^{14}N/^{15}N$ ratios of the nitrogen in the *N,N*-dimethylaniline formed after small extents of reaction, between 17 and 38% of completion, with this ratio in the ammonium nitrogen in the starting material. The latter was obtained by measuring this ratio of the nitrogen in the *N,N*-dimethylaniline from a reaction taken to completion (16).

The *N,N*-dimethylaniline was recovered from the reaction mixture and decomposed in a kjeldahl digestion to ammonium sulfate using the procedure described in the section titled product identification and analysis. Finally, the ammonium ions were oxidized to nitrogen gas for mass spectrometric analysis (17). The magnitudes of the isotope effects shown in Table 2 do not vary either directly or indirectly with the extent of reaction. This indicates that the samples are not contaminated with traces of nitrogen containing impurities since impurities of this type would contaminate the samples of varying $^{14}N/^{15}N$ ratio with some nitrogen of constant isotopic ratio and thus would alter the observed effect in a way that would be related to the extent of reaction.

The authors are greatly indebted to President E. J. Monahan of Laurentian University for the financial support required to complete this study. We also wish to acknowledge the contribution of Mr. G. Alexiuk who helped to work out many of the techniques required in this investigation.

1. S. D. Ross, M. Finkelstein, and R. C. Petersen. J. Am. Chem. Soc. **82**, 5335 (1960).
2. S. D. Ross, M. Finkelstein, and R. C. Petersen. J. Am. Chem. Soc. **83**, 4853 (1961).
3. R. C. Petersen, M. Finkelstein, and S. D. Ross. J. Am. Chem. Soc. **84**, 2222 (1962).
4. K. Mulkerjee, J. N. Kar, G. B. Behera, R. C. Acharya, and M. K. Rout. Indian J. Chem. **9**, 947 (1971).
5. K. T. Leffek and F. H. C. Tsao. Can. J. Chem. **46**, 1215 (1968).
6. E. C. F. Ko and K. T. Leffek. Can. J. Chem. **49**, 129 (1971).
7. E. C. F. Ko and K. T. Leffek. Can. J. Chem. **50**, 1297 (1972).
8. R. A. Sneen and J. W. Larsen. J. Am. Chem. Soc. **91**, 362 (1969).
9. R. A. Sneen and J. W. Larsen. J. Am. Chem. Soc. **91**, 6032 (1969).
10. F. G. Bordwell and T. G. Mecca. J. Am. Chem. Soc. **94**, 2119 (1972).
11. C. A. Bunton. Nucleophilic substitution reactions at a saturated carbon atom. Elsevier, New York. 1963. p. 9; E. Gelles, E. D. Hughes, and C. K. Ingold. J. Chem. Soc. 2918 (1954).
12. V. F. Raaen, T. Juhlke, F. J. Brown, and C. J. Collins. J. Am. Chem. Soc. **96**, 5928 (1974).
13. S. Dal Nogare and R. S. Juvet, Jr. Gas-liquid chromatography. Interscience, New York. 1962. p. 256.
14. K. C. Westaway and A. N. Bourns. Can. J. Chem. **50**, 2332 (1972).
15. D. C. Gregg, P. E. Bouffard, and R. Barton. Anal. Chem. **33**, 269 (1961).
16. E. Buncel and A. N. Bourns. Can. J. Chem. **38**, 2457 (1960).
17. G. Ayrey, A. N. Bourns, and V. A. Vyas. Can. J. Chem. **41**, 1759 (1963).
18. J. T. Burns and K. T. Leffek. Can. J. Chem. **47**, 3725 (1969).
19. K. B. Wiberg. Physical organic chemistry. J. Wiley and Sons, New York. 1964. (*a*) p. 290; (*b*) pp. 404–406; (*c*) pp. 273–275.
20. K. Yates and G. Welch, Can. J. Chem. **50**, 474 (1972).
21. L. Melander. Isotope effects on reaction rates. Ronald Press, New York. 1960. p. 20.
22. D. G. Graczyk and J. W. Taylor. J. Am. Chem. Soc. **96**, 3255 (1974).
23. P. J. Smith and A. N. Bourns. Can. J. Chem. **52**, 749 (1974).
24. J. March. Advanced organic chemistry; reactions, mechanisms and structure. McGraw-Hill, Toronto. 1968. pp. 281 and 284.
25. T. Kametani, K. Kigasawa, M. Hiiragi, N. Wagatsuma, and K. Wakisaka. Tetrahedron Lett. 635 (1969).

Can. J. Chem. Downloaded from www.nrcresearchpress.com by 210.87.254.42 on 09/05/12
For personal use only.

26. R. A. SNEEN and H. M. ROBBINS. J. Am. Chem. Soc. **94**, 7868 (1972).
27. R. A. CHAMBERS. Ph.D. Thesis, Vanderbilt University, Nashville, Tennessee. 1963. p. 92.
28. I. HORMAN and M. J. STRAUSS. J. Chem. Educ. **46**, 114 (1969).
29. R. L. SHINER, H. C. STRUCT, and W. J. JORISON. J. Am. Chem. Soc. **52**, 2066 (1930).
30. C. M. SUTER and H. L. HANSEN. J. Am. Chem. Soc. **54**, 4100 (1932).
31. G. F. GRILLOT and R. E. SCHAFFRATH. J. Org. Chem. **24**, 1035 (1959).
32. I. E. POLLAK and G. F. GRILLOT. J. Org. Chem. **32**, 2892 (1967).

Can. J. Chem. Downloaded from www.nrcresearchpress.com by 210.87.254.42 on 09/05/12
For personal use only.

Aziridines saturées et insaturées. Synthèses par réduction de cyclohexénones oximes et études spectroscopiques

LOUIS FERRERO,[1] SERGE GERIBALDI, MICHEL ROUILLARD ET MARCEL AZZARO

Laboratoire de Chimie Physique Organique, Université de Nice, Campus Valrose, 06034 Nice Cédex, France

Reçu le 24 janvier 1975

LOUIS FERRERO, SERGE GERIBALDI, MICHEL ROUILLARD et MARCEL AZZARO. Can. J. Chem. **53**, 3227 (1975).

Les réductions de plusieurs oximes de cyclohexénones par $LiAlH_4$ et $NaAlH_2(OCH_2CH_2OCH_3)_2$ (Red-Al) conduisent à des aziridines saturées et insaturées du type aza-7 bicyclo[4.1.0]-heptane, ainsi qu'à des cyclohexène-2 amines. L'utilisation d'oximes de configuration *E* ou (et) *Z* permet de mettre en évidence la régiosélectivité des réductions et de proposer les schémas réactionnels d'obtention des différents types de produits.

LOUIS FERRERO, SERGE GERIBALDI, MICHEL ROUILLARD, and MARCEL AZZARO. Can. J. Chem. **53**, 3227 (1975).

The reduction of several cyclohexenone oximes using lithium aluminum hydride and sodium dihydrobis-(2-methoxyethoxy)aluminate yields saturated and unsaturated aziridines with a 7-azabicyclo[4.1.0]heptane skeleton and cyclohex-2-ene amines. The use of oximes of *E* and/or *Z* configuration demonstrates the regioselectivity of the reduction and allows us to propose reaction schemes explaining the formation of the different types of products.

Si les réductions d'oximes saturées linéaires et cycliques ont fait l'objet d'un nombre considérable de travaux, il n'en est pas de même en série éthylénique. Récemment, divers auteurs se sont intéressés aux oximes α,β-éthyléniques cycliques (1–4); cependant, leurs travaux ne concernent qu'un nombre restreint d'oximes, réduites avec un seul réducteur, $LiAlH_4$. L'utilisation de cyclohexène-2 one oximes diversement substituées et de deux réducteurs aluminiques, $LiAlH_4$ et $NaAlH_2(OCH_2CH_2OCH_3)_2$ (Red-Al) nous permet d'accéder à des séries d'aziridines saturées et insaturées de structures inédites, ainsi qu'à des amines primaires éthyléniques et secondaires transposées (schéma 1).

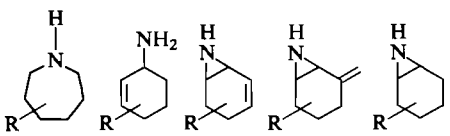

R = alkyle

SCHÉMA 1

Le phénomène de régiosélectivité des réductions, depuis longtemps démontré en série saturée et observé en série insaturée (5), peut être généralisé pour les oximes α,β-éthyléniques. Les études en résonance magnétique nucléaire du proton et en infrarouge permettent de préciser les structures des composés azotés synthétisés. Par ailleurs, les configurations des aziridines substituées sont confirmées par hydrogénation catalytique en amine primaire (6). Les études spectroscopiques font l'objet de la seconde partie de ce mémoire.

[1]Ce travail fait partie de la thèse de 3ème cycle de L. Ferrero présentée à Nice, le 15 octobre 1974.

Resultats et discussion

Toutes les réductions ont été menées sur trois types de cyclohexénone oximes choisies d'après un critère configurationnel (schéma 2) : (*i*) isomérie *E* et *Z* possibles sur le même type d'oxime: isophorone oxime **1** et méthyl-3 cyclohexène-2 one-1 oxime **2**; (*ii*) isomérie *E* seule possible: carvone oxime **3** et méthyl-2 cyclohexène-2 one-1 oxime **4**; (*iii*) isomérie *Z* seule possible: pipéritone oxime **5**.

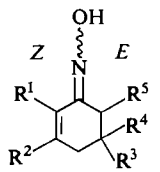

1: $R^1 = R^5 = H$ $R^2 = R^3 = R^4 = CH_3$
2: $R^1 = R^3 = R^4 = R^5 = H$ $R^2 = CH_3$
3: $R^1 = CH_3$ $R^2 = R^4 = R^5 = H$ $R^3 = C(=CH_2)(CH_3)$
4: $R^1 = CH_3$ $R^2 = R^3 = R^4 = R^5 = H$
5: $R^1 = R^3 = R^4 = H$ $R^2 = CH_3$ $R^5 = CH(CH_3)_2$

SCHÉMA 2

Can. J. Chem. Downloaded from www.nrcresearchpress.com by 210.87.254.5 on 09/05/12
For personal use only.

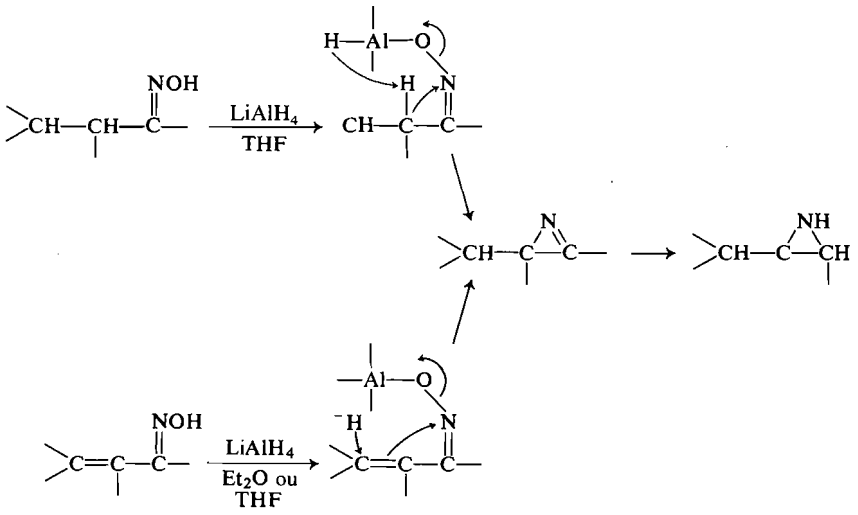

SCHÉMA 3

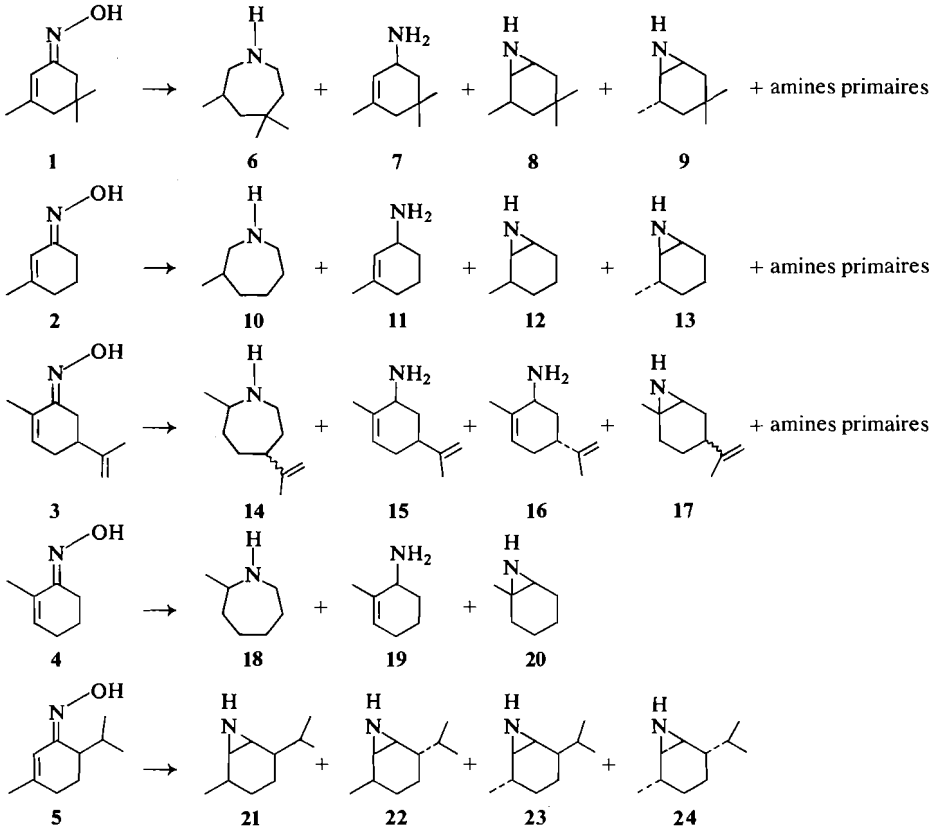

SCHÉMA 4

Réduction par $LiAlH_4$ dans l'éther diéthylique

Si la réduction des oximes saturées par $LiAlH_4$ dans l'éther ne peut conduire qu'à des amines primaires et secondaires, il n'en est pas de même en série insaturée où des aziridines peuvent être obtenues (1–4). En effet, les processus généraux d'obtention d'aziridines par réduction d'oxime s'effectuent, soit par arrachement d'un proton

Can. J. Chem. Downloaded from www.nrcresearchpress.com by 210.87.254.5 on 09/05/12
For personal use only.

Can. J. Chem. Downloaded from www.nrcresearchpress.com by 210.87.254.5 on 09/05/12
For personal use only.

mobile (cas des oximes saturées), soit par addition d'un ion hydrure (cas des oximes éthyléniques) (schéma 3).

Dans le premier cas, l'utilisation du tétrahydrofurane facilite le départ du proton; dans le second cas, un tel solvant n'est plus nécessaire. Ainsi, dans l'éther diéthylique, l'addition d'un ion hydrure est nettement favorisée par rapport à l'arrachement d'un proton aliphatique; le cours de la réaction est donc simplifié, ce qui nous a permis de mettre en évidence un phénomène de régiosélectivité. Toutes les réductions ont été opérées en respectant les conditions suivantes : (*i*) $LiAlH_4$ en excès : de 4 à 5 moles de réducteur par mole d'oxime; (*ii*) solvant : éther diéthylique; concentration en oxime : 10^{-1} *M*; (*iii*) température : au reflux du solvant; (*iv*) temps de réaction : jusqu'à disparition totale de l'oxime, soit de 24 à 72 h.

Les différentes réductions peuvent être schématisées comme suit (schéma 4). Les pourcentages en produits de réaction, obtenus à partir des données de la c.p.v. analytique, sont notés dans le tableau 1.

Trois conclusions principales se déduisent de ces résultats:

1. Avant le début de nos travaux, la formation d'aziridines dans l'éther n'avait été observée qu'à partir d'oximes éthyléniques substituées par des noyaux phényles. Nous constatons donc que l'obtention de tels composés est possible même en l'absence d'une telle substitution. Ces résultats sont en accord avec les observations de C. Glacet et ses collaborateurs (2).

2. Parmi les autres produits, nous trouvons des amines β,γ-éthyléniques et secondaires. Il est à noter que ces structures n'avaient été que très rarement observées dans des réductions analogues (1, 2).

3. Nous constatons que quelle que soit la substitution des oximes de départ, l'isomère *Z* (*syn*) conduit toujours préférentiellement à la formation d'aziridines, alors que l'isomère *E* (*anti*) favorise l'obtention des amines.

Ce dernier résultat nous permet donc de conclure que le phénomène de régiosélectivité déjà observé en série saturée (7) peut être étendu aux oximes α,β-éthyléniques (5). L'interprétation de ce phénomène peut être faite sur la base des études mécanistiques menées par Kotera et ses collaborateurs (7) et par Dimmock et al. (1). Le processus de formation des aziridines à partir des isomères *Z* peut se concevoir à partir du chemin réactionnel suivant (schéma 5):

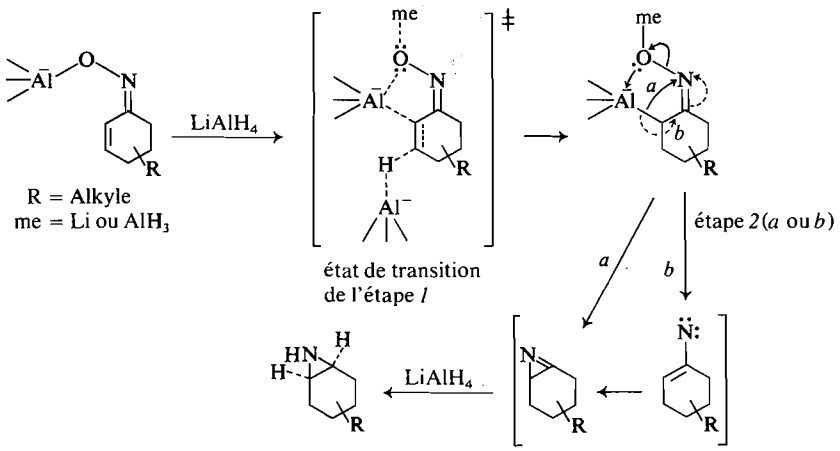

SCHÉMA 5

La régiosélectivité est commandée à la fois par les étapes *1* et *2*. La délocalisation électronique du complexe d'isomérie *Z* favorise l'addition de la seconde molécule d'hydrure métallique. La seconde étape est la *cis*-élimination intramoléculaire avec participation d'un doublet libre de l'oxygène.

Il est à remarquer que l'état de transition proposé pour mener à l'organo-métallique intermédiaire possède déjà la structure nécessaire au processus de *cis*-élimination. Les étapes *1* et *2* peuvent donc être confondues, ce qui expliquerait le fait que nous n'ayons jamais pu isoler d'oxime saturée résiduelle.

TABLEAU 1. Réductions par $LiAlH_4$ dans Et_2O

Oximes	Rapport Z:E	Amines				Aziridines			
		Primaires	Secondaires		Ethylénique				
			6		**7**	**8**			**9**
1	1:1		6%		40%	24%			30%
	1:2		6%		54%	18%			22%
			10		**11**	**12**			**13**
2	1:0	8%	4%		12%	42%			34%
	1:2	13%	16%		31%	21%			19%
			14	**15**	**16**		**17**		
3	0:1	13%	8%	42%	13%		24%		
			18		**19**		**20**		
4	0:1	0%	42%		34%		24%		
						21	**22**	**23**	**24**
5	1:0	0%	0%		0%	34%	20%		46%

L'étude détaillée de cette régiosélectivité a fait l'objet d'une récente étude (8).

Réduction par $LiAlH_4$ dans le tétrahydrofurane

Comme nous l'avons déjà fait remarquer précédemment, l'utilisation du THF favorisant l'élimination des protons mobiles, du fait de l'augmentation de la température de réaction et de l'accroissement de la polarité du solvant (9), la cyclisation en aziridines peut suivre les deux voies distinctes (*a*) et (*b*) (schéma 6) : (*a*) addition

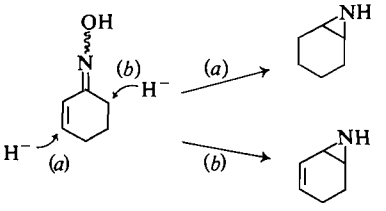

SCHÉMA 6

de l'ion hydrure sur le carbone éthylénique C_3 comme dans l'éther diéthylique; (*b*) élimination d'un proton mobile aliphatique en α de la fonction oximino comme dans le cas des oximes saturées (7).

Les conditions de réductions sont semblables à celles menées dans l'éther. Les temps de réactions varient de 3 à 6 h; les oximes *E* réagissant plus lentement que les isomères *Z*. Les composés obtenus à partir des cinq oximes de cyclohexénones sont identiques à ceux précédemment décrits, sauf en ce qui concerne l'isophorone oxime **1** et la carvone oxime **3** qui conduisent en plus aux aziridines éthyléniques **25** et **31**, et l'oxime **4** qui donne l'imine **35** (schéma 7).

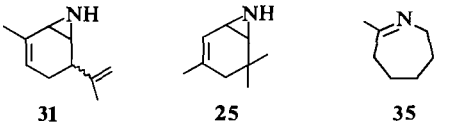

31 **25** **35**

SCHÉMA 7

Comme précédemment, les proportions en produits azotés varient principalement en fonction de la configuration des oximes de départ. Toutefois, pour des oximes de même configuration, l'influence de la substitution sur le carbone 5 n'est pas à négliger. Les résultats sont résumés dans le tableau 2.

La réduction des oximes α,β-éthyléniques par $LiAlH_4$ est fortement influencée par l'emploi du THF à 66 °C. Comme l'a déjà fait observer G. Ricart (9), cette influence peut avoir deux origines, d'une part, l'augmentation de la polarité du solvant et d'autre part, un accroissement de la température de réaction. Il est toutefois difficile d'évaluer l'apport de ces deux effets puisque les réductions menées dans le THF à 35 °C sont beaucoup plus lentes qu'à 66 °C et que le rendement global est nettement plus faible (9). Ces effets de solvant et de température sont fortement marqués dans le cas de l'isophorone oxime **1** et se traduisent par l'apparition d'un composé nouveau, l'aza-7 triméthyl-3,5,5 bicyclo[4.1.0]heptène-2, **25**. Cependant, cette constatation ne peut être généralisée aux autres cyclohexénones oximes où l'emploi du THF à 66 °C provoque principalement une diminution des temps de réaction et une augmentation sensible des proportions en aziridines saturées. Remarquons que la formation de **25** est prépondérante lorsque

Can. J. Chem. Downloaded from www.nrcresearchpress.com by 210.87.254.5 on 09/05/12
For personal use only.

TABLEAU 2. Réductions par $LiAlH_4$ dans le THF

Oximes	Rapport Z:E	Amines																							
		Primaires		Secondaires			Ethyléniques			Aziridines															
				6			**7**			**8**			**9**			**25**									
	1:1			6%			24%			17%			27%			26%									
1	1:2			6%			24%			12%			19%			39%									
	0:1			10%			28%			2%			4%			56%									
				10			**11**					**12**			**13**										
2	1:0	8%		7%			12%					38%			35%										
	1:2	19%		10%			24%					24%			23%										
				14		**15**		**16**				**17**			**31**										
3	0:1			0%		34%		9%				49%			8%										
				18			**19**						**20**												
4	0:1	0%		10%			19%						58%*												
										21		**22**			**23**			**24**							
5	1:0	0%		0%			0%			26%			26%			48%									

*+13% de l'imine **35**.

l'oxime **1** est de configuration *E*, ce qui est conforme au phénomène de régiosélectivité observé sur les oximes saturées, déjà interprété par Kotera et ses collaborateurs (7).

Réduction par le Red-Al '$NaAlH_2(OCH_2CH_2OCH_3)_2$' dans le tétrahydrofurane

Avant nos travaux, ce réactif avait été employé avec succès dans la réduction de deux oximes : une aldoxime aromatique et la cyclohexanone oxime (10); cependant, seule la formation d'amines primaires avait été observée. L'utilisation de ce réducteur avec l'isophorone oxime **1** a montré que des aziridines éthyléniques pouvaient être obtenues (11). Ceci nous a incité à généraliser ce type de réduction à une série d'oximes de cyclohexénones.

Les conditions de réactions sont identiques à celles précédemment décrites. Les temps de réaction varient de 1 à 3 h. La complexité des bilans réactionnels est résumée dans le schéma 8. Les proportions en composés azotés obtenues

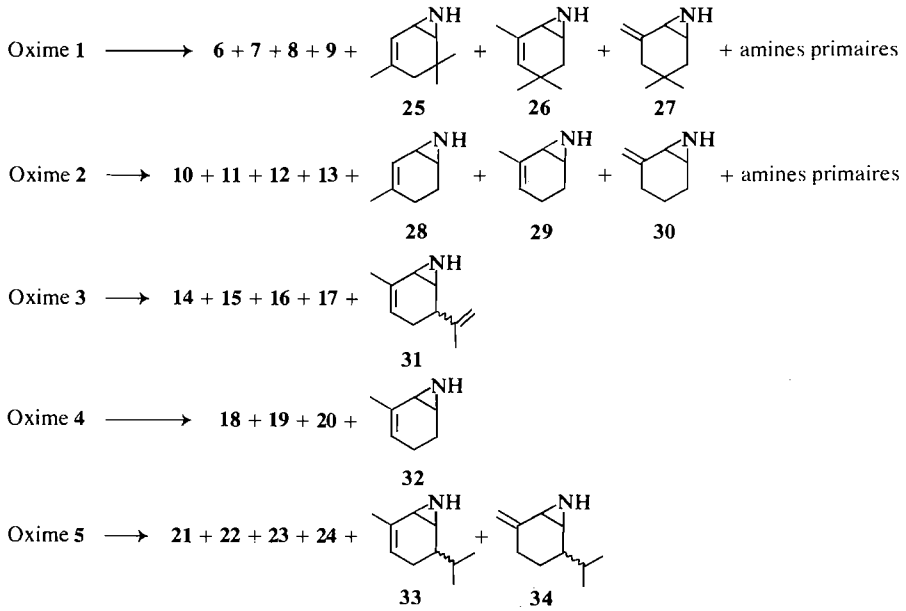

SCHÉMA 8

Can. J. Chem. Downloaded from www.nrcresearchpress.com by 210.87.254.5 on 09/05/12
For personal use only.

Can. J. Chem. Downloaded from www.nrcresearchpress.com by 210.87.254.5 on 09/05/12
For personal use only.

TABLEAU 3. Réductions par le Red-Al dans le THF

Oximes	Rapport $Z:E$	Amines			Aziridines			
		Primaires	Secondaires	Ethyléniques	Saturées		Ethyléniques	
			6	**7**	**8**		**9**	**25**	**26**	**27**
	1:1		≃0%	5%	1%		2%	45%	15%	32%
1	1:2		3%	4%	1%		2%	55%	11%	24%
	0:1		≃0%	≃0%		≃0%		88%	4%	8%
			10	**11**	**12**		**13**	**28**	**29**	**30**
2	1:0	3%	3%	2%	13%		10%		31%	37%
	1:2	4%	4%	20%	11%		9%	18%	15%	16%
			14	**15** **16**		**17**			**31**	
3	0:1		0%	39% 6%		10%			45%	
			18	**19**		**20**			**32**	
4	0:1		0%	18%		19%			40%*	
					21	**22** **23**	**24**	**33**		**34**
5	1:0	0%	0%	0%	5%	3%	16%	50%		26%

*+23% de l'imine **35**.

Can. J. Chem. Downloaded from www.nrcresearchpress.com by 210.87.254.5 on 09/05/12
For personal use only.

par c.p.v. analytique sont données dans le tableau 3.

Ces résultats confirment bien la spécificité de ce nouveau réducteur. En effet, toutes les cyclohexénone oximes traitées par le Red-Al donnent des taux importants d'aziridines α,β-éthyléniques, alors que $LiAlH_4$ n'a jamais permis l'obtention de ces produits (sauf cas de **1** dans le THF) de façon prépondérante. Nous observons à nouveau la régiosélectivité de la réaction qui est parfaitement démontrée dans le cas des oximes **1** et **2**, où les aziridines éthyléniques **25** et **28** ne sont formées qu'à partir d'oximes de configuration *E* par cyclisation sur le carbone aliphatique (7), alors que les aziridines insaturées **26**, **27** et **29**, **30** dérivent essentiellement des oximes de configuration *Z* suivant le processus réactionnel suivant (schéma 9).

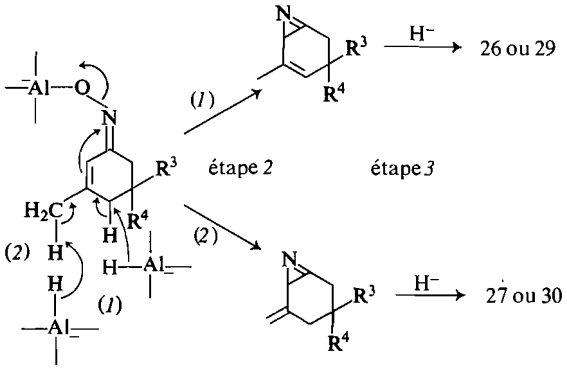

1: $R^3 = R^4 = CH_3$

2: $R^3 = R^4 = H$

SCHÉMA 9

Le Red-Al diffère donc de $LiAlH_4$ par son aptitude à favoriser les réactions procédant par élimination d'un proton mobile en α d'une insaturation. Cette propriété peut être expliquée par la conjugaison des deux facteurs suivants: (*i*) le facteur stérique inhérent à la taille du groupement méthoxy-2 éthoxy qui s'oppose à une approche suffisante de l'oxime par la molécule de Red-Al chargée d'additionner l'ion hydrure sur la liaison éthylénique (12); (*ii*) la basicité ou dureté du réducteur, c'est-à-dire l'aptitude du Red-Al à éliminer les protons aliphatiques mobiles.

Par ailleurs, il est important de noter que la réactivité du Red-Al se manifeste de façon analogue dans l'éther diéthylique et le tétrahydrofurane. Ceci peut être vérifié, par exemple, sur l'oxime **1**, dont les résultats comparatifs sont rapportés dans le tableau 4. Il semble donc que l'influence de ce réducteur est telle qu'elle masque pratiquement les effets du solvant et de la température qui ne sont, dans ce cas, que minimes.

Conclusion

Les réductions de cyclohexénone oximes de configuration *E* ou (et) *Z* par $LiAlH_4$ et $NaAlH_2(OCH_2CH_2OCH_3)_2$ ont permis de synthétiser un grand nombre d'aziridines et, en particulier, avec le dernier réactif, d'accèder à une nouvelle série de composés inédits qui sont des aziridines α,β-éthyléniques du type aza-7 bicyclo[4.1.0] heptane. Parmi les nombreux facteurs qui déterminent les voies de réduction suivies, notre étude en fait ressortir les quatre plus importants, à savoir, l'influence du solvant, de la température de réaction, la nature de l'agent réducteur et l'effet de la configuration de l'oxime. Nos travaux ont été axés plus particulièrement sur ce dernier facteur; en effet, le phénomène de régiosélectivité déjà connu sur les oximes saturées a pu être étendu en série α,β-éthylénique.

Il nous paraîtrait donc intéressant d'essayer d'appliquer, dès à présent, ce type de réduction par le Red-Al à la synthèse d'aziridines α,β-éthyléniques. Nos travaux actuels ont pour but de rechercher les conditions réactionnelles optimales afin d'orienter le cours des réductions essentiellement vers la formation de telles aziridines, en particulier par l'emploi d'autres hydrures complexes, ainsi qu'une méthode de séparation efficace permettant d'isoler ces composés avec de meilleurs rendements.

Etudes spectroscopiques r.m.n. et i.r.

Les structures des composés azotés nouveaux dont la synthèse a été décrite précédemment, ont été établies, d'une part, par transformations chimiques (hydrogénolyse des aziridines en amines primaires (6)), et d'autre part, par analyse spectroscopique, en particulier par résonance magnétique nucléaire du proton et par infra-rouge. Nous ne donnerons ici que les signaux caractéristiques nécessaires à l'identification des structures. Les déplacements chimiques et constantes de couplages relatifs à chaque produit sont donnés dans la partie expérimentale.

Les aziridines bicycliques α,β-insaturées étant les plus riches en information de par la présence des protons éthyléniques, seront étudiées en premier lieu.

TABLEAU 4. Comparaison entre les réductions dans l'éther et le THF (pour l'isophorone avec le Red-Al)

Solvant	Rapport Z:E	Amines			Aziridines				
		Primaires	Secondaires	Ethyléniques	Saturées		Ethyléniques		
			6	**7**	**8**	**9**	**25**	**26**	**27**
THF	1:1	0%		5%	1%	2%	45%	15%	32%
	1:2	3%		4%	1%	2%	55%	11%	24%
Et_2O	1:1	2%		12%	6%	7%	42%	10%	21%
	1:2	2%		9%	4%	5%	58%	7%	15%

Etudes des aziridines α,β-éthyléniques

Les spectres r.m.n. des aziridines éthyléniques présentent plusieurs types de signaux caractéristiques : (*i*) entre 4 et 6 p.p.m., les protons éthyléniques ; (*ii*) entre 1.8 et 2.5 p.p.m., les protons des carbones tête de pont en position 1 et 6 ; ces signaux, plus ou moins séparés, permettent de confirmer la position *cis* de ces deux protons (constante de couplage classique $J_{1,6}$ = 6 Hz) (13) ; leurs déplacements chimiques et les autres constantes de couplage sont caractéristiques de la structure de la molécule ; (*iii*) entre 0.5 et 0.8 p.p.m., le proton de la fonction aziridine; (*iv*) les signaux des autres protons du cycle ne sont que très rarement exploitables.[2]

Les aziridines éthyléniques à double liaison exocyclique sont de plus, caractérisées par le système vinylique, observable en infra-rouge (3080, 1650 et 880 cm^{-1}). L'ensemble des signaux caractérisant les aziridines insaturées étudiées et leurs évolutions pour les différents isomères sont résumés dans le schéma 10.

Nous noterons en particulier : (*i*) les protons éthyléniques résonnant pour chaque type de structure à des champs bien différenciés (5.60, 5.20, 4.94 et 4.80 p.p.m.); (*ii*) les protons en tête de pont et en particulier, le proton en C_1 faiblement sensible aux effets de substitution.

Etudes des aziridines bicycliques saturées

Du fait de l'absence de liaison éthylénique, les protons résonnent à des champs très voisins, ce qui rend les spectres r.m.n. de composés

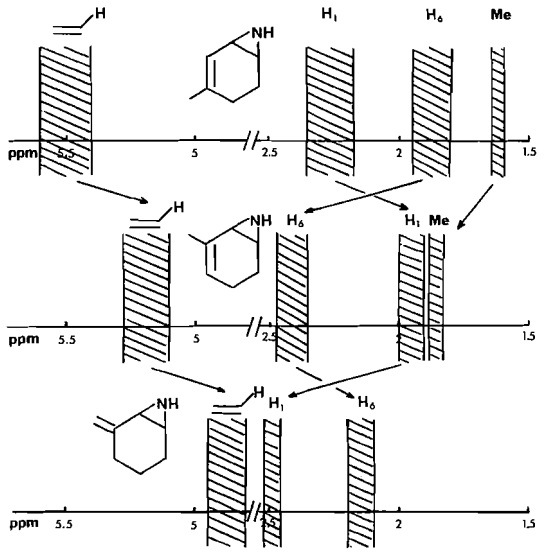

SCHÉMA 10

beaucoup plus complexes que ceux précédemment décrits. De plus, un nouveau problème apparaît : la position *cis* ou *trans* des différents substituants par rapport au cycle aziridinique. Ce problème d'isomérie ayant été résolu par hydrogénolyse (6) (voir partie expérimentale); il nous a donc été possible de relever les principales caractéristiques r.m.n. des différentes aziridines saturées.

Les cyclohexénimines méthylées en tête de pont présentent peu de signaux exploitables, le méthyle tête de pont blindant le proton voisin en C_6. Seul, le déblindage de ce méthyle (1.20 p.p.m.) est notable.

Les isomères *cis* et *trans* des différentes cyclohexénimines méthylées en position 2 présentent des spectres r.m.n. voisins; cependant, nous pouvons dégager des valeurs observées un certain nombre de résultats caractéristiques. La substitution en C_2 ou C_5 entraîne un blindage

[2]Il a cependant été possible, pour certains composés, en particulier pour les dérivés de l'isophorone oxime **1**, d'attribuer un grand nombre de signaux et dans certains cas, de mettre en évidence l'existence de conformations privilégiées. Nous ne développerons pas ici ce problème conformationnel, bien que le simple spectre r.m.n. (Varian A 60A, température ambiante, sans découplage) permette sa mise en évidence; ces différents problèmes seront exposés dans un prochain mémoire.

Can. J. Chem. Downloaded from www.nrcresearchpress.com by 210.87.254.5 on 09/05/12
For personal use only.

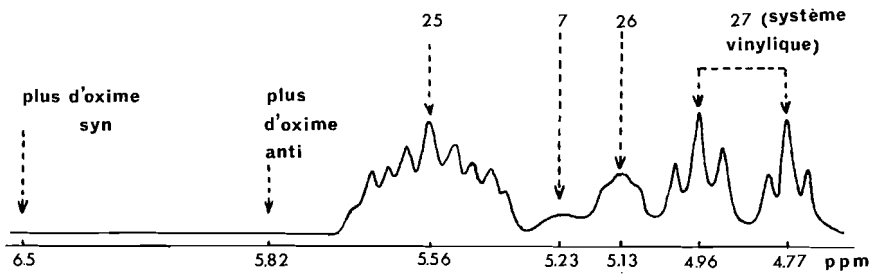

SCHÉMA 11

des protons en tête de pont lorsqu'elle s'effectue en *trans* du petit cycle, tandis que la substitution en *cis* provoque des effets négligeables. Les couplages vicinaux des protons en C_1 et C_6 sont un critère valable (s'ils sont mesurables). Nous noterons en particulier le couplage $J_{1,2}$ nul, caractéristique des composés **9** et **13**, tous deux *trans* méthylés.

Etudes des amines éthyléniques

Dans cette série, trois types de signaux sont exploitables : (*i*) à champ faible, le proton éthylénique centré vers 5.35 p.p.m.; (*ii*) vers 3.2 p.p.m., le proton en α du NH_2 fonctionnel; (*iii*) vers 1.65 p.p.m., le méthyle éthylénique.

Il est, de plus, possible de différencier les amines méthylées, soit en C_2, soit en C_3; en effet, le signal des protons du méthyle est légérement déblindé lorsque ce dernier est en C_2 (1.70 p.p.m. au lieu de 1.63 p.p.m. en position C_3). Inversement, le proton éthylénique en C_2 (5.25 p.p.m.) est blindé par rapport à un proton en C_3 (5.33 p.p.m.). Cependant, la largeur à mi-hauteur du signal de ce proton éthylénique reste le critère le plus significatif : elle est d'environ 6 Hz pour le proton en C_2 (un seul couplage vicinal $J_{1,2}$) et d'environ 10 Hz pour le proton en C_3 (deux couplages vicinaux).

Etudes des amines secondaires transposées et de l'imine 35

Les spectres r.m.n. des amines secondaires transposées sont assez peu explicites, la plupart des signaux étant superposés. La seule partie intéressante du spectre (entre 2.40 et 3.0 p.p.m.) concerne les protons portés par les carbones C_2 et C_7 en α de la fonction amine. L'intégration des signaux de cette région du spectre est liée au nombre de ces protons; trois protons pour les composés **14** et **18**, méthylés en C_2; quatre protons pour le composé **10**, confirmant l'absence de substitution en α de l'azote.

Pour le composé **35**, la présence d'une double liaison, l'absence de proton éthylénique et de proton fonctionnel lié à l'azote sont en bon accord avec la structure proposée pour ce composé basique. Ce produit disparaît du mélange réactionnel (avec l'amine β,γ-éthylénique) par simple lavage avec une solution de chlorure d'ammonium, ce qui n'est pas le cas pour les aziridines moins basiques et plus stables. Bien que l'hydrogénolyse en amine **18** n'ait pu être réalisée, les données i.r., r.m.n., masse et les travaux de C. Glacet et ses collaborateurs (2) confirment la structure proposée.

Cette étude r.m.n. nous a permis de confirmer les structures de tous les composés azotés synthétisés ainsi que d'envisager un dosage des mélanges réactionnels : les composés insaturés présentent tous, à champ faible, des signaux qui caractérisent leur appartenance à une série de composés bien déterminée, de plus, dans une même série, ces déplacements permettent de déduire directement la substitution. Une telle spécificité des déplacements chimiques et surtout l'absence de toute superposition de signaux, permet, pour chaque oxime réduite, un dosage du mélange réactionnel par intégration des signaux des protons éthyléniques (schéma 11), confirmant ainsi les résultats des chromatographies en phase gazeuse.

Partie expérimentale

Conditions générales

Les spectres i.r. ont été enregistrés sur un appareil Perkin-Elmer 457. Les masses des composés ont été mesurées à l'aide d'un spectromètre Varian MAT 111 (14).

Les caractéristiques r.m.n. ont été obtenues sur appareil Varian A 60A en utilisant le tétrachlorure de carbone et le chloroforme deutérié comme solvants et le tétraméthylsilane comme référence interne.

La pureté des oximes a été vérifiée par c.p.v. sur appareil Perkin-Elmer F 11, équipé d'une colonne analytique de 1.60 m (diamètre $\frac{1}{8}$ po) imprégnée d'une

Can. J. Chem. Downloaded from www.nrcresearchpress.com by 210.87.254.5 on 09/05/12
For personal use only.

TABLEAU 5. Résultats des différentes oximations

Cétones de départ	p*H* d'oximation	Oximes synthétisées			Point de fusion (°C)	Rendement (%)	M⁺ *m/e*
Isophorone	basique	33%*Z*	**1**	67%*E*	73–75	87	153
	acide	50%*Z*		50%*E*	73–75	58	
Méthyl-3 cyclohexène-2 one-1	basique	33%*Z*	**2**	67%*E*	49	75	125
	acide	100%*Z*		0%*E*	82	37	
Carvone	basique		**3**	*E*	71	75	165
Méthyl-2 cyclohexène-2 one-1	basique		**4**	*E*	63	76	125
Pipéritone	acide		**5**	*Z*	98–99	45	167

phase Carbowax 20 M à 10% sur support Chromosorb WDMCS, température 130 °C, vecteur azote.

La chromatographie gazeuse des aziridines a été effectuée sur deux colonnes différentes : (*1*) colonne analytique A : 3 m (diamètre $\frac{1}{8}$ po), Chromosorb P80/100 imprégné de 2% de potasse et 12.5% d'Hyprose; vecteur azote 3 cm/s; température de 100 à 120 °C; (*2*) colonne analytique B : 3 m (diamètre $\frac{1}{8}$ po), Chromosorb WDMCS 80/100 imprégné de 5% de potasse et de 10% de Carbowax 20M; vecteur azote 3 m/s; température de 95 à 125 °C.

La séparation des amines et des aziridines a été faite par chromatographie préparative en phase gazeuse sur un appareil Carlo Erba Fractovap 2400V : (*1*) colonne A préparative : 2 m (diamètre $\frac{3}{8}$ po), Chromosorb P80/100 imprégné de 2% de potasse et de 12% d'Hyprose; vecteur azote 4 cm/s; température de 110 à 130 °C; (*2*) colonne B préparative : 4 m (diamètre $\frac{3}{8}$ po), Chromosorb P80/100 imprégné de 5% de potasse et de 12.5% de Carbowax 20M; vecteur azote 4 cm/s; température 140 °C.

Les séparations de certains composés étant améliorées sur Carbowax ou sur hyprose, l'emploi de deux types de colonne nous a paru préférable.

Procédés généraux de préparation des oximes

Les méthodes de synthèses d'oximes α,β-éthyléniques, décrites par Sato et al. (15) ont toujours été employées. Cependant, si trois cyclohexénones ne peuvent conduire qu'à des oximes d'un seul type de configuration *E* ou *Z*, à cause de la substitution en α de la fonction carbonyle (cas des oximes **3**, **4** et **5**), il n'en est pas de même pour l'isophorone et la méthyl-3 cyclohexéne-2 one-1 dont les oximes peuvent être *Z* et *E* et où il est important d'obtenir des proportions variables d'isomères. En fait, le p*H* du milieu réactionnel oriente la synthèse vers la formation préférentielle d'un des isomères *syn* ou *anti* de l'oxime. Ainsi:

(*a*) Synthèse à p*H* basique : suivant (15), on obtient pour **1** un mélange d'isomères *Z* et *E* en proportion 1:2. Ce mélange peut être réduit tel quel ou être préalablement cristallisé dans un mélange éthanol–eau (90:10) de manière à isoler l'isomère *E* majoritaire (p.f. 98 °C). De même, les isomères *Z* et *E* de l'oxime **2** sont obtenus en proportion 1:2 avec un rendement de 75%.

(*b*) Synthèse à p*H* acide : on obtient le chlorhydrate des oximes. Celles-ci sont régénérées par lavage de leur chlorhydrate avec une solution aqueuse de soude. L'oxime **1** est présente sous la forme des deux isomères *Z* et *E* en proportions égales (1:1) tandis que l'oxime **2** n'est isolée que sous la forme *Z*.

Le tableau 5 résume les résultats des différentes oximations.

Les études r.m.n. des oximes de cyclohexénones ayant été déjà décrites pour la plupart (15, 16, 17), l'identification des oximes **3** et **4** d'isomérie *E* et de l'oxime **5** d'isomérie *Z*, n'offre aucune difficulté. Cependant, les spectres r.m.n. des oximes **1** et **2** existant sous les formes *Z* et *E* permettent d'établir les proportions exactes d'isomères grâce aux déplacements chimiques du proton éthylénique qui est fortement influencé par la position du groupement hydroxyle (tableau 6).

Par ailleurs, les spectres i.r. (KBr) de ces oximes présentent toutes les bandes caractéristiques du groupement oximino: 3290–3180 cm^{-1} (ν —OH), 1640 cm^{-1} (ν C=N), 930–970 cm^{-1} (ν N—O).

Procédés généraux de réduction

Réduction par $LiAlH_4$ dans l'éther diéthylique

Les réductions sont menées dans un ballon bicol de 250 cm^3 équipé d'un réfrigérant, surmonté d'un tube desséchant et d'une agitation magnétique. A une suspension de 1.90 g (50 mmol) de $LiAlH_4$ dans 80 cm^3 d'éther anhydre, refroidie à 0 °C, on ajoute sous agitation, une solution de 10 mmol d'oxime dans 20 cm^3 de ce solvant. A la fin de l'addition, la solution est portée au reflux. La fin de la réaction est indiquée par la disparition de l'oxime en c.p.v. et c.c.m. (hexane, benzène, éther, 5:3:2). Le mélange réactionnel est alors hydrolysé à 0 °C par addition d'eau. Les produits de la réaction sont alors extraits au pentane ou à l'éther, puis séchés sur carbonate de sodium. Le solvant est évaporé sous pression réduite et le mélange réactionnel est soumis aux différentes analyses.

Réduction par $LiAlH_4$ dans le tétrahydrofurane

Les conditions opératoires sont identiques aux précédentes, à l'exception de l'étape finale. Lorsque l'oxime a entièrement réagi, le THF est évaporé sous pression réduite entre 45 et 50 °C. Le résidu est repris par un volume égale d'éther diéthylique et hydrolysé dans ce solvant par addition d'eau à 0 °C. Cette technique a pour but d'éviter que des produits de réduction volatils soient

Can. J. Chem. Downloaded from www.nrcresearchpress.com by 210.87.254.5 on 09/05/12
For personal use only.

TABLEAU 6. Déplacements chimiques des protons éthyléniques des oximes **1**, **2** et **5** ($\delta_2H - \delta_1H$ mesure à la fois l'effet de solvant et l'effet résultant de la protonation)

Oximes	δ_1H Éthylénique (oxime) (CCl_4 réf. TMS)		δ_2H éthylénique (chlorhydrate de l'oxime) ($CDCl_3$ réf. TMS)		$\delta_2H - \delta_1H$	
	Z	*E*	*Z*	*E*	*Z*	*E*
1	6.62	5.91	6.66 ou* 6.77 6.77 ou* 6.66		0.04 ou* 0.86 0.15 ou* 0.75	
2	6.61	5.90	6.73	6.84	0.12	0.94
5	6.54		6.61		0.07	

*Le chlorhydrate de l'oxime **1** *syn* (ou *anti*) n'a pas été isolé pur.

perdus lors de l'élimination du solvant de la réaction.

Réduction par le Red-Al dans le tétrahydrofurane

Les réductions sont effectuées dans un ballon bicol de 250 cm^3 équipé d'un réfrigérant surmonté d'un tube desséchant et d'une agitation magnétique. La quantité appropriée de Red-Al (solution commerciale à 70% dans le benzène), soit 14.4 g pour 50 mmol est d'abord concentrée sous vide à 50 °C afin d'éliminer le benzène. Le réactif est ensuite dilué dans 80 cm^3 de THF anhydre; 10 mmol d'oxime dissoutes dans 20 cm^3 de ce solvant sont alors additionnées lentement à cette solution refroidie à 0 °C et agitée magnétiquement. A la fin de l'addition, le mélange réactionnel est porté au reflux. La réduction de l'oxime est suivie par c.p.v. et c.c.m. La phase finale de la manipulation est identique à celle déjà décrite pour $LiAlH_4$: le THF est remplacé par de l'éther sulfurique anhydre avant l'hydrolyse. Celle-ci est effectuée par une solution aqueuse de soude 5 *N* à 0 °C. Les produits de la réaction sont extraits au pentane ou à l'éther. La phase organique est lavée plusieurs fois à l'eau afin d'éliminer le glyme (produit d'hydrolyse du Red-Al). Elle est ensuite séchée sur carbonate de sodium. Enfin, le solvant est évaporé sous vide et le mélange réactionnel est soumis aux différentes analyses.

Analyses et identifications des produits de réduction

Dans tous les cas, les rendements des réductions en produits azotés varient de 60 à 70%. Ceux-ci ont été calculés approximativement à partir du poids du résidu réactionnel sur la base des masses moléculaires des composés obtenus, de leurs proportions chromatographiques et à l'aide de la technique des références internes.

Les études spectroscopiques, et en particulier, la résonance magnétique nucléaire du proton, nous ont permis d'identifier sans ambiguité les structures de tous les composés isolés. Ces études détaillées font l'objet de la seconde partie de ce mémoire.

Cependant, afin de préciser avec une certitude absolue la configuration de chaque aziridine isomère, nous avons été conduits à pratiquer une analyse chimique pour chaque diastéréoisomère. Les méthodes d'analyses chimiques appropriées à l'étude structurale des aziridines sont basées sur l'ouverture de l'hétérocycle azoté; l'ouverture par hydrogénolyse catalytique est la plus commode (6) : l'aziridine ne peut donner que deux amines primaires, isomères de position qui ont même configuration que l'aziridine de départ.

L'hydrogénolyse sur nickel de Raney des différentes aziridines isolées, suivant la méthode de Takano et ses collaborateurs (6) conduisent à des amines primaires connues (17). Ainsi, les caractéristiques r.m.n. des amines obtenues, comparées à celles décrites dans la littérature, nous ont permis d'assigner toutes les configurations.

Absorption r.m.n. et i.r.

Nous utilisons les dénominations suivantes : s, singulet; d, doublet; t, triplet; q, quadruplet; m, multiplet.

Aziridines α,β-éthyléniques à double liaison intracyclique

Composé **25** : r.m.n. δ (p.p.m.) 5.56 (H en C_2, d de d déquadruplé, $J_{1,2} = 4.5$ Hz, $J_{2,4a} = 3$ Hz, $J_{2,CH_3} = 1.5$ Hz), 2.16 (H en C_1, d de d, $J_{1,2} = 4.5$ Hz, $J_{1,6} = 6$ Hz), 1.90 (H axial en C_4, d, $J_{4,4} = 17$ Hz), 1.86 (H en C_6, d de d, $J_{1,6} = 6$ Hz, $J_{6,4e} = 1.6$ Hz), 1.62 (CH_3 en C_3, d, $J_{2,CH_3} = 1.5$ Hz), 1.35 (H équatorial en C_4, d de d, $J_{4,4} = 17$ Hz, $J_{4e,6} = 1.6$ Hz), 1.10 et 0.85 ($2CH_3$ équatorial et axial en C_5, 2s), 0.58 (H fonctionnel); i.r. (cm^{-1}) 3230 (ν NH), 3030 et 835 (CH éthylénique), 1665 (ν C=C) 1370 et 1360 (*gem*-diméthyle).

Composé **26** : r.m.n. δ (p.p.m.) 5.13 (H en C_3, m, $J_{3,CH_3} = 1.2$ Hz), 2.40 (H en C_6, m, $J_{1,6} = 6$ Hz, $J_{5a,6} \simeq J_{5e,6} \simeq 3$ Hz), 2.03 (H en C_1, d, $J_{1,6} = 6$ Hz), 1.84 (CH_3 en C_2, d, $J_{3,CH_3} = 1.2$ Hz), 1.01 et 0.96 ($2CH_3$ en C_4, 2s), 0.50 (H fonctionnel); i.r. (cm^{-1}) 3250 (ν NH), 3010 et 800 (CH éthylénique), 1650 (ν C=C), 1380 et 1360 (*gem*-diméthyle).

Composé **28** : r.m.n. δ (p.p.m.) 5.64 (H en C_2, m. $J_{1,2} = 4.5$ Hz, $J_{2,CH_3} = 1$ Hz), 2.25 (H en C_1, $J_{1,2} = 4.5$ Hz, $J_{1,6} = 6$ Hz), 1.90 (H en C_6, m, $J_{1,6} = 6$ Hz), 1.63 (CH_3 en C_3, d, $J_{2,CH_3} = 1$ Hz), 0.72 (H fonctionnel); i.r. (cm^{-1}) 3250 (ν NH), 3075 et 830 (CH éthylénique), 1643 (ν C=C).

Composé **29** ≡ **32**: r.m.n. δ (p.p.m.) 5.25 (H en C_3, m, $J_{1,3} = 1$ Hz), 2.38 (H en C_6, m, $J_{1,6} = 6$ Hz), 1.96 (H en C_1, m, $J_{1,3} = 1$ Hz, $J_{1,6} = 6$ Hz), 1.84 (CH_3 en C_2), 0.72 (H fonctionnel); i.r. (cm^{-1}) 3350, 3250 (ν NH), 3010 et 815 (CH éthylénique), 1665 (ν C=C).

Composé **31** (2 isomères): r.m.n. δ (p.p.m.) 5.24 (H en C_3), 4.83 et 4.73 (CH_2 isopropényle), 2.66 (H en C_5), 2.40 (H en C_6), 1.90, 1.83 et 1.71 (CH_3 en C_2 et CH_3 isopropényle), 0.73 (H fonctionnel); i.r. (cm^{-1}) 3240 (ν NH), 3085, 3075 (ν C=CH_2), 1650 (ν C=C), 885 et 820 (CH éthyléniques), 3040 (γ C=C—H).

Composé **33** (2 isomères): r.m.n. δ (p.p.m.) 5.24 (H en

Can. J. Chem. Downloaded from www.nrcresearchpress.com by 210.87.254.5 on 09/05/12
For personal use only.

Can. J. Chem. Downloaded from www.nrcresearchpress.com by 210.87.254.5 on 09/05/12
For personal use only.

C_3, m, $J_{1,3} = 0.5$ Hz), 2.28 (H en C_6, m, $J_{1,6} = 6$ Hz, $J_{5,6} = 6$ Hz), 1.95 (H en C_1, m, $J_{1,6} = 6$ Hz, $J_{1,3} = 0.5$ Hz), 1.84 (CH_3 en C_2), 0.99 et 0.90 ($2CH_3$ isopropyle, 2s, $J_{\text{isopropyle H,CH}_3} = 6$ Hz), 0.80 (H fonctionnel); i.r. (cm^{-1}) 3240 (ν NH), 3010–818 (CH éthylénique), 1650 (ν C=C), 1385–1370 (*gem*-diméthyle).

Aziridines α,β-éthyléniques à double liaison exocyclique

Composé **27**: r.m.n. δ (p.p.m.) 4.90 et 4.77 (2H éthyléniques, d de d, $J_{7,7} = 1.7$ Hz, $J_{7\alpha,3a} \simeq J_{7\beta,3a} = 1.5$ Hz), 2.51 (H en C_1, d, $J_{1,6} = 6$ Hz), 2.22 (H en C_6, d de t, $J_{1,6} = 6$ Hz, $J_{5e,6} = 6$ Hz, $J_{5a,6} = 3$ Hz), 2.10 (H axial en C_5, d de d, $J_{5,5} = 13$ Hz, $J_{5a,6} = 3$ Hz), 1.60 (H équatorial en C_5 et 2H en C_3), 0.88 et 0.77 ($2CH_3$ en C_4, s), 0.50 (H fonctionnel); i.r. (cm^{-1}) 3250 (ν NH), 3080 et 880 (CH_2 vinylique), 1650 (ν C=C) 1390 et 1367 (*gem*-diméthyle).

Composé **30**: r.m.n. δ (p.p.m.) 4.94 et 4.84 (2H éthyléniques), 2.49 (H en C_1, $J_{1,6} = 6$ Hz), 2.30 (H en C_6, m, $J_{1,6} = 6$ Hz, $J_{5,6\ \text{moyen}} = 3$ Hz), 0.73 (H fonctionnel); i.r. (cm^{-1}) 3240 (ν NH), 3085, 880 (CH_2 vinylique), 1655 (ν C=C).

Composé **34** (2 isomères) : r.m.n. δ (p.p.m.) 4.90 et 4.77 (2H éthyléniques), 2.49 (H en C_1, m, $J_{1,6} = 6$ Hz), 2.10 (H en C_6, m, $J_{1,6} = 6$ Hz, $J_{5,6\ \text{moyen}} = 3$ Hz), 1.01 et 0.85 ($2CH_3$ isopropyle, 2d, $J_{\text{H-CH}_3} = 7$ Hz), 0.50 (H fonctionnel); i.r. (cm^{-1}) 3230 (ν NH), 3075–880 (CH_2 vinylique), 1645 (ν C=C), 1385–1370 (*gem*-diméthyle).

Cyclohexénimines méthylées en tête de pont

Composé **17** (2 isomères): r.m.n. δ (p.p.m.) 4.60 (CH_2 isopropényle), 1.80 (H en C_6), 1.65 (CH_3 isopropényle), 1.22 (CH_3 en tête de pont C_1), 0.90 (H fonctionnel); i.r. (cm^{-1}) 3282–3275 (ν NH), 3080 et 870 (CH_2 éthylénique), 1645 (ν C=C).

Composé **20**: r.m.n. δ (p.p.m.) 1.80 (H en C_6), 1.20 (CH_3 en tête de pont C_1), 0.18 (H fonctionnel); i.r. (cm^{-1}) 3250 (ν NH).

Cyclohexénimines trans méthylées en position 2

Composé **9** *trans*: r.m.n. δ (p.p.m.) 2.12 (H en C_6, m, $J_{1,6} = 6$ Hz, $J_{6,5a} = 4$ Hz, $J_{6,5e} = 1.5$ Hz), 1.75 (H en C_1, d, $J_{1,2} = 0$ Hz, $J_{1,6} = 6$ Hz), 1.05 (CH_3 en C_2, d, $J_{2,\text{CH}_3} = 7$ Hz), 0.92 et 0.86 ($2CH_3$ en C_4, 2s), 0.50 (H fonctionnel); i.r. (cm^{-1}) 3250 (ν NH), 1390–1370 (*gem*-diméthyle).

Composé **13** *trans*: r.m.n. δ (p.p.m.) 2.09 (H en C_6, $J_{1,6} = 6$ Hz), 1.73 (H en C_1, d, $J_{1,2} = 0$ Hz, $J_{1,6} = 6$ Hz), 1.05 (CH_3 en C_2, d, $J_{2,\text{CH}_3} = 7$ Hz), 0.30 (H fonctionnel); i.r. (cm^{-1}) 3250 (ν NH).

Composé **24** *trans-trans*: r.m.n. δ (p.p.m.) 1.87 (2H en C_1 et C_6), 1.03 (CH_3 en C_2, d, $J_{2,\text{CH}_3} = 7$ Hz), 0.98 et 0.95 ($2CH_3$ isopropyle, 2d, $J_{\text{H,CH}_3} = 6.5$ Hz), 0.61 (H fonctionnel); i.r. (cm^{-1}) 3250 (ν NH), 1387–1370 (*gem*-diméthyle).

Cyclohexénimines cis méthylées en position 2

Composé **8** *cis*: r.m.n. δ (p.p.m.): 2.00 (2H en C_1 et C_6), 0.99 (CH_3 en C_2, d, $J_{2,\text{CH}_3} = 7$ Hz), 0.83 et 0.80 (2 CH_3 en C_4), 0.57 (H fonctionnel); i.r. (cm^{-1}) 3280 (ν NH), 1385–1360 (*gem*-diméthyle).

Composé **12** *cis*: r.m.n. δ (p.p.m.) 2.00 (2H en C_1 et C_6), 0.99 (CH_3 en C_2, d, $J_{2,\text{CH}_3} = 7$ Hz), 0.70 (H fonctionnel); i.r. (cm^{-1}) 3260 (ν NH).

Composé **21** *cis-cis*: r.m.n. δ (p.p.m.) 2.10 (2H en C_1 et C_6), 0.98 (CH_3 en C_2, d, $J_{2,\text{CH}_3} = 7$ Hz), 1.00 et 0.95 (2 CH_3 isopropyle, 2d, $J_{\text{H,CH}_3} = 6.5$ Hz), 0.30 (H fonctionnel); i.r. (cm^{-1}) 3245 (ν NH), 1385–1367 (*gem*-diméthyle).

Amines éthyléniques

Composé **7**: r.m.n. δ (p.p.m.) 5.23 (H en C_2), 3.20 (H en C_1), 1.62 (CH_3 en C_3), 1.23 (2H fonctionnels), 0.95 et 0.85 (2 CH_3 en C_5); i.r. (cm^{-1}) 3370–3300 (ν NH_2), 3030–815 (CH éthylénique), 1590 (ν C=C), 1380–1360 (*gem*-diméthyle).

Composé **11**: r.m.n. δ (p.p.m.) 5.28 (H en C_2), 3.20 (H en C_1), 1.63 (CH_3 en C_3), 0.91 (2H fonctionnels); i.r. (cm^{-1}) 3360–3300 (ν NH_2), 3025–810 (CH éthylénique), 1610 (ν C=C).

Composé **15** *cis*: r.m.n. δ (p.p.m.) 5.39 (H en C_3), 4.70 (CH_2 isopropényle), 3.25 (H axial en C_1), 1.70 (CH_3 en C_2 et CH_3 isopropényle), 1.00 (2H fonctionnels); i.r. (cm^{-1}) 3370–3300 (ν NH_2), 3085–3077 (ν C=CH_2), 3010 (ν C=CH), 1648–1600 (ν C=C), 885–800 (CH éthylénique).

Composé **16** *trans*: r.m.n. δ (p.p.m.) 5.34 (H en C_3), 4.64 (CH_2 isopropényle), 3.12 (H en C_1, t, $J_{1,6a} = J_{1,6e} = 4$ Hz), 1.70 (CH_3 en C_2 et CH_3 isopropényle), 1.70 (2H fonctionnels); i.r. (cm^{-1}) 3370–3290 (ν NH_2), 3080–3075 (ν C=CH_2), 3010 (ν C=CH), 1648–1610 (ν C=C), 885–805 (CH éthylénique).

Composé **19**: r.m.n. δ (p.p.m.) 5.33 (H en C_3), 3.02 (H en C_1), 1.70 (CH_3 en C_2), 0.95 (2H fonctionnels); i.r. (cm^{-1}) 3360–3290 (ν NH_2), 3020–795 (CH éthylénique), 1600 (ν C=C).

Amines secondaires transposées. Imine 35

Composé **10**: r.m.n. δ (p.p.m.) 2.95 (H équatorial en C_2, $J_{2,2} = 13$ Hz, $J_{2e,3} = 4$ Hz), 2.46 (H axial en C_2, d de d, $J_{2,2} = 13$ Hz, $J_{2a,3} = 9$ Hz), 2.30 (H fonctionnel), 0.92 (CH_3 en C_3, d, $J_{3,\text{CH}_3} = 7$ Hz); i.r. (cm^{-1}) 3320 (ν NH).

Composé **14** (2 isomères): r.m.n. δ (p.p.m.) 4.60 (CH_2 isopropényle), 3.00 (H fonctionnel), 3.05 (H équatorial en C_7, $J_{7,7} = 13$ Hz, $J_{7e,6a} = J_{7e,6e} = 4$ Hz), 2.57 (H axial en C_7, $J_{7,7} = 13$ Hz, $J_{7a,6a} = 13$ Hz, $J_{7a,6e} = 4$ Hz), 1.66 (CH_3 isopropényle), 1.02 (CH_3 en C_2, d, $J_{2,\text{CH}_3} = 7$ Hz); i.r. (cm^{-1}) 3360 (ν NH), 3090–885 (CH_2 éthylénique), 1630 (ν C=C).

Composé **18**: r.m.n. δ (p.p.m.) 1.90 (H fonctionnel), 1.04 (CH_3 en C_2, d, $J_{2,\text{CH}_3} = 7$ Hz); i.r. (cm^{-1}) 3350 (ν NH).

Composé **35** (imine): r.m.n. δ (p.p.m.) 3.40 (2H en C_7), 2.28 (2H en C_3), 1.92 (CH_3 en C_2); i.r. (cm^{-1}) 1662 (ν C=N).

Procédé général d'hydrogénolyse des aziridines

L'hydrogénolyse des aziridines se fait sous atmosphère d'hydrogène dans un hydrogénateur de Brown. A une suspension de 0.9 g de nickel de Raney dans 10 cm^3 de méthanol anhydre sont ajoutées 2 mmol d'aziridine. Après introduction de l'hydrogène dans le réacteur, le mélange est agité magnétiquement. La réaction est terminée lorsqu'il n'y a plus absorption d'hydrogène. Les produits formés sont analysés par c.p.v. sur colonne analytique B. Une première identification des amines formées est effectuée par comparaison des temps de rétention avec des échantillons purs. La solution méthanolique est ensuite filtrée; 2 mmol d'acide acétique sont ajoutées à froid afin de former les acétates des produits de réduction. Le méthanol est alors évaporé sous vide. Les acétates sont dissouts dans 2 cm^3 d'eau et basicifiés par une solution de soude 5 *N*. Les amines sont extraites au pentane et séchées sur carbonate de sodium. Le mélange réactionnel obtenu par évaporation du solvant

est analysé par r.m.n. Les spectres obtenus, comparés à ceux de Feltkamp et al. (18), ont permis de préciser toutes les configurations. Notons qu'il est parfois possible d'isoler l'une des deux amines formées par cristallisation sélective de son acétate dans l'éther anhydre. Le rendement des réactions, mesuré après passage à l'acétate, basification et extraction au pentane, est de l'ordre de 90%. L'analyse par c.p.v. montre que toute l'aziridine de départ est réduite au bout d'un jour de réaction, environ.

Les auteurs remercient Monsieur J. Cassan pour l'enregistrement des spectres de masse et Mademoiselle Y. Girault qui leur a fourni la plupart des échantillons d'amines primaires authentiques.

1. J. R. DIMMOCK, W. A. TURNER, P. J. SMITH et R. G. SUTHERLAND. Can. J. Chem. **51**, 427 (1973).
2. G. RICART, D. COUTURIER et C. GLACET. C.R. Acad. Sci. Ser. C. **277**, 519 (1973).
3. M. Y. SHANDALA, M. D. SALOMON et E. S. WAIGHT. J. Chem. Soc. 892 (1965).
4. K. KOTERA, Y. TAKANO, A. MATSUMURA et K. KITAHONOKI. Tetrahedron, **26**, 539 (1970).
5. L. FERRERO, M. DECOUZON et M. AZZARO. Tetrahedron Lett. 4151 (1973).
6. K. KITAHONOKI, Y. TAKANO et H. TAKAHASHI. Tetrahedron, **24**, 4605 (1968).
7. H. TANIDA, T. OKADA et K. KOTERA. Bull. Chem. Soc. Jpn. **46**, 934 (1973).
8. L. FERRERO, S. GERIBALDI et M. AZZARO. Rev. Roum. Chim. **8** (1975).
9. G. RICART. Bull. Soc. Chim. Fr. 2607 (1974).
10. M. CERNY, J. MALEK, M. CAPKA et V. CHUALOVSKY. Tetrahedron Lett. 1033 (1969).
11. L. FERRERO, M. ROUILLARD, M. DECOUZON et M. AZZARO. Tetrahedron Lett. 131 (1974).
12. O. KRIZ, B. CASENSKY et O. SROUF. Collect. Czech. Chem. Commun. **38**, 842 (1973).
13. G. SWIFT et D. SWERN. J. Org. Chem. **32**, 511 (1967).
14. J. CASSAN, M. DECOUZON, L. FERRERO et M. AZZARO. C.R. Acad. Sci. Ser. C. **280**, 33 (1975).
15. T. SATO, H. WAKATSULA et K. AMANO. Tetrahedron, **29**, 5381 (1971).
16. A. ZABZA, C. WAWRZENCZYK et M. KUCZYNSKI. Bull. Acad. Pol. Sci. Ser. Sci. Chim. **20**, 631 (1972).
17. B. L. FOX, J. E. REBOULET, R. E. RONDEAU et H. M. ROSENBERG. J. Org. Chem. **35**, 4234 (1970).
18. H. FELTKAMP, F. KOCH et T. N. THANH. Justus Liebigs Ann. Chem. **95**, 707 (1967).

Can. J. Chem. Downloaded from www.nrcresearchpress.com by 210.87.254.5 on 09/05/12
For personal use only.

On the Mechanism of Oxetan Formation in the Photocycloaddition of *p*-Benzoquinone to Alkenes[1]

NIGEL J. BUNCE AND MARY HADLEY

Guelph-Waterloo Centre for Graduate Work in Chemistry, University of Guelph, Guelph, Ontario N1G 2W1

Received May 26, 1975

NIGEL J. BUNCE and MARY HADLEY. Can. J. Chem. **53**, 3240 (1975).

Photochemical oxetan formation from *p*-benzoquinone and simple alkenes takes place from the lowest $^3n,\pi^*$ state of the quinone. It is suggested that an exciplex is formed between the alkene and the excited quinone, but that a biradical is nevertheless the immediate precursor of the oxetan.

NIGEL J. BUNCE et MARY HADLEY. Can. J. Chem. **53**, 3240 (1975).

La formation photochimique d'oxétannes à partir de *p*-benzoquinone et d'alcènes simples se produit à partir de l'état $^3n,\pi^*$ le plus bas de la quinone. On suggère qu'un exciplex est formé entre l'alcène et la quinone excitée mais on croit toutefois qu'un biradical est le précurseur immédiat de l'oxétanne.

[Traduit par le journal]

In common with other saturated and unsaturated carbonyl compounds, *p*-quinones afford cycloaddition products upon irradiation with alkenes (1). With *p*-benzoquinone, addition to the carbonyl group is the only mode of cyclization that has so far been observed (Eq. 1), although reaction at the olefinic linkage to give a cyclobutane might have been possible, and indeed is found with other *p*-quinones.

[1] 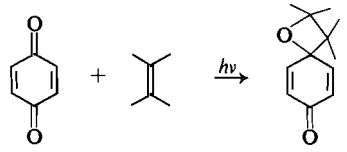

The resulting spirooxetan adducts are often formed in high yield, and the scope and preparative value of this reaction have been examined in some detail (2). To date, however, little is known about its mechanism; Bryce-Smith and his colleagues noted that oxetan production was more efficient upon irradiation into the $^1n,\pi^*$ band of the quinone rather than into either of the accessible $^1\pi,\pi^*$ bands, and that the yield of oxetan was reduced in the presence of oxygen. They suggested that a $^3n,\pi^*$ state might be the reactive intermediate, but the following observations may vitiate the basis for this interpretation. Short wavelength radiation destroys the product oxetan, optimal yields being obtained when wavelengths shorter than 400 nm are excluded. Additionally, recent findings by Wilson and his co-workers suggest that oxygen may participate chemically in the reaction rather than act as a triplet quencher; illumination of *p*-benzoquinone with alkenes under oxygen using an argon ion laser source affords trioxan adducts in addition to oxetans (3). The ratio of trioxan to oxetan is increased upon raising the oxygen pressure (4), suggesting that both adducts are formed competitively from a common precursor (Eq. 2). On these grounds,

[2] 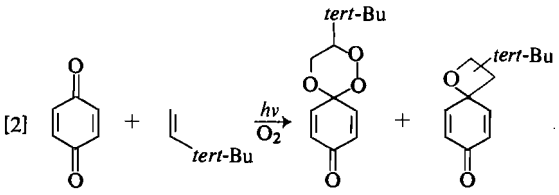

we considered the mechanism of oxetan formation to be incompletely established, and in this paper we report our findings on the mechanism of the reaction under anaerobic conditions.

Assignment of the Excited State

Participation of a triplet excited state of *p*-benzoquinone in the cycloaddition was demonstrated by various sensitization and quenching studies. In this respect, the quinone behaves like most other carbonyl compounds, but due to the equivocal nature of some of the results, the experiments are discussed in a little detail.

[1]Abstracted in part from the M.Sc. thesis of M. Hadley, University of Guelph, 1974.

Can. J. Chem. Downloaded from www.nrcresearchpress.com by 210.87.254.5 on 09/05/12
For personal use only.

Can. J. Chem. Downloaded from www.nrcresearchpress.com by 210.87.254.5 on 09/05/12
For personal use only.

In solutions containing benzophenone (E_T = 69 kcal/mol) where the ketone absorbed >90% of the incident light, the disappearance of *p*-benzoquinone (E_T = 50 kcal/mol) in the presence of cyclooctene was as fast as in solutions containing no sensitizer. Correspondingly, in the presence of 9,10-dibromoanthracene (E_T = 47 kcal/mol) under conditions where no light was absorbed by the quencher, the rate of reaction was markedly reduced. This result is not unambiguous because the quinone and the quencher form a charge transfer complex, a process known to decrease triplet lifetimes (5). This would have the same effect as quenching by energy transfer; in addition, the range of possible quencher concentrations is limited because at high dibromoanthracene concentrations, it is the complex rather than the free quinone that absorbs. In our experiments at least 85% of the light was absorbed by the free quinone. Consequently, it was not possible to quench oxetan formation completely, so that while we believe that the reaction is mainly triplet in character, a competing singlet pathway cannot be excluded, especially since dibromoanthracene may also be able to quench singlet states directly. Attempts to find other quenchers were limited by the low triplet energy of *p*-benzoquinone itself and by charge transfer complexation (*e.g.* pyrene, E_T = 49 kcal/mol, could not be used).

Recently, 2,2,3,3,-tetramethylazetine-*N*,*N*-dioxide has been suggested as a low energy quencher ($E_T \sim 40$ kcal/mol) that is capable of quenching triplet but not singlet states (6). This compound failed to quench oxetan formation from *p*-benzoquinone and cyclooctene, which seems to suggest a singlet state pathway to oxetan, since we were able to rule out a specific and preferential reaction of the quencher with the quinone. Alternatively, quenching may be ineffective due to the extremely short lifetime of *p*-benzoquinone in solution (7). In view of the high quantum yield for oxetan formation (2), we believe a wholly singlet pathway to be unlikely since intersystem crossing yields for carbonyl compounds are usually so high. Unfortunately, it is difficult to measure the intersystem crossing yield for *p*-benzoquinone experimentally, because its low triplet energy and oxetan formation preclude measurements based on photoisomerization of alkenes (*cf.* ref. 8). Certainly a triplet state pathway is possible in view of the photosensitization results, and since the direct and photosensitized reactions occur at equal rates, it would be coincidental if both singlet and triplet reactions proceeded with equal quantum yield. Consequently, we are inclined to favor a triplet state pathway for oxetan formation.

Phosphorescence measurements (in 3-methylpentane, 77 K) supported the triplet state assignment. *p*-Benzoquinone quenched the phosphorescence spectrum of benzophenone, and although the quinone itself did not phosphoresce at the concentrations used, illumination of the quinone in the presence of dibromoanthracene caused emission from the quencher.

Having implicated a triplet state for at least the major reaction pathway, we reasoned that the state was $^3n,\pi^*$ as follows. The phosphorescence spectrum of *p*-benzoquinone shows fine structure and has been attributed (9) to emission from a lowest $^3n,\pi^*$ state, although its lifetime is unusually short (7). We have found that oxetan formation from cyclooctene and either *p*-benzoquinone or its d_4 analog proceed at almost equal rates; Brus and McDonald (10) found that these two quinones have very similar triplet lifetimes. This seems to be typical of $^3n,\pi^*$ lifetimes of carbonyl compounds (11), whereas deuteration usually increases $^3\pi,\pi^*$ lifetimes appreciably (12); in that case an increase in the quantum yield for oxetan formation would have been expected upon deuteration.

A $^3n,\pi^*$ reactive state implies an electron deficient oxygen atom; if, as is believed to be the case for ketones (13), oxetan production is initiated by bond formation between oxygen and the alkene, electron withdrawing substituents in the alkene should disfavor this initial attack by oxygen. This was demonstrated for a series of chloro-substituted ethylenes which reacted in the order: cyclooctene $\gg$ $CH_2{=}CHCl$ > $CCl_2{=}CHCl$ > $CH_2{=}CCl_2$ > $CHCl{=}CHCl$ > $CCl_2{=}CCl_2$, although this reactivity order cannot be interpreted only in terms of progressive electron withdrawal by chlorine.[2]

[2]Whether this reactivity order would also be observed for addition of alkoxy radicals to these olefins is unknown. The obvious model radical, *tert*-butoxy, does not add to alkenes (14); recently, the perfluoro-*tert*-butoxy radical has been shown to add to alkenes (15) but no comparative data are yet available. Copolymerization studies (16) indicate that carbon based radicals add to these alkenes at rates that depend mainly upon the number of chlorine substituents present.

Can. J. Chem. Downloaded from www.nrcresearchpress.com by 210.87.254.5 on 09/05/12
For personal use only.

Possibility of Exciplex Intermediates

At this point our efforts were directed towards the establishment of a simple biradical mechanism, such as has been outlined for the photoaddition of several ketones with alkenes (13). The participation of a triplet excited state makes it improbable that the reaction is concerted, since a triplet excited state of the spirooxetan would then be produced. This is unlikely, especially considering the instability of the spirooxetan towards photolysis and by analogy with the arguments of Salem (17) on the course of ketone/alkene cycloadditions. The work of Barltrop and Hesp (18) provides some support for the intermediacy of a biradical which must close with spin-inversion before the product is obtained; illumination of benzoquinone with butadiene gave the spiropyran **1** and a macrocyclic ether **2**. The latter compound may be imagined as arising by attack of the allylic biradical **i** upon another molecule of diene rather than ring closure.[3]

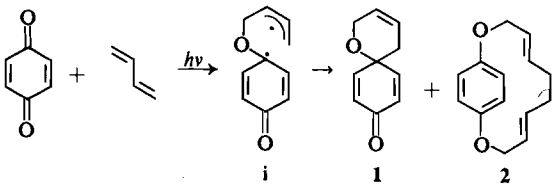

Support for the intermediacy of a biradical was obtained by photolyses of *p*-benzoquinone with *cis*- and *trans*-2-butene. Both geometric isomers afforded the same mixture of spirooxetans, suggesting that the biradical intermediate is sufficiently long lived that its stereochemical integrity is lost. Control experiments showed that negligible isomerization of the isomeric alkenes occurred during the photolyses. The trapping experiments of Wilson and Wunderly (4) provide strong additional evidence for the intermediacy of 1,4-biradicals in *p*-benzoquinone/olefin photoreactions.

Reactions proceeding by way of biradicals commonly afford predominantly the product derived from the more stable biradical when there is more than one possible orientation. An example is the reaction of benzophenone with 2-methylpropene (19). It was therefore anticipated that the irradiation of *p*-benzoquinone with 2-methyl-1-butene would afford **3** (derived from the tertiary biradical **ii**) as the major product with **4** in only small amounts. Unexpectedly, in both direct and benzophenone-sensitized photolyses, almost equal quantities of oxetans **3** and **4** were formed.

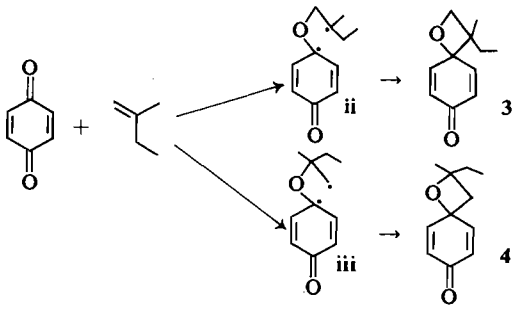

Possible explanations for this behavior are: (*i*) attack upon the alkene is indiscriminate, *i.e.*, radicals **ii** and **iii** are not formed under thermodynamic control; (*ii*) the alkene and the quinone are randomly (or possibly, symmetrically, *cf.* ref. 20) aligned before the first bond is formed; (*iii*) radical **ii** is formed in greater amount, but because of greater steric hindrance towards closure, it reverts to starting material more often than **iii**. The equivalent yields of **3** and **4** are thus fortuitous.

We believe explanation (*iii*) to be a likely possibility since we have demonstrated that oxetan formation proceeds with low quantum efficiency with this olefin. However, it may be more than coincidental that Bryce-Smith and his associates also observed an exactly 1:1 formation of isomeric oxetans in the photocycloaddition of 1-octene to benzoquinone (2), just as we did with 2-methyl-1-butene. This could support an exciplex intermediate if the exciplex had the geometry proposed by Caldwell *et al.* (20) for the benzophenone/2-butene cycloaddition, and collapse of the exciplex to biradical led to bond formation at either end of the alkene linkage with equal probability. This would imply that the relative stabilities of the resultant biradicals were unimportant at the transition state for bond formation.

Tenuous support for the participation of exciplex intermediates in oxetan formation comes from photo-CIDNP studies;[4] these were

[3]Actually, **1** and **2** may not be formed competitively from **i**, since it has been shown that allylic radicals maintain their geometry (14). Possibly the *s-cis* form of **i** closes to **1** while the *s-trans* is unable to do so, and consequently affords **2**.

[4]These experiments were carried out in collaboration with Drs. M. Cocivera and H. Chen, to whom we express our thanks.

Can. J. Chem. Downloaded from www.nrcresearchpress.com by 210.87.254.5 on 09/05/12
For personal use only.

undertaken in the hope of observing nuclear polarization in the oxetan and hence of providing evidence for polarization in 1,4-biradicals. Previously, the phenomenon has been observed only in 1,5 and longer biradicals (21). Nuclear magnetic resonance spectra run during the photolysis of *p*-benzoquinone with a variety of alkenes in benzene-d_6 showed polarization in only two cases. With cyclooctene and with trichloroethylene, the benzoquinone resonance was seen in emission, but polarization of neither the alkene nor the oxetan was observed. Polarization was not found when either reactant was photolyzed separately in benzene-d_6, nor when the benzoquinone–cyclooctene adduct was irradiated to destruction.

Observation of the CIDNP phenomenon definitely establishes the presence of radical pairs (or biradicals) in the photolyzing solution, but identification of the species causing the polarization is more difficult. The results do not support a simple biradical mechanism with polarization occurring at the biradical, for that would have also caused polarization of the adduct. One possibility is the involvement of a polarization-inducing intermediate that can either revert to reactants, or be transformed to the biradical, where the polarization is lost and hence not observed in the final product. An exciplex would be an attractive candidate for the polarization-inducing intermediate. There is however the possibility, since CIDNP is such a sensitive technique, that the source of the polarization is a reversible side reaction altogether unconnected with the main pathway leading to oxetan.

The following evidence points to an exciplex intermediate much more strongly. Solvation of the components of the exciplex should be much more efficient in a polar solvent, allowing them to separate. Separation should therefore reduce the likelihood of oxetan production and, consistent with this suggestion, oxetan formation was found to proceed much more slowly in acetonitrile than in benzene. Yomosa (22) has suggested that exciplexes have a large polar contribution to the total wave function (unlike Mulliken's (23) view of ground state charge transfer complexes in their ground states) and hence have a strong tendency to dissociate in polar solvents. In addition, we obtained traces of methoxycyclooctane from irradiations of *p*-benzoquinone and cyclooctene in methanol or acetonitrile/methanol. This product represents entrapment of a cyclooctene radical cation by methanol, and is analogous to the alcohol/alkene adducts obtained by Neunteufel and Arnold (24) in reactions sensitized by methyl benzoates. In our studies, however, the quantity of the methanol adduct was always very small. As to the multiplicity of the proposed exciplex, we believe it to be of the triplet configuration since the benzoquinone/2-methyl-1-butene photolyses gave the same 1:1 mixture of products whether or not the reaction was photosensitized. Had a singlet exciplex been involved, it would have been bypassed in the benzophenone assisted reaction.

In conclusion, our experiments suggest that oxetan formation from *p*-benzoquinone and simple alkenes involves the lowest $^3n,\pi^*$ excited state. The details of the subsequent chemical events are complex, but some features are clear. First, a biradical intermediate is likely the immediate precursor of the oxetan, as shown by the similarity of the products from *cis*- and *trans*-2-butene. Second, an excited state species with considerable polar character is present on the evidence of the methanol trapping experiment, the effect of acetonitrile as solvent on the reaction rate and possibly, by the CIDNP results. What is not clear is the relationship between these two species; several possibilities exist, and our data permit no distinction to be drawn between them.

(*i*) The exciplex is not on the reaction path to oxetan (Eq. 3). Here Q, A, $[Q^{\cdot}A]^{\pm}$, and $^{\cdot}Q—A^{\cdot}$ represent respectively quinone, alkene, exciplex, and biradical and it is to be inferred that all excited intermediates may also revert to ground state reactants.

$$[3]\quad Q \xrightarrow{h\nu} {}^1Q \xrightarrow{\text{i.s.c.}} {}^3Q \begin{cases} \xrightarrow{A} {}^3[Q—A]^{\pm} \rightleftharpoons Q^{-} + A^{\cdot+} \\ \xrightarrow{A} {}^{\cdot}Q—A^{\cdot} \rightarrow \text{Product} \end{cases}$$

(*ii*) The exciplex is on the main reaction pathway (Eq. 4), and has a stereochemical structure different from that of the biradical. Caldwell's proposed structure is one such possibility.

$$[4]\quad Q \xrightarrow{h\nu} {}^1Q \xrightarrow{\text{i.s.c.}} {}^3Q \xrightarrow{A} \begin{cases} \rightleftharpoons Q^{-} + A^{\cdot+} \\ [Q^{\cdot}A]^{\pm} \\ \rightarrow {}^{\cdot}Q—A^{\cdot} \rightarrow \text{Product} \end{cases}$$

(*iii*) An extreme form of proposal (*ii*) would arise if the geometry of the exciplex and the biradical were the same (Eq. 5). Under these circumstances there would be two exciplexes when the alkene was unsymmetrical, and the exciplex and biradical could then be viewed as different valence-bond descriptions of the same species.

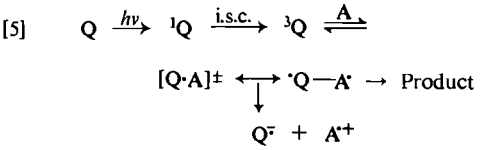

Experimental

Solvents were of reagent or spectroscopic grade, used as supplied except for benzene (dried over sodium). Chromatographic separations on columns employed silica gel (Davison Grade 12, 28–200 mesh) or alumina (Fisher, Brockman Activity I, 80–280 mesh). Reaction mixtures and chromatographic separations were analyzed qualitatively by t.l.c. using alumina (J. T. Baker, type 9F) or silica gel (E. Merck PF_{254} #7747) both of which contained a fluorescer to aid in locating the spots.

Compounds were identified using the usual spectroscopic methods; instruments used included Beckman IR5A and IR12 infrared, Unicam SP 800 and Beckman DB u.v.–visible, Varian Associates A60-A n.m.r., and Varian-MAT model CH7 mass spectrometer operated at 70 eV ionizing voltage. Microanalyses on purified samples were carried out by Mr. H. S. McKinnon of this department.

Preparative Irradiations

Benzoquinone (BDH) was sublimed before use and stored protected from the light. Cyclooctene (Matheson Coleman and Bell) was dried over molecular sieves, type 3A; 2-methyl-1-butene (Baker), and *cis*- and *trans*-2-butene (Matheson) were used as supplied. Reactions were carried out in the absence of oxygen, either in an immersion well apparatus of 300 ml capacity equipped with a nitrogen flush, or in Pyrex glass ampoules of various capacities which were degassed at $< 10^{-3}$ Torr by three freeze–pump–thaw cycles. The Hanovia model 679A 450W mercury arc source was cooled by the cooling jacket of the immersion well apparatus in the latter case, the distance from the source to the ampoules being about 2–3 in. Unless specified the radiation used was filtered through Pyrex glass ($\lambda > 300$ nm); when light input was to be restricted to $\lambda > 400$ nm an additional filter was used, either a nitrite–biphthalate filter solution (25), filter A, or a 3 in. × 6 in. Corning glass filter CS3-73 #3389, filter B.

Benzoquinone with Cyclooctene

In Benzene—The method was similar to that of Bryce-Smith *et al.* (2) except that after washing the crude photolysate with aqueous NaOH, the product was purified by chromatography over neutral alumina rather than by vacuum distillation. Infrared (cyclohexane) ν_{max} 1700 (s), 1665 (s), 1630 (s), 1605 (m), 1495 (m), 975 (m); n.m.r. identical to that reported (2); M^+ 218.

In Methanol—Benzoquinone (1 g) and methanol were irradiated through filter B in the presence of cyclooctene. After removal of methanol, the residue was examined by v.p.c. on columns of SE30, Carbowax 20M, and DEGS (diethylene glycol succinate). In each case a small peak was observed with a retention time identical to that of an authentic sample of methoxycyclooctane, prepared by the Williamson synthesis from cyclooctanol. Similar results were obtained when an equal volume mixture of methanol and acetonitrile was used as the solvent.

Benzoquinone with 2-Methyl-1-butene

(*i*) Freshly sublimed benzoquinone (2 g), 2-methyl-1-butene (20 ml), and benzene (40 ml) were irradiated under a nitrogen flush through the filter glass B for 220 h. After extraction with 0.1 *M* NaOH solution, the dried organic phase was evaporated and the residue chromatographed over basic alumina, when the mixture of oxetans **3** and **4** was obtained as a yellow oil: λ_{max} (cyclohexane) 233 (ε 14 000), 359 nm (ε 800); i.r. (cyclohexane) ν_{max} 1695 (s), 1640 (s); n.m.r. (CCl_4) δ 0.46, 0.68 (2 triplets, $J = 7$ Hz, $2CH_3$ groups), 1.0, 1.2 (2 singlets, ratio 1:1, $2CH_3$ groups), 1.4, 1.5 (2 overlapping quartets, $J = 7$ Hz, $2CH_2$ groups), 2.1–2.4, 3.9–4.1 (multiplets, ratio 1:1, $2CH_2$ groups), 5.7–5.8, 6.7–7.1 (ring protons); M^+ 178. Attempts to separate the isomers by t.l.c. or by gas chromatography were unsuccessful.

Anal. Calcd. for $C_{11}H_{14}O_2$: C, 74.12; H, 7.93. Found: C, 73.72; H, 7.91.

(*ii*) The reaction was repeated using benzoquinone (1 g), the alkene (12 ml), benzophenone (2.3 g), and benzene (170 ml) in the immersion well apparatus. After irradiation for 45 min, the mixture was evaporated and the n.m.r. spectrum run on the crude residue. In the region δ 0–6 not obscured by benzophenone, the spectrum was essentially unaltered from that previously observed.

Benzoquinone with cis- and with trans-2-Butene

The procedure is exemplified for the *cis* isomer. On to *p*-benzoquinone (1 g) in a Pyrex ampoule was condensed *cis*-2-butene (1.2 ml), and benzene (50 ml) was added. The ampoule was evacuated and sealed and irradiated through filter B for 24 h. The cooled ampoule was opened, and after reservation of a sample for v.p.c. analysis, the reaction mixture was washed with 0.5 *M* NaOH, dried, and evaporated. After obtaining an n.m.r. spectrum of the crude material, the residue was dried in a drying pistol. The n.m.r. spectrum of the purified material was indicative of two oxetans in the approximate ratio of 1:9.[5] Major isomer: δ 0.82 (doublet, $J = 7$ Hz, CH_3), 1.30 (doublet, $J = 7$ Hz, CH_3), 2.1–2.6 (quartet, each line further split once, CH), 4.2–4.6 (quartet, each line further split once, CH), 5.9–6.3 (multiplet, 2 ring CH), 6.7–7.2 (multiplet, 2 ring CH); minor isomer: same except that oxetan CH resonances appear at δ 2.5–3.0 and 4.5–5.1; i.r. ($CHCl_3$) ν_{max} 1680 (s), 1640 (s), 1610 (m); M^+ 164.

[5]By analogy with the benzophenone/2-butene photocycloaddition and from steric considerations, we presume the *trans* isomer predominates (see ref. 20).

Can. J. Chem. Downloaded from www.nrcresearchpress.com by 210.87.254.5 on 09/05/12
For personal use only.

TABLE 1. Photochemical reactivity of *p*-benzoquinone under various conditions

Reagents and conditions	Filter	Relative rates
PBQ + C_8H_{14}, benzene: no Ph_2CO *vs.* Ph_2CO	Pyrex	1:1.06 ± 0.13
PBQ + C_8H_{14}, benzene: no DBA *vs.* DBA	A	1:0.43 ± 0.02
PBQ + C_8H_{14}, benzene: no TMD *vs.* TMD	A	1:1.00 ± 0.03
C_8H_{14}, benzene: PBQ-d_0 *vs.* PBQ-d_4	Pyrex	1:0.94 ± 0.15
PBQ, benzene: C_8H_{14} *vs.* 2-methyl-1-butene	A	1:0.24 ± 0.05[a]
PBQ + C_8H_{14}: in benzene *vs.* CH_3CN	Pyrex	1:0.63 ± 0.10

[a]Since ϕ_r for cyclooctene ($\lambda > 400$ nm) is 0.55 ± 0.05 (2), this gives ϕ_r as 0.13 ± 0.05 in the case of 2-methyl-1-butene.

Anal. Calcd. for $C_{10}H_{12}O_2$: C, 73.11; H, 7.37. Found: C, 73.09; H, 7.50.

A mixture with identical spectroscopic properties was obtained from a similar irradiation using *trans*-2-butene.

Sensitization, Quenching, and Relative Rate Experiments

In these experiments, several reaction mixtures were irradiated simultaneously with the 450 W source using a rotating 'merry-go-round' apparatus to ensure equal illumination. These studies were all monitored by following the disappearance of the n,π^* absorption band of *p*-benzoquinone. The solutions were contained in Pyrex ampoules 1 × 1 × 5.5 cm of square cross-section, joined to 8 mm tubing for attachment to the vacuum line to permit degassing and sealing. The ampoules fitted directly into the sample chamber of the Beckman DB spectrophotometer. Before use, the ampoules were cleaned in chromic acid, rinsed several times (H_2O, NH_4OH, H_2O) and dried at 110 °C overnight. The results of the studies are given in Table 1. In each case the values quoted are the average of several runs at slightly different concentrations. Typical ranges of concentration were quinone (PBQ), 4–8 × 10^{-2} *M*; quenchers, dibromoanthracene (DBA) or 3,3,4,4-tetramethyl-1,2-diazetine-1,2-dioxide (TMD),[6] 10^{-3} *M*; alkene 0.9 *M*.

In the case of relative reactivities of chloroethylenes, the results were irreproducible from run to run and the average values are not quoted. Part of the problem seems to be polymerization of the alkene (purified by distillation). Various phenols were added to the reaction mixtures as radical traps, but because of charge transfer complexation between phenol and quinone, only modest success was achieved.

For the isotopic study, benzoquinone-d_4 was prepared from hydroquinone as follows. Hydroquinone-d_6 was obtained by exchange using D_2O/H_2SO_4 then D_2O/D_2SO_4 giving > 95% deuterium incorporation. Oxidation to the quinone was effected using silver carbonate on Celite (26) without loss of deuterium.

Phosphorescence Studies

The phosphorimeter was based on the Farrand Mark I fluorometer, modified with the manufacturer's accessories for phosphorescence. As supplied, the sample chamber did not permit degassing of samples, so it was redesigned to accommodate quartz ampoules of 8 mm o.d. 3-Methylpentane (Matheson, Coleman and Bell) was used as the glass medium; it was purified by treatments with oleum, water, and distillation under nitrogen after the method of Parker (27), then stored under nitrogen at −40 °C.

As a check on the effectiveness of the design of the new sample chamber, the phosphorescence spectrum of benzophenone was obtained: λ 419, 450, 486, 531, 570 nm as reported (28). The lifetime of the phosphorescence (Tektronix 2B67 oscilloscope) was 5.0 ms (lit. (28) 5.2 ms).

Benzoquinone samples for phosphorescence were triply sublimed; the samples were degassed and sealed after three freeze–pump–thaw cycles at 10^{-4} Torr. All samples were stored at −40 °C until the phosphorescence spectrum was run, and were carefully protected from the light throughout.

Photo-CIDNP Studies

The experimental arrangement was that described by Tomkiewicz *et al.* (29) employing a Varian Associates HA100 spectrometer, and a 1000W Hanovia high pressure mercury–xenon arc which was focussed onto the samples while the spectrum was recorded. Both degassed and aerated samples were examined. Benzene-d_6 solutions of benzoquinone (0.05 *M*) were studied with the following alkenes (~0.1 *M*): cyclooctene, trichloroethylene, vinyl chloride, 1,1- and 1,2-dichloroethylene, tetrachloroethylene, vinyl acetate, methyl vinyl ether, acrylonitrile, and fumaronitrile. Negative results were obtained with all but the first two olefins mentioned.

We acknowledge gratefully the help of Drs. M. Cocivera and H. Chen for running the photo-CIDNP spectra. We also thank Drs. P. de Mayo and D. R. Arnold for helpful discussions, and the National Research Council of Canada for financial support.

1. J. M. BRUCE. Quart. Rev. **21**, 405 (1967).
2. D. BRYCE-SMITH, A. GILBERT, and M. G. JOHNSON. J. Chem. Soc. C, 383 (1967).
3. E. J. GARDNER, R. H. SQUIRE, R. C. ELDER, and R. M. WILSON. J. Am. Chem. Soc. **95**, 1695 (1973); R. M. WILSON, E. J. GARDNER, R. C. ELDER, R. H. SQUIRE, and L. R. F. FLORIAN. J. Am. Chem. Soc. **96**, 2955 (1974).

[6]The absence of a specific reaction between the quinone and TMD was demonstrated in experiments where the two components, each 2 × 10^{-2} *M* were photolyzed in benzene. The rate of disappearance of quinone was very slow, and was no faster than in control experiments where the TMD was omitted.

Can. J. Chem. Downloaded from www.nrcresearchpress.com by 210.87.254.5 on 09/05/12
For personal use only.

4. R. M. WILSON and S. W. WUNDERLY. J. Chem. Soc. Chem. Commun. 461 (1974); R. M. WILSON and S. W. WUNDERLY. J. Am. Chem. Soc. **96**, 7350 (1974).
5. K. B. EISENTHAL and M. A. El-SAYED. J. Chem. Phys. **42**, 294 (1965).
6. E. F. ULLMAN. J. Am. Chem. Soc. **94**, 5077 (1972).
7. D. R. KEMP and G. PORTER. Proc. R. Soc. London, A **326**, 117 (1971).
8. W. G. HERKSTROETER and G. S. HAMMOND. J. Am. Chem. Soc. **88**, 4769 (1966) and references cited therein; L. M. COYNE. Diss. Abstr. Int. B, **28**, 515 (1967).
9. M. SEBTI, F. DUPUY, G. NOUCHI, and Y. ROUSSET. C.R. Acad. Sci. Ser. B, **270**, 1477 (1970); M. CHOWDHURY and D. S. MCCLURE. Chem. Abstr. **65**, 11563h (1966); W. HERRE and P. WEIS. Spectrochim. Acta. Part A, **29**, 203 (1973).
10. L. E. BRUS and J. R. MCDONALD. J. Chem. Phys. **58**, 4223 (1973).
11. J. C. MILLER and R. F. BORKMAN. J. Chem. Phys. **56**, 3727 (1972).
12. D. PHILLIPS. Photochemistry I. Specialist periodical report. The Chemical Society, London. 1970. Ch. 1.
13. D. R. ARNOLD. Adv. Photochem. **6**, 301 (1970).
14. C. WALLING and W. A. THALER. J. Am. Chem. Soc. **83**, 3877 (1961).
15. A. G. DAVIES, R. W. DENNIS, B. P. ROBERTS, and R. E. DOBBIE. J. Chem. Soc. Chem. Commun. 468 (1974); I. H. ELSON, S. W. MAO, and J. K. KOCHI. J. Am. Chem. Soc. **97**, 335 (1975).
16. C. WALLING. Free radicals in solution. John Wiley and Sons, Inc., New York. 1957. pp. 118, 132–40.
17. L. SALEM. J. Am. Chem. Soc. **96**, 3486 (1974).
18. J. A. BARLTROP and B. HESP. J. Chem. Soc. 5182 (1965).
19. D. R. ARNOLD, R. L. HINMAN, and A. H. GLICK. Tetrahedron Lett. 1425 (1964).
20. R. A. CALDWELL, G. W. SOVOCOOL, and R. P. GAJEWSKI. J. Am. Chem. Soc. **95**, 2549 (1973).
21. H. D. ROTH. Mol. Photochem. **5**, 91 (1973).
22. S. YOMOSA. Bull. Phys. Soc. Jpn. **36**, 1655 (1974).
23. R. S. MULLIKEN. J. Am. Chem. Soc. **74**, 811 (1952).
24. R. A. NEUNTEUFEL and D. R. ARNOLD. J. Am. Chem. Soc. **95**, 4080 (1973).
25. J. A. BARLTROP and B. HESP. J. Chem. Soc. C, 1625 (1967).
26. V. BALOGH, M. FETIZON, and M. GOLFIER. J. Org. Chem. **36**, 1339 (1971).
27. C. A. PARKER. Adv. Photochem. **2**, 305 (1964).
28. J. FERGUSON and H. J. TINSON. J. Chem. Soc. 3083 (1952); A. KUBOYAMO and S. YABE. Bull. Chem. Soc. Jpn. **40**, 2475 (1967).
29. M. TOMKIEWICZ, A. GROEN, and M. COCIVERA. J. Chem. Phys. **56**, 5850 (1972).

Can. J. Chem. Downloaded from www.nrcresearchpress.com by 210.87.254.5 on 09/05/12
For personal use only.

The Isolation and Synthesis of *E*-24-Ethylidene-5α-lanost-8-en-3β-yl Acetate

S. SAFE AND L. M. SAFE

Department of Chemistry, University of Guelph, Guelph, Ontario N1G 2W1

Received June 9, 1975

S. SAFE and L. M. SAFE. Can. J. Chem. **53**, 3247 (1975).

Extraction of the fungus *Mucor rouxii* gave small amounts of a 32 carbon triterpene (M^+ 454). Spectroscopic studies suggested a lanosterol ring skeleton with a 24-ethylidene group introduced into the side chain. The structure was confirmed by synthesis and shown to be *E*-24-ethylidene-5α-lanost-8-en-3β-yl acetate.

S. SAFE et L. M. SAFE. Can. J. Chem. **53**, 3247 (1975).

L'extraction du mycite *Mucor rouxii* permet d'isoler des petites quantités d'un triterpène de masse 454 possédant 32 atomes de carbone. Des études spectroscopiques ont suggéré que la structure de ce dérivé comporte un squelette de lanosterol auquel un groupe éthylidène a été attaché en position 24. On a confirmé la structure par synthèse et démontré ainsi qu'il s'agit de l'acétate du *E* éthylidène-24 (5α) lanostène-8 yl-3β.

[Traduit par le journal]

Mucor rouxii is a fungus capable of growth under a wide variety of environmental conditions; aerobic cultivation of the fungus gave filamentous mycelium whereas under oxygen-limiting conditions or in the presence of phenethyl alcohol, spherical budding yeast-like cells are produced (1, 2). The morphological changes in the cells are also accompanied by both quantitative and qualitative variations in the lipid levels with respect to fatty acids, sterols and triterpenes (3, 4). Examination of the triterpene fractions obtained from the yeast-like and filamentous cells indicated that lanosterol was the major component and this was accompanied by lower levels of 24-methylene-5α-lanost-8-en-3β-ol (3, 4). The triterpene fraction also contained trace quantities of a third component whose mass spectrum exhibited a molecular ion at *m/e* 454 and this paper describes the isolation, structure proof, and synthesis of this compound.

Results and Discussion

The mycelia of *Mucor rouxii* (5) obtained from 500 l of media were extracted with chloroform–methanol and the triterpene fraction was isolated by thin layer chromatographic (t.l.c.) procedures. Acetylation of the triterpene fraction and subsequent purification by argentation t.l.c. gave 3 bands. The least polar band gave material which was identified as lanosteryl acetate whereas the most polar band contained 24-methylene-5α-lanost-8-en-3β-yl acetate (3, 4). The band of intermediate polarity (5.5 mg) gave a single peak on gas-liquid chromatography (g.l.c., R_c = 7.65 retention time relative to the internal standard 5α-cholestane) and exhibited a molecular ion at *m/e* 496. Hydrolysis of the unknown acetate gave an alcohol for which high resolution mass measurement of the molecular ion indicated a molecular formula of $C_{32}H_{54}O$.

The mass spectrum of the acetate gave major fragment ions at *m/e* 481 ($M^+ - CH_3$) and 421 ($M^+ - CH_3 - HOAc$). The mass spectra of both lanosteryl acetate and 24-methylene-5α-lanost-8-en-3β-yl acetate also exhibited the corresponding ions for the losses of CH_3 and (CH_3 + HOAc) from the molecular ion. In addition the ion abundance data below *m/e* 340 for the three triterpene acetates were remarkably similar, suggesting a common lanostane ring skeleton.

The 220 MHz nuclear magnetic resonance (n.m.r.) spectrum of the 32 carbon triterpene acetate integrated for 56 protons using the proton at 5.19 p.p.m. as a 1H standard. The spectrum exhibited several signals between 0.5–1.6 p.p.m. which could be assigned to the 5 CH_3 groups on the ABCD rings of the lanostane skeleton as well as the C_{21}, C_{26}, and C_{27} methyl groups on the side chain (see Table 1). A three proton doublet was observed at 1.58 p.p.m. (J = 6 Hz) and this indicated a methyl group adjacent to an olefinic double bond and coupled to the olefinic proton. The low field quartet observed at 5.19 p.p.m. supported this assignment and since this olefinic proton was coupled only to the methyl group this was evidence for a trisubstituted double bond (*e.g.* CH_3—CH=C). Fucosterol and isofucosterol

TABLE 1. Nuclear magnetic resonance data for the natural and synthetic triterpene acetates

Assignment	Triterpene (chemical shifts, p.p.m.) Natural	Grignard product*	Wittig product†
C_{18}—CH_3	0.69	0.69	0.69
$C_{4\alpha,4\beta,14}$—CH_3	0.87	0.87	0.87
C_{21}—CH_3	0.95	0.95	0.92
C_{19}—CH_3	1.00	1.0	0.99
$C_{26,27}$—CH_3	0.97	0.97	0.99
C_{29}—CH_3	1.58	1.58	1.60
3-β-O—$COCH_3$	2.05	2.05	2.07
C_{25}—H	2.19	2.19	2.85
3α-H	4.50	4.50	4.52
C_{28}—H	5.19	5.19	5.13

*Major product (R_c 7.65) from Grignard reaction.
†Major product (R_c 7.95) from Wittig reaction.

both contain 24-ethylidene moieties and the chemical shift and coupling constants for the ethylidene protons in the respective sterols were similar to the triterpene data (6–8). Since the n.m.r. and mass spectral data suggested a conventional lanostane ring skeleton a possible site for the trisubstituted double bond in the side chain would be at C_{24} since this position is biogenetically favored for side chain alkylation.

The structure of the 32 carbon triterpene acetate was confirmed by synthesis of 24-ethylidene-5α-lanost-8-en-3β-yl acetate from 24-keto-5α-lanost-8-en-3β-yl acetate using both the Grignard (9) and Wittig (10) condensation reactions. Both synthetic schemes gave two major reaction products as indicated by g.l.c. analysis (R_c 7.65 and 7.95) with the R_c 7.65 compound having the same retention time as the natural 32 carbon acetate. This material was the major component in the Grignard reaction and repeated argentation t.l.c. gave >98% pure fraction of this compound whose mass and n.m.r. spectra (see Table 1) were identical to the spectra of the natural product.

Previous studies on the n.m.r. spectra of 24-ethylidenecholest-5-en-3β-ol have shown that the orientation of the substituents about the C_{24}—C_{28} olefinic bond influences the chemical shift of the C_{25} proton (6–8). The signal for this proton appears as a heptet at 2.80 p.p.m. for the *Z* configuration (*i.e.* isofucosterol) whereas the resonance shifts upfield to 2.20 p.p.m. for the *E* configuration (*i.e.* fucosterol). These differences in chemical shift were also observed in the n.m.r. spectra of the geometrical isomers of 24-ethylidene-5α-lanost-8-en-3β-ol. The n.m.r. spectra of the natural product and the major component of the Grignard reaction (R_c = 7.65) exhibited the heptet at 2.19 p.p.m. whereas the corresponding signal appeared at 2.85 p.p.m. in the n.m.r. spectrum of the major product of the Wittig reaction (R_c = 7.95). These data thus indicate that the structure of the 32 carbon triterpene acetate from *M. rouxii* is *E*-24-ethylidene-5α-lanost-8-en-3β-yl acetate which is presumably formed by two successive alkylations of lanosterol at C_{24} in the side chain (9).

Experimental

Spectroscopic and Chromatographic Procedures

Mass spectra were obtained with a Dupont CEC 21-110B double-focussing high resolution mass spectrometer at 70 eV. Nuclear magnetic resonance spectra were recorded on a Varian HR220 instrument and the samples were dissolved in deuteriochloroform.

Gas chromatographic analyses of the triterpene acetates were carried out with a Hewlett Packard 700 gas chromatograph on a ⅛ in. × 6 ft glass column packed with 2% OV-17 (100–120 mesh) at 260 °C.

Isolation of the 32 Carbon Triterpene Acetate

Cultivation and growth of *M. rouxii* (Calmette) Wehmer (HLX 1093) from sheep rumen contents have been described (5). The mycelia from 500 l of aerobically grown *M. rouxii* were freeze-dried, macerated with chloroform–methanol (2:1) in a Waring blender and the triterpene fraction isolated by t.l.c. as described. The crude triterpene acetates were prepared and the three components were separated by argentation t.l.c. (3, 4). The isolation of lanosteryl acetate and 24-methylene-5α-lanost-8-en-3β-yl acetate have been described (3, 4). In this large scale extraction a third triterpene acetate (5.5 mg) was also isolated and gave: n.m.r. spectrum ($CDCl_3$), (see Table 1); *m/e* 496, 481, 421; m.p. 135–138 °C; R_c 7.65 (relative to 5α-cholestane). Hydrolysis of the acetate gave the sterol:

high resolution mass measurement; calculated for $C_{32}H_{54}O$, 454.4174; found, 454.4169; n.m.r. ($CDCl_3$) 0.60 (3H, s, C_{18}—CH_3), 0.81 and 0.87 (6H, s, $C_{4\alpha,4\beta}$—CH_3), 0.96–1.02 (15H, m, C_{19}, C_{14}, C_{21}, C_{26}, and C_{27}—CH_3), 1.57 (3H, d, J = 6 Hz, C_{29}—CH_3), 2.29 (1H, heptet, J = 6 Hz, C_{25}—H), 3.24 (1H, q, J = 5 Hz, 3α-H), 5.29 (1H, q, J = 6 Hz, C_{28}—H).

Syntheses of Z- and E-24-Ethylidene-5α-lanost-8-en-3β-yl Acetate

Grignard Reaction—The condensation reaction of 24-keto-5α-lanost-8-en-3β-yl acetate (100 mg) and vinyl magnesium bromide was carried out as described by Sucrow and Raduchel (10) to give the crude condensation product. This compound was converted into the 29-bromo derivative by treatment with phosphorus tribromide (9); the reaction of the crude bromide with lithium aluminum hydride followed by reacetylation gave a mixture of *E*- and *Z*-24-ethylidene-5α-lanost-8-en-3β-yl acetate (18 mg). Gas-liquid chromatographic analysis indicated a 3:1 mixture of the *E* and *Z* isomers respectively (R_c 7.65 and 7.95). Argentation t.l.c. gave a fraction enriched in the *E* isomer, m.p. 135–138 °C, n.m.r. as given in Table 1.

Wittig Reaction—The condensation of 24-keto-5α-lanost-8-en-3β-yl acetate (40 mg) and the phosphonium salt of ethyl bromide was carried out as described by Fryberg *et al.* (11) except that ethyl lithium was used instead of butyl lithium. Gas-liquid chromatographic analysis of the crude *Z*- and *E*-24-ethylidene-5α-lanost-8-en-3β-yl acetate (12 mg) gave two peaks (R_c 7.65 and 7.95) in a ratio of 4:1 *Z*:*E*. Argentation t.l.c. gave an enriched fraction (>95% pure) of the *Z*-isomer, m.p. 131–134 °C; n.m.r. as given in Table 1.

The financial assistance of the Guelph Research Advisory Board is gratefully acknowledged.

1. S. Bartnicki-Garcia and W. J. Nickerson. Biochim. Biophys. Acta, **58**, 102 (1962).
2. H. F. Terenzi and R. Storck. J. Bacteriol. **97**, 1248 (1969).
3. S. Safe. Biochim. Biophys. Acta, **336**, 471 (1973).
4. S. Safe and J. Caldwell. Can. J. Microbiol. **21**, 79 (1975).
5. D. Brewer, J. M. Duncan, S. Safe, and A. Taylor. Can. J. Microbiol. **18**, 1119 (1972).
6. D. J. Frost and J. P. Ward. Tetrahedron Lett. 3779 (1969).
7. R. B. Bates, A. D. Brewer, B. A. Knights, and J. W. Rowe. Tetrahedron Lett. 6163 (1968).
8. D. R. Idler, L. M. Safe, and E. F. MacDonald. Steroids, **18**, 548 (1971).
9. E. A. Mercer and S. M. Russel. Phytochemistry, **14**, 451 (1975).
10. W. Sucrow and B. Raduchel. Chem. Ber. **103**, 2711 (1970).
11. M. Fryberg, A. C. Oehlschlager, and A. M. Unrau. Tetrahedron, **27**, 1261 (1971).

Formation et stabilité de lyato-complexes de l'argent(I) en solution hydro-méthanolique[1]

JEAN PIUZE[2] ET A. OTTO GÜBELI

Département de Chimie, Université Laval, Québec, Québec G1K 7P4

Reçu le 10 fevrier 1975

JEAN PIUZE et A. OTTO GÜBELI. Can. J. Chem. **53**, 3250 (1975).

La solubilité totale de l'oxyde d'argent en fonction du pH^* non-aqueux dans un mélange contenant 52.1% de méthanol en poids dans l'eau a été déterminée pour une force ionique constante décimolaire ($NaNO_3$) à 25 °C et à pression atmosphérique. La prise en considération des divers équilibres en jeu dans le milieu hydro-méthanolique a conduit à un traitement mathématique permettant d'identifier les complexes formés par solvolyse avec les ions lyate, c'est-à-dire OH^- et CH_3O^-, et de calculer les constantes de stabilité molaires pertinentes. La corrélation entre ces résultats et ceux de travaux antérieurs sur la solubilité de $Ag_2O(s)$ en milieu aqueux a été examinée.

JEAN PIUZE and A. OTTO GÜBELI. Can. J. Chem. **53**, 3250 (1975).

The total solubility of silver oxide as a function of the nonaqueous pH^* in a mixture containing 52.1 wt.% methanol in water was measured for a constant decimolar ionic strength ($NaNO_3$) at 25 °C and at atmospheric pressure. After examination of the different equilibria involved in the hydro-methanolic medium, mathematical expressions were derived, leading to the identification of the complex species formed through solvolysis phenomena with the lyate ions, *i.e.* OH^- and CH_3O^-, and to the calculation of the relevant molar stability constants. The correlation between these results and those from previous publications on the aqueous solubility of $Ag_2O(s)$ was investigated.

Introduction

La littérature chimique compte bon nombre de travaux sur la stabilité de complexes de cations de métaux avec une multitude de ligands inorganiques et organiques dans des mélanges hydro-méthanoliques de divers pourcentages (1, 2). Toutefois, à notre connaissance, aucun auteur[3] ne traite de la solvolyse de ces ions métalliques pour donner des hydroxo- ou des méthoxo-complexes, chacun s'attachant uniquement à examiner les espèces formées avec un ligand, autre que OH^- ou CH_3O^-, ajouté à la solution. Aussi, afin d'examiner cette possibilité inexplorée de formation de complexes par solvolyse non-aqueuse, avons-nous entrepris l'étude de la solubilité de $Ag_2O(s)$ dans un mélange eau–méthanol.

Cependant, la plupart des méthodes de détermination de constantes de stabilité, y compris la méthode de solubilité, ne permettent pas de distinguer un complexe d'une paire d'ions (5). C'est pourquoi, lorsqu'on désire considérer uniquement la formation de complexes, il faut toujours s'assurer que la constante diélectrique (permittivité relative, ε_r) du solvant est supérieure à 40, car on peut alors supposer le comportement d'électrolyte fort et négliger la formation de paires d'ions, tout au moins en solution suffisamment diluée (6). Dans le cas du mélange à 52.1% de méthanol en poids dans l'eau choisi, une interpolation des données de ε_r pour le système binaire H_2O–CH_3OH à 25 °C (7) fournit une valeur de 55.4, indiquant donc que l'association d'ions devrait pouvoir y être négligée, étant donné la force ionique relativement faible de 0.1 (M) maintenue.

Considérations théoriques

La méthode adoptée pour le traitement des données de solubilité a été élaborée par Ste-Marie (8) à la suite de travaux comme ceux de Schwarzenbach et Widmer (9). L'applicabilité de cette méthode graphique, dite "des pentes", à l'identification de complexes prédominants en milieu hydro-méthanolique requiert toutefois la prise en considération de certains éléments nouveaux.

Dans un solvant mixte constitué d'eau et de méthanol, si l'on ne tient pas compte des divers modes de solvatation des ions, on trouve qu'il y a six espèces chimiques à considérer: H_2O, CH_3OH, H_3O^+, $CH_3OH_2^+$, OH^- et CH_3O^- (10). L'acti-

[1]Travail présenté en partie au 55ième Congrès de l'Institut de Chimie du Canada, Québec, Québec, juin 1972.

[2]Adresse actuelle: Laboratoire de Chimie de l'Océan, Environnement Canada, Victoria, Colombie-Britannique.

[3]A l'exception de quelques travaux (3, 4) où la seule formation d'hydroxo-complexes a été envisagée.

Can. J. Chem. Downloaded from www.nrcresearchpress.com by 210.87.254.6 on 09/05/12
For personal use only.

Can. J. Chem. Downloaded from www.nrcresearchpress.com by 210.87.254.6 on 09/05/12
For personal use only.

vité des molécules du solvant étant invariante en solution diluée, il est possible de relier ces différentes particules en définissant des constantes apparentes, valables pour un mélange donné:

$$[1] \qquad k_1 = \{H_3O^+\}\{OH^-\}$$

$$[2] \qquad k_2 = \{CH_3OH_2^+\}\{CH_3O^-\}$$

$$[3] \qquad k_3 = \frac{\{H_3O^+\}}{\{CH_3OH_2^+\}}$$

$$[4] \qquad k_4 = \frac{\{OH^-\}}{\{CH_3O^-\}}$$

où les accolades dénotent une activité molaire. On pose ensuite le produit ionique du solvant,

$$[5] \quad K_a = \{H_3O^+\}(\{OH^-\} + \{CH_3O^-\})$$

où le terme $\{CH_3OH_2^+\}$ ne figure plus puisque les ions méthoxonium sont négligeables dans les mélanges contenant plus de 10% d'eau (10). Le pH^* dans ce solvant mixte est donc égal au cologarithme de $\{H_3O^+\}$.

Afin d'exprimer le produit de solubilité de l'oxyde d'argent en milieu aqueux, on peut supposer qu'une réaction d'hydrolyse à la surface de Ag_2O(s) amène d'abord la formation d'un film d'hydroxyde, AgOH(s) (11). Parallèlement, une réaction de solvolyse en surface du solide dans le solvant mixte devrait mener soit à AgOH(s), soit à $AgOCH_3$(s); mais Bradley (12) mentionne que les alcoxydes de métaux sont tous très facilement hydrolysés, même par des traces d'eau. Par conséquent, il semble fort plausible que la solubilisation de Ag_2O(s) dans le mélange eau–méthanol se fasse également par l'intermédiaire de AgOH(s) dont le produit de solubilité s'écrit

$$[6] \qquad K_{s0} = [Ag^+]\{OH^-\}$$

où les crochets dénotent une concentration molaire.

Hydroxo-méthoxo complexes

Lorsqu'on choisit des conditions telles qu'on puisse négliger les espèces polynucléaires, la formation de complexes de l'argent(I) en solution hydro-méthanolique peut être représentée par un équilibre menant à la définition de la constante cumulative de formation,

$$[7] \qquad \beta_{xy} = \frac{[Ag(OH)_x(OCH_3)_y{}^{1-x-y}]}{[Ag^+]\{OH^-\}^x\{CH_3O^-\}^y}$$

Après l'introduction des éqs 4, 5 et 6 dans l'éq. 7, on peut écrire la relation exprimant la concentration totale d'argent en solution en équilibre avec l'oxyde précipité:

$$[8] \quad [\Sigma Ag] = \sum_{x=0}^{n} \sum_{y=0}^{n-x} \beta_{xy} K_{s0} K_a{}^{x+y-1} k_4{}^{x-1} \times (1 + k_4)^{1-x-y}\{H_3O^+\}^{1-x-y}$$

où n représente l'indice de coordination usuel du métal en solution.

Si l'on pose qu'un seul complexe existe en concentration prédominante dans un intervalle de pH^* assez restreint, les deux symboles de sommation de l'éq. 8 disparaissent et $[\Sigma Ag]$ correspond à la concentration du seul complexe important dans cette région. La dérivation subséquente par rapport au pH^* de la forme cologarithmique de l'éq. 8 réduite à un seul terme nous révèle que la pente $(1 - x - y)$ d'une courbe de solubilité de $p[\Sigma Ag]$ en fonction du pH^* sera caractéristique d'une espèce prédominante de charge $(1 - x - y)$, comme on peut le constater au tableau 1. Il ressort clairement de ce tableau qu'une pente de (-1), par exemple, sur la courbe de solubilité permettra de conclure qu'on se trouve en présence d'un complexe contenant un total de deux ligands parmi OH^- et CH_3O^-, sans qu'on puisse distinguer entre $Ag(OH)_2^-$, $Ag(OH)(OCH_3)^-$ et $Ag(OCH_3)_2^-$. D'ailleurs, comment pourrait-il en être autrement lorsqu'on ne détermine expérimentalement qu'une seule variable, soit $\{H_3O^+\}$? Il est en effet bien évident, à la lumière des éqs 4 et 5, que la courbe de solubilité en fonction du pH^* ne pourra livrer des renseignements que sur la somme des ligands OH^- et CH_3O^-, non sur chacun d'eux.

Hydroxo-complexes simples

Cependant, si l'on pouvait démontrer l'absence de méthoxo-complexes prédominants dans le mélange eau–méthanol, c'est-à-dire ($y = 0$), l'éq. 8 résultante serait alors l'expression de la somme des concentrations de Ag^+ et des seuls hydroxo-complexes en solution.

Le fait que les alcoxydes solides soient immédiatement hydrolysés par des traces d'eau (12) suggère que les méthoxo-complexes pourraient peut-être eux aussi être transformés en hydroxo-complexes dans le solvant mixte. Ainsi, Jørgensen (13) rapporte que, dans une solution de Fe^{3+} dans du méthanol rendue alcaline à l'aide de KOH, il est difficile de savoir si $Fe(OCH_3)_6^{3-}$ ou $Fe(OH)_6^{3-}$ ou encore un complexe mixte se

TABLEAU 1. Espèces pouvant théoriquement résulter de la solvolyse de Ag^+ en solution hydro-méthanolique

Pente $dp[\Sigma Ag]/dpH^*$ $(1-x-y)$	$x+y$	x	y	Espèce $Ag(OH)_x(OCH_3)_y^{1-x-y}$
1	0	0	0	Ag^+
0	1	1	0	$Ag(OH)$
0	1	0	1	$Ag(OCH_3)$
−1	2	2	0	$Ag(OH)_2^-$
−1	2	1	1	$Ag(OH)(OCH_3)^-$
−1	2	0	2	$Ag(OCH_3)_2^-$

forme, mais qu'on peut faire cristalliser de cette solution un produit jaune ne contenant pas de carbone, peut-être $K_3Fe(OH)_6$. A plus forte raison, lorsqu'il y a une quantité d'eau importante dans le solvant, la formation d'hydroxo-complexes pourrait-elle être favorisée. Toutefois, il importe de remarquer que la connaissance des espèces précipitées ne permet pas de tirer des conclusions sur la nature des espèces effectivement présentes en solution.

Du point de vue de la solvatation, dans les mélanges contenant jusqu'à 80% de méthanol, c'est l'eau qui de loin joue le rôle prépondérant (14 à 16). De plus, Jørgensen (13) mentionne que les ions des éléments de transition préfèrent l'eau aux alcools dans leur première sphère de coordination. Il apparaît donc vraisemblable que solvatation soit synonyme d'hydratation dans le mélange contenant 52.1% de méthanol en poids. Par conséquent, si l'on postule que la solvatation des cations métalliques constitue une étape du mécanisme de formation des complexes en solution par solvolyse, on peut s'attendre à ce que la solvatation préférentielle de Ag^+ par l'eau favorise la formation d'hydroxo-complexes simples.

Finalement, si l'on savait le lien Ag—OH beaucoup plus fort que la liaison Ag—OCH_3, ou vice-versa, on pourrait en tirer des conclusions quant à la nature des complexes existant en solution. Toutefois, il y a peu d'information disponible à ce sujet, si ce n'est que le lien métal–alcool est plus faible que le lien métal–eau dans les ions métalliques solvatés (17) mais que la différence d'énergie entre ces deux liaisons est petite (18).

Il semble donc que la formation d'hydroxo-complexes simples soit favorisée par rapport à celle de méthoxo-complexes, mais aucun des arguments invoqués n'en constitue une preuve expérimentale formelle.

Lyato-complexes

Il ressort de ce qui précède que, même si la formation d'hydroxo-complexes simples prédominants semble plus probable, la présence de méthoxo-complexes n'en demeure pas moins possible. C'est pourquoi nous avons choisi d'interpréter nos résultats en termes plus généraux qui incluent toutes les possibilités. Pour ce faire, nous utilisons une nomenclature où l'acide conjugué d'une molécule du solvant est appelé ion lyonium et la base conjuguée, ion lyate (19). Dans notre milieu hydro-méthanolique, ion lyonium est synonyme de H_3O^+ tandis que l'ion lyate, symbolisé par OL^-, désigne à la fois OH^- et CH_3O^-. La constante d'autoprotolyse du solvant peut donc s'écrire

$$[9] \qquad K_a = \{H_3O^+\}\{OL^-\}$$

La formation de lyato-complexes dans ce milieu peut alors être représentée par un équilibre général dont la constante cumulative de formation s'écrit

$$[10] \qquad \beta_r = \frac{[Ag(OL)_r^{1-r}]}{[Ag^+]\{OL^-\}^r}$$

La combinaison des éqs 4 et 5 fournit une expression pour $\{OH^-\}$:

$$[11] \qquad \{OH^-\} = \frac{K_a k_4}{(1+k_4)\{H_3O^+\}}$$

Et si l'on introduit tour à tour les éqs 6, 9 et 11 dans l'éq. 10, on obtient comme expression de la solubilité totale de l'oxyde d'argent en solution hydro-méthanolique:

$$[12] \quad [\Sigma Ag] = \sum_{r=0}^{n} \beta_r K_{s0} K_a^{r-1} k_4^{-1} \times (1+k_4)\{H_3O^+\}^{1-r}$$

Selon un raisonnement identique à celui qui faisait suite à l'éq. 8, l'examen du tableau 1, où

Can. J. Chem. Downloaded from www.nrcresearchpress.com by 210.87.254.6 on 09/05/12
For personal use only.

Can. J. Chem. Downloaded from www.nrcresearchpress.com by 210.87.254.6 on 09/05/12
For personal use only.

$(x + y)$ est égal à r, révèle que la pente $(1 - r)$ de la courbe de solubilité en fonction du pH^* indique quelle espèce $Ag(OL)_r^{1-r}$ prédomine dans une région donnée.

Méthode expérimentale

Le solvant mixte a toujours été préparé par pesée d'eau bidistillée et de méthanol pur (Fisher A-412) et tous les réactifs chimiques utilisés étaient de pureté garantie. Dans des fioles de 100 ml, nous avons introduit quelques millilitres d'une solution mère de $AgNO_3$ contenant une petite quantité du traceur radioactif ^{110}Ag. Le pH^* a ensuite été ajusté à l'aide de NaOH et HNO_3 de telle sorte qu'il y avait toujours un précipité en équilibre avec la solution. Enfin, les solutions ont été complétées avec les quantités de $NaNO_3$ nécessaires dans le solvant pour maintenir une force ionique décimolaire. Puis elles ont été placées à l'abri de la lumière à 25 °C et agitées régulièrement au cours des premiers jours. Au bout d'un mois, après avoir vérifié par échantillonnage périodique que l'équilibre était atteint, nous avons procédé aux analyses.

Le solide précipité a été identifié par diffraction des rayons X à l'aide d'une caméra Guinier: dans tous les cas, il s'agissait de Ag_2O, quoique la présence d'un peu d'argent métallique ait aussi été observée. En outre, la formation d'un miroir d'argent très mince sur la paroi intérieure des fioles a été notée dans la plupart des cas. Toutefois, le métal déposé n'affectait pas l'équilibre puisqu'il restait toujours un grand excès d'oxyde d'argent précipité.

La concentration totale d'argent en solution a été mesurée par radiométrie γ à l'aide d'un compteur à scintillations de marque Philips. Un couple d'électrodes argent–calomel (saturée dans l'eau), dont la jonction était assurée par un pont d'agar–agar dans $NaNO_3$ 0.1 M, a été utilisé pour déterminer la concentration d'argent cationique.

Nous ne mentionnerons ici que les grandes lignes de notre façon d'aborder la mesure du pH^* en milieu non-aqueux (20), tant du point de vue théorique que pratique, puisque tout cela a été décrit en détail ailleurs (21). Nous avons obtenu le pH^* de chaque solution au moyen du couple d'électrodes mentionné plus haut, dans lequel une électrode de verre (Metrohm UX) avait été substituée à l'électrode d'argent, puis étalonnée à l'aide des tampons précis mis au point par Bates et ses collaborateurs (22) pour les pH^* jusqu'à 11.5 environ dans ce solvant. Pour les quelques valeurs supérieures à 11.5, l'étalonnage des électrodes a été réalisé à l'aide de solutions de NaOH dans le solvant non-aqueux pour lesquelles on était arrivé à une assez bonne valeur de pH^* en soustrayant un terme constant δ de la lecture de pH obtenue après avoir utilisée des solutions-tampons aqueuses pour étalonner la chaîne de mesure (20 à 22). Il est primordial de remarquer que l'échelle de pH^* définie pour un mélange hydro-méthanolique n'est pas reliée à celle du pH dans l'eau (22, 23). On ne peut en effet utiliser, pour tous les mélanges eau–méthanol, une seule échelle universelle d'activité protomique se référant à l'eau, à moins d'être en mesure d'évaluer l'effet de milieu (24) avec précision, ce qui n'a pas encore été réalisé de façon pratique (20).

Résultats

La courbe de solubilité de l'oxyde d'argent dans le mélange eau–méthanol apparaît à la fig. 1, tandis que la variation de la concentration de Ag^+ en fonction du pH^* est présentée à la fig. 2. L'examen de la courbe de $p[\sum Ag]$ en fonction du pH^* révèle une pente $(dp[\sum Ag]/dpH^*)$ de l'ordre de $(+1)$ dans la région de pH^* comprise entre 6.5 et 9.5, suivie d'un plateau (pente 0) entre pH^* = 11 et 12.5, puis d'un début de remontée qui semble s'amorcer selon une pente voisine de (-1). En consultant le tableau 1, on

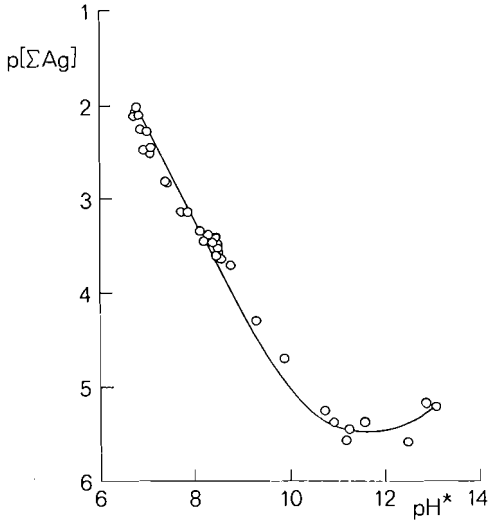

FIG. 1. Solubilité totale de $Ag_2O(s)$ en fonction du pH^* dans le solvant hydro-méthanolique.

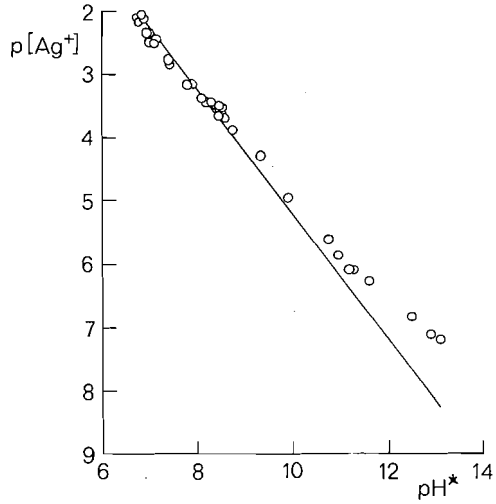

FIG. 2. Solubilité cationique de l'oxyde d'argent en fonction du pH^* dans le mélange eau–méthanol.

Can. J. Chem. Downloaded from www.nrcresearchpress.com by 210.87.254.6 on 09/05/12
For personal use only.

conclut donc que l'allure de la courbe de solubilité s'explique par la prédominance successive des espèces Ag^+, $Ag(OL)$ et $Ag(OL)_2^-$.

L'introduction des valeurs expérimentales de $[\sum Ag]$ et de $\{H_3O^+\}$ dans l'éq. 12 permettrait de résoudre des systèmes de trois équations à trois inconnues (K_{s0}, β_1 et β_2), à condition de connaître K_a et k_4. Cependant, il est important de pouvoir d'abord caractériser les équilibres en solution étudiés par des constantes de solubilité précises ne faisant appel ni à l'évaluation approximative de k_4, ni même à K_a. Pour ce faire, on peut considérer le processus global suivant de formation de lyato-complexes à partir de la phase intermédiaire solide AgOH:

$$[13]\quad AgOH(s) + H_3O^+ + rOL^- \rightleftharpoons Ag(OL)_r^{1-r} + 2H_2O$$

équilibre pour lequel la constante s'écrit

$$[14]\qquad {}^*K_{sr} = \frac{[Ag(OL)_r^{1-r}]}{\{H_3O^+\}^{1-r}}$$

après qu'on y ait exprimé $\{OL^-\}$ en termes de $\{H_3O^+\}$ en utilisant l'éq. 9.

Comme la solubilité totale de l'argent est égale à la somme des trois espèces chimiques identifiées, on peut écrire

$$[15]\quad [\sum Ag] = {}^*K_{s0}\{H_3O^+\} + {}^*K_{s1} + {}^*K_{s2}\{H_3O^+\}^{-1}$$

Les constantes ${}^*K_{sr}$ suivantes et leur écart type (σ) ont été calculés et raffinés en langage APL:

$$\log {}^*K_{s0} = 4.8 \quad (\sigma = \pm 0.2)$$

$$\log {}^*K_{s1} = -5.5 \quad (\sigma = \pm 0.1)$$

$$\log {}^*K_{s2} = -18.6 \quad (\sigma = \pm 0.2)$$

pour une force ionique de 0.1 ($NaNO_3$) à 25 °C. L'introduction de ces constantes dans l'éq. 15 permet alors de calculer la courbe tracée à la fig. 1.

De plus, les résultats de $p[Ag^+]$ assurent un contrôle de la valeur obtenue plus haut pour ${}^*K_{s0}$. En effet, partant de l'éq. 14, on peut écrire

$$[16]\qquad \log {}^*K_{s0} = pH^* - p[Ag^+]$$

Si l'on se reporte à la fig. 2, on constate que seuls les points de pH^* inférieur à 11 peuvent vérifier l'équation de cette droite de pente unitaire positive en fonction du pH^*. Insérés dans l'éq. 16, ils fournissent la valeur moyenne suivante:

$$\log {}^*K_{s0} = 4.77 \ (\sigma_m = \pm 0.04)$$

σ_m étant l'écart moyen. Cette dernière constante introduite dans l'éq. 16 permet de calculer la droite tracée à la fig. 2.

De la comparaison des éqs 12 et 14 découle la relation

$$[17]\quad {}^*K_{sr} = \beta_r K_{s0} K_a^{r-1} k_4^{-1}(1 + k_4)$$

Sachant que β_0 est égal à l'unité, il est possible de calculer K_{s0} à l'aide de l'éq. 17 si l'on connaît les valeurs de K_a et de k_4. On pourra ensuite utiliser K_{s0} calculé pour obtenir β_1 et β_2. La valeur de pK_a pour le solvant hydro-méthanolique (14.19 à 25 °C sur l'échelle molaire) peut être interpolée à partir des données expérimentales de Koskikallio (25). Ce dernier auteur a également obtenu la valeur d'une constante k_4' reliée à k_4 de l'éq. 4 par

$$[18]\qquad k_4 = k_4' \frac{\{H_2O\}}{\{CH_3OH\}}$$

Du point de vue thermodynamique, une des meilleures approximations du rapport des activités des composants du solvant mixte consiste à remplacer, tout comme l'a fait Oiwa (26), $\{H_2O\}$ par (p_1/p_1^0) et $\{CH_3OH\}$ par (p_2/p_2^0) où p_1 et p_2, les tensions de vapeur partielles respectives de l'eau et du méthanol au-dessus du mélange de solvants, sont calculés par interpolation des données de Butler et collaborateurs (27) et où les tensions de vapeur p_1^0 et p_2^0 de chacun des solvants à l'état pur sont respectivement égales à 23.76 Torr (26) et 126.6 Torr (27). La valeur de k_4 calculée par l'éq. 18 est alors 0.19. L'introduction des valeurs appropriées des diverses constantes dans une forme logarithmique de l'éq. 17 conduit ensuite aux résultats suivants: $pK_{s0} = 10.2$, $\log \beta_1 = 3.9$, $\log \beta_2 = 5.0$.

Discussion

La précision de la constante ${}^*K_{s0}$ paraît certainement satisfaisante lorsque l'on considère que deux méthodes d'analyse différentes, l'une radiométrique et l'autre potentiométrique, en ont fourni la même valeur logarithmique, soit 4.8. Notons ici qu'on peut expliquer, à la suite de Côté (11), la déviation positive des résultats potentiométriques en milieu alcalin, observée à la fig. 2, par le fait que la formation d'une couche d'oxyde d'argent à la surface de l'électrode d'argent en solution basique (28) peut causer un abaissement du pH^* local de la portion de solution en contact direct avec l'électrode.

D'après la définition physique même de la constante diélectrique, on sait que, si l'on peut

TABLEAU 2. Produit de solubilité de $Ag_2O(s)$ et constantes cumulatives de formation des lyato-complexes de l'argent(I) dans l'eau et dans le mélange eau–méthanol à 25 °C

Milieu (force ionique, μ)	pK_{so}	$\log \beta_1$	$\log \beta_2$	Référence
H_2O ($\mu = 0$)	7.71	2.0	3.99	Biedermann et Sillén (30)
H_2O ($NaClO_4$ 1 *M*)	7.82	2.57	4.04	Côté (11)
CH_3OH 52.1% (poids) ($\mu = 0.1$ ($NaNO_3$))	10.2	3.9	5.0	Présent travail

assimiler les ions en solution à des sphères chargées dans un milieu fluide continu (29), la stabilité d'espèces ioniques solubles sera d'autant plus grande que ε_r sera élevé. Il est donc possible de prévoir à peu près l'effet d'un changement de solvant sur une réaction chimique équilibrée en considérant la charge z de toutes les particules y prenant part afin d'appliquer la règle de Δz^2 (29):

$$[19] \quad \Delta z^2 = \sum z^2 \text{ (produits)} - \sum z^2 \text{(réactifs)}$$

Il ressort de ce qui précède que la diminution de la constante diélectrique macroscopique, lorsqu'on passe de l'eau ($\varepsilon_r = 78.5$ (7)) au mélange eau–méthanol utilisé ($\varepsilon_r = 55.4$), devrait faire augmenter ou diminuer la constante d'équilibre d'une réaction selon que Δz^2 est négatif ou positif. Lorsqu'on applique cette règle aux trois réactions dont les constantes d'équilibre sont K_{s0}, β_1 et β_2 (voir les éqs 6 et 10), on trouve des valeurs respectives de (+2), (−2) et (−2) pour Δz^2. Ceci signifie que la valeur de K_{s0} devrait décroître et que celles de β_1 et β_2 devraient s'accroître dans le solvant mixte par rapport au milieu aqueux, ce qui est effectivement le cas pour les données comparatives du tableau 2. C'est pourquoi on peut parler de solubilité plus faible de l'oxyde d'argent et de stabilité accrue des lyato-complexes de Ag(I) dans le solvant hydro-méthanolique. Il est à noter que le raisonnement qui précède ne tient pas compte des effets non électrostatiques, plus difficiles à évaluer, qui peuvent résulter des changements dans les interactions soluté–solvant (24).

A la fig. 3, la courbe de solubilité de $Ag_2O(s)$ pour le mélange de solvants est mise en parallèle avec les tracés pour le milieu aqueux calculés à l'aide des constantes qui apparaissent au tableau 2. Il est essentiel de mentionner que si l'ordonnée est la même dans le cas des trois courbes de la fig. 3, il n'en va pas de même de l'abscisse qui correspond au pH ($pK_a = 14.00$ (1, 2)) pour le milieu aqueux et au pH^* ($pK_a = 14.19$) pour le

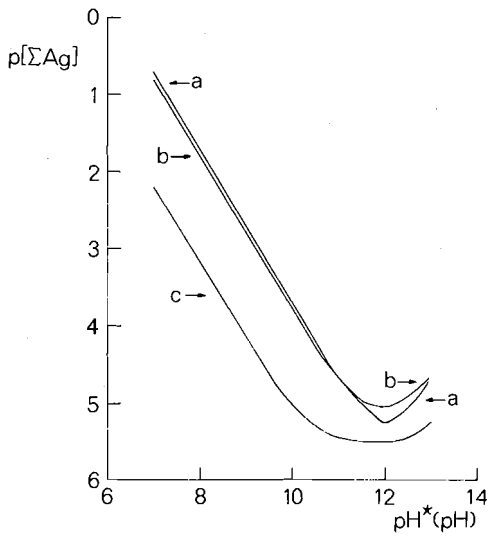

FIG. 3. Solubilité totale calculée pour l'oxyde d'argent: (*a*) en milieu aqueux d'après les constantes de Biedermann et Sillén (30), et (*b*) d'après celles de Côté (11); (*c*) en milieu hydro-méthanolique, d'après le présent travail.

milieu non-aqueux. Deux conséquences logiques de la diminution de la constante diélectrique ressortent ici: dans le mélange eau–méthanol, la solubilité complexe de $Ag_2O(s)$ est plus faible et l'intervalle de prédominance de l'espèce neutre Ag(OL), plus grand.

L'utilisation de l'éq. 15 pour exprimer la concentration totale d'argent en solution n'est justifiable que dans la mesure où la formation de nitrato-complexes de Ag(I) peut être négligée. Or il semble que $Ag(NO_3)$ soit la seule espèce soluble susceptible de se former de façon importante (1, 2). Fritz et Waki (31) ont obtenu des valeurs de 0.27 et 0.53 pour la constante de stabilité à 25 °C de $Ag(NO_3)$ respectivement dans l'eau et dans le 2-propanol à 40% en poids dans l'eau ($\varepsilon_r = 49.7$ (32)). Il est donc plausible de supposer que, dans le mélange eau–méthanol ($\varepsilon_r = 55.4$), la constante

Can. J. Chem. Downloaded from www.nrcresearchpress.com by 210.87.254.6 on 09/05/12
For personal use only.

de stabilité est de l'ordre de grandeur de 0.5. On peut alors écrire

$$[20]^{\ddagger} \qquad \frac{[AgNO_3]}{[Ag^+]} \cong 0.5[NO_3^-]$$

Dans le présent travail, le fait que la concentration totale maximum de nitrate soit égale à 0.1 signifie que $[AgNO_3]$ sera inférieur à 5% de $[Ag^+]$ et que ce nitrato-complexe pourra être négligé, même aux pH* auxquels Ag^+ prédomine.

En outre, l'utilisation de l'éq. 15 exige que les espèces polynucléaires en solution soient négligeables. D'une part, comme ces dernières peuvent être négligées lors de l'étude de la solubilité de $Ag_2O(s)$ dans l'eau (30), il est légitime de penser qu'elles peuvent également l'être dans le solvant mixte où la concentration totale d'argent est encore plus faible. D'autre part, il n'y a pas lieu de croire que le processus de formation d'espèces polynucléaires doive être nettement favorisé par la constante diélectrique inférieure du milieu hydrométhanolique, puisque l'on constate, d'après les pentes observées à la fig. 1, que les seuls complexes polynucléaires prédominants possibles devraient posséder la même charge que les espèces mononucléaires identifiées précédemment.

Les auteurs désirent remercier le Conseil national de recherches du Canada de son aide financière qui a permis la réalisation de ce travail.

1. L. G. Sillén et A. E. Martell. Stability constants. Special publication no. 17, The Chemical Society, Londres. 1964.
2. L. G. Sillén et A. E. Martell. Stability constants, supplement no. 1. Special publication no. 25, The Chemical Society, Londres. 1971.
3. E. J. Bowers et H. D. Weaver. Proc. Indiana Acad. Sci. **71**, 101 (1961).
4. G. Popa, C. Luca et E. Iosif. Z. Phys. Chem. Leipzig, **222**, 49 (1963).
5. W. Stumm et J. J. Morgan. Aquatic chemistry, an introduction emphasizing chemical equilibria in natural waters. Wiley-Interscience, New York. 1970. chap. 6.
6. B. Trémillon. La chimie en solvants non-aqueux. Presses Universitaires de France, Paris. 1971. chap. I.
7. P. S. Albright et L. J. Gosting. J. Am. Chem. Soc. **68**, 1061 (1946).
8. J. Ste-Marie. Thèse de doctorat, Université Laval, Québec, Québec. 1966.
9. G. Schwarzenbach et M. Widmer. Helv. Chim. Acta, **46**, 2613 (1963); **49**, 111 (1966).
10. R. Gaboriaud. Ann. Chim. Paris, Série 14, **2**, 201 (1967).
11. P. A. Côté. Thèse de doctorat, Université Laval, Québec, Québec. 1973.
12. D. C. Bradley. Progress in inorganic chemistry, vol. 2. *Dirigé par* F. A. Cotton. Interscience, New York. 1960. p. 303.
13. C. K. Jørgensen. Inorganic complexes. Academic Press, Londres. 1963. chap. 5.
14. P. K. Migal' et V. A. Tsiplyakova. Russ. J. Inorg. Chem. 333 (1964).
15. V. V. Alexandrov et N. A. Izmailov. Zh. Fiz. Khim. **32**, 404 (1958).
16. N. A. Kostromina et E. D. Romanenko. Russ. J. Inorg. Chem. 598 (1966).
17. P. K. Migal' et E. D. Ivanova. Russ. J. Inorg. Chem. 1270 (1969).
18. P. K. Migal' et N. Kh. Grinberg. Russ. J. Inorg. Chem. 369 (1961).
19. E. Grunwald et L. J. Kirschenbaum. Introduction to quantitative chemical analysis. Prentice-Hall, Englewood Cliffs, N.J. 1972. chap. 6.
20. R. G. Bates. Determination of pH, theory and practice. 2ième édition. Wiley-Interscience, New York. 1973. chap. 8.
21. J. Piuze. Thèse de doctorat, Université Laval, Québec, Québec. 1973.
22. R. G. Bates, M. Paabo et R. A. Robinson. J. Phys. Chem. **67**, 1833 (1963).
23. M. Alfenaar et C. L. de Ligny. Rec. Trav. Chim. **86**, 1185 (1967).
24. O. Popovych. Crit. Rev. Anal. Chem. **1**, 73 (1970).
25. J. Koskikallio. Suom. Kemistil. B, **30**, 111 (1957).
26. I. T. Oiwa. J. Phys. Chem. **60**, 754 (1956).
27. J. A. V. Butler, D. W. Thomson et W. H. Maclennan. J. Chem. Soc. 674 (1933).
28. M. Blanc et J. Guitton. C.R. Acad. Sci. Ser. C, **279**, 21 (1974).
29. E. Grunwald et L. J. Kirschenbaum. Introduction to quantitative chemical analysis. Prentice-Hall, Englewood Cliffs, N.J. 1972. chap. 5.
30. G. Biedermann et L. G. Sillén. Acta Chem. Scand. **14**, 717 (1960).
31. J. S. Fritz et H. Waki. J. Inorg. Nucl. Chem. **26**, 865 (1964).
32. G. Åkerlöf. J. Am. Chem. Soc. **54**, 4125 (1932).

Can. J. Chem. Downloaded from www.nrcresearchpress.com by 210.87.254.6 on 09/05/12
For personal use only.

Hydrogen–Water Deuterium Exchange Over Metal Oxide Promoted Nickel Catalysts[1,2]

NORMAN H. SAGERT, PAUL E. SHAW-WOOD, AND RITA M. L. POUTEAU

Research Chemistry Branch, Atomic Energy of Canada Limited, Whiteshell Nuclear Research Establishment, Pinawa, Manitoba R0E 1L0

Received April 11, 1975

NORMAN H. SAGERT, PAUL E. SHAW-WOOD, and RITA M. L. POUTEAU. Can. J. Chem. **53**, 3257 (1975).

Specific rates have been measured for hydrogen–water deuterium isotope exchange over unsupported nickel promoted with about 20% of various metal oxides. The oxides used were Cr_2O_3, MoO_2, MnO, WO_2–WO_3, and UO_2. Nickel surface areas, which are required to measure the specific rates, were determined by hydrogen chemisorption. Specific rates were measured as a function of temperature in the range 353 to 573 K and as a function of the partial pressure of hydrogen and water over a 10-fold range of partial pressure.

The molybdenum and tungsten oxides gave the highest specific rates, and manganese and uranium oxides the lowest. Chromium oxide was intermediate, although it gave the highest rate per gram of catalyst. The orders with respect to hydrogen and water over molybdenum oxide and tungsten oxide promoted nickel were consistent with a mechanism in which nickel oxide is formed from the reaction of water with the catalyst, and then is reduced by hydrogen. Over manganese and uranium oxide promoted catalysts, these orders are consistent with a mechanism in which adsorbed water exchanges with chemisorbed hydrogen atoms on the nickel surface. Chromium oxide is intermediate. It was noted that those oxides which favored the nickel oxide route had electronic work functions closest to those of metallic nickel and nickel oxide.

NORMAN H. SAGERT, PAUL E. SHAW-WOOD et RITA M. L. POUTEAU. Can. J. Chem. **53**, 3257 (1975).

On a mesuré les vitesses spécifiques d'échange isotopique H/D entre de l'hydrogène et de l'eau sur du nickel sans support mais activé par environ 20% de divers oxydes de métaux. On a utilisé les oxydes suivants: Cr_2O_3, MoO_2, MnO, WO_2–WO_3 et UO_2. On a déterminé, par chemisorbtion de l'hydrogène, les surfaces disponibles du nickel nécessaires pour mesurer les vitesses spécifiques. On a mesuré les vitesses spécifiques en fonction de la température entre 353 et 573 K et aussi en fonction des pressions partielles d'hydrogène et d'eau alors que l'on a fait varier les pressions partielles par un facteur de 10.

Les oxydes de molybdène et de tungstène donnent les vitesses spécifiques les plus élevées alors que les oxydes de manganèse et d'uranium donnent les plus basses. L'oxyde de chrome est intermédiaire mais il donne la plus haute vitesse par gramme de catalyseur. Les ordres des réactions par rapport à l'hydrogène et à l'eau pour les réactions sur du nickel activé par MO_2 et WO_2–WO_3 sont en accord avec un mécanisme dans lequel de l'oxyde de nickel, formé par réaction de l'eau avec le catalyseur, est ensuite réduit par l'hydrogène. Sur des catalyseurs activés par des oxydes de manganèse et d'uranium, les ordres sont en accord avec un mécanisme dans lequel il y aurait échange des molécules d'eau adsorbées à la surface du nickel avec des atomes d'hydrogène qui y seraient attachés par chemisorbtion. L'oxyde de chrome est intermédiaire. On a noté que les oxydes qui favorisent la route impliquant l'oxyde de nickel ont des fonctions électroniques de travail les plus rapprochées de celles du nickel soit métallique et soit sous forme d'oxyde.

[Traduit par le journal]

Introduction

Nickel, promoted with chromia, is known to be a good catalyst for hydrogen–water deuterium exchange (1–3). The chromia has two functions. It protects the metallic nickel particles against sintering during reduction and use, so that the nickel surface area is much higher than it would be in the absence of chromia (2). This may be called structural promotion. At the same time, the rate per unit surface area of exposed nickel, the so-called specific rate, is much higher than it would be in the absence of chromia (2). This promotion may be called chemical, or electronic, promotion.

Although it is generally conceded that a chemical, or electronic, interaction between the

[1]AECL No. 5211.

[2]Presented in part at 57th Canadian Chemical Conference, Regina, Saskatchewan, June, 1974.

Can. J. Chem. Downloaded from www.nrcresearchpress.com by 210.87.254.42 on 09/05/12
For personal use only.

Can. J. Chem. Downloaded from www.nrcresearchpress.com by 210.87.254.42 on 09/05/12
For personal use only.

oxide and the metal is responsible for chemical promotion (4–6), the way in which electronic promotion occurs has not been clearly established. We, therefore, examined the kinetics of hydrogen–water deuterium exchange using nickel catalysts promoted with various oxides, and have looked for correlations of specific rates with oxide properties.

Although one mechanism for this exchange over nickel–chromia catalysts, involving the formation and reduction of nickel oxide on the catalyst surface, is generally favored (3, 7), this mechanism is not universally accepted (8, 9). We measured kinetic parameters over all the catalysts used in an attempt to establish the mechanism over these catalysts.

Experimental

Rates were measured in a flow system at a total pressure of 110 ± 10 kPa as previously described (10, 11). Purified argon was used as a diluent to reduce the partial pressure of hydrogen, and the partial pressure of water was controlled by varying the saturator temperature (10, 11). Catalysts as mixed carbonates were evacuated for 2 h at 423 K. They were then reduced *in situ* in flowing hydrogen for 18 h at 530 K and cooled to room temperature in flowing hydrogen. Their activity became constant after about 30 min conditioning in a hydrogen–water stream and remained constant (±5%) indefinitely, provided that they were kept in flowing hydrogen at ~400 K when runs were not being performed.

Metal surface areas were measured by hydrogen chemisorption at room temperature as previously described (12). Total surface areas were measured by nitrogen adsorption at 77 K using a Perkin-Elmer Sorptometer. Catalysts were evacuated and reduced in the same way as those used for rate measurements, and were evacuated at 550 K for 16 h to at least 1.5×10^{-4} Pa before adsorption isotherms were measured. X-Ray diffraction patterns were measured as described previously (12) and thermograms were done in hydrogen using a Perkin-Elmer thermobalance.

The sources and means of purifying water, deuterium oxide, hydrogen, and argon have been described (12). Catalysts were prepared by coprecipitation. For most preparations, a solution containing 2 mol/kg $Ni(NO_3)_2$ plus the promoter as the nitrate was slowly added to an equal volume of solute containing 3.5 mol/kg of ammonium carbonate. The precipitate of mixed carbonates was aged overnight, filtered, washed, and dried. It was then lightly crushed and sieved, retaining the 40–80 mesh size. The manganese promoted catalyst was prepared from $MnCl_2 \cdot 4H_2O$ using a similar procedure. The tungsten promoted catalyst was made using $Na_2WO_4 \cdot 2H_2O$. In this case the tungstate was present in the ammonium carbonate solution. The molybdenum promoted catalyst was prepared using separate $(NH_4)_6Mo_7O_{24} \cdot 4H_2O$ and $NiCl_2$ solutions which were added simultaneously to the ammonium carbonate solution.

TABLE 1. Surface area of the catalysts

Catalyst	Total surface area (10^3 m^2/kg)	Nickel surface area (10^3 m^2/kg)
20/80 Cr/Ni	104	34.7
20/80 W/Ni	57	0.62
20/80 Mo/Ni	79	0.07
20/80 Mn/Ni	62	11.5
20/80 U/Ni	18	10.5
Ni	—	1.54

Results

Total surface areas and nickel surface areas are shown in Table 1. Total surface areas were calculated using the standard BET equation, taking the area of a nitrogen molecule to be 1.58×10^{-19} m^2. Metal surface areas were calculated by extrapolating the volume of hydrogen adsorbed at pressures between 1 and 5 kPa to zero pressure and using this volume as a measure of chemisorbed hydrogen. Nickel surface areas were then calculated, assuming that one hydrogen atom covers one nickel atom, and taking the area of an exposed nickel atom[3] as 6.76×10^{-20} m^2. The technique of extrapolating the volume of hydrogen to zero pressure should eliminate physically adsorbed hydrogen on the support. Nevertheless, the possibility remains that some chemisorption takes place on the oxides, although this has been shown not to be significant with nickel–chromia catalysts (2). Thus the metal surface areas are maximum areas, and the specific rates (see below) are minimum specific rates.

All rates and surface areas are quoted on the basis of the weight of mixed carbonate loaded into the reactor or surface area cell. This procedure was adopted for convenience. For nickel–chromia catalysts, the weight loss as the catalysts were heated in hydrogen corresponded within 5% to conversion to nickel metal plus Cr_2O_3.

We calculated the stable form of the oxide in hydrogen at 523 K using known free energies and entropies at 298 K and a three coefficient expression for heat capacities as a function of temperature (13). Thermochemically, the stable oxides are MoO_2, WO_2 in equilibrium with WO_3, UO_2, MnO, and Cr_2O_3. Nickel would be present as the metal. Recently Cr_2O_3 has been identified as the oxide present when chromium is the promoter (14) and nickel is present as the

[3]J. H. Rolston, private communication.

Can. J. Chem. Downloaded from www.nrcresearchpress.com by 210.87.254.42 on 09/05/12
For personal use only.

metal. X-Ray analysis showed the metallic nickel was present and that nickel particle sizes were in the range 5 to 30 nm. No distinct lines were seen for the oxide. Either the oxide is amorphous or the oxide particles are so small that the lines are too broad to be apparent.

The reaction rate coefficient, k, in mol of HD per kg of catalyst per s, can be calculated from [1] provided that deuterium concentrations are less than 5% (2, 12)

$$[1] \qquad k = \frac{F}{(\alpha + 1/\beta)W} \ln\left(\frac{n_e - n_0}{n_e - n}\right)$$

In this equation, F is the flow rate of hydrogen in mol/s, α is the reciprocal of the equilibrium constant for [2], β is the ratio of water to hydrogen partial pressures, W is the catalyst weight in kg, and the n's are HD concentrations in the incoming hydrogen (n_0), at the reactor exit (n), and at equilibrium (n_e)

$$[2] \qquad HDO + H_2 = H_2O + HD$$

Specific rates were calculated by dividing the rate coefficient, k, by the nickel surface area per kg of catalyst. To avoid confusion, it should be emphasized that the specific rates are reported in terms of the nickel surface area rather than the total surface area. The specific rates are shown in Fig. 1 as a function of reciprocal temperature in the Arrhenius fashion. The rates were all calculated from measurements made at several flow rates by taking initial slopes to plots of $\ln (n_e - n_0)/(n_e - n)$ against W/F. This procedure should eliminate the effects of external diffusion. Previously, it was shown (15) that with Graphon supported platinum catalysts, external diffusion was eliminated if the catalyst particles were smaller than 0.35 mm. The rates over the most active nickel catalyst were of the same order as those over the Graphon supported platinum, although the surface areas of the nickel catalysts were higher by a factor of 2. Thus external diffusion should not be important. The specific rates shown in Fig. 1 were all measured at a hydrogen pressure of 78 kPa and a water pressure of 24 kPa. Apparent activation energies, taken from the slopes of the lines in Fig. 1 are shown in Table 2. Unfortunately, the low rate over unpromoted nickel meant that rates could only be measured at the higher temperatures and even then with low precision. Thus kinetic parameters are not quoted for unpromoted nickel.

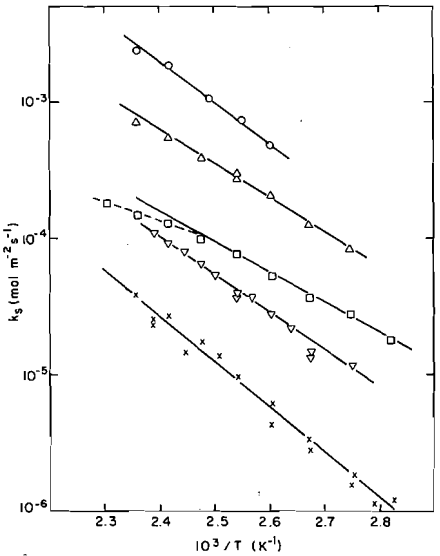

FIG. 1. Arrhenius plots of specific rates, measured with P_{H_2} = 78 kPa and P_{H_2} = 24 kPa, ○, MoO_2/Ni; △, WO_3/Ni; □, Cr_2O_3/Ni; ▽, UO_2/Ni; ×, MnO/Ni.

Rates were studied as a function of hydrogen and water pressure. Double logarithmic plots of the rate against hydrogen pressure were linear and the slopes, *i.e.* the orders with respect to hydrogen, are shown in Table 2. Double logarithmic plots of rate against water pressure are shown in Fig. 2 for all the catalysts except the uranium oxide promoted one. The order with respect to water was 0.1 for the uranium oxide promoted catalyst, but for the other catalysts, curved lines were obtained.

Discussion

The results will be discussed initially in terms of the mechanism proposed by Temkin and co-workers (7, 16, 17) for hydrogen–water exchange over nickel–chromia catalysts. This mechanism assumes that exchange takes place

TABLE 2. Kinetic parameters for H_2–HDO exchange over promoted nickel catalysts

Catalyst	E_{app} (kJ/mol)	Order in hydrogen (±0.1)	Specific rate at 393 K (10^{-5} mol HD m^{-2} s^{-1})
20/80 Cr/Ni	43.5	0.3	7.61
20/80 W/Ni	53.1	0.4	26.6
20/80 Mo/Ni	52.3	0.45	130
20/80 Mn/Ni	67.0	0.0	1.1
20/80 U/Ni	55.6	0.0	4.19
Ni	—	—	0.002

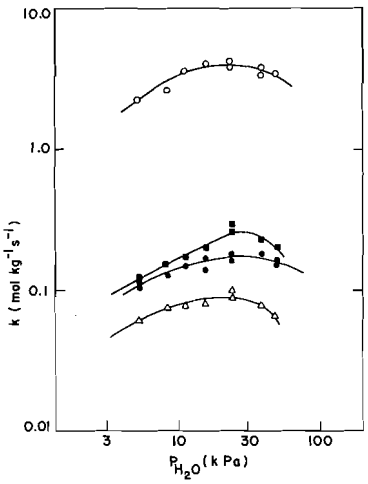

FIG. 2. Variation of the rate with water pressure measured with P_{H_2} = 78 kPa and at 393 K except for 20% Mn/Ni which was measured at 418 K. ○, Cr_2O_3; ■, MnO; ●, WO_3; △, MoO_3.

by the formation and subsequent reduction of an oxide film on the nickel surface (reactions 3 and 4).

[3] $$HDO + S = SO + HD$$

[4] $$H_2 + SO = H_2O + S$$

where S is a vacant surface site. The rate expression has been derived in detail by Temkin (16) but the steps in this derivation will be described here for convenience.

The virtual, or effective partial pressure of oxygen, P_{O_2}*, in equilibrium with the oxide film is given by [5].

[5] $$2P_{H_2O} = 2P_{H_2} + P_{O_2}^*$$

If the oxygen adsorption is described by a Freundlich isotherm, then

[6] $$\theta_0 = (a_0 P_{O_2}^*)^{m/2}$$

where a_0 is a constant and m equals RT/q, q being the heat of adsorption. Thus

[7] $$\theta_0 = \left(\frac{a_0}{K_5}\right)^{m/2}\left(\frac{P_{H_2O}}{P_{H_2}}\right)^m = a\left(\frac{P_{H_2O}}{P_{H_2}}\right)^m$$

where $(a_0/K_5)^{m/2} = a$. At equilibrium

[8] $$k_3 P_{HDO} f(O) = k_{-3} a P_{HD}\left(\frac{P_{H_2O}}{P_{H_2}}\right)^m$$

where $f(O)$ is a function giving the variation of the oxygen coverage with the partial pressures of hydrogen and water. Also from [4] at equilibrium

[9] $$ak_4 P_{H_2}\left(\frac{P_{H_2O}}{P_{H_2}}\right)^m = k_{-4} P_{H_2O} f(O)$$

Thus, recalling that $1/\alpha = K_3K_4$, where α is the reciprocal of K_2, and taking the net rate of reaction v as the forward rate minus the backward rate

[10] $$v = ak_3k_4 P_{HDO}\left(\frac{P_{H_2}}{P_{H_2O}}\right)^{1-m} - ak_3k_4\alpha P_{HD}\left(\frac{P_{H_2O}}{P_{H_2}}\right)^m$$

Furthermore, the derivation of [1] (3, 9) makes it clear that also

[11] $$v = k(N - \alpha n)$$

where N and n are the mole fractions of HDO and HD in the H_2O and H_2 respectively.

Comparing [10] and [11] it follows that

[12] $$k = ak_3k_4 P_{H_2O}\left(\frac{P_{H_2}}{P_{H_2O}}\right)^{1-m} = k_0 P_{H_2O}\left(\frac{P_{H_2}}{P_{H_2O}}\right)^{1-m}$$

where $k_0 = ak_3k_4$.

For this mechanism to be valid, a double logarithmic plot of k/P_{H_2O} against P_{H_2}/P_{H_2O}, *i.e.* k/P_{H_2O} against $1/\beta$, should be linear with a slope of $(1 - m)$. This should be so regardless of whether the hydrogen or the water pressure is varied.

The results over tungsten oxide and uranium oxide promoted nickel are shown as a double logarithmic plot of k/P_{H_2O} against $1/\beta$ in Figs. 3 and 4 respectively. For convenience, $k(P_T/P_{H_2O})$

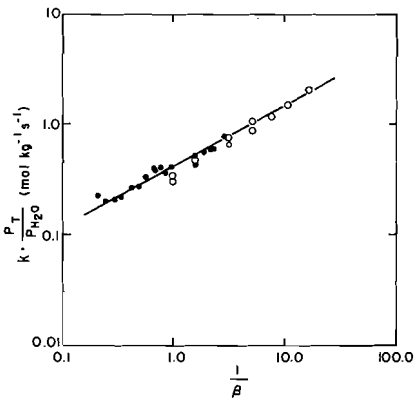

FIG. 3. Test for validity of Temkin mechanism with the 20% W/Ni catalyst, measured at 393 K. A single line indicates that Temkin kinetics are possible. ●, Hydrogen pressure varied; ○, water pressure varied.

Can. J. Chem. Downloaded from www.nrcresearchpress.com by 210.87.254.42 on 09/05/12
For personal use only.

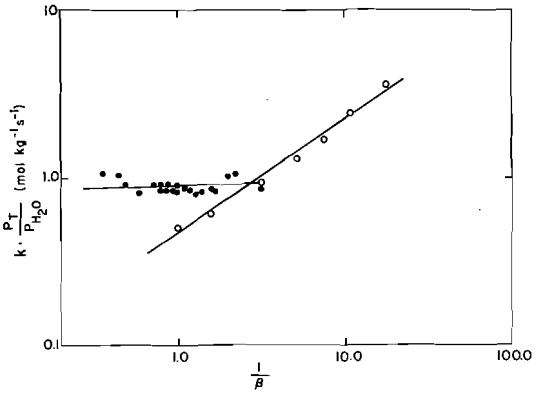

FIG. 4. Test for validity of Temkin mechanism with the 20% U/Ni catalyst, measured at 378 K. The points fall on two lines, so Temkin kinetics are not followed. ●, Hydrogen pressure varied; ○, water pressure varied.

is plotted as the ordinate where P_T is the total pressure which was always in the range 110 ± 10 kPa. A distinction is made between those runs where 1/β was changed by varying P_{H_2O} (from 5 to 41 kPa with hydrogen making up the difference), and those where 1/β was changed by varying the H_2 pressure by lowering the hydrogen pressure using argon as the diluent, and keeping P_{H_2O} constant at 27.3 kPa. For the tungsten oxide promoted catalyst, the data can be described by a single line, although if the best straight line is drawn through the two sets of points, slightly different slopes are obtained. For the uranium oxide promoted catalyst, the data points clearly fall on separate lines. Thus the Temkin mechanism may apply over the tungsten oxide promoted catalyst, but it clearly does not apply over the uranium oxide promoted catalyst.

Figure 5 shows ($m_{H_2} - m_{H_2O}$) plotted against

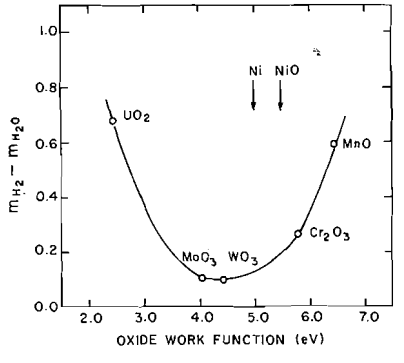

FIG. 5. Difference in Temkin m parameters for P_{H_2} variation and P_{H_2O} variation, plotted as a function of oxide work function. If the Temkin mechanism were obeyed m_{H_2} would equal m_{H_2O}.

the oxide work functions. The values for the work functions of Ni, NiO, MnO, and Cr_2O_3 were obtained from Krylov's monograph (18), that for UO_2 was taken from the work of Riviere (19), and that for MoO_2 was taken to be the same as that of MoO_3. The values of m_{H_2O} and m_{H_2}, in Fig. 5, were determined by varying the water and hydrogen pressures respectively as described. If the Temkin mechanism were followed exactly, this difference should be zero. Figure 5 shows that for the molybdenum oxide and tungsten oxide promoted catalysts, the difference is close to zero, so the Temkin mechanism may apply. For the uranium oxide and manganese oxide promoted catalysts, we can definitely say that the Temkin mechanism does not apply. For the 20% Cr_2O_3 catalyst shown in Fig. 5, the difference of 0.26 is somewhat greater than the assumed experimental error of ±0.2 if m can be determined to ±0.1. Therefore this case is unresolved.

The Temkin mechanism involves one adsorbed species, the oxygen atom, whose coverage is controlled by the ratio of hydrogen to water pressures. Thus the effects of changing hydrogen and water pressures are coupled. For the catalysts which do not follow the Temkin mechanism, the effects of changing the hydrogen and water pressures are not coupled. It seems likely that the mechanism in the cases involves exchange between adsorbed hydrogen atoms and adsorbed water (or OH groups) as has been previously proposed for supported noble metal catalysts (9, 11). If the adsorption–desorption steps are in equilibrium and the exchange is controlled by [13]

$$[13] \qquad H_{ads} + HDO_{ads} \rightarrow H_2O_{ads} + D_{ads}$$

then the rate expression is given by

$$[14] \qquad k_4 = k_{13}\theta_{H_2O}\theta_H$$

Assuming a Freundich isotherm for adsorption of hydrogen and water leads to

$$[15] \qquad k = k^1 P_{H_2O}{}^a P_{H_2}{}^b$$

The relationship is obeyed for the uranium oxide promoted catalyst and it is obeyed at all except the highest water pressures for the manganese oxide promoted catalysts. For these catalysts a and b are independent of each other.

Thus we have case A where an exchange type mechanism dominates with promotors such as manganese and uranium oxides and case B

Can. J. Chem. Downloaded from www.nrcresearchpress.com by 210.87.254.42 on 09/05/12
For personal use only.

where either the exchange type or the Temkin mechanism may dominate with promotors such as tungsten and molybdenum. Furthermore, the specific rate is higher (see Table 2) in case B.

The specific rates, shown in Table 2, vary considerably. This means that there are large chemical promotion effects, and it is natural to look for the source of these effects in the electronic interaction of the nickel and the promotor. This has already been attempted in Fig. 5, where $m_{H_2} - m_{H_2O}$, a parameter which indicates the relative importance of the oxidation–reduction mechanism and the exchange mechanism, is plotted as a function of the promotor oxide electronic work function. It is evident that the oxide film reduction mechanism predominates where the promotor oxide work function is close to the work function of nickel and nickel oxide. If the work function of the oxide is much higher than that of nickel, the Fermi level in the nickel will be lowered by donation of electrons to the oxide. Since oxygen adsorption adds electrons to the nickel, it is likely that the oxide film formed by water adsorption will be too strongly held to be reduced easily by hydrogen. Conversely, if the work function of the oxide is much lower than that of nickel, an oxide film will not be formed.

The exchange mechanism, as opposed to the oxide reduction mechanism, occurs with equal facility on both sides of the maximum. Thus, at first glance, it does not seem to be affected by variations in the nickel Fermi level. Nevertheless, the specific rates obtained over catalysts where the exchange mechanism is clearly dominant are still much higher than those over bulk nickel (Table 2). Clearly, the promoting oxide must have some chemical effect on the exchange mechanism. For the small particles of nickel present in these catalysts (20) adsorption of hydrogen and water could result in very large changes in the Fermi level. One suggestion is that the promotor acts as a sink and source for electrons to keep the Fermi level of the nickel from changing too much.

We had originally hoped that kinetic parameters such as true surface activation energies and frequency factors could be obtained and compared. However, as at least two mechanisms are involved, and for some catalysts these may occur simultaneously, it seems premature to attempt such analyses at the present time.

We thank A. M. Soulodre for measuring the BET surface areas, and R. E. Von Massow for the use of programs to calculate oxide stabilities. Useful discussions with G. G. Strathdee and H. C. Chen are also gratefully acknowledged.

1. E. H. TAYLOR. *In* Production of heavy water. *Edited by* G. M. Murphy, H. C. Urey, and I. Kirshenbaum. McGraw-Hill, New York. 1955. pp. 154–221.
2. P. MARGINEANU and A. OLARIU. J. Catal. **8**, 359 (1967).
3. T. FODOR, P. MARGINEANU, and A. OLARIU. Stud. Cercet. Fiz. **22**, 697 (1970).
4. D. TARINA, E. WEISSMANN, and D. BARB. J. Catal. **11**, 348 (1968).
5. A. OLARIU. Stud. Cercet. Fiz. **22**, 953 (1970).
6. I. INTA and P. MARGINEANU. Rev. Roum. Chim. **18**, 347 (1972).
7. M. L. NAKHMANOVICH, N. M. MOROZOV, L. G. BUADZE, and M. I. TEMKIN. Dokl. Akad. Nauk SSSR, **148**, 1346 (1963).
8. F. ABOU EL-NOUR and H. SCHUTZE. Istotopenpraxis, **10**, 391 (1972).
9. J. H. ROLSTON and J. W. GOODALE. Can. J. Chem. **50**, 1900 (1972).
10. N. H. SAGERT and R. M. L. POUTEAU. Can. J. Chem. **51**, 4031 (1973).
11. N. H. SAGERT and R. M. L. POUTEAU. Can. J. Chem. **52**, 2960 (1974).
12. N. H. SAGERT and R. M. L. POUTEAU. Can. J. Chem. **49**, 3411 (1971).
13. O. KUBASCHEWSKI and E. L. EVANS. Metallurgical thermodynamics. Pergamon Press, Oxford. 1958.
14. N. S. MCINTYRE, N. H. SAGERT, R. M. L. POUTEAU, and W. G. PROCTOR. Can. J. Chem. **51**, 1670 (1973).
15. N. H. SAGERT and R. M. L. POUTEAU. Can. J. Chem. **50**, 3686 (1972).
16. M. I. TEMKIN. Zh. Fiz. Khim. **31**, 3 (1957).
17. M. I. TEMKIN, M. L. NAKHMANOVICH, and N. M. MOROZOV. Kinet. Katal. **2**, 722 (1961).
18. O. V. KRYLOV. Catalysis by nonmetals – rules for catalyst selection. Academic Press, New York. 1970. pp. 247–258.
19. J. C. RIVIERE. Brit. J. Appl. Phys. **15**, 1341 (1964).
20. I. HODOR. Rev. Roum. Phys. **15**, 425 (1969).

Can. J. Chem. Downloaded from www.nrcresearchpress.com by 210.87.254.42 on 09/05/12
For personal use only.

Volumes and Heat Capacities of Dimethylsulfoxide, Acetone, and Acetamide in Water and of some Electrolytes in these Mixed Aqueous Solvents

OSAMU KIYOHARA, GÉRALD PERRON, AND JACQUES E. DESNOYERS[1]

Department of Chemistry, Université de Sherbrooke, Sherbrooke, Quebec J1K 2R1

Received May 15, 1975

OSAMU KIYOHARA, GÉRALD PERRON, and JACQUES E. DESNOYERS. Can. J. Chem. **53**, 3263 (1975).

The densities and volumetric specific heats of binary mixtures of dimethylsulfoxide (DMSO), acetone (ACT), and acetamide (ACM) in water were measured at 25 °C with a flow densimeter and a flow microcalorimeter. The same properties were also determined for ternary mixtures of 0.1 *m* LiCl, NaCl, Me_4NBr, and Bu_4NBr in ACT–water and DMSO–water mixtures, and volumes for 0.1 *m* Bu_4NBr in ACM–water and urea–water mixtures. The derived apparent molal volumes and heat capacities of nonelectrolytes in water and the transfer functions of the electrolytes from water to the mixed solvents suggest that, contrary to urea, the present nonelectrolytes are slightly hydrophobic but, with the possible exception of ACT, their overall influence on water structure has practically no influence on the various solute–solute interactions.

OSAMU KIYOHARA, GÉRALD PERRON et JACQUES E. DESNOYERS. Can. J. Chem. **53**, 3263 (1975).

Les masses volumiques et capacités calorifiques du diméthylsulfoxyde (DMSO), de l'acétone (ACT) et de l'acétamide (ACM) ont été mesurées dans l'eau à 25 °C avec un densimètre et un microcalorimètre à écoulement continu. Les mêmes propriétés ont été obtenues pour LiCl, NaCl, Me_4NBr et Bu_4NBr à 0.1 *m* dans les mélanges eau–ACT et eau–DMSO et les volumes pour Bu_4NBr (0.1 *m*) dans les mélanges eau–ACM et eau–urée. Les capacités calorifiques et volumes apparents molaires des nonélectrolytes dans l'eau et les fonctions de transfert des électrolytes de l'eau aux mélanges de solvants suggèrent que ACM, ACT et DMSO sont, par opposition à l'urée, légèrement hydrophobes dans l'eau mais que l'effet structural global n'a practiquement pas d'influence sur les interactions soluté–soluté, sauf peut-être dans le cas de l'ACT.

Introduction

The aqueous solutions of dimethylsulfoxide (DMSO), are amongst the best-known mixed solvents and reaction media. However, despite the extensive studies of their properties, the nature of the interactions between DMSO and water is still far from being fully understood (1–4). On the other hand, acetone (ACT), which has a molecular structure similar to DMSO, is usually considered to be hydrophobic in water (5, 6). Urea (U), which also has a similar geometry, is usually assumed to be a structure breaker. We therefore felt that a comparative study of acetamide (ACM), ACT, and DMSO in water, combined with data previously obtained with U (7–9), might give us a better understanding of the interactions between DMSO and water.

Another approach which has been found useful in the study of mixed aqueous solvents is to study the transfer functions of well-characterized electrolytes from water to the mixed solvent (9–11). As in previous work (11), the four electrolytes chosen are LiCl, NaCl, Me_4NBr, and Bu_4NBr so as to cover typical hydrophilic and hydrophobic electrolytes.

The properties chosen for these investigations are the volumes and heat capacities, since they are readily measurable and have proven sensitive to changes in the structure of the mixed solvents (7–11).

Experimental

The instruments and techniques used for density (12) and specific heat (13) measurements have been described previously. The difference between the density of the solution and that of the solvent $d - d_0$ can be determined to $\pm 3 \times 10^{-6}$ g cm^{-3}, and the change in volumetric specific heat $\sigma - \sigma_0$ to $\pm 7 \times 10^{-5}$ J K^{-1} cm^{-3} for a temperature increment of 1.8 K and a flow rate of 0.7 cm^3 min^{-1}.

The origin and purification of the electrolytes (LiCl, NaCl, Me_4NBr, and Bu_4NBr) have been given elsewhere (14, 15). The nonelectrolytes were purified as follows: ACT and DMSO (Certified A.C.S., Fisher Scientific Co.) were dried with a molecular sieve (Davidson Chemical, grade 564, 8–12 mesh beads), ACM (Baker Analytical

[1]To whom correspondence should be addressed.

Can. J. Chem. Downloaded from www.nrcresearchpress.com by 210.87.254.105 on 09/05/12
For personal use only.

Can. J. Chem. Downloaded from www.nrcresearchpress.com by 210.87.254.105 on 09/05/12
For personal use only.

Reagent) was recrystallized from absolute methanol and dried under vacuum.

All solutions were prepared by weight with deionized (Continental Deionized Water System) distilled water. All measurements were made at a mean temperature of 25.00 ± 0.01 °C.

Results

The apparent molal volumes ϕ_V and heat capacities ϕ_C of the nonelectrolytes in water and of the electrolytes in the mixed solvent were calculated in the usual way from the densities and volumetric specific heats (10). The results[2] for ACM, ACT, and DMSO are plotted in Figs. 1 and 2 against the molality and compared with the literature values (4, 16–20). In general, the present ϕ_V are in excellent agreement with the literature values but show less scatter, especially at low concentration. The good agreement in the case of ϕ_V and the proven reliability of the flow technique for differential specific heat measurements gives us confidence that the ϕ_C data are probably also reliable within an experimental uncertainty of ± 1 J K^{-1} mol^{-1}. The only heat capacity data reported in the literature for ACT and DMSO are those of Arnaud *et al.* (21); these data show a much larger scatter than the present ones and have not been included in Fig. 2.

The ϕ_V and ϕ_C data were fitted with a polynomial equation in molality

$$[1] \qquad \phi_Y = \phi_Y^0 + A_Y m + B_Y m^2 + \ldots$$

where Y stands for V or C_p. The parameters of [1] are listed in Table 1. The values for U which have been published elsewhere (8, 13) are also included for comparison.

The standard functions of transfer of an electrolyte E from water (W) to a mixed solvent (W + N) are given by

$$[2] \quad \Delta Y_E(W \rightarrow W + N) = \bar{Y}_E^0(W + N) - \bar{Y}_E^0(W)$$

where $\bar{Y}_E^0$ are the standard partial molal quantities. It has been shown previously (10) that the transfer functions obtained from the apparent molal quantities for electrolytes at 0.1 m were very close to the infinite dilution values. The functions ϕ_V and ϕ_C were therefore measured at 0.1 m electrolyte concentration[2]

[2]Complete set of tabular data is available, at a nominal charge, from the Depository of Unpublished Data, CISTI, National Research Council of Canada, Ottawa, Canada K1A 0S2.

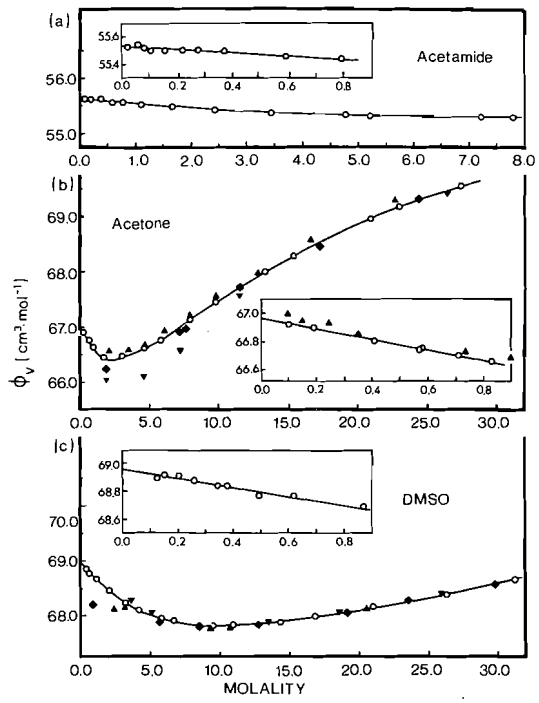

FIG. 1. Apparent molal volumes of nonelectrolytes in water at 25 °C. (*a*) Acetamide, ○, present results; (*b*) acetone, ○, present results; ▲, Pøge and Hvidt (20); ▼, Kurtz *et al.* (18); ◆, Griffiths (19); (*c*) DMSO, ○, present results; ◆, Kenttämaa and Lindberg (16); ▼, Cowie and Toporocoski (17); ▲, Kiyohara *et al.* (4).

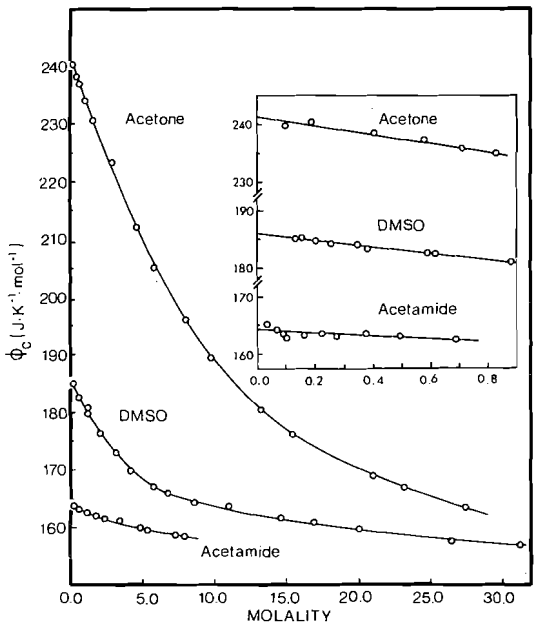

FIG. 2. Apparent molal heat capacity of acetamide, acetone, and DMSO in water at 25 °C.

Can. J. Chem. Downloaded from www.nrcresearchpress.com by 210.87.254.105 on 09/05/12
For personal use only.

TABLE 1. Apparent molal volumes (cm mol^{-1}) and heat capacities (J K^{-1} mol^{-1}) of nonelectrolytes in water at 25 °C, parameters of [1]

Substances	ϕ_V^0 Observed	ϕ_V^0 Literature	A_V	B_V	Concentration range	ϕ_C^0 Observed	ϕ_C^0 Literature	A_C	B_C	C_C	D_C	Concentration range
Urea*	44.24		0.116	−0.003	< 10	87.5		5.57	−0.33			< 10
Acetamide	55.61		−0.123	0.013	< 2.4	163.8		-1.3_8	0.12			< 2.4
Acetone	66.92	67.0†	−0.370	0.056	< 1.6	241.3	225‡	-7.6_4	0.27_9	-0.003_8		< 27
DMSO	68.92		−0.262	0.015	< 11	185.7	210‡	-5.3_4	0.46_1	-0.017_6	0.0002_4	< 31

*References 8 and 13.
†Reference 20.
‡Reference 21.

in ACT–water and DMSO–water mixtures, and the corresponding data in pure water at 25 °C were taken from the literature (14, 22–24): at 0.1 *m*, ϕ_V of the electrolytes LiCl, NaCl, Me_4NBr, and Bu_4NBr are respectively 17.46, 17.21, 114.80, and 300.00 $cm^3\ mol^{-1}$ and the corresponding ϕ_C are −53.3, −70.4, 129.2, and 1213 $J\ K^{-1}\ mol^{-1}$ respectively. The ϕ_V of Bu_4NBr was also measured in ACM–water and urea–water mixtures.[2]

The transfer functions of the four electrolytes from W to W + ACT and from W to W + DMSO are plotted in Figs. 3 and 4 against the cosolvent molality. The volumes of transfer of Bu_4NBr from water to aqueous solutions of U, ACM, and ACT at low cosolvent concentration are also shown in Fig. 5. Macdonald and Hyne (25) have measured $\overline{V}^0$ of tetraalkylammonium chlorides in aqueous ACT and DMSO solutions and their results agree qualitatively with the present results of Me_4NBr and Bu_4NBr. Mohanty *et al.* (26) have derived $\Delta C_{Bu_4NBr}{}^0(W \rightarrow W + ACT)$ from the temperature dependence of heats of solutions and found a maximum at about 0.04 mole fraction

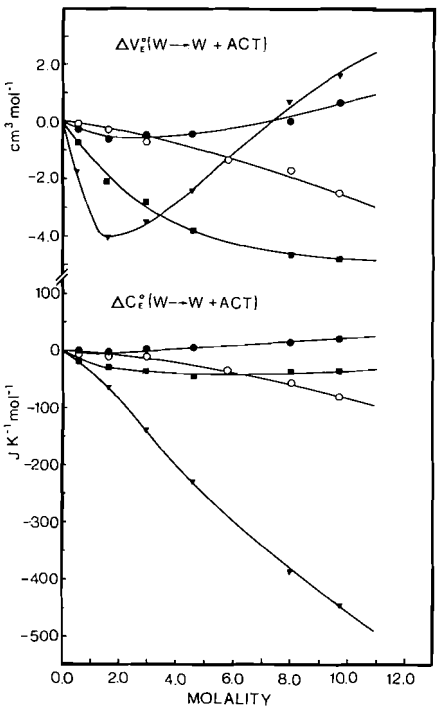

FIG. 3. Transfer functions of 0.1 *m* LiCl, NaCl, Me_4NBr, and Bu_4NBr from water to water–acetone mixed solvents at 25 °C. ○, LiCl; ●, NaCl; ■, Me_4NBr; ▼, Bu_4NBr.

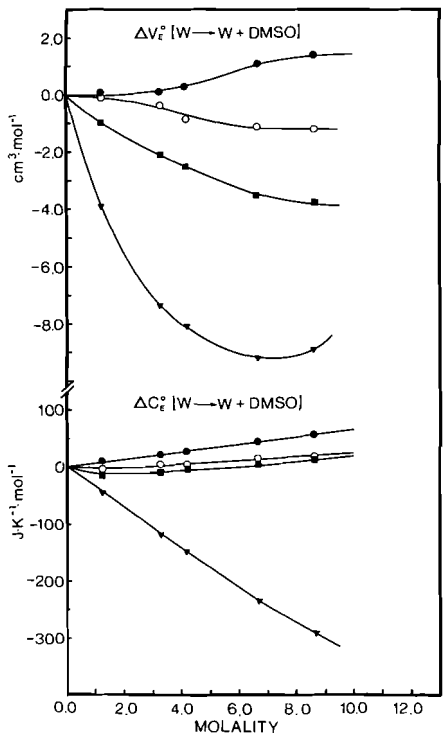

FIG. 4. Transfer function of 0.1 *m* LiCl, NaCl, Me_4NBr, and Bu_4NBr from water to water–DMSO mixed solvents at 25 °C. ○, LiCl; ●, NaCl; ■, Me_4NBr; ▼, Bu_4NBr.

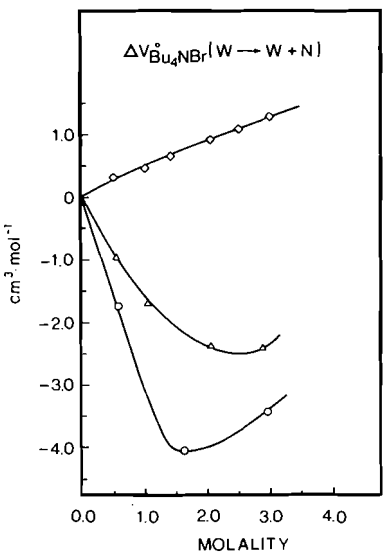

FIG. 5. Transfer functions of volume of 0.1 *m* Bu_4NBr from water to aqueous mixed solvents at 25 °C. ◇, U; △, ACM; ○, ACT.

Can. J. Chem. Downloaded from www.nrcresearchpress.com by 210.87.254.105 on 09/05/12
For personal use only.

Can. J. Chem. Downloaded from www.nrcresearchpress.com by 210.87.254.105 on 09/05/12
For personal use only.

($\sim$2.3 *m*) of ACT. The present results do not show such a concentration dependence.

Discussion

Group Additivity

Group additivity can often be used as a means of verifying the self-consistency of data and of predicting data of more complicated molecules. For the binary systems, the differences $\bar{V}_{ACM}^0 - \bar{V}_U^0$ and $\bar{V}_{ACT}^0 - \bar{V}_{ACM}^0$ are respectively 11.37 and 11.31 $cm^3\ mol^{-1}$ for $\bar{V}^0$ and 76.3 and 77.5 $J\ K^{-1}\ mol^{-1}$ for $\bar{C}_p^0$. This additivity being comparable with the expected uncertainties ($\pm 0.05\ cm^3\ mol^{-1}$ and $\pm 1\ J\ K^{-1}\ mol^{-1}$), it seems that the degree of substitution has little effect on the hydration of each group with these simple molecules in water. If the CH_3— group contribution to $\bar{V}^0$ and $\bar{C}_p^0$ is taken as 26.6 and 178 (27), then the —NH_2 contribution is 15.3 $cm^3\ mol^{-1}$ and 101 $J\ K^{-1}\ mol^{-1}$ for aliphatic molecules in water at 25 °C.

Binary Systems

An examination of Table 1 shows that $\bar{V}^0$ and $\bar{C}_p^0$ increase in the order U → ACM → ACT; DMSO has the largest $\bar{V}^0$ but its $\bar{C}_p^0$ is only slightly larger than ACM. The difference between $\bar{C}_p^0$ and the intrinsic heat capacity is often used as a criterion for the overall effect of a solute on water (23, 28). The intrinsic heat capacities can be taken as approximately equal to those of the pure substances: 93 (29) for U, 125 (30) for ACT, and 153 (31) for DMSO. Since there are little data in the literature for pure ACM at 25 °C, its densities and specific heats were measured in a polar organic solvent; 1-propanol was found to be convenient for this purpose. Up to approximately 3 *m*, ϕ_V (56.3 $cm^3\ mol^{-1}$) and ϕ_C (165 $J\ K^{-1}\ mol^{-1}$) are essentially independent of concentration. It therefore seems that $\bar{C}_p^0$ in water is significantly larger than the intrinsic heat capacity with ACT, slightly larger with DMSO, approximately equal with ACM, and slightly smaller with U. The concentration dependence of ϕ_C of the nonelectrolytes in water (Fig. 2) also shows that ϕ_C is rapidly decreasing to the intrinsic value with ACT, DMSO, and ACM while with U, ϕ_C increases with concentration (13). Again this change is significant with ACT but very small with ACM. On the other hand, even with ACT, there is little evidence of any structural hydrophobic–hydrophobic interactions; with strongly hydrophobic solutes, these hydrophobic interactions produce a positive contribution to the excess heat capacity which opposes the decrease of ϕ_C towards the intrinsic values, the net effect being a maximum or a positive hump in ϕ_C (10). No such behavior is apparent with these solutes. These nonelectrolytes are therefore affecting water in a way similar to dioxane, morpholine, and piperazine (11); whatever is causing the high heat capacity at infinite dilution is disappearing at higher concentration.

The increase in $\bar{V}^0$ when going from U to DMSO is reflecting primarily the increasing intrinsic volume and cannot give us much information on the overall structural hydration. On the other hand, ϕ_V of ACT and DMSO show a minimum typical of hydrophobic solutes. Presumably a minimum would also be observed with ACM if data were available at higher concentrations. These minima occur at rather high concentrations, especially with DMSO (and probably ACM) suggesting again that the hydrophobic character is rather small.

An examination of the binary system data therefore suggests that ACM, DMSO, and ACT are slightly hydrophobic in water in contrast with U, but the overall structural change is certainly not large, especially with ACM. The increasing hydrophobic character from U to ACT comes from the substitution of an hydrophilic —NH_2 by the hydrophobic —CH_3 and the much smaller hydrophobic character of DMSO compared with ACT comes from the higher dipole moment (3.96 compared with 2.88 D).

Ternary Systems

The transfer functions $\Delta Y_E^0(W \rightarrow W + N)$ are not simple to interpret since, at high cosolvent concentration, they must tend to $\Delta Y_E^0(W \rightarrow N)$, where N represents the pure liquid cosolvent. Since the ions are solvated differently in water and in the pure cosolvent, $\Delta Y_E^0(W \rightarrow W + N)$ will change gradually from one state to another. If in addition to a mean solvation there are new interactions which occur in the ternary system, this will result in some anomalies in the shape of the concentration dependence of $\Delta Y_E^0(W \rightarrow W + N)$, usually in the water-rich region.

The transfer functions $\Delta Y_E^0(W \rightarrow W +$ DMSO) in Fig. 4 are all changing in a regular

Can. J. Chem. Downloaded from www.nrcresearchpress.com by 210.87.254.105 on 09/05/12
For personal use only.

way with DMSO concentration, suggesting that at any concentration $\Delta Y_E^0(W \rightarrow W + N)$ is reflecting primarily some mean solvation of the ions. As seen from Fig. 5, $\Delta V_{Bu_4NBr}^0(W \rightarrow W +$ ACM) is also fairly regular. On the other hand, if we compare $\Delta Y_E^0(W \rightarrow W +$ ACT) in Fig. 3 with $\Delta Y_E^0(W \rightarrow W +$ *tert*-butyl alcohol) (10) or $\Delta Y_E^0(W \rightarrow W +$ piperidine) (11), the slight hump in the concentration dependence of $\Delta C_{Bu_4NBr}^0(W \rightarrow W +$ ACT), minimum with $\Delta V_{Bu_4NBr}^0(W \rightarrow W +$ ACT), and the slight minima with $\Delta Y_{NaCl}^0(W \rightarrow W +$ ACT) suggest that with ACT there are some specific structural interactions which are in the direction we would expect if ACT was slightly hydrophobic. The value of $\bar{C}_p^0$ of ACT in water was larger than its intrinsic heat capacity but the concentration dependence of ϕ_C did not show any maximum or hump characteristic of hydrophobic–hydrophobic interactions. It therefore seems that the hydrophobic–hydrophobic interaction between Bu_4N^+ and ACT and hydrophilic–hydrophobic ones between NaCl and ACT are somewhat larger than the structural interactions between two ACT molecules.

Little can be said on the transfer functions of Me_4NBr and LiCl. Even in ACT the transfer functions are all fairly regular. The overall structural hydration of these electrolytes is probably too weak to cause any significant change in structural electrolyte–nonelectrolyte interactions.

Conclusion

The present volume and heat capacity data suggest that the hydrophobic character of the nonelectrolytes decreases in the order ACT, DMSO, ACM but only in the case of ACT is there any evidence of some structural solute–solute structural interaction between a reference ion and the cosolvent. Like dioxane (11), DMSO is therefore an ideal cosolvent for water in the study of the influence of macroscopic properties such as dielectric constant and viscosity on various equilibria or reaction rates in aqueous medium.

We are grateful to the National Research Council of Canada and to Environment Canada for financial support.

1. K. J. Packer and D. J. Tomlinson. Trans. Faraday Soc. **67**, 1302 (1971).
2. G. J. Safford, P. C. Schaffer, D. S. Leung, G. F. Doebbler, G. W. Brady, and E. F. X. Lyden. J. Chem. Phys. **50**, 2140 (1969).
3. T. Tokuhiro, L. Menafra, and H. H. Samant. J. Chem. Phys. **61**, 2275 (1974).
4. O. Kiyohara, N. Takenaka, and K. Arakawa. To be published.
5. M. F. Fox. J. Chem. Soc. Faraday Trans. I, **68**, 1294 (1972).
6. D. N. Glew, H. D. Mak, and N. S. Rath. *In* Hydrogen-bonded solvent systems. *Edited by* A. K. Covington and P. Jones. Taylor and Francis, London. 1968.
7. P. R. Philip, J. E. Desnoyers, and A. Hade. Can. J. Chem. **51**, 187 (1973).
8. P. R. Philip, G. Perron, and J. E. Desnoyers. Can. J. Chem. **52**, 1709 (1974).
9. N. Desrosiers, G. Perron, J. G. Mathieson, B. E. Conway, and J. E. Desnoyers. J. Solution Chem. **3**, 789 (1974).
10. L. Avédikian, G. Perron, and J. E. Desnoyers. J. Solution Chem. **4**, 331 (1975).
11. O. Kiyohara, G. Perron, and J. E. Desnoyers. Can. J. Chem. **53**, 2591 (1975).
12. P. Picker, E. Tremblay, and C. Jolicoeur. J. Solution Chem. **3**, 377 (1974).
13. P. Picker, P. A. Leduc, P. R. Philip, and J. E. Desnoyers. J. Chem. Thermodyn. **3**, 631 (1971).
14. J. E. Desnoyers, M. Arel, G. Perron, and C. Jolicoeur. J. Phys. Chem. **73**, 3346 (1969).
15. J. E. Desnoyers and G. Perron. J. Solution Chem. **1**, 199 (1972).
16. J. Kenttämaa and J. J. Lindberg. Suom. Kemistil. B, **33**, 32 (1960).
17. J. M. C. Cowie and P. M. Toporocoski. Can. J. Chem. **39**, 2240 (1961).
18. S. S. Kurtz, Jr., A. E. Wilkingson, D. L. Lamin, and A. R. Thompson. J. Chem. Eng. Data, **10**, 3301 (1965).
19. U. S. Griffiths. J. Chem. Soc. 1326 (1952).
20. L. Pøge and A. Hvidt. J. Chem. Thermodyn. **3**, 663 (1971).
21. P. Arnaud, L. Avédikian, and J. P. Morel. J. Chim. Phys. **1**, 45 (1972).
22. P. R. Philip and J. E. Desnoyers. J. Solution Chem. **1**, 353 (1972).
23. J. L. Fortier, P. A. Leduc, and J. E. Desnoyers. J. Solution Chem. **3**, 323 (1974).
24. G. Perron and J. E. Desnoyers. J. Chem. Eng. Data, **17**, 136 (1972).
25. D. D. Macdonald and J. B. Hyne. Can. J. Chem. **48**, 2416 (1970).
26. R. K. Mohanty, T. S. Sarma, S. Subramanian, and J. C. Ahluwalia. Trans. Faraday Soc. **69**, 305 (1971).
27. C. Jolicoeur and G. Lacroix. To be published.
28. T. S. Sarma and J. C. Ahluwalia. Chem. Soc. Rev. **2**, 203 (1973).
29. Selected values of chemical thermodynamic properties. Circular of the National Bureau of Standards 500. Washington D.C. 1952.
30. Handbook of Chemistry and Physics, 49th ed. The Chemical Rubber Co., Cleveland, Ohio.
31. H. L. Clever and E. F. Westrum, Jr. J. Phys. Chem. **74**, 1309 (1970).

Phenyl Substitution Effects on Triplet–Triplet Absorption Spectra: I. Study of 1,3,6,8-Tetraphenylpyrene[1]

C. RULLIÈRE[2]

Laboratoire de Recherches en Optique et Laser, Département de Physique, Université Laval, Québec, Québec G1K 7P4

AND

E. C. COLSON AND P. C. ROBERGE,

Groupe de Dynamique Moléculaire, Département de Chimie, Université Laval, Québec, Québec G1K 7P4

Received May 5, 1975

C. RULLIÈRE, E. C. COLSON, and P. C. ROBERGE. Can. J. Chem. **53**, 3269 (1975).

The triplet–triplet (T–T) absorption spectrum of 1,3,6,8-tetraphenylpyrene (TPP) was measured from 400 to 620 nm. The data obtained are compared with theoretical calculations using the Ruedenberg–Scherr FEMO model. A planar triplet state is evidenced by fine vibrational structure. The T–T quenching rate constant measured ($1.3 \pm 0.1 \times 10^9\ M^{-1}\ s^{-1}$) is 20% of the expected diffusion-controlled value.

C. RULLIÈRE, E. C. COLSON et P. C. ROBERGE. Can. J. Chem. **53**, 3269 (1975).

Le spectre d'absorption triplet–triplet (T–T) du tétraphényl-1,3,6,8 pyrene (TPP) a été obtenu dans le domaine de 400 à 620 nm. Le calcul des énergies de transition T–T utilisant le modèle de Ruedenberg et Scherr permet de vérifier l'interprétation suggérée des résultats expérimentaux. Une structure plane du premier état triplet permet d'expliquer la structure vibrationnelle observée. La valeur de la constante d'annihilation T–T mesurée ($1.3 \pm 0.1 \times 10^9\ M^{-1}\ s^{-1}$) est cinq fois plus faible que la valeur prévisible pour une réaction limitée par diffusion.

Introduction

There are very few experimental data available on the effect of substituents on T–T absorption spectra of aromatic molecules (1). In the framework of a general study of the phenyl substituent effect on T–T absorption spectra, we report here results on 1,3,6,8-tetraphenylpyrene (TPP). Unsubstituted pyrene has been extensively studied: $S_n \leftarrow S_0$ and $T_n \leftarrow T_1$ absorption spectra are available (2–5).

Berlman (2) has measured the $S_n \leftarrow S_0$ absorption and fluorescence spectra of both pyrene and TPP. Whereas pyrene spectra show fine vibrational structure, TPP spectra are very diffuse. This finding can be attributed to a nonplanar ground state of TPP (6). In pyrene, fluorescence originates from the ^1L_b state. The transition $^1B_{1u}^- \leftarrow {}^1A_g^-$, oriented along the short axis of the molecule, is parity forbidden and the ^1L_b state is longlived (300 ns) (7). TPP fluorescence lifetime is however much shorter (2.68 ns) (2) and TPP fluorescence must originate from the ^1L_a state. Introduction of the phenyl substituents in the 1,3,6 and 8 positions red shifts the $^1B_{2u}^+ \leftarrow {}^1A_{1g}^-$ transition by 4000 cm^{-1}, causing at the same time an hyperchromic effect on the corresponding absorption band. The small overall fluorescence red shift ($\sim$900 cm^{-1}) indicates that the ^1L_b state is not much affected by the substitution. This interpretation of Berlman's results implies that phenyl substitution in the 1,3,6, and 8 positions affects mainly the long-axis oriented transitions of pyrene. This conclusion, which can easily be reached on geometrical grounds, will be very important for the interpretation of the T–T absorption spectrum of TPP. Of course, the possibility of having, upon phenyl substitution, new transitions of TPP as a whole must not be overlooked.

Experimental

Flash Apparatus

A flash of 15 μs duration ($t_{1/e}$) is obtained by discharging a set of capacitors (max. 3.0 kJ) through two oxygen-filled linear flash lamps of the type B described by Claesson and Lindqvist (8). The condenser bank consists of ten 1-μF high voltage, low inductance Hivotronic capacitors; the connections are such that three units of 2, 5, and 10 μF respectively can be formed. These units can be charged at variable voltages from 13 to 25 kV. The discharge is initiated by applying a 30 kV pulse at a spark gap in nitrogen. The lamps are placed along a jacketted, cylindrical silica cell with end windows (length

[1]This work, presented at the ACFAS meeting (Montreal, May 1973), is part of C. Rullière's D.Sc. thesis (21).

[2]Present address: Laboratoire de Chimie Physique A, Université de Bordeaux, 351 Cours de La Libération, 33405 Talence, France.

Can. J. Chem. Downloaded from www.nrcresearchpress.com by 210.87.254.6 on 09/05/12
For personal use only.

Can. J. Chem. Downloaded from www.nrcresearchpress.com by 210.87.254.6 on 09/05/12
For personal use only.

20 cm, i.d. 1.3 cm). A $CuSO_4$ solution was circulated through the cell jacket. Transient changes in light transmission of the solution contained in the cell were measured at selected wavelengths. Either a quartz–iodine lamp (FCR 100W-12V) or a d.c. xenon discharge lamp (Osram XB0 150 W/1) can be used as analytical light source; appropriate glass filters reduce photochemical effects of the measuring light. The light transmitted by the cell passes through a monochromator (Jarrell-Ash 82-410, 150 μm slit width, 0.6 nm resolution) and is measured using a photomultiplier (RCA 931 A or RCA 4832). The anode current of the photomultiplier is amplified either by a differential probe (Tektronix P6046) or by a cathode follower built according to Lindqvist (9). With both types of amplifiers, the signal resulting from exposure of the detector to light of constant intensity can be adjusted to zero with the aid of a calibrated d.c. offset (Hewlett-Packard 1803A plug-in) thus allowing a high amplification of small changes in signal. The amplified signal is fed either to a storage oscilloscope (Hewlett-Packard 181-A equipped with 1822A and 1083A plug-ins) or to a transient recorder (Biomation 610B). The sweep triggering pulse for the oscilloscope or the transient recorder is obtained from a photocell exposed to the flash lamps through a pinhole.

The data reported here have been obtained using the RCA 931A photomultiplier, the Tektronix differential probe, and the storage oscilloscope. Transmission changes of 0.4% were detectable over most of the wavelength range studied (400–620 nm). The rise time of the total detection system was 0.1 μs.

Preparation of Solutions

1,3,6,8-Tetraphenylpyrene (K & K) was purified by chromatography on alumina and absorption and emission spectra compared with Berlman's spectra (2). Cyclohexane (Fisher spectroanalyzed) was used without further purification. The solutions were outgassed by six cycles of freezing, pumping, thawing, and saturation with oxygen-free argon (Linde) after which the cell was sealed under vacuum (10^{-5} mm Hg). The use of the $CuSO_4$ filter restricted the excitation to the first absorption band of TPP and in these conditions there was no photodecomposition of the solution. All experiments were done at room temperature (21 ± 2 °C).

Results and Discussion

Flash excitation of solutions of TPP in cyclohexane produced a transient decrease of ground state TPP absorption and the appearance of a structured absorption lasting a few milliseconds (*ca.* 3–7 ms). This transient absorption is attributed to the triplet state of TPP. It is shown in Fig. 1, that the transient triplet absorption reaches a limit at electrical discharge energies higher than *ca.* 2 kJ for low TPP concentration. Since triplet absorption lasted much longer than the flash, this light saturation effect indicates that all TPP was converted to the triplet state at the higher flash energies, thus making possible the determination of triplet extinction coefficient.

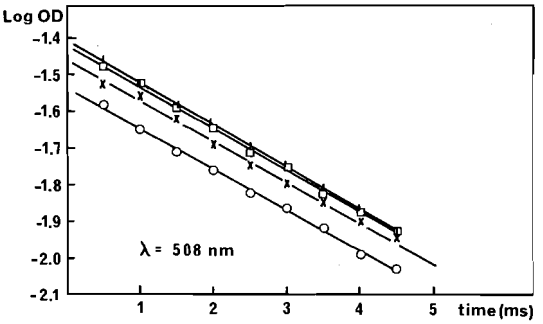

FIG. 1. Decay of the transient absorbance observed at 508 nm through a 20 cm cell containing a solution 1.08×10^{-7} *M* TPP in cyclohexane (21 ± 2 °C) exposed to flashes of varying discharge energy. ○, 1300 J; ×, 1600 J; □, 1800 J; |, 2000 J (saturation).

Before we discuss the T–T absorption spectrum of TPP, let us review the information available on T–T absorption of pyrene. In the region from 350 to 600 nm, there are two main absorption bands (3–5). The first progression at 19 200, 20 600, and 22 000 cm^{-1} ($f = 0.14$) is polarized along the short axis of pyrene and has been attributed to a ${}^3B_{3g}^- \leftarrow {}^3B_{2u}^+$ transition (3, 4). The second and more intense progression with peaks at 24 200, 25 500, and 27 000 cm^{-1} ($f = 0.31$) shows long-axis polarization and has been assigned to a ${}^3A_g^- \leftarrow {}^3B_{2u}^+$ transition (3, 4). The assignment is in agreement with Orloff's theoretical calculations (10). However, the polarization measurements indicate the presence of a hidden short-axis polarized absorption around 24 000 cm^{-1} which would correlate with the weak ${}^3B_{3g}^- \leftarrow {}^3B_{2u}^+$ transition calculated by Orloff at 27 000 cm^{-1}.

The T–T absorption spectrum of TPP is shown in Fig. 2; the absorption maxima are gathered in Table 1. This spectrum is the result of more than 400 flashes. Peaks have been numbered in Fig. 2 in order to facilitate the discussion. At first sight, the location of the two absorption bands is very similar to the pyrene case. However there is an inversion of the intensity of the two absorption bands in going from pyrene to TPP. The system of axes chosen is given in Fig. 2.

Assignment of the Spectrum

As already noticed, phenyl substitution in the 1,3,6 and 8 positions of pyrene should produce an important bathochromic shift of the long-axis polarized transitions, the short-axis oriented transitions being virtually unaffected by such a

Can. J. Chem. Downloaded from www.nrcresearchpress.com by 210.87.254.6 on 09/05/12
For personal use only.

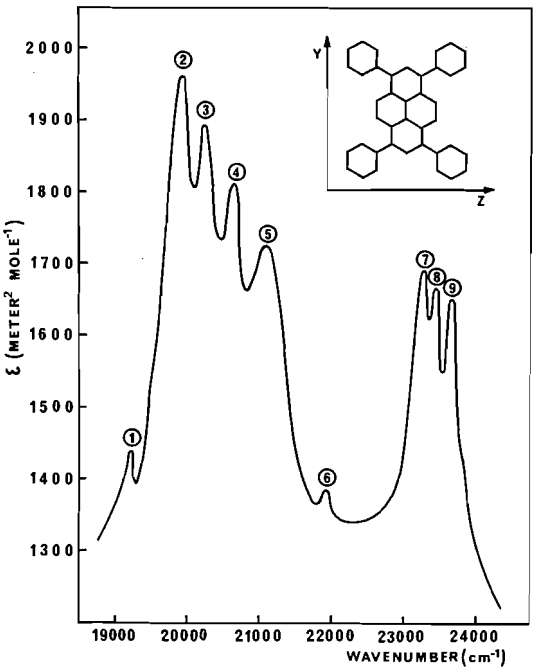

FIG. 2. Absorption spectrum of triplet TPP in cyclohexane.

substitution. Therefore, peaks 1 and 6 at 19 030 and 21 740 cm^{-1} are attributed to the first and third member of the progression corresponding to the short-axis polarized $^3B_{3g}^- \leftarrow {}^3B_{2u}^+$ transition, the second member of this progression being hidden under the absorption starting at $\sim$19 400 cm^{-1}. These two peaks are only very slightly red shifted ($\sim$200 cm^{-1}) when compared with the equivalent absorption maxima of the first T–T band of pyrene (3). This red shift is not significant and could be a trivial solvent effect. The progression involves the same 1400 cm^{-1} vibrational mode in both pyrene and TPP.

Peaks 2, 3, 4, and 5 are attributed to the long-axis polarized $^3A_g^- \leftarrow {}^3B_{2u}^+$ transition. This assignment implies a 4300 cm^{-1} red shift of the $^3A_g^- \leftarrow {}^3B_{2u}^+$ pyrene transition upon phenyl substitution, which is consistent with the expected phenyl substituent effect. Polarization measurements would allow this assignment to be checked. The progression involves a 450 cm^{-1} vibrational mode. The red shift of the $^3A_g^- \leftarrow {}^3B_{2u}^+$ transition clears the absorption region above 23 000 cm^{-1}. The three peaks at 23 095, 23 280, and 23 475 cm^{-1} could therefore correspond to the second $^3B_{3g}^- \leftarrow {}^3B_{2u}^+$ transition ($I^-(z)$) calculated by Orloff at 27 000 cm^{-1}. This attribution fits nicely with the suggestion of a weak hidden z-polarized transition around 24 000 cm^{-1} in pyrene (3). The vibrational progression in this third transition is $\sim$200 cm^{-1}.

Another weak band at 16 300 cm^{-1} was observed. However, as the lifetime of the species giving rise to this absorption was much shorter than the triplet lifetime, this band is not included in Fig. 2 and Table 1.

Vibrational Structure

In contrast to the $S_n \leftarrow S_0$ spectrum, the $T_n \leftarrow T_1$ spectrum of TPP shows very fine vibrational structure. This suggests a planar or quasi-planar $^3B_{2u}^+$ state. Orloff has shown that using an aromatic resonance integral (β) for the ring–ring bond in the first triplet state of 1-phenylnaphthalene gives the best fit to experimental data for zero-field splitting and triplet energy (11). Steric hindrance of the phenyl substituents in 1,3,6,8-tetraphenylpyrene is identical to the steric hindrance of the phenyl group in 1-phenylnaphthalene and it is expected that TPP lowest triplet state is also planar.

Assuming that TPP has the same symmetry (D_{2h}) in the equilibrium positions of higher and lowest triplet states, only excitations of totally symmetric vibrations should occur accompanying the $T_n \leftarrow T_1$ allowed electronic transitions (6). The appearance of fine vibrational structure ($\sim$450 cm^{-1}) in T–T absorption upon phenyl substitution seems to be a current phenomenon; it does show up in phenyl oxadiazoles,[3] as well as in 9,10-diphenylanthracene (12). The sole A_g vibration in substituted benzenes in the right energy range is the c type vibration (13–15). This substituent-sensitive vibration is mode 18a of benzene which involves appreciable coupling with the ring–ring C—C stretching frequency in phenyl substituted aromatic compounds. The displacement of the frequency of this vibration, from the value of 512 cm^{-1} in toluene, has already been suggested as an indication of the importance of the coupling between phenyl rings in biphenyl (315 cm^{-1}) and polyphenyl methanes (14). The c type vibration could therefore be responsible for the vibrational progressions of 450 cm^{-1} and 200 cm^{-1} in the $^3A_g^- \leftarrow {}^3B_{2u}^+$ and second $^3B_{3g}^- \leftarrow {}^3B_{2u}^+$ transitions, respectively.

[3]C. Rullière and P. C. Roberge, to be published.

Can. J. Chem. Downloaded from www.nrcresearchpress.com by 210.87.254.6 on 09/05/12
For personal use only.

TABLE 1. Triplet–triplet absorption peaks of pyrene and 1,3,6,8-tetraphenylpyrene and proposed assignments (lower state $^3B_{2u}^+$)

1,3,6,8-Tetraphenylpyrene					Pyrene					
Observed absorption peaks		Assignments			Observed absorption peaks[a]		Assignments[a]			Calculated frequency[b]
ν (cm^{-1})	ε ($m^2\ M^{-1}$)	Upper state	Configuration	Vibrational	ν (cm^{-1})	Polarization	Upper state	Configuration	Vibrational	ν (cm^{-1})
19 030	1440	$^3B_{3g}^-$	$I_2^-(z)$	0	19 230	z	$^3B_{3g}^-$	$I_2^-(z)$	0	18 200
19 570	1970	$^3A_g^-$	$I_3^-(y)$	0						
20 050	1890			+ 450	20 600	z			+ 1400	
20 470	1810			+2×450						
20 900	1680			+3×450						
21 740	1390	$^3B_{3g}^-$	$I_2^-(z)$	+2×1400	22 200	z			+2×1400	
23 050	1690	$^3B_{3g}^-$	$I_4^-(z)$	0	24 200	$y(+z)$	$^3A_g^-$	$I_3^-(y)$	0	24 900
23 280	1670		or	+ 200	25 500	$y(+z)$	+		+ 1400	
23 475	1650		$B_1^-(z)$	+2×200			$^3B_{3g}^-$	$I_4^-(z)$		27 000
			or				(hidden)			
			$I_\phi^-(z)$		27 000	$y(+z)$			+2×1400	

[a]Reference 4.
[b]Reference 10.

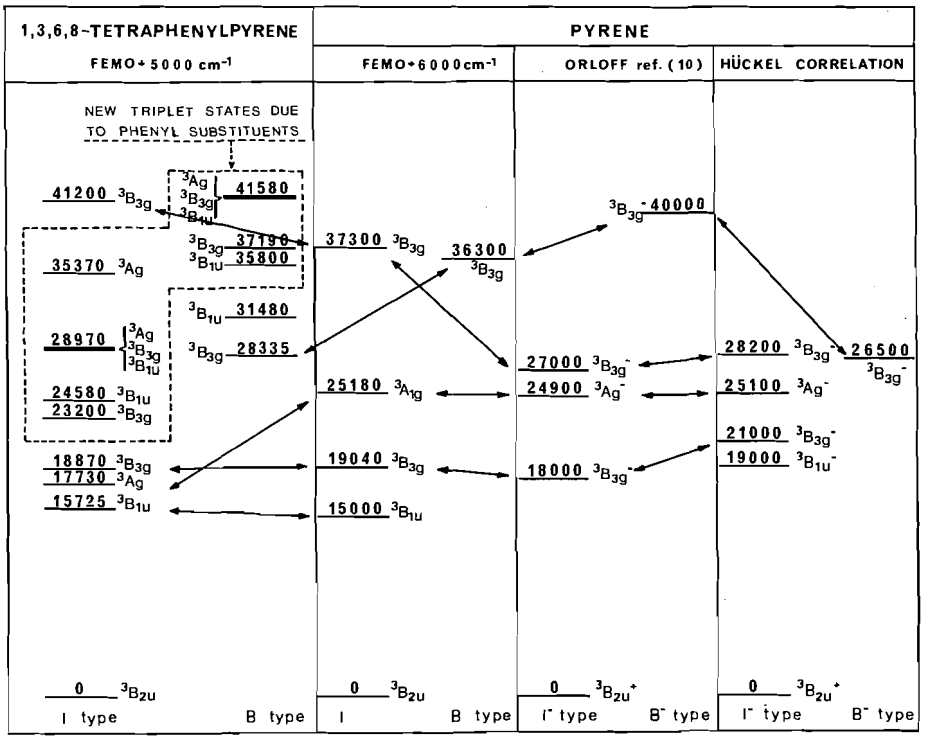

FIG. 3. Correlation of the calculated triplet energies (referred to the lowest ${}^3B_{2u}{}^+$) for pyrene and TPP.

However, if the T_n states are not planar and have lower symmetry than the lowest triplet, excitation of the torsional mode can occur accompanying the electronic transitions. If this is so, excitation of the torsional frequency does not blur the fine structure of the T–T spectrum as it does in the $S_n \leftarrow S_0$ spectrum. The 450 and 200 cm^{-1} vibrational modes could therefore be the torsional frequencies in the corresponding higher triplet states. Due to the aromatic character of the ring–ring bond, these frequencies would be of much higher energy than in the ground state ($\sim$110 cm^{-1} in biphenyl (14, 15)).

FEMO Calculated Transition Energies

FEMO calculations using the Ruedenberg–Scherr model (16) have been done to evaluate the T–T transition energies in TPP. This model is very simple and should be quite convenient for planar, phenyl substituted aromatic molecules, especially if, as suggested here for TPP in the triplet state, the ring–ring bonds are nearly aromatic. As the singlet–triplet splits are neglected in this model, the barycenter of the singlet–triplet energy is obtained for each state. However, except for the lowest triplet, the triplet states of interest (mainly I^- states according to Hoÿtink's notation (17)) are degenerate or nearly degenerate with the corresponding singlet states (18). Therefore, after a correction has been applied for the energy of the lowest triplet state (${}^3B_{2u}{}^+$), the Ruedenberg–Scherr model should give good approximations to the T–T transition energies. As a check, a calculation on pyrene has been undertaken. The results are presented in Fig. 3. A scaling factor of 6000 cm^{-1} has been added to the calculated energies in order to fit the first ${}^3B_{3g}{}^- \leftarrow {}^3B_{2u}{}^+$ transition energy with experiment. This scaling factor is very close to the energy difference (4500 cm^{-1}) between the ${}^3B_{2u}{}^+$ experimental energy and the calculated barycenter of the ${}^3B_{2u}{}^+$ and ${}^1B_{2u}{}^+$ energies. The FEMO predictions are compared in Fig. 3 with Orloff's calculations as well as with predictions using a semiempirical Hückel correlation (19, 20). Except for the second ${}^3B_{3g}{}^- \leftarrow {}^3B_{2u}{}^+$ transitions ($I_4{}^-(z)$), there is a good agreement between the different calculations. FEMO calculations also give remarkable agreement with experiment for triplet energies of *trans*-stilbene and 1,4-diphenyl-1,3-butadiene (21).

The FEMO calculated triplet energies for TPP

Can. J. Chem. Downloaded from www.nrcresearchpress.com by 210.87.254.6 on 09/05/12
For personal use only.

and a correlation with pyrene are given in Fig. 3, the scaling factor here being 5000 cm^{-1}. The calculation evidences the important bathochromic shift of the $^3A_{1g}^- \leftarrow {}^3B_{2u}^+$ transition and supports the assignment given previously. However, in the region above 23 000 cm^{-1}, new transitions due to phenyl substitution are predicted. The absorption band experimentally observed at 23 095 cm^{-1} was previously assigned to the $I_4^-(z)$ transition calculated by Orloff at 27 000 cm^{-1} in pyrene (FEMO calculation gives 41 200 cm^{-1} for this transition in TPP). This band could very well be attributed either to the $B_1^-(z)$ transition calculated at 28 335 cm^{-1} (40 000 cm^{-1} by Orloff) or to a new $I_\phi^-(z)$ transition appearing upon phenyl substitution and calculated at 23 200 cm^{-1}. As all three transitions are short-axis polarized, polarization studies would not help clarify this point.

Triplet Decay Kinetics

The triplet decay kinetics were measured over the whole range of wavelengths and over a wide range of concentrations and flash energies. The results are satisfactorily accounted for by the following scheme:

$$[1] \qquad T \xrightarrow{k_1} S_0$$

$$[2] \qquad T + Q \xrightarrow{k_2} S_0 + Q$$

$$[3] \qquad T + T \xrightarrow{k_3} \begin{cases} T + S_0 \\ S_1 + S_0 \\ 2S_0 \\ D^* \end{cases}$$

where T designates the lowest triplet state, S_0 and S_1 respectively the ground state and the first excited state of TPP, D* the excimer, and Q any impurity quencher. The decay of triplet absorption was found to be pseudo first-order at low triplet concentrations. The corresponding triplet lifetime (~2–7 ms) is probably limited by oxygen quenching ($Q = O_2$). Process 3 occurred at higher TPP concentrations and high flash energies. Under these conditions the triplet decay curves deviate from the first-order decay mode observed at lower energies, as shown on Fig. 4. The decay law can be written:

$$[4] \qquad -\frac{d[T]}{dt} = (k_1 + k_2[Q])[T] + k_3[T]^2$$

At high enough flash energies and at short times after excitation, the decay is controlled by

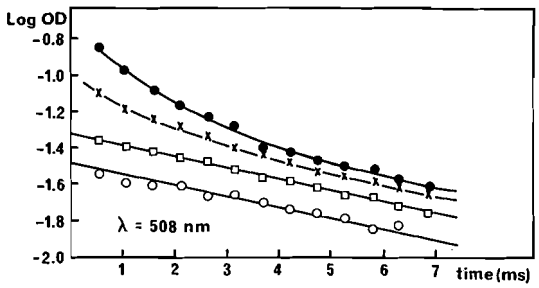

FIG. 4. Decay of the transient absorbance observed at 508 nm through a 20 cm cell containing a solution 5.4×10^{-7} *M* TPP in cyclohexane (21 ± 2 °C) exposed to flashes of varying discharge energy. ○, 1000 J; □, 1300 J; ×, 1500 J; ●, 2200 J.

T–T quenching (process 3). Integration of [4] under these conditions gives:

$$[5] \qquad [[T](t)]^{-1} = [[T](0)]^{-1} + k_3 t$$

or

$$[6] \qquad [OD_\lambda(t)]^{-1} = [OD_\lambda(0)]^{-1} + k_3/\varepsilon_\lambda l t$$

where OD_λ is the absorbance at wavelength λ, ε_λ is the triplet extinction coefficient at this wavelength, and l is the length of the cell. A representative curve obtained at 508 nm is given in Fig. 5. The mean determined value of k_3 is $1.3 \pm 0.1 \times 10^9\ M^{-1}\ s^{-1}$. This value is 20% of the diffusion controlled rate constant for pyrene in cyclohexane (7×10^9 at 22 °C (22)).

Conclusion

On experimental and theoretical grounds, we assigned the first observed T–T absorption band of TPP (peaks 1–6 in Fig. 1) to a superposition of the $I_2^-(z)$ and $I_3^-(y)$ transitions. This last transition is red shifted by as much as 4300 cm^{-1} when compared to pyrene. The second band (peaks 7–9 in Fig. 1) is due to a $^3B_{3g}^- \leftarrow {}^3B_{2u}^+$ transition, but it might correspond to $I_4^-(z)$, $B_1^-(z)$, or $I_\phi^-(z)$. This second T–T band seriously overlaps with the fluorescence of TPP. If it were not for this second band appearing upon phenyl substitution, pyrene could be considered as a perfect case of the $A_2{}^1a$ constellation, according to Pavlopoulos and Hammond's notation for laser dyes (23). As a matter of fact, laser action was easily obtained with TPP in cyclohexane (21, 24). Laser action was even obtained using the window of the cell as sole cavity mirrors, indicating a high gain in this system. However, the effect of T–T absorption on the laser action was clearly evidenced (21). It surely limits the

Can. J. Chem. Downloaded from www.nrcresearchpress.com by 210.87.254.6 on 09/05/12
For personal use only.

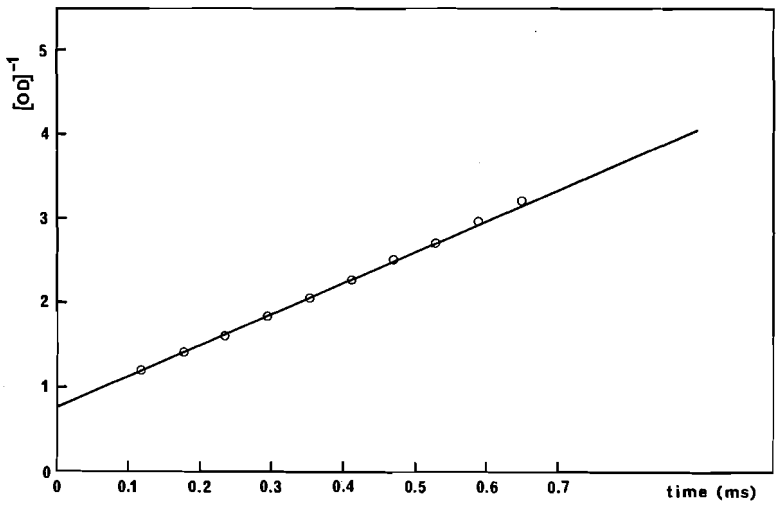

FIG. 5. Second order decay of the transient absorption observed at 508 nm through a 20 cm cell containing a solution of 2.7×10^{-6} *M* TPP in cyclohexane (21 ± 2 °C) exposed to a flash of 2400 J discharge energy ($k_3 = 1.3 \times 10^9$ $M^{-1}s^{-1}$).

efficiency of TPP laser and prevents any flash-lamp pumping of this system.

If the second T–T absorption band corresponded to the $I_\phi^-(z)$ transition, pyrene would be a member of the $A_2{}^1a$ constellation. Replacement of the phenyl substituents in TPP by auxochromic groups (*e.g.* $N(C_2H_5)_2$) should allow good improvement of the laser efficiency. On the other hand, if that band corresponds to $I_4^-(z)$ or $B_1^-(z)$, there is not much hope that changing the substituent will improve the laser efficiency.

We wish to thank the National Research Council of Canada and the Ministère de l'Education de la Province de Québec (FCAC) for financial support.

1. T. G. PAVLOPOULOS. Chem. Phys. Lett. **20**, 207 (1973).
2. I. B. BERLMAN. Handbook of fluorescence spectra of aromatic molecules. Academic Press, New York, New York. 1971.
3. T. G. PAVLOPOULOS. J. Chem. Phys. **52**, 3307 (1970).
4. J. LANGELAAR, J. WEGDAM-VAN BEEK, H. TEN BRINK, and J. D. W. VAN VOORST. Chem. Phys. Lett. **7**, 368 (1970).
5. D. LAVALETTE. J. Chim. Phys. **66**, 1853 (1969).
6. H. SUZUKI. Electronic absorption spectra and geometry of organic molecules. Academic Press, New York, New York. 1967.
7. C. A. PARKER and C. G. HATCHARD. Trans. Faraday Soc. **59**, 284 (1963).
8. S. CLAESSON and L. LINDQVIST. Ark. Kemi, **11**, 535 (1957).
9. L. LINDQVIST. Ark. Kemi, **16**, 79 (1960).
10. M. K. ORLOFF. J. Chem. Phys. **47**, 235 (1967).
11. M. K. ORLOFF and J. S. BRINEN. Int. J. Quantum Chem. **3**, 225 (1969).
12. Y. MEYER. DSc. Thesis, Faculté des Sciences de Paris. Université de Paris, Paris, France. 1970.
13. J. M. SALMON et P. VIALLET. Bull. Soc. Chim. **7–8**, 2188 (1973).
14. B. PASQUIER and J. M. LEBAS. J. Chim. Phys. **64**, 765 (1967).
15. D. H. WHIFFEN. J. Chem. Soc. 1350 (1956).
16. K. RUEDENBERG and C. W. SCHERR. J. Chem. Phys. **21**, 1565 (1953); C. W. SCHERR. J. Chem. Phys. **21**, 1582 (1953).
17. G. J. HOŸTINK. Pure Appl. Chem. **11**, 393 (1965).
18. R. PARISER. J. Chem. Phys. **24**, 250 (1956).
19. D. LAVALETTE. Chem. Phys. Lett. **3**, 264 (1969).
20. C. HELLNER, L. LINDQVIST, and P. C. ROBERGE. J. Chem. Soc. Faraday Trans. II, **68**, 1928 (1972).
21. C. RULLIÈRE. DSc. Thesis, Laval University, Quebec, Quebec. 1974.
22. J. B. BIRKS, D. J. DYSON, and I. H. MUNRO. Proc. R. Soc. A, **275**, 575 (1963).
23. T. G. PAVLOPOULOS and P. R. HAMMOND. J. Am. Chem. Soc. **96**, 6568 (1974).
24. C. RULLIÈRE and M. M. DENARIEZ-ROBERGE. Opt. Commun. **7**, 166 (1973).

Can. J. Chem. Downloaded from www.nrcresearchpress.com by 210.87.254.6 on 09/05/12
For personal use only.

5-Allyl-9-oxobenzomorphans. Part 2. The Crystal and Molecular Structure of an Unusual Product of Dequaternization of 5-Allyl-9-oxobenzomorphan Methobromide[1,2]

FARID R. AHMED

Division of Biological Sciences, National Research Council of Canada, Ottawa, Canada K1A 0R6

AND

MICHEL SAUCIER[3] AND IVO MONKOVIĆ[4]

Bristol Laboratories of Canada, 100 Industrial Blvd., Candiac, Quebec J5R 1J1

Received June 19, 1975

FARID R. AHMED, MICHEL SAUCIER, and IVO MONKOVIĆ. Can. J. Chem. **53**, 3276 (1975).

The synthesis of 5-allyl-2′-methoxy-9-oxo-6,7-benzomorphan (**5***b*) is described. The 10-hydroxy-2-methyl-1,11-propano-9*H*-indeno-1,2,10,11-tetrahydro[2,1-*c*]pyridine (**7***a*) and the corresponding 6-methoxy derivative (**7***b*) are unexpected products of pyrolysis of 5-allyl-2-methyl-9-oxobenzomorphan methobromide (**4***a*) and 5-allyl-2′-methoxy-2-methyl-9-oxobenzomorphan methobromide (**4***b*) respectively. The molecular structure of **7***a* ($C_{16}H_{19}NO$) has been determined from spectral and microanalytical data, and confirmed by X-ray single crystal analysis on its hydrobromide salt using the heavy atom technique. The crystals of $[C_{16}H_{20}NO]^+Br^-$ are monoclinic, $P2_1/a$, with $a = 13.724(2)$, $b = 14.022(3)$, $c = 7.495(2)$ Å, $\beta = 97.33(5)°$, and $Z = 4$. The crystal structure has been refined by block-diagonal least-squares calculations to R and $R_w = 0.036$ for the 2197 observed reflections. The N atom has planar trigonal coordination, and forms one double and two single C—N bonds of lengths 1.273(4), 1.465(4), and 1.474(4) Å, respectively. The Br is hydrogen-bonded to O. The N and O atoms are *trans*.

FARID R. AHMED, MICHEL SAUCIER et IVO MONKOVIĆ. Can. J. Chem. **53**, 3276 (1975).

On décrit la synthèse de l'allyl-5 méthoxy-2′ oxo-9 benzo-6,7 morphane (**5***b*). L'hydroxy-10 méthyl-2 propano-1,11 9*H*-indènotétrahydro-1,2,10,11[2,1-*c*]pyridine (**7***a*) et le dérivé méthoxy-6 correspondant (**7***b*) sont des produits inattendus des pyrolyses respectives des méthobromures de l'allyl-5 méthyl-2 oxo-9 benzomorphane (**4***a*) et de l'allyl-5 méthoxy-2′ méthyl-2 oxo-9 benzomorphane (**4***b*). On a déterminé la structure moléculaire de **7***a* ($C_{16}H_{19}NO$) à partir de données spectroscopiques et microanalytiques et on l'a confirmée par rayons-X sur un cristal unique de bromhydrate utilisant la technique des atomes lourds. Les cristaux de $[C_{16}H_{20}NO]^+Br^-$ sont monocliniques, $P2_1/a$, avec $a = 13.724(2)$, $b = 14.022(3)$, $c = 7.495(2)$ Å, $\beta = 97.33(5)°$ et $Z = 4$. On a affiné la structure cristalline par la méthode des moindres carrés blocs diagonaux jusqu'à des valeurs de R et R_w de 0.036 pour 2197 réflexions observées. L'atome d'azote a une coordination trigonale planaire et forme un lien double et deux liens C—N simples avec des longueurs respectives de 1.273(4), 1.465(4) et 1.474(4) Å. Le brome est lié à l'oxygène par un pont hydrogène. Les atomes d'azote et d'oxygène sont *trans*.

[Traduit par le journal]

Introduction

A research project designed to study the synthesis and pharmacological properties of various 5,9-disubstituted-2′,9-dihydroxybenzomorphans required 5-allyl-2′-methoxy-2-methyl-9-oxobenzomorphan **5***b* (Scheme 1) as starting material. In part one of this series, we have reported the synthesis of benzomorphanone **5***a* starting with 2-tetralone (1). We now report the synthesis of **5***b* via the same reaction sequence (**1***b*–**4***b*) starting with 7-methoxy-2-tetralone. We should also like to report on the isolation and structure determination of certain unexpected products (**7***a*, **7***b*) of pyrolytic dequaternization of methobromides **4***a* and **4***b* respectively.

Results and Discussion

Chromatographic separation of the reaction mixture obtained by thermal dequaternization of **4***a* has been described earlier (1). In addition to the expected products due to the *N*-demethylation (**5***a*) and Hofmann elimination (**6***a*) there was obtained in 11% yield another unknown basic constituent (**7***a*). The pure base crystallized

[1]NRCC No. 9675.

[2]For part 1 see ref. 1.

[3]Present address: Hoffmann–La Roche Limitée, 1000 Roche, Vaudreuil, Quebec.

[4]To whom correspondence regarding this paper should be addressed.

Can. J. Chem. Downloaded from www.nrcresearchpress.com by 210.87.254.5 on 09/05/12
For personal use only.

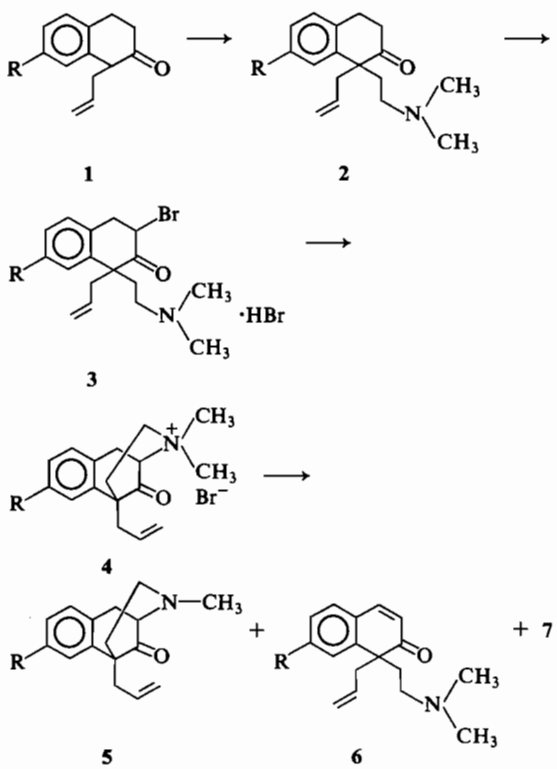

(*a*) R = H (*b*) R = OCH_3

SCHEME 1

from aqueous methanol as a white solid (slightly orange colored), m.p. 96–97 °C. The molecular formula of $C_{16}H_{19}NO$ (same as that of **5***a*) was obtained by microanalytical data and confirmed by mass spectrometry. However, its spectral properties were strikingly different from either **5***a* or **6***a* indicating a deep seated structural change with multiple bond breaking and bond formation. The least affected part of the molecule appeared to be the aromatic ring as seen in the n.m.r. spectrum (Table 1). An AX system (2H, doublets centered at 5.84 and 3.45 δ) whose upfield proton is labile and exchanges on shaking with D_2O with concomitant collapse of the downfield doublet (5.84 δ) to a singlet, is characteristic of an enamine function (2), which is attached to a quaternary carbon atom (C^t indicates a quaternary carbon atom). An AB quartet (doublets centered at 3.28 and 2.44 δ) is indicative of an isolated pair of benzylic protons bonded to a quaternary carbon atom. The singlet at 3.4 δ is characteristic of an N—CH_3 group and it signifies loss of one of the original *N*-methyl groups. The most conspicuous n.m.r. spectral feature is the disappearance of the signals due to allylic double bond, and the absence of a terminal methyl group, suggesting that a terminal bonding to the allylic double

TABLE 1. The 100 MHz proton n.m.r. spectrum of **7***a* in CCl_4 and chemical shifts induced by Eu(fod)$_3$ lanthanide shift reagent

δ	Spectrum characteristics		Δδ[a]	Molecular fragment
			1.18 (1H)	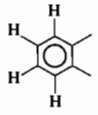
6.9–7.2	4H, m, aromatic protons		~0.4 (3H)	
5.84	1H, d, J = 8 Hz, collapses to a singlet upon exchange with D_2O	AX q	2.39	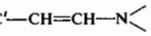
3.45	1H, d, J = 8 Hz, exchanges with D_2O	AX q	1.98	
3.28	1H, d, J = 15 Hz	AB q	3.60	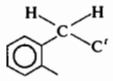
2.44	1H, d, J = 15 Hz	AB q	3.71	
3.41	3H, s		0.61	
3.08	1H, unresolved m		4.95	
1.4–2.4	7H, m		3.0	—$CH_2CH_2CH_2$—, OH

[a]Enough Eu(fod)$_3$ was added to induce tabulated displacements of the chemical shifts.

Can. J. Chem. Downloaded from www.nrcresearchpress.com by 210.87.254.5 on 09/05/12
For personal use only.

bond must have taken place. Such bonding would be expected to give rise to a propylene envelope in the n.m.r. spectrum and indeed it is present at 1.4–2.4 δ mixed with an exchangeable proton, presumably due to OH. Another significant spectral feature is the lack of a carbonyl absorption and presence of an hydroxyl absorption (3570 cm^{-1}) in the i.r. spectrum, which was assumed to be due to a tertiary OH (C′—OH); a secondary or primary OH would have deshielded the adjacent proton(s) in the n.m.r. spectrum. Thus based on the above spectral evidence, the following molecular fragments emerged:

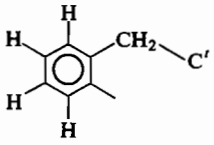

$CH_3N—CH=CH—C'$,

$—CH_2CH_2CH_2—$, C′—OH

accounting possibly for all, or all but one carbon, and one hydrogen atom. The absorption in the n.m.r. spectrum due to the missing proton appears at 3.08 δ as an unresolved multiplet (almost a singlet), and it is characteristic of either an isolated benzylic proton or a methine proton adjacent to nitrogen (>CH—N<). Its correct assignment was made possible by analysis of the lanthanide induced shifts (l.i.s.) in the n.m.r. spectrum. The utility of lanthanide shift reagents in the analysis of n.m.r. spectra of bifunctional compounds is well established (3). The recorded l.i.s. in Table 1 suggest that the primary site of coordination of the europium complex is the hydroxyl rather than the enamine function since there are a number of protons which are more deshielded than the ones attached to carbons adjacent to the nitrogen. Furthermore, the greater l.i.s. for the isolated methine proton ($\Delta\delta = 4.95$) than for any other one in the spectrum indicates that it is surrounded by a highly complexed environment. Such an environment would exist in a molecular fragment *A* (Scheme 2) in which coordination on the nitrogen as well as on the oxygen would influence its l.i.s. The atomic arrangement in *A* also accounts for the observed n.m.r. pattern, chemical shifts and l.i.s. due to the isolated pair of benzylic protons. At this point, out of two possible bonding combinations for the two out of three unattached bonds on the quaternary carbon atom in *A* (C′—) the only likely one appeared to be that represented by *B*. Finally, insertion of the propylene group

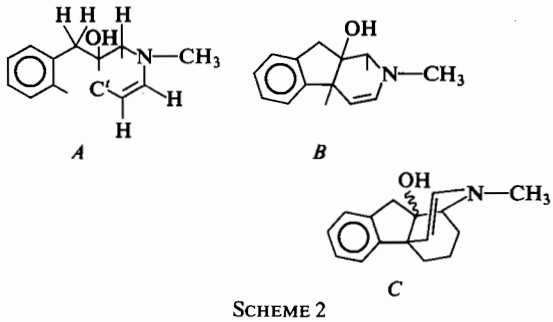

SCHEME 2

gave the complete structure for **7***a* as that shown by *C*.

Additional support for the proposed structure was obtained by chemical transformation and mass spectral evidence. Treatment of **7***a* with sodium borohydride in ethanol afforded a saturated base $C_{16}H_{21}NO$, whose n.m.r. and i.r. spectra were consistent with the structure **8***a*. The mass spectra of both **7***a* and **8***a* have peaks at $M - 17$, $M - 42$, and $M - 59$ formed by elimination of the OH and/or propylene bridge (Table 2). In addition, **8***a* has a peak at $M - 25$ formed by elimination of the ethylene bridge.

The remaining questions to be solved were the stereochemistry of the hydroxyl function and the reaction mechanism which could account for this remarkable transformation of **4***a* to **7***a*. We suggest that **7***a* is formed by the sequence shown in Scheme 3. The quaternary base undergoes homolytic $C_1—C_8$ fission to give diradical *i* followed by an intramolecular attack of this diradical on the carbonyl and allyl groups to give another diradical, *ii*, in which a new molecular skeleton is already formed. Next, one inter-

TABLE 2. Mass spectra[a] of **7***a* and **8***a*

7*a*		**8***a*	
m/e	Relative intensities[b]	*m/e*	Relative intensities
241	100	243	100
224	19	226	100
212	7	214	23
198	23	202	16
184	11	201	33
182	15	199	8
181	9	186	13
		184	34
		182	14

[a]Measured with an LKB 9000 instrument using an ionization energy of 70 eV and 43 °C temperature.
[b]Peaks below *m/e* 181 and those with relative intensities of less than 7% were not tabulated.

Can. J. Chem. Downloaded from www.nrcresearchpress.com by 210.87.254.5 on 09/05/12
For personal use only.

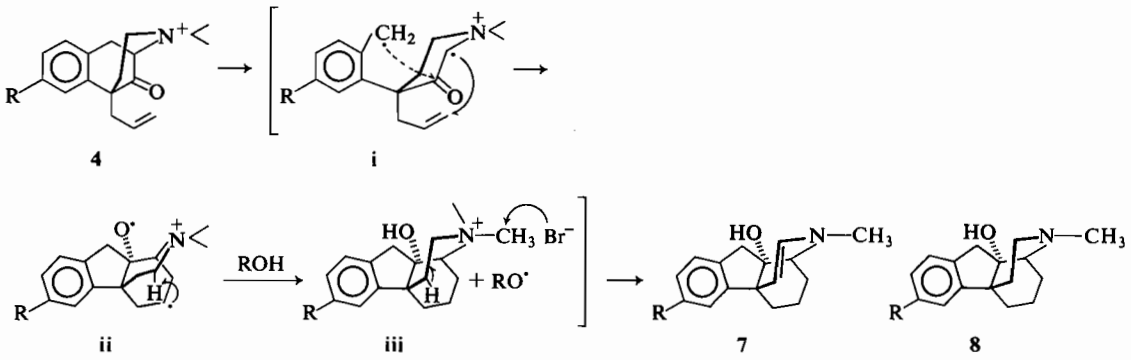

(*a*) R = H, (*b*) R = OCH_3, (*c*) R = OH

SCHEME 3

molecular and one intramolecular (1–5) hydrogen transfer give the immoniun radical *iii*, and the sequence is completed by demethylation and abstraction of a proton by the solvent. Radical mechanisms have been demonstrated in nitrogen (4) and sulfur (5) ylide rearrangements,[5] although we are unaware of any example in the literature of the next step postulated in Scheme 3, *i.e.* radical attack on the carbonyl carbon. The reverse reaction *i.e.* radical oxidation of a secondary alcohol to give a ketone is well documented (6). The alternative ionic mechanism is considered less likely to be operative, since it would have to involve an unlikely electrophilic attack by a benzylic carbo-cation on the carbonyl carbon.

If the reaction sequence shown in Scheme 3 was indeed to take place, then the stereochemistry of the hydroxyl group should be α or *trans* in relation to the nitrogen atom. This, as well as the overall structure has been verified by an X-ray crystallographic study of the hydrobromide salt of **7***a* (*vide infra*).

The synthesis of benzomorphanon **5***b*, an important intermediate for the investigations in the field of analgesics and narcotic antagonists was accomplished analogously to that of **5***a* (1). Pyrolysis of **4***b* again gave a mixture of **5***b*, **6***b*, and **7***b*, which was similarly separated by column chromatography. Reduction of **7***b* with lithium aluminum hydride yielded saturated base **8***b*, which was further transformed to the phenolic base **8***c* by treatment with boron tribromide.

Crystal Structure

The molecular structure, as viewed along the normal to the benzene ring, is presented in Fig. 1. The same conformation was also deduced from the spectroscopic data. The bond lengths and valency angles (uncorrected for thermal vibration) for the non-hydrogen atoms are listed in Table 3. The C—H lengths are in the range 0.88–1.04(3) Å, mean = 0.96 Å, and O—H = 0.87(4) Å. All the bond lengths are in the range of their expected values.

The conformation of the rings, described in terms of the torsion angles of the bonds and the deviations of the atoms from some selected mean planes, is presented in Fig. 2. The benzene ring is planar, the five-membered ring is near envelope, the six-membered ring containing the N atom is an approximate sofa, and the remaining six-membered ring is a slightly distorted chair. The three C—N bonds are coplanar, and form C—N—C angles of 121.8(7), 121.5(8), and 116.7(2)°, where the smallest angle is opposite the double bond.

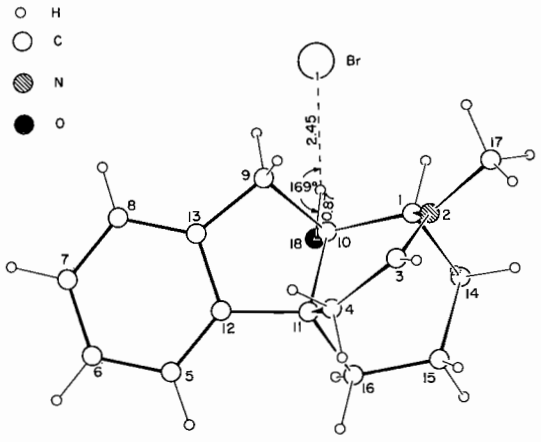

FIG. 1. A view of $C_{16}H_{19}NO{\cdot}HBr$ normal to the benzene ring, showing the conformation and the Br...H—O hydrogen bond. The interatomic distances are in Å.

[5]For a review on related rearrangements see ref. 13.

Can. J. Chem. Downloaded from www.nrcresearchpress.com by 210.87.254.5 on 09/05/12
For personal use only.

TABLE 3. Bond lengths (Å), valency angles (deg) and their estimated standard deviations in parentheses

Bond	Distance	Bonds	Angle
C—C single		N(2)—C(1)—C(10)	110.7(2)
C(1)—C(10)	1.535(4)	N(2)—C(1)—C(14)	107.9(2)
C(1)—C(14)	1.547(4)	C(10)—C(1)—C(14)	109.4(2)
C(3)—C(4)	1.466(4)[a]	C(1)—N(2)—C(3)	121.8(2)
C(4)—C(11)	1.559(4)	C(1)—N(2)—C(17)	116.7(2)
C(9)—C(10)	1.528(4)	C(3)—N(2)—C(17)	121.5(3)
C(9)—C(13)	1.520(4)[b]	C(2)—C(3)—C(4)	124.0(3)
C(10)—C(11)	1.542(4)	C(3)—C(4)—C(11)	116.8(3)
C(11)—C(12)	1.513(4)[b]	C(6)—C(5)—C(12)	118.7(3)
C(11)—C(16)	1.525(4)	C(5)—C(6)—C(7)	120.2(3)
C(14)—C(15)	1.527(5)	C(6)—C(7)—C(8)	121.3(3)
C(15)—C(16)	1.526(5)	C(7)—C(8)—C(13)	118.9(3)
		C(10)—C(9)—C(13)	100.5(2)
C—C aromatic		C(1)—C(10)—C(9)	120.8(2)
C(5)—C(6)	1.393(5)	C(1)—C(10)—C(11)	108.7(2)
C(5)—C(12)	1.377(5)	C(1)—C(10)—O(18)	107.4(2)
C(6)—C(7)	1.372(5)	C(9)—C(10)—C(11)	103.8(2)
C(7)—C(8)	1.386(5)	C(9)—C(10)—O(18)	108.5(2)
C(8)—C(13)	1.382(4)	C(11)—C(10)—O(18)	106.9(2)
C(12)—C(13)	1.394(4)	C(4)—C(11)—C(10)	107.9(2)
		C(4)—C(11)—C(12)	106.8(2)
C—N single		C(4)—C(11)—C(16)	110.5(2)
C(1)—N(2)	1.474(4)[a]	C(10)—C(11)—C(12)	100.4(2)
C(17)—N(2)	1.465(4)[a]	C(10)—C(11)—C(16)	110.4(2)
		C(12)—C(11)—C(16)	120.0(2)
C—N double		C(5)—C(12)—C(11)	129.7(3)
C(3)—N(2)	1.273(4)	C(5)—C(12)—C(13)	121.1(3)
		C(11)—C(12)—C(13)	109.2(2)
C—O single		C(8)—C(13)—C(9)	130.0(3)
C(10)—O(18)	1.433(3)	C(8)—C(13)—C(12)	119.8(3)
		C(9)—C(13)—C(12)	110.2(2)
		C(1)—C(14)—C(15)	112.9(3)
		C(14)—C(15)—C(16)	114.1(3)
		C(11)—C(16)—C(15)	110.2(3)

[a]Next to C=N bond.
[b]Type C(sp^3)—C(sp^2).

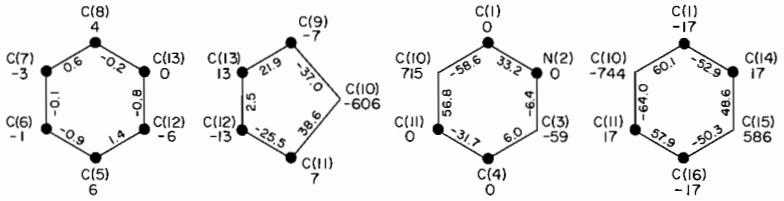

FIG. 2. The torsion angles (deg), and the distances (10^3 Å) of the atoms from the mean planes through those atoms identified by circles. The standard deviation of the distances is 0.003 Å.

The Br at ($\frac{1}{2} - x$, $\frac{1}{2} + y$, $1 - z$) is hydrogen bonded to O(18), where Br...H(18) = 2.45(3), Br...O(18) = 3.307(2) Å, Br...H(18)—O(18) = 168.9°, and Br...O(18)—H(18) = 8.2°. The observed Br...H distance is considerably shorter than the normal van der Waals contact (11) of 3.15 Å. There are no other short intermolecular contacts in the crystal structure.

Experimental

X-ray Analysis of 10-Hydroxy-2-methyl-1,11-propano-9H-indeno-3,4,10,11-tetrahydro[2,1-c]pyridinium Bromide, 7a

Crystal Data

$C_{16}H_{19}NO \cdot HBr$ f.w. = 322.25

Unit cell: monoclinic, $P2_1/a$, $Z = 4$, $a = 13.724(2)$, $b = 14.022(3)$, $c = 7.495(2)$ Å, $\beta = 97.33(5)°$, $V = 1433.55$ Å^3, $D_x = 1.493$ g cm^{-3}, $D_o = 1.491$ g cm^{-3} (by

Can. J. Chem. Downloaded from www.nrcresearchpress.com by 210.87.254.5 on 09/05/12
For personal use only.

Can. J. Chem. Downloaded from www.nrcresearchpress.com by 210.87.254.5 on 09/05/12
For personal use only.

flotation in toluene and carbon tetrachloride solution at 25 °C). Radiation: CuKα and Ni filter, $\lambda(K\alpha_1) = 1.54050$, $\lambda(K\alpha_2) = 1.54434$ Å, $\mu(Cu) = 42.34$ cm^{-1}. Crystal shape: slightly oblique prism of length 0.53 mm, and a hexagonal cross section of sides 0.23, 0.23, and 0.33 mm.

Intensities

The intensities were measured on an automatic diffractometer by the θ–2θ scan method, up to a limit of 125° in 2θ. Of the 2280 reflections scanned, 2197 (96%) were observed above threshold, thus giving 8.7 observations per parameter. The measured net intensities were corrected for L*p*, absorption (7), and extinction based on the linear plot of (I_o/I_c) against I_o.

Structure Determination

The position of Br was derived from a sharpened Patterson map, then the other non-hydrogen atoms were located from a vector superposition map. After some preliminary refinement of the atomic parameters by block-diagonal least-squares calculations, the *R* index was reduced to 0.07. The H atoms were then identified from a difference map and the refinement was continued until the parameter shifts were reduced to an average of 0.2σ and a maximum of 1.0σ. For the final parameters listed in Table 4, both *R* and R_w were 0.036 for the 2197 observed reflections,[6] and all the unobserved reflections were calculated less than 1.8 times their threshold amplitudes. The residual electron density in the final difference map was −0.7 to 0.4 e $Å^{-3}$ near Br and within ±0.3 e $Å^{-3}$ elsewhere.

The quantity minimized in the least-squares refinement was $\Sigma w(|F_o| - |F_c|)^2$, where $w = 1/\{1 + [(|F_o| - 35)/30]^4\}$ and $1.5 \leq |F_o| \leq 176.3$. The scattering factor curves were those of refs. 8 and 9 except that the curves for N and Br were modified to allow for the state of ionization (N^+ and Br^-) and to include the $\Delta f'$(Br) anomalous contribution. All calculations were carried out with the NRCC set of crystallographic programs (10).

Synthetic Procedures

The melting points were determined on a Gallenkamp apparatus, and are uncorrected. The infrared (i.r.) spectra were recorded on a Unicam Sp-200G grating i.r. spectrometer. The n.m.r. spectra were recorded on a Varian A-60A spectrometer. In addition, spectra of **7***a* were recorded on a 100 Mc spectrometer (Table 1). The chemical shifts are expressed in δ values using tetramethylsilane as internal reference. Microanalyses were performed by Micro-Tech Laboratories Inc., Skokie, Illinois.

10-Hydroxy-2-methyl-1,11-propano-9H-indeno-1,2,10,11-tetrahydro[2,1-c]pyridine, 7a

The chromatographic separation of a mixture of **5***a* and **6***a*, obtained by thermal decomposition of methiodide **4***a* was described earlier (1). The first fraction (255 mg, 11% based on **4***a*) which is now shown to be enamine **7***a* was purified by recrystallization from aqueous methanol to give a slightly orange solid; m.p. 96–97 °C; i.r. (CCl_4) 3570 (strong), 3515 (weak), 3430 (broad), 1632 cm^{-1}; n.m.r. (CCl_4) δ 7.2–7.5 (4H, m), 6.1 (1H, d, $J = 8$ Hz), 3.83 (1H, d, $J = 8$ Hz, exchanges with D_2O with collapse of a d at δ 3.45 to a s), 3.42 (1H, d, $J = 15$ Hz), 3.24 (1H, unresolved m), 2.88 (3H, s), 2.58 (1H, d, $J = 15$ Hz), 1.5–2.3 (7H, m).

Anal. Calcd. for $C_{16}H_{19}NO$: C, 79.63; H, 7.93; N, 5.80. Found: C, 79.72; H, 8.08, N, 5.62.

The hydrobromide salt was recrystallized from methanol acetone; m.p. 246–248 °C.

Anal. Calcd. for $C_{16}H_{19}NO{\cdot}HBr$: C, 59.63; H, 6.25; N, 4.35. Found: C, 59.33; H, 6.21; N, 4.27.

10-Hydroxy-2-methyl-1,11-propano-9H-indeno-1,2,3,4,10,11-hexahydro[2,1-c]pyridine, 8a

A mixture of enamine **7***a* (100 mg) ethanol (10 ml, 99%) and sodium borohydride (10 mg) was heated under reflux for 30 min. After cooling, it was treated with dilute hydrochloric acid, made alkaline with sodium bicarbonate, and extracted with ether to give after drying and evaporation of solvent 90 mg of crude solid **8***a*. An analytical sample was prepared by recrystallization from aqueous methanol; m.p. 99–100 °C; i.r. ($CHCl_3$) 3545 (sharp), 3430 (broad); n.m.r. ($CDCl_3$) δ 7.0–7.4 (4H, m), 3.83 (1H, d, $J = 16$ Hz), 2.58 (1H, d, $J = 16$ Hz), 2.55–3.0 (3H, m), 2.45 (3H, s), 1.5–2.4 (7H, m).

Anal. Calcd. for $C_{16}H_{21}NO$: C, 78.97; H, 8.69; N, 5.75. Found: C, 78.81; H, 8.59; N, 5.69.

3,4-Dihydro-7-methoxy-1-allyl-2(1H)-naphthalenone, 1b

To a stirred solution of 7-methoxy-2-tetralone (50 g, 0.284 mol) in dry benzene (200 ml) was added during 5 min under nitrogen a solution of pyrrolidine (40.5 g, 0.5 mol) in benzene (50 ml). The mixture was heated under reflux for 1 h (5 ml of water was collected in a Dean–Stark apparatus) and after cooling, it was added cautiously under nitrogen to a solution of allyl bromide (60.5 g, 0.5 mol) in benzene (300 ml). The resulting mixture was heated under reflux for 3 h. Then water (200 ml) was added and heating resumed for another 30 min. After cooling, the benzene layer was separated, washed with water, followed by water saturated with sodium chloride, dried, and evaporated to dryness. The residue was distilled to give **1***b* (52.2 g, 85% yield); b.p. 106–112 °C/0.05 Torr; i.r. (neat) 1715 cm^{-1}; n.m.r. (CCl_4) δ 6.6–7.4 (3H, m), 4.8–6.2 (3H, m), 3.8 (3H, s), 3.3–3.6 (1H, m), 2.4–3.21 (6H, m).

Anal. Calcd. for $C_{14}H_{16}O_2$: C, 77.74; H, 7.45. Found: C, 77.47; H, 7.50.

3,4-Dihydro-1-allyl-1-(2-dimethylaminoethyl)-7-methoxy-2(1H)-naphthalenone Hydrobromide, 2b

A mixture of dry benzene (400 ml), *tert*-pentyl alcohol and sodium hydride (10.62 g of a 55% suspension in mineral oil, 0.25 mol) was heated under reflux under nitrogen until all the hydride was consumed (*ca.* 30 min). Then a solution of allyltetralone **1***b* (47.2 g, 0.22 mol) in benzene (100 ml) was added slowly while distilling off the excess of *tert*-pentanol. Another 100 ml of benzene was added and distilled off followed by dropwise addition of a solution of 2-chloro-*N*,*N*-dimethylethylamine (28 g, 0.3 mol) in benzene (100 ml). The reaction mixture was heated under reflux for 20 h, and after cooling, washed twice with water, diluted with ether, and extracted with 1 *N* hydrochloric acid. The acidic extract was warmed to 60 °C for 1 h, cooled and extracted with ether to recover after drying and evaporation of ether 15 g of allyl tetralone **1***b*. The acidic extract was cooled, made alkaline with ammonium

[6]A complete set of tables is available, at a nominal charge, from the Depository of Unpublished Data, CISTI, National Research Council of Canada, Ottawa, Canada K1A 0S2.

Can. J. Chem. Downloaded from www.nrcresearchpress.com by 210.87.254.5 on 09/05/12
For personal use only.

TABLE 4. Atomic fractional coordinates, and thermal parameters as in the expression $T = \exp[-2\pi^2(U_{11}a^{*2}h^2 + ... + 2U_{23}b^*c^*hl + ...)]$. These parameters are $\times 10^4$, and the isotropic B values are in Å^2

Atom	x	y	z	U_{11}	U_{22}	U_{33}	$2U_{23}$	$2U_{13}$	$2U_{12}$
Br	147(0)	1915(0)	2205(0)	380(2)	502(2)	445(2)	276(3)	79(3)	79(3)
C(1)	3527(2)	4181(2)	6902(4)	325(15)	286(15)	312(15)	−29(25)	71(25)	−27(25)
N(2)	3728(2)	3257(2)	6086(3)	347(13)	268(13)	320(13)	70(20)	161(21)	−11(20)
C(3)	3192(2)	2937(2)	4703(4)	425(17)	256(15)	413(17)	−37(26)	244(28)	−68(26)
C(4)	2394(2)	3478(2)	3679(4)	382(17)	300(16)	389(17)	−122(26)	53(27)	−126(26)
C(5)	1091(2)	5350(2)	1803(4)	441(19)	406(19)	441(19)	−120(30)	−64(30)	111(30)
C(6)	1118(3)	5986(2)	384(4)	630(23)	418(19)	385(18)	−115(30)	−204(32)	320(34)
C(7)	1993(3)	6386(2)	67(4)	802(25)	362(18)	300(17)	−2(29)	132(33)	255(36)
C(8)	2865(3)	6169(2)	1137(4)	624(22)	314(17)	324(17)	−35(27)	169(30)	−42(31)
C(9)	3671(2)	5192(2)	3939(4)	319(15)	288(15)	347(16)	−26(25)	139(25)	−92(25)
C(10)	3092(2)	4890(2)	5456(4)	284(14)	238(14)	283(14)	−74(23)	81(23)	−27(23)
C(11)	2138(2)	4464(2)	4461(4)	291(14)	267(15)	365(16)	−60(25)	78(24)	−58(24)
C(12)	1953(2)	5144(2)	2886(4)	379(16)	280(15)	320(15)	−108(25)	51(26)	55(26)
C(13)	2842(2)	5544(2)	2558(4)	405(17)	258(15)	325(16)	−82(24)	134(26)	37(25)
C(14)	2780(3)	4006(2)	8248(4)	576(21)	339(17)	315(16)	28(26)	267(29)	50(30)
C(15)	1768(2)	3713(2)	7328(5)	453(19)	454(19)	494(20)	90(32)	451(32)	−97(32)
C(16)	1370(2)	4348(2)	5747(4)	342(17)	392(18)	501(19)	−13(30)	255(29)	−64(28)
C(17)	4569(3)	2715(2)	6960(5)	456(20)	375(18)	494(19)	193(30)	90(31)	158(30)
O(18)	2819(1)	5729(1)	6364(3)	406(11)	278(11)	384(11)	−190(18)	135(18)	−24(18)

Atom	x	y	z	B	Atom	x	y	z	B
H(1)	4159(21)	4401(22)	7532(40)	2.8(0.7)	H(14,1)	3020(20)	3547(20)	9141(37)	2.3(0.6)
H(3)	3306(27)	2299(27)	4319(49)	4.8(0.9)	H(14,2)	2731(23)	4535(23)	8871(42)	3.1(0.7)
H(4,1)	1832(26)	3144(26)	3601(49)	4.7(0.8)	H(15,1)	1304(25)	3737(25)	8192(46)	4.5(0.8)
H(4,2)	2600(22)	3524(21)	2542(40)	2.7(0.6)	H(15,2)	1799(22)	3083(21)	6957(40)	2.8(0.6)
H(5)	491(25)	5050(26)	2043(46)	4.0(0.8)	H(16,1)	1219(24)	4960(25)	6141(45)	3.8(0.8)
H(6)	500(24)	6108(23)	−398(43)	3.5(0.7)	H(16,2)	731(23)	4069(23)	5041(42)	3.4(0.7)
H(7)	2025(32)	6857(30)	−910(58)	6.7(1.1)	H(17,1)	4424(32)	2076(29)	6693(58)	6.2(1.0)
H(8)	3456(23)	6378(23)	863(42)	3.0(0.7)	H(17,2)	4636(23)	2796(22)	8234(41)	2.9(0.7)
H(9,1)	4151(20)	5652(20)	4310(37)	2.1(0.6)	H(17,3)	5193(30)	3000(29)	6559(57)	6.1(1.0)
H(9,2)	4009(20)	4660(20)	3493(36)	2.0(0.6)	H(18)	3390(26)	5961(25)	6772(47)	4.5(0.8)

Can. J. Chem. Downloaded from www.nrcresearchpress.com by 210.87.254.5 on 09/05/12
For personal use only.

hydroxide, and extracted with ether. The extract was dried and filtered with charcoal, followed by treatment with dry hydrogen bromide to give **2***b* (33.8 g, 61.5%) as a white solid. A sample recrystallized from methanol–ether melts at 139–140 °C; i.r. (free base neat) 1710 cm^{-1}; n.m.r. (free base, CCl_4) δ 6.65–7.2 (3H, m), 4.7–5.8 (3H, m), 3.82 (3H, s), 2.0 (6H, s), 1.5–3.2 (10H, m).

Anal. Calcd. for $C_{18}H_{25}NO_2 \cdot HBr$: C, 58.69; H, 7.11; N, 3.80. Found: C, 58.63; H, 7.16; N, 3.59.

3-Bromo-3,4-dihydro-1-allyl-1-(2-dimethylaminoethyl)-7-methoxy-2(1H)-naphthalenone Hydrobromide, 3b

To a stirred solution of aminotetralone **2***b* (15 g, 41 mmol) in dichloromethane (100 ml) and THF (300 ml) was added dropwise in the dark over a period of 4 h a solution of pyrrolidone hydrotribromide (20.58 g, 41.5 mmol) in THF (300 ml). After the addition, the reaction mixture was allowed to stand overnight at room temperature, and then it was concentrated *in vacuo* and the solid residue recrystallized from 2-propanol (700 ml) to give 17.7 g (68.5%) of bromotetralone hydrobromide **3***b*; m.p. 149–150 °C; i.r. (Nujol) 1725 cm^{-1}.

Anal. Calcd. for $C_{18}H_{24}BrNO_2 \cdot HBr$: C, 48.34; H, 5.63; N, 3.13. Found: C, 48.64; H, 5.70; N, 3.14.

5-Allyl-2′-methoxy-2-methyl-9-oxo-6,7-benzomorphan Methobromide, 4b

The hydrobromide salt **3***b* (12.6 g, 28 mmol) was dissolved in ice cold water, made alkaline with ammonium hydroxide, and extracted with ether. The layers were separated as rapidly as possible, and the organic layer was concentrated *in vacuo*. The residual oil was dissolved in acetone and the solution was allowed to stand overnight. The deposited solid was collected by filtration to give 6.55 g (64%) of **4***b* containing ½ mol of water of crystallization. An analytical sample was prepared by recrystallization from 2-propanol; m.p. 175–177 °C; i.r. (Nujol) 1735 cm^{-1}; n.m.r. ($CDCl_3$–DMSO) δ 6.8–7.4 (3H, m), 5.0–6.0 (3H, m), 4.62 (1H, d, J = 4 Hz), 3.83 (3H, s), 3.77 (3H, s), 3.48 (3H, s), 1.9–4.3 (8H, m).

Anal. Calcd. for $C_{17}H_{21}NO_2 \cdot CH_3Br \cdot \frac{1}{2}H_2O$: C, 57.60; H, 6.71; N, 3.73. Found: C, 57.44; H, 6.78; N, 3.58.

5-Allyl-2′-methoxy-2-methyl-9-oxo-6,7-benzomorphan, 5b and 10-Hydroxy-6-methoxy-2-methyl-1,11-propano-9H-indeno-1,2,10,11-tetrahydro[2,1-c]-pyridine, 7b

The procedure for thermal dequaternization of **4***b* (2 g) was similar to that of **4***a* (1). The product, an oil (1.23 g) was chromatographed on a silica gel column (100 g). Elution with ether gave at first **7***b* as an oil, which was treated with dry hydrogen chloride in ether to afford 415 mg (16%) of the salt. It was purified by recrystallization from methanol–acetone; m.p. 241–243 °C; free base, m.p. 105–107 °C (from CH_2Cl_2); i.r. ($CHCl_3$) 3555, 1632 cm^{-1}; n.m.r. (CCl_4) δ 6.4–7.2 (3H, m), 5.85 (1H, d, J = 7 Hz), 3.7 (3H, s), 3.64 (1H, d, J = 7 Hz,) 3.2 (1H, d, J = 15 Hz), 3.0 (1H, unresolved m), 2.75 (3H, s), 2.31 (2H, d, J = 15 Hz), 1.3–2.3 (7H, m).

Anal. Calcd. for $C_{17}H_{21}NO_2 \cdot HCl$: C, 66.32; H, 7.20; N, 4.55. Found: C, 65.96; H, 7.27; N, 4.38.

A second product to emerge from the column was benzomorphanone **5***b* (735 mg, 50%) as an oil; i.r. (neat) 1730 cm^{-1}; n.m.r. (CCl_4) δ 6.55–7.2 (3H, m), 4.8–6.2 (3H, m), 3.75 (3H, s), 2.98–3.7 (3H, m), 2.37 (3H, s), 1.8–2.9 (3H, m), 1.56 (1H, unresolved d, J = 12 Hz). The oil was treated with an aqueous solution of oxalic acid to yield monohydrate oxalate salt, m.p. 115–120 °C with solidification and subsequent melting at 160–161 °C.

Anal. Calcd. for $C_{17}H_{24}NO_2 \cdot C_2H_2O_4 \cdot H_2O$: C, 60.15; H, 6.64; N, 3.69. Found: C, 60.52; H, 6.72; N, 3.70.

Continued elution of the column with a mixture of ether and methanol gave a small amount of the Hofmann elimination product **6***b* as judged by its n.m.r. spectrum, which was similar to that of **6***a*.

10-Hydroxy-6-methoxy-2-methyl-1,11-propano-9H-indeno-1,2,3,4,10,11-hexahydro[2,1-c]pyridine, 8b

To a solution of lithium aluminum hydride (100 mg) in dry ether, was added in small portions enamine **7***b* (450 mg) and the mixture was stirred and heated under reflux for 1 h. After work up in the usual manner, there was obtained 410 mg of **8***b* as an oil; i.r. (CCl_4) 3545, 3430 cm^{-1}; n.m.r. (CCl_4) δ 6.5–7.2 (3H, m), 3.65 (3H, s), 3.62 (1H, d, J = 15 Hz), 2.44 (3H, s), 2.33 (1H, d, J = 15 Hz), 1.5–3.1 (11H, m). A sample for analysis was purified as the hydrochloride salt by recrystallization from aqueous ethanol (80%); m.p. 270–272 °C.

Anal. Calcd. for $C_{17}H_{23}NO_2 \cdot HCl$: C, 65.90; H, 7.81; N, 4.52. Found: C, 66.04; H, 7.94; N. 4.38.

6,10-Dihydroxy-2-methyl-1,11-propano-9H-indeno-1,2,3,4,10,11-hexahydro[2,1-c]pyridine, 8c

A solution of **8***b* (546 mg, 2 mmol) in dry dichloromethane (10 ml) was added dropwise to a cooled (ice) and stirred solution of boron tribromide (1.8 g, 7.1 mmol) in dichloromethane (4 ml). The mixture was stirred at room temperature for 1 h, and then worked up in the usual manner (12) to give 420 mg (82% yield) of crude solid **8***c*; m.p. 198–204 °C. An analytical sample was prepared by recrystallization from methanol; m.p. 208–211 °C; i.r. (Nujol) 3250, 3180 cm^{-1}; n.m.r. ($CDCl_3$–DMSO) δ 6.4–7.2 (3H, m), 3.63 (1H, d, J = 15 Hz), 2.5 (1H, d, J = 15 Hz), 2.42 (3H, s), 1.5–3.0 (11H, m).

Anal. Calcd. for $C_{16}H_{21}NO_2$: C, 74.10; H, 8.16; N, 5.40. Found: C, 74.33; H, 8.11; N, 5.60.

The authors are grateful to Mrs. M. E. Pippy of NRCC for valuable assistance with the computations, and to Dr. D. N. McGregor and Dr. H. Brown of Bristol Laboratories, Syracuse, N.Y. for 100 MHz n.m.r. spectra and mass spectra respectively.

1. I. Monković. Can. J. Chem. **53**, 1189 (1975).
2. A. G. Cook. Enamines: synthesis, structure and reactions. M. Dekker, New York. 1969.
3. G. Montaudo and P. Finocchiaro. J. Org. Chem. **37**, 3434 (1972); H. Hart and G. M. Love. Tetrahedron Lett. 625 (1971).
4. G. Ostermann and U. Schollkopf. Ann. Chem. **737**, 170 (1970).
5. J. E. Baldwin, W. F. Erickson, R. E. Hackler, and R. M. Scott. Chem. Commun. 170 (1970).
6. D. C. Neckers. Mechanistic organic photo chemistry. Reinhold Publishing Company, New York. 1967. p. 166.
7. F. R. Ahmed. Crystallographic computing. Munksgaard, Copenhagen. 1970. p. 279.

8. H. P. HANSON, F. HERMAN, J. D. LEA, and S. SKILLMAN. Acta Crystallogr. **17**, 1040 (1964).
9. R. F. STEWART, E. R. DAVIDSON, and W. T. SIMPSON, J. Chem. Phys. **42**, 3175 (1965).
10. F. R. AHMED, S. R. HALL, M. E. PIPPY, and C. P. HUBER. NRCC crystallographic programs for the IBM 360 system. Accession Nos. 133–147; J. Appl. Crystallogr. **6**, 309 (1973).
11. L. PAULING. The nature of the chemical bond. Cornell University Press, Ithaca, New York. 1960. p. 260.
12. I. MONKOVIĆ, H. WONG, B. BELLEAU, I. J. PACHTER, and Y. G. PERRON. Can. J. Chem. **53**, 2515 (1975).
13. A. R. LEPLEY and A. G. GIUMANINI. *In* Mechanisms of molecular migration, Vol. 3. *Edited by* T. S. Thyagarajan. Wiley-Interscience, New York. 1971. p. 297.

Can. J. Chem. Downloaded from www.nrcresearchpress.com by 210.87.254.5 on 09/05/12
For personal use only.

Four New Sesquiterpene Analogs of Common Monoterpenes

STUART J. TERHUNE, JAMES W. HOGG, A. CHRISTINE BROMSTEIN, AND BRIAN M. LAWRENCE

Stange Canada Ltd., 3340 Orlando Drive, Mississauga, Ontario L4V 1C7

Received September 11, 1974[1]

STUART J. TERHUNE, JAMES W. HOGG, A. CHRISTINE BROMSTEIN, and BRIAN M. LAWRENCE. Can. J. Chem. **53**, 3285 (1975).

Four new sesquiterpenes: sesquithujene, *cis*-sesquisabinene hydrate, and 2-methyl-6-(*trans*-4′-methyl-4′-hydroxycyclohex-2′-enyl)-hept-2-ene (zingiberenol) from *Zingiber officinale* and sesquisabinene from *Piper nigrum* are reported. Similarities in the i.r. and n.m.r. spectra between monoterpenes and their sesquiterpene analogs are used to assist in the structural elucidation.

STUART J. TERHUNE, JAMES W. HOGG, A. CHRISTINE BROMSTEIN et BRIAN M. LAWRENCE. Can. J. Chem. **53**, 3285 (1975).

On a isolé quatre nouveaux sesquiterpènes: le sesquithujène, l'hydrate du sesquisabinène *cis* et le méthyl-2 (méthyl-4′ hydroxy-4′ cyclohexène-2′ yl *trans*)-6 heptène-2 (zingibérénol) à partir du *Zingiber officinale* et le sesquisabinène à partir du *Piper nigrum*. On a utilisé les similarités qui existent entre les spectres i.r. et r.m.n. des monoterpènes et des sesquiterpènes correspondants pour élucider les structures de ces derniers.

[Traduit par le journal]

Introduction

During the analysis of the essential oils of *Zingiber officinale* Rosc. and *Piper nigrum* L., four previously uncharacterized sesquiterpenes were isolated. It was during the analysis of the structure yielding information of these compounds that we noticed strong similarities between the i.r. and n.m.r. spectra of a given monoterpene and its corresponding sesquiterpene analog, which is obtained by the addition of an isopentylidene (3-methyl-2-butenyl) group to one of the monoterpene's geminal methyls. We will describe the nature of these similarities and show how they were used to assist in the identification of sesquisabinene, sesquithujene, *cis*-sesquisabinene hydrate, and zingiberenol.

Experimental

Dried *Zingiber officinale* rhizomes (6.7 kg) from Kerala, India were ground (60–180 mesh) and immediately steam distilled for 12 h. The resulting essential oil (130 g) was subsequently vacuum distilled through a 35 theoretical plate, spinning band column until the head and pot temperatures reached 65 and 128 °C, respectively, under a maximum vacuum of 150 μ. The distillation residue was then column chromatographed over neutral alumina (Brockman Activity II) using 30–60 petroleum ether, diethyl ether, and methanol as solvents. The sesquiterpenes, which were eluted with petroleum ether, were rechromatographed using the same three solvents, over neutral alumina which had been coated with silver nitrate (5:1 w/w). Each fraction from the silver nitrate alumina column was then analyzed by temperature programmed (60–180 °C at 4 °C/min) preparative g.l.c. using a 6 ft × ¼ in. Carbowax 20M column (19% on 80/100 Chromasorb W). If the compound collected was still impure, a 10 ft × ¼ in. SF96 column (12% on 80/100 Chromosorb W) was then used to purify it. The sesquiterpene alcohols were eluted from the alumina column with ether–methanol and rechromatographed using a silver nitrate–alumina column if further purification was necessary before preparative g.l.c. *Piper nigrum* fruits (14.6 kg) obtained from the same source were also distilled and analyzed using the above procedure.

Analytical g.l.c. was used throughout to monitor the isolation and purification of each component. This system consists of two 150 ft × 0.01 in. stainless steel capillary columns, one coated with Carbowax 6000 and the other with SF96. Temperature programming (4 °C/min 60–170 °C) and flow programming (2 p.s.i./min 15–65 p.s.i.) were used throughout.

As a precaution against unknown rearrangements occurring during steam distillation, a carbon disulphide extract of each plant was prepared at room temperature. The analytical chromatograms of these extracts were then compared with those of the steam distilled oil. During these tests, the injector and detector temperatures were lowered from 195 to 150 °C and the rate of flow programming was increased to test for possible thermal rearrangements during analytical g.l.c. Furthermore, each fractionation step was checked for possible artifacts by taking aliquots of each resulting subfraction, recombining them, and comparing the resulting chromatogram with that of the initial mixture.

The n.m.r. spectra were done at the Canadian 220 n.m.r. Centre, Ontario Research Foundation, Sheridan Park, Ontario. The solvents were either deuterated chloroform or carbon tetrachloride using TMS as an

[1]Revision received July 16, 1975.

Can. J. Chem. Downloaded from www.nrcresearchpress.com by 210.87.254.42 on 09/05/12
For personal use only.

TABLE 1. Nuclear magnetic resonance comparison of sesquithujene (**1**) and α-thujene

Sesquithujene					α-Thujene			
δ	Number of H	Multiplicity	*J* (Hz)	Inference	δ	Number of H	Multiplicity	*J* (Hz)
0.096	1	t (d × d)	3 & 3	endo cyclopropyl proton	0.0	1	t (d × d)	3 & 3
0.755	1	d × d	3 & 8	exo cyclopropyl proton	0.704	1	d × d	3 & 7.5
0.928	3	d	7	CH_3—CH<	0.905	3	d	7
—	—	—	—	CH_3—CH<	0.950	3	d	7
1.1	2	m	?	H on C5	—	—	—	—
1.31	1	m × d	8 & ?*	cyclopropyl proton	1.32	1	d × d	3 & 7.5
1.4	1	m	6–7	H on C6	—	—	—	—
—	—	—	—	$(CH_3)_2$—CH<	1.41	1	sept.	7
1.61	3	s	—	(CH_3)—C=	—	—	—	—
1.68	3	s	—	(CH_3)—C=	—	—	—	—
1.76	3	d × t	2	CH_3—C(H)=C—CH_2	1.74	3	d × t	2
2.04	2	d × t	7	H on C4	—	—	—	—
2.11	1	d × m	16 & 2	H on C8	2.12	1	d × m	17 & 2
2.38	1	d × m	16 & 2	H on C8	2.35	1	d × m	17 & 2
4.95	1	broad s	—	H on C9	4.89	1	broad s	—
5.12	1	t	7	H on C3	—	—	—	—

*Long range couplings present made accurate measurement impossible.

internal standard. The mass spectra were done with a Varian Aerograph EM-600 using an internal standard of *n*-alkyl benzenes. The infrared spectra were obtained using a Beckman IR 8 and/or a Perkin Elmer 237B on neat liquids between sodium chloride plates. Spacer thickness was varied between 0.013 and 0.05 mm in order to obtain a spectrum of reasonable definition in the fingerprint region. Polystyrene was used to calibrate the instruments. Published i.r. spectra were used as standards for the following monoterpenes: α-thujene and sabinene (1), *cis*- and *trans*-*p*-menth-2-en-1-ol (2), and *cis*- and *trans*-sabinene hydrate (3).[2]

The sesquiterpene alcohols were dehydrated using thionyl chloride in pyridine at 0 °C (4). Dehydration was also accomplished using a 6 ft × ¼ in. Carbowax 20M column isothermally at 200 °C with an injector temperature of 230 °C. All reaction products were isolated by preparative g.l.c. and were identified by their g.l.c. retention times and their i.r. spectra. For further information on the techniques used, refer to a detailed description previously published (5).

Results and Discussion

Sesquithujene (1)

When silver nitrate – alumina column chromatography was performed on the sesquiterpenes from *Zingiber officinale*, an unknown sesquiterpene hydrocarbon, **1**, (M^+ 204, $C_{15}H_{24}$) was found in the same fraction as *trans*-α-bergamotene. Since compounds with the same number and type of double bonds tend to elute together from this type of column, **1** can be suspected of having two internal double bonds.

A comparison of the n.m.r. spectra of **1** and α-thujene is given in Table 1. The addition of an isopentylidene group to one of the geminal methyls of α-thujene can be seen quite clearly: one tertiary methyl absorption in the spectrum of α-thujene (δ 0.950) is replaced with an ethano group (δ 1.1) in the spectrum of **1**. Similarly, the *gem*-dimethyl proton (δ 1.41) changes from a septet to a multiplet (δ 1.4). The isopentylidene group contributes one ethano group α to a double bond (δ 2.04), one vinyl proton (δ 5.12), and two tertiary vinyl methyls (δ 1.61 and 1.68). The remaining protons common to both structures show very similar chemical shifts and multiplicity.

After the n.m.r. spectrum was completed, the solution of **1** and deuterated chloroform –

[2]All monoterpenes named according to 'Nomenclature for Terpene Hydrocarbons' American Chemical Society, 1955.

Can. J. Chem. Downloaded from www.nrcresearchpress.com by 210.87.254.42 on 09/05/12
For personal use only.

TMS was stored in a sealed glass tube for 80 days at −10 °C. On re-examination, it was found to contain **1** (60%), β-curcumene (**2**) (37%), and aromatic curcumene (**3**) (10%). The formation of these two compounds is in agreement with the proposed structure.

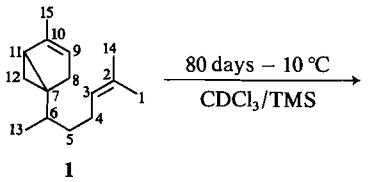

1

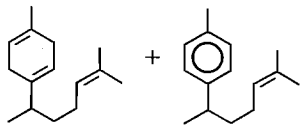

2 **3**

As with the n.m.r. spectra, the i.r. spectra of sesquithujene and α-thujene (Fig. 1) show only small and for the most part, interpretable, differences. The *gem*-dimethyl split (6) in α-thujene's i.r. spectrum (7.26 and 7.35 μ) is replaced with a single absorption at 7.25 μ in sesquithujene's spectrum. This spectrum also has two additional absorptions at 8.96 and 12.04 μ due to the isopentylidene group. The latter absorption is due to the out of plane deformation of the vinyl hydrogen (7). Based on the above information, it is proposed that sesquithujene has structure **1**.

cis-Sesquisabinene Hydrate (4)

Also isolated from the essential oil of *Zingiber officinale* was a sesquiterpene alcohol **4** (M^+ 222, $C_{15}H_{26}O$). It was found in the same alumina column fraction as α-cadinol and was purified

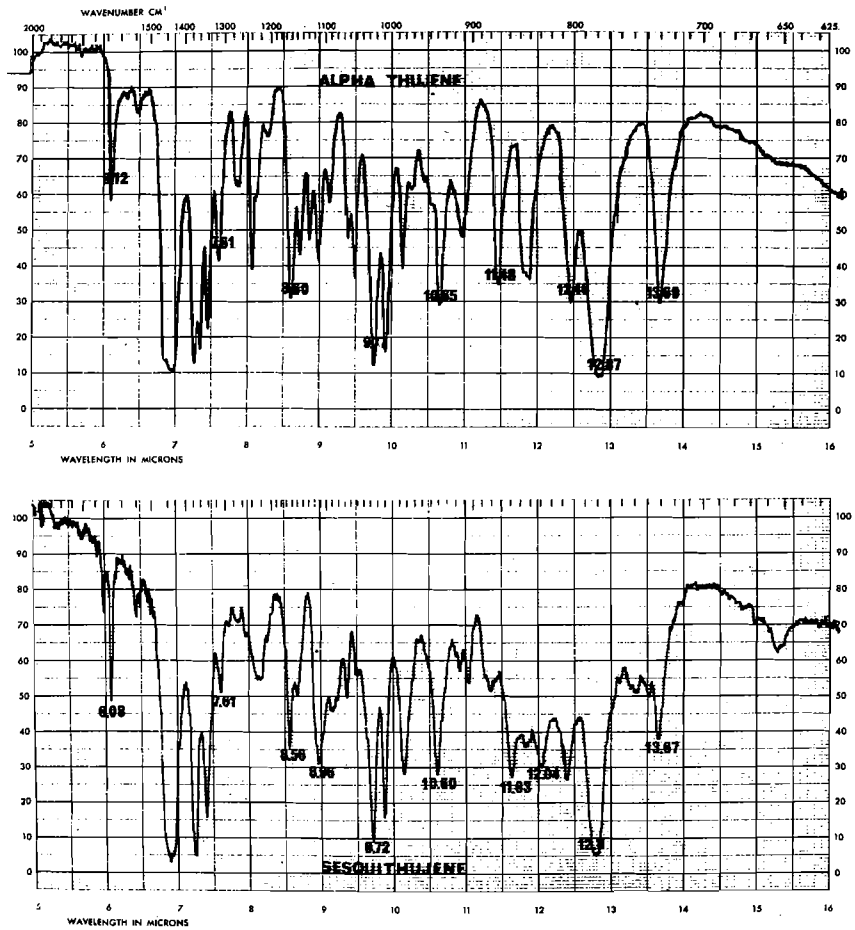

FIG. 1. The infrared spectra of α-thujene and sesquithujene.

Can. J. Chem. Downloaded from www.nrcresearchpress.com by 210.87.254.42 on 09/05/12
For personal use only.

TABLE 2. Nuclear magnetic resonance comparison of *cis*-sesquisabinene hydrate (**4**) and *cis*-sabinene hydrate

cis-Sesquisabinene hydrate					*cis*-Sabinene hydrate			
δ	Number of H	Multiplicity	*J* (Hz)	Inference	δ	Number of H	Multiplicity	*J* (Hz)
0.339	1	d × d	5 & 8	cyclopropyl H	0.318	1	d × d	5 & 8
0.732	1	d × d	4 & 5	cyclopropyl H	0.645	1	d × d	4 & 5
0.991	1	d × d	4 & 8	cyclopropyl H	1.05	1	d × d	4 & 8
—	—	—	—	CH_3—CH<	0.882	3	d	7
0.927	3	d	6	CH_3—CH<	0.926	3	d	7
1.33	3	s	—	CH_3—C(OH)<	1.32	3	s	—
1.60	3	s	—	CH_3—C=C	—	—	—	—
1.68	3	s	—	CH_3—C=C	—	—	—	—
2.00	2	d × t	7–8	CH_2—CH_2—CH=	—	—	—	—
5.09	1	t	7–8	—C=C*H*—CH_2	—	—	—	—

by g.l.c. using both the Carbowax and SF96 columns at reduced temperatures (160 °C) and increased flow (115 ml/min) to decrease the possibility of thermal dehydration.

A comparison of the n.m.r. data of **4** and *cis*-sabinene hydrate is given in Table 2. Again, the similarity in chemical shifts of common protons can be seen as well as the effect of the isopentylidene group; the loss of one geminal methyl absorption (δ 0.882), the addition of two vinyl methyl groups (δ 1.60, 1.68), one ethano group α to a double bond (δ 2.00), and a single vinyl proton (δ 5.09) are all consistent with the addition of an isopentylidene group to *cis*-sabinene hydrate. Due to absorption overlap, no definite conclusions about the *gem*-dimethyl proton or the C_5 ethano group can be drawn.

Dehydration of **4** using thionyl chloride produced **2** (45%) and **1** (40%). Thermal dehydration yielded **1** (2.8%), **2** (8.7%), zingiberene (**5**) (11%), β-sesquiphellandrene (**6**) (14%), sesquisabinene (**7**) (11%), γ-curcumene (**8**) (9.1%), and unreacted **4** (43%). The gross structure of this alcohol can thus be proposed as being the sesquiterpene analog of sabinene hydrate. The n.m.r. comparison suggests that the sesquiterpene has, in fact, *cis* stereochemistry. Further evidence in favor of this proposal can be found

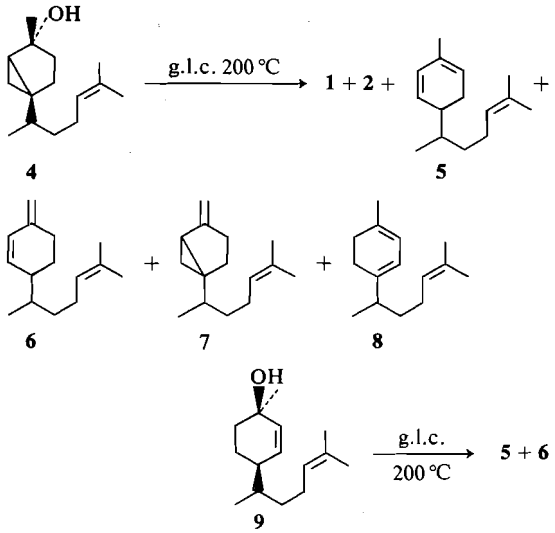

in the comparison of the i.r. spectrum of **4** with those of *cis*- and *trans*-sabinene hydrate (Fig. 2). The i.r. spectrum of **4** is virtually identical to that of *cis*-sabinene hydrate (with additional absorptions at 9.1 and 12.06 μ due to the isopentylidene group) and is considerably different from the i.r. spectrum of *trans*-sabinene hydrate. The i.r. spectrum of the sesquiterpene also shows no evidence of a *gem*-dimethyl split

Can. J. Chem. Downloaded from www.nrcresearchpress.com by 210.87.254.42 on 09/05/12
For personal use only.

Can. J. Chem. Downloaded from www.nrcresearchpress.com by 210.87.254.42 on 09/05/12
For personal use only.

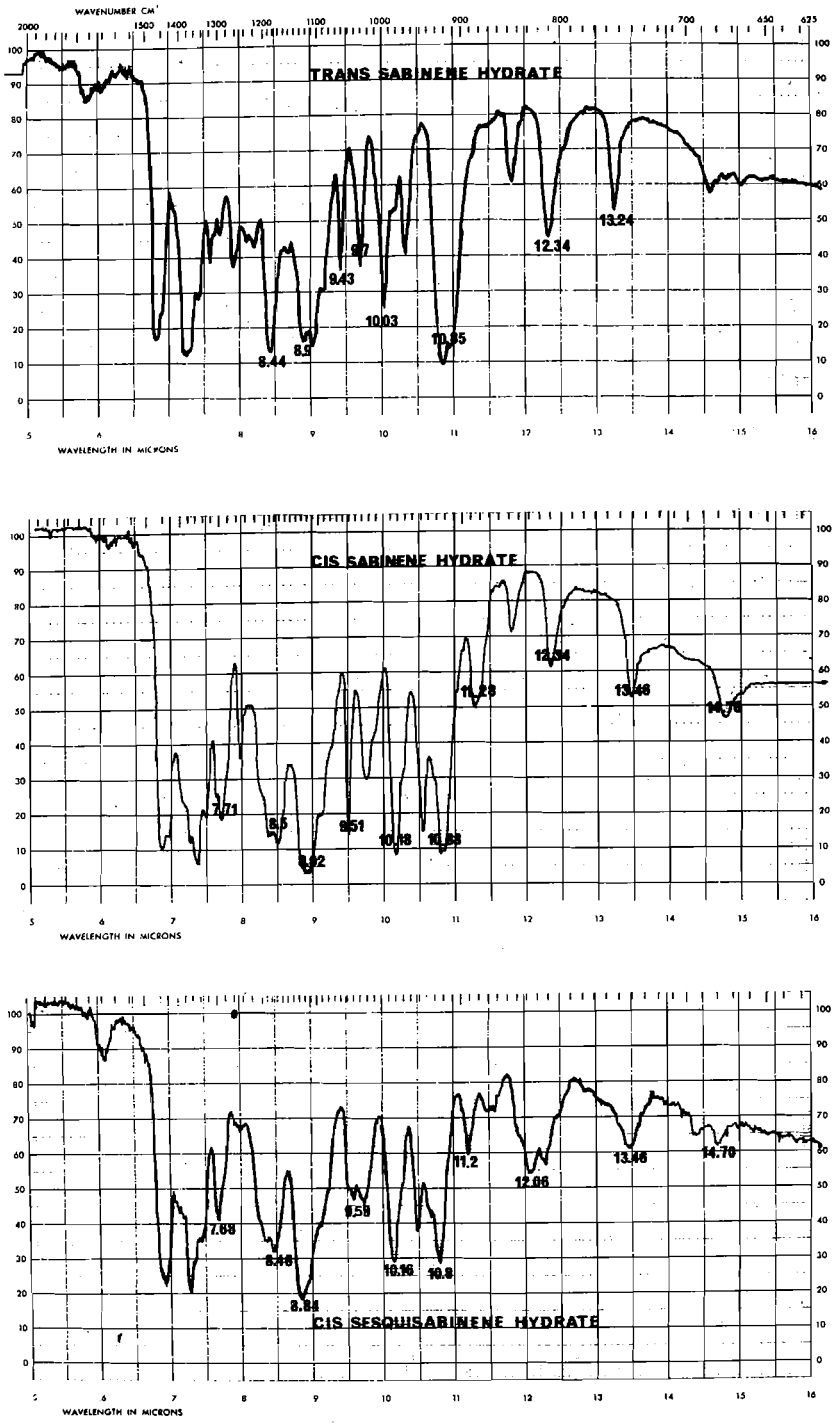

FIG. 2. The infrared spectra of *trans*-sabinene hydrate, *cis*-sabinene hydrate, and *cis*-sesquisabinene hydrate.

TABLE 3. Nuclear magnetic resonance comparison of sesquisabinene (7) and sabinene

Sesquisabinene					Sabinene			
δ	Number of H	Multiplicity	*J* (Hz)	Inference	δ	Number of H	Multiplicity	*J* (Hz)
0.628	1	d × d	8 & 4	cyclopropyl proton	0.618	2	m	?
0.728	1	d × d	4 & 4	cyclopropyl proton				
—	—	—	—	CH_3—CH<	0.882	3	d	7
0.959	3	d	7	CH_3—CH<	0.959	3	d	7
—	—	—	—	$(CH_3)_2$—CH	1.48	1	7	7
1.47	1	d × d	8 & 4	cyclopropyl proton	1.53	1	d × d	4 & 8
1.58	3	s	—	CH_3—C=	—	—	—	—
1.66	3	s	—	CH_3—C=	—	—	—	—
2.0	2	m	?	CH_2—CH_2—CH=	—	—	—	—
4.52	1	s	—	CH_2=C<	4.52	1	s	—
4.70	1	s	—	CH_2=C<	4.70	1	s	—
5.01	1	t	7–8	CH_2—CH=C<	—	—	—	—

(7.3 μ). Not shown in Fig. 2 is the typical —OH stretching absorption (3.0 μ) present in all three alcohols. The above evidence suggests that **4** has *cis* stereochemistry and is, in fact, *cis*-sesquisabinene hydrate.

Sesquisabinene (7)

Another sesquiterpene hydrocarbon **7**, (M^+ 204, $C_{15}H_{24}$) was isolated from the essential oil of *Piper nigrum* in the same silver nitrate – alumina column fraction as β-sesquiphellandrene, indicating the presence of one exocyclic and one endocyclic double bond. An examination of the n.m.r. data comparison between **7** and sabinene (Table 3) suggests that **7** is the sesquiterpene analog of sabinene. The presence of the isopentylidene group in **7** is indicated by two vinyl methyl groups (δ 1.58, 1.66) and one vinyl hydrogen at δ 5.01. Of the two additional ethano groups, the one α to the double bond is a poorly resolved multiplet at δ 2.0 and the other's location is uncertain. The remainder of the protons, common to both structures have, again, very similar chemical shifts. The i.r. comparison in Fig. 3 shows that the spectrum of **7** is similar to that of sabinene. The loss of the *gem*-dimethyl split and the two additional absorptions due to the isopentylidene group at 8.99 and 12.08 μ can be seen in the spectrum of **7**. Further structural evidence for **7** is the previously mentioned dehydration of **4**.

Zingiberenol (2-Methyl-6-(trans-4'-methyl-4'-hydroxy-cyclohex-2'-enyl)-hept-2-ene) (9)

During the analysis of the essential oil of *Zingiber officinale*, another sesquiterpene alcohol, **9** (M^+ 222, $C_{15}H_{26}O$) was found in a slightly later alumina column fraction than *cis*-sesquisabinene hydrate. As the fraction in which **9** was found was quite complex, silver nitrate – alumina column chromatography followed by preparative g.l.c. was needed to purify it. The n.m.r. data (Table 4) indicates that **9** could be the sesquiterpene analog of *cis*- or *trans-p*-menth-2-en-1-ol. The two vinyl methyls at δ 1.60 and

Can. J. Chem. Downloaded from www.nrcresearchpress.com by 210.87.254.42 on 09/05/12
For personal use only.

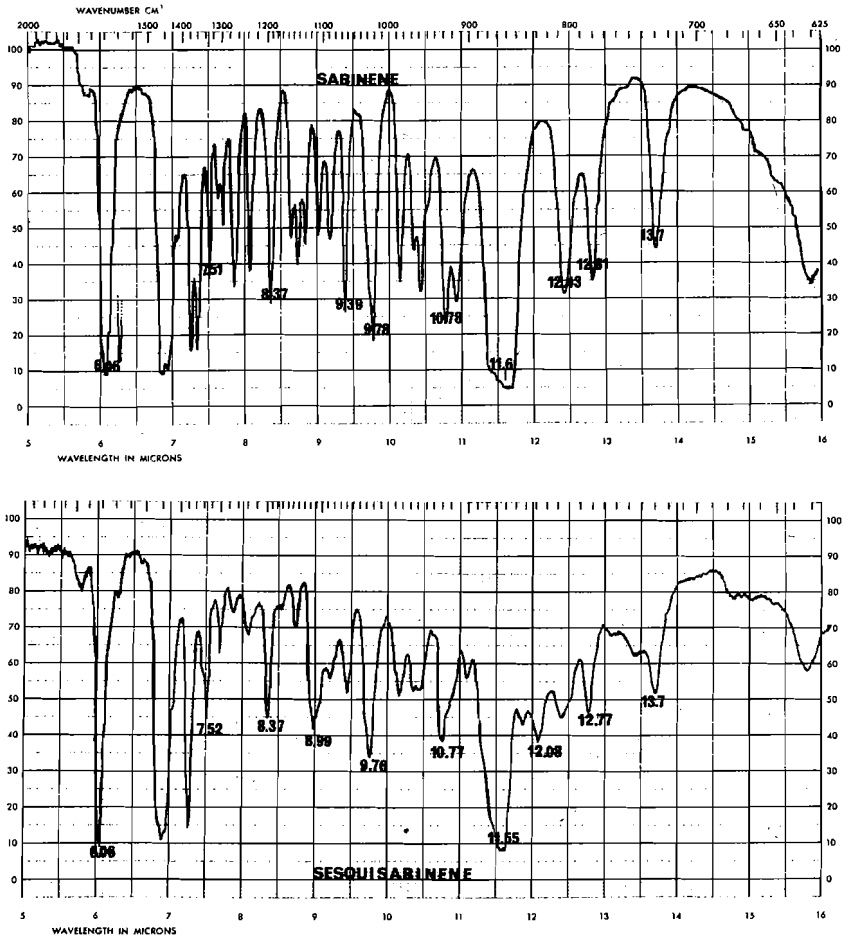

FIG. 3. The infrared spectra of sabinene and sesquisabinene.

1.68 and the vinyl hydrogen triplet at δ 5.1 are, once again, indicative of an isopentylidene group. Unfortunately, no suitable n.m.r. data for either *cis*- or *trans*-*p*-menth-2-en-1-ol could be obtained but the remaining absorptions in Table 4 are approximately what one would predict. Additional evidence for the gross structure of **9** was obtained by dehydration on g.l.c. which produced **5** (16%), **6** (20%), and unreacted **9** (60%).

To determine if **9** has *cis* or *trans* stereochemistry, a comparison of its i.r. spectrum to those of *cis*- and *trans*-*p*-menth-2-en-1-ol was made (Fig. 4). It can be seen that the i.r. spectrum of **9** is very similar to that of *trans*-*p*-menth-2-en-1-ol and it was on this evidence that the *trans* stereochemistry was assigned to **9**. Again, the loss of the *gem*-dimethyl split (7.3 μ)

TABLE 4. Nuclear magnetic resonance data of zingiberenol (**9**)

δ	Number of H	Multiplicity	*J* (Hz)	Inference
0.809	3	d	7	CH_3—CH—
1.27	3	s	—	CH_3—C(OH)—
1.60	3	s	—	CH_3—C=
1.68	3	s	—	CH_3—C=
5.1	1	broad t	6	CH_2—C*H*=C
5.53	1	broad d	11	C*H*=CH
5.63	1	broad d	11	CH=C*H*

Can. J. Chem. Downloaded from www.nrcresearchpress.com by 210.87.254.42 on 09/05/12
For personal use only.

Can. J. Chem. Downloaded from www.nrcresearchpress.com by 210.87.254.42 on 09/05/12
For personal use only.

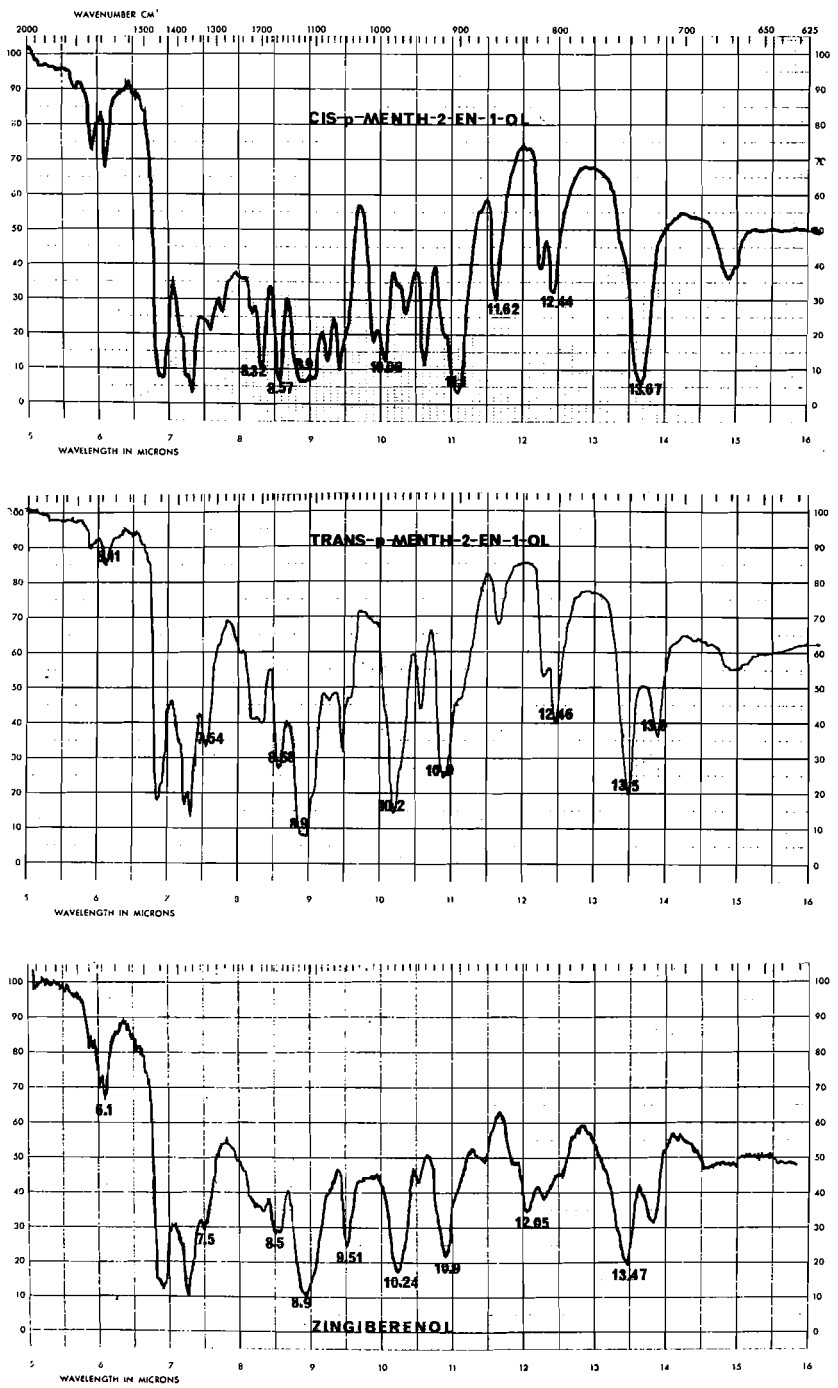

FIG. 4. The infrared spectra of *cis*-*p*-menth-2-en-1-ol, *trans*-*p*-menth-2-en-1-ol, and zingiberenol.

and the presence of the isopentylidene group (12.05 μ) can be seen in the spectrum of **9**. The additional peak at 9 μ in the spectrum of the sesquiterpene cannot be observed due to the C—O stretching absorption.

Conclusion

The effect of the isopentylidene group on the i.r. or n.m.r. spectra, when comparing analogous monoterpenes and sesquiterpenes, is usually either predictable or negligible. The i.r. spectrum of the sesquiterpene consistently contains two additional peaks of weak to moderate intensity at 9.12 ± 0.17 μ and 12.05 ± 0.1 μ. The 10–16 μ region is otherwise very similar to that of the monoterpene in both peak intensity and position. The fingerprint region, 7.5–10 μ, as expected, shows less similarity but there is generally some correlation between the two spectra. The 'geminal dimethyl split', very often present in the monoterpene spectrum, is not present in that of the sesquiterpene as no geminal dimethyl group exists. The n.m.r. spectrum of the sesquiterpene will contain easily identifiable additional absorptions due to the two vinyl methyl groups (about δ 1.6) and an extra vinyl proton which appears as a triplet (about δ 5.1). The loss of one secondary methyl absorption (monoterpene to sesquiterpene) as well as the addition of two ethano groups can also be observed.

It is generally recognized that the use of n.m.r. and particularly i.r. spectra to assign structures and even stereochemistry to unknown compounds can by no means be regarded as an absolute proof of those structures. The authors have, however, examined 29 sets of i.r. spectra of monoterpenes and their sesquiterpene analogs and have found that they all support the proposed theory. It must be emphasized that the spectra, particularly the i.r. spectra, must have absorptions of reasonable intensity and definition before any comparisons can be made.

The one remaining commonly occurring monoterpene for which the analogous sesquiterpene has not been found is car-3-ene. There are, however, many monoterpene alcohols, ketones, etc. for which analogous sesquiterpenes have not been found. It is hoped that the techniques described in this paper may aid in the identification of some of these.

1. B. M. MITZNER, E. T. THEIMER, and S. K. FREEMAN. Appl. Spectrosc. **19**, 169 (1965).
2. B. M. MITZNER, V. J. MANCINI, S. LEMBERG, and E. T. THEIMER. Appl. Spectrosc. **22**, 34 (1968).
3. J. W. DALY. Ph.D. Thesis (1958) Stanford University.
4. J. LEVISALLES and H. RUDLER. Bull. Soc. Chim. Fr. **6**, 2059 (1967).
5. B. M. LAWRENCE. Can. Inst. Food Technol. J. **4**, A 44 (1971).
6. L. J. BELLAMY. Advances in infrared group frequencies. Methuen and Co. Ltd, London. 1968. p. 9.
7. H. A. SZYMANSKI. Interpreted infrared spectra, Vol. 1. Plenum Press, New York. 1964. p. 35.

Can. J. Chem. Downloaded from www.nrcresearchpress.com by 210.87.254.42 on 09/05/12
For personal use only.

Synthèse et propriétés des pentaméthyl-2,3,3,5,5 et tétraméthyl-3,3,5,5 *N*-pipéridinométhyl-2 cyclohexanones et de leurs dérivés

JEAN-CLAUDE RICHER ET RAPHAEL ARLOTTO[1]

Département de Chimie, Université de Montréal, B.P. 6210, Montréal, Québec H3C 3V1

Reçu le 25 novembre 1974[2]

JEAN-CLAUDE RICHER et RAPHAEL ARLOTTO. Can. J. Chem. **53**, 3294 (1975).

On rapporte la préparation des méthylène-2 et butylthiométhylène-2 tétraméthyl-3,3,5,5 cyclohexanones et leur transformation en pentaméthyl-2,3,3,5,5 cyclohexanone. On rapporte aussi la synthèse de la *N*-pipéridinométhyl-2 tétraméthyl-3,3,5,5 cyclohexanone. Les propriétés des cétones ainsi que la stéréochimie de leur réduction par les hydrures complexes sont examinées.

JEAN-CLAUDE RICHER and RAPHAEL ARLOTTO. Can. J. Chem. **53**, 3294 (1975).

The preparation is reported of 2-methylene- and of 2-butylthiomethylene-3,3,5,5-tetramethylcyclohexanone as is their transformation into 2,3,3,5,5-pentamethylcyclohexanone. The synthesis of 2-*N*-piperidinomethyl-3,3,5,5-tetramethylcyclohexanone is described. The properties of the ketones as well as the stereochemistry of their reduction by complex hydrides was examined.

[Journal translation]

Introduction

Dans le cadre de nos travaux sur la réduction, par les hydrures complexes, de méthylène-2 cycloalkanones substituées (1) et sur la stéréochimie des additions sur les cétones cycliques (2), nous avons été amenés (*a*) à préparer, à titre de produits de référence, des tétraméthyl-3,3,5,5 méthylène-2 cyclohexanones (**1**) de même que quelques-uns de leurs produits de réduction comme le tétraméthyl-3,3,5,5 méthylène-2 cyclohexanol (**2***a*) et les cétones saturées (**3**) et (*b*) à examiner la stéréochimie de la réduction, par les hydrures complexes, des cétones saturées (**5**). Ce sont les résultats obtenus au cours de ces études qui font l'objet de la présente note.

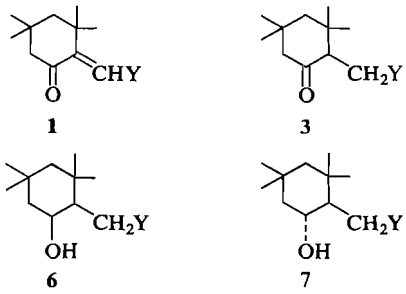

1 **3** **6** **7**

(*a*) Y = H

(*b*) Y = N

(*c*) Y = O—Bu
(*d*) Y = S—Bu
(*e*) Y = OH

Résultats et discussion

On a préparé l'hydroxyméthylène-2 tétraméthyl-3,3,5,5 cyclohexanone (**1***e*) à l'aide de réactions connues (3) appliquées à la cétone saturée **4**. Le produit ainsi obtenu présente les caractéristiques qui lui ont été attribuées par Vonderwahl et Schinz (4). Le spectre r.m.n. de **1***e* ne présente à bas champ qu'un pic à 8.93 p.p.m. (J = 3 Hz) et un autre à 15.16 p.p.m. (J = 3 Hz) qui deviennent tous les deux des singulets par addition de D_2O et c'est sur la base de ces données que la forme hydroxyméthylénique est proposée; Garbisch (5) a déjà noté que des systèmes tendus favorisent ces formes. Plus récemment Barker et Bartley (6) ont suggéré que la constante de couplage *H*—O—C—*H* dépend de l'angle dièdre formé par ces protons; la constante de 3 Hz observée dans le cas présent suggèrerait que cet angle est d'environ 120°.

On peut transformer **1***e* en **1***a* en appliquant la technique de Manson et Wood (7); comme il a pu être démontré antérieurement (8) pour d'autres systèmes, **1***e* se dimérise pour donner **4**. Par ailleurs on a obtenu **1***b*, **1***c* et **1***d* en soumettant **1***e* à des réactions bien connues (9, 10); les spectres r.m.n. de ces dérivés ne montrent la présence que d'un seul proton éthylénique pour

[1]Les résultats rapportés dans cette communication sont extraits de la thèse soumise par M. Raphael Arlotto en vue de l'obtention du grade de Ph.D. (Faculté des sciences, Université de Montréal, octobre 1969.)

[2]Revision reçue le 22 juillet 1975.

Can. J. Chem. Downloaded from www.nrcresearchpress.com by 210.87.254.5 on 09/05/12
For personal use only.

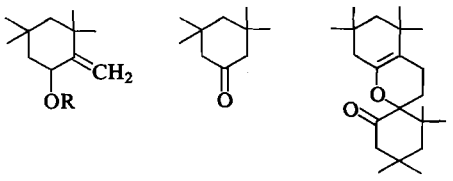

2 4 5

(*a*) R = H
(*b*) R = CO—$C_6H_4NO_2$-*p*

les composés **1***b* et **1***c* et de deux types de protons éthyléniques (rapport 0.65:0.35) pour le composé **1***d*. En se basant sur la règle d'additivité (11)

$$\delta = 5.25 + \delta\ gem + \delta\ cis + \delta\ trans$$

on a construit le tableau 1 grâce auquel on a déduit que le groupe OBu est *trans* par rapport au carbonyle et que le groupe $-NC_5H_{10}$ est *cis* par rapport au groupement carbonyle. Dans le cas du thioéther énolique, 65% du SBu serait *cis* et 35% du SBu serait *trans* par rapport au carbonyle. Le tableau 2 met en relief l'influence stérique des substituants en α de la double liaison sur la position de l'équilibre *cis–trans* autour de la double liaison de thioéthers énoliques préparés au cours des dernières années dans notre laboratoire (12–14).

TABLEAU 1. Déplacements chimiques des protons vinyliques des cétones **1**

Produits	Isomères	Calculé	Observé	Pourcentage
1*c*	*cis*	7.09	—	—
	trans	7.31	7.33	100
1*d*	*cis*	6.98	6.90	65
	trans	7.20	7.53	35
1*b*	*cis*	6.67	6.30	100
	trans	6.92	—	—

Cette observation suggère que les variations notées dans le tableau 1 relativement à la position de l'équilibre *cis–trans* autour de la double liaison sont probablement dues à des effets stériques; par exemple, la présence dans **1***d* par rapport à **1***c*, d'une grande proportion d'isomère *cis* pourrait provenir du fait que le lien C—S est plus long que le lien C—O et que le groupe SBu, par opposition au groupe OBu, peut s'accommoder plus facilement, au point de vue stérique, avec la présence de l'oxygène voisin.

Le spectre u.v. du dérivé **1***b*, déterminé dans l'éthanol 95%, montre deux bandes d'absorption: l'une à 288 nm avec log ε = 3.84 et l'autre à 356 nm avec log ε = 3.24. Si le solvant contient une trace d'acide chlorhydrique, une seule bande est observée à 288 nm avec un log ε = 3.87; cette absorption serait due à la transition $\pi \rightarrow \pi^*$ des électrons π du carbonyle et de la double liaison conjuguée. L'autre absorption qui disparait en présence d'acide serait due aux électrons du système conjugué: carbonyle, double liaison et doublet libre sur l'atome d'azote.

La réduction de la cétone **1***a*, selon la méthode de Meerwein–Pondorff–Verley (15), conduit au tétraméthyl-3,3,5,5 méthylène-2 cyclohexanol (**2***a*) qui par traitement en milieu acide chlorhydrique (10) fournit la pentaméthyl-2,3,3,5,5 cyclohexanone (**3***a*). On peut obtenir la même cétone **3***a* plus aisément par désulfurisation du thioéther énolique **1***d* en présence de nickel de Raney (10). Par ailleurs, l'hydrogénation catalytique des méthylènecétones **1***b* et **1***c* en présence de palladium à 5% sur charbon fournit les cétones saturées correspondantes **3***b* et **3***c*.

La réduction, par $LiAlH_4$, des cétones saturées **3***a* et **3***b* conduit dans le premier cas à 94% d'alcool *cis* (**6***a*) et dans le deuxième cas à 80%

TABLEAU 2. Pourcentage d'isomères *cis* et *trans*[a] présents dans diverses butylthiométhylène-2 cyclohexanones

	Isomères *trans*		Isomères *cis*	
Produits	Observé	Pourcentage	Observé	Pourcentage
Diméthyl-4,4 (réf. 14)	7.60	100	—	—
Diméthyl-5,5 (réf. 13)	7.50	100	—	—
Triméthyl-3,5,5 (réf. 12)	7.45	78.8	6.85	21.2
Tétraméthyl-3,3,5,5	7.53	35	6.90	65

[a]La notation *trans* ou *cis* se réfère à la position du groupe butylthio- par rapport au groupement carbonyle.

Can. J. Chem. Downloaded from www.nrcresearchpress.com by 210.87.254.5 on 09/05/12
For personal use only.

d'alcool *cis* (**6***b*); ces résultats impliquent que, dans chaque cas, le facteur principal influençant la stéréochimie de la réduction est la présence de méthyles axiaux en position β du centre réactionnel (16). La différence notable entre les résultats stéréochimiques obtenus, lors de la réduction de **3***a* et de **3***b*, pourrait être attribuée à la présence du groupe méthylpipéridine attaché au carbone en position 2; dans la conformation énergétiquement privilégiée, le groupe pipéridine vient masquer la face équatoriale du groupement carbonyle et force la réduction à se produire en partie par la face axiale. Ces résultats pourraient être utilisés pour déduire qu'il n'y a pas de complexation entre le réducteur et l'amine; en effet si tel était le cas, la conformation privilégiée de la chaîne latérale favoriserait une entrée encore plus grande de l'hydrure par la face équatoriale de la cétone **3***b*.

Partie expérimentale

Les techniques expérimentales générales ont déjà été rapportées (17). Les analyses par chromatographie en phase gazeuse (c.p.g.) ont été effectuées avec des chromatographes F et M, modèles 700 et 810; les conditions utilisées sont les suivantes: colonne de diglycérol à 14% avec 2% d'eau sur Chromosorb W 60–80 mesh, de 7 pieds × ¼ po; colonne de Zonyl E-7 à 10% sur Chromosorb W 60–80 mesh, lavé à l'acide et traité au diméthyldichlorosilane de 7 pieds × ¼ po; colonne de succinate de butanediol-1,4 à 10% sur Chromosorb P 60–80 mesh de 7 pieds × ¼ po; colonne d'hyprose à 15% sur Chromosorb P 30–60 mesh de 7 pieds × ¼ po; colonne de Carbowax 4000 à 10% sur Chromosorb W 60–80 lavé à l'acide et traité audi méthyldichlorosilane de 7 pieds × ¼ po; colonne de UCW-98 à 10% sur Chromosorb W 80–100 de 6 pieds × ⅛ po; le gaz vecteur utilisé est l'azote.

Méthylène-2 tétraméthyl-3,3,5,5 cyclohexanones substituées (1)

Hydroxyméthylène-2 tétraméthyl-3,3,5,5 cyclohexanone (1e)

Obtenu avec 95% de rendement, en suivant les indications de Johnson et Posvic (3), **1***e* présente les caractéristiques suivantes: p.é. 120–121 °C/24 Torr (litt.(3) p.é. 104 °C/11 Torr); n_D^{24} 1.4905 (litt.(4) n_D^{20} 1.4940); i.r. bande large entre 1640 et 1570 cm^{-1} due au carbonyle conjugué; u.v. (EtOH 95%) λ_{max} à 293 nm, log ε de 3.80; r.m.n. (CCl_4), signaux à 1.00 (singulet, deux méthyles), 1.26 (singulet, 2 méthyles), 1.43 singulet, —CH_2— en position 4), 2.11 (—CH_2— en position 6), 8.93 (doublet, J = 3 Hz., proton vinylique qui devient singulet dans D_2O) et 15.16 p.p.m. (doublet, J = 3 Hz, proton hydroxylique qui disparait dans D_2O); spectre de masse, ion moléculaire à *m/e* de 182.

Méthylène-2 tétraméthyl-3,3,5,5 cyclohexanone (1a)

Suivant la technique décrite par Manson et Wood (7), 4 g (22 mmol) de **1***e*, 16 g de carbonate de potassium et 16 ml de formaldéhyde à 37% sont agités à la température ambiante durant 30 min. L'extraction à la manière habituelle conduit, avec un rendement de 85%, à **1***a* qui présente les caractéristiques suivantes: p.é. 48 °C/0.05 Torr; n_D^{26} 1.4670; i.r. bandes à 1690 (carbonyle conjugué), 1610–1580 (double liaison) et 930 cm^{-1} (méthylène exocyclique); u.v. (EtOH 95%) λ_{max} à 230 nm et log ε = 3.69; r.m.n. (CCl_4) signaux à 1.01 (singulet, deux méthyles), 1.22 (singulet, deux méthyles), 1.60 (singulet, —CH_2— en position 4), 2.26 (singulet, —CH_2— en position 6), 5.22 (doublet, J = 1.5 Hz, proton vinylique *trans* par rapport au carbonyle) et 5.90 p.p.m. (doublet, J = 1.5 Hz, proton vinylique *cis* par rapport au groupe carbonyle); spectre de masse, ion moléculaire à *m/e* de 166.

La tétraméthyl-3,3,5,5 méthylène-2 cyclohexanone (**1***a*) ainsi obtenue, conservée quelques jours à la température ambiante, se transforme, avec un rendement quantitatif, en un solide blanc (**5**) qui, recristallisé de l'éther de pétrole, possède les caractéristiques suivantes: p.f. 53–54 °C; p.é. 80–85 °C/0.3 Torr; i.r. bandes à 1720 (carbonyle saturé), 1680 (double liaison), 1290, 1225, 1150 et 1070 cm^{-1} (C—O); r.m.n. (CCl_4) signaux de 0.9–1.05 (8 groupes méthyles), 1.30 (singulet, deux méthylènes entre les *gem*-diméthyles), 1.4–2.0 (massif de 6 protons des trois groupes méthylènes) et 2.40 p.p.m. (quadruplet, J = 11.25 et J = 36 Hz pour le méthylène en α du carbonyle); spectre de masse, ion moléculaire à *m/e* de 332.

Butoxyméthylène-2 tétraméthyl-3,3,5,5 cyclohexanone (1c)

La réaction de 5 g de l'énol **1***e* avec 9 ml de butanol en présence d'une quantité catalytique d'acide *p*-toluènesulfonique dans 20 ml de benzène, en suivant les indications de Seifert et Schinz (9), conduit à 6.4 g (98% du rendement théorique) de l'éther **1***c* qui présente les caractéristiques suivantes: p.é. 120 °C/0.7 Torr: n_D^{27} 1.4798; i.r. bandes à 1670 (carbonyle conjugué) et 1577 cm^{-1} (double liaison); u.v. (EtOH 95%) λ_{max} à 278 nm et log ε = 4.19; r.m.n. (CCl_4) signaux à 1.00 (singulet, trois méthyles), 1.26 (deux méthyles), 1.50 (singulet, —CH_2— en position 4), 2.04 (singulet, —CH_2— en position 6) et 7.33 p.p.m. (singulet, proton vinylique); spectre de masse, ion moléculaire à *m/e* de 238.

Butylthiométhylène-2 tétraméthyl-3,3,5,5 cyclohexanone (1d)

Ce dérivé est préparé avec un rendement de 93% en suivant la méthode décrite par Ireland et Marshall (10); il se présente sous forme de liquide de p.é. 130 °C/0.4 Torr; n_D^{27} 1.5245; i.r. bandes à 1665 (carbonyle conjugué) et 1520 cm^{-1} (double liaison); u.v. (EtOH 95%) λ_{max} à 320 nm et log ε = 4.33; r.m.n. (CCl_4) signaux à 1.07 (singulet, trois méthyles), 1.23 (singulet, deux méthyles), 2.10 et 2.19 (singulets d'intensités relatives 0.35:0.65 dus aux —CH_2— *syn* et *anti* en position 6) et 6.90 et 7.53 p.p.m. (singulets d'intensités relatives de 0.65 et 0.35, dus aux protons vinyliques des isomères *cis* et *trans* autour de la double liaison); spectre de masse, ion moléculaire à *m/e* de 254.

N-Pipéridinométhylène-2 tétraméthyl-3,3,5,5 cyclohexanone (1b)

Préparé avec un rendement de 75% par action de la pipéridine sur l'énol **1***e* en présence d'acide *p*-toluènesulfonique et de benzène, ce dérivé se présente sous

Can. J. Chem. Downloaded from www.nrcresearchpress.com by 210.87.254.5 on 09/05/12
For personal use only.

Can. J. Chem. Downloaded from www.nrcresearchpress.com by 210.87.254.5 on 09/05/12
For personal use only.

forme de solide de p.f. 73–74 °C; p.é. 135 °C/0.5 Torr; i.r. bandes à 1620 (carbonyle conjugué) et 1515 cm^{-1} (double liaison); u.v. (EtOH 95%) λ_{max} à 288 (log ε de 3.84) et 356 nm (log ε de 3.24) et dans EtOH 95% contenant des traces d'acide chlorhydrique, λ_{max} à 286 nm avec log ε de 3.87; r.m.n. (CCl_4) signaux à 0.97 (singulet, deux méthyles), 1.17 (singulet, deux méthyles), 1.47 (singulet, —CH_2— en position 4), 1.99 (singulet, —CH_2— en position 6) et 6.30 p.p.m. (singulet, proton vinylique); spectre de masse, ion moléculaire à *m/e* de 249.

Méthylène-2 tétraméthyl-3,3,5,5 cyclohexanol (2a)

La réduction de 3 g (18 mmol) de la cétone **1***a*, par 6 g d'isopropylate d'aluminium en présence de 100 ml d'alcool isopropylique selon la méthode de Meerwein–Pondorff–Verley (15), conduit, après extractions habituelles, à 2.35 g (84% rendement) d'alcool purifié par l'intermédiaire de son *p*-nitrobenzoate (**2***b*) de p.f. 108 °C; i.r. bandes à 1725 (carbonyle de l'ester), 1640 (double liaison), 1608 et 1520 (noyau aromatique) et 880 cm^{-1} (double liaison exocyclique); r.m.n. (CCl_4), signaux à 1.02 (singulet, groupe méthyle), 1.18 (singulet, groupe méthyle), 1.27 (singulet, deux groupes méthyles), 1.40 (singulet, —CH_2— en position 4), 1.57 et 1.87 (hydrogènes en position 6), 4.91 (massif, =CH_2), 5.86 (quadruplet, J = 12 et 4.8 Hz, C*H*O—) et 8.25 p.p.m. (singulet, 4 protons aromatiques); spectre de masse, ion moléculaire à *m/e* de 317. La saponification de ce dérivé conduit à l'alcool **2***a* pur (par c.p.g. sur colonne de butanediol-1,4 succinate) de p.é. 126 °C/38 Torr; n_D^{26} 1.4758; i.r. bandes à 3350 (hydroxyle), 1640 (double liaison), 1050 (C—O) et 900 cm^{-1} (double liaison exocyclique); r.m.n. (benzène) signaux à 0.82 (singulet, groupe méthyle), 1.00 (singulet, méthyle), 1.08 (singulet, deux groupes méthyles), 1.10–2.00 (massif, méthylènes en position 4 et 6 et proton hydroxylique), 4.10–4.60 (massif, C*H*OH), 4.94 et 5.32 p.p.m. (protons vinyliques); spectre de masse, ion moléculaire à *m/e* de 168.

Pentaméthyl-2,3,3,5,5 cyclohexanones (5)

Pentaméthyl-2,3,3,5,5 cyclohexanone (5a)

Par désulfurisation de la butylthiométhylène-2 tétraméthyl-3,3,5,5 cyclohexanone (1d)—La désulfurisation de 4.4 g (17 mmol) de l'éther **1***d* par 22 g de nickel de Raney en présence de 80 ml d'éthanol en suivant les indications de Ireland et Marshall (10), conduit, après extractions habituelles, à 2.25 g (78% rendement) de la cétone désirée **5***a* de p.é. 92 °C/15 Torr; n_D^{28} 1.4538; i.r. bandes à 1705 (carbonyle) et 1375 cm^{-1} (*gem*-diméthyles); r.m.n. (100 MHz, CCl_4) signaux à 0.81 (singulet, groupe méthyle), 0.89 (doublet, J = 6.5 Hz, méthyle en position 2), 0.98 (singulet, groupe méthyle), 1.04 (singulet, deux groupes méthyles), 1.48 (quadruplet, J = 14 et 1.25 Hz, proton équatorial en position 4), 1.70 (doublet, J = 14 Hz, proton axial en position 4), 2.03 (quadruplet, J = 12.5 et 1.25 Hz, proton équatorial en position 6), 2.18 (doublet, J = 12.5 Hz, proton axial en position 6) et 2.19 p.p.m. (quadruplet, J = 6.5 Hz, proton axial en position 2); spectre de masse, ion moléculaire à *m/e* de 168. La semicarbazone de cette cétone se présente sous forme de solide de p.f. 186–188 °C; spectre de masse, ion moléculaire à *m/e* de 225. La dinitro-2,4 phénylhydrazone dérivée de **5***a* se présente sous forme de solide de p.f. 157–158 °C, r.m.n. ($CDCl_3$) signaux à 0.83 (singulet, méthyle), 0.95 (singulet, méthyle), 1.17 (singulet et doublet, trois méthyles), 1.50 (singulet, méthylène en position 4), 1.9–2.7 (multiplet, trois protons du méthylène en position 6 et du proton en position 2), 7.88 (doublet, J = 10 Hz, proton aromatique en position 6), 8.68 (quadruplet, J = 10 et 2.5 Hz, proton aromatique en position 5), 9.83 (doublet, J = 2.5 Hz, proton aromatique en position 3) et 11.10 p.p.m. (singulet du —N*H*—); spectre de masse, ion moléculaire à *m/e* de 348.

Par transposition en milieu acide du tétraméthyl-3,3,5,5 méthylène-2 cyclohexanol (2)—On chauffe à reflux, durant 70 h, une solution éthanolique de HCl à 10% et 0.5 g d'un mélange (74:26) de cétone **5***a* et d'alcool **2***a*. On obtient alors 0.45 g (90% du rendement) de cétone **5***a* chromatographiquement pure qui possède les mêmes constantes physiques et données spectrales que la cétone **5***a* obtenue dans la section précédente.

Tétraméthyl-3,3,5,5 N-pipéridinométhyl-2 cyclohexanone (5b)

L'hydrogénation de 0.5 g de cétone **1***b*, en solution dans 10 ml d'éthanol absolu en présence de 60 mg de Pd/C à 5%, conduit à 0.45 g (90% rendement) de la cétone **5***b* présentant les caractéristiques suivantes: p.f. 86.5 °C; i.r. bandes de Bohlmann à 2793, 2750 et 2705 et C=O à 1705 cm^{-1}; r.m.n. (C_6H_6) signaux à 0.71 (singulet, CH_3), 0.81 (singulet, CH_3), 0.86 (singulet, CH_3), 0.98 (singulet, CH_3), 1.27 (singulet, CH_2 en position 4), 1.20–1.70 (massif, 6 protons, —CH_2—CH_2—CH_2), 1.70–2.50 (massif, 7 protons soit CH_2—N—CH_2, CH_2—C—CH), 2.83 et 2.93 p.p.m. (N—CH_2 sous forme

ABX avec J_{AB} = 21, J_{AX} = 10 et J_{BX} = 11.2 Hz); spectre de masse, ion moléculaire à *m/e* de 251.

Butoxyméthyl-2 tétraméthyl-3,3,5,5 cyclohexanone (5c)

L'hydrogénation de 900 mg d'éther **1***c*, en solution dans 5 ml d'éthanol absolu et en présence de 60 mg de Pd/C à 5%, conduit à l'absorption d'une mole d'hydrogène et fournit 750 mg (83% rendement) de cétone **5***c* présentant les caractéristiques suivantes: p.é. 138 °C/10 Torr; n_D^{26} 1.4587; i.r. bandes à 1710 (C=O); r.m.n. (C_6H_6) signaux à 1.88 (doublet, J = 12 Hz, proton C), 2.10 (doublet, J = 12 Hz, proton D), 2.34 (quadruplet, J_{AX} = 3.91 et J_{BX} = 8.09 Hz, proton X), 2.30 (triplet, J = 6.4 Hz des hydrogènes), 3.35 (quadruplet, J_{AX} = 3.91 et J_{AB} = 9.23 Hz, proton A) et 3.83 p.p.m. (quadruplet, J_{BX} = 8.09 et J_{AB} = 9.23 Hz, proton B). Le spectre a pu être reproduit par un ordinateur à partir des données suivantes: J_{AB} = 9.23, J_{BX} = 8.09 et J_{AX} = 3.91 Hz, et δ_X = 140.75, δ_A = 201.2 et δ_B = 230.3 Hz; spectre de masse, ion moléculaire *m/e* à 240 trop peu intense pour être mesuré.

Cyclohexanols 6 et 7

Pentaméthyl-2,3,3,5,5 cyclohexanols (6a et 7a)

Réduction de la cétone 5a par $LiAlH_4$—La réduction de 0.7 g (4 mmol) de cétone **5***a* par 0.02 g (5 mmol) de $LiAlH_4$ dans 10 ml d'éther anhydre, conduit à 0.68 g (96% rendement) d'alcools correspondants qui peuvent être analysés en c.p.g. sur une colonne de Zonyl à 110 °C ou de diglycérol à 105 °C; la quantité d'alcool *cis* **6***a* est de 95 ± 1% et cet alcool est purifié par l'intermédiaire de

son *p*-nitrobenzoate qui, recristallisé dans le méthanol, présente les caractéristiques suivantes: p.f. 92 °C; i.r. bandes à 1740 (C=O) et 1285 cm^{-1} (C—O); r.m.n. (CCl_4) 0.9–1.15 (massif, cinq méthyles), 1.15–2 (massif, 5 protons), 5.40 (proton carbinolique) et 8.18 p.p.m. (massif, 4 protons aromatiques); spectre de masse, pas d'ion moléculaire; poids moléculaire (osmométrie, dans $CHCl_3$), trouvé 313 et calculé 319.

L'hydrolyse de ce dérivé conduit, avec un rendement de 90%, au pentaméthyl-2,3,3,5,5 cyclohexanol *cis* (**6***a*) pur qui, après recristallisation dans l'éther de pétrole, se présente sous forme d'aiguilles fines ayant les caractéristiques suivantes: p.f. 72 °C; p.é. 110 °C/17 Torr; i.r. bandes à 3290 (OH), 1070 et 1022 cm^{-1} (C—O); r.m.n. (100 MHz, CCl_4) signaux à 0.93–1.1 (massif, 15 protons de 5 groupes méthyles), 1.22–1.40 (massif, 5 protons), 2.90 (singulet du OH, échange avec D_2O) et 4.03 p.p.m. (octuplet, J = 4.25, 5.5 et 8.5 Hz, proton carbinolique); spectre de masse, l'ion moléculaire n'est pas observé.

Réduction de la cétone **5***a par le sodium et l'éthanol*—La cétone **5***a* (1 g 6 mmol), réduite par du sodium (1 g, 44 mmol) et 25 ml d'éthanol, conduit à 0.9 g (90% rendement) d'un mélange d'alcools dans lequel **6***a* et **7***a* sont présents dans le rapport 22:78. La chromatographie sur alumine permet d'enrichir le mélange en produit *trans* (**7***a*) qui est ensuite purifié par l'intermédiaire de son dérivé *p*-nitrobenzoate présentant les caractéristiques suivantes: p.f. 102.5–103.5 °C; i.r. bandes à 1705 (C=O) et 1205 cm^{-1} (C—O); r.m.n. (CCl_4) 0.87–1.01 (massif, 4 méthyles), 1.15 (singulet, méthyle), 1.3–2.1 (massif, 5 protons), 5.07 (proton carbinolique) et 8.22 p.p.m. (massif, 4 protons aromatiques); spectre de masse, pas d'ion moléculaire; poids moléculaire (osmométrie avec $CHCl_3$), trouvé 318 et calculé 319.

L'hydrolyse de ce dérivé conduit au pentaméthyl-2,3,3,-5,5 cyclohexanol *trans* (**7***a*) pur présentant les caractéristiques suivantes: p.f. 46 °C; p.é. 110 °C/20 Torr; i.r. bandes à 3300 (OH) et 1025 cm^{-1} (C—O); r.m.n. (100 MHz, CCl_4) pics à 0.85–1.00 (massif, 4 méthyles), 1.01 (singulet, méthyle), 1.05–1.54 (massif, 4 protons), 2.09 (singulet, OH échange avec D_2O) et 3.39 p.p.m. (proton carbinolique); spectre de masse, ion moléculaire à *m/e* de 170.

Tétraméthyl-3,3,5,5 N-pipéridinométhyl cyclohexanols **6***b et* **7***b*

Réduction de la cétone **5***b par* $LiAlH_4$—La réduction de 200 mg (0.8 mmol) de cétone **5***b*, par 120 mg (3 mmol) de $LiAlH_4$, conduit, avec un rendement quantitatif, à un mélange d'amino-alcools qui peut être analysé par c.p.g. à l'aide d'une colonne U.C.W. 98 à 170 °C; les alcools **6***b* et **7***b* sont présents dans le rapport 80:20. Deux recristallisations, dans l'éther de pétrole 30–60, permettent d'isoler l'alcool **6***b* pur présentant les caractéristiques suivantes: p.f. 62–63 °C; p.é. 160 °C/7 Torr; i.r. bandes à 3200 (OH), 2800 et 2600 (bandes de Bohlmann), 1110 et 1055 cm^{-1} (C—O); r.m.n. signal à 4.00 p.p.m. (massif du proton carbinolique); spectre de masse, ion moléculaire à *m/e* de 253.

Réduction de la cétone **5***b par le sodium dans l'éthanol*—La réduction de 2 g de cétone **5***b*, par 0.6 g de sodium en présence de 100 ml d'éthanol, fournit 2 g d'un mélange d'amino-alcools dans lequel les alcools **6***b* et **7***b* sont présents dans le rapport 14:86. On peut déduire des propriétés de ce mélange que le proton carbinolique de l'alcool *trans* **7***b* apparaît à 3.5 p.p.m.

Les auteurs remercient vivement le Conseil National de Recherches du Canada ainsi que les autorités chargées d'administrer les échanges franco-québécois pour l'aide financière accordée sous forme de bourses et d'octrois de recherches et de frais de mission.

1. J.-C. Richer et Y. Pepin. Can. J. Chem. **48**, 1226 (1970).
2. J.-C. Richer. J. Org. Chem. **30**, 324 (1965).
3. W. J. Johnson et H. Posvic. J. Am. Chem. Soc. **69**, 1391 (1947).
4. R. Vonderwahl et H. Schinz. Helv. Chim. Acta, **35**, 2368 (1952).
5. E. W. Garbisch Jr. J. Am. Chem. Soc. **85**, 1696 (1963).
6. K. M. Barker et J. P. Bartley. Tetrahedron, **24**, 1651 (1968).
7. A. J. Manson et D. Wood. J. Org. Chem. **32**, 3434 (1967).
8. C. Mannich. Chem. Ber. **74B**, 557 (1941).
9. P. Seifert et H. Schinz. Helv. Chim. Acta, **34**, 728 (1951).
10. R. E. Ireland et J. A. Marshall. J. Org. Chem. **27**, 1620 (1962).
11. U. E. Matter, C. Pascual, E. Pretsch, A. Pross, W. Simon et S. Sternhell. Tetrahedron, **25**, 691 (1969) et **25** 2023 (1969).
12. J. M. Hachey. Mémoire de maîtrise. Université de Montréal, Montréal, Québec.
13. M. Forest. Mémoire de maîtrise. Université de Montréal, Montréal, Québec. 1967.
14. D. Perelman. Mémoire de maîtrise. Université de Montréal, Montréal, Québec. 1965.
15. A. L. Wilds. *Dans* Organic reactions, Vol. II. R. Adams, *éditeur*. Wiley, New York. 1946. p. 178.
16. A. V. Kamernitzky et A. A. Akhrem. Tetrahedron, **18**, 705 (1962).
17. J.-C. Richer et C. Lamarre. Can. J. Chem. **53**, 556 (1975).

Can. J. Chem. Downloaded from www.nrcresearchpress.com by 210.87.254.5 on 09/05/12
For personal use only.

Vapor Pressures of Triethylamine + Chloroform and of Diethyl Ether + Chloroform at 298.15 K

YASH PAUL HANDA AND DAVID EDWARD JONES[1]

Department of Chemistry, University of Otago, Dunedin, New Zealand

Received April 2, 1975

YASH PAUL HANDA and DAVID EDWARD JONES. Can. J. Chem. 53, 3299 (1975).

Vapor pressures of triethylamine + chloroform and of diethyl ether + chloroform were measured at 298.15 K with a calibrated quartz spiral. The ideal associated solution model has been used to determine the equilibrium constants and standard enthalpies of formation of the complexes from the thermodynamic properties derived from the vapor pressure measurements and from earlier calorimetric measurements. These complex formation constants are compared with values obtained by calorimetric and spectroscopic methods.

YASH PAUL HANDA et DAVID EDWARD JONES. Can. J. Chem. 53, 3299 (1975).

On a mesuré, à 298.15 K et à l'aide d'une spirale en quartz calibrée, les tensions de vapeur de mélange de triéthylamine + chloroforme et d'éther éthylique + chloroforme. On a utilisé le modèle de la solution associée idéale pour déterminer les constantes d'équilibre et les enthalpies standards de formation des complexes à partir des propriétés thermodynamiques obtenues à l'aide des mesures de tension de vapeur et aussi en faisant appel à des mesures calorimétriques antérieures. On compare ces constantes de formation de complexes avec celles obtenues par des méthodes calorimétriques et spectroscopiques.

[Traduit par le journal]

Introduction

The experimental investigation of liquid mixtures which form complexes has in the past been largely the domain of spectroscopic and other nonthermodynamic measurements. Often there is evidence for complex formation in the system of interest from solid–liquid phase equilibrium studies. Recently, thermodynamic measurements (1, 2) have been used with considerable success both to supplement the results obtained independently and to improve their precision.

In particular triethylamine (A) + chloroform (B) has been studied extensively and there is considerable spectroscopic and thermodynamic evidence for the chemical reaction

$$[1] \qquad A + B = AB$$

The molar excess enthalpies (3), partial molar enthalpies of solution (4) at 298 K, and the vapor pressures (2) at 283.15 K of this system have been used in conjunction with the ideal associated solution model to determine the equilibrium constant and standard enthalpy of formation of the complex AB. The same model has been used to explain the sign of the temperature coefficient of the molar excess volume for this system and other systems containing chloroform (5).

Complete application of the theory of the ideal associated solution model to triethylamine + chloroform has not been entirely satisfactory since the vapor pressures were measured with a mercury manometer (2) and restricted in the temperature range studied. We report here the vapor pressures of triethylamine + chloroform at 298.15 K measured with an apparatus which uses a calibrated quartz spiral as the pressure sensor.

Thermodynamic and spectroscopic evidence suggests that diethyl ether (A) + chloroform (B) mixtures consist of A, B, and the complex AB. Molar excess enthalpies of ethers + chloroform at 298 K (6) have been used with the ideal associated solution model to determine the complex formation constants (7). Constant pressure liquid–vapor equilibrium results for diethyl ether + chloroform at higher temperatures were analyzed using the ideal associated solution model (7). The equilibrium constant at 298 K (obtained by extrapolation) was in good agreement with that obtained from calorimetric and spectroscopic measurements but the scatter in the experimental results precluded determination of the standard enthalpy of formation of

[1]Author to whom correspondence should be addressed.

Can. J. Chem. Downloaded from www.nrcresearchpress.com by 210.87.254.40 on 09/05/12
For personal use only.

the complex AB. We report measurements of the vapor pressures of diethyl ether + chloroform at 298.15 K.

Experimental

Materials

Chloroform and triethylamine were purified as reported previously (2).

Diethyl ether (Baker, anhydrous A.R. grade) was shaken with one-tenth its volume of a 10% (by mass) $NaHSO_3$ solution intermittently for a period of 1 h. The aqueous phase was withdrawn and the ether washed with a saturated NaCl solution containing 0.5% (by mass) NaOH. Diethyl ether was then washed initially with a saturated NaCl solution containing a small amount of H_2SO_4, and subsequently with two portions of saturated NaCl solution. Storage of diethyl ether overnight over lithium aluminum hydride was followed by refluxing for 2 h in the presence of lithium aluminum hydride and then by fractional distillation in a column of 15 theoretical plates at a reflux ratio of 20. Dry and oxygen free nitrogen was bubbled through during the treatment with lithium aluminum hydride and the distillation. The distillation apparatus was wrapped in black cloth to exclude light.

All materials were thoroughly degassed by vacuum sublimation (8) and then by successive freezing (using a Dry Ice – acetone mixture), pumping, and distillation cycles. The degassed liquids were distilled under vacuum and the middle fractions collected in preweighed ampoules. The ampoules were sealed under vacuum and stored in the dark.

Constant values of the vapor pressure of a given liquid sample resulted when successive amounts of material were distilled from it and this is good evidence for the purity of each of the liquids used.

Vapor Pressure Measurements

Vapor pressures of mixtures of known total composition and volume were measured in a vacuum system similar to one used previously (9). A quartz spiral mounted in a pressure gauge (Texas Instruments Model 145) was used as the pressure sensor. The quartz spiral was calibrated with a precision Hg manometer over the pressure range covered by each system studied. The equilibrium cell was thermostatted to 298.15 K with a probe and temperature controller (Tronac Model 40).

Material was added to the equilibrium cell from ampoules on a line external to the thermostat bath. For each system two sets of measurements were done in order to cover the entire mole fraction range with some overlap about the midregion of the mole fraction scale.

Table 1 gives a comparison of the measured and literature values of the vapor pressures of triethylamine, chloroform, and diethyl ether at 298.15 K.

TABLE 1. Vapor pressures p of pure materials at 298.15 K

Material	p (kPa)	Reference
Triethylamine	8.942	This work
	8.911	Copp and Findlay (10), extrapolated value
	8.91	Chun and Davison (11)
Chloroform	26.231	This work
	26.236	Philippe *et al.* (12)
	26.222	Boublik *et al.* (13)
Diethyl ether	71.557	This work
	71.622	Ambrose *et al.* (14)
	71.317	Boublik *et al.* (13), extrapolated value

Results

The vapor pressures p of triethylamine + chloroform and of diethyl ether + chloroform at 298.15 K are given in Table 2. Errors in the

TABLE 2. Vapor pressures of $[x_A(C_2H_5)_3N + x_BCHCl_3]$ (l) = $[y_A(C_2H_5)_3N + y_BCHCl_3]$ (g) and of $[x_A(C_2H_5)_2O + x_BCHCl_3]$ (l) = $[y_A(C_2H_5)_2O + y_BCHCl_3]$ (g) at 298.15 K

		p (kPa)				p (kPa)	
x_B	y_B	Calculated	Experimental	x_B	y_B	Calculated	Experimental
			Triethylamine + chloroform				
0.1342	0.1361	8.850	8.847	0.5211	0.7699	12.568	12.602
0.2465	0.2988	9.045	9.055	0.6023	0.8594	14.682	14.685
0.3415	0.4695	9.652	9.658	0.7085	0.9321	17.919	17.940
0.4183	0.6102	10.585	10.576	0.8374	0.9761	21.919	21.894
0.4940	0.7326	11.964	11.920	0.9281	0.9918	24.442	24.426
			Diethyl ether + chloroform				
0.1383	0.0247	61.973	61.911	0.5520	0.3445	33.080	32.964
0.2668	0.0695	52.090	52.092	0.6346	0.4797	29.805	29.768
0.3789	0.1413	43.581	43.575	0.7218	0.6321	27.596	27.588
0.4772	0.2416	37.074	37.189	0.8182	0.7885	26.391	26.416
0.5291	0.3106	34.207	34.242	0.9138	0.9023	26.090	26.139

Can. J. Chem. Downloaded from www.nrcresearchpress.com by 210.87.254.40 on 09/05/12
For personal use only.

TABLE 3. Molar mass M_k, molar volumes V_k^0, and second virial coefficients B_{kk} of the pure fluids at 298.15 K

Material	M_k (g mol^{-1})	V_k^{0a} (cm^3 mol^{-1})	$-B_{kk}^b$ (cm^3 mol^{-1})
Triethylamine	101.191	140.3	2000
Chloroform	119.378	80.7	1209
Diethyl ether	74.122	104.7	1165

[a]Reference 16.
[b]Reference 17.

TABLE 4. Coefficients in [3], the standard deviations of these coefficients, and standard deviations $\sigma(p)$ defined by [4]

	g_1	g_2	g_3	$\sigma(p)$ (kPa)
Triethylamine + chloroform	−3.632 ±0.012	−0.071 ±0.023	0.570 ±0.034	0.026
Diethyl ether + chloroform	−3.013 ±0.010	−0.060 ±0.021	0.306 ±0.032	0.072

TABLE 5. Molar excess thermodynamic properties of $[x_A(C_2H_5)_3N + x_BCHCl_3]$(I) and of $[x_A(C_2H_5)_2O + x_BCHCl_3]$(II) at 298 K

	$-H_m^E$ (kJ mol^{-1})		$-G_m^E$ (kJ mol^{-1})		$-TS_m^E$ (kJ mol^{-1})	
x_B	I	II	I	II	I	II
0.1	1.14	0.86	0.30	0.26	0.84	0.60
0.2	2.29	1.53	0.56	0.47	1.73	1.06
0.3	3.25	2.08	0.75	0.63	2.50	1.45
0.4	3.87	2.48	0.87	0.72	3.00	1.76
0.5	4.07	2.65	0.91	0.75	3.16	1.90
0.6	3.83	2.53	0.86	0.72	2.97	1.81
0.7	3.18	2.14	0.74	0.62	2.44	1.52
0.8	2.21	1.54	0.54	0.46	1.67	1.08
0.9	1.08	0.82	0.29	0.25	0.79	0.57

mole fractions are less than ±0.004 and those in the vapor pressures arising both from random and systematic errors in the cathetometer and from fluctuations in the thermostat are ±0.015 kPa or less.

The liquid and vapor compositions and the calculated vapor pressures in Table 2 were determined from a set of equilibrium pressures, known total amounts of each component, and known total volume of the equilibrium cell line by using a modified form of Barker's analysis (15). The properties of the pure components listed in Tables 1 and 3 were used in the analysis.

The molar excess Gibbs free energy, G_m^E of a binary mixture of mole fractions x_k (liquid) and y_k (vapor) is given by

$$[2]\quad G_m^E = \sum_k x_k[RT \ln (y_k p/x_k p_k^0) + (B_{kk} - V_k^0)(p - p_k^0) + \delta(1 - y_k)^2 p]$$

where k = A, B, and p_k^0 and V_k^0 are respectively the saturated vapor pressure and the molar volume of liquid k at temperature T. The term δ is given by $2B_{AB} - B_{AA} - B_{BB}$, where B_{kj} is a second virial coefficient.

An iterative technique (9) was used to determine the liquid and vapor compositions and the coefficients in the series

$$[3]\quad G_m^E/\text{kJ mol}^{-1} = x_A x_B \sum_{i=1}^{m} g_i(1 - 2x_B)^{i-1}$$

with x_B the mole fraction of chloroform, were

Can. J. Chem. Downloaded from www.nrcresearchpress.com by 210.87.254.40 on 09/05/12
For personal use only.

adjusted to minimize the difference in the observed and calculated pressures. Use of reasonable estimates (18) for B_{AB}, the cross virial coefficient of the mixture, had no significant effect on the calculated values for G_m^E, hence the results given in Table 2 are obtained by setting δ equal to zero.

The results for both systems were fitted satisfactorily using $m = 3$ in [3] and the coefficients g_i and their respective standard deviations are listed in Table 4. Included in Table 4 are the values of $\sigma(p)$ the standard deviation in the vapor pressure given by

$$[4] \qquad \sigma(p) = \{\sum(\Delta p)^2/(N - m)\}^{1/2}$$

where Δp is the deviation of the calculated from the observed vapor pressure and N is the number of experimental points. The calculated liquid and vapor compositions and vapor pressures listed in Table 2 were determined using the values of g_i given in Table 4.

The values of G_m^E obtained from our vapor pressure measurements at 298.15 K were combined with published values of the molar excess enthalpy, H_m^E at 298 K (3, 6) to give TS_m^E at 298 K, where S_m^E is the molar excess entropy. Table 5 lists the excess thermodynamic properties of triethylamine + chloroform and of diethyl ether + chloroform at 298 K.

Discussion

With the notation given in Table 6 the equilibrium constant K for [1] can be expressed as

$$[5] \qquad K = r(1 - r)/(x_A x_B - r + r^2)$$

where $r = n/(N_A + N_B)$.

Previously, McGlashan and Rastogi have shown (19) that K can be related to the activities a_A and a_B by

$$[6] \qquad K = (1 - a_A - a_B)/a_A a_B$$

which is a contracted form of the more general expression

$$[7] \qquad K_1 + K_2 a_B = (1 - a_A - a_B)/a_A a_B$$

derived for systems in which there was an additional equilibrium resulting in the formation of complex AB_2.

Expressions for molar excess thermodynamic properties X_m^E of mixtures which form complexes have been derived (1, 2) using the ideal associated solution model with the following thermodynamic cycle (p^θ = 101.325 kPa)

$$[8] \qquad \begin{array}{ccc} A(1)\,[N_A,T,p^\theta] + B(1)\,[N_B,T,p^\theta] & \xrightarrow{(N_A + N_B)\Delta X_m} & \text{Mixture}(1)\,[N_A + N_B,T,p^\theta] \\ \downarrow n\Delta X^\theta & & \uparrow \Delta X^* \\ A(1)\,[N_A - n,T,p^\theta] + B(1)\,[N_B - n,T,p^\theta] + AB(1)\,[n,T,p^\theta] & & \end{array}$$

where X is any extensive thermodynamic property. The notation used is summarized in Table 6.

The molar X of mixing, ΔX_m is related to the standard X of complex formation ΔX^θ by

$$[9] \qquad (N_A + N_B)\Delta X_m = n\Delta X^\theta + \Delta X^*$$

Use of the ideal associated solution model allows representation of ΔX^* by the appropriate ideal solution expression.

The equation for H_m^E has been derived previously (3) and applied to various systems (1) and will not be discussed here. The following expressions were obtained for G_m^E and S_m^E (2)

$$[10] \qquad G_m^E = RT[x_A \ln(1 - r/x_A) + x_B \ln(1 - r/x_B) - \ln(1 - r)]$$

$$[11] \qquad S_m^E = r\Delta H^\theta/T - R[x_A \ln(1 - r/x_A) + x_B \ln(1 - r/x_B) - \ln(1 - r)]$$

The equation for V_m^E, the molar excess volume

$$[12] \qquad V_m^E = r\Delta V^\theta$$

has been applied and discussed elsewhere (5).

The methods used to calculate K and ΔH^θ have been described (2) and can be summarized as follows: (*i*) the term $(1 - a_A - a_B)/a_A a_B$ calculated from the smoothed activities, which were in turn derived from the vapor pressure results, was plotted against a_B as indicated by [7], (*ii*) [10] was solved for r and the value of r obtained was substituted in [5] to obtain K, (*iii*) values of S_m^E derived from Table 5 were used in [11] and

Can. J. Chem. Downloaded from www.nrcresearchpress.com by 210.87.254.40 on 09/05/12
For personal use only.

TABLE 6. Notation used for a liquid mixture in which [1] takes place

	A	B	AB
Stoichiometric amount	N_A	N_B	
Stoichiometric mole fraction	x_A	x_B	
Equilibrium amount	$N_A - n$	$N_B - n$	n
Equilibrium mole fraction	$(x_A - r)/(1 - r)$	$(x_B - r)/(1 - r)$	$r/(1 - r)$

TABLE 7. Complex formation constants for the triethylamine–chloroform complex at 298 K

Method	K	$-\Delta H^\theta$ (kJ mol^{-1})
Spectroscopic	3–4.7[a]	17[a]
Calorimetric	4.8 ± 2.5[a]	14.2 ± 1.1[a]
Partial molar enthalpies	3.3 ± 2.1[b]	15.8 ± 2.3[b]
Equation 7	2.50 ± 0.01 (slope = 0.16 ± 0.02)	
Equation 10	2.6 ± 0.4	
Equation 11	3.0 ± 1.0	16.4 ± 1.0

[a]Reference 3, K value of 4.7 based on n.m.r. measurements in c-C_6H_{12} solution.
[b]Reference 4.

r values were adjusted to give the most constant value of ΔH^θ over the entire mole fraction range.

The values of K and ΔH^θ (where determined) at 298 K for triethylamine + chloroform are given in Table 7. These values are compared with values previously reported and obtained by calorimetric or spectroscopic methods. With the exception of those values of K derived directly from the vapor pressure measurements there is satisfactory agreement. The low values of K which result from the use of [7] and [10] may be attributed to failings in the ideal associated solution model. A reasonable estimate of the 'physical' contribution to G_m^E would increase the value of K.

Bertrand (20) has discussed the effect of an estimation of the physical contribution on the results obtained for triethylamine + chloroform.[2] The values of K and ΔH^θ derived by application of this extension of the ideal associated solution model to the calorimetric results (3, 4) are respectively 2.0 ± 0.5 and -20.4 ± 2 kJ mol^{-1}. These values are claimed to be in better agreement with those derived from spectroscopic studies (Table 7). Use of the same values for the weighting and interaction parameters introduced by Bertrand gives a physical contribution to G_m^E of approximately 200 J mol^{-1} and $K/K_{id} = 1.4$ where K_{id} is given by [5]. The approximations involved in using (*i*) the solubility parameters to estimate the interaction parameter and (*ii*) the same weighting and interaction parameters as used for the calorimetric results indicate the qualitative nature of these calculations. The range of K values and their respective uncertainties in Table 7 includes the possible variation in K from an estimate of the physical contribution to X_m^E.

The values of K (and ΔH^θ where determined) at 298 K for diethyl ether + chloroform are summarized in Table 8. For comparison values previously obtained by spectroscopy, calorimetry, and liquid–vapor equilibrium are also listed.

Application of Bertrand's procedure (20) for estimation of the physical contribution to G_m^E

[2]We are indebted to one of the referees for bringing this paper to our attention.

Can. J. Chem. Downloaded from www.nrcresearchpress.com by 210.87.254.40 on 09/05/12
For personal use only.

TABLE 8. Complex formation constants for the diethyl ether – chloroform complex at 298 K

Method	K	$-\Delta H^0$ (kJ mol^{-1})
Spectroscopic	1.46 ± 0.04, 3.76 ± 0.10[a]	
Calorimetric	1.46 ± 0.37[a]	14.5 ± 1.2
Liquid–vapor equilibrium	1.4[a]	
Equation 7	1.91 ± 0.01 (slope = 0.12 ± 0.02)	
Equation 10	1.9 ± 0.3	
Equation 11	2.0 ± 0.5	12.6 ± 0.3

[a]Reference 7, K values of 1.46 and 3.76 based on n.m.r. measurements in CCl_4 and c-C_6H_{12} solutions respectively.

(using the solubility parameters to estimate the interaction parameter) gives qualitatively the same results as obtained for triethylamine + chloroform. In view of the magnitude of G_m^E and the effect of an estimation of the physical contribution on the value of K, the values of K obtained directly from the vapor pressure results using [7] and [10] are unexpectedly large and in direct contrast with the corresponding results for triethylamine + chloroform.

Furthermore, the values of $(\partial V_m^E/\partial T)_p$ are of opposite sign for diethyl ether + chloroform (21) and for triethylamine + chloroform (5). In the former system $(\partial V_m^E/\partial T)_p$ is positive, as expected for a system in which there is complex formation. The term involving the variation in extent of complex formation with temperature is necessarily positive and for diethyl ether + chloroform is larger in magnitude than that which includes the temperature dependence of ΔV^0, the molar volume of complex formation.

NOTE ADDED IN PROOF: Becker *et al.* (22) reported vapor pressure measurements for diethyl ether and chloroform at 298.15 K and found K = 1.742 from application of the ideal associated solution model to their results.

We acknowledge the assistance of Dr. D. V. Fenby and the financial support of the New Zealand Universities Grants Committee. Y.P.H. acknowledges the award of a Mellor Postgraduate Scholarship.

1. D. V. FENBY and L. G. HEPLER. Chem. Soc. Rev. **3**, 193 (1974).
2. Y. P. HANDA, D. V. FENBY, and D. E. JONES. J. Chem. Thermodyn. **7**, 337 (1975).
3. L. G. HEPLER and D. V. FENBY. J. Chem. Thermodyn. **5**, 471 (1973).
4. T. MATSUI, L. G. HEPLER, and D. V. FENBY. J. Phys. Chem. **77**, 2397 (1973).
5. A. CHAND, Y. P. HANDA, and D. V. FENBY. J. Chem. Thermodyn. **7**, 401 (1975).
6. L. A. BEATH and A. G. WILLIAMSON. J. Chem. Thermodyn. **1**, 51 (1969).
7. N. F. PASCO, D. V. FENBY, and L. G. HEPLER. Can. J. Chem. **52**, 2139 (1974).
8. T. N. BELL, E. L. CUSSLER, K. R. HARRIS, C. N. PEPELA, and P. L. DUNLOP. J. Phys. Chem. **72**, 4693 (1968).
9. J. SINGH and G. C. BENSON. Can. J. Chem. **46**, 1249 (1968).
10. J. L. COPP and T. J. V. FINDLAY. Trans. Faraday Soc. **56**, 13 (1960).
11. K. W. CHUN and R. R. DAVISON. J. Chem. Eng. Data, **17**, 307 (1972).
12. R. PHILIPPE, C. JAMBON, and P. CLECHET. J. Chem. Thermodyn. **5**, 431 (1973).
13. T. BOUBLIK, V. FRIED, and E. HALA. The vapour pressures of pure substances. Elsevier, Amsterdam. 1973.
14. D. AMBROSE, C. H. S. SPRAKE, and R. TOWNSEND. J. Chem. Thermodyn. **4**, 247 (1972).
15. J. A. BARKER. Aust. J. Chem. **6**, 207 (1953).
16. J. TIMMERMANS. Physico-chemical constants of pure compounds. Elsevier, New York. 1950.
17. J. H. DYMOND and E. B. SMITH. The virial coefficients of gases. Clarendon Press, Oxford. 1969.
18. J. P. O'CONNELL and J. M. PRAUSNITZ. Ind. Eng. Chem. Process Des. Dev. **6**, 245 (1967).
19. M. L. MCGLASHAN and R. P. RASTOGI. Trans. Faraday Soc. **54**, 496 (1958).
20. G. L. BERTRAND. J. Phys. Chem. **79**, 48 (1975).
21. R. BATTINO. Chem. Rev. **71**, 5 (1971).
22. F. BECKER *et al.* Z. Phys. Chem. **92**, 196 (1974).

Can. J. Chem. Downloaded from www.nrcresearchpress.com by 210.87.254.40 on 09/05/12
For personal use only.

Mechanism of Electron Capture and Hydrogen Formation by HBr Irradiated in Mixtures with C_2F_6, CO_2, and Xe

SURJIT S. NAGRA AND DAVID A. ARMSTRONG
Department of Chemistry, University of Calgary, Calgary, Alberta T2N 1N4

Received April 16, 1975

SURJIT S. NAGRA and DAVID A. ARMSTRONG. Can. J. Chem. **53**, 3305 (1975).

The gas phase ^{60}Co γ-radiolysis of HBr in mixtures with C_2F_6 and CO_2 has been studied at room temperature, using doserates determined from ionization chamber measurements. A new value of $W_{C_2F_6} = 32.7$ eV is reported, but W_{CO_2} was in agreement with earlier work. Ionization yields and hydrogen yields in the mixtures followed a linear energy partitioning equation.

The increase in the fraction of scavengable electrons with increasing pressure of buffer gas can be satisfactorily explained by enhanced moderation of the energies of subexcitation electrons. A study of the competition for thermal electrons between SF_6 and HBr indicates that the rate of electron capture by HBr maintains a second order dependence on HBr pressure over the 50 to 600 Torr range both in the presence and absence of buffer gas. There was no evidence for the collisional stabilization of HBr^{-*} by the buffer gases and it is pointed out that thermal electron capture may involve $(HBr)_2$ dimers.

SURJIT S. NAGRA et DAVID A. ARMSTRONG. Can. J. Chem. **53**, 3305 (1975).

On a étudié, à la température de la pièce, la radiolyse-γ (^{60}Co) en phase gazeuse du HBr en mélange avec C_2F_6 et du CO_2; pour ces études on a utilisé des vitesses de dose déterminés à partir de mesures de chambre à ionisation. Une nouvelle valeur de $W_{C_2F_6} = 32.7$ eV est obtenue mais la valeur de W_{CO_2} est en accord avec cette détermination lors de travaux antérieurs. Des rendements en ionisation et des rendements en hydrogène dans les mélanges suivent une équation de partitionnement d'énergie qui est linéaire.

Une augmentation dans la fraction d'électrons piégeables avec une augmentation de la pression du gaz tampon peut être expliquée facilement par une modération accrue des énergies des électrons sous-excités. Une étude de la compétition pour les électrons thermiques entre SF_6 et HBr indique que la vitesse de capture des électrons par HBr maintient une dépendance du second ordre sur la pression de HBr entre 50 et 600 Torr en présence et en absence de gaz tampon. Il n'y a pas d'indication pour une stabilisation provenant de collision de HBr^{-*} avec les gaz tampons et on indique que la capture d'électron thermique peut impliquer des dimères de $(HBr)_2$.

[Traduit par le journal]

Introduction

Electron capture reactions in HBr have previously been studied by both physical and chemical techniques. Low pressure beam experiments (ref. 1, chapt. 6) have established the existence of a resonance capture reaction

$$[1] \qquad e + HBr \rightarrow H + Br^-$$

having a peak cross section of 2.7×10^{-16} cm^2 molecule^{-1} at 0.3 eV. Chemical studies of the competition for thermal electrons between HBr and CCl_4 (2) and HBr and SF_6 (3) have demonstrated that there is a second reaction occurring at thermal or near thermal electron energies and with a rate which is second order in HBr. As in the case of related experiments with HCl (4, 5) these studies are consistent with the formation of one molecule of hydrogen per electron captured. The purpose of the present work was to extend the competition-kinetic studies to systems containing large amounts of buffer gases so that measurable electron yields could be obtained at lower HBr pressures and the effects of stabilizing 'third bodies' on the rate of capture examined. Sulfur hexafluoride was used as the electron scavenger since it does not react with hydrogen atoms (5) and the kinetics of its electron capture reactions have been extensively studied (1). Also its electron capture cross section peaks sharply near zero, making it highly selective for low energy electrons.

Hexafluoroethane, carbon dioxide, and xenon were chosen as buffer gases since they are chemically inert to thermal electrons (see refs. 1, 6–8) and cannot themselves produce hydrogen. Furthermore the radiolyses of C_2F_6 (9, 10) and

Can. J. Chem. Downloaded from www.nrcresearchpress.com by 210.87.254.6 on 09/05/12
For personal use only.

Can. J. Chem. Downloaded from www.nrcresearchpress.com by 210.87.254.6 on 09/05/12
For personal use only.

CO_2 (11, 12) have been studied and the yields and reactions of primary free radicals and ions are reasonably well understood.

The electrons were produced by irradiating the HBr – buffer gas mixture with ^{60}Co γ rays. Since the radiation ionizes and excites both the HBr and the buffer gas molecules, the product yields can also be used to obtain information concerning the partition of energy in the mixtures. For the HBr–C_2F_6 and HBr–CO_2 systems the energy partitioning was relatively straightforward and it is discussed here. For the HBr–Xe system there was concrete evidence for complex interactions between the excited species of the two components. The results dealing with this will be presented and discussed in detail elsewhere. Only the competition for thermal electrons in the HBr–Xe system is considered here.

Experimental

Materials

Hydrogen bromide (99.8% minimum purity), carbon dioxide (99.6% minimum purity), SF_6 (99.99% pure), and hexafluoroethane (99.6% pure) were all obtained from the Matheson company. The hydrogen bromide was purified by irradiation with X-rays and distillation through Cu turnings and a trap at 170 K before being stored at liquid nitrogen temperature. All other gases were condensed in liquid nitrogen and thoroughly degassed before distillation through the trap at 170 K. Middle fractions were stored in bulbs attached to the mercury free preparation line.

Apparatus and Procedure

Samples for product yield determinations were irradiated in 10 cm diameter cylindrical Pyrex cells of volume 354 cm^3 at a dose rate of $\sim 2.6 \times 10^{18}$ eV g^{-1} h^{-1} to total doses of 1 to 6×10^{18} eV g^{-1}. The cells were sealed during irradiation by Hoke high vacuum metal valves with Teflon seats. Prior to this they were filled with the required quantities of each gas measured in standard bulbs with a Wallace-Tiernan precision dial manometer.

After ^{60}Co radiolysis with an AECL γ cell 220 the condensible gases were condensed in a small liquid nitrogen trap attached to the radiation cell. Noncondensible gases were pumped into a calibrated volume and the hydrogen content established by the fall in pressure on diffusion through a heated palladium thimble as previously described (3).

Samples for ionization yield determinations were prepared on the same vacuum line and transferred to cylindrical Pyrex cells fitted with coaxial electrodes (3) and having the same 10 cm diameter as those used for product yield determinations. However, these cells had a volume of 230 ml and were irradiated at a somewhat lower dose rate of about 5.2×10^{16} eV g^{-1} h^{-1} to facilitate complete ion collection. Saturation ionization currents were obtained with a Keithly model 621 electrometer connected to the center electrode and a 0–6000 V high voltage power supply attached to the outer one. Good current–voltage plateaus, which were independent of polarity, were obtained in all cases.

Dose Rate Determinations

As in previous work with CO_2, C_2F_6, and several other gases (13, 14), plots of saturation ionization current, I^s, *vs.* pressure were linear over the range 50 to 700 Torr, see Fig. 1. The dose rate, D_m, in eV per h for each mixture in the ionization chamber was calculated from the sum of the dose rates of the two components, each taken as $(3600 I^s W/e)$, where I^s is the saturation ionization current read from Fig. 1 for the required partial pressure of the component, e is the electron charge, and W the energy required to create an ion pair in the pure component (13–15, ref. 1, Table 2.1).

The dose rates used in the determination of product yields were obtained in the following way. The total dose expected for a mixture of the same composition in the ionization chamber was calculated as described above and then multiplied by a constant factor to correct for the increased γ ray intensity. The hydrogen yield from pure HBr irradiated at the higher intensity and the known value of $G(H_2)_{HBr} = 9.8 \pm 0.1$ (5) molecules per 100 eV were used to calculate the dose rate in HBr. The intensity factor was obtained by comparing this to the dose rate in HBr in the ionization chamber calculated from the saturation ionization currents and W_{HBr}.

Results

W Values and Ionization Yields

The Bragg–Gray cavity ionization principle has been shown to hold for low atomic number gases ($Z \gtrsim 20$) in Pyrex cells irradiated by ^{60}Co γ rays under the conditions which applied in our cells (14, 15). Therefore for two such gases, with properties denoted by the subscripts 1 and 2, the W values and ionization currents per unit pressure or J values should be accurately related by the expression $W_2 = W_1 \times \overline{\rho_1^2} \times J_1/J_2$. The symbol $\overline{\rho_1^2}$ is the weighted mean stopping power ratio for the spectrum of energies of the electrons

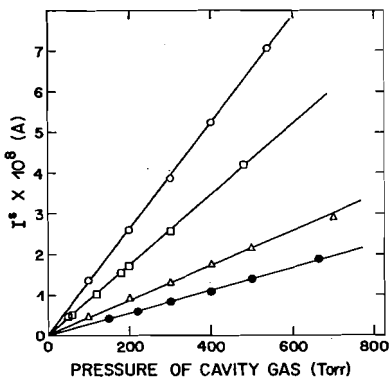

FIG. 1. Dependence of saturation ionization current (I^s) on pressure of cavity gas: ●, air; △, CO_2; □, HBr; ○, C_2F_6.

Can. J. Chem. Downloaded from www.nrcresearchpress.com by 210.87.254.6 on 09/05/12
For personal use only.

traversing the Pyrex chamber. It is equal to $S_A(BG)_1/S_A(BG)_2$ in Huyton and Woodward's notation and was obtained from their tables (14). Using air as a standard gas with $W = 33.8$ eV (ref. 1, Table 2.1) the ratios of J values in our ionization chamber gave $W_{CO_2} = 33.3$ eV and $W_{C_2F_6} = 32.7$ eV. The former value agrees within 1.5% with 32.8 recommended by Christophorou (ref. 1, Table 2.1), while $W_{C_2F_6} = 32.7$ is 9% less than 35.7 eV reported by Cooper and Mooring (13). Our value of $W_{C_2F_6}$ was used throughout the present work, both for self consistency and also because the stopping power ratios employed in the present calculation of $\overline{\rho_1^2}$ are averaged over the electron energy spectrum while Cooper and Mooring's were for 0.7 MeV electrons. W_{CO_2} and W_{HBr} were taken as 32.8 eV (ref. 1, Table 2.1) and 24.4 eV (15) respectively.

Using the dose rates, D_m, calculated for the mixtures and the observed saturation ionization currents, I_m^s, the values of the ionization yields in ion pairs per 100 eV in the mixtures were calculated from the relationship $G_m^i = 3600 I_m^s/eD_m$. They are plotted in Fig. 2 *a* and *c* as a function of Z, the stopping power fraction of HBr in the mixture. The value of Z is given by the relation $Z = (1 + \overline{\rho_{HBr}^2} P_2/P_{HBr})^{-1}$, where $\overline{\rho_{HBr}^2}$ is the ratio of the weighted mean stopping powers taken from ref. 14 and P_2 and P_{HBr} are the pressures of the added gas and HBr respectively.

Product Yields

Figure 2 *b* and *d* show values of the total hydrogen yields, G_m(total H_2), for mixtures of HBr with C_2F_6 and CO_2 plotted as a function of Z. The points on the lowest lines are values of (G_m(total H_2) $- G_m^i$) and are expected to represent the hydrogen yield from excited HBr molecules (see below).

The effects of the electron scavenger SF_6 on the hydrogen yields for C_2F_6 and CO_2 mixtures with HBr are shown in Figs. 3*a* and 4*a*. The reductions in hydrogen yield are due to the scavenging of thermal (or near thermal) electrons in [2]

$$[2] \qquad e + SF_6 \rightarrow SF_6^-$$

The competition may be described in terms of the expression $\Delta G(H_2) = G_m^s\{1 +$ (rate of e capture by HBr)/(rate of e capture by SF_6)$\}^{-1}$, where G_m^s is the yield of scavengable electrons. This can be rearranged to $(\Delta G(H_2))^{-1} = \{1 +$

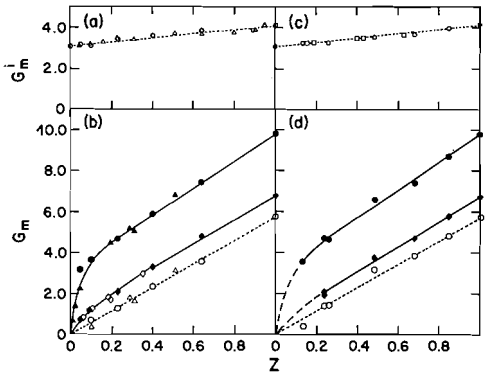

FIG. 2. Ionization yields, G_m^i, and hydrogen yields, G_m, in C_2F_6–HBr mixtures (*a* and *b*) and CO_2–HBr mixtures (*c* and *d*) plotted as a function of stopping power fraction, Z. Total pressures were: ○, ●, ◆, 600 Torr; △, ▲, ◇, 200 Torr; □, a constant pressure of 120 Torr HBr with varying pressure of buffer gas up to 900 Torr. In *b* and *d*: ●, ▲, total hydrogen yields; ◇, ◆, hydrogen yields observed in the presence of 3 mol% SF_6; ○, △, total hydrogen yields less G_m^i.

(rate of e capture by HBr)/$k_2[SF_6][e]\}/G_m^s$. Plots of $(\Delta G(H_2))^{-1}$ against $[SF_6]^{-1}$ were made for the data in Figs. 3*a* and 4*a* and the (rate of e capture by HBr)/[e] was calculated for each mixture by multiplying the ratio of the slopes to the intercepts by 2×10^{-7} cm^3 molecule^{-1} s^{-1}, which is the mean value observed for k_2 in a great variety of gases (16). The results from additional experiments with pure HBr at 360 Torr and from a mixture of 200 Torr of xenon and 50 Torr of HBr were treated similarly. The

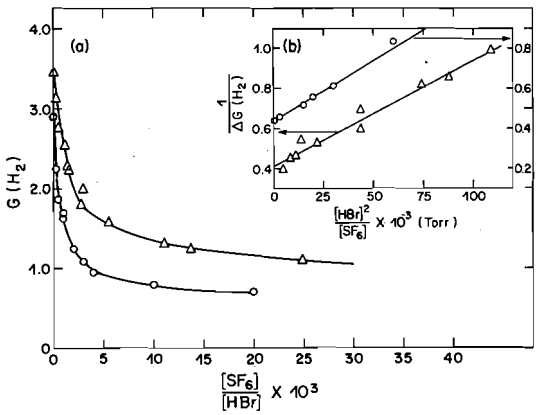

FIG. 3. Effect of SF_6 on hydrogen yields from C_2F_6–HBr mixtures (*a*) $G(H_2)$ *vs.* $[SF_6]/[HBr]$; (*b*) $1/\Delta G(H_2)$ *vs.* $[HBr]/[SF_6]$; △, 540 Torr C_2F_6 and 120 Torr HBr, dose rate = 2.89×10^{18} eV g^{-1} h^{-1}; ○, 540 Torr C_2F_6 and 60 Torr HBr, dose rate = 2.92×10^{18} eV g^{-1} h^{-1}.

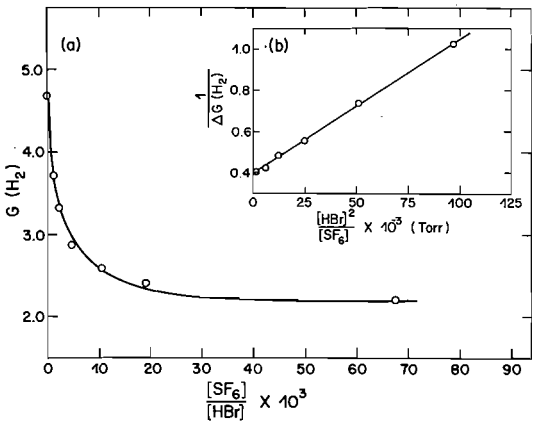

FIG. 4. Effect of SF_6 on hydrogen yields for a CO_2–HBr mixture: (*a*) $G(H_2)$ *vs.* $[SF_6]/[HBr]$; (*b*) $1/\Delta G(H_2)$ *vs.* $[HBr]^2/[SF_6]$; 540 Torr CO_2 and 120 Torr HBr, dose rate = 2.54×10^{18} eV g^{-1} h^{-1}.

data for the xenon HBr mixture are shown in Fig. 5.

Figure 6 shows a log–log plot of the rate of electron capture by HBr against the pressure of HBr. The line passing through the points for the present study was drawn with a slope of two. The earlier results of Chen and Armstrong (3) lie above it by 20% which is well within the combined uncertainties of the two measurements. It is evident from the overall behavior in Fig. 6 that the electron capture rate maintains a second order dependence on HBr pressure over the 50 to 600 Torr range, both in the presence and absence of diluent gases. The term $k_s[e][HBr]^2$

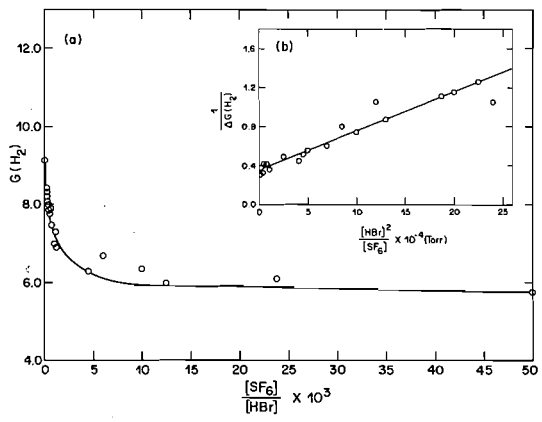

FIG. 5. Effect of SF_6 on hydrogen yields for a Xe–HBr mixture: (*a*) $G(H_2)$ *vs.* $[SF_6]/[HBr]$; (*b*) $1/\Delta G(H_2)$ *vs.* $[HBr]^2/[SF_6]$; 200-Torr Xe and 50 Torr HBr, dose rate = 2.4×10^{18} eV g^{-1} h^{-1}.

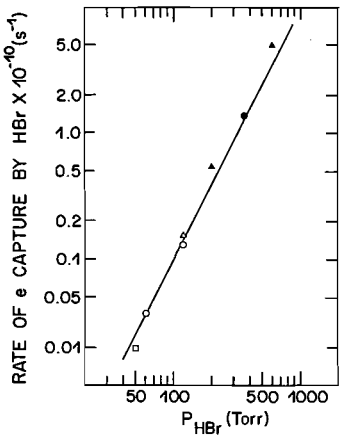

FIG. 6. Log–log plot of the rate of electron capture by HBr as a function of HBr pressure at 298 K. ▲, Data of ref. 3 for pure HBr in the 200 to 600 Torr pressure region; present data: — pure HBr; ●, HBr with buffer gases; ○, CO_2 at 540 Torr; △, C_2F_6 at 540 Torr; □, xenon at 200 Torr.

TABLE 1. Competition kinetic data for scavengable electrons

Mixture composition		$(k_s/k_2) \times 10^{22}$ (cm^3 $molecule^{-1}$) (uncertainty = ±1)
P_{HBr} (Torr)	P_2 (Torr)	
360	0	5.12
120	540(C_2F_6)	4.53
60	540(C_2F_6)	4.87
120	540(CO_2)	5.03
50	200(Xe)	3.74

was therefore substituted for (rate of e capture by HBr) to give:

$$[3] \quad (\Delta G(H_2))^{-1} = \{1 + k_s[HBr]^2/k_2[SF_6]\}/G_m^s$$

The values k_s/k_2 shown in Table 1 were then obtained from the ratios of slopes to intercepts of plots according to [3] as shown in Figs. 3*b*, 4*b*, and 5*b* for the C_2F_6, CO_2, and Xe mixtures respectively.

The diamonds in Fig. 2 *b* and *d* are hydrogen yields observed in mixtures containing 3 mol% SF_6. Except for those systems with more than 100 Torr of HBr this SF_6 concentration was sufficient to completely suppress the yield of hydrogen from thermal electrons. Corrections were made on the basis of $k_s/k_2 = 5 \times 10^{-22}$ cm^3 $molecule^{-1}$ from Table 1 where it was not. Subtraction of these yields from G_m(total H_2) therefore gives the yields of electrons scavengable by SF_6. The magnitudes of G_m^s obtained in

Can. J. Chem. Downloaded from www.nrcresearchpress.com by 210.87.254.6 on 09/05/12
For personal use only.

TABLE 2. Yields of scavengable electron

P_{CO_2}/P_{HBr}	G_m^s	G_m^i	G_m^s/G_m^i	$P_{C_2F_6}/P_{HBr}$	G_m^s	G_m^i	G_m^s/G_m^i
0.00	3.00	4.09	0.73	0.00	3.00	4.09	0.73
0.24	2.95	3.90	0.75	0.26	2.64	3.70	0.71
0.65	2.79	3.76	0.74	0.69	2.58	3.47	0.74
1.46	2.88	3.60	0.79	0.85	2.61	3.40	0.77
4.35	2.68	3.30	0.81	1.53	2.63	3.30	0.80

this way for several compositions are given in Table 2, where they are also expressed as fractions of G_m^i.

Discussion

The ionization yield in a mixture of two gases can be related to the yields in the pure components, G_1 and G_2 by the expression $G_m^i = G_1(1 + aP_2/P_1)^{-1} + G_2(1 + P_1/aP_2)^{-1}$ (17). The symbol a is an energy partition parameter and P_1 and P_2 the pressures of the two components. The mixture is said to behave ideally when a is equal to the ratio of the stopping powers, $\overline{\rho_1^2}$. This is seen to be the case within our precision of $\pm 3\%$ in Fig. 2 *a* and *c*, where the experimental points may be compared with the dashed line calculated for $a = \overline{\rho_{HBr}^2}$.

The occurrence of a linear energy partitioning in the ionization yields as in Fig. 2 *a* and *c* indicates the absence of any 'Jesse effect' and of interactions which prevent ionization of preionizing states of either component. It is also a strong indication that the electron energy degradation spectra in the mixtures are similar to those in the pure components (18), and under these circumstances one expects that the yields of products produced from excited molecules of each component should obey a linear energy partitioning expression with a similar a value. For the hydrogen yield G(ex. H_2) from excited HBr molecules the relationship would be: $G_m(\text{ex. } H_2) = G_{HBr}(\text{ex. } H_2)\{1 + \overline{\rho_{HBr}^2}P_2/P_{HBr}\}^{-1}$.

Previous studies of hydrogen formation from pure HBr at 23 °C (3) are consistent with a yield of one hydrogen molecule per electron and there is no evidence for hydrogen production in ion recombination (5). Taking the total electron yield as being equal to G^i, then G(ex. H_2) should be given by $G(\text{total } H_2) - G^i$. The bottom lines in Fig. 2 *b* and *d* are the values of G_m(ex. H_2) calculated from the relationship $G_m(\text{ex. } H_2) = \{G_m(\text{total } H_2) - G_m^i\} = \{G_{HBr}(\text{total } H_2) - G_{HBr}^i\}(1 + \overline{\rho_{HBr}^2}P_2/P_{HBr})^{-1}$, where the G terms with subscripts m and HBr refer respectively to yields in the mixtures and in pure HBr. The experimental values of $\{G_m(\text{total } H_2) - G_m^i\}$ are seen to conform to this expression.

Yields of the noncondensible products CO and O_2 from CO_2 were not separately identified and are not reported in detail. However, it may be noted that in the CO_2–HBr mixtures the total yields of noncondensible gas other than hydrogen were observed to follow a linear relationship of the form: $G_m(\text{noncondensible}) = (5.1 \pm 0.5)\{1 + P_{HBr}/\overline{\rho_{HBr}^{CO_2}}P_{CO_2}\}^{-1}$. The intercept of 5.1 ± 0.5 for pure CO_2 is consistent with values of G(CO) in the range 4.5 to 5.2 observed at low dose rates or in the presence of electron scavengers (12). Oxygen formation from atom combinations

[4] $$O(^3P) + O(^3P) \rightarrow O_2 + M$$

is probably suppressed by reactions 5 and 6:

[5] $$O(^3P) + HBr \rightarrow OH + Br$$

[6] $$OH + HBr \rightarrow H_2O + Br$$

which have rate constants of 4.4×10^{-14} and 5.1×10^{-12} cm^3 molecule^{-1} s^{-1} at 23 °C respectively (19). Radicals produced from C_2F_6 would also abstract hydrogen atoms from HBr (9). However, at low doses the products of these reactions are not expected to interfere with hydrogen formation, and no dose dependence was observed over the range employed in this work.

Reference to Fig. 2*b* shows that G_m(total H_2) rises very rapidly below $Z = 0.1$ and above $Z = 0.2$ becomes a linear function in Z, which extrapolates to G_{HBr}(total H_2) at $Z = 1.0$. This suggests that for Z between 0.2 and 1.0 all electrons form H_2. Although the data are less extensive it is evident that a similar behavior occurs with CO_2.

The fact that G^s in HBr (see Table 2) is only $\sim 73\%$ of G^i has been attributed to the occurrence of reaction 1 since the average initial

Can. J. Chem. Downloaded from www.nrcresearchpress.com by 210.87.254.6 on 09/05/12
For personal use only.

Can. J. Chem. Downloaded from www.nrcresearchpress.com by 210.87.254.6 on 09/05/12
For personal use only.

energy of subexcitation electrons in HBr (~2.5 eV (5)) far exceeds the peak energy of the reaction (~0.3 eV (1)) and also the SF_6 capture cannot compete with HBr at this energy. According to Magee and Burton (20), in pure HBr the fraction of electrons escaping capture in reaction 1 (*i.e.* (G^s/G_i)) is given by

$$[7] \qquad -\ln (G^s/G^i) = \int_{E_s}^{E_i} \frac{\sigma_c(E) \cdot dE}{\frac{\sigma_{HBr}(E) \cdot E}{\eta_{HBr}(E)}}$$

where E_i and E_s are the initial and final energies of the electrons, $\eta_{HBr}(E)$ is the mean energy lost per collision of the electron at energy E and $\sigma_c(E)$ and $\sigma_{HBr}(E)$ are the capture and total collision cross sections respectively. Since the resonance capture processes in CO_2 (1, 8) and C_2F_6 (21) occur at much higher energies than in HBr and have relatively low cross sections, the only effect of these gases on G^s/G^i should be through an increase in the number of moderating collisions giving for mixtures

$$[8] \qquad -\ln \left\{\frac{G_m{}^s}{G_m{}^i}\right\} = \int_{E_s}^{E_i} \frac{f_{HBr} \frac{\sigma_c(E)}{\sigma_{HBr}(E)} \frac{dE}{E}}{f_{HBr}\eta_{HBr}(E) + f_2\eta_2(E)}$$

Here the f refer to collision fractions, for example

$$f_{HBr} = \frac{\sigma_{HBr}(E)[HBr]}{\sigma_{HBr}(E)[HBr] + \sigma_2(E)[2]}$$

with [2] signifying the concentration of the added moderating gas. In the absence of detailed information concerning $\eta_{HBr}(E)$ and $\sigma_{HBr}(E)$ we make the assumption that they are energy independent from 0.15 to 0.7 eV where $\sigma_c(E)$ is significant. Simplifying and rearranging the above expression one then has[1]

$$[9] \qquad \frac{1}{-\ln \left\{\frac{G_m{}^s}{G_m{}^i}\right\}} = \frac{\sigma_{HBr}\eta_{HBr}}{I} + \frac{\sigma_2\eta_2}{I} \times \frac{[2]}{[HBr]}$$

in which

$$[10] \qquad I = \int_{E_s}^{E_i} \frac{\sigma_c(E)\, dE}{E}$$

A linear plot of $1/-\ln\{G_m{}^s/G_m{}^i\}$ *vs.* $[CO_2]/[HBr]$ was made from the data in Table 2. It exhibited a slope of 0.45 and an intercept of 3.2. The ratio of these leads to $\sigma_{CO_2}\eta_{CO_2}/\sigma_{HBr}\eta_{HBr} = 0.14$. From Figs. 4.37 and 4.4 of ref. 1 one can obtain $\eta_{CO_2} = 0.05$ and $\sigma_{CO_2} = 2 \times 10^{-15}$ cm^2 molecule^{-1} respectively at 0.35 eV. Therefore $\sigma_{HBr}\eta_{HBr} \sim 0.05 \times 2 \times 10^{-15}/0.14 \sim 7 \times 10^{-16}$ cm^2 molecule^{-1}, which is similar to 3×10^{-16} cm^2 molecule^{-1} for HCl calculated from earlier data (5).

Since $\sigma_{HBr}\eta_{HBr}/I = 3.2$ we find $I \sim 7 \times 10^{-16}/3.2 = 2.2 \times 10^{-16}$ cm^2 molecule^{-1}. One may evaluate I using an energy dependent cross section fitted to the data in Fig. 6.15 of ref. 1. Taking $\sigma_1 = 2 \times 10^{-16}$ for 0.15 to 0.3 eV and $2.75 \times 10^{-17}(E - 0.2)^{-1}$ for 0.3 to 0.7 eV,[2] I was calculated to be 2.4×10^{-16} cm^2 molecule^{-1} in good agreement with 2.2×10^{-16} cm^2 molecule^{-1} from the experimental data. Thus the differences between G^s and G^i and the increase in $G_m{}^s/G_m{}^i$ for increasing $[CO_2]/[HBr]$ in Table 2 can be satisfactorily explained by the occurrence of reaction 1 and by the enhanced moderation of the energies of subexcitation electrons by CO_2 molecules. A similar explanation should hold for C_2F_6, but there are at present no data on η or σ to facilitate quantitative comparisons for this molecule.

It may also be noted here that application of [9] and [10] to the capture of 'hot' electrons by SF_6 shows that fewer than 3% would be captured above 0.15 eV for $[SF_6]/[HBr] \leq 0.01$. This calculation was based on $\sigma_{HBr}\eta_{HBr} = 7 \times 10^{-16}$ cm^2 molecule^{-1} and $\sigma_2 = 3.24 \times 10^{-16} E^{-2.37}$ for the 0.15 to 0.4 eV electron energy range and $1.03 \times 10^{-16}E^{-3.6}$ for the 0.4 to 0.8 eV range. These values were obtained by trial fits to the results in Fig. 4*a* of ref. 23. Since the values of $[SF_6]/[HBr]$ used in finding k_s/k_2 in the present mixtures were normally less than 0.01 errors introduced by SF_6 competing with [1] are negligible. The values of $G_m{}^s$ obtained from hydrogen yields in mixtures with 3% SF_6 will be slightly high (~2%), but the errors are close to experimental uncertainties and also tend to compensate for the slight increase in $G_m{}^i$ caused by the addition of SF_6. Thus no corrections for them were made.

Returning to the reactions of scavengable electrons we note that the magnitudes of k_s/k_2 in Table 1 are within experimental error the same in pure HBr and in all the buffer gases except xenon. This is of interest, since the mech-

[1]This is analogous to Wolfgang's treatment of the reaction and moderation of kinetically hot atoms (see for example ref. 22).

[2]The accuracy of the fit to the overall shape of σ_1 ($= \sigma_c$) was checked by evaluating $\int_0^\infty \sigma_c(E)dE$. The result was 7.4×10^{-17} cm^2 eV, in agreement with the value in ref. 24.

Can. J. Chem. Downloaded from www.nrcresearchpress.com by 210.87.254.6 on 09/05/12
For personal use only.

anism of the overall reaction 2 is considered to be (1)

[11] $$e + SF_6 \leftrightarrows SF_6^{-*}$$

[12] $$SF_6^{-*} + M \rightarrow SF_6 + M + e$$

Thus k_2 is equal to $k_{11}k_{12}(k_{-11} + k_{12})^{-1}$, and with k_{11} being dependent on the -0.62 power of the electron kinetic energy in the thermal energy range (1), buffer gases may modify k_2 by either failing to moderate the electrons to thermal energy or by virtue of different rate constants (*i.e.*, k_{12}) for stabilizing the vibrationally excited SF_6^{-*} ion initially produced. The lower value of k_s/k_2 for the xenon–HBr mixture in Table 1 cannot be due to a smaller value of k_{12}. It may be due to incomplete thermalization of the electrons, since the inert gases are very poor moderators for electrons (25). However, if this effect is important then the capture reaction for HBr must have a stronger inverse dependence on electron energy than [11], since k_s/k_2 is *smaller* in xenon than in the other gaseous mixtures.

Actually there is reason to believe that the scavengable electrons are reacting at thermal energies for most if not all of the conditions of the present study. From a recent analysis of electron thermalization in gases Warman and Sauer (25) give a thermalization rate coefficient, K_u, of 6×10^{-9} cm^3 s^{-1} for CO_2. Thus based on the CO_2 alone the thermalization rate (*i.e.* d(electron excess kinetic energy)/dt) for the CO_2–HBr mixture in Table 1 would have been 3×10^{10} s^{-1} which is 20 times the rate of electron capture calculated from the competition with SF_6 using $k_2 = 2 \times 10^{-7}$ cm^3 molecule^{-1} s^{-1}. Measured values of K_u are not available for C_2F_6 or for HBr itself. However, for the latter one expects a somewhat higher value than for CO_2 due to (*a*) its larger dipole moment (25) and (*b*) vibrational and/or rotational excitation due to temporary negative ion formation and auto detachment (1, 26). Taking K_u for HBr = 6×10^{-9} cm^3 molecule^{-1} s^{-1} one finds minimum thermalization rates which exceed the capture rates for the mixtures in Table 1 by a factor of four or more. Only for pure HBr at 360 and 600 Torr do the calculated minimum thermalization rates approach the capture rates. The absence of marked differences in k_s/k_2 for these conditions and for the mixtures suggests that thermalization is essentially complete under all conditions, K_u for HBr being somewhat larger than for CO_2. This indeed was suggested by the preceding analysis which lead to $\sigma_{HBr}\eta_{HBr} \sim 6\sigma_{CO_2}\eta_{CO_2}$ for the 0.15 to 0.7 eV region of electron energies.

The present investigation has shown that the second order dependence on HBr of the electron capture rate persists in the presence of a five- to tenfold excess of buffer gas, and k_s/k_2 is $5 \pm 1 \times 10^{-22}$ cm^3 molecule^{-1} for all our conditions. Taking $k_2 = 2 \times 10^{-7}$ we find $k_s = 1 \times 10^{-28}$ cm^6 molecule^{-2} s^{-1}. There are two mechanisms which must be considered in attempting to explain this. One involves a transitory HBr^{-*} species:

[13] $$e + HBr \underset{k_{-13}}{\overset{k_{13}}{\rightleftarrows}} HBr^{-*}$$

[14′] $$HBr^{-*} + M \overset{k_{14}'}{\rightarrow} HBr^- + M$$

[15′] $$HBr^{-*} + M \overset{k_{15}'}{\rightarrow} HBr + M + e$$

[14] $$HBr^{-*} + HBr \overset{k_{14}}{\rightarrow} HBr^- + HBr$$

[15] $$HBr^{-*} + HBr \overset{k_{15}}{\rightarrow} 2HBr + e$$

[16] $$HBr^{-*} + HBr \overset{k_{16}}{\rightarrow} H_2 + Br_2^- \text{ or } H + Br{-}H{-}Br^-$$

[17] $$HBr^- + HBr \overset{k_{17}}{\rightarrow} H_2 + Br_2^- \text{ or } H + Br{-}H{-}Br^-$$

Since [18] is fast (5) each HBr^{-*} undergoing [16]

[18] $$H + HBr \rightarrow H_2 + Br$$

and each HBr^- consumed in [17] will eventually produce a hydrogen molecule. Hence, the rate of hydrogen formation

$$\left(\frac{d[H_2]}{dt}\right)_s$$

from scavengable electrons is given by:

$$\left(\frac{d[H_2]}{dt}\right)_s = -\frac{d[e]}{dt} = k_s[e][HBr]^2$$

$$= \frac{k_{13}\{k_{14} + k_{16} + k_{14}'[M]/[HBr]\}}{k_{-13} + (k_{14} + k_{15} + k_{16})[HBr] + (k_{14}' + k_{15}')[M]}[e][HBr]^2$$

The second order dependence on [HBr] in the absence of M requires k_{-13} to be very large, and on simplifying one obtains

$$k_s = \frac{k_{13}\{k_{14} + k_{16} + k_{14}'[M]/[HBr]\}}{k_{-13}}$$

Taking $k_{13} \simeq 10^{-7}$ cm^3 molecule^{-1} s^{-1}, $k_{14} + k_{16}$ = a typical ion–molecule rate constant of 10^{-9} cm^3 molecule^{-1} s^{-1} and $k_{-13} = 10^{12}$ s^{-1} as for O_2^{-*} (27), the value of $k_{13}(k_{14} + k_{16})/k_{-13} = 10^{-28}$ cm^6 molecule^{-2} s^{-1} in pure HBr can be rationalized. However the fact that any contribution from $k_{14}'[M]$ constituted less than the 20% uncertainty in k_s shows that k_{14}' for CO_2 is $\leq (k_{14} + k_{16})/25$ and k_{14}' for C_2F_6 is $\leq (k_{14} + k_{16})/40$. Although they do not completely vitiate it, the small magnitudes of these rate constant ratios cast considerable doubt on the possible importance of the foregoing mechanism and lead to the consideration of an alternative involving dissociative electron capture by an HBr dimer:

[19] $$HBr + HBr + M \leftrightarrows (HBr)_2 + M$$

[20] $$e + (HBr)_2 \rightarrow H + Br—H—Br^- \text{ or } H_2 + Br_2^-$$

For this mechanism $k_s = k_{20}K_{19}$ and the capture rate has no dependence on buffer gas concentration. Also the value of $k_s = 1 \times 10^{-28}$ cm^6 molecule^{-1} s^{-1} can be satisfactorily accounted for if $K_{19} = 3 \times 10^{-22}$ cm^3 molecule^{-1} as calculated from the PVT data (28, 29) for HBr, and $k_{20} \simeq 3 \times 10^{-7}$ cm^3 molecule^{-1} s^{-1}, which is comparable to k_2 and the electron capture rate constant for CCl_4 (6).

Further work will be required to establish the precise mechanism for the thermal electron capture by HBr and the application of physical techniques is clearly of great importance. However, since many physical techniques employ relatively low reagent concentrations it is important that the second order dependence of the capture rate be taken into account. For example to observe an electron half-life of 10^{-3} s one would require an HBr concentration of 3×10^{15} molecules cm^{-3} as opposed to about 3×10^9 for SF_6. Furthermore the apparent two body capture rate coefficient would be about 2×10^{-13} cm^3 molecule^{-1} s^{-1}. This is much smaller than rate coefficients previously reported for swarm and e.c.r. experiments at about this concentration (see refs. 30 and 31 and comment about them in ref. 6). It is therefore doubtful that the same capture reaction was being observed in those experiments.

This work was supported by N.R.C.C. grant number A 3571.

1. L. G. Christophorou. *In* Atomic and molecular radiation physics. Wiley, New York. 1971.
2. D. R. McCracken and D. A. Armstrong. J. Chem. Phys. **55**, 982 (1971).
3. J. D. Chen and D. A. Armstrong. J. Chem. Phys. **48**, 2310 (1968).
4. G. R. A. Johnson and J. L. Redpath. Trans. Faraday Soc. **66**, 861 (1970).
5. D. E. Wilson and D. A. Armstrong. Radiat. Res. Rev. **2**, 297 (1970).
6. F. J. Davis, R. N. Compton, and D. R. Nelson. J. Chem. Phys. **59**, 2324 (1973).
7. R. D. Hake and A. V. Phelps. Phys. Rev. **158**, 70 (1967).
8. P. J. Chantry. J. Chem. Phys. **57**, 3180 (1972).
9. R. Cooper and H. R. Haysom. J. Chem. Soc. Faraday Trans. **69**(5), 904 (1973).
10. L. Sieck, R. Gorden, and P. Ausloos. J. Res. Natl. Bur. Stand. A, **78A**, 151 (1974).
11. A. R. Anderson and D. A. Dominey. Radiat. Res. Rev. **1**, 269 (1968).
12. C. Willis and A. W. Boyd. To be published.
13. R. Cooper and R. M. Mooring. Aust. J. Chem. **21**, 2417 (1968).
14. D. W. Huyton and T. W. Woodward. Radiat. Res. Rev. **2**, 205 (1970).
15. R. S. Davidow and D. A. Armstrong. Radiat. Res. **28**, 143 (1966).
16. F. J. Davis and D. R. Nelson. Chem. Phys. Lett. **6**, 277 (1970).
17. D. W. Huyton and T. W. Woodward. J. Chem. Soc. Faraday Trans. II, **68**, 144 (1972).
18. C. E. Klots. J. Chem. Phys. **39**, 1571 (1963).
19. G. A. Takacs and G. P. Glass. J. Phys. Chem. **77**, 1182 (1973).
20. J. L. Magee and M. Burton. J. Am. Chem. Soc. **73**, 523 (1951).
21. P. W. Harland and J. L. Franklin. J. Chem. Phys. **61**, 1621 (1974).
22. R. Wolfgang. Prog. React. Kinet. **3**, 97 (1965).
23. L. G. Christophorou, D. L. McCorkle, and J. G. Carter. J. Chem. Phys. **54**, 253 (1971).
24. L. G. Christophorou and J. A. D. Stockdale. J. Chem. Phys. **48**, 1956 (1968).
25. J. M. Warman and M. C. Sauer. J. Chem. Phys. **62**, 1971 (1975).
26. R. E. Center and H.-L. Chen. J. Chem. Phys. **61**, 3785 (1974).
27. R. E. Goans and L. G. Christophorou. J. Chem. Phys. **60**, 1036 (1974).
28. O. K. Rice. Statistical mechanics, thermodynamics and kinetics. W. H. Freeman and Co., San Francisco. 1966. Chapt. 8; A. A. Passilier and N. W. Gregory. J. Phys. Chem. **72**, 2697 (1968).
29. Handbook of Chemistry and Physics. 53rd ed., CRC Press, D-146. 1973.
30. L. G. Christophorou, R. N. Compton, and H. W. Dickson. J. Chem. Phys. **48**, 1949 (1968).
31. K. G. Mothes, E. Schultes, and R. N. Schindler. J. Phys. Chem. **76**, 3758 (1972).

Can. J. Chem. Downloaded from www.nrcresearchpress.com by 210.87.254.6 on 09/05/12
For personal use only.

Can. J. Chem. Downloaded from www.nrcresearchpress.com by 210.87.254.42 on 09/05/12
For personal use only.

COMMUNICATIONS

A Differential Spectroscopic Technique for Obtaining the Spectra of Chemisorbed Molecules

M. MOSKOVITS, C. J. HOPE, and B. JANTZI

Lash Miller Laboratories and Erindale College, University of Toronto, Toronto, Ontario M5S 1A1

Received July 25, 1975

M. MOSKOVITS, C. J. HOPE, and B. JANTZI. Can. J. Chem. 53, 3313 (1975).

A technique for recording the first derivative with respect to wavelength of the infrared spectrum of a substance is described. Its use allows one to detect with enhanced sensitivity a weak spectrum superimposed upon a strong, featureless background such as is encountered in the specular reflectance spectra of monolayers adsorbed on metal surfaces. The method is illustrated by the infrared spectrum of CO adsorbed on deposited copper.

M. MOSKOVITS, C. J. HOPE et B. JANTZI. Can. J. Chem. 53, 3313 (1975).

On décrit une technique pour l'enregistrement de la première dérivée, par rapport à la longueur d'onde, du spectre infrarouge d'une substance. Son utilisation permet de détecter, avec une sensibilité accrue, un spectre faible superposé à un fond fort et sans caractéristique tel qu'on le rencontre dans les spectres de réflexion spéculaire de couches monoléculaires adsorbées sur des surfaces métalliques. On illustre la méthode par le spectre infrarouge du CO adsorbé sur du cuivre déposé.

[Traduit par le journal]

Introduction

The use of infrared spectroscopy in observing vibrations due to molecules adsorbed on metals and oxides is now well established. By far the largest part of the literature in this field has been devoted to the observation of CO, hydrogen, and olefins chemisorbed on metal particles suspended in a support material such as silica or alumina. These systems approximate, more or less, commercial catalysts and are therefore of considerable interest. The spectra obtained in these systems are, however, characteristic of the heterogeneous nature of the metal surface as a result of the distribution of surface sites on particles of various sizes. This gives rise to many bands usually coalescing into broad envelopes. The spectra are, moreover, sensitive to the nature of the support. These facts have led workers such as Pritchard and Sims (1), Tompkins and Greenler (2), and Dignam *et al.* (3) to measure the specular reflectance spectra (or as Greenler refers to them, the reflectance absorption spectra) of molecules adsorbed on metal surfaces using multiple external reflection to enhance the signal. Recently Pritchard and co-workers (4) have reported spectra of CO adsorbed on several single-crystal faces of copper obtained with one single reflection only. The study of adsorption onto single-crystal faces demands the use of single reflection spectroscopy.

Pritchard has also recently published preliminary data for CO absorbed on Cu using wavelength modulation infrared spectroscopy (5).

Infrared reflectance spectra of monolayers adsorbed on metal substrates are characterized by a large, almost featureless background on which is superimposed a weak (<2% absorbance) absorption due to the adsorbate. In order to improve the sensitivity with which one observes the adsorbate absorption one must reject the large background reflection. In this paper we describe a technique for doing this by taking the derivative of the infrared reflectance spectrum. The derivative of the slowly varying background is, of course, small compared with that of the relatively sharp absorption peaks making it easier to amplify and observe the latter. We illustrate the method with a single-reflection spectrum of CO adsorbed on polycrystalline copper.

Experimental

The apparatus is described in detail elsewhere (6). Briefly, it consists of an ion-pumped ultrahigh vacuum

system fitted with CaF_2 windows. Copper is deposited from a tantalum filament onto a Pyrex slide. The spectrometer consists of a Nernst glower source, and mirrors which focus the source radiation onto the sample; another mirror focuses the reflected light (the angle of incidence is approximately 80°) onto the slit of a Spex Minimate grating monochromator. The derivative spectrum is obtained by vibrating a sodium chloride disc about an axis parallel to the exit slit using a vibrating galvanometer in front of the exit slit of the monochromator. The dispersed bean is thereby periodically swept across the slit and the outgoing radiation is detected by means of a cooled indium antimonide detector whose output is amplified and measured on a lock-in amplifier. A synchronous reference signal from the galvanometer amplifier is provided to the lock-in amplifier.

Theory

The theory of derivative spectroscopy has been previously discussed by others (7–9). We shall therefore give only a brief account of it.

Assume the combined spectrum resulting from the source radiation, optics and detector response function in the system described is given by $S(\lambda)$. The intensity of the radiation specularly reflected from the sample at wavelength λ is therefore

$$[1] \qquad I_0(\lambda) = S(\lambda)R_0(\lambda)$$

when the sample surface is bare and

$$[2] \qquad I(\lambda) = S(\lambda)[R_0(\lambda) + \Delta R(\lambda)]$$

when the sample surface is covered with a layer of adsorbate.

If the beam falling on the exit slit of the monochromator is deflected by a small amount $\delta\lambda$ the measured intensity is then given by

$$[3] \quad I(\lambda + \delta\lambda) \simeq I(\lambda) + \delta\lambda\frac{dI}{d\lambda} + \tfrac{1}{2}(\delta\lambda)^2\frac{d^2I}{d\lambda^2} + \ldots$$

If $\delta\lambda$ varies sinusoidally with time so that

$$[4] \qquad \delta\lambda = \delta\lambda_{max} \sin \omega t$$

then the Fourier component of $I(\lambda)$ having frequency ω has an amplitude proportional to $dI/d\lambda$ as given by [3]. From [2]

$$[5] \quad \frac{dI}{d\lambda} = \frac{d[S(\lambda)R_0(\lambda)]}{d\lambda} + S(\lambda)\frac{d\Delta R}{d\lambda} + \Delta R\frac{dS(\lambda)}{d\lambda}$$

The first term of [5] is small if $S(\lambda)R_0(\lambda)$ is a slowly varying function of λ while the last term is small for small values of ΔR. Equation 5 is therefore dominated by the term $S(\lambda)(d\Delta R/d\lambda)$ which is proportional to the first derivative of the absorption due to the presence of the adsorbate, as required. The first term in [5] can also be subtracted out by first recording the first derivative spectrum of the bare substrate. Thus

$$[6] \qquad S(\lambda)\frac{d\Delta R}{d\lambda} = \frac{dI}{d\lambda} - \frac{dI_0}{d\lambda}$$

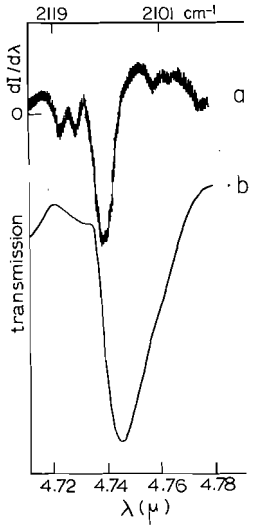

FIG. 1. (*a*) The difference between the first derivative single-reflection spectrum of CO adsorbed on polycrystalline copper and that of the bare substrate. (*b*) The integral of the above.

Results

Using this technique we have succeeded in recording the single-reflection reflectance spectrum of CO on copper. The CO pressure was approximately 0.5 μ.

Figure 1*a* shows the difference in derivative spectra with CO covered and bare copper surfaces as stated by [6]. Figure 1*b* is a digitally integrated spectrum of the data displayed in Fig. 1*a*, giving a conventional transmission spectrum except that the large reflection background has been suppressed. The observed spectrum has a maximum absorbance at 2107 cm^{-1} with a shoulder at lower wavenumbers as reported by Pritchard and Sims (1). The absorbance of the feature at its maximum is approximately 0.5% and it was not observable by direct reflectance.

Can. J. Chem. Downloaded from www.nrcresearchpress.com by 210.87.254.42 on 09/05/12
For personal use only.

This demonstrates the usefulness of the described technique.

We thank the National Research Council of Canada for financial support and the Connaught Fund for a grant.

1. J. PRITCHARD and M. L. SIMS. Trans. Faraday Soc. **66**, 427 (1970).
2. H. G. TOMPKINS and R. G. GREENLER. Surf. Sci. **28**, 194 (1971).
3. M. J. DIGNAM, B. RAO, and R. W. STOBIE. Surf. Sci. **46**, 308 (1974).
4. M. A. CHESTER, J. PRITCHARD, and M. L. SIMS. Chem. Commun. 1454 (1970); J. PRITCHARD. J. Vac. Sci. Technl. **9**, 895 (1972).
5. J. PRITCHARD. *In* Modern methods of surface analysis. Dechema-Monographicu. Vol. 78. 1975. p. 231.
6. M. MOSKOVITS and C. J. HOPE. To be published.
7. M. CARDONA. Modulation spectroscopy solid state physics supplement. Vol. 11. Academic Press. 1969. Chapt. 4.
8. G. BONFIGLIOLI and P. BROVETTO. Appl. Opt. **3**, 1417 (1964).
9. T. C. O'HAVER and G. L. GREEN. Internat. Lab. 1975. May/June issue, p. 11.

Can. J. Chem. Downloaded from www.nrcresearchpress.com by 210.87.254.42 on 09/05/12
For personal use only.

Librations Around the C(S)—Phenyl Bond in *N*-Thiobenzoylmorpholines Observed by 220 MHz Proton Magnetic Resonance Spectroscopy

ADRIAN O. FULEA[1] AND PETER J. KRUEGER

Department of Chemistry, University of Calgary, Calgary, Alberta T2N 1N4

Received April 18, 1975

ADRIAN O. FULEA and PETER J. KRUEGER. Can. J. Chem. **53**, 3315 (1975).

The 220 MHz p.m.r. spectra of 4-(4′-nitrothiobenzoyl)-2,6-dimethylmorpholine (**1**) provide evidence for the progressive freezing of the librations of the thioamide group around the C(S)—Ph bond as the temperature is lowered. This is supported by spectral data on related compounds in which the aromatic and hetero-ring substituents are altered.

ADRIAN O. FULEA and PETER J. KRUEGER. Can. J. Chem. **53**, 3315 (1975).

Le spectre r.m.p. à 220 MHz du (nitro-4′ thiobenzoyl)-4 diméthyl-2,6 morpholine (**1**) fournit une preuve qu'il y a un arrêt progressif de la libration du groupe thioamide autour du lien C(S)—Ph au fur et à mesure que la température est abaissée. Cette conclusion est supportée par des données spectrales sur des composés connexes dans lesquels les substituants du cycle aromatique et de l'hétérocycle sont changés.

[Traduit par le journal]

Previously we have shown (1) that the librations around the C—N bond, *i.e.* oscillations about the local potential energy minimum for intramolecular rotation, in 1-(2′-hydroxythiobenzoyl)-piperidine and 4-(2′-hydroxythiobenzoyl)-morpholine can be investigated by p.m.r. spectroscopy, using the magnetically nonequivalent NCH_2 protons as sensors in a system where an intramolecular OH···S hydrogen bond locks the internal motions of the thiobenzoyl group. It has also been demonstrated that torsional librations can decouple spin systems, and sharpen or broaden p.m.r. signals (2).

[1]Izaak Walton Killam Scholar.

The 220 MHz p.m.r. signal patterns for the 2′ and 6′ protons of **1** at different temperatures in CS_2, acetone-d_6, and $CDCl_3$ solution are shown in Fig. 1.[2] At or below −30 °C all rotations around the C(S)—Ph bond in **1** are frozen on the 220 MHz scale (Fig. 1*b* and 1*c*); we believe this to be the first case where freezing of the rotation around this bond has been observed in thiobenzamides which are not *o*-substituted (3).

Two rotational energy barriers can be envisaged for rotation about the C(S)—Ph bond:

[2]We thank Mrs. C. Fulea for the synthesis of this compound. Proton magnetic resonance spectra were obtained at the Canadian 220 MHz n.m.r. Centre, Sheridan Park, Ontario, under the direction of Dr. A. E. Grey.

This demonstrates the usefulness of the described technique.

We thank the National Research Council of Canada for financial support and the Connaught Fund for a grant.

1. J. PRITCHARD and M. L. SIMS. Trans. Faraday Soc. **66**, 427 (1970).
2. H. G. TOMPKINS and R. G. GREENLER. Surf. Sci. **28**, 194 (1971).
3. M. J. DIGNAM, B. RAO, and R. W. STOBIE. Surf. Sci. **46**, 308 (1974).
4. M. A. CHESTER, J. PRITCHARD, and M. L. SIMS. Chem. Commun. 1454 (1970); J. PRITCHARD. J. Vac. Sci. Technl. **9**, 895 (1972).
5. J. PRITCHARD. *In* Modern methods of surface analysis. Dechema-Monographicu. Vol. 78. 1975. p. 231.
6. M. MOSKOVITS and C. J. HOPE. To be published.
7. M. CARDONA. Modulation spectroscopy solid state physics supplement. Vol. 11. Academic Press. 1969. Chapt. 4.
8. G. BONFIGLIOLI and P. BROVETTO. Appl. Opt. **3**, 1417 (1964).
9. T. C. O'HAVER and G. L. GREEN. Internat. Lab. 1975. May/June issue, p. 11.

Can. J. Chem. Downloaded from www.nrcresearchpress.com by 210.87.254.5 on 09/05/12
For personal use only.

Librations Around the C(S)—Phenyl Bond in *N*-Thiobenzoylmorpholines Observed by 220 MHz Proton Magnetic Resonance Spectroscopy

ADRIAN O. FULEA[1] AND PETER J. KRUEGER

Department of Chemistry, University of Calgary, Calgary, Alberta T2N 1N4

Received April 18, 1975

ADRIAN O. FULEA and PETER J. KRUEGER. Can. J. Chem. **53**, 3315 (1975).

The 220 MHz p.m.r. spectra of 4-(4′-nitrothiobenzoyl)-2,6-dimethylmorpholine (**1**) provide evidence for the progressive freezing of the librations of the thioamide group around the C(S)—Ph bond as the temperature is lowered. This is supported by spectral data on related compounds in which the aromatic and hetero-ring substituents are altered.

ADRIAN O. FULEA and PETER J. KRUEGER. Can. J. Chem. **53**, 3315 (1975).

Le spectre r.m.p. à 220 MHz du (nitro-4′ thiobenzoyl)-4 diméthyl-2,6 morpholine (**1**) fournit une preuve qu'il y a un arrêt progressif de la libration du groupe thioamide autour du lien C(S)—Ph au fur et à mesure que la température est abaissée. Cette conclusion est supportée par des données spectrales sur des composés connexes dans lesquels les substituants du cycle aromatique et de l'hétérocycle sont changés.

[Traduit par le journal]

Previously we have shown (1) that the librations around the C—N bond, *i.e.* oscillations about the local potential energy minimum for intramolecular rotation, in 1-(2′-hydroxythiobenzoyl)-piperidine and 4-(2′-hydroxythiobenzoyl)-morpholine can be investigated by p.m.r. spectroscopy, using the magnetically nonequivalent NCH_2 protons as sensors in a system where an intramolecular OH···S hydrogen bond locks the internal motions of the thiobenzoyl group. It has also been demonstrated that torsional librations can decouple spin systems, and sharpen or broaden p.m.r. signals (2).

[1]Izaak Walton Killam Scholar.

The 220 MHz p.m.r. signal patterns for the 2′ and 6′ protons of **1** at different temperatures in CS_2, acetone-d_6, and $CDCl_3$ solution are shown in Fig. 1.[2] At or below −30 °C all rotations around the C(S)—Ph bond in **1** are frozen on the 220 MHz scale (Fig. 1*b* and 1*c*); we believe this to be the first case where freezing of the rotation around this bond has been observed in thiobenzamides which are not *o*-substituted (3).

Two rotational energy barriers can be envisaged for rotation about the C(S)—Ph bond:

[2]We thank Mrs. C. Fulea for the synthesis of this compound. Proton magnetic resonance spectra were obtained at the Canadian 220 MHz n.m.r. Centre, Sheridan Park, Ontario, under the direction of Dr. A. E. Grey.

Can. J. Chem. Downloaded from www.nrcresearchpress.com by 210.87.254.5 on 09/05/12
For personal use only.

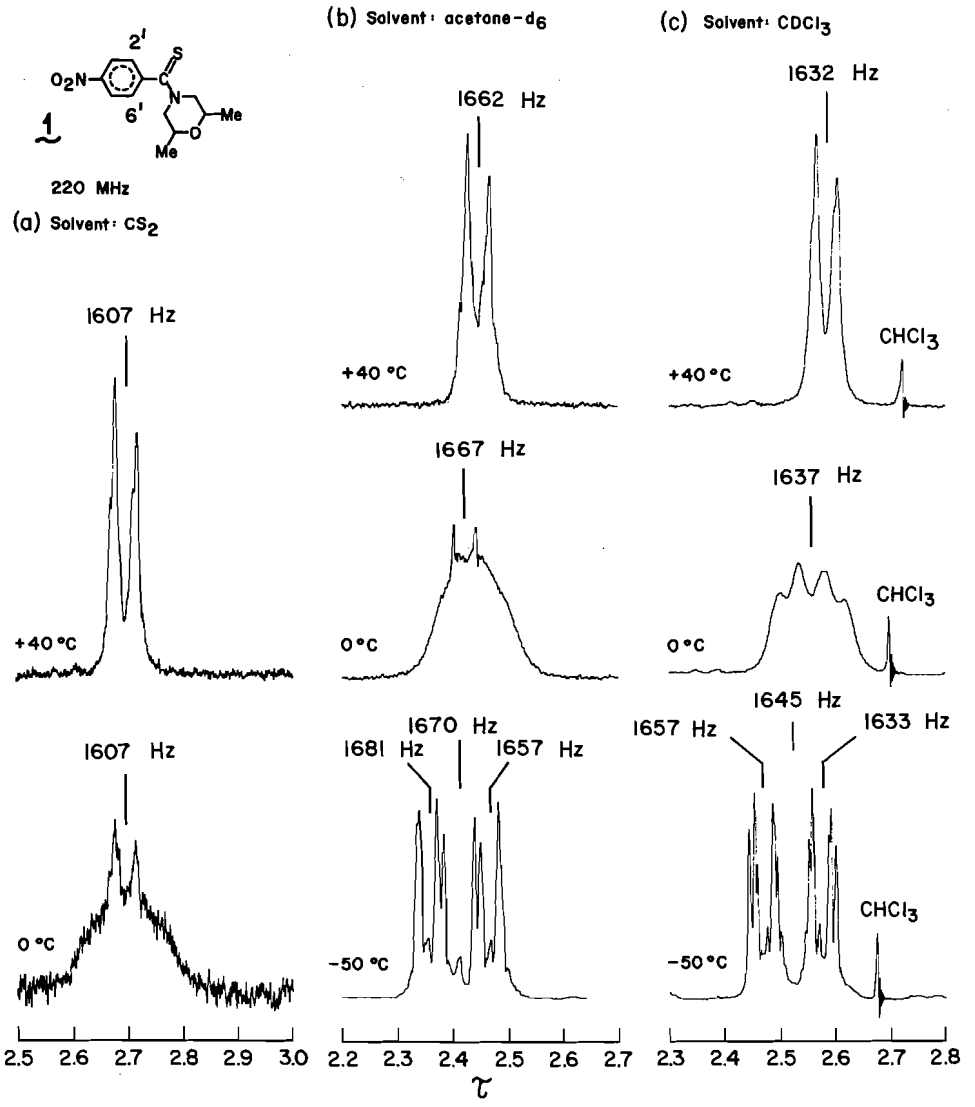

FIG. 1. 220 MHz p.m.r. spectra of **1** in (*a*) CS_2, (*b*) acetone-d_6, and (*c*) $CDCl_3$ solutions. Internal TMS reference.

E_{steric} for the process by which *o*-protons would pass through the thioamide plane, and E_π for the process by which the phenyl ring passes through a plane perpendicular to the thioamide plane (the barrier in this case arising from the breaking of conjugation); the relative magnitudes would be $E_{steric} > E_\pi$. The spectral features observed cannot be explained by the freezing of the rotation due to the E_{steric} barrier, since the chemical shift of the *syn* and *anti* *o*-protons will still be equalized by passage over the E_π barrier, *i.e.* a given *o*-proton oscillates between *syn* and *anti* positions on the same side of the thioamide plane.[3] Rotation over the E_{steric} barrier (and rotation around the CN bond) is frozen for these compounds throughout the temperature range under consideration. Nevertheless, as can be seen from Fig. 1*a*, part of the *o*-proton signal is unchanged when the temperature drops from 40 to 0 °C, whereas the

[3]The *o*-protons would both have the same chemical shift:

$$\tau = \tfrac{1}{2}(\tau_{anti} + \tau_{syn})$$

Can. J. Chem. Downloaded from www.nrcresearchpress.com by 210.87.254.5 on 09/05/12
For personal use only.

other part broadens, but with good approximation still has the same chemical shift of 1607 Hz on the 220 MHz scale.[4]

We presume that the rotation over the E_π barrier in **1** freezes above 0 °C on the n.m.r. scale, based on the chemical shift difference between *syn* and *anti* *o*-protons at −30 °C in both CS_2 and acetone-d_6 solution. The chemical shift of the *syn* and *anti* *o*-protons in CS_2 is unchanged relative to their chemical shift when this rotation is rapid, because relatively high amplitude librations move the *syn* and *anti* protons in regions with the same chemical shift. The broadening of *half* of the signal is attributed to the freezing of the higher energy liberations of the thioamide group around the C(S)—Ph bond.[5] The two parts of the molecule will oscillate in opposite directions around this bond, with different amplitudes, the part with the lower moment of inertia around the axis of rotation (*i.e.* the aromatic ring) having the higher amplitude. On decreasing the temperature the librations with high amplitude begin to freeze and the average angle between the aromatic ring and the C(S)—N plane (when both are in their equilibrium position, *i.e.* most of the time) decreases.[6] The sharp peaks in CS_2 and acetone-d_6 solution at 0 °C are due to the *o*-proton *anti* to the C=S bond. The broadened peaks are due to the *o*-proton *syn* to the C=S bond, where the gradient of deshielding is higher. To explain this broadening by librational transitions, which usually are between levels differing little in energy, we envisage that the degree of steric interaction between the 5 and 6′ protons in **1** depends on the torsional amplitude (torsional state with angular amplitude θ, measured from the equilibrium position in the torsional ground state). Some θ states will be highly unfavorable energetically because of steric hindrance, and hence will be unpopulated, increasing the difference between populated levels, which correspond to amplitudes accompanied by a 'cogwheel' configuration of the three hydrogen atoms (5). For these states the energy difference may be approximately equal to the difference in the resonance energies that correspond to the two dihedral angles, respectively. On the n.m.r. scale, the signal averaging will thus take place over a smaller number of states, but which have a larger energy separation between them. The chemical shift of the *syn* aromatic *o*-protons will be different in two populated 'cogwheel' torsional states, and this leads to the broadening of their signal.

A change in the chemical shift of *o*-protons due to librational movement has been observed previously in biphenyls (6).

In $CDCl_3$ solution the rotation around the C(S)—Ph bond involving the E_π barrier is also frozen, but here the librations of the phenyl part of the molecule cannot equalize the chemical shift of the *o*-protons at 0 °C, presumably due to the higher bond order of the C(S)—Ph bond in this solvent as a result of intermolecular CD···S hydrogen bond formation.

In $CDCl_3$ and acetone-d_6 solutions the chemical shift of the *o*-protons in **1** moves downfield with decreasing temperature, *e.g.* in $CDCl_3$ (Fig. 1*c*) from 1632 Hz at 40 °C to 1645 Hz at −50 °C, due to the progressive freezing of higher energy (and amplitude) librations around the C(S)—Ph bond as the temperature is lowered, since the angle between the phenyl ring and thioamide planes decreases.

In marked contrast, the 220 MHz spectrum of 4-(4′-nitrothiobenzoyl)-morpholine, **2**, exhibits no change in the aromatic *o*-proton signal from +40 to −50 °C. Following the usual interpretation a rotational barrier of about 14 kcal/mol might be implied for **1**, and a barrier of less than 11 kcal/mol for **2**. This is extremely unlikely, since the basic structural features of **1** and **2** are the same, dictating virtually identical barriers to rotation for the process which would equalize *syn* and *anti* protons,[7] and the

[4]We thank one of the referees for helpful comments regarding line-widths.

[5]Strictly speaking, this liberation will take place around an intramolecular axis through the center of mass, and not coincident with the C(S)—Ph bond.

[6]Due to steric hindrance the aromatic ring and the C(S)—N group cannot be coplanar if the conjugation in the thioamide group is maximized. A phenyl ring twist angle of about 50° is estimated from Dreiding models. Twisting in thiobenzamides has recently been discussed in the literature (4). The high rotational barrier E_π for **2** can be explained by a smaller phenyl ring twist angle out of the thioamide plane in the ground state than is envisaged from a Dreiding model, with steric interactions accommodated to some extent by distortion of bond angles.

[7]The barrier E_{steric} for rotation around the C(S)—Ph bond differs in **1** and **2** due to the 'cogwheeling' effect in the latter, but this barrier cannot be determined by observation of the *o*-proton signal.

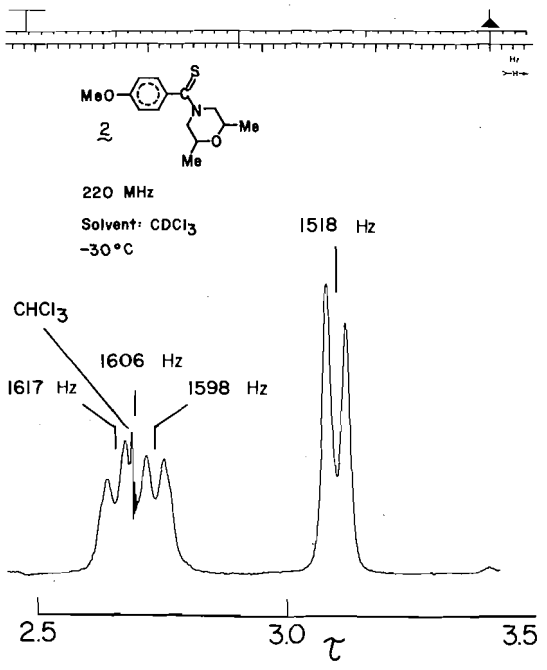

FIG. 2. 220 MHz p.m.r. spectrum of **2** in $CDCl_3$.

same chemical shift for the *o*-proton in the ground state. The much lower moment of inertia of the thioamide group about the internal axis in **2** is the principal feature which differentiates **2** from **1**. Thus the librations of the thioamide group in **2** have a much higher amplitude than in **1**, equalizing the *syn* and *anti* *o*-protons down to -50 °C. Even for **1** the coalescence point cannot be determined precisely,[8] and thus the E_π barrier cannot be determined accurately.

Similar observations have been made for other selected *N*-benzoyl morpholines, piperidines, and piperazines. Compound **1** is an excellent choice for this study because the *o*-protons are well separated in the p.m.r. spectrum, the two methyl groups on the morpholine ring increase the moment of inertia of the thioamide group, and the strongly electron-withdrawing *p*-NO_2 substituent enhances the C—N bond order because the N atom is more responsive to this effect than the S atom (7). This makes the thioamide frame stiffer and precludes interference from torsional oscillations about the C—N bond. In 4-(4′-methoxythiobenzoyl)-2,6-dimethylmorpholine, **3**, where the thioamide frame is not as stiff as in **1** (*i.e.* lower CN bond order) the *o*-proton signal is a sharp doublet in $CDCl_3$ at 0 °C, and only by -30 °C (Fig. 2) does the observed pattern resemble that seen for **1** at 0 °C.

The hitherto puzzling finding that sometimes one of the magnetically nonequivalent geminal protons in sterically crowded molecules exhibits a broad p.m.r. signal pattern whereas that of the other proton is sharp (8) can now be explained in the light of this study and our earlier work (1). The broadening of the signal from only one geminal proton can be due to the freezing of a libration in which this proton moves in a very high gradient of deshielding.

Financial support for this work by the National Research Council of Canada is gratefully acknowledged.

1. A. O. FULEA and P. J. KRUEGER. Spectrosc. Lett. In press.
2. A. O. FULEA and P. J. KRUEGER. Chem. Phys. Lett. In press.
3. S. L. SPASOV, V. S. DIMITROW, and I. KANTSCHOVSKA. Org. Magn. Reson. **6**, 20 (1974).
4. G. A. BARAMKI, G. DERDALL, and J. T. EDWARD. Can. J. Spectrosc. **18**, 160 (1973).
5. F. SUZUKI, M. OKI, and H. NAKANISHI. Bull. Chem. Soc. Jpn. **47**, 3114 (1974).
6. R. J. KURLAND and W. B. WISE. J. Am. Chem. Soc. **86**, 1877 (1964).
7. P. J. KRUEGER and A. O. FULEA. Tetrahedron, **31**, 1813 (1975).
8. T. H. SIDDALL and C. A. PROHASKA. J. Am. Chem. Soc. **88**, 1172 (1966); J. C. RANDALL, J. J. MCLESKEY III, P. SMITH, and M. E. HOBBS, J. Am. Chem. Soc. **86**, 3229 (1964).

[8]For 4-thiobenzoyl-2,6-dimethylmorpholine in $CDCl_3$ solution the coalescence temperatures for the two parts of the *o*-proton signal differ by more than 20 °C.

Can. J. Chem. Downloaded from www.nrcresearchpress.com by 210.87.254.5 on 09/05/12
For personal use only.

Can. J. Chem. Downloaded from www.nrcresearchpress.com by 210.87.254.105 on 09/05/12
For personal use only.

Canadian Journal of Chemistry

Published by
THE NATIONAL RESEARCH COUNCIL OF CANADA

Journal canadien de chimie

Publié par
LE CONSEIL NATIONAL DE RECHERCHES DU CANADA

Volume 53 Number 22 November 15, 1975

Volume 53 numéro 22 15 novembre 1975

Kinetics and Mechanism of the Oxidation of Thiocyanate by Tris(1,10-phenanthroline)iron(III) and its Derivatives

FLORA T. T. NG AND PATRICK M. HENRY

Guelph-Waterloo Centre for Graduate Work in Chemistry, University of Guelph, Guelph, Ontario N1G 2W1

Received May 8, 1975

FLORA T. T. NG and PATRICK M. HENRY. Can. J. Chem. **53**, 3319 (1975).

Oxidation of thiocyanate by tris(1,10-phenanthroline)Fe(III) to give cyanide and sulfate ions was studied at 25 °C in both H_2SO_4 and $HClO_4$ media. The rate of oxidation showed a first order dependence on the Fe(III) complex and a second order dependence on potassium thiocyanate at $\geq 4.0 \times 10^{-4}$ *M* potassium thiocyanate. The value of k_{obs} decreased with increasing $[H^+]$. This acid inhibition is consistent with the protonation of SCN^- to give an inactive HSCN species. A mechanism consistent with the data involved an initial equilibrium formation of $[Fephen_3SCN]^{2+}$ which subsequently undergoes an outer-sphere electron transfer with SCN^- to eventually give Fe(II)$phen_3$, CN^-, and SO_4^{2-}. Similar kinetic behavior was found with the substituted tris(1,10-phenanthroline)Fe(III) complexes. The value of the third order rate constant was found to increase with the increase in the reduction potential of the complexes. This result indicates a direct dependence of the standard free energy of the reaction and the free energy of activation.

FLORA T. T. NG et PATRICK M. HENRY. Can. J. Chem. **53**, 3319 (1975).

On a étudié, à 25 °C, dans des milieux H_2SO_4 et $HClO_4$, l'oxydation du thiocyanate par le tris(phénanthroline-1,10)Fe(III) conduisant aux ions cyanure et sulfate. A des concentrations $\geq 4.0 \times 10^{-4}$ *M* en thiocyanate de potassium, la vitesse d'oxydation est du premier ordre en complexe ferrique et du deuxième en thiocyanate de potassium. La valeur de k_{obs} diminue avec une augmentation de $[H^+]$. Cette inhibition par les acides est en accord avec une protonation du SCN^- conduisant à une espèce HSCN inactive. Un mécanisme en accord avec les données implique une formation initiale en équilibre de $[Fephen\ SCN]^{2+}$ qui subit d'une façon subséquente un transfert d'électron avec SCN^- dans la sphère extérieure puis finalement donne du Fe(II) $phen_3$, du CN^- et SO_4^{2-}. On a trouvé des comportements cinétiques semblables pour des complexes de tris(phénanthroline-1,10)Fe(III) substitués. On a trouvé que la constante de vitesse du troisième ordre augmente avec une augmentation des potentiels de réduction de ces complexes. Ce résultat indique qu'il existe une relation directe entre l'énergie libre standard de la réaction et l'énergie libre d'activation.

[Traduit par le journal]

Introduction

There have been recent reports of thiocyanate assisted outer-sphere electron transfer reactions between inorganic complexes (1, 2). Similarly, thiocyanate has been found to catalyze electron transfer in cytochrome C and porphyrin complexes (3–5). We are interested in the effect of anions on the rate of oxidation of organics by tris(1,10-phenanthroline)Fe(III).[1] In the absence of organic, tris(1,10-phenanthroline)Fe(III) was reduced by SCN^- at an appreciable rate. We studied the reaction in the absence of any organics in some detail since this might elucidate the mechanism of the SCN^- assisted outer-sphere electron transfer reactions.

[1]F. T. T. Ng and P. M. Henry, unpublished data.

TABLE 1. Data for determination of stoichiometry of the reaction in 0.75 M H_2SO_4

[Fe(III)phen$_3$] $\times 10^3$ (M)	[SCN]$_T$ $\times 10^4$ (M)	Final O.D. in 1 mm cell after correction for unreacted Fe(III)phen$_3$	[Fe(II)phen$_3$]^a $\times 10^3$ (M)	[Fe(III)phen$_3$] / [SCN]$_T$
1.0	1.0	0.59	0.59	5.9
2.0	2.0	1.20	1.2	6.0
3.0	2.0	1.12	1.12	5.6
3.0	3.0	1.71	1.7	5.7

^{a}Literature value (ref. 6, p. 55) for extinction coefficient of Fe(II)phen$_3$ is 1.1×10^4 at 510 nm O.D. measured for a 1.2×10^{-3} M Fe(II)phen$_3$ in 0.75 M H_2SO_4 is 1.24 in 1 mm cell. We have chosen the latter standard ($\varepsilon = 1.03 \times 10^4$) as reference for calculating the concentration of Fe(II)phen$_3$.

Results

Stoichiometry and Products

Reduction of tris(1,10-phenanthroline)Fe(III), commonly known as ferriin, Fe(III)phen$_3$, by KSCN in acid yielded tris(1,10-phenanthroline)Fe(II), also known as ferroin, Fe(II)phen$_3$. Fe(II)phen$_3$(ClO_4)$_2$ was identified by microanalysis and comparison of its infrared and visible spectrum with an authentic sample of Fe(II)phen$_3$(ClO_4)$_2$. Cyanide was identified as the oxidation product via precipitation as AgCN and comparison of its —C≡N stretch with an authentic sample of AgCN. The presence of SO_4^{2-} was indicated by immediate formation of a white precipitate of $BaSO_4$ on addition of $BaCl_2$ to a reaction mixture in which the ferriin has been completely reduced. The weight of the precipitate of $BaSO_4$ was approximately that expected from the initial concentration of ferriin.

Stoichiometry of the reaction was determined in the presence of excess Fe(III)phen$_3$. The formation of Fe(II)phen$_3$ was followed at 510 nm as shown in Table 1. For every mole of KSCN present in the reaction mixture, an average of 5.8 ± 0.2 mol of Fe(II)phen$_3$ was produced at the end of the reaction. Thus, the stoichiometry of the reaction is as follows

[1] $6Fe(III)phen_3 + SCN^- + 4H_2O \rightarrow 6Fe(II)phen_3 + CN^- + SO_4^{2-} + 8H^+$

Kinetics of the Oxidation of Thiocyanate by Ferriin in $HClO_4$

In the presence of excess KSCN, good pseudo first order kinetics was observed over at least two half lives. The pseudo first order rate constant, k_{obs}, was found to be second order in total thiocyanate concentration, [SCN]$_T$, at $\geq 4.0 \times 10^{-4}$ M KSCN in 1 M $HClO_4$ (Fig. 1). The value of k_3'', $k_{obs}/[SCN]_T^2$, was $(5.5 \pm 0.6) \times 10^3$ M^{-2} s^{-1} at 25 °C.

Wilmarth and co-workers (7) reported a rate law of the form

[2] $k_{obs} = k_1[SCN^-] + k_2[SCN^-]^2$

in the oxidation of SCN^- by tris(2,2′-bipyridyl)Fe(III) at 0.1 M ionic strength and 25 °C where $k_1 = 11\ M^{-1}\ s^{-1}$ and $k_2 = 1.5 \times 10^4\ M^{-2} s^{-1}$. Oxidation of thiocyanate at low [SCN]$_T$ was carried out under our reaction conditions to determine if the k_1 term existed. In the absence of thiocyanate, a freshly prepared 5.0×10^{-4} M stock solution of ferriin in concentrated $HClO_4$ when diluted with H_2O to 1 M [H^+] was reduced to ferroin with a k_0 value comparable to the k_{obs} value at low [SCN]$_T$ (Table 2). The origin of the k_0 term was not clear and appeared to be dependent on the 'age' of the stock solution. Results in Table 2 represent data obtained from a same stock solution of ferriin. When k_0 was subtracted from k_{obs} to give k_{obs}', the experimental value of

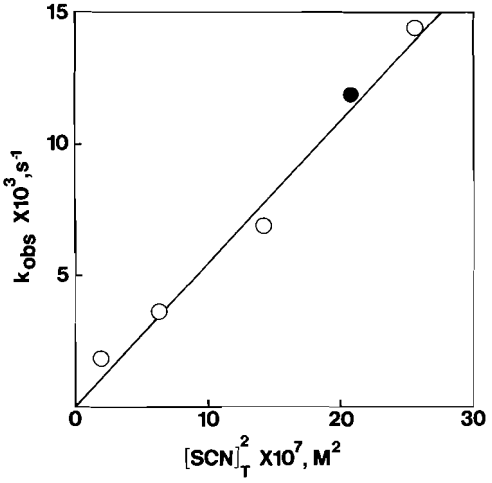

FIG. 1. Variation of k_{obs} with $[SCN]_T^2$ at 25 °C and 1 M $HClO_4$. ○, [Ferriin] = 1.00×10^{-4} M; ● [Ferriin] = 1.12×10^{-4} M.

Can. J. Chem. Downloaded from www.nrcresearchpress.com by 210.87.254.105 on 09/05/12
For personal use only.

TABLE 2. Kinetic data for the oxidation of thiocyanate in 1 M $HClO_4$ at low $[SCN]_T$. [Ferriin] = 4.10×10^{-5} M, $T = 25$ °C

$[SCN]_T \times 10^4$ (M)	$k_o \times 10^4$ (s^{-1})	$k_{obs} \times 10^4$ (s^{-1})	$k_{obs}' = k_{obs} - k_o \times 10^4$ (s^{-1})	$\frac{k_{obs}'}{[SCN]_T}$ (M^{-1} s^{-1})	
				Experimental	Calculated
0	8.6				
1.0		9.2	0.6	0.6	0.55
2.0		11	2.4	1.2	1.1
4.0		17	8.4	2.1	2.2

$k_{obs}'/[SCN]_T$ compared well with the calculated value of $k_{obs}/[SCN]_T$, assuming the presence of only a second order term in $[SCN]_T$. When $k_{obs}'/[SCN]_T$ was plotted against $[SCN]_T$, a straight line with an intercept of 0 ± 0.3 M^{-1} s^{-1} was found. Such a k_1 value is considerably lower than the k_1 value of 11 M^{-1} s^{-1} reported by Wilmarth and co-workers. Although the first order term in $[SCN]_T$ cannot be ruled out completely, this term is of negligible significance under most of our reaction conditions.

k_{obs} appears to have a complicated $[H^+]$ dependence. At 1 M ionic strength, k_{obs} was practically independent of $[H^+]$ at $[H^+] \leq 0.06$ M and then decreased with increasing $[H^+]$. At 2 M ionic strength, k_{obs} was practically independent of $[H^+]$ up to $[H^+] \leq 1$ M and then decreased with increasing $[H^+]$. At 4 M ionic strength, the value of k_{obs} decreased with increasing $[H^+]$ (Table 3).

TABLE 3. Variation of k_{obs} with $[H^+]$ in $HClO_4$ at different ionic strengths at 25 °C. Ionic strength kept constant by adding $NaClO_4$. [Ferriin] = 1.00×10^{-4} M; [KSCN] = 8.00×10^{-4} M

μ (M)	$[H^+]$ (M)	$k_{obs} \times 10^3$ (s^{-1})	$k_{obs}^{-1/2}$ ($s^{1/2}$)
1.0	0.2	7.2	11.8
1.0	0.6	7.3	11.7
1.0	0.8	6.0	12.9
1.0	1.0	4.1	15.8
2.0	0.2	3.3	17.4
2.0	0.4	3.6	16.7
2.0	0.6	3.4	17.1
2.0	0.8	3.6	16.7
2.0	1.0	2.7	19.2
2.0	1.4	2.8	18.9
2.0	2.0	2.2	21.3
4.0	0.2	1.7	24.0
4.0	0.6	1.6	25.3
4.0	1.0	1.3	27.6
4.0	2.0	0.8	35.8

Oxidation of Thiocyanate by Ferriin in H_2SO_4

The reaction was found to be first order in $Fe(III)phen_3$ and second order in $[SCN]_T$ where $[SCN]_T$ was varied from 7.2×10^{-4} to 1.44×10^{-3} M. The value of k_3'' was $(2.8 \pm 0.5) \times 10^4$ M^{-2} s^{-1} in 1 M H_2SO_4 at 25 °C. At ≤ 0.2 M $[H^+]$ and ionic strength of 2 M, k_{obs} was found to increase with increasing $[SO_4^{2-}]$ (Table 4).

Oxidation of Thiocyanate by 5-Methylferriin in H_2SO_4

Oxidation of thiocyanate by 5-methylferriin, $Fe(III)(Mephen)_3$, was carried out in H_2SO_4 medium because $Fe(II)(Mephen)_3$ is only slightly soluble in $HClO_4$ and precipitation occurred during the reaction. The value of k_{obs} showed a second order dependence on $[SCN]_T$ (Table 5) and the value of k_3'' was found to be $(1.4 \pm 0.4) \times 10^4$ M^{-2} s^{-1} at 25 °C. Air did not affect the reaction (Table 5).

Variation of k_{obs} with $[H^+]$ was studied in HBF_4 medium. k_{obs} decreased slightly as $[H^+]$ was increased from 0.25 to 1.0 M (Table 6).

Variation of k_3'' with the Reduction Potential, E^0, for the Substituted Ferriin Complexes

Oxidation of thiocyanate by a number of other substituted ferriin complexes was studied in 1 M H_2SO_4 since the methyl substituted ferriin com-

TABLE 4. Variation of k_{obs} with addition of Na_2SO_4 at 0.2 M $HClO_4$ and ionic strength of 2 M, adjusted with $NaClO_4$. [Ferriin] = 1.00×10^{-4} M, [KSCN] = 8.00×10^{-4} M

$[Na_2SO_4]$ (M)	$[SO_4^{2-}]^a$ (M)	$[H^+]^a$ (M)	$k_{obs} \times 10^3$ (s^{-1})
0	0	0.200	3.5
0.2	0.034	0.034	6.0
0.3	0.118	0.018	9.85
0.5	0.306	0.006	12.3
0.6	0.406	0.006	13.8

[a] $[SO_4^{2-}]$ and $[H^+]$ were calculated using the following equilibrium value: $HSO_4^- \rightleftharpoons H^+ + SO_4^{2-}$, $K = 0.012$ (31).

Can. J. Chem. Downloaded from www.nrcresearchpress.com by 210.87.254.105 on 09/05/12
For personal use only.

Can. J. Chem. Downloaded from www.nrcresearchpress.com by 210.87.254.105 on 09/05/12
For personal use only.

TABLE 5. Kinetic data for the reduction of 5-Meferriin by potassium thiocyanate at 25 °C and 1 M H_2SO_4, [5-Meferriin] = 6.92×10^{-5} M

$[SCN]_T$ $\times 10^4$ (M)	k_{obs} $\times 10^3$ (s^{-1})	$[SCN]_T^2$ $\times 10^7$ (M^2)	$k_3'' = \frac{k_{obs}}{[SCN]_T^2}$ $\times 10^{-4}$ (M^{-2} s^{-1})
3.0	1.4	0.9	1.60
5.0	2.8	2.5	1.10
6.0	3.8	3.6	1.04
7.0[a]	6.4	4.9	1.31
8.0	8.9	6.4	1.38
8.0	8.9	6.4	1.38
9.0	11.3	8.1	1.40
9.0	12.8	8.1	1.58
11.0	17.3	12.1	1.43
12.0	19.7	14.4	1.37
13.0	24.2	16.9	1.43
100.0[b]	1060.0	1000.0	1.06
100.0[c]	9600.0	1000.0	0.96

[a][5-Meferriin] = 2.78×10^{-5} M.
[b][5-Meferriin] = 1.00×10^{-4} M.
[c][5-Meferriin] = 1.00×10^{-4} M anaerobic conditions.

plexes are not very soluble in 1 M $HClO_4$. In addition, the reduction potentials (ref. 6, p. 113) of these complexes were reported in H_2SO_4 medium. The value of k_3'' increased as the E^0 value of the complexes increased (Table 7, Fig. 2).

Discussion

Identification of $Fe(II)phen_3$ at the end of the reaction suggested an outer-sphere electron transfer mechanism. If dissociation of phenanthroline occurred during the reaction, substitution of SCN^- into the first coordination sphere of the Fe(III) complex might be expected to occur to give $Fe(III)phen_2(SCN)_3$ which was reported to be a dark red solid (8). Although oxidation of SCN^- by Fe(III) in acetonitrile produced $(SCN)_2$ (9), we are not surprised that CN^- and SO_4^{2-} are the oxidation products since $(SCN)_2$ is known to decompose readily in aqueous medium (10). Oxidation of SCN^- by $Fe(H_2O)_6^{3+}$ (11) and H_2O_2 (12) in acidic medium was reported to produce CN^- and SO_4^{2-}.

TABLE 6. Oxidation of KSCN by 5-methylferriin at 25 °C. Variation of k_{obs} with $[H^+]$ in HBF_4 medium. [5-Meferriin] = 1.00×10^{-4} M, $[SCN]_T$ = 8.00×10^{-4} M, μ = 1 M

$[H^+]$ (M)	k_{obs} $\times 10^2$ (s^{-1})	$k_{obs}^{-1/2}$ ($s^{1/2}$)
0.25	1.33	8.65
0.50	1.13	9.40
0.75	1.10	9.55
1.00	0.91	10.50

TABLE 7. Third order rate constant for the oxidation of thiocyanate by substituted ferriin complexes at 25 °C and 1 M H_2SO_4

Complex	E^{0a}	$k_{obs}[SCN]_T^2$ $\times 10^{-4}$ (M^{-2} s^{-1})
4,7-Dimethylferriin	0.86	0.012
5-Methylferriin	1.02	1.4
Ferriin	1.06	2.8
5-Chloroferriin	1.12	37.4
5-Bromoferriin	1.13	35.0 ± 10.0
5-Nitroferriin	1.25	100.0 ± 50.0

[a]Reference 6, p. 113.

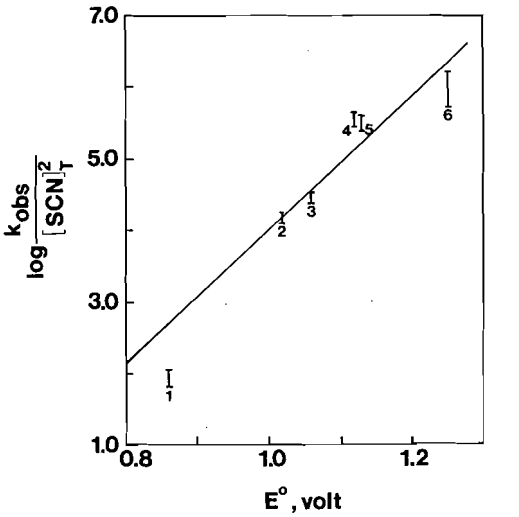

FIG. 2. Plot of log ($k_{obs}/[SCN]_T^2$) *vs.* E^0 for the substituted ferriin complexes at 25 °C and 1 M H_2SO_4: *1*, 4,7-dimethylferriin; *2*, 5-methylferriin; *3*, ferriin; *4*, 5-chloroferriin; *5*, 5-bromoferriin; *6*, 5-nitroferriin.

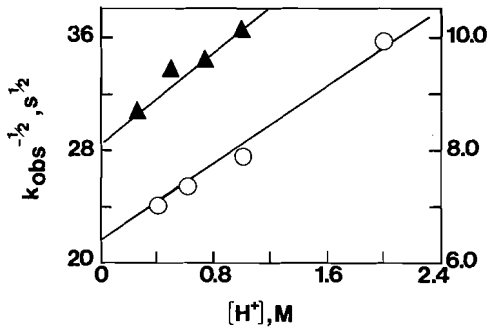

FIG. 3. Plot of $k_{obs}^{-1/2}$ *vs.* $[H^+]$, [Fe(III)] = 1.00 × 10^{-4} *M*, [KSCN] = 8.00 × 10^{-4} *M*, 25 °C. ○, Ferriin in $HClO_4$ at 4 *M* ionic strength (left hand scale); △, 5-methylferriin in HBF_4 at 1 *M* ionic strength (right hand scale).

Our data indicated that under our reaction conditions, 1 *M* $[H^+]$ and ionic strength of 1 *M*, the important term in the oxidation is given by the second order term. Thus, the rate law at constant $[H^+]$ is shown in [3].

$$[3] \quad \frac{d[Fe(II)phen_3]}{dt} = k_3''[SCN]_T^2[Fe(III)phen_3]$$

Inverse dependence on $[H^+]$ suggests that SCN^- is the reactive species which was protonated at higher acidity. Since k_{obs} showed a second order dependence on $[SCN]_T$ and an inverse dependence on $[H^+]$, the dependence of k_{obs} on $[H^+]$ is as follows:

$$[4] \quad k_{obs} = \frac{k_3'[SCN]_T^2}{\left(1 + \frac{[H^+]}{K_a}\right)^2}$$

Equation 4 can be rearranged to

$$[5] \quad k_{obs}^{-1/2} = \frac{1}{k_3'^{1/2}[SCN]_T} + \frac{[H^+]}{K_a k_3'^{1/2}[SCN]_T}$$

Thus, a plot of $k_{obs}^{-1/2}$ *vs.* $[H^+]$ should give a straight line at constant $[SCN]_T$ and from the ratio of intercept/slope, the value of K_a could be obtained and compared with literature data.

The data for $[H^+]$ dependence in $HClO_4$ for ferriin was analyzed according to [5] where $k_{obs}^{-1/2}$ was plotted against $[H^+]$. A reasonable straight line was obtained at 4 *M* ionic strength (Fig. 3) and K_a was evaluated as 3.3 ± 0.4 *M*. There was considerable scatter for the data at 1 and 2 *M* ionic strength, however, reasonable values of K_a, 3.5 ± 0.8 and 3.4 ± 2.0 *M* at 2 and 1 *M* ionic strength were obtained respectively. From the intercept of graphs plotted as in [5], values of k_3' at 1, 2, and 4 *M* ionic strength were 1.44 ± 0.5 × 10^4, 7.7 ± 1.2 × 10^3, and 3.3 ± 0.2 × 10^3 M^{-2} s^{-1} respectively. A plot of log k_3' *vs.* $\sqrt{I}$ gave a straight line with a slope of −0.66 (Fig. 4).

The $[H^+]$ dependence data for 5-methylferriin were also analyzed according to [5] (Fig. 3). The value of K_a was found to be 3.3 ± 0.4 *M*.

Literature values of K_a varied from 0.1 to 100 (13). However, a K_a value of 5 *M* is believed to be the best value (14). Thus, values of K_a obtained from analysis of our data appeared to be in fair agreement with literature data. Apparently K_a does not vary much with ionic strength, which was a little surprising.

A mechanism consistent with the kinetic data is as follows:

$$[6] \quad Fe(III)phen_3 + SCN^- \underset{k_{-1}}{\overset{k_1}{\rightleftharpoons}} [Fephen_3SCN]^{2+} \quad \mathbf{1}$$

$$[7] \quad [Fephen_3SCN]^{2+} + SCN^- \xrightarrow{k_3} Fe(II)phen_3 + (SCN)_2^{\cdot-}$$

$$[8] \quad SCN^- + H^+ \overset{K_a^{-1}}{\rightleftharpoons} HSCN$$

The initial step of the reaction involves formation of a reactive intermediate **1**. **1** then reacts with another molecule of SCN^- to give Fe(II)-$phen_3$ and $(SCN)_2^{\cdot-}$ radical. Subsequent fast reaction of $(SCN)_2^{\cdot-}$ with $Fe(III)phen_3$ or H_2O produces $Fe(II)phen_3$, CN^-, and SO_4^{2-}.

Applying steady state approximation for the formation of the intermediate **1**, the following rate expression was obtained.

$$[9] \quad \frac{d[Fe(II)phen_3]}{dt} = \frac{k_1k_3[SCN^-]^2[Fe(III)phen_3]}{k_{-1} + k_3[SCN^-]}$$

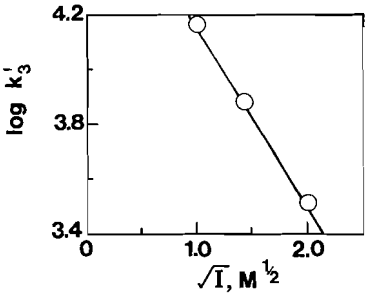

FIG. 4. Plot of log k_3' *vs.* $\sqrt{I}$ at 25 °C.

Can. J. Chem. Downloaded from www.nrcresearchpress.com by 210.87.254.105 on 09/05/12
For personal use only.

Can. J. Chem. Downloaded from www.nrcresearchpress.com by 210.87.254.105 on 09/05/12
For personal use only.

Fairly good second order dependence on $[SCN]_T$ was observed over a wide range of thiocyanate concentration, hence under the reaction conditions, $k_{-1} \gg k_3[SCN^-]$ and [9] reduces to

$$[10] \quad \frac{d[Fe(II)phen_3]}{dt} = \frac{k_1 k_3 [Fe(III)phen_3][SCN^-]^2}{k_{-1}} = k_3'[Fe(III)phen_3][SCN^-]^2$$

The concentration of free SCN^- may be expressed in terms of total thiocyanate such that

$$[11] \quad [SCN^-]_T = [SCN^-] + [HSCN] = [SCN^-]\left(1 + \frac{[H^+]}{K_a}\right)$$

Therefore

$$[12] \quad \frac{d[Fe(II)phen_3]}{dt} = \frac{k_3'[Fe(III)phen_3][SCN^-]_T^2}{\left(1 + \frac{[H^+]}{K_a}\right)^2}$$

where

$$[13] \quad k_3' = \frac{k_1 k_3}{k_{-1}}$$

Thus, the derived rate expression 12 is consistent with our kinetic data.

Possible mechanisms for the formation of the intermediate $(Fephen_3SCN)^{2+}$ are discussed below.

The initial complex formation could simply be an ion-pairing formation to give $(Fephen_3^{3+}, SCN^-)$ whereby the SCN^- molecule acts as a bridge for intramolecular electron transfer from another SCN^- to the ion pair and subsequently produces $Fe(II)phen_3$ and $(SCN)_2^{\cdot-}$. Existence of the radical anion has been documented (15) and was proposed to be an intermediate in the oxidation of SCN^- by $Fe(H_2O)_6^{3+}$ (11). Alternatively, the 'soft' sulfur atom in the SCN^- molecule in the ion pair may be polarized to give $Fe(III)phen_3...^{\delta-}SCN^{\delta+}$. The polarized $^{\delta-}SCN^{\delta+}$ molecule may induce electron transfer from another SCN^- molecule to give $(SCN)_2^{\cdot-}$. A third possibility is the formation of a radical cation intermediate, $(Fe(II)phen_3SCN^{\cdot}) \equiv (Fephen_3SCN)^{2+}$, via the interaction of filled π orbitals of the sulfur atom with the π^* orbitals of the phenanthroline or by nucleophilic attack of the sulfur on the carbon bearing a partial positive charge. The latter mode of attack is less likely because substituents on the phenanthroline ring which block positions for nucleophilic attack have little effect on the rate. The radical cation intermediate will readily oxidize a SCN^- molecule to give $Fe(II)phen_3$ and $(SCN)_2^{\cdot-}$. Relatively stable precursor complexes have been postulated to exist for $Co(phen)_3^{2+,3+}$, and $Fe(phen)_3^{3+,2+}$ reactions involving thiocyanate (1, 2). The preferred mechanism for their formation involved interaction of the π orbitals on the thiocyanate with the π^* orbitals of the phenanthroline ring. On the basis of the present data, it is not possible to distinguish whether the initial complex formation is an ion-pair formation, ion pair formation prior to radical cation formation, or radical cation formation. However, we found that in the presence of acetone, a limiting value of k_{obs} was found at $\sim 2\ M$ [acetone] and k_1 was estimated to be $\sim 55\ M^{-1}\ s^{-1}$.[1] In the absence of SCN^-, acetone did not appear to be oxidized.[1] The rate constant for ion-pairing is documented to approach the diffusion limit, 10^9–$10^{10}\ M^{-1}\ s^{-1}$ (16). Thus, radical cation intermediate formation is favored. However, ion-pairing prior to radical cation formation could not be ruled out. Formation of an intermediate, $[Fephen_3HSO_3]^{2+}$ between HSO_3^- and $Fe(III)phen_3$ prior to electron transfer from S(IV) to Fe(III) has been proposed (17), but the question exists whether it is only an ion pair or if a more specific interaction exists.

It is interesting to note that simple electron transfer from SCN^- to $Fe(III)phen_3$ to give a $SCN^{\cdot}$ radical is not favored thermodynamically. The E^0 value for $Fe(III)phen_3 \rightarrow Fe(II)phen_3$ is 1.06 V (ref. 6, p. 113), while that for $SCN^- \rightarrow SCN^{\cdot}$ is 1.8 V (18). The initial complexation as represented in [6] probably serves to lower the potential energy for subsequent electron transfer. The first order term reported by Wilmarth and co-workers (7) could result from decomposition of **1** to give $Fe(II)phen_3$ and $SCN^{\cdot}$. In the present study this pathway was found to be unimportant compared to the path second order in thiocyanate. The reason that **1** does not prefer to decompose to thiocyanate radical directly is probably related to the fact that $SCN^{\cdot}$ is a very high energy species.

An estimate of the equilibrium constant K_2 for production of free $SCN^{\bullet}$ *i.e.*

$$[14] \quad Fe(III)phen_3 + SCN^- \underset{}{\overset{K_2}{\rightleftarrows}} Fe(II)phen_3 + SCN^{\bullet}$$

Can. J. Chem. Downloaded from www.nrcresearchpress.com by 210.87.254.105 on 09/05/12
For personal use only.

is of the order of 10^{-12}. The equilibrium value, K_1, for the initial complex formation to give radical cation intermediate must be greater than 10^{-12} since there is extra stabilization energy due to π complex formation. The experimental value for K_1k_3 is $\sim 10^4\ M^{-2}\ s^{-1}$ for ferriin (Table 6). Since k_3 cannot exceed the diffusion controlled limit of $10^{10}\ M^{-1}\ s^{-1}$, K_1 is $\sim \geq 10^{-6}$ which is greater than 10^{-12}. Unfavorable energy requirements are suggested to account for the complicated mechanism in the oxidation of I^- and CN^- by $Fe(H_2O)_6^{3+}$ (19) and $Fe(CN)_6^{3-}$ (20) and radical anions such as $I_2^{\cdot-}$ (21) and $(CN)_2^{\cdot-}$ (21) were thought to be involved.

The plot of $\log k_3'$ *vs.* E^0 (Fig. 2) does not give a good straight line through all the points. However, if points **1** or **6** are eliminated, reasonably good straight lines can be drawn through the other five points. If **6** is eliminated a line with a slope higher than the theoretical slope predicted by the Marcus theory (22) is obtained. If **1** is eliminated a line with a theoretical slope of 0.5 can be drawn. This line is shown in Fig. 2. If in fact, the Marcus relationship does hold and **1** is off the line the reason could arise from the fact that this complex has 4,7-substituents while the others have 5-substituent. The 4,7-substituents could provide steric hindrance to positions at which the thiocyanate prefers to approach to form intermediate **1** or it could be these positions are the preferred points for electron transfer through the phenanthroline ring. Electron density has been calculated to be different at the different carbons of the phenanthroline ring (23). In any case, the present results do not justify a further discussion of this plot.

Since the rate determining step is preceded by equilibrium two potential surfaces are involved. If the equilibrium constant represented by [6] does not change markedly between each complex, the value of k_3'' will be proportional to k_3 and hence we might expect to get a linear free energy dependence. It is not unreasonable that rates of reaction would increase as ΔG^0 becomes more positive, regardless of mechanism. The fact that ΔG^0 does enter into the rate equation has been interpreted physically in that where there is an overall decrease in free energy, the requirement for any atomic rearrangement prior to electron transfer is reduced since the product can be formed in a vibrationally excited state (24).

Oxidation of $S_2O_8^{2-}$ by substituted ferriin complexes have been found to show a direct dependence of $\log k$ *vs.* E^0 and the expected slope for the Marcus correlation (25). Oxidation of thiourea and *N*-substituted derivatives by cerium(IV) (26) has been reported to have a linear free energy plot with a slope of -0.14 ± 0.2 in the opposite sense to that of $+0.5$ predicted by theory. The deviation from Marcus theory was attributed to the strong interactions between the reactants involved in the formation of radicals, change in formal reduction potentials of the reacting species or that an inner-sphere mechanism occurs. However, there are instances of inner-sphere electron transfer found to give a linear free energy plot (27).

The specific catalytic effect of SO_4^{2-} on the value of k_{obs} (Table 4) in the ferriin case is not clear. Ion pairing is expected to occur (28) but the ion pair, $Fe(III)phen_3,SO_4^{2-}$, may be expected to be less reactive than $Fe(III)phen_3$ towards interaction with SCN^- on electrostatic grounds. Almost identical values of k_3'', $1.44 \times 10^4\ M^{-2}\ s^{-1}$ in 1 *M* H_2SO_4 and $1.42 \times 10^4\ M^{-2}\ s^{-1}$ in 1 *M* HBF_4, were observed for the 5-methylferriin complex. BF_4^- is less effective for ion-pairing compared with SO_4^{2-}, partly because of its univalent positive charge. It is not clear what specific roles the anions, ClO_4^-, SO_4^{2-}, BF_4^- are playing in the oxidation. Specific salt effect (29) is expected to be of importance since high ionic strengths were used in these studies.

The slope of the ionic strength dependence plot (Fig. 4) has the right sign ($-$ve) for reaction between two oppositely charged species. The absolute value of the slope is immaterial since the Debye–Hückel relationship only holds for dilute solutions (<0.01 *M*).

Experimental

1,10-Phenanthroline and the substituted 1,10-phenanthroline derivatives were purchased from G. Frederick Smith Chemical Company. Potassium thiocyanate was AnalaR grade purchased from BDH chemicals and was recrystallized from H_2O before use. Perchloric acid was purchased from G. Frederick Smith Chemical Company. H_2SO_4 was obtained from Matheson, Coleman and Bell Manufacturing Company.

Tris(1,10-phenanthroline)Fe(II), ferroin, and the substituted ferroin complexes were prepared by a published procedure (30) which consists of adding an equivalent amount of appropriate ligand to a solution of $FeSO_4 \cdot 7H_2O$ in a 3:1 molar ratio. The Fe(III) complexes were obtained by oxidation of the Fe(II) complexes with PbO_2 in $\sim 1\ M$ H_2SO_4. The Fe(III) complexes were precipitated as perchlorate salts. Stock solutions of the Fe(III) complexes were made up in concentrated H_2SO_4

Can. J. Chem. Downloaded from www.nrcresearchpress.com by 210.87.254.105 on 09/05/12
For personal use only.

or $HClO_4$ medium. Such solutions were diluted with water to the desired acid strength immediately before each kinetic run.

Kinetic Studies

The Fe(II) complexes have extinction coefficients of the order of 10^4 in the region of 510 nm while the corresponding Fe(III) complexes are practically transparent at this wavelength. Thus, the rate of oxidation of SCN^- was conveniently monitored by following the increase in optical density at ~510 nm with time.

Kinetic studies for the oxidation were carried out on a Durrum stopped-flow spectrophotometer, Unicam SP 800, Unicam SP 1700, and Cary 118 spectrophotometers. The reaction was carried out under pseudo first order conditions with excess KSCN and reasonably good pseudo first order kinetics were obtained. The pseudo first order rate constants were obtained by plotting log $(O.D._\infty - O.D._t)$ against time.

The concentration of the stock KSCN solution was determined by titration with standard $AgNO_3$ using ferric ammonium sulfate as indicator. Stock solutions of KSCN kept in deionized water were stable for several months. However, acidic solutions of KSCN were not stable for a long period of time due to the production of H_2S (11).

Product Analysis

$Fe(II)phen_3(ClO_4)_2$ is less soluble than $Fe(III)phen_3(ClO_4)_3$. In experiments designed for product analysis, a high concentration of $Fe(III)phen_3(ClO_4)_3$, 10^{-2} *M*, was used and during the reduction, an orange red precipitate was observed. The orange red precipitate was washed with water and collected. The infrared spectrum was identical to a standard $Fe(II)phen_3(ClO_4)_2$ sample. Satisfactory microanalysis for C, H, N were also found.

Anal. Calcd. for $Fe(II)phen_3(ClO_4)_2$: N, 10.95; C, 54.53; H, 2.87. Found N, 10.6; C, 54.5; H, 3.02.

The visible spectrum of the orange red precipitate also resembled that of $Fe(II)phen_3(ClO_4)_2$.

CN^- was determined by precipitation as AgCN. A solution containing 4.56×10^{-3} mol of $Fe(III)phen_3$ and 7.6×10^{-4} mol of KSCN in 3 *M* H_2SO_4 was stirred in a closed system. Argon was passed slowly into the solution to purge any HCN produced into a $AgNO_3$ solution. After a period of 2 d, there was sufficient white precipitate for a spectrum. The solid was collected from the $AgNO_3$ solution and the infrared spectrum of the white solid was recorded using a Beckman IR12 spectrophotometer. The spectrum showed an intense absorption at 2168 cm^{-1} which is characteristic of the —C≡N stretch of AgCN. The characteristic —C≡N absorption for AgSCN is at 2152 cm^{-1}.

A solution containing 4×10^{-4} mol of ferriin was suspended in 10 ml 6 *M* $HClO_4$ and 2.4×10^{-4} mol of KSCN were added. The solution was stirred for a day and the red precipitate of $Fe(II)phen_3$ was filtered. The solution was made basic with NaOH and the dissociated phenanthroline was precipitated and filtered. The resulting solution was acidified with $HClO_4$ and a white precipitate of $BaSO_4$ was obtained on adding a solution of $BaCl_2$.

We wish to thank Defence Research Board of Canada and National Research Council of Canada for financial support. Technical assistance by E.J. Makowsky is also gratefully acknowledged.

1. N. Sutin and A. Foreman. J. Am. Chem. Soc. **93**, 5274 (1971).
2. T. J. Przystas and N. Sutin. J. Am. Chem. Soc. **95**, 5545 (1973).
3. J. K. Yandell, D. P. Fay, and N. Sutin. J. Am. Chem. Soc. **95**, 1131 (1973).
4. P. Hambright and E. B. Fleisher. Inorg. Chem. **4**, 912 (1965).
5. C. E. Castro and H. F. Davies. J. Am. Chem. Soc. **91**, 3505 (1969).
6. A. A. Schilt. Analytical application of 1,10-phenanthroline and related compounds. Pergamon Press, London. 1969.
7. J. E. Byrd, Jia Yong Chen, Henry Po, Chee-Peng Chua, and W. K. Wilmarth. Abstracts of the 167th ACS National Meeting, Los Angeles, California. April, 1974. Paper INOR 102.
8. P. G. David. J. Inorg. Nucl. Chem. **35**, 1463 (1973).
9. B. Kratochvil and R. Lang. Anal. Chem. **42**, 43 (1970).
10. C. E. Vanderzee and A. S. Quist. Inorg. Chem. **5**, 1238 (1966).
11. R. H. Betts and F. S. Dainton. J. Am. Chem. Soc. **75**, 5721 (1953).
12. I. R. Wilson and G. M. Harris. J. Am. Chem. Soc. **83**, 286 (1961).
13. C. T. Lin and J. K. Beattie. J. Am. Chem. Soc. **94**, 3011 (1972).
14. K. A. Muirhead and G. P. Haight, Jr. Inorg. Chem. **12**, 1116 (1973).
15. J. H. Baxendale, P. L. T. Bevan, and D. A. Stott. Trans. Faraday Soc. **64**, 2389 (1968).
16. F. Basolo and R. G. Pearson. Mechanisms of inorganic reactions, 2nd ed. John Wiley and Sons Inc., New York. 1967. p. 154.
17. D. W. Carlyle. J. Am. Chem. Soc. **94**, 4525 (1972).
18. S. D. Malone and J. F. Endicott. J. Phys. Chem. **76**, 2223 (1972).
19. A. J. Fudge and K. W. Sykes. J. Chem. Soc. 119 (1952).
20. A. W. Adamson. J. Phys. Chem. **56**, 858 (1952).
21. J. Silverman and R. W. Dobson. J. Phys. Chem. **56**, 846 (1952).
22. R. A. Marcus. J. Chem. Phys. **26**, 867 (1957).
23. H. C. Longuet-Higgens and C. A. Coulson. J. Chem. Soc. 1534 (1954).
24. J. Halpern. Q. Rev. 207 (1961).
25. D. H. Irvine. J. Chem. Soc. 2977 (1959).
26. M. D. Gomwalk and A. McAuley. J. Chem. Soc. A, 2948 (1968).
27. R. A. Marcus. J. Phys. Chem. **72**, 891 (1968); A. O. Cohen and R. A. Marcus. J. Phys. Chem. **72**, 4249 (1968).
28. J. E. Dickens, F. Basolo, and H. M. Neumann. J. Am. Chem. Soc. **79**, 1286 (1956).
29. A. A. Frost and R. G. Pearson. Kinetics and mechanism, 2nd ed. John Wiley and Sons Inc., New York. 1961. p. 151.
30. M. H. Ford-Smith and N. Sutin. J. Am. Chem. Soc. **83**, 1830 (1961).
31. Handbook of Chemistry and Physics, 49th ed. The Chemical Rubber Company, Cleveland, Ohio. 1968. p. D-61.

Consumption of Cetyl Trimethyl Ammonium Bromide (CTAB) during Electrodeposition of Lead Dioxide

KAPISTHALAM CHETLUR NARASIMHAM, SRINIVASARAGHAVAN VASUNDARA, AND HANDADY VENKATAKRISHNA UDUPA

Central Electrochemical Research Institute, Karaikudi 623 006, India

Received February 3, 1975

KAPISTHALAM CHETLUR NARASIMHAM, SRINIVASARAGHAVAN VASUNDARA, and HANDADY VENKATAKRISHNA UDUPA. Can. J. Chem. **53**, 3327 (1975).

The beneficial effect of the addition of CTAB during electrodeposition of lead dioxide led to the investigations on the necessity to control the concentration of the addition agent for obtaining a smooth and adherent deposit of the same on a stationary graphite anode. To achieve this, it is important to know the consumption pattern of the addition agent. It has been observed that the CTAB is consumed not only for cathodic reaction but also for anodic reaction. Increasing temperature lowers the consumption of CTAB.

KAPISTHALAM CHETLUR NARASIMHAM, SRINIVASARAGHAVAN VASUNDARA et HANDADY VENKATAKRISHNA UDUPA. Can. J. Chem. **53**, 3327 (1975).

L'effet advantageux qu'on obtient par l'addition de CTAB pendant le dépôt electrolytique de dioxyde de plomb conduit à examiner la necessité d'asservir le concentration avec le but d'obtenir un dépôt uniforme et adhérent de dioxyde de plomb sur un anode stationnaire de graphite. Pour cela, c'est important de savoir la maquette de consommation de l'agent actif. Il a été observé que la consommation de CTAB est non seulement lors de la réaction cathodique mais aussi lors de la réaction anodique. L'accroissement de la temperature abaisse la consommation de CTAB.

Introduction

In the course of the study on the measurement of internal stress in electrodeposited lead dioxide from lead nitrate – copper nitrate bath, Gnanasekaran *et al.* (1) found that the addition of CTAB not only lowered the stress but also helped in getting a deposit free from pinholes under stationary condition. The beneficial effect of addition of CTAB and other alkyl trimethyl ammonium bromide during electrodeposition of lead dioxide has been studied in detail and found to give a smooth and adherent deposit of lead dioxide on a stationary graphite anode (2, 3). In order to obtain a desirable deposit of lead dioxide it is necessary to control the concentration of addition agent. To achieve this, it is important to know the consumption pattern of the addition agent. A suitable analytical procedure for the determination of alkyl trimethyl ammonium bromide in the presence of lead and copper nitrates has earlier been reported by Narasimham *et al.* (4) and using this method the consumption of CTAB during deposition has been estimated and the results are presented in this paper.

Experimental

Cell Assembly

A 1 l Pyrex beaker fitted with a PVC cover containing suitable holes to introduce anode, cathode, and thermometer, acted as cell container. Two rectangular stainless steel plates (14 × 3 × 0.1 cm each) placed on either side of the anode acted as cathode. A graphite rod (1 cm diameter × 15 cm long) with the lower end rounded off served as anode. Before electrolysis the anode was given the usual pretreatment (5).

The electrolyte was an aqueous solution of lead nitrate (350 ± 10 g/l) and copper nitrate (25 ± 2 g/l) containing CTAB. For determining CTAB consumption during copper deposition from copper nitrate solution alone, copper nitrate of 25 ± 2 g/l concentration was used. To determine the consumption of CTAB in pure lead nitrate solution (350 ± 10 g/l) a porous pot was introduced in which 5% (v/v) nitric acid was taken as catholyte to prevent the deposition of lead at the cathode. CTAB (1.2 g/l) was added in all the cases.

Electrolysis

The p*H* of the electrolyte before starting the deposition was adjusted to 4 and 850 ml of this solution was then taken for the experiment. Both anode and cathode were kept stationary during electrolysis. Direct current was supplied from a selenium rectifier (0–12 V and 50 A). The deposition of lead dioxide or copper or both was carried out for different durations and the amount of CTAB consumed was determined. Similarly, the consumption of CTAB was determined at different tempera-

Can. J. Chem. Downloaded from www.nrcresearchpress.com by 210.87.254.42 on 09/05/12
For personal use only.

TABLE 1. Consumption of CTAB for different durations. Electrolyte: lead nitrate 350 ± 10 g/l and copper nitrate 25 ± 2 g/l, either present individually or together; initial pH = 4; initial CTAB concentration 1.2 g/l; anode current density 5 A/dm^2; temperature 30 ± 1 °C; volume of electrolyte 850 ml

			Consumption of CTAB in			
					$Pb(NO_3)_2$ + $Cu(NO_3)_2$	
Sample number	Duration (h)	Quantity of electricity (A h)	$Pb(NO_3)_2$* (g)	$Cu(NO_3)_2$ (g)	On the same anode (g)	On fresh anodes† (g)
1	2	3.26	0.16	0.31	0.47	0.47
2	4	6.52	0.22	0.48	0.65	0.65
3	6	9.78	0.27	0.62	0.88	0.87
4	8	13.05	0.37	0.71	0.96	0.96

*Porous pot was used to prevent lead deposition.
†Fresh anode was used every two hours of electrolysis.

tures. Experiments were conducted in duplicate and the results varied within 1%.

Internal Stress

The internal stress of the electrodeposited lead dioxide obtained from lead nitrate – copper nitrate bath containing various concentrations of CTAB (due to consumption for different durations) was measured employing a Hoar and Arrowsmith balance (6, 7) and using the procedure described by Gnanasekaran *et al.* (1) earlier.

Analysis

Lead and copper concentrations in the electrolyte were estimated by EDTA method (8) and iodometric (9) method respectively. The single-phase titration of CTAB in presence of lead and copper nitrates, with sodium tetraphenyl boron at pH 3 using methyl yellow as indicator, as reported by Narasimham *et al.* (4), was the method adopted for the determination of the consumption of CTAB in the electrolyte.

Results and Discussion

Table 1 shows the results of experiment. It is seen that CTAB is being consumed both for anodic and cathodic reactions, the consumption for the latter being greater. Since CTAB is a cationic surfactant, its consumption for cathodic reaction can very well be expected. However, the consumption of CTAB for the anodic reaction cannot normally be expected, but the results obtained are similar to the observations made by Lorking (10) in the experiments on anodic polishing of copper. The consumption of CTAB can be attributed to depletion arising out of adsorption and/or oxidation of the organic molecule itself. The consumption of CTAB in lead nitrate – copper nitrate mixture almost corresponds to the total consumption of the surfactant in lead nitrate and copper nitrate present separately.

The consumption of CTAB in the mixture of lead nitrate – copper nitrate decreases with increase in temperature as can be seen from Fig. 1. Thus at higher temperature not only is the consumption of CTAB less but there is also the practical advantage that the deposit obtained is adherent, smooth, and free from pinholes. However this observation is not in conformity with the usual expectation of increased consumption of organic molecule with increased temperature. Aspects relating to the mechanism of consumption and the anomalous temperature effect on the consumption of CTAB are not studied in detail in this paper, since the primary

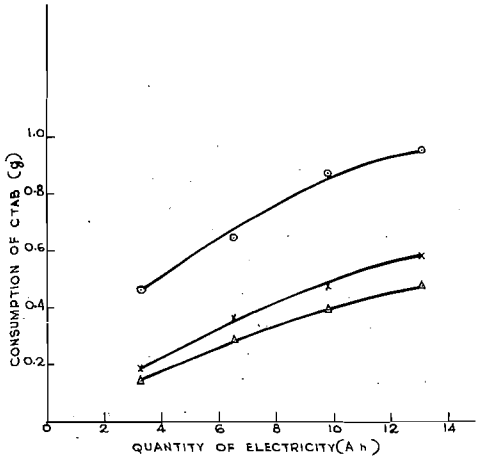

FIG. 1. Consumption of CTAB with quantity of electricity passed at different temperatures. ○, 30 °C; ×, 45 °C; △, 60 °C.

Can. J. Chem. Downloaded from www.nrcresearchpress.com by 210.87.254.42 on 09/05/12
For personal use only.

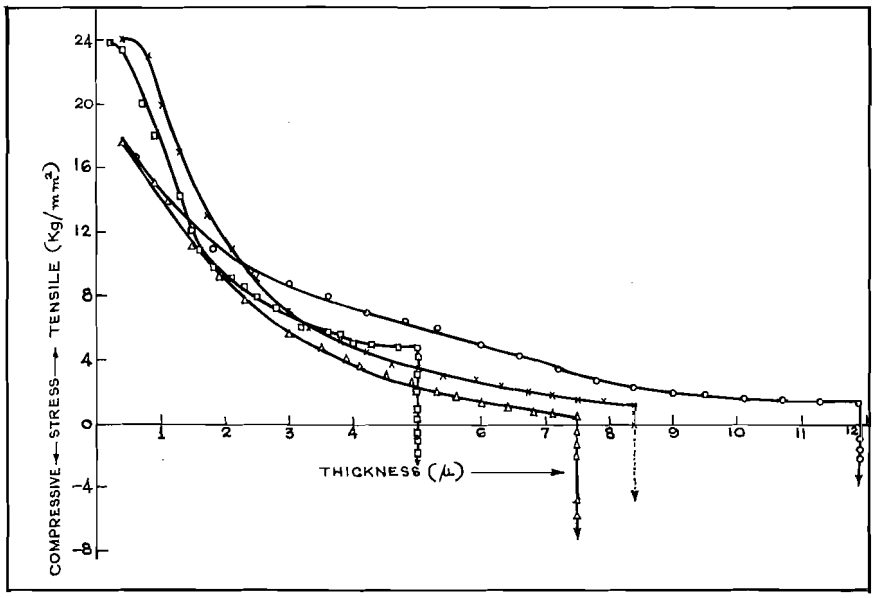

FIG. 2. Variation of internal stress due to consumption of CTAB. ○, at start; ×, after 2 h; △, after 4 h; □, after 6 h.

aim of this investigation is to ascertain the consumption pattern of the surfactant during the deposition.

From Fig. 2, it can be seen that the peak stress of fresh bath is lower. The mean stress remains tensile even with the electrolyte used for 6 h of electrolysis without replenishing CTAB. The compressive aftereffect is seen in all the solutions as observed earlier (1). The lead dioxide deposits obtained were shiny, smooth, adherent, and free from pinholes.

Conclusion

The beneficial effect of a cathodic surface active agent like CTAB, which is a typical example of quaternary ammonium surfactants, on the anodic deposition of lead dioxide offers an interesting study. It is now well established that the cationic surfactant is also consumed, perhaps by adsorption/oxidation at the anode during the deposition of lead dioxide, and these results are similar to the observations of Lorking (10). The lower consumption of CTAB in the electrolyte coupled with the obtaining of the desired deposit at higher temperature during the deposition of lead dioxide make the process interesting and attractive from a practical point of view.

1. K. S. A. GNANASEKARAN, K. C. NARASIMHAM, and H. V. K. UDUPA. Electrochim. Acta, **15**, 1615 (1970).
2. H. V. K. UDUPA, K. C. NARASIMHAM, and K. S. A. GNANASEKARAN. Indian patent 124 215. 1969.
3. K. S. A. GNANASEKARAN, K. C. NARASIMHAM, and H. V. K. UDUPA. Addition of cetyl trimethyl ammonium bromide in electrodeposition of lead dioxide. Presented at the 10th Seminar on Electrochemistry held in CECRI, Karaikudi, India. 1969.
4. K. C. NARASIMHAM, S. VASUNDARA, and H. V. K. UDUPA. Analyst, **97**, 260 (1972).
5. K. C. NARASIMHAM and H. V. K. UDUPA. Proc. Symp. Electrolytic Cells. Central Electrochemical Research Institute, Karaikudi, India. 1961. p. 22.
6. T. P. HOAR and D. J. ARROWSMITH. Trans. Inst. Metal Finish. **34**, 354 (1957).
7. D. R. GABE and J.M. WEST. Trans. Inst. Metal Finish. **40**, 197 (1963).
8. F. J. WELCHER. The analytical uses of ethylene diamine tetraacetic acid. D. Van Nostrand Co. Inc., London. 1958. p. 193.
9. A. I. VOGEL. A text book of quantitative inorganic analysis including elementary instrumental analysis. III ed. Longmans, Green & Co., London. 1964. p. 358.
10. K. F. LORKING. J. Electrochem. Soc. **102**, 479 (1955).

Can. J. Chem. Downloaded from www.nrcresearchpress.com by 210.87.254.42 on 09/05/12
For personal use only.

A Kinetic Determination of the Dissociation Energy of the C—O Bond in Anisole

S. PAUL AND M. H. BACK

Chemistry Department, University of Ottawa, Ottawa, Canada K1N 6N5

Received June 12, 1975

S. PAUL and M. H. BACK. Can. J. Chem. **53**, 3330 (1975).

The rate of dissociation of anisole into phenoxy and methyl radicals has been measured using a toluene scavenging technique. The rate was measured by the production of methane over the range of temperature 720–795 K and was shown to be first order in anisole concentration and homogeneous. The rate constant, expressed in the Arrhenius form, was

$$\log k\,(s^{-1}) = 13.7 \pm 0.3 - \frac{58000 \pm 2000}{2.3RT}$$

The dissociation energy, $D_{298}(C_6H_5O—CH_3)$, therefore equals 57 ± 2 kcal/mol, giving $\Delta H_f(C_6H_5O) = 5$ kcal/mol. The stabilization energy of the phenoxy radical is discussed.

S. PAUL et M. H. BACK. Can. J. Chem. **53**, 3330 (1975).

On a mesuré le taux de dissociation de l'anisole en radicaux phénoxy et méthyle en utilisant la technique de piégeage au toluène. On a mesuré la vitesse par la production de méthane à des températures allant de 720 à 795 K et on a montré que cette vitesse est du premier ordre en concentration d'anisole et qu'elle est homogène. La constante de vitesse, exprimée sous une forme d'Arrhénius, est

$$\log k\,(s^{-1}) = 13.7 \pm 0.3 - \frac{58000 \pm 2000}{2.3RT}$$

L'énergie de dissociation $D_{298}(C_6H_5O—CH_3)$ est donc égale à 57 ± 2 kcal/mol donnant un $\Delta H_f(C_6H_5O) = 5$ kcal/mol. On discute de l'énergie de stabilisation du radical phénoxy.

[Traduit par le journal]

Introduction

There is an abundance of evidence that the thermal decomposition of dialkyl, diaryl, and alkyl aryl ethers occurs by an initial dissociation into radicals, followed by radical chain processes (1, 2). Some cyclic ethers, such as dioxalane (3) and tetrahydrofuran (4) also decompose in this way. Nevertheless there are no direct measurements of the dissociation energy of the C—O bond in ethers.[1] These values are available only through the heats of formation of the alkoxy radicals, and few of these are known with confidence (6). In order to provide a direct measurement of the dissociation energy of an ether linkage, the present study of the thermal decomposition of anisole was undertaken.

Anisole was the ether chosen for study because it was expected that the $C_6H_5O—CH_3$ bond would be considerably weakened due to the stabilization of the phenoxy radical. Toluene would therefore provide a suitable scavenger so that the rate of the initial dissociation could be measured. The technique involved the pyrolysis of mixtures of anisole and toluene in a static system. The following reactions would be expected to occur.

[1] $$C_6H_5OCH_3 \rightarrow C_6H_5O + CH_3$$

[2] $$CH_3 + C_6H_5CH_3 \rightarrow CH_4 + C_6H_5CH_2$$

[3] $$C_6H_5O + C_6H_5CH_3 \rightarrow C_6H_5OH + C_6H_5CH_2$$

[4] $$2C_6H_5CH_2 \rightarrow (C_6H_5CH_2)_2$$

From the measurement of the rate of formation of methane or phenol, the rate of bond fission in anisole may be obtained. With certain assumptions, the temperature-dependence of this rate may be equated to the bond dissociation energy.

Experimental

The experiments were performed in a conventional glass vacuum apparatus which included a 3-l mixing vessel, a 342-cc quartz reaction vessel, and a series of traps for fractionation of the products of the reaction. The mixing vessel and storage flasks were enclosed in an oven maintained at 110 °C, to ensure sufficient pressure

[1] In a concurrent study by Pacey (5) a value for $D(CH_3—OCH_3)$ has been determined.

Can. J. Chem. Downloaded from www.nrcresearchpress.com by 210.87.254.5 on 09/05/12
For personal use only.

Can. J. Chem. Downloaded from www.nrcresearchpress.com by 210.87.254.5 on 09/05/12
For personal use only.

of the reactants. The pressure in the mixing vessel was measured with a glass diaphragm gauge operated as a null measurement. A second reaction vessel, packed with glass tubes to give a S/V ratio of 9 cm^{-1} was used for several series of experiments to test for a heterogeneous reaction. The reaction vessel was enclosed in an electrically heated iron cylinder and the temperature was controlled within $\pm 0.5°$. Mixtures of reactants were allowed to equilibrate for at least 18 h and were admitted to the reaction vessel through heated capillary tubing. The final pressure in the mixing vessel was the initial pressure of the reactants in the reaction vessel. Several series of experiments were done for a fixed reaction time with the same mixture in the mixing vessel, but with a continuously decreasing pressure in the reaction vessel, corresponding to the ratio of volumes of the reaction vessel and the mixing vessel.

Toluene was research grade (99.9%) obtained from Phillips Petroleum Co. Anisole was reagent grade from Fisher Scientific Co. Analysis by gas chromatography showed that the most probable impurities, benzene, toluene, methyl anisole, and phenetole, if present, were less than 0.1% of the anisole. Hydrogen, methane, carbon monoxide, and ethane, used for calibrations, were research grade from Phillips Petroleum Co. Other compounds used for calibration were research grade from various suppliers.

At the end of an experiment, the products and reactants were fractionated through traps at −78 and −196 °C. The noncondensable gases were collected and the total amount measured in the gas burette. These products, which consisted of hydrogen, carbon monoxide, and methane, were analyzed by gas chromatography using a silica gel column (9 ft × 1/4 in.) at −35 °C. The carrier gas was He and a thermal conductivity detector was used. Under these conditions the sensitivity for detection of hydrogen is not great and in some experiments, where the amount of hydrogen was small, the yield of hydrogen was calculated as the difference between the yields of methane and carbon monoxide and the total yield of noncondensable products. The fraction collected at −196 °C was analyzed on the same silica gel column maintained at 30 °C. The fraction collected at −78 °C was weighed and the volume calculated by assuming a density equal to that of toluene. Aliquot samples were taken for analysis by gas chromatography. The column used was 4% silicone grease SE 30 on chromosorb G (9 ft × 1/4 in.) maintained initially at 100 °C. After the major products, phenol and xylenes, together with the reactants anisole and toluene, were eluted, the temperature was quickly raised to 170 °C and, after stabilization, dibenzyl and other dimers were eluted. Calibrations of the liquid products were made from solutions in toluene. The reproducibility was about ±4%.

Results

The reaction was studied over the temperature range 720–795 K and at pressures of anisole from 16 to 4 Torr. The major products were methane, phenol, dibenzyl, and hydrogen. Carbon monoxide, ethylbenzene, xylenes, and benzyl phenyl ether were minor products.

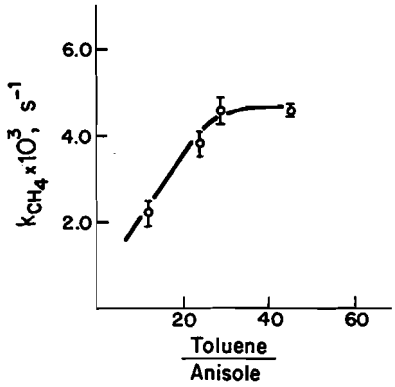

FIG. 1. Variation of the rate constant for the formation of methane as a function of the ratio toluene/anisole at 795 K. Range of anisole pressure, 4–13 Torr.

Ethane, benzaldehyde, and cresols were shown to be absent. Identification was made by coincidence of retention time with pure samples on two different columns. A small amount of product was tentatively identified as $C_6H_5CH_2$-OC_6H_5, the cross-combination product, because its retention time was intermediate between that of diphenyl ether and dibenzyl ether. The yield of xylenes and ethyl benzene was always less than 5% of the yield of methane or phenol. The yield of methane and hydrogen from the decomposition of toluene itself was shown to be negligible in the temperature range studied.

The rate of formation of methane from the decomposition of anisole was first studied as a function of the ratio of toluene to anisole, in order to determine the pressure of toluene necessary to scavenge all the radicals formed in the initial dissociation. The rate constant for the formation of methane is shown as a function of the ratio of toluene/anisole in Fig. 1. For this calculation, the rate of formation of methane was assumed to be first order with respect to anisole; evidence to support this will be presented later. Complete scavenging of the methyl radicals occurs at a ratio of toluene/anisole above 30. In most of the subsequent series of experiments, the ratio of toluene/anisole was kept at 30. In a few series, the ratio was increased to 45 and no change in the rate constant was observed.

The Primary Products, Methane, Phenol, and Dibenzyl

The yields of methane, phenol, and dibenzyl are shown as a function of initial pressure of anisole for a given time of reaction in Fig. 2.

Can. J. Chem. Downloaded from www.nrcresearchpress.com by 210.87.254.5 on 09/05/12
For personal use only.

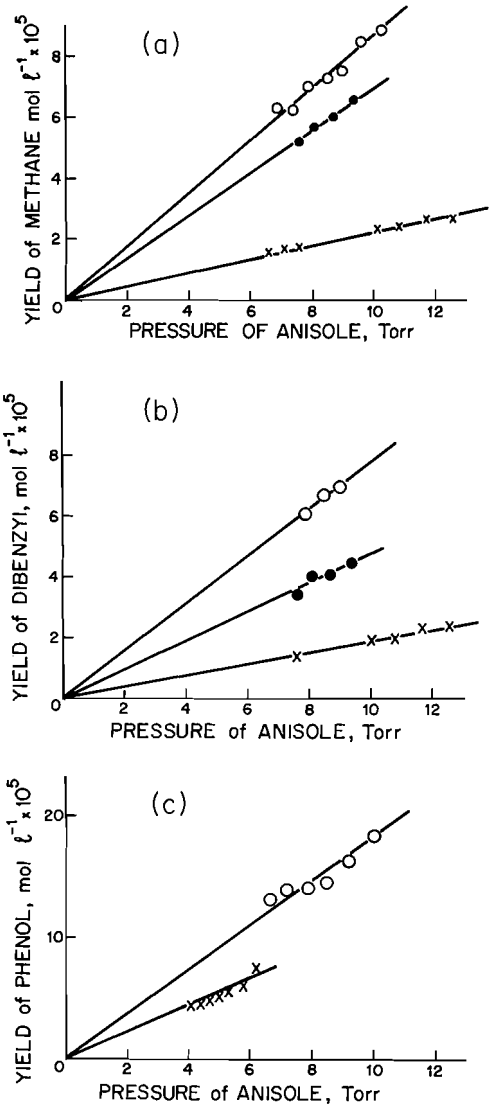

FIG. 2. Yields of the major primary products as a function of initial pressure of anisole. (*a*) Methane, 762 K; (*b*) dibenzyl, 762 K; (*c*) phenol, 795 K. ○, 500 s; ●, 400 s; ×, 100 s.

The linearity of these plots, extrapolating to the origin, shows that the rates of formation of these products are first order with respect to anisole. Yield–time plots for each of these products were obtained by interpolation for a particular pressure of anisole from series of experiments such as given in Fig. 2. An example is shown in Fig. 3. The integrated first order rate equation for methane at 762 and 795 K is shown in Fig. 4. Thus, both the concentration dependence and the time dependence show that

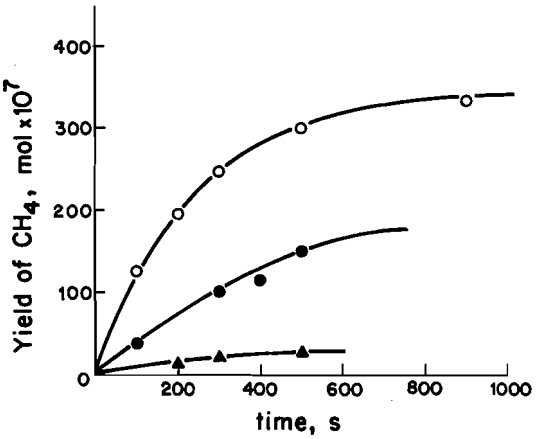

FIG. 3. Yield of methane as a function of time. Anisole pressure = 5 Torr. ○, 795 K; ●, 762 K; ▲, 740 K.

the rate of formation of methane is first order with respect to anisole.

In previous studies of dissociation reactions using the toluene-carrier technique, one of the most serious errors was caused by the fact that under the conditions of high temperature and low pressure, the dissociation was often in its pressure-dependent region (6). In the flow system used for these studies, a suitable test for order could not always be achieved. In the present technique, using toluene as a scavenger in a static system, this error is not important. At the lower temperatures, the measured rate constants are 100–1000 times less than typical values measured by the toluene-carrier technique. This, combined with the higher pressures of the static system, ensures that the rate constants for dissociation are truly first order.

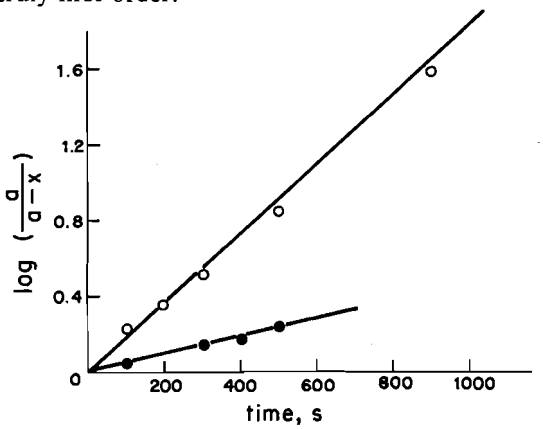

FIG. 4. Log $a/(a - x)$ as a function of time. ○, 762 K; ●, 795 K.

TABLE 1. Yields and ratios of products

T (K)	Pressure of anisole (Torr)	Time (s)	CH_4 (mol $l^{-1} \times 10^5$)	Phenol / Methane	Dibenzyl / Methane	Hydrogen / Methane
720	10.0	600	1.46	0.97	0.84	0.07
	9.3	600	1.43	0.91	0.80	0.06
	8.7	600	1.32	0.90	0.86	
	8.1	600	1.29	0.81	0.86	0.06
	7.5	600	1.20	1.00	0.90	
	12.4	600	1.29	0.90	1.17	
	11.6	600	1.23	0.96	1.00	
	10.7	600	1.14	0.87	1.00	
	10.0	600	1.02	0.97	1.00	
740	10.2	300	1.72	0.72	0.74	
	9.5	300	1.61	0.79	0.64	0.11
	8.8	300	1.49	0.94	0.82	0.11
	8.3	300	1.46	0.83	0.92	
	7.7	500	2.25	1.03	0.80	
	7.2	500	2.22	0.90	0.74	
	6.7	500	2.02	0.89	0.83	
	6.3	500	2.02	0.89	0.71	
762	9.4	300	5.73	0.89	0.75	0.13
	8.8	300	5.50	0.87	0.69	0.06
	8.2	300	5.15	0.90	0.76	0.12
	12.6	100	2.66	0.90	0.87	0.01
	11.7	100	2.60	0.84	0.89	
	10.8	100	2.34	0.86	0.83	0.02
	10.1	100	2.28	0.84	0.83	0.02
	9.4	400	6.68	1.16	0.68	0.16
	8.1	400	5.76	1.09	0.70	0.16
	7.6	400	5.30	1.02	0.65	0.18
795	10.0	500	16.90	1.08	0.38	0.30
	9.2	500	15.92	1.02	0.43	0.29
	8.5	500	15.0	0.97	0.33	
	7.9	500	13.3	1.05	0.44	0.32
	7.2	500	12.8	1.09	0.46	0.26
	6.7	500	11.2	1.17	0.52	0.33
721P	13.5	1800	4.95	0.98	0.60	
	12.2	1800	5.12	0.88	0.65	
741P	14.4	600	4.65	0.95	0.74	

According to the simple mechanism given by [1]–[4], the yields of phenol and methane should be equal and the yield of methane or of phenol should equal the yield of dibenzyl. Some of the results, showing the stoichiometry, are given in Table 1. The ratio of phenol/methane is close to one under most conditions and is independent of time, further evidence that phenol is a primary product. The ratio dibenzyl/methane is close to one at the lowest temperature, 720 K, but becomes less than one as the temperature is increased. Dibenzyl is relatively unstable at these temperatures and might be expected to undergo secondary decomposition. That this is the case is shown by the decrease in the ratio of dibenzyl/methane with time, illustrated in Fig. 5. Complementing the loss of dibenzyl with time is the appearance of hydrogen as a product. Ratios of hydrogen/methane as a function of time are shown in Fig. 6, which clearly indicates that hydrogen is a secondary product.

It seems reasonable to suggest that secondary decomposition of dibenzyl yields hydrogen. Two possible mechanisms for this decomposition may be suggested: (*a*) molecular decomposition to give hydrogen and stilbene; (*b*) dissociation by C—H bond rupture followed by hydrogen-

Can. J. Chem. Downloaded from www.nrcresearchpress.com by 210.87.254.5 on 09/05/12
For personal use only.

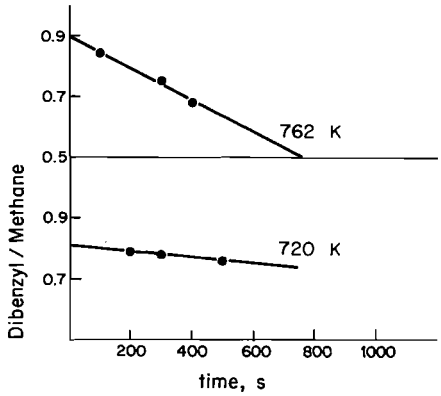

FIG. 5. The ratio of dibenzyl/methane as a function of time. Range of total pressure = 180 − 300 Torr.

atom abstraction. An early study of the thermal decomposition of dibenzyl (7) in the region of 1000 K at low pressure showed that, in the absence of a scavenger, hydrogen was a minor product. Blades *et al.* (8), however, found that when dibenzyl was pyrolyzed in the presence of toluene, hydrogen was an important product. It appears reasonable to conclude that in the present study, secondary decomposition of dibenzyl yields hydrogen as a main product.

The extrapolation of the ratio dibenzyl/methane to zero time was always less than one and usually varied between 0.9 and 0.8. The complete collection of dibenzyl was difficult because of its low volatility and it may be assumed that some loss occurred in this way. Because of the temperature-programming required for the analysis of dibenzyl, the error in its calibration, ±5%, was larger than that of

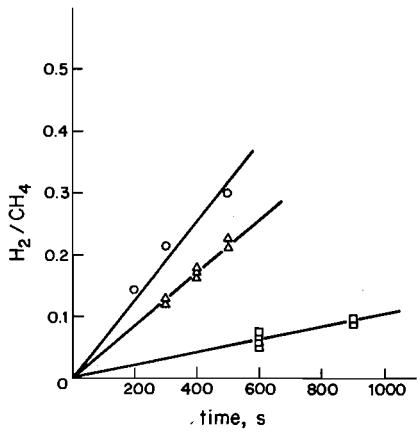

FIG. 6. The ratio of hydrogen/methane as a function of time. Range of total pressure 200–300 Torr. ○, 795 K; △, 762 K; □, 720 K.

TABLE 2. Rate constants

T (K)	Average k ($s^{-1} \times 10^3$)	Number of series averaged
795	4.82±0.2	1
762	1.10±0.05	3
740	0.30±0.02	3
720	0.12±0.005	2
721P	0.11±0.01	1
741P	0.28±0.01	1
752P	0.54±0.01	1

the other major products. The low ratio of dibenzyl/methane observed in the present study may be attributed to experimental error, compounded by the loss by secondary decomposition, and not to any serious complication to the simple series of reactions 1 to 4. That complete scavenging of the methyl and phenoxy radicals occurred seems a reasonable conclusion in view of the fact that combination products of the methyl radical, such as ethyl benzene and xylenes were never more than 5% of the methane.

Calculation of Rate Constants

The rate constants were calculated from the yield of methane, using the integrated first order rate equation, since the measurement of this product was judged to be the most accurate. An average rate constant was obtained from each series of experiments, usually comprising six or seven measurements, such as illustrated in Fig. 2. Each of these rate constants were again averaged to obtain a final value for each temperature. A summary of the rate constants obtained in the packed and unpacked vessels, with the number of series used to obtain the average, is given in Table 2. The Arrhenius plot of the rate constants is shown in Fig. 7. From these results, the activation energy of the reaction is 58 ± 2 kcal/mol and log A (s^{-1}) is 13.7 ± 0.3.

Minor Products

The minor products, which amounted to about 5% of the yield of methane, were xylenes, ethylbenzene, and carbon monoxide. The formation of xylenes suggests that in the reaction of radicals with toluene, there was some interaction with the ring, either as abstraction or as addition.

[5] $CH_3 + C_6H_5CH_3 \rightarrow CH_4 + C_6H_4CH_3$

$C_6H_4CH_3 + CH_3 \rightarrow$ xylenes

Can. J. Chem. Downloaded from www.nrcresearchpress.com by 210.87.254.5 on 09/05/12
For personal use only.

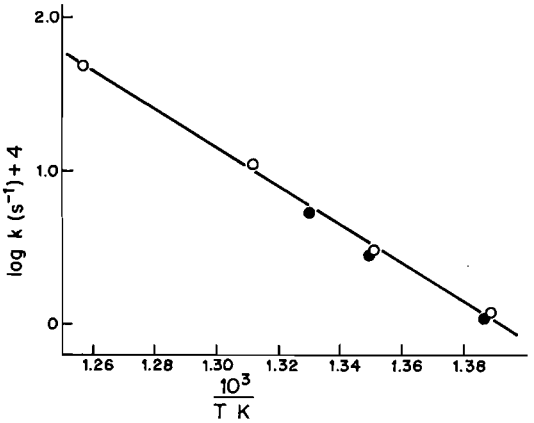

FIG. 7. Arrhenius plot of log k_{CH_4} as a function of $1/T$(K). Filled circles denote experiments in the packed reaction vessel.

[6] $CH_3 + C_6H_5CH_3 \rightarrow$ 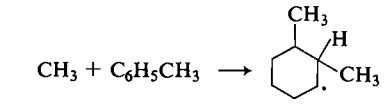

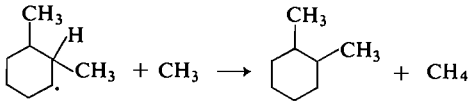

and other isomers

Similarly, ethylbenzene may be formed by the combination of benzyl and methyl radicals. The formation of these products represents a loss of methane and dibenzyl. A correction was therefore applied to the yield of methane equivalent to the sum of the yields of xylenes and ethylbenzene. The maximum correction at the highest temperature was not more than 5% of the yield of methane and was negligible at the other temperatures.

A small amount of carbon monoxide, about 2% of the yield of phenol, was detected at the highest temperature. The rate of formation of carbon monoxide was first order in anisole and the most likely reaction leading to its formation is the decomposition of the phenoxy radical

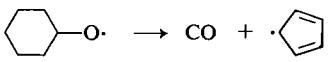

This reaction was suggested as the source of carbon monoxide formation in the pyrolysis of anisole at 1223 K, where it was a major product (9). In the present experiments the ratio toluene/anisole was constant for the determination of the order.

Discussion

The identification of the activation energy for the rate of formation of methane with the bond dissociation energy $D(C_6H_5O—CH_3)$ in anisole is substantiated by the following results: (*1*) The rate of formation of methane is first order with respect to anisole. (*2*) The ratio of dibenzyl/methane is close to one. (*3*) Other products formed from methyl radicals, for example, xylenes and ethylbenzene, are a small fraction of the methane and a correction for loss of methyl radical may be made with reasonable accuracy. (*4*) The formation of methane is a homogeneous reaction. (*5*) The frequency factor is in the range expected for this type of dissociation reaction.

Thus, we may conclude that the rate of formation of methane may be equated to the rate of the homogeneous unimolecular dissociation of anisole into phenoxy and methyl radicals and, with the assumption that the combination of phenoxy and methyl radicals requires no activation energy, the activation energy of the rate may be equated to the dissociation energy of the bond broken.

The uncertainty in the measurement of k is largely the result of errors in recovery and analysis of the products and in the temperature control. The largest average deviation of the rate constant was $\pm 5\%$ at the highest temperature. A reasonable estimate for the random error in the activation energy is therefore ± 2 kcal/mol.

The measured value of the frequency factor for [1] may be combined with the entropy change of the reaction to obtain a value for the frequency factor for the reverse reaction, which, if no activation energy is involved, is the rate constant for combination of the phenoxy and methyl radicals. Although entropy data are not available for the phenoxy radical, the entropy change of the reaction may be assumed to be similar to that for the dissociation of *N*-methylaniline, $C_6H_5NHCH_3$, for which $\Delta S^0 = 36.5$ cal deg^{-1} mol^{-1} (10). A value for k_{-1} of 6×10^7 l mol^{-1} s^{-1} is thus obtained.

The measured values for the combination rate constants for small radicals in the gas phase lie between 10^9 and 10^{10} l mol^{-1} s^{-1}, while the estimated values for resonance-stabilized radicals appear lower, in the range 10^8 to 10^9 l mol^{-1} s^{-1} (10). Although no direct measurement has been made in the gas phase, measurements of the

Can. J. Chem. Downloaded from www.nrcresearchpress.com by 210.87.254.5 on 09/05/12
For personal use only.

TABLE 3. Heats of formation and bond dissociation energies

Compound	ΔH_{f298} (kcal/mol)	Reference	Bond	Dissociation energy (kcal/mol)	Reference
$C_6H_5OCH_3$	−18.0	22	$C_6H_5O—CH_3$	57	This work
$C_6H_5OC_2H_5$	−26.3	23	$C_6H_5O—C_2H_5$	57	This work
$C_6H_5OC_6H_5$	11.9	23	$C_6H_5O—C_6H_5$	73	This work
C_6H_5OH	−23.1	23	$C_6H_5O—H$	80	This work
Radical					
C_6H_5O	+5	This work			
CH_3	34.0	22			
H	52.1	22			
C_2H_5	26.0	22			
C_6H_5	80	22			

rate constant for dimerization of phenoxy radicals in solution (11) indicate a value of 8×10^8 l mol^{-1} s^{-1} and for the combination of phenoxy and alkyl peroxy radicals (12), a similar value. On the other hand, a recent measurement of the rate of disappearance of phenoxy radicals in aqueous solution (13) gave a value for the rate constant of about 10^7–10^8 l mol^{-1} s^{-1}. Although the value of k_{-1} calculated from the present results appears low, it may be concluded, in view of the lack of direct measurements of combination rate constants for large radicals and the uncertainties in comparing rate constants measured in liquid and gas phase, that the value lies within an acceptable range. It should be pointed out that some of the errors associated with the toluene carrier technique, for example, pressure-dependence of the rate constant or chain propagation by benzyl radicals, have in the past sometimes led to low values of the activation energy and frequency factor for bond fission reactions (10). These errors should have been eliminated under the conditions of lower temperature and higher pressure used in the present experiments. In the following tables, therefore, the activation energy measured in the present experiments will be the value given for the dissociation energy of the C—O bond in anisole.

Taking ΔC_p for [1] as approximately equal to RT, the present result gives the dissociation energy of the C—O bond, $D_{298}(C_6H_5O—CH_3) = 57 \pm 2$ kcal/mol. Using this value, the heat of formation of the phenoxy radical may be calculated from the equation

$$\Delta H_f(C_6H_5OCH_3) + D_{298}(C_6H_5O—CH_3) = \Delta H_f(C_6H_5O) + H_f(CH_3)$$

This value and related bond dissociation energies are given in Table 3.

The Stabilization Energy of the Phenoxy Radical

In a qualitative sense the phenoxy radical has long been recognized as being particularly stable. The kinetics and thermodynamics of its reactions in solution (14), its inhibitory effect on the oxidation of hydrocarbons (12), and the energetics of its oxidation–reduction system (15), combined with the fact that aromatic peroxides are not stable at room temperature (16), all indicate a large resonance stabilization. Nevertheless, an unambiguous value for its heat of formation has been difficult to obtain.

From measurements of the critical potentials of oxidation–reduction systems, Hush (15) estimated a value for $D(C_6H_5O—H)$ of 84 kcal/mol, which leads to a value of +9 kcal/mol for $\Delta H_f(C_6H_5O)$. In a study of the kinetics and thermodynamics of reactions of substituted phenoxy radicals with their parent phenol molecule, Mahoney and DaRooge (14) obtained values for the difference in heats of formation between the radicals and parent molecules. The heats of formation of the substituted phenoxy radicals obtained in this way were grouped around the value of +9 kcal/mol for phenoxy estimated by Hush. From the measurement of the ionization potential of the phenoxy radical, Fisher *et al.* (17) calculated a value for $\Delta H_f(C_6H_5O) < 20$ kcal/mol, but suggested that this was probably high by about 10 kcal/mol. Natalis and Franklin (18) reached a similar conclusion from a study of the appearance potential of the $C_6H_5CO^+$ ion from several different sources. Their value of $\Delta H_f(C_6H_5CO^+)$ when combined with relevant thermochemical

Can. J. Chem. Downloaded from www.nrcresearchpress.com by 210.87.254.5 on 09/05/12
For personal use only.

TABLE 4. Comparison of C—H, N—H, and O—H bond dissociation energies

Bond	Dissociation energy (kcal/mol)	Reference	δD
CH_3—H	104	10	
			6
C_2H_5—H	98	6	
			13
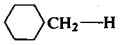	85	6	
		Total decrease	19
NH_2—H	109	24, 25	
			11
CH_3NH—H	98	10	
			13
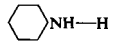	85	10	
		Total decrease	24
HO—H	118	6	
			16
CH_3O—H	102	6	
			22
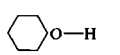	80	This work	
		Total decrease	38

and appearance potential data, gave $\Delta H_f(C_6H_5O) = 9$ kcal/mol. These estimates are about 4–5 kcal/mol higher than the present measurement, but scarcely outside the combined errors of each technique.

The heat of formation of a radical in itself is not a quantitative measure of its stability. Bond dissociation energies involving the radical, however, provide a direct means of estimating its stabilization energy (19). The difference in dissociation energies of two bonds, one of which, on dissociation, gives a stabilized radical while the other gives an unstabilized radical, may be taken as the stabilization energy. If the present measurement of $D(C_6H_5O—CH_3)$ (57 kcal/mol) is compared to the dissociation energy of the C—O bond in dimethyl ether (77 kcal/mol) (5), a stabilization energy of 20 kcal/mol for the phenoxy radical is indicated. A similar value was suggested by Thomas (12) from a study of the inhibition of the oxidation of hydrocarbons by phenol. He concluded that the phenoxy radical was only slightly less stabilized than the alkyl peroxide radical, RO_2, which was estimated to be stabilized by as much as 25 kcal/mol.

To compare the stabilization of the phenoxy radical with the isoelectronic benzyl and anilino radicals, a group of C—H, N—H, and O—H bond dissociation energies are compared in Table 4. The group of three values is shown in order to minimize the effect of uncertainties in individual values. The total decrease through the series is largest for the O—H bonds and smallest for the C—H bonds. In each case, the energy decrease observed when the phenyl group replaces the methyl group is larger than the decrease observed when a methyl group replaces a hydrogen atom. With the N—H bonds, the difference is not large, but these values should be accepted with caution since dissociation energies of bonds containing nitrogen are not, except for a few cases, well established.

Calculations of the spin density distribution and measurements of the e.p.r. hyperfine splittings have been interpreted to indicate a trend toward a more symmetric ring in going from benzyl to phenoxy (20). This is in accord with the suggestion that the ionic form of the phenoxy radical makes a substantial contribution to the total structure. In a kinetic study of reactions involving the phenoxy and the benzyl radicals (21) the results indicated a greater tendency of the phenoxy radical to undergo reaction at a ring site. These interpretations suggest that the stabilization energy should increase in going from benzyl to phenoxy and the present results bear out these expectations.

The authors thank the National Research Council of Canada for financial support of this work.

1. K. J. LAIDLER and D. J. MCKENNEY. The chemistry of the ether linkage. *Edited by* S. Patai. Interscience, New York. 1967. Chapt. 4.
2. W. H. RICHARDSON and H. E. O'NEAL. Decomposition and isomerization of organic compounds. *Edited by* C. H. Bamford and C. F. H. Tipper. Elsevier Publishing Co., London. 1972. Chapt. 4.
3. W. B. GUENTHER and W. D. WALTERS. J. Am. Chem. Soc. **73**, 2127 (1951).
4. C. H. KLUTE and W. D. WALTERS. J. Am. Chem. Soc. **68**, 506 (1946).
5. P. D. PACEY. 58th Canadian Chemical Conference, Toronto, May 1975; Can. J. Chem. **53**, 2742 (1975).
6. J. A. KERR. Chem. Rev. **66**, 465 (1966).
7. C. HORREX and S. E. MILES. Discuss. Faraday Soc. **10**, 187 (1951).
8. H. BLADES, A. T. BLADES, and E. W. R. STEACIE. Can. J. Chem. **32**, 298 (1954).
9. A. G. HARRISON, L. R. HONNEN, H. J. DAUBEN, and F. P. LOSSING. J. Am. Chem. Soc. **82**, 5593 (1960).
10. S. W. BENSON and H. E. O'NEAL. Kinetic data on gas phase unimolecular reactions, NSRDS-NBS21. 1970. Chapt. V.

Can. J. Chem. Downloaded from www.nrcresearchpress.com by 210.87.254.5 on 09/05/12
For personal use only.

11. E. J. LAND and G. PORTER. Trans. Faraday Soc. **59**, 2016 (1963).
12. J. R. THOMAS. J. Am. Chem. Soc. **86**, 4807 (1964).
13. I. V. KHUDYAKOV and V. A. KUZ'MIN. Khim. Vys. Energ. **7**, 331 (1973).
14. L. R. MAHONEY and M. A. DAROOGE. J. Am. Chem. Soc. **92**, 890 (1970).
15. N. S. HUSH. J. Chem. Soc. 2375 (1953).
16. DANIEL SWERN. (*Editor*). Organic peroxides. Wiley-Interscience, New York. 1970.
17. I. P. FISHER, T. F. PALMER, and F. P. LOSSING. J. Am. Chem. Soc. **86**, 2741 (1964).
18. P. NATALIS and J. L. FRANKLIN. J. Phys. Chem. **69**, 2943 (1965).
19. A. STREITWIESER. Molecular orbital theory. Wiley, New York. 1961.
20. R. V. LLOYD and D. E. WOOD. J. Am. Chem. Soc. **96**, 659 (1974).
21. M. F. R. MULCAHY, D. J. WILLIAMS, and J. R. WILMHURST. Aust. J. Chem. **17**, 1329 (1964).
22. S. W. BENSON. Thermochemical kinetics. Wiley, New York. 1968.
23. J. D. COX and G. PILCHER. Thermochemistry of organic and organometallic compounds. Academic Press, New York. 1970.
24. W. TSANG. Interim report on the thermodynamics of chemical species important in aerospace technology. N.B.S. Report #10904, U.S. Government Printing Office, Washington, D.C. 1972.
25. D. M. GOLDEN, R. K. SOLLY, N. A. GAC, and S. W. BENSON. J. Am. Chem. Soc. **94**, 363 (1972).

Can. J. Chem. Downloaded from www.nrcresearchpress.com by 210.87.254.5 on 09/05/12
For personal use only.

Stereochemistry of the Bucherer–Bergs and Strecker Reactions of 4-*tert*-Butylcyclohexanone

JOHN T. EDWARD AND CHOTE JITRANGSRI

Department of Chemistry, McGill University, P.O. Box 6070, Station A, Montreal, Quebec H3C 3G1

Received May 16, 1975

JOHN T. EDWARD and CHOTE JITRANGSRI. Can. J. Chem. **53**, 3339 (1975).

The spirohydantoin (α-isomer) obtained from 4-*tert*-butylcyclohexanone by the Bucherer–Bergs reaction has been shown by n.m.r., u.v., and considerations of steric hindrance to have the *tert*-butyl group and 1′-nitrogen atom *cis*; the β isomer obtained via the Strecker reaction, or via modified Bucherer–Bergs reactions employing carbon disulfide or carbon oxysulfide, has these groups *trans*. The differing stereochemical courses of the various reactions can be explained by a detailed consideration of their mechanisms.

JOHN T. EDWARD et CHOTE JITRANGSRI. Can. J. Chem. **53**, 3339 (1975).

On montre par des études r.m.n., u.v., et chimiques que dans la spirohydantoïne (α) fournie par la *tert*-butyl-4 cyclohexanone dans la réaction de Bucherer–Bergs il y a une relation *cis* entre le groupement *tert*-butyle et le 1′-N de l'anneau hydantoïne. Les composés *spiro* fournis par la réaction de Strecker, ou par les réactions modifiées de Bucherer–Bergs utilisant le disulfide de carbone ou l'oxysulfide de carbone, montrent une relation *trans* entre ces groupements. Par une considération en détail des mécanismes de ces réactions, on peut expliquer les résultats stéréochimiques différents.

Introduction

One of the most convenient routes to α-amino acids involves the reaction of aldehydes or ketones with ammonium carbonate and sodium cyanide to form hydantoins (the Bucherer–Bergs reaction), followed by hydrolysis of the latter to amino acids. The alternative route from ketones via amino nitriles (the Strecker reaction) generally gives the same products, but in poorer yields. However, with some ketones the two routes lead to different products. Thus Munday (1) found that the Bucherer–Bergs reaction of 4-*tert*-butylcyclohexanone (**1**) gave preponderantly one isomeric hydantoin (designated α (2)), accompanied by only a trace of a second (β) isomer. These must have the structures **2** and **3** (X = Y = O). Hydrolysis of the hydantoins furnishes two isomeric amino acids (**4** and **5**). While the amino acid of the α series is the major product by this route, only the amino acid of the β series could be obtained from the amino nitrile furnished by the Strecker reaction (1).

Carrington and co-workers discovered two modifications of the Bucherer–Bergs reaction: one in which the ammonium carbonate of the usual reaction is replaced by ammonium chloride and carbon disulfide (3); a second in which it is replaced by ammonium chloride and carbon oxysulfide (4). These reactions give a 2,4-dithiohydantoin and a 4-thiohydantoin, respectively.

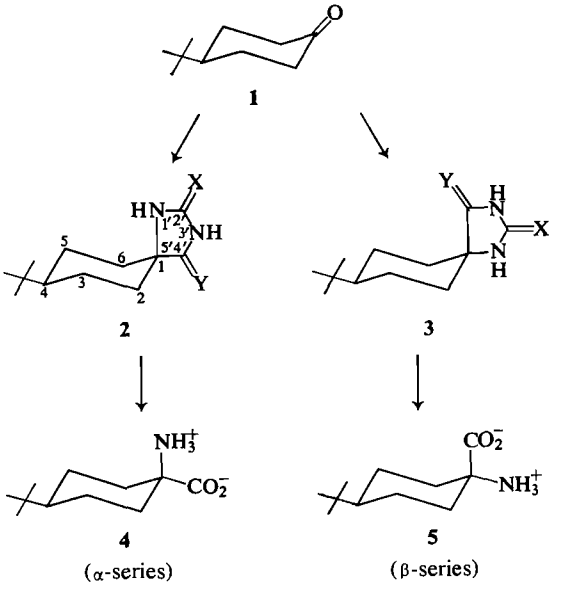

SCHEME 1

We have now found that 4-*tert*-butylcyclohexanone (like many other substituted cyclohexanones studied by Carrington (3)) furnishes exclusively spiro compounds of the β series by these reactions. This was proved by treating the major (α) hydantoin from the normal Bucherer–Bergs reaction with phosphorus pentasulfide (5) and converting it into a 2,4-dithiohydantoin

Can. J. Chem. Downloaded from www.nrcresearchpress.com by 210.87.254.6 on 09/05/12
For personal use only.

Can. J. Chem. Downloaded from www.nrcresearchpress.com by 210.87.254.6 on 09/05/12
For personal use only.

which turned out to differ from the product afforded by Carrington's procedure. On the other hand, 2,4-dithiohydantoin produced by treating with phosphorus pentasulfide the spiro-4-hydantoin afforded by his second modified procedure using carbon oxysulfide, was identical to the compound produced by using carbon disulfide.

The configurations of the α- and β-isomeric compounds obtained from 4-*tert*-butylcyclohexanone have up until now remained unsettled. On the basis of various physical and chemical properties, Munday (1) assigned the structure **2** (X = Y = O) to the α-hydantoin and **3** (X = Y = O) to the β-hydantoin. On the basis of other properties, Cremlyn and Chisholm (6) reversed this assignment. More recently, Maki and Masugi (7) obtained two isomeric 4-benzoyloxycyclohexane-1-spiro-5′-hydantoins (**2** and **3**; X = Y = O; PhCOO in place of *tert*-Bu) from 4-benzoyloxycyclohexanone (**1**; PhCOO in place of *tert*-Bu) by the Bucherer–Bergs reaction, and established by unequivocal chemical evidence that the minor (β) isomer had the structure **3** (X = Y = O; PhCOO in place of *tert*-Bu). This supports, by analogy, Munday's assignment.

In the present paper we offer more direct evidence for this assignment, which is the one shown in Scheme 1. Furthermore, our preliminary studies of the mechanism of the Bucherer–Bergs reaction in its various modifications enable us to explain the curious dependence of the stereochemistry of the product on whether carbon dioxide (in the form of ammonium carbonate), carbon oxysulfide, or carbon disulfide are used.

Experimental

All melting points are in degrees Centigrade and are uncorrected. The proton n.m.r. spectra were determined in the specified solvents with tetramethylsilane as internal standard on a Varian T-60 spectrometer. The carbon-13 n.m.r. spectra were determined on a Bruker 22.63 MHz spectrometer. The infrared spectra were measured on a Perkin-Elmer 257 spectrophotometer. The ultraviolet spectra were obtained with a Unicam SP800 spectrophotometer. Analyses were done by Dr. C. Daessle of Montreal.

*1-Amino-4-tert-butylcyclohexanecarboxynitrile (**14**)*

A solution of 4-*tert*-butylcyclohexanone (30 g), potassium cyanide (13 g), ammonium chloride (11 g) in methanol (150 ml) and water (100 ml), on standing at room temperature for 6 d, deposited a white solid (27.2 g, 77%); ν_{max} (KBr): 3330, 3140 (ν_{N-H}), 2225 (ν_{CN}), and 1615 cm^{-1} (δ_{NH}); δ ($CDCl_3$) 0.91 (s, 9H, *t*-Bu), 1.0–2.2 (m, 9H, cyclohexane), 2.2 (s, 2H, NH_2).

A small amount of this crude aminonitrile was suspended in water, the solution was acidified with hydrochloric acid and the mixture was extracted with ether. The aqueous layer was neutralized with sodium hydroxide and precipitated a white solid having an infrared spectrum identical with that of the crude product. The small amount of neutral compound obtained by evaporating the ether layer showed infrared absorption bands (KBr) at 3400 (ν_{O-H}) and 2225 cm^{-1} (ν_{CN}), but no band at about 1620 cm^{-1} (N—H deformation), and was probably the cyanohydrin **9**.

*4-tert-Butylcyclohexane-1-spiro-5′-hydantoin (α-Isomer, **2**, X = Y = O)*

(a) Normal Bucherer–Bergs Hydantoin Synthesis Using Ammonium Carbonate

A solution of 4-*tert*-butylcyclohexanone (15 g), potassium cyanide (6.8 g), and ammonium carbonate (42 g) in ethanol (220 ml) and water (220 ml) was heated under reflux at 50–55 °C for 5 h, then diluted with water and cooled. The precipitated solid was filtered off, washed with water, and recrystallized from absolute ethanol, giving the α-hydantoin as shiny white crystals; m.p. 315–318 °C (lit. (1) 322 °C; (2) 330 °C) (14.7 g, 68%); ν_{max} (KBr) 3265, 3180 (ν_{N-H}), 1773 ($\nu_{C=O}$), and 1730 cm^{-1} ($\nu_{C=O}$); δ (DMSO-d_6) 0.85 (s, 9H, *t*-Bu), 1.0–2.0 (m, 9H, cyclohexane), 8.62 (s, 1H, 1′), and 10.65 (s, 1H, 3′).

Anal. Calcd. for $C_{12}H_{20}N_2O_2$: C, 64.2; H, 9.0; N, 12.5. Found: C, 64.0; H, 8.9; N, 12.4.

(b) Using Carbon Dioxide

The mixture of 4-*tert*-butylcyclohexanone (5 g), potassium cyanide (2.5 g), and ammonium chloride (2.2 g) in methanol (140 ml) and water (100 ml) was heated to 50–55 °C with stirring. Carbon dioxide was passed into the solution over 4 h. The mixture was diluted with water and cooled. The crude product (5.34 g) was recrystallized from ethanol, and yielded the α-form of the hydantoin, identified by its infrared spectrum.

(c) From 1-Amino-4-tert-butylcyclohexanecarboxynitrile and Ammonium Carbonate

A solution of aminonitrile **18** (1.0 g) and ammonium carbonate (0.52 g) in ethanol–water 20:3 (v/v) (46 ml) was heated to 50–55 °C for 10 h. The crude product (0.32 g) was recrystallized from ethanol, giving the pure α-hydantoin, identified by its infrared spectrum.

(d) From 1-Amino-4-tert-butylcyclohexanecarboxynitrile and Carbon Dioxide

Carbon dioxide was passed into an aqueous ethanol solution of the aminonitrile at 50–55 °C for 4 h. The mixture was treated as above, and yielded a product containing only the α-hydantoin, identified by infrared spectrum.

*4-tert-Butylcyclohexane-1-spiro-5′-hydantoin (β-Isomer, **3** X = Y = O)*

A solution of 1-amino-4-*tert*-butylcyclohexanecarboxynitrile (14) hydrochloride (8 g) and potassium cyanate (14 g) in acetic acid (120 ml) and water (60 ml) was heated at 100 °C under reflux for 1 h. The mixture was cooled and diluted with water, and a white solid filtered off. This was heated with concentrated hydrochloric acid (60 ml) for 30 min. The reaction mixture was diluted with water, cooled, and the crude product was filtered off and was recrystallized from absolute methanol: shiny colorless crystals; m.p. 335–338 °C (dec.); lit. (6) 346–350 °C (3.8

Can. J. Chem. Downloaded from www.nrcresearchpress.com by 210.87.254.6 on 09/05/12
For personal use only.

g, 46%); ν_{max}(KBr) 3200 (ν_{N-H}), 1772 ($\nu_{C=O}$), and 1720 cm^{-1} ($\nu_{C=O}$); δ (DMSO-d_6) 0.87 (s, 9H, *t*-Bu), 1.1–2.1 (m, 9H, cyclohexane) 7.8 (s, 1H, 1′), and 10.55 (s, 1H, 3′).

Anal. Calcd. for $C_{12}H_{20}N_2O_2$: C, 64.2; H, 9.0; N, 12.5. Found: C, 64.2; H, 9.3; N, 12.4.

4-tert-Butylcyclohexane-1-spiro-5′-(2′,4′-dithiohydantoin) (α-Isomer, 2, X = Y = S)

A mixture of 4-*tert*-butylcyclohexane-1-spiro-5′-hydantoin (α-form, m.p. 315–318 °C) (4 g), phosphorus pentasulfide (4 g), and tetralin (150 ml) was heated under reflux for 2 h. The hot solution was decanted from some tar and was allowed to cool. The crude product was removed by filtration and washed with a small amount of cold benzene. It crystallized from methanol as colorless crystals; m.p. 305–306 °C (1.9 g, 42%); ν_{max}(KBr) 3165, 3095 (ν_{N-H}), 1525 cm^{-1} (—N—C=S I band); δ (DMSO-d_6) 0.89 (s, 9H, *t*-Bu), 1.1–2.1 (m, 9H, cyclohexane), 11.5 (s, 1H, 1′), and 13.5 (s, 1H, 3′).

Anal. Calcd. for $C_{12}H_{20}N_2S_2$: C, 56.2; H, 7.8; N, 10.9; S, 25.0. Found: C, 56.4; H, 7.9; N, 10.9; S, 24.7.

4-tert-Butylcyclohexane-1-spiro-5′-(2′,4′-dithiohydantoin) (β-Isomer, 3, X = Y = S)

(a) Carbon Disulfide Modification of the Bucherer–Bergs Hydantoin Synthesis

A solution of 4-*tert*-butylcyclohexanone (4 g), sodium cyanide (2 g), ammonium chloride (2.1 g), and carbon disulfide (2.6 ml) in ethanol (25 ml) and water (10 ml) was heated under reflux to 50–55 °C for 24 h. The mixture was cooled and the crude product was recrystallized from aqueous ethanol, yielding the β-form of the dithiohydantoin as bright yellow crystals; m.p. 277–279 °C (dec.) (3.8 g, 57%); ν_{max}(KBr) 3125 (ν_{N-H}), and 1555 cm^{-1} (—N—C=S I band); δ (DMSO-d_6) 0.90 (s, 9H, *t*-Bu), 1.1–2.4 (m, 9H, cyclohexane), 10.70 (s, 1H, 1′), and 13.28 (s, 1H, 3′).

Anal. Calcd. for $C_{12}H_{20}N_2S_2$: C, 56.2; H, 7.8; N, 10.9; S, 25.0. Found: C, 56.1; H, 7.8; N, 10.7; S, 24.8.

(b) From the Aminonitrile and Carbon Disulfide in Ethanol

A solution of 1-amino-4-*tert*-butylcyclohexanecarboxynitrile (β-isomer) (1 g), and carbon disulfide (1.5 ml) in ethanol (15 ml) was heated under reflux at 50–55 °C for 14 h. The solution was cooled and the bright yellow crystals were removed by filtration and recrystallized from aqueous ethanol, giving the pure β-dithiohydantoin (0.6 g, 42%), i.r. spectrum identical with that of the product from method (*a*).

(c) Replacement of Oxygen in 4-tert-Butylcyclohexane-1-spiro-5′-(4′-thiohydantoin) (β-Isomer, 3, X = O, Y = S) by Sulfur

4-*tert*-Butylcyclohexanespiro-5′-(4′-thiohydantoin) (β-form, m.p. 339–341 °C) (see below) was heated with phosphorus pentasulfide in tetralin for 2 h. The dithiohydantoin thus obtained was identical (i.r.) with the product from method (*a*).

4-tert-Butylcyclohexane-1-spiro-5′-(2′-thiohydantoin) (α-Isomer, 2, X = S, Y = O)

4-*tert*-Butylcyclohexane-1-spiro-5′-(2′,4′-dithiohydantoin) (α-form, m.p. 305–306 °C) (0.6 g), 2-aminoethanol (2 ml), and water (4 ml) were heated under reflux for 1 h. The 4′-β′-hydroxyethylimino derivative was removed by filtration of the cooled solution and was heated with concentrated hydrochloric acid (25 ml) and water (20 ml) under reflux for 45 min. After cooling, the crude product was removed and recrystallized from absolute ethanol: colorless crystals; m.p. 358 °C (sublimes) (0.2 g, 36%); ν_{max}(KBr) 3175 (ν_{N-H}), 1735 ($\nu_{C=O}$), and 1517 cm^{-1} (—N—C=S I band); δ (DMSO-d_6) 0.87 (s, 9H, *t*-Bu) 1.0–2.0 (m, 9H, cyclohexane), 10.85 (s, 1H, 1′), and 11.85 (s, 1H, 3′); λ_{max} (EtOH) 265 nm (ε 18 400), 225 nm (ε 7460).

Anal. Calcd. for $C_{12}H_{20}N_2OS$: C, 59.9; H, 8.4; N, 11.6; S, 13.3. Found: C, 60.3; H, 8.3; N, 11.6; S, 13.6.

4-tert-Butylcyclohexane-1-spiro-5′-(2′-thiohydantoin) (β-Isomer, 3, X = S, Y = O)

4-*tert*-Butylcyclohexane-1-spiro-5′-(2′,4′-dithiohydantoin) (β-form, m.p. 277–279 °C) (1.5 g), 2-aminoethanol (2 ml), and water (2 ml) were heated under reflux for 1 h. The crude product was removed and heated with concentrated hydrochloric acid (20 ml) and water (10 ml) for 45 min. The solution was allowed to cool and a pale yellow solid crystallized out. It was washed with water and recrystallized from aqueous ethanol, giving colorless crystals; m.p. 310–313 °C (dec.) (0.6 g, 43%); ν_{max} (KBr) 3235, 3125 (ν_{N-H}), 1760 ($\nu_{C=O}$), and 1564 cm^{-1} (—N—C=S I band); δ (DMSO-d_6) 0.87 (s, 9H, *t*-Bu), 1.2–2.3 (m, 9H, cyclohexane), 10.13 (s, 1H, 1′), and 11.71 (s, 1H, 3′); λ_{max} (EtOH) 267 nm (ε 19 800), 227 nm (ε 7340).

Anal. Calcd. for $C_{12}H_{20}N_2OS$: C, 59.9; H, 8.4; N, 11.6; S, 13.3. Found: C, 60.5, H, 8.4; N, 11.7; S, 13.0.

4-tert-Butylcyclohexane-1-spiro-5′-(4′-thiohydantoin) (β-isomer, 3, X = O, Y = S)

(a) Carbon Oxysulfide Modification of the Bucherer–Bergs Hydantoin Synthesis

A solution of 4-*tert*-butylcyclohexanone (2.5 g), potassium cyanide (2.1 g), and ammonium chloride (1.8 g) in ethanol (50 ml) and water (15 ml) was heated to 50–55 °C under reflux. Carbon oxysulfide was passed into the solution for 3 h while stirring. The solution was cooled and a pale yellow solid removed and recrystallized from absolute ethanol: pale yellow needles; m.p. 339–341 °C (2.1 g, 54%); ν_{max} (KBr) 3200, 3075 (ν_{N-H}), 1740 cm^{-1} ($\nu_{C=O}$); δ (DMSO-d_6) 0.90 (s, 9H, *t*-Bu) 1.1–2.4 (m, 9H, cyclohexane), 8.5 (s, 1H, 1′), and 12.4 (s, 1H, 3′).

Anal. Calcd. for $C_{12}H_{20}N_2OS$: C, 59.9; H, 8.4; N, 11.6; S, 13.3. Found: C, 60.1; H, 8.5; N, 11.8; S, 13.5.

(b) From the Aminonitrile 14 and Carbon Oxysulfide

Carbon oxysulfide was passed into a stirred solution of 1-amino-4-*tert*-butylcyclohexanecarboxynitrile (5 g) in ethanol (100 ml) at 50–55 °C for 4 h. The mixture was cooled and the solid product was recrystallized from absolute ethanol; pale yellow needles (1.8 g, 27%). These had an i.r. spectrum identical with that of the 4′-thiohydantoin obtained above by method (*a*).

4-tert-Butylcyclohexane-1-spiro-5′-(3′-methyl-2′,4′-dithiohydantoin) (α-Isomer)

4-*tert*-Butylcyclohexane-1-spiro-5′-(2′,4′-dithiohydantoin) (**2**, X = Y = S) (0.92 g) was dissolved in ether (50 ml) and cooled in an ice-bath. The solution was

Can. J. Chem. Downloaded from www.nrcresearchpress.com by 210.87.254.6 on 09/05/12
For personal use only.

treated with a cooled ethereal solution containing about 0.15 g of diazomethane, and the clear yellow solution was left overnight at room temperature.

The ether was evaporated and the residue was recrystallized from aqueous methanol, giving pale yellow needles; m.p. 258 °C (dec.) (0.31 g, 31.9%); ν_{max} (KBr) 3200 (ν_{N-H}), 1520 cm^{-1} (—N—C=S); δ ($CDCl_3$) 0.90 (s, 9H, *t*-Bu), 1.0–2.3 (m, 9H, cyclohexane), 3.60 (s, 3H, 3′-CH_3), 8.5 (broad, 1H, 1′).

Anal. Calcd. for $C_{13}H_{22}N_2S_2$: C, 57.7; H, 8.2. Found: C, 57.6; H, 8.3.

4-tert-Butylcyclohexane-1-spiro-5′-(3′-methyl-2′,4′-dithiohydantoin) (β-Isomer)

4-*tert*-Butylcyclohexane-1-spiro-5′-(2′,4′-dithiohydantoin) (**3**, X = Y = S) (0.58 g) in ether (60 ml) was treated with an ethereal solution containing about 0.15 g of diazomethane, and worked up by the same procedure as above: yellow crystals; m.p. 215–217 °C (0.2 g, 32.7%); ν_{max} (KBr) 3200 (ν_{N-H}), 1539 cm^{-1} (—N—C=S I band); δ ($CDCl_3$) 0.96 (s, 9H, *t*-Bu), 1.2–2.3 (m, 9H, cyclohexane), 3.60 (s, 3H, 3′-CH_3), 7.9 (broad, 1H, 1′).

Anal. Calcd. for $C_{13}H_{22}N_2S_2$: C, 57.7; H, 8.2. Found: C, 57.6; H, 8.4.

Dissociation Constants of α- and β-isomers of 4-tert-Butylcyclohexane-1-spiro-5′-(3′-methyl-2′,4′-dithiohydantoin)

The ultraviolet absorption spectra of the α- and β-isomers were obtained in 50% (v/v) aqueous ethanol, in 0.1 *N* aqueous sodium hydroxide, and in phosphate buffer of p*H* 11.0 in 50% (v/v) aqueous ethanol, and analyzed by conventional methods (8) to give the following pK_a values: α-isomer, 10.8 ± 0.1; β-isomer, 10.85 ± 0.15.

4-tert-Butylcyclohexane-1-spiro-5′-(1′,3′-dimethyl-2′,4′-dithiohydantoin) (α-Isomer)

4-*tert*-Butylcyclohexane-1-spiro-5′-(2′,4′-dithiohydantoin) (α-form, m.p. 305–306 °C) (0.45 g), dissolved in ether (50 ml), was treated with an excess of ethereal diazomethane and left overnight at room temperature. The solvent was removed, the residue was washed with sodium hydroxide solution and was taken up in ether. The ether was evaporated and the oily yellow residue was recrystallized from aqueous ethanol: colorless needles; m.p. 101–105 °C (0.25 g, 51%); ν_{max} (KBr) 1580 cm^{-1} (—N—C=S I band); δ ($CDCl_3$) 0.91 (s, 9H, *t*-Bu), 1.1–2.2 (m, 9H, cyclohexane), 2.63 (s, 3H, 1′-CH_3), and 3.40 (s, 3H, 3′-CH_3).

Anal. Calcd. for $C_{14}H_{24}N_2S_2$: C, 59.1; H, 8.5; N, 9.8; S, 22.5. Found: C, 59.4; H, 8.5; N, 10.0; S, 22.8.

4-tert-Butylcyclohexane-1-spiro-5′-(1′,3′-dimethyl-2′,4′-dithiohydantoin (β-Isomer)

4-*tert*-Butylcyclohexane-1-spiro-5′-(2′,4′-dithiohydantoin) (β-form, m.p. 277–279 °C) (0.60 g) in ether (30 ml) was treated with an excess of ethereal diazomethane, and worked up as above: pale yellow crystals; m.p. 116–123 °C (0.4 g, 60%); ν_{max} (KBr) 1586 cm^{-1} (—N—C=S I band); δ ($CDCl_3$) 0.93 (s, 9H, *t*-Bu), 1.2–2.4 (m, 9H, cyclohexane), 2.60 (s, 3H, 1′-CH_3), and 3.33 (s, 3H, 3′-CH_3).

Anal. Calcd. for $C_{14}H_{24}N_2S_2$: C, 59.1; H, 8.5; N, 9.8; S, 22.5. Found: C, 58.9; H, 8.7; N, 9.7; S, 22.4.

4-tert-Butylcyclohexane-1-spiro-5′-(3′-acetylhydantoin) (α-Isomer)

A solution of 4-*tert*-butylcyclohexane-1-spiro-5′-hydantoin (**2**; X = Y = O) (m.p. 320 °C) (1.05 g) in acetic anhydride (100 ml) was heated under reflux for 42 h. The solvent was evaporated off under reduced pressure and the residue was recrystallized from aqueous ethanol, giving pale-cream crystals; m.p. 180–184 °C (0.85 g, 74%); ν_{max} (KBr) 3220 (ν_{N-H}), 1787 ($\nu_{C=O}$), 1770 ($\nu_{C=O}$), and 1720 cm^{-1} ($\nu_{C=O}$); δ ($CDCl_3$) 0.91 (s, 9H, *t*-Bu), 1.4–2.4 (m, 9H, cyclohexane), 2.63 (s, 3H, acetyl), and 9.2 δ (s, 1H, 1′).

Anal. Calcd. for $C_{14}H_{22}N_2O_3$: C, 63.1; H, 8.3; N, 10.5. Found: C, 63.5; H, 8.5; N, 10.8.

The 3′-acetyl compound (0.27 g) was boiled with 10 ml of 0.1 *N* NaOH for 30 min. The mixture was cooled, filtered and the white residue was washed with water. The crude solid was shown by i.r. to be the α-form of 4-*tert*-butylcyclohexane-1-spiro-5′-hydantoin (**2**; X = Y = O).

4-tert-Butylcyclohexane-1-spiro-5′-(1′,3′-diacetylhydantoin) (β-Isomer)

A solution of 4-*tert*-butylcyclohexane-1-spiro-5′-hydantoin (β-form) (1.34 g) in acetic anhydride (100 ml) was heated under reflux for 12 h. After the solvent was removed by evaporation under reduced pressure, the residue was crystallized from absolute ethanol, giving pale-cream needles; m.p. 155–160 °C (0.87 g, 51%); ν_{max} (KBr) 1811 ($\nu_{C=O}$), 1764 ($\nu_{C=O}$), and 1704 cm^{-1} ($\nu_{C=O}$); δ ($CDCl_3$) 0.95 (s, 9H, *t*-Bu), 1.2–2.1 (m, 9H, cyclohexane), and 2.65 δ (d, 6H, two acetyls).

Anal. Calcd. for $C_{16}H_{24}N_2O_4$: C, 62.3; H, 7.8; N, 9.1. Found: C, 62.6; H, 8.1; N, 9.1.

4-tert-Butylcyclohexane-1-spiro-5′-(1′-acetylhydantoin) (β-Isomer)

4-*tert*-Butylcyclohexane-1-spiro-5′-(1′,3′-diacetylhydantoin) (0.31 g) was boiled with 10 ml 0.1 *N* NaOH for 30 min. The mixture was cooled and filtered, and the residue was washed with water and recrystallized from aqueous ethanol, giving colorless needles of 4-*tert*-butylcyclohexane-1-spiro-5′-(1′-acetylhydantoin); m.p. 252–255 °C (0.25 g, 93%); ν_{max} (KBr) 3220 (ν_{N-H}), 1790, 1745, ($\nu_{C=O}$), 1615 cm^{-1}; δ ($CDCl_3$) 0.90 (s, 9H, *t*-Bu), 1.5–2.1 (m, 9H, cyclohexane), 2.6 (s, 3H, acetyl), 8.4 (broad, 1H, 3′).

Anal. Calcd. for $C_{14}H_{22}N_2O_3$: C, 63.1; H, 8.3. Found: C, 63.0; H, 8.4.

1-Amino-trans-4-tert-butylcyclohexane Carboxylic Acid (4)

The amino acid was prepared by the method described by Munday (1). 4-*tert*-Butylcyclohexane-1-spiro-5′-hydantoin (**2**; X = Y = O) (2.4 g) was heated with 70% sulfuric acid (20 ml) at 150 °C for 24 h. The mixture was diluted with water and cooled. The precipitated solid was dissolved in ammonium hydroxide and was decolorized by boiling with animal charcoal. The ammonium hydroxide was evaporated off, and the residue was recrystallized from aqueous acetic acid: m.p. 354–356 °C (sublimes) (lit. (1) 300–304 °C, (6) 360 °C (sublimes)) (1.0 g, 46%); ν_{max} (KBr) 3300 (ν_{N-H}), 1664 (asym. $\delta_{NH_3^+}$), 1585 (asym. ν_{C-O}), and 1530 cm^{-1} (sym. $\delta_{NH_3^+}$).

Can. J. Chem. Downloaded from www.nrcresearchpress.com by 210.87.254.6 on 09/05/12
For personal use only.

Anal. Calcd. for $C_{11}H_{21}NO_2 \cdot \frac{1}{2}H_2O$: C, 63.4; H, 10.6; N, 6.7. Found: C, 63.6; H, 10.6; N, 6.9.

1-Amino-cis-4-tert-butylcyclohexane Carboxylic Acid (5)

1-Amino-4-*tert*-butylcyclohexanecarboxynitrile (**14**) (1.57 g) was heated with 65% sulfuric acid (20 ml) at 140 °C for 40 h. The mixture was diluted with water and was cooled. The solid removed by filtration from the cooled solution was dissolved in ammonium hydroxide and treated with animal charcoal. The solution was concentrated to 100 ml, and the precipitate which deposited was recrystallized from aqueous acetic acid, giving a solid (0.88 g, 61%) melting above 360 °C (sublimes) (lit. (1) 345–350 °C, (6) 356 °C (sublimes)); ν_{max} (KBr) 3245 (ν_{N-H}), 1658 (asym. $\delta_{NH_3^+}$), 1598 (asym. ν_{C-O}), and 1537 cm^{-1} (sym. $\delta_{NH_3^+}$).

Anal. Calcd. for $C_{11}H_{21}NO_2$: C, 66.3; H, 10.6; N, 7.0. Found: C, 66.7; H, 10.8; N, 7.1.

Results and Discussion

Configurations of α and β-Isomers

The evidence for assigning structure **2** to hydantoins and thiohydantoins of the α series, and structure **3** to compounds of the β series, comes from the following lines of evidence:

(a) ^{13}C *n.m.r.*

Compounds **2** and **3** (X = Y = S) differ in having the 4′-carbon atom equatorial and axial, respectively, so that in **2** this atom will be *gauche* with respect to all four hydrogen atoms at C-2 and C-6, but in **3** it will be *anti* with respect to two of them. Recent work (9) indicates that the vicinal coupling constants, $^3J_{(^{13}C-^1H)}$, should be greater in the latter case, so that one should expect a wider ^{13}C peak for the axial carbon of **3** than the equatorial carbon of **2**.

In order to apply these ideas, it is necessary to identify the different peaks in the spectra. These are listed in Table 1 and their assignments shown. The resonance of the thiocarbonyl carbon of thioacetamide is at 207.2 p.p.m. (10*a*) (relative to tetramethylsilane), and so the peaks at lowest field in **2** and **3** (X = Y = S) can be assigned to the 4′-carbon atom. The next lowest peaks will be due to the thiourea 2′-carbon atoms (*cf.* δ 182.8 for thiocarbonyl carbon of Et-NHCSNHEt (10*a*)). The peaks at higher field come from the cyclohexane (11) and *tert*-butyl carbon atoms and can be assigned by noting the splitting patterns caused by the hydrogen atoms attached to them.

The C-4′ peak of the β-compound shows a half-width of 18.0 Hz, while the corresponding peak of the α-compound shows a half-width of 9.5 Hz (Table 2). Consequently, we can assign the structure **3** (X = Y = S) to the β compound and **2** (X = Y = S) to the α compound.

The hydantoins **2** and **3** (X = Y = O) would be expected to have 2′ and 4′ peaks at higher fields (*cf.* CH_3CONH_2 carbonyl: 172.7 (10*b*) urea, 161.2 p.p.m. (10*c*)). However, both α- and β-forms proved insoluble in the usual n.m.r. solvents and so the spectra were obtained using deuterated sulfuric acid (95%) as solvent. In acid of this strength it is likely that both carbonyl oxygen atoms are deuterated (12) so that, for example, **3** (X = Y = O) exists as **6** with both C-2′ and C-4′ shifted downfield, but with their relative chemical shifts unaltered. In fact, it can be seen from Table 1 that any downfield shift must be modest. Again the 4′-carbon atom of the β-compound shows the greatest half-width, indicating the structure **3** (X = Y = O) for it.

Finally, the n.m.r. spectra of trifluoroacetic acid solutions of the α- and β-forms of the amino acids (**4** and **5**) were obtained (Tables 1 and 2), and the half-widths of the carboxyl carbon peaks indicated the α-compound to be **4** and the β-compound to be **5**.

The other n.m.r. evidence, summarized in Table 1, also supports (albeit less decisively) the structural relations indicated in Scheme 1. The distance between the 1′-hydrogen atom of the hydantoin ring and the 3,5-axial hydrogen atoms of the cyclohexane ring in **2** can be calculated by trigonometry to be 2.10 Å, assuming tetrahedral angles for the cyclohexane ring (*cf.* cyclohexylamine hydrochloride (13*a*)) and the ring angles of creatinine (13*b*) for the hydantoin ring. This compares with a distance of 2.40 Å when the van der Waals surfaces of the atoms are in contact (14), or a compression of 0.30 Å if the cyclohexane ring remained undistorted from its normal shape. Similar calculations for **3** (X = Y = O) show a more serious compression (0.54 Å) between the 3,5-axial hydrogens and the 4′-oxygen atom, which becomes further aggravated (compression 1.01 Å) in **3** (X = Y = S). This compression of the axial hydrogen atoms should lead to shifts in electron density, causing C-3 and C-5 of **3** (X = Y = O or X = Y = S) to resonate at higher field than these atoms in **2** (X = Y = O or X = Y = S); again, this supports the identification of the compounds of the β-series with **3** (see Table 1). On the other hand, for the amino acids **4** and **5** the reverse should be true: now the axial hydrogens of **4** are subjected to greater compression, when account is taken

Can. J. Chem. Downloaded from www.nrcresearchpress.com by 210.87.254.6 on 09/05/12
For personal use only.

TABLE 1. ^{13}C chemical shifts (p.p.m., downfield from TMS) of Bucherer–Bergs and Strecker products

Compounds	Isomer	Solvent	Cyclohexane ring carbons						Other carbons			
			C-1	C-2	C-3	C-4	C-5	C-6	$(CH_3)_3C$	$(CH_3)_3C$	C′-2′	C′-4′
4-*tert*-Butylcyclohexane-1-spiro-5′-(2′,4′-dithiohydantoin)	α	DMSO-d_6	77.5	38.3	22.9	47.3	22.9	38.3	32.9	28.2	180.3	211.8
	β	DMSO-d_6	73.9	35.8	21.1	46.3	21.1	35.6	32.8	28.1	179.1	211.2
4-*tert*-Butylcyclohexane-1-spiro-5′-hydantoin	α	D_2SO_4	71.3	34.1	24.5	47.7	24.5	34.1	34.8	29.2	162.4	180.6
	β	D_2SO_4	69.6	34.5	23.9	48.1	23.9	34.5	35.1	29.5	162.1	179.3
1-Amino-4-*tert*-butylcyclohexane-1-carboxylic acid	α	CF_3CO_2D	59.8	30.6	20.0	45.4	20.0	30.6	30.8	25.0	—	173.4
	β	CF_3CO_2D	59.3	32.2	21.9	45.3	21.9	32.3	30.9	25.6	—	172.6

TABLE 2. ^{13}C coupling constants of Bucherer–Bergs and Strecker products

Compounds			$^1J_{(^{13}C-^1H)}$ (Hz)				$^3J_{(^{13}C-^1H)}$ (Hz)*	
			C-2,6	C-3,5	C-4	(*t*-Bu)CH_3	C-2′	C-4′
2	(X = Y = S)	(α)	132.0	132.0	132.0	125.0	6.5	9.5
3	(X = Y = S)	(β)	135.0	125.0	125.0	123.0	11.0	18.0
2	(X = Y = O)	(α)	120.0	120.0	123.8	120.0	~3.5	7.0
3	(X = Y = O)	(β)	131.3	123.8	120.0	120.0	~6.0	15.0
4		(α)	146.3	127.5	120.0	125.3	—	6.0†
5		(β)	127.5	127.5	123.8	123.8	—	15.0†

*Half-widths of peaks.
†Carboxyl carbons.

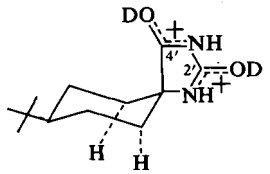

6

of the relative conformational free energies of the axial ammonium and carboxyl groups (15). Again, the experimental results (Table 1) support the assignments shown in Scheme 1.

In summary, n.m.r. evidence from a variety of compounds points unequivocally to the structures indicated in Scheme 1.

(b) Ultraviolet Absorption Spectra

The ultraviolet absorption characteristics of some mono- and dithiohydantoins in ethanol solution are given in Table 3, the absorption bands being classified according to Janssen (16). The band of low intensity and at longest wavelength (Band I) is due to an n → π* transition of the 4-thiocarbonyl group in 4-thiohydantoins or 2,4-dithiohydantoins (8). Such transitions are sensitive to solvent, the band undergoing a red shift when the solvent is changed from ethanol (which stabilizes the ground state by hydrogen bonding) to hydrocarbon (16). Hence we can expect Band I of **3** (X = Y = S) in ethanolic solution to be at longer wavelength than Band I of **2** (X = Y = S), because of the greater accessibility of the 4-thiocarbonyl sulfur to solvent in the latter compound. The relative positions of Band I (Table 3) again indicate the α-isomer to be **2** (X = Y = S) and the β-isomer to be **3** (X = Y = S).

Cyclohexane-spiro-5′-(2′,4′-dithiohydantoin) (**7**, X = S) lacks the anchoring *tert*-butyl group, and hence can exist in the two conformations **7**α and **7**β (X = S). The latter would be expected to be extremely disfavored because of the much greater steric compression between the 3,5-axial hydrogen atoms and the 4′-sulfur atom of **7**β than between the 3,5-axial hydrogen atoms and the 1′-hydrogen atom of **7**α, as discussed above. This is confirmed by the position of Band I (Table 3), which is closer to that of **2** (X = Y =

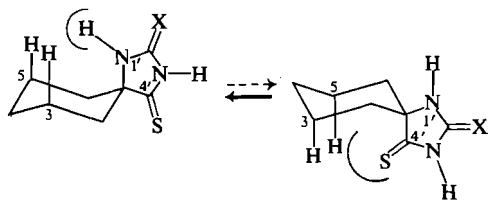

7α **7**β

TABLE 3. Ultraviolet absorption bands of mono- and dithiohydantoins in ethanol

Compounds	Isomer	Band I		Band II		Band IV	
		λ_{max}(nm)	ε_{max}	λ_{max}(nm)	ε_{max}	λ_{max}(nm)	ε_{max}
2 or **3** (X = Y = S)	α	390	55	299	28 000	227	6100
2 or **3** (X = Y = S)	β	405	45	301	29 000	226	6500
7α ⇄ **7**β (X = Y = S)*	—	393	45	297	31 000	227	5540
2 or **3** (X = O, Y = S)	β	390	18	281	13 300	232	6010
7α ⇄ **7**β (X = O, Y = S)*	—	375	26	277	14 800	228	4800

*From ref. 8.

Can. J. Chem. Downloaded from www.nrcresearchpress.com by 210.87.254.6 on 09/05/12
For personal use only.

Can. J. Chem. Downloaded from www.nrcresearchpress.com by 210.87.254.6 on 09/05/12
For personal use only.

S), the α isomer. For similar reasons, **7**α would be expected to be the favored conformation of cyclohexanespiro-5′-(4′-thiohydantoin) (**7**, X = O), and again this is supported by the spectral evidence (Table 3).

(c) Acetylation of α- *and* β-*Hydantoins*

Acetylation of hydantoin at both 1- and 3-positions is reported to take place readily (17). Consequently it would be expected that acetylation at both the 1′- and 3′-positions of **3** (X = Y = O) would also take place readily, but that **2** (X = Y = O) would be acetylated only at the 3′-position, because of the extreme steric pressures for an acetyl group at the 1′-position. In fact, the β-compound was diacetylated by treatment for 12 h in refluxing acetic anhydride,[1] while the α-compound was only monoacetylated after 42 h under these conditions. The diacetyl derivative of the β compound readily lost one acetyl group by mild alkaline hydrolysis: this was probably from the more labile 3′-position (17).

From a similar consideration of steric effects, it might be expected that **3** (X = Y = S) would react with diazomethane to form the 1′,3′-dimethyl derivative, but that **2** (X = Y = S) would form only the 3′-monomethyl derivative. In fact, with an excess of diazomethane both α- and β-compounds formed a dimethyl derivative, and with one mole of diazomethane both formed a monomethyl derivative which could be expected to be the 3′-derivative (19); this was confirmed by the pK_a values of the compounds (8). The α- and β-isomers proved to be essentially identical in acid strength although one has its ionizing group in an axial position and the other in an equatorial position (*cf.* refs. 20, 21). However, apart from the steric complexities of these compounds, it is becoming apparent (22) that relations between axial or equatorial configuration and acid or base strength are not straightforward.

The 2-thiohydantoins **2** and **3** (X = S, Y = O) were prepared from the 2,4-dithiohydantoins **2** and **3** (X = Y = S) by reaction with ethanolamine to form the 2-hydroxyethylimino derivatives **2** and **3** (X = S, Y = $HOCH_2CH_2N$) followed by hydrolysis of the latter with concentrated hydrochloric acid (23). Again, it was expected that **3** (X = Y = S) would react much more slowly than **2** (X = Y = S), because of the strain to be expected in the tetrahedral intermediates issuing from the former, but the yields from the two compounds were similar. Possibly if milder reaction conditions were investigated, pronounced differences in reactivity of the two isomers **2** and **3** (X = Y = S) might become apparent.

In summary, the different lines of physical and chemical evidence outlined above cohere in supporting the configurational assignments shown in Scheme 1, originally advanced on other grounds by Munday (1). Some of the counter-arguments advanced by Cremlyn (6) seem very plausible: in particular, that based on the effect to be expected from changing solvent composition on the pK_a of axial and equatorial groups (24). We are currently reexamining this effect.

Mechanistic Considerations: the Strecker Reaction

The sole amino acid obtained from the Strecker reaction of 4-*tert*-butylcyclohexane (**1**) was the β-compound **5**. Examination of the infrared spectrum of the hydrolysis product of the amino nitrile showed no trace of a peak at 675 cm^{-1}, characteristic of the α-isomer **4**.[2]

If equilibrium is established between the various compounds of Scheme 2, it would be expected, on the basis of the ΔG^0 values of axial amino and nitrile groups (15), that the crude amino nitrile would be made up of 7% of **13** (of the α-series) and 93% of **14** (β). Our cursory examination of the crude amino nitrile indicates the presence also of a small amount of cyanohydrin, presumably **9** (25) and some **8**. The amino nitrile and its hydrochloride are quite unstable to recrystallization, and the various equilibria of Scheme 2 merit further investigation. On mechanistic grounds it seems reasonable that the various equilibria of Scheme 2 are established rapidly in alkaline solution (through the intermediacy of **10** and **12**) but not in acid solution. This assumption, which is crucial to our further discussions of mechanism, receives some support from observations of Tager and Christen-

[1]These conditions are considerably more drastic than those reported in the literature for hydantoin (17), possibly because the acetic anhydride of 70 years ago contained acidic impurities which catalyzed the reaction: *cf.* W. J. Chute *et al.* (18) for a parallel case.

[2]The total recovery of amino acid was only 60% of theoretical, so that the α-isomer expected as a minor product in this reaction was probably lost in the isolation process.

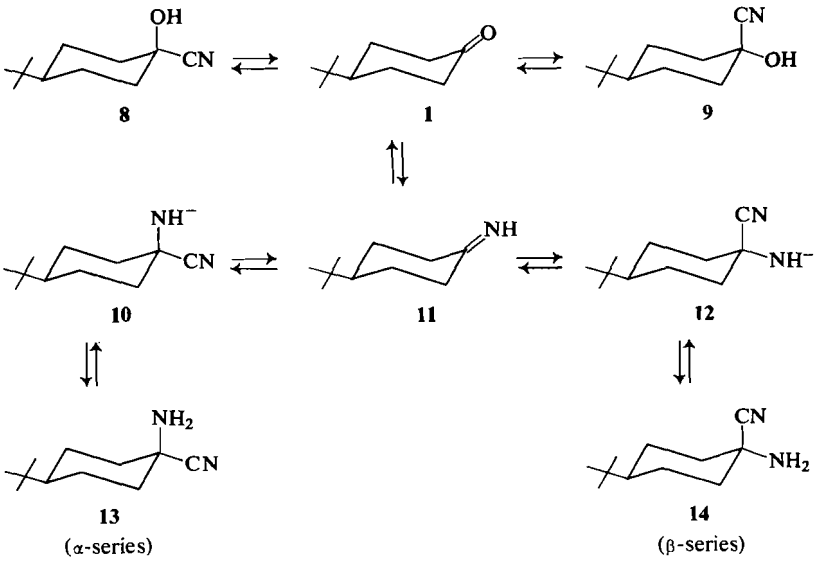

SCHEME 2

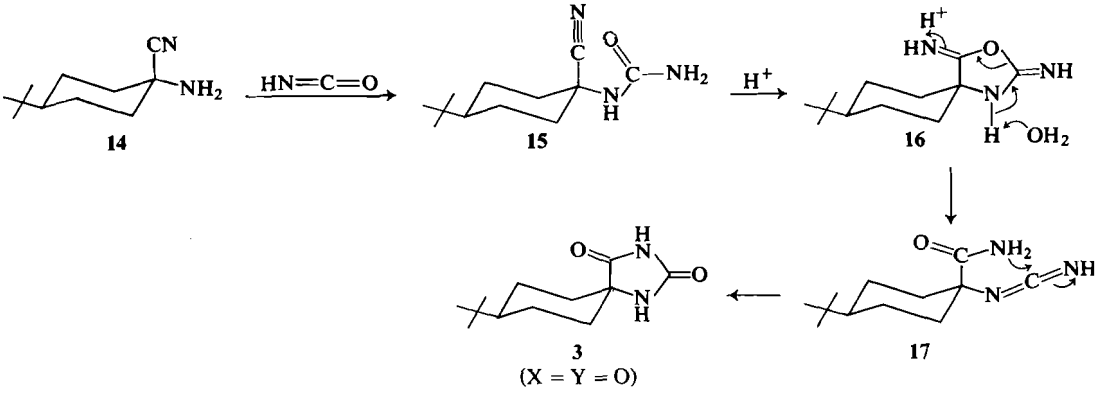

SCHEME 3

sen (22); we hope to study the effect of p*H* on the equilibria of Scheme 2 in the future. The evidence discussed below indicates that even in the weakly alkaline solution produced by dissolving the crude amino nitrile (**14** and some **13**; $pK_a \sim 7$ (26)) in aqueous ethanol the rates for the interconversion **13** ⇌ **14** are very fast.

Mechanistic Considerations: the Bucherer–Bergs Reaction

With these assumptions it now becomes possible to explain how the same amino nitrile can yield either the α- or the β-hydantoin, according to reaction conditions. Thus Cremlyn and Chisholm (6) found, and we have confirmed, that the amino nitrile (mostly **14**) reacts with cyanic acid in acetic acid to form a urea (**15**) which can then by cyclized to the β-hydantoin **3** (X = Y = O). A possible reaction sequence is given in Scheme 3, although variations of this sequence can be envisaged. The important fact is that the reaction is conducted under acidic conditions, so that the interconversion **13** ⇌ **14** does not take place, and hence the β-isomer **3** (X = Y = O) is the main product of the reaction.

On the other hand, the same amino nitrile treated with carbon dioxide in aqueous ethanol gives the α-hydantoin **2** (X = Y = O). Under

Can. J. Chem. Downloaded from www.nrcresearchpress.com by 210.87.254.6 on 09/05/12
For personal use only.

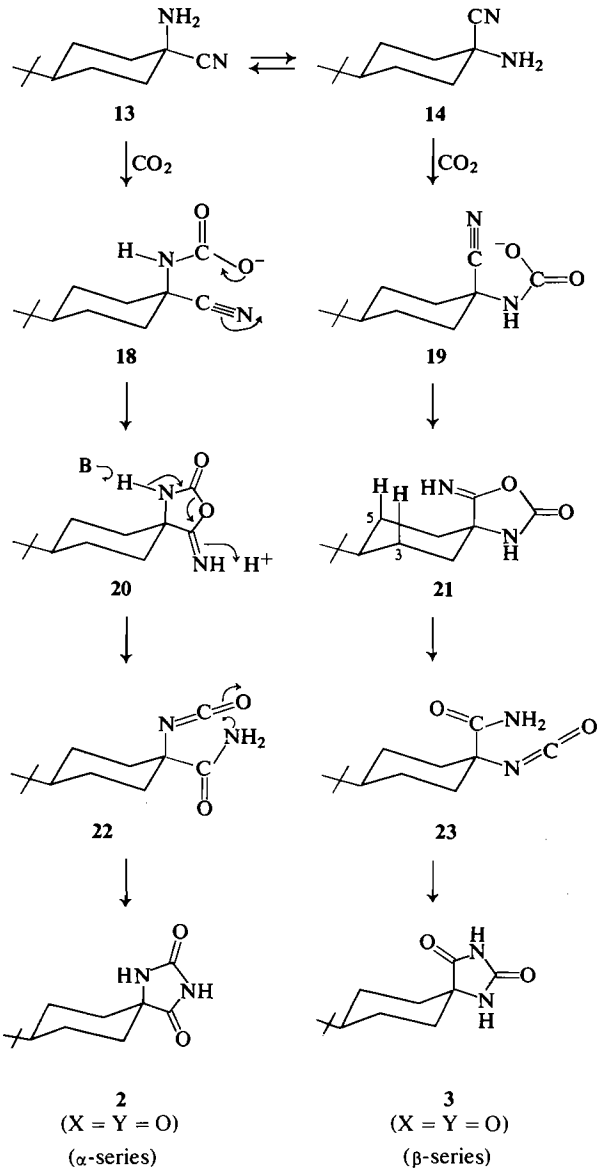

SCHEME 4

these conditions we assume the interconversion **13** ⇌ **14** to be rapid. The mechanism for this reaction shown in Scheme 4 is an elaboration of that of Bucherer and Steiner (27). The fact that the α-hydantoin is formed in preference to the β-hydantoin indicates that the former route involves a lower overall energy barrier in going from reactants to the rate-determining step than does the latter. It seems likely that the rate-determining step on the path to **3** (X = Y = O) is **19** → **21**. If this is endothermic, the transition state will resemble **21** (Hammond principle (28)), and hence be subject to severe steric hindrance because of the compression between the developing C═NH group and the 3,5-axial hydrogen atoms. (In **21** the van der Waals surfaces are compressed by 0.65 Å). Consequently, this path is a highly disfavored one. The other path (**14** → **13** → **18** → **20** → **22** → **2** (X = Y = O)) leading to the α-compound should be less favored in its

Can. J. Chem. Downloaded from www.nrcresearchpress.com by 210.87.254.6 on 09/05/12
For personal use only.

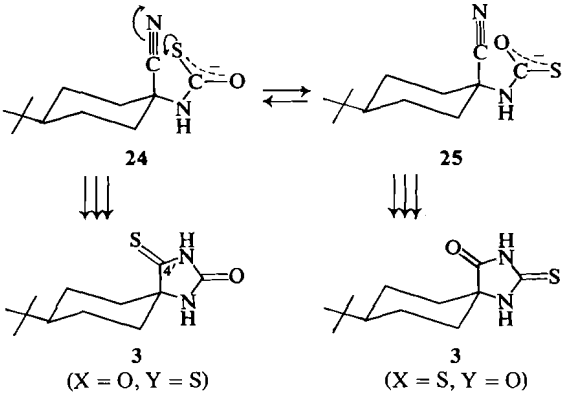

SCHEME 5

earlier, pre-equilibrium steps: for steric reasons, **13** → **18** should be less favored than **14** → **19**; but by the Hammett–Curtin principle, the relative rates by the α- and β-paths depend upon the *overall* barrier between **14** and the intermediate after the rate-determining step, and this should, for steric reasons, be larger on the β-path.

Why should the replacement of carbon dioxide by carbon disulfide cause the reaction now to take the β-path? If the sulfur atom is very much more nucleophilic than the oxygen atom, the reaction **19** → **21** (S in place of O) should be exothermic and should have a transition state resembling **19** rather than **21** (S in place of O). In that case, the bending of the nitrogen atom towards the 3,5-axial hydrogen atoms should have progressed by only a small amount when the transition state is reached. Consequently, the steric barrier impeding the β-path to the hydantoin is missing on the β-path to the 2,4-dithiohydantoin, whereas the various steric factors disfavoring the α-path, and mentioned above, are still present.

A similar rationale can be offered for the formation of the β- rather than the α-4′-thiohydantoin when carbon dioxide is replaced by carbon oxysulfide. It may be remarked that the fact that this reaction affords the 4′-thiohydantoin (**3**, X = O, Y = S) rather than the 2′-thiohydantoin (**3**, X = S, Y = O) shows that the thiocarbamic acid intermediate cyclizes when in the conformation **24** and not **25** (Scheme 5): a further example of the superior reactivity of the sulfur over the oxygen atom in attacking the nitrile group.

Conclusion

These mechanisms, which explain for the first time the differing stereochemical courses of the Strecker and Bucherer–Bergs reactions (2), require a pre-equilibrium **13** ⇌ **14** which is susceptible to experimental proof or disproof. Further, they can serve to predict the stereochemical outcome for the reaction of various ketones, such as norbornanone (22), *cis*- and *trans*-(1- and 2-)decalone (6), and 5α-cholestan-3-one (29), which have been submitted to some but not all of the various reactions discussed here. In particular, it can be expected that one of the two possible epimeric amino acids may be accessible by a modified Bucherer reaction when it is not accessible by a Strecker reaction (6).

We hope to explore some of these possibilities in future work.

We are most grateful to Professor A. S. Perlin for suggesting the ^{13}C n.m.r. studies, and for much help in interpreting spectra, to Dr. N. Cyr for the ^{13}C n.m.r. measurements, to Dr. P. G. Farrell for advice and assistance, to the Canadian government for a C.I.D.A. Scholarship (to C. Jitrangsri), and to the National Research Council of Canada for financial support.

1. L. MUNDAY. J. Chem. Soc. 4372 (1961).
2. H. C. BRIMELOW, H. C. CARRINGTON, C. H. VASEY, and W. S. WARING. J. Chem. Soc. 2789 (1962).
3. H. C. CARRINGTON. J. Chem. Soc. 681 (1947).
4. H. C. CARRINGTON, C. H. VASEY, and W. S. WARING. J. Chem. Soc. 396 (1959).
5. H. R. HENZE and P. E. SMITH. J. Am. Chem. Soc. **65**, 1090 (1943).
6. R. J. W. CREMLYN and M. CHISHOLM. J. Chem. Soc. C, 2269 (1967).
7. Y. MAKI and T. MASUGI. Chem. Pharm. Bull. (Tokyo), **21**, 685 (1973).
8. J. T. EDWARD and J. K. LIU. Can. J. Chem. **47**, 1117 (1969).
9. J. FEENEY, P. E. HANSEN, and G. C. K. ROBERTS. J. Chem. Soc. Chem. Commun. 465 (1974). A. S. PERLIN, N. CYR, R. G. S. RITCHIE, and A. PARFONDRY. Carbohydr. Res. **37**, Cl (1974) and references therein.
10. G. C. LEVY and GORDON L. NELSON. Carbon-13 nuclear magnetic resonance for organic chemists. Wiley-Interscience, New York. 1972. (*a*) p. 133, (*b*) p. 123, (*c*) p. 126.
11. J. D. ROBERTS, F. J. WEIGERT, J. I. KROSCHWITZ, and H. J. REICH. J. Am. Chem. Soc. **92**, 1338 (1970).
12. W. I. CONGDON and J. T. EDWARD. J. Am. Chem. Soc. **94**, 6096 (1972).
13. L. E. SUTTON (*Editor*). Interatomic distances. Chem. Soc. Special Publication, London. 1958. (*a*) M. 207, (*b*) M. 168.
14. A. MACCOLL. *In* Progress in stereochemistry. *Edited by* W. Klyne. Butterworths, London. 1954. p. 361.

Can. J. Chem. Downloaded from www.nrcresearchpress.com by 210.87.254.6 on 09/05/12
For personal use only.

15. E. L. ELIEL, N. L. ALLINGER, S. J. ANGYAL, and G. A. MORRISON. Conformational analysis. John Wiley, New York. 1967. p. 44.
16. M. J. JANSSEN. Rec. Trav. Chim. **79**, 454 (1960); **79**, 464 (1960); **79**, 1066 (1960).
17. L. SIEMONSON. Ann. **333**, 101 (1904).
18. W. J. CHUTE, K. G. HERRING, L. E. TOOMBS, and G. F. WRIGHT. Can. J. Res. B **26**, 89 (1948).
19. H. C. CARRINGTON and W. S. WARING. J. Chem. Soc. 354 (1950).
20. C. W. BIRD and R. C. COOKSON. J. Chem. Soc. 2343 (1960).
21. R. D. STOLOW. J. Am. Chem. Soc. **81**, 5806 (1959).
22. H. S. TAGER and H. N. CHRISTENSEN. J. Am. Chem. Soc. **94**, 968 (1972).
23. H. C. CARRINGTON. J. Chem. Soc. 684 (1947).
24. M. CHISHOLM, R. J. W. CREMLYN, and P. J. TAYLOR. Tetrahedron Lett. 1373 (1967).
25. L. MUNDAY. J. Chem. Soc. 1413 (1964).
26. H. C. BROWN, D. H. MCDANIEL, and O. HÄFLIGER. *In* Determination of organic structures by physical methods. *Edited by* E. A. Braude and F. C. Nachod. Academic Press, New York. 1955. p. 567.
27. H. T. BUCHERER and W. STEINER. J. Prakt. Chem. **140**, 291 (1934).
28. G. S. HAMMOND. J. Am. Chem. Soc. **77**, 334 (1955).
29. Y. MAKI, M. SATO, and K. OBATA. Chem. Pharm. Bull. (Tokyo), **13**, 1377 (1965).

Can. J. Chem. Downloaded from www.nrcresearchpress.com by 210.87.254.6 on 09/05/12
For personal use only.

The Structures of some Stress Metabolites from *Solanum melongena*[1,2]

A. STOESSL, J. B. STOTHERS, AND E. W. B. WARD

Agriculture Canada Research Institute and the Chemistry Department, University of Western Ontario, London, Ontario N6A 3K7

Received May 28, 1975

A. STOESSL, J. B. STOTHERS, and E. W. B. WARD. Can. J. Chem. **53**, 3351 (1975).

The structures of the acyclic sesquiterpenes **1–5** and the bicyclic sesquiterpenes **6** and **7**, all isolated from eggplant fruit inoculated with fungi, were elucidated with the aid of ^1H and ^{13}C n.m.r. studies. Trienone **1** was found to be identical to 9-oxonerolidol from camphor leaf oil while **2** and **3** are isomeric alcohols derived from **1**. Compounds **4** and **5** are probably artifacts. The hydroxyaldehyde **6** is identical with the potato phytoalexin lubimin, originally represented by a structure shown here to be incorrect. Enone **7** is a novel eudesmane. The stereochemistries of these compounds are discussed.

A. STOESSL, J. B. STOTHERS et E. W. B. WARD. Can. J. Chem. **53**, 3351 (1975).

Utilisant des études de r.m.n. du ^1H et du ^{13}C, on a étudié les structures des sesquiterpènes acycliques **1–5** et des sesquiterpènes bicycliques **6** et **7**, tous isolés d'aubergines inoculées avec des champignons. On a trouvé que la triènone **1** est identique à l'oxo-9 nérolidol obtenu à partir de l'huile de la feuille du camphrier alors que **2** et **3** sont des alcools isomères dérivés de **1**. Les composés **4** et **5** sont probablement des 'artefacts'. L'hydroxyaldéhyde **6** est identique avec la phytoalexine lubimin de la pomme de terre qui avait été représentée antérieurement par une structure qui s'avère fausse. L'énone **7** est un nouvel eudesmane. On discute de la stéréochimie de ces composés.

[Traduit par le journal]

Incubation of fruit of the eggplant (*Solanum melongena*) with spore suspensions of *Monilinia fructicola* or other fungi results in the production of a complex mixture of compounds which are not found in fruit incubated with water alone (1). Seven, essentially pure, compounds were isolated from this mixture but, of these, two are probably artifacts. The other five substances, however, are stress metabolites and may function as agents, 'phytoalexins', in the natural defense of the plant against disease (1). Details of the isolation and biological significance of these materials have been reported (1) while structures and biogenetic relationships for the five stress metabolites have been presented in preliminary form (2). In this paper we wish to present the full spectroscopic and experimental data which led to structural assignments for compounds **1–7** and to discuss the stereochemistry of these substances briefly.

Compound **1** was formulated as 9-oxonerolidol on the basis of its i.r., u.v. and ^1H n.m.r. spectra. While our work was in progress the same structure was assigned to a compound isolated from the nonvolatile terpenoids in the leaf oil of the camphor tree (3). In a direct comparison,[3] the two substances were indistinguishable in all essential aspects (see Experimental). A slight difference between the optical activities of our preparation ($[\alpha]_D^{23}$ +24; *c*, 1.0, CCl_4) and that of Hiroi ($[\alpha]_D^{23}$ +19), as determined in these laboratories, is attributable to the presence of small amounts of different impurities in the two specimens (~6% in each, by g.l.c.). Thus, the two substances have identical configurations. The stereochemistry, as depicted in **1**, has been assigned by Hiroi on the basis of the ^1H n.m.r. and o.r.d. data (4). The *trans* geometry of the central double bond (Δ^6) is supported by the ap-

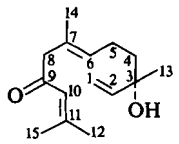

1

[1]Part 51 of ^{13}C Nuclear Magnetic Resonance Studies. For Pt. 50 see ref. 24, for Pt. 49, ref. 25, and for Pt. 48 ref. 26.

[2]Part 22 in the series, Post-infectional Inhibitors from Plants. For Pt. 21, see ref. 27. Contribution No. 622 from the Research Institute.

[3]We thank Prof. Hiroi for kindly providing a generous sample of his 9-oxonerolidol.

Can. J. Chem. Downloaded from www.nrcresearchpress.com by 210.87.254.6 on 09/05/12
For personal use only.

Can. J. Chem. Downloaded from www.nrcresearchpress.com by 210.87.254.6 on 09/05/12
For personal use only.

TABLE 1. ^{13}C shieldings* of sesquiterpenes **1–3**, **6**, and **7**

Compound	C-1	C-2	C-3	C-4	C-5	C-6	C-7	C-8	C-9	C-10	C-11	C-12	C-13	C-14	C-15
1	111.6	144.8	73.2	41.8	23.0	122.8	129.6	55.2	198.9	129.2	155.4	27.6	27.9	16.4	20.7
2†	111.8	144.9	73.5	41.8	23.0	127.7	134.8	48.1	66.0	128.5_4	131.8	25.7	28.0	16.2	18.2
	111.7	145.1	73.4		22.9					128.4_8	131.9		28.2		
3	111.7	144.9	73.4	42.1	22.9	(125.0)	134.1	42.4	(125.2)	139.4	70.6	29.9	27.9	16.2	29.9
6	33.3	41.0	32.6	25.9	46.9	58.4	41.8	69.3	40.3	47.4	147.3	108.8	21.2	204.9	16.4
7	160.9	125.9	204.0	(49.1)	(45.3)	26.1	(44.5)	22.4	40.0	36.2	13.4	72.6	(27.2)	(27.6)	20.8
16	156.7	128.5	201.9	(48.6_4)	(48.5_6)	24.5	(42.1)	23.9	41.0	38.2	12.0	72.7	27.1	27.1	27.1

*In p.p.m. from internal TMS for $CDCl_3$ solutions. Similar values in parenthesis may be interchanged.
†The complete results for **2** from eggplant are listed, while the shieldings for the diastereomer (see text) which differ are given below the former.

Can. J. Chem. Downloaded from www.nrcresearchpress.com by 210.87.254.6 on 09/05/12
For personal use only.

pearance of a methyl signal at 16.4 p.p.m. in the ^{13}C spectrum of **1**; a similar signal was found in the spectra of **2** and **3** (see Table 1). Its assignment to C-14 in this series followed from a comparison with the data for geraniol (**8***a*), nerol (**8***b*), citral *a* (**8***c*), and citral *b* (**8***d*) (5, 6). For these pairs of isomers the geometry about the 6–7 double bond is clearly revealed by the C-10 methyl carbon shielding difference of ~7 p.p.m. In **8***a* and **8***c*, the *cis* relation between this methyl and the terminal group shifts the methyl signal to 16–17 p.p.m. while in the *trans* cases, **8***b* and **8***d*, this methyl carbon absorbs near 24 p.p.m. This is a general tendency in olefinic systems (6) and has been exploited for stereochemical assignments in a variety of systems (7), for example, in a distinction between *cis*- and *trans*-phytoene isomers (8) which also serves as a model for the present case.

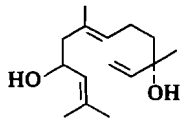

2

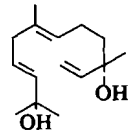

3

The quaternary methyl signal near 28 p.p.m. in **1–3** was assigned by comparison with the corresponding absorption for linalool and dihydrolinalool (9). The remaining methyl signals, therefore, arise for C-12 and C-15 with the more shielded of the two, in **1** and **2** assigned to the methyl *cis* to C-9, for the reasons given above; it may be noted that the geminal methyl shieldings differ by 7 p.p.m. in each case, in good agreement with expectations. For similar reasons, the methylene signal near 23 p.p.m. was assigned to C-5. Each compound gave rise to a methylene signal near 42 p.p.m. which was readily assigned to C-4, since structural changes at C-9 and beyond would not be expected to affect this carbon significantly. The carbonyl carbon, at 198.9 p.p.m., was easily assigned and its shielding clearly indicates its conjugated nature (10). Of the two signals from fully substituted olefinic carbons, that at 155.4 p.p.m. arises from C-11 since it is β to the carbonyl group. The consistent appearance of a signal at 145 p.p.m. in the spectra of **1–3** for an olefinic carbon with one directly bonded proton led to its assignment as the C-2 signal, while the remaining assignments for **1** appear to be the most probable on the basis of comparison with model systems (9, 10).

Eggplant metabolite **2** was characterized as 9-hydroxynerolidol by its spectroscopic properties and by oxidation with manganese dioxide in benzene to **1**. Also, a sample of 9-oxonerolidol (**1**) obtained by Hiroi[3] gave a diol upon reduction with sodium borohydride which was identical by i.r., t.l.c. and g.l.c. with eggplant metabolite **2**, except for the presence of an unidentified impurity (3.5% by g.l.c.) in the reduction product. The o.r.d. curves of the two substances showed virtually no optical activity between 350 and 700 nm. As noted by Hiroi and Takaoka (3), the reduction product was expected to be a mixture of diastereoisomers and the proton spectrum suggested this to be the case, although no separation was achieved by t.l.c. A comparison of the ^{13}C spectra of natural **2**, and **2** obtained by reduction of **1**, however, revealed slight differences (0.05–0.2 p.p.m.) in the shieldings of seven of the carbons. In the ^{13}C spectrum of the reduction product, these seven carbons each gave rise to a pair of signals of essentially equal intensity while the ^{13}C spectrum of natural **2** contained a predominant set for one diastereomer with a second set of weaker signals indicating the presence of ~20% of the second stereoisomer. The fact that the natural metabolite is a mixture (~4:1) of diastereomers suggests that **2** and **3** may be interconverted in the plant or during the isolation. The assignment of the ^{13}C signals for the diastereomeric pair followed from considerations analogous to those outlined above for **1**. The observed doubling of the signal near 132 p.p.m. for a fully substituted olefinic carbon was taken to distinguish C-11 from C-7, but this is not unequivocal. Similar reasoning led to the assignments for C-6 and C-10. The small but measurable, shielding differences for C-1, -2, -3, -5, -11, -12, and -13 indicate that the two diastereomers favor significantly different conformations since it seems most probable that the C-3 configuration is the same in each, but the observed shielding changes cannot be interpreted in any further detail. Since Hiroi's specimen of **1** was used for the reduction, this experiment further confirmed the identity of the eggplant and camphor tree metabolites.

Compound **3** showed neither carbonyl absorption in its infrared spectrum nor u.v. absorption above 220 nm. The ^{1}H spectrum, however, was particularly revealing containing the absorptions for six olefinic protons, four methyl

Can. J. Chem. Downloaded from www.nrcresearchpress.com by 210.87.254.6 on 09/05/12
For personal use only.

groups, and a methylene group as the readily assigned features. The ABX pattern characteristic of the vinyl group in **1** and **2** was evident together with a triplet of sextets ($J \sim 7$ and 2 Hz, respectively) centered at 5.16 p.p.m. Simultaneous irradiation of the olefinic methyl doublet at 1.63 changed this pattern to a triplet of triplets while irradiation of the broadened doublet at 2.65 p.p.m., arising from two protons of a methylene group, changed it to a triplet of quartets. The latter experiment also collapsed the absorption of the two remaining olefinic protons to a singlet, presumably the central lines of an AB system produced by the decoupling. The results indicated the pattern at 5.16 p.p.m. to arise from H-6 having long range coupling to the olefinic methyl on C-7 and the C-8 methylene protons (2.65 p.p.m.). Simultaneous irradiation at 1.63 and 2.65 p.p.m. indeed reduced the pattern at 5.16 p.p.m. to a triplet which was then collapsed to a singlet by irradiation at 2.04 p.p.m. The remaining olefinic absorption was that of H-9 and H-10, which are nearly equivalent. To simplify the spectrum and to confirm the above analysis, a spectrum of **3** in $CDCl_3$ containing $Eu(fod)_3$ was recorded. Upon irradiation of the methylene doublet, which was shifted to 3.06 p.p.m., H-9 and H-10 gave rise to a well-defined AB pattern with $J_{AB} = 16$ Hz. These results led directly to structure **3**, an allylic isomer of **2**, and the ^{13}C data are entirely consistent with this formulation. Although the signals for C-6 and C-9 cannot be unequivocally assigned, their similarity indicates that both double bonds are *trans*. The presence of a moderately strong band at 978 cm^{-1} in the i.r. spectrum of **3** but absent in those of **1** and **2** also suggested that the C-9–C-10 double bond is *trans* (11). The proton–proton coupling constant, however, proved the point.

It must be pointed out that while **3** was always detected in appreciable amounts in freshly prepared extracts from *S. melongena* diffusates, it could, nevertheless, have been formed by a nonenzymatic allylic rearrangement of **2**, either during incubation of the diffusates or during extraction, despite the mildness of the conditions employed (1). Some evidence to support this possibility comes from the fact that **2** from eggplants, was partially racemized at C-9, as discussed above. There can be little doubt that compounds **4** and **5** are such artifacts, generated during work-up, since neither could be detected in freshly prepared ether extracts. Although only small amounts of these materials (1.5 and 2 mg respectively) were available for n.m.r. analysis their structures were readily deduced from spectral data.

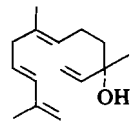

4

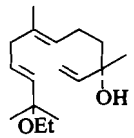

5

Both compounds exhibited in their ^1H n.m.r. spectra the bands attributable to the C-1 to C-8 moiety, as found in **1–3**. In addition **4** clearly contained a diene system, incorporating a new terminal methylene and an olefinic methyl group, from the proton spectrum and the u.v. absorption, λ_{max} 230 nm (ε 19 600). Apparently dehydration of **2** during work-up is responsible for the formation of **4**. The proton spectrum of **5** was remarkably similar to that of **3** with the significant addition of the characteristic absorption of an ethoxyl group. Like **2** and **3**, **5** is transparent in the near ultraviolet. Presumably **5** arises by an allylic rearrangement of **2** in ethanol-containing solvents.

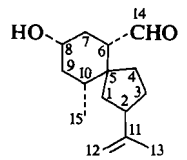

6

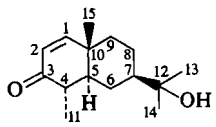

7

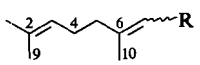

8*a* R = *E*—CH_2OH
b R = *Z*—CH_2OH
c R = *E*—CHO
d R = *Z*—CHO

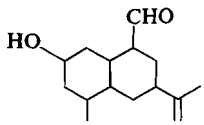

9

Compound **6** accounted for much of the antifungal activity of the diffusate extract from which it was isolated as a major constituent (1). Our results from infrared, proton and mass spectra virtually coincided with those published for lubimin, a phytoalexin from potatoes, which has been described by Metlitskii and co-workers in a series of studies (12). To confirm the identity of the eggplant metabolite **6**, we isolated lubimin from potatoes essentially as described by the Russian

Can. J. Chem. Downloaded from www.nrcresearchpress.com by 210.87.254.6 on 09/05/12
For personal use only.

workers. The two compounds were found to be identical in every respect. However, their ^{13}C spectra showed clearly that structure **9**, originally proposed for lubimin, was untenable. The key feature was an absorption for a quaternary sp^3 carbon which is incompatible with **9**. The ^{13}C spectrum also contained signals for two methyl, five methylene and three methine carbons in addition to those for an aldehydic carbonyl, one carbinyl and two olefinic carbons; these shieldings are listed in Table 1. This array of signals suggested the spiro structure **8** having the vetispirane skeleton. The shieldings of the carbinyl and secondary methyl carbons indicated that the hydroxyl and methyl groups were equatorial and this was confirmed by the ^1H spectrum, which was also utilized to establish the orientation of the formyl group. Irradiation of the formyl proton doublet (J = 3.5 Hz) at 9.79 p.p.m. collapsed a doublet of triplets at 2.26 p.p.m. to a doublet of doublets (J = 8 and 3.5 Hz) while irradiation at 1.60 p.p.m. eliminated the larger coupling of 8 Hz in the 2.26 p.p.m. pattern. In the latter experiment, the carbinyl absorption was also narrowed by ~8 Hz. This indicated that the proton vicinal to the formyl group is axial and is coupled to an axial proton near 1.60 p.p.m. which, in turn, is coupled to the axial carbinyl proton. A second large coupling in the carbinyl absorption was eliminated by irradiation at 1.40 p.p.m. Spin decoupling also revealed that the secondary methyl protons (0.94 p.p.m.) were coupled to a proton at 1.55 p.p.m. Spin decoupling at 1.55 and 2.26 p.p.m. did not affect the carbinyl absorption. Thus, these results indicated the presence of the fragment $-CH_2-CH(OH)-CH_2-CH(CHO)-C<$. A precise mass determination gave the formula $C_{15}H_{24}O_2$ showing the compound to be bicyclic. While these results can be accommodated by a number of structures only **6** incorporates a known sesquiterpenoid skeleton and is plausible on biogenetic grounds. Subsequent to our preliminary communication (2), the same conclusion was reached independently by other workers (13).

Compound **7** has the formula $C_{15}H_{24}O_2$, as shown by a precise mass determination and contains a six- or higher-membered cyclic enone with λ_{max} 227 nm (ε 8650) and ν_{max} 1667 cm^{-1}, as well as a *tert*-hydroxyl group (ν_{max} 3455 cm^{-1}). The ^1H n.m.r. pattern for the olefinic protons was a simple AB system (J_{AB} = 10 Hz, δ_A = 5.86, δ_B = 6.78) showing that the adjacent carbon is fully substituted. These data for the enone moiety are remarkably similar to those reported for the enone fragment in tuberiferine (**10**): λ_{max} 224 nm (ε 11 200), ν_{max} 1680 cm^{-1}, J_{AB} = 9.9 Hz, δ 5.90 and 6.75 (14). In addition, the proton spectrum contained a singlet (6H, δ 1.40) a secondary methyl doublet (δ 1.13, J = 8.5 Hz), and a singlet (3H, δ 1.16). In C_6D_6 solution these methyl signals were shifted to 1.02, 1.01, and 0.83 p.p.m., respectively, which indicated that the secondary methyl is α to the carbonyl and equatorial while the lone *tert*-methyl is γ to the carbonyl (15). The two equivalent methyl groups could be assigned to an oxyisopropyl group. In addition the proton spectrum contained a well-defined doublet of quartets centered at 2.45 p.p.m. ($CDCl_3$). Upon irradiation at 1.13 p.p.m. this pattern collapsed to a doublet (J ~6 Hz) from which it was clear that this absorption arose from the proton vicinally coupled to the secondary methyl protons and to one other proton. The ^{13}C spectrum of **7** contained fifteen signals comprised of four methyl, three methylene, three methine, two quaternary (one of which was carbinyl at 72.6 p.p.m.), two monoprotonated olefinic, and a carbonyl carbon (see Table 1). Selective decoupling using a C_6D_6 solution of **7**, identified the individual signals for the angular and secondary methyl carbons and the latter's shielding (13.4 p.p.m.) is as expected for methyl α to carbonyl (16) while the value for the angular methyl seemed to be in good agreement with that expected for C-15 in structure **7** on the basis of the available data for angular methyl carbons in related *trans*-decalones (17). However, it seemed worthwhile to determine the methyl shielding in a better model system and to this end we prepared olefin **11** as described in the accompanying paper (18). Its methyl carbon absorbed at 18.9 p.p.m. or 2 p.p.m. upfield from the corresponding signal for **7**. This difference agreed very nicely with that predicted from the results for **12** and **13** (17). The angular methyl shieldings for the latter pair differ by 3 p.p.m. with **12** at higher field. Since it is known that the equatorial hydroxyl in **12** deshields the angular methyl by 1 p.p.m. in the *trans*-decalin system (19), the effect of the 3-carbonyl group on the angular methyl shielding is *ca.* 2 p.p.m., as was observed for **7** *vs.* **11**. Equatorial alkyl substituents on the

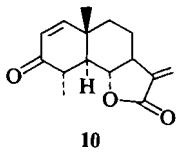

10

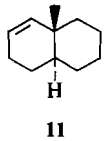

11

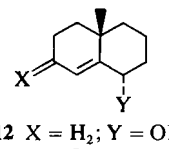

12 X = H_2; Y = OH
13 X = O; Y = H

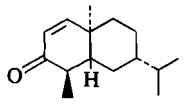

14

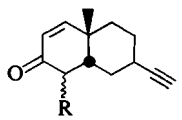

15*a* R = α-CH_3
b R = β-CH_3

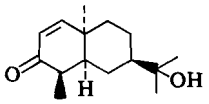

16

trans-decalin ring system are not expected to influence the angular methyl shielding appreciably. Thus, the n.m.r. results led to **7** as the formulation best representing the eggplant metabolite. It may be noted that, on biogenetic grounds, this structure fits in very nicely with the other bicyclic sesquiterpenoidal stress compounds of the *Solanaceae* (2).

Enone **14**, which has been synthesized (20), differs from **7** only by the absence of the C-12 hydroxyl and the spectral properties of **7** and **14** are closely similar, confirming our structural deductions. The absolute configuration of **14** is known and its o.r.d. curve, exhibits a complex positive Cotton effect and bears an essentially mirror image relation to that of **7** apart from constant amplitude differences, presumably due to the low optical purity reported (20). A complex positive Cotton effect has been reported for **15***a* while **15***b* exhibits a negative effect (21). These results were readily interpreted in terms of the different conformational preferences produced by the changes in orientation of the α-methyl group. It should also be noted that the olefinic β proton (H-1) was spin coupled to H-5 in **15***a* but not in **15***b*. In the former H-1 and H-5 are in a nearly planar W orientation which is ideal for long range coupling between protons separated by four bonds. As an additional model compound for comparison with **7**, we have recorded the n.m.r. spectra for **16**,[4] an intermediate in the synthesis of occidentalol described by Deslongchamps and co-workers (22). The ^{13}C data are listed in Table 1 and the main feature is the markedly lower shielding observed for the angular methyl carbon (C-15) relative to that for **7**, a difference of 6.3 p.p.m. which is entirely consistent with the change in geometry at the ring junction (7). In the proton spectrum the β olefinic proton showed long range coupling (2 Hz) with H-5, analogous to that noted above for **15***a*, since protons 1 and 5 are in a nearly planar W arrangement. If the ring junction in **7** was *cis*, *i.e.* the 5β-form with 3α-methyl substitution, the same long range coupling should occur and the vicinal coupling (H_4–H_5) would be expected to be smaller than 6 Hz as observed. All of this evidence strongly supports structure **7** for the eggplant metabolite.

The biogenetic interrelationships between **6**, **7**, and other bicyclic sesquiterpenes of the *Solanaceae* have been outlined (2) and we are currently exploring these in further detail.

[4]We are grateful to Professor Deslongchamps and Mrs. M. Sergent-Guay for specially preparing a sample of **16** for our examination, and to Dr. J. S. Roberts for drawing our attention to this compound.

Experimental

General

Melting points were determined on a Kofler hot-stage. Infrared spectra were recorded for liquid films with a Unicam SP 1000 instrument; ultraviolet spectra were obtained in 96% ethanol using either a Beckman DK or a Pye-Unicam SP 8000 spectrophotometer. Optical rotatory dispersion curves were obtained with a Jasco ORD-UV5 spectropolarimeter using a 0.1 dm path length. For optical activity measurements at 589 nm only, a Schmidt-Haensch polarimeter was used with a 1 dm path length. Proton n.m.r. spectra were obtained with Varian A60A and HA100 instruments, using $CDCl_3$ as solvent and TMS as the internal reference. The ^{13}C n.m.r. spectra were recorded with a Varian XL-100-15 system operating in the Fourier transform mode. Mass spectra were determined on a Varian M-66 spectrometer at 70 eV. Camag DF5 silica gel, activated at 110 °C, was used for thin layer (300 μ) chromatography. Gas chromatography was done with a Hewlett-Packard 5750 instrument, equipped with a digital integrator, using a 6 ft glass column, 0.25 in. diameter, packed with 3% SE-30 on Gas-Chrom Q (80–120 mesh) at 160 °C with a nitrogen flow of 40 ml/min. Low boiling petroleum ether (30–60 °C) was used and all solvents were redistilled before use.

All compounds **1**–**7** were obtained as essentially colorless syrups. Their isolation and purification, by repeated preparative t.l.c., have been described in detail (1).

9-Oxonerolidol (1)

Both the eggplant metabolite and Hiroi's sample had λ_{max}^{EtOH} 238 nm (ε 12 000), ν_{max} 3490, 3140, 1690, 1625, and 923 cm^{-1}. Infrared and mass spectra of the samples differed only in a few minor bands which apparently arose from small amounts of different impurities as revealed by g.l.c. analyses. The retention times in minutes (and rela-

Can. J. Chem. Downloaded from www.nrcresearchpress.com by 210.87.254.6 on 09/05/12
For personal use only.

Can. J. Chem. Downloaded from www.nrcresearchpress.com by 210.87.254.6 on 09/05/12
For personal use only.

tive peak areas, %) were: eggplant specimen; 1.1(0.14), 3.9(0.21), 4.3(0.10), 4.8(5.1), 6.1(94.4), and 7.5(0.08). Hiroi's specimen: 4.0(0.16), 5.2(6.1), 6.1(93.6), and 8.2-(0.11). The proton spectra were essentially identical and have been described (3).

9-Oxynerolidol (2)

This diol had ν_{max} 3420, 3130, and 922 cm^{-1}; *m/e* 239(M + 1), 238(M), 236, 221, 220, 85, and was transparent in the near u.v. It was identical by i.r., ^1H n.m.r., t.l.c. (methanol–chloroform, 5:95; *sec*-butanol – ethyl acetate, 5:95) and g.l.c. (retention time 6.3 min (98%)) with the product obtained from Hiroi's sample of **1** upon reduction with $NaBH_4$ in methanol (3) except that the reduction product, despite purification by preparative t.l.c., contained 3.5% of an impurity (retention time, 5.5 min). The o.r.d. curves of the two substances (5 mg/ml in EtOH) showed virtually no optical activity between 350 and 700 nm. The two samples exhibited slightly different ^{13}C n.m.r. spectra in that seven carbons each gave rise to two closely spaced signals (see Table 1) which were of approximately the same intensity in the spectrum of the reduction product but in a ratio of ~4:1 for the natural product.

Diol **2** (7 mg, eggplant specimen) was shaken with a large excess of manganese dioxide in benzene at room temperature for 48 h (23). The main product (40% yield), isolated by preparative t.l.c. (MeOH–Et_2O, 1:9) was identical with **1** by t.l.c. and g.l.c. as well as i.r. and u.v. spectra.

Triendiol 3 (3,11-Dihydroxy-3,7,11-trimethyldodeca-1,6,9-triene)

This compound had $[\alpha]_D^{23}$ +14 (*c*; 1.0, CCl_4), ν_{max} 3420, 3120, 978, 926, and 692 cm^{-1} and *m/e* 239(M + 1), 238(M), 221, 220, 205, 202, 193, 187, and 138 (base). The proton spectrum ($CDCl_3$) contained an ABX pattern, δ_A 5.190, δ_B 5.051, J_{AB} = 1.5 Hz (H-1), δ_X 5.936 (H-2), J_{AX} = 17.4, J_{BX} = 10.6 Hz, an ABX_2 pattern δ_A 5.625 (H-10), δ_B 5.605 (H-9), J_{AB} = 16 Hz, δ_X 2.65 (H-8), J_{BX} = 4.5 Hz and an olefinic proton at 5.16 p.p.m. (H-6), $J_{5,6}$ = 7 Hz, $J_{6,8}$ = 1.5 Hz. Methyl absorption occurred at δ 1.30 (3-Me), 1.33 (11-Me's), and 1.62 (7-Me, J ~ 1.5 Hz).

Tetraenol 4 (3-Hydroxy-3,7,11-trimethyldodeca-1,6,9,10-tetraene)

This unsaturated alcohol exhibited λ_{max}^{EtOH} 230 nm (ε 19 600) and ν_{max} 3450, 3095, 1610, 970, 927, and 889 cm^{-1}. The proton spectrum contained an ABX pattern; δ_A 5.195, δ_B 5.055, J_{AB} = 1.5 (H-1), δ_X 5.93 (H-2), J_{AX} = 10.5, J_{BX} = 17.5 Hz; an ABX_2 pattern δ_A 6.146, (H-10), δ_B 5.610 (H-9), J_{AB} = 15.5 Hz, J_{BX} = 7.5 Hz, δ_X 2.80 (H-8); a triplet (J ~7 Hz) of closely spaced multiplets δ 5.16 (H-6) and a multiplet at δ 4.85 (2H, H-12). Methyl absorption appeared at δ 1.30 (3-Me), 1.63 (7-Me), and 1.86 (11-Me).

Hydroxyether 5 (11-Ethoxy-3-hydroxy-3,7,11-trimethyldodeca-1,6,9-triene)

This compound was transparent in the ultraviolet spectrum and exhibited ν_{max} 3450, 3100, 985, 828, and 695 cm^{-1}. The proton spectrum had an ABX pattern δ_A 5.30, δ_B 5.14, J_{AB} = 1.5 (H-1), δ_X 6.08 (H-2), J_{AX} = 18, J_{BX} = 10 Hz; δ 5.26 (t, J ~7) for H-6 and the AB part (δ_A 5.60, δ_B 5.58, H-10 and H-9, respectively) of an ABX_2, δ_X 2.72 (H-8). Methyl absorption occurred at δ 1.28 (3-Me), 1.26 (6H, 11-Me's), 1.60 (6-Me), and the triplet, δ 1.14, for the methyl of the ethoxyl group (—CH_2—O, δ 3.40).

Lubimin (6)

From Eggplants

The isolation of **6** has been described (1). An o.r.d. curve was recorded at 32 °C in ethanol: $[\phi]_{589}$ +92, $[\phi]_{450}$ +203, $[\phi]_{350}$ +762, $[\phi]_{322}$ +1680, $[\phi]_{299}$ 0, and $[\phi]_{280}$ −920. Mol. Wt. Calcd. for $C_{15}H_{24}O_2$: 236.1775. Found: 236.1762.

The proton spectrum contained formyl proton absorption δ 9.79, J = 3.5 Hz coupled to a doublet (J ~8) of triplets (J ~3.5) at δ 2.26 and carbinyl absorption as a triplet (J ~10.5) of triplets (J ~4.5) at δ 3.69. Double irradiation at 1.60 p.p.m. removed one large coupling in each of the patterns at 2.26 and 3.69 p.p.m. while triple irradiation at 1.40 and 1.60 p.p.m. reduced the carbinyl pattern to a triplet (J ~4.5 Hz). Methyl absorption appeared at δ 1.70 (olefinic methyl) and δ 0.93 (d, J ~7 Hz); the doublet was collapsed to a singlet upon irradiation at 1.55 p.p.m.

From Potatoes

Potato tubers (*ca.* 130 lb) were cleaned and cut into slices ~2 cm thick under sterile conditions. Circular wells (2 cm diameter, 1 cm deep) were scooped out from one side of each slice and filled with spore suspensions of *Monilinia fructicola* (Wint.) Honey (5 × 10^5 spores/ml). After incubation in covered trays at room temperature for 48 h, the liquid was collected from the wells (*ca.* 5 l) and extracted with petroleum ether (3 × 2.5 l). The residue (150 mg) obtained by evaporation of the washed and dried extracts was chromatographed over a column of silica gel (100 g, unactivated Camag DF 5) packed in MeOH–$CHCl_3$ (5:95). Elution with the same solvent in 5 ml fractions gave an oil (44 mg, fractions 16–21) which had the spectral properties reported for lubimin (i.r., ^1H n.m.r., mass spectra); $[\alpha]_D^{32}$ 46 (lit. (12) $[\alpha]_D^{20}$ 27).

This product was identical with the material isolated from eggplant as judged by i.r., ^1H and ^{13}C n.m.r., o.r.d. and mass spectra as well as by t.l.c. (in 3 systems), g.l.c., m.p. and mixture m.p. (137–141 °C) of the 2,4-dinitrophenylhydrazones (lit. (12) m.p. 124–127 °C).

Reduction of the substance (34 mg) with sodium borohydride (6 mg) in methanol (3 ml) at 10 °C gave a diol (33 mg, m.p. 127–128 °C) which has since been described (lit. (13) m.p. 128–130 °C).

Enone 7

A small amount of the enone, whose isolation has been described (1), was sublimed *in vacuo* at 70 °C and was found to crystallize slowly when kept at −10 °C, m.p. 65–68 °C; λ_{max} 227 nm (ε 8650) with a weak shoulder at 310 nm (ε 54); ν_{max} 3455, 2990, 2955, 2890, 1667, 920, 827, and 756 cm^{-1}; *m/e*, 236(M), 221, 203, 178, 163, and 59 (base). Mol. Wt. Calcd. for $C_{15}H_{24}O_2$: 236.1775. Found: 236.1772.

An o.r.d. curve was recorded at 32 °C in ethanol: $[\phi]_{589}$ 0, $[\phi]_{500}$ 0, $[\phi]_{450}$ −94, $[\phi]_{400}$ −470, $[\phi]_{370}$ −1605, $[\phi]_{365}$ −1790, $[\phi]_{359}$ −1628, $[\phi]_{345}$ 0, $[\phi]_{312}$ +3900, $[\phi]_{285}$ +3350, and $[\phi]_{270}$ +3870.

We wish to thank D. Hairsine, R. Lazier, G. L. Rock, H. Schroeder, I. Grikis, and Dr. M. B. Rampersad for

technical assistance. We are grateful to Profs. Hiroi and Deslongchamps for so kindly providing generous samples of **1** and **16**, respectively, for comparisons with our materials.

We acknowledge with thanks, the financial support of the National Research Council of Canada.

1. E. W. B. WARD, C. H. UNWIN, J. HILL, and A. STOESSL. Phytopathology, **65**, 859 (1975).
2. A. STOESSL, J. B. STOTHERS, and E. W. B. WARD. J. Chem. Soc. Chem. Commun. 709 (1974).
3. M. HIROI and D. TAKAOKA. Chem. Lett. 1213 (1974).
4. M. HIROI and D. TAKAOKA. Nippon Kagaku Kaishi, 762 (1974).
5. M. JAUTELAT, J. B. GRUTZNER, and J. D. ROBERTS. Proc. Nat. Acad. Sci. U.S.A. **65**, 288 (1970).
6. J. W. DE HAAN and L. J. M. VAN DE VEN. Org. Magn. Reson. **5**, 147 (1973).
7. N. K. WILSON and J. B. STOTHERS. *In* Topics in stereochemistry, Vol. 8. *Edited by* E. L. Eliel and N. L. Allinger. Wiley-Interscience, New York. 1974. Chpt. 1.
8. P. GRANGER, B. MAUDINAS, R. HERBER, and J. VILLOUTREIX. J. Magn. Reson. **10**, 43 (1973).
9. E. BREITMAIER and W. VOELTER. ^{13}C NMR spectroscopy. Verlag Chemie, Gmb. H. Düsseldorf. 1974. p. 199.
10. J. B. STOTHERS. Carbon-13 NMR spectroscopy. Academic Press, New York. 1972.
11. L. J. BELLAMY. The infrared spectra of complex molecules. Methuen and Co., London. 1958. p. 45.
12. L. V. METLITSKII, O. L. OZERETSKOVSKAYA, N. S. VUL'FSON, and L. I. CHALOVA. Dokl. Akad. Nauk S.S.S.R. **200**, 1470 (1971) and references therein.
13. N. KATSUI, A. MATSUNAGA, and T. MASAMUNE. Tetrahedron Lett. 4483 (1974).
14. J. B. BARRERA, J. L. BRETON, M. FAJARDO, and A. G. GONZALES. Tetrahedron Lett. 3475 (1967).
15. P. LASZLO. *In* Progress in nuclear magnetic resonance spectroscopy, Vol. 3. *Edited by* J. W. Emsley, J. Feeney, and L. H. Sutcliffe. Pergamon Press, London. 1967. Chpt. 6.
16. J. B. STOTHERS and C. T. TAN. Can. J. Chem. **52**, 308 (1974).
17. G. I. BIRNBAUM, A. STOESSL, S. H. GROVER, and J. B. STOTHERS. Can. J. Chem. **52**, 993 (1974).
18. A. STOESSL and J. B. STOTHERS. Can. J. Chem. This issue.
19. S. H. GROVER and J. B. STOTHERS. Can. J. Chem. **52**, 870 (1974).
20. S. J. STEINDEL. Ph.D. thesis, Georgia Institute of Technology, Atlanta, Ga. 1973; L. H. ZALKOW, S. J. STEINDEL, N. G. SCHNAUTZ, and C. K. KELLOG. Tetrahedron Lett. 3337 (1973).
21. T. TODA, M. C. WOODS, and K. TAKAHASHI. Tetrahedron, **27**, 5391 (1971).
22. M. SERGENT, M. MONGRAIN, and P. DESLONGCHAMPS. Can. J. Chem. **50**, 336 (1972).
23. J. ATTENBURROW, A. F. B. CAMERON, J. H. CHAPMAN, R. M. EVANS, B. A. HEMS, A. B. A. JANSEN, and T. WALKER. J. Chem. Soc. 1094 (1952).
24. A. STOESSL, J. B. STOTHERS, and E. W. B. WARD. J. Chem. Soc. Chem. Commun. 431 (1975).
25. M. L. CASPAR, J. B. STOTHERS, and N. K. WILSON. Can. J. Chem. **53**, 1958 (1975).
26. S. H. GROVER, D. H. MARR, J. B. STOTHERS, and C. T. TAN. Can. J. Chem. **53**, 1351 (1975).
27. D. R. JONES, C. H. UNWIN, and E. W. B. WARD. Phytopathology, In press.

Can. J. Chem. Downloaded from www.nrcresearchpress.com by 210.87.254.6 on 09/05/12
For personal use only.

On the Alkaline Degradation of 2-Furfurylidene-10-methyl-*trans*-1-decalone[1]

A. STOESSL AND J. B. STOTHERS

Agriculture Canada Research Institute and the Chemistry Department, University of Western Ontario, London, Ontario N6A 3K7

Received May 28, 1975

A. STOESSL and J. B. STOTHERS. Can. J. Chem. **53**, 3359 (1975).

The reaction of 2-furfurylidene-10-methyl-*trans*-1-decalone with base (NaOH – aqueous $HOCH_2CH_2OH$) has been reinvestigated and found to give nine products. Elucidation of the structures of eight of these products, which accounted for *ca.* 80% of the process, was accomplished from their spectroscopic data and confirmed by chemical interconversions. The product mixture obtained shows that the reaction involves competition between the retroaldol process and various hydride reductions with some allylic isomerization.

A. STOESSL et J. B. STOTHERS. Can. J. Chem. **53**, 3359 (1975).

On a réétudié la réaction de la furfurylidène-2 méthyl-10 décalone-1 *trans* avec les bases (NaOH – $HOCH_2CH_2OH$ aqueux) et on a trouvé qu'il y a formation de neuf produits. On a élucidé la structure de huit de ces composés (représentant environ 80% de la réaction) à l'aide de données spectroscopiques et on les a confirmés par des interconversions chimiques. Le mélange de composés obtenus montre que la réaction implique une compétition entre la réaction rétroaldolique et diverses réductions par des hydrures avec un peu d'isomérisation allylique.

[Traduit par le journal]

As a model compound for the structural elucidation of some stress metabolites reported elsewhere in this issue (1) we required 10-methyl-Δ^1-*trans*-decalin (**1**). Since a quantity of 2-furfurylidene-10-methyl-*trans*-1-decalone (**2**) was on hand from an earlier study (2), we elected to prepare 10-methyl-*trans*-decal-1-ol (**3**) as a precursor for **1** from **2** as described in the literature (3). In our hands, the latter procedure gave in addition to **3**, seven compounds (**4**–**10**) which have been characterized. In our attempts to prepare **1**, recently described for the first time by Heathcock *et al.* (4) we found that **4**, the 1α epimer of **3**, is a much better precursor for **1**.

In the original description of the preparation of **3** from **2** (3), the product was isolated by distillation of the steam volatile fraction. However, since thin layer chromatography (t.l.c.) of the latter material showed the presence of nine distinct components, we chromatographed it preparatively on silica gel to obtain eight major fractions. Rechromatography of some of these fractions led to the isolation of eight compounds, **3**–**10**. One additional component, observable on analytical t.l.c., apparently decomposed during preparative chromatography. The isolated products accounted for 80% of the reaction, with **3** and **4** obtained in 33% and 17% yields, respectively, which may be compared with the 31% yield originally reported for the alcohol product of unspecified stereochemistry. The remaining six components included two ketones (**5** and **8**) and four alcohols, as shown by their i.r. and ^{13}C n.m.r. spectra; further, each was found to contain a furan moiety from the u.v. and n.m.r. spectra. The latter data also showed that **10** retained the furfurylidene

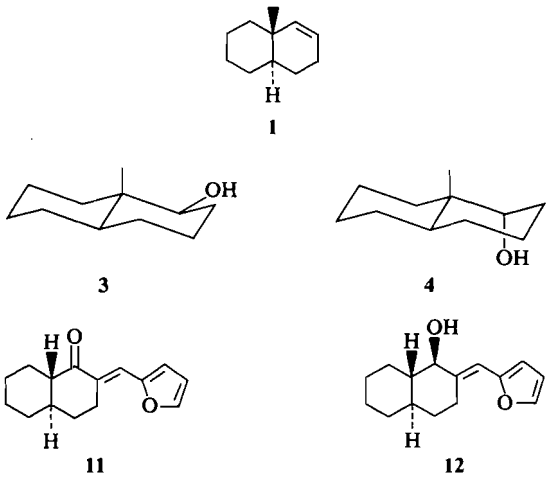

1 3 4 11 12

[1]Part 52 of ^{13}C Nuclear Magnetic Resonance Studies. For Pt. 51 see ref. 1. Contribution No. 623 from the Research Institute.

Can. J. Chem. Downloaded from www.nrcresearchpress.com by 210.87.254.5 on 09/05/12
For personal use only.

Can. J. Chem. Downloaded from www.nrcresearchpress.com by 210.87.254.5 on 09/05/12
For personal use only.

TABLE 1. ^{13}C shieldings* of **2** and **5–12**

Compounds	C-1	C-2	C-3	C-4	C-5	C-6	C-7	C-8	C-9	C-10	C-11	C-12	C-13	C-14	C-15	C-16
2	205.8	132.3	27.4	25.6	41.2	28.5	26.0	21.6	33.7	46.2	15.9	123.1	152.7	112.1	115.1	144.0
11	201.7	132.8	27.8	30.7	39.6	34.2	26.0	25.7	26.7	54.2	—	122.4	152.6	112.2	115.5	144.2
5	215.6	44.4	33.4	28.0	47.2	28.4	26.2	21.3	32.7	48.5	15.7	28.0	154.6	110.2	106.1	140.9
8	206.5	134.4	143.5	30.5	41.6	28.4	25.8	21.5	32.5	44.5	14.3	28.0	153.5	110.3	106.4	141.2
6	83.1	39.1	30.6	28.0	44.3	28.0	26.5	21.6	37.5	39.3	10.6	31.7	155.1	110.1	106.2	140.9
7	77.3	37.3	26.8	28.5	36.5	28.6	26.8	21.7	34.9	38.7	15.9	32.0	155.3	110.1	105.8	140.9
9	79.2	136.2	124.8	30.3	39.6	28.4	26.3	21.9	37.6	37.6	10.3	32.2	154.8	110.3	105.8	141.1
10	81.6	141.2	29.2	27.9	44.2	28.4	26.4	21.7	37.3	41.3	10.2	108.3	153.3	110.8	109.1	140.6
12	76.8	143.8	28.4	30.0	41.6	33.3	26.2	25.9	34.5	52.1	—	108.5	153.5	110.9	107.4	140.9

*In p.p.m. from TMS for $CDCl_3$ solutions.

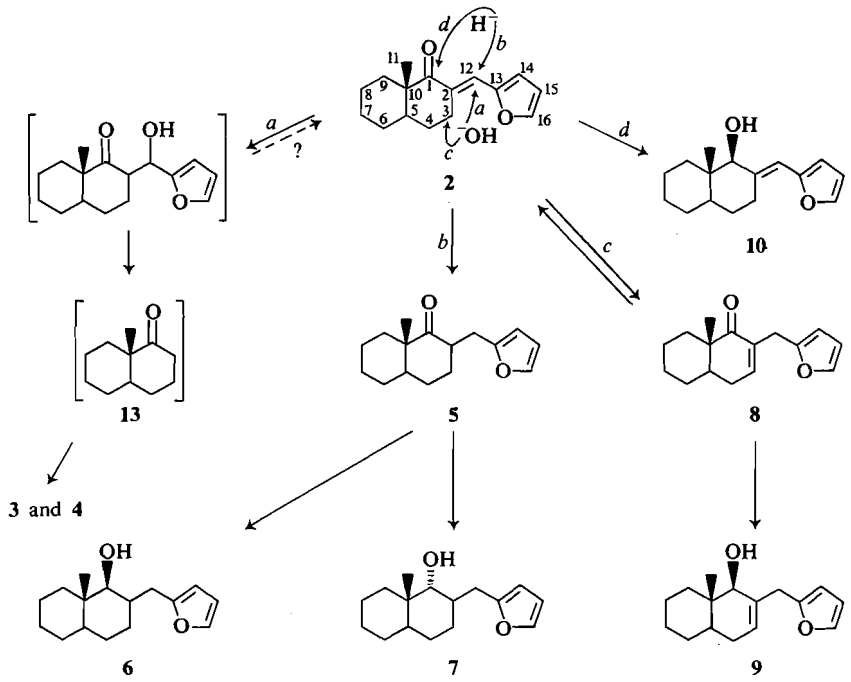

SCHEME I

group while **8** and **9** contained a trisubstituted double bond which in **8** was conjugated with the carbonyl group, thereby placing it at C-2,3 in the decalin skeleton. Conversion of **8** → **9** and **2** → **10** was readily accomplished by $NaBH_4$ reduction. A similar reduction of **5** gave a mixture of **6** and **7** with **6** as the major component. An examination of the ^1H and ^{13}C n.m.r. spectral data for the series led to the assigned structures; the ^{13}C data are collected in Table 1, including the results for models **11** and **12**.

A comparison of the noise decoupled and off-resonance decoupled ^{13}C spectra readily distinguished the signals for the methyl, methylene, methine and fully substituted carbons from which it was apparent that the decalin and furan moieties were intact in all cases. The methyl and carbonyl shieldings for **5** were identical to those for 10-methyl-*trans*-1-decalone (5), thus indicating its structure since an equatorial α alkyl substituent is not expected to affect these shieldings appreciably (6). Firm support for the location of the carbonyl group was provided by the spectra of the epimeric alcohols **6** and **7** formed from **5**. The carbinyl protons in each gave rise to a doublet, $J = 10.3$ and 2.0 Hz, respectively, while the carbinyl carbons absorbed at 83.1 and 77.3 p.p.m. with the corresponding methyl signals at 10.6 and 15.9 p.p.m.; these ^{13}C data are comparable to those for **3** and **4** (2). These results established **6** as the β-epimer while **7** has an α-hydroxyl group. The methyl shieldings of **9** and **10** at 10.3 and 10.2 p.p.m., respectively, similarly indicated the presence of a β-hydroxyl group in each of these alcohols. The remaining assignments of the carbon resonances as set out in Table 1 are entirely in agreement with the proposed structures with the noteworthy consistency of the shifts for the furan ring and C-6–C-9 of the decalin skeleton.

The major course of the overall process is the crossed Cannizzaro reaction with **13** as the presumed intermediate formed by a retro aldol reaction after hydroxide attack at C-12 of **2** (route *a* in Scheme 1). The presence of ketone **5** shows that hydride ion attack at C-12 is a competitive process (route *b* in Scheme 1). Presumably proton abstraction by hydroxide ion at C-3 in **2** leads to its conversion to **8** (route *c*) while hydride ion attack directly at the carbonyl group of **5**, **8**, and **2** led to the formation of **6**, **7**, **9**, and **10**. The ratios of the products obtained under the original conditions indicated that route *a* constituted ~67% of the overall process,

Can. J. Chem. Downloaded from www.nrcresearchpress.com by 210.87.254.5 on 09/05/12
For personal use only.

TABLE 2. Composition of the product from **2**

Fractions	Weight (mg)	Major component(s)	Approximate mole ratio (%)*
36–53	202	**5**	9.5
54–63	54	**8**	2.5
64–83	263†	**10**	6.5
		7	6.0
84–101	169	**6**	3.5
		9	4.5
102–119	163‡	**6**	5.0
		4	4.0
120–141	208	**4**	14.5
142–157	107	**4**	2.5
		3	5.5
158–216	513	**3**	36.0

*Total product represented *ca.* 80% conversion of **2**.
†Contained traces of **8** and **9**.
‡Contained a trace of **9**.

b ~18%, *c* ~9%, and *d* ~6%. However, under slightly less severe conditions, the product composition differed somewhat having a higher proportion of **8** and smaller amounts of **3** and **4**, indicating a reversible allylic isomerization, **2** ⇄ **8**. This was confirmed by the formation of **3**–**10** from **8** upon treatment of the latter under the milder conditions.

A second point of interest in this study is that olefin **1** is much more readily accessible from **4** than **3** presumably because **4** has an axial hydroxyl function. Heathcock *et al.* (4) obtained **1** in 43% yield by heating the tosylate of **3** in lithium chloride – dimethylacetamide to 100 °C, and these authors found that several other reagents gave zero yields. We found, similarly, that the treatment of **3** with (*a*) phosphorus oxychloride in pyridine, (*b*) thionyl chloride in pyridine, (*c*) aluminum oxide – pyridine (7), and (*d*) heating the mesylate of **3** in pyridine or in quinoline at 210–222 °C, gave products essentially devoid of the desired olefin. We obtained **1** in only moderate yields as a component of a complex mixture by pyrolysis of the acetate of **3** as well as in the solvolysis of the tosylate of **3** (4). In contrast **1** was prepared very conveniently and in 80% purity by the treatment of **4** with phosphorus oxychloride in pyridine at 0 °C. Presumably the dehydration of **4** proceeds more readily to **1** than with **3** because one of the vicinal hydrogens is axial and periplanar to the axial hydroxyl as required for facile elimination.

Experimental

General experimental procedures and the instrumentation employed were as described in the accompanying paper (1), except that infrared spectra were recorded for solutions (2% in CCl_4) with a Beckman IR 20 spectrophotometer. Unless otherwise noted, both column and thin layer chromatography employed Camag DF5 silica gel as adsorbent with methylene chloride as irrigant, but the adsorbent was activated (by heating to 110 °C) only for t.l.c.

Reaction of 2-Furfurylidene-10-methyl-trans-1-decalone (2) with Base

Ketone **2** (2.62 g) was added to a solution of NaOH (30 g) in freshly distilled ethylene glycol (150 ml) and water (15 ml) at 110 °C. The temperature of the mixture was raised to approximately 150 °C during 2 h, maintained near 150 °C for the next 7 h, and then raised to 175 °C for another 2 h. The product was allowed to cool to room temperature, diluted with water, and distilled in steam until the distillate was no longer cloudy (3.6 l). After saturation with sodium chloride, the distillate was extracted with ether (2 × 750, 1 × 200 ml); the combined extracts were dried over sodium sulfate, filtered, and evaporated to dryness, the remaining traces of moisture being removed by re-evaporation from absolute ethanol. The product (1.84 g) was eluted from a column of silica gel (500 g) in 25 ml fractions (see Table 2). A compound just slower than **3** was observed on analytical t.l.c. but apparently decomposed during preparative chromatography. Fractions 84–101 were further separated into crude **9** (52 mg) and **6** (36 mg) by preparative t.l.c.; fractions 102–119 afforded **9** (2 mg), **6** (87 mg), and **4** (50 mg) on rechromatography over a column of silica (100 g).

Compound **5**, after repeated recrystallization from petroleum ether (30–60 °C) at −10 °C, had m.p. 73 °C, λ_{max} 217 nm (log ε 3.94), and ν_{max} 1711 cm^{-1}.

Anal. Calcd. for $C_{16}H_{22}O_2$ (mol. wt. 246.1619): C, 78.01; H, 9.00. Found (246.1628): C, 77.82; H, 9.03.

The ketone **5** (86 mg) in ethanol (8.6 ml) was treated

Can. J. Chem. Downloaded from www.nrcresearchpress.com by 210.87.254.5 on 09/05/12
For personal use only.

Can. J. Chem. Downloaded from www.nrcresearchpress.com by 210.87.254.5 on 09/05/12
For personal use only.

with $NaBH_4$ for 10 min at 25 °C. The product was poured onto ice, extracted into chloroform, washed, dried, and chromatographed over silica (100 g). Elution with methylene chloride (5 ml fractions) gave **7** (14 mg; fractions 17–21) and **6** (53 mg; fractions 22–27), both identified by ^1H n.m.r., i.r., and t.l.c.

Compound **8** was a syrup, λ_{max} 220, λ_{sh} 236 nm (log ε 4.05, 3.83), ν_{max} 1676 cm^{-1}. Calcd. for $C_{16}H_{20}O_2$: 244.1462; found *m/e*: 244.1446. The ketone accrued in much greater yield (approx. 250 mg from 2.75 g of **1**) under slightly less vigorous conditions (termination after 7.5 h and the temperature not exceeding 155 °C). The alcohols **3** and **4** obtained in this run, together amounted to only 760 mg compared to the 900 mg yield for the first run.

Enone **8** (34 mg) was heated at 156 °C in ethylene glycol (1.5 ml) containing water (0.15 ml) and sodium hydroxide (0.3 g) for 7.5 h. The product (14 mg), isolated by steam distillation and having the odor characteristic of alcohol **3**, was found by t.l.c. to contain compounds **3**–**10** in proportions similar to those in the product obtained by the alkaline degradation of **2**.

Compound **10** (119 mg) crystallized on cooling a concentrated solution of fractions 64–83 in petroleum ether (30–60 °C) to −10 °C. Repeated recrystallizations gave material melting at 88–95 °C, invariably contaminated with decomposition products formed during the process. A pure sample, m.p. 99–101.5 °C, for a precise mass determination was obtained by sublimation *in vacuo* at 65–70 °C. Larger amounts of material, sufficiently pure for n.m.r. and i.r. spectroscopy, were obtained by extracting crystalline material at room temperature with a moderate excess of petroleum ether (30–60 °C), filtration from the insoluble decomposition products, and rapid removal of the solvent *in vacuo*, immediately before use. The compound was stable in dilute solution in deuteriochloroform at room temperature for several days, and also when purified by sublimation, but was unstable if concentrated or when kept in inadequately purified form, even at −10 °C. Essentially pure material exhibited λ_{max} 265, 271, and 283 nm (log ε 4.37, 4.41, and 4.23) and ν_{max} 3640 cm^{-1}. Calcd. for $C_{16}H_{22}O_2$: 246.1619; found *m/e*: 246.1618.

Ketone **2** (59 mg) in ethanol (6 ml) was treated with sodium borohydride (16 mg + 6 mg after 60 min) at room temperature for 70 min. The product was taken up in ice water (50 ml), acidified with a few drops of acetic acid and exhaustively extracted with chloroform (9 × 20 ml). Evaporation of the washed and dried extracts gave a quantitative yield of crystalline **10** identified by m.p., mixture m.p., t.l.c., and ^1H n.m.r. and i.r. spectra. The material, though obtained pure originally, commenced to decompose during recovery from spectroscopic solutions, at a rate which appeared to accelerate during subsequent recrystallization.

Compound **7** (45 mg) was isolated as a syrup (ν_{max} 3640 cm^{-1}) by rechromatography over silica gel (100 g) of the mother liquors from which **10** had crystallized. Except for the presence of a little of the latter, it was identical (^1H n.m.r., i.r., t.l.c.) with the minor reduction product from compound **5**. The mass spectrum was almost indistinguishable from that of compound **6**.

Compound **9**, λ_{max} 218 nm (log ε 3.96), ν_{max} 3620 and 3598 cm^{-1}, was obtained as a syrup by preparative t.l.c. of the crude substance on aluminum oxide (Camag DSF 5) with carbon tetrachloride as irrigant.

The same compound (^1H n.m.r., i.r., t.l.c.) was obtained as the main product (28 mg) of the reduction of compound **8** (70 mg) in ethanol (7 ml) with sodium borohydride (124 mg, added in portions during 60 min) by chromatography of the crude product over silica (50 g).

Compound **6** was a syrup, λ_{max} 218 nm (log ε 3.96), ν_{max} 3640 and 3620 cm^{-1}, identical by ^1H n.m.r., i.r., and t.l.c. with the major borohydride reduction product from compound **5**. Calcd. for $C_{16}H_{24}O_2$: 248.1775; found *m/e*: 248.1737.

Compound **4**, purified by recrystallization from petroleum ether (30–60 °C) at −10 °C or by sublimation at 30–40 Torr at *ca.* 55 °C, had m.p. 61–62.5 °C and ν_{max} 3630 and 3490 cm^{-1}. The pure material was almost odorless.

Anal. Calcd. for $C_{11}H_{20}O$: C, 78.51; H, 11.98. Found: C, 78.14; H, 12.29.

Compound **3**, recrystallized from petroleum ether (30–60 °C) at −10 °C, had m.p. 53–54 °C (lit. (4) m.p. 52–56 °C), ν_{max} 3620 and 3490 cm^{-1}, and a strong odor of peppermint. The derived tosylate, filtered from carbon tetrachloride insoluble impurities and recrystallized from petroleum ether (30–60 °C), had m.p. 93–95 °C (lit. (4) m.p. 95–102 °C). The ^1H n.m.r. data for **3** and its tosylate were in close accord with those published (2).

*Oxidation of **3** and **4** to 10-Methyl-trans-decalone (**13**)*

Fractions 142–157 (Table 2) (105 mg), containing compounds **3** and **4** in the ratio 70:30 (g.l.c. on a Carbowax column (10%) at 130 °C), in acetic acid (1 ml) were treated dropwise during 5 min with a solution of $Na_2Cr_2O_7 \cdot 2H_2O$ (*ca.* 65 mg) in acetic acid (2 ml). After stirring at room temperature for another 30 min, the mixture was poured on ice, neutralized with solid sodium carbonate, and the product extracted into chloroform. Apart from unreacted **3** (16 mg), the extract (69 mg) contained only a single product (44 mg), which was eluted from silica gel (5 g) by methylene chloride–petroleum ether (30–60 °C) (3:7) and proved identical with **13** by ^1H n.m.r. and t.l.c.

*2-Furfurylidene-trans-1-decalol (**12**)*

A solution of **11** (3) (60 mg) in ethanol (6 ml) was treated with $NaBH_4$ (18 mg + 9 mg after 10 min) to give the pure decalol, m.p. 155–156 °C, λ_{max} 263, 270, and 281 nm (log ε 4.34, 4.38, and 4.20), ν_{max} 3630, ν_{sh} 3595 cm^{-1}, and M^+ 232. The compound was as unstable as **10** to recrystallization from petroleum ether (30–60 °C). An analytical sample was prepared by sublimation.

Anal. Calcd. for $C_{15}H_{20}O_2$: C, 77.55; H, 8.68. Found: C, 77.20; H, 8.66.

*Dehydration of Compound **3** to Olefin **1***

(*a*) Treatment of **3** with phosphorus oxychloride or with thionyl chloride in pyridine at 0 °C; or heating the derived mesylate (methanesulfonylchloride–pyridine at room temperature) in pyridine (no reaction) or in quinoline at 210–222 °C during 2 h, gave products which

did not show the singlet absorption at δ 5.47 which is characteristic of olefin **1** (4). Treatment with aluminum oxide – pyridine (7) at 175 or at 230 °C gave a product, also free of the desired olefin, whose main components were starting material and ketone **13** (^{1}H n.m.r., t.l.c., borohydride reduction to starting material).

(*b*) Pyrolysis of the derived acetate at 500 °C for 0.5 h, in a sealed pyrex tube filled with nitrogen, gave a complex product which contained a small proportion (20–30%) of olefin **1** (^{1}H n.m.r.).

(*c*) Treatment of the tosyl derivative with lithium chloride in dimethylacetamide as in the literature (4) gave a mixture containing a similarly small proportion of the olefin.

*Dehydration of **4** to Olefin **1***

Alcohol **4** (208 mg) in pyridine (2 ml) at 0 °C was treated dropwise with phosphorus oxychloride (0.5 ml) in pyridine (2 ml) during about 2 min. After 4 days at 5 °C, the mixture was poured onto ice (20 g), and extracted with several portions of ice-cold ether. The extracts were washed in turn with water, 2 *N* sulfuric acid, water, 5% sodium hydrogen carbonate solution, and water, all at 0 °C. The ether layers were combined, dried over sodium sulfate at 5 °C, filtered, and evaporated *in vacuo*. The product (92 mg), comprising olefin **1** (*ca.* 80%) and two unidentified compounds (*ca.* 10% each by g.l.c. on a Carbowax column (10%) at 130 °C) was suitable for n.m.r. spectroscopy without purification.

We thank G. L. Rock for experimental assistance, H. Schroeder for the determination of 100 MHz proton spectra, and R. Lazier and D. Hairsine for the mass spectra. We are grateful to the National Research Council of Canada for financial support.

1. A. Stoessl, J. B. Stothers, and E. W. B. Ward. Can. J. Chem. This issue.
2. S. H. Grover and J. B. Stothers. Can. J. Chem. **52**, 870 (1974).
3. W. S. Johnson, I. A. David, H. C. Dehm, R. J. Highet, E. W. Warnhoff, W. D. Wood, and E. T. Jones. J. Am. Chem. Soc. **80**, 661 (1958).
4. C. H. Heathcock, R. Ratcliffe, and J. Van. J. Org. Chem. **37**, 1796 (1972).
5. S. H. Grover, D. H. Marr, J. B. Stothers, and C. T. Tan. Can. J. Chem. **53**, 1351 (1975).
6. J. B. Stothers and C. T. Tan. Can. J. Chem. **52**, 308 (1974).
7. E. v. Rudloff. Can. J. Chem. **39**, 1860 (1961).

Can. J. Chem. Downloaded from www.nrcresearchpress.com by 210.87.254.5 on 09/05/12
For personal use only.

The Structure of Acetaldehyde Enolate Anion

SAUL WOLFE AND H. BERNHARD SCHLEGEL[1]
Department of Chemistry, Queen's University, Kingston, Ontario K7L 3N6
IMRE G. CSIZMADIA
Department of Chemistry, University of Toronto, Toronto, Ontario M5S 1A1
AND
FERNANDO BERNARDI
Istituto di Chimica Organica, Universita di Bologna, 40136-Bologna, Italy
Received May 29, 1975

SAUL WOLFE, H. BERNHARD SCHLEGEL, IMRE G. CSIZMADIA, and FERNANDO BERNARDI. Can. J. Chem. **53**, 3365 (1975).

Non-empirical SCF–MO computations have been performed on $[CH_2CHO]^-$, the simplest enolate anion. Following a preliminary search of the conformational hypersurface using an STO-3G basis set to determine the C—C and C—O bond lengths as a function of rotation about the C—C bond, the rotation–inversion surface has been generated with an STO-4G basis set. The energy minimum of this surface is the all-planar anion whose C—C and C—O bond lengths are entirely compatible with the usual description $^-CH_2CHO \leftrightarrow CH_2{=}CHO^-$. The planar structure results from extensive conjugative stabilization amounting to over 30 kcal/mol (based on the C—C rotational barrier). When the CH_2 plane is perpendicular to the CHO plane, the conjugative interaction is symmetry forbidden and the electron-withdrawing inductive effect of the formyl substituent leads to a pyramidal carbanion. Experimental implications of these results are discussed.

SAUL WOLFE, H. BERNHARD SCHLEGEL, IMRE G. CSIZMADIA et FERNANDO BERNARDI. Can. J. Chem. **53**, 3365 (1975).

On a effectué des calculs SCF–MO non-empiriques sur $[CH_2CHO]^-$, l'anion énolate le plus simple. On a effectué une étude préliminaire de l'hypersurface conformationnelle utilisant une base STO-3G afin de déterminer les longueurs des liaisons C—C et C—O en fonction de la rotation du lien C—C; on a ensuite généré la surface de rotation–inversion utilisant une base STO-4G. Le minimum d'énergie de cette surface correspond à l'anion complètement plan pour lequel les longueurs des liaisons des liens C—C et C—O sont compatibles avec la description usuelle $^-CH_2CHO \leftrightarrow CH{=}CHO^-$. La structure planaire est le résultat d'une stabilisation importante provenant de la conjugaison et correspondant à plus de 30 kcal/mol (en se basant sur la barrière à la rotation C—C). Quand le plan du CH_2 est perpendiculaire au plan CHO, l'interaction de conjugaison n'est pas permise par la symétrie et l'effet inductif d'attraction des électrons par le groupe formyle conduit à un carbanion pyramidal. On discute des implications expérimentales de ces résultats.

[Traduit par le journal]

Introduction

"The generally-accepted mechanism of racemization, hydrogen isotope exchange, and halogenation of carbonyl compounds is rate-determining enolization followed by fast reaction of the enol or enolate ion" (1) (Eq. 1). The classic experiments upon which this mechanism rests (2, 3) were designed to demonstrate that "if the carbon atom bearing mobile hydrogen is an asymmetric center of optical activity, and is the only one present in the molecule, then optical activity must be lost in the mesomeric anion" (4).

[1] 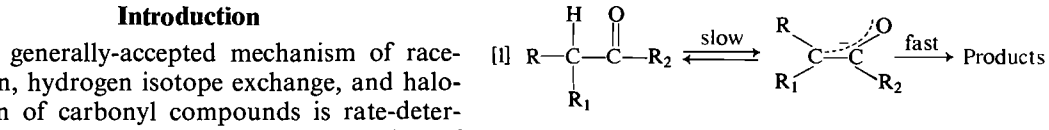

The purpose of the present investigation is to examine theoretically the circumstances under which an enolate anion will have trigonal planar geometry at carbon and will, therefore, be achiral. The work was initiated because of the implications that may be drawn from three types of study: (*i*) the extensive literature on the symmetry properties of tricoordinated species (5) indicates that attachment of a carbonyl group to a carbanionic center will cause a lowering of the barrier to pyramidal inversion at

[1]Holder of a National Research Council of Canada 1967 Science Scholarship.

Can. J. Chem. Downloaded from www.nrcresearchpress.com by 210.87.254.40 on 09/05/12
For personal use only.

Can. J. Chem. Downloaded from www.nrcresearchpress.com by 210.87.254.40 on 09/05/12
For personal use only.

carbon if the conjugative effect of the carbonyl group dominates; however, the electron-withdrawing *inductive* effect of the carbonyl group operates in the opposite direction and will tend to increase the inversion barrier. Depending upon the balance between conjugative and inductive effects in this system, the barrier to pyramidal inversion at carbon in the anion of acetaldehyde (**1**) might be higher, lower, or equal to that in methylcarbanion. (*ii*) Although several claims that conjugated asymmetric carbanions had been generated (6) could not be confirmed (7), Marquet and co-workers (8) have succeeded in repeating and extending the observations of Leuchs (9). Thus the ketone **2** undergoes chlorination and bromination with retention of configuration at the asymmetric center, the degree of asymmetric induction depending upon the nature of the halogenating agent and the solvent. (*iii*) A number of examples now exist (10) of large differences in the rates of appearance of deuterium at the *exo* and *endo* methylene positions of certain bicyclic ketones (*e.g.* **3**), when these compounds are subjected to base catalyzed hydrogen–deuterium exchange.

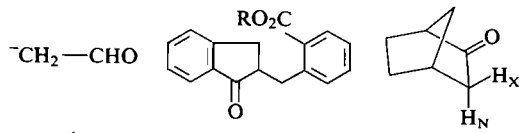

1 **2** **3**

These latter observations have been interpreted in terms of a kinetic model which assumes a difference in the rates of protonation (deuteration) of an achiral intermediate (the enol or enolate anion) from *exo* and *endo* faces. However, there is an alternative interpretation of such observations if it is supposed that the asymmetry resides in the anionic intermediate itself, and not in the capture of this intermediate. In this event, the experimental observations would be consistent with either a greater rate of *abstraction* of the *exo* proton, or with exchange of the *exo* proton with retention of configuration and exchange of the *endo* proton with *inversion* of configuration (11). Analysis of experimental data in terms of such a mechanism would require a more complex kinetic model (12).

To assess the validity of these views, and the possible role of conformational effects in creating and maintaining asymmetry (*i.e.*, non-planar geometry at carbon) in an enolate anion, we have carried out a theoretical study of a portion of the conformational hypersurface of **1** corresponding to rotation about the carbon–carbon bond and pyramidal inversion at the carbanionic center. We were aware of the fact that formamide, H_2NCHO, which is isoelectronic with **1**, may have a non-planar configuration at nitrogen (13).

Method

The Hartree–Fock–Roothaan equations were solved using the Gaussian 70 program system (14). A preliminary search of the energy hypersurface was performed with an STO-3G basis set (15) and detailed investigation of the rotation–inversion surface was then carried out with the STO-4G basis set.[2] As a result of convergence problems, the computations could not be extended to the 4-31G level (16).

All computations were performed on a CDC 6600 computer at the University of Bologna.

Calculations

Because of the low (*ca.* 1 kcal/mol) inversion barrier in formamide (13), it was recognized that a crude optimization of the out-of-plane angle of **1** could well overlook a non-planar anion. In addition, the degree of non-planarity was expected to depend strongly upon both the C—C and C—O bond lengths. For example, shorter C—C and longer C—O bonds should enhance the conjugative effect and diminish any tendency towards a non-planar anion. The computations were, therefore, carried out in three stages.

In the first stage, the C—C and C—O bond lengths were varied with the carbanionic center non-planar (C—H = 1.09 Å; $\angle$CCO = $\angle$OCH = 120°; $\angle$HCH = $\angle$HCC = 115°; HCCO dihedral angle = 20° and both methylene hydrogens on the same side of the CCHO plane). These results are summarized in Table 1, together with a similar optimization with the carbanionic center planar. The second stage consisted of a complete optimization beginning with a slightly non-planar structure. Starting from $\angle$HCH = $\angle$HCC = 119°, all bond lengths and angles were optimized, with the inversion coordinate varied last. This led to a fully planar structure for the energy minimum. In the third stage of the work, this optimized structure represented the starting point for the STO-4G calcu-

[2]Minimal basis sets tend to overestimate barriers to pyramidal inversion. Therefore, energy differences in this paper which deal with changes in the inversion coordinate should be regarded as upper limits of these values.

Can. J. Chem. Downloaded from www.nrcresearchpress.com by 210.87.254.40 on 09/05/12
For personal use only.

TABLE 1. Optimization of the C—C and C—O bond lengths of **1** with an STO-3G basis set

Bond length (Å)		Energy (hartree[a])	
C—O	C—C	Non-planar[b]	Planar[c]
1.43	1.45	−150.102438	
1.35	1.50	−150.114595	
1.35	1.45	−150.121671	
1.35	1.40	−150.124948	−150.122763
1.25	1.50	−150.124957	
1.25	1.45	−150.130463	−150.129779
1.25	1.40	−150.132067	−150.133724
1.25	1.35	−150.128540	−150.132561
1.15	1.40	−150.106068	−150.106199

[a]1 hartree = 627.71 kcal/mol.
[b]Optimum structure: C—O = 1.279 Å; C—C = 1.409 Å; E = −150.133502.
[c]Optimum structure: C—O = 1.272 Å; C—C = 1.386 Å; E = −150.134805.

lations of the rotation–inversion surface. The coordinates are defined as shown in **4**; in this structure, the point X is included to facilitate the definition of the inversion coordinate.

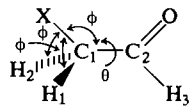

4

Thus $\phi = 90$, $\theta = 0$ defines the all-planar conformation.

At each of three dihedral angles ($\theta = 0$, 45, and 90°), the C—C and C—O bond lengths and the HC_1C_2 valence angles were reoptimized with ϕ maintained at 90°. Then the inversion cross-sections were scanned by permitting ϕ to vary. The relationship between the HC_1C_2 angles and

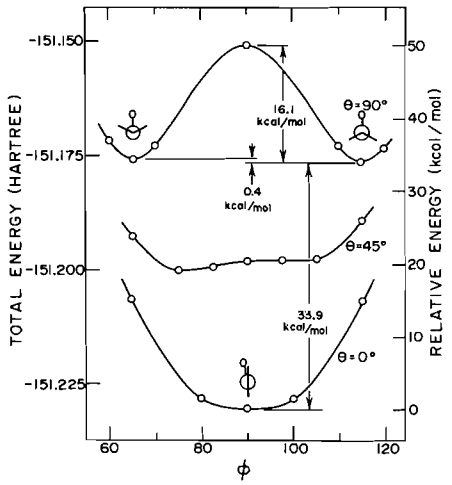

FIG. 1. Cross-sections of the rotation–inversion surface of **1** corresponding to $\theta = 0°$ (the all-planar conformation), $\theta = 45°$, and $\theta = 90°$.

ϕ is given in Eq. 2, and corresponds to the assumption that the projected HC_1C_2 angle about the C_1X axis remains constant.

$$[2]\quad \cos(\angle HC_1C_2)_\phi = \cos^2\phi + \cos(\angle HC_1C_2)_{90}\sin^2\phi$$

These latter cross-sections are displayed in Fig. 1 and summarized in Table 2.

An analytical expression having the form shown in Eq. 3 was then fitted to the data of Table 2. The coefficients of Eq. 3 are given in Table 3. With the aid of this equation, a perspective view of the final rotation–inversion surface was generated, and is presented in Fig. 2.[3]

$$[3]\quad \begin{aligned} E = {} & C_0 + C_1(\phi - 90)^2 + C_2\exp[-1.05(\phi - 90)^2] \\ & + C_3\sin\theta\cdot(\phi - 90) + C_4\sin\theta\cdot(\phi - 90)^3 \\ & + C_5\sin^2\theta + C_6\sin^2\theta\cdot(\phi - 90)^2 \\ & + C_7\sin\theta\cdot\exp[-1.05(\phi - 90)^2] + C_8\sin^3\theta\cdot(\phi - 90) \\ & + C_9\sin^3\theta\cdot(\phi - 90)^3 + C_{10}\sin^4\theta \\ & + C_{11}\sin^4\theta\cdot(\phi - 90)^2 + C_{12}\sin^4\theta\cdot\exp[-1.05(\phi - 90)^2] \end{aligned}$$

Discussion

The all-planar structure is the minimum point on the rotation–inversion surface because of the overriding effect of the conjugative stabilization that is present in this conformation. The magnitude of this conjugative effect may be gauged from the 33.9 kcal/mol barrier to rotation about the C_1—C_2 bond and the decrease in this bond length from 1.472 Å at $\theta = 90°$ to 1.379 Å at

[3]This surface is generated by a series of computer programmes SURFPLOT, which may be obtained from the authors.

Can. J. Chem. Downloaded from www.nrcresearchpress.com by 210.87.254.40 on 09/05/12
For personal use only.

TABLE 2. Rotation–inversion surface of **1** with an STO-4G basis set

Geometry[a]						
θ (deg.)	φ (deg.)	r_{CO} (Å)	r_{CC} (Å)	$\angle H_1C_1C_2$ (deg.)	$\angle H_2C_1C_2$ (deg.)	Energy[b]
0	90[c]	1.270	1.379	122.4	121.7	−151.230542
0	100	1.270	1.379	119.3	118.7	−151.228334
0	115	1.270	1.379	105.2	104.7	−151.206895
45	90	1.261	1.404	122.5	121.2	−151.198504
45	65	1.261	1.404	105.2	104.3	−151.192742
45	75	1.261	1.404	115.7	114.6	−151.200313
45	82.5	1.261	1.404	120.7	119.5	−151.199681
45	97.5	1.261	1.404	120.7	119.5	−151.198338
45	105	1.261	1.404	115.7	114.6	−151.197877
45	115	1.261	1.404	105.2	104.3	−151.189213
90	90	1.233	1.472	119.8	119.8	−151.150814
90	60	1.233	1.472	97.0	97.0	−151.171749
90	65	1.233	1.472	103.2	103.2	−151.175878
90	70	1.233	1.472	108.8	108.8	−151.172916
90	110	1.233	1.472	108.8	108.8	−151.172703
90	115	1.233	1.472	103.2	103.2	−151.176521
90	120	1.233	1.472	97.0	97.0	−151.173670

[a]Additional parameters: $r_{C_2H_3} = 1.12$ Å; $r_{C_1H} = 1.075$ Å; $\angle C_1C_2O = 126.8°$; $\angle H_3CO = 118.0°$.
[b]In hartree units.
[c]Planar structure.

TABLE 3. The parameters of Eq. 3, employed in the generation of the rotation–inversion surface[a,b]

Parameter	Value
C_0	−151.863773
C_1	0.726856
C_2	0.633231
C_3	0.012411
C_4	−0.001579
C_5	0.177172
C_6	−0.203588
C_7	−0.128697
C_8	−0.010458
C_9	−0.012292
C_{10}	−0.833062
C_{11}	0.645908
C_{12}	0.864296

[a]θ, φ in radians; E in hartree units.
[b]Maximum deviation 0.000081. Root mean square deviation 0.000031.

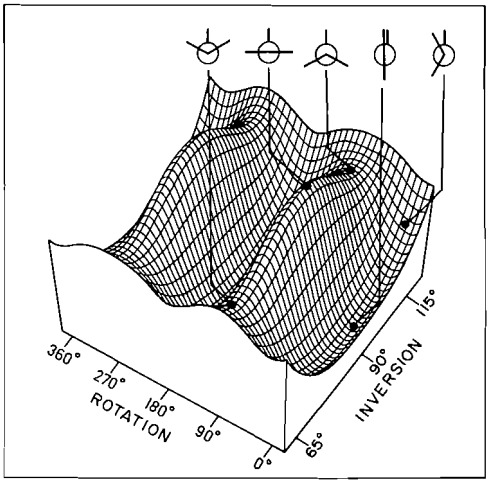

FIG. 2. The rotation–inversion surface of **1**.

θ = 0°, accompanied by a lengthening of the C_2—O bond from 1.233 to 1.270 Å. Inspection of the π-type molecular orbitals (Fig. 3) reveals that conjugation is achieved by a four-electron three-orbital interaction between the carbon lone pair and the π and π* C_2—O orbitals. Even when the methylene group is rotated 45° out of the plane of the formyl group, substantial conjugation remains, as indicated by the short C_1—C_2 bond (1.404 Å). However, at θ = 90°, this conjugative interaction is now symmetry forbidden and the methylene group behaves normally, *i.e.*, it is pyramidal. The inversion barrier is 16.1 kcal/mol, which may be compared to the 21.7 kcal/mol barrier computed for CH_3^- with the same basis set.

Our expectation that the electron-withdrawing formyl substituent might bring about some stabilization of the pyramidal configuration at the methylene group is thus not confirmed, either at θ = 0° (the all-planar structure) or at θ = 90°. The reason for this can be seen upon considera-

Can. J. Chem. Downloaded from www.nrcresearchpress.com by 210.87.254.40 on 09/05/12
For personal use only.

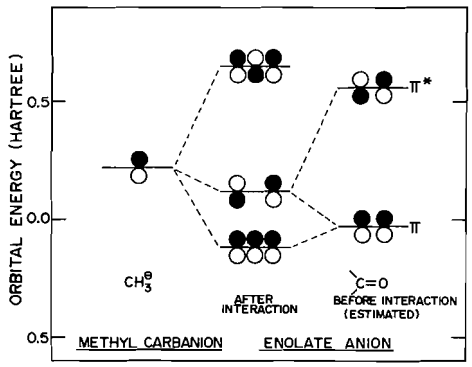

FIG. 3. Interaction of the π-type molecular orbitals in the energy minimum of **1**.

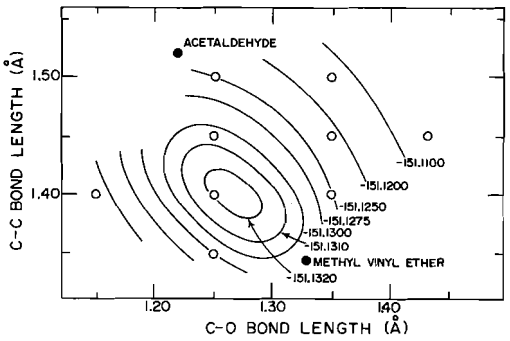

FIG. 4. The relationship between the computed (STO-3G) C—C and C—O bond lengths of **1**. Experimental data for methyl vinyl ether and acetaldehyde are indicated by ●.

tion of the nature of the charge transfer between the methylene and formyl groups. Within the framework of the Mulliken population analysis, there is, in the all-planar structure, a π charge transfer of 0.47 electron from CH_2^- to CHO, and a σ charge transfer of only 0.04, illustrative of the dominating influence of the conjugative interaction. In the θ = 90° conformation, the σ charge transfer is 0.27 electron from CH_2^- to CHO, but some π charge transfer, amounting to 0.05 electron in the same direction, or 18% of the σ charge transfer, remains. This is caused by a hyperconjugative interaction between the methylene group and the formyl group. This hyperconjugative interaction works against the inductive (*i.e.* σ) effect of the formyl group, and it leads to a net destabilization of the pyramidal configuration, as compared to CH_3^-.

The C—C and C—O bond lengths are strongly coupled to each other (*cf.* Table 1). The contour plot of Fig. 4 shows this coupling for the STO-3G calculations. For comparison, the experimental bond lengths of acetaldehyde (C—C and C=O) and methyl vinyl ether (C=C and C—O) are included in this figure. It is clear that the structure of acetaldehyde enolate anion is very well represented by the usual resonance description

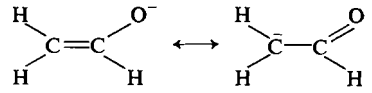

The C—C and C—O bond lengths are also coupled to the out-of-plane bending of the methylene group. In the 0° rotational structure, for instance, the out-of-plane bending allows the orbitals of H_1 and H_2 to mix with the π orbitals and withdraw charge from them. In doing so, the π conjugation is reduced and the net effect is to lengthen both the C—C bond and the C—O bond as the geometry at C_1 is made non-planar. However, the stabilization gained by this out-of-plane bending is unable to overcome the concomitant destabilization of the π system.

The rotation–inversion surface shows in some detail the dependence of the energy on the rotation and inversion coordinates. It is noteworthy that the more stable of the two pyramidal structures has the Y conformation **5**. Such behavior has been found previously in $^-CH_2OH$ (17), whose C—O bond length is similar to the C_1—C_2 bond length of the enolate anion. The Y conformation is favored when the structure is dominated by the nuclear component of the total energy. However, in the θ = 45° cross-section, the structure is dominated by the electronic component of the total energy (*i.e.*, the conjugative effect), and the more crowded W conformation (**6**) is favored.

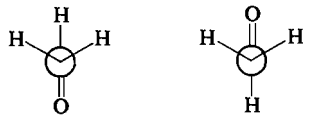

5 **6**

Conclusions

The suggestion that the simplest enolate anion might have non-planar geometry at carbon has not been supported. Although the electron-withdrawing effect of the carbonyl group can be shown to exist, in the absence of conformational constraint it does not overcome the conjugative interaction leading to a planar carbanion. The

Can. J. Chem. Downloaded from www.nrcresearchpress.com by 210.87.254.40 on 09/05/12
For personal use only.

required conformational constraint is found in the ketone **7** (18). The observation that the bridgehead protons of this compound undergo base-catalyzed exchange demonstrates that, as computed for the $\theta = 90°$ structure, a pyramidal enolate anion has some stability. However, since the pyramidal conformation is much higher in energy than the all-planar conformation, the exchange is extremely slow.

In each of the bicyclic ketones (*e.g.*, **3**, **8–12**) for which stereoselective hydrogen exchange has been reported (10) a planar enolate anion is possible. Consequently it is valid to analyze stereoselective exchange in such compounds in terms of a kinetic model which assumes asymmetric capture of an inherently symmetrical intermediate. For stereoselective exchange of methylene protons adjacent to a carbonyl group to proceed via an asymmetric intermediate it will be necessary to employ a substrate containing diastereotopic methylene protons which cannot achieve a planar conformation in the enolate anion. Inspection of molecular models suggests that the ketone **13** may be suitable for such a study.

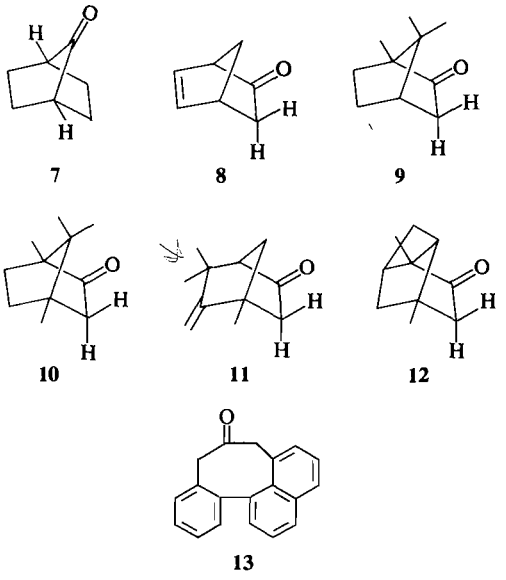

We thank the National Research Council of Canada, the Italian C.N.R., and the donors of the Petroleum Research Fund, administered by the American Chemical Society, for financial support of this work.

1. J. W. Thorpe and J. Warkentin. Can. J. Chem. **50**, 3229 (1972).
2. C. K. Ingold and C. L. Wilson. J. Chem. Soc. 93 (1934).
3. S. K. Hsü, C. K. Ingold, and C. L. Wilson. J. Chem. Soc. 1778 (1935).
4. C. K. Ingold. Structure and mechanism in organic chemistry. 2nd Edition. Cornell University Press. 1969. p. 829.
5. J. M. Lehn. Top. Curr. Chem. **15**, 311 (1970); A. Rauk, L. C. Allen, and K. Mislow. Angew. Chem. Int. Ed. Engl. **9**, 400 (1970); J. B. Lambert. Top. Stereochem. **6**, 19 (1971); H. A. Bent. Chem. Rev. **61**, 275 (1961).
6. R. Kuhn and H. Albrecht. Chem. Ber. **60**, 1297 (1927); R. L. Shriner and J. H. Young. J. Am. Chem. Soc. **52**, 3332 (1930); C. Rappe. Acta Chem. Scand. **21**, 1823 (1967).
7. N. Kornblum, J. T. Patton, and J. B. Woodman. J. Am. Chem. Soc. **70**, 746 (1948); G. Wittig, F. Vidal, and E. Bohnert. Chem. Ber. **83**, 359 (1950); J. Warkentin and C. Barnett. J. Am. Chem. Soc. **90**, 4629 (1968).
8. M. J. Ronteix and A. Marquet. Tetrahedron Lett. 5801 (1966); M. Dvolaitzky, M. J. Luche, and A. Marquet. Compt. Rend. Ser. C. **266**, 1797 (1968); M. J. Luche and A. Marquet. Compt. Rend. Ser. C. **267**, 420 (1968).
9. H. Leuchs. Chem. Ber. **46**, 2435 (1913); **48**, 1015 (1915).
10. A. F. Thomas and B. Willhalm. Tetrahedron Lett. 1309 (1965); J. M. Jerkunica, S. Borčić, and D. E. Sunko. Tetrahedron Lett. 4465 (1965); A. F. Thomas, R. A. Schneider, and J. Meinwald. J. Am. Chem. Soc. **89**, 68 (1967); T. T. Tidwell. J. Am. Chem. Soc. **92**, 1448 (1970); N. H. Werstiuk and R. Taillefer. Can. J. Chem. **48**, 3966 (1970); G. Lamaty, A. Roques, and L. Fonzes. Compt. Rend. Ser. C. **273**, 521 (1971); G. A. Abad, S. P. Jindal, and T. T. Tidwell. J. Am. Chem. Soc. **95**, 6326 (1973).
11. R. R. Fraser, F. J. Schuber, and Y. Y. Wigfield. J. Am. Chem. Soc. **94**, 8795 (1972).
12. T. F. Garrard. M.Sc. Thesis, Queen's University, Kingston, Ont. 1974.
13. D. H. Christensen, R. N. Kortzeborn, B. Bak, and J. J. Led. J. Chem. Phys. **53**, 3912 (1970).
14. W. J. Hehre, W. A. Lathan, R. Ditchfield, M. D. Newton, and J. A. Pople. GAUSSIAN 70. Quantum Chemistry Program Exchange. Indiana University, Bloomington, Ind. No. 236.
15. W. J. Hehre, R. F. Stewart, and J. A. Pople. J. Chem. Phys. **51**, 2657 (1969).
16. R. Ditchfield, W. J. Hehre, and J. A. Pople. J. Chem. Phys. **54**, 724 (1971).
17. S. Wolfe, L. M. Tel, and I. G. Csizmadia. Can. J. Chem. **51**, 2423 (1973).
18. P. G. Gassman and F. V. Zalar. J. Am. Chem. Soc. **88**, 3070 (1966).

^{119}Sn Mössbauer Spectra of some Tin(II)–Oxygen Compounds

JACK G. BALLARD AND THOMAS BIRCHALL
Department of Chemistry, McMaster University, Hamilton, Ontario L8S 4M1
Received June 27, 1975

JACK G. BALLARD and THOMAS BIRCHALL. Can. J. Chem. **53**, 3371 (1975).
Mössbauer data for α- and β-$SnWO_4$ and $Sn(SO_3X)_2$ are reported and the spectrum of $SnCl_2$ re-examined.

JACK G. BALLARD et THOMAS BIRCHALL. Can. J. Chem. **53**, 3371 (1975).
On rapporte des données Mössbauer pour les $SnWO_4$ α et β et pour le $Sn(SO_3X)_2$ et on a réexaminé le spectre du $SnCl_2$.

Can. J. Chem. Downloaded from www.nrcresearchpress.com by 210.87.254.105 on 09/05/12
For personal use only.

Results and Discussion

Several attempts have been made to estimate the ^{119}Sn Mössbauer isomer shift that a bare stannous ion ($5s^2$ configuration) would have. These estimates range from 4.76 mm/s (1) to 7.7 mm/s (2) and while the approach used for the former estimate has been shown to be incorrect (3, 4), isomer shift values for compounds containing Sn(II) are all lower than 4.76 mm/s. This either means that none of the compounds so far examined contain a bare $5s^2$ or that Lees and Flinn's approach (1) fortuitously gives the correct estimate. Very large shift values accompanied by zero quadrupole splitting have been taken to indicate that the $5s^2$ electrons are not involved in the metal–ligand bonds (5) and this is supported by crystallographic evidence for the $[SbX_6]^{3-}$ system (6). The analogous Sn(II) compound $[SnCl_6]^{4-}$ has not yet been prepared but such an ion might have a stereochemically inactive 5s electron pair and give a large positive isomer shift.

The only compound of Sn(II) known to exist in a cubic environment is SnTe (7). Its isomer shift (3.28 mm/s) is more positive than one might have expected from the electronegativity of Te and furthermore has no resolvable quadrupole splitting (2). However, SnTe cannot be considered to contain a bare Sn(II) ion since this is only likely to be achieved with the most electronegative ligands. Fluorine, being the most electronegative element, might have been expected to have the desired effect on a tin atom and produce a compound with a very high isomer shift. Invariably, however, tin(II) fluorides have distorted tin environments (8–11) and this is reflected in their Mössbauer parameters (Table 1) (12). $Sn(SbF_6)_2$ does have a very large positive isomer shift with no resolvable quadrupole splitting (Table 1) and might be considered an example of a compound containing a bare stannous ion, but other spectroscopic evidence suggests (13) that there is interaction between the Sn^{2+} and the SbF_6^- ions. Crystallographic data is not available on this compound to clarify this point.

TABLE 1. Mössbauer data for some tin(II) compounds

Compound	Isomer shift δ (mm/s)	Quadrupole splitting Δ (mm/s)
$Sn(SbF_6)_2$*	4.40	—
$Sn(SO_3F)_2$	4.06	0.69
$Sn(SO_3Cl)_2$	4.09	0.97
$SnSO_4$†	3.90	1.00
β-$SnWO_4$	3.53	1.38
α-$SnWO_4$	3.48	1.15
SnF_2(*ortho*)	3.30	2.15
$SnCl_2$	4.04	0.60

*Reference 17.
†Reference 18.

Stannous chloride has a large positive isomer shift (14, 15) but it is polymeric in the solid state (16) and cannot be considered an ionic compound. We have repeated Mössbauer measurements on this compound and while our isomer shift agrees with the literature value we find that the spectrum could only be satisfactorily analyzed in terms of a quadrupole split doublet rather than a single line. Figure 1 shows these fits with χ^2 values of 334 and 192 for the one and two line fits respectively. A quadrupole split absorption is more consistent with the distorted octahedral environment about the tin (16).

The tin(II)–oxygen systems appear to offer the best chance of obtaining the stannous ion in a

Can. J. Chem. Downloaded from www.nrcresearchpress.com by 210.87.254.105 on 09/05/12
For personal use only.

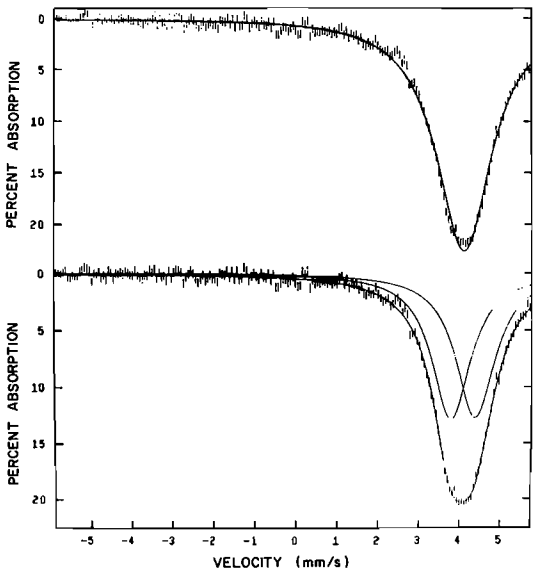

FIG. 1. ^{119}Sn Mössbauer spectra of $SnCl_2$ using one and two line fits.

regular octahedral environment with the oxygen ligand being sufficiently electronegative to leave the tin with a bare $5s^2$ configuration. We report in Table 1 data for α- and β-$SnWO_4$ and $Sn(SO_3X)_2$ which, when we began this work, we thought might contain Sn(II) in regular octahedral environments. If this had been the case very high isomer shifts with zero quadrupole splitting would have been observed. Both of the tungstates are now known to have distorted tin environments with the 5s electron pair clearly stereochemically active (17, 18). The bonding participation of the 5s electrons is reflected in the Mössbauer parameters where the isomer shift is lower than expected with a clearly resolved quadrupole splitting. The isomer shifts for these two compounds are not very different but are in the order one would expect from a comparison of their average Sn—O bond lengths. If one considers that the average of the Sn—O bond lengths is a measure of s electron withdrawal, and/or p–d electron donation, and that both have six significantly bonded oxygens, then α-$SnWO_4$ having Sn—O(average) = 2.47 Å should have a lower isomer shift then β-$SnWO_4$ (Sn—O(average) = 2.51 Å), as is observed. $SnSO_4$ has Sn—O(average) > 2.64 Å, longer than either of the tungstates, and it has a more positive isomer shift. Examination of the crystallographic data for these tungstates shows that the immediate tin environment in α-$SnWO_4$ is more distorted than in the β form, yet the quadrupole splitting is largest for the β form. It must be remembered however that the splitting is made up of a lattice as well as a valence contribution and the smaller value for α-$SnWO_4$ may be the result of a larger lattice contribution, which is likely to be of opposite sign to the valence contribution (19).

The Sn(II) halosulfonates are somewhat closer to the Sn^{2+} ideal, having very positive isomer shifts but still significant quadrupole splittings (Fig. 2). This again suggests participation of the 5s electron pair in the bonding, probably to about the same extent as in $SnCl_2$. The structures of these halosulfonates are almost certainly similar to that of $SnCl_2$ with the Sn atoms being linked by halosulfonate bridges to form polymeric chains. The bridging would, by analogy to $(CH_3)_2Sn(SO_3F)_2$ (20), be through the SO_3X^- oxygens rather than the halogen and the immediate tin environment would have one short and two longer Sn—O bonds on one side of the tin with the distorted octahedron probably being completed by two oxygens and a halogen on the lone pair side. Based upon a comparison of the isomer shift data for the Sn—O compounds of known structure one would anticipate that the

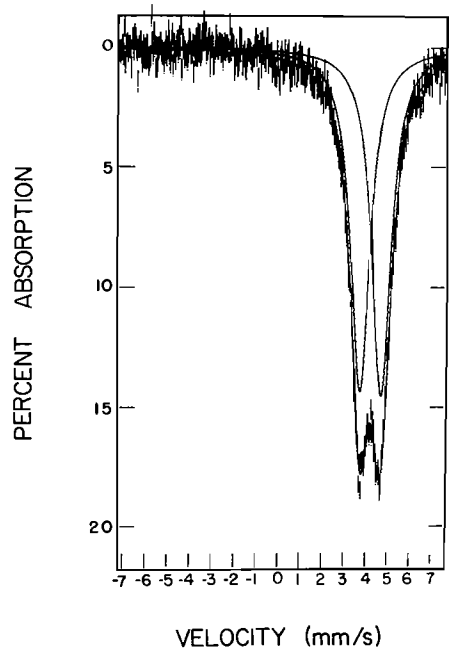

FIG. 2. ^{119}Sn Mössbauer spectra of $Sn(SO_3Cl)_2$ at 77 K.

Sn—O bonds would be longer than in $SnSO_4$ by ~0.1 Å. We are currently attempting crystallographic analyses of these $Sn(SO_3X)_2$ compounds.

Experimental

The Mössbauer spectra were recorded and computer fitted by procedures already described (21). Samples contained ~10 mg Sn/cm^2 and were cooled to 77 K. Isomer shifts are reported relative to $BaSnO_3$ at room temperature and are accurate to ±0.05 mm/s. Raman spectra were recorded on a Spex Industries Model 1400 Spectrometer with Ar^+ excitation (5145 or 4880 Å) from a Spectra Physics 164 Laser. α- and β-$SnWO_4$ were kindly supplied by Dr. A. W. Sleight, E.I. duPont de Nemours Co. Ltd., Wilmington, Delaware and have been fully characterized (17, 18).

Preparation of $Sn(SO_3X)_2$

$Sn(SO_3Cl)_2$

Pure dry SO_2 was condensed onto a pure sample of $SnCl_2$ at −63.5 °C in a glass apparatus which has been described (13). Liquid SO_3 in excess was added and the tube sealed. On removing the tube from the cold bath and warming to room temperature a vigorous reaction occurred. All of the stannous chloride went into solution and after a time a white precipitate formed, which was filtered, and washed with liquid SO_2 and then dried under vacuum.

Anal. Calcd. for $Sn(SO_3Cl)_2$: Sn, 33.94. Found: Sn, 33.88, 33.12.

$Sn(SO_3F)_2$

An excess of freshly distilled HSO_3F was condensed onto pure dry $SnCl_2$ in the apparatus described (13). Hydrogen chloride was evolved and a white precipitate formed. SO_2 was condensed in and the reaction mixture was for some time. The precipitate was filtered, washed with SO_2, and dried under vacuum.

Anal. Calcd. for $Sn(SO_3F)_2$: Sn, 37.48. Found: 37.46, 37.76.

The Raman spectrum showed that this compound was identical with that prepared from SnF_2 though the Mössbauer isomer shift is slightly smaller than reported previously (13).

The National Research Council of Canada is thanked for financial support.

1. J. Lees and P. A. Flinn. Phys. Lett. **19**, 186 (1965).
2. J. D. Donaldson and B. J. Senior. J. Chem. Soc. (A), 1796 (1966).
3. J. D. Donaldson. Prog. Inorg. Chem. **8**, 287 (1967).
4. T. C. Gibb, B. A. Goodman, and N. N. Greenwood. Chem. Commun. 774 (1970).
5. J. G. Ballard, T. Birchall, J. B. Milne, and W. D. Moffett. Can. J. Chem. **52**, 2375 (1974).
6. D. R. Schroeder and R. A. Jacobson. Inorg. Chem. **12**, 210 (1973).
7. K. Schubert and H. Friche. Z. Metallkd. **44**, 457 (1953).
8. M. F. A. Dove, R. King, and T. J. King. Chem. Commun. 944 (1973).
9. G. Bergerhoff. Acta Crystallogr. **15**, 509 (1962).
10. J. D. Donaldson and R. Oteng. Inorg. Nucl. Chem. Lett. **3**, 163 (1967).
11. R. R. McDonald, A. C. Larson, and D. T. Cromer. Acta Crystallogr. **17**, 1104 (1964).
12. T. C. Gibb and N. N. Greenwood. Mössbauer spectroscopy. Chapman and Hall, London. 1971.
13. T. Birchall, P. A. W. Dean, and R. J. Gillespie. J. Chem. Soc. (A), 1777 (1971).
14. J. D. Donaldson and B. J. Senior. J. Chem. Soc. (A), 2358 (1969).
15. J. D. Donaldson and D. G. Nicholson, and B. J. Senior. J. Chem. Soc. (A), 2928 (1968).
16. J. M. van den Berg. Acta Crystallogr. **14**, 1002 (1961).
17. W. Jeitschke and A. W. Sleight. Z. Naturforsch. **27b**, 203 (1972).
18. W. Jeitschke and A. W. Sleight. Acta Crystallogr. Sect. B, **28**, 3174 (1972).
19. J. D. Donaldson, D. C. Puxley, and M. J. Tricker. Inorg. Nucl. Chem. Lett. **8**, 845 (1972).
20. F. H. Allen, J. A. Lerbscher, and J. Trotter. J. Chem. Soc. (A), 2507 (1971).
21. T. Birchall. Can. J. Chem. **49**, 1351 (1969); T. Birchall and A. W. Sleight. J. Solid State Chem. **13**, 118 (1975).

Can. J. Chem. Downloaded from www.nrcresearchpress.com by 210.87.254.105 on 09/05/12
For personal use only.

Rates of OH Radical Reactions. I. Reactions with H_2, CH_4, C_2H_6, and C_3H_8 at 295 K[1]

R. P. OVEREND, G. PARASKEVOPOULOS, AND R. J. CVETANOVIĆ

Division of Chemistry, National Research Council of Canada, Ottawa, Canada K1A 0R9

Received June 20, 1975

R. P. OVEREND, G. PARASKEVOPOULOS, and R. J. CVETANOVIĆ. Can. J. Chem. **53**, 3374 (1975).

A fast flash photolysis kinetic spectrophotometer capable of measuring rates of up to 10^5 s^{-1} is described. The rates of hydrogen abstraction from H_2, CH_4, C_2H_6, and C_3H_8 by OH radicals at 295 ± 2 K, have been measured in the gas phase by hydroxyl resonance absorption spectrophotometry. The influence of secondary reactions on the measured rates and the derivation of the absolute rate constants is discussed in detail.

The absolute rate constants in units of cm^3 mol^{-1} s^{-1} were found to be: $k_{H_2} = 3.49 \pm 0.16 \times 10^9$, $k_{CH_4} = 3.92 \pm 0.16 \times 10^9$, $k_{C_2H_6} = 1.59 \pm 0.10 \times 10^{11}$, and $k_{C_3H_8} = 12.17 \pm 0.63 \times 10^{11}$.

R. P. OVEREND, G. PARASKEVOPOULOS et R. J. CVETANOVIĆ. Can. J. Chem. **53**, 3374 (1975).

Nous décrivons un spectrophotomètre à photolyse-éclair et à cinétique rapide capable de mesurer des vitesses de réaction de l'ordre de 10^5 s^{-1}. Les vitesses d'abstraction des atomes d'hydrogène de H_2, CH_4, C_2H_6 et C_3H_8 par des radicaux OH, à 295 ± 2 K ont été mesurées en phase gazeuse par spectrophotométrie d'absorption de résonance du radical hydroxyle. L'influence de réactions secondaires sur les vitesses mesurées et l'obtention des constantes de vitesse absolues sont discutées en détail.

Nous avons trouvé que les constantes de vitesse absolues en unités de cm^3 mol^{-1} s^{-1} sont: $k_{H_2} = 3.49 \pm 0.16 \times 10^9$, $k_{CH_4} = 3.92 \pm 0.16 \times 10^9$, $k_{C_2H_6} = 1.59 \pm 0.10 \times 10^{11}$ et $k_{C_3H_8} = 12.17 \pm 0.63 \times 10^{11}$.

Introduction

Hydroxyl radicals have long been recognized as being a chain carrier in the oxidative combustion of hydrogen and hydrocarbons; they also play an important role in the chemistry of the upper and lower atmosphere where they act as an oxidant. There is, therefore, a need for accurate values of the rate parameters of the reactions of OH with hydrogen, hydrocarbons, and atmospheric gases for use in numerical modelling of the above processes. Such reactions have been widely studied by various experimental techniques. However, data from earlier studies using flame, shock tube, and flow system experiments showed large discrepancies in the reported values of the kinetic parameters. More recently direct techniques have been developed, using spectroscopic, e.s.r., and resonance fluorescence detection of OH, which have improved the accuracy and precision of the data, so that at present the rate constants of some of the reactions (*e.g.*, H_2, CH_4) are established within a 20% range. The data for OH reactions have been reviewed by Drysdale and Lloyd (1) and Wilson (2), and it appears that further work is necessary, in particular using direct determinations.

In the present paper we describe a fast flash photolysis apparatus coupled with time resolved resonance absorption detection of OH. Signal averaging is employed to improve the signal-to-noise ratio. The apparatus is capable of measuring first order rates of up to 10^5 s^{-1}, thus enabling a more complete range of experimental conditions to be examined than hitherto.

We have in progress an extensive program of study on both abstraction and addition reactions of OH radicals in the gas phase. In this paper, the first of a series, we describe in detail the method used and report the rate constants of abstraction of hydrogen from H_2, CH_4, C_2H_6, and C_3H_8 at room temperature. The reaction of OH + H_2 is much studied and serves as a standard against which we compare our technique. We have also examined the effect of secondary radical reactions on the rate measurements by numerical simulation, and established the conditions for which such an effect is negligible.

[1]Issued as NRCC No. 14847.

Can. J. Chem. Downloaded from www.nrcresearchpress.com by 210.87.254.105 on 09/05/12
For personal use only.

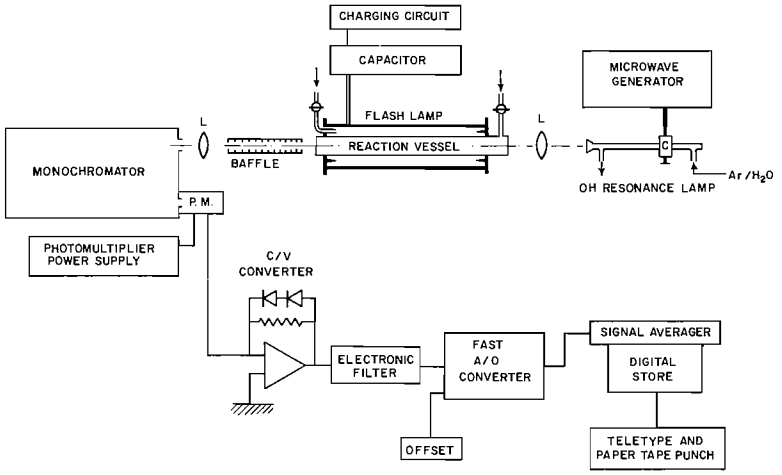

FIG. 1. Block diagram of the apparatus. L, lenses; P.M., photomultiplier; C/V converter, current-to-voltage converter; A/D converter, analog-to-digital converter.

Experimental

The apparatus consists of a fast flash photolysis system coupled with a spectrophotometric detection system. The block diagram of the experimental arrangement is given in Fig. 1. The flash lamp and reaction vessel are a low inductance coaxial assembly based in part on the design concepts of Furumoto and Ceccon (3). The 30 cm length flash discharge is in an annulus 1 mm deep around the 25 mm diameter reaction vessel. The electrodes are polished stainless-steel knife-edged rings. The flash lamp is discharged by lowering the pressure of dry air within the annulus. A range of energies from 100–600 J is obtained by charging either a 1.5 μF or a 5.1 μF capacitor to the appropriate voltage (10–16 kV). With the smaller capacitor the flash peaks at 650 ns and has a decay ($1/e$) time of 850 ns.

Two 50 cm long, 25 mm diameter reaction vessels were used, both made of Suprasil quartz. The first vessel was a simple tube; the second was a double wall tube in which the reaction mixture occupied the 10 mm diameter inner tube and could be surrounded by a suitable optical shield placed in the outer tube.

The OH concentration in the vessel is monitored by following the time resolved attenuation of the OH resonance radiation ($A^2\Sigma^+ \rightarrow X^2\Pi$) produced by a 2.45 GHz microwave discharge in a low pressure (~1 Torr) Ar/H_2O mixture (~5% H_2O). The resonance lamp is similar to that described by Carrington and Broida (4). After each flash attenuation of either the Q_1^3 or Q_1^4 rotational lines of the (0,0) band is followed by means of a 1 m Czerny-Turner spectrophotometer (Jarrell-Ash) and a S-5 photo cathode photomultiplier. The spectrometer has a resolution of 0.87 nm/mm and is operated at a band pass of 0.05–0.2 nm.

The photomultiplier voltage divider is wired for fast pulse response and high peak-current capability. The dynode voltage supply is a well regulated high current supply. Together these ensure fast recovery (≃5–10 μs) after the flash. To further protect the electronics after the photomultiplier from the flash pulse, two high speed signal diodes were wired across the load resistor in the current-to-voltage converter.

The signal is then passed to a variable low pass electronic filter which has a 4 pole Bessel response. The cutoff frequency of the filter was set at >2 × rate to be measured in the experiment; this provides adequate filtering of high frequency noise with a tolerable distortion of the rise to maximum OH absorption. The filtered signal is then accumulated by the fast analog-to-digital (A/D) converter and signal averager combination. Signal averaging techniques are required on account of the low intensity of the resonance lamp and the large electronic instrument bandwidth required to measure rates of 10^5 s^{-1}. The signal-to-noise (S/N) ratio of the system is 10 at 1 MHz and 30 at 100 kHz. With signal averaging the S/N ratio improves to 100 with less than 64 flashes.

The main source of OH radicals was the photolysis of water vapor mixed with the reactant and, in a few experiments with H_2 and CH_4, the photolysis of N_2O followed by the reactions:

$$N_2O + h\nu \rightarrow N_2 + O(^1D)$$

$$O(^1D) + H_2 \rightarrow H + OH$$

$$O(^1D) + CH_4 \rightarrow CH_3 + OH$$

The results with both sources of OH radicals were the same within the experimental error.

The gases were handled in a conventional mercury-free vacuum line provided with a Cellows gauge and an oil manometer. The experimental procedure was to prepare an accurately measured mixture made up from the hydroxyl source, the reactant, and the diluent gas (He). The mixture was mixed with a magnetic stirrer before transfer to the reaction vessel, where it was flashed the required number of times to achieve a satisfactory S/N ratio.

Can. J. Chem. Downloaded from www.nrcresearchpress.com by 210.87.254.105 on 09/05/12
For personal use only.

Can. J. Chem. Downloaded from www.nrcresearchpress.com by 210.87.254.105 on 09/05/12
For personal use only.

The materials were of the highest available purity and in all cases except H_2 and He were subjected to degassing and bulb-to-bulb distillation *in vacuo* before use.

Results

Experiments with varying low water vapor pressures and a constant flash energy showed the expected logarithmic dependence of the maximum OH absorption on the pressure of water, *i.e.*, $\ln I_0/I = KP_{H_2O}$, for absorptions of up to ~40%. The absorption decreased by about 40% when the total pressure in the vessel increased from 100 to 760 Torr; this was attributed to pressure broadening of the rotational line. Trainor and von Rosenberg (5) have discussed in detail the effect of pressure on absorption. In our experiments, in which we measure relative absorption with time, there should be no effect of pressure broadening on the measured rates. In the majority of our experiments the pressure of H_2O was such that the maximum absorption of OH was less than 10%. Using the formula of Kaufman and co-workers (6) and their suggested value of 8×10^{-4} for the oscillator strength of the hydroxyl $A^2\Sigma \rightarrow X^2\Pi$ transition we calculate that 25% absorption in 30 cm path length corresponds to a concentration of $[OH] \approx 1.3 \times 10^{-10}$ mol cm^{-3}. In our experiments the average initial absorption of OH was ~7–12% corresponding to an average concentration of ~3.3–5.8 $\times 10^{-11}$ mol cm^{-3}.

At the wavelengths used >160 nm the OH($X^2\Pi$) is formed without vibrational or rotational excitation (such excited OH, if present, might relax thereby producing an apparent decrease in the measured rates). The absence of OH with vibrational and rotational excitation has been shown experimentally by Welge and Stuhl (7) who found that throughout the 186–140 nm continuum the energy of the photons, in excess of that required to break the H—OH bond appears mainly as translational energy of the H and OH fragments, *i.e.* they found that the intensity of the $v'' = 1$ bands was only a few percent of the (0,0) band, and that the rotational distribution of OH($X^2\Pi$) was practically the room temperature equilibrium distribution.

The alternative source of hydroxyl radicals (*i.e.*, $N_2O + h\nu \rightarrow O(^1D) + N_2$, $O(^1D) + H_2 \rightarrow OH^* + H$) produced results in agreement with those from the photolysis of water. Thus, although the $O(^1D) + H_2$ reaction has been shown to produce vibrationally excited OH^* (8), the excited species have evidently relaxed by the time our measurements commence.

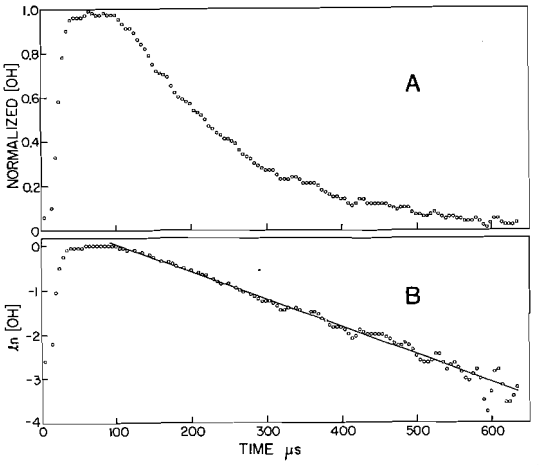

FIG. 2. Example of computer plots of (*A*) normalized [OH], and (*B*) ln [OH] against time for OH + H_2. The conditions of the experiment were: H_2 = 21.36 Torr, H_2O = 2.68 Torr, He = 499.3 Torr, time = 5 μs per channel.

In our experiments the concentration of the second reactant was always made much greater than the initial OH concentration. Under these conditions the reaction is pseudo-first order.

The digital data recorded on the paper tape consist of values of $\Delta I = I_0 - I$ at various time intervals and were processed on an off-line IBM 360 computer. The data were smoothed using a nine-point quadratic approximation suggested by Savitzky and Golay (9). The OH concentration, $[OH] = \ln (I_0/I)$, expressed in normalized

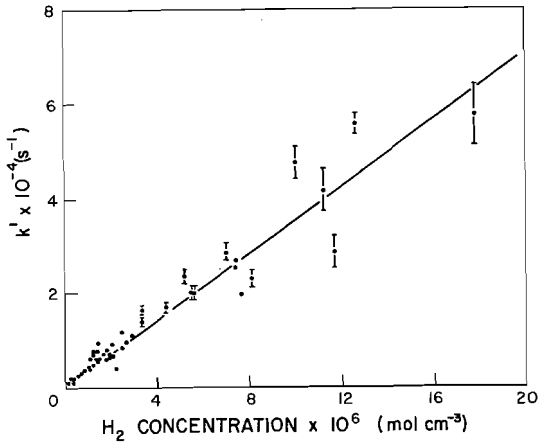

FIG. 3. Plot of pseudo-first order rate constant, k' against the H_2 concentration for the reaction OH + $H_2 \rightarrow H_2O$ + H.

Can. J. Chem. Downloaded from www.nrcresearchpress.com by 210.87.254.105 on 09/05/12
For personal use only.

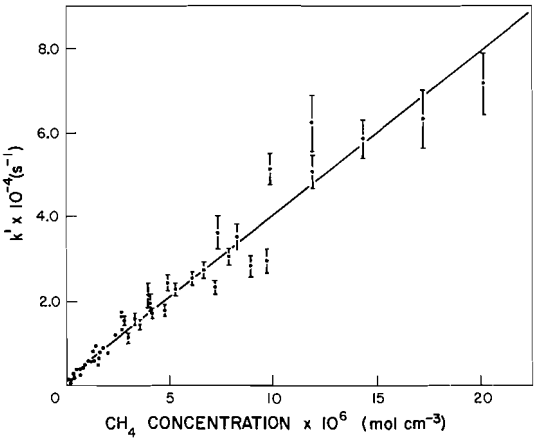

FIG. 4. Plot of pseudo-first order rate constant, k', against the CH_4 concentration for the reaction OH + $CH_4 \rightarrow H_2O + CH_3$.

units (*i.e.* as fraction of the concentration at maximum absorption), as well as ln [OH] = ln (ln (I_0/I)) were plotted against time. Such plots are shown in Fig. 2. The latter plots (pseudo-first order plots) were linear over 2–5 half-lives depending on the conditions.

The pseudo-first order rate constant for the OH decay k', was obtained from the slopes of the linear plots. The data had sometimes superimposed on them a sporadic spike noise which occurred in only one direction, as will be illustrated in the next section. The effect was easily filtered out by eye and the slope drawn by hand.

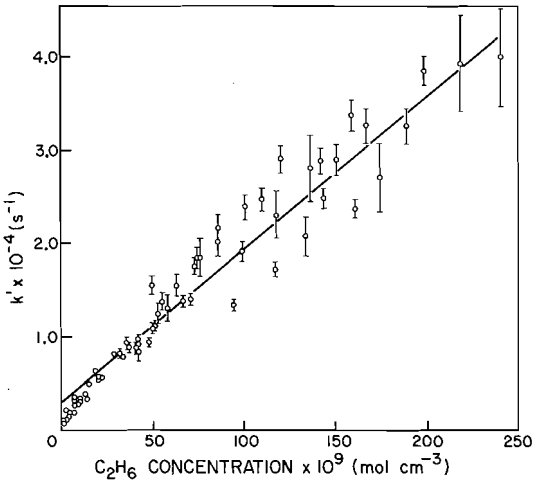

FIG. 5. Plot of pseudo-first order rate constant, k', against the C_2H_6 concentration for the reaction OH + $C_2H_6 \rightarrow H_2O + C_2H_5$.

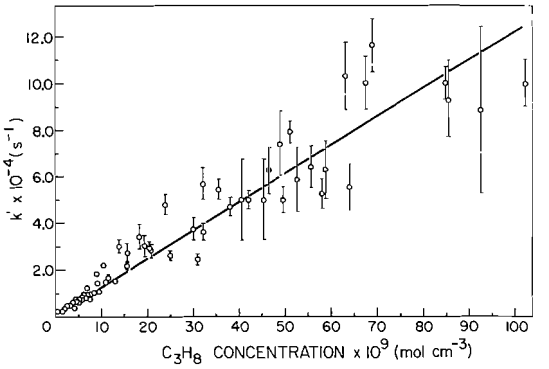

FIG. 6. Plot of pseudo-first order rate constant, k', against the C_3H_8 concentration for the reaction OH + $C_3H_8 \rightarrow H_2O + C_3H_7$.

The pseudo-first order rate constant k' obtained over a range of reactant [RH] concentrations is related to the bimolecular rate constant k by the equation $k' = \alpha + k[RH]$. Plots of k' against [RH] are shown in Figs. 3–6, for RH = H_2, CH_4, C_2H_6, and C_3H_8, respectively. The bimolecular rate constants, k, were evaluated from the slope of these plots. The slopes were obtained from least square fits of the equation $k' = \alpha + k[RH]$ to the points with weights of $1/\sigma^2$ where σ is the error in k' evaluated separately as described below. The least square values of the bimolecular rate constants and the standard deviation of the fit are listed in Table 1.

The total pressure in the experiments with all four reactants was varied between 40 and 760 Torr. The measured rate constants were found to be independent of the total pressure.

The effect of accumulation of reaction products (*e.g.* C_2H_6 in the reaction $CH_4 + OH \rightarrow CH_3 + H_2O$) on the measured rates was considered. The reaction mixture in a representative experiment was irradiated repeatedly and the data collected in consecutive batches of four flashes. Comparison of the signal for the first 4 and last 4 in 32 flashes showed no significant difference. A simple calculation shows that in the

TABLE 1. Bimolecular rate constants of the reaction OH + RH → H_2O + R at 295 ± 2 K

Reactant RH	k ($cm^3\ mol^{-1}\ s^{-1}$)	Number of experiments
H_2	$3.4_9 \pm 0.1_6 \times 10^9$	72
CH_4	$3.9_2 \pm 0.1_6 \times 10^9$	60
C_2H_6	$1.5_9 \pm 0.1_0 \times 10^{11}$	42
C_3H_8	$12.1_7 \pm 0.6_3 \times 10^{11}$	59

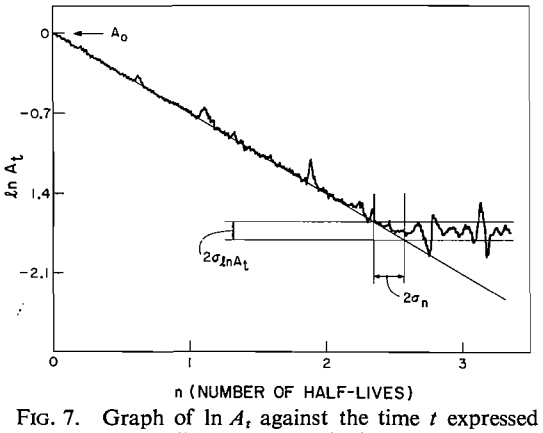

FIG. 7. Graph of ln A_t against the time t expressed as number of half-lives. (The graph shows the unidirectional noise and the error $\sigma_{\ln A_t}$ expressed as uncertainty in the number of half-lives $n \pm \sigma_n$.)

case of CH_4 the effect of accumulation of C_2H_6 from recombination of CH_3 radicals will not perturb the measurements. (It is calculated that after 32 flashes the ratio of the rate of OH with the accumulated C_2H_6 and with CH_4 is about 5×10^{-3}.) In the case of propane the calculation shows that the accumulation of products could possibly affect the measurements. The test described above was carried out more frequently with propane and the total number of flashes was kept at a minimum.

Evaluation of Error

The method of estimation of the error, σ, of the individual values of pseudo-first order rate constant, k', has been described in detail in Appendix I of ref. 10, and will be outlined only briefly here. As mentioned above the slope $\Delta \ln [OH]/\Delta t$ of the graph of the decay curve of ln [OH] against time expressed as number of half-lives and shown in Fig. 7 was drawn by hand. Figure 7 shows also the previously mentioned sporadic unidirectional noise. The error in the slope can be determined from the two extremes of the line

$$k' = \Delta(\ln [OH])/\Delta t = \ln (A_0/A_t)/\Delta t$$

where A_0 = absorbance at $t = 0$, A_t = absorbance at $t = t$, and $\Delta t = t - t_0$ or

$$R_f = \Delta t \times k' = \ln (A_0/A_t)$$

where R_f is defined as rate function. By determining or assessing the experimental precisions at each stage of the measurement of the quantities on the graph of ln A_t against t and using the propagation of error equation we obtain (10)

$$\sigma_{A_t}^2 = \exp(-1.4n)[\sigma_{A_0}^2 + (0.693 A_0 \sigma_n)^2]$$

where n = the number of half-lives over which the straight line in Fig. 7 fits the experimental line; σ_n was estimated from the experimental plots. Graphs of fractional error σ_{R_f}/R_f at constant n's against A_0 are shown in Fig. 8. It may be seen from the graphs that the fractional error, *i.e.*, precision of the pseudo-first order rate constant, k', is $\sim 3\%$ for high A_0 and good straight lines of several half-lives. On the other hand a low A_0 and low n combine to give very poor precision. The errors in k' are shown as error bars of length 1σ in Figs. 3–6.

The time base of the ADC/signal averager was calibrated with an accurate frequency standard. The accuracy is about 1 part in 10^4. The measurement of pressures and concentrations was considered to be both accurate and precise to about 1%. Under these conditions the contribution of these sources to the overall error in the bimolecular rate constant k (evaluated from the slope of the plot of k' against concentration, [RH]) is negligible in comparison to that of spectrophotometry. The overall precisions of the bimolecular rate constants in Table 1 are 10–15% at one standard deviation. The accuracy

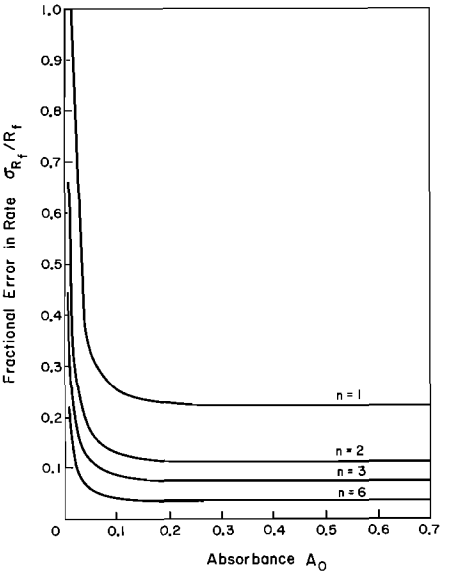

FIG. 8. Graphs of fractional error σ_{R_f}/R_f at constant n against initial absorbance, A_0, for various values of n. (The graphs illustrate the variation of the fractional error with A_0 and with the number of half-lives n.)

Can. J. Chem. Downloaded from www.nrcresearchpress.com by 210.87.254.105 on 09/05/12
For personal use only.

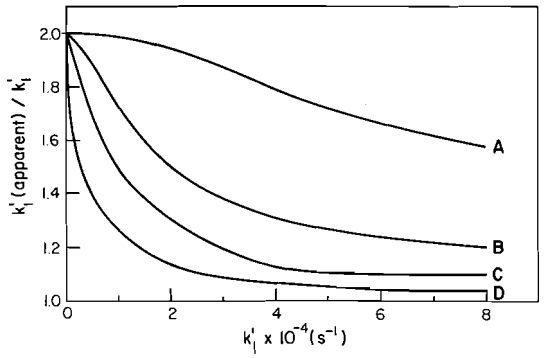

FIG. 9. Effect of the initial OH concentration on the dependence of the k_1'(apparent)/k_1' ratio on k_1' (*i.e.* on the RH concentration) at constant k_2. (The curves were calculated for $k_2 = Z$ (collision frequency) and initial [OH] in mol cm^{-3}: (*A*), 5×10^{-10}; (*B*), 10^{-10}; (*C*), 5×10^{-11}; and (*D*), 2×10^{-11}.)

was estimated to be in the region $\pm 5\%$; this value was estimated from the influence of the flash period, electronic bandwidth, system linearity, and A/D converter resolution on the measured rates.

Discussion

The following reactions were considered for the discussion and interpretation of our experimental results

$$H_2O + h\nu \rightarrow OH + H$$

[1] $$OH + RH \rightarrow H_2O + R$$

[2] $$OH + R \rightarrow \text{Products}$$

[3] $$OH + OH + M \rightarrow H_2O_2 + M$$

[4] $$OH + H + M \rightarrow H_2O + M$$

[5] $$OH + OH \rightarrow H_2O + O$$

where RH = H_2, CH_4, C_2H_6, and C_3H_8. We will examine first if (and to what extent) side reactions of OH affect our results and then we will compare them with other results in the literature.

Effect of Radical–Radical Reactions of OH

The effect of the radical–radical reactions of OH, reactions 2, 3, 4, and 5, was tested by a numerical simulation model in which the differential equations describing the system were integrated numerically for the following initial conditions: (*1*) Since [RH] is present in large excess over OH, reaction 1 was taken as a first order reaction of the form $-d[OH]/dt = k_1'[OH]$ where $k_1' = k_1[RH]$, and k_1' was varied in the model over a range 10^3 to 10^5 s^{-1}. (*2*) The rate of reaction 2 was taken initially to be the collisional rate. (*3*) Other rate constants were taken from the reviews of Drysdale and Lloyd (1) and Wilson (2). (*4*) The initial concentration of OH radicals was taken to be that estimated earlier using the value of 0.8×10^{-3} for the oscillator strength of OH.

The simulation results showed for measured pseudo-first order rate constants larger than 5×10^3 s^{-1} a negligible influence of radical–radical reactions other than reaction 2, *i.e.* the influence of reactions 3, 4, and 5 was negligible. The plots of ln [OH] against t were curved only in the time region below 5×10^3 s^{-1} showing a second order contribution from reactions 3 and 4. Similarly plots of k_1' against concentration in this time region (very low reactant pressures) were not entirely linear for H_2, and the effect became more pronounced for the C_1–C_3 hydrocarbons. In view of this result and in order to speed the numerical calculations a simplified scheme consisting only of reactions 1 and 2 was modelled over the experimental range. In this model a series of values of k_1 and k_2 were used as input to calculate concentrations of OH at various time intervals. It was found that the scheme nearly always produced linear plots of the ln [OH] against time. From these plots apparent pseudo-first order rate constants, k_1'(apparent), were obtained. The simple model results plotted as a ratio, k_1'(apparent)/k_1', against k_1', (*i.e.* against the RH concentration), are shown in Figs. 9 and 10. Figure 9 shows the influence on the ratio of the initial concentration of OH at constant $k_2 = Z$ (Z = collision frequency) and Fig. 10 shows the influence of k_2

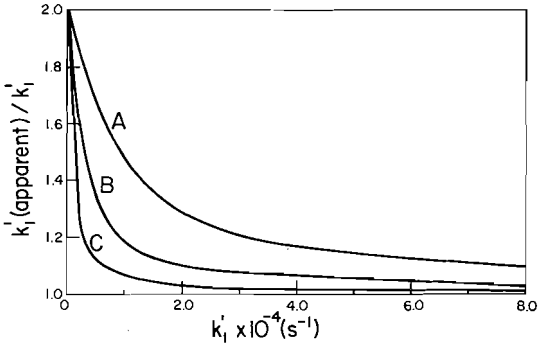

FIG. 10. Effect of the value of k_2 on the dependence of the k_1'(apparent)/k_1' ratio on k_1' (*i.e.* on the RH concentration) at constant initial OH concentration of 5×10^{-11} mol cm^{-3}. (The curves were calculated for k_2 expressed as fraction of the collision frequency Z, (*A*), $k_2 = Z$; (*B*), $k_2 = Z/3$; (*C*), $k_2 = Z/10$.)

Can. J. Chem. Downloaded from www.nrcresearchpress.com by 210.87.254.105 on 09/05/12
For personal use only.

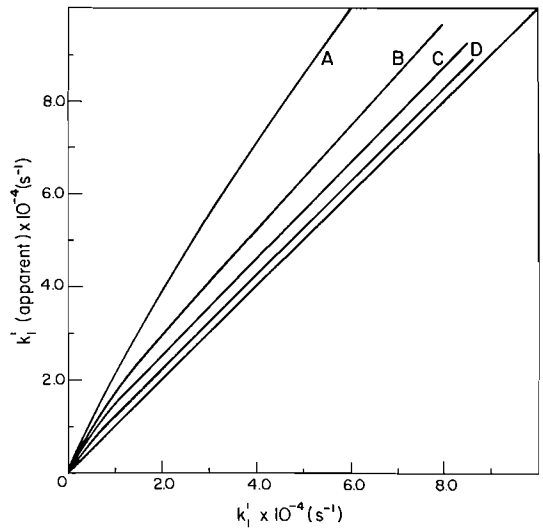

FIG. 11. Dependence of k_1'(apparent) on k_1' (*i.e.* on the RH concentration) at different initial OH concentrations and constant $k_2 = Z$. (The lines were calculated for $k_2 = Z$ and initial OH concentration in mol cm^{-3}; (*A*), 5×10^{-10}; (*B*), 10^{-10}; (*C*), 5×10^{-11}; (*D*), 2×10^{-11}.)

on the ratio at a constant initial concentration of [OH] = 5×10^{-11} mol cm^{-3}. Thus, the simple model indicates that at high measured rates and low initial concentrations of OH the ratio is close to unity, *i.e.* the measured rates will not be appreciably affected by reaction 2. On the other hand at low overall rates and high initial OH concentrations the model predicts an apparent rate increase by almost a factor of two, *i.e.* the plot of the pseudo-first order rate *vs.* concentration is still linear but the slope is almost twice the true bimolecular rate, since the radical R can be considered to be in a steady state. This is illustrated in Fig. 11, where k_1'(apparent) is plotted against k_1', for $k_2 = Z$ and at various values of the initial OH concentration. It may be seen in Fig. 11 that for OH concentrations of 2–5 $\times$ 10^{-11} mol cm^{-3} and rates larger than 5–10 $\times$ 10^3 s^{-1} the lines are almost parallel to the 45° line, *i.e.*, for these conditions the measured slopes are not affected. Subsequent experiments with propane verified this behavior. The general behavior of the series H_2 to C_3H_8 suggests that the rate of reaction of the smaller radicals with OH, *i.e.*, k_2 may be appreciably smaller than that of the propyl radical. The combination of low measured rates and high initial OH concentration, is probably the reason that the rates of OH with CH_4 and C_2H_6 obtained by Horne and Norrish (11) are almost a factor of two larger than the currently accepted values.

Similar considerations apply to the measurement of OH rate constants by the resonance fluorescence technique, where the bimolecular rate constant is obtained from plots of k_1' *vs.* the concentration of RH. A single simulation was made using typical experimental conditions of this technique (12, 13) (*i.e.* initial [OH] = 5×10^{-13} mol cm^{-3} and k_1' = 25–300 s^{-1}). The simulation indicated that k_1'(apparent)/k_1' assumes values close to 2 for low k_1', but decreases with increasing k_1' and approaches 1 at high k_1'.

In the OH concentration range of the present work, the points corresponding to small concentrations of RH on the plots of the first order rate constant *vs.* RH concentration will indicate twice the true bimolecular rate constant, but as the RH concentration increases will gradually assume the true value. Plots of bimolecular rate constants against the RH concentration served to indicate the concentration region in which the points have a large dependence on RH concentration, and these points were not used in the evaluation of the slope so that the measured slopes correspond closely to the true value of the bimolecular rate constant. As a result the small intercepts in Figs. 3–6 cannot be ascribed to a single predominant cause. In the two limiting cases the intercept should be zero, *i.e.* when re-

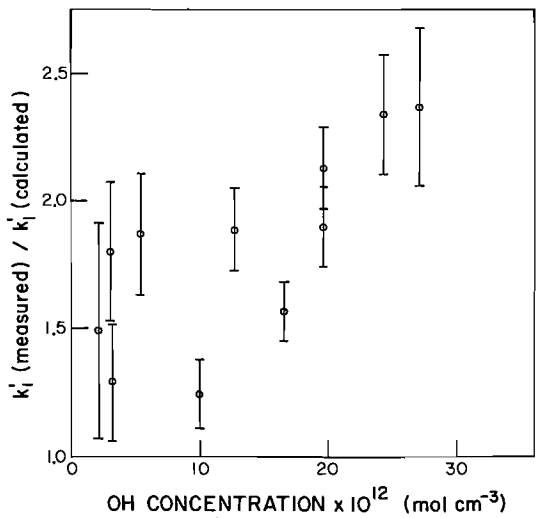

FIG. 12. Variation of k_1'(measured)/k_1'(calculated) with the OH concentration, for k_1'(calculated) of 1.53 $\times$ 10^3 s^{-1} (*i.e.* k_1 = 12.17 $\times$ 10^{11} and [C_3H_8] = 1.26 $\times$ 10^{-9} mol cm^{-3}.)

Can. J. Chem. Downloaded from www.nrcresearchpress.com by 210.87.254.105 on 09/05/12
For personal use only.

TABLE 2. Comparison of the room temperature rate constants for the reaction RH + OH → H_2O + R determined by different techniques

Reactant	k (cm^3 mol^{-1} s^{-1}) This work	Literature values	Reference
H_2	$3.49 \pm 0.16 \times 10^9$	$3.96 \pm 1.2 \times 10^9$	2
		$3.92 \pm 0.78 \times 10^9$	17
		$4.28 \pm 0.64 \times 10^9$	12
		$4.60 \pm 0.46 \times 10^9$	18
		$4.28 \pm 0.60 \times 10^9$	19
		$4.20 \pm 0.42 \times 10^9$	20
CH_4	$3.92 \pm 0.16 \times 10^9$	$6.85 \pm 4.80 \times 10^9$	2
		$4.51 \pm 0.06 \times 10^9$	13
C_2H_6	$1.59 \pm 0.10 \times 10^{11}$	1.61×10^{11}	2
		$1.79 \pm 0.17 \times 10^{11}$*	16
C_3H_8	$12.17 \pm 0.63 \times 10^{11}$	$6.81 \pm 0.67 \times 10^{11}$*	16
		$5.10 \pm 1.0 \times 10^{11}$	21
		$13.25 \pm 3.6 \times 10^{11}$	22

*These values are our estimates of the weighted means of the corrected rate constants, at room temperature, given in Table II of ref. 16; the weights w were taken to be equal to $1/\sigma^2$ where σ is the reported error of each rate constant.

action 2 causes no interference, and when the concentration of the radical R is in steady state.

Examination of Fig. 9 shows that at a low true rate k_1', for example a rate of 2–3 × 10^3 s^{-1}, the dependence of k_1'(apparent)/k_1' on the concentration of [OH] will be very marked. Figure 12 shows results for propane in this region. The trend in increasing relative rate with OH concentration is evident. The large error bars reflect the difficulty of the measurements at low OH concentrations (*i.e.* poor *S/N* ratios). The apparent trend of the ratio k_1'(measured)/k_1'(calculated) to a value larger than 2 may well be correct, as the simple model discussed above may have shortcomings in this concentration/rate region.

The values of 2–2.5 for the measured to calculated ratio of k_1' led us to consider that photolysis of propane was producing an excessive initial concentration of radicals. In the case illustrated in Fig. 12 where the concentration of propane is 1.26×10^{-9} mol cm^{-3} and that of OH is 25–30 × 10^{-12} mol cm^{-3}, the reported absorption coefficients of propane (14) and water (15) and the path length suggest that the extent of propane photolysis and thus the concentration of radicals formed will be less than 0.001% of the total OH produced (*i.e.* less than 3 × 10^{-16} mol cm^{-3}). This would make a negligible contribution to the rate in the presence of 1.26×10^{-9} mol cm^{-3} of propane.

Comparison of Rate Constant Values

As mentioned in the introduction the reactions of OH with hydrogen and hydrocarbons have been studied widely by a variety of indirect and direct techniques. Prominent among the direct studies is the pioneering work of Greiner (ref. 16 and references therein) who used the flash photolysis kinetic spectroscopy technique. The rate constant of the H_2 reaction, in particular, is more reliably known and is used to test our technique. On the other hand there are few direct determinations of rate constants for the C_2H_6 and C_3H_8 reactions. The rate constants determined in this work together with literature values are given in Table 2. The first entry for H_2, CH_4, and C_2H_6 is the recommended value from the review of Wilson (2), the second entry for H_2 is from the review of Baulch *et al.* (17). Both reviews have summarized work up to 1972; the other entries are values reported after that date.

Our values for H_2 and CH_4 although somewhat lower are, within experimental error, in reasonable agreement with those in the literature. The value for C_2H_6 agrees well with both the recommended value and the value of Greiner (16). The reported values for C_3H_8 (16, 21, 22) differ by over a factor of 2. Our value agrees well with the higher value of Gorse and Volman (22), determined indirectly, relative to the rate constant of the reaction OH + CO.

Can. J. Chem. Downloaded from www.nrcresearchpress.com by 210.87.254.105 on 09/05/12
For personal use only.

The authors are grateful to Drs. A. R. Gibbons and H. A. Wiebe for the early work on the development of the apparatus.

1. D. D. DRYSDALE and A. C. LLOYD. Oxid. Combust. Rev. **4**, 157 (1970).
2. W. E. WILSON, JR. J. Phys. Chem. Ref. Data, **1**, 535 (1972).
3. H. W. FURUMOTO and H. L. CECCON. Appl. Opt. **8**, 1613 (1969).
4. T. CARRINGTON and H. P. BROIDA. J. Mol. Spectrosc. **2**, 273 (1958).
5. D. W. TRAINOR and C. W. VON ROSENBERG, JR. J. Chem. Phys. **61**, 1010 (1974).
6. D. M. GOLDEN, F. P. DEL GRECO, and F. KAUFMAN. J. Chem. Phys. **39**, 3034 (1963).
7. K. H. WELGE and F. STUHL. J. Chem. Phys. **46**, 2440 (1967).
8. N. BASCO and R. G. W. NORRISH. Proc. R. Soc. (London) Ser. A, **260**, 293 (1961).
9. A. SAVITSKY and M. J. E. GOLAY. Anal. Chem. **36**, 1627 (1964).
10. R. J. CVETANOVIĆ, R. P. OVEREND, and G. PARASKEVOPOULOS. *In* Proceedings of the Symposium on Chemical Kinetics Data for the Lower and Upper Atmosphere. *Edited* by S. W. Benson. Int. J. Chem. Kinet. Supplement to Vol. 7, 249 (1975).
11. D. G. HORNE and R. G. W. NORRISH. Nature (London), **215**, 1373 (1967).
12. F. STUHL and H. NIKI. J. Chem. Phys. **57**, 3671 (1972).
13. D. D. DAVIS, S. FISCHER, and R. SCHIFF. J. Chem. Phys. **61**, 2213 (1974).
14. H. OKABE and D. A. BECKER. J. Chem. Phys. **39**, 2549 (1963).
15. K. WATANABE, M. ZELIKOFF, and E. C. Y. INN. Absorption coefficients of several atmospheric gases. Geophysics Research Directorate, Air Force Cambridge Research Center, Cambridge, Mass., Technical Report No. 53-23, 1953.
16. N. R. GREINER. J. Chem. Phys. **53**, 1070 (1970).
17. D. L. BAULCH, D. D. DRYSDALE, D. G. HORNE, and A. C. LLOYD. Evaluated kinetic data for high temperature reactions, Vol. 1. Butterworths, London. 1972. p. 77.
18. A. A. WESTENBERG and N. DE HAAS. J. Chem. Phys. **58**, 4061 (1973).
19. I. W. M. SMITH and R. ZELLNER. J. Chem. Soc. Faraday Trans. 2, **70**, 1045 (1974).
20. R. ATKINSON, D. A. HANSEN, and J. N. PITTS, JR. J. Chem. Phys. **62**, 3284 (1975).
21. J. N. BRADLEY, W. HACK, K. HOYERMANN, and H. G. WAGNER. J. Chem. Soc. Faraday Trans. 1, **69**, 1889 (1973).
22. R. A. GORSE and D. H. VOLMAN. J. Photochem. **3**, 115 (1974).

Can. J. Chem. Downloaded from www.nrcresearchpress.com by 210.87.254.105 on 09/05/12
For personal use only.

Crystal and Molecular Structure of Dithiocyanato(triphenylarsine)mercury(II)

JOSEPH HUBERT, ANDRÉ L. BEAUCHAMP, AND ROLAND RIVEST

Département de Chimie, Université de Montréal, C.P. 6210, Montréal, Québec H3C 3V1

Received May 29, 1975

JOSEPH HUBERT, ANDRÉ L. BEAUCHAMP, and ROLAND RIVEST. Can. J. Chem. **53**, 3383 (1975).

The crystal and molecular structure of dithiocyanato(triphenylarsine)mercury(II) has been determined from X-ray diffraction data. The crystals are monoclinic, space group $P2_1/c$, with $a = 10.290(7)$, $b = 21.199(23)$, $c = 10.719(7)$ Å, $\beta = 112.00(2)°$, and $Z = 4$. The structure has been solved by the heavy-atom method and refined by block-diagonal least-squares calculations. The agreement factor R obtained for 2607 'observed' reflections is 0.030. The crystal consists of single molecules. The 'characteristic' coordination number of mercury is three, with two sulfur and one arsenic atoms at the apexes of a triangle. The nitrogen atoms of the thiocyanate groups are at 2.67 and 2.74 Å from the adjoining mercury atoms and therefore link the dif ferent molecules together.

JOSEPH HUBERT, ANDRÉ L. BEAUCHAMP et ROLAND RIVEST. Can. J. Chem. **53**, 3383 (1975).

Les structures cristalline et moléculaire du dithiocyanato(triphénylarsine)mercure(II) ont été déterminées par diffraction de rayons X. Les cristaux sont monocliniques, de groupe d'espace $P2_1/c$ et de paramètres de maille: $a = 10.290(7)$, $b = 21.199(23)$, $c = 10.719(7)$ Å, $\beta = 112.00(2)°$ et $Z = 4$. La structure a été résolue par la méthode de l'atome lourd et affinée par moindres carrés (matrice à blocs diagonaux). Le facteur d'accord R obtenu pour les 2607 réflexions 'observées' est de 0.030. Le cristal est constitué de molécules monomères. Le nombre de coordination 'caractéristique' du mercure est de trois, et la coordination est assurée par deux atomes de soufre des thiocyanates et l'atome d'arsenic. Les atomes d'azote des groupements thiocyanates se trouvent à des distances de 2.67 et 2.74 Å d'atomes de mercure voisins et relient les diverses molécules entre elles.

Can. J. Chem. Downloaded from www.nrcresearchpress.com by 210.87.254.40 on 09/05/12
For personal use only.

Introduction

Reactions of mercuric halides with monodentate ligands often lead to dimeric halide-bridged 1:1 complexes in which mercury has a tetrahedral coordination. Several examples of similar thiocyanate complexes are also known. On the basis of preliminary X-ray results (1), we recently reported that mercury is three-coordinated in $Hg(SCN)_2 \cdot As(C_6H_5)_3$. The complete crystal structure analysis on that compound is described in the present paper.

Experimental Section

Crystal data

$C_{20}H_{15}AsHgN_2S_2$ f.w. = 622.99

Monoclinic, $P2_1/c$, $a = 10.290(7)$, $b = 21.199(23)$, $c = 10.719(7)$ Å, $\beta = 112.00(2)°$, $V = 2168$ Å^3, $\rho_o = 1.90(1)$, $Z = 4$, $\rho_c = 1.909$ g cm^{-3}, $\mu = 90.72$ cm^{-1} (23 °C; $MoK_{\bar{\alpha}}$, $\lambda = 0.71069$ Å).

The complex was prepared by reaction of 1.9 mmol of $Hg(SCN)_2$ and 2.1 mmol of $As(C_6H_5)_3$ in 125 ml of ethanol. By slow evaporation of the solution, well-shaped crystals were obtained.

The set of data used to solve the structure (1) was collected with CuK_α radiation on a relatively large crystal of complicated geometry. Refined values of some temperature factors were high, presumably because of the high absorption coefficient for copper radiation and problems in describing the crystal faces. For those reasons, another crystal of simpler geometry was selected and a new set of data was collected with MoK_α radiation. This crystal had dimensions $0.35 \times 0.12 \times 0.20$ mm perpendicular to [011], [010], and [110] respectively. The crystal was mounted on a Picker FACS-1 automatic four-circle diffractometer equipped with a graphite monochromator. The lattice parameters were calculated by least-squares refinement (2) on the setting angles of 12 MoK_α reflections ($12 < 2\theta \leqslant 30°$).

A total of 3046 MoK_α reflections (hkl and $hk\bar{l}$) were measured up to a 2θ value of 48°. The intensities were collected by the $\theta/2\theta$ scan technique at a constant speed of 1° per min. The scan range was 1.75° symmetrically disposed with respect to the calculated peak center and backgrounds were counted for 20 s on each side of the scanning range. During data collection, three standard reflections were measured every 50 reflections as a test on crystal and instrument stability. No systematic changes were observed and the intensity fluctuations were within ±5%.

Integrated intensities $I = N - (B_1 + B_2) \times T/2t$ were calculated and standard deviations $\sigma(I)$ were estimated according to the formula

$$\sigma^2(I) = N + 0.25 \times (T/t)^2 \times (B_1 + B_2) + (cI)^2$$

where N is the total counts from scanning for T s, B_1 and B_2 are the background counts measured during t s each, and c, the instability factor, is 0.05.

A set of 2607 reflections for which $I \geqslant 2.5\sigma(I)$ were considered as observed and later used in least-squares refinement.

Can. J. Chem. Downloaded from www.nrcresearchpress.com by 210.87.254.40 on 09/05/12
For personal use only.

TABLE 1. Final fractional coordinates ($\times 10^4$), and thermal parameters ($\times 10^3$) in $Hg(SCN)_2 \cdot As(C_6H_5)_3$[a]

Atom	X	Y	Z	U_{11}	U_{22}	U_{33}	U_{12}	U_{13}	U_{23}
Hg	4162.9(4)	506.5(2)	2148.1(3)	76.4(2)	67.8(2)	56.3(2)	3.1(2)	25.7(1)	3.8(1)
As	2588.3(7)	1421.9(4)	909.9(7)	54.2(4)	58.5(4)	47.6(4)	−6.0(3)	20.1(3)	0.1(3)
S(1)	6604(2)	575(1)	3757(3)	60(1)	155(2)	108(1)	−10(1)	24(1)	64(1)
S(2)	2993(2)	−514(1)	1146(2)	109(1)	72(1)	118(1)	−19(1)	79(1)	−15(1)
C(1)	6613(7)	91(3)	4980(7)	44(3)	74(5)	61(4)	−1(3)	15(3)	−5(3)
N(1)	6698(7)	−233(3)	5851(6)	75(4)	87(6)	55(3)	−2(3)	20(3)	7(3)
N(2)	4427(8)	−824(4)	−523(7)	100(5)	124(6)	87(5)	−17(5)	57(4)	−24(5)
C(2)	3842(8)	−678(3)	148(7)	59(4)	71(5)	60(4)	−10(3)	18(3)	2(3)
C(10)	3562(7)	2199(3)	997(6)	55(4)	61(4)	51(3)	−0(3)	22(3)	−0(3)
C(11)	3125(9)	2632(4)	−32(7)	101(6)	71(5)	55(4)	−14(4)	24(4)	6(3)
C(12)	3853(11)	3196(4)	61(9)	137(8)	70(5)	76(5)	−18(5)	45(5)	3(4)
C(13)	5024(11)	3315(4)	1182(10)	130(8)	66(5)	111(7)	−31(5)	61(6)	−5(5)
C(14)	5475(10)	2889(4)	2219(10)	94(7)	84(6)	99(6)	−25(5)	23(5)	−15(5)
C(15)	4760(8)	2323(4)	2116(8)	69(5)	71(5)	76(5)	−4(4)	22(4)	6(4)
C(20)	1037(7)	1611(4)	1458(7)	58(4)	81(5)	55(4)	−8(3)	22(3)	−10(3)
C(21)	524(9)	1120(5)	2013(8)	67(5)	132(8)	61(5)	−2(5)	28(4)	10(5)
C(22)	−635(10)	1232(7)	2342(10)	79(6)	198(13)	93(7)	−6(7)	51(5)	20(7)
C(23)	−1251(11)	1805(7)	2148(12)	78(7)	207(14)	129(9)	−4(8)	61(6)	−46(9)
C(24)	−729(12)	2279(6)	1647(16)	103(8)	128(10)	200(13)	8(7)	79(9)	−53(9)
C(25)	427(10)	2189(4)	1274(12)	92(7)	86(6)	145(9)	−0(5)	61(7)	−17(6)
C(30)	1671(8)	1222(3)	−977(7)	74(5)	64(4)	55(4)	−6(3)	23(3)	−2(3)
C(31)	291(10)	1051(6)	−1494(9)	92(7)	173(11)	70(5)	−64(7)	34(5)	−28(6)
C(32)	−329(14)	874(8)	−2797(10)	128(9)	242(16)	72(6)	−115(11)	30(6)	−55(8)
C(33)	385(13)	853(6)	−3624(9)	143(10)	136(9)	57(5)	−47(8)	21(5)	−22(6)
C(34)	1748(12)	1028(5)	−3148(9)	132(8)	127(9)	59(5)	−6(7)	47(5)	−21(5)
C(35)	2423(9)	1223(5)	−1809(8)	79(5)	114(7)	63(5)	−3(5)	26(4)	−2(4)

[a]The expression for the anisotropic temperature factor is $\exp[-2\pi^2(U_{11}h^2a^{*2} + U_{22}k^2b^{*2} + U_{33}l^2c^{*2} + U_{12}hka^*b^* + U_{13}hla^*c^* + U_{23}klb^*c^*]$.

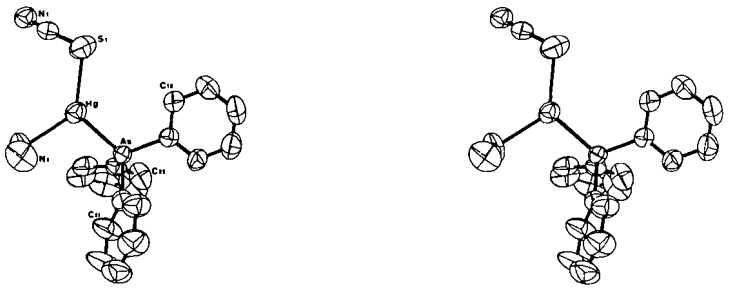

FIG. 1. The molecular structure of $Hg(SCN)_2 \cdot As(C_6H_5)_3$.

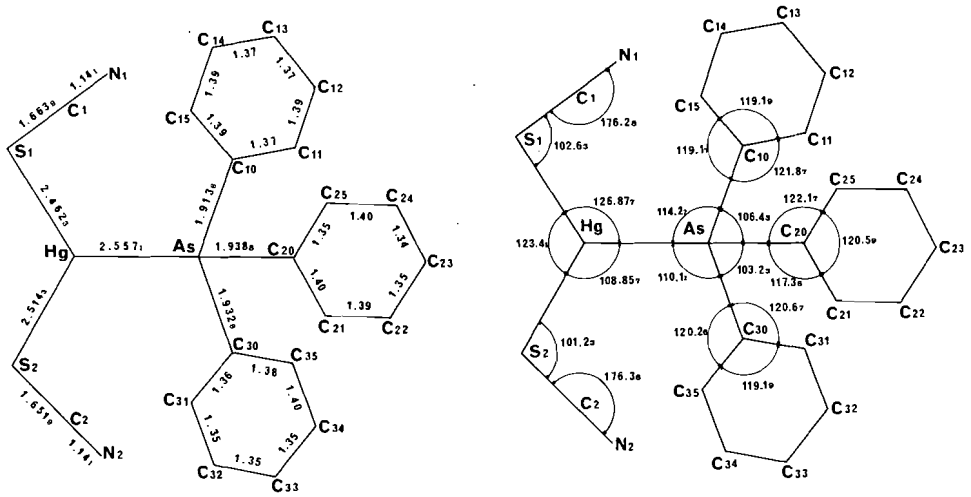

FIG. 2. Bond lengths and angles in $Hg(SCN)_2 \cdot As(C_6H_5)_3$. The values for Hg—As—C(20) and C(10)—As—C(30) are 115.7(2) and 106.3(3)° respectively. Standard deviations are given as subscripts.

An absorption correction based on the crystal faces was applied.[1] The calculated transmission factor ranged from 0.16 to 0.37. The usual corrections for polarization and Lorentz effects were finally applied. During the absorption correction the coefficient $dA^*/d\mu$ was evaluated for secondary extinction correction (3).

Mercury was located from an origin-removed sharpened Patterson map. After two cycles of least-squares refinement, a difference Fourier map revealed all nonhydrogen atoms. Block-diagonal least-squares refinement with unit weights, of the scale factor, the positional and individual isotropic temperature factors led to $R = (\Sigma||F_o| - |F_c||)/\Sigma|F_o| = 0.089$. The R factor reduced to 0.033 by introducing and refining anisotropic temperature factors and a secondary extinction coefficient (4). At this stage, the phenyl hydrogen atoms were placed at the calculated position (C—H = 0.95 Å) and were included in structure factor calculations with fixed isotropic factors ($B = 7$ Å^2). The function minimized in least-squares refinements was $\Sigma w(|F_o| - |F_c|)^2$, where $w = 1/\sigma^2$ and $\sigma = a + bF_o + cF_o^2$ (5). After three additional least-squares cycles the final R and $Rw = [\Sigma w(F_o - F_c)^2/\Sigma wF_o^2]^{1/2}$ were respectively 0.030 and 0.040. The values of a, b, and c were adjusted in order to minimize the variations of the $\Sigma w\Delta F^2$ function *vs.* F_o (final values $a = 5.38$, $b = -0.08$, and $c = 0.0006$). The standard deviation of an observation of unit weight was 1.65. In the final least-squares cycle the highest and the average shifts were respectively 0.6σ and 0.4σ.

On the final difference Fourier map, the highest peaks had an intensity of $+0.6$ e/Å^3 and were located at less than 1 Å from the mercury atom.

The scattering factors used for the nonhydrogen atoms were taken from Cromer and Waber (6), the scattering curve of hydrogen was from Stewart *et al.* (7), and the anomalous dispersion coefficients for the heavy atoms (Hg, As, S) from Cromer (8).

The final positional and thermal parameters are given in Table 1. The carbon atoms belonging to phenyl rings are identified with labels of the type $C(ij)$, where i is the

[1]The computer programs used were locally modified versions of the following: F. R. Ahmed and C. P. Huber, NRC-2 (data reduction); F. R. Ahmed and P. Singh, NRC-3 (absorption correction); R. J. Doedens and J. A. Ibers, NUCLS (least-squares refinement with block diagonal option); A. Zalkin, FORDAP (Fourier, Patterson) and C. K. Johnson, ORTEP (drawings).

Can. J. Chem. Downloaded from www.nrcresearchpress.com by 210.87.254.40 on 09/05/12
For personal use only.

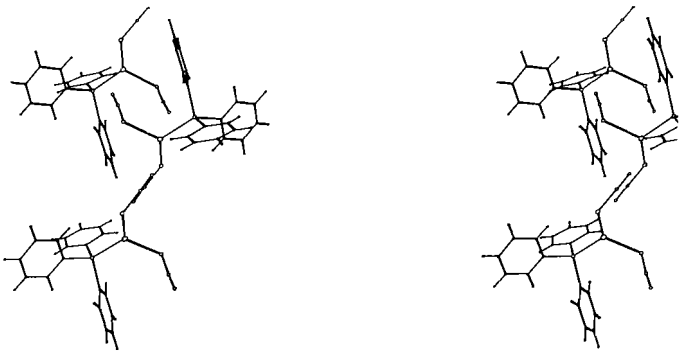

FIG. 3. Stereoscopic drawings of the molecular packing in $Hg(SCN)_2 \cdot As(C_6H_5)_3$.

TABLE 2. Selected intermolecular distances and angles

Atoms	Distance (Å)	Bonds	Angle (deg)
Hg–N(1)[a]	2.673(7)	As–Hg–N(1)[a]	104.2(2)
Hg–N(2)[b]	2.736(9)	As–Hg–N(2)[b]	82.3(2)
N(1)–H(12)[c]	2.68	S(1)–Hg–N(1)[a]	90.5(2)
N(1)–H(21)[a]	2.74	S(1)–Hg–N(2)[b]	77.6(2)
N(2)–H(35)[b]	2.70	S(2)–Hg–N(1)[a]	84.6(2)
		S(2)–Hg–N(2)[b]	102.9(2)
		N(1)[a]–Hg–N(2)[b]	168.1(3)

[a] $1 - x, -y, 1 - z$.
[b] $1 - x, -y, -z$.
[c] $1 - x, -\frac{1}{2} + y, \frac{1}{2} - z$.

ring number and j corresponds to sequential numbering of the ring vertices with $j = 0$ for the atom bound to arsenic. The structure factor table is available.[2]

Results and Discussion

The crystal consists of single molecules as shown in Fig. 1. Intramolecular bond lengths and angles are given in Fig. 2.

Molecular Structure

Mercury forms strong bonds to one arsenic and two sulfur atoms and its so-called 'characteristic' coordination number (9) is three. The Hg—S bonds are significantly different (2.514(3) and 2.462(3) Å) but still in the range observed for $[(C_6H_5)_4P][Hg(SCN)_3]$, another (12) three-coordinate mercury complex. Mercury is shifted toward N(1) of another molecule and is only 0.14 Å above the plane defined by As, S(1), and S(2). Intramolecular nonbonded interactions with the phenyl rings of triphenylarsine could be partly responsible for the angular distortions around the mercury atom. S(1) lies close to the plane of ring (1) and increasing the S(1)—Hg—As angle to 126.9° probably helps to minimize S(1)... H(15) (3.3 Å) repulsions. Ring (3) which is closest to S(2), is approximately perpendicular to the coordination plane and S(2)—Hg—As can reduce to 108.9° before appreciable S(2)... C(31) (3.04 Å) repulsions are experienced. The S(1)—Hg—S(2) angle is normal at 123.4°.

As commonly observed in mercury–thiocyanate compounds, the SCN groups are linear, the Hg—S—C angles are close to 100°, and the S—C and C—N bond lengths are 1.65–1.66 and 1.14 Å respectively.

The three As—C bonds (1.91–1.93 Å) in triphenylarsine are equal within experimental errors and the expected tetrahedral geometry is observed with some distortions. The phenyl rings are planar within 1σ. Their C—C distances and bond angles range from 1.34 to 1.40 Å (average = 1.37(1) Å) and 118.5 to 121.5° (average = 120(1)°) respectively.

[2]Complete set of tabular data is available, at a nominal charge, from the Depository of Unpublished Data, CISTI, National Research Council of Canada, Ottawa, Canada K1A 0S2.

Can. J. Chem. Downloaded from www.nrcresearchpress.com by 210.87.254.40 on 09/05/12
For personal use only.

Molecular Packing

The molecules are linked in infinite zigzag chains along the *c* direction by weakly bridging SCN groups (Fig. 3).

The Hg–N distances (2.67 and 2.74 Å, Table 2), although shorter than the sum of the van der Waals radii (3.0 Å), correspond to the weak intermolecular contacts found in $Hg(SCN)_2$ (10) and $Hg(CN)_2$ (11). The type of bridging reported for $[Hg(SCN)_3]^-$ ions (12), though geometrically similar, involves much greater participation of the terminal nitrogens, with Hg–N distances of 2.40 Å.

When the two Hg–N contacts are taken into account, the effective coordination of mercury corresponds to a very distorted trigonal bipyramid (Table 2).

The chains are held together by normal van der Waals contacts.

We wish to thank the National Research Council of Canada for a research grant.

1. R. C. MAKHIJA, A. L. BEAUCHAMP, and R. RIVEST. Chem. Commun. 1043 (1972).
2. W. R. BUSING and H. A. LEVY. Acta Cryst. **22**, 457 (1967).
3. S. ÅSBRINK and P. E. WERNER. Acta Cryst. **20**, 407 (1966).
4. W. H. ZACHARIASEN. Acta Cryst. **16**, 1139 (1963).
5. G. H. STOUT and L. H. JENSEN. X-Ray structure determination. Macmillan Co., New York. 1968. p. 457.
6. D. T. CROMER and J. T. WABER. Acta Cryst. **18**, 104 (1965).
7. J. STEWART, R. DAVIDSON, and A. SIMPSON. J. Chem. Phys. **42**, 3175 (1965).
8. D. T. CROMER. Acta Cryst. **18**, 17 (1965).
9. D. GRDENIC. Q. Rev. **19**, 303 (1965).
10. A. L. BEAUCHAMP and D. GOUTIER. Can. J. Chem. **50**, 977 (1972).
11. R. C. SECCOMBE and C. H. L. KENNARD. J. Organomet. Chem. **18**, 243 (1969).
12. A. L. BEAUCHAMP and A. SAKHRI. Inorg. Chem. **14**, 740 (1975).

Can. J. Chem. Downloaded from www.nrcresearchpress.com by 210.87.254.40 on 09/05/12
For personal use only.

Synthesis and Spectral Properties of $[Cr(en)_2NH_3X]^{n+}$ Compounds

CARL F. C. WONG AND A. D. KIRK

Department of Chemistry, University of Victoria, Victoria, British Columbia V8W 2Y2

Received June 5, 1975

CARL F. C. WONG and A. D. KIRK. Can. J. Chem. **53**, 3388 (1975).

Preparation of the compounds *cis*- and *trans*-$[Cr(en)_2NH_3F](ClO_4)_2$, $[Cr(en)_2NH_3NO_2]BrClO_4$, *cis*- and *trans*-$[Cr(en)_2NH_3Cl](ClO_4)_2$, *cis*-$[Cr(en)_2NH_3Br](ClO_4)_2$, *trans*-$[Cr(en)_2NH_3H_2O]Br_3$, *trans*-$[Cr(en)_2NH_3H_2O]Cl_3 \cdot xH_2O$, and *trans*-$[Cl(en)_2CrOHCr(en)_2Cl](ClO_4)_3$ is described. The compounds have been characterized by analysis and u.v.–visible and i.r. spectral data. Spectral criteria for establishing *cis* and *trans* configuration are discussed.

CARL F. C. WONG et A. D. KIRK. Can. J. Chem. **53**, 3388 (1975).

On décrit la préparation des composés suivants: $[Cr(en)_2NH_3F](ClO_4)_2$-*cis* et *trans*, $[Cr(en)_2NH_3NO_2]BrClO_4$, $[Cr(en)_2NH_3Cl](ClO_4)_2$-*cis* et *trans*, $[Cr(en)_2NH_3Br](ClO_4)_2$-*cis*, $[Cr(en)_2NH_3H_2O]Br_3$-*trans*, $[Cr(en)_2NH_3H_2O]Cl_3 \cdot xH_2O$-*trans* et $[Cl(en)_2CrOHCr(en)_2Cl](ClO_4)_3$-*trans*. On les a caractérisés par analyse et par spectroscopie u.v.–visible et i.r. On discute des critères spectraux utilisés pour attribuer les configurations *cis* et *trans*.

[Traduit par le journal]

Can. J. Chem. Downloaded from www.nrcresearchpress.com by 210.87.254.5 on 09/05/12
For personal use only.

Although an extensive series of mixed amine complexes of Co(III) has been known for a considerable time (1), few analogous Cr(III) complexes have been reported (2). In particular, cobalt complexes of the type $[Co(en)_2NH_3X]^{2+}$, where en is ethylenediamine and X is an acido ligand, were prepared by Werner, and others, and have been studied kinetically in attempts to establish the stereochemistry of Co(III) solvation reactions (3–6).

Despite the superficial similarities between the chemistries of Co(III) and Cr(III) complexes no reports of any of the Cr(III) analogs appeared until recently when the synthesis of *cis*- and *trans*-$[Cr(en)_2NH_3NCS](NCS)_2$ was reported (7). Because of their great potential to yield detailed stereochemical information about Cr(III) photo-solvations, we have continued to attempt to find synthetic methods for other complexes of this type.

Results and Discussion

Synthetic Methods

In order to develop a fairly general synthetic method several approaches were tried. By analogy with synthetic methods for the cobalt compounds the first attempts involved oxidation of the *N*-bonded thiocyanate ligand with Cl_2 or H_2O_2 to convert the ligand to NH_3. The method has the advantage, in principle, of conserving the stereochemistry around the Cr(III) center. Attempts to oxidize, for example, *trans*-$[Cr(en)_2NCSCl]^{2+}$ to *trans*-$[Cr(en)_2NH_3Cl]^{2+}$ failed completely. Invariably complete loss of thiocyanate occurred, leading to aquo or acido complexes depending on conditions. This was presumably a reflection of the greater lability of Cr(III) complexes and the affinity of Cr(III) for oxygen-bonding ligands.

The only reasonably general approach found was reaction of *cis*- or *trans*-$[Cr(en)_2XY]^+$ with liquid ammonia, where, of the X and Y acido ligands, Y is the more readily substituted by ammonia. This procedure enabled the successful preparation of *cis*- and *trans*-$[Cr(en)_2NH_3NCS](NCS)_2$ (7), *cis*- and *trans*-$[Cr(en)_2NH_3F](ClO_4)_2$ and *cis*- and *trans*-$[Cr(en)_2NH_3NO_2]BrClO_4$, although in the last case the lability of the product mixture prevented isolation of the separate isomers.

The method failed to be completely general, however, owing to a number of problems, not the least of which was the preparation of the required starting materials. Also, while *cis* starting materials gave *cis* products, the *trans* compounds reacted to produce *cis*/*trans* product mixtures in unpredictable proportions, it proved difficult to isolate the *trans* isomer from some of these mixtures. Some compounds, *e.g.* *trans*-$[Cr(en)_2ClBr]^+$, gave rise to both chloride and bromide substitution, and once one halide had been replaced the second was more readily substituted. Thus the reaction yielded a mixture of *cis* and *trans* isomers of $[Cr(en)_2NH_3Cl]^{2+}$, $[Cr(en)_2$-

Can. J. Chem. Downloaded from www.nrcresearchpress.com by 210.87.254.5 on 09/05/12
For personal use only.

$NH_3Br]^{2+}$, and $[Cr(en)_2(NH_3)_2]^{3+}$ together with unreacted starting material. It proved to be impossible to obtain pure samples of the desired complexes from such a mixture.

Attempts were made to overcome the problem of substitution of both acido ligands by carrying out the ammonolysis in nonaqueous solvents such as acetonitrile, but these failed as the desired product was more soluble than the starting material (as perchlorates or halide salts) and therefore again reacted all the way to the $[Cr(en)_2(NH_3)_2]^{3+}$ compounds. This gave a cleaner synthesis of these compounds but left the problem of preparing $[Cr(en)_2NH_3X]^{2+}$ for X = Cl, Br.

Consequently the possibility of preparing these from compounds already prepared was considered. Reaction of *cis*-$[Cr(en)_2NH_3F]^{2+}$ with concentrated HCl or HBr was found to give a clean substitution of the fluoride, but this reaction failed to go for the desired *trans* isomer. As a second approach *trans*-$[Cr(en)_2NH_3NCS]^{2+}$ was treated in aqueous solution with mercuric chloride, but no reaction occurred. Crude $[Cr(en)_2NH_3NO_2]BrClO_4$ was reacted with HCl and HBr; depending on conditions mainly *trans*-$[Cr(en)_2NH_3H_2O]^{3+}$ and *cis*-$[Cr(en)_2NH_3Br]^{2+}$ or *cis*-$[Cr(en)_2NH_3Cl]^{2+}$ would be isolated; either no anation of *trans*-$[Cr(en)_2NH_3H_2O]^{3+}$ occurred, or the *trans* products, once formed, decomposed too readily.

A successful approach to these elusive *trans* compounds was finally found through preparation of *trans*-$[Cr(en)_2NH_3H_2O]^{3+}$ and its subsequent anation. First attempts to prepare this compound by reaction of *trans*-$[Cr(en)_2ClH_2O]^{2+}$ with ammonia failed (probably the ammonolysis is base catalyzed and was vanishingly slow in the strongly acid solution of the complex). The compound *trans*-$[Cl(en)_2CrOHCr(en)_2Cl](ClO_4)_3$ was therefore prepared and reacted with liquid ammonia in the presence of a small amount of lithium amide. Acidification of the product (with HBr) yielded *trans*-$[Cr(en)_2NH_3H_2O]Br_3$ in good yield. Since it was found that *trans*-$[Cr(en)_2NH_3H_2O]^{3+}$ was not anated by concentrated HBr in aqueous solutions, and solubility difficulties were anticipated for anation in nonaqueous solvents, the haloammines were prepared by heating of the solid halide salt even though this led to some isomerization, and some loss of NH_3 rather than H_2O. This enabled us to prepare *trans*-$[Cr(en)_2NH_3Cl](ClO_4)_2$; the pure bromo analog has not yet been obtained by this technique. It is likely that this same procedure could be used to prepare other $[Cr(en)_2NH_3X]^{2+}$ compounds.

Characterization of Compounds

The compounds were characterized by analysis and their u.v.–visible and i.r. spectra. In the main the characterization was straightforward and the only difficulties were with establishing the geometric configuration of the compounds and their isomeric purity.

Hughes and McWhinnie (8) considered the problem of distinguishing *cis* and *trans* isomers of Cr(III) bisethylenediamine compounds by infrared spectra and concluded that the best criterion lay in the band pattern between 550 and 395 cm^{-1}. They used compounds having a variety of anions, and found that *cis* compounds always had a pattern of four bands: one strongly split, at 545–535 cm^{-1}, two other strong bands at approximately 480 and 430 cm^{-1} and one much weaker band at about 405 cm^{-1}. *Trans* complexes showed three strong bands in this region, at about 540 (sometimes split), 490, and 440 cm^{-1}. These criteria were found to be met by the spectra of *cis*- and *trans*-$[Cr(en)_2NH_3NCS](NCS)_2$ (7). However, the data shown in Table 1 for the complexes of this work lead to some doubt about the absolute reliability of these criteria for these compounds. All the *cis* compounds show the expected band pattern, but the *trans* complexes in three cases show a band at *ca.* 400 cm^{-1}, depending on the nature of the anion. The observed influence of the anion suggests that the criterion of the band at 400 cm^{-1} should be used with caution. Other than this the band patterns are as suggested by the above authors and the band positions support the geometric assignments made in drawing up Table 1.

Table 2 compares the wavelength maxima and minima and molar absorptivities for the compounds. Our earlier work (7) showed that, like the cobalt analogs, the *cis* and *trans* isomers of $[Cr(en)_2NH_3NCS]^{2+}$ had the same λ_{max} value but the molar absorptivity of the *cis* isomer was 50% higher than the *trans*, due to the lower symmetry of the former. The data in Table 2 show that this criterion is valid for these new compounds. It is clear that, particularly for the low energy ligand field band, the *trans* isomer has roughly the same molar absorptivity as the pentammine, while that of the *cis* isomer is on

TABLE 1. Infrared spectral data for the $[Cr(en)_2NH_3X]^{n+}$ complexes

Complex	Band frequencies*					
cis-$[Cr(en)_2NH_3F](ClO_4)_2$	540s	519m	475w	440m		387w
cis-$[Cr(en)_2NH_3Cl]Br_2$†	537s		476m	447w	420w	395w
cis-$[Cr(en)_2NH_3Br]Br_2$	548s	535s	474m	446w	421w	396w
trans-$[Cr(en)_2NH_3F](ClO_4)_2$	551s	522m	491w		434w	
trans-$[Cr(en)_2NH_3Cl]Br_2$	540s		487s	457w	438m	384w
trans-$[Cr(en)_2NH_3Cl](ClO_4)_2$	554s	535s	481s		439m	
trans-$[Cr(en)_2NH_3H_2O]Cl_3$	542s		495m		446w	398w
trans-$[Cr(en)_2NH_3H_2O]Br_3$	543s		494m		445w	400w
trans-$[Cr(en)_2NH_3H_2O]Br_2ClO_4$	542s		495m		446w	398w

*All frequencies are precise to ± 3 cm^{-1}. The letters following the band frequencies denote the relative intensities of the bands: s, strong; m, medium; w, weak.
†This compound showed splitting of the 537 cm^{-1} band in the $BrClO_4$ salt.

TABLE 2. Ultraviolet–visible spectral data for *cis*- and *trans*-$[Cr(en)_2NH_3X]^{n+}$ and analogous $[Cr(NH_3)_5X]^{n+}$ complexes*

Complex	λ_{max}†	λ_{min}	λ_{max}	Reference
cis-$[Cr(en)_2(NH_3)H_2O]^{3+}$	359(46.6)	406(16.8)	473(59.2)	This work
trans-$[Cr(en)_2(NH_3)H_2O]^{3+}$	354(35.7)	400(14.0)	466(40.2)	This work
$[Cr(NH_3)_5H_2O]^{3+}$	360(29)		479(34)	2
cis-$[Cr(en)_2NH_3F]^{2+}$	360(34.4)	417(16.6)	494(64.9)	This work
trans-$[Cr(en)_2NH_3F]^{2+}$	356(24.1)	409(12.8)	490(45.7)	This work
$[Cr(NH_3)_5F]^{2+}$	366(20.4)		503(41.7)	12
cis-$[Cr(en)_2NH_3Cl]^{2+}$	374(58.9)	424(18.2)	506(54.0)	This work
trans-$[Cr(en)_2NH_3Cl]^{2+}$	371(45.0)	417(17.5)	504(39.9)	This work
$[Cr(NH_3)_5Cl]^{2+}$	376(38.2)	426(10.0)	513(36.5)	13
cis-$[Cr(en)_2NH_3Br]^{2+}$	377(66.2)	427(22.1)	517(60.1)	This work
$[Cr(NH_3)_5Br]^{2+}$‡	380(38)	430(11)	526(36)	14

*All $[Cr(en)_2NH_3X]^{n+}$ spectra were obtained in 0.10 *N* $HClO_4$.
†The values in parentheses are the corresponding molar absorptivities (l mol^{-1} cm^{-1}). All wavelengths are in nm.
‡Estimated from spectral curve in ref. 14.

average about 40% higher. The λ_{max} for both *cis* and *trans* are more or less the same and shifted to slightly higher energy than the pentammine. Taken together with chemical analysis and ion-exchange determination of isomer purity we believe the u.v.–visible data to be the best available criterion of geometric configuration and, by means of repeated fractional crystallization and measurement of molar absorptivity, a good criterion of isomer purity. Figures 1 through 3 give the spectra of the compounds for easy reference.

In addition to the above checks, where the isomer purity was questionable, as in the case of *trans*-$[Cr(en)_2NH_3Cl](ClO_4)_2$ which was isolated from a mixture containing at least six complexes, ion-exchange chromatography was carried out. For the case cited, the complex was found to be virtually 100% pure (no *cis* isomer or 1+ ions were present, small amounts of 3+ ions would have remained on the column undetected).

Experimental

Starting Materials

trans-$[Cr(en)_2FBr]ClO_4$ was prepared by the method of Wirth *et al.* (9) except that the anation of *trans*-$[Cr(en)_2(H_2O)F]^{2+}$ with NH_4Br in methanol was found to be very much accelerated by refluxing at 70 °C. A reaction time of 45 min was found to give optimum yields (*ca.* 40% after crystallization as the perchlorate). Too long a reaction time caused production of a rather insoluble pinkish solid in addition to the desired product.

trans-$[Cr(en)_2(NO_2)Br]ClO_4$ and *trans*-$[Cr(en)_2(H_2O)Cl]Br_2$ were prepared as described by Fee *et al.* (10).

trans-[Cl(en)$_2$CrOHCr(en)$_2$Cl](ClO$_4$)$_3$

trans-$[Cr(en)_2H_2OCl]Br_2$ (10 g) was dissolved in 10 ml of water. Saturated $NaClO_4$ (10 ml) was added to the filtered solution, and, after cooling to 0 °C, 10 ml of 1.0 *M* NaOH were added dropwise over a 10-min period to the continuously stirred solution. The red crystals

Can. J. Chem. Downloaded from www.nrcresearchpress.com by 210.87.254.5 on 09/05/12
For personal use only.

Can. J. Chem. Downloaded from www.nrcresearchpress.com by 210.87.254.5 on 09/05/12
For personal use only.

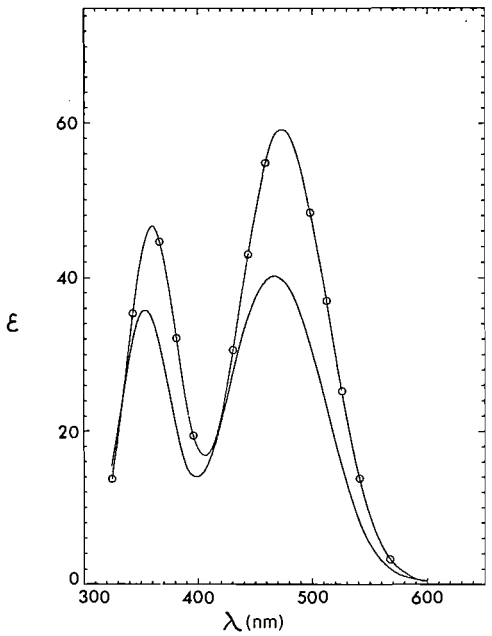

FIG. 1. Ultraviolet–visible spectra of *trans*(—) and *cis*-$[Cr(en)_2NH_3H_2O]^{3+}$ (○—○—○). The circles in the figure (as in the other figures) are not experimental points, but are added to distinguish the spectra.

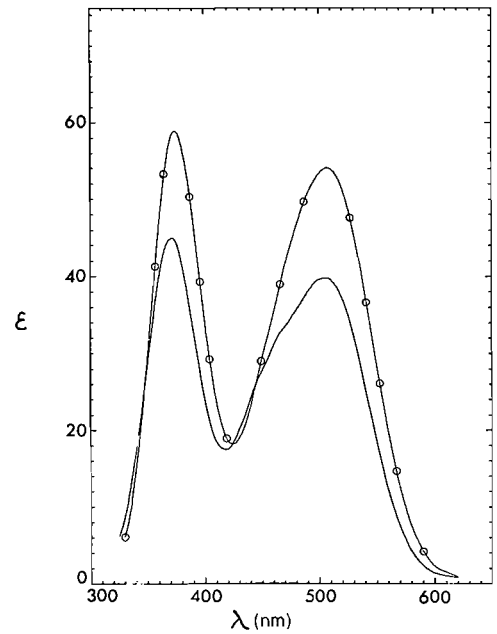

FIG. 2. Ultraviolet–visible spectra of *trans*(—) and *cis*-$[Cr(en)_2NH_3Cl]^{2+}$ (○—○—○).

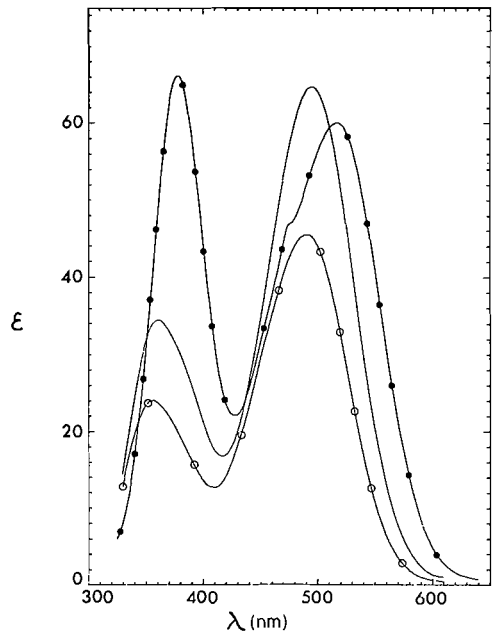

FIG. 3. Ultraviolet–visible spectra of *cis*(—) and *trans*-$[Cr(en)_2NH_3F]^{2+}$ (○—○—○) and *cis*-$[Cr(en)_2NH_3Br]^{2+}$ (●—●—●).

(with a slight purple tint) were filtered and washed with methanol and acetone (yield 7–8 g, 81–93%).

The method used was an attempt to make *trans*-$[Cr(en)_2OHCl]ClO_4$. That the product was a binuclear species was indicated by its u.v.–visible spectrum in 1 *M* HCl. The spectrum in acid medium is identical to that of *trans*-$[Cr(en)_2H_2OCl]^{2+}$ but the absorbances at its λ_{max} values (as compared with the ε_{max} values of Quinn and Garner (11)) were consistent with a chromium content for the solid product of 13.8 ± 0.1%. This differs significantly from that for $[Cr(en)_2OHCl]ClO_4$ (16.04%), but agrees reasonably with that for the hydroxyl bridged binuclear compound (14.23%). A third possibility, $[Cl(en)_2CrOCr(en)_2Cl](ClO_4)_2$, should also be considered, but the chromium content for this compound, 16.54%, is too high. It should be noted that the analytical C, H, and N values are also somewhat low, but as this compound was to be used only as an intermediate, no further attempts were made to identify any impurities.

Anal. Calcd. for $[Cl(en)_2CrOHCr(en)_2Cl](ClO_4)_3$: C, 13.16; N, 15.34; H, 4.55. Found: C, 12.7; N, 14.8; H, 4.3.

Preparation of $[Cr(en)_2NH_3X]^{2+}$ Compounds

Crude $[Cr(en)_2NH_3F]BrClO_4$

An 8-g sample of dried *trans*-$[Cr(en)_2FBr]ClO_4$ with about 1 mg of NH_4ClO_4 was reacted with about 20 ml of distilled, potassium-dried ammonia for 2 h at 0 °C in a sealed 200 ml Carius tube (7). The crude product was an approximately 60%/40% mixture of *cis*/*trans*-$[Cr(en)_2NH_3F]BrClO_4$ as evidenced by the u.v.–visible and i.r. spectra.

Can. J. Chem. Downloaded from www.nrcresearchpress.com by 210.87.254.5 on 09/05/12
For personal use only.

Separation of cis- and trans-[Cr(en)$_2$NH$_3$F](ClO$_4$)$_2$

An 8-g sample of crude [Cr(en)$_2$NH$_3$F]BrClO$_4$ was dissolved in 8 ml of 0.1 *M* HCl at room temperature. On cooling to 0 °C, large orange prisms of *trans*-[Cr(en)$_2$NH$_3$F](ClO$_4$)$_2$ precipitated and were filtered, washed with methanol, and dried. A second fraction was obtained by adding 2 ml of 60% HClO$_4$ to the filtrate, and cooling to 0 °C. The total yield of pure *trans*-[Cr(en)$_2$NH$_3$F](ClO$_4$)$_2$ was 3 g. Third and fourth fractions were similarly obtained by stepwise 2-ml additions of HClO$_4$ (4.0 and 0.5 g, respectively). Fraction 3 was a mixture of *cis* and *trans* material, but fraction 4 was practically pure *cis*-[Cr(en)$_2$NH$_3$F](ClO$_4$)$_2$. Further purification of both the *trans* and *cis* products was carried out by repeated fractional recrystallizations.

Anal. Calcd. for [Cr(en)$_2$(NH$_3$)F](ClO$_4$)$_2$: C, 11.80; N, 17.2; H, 4.70. Found for the *trans* product: C, 11.9; N, 17.0; H, 4.75. Found for the *cis* product: C, 11.9; N, 17.0; H, 4.65.

Crude [Cr(en)$_2$NH$_3$NO$_2$]BrClO$_4$

A 10-g sample of dried *trans*-[Cr(en)$_2$(NO$_2$)Br]ClO$_4$, *ca.* 1 mg of NH$_4$ClO$_4$, and dried liquid ammonia (*ca.* 10 ml) were reacted for 20 min at 0 °C in a sealed Carius tube. The dried product is very heat sensitive and inflames violently on heating with a hot glass rod. The crude product appears to be about 60% *cis* isomer. No attempt was made to separate the isomers due to the lability of the complex in aqueous solution.

cis-[Cr(en)$_2$NH$_3$Cl]Br$_2$

A 2-g sample of crude [Cr(en)$_2$(NH$_3$)NO$_2$]BrClO$_4$ was slurried with 10 ml of concentrated HCl. After evolution of NO$_2$ had stopped, 2 ml of water were added to completely dissolve the aquo-product(s). The solution was filtered, left to anate for 2 h, cooled to precipitate the small amount of unreacted aquo-product(s), and filtered off. Concentrated HBr (3 ml), 2 volumes of isopropanol, and excess ether were added to the filtrate to yield a red oil. After decanting the pale orange supernatant, the oil was taken up with 2 ml of 5 *M* HBr. Upon dropwise addition of isopropanol to cloudiness and overnight cooling at 0 °C, a pink–red precipitate was filtered off. The crude product was recrystallized by dissolving in a minimum of HBr-acidified water, adding isopropanol until just cloudy, and cooling in ice. The orange–red crystals were filtered, washed with isopropanol and acetone, and dried under vacuum. This procedure yielded only the *cis*-product (yield, about 20%).

Anal. Calcd. for [Cr(en)$_2$(NH$_3$)Cl]Br$_2$: C, 12.50; N, 18.22; H, 4.98. Found: C, 12.6; N, 18.2; H, 5.1.

cis-[Cr(en)$_2$NH$_3$Br]Br$_2$ was prepared from crude [Cr(en)$_2$(NH$_3$)NO$_2$]BrClO$_4$ as for the chloro-complex except that HBr was used instead of HCl for the anation. Only the *cis* product was obtained.

Anal. Calcd. for [Cr(en)$_2$NH$_3$Br]Br$_2$: C, 11.20; N, 16.32; H, 4.46. Found: C, 11.1; N, 15.8; H, 4.4.

trans-[Cr(en)$_2$(NH$_3$)H$_2$O]Br$_3$

trans-[Cl(en)$_2$CrOHCr(en)$_2$Cl](ClO$_4$)$_3$ (10 g) was reacted with about 20 ml of liquid NH$_3$ containing a trace of LiNH$_2$ for 1 h at 20 °C in a sealed Carius tube. (The reaction appears to be 100% stereoretentive as determined by the molar absorptivity of the crude product.) After removal of the unreacted NH$_3$, first by evaporation and then by pumping, the purple product was taken up with 5 ml of 1 *M* HBr and reprecipitated with 10–15 ml 48% HBr. During the acidification, the hydroxyl bridge is presumably cleaved and both the solution and any solid product becomes yellow–orange in color. The crude product was filtered and washed with 10 ml of methanol and acetone. A second crop could be obtained by adding isopropanol to the filtrate (total yield, about 9 g (74%)).

The crude bromide salt was recrystallized by dissolving 1.0 g in 2 ml of water and adding, dropwise, 3 ml 48% HBr and 3 ml isopropanol to the filtered solution while it was continuously stirred and cooled in ice (yield, 95%).

Anal. Calcd.: C, 10.75; N, 15.67; H, 4.74. Found: C, 10.5; N, 15.1; H, 4.7.

trans-[Cr(en)$_2$NH$_3$H$_2$O]Br$_2$ClO$_4$

Crude *trans*-[Cr(en)$_2$NH$_3$H$_2$O]Br$_3$ was dissolved in a minimum amount of water, 60% HClO$_4$ was added dropwise until cloudy and the solution cooled to 0 °C. The product was filtered and washed with methanol and acetone.

The method used was an attempt to make the triperchlorate salt. That the salt obtained is the one indicated was suggested by the λ_{max} absorbances of its u.v.–visible spectrum and by its i.r. spectrum. The u.v.–visible spectrum indicated the salt to have a formula weight of 464 ± 3, agreeing well with that of 466.5 for the Br$_2$(ClO$_4$) salt. That the sample is not a mixture of the tribromide and triperchlorate salts is suggested by a slight difference between its infrared spectrum and that of the tribromide; no band at ~400 cm^{-1} is observed in the former (see Table 1).

trans-[Cr(en)$_2$(NH$_3$)H$_2$O]Cl$_3$·xH$_2$O

A 2.0 g sample of *trans*-[Cr(en)$_2$(NH$_3$)H$_2$O]Br$_3$ was dissolved in 3 ml of water at 30–35 °C and quickly filtered. Concentrated HCl (6 ml) was then added dropwise to the stirred solution. After cooling, the yellow crystals (pale orange tint) were filtered and washed with 2–3 ml of methanol and acetone. The product was recrystallized by dissolving the crude chloride in 2 ml of water, adding 4 ml of concentrated HCl to the stirred solution, and cooling in ice (yield, 1.1 g, 80%). The filtrate may be treated with HBr and isopropanol to recover most of the complex still in solution.

trans-[Cr(en)$_2$NH$_3$Cl]Br$_2$

Gently ground solid *trans*-[Cr(en)$_2$NH$_3$H$_2$O]Cl$_3$ was heated for 1 h with periodic mixing at 95–100 °C. The crude product was examined by ion-exchange chromatography and found to contain about 65–70% *trans*-[Cr(en)$_2$NH$_3$Cl]$^{2+}$, 25–30% *cis*-[Cr(en)$_2$NH$_3$Cl]$^{2+}$, and traces of *cis*- and *trans*-[Cr(en)$_2$H$_2$OCl]$^{2+}$ and *cis*- and *trans*-[Cr(en)$_2$Cl$_2$]$^+$. For crystallization, a 2.0 g sample of the crude product was dissolved in 4 ml of water and 1 ml of 40% HBr was added. Acetone (50 ml) was then added dropwise to the rapidly-stirred solution at room temperature. It should be noted that acetone must be added very slowly (~ one drop every second) after precipitation begins or a gum may result. The orange-red crystals were filtered off and washed with acetone (yield, 2.0 g (55%)). The product may be recrystallized by dissolving in water, adding about a one-half volume of 48% HBr, and adding acetone.

trans-[Cr(en)$_2$NH$_3$Cl](ClO$_4$)$_2$

trans-$[Cr(en)_2NH_3Cl]Br_2$ (2.0 g) was dissolved in 3 ml of water at ~30 °C, 1 ml of 60% $HClO_4$ was added to the filtered solution and then left for a few minutes in an ice-bath. The orange–red crystals were filtered off, washed with 2 ml of methanol and ether (yield, 1.2 g (55%)). The filtrate was treated with HBr and acetone to recover most of the complex still in solution. Repeated recrystallizations are necessary to obtain a bromide-free sample.

Anal. Calcd.: C, 11.34; N, 16.53; H, 4.52. Found: C, 11.6; N, 16.6; H, 4.6.

cis-[Cr(en)$_2$NH$_3$H$_2$O]$^{3+}$

Although this complex is present in the aquo-product obtained in the nitrito destruction of the crude $[Cr(en)_2NH_3NO_2]BrClO_4$ product; isolation was not attempted. For the purpose of u.v.–visible spectral characterization, this ion was produced in solution by aquating *cis*-$[Cr(en)_2NH_3Br]^{2+}$ in 0.1 *N* $HClO_4$ for about 3 h at 40 °C (such reactions are known to be stereoretentive). The reaction was followed spectrally and the sharp isobestic points observed at 359, 422, and 492 nm suggest that secondary aquation of *cis*-$[Cr(en)_2NH_3H_2O]^{3+}$ occurs at a rate slow enough that a satisfactory spectrum of the desired ion is obtainable by this method.

Spectral Measurements

All u.v.–visible spectra were obtained using a Cary 17 spectrophotometer and infrared spectra using a Beckman IR-20 spectrometer.

Ion Exchange Chromatography

Ion-exchange chromatography was carried out using Baker analyzed CGC-241 cation exchange resin (200–400 mesh) and solutions of $(NH_4)_2SO_4$ as eluent. For a typical run involving separation of *cis* and *trans* isomers of 2+ charge, a 10-cm column was used, at 20 °C, and eluent, 0.5 → 1.0 *M* $(NH_4)_2SO_4$, was pumped through at 100 ml per h. Eluted complexes were detected, after oxidation with basic peroxide, as chromate ion.

The authors wish to thank the National Research Council of Canada and the University of Victoria Faculty Research Fund for financial support. C.F.C.W. wishes to acknowledge a University of Victoria Scholarship.

1. Gmelin Handbuch der Anorganische Chemie, Kobalt, Teil B. Verlag Chemie, Weinheim. 1930.
2. C. S. Garner and D. A. House. Transition metal chemistry. Vol. 6. *Edited by* R. L. Carlin. Marcel Dekker Inc., New York. 1970. p. 59.
3. R. S. Nyholm and M. L. Tobe. J. Chem. Soc. 1707 (1956).
4. M. L. Tobe. J. Chem. Soc. 3776 (1959).
5. D. A. Buckingham, I. I. Olsen, and A. M. Sargeson. J. Am. Chem. Soc. **90**, 6654 (1968).
6. D. A. Buckingham, I. I. Creaser, W. Marty, and A. M. Sargeson. Inorg. Chem. **11**, 2738 (1972).
7. A. D. Kirk and T. L. Kelly. Inorg. Chem. **13**, 1613 (1974).
8. M. N. Hughes and W. R. McWhinnie. J. Chem. Soc. A, 592 (1967).
9. G. Wirth, C. Bifano, R. T. Walters, and R. G. Linck. Inorg. Chem. **12**, 1955 (1973).
10. W. W. Fee, J. N. Mac. B. Harrowfield, and W. G. Jackson. J. Chem. Soc. A, 2612 (1970).
11. L. P. Quinn and C. S. Garner. Inorg. Chem. **3**, 1348 (1964).
12. E. Zinato, R. Lindholm, and A. W. Adamson. J. Inorg. Chem. **31**, 449 (1969).
13. C. Wong and A. D. Kirk. Can. J. Chem. **53**, 419 (1975).
14. P. Riccieri and H. L. Schläfer. Inorg. Chem. **9**, 727 (1970).

Can. J. Chem. Downloaded from www.nrcresearchpress.com by 210.87.254.5 on 09/05/12
For personal use only.

Infrared Spectra of the Ammonium Ion in Crystals. II. The Ammonium Ion in Trigonal Environments, with a Consideration of Hydrogen Bonding[1,2]

IAN A. OXTON AND OSVALD KNOP

Department of Chemistry, Dalhousie University, Halifax, Nova Scotia B3H 4J3

AND

MICHAEL FALK

Atlantic Regional Laboratory, National Research Council of Canada, Halifax, Nova Scotia B3H 3Z1

Received June 26, 1975

IAN A. OXTON, OSVALD KNOP, and MICHAEL FALK. Can. J. Chem. **53**, 3394 (1975).

Infrared spectra of polycrystalline $(NH_4)_2GeF_6$, β-$(NH_4)_2SiF_6$, and $(NH_4)_2Pb(SO_4)_2$ have been recorded at room and liquid-nitrogen temperatures. The N—D stretching and bending fundamentals of the isotopically dilute NH_3D^+ ion in these compounds have been studied with particular attention. The occurrence of N—D stretching doublets and bending triplets, of approximate intensity ratios 1:3 and 2:3:3 respectively, confirms the C_{3v} symmetry of the ammonium ion and suggests that the isotopic dilution technique will prove useful as a diagnostic tool for ascertaining site symmetries of the ammonium ion. The spectra are consistent with non-rotating ammonium ions. The frequencies of dilute NH_3D^+ ions suggest that for the ammonium ion in $(NH_4)_2Pb(SO_4)_2$ a trifurcated hydrogen bond is stronger than a normal hydrogen bond.

IAN A. OXTON, OSVALD KNOP et MICHAEL FALK. Can. J. Chem. **53**, 3394 (1975).

On a enregistré les spectres infrarouge des $(NH_4)_2GeF_6$, β-$(NH_4)_2SiF_6$ et $(NH_4)_2Pb(SO_4)_2$ polycristallins à températures de la pièce et de l'azote liquide. Dans ces composés on a étudié avec une attention particulière les vibrations fondamentales de valence et de déformation de l'ion NH_3D^+ isotopiquement dilué. La présence de *deux* bandes N—D de valence, dans des proportions relatives 1:3, et de *trois* bandes de déformation, dans des proportions relatives 2:3:3, dans les spectres confirme que l'ion ammonium existe dans la symétrie C_{3v}. Cette charactéristique laisse prévoir l'utilisation de la dilution isotopique comme moyen diagnostique pour déterminer la symétrie de site de l'ion ammonium. Les spectres sont en accord avec l'absence de rotation libre dans l'ion NH_4^+. Les fréquences de l'ion NH_3D^+ dilué suggèrent que pour l'ion ammonium dans le $(NH_4)_2Pb(SO_4)_2$ une liaison hydrogène trifurquée est plus forte qu'une liaison hydrogène normale.

In the first paper of this series (1) we described the i.r. spectra of the partially deuterated ammonium ion species in $(NH_4)_2PtCl_6$ and $(NH_4)_2TeCl_6$, at sites of tetrahedral symmetry. The present paper is concerned with the spectroscopic behavior of the ammonium ion in trigonal surroundings, more precisely at sites of C_{3v} symmetry, and with the manifestations of hydrogen bonding in the spectra of the isotopically isolated NH_3D^+ ion in such situations.

The first systematic criterion for the presence of hydrogen bonding in ammonium salts was advanced by Waddington (2), who suggested that the appearance of the combination band $\nu_4 + \nu_6$ in the i.r. spectrum, where ν_6 is a librational mode, indicated the presence of hydrogen bonding. Waddington also considered that the existence of K or Rb isomorphs of a particular ammonium salt was indicative of the absence of hydrogen bonding in that salt. The validity of this latter criterion has been questioned (3). For example, cubic $(NH_4)_2SiF_6$ has K, Rb, and even Cs isomorphs (4), yet it has been reported to contain hydrogen bonds (5). Mathieu and Poulet (6) have discussed the problem of hydrogen bonding in ammonium salts in terms of the lowering of the N—H stretching frequencies from their hypothetical "free ion" values but introduced no new criteria. In a study of the vibrational spectra of a series of complex ammonium halides Dunsmuir and Lane (3) re-examined Waddington's criteria and recommended the detection of hydrogen bonding in such compounds by (*i*) the observation of *both* $\nu_4 + \nu_6$ and $\nu_2 + \nu_6$ in the i.r. spectrum; (*ii*)

[1]For Part I, see ref. 1.

[2]NRCC No. 14881.

Can. J. Chem. Downloaded from www.nrcresearchpress.com by 210.87.254.105 on 09/05/12
For personal use only.

Can. J. Chem. Downloaded from www.nrcresearchpress.com by 210.87.254.105 on 09/05/12
For personal use only.

the broadening of lattice-mode absorptions; and (*iii*) the frequency of ν_4. They also suggested that the converse of Waddington's second rule might be true, *viz.* where the NH_4 salt is *not* isomorphous with the K and Rb analogs, the dissimilarity of the crystal structure of the ammonium salt is likely to be the result of hydrogen bonding.

In the present study we have examined examples of trigonally coordinated ammonium ions with reference to some of the criteria of hydrogen bonding. The term hydrogen bonding, as applied in the following to the ammonium ion, shall include all factors which restrict rotation of the ion to torsional oscillations.

Infrared spectra of undeuterated, or fully deuterated, ammonium salts have proved intractable for such purposes as the diagnosis of site symmetries of the ammonium ion (for discussion, see ref. 1). The i.r. spectra of isotopically dilute NH_3D^+, on the other hand, have been found to yield considerable information even for high site symmetry (T_d, ref. 1), and it was hoped that this would also prove to be the case in environments of lower symmetry. We have also attempted to correlate the i.r. spectra of isotopically dilute NH_3D^+ ions with the known structural features of the compounds studied.

Consider the simplest case of a trigonally distorted NH_4^+ ion, *i.e.* an ion of symmetry C_{3v} held in a fixed orientation by hydrogen bonds to four acceptor atoms. Suppose one of the H atoms is exchanged for a D atom. The four equally probable orientations of the NH_3D^+ ion will produce two distinguishable configurations, with an abundance ratio of 1:3. We will refer to these as *axial* (*a*-NH_3D^+, of symmetry C_{3v}) and *non-axial* (*n*-NH_3D^+, of symmetry C_s). Consequently, at low deuteration, two $\nu_1(NH_3D^+)$ bands should appear. The separation of this doublet should be a measure of the difference in the hydrogen bonding of the on-axis and off-axis H atoms. If this difference is small, the doublet would be expected to exhibit integrated intensities in the approximate ratio 1:3. Prediction of the expected absorptions in the bending region of NH_3D^+ follows a similar argument. Absorptions arising from *a*-NH_3D^+ will be qualitatively similar to those of a NH_3D^+ ion at a site of tetrahedral symmetry (1), whilst those arising from *n*-NH_3D^+ will be as expected from Table 1. Thus for a bending mode such as

TABLE 1. Correlation of vibrational modes for axial and non-axial NH_3D^+ ions at sites of C_{3v} symmetry*

Mode of "free" NH_3D^+	Axial (*a*) NH_3D^+	Non-axial (*n*) NH_3D^+
$\nu_1(a_1)$	$\nu_1(a_1)$	$\nu_1(a')$
$\nu_2(e)$	$\nu_2(e)$	$\nu_{2a}(a') + \nu_{2b}(a'')$
$\nu_{3a}(a_1)$	$\nu_{3a}(a_1)$	$\nu_{3a}(a')$
$\nu_{3bc}(e)$	$\nu_{3bc}(e)$	$\nu_{3b}(a') + \nu_{3c}(a'')$
$\nu_{4a}(a_1)$	$\nu_{4a}(a_1)$	$\nu_{4a}(a')$
$\nu_{4bc}(e)$	$\nu_{4bc}(e)$	$\nu_{4b}(a') + \nu_{4c}(a'')$

*Designation of fundamental modes as in Herzberg (7) and ref. 1.

$\nu_{4bc}(NH_3D^+)$ we may expect three bands in the approximate intensity ratio of 2:3:3.

In contrast, the spectrum of a *freely rotating* NH_3D^+ ion should be qualitatively similar to that of an NH_3D^+ ion at a site of full tetrahedral symmetry (1). Absorption arising from $\nu_1(NH_3D^+)$ should then consist of a single band, probably broadened by unresolved rotational fine structure.

In the intermediate case of an NH_3D^+ ion which undergoes frequent reorientation but does not rotate freely, the spectrum would be qualitatively similar to that of the non-rotating ion. At high rates of reorientation the absorption bands would be broadened by the short lifetime of the upper vibrational state.

Choice of Test Compounds

Our first choice was β-$(NH_4)_2SiF_6$. This is an example *par excellence* of a compound containing trigonally coordinated ammonium ions: all ammonium ions in the structure are equivalent and located at sites of C_{3v} symmetry (Table 2). However, we did not succeed in obtaining spectra completely free from bands of the cubic α-$(NH_4)_2SiF_6$ (see Results).[3] Even though these parasitic bands were uniquely identifiable by comparison with the spectra of the pure α form, we decided to use as our main example $(NH_4)_2GeF_6$, which is isostructural with β-$(NH_4)_2SiF_6$ (Table 2) and gives clean i.r. spectra.

In β-$(NH_4)_2SiF_6$ and $(NH_4)_2GeF_6$, an ammonium ion has 12 nearest F neighbors arranged in four triangles: three isosceles, related by the threefold axis containing the N atom, and one equilateral, with the threefold axis as its own symmetry axis (Fig. 1). If the NH_4^+ ion were

[3]Both forms of $(NH_4)_2SiF_6$ occur in nature, α as the mineral *cryptohalite*, β as the mineral *bararite*.

Can. J. Chem. Downloaded from www.nrcresearchpress.com by 210.87.254.105 on 09/05/12
For personal use only.

TABLE 2. Crystallographic data for the compounds

Atom	Equipoint	Site symmetry	x	y	z
		β-$(NH_4)_2SiF_6$, $P\bar{3}m1$ (No. 164) (8)*			
Si	1(*a*)	$\bar{3}m$–D_{3d}	0	0	0
N	2(*d*)	$3m$–C_{3v}	1/3	2/3	0.670
F	6(*i*)	m–C_s	0.139	−0.139	0.201
		$(NH_4)_2GeF_6$, $P\bar{3}m1$ (No. 164) (9)†			
Ge	1(*a*)	$\bar{3}m$–D_{3d}	0	0	0
N	2(*d*)	$3m$–C_{3v}	1/3	2/3	0.695(15)
F	6(*i*)	m–C_s	0.143	−0.143	0.220
		$(NH_4)_2Pb(SO_4)_2$, $R\bar{3}m$ (No. 166) (10)‡			
Pb	3(*a*)	$\bar{3}m$–D_{3d}	0	0	0
N	6(*c*)	$3m$–C_{3v}	0	0	0.200
S	6(*c*)	$3m$–C_{3v}	0	0	0.394
O(1)	6(*c*)	$3m$–C_{3v}	0	0	0.325
O(2)	18(*h*)	m–C_s	0.820	−0.820	0.083

*a_0 = 5.784(5) Å, c_0 = 4.796(6) Å (8).
†a_0 = 5.86 Å, c_0 = 4.79 Å (9) (converted from kX); a_0 = 5.862 Å, c_0 = 4.817 Å (11).
‡a_0 = 5.58(1) Å, c_0 = 21.84(5) Å (10).

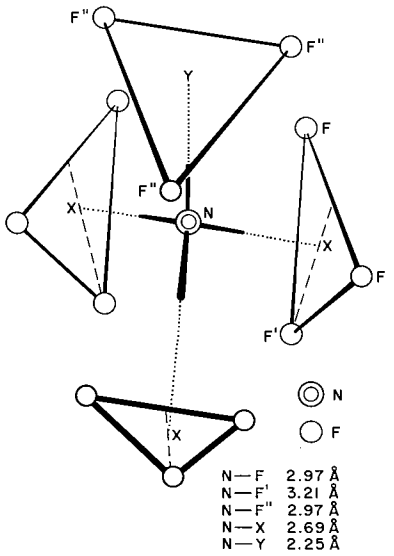

FIG. 1. The fluorine environment of an ammonium ion in β-$(NH_4)_2SiF_6$ and $(NH_4)_2GeF_6$. The nitrogen atom and point Y lie on a threefold axis. The interatomic distances shown are for the silicate (*cf.* footnote 4).

rigid and at rest, the *on-axis* N—H vector would most likely point to the center of the equilateral triangle, Y. If in addition the ion preserved the *internal* T_d symmetry, the three *off-axis* N—H vectors would most likely point to positions X on the symmetry axes of the isosceles triangles, somewhat below the center of gravity of the triangles. In the silicate the N—X distance is 2.69 Å and the N—Y distance is 2.25 Å. The uncertainties in the corresponding distances in the germanate, as calculated from the data of refs. 9 and 11, are so large that no distinction can be made in this respect between the β form of the silicate and the germanate at present. With the N—H vectors pointing towards X and Y all four H atoms may be considered as forming trifurcated hydrogen bonds. The fluorine environment of an NH_4^+ ion in β-$(NH_4)_2SiF_6$ and in $(NH_4)_2GeF_6$ is topologically equivalent to that in the cubic α-$(NH_4)_2SiF_6$, in which the ion is at a site of symmetry T_d; Fig. 1 of ref. 1 shows the analogous Cl environment in $(NH_4)_2PtCl_6$, which is isostructural with α-$(NH_4)_2SiF_6$.

In the third compound chosen, $(NH_4)_2Pb(SO_4)_2$, the ammonium ions again are all equivalent and in sites of symmetry C_{3v} (Table 2). However, out of the ten nearest oxygen neighbors of an ammonium ion, nine, O(2), are arranged in three isosceles triangles related by the threefold axis containing the N atoms, and the tenth, O(1), is on the threefold axis (Fig. 2). The N—O(1) distance would thus correspond to a "normal", *i.e.* straight, hydrogen bond, while the three N—X distances, along the N—H vectors of the rigid tetrahedral NH_4^+ ion, would correspond to trifurcated hydrogen bonds.

Experimental

The low-deuterium samples of $(NH_4)_2GeF_6$ were obtained from commercial material (Alfa Chemicals) by

TABLE 3. Infrared frequencies of isotopically dilute NH_3D^+ in $(NH_4)_2GeF_6$, β-$(NH_4)_2SiF_6$, and $(NH_4)_2Pb(SO_4)_2$ at liquid-nitrogen temperature

Assignment*	Frequency (cm^{-1})		
	$(NH_4)_2GeF_6$	β-$(NH_4)_2SiF_6$†	$(NH_4)_2Pb(SO_4)_2$
$2\nu_{4bc}(a)$, $2\nu_{4b}(n)$, $2\nu_{4c}(n)$	2513	2510, 2550	2436
$\nu_1(a)$	2419.5	2425	2311.5
$\nu_1(n)$	2411.5	2413.5	2290.5
$\nu_{4bc}(a)$	1266.1	1275.3 sh	1271.6
$\nu_{4b}(n)$, $\nu_{4c}(n)$	1272.9, 1258.9	1278.2, 1256.8	1286.1, 1262.0

*a, NH_3D^+ in axial orientation; n, in non-axial orientation.
†The spectrum of β-$(NH_4)_2SiF_6$(1% D) contained two bands, at 2437 and 1262.1 cm^{-1}, arising from an α-$(NH_4)_2SiF_6$ impurity (see text). In the spectrum of pure α-$(NH_4)_2SiF_6$ these bands appear at 2437 and 1261.3 cm^{-1} respectively (13).

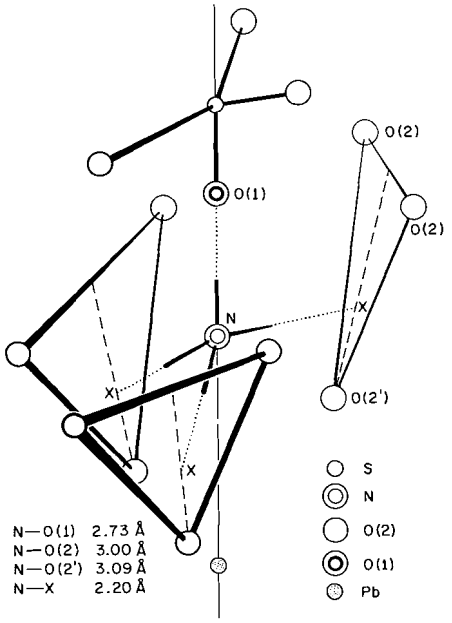

FIG. 2. The oxygen environment of an ammonium ion in $(NH_4)_2Pb(SO_4)_2$. The threefold axis which passes through the nitrogen atom is indicated as a thin solid line.

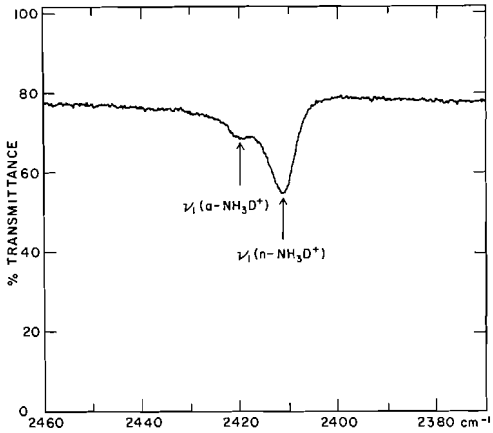

FIG. 3. The N—D stretching region of the i.r. spectrum of $(NH_4)_2GeF_6$(1% D) measured at liquid-nitrogen temperature.

recrystallization from dilute HF containing 1% D. Samples of the trigonal β-$(NH_4)_2SiF_6$ were prepared by recrystallizing cubic α-$(NH_4)_2SiF_6$ at 3 °C from water containing 1% D. $(NH_4)_2Pb(SO_4)_2$ was prepared as in ref. 10, as was the sample of low D content.

Spectra were recorded at room temperature and liquid-nitrogen temperature as Nujol mulls on a Perkin–Elmer model 180 spectrophotometer thoroughly purged with dry air. Frequencies are believed to be accurate to ± 0.5 cm^{-1}.

Results

The observed vibrational frequencies of the NH_3D^+ ion isotopically isolated in $(NH_4)_2GeF_6$, β-$(NH_4)_2SiF_6$, and $(NH_4)_2Pb(SO_4)_2$, at liquid-nitrogen temperature, are shown in Table 3. The corresponding room-temperature frequencies could not be determined with any accuracy, as has previously been found to be the case with $(NH_4)_2PtCl_6$ (1).

Two sharp bands are present in the N—D stretching region of the i.r. spectrum of isotopically dilute NH_3D^+ in $(NH_4)_2GeF_6$ (Fig. 3). Unfortunately their frequency separation, 8 cm^{-1}, is small compared to their half-widths and an accurate estimate of their relative intensities is not possible. The more intense band is assigned to $\nu_1(n\text{-}NH_3D^+)$ and the weaker band, to $\nu_1(a\text{-}NH_3D^+)$. The 1300 to 1220 cm^{-1} region of the spectrum (Fig. 4), in which we expect to observe bands due to $\nu_{4bc}(NH_3D^+)$ (1, 12), contains three bands. The highest- and lowest-fre-

Can. J. Chem. Downloaded from www.nrcresearchpress.com by 210.87.254.105 on 09/05/12
For personal use only.

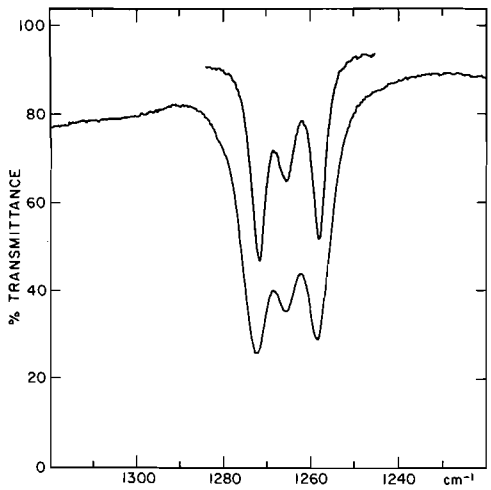

FIG. 4. The N—D bending region of the i.r. spectrum of $(NH_4)_2GeF_6$(1% D) measured at liquid-nitrogen temperature.

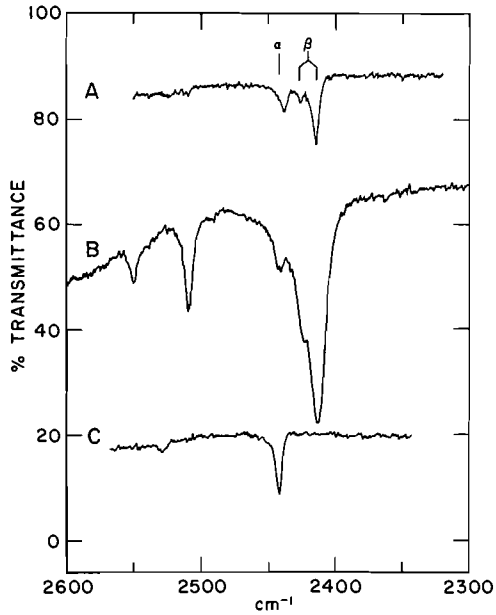

FIG. 5. The N—D stretching region of the i.r. spectrum of $(NH_4)_2SiF_6$(1% D) measured at liquid-nitrogen temperature. Spectra *A* and *B* refer to the β-form contaminated with different concentrations of the α-form. Spectrum *C* is that of the pure α-form.

quency bands are of approximately equal intensity, whilst the central band is of lower intensity. We thus assign the central band to $\nu_{4bc}(a\text{-}NH_3D^+)$.

The corresponding regions of the spectrum of β-$(NH_4)_2SiF_6$(1% D) are found to be similar, with the addition of a weak band in each region. It was, however, noted that the frequencies of the extra bands were very close to those of the corresponding modes in α-$(NH_4)_2SiF_6$(1% D) (13). The relative intensities of the extra bands varied with the amount of grinding during mull preparation, and it was concluded that grinding induced the β-to-α phase change in a small quantity of the material. Subsequently it was found that even the gentlest grinding introduced a small amount of the cubic impurity and that complete elimination of the extraneous bands could not be effected. The N—D stretching regions of the i.r. spectra of cubic and trigonal $(NH_4)_2SiF_6$(1% D) are shown in Fig. 5.

The bands arising from $\nu_1(NH_3D^+)$ of $a\text{-}NH_3D^+$ and $n\text{-}NH_3D^+$ in $(NH_4)_2Pb(SO_4)_2$-(1% D) were the best-resolved of the examples chosen, with a separation of 21.0 cm^{-1}, and the relative intensities of these bands were in the ratio (2.9 ± 0.2):1 (Fig. 6). Three bands were present in the 1300 to 1220 cm^{-1} region. They were assigned by analogy with those of the hexafluorogermanate.

In order to apply to these salts the criterion

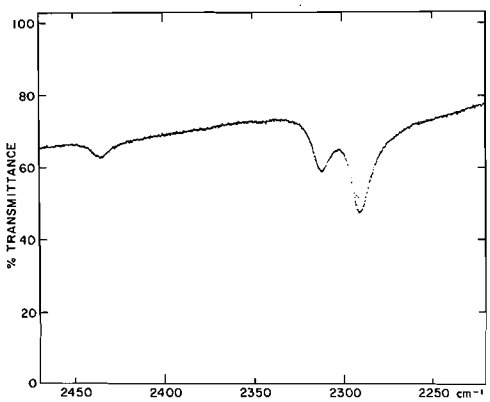

FIG. 6. The N—D stretching region of the i.r. spectrum of $(NH_4)_2Pb(SO_4)_2$(1% D) measured at liquid-nitrogen temperature.

of Waddington (2, 3), the i.r. spectra of the undeuterated salts were examined for the presence of bands attributable to combination modes involving the librational mode ν_6. The vibrational frequencies of these bands, where observed, are listed in Table 4. The observed frequencies were practically independent of temperature.

Can. J. Chem. Downloaded from www.nrcresearchpress.com by 210.87.254.105 on 09/05/12
For personal use only.

Can. J. Chem. Downloaded from www.nrcresearchpress.com by 210.87.254.105 on 09/05/12
For personal use only.

TABLE 4. Infrared frequencies of combination modes involving the torsional mode ν_6 of NH_4^+ at room and liquid-nitrogen temperatures

Compound	Frequency (cm^{-1})	
	$\nu_2 + \nu_6$	$\nu_4 + \nu_6$
$(NH_4)_2GeF_6$	—	1730
β-$(NH_4)_2SiF_6$	—	1730
$(NH_4)_2Pb(SO_4)_2$	2150–2000*	1780

*$2\nu_3$ of the sulfate ion also occurs in this region.

Discussion

The i.r. spectra of the NH_3D^+ ion in the trigonal environments investigated in this work are in good agreement with the spectrum predicted, in the introduction, for the hypothetic H-bonded ion of C_{3v} symmetry. We shall now consider the possible rotational motions of the ammonium ion in the three compounds.

The i.r. spectra of isolated NH_3D^+ ions are not consistent with a freely rotating ammonium ion in any of the three cases: a *freely* rotating ion would yield a single ν_1 frequency, the four H atoms being equivalent. The presence of two distinct $\nu_1(NH_3D^+)$ bands in the low-temperature spectra does not rule out the possibility of free rotation about one hydrogen bond, of the type suggested to occur in the high-temperature form (phase *I*, CsCl type) of ammonium iodide (14–16).[4] However, the frequency differences $\nu_1(a\text{-}NH_3D^+) - \nu_1(n\text{-}NH_3D^+)$ for $(NH_4)_2GeF_6$, β-$(NH_4)_2SiF_6$, and $(NH_4)_2Pb(SO_4)_2$ are 8.0, 11.5, and 21.0 cm^{-1}, respectively (Table 3) and thus only a small fraction of the total range, 135 cm^{-1}, of isolated N—D stretching frequencies encountered in these compounds. It thus appears that the environments of the axial and non-axial H atoms *within* each compound are sufficiently similar to preclude the possibility of free rotation about a preferred single axis. The comparable half-widths of the $\nu_1(a)$ and $\nu_1(n)$ bands in each compound rule out the possibility of rapid reorientation about the threefold axis.

The existence of *two* $\nu_1(NH_3D^+)$ frequencies and the occurrence of i.r. bands arising from combination modes involving ν_6 are evidence that in the three cases considered the ammonium ions are fixed in position at their lattice sites and that, *at least during the life-time of a vibrationally excited state*, the only rotational motions are librational.

The structural features (Fig. 1) suggest that the orientation of the NH_4^+ ion in $(NH_4)_2GeF_6$ and β-$(NH_4)_2SiF_6$ is maintained by four trifurcated hydrogen bonds, three of which are equivalent and the fourth involving a distance N—*Y* shorter than N—*X*. If N—*X* and N—*Y* measure the length of a trifurcated hydrogen bond, and if it is assumed that this "effective" length is the dominant factor affecting the $\nu_1(NH_3D^+)$ frequency, $\nu_1(a\text{-}NH_3D^+)$ would be expected to occur at a lower frequency than $\nu_1(n\text{-}NH_3D^+)$. Although two bands arising from $\nu_1(NH_3D^+)$ are observed for each compound, in approximately the expected intensity ratio, the order of frequency is the reverse of the expectation. This indicates that other factors exist which influence the strength of the N—H...F bond, at least as important as the "effective" length. We intend to discuss the apparent anomalies found for these two compounds more fully when we have accumulated ampler experimental evidence from other ammonium compounds.

In $(NH_4)_2Pb(SO_4)_2$ the oxygen closest to the nitrogen is the O(1) on the threefold axis (Fig. 2). From the $\nu_1(NH_3D^+)$ frequencies for the sulfate, however, it is apparent that the stronger hydrogen bonds are formed by the off-axis H atoms, hence a trifurcated hydrogen bond is stronger than a normal bond when the acceptor atoms are situated at comparable distances from the nitrogen.

The importance of this conclusion to the structural role of the ammonium ion in crystals is illustrated by Khan and Baur's (18) observation that out of thirty ammonium oxo-salts they reviewed only six contained the ion in approximately tetrahedral, fourfold coordination, *i.e.* capable of forming nearly straight N—H...O contacts. With the exception of the cubic phases of the ammonium halides, the straight H bond, as found in the structure of $(NH_4)_2Pb(SO_4)_2$, appears to be something of a rarity. It would seem that any meaningful correlation of N—H stretching frequency (or isolated $\nu_1(NH_3D^+)$ frequency in the approach adopted here) and N—H...*X* distance would require the separate

[4]Recent re-interpretation of Levy and Peterson's (14) neutron-diffraction intensities of phase *I* of ND_4Br by Press (17) supports the existence of a librational motion of the ND_4^+ ion rather than free rotation about a single axis.

Can. J. Chem. Downloaded from www.nrcresearchpress.com by 210.87.254.105 on 09/05/12
For personal use only.

consideration of each type of H bond, *i.e.* separate correlations for normal, bifurcated etc. H bonds.

We may now apply the criteria suggested at the beginning of this paper to the three examples studied.

$(NH_4)_2GeF_6$ is isomorphous with the corresponding K and Rb salts (19). This observation would suggest, on Waddington's idea (2), that no H bonding exists in its structure. A band corresponding to $\nu_4 + \nu_6$ is, however, observed in the i.r. spectrum of the hexafluorogermanate. Previous authors (2, 3) are in agreement that the appearance of this combination band confirms the presence of H bonding. The spectral data from isolated NH_3D^+ in $(NH_4)_2GeF_6$ support that conclusion.

K and Rb analogs of β-$(NH_4)_2SiF_6$ have not been reported and may not exist under normal circumstances. A band arising from the combination mode $\nu_4 + \nu_6$ is found in the i.r. spectrum of the ammonium compound at room temperature. This example thus appears to bear out Dunsmuir and Lane's (3) suggestion that any departure by the ammonium salt from the structure of the K and Rb analogs might be attributed to the presence of H bonding in the ammonium salt. This conclusion is supported by the isotopically dilute NH_3D^+ spectra of β-$(NH_4)_2SiF_6$.

The double sulfates $M_2Pb(SO_4)_2$ (M = K, Rb, NH_4) form an isomorphous series (4), which would suggest, on Waddington's criterion, the absence of H bonding. Infrared bands are, however, found corresponding to the combination modes $\nu_4 + \nu_6$ *and* $\nu_2 + \nu_6$ in the room-temperature spectrum of the ammonium compound. This provides evidence in favor of a H-bonded ammonium ion. The isolated $\nu_1(NH_3D^+)$ results presented above confirm the existence of H bonding; in addition, they lead to indications of the relative strengths of the H bonds present in the sulfate structure.

Summary

The i.r. spectra of isotopically dilute NH_3D^+ ions at crystal sites of C_{3v} symmetry in $(NH_4)_2GeF_6$, β-$(NH_4)_2SiF_6$, and $(NH_4)_2Pb(SO_4)_2$ at liquid-nitrogen temperature, have been shown to be consistent with non-rotating ammonium ions. This conclusion is in agreement with the observation of at least one band, in the i.r. spectrum of each compound, which may be assigned to a combination mode involving the libration ν_6.

The results of this study demonstrate the usefulness of isotopically dilute NH_3D^+ ions as a diagnostic tool for the spectroscopic recognition of trigonal site symmetry of ammonium ions in crystal structures. For the site symmetries C_{3v} and C_3 the orientation of the ammonium ion is uniquely determined, while for the other trigonal site symmetries (D_{3h}, D_{3d}, D_3, C_{3h}, C_{3i}) orientational disorder may occur. The spectra of isolated NH_3D^+ provide for a ready investigation of the rotational behavior of ammonium ions in crystals and for a more reliable detection of H bonding in ammonium salts than has been proposed previously.

This investigation was supported by the National Research Council of Canada through a grant-in-aid of research to one of us (O.K.).

1. I. A. Oxton, O. Knop, and M. Falk. Can. J. Chem. **53**, 2675 (1975).
2. T. C. Waddington. J. Chem. Soc. 4340 (1958).
3. J. T. R. Dunsmuir and A. P. Lane. Spectrochim. Acta, **28A**, 45 (1970).
4. R. W. G. Wyckoff. Crystal structures. Vol. 3. 2nd ed. Interscience, New York. 1965.
5. E. O. Schlemper, W. C. Hamilton, and J. J. Rush. J. Chem. Phys. **44**, 2499 (1966).
6. J.-P. Mathieu and H. Poulet. Spectrochim. Acta, **16**, 696 (1960).
7. G. Herzberg. Infrared and Raman spectra of polyatomic molecules. Van Nostrand, New York. 1945. p. 238.
8. E. O. Schlemper and W. C. Hamilton. J. Chem. Phys. **45**, 408 (1966).
9. J. L. Hoard and W. B. Vincent. J. Am. Chem. Soc. **61**, 2849 (1939).
10. C. Knakkergaard Møller. Acta Chem. Scand. **8**, 81 (1954).
11. H. E. Swanson, N. T. Gilfrich, and M. I. Cook. U.S. Natl. Bur. Stand. Circ. 539, **6**, 8 (1956).
12. L. L. Oden and J. C. Decius. Spectrochim. Acta, **20**, 667 (1964).
13. I. A. Oxton. Unpublished results.
14. H. A. Levy and S. W. Peterson. J. Am. Chem. Soc. **75**, 1536 (1953).
15. H. A. Levy and S. W. Peterson. J. Chem. Phys. **21**, 366 (1953).
16. R. C. Plumb and D. F. Hornig. J. Chem. Phys. **21**, 366 (1953).
17. W. Press. Acta Cryst. A**29**, 257 (1973).
18. A. A. Khan and W. Baur. Acta Cryst. B**28**, 683 (1972).
19. H. Bode and R. Brockmann. Z. Anorg. Allg. Chem. **269**, 173 (1952).

Group VI Metal Carbonyl Derivatives of *cis*-$(CH_3)_2AsC(CF_3)=C(CF_3)As(CH_3)_2$

WILLIAM R. CULLEN AND LYNN MIHICHUK

Chemistry Department, University of British Columbia, Vancouver, British Columbia V6T 1W5

Received June 16, 1975

WILLIAM R. CULLEN and LYNN MIHICHUK. Can. J. Chem. **53**, 3401 (1975).

The carbonyls $M(CO)_6$ (M = Cr, Mo, W) react with *cis*-$(CH_3)_2AsC(CF_3)=C(CF_3)As(CH_3)_2$ (L—L) to give the chelate derivatives (L—L)$M(CO)_4$. These react with excess (L—L) on ultraviolet irradiation affording *cis*-(L—L)$_2M(CO)_2$ and *trans*-(L—L)$_2M(CO)_2$ and two isomers of *fac*-(L—L)$_2M(CO)_3$ where one (L—L) is acting as a monodentate ligand, and is either the *cis* ligand or its *trans* isomer.

WILLIAM R. CULLEN et LYNN MIHICHUK. Can. J. Chem. **53**, 3401 (1975).

Les carbonyles $M(CO)_6$ (M = Cr, Mo, W) réagissent avec le $(CH_3)_2AsC(CF_3)=C(CF_3)As(CH_3)_2$-*cis* (L—L) pour conduire aux chélates (L—L)$M(CO)_4$. Par irradiation u.v., ces derniers réagissent avec un excès de L—L pour fournir (L—L)$_2M(CO)_2$-*cis* et (L—L)$_2M(CO)_2$-*trans* et deux isomères du (L—L)$_2M(CO)_3$-*fac* où un (L—L) agit comme ligand monodentate; il est soit le ligand-*cis* ou son isomère-*trans*.

[Traduit par le journal]

Although chelate derivatives of the Group VI hexacarbonyls of formula (bidentate)$M(CO)_4$ are well known (M = Cr, Mo, W; bidentate is a ligand such as diphos, $(C_6H_5)_2PCH_2CH_2P(C_6H_5)_2$ which contains two Group V donor atoms), there is a surprising lack of knowledge about derivatives of the type (bidentate)$_2M(CO)_2$ and (bidentate)$_2M(CO)_3$ (1–3). In the latter case one ligand is coordinated by only one of the two potential donor atoms.

The ligand *cis*-$(CH_3)_2AsC(CF_3)=C(CF_3)As(CH_3)_2$ (L—L) is readily available from the reaction of tetramethyldiarsine with hexafluoro-2-butyne (4) and is closely related to the versatile $f_4$fars, $(CH_3)_2AsC=CAs(CH_3)_2CF_2CF_2$ (5). The 'bite' of (L—L) is expected to be less than that of $f_4$fars and so the former should tend to form chelate complexes rather than the bridged derivatives such as $f_4farsFe_3(CO)_{10}$ (6–8) characteristic of the fluoroalicylic-bridged ligand.

The present paper is concerned with a study of the reactions of L—L with the Group VI hexacarbonyls.

TABLE 1. Analytical data for (L—L) derivatives of $M(CO)_6$

Compound*	Color	Melting point (°C)	C (%)		H (%)	
			Calculated	Found	Calculated	Found
(L—L)$Cr(CO)_4$	Amber	138–140	26.87	26.80	2.24	2.30
(L—L)$Mo(CO)_4$	Yellow	141–143	24.83	25.08	2.07	2.20
(L—L)$W(CO)_4$	Yellow	155–157	21.56	21.76	1.80	1.95
fac-(L—L)^b(L-L)$_c{}^m$Cr(CO)$_3$	Pale orange	150–155†	25.91	25.98	2.73	2.91
fac-(L—L)^b(L-L)$_t{}^m$Cr(CO)$_3$	Orange	115–118	25.91	25.60	2.73	2.79
cis-(L—L)$_2$Cr(CO)$_2$	Brown-red	168–170	25.35	25.50	2.82	3.00
trans-(L—L)$_2$Cr(CO)$_2$	Brown-red	141–143	25.35	25.21	2.82	3.02
fac-(L—L)^b(L-L)$_c{}^m$Mo(CO)$_3$	Yellow	167–170†	24.67	24.45	2.60	2.72
fac-(L—L)^b(L-L)$_t{}^m$Mo(CO)$_3$	Orange	118–120	24.67	24.66	2.60	2.81
cis-(L—L)$_2$Mo(CO)$_2$	Orange	160–162	24.11	24.33	2.68	2.76
trans-(L—L)$_2$Mo(CO)$_2$	Orange	152–154	24.11	24.28	2.68	2.86
fac-(L—L)^b(L-L)$_c{}^m$W(CO)$_3$	Yellow	168–170†	22.53	22.30	2.37	2.31
fac-(L—L)^b(L-L)$_t{}^m$W(CO)$_3$	Orange	136–137	22.53	22.43	2.37	2.55
cis-(L—L)$_2$W(CO)$_2$	Red-orange	177–179	21.95	21.70	2.44	2.61

*The subscripts *c* and *t* are abbreviations for *cis* and *trans*.
†Complex melted with decomposition.

Can. J. Chem. Downloaded from www.nrcresearchpress.com by 210.87.254.105 on 09/05/12
For personal use only.

Can. J. Chem. Downloaded from www.nrcresearchpress.com by 210.87.254.105 on 09/05/12
For personal use only.

TABLE 2. Reactions of (L—L)$M(CO)_4$ and $M(CO)_6$ with excess (L—L)

Carbonyl	(L—L)	Conditions	Products*	Yield	Purification†
$Cr(CO)_6$ 0.2 g, 0.90 mmol	0.82 g, 2.2 mmol	Pyrolysis in benzene (15 ml) at 195 °C for 22 h	(L—L)$Cr(CO)_4$	70%	C (1)
(L—L)$Cr(CO)_4$ 0.3 g, 0.56 mmol	0.82 g, 2.2 mmol	Pyrolysis in benzene (15 ml) at 190 °C for 46 h	(L—L)$Cr(CO)_4$ *cis*-(L—L)$_2Cr(CO)_2$	0.060 g Trace	C (1) C (2)
(L—L)$Cr(CO)_4$ 1.2 g, 2.2 mmol	4.5 g, 12.0 mmol	Ultraviolet irradiation (450 W) in benzene (350 ml) for 85 min	(L—L)$Cr(CO)_4$ *cis*-(L—L)$_2Cr(CO)_2$ *fac*-(L—L)^b(L—L)$_c{}^mCr(CO)_3$ *fac*-(L—L)^b(L—L)$_t{}^mCr(CO)_3$	Trace 32% 3% Trace	C (1) C (2) C (4) C (3)
(L—L)$Cr(CO)_4$ 0.6 g, 1.1 mmol	2.3 g, 6 mmol	Ultraviolet irradiation (450 W) in benzene (350 ml) for 20 min	(L—L)$Cr(CO)_4$ *cis*-(L—L)$_2Cr(CO)_2$ *fac*-(L—L)^b(L—L)$_c{}^mCr(CO)_3$ *fac*-(L—L)^b(L—L)$_t{}^mCr(CO)_3$	0.030 g 26% 9% Trace	C (1) C (2) C (4) C (3)
$Mo(CO)_6$ 0.2 g, 0.76 mmol	0.70 g, 1.88 mmol	Pyrolysis in benzene (15 ml) at 175 °C for 23 h	(L—L)$Mo(CO)_4$ *cis*-(L—L)$_2Mo(CO)_2$	46% 30%	C (1) C (2)
(L—L)$Mo(CO)_4$ 0.36 g, 0.62 mmol	0.24 g, 0.62 mmol	Pyrolysis in benzene (15 ml) at 175 °C for 20 h	(L—L)$Mo(CO)_4$ *cis*-(L—L)$_2Mo(CO)_2$	Trace 36%	C (1) C (2)
$Mo(CO)_6$ 0.4 g, 1.52 mmol	2.8 g, 7.60 mmol	Ultraviolet irradiation (200 W) in benzene (15 ml) for 266 h	(L—L)$Mo(CO)_4$ *cis*-(L—L)$_2Mo(CO)_2$ *fac*-(L—L)^b(L—L)$_c{}^mMo(CO)_3$	Trace Trace 20%	C (1) C (2) C (4)
(L—L)$Mo(CO)_4$ 1 g, 1.7 mmol	3.0 g, 8.0 mmol	Ultraviolet irradiation (450 W) in benzene (300 ml) for 65 min	*cis*-(L—L)$_2Mo(CO)_2$ *fac*-(L—L)^b(L—L)$_c{}^mMo(CO)_3$ *fac*-(L—L)^b(L—L)$_t{}^mMo(CO)_3$	26% 19% 3%	C (2) C (4) C (3)
$Mo(CO)_6$ 0.6 g, 2.3 mmol	4 g, 10.8 mmol	Ultraviolet irradiation (450 W) in benzene (350 ml) for 1.5 h	(L—L)$Mo(CO)_4$ *cis*-(L—L)$_2Mo(CO)_2$ *fac*-(L—L)^b(L—L)$_c{}^mMo(CO)_3$ *fac*-(L—L)^b(L—L)$_t{}^mMo(CO)_3$	Trace 15% 33% 3%	C (1) C (2) C (4) C (3)
$W(CO)_6$ 0.4 g, 1.1 mmol	1.0 g, 2.8 mmol	Pyrolysis in benzene (10 ml) at 185 °C for 69 h	(L—L)$W(CO)_4$	70%	C (1)
(L—L)$W(CO)_4$ 0.2 g, 0.30 mmol	0.12 g, 0.30 mmol	Pyrolysis in benzene (15 ml) at 195 °C for 66 h Pyrolysis in benzene (15 ml) at 210 °C for 48 h	(L—L)$W(CO)_4$ *cis*-(L—L)$_2W(CO)_2$ Complete decomposition	0.1 g Trace	C (1) C (2)
(L—L)$W(CO)_4$ 0.4 g, 0.6 mmol	1.1 g, 2.9 mmol	Ultraviolet irradiation (200 W) in benzene (15 ml) for 141 h	(L—L)$W(CO)_4$ *fac*-(L—L)^b(L—L)$_c{}^mW(CO)_3$	0.15 g 17%	C (1) C (4)

Can. J. Chem. Downloaded from www.nrcresearchpress.com by 210.87.254.105 on 09/05/12
For personal use only.

TABLE 2. (*Concluded*)

Carbonyl	(L—L)	Conditions	Products*	Yield	Purification†
$W(CO)_6$ 0.6 g, 1.7 mmol	2.7 g, 7.3 mmol	Ultraviolet irradiation (450 W) in benzene (350 ml) for 29 h	(L—L)$W(CO)_4$	9%	C (1)
			cis-(L—L)$_2W(CO)_2$	2%	C (2)
			fac-(L—L)^b(L—L)$_c{}^m W(CO)_3$	20%	C (4)
			fac-(L—L)^b(L—L)$_t{}^m W(CO)_3$	6%	C (3)
(L—L)$W(CO)_4$ 1 g, 1.5 mmol	2 g, 5.4 mmol	Ultraviolet irradiation (450 W) in benzene (300 ml) for 6.5 h	(L—L)$W(CO)_4$	Trace	C (1)
			cis-(L—L)$_2W(CO)_2$	10%	C (2)
			fac-(L—L)^b(L—L)$_c{}^m W(CO)_3$	13%	C (4)
			fac-(L—L)^b(L—L)$_t{}^m W(CO)_3$	2%	C (3)

*Not including excess ligand which was recovered in each experiment. Irradiation (450 W) of *cis*-(L—L)$_2Cr(CO)_2$ for 85 min gave *trans*-(L—L)$_2Cr(CO)_2$ and irradiation (450 W) of *cis*-(L—L)$_2Mo(CO)_2$ for 3.5 h gave *trans*-(L—L)$_2Mo(CO)_2$. In each case, the *trans*-isomer was recrystallized from a methylene chloride – hexane mixture at −20 °C. *cis*-(L—L)$_2W(CO)_2$ did not isomerize. (L—L)^b denotes bidentate ligand, (L—L)$_c{}^m$ denotes monodentate ligand in a *cis* configuration and (L—L)$_t{}^m$ monodentate ligand in a *trans* configuration.

†C indicates chromatography on Florisil. The arabic numeral indicates the solvent required to elute the product: (1) is 99% petroleum ether (b.p. 30–60 °C), 1% diethyl ether, (2) is 98% petroleum ether, 2% diethyl ether, (3) is 95% petroleum ether, 5% diethyl ether, (4) is 90% petroleum ether, 10% diethyl ether.

Can. J. Chem. Downloaded from www.nrcresearchpress.com by 210.87.254.105 on 09/05/12
For personal use only.

Experimental

Air-sensitive starting materials were handled in a nitrogen atmosphere. A standard vacuum system was used for the manipulation of volatile reactants. Infrared spectra were recorded on a Perkin-Elmer 457 double beam spectrophotometer and calibrated using polystyrene and cyclohexane. Nuclear magnetic resonance (n.m.r.) spectra were run on Varian T-60 and HA-100 spectrometers with chemical shifts given in p.p.m. downfield from internal TMS for ^1H spectra and upfield from internal $CFCl_3$ for ^{19}F spectra. Melting points were determined in open capillaries using a Gallenkamp melting point apparatus and are uncorrected.

Ultraviolet irradiations were performed using a 200 W Hanovia 654A-36 lamp situated 20 cm from the sealed reaction tube. The tube was continuously shaken and cooled by an air stream. In some cases irradiations were performed using a 450 W Hanovia lamp placed in a water cooled quartz jacket. This was inserted into a larger glass jacket containing the solution to be irradiated. Nitrogen was bubbled through the solution during the course of the reactions.

Microanalyses were performed by P. Borda of this department.

The Group VI metal hexacarbonyls were purchased from Strem Chemical Company and were used without further purification. The ligand *cis*-2,3-bis(dimethylarsino)-1,1,1,4,4,4-hexafluorobut-2-ene (L—L) has been previously described (4, 8).

Preparation of (L—L)M(CO)$_4$ Complexes

The following general method was used for the preparation of all new (L—L)M(CO)$_4$ complexes from the reaction of (L—L) with the Group VI hexacarbonyls.

A benzene solution (15–20 ml) containing a 1:1 mole ratio of ligand to hexacarbonyl was heated at 150 °C in an evacuated Carius tube for 19–42 h. At the end of the reaction period the solution (initially pale yellow) was dark yellow (except for (L—L)Cr(CO)$_4$ which was amber). The solvent was removed under reduced pressure and the resulting solid residue chromatographed on Florisil. Petroleum ether (b.p. 30–60 °C) eluted a yellow band which upon recrystallization from a methylene chloride – hexane mixture afforded the (L—L)M(CO)$_4$ complexes.

Analytical, preparative, and spectroscopic data for the new complexes are listed in Tables 1, 2, and 3.

Reactions of (L—L)M(CO)$_4$ and M(CO)$_6$ with Excess (L—L)

A number of reactions between M(CO)$_6$ and the (L—L)M(CO)$_4$ complexes with (L—L) are given in tabular form in Table 2. All pyrolysis reactions were performed in sealed evacuated Carius tubes; ultraviolet irradiations (200 W) were performed in evacuated quartz tubes. In all cases the crude reaction mixture was evaporated to dryness and the residue was chromatographed on Florisil using nitrogen saturated solvents as indicated in Table 2. All complexes were recrystallized from a degassed methylene chloride – hexane mixture at −20 °C.

Analytical and spectroscopic data for the new complexes are listed in Tables 1 and 3.

Results and Discussion

(L—L)M(CO)$_4$ Complexes

Reaction of the Group VI metal hexacarbonyls with an equimolar amount of (L—L) for 1–2 d in a sealed evacuated Carius tube, yields in the usual manner (1–3) the disubstituted chelate complexes (L—L)M(CO)$_4$. The complexes are yellow (except for the chromium derivative which is amber), air-stable, crystalline solids moderately soluble in nonpolar organic solvents and very soluble in polar organic solvents.

The infrared spectra are as expected for chelate derivatives and the ^1H and ^{19}F n.m.r. spectra show one arsenic methyl singlet and one trifluoromethyl singlet. This data indicates that either the five-membered ring (determined by the metal, two arsenic, and two carbon atoms of the ligand) is planar in solution (*i.e.* a symmetric structure), or the ring is involved in a rapid conformational equilibrium between two envelope forms.

fac-(L—L)^b(L—L)$^m{}_{cis}$M(CO)$_3$ and fac-(L—L)^b(L—L)$^m{}_{trans}$M(CO)$_3$[1]

These tricarbonyl complexes are best prepared by photolyzing a benzene solution of the parent hexacarbonyl or tetracarbonyl derivative and excess (L—L). Pyrolysis at temperatures of 150–200 °C does not yield the tricarbonyl derivative.

Hitherto no tricarbonyl complex containing two bidentate ligands has been reported from the reaction of a Group VI metal hexacarbonyl with an excess amount of a potentially bidentate ligand. However, the literature relating to complexes of the type (L$_2$)(L)M(CO)$_3$ (M = Cr, Mo, W; L$_2$ is a bidentate ligand; L is a monodentate ligand) has been well documented (9, 10).

Two isomeric tricarbonyl derivatives are obtained from the 450 W photochemical reaction. Analytical data suggest the formula (L—L)$_2$-M(CO)$_3$.

The i.r. spectra of the two isomers are identical in the carbonyl region; hence, the configuration of the carbonyl groups is probably the same in both isomers. The band intensities suggest both isomers are *fac* isomers (9, 10).

The basic difference in the n.m.r. spectra of the two isomeric *fac* complexes is the magnitude

[1] b and m denote bidentate and monodentate.

Can. J. Chem. Downloaded from www.nrcresearchpress.com by 210.87.254.105 on 09/05/12
For personal use only.

TABLE 3. Infrared and nuclear magnetic resonance data for (L—L)M(CO)$_4$ complexes*

Compound	^{1}H (p.p.m.)	^{19}F (p.p.m.)	ν(CO) (cm^{-1})
(L—L)Cr(CO)$_4$†	1.85	50.2	2020 (m), 1931 (s), 1911 (vs)
(L—L)Mo(CO)$_4$†	1.85	50.6	2036 (m), 1939 (s), 1921 (vs)
(L—L)W(CO)$_4$†	1.97	50.6	2036 (m), 1931 (s), 1911 (vs)
fac-(L—L)^b(L—L)$_c{}^m$Cr(CO)$_3$	1.33, 1.68, 1.80.	52.0, quartets centered at 53.6 and 54.6, J(F, F) = 12.0 Hz	1953 (vs), 1873 (s), 1863 (s)
fac-(L—L)^b(L—L)$_t{}^m$Cr(CO)$_3$	1.31, 1.70, 1.82	51.6, quartets centered at 50.4 and 52.0, J(F, F) = 2.2 Hz	1953 (vs), 1873 (s), 1863 (s)
cis-(L—L)$_2$Cr(CO)$_2$	1.30, 1.70, 1.82, 1.88	50.6	1883 (vs), 1829 (s)
trans-(L—L)$_2$Cr(CO)$_2$	1.83	49.8	1829
fac-(L—L)^b(L—L)$_c{}^m$Mo(CO)$_3$	1.33, 1.70, 1.82	50.8, quartets centered at 52.9 and 53.0, J(F, F) = 11.3 Hz	1963 (vs), 1885 (s), 1873 (s)
fac-(L—L)^b(L—L)$_t{}^m$Mo(CO)$_3$	1.30, 1.68, 1.80.	50.2, quartets centered at 49.2 and 50.3, J(F, F) = 2.3 Hz	1963 (vs), 1885 (s), 1873 (s)
cis-(L—L)$_2$Mo(CO)$_2$	1.37, 1.70, 1.83, 1.90	50.6	1899 (vs), 1845 (s)
trans-(L—L)$_2$Mo(CO)$_2$	1.87	49.6	1845
fac-(L—L)^b(L—L)$_c{}^m$W(CO)$_3$	1.33, 1.77, 1.83, 1.93	50.8, quartets centered at 52.7 and 53.0, J(F, F) = 13.5 Hz	1959 (vs), 1879 (s), 1867 (s)
fac-(L—L)^b(L—L)$_t{}^m$W(CO)$_3$	1.27, 1.72, 1.77, 1.90	Singlet (br) at 50.8, quartet centered at 49.6, J(F, F) = 2.2 Hz	1959 (vs), 1879 (s), 1867 (s)
cis-(L—L)$_2$W(CO)$_2$	1.43, 1.80, 1.97, 2.05	50.2	1890 (vs), 1839 (s)

*Unless otherwise indicated ^{1}H n.m.r. spectra from $CDCl_3$ solutions and ^{19}F n.m.r. spectra from CH_2Cl_2 solutions, all resonances are singlets: i.r. spectra from C_6H_{12} solutions.
†Nuclear magnetic resonance spectra from CS_2 solutions.

Can. J. Chem. Downloaded from www.nrcresearchpress.com by 210.87.254.105 on 09/05/12
For personal use only.

of the ^{19}F–^{19}F coupling constants of the resonances assigned to the monodentate ligand. This indicates that the two isomers differ in the configuration of the monodentate ligand since the bidentate ligand in each isomer *must* possess a *cis* configuration to form a chelate complex.

The structural assignments indicated in the tables are based on the well established result

$$\begin{matrix} & X & Y \\ & | & | \\ cis\text{-}CF_3— & C= & C—CF_3 \end{matrix}$$

(11) that $^5J_{FF}$ for *cis*-CF_3—C=C—CF_3 is ~12 Hz whereas for the *trans* geometry it is ~2 Hz. The ^1H n.m.r. spectrum of each complex is in agreement with this interpretation. Independent experiments show that the source of the *trans* ligand in these $M(CO)_3$ derivatives is an isomerization of (L—L) that occurs in the 450 W photochemical reaction such that the *cis* and *trans* forms of the ligand are in equilibrium, with the ratio of *cis* to *trans* being 9:1 as shown by ^{19}F n.m.r. spectroscopy.

The tricarbonyl complexes are unstable in nondegassed solvents but indefinitely stable in the solid state. The monodentate ligand in the two isomeric tricarbonyl derivatives is easily displaced by carbon monoxide, resulting in the formation of the tetracarbonyl complexes $(L—L)M(CO)_4$.

cis$(L—L)_2M(CO)_2$ *(M = Cr, Mo, W) and* *trans*-$(L—L)_2M(CO)_2$ *Complexes (M = Cr, Mo)*

The *cis* dicarbonyl complexes are best prepared by irradiating (450 W) a benzene solution of the tetracarbonyl complex and excess ligand (L—L). Heating the reactants at 175 °C yields the molybdenum dicarbonyl complex. Trace amounts of the chromium and tungsten derivatives are obtained at higher temperatures (190–210 °C) after prolonged heating and occasional removal of the accumulated carbon monoxide.

Further irradiation of *cis*-$(L—L)_2M(CO)_2$ (M = Cr, Mo) gives the isomeric *trans*-$(L—L)_2M(CO)_2$ derivatives.

The *cis* dicarbonyl complexes show the expected two bands (at considerably lower frequencies than the $(L—L)M(CO)_4$ complexes) in the ν(CO) region consistent with other characterized Group VI *cis* dicarbonyl complexes (12–15). Their ^1H n.m.r. spectra show four arsenic methyl singlets of equal area in accordance with the *cis* dicarbonyl structure. However the ^{19}F n.m.r. spectra consist of singlets rather than the anticipated doublet of quartets. Presumably the trifluoromethyl groups are insensitive to the different methyl environments about each arsenic atom. This has been noted in cobalt carbonyl complexes of $f_4$fars and related ligands (16, 17).

The i.r. spectra of the *trans* derivatives show the expected one carbonyl band and have the appropriate n.m.r. spectra.

The *cis* complexes are thermodynamically more stable than the isomeric *trans* complexes. Complete *trans* to *cis* isomerization occurs for the molybdenum derivative upon refluxing in benzene for 44 h and the chromium derivative upon refluxing for 1.5 h.

Trans to *cis* isomerization is also found when the molybdenum and chromium derivatives are chromatographed on Florisil and the *trans* chromium complex even isomerizes in the solid state.

Bond and co-workers (15, 18) have recently reported on an electrochemical investigation of the complexes $[M(CO)_2(bidentate)_2]^{0,+1,+2}$ (bidentate = $(C_6H_5)_2PCH_2CH_2P(C_6H_5)_2$ and $(C_6H_5)_2PCH_2P(C_6H_5)_2$). They find that for the neutral complexes, where both *cis* and *trans* isomers can be identified, the *cis* isomer is the more stable. However, oxidation results in increased stability of the *trans* species.

The authors are grateful to the National Research Council of Canada for financial support of this work in the form of operating grants to W.R.C. and scholarships to L.M.

1. G. R. Dobson, I. W. Stolz, and R. K. Sheline. Adv. Inorg. Chem. Radiochem. **8**, 1 (1966).
2. F. Calderazzo, R. Ercoli, and G. Natta. *In* Organic syntheses via metal carbonyls, Vol. 1. *Edited by* I. Wender and P. Pino. Wiley-Interscience, New York. 1968. p. 147.
3. C. A. McAuliffe. (*Editor*). Transition metal complexes of phosphorus, arsenic, and antimony ligands. Wiley and Sons, New York, New York. 1973.
4. W. R. Cullen and G. E. Styan. J. Organomet. Chem. **4**, 151 (1965).
5. W. R. Cullen. Adv. Inorg. Chem. Radiochem. **15**, 323 (1972).
6. W. R. Cullen, D. A. Harbourne, B. V. Liengme, and J. R. Sams. Inorg. Chem. **9**, 702 (1970).
7. P. J. Roberts, B. R. Penfold, and J. Trotter. Inorg. Chem. **9**, 2137 (1970).
8. W. R. Cullen and L. Mihichuk. Can. J. Chem. **51**, 936 (1973).

9. G. R. DOBSON and L. W. HOUK. Inorg. Chim. Acta, **1**, 287 (1967).
10. W. R. CULLEN and R. K. POMEROY. J. Organomet. Chem. **85**, 217 (1975).
11. W. R. CULLEN, D. S. DAWSON, and G. E. STYAN. Can. J. Chem. **43**, 3392 (1965).
12. J. CHATT and H. R. WATSON. J. Chem. Soc. 4980 (1961).
13. H. L. NIGAM, R. S. NYHOLM, and M. H. B. STIDDARD. J. Chem. Soc. 1803 (1960).
14. P. F. CROSSING and M. R. SNOW. J. Chem. Soc. A, 610 (1971).
15. A. M. BOND, R. COLTON, and J. J. JACKOWSKI. Inorg. Chem. **14**, 274 (1975).
16. L. S. CHIA and W. R. CULLEN. Inorg. Chem. **14**, 482 (1975).
17. L. S. CHIA, W. R. CULLEN, M. FRANKLIN, and A. R. MANNING. Inorg. Chem. In press.
18. F. L. WIMMER, M. R. SNOW, and A. M. BOND. Inorg. Chem. **13**, 1617 (1974).

Can. J. Chem. Downloaded from www.nrcresearchpress.com by 210.87.254.105 on 09/05/12
For personal use only.

Kinetic Study of the Reaction between Substituted Triphenylmethyl Perchlorates with Pyridines in Nitromethane and 1,2-Dichloroethane Solvents[1]

CHANG B. KIM[2] AND KENNETH T. LEFFEK

Chemistry Department, Dalhousie University, Halifax, Nova Scotia B3H 4H6

Received April 28, 1975

CHANG B. KIM and KENNETH T. LEFFEK. Can. J. Chem. 53, 3408 (1975).

Second-order rate constants at 25 °C have been measured for the reaction of triphenylmethyl carbonium ion with pyridine and substituted pyridines in nitromethane and 1,2-dichloroethane solvent. The activation parameters are in the range 1 to 3 kcal mol^{-1} for the enthalpies of activation and -20 to -45 cal mol^{-1} deg^{-1} for the entropies of activation. The results are compared to the analogous measurements for Menschutkin reactions and it is concluded that the enthalpy of activation of a Menschutkin reaction results mainly from the bond breaking process and solvation changes associated with it, since the carbon–nitrogen bond making process seems to be entropy controlled.

Rate measurements have also been made for 2-methylpyridine reacting with a series of *para*-substituted triphenylmethyl carbonium ion substrates in 1,2-dichloroethane solvent. A plot of $\log k_2$ *vs.* $\Sigma\sigma^+$ is non-linear and the curvature is interpreted as a saturation effect.

CHANG B. KIM et KENNETH T. LEFFEK. Can. J. Chem. 53, 3408 (1975).

On a mesuré les contantes de vitesse du deuxième ordre à 25 °C pour la réaction du carbocation triphénylméthyle avec la pyridine et des pyridines substituées; le nitrométhane et le dichloro-1,2 éthane ont été utilisés comme solvant. Les paramètres d'activations sont de l'ordre de 1 à 3 kcal mol^{-1} pour les enthalpies d'activation et de -20 à -45 cal mol^{-1} deg^{-1} pour les entropies d'activation. On compare ces résultats avec des mesures analogues pour des réactions de Menschutkin et on en conclut que l'enthalpie d'activation d'une réaction de Menschutkin provient principalement du processus de bris de lien et de changements de solvatation qui lui sont associés; cette conclusion est basée sur le fait que le processus de formation du lien C—N semble être contrôlé par l'entropie.

On a aussi mesuré, dans le dichloro-1,2 éthane, des vitesses de réaction de la méthyl-2 pyridine avec une série de carbocations triphénylméthyles substitués en *para*. La relation $\log k_2$ *vs.* $\Sigma\sigma^+$ n'est pas linéaire et on interprète la courbature en fonction d'un effet de saturation.

[Traduit par le journal]

Introduction

It has been known for a long time (1) that the triphenylmethyl (trityl) carbonium ion in dipolar aprotic solvents very rapidly loses its characteristic yellow color upon addition of reagents with lone pair electrons such as ethers and tertiary amines. The strength of the bond between the electron deficient carbon atom and the electron rich basic atom should depend upon the pK_a of the base and be stronger for tertiary amines than for ethers (2). Gelles, Hughes, and Ingold (3) observed an immediate discharge of the yellow color of trityl chloride in nitromethane upon the addition of pyridine which they described as the formation of a complex between the pyridine and the trityl chloride carbonium ion-pairs. They represented this complex as the tritylpyridinium ion, $(C_6H_5)_3C\overset{+}{N}C_5H_5$. Streitwieser (4) also favored the formation of triphenylmethylpyridinium chloride as the explanation of this reaction, despite the fact that there had been several unsuccessful attempts to synthesize this compound (5–11). However, in 1970, the preparation of the compound was reported by Okamoto and Shimakawa (12) using a pressure of 4000–5000 atm at 60–70 °C. In contrast, these workers prepared tritylpyridinium perchlorate and tetrafluoroborate in acetonitrile solvent at room pressure and temperature in 10 min.

Some experiments have been reported on the equilibrium constants for the reaction of trityl carbonium ion with diethyl ether in nitromethane and in acetic anhydride (13), which gave

[1]Presented in part at the 57th Canadian Chemical Conference of the Chemical Institute of Canada, Regina, Saskatchewan, June 1974.

[2]Postdoctoral Fellow 1973–1974.

Can. J. Chem. Downloaded from www.nrcresearchpress.com by 210.87.254.40 on 09/05/12
For personal use only.

Can. J. Chem. Downloaded from www.nrcresearchpress.com by 210.87.254.40 on 09/05/12
For personal use only.

an equilibrium constant of 0.8×10^{-4} l mol^{-1} in nitromethane, and of trityl bromide carbonium ion-pairs with pyridine in 1,1,2,2-tetrachloroethane (14), which gave $K = 3 \times 10^5$ l mol^{-1}. These values reflect the different basicities of ether and pyridine. However, due to the high velocity of the reactions, no kinetic measurements have been made. The kinetics of the reaction of carbonium ions with tertiary amines are of interest because this type of reaction is analogous to a Menschutkin reaction in which there is no carbon–halogen bond breaking component. Therefore, the rates and activation parameters for such a reaction should allow a more meaningful interpretation of analogous parameters in Menschutkin reactions.

In the present study, the perchlorates were selected as the substrate molecules since triphenylmethyl perchlorate is an ionic compound in the solid state (2, 15) and in solution (16), and is known to react readily with pyridine to give the quaternary ammonium salt (12). Pyridine, 2-picoline, and 2,6-lutidine were used as the nucleophilic reagents with unsubstituted triphenylmethyl perchlorate in order to make a comparison of the steric effect of the methyl group substituents in the amines in this reaction with that effect in the Menschutkin reaction. A second series of experiments was made with substituted triphenylmethyl perchlorates with the base 2-picoline.

Results and Discussion

Reaction of Triphenylmethyl Perchlorate with Substituted Pyridines

Pseudo first-order rate constants for the disappearance of the yellow color due to the trityl carbonium ion by reaction with an excess of tertiary amine were just slow enough to be determined using a stopped-flow spectrophotometer. These rate constants, measured at 25 °C, are shown in Table 1 for the two solvents nitromethane and 1,2-dichloroethane.

Similar measurements to those in Table 1 were made at several other temperatures in an attempt to measure the activation parameters. The second-order rate constants derived from these measurements, calculated by a least squares computation from the reaction $k_1 = k_2$[Amine], are shown in Table 2. It can be seen that the second-order rate constants have large standard deviations compared to the range of k_2 values for the 25 °C temperature spread. Nevertheless,

TABLE 1. Reaction of triphenylmethyl perchlorate with substituted pyridines

(*a*) First-order rate constants in nitromethane solvent at 25 °C
Initial $[(C_6H_5)_3C^+ClO_4^-] = 4.65 \times 10^{-5}$ *M*

Substituted pyridine	Concentration ($M \times 10^4$)	k_1 (s^{-1})
Pyridine	0.60	211
	0.81	423
	1.21	622
	1.41	843
	1.62	908
2-Methylpyridine	3.24	18.1
	4.87	17.9
	6.3	22.9
	8.1	52.3
	9.8	47.6
2,6-Dimethylpyridine	13.2	0.337
	19.8	0.413
	26.4	0.563
	33.1	0.641
	39.7	0.709

(*b*) First-order rate constants in 1,2-dichloroethane at 25 °C
Initial $[(C_6H_5)C^+ClO_4^-] = 0.75 \times 10^{-5}$ *M*

Substituted pyridine	Concentration ($M \times 10^5$)	k_1 (s^{-1})
Pyridine	0.70	123
	1.39	245
	1.86	345
	2.32	420
2-Methylpyridine	50	2.18
	100	3.91
	150	4.83
	200	7.8
2,6-Dimethylpyridine	66	0.73
	99	1.01
	132	1.08
	166	1.30

the activation parameters obtained from plots of $\ln (k_2/T)$ *vs.* $1/T$, given in Table 3, show that the enthalpies of activation for triphenylmethyl perchlorate reacting with all three amines are in the range of 1 to 3 kcal mol^{-1} in both solvents and that the entropies of activation are in the order of -20 to -45 cal mol^{-1} deg^{-1}. The enthalpies of activation are probably reliable to within 1 kcal mol^{-1}, with corresponding uncertainty in the entropies of activation.

In each solvent, the free energy of activation increases from pyridine to 2,6-lutidine, as has been observed for Menschutkin reactions. The

Can. J. Chem. Downloaded from www.nrcresearchpress.com by 210.87.254.40 on 09/05/12
For personal use only.

TABLE 2. Second-order rate constants for the reaction of triphenylmethyl perchlorate with substituted pyridines

(*a*) Nitromethane solvent

Temperature (°C)	$k_2 \pm$ std. dev. (l mol^{-1} s^{-1})		
	Pyridine	2-Picoline	2,6-Lutidine
10.0	$(5.2\pm0.6)\times10^6$	$(4.1\pm0.8)\times10^4$	$(1.3\ \pm0.1)\times10^2$
15.0	$(6.7\pm0.4)\times10^6$	$(5.5\pm1.0)\times10^4$	$(1.2\ \pm0.1)\times10^2$
20.0	$(7.2\pm0.6)\times10^6$	$(5.4\pm0.8)\times10^4$	$(1.2_5\pm0.1)\times10^2$
25.0	$(6.6\pm0.6)\times10^6$	$(5.2\pm0.8)\times10^4$	$(1.6\ \pm0.1)\times10^2$
30.0	$(6.7\pm0.5)\times10^6$	—	$(1.8\ \pm0.1)\times10^2$
35.0	$(7.2\pm0.5)\times10^6$	$(5.6\pm1.2)\times10^4$	$(1.9\ \pm0.1)\times10^2$

(*b*) 1,2-Dichloroethane solvent

Temperature (°C)	$k_2 \pm$ std. dev. (l mol^{-1} s^{-1})		
	Pyridine	2-Picoline	2,6-Lutidine
10.0	$(1.6\pm0.2)\times10^7$	—	$(4.9\pm0.4)\times10^2$
15.0	$(1.9\pm0.2)\times10^7$	$(3.3\pm0.2)\times10^3$	$(4.7\pm0.3)\times10^2$
20.0	$(1.7\pm0.1)\times10^7$	$(4.0\pm0.1)\times10^3$	$(5.9\pm0.2)\times10^2$
25.0	$(1.8\pm0.1)\times10^7$	$(4.2\pm0.3)\times10^3$	$(4.9\pm0.8)\times10^2$
30.0	$(2.1\pm0.1)\times10^7$	$(4.5\pm0.2)\times10^3$	—
35.0	—	$(5.2\pm0.4)\times10^3$	$(5.8\pm0.4)\times10^2$

TABLE 3. Activation parameters for the reaction of triphenylmethyl perchlorate with substituted pyridines

Substituted pyridine	ΔH^* (kcal mol^{-1})	ΔS^* (cal deg^{-1} mol^{-1})
(*a*) Nitromethane solvent		
Pyridine	1.6	−22
2-Picoline	1.0	−34
2,6-Lutidine	2.3	−41
(*b*) 1,2-Dichlorochloroethane solvent		
Pyridine	1.3	−21
2-Picoline	2.8	−33
2,6-Lutidine	1.0	−43

reactions with pyridine and with 2,6-lutidine are about 3 times faster in 1,2-dichloroethane than they are in nitromethane, but for 2-picoline the reaction is about 10 times slower in 1,2-dichloroethane than in nitromethane. We have no explanation for this irregular behavior.

Since the reaction involves more delocalization of the positive charge in the transition state relative to the initial state, it would be expected to proceed faster in the less polar solvent (17), that is, faster in 1,2-dichloroethane than in nitromethane.

The rate changes with *ortho*-methyl substitution of pyridine which we have observed are large (*ca.* 1000) compared to similar changes observed in Menschutkin reactions (generally less than 10) in similar solvents (18, 19). In the latter reactions, changes in ΔH^* are less than 1 kcal and changes in ΔS^* are 1 to 2 cal mol^{-1} deg^{-1}. Although we may have ΔH^* changes of 1 kcal, the major change in k_2 in Table 2 results from ΔS^* changing by about 20 cal mol^{-1} deg^{-1}.

It is concluded, therefore, that most of the enthalpy of activation of a Menschutkin reaction is due to the bond breaking process and solvation changes associated with it. The carbon–nitrogen bond making process, judged from

Can. J. Chem. Downloaded from www.nrcresearchpress.com by 210.87.254.40 on 09/05/12
For personal use only.

TABLE 4. First-order rate constants for the reaction of 2-methylpyridine with *para*-substituted triphenylmethyl perchlorates in 1,2-dichloroethane at 25 °C

(*a*) Initial [*p*-Tolyldiphenylmethyl perchlorate] = 2.72×10^{-5} *M*

[2-Methylpyridine] ($M \times 10^3$)	k_1 (s^{-1})
0.30	0.172
0.60	0.193
0.90	0.298
1.2	0.284
1.8	0.478

(*b*) Initial [Di-*p*-tolylphenylmethyl perchlorate] = 4.65×10^{-5} *M*

[2-Methylpyridine] ($M \times 10^2$)	k_1 (s^{-1})
0.50	0.215
1.0	0.394
2.0	0.825
3.0	1.12
4.0	1.64
5.0	2.00

(*c*) Initial [Tri-*p*-tolylmethyl perchlorate] = 1.46×10^{-5} *M*

[2-Methylpyridine] ($M \times 10^2$)	k_1 (s^{-1})
1.0	0.167
1.5	0.291
2.0	0.423
2.5	0.617
3.0	0.792
4.0	1.15

(*d*) Initial [*p*-Anisyldiphenylmethyl perchlorate] = 2.60×10^{-5} *M*

[2-Methylpyridine] ($M \times 10^{-2}$)	k_1 (s^{-1})
1.0	0.122
2.0	0.298
4.8	0.954
7.5	2.16
10.0	2.72
20.0	5.27

the present measurements, is entropy controlled, requiring only the reorientation of the reacting and solvent molecules with very little energy input.

Reaction of 2-Methylpyridine with Substituted Triphenylmethyl Perchlorates

The reaction of 2-methylpyridine with a series of *para*-substituted triphenylmethyl perchlorates was studied in 1,2-dichloroethane by measuring pseudo first-order rate constants with the nucleophile in large excess. Second-order rate constants were calculated as before. The results are given in Tables 4 and 5.

A plot of $\log k_2$ *vs.* $\sum\sigma^+$ shown in Fig. 1 is seen to be non-linear. The values of σ^+ used are those calculated by Deno and Evans (20) for triarylmethyl cation equilibria. The slope of the graph indicates a positive ρ value as expected for a reaction in which negative charge is accumulated adjacent to the benzene ring and ρ becomes smaller as the electron releasing power of the substituent increases. The value of ρ drops from about 5.5 to about 0.7 indicating a decreasing sensitivity to negative charge accumulation. This has been described as a saturation effect (2, 21, 22): the more the positive charge on the carbonium ion is delocalized in the initial state, the smaller the extra delocalization is obtained from an additional *para*-methyl substituent. The delocalization of positive charge in the initial state parallels the decrease in reactivity. 4,4′-Dimethylaminotriphenylmethyl carbonium ion does not react at all with pyridine in methanol solution (23).

The kinetic Hammett plot is not unique. The plot of $\Delta F_{R+}{}^0$, the thermodynamic stability of carbonium ions derived from alcohols, against $\sum\sigma^+$ which is given by Freedman (24) shows very similar behavior for the same compounds when plotted on the same scale, although the ρ value is negative in this case. However, the curvature is less pronounced and over a $\sum\sigma^+$ range of more than 5 the plot is almost linear. Thus, although the saturation effect is smaller for the thermodynamic stability case, qualitatively the same phenomenon is seen. If the curvature of the plot is ignored a least squares treatment yields $\rho = 2.9 \pm 0.6$ somewhat less than the value of 4.0 ± 0.15 found for substituted triphenylmethyl carbonium ions reacting with water at 25 °C (25).

Experimental

Materials

Triphenylmethyl perchlorate was prepared from the carbinol and 70% perchloric acid in acetic anhydride solvent as described by Dauben *et al.* (26). The yellow crys-

Can. J. Chem. Downloaded from www.nrcresearchpress.com by 210.87.254.40 on 09/05/12
For personal use only.

TABLE 5. Second-order rate constants for the reaction of 2-methylpyridine with *para*-substituted triphenylmethyl perchlorates in 1,2-dichloroethane at 25 °C

Substrate	k_2 (l mol^{-1} s^{-1})
Triphenylmethyl perchlorate	4200 ± 300
p-Tolyldiphenylmethyl perchlorate	195 ± 40
Di-*p*-tolylphenylmethyl perchlorate	40 ± 2
Tri-*p*-tolylmethyl perchlorate	33 ± 3
p-Anisyldiphenylmethyl perchlorate	28 ± 2
p-Chlorophenyldiphenylmethyl perchlorate	ca.10^6

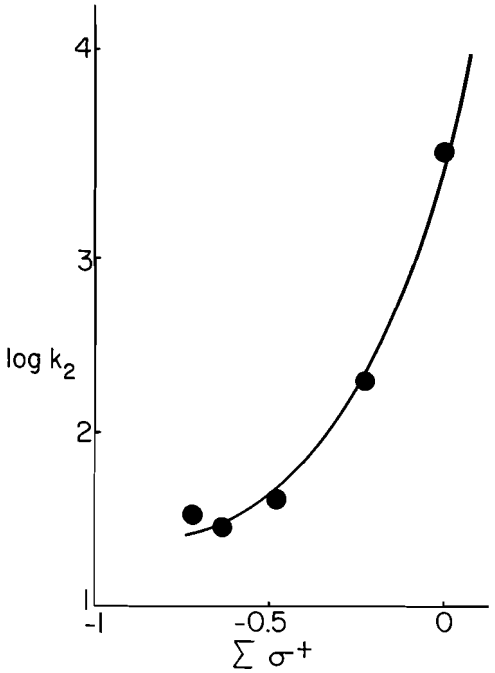

FIG. 1. Plot of the logarithm of the second-order rate constant *vs.* $\Sigma\sigma^+$ for the reaction of *para*-substituted triphenylmethyl perchlorate with 2-methylpyridine in 1,2-dichloroethane at 25 °C

tals, after vacuum drying for 5 h, had m.p. 143 °C in a sealed tube (lit. (26, 27) 143–144 °C). *p*-Tolyldiphenylmethyl carbinol was prepared by a Grignard reaction of *p*-tolylmagnesium bromide and benzophenone. After 4 h under reflux, 0.1 *M* H_2SO_4 was used to generate the alcohol which was recovered as an oil. The middle cut of a vacuum distillation gave a viscous oil, which crystallized after several hours. Recrystallization from petroleum ether (30–60 °C) gave crystals m.p. 75 °C (lit. (28) 73–74 °C). Di-*p*-tolylphenylmethyl carbinol was prepared by a Grignard reaction of *p*-tolylmagnesium bromide and methyl benzoate. The product was vacuum distilled and recrystallized from petroleum ether, m.p. 74 °C (lit. (29) 76.5–77.5 °C).

Tri-*p*-tolylmethyl carbinol was prepared by a Grignard reaction of *p*-tolylmagnesium bromide and ethyl *p*-toluate. The product was vacuum distilled and the middle cut was esterified with glacial acetic acid. The ester crystallized at low temperature and was recrystallized from petroleum ether. The carbinol was obtained by treatment with NaOH and recrystallized from petroleum ether, m.p. 97 °C (lit. 96.5 °C (30), 93 °C (31)).

p-Methoxyphenyldiphenylmethyl carbinol was prepared by a Grignard reaction of *p*-methoxyphenylmagnesium bromide and benzophenone. The high boiling fraction of a vacuum distillation was recrystallized with some difficulty from petroleum ether, m.p. 57 °C, (lit. (32) 58–61 °C).

p-Chlorophenyldiphenylmethyl carbinol was prepared by a Grignard reaction of *p*-chlorophenylmagnesium bromide and benzophenone. The product was recrystallized from petroleum ether, m.p. 85 °C (lit. (33, 34) 84.8–85.5 °C).

Each of the substituted triphenylmethyl carbinols was converted to the perchlorate by treating a solution of the alcohol in glacial acetic acid with concentrated $HClO_4$. After removal of solvent under vacuum, the product was recrystallized from glacial acetic acid.

Reagent grade pyridine and 2-picoline were fractionally distilled over NaOH pellets and 2,6-lutidine was distilled from zinc dust.

Reagent grade nitromethane was purified by the procedure of Thompson *et al.* (35), which consists of successive washings with sodium bicarbonate, sodium bisulfite, and sulfuric acid solutions, followed by drying with P_2O_5 and distillation at reduced pressure. We added the additional step of passing the solvent through a column of molecular sieve Linde Type 4A before the distillation.

Reagent grade 1,2-dichloroethane was washed with KOH solution and water, dried over Driente, passed through a molecular sieve column and fractionally distilled at atmospheric pressure. Only material boiling at 83.5 °C was collected since the azeotropic mixture with water boils at 81–83 °C.

Kinetic Measurements

The reaction rates were measured using a Durrum stopped-flow spectrophotometer using an optical cell with a 2 mm pathlength according to the standard procedure described previously (36, 37). The increase in transmittance was observed over the 90–100% range at 430 nm wavelength. Several individual runs were superimposed on the oscilloscope screen and first order rate constants were calculated from the composite trace.

It is well known that very small amounts of impurity in nitromethane react rapidly with triphenylmethyl car-

bonium ion (38, 39). However, in carefully purified nitromethane, the carbonium ion is stable for 24 h (13, 40). We verified the latter statement and used in our kinetic experiments only nitromethane in which the carbonium ion was stable for at least 7 h.

The authors are grateful for financial support by the National Research Council of Canada.

1. C. D. NENITZESCU. *In* Carbonium ions. Vol. 1. *Edited by* G. A. Olah and P. v. R. Schleyer. Wiley-Interscience, New York. 1968. Chapt. 1.
2. H. H. FREEDMAN. *In* Carbonium ions. Vol. IV. *Edited by* G. A. Olah and P. v. R. Schleyer. Wiley-Interscience, New York 1973. Chapt. 28.
3. E. GELLES, E. D. HUGHES, and C. K. INGOLD. J. Chem. Soc. 2918 (1954).
4. A. STREITWIESER, JR. Solvolytic displacement reactions. McGraw-Hill Book Co. Inc., New York. 1962. p. 82.
5. J. F. NORRIS and L. R. CULVER. Am. Chem. J. **29**, 129 (1903).
6. C. A. KRAUS and R. ROSEN. J. Am. Chem. Soc. **47**, 2739 (1925).
7. B. HELFERICH and H. SIEBER. Ber. **59B**, 600 (1926).
8. M. REBEK and G. MANDRINO. Ber. **62B**, 2508 (1929).
9. E. D. HUGHES. J. Chem. Soc. **75** (1933).
10. C. G. SWAIN and E. E. PEGUES. J. Am. Chem. Soc. **80**, 812 (1958).
11. C. G. SWAIN and Y. OKAMOTO. J. Am. Chem. Soc. **92**, 3409 (1970).
12. Y. OKAMOTO and Y. SHIMAKAWA. J. Org. Chem. **35**, 3752 (1970).
13. W. B. SMITH and P. S. RAO. J. Org. Chem. **26**, 254 (1961).
14. G. BRIEGLEB, W. RUTTIGER, and W. JUNG. Angew. Chem. Int. Ed. **2**, 545 (1963).
15. A. H. GOMES DE MESQUITA, C. H. MACGILLAVRY, and K. ERIKS. Acta Crystallogr. **18**, 437 (1965).
16. W. R. LONGWORTH and C. P. MASON. J. Chem. Soc. A, 1164 (1966).
17. C. K. INGOLD. Structure and mechanism in organic chemistry. 2nd ed. Cornell Univ. Press, Ithaca, New York. 1969. p. 460.
18. H. C. BROWN and A. CAHN. J. Am. Chem. Soc. **77**, 1715 (1955).
19. K. CLARKE and K. ROTHWELL. J. Chem. Soc. 1885 (1960).
20. N. C. DENO and W. L. EVANS. J. Am. Chem. Soc. **79**, 5804 (1957).
21. J. HINE. Physical organic chemistry. 2nd ed. McGraw-Hill, New York. 1962. p. 101.
22. L. D. MCKEEVER and R. W. TAFT. J. Am. Chem. Soc. **88**, 4544 (1966).
23. K. T. LEFFEK and A. SUSZKA. Unpublished work.
24. H. H. FREEDMAN. *In* Carbonium ions. Vol. IV. *Edited by* G. A. Olah and P. v. R. Schleyer. Wiley-Interscience. New York. 1973. p. 1549.
25. P. R. WELLS. Linear free energy relationships. Academic Press, New York. 1968. p. 13.
26. H. J. DAUBEN, JR., L. R. HONNEN, and K. M. HARMAN. J. Org. Chem. **25**, 1442 (1960).
27. K. A. HOFMANN and H. KIRMREUTHER. Ber. **42**, 4856 (1909).
28. S. F. ACREE. Ber. **37**, 990 (1904).
29. A. KLIEGL. Ber. **38**, 84 (1905).
30. A. MOTHWURF. Ber. **37**, 3153 (1904).
31. A. BENTLEY and A. G. EVANS. J. Chem. Soc. 3468 (1952).
32. A. BAEYER and V. VILLIGER. Ber. **35**, 3027 (1902).
33. M. GOMBERG and L. H. CONE. Ber. **39**, 3274 (1906).
34. N. N. LICHTIN and M. J. VIGNALE. J. Am. Chem. Soc. **79**, 579 (1957).
35. C. J. THOMPSON, H. J. COLEMAN, and R. HELM. J. Am. Chem. Soc. **76**, 3445 (1954).
36. A. JARCZEWSKI and K. T. LEFFEK. Can. J. Chem. **50**, 24 (1972).
37. J.-H. KIM and K. T. LEFFEK. Can. J. Chem. **51**, 2805 (1973).
38. E. PRICE and N. N. LICHTIN. Tetrahedron Lett. **10**, 18 (1960).
39. Y. POCKER. J. Chem. Soc. 240 (1958).
40. B. B. SMITH and J. E. LEFFLER. J. Am. Chem. Soc. **77**, 1700 (1955).

Can. J. Chem. Downloaded from www.nrcresearchpress.com by 210.87.254.40 on 09/05/12
For personal use only.

Effect of Pressure on the Alkaline Hydrolysis of Ethyl Acetate in Acetone–Water Solutions. Parameters of Activation at Constant Volume[1]

M. L. TONNET[2] AND E. WHALLEY

Division of Chemistry, National Research Council of Canada, Ottawa, Canada K1A 0R9

Received October 28, 1974[3]

M. L. TONNET and E. WHALLEY. Can. J. Chem. **53**, 3414 (1975).

The effect of pressures up to 3 kbar on the rate of the base-catalyzed hydrolysis of ethyl acetate in acetone–water mixtures has been measured. From these measurements and the enthalpy and entropy of activation at constant pressure measured by others, the internal energy and entropy of activation at constant volume have been obtained as a function of solvent composition. The constant-volume parameters of activation vary with composition in a simpler way than the constant-pressure parameters. It seems likely that theoretical discussions of the solvent effect are easier if they are based on the constant-volume parameters. At low acetone concentrations, the addition of acetone reduces the rate constant at low pressure, but increases it at 3 kbar.

M. L. TONNET et E. WHALLEY. Can. J. Chem. **53**, 3414 (1975).

On a mesuré l'effet de pressions allant jusqu'à 3 kbar sur la vitesse d'hydrolyse basique de l'acétate d'éthyle dans des mélanges d'eau-acétone. A partir de ces mesures et aussi utilisant l'enthalpie et l'entropie d'activation à pression constante mesurées par d'autres, on a pu obtenir l'énergie interne et l'entropie d'activation à volume constant en fonction de la composition du solvant. Les paramètres d'activation à volume constant varient en fonction de la composition d'une façon beaucoup plus simple que les paramètres à pression constante. Il semble probable que les discussions théoriques de l'effet de solvant sont plus simples si elles sont basées sur des paramètres à volume constant. A des concentrations d'acétone basses, l'addition d'acétone réduit la constante de vitesse à basse pression; toutefois à 3 kbar, elle l'augmente.

[Traduit par le journal]

Can. J. Chem. Downloaded from www.nrcresearchpress.com by 210.87.254.6 on 09/05/12
For personal use only.

Introduction

Many reactions in aqueous organic solvents have minima in the constant-pressure enthalpy $\Delta H_p^{\ddagger}$ and entropy $\Delta S_p^{\ddagger}$ of activation as a function of solvent composition. This minimum is frequently interpreted as indicating changes in the structure of the solvent at the location of the minimum (1).

But there are two major causes of extrema in physical properties; those due to causes inherent in a single phenomenon, such as the maximum in the light absorption due to an energy transition, and those due to the opposing effects of several independent or partially independent causes. For example, a particular measurement a may be considered as the result of two more fundamental processes a_1 and a_2

$$a = a_1 + a_2$$

and a maximum in a as a function of a parameter x will occur where

$$\partial a_1/\partial x = -\partial a_2/\partial x$$

In this case, the reasons for the location of the maximum must be sought in the reasons for the values of the parameters controlling $a_1(x)$ and $a_2(x)$. The simplest example of this phenomenon occurs when $a_1 = b_1x$, $a_2 = b_2x^2$, and an extremum in a occurs at $x = -b_1/2b_2$.

As was mentioned, minima in $\Delta H_p^{\ddagger}$ and $\Delta S_p^{\ddagger}$ as a function of solvent composition have often been used to infer specific changes in the solvent at this composition. But the minima may be due to two or more opposing effects as outlined above. An examination of the same results in another coordinate system, (a change of coordinate system is a well-known scientific technique for denying or confirming inferences) might help to decide whether the minima are due to specific changes in the structure of the solvent at the composition of the minimum, or are due to opposing effects which do not imply such specific changes in the structure.

When the temperature is changed to measure an activation energy, the way in which the pressure and volume change must be specified, because the pressure, volume, and temperature of a

[1]NRCC No. 14846.

[2]NRCC Post-doctorate Fellow, 1968–1969.

[3]Revision received July 21, 1975.

Can. J. Chem. Downloaded from www.nrcresearchpress.com by 210.87.254.6 on 09/05/12
For personal use only.

homogenous system are related by an equation of state, and two of them must be specified to specify the state.

Because we live in a nearly constant-pressure world, it is usual to keep the pressure constant when reactions in solution are studied and the enthalpy and entropy of activation at constant pressure are determined. An alternative possibility is to keep the volume constant, and then the energy and entropy of activation at constant volume are determined. The relation between the constant-volume and constant-pressure parameters is (2)

$$\Delta U_v^{\ddagger} = \Delta H_p^{\ddagger} - T\alpha\Delta V^{\ddagger}/\kappa$$

$$T\Delta S_v^{\ddagger} = T\Delta S_p^{\ddagger} - T\alpha\Delta V^{\ddagger}/\kappa$$

It does not appear to be possible to argue *a priori* whether constant-pressure or constant-volume conditions are to be preferred for a theoretical interpretation (3).

In a number of papers from this laboratory, the effect of solvent composition in aqueous organic solvents on the enthalpy and entropy of activation for the neutral hydrolysis of benzyl (4*a*, 5, 6) and *tert*-butyl (4*b*) chlorides, the acid-catalyzed enolization of acetone and acetophenone (7), the acid-catalyzed hydrolysis of methyl acetate and ethylene oxide (8), and the base-catalyzed decomposition of diacetone alcohol (9, 10), have been found to appear simpler after the coordinate transformation from constant-pressure conditions to constant-volume conditions. In particular, the minima that occur in the constant-pressure parameters are much smaller or are nonexistent in the constant-volume parameters. The main reason for the difference, with the commoner aqueous organic solvents, is that the thermal expansivity α changes greatly with solvent composition because the thermal expansivity of water at ordinary temperatures is much smaller than that of the organic solvents. When a solvent system for which the thermal expansivity changes only slightly is used, such as aqueous glycerol, both the constant-pressure and constant-volume parameters vary in a relatively simple way (5, 6).

It would appear from these results that there is no need to invoke specific structural changes at the location of the minimum in $\Delta H_p^{\ddagger}$ and $\Delta S_p^{\ddagger}$, because it disappears if the coordinate system is changed. It was concluded that the minimum could be interpreted as a relatively simple behavior of $\Delta U_v^{\ddagger}$ (a curve with a small slope at low concentrations of organic solvent and a concave upward curvature, which would occur if transition states solvated wholly by water carried the reaction in dilute organic solutions) and a strong effect of composition on the thermal expansivity and to a lesser extent on the activation volume.

The purpose of the present work is to inquire whether a base-catalyzed ester hydrolysis behaves in the same way, and the hydrolysis of ethyl acetate in acetone–water mixtures was chosen.

Experimental Methods and Results

Reagent grade ethyl acetate was used after drying over potassium carbonate and distilling under reduced pressure. It contained no detectable acid.

The reaction solutions were made by adding 25, 37.5, and 50 cm^3 of acetone to suitable solutions of ethyl acetate and sodium hydroxide and making up to 100 cm^3 to produce solutions that were 5 mM in both ethyl acetate and sodium hydroxide. The acetone concentrations in the three solutions were 24.0, 32.0, and 42.4% by weight.

The reaction was followed conductimetrically using a General Radio 1680-A automatic capacitance–conductance bridge and digital readout. About 10 conductances were measured during each run, and during a run the concentrations of sodium hydroxide and ethyl acetate dropped from about 2.5 to about 0.2 mM. The pressure equipment and conductance cells were similar to those used earlier (6, 11). They had a capacity of about 15 cm^3, and two were placed in the vessel at the same time. The thermostat temperature was controlled to 20 mK by a mercury contact regulator and was measured with a platinum resistance thermometer.

The first conductance readings were taken after allowing an hour for the system to reach thermal equilibrium, by which time about half the reaction had gone. The reactions were then followed for periods of 5–6 h.

The rate constants were calculated from the integrated form of the second-order rate equation with equal concentrations. Because of the time required for thermal equilibrium after pressurizing the sample, an arbitrary starting time t_0 at which some reaction has already occurred must be used. The ionic concentration remains constant at 5 mM during the run, although hydroxide ions are replaced by acetate ions. A linear relation between conductance and extent of reaction is therefore

Can. J. Chem. Downloaded from www.nrcresearchpress.com by 210.87.254.6 on 09/05/12
For personal use only.

TABLE 1. Rate constants for the alkaline hydrolysis of ethyl acetate in acetone–water mixtures at 10.02 °C in the range 10 to 3000 bar

% by weight acetone in water	p/bar	$10^3 k/M^{-1}s^{-1}$ [a]	
0	10	35.8	35.6
	250	38.9	39.1
	925	47.4	
	1500	54.5	52.8
	2000	61.6	
	2800	68.8	70.5
20.4	10	32.0	
	500	38.3	
	1000	45.0	
	1500	51.3	
	2000	61.9	
	2800	83.2	
	3000	86.4	
32.0	10	31.1	31.3
	500	41.0	
	1000	48.9	
	1500	65.5	
	2000	81.5	
	2800	104.5	
	3000	111.0	
42.4	10	21.5	
	500	30.2	29.7
	1000	38.7	
	1500	46.1	47.6
	2000	59.0	
	3000	77.2	76.3

[a]The volume concentration units are those at 1 atm; see the text.

valid to a good accuracy. The integrated form of the rate equation is then

$$[1] \qquad G_t = \left(\frac{1}{kc_{t_0}}\right)\frac{G_{t_0} - G_t}{t - t_0} + G_\infty$$

where G_{t_0}, G_t, and G_∞ are the conductances at times t_0, t, and ∞, and c_{t_0} is the concentration of hydroxide ion and of ethyl acetate at time t_0.

The value c_{t_0} was obtained from the conductance G_{t_0} by comparing it with the conductance of various mixtures of sodium hydroxide and sodium acetate of total concentration 5 mM at various pressures. In the kinetic runs, c_{t_0} was 2.5 mM or less. No allowance was made for the reaction of acetone and sodium hydroxide as it is negligible under the experimental conditions. The measured conductances were fitted to Eq. 1 by least squares, minimizing the sum of squares of $G_{t_0} - G_t$. The standard deviation was about 0.5%.

The rate constants are summarized in Table 1 and are plotted against pressure at constant composition and against composition at constant pressure in Figs. 1 and 2. The concentration units are those at 1 bar because in the expression for the volume of activation $(\partial \ln k/\partial p)_T = -\Delta V^{\ddagger}/RT$, the rate constants must be expressed in suitable pressure-independent units.

The rate constants at 1 bar are lower than those

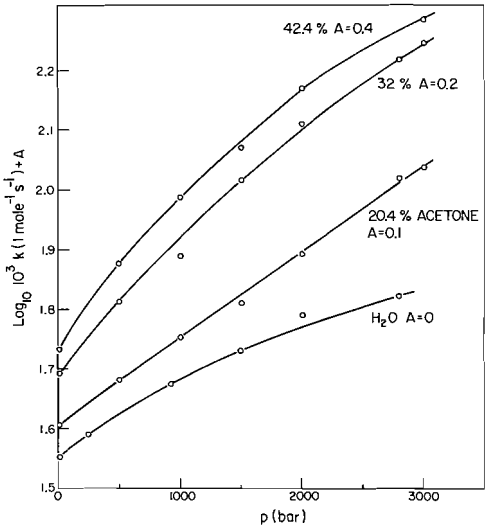

FIG. 1. Graph of log k against the pressure for the alkaline hydrolysis of ethyl acetate in acetone–water mixtures at 10.02 °C at the solvent composition in % w/w indicated on the graph. The data are from Table 2.

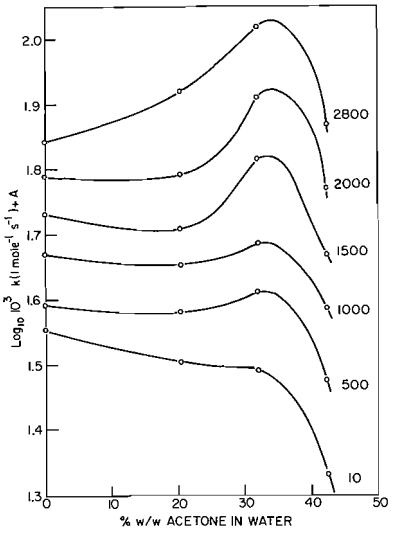

FIG. 2. Graph of log k against solvent composition for the alkaline hydrolysis of ethyl acetate at the pressures in bars indicated on the graph. The data are from Table 2.

TABLE 2. Volumes of activation and parameters of activation at constant volume for the alkaline hydrolysis of ethyl acetate in acetone–water mixtures at 10.02 °C

% w/w acetone in water	$\Delta V^{\ddagger}$ / cm^3 mol^{-1}	$T\alpha\Delta V^{\ddagger}/\kappa$ / kcal mol^{-1}	$\Delta H_p^{\ddagger a}$ / kcal mol^{-1}	$-T\Delta S_p^{\ddagger a}$ / kcal mol^{-1}	$\Delta U_v^{\ddagger}$ / kcal mol^{-1}	$-T\Delta S_v^{\ddagger}$ / kcal mol^{-1}
0	−7.6±0.5	−0.10	10.81	7.59	10.94	7.46
20.4	−8.9±0.5	−0.67	9.88	8.56	10.64	7.80
31.0	−13.1±0.7	−1.41	9.85	8.75	11.42	7.19
42.8	−16.8±1.0	−2.29	10.12	8.58	12.41	6.29

[a]To ensure at least internal consistency, all values of $\Delta H_p^{\ddagger}$ and $\Delta S_p^{\ddagger}$ were taken from ref. 8.

TABLE 3. Thermal expansivity and compressibility of acetone–water mixtures at 10.02 °C

Acetone in water (% w/w)	α/MK^{-1}	κ/Mbar^{-1}
0	91.9	47.9
20.4	495	44.7
31.0	745	46.8
42.8	967	48.0

previously reported (12, 13) probably because of the strong effect of the ionic strength (14, 15) on the rate constant.

The volume of activation was determined graphically by plotting $(\log k_i/k_j)/(p_i - p_j)$ against $\frac{1}{2}(p_i + p_j)$, where p_i and p_j are pressures corresponding to the rate constants k_i and k_j (8). The results are summarized in Table 2.

The volume of activation in water agrees well with the value −8.8 cm^3 mol^{-1} at 25 °C reported by Laidler and Chen (13) but less well with the values of $-4.5 \pm \sim 1$ cm^3 mol^{-1} calculated (2) from Cohen and Kaiser's (16) data at 2.4 °C and −5.6 and −6.4 cm^3 mol^{-1} reported by Andersen *et al.* (17) at 20 and 30 °C. The rate measurements of Andersen *et al.* were made at 0, 5, and 8 kbar only. Because of the curvature of the plot of log k *vs.* p in Fig. 1, these pressure intervals are quite inadequate (2, 18) and will yield a value numerically too low.

The energy and entropy of activation at constant volume, $\Delta U_v^{\ddagger}$ and $\Delta S_v^{\ddagger}$, were calculated from the enthalpy and entropy of activation at constant pressure, $\Delta H_p^{\ddagger}$ and $\Delta S_p^{\ddagger}$, by the relations

$$\Delta U_v^{\ddagger} = \Delta H_p^{\ddagger} - T\alpha\Delta V^{\ddagger}/\kappa$$

$$T\Delta S_v^{\ddagger} = T\Delta S_p^{\ddagger} - T\alpha\Delta V^{\ddagger}/\kappa$$

where T is the temperature and α and κ the thermal expansivity and compressibility of the solution. The compressibility and thermal expansivity

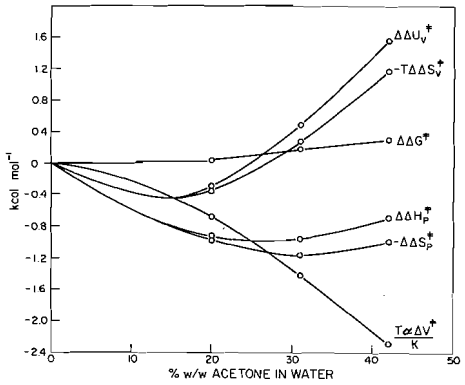

FIG. 3. Graph of the change, from the values in pure water, of the parameters of activation at constant pressure and at constant volume for the alkaline hydrolysis of ethyl acetate in acetone–water mixtures. The data are from Table 2.

were determined from literature values, (19–23) with interpolation and extrapolation as required. The errors of the values should cause no significant error for our purpose. The values of α and κ are listed in Table 3 and the constant-volume parameters are listed in Table 2. The constant-pressure and constant-volume parameters are plotted against solvent composition in Fig. 3.

Discussion

Energy and Entropy of Activation at Constant Volume

Both $\Delta H_p^{\ddagger}$ and $-T\Delta S_p^{\ddagger}$ have a minimum at about 25% w/w acetone in water, as shown in Fig. 3, as do many other reactions in this and related solvents. The depth of the minimum is reduced to about one third by the coordinate transformation to the constant-volume parameters. The addition of a small amount of acetone to the reaction mixture should change the energy of activation for the reaction only slightly, because

Can. J. Chem. Downloaded from www.nrcresearchpress.com by 210.87.254.6 on 09/05/12
For personal use only.

reactant molecules solvated by water will react faster than those solvated partly by acetone. But the low reactivity of some of the molecules increases the entropy of activation. At higher concentrations of acetone, molecules solvated partly by acetone begin to carry an appreciable part of the reaction, and the activation energy increases and at the same time the activation entropy starts to decrease. It appears, therefore, that constant-volume parameters vary with acetone concentration in a way more as expected on simple grounds than the constant-pressure parameters do. This is true of several other reactions also, which are reviewed in the Introduction.

When phenomena look simpler after a coordinate transformation, it is usual to think that the theoretical interpretation of the simpler-looking phenomena is simpler, unless there is strong reason to think otherwise. It is concluded therefore, until there is evidence to the contrary, that the constant-volume parameters are the simpler to understand.

The difference between the constant-pressure and constant-volume parameters is, of course $T\alpha\Delta V^{+}/\kappa$. The quantity that varies the most in our solvent range is the thermal expansivity, which as Table 3 shows, changes by a factor of about ten. The volume of activation changes by a factor of about 1.8, and the compressibility hardly changes at all. The minimum in the constant-pressure parameters can be ascribed largely to a relatively simple variation of the constant-volume parameters complicated by the large variation in the thermal expansivity.

If this is so, then in solvent mixtures that have only a small variation of the thermal expansivity with composition, even the constant-pressure parameters should be relatively simple. This prediction has been verified for the spontaneous hydrolysis by benzyl chloride in water-glycerol mixtures (5, 6).

We are greatly indebted to A. Lavergne for help with the high-pressure equipment.

1. E. M. Arnett. *In* Physico chemical processes in mixed aqueous solvents. *Edited by* F. Franks. Heinemann, London. 1963.
2. E. Whalley. Adv. Phys. Org. Chem. **2**, 93 (1964).
3. E. Whalley. Adv. High Pressure Res. **1**, 143 (1966).
4. (*a*) B. T. Baliga and E. Whalley. J. Phys. Chem. **71**, 1166 (1967); (*b*) B. T. Baliga and E. Whalley. Can. J. Chem. **48**, 528 (1970).
5. D. L. Gay and E. Whalley. J. Phys. Chem. **72**, 4145 (1968).
6. D. L. Gay and E. Whalley. Can. J. Chem. **48**, 2021 (1970).
7. B. T. Baliga and E. Whalley. Can. J. Chem. **42**, 1835 (1964).
8. B. T. Baliga, R. J. Withey, D. Poulton, and E. Whalley. Trans. Faraday Soc. **61**, 517 (1965).
9. T. Morioyoshi. Rev. Phys. Chem. Jpn. **41**, 22 (1971).
10. T. Morioyoshi. Rev. Phys. Chem. Jpn. **40**, 102 (1970).
11. B. T. Baliga and E. Whalley. J. Phys. Chem. **73**, 654 (1969).
12. E. Tommila, A. Koivisto, J. P. Lyyra, K. Antell, and S. Heimo. Ann. Acad. Sci. Fenn. Ser. A, **47**, (1952).
13. K. J. Laidler and D. Chen. Trans. Faraday Soc. **54**, 1026 (1958).
14. J. E. Potts and E. S. Amis. J. Am. Chem. Soc. **71**, 2112 (1949).
15. E. S. Amis and S. Siegel. J. Am. Chem. Soc. **72**, 674 (1950).
16. E. Cohen and H. F. G. Kaiser. Z. Phys. Chem. **89**, 338 (1915).
17. B. Andersen, F. Grønlund, and I. Olsen. Acta Chem. Scand. **23**, 2458 (1969).
18. S. D. Hamann. Aust. J. Chem. **9**, 533 (1956).
19. K. T. Thomas and R. A. McAllister. Am. Inst. Chem. Eng. **3**, 161 (1957).
20. J. Timmermans. The physico-chemical constants of binary systems in concentrated solutions. Vol. 4. Interscience, New York. 1960.
21. G. S. Kell and E. Whalley, Philos. Trans. R. Soc. London Ser. A **258**, 565 (1965).
22. R. C. Weast. (*Editor*). Handbook of Chemistry and Physics. 49th ed. Chemical Rubber Co., Cleveland. 1968. p. F12.
23. D. M. Newitt and K. E. Weale. J. Chem. Soc. 3092 (1951).

Can. J. Chem. Downloaded from www.nrcresearchpress.com by 210.87.254.6 on 09/05/12
For personal use only.

^{13}C Fourier Transform Nuclear Magnetic Resonance. XI. Pyridine *N*-Oxide Derivatives

ROBERT J. CUSHLEY, DAVID NAUGLER, AND CARLOS ORTIZ
Department of Chemistry, Simon Fraser University, Burnaby, British Columbia V5A 1S6

Received October 8, 1974[1]

ROBERT J. CUSHLEY, DAVID NAUGLER, and CARLOS ORTIZ. Can. J. Chem. **53**, 3419 (1975).

Formation of the *N*-oxide for several pyridine derivatives results in a large upfield shift of the 2-, 4-, and 6-carbons and a significant downfield shift of the 3- and 5-carbons. The chemical shifts ($\Delta\delta$) are consistent with a resonance and electric field mechanism. Molecular orbital calculations using CNDO/2 show a qualitative correlation between excess charge density and $\Delta\delta$.

ROBERT J. CUSHLEY, DAVID NAUGLER et CARLOS ORTIZ. Can. J. Chem. **53**, 3419 (1975).

La transformation de plusieurs dérivés de la pyridine en *N*-oxyde conduit à de grands déplacements vers les hauts champs pour les carbones 2, 4 et 6 et à des déplacements importants vers les bas champs pour les carbones 3 et 5. Les déplacements chimiques ($\Delta\delta$) sont en accord avec un mécanisme de résonance et de champ électrique. Des calculs d'orbitale moléculaire CNDO/2 montrent qu'il y a une corrélation qualitative entre l'excès de la densité de charge et le $\Delta\delta$.

[Traduit par le journal]

Introduction

The *N*-oxide group has become increasingly more important as a biological functionality. Aliphatic *N*-oxides were recognized as early as 1945, when it was discovered that trimethylamine was oxidized to trimethylamine *N*-oxide in hog liver microsomes (1). Aromatic *N*-oxides were found to be biologically active when Neuberg (2) conducted his classic studies with pyridine *N*-oxide. Chemically, the $N \rightarrow O$ group s analogous to OH^+, hence, protonated *N*-oxides represent possible electrophilic reagents. Much more important however, is their role as a biological oxygenating agent. *N*-oxides have been depicted as the main moiety responsible for biological demethylation of *N*-methyl derivatives (3, 4). Nicotinamide *N*-oxide has been shown to be an intermediate in uric acid formation, being first converted to xanthine with xanthine oxidase (5). Many *N*-oxides have been found in nature. For instance, substituted quinoline *N*-oxides and quinoxalin *N*,*N*-dioxides have been found to be antiviral agents (6) and a large number of *N*-oxides have been shown to have antibacterial activity including the antibiotics aspergillic acid, emimycin, iodinin, and myxin. The latter compounds are all formally related to diketopiperazines.

Finally, several pyrrolizidine alkaloids such as senecionine *N*-oxide have been demonstrated to be the tumor inhibitory principals of plant extracts (7). It must be added, however that purine *N*-oxides have proven to be potent oncogenic[2] agents.

In order to gather insight into the structures and electronic configurations of this class of biologically important compounds, we have determined the ^{13}C chemical shift parameters of a series of pyridines and their *N*-oxides. ^{13}C chemical shifts have been shown to be an effective means for calculation of electron densities and *vice versa*. The sensitivity of the method derives from the fact that in the ^{13}C shielding constant tensor (8)

$$[1] \qquad \sigma = \sigma_d + \sigma_p + \sigma'$$

the paramagnetic term, σ_p, dominates, hence, the large dispersion of ^{13}C shifts results.

Pugmire and Grant (9) have reported that carbons α to the nitrogen in various five-membered nitrogen heterocycles are strongly shielded on protonation of the nitrogen, by about 9.0 p.p.m. Explanations of this phenomenon differ; Grant has proposed a change in the N—C bond order, while Adam *et al.* (10) have considered changes in the average excitation energy. This protona-

[1]Revision received July 28, 1975.

[2]An agent which induces any form of neoplasm is oncogenic. Carcinogenic should be reserved for agents inducing carcinomas.

Can. J. Chem. Downloaded from www.nrcresearchpress.com by 210.87.254.5 on 09/05/12
For personal use only.

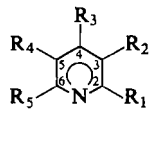

1 R_1–R_5 = H
3 R_1 = CH_3; R_2–R_5 = H
5 R_2 = CH_3; R_1, R_3–R_5 = H
7 R_3 = CH_3; R_1, R_2, R_4, R_5 = H
9 R_3 = CN; R_1, R_2, R_4, R_5 = H
10 R_1, R_5 = CH_3; R_2–R_4 = H

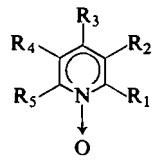

2 R_1–R_5 = H
4 R_1 = CH_3; R_2–R_5 = H
6 R_2 = CH_3; R_1, R_3–R_5 = H
8 R_3 = CH_3; R_1, R_2, R_4, R_5 = H

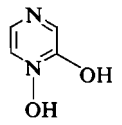

Aspergillic acid

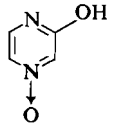

Enimycin

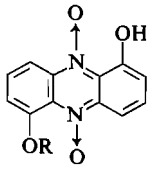

R = H; Iodinin
R = CH_3; Myxin

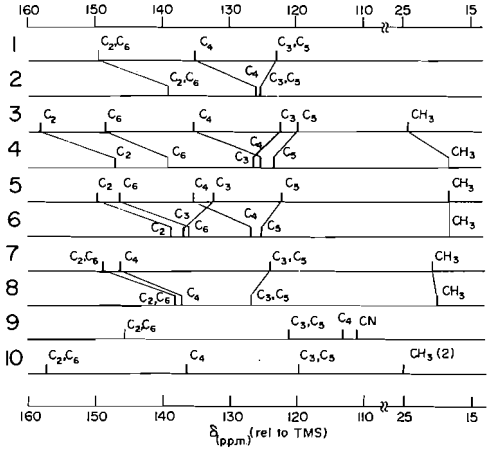

FIG. 1. ^{13}C chemical shifts of pyridines and pyridine *N*-oxide derivatives.

tion of a heterocycle has been envisioned as primarily a σ-bond change (10*a*). However, ^{13}C chemical shifts must be correlated with total (σ and π) electron density distributions (11, 12).

Results and Discussion

We have studied pyridine (**1**), α-, β-, and γ-picolines (2-, 3-, and 4-methylpyridines, **3**, **5**, **7**) and their *N*-oxides (**2**, **4**, **6**, **8**). The model compounds 4-cyanopyridine (**9**) and 2,5-dimethylpyridine (**10**) were also studied. The complete ^{13}C chemical shift assignments for compounds **1–10** are contained in Fig. 1 and Table 1 contains the chemical shifts for the pyridine – pyridine *N*-oxide pairs **1–8**. The ^{13}C assignments were made on the basis of previous literature values (13–15), model studies, and single resonance spectra. In

TABLE 1. ^{13}C chemical shifts of pyridines and their *N*-oxides*

	Position					
Compound	2	3	4	5	6	Me
1	149.59	123.46	135.58	123.46	146.59	—
2	139.09	125.65	126.10	125.65	139.09	—
3	158.10	123.01	135.95	120.46	148.88	24.36
4	148.83	126.43	125.30	123.52	139.21	17.75
5	150.06	132.84	136.15	122.93	146.73	18.34
6	138.92	136.74	127.22	125.37	136.26	18.19
7	149.33	124.43	146.72	124.43	149.33	20.89
8	138.44	126.63	137.46	126.63	138.44	20.20

*Chemical shifts are downfield from internal TMS.

Can. J. Chem. Downloaded from www.nrcresearchpress.com by 210.87.254.5 on 09/05/12
For personal use only.

Can. J. Chem. Downloaded from www.nrcresearchpress.com by 210.87.254.5 on 09/05/12
For personal use only.

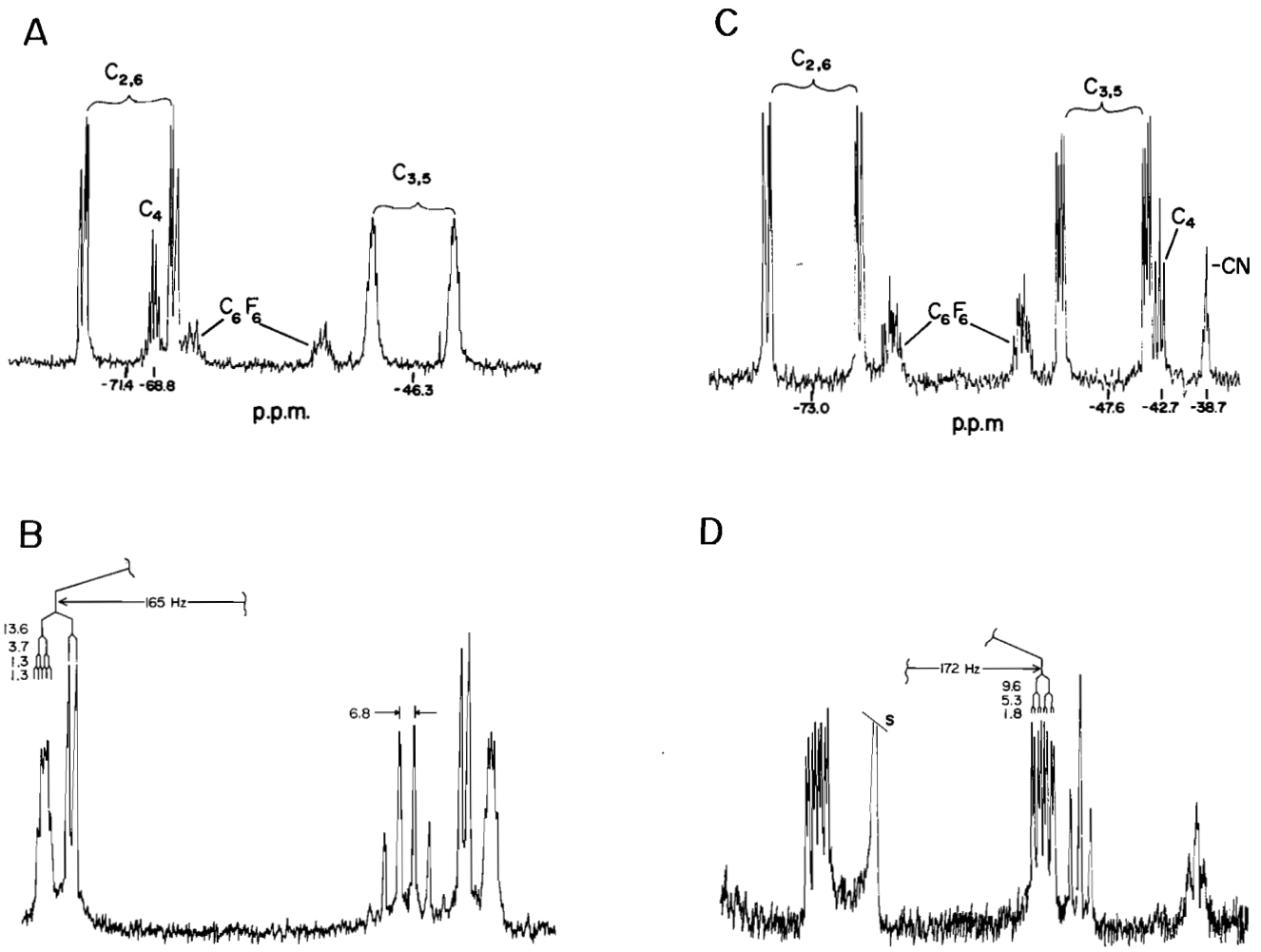

FIG. 2. (*A*) Pulsed double resonance ^{13}C spectrum of 20% 4-methylpyridine, **7**, in $CHCl_3$; 1.25 Hz resolution; (*B*) expansion of spectrum *A*, 65–78 p.p.m.; 0.31 Hz resolution; (*C*) pulsed double resonance ^{13}C spectrum of 20% 4-cyanopyridine, **9**, in $CHCl_3$; 1.25 Hz resolution; (*D*) expansion of spectrum *C*, 36–52 p.p.m.; 0.31 Hz resolution (s = solvent line).

Can. J. Chem. Downloaded from www.nrcresearchpress.com by 210.87.254.5 on 09/05/12
For personal use only.

order to obtain the single resonance spectra we utilized gated proton decoupling. Our needs were the usual, to observe small ^{13}C–^{1}H splittings while cutting down scanning time by utilizing Overhauser enhanced signals due to pulsed double resonance effects (16). To this end we have had cause to construct a Digital Gate Width Control unit for pulsed double resonance studies (see Experimental).

The first pulsed double resonance ^{13}C–Fourier transform (FT) spectrum, shown in Fig. 2*A*, is that of 4-picoline (4-methylpyridine, **7**). In Fig. 2*A* the spectrometer resolution is 1.25 Hz. The C_2,C_6 peaks on either side of the C_4 sextet show a *unique* coupling pattern. The same pattern is seen in the splitting pattern for 4-cyanopyridine, **9**, Fig. 2*C*. The FT resolution of **7** was increased as shown in Fig. 2*B* for the region 65–78 p.p.m. downfield from the solvent peak, $CHCl_3$. The resolution was increased to 0.31 Hz (8K data set; 2.5 kHz digitizing rate) and clearly shows the outermost lines as pentets while the innermost lines remain doublets. The C_3,C_5 peaks, not shown, resolve into 15 line doublets indicating a 4-bond coupling to the methyl protons. As well, the methyl resonance consists of broadened quartets of triplets, indicating a small (<0.3 Hz) 4-bond coupling between the side-chain methyl carbon and the 2,6-protons.

The single resonance ^{13}C spectrum of the 4-cyano compound **9** shows an altered C_3,C_5 region, illustrated in the following 0.31 Hz resolution segment, Fig. 2*D*. The expected eight line multiplet for each peak of the doublet is shown and reinforces the assignment for 4-picoline, **7**. The ^{13}C resonance for the cyano group, although broadened by the quadrupolar nitrogen, does show a triplet of triplets indicating side chain carbon to ring hydrogen coupling of 4-bonds.

Although several examples of long range cross-ring coupling have appeared in the literature there is a paucity of information on ring to side-chain coupling. Thus, while cross-ring coupling has been reported for pyrrole and 2,5-dimethylpyrrole by Weigert and Roberts (17), no data was reported for side-chain to ring ^{13}C–^{1}H coupling.

We have previously reported on ring to side-chain long range couplings in pyrroles (18) and the present single resonance work provides further evidence for such interactions.

Figure 1 lists the chemical shift behavior of the pyridines upon *N*-oxide formation as well as their assignments. In all cases, upon *N*-oxide formation, the *ortho* and *para* positions undergo an upfield ^{13}C shift of up to 10 p.p.m. (225 Hz), while the *meta* positions undergo a smaller but still substantial downfield shift. The significant changes in ^{13}C shifts represent a substantial change in the electronic configuration of *N*-oxides as compared to the unoxidized parent compound. The results agree qualitatively with the canonical forms by which pyridine *N*-oxide may be represented, *viz.*

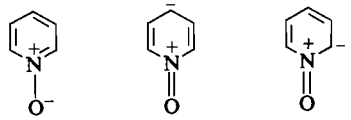

Increased electron density at the C_2,C_6 and C_4 carbons due to the oxygen function cause a paramagnetic shift. The lesser downfield shift of C_3,C_5 may be explained by a resonance polar effect (19) wherein the increased electron density at C_2,C_6 or C_4 causes a decrease in electron density at C_3,C_5, hence, the 3- and 5-carbons shift downfield. Such an effect is a π (resonance) effect or an electric field effect. Support both for and against resonance quinoid forms for the *N*-oxides has been suggested by a very recent molecular structure determination of **2** (20) which shows a shortened C=N bond distance, and the X-ray data of Ulku *et al.* (21) who suggest N—O and C_2—C_3 bond distances disfavor quinoid forms.

To shed further light on the situation we have calculated the electron densities of our series of *N*-oxides *vs.* unoxidized substrates by means of CNDO/2 calculations using the Dobosh modification of the CNDO/MO computer program (22). Calculations were performed on an IBM 370-155 computer. The charge densities are given in Table 2.

The shielding tensor for ^{13}C can be represented by

$$\sigma = \sigma_d + \sigma_p$$

where σ_d is given by the formula

$$\sigma_d = (e^2/3mc^2) \sum_i \langle r_i^{-1} \rangle$$

where $\langle r_i^{-1} \rangle$ is the mean inverse distance of the ith electron from the nucleus (23).

$$\sigma_p^A = (2e^2h^2/3m^2c^2)(\Delta E)\langle r^{-3} \rangle_{2p}(P_1 - P_2 - P_3)$$

$$P_1 = (P_{xx} + P_{yy} + P_{zz})_{AA}$$

TABLE 2. Charge densities calculated by CNDO/2

Compound	Position 2	3	4	5	6	Me
1	3.8450	4.0278	3.9304	4.0278	3.8450	—
2	3.9996	3.9497	4.0040	3.9497	3.9996	—
3	3.8422	4.0385	3.9276	4.0336	3.8432	3.9780
4	3.9704	3.9671	3.9978	3.9584	3.9944	3.9401
5	3.8574	4.0110	3.9428	4.0240	3.8517	3.9415
6	4.0148	3.9384	4.0172	3.9471	4.0068	3.9543
7	3.8420	4.0403	3.9215	4.0406	3.8420	3.9594
8	3.9949	3.9648	3.9834	3.9645	3.9944	3.9450

$$P_2 = (P_{xx}P_{yy} + P_{yy}P_{zz} + P_{zz}P_{xx})_{AA}/2$$

$$P_3 = \sum_{B \neq A} (P_{xx}P_{yy} + P_{yy}P_{zz} + P_{zz}P_{xx})_{AB}/2$$

where

$$(P_{xx})_{AB} = 2\sum_{i}^{occ} C_{xA}{}^{i}C_{xB}{}^{i}$$

and $C_{xA}{}^{i}$ is the coefficient of the $2P_x$ atomic orbital of carbon A in the ith MO. Here the principal simplifications are neglect of two center integrals and substitution of the average excitation energy, ΔE, for the electronic excitation energies (23). Thus, this semiempirical calculation is dependent on the choice of ΔE (10*b*), however, a recent study by Strong *et al.* (24) has shown that the use of ΔE (=10 eV) is a good approximation of the sum over all energy states, $\sum_{n \neq 0}(E_n - E_0)$, for a variety of compounds. The above treatment predicts a proportionality between the ^{13}C chemical shifts, $\Delta\sigma$, and the excess charge density, ΔQ_{2p}, calculated by CNDO/2 if $\Delta\delta$ is due to a total electron density change. A plot of $\Delta\delta$ *vs.* ΔQ_{2p} is shown in Fig. 3 for the compound pairs **1–8** based on the chemical shifts contained in Table 1 and the charge densities contained in Table 2.

In the cases of picolines and picoline *N*-oxides, the minimum interaction between the methyl group and heteroaromatic ring has been calculated before evaluating MO's. This was performed using the perturbation treatment of configuration interaction, PCILO (25). Thus, molecular geometries from X-ray, microwave, or

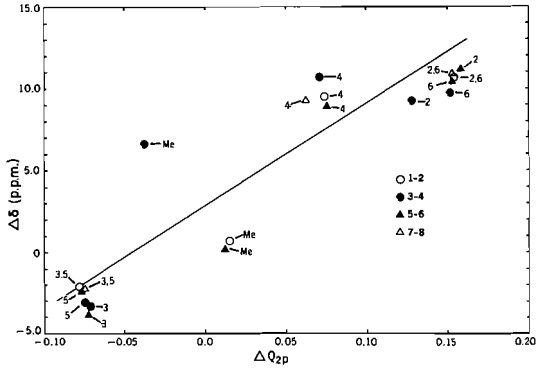

FIG. 3. Plot of ^{13}C chemical shifts between pyridines and their *N*-oxides *vs.* excess charge density. The solid line is represented by $\Delta\delta = \beta\Delta Q_{2p} + \alpha$ where $\beta = 58.85$ ($\sigma = 6.11$) and $\alpha = 2.539$ ($\sigma = 0.612$).

standard geometries are treated by PCILO. The output includes a new set of atomic coordinates corresponding to the minimum energy conformation which are used directly as the input data for the CNDO calculation.

Minimum energy calculations for compounds **3–8** predict essentially free rotation of the methyl substituent on the heteroaromatic ring except in the case of 2-picoline *N*-oxide (**3**). In the case of **3** a nonbonded interaction between N–O and C_2–CH_3 leads to a preferred conformation **A** where a methyl C—H eclipses the C_3—H bond. Conformation **A** is more stable by 3.2 kcal than conformation **B** where the methyl C—H would eclipse the N → O, and 1.2 kcal more stable than the staggered form (CH_3 rotated 90°).

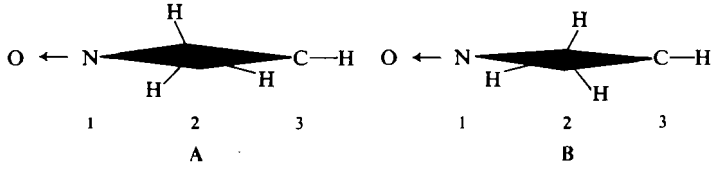

Can. J. Chem. Downloaded from www.nrcresearchpress.com by 210.87.254.5 on 09/05/12
For personal use only.

Evidence of a steric interaction between the methyl group and oxygen probably accounts for the failure of the C_2 methyl group to conform to the plot in Fig. 3. A nonbonded interaction of this sort might result in bond length or bond angle changes not accounted for in the CNDO calculations but reflected in the lower $^{13}CH_3$ chemical shift in compound **3** (Fig. 1 and Table 1).

Experimental

Compounds **1–10** were obtained commercially (K and K Chemicals, ICN, Eastman, and MCB), and used without further purification.

Spectra were obtained using a Computer Controlled Fourier Transform system described previously (26) and samples composed of 20% w/v solutions in $CHCl_3$ containing 20% C_6F_6 for field frequency locking and with TMS as internal standard. For the proton noise decoupled spectra FT system settings were: data set = 8192; pulse width = 50 μs; receiver skip = 100 μs; digitizing rate = 10 kHz. For pulsed double resonance spectra FT system settings were: data set = 8192; pulse width = 50 μs; receiver skip = 100 μs; IRRAD[3] = 1.0 s; program delay = 1.0 s; digitizing rate = 2.5 kHz.

The chemical shift values in Table 1 were obtained using a Varian XL-100 spectrometer fitted with a 20K TT100 Fourier transform accessory. Samples were 20% w/v in $CDCl_3$ (deuterium internal lock) using internal TMS as a standard. Settings were: data set = 16K; pulse width 22 μs; receiver skip = 100 μs; digitizing rate = 10 kHz.

1. E. R. Norris and C. J. Benoit. J. Biol. Chem. **158**, 443 (1965).
2. C. Neuberg. Bull. Res. Counc. Isr., **4**, 12 (1954).
3. M. S. Fish, W. M. Johnson, E. P. Lawrence, and E. C. Horning. Biochim. Biophys. Acta, **18**, 564 (1955).
4. B. B. Brodie, J. R. Gillette, and S. N. LaDu. Annu. Rev. Biochem. **57**, 427 (1958).
5. K. N. Murray, J. E. Watson, and S. Chayki. J. Biol. Chem. **241**, 4798 (1966).
6. J. K. Landquist. J. Chem. Soc. 2816 (1953).
7. S. M. Kupchan and M. J. Suffness. J. Pharm. Sci. **56**, 541 (1967).
8. A. Saika and C. P. Slichter. J. Chem. Phys. **23**, 26 (1954).
9. R. J. Pugmire and D. M. Grant. J. Am. Chem. Soc. **90**, 697 (1968).
10. (*a*) W. Adam, A. Grimison, and G. Rodriguez. Tetrahedron, **23**, 2513 (1967); (*b*) W. Adam, A. Grimison, and G. Rodriguez. J. Chem. Phys. **50**, 645 (1969).
11. J. E. Bloor and D. L. Breen. J. Am. Chem. Soc. **89**, 6835 (1967).
12. T. Tokuhiro, N. K. Wilson, and G. Fraenkel. J. Am. Chem. Soc. **90**, 3622 (1968).
13. P. C. Lauterbur. J. Chem. Phys. **43**, 360 (1965).
14. G. Miyajima, Y. Sasaki, and M. Suzaki. Chem. Pharm. Bull. **20**, 429 (1972).
15. (*a*) H. L. Retcofsky and R. A. Friedel. J. Phys. Chem. **71**, 3592 (1967); (*b*) Y. Takeuchi and N. Dennis. J. Am. Chem. Soc. **96**, 3657 (1974).
16. R. Freeman and H. D. W. Hill. J. Magn. Reson. **5**, 278 (1971).
17. F. J. Weigert and J. D. Roberts. J. Am. Chem. Soc. **90**, 3543 (1968).
18. R. J. Cushley, R. J. Sykes, C.-K. Shaw, and H. H. Wasserman. Can. J. Chem. **53**, 148 (1975).
19. R. W. Taft and M. S. Newman. Steric effects in organic chemistry. Wiley, New York. 1956. pp. 570, 578.
20. J. F. Chiang. J. Chem. Phys. **61**, 1280 (1974).
21. D. Ulku, B. P. Huddle, and J. C. Morrow. Acta. Crystallogr. Sect. B, **27**, 432 (1971).
22. P. A. Dobosh. Carnegie-Mellon University, Pittsburgh, Pa. CNINDO Molecular Orbital Program, Quantum Chemistry Exchange Program 141.
23. M. Karplus and J. A. Pople. J. Chem. Phys. **38**, 2803 (1963).
24. A. B. Strong, D. Ikenberry, and D. M. Grant. J. Magn. Reson. **9**, 145 (1973).
25. P. Claverie *et al.* Laboratoire de Chimie Quantique, Institut de Biologie Physiochimique. 13 rue P. et M. Curie, Paris 53, France. Perturbation Configuration Interaction using Localized Orbitals Method (PCILO). Quantum Chemistry Exchange Program 220/221.
26. R. J. Cushley, D. R. Anderson, and S. R. Lipsky. Anal. Chem. **43**, 1281 (1971).

[3]The pulse for gating the proton noise-decoupling frequency (IRRAD) is created when the leading edge of the receiver gating pulse (26) triggers a Gate Width Control Unit whose pulse length is selected by thumb wheels. The IRRAD pulse is delayed for a period just greater than required to accumulate 8192 data points at rates (in the present instance) as low as 2.5 kHz. Concomitant with the IRRAD pulse, the next r.f. pulse is delayed by a time greater than the IRRAD pulse length, using the program delay inherent in the routine NIN10 (26).

Can. J. Chem. Downloaded from www.nrcresearchpress.com by 210.87.254.5 on 09/05/12
For personal use only.

Diprotonation of 5-Acyl-1,2,3,4,5-pentamethylcyclopentadienes

RONALD F. CHILDS AND MAUNG ZEYA
Department of Chemistry, McMaster University, Hamilton, Ontario L8S 4M1

Received June 17, 1975

RONALD F. CHILDS and MAUNG ZEYA. Can. J. Chem. **53**, 3425 (1975).

5-Acyl-1,2,3,4,5-pentamethylcyclopentadienes could potentially be protonated on either or both of two sites, the diene moiety in the five-membered ring or the carbonyl oxygen. The protonation of a series of 5-acylpentamethylcyclopentadienes has been examined and evidence is presented which shows that the former site is essentially completely protonated in FSO_3H and that the carbonyl oxygen is also partially protonated. The extent of diprotonation is shown to be dependent both on the nature of the acyl groups and also the acidity of the medium. At temperatures above 40 °C these protonated species undergo a clean fragmentation to give protonated pentamethylcyclopentadiene from which pentamethylcyclopentadiene can be recovered in good yield on quenching the acid solution.

RONALD F. CHILDS et MAUNG ZEYA. Can J. Chem. **53**, 3425 (1975).

En théorie, les acyl-5 pentaméthyl-1,2,3,4,5 cyclopentadiènes peuvent se protoner sur l'un ou l'autre ou sur deux sites soit la portion diénique du cycle à cinq chainons ou l'oxygène du carbonyle. On a étudié la protonation d'une série d'acyl-5 pentaméthylcyclopentadiènes et on présente des données qui démontrent que le premier site est pratiquement complètement protoné dans le FSO_3H et que l'oxygène du carbonyle est aussi partiellement protoné. On montre que la quantité de diprotonation dépend à la fois de la nature des groupes acyles et aussi de l'acidité du milieu. A des températures supérieures à 40 °C, les espèces protonées subissent une fragmentation propre pour conduire au pentaméthylcyclopentadiène protoné à partir duquel on peut recupérer du pentaméthylcyclopentadiène avec de bons rendements en diluant la solution acide dans de l'eau.

[Traduit par le journal]

Introduction

In order to extend our studies on the bicyclo-[3.1.0]hexenyl cations and to explore the importance of the related cyclopentadienylcarbinyl cations in their five-fold degenerate rearrangement (1), it became necessary to prepare examples of these cations with an oxygen substituent at C_6. As it has been previously shown that ionization of the cyclopentadienyl ester **1** takes place with anchimeric assistance to give the bicyclohexenyl cations **2** (2), one obvious synthetic route to these cations would be the reaction of the carbonyl oxygen of a 5-acylcyclopentadiene with a suitable electrophile. When Lewis acids are used as the electrophile this approach works well (3), however the situation is much more complex when a proton is employed. We describe here the results of a study of the protonation of several 5-acylpentamethylcyclopentadienes in FSO_3H and show that protonation of the diene moiety occurs in addition to protonation of the carbonyl oxygen.

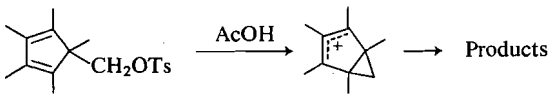

1 **2**

Results and Discussion

5-Acetylpentamethylcyclopentadiene, **3**, was protonated by extraction from CH_2Cl_2 into FSO_3H at −78 °C. From the complexity of the low temperature n.m.r. spectrum of the resulting solution, Fig. 1, it was quite clear that protonation was not simply occurring on the carbonyl oxygen. So as to ensure that the n.m.r. spectrum obtained derived simply from products of protonation of **3** and not subsequent rearrangements or fragmentations, the acid solution was quenched in an ether–HCO_3^- suspension to yield **3** in greater than 90% recovery.

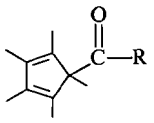

3 R = CH_3
4 R = CH_2CH_3
5 R = C_6H_5
6 R = *p*-MeO—C_6H_4

In order to identify the resonance attributable to the C_6 methyl group, the related ketones **4**, **5**, and **6** were protonated with FSO_3H. Examination of the n.m.r. spectra of the solutions so obtained, showed that in each case a similar product to that obtained from **3** was formed. It was apparent that the resonance at 3.07 δ in the

Can. J. Chem. Downloaded from www.nrcresearchpress.com by 210.87.254.42 on 09/05/12
For personal use only.

TABLE 1. Proton chemical shifts for protonated ketones and related materials

Compound protonated	Acid medium	Position* C_1/C_3 Me	C_2 Me	C_4 Me	H	C_5 Me	C_6 substituent
3	FSO_3H	3.07 2.90	2.27	1.46d	3.8m	1.89	3.07
		3.08 2.99	2.27	1.63d	3.8m	1.77	2.99
3	FSO_3H–SbF_5	3.08 2.94	2.28	1.48d	3.9m	1.95	3.31
		— —	2.28	1.6d	—	1.83	3.21
4	FSO_3H	3.06 2.93	2.27	1.59d	3.7m	1.75	2.98q 1.32t
		— —	—	1.16d	—	1.85	— —
5	FSO_3H	3.19 2.89	2.42	1.57d	4.3m	2.07	7.79–8.17
		— —	—	1.76d	—	1.92	—
6	FSO_3H	3.12 2.88	2.40	1.68d	4.1m	1.83	4.19, 7.27–7.84
		— —	—	1.45d	—	1.98	—
7	FSO_3H	2.89 2.89	2.22	1.50d	3.56m	1.50	—
		2.89 2.89	2.22	1.43d	3.56m	1.43	—

*In p.p.m. measured from internal CH_2Cl_2 taken as 5.30 δ. All spectra recorded at −25 °C; d, doublet; t, triplet; q, quartet; m, multiplet.

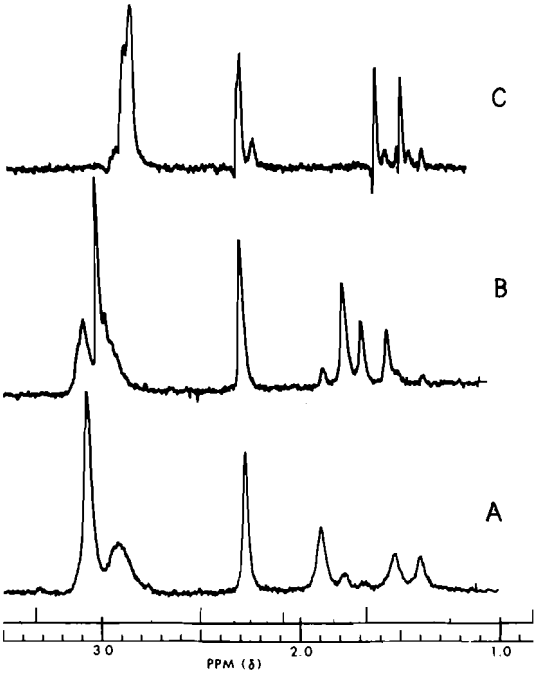

FIG. 1. Protonated 5-acetylpentamethylcyclopentadiene; *A*, initial protonation at −25 °C; *B*, after equilibration at 0 °C; *C*, after thermal fragmentation at 44 °C.

spectrum of protonated **3** was due to the C_6 methyl group and that the rest of the signals must be due to the methyl groups on the five-membered ring.

The high field doublets present in the n.m.r. spectra of these protonated ketones suggested that protonation on the five-membered ring had occurred. Consistent with this is presence of a broad resonance 3.7–4.0 δ, which is in a similar position to that found for a methine proton adjacent to an allylic cation in a five-membered ring (4). Confirmation of this ring protonation was obtained by solution of **6** in FSO_3D when the n.m.r. spectrum so obtained differed from that of **6** in FSO_3H in that the two high field doublets at 1.68 δ and 1.45 δ were now singlets and the resonance at 4.10 δ was absent.

There are two possible structural isomers that could result from protonation of the diene moiety; the proton could be situated either *cis* or *trans* with respect to the acyl group. A similar situation has been found for the protonation of pentamethylcyclopentadiene **7** (5), which gives both **8** and **9** upon solution in super acids. The cations **8** and **9** indeed serve as good models for what would be expected for the positions of the ring methyl resonances of the ketones if protonation of the diene were occurring. Thus while the cations derived from **3**, **4**, **5**, and **6** lack the inherent symmetry of **8** and **9**, it can be seen from Table 1 that the n.m.r. spectra of these two sets of cations are very similar. It would appear clear that protonation of these ketones is taking place on the five-membered ring and that the products can be at least partially represented as being made up of a mixture of **10** and **11**.

While it has not been possible to distinguish between **10** and **11** on the basis of their spectra, it is apparent that they are not produced in

Can. J. Chem. Downloaded from www.nrcresearchpress.com by 210.87.254.42 on 09/05/12
For personal use only.

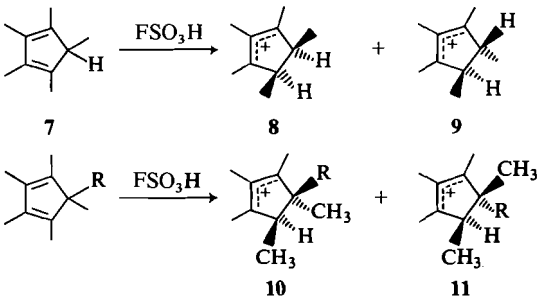

7 8 9

10 11

R = Acyl R = Acyl or protonated acyl

equal amounts on protonation of **3** at low temperatures. As is shown in Fig. 1*A*, the two isomers were initially present in a ratio of 80:20. At higher temperatures **10** and **11** interconverted and a thermodynamic product distribution was eventually reached in which the ratio was 15:85, Fig. 1*B*, which was the inverse of the initial kinetic distribution of products. This interconversion of the two isomers was rapid at 0 °C (pseudo first-order rate constant *ca.* 10^{-2} s^{-1}). When **3** was protonated in FSO_3H–SbF_5 (4:1), the same 80:20 kinetic distribution of products was observed, however in this stronger acid medium (6) no interconversion of the isomers **10** and **11** could be detected up to 40 °C, when other rearrangements and a general decomposition occurred. Comparable kinetic and thermodynamic product distributions have been reported with the cations **8** and **9** derived by protonation of **7** (5).

It is not unexpected that protonation of the diene moiety of these ketones is occurring in FSO_3H. 3-Methylene-1,4,4,5,5-pentamethylcyclopent-1-ene is sufficiently basic to be 50% protonated in 33% H_2SO_4 ($pK_a = -1.8$) (7) and other similarly alkylated cyclopentenyl cations are formed in acid of about the same strength. The carbonyl function, however, would be expected to be much less basic than the diene. Pinacolone, which is a reasonable model for **3**, is half protonated in 81% H_2SO_4 ($pK_a = -7.1$) (8). Even the aryl substituted carbonyl groups of **5** and **6**, are expected to be less basic than the diene. Acetophenone is half protonated in 74% H_2SO_4 ($pK_a = -6.15$) and *p*-methoxyacetophenone in 63% H_2SO_4 ($pK_a = -4.71$) (9). Fluorosulfuric acid is a much stronger acid than any of these aqueous sulfuric acid solutions (6) and it is sufficiently acidic to essentially completely protonate either of the two possible sites, the diene or the carbonyl oxygen. From the results presented above it is apparent that protonation of the diene to give a cyclopentenyl cation has taken place. The question arises, however, as to whether the carbonyl oxygen is also protonated in FSO_3H, either in competition with, or in addition to that of the diene.

In the unprotonated ketone **3**, the resonance attributable to the C_6 methyl group occurs at 1.50 δ. When dissolved in FSO_3H, the signal due to this methyl is shifted very considerably further downfield and appears at 3.07 δ. Typically the resonance of a methyl group adjacent to a protonated carbonyl group of an aliphatic ketone occurs at *ca.* 3.0 δ (10), for example, those of acetone and pinacolone occurring at 2.97 δ and 2.90 δ respectively.[1] The large downfield shift of the C_6 methyl group of **3** and the close similarity in its position to other protonated ketones is suggestive that the carbonyl oxygen of **3** is at least partially protonated in FSO_3H. Additional support for this suggestion can be found by examining the changes that occur in the aryl regions of the n.m.r. spectra of **5** and **6** on protonation and comparing them with those observed on protonation of acetophenone and *p*-methoxyacetophenone (11), Table 2.

It is conceivable that instead of protonation on oxygen some interaction of the carbonyl oxygen with the cyclopentenyl cation such as is shown with **12** or **13**, could account for the observed deshielding of the C_6 groups. However, the magnitude of this deshielding and the similarity of the resonance positions of the C_6 substituents with model protonated ketones would render this suggestion unlikely.

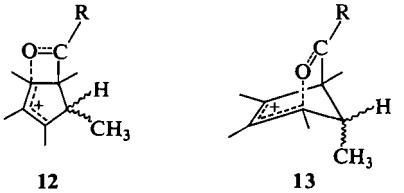

12 13

Further, definitive evidence for the protonation of the carbonyl group comes from the observation of an OH resonance in the n.m.r. spectrum of protonated **6**. The spectrum of **6**

[1]Care has to be taken in simply taking published literature values for the chemical shifts of cations as different standards are used as references. The values quoted in this paper are all based upon internal CH_2Cl_2 taken as 5.30 δ.

Can. J. Chem. Downloaded from www.nrcresearchpress.com by 210.87.254.42 on 09/05/12
For personal use only.

TABLE 2. Comparison of proton chemical shifts of some protonated and unprotonated ketones*

	Position			
	Neutral ($CDCl_3$)		Protonated (FSO_3H)	
Ketone	Aryl H	OCH_3	Aryl H	OCH_3
Acetophenone	7.23–7.80	—	7.71–8.64	—
5	7.14–7.60	—	7.79–8.17	—
p-Methoxyacetophenone	6.79–7.91	3.86	7.18–8.57	4.12
6	6.63–7.74	3.76	7.27–7.84	4.19

*In p.p.m., measured from internal CH_2Cl_2 taken as 5.30 δ for protonated species.

when protonated in a FSO_3H–SbF_5–SO_2ClF (4:1:4) medium was identical to that observed in FSO_3H with the exception that at low temperatures (−70 °C) an additional singlet at 12.70 δ was found. On warming the solution, this peak moved upfield and appeared to average with the solvent peak. The position of this low field resonance is just that expected for the OH signal of a protonated *p*-methoxyphenyl substituted ketone (11, 12). Thus, protonation of **6** would seem to be occurring both on the five-membered ring and also on the carbonyl oxygen. Either this could be taking place at the same time, resulting in the formation of two dications, or there could be an equilibrium between C and O protonated monocations. The latter possibility can be ruled out on several counts. Firstly, as has been previously pointed out, the resonance positions of both the ring methyls and also C_6 substituents are not consistent with a mixture of monoprotonated species being present. More importantly, in FSO_3H–SbF_5–SO_2ClF, observation of both hydroxy proton and methine proton resonances of protonated **6** at the same time shows that if two separate cations were responsible for these resonances, then their rate of interconversion must be slow on the n.m.r. time scale. However as the rest of the spectrum is not compatible with a slow equilibration between O and C monoprotonated cations, it can only be concluded that the hydroxy and methine proton resonances originate from the same species, dications **14** and **15**.[2]

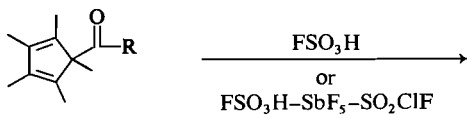

6 R = *p*-$MeOC_6H_4$—

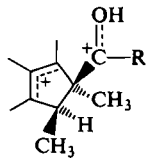

14 R = *p*-$MeOC_6H_4$—

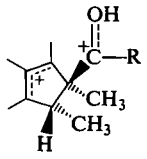

15 R = *p*-$MeOC_6H_4$—

As was pointed out earlier, the n.m.r. spectra of the cations derived by solution of **3** in FSO_3H cannot be simply accounted for on the sole basis of protonation of the five-membered ring. It was not possible however, to detect any —O*H* proton resonance in the low temperature n.m.r. spectra of **3** in FSO_3H–SbF_5 media, although the addition of SbF_5 to the acid did produce an effect on the positions of the methyl resonances. In particular, it will be noted in Table 1 that the resonance attributed to the C_6 methyl moved downfield by 0.24 p.p.m. in going from FSO_3H to a FSO_3H–SbF_5 mixture. This would imply that diprotonation of **3** is not complete in FSO_3H, and that the system exists as a fast equilibrating mixture of mono- and diprotonated species, Scheme 1. As the acidity of the medium is enhanced by the addition of SbF_5, the equilibrium position would be expected to be displaced further in favor of the diprotonated forms, resulting in a downfield shift of the C_6-methyl group.

Thermal Fragmentation

While FSO_3H solutions of ketones **3–6** were stable for long periods of time when kept below

[2]While the two dications **14** and **15** should give rise to two *OH* resonances, only one such signal could be detected. The second *OH* resonance would be expected to be only some 20–25% of the one observed and could be either lost in baseline noise or coincident with the peak at 12.70 δ.

Can. J. Chem. Downloaded from www.nrcresearchpress.com by 210.87.254.42 on 09/05/12
For personal use only.

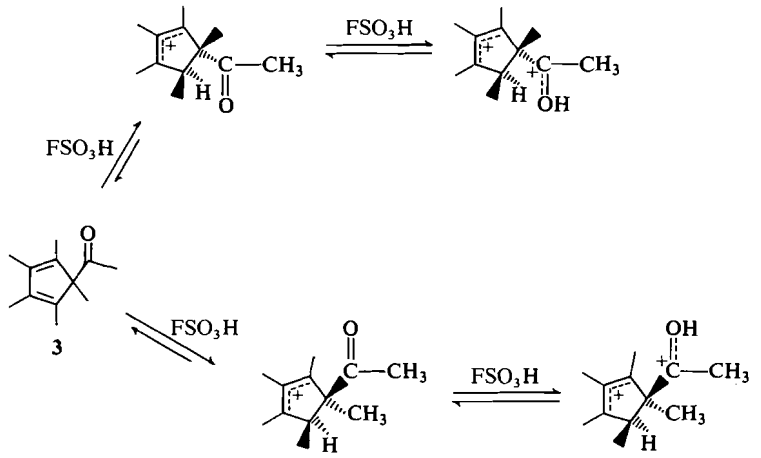

SCHEME 1

room temperature, at higher temperatures they underwent a thermal fragmentation to give protonated pentamethylcyclopentadiene. Thus **3** in FSO_3H reacted at 44 °C (half life 45 min) to give a mixture of **8** and **9**, Fig. 1*C*. Reaction of this acid solution with ether–HCO_3^- at −78 °C gave pentamethylcyclopentadiene **7** in high recovery.

$$\mathbf{3} \xrightarrow[\substack{44\,^\circ C \\ t_{1/2}\ 45\ min}]{FSO_3H} \mathbf{8} + \mathbf{9} \xrightarrow[\substack{ether \\ -78\,^\circ C}]{NaHCO_3} \mathbf{7}$$

The n.m.r. spectrum, Fig. 1*C*, of the products of this fragmentation reaction differed from that of authentic protonated pentamethylcyclopentadiene by the presence of an additional methyl resonance at 2.80 δ. Acyl cations are known to be stable in super acid media such as FSO_3H–SbF_5, and in the case of the fragmentation of protonated **3**, a methyl resonance attributable to the methyloxocarbonium ion at *ca.* 4 δ would be expected (13). The fragmentation of protonated **3** did not take place cleanly in FSO_3H–SbF_5, however the addition of SbF_5 to a FSO_3H solution after fragmentation caused a resonance corresponding to three protons, formally at 2.80 δ, to be shifted to 3.91 δ. It would appear that the acylium cation formed on fragmentation of **3** in FSO_3H must react with a nucleophile present in the acid medium to form a protonated acetic acid derivative, a reaction which is reversed upon the addition of SbF_5.

As pentamethylcyclopentadiene is not a readily available material (14) and acetylpentamethylcyclopentadiene can be obtained in one step from the commercially available hexamethylbicyclo[2.2.0]hex-2,5-diene (15, 16) the scale up of this fragmentation reaction in FSO_3H seemed attractive. However, whereas we have been able to carry out this reaction with up to 200 mg of material at a time, the yields drop as the reaction size is increased and these reactions do not as yet provide a viable alternate synthetic route to **7**.

Experimental

Nuclear magnetic resonance spectra were obtained on Varian HA-100 and A-60 spectrometers fitted with variable temperature probes. Probe temperature was measured with a copper–constantan thermocouple and Leeds and Northrup 8692 temperature potentiometer. The thermocouple was mounted at the appropriate depth in a nonrotating sample tube. Chemical shifts are referred to TMS or in the case of the cations, internal CH_2Cl_2 taken as 5.30 δ. Vapor phase chromatographic analyses were performed on an Aerograph 204B instrument, using 8 ft × $\frac{1}{8}$ in. columns packed with 15% SE-30 on 60–80 Chromosorb W and 20% Carbowax on 60–80 Chromosorb W.

Materials

Pentamethylcyclopentadiene was prepared by the method of de Vries (14). 5-Acylpentamethylcyclopentadienes were obtained by reaction of lithium pentamethylcyclopentadienide (15) with the appropriate acid halide (17). FSO_3H was distilled from a small quantity of NaF and stored in sealed glass ampoules until used. SbF_5 was doubly distilled and stored under nitrogen in a dry box. FSO_3H–SbF_5 solutions were prepared under nitrogen.

Preparation of Cations

Protonations in FSO_3H and FSO_3H–SbF_5 were carried out by slowly adding a CH_2Cl_2 solution (0.2 ml)

Can. J. Chem. Downloaded from www.nrcresearchpress.com by 210.87.254.42 on 09/05/12
For personal use only.

of the appropriate compound (20 mg) down the side of an n.m.r. tube which contained FSO_3H at −78 °C. After 15 s the two phases were mixed with a glass rod.

Preparation of Pentamethylcyclopentadiene, 7, from 5-Acetylpentamethylcyclopentadiene, 3

5-Acetyl-1,2,3,4,5-pentamethylcyclopentadiene, **3**, (178 mg) in methylene chloride (1 ml) was extracted into $HFSO_3$ (2 ml) kept at −78 °C. The sample was gradually warmed to 40 °C and kept for 3–4 h, complete reaction being checked for by n.m.r.

A suspension of sodium bicarbonate (5 g) in ether (25 ml) was stirred at −78 °C while the acid solution was added dropwise. The resulting mixture was warmed to 0 °C. Ice-water was added to the mixture and the stirring was continued for 15 min. The resulting solution was filtered *in vacuo* and the filtrate extracted with ether (3 × 25 ml). The extract was dried (Na_2CO_3) and evaporation of ether *in vacuo* yielded 148 mg of organic material.

The product was characterized as pentamethylcyclopentadiene by the comparison of its n.m.r. spectrum with that of an authentic sample. No other signal was observed in the n.m.r. spectrum of the product. Only two peaks were observed on the chromatogram when the product was subjected to v.p.c. analysis. The ratio of the amount of the major product to that of the minor was 19:1. The major product was collected and identified as pentamethylcyclopentadiene by the comparison of the n.m.r. spectra with an authentic sample.

This work was supported by a grant from the National Research Council of Canada. One of us (MZ) acknowledges the award of a scholarship from the Canadian International Development Agency.

1. R. F. Childs and S. Winstein. J. Am. Chem. Soc. **96**, 7146 (1968); D. W. Swatton and H. Hart. J. Am. Chem. Soc. **89**, 5075 (1967); H. Hart, T. R. Rodgers, and J. Griffiths. J. Am. Chem. Soc. **91**, 754 (1969); P. Vogel, M. Saunders, N. Hasty, Jr., and J. A. Berson, J. Am. Chem. Soc. **93**, 1551 (1971); I. S. Isaev, V. I. Mamatyuk, L. I. Kuzubova, T. A. Gordymova, and V. A. Koptyug. Zh. Org. Khim. **6**, 2482 (1970); V. A. Koptyug, L. I. Kuzubova, I. S. Isaev, and V. I. Mamatyuk. J. Chem. Soc. Chem. Commun. 389 (1969) and Zh. Org. Khim. **6**, 2258 (1970).
2. S. Winstein and M. Battiste. J. Am. Chem. Soc. **82**, 5244 (1960); L. de Vries. J. Am. Chem. Soc. **82**, 5242 (1960).
3. R. F. Childs and M. Zeya. J. Am. Chem. Soc. **96**, 6418 (1974).
4. N. C. Deno, H. G. Richey, Jr., N. Freidman, J. D. Hodge, J. J. Houser, and C. U. Pittman, Jr. J. Am. Chem. Soc. **85**, 2991 (1963); T. S. Sorensen. Can. J. Chem. **42**, 2768 (1964).
5. P. H. Campbell, N. W. K. Chiu, K. Deugau, I. J. Miller, and T. S. Sorensen. J. Am. Chem. Soc. **91**, 6404 (1969); T. S. Sorensen, I. J. Miller, and C. M. Urness. Can. J. Chem. **48**, 3374 (1970); D. M. Brouwer and J. A. van Doorn. Rec. Trav. Chim. Pays-Bas, **89**, 333 (1970).
6. R. J. Gillespie and T. E. Peel. Adv. Phys. Org. Chem. **9**, 1 (1971).
7. N. C. Deno, J. Bollinger, N. Friedman, K. Hafer, J. D. Hodge, and J. J. Houser. J. Am. Chem. Soc. **85**, 2998 (1963).
8. H. J. Campbell and J. T. Edward. Can. J. Chem. **38**, 2109 (1960).
9. R. Stewart and K. Yates. J. Am. Chem. Soc. **80**, 6355 (1958).
10. D. M. Brouwer. Rec. Trav. Chim. Pay-Bas, **86**, 879 (1967); G. A. Olah, A. M. White, and D. H. O'Brien. *In* Carbonium ions, Vol. **4**. Wiley-Interscience, Toronto. 1973. p. 1697.
11. T. Birchall and R. J. Gillespie. Can. J. Chem. **43**, 1045 (1965).
12. M. Brookhart, G. C. Levy, and S. Winstein. J. Am. Chem. Soc. **89**, 1735 (1967).
13. G. A. Olah and A. M. White. J. Am. Chem. Soc. **89**, 3591 (1967); N. C. Deno, C. U. Pittman, Jr., and M. J. Wisotsky. J. Am. Chem. Soc. **86**, 4370 (1964).
14. L. de Vries. J. Org. Chem. **25**, 1838 (1960); *Cf.* U. Burger, A. Delay, and F. Mazenoid. Helv. Chim. Acta, **57**, 2106 (1974).
15. H. N. Junker, W. Schäfer, and H. Neidenbrück. Chem. Ber. **100**, 2508 (1967).
16. R. B. King and A. Efraty. J. Am. Chem. Soc. **94**, 3773 (1972).
17. R. B. King and M. B. Bisnette. J. Organomet. Chem. **8**, 287 (1967).

Can. J. Chem. Downloaded from www.nrcresearchpress.com by 210.87.254.42 on 09/05/12
For personal use only.

Hindered Internal Rotation About Aryl C—N Bonds in Aryl Substituted Heterocyclic Compounds: 3-Aryl-2-benzyl-4(3*H*)-quinazolinones

LAWRENCE D. COLEBROOK AND H. GWYNNE GILES
Department of Chemistry, Sir George Williams Campus, Concordia University, Montreal, Quebec H3G 1M8

Received November 13, 1974[1]

LAWRENCE D. COLEBROOK and H. GWYNNE GILES. Can. J. Chem. **53**, 3431 (1975).

The proton magnetic resonance spectra of a number of 3-aryl substituted 2-benzyl-4(3*H*)-quinazolinones indicate that internal rotation about the aryl C—N bond is highly hindered. Substantial free energy barriers (18.9–19.8 kcal/mol) have been measured even when the aryl groups lack bulky *ortho* substituents.

LAWRENCE D. COLEBROOK et H. GWYNNE GILES. Can. J. Chem. **53**, 3431 (1975).

Les spectres r.m.n. d'un certain nombre d'aryl (substitués)-3 benzyl-2 (3*H*)-quinazolinones-4 indiquent que la rotation interne autour du lien C(aryl)—N est très empêchée. On a mesuré des barrières importantes (18.9–19.8 kcal/mol) d'énergie libre même lorsque les groupes aryles ne portent pas de substituants *ortho* volumineux.

[Traduit par le journal]

As part of a study of restricted internal rotation about aryl C—N bonds in aryl substituted heterocyclic compounds (1–5)[2], we have prepared a series of 3-aryl substituted 2-benzyl-4(3*H*)-quinazolinones and have investigated their proton magnetic resonance spectra. Of particular interest are the barriers to internal rotation of the 3-aryl groups and their dependence on the nature of the 3-aryl group substituents. The steric barriers to aryl group rotation in these compounds are expected to be high, since, in the transition states for rotation there should be severe crowding between the *ortho* substituents on the 3-aryl group and the heterocyclic ring substituents adjacent to the 3-position, *i.e.* the benzyl group in the 2-position, and the oxygen atom of the carbonyl group. Large dihedral angles between the 3-aryl and the heterocyclic moieties are expected in the conformational ground states (4), which are enantiomeric in the compounds studied.

The 3-aryl-2-benzyl-4(3*H*)-quinazolinones are stereochemically analogous to biphenyls, and undergo similar interconversion processes between enantiomeric rotational isomers. Other examples of compounds in which the biphenyl-like restriction to rotation about C—N bonds linking two cyclic moieties is predominantly steric in origin have been reported: 2-aryl-1,4-dihydro-3(2*H*)-isoquinolinones (6), 3-aryl-3,4-dihydro-2*H*-1,3-benzoxazines (7), 2-methyl- and 2,2-dimethyl-1-aryl-1,2-dihydro-4,6-diamino-*s*-triazines (1, 2), 3-arylhydantoins and 3-aryl-2-thiohydantoins (1–5), and 1-arylhydantoins (3, 5). The stereochemistry, based on the biphenyl model, of the process of torsion about the C—N pivot bonds of such compounds has been discussed in detail by Shvo *et al.* (6).

In addition to acting as a steric blocking group to rotation of the 3-aryl group, the 2-benzyl substituent functions as a 'probe' to enable the restricted rotational process to be detected in the proton magnetic resonance spectrum. Provided that the substitution pattern on the 3-aryl group is unsymmetric, the benzylic methylene protons in these compounds are diastereotopic, and may be expected to give rise to an AB quartet if rotation of the 3-aryl group is slow on the n.m.r. time scale. If aryl group rotation is fast on the n.m.r. time scale, the AB quartet should collapse to a singlet. Rate constants should be obtainable by complete line shape analysis of the partially collapsed methylene group signals at intermediate rates of rotation (8), providing that the chemical shift difference is sufficiently large. Rotation of the 3-aryl group is the only conformational exchange process in these compounds which can result in exchange of the environments of the benzylic methylene protons, causing collapse of the AB quartets.

[1]Revision received August 1, 1975.

[2]Reference 2 contains a preliminary report of some of the material in this paper.

Can. J. Chem. Downloaded from www.nrcresearchpress.com by 210.87.254.5 on 09/05/12
For personal use only.

Can. J. Chem. Downloaded from www.nrcresearchpress.com by 210.87.254.5 on 09/05/12
For personal use only.

Results and Discussion

With a suitable choice of solvent, all eight compounds prepared for this investigation exhibited AB quartets, arising from the benzylic methylene protons, in their 100 MHz n.m.r. spectra at normal probe temperatures (about 26 °C), indicating that rotation of the 3-aryl group about the aryl C—N bond was slow on the n.m.r. time scale. The chemical shifts between the benzylic methylene protons showed a strong solvent dependence, which is not easily predictable. Thus, the 3-(2-tolyl), **4**, and the 3-(2-fluorophenyl), **5**, compounds exhibited

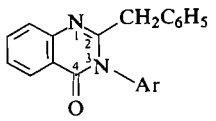

1 Ar = 2-chloro-6-methylphenyl
2 Ar = 2-bromophenyl
3 Ar = 2-chlorophenyl
4 Ar = 2-tolyl
5 Ar = 2-fluorophenyl
6 Ar = β-naphthyl
7 Ar = 3-bromophenyl
8 Ar = 3-acetylphenyl

no chemical shift difference between the benzylic methylene protons in nitrobenzene solution. The chemical shift differences for the remaining six compounds ranged from 0.088–0.295 p.p.m. These two compounds showed chemical shift differences of 0.057 and 0.143 p.p.m., respectively, in bromoform solution. In view of the high rotational barriers exhibited in nitrobenzene solution by all the other compounds (**1–3**) with *ortho*-substituted 3-aryl groups, and the behavior of these two compounds in bromoform solution, the observation of a singlet for the benzylic methylene protons cannot be attributed to the effects of fast rotation of the 3-aryl group.

Compounds with ortho-Substituted 3-Aryl Groups

Attempts to measure the rate of rotation of the 3-aryl groups by line shape analysis of the AB quartets at elevated temperatures failed for all those compounds (**1–5**) with *ortho*-substituted 3-aryl groups. No indications of collapse of the AB quartets through time averaging were detectable at the highest temperatures employed (150–187 °C), even for compounds with small blocking substituents, such as fluoro, in an *ortho* position.

Minimal possible values for the free energies of activation (Table 1) were estimated from rate constants (9) calculated from the chemical shifts and coupling constants (10) on the assumption that the spectra had collapsed to the coalescence points at the highest temperatures employed. Since no signs of incipient temperature dependence were observed at these sample temperatures, it may safely be assumed that the true free energies of activation for 3-aryl group rotation in these compounds are considerably higher than those shown in Table 1. These figures suggest that compounds of this type should be resolvable and have substantial optical stability at normal temperatures.

Compounds with meta-Substituted 3-Aryl Groups

In view of the high barriers to internal rotation in those compounds with blocking substituents in the ortho positions of the 3-aryl groups, three compounds (**6–8**) were prepared in which the only blocking substituents present in the *ortho*-positions are hydrogen atoms (2). Barriers to internal rotation in these compounds would be expected to be much lower than in the other series. The steric requirements of one of the *ortho* hydrogen atoms may be increased by buttressing with the adjacent substituent. This situation is unavoidable since an unsymmetrical substitution pattern on the 3-aryl group is necessary to render the benzylic methylene protons diastereotopic.

These compounds showed well resolved AB quartets arising from the benzylic methylene protons, with chemical shift differences of 0.088–0.132 p.p.m. (nitrobenzene solutions). When the samples were warmed the AB quartets collapsed to singlets, with coalescence temperatures in the range 94–116 °C (Table 1), indicating fast internal rotation about the aryl C—N bonds on the n.m.r. time scale. The original spectra reappeared when the samples were cooled.

Although, in principle, a complete set of activation parameters should be obtainable by complete line shape analysis of the partially collapsed AB quartets over a range of temperatures, this was not considered practicable in the present case. The chemical shifts between the diastereotopic methylene protons are small, and the nuclei tightly coupled (Table 1), limiting the temperature range over which the spectra show sufficient temperature dependence for accurate line shape analysis. In such cases only

TABLE 1. Proton magnetic resonance[a] and activation parameters for 2-benzyl-3-aryl-4(3*H*)-quinazolinones

Compound	Solvent	Benzylic protons δ_B[d]	Benzylic protons δ_A[d]	Benzylic protons $\lvert J_{AB}\rvert$(Hz)	Coalescence temperature (°C)	$\Delta G^{\ddagger}$ (kcal/mol)
1	Nitrobenzene	3.916	3.621	14.7	187[b]	23.7[c]
2	Nitrobenzene	3.919	3.709	14.8	177[b]	23.3[c]
3	Nitrobenzene	3.923	3.754	15.0	177[b]	23.3[c]
4	Bromoform[e]	3.833	3.776	14.5		[f]
5	Bromoform[e]	3.966	3.823	15.1	150[b]	21.9[c]
6	Nitrobenzene	3.958	3.826	15.1	116	19.8±0.3
7	Nitrobenzene	3.854	3.766	15.1	94	18.9±0.3
8	Nitrobenzene	3.966	3.861	15.0	102	19.2±0.3

[a]100 MHz.
[b]Highest temperature employed. No collapse observed.
[c]Minimum value of $\Delta G^{\ddagger}$ at the specified temperature.
[d]Chemical shifts in p.p.m. from TMS.
[e]The benzylic protons give rise to singlets in nitrobenzene solution.
[f]Not calculated because of the small chemical shift difference.

TABLE 2. Melting points, yields, elemental analyses, and carbonyl stretching frequencies of 3-aryl-2-benzyl-4(3*H*)-quinazolinones

Compound	Melting point (°C)	Yield (%)	Formula	Calculated (%) C	Calculated (%) H	Calculated (%) N	Found (%) C	Found (%) H	Found (%) N	C=O stretch (cm^{-1})[a]
1	152	6	$C_{22}H_{17}ClN_2O$	73.23	4.75	7.76	72.97	4.15	7.69	1670
2	130	50	$C_{21}H_{15}BrN_2O$	64.46	3.86	7.16	64.77	3.73	6.93	1685
3	111	12	$C_{21}H_{15}ClN_2O$	72.73	4.36	8.08	72.45	4.42	7.97	1690
4	113	30	$C_{22}H_{18}N_2O$	80.96	5.56	8.58	81.05	5.37	8.58	1665
5	133	15	$C_{21}H_{15}FN_2O$	76.35	4.58	8.48	76.46	4.73	8.60	1675
6	136	20	$C_{25}H_{18}N_2O$	82.85	5.01	7.73	83.11	4.81	7.69	1675
7	110	8	$C_{21}H_{15}BrN_2O$	64.46	3.86	7.16	64.28	3.66	7.15	1675
8	129	6	$C_{23}H_{18}N_2O_2$	77.95	5.12	7.90	78.10	5.17	7.80	[b]

[a]KBr discs.
[b]Overlapped by acetyl carbonyl band.

free energies of activation are likely to be accurate. Values of $\Delta G^{\ddagger}$ at the coalescence temperatures, calculated from rate constants (9) obtained by computer simulation of the line shapes (11) in the coalescence region, are reported in Table 1.

Compensation for the poor blocking ability of the *ortho* hydrogen atoms in these compounds is provided by the high steric requirements of the 2-benzyl group and the oxygen atom of the carbonyl group in the 4-position, resulting in severe steric interaction between the two moieties in the transition states for aryl group rotation. A large contribution to the steric barrier to rotation appears to result from the geometry at the 2-position of the hetero ring. Coplanarity between the bond joining the benzylic carbon and C-2 with the hetero ring maximizes steric interaction between the benzyl group and the ortho substituents on the 3-aryl group in the transition states for rotation (assumed to be approximately planar). In closely related compounds with the N-1—C-2 bond reduced, so that the hydridization at C-2 is formally sp^3, the barriers to rotation are considerably lower (12).

Experimental

Preparation of Materials

The 2-benzyl-3-aryl-4(3*H*)-quinazolinones were prepared by an adaptation of the method of Klosa (13). *N*-(Phenylacetyl)anthranilic acid (prepared by the method of de Diesbach *et al.* (14)) was employed as the precursor in all cases. Reaction of this compound with the appropriate aryl amine was carried out in the presence of polyphosphoric acid. Normally, two recrystallizations from methanol yielded analytically pure products. However, **8** required chromatography before the pure material was obtained.

Experimental details of two representative syntheses are given. No attempts were made to maximize yields. Analytical data are shown in Table 2. The structures were confirmed by n.m.r. and i.r. spectra. Elemental analyses were performed either by Galbraith Laboratories, Knoxville, Tennessee, U.S.A., or by Alfred Bernhardt, Mikroanalytisches Laboratorium, West Ger-

Can. J. Chem. Downloaded from www.nrcresearchpress.com by 210.87.254.5 on 09/05/12
For personal use only.

Can. J. Chem. Downloaded from www.nrcresearchpress.com by 210.87.254.5 on 09/05/12
For personal use only.

many. Infrared spectra were taken (KBr discs) on a Perkin-Elmer 457 spectrophotometer, and melting points on a Mettler FP1 apparatus.

2-Benzyl-3-(2-naphthyl)-4-(3H)-quinazolinone, **6**

N-(Phenylacetyl)anthranilic acid (10.0 g, 0.0392 mol), 2-naphthylamine (Eastman) (3.26 g, 0.0228 mol) and polyphosphoric acid (40 g) were heated to 180 °C with stirring, and kept at that temperature for 30 min. After cooling, the solution was poured into a concentrated sodium carbonate solution. When neutralization was complete, the product was extracted with chloroform (100 ml). When the resulting solution was washed with hydrochloric acid (6 *N*, 50 ml) a white precipitate (probably the amine salt) formed in the organic layer. This precipitate was removed by filtration. The process of washing with hydrochloric acid was repeated until no more precipitate formed. The chloroform layer was then neutralized with sodium carbonate solution, washed, and dried over molecular sieves (British Drug Houses, type 4A). The chloroform was removed under vacuum to yield an oil that solidified after standing for 30 min. The crude product was recrystallized three times from methanol to give pale needles that were then dried under vacuum.

2-Benzyl-3-(3-acetylphenyl)-4(3H)-quinazolinone, **8**

N-(Phenylacetyl)anthranilic acid (10.0 g, 0.0392 mol), *m*-aminoacetophenone (K and K) (5.29 g, 0.0392 mol), and polyphosphoric acid (44 g) were heated to 180 °C with stirring and kept at that temperature for 25 min. After cooling, the solution was poured into a concentrated sodium carbonate solution. When neutralization was complete the product was extracted with chloroform (100 ml) and the resulting solution was washed with hydrochloric acid (6 *N*, 50 ml) to remove any unreacted amine, and was then washed with sodium bicarbonate solution. The organic layer was separated and the chloroform solvent was removed under vacuum, yielding a brown oil. The oil was dissolved in an ether–ethanol (50:50) mixture and was chromatographed on silica gel (100 g, 60–120 mesh, British Drug Houses). The column was first eluted with ether (fraction 1, 120 ml, orange; fraction 2, 80 ml, black; fraction 3, 130 ml, orange), then ethanol (fraction 4, 60 ml, yellow; fraction 5, 120 ml, orange), and finally chloroform (fraction 6, 500 ml, yellow). The solvent was evaporated from fraction 2 to yield a red oil. The oil was dissolved in acetone and the solution was poured into water, yielding a yellow suspension. After 2 days a yellow solid which had formed was filtered off and dried under vacuum, then recrystallized from methanol.

Magnetic Resonance Measurements

Proton magnetic resonance spectra were taken using a Varian HA-100 spectrometer operating in the field sweep mode and employing the standard variable temperature equipment. The AB quartets arising from the benzylic methylene protons of the substituent in the 2-position were recorded at maximum convenient scale expansion. Temperatures, believed to be accurate to ± 2°C, were determined immediately after each spectrum was taken by measuring the peak separation of a standard Varian ethylene glycol sample.

Because of the high barriers to internal rotation in this series of compounds and the consequent high temperatures at which spectral measurements must be made, it is necessary to use high boiling solvents. The choice of solvent is important, since the chemical shift differences resulting from anisotropic shielding by the aryl groups may be small and solvent dependent. For example, the room temperature spectrum of the 3-(3-bromophenyl) compound, **7**, in bromoform solution shows a singlet rather than an AB quartet in the methylene region at $\delta 3.85$, although quartets appear when nitrobenzene or deuterochloroform solutions are used. In the case of the 3-(2-fluorophenyl) compound, **5**, AB quartets were exhibited by deuterochloroform and bromoform solutions, and singlets by nitrobenzene, DMSO-d_6, and 2-chloropyridine solutions. Nitrobenzene was found to be a useful high boiling solvent for this series, but, as noted, it could not be used in all cases.

This work was supported by grants from the National Research Council of Canada.

1. W. E. Bentz, L. D. Colebrook, J. R. Fehlner, and A. Rosowsky. Chem. Commun. 974 (1970).
2. L. D. Colebrook, H. G. Giles, and A. Rosowsky. Tetrahedron Lett. 5239 (1972).
3. L. D. Colebrook, H. G. Giles, A. Granata, S. Icli, and J. R. Fehlner. Can. J. Chem. **51**, 3635 (1973).
4. P. H. Bird, L. D. Colebrook, A. R. Fraser, and H. G. Giles. Chem. Commun. 225 (1974).
5. L. D. Colebrook, S. Icli, and F. H. Hund. Can. J. Chem. **53**, 1556 (1975).
6. Y. Shvo, E. C. Taylor, K. Mislow, and M. Raban. J. Am. Chem. Soc. **89**, 4910 (1967).
7. S. Brownstein, E. C. Horswill, and K. U. Ingold. Can. J. Chem. **47**, 3243 (1969).
8. G. Binsch. *In* Topics in stereochemistry. Vol. III. *Edited by* E. R. Eliel and N. L. Allinger. Interscience Publishers, New York. 1968. p. 97.
9. W. J. Moore. Physical chemistry. 3rd ed. Prentice-Hall, Inc., Englewood Cliffs, New Jersey. 1964. Chapt. 8.
10. R. J. Kurland, M. B. Rubin, and W. B. Wise. J. Chem. Phys. **40**, 2426 (1964).
11. S. Alexander. J. Chem. Phys. **37**, 967 (1962).
12. J. R. Fehlner. Ph.D. Thesis, University of Rochester, Rochester, New York. 1970.
13. J. Klosa. J. Prakt. Chem. **20**, 283 (1963).
14. H. de Diesbach, J. Gross, and W. Tschannen. Helv. Chim. Acta, **34**, 1050 (1951).

A Novel Base-promoted Rearrangement of Penicillin G

SAUL WOLFE, JEAN-BERNARD DUCEP, AND JOHN DWAYNE GREENHORN
Department of Chemistry, Queen's University, Kingston, Ontario K7L 3N6

Received June 30, 1975

SAUL WOLFE, JEAN-BERNARD DUCEP, and JOHN DWAYNE GREENHORN. Can. J. Chem. **53**, 3435 (1975).

The cleavage of methyl benzoate by alkyl-oxygen fission is just as efficient with lithium isopropyl and *tert*-butylmercaptide as with lithium *n*-propylmercaptide when hexamethylphosphoric triamide is employed as the solvent. The reaction of methyl benzylpenicillinate with lithium *tert*-butylmercaptide does not lead to cleavage of the ester but, rather, to a dehydration product having a thiazole structure.

SAUL WOLFE, JEAN-BERNARD DUCEP et JOHN DWAYNE GREENHORN. Can. J. Chem. **53**, 3435 (1975).

Lorsque le HMPT est utilisé comme solvant, la fission alkyl-oxygène du benzoate de méthyle est aussi efficace avec les isopropylthiolate et *tert*-butylthiolate de lithium qu'avec le *n*-propylthiolate de lithium. La réaction de benzylpenicillinate de méthyle avec le *tert*-butylthiolate de lithium ne conduit pas à la coupure de l'ester mais plutôt à un produit de déshydratation possédant la structure d'un thiazole.

[Traduit par le journal]

A number of base-catalyzed reactions of penicillin derivatives have been reported recently. These include epimerization at C6 (1), and rearrangement to anhydropenicillins (2), to 1,3-thiazines (3), to 1,4-thiazines (4), and to 1,4-thiazepines (5).

We report here a novel rearrangement of **1**, the methyl ester of Penicillin G. The rearrangement was encountered in the course of an unsuccessful attempt to effect hydrolysis of the

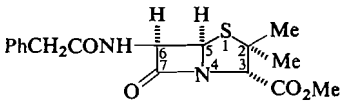

1

ester by a modification of the method of Bartlett and Johnson (6). These workers found that lithium *n*-propylmercaptide (**2**), in hexamethylphosphoric triamide (HMPT), effects efficient nucleophilic displacement of carboxylate anions from methyl esters at room temperature. Because the β-lactam carbonyl group of a penicillin ester seemed likely to offer a ready alternative site for attack by a nucleophilic reagent, it was considered that a bulkier nucleophile than *n*-propylmercaptide would be required.

To check that cleavage of a methyl ester is not impaired by such a modification, the cleavage of methyl benzoate was examined using **2**, lithium isopropylmercaptide (**3**), and lithium *tert*-butylmercaptide (**4**). All reactions were performed, as described by Bartlett and Johnson, in dry oxygen-free HMPT, with the additional modification that *n*-butyllithium was employed in place of lithium hydride to generate the reagent. This procedure permitted the filtration step to be avoided and, in each case, afforded a clear, pale yellow solution which was stable in the cold for at least one month and from which aliquots could be withdrawn for reaction as required.

After 1 h at room temperature, the yields of benzoic acid from methyl benzoate were 89%, 98%, and 99%, using **2**, **3**, and **4**, respectively. No ester cleavage was observed when the HMPT solvent was replaced by tetrahydrofuran.

The ester **1** was recovered unchanged following exposure to excess *tert*-butylmercaptan in HMPT for 2 days. However, it reacted rapidly with the lithium salt of the mercaptan. One equivalent of **4** was added dropwise to **1** during 2.5 h. As the addition proceeded, a transient orange color appeared, which slowly faded to a pale yellow. Only traces of unidentified, biologically inactive, acidic material were obtained, most of the product remaining in the neutral phase. From this phase was obtained, in 80% yield, an optically inactive crystalline compound,

Can. J. Chem. Downloaded from www.nrcresearchpress.com by 210.87.254.6 on 09/05/12
For personal use only.

Can. J. Chem. Downloaded from www.nrcresearchpress.com by 210.87.254.6 on 09/05/12
For personal use only.

m.p. 128–129 °C, which analyzed as $C_{17}H_{18}N_2O_3S$, *i.e.*, **1** *minus* H_2O.

The nuclear magnetic resonance (n.m.r.) spectrum showed a broad one proton singlet at δ 8.58, and sharp singlets at 7.98 (1H), 7.30 (5H), 4.32 (2H), 3.74 (3H), 2.20 (3H), and 1.92 (3H). The compound thus retains the benzyl and methoxycarbonyl groups, and the C2 methyl groups have become vinylic.

The infrared (i.r.) spectrum displayed a sharp N—H peak at 2.97 μm, ester absorption at 5.80 μm, and, in addition, strong peaks at 5.95, 6.50, and 6.71 μm, the latter being assigned to the isopropylidene group. The peaks at 5.95 and 6.50 are characteristic of α, β-unsaturated γ-thiolactones (2*a*) and strained thiazolines, respectively.[1] They also correspond to the 'I' and 'II' peaks of thiazoles (7). The one proton singlet at 7.98 in the n.m.r. is reminiscent of peaks in the same region in the thiazepines **5** (H7) (8) and **6** (H5) (5); the H5 proton of thiazoles is also found in this region (9).

The spectral data are consistent with structures **7** and **8** as the rearrangement products. The formation of **7** can be rationalized using various precedents in the literature. Thus, thiazepines of type **6** are known products of base-promoted rearrangement of the penicillin nucleus (5), and both **5** and **6** (3, 5, 10) undergo ready β-elimination (**5** → **9**; **6** → **10**). In the case of the ester **1**, these two reactions lead to an intermediate **11**, which can cyclize in the manner indicated to the thiazolone **7**.

The formation of **8** can be rationalized in terms of the chemistry of mercaptoazetidinones (**12**) (11) and related (12) compounds. In this case, the rearrangement would be initiated by the β-elimination **1** → **12**(R = $PhCH_2$) → **13** ⇄ **14** and the thiazole would be produced following cyclization of this latter intermediate. Alterna-

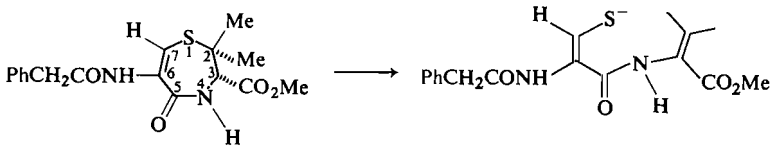

5 **9**

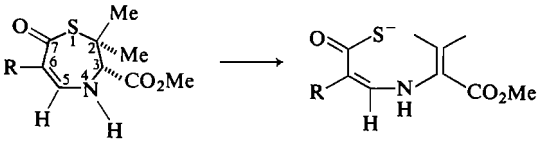

6 **10**

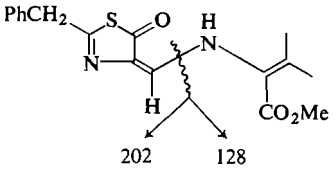

202 128

7

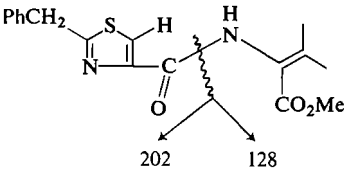

202 128

8

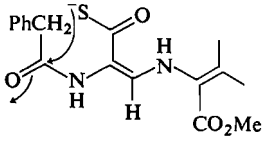

11

[1]S. Wolfe and J. M. Dodsworth, unpublished results.

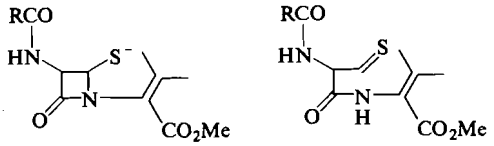

12

13

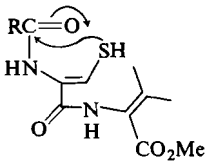

14

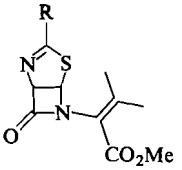

15

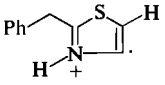

16

tively, **12** might cyclize to the thiazoline **15**. Such thiazolines are known (13) to undergo prototropic rearrangement to thiazoles of type **8**.

A distinction between the two proposed structures **7** and **8** could be obtained on the basis of the mass spectrum, which showed prominent peaks at 330 (M^+), 202, 175, and 128. The peaks at 202 and 128 are compatible with either structure, by the fragmentations indicated, but the peak at 175 corresponds to a fragment **16** (calcd. 175.0456; found 175.0456), which must originate from the thiazole **8**.

To check this assignment, methyl 2-benzylthiazole-4-carboxylate (**17**) was prepared by the Hantzsch synthesis shown in Scheme 1. Its mass spectrum contained a prominent peak at 175. Attempts to convert **17** to **8**, or to isolate **17** following ethanolysis of the unknown compound were unsuccessful. The thiazole **8** was, therefore, synthesized from **1** by the route shown in Scheme 2, which is the method employed by Cooper and

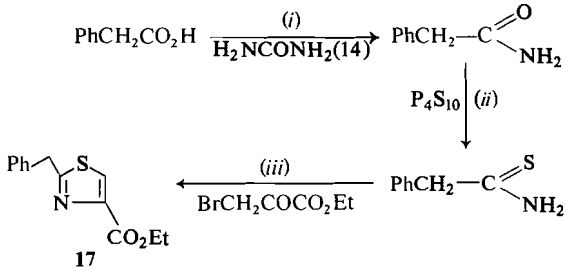

SCHEME 1

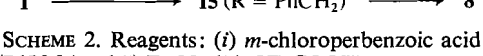

SCHEME 2. Reagents: (*i*) *m*-chloroperbenzoic acid; (*ii*) $\Delta/P(OMe)_3$; (*iii*) Et_3N; (*iv*) CF_3COOH.

José (13) to prepare the analogous thiazole derivative of Penicillin V. The compound obtained from the thiazoline **15** was identical in all respects with the lithium *tert*-butylmercaptide rearrangement product. The intriguing possibility that **8** is formed via **15** in this latter rearrangement remains to be established.

Experimental

Hexamethylphosphoric triamide was distilled from lithium aluminum hydride or lithium hydride at 116–117 °C/19–20 Torr and, after degassing, was stored under nitrogen over 4A molecular sieves in a flask fitted with a rubber septum. *n*-Butyllithium in hexane, obtained from Ventron Inc., was determined by acid–base titration to be 2.28 *M*. Commercial isopropylmercaptan was distilled before use; *n*-propyl (15) and *tert*-butyl mercaptan (16) were prepared by the literature methods. All reactions with organometallic reagents were performed under an atmosphere of dry nitrogen.

The i.r. spectra were recorded on a Beckmann 5A spectrometer; n.m.r. spectra were obtained on Varian A60 or T60 spectrometers, in $CDCl_3$, with internal TMS. The mass spectra were obtained on a JEOL-JMS-O1SC instrument.

Reaction of Methyl Benzoate with Lithium n-Propylmercaptide

To HMPT (10 ml) were added successively, at room temperature, *n*-propylmercaptan (0.8 ml, 8.9 mmol) and *n*-butyllithium (3.5 ml, 8 mmol). To the resulting pale yellow solution was added methyl benzoate (300 mg, 2.2 mmol). There was no significant color change. The reaction mixture was stirred for 1 h, then poured into cold *N* HCl (150 ml) and extracted with ether. The crystalline residue obtained following evaporation of the dried ether solution was shaken with a mixture of ether and 2 *N* sodium hydroxide. Acidification of the aqueous phase then afforded 238 mg (89%) of benzoic acid, m.p. 121–122 °C, identified by i.r., n.m.r. and a mixture melting point with authentic material.

Repetition of this experiment, using isopropyl and *tert*-butylmercaptan in place of *n*-propylmercaptan, led to benzoic acid in 98% and 99% yields, respectively.

Reaction of 1 with Lithium tert-Butylmercaptide

The methyl ester of penicillin G (215 mg, 0.62 mmol), in HMPT (1.5 ml), was treated dropwise during 2.5 h with 1.4 ml (0.66 mol) of a 0.47 *M* solution of lithium *tert*-butylmercaptide in HMPT. An orange color was produced with each drop of the reagent, and this color faded slowly to a pale yellow. The final yellow solution was allowed to stand for 2 h and then diluted with ice-cold water, acidified to p*H* 2.5, and extracted with ether. The ether extract was washed with bicarbonate, dried, and evaporated to yield a solid residue. Recrystallization from ethyl acetate – hexane afforded 170 mg (80%) of **8**, m.p. 128–129 °C.

Can. J. Chem. Downloaded from www.nrcresearchpress.com by 210.87.254.6 on 09/05/12
For personal use only.

Can. J. Chem. Downloaded from www.nrcresearchpress.com by 210.87.254.6 on 09/05/12
For personal use only.

Anal. Calcd. for $C_{17}H_{18}N_2O_3S$: C, 61.79; H, 5.49; N, 8.48; S, 9.66. Found: C, 62.02; H, 5.42; N, 8.52; S, 9.77.

Synthesis of Methyl 2-Benzylthiazole-4-carboxylate

Phenylacetic acid (35 g) and urea (15 g) were ground together and the mixture was heated at 160 °C for 2 h. It was then cooled, triturated with water, and filtered. The resulting solid was washed successively with *N*/10 NaOH and water, and dried overnight *in vacuo* at 70 °C. The resulting material was then recrystallized from hot ethanol to give 14.8 g (42%) of phenylacetamide, m.p. 154–157 °C. To this 14.8 g (0.11 mol) of material, in 120 ml of refluxing dry xylene, was added P_4S_{10} (7.5 g) during a 20 min period, and the refluxing was continued for an additional 1.5 h. The mixture was then allowed to stand for 24 h, and the supernatant material was decanted from the precipitated polymer and washed with 2 *N* NaOH and water, dried, and evaporated. The phenylthioacetamide was used directly in the next step.

To ethyl bromopyruvate (9.75 g, 0.05 mol), cooled in an ice bath, was added phenylthioacetamide (7.55 g, 0.05 mol). When the addition was complete, the mixture was heated cautiously to 100 °C and maintained at this temperature for 1 h. The sticky brown residue was triturated with hot chloroform, filtered to remove some insoluble material, and the chloroform solution was evaporated to dryness. The residue, in the minimum amount of methylene chloride, was filtered through a column of 200 g of silica gel. Elution with methylene chloride and evaporation of the eluate afforded a crystalline residue. Recrystallization from hot ethyl ether gave 2.24 g of long white fluffy needles, m.p. 68.0–69.5 °C. Nuclear magnetic resonance: 8.03 (1H, s), 7.28 (5H, s), 5.27 (2H, s), 4.42 (2H, q), 4.37 (3H, s), and 1,37 (3H, t).

Anal. Calcd. for $C_{13}H_{13}NO_2S$: C, 63.13; H, 5.30. Found: C, 63.20; H, 5.26.

Conversion of 1 to 8 via the Sulfoxide

The methyl ester of Penicillin G (1.23 g, 3.54 mmol), in methylene chloride (36 ml), was treated, dropwise with stirring during 1.5 h, with a cooled (0 °C) solution of 85% *m*-chloroperbenzoic acid (0.72 g, 3.54 mmol) in methylene chloride (28 ml). The solution was then warmed to room temperature and stirred overnight. It was then washed with saturated bicarbonate (2 × 15 ml), 5% bisulfite (2 × 15 ml), bicarbonate again (2 × 10 ml), dried, and evaporated to give a pale yellow solid (1.08 g, 84%). A portion (0.62 g) was recrystallized from ethyl acetate – petroleum ether to give fine white plates (0.44 g, 52% overall yield), m.p. 122–123 °C.

The sulfoxide (0.33 g, 0.916 mmol) and trimethylphosphite (0.12 ml, 0.124 g, 1.0 mmol) were refluxed in 12 ml of dry benzene. The reaction was followed by thin layer chromatography until the sulfoxide had disappeared (42 h). The solution was then evaporated to give a white amorphous solid in quantitative yield. A portion (0.082 g) was recrystallized from ethyl acetate – petroleum ether to give fine elongate prisms (0.060 g, 73%), m.p. 98–99 °C. Nuclear magnetic resonance 7.23 (5H, s), 5.90 (2H, s), 4.92 (3H, m), 3.85 (2H, s), 3.72 (3H, s), and 1.68 (3H, s). This β,γ-olefin (0.23 g, 0.76 mmol) and triethylamine (0.08 g, 0.79 mmol) were stirred in absolute methanol (15 ml) for 25 min, and the solution was then evaporated to give the thiazoline **15** (R = $PhCH_2$) as a sticky solid. The n.m.r. spectrum suggested sufficient purity to proceed to the next step: 7.17 (5H, s), 5.98 (1H, d, J = 4 Hz), 5.80 (1H, d, J = 4 Hz), 3.88 (2H, s), 3.72 (3H, s), 2.18 (3H, s), and 1.62 (3H, s).

The oily thiazoline **15** (0.23 g, 0.70 mmol) was refluxed with trifluoroacetic acid (6 ml) in chloroform (15 ml) for 2 h, at which time the n.m.r. spectrum showed the presence of **8** and **15** in an approximately 1:1 ratio. Further refluxing did not increase the proportion of **8**. The solvent was, therefore, removed and a portion of the residue (0.19 g) was subjected to preparative layer chromatography (Merck silica gel 60 F-254, 2 mm) using benzene – ethyl acetate (3:1) as eluant. The fraction containing the thiazole **8** weighed 0.0625 g (27%). Recrystallization from ethyl acetate – hexane gave fine white needles, m.p. 129–130 °C. The i.r. and n.m.r. spectra were identical to those of material prepared in the lithium *tert*-butylmercaptide rearrangement.

We thank the National Research Council of Canada for financial support of this research, and Dr. R. D. G. Cooper for suggesting the synthesis shown in Scheme 2.

1. S. Wolfe and W. S. Lee. J. Chem. Soc. D, 242 (1968); D. A. Johnson, D. A. Mania, C. A. Panetta, and H. H. Silvestri. Tetrahedron Lett. 1903 (1968).
2. (*a*) S. Wolfe, J. C. Godfrey, C. T. Holdrege, and Y. G. Perron. Can. J. Chem. **46**, 2549 (1968); (*b*) D. H. R. Barton, M. Girijavallabhan, and P. G. Sammes. J. Chem. Soc. Perkin Trans. 1, 929 (1972).
3. J. R. Jackson and R. J. Stoodley. J. Chem. Soc. Perkin Trans. 1. 1063 (1972).
4. R. J. Stoodley. J. Chem. Soc. C, 2891 (1968).
5. O. K. J. Kovacs, B. Ekström, and B. Sjöberg. Tetrahedron Lett. 1863 (1969).
6. P. A. Bartlett and W. S. Johnson. Tetrahedron Lett. 4459 (1970).
7. M. P. V. Mijovic and J. Walker. J. Chem. Soc. 3381 (1961).
8. N. J. Leonard and G. E. Wilson, Jr. J. Am. Chem. Soc. **86**, 5307 (1964).
9. E. J. Vincent, R. Phan-tan-luu, J. Metzger, and J. M. Surzor. Bull. Soc. Chim. Fr. 3524 (1966).
10. N. J. Leonard and R. Y. Ning. J. Org. Chem. **32**, 677 (1967).
11. S. Kukolja, R. D. G. Cooper, and R. B. Morin. Tetrahedron Lett. 3381 (1969).
12. S. Wolfe, S. L. Lee, J. B. Ducep, G. Kannengiesser, and W. S. Lee. Can. J. Chem. **53**, 497 (1975).
13. R. D. G. Cooper and F. L. José. J. Am. Chem. Soc. **92**, 2575 (1970).
14. E. Cherbuliez and F. Landolt. Helv. Chim. Acta, **29**, 1315 (1946).
15. M. B. Evans, G. M. C. Higgins, B. Saville, and A. A. Watson. J. Chem. Soc. 5045 (1962).
16. H. J. Backer and P. L. Stedehouder. Rec. Trav. Chim. Pays-Bas, **52**, 437 (1933).

A Photoelectron Investigation of the Peroxide Bond

R. S. BROWN

Department of Chemistry, University of Alberta, Edmonton, Alberta T6G 2E1

Received March 14, 1975

R. S. BROWN. Can. J. Chem. **53**, 3439 (1975).

The photoelectron spectra of several peroxides and their interpretation is presented. The effects of substituents is separated from vicinal orbital interactions using as a guideline the effect of similar substitution on the ether analogues. It is found that by comparison of Raman spectroscopic frequencies of the peroxide ground state, and vibrational frequencies for the ion (via pes), that the HOMO of peroxides is antibonding with respect to the O—O linkage. Additionally, the dependence of the splitting of the two highest occupied molecular orbitals on dihedral angle is verified by the pe spectra of several well-defined cyclic peroxides. Finally, the pe spectrum of tetramethyl-1,2-dioxacyclobutane (tetramethyl dioxetane) is presented indicating that it is not unlike other cyclic peroxides.

R. S. BROWN. Can. J. Chem. **53**, 3439 (1975).

On présente les spectres photoélectroniques de plusieurs péroxydes ainsi que leur interprétation. On sépare les effets des substituants des interactions orbitalaires vicinales en faisant appel comme référence les effets de substitutions semblables sur des éthers similaires. On a trouvé par comparaison des fréquences de vibration spectroscopique de l'état fondamental du peroxyde en Raman et les fréquences de vibration de l'ion (par l'intermédiaire de spe) que l'HOMO des peroxydes est antiliante par rapport au lien O—O. De plus on a vérifié, à l'aide de spectres pe de plusieurs peroxydes cycliques bien définis, la relation qui existe entre le dédoublement des deux HOMO et l'angle dièdre. Finalement on présente le spectre pe du tétraméthyldioxa-1,2 cyclobutane (tétraméthyl dioxétanne); il n'est pas dissimilaire de ceux d'autres peroxydes cycliques.

[Traduit par le journal]

Recently photoelectron (pe) spectroscopic studies have been conducted on lone pair – lone pair interactions occurring in such molecules as hydrazines (1) and disulfides (2). The situation for hydrazines has proved interesting and a clearer understanding for the n–n interactions as a function of dihedral angle has emerged.

Very recently, initial work of Batich and Adam (3) on some alkyl peroxides, and Osafune and Kimura (4) on hydrogen peroxide has provided some information about the n–n interactions within peroxides. Unlike the hydrazines in which there is only one 'non-bonded' pair of electrons per nitrogen yielding an n^+ and n^- combination which are easily identified, the peroxides present a rather more complex situation in that each oxygen formally possesses two n_0 pairs of electrons. Additionally, the greater electronegativity of oxygen places the n^+ combination(s) at relatively high ionization potentials (ip) making their accurate location difficult.

While peroxides represent an important class of compounds, little of the wide variety of information available on such molecules (5) relates to their electronic structure. The following study was undertaken to investigate electronic interactions within peroxides.

In particular, two areas were investigated concerning the distinction of substituent effects from n-orbital interactions, and the relationship of ionization potential and dihedral angle.

The first section of the following deals with the changes in ip of an isolated oxygen 2p orbital when the substitution on that oxygen atom changes from two hydrogens to two *tert*-butyl groups. With this guideline in hand we will then turn our attentions to an investigation of the additional perturbations in effect when two oxygens are linked together and symmetrically substituted.

Experimental

Photoelectron spectra were recorded using a MacPherson Model 36 ESCA spectrometer equipped with a He(I) ionization source. All spectra were run using argon as an internal calibrating gas. While under optimum conditions the resolution of the $Ar_{3/2}$–$Ar_{1/2}$ doublet was 17 meV at 60 000 Hz, a resolution of 24 to 28 meV was noticed during actual recording of spectra.

Raman spectra were determined on neat samples using a SPEX 1401 Laser Raman Spectrometer. Repeated runs showed no laser decomposition of the samples.

Can. J. Chem. Downloaded from www.nrcresearchpress.com by 210.87.254.42 on 09/05/12
For personal use only.

Can. J. Chem. Downloaded from www.nrcresearchpress.com by 210.87.254.42 on 09/05/12
For personal use only.

TABLE 1. Ionization potentials for water,[a] dimethyl ether,[b] and and di-*tert*-butyl ether[c]

Compound	Assignment	Ionization potential (eV) Vertical	Adiabatic
H_2O	$b_1(n_0)$	12.62	12.61
	$a_1(O_{2p_z})$	14.73	13.7
	$b_2(O_{2p_x})$	18.55	17.22
CH_3OCH_3	$b_1(n_0)$	10.04	
	$a_1(O_{2p_z})$	11.91	
	$b_2(O_{2p_x})$	13.43	
$((CH_3)_3C)_2O$	$b_1(n_0)$	9.16	8.81
	$a_1(O_{2p_z})$	10.24	9.76
	$b_2(O_{2p_x})$	10.95	

[a]Reference 10.
[b]Reference 13.
[c]This work. An adiabatic ionization potential for di-*tert*-butyl ether of 8.94 eV was previously reported (14).

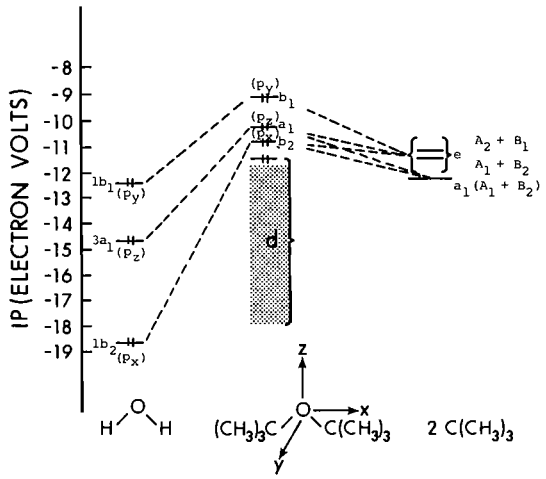

FIG. 1. Energy level diagram for H_2O and di-*tert*-butyl ether (I) utilizing vertical ip's determined by pe spectra. The two *tert*-butyl groups of local C_{3v} symmetry each contain an *e* orbital and an a_1 orbital. Utilizing Koopmans' theorem (11) one can assign the energy level of the *e* orbital as being roughly equal to the average value for the Jahn–Teller splitting of the $3t_2$ orbital in $C(CH_3)_4$ of 11.2 eV (12). The a_1 orbital is *assumed* to be at somewhat higher binding energy. If one treats each of the two components of the *e* orbital on both *tert*-butyl groups as a pseudo orbital, the p_y pseudo orbitals transform as $A_2 + B_1$ under the C_{2v} point group while the p_x pseudo orbitals transform as $A_1 + B_2$. The a_1 orbital of the *tert*-butyl groups transforms as $A_1 + B_2$ under the C_{2v} point group. The shaded area represents an unresolvable series of ionizations presumably arising from σ bonds.

Hydrogen peroxide was commercially obtained from the Food Machinery and Chemical Corporation in 98% purity. Initial determination of the pe spectrum of 98% H_2O_2 indicated a large proportion of water in the vapor state; however, after 10 to 12 h of periodically monitoring the spectra, only small peaks which may be attributed to water remained. The reported spectrum below was obtained after no further diminution of the assumed H_2O peak at 12.61 eV.

Di-*tert*-butyl ether (I) was prepared by the method of West, Powell, Lee, and Whatley (6).

Ascaridole (IV) was obtained from the Fluka A.G. Chemische Fabrik (Switzerland) and was purified by low temperature recrystallization from isopentane at −78 °C to a constant melting point of 3 °C (lit. m.p. 3.3 °C (7)). Dihydroascaridole (V) was prepared via the procedure of Paget (8) and recrystallized from pentane to a constant melting point of 19 °C (lit. m.p. (8) 19.5 °C).

3,3,5,5-Tetramethyl-1,2-dioxacyclopentane (VIII) and 3,3,6,6-tetramethyl-1,2-dioxacyclohexane (IX) were prepared according to literature procedures (9).

Results and Discussion

Before discussing the actual peroxides, it would be of benefit to distinguish those perturbations caused by the presence of the alkyl substituents, from n-orbital interactions by examining systems in which the latter complications are absent. A comparison of H_2O and di-*tert*-butyl ether (I) ought to provide an estimate of the substituent effect of two *tert*-alkyl groups on the oxygen orbitals. The energy level diagram for H_2O and I is shown in Fig. 1, while the corresponding data are provided in Table 1.

Substitution of two *tert*-butyl groups lowers the first ip ($1b_1$ orbital (n_0)) from 12.62 eV in H_2O (10) to 9.16 eV in I. Decreasing ip of the $1b_1$ orbital with increasing substitution is well known (13–15) and results from the greater electron releasing ability of these alkyl groups relative to hydrogen. The difference of 3.46 eV in passing from H_2O to I is observed to be some-

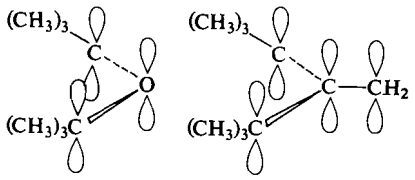

I II

what greater than the analogous substitution on carbon as indicated by values of 10.52 and 8.80 eV for ethylene and 1,1-di-*tert*-butylethylene (**II**), respectively (15). We assume that there must be significant buttressing between the two *tert*-butyl groups in both **I** and **II**, based upon inspection of molecular models. We can perhaps observe this distortion by observing changes in the $1b_1$ orbital and highest occupied a_1 orbital in passing from H_2O, to dimethyl ether, to di-*tert*-butyl ether. Figure 2 shows the orbitals in terms of their dominant oxygen atomic component.

From water (R = H) to dimethyl ether (R = CH_3) the change in the vertical ip of the $1b_1$ and a_1 orbitals is 2.58 and 2.82 eV, respectively. The corresponding change in these orbitals from water to di-*tert*-butyl ether (R = $C(CH_3)_3$) is 3.46 and 4.97 eV, respectively, indicating that the a_1 orbital is more sensitive to *tert*-butyl substitution than the $1b_1$ orbital. Were any of the above molecules linear, the $1b_1$ and highest occupied a_1 orbital would be degenerate. In part then, the splitting of these two orbitals reflects the non-linearity of the molecule which causes a_1 to become more bonding and hence of lower energy than $1b_1$. The $1b_1$–a_1 splitting for **I** is 1.08 eV, while that for water and dimethyl ether is 2.1 and 1.87 eV, respectively, and using the above argument, one predicts that di-*tert*-butyl ether is "more linear" than either H_2O or dimethyl ether.

The important point for this discussion, is that dialkyl substitution lowers the first ip of the oxygen non-bonding orbital by 3.46 eV in changing from H_2O to **I**. Such substitution also lowers the ip of other occupied orbitals but of a magnitude dependent upon steric interactions of the alkyl groups.

Vicinal n-orbital interactions independent of substituent effects can be illustrated by investigating the simplest peroxide. The pe spectrum of H_2O_2 was determined and is presented in Fig. 3 while the corresponding data are displayed in Table 2. While the gross spectrum is similar to that presented by Osafune and Kimura (4) the

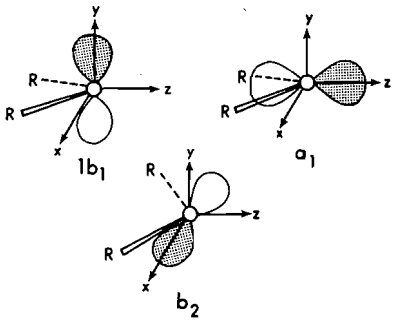

FIG. 2. The three highest occupied molecular orbitals of R_2O illustrating oxygen 2p components (ref. 10).

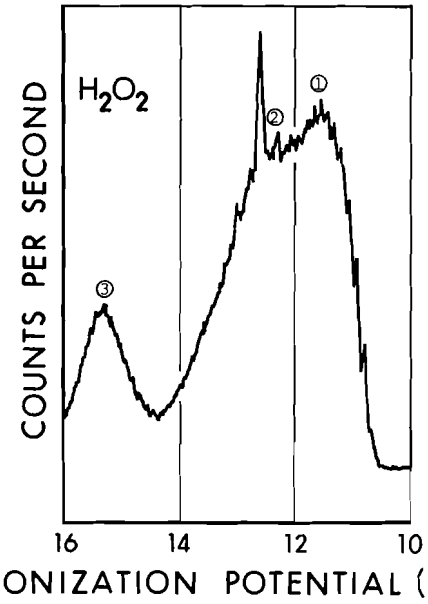

FIG. 3. Photoelectron spectrum of H_2O_2 between 16 and 10 eV. Peak at 12.61 eV is H_2O impurity.

resolution here is superior and allows us to draw some conclusions about the HOMO.

Ab initio calculations for H_2O_2 (16) have predicted that the HOMO is an antisymmetric combination of the n_0 orbitals (n^-), illustrated for visualization in Fig. 4. While this assignment has been made before (4), the spectrum provided here gives additional confirming vibrational evidence. Raman investigations of H_2O_2 have placed the O—O stretch at 880 cm^{-1} (17) which, in conjunction with our value of 1080 ± 50 cm^{-1} for the O—O stretch of $H_2O_2^+$, indicate that the orbital from which the first electron comes must be antibonding (18) with respect to the O—O linkage.

Can. J. Chem. Downloaded from www.nrcresearchpress.com by 210.87.254.42 on 09/05/12
For personal use only.

TABLE 2. Experimentally determined ionization potential for H_2O_2

Ionization potential (eV)				
	This work		Vibrational spacing	
Literature[a]	Vertical	Adiabatic	(cm^{-1})	Assignment
11.69	11.51	10.54	1080 ± 50	$4b(n^-)$
12.69	12.56			$5a$
15.33	15.26			$4a$
17.40	17.35			$3a$, $3b$

[a]Reference 4. Note that these values differ slightly from those in ref. 4, probably due to difficulties arising in assignment of the maxima of such broad bands. Electron impact studies place the first ip of H_2O_2 at 10.92 ± 0.05 eV (26).

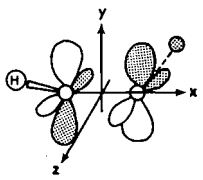

$4b(n^-)$

$-0.23(P_zO_1 + P_zO_2) + 0.66(P_yO_1 - P_yO_2)$

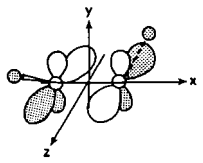

$5a$

$+ 0.55(P_zO_1 - P_zO_2) - 0.22(P_yO_1 + P_yO_2)$

FIG. 4. Two highest occupied molecular orbitals of H_2O_2 showing their dominant components. Data are from ref. 16*d*. Calculations above refer to equilibrium dihedral angle of 111°30′.

Band *2*, according to calculations (16), arises from an orbital containing predominant antisymmetric combinations of the OH σ-bonds as shown in Fig. 4. This band is obscured by bands from slight impurities which from their regular progression can certainly be assigned to water and oxygen. Even after repeated experiments with 98% H_2O_2 we were unable to eliminate these impurities which suggest that a metathesis reaction of H_2O_2 was occurring within the spectrometer.

If H_2O_2 were linear then the top two orbitals (*4b* and *5a*) would be degenerate, however, the non-linearity of H_2O_2 with a dihedral angle of $\theta = 111°30'$ (19) effectively removes the degeneracy, making *5a* more bonding than *4b*.

The important feature of the above is that while the assignments for the HOMO of peroxides had been given (3, 4) this spectrum, to our knowledge, provides the first confirmatory pe data for the antibonding nature of the HOMO.

The effect of introducing the second oxygen atom to produce H_2O_2 from water apparently lowers the HOMO by 1.1 eV. It is difficult to compare these two orbitals however, since the $1b_1$ orbital (HOMO) in H_2O is non-bonding, while that in H_2O_2 is antibonding with respect to the O—O bond.

Alkyl Peroxides

As a guide in assigning the spectra of some dialkyl peroxides, we have extensively used the *ab initio* calculations of Fink and Allen (16*c*) and Kaldor and Shavitt (16*d*) concerning H_2O_2. While it is recognized that this extrapolation may be simplistic with regard to the additional perturbations introduced by the alkyl groups which may alter or even invert some of the molecular orbitals, less sophisticated computations (3) per-

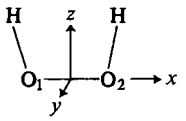

III

cis-H_2O_2; dihedral angle $\theta = 0°$

LUMO $5a_1 = 0.46(O_12S + O_22S) + 0.57(O_12P_z + O_22P_z) - 0.71(H_1 + H_2)$

HOMO $1a_2 = 0.73(O_12P_y - O_22P_y)$

$4a_1 = -0.22(O_12S + O_22S) + 0.62(O_1P_x - O_2P_x) + 0.17(O_1P_z + O_2P_z)$

$3b_2 = 0.38(O_12S - O_22S) - 0.51(O_1P_z - O_2P_z) - 0.44(H_1S - H_2S)$

FIG. 5. The three highest and lowest unoccupied molecular orbitals of *cis*-H_2O_2.

Can. J. Chem. Downloaded from www.nrcresearchpress.com by 210.87.254.42 on 09/05/12
For personal use only.

TABLE 3. Ionization potentials for ascaridole (IV) and dihydroascaridole (V)

Compound	Assignment	Ionization potential (eV) Vertical	Adiabatic
IV	n^- (band *1*)	8.42[a]	8.07
	π(C—C)	9.70	9.35
	σ^-(C—O) (band *2*)	10.71	10.26
V	n^- (band *1*)	8.50	8.09
	σ^-(C—O) (band *2*)	10.36	9.83

[a]Band *1* of IV exhibits a vibrational progression of 1008 ± 50 cm^{-1}.

formed on dimethyl peroxide show similar trends to those found for H_2O_2. At least this extrapolation can serve to assign the HOMO, and offer a tentative suggestion about the second highest molecular orbital.

If we are allowed to use these computations (16) then the *cis*-dialkyl peroxides may be analyzed in terms of the corresponding orbitals calculated for *cis*-H_2O_2 (**III**, C_{2v} symmetry). The three highest, and lowest unoccupied molecular orbitals are presented in Fig. 5.

Ascaridole (**IV**) is a *cis*-dialkyl peroxide with a dihedral angle of 0°.[1]

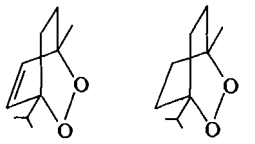

IV $\theta = 0° \pm 5°$ **V** $\theta = 15° \pm 5°$

Ionization potentials for **IV** and **V** are presented in Table 3, while the spectra from which the data were obtained are presented in Fig. 6.

Band *1* in both **IV** and **V** is assigned to the removal of an electron from an antisymmetric π^* combination (n^-). That this band in effect corresponds to ionization of an antibonding electron is evidenced by the vibrational spacing of 1008 ± 50 cm^{-1} appearing on band *1* of **IV**. Raman studies of **IV** and **V** indicate an O—O stretching frequency of 730 ± 2 cm^{-1} in both species. An appreciable interaction of this orbital with the double bond can be ruled out on symmetry grounds and by noting that band *1* appears at roughly the same position in both **IV** and **V**.

The second peak in the pe spectrum of **IV** can be assigned to ionization of the C—C π-bond. A

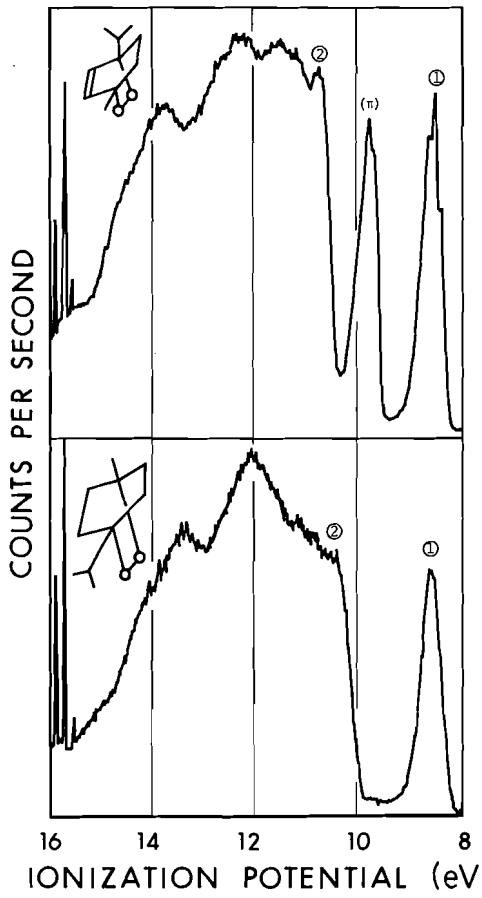

FIG. 6. Photoelectron spectra of ascaridole (**IV**) and dihydroascaridole (**V**) using argon as a calibrating gas.

[1]Dreiding models suggest **IV** possesses a dihedral angle of 0°. While these models are unable to assess the contribution of tortional effects on the dihedral angle, **IV** is sufficiently rigid so that little distortion from 0° is expected. Dihydroascaridole (**V**) exhibits slightly more flexibility and thus an angle of 15° ± 5° is assumed based upon the models.

Can. J. Chem. Downloaded from www.nrcresearchpress.com by 210.87.254.42 on 09/05/12
For personal use only.

Can. J. Chem. Downloaded from www.nrcresearchpress.com by 210.87.254.42 on 09/05/12
For personal use only.

comparison of the ip of 9.70 eV with that of bicyclooctene (9.05 eV (20)) indicates a significant stabilizing perturbation in the former. While we cannot exclude the possibility of an interaction of the π-bond with the *bonding* σ-framework as shown in **VI**, such an interaction would be expected to raise the π-level rather than lower it.

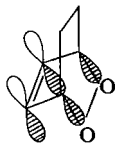

VI

Of the effects which could be contributing to the stabilization of the π-bond in **IV**, perhaps the simplest to visualize is an inductive withdrawal of electron density from the π-bond by the electronegative oxygens. Alternatively, if we are allowed to extrapolate the calculated orbitals for *cis*-H_2O_2 (16*d*) to the peroxide linkage in **IV**, a through-bond type of stabilization can be envisioned. The only orbital of appropriate symmetry localized on the peroxide portion of **IV** which can interact with the π-bond is the LUMO (*cf.* **III**), which is predominantly a symmetric combination of antibonding σ-orbitals. Hence one could envision an interaction between the π-bond and σ^{*+} as shown in **VII**, which effectively transfers electron density from the π-bond to the unoccupied C—O orbitals, exerting a net stabilizing influence on the double bond. The present study offers no solution to the mechanism of stabilization, and further work will be required to provide an answer.

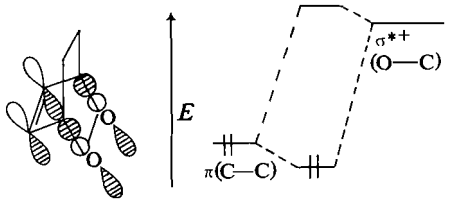

VII

Band *2* in both **IV** and **V** can be assigned on the basis of calculations (16) of *cis*-H_2O_2 to ionization occurring from either an orbital consisting of an antisymmetric combination of C—O σ-bonds (σ^-) or an O—O σ-bond. The calculations indicate that these two orbitals are very close in energy, and certainly the pe data cannot clearly distinguish the two ionizations.

As has been noted before (4) the separation of the two highest occupied molecular orbitals of peroxides should have maximum (but not necessarily equal) values at θ = 0° and 180°, and become degenerate at θ = 90° where the two orbitals cross each other (3, 4, 16*c*, 16*d*).

While alkyl substitution undoubtedly affects this dependence, qualitatively one expects to observe a decrease in the separation of the first two peroxide bands as the dihedral angle progresses from 0° to 90°. An extension of the plot of Δip *vs.* dihedral angle (3) for compounds **IV**, **V**, **VIII**, and **IX** is presented in Fig. 6. While it is not certain what the exact dependence should be, it can be seen that there appears to be a steady decrease from ascaridole (**IV**, θ = 0° ± 5°), Δip = 2.29 eV to 3,3,6,6-tetramethyl-1,2-dioxacyclohexane (**IX**, θ = 75° ± 5°), Δip = 0.41 eV.

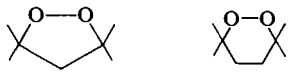

VIII $\theta = 30° \pm 5°$[2] **IX** $\theta = 75° \pm 5°$[2,3]

Vertical ip { 9.26 eV (n^-), 10.47 eV (σ^-) } 9.56 eV { 9.35 eV (n^-), 9.76 eV (σ^-) }

Computations (3, 4, 16*c*, 16*d*) suggest a similar dependence upon dihedral angle from 180° to 90°, although there is no experimental evidence that the 90° to 180° section should mirror that from 0° to 90°. In fact, while electric-dipole measurements in solution indicate that di-*tert*-butyl peroxide possesses a dihedral angle of 123° (21), the splitting observed as 1.75 eV corresponds more to a gas phase angle of 160° to 180° if Fig. 6 is mirrored from 90° to 180°.

In view of the recent interest in dioxetanes (22) the pe spectrum of tetramethyl-1,2-dioxacyclobutane **X** was obtained. Initial attempts to obtain this spectrum gave only that of the decomposition product acetone, however, suitable modification of the spectrometer inlet system allowed the recording of the spectrum listed in

[2]In a fashion similar to that used for **IV** and **V**[1], Dreiding models suggest to us angles for **VIII** and **IX** of 30° ± 5° and 75° ± 5°, respectively, slightly different than those assumed in ref. 3.

[3]Curve resolution of the broad intense peak at 9.56 eV indicates two peaks of equal dimensions centered at 9.35 and 9.76 eV. It is felt that the breadth and intensity of this peak relative to the σ-framework indicates the presence of two overlapping bands.

TABLE 4. Ionization potentials for tetramethyl-1,2-dioxacyclobutane (X)

Band	Vertical ip (eV)	Assignment[b]	Major orbital components
1	8.98[a]	$2a_2(\pi^*_y)$	$-(\pi^*_yO + \pi^*_yC)$
2	10.94	$3b_1$	$-(\pi^*_zC + \pi^*_zO)$
3	11.41	$5a_1$	$-(\sigma_xO + \sigma_xC)$
4	12.09	$1a_2$	$\pi^*_yO - \pi^*_yC$

[a]Onset potential for band *1* is 8.53 eV. FWHM = 0.53 eV.
[b]Reference 23. Assignments proposed here are extensions of those given for 1,2-dioxetane.

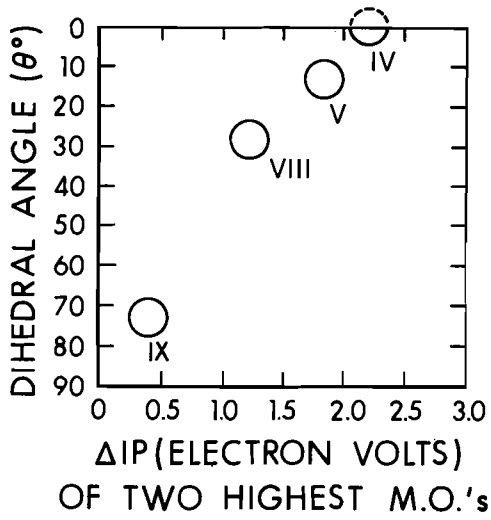

FIG. 7. A graphical presentation of the Δip for the two highest bands in dialkyl peroxides as a function of dihedral angle θ. Refer to footnotes 1 and 2.

Fig. 7. Table 4 lists the corresponding ip's and assignments for **X**.

Molecular models indicate that dioxetane **X**, like ascaridole (**IV**), should possess a dihedral

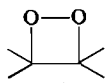

X
$\theta = 0° \pm 5°$

angle of 0°.[1] Although **X** contains a peroxide linkage it is possible that the extra strain in the four-membered ring (estimated at 26 kcal/mol (22*c*)) alters the orbitals such that **X** is an abnormal peroxide in terms of its electronic structure. Inspection of Fig. 7 shows that the pe spectrum of **X** is similar to that of other cyclic peroxides, particularly the appearance of the first band.

Assignment of the orbitals giving rise to the pe spectrum is based largely upon the CNDO/2 calculations of Barnett for the parent compound 1,2-dioxacyclobutane (23). Band *1* (vip 8.98 eV) is assigned to removal of an electron from an antisymmetric π^*_y orbital. While there is little well-resolved vibrational structure on this band, it is expected that the orbital giving rise to it is similar in character to the HOMO of ascaridole (**IV**) or dihydroascaridole (**V**). Band *2* is suggested (23) to arise from an antisymmetric combination of C—O σ*-orbitals, while band *3* corresponds to a symmetric combination of O—O and C—C σ-bonds. Calculations (23) predict *2* and *3* to be very close in energy, in good agreement with our observation. Additionally, the computed splitting between the two highest occupied molecular orbitals ($3b_1$–$2a_2$) is 2.17 eV while the experimental value determined for **X** is 1.96 eV. Interestingly, if one naively places the latter value on the plot shown in Fig. 6 it falls gratifyingly close to that expected for a peroxide with a 0° dihedral angle.[4]

Based upon this experimental data and the application of Koopman's theorem (11), one can draw a correlation diagram for the construction of **X** from O_2 and tetramethylethylene under C_{2v} point group symmetry as shown in Fig. 8.

We have been careful to include in our study of alkyl peroxides only tertiary dialkyl peroxides. While one could have chosen to study the hydroperoxides, the lack of symmetry in these molecules precludes group theoretical analysis. The dialkyl peroxides at least preserve the local C_2 symmetry about the peroxide portion. Additionally, since each peroxide contains di-*tert*-

[4]The second highest occupied molecular orbital of **X** ($3b_1$) is described (23) as an antisymmetric combination of σ* orbitals, while the analogous orbital of *cis*-H_2O_2 ($3b_2$) is suggested to be an antisymmetric combination of the O—H σ-bonds. Since these two orbitals are unlike in their overall character, it leads to some question about the comparison of **X** with other peroxides in terms of Fig. 6. However, the Δip of bands *1* and *2* in **X** is still an experimental observation regardless of the nature of the orbital giving rise to band *2*.

Can. J. Chem. Downloaded from www.nrcresearchpress.com by 210.87.254.42 on 09/05/12
For personal use only.

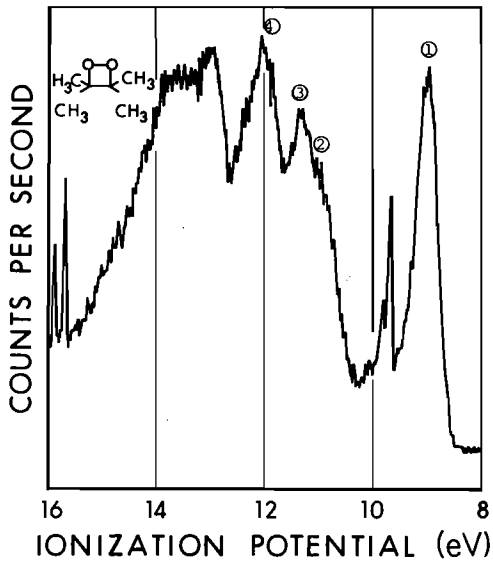

FIG. 8. Photoelectron spectrum of tetramethyl-1,2-dioxacyclobutane (**X**) using argon as an internal calibrating gas. Band centered at 9.70 eV is attributable to acetone formed from the decomposition of **X**.

alkyl substitution, to a first approximation the substituent effects on the HOMO might be expected to be similar.[5] The difference between a methyl group and an isopropyl group is not expected to markedly alter the substituent effect.

Since di-*tert*-butyl ether (**I**) has the ip of its HOMO ($1b_1$) 3.46 eV lower in energy than H_2O, one might expect to find such a lowering in the peroxides as well. Indeed, substitution of two *tert*-alkyl groups for H lowers the ip of the HOMO in all the dialkyl peroxides studied as can be seen from Table 5.

Table 5 indicates that the ip of the HOMO of these dialkyl peroxides is not constant. As expected from the calculations (3, 4, 16) those peroxides in which the dihedral angle tends toward 0° (or 180°) are the ones which exhibit the lowest ip, presumably due to increasing the antisymmetric vicinal orbital interactions. Rotation about the O—O bond apparently lessens these repulsive interactions and hence allows the HOMO to reach higher binding energy as evidenced by the ip of **IX** (9.35 eV). Assuming **IX**

[5]Substituent effects of the alkyl groups may be due to a hyperconjugative interaction of the appropriate symmetry orbitals located on the alkyl residue with the adjacent oxygen orbitals, and/or a difference in the group electronegativity relative to H, which alters its electron-releasing ability. We cannot distinguish between these two possibilities in this study.

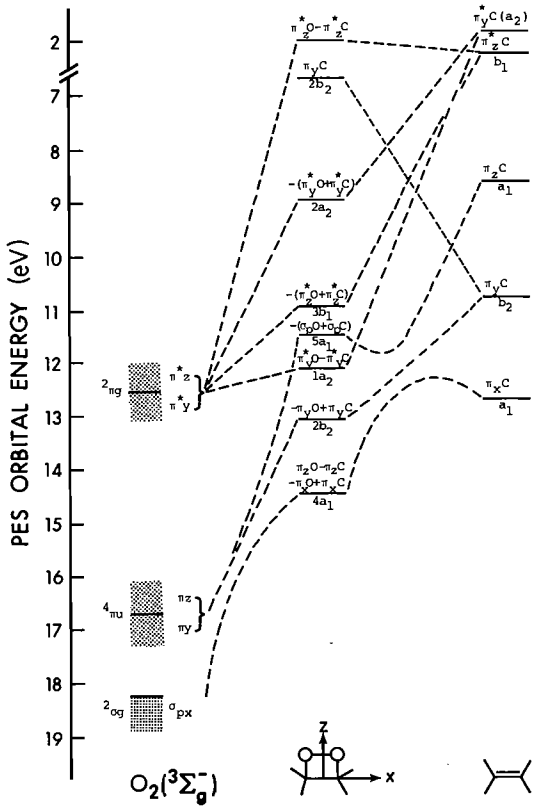

FIG. 9. Partial correlation diagram for tetramethyl-1,2-dioxacyclobutane from O_2 and tetramethylethylene under the C_{2v} point group. C_{2v} symmetry. Assignments for orbitals of the tetramethyl dioxetane based upon those given in ref. 23. O_2 assumed to be in $^3\Sigma_g^-$ state (27). π^*_zC calculated from the $\pi \rightarrow \pi^*$ absorption energy for tetramethylethylene as found in ref. 28.

to be our best *experimental* case for the minimization of vicinal orbital effects ($\theta = 75° \pm 5°$) it appears that in the absence of other effects, substitution of two *tert*-alkyl groups for hydrogens raises the HOMO of the peroxide linkage by at least 2 eV relative to H_2O_2.

Assuming this substitution effect to be constant at roughly 2 eV, the rotational dependence between 90° and 0° of this orbital is seen to be roughly 1 eV. While this is undoubtedly oversimplified (particularly since the gas phase geometry of H_2O_2 is *not* 90° but 111°30′ (19), and the ip of the HOMO of H_2O_2 is suspected to show rotational dependence), it does serve to demonstrate that the substituent caused lowering of the HOMO in the peroxides studied is less than that experienced in passing from H_2O to **I**.

One will notice that dioxetane **X** does not fit this expectation well. It is expected that if **X**

Can. J. Chem. Downloaded from www.nrcresearchpress.com by 210.87.254.42 on 09/05/12
For personal use only.

TABLE 5. A comparison of the ip of the HOMO in several dialkyl peroxides

Peroxide	ip of HOMO (eV)	$\Delta(ip_{H_2O_2} - ip_{peroxide})$ (eV)
H_2O_2	11.51	0.0
Ascaridole (**IV**)	8.42	3.09
Dihydroascaridole (**V**)	8.50	3.02
Tetramethyl-1,2-dioxacyclobutane (**X**)	8.98	2.54
3,3,5,5-Tetramethyl-1,2-dioxacyclopentane (**VIII**)	9.26	2.26
3,3,6,6-Tetramethyl-1,2-dioxacyclohexane (**IX**)	9.35	2.17
Di-*tert*-butyl ether peroxide	8.79	2.73

were a "normal" peroxide with a dihedral angle of 0°, it ought to have a first vip of ~8.5 eV. That the observed ip is somewhat greater (8.98 eV) can perhaps be best related to the internal strain of the molecule. By analogy, decreasing the endocyclic angles in the cyclic ethers causes a marked increase in ip. Hence the vip of tetrahydrofuran (**XI**) is 8.89 eV (18) while that of the four-membered oxetane (**XII**) is 9.67 eV (24) and that of ethylene oxide (**XIII**) is 10.57 eV (25).

XI **XII** **XIII**

The author gratefully acknowledges the financial support of the University of Alberta and the National Research Council of Canada. He is grateful to Professor K. R. Kopecky for stimulating discussions as well as gifts of ascaridole and tetramethyl-1,2-dioxacyclobutane, and to Mr. R. N. Swindlehurst for the determination of Raman spectra.

1. (*a*) S. F. NELSEN and J. M. BUSCHEK. J. Am. Chem. Soc. **95**, 2011 (1973). (*b*) S. F. NELSEN, J. M. BUSCHEK, and J. P. HINTZ. J. Am. Chem. Soc. **95**, 2013 (1973). (*c*) N. BODOR, M. J. S. DEWAR, W. B. JENNINGS, and S. D. WORLEY. Tetrahedron, **26**, 4109 (1970).
2. G. WAGNER and H. BOCK. Chem. Ber. **107**, 68 (1974).
3. C. BATICH and W. ADAM. Tetrahedron Lett. **16**, 1467 (1974).
4. K. OSAFUNE and K. KIMURA. Chem. Phys. Lett. **25**, 47 (1974).
5. D. SWERN (*Editor*). Organic peroxides. Wiley-Interscience, New York. 1970.
6. R. WEST, D. L. POWELL, M. K. T. LEE, and L. S. WHATLEY. J. Am. Chem. Soc. **86**, 3227 (1964).
7. R. C. WEAST (*Editor*). Handbook of chemistry and physics. 50th ed. Chemical Rubber Co. Press. 1969–1970.
8. H. PAGET. J. Chem. Soc. 829 (1938).
9. R. CRIEGEE and G. PAULING. Chem. Ber. **88**, 712 (1955).
10. C. R. BRUNDLE and D. W. TURNER. Proc. R. Soc. London, A, **27**, 307 (1968).
11. T. KOOPMANS. Physica, **1**, 104 (1934).
12. A. E. JONAS, G. K. SCHWEITZER, F. A. GRIMM, and T. A. CARLSON. J. Electron Spectrosc. **1**, 29 (1972/73).
13. S. CRADOCK and R. A. WHITEFORD. J. Chem. Soc. Faraday Trans. 2, **68**, 281 (1972).
14. B. J. COCKSEY, J. H. D. ELAND, and C. J. DANBY. J. Chem. Soc. B, 790 (1971).
15. P. MASCHET, D. GROSJEAN, G. MOUVIER, and J. DUBOIS. J. Electron Spectrosc. **2**, 225 (1973).
16. (*a*) C. GUIDOTTI, U. LAMANNA, M. MAESTRO, and R. MOCCIA, Theor. Chim. Acta, **27**, 55 (1972). (*b*) A. VEILLARD. Theor. Chim. Acta, **18**, 21 (1970). (*c*) W. H. FINK and L. C. ALLEN. J. Chem. Phys. **46**, 2261 (1967). (*d*) U. KALDOR and I. SHAVITT. J. Chem. Phys. **44**, 1823 (1966).
17. R. L. MILLER and D. F. HORNING. J. Chem. Phys. **34**, 265 (1961).
18. D. W. TURNER, C. BAKER, A. D. BAKER, and C. R. BRUNDLE. Molecular photoelectron spectroscopy. Wiley-Interscience, New York. 1970.
19. R. H. HUNT, R. A. LEACOCK, C. W. PETERS, and K. T. HECHT. J. Chem. Phys. **42**, 1931 (1965).
20. P. BISCHOF, J. A. HASHMALL, E. HEILBRONNER, and V. HORNING. Helv. Chim. Acta, **52**, 1745 (1969).
21. (*a*) W. LOBUNEZ, J. R. RITTENHOUSE, and J. G. MILLER. J. Am. Chem. Soc. **80**, 3505 (1958). (*b*) M. T. ROGERSAND, T. W. CAMPBELL. J. Am. Chem. Soc. **74**, 4742 (1952).
22. (*a*) K. R. KOPECKY and C. MUMFORD. Can. J. Chem. **47**, 709 (1969). (*b*) H. E. O'NEAL and W. H. RICHARDSON. J. Am. Chem. Soc. **92**, 6553 (1970). (*c*) N. J. TURRO and P. LECHTKEN. J. Am. Chem. Soc. **95**, 264 (1973). (*d*) T. WILSON, M. E. LANDIS, A. L. BAUMSTARK, and P. D. BARTLETT. J. Am. Chem. Soc. **95**, 4765 (1973).
23. G. BARNETT. Can. J. Chem. **52**, 3837 (1974).
24. P. D. MOLLERE. Tetrahedron Lett. 2791 (1973).
25. H. BASCH, M. B. ROBIN, N. A. KUEBLER, C. BAKER, and D. W. TURNER. J. Chem. Phys. **51**, 52 (1969).
26. S. N. FONER and R. L. HUDSON. J. Chem. Phys. **36**, 2676 (1962).
27. D. W. TURNER and D. P. MAY. J. Chem. Phys. **45**, 471 (1966).
28. J. W. ROBINSON (*Editor*). Handbook of spectroscopy. Vol. II. C.R.C. Press. 1974.

Can. J. Chem. Downloaded from www.nrcresearchpress.com by 210.87.254.42 on 09/05/12
For personal use only.

Conductance Study of Ion Pairing of Alkali Metal Tetrafluoroborates and Hexafluorophosphates in Acetonitrile

H. L. YEAGER

Department of Chemistry, University of Calgary, Calgary, Alberta T2N 1N4

AND

B. KRATOCHVIL

Department of Chemistry, University of Alberta, Edmonton, Alberta T6G 2E1

Received June 25, 1975

H. L. YEAGER and B. KRATOCHVIL. Can. J. Chem. **53**, 3448 (1975).

High precision conductance measurements are reported for sodium, potassium, and rubidium tetrafluoroborate and hexafluorophosphate in acetonitrile at 25 °C. The results are analyzed using the expanded form of the Fuoss–Hsia conductance equation. The ion size parameter, *d*, was systematically varied to obtain the value which gave best fit of the data to the equation. All salts were found to be associated, and the trends in association are discussed in terms of the ability of acetonitrile to solvate cations and anions.

H. L. YEAGER et B. KRATOCHVIL. Can. J. Chem. **53**, 3448 (1975).

On rapporte des mesures de conductivité de haute précision qui ont été effectuées à 25 °C, sur des solutions, dans l'acétonitrile, de tétrafluoroborates et d'hexafluorophosphates de sodium, de potassium et de rubidium. On analyse les résultats en faisant appel à une forme étendue de l'équation de Fuoss–Hsia pour la conductivité. On a fait varier d'une façon systématique le paramètre, *d*, ayant trait à la grosseur de l'ion; on a ainsi obtenu la valeur qui permet d'arriver à la meilleur corrélation entre nos données et l'équation. On a trouvé que tous les sels sont associés et on discute des tendances dans l'association en termes de l'habilité de l'acétonitrile à solvater les cations et les anions.

[Traduit par le journal]

Introduction

Acetonitrile has served for a number of studies of nonaqueous electrolyte solutions. It is a dipolar aprotic solvent of moderate cation solvating ability and rather weaker anion solvating ability (1, 2). Results of several conductance investigations (3, 4) indicate that many 1:1 univalent salts are at most only slightly associated in acetonitrile, in accordance with this solvent's dielectric constant of 35.95 (5). In recent years increasing interest has developed in obtaining information on solvation, ion-pairing, and complexation of alkali metals, especially sodium and potassium. Part of this interest is a result of the synthesis of new ligands that form complexes of appreciable stability with these ions, and part is due to studies of the role of these ions in biological systems and of the mechanisms by which they are transported through cell membranes, especially as complexes with macrotetrolide antibiotics (see for example, ref. 6, which contains four review articles on complexation of alkali and alkaline earth cations).

Techniques used to gain the needed information include ^{23}Na and ^{7}Li n.m.r. spectroscopy in a range of solvents (7), infrared spectroscopy (8), and electrical conductance (9). By a combination of conductance and n.m.r. spectroscopic measurements it is often possible to identify contact and solvent-separated ion pairs, and to calculate the fraction of metal ion present in each form. Since many interesting ligands are not water soluble, the use of other solvents such as acetonitrile is often necessary. To provide adequate solubility and minimal interaction, anions of large radius and low charge density are often employed. We report here high precision conductance measurements for several alkali metal tetrafluoroborates and hexafluorophosphates in acetonitrile. These two anions are spherically symmetrical and noncoordinating, and therefore ion pair association constant trends for their salts may be considered in

Can. J. Chem. Downloaded from www.nrcresearchpress.com by 210.87.254.42 on 09/05/12
For personal use only.

Can. J. Chem. Downloaded from www.nrcresearchpress.com by 210.87.254.42 on 09/05/12
For personal use only.

terms of anion size and simple ion–dipole interaction. These results are compared with previously reported conductance data for alkali metal perchlorates and tetraphenylborides (10) to demonstrate ion pairing trends with increasing cation and anion size.

Experimental Section

Sodium tetrafluoroborate (Ventron) was recrystallized from an 80:20 ethanol–water mixture and dried under vacuum at 120 °C for 15 h. Sodium hexafluorophosphate (Ventron) was recrystallized from absolute ethanol and dried under vacuum at 25 °C for 8 h. Potassium tetrafluoroborate (Ventron) was recrystallized from a 50:50 water–ethanol mixture and dried under vacuum at 25 °C for 8 h and then at 120 °C for 8 h. Potassium hexafluorophosphate (Matheson, Coleman, Bell) was recrystallized four times from water and dried under vacuum at 25 °C for 10 h before the first conductance run. As a check on the purity of the salt and reproducibility of the conductance measurements, the salt was recrystallized from water a fifth time, redried another 10 h, and a second conductance run made. Rubidium bromide was prepared by combining a slight excess of hydrobromic acid (Baker Analyzed Reagent) with rubidium carbonate (A. D. Mackay Inc.). This product was dissolved in water and slowly mixed with an aqueous solution of sodium tetrafluoroborate to produce rubidium tetrafluoroborate. The precipitate was recrystallized twice from a 50:50 water–methanol mixture and dried under vacuum at 25 °C for 4 h and then at 105 °C for 6 h. Rubidium hexafluorophosphate was prepared in similar fashion, except that sodium hexafluorophosphate was used in the second step. The product was recrystallized two times from water and dried under vacuum at 50 °C for 12 h before the first conductance run. As a check on the purity, the material was recrystallized a third time from water, redried at 55 °C for 11 h under vacuum, and a second conductance run made. Accurate analysis of these salts is difficult, but an estimate of purity can be obtained from the limiting equivalent conductances, which should equal the sum of the limiting ionic conductivities (4). On this basis, the purities of the salts in percent are: $NaBF_4$, 99.4; KBF_4, 100.1; $RbBF_4$, 99.6; $NaPF_6$, 98.6; KPF_6, 99.9; and $RbPF_6$, 99.5. In two instances (potassium and rubidium hexafluorophosphate), an additional recrystallization was performed prior to a second conductance run; the change in the limiting equivalent conductance was slight in each case. Excessive drying temperatures cause decomposition of many of these salts, as does prolonged storage.

The method of acetonitrile purification, the apparatus, and the experimental procedure are described in ref. 11. Values used for the physical properties of acetonitrile were: density, 0.7767 g/ml (11); viscosity, 0.003412 P (11); and dielectric constant, 35.95 (5).

Results and Discussion

The measured equivalent conductances and corresponding electrolyte concentrations have been placed in the Depository of Unpublished Data.[1] The data were analyzed using the expanded form of the Fuoss–Hsia equation (12, 13)

$$\Lambda = \Lambda_0 - S(C\gamma)^{1/2} + EC\gamma \log C\gamma + J_1 C\gamma - J_2(C\gamma)^{3/2} - K_A C\gamma f_\pm^2 \Lambda$$

where all symbols have their usual meaning. This equation and the comparable expanded Pitts equation (13*a*, 14) have been shown to be superior to the earlier Fuoss–Onsager equation (15) in fitting conductance data (13*b*, 16, 17). In order to evaluate the limiting equivalent conductance and ion pair association constant for a set of conductance data the third parameter in the equation, distance of closest approach of the ions, d, must also be evaluated. The d parameter appears in the J_1, J_2, and $f_\pm$ terms, and several approaches have been taken to optimize its value in the equation. These include assigning a value of the Bjerrum distance (18, 19) or some other value to d in the J_1 and $f_\pm$ terms and performing a three-parameter fit for Λ_0, K_A, and J_2, or assigning a value of d in J_1, J_2, and $f_\pm$ and performing a two-parameter fit (20). Perhaps a more reasonable approach is to perform several two-parameter analyses of the data using a series of values for d (16, 21). The distance parameter which yields a minimum standard deviation of fit, $\sigma\Lambda$, to the conductance data along with the corresponding Λ_0 and K_A values is chosen as the optimized parameter. We have employed the latter approach in this work.

A computer program which provided a two-parameter least-squares fit of conductance data was employed. Values of d were varied from 2.0 to 20.0 Å in 0.2 Å steps, and the least-squares fit was performed several times for each salt. Two types of behavior were observed in the results. Either a broad minimum in $\sigma\Lambda$ was observed over a range in d values, or two minima were found. In the latter case one d value would be in the range of 2–4 Å, and for salts with slight association would yield a corresponding K_A value which was negative. Similar results

[1]Complete set of tabular data is available, at a nominal charge, from the Depository of Unpublished Data, CISTI, National Research Council of Canada, Ottawa, Canada K1A 0S2.

Can. J. Chem. Downloaded from www.nrcresearchpress.com by 210.87.254.42 on 09/05/12
For personal use only.

TABLE 1. Optimized conductance parameters for alkali metal ion salts in acetonitrile at 25 °C

Salt	Concentration range ($\times 10^4$ C)	Λ_0	K_A	d	$\sigma\Lambda$
$NaBF_4$	5–34	184.49 ± 0.05	45.4 ± 0.2	6.6	0.06
	4–32	184.17 ± 0.02	50.10 ± 0.09	10.0*	0.02
KBF_4	3–18	192.34 ± 0.03	55.8 ± 0.2	7.2	0.03
$RbBF_4$	3–16	193.39 ± 0.05	60.4 ± 0.4	16.2	0.05
$NaPF_6$	3–34	178.60 ± 0.02	13.89 ± 0.07	10.8*	0.02
KPF_6	6–35	187.62 ± 0.02	21.16 ± 0.06	9.6*	0.02
	6–42	187.52 ± 0.01	20.75 ± 0.04	9.2*	0.01
$RbPF_6$	3–26	188.78 ± 0.02	25.5 ± 0.1	11.6*	0.02
	3–24	188.90 ± 0.02	24.72 ± 0.09	10.4*	0.02

*Two minima are found; the one at larger d is listed.

TABLE 2. Ion pair association constants for alkali metal ion salts in acetonitrile at 25 °C*

Cation	Association constants			
	BF_4^-	ClO_4^-†	PF_6^-	BPh_4^-†
Na^+	48(47)	16(20)	14(10)	4(4)
K^+	56(57)	28(27)	21(18)	2(3)
Rb^+	60(52)	31(31)	25(20)	7(5)
Cs^+	—	34(34)	—	19(17)

*Averaged values from Table 1. Values in parentheses are those obtained using d = 7.8 Å.
†Reanalysis of data from ref. 10.

have been found by other workers using this method of data treatment in different solvents (16, 17, 21). Table 1 lists the results of the least-squares fitting. When two minima were observed, the results for the larger d are given. The optimized Λ_0 and K_A values are included, along with standard deviations of fit and the d value used.

Kohlrausch differences calculated for the tetrafluoroborate and hexafluorophosphate salts of sodium, potassium, and rubidium are 5.73, 4.77, and 4.55. These values can be compared to the difference for the corresponding purified silver salts of 4.50 (11). The high value for the sodium salts can be attributed to quality of the hexafluorophosphate, which decomposes readily upon drying.

In Table 2 are listed association constants from Table 1 along with values for the alkali metal perchlorates and tetraphenylborides obtained by reanalysis of the data from ref. 10 by the method described here. Again, several sets of data for these salts showed two minima in $\sigma\Lambda$ with changing d. As before, the K_A value at the larger d is reported in each instance.

Although the limiting equivalent conductances from our reanalyses are virtually identical to those obtained by Kay *et al.* (10), the K_A values are systematically larger. The original treatment used the Fuoss–Onsager conductance equation (15), and similar trends in limiting equivalent conductance and K_A values upon reanalysis have been observed and discussed (16, 17). Association trends are not affected by the equation used however. Kay *et al.* found that the only tetraphenylboride salt which indicated association was the cesium salt. Reanalysis by the improved conductance equation confirms that only this salt has significant association behavior.

The association trends in Table 2 may be explained by assuming that the alkali metal ions are solvated by acetonitrile, while the larger anions are not. This assumption is reasonable not only on a size basis but also in terms of the ability of acetonitrile to function as a better Lewis base than Lewis acid. Therefore association increases with increasing crystallographic radii of the alkali metal ions due to decreasing cation solvation. Alternately, association decreases in the order $BF_4^- > ClO_4^- > PF_6^- > BPh_4^-$ due to the increase in size of the relatively unsolvated anion. The results in Table 2 illustrate a smooth trend in association with anion size for these spherically symmetrical noncoordinating anions.

To test whether the data analysis procedure affects the trends shown in Table 2, association constants are also listed for each salt when the ion size parameter is fixed at 7.8 Å, the Bjerrum distance in acetonitrile. With the possible exception of $RbBF_4$, the association constants do not change substantially.

Financial support by the National Research Council of Canada, the University of Alberta, and the University of Calgary is gratefully acknowledged.

1. J. F. COETZEE and J. J. CAMPION. J. Am. Chem. Soc. **89**, 2517 (1967).
2. C. H. SPRINGER, J. F. COETZEE, and R. L. KAY. J. Phys. Chem. **73**, 471 (1969).
3. G. J. JANZ and R. P. T. TOMKINS (*Editors*). Nonaqueous electrolytes handbook. Vol. 1. Academic Press, New York, N.Y. 1972.
4. B. KRATOCHVIL and H. L. YEAGER. *In* Topics in current chemistry. Vol. 27. Springer-Verlag, New York, N.Y. 1972.
5. G. P. CUNNINGHAM, G. A. VIDULICH, and R. L. KAY. J. Chem. Eng. Data, **12**, 336 (1967).
6. D. DUNITZ *et al.* (*Editors*). Structure and bonding. Vol. 16. Springer-Verlag, New York. 1973.
7. M. S. GREENBERG, R. L. BODNER, and A. I. POPOV. J. Phys. Chem. **77**, 2449 (1973); M. S. GREENBERG, D. M. WEID, and A. I. POPOV. Spectrochim. Acta, Part A **29**, 1927 (1973); Y. M. COHEN, P. R. HANDY, E. T. ROACH, and A. I. POPOV. J. Phys. Chem. **79**, 80 (1975).
8. W. F. EDGELL, J. LYFORD, R. WRIGHT, W. RISEN, and A. WATTS. J. Am. Chem. Soc. **92**, 2240 (1970).
9. D. F. EVANS, S. L. WELLINGTON, J. A. NADIS, and E. L. CUSSLER. J. Solution Chem. **1**, 499 (1972).
10. R. L. KAY, J. B. HALES, and G. P. CUNNINGHAM. J. Phys. Chem. **71**, 3925 (1967).
11. H. L. YEAGER and B. KRATOCHVIL. J. Phys. Chem. **73**, 1963 (1969).
12. (*a*) R. M. FUOSS and K.-L. HSIA. Proc. Natl. Acad. Sci. USA, **57**, 1550 (1967); **58**, 1818 (1968); (*b*) K.-L. HSIA and R. M. FUOSS. J. Am. Chem. Soc. **90**, 3055 (1968).
13. (*a*) R. FERNÁNDEZ-PRINI and J. E. PRUE. Z. Phys. Chem. (Leipzig), **228**, 373 (1965); (*b*) R. FERNÁNDEZ-PRINI. Trans. Faraday Soc. **65**, 3311 (1969).
14. (*a*) E. PITTS. Proc. R. Soc. Ser. A, **217**, 43 (1953); (*b*) E. PITTS, B. E. TABOR, and J. DALY. Trans. Faraday Soc. **65**, 849 (1969).
15. (*a*) R. M. FUOSS and L. ONSAGER. J. Phys. Chem. **61**, 668 (1957); (*b*) R. M. FUOSS and F. ACCASCINA. Electrolytic conductance. Interscience, New York, N.Y. 1959.
16. E. M. HANNA, A. D. PETHYBRIDGE, and J. E. PRUE. Electrochim. Acta, **16**, 677 (1971).
17. B. J. BARKER, H. L. HUFFMAN, JR., and P. G. SEARS. J. Phys. Chem. **78**, 2689 (1974).
18. J. C. JUSTICE. Electrochim. Acta, **16**, 701 (1971).
19. R. M. FUOSS. J. Phys. Chem. **78**, 1383 (1974).
20. R. FERNÁNDEZ-PRINI. Trans. Faraday Soc. **64**, 2146 (1968).
21. (*a*) E. M. HANNA, A. D. PETHYBRIDGE, and J. E. PRUE. J. Phys. Chem. **75**, 291 (1971); (*b*) W. C. DUER, R. A. ROBINSON, and R. G. BATES. J. Chem. Soc. Faraday Trans. 1, **68**, 716 (1972); (*c*) E. M. HANNA, A. D. PETHYBRIDGE, J. E. PRUE, and D. J. SPIERS. J. Solution Chem. **3**, 563 (1974).

Can. J. Chem. Downloaded from www.nrcresearchpress.com by 210.87.254.42 on 09/05/12
For personal use only.

Apparent Molal Volumes and Heat Capacities of Some Tetraalkylammonium Bromides, Alkyltrimethylammonium Bromides, and Alkali Halides in Aqueous Glycerol Solutions

GIUSEPPA DIPAOLA[1] AND BERNARD BELLEAU

Department of Chemistry, McGill University, Montreal, Quebec H3C 3G1

Received July 24, 1975

GIUSEPPA DIPAOLA and BERNARD BELLEAU. Can. J. Chem. **53**, 3452 (1975).

The densities and volumetric specific heats of some tetraalkylammonium bromides, alkyltrimethylammonium bromides, and some alkali halides (0.02 to 0.5 aquamolal) were measured in 0 to 30 wt.% glycerol in water with a flow densimeter connected in series with a flow microcalorimeter at 24 and 25 °C respectively. The derived volumes and heat capacities of transfer of the electrolytes from water to glycerol–water mixtures are consistent with the corresponding transfer functions from water to D_2O and from water to urea–water mixtures, and suggest that structural interactions are reduced in aqueous glycerol solutions. The volumes and heat capacities of micellization of *n*-nonyltrimethylammonium bromide were determined in water, glycerol–water mixtures, urea–water mixtures, and in D_2O. Both the transfer and the micellization study indicate that glycerol behaves in an analogous manner to urea. An effect other than a simple alteration of the water structure must be invoked to account for their different effects on protein stability.

GIUSEPPA DIPAOLA et BERNARD BELLEAU. Can. J. Chem. **53**, 3452 (1975).

Les densités et les chaleurs spécifiques volumiques des bromures de tetra-alkylammonium, alkyl-trimethylammonium et des halogénures d'alkalis (0.02–0.5 aquamolal) ont été mesurées dans des mélanges eau–glycérol (0–30 wt.%) à 24 et 25 °C respectivement au moyen d'un densimètre et d'un microcalorimètre dynamique. Les volumes et capacités calorifiques de transfert de l'eau aux mélanges eau–glycérol sont en accord avec les fonctions de transfert correspondantes de l'eau à D_2O et de l'eau aux mélanges eau–urée, et suggèrent que les effets structuraux d'hydration sont moins prononcés dans les mélanges eau–glycérol que dans l'eau. On a mesuré les volumes et capacités calorifiques de micellisation du bromure de *n*-nonyl-trimethylammonium dans des mélanges eau–glycerol, eau–urée et dans D_2O. L'étude des fonctions de transfert et l'étude de micellisation indiquent que le glycérol agit comme l'urée. Pour expliquer la différence entre l'urée et le glycérol sur la stabilité des protéines, il faut invoquer d'autres effets que la modification de la structure de l'eau.

Introduction

The ability of glycerol and other polyhydroxy compounds to stabilize highly organized biological substances is a widely recognized phenomenon (1–8). However, postulated mechanisms on the nature of these effects belong to the realm of speculation. Glycerol is one of the more effective of the polyhydroxy compounds in the protection of enzymes against the denaturing effects of cooling (2, 3) and urea (3), and against heat inactivation (4, 5). The minimum concentration of glycerol required is usually 20% (v/v). It has been suggested (1, 3, 6, 7) that a possible reason for glycerol's mechanism of action is its effect on water structure. However, no definitive conclusions could yet be reached.

Many physicochemical properties of glycerol and its aqueous solutions are now known, such as dielectric constants (9, 14), densities (10, 14), heats of dilution (11, 12, 14), and specific heats (13, 14).

We are presently in the process of studying the calorimetric and volumetric behavior of aqueous solutions of a homologous series of polyhydric alcohols. It is hoped that such a study might give some insight into the problem at hand. This paper reports the volumes and heat capacities of binary and ternary systems containing glycerol.

Experimental

Heat capacities were measured with a flow microcalorimeter described by Picker *et al.* (15). The instrument used can detect differences between the volumetric specific heat of a solution (σ) and that of a reference solvent (σ_0) to $\pm 3 \times 10^{-5}$ J K^{-1} cm^{-3}, during a temperature rise of 2 °C and a liquid flow rate of 0.80 cm^3

[1]Holder of a Centennial Predoctoral Scholarship of the National Research Council of Canada 1972–1976.

Can. J. Chem. Downloaded from www.nrcresearchpress.com by 210.87.254.6 on 09/05/12
For personal use only.

Can. J. Chem. Downloaded from www.nrcresearchpress.com by 210.87.254.6 on 09/05/12
For personal use only.

min^{-1}. The overall precision on $\Delta\sigma/\sigma_0$ is 0.3% (16). Densities were determined with a flow digital densimeter (17) sensitive to $\pm 3 \times 10^{-6}$ g cm^{-3}, connected in series with the microcalorimeter. Thermostatic control of the instrument was achieved with a closed-loop bath (18) whose stability was better than 0.001 °C.

Apparent molal volumes (ϕ_v) and heat capacities (ϕ_c) were derived from

$$[1] \qquad \phi_v = M/d - W_{55.51}(d - d_0)/dd_0m$$

and

$$[2] \qquad \phi_c = MC_p + W_{55.51}(C_p - C_{p0})/m$$

where all symbols have their usual meaning (19). The weight specific heats (C_p and C_{p0}) are calculated from the volumetric specific heats (σ and σ_0); thus

$$[3] \qquad C_p/C_{p0} = (\sigma/\sigma_0)(d_0/d)$$

All heat capacity measurements were made at 25.00 °C. Because of the experimental setup, density measurements were obtained at 24.00 °C. The values for C_{p0} and d_0 of pure water were taken as 4.1793 J K^{-1} g^{-1} (20) and 0.997299 g cm^{-3} (21). The error introduced by taking the ratio of densities at 24 °C rather than at 25 °C is negligible.

Transfer functions are defined as follows:

$$\Delta\phi_x = \phi_{x(\text{soln})} - \phi_{x(H_2O)}$$

where ϕ_x represents the appropriate molal quantity at a specific concentration.

The tetraalkylammonium bromide salts (Eastman Kodak Reagents) were purified as described in the literature (22). The alkyltrimethylammonium bromide salts used were reported previously (23). Urea (Schwarz/Mann Ultra Pure Reagents) was dried under vacuum at 60 °C for several hours. The following were used without further purification: NaF, NaBr (Anachemia Reagents); NaCl, NaI, KBr (Fisher Certified Reagents); glycerol (Fisher Certified Spectranalyzed); glycerol-d_3 and D_2O (99.7%) (Merck, Sharp and Dohme); and D_2O (99.7%) (Aldrich).

All solutions were prepared by weight with double-distilled, deionized water and used the same day. To facilitate comparison in different solvents, all salt concentrations are expressed in aquamolalities (m).

Results

Densities and heat capacities were determined for the following systems:[2] (*1*) glycerol–water and glycerol-d_3–D_2O from 0 to 30 wt.%, (*2*) Me_4NBr, NaCl, NaF in the concentration range of 0.02 to 0.5 m at a fixed glycerol concentration (0 and 20 wt.%), (*3*) Me_4NBr, n-Bu_4NBr, NaCl, NaF at a fixed aquamolality of 0.05 m in a variable glycerol concentration (0 to 30 wt.%), (*4*) homologous series of n-alkyltrimethylammonium bromide salts, NaBr, NaI, KBr at a fixed aquamolality (0.05 m) and a fixed glycerol concentration (20 wt.%), and (*5*) n-nonyltrimethylammonium bromide salt (0.02 to 0.6 m) in water, 10 and 20 wt.% glycerol–water, 1 and 3 m urea, D_2O and in a solution containing molar ratios of glycerol:urea:water of 1:1:50.

All experimental measurements of σ/σ_o were determined in duplicate or more. Since the densities are known to better than 1 part in 10^5, the uncertainty in ϕ_c depends mainly on the error in the difference (or ratio of) in volumetric specific heats, which is of the order of 0.3% under the best conditions. The values of ϕ_c are thus reliable to 1 to 5 J K^{-1} mol^{-1} at low aquamolalities, and better than 1 J K^{-1} mol^{-1} above 0.1 m (24).

The concentration dependence of ϕ_c and ϕ_v for glycerol in water and for glycerol-d_3 in D_2O is similar (Table 1). There is a slight but significant[3] decrease in ϕ_c accompanied by an increase in ϕ_v. The infinite dilution water to D_2O transfer functions are found by graphical extrapolation of a ϕ_c or ϕ_v *vs.* m plot (not shown) to be $\Delta\phi_{ctr}^0 = 5 \pm 2$ J K^{-1} mol^{-1} and $\Delta\phi_{vtr}^0 = -0.15 \pm 0.1$ cm^3 mol^{-1}. In this case, no significance can be attached to the transfer functions due to the given uncertainties.

Apparent molal heat capacities and volumes at infinite dilution were obtained for Me_4NBr, n-Bu_4NBr, NaCl, and NaF in water by graphical extrapolation of a plot of the apparent molal quantity (corrected for the Debye–Hückel limiting law contribution) *vs.* aquamolality to $m = 0$ (not shown). Results for ϕ_c^0 at 25 °C are 123, 1221, −81, and −77 J K^{-1} mol^{-1} respectively. There is good agreement with corresponding literature values of 109, 1209 (25), and −81 and −73 J K^{-1} mol^{-1} (16) at 25 °C. Results for ϕ_v^0 at 24 °C are 114.35, 300.30, 16.75, and −2.50 cm^3 mol^{-1} which are in reasonable agreement with literature values 114.26 (26), 300.59 (27), 16.62 and −2.48 cm^3 mol^{-1} (28). Only recent literature data of comparable precision have been included.

The concentration dependence of the salts studied in 20 wt.% glycerol–water follows a similar behavior pattern to that observed in water. The Debye–Hückel limiting law coefficients for ϕ_v and ϕ_c are not known for electrolytes

[2]Complete set of tabular data for d_0/d, σ/σ_0, ϕ_v, and ϕ_c is available, at a nominal charge, from the Depository of Unpublished Data, CISTI, National Research Council of Canada, Ottawa, Canada K1A 0S2.

[3]Uncertainty on ϕ_c for a 0.1, 1, 2 m solution is 1–2, 0.1–0.2, and 0.05–0.1 J K^{-1} mol^{-1} respectively.

Can. J. Chem. Downloaded from www.nrcresearchpress.com by 210.87.254.6 on 09/05/12
For personal use only.

TABLE 1. Volumes and heat capacities of glycerol–water and glycerol-d_3–D_2O systems at 24 and 25 °C respectively

Aquamolality	Weight percent	σ/σ_0*	d_0/d†	ϕ_c‡ ($J\,K^{-1}\,mol^{-1}$)	ϕ_v ($cm^3\,mol^{-1}$)
Glycerol–H_2O					
0.1220	1.111	0.998390	0.997429	239.8	70.98
0.2205	1.991	0.997111	0.995387	240.0	70.95
0.5672	4.964	0.992711	0.998517	239.8	70.99
0.7988	6.853	0.989622	0.984150	238.4	70.99
1.1209	9.357	0.985594	0.978370	237.8	71.00
1.7295	13.740	0.978204	0.968288	236.9	71.03
2.1989	16.841	0.972375	0.961198	235.5	71.07
3.4552	24.140	0.958116	0.944536	233.3	71.13
4.4979	29.291	0.947422	0.932891	232.2	71.19
Glycerol-d_3–D_2O§					
0.07348	0.6255	0.990643	0.998881	240.6	70.72
0.1708	1.442	0.996960	0.997477	246.0	71.05
0.3098	2.585	0.994533	0.995423	245.0	70.87
0.6556	5.317	0.988637	0.990609	244.7	70.90
0.8602	6.863	0.985247	0.987841	244.2	70.86
1.2823	9.898	0.978391	0.982510	243.6	70.89
2.2968	16.441	0.962928	0.971204	242.4	71.03
3.7648	24.387	0.942967	0.957516	240.9	71.11

*To eliminate rounding-off errors, at least one extra digit is included.
†Value of d_0 is taken as 0.997299 g cm^{-3} in H_2O (20).
‡Values calculated using C_{p0} = 4.1793 J K^{-1} g^{-1} (19).
§Measured values for D_2O (Merck, Sharp and Dohme): C_{p0}(25 °C) = 4.2094 J K^{-1} g^{-1}; d_0(24 °C) = 1.10404 g cm^{-3}.

in glycerol–water mixtures. Since the dielectric properties of glycerol–water mixtures (14) are close to those of water, one can assume that as a first approximation, the limiting Debye–Hückel slopes are about equal. Since we are interested in trends rather than in absolute values, any systematic differences that would be encountered by treating the data in a more quantitative manner will be ignored.

The heat capacities of transfer of 0.05 *m* tetraalkylammonium bromides from water to glycerol–water mixtures up to 30 wt.% are shown in Fig. 1 (the volumes of transfer are not shown). The transfer functions of *n*-Bu_4NBr are linear functions of the glycerol concentration, and are negative. No definitive conclusion could be reached regarding the sign of the transfer functions for Me_4NBr especially $\Delta\phi_{vtr}$, due to the proximity of the values to zero.

The transfer functions of 0.05 *m* alkyltrimethylammonium salts from water to 20 wt.% glycerol–water are negative. The heat capacities of transfer are linear functions of the alkyl chain length, *i.e.*, the absolute magnitude increases as the hydrophobicity of the molecule increases (Fig. 2). A regularity is observed in the variation of ϕ_c with increasing chain length of the alkyl group of the trimethylammonium salts (0.05 *m*) in water (Fig. 3), and in 20 wt.% glycerol–water. Both ϕ_c and ϕ_v increase linearly with the number of carbon atoms in the chain. The average incremental group contribution of each $-CH_2$ group in water was found to be 88 ± 6 J K^{-1}

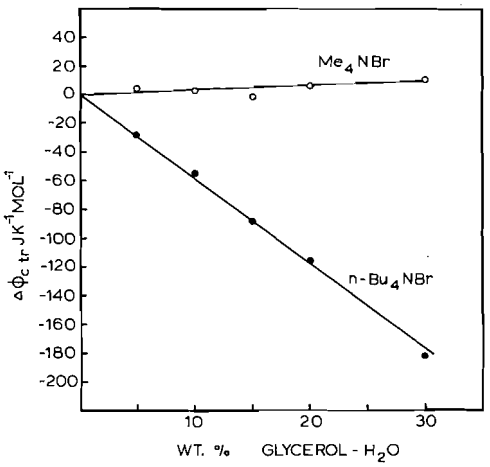

FIG. 1. Apparent molal heat capacities of transfer of 0.05 *m* tetraalkylammonium bromides from water to glycerol–water mixtures at 25 °C.

Can. J. Chem. Downloaded from www.nrcresearchpress.com by 210.87.254.6 on 09/05/12
For personal use only.

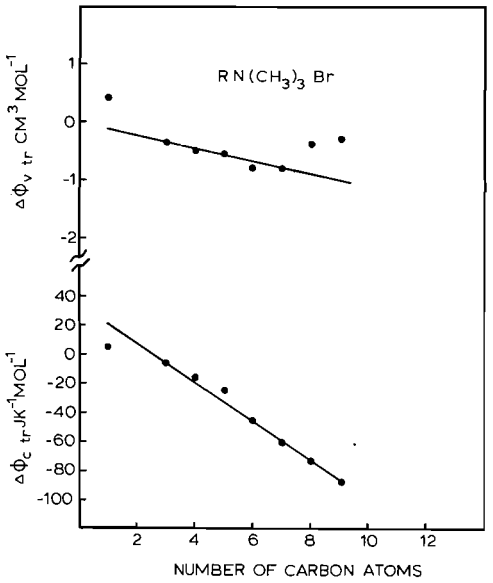

FIG. 2. Apparent molal volumes and heat capacities of 0.05 *m* alkyltrimethylammonium bromides from water to 20 wt.% glycerol–water at 24 and 25 °C respectively.

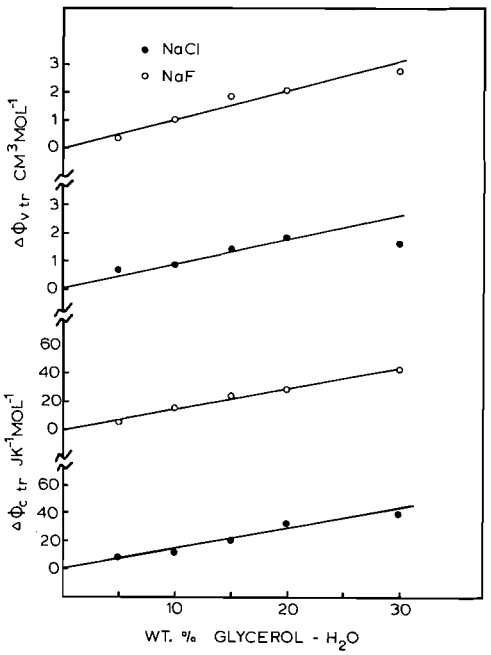

FIG. 4. Apparent molal volumes and heat capacities of transfer 0.05 *m* NaF and NaCl from water to glycerol–water mixtures at 24 and 25 °C respectively.

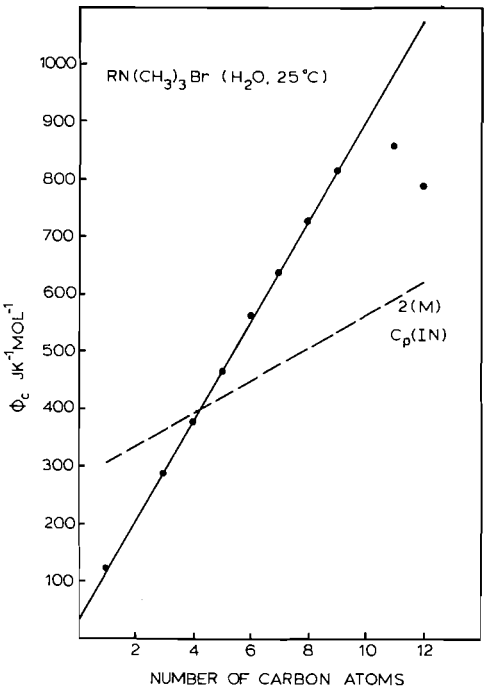

FIG. 3. Apparent molal heat capacities of 0.05 *m* alkyltrimethylammonium bromides in water at 25 °C. (Deviations for $C_{11}H_{23}N(CH_3)_3Br$ and $C_{12}H_{25}N(CH_3)_3$-Br are due to micellization.)

mol^{-1} (Fig. 3) and 15.8 ± 0.2 cm^3 mol^{-1} at 25 and 24 °C respectively. This agrees with the corresponding values that have been obtained for other homologous series in H_2O at 25 °C, such as the *n*-alkylamine hydrobromides (ref. 29 and references cited therein, 30).

The volumes and heat capacities of transfer of 0.05 *m* NaCl and NaF are positive (Fig. 4) and are linear functions of the glycerol concentration. A mirror-image relationship is observed on comparing the slopes for the transfer from water to glycerol–water, and urea–water (31) systems to transfer to the D_2O system (28).

The apparent molal volumes and heat capacities of *n*-nonyltrimethylammonium bromide were determined as a function of salt concentration in different glycerol–water mixtures (Fig. 5). For comparative purposes, the study was extended to include 1 and 3 *m* urea and D_2O. For each system studied, there is a sharp increase in ϕ_v and decrease in ϕ_c at the critical micelle concentration (c.m.c.) of the surfactant. If the c.m.c. is associated with the beginning of micellization, the c.m.c. of *n*-nonyltrimethylammonium bromide in water is approximately 0.12 *m* (Fig. 6) which is in very good agreement

Can. J. Chem. Downloaded from www.nrcresearchpress.com by 210.87.254.6 on 09/05/12
For personal use only.

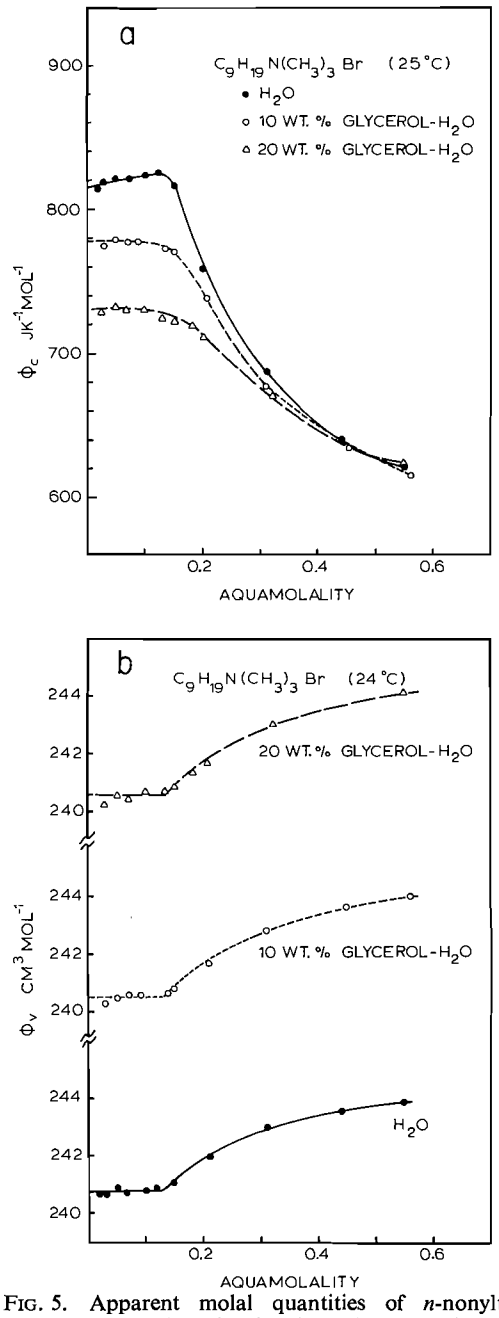

FIG. 5. Apparent molal quantities of *n*-nonyltrimethylammonium bromide in glycerol–water mixtures: (*a*) apparent molal heat capacities at 25 °C; (*b*) apparent molal volumes at 24 °C.

with the value of 0.13 *M* found by Musbally *et al.* at 25 °C (32). The c.m.c. in 10 and 20 wt.% glycerol–water is slightly decreased to 0.10 *m*. The c.m.c. in 1 and 3 *m* urea is approximately

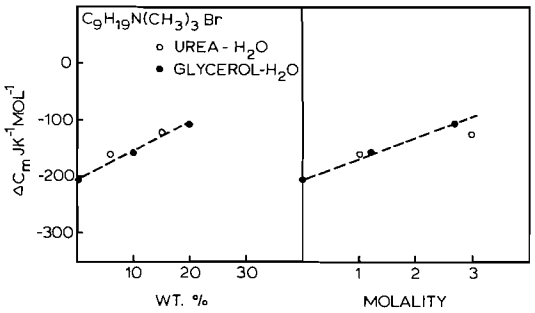

FIG. 6. The concentration dependence of the heat capacity of micellization of *n*-nonyltrimethylammonium bromide in glycerol–water and urea–water mixtures at 25 °C.

0.15 and 0.20 *m* respectively; that in D_2O is 0.10 *m*. The changes in volume (ΔV_m) and heat capacities (ΔC_m) on micellization were determined. These thermodynamic functions are not easily evaluated since the micellization region is not very sharp. They were approximated from the differences in the functions at 0.6 *m* and the corresponding values just below the c.m.c. The estimated uncertainties on ΔC_m and ΔV_m are ± 10 J K^{-1} mol^{-1} and ± 0.5 cm^3 mol^{-1} respectively (Table 4).

Discussion

Much of the recent work on aqueous solutions seems to indicate the presence of structural interactions in all solutions, which affect both the solute–solvent and solute–solute interactions. Since the apparent molal heat capacity is related to the second derivative of the chemical potential with respect to temperature, it is particularly sensitive to structural effects (16). Because of various contributions to ϕ_v this quantity is not easily explained (30, 33, 34). Studies of apparent molal quantities in dilute solution and of their concentration dependence have been shown to be useful tools in the study of solute–solvent and solute–solute interactions (25, 29, 35).

The predominance of structural interactions can best be illustrated through a study of transfer functions. The dielectric properties of water (36) and those of low concentrations of glycerol in water (14) are similar. The dipole moments of water and glycerol are respectively 1.83 (36) and 2.68 D (37). As a first approximation, all electrostatic ion–solvent interactions will be equal in both water and aqueous glycerol. Although the electrostatic contribution will be larger for simple ions as compared to larger hydrophobic ions, it

Can. J. Chem. Downloaded from www.nrcresearchpress.com by 210.87.254.6 on 09/05/12
For personal use only.

will be negligible for both when the transfer quantities are considered. The contribution due to the intrinsic quantities C_p(in) and $\overline{V}$(in) disappears when these functions are considered. Therefore, the transfer functions (as a first approximation) primarily reflect structural changes.

No marked concentration dependence is seen in the apparent molal volumes and heat capacities of glycerol in water (0 to 30 wt.%). This indicates that solute–solute interactions play a minor (and negligible) role in the glycerol–water system and that no long-range effects should therefore be expected. Similar suggestions have been made by Franks *et al.* (38). The difference between ϕ_c^0 of glycerol in water and the heat capacity of pure glycerol in the liquid state should reflect the structural influence of glycerol on water (35, 38). The specific heat capacity of pure glycerol at 25 °C is approximately 220 J K^{-1} mol^{-1} (14); ϕ_c^0 is 240 J K^{-1} mol^{-1}. The similar values suggest only a small structural effect on water. Similar conclusions have been reached by other workers (39, 40). The solvent isotope effect (as shown by $\Delta\phi_{vtr}^0$ and $\Delta\phi_{ctr}^0$ from water to D_2O) shows only negligible differences. An attempt at interpretation would be unjustified since any exchange (D–H) would contribute to masking possible differences between the two systems. The slight trends in the concentration dependence of ϕ_v and ϕ_c observed for the glycerol–water system are repeated for the glycerol-d_3–D_2O system.

An abnormally large ϕ_c in comparison with C_p(in) is usually associated with structure making and a small ϕ_c with structure breaking. The intrinsic heat capacity (C_p(in)) is not known for these solutes (Fig. 3). Since most organic liquids have specific heats of the order of 2 J K^{-1} g^{-1}, C_p(in) can be estimated as 2 × mol. wt. (29).[4] A comparison of the estimated C_p(in) values with the experimental ϕ_c values for the trimethylammonium bromide salts in water (Fig. 3) shows that there is a negative hydration contribution with the lower homologs and a positive hydration contribution (extra heat capacity) with the higher homologs. A crossover point is obtained at *n*-butyl-$N(CH_3)_3Br$. Leduc *et al.* (29) also obtained a crossover point at *n*-butyl-NH_3Br for a similar study in water. The apolar portion of the molecule again apparently dominates the heat capacity behavior in aqueous solution. An intuitive expectation is a group contribution dependent on the distance from the $N^+(CH_3)_3$ and the CH_3 groups. No such dependence is noted here. The constancy of the incremental group contribution (—CH_2) suggests an additive effect on water structure *i.e.* the environment of each —CH_2 group is similar and independent of effects from the previous group. The average incremental group contribution in 20 wt.% glycerol–water is 76 ± 6 J K^{-1} mol^{-1}, approximately 12 J K^{-1} mol^{-1} lower than the value in water. This suggests a reduction in structural hydration effects as compared to those in water.

The negative apparent molal heat capacities of transfer of *n*-Bu_4NBr, and *n*-propyl- to *n*-nonyl-$N(CH_3)_3Br$ from water to aqueous glycerol (Table 2 and Figs. 1 and 2) suggest that the structure-making propensity possessed by these hydrophobic salts in pure water is reduced in glycerol–water mixtures, and decreases regularly as the concentration of glycerol increases (0–30 wt.%). This effect on structural interactions also increases in absolute magnitude with increasing hydrophobic character of the molecules.

Based on these results, the volumes of transfer are expected to be positive if the cavity effect predominates as has been suggested in the literature (30, 33, 34). However, negative values are observed for the transfer of the hydrophobic salts. This apparent anomaly can be accounted for as follows. Warner (41) has pointed out that the glycerol molecule can adopt a conformation in which the oxygen atoms are spaced at a distance of 4.8 Å. The oxygen spacings are thus compatible with the second nearest neighbor distance of the oxygens in liquid water. Because of this structural compatibility, the dimensions of icelike aggregates formed would be similar, and the cavity-filling effect might be about the same in both water and dilute aqueous glycerol solutions. The negative value of $\Delta\phi_{vtr}$ of the large hydrophobic salts therefore reflects primarily the change in icelikeness of the hydrophobic hydration cosphere.[5] A similar proposal was put

[4] A list of other references can be found in ref. 29.

[5] The structural contribution is negative in the presence of structure breakers and positive with structure makers. The cavity effect for hydrophobic hydration is negative. If $\Delta\phi_{vtr}$ primarily reflects the structural contribution then ϕ_v in the less-ordered (glycerol–water) would be less than ϕ_v in a more ordered, more icelike environment (water). Therefore, $\Delta\phi_{vtr}$ for the hydrophobic probes is negative.

TABLE 2. Volumes and heat capacities of transfer from $H_2O \rightarrow$ 20 wt.% glycerol–H_2O at 24 and 25 °C respectively of 0.05 *m*

Alkylammonium bromides			Alkali halides		
Solute	$\Delta\phi_{ctr}$ (J K^{-1} mol^{-1})	$\Delta\phi_{vtr}$ (cm^3 mol^{-1})	Solute	$\Delta\phi_{ctr}$ (J K^{-1} mol^{-1})	$\Delta\phi_{vtr}$ (cm^3 mol^{-1})
Me_4NBr	+5	+0.44	NaF	28	2.05
propyl-$N(Me)_3Br$	−6	−0.34	NaCl	34	1.78
butyl-$N(Me)_3Br$	−16	−0.47	NaBr	35	1.53
pentyl-$N(Me)_3Br$	−25	−0.52	NaI	40	1.46
hexyl-$N(Me)_3Br$	−46	−0.79	KBr	39	2.09
heptyl-$N(Me)_3Br$	−62	−0.77			
octyl-$N(Me)_3Br$	−74	−0.37			
nonyl-$N(Me)_3Br$	−90	−0.27			
n-Bu_4NBr	−115	−1.82			

TABLE 3. Thermodynamic functions of transfer of tetraalkylammonium bromides and alkali halides at 25 °C

	$H_2O \rightarrow D_2O$		$H_2O \rightarrow$ 3 *m* urea	
	$\Delta\phi_{ctr}^0$ (J K^{-1} mol^{-1})	$\Delta\phi_{vtr}^0$ (cm^3 mol^{-1})	$\Delta\phi_{ctr}^0$ (J K^{-1} mol^{-1})	$\Delta\phi_{vtr}^0$ (cm^3 mol^{-1})
Me_4NBr	−14*	−0.21†	+37‡	+1.5‡
n-Bu_4NBr	+37*	+1.31†	−153‡	+1.1‡
NaF	−47§	−1.32§	+48.2‖	+2.14‖
NaCl	−40§	−0.87§	+51.6‖	+2.05‖

*From ref. 22.
†From ref. 25.
‡From ref. 19.
§From ref. 16.
‖From ref. 29.

forward by Philip and Desnoyers (25) to explain the apparent anomaly in $\Delta\phi_{vtr}^0$ of *n*-Bu_4NBr from water to D_2O.

The thermodynamic parameters of transfer for the alkali halides (electrostrictive structure breakers) are also consistent with a decrease in structural interactions in aqueous glycerol. The small dependence of the transfer functions on ionic size are in the same direction and of the same order of magnitude as that observed in the urea–water system (31).

A comparison of our present results for the transfer of several ionic probes from water to glycerol–water mixtures and literature data for transfer to D_2O and 3 *m* urea systems is summarized in Tables 2 and 3. The transfer behavior is qualitatively and quantitatively similar to transfers to 3 *m* urea, and opposite in sign from those to the D_2O system. This comparison suggests that there is less structural order in glycerol–water than in pure water. Of the available models describing the thermodynamic behavior of aqueous solutions of hydrophilic solutes, the specific site hydration model proposed by Tait *et al.* (42) seems to be the most appropriate in describing the behavior of the glycerol–water system.

Micellization Study

Micelle formation can serve as a model system for hydrophobic bonding and for understanding more complex solution phenomena. It is usually considered to be an entropy-driven process in which hydrocarbon chains associate to minimize the overall hydrophobic hydration. Determination of heat capacities (29, 43–46) and volumes (29, 30, 47–49) for micelle formation are rather scarce. In all cases, ΔC_m has been found to be negative and ΔV_m found to be positive. The signs of these thermodynamic functions are consistent with a decrease in hydrophobic hydration during association. The positive structural heat capacity

Can. J. Chem. Downloaded from www.nrcresearchpress.com by 210.87.254.6 on 09/05/12
For personal use only.

TABLE 4. Solvent effects on thermodynamic parameters of micellization of *n*-nonyltrimethylammonium bromide

Solvent	ϕ_c^{0*} (J K^{-1} mol^{-1})	ΔC_m†	ϕ_v^{0*} (cm^3 mol^{-1})	ΔV_m‡
H_2O	816	−205	240.7	3.4
D_2O	814	−226	240.0	3.5
Glycerol–H_2O				
10 wt.%	776	−161	240.5	3.5
20 wt.%	731	−110	240.6	3.6
Urea–H_2O				
1 *m*	789	−162	241.5	2.6
3 *m*	746	−125	242.5	2.0
Glycerol:urea:H_2O				
molar ratios 1:1:50	754	−124	241.0	4.1

*Values obtained by linear extrapolation (Fig. 5); they are uncorrected for Debye–Hückel limiting law contribution. ϕ_c^0 values are at 25 °C, and ϕ_v^0 values at 24 °C.
†Estimated uncertainty is ±10 J K^{-1} mol^{-1}.
‡Estimated uncertainty is ±0.5 cm^3 mol^{-1}.

contribution to ϕ_c^0 of the hydrophobic monomer is lost, and the reappearance of free space around the solute causes a positive contribution to the volume. Addition of cosolvents (glycerol, urea) to water, or replacement of water by D_2O affects the monomeric state (pre-c.m.c.) rather than the micellular state (post-c.m.c.) (Fig. 6). Quantitative differences exist between effects of various additives. However, post-c.m.c. values tend toward a common value which is of the same order of magnitude as the molar heat capacity for the pure organic liquid (estimated C_p(in) of *n*-nonyl-N$(CH_3)_3$Br is 532 J K^{-1} mol^{-1}). This suggests that the interior of the micelle resembles the organic liquid. The ΔC_m values observed are negative and the ΔV_m values are positive. The heat capacity of micellization is much more sensitive to solvent effects than the volume of micellization. Examination of the data reveals that ΔC_m is much more positive in the glycerol–water and urea–water mixtures than in water alone. The values of ΔC_m decrease in absolute magnitude with increasing cosolvent concentration. In the glycerol–water system the ΔC_m is a linear function of the glycerol concentration (Fig. 6). The largest ΔC_m occurs in D_2O. It is possible that the relative magnitudes of ΔC_m can be used to differentiate between so-called 'structured' and 'unstructured' solvents. The ΔV_m values are constant in H_2O, D_2O, and aqueous glycerol. Lower values are ΔV_m are observed in urea, suggesting that less icelike water of hydration is released upon micellization in this solvent mixture.

It would be unjustifiable to emphasize the small effects on the c.m.c. observed in D_2O and in glycerol–water. Complications arising from solvent penetration of the micelle by glycerol are not expected. Emerson and Holtzer (50) have pointed out that the numerical value of the c.m.c. should not be taken as a single criterion for hydrophobic bond strength in micelles. Micelles may contain different number of monomers for different additives. There is a 67% increase in the c.m.c. on addition of 3 *m* urea. This large effect points to a decrease in the hydrophobic bond strength and destabilization of the micelle.

The results for micellization for a system containing 1:1:50 molar ratio of glycerol:urea:water are found in Table 4. The effects of glycerol and urea on the heat capacity of micellization are additive. The molalities of glycerol and urea in the solvent are approximately 1 *m* each. The result for ΔC_m can be predicted from Fig. 6 by considering the value of ΔC_m to be analogous to either a 2 *m* glycerol–water or a 2 *m* urea–water solvent system. They are apparently affecting the water structure independently of one another and leaving their respective 'structure-altering' properties unchanged. The value of ΔV_m resembles that in glycerol–water. The c.m.c. is identical to value in 1 *m* urea.

Conclusion

The transfer studies have shown that there is little difference between the effect of urea and that of glycerol on water structure. Structural interactions are reduced in both systems. The

Can. J. Chem. Downloaded from www.nrcresearchpress.com by 210.87.254.6 on 09/05/12
For personal use only.

micellization study also shows that urea and glycerol behave in very much the same way. The model system used shows no specific correlations.

Glycerol and urea, however, have very different effects on protein conformation. Glycerol protects proteins against urea inactivation. There have been several attempts in the past to correlate the denaturing ability of a compound and its effect on water structure (51–55). These have met with little success. Our results lead us to believe that an effect other than a simple alteration of the water structure must be postulated to explain the stabilizing influence of glycerol. Unpublished model evidence from our laboratories indicates that glycerol and related polyols may directly interact with centers of nucleation for protein unfolding and thus stabilize the native conformation through an enhancement of the freezing effect of water (56) on the rotation of strategic peptide linkages.

This work was generously supported by the National Research Council of Canada.

1. M. A. LAUFFER and C. L. STEVENS. Advances in virus research. Vol. 13. *Edited by* K. M. Smith and M. A. Lauffer. Academic Press, New York. 1968. p. 1.
2. S. L. BRADBURY and W. B. JAKOBY. Proc. Natl. Acad. Sci. USA, **69**, 2373 (1972).
3. J. JARABAK, A. E. SEEDS, JR., and P. TALALAY. Biochemistry, **5**, 1269 (1966).
4. L. J. LANGER and L. L. ENGEL. J. Biol. Chem. **233**, 583 (1958).
5. J. JARABAK, J. A. ADAMS, H. G. WILLIAMS-ASHMAN, and P. TALALAY. J. Biol. Chem. **237**, 345 (1962).
6. I. FRIDOVICH. J. Biol. Chem. **238**, 592 (1963).
7. M. L. SHELANSKI, F. GASKIN, and C. R. CANTOR. Proc. Natl. Acad. Sci. USA, **70**, 765 (1973).
8. J. S. MYERS and W. B. JAKOBY. Biochem. Biophys. Res. Commun. **51**, 631 (1973).
9. G. E. MCDUFFIE, JR., R. G. QUINN, and T. A. LITOVITZ. J. Chem. Phys. **37**, 239 (1962).
10. G. E. MCDUFFIE, J. W. FORBES, W. M. MADIGOSKY, J. J. VON BRETZEL. J. Chem. Eng. Data, **14**, 176 (1969).
11. L. GOUDARD and P. LEYDET. C. R. Acad. Sci. Paris, **261**, (Groupe 7), 4063 (1965).
12. L. GOUDARD. C. R. Acad. Sci. Ser. C. **262**, 1827 (1966).
13. S. P. SUKHATME and N. SAIKEDKAR. Indian J. Technol. **7**, 1 (1969).
14. C. S. MINER and N. N. DALTON (*Editors*). Glycerol. Reinhold Publishing Corp., New York. 1953.
15. P. PICKER, P.-A. LEDUC, P. R. PHILIP, and J. E. DESNOYERS. J. Chem. Thermodyn. **3**, 631 (1971).
16. J.-L. FORTIER, P.-A. LEDUC, and J. E. DESNOYERS. J. Solution Chem. **3**, 323 (1974).
17. P. PICKER, E. TREMBLAY, and C. JOLICOEUR. J. Solution Chem. **3**, 377 (1974).
18. P. PICKER, C. JOLICOEUR, and J. E. DESNOYERS. J. Chem. Educ. **45**, 614 (1968).
19. P. R. PHILIP, J. E. DESNOYERS, and A. HADE. Can. J. Chem. **51**, 187 (1973).
20. H. F. STIMSON. Am. J. Phys. **23**, 614 (1955).
21. G. S. KELL. J. Chem. Eng. Data, **12**, 66 (1967).
22. B. E. CONWAY, R. E. VERRALL, and J. E. DESNOYERS. Trans. Faraday Soc. **62**, 2738 (1966).
23. B. BELLEAU, H. TANI, and F. LIE. J. Am. Chem. Soc. **87**, 2283 (1965).
24. H. S. HARNED and B. B. OWEN. The physical chemistry of electrolytic solutions. 3rd ed. Reinhold Publishing Corp., New York. 1958. p. 352.
25. P. R. PHILIP and J. E. DESNOYERS. J. Solution Chem. **1**, 353 (1972).
26. B. E. CONWAY and L. H. LALIBERTÉ. Trans. Faraday Soc. **66**, 3032 (1970).
27. G. PERRON and J. E. DESNOYERS. J. Chem. Eng. Data, **17**, 136 (1972).
28. J.-L. FORTIER, P. R. PHILIP, and J. E. DESNOYERS. J. Solution Chem. **3**, 523 (1974).
29. P.-A. LEDUC, J.-L. FORTIER, and J. E. DESNOYERS. J. Phys. Chem. **78**, 1217 (1974).
30. J. E. DESNOYERS and M. AREL. Can. J. Chem. **45**, 359 (1967).
31. N. DESROSIERS, G. PERRON, J. G. MATHIESON, B. E. CONWAY, and J. E. DESNOYERS. J. Solution Chem. **3**, 789 (1974).
32. G. M. MUSBALLY, G. PERRON, and J. E. DESNOYERS. J. Colloid Interface Sci. **48**, 494 (1974).
33. F. J. MILLERO. Water and aqueous solutions. *Edited by* R. A. Horne. Wiley Interscience, New York. 1972. p. 519; W.-Y. WEN. Water and aqueous solutions. *Edited by* R. A. Horne. Wiley Interscience, New York. 1972. p. 613.
34. P. R. PHILIP and C. JOLICOEUR. J. Phys. Chem. **77**, 307 (1973).
35. F. FRANKS and D. S. REID. Water: a comprehensive treatise. Vol. II. *Edited by* F. Franks. Plenum Press, New York. 1973. p. 323.
36. D. EISENBERG and W. KAUZMANN. The structure and properties of water. Oxford University Press, New York. 1969. p. 12.
37. H. A. RIZK and I. M. ELANWAR. Can. J. Chem. **46**, 507 (1968).
38. F. FRANKS, D. S. REID, and A. SUGGETT. J. Solution Chem. **2**, 99 (1973).
39. G. WADA and S. UMEDA. Bull. Chem. Soc. Jpn. **35**, 646 (1962).
40. J. L. NEAL and D. A. I. GORING. J. Phys. Chem. **74**, 658 (1970).
41. D. T. WARNER. Nature, **196**, 1055 (1962).
42. M. J. TAIT, A. SUGGETT, F. FRANKS, S. ABLETT, and P. A. QUICKENDEN. J. Solution Chem. **1**, 131 (1972).
43. G. C. KRESCHECK and W. A. HARGRAVES. J. Colloid Interface Sci. **48**, 481 (1974).
44. G. M. MUSBALLY, G. PERRON, and J. E. DESNOYERS. J. Colloid Interface Sci. **48**, 494 (1974).
45. E. D. GODDARD, C. A. J. HOEVE, and G. C. BENSON. J. Phys. Chem. **61**, 593 (1957).
46. P. WHITE and G. C. BENSON. J. Phys. Chem. **64**, 599 (1960).
47. K. SHINODA and S. TOSHIRO. J. Phys. Chem. **67**, 2072 (1963).

Can. J. Chem. Downloaded from www.nrcresearchpress.com by 210.87.254.6 on 09/05/12
For personal use only.

48. H. LAL. J. Colloid Sci. **8**, 414 (1953).
49. G. M. BROWN. P. DUBREUIL, F. M. ICHHAPORIA, and J. E. DESNOYERS. Can. J. Chem. **48**, 2525 (1970).
50. M. F. EMERSON and A. HOLTZER. J. Phys. Chem. **71**, 3320 (1967).
51. W. P. JENCKS. Fed. Proc. Suppl. **15**, S-50 (1965).
52. J. A. GLASEL. J. Am. Chem. Soc. **92**, 372 (1970).
53. G. BARONE, E. RIZZO, V. VITAGLIANO. J. Phys. Chem. **74**, 2230 (1970).
54. S. SUBRAMANIAN, T. S. SARMA, D. BALASIBRAMANIAN, J. C. AHBWALIA. J. Phys. Chem. **75**, 815 (1971).
55. M. J. MASTROIANNI, M. J. PIKAL, and S. LINDENBAUM. J. Phys. Chem. **76**, 3050 (1972).
56. F. SCHUBER and B. BELLEAU. Bioorg. Chem. **2**, 111 (1973).

Can. J. Chem. Downloaded from www.nrcresearchpress.com by 210.87.254.6 on 09/05/12
For personal use only.

Some Reactions of *trans*-Hydridochlorobis(tricyclohexylphosphine)nickel(II), *trans*-Ni(Cl)(H)[P(C_6H_{11})$_3$]$_2$[1]

HOWARD C. CLARK AND ALAN SHAVER[2]

Department of Chemistry, University of Western Ontario, London, Ontario N6A 5B7

Received June 10, 1975

HOWARD C. CLARK and ALAN SHAVER. Can. J. Chem. **53**, 3462 (1975).

Some reactions of the title compound with several ligands, including olefins and acetylenes have been conducted and the new complexes *trans*-[NiH{P(C_6H_{11})$_3$}$_2$L]BF_4, L = methylpyridine or acetonitrile have been isolated. Although the bulky phosphine apparently hinders reaction sterically, with hexafluoro-2-butyne a product is obtained which is tentatively characterized as Ni($CF_3C{\equiv}CCF_3$)$_3$P(C_6H_{11})$_3$. This compound is thought to contain the seven-membered ring nickelahexakis(trifluoromethane)cyclohepta-*cis,cis,cis*-triene. Pyrolysis of this compound yields hexakis(trifluoromethyl)benzene. A reaction of the nickel hydride also occurs with carbon monoxide in the presence of $TlBF_4$ to give Ni(CO)$_3$P(C_6H_{11})$_3$ and [P(H)(C_6H_{11})$_3$]BF_4. This reaction can be considered to result from the reductive elimination of [P(H)(C_6H_{11})$_3$]Cl.

HOWARD C. CLARK et ALAN SHAVER. Can. J. Chem. **53**, 3462 (1975).

On a effectué quelques réactions du composé mentionné dans le titre avec plusieurs ligands y compris des alcènes et des alcynes et on a isolé les nouveaux complexes [NiH{P(C_6H_{11})$_3$}$_2$L]BF_4-*trans*, où L = méthylpyridine ou acétonitrile. Quoique la volumineuse phosphine semble empêcher la réaction pour des raisons stériques, on a obtenu, avec l'hexafluorobutyne-2, un produit auquel on attribue provisoirement la structure Ni($CF_3C{\equiv}CCF_3$)$_3$P(C_6H_{11})$_3$. On croit que ce composé contient le cycle à sept chaînons nickelahexakis(trifluorométhane)-cycloheptatriène-*cis,cis,cis*. La pyrolyse de ce composé fournit l'hexakis(trifluorométhyl) benzène. Une réaction de l'hydrure de nickel se produit aussi avec le monoxyde de carbone en présence de $TlBF_4$; il y a alors formation de Ni(CO)$_3$P(C_6H_{11})$_3$ et de [P(H)(C_6H_{11})$_3$]BF_4. On peut considérer que cette réaction provient d'une élimination réductive de [P(H)(C_6H_{11})$_3$]Cl.

[Traduit par le journal]

As part of a general interest in metal hydrides, we have been particularly concerned with the chemistry of neutral and cationic platinum hydrides (1, 2). The previously reported (3, 4) compound *trans*-Ni(Cl)(H)(Cy_3P)$_2$, where Cy_3P = P(C_6H_{11})$_3$, was chosen for study in an attempt to supply some comparisons to these platinum systems.

We hoped that the presence of the bulky phosphine ligands would help to stabilize reaction products, since σ-bonded hydride and carbon derivatives of nickel are often air sensitive and unstable at room temperature (3, 5).

Experimental

Inert atmosphere techniques were used. Solvents were generally dried over molecular sieves and purged with dry nitrogen before use; tetrahydrafuran and toluene were distilled from sodium–benzophenone under dry nitrogen just before use. *trans*-Ni(Cl)(H)(Cy_3P)$_2$ was prepared as previously reported (3).

Hydrido-4-methylpyridinebis(tricyclohexylphosphine)-nickel Tetrafluoroborate

trans-Ni(Cl)(H)(Cy_3P)$_2$, 0.378 g (0.50 mmol), was dissolved in 40 ml THF. 4-Methylpyridine, 0.6 ml (6.3 mmol) was added and a slight color change from yellow–brown to yellow occurred. $TlBF_4$, 0.146 g (0.50 mmol) was added in one portion and a white precipitate of TlCl formed immediately. The yellow reaction mixture was stirred at room temperature for 1 h, then filtered and stripped to a yellow oil which gave crystals upon pumping. These were extracted with 10 ml acetone and the solution filtered. Addition of ether and cooling to −78 °C caused the product to crystallize. It was collected on a fritte and washed with ether. Yield = 0.266 g (66.5%); decomposes at 165 °C *in vacuo*; i.r. ν(Ni—H) 1995 cm^{-1} (Nujol mull); n.m.r. (acetone) τ(Ni—H) 33.4 (triplet, J(P–H) = 139 Hz), τ(CH_2) 8.48 (multiplet), τ(CH_3) 7.50 (singlet), τ($NC_5H_4CH_3$) 2.48 and 1.16 (doublets, J = 6 Hz).

Anal. Calcd. for $C_{42}H_{72}NP_2NiBF_4$: C, 63.0; H, 9.25. Found: C, 63.2; H, 9.31.

Hydridoacetonitrilebis(tricyclohexylphosphine)nickel Tetrafluoroborate

This compound was prepared in an analogous manner. It was noted that if the $TlBF_4$ was added to the nickel

[1]Part XVI of the series, Chemistry of Metal Hydrides (for Part XV, see ref. 13).

[2]Present address: Department of Chemistry, McGill University, P.O. Box 6070, Station A, Montreal, Quebec.

Can. J. Chem. Downloaded from www.nrcresearchpress.com by 210.87.254.6 on 09/05/12
For personal use only.

Can. J. Chem. Downloaded from www.nrcresearchpress.com by 210.87.254.6 on 09/05/12
For personal use only.

complex in the absence of acetonitrile there was no reaction. However, addition of acetonitrile caused a rapid formation of TlCl. The product, isolated as above, decomposes above 150 °C; i.r. ν(Ni—H) 1992 cm^{-1} (Nujol mull); n.m.r. (acetone) τ(Ni—H) 31.6 (triplet, J(P–H) = 153 Hz), τ(CH_2) 8.42 (multiplet), τ(CH_3) 7.49 (singlet).

Anal. Calcd. for $C_{38}H_{70}NP_2NiBF_4$: C, 61.0; H, 9.37. Found: C, 61.0; H, 9.49.

Tricyclohexylphosphinetricarbonylnickel and Tricyclohexylphosphonium Tetrafluoroborate

trans-Ni(Cl)(H)(Cy_3P)$_2$ (0.5 mmol) was dissolved in 20 ml THF. $TlBF_4$ (0.50 mmol) was added and carbon monoxide was bubbled into the yellow–brown slurry. There was an immediate precipitation of TlCl. The color changed first to lemon green, then after ½ h treatment with CO, to pale blue. The reaction mixture was filtered and concentrated to about 2 ml. Addition of ether caused precipitation of a white product identified as P(H)-$(C_6H_{11})_3 \cdot BF_4$ (yield = 0.14 g, 76%). It was recrystallized from THF–ether, m.p. = 163 °C.

Anal. Calcd. for $C_{18}H_{34}PBF_4$: C, 58.7; H, 9.24. Found: C, 58.8; H, 9.26.

The THF–ether mother liquors from the reaction solution were stripped to dryness and recrystallized from a minimum of ether at −70 °C to give $Ni(CO)_3P(C_6H_{11})_3$, (yield > 60%, decomposes at 96 °C), which was identified by its infrared spectrum (6) and analysis.

Anal. Calcd. for $C_{21}H_{33}NiPO_3$: C, 59.6; H, 7.80. Found: C, 59.9; H, 8.00.

Reaction with Hexafluoro-2-butyne

trans-Ni(Cl)(H)(Cy_3P)$_2$, 0.514 g (0.68 mmol) was dissolved in 20 ml toluene. The yellow–brown solution was frozen, the flask evacuated, isolated from the vacuum line, and allowed to warm at room temperature. Then $CF_3C{\equiv}CCF_3$ was admitted and the pressure adjusted to about 0.9 atm. The uptake of acetylene was monitored by means of a manometer and the pressure was readjusted to 0.9 atm by the admission of more acetylene as the reaction progressed. After stirring for about 1 h, an orange precipitate formed. After 3 h the reaction was complete and uptake of acetylene had ceased. The reaction mixture was filtered and the orange precipitate collected. The red mother liquors were concentrated to about 5 ml and cooled to −20 °C overnight to give 0.25 g of white crystals. These were readily sublimed at room temperature (10^{-2} Torr) (m.p. 206 °C (sealed capillary)) and were identified as hexakis(trifluoromethyl)benzene by means of the mass spectrum, infrared, and ^{19}F n.m.r. spectra (7) (yield = 76% based on Ni).

The orange precipitate was extracted with 10 ml CH_2Cl_2 and the solution filtered. Hexane (*ca.* 15 ml) was added and the solution cooled at −20 °C overnight and then to −40 °C for a further 4 h. Well-formed orange crystals were isolated by removing the mother liquors with a syringe and washing the crystals with cold hexane; yield = 0.28 g (50% assuming the formula $NiP(C_6H_{11})_3(C_4F_6)_3$). The compound melts with decomposition at 128 °C. When a sample was heated to this temperature in an evacuated flask white crystals collected on a sublimation probe and were identified as hexakis(trifluoromethyl)benzene. Despite several attempts, reproducible analytical results for the complex could not be obtained. Analyses were conducted by Chemalytics, Tempe, Arizona; Spang Microanalytical Laboratory, Ann Arbor, Michigan; Midwest Microlab Indianapolis, Indiana, and Alfred Bernhardt, Elbach uber Engelskirchen, West Germany. The complex showed: i.r. (Nujol mull) 1675(w), 1645(m), 1616(w), 1330(s), 1300(s), 1262(vs), 1233(vs), 1195(vs), 1150(vs), 1100(s), 1005(w), 941(w), 730(m), 684(m), 663(m), 638(m); ^{19}F n.m.r. (CH_2Cl_2): peak A 50.1 p.p.m. (multiplet), peak B 54.9 p.p.m. (quartet, J = 8.8 Hz), peak C 59.6 p.p.m. (multiplet); A:B:C = 1:1:1. Double irradiation of C reduced A and B to singlets. Double irradiation of A reduced C to a quartet J = 8.8 Hz.

$NiP(C_6H_{11})_3(C_4F_6)_3$ analysis

	Calculated	Found*			
		A	*B*	*C*	*D*
C	43.7	42.6, 42.9	40.8, 41.7	40.2	40.0
H	4.00	3.74, 3.52	3.51, 3.48	3.77	3.8
F	41.5	—	48.1, 44.1	42.1	44.9
Molecular weight	824	—	841		

*The letters *A* to *D* represent different microanalytical laboratories.

Results and Discussion

The first reactions were attempts to remove the chloride ligand from *trans*-Ni(Cl)(H)(Cy_3P)$_2$ and generate a solvated cationic metal hydride. In platinum systems this type of complex is quite reactive (1, 2, 8–10). Extensive decomposition occurred with $AgPF_6$ so $TlBF_4$ was used. However in contrast to the analogous platinum complex (9), the chloride could not be removed in THF or acetone solution. Instead the presence of a small, highly coordinating ligand was necessary to cause precipitation of TlCl and formation of complexes of the type *trans*-[Ni(H)(L)(Cy_3P)$_2$]BF_4, where L = acetonitrile or 4-methylpyridine.

A color change from yellow–brown to yellow

Can. J. Chem. Downloaded from www.nrcresearchpress.com by 210.87.254.6 on 09/05/12
For personal use only.

was observed when 4-methylpyridine was added to a solution of *trans*-Ni(Cl)(H)(Cy_3P)$_2$. Also there was no precipitation of TlCl from a slurry of $TlBF_4$ and *trans*-Ni(Cl)(H)(Cy_3P)$_2$ until one or two drops of acetonitrile were added. These two facts seem to imply coordination of the incoming ligand before the chloride is displaced. This is surprising since we felt that the large cone angle (11) of Cy_3P (180°) might inhibit the formation of a five-coordinate intermediate. This is apparently not the case, at least for small or narrow bases. Several other ligands were tested but all failed to displace the chloride under similar reaction conditions. These included trialkyl and aryl phosphines and some acetylenes. Attempts to displace the coordinated acetonitrile with some acetylenes were also unsuccessful.

The reaction with carbon monoxide probably proceeds initially in the same way as the acetonitrile reaction. The first step is displacement of chloride and formation of *trans*-[Ni(H)(CO)(Cy_3P)$_2$]BF_4. In the presence of excess CO a reductive elimination occurs to give Ni(CO)$_3$(Cy_3P) and [PCy_3(H)]BF_4.

Since a labile cationic nickel hydride complex could not be produced by abstraction of chloride from *trans*-Ni(Cl)(H)(Cy_3P)$_2$ a number of reactions of the complex itself with olefins and acetylenes were conducted. Again the complex proved somewhat unreactive; in most cases it was recovered unchanged. Although dimethylcarboxylate acetylene seemed to polymerize readily in the presence of the complex, no nickel–acetylene complex formation could be detected and starting material was recovered. However, hexafluoro-2-butyne reacts readily with the complex to give a mixture of products.

The mechanics of the reaction with C_4F_6 are important. In one experiment an excess of the acetylene was condensed onto the frozen toluene solution of the nickel complex and the mixture allowed to warm. As it became soft the acetylene layer was polymerized into a white perforated disk. The reaction was continued as usual and the normal products were obtained (see Experimental). The disk was removed from the flask with tweezers and found to be quite resistant to tearing. It was also insoluble in an assortment of common solvents. In another experiment the toluene was not allowed to warm sufficiently and C_4F_6 condensed in the liquid. The rapid stirring dispersed the liquid acetylene into fine droplets which polymerized to form tough white beads. After this polymerization, reaction continued normally.

In the usual reaction, the complex was dissolved in toluene at room temperature and exposed to 0.9 atm of C_4F_6. There was a smooth uptake of acetylene that gradually stopped over a period of 3 h. Much of this acetylene was converted to hexakis(trifluoromethyl)benzene (0.75 mol per mol of nickel). The gradual slowing of acetylene uptake was accompanied by the production of the orange nickel complex (50% yield).

Although we have experienced difficulty in obtaining reproducible analyses, the characterization of this complex has been aided by the report of a nickel complex (12) containing a nickelahexakis(trifluoromethyl)cyclohepta-*cis,trans,cis*-triene ring, whose stereochemistry was proven by X-ray analysis. The close similarity of the ^{19}F n.m.r. spectra of the two compounds leads us to propose a similar seven-membered ring for our complex. The exact stereochemistry must be decided by a crystal structure determination. However, since our orange complex yields hexakis(trifluoromethyl)benzene at 130 °C it seems reasonable to propose a *cis,cis,cis* structure as shown in **1**. A possible interaction (12)

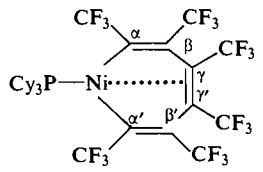

1

between nickel and the olefin across the ring is indicated with a dotted line. The quartet in the ^{19}F n.m.r. is assigned to the CF_3 in the α position while peaks C and A are assigned to the β and γ positions respectively.

The fact that hexakistrifluorobenzene (HTFB) and **1** are produced in 125% yield from starting nickel hydride is notable. **1** does not polymerize C_4F_6 when treated with the acetylene in freshly made THF or CH_2Cl_2 solutions. It is probable that a different nickel species acts as a cyclotrimerization catalyst and is also a precursor to **1**. As **1** is produced the concentration of the proposed catalyst decreases until all the nickel is converted to unreactive species. We have been

unable to isolate compounds other than **1** and HFTB from the reaction mixture.

The demonstration that **1** is an intermediate in the production of HFTB is significant since similar structures are often proposed in the mechanism of cyclotrimerization of acetylenes by transition metals.

The financial support of the National Research Council of Canada and the award of an NRCC Postdoctorate Fellowship (to A.S. 1972–1974) are gratefully acknowledged.

1. H. C. CLARK and C. R. JABLONSKI. Inorg. Chem. **13**, 2213 (1974).
2. H. C. CLARK and C. S. WONG. J. Am. Chem. Soc. **96**, 7213 (1974).
3. M. L. H. GREEN, T. SAITO, and P. J. TANFIELD. J. Chem. Soc. A, 152 (1971).
4. K. JONAS and G. WILKE. Angew. Chem. Int. Ed. Engl. **8**, 519 (1969).
5. D. R. FAHEY. J. Organomet. Chem. Rev. A, **7**, 245 (1972).
6. C. A. TOLMAN. J. Am. Chem. Soc. **92**, 2953 (1970).
7. J. F. HARRIS, JR., R. J. HARDER, and G. N. SAUSEN. J. Org. Chem. **25**, 633 (1960).
8. H. C. CLARK and H. KUROSAWA. Inorg. Chem. **11**, 1275 (1972); **12**, 357 (1973); **12**, 1566 (1973).
9. T. G. ATTIG and H. C. CLARK. Can. J. Chem. This issue.
10. H. C. CLARK, C. R. JABLONSKI, and C. S. WONG. Inorg. Chem. **14**, 1332 (1975).
11. C. A. TOLMAN. J. Am. Chem. Soc. **92**, 2956 (1970).
12. J. BROWNING, M. GREEN, B. R. PENFOLD, J. L. SPENCER, and F. G. A. STONE. J. Chem. Soc. Chem. Commun. 31 (1973).
13. H. C. CLARK and H. KUROSAWA. Inorg. Chem. **12**, 1566 (1973).

Can. J. Chem. Downloaded from www.nrcresearchpress.com by 210.87.254.6 on 09/05/12
For personal use only.

The Preparation of Some Hydridotricyclohexylphosphine Platinum(II) Complexes

THOMAS G. ATTIG[1] AND HOWARD C. CLARK

Department of Chemistry, University of Western Ontario, London, Ontario N6A 5B7

Received June 10, 1975

THOMAS G. ATTIG and HOWARD C. CLARK. Can. J. Chem. **53**, 3466 (1975).

The reaction of the platinum(II) hydride containing bulky tricyclohexylphosphine ligands, *trans*-$PtHCl(PCy_3)_2$, PCy_3 = tricyclohexylphosphine, with $AgPF_6$ in methanol affords the air-stable cationic hydrido complex [*trans*-$PtH(CH_3OH)(PCy_3)_2]^+PF_6^-$, **1**, The reaction of **1** with a number of neutral molecules, L, leads to simple substitution of the coordinated methanol molecule by L. The reaction of **1** with terminal acetylenes in methanol affords hydrido–methoxycarbene complexes rather than vinylic derivatives. The role of the bulky tricyclohexylphosphine ligand in these reactions is discussed. The reactions of **1** are compared to those of cationic platinum(II) hydrides containing other phosphines.

THOMAS G. ATTIG et HOWARD C. CLARK. Can. J. Chem. **53**, 3466 (1975).

La réaction de $AgPF_6$ dans le méthanol avec l'hydrure de platine(II) contenant le ligand volumineux tricyclohexylphosphine, *trans*-$PtHCl(PCy_3)_2$ dans lequel PCy_3 = tricyclohexylphosphine, conduit au complexe hydrido cationique stable en présence d'air [*trans*-$PtH(CH_3OH)(PCy_3)_2]^+PF_6^-$, **1**. La réaction de **1** avec une variété de molécules neutres, L, conduit à une substitution simple de la molécule de méthanol par L. La réaction de **1** en solution dans le méthanol avec des acétylènes vrais fournit des complexes hydrido–méthoxy carbènes plutôt que des dérivés vinyliques. On discute du rôle du ligand volumineux tricyclohexylphosphine dans ces réactions. On compare la réactivité de **1** avec celles d'hydrures cationiques de platine(II) contenant d'autres phosphines.

[Traduit par le journal]

Introduction

Our interest in the reactivity of platinum(II) hydrides has prompted us to examine the reactions of those containing very bulky phosphines (*e.g.*, tricyclohexylphosphine) with acetylenes, olefins, and a number of other neutral molecules.

While frequent use is made of steric constraints to rationalize unusual chemical behavior or unexpected spectroscopic parameters, a more precise understanding of the steric requirements of different types of ligands has yet to be developed. Tertiary phosphines and phosphites comprise a large and important class of closely related ligands for which the concept of 'cone angle' is frequently cited as a description of their steric requirements. This concept, developed by Tolman *et al.* (1, 2), provides a quantitative measure of steric effects in phosphorus – transition metal complexes, based on measurements on atomic models. With some allowance for ligand flexibility, these cone angles were estimated to be in the range of 87 ± 2° (for PH_3) to 194 ± 6° (for $P(o\text{-}C_6H_4CH_3)_3$). As Tolman pointed out, to the extent that these phosphorus ligands approach cylindrical symmetry about the M—P bond, coordination of six, four, three, or two such ligands should not be possible for cone angles larger than 90, 109.5, 120, or 180°, respectively, although this takes no account of any possible 'meshing' of the ligands. The large cone angle of 179 ± 10° for tricyclohexylphosphine suggests that square planar platinum(II) complexes containing two *cis* PCy_3 ligands would not exist. On the other hand, the existence of low coordination complexes of Pt(0) and Pd(0) (*e.g.*, $Pt(PCy_3)_2$ (3) and $Pd(PCy_3)_2$ (4) has been attributed to the bulk of the PCy_3 ligand.

We felt that the use of PCy_3 as a ligand might allow the isolation of different types of products from the reactions of platinum(II) hydrides with a variety of substrates. For example, we hoped to isolate hydrido–acetylene complexes by the following sequence

[1] *trans*-$PtHCl(PCy_3)_2 + RC{\equiv}CR + AgPF_6 \rightarrow$ [*trans*-$PtH(RC{\equiv}CR)(PCy_3)_2]^+PF_6^- + AgCl$

[1]Present address: Department of Chemistry, University of Kentucky, Lexington, Kentucky 40506.

Can. J. Chem. Downloaded from www.nrcresearchpress.com by 210.87.254.40 on 09/05/12
For personal use only.

Can. J. Chem. Downloaded from www.nrcresearchpress.com by 210.87.254.40 on 09/05/12
For personal use only.

analogous to the isolation of [*trans*-$PtCH_3(RC{\equiv}CR)L_2]^+PF_6^-$ from the reaction of *trans*-$PtCH_3ClL_2$ with acetylenes in the presence of $AgPF_6$ (5). It was our feeling that the bulkiness of the two PCy_3 ligands would prevent the insertion of the acetylene into the Pt—H bond, since the Pt—H bond and the acetylene could not easily come into close proximity.

Herein we describe the reaction of [*trans*-$PtH(CH_3OH)(PCy_3)_2]^+PF_6^-$ with terminal acetylenes as well as with a number of other neutral molecules.

Results and Discussion

It has been shown that the hydridoplatinum cations [*trans*-$PtH(solvent)L_2]^+$, where solvent = acetone or methanol, are useful as synthetic intermediates in the reactions of olefins and acetylenes with platinum(II) hydrides (6–9). The complex *trans*-$PtHCl(PCy_3)_2$ readily reacts with $AgPF_6$ in methanol to give, after removal of the precipitated AgCl, colorless solutions of [*trans*-$PtH(CH_3OH)(PCy_3)_2]^+PF_6^-$, **1**. Methanolic solutions of **1** are particularly stable for long periods of time (greater than one month without yellowing). Solutions of [*trans*-$PtH(solvent)L_2]^+PF_6^-$ where $L \neq PCy_3$, on the other hand, are only stable for several hours (9). White, air-stable crystals of **1** were obtained upon cooling a concentrated methanolic solution of **1**. However, good analytical characterization was not possible, presumably due to the difficulty of obtaining exact stoichiometric content of methanol. By comparison, the corresponding hydridonickel(II) complex [*trans*-$NiH(solvent)(PCy_3)_2]^+PF_6^-$ cannot be prepared from the reaction of *trans*-$NiHCl(PCy_3)_2$ and $AgPF_6$ (10).

The methanol molecule in **1** exhibits a weak *trans influence* as is evidenced by the high values for ν(Pt—H), τ(Pt—H), and *J*(Pt—H) (11). It is readily displaced by neutral molecules such as CO, γ-picoline, and triethylphosphine to afford the complexes [*trans*-$PtH(PCy_3)_2L]^+PF_6^-$, **2**, according to [2].

[2] [*trans*-$PtH(CH_3OH)(PCy_3)_2]^+PF_6^-$ + L → [*trans*-$PtH(PCy_3)_2L]^+PF_6^-$ + CH_3OH

where L = CO, γ-pic, PEt_3.

While the isolation of **2** where L = CO and γ-picoline was expected, the isolation of **2** where L = PEt_3 was not. The recently determined crystal structure of *trans*-$PtI_2(PCy_3)_2$ shows it to be a highly crowded molecule (12). From cone angle values of 179 ± 10° and 134 ± 2° for PCy_3 and PEt_3, respectively, it would seem unlikely that a large ligand such as PEt_3 could be easily accommodated between the two *trans* PCy_3 ligands of **2**. Our results suggest that there must be considerable meshing of the three phosphines and that the absolute value for the cone angle of 179 ± 10° does not accurately describe the steric bulk of the PCy_3 ligand.

The reaction of **1** with terminal acetylenes such as $CH{\equiv}CCH_3$ and $CH{\equiv}CC_6H_5$ in methanol leads to the formation of the hydrido–alkoxycarbene complexes [*trans*-$PtH[C(OCH_3)(CH_2R)](PCy_3)_2]^+PF_6^-$, **3** according to [3], rather than the vinylic insertion products which might have been expected according to [4].

[3] [*trans*-$PtH(CH_3OH)(PCy_3)_2]^+PF_6^-$ + $CH{\equiv}CR$

$$\xrightarrow{R'OH} \left[H{-}Pt(PCy_3)_2{-}C(OR')(CH_2R) \right]^+ PF_6^-$$

The reaction of **1** with $CH{\equiv}CCH_2CH_2OH$ in dichloromethane afforded the cyclic carbene complex [*trans*-$PtH(:\overline{COCH_2CH_2CH_2})(PCy_3)_2]^+PF_6^-$.

[4] [*trans*-$PtH(CH_3OH)(PCy_3)_2]^+PF_6^-$ + $RC{\equiv}CR'$ → [*trans*-$Pt(CR{=}CHR')(CH_3OH)(PCy_3)_2]^+PF_6^-$

The reactions in [3] are analogous to those reported for *trans*-$PtCH_3ClL_2$ with terminal acetylenes in methanol or ethanol in the presence of $AgPF_6$ (13).

[5] *trans*-$PtCH_3ClL$ + $CH{\equiv}CR$ + $AgPF_6$

$$\xrightarrow{R'OH} \left[CH_3{-}Pt(L)_2{-}C(OR')(CH_2R) \right]^+ PF_6^- + AgCl$$

The formation of the alkoxycarbene complexes according to [5] is believed to proceed via the formation of the 'metal-induced carbonium' ion, $CH_3{-}Pt{-}C^+{=}CHR$, which is subsequently attacked by methanol or ethanol to afford the alkoxycarbene ligand (14).

The formation of vinylic complexes from insertion of the acetylene into the Pt—H bond according to [4], was not observed. Thus, the rate of carbene formation is very much greater

TABLE 1. Analytical data and melting points of [*trans*-$PtH(PCy_3)_2L]^+PF_6^-$ complexes

L	Analysis (%) Calculated C	Calculated H	Found C	Found H	Melting point (°C)
CO	47.79	7.26	48.10	7.63	226–228
γ-picoline	50.70	7.50	50.88	8.13	239–241
PEt_3	49.45	8.10	49.15	8.09	203–205
$:C(OCH_3)(C_2H_5)$	49.32	7.76	49.57	7.78	203–205
$:C(OCH_3)(CH_2C_6H_5)$	52.17	7.49	52.16	7.61	206–208
$:\overline{COCH_2CH_2CH_2}$	49.43	7.57	49.45	8.20	207–208

Can. J. Chem. Downloaded from www.nrcresearchpress.com by 210.87.254.40 on 09/05/12
For personal use only.

than the rate of insertion; the rate difference perhaps being influenced by the bulkiness of the PCy_3 ligands which prevents the coordinated acetylene and Pt—H bond from coming into close proximity, thus preventing insertion. Such a difference between the rate of carbene formation and the rate of insertion may be quite general. For example, the acetylene $CH{\equiv}CC_6H_5$ inserts into the Pt—H bond of [*trans*-$PtH(CH_3OH)(PEt_3)_2]^+PF_6^-$ but only in low yields (~20%).[2] It is likely that in such systems most of the hydride is consumed in carbene formation, the latter products being undetected due to the reaction conditions employed.

The infrared and proton n.m.r. spectra of some hydridotricyclohexylphosphine platinum(II) complexes are tabulated in Tables 1 and 2 respectively. The Pt—H proton, except when L = PEt_3, appears as a 1:2:1 triplet accompanied by ^{195}Pt satellites, indicating the *trans* geometry of the PCy_3 ligands. When L = PEt_3 a doublet of triplets with ^{195}Pt satellites was observed. Although the geometry of **2** when L = PEt_3 cannot be unequivocally determined from the proton n.m.r. spectrum, it has been assigned a *trans* geometry based on the *trans* geometries of the other compounds prepared in this and in other studies (15).

The value of ν(Pt—H) and J(Pt—H) for the hydrido proton reflects the relative *trans influence* of the ligand L (11). The carbene ligand in **3** exhibits the lowest values for ν(Pt—H) and J(Pt—H) as reflective of the large *trans influence* of this ligand. The large *trans influence* of carbene ligands has been previously reported for the complexes [*trans*-$PtCH_3$(carbene)$L_2]^+$ (13), as well as [*trans*-$PtH[C\overline{N(CH_3)CH_2CH_2}N(CH_3)]PEt_3)_2]^+BF_4^-$ (16). The high values for ν(Pt—H) and J(Pt—H) where L = CH_3OH, conversely, indicate the relative low *trans influence* of methanol.

The reactions and products described above reveal several characteristics of tricyclohexylphosphine as a ligand. Comparison of these results with those of analogous complexes containing other tertiary phosphine ligands reveals that:

(*a*) PCy_3 increases stability (including thermal stability). The ability of PCy_3 to stabilize the low-coordination complex $Pt(PCy_3)_2$ (3) has been described previously. The high thermal stability is exemplified by the high melting points of many products, *e.g.*, *trans*-$PtHCl(PCy_3)_2$ melts reversibly at 240 °C while *trans*-$PtHCl(PEt_3)_2$ melts reversibly at 82 °C (18). Similarly, the general stability of the salt containing the methanol cation, [*trans*-$PtH(CH_3OH)(PCy_3)_2]^+PF_6^-$, compared to those containing other [*trans*-PtH(solvent)$L_2]^+$ cations reflects the increased stability due to the PCy_3 ligand. The cyclic carbene complex [*trans*-$PtH(:\overline{COCH_2CH_2CH_2})L_2]^+PF_6^-$ where L = PCy_3 is an air-stable white compound, while the analogous complex when L = PEt_3 is found to decompose slowly to a black tar.[3]

(*b*) The cone angle of a tertiary phosphine is only a crude measure of steric requirements and, since it makes no allowance for meshing of

[2]H. C. Clark and P. L. Feiss, unpublished results.

[3]H. C. Clark and C. S. Wong, unpublished results.

TABLE 2. Infrared and proton n.m.r. data for some hydridotricyclohexylphosphine platinum(II) complexes

trans-PtH(PCy_3)$_2$(L)]$^+PF_6^-$ for L =	ν(Pt—H)* (cm^{-1})	Hydrido proton† τ	*J*(Pt—H)	*J*(P—H)	Other
CH_3OH	2308	37.8	1590	14	
CO	2170‡	14.66	916	11	
γ-picoline	2237	29.59	1069	14	γ-CH_3 7.49; α 1.29 *J*(Pt—H) = 11 Hz; β 2.38 *J*(H—H) = 6 Hz
PEt_3	2102	17.80	700	15 153	
:$C(OCH_3)(C_2H_5)$	2057	18.06	492	19	OCH_3, 5.14, *J*(Pt—H) = 9 Hz; CH_2, 7.02, *J*(H—H) = 7 Hz
:$C(OCH_3)(CH_2C_6H_5)$	2076	18.00	470	18	OCH_3, 5.16, *J*(Pt—H) = 8 Hz; CH_2, 5.73
:$COCH_2CH_2CH_2$	2068	17.63	552	17	CH_2, 4.92, *J*(H—H) = 7.5 Hz, *J*(Pt—H) = 7.5 Hz; CH_2, 6.70
trans-PtHCl(PCy_3)$_2$	2177	28.79	1284	13	

*Nujol mull.
†$CDCl_3$ solution.
‡CH_2Cl_2 solution; ν(CO) = 2058 cm^{-1}.

organic substituents, it cannot be used in any predictive sense.

(*c*) The steric bulk of the PCy_3 ligands may be the dominant factor in determining product distributions when more than one reaction pathway is available for a reaction intermediate. For example, in the reaction of **1** with terminal acetylenes the initial intermediate is probably [*trans*-PtH(CH≡CR)(PCy_3)$_2$]$^+PF_6^-$ obtained by the displacement of the coordinated methanol by the acetylene (5). This intermediate can lead to (*1*) vinylic products via insertion of the coordinated acetylene into the Pt—H bond, or (*2*) carbene products via a 'metal-induced carbonium' ion. If one of the steps necessary for insertion is a *trans* to *cis* isomerization (18) of the two PCy_3 ligands, the rate will be slow relative to carbene formation, since the PCy_3 ligands cannot readily reside in a *cis* geometry because of their bulkiness. Not unexpectedly then, the only products isolated from these reactions are carbene complexes in high yields.

The reactions of **1** with *non*terminal activated acetylenes such as $CH_3CO_2C{\equiv}CCO_2CH_3$ are found to afford vinylic products; however, these reactions were shown to proceed via a mechanism other than insertion.[4]

Experimental

The following chemicals were obtained commercially and were used without further purification: $AgPF_6$ from Cationics, Inc., $PCy_3 \cdot CS_2$ from Strem Chemicals, Inc., PEt_3 and $CH{\equiv}CCH_2CH_2OH$ from Aldrich Chemical Co., $CH{\equiv}CCH_3$ from Matheson, $CH{\equiv}CC_6H_5$ from BDH Chemicals, and γ-picoline from Eastman. Tricyclohexylphosphine was prepared by decomposing $PCy_3 \cdot CS_2$ in boiling ethanol under a nitrogen atmosphere. The complexes *trans*-PtHCl(PEt_3)$_2$ (17) and *trans*-PtHCl(PCy_3)$_2$ (19) were prepared according to the literature. We have also prepared *trans*-PtHCl(PCy_3)$_2$ from the $NaBH_4$ reduction of *cis*-$PtCl_2(Et_2S)PCy_3$ in the presence of 1 mol at PCy_3. With a large excess of $NaBH_4$, the dihydride *trans*-$PtH_2(PCy_3)_2$ was also isolated.

Infrared spectra were recorded on a Perkin-Elmer 621 spectrophotometer as Nujol mulls or in dichloromethane solution and were calibrated with a polystyrene film. Proton n.m.r. spectra were obtained on a Varian T-60 or Varian HA-100 spectrometer with TMS as an internal standard. Elemental analyses were performed by Midwest Microlab, Ltd., Indianapolis, Indiana.

Preparation of [trans-PtH(CH$_3$OH)(PCy$_3$)$_2$]$^+PF_6^-$, 1

The methanol cation, **1**, was prepared by the slow addition of a methanolic solution of 1 equiv. of $AgPF_6$ to a rapidly stirred CH_2Cl_2 solution of *trans*-PtHCl(PCy_3)$_2$. After removal of the AgCl by centrifugation, the resulting clear solution was concentrated and upon cooling the white crystals of **1** precipitated and were subsequently recrystallized from dichloromethane–hexane. Generally **1** was not isolated, but was used *in situ*.

Reaction of 1 with Neutral Ligand L

L = CO

Carbon monoxide was bubbled through a dichloromethane solution of **1**, for 15 min. The solvent was evaporated to dryness and the residue was recrystallized from dichloromethane–hexane to give the white crystals of [*trans*-PtH(CO)(PCy_3)$_2$]$^+PF_6^-$ (82%).

L = γ-picoline

To a dichloromethane solution of **1** was added 1 equiv. of γ-picoline and the solution stirred for 15 min. The

[4]T. G. Attig and H. C. Clark, unpublished results.

Can. J. Chem. Downloaded from www.nrcresearchpress.com by 210.87.254.40 on 09/05/12
For personal use only.

solvent was evaporated and the residue was chromatographed on Florisil with dichloromethane. The eluent was concentrated and upon addition of hexane the white crystals of [*trans*-PtH(γ-pic)$(PCy_3)_2]^+PF_6^-$ (80%) were obtained.

$L = PEt_3$

The complex [*trans*-$PtH(PEt_3)(PCy_3)_2]^+PF_6^-$ was similarly prepared. Recrystallization from dichloromethane–ether afforded the white crystals of the product in 61% yield.

Reaction of ***1*** *with Terminal Acetylenes*

Preparation of [trans-$PtH\{:C(OCH_3)(C_2H_5)\}(PCy_3)_2]^+PF_6^-$

Propyne was bubbled through a 1:1 dichloromethane–methanol solution of **1** for 10 min. The solution was concentrated and product precipitated. Recrystallization from dichloromethane–methanol gave the white crystals of [*trans*-$PtH\{:C(OCH_3)(C_2H_2)\}(PCy_3)_2]^+PF_6^-$ (85%).

Preparation of [trans-$PtH\{:C(OCH_3)(CH_2C_6H_5)\}(PCy_3)_2]^+PF_6^-$

To a 1:1 dichloromethane–methanol solution of **1** was added 1 equiv. of phenylacetylene. The reaction was stirred for 30 min. The solvent was evaporated and the residue was recrystallized from dichloromethane–hexane to give the white crystals of [*trans*-$PtH\{:C(OCH_3)(CH_2C_6H_5)\}(PCy_3)_2]^+PF_6^-$ (74%).

Preparation of [trans-$PtH(:\overline{COCH_2CH_2CH_2})(PCy_3)_2]^+PF_6^-$

To a dichloromethane solution of **1** was added 1 equiv. of $CH{\equiv}CCH_2CH_2OH$. The solution was concentrated and upon addition of methanol the white crystals of [*trans*-$PtH(:\overline{COCH_2CH_2CH_2})(PCy_3)_2]^+PF_6^-$ (75%) were obtained.

We thank the National Research Council of Canada for continued financial support.

1. C. A. Tolman. J. Am. Chem. Soc. **92**, 2953 (1970).
2. C. A. Tolman, W. C. Seidel, and L. W. Gosser. J. Am. Chem. Soc. **96**, 53 (1974).
3. M. Green, J. A. Howard, J. L. Spencer, and F. G. A. Stone. J. Chem. Soc. Chem. Commun. 3 (1975).
4. A. Immirzi and A. Musco. J. Chem. Soc. Chem. Commun. 400 (1974).
5. M. H. Chisholm and H. C. Clark. Inorg. Chem. **10**, 2557 (1971).
6. H. C. Clark and C. R. Jablonski. Inorg. Chem. **13**, 2213 (1974).
7. H. C. Clark and H. Kurosawa. Inorg. Chem. **11**, 1275 (1972).
8. H. C. Clark and H. Kurosawa. Inorg. Chem. **12**, 357 (1973).
9. H. C. Clark and H. Kurosawa. J. Organomet. Chem. **36**, 399 (1972).
10. H. C. Clark and A. Shaver. Can. J. Chem. This issue.
11. T. G. Appleton, H. C. Clark, and L. E. Manzer. Coord. Chem. Rev. **10**, 335 (1973).
12. N. W. Alcock and P. G. Leviston. J. Chem. Soc. Dalton, 1834 (1974).
13. M. H. Chisholm and H. C. Clark. Inorg. Chem. **10**, 1711 (1971).
14. M. H. Chisholm and H. C. Clark. Acc. Chem. Res. **6**, 202 (1973).
15. M. J. Church and M. J. Mays. J. Chem. Soc. A, 3074 (1968).
16. B. Cetinkaya, E. Cetinkaya, and M. F. Lappert. J. Chem. Soc. Dalton, 906 (1973).
17. G. W. Parshall. Inorg. Synth. **12**, 28 (1970).
18. H. C. Clark and C. S. Wong. J. Organometal. Chem. In press.
19. B. L. Shaw and M. F. Uttley. Chem. Commun. 918 (1974).

Can. J. Chem. Downloaded from www.nrcresearchpress.com by 210.87.254.40 on 09/05/12
For personal use only.

Thermal Decomposition of EDTA, NTA, and Nitrilotrimethylenephosphonic Acid in Aqueous Solution[1]

A. E. MARTELL,[2] R. J. MOTEKAITIS, A. R. FRIED, J. S. WILSON, AND D. T. MACMILLAN

Department of Chemistry, Texas A & M University, College Station, Texas 77843

Received December 23, 1974[3]

A. E. MARTELL, R. J. MOTEKAITIS, A. R. FRIED, J. S. WILSON, and D. T. MACMILLAN. Can. J. Chem. **53**, 3471 (1975).

The decomposition of ethylenediaminetetraacetic acid (EDTA) in water solution at 200 and 260 °C, nitrilotriacetic acid (NTA) at 260 and 293 °C, and of nitrilotrimethylenephosphonic acid (NTPO) at 260 °C was studied by n.m.r. as a function of time at p*H* 9.5 and decomposition rates and products were determined. The primary (fast) decomposition reaction of EDTA involves the hydrolytic cleavage of the ethylenic C—N bond to produce the relatively stable pair: *N*-(2-hydroxyethyl)iminodiacetic acid and iminodiacetic acid. NTA does not cleave below 260 °C but decomposes at about 290 °C and above through a stepwise decarboxylation reaction. NTPO cleaves hydrolytically at 260 °C at two C—N bonds to produce aminomethylenephosphonic acid and 2 mol of hydroxymethylenephosphonic acid. The further breakdown of the primary products of EDTA at higher temperatures occurs by the loss of carbon dioxide producing the corresponding methylamines, concomitantly with the hydrolytic cleavage of the remaining CH_2CH_2—N bond giving ethylene glycol. The pseudo first order rate constant k_{obs} for NTA decarboxylation at 293 °C and p*H* 9.3 is 0.19 ± 0.01 h^{-1}. The value of k_{obs} for EDTA hydrolysis at 200 °C is 1.4 ± 0.2 h^{-1}.

A. E. MARTELL, R. J. MOTEKAITIS, A. R. FRIED, J. S. WILSON et D. T. MACMILLAN. Can. J. Chem. **53**, 3471 (1975).

On a étudié, par r.m.n. en fonction du temps à un p*H* de 9.5, la décomposition de l'acide éthylènediaminetétraacétique (EDTA) dans des solutions aqueuses à 200 et 260 °C de l'acide nitrilotriacétique (NTA) à 260 et 293 °C et de l'acide nitrilotrimethylenephosphonique (NTPO) à 260 °C et on a déterminé les vitesses de décompositions et la nature des produits formés. La réaction de décomposition initiale (rapide) de l'EDTA implique un clivage hydrolytique du lien C—N éthylénique pour conduire à la paire relativement stable: acide *N*-(hydroxy-2 éthyliminodiacétique) et acide iminodiacétique. Le NTA ne se coupe pas en-dessous de 260 °C mais se décompose à environ 290 °C et plus haut par l'intermédiaire d'une série de réaction successive de décarboxylation. Le NTPO se coupe d'une façon hydrolytique à 260 °C à deux des liens C—N; il y a formation d'acide aminométhylènephosphonique et de deux moles d'acide hydroxyméthylènephosphonique. Des coupures ultérieures des produits initiaux de l'EDTA à des températures plus élevées se produisent par perte de CO_2 conduisant aux méthylamines correspondants; il y a un clivage hydrolytique concomitant du lien CH_2CH_2—N risiduel conduisant à l'éthylène glycol. La constante de vitesse du pseudo premier ordre (k_{obs}) pour la décarboxylation de NTA, à 293 °C et un p*H* de 9.3, est de 0.19 ± 0.01 h^{-1}. La valeur de k_{obs} pour l'hydrolyse de EDTA à 200 °C est 1.4 ± 0.2 h^{-1}.

[Traduit par le journal]

Introduction

Among the many differing applications of the two organic chelating agents ethylenediaminetetraacetic acid (EDTA) and nitrilotriacetic acid (NTA) are their use in aqueous solution at high temperatures for metal oxide solubilization (*i.e.*, scale removal) (1). To understand the chemical processes that occur in such applications, it is essential to know the hydrolytic stabilities of these ligands, and to determine if the ligands present at the time of reaction are actually those introduced into the solution. Thus the determination of the breakdown of these ligands at high temperatures in aqueous solution is of considerable practical value, as well as being essential to a basic understanding of complexation reactions occurring at high temperatures. Indeed, it turns out that EDTA and NTA are not in fact stable in aqueous solution at high temperatures.

[1]This work was supported by a research contract G-9-2-D with the American Society of Mechanical Engineers, New York, N.Y.

[2]Author to whom correspondence should be addressed.

[3]Revision received July 2, 1975.

Can. J. Chem. Downloaded from www.nrcresearchpress.com by 210.87.254.40 on 09/05/12
For personal use only.

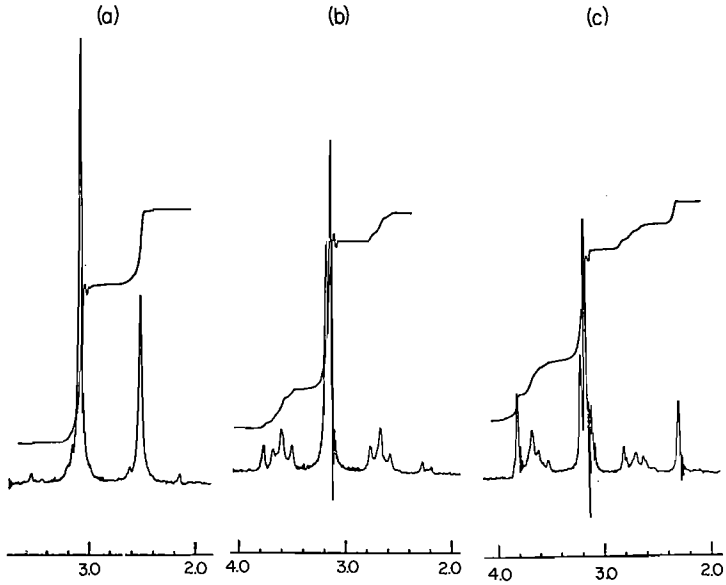

FIG. 1. Nuclear magnetic resonance spectra of EDTA samples heated at 260 °C at (*a*) $t = 0$, (*b*) $t = 0.5$ h, (*c*) $t = 7.5$ h. Solvent = 5% $NaOD/D_2O$.

This work results from a program of synthesis and testing (2, 3) of organic chelating ligands of potential use for the removal of scale deposits on heat transfer surfaces of high pressure boilers.

It had been proposed (4, 5) that at 200 °C, $EDTA^{4-}$ decomposes stepwise through the sequential loss of acetate groups. Likewise, it was concluded (6, 7) that both Na_3NTA and Na_2HNTA are exceptionally stable for at least 100 h at 200 °C. Later, the EDTA decomposition route was reinterpreted (8) to proceed through the hydrolysis of the ethylenic C—N link in agreement (2) with earlier findings in these laboratories.

This paper describes the sequential chemical reactions occurring in the aqueous decomposition of EDTA, NTA, and NTPO (nitrilotrimethylenephosphonic acid), and identifies the various decomposition products formed in each case. The p*H* of ~9.5 for this study represents a realistic working p*H* where the ligands would be efficient as scale removers yet at the same time the hydrolytic and boiler wall reactions would be kept reasonably low.

Experimental

A 2-l titanium Parr stirred autoclave was charged with 1.00 l of 0.015 *M* deoxygenated (< 1 p.p.m. O_2) solutions of EDTA, NTA, and NTPO adjusted to p*H* ~ 9.5 with NaOH and was heated rapidly with stirring to 200, 260, or 293 °C. Aliquots (10 ml) were withdrawn at periodic intervals and were evaporated to dryness under vacuum. The solvent was replaced by D_2O several times, followed by evaporation, and finally the solution was made up to 0.50 ml with 5% NaOD in D_2O. Precision n.m.r. tubes were employed and calibrated by integration of a standard EDTA solution. The n.m.r. spectra relative to TMS (trimethylsilylpropanesulfonic acid, sodium salt) were recorded and analyzed with a Varian T-60 n.m.r. spectrometer. The Varian HA-100 n.m.r. spectrometer was also used in earlier experiments on EDTA to identify and confirm the closely spaced peaks, but for routine measurements the T-60 resolution was found to be adequate.

Results and Discussion

Figure 1 shows that at 260 °C EDTA decomposes after about 30 min to its primary degradation products, *N*-(2-hydroxyethyl)iminodiacetic acid, **1**, and iminodiacetic acid, **2**. The two singlets in 2:1 ratio corresponding to the acetate methylenes and ethylene bridge protons of EDTA (Fig. 1*a*) have disappeared and were replaced by two closely spaced singlets at 3.1–3.2 p.p.m., and two triplets at 2.7 and 3.6 p.p.m. relative to TMS. At 200 °C, the $t_{1/2}$ for this transformation at p*H* 11.4, 0.15 *M* Na_4EDTA has been stated to be 15 h (6). Our calculations (Fig. 4) show that the half-life of EDTA at 200 °C under our conditions is ~0.5 h. The two singlets (Fig. 1*b*) are assigned to the acetate methylene protons of the cleaved

Can. J. Chem. Downloaded from www.nrcresearchpress.com by 210.87.254.40 on 09/05/12
For personal use only.

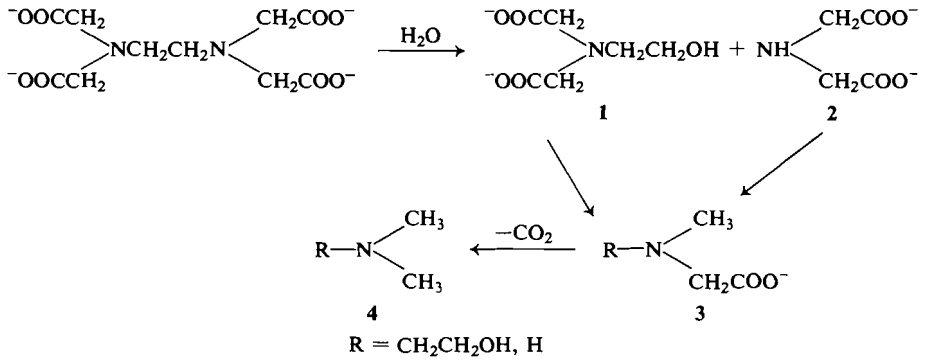

species **1** and **2**; their similar chemical shifts are caused by the difference in —H and —CH_2-CH_2OH substitution on the nitrogens. The two triplets represent the latter group with the absorption at 3.6 p.p.m. assigned to the methylene adjacent to the hydroxyl group. These assignments were confirmed by a direct comparison with the n.m.r. spectra of authentic samples of **1** and **2**.

After some time at 260 °C (Fig. 1*c*), the primary decay products of EDTA decarboxylate to the various substituted methylamines. This conclusion is reached both from the work on NTA and from an appreciation of the chemical shifts shown in Fig. 1*c*. The peak at approximately 2.3 p.p.m. is a methyl bound to nitrogen such as shown in **3** or **4**. The singlet that grows in at approximately 3.8 p.p.m. is indicative of further hydrolysis of *N*-(2-hydroxyethyl)iminodiacetic acid to ethylene glycol and iminodiacetic acid.

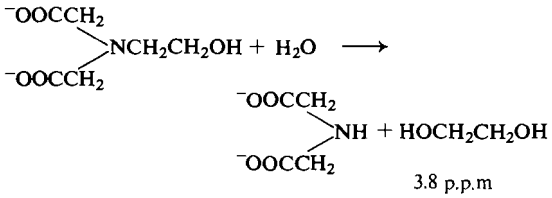

NTA apparently does not undergo hydrolytic cleavage, but does decompose at 293 °C via decarboxylation to *N*-methyliminodiacetic acid, **5**, methylsarcosine, **6**, and trimethylamine, **7**. Figure 2 shows the decay of NTA in 4 h, indicating a mixture of these products. The half-life of 4.0 h is appreciably longer than that associated with the initial decay of EDTA, but at this temperature is comparable to the decomposition rate of the primary decomposition products formed from EDTA. Indeed it has been estimated that at the lower temperature of 200 °C, the half-lives of NTA^{3-} and $HNTA^{2-}$ are both > 1000 h (7).

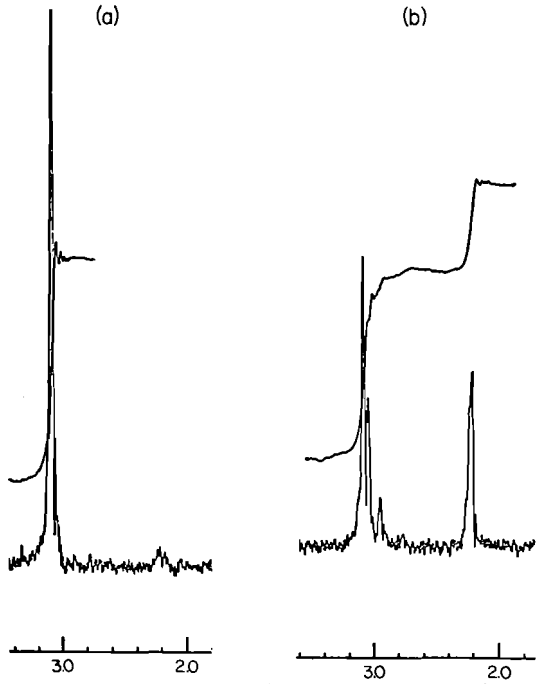

FIG. 2. Nuclear magnetic resonance spectra of NTA samples heated at 293 °C taken at (*a*) $t = 0$, (*b*) $t = 4.0$ h. Solvent is 5% $NaOD/D_2O$.

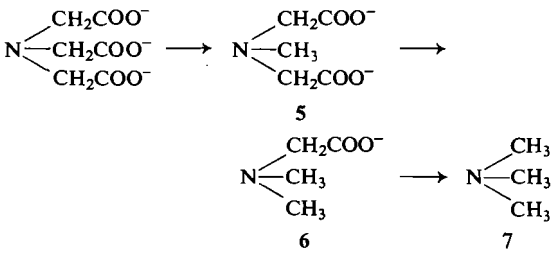

Can. J. Chem. Downloaded from www.nrcresearchpress.com by 210.87.254.40 on 09/05/12
For personal use only.

Can. J. Chem. Downloaded from www.nrcresearchpress.com by 210.87.254.40 on 09/05/12
For personal use only.

TABLE 1. Kinetic analysis of NTA decomposition at 293 °C and p*H* 9.3

Initial concentration of NTA (*M*)	Time (h)	*F* Fraction remaining	$1/t \ln F_0/F$ (h^{-1})
0.0025	1.0	0.80	0.22
	2.5	0.62	0.19
	4.0	0.45	0.20
	6.0	0.22	0.25
		Average	0.21
0.0050	1.0	0.82	0.20
	2.0	0.71	0.17
	4.0	0.51	0.17
	6.0	0.26	0.22
		Average	0.19
0.010	0.75*	0.93*	0.10*
	2.0	0.73	0.16
	4.0	0.50	0.17
	6.0	0.28	0.21
		Average	0.18
0.020	1.0	0.83	0.19
	2.0	0.64	0.22
	4.0	0.46	0.19
	6.0	0.37	0.17
		Average	0.19

Mean of averages: $k_{obs} = 0.19 \pm 0.01 \ h^{-1}$

*Discarded point.

The broadness of the 2.2 p.p.m. resonance (Fig. 2*b*) and the growth of closely spaced peaks at 3.0 p.p.m. support the composition of the mixture indicated in the equation above. Clearly, the 2.2 p.p.m. resonance represents three types of N—CH_3 groups (**5**–**7**), and the 3.0 p.p.m. peak shows the presence of three types of acetate methylenes (NTA, **5**, **6**).

Since the NTA decay rate at 293 °C was considerably slower that that of EDTA at the lower temperature investigated, a kinetic analysis for the initial NTA decomposition reaction was also undertaken in addition to the product analysis described above. Reaction kinetics was also obtained for EDTA hydrolysis within the limitation that a significant fraction of the starting substrate decomposes during heat-up time.

Table 1 summarizes the reaction conditions at four initial concentrations of NTA. It is seen that the observed rate constant does not vary with initial concentration. Thus the reaction rate at 293 °C and p*H* 9.3 for the decarboxylation of NTA follows pseudo first order kinetics with $k_{obs} = 0.19 \ h^{-1}$.

TABLE 2. Kinetic analysis of EDTA decomposition at 200 °C

EDTA initial concentration (*M*)	Time (h)	*F* Fraction remaining	$-\ln F$	k_{obs} (h^{-1})
0.0112	0.5	0.59	0.53	
	1.0	0.20	1.61	1.27
	2.0	0.08	2.53	
0.0056	0.5	0.40	0.92	
	1.0	0.18	1.71	1.37
	2.0	0.05	3.00	
0.0028	0.5	0.20	1.61	
	1.0	0.05	3.00	1.65
	2.0	0.015	4.20	
			Average	1.43 ± 0.20

Similarly, over a fourfold initial concentration range (Table 2) the pseudo first order rate constant for EDTA hydrolysis is found to be rather invariant within $\sigma = 0.2 \ h^{-1}$ with a value of $k_{obs} = 1.4 \ h^{-1}$.

The n.m.r. spectra of NTPO at 260 °C show the complete disappearance of the parent doublet ($J_{PCH} = 12$ Hz) after 0.25 h, replaced by two doublets with the same coupling constant and an intensity ratio of 2:1, both at lower field strength (Fig. 3*a*). The smaller doublet was determined to be aminomethylphosphonic acid (AMP) by the addition of an authentic sample

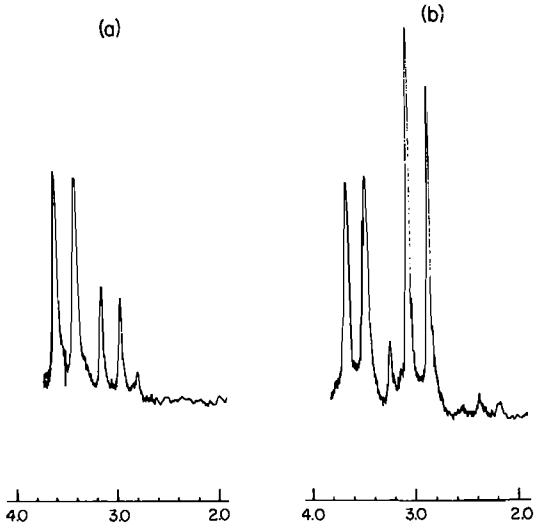

FIG. 3. Nuclear magnetic resonance spectra of NTPO sample at (*a*) $t = 0.25$, (*b*) $t = 0.25$ h, with aminomethylenephosphonic acid added. $T = 260$ °C, solvent = 5% $NaOD/D_2O$.

Can. J. Chem. Downloaded from www.nrcresearchpress.com by 210.87.254.40 on 09/05/12
For personal use only.

of AMP to the n.m.r. tube (Fig. 3*b*). The larger doublet is therefore hydroxymethylphosphonic acid. Thus the fast hydrolytic reaction may be concluded to proceed as

$$N(CH_2PO_3^{2-})_3 \xrightarrow{H_2O} H_2NCH_2PO_3^{2-} + 2HOCH_2PO_3^{2-}$$

This behavior is quite different from that found with NTA, which does not undergo carbon–nitrogen bond fission even at much higher temperatures. Since the presence of high negative charge resulting from the phosphonate groups would seem to repel hydroxide ions and thus decrease base-catalyzed carbon–nitrogen hydrolytic fission relative to what is observed in NTA, the question arises as to the special nature of the NTPO anion that would tend to promote hydrolytic splitting. In this connection, it should be noted that the basicity of the tertiary amino group in NTPO is at least two orders of magnitude greater than NTA (9). Hence, even at the high temperatures involved in these studies, a considerable proportion of the ligand must be in the *N*-protonated form, **8**.

The positive charge on the nitrogen would be expected to assist carbon–nitrogen bond fission by transfer of the bonding electron pair to nitrogen.

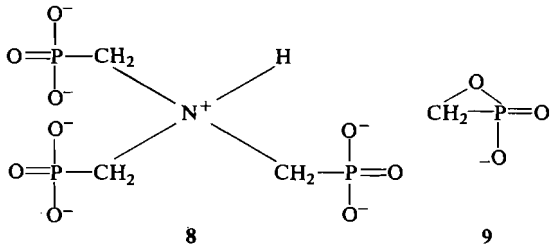

8

9

There is also the possibility that hydrolytic fission of **8** may be assisted by the formation of an intermediate **9** which would be rapidly converted by hydroxide ion attack to hydroxymethylenephosphonic acid, which has been demonstrated to be one of the reaction products.

Figure 4 shows the relatively fast decomposition rate for EDTA, when compared to NTA. This, taken together with the above discussion, explains that the coordinating activity of aqueous solutions of EDTA at high temperatures (*i.e.*, above 200 °C) is due not to EDTA itself, but is primarily due to the complexing ability of the more thermally stable primary breakdown products **1** and **2**. By virtue of its

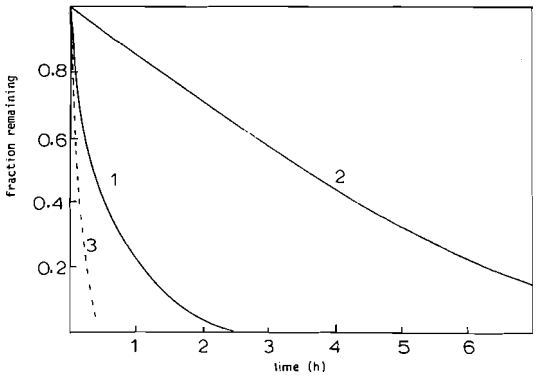

FIG. 4. Thermal decay plots of (*1*) EDTA at 200 °C, (*2*) NTA at 293 °C, (*3*) NTPO at 260 °C The decay in (*3*) is so rapid as to be difficult to measure. The decay of (*1*) was measured at $[EDTA]_0$ of 0.0112, 0.0056, and 0.0028 *M*; it showed no concentration dependence within the large experimental error induced by relatively long heat-up time compared to the rate of breakdown.

hydroxyethyl moiety **1** should be particularly suited for Fe^{3+} complexation, as is amply demonstrated in the literature and probably is the more active ingredient in such solutions. Both **1** and iminodiacetic acid, **2**, would be effective toward divalent transition metal ions. Thus from an economic point of view, as well as for the purpose of maintaining maximum chemical effectiveness, it would probably be reasonable to use *N*-hydroxyethyliminodiacetic acid as a sequestering agent for transition metals at elevated temperature (~200 °C and above) in place of more rapidly-hydrolyzed substances such as EDTA. At the present time NTA is the least expensive organic sequestering agent available. Since its slower breakdown leads to *N*-methyliminodiacetic acid which still retains considerable effectiveness, and since NTA is itself an order of magnitude more stable than EDTA, it may very well be the chelating agent of choice at the present time.

The above argument is based on the relative stabilities of the ligands themselves, rather than the metal chelates. While this is logical from the point of view of maintaining an effective concentration of ligands for the purposes of scale removal, the abilities of the metal chelates to resist hydrolytic breakdown is also important to prevent redeposition of metal hydroxides in aqueous solution at elevated temperatures.

1. J. R. METCALF. Proc. 31st International Water Conference, Engineers Society of Western Pennsylvania. Pittsburgh, Pa. October, 1970.

2. A. E. MARTELL, R. J. MOTEKAITIS, and D. MACMILLAN. Fourth Quarterly Progress Report to the Contract Research Department, Texas Division, Dow Chemical Company, Freeport, Texas. August, 1972.
3. O. OSBORN, J. S. WILSON, A. R. FRIED, and W. H. PRYOR, JR. The development of a method for in-service high pressure boiler cleaning. Phase I – synthesis and screening program". Final Report to the American Society of Mechanical Engineers. March, 1973.
4. D. L. VENEZKY and W. B. MONIZ. NRL Report 6747 Naval Research Laboratory, Washington, D.C. August, 1968.
5. D. L. VENEZKY and W. B. MONIZ. Anal. Chem. **41**, 11 (1969).
6. D. L. VENEZKY. Proc. 32nd International Water Conference, Engineers Society of Western Pennsylvania, Pittsburgh, Pa. November, 1971.
7. D. L. VENEZKY and W. B. MONIZ. NRL Report 7192, Naval Research Laboratory, Washington, D.C. November, 1970.
8. P. J. SNIEGOWSKI and D. L. VENEZKY. J. Chromatogr. Sci. **12**, 359 (1974).
9. A. E. MARTELL and R. M. SMITH. Critical stability constants, Vol. 2. Plenum Press, Inc., New York 1975.

Can. J. Chem. Downloaded from www.nrcresearchpress.com by 210.87.254.40 on 09/05/12
For personal use only.

A New Mode of Photorearrangement in the Azoxybenzene Series

NIGEL J. BUNCE

Guelph-Waterloo Centre for Graduate Work in Chemistry, University of Guelph, Guelph, Ontario N1G 2W1

Received May 26, 1975

NIGEL J. BUNCE. Can. J. Chem. **53**, 3477 (1975).

Both isomers of 4-methoxyazoxybenzene photorearrange to the same *o*-hydroxyazo compound. In the case of β-4-methoxyazoxybenzene, prior photoisomerization to the α-isomer is involved.

NIGEL J. BUNCE. Can. J. Chem. **53**, 3477 (1975).

Les deux isomères du méthoxy-4 azoxybenzène se réarrangent photochimiquement pour conduire au même composé *o*-hydroxyazo. Dans le cas du β-méthoxy-4 azoxybenzène il y a photoisomérisation préalable en isomère α.

[Traduit par le journal]

Can. J. Chem. Downloaded from www.nrcresearchpress.com by 210.87.254.40 on 09/05/12
For personal use only.

Photolysis of aromatic azoxy compounds causes them to isomerize into *o*-hydroxyazo compounds (1). The usual mode of rearrangement involves oxygen migration to the distant aromatic ring [1]. This was shown by analysis of the products of irradiation of unsymmetrically substituted azoxy compounds (2), and later confirmed by isotopic tracer experiments (3).

[1] 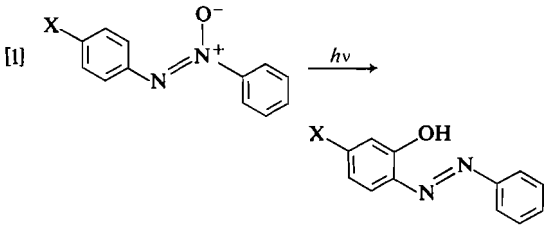

Concurrently with photorearrangement, *cis–trans* isomerization at the azoxy linkage may also be observed (4). In this paper is reported an instance in which both isomers of a monosubstituted azoxybenzene photorearrange to the same *o*-hydroxyazo compound.

Illumination of ethanolic solutions of either **1** or **2** through Pyrex glass afforded the same rearrangement product **3**. The identity of the samples was established by mixture m.p., u.v. and n.m.r. spectra, and also by mass spectrometry. Aromatic azo compounds are well known to fragment predominantly to the ions represented in [2] (5), so that the observation of major fragment ions at *m/e* 77, 105, 123, and 151 corresponding to $C_6H_5^+$, $C_6H_5N_2^+$, $CH_3OC_6H_3OH^+$, and $CH_3OC_6H_3(OH)N_2^+$ (and the absence of the alternative *m/e* 93, 107, 121, and 135) locates the hydroxy and methoxy substituents in the same ring.

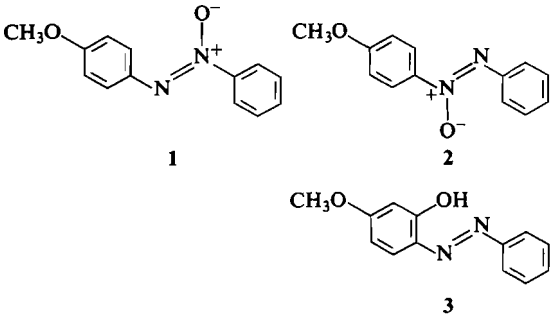

1 **2** **3**

[2] $Ar—N{=}N—Ar' \xrightarrow{e.i.} Ar^+, ArN_2^+, Ar'^+, Ar'N_2^+$

Formation of **3** on a photolysis of **2** appears to violate the generality of the photorearrangement pathway of [1], established by Badger and Buttery (2). That this is probably not so was revealed by examination of the azoxy compound remaining after photolysis; from the irradiation of **2**, its isomer **1** was recovered. Thus the 'abnormal' rearrangement product is unlikely to be formed directly from **2**, but rather results from prior isomerization of **2** to **1**. Consistent with this proposal, **3** was found to be produced more slowly from **2** than from **1**.

Although it has not proved possible to isolate or detect any intermediates in the transformation **2** → **1**, analogy with the work of Greene and Hecht (6) suggests **4** as a likely intermediate. Interestingly, when **2** is photolyzed in quartz equipment, the expected rearrangement product **5** is produced along with **3**, perhaps indicating

Can. J. Chem. Downloaded from www.nrcresearchpress.com by 210.87.254.40 on 09/05/12
For personal use only.

TABLE 1. Calculated charge densities and free valence indices for three azoxy compounds[a]

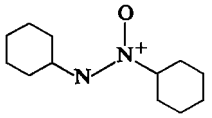

Compound	Electron densities N	Electron densities N^+	Electron densities O	Free valence N	Free valence O
Azoxybenzene					
Ground state	−0.05	+0.57	+0.18	0.61	1.42
n,π*	−0.46	+0.33	+0.09	0.96	1.56
π,π*	−0.41	+0.38	+0.17	0.93	1.50
1					
Ground state	−0.06	+0.54	+0.17	0.60	1.43
n,π*	−0.46	+0.31	+0.09	0.98	1.57
π,π*	−0.46	+0.38	+0.17	0.96	1.50
2					
Ground state	−0.07	+0.57	+0.18	0.63	1.42
n,π*	−0.47	+0.32	+0.09	0.97	1.56
π,π*	−0.40	+0.34	+0.11	0.94	1.55

[a]HMO parameters: $\alpha_N = \alpha + \beta$; $\alpha_{N^+} = \alpha + 2\beta$; $\alpha_{O^-} = \alpha + 1.5\beta$; $\alpha_{OCH_3} = \alpha + 2\beta$; $\beta_{C-N} = 0.7\beta$; $\beta_{N-N} = \beta$; $\beta_{N-O} = 0.8\beta$; $\beta_{C-O} = 0.8\beta$

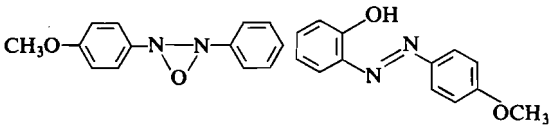

4 **5**

that **4** and **5** may be formed from different excited states of **2**.

A significant question is why position isomerization occurs for **2**, but not for **1** nor apparently for the unsymmetrical compounds studied by Badger and Buttery (2). Zero-order HMO calculations of the electron distributions in the π molecular orbitals of **1**, **2**, and unsubstituted azoxybenzene give no suggestion that the electron densities or free valence indices in the low lying excited states of **2** are significantly different from those in **1** or in unsubstituted azoxybenzene. Data for the n,π* states have been included since recent work suggests that this may be the reactive state for the azoxybenzene photorearrangement, rather than the π,π* as is usually assumed.[1] Table 1 notes these parameters for the nitrogen and oxygen atoms that would be involved if cyclization to **4** occurred. Another possibility might be the greater stability of **1** as compared with **2** arising from contributions from resonance structures such as **6**; this could

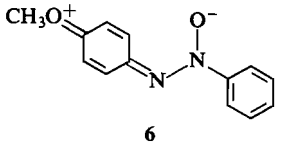

6

act as a driving force for the interconversion since no comparable structures can be drawn for **2**. Again, however, Table 1 suggests that this effect is small, judging by the very modest reduction in charge on the central nitrogen that results from interaction with the methoxy group.

At this point, we are unable to offer an explanation for the ability of **2** to photoisomerize in this new manner. However, position isomerization now joins photorearrangement and *cis–trans* photoisomerization as a possible and observed mode of photoreaction in the azoxybenzene series. It remains to be seen whether the new reaction occurs in other unsymmetrical aromatic azoxy compounds, though previous

[1]N. J. Bunce and M. C. Zerner, unpublished results.

Can. J. Chem. Downloaded from www.nrcresearchpress.com by 210.87.254.40 on 09/05/12
For personal use only.

TABLE 2. Relative rates of appearance of hydroxyazo compound **3** from azoxy compounds **1** and **2**

Concentration (*M*)	Rate (**2**)/rate (**1**)
5.5×10^{-5}	0.52
2.8×10^{-4}	0.50
5.5×10^{-4}	0.50

work (2, 3) indicates that it must usually be extremely inefficient.

Experimental

Solvents were reagent grade materials except ligroin for use in chromatography and preparative t.l.c., which was commercial hexane (fraction from petroleum). All were used without purification. Instrumentation included a Pye–Unicam SP 800 u.v.–visible spectrophotometer, a Varian Associates A-60A n.m.r. spectrometer, and a Varian-MAT CH7 mass spectrometer operated at 70 eV ionizing voltage. Melting points are uncorrected.

Isomeric 4-Methoxyazoxybenzenes

p-Hydroxyazobenzene (5 g) was methylated with dimethyl sulphate in aqueous alkaline solution, affording, after purification of the crude product by chromatography over alumina, *p*-methoxyazobenzene, m.p. 53–54 °C (lit. (7) 54 °C). The product (3 g) was oxidized in acetic acid solution with 30% H_2O_2 (5 ml) on a steam bath for 5 h. The crude product was purified by chromatography over alumina, eluting with ligroin, to give the isomeric *p*-methoxyphenylazoxybenzenes (2.23 g) as a pale yellow solid. Repeated fractional crystallization from methanol gave the pure isomers; the purest fractions were: 4-methoxyphenyl-*NNO*-azoxybenzene, **1**, m.p. 73–74 °C (lit. (8) 67 °C), and 4-methoxyphenyl-*ONN*-azoxybenzene, **2**, m.p. 39–40 °C (lit. (8) 42 °C).[2] Ultraviolet absorption maxima (EtOH) were respectively 348 and 337 nm (lit. (9) 350 and 338 nm).

Preparative Irradiations

These were carried out in ethanol solution in the presence of atmospheric amounts of oxygen, using a 450 W Hanovia medium pressure mercury arc and an immersion well apparatus. The outer jacket of the apparatus, which had a capacity of 325 ml with the immersion well in place, had a flat base to permit agitation of the solution using a magnetic stirrer. After photolysis, the solvent was removed and the residue resolved by preparative t.l.c. on silica gel PF_{254} (E. Merck #7747). The bands were scraped off and the compounds extracted into chloroform (Soxhlet extractor), which was filtered prior to evaporation and recrystallization of the residue from ethanol.

*Irradiation of **1**, Pyrex Filter*

The reactant (0.30 g) had m.p. 65–68 °C. The products were recovered **1**, (0.22 g), m.p. 70–72 °C, and 5-methoxy-2-phenylazophenol, **3**, (0.06 g), matted orange needles from ethanol, m.p. 111–112 °C (lit. (10) 115 °C). Ultraviolet λ_{max} (EtOH) 374 nm (ε 19 100) and 255 (6500); λ_{max} (EtOH–0.5 *M* KOH) 454 nm (ε 12 200), and 335 (11 000); n.m.r. (CCl_4) δ 13.4 (s, OH), 6.2–7.9 (m, ArH), and 3.85 (s, OCH_3); mass spectrum (70 eV): *m/e* 228 (M^+, 100%), 151 (61), 123 (83), 105 (23), and 77 (33).

*Irradiation of **2**, Pyrex Filter*

The reactant was **2**, (0.40 g), m.p. 37–41 °C. The products obtained were the azoxy compound **1**, (0.23 g), m.p. 61–65 °C, λ_{max} (EtOH) 346 nm, and the azo compound **3** (0.05 g), red needles from ethanol, m.p. 112–113.5 °C, not depressed by admixture with the product of irradiation of **1**. Mass spectrum *m/e* 228 (M^+, 100%), 151 (52), 123 (60), 105 (16), and 77 (36); u.v. and n.m.r. spectra identical to those reported above.

*Irradiation of **2**, Quartz Equipment*

The reactant was **2**, (0.35 g), m.p. 39–40 °C. After irradiation the products were the azoxy compound **1**, (7 mg), λ_{max} 345 nm, and two red substances. The more mobile on silica gel was 2-hydroxy-4′-methoxyazobenzene,[3] **5**, (36 mg), red needles from ethanol, m.p. 72–74 °C. Ultraviolet λ_{max} (EtOH) 380 nm (ε 19 000), 348 (20 500), and 248 (12 700); λ_{max} (EtOH–0.5 *M* KOH) 460 nm (ε 9700) and 317 (15 300); n.m.r. (CCl_4) δ 3.85 (s, OCH_3), 7.1–8.0 (m, ArH), and 15.9 (s, OH); mass spectrum *m/e* 228 (M^+, 63%), 135 (38), 121 (12), 107 (100), 93 (37), and 91 (35).

Anal. Calcd. for $C_{13}H_{12}N_2O_2$: C, 68.41; H, 5.30; N, 12.27. Found: C, 68.13; H, 5.55; N, 12.23.

The other red substance was the hydroxyazo compound **3**, (51 mg); red needles from ethanol, m.p. 113–114 °C. Nuclear magnetic resonance and mass spectra were identical to those reported above.

Anal. Calcd. for $C_{13}H_{12}N_2O_2$: C, 68.41; H, 5.30; N, 12.27. Found: C, 68.30; H, 5.51; N, 12.20.

Relative Rate Experiments

The 450 W mercury arc, cooled by the Pyrex immersion well, was surrounded by a filter solution (1 cm of 2×10^{-3} *M* K_2CrO_4 in 1% K_2CO_3) to restrict light absorption to 300–330 nm, where the reactants absorbed strongly. This assembly was placed in a constant temperature bath at 30 ± 0.2 °C. Corked Pyrex ampoules containing 4 ml aliquots of the azoxy compounds dissolved[4] in ethanol–0.5 *M* KOH were irradiated simultaneously using a 'Merry-go-round' to ensure equal illumination of samples. Samples were irradiated for specified times and then examined spectrophotometrically for the appearance of the anion of **3** (λ = 454 nm). The results are given in Table 2.

The author thanks the National Research Council of Canada for financial support.

[2]Compounds **1** and **2** are respectively the α and β isomers in the older system of nomenclature.

[3]The possible structure 4-hydroxy-4′-methoxyazobenzene is ruled out by the higher m.p., 142 °C (11), of the latter.

[4]The alkaline solution was used so that the hydroxyazo compound produced could be monitored as its anion. Experiments with azoxybenzene have shown that neither the rate nor the identity of the product is affected by using this solvent rather than pure ethanol.

1. G. G. SPENCE, E. C. TAYLOR, and O. BUCHARDT. Chem. Rev. **70**, 231 (1970); E. BUNCEL. *In* Mechanisms of molecular migrations. Vol. 1. *Edited by* B. S. Thyagarajan. Interscience, New York. 1969. pp. 104–110.
2. G. M. BADGER and R. G. BUTTERY. J. Chem. Soc. 2243 (1954).
3. S. OAE, T. FUKUMOTO, and M. YAMAGAMI. Bull. Chem. Soc. Jpn. **34**, 1873 (1961); M. M. SHEMYAKIN, T. E. AGADZHANYAN, V. I. MAIMIND, R. V. KUDRYAVTSEV, and D. N. KURSANOV. Dokl. Akad. Nauk. SSSR, **135**, 346 (1960), through Chem. Abstr. **55**, 11337d (1961); M. M. SHEMYAKIN, V. I. MAIMIND, and B. K. VAICHUNAITE. Chem. Ind. 755 (1958); Zh. Obshch. Khim. **28**, 1708 (1958), through Chem. Abstr. **53**, 1201f (1959).
4. R. TANIKAGA. Bull. Chem. Soc. Jpn. **41**, 2151 (1968).
5. J. H. BOWIE, G. E. LEWIS, and R. G. COOKS. J. Chem. Soc. B, 621 (1967).
6. F. D. GREENE and S. S. HECHT. J. Org. Chem. **35**, 2482 (1970).
7. H. GORKE, E. KÖPPE, and F. STAIGER. Ber. **41**, 1156 (1908).
8. C.-S. HAHN and H. H. JAFFÉ. J. Am. Chem. Soc. **84**, 949 (1962).
9. L. SZEGÖ. Ber. **61**, 2087 (1928).
10. J. BECHHOLD. Ber. **22**, 2374 (1889).
11. M. KRAUSE. Ber. **32**, 124 (1899).

Can. J. Chem. Downloaded from www.nrcresearchpress.com by 210.87.254.40 on 09/05/12
For personal use only.

The Mechanism for the Thermal Decomposition of *E*-Aldoxime Carbonates[1]

J. M. PROKIPCAK AND P. A. FORTE

Department of Chemistry, University of Guelph, Guelph, Ontario N1G 2W1

Received May 22, 1975

J. M. PROKIPCAK and P. A. FORTE. Can. J. Chem. **53**, 3481 (1975).

Pyrolysis of aldoxime carbonates at relatively low temperatures (100–120 °C) produced nitriles in excellent yields. These decompositions followed first-order kinetics and the decomposition rates showed little dependence on inductive effects or solvent polarity. Low entropy values along with the fact that the *E* and *Z*-isomers behaved quite differently led to the proposal of a cyclic transition state for the decompositions.

J. M. PROKIPCAK et P. A. FORTE. Can. J. Chem. **53**, 3481 (1975).

La pyrolyse des carbonates d'aldoxime à des températures relativement basses (100–120 °C) conduit aux nitriles avec d'excellents rendements. Ces décompositions se produisent suivant une cinétique du premier ordre et les vitesses de décomposition ne sont que peu affectées par les effets inductifs ou la polarité du solvant. En se basant sur le fait que les entropies sont basses et que les isomères *E* et *Z* se comportent très différemment, on suggère un état de transition cyclique pour ces décompositions.

[Traduit par le journal]

Can. J. Chem. Downloaded from www.nrcresearchpress.com by 210.87.254.40 on 09/05/12
For personal use only.

Introduction

It was shown in an earlier publication (1) that the thermal decomposition of *E*-benzaldoxime carbonates was a useful synthetic route in the preparation of nitriles. This route was particularly valuable since the conversion of the *E*-aldoxime carbonates to the corresponding nitriles required no acidic or basic reagents.

Other recent articles have appeared in the literature which describe the conversion of aldehydes to nitriles under mild conditions (2–4). These conversions are suggested to be fragmentation reactions but no real attempts were made to determine the mechanisms involved. A continuing study of the thermal fragmentation of aldoxime carbonates was carried out in an effort to allow some conclusions to be made with regard to the mechanism involved. It was felt that two possible modes for the decomposition were possible (Scheme 1) and that the investigation of inductive effects and solvent effects would allow a more conclusive picture to be made regarding the actual transition state involved in the decomposition. All the benzaldoximes used in this study were readily prepared from the respective aldehydes using standard methods. The benzaldoximes were treated with phenyl chloroformate (or a *p*-substituted phenyl chloroformate) in the presence of an equimolar amount of pyridine. The aldoxime carbonates were then heated to 100–120 °C giving the corresponding nitriles, phenols, and CO_2. The variation in the decomposition rate due to structural changes in the benzaldoxime and phenyl chloroformate portion of the molecule were examined. Also the effect of solvent polarity and nature of the oxime (*i.e.* whether the aldoxime was the *E*- or *Z*-form) was investigated. This report gives the results of these studies and a mechanism for the thermal decomposition is proposed.

Experimental

Synthesis of Chloroformates

Phenyl chloroformate, 4-methoxyphenyl chloroformate, and 4-nitrophenyl chloroformate were obtained commercially and used without further purification. The 4-methylphenyl and 4-chlorophenyl chloroformates were prepared by the reaction of the properly substituted phenol with phosgene according to the method of Zabik and Schuetz (5).

Synthesis of Benzaldoxime Carbonates

The general synthesis procedure used for the preparation of these compounds can be found in previous work (1). The complete list of *E*-benzaldoxime carbonates prepared and used in this study along with physical constants and elemental analyses is given in Table 1.

In addition to the *Z*-isomers, the *E*-isomer of benz-

[1]Taken from the thesis of P. A. Forte presented to the Faculty of Graduate Studies, University of Guelph, Guelph, Ontario, as part of the requirements for the degree of Ph.D.

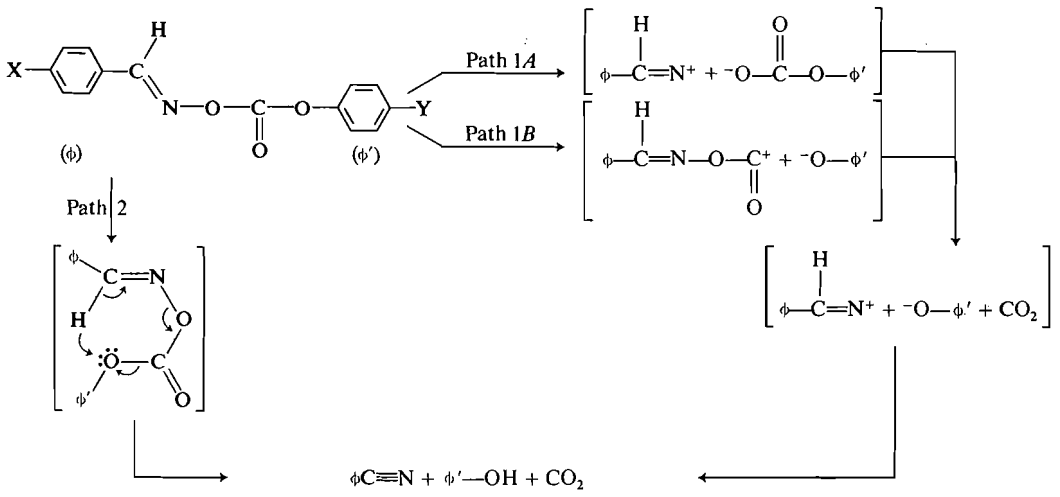

SCHEME 1

TABLE 1. The preparation of *E*-benzaldoxime carbonates[a]

Carbonate		Melting point[b]	Yield	Analyses					
				Calculated			Found		
X	Y	(°C)	(%)	C	H	N	C	H	N
NO_2	H	151–152	84	58.74	3.52	9.79	58.47	3.47	9.68
Cl	H[c]	115–116	74	60.99	3.66	5.08	60.66	3.70	4.95
H	H	83–85	84	69.70	4.50	5.80	69.64	4.48	5.70
CH_3	H	91–92	82	70.58	5.13	5.49	70.77	5.14	5.40
CH_3O	H	116–118	79	66.41	4.83	5.16	66.63	4.76	5.28
H	NO_2	135–137	70	58.74	3.52	9.79	58.57	3.57	9.70
H	Cl[d]	120–122	60	60.99	3.66	5.08	60.72	3.70	4.95
H	CH_3	88–90	72	70.58	5.13	5.49	70.42	4.98	5.42
H	CH_3O	104–106	64	66.41	4.83	5.16	66.58	4.90	5.21

[a]The general structure is 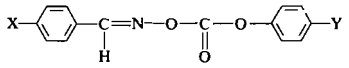

[b]All melting points were determined on the Fisher-Johns melting point apparatus and are uncorrected.
[c]Calculated for Cl, 12.86. Found, 12.79.
[d]Calculated for Cl, 12.86. Found, 12.76.

aldoxime was prepared (6). However, attempts to prepare the carbonate from the *E*-benzaldoxime failed and the reaction gave the nitrile directly.

Kinetics of the Decompositions

Since all the starting carbonates had a carbonyl group which gave a strong absorption band in the infrared over the region 1900–1700 cm^{-1} and since this absorption was not close to any other major absorptions, the base-line method was used to analyze each spectrum. Furthermore, earlier experiments with standard solutions of the carbonates in various solvents employed showed that the intensity of the carbonyl band did indeed obey Beer's Law and that a plot of $\log P_0/P$ (P = absorptions) *vs.* concentration resulted in a straight line. Thus all the decompositions carried out in this study were followed by means of i.r. using the following general method.

A solution of the carbonate (3–4 g) dissolved in a solvent (5–8 ml) such as diphenyl ether, benzonitrile, or dimethyl sulfoxide was made. Then using a syringe (1 ± 0.01 ml), equal aliquots (0.50 ml) of this solution were put into a series of reaction tubes which were placed simultaneously into a constant temperature oil bath which was maintained at a desired temperature (100–120 ± 0.05 °C). At spaced intervals of time, each tube was removed quickly from the oil bath and immediately quenched in an acetone – Dry Ice mixture. After all the reaction tubes had been quenched and allowed to return to room temperature, 0.7 ml of spectral grade chloroform was added to each tube to dilute the reaction mixture. The absorption of the carbonyl peak was measured on the IR-5A and the absorbance was obtained by the base-line method (7). The average absorbance was then multiplied by the slope of the Beer's

Can. J. Chem. Downloaded from www.nrcresearchpress.com by 210.87.254.40 on 09/05/12
For personal use only.

TABLE 2. Kinetics of the decomposition[a] of *E*-benzaldoxime carbonates[b]

X	Y	Solvent[c]	$k_1 \times 10^4$ [d] (s^{-1})	$\Delta H^{\ddagger}$ [e] (kcal mol^{-1})	$\Delta S^{\ddagger}$ (e.u.)
NO_2	H	DMSO	1.38±0.09	27.2±0.2	−3.8±1.8
Cl	H	DMSO	1.80±0.09		
H	H	DMSO	2.00±0.03	28.4±0.8	0.1±0.7
		DPE	1.81±0.00	28.8±0.4	1.2±0.7
		BN	1.58±0.05	28.8±0.9	0.9±0.8
CH_3	H	DMSO	2.24±0.06		
CH_3O	H	DMSO	2.45±0.05	29.1±0.9	2.5±0.9
H	NO_2	DMSO	7.56±0.12	28.4±0.4	0.1±1.0
		DPE	1.22±0.05	29.9±0.4	3.3±1.0
H	Cl	DMSO	12.1±0.20		
		DPE	1.60±0.05		
H	CH_3	DMSO	2.16±0.04		
		DPE	1.90±0.04		
H	CH_3O	DMSO	2.54±0.08	28.7±0.4	1.4±0.8
		DPE	2.04±0.03	28.4±0.3	0.1±0.4

[a]The decompositions were all carried out at 100 °C.

[b]The general structure is 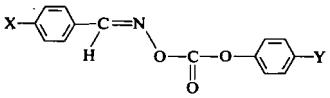

[c]DMSO (dimethylsulfoxide); DPE (diphenyl ether); BN (benzonitrile).
[d]Average of triplicate runs.
[e]Activation parameters were obtained using kinetic runs taken at 100, 110, 120, and 130 °C using the method of Purlee *et al.* (15).

Law plot to give the concentration of the sample. A plot of log concentration *vs.* time was made and the rate constant obtained.

Results and Discussion

Using the aforementioned method, the decompositions were found to exhibit good first-order kinetics and Table 2 summarizes the results of the various kinetic runs. The method of least squares was used to determine the slopes of the lines and in all cases, regression coefficients of at least 0.990 were obtained.

The first-order kinetics could be applied to three basic modes of decomposition; homolytic type, ionic heterolytic type, or concerted heterolytic type. Even though the latter two (heterolytic types) are the most probable reaction pathways for the reaction (Scheme 1), the possibility of a homolytic cleavage (or radical mechanism) could not be overlooked. This possibility was examined by means of a procedure called chemically induced dynamic nuclear polarization (CIDNP) (8, 9) which makes use of the fact that the presence of any radicals in the reaction flask would give rise to significant changes in the absorption intensities of a n.m.r. spectrum. When the progress of the decomposition of *E*-benzaldoxime phenyl carbonate was followed in a n.m.r. tube using DMSO as a solvent, the n.m.r. spectra showed no enhanced or unexplainable absorption or emmission lines. Even though this does not completely disprove the existence of nonpaired radicals, one can with reasonable confidence conclude that a dissociative radical mechanism is most likely not operative in this reaction whether the *E*- or *Z*-isomer is involved.

In heterolytic processes, transition states or intermediates often develop charge character and appropriate substituents at or near the reaction center may affect their formation. Also induced electron withdrawal or supply may influence the bond heterolysis taking place in the process. In order to examine the charge characteristics of the transition state or intermediate, the dependence of the decomposition rates on the inductive effect of substituents both on the benzaldoxime portion and chloroformate portion of the compounds was investigated. Figure 1 shows the results when Hammett plots were made for each series. The resultant plot of $\log k/k_0$ versus σ (10) for the *E*-4-substituted benzaldoxime carbonates gave a straight line with a ρ value of -0.249. This low negative ρ value indicates only small inductive

Can. J. Chem. Downloaded from www.nrcresearchpress.com by 210.87.254.40 on 09/05/12
For personal use only.

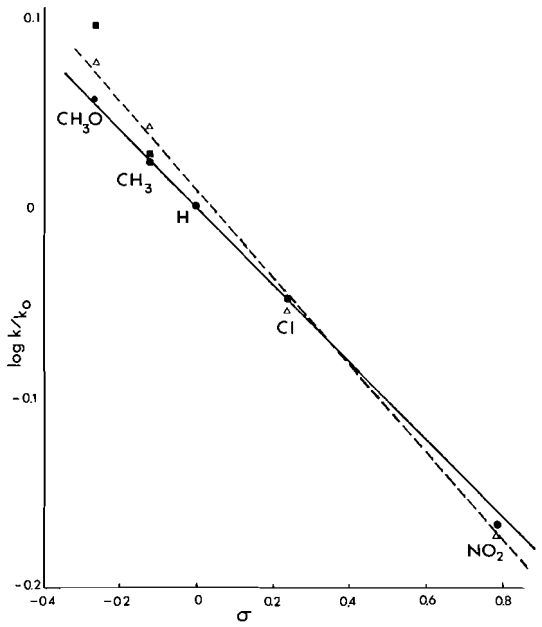

FIG. 1. Plot of $\log k/k_0$ for aldoxime carbonates *vs.* Hammett σ values: (*a*) —△—△—△— 4-substituted benzaldoxime phenyl carbonates in DMSO ($\rho = -0.249$); (*b*) —●—●—●— benzaldoxime 4-substituted phenyl carbonates in DPE ($\rho = -0.213$); (*c*) ■ values for benzaldoxime 4-substituted phenyl carbonates in DMSO. Note, for benzaldoxime 4-chlorophenyl carbonate $\log k/k_0 = 0.782$, and for benzaldoxime 4-nitrophenyl carbonate $\log k/k_0 = 0.578$.

effects operating and also that the transition state has a greater demand for electrons than the ground state. These results would be indicative of a small positive charge build-up on the nitrogen as the N—O bond begins to break.

The effect of substituents on the phenoxide portion of the molecule were next examined by measuring the rates of decomposition of *E*-benzaldoxime 4-substituted phenyl carbonates in DMSO. However, when the $\log k/k_0$ versus σ plot was made for this series, no orderly progression of electronic effects was found (Fig. 1). These substituents would be expected to appreciably affect the electron density around the phenoxide oxygen which should in turn affect the strength of the phenoxide–carbonyl bond and ultimately the stability of the phenoxide ion if it were formed. Electron-releasing groups such as CH_3O— and CH_3— had little effect on the decomposition rates; on the other hand, electron-withdrawing groups such as Cl and NO_2 did enhance the decompositions but to a much greater extent than was originally expected. It is possible that the electron-withdrawing groups affected the strength of the bonds around the carbonyl grouping thereby causing the appearance of a secondary mechanism which is more ionic in nature. Furthermore, the nitro and chloro groups could enhance breakdown of any intermediate to products and CO_2 by stabilizing the phenoxide once it has formed. This coupled with the ability of the solvent (DMSO) to support an ionic mechanism could explain the increased decomposition rate.

In order to substantiate the possible existence of a secondary ionic mechanism, the same *E*-benzaldoxime 4-substituted phenyl carbonates were pyrolyzed in diphenyl ether rather than DMSO and the substituent effects were observed. A Hammett plot in this case (Fig. 1, solid line) gave a straight line of slope −0.213 which indicates that a solvent which does not favor an ionic process returns the decomposition to an orderly dependence on electronic effects. Again the small negative slope indicates that electrons are needed in the transition state but only to a very small extent. A possible explanation for this dependence is that the electrons on the phenolic oxygen are required in the transition state or intermediate; electron-donating groups such as CH_3O— and CH_3— increase this electron density whereas electron-withdrawing groups such as Cl and NO_2 decrease it.

If a highly ionic intermediate or even an appreciable charge build-up were involved in the process, the decomposition rates should show a dependence on solvent polarity. When the decomposition of *E*-benzaldoxime phenyl carbonate was carried out in diphenyl ether, benzonitrile, and dimethyl sulfoxide, *i.e.* solvents of different polarity, the first-order rate constants were 1.81×10^{-4}, 1.5×10^{-4}, and $2.00 \times 10^{-4}\ s^{-1}$ respectively. These extremely close values indicate a very small or almost non-existent solvent effect and would not support the existence of a very charged intermediate. Indeed this lack of solvent effect is analogous to that reported for the Claisen rearrangement (11) of allylic ethers which has been shown to undergo rearrangement via a cyclic, concerted process.

The 4-substituted phenyl carbonates of *E*-benzaldoxime gave similar results when the decompositions were carried out in different solvents. The only variation occurred with the *E*-benzaldoxime-4-chlorophenyl and -4-nitro-

Can. J. Chem. Downloaded from www.nrcresearchpress.com by 210.87.254.40 on 09/05/12
For personal use only.

Can. J. Chem. Downloaded from www.nrcresearchpress.com by 210.87.254.40 on 09/05/12
For personal use only.

phenyl carbonates which decomposed approximately six times faster in dimethyl sulfoxide than in diphenyl ether. This difference in behavior, as already mentioned, could be a result of a change towards a more ionic mechanism and which is supported by the Eyring plots which indicated the appearance of a secondary mechanism in the case of the NO_2 substituted system.

The activation parameters for both the *p*-substituted-*E*-benzaldoxime and *p*-substituted phenyl series were calculated (Table 2) in an attempt to shed some light on the nature of the intermediate in the decomposition. In all cases (except the one given above), the Eyring plots gave straight lines which were used to calculate enthalpies of activation ($\Delta H^{\ddagger}$) and entropies of activation ($\Delta S^{\ddagger}$). The $\Delta H^{\ddagger}$ were approximately 28.4 kcal mol^{-1} for all the systems studied while the $\Delta S^{\ddagger}$ were all very small and mainly positive. The $\Delta S^{\ddagger}$ values were somewhat surprising at first since normally large positive values would be expected for an ionic process and negative values would be expected (11) for a concerted process where a certain amount of orientation is needed in the transition state. The small value for $\Delta S^{\ddagger}$ would seem to indicate that the orientation in the reactant or ground state is very close to that required in the transition state for the process to occur. Thus it would seem that little change in geometry of the molecule was required and the entropy did not change appreciably even when solvents of different polarity were used. This inherent desired orientation can probably be attributed to the imino double bond.

The presence of the imino double bond did present two questions that had to be considered. The first raised the possibility that isomerization was occurring between the *E*- and *Z*-isomers of the carbonates. However, work by Curtin *et al.* (12) on 4-chlorobenzophenone ketoxime methyl ether and by Philips (13) on benzaldoximes would indicate that this type of isomerization is very unlikely under the reaction conditions. The second involved seeing whether the *E*- and *Z*-isomers did actually behave differently *i.e.* was the geometry of the starting aldoxime important in the process. Investigation of this aspect gave some interesting results. When attempts were made to carry out the aldoxime to aldoxime carbonate to nitrile sequence on the *Z*-benzaldoxime, no intermediate carbonate could be isolated. Rather the *Z*-isomer was converted directly to the nitrile, CO_2 and phenol. Thus the *E*- and *Z*-isomers both gave the same final results but the *Z*-isomer required much milder conditions. Apparently two different decomposition paths are involved and a possible explanation for this difference can be found if one considers the various interactions that can occur which are a result of the stereochemistry around the imino double bond. The *E*-form of the benzaldoxime carbonate permits the intramolecular interaction of the phenolic oxygen **1** or carbonyl oxygen **2** with the imino

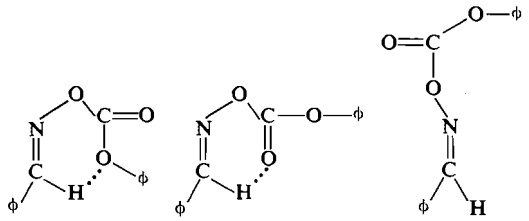

1 **2** **3**

hydrogen which can result in a cyclic transition state and eventually to decomposition. The *Z*-form **3** on the other hand offers no locations for similar major intramolecular overlap or interaction. Thus the imino hydrogen of the *Z*-form could be prone to attack from external reagents such as pyridine to give a simple base-catalyzed *trans* elimination. Banthrope (14) used this argument to explain the much greater ease with which base-promoted formation of nitriles occurred with *Z*-aldoxime acetates than with the *E*-isomers.

Conclusions

From the data obtained in this study, there is little support for the ionic mechanism given in Scheme 1, Path 1*A* or *B*. The low ρ values would not be expected if indeed there were an appreciable charge build-up in the transition state. Furthermore the general lack of dependence of decomposition rate on solvent polarity would not support the presence of an ionic intermediate. The low entropy values indicate the orientation in the ground state is very close to that in the transition state. This along with the difference in behavior between the *E*- and *Z*-isomers would indicate that the *E*-benzaldoxime carbonates undergo decomposition via a cyclic process as indicated in Scheme 1, Path 2.

The authors wish to thank the National Research Council of Canada for financial support of this research in the form of a NRCC Scholarship awarded to P. A. Forte.

1. J. M. PROKIPCAK and P. A. FORTE. Can. J. Chem. **49**, 1321 (1971).
2. D. L. J. CLIVE. Chem. Commun. 1015 (1970).
3. P. J. FOLEY, JR. J. Org. Chem. **34**, 2805 (1969).
4. H. G. FOLEY and D. R. DALTON. J. Chem. Soc. Chem. Commun. 628 (1973).
5. M. J. ZABIK and R. D. SCHUETZ. J. Org. Chem. **32**, 300 (1967).
6. A. PALM and H. WERBIN. Can. J. Chem. **31**, 1004 (1953).
7. H. H. WILLARD, L. L. MERRITT, JR., and J. A. DEAN. Instrumental methods of analysis. 4th ed. Van Nostrand Co. Inc., Toronto. 1965. pp. 152–153.
8. A. R. LEPLEY. J. Am. Chem. Soc. **91**, 1237 (1969).
9. H. R. WARD. Acc. Chem. Res. **5**, 18 (1972).
10. P. R. WELLS. Linear free energy relationships. Academic Press, London. 1968. p. 14.
11. S. J. RHOADS. Molecular rearrangements. *Edited by* P. DeMayo. John Wiley and Sons, New York. 1963. Chapt. 11.
12. D. Y. CURTIN, E. J. GRUBBS, and C. G. MCCARTY. J. Am. Chem. Soc. **88**, 2775 (1966).
13. W. D. PHILIPS. Ann. N.Y. Acad. Sci. **70**, 817 (1958).
14. D. V. BANTHROPE. Elimination reactions. Vol. 2. *Edited by* E. D. Hughes. Elsevier Publishing Co., New York. 1963. p. 143.
15. E. L. PURLEE, R. W. TAFT, JR., and C. A. DEFAZIO. J. Am. Chem. Soc. **77**, 837 (1955).

Can. J. Chem. Downloaded from www.nrcresearchpress.com by 210.87.254.40 on 09/05/12
For personal use only.

The Raman Spectra of some Tricoordinate Halogenocadmate(II) Anions in the Solid State

J. GUILLERMO CONTRERAS
Instituto de Quimica, Universidad de Concepciòn, Casilla 3-C, Concepciòn, Chile
AND
DENNIS G. TUCK
Department of Chemistry, University of Windsor, Windsor, Ontario N9B 3P4

Received June 2, 1975

J. G. CONTRERAS and D. G. TUCK. Can. J. Chem. **53**, 3487 (1975).

The Raman spectra of the solids *n*-$Pr_4N[CdX_3]$, where X is Cl, Br, or I, show that trihalogenocadmate anions possess C_{2v} symmetry in the solid state. Force constants have been calculated using the Urey–Bradley approximation and are correlated with the values reported for other tricoordinate species.

J. G. CONTRERAS et D. G. TUCK. Can. J. Chem. **53**, 3487 (1975).

Les spectres Raman des solides *n*-$Pr_4N(CdX_3)$, où X = Cl, Br ou I, montrent que les anions trihalogénocadmates possèdent une symétrie C_{2v} à l'état solide. On a calculé des constantes de force en faisant appel à l'approximation de Urey–Bradley et on les a reliées avec les valeurs rapportées antérieurement pour d'autres espèces tricoordonnées.

[Traduit par le journal]

Can. J. Chem. Downloaded from www.nrcresearchpress.com by 210.87.254.40 on 09/05/12
For personal use only.

Introduction

Like other d^{10} cations, cadmium(II) forms an interesting range of anionic complexes with halide ligands. The salt K_4CdCl_6 contains octahedral $CdCl_6^{4-}$ anions; (*1*), $CdCl_5^{2-}$ has D_{3h} symmetry; (*2*), and the CdX_4^{2-} complexes (X = Cl, Br, I) must clearly be tetrahedral. The information with respect to the solids $MCdX_3$ is more complicated. Vibrational spectra and X-ray diffraction studies (3, 4) have shown that salts of the type $MCdCl_3$, where M = K, Rb, NH_4, have structures containing anionic chains $(CdCl_3^-)_\infty$ of C_{2h} line group symmetry. On the other hand, the Raman spectra of aqueous and non-aqueous solutions of various $Cd^{2+}:X^-$ ratios (X = Cl, Br, or I) have been studied by Davies and Long (5), who identified CdX_3^- species. In each case, a medium-to-strong polarized Raman band was assigned to the symmetric cadmium–halogen stretching mode. Two depolarized emissions were assigned to the antisymmetric stretching and bending modes of the planar CdX_3^- anion, of D_{3h} symmetry. Sanyal and Singh (6) have calculated Urey–Bradley force constants, using the results reported by Davies and Long, and assuming D_{3h} symmetry.

In contrast, Macklin and Plane (7) studied the stepwise formation of cadmium/bromide complexes in aqueous solutions, and found three bands (173, 73, and 44 cm^{-1}), which they assigned to $CdBr_3^-$ species of C_{3v} symmetry. The failure to observe the other vibrations required for C_{3v} was attributed to the extensive overlap of various other bands. Clarke *et al.* (8) recently reported a Raman emission at 264 cm^{-1} in solutions of $Cd(NO_3)_2$ + KCl in molten sodium nitrate – potassium nitrate mixtures. This vibration was assigned to the $CdCl_3^-$ anion; no corresponding bands from the $CdBr_3^-$ species were detected, in keeping with the fact that $CdBr_4^{2-}$ is the predominant complex ion in solution in the cadmium/bromide melt system.

Some further study of these CdX_3^- systems seems called for, and we have accordingly prepared crystalline salts of these anions with the large tetrapropylammonium cation, and recorded their Raman spectra. Force constant calculations support the assignment of C_{2v} symmetry for the anions in these solids. The results lead to some interesting comparisons with those for the analogous complexes of other d^{10} ions.

Experimental

General

The Raman spectra were recorded on a Laser He/Ne Carry 81 spectrometer. Cadmium analyses were by atomic absorption spectroscopy; halide was analyzed gravimetrically.

TABLE 1. The Raman spectra of the $(C_3H_7)_4NCdX_3$ (X = Cl, Br, or I) species in the solid state (in cm^{-1})

Raman spectra						
$CdCl_3^{-a}$	$(C_3H_7)_4NCdCl_3$	$CdBr_3^{-a}$	$(C_3H_7)_4NCdBr_3^{-a}$	CdI_3^{-a}	$(C_3H_7)_4NCdI_3$	Assignment[b]
265	252 ms	168	164 s	124	118 s	$\nu_1(A_1)$
287	314 ms	184	201 ms	161	171 ms	$\nu_4(B_2)$
	294 s		187 m		162 ms	$\nu_2(A_1)$
90	98 mw	58	77 mw	51	74 w	$\nu_3(A_1)$
	76 mw		58 w		55 w	$\nu_5(B_2)$

[a]Raman spectra for the D_{3h} species in solution (5).
[b]Assignment based on a C_{2v} model.

Preparative

A general preparative method was used throughout this work. Cadmium dihalides were either dissolved or suspended in anhydrous methanol, the stoichiometric amount of the appropriate tetrapropylammonium salt added, and the solution left with stirring for 3–4 h. Solvent was then pumped off and the resulting solid dissolved in a 1:1 mixture of either acetone/acetonitrile or methanol/acetonitrile. Slow evaporation yielded colorless crystals which were recrystallized twice from the same solvent mixtures. Analyses and molar conductivities in acetonitrile (approximate m*M* concentration) are given below.

Anal. Calcd. for $(C_3H_7)_4N{\cdot}CdCl_3$: C, 35.6; H, 6.9; N, 3.5; Cd, 27.8; Cl, 26.3. Found: C, 35.4; H, 7.0; N, 3.4; Cd, 27.7; Cl, 26.3.

$\Lambda_M^{25} = 128\ ohm^{-1}\ cm^{-2}$; m.p. 190 °C.

Anal. Calcd. for $(C_3H_7)_4N{\cdot}CdBr_3$: C, 26.8; H, 5.2; N, 2.6; Cd, 20.9; Br, 44.5. Found: C, 26.9; H, 5.3; N, 2.6; Cd, 20.9; Br, 44.3.

$\Lambda_M^{25} = 131\ ohm^{-1}\ cm^{-2}$; m.p. 193 °C.

Anal. Calcd. for $(C_3H_7)_4N{\cdot}CdI_3$: C, 21.2; H, 4.1; N, 2.1; Cd, 16.6; I, 56.1. Found: C, 21.5; H, 4.1; N, 2.0; Cd, 16.6; I, 56.0.

$\Lambda_M^{25} = 124\ ohm^{-1}\ cm^{-2}$; m.p. = 234 °C.

Calculations

Since no molecular structure parameters are available for these anions, bond distances were taken from the literature (9); the values used were 2.62 and 2.40 Å for Cd—Br and 2.35 and 2.30 Å for the Cd—Cl bond distances. The X—Cd—X angles were all assumed to be 120°.

The normal coordinate analysis utilized the program described by Overend and Scherer (10), with local modifications. The program was set up in cartesian coordinates. Computations were carried out on the IBM 1620 computer of the Universidad de Concepciòn.

The calculations gave values for the five in-plane normal modes; the out-of-plane deformation mode was not calculated.

Results and Discussion

There are pronounced differences between the Raman spectra of $Pr_4N{\cdot}CdCl_3$ and those reported for the solids $MCdCl_3$, where M = K, Rb, NH_4, or Me_4N (3). Since the latter group of compounds involve halogen-bridged structures (3, 5), it is reasonable to assume that the anions are effectively individual units in the tetrapropylammonium salt, due to the effect of the large cation. In view of the agreement between our spectra and those reported for CdX_3^- species in solution (7, 8), we believe that we are observing the Raman emission from discrete CdX_3^- anions.

Table 1 shows the observed spectra, with assignments based on C_{2v} symmetry for the anions, following the work of Davies and Long (5). The splitting of the E' vibrational modes was ascribed to the effect of the site symmetry, which brings about a non-equivalence in one of the halide ligands, possibly through a long contact with another molecule in the unit cell. The molecular symmetry therefore cannot be D_{3h} (or D_3); although vibrational spectroscopy does not allow a differentiation between C_{2v} and C_s symmetries, the former was assumed for all three CdX_3^- species in the present work.

The correlation between the D_{3h} and C_{2v} irreducible representations of the fundamentals can be written as

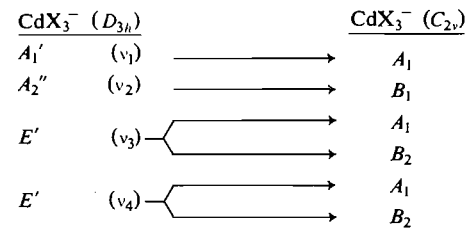

Can. J. Chem. Downloaded from www.nrcresearchpress.com by 210.87.254.40 on 09/05/12
For personal use only.

Can. J. Chem. Downloaded from www.nrcresearchpress.com by 210.87.254.40 on 09/05/12
For personal use only.

TABLE 2. Urey–Bradley force constants list for CdX_3^- complexes (X = Cl, Br, I) (values in 10^5 dyn cm^{-1})

Force constant number	Symbol	Value		
		$CdCl_3^-$	$CdBr_3^-$	CdI_3^-
1	K_I	0.920	0.639	0.574
2	K_{II}	1.348	0.877	0.774
3	H_I	−0.002	−0.017	0.009
4	H_{II}	0.023	0.010	0.057
5	F_I	0.102	0.165	0.115
6	F_{II}[a]	0.114	0.196	0.150

[a]Force constants transferred from ref. 6.

TABLE 3. The vibrational spectrum and potential energy distribution (PED) for the $CdCl_3^-$ anion

Mode	Frequency (cm^{-1})		PED (%) amongst force constants[a]
	Observed	Calculated	
ν_1 } A_1	252	251	80(1)+4(2)+1(6)+14(5)
ν_2 } A_1	294	296	8(1)+82(2)+1(5)+8(6)
ν_3 } A_1	98	98	31(4)−1(3)+22(5)+48(6)
ν_4 } B_2	314	312	97(2)+3(5)
ν_5 } B_2	76	77	1(2)−5(3)+104(5)

[a]Force constant number given in parentheses refers to list in Table 2.

The Raman bands of the solids were assigned by comparison with those reported for the same species in solution (7, 8). Table 1 shows the spectral bands for the solids $[(C_3H_7)_4N][CdX_3]$ (X = Cl, Br, or I) used in our calculations, and their assignments. The spectral results for solutions of CdX_3^- species are also given (5). Force constant calculations using the Urey–Bradley approximation for these species on a C_{2v} model support the conclusion that they possess such a symmetry in the solid state.

In each case we observed one very weak emission, located at 184, 143, and 105 cm^{-1} for the chloro, bromo, and iodo complexes, respectively. This band has been assigned to the $\nu_6(B_1)$ out-of-plane vibrational mode which was not included in the calculations. Since there are six unknown force constants to be calculated from the five vibrational modes, we have used the value of the repulsive force constant, $F_I(X_{II}...X_{II})$ of the corresponding D_{3h} species in solution as calculated by Sanyal and Singh (6). As usual F' was assumed to be equal to $-0.1F$. The set of force constants calculated on this basis are given in Table 2, and the potential energy distribution amongst the force constants is shown in Tables 3 to 5.

The calculated eigenvectors, and the potential energy distribution amongst the force constants, show that ν_4 and $\nu_5(B_2)$ are essentially pure antisymmetric Cd—X_{II} and X_I—Cd—X_{II} stretching and bending modes, respectively. For ν_1, however, there is a significant contribution of K_{II}, varying from 29% for CdI_3^- through 9% for $CdBr_3^-$ to 4% for $CdCl_3^-$, so that the coupling of the Cd—X_I and Cd—X_{II} stretching modes changes appreciably through this series. Similarly, the difference in the corresponding stretching force constants $K_I - K_{II}$ has the values 0.43, 0.24, and 0.20 for X = Cl, Br, and I, respectively; for D_{3h} symmetry, there is one such stretching force constant, so that the difference $K_I - K_{II}$ reflects the extent of the deviation from D_{3h} symmetry. Finally, the splitting of ν_3 mode of the D_{3h} CdX_3^- species into $\nu_2 + \nu_4$ (see Table 1) amounts to 20, 14, and 9 cm^{-1} for $CdCl_3^-$, $CdBr_3^-$, and CdI_3^-. Each of these three tests shows that the $CdCl_3^-$ anion is most strongly distorted from D_{3h} symmetry in the compounds studied, and CdI_3^- the least.[1] Both K_I and K_{II} show a smooth decrease from $CdCl_3^-$ to CdI_3^-,

[1]We are grateful to a referee for suggesting this argument.

Can. J. Chem. Downloaded from www.nrcresearchpress.com by 210.87.254.40 on 09/05/12
For personal use only.

TABLE 4. The vibrational spectrum and potential energy distribution (PED) amongst force constants for the $CdBr_3^-$ anion

Mode	Frequency (cm^{-1}) Observed	Calculated	PED (%) amongst force constants[a]
ν_1	164	162	57(1)+9(2)+27(5)+7(6)
ν_2 A_1	187	189	23(1)+65(2)+12(6)
ν_3	77	77	11(4)−10(3)+67(6)+31(5)
ν_4	201	199	97(2)−1(3)+6(5)−1(6)
ν_5 B_2	58	58	4(2)−51(3)+148(5)

[a]Force constant number given in parentheses refers to list in Table 2.

TABLE 5. The vibrational spectrum and potential energy distribution amongst force constant for the CdI_3^- anion

Mode	Frequency (cm^{-1}) Observed	Calculated	PED (%) amongst force constants[a]
ν_1	118	119	35(1)+29(2)+21(5)+13(6)
ν_2 A_1	162	163	42(1)+45(2)+7(4)+5(6)
ν_3	74	74	4(1)+3(3)+38(4)+19(5)+36(6)
ν_4	171	171	96(2)+1(3)+4(5)
ν_5 B_2	55	55	19(3)+81(6)

[a]Force constant number given in parentheses refers to list in Table 2.

as was found in calculations of the primary stretching force constants of the tetrahedral InX_4^- anions (X = Cl, Br, I) (11), where the values change from 0.760 for $InCl_4^-$ to 0.625 × 10^5 dyn cm^{-1} for InI_4^-. We have discussed previously (11) the dependence of these force constants upon the electronegativity difference $\Delta\chi$ ($= \chi_{halogen} - \chi_{metal}$); in the present work, K_1 and K_{11} clearly change monotonically with $\Delta\chi$. As in the earlier study, the inference that the cadium halide bond is ionic in character is more important than any discussion as to the exact nature of the relationship between K_1 (or K_{11}) and $\Delta\chi$. We also note, in this context, that the stretching force constants for the tetrahedral CdX_4^{2-} species (X = Cl, Br, I) also decrease with decreasing ligand electronegativity (f_r = 1.41, 1.19, and 0.98 × 10^5 dyn cm^{-1} for X = Cl, Br, and I, respectively (5)). These values are smaller than those for the isoelectronic InX_4^- species (11), in keeping with an ionic bonding model.

In our previous work (11), we showed that a linear relationship exists between the logarithim of the stretching force constant and the oxidation state of the metal in the tricoordinate isoelectronic InX_3^{2-}, SnX_3^-, and SbX_3 species. We have tested this relationship against our present results, and find that despite the difference in the symmetry and electronic configuration of the central atom, the values for CdX_3^- fit remarkably well onto the earlier curve. The conclusion is then that for the CdX_3^- and SnX_3^- anions, the difference in stereochemistry has little effect on the stretching force constants, a

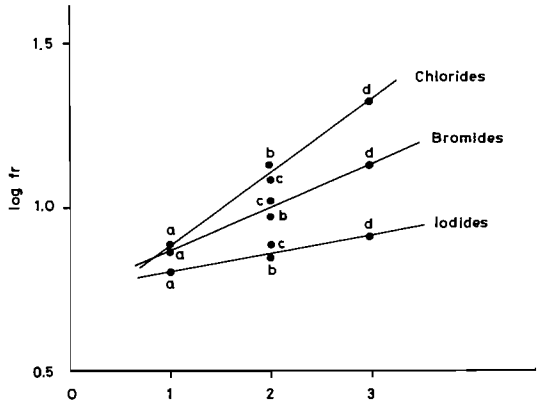

FIG. 1. The dependence of the stretching force constant upon oxidation state for some MX_3 species. *a*, indium; *b*, cadmium; *c*, tin; *d*, antimony.

conclusion which further supports the ionic character of the bonding in these species (Fig. 1).

In summary, the calculated stretching force constants for the CdX_3^- complexes depend on the electronegativity of the ligand in a manner which is very similar to that observed for other related species (11, 12), and which supports the concept of a significantly ionic type of bonding.

1. G. BERGERHOFF and O. SCHMITZ-DUMONT. Z. Anorg. Chem. **284**, 10 (1956).
2. T. V. LONG, A. W. HERLINGER, E. F. EPSTEIN, and I. BERNAL. Inorg. Chem. **9**, 459 (1970).
3. D. M. ADAMS and D. C. NEWTON. J. Chem. Soc. A, 3499 (1971).
4. C. H. MACGILLAVRY, H. NIJUELD, S. DIERDORP, and K. KARSTEN. Rec. Trav. Chim. **58**, 193 (1939).
5. J. E. D. DAVIES and D. A. LONG. J. Chem. Soc. A, 2054 (1968).
6. N. K. SANYAL and B. P. SINGH. J. Pure Appl. Phys. 758 (1971).
7. J. W. MACKLIN and R. A. PLANE. Inorg. Chem. **9**, 821 (1970).
8. J. H. R. CLARKE, P. J. HARTLEY, and Y. KURODO. Inorg. Chem. **11**, 29 (1972).
9. International Tables for X-ray Crystallography. Vol. III, The Kynoch Press, Birmingham, England. 1962.
10. J. OVEREND and J. R. SHERER. J. Chem. Phys. **32**, 1289 (1960).
11. J. G. CONTRERAS and D. G. TUCK. Inorg. Chem. **11**, 2967 (1972).
12. I. WHARF and D. F. SHRIVER. Inorg. Chem. **8**, 914 (1969).

Can. J. Chem. Downloaded from www.nrcresearchpress.com by 210.87.254.40 on 09/05/12
For personal use only.

Coordination Compounds of Indium. Part XXX. Pyrrole Complexes of Indium(III) and Dimethylindium(III)

HENRY L. CHUNG AND DENNIS G. TUCK

Department of Chemistry, University of Windsor, Windsor, Ontario N9B 3P4

Received June 18, 1975

H. L. CHUNG and D. G. TUCK. Can. J. Chem. **53**, 3492 (1975).

Preparative and spectroscopic studies show that the interaction of 2-formylpyrrole, $C_4H_4N{\cdot}CHO$, and 2-acetylpyrrole, $C_4H_4N{\cdot}COCH_3$ (=HL), with In(III) may involve the organic base as either a bidentate organic anion ligand to give InL_3 complexes, (L = 2-acetylpyrrolate only) or as a neutral monodentate species to form $InCl_3{\cdot}3HL$. The spectroscopic and kinetic properties of the organometallic derivatives Me_2InL are also discussed. The polarographic reduction of InL_3 (L = 2-acetylpyrrole anion) involves three one-electron reduction steps.

H. L. CHUNG et D. G. TUCK. Can. J. Chem. **53**, 3492 (1975).

Des études de préparation et de spectroscopie permettent de montrer que l'interaction du formyl-2 pyrrole, C_4H_4NCHO, et de l'acétyl-2 pyrrole, $C_4H_4N{\cdot}COCH_3$ (=HL), avec In(III) peut impliquer la base organique soit sous forme de ligand organique anionique bidentate conduisant à des complexes InL_3, (L = seulement l'acétyl-2 pyrrolate) ou sous forme d'espèces monodentates neutres amenant la formation de $InCl_3{\cdot}3HL$. On discute aussi des propriétés spectroscopiques et cinétiques des dérivés organométalliques Me_2InL. La réduction polarographique de InL_3 (L = anion acétyl-2 pyrrole) implique trois transferts d'un électron.

[Traduit par le journal]

Introduction

One of the interesting features of complexes of indium(III) with bidentate ligands is that polarographic reduction in nonaqueous solvents may take place via three one-electron steps, in contrast to the single three-electron reduction observed for simple In(III) species in aqueous solution. The details of such reduction processes for In(III)–dithiolate and In(III)–diketonate species have been discussed elsewhere (1–3). The original aim of the present work was to prepare complexes of indium(III) with 2-formylpyrrole (**1**; R = H) and related compounds in order to investigate the effect of the group R on the reduction to the formally In(II) and In(I) states, but this was not in fact achieved because the synthesis of the InL_3 complexes proved much more difficult than expected. The preparative and spectroscopic work did, however, reveal that pyrrole derivatives may coordinate as either neutral or anionic ligands. We have also prepared the corresponding Me_2InL complexes, examples of an increasing number of dimethylindium(III) derivatives of bidentate organic bases.

Previous work with pyrrole compounds as ligands has been entirely concerned with transition metals. Emmert *et al.* (4) reported the preparation of the copper(II) complex of 2-formylpyrrole; this compound, the cobalt(III) analog, and related compounds with R = CH_3, were studied spectroscopically by Perry and Weber (5). Davies and Gogan (6) obtained CrL_3 compounds of various pyrrole ligands, starting with $Cr(CO)_6$, and showed that in these compounds the ligand is bidentate and formally anionic, chelating through basic oxygen and nitrogen atoms. Later work by these authors (7), and others (8), established that pyrroles can also function as π-donors, in which the ligand donates electrons from the C_4H_4N ring. To these two modes of ligation can now be added a third, in which the basic oxygen bonds to the metal ion, with retention of the nitrogen acidic proton, which is involved in intramolecular hydrogen-bonding to a halide ligand also coordinated to the metal ion.

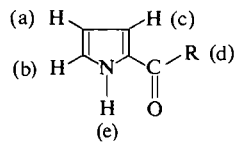

1

R = H; Hpyr.CHO
R = CH_3; Hpyr.$COCH_3$

Can. J. Chem. Downloaded from www.nrcresearchpress.com by 210.87.254.40 on 09/05/12
For personal use only.

TABLE 1. Analytical results for pyrrole derivatives of indium(III)

Compound	Found (%)			Calculated (%)		
	C	H	In	C	H	In
$Me_2In(pyr{\cdot}CHO)$*	35.1	4.1	48.1	35.2	4.2	48.2
$Me_2In(pyr{\cdot}COCH_3)$†	37.2	4.8	45.1	37.9	4.7	45.5
$In(pyr{\cdot}COCH_3)_3$‡	48.0	4.6	26.9	49.2	4.1	26.2
$InCl_3(Hpyr{\cdot}CHO)_3$§	36.0	3.0	22.3	35.5	3.0	22.7
$InCl_3(Hpyr{\cdot}COCH_3)_3$‖	—	—	21.5	—	—	21.0

*pyr·CHO = 2-formylpyrrole anion.
†pyr·$COCH_3$ = 2-acetylpyrrole anion.
‡N; found 9.0%, calculated 9.6%.
§Cl; found 21.1%, calculated 21.1%.
‖Cl; found 19.1%, calculated 19.5%.

Experimental

General, Materials

Spectroscopic and analytical methods were as described in previous work (1–3). Operations involving organoindium compounds were carried out in a dry oxygen-free glove box.

2-Formylpyrrole was prepared according to the method described by Silverstein *et al.* (9). 2-Acetylpyrrole was obtained by a modification of this method; *N,N*-dimethylacetamide (48 g) was treated with phosphorus oxychloride (85 g); after about 15 min, ethylene dichloride (125 ml) was added to the reaction mixture, followed by 34 g of freshly distilled pyrrole in ethylene dichloride (125 ml). This mixture was refluxed for 20 min, cooled to 25 °C, and aqueous sodium acetate (375 g in 500 ml) added. After refluxing for a further 20 min the organic phase was worked up to give a white crystalline material (m.p. 90 °C) which was sublimed *in vacuo*.

Trimethylindium was prepared by the reaction of indium(III) chloride and methyl lithium.

Preparation of Dimethylindium(III) Derivatives

When equimolar quantities of trimethylindium and 2-formylpyrrole were stirred together in dry ether at room temperature, a white precipitate formed after about 5 min. After 30 min, during which time the solution changed from colorless to yellow, the final precipitate was collected and dried *in vacuo*. The compound (dimethylindium(III)-2-formylpyrrolate) is soluble in acetone, methanol, ethanol, dimethylsulfoxide, chloroform, and hot benzene, but insoluble in ether, petroleum ether, carbon tetrachloride, carbon disulfide, and cyclohexane. The solid material darkened on standing over some weeks in a sealed tube. Analytical results for this and other compounds are given in Table 1. The preparation and properties of dimethylindium(III)-2-acetylpyrrolate were similar to those of the formyl compound.

An adduct of dimethylindium(III)-2-formylpyrrolate was prepared by mixing solutions of this compound and 2,2′-bipyridyl in acetone; addition of cyclohexane produced a yellow solid. We were unable to obtain this material in a form suitable for elemental analysis since attempted crystallization gave only gummy solids, but integration of the n.m.r. spectrum of the dissolved material showed that the bipy:pyrrole:CH_3 proton ratio was 8:4:6, as required for a $Me_2In(pyr{\cdot}CHO)(bipy)$ compound.

Attempted Preparations of $In(pyr{\cdot}CHO)_3$

Via Indium(III) Carbonate

Following the work of Emmert *et al.* (4), a suspension of indium(III) carbonate (prepared from the reaction of indium(III) chloride and sodium carbonate) was refluxed with 2-formylpyrrole in xylene. After about 15 min orange crystals were visible, but these proved to be merely contaminated indium carbonate. After longer refluxing (~10 h), the solution phase was evaporated to yield a purple solid which appeared to be polymer contaminated with pyrrole.

Via Solvent Extraction

Indium(III) chloride was dissolved in water and the p*H* adjusted to 6; this solution was then refluxed with a chloroform solution of 2-formylpyrrole. Although this method works successfully for $In(acac)_3$ (10), refluxing over periods from 2 h to 3 days yielded only unchanged pyrrole in the organic phase of the present experiments.

Via Lithium 2-Formylpyrrolate

The lithium derivative of 2-formylpyrrole, prepared by the reaction of the parent compound and methyl lithium suspended in chloroform, was treated with indium chloride in the same solvent. The color of the suspension changed from white through orange to red, but the solution phase did not yield the desired InL_3 compound.

Via $InCl_3(Hpyr{\cdot}CHO)_3$

This complex (see below) was treated with triethylamine in the hope of forming $Et_3NH{\cdot}Cl$ and $In(pyr{\cdot}CHO)_3$. Reaction of these materials in acetone produced an immediate white precipitate, insoluble in water, and containing 18.1% Cl (calculated for Et_3NHCl, 25.8% Cl); the n.m.r. spectrum showed the presence of ethyl groups in the solid. The filtrate from this reaction yielded 2-formylpyrrole as the only significant solid.

Via $Me_2In(pyr{\cdot}CHO)$

Dimethylindium(III)-2-formylpyrrolate and excess of 2-formylpyrrole in toluene were heated in a sealed tube at 110 °C for 10 min, after which the tube was opened and gaseous products removed by pumping. This cycle was repeated six times. The final solution produced brownish crystals on cooling, or on reduction in volume, but this material again proved to be 2-formylpyrrole, and contained no indium.

Preparation of $In(pyr{\cdot}COCH_3)_3$

Dimethylindium(III)-2-acetylpyrrolate and 2-acetylpyrrole (1:3 mole ratio) were heated in benzene in a

Can. J. Chem. Downloaded from www.nrcresearchpress.com by 210.87.254.40 on 09/05/12
For personal use only.

Can. J. Chem. Downloaded from www.nrcresearchpress.com by 210.87.254.40 on 09/05/12
For personal use only.

sealed tube for 10 min, after which the mixture was degassed *in vacuo*. After repeating this cycle six times, the solution was held at 110 °C for 3 days. The solvent was then pumped off, leaving a yellow residue of $In(pyr{\cdot}COCH_3)_3$. The mass spectrum of this solid had strong peaks at *m/e* 115 (In^+), 223 (InL^+), 331 (InL_3^+), and 439 (InL_3^+).

Preparation of $InCl_3(Hpyr{\cdot}CHO)_3$ and $InCl_3(Hpyr{\cdot}COCH_3)_3$

When ether solutions of $InCl_3{\cdot}3H_2O$ and 2-formylpyrrole (1:3 mole ratio) were mixed and stirred at room temperature, a white precipitate began to form after 5 min. After 30 min the solid material was collected, washed, and dried *in vacuo*. This material, $InCl_3(Hpyr{\cdot}CHO)_3$, m.p. 143 °C, is soluble in acetone, ethanol, and dimethylsulfoxide, but insoluble in carbon tetrachloride, benzene, ethylenedichloride, petroleum ether, and carbon disulfide.

The corresponding derivative of 2-acetylpyrrole was prepared by a similar reaction, but the resultant white crystalline solid decomposed very readily on removal of solvent at or below room temperature, so that only indium and chloride analyses were possible, and no spectroscopic results were obtained for this compound. This decomposition, which is not photodependent, involves the loss of a gas identified as hydrogen chloride. In a subsequent experiment, we collected the materials evaporating from the reaction mixture during the final removal of the solvent. No significant material was detected in the first (70 ml) or second (8 ml) fractions, but the final 2 ml contained both H^+ and Cl^-. We return to this point below.

Results and Discussion

Preparative Studies

The present work apparently represents the first attempt to prepare derivatives of pyrrole compounds with main group elements. It is clear that the indium(III) tris(2-formylpyrrolate) complex was not obtained by any of the five methods investigated, despite the fact that the corresponding 2-acetylpyrrole compound is reasonably stable. The reason for the differing behavior of the two compounds is not immediately obvious.

The difficulty in stabilizing indium(III), relative to transition metal species, may reflect extra stabilization in the latter due to delocalization in the metal–ligand ring system. The ready formation of dimethylindium(III) derivatives of both pyrrole anions shows that there can be no steric barrier to the chelation of these ligands to indium(III).

The delocalization has been discussed by Gogan and Davies (6, 7) in terms of the structure and to the extent that this structure depends upon the metal d_π-orbitals, the low stability of the indium(III) compounds may be due to charge being confined to the pyrrole ring.

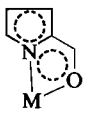

In addition to the difficulties experienced in the preparation of neutral InL_3 species with these pyrroles, we have the formation of unusual adducts in which the pyrrole is a protonated monodentate ligand. The spectroscopic evidence on the structure of these compounds is reviewed below.

Nuclear Magnetic Resonance Spectroscopy

The n.m.r. (^1H) spectra of 2-formyl- and 2-acetylpyrrole are given in Table 2; that for the 2-formylpyrrole is in good agreement with published material (11).

The spectrum of 2-formylpyrrole shows little dependence on solvent apart from a slight shift in the broad and readily identifiable N—H proton signal (e). Similarly, substitution of —CHO by $—COCH_3$ at the 2-position causes a small downfield shift of ~0.40 p.p.m. in the ring proton resonances. The formation of the dimethylindium complexes $Me_2In(pyr{\cdot}CHO)$ and $Me_2In(pyr{\cdot}COCH_3)$ produces a shift of ~0.1 p.p.m. in protons a, b, and c, corresponding to a deshielding associated with electron donation from the chelating oxygen atoms to the Me_2In group. Changes of similar magnitude were observed in the formation of γ-pyrone complexes of indium(III) (2).

It was necessary to obtain the spectrum of $In(pyr{\cdot}COCH_3)_3$ in benzene-d_6 and in consequence a direct comparison with that of $Me_2In(pyr{\cdot}COCH_3)$ in acetone-d_6 is not possible. The ring protons appear to be significantly more deshielded in the former (shifts ~0.3 p.p.m.), relative to the parent ligand. The compound formed by the direct addition of 2-formylpyrrole to indium(III) chloride shows virtually no shift in the resonance of any of the protons.

As part of the n.m.r. studies, we find that a solution of a mixture of $Me_2In(pyr{\cdot}CHO)$ and 2-formylpyrrole in acetone-d_6 at 0 °C shows two resonances in the 9.3 p.p.m. region (−CHO). These resonances coalesce at 35 °C, and from this, and the measured frequency difference of 22.2 Hz between ligand and complex at 0 °C, we calculate that the free energy of ligand exchange in this system is 14.8 kcal mol^{-1}. This value is in the same order as that reported previously for

TABLE 2. Nuclear magnetic resonance spectra of pyrrole derivatives of indium(III), (values in p.p.m. from TMS)

Compounds	Solvent	Assignment* a	b	c	d	e (all br)	Others
Hpyr·CHO	$CDCl_3$	6.37	7.00	7.16	9.53	10.6	
Hpyr·CHO	DMSO-d_6	6.09	6.78	7.02	9.31	11.5	
Hpyr·CHO	Acetone-d_6	6.15	6.83	7.09	9.33	11.2	
Hpyr·$COCH_3$	Benzene-d_6	5.99	6.55	6.78	—	10.99	keto CH_3 1.99
Hpyr·$COCH_3$	Acetone-d_6	5.78	6.48	6.67	—	9.63	keto CH_3 1.92
Me_2In(pyr·CHO)	Acetone-d_6	6.20	6.93	7.18	9.10	abs	CH_3(In) −0.35
Me_2In(pyr·$COCH_3$)	Acetone-d_6	5.67	6.40	6.54	—	abs	CH_3(In) 2.36 keto CH_3 1.78
$InCl_3$(Hpyr·CHO)$_3$	Acetone-d_6	6.15	6.88	7.10	9.29	11.2	
In(pyr·$COCH_3$)$_3$	Benzene-d_6	6.29	6.81	7.08	—	abs	keto CH_3 1.83

*For key to assignments, see 1; abs = sought, but not detected; br = broad; sh = sharp.

ligand exchange involving dimethylindium complexes of β-diketonates (12).

We note finally that solutions of dimethylindium pyrrole species are rather unstable, depositing white solids after some hours at room temperature. The spectra reported are for freshly prepared solutions.

Vibrational Spectra

The vibrational spectrum of 2-formylpyrrole has been analyzed and assigned by Lord and Miller (13). The most important features relevant to the present work are ν(N—H) at 3400 cm^{-1} (br) and ν(C=O) at 1650 cm^{-1}. From our work, the corresponding values in 2-acetylpyrrole are ν(N—H) 3275 and ν(C=O) 1649 cm^{-1}.

The infrared spectra of the two dimethylindium(III) derivatives show an absence of ν(N—H), and a lowering of approximately 50 cm^{-1} in ν(C=O). A band at 725 cm^{-1} in Me_2In(pyr·$COCH_3$), and a shoulder at 720 cm^{-1} in Me_2In(pyr·CHO), are assigned to δ(In—CH_3) by analogy with a number of other dimethylindium(III) derivatives. Both compounds have vibrations which can be assigned to ν(In—CH_3): Me_2In(pyr·CHO), 545s + 480m (i.r.); 546m + 482m (R); Me_2In(pyr·$COCH_3$), 541m + 489mw (i.r.); 544m + 490s (R). Again, these values are in keeping with previous work.

The only interesting features of the infrared spectrum of the complex In(pyr·$COCH_3$)$_3$ are the absence of ν(N—H) and the shift in ν(C=O) to 1640vs cm^{-1}. The latter is, on the face of it, surprisingly small, but mixing of vibrations is believed to hinder the analysis of vibrations in other bis- and tris-chelate systems (e.g. β-diketonates (14)) and the same phenomenon may well be important in the present case. Finally, in $InCl_3$(Hpyr·CHO)$_3$, ν(C=O) is at 1645vs cm^{-1}; ν(N—H) of the free ligand is absent, and a very broad absorption centered at about 2800 cm^{-1} may be the stretching mode of the N—H---Cl system (see below).

Structural Discussion

The spectroscopic and kinetic properties of Me_2In(pyr·CHO) and Me_2In(pyr·$COCH_3$) are in keeping with those of other dimethylindium(III) complexes with bidentate chelate ligands, and require no special comment. It is probable that the solid phase involves polymerization via intermolecular bonding as in Me_2In(OAc) (15). By analogy with the behavior of the latter, the adduct Me_2In(pyr·CHO) (bipy) should be one member of a series of adducts with neutral donors. The failure of the attempts to prepare In(pyr·CHO)$_3$ is puzzling and no specific reason is obvious. The compound In(pyr·$COCH_3$)$_3$ has the properties to be expected of a six-coordinate InO_3N_3 chelate complex.

Finally, we turn to the unusual compounds $InCl_3$(HL)$_3$ (HL = 2-formyl or 2-acetylpyrrole). The n.m.r. spectroscopic evidence (Table 2) shows unambiguously that there are five proton resonances per pyrrole in $InCl_3$(Hpyr·CHO)$_3$, in keeping with the presence of three chloride ligands in the molecule. The simplest assumption then is that intramolecular hydrogen bonding stabilizes the N—H proton. Hydrogen-bonding by pyrrole itself has been the subject of a number of studies. Infrared spectroscopy (16, 17) has been used to show that pyrrole interacts in

Can. J. Chem. Downloaded from www.nrcresearchpress.com by 210.87.254.40 on 09/05/12
For personal use only.

solution with various organic bases, and similar conclusions have been reached from dielectric polarization studies (18–20). Proton n.m.r. results in such systems have been discussed by Reeves (21), Freymann and Freymann (22), and Happe (23). None of these studies, unfortunately, refers to interactions in the solid state, or to pyrroles with substituted basic groups.

The structure

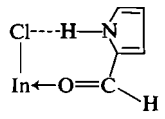

is proposed to explain the bonding in the solid state. Molecular models, based on reasonable interatomic distances, show that the overall molecular structure easily accommodates three such interactions, with three *cis* chlorides. The model appears free of significant strain. The intramolecular stabilization of acidic hydrogen atoms is not unusual; a relevant example is the molecule $[(Meen)_2Cu(CF_3{\cdot}CO{\cdot}CH{\cdot}CO{\cdot}CF_3)_2]$ (Meen = $(CH_3)_2N{\cdot}C_2H_4{\cdot}NH_2$) in which there are two monodentate β-diketonate ligands whose noncoordinated oxygens are each hydrogen-bonded to an NH_2 group of the diamine (24). The n.m.r. results (Table 2) are incompatible with the existence of the above structure in acetone solution, since the spectrum of a freshly prepared solution is almost identical with that of free Hpyr·CHO. This could imply that the solution decomposition process is

$$[1] \qquad InCl_3{\cdot}3HL \rightleftharpoons InCl_3 + 3HL$$

The broad resonance at +11.2 is clearly that of a hydrogen-bonded system, but unfortunately the resonance frequency is an unreliable structural guide in such cases.

An alternative decomposition could be

$$[2] \qquad InCl_3{\cdot}3HL \rightleftharpoons InL_3 + 3HCl$$

and the reality of this process for the 2-acetylpyrrole adduct of $InCl_3$ is illustrated by the loss of HCl in the final stages of the preparative procedure (see Experimental). In this latter system, the existence of a stable InL_3 compound serves to move the equilibrium completely to the right. A solution of $InCl_3(Hpyr{\cdot}CHO)_3$ in acetone turns red–brown on standing at room temperature, again suggesting decomposition by reaction 2. Thus we conclude that the failure to obtain a pure crystalline sample of $InCl_3(Hpyr{\cdot}COCH_3)_3$ is a consequence of the stability of $In(pyr{\cdot}COCH_3)_3$; equally the isolation of $InCl_3(Hpyr{\cdot}CHO)_3$ may in part reflect the instability of $In(pyr{\cdot}CHO)_3$.

The question of why substitution of H by CH_3 in the sidechain at the 2-position of pyrrole has such a pronounced effect on the ligating properties of these compounds must remain unanswered at the present time.

Polarographic Reduction

An initial aim of this work was to investigate polarographic reduction of In(III) pyrrole complexes; in the event we were only able to study $In(pyr{\cdot}COCH_3)_3$. In acetone solution containing the complex and 0.1 *M* $Et_4N{\cdot}ClO_4$, with Ag/AgCl and dropping mercury electrodes, we observed three one-electron reduction steps, with $E_{1/2}{}^{I}$ 0.37 V, $E_{1/2}{}^{II}$ −1.30 V, and $E_{1/2}{}^{III}$ −1.98 V. All three steps are polarographically irreversible (α^{I} 0.14, α^{II} 0.24, α^{III} 0.48). The reduction of 2-acetylpyrrole under the same conditions showed only one polarographic wave, $E_{1/2}$ = −1.60 V (α = 0.31), so that at least the first two reduction steps in InL_3 must be associated with reduction of the complex. In this respect then, $In(pyr{\cdot}COCH_3)_3$ behaves similarly to other neutral indium(III) complexes with bidentate chelating ligands.

This work was supported in part by Operating Grants from the National Research Council of Canada. Dr. J. J. Habeeb is thanked for carrying out the preparative work on $InCl_3(Hpyr{\cdot}COCH_3)_3$.

1. D. G. Tuck and M. K. Yang. J. Chem. Soc. A, 214 (1971).
2. D. G. Tuck and M. K. Yang. J. Chem. Soc. A, 3100 (1971).
3. A. F. Berniaz, G. Hunter, and D. G. Tuck. J. Chem. Soc. A, 3254 (1971).
4. B. Emmert, K. Diehl, and F. Gollwitzer. Ber. **62**, 1733 (1928).
5. C. L. Perry and J. H. Weber. J. Inorg. Nucl. Chem. **33**, 1031 (1971).
6. C. S. Davies and N. J. Gogan. J. Inorg. Nucl. Chem. **34**, 2791 (1972).
7. N. J. Gogan and C. S. Davies. J. Organomet. Chem. **39**, 129 (1972).
8. K. Ofele and E. Dotzauer. J. Organomet. Chem. **30**, 211 (1971).
9. R. M. Silverstein, E. E. Ryskiewicz, and C. Willard. Org. Synth. Coll. Vol. **4**, 831 (1963).
10. C. J. Morgan and H. D. K. Drew. J. Chem. Soc. 1058 (1921).
11. NMR spectra catalog. Varian Associates, Palo Alto, 1963.

Can. J. Chem. Downloaded from www.nrcresearchpress.com by 210.87.254.40 on 09/05/12
For personal use only.

12. H. L. CHUNG and D. G. TUCK. Can. J. Chem. **52**, 3944 (1974).
13. R. C. LORD and F. A. MILLER. J. Chem. Phys. **10**, 328 (1942).
14. K. NAKAMOTO. Infrared spectra of inorganic and coordination compounds, 2nd ed. John Wiley, New York. 1970.
15. F. W. B. EINSTEIN, M. M. GILBERT, and D. G. TUCK. J. Chem. Soc. Dalton Trans. 248 (1973).
16. C. M. HUGGINS and G. C. PIMENTAL. J. Phys. Chem. **60**, 1615 (1956).
17. M. S. NOZARI and R. S. DRAGO. J. Am. Chem. Soc. **92**, 7086 (1970).
18. M. VEYRET and M. GOMEL. C. R. **258**, 4506 (1964).
19. M. GOMEL. C. R. **261**, 403 (1965).
20. R. GIAVARINI and M. GOMEL. C. R. Acad. Sci. Ser. C, **267**, 1 (1968).
21. L. W. REEVES. Can. J. Chem. **35**, 1351 (1957).
22. M. FREYMANN and R. FREYMANN. C. R., **248**, 677 (1959).
23. J. A. HAPPE. J. Phys. Chem. **65**, 72 (1961).
24. M. A. BUSH, D. E. FENTON, R. S. NYHOLM, and M. R. TRUTER. Chem. Commun. 1335 (1970).

Can. J. Chem. Downloaded from www.nrcresearchpress.com by 210.87.254.40 on 09/05/12
For personal use only.

Can. J. Chem. Downloaded from www.nrcresearchpress.com by 210.87.254.105 on 09/05/12
For personal use only.

Acid-catalyzed Reactions of 3β-Acetoxy-9α-hydroxy-11-keto-5α-lanostane: 19(10→9β)*abeo*-lanostenes[1]

OLIVER E. EDWARDS AND ZDSISLAW PARYZEK[2]

Division of Biological Sciences, National Research Council of Canada, Ottawa, Canada K1A 0R6

Received September 9, 1975

OLIVER E. EDWARDS and ZDSISLAW PARYZEK. Can. J. Chem. **53**, 3498 (1975).

Acid-catalyzed dehydration of 3β-acetoxy-9-hydroxy-11-keto-5α-lanostane gave under varying conditions 3β-acetoxy-11-keto-14(13 → 12)*abeo*-lanost-12-ene, or the two cucurbitanes 3β-acetoxy-11-keto-19(10 → 9β)*abeo*-lanost-1(10)-ene and the corresponding 5(10)-ene.

OLIVER E. EDWARDS et ZDSISLAW PARYZEK. Can. J. Chem. **53**, 3498 (1975).

La déshydratation, en milieu acide, de l'acétoxy-3β hydroxy-9 oxo-11 5α-lanostane conduit, suivant les conditions, à l'acétoxy-3β oxo-11 14(13 → 12) *abéo*-lanostène-12 ou aux deux cucurbitanes acétoxy-3β oxo-11 19(10 → 9β) *abéo*-lanostène-1(10) et l'alcène correspondant avec une double liaison en 5,10.

[Traduit par le journal]

Attempts have been made without success in several laboratories to convert lanostane derivatives, by processes involving cationic carbon, into cucurbitanes (1–3).[3] We now report the first such transformation.

The ketol **1**, m.p. 183 °C, $[\alpha]_D$ 63° (*c*, 1.3 in chloroform), ν_{max} ($CHCl_3$) 1712, and 1691 cm^{-1}, was prepared from 3β-acetoxylanost-9(11)-ene(4) via the 9α,11α-diol, m.p. 164 °C. Its structure was confirmed by thionyl chloride – pyridine dehydration to 3β-acetoxy-11-keto-5α-lanost-8-ene. Under Westphalen dehydration conditions (sulfuric acid in acetic acid – acetic anhydride mixture at room temperature), **1** gave two olefinic products A and B in 19 and 15% yields respectively.

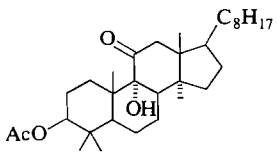

1

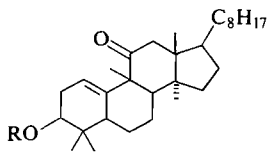

2

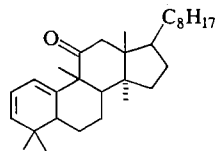

3

Compound A was a trisubstituted olefin, m.p. 84 °C, with ν_{max} ($CHCl_3$) 1725, and 1685 cm^{-1}. The following evidence established its structure as **2** (R = Ac). It gave ^1H n.m.r. signals at δ 5.14 (br s, 1H), 4.84 (dd, 1H), a pair of doublets (2H, Δδ 23 Hz, J = 15 Hz) centered at δ 2.59, and a 3H singlet at δ 2.06. It could be hydrolyzed to an alcohol (**2**, R = H) with c.d.$_{max}$ 300 nm, Δε 4.65 which gave ^{13}C n.m.r. signals at 214, 139, and 119.6 p.p.m. The action of pyridine on the tosylate of this alcohol produced a homo-annular diene **3**, m.p. 115 °C, ν_{max} ($CHCl_3$) 1695 cm^{-1}, M^+ 424, λ_{max} 270 nm, ε 6450. Its ^1H n.m.r. spectrum had a complex group of signals (3H) between δ 5.2 and 5.8.

Oxidation of **2** (R = H) with Jones' reagent gave an amorphous diketone with ν_{max} ($CHCl_3$) 1710 and 1690 cm^{-1}. This gave ^1H n.m.r. signals at δ 5.26 (m, 1H), 2.82 (m, 2H), and 2.62 (pair of doublets, 2H, Δδ 27 Hz, J = 14 Hz). Double irradiation showed that the olefinic proton was coupled with the methylene resonating at δ 2.82. The action of selenium dioxide in hot

[1]Issued as NRCC No. 14960.

[2]NRCC Postdoctorate Fellow. Present address: Instytut Chemii, Uniwersytet A. Mickiewicza, Poznan, Poland.

[3]The multifunctional cucurbitacins are derivatives of 19(10 → 9β)*abeo*-lanostane. We suggest that this skeleton be named cucurbitane.

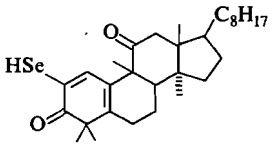

4

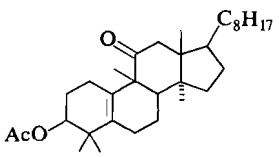

5

wet dioxane on the diketone produced pale yellow needles of a compound with possible structure **4**, m.p. 205 °C, λ_{max} 370 nm, ε 2340, ν_{max} 1690, 1646, and 1623 cm^{-1}, ^1H n.m.r. signals at δ 7.18 (1H) and 2.6 (2H).

Compound B was a tetrasubstituted olefin, m.p. 149 °C whose structure proved to be **5**. It had ν_{max} 1725 and 1690 cm^{-1}, ^1H n.m.r. signals at δ 4.65 (1H), 2.55 (2H), and 2.05 (3H), ^{13}C n.m.r. signals at 216, 180, 134, and 128 p.p.m. and c.d.$_{max}$ 300 nm, Δε 7.5. On hydrolysis this gave an amorphous keto alcohol (Δε 8.0 at 300 nm) which could be oxidized to an amorphous diketone with ν_{max} 1712 and 1693 cm^{-1}. This diketone was oxidized by selenium dioxide in hot wet dioxane to a mixture of a homoannular dienone **6** (36%) (λ_{max} 325 nm, ε 4750, ν_{max} 1690, 1660, and 1625 cm^{-1}) and a 16% yield of **4** thus relating it to A.

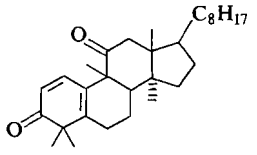

6

The action of anhydrous *p*-toluenesulfonic acid in hot benzene on B gave among other products a 20% yield of an amorphous aromatic compound with ν_{max} ($CHCl_3$), 1690 cm^{-1}; λ_{max} 271 nm (ε 178), 263 nm (ε 220) with intense end absorption. It had ^1H n.m.r. signals at δ 7.08 (s, 3H), 2.7 (t, 2H), 2.53 (s, 2H), 2.30 (s, 3H), and 2.23 (s, 3H). Its mass spectrum had M^+ 424 and intense peaks at *m/e* 317, 304, and 291 corresponding to loss of the aromatic ring and one or two extra carbons respectively. The use of $Eu(dpm)_3$ shift reagent caused rapid movement of both the signal from a methylene group which was originally at δ 2.5 (finally transforming it into a pair of doublets with Δδ 42 Hz and J = 16 Hz (—CH_2CO—)) and a broad signal for a third hydrogen (CHCO). A 3H doublet (CH_3-CHCO) moved with moderate speed as the shift reagent concentration increased. This evidence is consistent with structure **7**, formed in a mechanistically plausible way from a protonated species such as **8**.

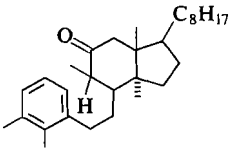

7

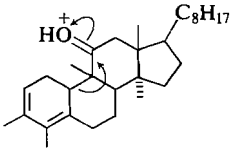

8

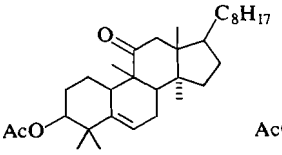

9

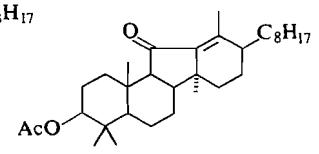

10

24-Deoxybryogenin acetate **9** was prepared from bryogenin. It had m.p. 140 °C, c.d.$_{max}$ 298 nm, Δε 6.6. When treated with *p*-toluenesulfonic acid in benzene as for B it gave a 60% yield of **7** thus interrelating A and B with an authentic cucurbitacin.

As far as we are aware, A and B are the first 19(10 → 9β)*abeo*-lanostane derivatives to be obtained by partial or total synthesis.

The action of *p*-toluenesulfonic acid hydrate in hot benzene on **1**, followed by alkaline hydrolysis, gave among other products the *C*-nor-*D*-homo derivative **10** (3β-hydroxy-11-keto-14(13 → 12)*abeo*-lanost-12-ene). It had m.p. 159 °C, ν_{max} (CH_2Cl_2) 1620 and 1695 cm^{-1}, and λ_{max} 255 nm (ε 15 000) and 356 nm (ε 100). Its ^1H n.m.r. spectrum contained a 3H singlet at δ 2.1. This appears to be the first report of a *C*-nor-*D*-homo lanostane derivative.

We thank Mr. R. Kolt for valuable technical assistance, Dr. R. E. Williams for the circular dichroism measurements, and Dr. I. C. P. Smith and co-workers for the ^{13}C n.m.r. spectra.

1. J. W. ApSimon and J. M. Rosenfeld. Chem. Comm. 1271 (1970). J. M. Rosenfeld. Ph.D. Thesis, Carleton University, Ottawa, Ont. 1970.
2. I. G. Guest and B. A. Marples. J. Chem. Soc. C, 1468 (1971).
3. E. C. Levy and D. Lavie. Isr. J. Chem. **8**, 677 (1970).
4. J. Fried, J. W. Brown, and M. Applebaum. Tetrahedron Lett. 849 (1965).

Can. J. Chem. Downloaded from www.nrcresearchpress.com by 210.87.254.105 on 09/05/12
For personal use only.

Polymerization *in situ* Accompanying Field Desorption Mass Spectrometry

GORDON WALTER WOOD AND DONNA LEE WADE
Department of Chemistry, University of Windsor, Windsor, Ontario N9B 3P4

Received August 11, 1975

GORDON WALTER WOOD and DONNA LEE WADE. Can. J. Chem. **53**, 3500 (1975).

Field desorption mass spectrometry of hydroxycarboxylic acids results in ions corresponding to condensation polymerization with water loss. The phenomenon is particularly marked with 3-hydroxypropanoic acid where at high anode temperatures the base peak corresponds to $6M - 5H_2O$ and ions up to $13M - 12H_2O$ are observed.

GORDON WALTER WOOD et DONNA LEE WADE. Can. J. Chem. **53**, 3500 (1975).

La spectrométrie de masse avec une source à désorption de champ, d'acides hydroxycarboxyliques provoque la formation d'ions correspondants à une polymérisation par condensation avec perte d'eau. Le phénomène est particulièrement marqué avec l'acide hydroxy-3 propanoïque, où à des températures élevées de l'anode, le pic de base correspond à $6M - 5H_2O$ et où on observe des ions jusqu'à $13M - 12H_2O$.

[Traduit par le journal]

We wish to report the first observation of a process in field desorption mass spectrometry (f.d.m.s.) which has the characteristics of thermal polymerization of a hydroxyacid to form polyester chains.

Field desorption mass spectrometry has undergone very rapid growth since its development in 1969, particularly in the 2 years since commercial instrumentation became available (1, 2). The initial emphasis on this technique for determining molecular weights of organic compounds not amenable to electron impact mass spectral study is still evident (3), but the scope of the method has been expanded to include a wide variety of compounds including salts, phospholipids, sugars, amino acids and oligopeptides, metal complexes, and DNA pyrolysis products. During this work it has been discovered that variation of anode heating current produces important changes in spectra. In particular, many compounds give structurally significant fragments at higher temperatures. On the other hand, hydrogen rearrangements and exchange processes frequently make difficult the assignment of structures to *m/e* peaks.

Further difficulty arises from the presence of cluster ions frequently involving several molecules and/or ions. The results to be reported here represent another process with potential for complicating the interpretation of f.d. spectra.

In connection with an extensive survey of the behavior of carboxylic acids and salts on f.d.m.s., we have determined the spectra of a number of hydroxyacids. The compounds tested thus far all show some evidence of condensation accompanied by water loss prior to ionization. For example, lactic, glycolic, and gluconic acids all show ions corresponding to $2M - H_2O$. Lactic acid shows oligomer peaks up to $5M - 4H_2O$, while the other two show 'lactide peaks' at $2M - 2H_2O$. The amino acids threonine and homoserine did not show appreciable evidence of this behavior. The only peak of any significance found was $2M - H_2O$ (3%) in homoserine (4).

Intensities of polymerization peaks are particularly high for 3-hydroxypropanoic acid as shown in Table 1. The base peak of this spectrum is *m/e* 235 which corresponds to $(3M - 2H_2O) + H$. The M + H ion (*m/e* 91) has a relative intensity of 8% and the only true cleavage peak occurs at *m/e* 59 (CH_2COOH). An extensive series of peaks corresponding to $[xM - (x - 1)H_2O] + H$ consists of ions for every value of x from 2 to 9 (*m/e* 163, 235, 307, 379, 451, 523, 595, 667). Of the remaining ions, six may be attributed to $[xM - (x - 2)H_2O] + H$ (*m/e* 470, 541, 613, 685, 756, 829), and another eight appear to be decarboxylation products of the above. About 13 ions are still unassigned; further work will be necessary to discover their origin and to confirm the tentative assignments already made.

An indication of the dependence of the degree of polymerization on anode temperature may be obtained from Table 2. It is apparent that spectra may be recorded over a wide temperature range (approximately 50–200°) with a fairly reg-

Can. J. Chem. Downloaded from www.nrcresearchpress.com by 210.87.254.6 on 09/05/12
For personal use only.

TABLE 1. Field desorption mass spectrum of 3-hydroxypropanoic acid (mol. wt. = 90)*

m/e	Relative intensity (%)	m/e	Relative intensity (%)
59	9	397	15
86	11	407	8
91	8	420	11
163	26	435	11
164	17	451	26
189	13	470	43
235	100†	496	11
236	20	497	17
237	20	522	17
260	9	523	15
291	17	541	22
292	12	562	11
307	78	587	12
308	30	595	17
309	15	613	22
310	15	624	15
335	16	667	13
336	17	675	57
350	12	685	20
353	15	756	22
361	22	784	12
362	17	829	15
379	43		

*Ethanol solution of sample applied to anode by dipping (5). Anode current, 10 mA. Ion source temperature, 45°. Field 10.5 kV. Spectra were obtained with a Varian MAT CH5 DF mass spectrometer equipped with electron impact/field ionization/field desorption source.
†Base peak.

TABLE 2. Effect of anode heating current on degree of polymerization

Current (mA)	Relative intensity (%) of $xM - (x-1)H_2O + H$ for $x =$											
	2	3	4	5	6	7	8	9	10	11	12	13
0	100	73	73	18	32	18						
6	100	75	67	50	58	30						
9	50	100	51	22	14	11	11					
10	26	100	78	43	26	17	17	13				
11	—	21	100	85	44	15	10	10				
12.5	2	21	100	45	18	11	5	2				
13	—	35	59	100	59	47	24	21	24	24		
15	3	3	31	100	38	27	16	8	8	6	5	6
16	—	4	27	100	29	16	14	9	8	3	4	
18	—	—	—	14	100	98	75	23	14	8	8	

ular progression of base peak and highest polymer detected as temperature is increased.[1]

[1]Following a referee's suggestion, we determined the effect on molecular weight distribution of heating the sample-coated anode before applying high voltage. Heating the sample to 15 mA prior to field desorption at 9 mA resulted in an increased degree of polymerization ($x = 4$ became base peak and other intensities were shifted accordingly), indicating that at least part of the observed effect of anode heating arises from thermal polymerization rather than a field effect.

It will be some time before the significance of these results is established, but it is apparent that care must be taken in interpretation of f.d.m.s. whenever molecules containing 2 or more functional groups capable of reaction are involved. Some support for the view that the conditioned field anode should be regarded as a micro-reactor is also provided. The focussing requirements for the polymer ions observed here suggest that ionization may occur outside the

Can. J. Chem. Downloaded from www.nrcresearchpress.com by 210.87.254.6 on 09/05/12
For personal use only.

condensed phase region. However, more detailed study will be required before a mechanism for this process can be proposed.

Support of this work by an Imperial Oil Limited University Research Grant and a major equipment grant from National Research Council of Canada is gratefully acknowledged.

1. G. W. A. MILNE and M. J. LACEY. Crit. Rev. Anal. Chem. **4**, 45 (1974).
2. H. D. BECKEY and H.-R. SCHULTEN. Angew. Chem. Int. Ed. Engl. **14**, 403 (1975).
3. J. O. PEZZANITE, J. CLARDY, P.-Y. LAU, G. WOOD, D. L. WALKER, and B. FRASER-REID. J. Am. Chem. Soc. In press.
4. D. E. SCHMIDT, JR. and S. ASANTE-POKU. Private communication.
5. H. D. BECKEY. Int. J. Mass Spectrom. Ion Phys. **2**, 500 (1969).

Can. J. Chem. Downloaded from www.nrcresearchpress.com by 210.87.254.6 on 09/05/12
For personal use only.

Can. J. Chem. Downloaded from www.nrcresearchpress.com by 210.87.254.42 on 09/05/12
For personal use only.

Canadian Journal of Chemistry

Published by
THE NATIONAL RESEARCH COUNCIL OF CANADA

Journal canadien de chimie

Publié par
LE CONSEIL NATIONAL DE RECHERCHES DU CANADA

Volume 53 Number 23 December 1, 1975

Volume 53 numéro 23 1 décembre 1975

Secondary β-Hydrogen Isotope Effects in Ketal Formation Equilibria[1]

VALERIE A. STOUTE AND MITCHELL A. WINNIK[2]

Erindale College and Lash Miller Laboratories, Department of Chemistry, University of Toronto, Toronto, Ontario M5S 1A1

Received June 5, 1975

VALERIE A. STOUTE and MITCHELL A. WINNIK. Can. J. Chem. **53**, 3503 (1975).

An n.m.r. technique was used to measure K_H/K_D of ketal formation in methylene chloride solution for acetone and phenylacetone. For acetone, $K_H/K_D = 0.95$ per D for methyl ketal formation. Phenylacetone-1,1-d_2, -3,3,3-d_3, and -1,1,1,3,3-d_5 were examined for both dimethyl and ethylene ketal formation. For both ketals, $K_H/K_D = 0.91$ per D, for each ketone. Liquid scintillation counting was used to examine K_H/K_T for ketal formation in methylene chloride. An extraordinarily large isotope effect was found for ethylene ketal formation in 1,3-diphenylacetone. Here $K_H/K_T = 0.67$ for one tritium atom. This isotope effect is too large to arise from hyperconjugative effects alone. It must have a substantial steric component.

VALERIE A. STOUTE et MITCHELL A. WINNIK. Can. J. Chem. **53**, 3503 (1975).

On a utilisé une technique de r.m.n. pour mesurer le K_H/K_D de la formation de cétals de l'acétone et de acétophénone en solution dans le chlorure de méthylène. Pour l'acétone, $K_H/K_D = 0.95$ par D pour la formation du cétal de méthyl. On a étudié les formations des diméthyl et éthylène cétals des phénylacétones -1,1-d_2, -3,3,3-d_3 et -1,1,1,3,3-d_5. Pour les deux cétals on a trouvé un $K_H/K_D = 0.91$ par D pour chaque cétone. On a utilisé le comptage par scintillation liquide pour étudier le K_H/K_T de la formation des cétals en solution dans le chlorure de méthylene. On a trouvé qu'il y a un effet isotopique très grand pour la formation de l'éthylène cétal de la diphényl-1,3 acétone. Dans ce cas, le $K_H/K_T = 0.67$ pour un atome de tritium. Cet effet isotopique est trop grand pour dériver uniquement d'effets d'hyperconjuguaison; il doit y avoir en plus une composante stérique.

[Traduit par le journal]

The wealth of secondary deuterium isotope data on the kinetics of nucleophilic addition to carbonyl compounds, (1) and hydrolysis of ketone adducts, (2) has not been accompanied by a similar effort to determine isotope effects on corresponding carbonyl addition equilibria (3). Equilibrium isotope effects serve as an important point of reference for kinetic isotope effects studies (3*c*). The latter are easier to carry out. Results can be obtained with greater precision, and, for the most part, that has been where the attention has been focused.

In the course of our studies of isotope effects in the Baeyer–Villiger reaction, (4) it became necessary to model the isotope effect on the pre-equilibrium step. This meant determining an equilibrium isotope effect for an appropriate reaction involving nucleophilic addition to a ketone. Since we were concerned with an oxygen nucleophile, hemiketal or ketal formation seemed appropriate. In our original communication (4) we reported application of the method of Jones and Bender (3*a*) to obtain the isotope effect for hemiketal formation in phenyl-2-pro-

[1]The experimental results in this paper are taken from the Ph.D. Thesis of V.A.S.

[2]Author to whom correspondence should be addressed.

Can. J. Chem. Downloaded from www.nrcresearchpress.com by 210.87.254.42 on 09/05/12
For personal use only.

panone (phenylacetone). In this approach, the ketone, in methanol–dioxane, is treated with an acid catalyst and the equilibrium concentrations of all species are inferred from the decrease in carbonyl absorbance. This approach is unsatisfying, not only because of scatter in the data, and not only because the data unexpectedly required extrapolation of equilibrium constants to zero ketone concentration, but also because the spectroscopic technique does not guarantee that one is looking only at hemiketal formation.

Lamaty and co-workers have published extensive studies of kinetic isotope effects in the addition of nucleophiles to ketones (1*c*, 1*d*, 3). Among the nucleophiles studied is bisulfite (3*b*). Here secondary deuterium isotope effects on the kinetics of dissociation of the bisulfite addition complex were measured. K_H/K_D has been measured in this system and k_H/k_D for formation of the complex calculated from these data.

Isotope effects on equilibria of addition to aldehydes have recently been reported (3*c*). These isotope effects derive from substitution of deuterium for the aldehyde proton, and are properly referred to as α-isotope effects. Our concern is the perturbation of ketone-addition equilibrium constants by deuterium and tritium substitution at carbons adjacent to the carbonyl. These are called β-isotope effects. These β-isotope effects are related to β-isotope effects in solvolysis reactions (5, Chapt. 2, 6).

From the work of Lamaty and co-workers (3*b*) and of Bender and co-worker (3*a*) it is clear that nucleophilic addition to carbonyls gives rise to inverse β-deuterium isotope effects, $K_H/K_D < 1$. The magnitude of these isotope effects (*i.e.* the degree to which K_H/K_D differs from 1.0) is significantly greater than kinetic isotope effects for addition to carbonyls (1, 3*c*). Much more is known about the variation of k_H/k_D with changes in ketone and nucleophile structure than about K_H/K_D. To understand kinetic isotope effects sufficiently to use them for inferring the position of the transition state along the reaction coordinate, corresponding values for k_H/k_D and K_H/K_D must be obtained. Lamaty has accomplished this for bisulfite additions to ketones (3*b*).

We have turned to an n.m.r. method to determine isotope effects in ketone–ketal equilibria in an unambiguous manner. What we wished to obtain was the ratio of equilibrium constants for reactions 1 and 2 under conditions in which hemiketal formation would be unimportant and the concentrations of all species at equilibrium could be monitored.

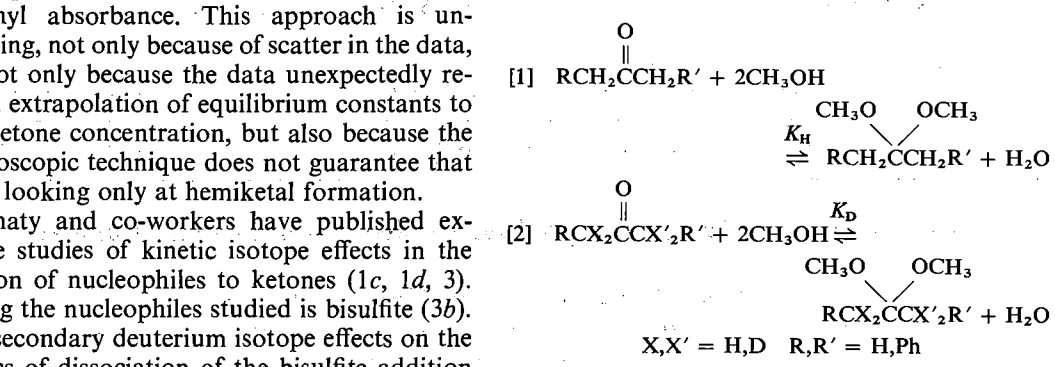

We recognized (5, p. 97) that the equilibrium constant for reaction 3 was equal to the isotope effect on reactions 1 and 2, $K_3 = K_H/K_D$. The isotope effect could be obtained by mixing solutions of the deuterated ketone and undeuterated ketal, effecting equilibrium by addition of an acid catalyst, and observing all species by n.m.r.

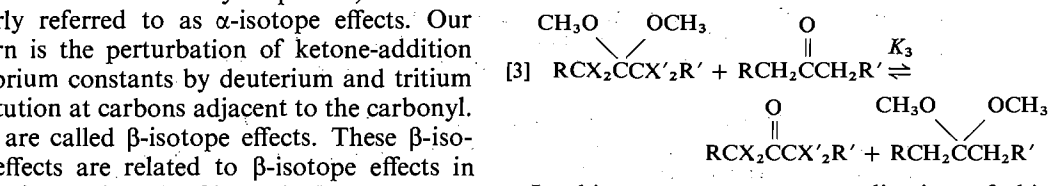

In this paper we report application of this method to determine K_H/K_D for acetone dimethyl ketal formation, and for formation of both dimethyl and ethylene glycol ketals of three specifically-deuterated phenylacetones. A modified approach allowed us to measure K_H/K_T, by scintillation counting, for formation of the ethylene glycol ketal of tritiated dibenzyl ketone.

Results

Most reactions were carried out in dry methylene chloride solution. Reactions of acetone were also examined in 1,1,2,2-tetrachloroethane (*sym*-TCE). $BF_3 \cdot Et_2O$ was used as the acid catalyst. For the reactions discussed here, equilibrium was achieved in 2–10 h at room temperature (22 ± 1 °C), although reactions in some cases were examined up to 48 h after adding catalyst. The catalyst could be quenched by removing solvent and catalyst at reduced pressure. Monitoring the n.m.r. intermittently after several hours gave identical results. For tritiated

Can. J. Chem. Downloaded from www.nrcresearchpress.com by 210.87.254.42 on 09/05/12
For personal use only.

dibenzyl ketone, the approach to equilibrium could not be followed by n.m.r. Instead, the reaction was examined at successive reaction times until K_H/K_D became constant.

Proton–deuterium and proton–tritium exchange was a constant source of concern. The methylene position in phenyl acetone and dibenzyl ketone exchanges readily in base, more slowly in acid. Strict controls were run in which deuterated, partially deuterated, and tritiated ketones were exposed to the reaction conditions and then examined by n.m.r. and mass spectrometry. No exchange was detectable under these reaction conditions. In addition, all ketals were unchanged when exposed to the reaction conditions.

One technique was used to measure the isotope effects in the phenylacetone and acetone systems. In these series of experiments, the equilibrium isotope effect is given by Eq. 4.

$$[4]\quad \frac{K_H}{K_D} = K_3 = \frac{[\text{ketone} - d_x]_{eq}[\text{ketal} - d_0]_{eq}}{[\text{ketone} - d_0]_{eq}[\text{ketal} - d_x]_{eq}}$$

(*i*) For phenylacetone, values of K_H/K_D were determined both for dimethyl ketal formation and for ethylene ketal formation. These were obtained for each of the three deuterated species $PhCD_2COCH_3(d_2)$, $PhCH_2COCD_3(d_3)$, and $PhCD_2COCD_3(d_5)$. Mixtures of the deuterated ketones and undeuterated ketals were dissolved in dry methylene chloride. $BF_3 \cdot Et_2O$ in dry methylene chloride was added as a catalyst. The reaction was monitored by n.m.r. Once equilibrium was established, the solvent and catalyst were distilled off at room temperature. The relative concentrations of the deuterated and nondeuterated species were calculated from the n.m.r. spectrum and substituted into Eq. 4 to yield K_H/K_D.

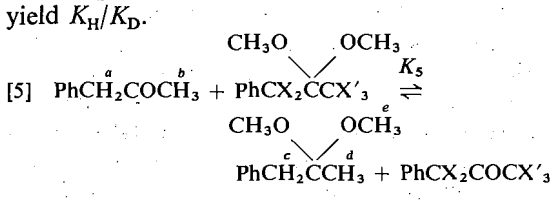

[5] $PhC\overset{a}{H}_2COC\overset{b}{H}_3 + PhCX_2CCX'_3 \overset{K_5}{\rightleftharpoons} PhC\overset{c}{H}_2C\overset{d}{C}H_3 + PhCX_2COCX'_3$

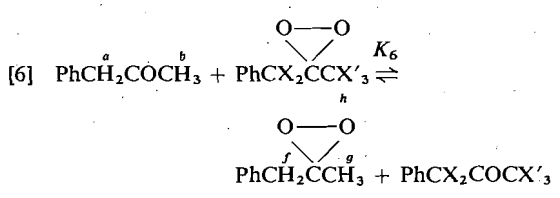

[6] $PhC\overset{a}{H}_2COC\overset{b}{H}_3 + PhCX_2CCX'_3 \overset{K_6}{\rightleftharpoons} PhC\overset{f}{H}_2C\overset{g}{C}H_3 + PhCX_2COCX'_3$

For the equilibrium mixtures in Eqs. 5 and 6 the equilibrium constants could be obtained by direct manipulation of the various n.m.r. intensities. The protons labelled by *a*, *b*, *c*, *d*, *e* and the phenyl hydrogens *p* in Eq. 5 all show discrete and resolved signals (see Table 1). The integrals for each signal were normalized by dividing the integral by the number of hydrogens contributing to the signal. These normalized values I_x were taken to be representative of the concentration of the species *x* in the mixture (Eqs. 7–14). Eq. 16 gives the equilibrium isotope effect for both d_3 and for d_5, while Eq. 17 allows K_H/K_D to be obtained for d_2 and d_5.

$$[7]\quad \text{Total } [\text{ketal}]_{eq} \propto I_e$$

$$[8]\quad [\text{ketal} - d_0]_{eq} \propto I_c \quad \text{or} \quad I_d$$

$$[9]\quad [\text{ketal} - d_x]_{eq} \propto (I_e - I_c) \quad \text{or} \quad (I_e - I_d)$$

$$[10]\quad \frac{[\text{ketal} - d_0]_{eq}}{[\text{ketal} - d_x]_{eq}} = \frac{I_c}{I_e - I_c} \quad \text{or} \quad \frac{I_d}{I_e - I_d}$$

$$[11]\quad \text{Total } ([\text{ketal}]_{eq} + [\text{ketone}]_{eq}) \propto I_p$$

$$[12]\quad \text{Total } [\text{ketone}]_{eq} \propto (I_p - I_e)$$

$$[13]\quad [\text{ketone} - d_0]_{eq} \propto (I_a \quad \text{or} \quad I_b)$$

$$[14]\quad [\text{ketone} - d_x]_{eq} \propto I_p - (I_e + I_a) \quad \text{or} \quad I_p - (I_e + I_b)$$

TABLE 1. Nuclear magnetic resonance shifts for the compounds in the ketal–ketone equilibrium mixtures

Compound	δ(p.p.m.)[a]
$PhC\overset{a}{H}_2COC\overset{b}{H}_3$	*a* 3.55 *b* 2.00
$CH_3O\ \ OC\overset{e}{H}_3$ $PhC\overset{c}{H}_2C\overset{d}{C}H_3$	*c* 2.80 *d* 1.00 *e* 3.15
$O\ \ O$ (h) $PhC\overset{f}{H}_2C\overset{g}{C}H_3$	*f* 2.80 *g* 1.15 *h* 3.65
$CH_3COC\overset{i}{H}_3$	*i* 2.10
$CH_3O\ \ OC\overset{k}{H}_3$ $CH_3C\overset{j}{C}H_3$	*j* 1.20 *k* 3.10

[a]Downfield from internal TMS.

Can. J. Chem. Downloaded from www.nrcresearchpress.com by 210.87.254.42 on 09/05/12
For personal use only.

$$[15]\quad \frac{[\text{ketone} - d_x]_{eq}}{[\text{ketone} - d_0]_{eq}} = \frac{I_p - (I_e + I_a)}{I_a} \quad \text{or} \quad \frac{I_p - (I_e + I_b)}{I_b}$$

$$[16]\quad \left(\frac{K_H}{K_D}\right) = \left(\frac{I_p - (I_e + I_b)}{I_b}\right)\left(\frac{I_d}{I_e - I_d}\right) \quad \text{for } d_3 \text{ and } d_5$$

$$[17]\quad \left(\frac{K_H}{K_D}\right) = \left(\frac{I_p - (I_e + I_a)}{I_a}\right)\left(\frac{I_c}{I_e - I_c}\right) \quad \text{for } d_2 \text{ and } d_5$$

For the ethylene ketals in reaction 6, the methylene signals a overlapped part of the ketal signals h. We were able to correct for the appropriate intensity of h and obtain I_a by difference. The equilibrium constants for reaction 6 are described by equations identical to 16 and 17 with I_h substituted for I_e, and I_f and I_g substituted respectively for I_c and I_d.

(*ii*) A small modification of this method was necessary for calculation of K_H/K_D for equilibria involving acetone. There is no way of obtaining, from the n.m.r. spectrum of the equilibrium mixture, the relative concentrations of the deuterated and non-deuterated acetone present. If the system is depicted by Eq. 18, K_H/K_D is given by Eq. 19.

[18]

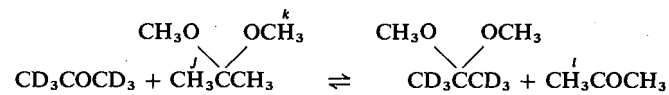

Initially:	$[a]$	$[b]$	0	$[c]$
At equilibrium:	$[a - x]$	$[b - x]$	$[x]$	$[c + x]$

$$[19]\quad \frac{K_H}{K_D} = \frac{[a - x][b - x]}{[c + x][x]}$$

The relative ketal concentrations can be calculated (Eqs. 20–23) from the n.m.r. spectrum as before. Equation 23 can be solved for x and this value, along with the known concentrations $[a]$, $[b]$, $[c]$, can be substituted into Eq. 19. The concentration $[c]$ derives from a small and unavoidable amount of acetone in the freshly distilled 2,2-dimethoxypropane.

$$[20]\quad \text{Total } [\text{ketal}]_{eq} \propto I_k$$

$$[21]\quad [\text{ketal} - d_0]_{eq} \propto I_j$$

$$[22]\quad [\text{ketal} - d_x]_{eq} \propto (I_k - I_j)$$

$$[23]\quad \frac{[\text{ketal} - d_0]}{[\text{ketal} - d_x]} = \frac{[b - x]}{[x]} = \frac{I_j}{I_k - I_j}$$

(*iii*) The equilibrium with dibenzyl ketone could not be monitored by n.m.r. Furthermore, once equilibrium was achieved and the catalyst removed under vacuum, problems arose in attempts to separate and purify ketone and ketal. The most serious problem was that chromatography of the ketone on Florisil, alumina, or silica gel resulted in loss of radiolabel. Control experiments indicated that dibenzyl ketone could be reduced to 1,3-diphenyl-2-propanol with lithium aluminum hydride in ether at −78 °C, without loss of molar activity, M.

[24]

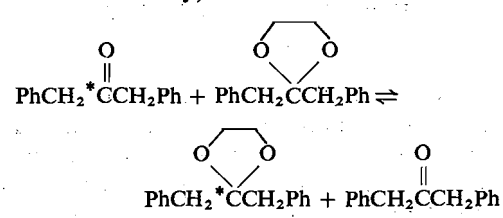

$$[25]\quad \frac{K_H}{K_T} = \frac{M_{ketone}}{M_{ketal}}$$

The equilibrium mixture of ketone and ketal in ether was treated with lithium aluminum hydride at −78 °C. The product diphenylpropanol and unreacted ketal were chromatographed on activity II alumina using methanol–hexane as the eluting solvents. Radioactivities of the purified compounds were measured by scintillation counting. Absolute molar activities were not calculated. The a.e.s. (automatic external standardization) ratios of the ketal, ketone, and alcohol were found to be identical. Relative molar activities were obtained; $M_{alcohol}$ was substituted for M_{ketone}; and K_H/K_T was obtained from Eq. 25.

Can. J. Chem. Downloaded from www.nrcresearchpress.com by 210.87.254.42 on 09/05/12
For personal use only.

TABLE 2. Equilibrium isotope effects

System	Ketone	Isotopic purity (%)	Ketal	K_H/K_D[a,b,c]
1.	$PhCD_2COCD_3$	96.8	$PhCH_2C(OCH_3)_2CH_3$	0.63±0.02
2.	$PhCD_2COCD_3$	96.8	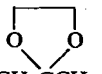	0.60±0.02
3.	$PhCD_2COCH_3$	85.6	$PhCH_2C(OCH_3)_2CH_3$	0.85±0.03
4.	$PhCD_2COCH_3$	85.6	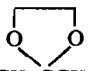	0.82±0.03
5.	$PhCH_2COCD_3$	90.5	$PhCH_2(OCH_3)_2CH_3$	0.74±0.05[d]
6.	$PhCH_2COCD_3$	90.5	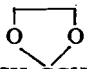	0.75±0.04
7.	$PhCH_2{}^*COCH_2Ph$	—	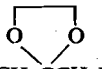	0.67±0.02[e]
8.	CD_3COCD_3	97.0	$CH_3C(OCH_3)_2CH_3$	0.72±0.05 0.70±0.03[f]

[a]All values of K_H/K_D were calculated from the n.m.r. spectra of equilibrium mixtures. These values are the averages of five experiments.
[b]In methylene chloride solution using $BF_3{\cdot}Et_2O$ as the catalyst.
[c]Corrected to 100% isotopic abundance.
[d]Calculated from $(K_H/K_D)_{d_3} = (K_H/K_D)_{d_5}/(K_H/K_D)_{d_2}$ = SYSTEM 1/SYSTEM 3.
[e]K_H/K_T, calculated from scintillation counting experiments.
[f]In *sym*-tetrachloroethane solvent using $BF_3{\cdot}Et_2O$ as a catalyst.

The extraordinary magnitude of the isotope effect in reaction 24 suggested special care in examining the validity of our experimental method. Since K_H/K_T is inverse, we were concerned that the number we obtained might be artificially too small. Two factors convince us that this is not the case. First, lithium aluminum hydride reduction of the ketone, followed by chromatography of the alcohol and distillation, gave diphenylpropanol with the same molar activity as that of the starting ketone. Second, the molar activity of the ketal plus that of the diphenylpropanol equalled that of the starting ketone. These controls demand that artifacts in K_H/K_T be less than one percent.

Discussion

Calculated equilibrium isotope effects are presented in Table 2. In each case, the isotope effects are strongly inverse, $K_H/K_D < 1.0$. Inverse β-deuterium isotope effects in carbonyl addition reactions are associated with decrease in the positive charge on the carbonyl carbon in rehybridization from sp^2 to sp^3 (3, 5, 6). The relationship between the magnitude of the β-deuterium isotope effect and the amount of positive charge at the adjacent carbon is well demonstrated by three examples taken from the literature. Protonation of acetophenone (7), (Eq. 26), occurs with a large isotope effect. Solvolysis of acetyl chloride (1*e*), (Eq. 27), in 10% and 20% aqueous acetone has a kinetic β-isotope effect in the opposite direction to that of the base catalysed hydrolysis of acetate esters (1*e*). The β-isotope effect is a useful probe of charge development at an adjacent center. This makes it particularly useful for studies of solvolysis reactions (8). Other factors, however, are involved.

[26] 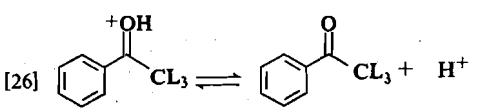

L = H, D $K_H/K_D = 0.76$

Can. J. Chem. Downloaded from www.nrcresearchpress.com by 210.87.254.42 on 09/05/12
For personal use only.

[27] $CL_3\overset{\overset{O}{\|}}{C}Cl \rightarrow [CL_3C{\equiv}\overset{+}{O}] \rightarrow CL_3CO_2H$

10% H_2O–acetone $k_H/k_D = 1.62$

[28] $CL_3\overset{\overset{O}{\|}}{C}OC_2H_5 + OH^- \rightarrow [CL_3C(O^-)(OH)OC_2H_5] \rightarrow CL_3CO_2^- + C_2H_5OH$

$k_H/k_D = 0.90$

Isotope effects arise from changes in zero-point energies for C—H and C—D vibrational modes in going from reactants to the transition state (k_H/k_D) or products (K_H/K_D). These changes derive from changes in force constants for the respective modes, which in turn are determined by the shapes of the potential energy wells associated with the C—H bonds at which attention is focused (ref. 5, Chapt. 4 and p. 138). Steeper wells give rise to larger force constants, with greater separation of C—H and C—D zero-point energies.

Isotopic substitution does not affect the shape of the electronic energy surface. The origin of secondary hydrogen isotope effects is purely vibrational. An explanation of the magnitude of isotope effects observed in an experiment must be couched in terms of the effect (steric, electronic) of the rest of the molecule on the C—H and C—D vibrations (ref. 5, Chapt. 4 and p. 138, and ref. 9).

V. J. Shiner has pointed out (ref. 5, p. 97) that there are two major contributors to β-isotope effects; the extent of nuclear attachment at the reactive carbon and the internal electronic distribution. The latter factor is sensitive to the dihedral angle between the β C—H or C—D bond and a p orbital at the electron deficient carbon. The charge induces a dipole into those adjacent C—H bonds with proper overlap. The C—H potential energy well is broadened, giving rise to weaker force constants, larger vibrational amplitudes, and decreased separation of C—H and C—D zero-point energies (ref. 5 Chapt. 4 and p. 138).

While the word 'hyperconjugation' is properly used to describe these dipole-induced dipole interactions, explanations which cite the greater polarizability of C—H bonds adjacent to a charge as the source of the β-isotope effect, focus on the wrong part of the potential energy surface. Hyperconjugation is a word commonly used. Keeping in mind its proper focus, we have found both the concept and the word convenient.

In these terms, the major contributor to the inverse isotope effects presented in Table 2 is the loss of hyperconjugative delocalization when the ketones react to form ketals. The most compelling evidence for this point of view is the nearly identical isotope effects observed for both dimethyl ketal and ethylene glycol ketal formation from the three different deuterated phenyl-2-propanones. Small changes in ketal structure apparently do not perturb the equilibrium isotope effects.

In the phenyl-2-propanones, the β-isotope effects are cumulative. For ethylene glycol ketal formation K_H/K_D for $d_2 = 0.82$, K_H/K_D for $d_3 = 0.75$, and their product $(0.75)(0.82) = 0.615$. This value compares favorably with the value 0.60 ± 0.02 measured for d_5. Cumulative kinetic isotope effects were observed for these three ketones in their Baeyer–Villiger oxidation (4). Both results imply that $PhCD_2$— and CD_3— make the same contribution to the isotope effect in d_5 and in d_2 and d_3, respectively.

From the tritium isotope effect K_H/K_T for dibenzyl ketone, one can calculate from the Swain–Schaad equation, [29], (10) the corresponding isotope effect associated with a single deuterium. For dibenzyl ketone we calculate $K_H/K_D = 0.76$

$$[29] \qquad \frac{K_H}{K_D} = \left[\frac{K_H}{K_T}\right]^{0.693}$$

The isotope effect for dimethyl ketal formation in acetone is significantly smaller than that for phenylacetone. On a per-deuterium basis, these differences become even more striking (see below).

In Table 3, our experimental results are presented in terms of the secondary β-isotope effect per deuterium. It is customary to present these results as $\Delta\Delta G/n$ values, where $\Delta\Delta G^0$ and $\Delta\Delta G^{\ddagger}$ are, respectively the change in standard free energy or activation free energy, in cal/mol, for substituting n hydrogens with deuteriums. Before commenting on the implications of the data, we ask the reader to note that small changes in K_H/K_D per D lead to large changes in $\Delta\Delta G/n$, and that the K_H/K_D values from which the $\Delta\Delta G^0/n$ values are calculated, for all examples in Table 3, are known only to about ± 0.01.

One obvious and important conclusion from the data in Table 3 is that deuterium substitution at CH_2 and CH_3 in phenylacetone contributes equally to the observed isotope effect.

TABLE 3. Equilibrium and kinetic isotope effects on ketone-addition reactions

Ketone	Ketal K_H/K_D per D	$\Delta\Delta G^\circ/n$ Ketal	$\Delta\Delta G^\circ/n$ Hemiketal	$\Delta\Delta G^\circ/n$ Bisulfite[a]	$\Delta\Delta G^*/n$ BH_4[b]	$\Delta\Delta G^*/n$ HSO_3^-[a]	$\Delta\Delta G^*/n$ NH_2OH[c]
CH_3COCH_3	0.95[d] 0.94[i]	32±2 35±4	26±5[f]	26	3.6	9	8
Ph$CH_2CO$$CH_3$	0.91[d] 0.90[e]	55±4 60±4	46±10[g]	28		14	21
Ph$CH_2$$COCH_3$	0.92[d] 0.91[e]	48±10 55±10	42±10[g]				
$PhCH_2CO$$CH_3$	0.90[d] 0.91[e]	60±13 55±11	47±15[g]				
Ph$CH_2$$COCH_2Ph$	0.76[h]	160±15					34
Cyclopentanone	—	—	54[f]	58		33	25

[a]Data from ref. 3*b*.
[b]Data from ref. 1*c*.
[c]Data from ref. 1*d*.
[d]Methyl ketal formation.
[e]Ethylene glycol ketal formation.
[f]Data from ref. 3*a*.
[g]Data from ref. 4.
[h]Calculated from corresponding K_H/K_T value, see text.
[i]*Sym*-tetrachloroethane solvent.

This result is somewhat surprising (3*b*). It is often found that β-isotope effects, per deuterium, are larger for methylene than for methyl (11). Note as an example the $\Delta\Delta G^0/n$ values for acetone and cyclopentanone hemiketal formation in Table 3, taken from experiments by Jones and Bender (3*a*). This empirical generalization does not yet have a sound theoretical basis. The observations probably reflect the effects of structural modification on either the C—H vibrational force constants or the preferred conformations of the molecule. The number of hydrogens adjacent to the reaction center, *per se*, may not be important.

A more difficult challenge is to understand how structural changes give rise to changes in $\Delta\Delta G^0/n$. For example $\Delta\Delta G^0/n$ nearly doubles for methyl ketal formation from 32 cal/mol in acetone to 55 cal/mol in phenylacetone. The same trend is seen in methyl hemiketal formation, with cyclopentanone having as large an effect as phenylacetone. Bisulfite addition is rather peculiar in that $\Delta\Delta G^0/n$ follows hemiketal formation for acetone and cyclopentanone, but is significantly smaller than for those reactions of phenylacetone (3*b*).

A complete normal coordinate analysis for proto- and deuteroketones, ketals, and bisulfite addition products is central to a complete understanding of these isotope effects. In its absence we can only speculate on the source of the isotope effects.

The larger isotope effect in cyclopentanone than acetone is probably related to the ketone conformations in solution. The most favorable

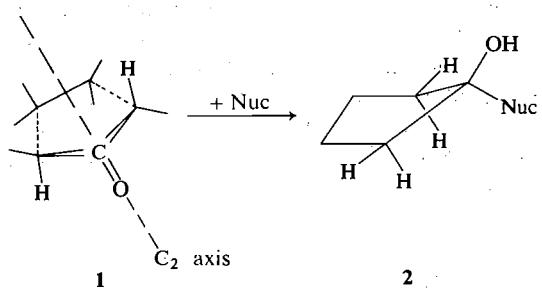

1 2

conformation of cyclopentanone is the half-chair form, which minimizes hydrogen eclipsing interactions (12). The pseudoaxial protons adjacent to the carbonyl overlap well with the ketone C=O p-orbital. Not only is this hyperconjugation lost on formation of a tetrahedral product, but there is significant increase in hydrogen-eclipsing interactions. If these interactions narrow the energy well in those cross-sections of the potential energy surface describing the C—H bonds on the β carbon, the isotope effect will increase over that in acetone, *almost irrespective of the reacting nucleophile*.

In tetrahedral phenylacetone addition prod-

Can. J. Chem. Downloaded from www.nrcresearchpress.com by 210.87.254.42 on 09/05/12
For personal use only.

Can. J. Chem. Downloaded from www.nrcresearchpress.com by 210.87.254.42 on 09/05/12
For personal use only.

ucts, coupling of the carbon–nucleophile vibrational modes with the β C—H modes must be important. The bisulfite adduct, with its relatively long C—S bond, contributes less to the isotope effect than does the shorter C—O bond in the ketal and hemiketal. Similar trends appear in kinetic isotope effects determined by Lamaty (*3b*) (*cf.* Table 3). A significantly smaller kinetic isotope effect is observed in the addition of bisulfite to phenylacetone when compared to hydroxylamine. These differences are not apparent for the addition of those nucleophiles to acetone and cyclopentanone. Comparison of the kinetic and equilibrium isotope effects give some indication of what fraction of the carbonyl character is lost in the transition state for nucleophilic addition.

The β-isotope effect of extraordinary magnitude is that for ketal formation in dibenzyl ketone. It is our belief that such a large isotope effect must reflect a preferred conformation in the ketone giving rise to a strong hyperconjugative interaction between the ketone and the β-hydrogens. In addition, steric crowding in the tetrahedral product must seriously perturb its C—H bending or stretching modes.[3] A comparison of phenylacetone and dibenzyl ketone is shown. Differences in ketone conformations and the energetics of ketal formation result primarily from phenyl–phenyl interactions in the latter. Space-filling molecular models suggest that the preferred conformation of dibenzyl ketone has a C—H bond parallel to the C=O π-bond. Phenylacetone has a slightly different geometry of lowest energy.

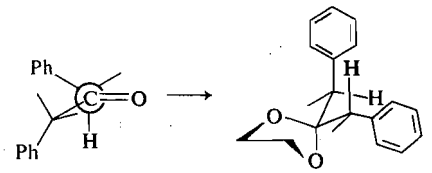

3 4

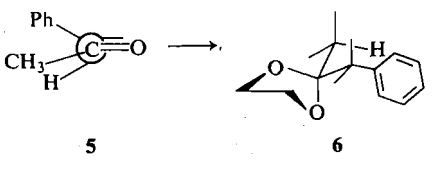

5 6

[3]We do not wish to imply that **4** is extraordinarily strained; **4** is more strained than any tetrahedral adduct for which equilibrium isotope effects have been measured.

In phenylacetone, as in most α-CH_2 ketones, the preferred geometry has a CH bond eclipsing C=O. This allows a staggered geometry between α-substituents of the ketone. Phenyl–phenyl repulsion is rather severe in dibenzyl ketone. Increasing the dihedral angle between these staggered substituents increases the overlap between one C—H bond and the C=O π-bond. In no way does it appear possible for two C—H bonds simultaneously to achieve such overlap.

In the corresponding ketals, 1–3 steric interactions appear to dominate conformational preferences. These are difficult to assess. In conformation **4** there are obvious destabilizing steric interactions involving the hydrogens at which the isotope effect is probed. There is no doubt, however, that the ketal derived from dibenzyl ketone is significantly more crowded than that derived from phenylacetone. With the increase in isotope effects paralleling the increasing difficulty (primarily steric) in forming tetrahedral addition products from ketones, (13), it is likely that these steric factors are in part responsible for the size of the β-deuterium isotope effect.

Experimental

Acetone-d_6 was purchased from Merck, Sharp, and Dohme. Specifically deuterated phenyl-2-propanones were prepared and purified by methods we reported previously (14). Methylene chloride was distilled fresh from phosphorus pentoxide. *Sym*-tetrachloroethane was washed with concentrated sulfuric acid, followed by aqueous sodium carbonate. $BF_3 \cdot Et_2O$ was freshly distilled. Nuclear magnetic resonance spectra were run on a Varian T-60 spectrometer. Peak areas were determined by repetitive integration. The details of the n.m.r. method and typical correlation coefficients have been reported (15). Scintillation counting in toluene-Omnifluor was carried out in a Packard-Tri-Carb liquid scintillation spectrometer, model 3375. Counting data were recorded by teletype. Sample counts per minute normally had standard deviations of 0.1%. Those with deviations greater than 0.2 were discarded. An automatic external standardization (a.e.s.) feature allowed a.e.s. ratios to be measured. These give an indication of the counting efficiency of each sample.

1,3-Diphenyl-2-propanone-1-t

A solution of 32.5 g (0.15 mol) of 1,3-diphenyl-2-propanone (J. T. Baker, recrystallized from petroleum ether 30–60 °C) in 50 ml of pyridine was prepared. To this was added a mixture of 1.5 ml tritiated water (New England Nuclear Co., 1 mCi/ml) and 15 ml distilled deionized water. The reaction mixture was refluxed for 10 h. The pyridine and water were distilled off, and the ketone was twice recrystallized from petroleum ether, m.p. 33–34 °C. The sample activity was 2.1×10^9 c.p.m./mol.

Can. J. Chem. Downloaded from www.nrcresearchpress.com by 210.87.254.42 on 09/05/12
For personal use only.

2,2-Dibenzyl-1,3-dioxolan (Dibenzyl Ketone Ethylene Ketal)

Dibenzyl ketone (10.5 g, 0.050 mol) was refluxed with ethylene glycol (0.049 mol) in toluene using 0.5 g *p*-toluenesulfonic acid as a catalyst. Water was removed via a Dean–Stark trap. After 5 h, the catalyst was quenched with powdered anhydrous potassium carbonate. After filtering, the solution was concentrated and then chromatographed on a column of activity II alumina. Hexane was used as the eluting solvent. Concentration of the hexane gave white crystals, m.p. 36–37 °C free of detectable traces of ketone. The overall yield was 88%.

2-Phenyl-2-methyl-1,3-dioxolan (Phenylacetone Ethylene Ketal)

An identical procedure gave the ketal as a liquid, which was distilled at 90 °C (pot temperature)/0.2 Torr through a 10 in. Vigreux column. The yield of product was 75%; however, it contained 5.5% phenylacetone by n.m.r. as the sole impurity. Further purification was unnecessary, as our analytical technique allowed us to monitor concentrations of all species at equilibrium.

1-Phenyl-2,2-dimethoxypropane (Phenylacetone Dimethyl Ketal)

Phenylacetone (2.08 g, 15.5 mmol) in 60 ml anhydrous methanol (distilled from magnesium) was treated with 10 ml 2,2-dimethoxypropane and 80 mg bis(*p*-nitrophenyl)phosphoric acid (Aldrich). After 15 min reflux, the acid was quenched with 10% aqueous sodium hydroxide. The solution was concentrated, taken up in hexane, washed with aqueous bicarbonate, dried with magnesium sulfate, and chromatographed on a 45 cm × 1 cm Florisil column. Benzene (10%) in hexane was used as the eluant. The dimethyl ketal was collected as a colorless oil, rechromatographed on Florisil and distilled at 60 °C (pot)/0.4 Torr. It was stored in a desiccator. The overall yield, 0.3 g, was poor, 11%, but the n.m.r. showed it to be free of ketone.

2,2-Dimethoxypropane (Aldrich) was fractionally distilled (82–83 °C) through a 10 in. Vigreux column. The compound decomposed in the g.l.c. on both DEGS and Carbowax columns. An n.m.r. analysis of the fraction used indicated that it contained 7.2% acetone. There was no detectable trace of methanol or other impurities in the n.m.r. spectrum. A suitable correction for this acetone impurity was applied to the calculation of isotope effects (see text).

Ketone–Ketal Equilibria

In general, the catalytic solution of $BF_3 \cdot Et_2O$ (freshly distilled) in dry methylene chloride or *sym*-tetrachloroethane was prepared and a 0–5 ml aliquot of this was added to a pre-weighed mixture of the labelled ketone and unlabelled ketal.

(*i*) *Acetone*—Acetone-d_6 (150 mg, 2.58 mmol) and 2,2-dimethoxypropane (210 mg, 2.0 mmol) were mixed together in 0.5 ml of solvent containing $BF_3 \cdot Et_2O$ (0.05 mmol). In separate experiments methylene chloride or *sym*-tetrachloroethane was used as the solvent. The reaction was monitored by n.m.r. and spectra, recorded between 2–15 h after the addition of catalyst, were used to calculate values for K_H/K_D.

(*ii*) *Phenylacetone*—Mixtures of the ketone (0.75 mmol) and the ketal (0.60 mmol) were stirred together in methylene chloride using $BF_3 \cdot Et_2O$ (0.05 mmol). The three deuterated species $PhCD_2COCD_3$, $PhCD_2COCH_3$, and $PhCH_2COCD_3$ were all examined in this way Mixtures of the d_5 and of the d_2 compounds with 2,2-dimethoxy phenylpropane and with phenylacetone ethylene ketal were studied. The d_3 species was equilibrated only with phenylacetone ethylene ketal. The solutions were concentrated at reduced pressure to remove solvent and catalyst. The n.m.r. spectra of these mixtures, recorded between 10–48 h after contact with the catalyst, were used to calculate values for K_H/K_D.

(*iii*) *Dibenzyl Ketone*—Tritium labelled dibenzyl ketone (0.75 mmol) and unlabelled dibenzyl ketone ethylene glycol ketal were dissolved in 0.5 ml dry methylene chloride, containing 0.010 mmol $BF_3 \cdot Et_2O$. The reaction mixture was stirred for 16 h. The methylene chloride and $BF_3 \cdot Et_2O$ were removed at room temperature under reduced pressure. The solid residue was dissolved in 5 ml of dry ether and added dropwise to three molar equiv. of lithium aluminum hydride in 10 ml ether at −78 °C. The reactants were stirred ten minutes at −78 °C. The stirring was continued for 1 h as the contents of the reaction flask warmed to room temperature.

The reaction was quenched by slowly adding a saturated aqueous solution of sodium sulfate until a white powdery precipitate formed. After filtering, the ether solution was washed with 5 ml water followed by an equal volume of saturated sodium chloride solution. The concentrate was applied to a small (3 in. × ½ in.) column of activity II alumina. The ketal came off the column in hexane, whereas addition of methanol to the hexane was necessary to recover the 1,3-diphenyl-2-propanol. The ketal was crystallized, and the alcohol was molecularly distilled at 110 °C (pot)/0.2 Torr. Radioactivities of each were measured by scintillation counting.

The authors wish to thank the National Research Council of Canada for its financial support, and Professor A. Guha for the use of the scintillation counter.

1. (*a*) V. F. RAAEN, T. K. DUNHAM, D. D. THOMPSON, and C. J. COLLINS. J. Am. Chem. Soc. **85**, 3497 (1963); (*b*) M. CHEREST, H. FELKIN, and C. FRAJERMAN. Tetrahedron Lett. 379 (1971); (*c*) P. GENESTE and G. LAMATY. Tetrahedron Lett., 4633 (1965); Bull. Soc. Chim. (Fr.), 669 (1968); (*d*) P. GENESTE, G. LAMATY, and J. P. ROQUE. Tetrahedron, **27**, 5561 (1971); (*e*) M. L. BENDER and M. S. FENG. J. Am. Chem. Soc. **82**, 6318 (1960).
2. (*a*) V. J. SHINER, JR. and S. CROSS. J. Am. Chem. Soc. **79**, 3599 (1957); (*b*) H. G. BULL, K. KOEHLER, T. C. PLETCHER, J. J. ORTIZ, and E. H. CORDES. J. Am. Chem. Soc. **93**, 3002 (1971); (*c*) J. ARCHILA, H. BULL, C. LAGENAUR, and E. H. CORDES. J. Org. Chem. **36**, 1345 (1971); (*d*) F. GUINOT and G. LAMATY. Tetrahedron Lett. 2569 (1972).
3. (*a*) J. M. JONES and M. C. BENDER. J. Am. Chem. Soc. **82**, 6322 (1960); (*b*) P. GENESTE, G. LAMATY, and J. P. ROQUE. Tetrahedron, **27**, 5539 (1971); (*c*) L. DO AMARAL, H. G. BULL, and E. H. CORDES. J. Am. Chem. Soc. **94**, 7579 (1972).

4. M. A. WINNIK, V. A. STOUTE, and P. FITZGERALD. J. Am. Chem. Soc. **96**, 1977 (1974).
5. C. J. COLLINS and M. S. BOWMAN. (*Editors*) Isotope effects in chemical reactions. Van Nostrand Reinhold, New York. 1970.
6. S. E. SCHEPPELE. Chem. Rev. **72**, 511 (1972); E. R. THORNTON. Annu. Rev. Phys. Chem. **17**, 349 (1966); E. A. HALEVI. Prog. Phys. Org. Chem. **1**, 109 (1966); C. J. COLLINS. Adv. Phys. Org. Chem. **2**, 1 (1964); L. MELANDER. Isotope effects on reaction rates. Ronald Press, New York. 1960.
7. E. M. ARNETT, T. COHEN, A. A. BOTHER-BY, and R. D. BUSHICK. Chem. Ind. (London) 473 (1961).
8. V. J. SHINER, JR. and W. DOWD. J. Am. Chem. Soc. **93**, 1029 (1971), and references therein.
9. W. P. JENCKS. Catalysis in chemistry and enzymology. McGraw-Hill, New York. 1969. pp. 253 ff.
10. C. G. SWAIN, E. C. STIVERS, J. F. REUWER, JR., and L. J. SCHAAD. J. Am. Chem. Soc. **80**, 5885 (1958).
11. V. J. SHINER, JR., B. L. MURR, and G. HEINEMANN. J. Am. Chem. Soc. **85**, 2413 (1963); V. J. SHINER, JR. J. Am. Chem. Soc. **83**, 240 (1961).
12. E. L. ELIEL. Stereochemistry of carbon compounds. McGraw-Hill, New York. 1962. pp. 250 ff.
13. O. H. WHEELER. J. Am. Chem. Soc. **79**, 4191 (1957); J. W. BAKER. Tetrahedron, **5**, 135 (1959); D. P. EVANS and J. R. YOUNG. J. Chem. Soc. 1310 (1954).
14. M. A. WINNIK. Synth. Commun. **3**, 299 (1973).
15. M. A. WINNIK and V. A. STOUTE. Can. J. Chem. **51**, 2788 (1973).
16. V. A. STOUTE. Ph.D. Thesis, University of Toronto, Toronto, Ontario. 1975.

Can. J. Chem. Downloaded from www.nrcresearchpress.com by 210.87.254.42 on 09/05/12
For personal use only.

Isotope Effect Studies on Elimination Reactions. XI. The Nature of the Transition State for the E2 Reaction of 2-Phenylethyldimethylanilinium Salts Containing Substituents in the Aniline Ring with Sodium Ethoxide in Ethanol[1]

PETER SCHMID AND ARTHUR NEWCOMBE BOURNS

Department of Chemistry, McMaster University, Hamilton, Ontario L8S 4M1

Received May 21, 1975

PETER SCHMID and ARTHUR NEWCOMBE BOURNS. Can. J. Chem. **53**, 3513 (1975).

Kinetic isotope effects have been determined for the E2 reactions of a series of 2-phenylethyldimethylanilinium salts containing substituents in the aniline ring with sodium ethoxide in ethanol at 40 °C. The nitrogen isotope effect, $(k^{14}/k^{15} - 1)100$, is not very sensitive to substituent changes but appears to increase slightly with increasing electron-withdrawing ability of the substituents, *i.e.*, 1.19 ± 0.07, 1.13 ± 0.06, 1.12 ± 0.08, 1.30 ± 0.07, and 1.32 ± 0.06 for *p*-OCH_3, *p*-CH_3, *p*-H, *p*-Cl, and, *m*-CF_3, respectively. The hydrogen–deuterium isotope effects pass through a minimum in the region of the unsubstituted compound and increase both with increasing electron-donating as well as with electron-withdrawing power of the substituents, *i.e.* k^H/k^D = 4.70 ± 0.06, 4.61 ± 0.04, 4.51 ± 0.04, 4.53 ± 0.09, 5.00 ± 0.07, and 5.39 ± 0.07 for *p*-OCH_3, *p*-CH_3, *p*-H, *p*-Cl, *m*-CF_3, and *p*-CF_3, respectively. The results are discussed in terms of recent theoretical treatments of the effect of structural variations in the reactants on the nature of the transition state of E2 elimination reactions. The conclusion is reached that the transition states in the present reaction series can be characterized as 'central with slight carbanion character' and that the effect of a change in the ability of the leaving group on the structure of the transition state manifests itself mainly in the direction perpendicular to the reaction coordinate. A simple novel hypothesis is formulated which emphasizes the importance of the location of the transition state in a More O'Ferrall-type potential energy diagram in determining its sensitivity to structural changes in the reactants.

PETER SCHMID et ARTHUR NEWCOMBE BOURNS. Can. J. Chem. **53**, 3513 (1975).

On a déterminé les effets isotopiques cinétique de réactions E2 d'une série de sels de phényl-2 éthyl diméthylanilinium (substitués sur le noyau de l'aniline) avec l'éthylate de sodium dans l'éthanol à 40 °C. L'effet isotopique de l'azote $(k^{14}/k^{15} - 1)100$ n'est pas très sensible aux changements de substituant mais il semble qu'il augmente légèrement avec la facilité qu'ont les substituants d'attirer les électrons soit respectivement 1.19 ± 0.07, 1.13 ± 0.06, 1.12 ± 0.08, 1.30 ± 0.07 et 1.32 ± 0.06 pour *p*-OCH_3, *p*-CH_3, *p*-H, *p*-Cl et *m*-CF_3. Les effets isotopiques de l'hydrogène passent par un minimum dans la région du composé non-substitué et augmentent avec une augmentation des effets électroaffinitaires et électrodonneurs des substituants soit respectivement k^H/k^D = 4.70 ± 0.06, 4.61 ± 0.04, 4.51 ± 0.04, 4.53 ± 0.09, 5.00 ± 0.07 et 5.39 ± 0.07 pour *p*-OCH_3, *p*-CH_3, *p*-H, *p*-Cl, *m*-CF_3 et *p*-CF_3. On discute de ces résultats en termes de traitements théoriques récents de l'effet de variations structuralles dans les réactifs sur la nature de l'état de transition des réactions d'élimination E2. On arrive à la conclusion que les états de transition de la série de réactions actuelles peuvent être caractérisés comme étant 'centrés avec un faible caractère carbanionique' et que l'effet d'un changement dans la capacité du nucléofuge sur la structure de l'état de transition se manifeste principalement dans la direction perpendiculaire des coordonnées de la réaction. On formule une nouvelle hypothèse simple qui met en relief l'importance de la position de l'état de transition dans un diagramme d'énergie potentielle du type More O'Ferrall pour déterminer sa sensibilité vis-à-vis des changements structuraux dans les réactifs.

[Traduit par le journal]

Introduction

A large body of evidence suggests that the nature of the transition state in an E2 elimination reaction is variable, *i.e.* that the reacting bonds can be broken or formed in varying degrees (for recent reviews see refs. 3 and 4). A number of sometimes conflicting theories concerning the effect of structural changes in the reactants on the nature (*i.e.* the structure and energy) of the transition state have been put forward (5–9).

Bunnett's theory (4, 5), which was developed mainly on an intuitive basis, suggests that a structural change which makes the cleavage of the C_β—H bond easier will lead to more exten-

[1]For part X see ref. 1.

Can. J. Chem. Downloaded from www.nrcresearchpress.com by 210.87.254.40 on 09/05/12
For personal use only.

Can. J. Chem. Downloaded from www.nrcresearchpress.com by 210.87.254.40 on 09/05/12
For personal use only.

sive breaking of this bond in the transition state while the C_α—X bond (where X is the leaving group) will be correspondingly less broken. In Thornton's treatment (6) substituent effects are considered as linear perturbations of the vibrational potentials for the normal coordinate motions both parallel to and perpendicular to the reaction coordinate. The effects on the parallel motion are expected to dominate in many, but not all, cases. This leads to the prediction that a structural change which makes the breaking of the C_β—H bond easier will cause this bond to be broken less in the transition state. The other bond (in our example the C_α—X bond) will then follow along in the direction of the coordinate motion set by the former one, and be shorter as well. Recently Thornton and co-worker (7) have expanded the theory to explain more recent data which indicate that in some cases the influence of a substituent change on the perpendicular motion outweighs the effect on the parallel one. A system where this is the case would appear to behave according to Bunnett's theory. A third approach has been developed by More O'Ferrall (8). In his model, reactants, products, and transition state are represented on a common potential energy surface, along with carbonium ion and carbanion intermediates of stepwise reaction paths.[2] He concludes that structural changes which mainly influence the stability of products and/or reactants are transmitted along the reaction coordinate, resulting in a more or less product-like or reactant-like transition state. This is in agreement with Thornton's theory (6) and the Hammond postulate (11). Structural changes affecting mainly the stability of the carbonium ion and/or the carbanion, however, are expected to exert their effect in the direction perpendicular to the reaction coordinate. Their effect, then, would correspond to what is expected on the basis of Bunnett's theory (4, 5). Jencks (12), in a recent paper, has arrived at essentially the same predictions for structure–reactivity relationships. A somewhat related model has been presented by Critchlow (9). It allows the prediction of the configuration and energy of the transition state of a concerted reaction from the energies required to form the intermediates of the hypothetical stepwise processes. Substitution in the attacking or leaving portion of a concerted reaction system should manifest itself only in changes in the more remote bond. Interestingly, this model suggests that the energetically less demanding part of the overall process has made greater progress at the transition state. This is in accordance with the principles stated in Bunnett's theory (4, 5), but contrary to the Hammond postulate (11).

In a recent report from this laboratory (2) it was suggested that the apparent contradiction between the theories of Bunnett (4, 5) and Thornton (6) might have its origin in a different sensitivity of the transition state to structural changes, depending on its position in More O'Ferrall's potential energy diagram (8). It was pointed out that in the studies of Bartsch and Bunnett (13) and Bartsch (14) which lend support to Bunnett's theory, the leaving group is always a 'good' one, namely a halogen. In systems which behave according to Thornton's theory, on the other hand, the leaving group is always a 'poor' one, *e.g.* trimethylamine. We may assume as a working hypothesis that compounds with relatively good leaving groups undergo elimination with strong bases by way of a central transition state in which the extent of C_β—H and C_α—X bond breaking is approximately equal. For elimination reactions with most quaternary ammonium salt substrates studied so far the transition states appear quite clearly to be strongly carbanion-like (considerably more C_β—H than C_α—X bond rupture). Reference to More O'Ferrall's potential energy diagram (Fig. 2) shows that a structural change influencing mainly the energy of the carbanion will exert its effect essentially through the perpendicular vibrational mode for a central transition state. For a transition state with considerable carbanion character, however, a similar effect may manifest itself to a greater extent in a direction along the reaction coordinate than perpendicular to it. In the latter case the curvature of the potential energy surface may well be considerably greater in the perpendicular than in the parallel direction whereas in the case of a central transition state the opposite may be true.

Even though there is no question that the leaving group is a very important factor in determining the structure of the transition state in an E2 reaction (ref. 15, p. 499; ref. 4, pp. 72, 73) there have been few systematic studies carried out in this area. In this paper we wish to report the results of such an investigation. We have

[2]Diagrams of this type have originally been proposed by Albery (10).

TABLE 1. Rate constants and primary β-hydrogen isotope effects in elimination reactions of $C_6H_5CY_2CH_2\overset{+}{N}(CH_3)_2C_6H_4X$ ions with sodium ethoxide in ethanol at 40 °C

X	Y	$k \times 10^2$ (l mol^{-1} s^{-1}) [EtO$^-$] = 0.0142 mol/l	$k \times 10^2$ (l mol^{-1} s^{-1}) [EtO$^-$] = 0.0121 mol/l	k^H/k^D [b]	σ^- [c]
p-OMe	H	1.22±0.01[a]	1.31±0.01[a]	4.70±0.06	−0.27
	D	0.259±0.002	0.279±0.002		
p-Me	H	1.34±0.01		4.61±0.04	−0.17
	D	0.291±0.002			
H	H	1.89±0.01	2.18±0.01	4.50±0.04	0
	D	0.421±0.003	0.483±0.004		
p-Cl	H	4.26±0.05	4.57±0.04	4.53±0.09	0.24
	D	0.931±0.019	1.01±0.02		
m-CF_3	H	8.81±0.05		5.00±0.07	0.49[d]
	D	1.74±0.02			
p-CF_3	H	9.32±0.10	10.05±0.10	5.39±0.07	0.65[d]
	D	1.73±0.01	1.86±0.02		

[a]Standard deviations.
[b]Ratio of specific rates of elimination; deviation $(\pm k^H/k^D)[(r^H/k^H)^2 + (r^D/k^D)^2]^{1/2}$, where r is the standard deviation in k.
[c]See ref. 19, p. 356.
[d]See ref. 20.

studied the reactions of a series of 2-phenylethyldimethylanilinium salts containing substituents in the aniline ring with ethoxide ion in ethanol. These substrates were chosen for a number of reasons. They are closely related to 2-phenylethylammonium ions which have been studied earlier in these laboratories (2, 16, 17). On the other hand, they contain a much better leaving group and may therefore allow us to test our hypothesis concerning the apparent discrepancies between the theories of Bunnett and Thornton. Furthermore, they contain substituents in the aromatic ring of the leaving group. This feature makes the compounds suitable for a systematic study of the influence of the leaving group by a method combining isotope and substituent effects.[3]

Results

Hydrogen–Deuterium Isotope Effects

Rate constants have been determined for the elimination reactions of a series of 2-phenylethyldimethylanilinium bromides containing substituents in the aniline ring and their 2,2-dideuterated analogs with sodium ethoxide in ethanol at 40 °C. All the reactions studied were found to be of second order overall, first order with respect to each reactant. The spectrophotometric procedure used to determine the kinetics is described in the experimental section. The measured rate constants are shown in Table 1.

The Hammett plots of log k/k_0 *vs.* σ^- which were obtained for the undeuterated and the deuterated series are reasonably linear. However, a small but apparently systematic deviation from linearity is noticeable in both plots. The slope, ρ, for the undeuterated series is $+1.07 \pm 0.08$, with a correlation coefficient, r, of 0.988. For the 2,2-dideuterated series ρ is $+1.01 \pm 0.08$, with a correlation coefficient of 0.985. The errors given are standard deviations.

The primary hydrogen–deuterium kinetic isotope effects calculated from the rate data and the σ^- substituent constants are also presented in Table 1.

It is interesting to note that the rates of the elimination reactions are subject to a strong salt effect while the kinetic isotope effects are independent of the ionic strength, at least in the narrow range studied.

Nitrogen Isotope Effects

The results of the nitrogen isotope effect study of the reaction of 2-phenylethyldimethylanilinium bromides with sodium ethoxide in ethanol at 40 °C are shown in Table 2. The nitrogen isotope effects were determined by comparing the $^{14}N/^{15}N$ ratio of the starting material of natural isotopic abundance with that of the dimethylaniline formed in the reaction carried to some

[3]For a discussion of the merits of this technique see ref. 18.

Can. J. Chem. Downloaded from www.nrcresearchpress.com by 210.87.254.40 on 09/05/12
For personal use only.

TABLE 2. Nitrogen isotope effects for the E2 reaction of $C_6H_5CH_2CH_2\overset{+}{N}(CH_3)_2C_6H_4X$ ions with sodium ethoxide in ethanol at 40 °C

Substituent X	Number of determinations	$(k^{14}/k^{15} - 1)100^a$
p-OCH_3	10	1.19±0.07
p-CH_3	9	1.13±0.06
H	8	1.12±0.08
p-Cl	7	1.30±0.07
m-CF_3	8	1.32±0.06

[a]The limits shown are the standard deviations.

known extent of completion. The experimental procedure is outlined in the experimental section.

Discussion

Inspection of the isotope effect data in Tables 1 and 2 shows that the reactions of 2-phenylethyldimethylanilinium salts with ethoxide ion in ethanol exhibit β-hydrogen and leaving group isotope effects of significant magnitude. The conclusion seems warranted that both effects are primary ones, *i.e.* that both bonds are being broken in the rate determining step of the reaction (ref. 21, p. 215). This then implies that the reactions occur by a genuine synchronous E2 mechanism, in analogy with the corresponding reactions of 2-phenylethyltrimethylammonium salts (2, 16, 17).

Interestingly, the variation in the nitrogen isotope effect is rather small, while the hydrogen isotope effect changes over a comparably larger range. Clearly, a substituent change in the leaving group has a considerable influence on the breaking of the more distant C_β—H bond. This indicates that there must be rather extensive coupling between the C_α—X and C_β—H bond breaking processes, an observation which has also been made by Willi (22) in his investigation of elimination reactions in 2,2-diphenylethylarenesulfonate systems. Intuitively, one might have expected the substituent change to manifest itself more strongly in the closer bond (ref. 6, p. 2919).

Of special interest is the striking similarity in the shape of the plots of the two isotope effects *vs.* the σ^- constants (Fig. 1). Both are clearly not linear but rather seem to level out in the direction of stronger electron-donating substituents, *i.e.* upon going to more basic ('poorer') leaving groups. The hydrogen isotope effect even appears to pass through a minimum. The slight increase

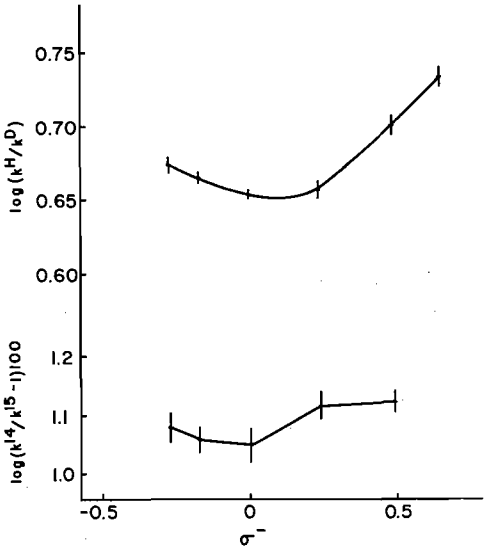

FIG. 1. Plot of log (k^H/k^D) and log ($k^{14}/k^{15} - 1$)100 *vs.* σ^- for the reaction of 2-phenylethyldimethylanilinium salts containing substituents in the aniline ring with sodium ethoxide in ethanol at 40 °C.

in the direction of decreasing σ^- values seems to be just outside the experimental error limits. The possible significance of this point will be discussed below.

Leaving Group Isotope Effects

Since the magnitude of the nitrogen isotope effect depends on the extent to which the composite force constant of the C_α—N^+ bond is decreased in going from the initial to the transition state, the effect will increase regularly in a reaction series with the extent of bond weakening in the transition state. The experimental results, therefore, indicate that the extent of carbon–nitrogen bond rupture in the transition state is greater the more electron-withdrawing the substituent, *i.e.* the 'better' the leaving group.

Can. J. Chem. Downloaded from www.nrcresearchpress.com by 210.87.254.40 on 09/05/12
For personal use only.

Can. J. Chem. Downloaded from www.nrcresearchpress.com by 210.87.254.40 on 09/05/12
For personal use only.

The numerical values of the nitrogen isotope effects are substantial, amounting to between 25 and 40% of the theoretical maximum value.[4] This implies that there is a fairly sizeable amount of C_α—N^+ bond stretching in the transition state of, perhaps, 25–50%. We shall not attempt to specify more accurately the extent of bond weakening at this point. Theoretical calculations by Saunders and co-workers (refs. 24 and 3*a*, pp. 76, 77) demonstrate that a general relationship between the value of the leaving group isotope effect and the absolute extent of bond stretching in the transition state is hardly a straightforward matter and depends greatly on the models on which the calculations are based. Further complications can occur when there is extensive coupling between the various atomic motions in the transition state, as seems to be the case in our system. In addition, the present treatment of isotope effects does not take into account solvation effects which, in the case of charged substrates, might be of considerable importance. In spite of these complications we feel that within our reaction series the qualitative interpretation of isotope effects in terms of bond rupture is justified, since the structural changes made in the reactants are only relatively minor and the solvent is the same in all cases.

β-*Hydrogen Isotope Effects*

The correlation of the magnitude of the hydrogen isotope effect with the degree of bond stretching in the transition state is somewhat more complicated because the reacting hydrogen is involved in a three-center reaction. In this situation the value of k^H/k^D is expected to reach a maximum when the force constants of the bonds being formed and broken are equal, *i.e.* the proton is half transferred, as has been pointed out by Melander (25), Westheimer (26) and others (27–29). The unambiguous interpretation of a measured isotope effect, which is smaller than the theoretical maximum, therefore, requires a knowledge of whether the proton is more or less than half transferred in the transition state. This can be obtained from the calculations and experimental results of Steffa and Thornton (30) on the secondary isotope effect k^{OD^-}/k^{OH^-}, for proton abstraction by OD^- in D_2O and OH^- in H_2O. The theoretical value of this isotope effect for a reaction with complete proton transfer at the transition state is 1.88 at 80 °C. For half transfer the effect is the square root of this maximum value, namely 1.37.

The results of Steffa and Thornton's study are presented in Table 3, along with primary hydrogen isotope effect data. One notes that all the secondary isotope effects are greater than 1.37 and, furthermore, that the decrease in k^{OD^-}/k^{OH^-} as one proceeds down the table is paralleled by an increase in primary isotope effect. The combination of these two findings establishes rather convincingly that the proton must be more than half transferred in all the cases listed (compare refs. 2 and 21, p. 272).

After taking into account the possibility of a fairly substantial solvent isotope effect Steffa and Thornton conclude that the reaction of the sulfonium ion represents a case where the proton is approximately half transferred in the transition state. The large value of the primary isotope effect is consistent with this view. Since the isotope effects for the dimethylanilinium salt are rather similar it is reasonable to conclude that in this case the proton is slightly more than half transferred in the transition state.

The Hammett ρ values listed in Table 4 lend further support to this conclusion. The ρ value for the dimethylanilinium leaving group is similar to that for chlorine and dimethylsulfonium leaving group.

On the basis of these findings it is possible to indicate the position of the transition state of the reaction of unsubstituted 2-phenylethyldimethylanilinium ion with ethoxide ion in ethanol in More O'Ferrall's potential energy diagram (Fig. 2). It appears to be located in the quadrant adjoining the carbanion intermediate, close to the center of the diagram. In other words, the transition state is a very central one with slight carbanion character. This is in contrast to what has been found for reactions of 2-phenylethyltrimethylammonium ions where the leaving group is much worse and the transition state is strongly carbanion-like in character (*i.e.* the C_β—H bond is much more stretched than the C_α—X bond) (2).

Furthermore, we can relate the trend in the magnitudes of k^H/k^D and k^{14}/k^{15} with relative amounts of bond rupture. On the side of positive σ^- values (*i.e.* upon going to better leaving groups) both k^H/k^D and k^{14}/k^{15} increase. This

[4]Biegeleisen and Wolfsberg (23) have calculated a theoretical maximum for the kinetic nitrogen isotope effect of 1.032. Saunders and Cockerill (ref. 3*a*, p. 89) mention a value of 1.040–1.045.

TABLE 3. Secondary and primary isotope effects in reactions of 2-phenylethyl derivatives

Substrate	k^{OD^-}/k^{OH^-} [a]	k^H/k^D [b]
$C_6H_5—CH_2—CH_2—\overset{+}{N}(CH_3)_3$	1.79	3.23[c]
$C_6H_5—CH_2—CH_2—\overset{+}{N}(CH_3)_2C_6H_5$	1.62	4.50[d]
$C_6H_5—CH_2—CH_2—\overset{+}{S}(CH_3)_2$	1.57	5.05[e]

[a]Secondary isotope effect for reaction with OD^- in D_2O and OH^- in H_2O, $T = 80$ °C, (see ref. 30).
[b]Primary isotope effect for reaction with EtO^- in EtOH.
[c]Smith and Bourns (2), $T = 40$ °C.
[d]This work, $T = 40$ °C.
[e]Saunders and Edison (31), $T = 30$ °C.

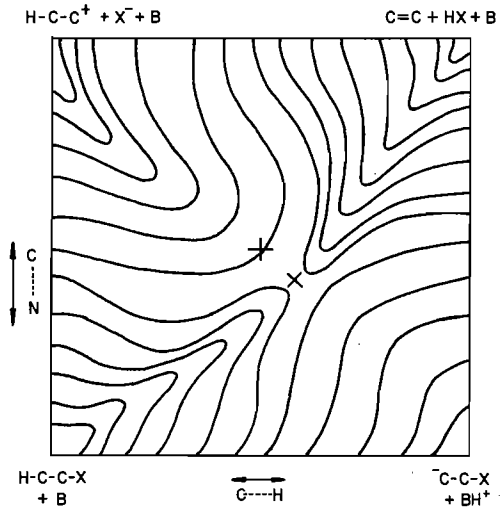

FIG. 2. Schematic potential energy diagram for concerted β-elimination reaction H—C—C—X + B → C=C + HX + B.

means that an increase in C_α—X bond length is coupled with a decrease in C_β—H bond length and indicates that the main effect of changing a substituent in the leaving group is felt in the direction perpendicular to the reaction coordinate. This finding is in contrast with what has been usually found in reactions with quaternary ammonium salts (2, 36, 37). Only recently one case has been found,[5] namely the E2 reaction of 9-(4-substituted-benzyl)-fluorene-9-trimethylammonium ions with ethoxide in ethanol, where substituents show their effect primarily in the direction perpendicular to the reaction coordinate, rather than parallel to it.

On the side of negative σ^- values (*i.e.* on going to 'poorer' leaving groups) there is relatively little change in the isotope effects and thus the bond lengths. The nitrogen isotope effect levels out (within experimental error), whereas k^H/k^D increases very slightly, indicating a decrease in C_β—H bond length.

A few cases reported in the literature represent interesting parallels to this situation: Banger *et al.* (15) investigated the reaction of substituted 2-phenylethylarenesulfonates with potassium-*tert*-butoxide in *tert*-butyl alcohol and found that substitution in the 2-phenyl ring has an effect on the Hammett ρ constant and thus the structure of the transition state which is uniform and linear over the entire range studied. This is in complete analogy with observations in 2-phenylethyl systems with trimethylammonium (2) and dimethylanilinium[6] leaving groups. The effect of substitution in the leaving group, on the other hand, only becomes notable for the stronger electron-withdrawing substituents (*i.e.* the better leaving groups), as is the case in our system. This is taken as an indication of a shift to transition states with less carbanion character. Similarly, Willi (22) observed in his study of elimination reactions of 2,2-diphenylethylarenesulfonates that a *para*-nitro substituent in the arenesulfonate leaving group gave rise to an unexpectedly large increase in the β-hydrogen isotope effect. Winey and Thornton (7), finally, also found in their study of secondary isotope effects in reactions of 2-(*p*-trimethylammoniophenyl)-ethyl derivatives with lyoxide ions in water and deuterium oxide, respectively, that the isotope effects become an increasingly more sensitive function of the leaving group as the leaving group ability increases. They, too, conclude that the transition state of the reaction becomes less carbanion-like (or more central) the 'better' the leaving group.

[5]P. J. Smith, private communication.

[6]A. N. Bourns and P. B. Barrett, unpublished results.

Can. J. Chem. Downloaded from www.nrcresearchpress.com by 210.87.254.40 on 09/05/12
For personal use only.

TABLE 4. Hammett reaction constants and kinetic β-hydrogen isotope effects for the reaction of 2-phenylethyl derivatives with sodium ethoxide in ethanol at 30 °C

Leaving group	Hammett ρ[a]	k^H/k^D [a]
I	2.07 (32)	
Br	2.14 (32)	7.1 (31)
OTs	2.27 (33)	5.7 (31)
Cl	2.61 (33)	
$\overset{+}{N}(CH_3)_2C_6H_5$	2.69[c]	
$\overset{+}{S}(CH_3)_2$	2.75 (34)	5.1 (31)
F	3.12 (35)	
$\overset{+}{N}(CH_3)_3$	3.66 (2)[b]	3.2 (2)[b]

[a]Reference in parentheses.
[b]$T = 40$ °C.
[c]A. N. Bourns and P. B. Barrett, unpublished results.

The results of our study, then, can be summarized as follows: (*i*) the transition state of the reaction of unsubstituted 2-phenylethyldimethylanilinium ion with ethoxide ion in ethanol is a fairly 'central' one; (*ii*) a substituent change in the leaving group manifests itself mainly in a direction perpendicular to the reaction coordinate; (*iii*) going to stronger electron-donating substituents, *i.e.* 'poorer' leaving groups, shifts the structure of the transition state towards the $E1_{cb}$-like extreme; (*iv*) with increasing $E1_{cb}$ character the transition state geometry becomes less sensitive to further changes in the leaving group.

A Comment on Theoretical Predictions of the Effect of Structural Variations on Transition State Geometry

Table 5 summarizes the effects of structural variations in the reactants on the geometry of the transition state as predicted by the several theories to which reference was made in the Introduction. The following discussion will be limited to the effect of changes in the leaving group.

Interestingly, all the theories agree in their predictions of the influence of a change in the leaving group on the (more distant) C_β—H bond. The better the leaving group, the less stretched is the C_β—H bond in the transition state, *i.e.* the less carbanion character is developed. A large body of evidence, including the kinetic isotope effects and the Hammett reaction constants listed in Table 4 and our own data, lends support to this view. Thornton's updated theory (7) suggests in addition that the C_β—H bond is less sensitive to changes in the leaving group in carbanion-like transition states than in central ones. This is precisely the behavior displayed by our reaction system as well as the ones studied by Banger *et al.* (15), Willi (22), and Winey and Thornton (7).

There is no agreement between the predictions of the various theories for the effect of a change in the leaving group on the C_α—X bond. Bunnett (4) and Thornton (6) come to exactly opposite conclusions. Clearly, Bunnett's and Thornton's views represent two extremes, one considering the effect on the perpendicular, the other one on the parallel motion only. If both effects are taken into account (as in More O'Ferrall's (8) and Critchlow's (9) models and in Thornton's updated theory (7)) an unambiguous prediction is no longer possible. The result of the present as well as various other studies (*e.g.* Bartsch and Bunnett (13), Bartsch (14), Banger *et al.* (15)) suggest that in general the effect on the perpendicular motion may be more important. However, the present data also indicate that the sensitivity of the C_α—X bond to further changes in the leaving group may be smaller when the leaving group is already a poor one and the transition state shows an appreciable degree of carbanion character.

One point emerges more and more clearly. The hope to find a unique general correlation between the effect of a substituent change on the C—H and C—X bonds in the transition state of an E2 reaction (such as 'any increase in C—H bond length is necessarily coupled with an increase in C—X bond length') is no longer realistic. A theory relating the effect of structural

Can. J. Chem. Downloaded from www.nrcresearchpress.com by 210.87.254.40 on 09/05/12
For personal use only.

TABLE 5. Effect of structural variations in the reactants on the extent of C_α—X and C_β—H bond stretching in the transition state of E2 reactions as predicted by various theories[a]

	Theoretical predictions											
					Winey and Thornton (7)							
	Bunnett (4)		Thornton (6)		Central tr. s.[b]		El_{cb}-like tr. s.[b]		More O'Ferrall (8)		Critchlow (9)	
Structural variation	C_α—X	C_β—H	C_α—X	C_β—H	C_α—X	C_β—H	C_α—X	C_β—H	C_α—X	C_β—H	C_α—X	C_β—H
Better leaving group	↑	↓	↓	↓	±	↓	↓	±	±	↓	±	↓
Stronger base	↓	↑	↓	↓	↓	±	±	↓	↓	±	↓	±
Electron-withdrawing substituent at C_α	↓	↑	↑	↑	↓	↑	↓	±	↓	↑	↓	↑
Electron-withdrawing substituent at C_β	↓	↑	↓	↓	↓	↑	↓	↓	↓	↑	↓	↑

[a]Symbols indicate the following: ↑ extent of bond stretching increased, ↓ extent of bond stretching decreased, ± no unambiguous prediction possible.
[b]Transition state, tr. s.

changes with transition state geometry must take into account both parallel and perpendicular effects if it is to explain all the experimental data available. The single most important factor determining whether the parallel or perpendicular effect will dominate in a particular case appears to be the position of the transition state in the potential energy diagram. However, Thornton's updated theory (7) is the only one which incorporates to some extent the concept of differential sensitivity of the transition state geometry towards structural changes, depending on the character of the transition state. We would therefore like to propose a simple new working hypothesis which, while relying essentially on Thornton's original ideas (6), emphasizes the importance of the location of the transition state in a potential energy diagram as it was developed by More O'Ferrall (8) for elimination reactions (see Fig. 2). It may be stated as follows.

1. The closer the transition state of a concerted reaction is located to a corner of the potential energy diagram, the larger will be the slope of the potential energy surface in the direction to the corner. This will be true as long as there is a considerable energy difference between the corner itself and the transition state. A larger slope very likely corresponds to a large curvature of the energy surface along the line defined by the transition state and the adjacent corner.

2. If the transition state is very reactant- or product-like, the curvature of the energy surface in the parallel direction, *i.e.* along the reaction coordinate, will be large. If, on the other hand, it is very carbanion- or carbonium ion-like the curvature will be large in the perpendicular direction. Implicit in these statements is the assumption that the curvature in the corresponding other direction will be smaller.

3. In accordance with Thornton's theory (6) a perturbation caused by a substituent change will produce a greater shift in bond lengths, the smaller the curvature of the unperturbed curve. For a reactant- or product-like transition state the effect of a structural change should therefore manifest itself more strongly in the perpendicular than in the parallel direction. Conversely, for a carbanion- or carbonium ion-like transition state the effect in the parallel direction should dominate.

4. For very central transition states it is not possible to predict *a priori* which of the two effects will outweigh the other.

Support for this hypothesis comes mainly from the studies of Smith and Bourns (1) and Smith (38)[5] in which the effect of structural variations on the C—H and C—N^+ bond was simultaneously studied. The transition state of the E2 reaction of 2-arylethyltrimethylammonium ions with ethoxide in ethanol has considerable El_{cb} character (2). In this system any structural change which causes one bond (C—H) to be weakened more in the transition state has a corresponding effect on the other bond (C—N^+). This is the result expected when the effect on the parallel motion dominates. The transition state of the E2 reaction of 9-(4-substituted-benzyl)-fluorene-9-trimethylammonium ions with ethoxide in ethanol appears to be reactant-like (38). In this case a trend towards more C—H bond rup-

Can. J. Chem. Downloaded from www.nrcresearchpress.com by 210.87.254.40 on 09/05/12
For personal use only.

Can. J. Chem. Downloaded from www.nrcresearchpress.com by 210.87.254.40 on 09/05/12
For personal use only.

ture is associated with a trend towards less C—N^+ bond rupture.[5] This combination is consistent with the assumption that the perpendicular motion is more important.[7] The reaction of 2-phenylethyldimethylanilinium ions with ethoxide in ethanol (this work) occurs via a fairly central transition state; the same probably holds true for reactions of 2-phenylethylarenesulfonates with potassium *tert*-butoxide in *tert*-butyl alcohol (15). In both these systems the perpendicular effect is predominant. However, as structural changes shift the transition state structure towards the $E1_{cb}$ extreme, the transition state geometry becomes less sensitive to or almost independent of further structural variations. It appears that in this region parallel and perpendicular effects more or less balance. Presumably the curvature of the potential energy surface in the two directions is of comparable magnitude. It is not unreasonable to assume that in this area we may encounter small changes in bond lengths which are not *a priori* predictable but reflect subtleties of the energy surface. The small increase in C—H bond weakening upon going from a dimethylanilinium to a dimethyl-*p*-anisidinium leaving group, which we observed in this work, may be interpreted on this basis.

Since our working hypothesis has been derived on purely geometrical grounds, which are not peculiar to carbon elimination reactions, the respective conclusions should be equally valid for any reaction which can be represented in a three-dimensional More O'Ferrall-type potential energy diagram.

Experimental

Materials

2-Phenylethyldimethylanilinium Bromide

A threefold excess of methyl bromide (15 g, 0.15 mol), cooled in an acetone – Dry Ice bath, was added to a similarly cooled solution of 11.1 g (0.05 mol) *N,N*-2-phenylethylmethylaniline in 50 ml of acetonitrile. The flask was sealed and the solution was allowed to stand for 60 h in the dark at room temperature. The quaternary salt was precipitated by addition of ether and recrystallized four times from ethanol–ether; yield 14.9 g (92%); m.p. 169–170 °C lit. (30) 169–170 °C).

N,N-2-Phenylethylmethylaniline

This compound was prepared using the method of Oki and Mutai (39): 27.75 g. 2-Bromoethylbenzene (0.15 mol) (Eastman) and 16.05 g (0.15 mol) *N*-methylaniline (Eastman) were treated with 45 ml of 20% aqueous sodium hydroxide for 30 min. Most of the unreacted halide and amine were removed by steam distillation. The residue was extracted with ether. The ethereal solution was dried over potassium carbonate. Removal of the solvent and distillation produced 11.1 g (35%) of the pure product; b.p. 98 °C/0.04 Torr (lit. (40) 124–128 °C/0.3 Torr, (41) 131–134 °C/0.75 Torr). Recrystallization from ethanol yielded a white solid, m.p. 42–43 °C (lit. (41) 42–43 °C, (42) 44 °C).

2-Phenylethyldimethyl-p-anisidinium Bromide

This compound was prepared from *N,N*-2-phenylethylmethyl-*p*-anisidine and methyl bromide by the same procedure as the unsubstituted compound; m.p. 181–182 °C.

Anal. Calcd. for $C_{17}H_{22}NOBr$: C, 60.72; H, 6.59; N, 4.17. Found: C, 60.74; H, 6.60; N, 3.98.[8]

N,N-2-Phenylethylmethyl-p-anisidine

This compound was prepared by means of the Eschweiler–Clarke (43) procedure. To 17 g (0.075 mol) of *N*-2-phenylethyl-*p*-anisidine were added 10 g (0.195 mol) of 90% formic acid and 7.5 g (0.085 mol) of 35% formaldehyde and the mixture heated on the steam bath for 10 h. After cooling and addition of 40 ml 4 *N* hydrochloric acid, the excess of formaldehyde and formic acid was removed by distillation under reduced pressure. The residue was rendered alkaline with 40% aqueous sodium hydroxide and extracted with ether. After drying over potassium carbonate and removal of the solvent 17.4 g (100%) of the crude product were recovered. Vacuum distillation produced 10 g (59%) of the pure wax-like yellowish white product; b.p. 118 °C/0.03 Torr.

N-2-Phenylethyl-p-anisidine

This compound was prepared by the same method as *N,N*-2-phenylethylmethylaniline. From 18.5 g (0.1 mol) 2-bromoethylbenzene and 12.3 g (0.1 mol) *p*-anisidine, 11 g (48%) of pure product were obtained; b.p. 140–142 °C/0.5 Torr.

2-Phenylethyldimethyl-p-toluidinium Bromide

This material was prepared from *N,N*-2-phenylethylmethyl-*p*-toluidine and methyl bromide by the procedure described for the unsubstituted compound; m.p. 177 °C.

Anal. Calcd. for $C_{17}H_{22}NBr$: C, 63.75; H, 6.92; N, 4.37. Found: C, 63.76; H, 6.75; N, 4.27.[8]

N,N-2-Phenylethylmethyl-p-toluidine

N-2-Phenylethyl-*p*-anisidine (12.3 g, 0.058 mol) was converted into 10.3 g (80%) of this compound by means of the Eschweiler–Clarke procedure described for the corresponding *p*-anisidine derivative. The material was quaternized without further purification.

N-2-Phenylethyl-p-toluidine

4′-Methyl-phenylacetanilide (12.3 g, 0.054 mol) was

[7]Smith's data (38)[5] represent a problem, however, and cannot be considered as final proof of the present hypothesis. Although they seem to indicate that a trend towards the shortening of one bond is associated with a trend towards the lengthening of the other one, they do not appear to represent an effect on the perpendicular motion as interpreted in Thornton's (6, 7) theory, since the sense of the variation is exactly opposite to the one predicted on the basis of this theory. We are currently trying to establish the causes and implications of Smith's results.

[8]Elemental analyses were performed by Galbraith Laboratories Inc., Knoxville, Tennessee.

Can. J. Chem. Downloaded from www.nrcresearchpress.com by 210.87.254.40 on 09/05/12
For personal use only.

placed in the thimble of a Soxleth extraction apparatus, the flask of which contained 5.2 g (0.135 mol) lithium aluminum hydride (BDH Chemicals) and 350 ml ether. The extraction and reduction was allowed to proceed for 24 h. After cooling, water was carefully added dropwise until the reaction mixture appeared white. The precipitated aluminum hydroxide was then filtered and washed with ether. Removal of the solvent yielded 11.5 g (100%) of the product, a white, wax-like solid. It was used for the next step without further purification.

4′-Methyl-phenylacetanilide

A solution of 27 g (0.25 mol) *p*-toluidine (Eastman) and 50 g triethylamine in 50 ml benzene was added slowly whilst stirring to a solution of 38.7 g (0.25 mol) of phenylacetylchloride in 100 ml benzene. After allowing the reaction mixture to stand for 1 h the triethylamine hydrochloride formed was removed by filtration. The benzene solution was concentrated on the rotary evaporator. The precipitated anilide was filtered and thrice recrystallized from ethanol; yield 12.3 g (22%), m.p. 130 °C. Additional crude product was obtained on concentration of the mother liquors.

2-Phenylethyldimethyl-4-chloroanilinium Bromide

This material was prepared from *N,N*-2-phenylethylmethyl-4-chloroaniline and methyl bromide by the procedure described for the unsubstituted compound; m.p. 170–171 °C.

Anal. Calcd. for $C_{16}H_{19}NClBr$: C, 56.40; H, 5.62; N, 4.11. Found: C, 56.22; H, 5.66; N, 4.04.[8]

N,N-2-Phenylethylmethyl-4-chloroaniline

N-2-Phenylethyl-4-chloroaniline was methylated by the Eschweiler–Clarke procedure described for the corresponding *p*-anisidine derivative with nearly quantitative yield. The product was purified by dissolving it in petroleum ether and filtering through aluminum oxide, followed by recrystallization from ethanol; m.p. 61–62 °C.

N-2-Phenylethyl-4-chloroaniline

This compound was prepared by reduction of 4′-chloro-phenylacetanilide with lithium aluminum hydride as described for the corresponding *p*-toluidine derivative. It was purified by vacuum distillation; b.p. 126–128 °C/0.15 Torr.

4′-Chloro-phenylacetanilide

This compound was prepared by the procedure described for 4′-methyl-phenylacetanilide; m.p. 163 °C (lit. (44) 163–164 °C).

2-Phenylethyldimethyl-3-trifluoromethylanilinium Bromide

This compound was prepared by quaternization of *N,N*-2-phenylethylmethyl-4-trifluoromethylaniline with methyl bromide, as described for the unsubstituted compound; m.p. 160–161 °C.

Anal. Calcd. for $C_{17}H_{19}NF_3Br$: C, 54.55; H, 5.12; N, 3.74. Found: C, 54.35; H, 5.10; N, 3.66.[8]

N,N-2-Phenylethylmethyl-4-trifluoromethylaniline

N-2-Phenylethyl-4-trifluoromethylaniline was methylated by the Eschweiler–Clarke procedure described for the corresponding *p*-anisidine derivative. The product was quaternized without further purification.

N-2-Phenylethyl-4-trifluoromethylaniline

This compound was prepared by heating 16.1 g (0.1 mol) 4-trifluoromethylaniline with 13 g (0.13 mol) triethylamine and 18.5 g (0.1 mol) 2-bromoethylbenzene in a sealed flask for 48 h. After addition of 100 ml water, the mixture was extracted with ether. After drying over potassium carbonate, removal of the solvent and distillation, 2.7 g (11%) of the pure product were obtained; b.p. 114 °C/0.03 Torr.

2-Phenylethyldimethylanilinium-2,2-d_2 Bromide

This material was prepared from *N,N*-2-phenylethylmethylaniline-2,2-d_2 and methyl bromide as described for the undeuterated compound and purified by recrystallization from isopropanol–ether; m.p. 168 °C.

Anal. Calcd. for $C_{16}H_{18}D_2NBr$: C, 62.34; H + D, 7.19; N, 4.54. Found: C, 62.30; H + D, 7.01; N, 4.60.[8] Deuterium content: 1.96 atoms D per molecule.[9]

N,N-2-Phenylethylmethylaniline-2,2-d_2

2-Bromoethylbenzene-1,1-d_2 (4.6 g, 0.025 mol) and 5.4 g (0.05 mol) *N*-methylaniline were heated in a sealed flask for 24 h on the steambath. The reaction product was extracted with ether. After drying of the ethereal solution over potassium carbonate, removal of the solvent and vacuum distillation 2.6 g (50%) of the pure product were obtained; b.p. 102 °C/0.02 Torr.

2-Bromoethylbenzene-1,1-d_2

2-Phenylethanol-2,2-d_2 (6.2 g, 0.05 mol) and 31 g (0.18 mol) 48% hydrobromic acid were heated to reflux for two hours. Extraction of the cool solution with ether, drying of the organic phase over sodium sulfate and removal of the solvent yielded 8.3 g (88%) of the desired bromide.

2-Phenylethanol-2,2-d_2

Phenylacetic acid-α,α-d_2 (8.2 g, 0.061 mol) dissolved in 50 ml ether was added dropwise to a solution of 2.64 g (0.07 mol) lithium aluminum hydride in 75 ml ether. After heating the resulting solution to reflux for 2 h, just enough water was added to transform all the lithium aluminum hydride into aluminum hydroxide, which was then filtered off and washed with anhydrous ether. After removal of the solvent 6.6 g (87%) of product were obtained.

Phenylacetic Acid-α,α-d_2

A solution of 93 g (0.39 mol) diethylphenylmalonate (Eastman) in 390 ml dry petroleum ether (30–60 °C) was filtered through a column of alumina (80–200 mesh, Brockman activity 1) and then added to a well-stirred mixture of 170 ml petroleum ether and 18.6 g (0.39 mol) of a 50% dispersion of sodium hydride in mineral oil (Metal Hydrides Inc).

The resulting white solid was removed by filtration and washed repeatedly with petroleum ether. The solvent was removed from the solid by pumping overnight in a vacuum desiccator. The dried sodium salt, 66 g (0.26 mol), was added to 70 ml deuterium oxide. The resulting solution was heated to reflux for 8 h in a dry nitrogen atmosphere. After cooling, the solution was acidified by adding thionyl chloride and heated again to reflux for 2 h to bring about decarboxylation. After extraction with ether, drying over sodium sulfate and removal of the solvent, 31 g of the crude product were obtained. Recrystallization from petroleum ether yielded 22 g (41%) of pure phenylacetic acid-α,α-d_2.

[9]Deuterium analyses were performed by Mr. J. Nemeth, 303 W. Washington Street, Urbana, Illinois.

Can. J. Chem. Downloaded from www.nrcresearchpress.com by 210.87.254.40 on 09/05/12
For personal use only.

2-Phenylethyldimethyl-p-anisidinium-2,2-d_2 Bromide

This salt was prepared from *N,N*-2-phenylethylmethyl-*p*-anisidine-2,2-d_2 and methyl bromide as described for the corresponding undeuterated unsubstituted material; m.p. 180 °C.

Anal. Calcd. for $C_{17}H_{20}D_2NOBr$: C, 60.36; H + D, 7.15; N, 4.14. Found: C, 60.28; H + D, 6.93; N, 4.13.[8] Deuterium content: 1.96 atoms D per molecule.[9]

N-2-Phenylethylmethyl-p-anisidine-2,2-d_2

N-2-Phenylethyl-*p*-anisidine-2,2-d_2 (1.65 g, 0.0073 mol) was transformed into 1.5 g (85%) of the corresponding *N*-methyl compound by the Eschweiler–Clarke procedure described for the undeuterated compound. The product was quaternized without further purification.

N-2-Phenylethyl-p-anisidine-2,2-d_2

4′-Methoxy-phenylacetanilide-α,α-d_2 (2.5 g, 0.024 mol) was reduced with lithium aluminum hydride to yield 2.1 g (89%) of the desired amine, using the procedure described for the corresponding undeuterated *p*-toluidine derivative.

4′-Methoxy-phenylacetanilide-2,2-d_2

A solution of 5 g (0.033 mol) phenylacetylchloride-α,α-d_2 in 10 ml dry benzene was added dropwise to a stirred solution of 4 g (0.033 mol) *p*-anisidine (Eastman) and 3.4 g (0.033 mol) triethylamine in 50 ml benzene. The mixture was allowed to stand for 1 h, after which time the white product was removed by filtration, washed with deuterium oxide and recrystallized from benzene; yield 4.5 g (57%); m.p. 122 °C.

Phenylacetyl Chloride-α,α-d_2

A mixture of 11 g (0.079 mol) phenylacetic acid-α,α-d_2 and 9.4 g (0.079 mol) thionyl chloride (BDH) was provided with a few boiling chips and allowed to stand at room temperature for 24 h. The reaction was quantitative and the product was used without further purification.

2-Phenylethyldimethyl-p-toluidinium-2,2-d_2 Bromide

This material was available from an earlier study.[10] It was recrystallized four times from ethanol–ether; m.p. 178 °C.

Anal. Calcd. for $C_{17}H_{20}D_2NBr$: C, 63.35; H + D, 7.50; N, 4.35. Found: C, 63.31; H + D, 7.06; N, 4.34.[8] Deuterium content: 1.94 atoms D per molecule.[9]

2-Phenylethyldimethyl-4-chloroanilinium-2,2-d_2 Bromide

This compound was prepared from *N,N*-2-phenylethylmethyl-4-chloroaniline-2,2-d_2 and methyl bromide as described for the unsubstituted, undeuterated material; m.p. 170 °C.

Anal. Calcd. for $C_{16}H_{17}D_2NClBr$: C, 56.07; H + D, 6.17; N, 4.09. Found: C, 56.15; H + D, 5.95; N, 3.95.[8] Deuterium content: 1.89 atoms D per molecule.[9]

N,N-2-Phenylethylmethyl-4-chloroaniline-2,2-d_2

N-2-Phenylethyl-4-chloroaniline-2,2-d_2 (2.6 g, 0.0113 mol) was transformed into the corresponding *N*-methylaniline by the Eschweiler–Clarke procedure described for the corresponding undeuterated *p*-methoxy compound; yield 2.46 g (88%). The product was quaternized without further purification.

N-2-Phenylethyl-4-chloroaniline-2,2-d_2

Phenylacetyl-4-chloroanilide-α,α-d_2 (3.7 g, 0.0151 mol) was reduced with lithium aluminum hydride to the desired amine, as described for the corresponding undeuterated *p*-toluidine derivative.

Phenylacetyl-4-chloroanilide-α,α-d_2

A solution of 5 g (0.033 mol) phenylacetylchloride-α,α-d_2 in 10 ml dry benzene was added dropwise to a stirred solution of 4.15 g (0.033 mol) 4-chloroaniline-*N,N*-d_2 and 3.4 g (0.033 mol) triethylamine (Eastman) in 50 ml benzene. The mixture was allowed to stand for 1 h, after which time the white product was removed by filtration, washed with deuterium oxide, and recrystallized from chloroform–ether; yield 3.8 g (47%); m.p. 163 °C.

4-Chloroaniline-N,N-d_2

A mixture of 10 g (0.079 mol) 4-chloroaniline (Eastman), 20 ml deuterium oxide and enough pyridine to bring all the aniline into solution was allowed to stand overnight at room temperature. Most of the solvent was then removed on the rotation evaporator. This treatment was repeated once. The product was then recrystallized from petroleum ether; m.p. 70 °C. Nuclear magnetic resonance analysis indicated a deuterium content of 1.92 atoms D per molecule.

2-Phenylethyldimethyl-3-trifluoromethylanilinium Bromide-2,2-d_2

This compound was available from an earlier study.[10] It was recrystallized three times from ethanol–ether; m.p. 125 °C.

Anal. Calcd. for $C_{17}H_{17}D_2NF_3Br$: C, 54.26; H + D, 5.62; N, 3.72. Found: C, 54.18; H + D, 5.52; N, 3.66.[8] Deuterium content: 1.89 atoms D per molecule.[9]

2-Phenylethyldimethyl-4-trifluoromethylanilinium Bromide-2,2-d_2

This material was available from an earlier investigation.[10] It was recrystallized twice from ethanol–ether; m.p. 159 °C. Nuclear magnetic resonance analysis indicated more than 90% deuteration in the benzyl position.

Absolute Ethanol

This solvent was dried by the method of Lund and Bjerrum (45) and stored under anhydrous conditions.

Sodium Ethoxide

Stock solutions of this base were prepared by dissolving clean sodium metal in ethanol under strictly anhydrous conditions in a nitrogen atmosphere.

Product Analyses

The appropriate undeuterated quaternary ammonium salt (300 to 500 mg) was dissolved in 25 ml of a 1.48 *N* solution of sodium ethoxide in ethanol and the solution allowed to stand for 18–24 h in a thermostatted bath at 40 °C. The solution was then diluted with 25 ml water and extracted three times with 50 ml portions of petroleum ether. After removal of the solvent under reduced pressure the mixture was analyzed by g.l.c., using a column packed with 15% silicon rubber SE30 on Chromosorb W. This procedure was applied to the *p*-Me, *p*-H, *p*-Cl, and *m*-CF_3 substrates. In all cases three peaks could be distinguished. The two large ones corresponded to the two products of the elimination reaction (styrene and a substituted *N,N*-dimethylaniline) the third very small one corresponded to the product of a competing substitution reaction, namely a substituted *N,N*-2-phenylethylmethylaniline. The various peaks were identified by comparing them with the peaks corresponding to authentic samples. A rough comparison of the peak areas indicated the

[10]A. N. Bourns and B. Wang, unpublished work.

TABLE 6. Ultraviolet absorption of substituted *N,N*-dimethylanilines and styrene in absolute ethanol, reference 95% ethanol

Compound	λ_{max}(nm)	$\varepsilon(\lambda_{max}) \times 10^4$	ε(248 nm) $\times 10^4$
N,N-Dimethyl-*p*-anisidine	249	1.12	1.11
N,N-Dimethyl-*p*-toluidine	252	1.22	1.12
N,N-Dimethylaniline	248	1.25	1.25
N,N-Dimethyl-*p*-chloroaniline	260	1.80	1.00
N,N-Dimethyl-*m*-trifluoromethylaniline	258	1.62	1.00
Styrene	248	1.40	1.40

following maximal amounts of substitution products: *p*-Me, 0.18%; *p*-H, 0.16%; *p*-Cl, 0.23%; *m*-CF_3, 0.85%. It appears that the percentage of substitution reaction is larger for stronger electron-withdrawing substituents in the leaving group, a trend which has also been observed by Willi (22).

A visual comparison of the u.v. spectra of the actual reaction solutions at infinite time gave no indication of any appreciable amounts of competing substitution reaction. Deuterated and undeuterated starting materials produced solutions with virtually identical spectra. Furthermore, the spectra of the reaction solutions at infinite time appeared identical to the spectra of solutions prepared from authentic samples. This, together with the fact that the infinity value of the optical density in the kinetic runs was within $\pm 1\%$ of the expected value, was taken as evidence that competition by substitution reactions was not important under the experimental conditions chosen.

Kinetic Measurements

The rate of reaction of undeuterated and deuterated 2-phenylethyldimethylanilinium salts with sodium ethoxide in ethanol was determined by spectrophotometrically monitoring the increase in the amount of reaction product (*i.e.* styrene and *N,N*-dimethylaniline) as a function of time. All the reactions were carried out directly in the spectrophotometer cell and followed to a minimum of 75% completion. Standard wavelength for all the measurements was 248 mm, the wavelength of the absorption maxima of styrene and unsubstituted dimethylaniline. At this wavelength absorption caused by the reactants was negligible. A compilation of the absorption maxima and molar extinction coefficients of the various reaction products as measured under the reaction conditions is given in Table 6.

A Hitachi–Perkin-Elmer model 139 spectrophotometer fitted with a thermostatted cell compartment was used throughout for the kinetic measurements. The temperature in the cell compartment was kept constant at 40 ± 0.05 °C. Ultraviolet–visible spectra were recorded on a Cary 14 spectrophotometer.

The reaction solutions were prepared by mixing appropriate amounts of thermostatted stock solutions of the quaternary anilinium salts and the base in 50 ml volumetric flasks. All reactions were measured under pseudo first-order conditions with the base in large excess (*ca.* 400 fold) over the quaternary salt. The same sodium ethoxide solution was used for a complete set of experiments. This ensured a constant ionic strength. The substrate concentration was chosen such that a convenient value of the optical density of the reaction solutions at infinite time would be obtained, *i.e.* $3\text{–}4 \times 10^{-5}$ mol/l. Reactions with undeuterated and deuterated substrates were always carried out simultaneously. Excellent first-order plots were obtained in all cases.

Solutions of the quaternary anilinium salts were entirely stable. Elimination was caused only by ethoxide ion, not by ethanol. No deuterium exchange was detected in solutions of the deuterated salts.

The pseudo first-order rate constants, k', were calculated as -2.3 times the slope of the first-order plots (46). This slope was determined either by visually drawing a straight line or by least-squares treatment, both methods giving the same result. The second-order rate constants, k_E, were then obtained by division of k' by the ethoxide ion concentration, *i.e.* $k_E = k'/[EtO^-]$. The rate constants given in Table 1 represent the average of 3 to 6 kinetic runs.

Nitrogen Isotope Effects

The nitrogen isotope effects were determined by comparing the nitrogen isotopic abundance of the dimethylaniline formed in reactions carried out to some known fractional extent (partial reactions) with the isotopic abundance in the starting material or in the product after complete reaction.

The desired extent of reaction was achieved by adding the appropriate amount of base to the quaternary salt solution and allowing the reaction to proceed for more than ten half lives. Runs were set up so that 0.2 mmol of dimethylaniline would be formed, a convenient quantity for the subsequent mass spectrometric analysis. The faster reactions were carried out in 50 ml volumetric flasks, the slower ones in evacuated ampoules. The concentrations were small enough to ensure that practically no reaction occurred during mixing of the reactants. The reaction vessels were kept in a thermostatted bath at 40 ± 0.02 °C.

After the reaction had proceeded for ten or more half lives, water (twice the amount of the alcoholic reaction solution) was added to the reaction mixture. The aqueous solution was extracted three times with 50 ml portions of petroleum ether (30–60); 2.5 ml of concentrated sulfuric acid were then added to the organic phase and the solvent removed on the rotary evaporator. The acid residue was washed with water into a Kjeldahl flask. After the water had been removed by gentle heating, 2 g potassium sulfate and 0.10 g mercuric oxide were added. This mixture was digested in the usual manner for 2.5–3 h. Ammonia was

Can. J. Chem. Downloaded from www.nrcresearchpress.com by 210.87.254.40 on 09/05/12
For personal use only.

Can. J. Chem. Downloaded from www.nrcresearchpress.com by 210.87.254.40 on 09/05/12
For personal use only.

then liberated by addition of sodium hydroxide and transferred into excess standard sulfuric acid by steam distillation. The overall yield was always over 90%, usually between 95 and 100%.

This extraction technique was used for partial and complete reactions. For the preparation of nitrogen samples from the quaternary salts it was necessary to remove the halogen by oxidation with hydrogen peroxide prior to digestion, as described by Ayrey *et al.* (47).

The ammonium sulfate solution resulting from the Kjeldahl digestion was concentrated and oxidized with sodium hypobromite to nitrogen gas, which was purified and then analyzed by mass spectrometry. Details of the procedure are given by Ayrey *et al.* (47).

The kinetic isotope effects were calculated as described previously (47).

Financial support for this work was provided by the National Research Council of Canada and McMaster University. We wish to thank Professors E. R. Thornton and W. H. Saunders, Jr. for discussions.

1. P. J. Smith, C. A. Pollock, and A. N. Bourns. Can. J. Chem. **53**, 1319 (1975).
2. P. J. Smith and A. N. Bourns. Can. J. Chem. **52**, 749 (1974).
3. (*a*) W. H. Saunders, Jr. and A. F. Cockerill. Mechanisms of elimination reactions. Wiley-Interscience, New York. 1973; (*b*) A. F. Cockerill. Elimination reactions. *In* Comprehensive chemical kinetics. Vol. 9. *Edited by* C. H. Bamford and C. F. H. Tipper. Elsevier, Amsterdam. 1973.
4. J. F. Bunnett. Surv. Prog. Chem. **5**, 53 (1969).
5. J. F. Bunnett. Angew. Chem. **74**, 731 (1962).
6. E. R. Thornton. J. Am. Chem. Soc. **89**, 2915 (1967).
7. D. A. Winey and E. R. Thornton. J. Am. Chem. Soc. **97**, 3102 (1975).
8. R. A. More O'Ferrall. J. Chem. Soc. B, 274 (1970).
9. J. E. Critchlow. J. Chem. Soc. Faraday Trans. 1, **68**, 1774 (1972).
10. W. J. Albery. Progr. reaction kinetics. *Edited by* G. Porter. **4**, 353 (1967).
11. G. S. Hammond. J. Am. Chem. Soc. **77**, 334 (1955).
12. W. P. Jencks. Chem. Rev. **72**, 705 (1972).
13. R. A. Bartsch and J. F. Bunnett. J. Am. Chem. Soc. **91**, 1382 (1969); **91**, 1376 (1969); **90**, 408 (1968).
14. R. A. Bartsch. J. Org. Chem. **35**, 1334 (1970).
15. J. Banger, A. F. Cockerill, and G. L. O. Davies. J. Chem. Soc. B, 498 (1971).
16. A. N. Bourns and A. C. Frosst. Can. J. Chem. **48**, 133 (1970).
17. P. J. Smith and A. N. Bourns. Can. J. Chem. **48**, 125 (1970).
18. A. Fry. Chem. Soc. Rev. **1**, 163 (1972).
19. L. P. Hammett. Physical organic chemistry. 2nd ed. McGraw Hill, New York. 1970.
20. W. A. Sheppard. J. Am. Chem. Soc. **87**, 2410 (1965).
21. E. K. Thornton and E. R. Thornton. *In* Isotope effects in chemical reactions. *Edited by* C. J. Collins and N. S. Bowman. Van Nostrand Reinhold, New York. 1970.
22. A. V. Willi. Helv. Chim. Acta, **49**, 1725 (1966).
23. J. Biegeleisen and M. Wolfsberg. Adv. Chem. Phys. **1**, 15 (1958).
24. (*a*) A. M. Katz and W. H. Saunders, Jr. J. Am. Chem. Soc. **91**, 4469 (1969); (*b*) W. H. Saunders, Jr. Chem. Scripta (Sweden). **8**, 27 (1975).
25. L. Melander. Isotope effects on reaction rates. Ronald Press, New York. 1960. pp. 24–32.
26. F. H. Westheimer. Chem. Rev. **61**, 265 (1961).
27. J. Biegeleisen. Pure Appl. Chem. **8**, 217 (1964).
28. R. A. More O'Ferrall and J. Kouba. J. Chem. Soc. B, 985 (1967).
29. R. P. Bell, W. H. Sachs, and R. L. Tranter. Trans. Faraday Soc. **66**, 1995 (1970).
30. L. J. Steffa and E. R. Thornton. J. Am. Chem. Soc. **89**, 138 (1967).
31. W. H. Saunders, Jr. and D. H. Edison. J. Am. Chem. Soc. **82**, 138 (1960).
32. C. H. de Puy and D. H. Froemsdorf. J. Am. Chem. Soc. **79**, 3710 (1957).
33. C. H. de Puy and C. A. Bishop. J. Am. Chem. Soc. **82**, 2532 (1960).
34. W. H. Saunders, Jr. and R. A. Williams. J. Am. Chem. Soc. **79**, 3712 (1957).
35. C. H. de Puy and C. A. Bishop. J. Am. Chem. Soc. **82**, 2535 (1960).
36. P. J. Smith and S. K. Tsui. Tetrahedron Lett., 61 (1973).
37. P. J. Smith and S. K. Tsui. Tetrahedron Lett., 917 (1972).
38. P. J. Smith and S. K. Tsui. J. Am. Chem. Soc. **95**, 4760 (1973).
39. M. Oki and K. Mutai. Bull. Chem. Soc. Jpn. **38**, 387 (1965).
40. M. S. Kharash, G. N. Williams, and W. Nudenberg. J. Org. Chem. **20**, 937 (1955).
41. G. C. Jones, W. Q. Beard, and C. R. Hauser. J. Org. Chem. **28**, 199 (1963).
42. J. V. Braun. Chem. Ber. **43**, 3209 (1910).
43. Houben-Weyl. Methoden der organischen Chemie, Band XI/1. Stickstoffverbindungen II. *Edited by* E. Mueller. Georg Thieme Verlag, Stuttgart. 1957. p. 650 ff.
44. Beilsteins Handbuch der organischen Chemie. Band XII. 4th ed. *Edited by* Deutsche Chemische Gesellschaft. Springer-Verlag, Berlin. 1929. p. 614.
45. H. Lund and J. Bierrum. Chem. Ber. **64B**, 210 (1931).
46. R. Livingston. Evaluation and interpretation of rate data. *In* Technique of organic chemistry, Vol. VIII, Part 1. *Edited by* A. Weissberger. Interscience, New York. 1961. p. 126.
47. G. Ayrey, A. N. Bourns, and V. A. Vyas. Can. J. Chem. **41**, 1759 (1963).

The Direct Formation of 3-Vinylthiophenes Using Butadienylphosphonium Salts[1]

JOHN M. MCINTOSH[2] AND FREDERICK P. SEGUIN
Department of Chemistry, University of Windsor, Windsor, Ontario N9B 3P4

Received June 9, 1975

JOHN M. MCINTOSH and FREDERICK P. SEGUIN. Can. J. Chem. **53**, 3526 (1975).

The reaction of α-mercaptoaldehydes and ketones with 1,3-butadien-1-yltriphenylphosphonium salts (**4**) unexpectedly leads to 3-vinylthiophenes and triphenylphosphine. This result is attributed to the retardation of the usual Wittig cyclization reaction which allows the competing reaction to occur.

JOHN M. MCINTOSH et FREDERICK P. SEGUIN. Can. J. Chem. **53**, 3526 (1975).

La réaction des α-mercaptoaldéhydes et cétones avec les sels du butadiène-1,3 yl-1 triphénylphosphonium (**4**) conduit d'une façon inattendue aux vinyl-3 thiophènes et à la triphénylphosphine. On attribue ce résultat à un retardement de la réaction de cyclisation de Wittig habituelle qui permet à la réaction compétitive de se produire.

[Traduit par le journal]

The concept of 'umpolung' (1) or reversed polarity synthons in organic synthesis has become a center of intense investigation since the principle was first enunciated by Corey (2). By far the most concentrated attention has been on the generation of the nucleophilic equivalent of a carbonyl carbon atom and several successful variations of this have been achieved (for an excellent review of methods, see ref. 3). In recent years, several groups have been concerned with the reaction of another type of compound which fits into this type of classification, *viz.* vinylphosphonium salts (**1**) (ref. 4 and previous papers in the series) which can be visualized as the equivalent of a reversed-polarity enolate ion (**2**). Our

1 **2**

particular interest has been in the use of **1** and α-mercaptoaldehydes and ketones as convenient routes to conjugated dienes (5) and thiophenes (6) via the intermediacy of 2,5-dihydrothiophenes (**3**) [1]. As part of our program to enlarge the scope of these reactions we decided to prepare and investigate the use of some functionalized phosphonium salts. One of the simplest, yet most interesting of these is 1,3-butadien-1-yltriphenylphosphonium chloride (**4**) which is readily available from either the bis-salt **5**[3] or the monophosphonium salt **6** (7) by the appropriate elimination reaction. It is evident that salt **4** is related to the enolate of crotonaldehyde in the same way that **1** is related to **2**. Although **4** is a well-known entity (8), until recently, little work on its chemistry has been reported. More results using the closely related diethyl 1,3-butadien-1-ylphosphonate (**7**) are available (9). Unlike the alkylations of extended enolate ions which occur at the β-carbon atom

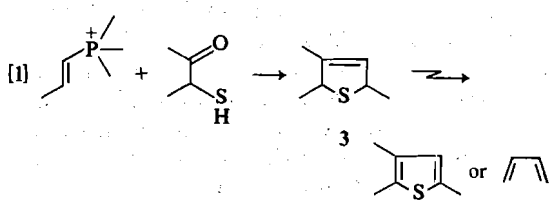

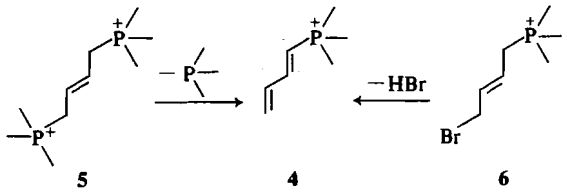

5 **4** **6**

[1]Presented in part at the annual meeting, Chemical Institute of Canada, Toronto, May 1975. Taken in part from the undergraduate research report of F.P.S., submitted April 1975.

[2]Author to whom correspondence should be addressed.

[3]The extreme ease of formation of **5** from triphenyl phosphine and 1,4-dichloro-2-butene contrasts sharply with the reported difficulty of forming the same salt from the dibromide (7).

Can. J. Chem. Downloaded from www.nrcresearchpress.com by 210.87.254.105 on 09/05/12
For personal use only.

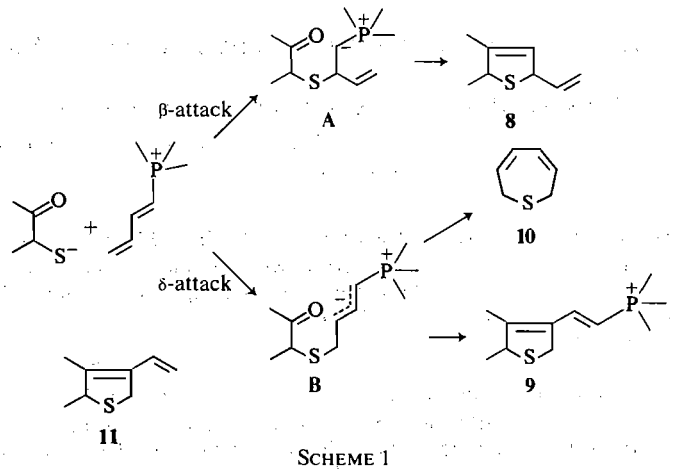

SCHEME 1

(10), all reports on the reactions of **4** and **7** implicate attack at the δ-position.

Depending on the site of initial attack on **4**, several products (**8–10**) can be envisioned as arising from its reaction with α-mercaptocarbonyl compounds (Scheme 1). A notable absence from this scheme is **11** which cannot arise by any simple loss of triphenylphosphine oxide from either of intermediates **A** or **B**.

Results and Discussion

When salt **4** was prepared *in situ* from **5** and reacted with 2-mercaptocyclohexanone (**12**) in pyridine solution, a single nonpolar compound was isolated in moderate yield after removal of triphenylphosphine. This was achieved by converting it into the sulfide using elemental sulfur (10) followed by chromatography. The n.m.r. spectrum of the remaining material clearly indicated the product was not of the expected type. The presence of a terminal vinyl group attached to an *aromatic* ring and one other low-field proton was clearly evident. The mass spectrum showed a molecular ion at *m/e* 164. All the data

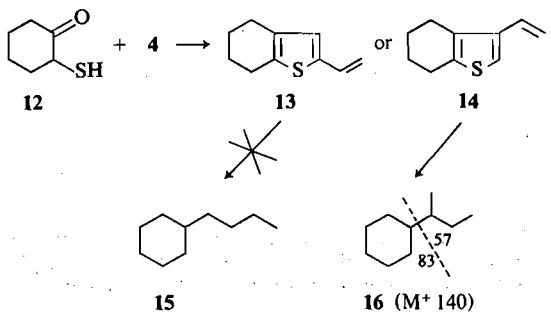

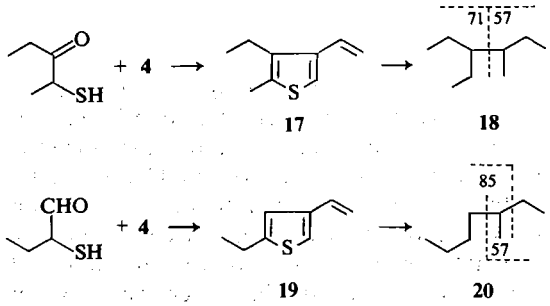

were in accord with either 2- or 3-vinyl-4,5,6,7-tetrahydrobenzo[*b*]thiophene (**13** or **14**). Attempts to reduce the product to the 2- or 3-ethyl compound using homogeneous catalysis (11) were unsuccessful. However, reductive desulfurization using Raney nickel (12) afforded a single saturated hydrocarbon, the mass spectrum of which coincided with that of **16**, but not its isomer **15** which established the structure of the product to be **14**. Similar results were obtained in the other two cases tried. In each instance, the 3-vinylthiophene (**17** and **19**) derivative was obtained. The yields of thiophene product were in the 30–40% range when pyridine was used as solvent. However, substitution of 2-picoline as solvent raised these to the 50–70% range.

These reactions of salt **4** produce a product in a higher formal oxidation state than those reactions of salts **1** previously investigated (5). The possibility of disproportionation of **3** to thiophene was eliminated by the absence of the corresponding tetrahydrothiophene from the reaction mixture and since all reactions were performed under a nitrogen atmosphere, aerial

Can. J. Chem. Downloaded from www.nrcresearchpress.com by 210.87.254.105 on 09/05/12
For personal use only.

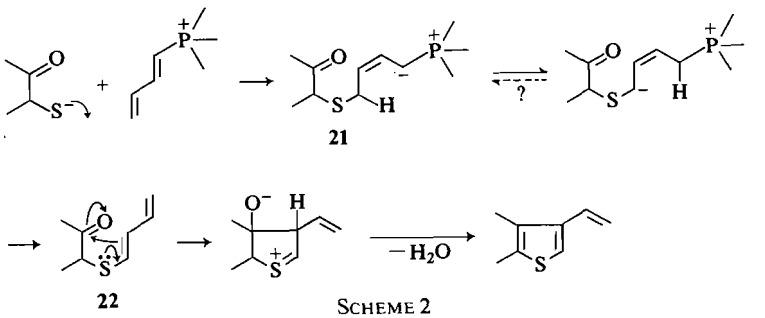

21

22

SCHEME 2

oxidation seems unlikely. The formation of large amounts of triphenylphosphine whether salt **5** or **6** was used as the starting material, and the total absence of triphenylphosphine oxide in the reaction mixture suggested an alternate mechanism might be operating (Scheme 2).[4] Acid catalysis of the cyclization–dehydration step, if necessary, could be provided by the amine hydrochloride present in the mixture. An analogous mechanism has recently been proposed (13) for the isomerization of a thiochromene to a benzothiophene. The *Z*-configuration of **21** required for proton transfer should be easily accessible.

In an attempt to verify this hypothesis, sulfide **23** was prepared and subjected to a variety of reaction conditions. In no case was any thiophene detected although **23** was consumed. The reactions uniformly turned black and decomposition of **23** leading to products other than **22** may account for this negative result.

In the reaction of 2-mercaptobutyraldehyde with **4**, a second product was isolated and identified as 2,4-diethylthiophene, **25**. This product appears to be formed from a decomposition product of the aldehyde dimer **24** since its formation depends on the purity of **24**. Attempted distillation or recrystallization of **24** leads to partial dehydration and the amount of **25** subsequently formed increases dramatically. Such extrusion reactions have previously been reported (14) for a variety of types of organic materials and the mechanisms suggested in those cases are clearly applicable here.

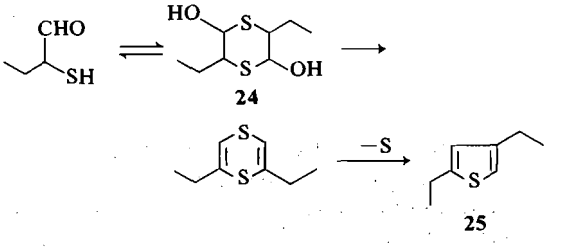

24

25

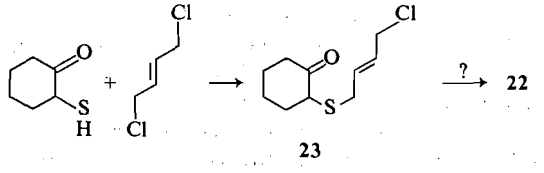

23

Why thiophenes and not dihydrothiophenes should be formed when salt **4** is used is not intuitively obvious. However, our experience has been that such factors as α-substitution of the vinyl salts which retard the rate of betaine formation generally increase the amount of thiophene in a mixture. It appears possible therefore, that the proton migration step is a competing side reaction in all cases, but only successfully competes with the intramolecular Wittig reaction when the latter is slow. Clearly the delocalized character of intermediate **B** (Scheme 1) and the unfavorable entropy term associated with the formation of **10** would be expected to result in a slower Wittig reaction and increased amounts of thiophene as is observed.

Experimental

Nuclear magnetic resonance spectra were run on Varian EM360 or JEOLCO C 60HL instruments and are reported in p.p.m. downfield from TMS as internal standard. Infrared spectra were recorded on a Beckmann IR 12 and mass spectra on a Varian MATCH-5DF spectrometer. Gas–liquid chromatographic analyses were carried out on

[4]A referee has suggested an alternative route from **21** involving proton transfer, cyclization, and dehydration to give **i**, followed by elimination of triphenylphosphine as shown.

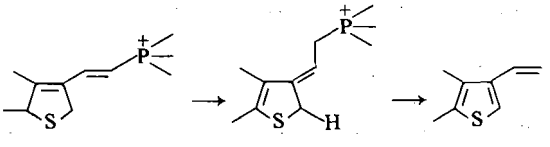

i

Can. J. Chem. Downloaded from www.nrcresearchpress.com by 210.87.254.105 on 09/05/12
For personal use only.

Can. J. Chem. Downloaded from www.nrcresearchpress.com by 210.87.254.105 on 09/05/12
For personal use only.

a Hewlett-Packard Model 5750 instrument using helium carrier gas at a flow rate of 1 ml/s. Unless otherwise noted, the drying agent was anhydrous magnesium sulfate and column chromatography was performed using Fisher acidic alumina, activity grade I. Pyridine was dried over solid sodium hydroxide and was decanted prior to use. Microanalyses were performed by A.B. Gygli, Microanalysis Laboratory, Toronto, Ontario.

2-Butenyl-1,4-bistriphenylphosphonium Dichloride (5)

A mixture of 12.4 g (0.1 mol) of 1,4-dichloro-2-butene and 52.4 g (0.2 mol) of triphenylphosphine in 400 ml acetonitrite was heated at reflux for 15 h. The cooled solution was filtered and the residue was washed well with ether and dried under vacuum at 85 °C. The yield was 64.5 g (98%), m.p. 255–258 °C.

When an attempt was made to prepare the mono-salt either in benzene or acetonitrite solvent, only the bis-salt **5** could be obtained.

3-Vinyl-4,5,6,7-tetrahydrobenzo[b]thiophene (14)

A solution of salt **5** in 150 ml dry pyridine and 10 ml of triethylamine was stirred at room temperature for 30 min. Mercaptoketone **12** (15) (4.2 g, 0.032 mol) was added all at once, the system was purged with nitrogen, and the solution was refluxed for 72 h. The cooled solution was diluted with 700 ml of water and extracted with ether (2 × 100 ml) and pentane (2 × 100 ml). The combined organic extracts were washed with 10% hydrochloric acid until the washings were acidic and then with water. Removal of the solvent from the dried solution gave a semisolid material which was dissolved in 300 ml of benzene containing excess sulfur flowers and the mixture was refluxed for 3.5 h. The benzene was removed, ice-cold pentane was added and the precipitated solids were removed by filtration. The filtrate was chromatographed on alumina using 10% ether in pentane as eluant. Thiophene **14** eluted rapidly and was pure to g.l.c. analysis; (20% SE 30, 160 °C); yield 2.51 g (51%); i.r. (CCl_4) 3090, 2930, 2850, 2840, 1630, 1440, 1420, 990, and 905 cm^{-1}; n.m.r. (CCl_4) 6.85 (1H, s), 6.46 (1H, dd, J = 17, 11 Hz), 5.36 (1H, dd, J = 17, 2 Hz), 501 (1H, dd, J = 11, 2 Hz), 2.6 (4H, m), and 1.82 (4H, m).

Anal. Calcd. for $C_{10}H_{12}S$: C, 73.12; H, 7.36. Found: C, 72.92; H, 7.01.

Increasing the reaction time did not raise the yield, but using 2-picoline as solvent increased the yield to 62%. The same product was obtained when phosphonium salt **6** was substituted for **5**.

2-Methyl-3-ethyl-4-vinylthiophene (17)

Working on a 0.03 mol scale and using pyridine as solvent the thiophene **17** was obtained in 31% yield; i.r. (CCl_4) 3090, 2970, 2930, 2870, 1625, 1450, 1420, 1375, 1190, 1065, 990, 950, 910, and 870 cm^{-1}; n.m.r. ($CDCl_3$) 7.03 (1H, s), 6.62 (1H, dd, J = 17, 10 Hz), 5.50 (1H, dd, J = 17, 1.5 Hz), 5.14 (1H, dd, J = 10, 1.5 Hz), 2.57 (2H, q, J = 7 Hz), 2.35 (3H, s), and 1.10 (3H, t, J = 7 Hz); λ_{max}(cyclohexane) 258 (6450), 231 (12 880), and 225 (14 650) nm.

Anal. Calcd. for $C_9H_{12}S$: C, 71.00; H, 7.94. Found: C 70.86; H, 8.03.

2-Ethyl-4-vinylthiophene (19) and 2,4-Diethylthiophene (25)

When 2-mercaptobutyraldehyde (16) was employed in pyridine solution, two compounds were isolated from the alumina chromatography. The g.l.c. analysis (20%, Carbowax 20M, 130 °C) separated these and gave **19** (35%); i.r. (CCl_4) 3095, 2970, 2930, 2870, 1630, 1460, 1210, 990, 900, 860, and 840 cm^{-1}; n.m.r. (CCl_4) 6.82 (2H, s), 6.53 (1H, dd, J = 16, 11 Hz), 5.43 (1H, dd, J = 16, 2 Hz), 5.08 (1H, dd, J = 11, 2 Hz), 2.82 (2H, q, J = 7.5 Hz), and 1.07 (3H, t, J = 7.5 Hz).

Anal. Calcd. for $C_8H_{10}S$: C, 68.55; H, 7.30. Found: C, 68.70; H, 7.24.

Also isolated was **25**; i.r. (CCl_4) 2960, 2930, 2870, 1455, and 790 cm^{-1}; n.m.r. (CCl_4) 6.55 (2H, s), 2.70 (4H, m), and 1.24 (6H, m).

Anal. Calcd. for $C_8H_{12}S$: C, 68.55; H, 8.63. Found: C 68.77; H, 8.63.

The ratio of **19** and **25** varied from experiment to experiment and the variation was traced to the use of different preparations of the aldehyde.

Desulfurization Experiments

The thiophene (0.5–2 g) was dissolved in 300 ml ethyl acetate (THF in the case of **19**) and 6–10 g W-2 Raney nickel (17) was added. The solution was stirred 1 h, and then refluxed for 1 h. The solution was filtered and the solvent removed by distillation at 1 atm through a 20 cm Vigreaux column. The residue was analyzed by g.l.c. (20% TCEP, 90 °C) and in each case consisted of a major product and two minor ones. The major products gave mass spectra identical to those recorded for **16** (18) **18** (19), and **20** (ref. 19, p. 419). The minor product in each case has a molecular weight (mass spectral) two units lower than the major fraction and fragmentation patterns consistent with unsaturated derivatives.

2-(4-Chloro-2-butenylthio)cyclohexanone (23)

A solution of 5 g of **12** in 50 ml of dimethyl formamide was added all at once to 4.4 g (1 equiv,) of potassium *tert*-butoxide in 50 ml of the same solvent. The reaction was stirred for 5 min at ambient temperature and then 5 ml of 1,4-dichloro-2-butene was added. The yellow color was immediately quenched. After stirring for 1 h at ambient temperature, the solution was poured into 300 ml of water and extracted with ether. The extracts were washed with water, dried, and evaporated to give a quantitative yield of a pale yellow oil. This oil could not be effectively purified, but the spectral characteristics of the crude material indicated it to be at least 90% pure **23**; n.m.r. ($CDCl_3$) 6.02–5.35 (2H, m), 4.03 (2H, m), 3.45–3.00 (3H, m), and 2.51–1.40 (8H, m).

Treatment of this material with pyridine and triethylamine with and without added triphenyl phosphine, or DBU in methylene chloride resulted in destruction of the starting material, but no identifiable products could be obtained.

The technical assistance of Mr. J. Lott and the financial assistance of the National Research Council of Canada and Hoffmann-LaRoche Co., Nutley, N.J. are very gratefully acknowledged.

1. D. SEEBACH and D. ENDERS. Angew. Chem. Int. Ed. Engl. **14**, 15 (1975); D. A. EVANS and G. C. ANDREWS. Acc. Chem. Res. **7**, 147 (1974).
2. E. J. COREY. Pure and Appl. Chem. **14**, 19 (1967).
3. J. E. BALDWIN, G. A. HOFLE, and O. W. LEVER. J. Am. Chem. Soc. **96**, 7125 (1974).

4. E. ZBIRAL. Synthesis. 775 (1974); E. E. SCHWEIZER, A. T. WEHMAN, and D. M. NYCZ. J. Org. Chem. **38**, 1583 (1973).
5. J. M. MCINTOSH, H. B. GOODBRAND, and G. M. MASSE. J. Org. Chem. **39**, 202 (1974); J. M. MCINTOSH and R. S. STEEVENSZ. Can. J. Chem. **52**, 1934 (1974); J. M. MCINTOSH and G. M. MASSE. J. Org. Chem. **40**, 1294 (1975).
6. J. M. MCINTOSH and H. KHALIL. Can. J. Chem. **53**, 209 (1975).
7. E. BUCHTA and F. ANDREE. Justus Liebig's Ann. Chem. **640**, 29 (1961).
8. G. BÜCHI and M. PAWLAK. J. Org. Chem. **40**, 100 (1975); J. A. FORD and C. V. WILSON. J. Org. Chem. **26**, 1433 (1961); P. L. FUCHS. Tetrahedron Lett. 4055 (1974).
9. S. D. DARLING, N. SUBRAMANIAN, and M. JENDRISAK. Abstracts of 167th National Am. Chem. Soc. Meeting, Los Angeles, April 1974. No. ORGN-72.
10. P. D. BARTLETT, E. COX, and R. E. DAVIES. J. Am. Chem. Soc. **83**, 109 (1961).
11. A. HORNFELDT, J. S. GRONOWITZ, and S. GRONOWITZ. Acta Chem. Scand. **22**, 2725 (1968).
12. G. R. PETTIT and E. E. VAN TAMELEN. Organic reactions. Vol. 12. Wiley, New York. 1962. p. 356.
13. D. D. MACNICOL and J. J. MCKENDRICK. J. Chem. Soc. Perkin Trans. 1, 2493 (1974).
14. R. GRIGG, R. HAYES, and J. L. JACKSON. Chem. Commun. 1167 (1969); B. STARK and A. J. DUKE. Extrusion reactions. Pergamon Press, Oxford. 1967; W. E. PARHAM and V. J. TRAYNELIS. J. Am. Chem. Soc. **76**, 4960 (1954).
15. F. ASINGER, M. THIEL, and H. KALTWASSER. Justus Liebig's Ann. Chem. **606**, 67 (1957).
16. A. KIRRMANN, J. CANTACUZENE, and L. VIO. Rev. Chim. Acad. Repub. Pop. Roum. **7**, 1011 (1962); Chem. Abstr. **61**, 8180a (1962).
17. R. MOZINGO. Organic synthesis. Vol. III. Wiley, New York, N.Y. 1955. p. 181.
18. ASTM Index of Mass Spectral Data (AMD-11). Am. Soc. for Testing and Materials, Philadelphia, Pa. 1969. p. 38.
19. E. STENHAGEN, S. ABRAHAMSSON, and F. W. MCLAFFERTY. Atlas of mass spectral data. Vol. 1. Interscience, New York, N.Y. p. 573.

Can. J. Chem. Downloaded from www.nrcresearchpress.com by 210.87.254.105 on 09/05/12
For personal use only.

Determination of the Rate Constant of the $O + H_2 \rightarrow OH + H$ Reaction using Atomic Oxygen Resonance Fluorescence and the Air Afterglow Techniques

RICHARD N. DUBINSKY AND DONALD J. MCKENNEY[1]

Department of Chemistry, University of Windsor, Windsor, Ontario N9B 3P4

Received May 12, 1975

RICHARD N. DUBINSKY and DONALD J. MCKENNEY. Can. J. Chem. **53**, 3531 (1975).

Measurements of the rate of the reaction

[1] $$O(^3P) + H_2(^1\Sigma_g^+) \rightarrow OH(^2\Pi) + H(^2S_{1/2})$$

were made over the temperature range of 347 to 832 K and a pressure range of 140 to 739 N m^{-2}. Experiments were carried out using a discharge fast-flow system with a fixed observation port. O atoms, generated by the $N + NO \rightarrow N_2 + O$ reaction, were reacted with H_2 added downstream under pseudo first-order conditions ($[H_2] \gg [O]$). Relative O atom concentrations were determined using two independent methods: atomic resonance fluorescence at 130.6 nm and the air afterglow technique. The rate coefficients derived from our data can be expressed as $k_1 = (8.3 \pm 3.8) \times 10^{-12} \exp\{-36.0 \pm 2.0 \text{ kJ mol}^{-1}/RT\}$ cm^3 $molecule^{-1}$ s^{-1} (by resonance fluorescence), and $k_1 = (8.8 \pm 5.0) \times 10^{-12} \exp\{-34.9 \pm 2.0 \text{ kJ mol}^{-1}/RT\}$ cm^3 $molecule^{-1}$ s^{-1} (by air afterglow method). Comparisons are made with selected published results.

The Arrhenius plot of our data shows no evidence of curvature at low temperature.

RICHARD N. DUBINSKY et DONALD J. MCKENNEY. Can. J. Chem. **53**, 3531 (1975).

On a mesuré la vitesse de la réaction

[1] $$O(^3P) + H_2(^1\Sigma_g^+) \rightarrow OH(^2\Pi) + H(^2S_{1/2})$$

à des températures allant de 347 à 832 K et à des pressions de 140 à 739 N m^{-2}. On a effectué des expériences impliquant un système de décharge à flux rapide avec un point d'observation fixe. On a fait réagir les atomes d'oxygène, générés par la réaction $N + NO \rightarrow N_2 + O$, avec de l'hydrogène additionné en aval sous des conditions de réaction de pseudo premier ordre $[H_2] \gg [O]$. On a déterminé les concentrations relatives d'atomes d'oxygène en faisant appel à deux méthodes indépendantes: la fluorescence de résonance atomique à 130.6 nm et la technique de la lueur de l'air.

Les coefficients de vitesse dérives de nos données peuvent etre exprimés sous la forme $k_1 = (8.3 \pm 3.8) \times 10^{-12} \exp\{-36.0 \pm 2.0 \text{ kJ mol}^{-1}/RT\}$ cm^3 $molécule^{-1}$ s^{-1} (par fluorescence de résonance) et $k_1 = (8.8 \pm 5.0) \times 10^{-12} \exp\{-34.9 \pm 2.0 \text{ kJ mol}^{-1}/RT\}$ cm^3 $molécule^{-1}$ s^{-1} (par la méthode de la lueur d'air). On fait des comparaisons avec des valeurs publiées choisies.

Le diagramme d'Arrhénius de nos données ne montre pas de courbature à basse température.

[Traduit par le journal]

Many studies (1*a*) of the rate of the $O + H_2 \rightarrow OH + H$ reaction have been made. Data obtained in discharge flow systems at temperatures of 400–900 K now appear to be fairly consistent. The low temperature end, however, is less well defined with very few data for temperatures below 400 K. Westenberg and de Haas (2) using e.s.r. detection of O atoms obtained curvature of their Arrhenius plot at temperatures from about 420 to 357 K. They attributed this behavior to quantum mechanical tunnelling.

In this paper we wish to report a series of experiments designed to measure the rate of the title reaction over a wide temperature range extending to temperatures as low as possible in our apparatus (832–347 K) and over a very wide range of O/H_2 ratio. Two methods of atom detection were employed: resonance fluorescence of atomic oxygen at 130.6 nm (3) and the well-known air afterglow technique (4). Results are compared with published work and an Arrhenius expression for k_1 is recommended for temperatures up to ~830 K. Published results obtained at high temperature ($T > 900$ K) from separate shock tube, ignition limit studies, etc. (1*a*) are much less consistent, but rate constants are generally higher than that predicted by extrapolation of the linear Arrhenius plot obtained at

[1]To whom correspondence should be addressed.

Can. J. Chem. Downloaded from www.nrcresearchpress.com by 210.87.254.42 on 09/05/12
For personal use only.

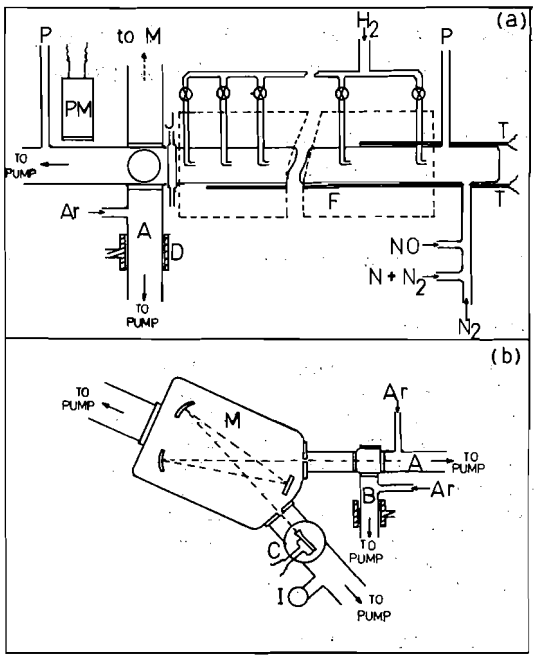

FIG. 1. (*a*) Schematic diagram of the quartz flow tube reactor. The first four jets closest to the observation cell are spaced 3 cm apart and the next five jets are 6 cm apart. Flow tube diameter is 2.50 cm i.d.; N + N_2, flow of N atoms in N_2 carrier from the discharge bypass; N_2, main carrier gas flow; P, connections to total pressure manometer; T, thermocouples (moveable); F, furnace; P M, photomultiplier tube; M, monochromator; J, cold water jacket; D, microwave discharge cavity; A, resonance fluorescence lamp. (*b*) Schematic top view of the observation cell and detector section. A and B, resonance fluorescence lamps; M, monochromator; C, Channeltron electron multiplier detector; I, ion gauge. Each section was separately pumped as described in the text.

low temperature. It has been suggested (5) that the O + H_2 reaction is therefore another example of a simple elementary process for which the rate coefficients at high temperature would be better represented on a curved Arrhenius plot. This point is discussed briefly.

Experimental

Flow System

A fast-flow discharge system was used for the production of $O(^3P)$ ground state atoms for reaction with ground state molecular hydrogen. Figure 1 shows a schematic diagram of the flow reactor and detection system. The $O(^3P)$ atoms were generated by the rapid reaction N + NO $\rightarrow$ N_2 + O, $k \simeq 3 \times 10^{-11}$ cm^3 molecule^{-1} s^{-1} (1*b*). The N atoms were formed by partial dissociation of molecular N_2 by passage through a 2.45 GHz microwave discharge (Microton 200) operated at 25–100 W power output. A discharge bypass arrangement as described by Clyne and Cruse (6) was used to obtain low [N]. Purified NO was added at known flows through a jet some 15 cm downstream of the discharge. The reactor flow tube was a 2.5 cm i.d. quartz tube provided with nine inlet jets spaced over a distance of 30 cm. Purified H_2 could be added through any of the jets or bypassed through an additional jet downstream of the observation ports.

For measurements at elevated temperatures a furnace was constructed around the reaction zone. The column was heated using Chromel heating element wire wound around the column in three sections, each of which was controlled by a variac auto transformer. Ceramic fiber held in place by asbestos board and covered with aluminum foil provided sufficient insulation. The temperature was measured at any point along the flow tube using two moveable chromel–alumel thermocouples located adjacent to the walls and on opposite sides of the flow tube. Simple adjustment of the variacs allowed temperature control to within ± 5 °C over the length of the reaction zone. A small water jacket surrounded the flow tube between the furnace and the observation port. The observation cell with its LiF windows was thus maintained at room temperature and protected from thermal shock.

The flow tube wall was coated with a mixture of CH_3SiCl_3 and $(CH_3)_2SiCl_2$ and baked at $\sim$400 K for several hours. This coating has been reported to inhibit atom removal on the wall (7).

Total pressure was measured at both ends of the flow tube, using a silicone oil manometer.

The downstream end of the flow tube led through a large bore (2.0 cm) stopcock to a liquid nitrogen-cooled high conductance trap to a Welch 500 l/min (model 1397) rotary pump.

Lamps and Detection Systems

The observation cell (Fig. 1*b*) was equipped with three polished LiF windows (Harshaw Manufacturing Co.). A fourth window of polished quartz which was positioned opposite Lamp B, (Fig. 1*b*), served to reduce scattered light entering the monochromator slit by multiple reflection. Lamps A and B were identical to each other and similar to that used by Bemand and Clyne (3). Cylinder argon dried by passage at low pressure through a liquid nitrogen-cooled trap packed with glass wool flowed through either lamp for excitation by means of a 2.45 GHz discharge operated at $\sim$25 W. Total pressure in the lamp was maintained at 1–2 $\times$ 10^2 N m^{-2} for a typical flow rate of $\sim$1 μmol s^{-1}. The conditions used were chosen to maximize the signal-to-noise ratio.

For those experiments in which relative [O] was measured from air afterglow intensities, the detector was an RCA 1P28 photomultiplier tube fitted with a Wratten No. 61 gelatin filter which transmits between 490.0–600.0 nm (maximum at 520.0 nm). The photomultiplier was fixed adjacent to the flow tube just below the observation cell. Signal currents were measured using a Keithley model 417 high speed picoammeter.

The detector system for the resonance fluorescence studies consisted of a McPherson monochromator (0.3 m, model 218) joined to the flow reactor by a simple tube collimator which directs emitted radiation to the entrance slit. The monochromator incorporated a 1200 line mm^{-1} MgF_2 coated diffraction grating (blazed at 500 nm). De-

Can. J. Chem. Downloaded from www.nrcresearchpress.com by 210.87.254.42 on 09/05/12
For personal use only.

Can. J. Chem. Downloaded from www.nrcresearchpress.com by 210.87.254.42 on 09/05/12
For personal use only.

tection was accomplished using a Bendix Channeltron electron multiplier operated at 2800 V d.c. (the power supply, Fluke, model 408B, specified line regulation of 0.001%). Signal pulses were amplified with a home-made preamplifier and Ortec timing filter amplifier (model 454). Counting rates were obtained after discrimination (Ortec integral discriminator, model 421) by either a rate meter (Ortec model 441) recorder system or a digital counter (Ortec model 775), coupled to a variable timer (Ortec model 719).

A pressure of $\sim 6.5 \times 10^{-5}$ N m^{-2} was maintained in the monochromator detector system by separate pumping (Fig. 1).

Reagents

Nitrogen (Liquid Carbonic) 99.996% stated purity was further purified by passage at ~ 101.3 kN m^{-2} pressure over divided copper (673 K), copper oxide powder (673 K), followed by a cold trap at 195 K. On the low pressure side of the flow-meter was another trap maintained at 77 K which contained silica gel on glass wool. Argon (Liquid Carbonic) was dried by passage at low pressure through a glass-wool packed cold trap (77 K). Hydrogen (Liquid Carbonic) was passed through a catalytic purifier (Deoxo-Engelhard Mfg.) and a silica gel glass wool trap (77 K). Nitric oxide (Matheson) was distilled repeatedly at 77–195 K under vacuum.

Procedure

The reaction was followed by monitoring the decay of relative [O] by either atomic resonance fluorescence or by the air afterglow method. In the former method resonance radiation emitted by the microwave-powered lamp, served to excite atomic resonance fluorescence of O(^{3}P) in the flow tube reactor. Measurements of the photon fluxes were made at λ 130.6 nm, corresponding to the transition O, 3s,$^3S_1$–2p^4,$^3P_0$. The air afterglow method involved the addition of a slight excess of NO beyond the nitrogen afterglow extinction point so that the greenish yellow emission from excited NO_2 could be readily measured. The emission intensity under the conditions employed in this work is directly proportional to [O] (4).

Kinetic Analysis

The removal of O atoms is considered with reference to the following processes:

[1] $$O + H_2 \rightarrow OH + H$$

[2] $$O + OH \rightarrow O_2 + H$$

[3] $$OH + H_2 \rightarrow H_2O + H$$

Assuming a steady-state concentration of OH the rate expression for O-atom consumption is

$$\frac{-d[O]}{dt} = k_1[O][H_2]\left(1 + \frac{1}{1 + \frac{k_3[H_2]}{k_2[O]}}\right)$$

$$= \alpha k_1[O][H_2]$$

where α corresponds to the term in parentheses. α, which must have values between 1 and 2, can be calculated for each run provided the ratio $[H_2]/[O]$ is known since k_2 and k_3 are both reasonably well established (8): $k_2 = (4.2 \pm 1.7) \times 10^{-11}$ cm^3 molecule^{-1} s^{-1} ($E = 0$), $k_3 = 3.8 \times 10^{-11}$ exp $\{-21.6$ kJ mol$^{-1}/RT\}$ cm^3 molecule^{-1} s^{-1}.

Most studies carried out in discharge flow systems have been studied under conditions such that only reactions 1 and 2 need be considered. In this work, however, the ratio $[H_2]_0/[O]_0$ was varied over a very wide range ($\sim$2000 to 40) partly because the resonance fluorescence work necessitated limiting [O] to values less than 2×10^{13} cm^{-3}. With very large $[H_2]_0/[O]_0$ ratios reaction 3 can be quite important relative to [2] for OH removal. Therefore, the contribution of reaction 3 was calculated for each run and the rate constant k_1 determined from plots of the equation

$$\log \{[O]_0/[O]\} = \frac{\alpha k_1}{2.303}[H_2]_0 t$$

A small correction ($\sim$5% maximum) was made for any pressure gradient along the length of the flow tube. Corrections for radial axial and back diffusion were found to be negligible.

Results

Heterogeneous Removal of H, OH, and O

A series of runs were carried out with the intention of obtaining k_1 by measuring the rate of production of H atoms. In this case Lyman-α resonance fluorescence at λ 121.6 nm was used to monitor relative [H] as a function of time. The data, which tended to show rather large scatter, indicated rapid loss at the wall. The H-atom fluorescence signal generally passed through a maximum with increasing reaction distance. Unfortunately, a quantitative comparison of H production to O loss was not possible. However, loss of H by heterogeneous processes is not expected to affect the kinetics of O decay (9).

If first-order OH removal on the wall was rapid enough, the apparent calculated value of k_1 may be too low by as much as a factor of two. This requires k_w^{OH} (rate coefficient for wall removal of OH) to be of the same magnitude or larger than $k_2[O]$. Thus, for $[O] = 10^{11}$–10^{13} cm^{-3}, k_w^{OH} would have to be greater than 10^2–10^3 s^{-1}. Recent estimates (10) of k_w^{OH} in similar systems have produced values of $\sim$10–100 s^{-1}. Although surface activity is often not compar-

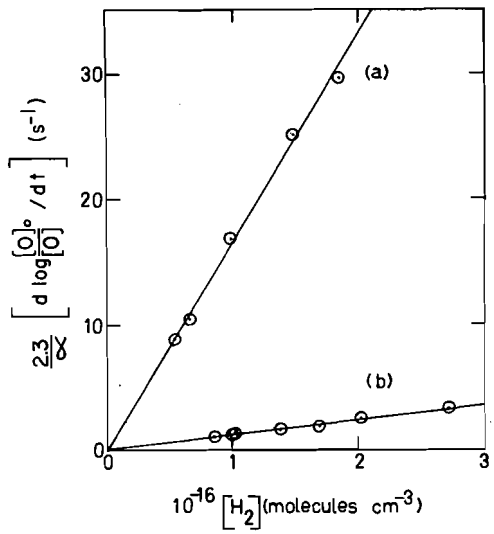

FIG. 2. Plot of $(2.3/\alpha)$[d log $\{[O]_0/[O]\}/dt$] *vs.* hydrogen concentration. (*a*) 508 K; by the resonance fluorescence technique. (*b*) 375 K; by the air afterglow method.

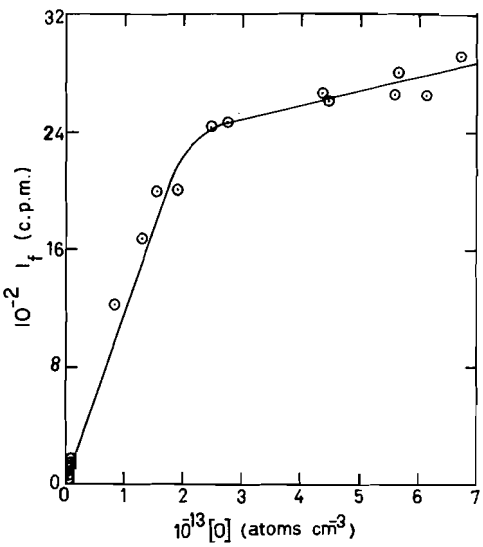

FIG. 3. Plot of fluorescence intensity (corrected for background) *vs.* oxygen atom concentration at λ 130.6 nm (unresolved) showing approximate linearity up to $\sim 2 \times 10^{13}$ cm^{-3}. (See ref. 3.)

able from one apparatus to another, the close agreement of our kinetic data (below) with those obtained by others suggests that heterogeneous removal of OH was not a serious problem in this work. Variation of $[O]_0$ over the range 10^{11}–10^{13} cm^{-3} produced no significant change in the value of k_1 calculated on the basis of negligible OH removal by heterogeneous processes.

Wall removal of O atoms does not interfere with the kinetic analysis provided that the removal is first-order and wall activity is not a function of added hydrogen (9). This assumption was verified by plots of [d log $[O]_0/[O]$)]/$dt \times (2.3/\alpha)$ *vs.* $[H_2]$ (Fig. 2). Within experimental scatter, these were straight lines with zero intercept, confirming that [1] is strictly first order with respect to $[H_2]$.

k_1 by Resonance Fluorescence

Pseudo first-order conditions were used throughout with H_2 in great excess ($[H_2]_0/[O]_0$ ~2000–40) (see Table 1*a*). The oxygen triplet emission from the source was readily resolved and showed considerable self-reversal typical of such lamps (3). Peak ratios were 1:2:2 which is to be compared with the theoretical ratios of 1:3:5 for the O $^3S_1$–$^3P_0$ (λ 130.6 nm), O $^3S_1$–$^3P_1$ (λ 130.5 nm), and O $^3S_1$–$^3P_2$ (λ 130.2 nm) respectively. In the fluorescence mode, however, loss of radiation necessitated the use of large slit widths (typically 100 μm) on the monochromator preventing full resolution under most conditions. Nevertheless, a few calibration runs showed that the intensity of the peak centered at λ 130.6 nm was approximately a linear function of [O] up to $\sim 2 \times 10^{13}$ cm^{-3} (Fig. 3). This result is consistent with the very extensive work of Bemand and Clyne (3) who obtained data for each line of the O $^3S_1$–^3P_J multiplet. Initial O atom concentrations[2] were kept below 2×10^{13} cm^{-3} to ensure linearity of fluorescence signal with [O].

Figure 4*a* shows a typical plot of log $[O]_0/[O]$ *vs.* time obtained by this technique. Table 1*a* summarizes all data obtained from resonance fluorescence measurements corrected for background levels of scattered light (typically ~50 Hz). The relatively low concentrations of O atoms required by this technique and the slow reaction rate restricted our measurements to temperatures above 495 K. Figure 5 shows an Arrhenius plot of all the data and the results are summarized in Table 2 in the form of Arrhenius parameters derived from a weighted least mean

[2] $[O]_0$ for the three runs done at 832 K (Table 1*a*) were slightly greater than 2×10^{13} cm^{-3}. At this temperature however, calculation shows that the concentration of O is reduced to $< 2 \times 10^{13}$ cm^{-3} in $< 7 \times 10^{-3}$ s (corresponding to < 10 cm). Thus, the relative changes in [O] for the jets within 10 cm of the observation cell were in error and were therefore ignored in determining the slope.

Can. J. Chem. Downloaded from www.nrcresearchpress.com by 210.87.254.42 on 09/05/12
For personal use only.

Can. J. Chem. Downloaded from www.nrcresearchpress.com by 210.87.254.42 on 09/05/12
For personal use only.

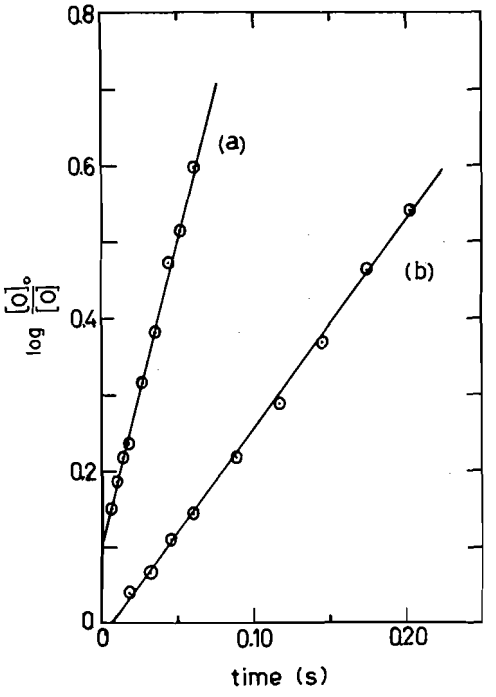

FIG. 4. Decay plots of relative [O]: (*a*) 508 K; resonance fluorescence technique, P_{tot} = 320 N m^{-2}, $[H_2]_0$ = 1.13 × 10^{16} molecules cm^{-3}, $[O]_0$ = 8.4 × 10^{12} atoms cm^{-3}; (*b*) 375 K; air afterglow technique. P_{tot} = 522 N m^{-2}, $[H_2]_0$ = 2.72 × 10^{16} molecules cm^{-3}, $[O]_0$ = 1.93 × 10^{14} atoms cm^{-3}. Zero of time scale differs from reaction time = 0.

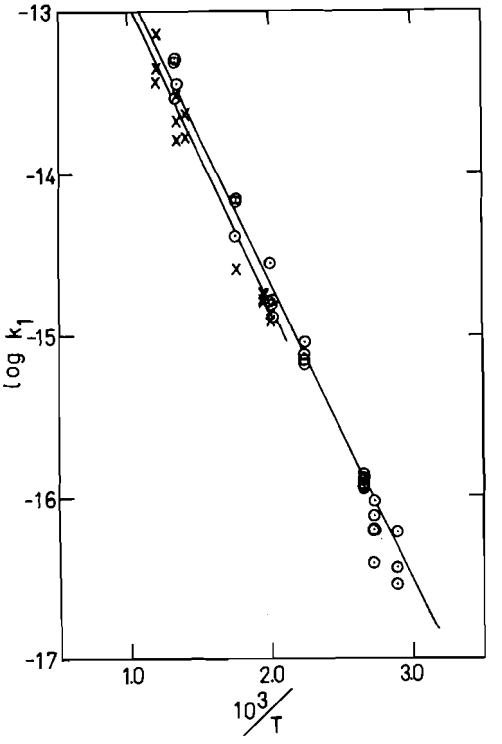

FIG. 5. Arrhenius plot of all data obtained in this work. ×, resonance fluorescence data; ○, air afterglow data.

squares analysis (see Appendix). Error limits quoted are 2σ (σ is the standard deviation). The statistical treatment applied to our resonance fluorescence data yields a 'best' line which is ~25% lower than that derived from our air afterglow results over the range 495–832 K. However, within the rather large uncertainty limits cited, the Arrhenius frequency factor and activation energy determined by both techniques are in reasonable agreement. Results also agree with those of Clyne and Thrush (11) but are significantly lower than those determined using the e.s.r. technique by other workers (12–14).

k_1 by the Air Afterglow Method

Measurements by this technique were carried out over the temperature range of 347–742 K which well overlaps the range studied by resonance fluorescence. The minimum ratio $[H_2]/[O]$ was approximately 40. At the lowest temperature $[H_2]/[O] \sim 1000$ with $[H_2] \sim 4 \times 10^{16}$ cm^{-3} (corresponding to a mole fraction $\chi_{H_2} \sim 0.2$).

Figure 4*b* shows a typical decay plot obtained by the air afterglow technique and results are listed in Table 1*b*. No significant contribution to the total emission photocurrent by HNO was expected using the Wratten No. 61 filter. Results are plotted, along with results from the resonance fluorescence experiments on Fig. 5. It can be seen that all the results are fairly consistent within experimental scatter. The derived Arrhenius parameters are shown in Table 2.

For comparison Table 2 and Fig. 6 also show results from other studies. Over approximately the same temperature range, all rate coefficients are generally in good agreement, but the Arrhenius parameters obtained from the data of Balakhnin *et al.* (14) are considerably higher than all others.

Discussion

The existing data on the O + H_2 reaction have been reviewed several times in recent years (1*a*).

Can. J. Chem. Downloaded from www.nrcresearchpress.com by 210.87.254.42 on 09/05/12
For personal use only.

TABLE 1

(*a*) Resonance fluorescence results

T (K)	Total pressure (N m^{-2})	$[H_2]_0$ (10^{15} molecule cm^{-3})	$[O]_0$ (10^{12} atom cm^{-3})	$\frac{d \log ([O]_0/[O])}{dt}$ (s^{-1})	α	k (cm^3 molecule^{-1} s^{-1})
832	208	1.69	22	39.7	1.25	4.33×10^{-14}
	273	1.00	29	21.5	1.42	3.49×10^{-14}
	366	1.98	33	78.4	1.30	7.01×10^{-14}
						Av. $(4.94 \pm 1.84) \times 10^{-14}$
742	335	5.80	16	42.1	1.09	1.53×10^{-14}
	334	4.41	12	62.1	1.09	2.98×10^{-14}
						Av. $(2.26 \pm 1.03) \times 10^{-14}$
734	156	2.53	11	25.8	1.14	2.06×10^{-14}
714	259	0.97	5.8	7.95	1.20	1.57×10^{-14}
	263	1.58	5.8	17.4	1.14	2.22×10^{-14}
						Av. $(1.90 \pm 0.46) \times 10^{-14}$
570	411	5.68	18	7.49	1.25	2.43×10^{-15}
508	230	5.40	7.8	4.64	1.21	1.64 ± 10^{-15}
	307	6.52	6.4	5.23	1.15	1.61×10^{-15}
	320	9.94	7.4	8.17	1.12	1.69×10^{-15}
	479	14.9	11	12.2	1.12	1.68×10^{-15}
	572	18.6	10	14.0	1.09	1.59×10^{-15}
						Av. $(1.64 \pm 0.04) \times 10^{-15}$
498	182	4.89	4.9	3.2	1.17	1.29×10^{-15}
	314	8.55	17	5.47	1.29	1.14×10^{-15}
						Av. $(1.22 \pm 0.11) \times 10^{-15}$

Can. J. Chem. Downloaded from www.nrcresearchpress.com by 210.87.254.42 on 09/05/12
For personal use only.

(*b*) Air afterglow results

T (K)	Total pressure (N m^{-2})	$[H_2]_0$ (10^{15} molecule cm^{-3})	$[O]_0$ (10^{12} atom cm^{-3})	$\frac{d \log [O]_0/[O]}{dt}$ (s^{-1})	α	k (cm^3 molecule^{-1} s^{-1})
742	337	5.37	18.2	73.8	1.11	2.85×10^{-14}
	333	4.41	10.8	103	1.08	4.98×10^{-14}
	224	2.97	10.1	70.5	1.11	4.92×10^{-14}
						Av. $(4.25 \pm 1.21) \times 10^{-14}$
734	156	2.43	12.5	42.8	1.16	3.50×10^{-14}
570	145	2.01	18.1	8.77	1.49	6.74×10^{-15}
	140	1.94	17.5	8.55	1.49	6.81×10^{-15}
	410	5.68	25.7	12.9	1.32	3.96×10^{-15}
						Av. $(5.84 \pm 1.63) \times 10^{-14}$
498	181	4.90	4.9	6.85	1.17	2.75×10^{-15}
	314	8.55	24.2	7.92	1.37	1.56×10^{-15}
						Av. $(2.16 \pm 0.84) \times 10^{-15}$
495	197	4.58	7.21	3.14	1.25	1.26×10^{-15}
	197	4.58	9.6	4.08	1.31	1.57×10^{-15}
	197	4.58	8.9	3.98	1.29	1.55×10^{-15}
						Av. $(1.46 \pm 0.17) \times 10^{-15}$
446	405	5.20	124	3.81	1.90	8.88×10^{-16}
	427	5.56	25	2.49	1.63	6.33×10^{-16}
	328	4.30	29.8	2.12	1.72	6.60×10^{-16}
	398	8.38	89.1	4.97	1.80	7.59×10^{-16}
						Av. $(7.35 \pm 1.15) \times 10^{-16}$
375	164	8.50	27.1	0.82	1.78	1.25×10^{-16}
	203	10.5	35.7	1.09	1.79	1.34×10^{-16}
	266	13.8	52.9	1.33	1.81	1.23×10^{-16}
	322	16.8	67.9	1.47	1.82	1.11×10^{-16}
	348	9.95	69.2	1.04	1.89	1.27×10^{-16}
	389	20.3	108	2.04	1.86	1.24×10^{-16}
	522	27.2	150	2.71	1.86	1.23×10^{-16}
						Av. $(1.24 \pm 0.07) \times 10^{-16}$
362	427	10.9	120	0.52	1.94	6.11×10^{-17}
	427	10.9	120	0.63	1.94	7.40×10^{-17}
	468	14.8	344	1.17	1.96	9.29×10^{-17}
	437	8.69	151	0.28	1.96	3.79×10^{-17}
						Av. $(6.65 \pm 2.31) \times 10^{-17}$
347	368	16.3	21.1	0.71	1.72	5.83×10^{-17}
	655	29.2	37.9	0.76	1.72	3.48×10^{-17}
	739	41.1	39.9	0.83	1.66	2.80×10^{-17}
						Av. $(4.04 \pm 1.59) \times 10^{-17}$

TABLE 2. Arrhenius parameters for the reaction $O + H_2 \rightarrow OH + H$

Method	T (K)	$A \times 10^{11}$ (cm^3 molecule^{-1} s^{-1})	E (kJ mol^{-1})	Reference
Air afterglow	347–742	0.88 ± 0.50	34.9 ± 2.0	This work
Resonance fluorescence	495–832	0.83 ± 0.38	36.0 ± 2.0	This work
Air afterglow	409–733	1.8 ± 0.6	38.4 ± 1.6	11
Electron spin resonance	423–910	3.5 ± 2.0	41.1 ± 2.8	12
Electron spin resonance and mass spectrometry	373–478	2.3 ± 0.8	39.5 ± 1.2	13
Electron spin resonance	408–520	9.4 ± 3.8	43.2 ± 1.4	14
All low temperature data[a]	347–832	1.6 ± 0.8	38.0 ± 2.0	

[a]Low temperature values were derived from averages at each temperature from this work and from refs. 11–14. A weighted least mean squares analysis of the Arrhenius plot yielded parameters cited (Appendix). Error limits are 2σ.

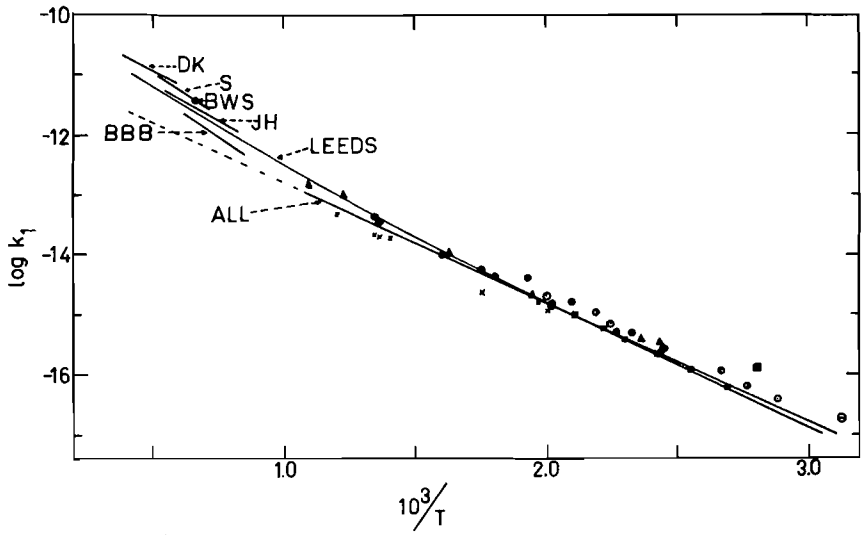

FIG. 6. Summary Arrhenius plot showing derived values of k_1, over the temperature range 320–~2600 K. DK, ref. 19; S, ref. 5; BWS, ref. 16; JH, ref. 17; BBB, ref. 18; LEEDS, ref. 1*a*; ALL, all low temperature data; △, ref. 12; ×, resonance fluorescence, this work; ○, air afterglow, this work; ◑, ref. 14; ●, ref. 11; ■, ref. 2; □, ref. 13; ⊖, ref. 15.

To our knowledge no new work at low temperature (<900 K) has appeared since the work of Balakhnin *et al.* in 1970 (14). Except for the few exceptions discussed in (1*a*) which for various reasons are not very reliable, the data reported is in fairly good agreement. In view of the variety of experimental techniques employed, considerable confidence can be placed in the results for the temperature range ~340–830 K.

Our data show no evidence of quantum mechanical tunnelling. We obtain a reasonably linear Arrhenius plot (Figs. 5 and 6) which (using the air afterglow technique) extrapolates to within ~11% of Campbell and Thrush's (15) value at 320 K. This linearity, however, is at variance with Westenberg and de Haas' results (2) which showed pronounced curvature at low temperature on their Arrhenius plot. The Westenberg and de Haas value at 357 K is approximately a factor of two higher than ours.

The last entry in Table 2 gives parameters derived from all low temperature data. It should be emphasized however that these values are not necessarily 'best' values. This is because a proper weighting of the data must take into account random and systematic errors in all data and this was not possible. On the other hand, data from all sources were statistically analyzed in the same way (Appendix). Therefore, the parameters derived from all low temperature data are probably the most reliable estimates which can be made at the present time. All the

Can. J. Chem. Downloaded from www.nrcresearchpress.com by 210.87.254.42 on 09/05/12
For personal use only.

Can. J. Chem. Downloaded from www.nrcresearchpress.com by 210.87.254.42 on 09/05/12
For personal use only.

low temperature (<900 K) results shown on Fig. 6, were selected as the most comprehensive and reliable, and nearly all values fall within about 50% of the 'all data' plot over the range 340–900 K. The discrepancy between our results and those of Westenberg and de Haas at low temperature is not readily explained. The excellent agreement of all workers over most of the temperature ranges studied probably rules out very serious systematic errors in flow calibrations etc. Assuming no large errors of this type, high values of k_1 would require enhancement of O decay, perhaps by heterogeneous processes involving H or OH.

Extrapolation of our results to the high temperature region (1000–2000 K) shows that a linear Arrhenius plot does not adequately describe the temperature dependence of this reaction over the extended temperature range. Figure 6 shows some of the more recent (post-1969) results acquired at high temperature in various shock tube and flame studies. The plot recommended by the Leeds group (Baulch *et al.* (1*a*) from an evaluation of selected low and high temperature results is also shown. The more recent data of Schott *et al.* would seem to indicate that the Baulch expression

$$k_1 = 3.0 \times 10^{-14} T \exp\{-37.2\ \text{kJ mol}^{-1}/RT\}\ \text{cm}^3\ \text{molecule}^{-1}\ \text{s}^{-1}$$

does not show quite enough curvature. Our low temperature results tend to bear out this conclusion.

There have been several other examples (20) of nonlinear Arrhenius behavior recently reported. Two different interpretations are usually made for this behavior. One, which has been applied in several cases (20), invokes transition state theory (t.s.t.). This was the approach taken by Schott *et al.* (5) to fit the low temperature results of Westenberg and de Haas (12) to their own high temperature data. In it the semiempirical bond-energy–bond-order (b.e.b.o.) method (21) which had earlier been applied to [1] by Mayer and Schieler (22) was combined with t.s.t. The computed values of k_1 fall along a smooth curve as expected, the curvature caused mainly by the changing contribution of a T^n term within the t.s.t. Gardiner *et al.* (23) have questioned the value of t.s.t. in this connection because of the large number of adjustable parameters required by the theory. Gardiner therefore prefers a second interpretation which in principle can be experimentally tested. This view suggests increasing participation of excited vibrational states of reactants with increasing temperature. The $O + H_2$ reaction presents an interesting test case. Because the energy separation between the first two vibrational levels in H_2 is very large (49.4 kJ (24)), the fraction of thermally produced vibrationally excited molecules ($H_2^{\ddagger}$) even at relatively high temperatures is quite small (*i.e.* $\sim 10^{-2}$ at 1500 K). Thus for reaction

[4] $$O + H_2^{\ddagger} \rightarrow OH + H$$

to contribute significantly to removal of O, an extremely large rate constant (at least equal to collision frequency) would be required if the high temperature results of Schott *et al.* (5) are to fit the low temperature data. We are now in the process of measuring k_4 in a newly designed apparatus by Lyman-α resonance fluorescence of H at λ 121.6 nm. Knowing k_1 the $O + H_2$ reaction can be used as a reliable calibration source for [H] (25) below 800 K.

We wish to thank the National Research Council of Canada for financial assistance in the form of an operating grant. We also wish to thank Dr. J. L. Hencher of this department for helpful discussions.

1. D. L. BAULCH, D. D. DRYSDALE, D. G. HORNE, and A. C. LLOYD. Evaluated kinetic data for high temperature reactions. Butterworths, London. (*a*) Vol. 1. 1972. p. 49; (*b*) Vol. 2. 1972. p. 171.
2. A. A. WESTENBERG and N. DE HAAS. J. Chem. Phys. **47**, 4241 (1967).
3. P. P. BEMAND and M. A. A. CLYNE. J. Chem. Soc. Faraday Trans. 2, **69**, 1643 (1973).
4. F. KAUFMAN. *In* Chemiluminescence and bioluminescence. *Edited by* M. J. Cormier, D. M. Hercules, and J. Lee. Plenum, New York. 1973. p. 83.
5. G. L. SCHOTT, R. W. GETZINGER, and W. A. SEITZ. Int. J. Chem. Kinet. **6**, 921 (1974).
6. M. A. A. CLYNE and H. W. CRUSE. J. Chem. Soc. Faraday Trans. 2, **68**, 1281 (1972).
7. J. P. WITTKE and R. H. DICKE. Phys. Rev. **103**, 620 (1956).
8. W. E. WILSON, JR. J. Phys. Chem. Ref. Data, **1**, 535 (1972).
9. A. A. WESTENBERG and N. DE HAAS. J. Chem. Phys. **46**, 490 (1967).
10. M. A. A. CLYNE and S. DOWN. J. Chem. Soc. Faraday Trans. 2, **70**, 253 (1974); J. G. ANDERSON, J. J. MARGITAN, and F. KAUFMAN. J. Chem. Phys. **60**, 3310 (1974); A. MCKENZIE, M. F. R. MULCAHY, and J. R. STEVEN. J. Chem. Phys. **59**, 3244 (1973).
11. M. A. A. CLYNE and B. A. THRUSH. Proc. R. Soc. London, Ser. A, **275**, 544 (1963).
12. A. A. WESTENBERG and N. DE HAAS. J. Chem. Phys. **50**, 2512 (1969).

Can. J. Chem. Downloaded from www.nrcresearchpress.com by 210.87.254.42 on 09/05/12
For personal use only.

13. K. HOYERMANN, H. Gg. WAGNER, and J. WOLFRUM. Ber. Bunsenges. Phys. Chem. **71**, 599 (1967).
14. V. P. BALAKHNIN, V. I. EGOROV, and V. N. KONDRATIEV. Dokl. Akad. Nauk. SSSR, **193**, 374 (1970).
15. I. M. CAMPBELL and B. A. THRUSH. Trans. Faraday Soc. **64**, 1265 (1968).
16. W. G. BROWNE, D. R. WHITE, and G. R. SMOOKLER. 12th Combust. Symp. The Combustion Institute, Pittsburgh, Pennsylvania. 1969. p. 557.
17. C. J. JACHIMOWSKI and W. M. HOUGHTON. Combust. Flame **15**, 125 (1970).
18. T. A. BRABBS, F. E. BELLES, and R. S. BROKAW. 13th Combust. Symp. The Combustion Institute, Pittsburgh, Pennsylvania. 1971. p. 129.
19. A. M. DEAN and G. B. KISTIAKOWSKI. J. Chem. Phys. **53**, 830 (1970).
20. A. A. WESTENBERG and N. DE HAAS. J. Chem. Phys. **58**, 4061 (1973); I. W. M. SMITH and R. ZELLNER. J. Chem. Soc. Faraday Trans. 2, **69**, 1617 (1973); W. C. GARDINER, JR., W. G. MALLARD, and J. H. OWEN. J. Chem. Phys. **60**, 2290 (1974); T. C. CLARK and J. E. DOVE. Can. J. Chem. **51**, 2147 (1973).
21. H. S. JOHNSTON. Gas phase reaction rate theory. Ronald Press Co., New York. 1966. p. 209.
22. S. W. MAYER and L. SCHIELER. J. Phys. Chem. **72**, 236 (1968); **72**, 2628 (1968).
23. W. C. GARDINER, JR., W. G. MALLARD, M. MCFARLAND, K. MORINAGA, J. H. OWEN, W. T. RAWLINS, T. TAKEYAMA, and B. F. WALKER. 14th Combust. Symp. The Combustion Institute, Pittsburgh, Pennsylvania. 1973. p. 61.
24. T. E. SHARP. At. Data, **2**, 119 (1971).
25. P. P. BEMAND, M. A. A. CLYNE, P. B. MONKHOUSE, and R. T. WATSON. Symposium on Chemical Kinetics Data for the Lower and Upper Atmosphere, Warrenton, Virginia, September 1974.
26. R. J. CVETANOVIĆ, R. P. OVEREND, and G. PARASKEVOPOULOS. Proceedings of the symposium in chemical kinetics data for the lower and upper atmosphere. *Edited* by S. W. Benson. Wiley Interscience, New York. 1975. p. 249.

Appendix

Evaluation of Arrhenius parameters from the familiar logarithmic form of the Arrhenius equation is usually done using an unweighted least mean squares treatment. However it has recently been pointed out (26)[3] that because the treatment involves a change in variable form k to $\ln k$ the low temperature data are in fact more heavily weighted. In order to compensate for this a weighted least squares treatment (26) is required where the weighting factor, $w_i' = w_i k_i^2$, is k^2/σ_k^2. (w_i are the statistical weights of the points.) In the case of the O + H_2 reaction, the k^2 term clearly dominates; *e.g.* $(k_{832}/k_{347})^2 \sim 10^6$. Thus the high temperature points are very heavily weighted. The standard deviation, σ_k, which is a measure of the precision of each k determination can be estimated from a complete assessment of the propagation of random errors. We have carried out this procedure for several experimental situations (below). Expected random errors generally fell in the range 9–28% using reasonable limits on each variable. This is to be compared with the observed scatter of 3–45% (σ) in the resonance fluorescence results and 6–40% (σ) in the air afterglow results. Such large scatter may indicate other sources of random error *e.g.* fluctuations in discharges, etc., which cannot easily be taken into account. We therefore used σ values from experimentally observed deviations for the weighting factors to derive the parameters cited in Table 2. (In cases where insufficient data were available estimates roughly equal to average σ's were made.) In two cases (refs. 13 and 14) rate constants were extracted from Arrhenius plots in order to apply the weighted least squares treatment, and in these cases the standard deviation for each point was arbitrarily (and optimistically) taken as 10%. Reference 11 gives average k's and corresponding deviations at each temperature. They were used 'as is'.

It is instructive to examine the consequences of the weighting procedure in detail on a set of apparently consistent data. Consider the most recent results of Westenberg and de Haas (12). They report the Arrhenius expression $k_1 = 5.3 \times 10^{11} \exp\{-42.7 \text{ kJ mol}^{-1}/RT\} \text{ cm}^3 \text{ molecule}^{-1} \text{ s}^{-1}$ for the range 500–900 K. Including their point at 423 K we obtain $k_1 = 3.2 \times 10^{-11} \exp\{-40.2 \text{ kJ mol}^{-1}/RT\} \text{ cm}^3 \text{ molecule}^{-1} \text{ s}^{-1}$. Both of these expressions were obtained using the unweighted least squares analysis. Using the weighted treatment with a weighting factor of $w_i' = k^2$ (which assumes all w_i are equal) we obtain the result, $k_1 = 8 \pm 4 \times 10^{-12} \exp\{-30.0 \pm 3.8 \text{ kJ mol}^{-1}/RT\} \text{ cm}^3 \text{ molecule}^{-1} \text{ s}^{-1}$! In this case the low temperature (and incidentally more precise) points are virtually ignored by the weighting treatment. Now taking $w_i' = k^2/\sigma^2$ and using standard deviations calculated from their data for each temperature we obtain $k_1 = 3.5 \pm 2.0 \times 10^{-11} \exp\{-41.1 \pm 2.8 \text{ kJ mol}^{-1}/RT\} \text{ cm}^3 \text{ molecule}^{-1} \text{ s}^{-1}$ which is the value cited in Table 2. While this is probably the best expression that can be derived from these data, it is clearly obvious that if accurate

[3]We thank one of the referees for drawing our attention to ref. 26 and for helpful suggestions.

Can. J. Chem. Downloaded from www.nrcresearchpress.com by 210.87.254.42 on 09/05/12
For personal use only.

Arrhenius parameters are to be obtained normal statistical distributions of data over a wide range of temperature must be available.

Propagation of Errors

Following Cvetanović *et al.* (26), estimates of random errors were made using the propagation of errors equation,

$$\sigma_Q = \left\{\sum_i \left(\frac{\partial F}{\partial M_i}\sigma_i\right)^2\right\}^{1/2}$$

where Q is the quantity being determined in the experiment from measurements, M_i. Q is a function F of M_i, $Q = F(M_i)$. σ_i are the standard deviations of the uncorrelated separate measurements M_i.

In this work k_1 was determined from

$$k_1 = \frac{2.303 \log ([O]_0/[O])}{\alpha[H_2]_0 t} = \frac{2.303(\text{slope})}{\alpha[H_2]_0}$$

The ratio $[O]_0/[O]$ is equal to the ratio of emission intensities measured, in the case of resonance fluorescence, as the number of photons less background counted over a 1 min period. In the air afterglow case it is measured as a current on a picoammeter. The rated time base accuracy is $< \pm 0.1\%$ for the Ortec (Model 719) timer. Statistical error in count rate amounts to $(\text{c.p.m.})^{1/2}$ which usually was $\sim \pm 2\%$. Rated error in current measurement is ± 2–3%. Nonlinearity of the resonance fluorescence signal *vs.* [O] at high [O] would contribute to the overall error. However, this is not expected to be a very serious problem since [O] is decreased quite rapidly in moderate reaction times.[2] At $[O] < 1 \times 10^{13}$ atom cm^{-3} linearity has been demonstrated for the λ 130.6 nm line (3).

Rapid deterioration of the LiF windows and consequent reduction of detection sensitivity was a serious practical problem since replacement of windows was not easily accomplished. For low signals the statistical error and spurious noise levels are relatively greater, possibly as large as 3%. Error in slope includes the random errors mentioned and also the error in t (s). The time, t, is calculated from $t = xAp/\sum F\,RT$ where x is the distance which defines the reaction zone, and A is the cross-sectional area of the flow tube, p is the total pressure, $\sum F$ is the total flow rate, R is the gas constant, and T is temperature. The errors in x and A are negligible and systematic. The error in T amounts to $\sim$1–1.5% (± 5 K). Pressures can generally be measured to at least ± 0.1 cm. For total pressures of 133–1000 N m^{-2} ($\sim$1–10 cm oil) the error amounts to 10–1%. The largest error in $\sum F$ probably arises from random fluctuations in flow rates but the error in flow meter readings can be significant for small Δp. We conclude that the combined error in t is of the order of $\pm$5–15% which generates a combined error of $\sim \pm$5–20% in the slope.

$$[H_2]_0 = \frac{f_{H_2}}{\sum F}\frac{p}{RT}$$

and therefore is considered precise to same limits as t ($\pm$5–15%). The error in $[O]_0$ can be quite large and contributes to the error in α. $[O]_0$ is equal to [NO] at the end point of the N + NO titration. This was usually determined visually. In addition the relatively low flows of NO are difficult to determine. Since $[NO] = f_{NO}p/(\sum F)RT$, errors in p, $\sum F$, and T also contribute. Limits of $\pm 30\%$ are therefore assumed. This, however, is not a large contributor to the overall error in k, because α is not very sensitive to small changes in $[O]_0$.

Substitution of all these limits into the propagation of errors equation leads to error values of $\pm$9–28% in k.

The Molecular Structure of Tetramethylgermane Determined by Gas Phase Electron Diffraction

J. LAWRENCE HENCHER AND FRANK J. MUSTOE

Department of Chemistry, University of Windsor, Windsor, Ontario N9B 3P4

Received May 8, 1975

J. LAWRENCE HENCHER and FRANCIS S. MUSTOE. Can. J. Chem. **53**, 3542 (1975).

The molecular structure of tetramethylgermane has been determined by vapor phase electron diffraction. The structural parameters, based on r_g interatomic distances are r(GeC) = 1.945 ± 0.003 Å, r(CH) = 1.12 ± 0.02 Å, and ∠(GeCH) = 108 ± 2°. Tetrahedral symmetry of the GeC_4 skeleton was preserved in the analysis by including a shrinkage correction for the C...C interatomic distance. The quoted uncertainties were estimated to include both systematic and random errors.

J. LAWRENCE HENCHER et FRANCIS S. MUSTOE. Can. J. Chem. **53**, 3542 (1975).

On a déterminé la structure moléculaire du tétraméthylgermane par diffraction électronique en phase vapeur. Les paramètres structuraux, basés sur des distances interatomiques r_g, sont r(GeC) = 1.945 ± 0.003 Å, r(CH) = 1.12 ± 0.02 Å et ∠(GeCH) = 108 ± 2°. La symétrie tétraédrique du squelette du GeC_4 est maintenue dans l'analyse en faisant intervenir une correction pour le raccourcissement de la distance interatomique C...C. On a estimé les incertitudes rapportées en incluant à la fois les erreurs systématiques et les erreurs dus au hasard.

[Traduit par le journal]

Introduction

The molecular structure of tetramethylgermane was first reported by Brockway and Jenkins (1). They reported a GeC bond length of 1.98 ± 0.03 Å which is longer than that observed in more recent structure determinat ons of CH_3GeH_3 (2), $(CH_3)GeH_2$ (3), and $(CH_3)_3GeH$ (4).

In view of the uncertainty in the GeC bond length, the structure of tetramethylgermane was redetermined as a necessary prelude to studies of the $(CH_3)_nGeX_{4-n}$ (X = F, Cl, Br, I) series.

Experimental

The sample of $(CH_3)_4Ge$ was obtained from Alfa Inorganics, Inc. and was used without further purification after checks of the gas phase infrared spectrum and the n.m.r. spectrum revealed no absorption peaks attributable to impurities.

Sectored electron diffraction patterns were recorded on the University of Windsor camera (5) on 4 × 5 in. Kodak Electron Image Plates for two nozzle-to-plate distances. The sample was maintained as vapor at 10 Torr in a 5 l flask. CS_2 patterns were recorded concurrently at each distance in order to calibrate the s scale ($s = (4\pi/\lambda)\sin(\theta/2)$ where λ is the electron wavelength and $\theta = \tan^{-1}$ (radius/camera length)). The parameters used for CS_2 in the calibration were those reported by Kuchitsu (6). The typical experimental conditions are given in Table 1.

The optical densities, $D(r)$, of the plates were samples at 0.1095 mm radial intervals, r, from the pattern center, on a specially constructed microdensitometer (5). Relative intensities were obtained by the emulsion linearity correction (7), $I(r) = D(r)[1 + 0.1D(r)]$. The experimental total intensity, obtained as $I_t(r) = I(r)/\Phi(r)$ where $\Phi(r)$ is the sector function,[1] was interpolated at $\pi/10$ Å^{-1} intervals in s by the Lagrange method (six point interpolation for long camera, three point for short camera), and converted to the levelled form $I_0(s) = s^4 I_t(s)$.

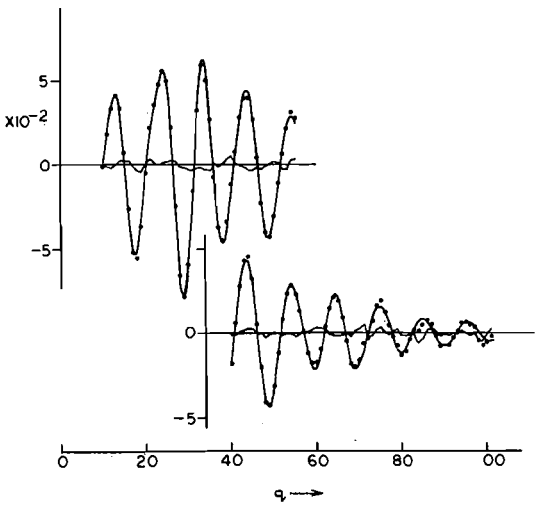

FIG. 1. The molecular intensity, $sI_m(s)$ of $(CH_3)_4Ge$. Experimental (dots), theoretical (solid curve), and difference curves from long camera and short camera diffraction patterns.

[1]The sector function, $\Phi(r)$, was calibrated to give a smooth $I(r)/\Phi(r)$ curve for experimental argon scattering.

Can. J. Chem. Downloaded from www.nrcresearchpress.com by 210.87.254.5 on 09/05/12
For personal use only.

Can. J. Chem. Downloaded from www.nrcresearchpress.com by 210.87.254.5 on 09/05/12
For personal use only.

TABLE 1. Experimental conditions[a]

Camera length (mm)	Wavelength (Å)	q^b Range (Å^{-1})	Exposure time (s)	Optical density range	Number of plates	Resolution factor[c]
296.16	0.05016	10–55	10–15	0.4–0.5	2	1.25±0.05
95.08	0.04965	40–101	40–60	0.2–0.4	2	1.33±0.12

[a]High voltage, 58 kV stabilized to $< 1 \times 10^{-4}$; beam current, 1×10^{-7} A; background pressure during exposures, $1–2 \times 10^{-5}$ Torr; sample pressure, 9–11 Torr; nozzle temperature, 21 °C.
[b]$q = (10/\pi)s$.
[c]The ratio of theoretical-to-experimental molecular intensity. The standard deviation was estimated to include both systematic and random errors.

TABLE 2. Correlation matrix of the refined parameters[a]

r(GeC) (0.003)	r(CH) (0.02)	∠(GeCH) (1.5)	l(GeC) (0.006)	l(CH) (0.018)	l(Ge...H) (0.018)	l(C...C) (0.024)	R_1[b] (0.045)	R_s[b] (0.126)
1.0								
−0.065	1.0							
0	−0.478	1.0						
0.143	0.269	0.075	1.0					
0.075	0.269	0.011	0.428	1.0				
0.127	−0.124	−0.017	−0.204	−0.176	1.0			
−0.007	0.018	−0.140	−0.076	−0.034	0.174	1.0		
0.109	−0.016	−0.032	0.195	0.091	0.208	0.135	1.0	
0.077	0.289	0.148	0.836	0.498	−0.353	−0.142	−0.140	1.0

[a]Estimated standard deviation in parentheses.
[b]Resolution factors for long and short camera, R_l and R_s. See Table 1.

TABLE 3. The molecular structure of tetramethylgermane[a]

Parameter	Value	l_{ij} Observed	l_{ij} Calculated	K_{ij}[d]	δ_{ij}[e]
r(GeC)	1.945±0.003	0.055±0.006	0.050	0.0057	
r(CH)	1.12 ±0.02	0.078±0.018	0.078		
∠(GeCH)	108.2 ±1.5	—			
∠(HCH)[b]	110.6 ±1.5	—			
r(C...C)[b]	3.176±0.004	0.11 ±0.024	0.11	0.0028	0.0065
r(Ge...H)[b]	2.527±0.01	0.12 ±0.018	0.12		
∠(CGeC)[c]	109.5	—			
R[f]		0.084			

[a]Distances in Å. Angles in degrees. Standard deviations estimated to include systematic and random errors.
[b]Dependent parameters.
[c]Parameter value fixed in the least squares analysis.
[d]The r.m.s. amplitude, l_{ij}, and perpendicular correction, K_{ij} calculated from normal coordinates for 298 K.
[e]Shrinkage correction, $-\delta(\text{C...C}) = K(\text{C...C}) - \frac{2}{3}\sqrt{6}\,K(\text{GeC})$ used in the analysis.
[f]$R = \{\sum_s [sI_m(s)_{exp} - sI_m(s)_{th}]^2 / \sum_s [sI_m(s)_{th}]^2\}^{1/2}$ is a measure of goodness of fit.

The molecular intensity, $I_m(s)$ was extracted by dividing $I_0(s)$ by its background (5, 7). The theoretical expression for $I_m(s)$ employed complex elastic scattering factors (8) and a correction for inelastic scattering (9).

The interatomic distances, r_g, were calculated from the independent parameters (10), r(CH), r(GeC), and ∠(GeCH). Tetrahedral symmetry was preserved by adding a shrinkage correction (11) to the C...C distance. This correction was calculated as $-\delta(\text{C...C}) \approx K(\text{C...C}) - \frac{2}{3}\sqrt{6}K(\text{GeC})$ from the perpendicular corrections, K_{ij}, which were obtained from the molecular force field by the method of Stölevik *et al.* (12). The force constants ($K_{CH} = 4.83$, $H_{HCH}/r_{CH}^2 = 0.44$, $H_{GeCH}/(r_{CH}r_{GeC}) = 0.22$, $K_{GeC} = 2.8$, and $H_{CGeC}/r_{GeC}^2 = 0.11$ mdyn Å^{-1}) were obtained from the frequency assignments of Lippincott and Tobin (13). Anharmonicity corrections of 2 Å^{-3} were assumed for the GeC and CH distances (14).

In the least squares analysis a diagonal (zeroth order)

weight matrix was assumed. The standard deviations in the refined parameters were estimated as three times the least squares values (15) in order to provide for systematic errors and the effect of the nonoptimum weighting on the random errors. The observed and calculated molecular intensity curves are presented in Fig. 1.[2] The correlation matrix for the refined parameters is given in Table 2. The principal interatomic distances, r_g, and the angles are presented in Table 3.

Results and Discussion

The GeC bond length determined here, 1.945 $\pm$ 0.003 Å, is substantially shorter than the earlier reported value of 1.98 $\pm$ 0.03 Å. The difference is probably a reflection of 40 years of development of the electron diffraction technique. The shorter bond length makes the $(CH_3)_4Ge$ structure consistent with CH_3GeH_3 (1.9453 $\pm$ 0.0005 Å) (2), $(CH_3)_2GeH_2$ (1.950 $\pm$ 0.003 Å) (3), and $(CH_3)_3GeH$ (1.947 $\pm$ 0.006 Å) (4). The shortness of the GeC bond compared to the sum of the covalent radii ($\frac{1}{2}(H_3Ge—GeH_3)$ + $\frac{1}{2}(H_3C—CH_3)$ = 1.97 Å (16)) is probably due to bond polarity.

Although the variation in angles through the above series is barely discernible, it appears that $\angle$(CGeC) is larger in dimethyl than in trimethyl germane as was observed for $(CH_3)_2GeF_2$ and $(CH_3)_3GeF$ (17).

This work was supported in part by an Operating Grant from the National Research Council of Canada.

[2]Tables of the molecular intensity for both camera lengths are available at a nominal charge, from the Depository of Unpublished Data, CISTI, National Research Council of Canada, Ottawa, Canada K1A 0S2.

1. L. O. Brockway and H. O. Jenkins. J. Am. Chem. Soc. **58**, 2036 (1936).
2. V. W. Laurie. J. Chem. Phys. **30**, 1210 (1959).
3. E. C. Thomas and V. W. Laurie. J. Chem. Phys. **50**, 3512 (1969).
4. J. R. Durig, M. M. Chen, Y. S. Li, and J. B. Turner. J. Phys. Chem. **77**, 227 (1973).
5. G. Barbe, J. L. Hencher, Q. Shen, and D. G. Tuck. Can. J. Chem. **52**, 3936 (1974).
6. K. Kuchitsu. Molecular vibrations and structure studies. *Edited by* S. J. Cyvin. Elsevier, Amsterdam. 1972. Chapt. 10.
7. L. S. Bartell. Physical methods in chemistry. 4th ed. Vol. 1. *Edited by* A. Weissberger and B. W. Rossiter. Interscience, New York. 1971.
8. L. Schäfer, A. C. Yates, and R. A. Bonham. J. Chem. Phys. **55**, 3055 (1971).
9. C. Tavard, D. Nicolas, and M. Rouault. J. Chim. Phys. **64**, 540 (1967).
10. R. L. Hilderbrandt. J. Chem. Phys. **51**, 1654 (1969).
11. Y. Morino, S. J. Cyvin, K. Kuchitsu, and T. Iijima. J. Chem. Phys. **36**, 1109 (1962).
12. R. Stölevik, H. M. Seip, and S. J. Cyvin. Chem. Phys. Lett. **15**, 263 (1972).
13. E. R. Lippincott and M. C. Tobin. J. Am. Chem. Soc. **75**, 4141 (1953).
14. K. Kuchitsu and L. S. Bartell. J. Chem. Phys. **35**, 1945 (1961).
15. H. M. Seip. Molecular structure by the diffraction methods. Vol. 1. *Edited by* G. A. Sim and L. E. Sutton. Specialist Periodical Reports, The Chemical Society, London. 1973. Chapt. 1.
16. B. Beagley. Molecular structure by the diffraction methods. Vol. 1. *Edited by* G. A. Sim and L. E. Sutton. Specialist Periodical Reports, The Chemical Society, London. 1973. Chapt. 3.
17. J. E. Drake, R. T. Hemmings, J. L. Hencher, F. J. Mustoe, and Q. Shen. J. Chem. Soc. Dalton Trans. In press.

Can. J. Chem. Downloaded from www.nrcresearchpress.com by 210.87.254.5 on 09/05/12
For personal use only.

Thiobinupharidines Epimeric at C-1 and C-1′

ROBERT THOMAS LALONDE AND CHUNFOOK WONG

Department of Chemistry, State University of New York, College of Environmental Science and Forestry, Syracuse, New York 13210

Received June 16, 1975

ROBERT THOMAS LALONDE and CHUNFOOK WONG. Can. J. Chem. **53**, 3545 (1975).

Thiobinupharidine epimers possessing axial methyl groups at C-1 and C-1′ have been isolated from extracts of *Nuphar luteum*. ^{13}C chemical shift data for the methyl and ring carbons demonstrate that both methyl groups are axial in 1-*epi*-1′-*epi*-thiobinupharidine and that one of two methyls is axial in 1-*epi*- and in 1′-*epi*-thiobinupharidine.

ROBERT THOMAS LALONDE et CHUNFOOK WONG. Can. J. Chem. **53**, 3545 (1975).

On a isolé à partir d'extraits du *Nuphar luteum* des épimères du thiobinupharidine possédant des groupes méthyles axiaux en C-1 et en C-1′. Les données de la résonance magnétique nucléaire du ^{13}C pour les groupes méthyles et les carbones du cycle démontrent que chacun des groupes méthyles est axial dans l'*épi*-1 *épi*-1′ thiobinupharidine et qu'un des deux méthyles est axial dans l'*épi*-1 et l'*épi*-1′ thiobinupharidine.

[Traduit par le journal]

In the course of a search for hemiaminal derivatives of neothiobinupharidine (1) we reduced a chromatographic fraction with sodium borodeuteride for the purpose of ascertaining the position of the hemiaminal hydroxyl group. Comparative thin layer chromatography of the product mixture indicated the presence of thiobinupharidine, **1**, neothiobinupharidine, and a component believed to be deoxynupharidine, but since determination of the position of the deuterium label was desired, the components were separated and their mass spectra were determined. Surprisingly, the component possessing the thin layer chromatographic behavior of deoxynupharidine (molecular weight 231) gave a mass spectrum showing a parent ion at *m/e* 495, a mass number consistent with a singly labelled thiaspirane Nuphar alkaloid. These observations led us to reexamine fractions of earlier separations containing the 'deoxynupharidine spot'. The reexamination has led to the isolation of 1-*epi*-1′-*epi*-thiobinupharidine, **2**, and a mixture of 1-*epi*-, **3**, and 1′-*epi*-thiobinupharidine, **4**. This paper discloses the details of isolation and the evidence for the structures, the latter relying heavily on ^{13}C n.m.r. and previous ^{13}C studies of quinolizidine compounds (2, 3).

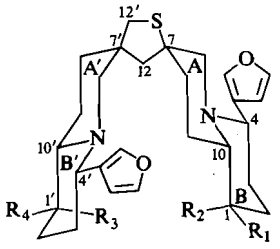

1 $R_1 = CH_3$(C-11); $R_4 = CH_3$(C-11′); $R_2 = R_3 = H$
2 $R_1 = R_4 = H$; $R_2 = CH_3$(C-11); $R_3 = CH_3$(C-11′)
3 $R_1 = R_3 = H$; $R_2 = CH_3$(C-11); $R_4 = CH_3$(C-11′)
4 $R_1 = CH_3$(C-11); $R_3 = CH_3$(C-11′); $R_2 = R_4 = H$

The mass spectra of **2** was typical of the C_{30} thiaspirane Nuphar alkaloids (4) and thus indicated the general skeletal characteristics. However, the presence of some of the separate structural features was clearly evident from other spectral characteristics. The i.r. absorption at 877 cm^{-1} and the ^{13}C n.m.r. signals in the 109–143 p.p.m. region (see Experimental) demonstrated the incorporation of two 3-furyl groups (3). The doublets at 1.11 and 1.14 p.p.m. in the ^1H n.m.r. and the separate lines at 13.6 and 13.7 p.p.m. in the ^{13}C n.m.r. indicated the presence of two methyls, involved as $HCCH_3$, the stereochemistry of which is discussed below. The AB quartet at 2.34 p.p.m. and the broad singlet found at 1.90 p.p.m. in the ^1H spectra were characteristic of methylenes in the thiolane ring (5). The ^1H n.m.r. absorption in the region 2.7–3.1 was typical of C-6 equatorial and C-4 axial protons in *trans*-fused quinolizidines that are substituted at C-4 by a 3-furyl group.

The stereochemical features of the ring systems were ascertained as follows. The i.r. Bohlmann bands, whose intensities were equivalent to those exhibited by thiobinupharidine, showed that *trans* quinolizidines were involved. The 2.34 p.p.m. AB quartet, attributed to the thiomethyl-

Can. J. Chem. Downloaded from www.nrcresearchpress.com by 210.87.254.40 on 09/05/12
For personal use only.

Can. J. Chem. Downloaded from www.nrcresearchpress.com by 210.87.254.40 on 09/05/12
For personal use only.

ene group, indicated that the new alkaloid belonged to either the thiobinupharidine or thionuphlutine B (**5**) families of thiaspiranes but not

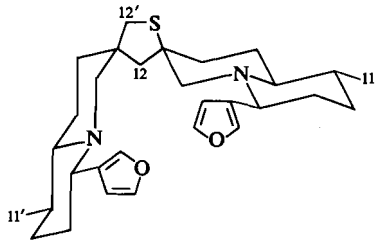

5

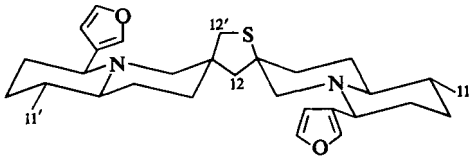

6

the neothiobinupharidine (**6**), nor a fourth as yet undiscovered stereochemical type, since neothiobinupharidine possesses an axial thiomethylene attached to the A′B′ quinolizidine moiety and this thiomethylene appears at 2.72 p.p.m. The thiomethylene in the fourth stereochemical possibility would also be axial and would be expected to appear in the 2.7 p.p.m. region but not the 2.3 p.p.m. region. However, the positions of the C-12 and C-12′ ^{13}C resonances, 44.4 and 42.6 p.p.m. respectively, are uniquely consistent with the thiobinupharidine lines appearing at 45.3 and 42.7 p.p m. (Fig. 1). The line positions of the C-12 and C-12′ methylenes are related to the number of axial and equatorial attachments in which these methylenes are involved (3). Thus the C-12′ thiomethylene carbon in neothiobinupharidine is axial with respect to the A′B′ quinolizidine ring and appears upfield at 39.1 p.p.m. The C-12 methylene in thiobinupharidine is axial to both the AB and A′B′ quinolizidines and is found further upfield than the corresponding signals of thionuphlutine B (50.6 p.p.m.) or neothiobinupharidine (54.5 p.p.m.) in which the C-12 methylenes are respectively equatorial to one or both quinolizidine systems. Therefore, the evidence from ^{1}H and ^{13}C n.m.r. establishes that the new alkaloid **2** belongs to the thiobinupharidine stereochemical family of thiaspirane Nuphar alkaloids.

The structural difference between **2** and thiobinupharidine, **1**, resides in the configuration of the C-1 and C-1′ methyls. The methyl ^{1}H n.m.r. signals appear somewhat downfield in **2** relative to the spectrum of **1** which exhibits them at 0.93 p.p.m. This observation in conjunction with the known chemical shift dependence (6) on the axial–equatorial disposition of the methyl group attached to the quinolizidine ring was the first indication that the C-1 methyls were axial.

In our earlier Nuphar alkaloid work, we employed an aromatic solvent induced shift of the methyl ^{1}H resonances to determine the axial or equatorial orientation of the methyl groups. Equatorial 1- and 3-methyl quinolizidines undergo upfield shifts whereas the axial methyls meet with a downfield shift (7). No significant solvent shift of methyl groups in **2** was observed and consequently no confirmation of methyl conformation was afforded. However, the ^{13}C n.m.r. spectrum in comparison with that of **1** clearly indicated the methyls in **2** were axial. Figure 1 shows that the highest field resonance of **2**, attributed to the coincidental methyl groups, is considerably shielded relative to the methyls of **1**. This chemical shift increment and those for the α, β and γ carbons are given in Table 1 which also compares the increments for corresponding carbon centers in model quinolizidines **7** and **8**.

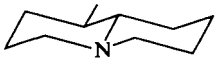

7

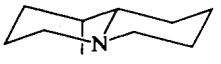

8

Table 1 illustrates that the shieldings of all of the various carbons, represented by the sign of the increments, is consistent with the known shift differences resulting from equatorial to axial changes of substituent groups in piperidine and quinolizidine rings (2, 8).

All of the spectral evidence important in determining that **2** belongs to the thiobinupharidine stereochemical family is given also (see Experimental) by the mixture of **3** and **4**, the components of which defied separation by conventional elution and thin layer chromatographic methods. Clearly the comparison of ^{13}C spectra given in Fig. 1 demonstrates that the mixture contains components with both axial and equatorial C-1 and C-1′ methyls. That the mixture consists of **3** and **4** and not **1** and **2** is apparent

Can. J. Chem. Downloaded from www.nrcresearchpress.com by 210.87.254.40 on 09/05/12
For personal use only.

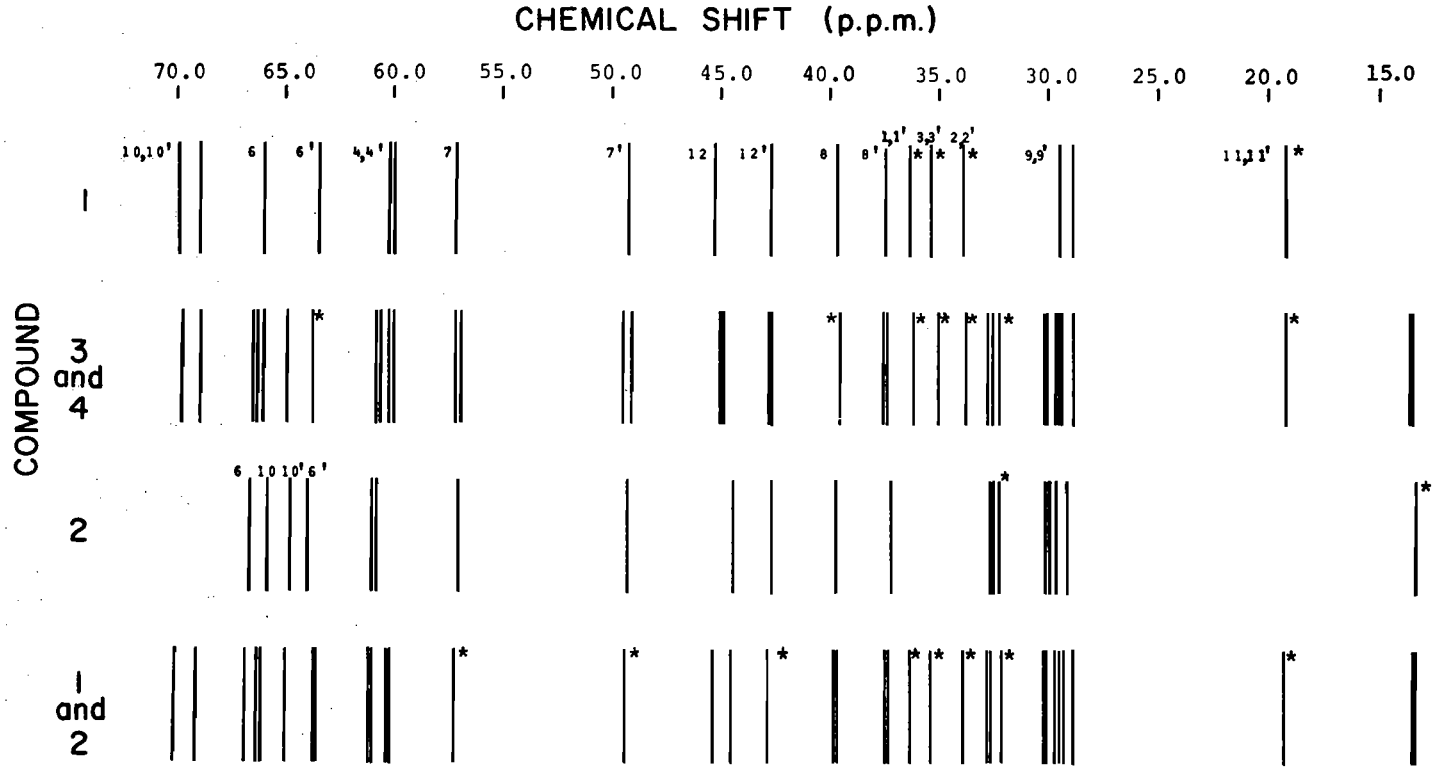

FIG. 1. ^{13}C n.m.r. line positions for saturated carbons in thiobinupharidine (**1**), 1-*epi*-1′-*epi*-thiobinupharidine (**2**), and 1-*epi*- (**3**) and 1′-*epi*-thiobinupharidine (**4**) based on correlation with thiobinupharidine (3), the axial methyl effect in quinolizidine systems (2) and, in the case of **1**, an off-resonance spectrum (the asterisk indicates intensity resulting from more than one carbon based on the average peak height and peak width at half height of C-8 and C-8′ in thiobinupharidine). Chemical shifts quoted in p.p.m. from TMS.

TABLE 1. Saturated carbon shieldings and a comparison of the stereochemical effect of axial and equatorial C-1 methyl groups in quinolizidine models (**7** and **8**) and C_{30} thiaspirane Nuphar alkaloids (**1** and **2**)

Effect at carbon	Chemical shifts (δ)[a,b] and increments (Δδ)[c]					
	Model compounds[d]			Thiaspirane alkaloids		
	7 (C-1, eq. Me)	**8** (C-1, ax. Me)	Δδ	**1**[e,f] (C-1, eq. Me)	**2**[f] (C-1, ax. Me)	Δδ
α						
C-1	36.6	33.3	−3.3	36.3	32.5	−3.8
					32.6	−3.7
β						
C-2	34.2	32.4	−1.8	33.8	32.2	−1.6
C-10	69.5	65.9	−3.6	69.9	65.7	−4.2
					64.6	−4.3
γ						
C-3	25.9	20.9	−5.0	35.3	29.9	−5.4
					30.1	−5.2
C-9	29.9	30.3	+0.4	28.8	29.1	+0.3
Me	18.7	13.8	−4.9	19.2	13.4	−5.8

[a]δ in p.p.m. from TMS.
[b]Chemical shift assignments for **2** are tentative and are based on the best fit of increment values to those of the model pair as well as the line separations of pairs of primed and non-primed carbon numbers in **1** (*e.g.* 10 and 10′, 6 and 6′ etc.).
[c]$\Delta\delta = \delta^{13c}$ (axial Me) − δ^{13c} (equatorial Me).
[d]Chemical shifts are taken from ref. 2.
[e]Chemical shifts are taken from ref. 3.
[f]Chemical shifts are given for primed and non-primed carbon numbers when separate resonances are observed.

from comparing the ^{13}C n.m.r. of these mixtures, especially in the regions occupied by C-7, C-7′, C-12, and C-12′ resonances. Moreover, the thin layer chromatographic behavior of thiobinupharidine, **1**, and the mixture of **3** and **4** are clearly distinguishable, the spot representing **1** being less mobile and widely separated from the spot, or on occasion the two spots, representing **3** and **4**. Therefore the isolated sample containing both axial and equatorial C-1 and C-1′ methyl groups must consist of two epimeric thiobinupharidines, the one possessing C-1 axial, C-1′ equatorial methyls, **3**, and the other C-1 equatorial and C-1′ axial methyls, **4**.

Evidence, primarily from ^1H n.m.r., indicates that the three piperidine Nuphar alkaloids nuphenine (9), 3-epinuphamine (10), and 3-epinupharamine (11) possess axial C-1 methyl groups. The newly isolated **2**, **3**, and **4** are the first quinolizidine Nuphar alkaloids possessing axial C-1 methyl groups. Also noteworthy is the previously mentioned isolation of the deuterium labelled material possessing both the mass spectral and thin layer chromatographic properties of the 1-*epi*- and 1′-*epi*-thiobinupharidines. This finding means that the 1-*epi*-thiobinupharidines are also present in the plant extracts as hemiaminals.

Experimental

Measurements and Methods

Spectra were determined as follows: mass spectra (m.s.) on a Hitachi–Perkin-Elmer RMU6E using a direct inlet probe, 70 eV and 120 °C; high resolution mass spectra (h.r.m.s.) were determined at the High Resolution Mass Spectrometry Laboratory, Battelle's Columbus Laboratories, Columbus, Ohio, using an AEI MS-9 spectrometer employing a direct inlet probe, 70 eV and 200 °C; infrared spectra (i.r.) in CCl_4 solution on Perkin-Elmer 137 and 621 spectrometers; ^1H n.m.r. in $CDCl_3$ and C_6D_6 (1% TMS, δ 0.00) as indicated on Varian A 60 and XL-100-15, the latter controlled by a VFT-100L computer and operating in the FT mode (m, s, d, t, q, and br referring to multiplet, singlet, doublet, triplet, quartet, and broad); ^{13}C n.m.r. in 5 mm tubes in $CDCl_3$, used also as a secondary reference (77.2 p.p.m. from TMS at δ 0.00 p.p.m.), on a Varian XL-100-15 operating at 25.16 MHz in the FT absorption mode employing 8192 data points. Field frequency lock was established on the deuterium resonance of $CDCl_3$. Fully decoupled spectra of **2** and the mixture of **3** and **4** were obtained from 71.5 and 74.4 K transients respectively. Chemical shifts are accurate to 0.1 p.p.m. Thin layer chromatography (t.l.c.) was performed on microscope slides uniformly coated (0.25 mm) with Alumina GF_{254} and using the solvent systems indicated.

Detection of Monodeuterated epi-Thiobinupharidines in a Reduction Mixture

A 2.1 mg chromatography fraction originating from *Nuphar luteum* from Poland had been obtained in the course of purifying 6- and 6′-hydroxythiobinupharidine

Can. J. Chem. Downloaded from www.nrcresearchpress.com by 210.87.254.40 on 09/05/12
For personal use only.

Can. J. Chem. Downloaded from www.nrcresearchpress.com by 210.87.254.40 on 09/05/12
For personal use only.

(1). This fraction was dissolved in 5 drops of methanol and the resulting solution was treated with 10 mg of sodium borodeuteride at ambient temperature for 30 min at the end of which time the product mixture was processed by the usual procedure to obtain 2 mg of colorless oil: t.l.c. (Et_2O–hexane, 1:9) R_f 0.12 (neothiobinupharidine), 0.39 (thiobinupharidine), and 0.56 ('Deoxynupharidine' (*epi*-thiobinupharidine)).

Chromatography of the above described mixture was effected on a column of 6 g of neutral Alumina (5% H_2O) eluted first with 30 ml of Et_2O–hexane (5:95); thereafter several 5-drop fractions of the same solvent were taken. Combined fractions 1–10 yielded ~1 mg of *epi*-thiobinupharidines: t.l.c. (Et_2O–hexane, 1:9) R_f 0.56; m.s. *m/e* (relative intensity, %) 495(21), 494(18), 360(11), 359(8), 231(43), 230(53), 179(100), 178(82), 136(21), 107(56), 94(91).

Isolation of 1-epi-1′-epi-Thiobinupharidine, 2, and a Mixture of 1-epi- and 1′-epi-Thiobinupharidine, 3 and 4

Three chromatographic fractions (5) which had been eluted with hexane, and previously designated A1, A2, and A3, were combined (219 mg) and chromatographed on 5 g of neutral alumina (activity 2) that was first eluted with 75 ml of hexane, to obtain 140 mg of u.v. active but Dragendorf inactive material, and then with 30 ml of Et_2O–hexane (5:95) to obtain 75 mg of material. The latter was dissolved in 15 ml of Et_2O and the resulting solution was shaken with 15 ml of 0.01 *N* aqueous HCl and then with water. The aqueous acid and water layers were combined, made alkaline with powdered sodium hydroxide, saturated with salt, and finally extracted several times with small portions of methylene chloride. The combined extracts were dried (Na_2SO_4) and the solvent removed at the rotary evaporator to obtain 58 mg of a colorless oily residue which was chromatographed on a column (1 cm o.d. × 15.5 cm) containing 20 g of neutral alumina (5% water) by eluting with: 75 ml of hexane (fraction A′1, 0 mg); Et_2O–hexane in eight 20-drop portions (combined fraction A′2, 4.4 mg); Et_2O–hexane in eighteen 30-drop portions (combined fractions A′3, 25 mg); 150 ml of Et_2O–hexane (fraction A′4, 20 mg). This chromatography and the one below were monitored by t.l.c. (Alumina GF_{254}, 0.25 mm). Combined fractions A′2 and A′3 were admixed and chromatographed on a similar column by eluting with: 10 ml of hexane (fraction B′1, 0 mg); six 20-drop fractions of hexane (combined fraction B′2, 9.3 mg); three 20-drop fractions of hexane (combined fraction B′3, 3.7 mg); ten 20-drop fractions of hexane (combined fraction B′4, 8.3 mg); 20 ml of methylene chloride (fraction B′5, 0.2 mg). Fraction B′2 was pure 1-*epi*-1′-*epi*-thiobinupharidine, **2**: t.l.c. (eluted three times with Et_2O–hexane, 5:95) R_f 0.65 (R_f thiobinupharidine, 0.33); $[\alpha]_D^{25}$ 30.9 (*c* 9 mg/ml, 95% EtOH); i.r. 2810–2490 cm^{-1} (Bohlmann band) and 877 cm^{-1} (3-furyl); ^1H n.m.r. (100 MHz, $CDCl_3$) δ 2.7–3.1 (m, 4H, C-6 eq., C-6′ eq., C-4, and C-4′), 2.34 (AB q, J = 12.5 Hz, 2H, CH_2S) 1.90 (br s, 2H, C-7 CH_2), and 1.11 and 1.14 (2d, 6H, C-1 and C-1′ CH_3); ^1H n.m.r. (100 MHz, C_6D_6) δ 3.12 (2d, J = 12.5 Hz, 2H, C-6 eq., and C-6′ eq.), 2.70 (m, 2H, C-4, and C-4′), 2.29 (AB q, J = 13 Hz, 2H, CH_2S), 2.13 (AB q, J = 13 Hz, 2H, C-7 CH_2), 1.13 (2d, 6H, C-1, and C-1′); ^{13}C n.m.r. (7 mg in 0.3 ml $CDCl_3$) δ 29.6, 37.2, 39.7, 42.6, 44.4, 49.2, 56.9, 60.6, 60.8, 63.8, 66.5, 109.7 (C-15 or C-15′) (3), 109.7 (C-15′ or C-15), 129.7 (C-13 or C-13′), 129.9 (C-13′ or C-13), 139.7 (C-14 and C-14′), 143.0 (C-16 and C-16′) and assigned resonances given in Table 1; h.r.m.s. obsvd/calcd mass (formula) 494.2957/494.2967 ($C_{30}H_{42}N_2O_2S$), 447.3021/447.3011 ($C_{29}H_{39}N_2O_2$), 359.2140/359.2157 ($C_{21}H_{31}N_2OS$), 230.1523/230.1545 ($C_{15}H_{20}NO$), 136.0868/136.0888 ($C_9H_{12}O$), 107.0497/107.0497 (C_7H_7O), 94.0413/94.0419 (C_6H_6O), and 81.0337/81.0340 (C_5H_5O).

Fractions A′4 and B′4 were combined to give 27 mg of a mixture of 1-*epi*- and 1′-*epi*-thiobinupharidine: t.l.c. (eluted three times with Et_2O–hexane, 5:95) R_f 0.61 (R_f thiobinupharidine, 0.33; R_f 1-*epi*-1′-*epi*-thiobinupharidine, 0.65); $[\alpha]_D^{25}$ 23.9 (*c* 27 mg/ml, 95% EtOH); i.r. 2810–2490 (Bohlmann bands, intensities equivalent to those exhibited by thiobinupharidine), 877 cm^{-1} (3-furyl); ^1H n.m.r. (60 MHz, $CDCl_3$) δ 2.6–3.15 (m, 4H, C-6 eq., C-6′ eq., C-4, and C-4′), 2.31 (AB q, J = 12.5 Hz, 2H, —CH_2S—), 1.88 (br s, 2H, C-7 CH_2), 1.13 (2d, J = 6.5 Hz, 3H), and 0.94 (2d, 3H); ^1H n.m.r. (60 MHz, C_6D_6) δ 3.2 (m, C-6 eq. and C-6′ eq.), 2.75 (m, C-4 and C-4′), 2.33 (AB q, J = 12.5 Hz, 2H, CH_2S), 2.17 (AB q, J = 12.5 Hz, 2H, C-7 CH_2), 1.12 (2d, J = 6.5 Hz, 3H), 0.84 (2d, 3H); ^{13}C n.m.r. (27 mg in 0.3 ml $CDCl_3$) δ 13.6, 13.7, 19.2, 28.8, 29.3, 29.4, 29.6, 30.0, 30.1, 32.2, 32.5, 32.7, 33.7, 35.2, 36.1, 37.3, 37.5, 39.5, 42.6, 42.7, 44.8, 44.9, 49.0, 49.4, 56.8, 57.1, 59.9, 60.1, 60.5, 60.7, 63.6, 64.8, 65.9, 66.2, 66.4, 68.8, 69.7, 109.7, 109.8, 129.6, 129.9, 139.7, and 143.0; h.r.m.s. obsvd/calcd mass (formula) 494.2950/494.2967 ($C_{30}H_{42}N_2O_2S$), 447.2976/447.3011 ($C_{29}H_{39}N_2O_2$), 359.2094/359.2157 ($C_{21}H_{31}N_2OS$), 230.1520/230.1545 ($C_{15}H_{20}NO$), 136.0907/136.0888 ($C_9H_{12}O$), 107.0497/107.0497 (C_7H_7O), 94.0414/94.0419 (C_6H_6O), and 81.0339/81.0340 (C_5H_5O).

Mixture of Thiobinupharidine, 1, and 1-epi-1′-epi-Thiobinupharidine, 2

^{13}C n.m.r. (5 mg of **1** and 5 mg of **2** in 0.3 ml $CDCl_3$) δ 13.4, 13.5, 19.3, 28.8, 29.3, 29.5, 29.7, 30.1, 30.2, 32.1, 32.4, 32.6, 32.8, 33.9, 35.4, 36.3, 37.3, 37.5, 39.7, 39.8, 42.8, 44.5, 45.3, 49.3, 57.1, 60.0, 60.2, 60.8, 61.0, 63.4, 64.0, 64.8, 65.9, 66.1, 66.6, 68.9, 109.9, 129.7, 130.5, 140.0, and 143.2.

Support of this work by the National Institutes of Health, U.S. Public Health Service (Grant No. AI-10188) is gratefully acknowledged. We also acknowledge the assistance of L. McCandless for determining the 100 MHz ^1H n.m.r. and the ^{13}C n.m.r. spectra. The authors are grateful to the National Science Foundation for an equipment grant to the Department of Chemistry, State University of New York, College of Environmental Science and Forestry toward the purchase of the XL-100-15 spectrometer and the VFT100 computer used in this study.

1. C. F. WONG and R. T. LALONDE. Experientia, **31**, 15 (1975).
2. R. T. LALONDE and T. N. DONVITO. Can. J. Chem. **52**, 3778 (1974).
3. R. T. LALONDE, T. N. DONVITO, and AMY I.-M. TSAI. Can. J. Chem. **53**, 1714 (1975).

4. R. T. LaLonde, C. F. Wong, J. T. Woolever, E. Auer, K. C. Das, and A. I.-M. Tsai. Org. Mass Spectrom. **9**, 714 (1974).
5. R. T. LaLonde, C. F. Wong, and K. C. Das. J. Am. Chem. Soc. **95**, 7342 (1973).
6. R. T. LaLonde, C. F. Wong, and H. G. Howell. J. Org. Chem. **36**, 3703 (1971).
7. R. T. LaLonde, T. N. Donvito, A. I.-M. Tsai, and C. F. Wong. Org. Magn. Reson. **7**, 191 (1975).
8. D. W. Cochran. Ph.D. Dissertation, Indiana University, Bloomington, Indiana. 1971.
9. R. Barchet and T. P. Forrest. Tetrahedron Lett. 4229 (1965).
10. C. F. Wong and R. T. LaLonde. Phytochem. **9**, 1851 (1970).
11. T. P. Forrest and S. Ray. Can. J. Chem. **49**, 1774 (1971).

Can. J. Chem. Downloaded from www.nrcresearchpress.com by 210.87.254.40 on 09/05/12
For personal use only.

Etudes conformationnelles de dérivés d'oligométhylène glycols et de composés apparentés. Partie II. Structure cristalline et moléculaire du di(parachlorobenzoate) d'éthylène glycol, $C_{16}H_{12}O_4Cl_2$

SERGE PÉREZ ET FRANÇOIS BRISSE

Département de Chimie, Université de Montréal, C.P. 6210, Succ. A, Montréal, Québec H3C 3V1

Reçu le 30 mai 1975

SERGE PÉREZ et FRANÇOIS BRISSE. Can. J. Chem. **53**, 3551 (1975).

Les cristaux de di(*para*-chlorobenzoate) d'éthylène glycol cristallisent dans le groupe spatial centrosymétrique $C2/c$ du système monoclinique. Les paramètres cristallins sont $a = 12.733(9)$, $b = 9.522(8)$, $c = 12.762(8)$ Å, $\beta = 79.63(10)°$ et $Z = 4$. Les intensités de 1206 réflexions indépendantes ont été mesurées sur un diffractomètre automatique Picker. La structure a été résolue par la méthode de multisolution. Un affinement anisotrope a conduit à un facteur de reliabilité final de 0.033.

La molécule est placée en position particulière: un axe cristallographique de rotation d'ordre 2 est perpendiculaire au milieu de la liaison CH_2—CH_2. Contrairement à la molécule de dibenzoate d'éthylène glycol qui se trouve dans la conformation *trans*, ce dérivé se présente dans la conformation *gauche*. Cette différence de conformation n'empêche néanmoins pas de retrouver le raccourcissement notable de la liaison CH_2—CH_2 dont la longueur est 1.493(2) Å. Les forces de van der Waals assurent la cohésion des molécules dans le cristal.

SERGE PÉREZ and FRANÇOIS BRISSE. Can. J. Chem. **53**, 3551 (1975).

Ethylene glycol di(*para*-chlorobenzoate) crystals are monoclinic, space group $C2/c$, with $a = 12.733(9)$, $b = 9.522(8)$, $c = 12.762(8)$ Å, $\beta = 79.63(10)°$, and $Z = 4$. The structure was solved by direct methods from 1206 independent reflections collected on a Picker diffractometer. An anisotropic refinement led to a final R factor of 0.033.

The molecule has a crystallographic twofold axis of rotation perpendicular to the middle of the CH_2—CH_2 bond. Unlike ethylene glycol dibenzoate which was shown to be in the *trans*-conformation, this derivative is nearly in the *gauche*-conformation. However the same significant shortening of the ethylene part of the molecule is observed: the CH_2—CH_2 distance is only 1.493(2) Å. The molecules are held in the crystal by van der Waals interactions only.

Introduction

Dans le cadre de notre étude systématique (1) sur les molécules modèles des polyesters, nous présentons ici la détermination de la structure cristalline du di(*para*-chlorobenzoate) d'éthylène glycol. Cette molécule, tout comme celle du dibenzoate d'éthylène glycol étudiée précédemment (2), sert de modèle partiel au polyéthylène téréphtalate.

Ce travail a aussi été entrepris pour obtenir des valeurs expérimentales en vue de confirmer les résultats de l'analyse conformationnelle menée sur le diacétate d'éthylène glycol (3).

Partie expérimentale

Le di(*para*-chlorobenzoate) d'éthylène glycol $C_{16}H_{12}O_4Cl_2$ a été préparé par réaction d'éthylène glycol et de chlorure de *para*-chlorobenzoyle en présence de pyridine (4). Le produit est ensuite recristallisé lentement dans le chloroforme à température ambiante. Les clichés obtenus sur chambres de Weissenberg et de précession ont permis de déterminer les conditions d'existences: hkl, $h + k = 2n$; $h0l$, $l = 2n$. Les deux groupes spatiaux Cc non-centrosymétrique et $C2/c$ centrosymétrique présentent les mêmes conditions d'extinctions systématiques. Il n'est pas possible de lever l'ambiguïté sur la détermination du groupe spatial. En effet, la détermination du nombre d'homologues $Z = 4$ est compatible avec les deux groupes spatiaux car l'existence d'une symétrie cristallographique de la molécule, composée de deux parties chimiquement équivalentes, ne peut être exclue.

L'affinement des dimensions de la maille a été effectué par la méthode des moindres-carrés appliquée à douze réflexions centrées sur le diffractomètre. Ces valeurs ainsi que les écarts-type correspondants sont groupés ci-dessous.

Données cristallographiques

$C_{16}H_{12}O_4Cl_2$ poids mol. = 339.27

p.f. = 140 °C, $F(000) = 694$, monoclinique, $C2/c$, $a = 12.733(9)$, $b = 9.522(8)$, $c = 12.762(8)$ Å, $\beta = 79.63(10)°$, $V = 1552$ Å^3, $Z = 4$, $d_{obs} = 1.48$, $d_{cal} = 1.452$ g cm^{-3}, $\mu(MoK\alpha) = 3.0$ cm^{-1}, $\lambda(MoK\bar{\alpha}) = 0.71069$ Å, $T = 20(1)$ °C.

Les intensités de 1472 réflexions indépendantes, à l'intérieur de la sphère limitée par $2\theta \leq 52°$, ont été mesurées sur le diffractomètre automatique Picker. La méthode de mesure θ–2θ a été utilisée avec une vitesse de

Can. J. Chem. Downloaded from www.nrcresearchpress.com by 210.87.254.6 on 09/05/12
For personal use only.

TABLEAU 1. Moyennes statistiques des facteurs de structure normalisés

	Centrosymétrique*	Expérimentale	Non-centrosymétrique*
$\langle\|E^2 - 1\|\rangle$	0.968	0.976	0.736
$\langle\|E\|\rangle$	0.798	0.796	0.886

*Voir ref. 12.

balayage de $1°(2\theta)\ mn^{-1}$ et une largeur de balayage de $1.75°(2\theta)$. Le temps de comptage du bruit de fond de part et d'autre de la réflexion (compteur fixe, cristal fixe) était de 20 s. La moyenne des intensités de trois réflexions témoins mesurées toutes les 30 réflexions a décru de 10% au cours de la durée de la collection des données. Toutes les intensités ont été corrigées du bruit de fond et ramenées à une même échelle. La réduction des données, par utilisation des programmes de Ahmed *et al.* (5), a été conduite de façon usuelle. Parmi les 1472 réflexions mesurées, 1206 d'entre elles telles que $I/\sigma(I) \geq 2.5$ ont été considérées comme observées (81%). $\sigma(I)$ a été calculé par la relation $\sigma(I) = [I_T + (t/40)^2B + (0.03I_N)^2]^{1/2}$, où I_T est le nombre total de coups, B est le bruit de fond total, I_N est le nombre net de coups et t la durée du balayage d'une réflexion.

Etant données les dimensions géométriques du cristal utilisé ($0.40 \times 0.35 \times 0.35$ mm), et la faible valeur du coefficient d'absorption pour la longueur d'onde utilisée, aucune correction d'absorption n'a été effectuée. Les valeurs des facteurs de diffusion des atomes C, O et Cl sont celles de Cromer et Waber (6) et celles de Stewart *et al.* (7) pour l'hydrogène. Les valeurs données par Cromer (8) ont été employées pour les parties réelle et imaginaire de la dispersion anomale du chlore.

Determination de la structure et affinement

Après correction de l'agitation thermique isotrope, les résultats de la moyenne statistique des facteurs de structure normalisés $|E|$ indiquaient une distribution centrosymétrique (tableau 1). Malgré ces indications, et pour les raisons expliquées précédemment, la recherche de la structure de départ a été effectuée dans le groupe spatial non-centrosymétrique *Cc*, par application du programme de multisolution MULTAN (9). Les différentes étapes de la recherche sont résumées ci-dessous.

On a utilisé 118 réflexions ayant $|E| \geq 1.90$, soit 5.3 réflexions par atome semi-lourd à déterminer, pour générer 680 relations $\Sigma 2$. La phase de la réflexion 060 a été déterminée par $\Sigma 1$ avec une probabilité de 1 tandis que l'origine a été fixée par les deux réflexions 12.4.5 et 773. Par ailleurs des symboles furent assignés aux phases des réflexions $66\bar{4}$, 2.6.12 et 2.10.3.

Les phases des 118 réflexions, correspondant au set possédant le meilleur ensemble de figures de mérite, ont permis de réaliser une carte de Fourier où tous les atomes semi-lourds de la molécule ont pu être localisés. A ce niveau, un affinement isotrope des 22 positions atomiques (groupe *Cc*) a conduit à un facteur de reliabilité $R = 0.113$. Comme cet affinement a été exécuté par la méthode de matrice entière, il a été possible de détecter de fortes corrélations existant entre les atomes correspondants des deux parties chimiquement équivalentes de la molécule. L'existence d'une symétrie moléculaire (groupe *C2/c*) a alors été de nouveau envisagée. A ce stade, les affinements par la méthode d'approximation par blocs diagonaux ont été menés parallèlement pour les groupes *C2/c* et *Cc*. Les principales étapes de ces affinements sont présentées dans le tableau 2. En fin d'affinement, les valeurs trouvées pour les facteurs de reliabilité et les grandeurs σ_F dans le cas des groupes *C2/c* ou *Cc* ne permettent pas de choisir sans ambiguïté le groupe spatial. L'application du test d'Hamilton (10, 11) aux facteurs de reliabilité pondérés donne pour vraisemblable l'hypothèse du groupe non-centrosymétrique *Cc* pour des niveaux d'acceptation α compris entre 0.50 et 0.005. Ce sont en fait des considérations d'ordre stéréochimique qui nous font pencher en faveur du groupe d'espace centrosymétrique.

En fin d'affinement dans le groupe *Cc*, le calcul des distances et des angles intramoléculaires conduisait à des résultats extrêmement incohérents. Les différences entre les longueurs de liens chimiquement équivalents étaient de l'ordre de 20 à 30 fois l'écart type. Par exemple, les distances Csp^2—Csp^2 à l'intérieur d'un même cycle aromatique variaient entre 1.250(3) et 1.450(3) Å. Comme de tels résultats sont chimiquement inacceptables et qu'il y avait des corrélations importantes entre les coordonnées d'atomes équivalents, l'hypothèse du groupe spatial *Cc* a été définitivement rejetée. Les poids $w = 1/\sigma^2(F)$ dérivés de $\sigma(I)$ ont été appliqués à chaque reflexion.

Un calcul de section différence effectué en fin d'affinement dans le groupe *C2/c* a montré que les maxima de densité électronique résiduelle variaient entre -0.19 et $+0.14\ e\ Å^{-3}$.

Figures de mérite (f.d.m.) du meilleur set et valeurs extrêmes

	f.d.m. absolue	ψ_0 (10^3)	*R*-Karle	f.d.m. combinée
Meilleur set	1.019	0.418	16.7	2.92
Valeur maximum	1.02	0.521	21.3	
Valeur minimum	0.948	0.409	16.5	

Can. J. Chem. Downloaded from www.nrcresearchpress.com by 210.87.254.6 on 09/05/12
For personal use only.

TABLEAU 2. Comparaison des affinements dans les groupes spatiaux *C*2/*c* et *Cc*

	Groupe spatial								
	*C*2/*c*				*Cc*				
Cycle	*n**	*R*	R_w	σ_F	*n*	*R*	R_w	σ_F	Commentaires
1–2	45	12.4		12.12	87	11.3		11.35	Affinement isotrope
3–5	101	7.2		8.92	199	6.3		7.63	Affinement anisotrope des atomes semi-lourds; localisation des hydrogènes
6–9	124	4.1		2.79	247	3.3		3.45	Affinement anisotrope des atomes semi-lourds; affinement isotrope des hydrogènes
10–12	124	3.3	3.4	2.40	247	3.3	3.0	3.40	Inclusion de la dispersion anomale du chlore et d'une pondération statistique

*$R = \Sigma\Delta F/\Sigma F_o$, $R_w = [\Sigma w\Delta F^2/\Sigma wF_o^2]^{1/2}$, $\sigma_F = [\Sigma w\Delta F^2/(m-n)]^{1/2}$, m = nombre de réflexions, n = nombre de paramètres affinés.

TABLEAU 3. Coordonnées atomiques et facteurs d'agitation thermique* (avec leurs écarts-type) du di(*para*-chlorobenzoate) d'éthylène glycol

Atome	*x*	*y*	*z*	U_{11}	U_{22}	U_{33}	U_{12}	U_{13}	U_{23}
Cl(01)	27411(3)	18193(5)	−20569(4)	640(2)	681(3)	650(3)	−122(2)	−70(2)	200(2)
O(11)	−4995(9)	−34002(12)	538(9)	712(7)	644(7)	536(7)	−192(6)	−251(6)	9(5)
O(12)	4140(8)	−29910(10)	13671(8)	590(6)	560(6)	346(5)	−105(5)	−110(5)	20(5)
C(11)	8391(11)	−16267(15)	−1867(11)	421(8)	430(8)	315(8)	42(6)	−55(6)	−70(6)
C(12)	16920(12)	−10098(17)	1860(12)	481(8)	558(9)	374(8)	5(7)	−109(7)	−1(7)
C(13)	22764(12)	527(17)	−3792(13)	467(9)	624(10)	487(9)	−58(8)	−126(8)	−9(8)
C(14)	20066(12)	4893(16)	−13259(12)	472(8)	512(9)	444(9)	16(7)	−6(7)	23(7)
C(15)	11654(12)	−1066(17)	−17170(12)	565(10)	582(10)	379(9)	21(8)	−124(7)	30(7)
C(16)	5836(12)	−11654(17)	−11453(12)	492(8)	524(9)	372(8)	7(7)	−130(7)	−50(7)
C(17)	1795(11)	−27581(15)	3963(12)	470(8)	467(9)	350(8)	61(7)	−90(7)	−90(7)
C(18)	−1485(13)	−41497(16)	19602(12)	624(10)	477(9)	403(9)	−54(8)	−61(8)	−11(7)
H(121)	1880(11)	−1347(14)	827(11)	46(4)					
H(131)	2853(12)	496(15)	−138(13)	59(5)					
H(151)	1008(11)	267(15)	−2368(12)	57(5)					
H(161)	−43(11)	−1615(13)	−1362(12)	50(5)					
H(181)	97(11)	−5051(14)	1569(12)	52(5)					
H(182)	−931(11)	−4015(16)	2006(12)	53(5)					

*Les coordonnées fractionnaires des atomes semi-lourds sont $\times 10^5$ et les facteurs thermiques anisotrope sont $\times 10^4$, les coordonnées des atomes d'hydrogène sont $\times 10^4$, les facteurs thermiques isotropes sont $\times 10^3$.

Résultats et discussion[1]

Les coordonnées atomiques, les facteurs d'agitation thermiques anisotropes et leurs écarts type sont présentés dans le tableau 3. Les facteurs thermiques sont les coefficients de l'expression $T = \exp[-2\pi^2(U_{11}a^{*2}h^2 + \ldots + 2U_{12}a^*b^*hk + \ldots)]$. La molécule de di(*para*-chlorobenzoate) d'éthylène glycol est représentée fig. 1.

[1]On peut obtenir la série complète des tableaux à un prix nominal, en s'adressant au Dépôt de données non publiées, ICIST, Conseil national de recherches du Canada, Ottawa, Canada K1A 0S2.

Distances et angles interatomiques

La fig. 2 rassemble schématiquement les distances et les angles d'une molécule de $C_{16}H_{12}O_4Cl_2$. Les erreurs estimées sont de 0.002 Å et de 0.15° pour les distances et angles entre atomes 'semi-lourds' respectivement; les erreurs correspondantes lorsque les atomes d'hydrogène sont impliqués sont de 0.015 Å et de 0.9° respectivement.

La molécule de di(*para*-chlorobenzoate) d'éthylène glycol est située sur l'axe cristallographique d'ordre 2, passant par le milieu de la liaison CH_2—CH_2. La géométrie du groupe chlorophenyle est en bon accord avec

Can. J. Chem. Downloaded from www.nrcresearchpress.com by 210.87.254.6 on 09/05/12
For personal use only.

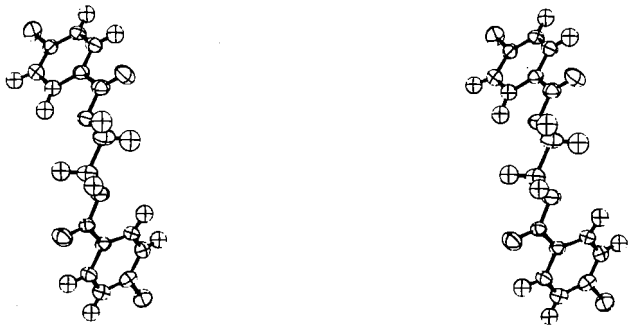

FIG. 1. Vue stéréoscopique d'une molécule de di(*para*-chlorobenzoate) d'éthylène glycol.

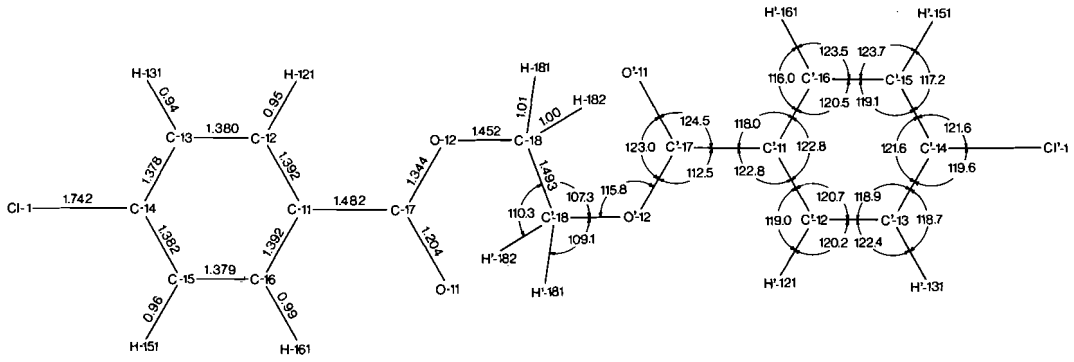

FIG. 2. Distances et angles dans la molécule de di(*para*-chlorobenzoate) d'éthylène glycol.

l'analyse faite récemment sur les groupes halogénophényles (13). La distance Csp^2—Cl de 1.742(2) Å est voisine de la moyenne de 1.736(2) Å calculée par Palenik *et al.* (14). La présence du chlore en *para* se manifeste par une légère augmentation de l'angle C(13)—C(14)—C(15) = 121.6° tandis que les deux angles C(11)—C(14)—C(13) et C(11)—C(14)—C(15) ont des valeurs proches de 119°. D'autre part on observe aussi que le chlore est légèrement en dehors du plan moyen du cycle. En ce qui concerne les distances C—H du cycle on observe une valeur moyenne de 0.96 Å tandis que les angles C—C—H sont tous voisins de 120°.

La géométrie du groupe carboxylate est comparable en tout points à celle trouvée pour le dibenzoate d'éthylène glycol (2).

La longueur de la liaison CH_2—CH_2 = 1.493(2) Å est significativement plus courte que la distance communément attendue de 1.537 Å pour une liaison Csp^3—Csp^3 (15). Afin de s'assurer que ce raccourcissement n'était pas dû aux mouvements de rotations moléculaires, nous avons entrepris l'analyse des mouvements thermiques par la méthode de Schomaker et Trueblood (16). La racine carrée de l'erreur quadratique moyenne des U_{ij}, $[\sum(\Delta U_{ij})^2/(r - s)]^{1/2}$, où r est le nombre de U_{ij} et s le nombre de paramètres du corps rigide, n'est que de 0.005 Å^2. Les corrections des longueurs de liaison sont au maximum de 0.002 Å, et la valeur corrigée du lien CH_2—CH_2, 1.494 Å, reste toujours significativement très courte. Une distance comparable de 1.499(2) Å avait été remarquée dans la structure du dibenzoate d'éthylène glycol (2). Afin d'élucider les raisons du raccourcissement de la liaison CH_2—CH_2 nous avons entrepris l'étude systématique de structures de composés de type (*a*) R—C_6H_4—CO—O—$(CH_2)_x$—O—CO—C_6H_4—R, où R = H, CH_3, NO_2, Cl et x = 2 à 6; (*b*) C_6H_5—R—$(CH_2)_2$—R—C_6H_5 où R = —O—CO, —CO—NH— et —CO—CH_2—.

L'angle[2] O(12)—C(18)—C′(18) a une valeur

[2]Les atomes primés (coordonnées $\bar{x}$, y, $\frac{1}{2} - z$) sont les équivalents, par rotation d'ordre 2, des atomes non primés (coordonnées x, y, z) portant le même numéro.

Can. J. Chem. Downloaded from www.nrcresearchpress.com by 210.87.254.6 on 09/05/12
For personal use only.

TABLEAU 4. Plans moyens†

Plan A atomes	$\chi^2 = 3.7$, déviations du plan (Å)	Plan B atomes	$\chi^2 = 4.7$, déviations du plan (Å)
C(11)	−0.001(2)	O(11)	−0.001(1)
C(12)	0.002(2)	O(12)	−0.001(1)
C(13)	−0.002(2)	C(11)	−0.001(2)
C(14)	0.001(2)	C(17)	0.003(2)
C(15)	0.001(2)		
C(16)	0.001(2)		
Cl(1)*	0.010(2)		
C(17)*	−0.014(2)		

*Ces atomes n'ont pas été inclus dans le calcul du plan moyen.
†Equations des plans moyens Plan A, $0.542X - 0.680Y - 0.495Z - 1.725 = 0$. Plan B, $0.622X - 0.678Y - 0.392Z - 1.780 = 0$. X, Y, Z sont les axes d'un référentiel orthogonal par rapport au référentiel cristallin.

TABLEAU 5. Angles de torsion

Liaisons	Angle (deg)
O(12)—C(18)—C′(18)—O′(12)	$\phi_2 = 74.5$
C(17)—O(12)—C(18)—C′(18)	$\phi_1 = -175.0$
C(18)—O(12)—C(17)—C(11)	$\omega = -176.0$
C(18)—O(12)—C(17)—O(11)	4.5

de 107.3(2)° alors que les angles correspondants du dibenzoate d'éthylène glycol sont encore plus refermés: 104.7(2) et 105.2(2)°.

Plans moyens et angles de torsion

Les équations des plans moyens du cycle aromatique (plan A) et du groupe carboxylique (plan B) sont données dans le tableau 4. Comme il a été indiqué précédemment, l'atome de chlore se trouve en dehors du plan moyen du cycle. Le groupement carboxylique est aussi situé légèrement en dehors du plan A et fait un angle de 7.5° avec ce dernier. Les angles de torsion[3] sont rassemblés dans le tableau 5. La conformation de la molécule est *trans–gauche*. Cette conformation diffère considérablement de la conformation *trans–trans* rapportée pour le dibenzoate d'éthylène glycol (2). Les projections de Newman le long du lien CH_2—CH_2 de ces deux molécules sont comparées à la fig. 3. Il est assez surprenant d'observer deux conformations radicalement différentes pour deux molécules qui somme toute ne diffèrent que par la présence d'un atome de chlore en para sur le groupe phényle.

Dans l'article suivant (3) Sundararajan *et al.* calculent l'énergie conformationnelle d'une

[3]L'angle de torsion pour la conformation *trans* est de 180° (17).

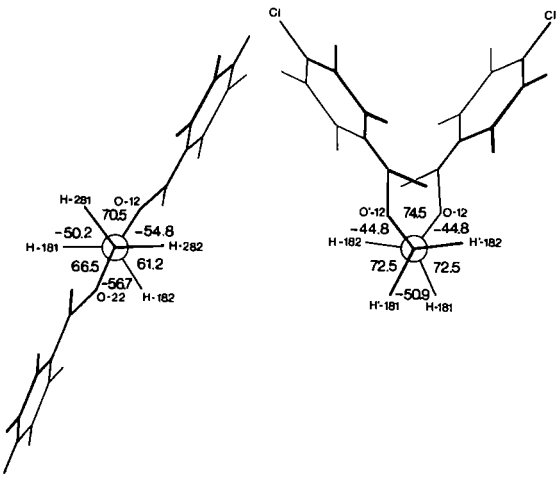

FIG. 3. Représentation de Newman du dibenzoate d'éthylène glycol (à gauche) et du di(*para*-chlorobenzoate) d'éthylène glycol (à droite). Projection le long du lien CH_2—CH_2.

molécule isolée de diacétate d'éthylène glycol en tenant compte de l'énergie électrostatique, de l'énergie d'interactions entre atomes non liés et de l'énergie de torsion.

Les deux conformations observées par diffraction des rayons-X se retrouvent parmi les conformations de basses énergies proposées par ces auteurs.

La conformation *trans–trans* du dibenzoate d'éthylène glycol correspond à la forme d'énergie minimum (1.10 kcal mol^{-1}) pour laquelle les angles de torsion calculés sont $\phi_1 = \phi_2 = 180°$. Les angles de torsion observés dans le di(*para*-chlorobenzoate) d'éthylène glycol (tableau 5) sont comparables aux angles calculés pour la forme *trans–gauche* ($\phi_1 = -179°$, $\phi_2 = 62°$). L'énergie calculée de la conformation *trans–gauche* ne diffère que de 300 cal mol^{-1} de celle de la forme *trans–trans*.

Les différences entre les valeurs observées et calculées des angles de torsion se manifestent surtout au niveau de l'angle ϕ_2, angle de torsion autour de la liaison CH_2—CH_2. Ces désaccords sont peut-être attribuables au fait que les valeurs standard des distances et des angles utilisées par Sundararajan *et al.* (3) sont assez différentes des distances et des angles observés ici, particulièrement en ce qui concerne le lien CH_2—CH_2 et l'angle O(12)—C(18)—C′(18).

Arrangement moléculaire

Une vue stéréoscopique (fig. 4) montre l'arrangement des molécules de di(*para*-chloro-

Can. J. Chem. Downloaded from www.nrcresearchpress.com by 210.87.254.6 on 09/05/12
For personal use only.

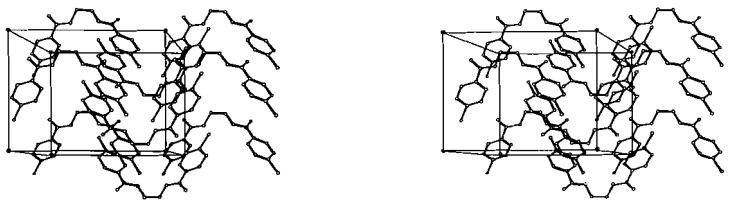

FIG. 4. Arrangement moléculaire.

TABLEAU 6. Contacts intermoléculaires à moins de 3.60 Å

De l'atome	à l'atome	Position*	Distance (Å)
Cl(1)	C(16)	4, $-c$	3.425
O(11)	O(11)	5, $-b$	3.295
	C(13)	3, $-a$, $-b$	3.325
	C(14)	5	3.589
	C(15)	4, $-c$	3.489
	C(18)	5, $-b$	3.459
O(12)	C(13)	7, $-b$	3.572
	C(15)	5	3.553

*Premier symbole: symétrie 1, x, y, z; 2, $-x, y, \frac{1}{2} - z$; 3, $\frac{1}{2} + x, \frac{1}{2} + y, z$; 4, $\frac{1}{2} - x, \frac{1}{2} + y, \frac{1}{2} - z$. Les symétries 5 à 8 sont les centrosymétriques des symétries 1 à 4. Deuxième symbole: translations de la maille.

benzoate) d'éthylène glycol dans le cristal. La distance qui sépare deux de ces cycles voisins et rigoureusement parallèles entre eux est de 3.45 Å. Une telle distance entre cycles aromatiques est comparable à ce que l'on observe pour le graphite, le triphénylène (18), le dibenzanthrone (19) et l'isodibenzanthrone (20) où cette distance est de 3.35, 3.37, 3.45 et 3.42 Å respectivement. Le tableau 6 rassemble les distances intermoléculaires inférieures à 3.60 Å impliquant les atomes de Cl et d'oxygène.

Les auteurs remercient vivement Alain Faure qui a préparé le composé étudié et MM. Marchessault et Sundararajan pour leur intérêt et commentaires sur le présent travail. Nous remercions également le Ministère de l'Education de la Province de Québec pour l'aide financière apportée à ce travail.

1. S. PÉREZ et F. BRISSE. Acta Crystallogr. Sous presse.
2. S. PÉREZ et F. BRISSE. Acta Crystallogr. Sous presse.
3. P. R. SUNDARARAJAN, P. LABRIE ET R. H. MARCHESSAULT. Can. J. Chem. Article suivant.
4. H. C. HEIM et C. P. POE. J. Org. Chem. **9**, 299 (1944).
5. F. R. AHMED, S. R. HALL, M. E. PIPPY et C. P. HUBER. NRC Crystallographic Programs for the IBM System. World List of Crystallographic Programs, 2nd ed. Appendix. 1966. p. 52.
6. D. T. CROMER et J. T. WABER. Acta Crystallogr. **18**, 104 (1965).
7. R. F. STEWART, E. R. DAVIDSON et W. T. SIMPSON. J. Chem. Phys. **42**, 3175 (1965).
8. D. T. CROMER. Acta Crystallogr. **18**, 17 (1965).
9. P. MAIN, M. N. WOOLFSON et G. GERMAIN. A computer program for the automatic solution of crystal structures. CECAM meeting, Parme, Italie. 1970.
10. International Tables for X-Ray Crystallography. Vol. IV. Kynoch Press, Birmingham. 1974.
11. W. C. HAMILTON. Acta Crystallogr. **18**, 502 (1965).
12. F. HANIC. Acta Crystallogr. **21**, 332 (1966).
13. F. BRISSE et J. SYGUSCH. Acta Crystallogr. Sect. B, **30**, 480 (1974).
14. G. J. PALENIK, J. DONOHUE et K. N. TRUEBLOOD. Acta Crystallogr. Sect. B, **24**, 1139 (1968).
15. L. E. SUTTON. Tables of interatomic distances and configuration in molecules and ions, Supplement 1956–1959. The Chemical Society, London. 1965.
16. V. SCHOMAKER et K. TRUEBLOOD. Acta Crystallogr. Sect. B, **24**, 63 (1968).
17. W. KLYNE et V. PRELOG. Experientia, **16**, 521 (1960).
18. F. R. AHMED et J. TROTTER. Acta Crystallogr. **16**, 503 (1963).
19. W. BOLTON et H. P. STAKLER. Acta Crystallogr. **17**, 1015 (1964).
20. W. BOLTON. Acta Crystallogr. **17**, 1020 (1964).

Can. J. Chem. Downloaded from www.nrcresearchpress.com by 210.87.254.6 on 09/05/12
For personal use only.

Can. J. Chem. Downloaded from www.nrcresearchpress.com by 210.87.254.5 on 09/05/12
For personal use only.

Conformational Studies on Oligomethylene Glycol Derivatives III. Ethylene Glycol Diacetate

PUDUPADI R. SUNDARARAJAN, PIERRE LABRIE, AND ROBERT H. MARCHESSAULT
Department of Chemistry, Université de Montréal, Montreal, Quebec H3C 3V1

Received May 30, 1975

PUDUPADI R. SUNDARARAJAN, PIERRE LABRIE, and ROBERT H. MARCHESSAULT. Can. J. Chem. **53**, 3557 (1975).

Conformational energies were calculated for the molecule ethylene glycol diacetate, using semiempirical methods. Several conformations corresponding to the *trans* and *gauche* states of the C—O and C—C single bonds are preferred. The $g^{\pm}$ state of the C—O bond is shifted from $\pm 120°$ by 10 to 32°. The relative energies of the various preferred conformations are found to depend on the value of the valence angle C—O—C. Calculations with C—O—C ranging from 110 to 124° showed that a value of 115° would be preferred for this angle. The predicted values of the torsion angles and bond angles are found to be in agreement with the crystal structure data on the benzoate derivatives of ethylene glycol.

PUDUPADI R. SUNDARARAJAN, PIERRE LABRIE et ROBERT H. MARCHESSAULT. Can. J. Chem. **53**, 3557 (1975).

Des calculs d'énergies de conformation, basés sur des méthodes semiempiriques, sont décrits pour le diacétate d'éthylène glycol. Plusieurs conformations correspondant aux formes *trans* et *gauche* des liaisons simples C—O et C—C sont les plus probables. La forme $g^{\pm}$ de la liaison C—O est déplacée de 10 à 32° par rapport à $\pm 120°$. Les énergies relatives des nombreuses conformations probables dépendent de la valeur de l'angle de valence C—O—C. En faisant varier cet angle de 110 à 124°, les calculs nous indiquent que la valeur de 115° serait la plus probable. Les valeurs trouvées pour les angles de torsion et les angles de valence sont en accord avec les données cristallines de la structure des dérivés benzoate de l'éthylène glycol.

[Traduit par le journal]

Introduction

Structural studies of aliphatic polyesters of the type $-[CO-(CH_2)_x-CO-O-(CH_2)_y-O]_n-$ derived from ethylene glycol ($y = 2$), trimethylene glycol ($y = 3$), and dekamethylene glycol ($y = 10$) were first made by Fuller *et al.* (1–4), using X-ray diffraction methods. Among the polyesters of the ethylene glycol series, these authors observed a shortening of the fiber repeat from the value expected for a fully extended chain. These are summarized in Table 1. A difference of 1.4 Å was observed for polyethylene succinate ($x = 2$, $y = 2$) and this was interpreted as due to a twist around the CH_2—CH_2 bond of the glycol portion of the chain, so as to bring the oxygen atoms towards each other, as in **1**. Later studies by Tadokoro and co-workers (5) showed that the dihedral angles around the two CH_2—CH_2 bonds in the repeat unit correspond to the g^+ and g^- *gauche* conformations. Turner-Jones and Bunn (6) studied the structures of polyethylene adipate ($x = 4$, $y = 2$) and polyethylene suberate ($x = 6$, $y = 2$), and attributed the shortening (of about 0.5 Å) of the fiber repeat to a rotation of 66° (see **2**) around the C—O bond, while the planar *trans* conformation is preserved around the CH_2—CH_2 bonds. As seen in **2**, a twist of 18° in the glycol portion, around the CO—O bond was also introduced, making the ester group nonplanar.

The vast amount of work on the conformational analysis of polypeptides, polysaccharides, and polynucleotides has shown that a knowledge

TABLE 1. Observed repeat distance for polyesters of the type $-[\overset{\overset{\displaystyle O}{\|}}{C}-(CH_2)_x-\overset{\overset{\displaystyle O}{\|}}{C}-O-(CH_2)_y-O]_n-$ and the corresponding theoretical repeat in the fully extended form

		Repeat (Å)		
x	y	Observed	Calculated	Reference
2	2	8.32	9.7	1, 5
4	2	11.71	12.21	1, 6
6	2	14.28	14.78	6
7	2	31.2	16.0 or 32.0	1
8	2	16.67	17.24	1

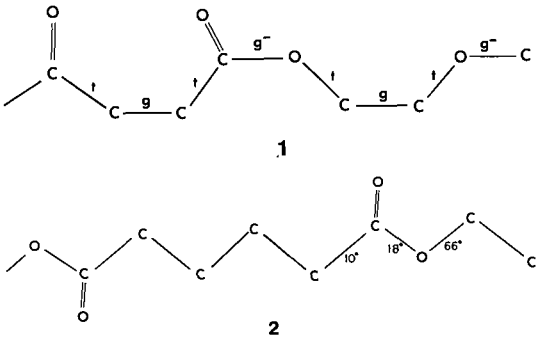

1

2

of the structural parameters (bond lengths, bond angles, and torsion angles) and the relative stability of several conformations of analogous small molecules is essential to derive reliable information on the conformations of a polymer (7–11). Hence, the conformational features of the molecule ethylene glycol diacetate (EGDA) were studied, since it can serve as a model compound for the class of polyesters mentioned above. This analysis predicts the probable rotational states of the various bonds in the molecule and the effect of varying the geometrical parameters, such as the bond angle, on the relative stability of these rotational states.

Geometrical Data

A schematic of EGDA is given in Fig. 1. The bond lengths and bond angles used in this study are given in Table 2, and were taken from previous studies on esters and acetates (12). The ester group is taken to be in the *trans* conformation. Any deviation from perfect planarity is measured by the angle ω. Several conformations of the molecule were generated by rotations ϕ_1, ϕ_2, and ϕ_3 around the single bonds, as shown in Fig. 1. Due to the chemical symmetry of the molecule, the dihedral angles ϕ_1 and ϕ_3 were taken to be equal. The all-*trans* planar conformation defines the starting position with $\phi_1 = \phi_2 = \phi_3 = 0°$. A positive increment in ϕ_1 and ϕ_3 is given by a clockwise rotation of the acetate groups on either side, viewing along the CH_2—O bonds. Looking along the CH_2—CH_2 bond from left to right, a clockwise rotation of the part of the molecule on the right hand side gives a positive increment in ϕ_2.

Parameters for Energy Calculations

Intrinsic torsional potentials with a threefold barrier of 2.8 kcal mol^{-1} and a twofold barrier of

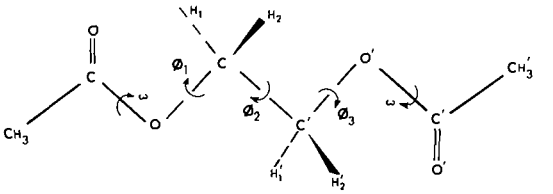

FIG. 1. Schematic of ethylene glycol diacetate (EGDA) molecule. The relevant torsion angles are marked.

8.75 kcal mol^{-1} were assigned to rotations about the CH_2—CH_2 bond (rotation ϕ_2) and the C═O bonds (rotation ω), respectively (12*a*). The torsional barrier for the C—O bond (rotations ϕ_1 and ϕ_3) was taken to be zero (12*a*).

Nonbonded interactions were computed using the Lennard-Jones function $E_{ij} = a_{ij}/r_{ij}^{12} - b_{ij}/r_{ij}^{6}$ for each pair of interacting atoms *i* and *j*, excluding the 1–3 interactions. The constants a_{ij} and b_{ij} were calculated according to the methods described previously (12, 13). The CH_3 group was treated as a spherical domain of van der Waals radius of 1.9 Å.

Coulombic interactions were evaluated (12*a*, 13) by assigning partial charges to the atoms, using bond moments of 0.82 D for C—O, 2.3 D for C═O, 0.74 D for C⋯O, and 0.38 D for C—H. An apparent dielectric constant of 2 was used (13).

The energy of deformation of the valence angles was estimated according to $V(\theta) = A(\Delta\theta)^2$ where $\Delta\theta$ is the distortion of an angle θ and *A* is half the force constant. A value of 80 kcal mol^{-1} was used for *A*, for the C—O—C and C—C—O valence angles whose standard value was taken to be 110°.

Results and Discussion

Iso-energy contours, plotted at intervals of 1 kcal mol^{-1} with respect to the minimum denoted by zero, are given in Fig. 2, as a function

TABLE 2. Geometrical data for calculations on ethylene glycol diacetate

Bond	Length (Å)	Bonds	Angle (deg)
C—C	1.53	C—C—O	100–114
C—O	1.42	C⋯O—C	110–124
C═O	1.26	O⋯C═O	125
C⋯O	1.36	O═C—CH_3	123
C—CH_3	1.53	O⋯C—CH_3	112
C—H	1.08	O—C—H	110

Can. J. Chem. Downloaded from www.nrcresearchpress.com by 210.87.254.5 on 09/05/12
For personal use only.

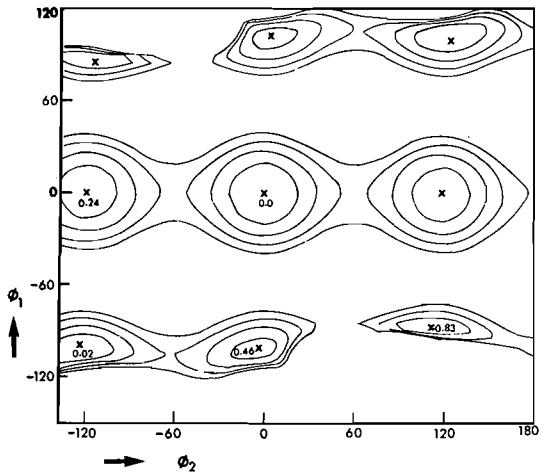

FIG. 2. Iso-energy contours for EGDA as a function of ϕ_1 and ϕ_2. Contours are drawn at intervals of 1 kcal mol^{-1} with respect to the minimum marked by 0.0. Values of $\omega = 0°$, $\angle COC = 112°$, and $\angle CCO = 110°$ are used here.

of $\phi_1 (= \phi_3)$ and ϕ_2. Energies were calculated at intervals of 1° in ϕ_1 and ϕ_2 in the neighborhood of the minima and at intervals of 10° elsewhere. Values of C—O—C = 112°, C—C—O = 110°, and $\omega = 0°$ were used here.

In addition to the *tt* conformation ($\phi_1 = \phi_2 = 0°$, *trans*), minima are recorded for the g^+ (*gauche*, +120°) and g^- (*gauche*, −120°) states of the bonds. The latter minima, in some conformations, are shifted significantly from the ideal ±120° position for perfect staggering. The values of ϕ_1 and ϕ_2 for all the minima are given in Table 3.

The relative energies of the minima show that the various possible conformations differ very little in energy from the *tt* state. The g^-g^- conformation is of equal energy to the *tt* state; the tg^- and g^-t states are only 0.24 and 0.45 kcal mol^{-1} higher in energy than the *tt* state. The g^-g^+ conformation, which is about 0.83 kcal mol^{-1} higher in energy, cannot be ruled out completely. The significant interactions which are relieved to some extent by a shift of the minima to nonstaggered conformations are given in Table 3. The higher energy of the perfectly staggered g^-g^+ conformation is due to the interactions involving carbonyl carbon and carbonyl oxygen. The severity of these interactions is reduced by a significant shift of ϕ_1 (to −88°) from perfect staggering. It is also to be noted that in all the conformations g^-g^+, g^-t, and g^-g^-, appreciable

TABLE 3. Preferred conformations, the energies, and the significant interactions for ethylene glycol diacetate ($t \approx 0°$, $g^+ \approx 120°$, $g^- \approx -120°$)

ϕ_1, ϕ_2 (deg)	Symbol	Energy (kcal mol^{-1})	Significant interactions		
			Atom pair*	Distance at perfect staggering (Å)	Distance† at the minimum energy position (Å)
0, 0	*tt*	1.10			
1, −118 or −1, 118	tg^- tg^+	1.34			
−88, 111 or 88, −111	g^-g^+ g^+g^-	1.93	$C_c \cdots C'$	2.80	3.13
			$C_c \cdots O'$	2.49	3.02
			$C_c \cdots C_c'$	1.67	2.93
			$C_c \cdots O_c'$	1.29	3.02
			$O \cdots O_c'$	1.83	2.81
			$CH_3 \cdots O_c'$	1.89	—
			$C \cdots O_c'$	2.69	—
			$CH_3' \cdots C'$	2.66	—
			$O_c \cdots O_c'$	1.92	—
−102, −5 or 102, 5	g^-t g^+t	1.56	$C_c \cdots C'$	2.80	2.99
			$C \cdots O_c'$	2.69	3.03
			$O_c \cdots H_1'$	1.96	2.47
−103, −124 or 103, 124	g^-g^- g^+g^+	1.12	$C_c \cdots C'$	2.80	2.98
			$C \cdots O_c'$	2.69	3.01
			$O_c \cdots H_2'$	1.97	2.44

*The subscript c denotes carbonyl.
†The dash in some entries denotes that the distance is more than the sum of the van der Waals radii.

Can. J. Chem. Downloaded from www.nrcresearchpress.com by 210.87.254.5 on 09/05/12
For personal use only.

Can. J. Chem. Downloaded from www.nrcresearchpress.com by 210.87.254.5 on 09/05/12
For personal use only.

shift from perfect staggering is recorded for ϕ_1 only, rather than for ϕ_2.

Though one would imagine that the *tt* conformation in which the C=O dipoles are antiparallel to each other would be most favored, examination of models would show that in all the conformations listed in Table 3, the dipoles are antiparallel. This is necessarily due to the fact that the parts of the molecule on either side of the CH_2—CH_2 bond are related by a twofold axis. This relationship is also borne out by the energy map shown in Fig. 2.

Effect of ω *Rotation*

As mentioned above, Turner-Jones and Bunn (6) proposed the torsional angle ω = 18° for the structures of polyethylene adipate and polyethylene suberate. A survey (14) of the crystallographic data on small molecules showed that the value of ω differs very little from 0°. In the present analysis, the value of ω was varied, from 0 to 10°, to examine its effect on the energy of the molecule.

Figure 3 shows the variation of energy as a function of ω, for the various preferred states of the molecule deduced from Fig. 2. The relative energy of the various conformations, compared to that of the *tt* state, remains almost the same through the range of ω presented here. These curves show that the energy of the molecule, in all the preferred conformations, does not decrease by choosing a value of ω other than 0°. The energy variation is negligible up to about ω = 2°, and thereafter an increase is noted. In all the conformations except g^-g^+, the increase in energy is mainly due to the torsional potential. The nonbonded distances show no significant variation. In the g^-g^+ conformation, the O...O′ (carbonyl) distance decreases from 2.8 to 2.7 Å as ω increases from 0 to 10°. The $CH_3\cdots C'$ (carbonyl) and $CH_3\cdots O'$ (carbonyl) distances are 3.56 and 3.20 Å respectively for ω = 10°. These two distances are greater than the sum of the van der Waals radii for ω = 0°. The increase in energy through the range of 0 to 10° is only of the order of 500 to 600 kcal mol^{-1}. However, a definite trend towards higher energy cannot be neglected. Hence, in the subsequent calculations, the value of ω was restricted to 0°.

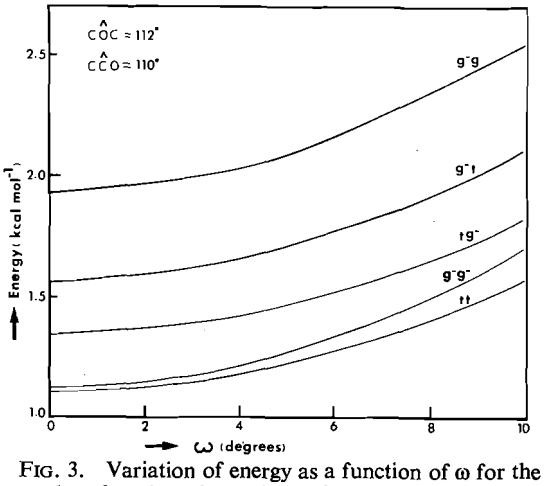

FIG. 3. Variation of energy as a function of ω for the several preferred conformations of EGDA.

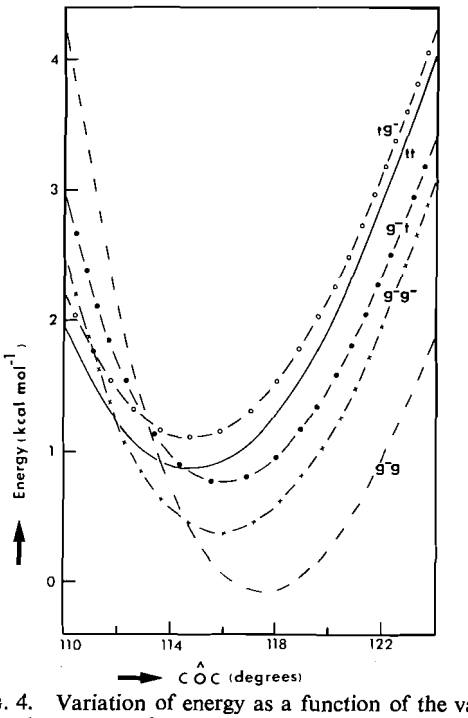

FIG. 4. Variation of energy as a function of the valence angle C—O—C for the following conformations: —, *tt*; ○, tg^-; ···, g^-t; ×, g^-g^-; and ---, g^-g^+.

Effect of Variation in the Angle C—O—C

The proper choice of the value for the valence angle C—O—C for conformational analysis of polymers is problematic. Studies on various types of small molecules have shown that the value of this angle varies from 110 to 122° depending upon the bulkiness of the group of atoms attached to the two carbons (7, 11).

The variation of energy of EGDA as a function of the angle C—O—C is shown in Fig. 4 for the five representative conformations. Consider-

Can. J. Chem. Downloaded from www.nrcresearchpress.com by 210.87.254.5 on 09/05/12
For personal use only.

able decrease in energy is noted as the angle is increased from 110°. For the *tt* and tg^- conformations, a minimum in the curves is observed at about 115°, and a further increase in the angle results in a sharp increase in energy due to the increasing contribution from $V(\theta)$. For the conformations g^-t and g^-g^-, the minimum is found at C—O—C = 116°. The preferred value is shifted to 118° for the g^-g^+ conformation. It would seem that the interaction between the carbonyl oxygens is relieved considerably by an increase in the value of the valence angle C—O—C. This is substantiated by a rather sharp decrease in energy with an increase of C—O—C from 110 to 118° for the g^-g^+ conformation, compared to the other curves in Fig. 4. Thus, the calculations show that with the exception of the g^-g^+ conformation, the most probable value of C—O—C would be 115° in EGDA.

The value of about 114–116° for C—O—C seems to be the range in which the relative stabilities of the conformations undergo a change. Throughout the range of C—O—C = 110 to 124°, the energy difference between the *tt* and tg^- states remains the same. However, beyond 114°, the energies of g^-t and g^-g^- conformations are found to be lower than that of *tt*. The g^-g^+ state, which is of highest energy for C—O—C = 110°, becomes the conformation of lowest energy beyond 115°.

Effect of Variation of Angle C—C—O

The iso-energy contours, as a function of the angles C—O—C and C—C—O are shown in Fig. 5 for the *tt* conformation. The minimum energy is observed for the values C—O—C = 115° and C—C—O = 109°. With C—O—C = 115°, as the value of C—C—O is decreased from 109 to 105°, the increase in energy is about 0.6 kcal mol^{-1}. Keeping C—C—O = 109°, the same amount of increase in energy results from a change of 3° in C—O—C, from 115 to 118°. Apart from this difference, the variation of energy seems to be equally sensitive to changes in both bond angles.

Comparison with Experimental Results

As seen from Table 3, various conformations are energetically possible for the EGDA molecule. These predictions are expected to be valid even if the CH_3 group is replaced by another kind of atom or group of atoms, *e.g.*, the aromatic moiety of van der Waals radius of 1.8 Å or the

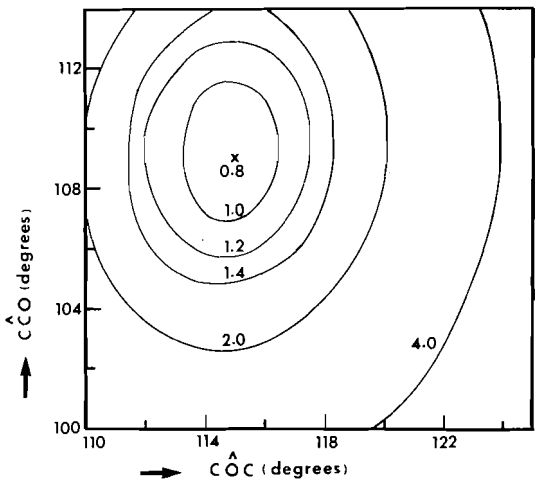

FIG. 5. Iso-energy contours as a function of the valence angles C—O—C and C—C—O for the *tt* state of EGDA. The minimum is marked by X. Energies are expressed in kcal mol^{-1}.

ethyl and propyl groups, should behave in the same way, the latter with a slightly larger van der Waals radius. In which of the predicted conformations these derivatives crystallize would depend upon the crystallization conditions and possibly packing requirements.

The crystal structure of ethylene glycol dibenzoate was reported previously (15). This molecule was found to be in the all-*trans* conformation, with $\phi_1 = 3.9°$ and $\phi_2 = 4.4°$. On the other hand, ethylene glycol di(*para*-chlorobenzoate) (16), crystallized under different conditions, was found to be in the tg^+ (or tg^-) conformation, with $\phi_1 = 5°$ and $\phi_2 = 105.5°$. The value of ω was found to be about 3° in these structures. In spite of the aromatic substitution (instead of CH_3), the values of the torsion angles ϕ_1, ϕ_2, and ω are in very good agreement with the values obtained for *tt* and $tg^{\pm}$ states theoretically. That remarkably similar values were obtained for the angle C—O—C, from the crystal structure analyses (115.5 to 115.9°) and the theoretical calculations (about 115°) is also very encouraging. The value of the angle C—C—O, in the crystal structure, is about 105°. This is rather small compared to the theoretical value of 108 to 110°. However, as seen from Fig. 5, the variation in energy as the angle C—C—O is reduced from 109 to 105° is only about 0.6 kcal mol^{-1}.

Table 4 shows a comparison of the atomic coordinates deduced from the crystal structure of the ethylene glycol di(*para*-chlorobenzoate)

TABLE 4. Comparison of the atomic coordinates (in Å) derived from calculations and the crystal structure

	Calculated coordinates for tg^+ conformation			Coordinates from crystal structure (ref. 16)		
Atom (Fig. 1)	x	y	z	x	y	z
O (carbonyl)	2.21	1.05	0.0	2.16	0.99	0.0
C (carbonyl)	1.53	0.0	0.0	1.48	0.0	0.0
O	2.04	−1.26	0.0	1.99	−1.24	−0.01
C	3.45	−1.36	0.0	3.44	−1.33	0.08
H_1	3.86	−0.88	0.9	3.72	−0.99	0.99
H_2	3.87	−0.82	−0.86	3.85	−0.77	−0.64
C′	3.88	−2.83	−0.05	3.81	−2.77	−0.07
H_1'	4.97	−2.90	0.01	4.79	−2.91	0.18
H_2'	3.47	−3.37	0.82	3.22	−3.35	0.48
O′	3.41	−3.43	−1.25	3.66	−3.11	−1.47
C′ (carbonyl)	3.68	−4.75	−1.40	3.85	−4.40	−1.78
O′ (carbonyl)	4.31	−5.46	−0.57	4.05	−5.25	−0.95

(which is in the tg^+ or tg^- conformation) and the atomic parameters derived from the present calculations for the tg^+ conformation of ethylene glycol diacetate. In spite of the minor differences in the angle C—C—O, there is a close agreement between the two sets of parameters. This demonstrates the potential of calculations of the type presented here to explain the occurrence of non-extended conformations for polyesters and model compounds based on ethylene glycol diesters.

Financial support from the National Research Council of Canada and the FCAC program of the Ministère de l'Education du Québec is gratefully acknowledged. The authors thank Professor F. Brisse and Mr. S. Pérez for helpful discussions.

1. C. S. FULLER and C. L. ERICKSON. J. Am. Chem. Soc. **59**, 344 (1937).
2. C. S. FULLER and C. J. FROSCH. J. Phys. Chem. **43**, 323 (1939).
3. C. S. FULLER and C. J. FROSCH. J. Am. Chem. Soc. **61**, 2575 (1939).
4. C. S. FULLER, C. J. FROSCH, and N. R. PAPE. J. Am. Chem. Soc. **64**, 154 (1942).
5. A. S. UEDA, Y. CHATANI, and H. TADOKORO. Polym. J. **2**, 387 (1971).
6. A. TURNER-JONES and C. W. BUNN. Acta Crystallogr. **15**, 105 (1962).
7. M. SUNDARALINGAM. Biopolymers, **6**, 189 (1968).
8. M. SUNDARALINGAM. Biopolymers, **7**, 821 (1969).
9. G. A. JEFFREY and R. D. ROSENSTEIN. Adv. Carbohydr. Chem. **19**, 7 (1964).
10. A. V. LAKSHMINARAYANAN, V. SASISEKHARAN, and G. N. RAMACHANDRAN. *In* Conformation of biopolymers. *Edited by* G. N. Ramachandran. Academic Press, New York. 1967. p. 61.
11. R. H. MARCHESSAULT and P. R. SUNDARARAJAN. Pure Appl. Chem. In press.
12. (*a*) J. CORNIBERT and R. H. MARCHESSAULT. J. Mol. Biol. **71**, 735 (1972); (*b*) S. M. GABBAY, P. R. SUNDARARAJAN, and R. H. MARCHESSAULT. Biopolymers, **11**, 79 (1972).
13. G. N. RAMACHANDRAN and V. SASISEKHARAN. Adv. Protein Chem. **23**, 283 (1968).
14. J. CORNIBERT, N. V. HIEN, F. BRISSE, and R. H. MARCHESSAULT. Can. J. Chem. **52**, 3742 (1974).
15. S. PÉREZ and F. BRISSE. Acta Crystallogr. In press.
16. S. PÉREZ and F. BRISSE. Can. J. Chem. Preceding paper.

Can. J. Chem. Downloaded from www.nrcresearchpress.com by 210.87.254.5 on 09/05/12
For personal use only.

Virtual Bond Method in Conformational Analysis of Polymers

PUDUPADI R. SUNDARARAJAN AND ROBERT H. MARCHESSAULT
Department of Chemistry, Université de Montréal, C.P. 6210, Succ. A, Montreal, Quebec H3C 3V1
Received May 13, 1975

PUDUPADI R. SUNDARARAJAN and ROBERT H. MARCHESSAULT. Can. J. Chem. **53**, 3563 (1975).

A detailed description of the virtual bond method is presented. Simple equations are set up to examine the various relative dispositions of the repeating units along the polymer helix, if the repeat distance and the screw symmetry are known from X-ray data. The method is demonstrated with the examples of β-D-1,4′-xylan helix and the α-helix. Due to the rapidity and simplicity of this procedure, the effect of using different geometries for the residues can be examined readily. Diagrams are presented, from which one can deduce the torsion angles ϕ, ψ for the various values of the valence angle at the bridge atom. This method does not involve a prior knowledge of ϕ, ψ and hence, derivation of atomic coordinates of the residue for Fourier transform or structure factor calculations is simple.

PUDUPADI R. SUNDARARAJAN et ROBERT H. MARCHESSAULT. Can. J. Chem. **53**, 3563 (1975).

La méthode d'analyse conformationnelle pour polymères employant le concept de la liaison virtuelle est décrite. Des équations simples permettent l'étude de conformations hélicoidales, si les symétries et les périodicités d'hélices sont déterminées auparavant par diffraction des rayons X. La méthode est appliquée à deux exemples: le polysaccharide β-D-1,4′ xylane et l'hélice α des polypeptides. La méthode permet facilement de faire varier la géométrie des unités de base. A partir de diagrammes, on peut déduire les angles de torsion: ϕ, ψ pour des valeurs données de l'angle de valence entre les unités de répétition. Cette méthode n'implique pas une connaissance préalable de ϕ, ψ, donc la détermination des coordonnées atomiques de l'unité de répétition pour le calcul de la transformée de Fourier, ou pour le calcul de facteurs de structure s'avère très simple.

[Traduit par le journal]

Conformational analysis of polymers in terms of rotations around single bonds connecting the repeat units is extensively used (1–3). Relative orientations of contiguous residues are described by the torsion angles ϕ and ψ which define the rotations around the bonds C(1)—O and O—C-(n') in a $1 \rightarrow n'$ linked polysaccharide, and around the bonds N_i—C_i^{α} and C_i^{α}—C_i' in the case of polypeptides. Energies for each relative orientation, computed as a sum of interactions between atoms of contiguous residues, are plotted as *iso*-energy contours in the (ϕ, ψ) plane and this defines the relative stability of the conformational regions accessible to the molecule. The *iso*-energy maps are employed for evaluation of the statistical mechanical average properties of macromolecules (3).

Methods are also available (2, 4) to evaluate the helical parameters n (the number of residues per turn of the helical chain) and h (the projected height of the residue along the helix axis), and again these parameters are plotted as *iso-n* and *iso-h* contours on a (ϕ, ψ) surface. Simultaneous use of the *iso* energy and the helical parameters maps aids in the selection of the most probable helical conformations of polymers in the solid state. In computing the *iso*-energy map and the helical parameters, the residue geometry as well as the angle τ at the bridge atom (τ = C(1)—O—C(n') for polysaccharides and N_i—C_i^{α}—C_i' for polypeptides) are fixed for any one particular map. Thus, for each polymer one should consider a family of maps, computed by varying τ over the range of acceptable values.

In order to generate the atomic coordinates of the atoms of the residues along a helix with a given set of n, h, and τ, one has to know the precise values of ϕ, ψ yielding the corresponding n, h and also the direction cosines of the helix axis in the defined coordinate system. This is usually achieved by interpolation of n, h values calculated at specific intervals of ϕ, ψ and while the interpolation may be graphical or computerized, in either case it is a tedious process. The task is multiplied if this has to be repeated for various values of τ. An alternate analytical method to deduce the

Can. J. Chem. Downloaded from www.nrcresearchpress.com by 210.87.254.5 on 09/05/12
For personal use only.

Can. J. Chem. Downloaded from www.nrcresearchpress.com by 210.87.254.5 on 09/05/12
For personal use only.

internal rotation angles was suggested by Nagai and Kobayashi (5), for structures with one, two, or three atom repeat units. The method presented here provides a simple way of deducing ϕ, ψ for a helical structure for various values of τ, in addition to serving as a tool to determine the best helical conformation.

A relatively simple method, that of rotation of the residue about the virtual bond was first applied to the analysis of cellulose conformation by Jones (6). Since then, the conformations of β-D-1,4′-xylan (7), acetyl amylose (8), and mycodextran (9) were treated by this procedure. Identical results have been reported in the case of β-D-1,4′-xylan (7, 10) and mycodextran (9), where the virtual bond method as well as the ϕ, ψ method were applied. A detailed description of the virtual bond method has not been presented so far. In this report, the details of the method will be set forth and the usefulness of this type of approach will be discussed.

The virtual bond method is applicable to a helix of given n, h, and chirality. It then examines the possible relative orientations of the contiguous residues, which obey the constraints imposed by the chosen n and h. Different conformations are generated by a rotation of the residue through angle θ around the virtual bond. The virtual bond itself is defined as the vector joining the contiguous bridge atoms (O(n') and O(1) atoms in polysaccharides, and C_{i-1}^{α} and C_i^{α} in polypeptides) with the residue geometry fixed.

The procedure will be illustrated with an example of the β-D-1,4′-xylan helix (7). Here $n = \pm 3$, and $h = 4.95$ Å. The negative sign of n applies for the left-handed helix. The angular twist about the helix axis relating two successive residues is then ± 120 ($360°/n$). The residue atoms are defined in the system (7) where the atom O(4) is at the origin and O(1) is along the positive Z axis. The starting position ($\theta = 0°$) is so chosen as to place the O(2) atom along the positive X-axis (Fig. 1*a*). In order to rotate the residue about the virtual bond, a counterclockwise rotation is applied to the residue, viewing towards the origin along the Z axis (*cf.* Fig. 1*a*). In order to transform the residue to the proper position along the helix, we have to do the following operations: (*i*) Viewing towards the origin along the X-axis rotate the residue clockwise through an angle μ (*cf.* Fig. 1*b*); this causes the residue to be at the proper tilt with respect to the helix axis (Z axis).

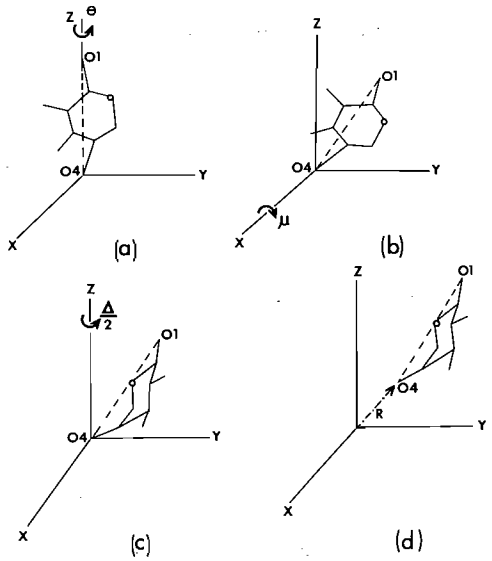

FIG. 1. Schematic representation of the virtual bond method, showing the (*a*) θ rotation, (*b*) μ tilt, (*c*) $\Delta/2$ rotation, and (*d*) translation through R. The virtual bond connecting O(4) and O(1) atoms is shown by dashed line.

(*ii*) Viewing towards the origin along Z axis, rotate the residue counterclockwise about the Z-axis through an angle $\pm\Delta/2$, the negative sign applying to left-handed helix (Fig. 1*c*). (*iii*) Translate the residue along the X-axis through $\pm R$, this being the radius of the atoms O(1) and O(4) with respect to the helix axis (Fig. 1*d*).

The parameters μ and R are calculated for the atoms O(1) and O(4) and the transformations involving these parameters are applied to all the atoms in the residue, since these are affine transformations. Thus, if $\boldsymbol{r}_1$ and $\boldsymbol{r}_2$ are the position vectors of an atom in the residue before and after transformation,

$$[1] \quad \boldsymbol{r}_2 = M_{0,0,1}^{\pm\Delta/2} M_{1,0,0}^{-\mu} \mathbf{M}_{0,0,1}^{\theta} [\boldsymbol{r}_1] \pm R$$

The matrices **M** have the general form described before (2). The subscripts denote the direction cosines of the axis of rotation: X or Z axis.

The parameter μ, which defines the tilt of the virtual bond with respect to the helix axis, and R are deduced from Fig. 2. In this figure, $\mu' = (90° - \mu)$. L represents the length of the virtual bond, h is the projected height of the residue, and Δ is the twist. From the diagram,

$$[2] \quad \mu = \cos^{-1}(h/L)$$

Can. J. Chem. Downloaded from www.nrcresearchpress.com by 210.87.254.5 on 09/05/12
For personal use only.

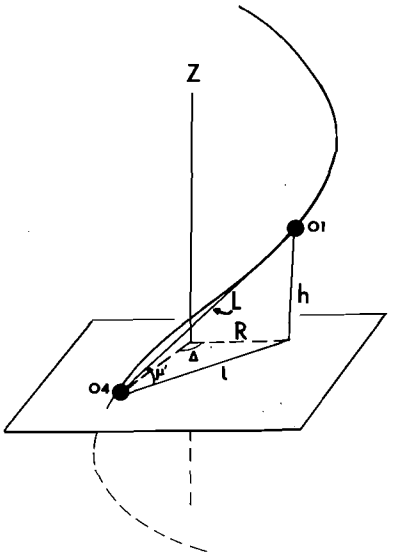

FIG. 2. Diagram showing the relationship between the virtual bond and the helix axis.

Since

$$[3] \qquad l = (L^2 - h^2)^{1/2}$$

and

$$[4] \qquad R = l/[2(1 - \cos \Delta)]^{1/2}$$

it follows that

$$[5] \qquad R = \frac{(L^2 - h^2)^{1/2}}{2 \sin\left(\frac{\Delta}{2}\right)}$$

After the rotation through μ described in step (*i*), the atom O(1) will have coordinates $x = 0$, $y = l$, $z = h$ (*cf.* Fig. 1*b*). It is essential that after translation through $\pm R$ along the X-axis (step *iii*), the radius of the atom O(1) with respect to the helix axis be R. Suppose that a clockwise rotation ε is applied to O(1) along Z axis, after step (*i*). Then, the coordinates of O(1) become

$$[6] \qquad x' = l \sin \varepsilon$$

$$y' = l \cos \varepsilon$$

After translation through R along the x-axis, the following condition should be satisfied

$$[7] \qquad (l \sin \varepsilon \pm R)^2 + l^2 \cos^2 \varepsilon = R^2$$

This equation simplifies to

$$[8] \qquad \sin \varepsilon = \pm \frac{l}{2R}$$

Since $l/2R = \sin(\Delta/2)$ (see eq. 5), it follows that a rotation $\varepsilon = \pm\Delta/2$ as described in step (*ii*) would transform O(1) to a position, which after step (*iii*), would place O(1) at a radius R with respect to the helix axis.

Once the residue is transformed to the correct helical orientation, the contiguous residue may be generated simply by the helix symmetry operation (rotation of the residue through $\pm\Delta$ about the helix axis and a translation h parallel to the helix axis). The angle C(1)—O—C(4′) at the bridge atom will vary as the value of θ is changed. From the coordinates of the atoms in a pair of residues generated as above, the value of τ can be readily obtained. The torsion angles ϕ and ψ are also easily deduced.

The variation of the angle τ as a function of the rotation θ is given in Fig. 3 for left-handed β-D-1,4′-xylan helix. The atomic coordinates given in ref. 7 were used. The angle τ varies from 113° to about 118° in the crystal structures of carbohydrates (11, 12). Figure 3 shows that, as we proceed along the solid curve (τ curve) the values of θ corresponding to the above range of τ are from 130 to 215°. Also given in Fig. 3 are the torsional angles ϕ = [H(1)—C(1)—O—C(4′)] and ψ = [C(1)—O—C(4′)—H(4′)]. It is seen that the values of ϕ and ψ for any given angle τ can be

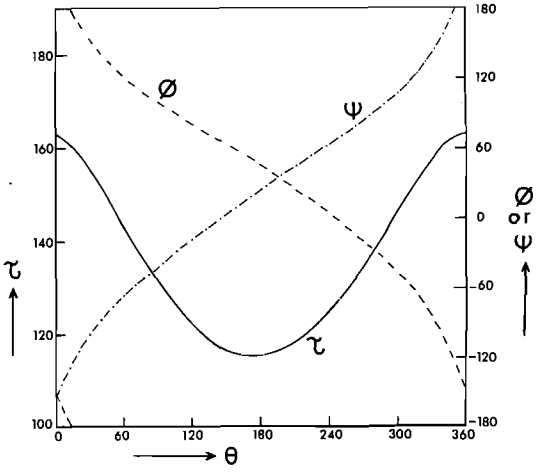

FIG. 3. Variation of τ (—, left ordinate), ϕ (---, right ordinate) and ψ (-·-·-, right ordinate) as a function of θ, the rotation about the virtual bond for left-handed β-D-1,4′-xylan helix.

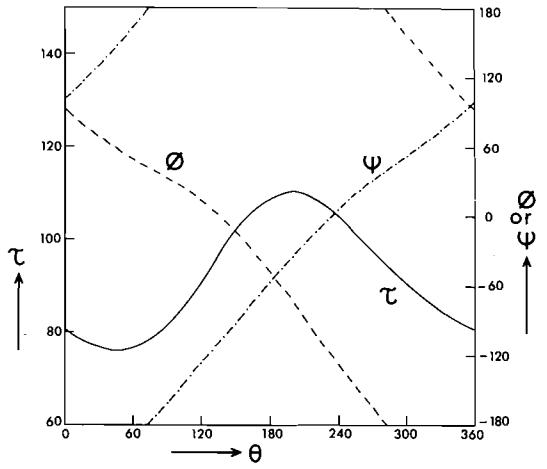

FIG. 4. Variation of τ (—, left ordinate), φ (---, right ordinate), and ψ (·····, right ordinate) as a function of θ, the rotation about the virtual bond for right-handed α-helix.

obtained from this figure in a straightforward manner. For example, with $\tau = 117.5$, the φ, ψ values which permit a 3_1 helix are: (66.1, −1.3) and (28.8, 40.5). From the φ, ψ energy map (10), it was shown that conformations similar to φ, ψ = 66.1, −1.3 are energetically favorable. The values of φ, ψ given here differ slightly from those in ref. 10 due to different residue geometries used in the two papers and due to differences in the definition of the starting position $\phi = \psi = 0$.

While two sets of values of φ, ψ are possible for values of τ such as 117.5°, only one set of φ, ψ is possible for the value of τ at the trough of the solid curve in Fig. 3. In this case, for $\tau = 115.4°$, the φ, ψ values are (48.7, 19.4). For $\tau < 115.4°$ it would be impossible to construct a xylan chain with the chosen residue geometry and the helical parameters. This value of τ which yields a unique φ, ψ for a helical conformation was termed (13) the 'critical τ' (τ_c).

One could evaluate the disaccharide energy (with due regard for the energy involved in changing τ) for each θ and plot a curve in Fig. 3. Such an energy curve would be of help in choosing the helix of minimum conformational energy.

A similar set of curves showing the variation of φ, ψ, and τ as a function of θ are given in Fig. 4 for the right-handed α-helix. The Pauling–Corey *trans* planar peptide geometry was used. It is seen that the critical τ_c in this case, at the apex of the solid curve, corresponds to a value of 110.4°, implying that an α-helix with $\tau > 110.4°$ cannot be generated with the planar peptide unit. For $\tau =$ 110° there are two sets of φ, ψ which satisfy the helix symmetry. These are (−58.4, −46.5) and (−86.3, −23.1). Only the former is the accepted α-helical conformation; the latter would fall in the disallowed area in the Ramachandran map, though dipeptide conformations with this value of φ, ψ are found in myoglobin and lysozyme (2).

The method and the results presented here show that for a given set of *n* and *h*, and the residue geometry, the values of φ and ψ can be evaluated rapidly for a series of values of τ. The critical τ is also made available immediately. In addition, comparison of the energy of the helices with varying τ is also possible. Due to its rapidity and simplicity, the effect of using different residue geometries can be examined easily. Since this procedure does not involve prior knowledge of φ, ψ or the direction cosines of the helix axis, derivation of atomic coordinates of the residue for calculations of Fourier transforms or structure factors is simplified.

Thus, while the φ, ψ approach looks at different possible helices with a given τ, the virtual bond method examines a chosen type of helix with varying τ, and in addition provides additional information which is of immediate use to the solid state conformational analyst.

Financial support from the National Research Council of Canada is gratefully acknowledged.

1. G. N. RAMACHANDRAN. *In* Structural chemistry and molecular biology. *Edited by* A. Rich and N. Davidson. W. H. Freeman and Co., San Francisco. 1967. p. 77.
2. G. N. RAMACHANDRAN and V. SASISEKHARAN. Adv. Protein Chem. **23**, 283 (1968).
3. P. J. FLORY. Statistical mechanics of chain molecules. Interscience, New York. 1969; J. Pure Appl. Chem. **26**, 309 (1971).
4. C. RAMAKRISHNAN. Proc. Indian Acad. Sci. **A59**, 327 (1964).
5. K. NAGAI and M. KOBAYASHI. J. Chem. Phys. **36**, 1268 (1962).
6. D. W. JONES. J. Polym. Sci. **32**, 371 (1958).
7. W. J. SETTINERI and R. H. MARCHESSAULT. J. Polym. Sci. C, **11**, 253 (1965).
8. A. SARKO and R. H. MARCHESSAULT. J. Am. Chem. Soc. **89**, 6454 (1967).
9. P. R. SUNDARARAJAN, R. H. MARCHESSAULT, G. J. QUIGLEY, and A. SARKO. J. Am. Chem. Soc. **95**, 2001 (1973).
10. P. R. SUNDARARAJAN and V. S. R. RAO. Biopolymers, **8**, 305 (1969).
11. M. SUNDARALINGAM. Biopolymers, **6**, 189 (1968).
12. R. H. MARCHESSAULT and P. R. SUNDARARAJAN. J. Pure Appl. Chem. In press.
13. P. R. SUNDARARAJAN and R. H. MARCHESSAULT. Can. J. Chem. **50**, 792 (1972).

Can. J. Chem. Downloaded from www.nrcresearchpress.com by 210.87.254.5 on 09/05/12
For personal use only.

On the Preparation of MoS_2 Catalysts from MoS_3

E. FURIMSKY AND C. H. AMBERG

Department of Chemistry, Carleton University, Ottawa, Canada K1S 5B6

Received May 29, 1975

E. FURIMSKY and C. H. AMBERG. Can. J. Chem. **53**, 3567 (1975).

We have examined the effect of reducing MoS_3 in hydrogen in the range 450–800 °C on the properties of the resulting MoS_2 catalyst. The appearance of rhombohedral MoS_2 at 800 °C is disputed. Instead, an 'overreduced' catalyst containing some Mo metal and hexagonal MoS_2 was formed. Catalytic activity in thiophene hydrodesulfurization was insensitive to pretreatment.

E. FURIMSKY et C. H. AMBERG. Can. J. Chem. **53**, 3567 (1975).

On a examiné l'effet de la réduction de MoS_3 par l'hydrogène à des températures de 450–800 °C sur les propriétés du catalyseur MoS_2 qui en résulte. On met en doute l'apparition de MoS_2 rhomboédrique à 800 °C. On suggère à la place de cette conclusion qu'il y a formation d'un catalyseur 'superréduit' contenant du Mo métallique et du MoS_2 hexagonal. L'activité catalytique vis-à-vis de l'hydrodésulfurisation du thiophène est insensible à un prétraitement.

[Traduit par le journal]

Can. J. Chem. Downloaded from www.nrcresearchpress.com by 210.87.254.42 on 09/05/12
For personal use only.

Introduction

MoS_2 is frequently used as a model catalyst in hydrodesulfurization (HDS) studies, and as such is often prepared from MoS_3. The activity of this catalyst in general is thought to depend on the temperature of reduction or pretreatment. For instance, it was shown earlier (1) that reduction of MoS_3 at 400 °C gave rise to significantly higher surface area and HDS activity per unit area than was found for the same MoS_2 catalyst sintered at 650 °C. Treatment at the higher temperature was said to have been responsible for improved reduction and/or thermal destruction of unstable surface states in the MoS_2 crystallites. A temperature increase to 800 °C resulted in a further decrease in surface area, but left the catalytic activity per unit surface area approximately unchanged.

There is conflicting evidence in the literature regarding the fate of MoS_2 catalysts subjected to thermal or reductive treatments. Ratnasamy and Léonard (2) in studying the structural evolution of MoS_2 concluded that the decrease in activity with increasing reduction temperatures was caused by a gradual build-up of rhombohedral MoS_2; this phase was presumed to be less active than hexagonal MoS_2. On the other hand, Wildervanck and Jellinek (3), who prepared MoS_2 by thermal dissociation of MoS_3, observed only hexagonal MoS_2 throughout the whole region of 350 to 1100 °C, with improved crystallinity detectable at the higher temperatures. Prolonged heating of the rhombohedral polymorph at 1000 °C effected the transition back to the hexagonal form. Silverman (4) demonstrated that rhombohedral MoS_2 can be prepared from its elements at temperatures higher than 1100 °C under ultrahigh pressures. Moreover, he observed that the hexagonal/rhombohedral transition occurs only in the neighborhood of 2000 °C, again under ultrahigh pressure.

Recently Aoshima and Wise (5) have studied the effect of varying the degree of reduction of a single crystal of hexagonal MoS_2 on the conversion of butanethiol. Through measurement of changes in electrical conductivity they were able to infer that with increasing reduction the number of S^{2-} ion vacancies in the crystal increased. In terms of the desulfurization of the thiol, an optimum region existed. However, beyond this, the crystal would be overreduced, and this caused loss of both activity and stability, some of which was due to an accumulation of carbon and sulfur species on the catalyst surface.

In view of these various observations a reexamination of several of the pertinent factors was thought to be worthwhile.

Experimental

Catalyst

MoS_3 was prepared by saturating a 200 g l^{-1} aqueous solution of ammonium paramolybdate with H_2S. After neutralizing with HCl, filtering, and washing, the brown precipitate which had formed was dried at 110 °C for 20 h. The material was then reduced in a quartz tube using a hydrogen stream (90 cc min^{-1}) near atmospheric

Can. J. Chem. Downloaded from www.nrcresearchpress.com by 210.87.254.42 on 09/05/12
For personal use only.

pressure at the temperatures 450, 600, and 800 °C and for various time periods. Fresh samples of MoS_3 were used for each reduction and time period.

Apparatus and Procedure

The microreactor and flow system were essentially the same as described previously (1). X-Ray analysis was carried out on a Siemens X-ray diffractometer using Cu K(α) radiation. Surface areas were determined in a volumetric B.E.T. apparatus using N_2 at liquid nitrogen temperature. Samples were outgassed at 200 °C.

Catalyst activity was tested at 400 °C, reactants consisting of a stream of hydrogen (30 cc min^{-1} near atmospheric pressure) containing a nominal partial pressure of thiophene of 21.4 Torr. The exact partial pressures, obtained by means of a thiophene bubble saturator which was kept at 0 °C, were measured on a routine basis during each test run. Thiophene conversion was analyzed by g.l.c. using a 6-ft squalane column (25% w/w) at 85 °C. Percent conversion was always expressed in terms of thiophene converted.

Results and Discussion

In the following we shall refer to the reaction which leads to the formation of MoS_2 as a reduction in hydrogen. It should be pointed out, however, that significant evolution of sulfur was observed at 600 and 800 °C, presumably through thermal dissociation of MoS_3. Sulfur deposits accumulated to a much smaller extent at 450 °C.

The change in crystallinity of our samples was examined by X-ray analysis throughout the time of reduction between 30 min and 20 h at constant temperature. No significant changes were observed at 450 and 600 °C, except for sharpening and intensification of the 002 band, indicating enhanced orientation around the *c*-axis at both these temperatures. Also, this band, as well as the broad 103, 101, and 105 reflections of the hexagonal MoS_2 lattice were sharper and more intense at 600 °C than at 450 °C, in agreement with the observations of Wildervanck and Jellinek (3). A marked increase in crystallinity appeared with reduction at 800 °C, as indicated by all lines of the spectrum, and this improved further with the time of reduction. In addition to this a new set of sharp lines was found after 8 h of reduction at 800 °C (Fig. 1*a*). As shown in Fig. 1*b*, these lines correspond closely with those of metallic molybdenum, in contradiction of the conclusions of Ratnasamy and Léonard (2) who interpreted their data in terms of the appearance of rhombohedral MoS_2. The experiments of the latter authors were performed under the same conditions as ours, except for possible differences in hydrogen flow rates, which were not cited in their paper. On reduction of highly crystalline and stoichiometric MoS_2 (Anachemia), again at 800 °C for 20 h, we were unable to detect any lines other than those of hexagonal MoS_2 (Fig. 1*c*).

Stubbles and Richardson (6) showed that the complete reduction of MoS_2 to Mo is possible via the following steps

$$[1] \qquad 2MoS_2 + H_2 \rightarrow Mo_2S_3 + H_2S$$

$$[2] \qquad \tfrac{1}{3}Mo_2S_3 + H_2 \rightarrow \tfrac{2}{3}Mo + H_2S$$

These authors used very pure synthetic MoS_2, and studied the equilibria obtained at temperatures between 850 and 1200 °C by circulating hydrogen over the powdered materials until constant H_2S pressures had been established. Reaction [1] was found to be much slower than [2]. Although our temperature was 50 °C below the bottom limit of their range, other conditions in our case were bound to favor further reduction of MoS_2. Thus, our reactor ensured a continuous supply of fresh hydrogen and removal of H_2S. Furthermore, our slightly sulfur-deficient MoS_2 of comparatively high surface area (Table 1) could be expected to be considerably more reactive than the 200-mesh powders of Stubbles and Richardson, the opposite extreme being represented by our inert Anachemia sample (surface area ~ 3 m^2 g^{-1}).

We have re-examined the data published by Ratnasamy and Léonard (2) for their 800 °C-sample, and found the X-ray lines to be consistent with the presence of both MoS_2 and Mo_2S_3; in other words, with 'overreduction' according to step [1] above. The X-ray diffractogram of these authors did not go to sufficiently high angles to permit us to establish the presence of molybdenum metal, because the four unique Mo lines at high angles (Fig. 1*b*) could not be seen.

In Table 1 we have recorded the surface area and sulfur content of all catalysts, as well as percent conversion and reaction rate per unit surface area in the hydrodesulfurization reaction.

At all temperatures, the initial reduction of MoS_3 resulted in a first steep increase in surface area to a maximum. The first entry at each temperature (1.0, 0.5, 0.5 h, respectively) represents this maximum. Thereafter, surface area decreased, reaching a steady value after 2–3 h at 600 °C, and after about 1 h at 800 °C. There was no sign of levelling off at 450 °C even after 20 h of reduction.

It is difficult to compare the initial surface

Can. J. Chem. Downloaded from www.nrcresearchpress.com by 210.87.254.42 on 09/05/12
For personal use only.

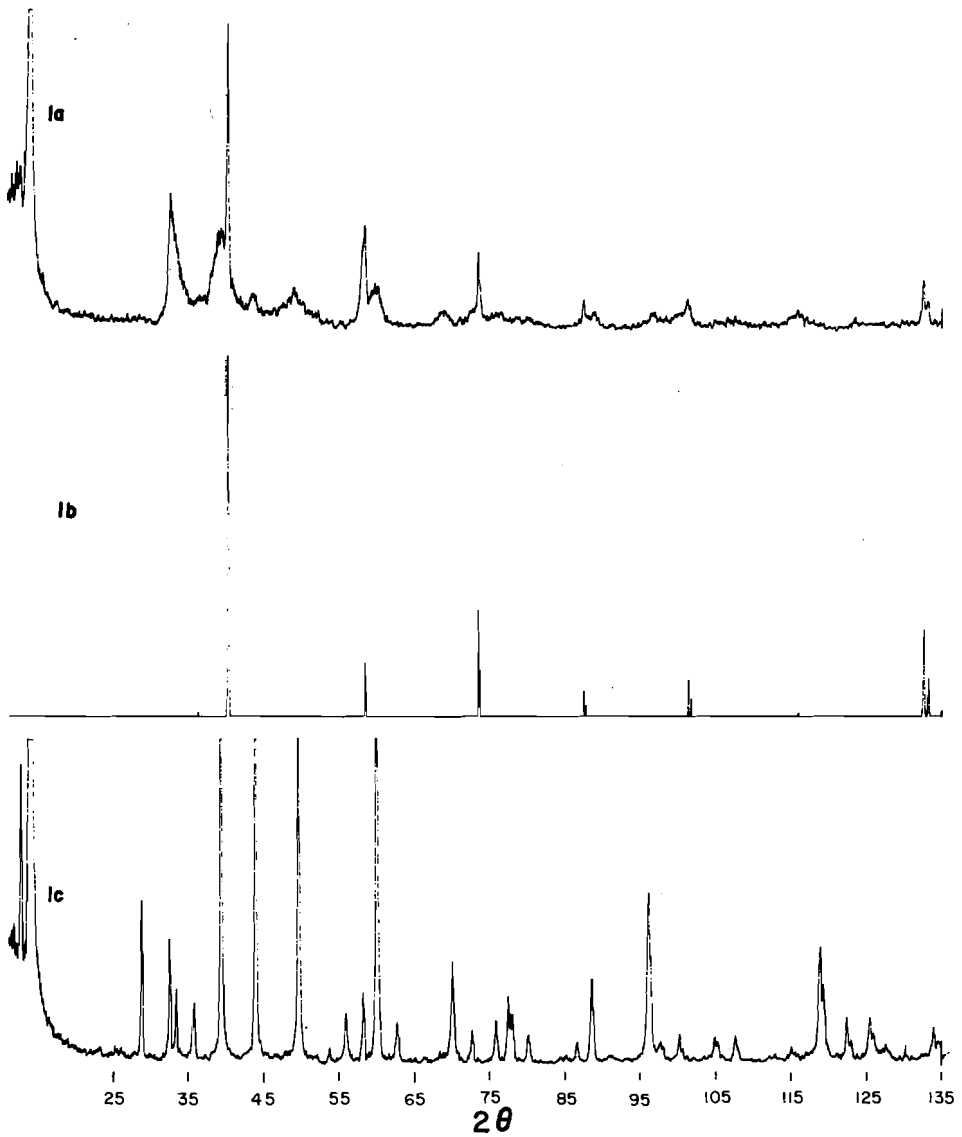

FIG. 1. X-Ray diffractograms of (*a*) catalyst prepared by the reduction of MoS_3 in hydrogen at 800 °C for 11 h, (*b*) Mo powder of better than 99.99% purity, (*c*) hexagonal MoS_2 (Anachemia).

areas (before reaction) with initial activities, because inevitably the first contact with the reaction stream leads to rapid sulfiding of what are presumed to be catalytically active S-vacancies. Nevertheless, by choosing an arbitrary 'initial' time of 10 min on stream one can see that percent conversion at this point parallels the decrease in surface area at 450 and 600 °C as expressed by the initial reaction rate. Thus the dominant feature in this temperature range would appear to be a decrease in area due to crystallization and sintering without significantly changing the number of catalytic sites per unit area. The initial reaction rate at 800 °C, however, is larger by a factor of 2 whereas surface area has decreased by 1/3 from the lowest value reached at 600 °C. This is consistent with 'overreduction' having created more vacancies, which have not yet been resulfided. Note, for instance, that initial S-content at 800 °C decreases with time of reduction at essentially constant surface area.

In earlier work (1) it had been demonstrated

TABLE 1. Surface area, catalytic activity, and sulfur contents of MoS_2 catalysts after various reductive pretreatments

Reduction conditions		Reaction time (h)	Surface area ($m^2\ g^{-1}$)		Conversion (%)		Reaction rate (mol $m^{-2}\ s^{-1}$)		Sulfur content[5] (wt.%)	
Temperature (°C)	Time (h)		Initial[1]	Final[2]	Initial[3]	Final[2]	Initial[4]	Final[2]	Initial[1]	Final[2]
450	1.0	24	55.8	33.9	78.0	31.5	7.7	5.3	—	—
450	20.0	24	32.5	26.3	53.4	20.5	8.1	5.1	36.4	38.8
600	0.5	10	36.6	25.3	60.6	28.0	7.1	4.7	—	—
600	10.0	24	30.7	20.0	59.4	22.7	8.2	4.8	35.7	38.2
800	0.5	10	19.9	16.5	57.0	17.9	14.1	4.4	36.5	38.5
800	11.0	24	18.6	13.8	55.1	15.9	13.9	4.9	35.3	37.2
800	20.0	24	19.1	13.6	57.2	17.0	13.7	5.5	33.4	35.2

[1]Before reaction.
[2]After reaction at 400 °C at atmospheric pressure (see Experimental section).
[3]After 10 min of reaction.
[4]Calculated from 'initial' conversion after 10 min, and initial surface area.
[5]Stoichiometric value for MoS_2: 40.1%S.

that the steady-state activity of a number of stabilized MoS_2 surfaces was surprisingly insensitive to their method of preparation. The same conclusion can be reached from the present final reaction rate data, even for the still relatively unstable catalyst reduced at 450 °C. In all cases the reaction rate decreased from its initial value; this is generally observed during the sulfiding stage of catalyst preparation. The detailed mechanism of this decrease is a combination of further crystallization (especially at 450 °C), electronic lattice modifications (5), and surface re-organization, the latter including strong sorption of inhibiting species such as polymeric carbon compounds (coking) and inactive sulfur species (5). Surface area losses during the reaction are least pronounced in the case of the 800 °C-samples, whereas their reaction rates experience the largest decrease. That this is not entirely due to resulfiding is reflected in the fact that with increasing time of reduction it becomes more difficult to replace the sulfur originally lost. This is probably due to the blocking of S-vacancies by inhibiting surface species, such as were suggested above.

We thank Mr. Gary Harris for technical assistance, and Professor George Chao of the Carleton University Geology Department for the use of his X-ray diffractometer. We are grateful to the National Research Council of Canada for financial support.

1. S. KOLBOE and C. H. AMBERG. Can. J. Chem. **44**, 2623 (1966).
2. P. RATNASAMY and A. J. LÉONARD. J. Catal. **26**, 352 (1972).
3. J. C. WILDERVANCK and F. JELLINEK. Z. Anorg. Allg. Chem. **328**, 309 (1964).
4. M. S. SILVERMAN. Inorg. Chem. **6**, 1063 (1967).
5. A. AOSHIMA and H. WISE. J. Catal. **34**, 145 (1974).
6. J. R. STUBBLES and F. D. RICHARDSON. Trans. Faraday Soc. **56**, 1460 (1960).

Can. J. Chem. Downloaded from www.nrcresearchpress.com by 210.87.254.42 on 09/05/12
For personal use only.

Pulse Radiolysis of Alkali Metal Solutions in Methylamine[1]

JOHN WALLACE FLETCHER, WILLIAM ARTHUR SEDDON, JOHN JOSEPH JEVCAK, AND FRED CHARLES SOPCHYSHYN

Physical Chemistry Branch, Atomic Energy of Canada Limited, Chalk River Nuclear Laboratories, Chalk River, Ontario K0J 1J0

Received May 5, 1975

JOHN WALLACE FLETCHER, WILLIAM ARTHUR SEDDON, JOHN JOSEPH JEVCAK, and FRED CHARLES SOPCHYSHYN. Can. J. Chem. **53**, 3571 (1975).

Pulse radiolysis studies of solutions of alkali metal methylamides (CH_3NHM) in methylamine indicate the formation of solvated electrons, e_s^-, ion-pairs (M^+, e_s^-), and alkali metal anions M^-. This paper compares the spectra, extinction coefficients, and yields of e_s^-, Li, Na, K, and Cs species, with those observed previously in other solvents. The overall reaction kinetics are complex and, in CH_3NHNa/NaI solutions, suggest the formation of a higher aggregate or triple ion species (Na_2^{2+}, e_s^-). A reaction mechanism, quantitatively consistent with experiment, is presented and discussed in detail for solutions containing Na^+.

JOHN WALLACE FLETCHER, WILLIAM ARTHUR SEDDON, JOHN JOSEPH JEVCAK et FRED CHARLES SOPCHYSHYN. Can. J. Chem. **53**, 3571 (1975).

Des études de radiolyse pulsée de solutions de méthylamidures de métaux alcalins dans la methylamine indiquent qu'il y a formation d'électrons solvatés, e_s^-, de paires d'ions (M^+, e_s^-) et d'anions de métaux alcalins, M^- Cette publication compare les spectres, les coefficients d'extinction et les rendements en espèces e_s^-, Li, Na, K et Cs avec ceux obtenus antérieurement dans d'autres solvants. La cinétique globale de la réaction est complexe et, pour des solutions dans CH_3NHNa/NaI, elle suggère qu'il y a formation d'un aggrégat supérieur ou d'espèces ioniques triples (Na_2^{2+}, e_s^-). On présente un mécanisme réactionnel en accord quantitatif avec l'expérience et on le discute en détail pour des solutions contenant du Na^+.

[Traduit par le journal]

Introduction

Extensive investigations (refs. 1–3 and references therein) on the optical, magnetic, and conductance properties of alkali metal solutions in liquid amines have shown that solvated electrons, e_s^-, ion-pairs (M^+, e_s^-), and alkali metal anions, M^-, coexist in equilibrium according to the reactions

$$[1] \qquad e_s^- + M^+ \underset{k_{-1}}{\overset{k_1}{\rightleftharpoons}} (M^+, e_s^-) \text{ or } M$$

$$[2] \qquad M + e_s^- \underset{k_{-2}}{\overset{k_2}{\rightleftharpoons}} M^-$$

Such solutions are intensely colored and stable but can be catalytically decomposed to give the corresponding alkali metal alkylamides as represented by the overall reaction

$$[3] \qquad RCH_2NH_2 + M \rightarrow RCH_2NHM + \tfrac{1}{2}H_2$$

A pulse radiolysis study of alkali metal ethylamides in ethylamine (4) showed three distinct optical bands attributed to e_s^-, (M^+, e_s^-), and M^-. Furthermore it was demonstrated that the rate and equilibrium constants for the formation of the species (M^+, e_s^-) and M^- were markedly dependent on the nature of the alkali metal amide.

This paper describes the spectra and more detailed kinetics for the corresponding species generated by pulse radiolysis of alkali metal methylamides in methylamine.

Experimental

Details of our pulse radiolysis facilities have been described elsewhere (5). Methylamine was obtained from Matheson Co. Ltd. The earlier paper on ethylamine (4) should be consulted for purification procedures and additional experimental details. Appropriate quantities of sodium iodide (Fisher Chemicals) were 'purified' by standing in dilute metal–methylamine solutions followed by solvent distillation.

Results

Spectra

Figure 1 shows the absorption spectrum observed at room temperature immediately after a 0.5 μs pulse in pure methylamine and in dilute

[1]AECL No. 5268.

Can. J. Chem. Downloaded from www.nrcresearchpress.com by 210.87.254.5 on 09/05/12
For personal use only.

Can. J. Chem. Downloaded from www.nrcresearchpress.com by 210.87.254.5 on 09/05/12
For personal use only.

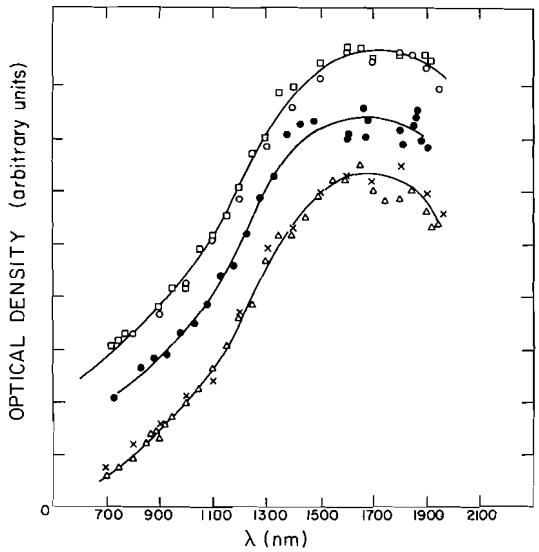

FIG. 1. Transient absorption spectra observed immediately after the pulse in pure methylamine and $\leq 10^{-5}$ *M* alkali metal methylamide solutions in methylamine; ●, pure CH_3NH_2; ○, Li; □, Na; △, K; ×, Cs. The curves are normalized to a common peak height of 6.9 divisions but arbitrarily displaced for clarity.

solutions ($\leq 10^{-5}$ *M*) containing Li, Na, K, or Cs methylamide. In all cases the absorption maximum occurs at ~1700 nm. In pure methylamine the absorption decays completely on a μs time scale whereas in methylamide solutions an additional growth in absorption is observed after the pulse.

Figure 2 shows the spectra observed 400 μs after the pulse for $\geq 10^{-3}$ *M* solutions of Li, Na, K, and Cs methylamide. Apart from the post pulse increase in intensity the infrared peak at ~1700 nm remains independent of the alkali metal for Li, Na, and K, and shows no distinct shift from that observed immediately after the pulse (Fig. 1). A blue shift to 1500 nm is observed with Cs. With the exception of Na solutions (see below) the infrared absorption is quite stable showing no decay over a period of ≤1 ms.

In K solutions the long time scale spectrum also exhibits a slight shoulder at ~900 nm. By repetitively flashing the analyzing light, after the electron pulse, it could be shown that the peak at ~1700 nm decayed with a $t_{1/2}$ ~ 60 s producing at the same time a relative increase in the peak at 900 nm.

In the Na solutions the infrared absorption band decays on a μs time scale forming a long-lived species with an absorption maximum at 690 nm.

Effect of Added "Crown Ether"

Earlier studies (2, 3) have shown that the addition of a cyclic polyether such as dicyclohexyl-18-crown-6 ("crown ether") complexes alkali metal cations and enhances their solubility in a variety of amines and ethers. Figure 3 shows the optical spectra and transient signals observed from solutions containing ~10^{-3} *M* potassium methylamide and ~10^{-3} *M* crown ether.

At low doses, $\leq 6 \times 10^{18}$ eV/l per pulse, the transient absorption shows no sign of a growth or decay over a period of ≥40 μs. At higher doses the absorption consists of an initial rapid decay followed by a long-lived residual component. Both the initial and long-lived species have identical spectra with an absorption maximum at ≥1800 nm.

Dose Dependence and Kinetics

The transient absorptions show a marked dose dependence in both the yield and in the decay kinetics. Plots of optical density as a function of dose per pulse are presented in Fig. 4 for Na methylamide solutions. In any given solution

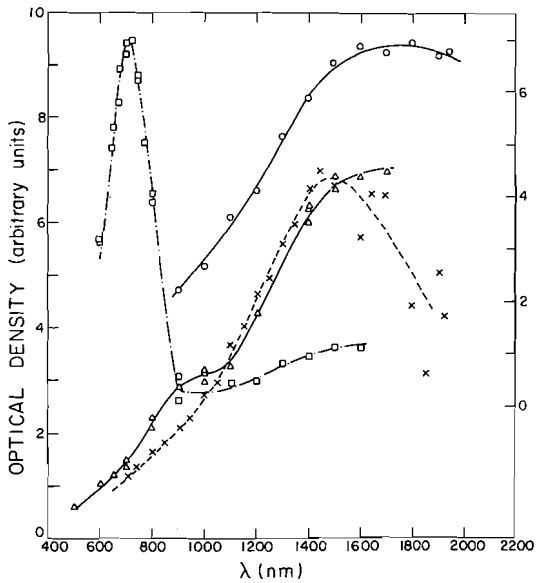

FIG. 2. Absorption spectra observed 400 μs after the pulse in $\geq 10^{-3}$ *M* alkali metal methylamide solutions in methylamine; ○, Li; □, Na; △, K; ×, Cs. The curves are normalized to a peak height of 6.9 units but with ○ and □ displaced 2.5 units for clarity (right hand scale).

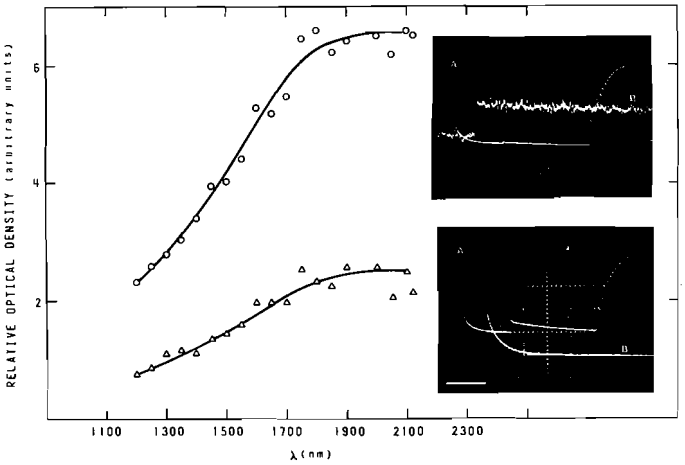

FIG. 3. Transient absorption spectrum observed in solutions containing $\sim 10^{-3}$ *M* CH_3NHK, and $\sim 10^{-3}$ *M* crown ether, ○, immediately after the pulse; △, 35 μs after the pulse. Upper curve *B*, dose 6.1×10^{18} eV/l; 1% absorption/division, 5 μs/division. Lower curve *B*, dose 1.52×10^{20} eV/l, 10% absorption/division, 5 μs/division. Wavelength 1650 nm and cell length 1.0 cm in both cases. Trace *A* shows the profile of the analyzing light at lower gain and a sweep speed of 500 μs/division.

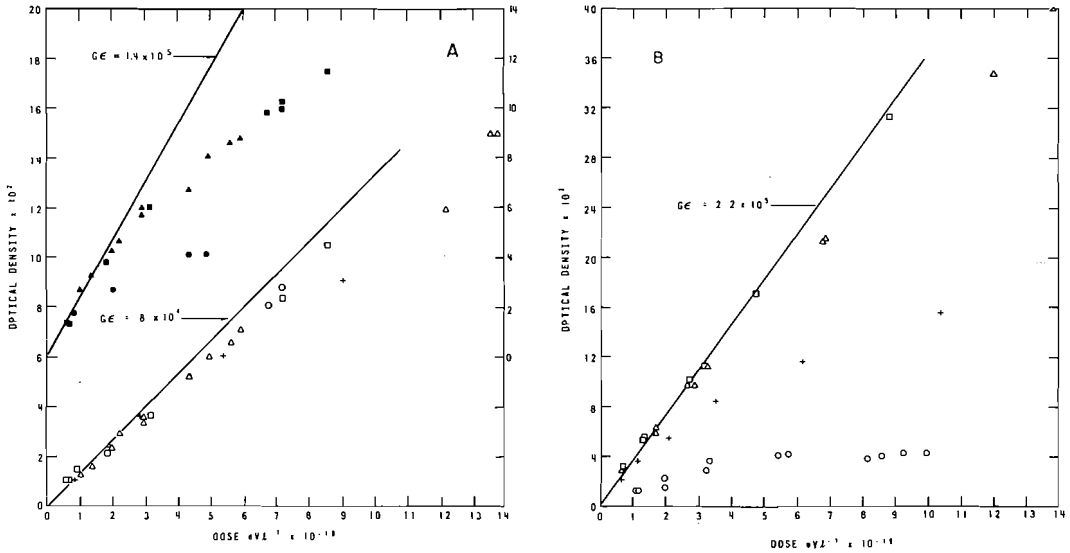

FIG. 4. (*A*) Effect of increasing dose per pulse on the transient absorptions observed at 1485 nm in sodium methylamide solutions: immediately after the pulse; +, 2×10^{-4} *M* (plus 10^{-3} *M* NaI); △, 1.1×10^{-3} *M*, □, 1.3×10^{-2} *M*: maximum absorption; ●, 1.0×10^{-4} *M* (100 μs); ▲, 1.1×10^{-3} *M* (50 μs); ■, 1.3×10^{-2} *M* (15 μs). Values in parentheses refer to the time required after the pulse to reach the maximum. (*B*) Effect of increasing dose per pulse on the absorption due to Na^- as observed at 700 nm ~ 400 μs after the pulse; +, 2×10^{-4} *M* (plus 10^{-3} *M* NaI); ○, 1.0×10^{-4} *M*; △, 1.1×10^{-3} *M*; □, 1.3×10^{-2} *M*. Cell length in both *A* and *B*, 1.0 cm.

the departure from linearity decreases with increasing methylamide concentration but increases again with the addition of NaI.

Similar plots were obtained for the other metals in the series. At corresponding concentrations Li solutions exhibit the most, and Cs solutions the least, dose effect of the series.

In the Na solutions the infrared absorption decays by a second order process with the concomitant formation of the 690 nm band. The latter is stable for times ≥ 10 s.

Potassium solutions appear to behave similarly but the rate is much too slow to deduce the kinetic order by our existing technique.

Can. J. Chem. Downloaded from www.nrcresearchpress.com by 210.87.254.5 on 09/05/12
For personal use only.

Can. J. Chem. Downloaded from www.nrcresearchpress.com by 210.87.254.5 on 09/05/12
For personal use only.

Discussion

Spectral Assignments

The spectra obtained in methylamine are similar to those observed in ethylamine and the reader is referred to the earlier paper (4) for background information and a general introduction. In pure methylamine, dilute methylamide solutions ($\leq 10^{-5}$ *M*), and solutions containing "crown ether", the spectrum observed immediately after the pulse (Figs. 1 and 3) is attributed to e_s^-. As a consequence of solvent absorption the maximum is difficult to resolve and therefore the observed peak may not be real. However, as in ethylamine, the maximum does occur at $\geq$1700–1800 nm.

On longer time scales the infrared band (Fig. 2) is more intense but very similar to the initial absorption. Its rate of formation is first order in methylamide concentration and dependent on the nature of the cation. In common with other recent work (4, 6, 7) we propose that this enhanced absorption is due to the formation of an ion-pair (M^+, e_s^-) or monomer species of stoichiometry M.

The lack of a significant change in the spectral shape of the infrared band with ion-pair formation is comparable to the situation observed in ethylenediamine (8, 9) and liquid ammonia (3, 10, 11). In ethylamine the ion-pair band for Na, K, and Cs is distinctly shifted but only about 400 nm below that of e_s^- (4).

In addition to the ion-pair peak at ~1700 nm it is evident that underlying absorptions are also present. This is most clear for sodium solutions where the predominant long-lived absorption occurs at 690 nm and is undoubtedly due to the species Na^- (1, 3, 12, 13).

In the case of potassium solutions the shoulder at 900 nm can likewise be assigned to K^- (1, 3, 12, 13). The relative predominance and stability of the infrared band is consistent with absorption spectra observed in potassium methylamine solutions (14) and contrasts sharply with ethylamine solutions (4, 14). For cesium solutions the slight blue shift to ~1500 nm may be due to the presence of some unresolved Cs^- which has a maximum at 1100 nm (2, 3, 12). Alternatively, since in methylamine only Cs and Rb show hyperfine splitting (15) the optical shift may be associated with the higher electron density for the Cs ion-pair (or monomer) as compared to the Li, Na, or K ion-pairs.[2]

[2]We acknowledge one of the referees for pointing out this possibility.

It is worth noting that the above results contrast sharply with ion-pair spectra observed in ethers (6, 7) where marked differences occur in the ion-pair and e_s^- absorption bands. For example, λ_{max} for e_s^- in tetrahydrofuran (THF) is given as 2120 nm (16, 17) whereas the corresponding maxima for (Na^+, e_s^-), (K^+, e_s^-), and (Cs^+, e_s^-) occur at 890, 1125, and 1400 nm, respectively (6, 7).

Formation of (M^+, e_s^-)

Studies of dilute solutions of Li, Na, K, and Cs methylamides ($\leq 6 \times 10^{-3}$ *M*) monitored at 1485 nm indicate that the rate of formation of (M^+, e_s^-) is first order and consistent with [1]. However very little information exists on the dissociation constants of alkali metal methylamides in methylamine. Data obtained for the potassium salt at -62.2 and -90 °C give values of 4×10^{-7} and 3×10^{-7} *M*, respectively, between 10^{-3} and 10^{-2} *M* (18). It is likely therefore that the methylamides are largely associated in methylamine at room temperature. Consequently, we have made no attempt to differentiate between [1] and those conceivably involving the undissociated salt CH_3NHM.

$$[4] \quad CH_3NHM + e_s^- \rightleftharpoons CH_3NH^- + (M^+, e_s^-)$$

The kinetic analysis suffers the same complications as noted previously (4). Quoted values for the rate constant k_1 in Table 1 are based on the total concentration of methylamide in solution and are not corrected for any back reaction.

As a general observation such rate constants are an order of magnitude slower than for the corresponding reactions in ethylamine (see Table 1). This may simply be due to the different degrees of dissociation of the various alkyl amides in the respective solvents. In either case the values are low in comparison with the diffusion controlled rates in THF, where for example, $k(e_s^- + Na^+) = 7.8 \times 10^{11}\ M^{-1}\ s^{-1}$ (6, 7). Until dissociation constants are established in the amines these details cannot be resolved.

Formation of M^-

The most notable feature of the results is that, with the exception of sodium solutions, the lifetime of the ion-pair is considerably longer than was observed in ethylamine (4). Consequently information relating to the formation of M^- can be obtained only for sodium solutions since in all other cases the reaction is too slow to be followed by our present technique. The kinetics were monitored either by observing the

TABLE 1. Rate constants for the formation of (M^+, e_s^-) in methylamine

Alkali metal	Methylamide concentration (M)	k_1 (M^{-1} s^{-1}) In methylamine	k_1 (M^{-1} s^{-1}) In ethylamine*
Li	$\sim 1 \times 10^{-3}$	5×10^6	4×10^6 ($\sim 1 \times 10^{-3}$)
Na	1×10^{-4}	2.1×10^8	1.2×10^9 (2.5×10^{-4})
	1×10^{-3}	7×10^7	
K	6×10^{-3}	1.2×10^7	1.6×10^8 (4.5×10^{-4})
Cs	7×10^{-5}	1×10^9	2×10^{10} ($\sim 3.5 \times 10^{-6}$)

*Values in parentheses give the appropriate ethylamide concentrations (M) obtained from ref. 4.

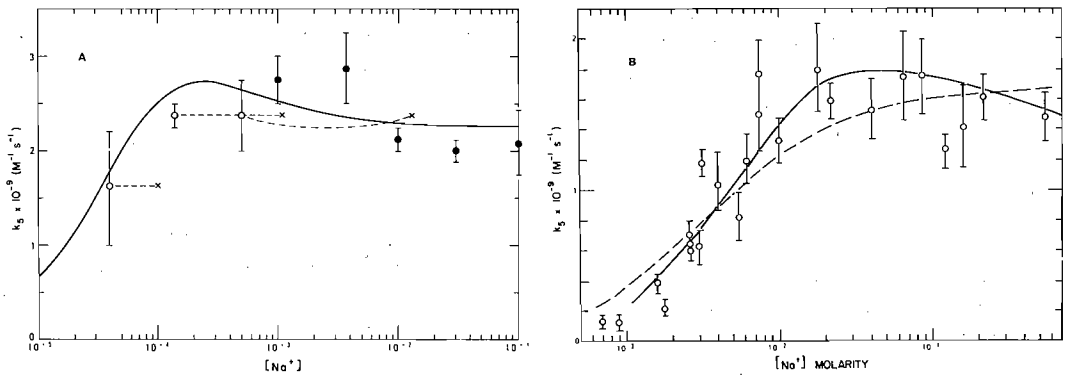

FIG. 5. Pseudo second order rate constants for the formation of Na^- in methylamine and ethylenediamine. (*A*) Methylamine; ○, Na^+ added as CH_3NHNa taking $K_{diss} = 2 \times 10^{-5} M$; ×, assumes CH_3NHNa is fully dissociated, dotted lines show relative displacement; ●, Na^+ added as $\sim 5 \times 10^{-4} M$ CH_3NHNa + NaI, assumes NaI fully dissociated. The solid line represents the calculated 'best fit' as described in the text. (*B*) Ethylenediamine (Na^+ added as NaBr plus sodium, potassium, or cesium ethylenediamide) see ref. 9 for specific details. The dotted line was calculated (9) on the basis of [7] and [8] and the solid line according to our mechanism (see text).

build up of Na^- at 690 nm or via the concomitant decay of (Na^+, e_s^-) at 1485 nm. As in the case of ethylamine (4) and ethylenediamine (9) the kinetics are pseudo second order and consistent with the overall stoichiometry represented by [5],

$$[5] \qquad e_s^- + e_s^- \overset{M^+}{\rightleftharpoons} M^-$$

Again it is important to note that the precise determination of the pseudo second order rate constant, represented by k_5, is difficult. Large errors in the kinetic analysis arise from the uncertainties in determining the optical densities corresponding to the complete formation of either (Na^+, e_s^-) or Na^-. Since the equilibria lie predominantly to the right the best values are deduced by monitoring the build up of absorption of Na^- at 690 nm. Assuming $\varepsilon_{M^-} = 1 \times 10^5 M^{-1}\,cm^{-1}$ (4) values increase, as a function of Na^+ concentration, from $4k_5 = 6.4 \times 10^9$ to 11.6×10^9 M^{-1} s^{-1} (Fig. 5*A*).

In ethylenediamine Dye *et al.* (9) considered a reaction scheme previously proposed from e.s.r. studies in dimethoxyethane (13)

$$[1] \qquad e_s^- + Na^+ \rightleftharpoons (Na^+, e_s^-)$$

$$[2] \qquad (Na^+, e_s^-) + e_s^- \rightarrow Na^-$$

with the modification that [2] be written as equivalent to [6]

$$[6] \qquad (Na^+, e_s^-) + (Na^+, e_s^-) \rightarrow Na^- + Na^+$$

Reactions 1 and 2 are, by themselves, inadequate to explain the results since the equilibrium for [1] lies to the right and, at high Na^+ concentrations, would result in a marked decrease in the rate of formation of Na^-.

This mechanism was then ruled out since the rate of Na^- formation was independent of other cations (K^+ or Cs^+) present in excess. Consequently they concluded that the formation of a species containing two electrons occurred prior to the formation of Na^-

$$[7] \qquad e_s^- + e_s^- \rightleftharpoons e_2^{2-}$$

$$[8] \qquad e_2^{2-} + Na^+ \rightarrow Na^-$$

Can. J. Chem. Downloaded from www.nrcresearchpress.com by 210.87.254.5 on 09/05/12
For personal use only.

Can. J. Chem. Downloaded from www.nrcresearchpress.com by 210.87.254.5 on 09/05/12
For personal use only.

It was also noted that [9] and [10] were considered equivalent to [7] and [8]

[9] $(M^+, e_s^-) + (M^+, e_s^-) \rightleftharpoons (M^+, e_s^-)_2$

[10] $(M^+, e_s^-)_2 + Na^+ \rightarrow Na^- + 2M^+$

However, from studies on mixed sodium–potassium solutions in ethylamine (19) we have deduced that the formation of Na^- can occur via [11]

[11] $$K^- \xrightarrow{Na^+} Na^- + K^+$$

at an overall rate not significantly different from pure sodium solutions. Furthermore, in sodium aluminum hydride solutions in tetrahydrofuran (7), [1], [2], and [6] are essential to explain the formation of Na^-. The analogous potassium reaction 6 is apparently much slower with K^- formation occurring via the corresponding reaction 2.

We therefore conclude that [1], [2], and [6] are also applicable to the amine–amide systems. It was pointed out that for this to be valid in ethylenediamine (9), the equilibrium constant for the formation of a species of stoichiometry Na must be much greater than the corresponding reaction to form Cs or K, and furthermore the spectrum of Na must be nearly the same as e_s^-. The latter is now thought to be the case whereas the former is still unknown. A comparison of the observed pseudo second order rate constants for methylamine (this work) with ethylenediamine (9) is given in Fig. 5. In the case of ethylenediamine the Na^+ concentration refers to the total concentration of added sodium (metal plus salt). In methylamine we have assumed that NaI is fully dissociated. A value of 2×10^{-5} M was chosen for the dissociation constant of CH_3NHNa since this gave the 'best fit' as judged by the initial slope in Fig. 5*A*. This compares well with that for $NaNH_2$ in liquid NH_3 (2.24×10^{-5} M at -33.5 °C (20)) but is greater than that for CH_3NHK in methylamine (4×10^{-7} M at -62.2 °C (18)).

The solid curves in Fig. 5 represent the calculated 'best fit' to the data where k_5 is given by

[12] $$k_{obs(Na^-)/4} \equiv k_5 = (k_2K' + k_6)/(1 + K')^2$$

and

$$K' = k_{-1}/k_1[Na^+]$$

Values for k_1 and k_{-1} for methylamine were estimated from the observed rate of formation of (Na^+, e_s^-) as a function of Na^+ concentration.

$$k_{obs(Na^+, e_s^-)} = k_{-1} + k_1[Na^+]$$

At high concentrations ($\geq 10^{-3}$ M) k_{-1} becomes unimportant and

$$k_{obs(Na^+, e_s^-)} \sim k_1[Na^+]$$

On this basis $k_1 = 1 \times 10^8$ M^{-1} s^{-1} and $k_{-1} = 8 \times 10^3$ s^{-1}. The equilibrium constant $K_{-1} = 1.2 \times 10^{-4}$ M as determined from the relative (Na^+, e_s^-) yield as a function of $[Na^+]$. This leads to a slightly higher, but comparable value for $k_{-1} = 1.2 \times 10^4$ s^{-1}.

At low concentrations ($\leq 10^{-4}$ M) k_6 becomes negligible and

$$k_{obs(Na^-)} \sim k_2K'/(1 + K')^2$$

Therefore k_6 was estimated via [12] from the decrease in $k_{obs(Na^-)}$ with increasing Na^+ concentration.

A similar iterative procedure was adopted for ethylenediamine using the original data from ref. 9. The appropriate constants deduced for both systems are summarized in Table 2. It can be seen that this mechanism composed of [1], [2], and [6] fits the ethylenediamine results equally as well as the mechanism (dotted line) composed of [7] and [8] (9).

These calculations also indicate that K_{-1} for methylamine is about two orders of magnitude less than that for ethylenediamine. Values for K_{-1} have been determined by conductance measurements for Li, K, Cs, and Rb in ethylenediamine (8), and Cs in methylamine (21), and are typically about 1×10^{-4} M. The conductance behavior of Na solutions differ markedly from the other alkali metals and therefore the corresponding values are not available for comparison.

Using the computer program WR 20 (7, 22, 23) we therefore sought to check the validity of this reaction sequence by comparing with experiment the calculated formation and decay of (Na^+, e_s^-) and Na^- (in methylamine) as a function of $[Na^+]$ and dose per pulse. Initial calculations demonstrated that the mechanism fails to predict observed effects of Na^+ concentration. While changes in rate constants could produce agreement in dilute solutions, such revised values would be inconsistent at higher concentrations, and vice versa.

Firstly, in dilute methylamide solutions ($\leq 10^{-4}$ M Na^+), the calculations did not predict

TABLE 2. Reactions and rate constants used to calculate the 'best fit' solid lines shown in Fig. 5

Reaction	Rate constant: Methylamine	Rate constant: Ethylenediamine
[1] $e_s^- + Na^+ \rightarrow (Na^+, e_s^-)$	$1 \times 10^8\ M^{-1}\ s^{-1}$	$3.3 \times 10^7\ M^{-1}\ s^{-1}$
[−1] $(Na^+, e_s^-) \rightarrow e_s^- + Na^+$	$1.2 \times 10^4\ s^{-1}$	$5 \times 10^5\ s^{-1}$
[2] $(Na^+, e_s^-) + e_s^- \rightarrow Na^-$	$6.7 \times 10^9\ M^{-1}\ s^{-1}$	$5 \times 10^9\ M^{-1}\ s^{-1}$
[6] $(Na^+, e_s^-) + (Na^+, e_s^-) \rightarrow Na^- + Na^+$	$2.0 \times 10^9\ M^{-1}\ s^{-1}$	$1.5 \times 10^9\ M^{-1}\ s^{-1}$

a sufficient build up of (Na^+, e_s^-). The appropriate increase in absorption could only be approximated by reducing k_{-1} effectively to zero, implying that (Na^+, e_s^-) is not dissociated. This in turn requires Na^- to be formed entirely by [6], the rate of which would then be independent of $[Na^+]$ and hence inconsistent with experiment.

Secondly, the equilibrium constant $K_{-6} = [Na^+, e_s^-]^2/[Na^-][Na^+]$ and, as a first approximation, $K_{-6}[Na^+] \propto \text{o.d.}^2_{1485}/\text{o.d.}_{690}$ (4), where o.d._{1485} and o.d._{690} are the optical densities observed ~400 μs after the pulse at 1485 nm and 690 nm, respectively. Experimentally it is found that this ratio decreases from 22×10^{-3} to 1.2×10^{-3} with increasing $[Na^+]$ from 1×10^{-4} to $1 \times 10^{-1}\ M$, respectively. With $k_{-1} = 0$, one would expect an increase in the ratio $\text{o.d.}^2_{1485}/\text{o.d.}_{690}$ with increasing $[Na^+]$. Alternatively, if Na^- dissociates exclusively via [−2], then the ratio would be independent of $[Na^-]$. Again, therefore, $k_{-1} \neq 0$.

Finally, at high $[Na^+]$ (sodium methylamide solutions containing $\geq 10^{-3}\ M$ NaI), the calculations predict an initial absorption due to (Na^+, e_s^-) about double that observed experimentally, but at the same time correctly predict the rate of formation and final yield of Na^-. In other words the observed lower initial absorption is not reflected by a stoichiometric reduction in the final product Na^-.

These discrepancies in detail can be resolved if we postulate at the higher concentrations a second order dependence on Na^+ involving the formation of a triple ion (24–26), such as (Na_2^{2+}, e_s^-). This can perhaps be regarded as analogous to the triple ions suggested in polymerization processes (27, 28) or in the reduction of semiquinones (29–32).

[13] $(Na^+, e_s^-) + Na^+ \rightleftharpoons (Na_2^{2+}, e_s^-)$

This additional species must also absorb in the infrared with an extinction coefficient about one-half that of (Na^+, e_s^-) at 1485 nm and be formed with $k_{13} \sim 5 \times 10^7\ M^{-1}\ s^{-1}$ and $K_{-13} \sim 2 \times 10^{-2}\ M$. Likewise it must also react at a rate and manner similar to (Na^+, e_s^-), reactions 14–16, to produce Na^-.

[14] $(Na_2^{2+}, e_s^-) + e_s^- \rightarrow Na^- + Na^+$

[15] $(Na_2^{2+}, e_s^-) + (Na^+, e_s^-) \rightarrow Na^- + 2Na^+$

[16] $(Na_2^{2+}, e_s^-) + (Na_2^{2+}, e_s^-) \rightarrow Na^- + 3Na^+$

Additional refinements are necessary, however, since at low methylamide concentrations and/or high doses per pulse an initial rapid decay is observed in the transient absorptions. As noted previously (4), and established in THF (7), we attribute this behavior to reaction with radiolytically produced radicals. For example, [17] to [19] in competition with [20].

[17] $e_s^- + R \rightarrow \text{product}$

[18] $(Na^+, e_s^-) + R \rightarrow \text{product}$

[19] $Na^- + R \rightarrow \text{product}$

[20] $R + R \rightarrow \text{product}$

For a given dose per pulse the effect decreases with increasing concentrations of methylamide suggesting, in a manner analogous to ethanol (33, 34), that the solvent base converts the radicals into a less reactive basic form, *e.g.*

[21] $\dot{C}H_2NH_2 + CH_3NH^- \rightarrow CH_2{=}NH^- + CH_3NH_2$

Estimates for k_{17} and k_{19} of ~6 and $1 \times 10^{10}\ M^{-1}\ s^{-1}$, respectively, were obtained from the initial rapid second order decays observed at high doses at 1485 and 720 nm, respectively.

At high [NaI] the situation is further complicated by ionic strength and common ion effects. The latter restricts the dissociation of CH_3NHNa and hence the significance of [21]. The observation of increased dose effects in solutions containing NaI is explicable on this basis.

Finally, the reactions by which $G_{e_s^-}$ increases from 2.2 in the pure solvent to 4.8 in basic

Can. J. Chem. Downloaded from www.nrcresearchpress.com by 210.87.254.5 on 09/05/12
For personal use only.

TABLE 3. Experimentally determined values of $G\varepsilon$ in various methylamide solutions

	Methylamide concentration ($\times 10^4$ M)	λ (nm)	$G\varepsilon$ ($\times 10^{-5}$)†		
			e_s^-	M	M^-
Li	10	1900	0.8	1.2	
Na	1 → 130	1485	0.8	1.4 1.6*	
	11 → 1000	700			2.2 2.4*
K	2	1600	0.7		
K (+'Crown')		1600	0.7		
Cs	0.7	1800	0.8	1.77 2.1*	
	20	1700	0.6	1.4	

*Extrapolated by curve fitting.
†Extinction coefficients can be estimated by taking $G_{e_s^-} = 2.2$, $G_M = 4.8$, and $G_{M^-} = 2.4$.

solution are not clear (35). The build up of the ion-pair absorption may be associated with such processes since the alternative of an extinction coefficient for (Na^+, e_s^-) about twice that for e_s^- would, since the spectra are the same, be inconsistent with oscillator strengths of ~1 for each species (6, 9). However, since the final yields of Na^- are only compatible with $G_{e_s^-} = 4.8$ it is necessary to adopt this value in the computer calculations[3] and simulate the build up by using an extinction coefficient for $e_s^- \sim (Na^+, e_s^-)/2$ to be consistent with measured $G\varepsilon$ values (Table 3).

In summary more information is needed on solute and ion-pair dissociation constants and the effect of base before further detail is justified. However, we believe that an additional intermediate such as (Na_2^{2+}, e_s^-) best explains all the data and that radical reactions with e_s^- and metal–electron species are an additional complication in the radiolytic system.

Kinetics in the Presence of "Crown Ether"

The results obtained in this study are very similar to those obtained in ethylamine (4). This earlier paper should be consulted for a general discussion. Again there is no evidence for the formation of either (M^+, e_s^-) or M^-. The solvated electron or e_s^-–crown complex thus becomes the predominant reactive species and at low doses is stable for ≥50 μs.

Yields and Extinction Coefficients

Figure 4 shows examples of the formation of the various sodium species as a function of dose per pulse. Because of the dose dependence the initial yields, and hence the corresponding $G\varepsilon$ values, are estimated from the linear portion of such curves. Values for Li, Na, K, and Cs solutions are summarized in Table 3 and, again, these are very similar to those observed in ethylamine (4). However, in the case of e_s^- the $G\varepsilon$ values of 8×10^4 are about four times greater than in ethylamine. This difference is not understood but may imply that the true absorption maximum for e_s^- in methylamine is closer toward the visible than is the case for ethylamine.

The points on the dose curves are taken directly from the original photographs. If the buildups in absorption are curve fitted to infinite time then slightly higher values are obtained (Table 3). Such fitting takes into account the decay of (Na^+, e_s^-) and Na^- concurrent with their formation and hence requires a larger value of $G\varepsilon(Na^+, e_s^-)$ and $G\varepsilon(Na^-)$ to give the best fit with experiment.

To calculate the extinction coefficients we have taken the value $G_{e_s^-} = 2.2$ and 4.8 in neutral and basic solution, respectively (35). On this basis we estimate $\varepsilon_{e_s^-} = 3.6 \times 10^4$, $\varepsilon_{(M^+, e_s^-)} = 3.0 \times 10^4$, and $\varepsilon_{Na^-} = 9.2 \times 10^4\ M^{-1}\ cm^{-1}$. These values are comparable with values of $\varepsilon_{e_s^-} = 2 \times 10^4$ in ethylenediamine (9, 36), $\varepsilon_{(M^+, e_s^-)} = 2.4$–$2.9 \times$

[3]Additional details showing comparisons with oscilloscope traces over a range of dose and $[Na^+]$ are available, at a nominal charge, from the Depository of Unpublished data, CISTI, National Research Council of Canada, Ottawa, Canada K1A 0S2.

Can. J. Chem. Downloaded from www.nrcresearchpress.com by 210.87.254.5 on 09/05/12
For personal use only.

10^4 in THF (6, 7), and $\varepsilon_{Na^-} = 8.2–12.0 \times 10^4$ (4, 36).

Conclusions

As in the case of ethylamine the results of this study are consistent with the formation of three distinct species e_s^-, (M^+, e_s^-), and M^-. However, in sodium solutions the more detailed kinetic analysis indicates the formation of an additional metal–electron species suggested to be (Na_2^{2+}, e_s^-). In general the overall rates of reactions are much slower in methylamine and, with the exception of Na^-, the equilibria appear to lie more in favor of (M^+, e_s^-) than M^-.

1. I. Hurley, T. R. Tuttle, Jr., and S. Golden. Metal ammonia solutions. I.U.P.A.C., Colloque Weyl II, Butterworth & Co., London. 1970. p. 449.
2. M. T. Lok, F. J. Tehan, and J. L. Dye. J. Phys. Chem. **76**, 2975 (1972).
3. J. L. Dye. Electrons in fluids. Colloque Weyl III, Springer-Verlag, West Berlin. 1973. p. 77.
4. J. W. Fletcher, W. A. Seddon, and F. C. Sopchyshyn. Can. J. Chem. **51**, 2975 (1973).
5. W. A. Seddon, C. Willis, M. J. Young, and E. B. Selkirk. Atomic Energy of Canada Limited, report no. AECL-3853.
6. B. Bockrath and L. M. Dorfman. J. Phys. Chem. **77**, 1002 (1973).
7. G. A. Salmon, W. A. Seddon, and J. W. Fletcher. Can. J. Chem. **52**, 3259 (1974).
8. R. R. Dewald and J. L. Dye. J. Phys. Chem. **68**, 128 (1964).
9. J. L. Dye, M. G. DeBacker, J. A. Eyre, and L. M. Dorfman. J. Phys. Chem. **76**, 839 (1972).
10. J. L. Dye. Metal ammonia solutions. I.U.P.A.C., Colloque Weyl II, Butterworth & Co., London. 1970. p. 1.
11. W. A. Seddon, J. W. Fletcher, J. Jevcak, and F. C. Sopchyshyn. Can. J. Chem. **51**, 3653 (1973).
12. S. Matalon, S. Golden, and M. Ottolenghi. J. Phys. Chem. **73**, 3098 (1969).
13. S. H. Glarum and J. H. Marshall. J. Chem. Phys. **52**, 5555 (1970).
14. K. Bar-Eli and G. Gabor. J. Phys. Chem. **77**, 323 (1973).
15. K. D. Vos and J. L. Dye. J. Chem. Phys. **38**, 2033 (1963).
16. L. M. Dorfman, F. Y. Jou, and R. Wageman. Ber. Bunsenges. Phys. Chem. **75**, 681 (1971).
17. F. Y. Jou and L. M. Dorfman. J. Chem. Phys. **58**, 4715 (1973).
18. E. Rochard and J. Ravoire. J. Chim. Phys. **68**, 1183 (1971).
19. W. A. Seddon, J. W. Fletcher, and F. C. Sopchyshyn. To be published.
20. R. Delmas, P. Courvoisier, and J. Ravoire. Adv. Chem. Ser. **89**, 25 (1969); R. Delmas. Report CEA-R-3377, CEN Saclay.
21. R. R. Dewald and K. W. Browall. J. Phys. Chem. **74**, 129 (1970).
22. K. H. Schmidt. Argonne National Laboratory report, ANL-7693.
23. W. A. Seddon, J. W. Fletcher, and F. C. Sopchyshyn. Can. J. Chem. **51**, 1123 (1973).
24. R. M. Fuoss and C. A. Kraus. J. Am. Chem. Soc. **55**, 21, 476, 1019, 2387 (1933).
25. N. L. Cox, and C. A. Kraus, and R. M. Fuoss. Trans. Faraday Soc. **31**, 749 (1935).
26. C. A. Kraus. J. Phys. Chem. **58**, 673 (1954).
27. D. N. Bhattacharyya, J. Smid, and M. Szwarc. J. Am. Chem. Soc. **86**, 5024 (1964).
28. D. N. Bhattacharyya, C. L. Lee, J. Smid, and M. Szwarc. J. Phys. Chem. **69**, 612 (1965).
29. J. V. Acrivos. J. Chem. Phys. **47**, 5389 (1967).
30. T. E. Gough and P. R. Hindle. Can. J. Chem. **47**, 1698 (1969).
31. T. E. Gough and P. R. Hindle. Can. J. Chem. **47**, 3393 (1969).
32. R. F. Adams, T. L. Staples, and M. Szwarc. **5**, 474 (1970).
33. J. W. Fletcher, P. J. Richards, and W. A. Seddon. Can. J. Chem. **48**, 3765 (1970).
34. D. W. Johnson and G. A. Salmon. J. Chem. Soc. Faraday Trans. **1**, **71**, 583 (1975).
35. W. A. Seddon, J. W. Fletcher, F. C. Sopchyshyn, and J. Jevcak. Can. J. Chem. **52**, 3629 (1974).
36. M. G. DeBacker and J. L. Dye. J. Phys. Chem. **75**, 3092 (1971).

Can. J. Chem. Downloaded from www.nrcresearchpress.com by 210.87.254.5 on 09/05/12
For personal use only.

The Thermal Decomposition of Methane. I. Kinetics of the Primary Decomposition to $C_2H_6 + H_2$; Rate Constant for the Homogeneous Unimolecular Dissociation of Methane and its Pressure Dependence[1,2]

C.-J. CHEN AND M. H. BACK

Chemistry Department, University of Ottawa, Ottawa, Canada K1N 6N5

AND

R. A. BACK

Chemistry Division, National Research Council of Canada, Ottawa, Canada K1A 0R9

Received July 11, 1975

C.-J. CHEN, M. H. BACK, and R. A. BACK. Can. J. Chem. **53**, 3580 (1975).

The pyrolysis of methane has been studied in a static system at temperatures of 995, 1038, 1068, and 1103 K and pressures from 25 to 700 Torr. It was concluded that the initial stages of the reaction can be described by a simple homogeneous, nonchain radical mechanism:

[1] $CH_4 \rightarrow CH_3 + H$

[2] $H + CH_4 \rightarrow CH_3 + H_2$

[3] $2CH_3 \rightarrow C_2H_6$

[4] $CH_3 + C_2H_6 \rightarrow CH_4 + C_2H_5$

[5] $C_2H_5 \rightarrow C_2H_4 + H$

Initial rates of reaction were measured, based on analysis of hydrogen, ethane, and ethylene, and k_1 was found to be pressure dependent and homogeneous. Quantitative agreement was obtained with values of k_1 calculated by R.R.K.M. theory. Values of $A^\infty = 2.8 \times 10^{16}$ s^{-1} and $E^\infty = 107.6$ kcal/mol were obtained, the latter appreciably greater than the value of $E_0 = 103$ kcal/mol used in the calculations. Comparison of previous shock-tube and flow-system data at temperatures up to 2200 K showed good agreement with values of k_1 obtained by extrapolation of the present R.R.K.M. calculations. It was concluded that in all previous studies, the initial dissociation was in its pressure-dependent region. Estimates were also made of the rate constant for the reverse of [1] and showed fair agreement with recent experimental measurements.

C.-J. CHEN, M. H. BACK et R. A. BACK. Can. J. Chem. **53**, 3580 (1975).

On a étudié la pyrolyse du méthane dans un système statique à des températures de 995, 1038, 1068 et 1103 K et à des pressions allant de 25 à 770 Torr. On en conclut que les étapes initiales de la réaction peuvent être décrites par un mécanisme simple, homogène et n'impliquant pas de chaîne radicalaire:

[1] $CH_4 \rightarrow CH_3 + H$

[2] $H + CH_4 \rightarrow CH_3 + H_2$

[3] $2CH_3 \rightarrow C_2H_6$

[4] $CH_3 + C_2H_6 \rightarrow CH_4 + C_2H_5$

[5] $C_2H_5 \rightarrow C_2H_4 + H$

On a mesuré les vitesses initiales en se basant sur l'analyse de l'hydrogène, de l'éthane et de l'éthylène et on a trouvé que k_1 dépend de la pression et est homogène. On a obtenu une corrélation quantitative avec les valeurs de k_1 calculées d'après la théorie R.R.K.M. On a obtenu des valeurs de $A^\infty = 2.8 \times 10^{16}$ s^{-1} et $E^\infty = 107.6$ kcal/mol; cette dernière est supérieure à la valeur de $E_0 = 103$ kcal/mol utilisée dans les calculs. Un bon accord existe entre des données obtenues antérieurement à des températures allant jusqu'à 2200 K, et les valeurs k_1 obtenues par extrapolation des calculs R.R.K.M. actuels. On en conclut que dans toutes les études antérieures, la dissociation initiale se faisait dans une région dépendante de la température. On a aussi fait des évaluations de la vitesse de la réaction inverse à [1] et on a montré qu'il y a un bon accord avec des mesures expérimentales récentes.

[Traduit par le journal]

[1]NRCC No. 14880.

[2]This paper is dedicated to Professor C. A. Winkler of McGill University on the occasion of his sixty-fifth birthday by two of his former students (M.H.B. and R.A.B.).

Can. J. Chem. Downloaded from www.nrcresearchpress.com by 210.87.254.6 on 09/05/12
For personal use only.

Can. J. Chem. Downloaded from www.nrcresearchpress.com by 210.87.254.6 on 09/05/12
For personal use only.

Introduction

Although the pyrolysis of methane has been studied many times before, important details of the reaction mechanism have remained obscure (1–5). It is well established that the initial products are C_2H_6 and H_2, and in some shock-tube experiments the pyrolysis has been effectively limited to this stage and initial rates measured. Even in these systems, however, the reaction mechanism is uncertain; it has not been shown clearly whether methane dissociates initially into $CH_3 + H$ or $CH_2 + H_2$, and the pressure dependence of the primary dissociation has not been established. In static and flow systems at lower temperatures the mechanism is even less well understood, because rapid secondary reactions set in at extremely low conversions, yielding successively ethylene, acetylene, and finally carbon. Induction periods and autocatalysis have been observed; activation energies generally lie between 75 and 90 kcal/mol, and because these are well below the bond dissociation energy of methane, radical chain reactions have been suggested; these have never been proven. Neither the primary dissociation process nor the secondary reactions leading to the formation of C_2 hydrocarbons and carbon has been established.

The present work was undertaken to resolve some of these uncertainties, particularly those of the low-temperature pyrolysis, by a careful study of the static pyrolysis in its very early stages. The present paper is concerned chiefly with the primary dissociation process and its pressure dependence, while subsequent papers deal with the secondary reactions.

Experimental

Apparatus

A conventional glass vacuum apparatus was used with Hoke metal valves in the portions having contact with methane and the reaction products. The apparatus could be evacuated to about 10^{-6} Torr measured with a McLeod gauge. The reaction vessel was a quartz cylinder of 478 cc, 20.4 cm long, and 6.0 cm o.d. Capillary tubing connected the vessel to a quartz spiral pressure gauge and through valves to the vacuum line. The reaction vessel was enclosed in a quartz tube of 7.0 cm o.d. and nitrogen gas was continuously passed through this annular space at a pressure of about 20 Torr above atmospheric and a flow rate of 3 cc per min. This eliminated the possibility of diffusion of oxygen through the wall of the reaction vessel at high temperatures. Some experiments were done with air replacing nitrogen in the jacket around the reaction vessel; this had no effect on the reaction rates. It appears therefore that diffusion of oxygen through the vessel wall is not a factor in the methane pyrolysis. Its greater effect in the thermal H_2–D_2 exchange reaction, where it doubled the rate at about 1000 K (6), must be due to the long chain character of the reaction. A quartz tube, 6 mm i.d., sealed through the center of the vessel, served as a thermocouple well and was also flushed with nitrogen. Before installation the vessel was treated with hot concentrated nitric acid and washed with distilled water. A vessel of the same dimensions packed with quartz tubes, which increased the S/V ratio by a factor of 10, was used to test for heterogeneous processes.

An Autoclave High Temperature cylindrical furnace with matching control unit gave a maximum variation in temperature of 1.5 deg. The heating element was tapped to allow adjustment of the temperature gradient along the reaction vessel which was less than 0.3 deg within 8 cm of the center and less than 1 °C in the last 2 cm. The thermocouple was calibrated at the melting point of sodium chloride.

Materials

Research grade methane was obtained from Matheson, Canada Ltd; the impurities were 6 p.p.m. oxygen, 20 p.p.m. ethane, and 100 p.p.m. nitrogen. Oxygen was removed by passing the methane through a column containing 3 kg of Ridox reagent (Fisher Scientific), activated with hydrogen at 230 °C. The ethane was removed by a 3 m column of activated charcoal maintained at −78 °C which was activated by heating under vacuum at 300 °C for 24 h. The purified methane contained less than 1 p.p.m. oxygen and 0.1 p.p.m. ethane, the limits detectable by the analytical system. Methane-d_4 was obtained from Merck, Sharp and Dohme, Canada Ltd., and oxygen was removed with Ridox reagent. Mass spectrometric analysis showed a D-atom purity of 99%. Research grade ethane, ethylene, and acetylene from Matheson, Canada Ltd., were used for calibrations.

Analysis

The products hydrogen, ethane, ethylene, acetylene, and the oxygen impurity were analyzed by gas chromatography. A separation of hydrogen, oxygen, argon, nitrogen, and methane was achieved with a 3 m × 6 mm column of molecular sieve 5A at room temperature, activated by heating at 370 °C for 12 h. Hydrogen was converted to water in a copper oxide furnace before entering the thermal conductivity detector. Larger amounts of hydrogen from longer experiments were collected through a solid nitrogen trap in series with a silica gel column at −196 °C, passed through a palladium thimble, and measured in a gas burette. A partial separation of the large quantities of methane from the small amounts of higher molecular weight products was achieved with a 30 cm × 3 mm silica gel column held at −78 °C. After most of the methane was removed the column was warmed to room temperature and the effluent injected into a second silica gel column composed of 30 cm × 3 mm plus 120 cm × 9 mm maintained at room temperature. H_2, HD, and D_2 were analyzed on a 2 m column of alumina treated with $MnCl_3$ and operated at the temperature of liquid nitrogen (7). Deuterated methanes were analyzed by mass spectrometer.

Experimental Procedure

Methane was admitted to the reaction vessel from a calibrated volume. The pressure and temperature were recorded during the experiment. At the end of the re-

Can. J. Chem. Downloaded from www.nrcresearchpress.com by 210.87.254.6 on 09/05/12
For personal use only.

action methane and products were condensed in solid nitrogen traps and analyzed as described. Prolonged pyrolysis (several hours) led to the deposition of carbon on the surface, which enhanced the rate of decomposition. This effect was negligible in the much shorter reaction times used in the kinetic studies. Nevertheless, to avoid accumulation of carbon from repeated experiments, air was admitted to the vessel after each experiment to burn off any carbon deposit. To ensure that no traces of oxygen remained after this procedure a small amount of methane was pyrolyzed for a few seconds before the experiment, then pumped away.

Results and Discussion

Initial Rate of Formation of Products

The products hydrogen, ethane, ethylene, propylene, and acetylene were analyzed as a function of time at the temperatures 995, 1038, 1068, and 1103 K over the pressure range 25–740 Torr. Typical yield–time plots are shown in Figs. 1 and 2. The results show clearly that in the initial stage of the reaction hydrogen and ethane are the only products. No pressure change was observed at this stage of the reaction and the rate of formation of ethane in the packed vessel was identical to that measured in the unpacked vessel. It may be concluded that the initial rate of formation of ethane is a measure of the initial homogeneous rate of decomposition of methane.

As the concentration of ethane builds up in the system, but while the conversion is still less

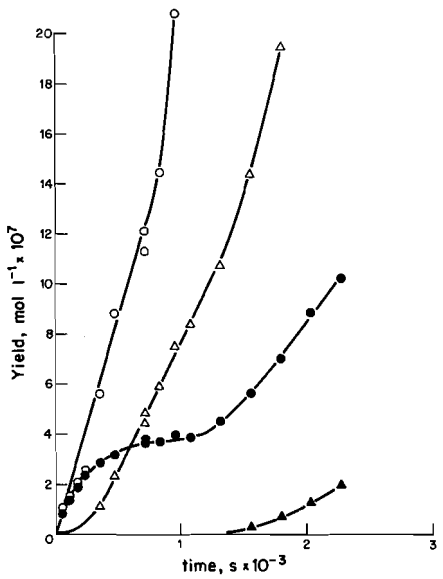

FIG. 1. Yield of the principal products as a function of time. ○, H_2; ●, C_2H_6; △, C_2H_4; ▲, C_2H_2; T = 1038 K.

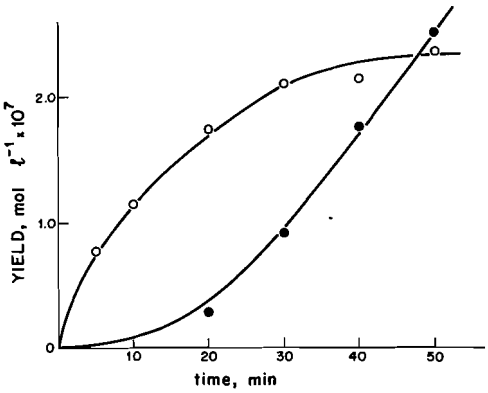

FIG. 2. Yield of ethane and ethylene in the initial stages of the reaction. ○, C_2H_6; ●, C_2H_4; T = 995 K.

than 0.01%, ethane begins to be consumed in secondary reactions and its concentration gradually approaches a steady value. Ethylene is clearly a secondary product and propylene and acetylene are tertiary, appearing only after the concentration of ethylene has surpassed that of ethane. As the reaction proceeds still further a marked increase in the rate of formation of ethane and the other products was observed. Mechanisms for this autocatalysis, which may involve, at least partially, the formation of carbon, will be discussed in a subsequent paper. In the present study, where any carbon deposit was burned off before each experiment, we have been able to measure the rates of product formation in the initial stages of the reaction well before the autocatalysis became significant. In almost all previous studies in static and flow systems rates were measured at conversions where the autocatalysis was important. This is particularly true of kinetic studies based on pressure measurements, since measurable pressure increase occurs only in the region of secondary acceleration.

The Mechanism of the Decomposition

The Initiation Step

Two initial dissociation reactions have been suggested in methane,

[1*a*] $$CH_4 \rightarrow CH_3 + H$$

and

[1*b*] $$CH_4 \rightarrow CH_2 + H_2$$

The endothermicity of [1*a*] has long been established as about 102–104 kcal/mol (3, 5, 8). The endothermicity of [1*b*] has been much more un-

TABLE 1. Comparison of measured rate constant and calculated value of k_{1b}[a]

	ΔH_f^0 (298) (kcal mol^{-1})	S^0 (cal deg^{-1} mol^{-1})	C_p (298–1000) (cal deg^{-1} mol^{-1})
CH_4	−17.9	44.5	12.87
CH_3	34.0	46.1	11.7
CH_2	93	43.3	9.3
H_2	0	31.2	7.05
H	52.1	27.4	5.0

	log A (l mol^{-1} s^{-1} or s^{-1})	E (kcal/mol)	log k (1000 K) (s^{-1})
Reaction −1b	9.62		
Reaction 1b	14.8	113.3	−10.03
Measured rate	16.4	106.7	−6.9

[a]All values are taken from ref. 14 except $\Delta H_f(CH_2)$ which is from ref. 12.

certain; at one time it was thought to be substantially (10 to 20 kcal) less than that of [1a], and in a number of studies of the methane pyrolysis where the activation energy was less than 103 kcal, it was concluded that [1b] must be predominant (1, 9, 10); conversely in other experiments, mostly in shock tubes, where the activation energy was about 103 kcal it was concluded that only [1a] was important (11). Subsequently it became evident that the endothermicity of [1b] was probably equal to or greater than that of [1a], so that all the earlier conclusions about the initial dissociation process based on activation energy had to be discounted (5). There now appears to be convincing evidence (12) for a value of $\Delta H_f^0(CH_2)$ of about 93 kcal/mol, which makes [1b] endothermic by about 109 kcal. The rate constant for reaction of CH_2 with H_2, the reverse of [1b], has been measured recently (13) and it thus becomes possible to calculate the rate constant for [1b]. Thermochemical data used in these and later calculations are given in Table 1 together with the rate constant for [1b] at 1000 K and the rate constant for the initial dissociation measured in the present study. It should be noted that both these values refer to the limiting high-pressure region. In the measurement by Braun *et al.* (13), singlet CH_2 was consumed in the reaction with hydrogen irrespective of whether the resulting CH_4* was stabilized, since the latter should have decomposed preferentially to $CH_3 + H$ rather than reforming $CH_2 + H_2$.

It is clear from Table 1 that [1b] should be of negligible importance in the pyrolysis of methane. This conclusion is further strengthened by the fact that in several respects the calculations in Table 1 probably overestimate the magnitude of k_{1b}, so that the values obtained should be regarded as upper limits. In particular, the rate constant measured by Braun *et al.* (13) for the reverse reaction was for CH_2 in its excited singlet state; the corresponding reaction of the ground-state triplet is undoubtedly much slower. On the other hand, the heat of formation of 93 kcal/mol is presumably for ground-state CH_2 and there appear to be convincing arguments (15) that the singlet state lies from 6 to 10 kcal higher in energy than the triplet ground state. It is not clear whether singlet or triplet CH_2 would be produced in [1b]; production of the former conserves spin, but if the energy barrier is much higher than for triplet formation, the latter may occur but with a reduced frequency factor associated with the spin violation. By using ΔH_f for the triplet in our calculation, and the reverse rate constant for the singlet, our estimate of k_{1b} is clearly an upper limit, and the true value may be much lower. It may also be noted that if there is an appreciable activation energy for the reaction of CH_2 with H_2 or if the CH_2 radicals in the experiments by Braun *et al.* were vibrationally excited, k_{1b} would be further overestimated in our calculation.

Experimentally it is not easy to distinguish between [1a] and [1b]. It will be seen later that the secondary reactions observed in the system point strongly to the presence of CH_3 radicals, but these could be generated from the reaction of CH_2 with CH_4 even if [1a] did not occur. Analysis of the isotopic composition of hydrogen produced in the initial stage of the pyrolysis of a

Can. J. Chem. Downloaded from www.nrcresearchpress.com by 210.87.254.6 on 09/05/12
For personal use only.

TABLE 2. The isotopic composition of the product hydrogen from pyrolysis of 1:1 mixture of CH_4 and CD_4; total pressure, 443 Torr

$T = 1068$ K			$T = 1103$ K		
t (min)	$\frac{[C_2H_6]}{[C_2H_4]}$	$\frac{[HD]^2}{[H_2][D_2]}$	t (min)	$\frac{[C_2H_6]}{[C_2H_4]}$	$\frac{[HD]^2}{[H_2][D_2]}$
0.50	23.2	5.02	0.26	14.7	5.24
1.01	20.3	5.36	0.40	6.4	5.13
2.00	3.00	3.84	0.51	4.3	4.48
3.51	1.25	4.51	0.77	1.95	3.63
5.01	0.81	4.95	1.01	1.36	4.59
	Average	4.7 ± 0.5	1.51	0.84	4.15
				Average	4.5 ± 0.5

mixture of CH_4 and CD_4 should reveal the occurrence of [1*b*]. This has been done recently in the shock pyrolysis at 1560 K (16), in which it was found that the ratio $[HD]^2/[H_2][D_2]$ was close to the value expected for hydrogen formation by atomic reactions only. Similar experiments have been performed in the present study, with similar results, shown in Table 2. The ratio $[C_2H_6]/[C_2H_4]$ corresponds to the ratio of primary to secondary hydrogen, so that at the shortest times greater than 90% of the hydrogen should have come from the primary reactions. It can be shown by comparison with the CH_3–CD_3 radical exchange[3] that molecular hydrogen should not have been appreciably exchanged after its formation. The data in Table 2 are scattered because the amounts of hydrogen, and particularly deuterium, analyzed were necessarily small, but within this scatter there is no significant deviation from a value of about four expected for hydrogen formed by an atomic mechanism. Reaction 1*b* should of course yield a $[HD]^2/[H_2][D_2]$ ratio of zero. From these experiments and from the calculations in Table 1, it can be concluded that [1*a*] is the only initial dissociation of importance. It will be seen later that all our experimental observations are quantitatively in accord with this conclusion.

Secondary Reactions

The initial stages of the reaction before propylene and acetylene are formed may be explained by a very simple mechanism

[1] $$CH_4 \rightarrow CH_3 + H$$

[2] $$H + CH_4 \rightarrow H_2 + CH_3$$

[3] $$2CH_3 \rightarrow C_2H_6$$

[4] $$CH_3 + C_2H_6 \rightarrow CH_4 + C_2H_5$$

[5] $$C_2H_5 \rightarrow C_2H_4 + H$$

In the earliest stages where only [1], [2], and [3] are important the yield of hydrogen was equal to the yield of ethane and no pressure increase was observed. As [4] and [5] became important ethane was converted to ethylene and hydrogen. During this period the quantities $[C_2H_4] + [C_2H_6]$ and $([H_2] + [C_2H_6])/2$ were both linear functions of time, showing that these were the only products at this stage of the reaction. The yield of ethane as it approaches its steady-state value can in fact be quantitatively accounted for by [4] and [5].[3] These and other subsequent secondary reactions will not be discussed further in the present paper which is concerned chiefly with the rate of [1].

Measurement of k_1

From the proposed mechanism it follows that

[6] $$k_1[CH_4] = R^0_{C_2H_6} = R^0_{H_2}$$

where R^0 signifies an initial rate of formation. Values of R^0 for ethane and hydrogen can be obtained directly from yield–time plots, but because [4] and [5] set in at very low conversion, accurate initial rates could not always be measured. $R^0_{C_2H_6}$ may also be equated to $R_{(C_2H_6+C_2H_4)}$ or to $\frac{1}{2}R_{(H_2+C_2H_6)}$, which corrects for loss of ethane in [4], and k_1 can be obtained from linear plots of these functions. While these various measurements of initial rates were in substantial agreement, the most accurate and consistent measurements of $R^0_{C_2H_6}$ and hence of k_1 were obtained from the yield–time plot of ethane alone by fitting the experimental points to a theoretical curve based on the proposed simple mechanism for loss of ethane, using a computer to obtain

[3]C.-J. Chen, M. H. Back, and R. A. Back, to be published.

Can. J. Chem. Downloaded from www.nrcresearchpress.com by 210.87.254.6 on 09/05/12
For personal use only.

Can. J. Chem. Downloaded from www.nrcresearchpress.com by 210.87.254.6 on 09/05/12
For personal use only.

TABLE 3. Measured values of k_1 and calculated values for k_1^∞, k_1^0, E^∞, and $A^{\infty a}$

T (K)	P (Torr)	k_1 (s^{-1})
995	741	2.82×10^{-8}
	640	2.95×10^{-8}
	540	2.34×10^{-8}
	440	2.40×10^{-8}
	333	1.32×10^{-8}
	230	1.58×10^{-8}
	162	1.07×10^{-8}
	108	1.07×10^{-8}
	51	0.74×10^{-8}
	$k_1^\infty = 6.66 \times 10^{-8}\ s^{-1}$	
	$k_1^0 = 1.23 \times 10^{-5}\ l\ mol^{-1}\ s^{-1}$	
1038	741	2.57×10^{-7}
	642	2.29×10^{-7}
	542	1.95×10^{-7}
	441	1.86×10^{-7}
	338	1.38×10^{-7}
	236	1.26×10^{-7}
	188	1.12×10^{-7}
	109	0.81×10^{-7}
	96	0.74×10^{-7}
	66	0.71×10^{-7}
	43	0.51×10^{-7}
	32	0.39×10^{-7}
	$k_1^\infty = 6.50 \times 10^{-7}\ s^{-1}$	
	$k_1^0 = 1.12 \times 10^{-4}\ l\ mol^{-1}\ s^{-1}$	
1068	742	8.71×10^{-7}
	440	7.08×10^{-7}
	233	4.90×10^{-7}
	154	3.72×10^{-7}
	104	3.58×10^{-7}
	75.5	2.34×10^{-7}
	48.6	1.70×10^{-7}
	25.2	0.98×10^{-7}
	$k_1^\infty = 2.74 \times 10^{-6}\ s^{-1}$	
	$k_1^0 = 4.53 \times 10^{-4}\ l\ mol^{-1}\ s^{-1}$	
1103	743	3.86×10^{-6}
	602	4.06×10^{-6}
	440	3.02×10^{-6}
	233	2.06×10^{-6}
	121	1.27×10^{-6}
	49	0.69×10^{-6}
	$k_1^\infty = 1.37 \times 10^{-5}\ s^{-1}$	
	$k_1^0 = 2.14 \times 10^{-3}\ l\ mol^{-1}\ s^{-1}$	
	$E^\infty = 107.6$ kcal mol^{-1}	
	$A^\infty = 2.8 \times 10^{16}\ s^{-1}$.	

the best fit, and this was the method finally employed. Values of the rate constant, k_1, obtained in this way over a range of temperature and pressure are given in Table 3. Error limits based on the values obtained by the various methods are indicated in Fig. 3 by vertical bars.

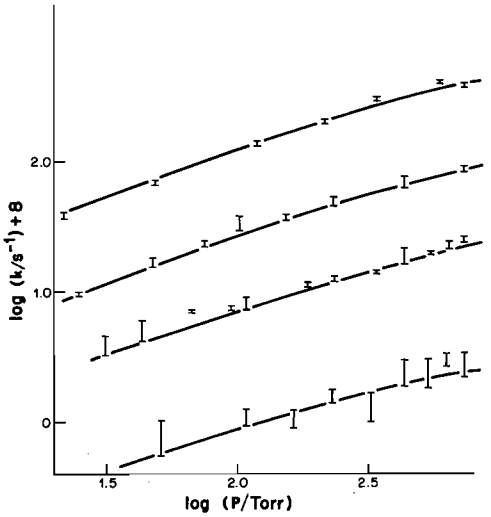

FIG. 3. The variation of k_1 with pressure. The experimental results are shown as vertical bars, indicating the error limits, while the solid lines are the calculated values. The temperatures are: 995, 1038, 1068, and 1103 K.

The Pressure Dependence of k_1

log k_1 is shown in Fig. 3 as a function of log (methane pressure). It is clear that k_1 depends markedly on the pressure of methane under the conditions of the present experiments. The obvious and simplest explanation of this behavior is that [1] is a unimolecular reaction in its pressure-dependent region. Such a pressure dependence is indeed expected for a molecule as small as methane (3), although it has not been clearly demonstrated before at these temperatures. Alternatively, it might be suggested that the dependence of k_1 on methane pressure could arise from a complex radical-chain mechanism. The only possible propagation step in pure methane appears to be

[7] $$CH_3 + CH_4 \rightarrow C_2H_6 + H$$

This has frequently been suggested in the past (1), and together with [2] constitutes a chain yielding C_2H_6 and H_2. There are several arguments against such a chain in the methane pyrolysis. First, [7], an inversion reaction at a simple saturated carbon atom, is without precedent in gas-phase radical reactions and would have a high activation energy (14). The chain mechanism in fact would require E_7 to be about 50 kcal to give the overall observed activation energy, and therefore [7] although unlikely, probably cannot be ruled out *a priori*. Second, if

Can. J. Chem. Downloaded from www.nrcresearchpress.com by 210.87.254.6 on 09/05/12
For personal use only.

[7] occurred, the rate of reaction would be given by the expression

$$[8]\quad R^0_{C_2H_6} = R^0_{H_2} = k_1[CH_4] + k_7[CH_4](k_1[CH_4]/k_3)^{1/2}$$

with the right hand side consisting of two terms, the first for the nonchain process, the second for the chain reaction. Recognizing that both k_1 and k_3 may be pressure dependent, it can be seen that their dependence on methane pressure will cancel at low pressure and disappear at high pressure, leaving a simple overall dependence of the chain process on $[CH_4]^{3/2}$ in the high and low pressure limits. At intermediate pressures when both k_1 and k_3 are pressure dependent, the order will rise above $\frac{3}{2}$ because k_4 would reach its high-pressure limit well before k_1. The result on a log–log plot of k_1 against CH_4 pressure would be two parallel lines at high and low pressure with slope $\frac{1}{2}$, displaced laterally and joined by a sigmoid curve at intermediate pressure. This prediction may be compared with Fig. 3, in which the slope in fact decreases monotonically from about 0.6 at the lowest pressure to 0.4 at the highest. Finally, and most convincingly, it will be seen that the measured values of k_1 over the whole range of pressure and temperature are quantitatively in accord with theoretical calculations for the simple unimolecular dissociation of methane in its pressure-dependent region. Thus while the occurrence of [7] cannot be ruled out completely, the present evidence weighs heavily against it, and it seems most unlikely that it is of any importance in the methane pyrolysis.

Theoretical Calculations of k_1 and its Pressure Dependence

Calculations of k_1 were based on the R.R.K.M. theory, well described by Robinson and Holbrook (17). The general expression for the unimolecular rate constant is

$$[9]\quad k_{uni} = \frac{L^{\ddagger}Q_1^{+}}{hQ_1Q_2}\exp(-E_0/RT) \times \int_0^{\infty} \frac{\sum_{E^+_{v=0}}^{E^+} P(E_v^{+})\exp(-E^{+}/RT)\,dE^{+}}{1 + k_a(E^* + \langle\Delta E_J\rangle)/k_2[M]}$$

where

$$[10]\quad k_a(E^* + \langle\Delta E_J\rangle) = \frac{L^{\ddagger}\sum_{E^+_{v=0}}^{E^+} P(E_v^{+})}{hFN^*(E^*)}$$

The sum of states, $\sum P(E_v^{+})$, was evaluated by the direct count method. The density of states, $N^*(E^*)$, was calculated using the approximation described by Tardy *et al.* (18). The centrifugal correction factor, F, was given by Marcus (19) and by Waage and Rabinovitch (20) as follows

$$[11]\quad N^*(E^* + \langle\Delta E_j\rangle) = FN^*(E^*)$$

where

$$[12]\quad F = \frac{\left[E^* + aE_z - \left(\frac{I^+}{I} - 1\right)RT\right]^{s-1}}{(E^* + aE_z)^{s-1}}$$

A constant energy increment of 0.5 kcal/mol was used in the computations. The symbols follow the nomenclature used by Robinson and Holbrook: $\sum P$ = sum of states of the transition state for energy = E^+; $N^*(E^*)$ = density of states of molecules of energy E^*; Q_1^{+} = partition function of inactive modes of activated complex; Q_1, Q_2 = partition functions of rotation and vibrational modes of the molecule; E^+ = total nonfixed energy in the active degrees of freedom of the activated complex; E_0 = critical energy; E^* = nonfixed energy in the energized molecule; E_z = total zero-point energy; $L^{\ddagger}$ = reaction path degeneracy. Values for k_1^{∞} were not obtained in the present study but are not necessary for the calculation since the bond dissociation energy, E_0, for methane is well established. A value of E_0 of 103 kcal/mol gave agreement with the magnitude of the measured value of k_1 while the dependence on pressure was matched by adjustment of the bending frequencies and of the moment of inertia of the activated complex. The methyl radical was assumed to be planar in the complex. All rotations were taken as adiabatic and centrifugal corrections were applied to the two external rotations. The complex is similar to the Model 4 described by Placzek *et al.* (21). The values used in the calculations are shown in Table 4. The vibrational frequencies of the molecule and of the methyl radical were taken from JANAF (22).

The results of the calculations are shown in Fig. 3 as the solid lines. The calculated values for k_1 are seen to represent both the pressure dependence and the absolute value for k_1 found experimentally. This provides strong confirmation of the interpretation of the present results in terms of the simple mechanism described by [1]–[5].

Values of k_1^{∞} obtained from [9] are listed in Table 3 together with the corresponding values

TABLE 4. Values used in calculations

Molecule		Activated complex	
Designation	Frequency (cm^{-1})	Designation	Frequency[a] (cm^{-1})
ν_1	2914	ν_1	3002
ν_2	1526 (2)	ν_2	580
ν_3	3020 (3)	ν_3	3184 (2)
ν_4	1306	ν_4	1380 (2)
		bending modes of dissociating bond	280 (2)

Parameter	Value
Collision diameter	3.8 Å
E_0	103.0 kcal/mol
Number of rotations for centrifugal correction	2
Collision efficiency, λ	1
Statistical factor, L^*	4
Moments of Inertia	
for molecule	$I_a = I_b = I_c = 5.33 \times 10^{-40}$ g cm^2
for complex	$I_a = 5.84 \times 10^{-40}$ g cm^2
	$I_b = I_c = 17.0 \times 10^{-40}$ g cm^2

[a]For purposes of calculation γ_1 and γ_3 were combined as 3122 cm^{-1}.

of A^∞ and E^∞ calculated at each temperature. The striking feature of these results is the large difference (4.6 kcal/mol) between E^∞ and E_0. For a dissociation reaction in the high-pressure region, the experimental activation energy is always larger than E_0, which is defined as the difference in zero-point energies of the reactants and the activated complex because the population of excited vibrational levels will always be larger in the activated complex than in the reactant. The difference between E^∞ and E_0 has commonly been found to be about 2 kcal/mol. For example for the isomerization of 1,1-dichlorocyclopropane, $E^\infty = 57.7$ and $E_0 = 55.5$ kcal/mol (17). Most of the unimolecular decompositions which have been studied have activation energies in this range. The critical energy for decomposition of methane is much larger and the temperature at which decomposition occurs is correspondingly higher. Taking into account as well the very low vibrational frequencies of three of the normal modes of the complex as compared to the reactant, a relatively large population of excited vibrational levels in the activated molecule will be expected. The result is a large difference between E^∞ and E_0, larger than has previously been reported.

Comparison of k_1 Measured in Static, Flow, and Shock Tube Pyrolysis

Using the parameters for the unimolecular dissociation of methane determined in the preceding section, the rate constant may be calculated for a wide range of temperature and pressure. These values are shown as solid lines in Fig. 4. The values of k_1 obtained at the highest temperature in the present work are shown together with recent values of k_1 obtained from shock tube pyrolysis and studies in a flow system. In most of these studies argon was used as diluent. To compute a total equivalent pressure of methane, Ar was assumed to be one-third as efficient as methane as a collision partner (17). The same efficiency was assumed for other inert diluents. For comparison purposes only representative data were chosen from the range of values reported by most authors.

The data of Palmer and Hirt (5) obtained in a flow system at 1200 and 1400 K are in good agreement with the calculated values. From shock tube studies, the results of Skinner and Ruehrwein (11) at 1200 and 1400 K, Kozlov and Knorre (23) at 1800 and 2000 K, and Glick (9) at 2000 K are in very close agreement; those of Kevorkian *et al.* (10) at 1670 K and Glick (9) at 2200 K are slightly higher, and those of Napier and Subrahmanyam (24) at 2000 K slightly lower, than the calculated values. In all of these studies the authors assumed that the rate constant was not pressure dependent. However, the scatter in the rate constants obtained by Glick at 2200 K and by Kozlov and Knorre at 1800 K would encompass the variation with pressure which we predict, and their data are therefore

Can. J. Chem. Downloaded from www.nrcresearchpress.com by 210.87.254.6 on 09/05/12
For personal use only.

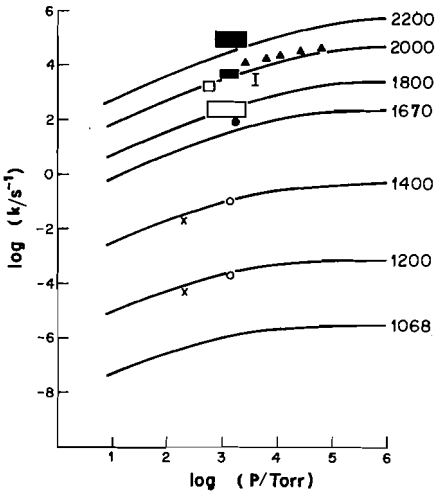

FIG. 4. The variation of k_1 with pressure for temperatures up to 2200 K. The solid lines are calculated from [9] and the experimental results were obtained in shock-tube studies or flow-system pyrolysis. ○, ref. 11; ×, ref. 5; ●, ref. 10; □, ref. 23; I, ref. 24; ■, ref. 9; ▲ ref. 25.

compatible with the present results. In only one shock-tube study, that of Hartig *et al.* (25), was the rate constant shown to be pressure dependent. This dependence is also close to that predicted by the present model but the measured value of k_1 is about six times lower than the calculated value; the reason for this discrepancy is not obvious. Agreement between observed and calculated rate constants is on the whole very good, especially as it is well known that the uncertainty in the measurement of temperature in a shock tube may easily be 50 deg. All the results except those of Hartig *et al.* fall within this range of the calculated values.

The most interesting aspect of these comparisons is the demonstration that all the measurements of the rate constant for dissociation of methane reported so far have been made in the pressure-dependent region. This fact was recognized in only one study, that of Hartig *et al.* An Arrhenius plot of rate constants in the pressure-dependent region is not very meaningful because the activation energy in this region is not simply related to the bond dissociation energy and because the ratio k/k^∞ is itself a function of temperature. Indeed a wide range of values for the activation energy of k_1 has been reported (85–103 kcal/mol) and the reason for the disagreement may be traced to the pressure dependence of k_1. Fortuitously, however, the measured activation energy from several studies of about 103 kcal/mol appeared close to the bond dissociation energy and the authors were led to believe that a high-pressure value for k_1 had been measured. The present calculations show that the activation energy of k_1 in the pressure-independent region, E^∞, of 107 kcal/mol, is in fact several kcal/mol higher than $D^0(CH_3—H)$, which was taken as 103 kcal/mol. The observed activation energy of k_1 in its pressure-dependent region is therefore lower than the value of E^∞ as predicted by unimolecular theory.

Calculations of k_{-1} and Comparison with Measured Values

Using the value of the equilibrium constant for [1] and the expression obtained for k_1, values of k_{-1}, the rate constant for the combination of a methyl radical and a hydrogen atom, were calculated over a range of pressures at 500, 700, and 1038 K. The results are shown in Fig. 5 and are listed in Table 5 together with the thermodynamic values used in the calculation. The results of three recent measurements of k_{-1} are also included. These measurements were made in an Ar or He carrier and the total pressure has therefore been reduced by a factor of three to correct for the efficiency of these gases as third bodies relative to methane (17). The measurements of Camilleri *et al.* (26) in the range 500–700 K are in good agreement with the present calculations. Comparison with the data of Dodonov *et al.* (27), Pratt and Veltman (28), and Halstead *et al.* (29) all at about 295–300 K is less certain because extension of [9] to this tempera-

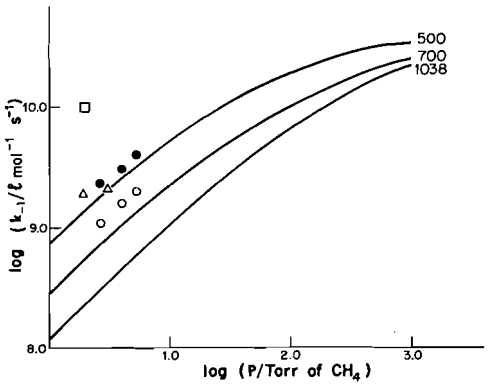

FIG. 5. The variation of $\log k_{-1}$ with pressure. The solid lines are calculated as described in the text and the experimental points are recent measurements of k_{-1}. ○, ref. 26; △, ref. 28; ●, ref. 29; □, ref. 27.

Can. J. Chem. Downloaded from www.nrcresearchpress.com by 210.87.254.6 on 09/05/12
For personal use only.

TABLE 5. Equilibrium constant and rate constants for the reaction[a] $CH_4 \underset{-1}{\overset{1}{\rightleftarrows}} CH_3 + H$

T(K)	ΔH (kcal/mol)	ΔS_p^b (cal mol^{-1} deg^{-1})	log K_c^c	log k_1	log k_{-1}	log P (Torr)
500	105.0	31.5	−40.62	−31.76	8.86	0
				−30.89	9.73	1
				−30.34	10.28	2
				−30.10	10.52	3
700	105.8	32.76	−27.64	−19.19	8.45	0
				−18.29	9.35	1
				−17.63	10.01	2
				−17.25	10.39	3
1038	106.6	33.53	−16.96	−8.88	8.08	0
				−7.93	9.03	1
				−7.16	9.80	2
				−6.62	10.34	3

[a]Units mol l^{-1} where applicable. Data are taken from ref. 14.
[b]Standard state 1 atm of ideal gas.
[c]$K_p = K_c(RT)^{\Delta n}$.

ture presented some computational difficulties and was not pursued. If the trend at the three higher temperatures continues, the value of Dodonov *et al.* appears rather high; the other data are somewhat lower than predicted, but in reasonable agreement. The value of k_{-1}^{∞} obtained in these calculations is 2.5×10^{11} l mol^{-1} s^{-1}, which is about one-quarter of the collision number for these radicals.

The extension of [9], with the model of the activated complex for methane described herein, down to 500 K and up to 2200 K provides a stringent test for the theory. The agreement with other measurements at both ends of the temperature range is strong support for the validity of this method. There are several approximations in these calculations which might be expected to limit the range of applicability of any particular model. For example, in the calculation of the density of states the harmonic oscillator approximation has been used. The limitations of this assumption have been discussed by Forst (30) and Forst and Prášil (31) have investigated the dependence on energy of the density of states and of the unimolecular rate constant k_a, eq. 10, for a small molecule, hydrogen peroxide. Their results showed that the unimolecular rate constant calculated using Morse oscillators is lower by about a factor of two than the rate constant calculated using purely harmonic oscillators, in the 'low energy' region applicable to thermal systems. The ratio of the two rate constants, however, did not change appreciably with an increase in the excitation energy in the low energy region. The excitation energy of the activated complex for the thermal dissociation of methane lies well within this low energy region considered by Forst and Prášil (31) and it may be concluded that inclusion of anharmonic effects in the present calculations will not change the relative values of the rate constants over the temperature range considered here.

The model of the activated complex is itself an approximation and modifications to it could be explored for better agreement over the whole temperature range. For example, Forst and Prášil (31) have calculated the effect on k_a of a complex in which one oscillator is coupled with a two-dimensional rotor, taking hydrogen peroxide as the dissociating molecule. Some lowering of k_a was observed as the excitation energy and the rotational quantum number was increased. The effect, however, was not large in the low range of excitation energy encountered in thermal systems, and taking into account the large uncertainties in the values of k_1 in the region of 2000 K and of k_{-1} at the low temperature end it was not considered profitable to pursue such calculations. It may be concluded that the model chosen for the activated complex provides a reasonable agreement with other measurements in the temperature range 500–2000 K.

The present system demonstrates some of the advantages gained from pyrolysis studies in a static system. Precise control of temperature, reaction time, and reactant concentration are of

Can. J. Chem. Downloaded from www.nrcresearchpress.com by 210.87.254.6 on 09/05/12
For personal use only.

prime importance in the measurement of rate constants. Sufficient precision for comparison of experimental and calculated unimolecular rate constants can probably be achieved only in a static system.

The authors thank the National Research Council of Canada for generous financial support.

1. E. W. R. STEACIE. Atomic and free radical reactions. Reinhold, New York. 1954.
2. M. S. KHAN and B. L. CRYNES. Ind. Eng. Chem. **62**, 54 (1970).
3. S. W. BENSON and H. E. O'NEAL. Kinetic data on gas phase unimolecular reactions. NSRDS-NBS 21. Washington, D.C. 1970.
4. H. B. PALMER, J. LAHAYE, and K. C. HOU. J. Phys. Chem. **72**, 348 (1968).
5. H. B. PALMER and T. J. HIRT. J. Phys. Chem. **67**, 709 (1963).
6. G. BOATO, G. CARERI, A. CIMINO, E. MOLINERI, and G. G. VOLPI. J. Chem. Phys. **24**, 783 (1956).
7. T. TERAO and R. A. BACK. J. Phys. Chem. **73**, 3884 (1969).
8. J. A. KERR. Chem. Rev. **66**, 465 (1966).
9. H. S. GLICK. 7th Combustion Symposium, Butterworth, London. 98. 1959.
10. V. KEVORKIAN, C. E. HEATH, and M. BOUDART. J. Phys. Chem. **64**, 964 (1960).
11. G. B. SKINNER and R. A. RUEHRWEIN. J. Phys. Chem. **63**, 1736 (1959).
12. P. WARNECK. Z. Naturforsch. Teil A, **26**, 2047 (1971); W. A. CHUPKA and C. LIFSHITZ. J. Chem. Phys. **48**, 1109 (1968).
13. W. BRAUN, A. M. BASS, and M. PILLING. J. Chem. Phys. **52**, 5131 (1970).
14. S. W. BENSON. Thermochemical kinetics. Wiley & Sons, New York. 1968.
15. H. M. FREY. J. Chem. Soc. Chem. Commun. 1024 (1972).
16. T. YANO. Bull. Chem. Soc. Jpn. **46**, 1619 (1973).
17. P. J. ROBINSON and K. A. HOLBROOK. Unimolecular reactions. Wiley-Interscience, New York. 1972.
18. D. C. TARDY, B. S. RABINOVITCH, and G. Z. WHITTEN. J. Chem. Phys. **48**, 1427 (1968).
19. R. A. MARCUS. J. Chem. Phys. **43**, 2658 (1965).
20. E. V. WAAGE and B. S. RABINOVITCH. Chem. Rev. **70**, 377 (1970).
21. D. W. PLACZEK, B. S. RABINOVITCH, and G. Z. WHITTEN. J. Chem. Phys. **43**, 4071 (1965).
22. JANAF Thermochemical Tables. 2nd ed. NSRDS-NBS37. Washington, D.C. 1970.
23. G. I. KOZLOV and V. G. KNORRE. Combust. Flame, **6**, 253 (1960).
24. D. H. NAPIER and N. SUBRAHMANYAM. J. Appl. Chem. Biotechnol. **22**, 303 (1972).
25. R. HARTIG, J. TROE, and H. G. G. WAGNER. 13th Comb. Sym. Combustion Institute, Pittsburgh. 1971. p.147.
26. P. CAMILLERI, R. M. MARSHALL, and J. H. PURNELL. J. Chem. Soc. Faraday Trans. 1, **70**, 1434 (1974).
27. A. F. DODONOV, G. K. LAVROVSKAYA, and V. L. TAL'ROZE. Kinet. Katal. **10**, 477 (1969).
28. G. PRATT and I. VELTMAN. J. Chem. Soc. Faraday Trans. 1, **70**, 1840 (1974).
29. M. P. HALSTEAD, D. A. LEATHARD, R. M. MARSHALL, and J. H. PURNELL. Proc. R. Soc. London, Ser. A, **316**, 575 (1970).
30. W. FORST. Theory of unimolecular reactions. Academic Press, New York. 1973.
31. W. FORST and Z. PRÁŠIL. J. Chem. Phys. **53**, 3065 (1970).

Can. J. Chem. Downloaded from www.nrcresearchpress.com by 210.87.254.6 on 09/05/12
For personal use only.

Stereochemical Determination of Key Substrates of the Cope Rearrangement by ^{13}C Nuclear Magnetic Resonance Spectroscopy

DONALD C. WIGFIELD AND KEVSER TAYMAZ

Department of Chemistry, Carleton University, Ottawa, Canada K1S 5B6

Received July 15, 1975

DONALD C. WIGFIELD and KEVSER TAYMAZ. Can. J. Chem. **53**, 3591 (1975).

The ^{13}C n.m.r. spectra of two key substrates of the Cope rearrangement (compounds **3** and **5**) have been assigned and compared with those of their monosaturated analogs. The spectra are consistent with the substrates being stereochemically homogeneous and with the *E* configuration around the trisubstituted double bond.

DONALD C. WIGFIELD et KEVSER TAYMAZ. Can. J. Chem. **53**, 3591 (1975).

On a attribué les spectres r.m.n. du ^{13}C de deux (composés **3** et **5**) substrats-clé du réarrangement de Cope et on les a comparés avec ceux de leurs analogues monosaturés. Les spectres sont en accord avec le fait que les substrats sont stéréochimiquement homogènes et de configuration *E* autour de la liaison double trisubstituée.

[Traduit par le journal]

Since its discovery in 1940 (1), the Cope rearrangement has been the subject of exhaustive mechanistic study. Kinetic studies have figured prominently in these mechanistic determinations and, due to both synthetic and kinetic convenience, these studies, both originally (2, 3), and more recently (4–6), have frequently utilized the type of substrates indicated in Scheme 1 where X and Y are most frequently CN or COOEt (originating in the synthesis from malononitrile, ethyl cyanoacetate, or diethyl malonate) and Z is either H or an aromatic group.

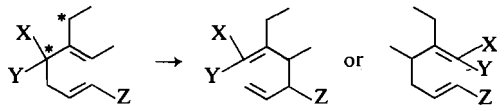

SCHEME 1. Substrates for the Cope rearrangement.

We have previously pointed out (7) that, in this type of Cope rearrangement substrate, a major stereochemical ambiguity exists. While the geometrical configuration around the double bond to which the group Z is attached is easily assigned (7), the configuration around the other double bond has always remained obscure, being either *E* (as written) (8) or *Z*, or a mixture of both diastereomers. The absence of any evidence of heterogeneity in such samples does not aid the stereochemical assignment; indeed it hinders it, as almost all methods of such determination require the comparison of both stereoisomers (see refs. 19–26 of ref. 7). It is somewhat disquieting that much of the fundamental kinetic work on the Cope rearrangement thus rests on the kinetics of samples of unknown stereochemical homogeneity, and one cannot help but wonder whether it was entirely fortuitous that Cope and his co-workers reported their most satisfactory kinetic data on a different but related compound, one devoid of this particular ambiguity (see ref. 2, footnote 6).

One method for making this type of stereochemical distinction, not necessarily requiring the possession of both stereoisomers, and one that has not previously been applied to these substrates, is ^{13}C n.m.r. spectroscopy. It is now well established that the α-carbons in *trans*-isomers are generally deshielded (by 2–5 p.p.m.) whereas the α-carbons in *cis*-isomers are shielded (by 1–3 p.p.m.) relative to the saturated analogs (9). Examination of the shifts of the starred atoms (Scheme 1) upon insertion of the double bond, therefore, provides the desired analysis. Accordingly, we have conducted a program to assign the ^{13}C signals in two representative Cope rearrangement substrates, and thereby determine the double bond stereochemistry in these compounds.

Results and Discussion

The two substrates chosen for examination in this study were compounds **3** and **5**, **3** being representative of the kinetically studied substrates (2–6) and **5** being the compound whose rearrangement has provided evidence of the ionic Cope rearrangement (7). (In the literature these

Can. J. Chem. Downloaded from www.nrcresearchpress.com by 210.87.254.6 on 09/05/12
For personal use only.

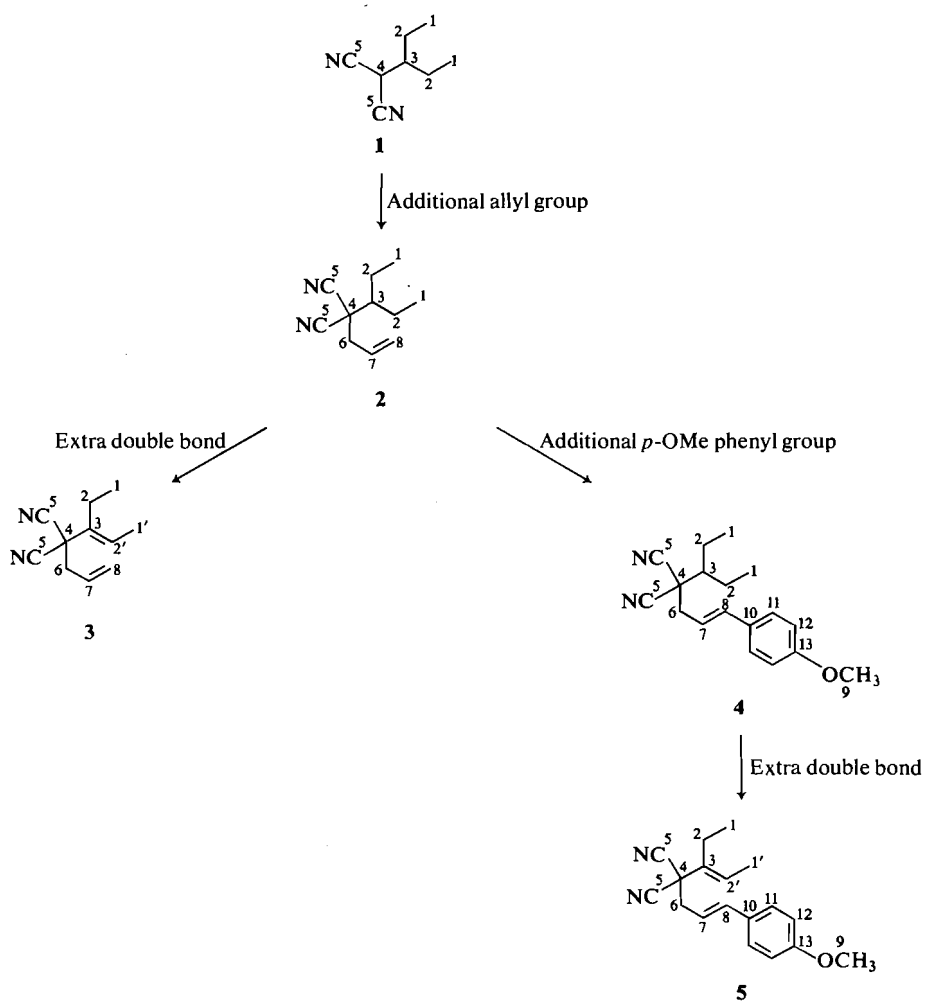

1 2 3 4 5

SCHEME 2. Peak assignment sequence for compounds examined by ^{13}C n.m.r. spectroscopy, and carbon numbering scheme used.

compounds have always been drawn in the *E* configuration; we arbitrarily continue this practice here.)

In order to facilitate unambiguous peak assignment, the series of compounds indicated in Scheme 2 were examined, the peaks of the simplest compound, 2-(1-ethylpropyl)malononitrile **1** being easily assigned. Addition of the allyl group and application of the alkane additivity shielding effects (ref. 9, p. 58) yields the assignments for compound **2**, which differs from compound **3** only by insertion of the double bond. Compound **2** is also instrumental in peak assignment of compound **4**, the two differing only by the *p*-methoxyphenyl group at C-8; and insertion of the double bond gives the assignments to compound **5**. Comparison of the shifts of C-2 and of C-4 in both compounds **2** and **3**, and in compounds **4** and **5** is the desired stereochemical analysis. Although clearly the assignment of many peaks is irrelevant to the question at hand, the complete peak assignments for all compounds have been made. These assignments are shown in Table 1.

Synthesis of Substrates

The synthetic sequence to compounds **1**–**5**, is shown in Scheme 3. 2-(1-Ethyl-propylidene)malononitrile was prepared, as previously (5, 10), by condensation of malononitrile with 3-pentanone, and this was then condensed with the appropriate allyl chloride to yield hexadienes **3** and **5**

Can. J. Chem. Downloaded from www.nrcresearchpress.com by 210.87.254.6 on 09/05/12
For personal use only.

TABLE 1. ^{13}C shieldings for compounds **1–5** ($\delta_C \pm 0.1$ from TMS)

	Compound				
Position	**1**	**2**	**3**	**4**	**5**
C-1	10.9	11.6	13.7	11.6	13.8
C-2	24.1	23.2	21.3	23.2	21.4
C-1′	—	—	13.7	—	13.8
C-2′	—	—	127.6	—	127.8
C-3	43.1	46.6	132.0	46.5	132.0
C-4	26.9	42.4	42.5	43.0	44.6
C-5	112.9	115.5	114.7	114.6	114.8
C-6	—	39.8	42.0	39.3	42.3
C-7	—	129.4	129.1	117.6	117.2
C-8	—	122.6	122.7	137.0	137.1
C-9	—	—	—	55.3	55.3
C-10	—	—	—	128.9	128.8
C-11	—	—	—	128.0	128.0
C-12	—	—	—	114.2	114.2
C-13	—	—	—	160.0	159.9

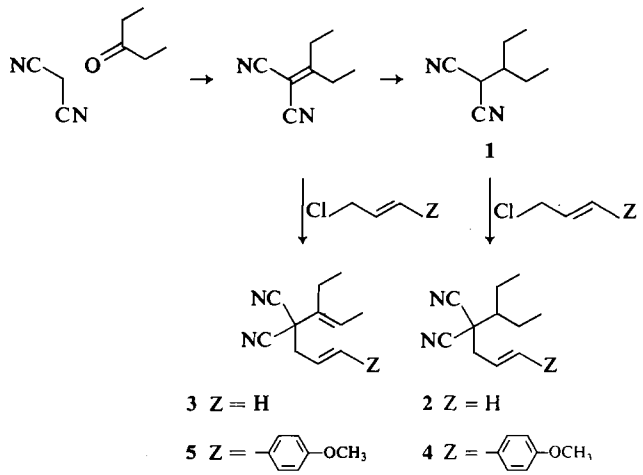

SCHEME 3. Synthetic procedure.

(7). Attempts to prepare 2-(3-pentyl)malononitrile **1** by condensation of malononitrile with 3-bromopentane were not successful, and compound **1** was therefore prepared by reduction of 2-(1-ethylpropylidene)malononitrile, this reduction being accomplished very conveniently by aluminum amalgam, a reagent of some antiquity (11). Condensation of compound **1** with the appropriate allyl chloride yielded the reference compounds **2** and **4**.

Peak assignments (see Table 1 and Scheme 2)

Compound 1

The ^{13}C spectrum of compound **1** consists of five peaks of which the peak at 112.9 p.p.m. is clearly due to the nitrile carbons. The other assignments made were confirmed by selective decoupling at δ 3.88 p.p.m. (C4-H), under which conditions the peak for C-1 became a quartet, that for C-2 a triplet, and that for C-3 a doublet, while C-4 remained a singlet.

Compound 2

Peak assignments for compound **2** were made with reference to the assignments for compound **1** utilizing the alkane α–ε additivity factors for the additional allyl group (ref. 9, p. 58). This gave the following calculated values for the peak positions of C-1–C-4 (observed position in parentheses): C-1, 11.3 (11.6); C-2, 22.0 (23.2);

Can. J. Chem. Downloaded from www.nrcresearchpress.com by 210.87.254.6 on 09/05/12
For personal use only.

Can. J. Chem. Downloaded from www.nrcresearchpress.com by 210.87.254.6 on 09/05/12
For personal use only.

C-3, 50.3 (46.6); C-4, 42.9 (42.4). Possible confusion between the assignments for C-4 and C-6 was eliminated by selective decoupling at δ 2.68 p.p.m. (C6-H), under which conditions the peak at 39.8 p.p.m. remained a singlet.

Compound 3

Assignments for compound **3** were made in comparison with those for compound **2**, the introduction of the double bond having little effect on carbon nuclei separated by two or more σ bonds (9). It is noteworthy that C-1 and C-1′ have almost identical chemical shifts. Rigorous distinction of the assignments for C-1′ and C-2 was made by selective decoupling at δ 1.78 p.p.m. (C1′-H), under which conditions the possible ambiguity between assignments for C-4 and C-6 was also resolved, the peak at 42.0 p.p.m. (C-6) degenerating to a triplet.

Compound 4

Assignments of the high-field peaks of compound **4** were made by comparison to those of compound **2**, the introduction of the *p*-methoxyphenyl group having little effect on these shifts. Confirmation of the assignments for C-1–C-4, C-6, and C-9 was also obtained by the appropriate multiplicity changes on selective decoupling at δ 2.77 p.p.m. (C6-H). The aromatic carbon peaks were identified by a combination of calculation (ref. 9, p. 197) and comparison with the known spectrum of *p*-methoxystyrene (12). Carbons 11 and 12 are easily identified as high intensity peaks that are split into doublets upon selective decoupling at other hydrogens. The shift for C-11 of 128.0 p.p.m. compares with the calculated (ref. 9, p. 197) value of 126.7 p.p.m. and the shift of the corresponding carbon in *p*-methoxystyrene of 126.8 p.p.m. (12). For C-12 (114.2 p.p.m.) the corresponding shifts are 113.4 and 113.6 p.p.m. respectively. Similar comparisons on the smaller peaks due to C-10 (calculated 129.3 p.p.m., comparison 130.4 p.p.m., observed 128.9 p.p.m.) and C-13 (calculated 158.4 p.p.m., comparison 159.0 p.p.m., observed 160.0 p.p.m.) allowed their assignment. These assignments leave, by difference, the peaks at 117.6 and 137.0 p.p.m. as C-7 and C-8 respectively; the assignments appear reasonable by comparison with the spectra of compounds **2** and **3**, bearing in mind that an α substituent is deshielding but an α′ substituent shielding (ref. 9, p. 72). Multiplicity changes on selective decoupling at δ 2.77 p.p.m. were consistent with all the above assignments.

Compound 5

With the assignments for compounds **3** and **4** in hand, the assignments of the 15 signals of compound **5** are straightforward. Inspection of Table 1 reveals that the low-field portion of the spectrum is virtually identical with that of compound **4**, with the addition of two signals due to C-2′ and C-3 which have the characteristic shifts exhibited by the corresponding carbons in compound **3**. As in compound **3**, there is barely any distinction between carbons 1 and 1′, and, as before, rigorous distinction between the shifts of C-4 and C-6 was made by selective decoupling at δ 1.73 p.p.m. (C1′-H) and at δ 2.82 p.p.m. (C6-H), all other multiplicity changes being consistent with assignment.

Stereochemical Analysis

Comparison of the chemical shifts of C-2 in compounds **2** and **3**, and in compounds **4** and **5** (Table 1) show that an upfield shift of 1.85 and 1.71 p.p.m. respectively occurs upon insertion of the double bond, this shift being indicative of C-2 being *cis* to the methyl group in both compounds **3** and **5**. Similarly the shift of the

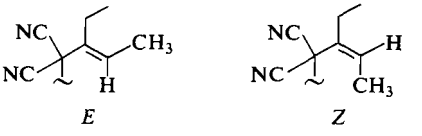

E *Z*

quaternary carbon C-4 is downfield in both comparisons (compounds **2** and **3**, 0.12 p.p.m.; compounds **4** and **5**, 1.61 p.p.m.), consistent with C-4 being *trans* to the methyl group. These shifts appear to demand the *E* configuration for the trisubstituted double bond of both compounds **3** and **5**. One curious feature of the spectra is that the methyl group (C-1, C-1′) in both cases undergoes a downfield shift (2.04, 2.15 p.p.m.) upon insertion of the double bond despite the fact that the methyl clearly must be *cis* to one group or the other. This may be a case, however, of electronic factors being superimposed on steric factors, the methyl becoming conjugated in a homoallylic sense with the nitrile groups on insertion of the double bond.

Conclusions

The ^{13}C chemical shifts of C-2 and C-4 in compounds **2–5** are consistent with compounds **3** and **5** having the *E* configuration around the trisubstituted double bond which has been implicitly assumed for many years. No extra

Can. J. Chem. Downloaded from www.nrcresearchpress.com by 210.87.254.6 on 09/05/12
For personal use only.

spurious peaks suggestive of an *E–Z* mixture are evident. This result lends support to the validity of numerous kinetic studies on Cope rearrangements of this type of substrate, and thus to the various mechanistic deductions drawn therefrom.

Experimental

2-(1-Ethylpropylidene)malononitrile was prepared as previously described (5, 13).

2-(1-Ethylpropyl)malononitrile ***1***

Aluminum amalgam (prepared according to Fieser and Fieser (13)) (15 g) was added to a solution of 2-(1-ethylpropylidene)malononitrile (13.4 g, 0.1 mol) in ether (200 ml). Water (200 ml) was added and the mixture heated under reflux until reduction was complete, the reaction being monitored by measuring the n.m.r. spectrum of the ether layer. Fresh amalgam (10 g) was added after 3 days, and the reaction was complete after 1 week. The ether layer was removed, 100 ml of ice-cold hydrochloric acid added to the aqueous layer, and the aqueous layer extracted with ether (3 × 100 ml). The combined ether extracts were dried (Na_2SO_4), evaporated, and distilled (80 °C, 0.14 Torr) to give the title compound (9.2 g, 67%), n_D^{20} 1.4431; ν_{max}(film) 2986, 2950, 2251, 2214, and 1463 cm^{-1}; δ 0.99 (6H, t, J = 5 Hz, CH_3), 1.37–2.20 (5H, m, CH_2 and adjacent CH), and 3.9 p.p.m. (1H, d, J = 5 Hz, $CH(CN)_2$).

Anal. Calcd. for $C_8H_{12}N_2$: C, 70.56; H, 8.87; N, 20.57. Found: C, 70.61; H, 9.00; N, 20.64.

2-Allyl-2-(1-ethylpropyl)malononitrile ***2***

A solution of sodium isopropoxide was prepared by dissolving sodium (0.23 g, 0.01 mol) in 2-propanol (25 ml) at 50 °C. The solution was then cooled in an ice–water bath and 2-(1-ethylpropyl)malononitrile **1** (1.36 g, 0.01 mol) added dropwise to give a clear yellow solution. Allyl chloride (0.76 g, 0.01 mol) was added in one portion and the mixture stirred at room temperature for 1 h. Water (100 ml) was added and the solution extracted with benzene (3 × 30 ml). The combined extracts were washed with water (2 × 25 ml), dried (Na_2SO_4), and evaporated to give a yellow liquid (1.7 g). Preparative layer chromatography (silica gel; 25% ether in benzene) yielded the pure compound (0.8 g, 45%), n_D^{20} 1.4512; ν_{max}(film) 3000, 2970, 2255, 1470, 975, 910 cm^{-1}; δ 1.06 (6H, t, J = 5 Hz, CH_3), 1.64 (5H, m, —CH—$(CH_2—)_2$), 2.65 (2H, d, J = 6 Hz, allylic CH_2), and 5.06–6.32 p.p.m. (3H, m, olefinic H); high resolution mass spectrometry m/e 176.1313, calcd. for $C_{11}H_{16}N_2$, 176.1313.

Anal. Calcd. for $C_{11}H_{16}N_2$: C, 74.95; H, 9.16; N, 15.89. Found: C, 74.89; H, 9.20; N, 15.07.

2-Allyl-2-(1-ethyl-1-propenyl)malononitrile **3** was prepared as described previously (2, 5).

2-(3-p-Methoxyphenylallyl)-2-(1-ethylpropyl)malononitrile ***4***

2-(1-Ethylpropyl)malononitrile **1** (1.36 g, 0.01 mol) was added dropwise at 0 °C to a solution of sodium isopropoxide (0.01 mol) in isopropanol (25 ml). *p*-Methoxycinnamyl chloride (1.82, 0.01 mol) was added in one portion, and the mixture stirred at room temperature for 1 day, and then refluxed for 1 h. Water (100 ml) was added and the solution extracted with benzene (3 × 30 ml). The combined extracts were washed with water (2 × 25 ml), dried (Na_2SO_4), and evaporated giving a dark yellow viscous liquid (2.8 g). Preparative layer chromatography (silica gel; 10% ether in benzene, and then repurification using 50% ether in petroleum ether (b.p. 30–60 °C)) yielded the pure product (0.6 g, 21.3%), n_D^{20} 1.5982; ν_{max}(film) 3000, 2230, 1610, 1510, 1255, and 1040 cm^{-1}; δ 1.10 (6H, t, J = 5 Hz, CH_3), 1.66 (5H, m, —CH—$(CH_2—)_2$), 2.77 (2H, d, J = 7 Hz, allylic CH_2), 3.72 (3H, s, OCH_3), 5.88–6.50 (2H, m, olefinic H), and 6.68–7.46 p.p.m. (4H, m, aromatic H); high resolution mass spectrometry m/e 282.1734, calcd. for $C_{18}H_{22}N_2O$, 282.1732.

Anal. Calcd. for $C_{18}H_{22}N_2O$: C, 76.59; H, 7.85; N, 9.92. Found: C, 76.61; H, 7.86; N, 9.25.

2-(1-Ethyl-1-propenyl)-2-(3-*p*-methoxyphenylallyl)malononitrile **5** was prepared as described previously (7).

Spectral Measurements

Infrared spectra were obtained on a Perkin-Elmer 257 spectrophotometer, and p.m.r. spectra in $CDCl_3$, with TMS as internal standard on a Varian T-60 instrument. ^{13}C spectra (natural abundance) were obtained on a Varian XL-100-12 n.m.r. spectrometer equipped with a Nicolet Technology Corporation Fourier Transform data system. High resolution mass spectra were obtained through the courtesy of J. P. Kutney and G. Eigendorf, University of British Columbia.

It is a pleasure to acknowledge the helpful advice provided by Dr. G. W. Buchanan of this Department at various stages of the work. The financial support of the National Research Council of Canada is also gratefully acknowledged.

1. A. C. Cope and E. M. Hardy. J. Am. Chem. Soc. **62**, 441 (1940).
2. A. C. Cope, K. E. Hoyle, and D. Heyl. J. Am. Chem. Soc. **63**, 1843 (1941).
3. E. G. Foster, A. C. Cope, and F. Daniels. J. Am. Chem. Soc. **69**, 1893 (1947).
4. K. Humski, T. Strelkov, S. Borcic, and D. E. Sunko. Chem. Commun. 693 (1969).
5. D. C. Wigfield and S. Feiner. Can. J. Chem. **48**, 855 (1970).
6. K. Humski, R. Malojcic, S. Borcic, and D. E. Sunko. J. Am. Chem. Soc. **92**, 6534 (1970).
7. D. C. Wigfield, S. Feiner, G. Malbacho, and K. Taymaz. Tetrahedron, **30**, 2949 (1974).
8. J. E. Blackwood, C. L. Gladys, K. L. Loening, A. E. Petrarca, and J. E. Rush. J. Am. Chem. Soc. **90**, 509 (1968).
9. J. B. Stothers. Carbon-13 NMR spectroscopy. Academic Press Inc., New York. 1972. pp. 80–82, 406 *et seq*.
10. A. C. Cope and K. E. Hoyle. J. Am. Chem. Soc. **63**, 733 (1941).
11. H. Wislicenus and L. Kaufmann. Chem. Ber. **28**, 1323 (1895).
12. K. S. Dharmi and J. B. Stothers. Can. J. Chem. **43**, 510 (1965).
13. L. F. Fieser and M. Fieser. Reagents for organic synthesis. Vol. 1. John Wiley and Sons Inc., New York. 1967.

Sur la structure cristalline des diméthyl-1,1 germa-1 (et sila-1) cycloundécanediols-6,7

FRANÇOIS BRISSE, AVIVA BATTAT ET JEAN-CLAUDE RICHER
Département de Chimie, Université de Montréal, B.P. 6210, Montréal, Québec H3C 3V1
ET
PIERRE MAZEROLLES ET ALFREDA FAUCHER
Laboratoire des Organométalliques, Université Paul Sabatier, 118 Route de Narbonne, 31077 Toulouse, France

Reçu le 22 avril 1975

FRANÇOIS BRISSE, AVIVA BATTAT, JEAN-CLAUDE RICHER, PIERRE MAZEROLLES et ALFREDA FAUCHER. Can. J. Chem. **53**, 3596 (1975).

Les diméthyl-1,1 germa-1 (et sila-1) cycloundécanediols-6,7 ($C_{12}H_{26}O_2Ge$ et $C_{12}H_{26}O_2Si$) sont caractérisés par leurs diagrammes de poudres; ces composés sont isostructuraux. Les dimensions des mailles tricliniques sont $a = 10.53$, $b = 12.45$ et $c = 12.43$ Å, $\alpha = 81.5°$, $\beta = 67.0°$ et $\gamma = 76.3°$ pour le dérivé silicié et $a = 10.56$, $b = 12.50$ et $c = 12.58$ Å, $\alpha = 82.1°$, $\beta = 67.8°$ et $\gamma = 76.1°$ pour le dérivé germanié. Si le groupe spatial est $P\bar{1}$, il y aura deux molécules indépendantes par unité asymétrique.

FRANÇOIS BRISSE, AVIVA BATTAT, JEAN-CLAUDE RICHER, PIERRE MAZEROLLES, and ALFREDA FAUCHER. Can. J. Chem. **53**, 3596 (1975).

1,1-Dimethyl-1-germa (and -1-sila) -6,7-cycloundecanediol ($C_{12}H_{26}O_2Ge$ and $C_{12}H_{26}O_2Si$) are isostructural as established by their X-ray powder patterns. The dimensions of the triclinic cells are as follows: for the silicon derivative, $a = 10.53$, $b = 12.45$, and $c = 12.43$ Å, $\alpha = 81.5°$, $\beta = 67.0°$, and $\gamma = 76.3°$; for the germanium derivative, $a = 10.56$, $b = 12.50$, and $c = 12.58$ Å, $\alpha = 82.1°$, $\beta = 67.8°$, and $\gamma = 76.1°$. If the space group is $P\bar{1}$, there will be two independent molecules in each asymmetric unit.

[Journal translation]

Introduction

Dans le cadre de nos travaux (1) sur la synthèse et les propriétés de cycles moyens contenant du germanium et du silicium, nous avons été amenés à examiner la structure cristalline du diméthyl-1,1 germacycloundécanediol-6,7 (**1***a*) et de son analogue silicié **1***b* dont la préparation a été décrite antérieurement (2). On a établi précédemment (1) que le méthyl-1 germacycloundécanol-6 (**2**) perd de l'hydrogène pour conduire,

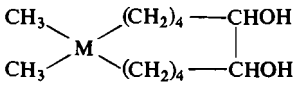

1*a* M = Ge
1*b* M = Si

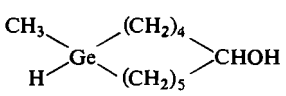

2

par une réaction de cyclisation intramoléculaire, à la formation du méthyl-1 oxa-12 germa-1 bicyclo[5.4.1]dodécane (**3**) qui résulte aussi de la cyclisation intramoléculaire, en présence de zinc, de la méthyl-1 germacycloundécanone-6 (**4***a*) formée transitoirement par réduction partielle de la chloro-1 méthyl-1 germacyclodécanone (**4***b*). Ces cyclisations intramoléculaires résulteraient d'un effet de proximité semblable à celui mis en évidence par Prelog et Schenler (3) et par Cope *et al.* (4) pour divers composés contenant des cycles moyens. Ces réactions laissent supposer que, dans les composés **2** et **4***a*,

TABLEAU 1. Données cristallographiques

	$C_{12}H_{26}O_2Si$	$C_{12}H_{26}O_2Ge$
Poids mol.	230.42	274.93
a	10.53(2) Å	10.56(2) Å
b	12.45(2) Å	12.50(2) Å
c	12.43(2) Å	12.58(2) Å
α	81.5(2)°	82.1(2)°
β	67.0(2)°	67.8(3)°
γ	76.3(2)°	76.1(2)°
V	1454 Å^3	1489 Å^3
ρ_{obs}	1.08 g cm^{-3}	1.27 g cm^{-3}
ρ_{cal}	1.05 g cm^{-3}	1.23 g cm^{-3}
Z	4	4

Can. J. Chem. Downloaded from www.nrcresearchpress.com by 210.87.254.5 on 09/05/12
For personal use only.

Can. J. Chem. Downloaded from www.nrcresearchpress.com by 210.87.254.5 on 09/05/12
For personal use only.

TABLEAU 2. Distances réticulaires

	$C_{12}H_{26}O_2Si$			$C_{12}H_{26}O_2Ge$		
hkl	d_{obs}	d_{cal}	I_{obs}	d_{obs}	d_{cal}	I_{obs}
010	12.2	12.1	70	12.3	12.1	20
001	11.0	11.4	50			
100				9.40	9.56	2
011	8.68	8.57	50	8.76	8.62	10
$0\bar{1}1$	7.67	8.05	50			
$\bar{1}10$	6.76	6.84	15	6.77	6.85	40
$1\bar{1}1$	6.43	6.58	15	6.55	6.60	20
$10\bar{1}$	6.30	6.25	80	6.33	6.35	60
020	6.07	6.03	20	6.08	6.06	20
120	5.611	5.622	60	5.662	5.670	25
012	5.300	5.283	5			
$0\bar{2}1$				5.261	5.261	15
201		5.109		5.109	5.115	100
	5.088		100			
$0\bar{1}2$		5.042				
$1\bar{1}2$				5.031	5.035	20
210		4.753		4.816	4.797	20
	4.751		50			
200		4.752				
221	4.466	4.463	50	4.474	4.481	50
$2\bar{1}1$	4.355	4.346	75	4.362	4.350	60
$\bar{1}12$		4.062				
	4.059		50			
131		4.059		4.070	4.071	20
$2\bar{1}2$				3.992	3.988	5
031	3.869	3.869	5			
003		3.805				
	3.799		70			
213		3.788		3.804	3.806	50
$0\bar{3}1$		3.721				
	3.719		15			
203		3.717				
123	3.653	3.654	20		3.681	
				3.682		25
132					3.680	
$\bar{1}22$		3.405				
	3.399		40			
$1\bar{3}1$		3.396		3.400	3.401	20
$0\bar{2}3$	3.136	3.134	20			
$21\bar{2}$	3.100	3.103	10			
$\bar{1}13$		3.039				
	3.040		25			
$31\bar{2}$		3.038				
$2\bar{2}3$	2.902	2.900	20			
242					2.861	
				2.860		20
$14\bar{1}$		2.827			2.856	
	2.836		35			
311		2.826				
$2\bar{3}2$					2.727	
				2.726		15
$0\bar{3}3$					2.726	
$\bar{3}11$		2.634				
	2.633		25			
243		2.633				

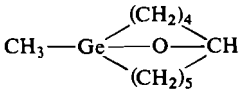

3

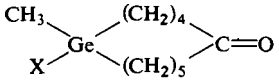

4*a* X = H
4*b* X = Cl

les distances interatomiques entre le germanium et les atomes d'oxygène de l'alcool ou de la cétone sont courtes. C'est dans le but de vérifier si cette hypothèse est valable à l'état solide que les travaux actuels ont été entrepris.

Résultats et discussion

L'étude des cristaux uniques des deux composés **1***a* et **1***b* entreprise sur la caméra de précession a révélé que tous les cristaux observés étaient maclés et que les intensités diffractées s'atténuaient très rapidement en fonction de l'angle de diffraction. Les dimensions approchées des mailles tricliniques ont été obtenues à partir des films de précession. Ces mailles ont été réduites (5) et les nouvelles dimensions ont servi comme valeurs initiales pour l'indexation des films de poudres. Les paramètres des mailles élémentaires affinés par moindres carrés selon la méthode de Cohen (6) sont présentées (tableau 1). Les distances réticulaires et les intensités observées pour les deux composés sont présentées (tableau 2).

Le volume de la maille du composé germanié est légèrement supérieur à celui du dérivé silicié correspondant. Les densités déterminées expérimentalement par flottaison indiquent qu'il y a quatre molécules par maille triclinique. Si l'on suppose que le groupe spatial est centrosymétrique il y aurait donc deux molécules indépendantes par unité asymétrique. Le nombre de paramètres structuraux est au moins doublé rendant les chances de détermination de ces structures très peu probables compte tenu du maclage et du petit nombre de réflexions observables. Aucun travail ultérieur n'est donc prévu sur ces composés particuliers.

Partie expérimentale

Les cristaux uniques ont été étudiés sur la caméra de précession en se servant de la radiation du cuivre tandis que les diagrammes de poudres ont été pris à l'aide d'une caméra Debye-Scherrer de 114.5 mm de diamètre en utilisant la radiation du chrome (λ CrK$\bar{\alpha}$ 2.29092 Å) filtrée par le vanadium. Les échantillons ont été introduits dans des capillaires de Lindemann de 0.3 mm de diamètre. Les intensités ont été estimées visuellement.

Les auteurs remercient vivement le Conseil National de Recherches du Canada et les autorités chargées d'administrer les accords scientifiques franco-québécois pour l'aide financière apportée sous forme d'octrois de recherches (CNR A-1295, A-5968) et de frais de mission.

1. Pierre Mazerolles et Alfreda Faucher. J. Organomet. Chem. **63**, 195 (1973).
2. Pierre Mazerolles et Alfreda Faucher. Bull. Soc. Chim. Fr. 2134 (1967).
3. V. Prelog et K. Schenler. Helv. Chim. Acta, **35**, 2044 (1952).
4. A. C. Cope, S. W. Fenton et C. F. Spencer. J. Am. Chem. Soc. **74**, 5882 (1952).
5. International tables for X-ray crystallography. Vol. 1. Kynoch Press, Birmingham. 1969. p. 530.
6. M. U. Cohen. Rev. Sci. Instrum. **6**, 68 (1935).

Can. J. Chem. Downloaded from www.nrcresearchpress.com by 210.87.254.5 on 09/05/12
For personal use only.

Ab Initio Computation of Force Constants. II. The Estimation of Dissociation Energies from *ab initio* SCF Calculations

H. BERNHARD SCHLEGEL[1] AND SAUL WOLFE

Department of Chemistry, Queen's University, Kingston, Ontario K7L 3N6

AND

FERNANDO BERNARDI

Istituto di Chimica Organica, Universita di Bologna, 40136-Bologna, Italy

Received May 27, 1975

H. BERNHARD SCHLEGEL, SAUL WOLFE, and FERNANDO BERNARDI. Can. J. Chem. **53**, 3599 (1975).

The dissociation energies of second and third period hydrides have been estimated by fitting a Morse potential to the harmonic and cubic stretching force constants computed from *ab initio* wavefunctions. The estimates thus obtained are superior to dissociation energies computed by direct differences of Hartree–Fock energies.

H. BERNHARD SCHLEGEL, SAUL WOLFE et FERNANDO BERNARDI. Can. J. Chem. **53**, 3599 (1975).

On a estimé les énergies de dissociation des hydrures de la deuxième et de la troisième période en ajustant un potentiel de Morse aux potentiels de vibration harmonique et cubique calculés à l'aide de fonction d'ondes *ab initio*. Ces estimés sont supérieurs aux énergies de dissociation calculés par les différences directes des énergies de Hartree et Fock.

[Traduit par le journal]

The calculation of bond dissociation energies *ab initio* has proved to be a virtually intractable theoretical problem. Reasonable agreement with experiment has been achieved only in a relatively small number of cases because large and complicated wavefunctions that take electron correlation specifically into account must be employed. The purpose of this paper is to outline a method for the estimation of the dissociation energies of hydride bonds which requires only SCF wavefunctions computed with a moderate size basis set.

The general shapes of interatomic potentials are well known from studies of the band spectra of diatomic molecules (1). In favorable cases the R.K.R. method (2) allows the exact shape of the potential curve to be deduced directly from the vibrational spectrum. When the vibrational spectrum is insufficiently well known for the computation of an R.K.R. potential, it is possible to fit the experimental data to one of a number of empirical curves. The best known of these is the Morse function (3),

$$[1] \qquad V(r) = D_e[1 - \exp(-\alpha(r - r_e))]^2$$

in which D_e is the dissociation energy and r_e is the equilibrium bond length. The parameter α is usually adjusted by fitting the potential V to the harmonic force constant k_2. A particular advantage of the Morse function is its ability to reproduce the cubic and quartic force constants, k_3 and k_4. Thus, when the dissociation energy D_e is unobtainable or unreliable, the potential can be fitted to the observed cubic force constant by the use of [2*a*] and [2*b*].

$$[2a] \qquad \left.\frac{\partial^2 V}{\partial r^2}\right|_{r_e} = k_2$$

$$[2b] \qquad \left.\frac{\partial^3 V}{\partial r^3}\right|_{r_e} = k_3$$

In a recent study of the force fields of second and third period hydrides (4), it was found that harmonic and cubic stretching force constants computed by the force method (5) are in excellent agreement with experiment. This suggested that, as has been done experimentally, it might be possible to estimate dissociation energies by fitting a three-parameter potential to the bond length and the calculated harmonic and cubic force constants. A number of possible functions have been evaluated (6, 7). Those due to Morse eq. 1, Rydberg (2*a*) eq. 3, Varshni (6) eq. 4, and

[1]Holder of a National Research Council of Canada 1967 Science Scholarship.

Can. J. Chem. Downloaded from www.nrcresearchpress.com by 210.87.254.5 on 09/05/12
For personal use only.

Can. J. Chem. Downloaded from www.nrcresearchpress.com by 210.87.254.5 on 09/05/12
For personal use only.

TABLE 1. Estimated and experimental[a] dissociation energies[b]

	Molecule	r^c	Computed force constants[d] k_2	k_3	Dissociation energy, D_e [8a]	[9a]	[7]	[6]	Exp.[e]	SCF	Hartree–Fock[f]
1	H_2	0.7420	6.054	−38.88		90.4	84.5	95.1	104.2[d]	80.5	83.9
2	HF	0.9170	9.874	−70.11	112.9	111.8	112.8	126.9	135.9	76.9	101.4
3	H_2O	0.9568	8.707	−61.40	97.7	99.2	100.9	113.5	119.0	64.2	78.5
4	NH_3	1.0080	7.505	−49.17	99.4	99.5	100.7	113.3	110.0	58.0	68.1
5	CH_4	1.0930	5.488	−32.14	94.0	91.6	92.2	103.7	104.0	79.3	80.1
6	HCl	1.2744	5.183	−29.37	86.1	90.3	93.0	104.6	103.1	57.8	77.7
7	H_2S	1.3552	3.903	−20.82	73.1	76.7	79.0	88.9	90.0	48.2	64.4
8	PH_3	1.4332	2.994	−13.89	78.6	79.1	80.1	90.1	77.0	43.5	55.5
9	SiH_4	1.4780	2.906	−12.50	93.0	90.1	90.5	101.8	94.0	61.3	63.3
10	CO	1.1280	21.739	−146.88	247.8	263.9	274.3	308.6	256.7	131.7	182.7
11	N_2	1.0940	27.396	−191.56	291.2	310.4	322.8	363.1	226.8	61.4	121.6
12	F_2	1.4350	7.425	−36.91	161.3	168.5	173.1	194.7	37.7	−45.5	−31.6

[a]Zero point vibrational effects have not been taken into account.
[b]Bond lengths in Å; quadratic and cubic force constants in mdyn/Å and mdyn/Å^2; dissociation energies in kcal/mol.
[c]Bond length at which the force constants were computed (see ref. 4).
[d]Force constant data for molecules 2–9 were computed in ref. 4; 1, 10–12 in the present work.
[e]Reference 9.
[f]Calculated from data presented in ref. 10 (compounds 1–5, 10–12) and ref. 11 (6–9).

Can. J. Chem. Downloaded from www.nrcresearchpress.com by 210.87.254.5 on 09/05/12
For personal use only.

Lippincott and co-worker (8) eq. 5 were considered to be the most suitable (7).

$$[3]\quad V(r) = D_e[1 - (1 + \beta(r - r_e)) \times \exp(-\beta(r - r_e))]$$

$$[4]\quad V(r) = D_e\left[1 - \frac{r_e}{r}\exp(-\beta(r^2 - r_e^2))\right]^2$$

$$[5]\quad V(r) = D_e[(1 - \exp(-x)) \times (1 - ab\sqrt{x}\exp(-b\sqrt{xr/r_e}))]$$

$$b = 1.065$$

$$x = k_2 r_e(r - r_e)^2/2D_e r$$

For the Morse and Rydberg potentials the resulting expressions for dissociation energy have the simple form shown in [6] and [7].

$$[6]\quad D_e(\text{Morse}) = 9k_2^3/2k_3^2$$

$$[7]\quad D_e(\text{Rydberg}) = 4k_2^3/k_3^2$$

For the Varshni potential, the dissociation energy is given by [8*a*].

$$[8a]\quad D_e(\text{Varshni}) = 2C^3/(B^2 + 2BC - 3C^2 - (C + B)\sqrt{(C + B)^2 - 8C^2})$$

in which

$$[8b]\quad B = -k_3 r_e^3/6$$

$$[8c]\quad C = k_2 r_e^2/2$$

In the case of the Lippincott potential, the procedure of ref. 8 is adopted, *i.e.*,

$$[9a]\quad D_e(\text{Lippincott}) = (b^2/2)k_2 r_e^2(1 - 5a/4)$$

in which

$$[9b]\quad a = F/(1 + 5F/4)$$

$$[9c]\quad F = B/C - 1$$

(*i.e.* F is defined as in ref. 6)

Table 1 summarizes the results. The computed k_2 and k_3 were used in [6]–[9] to estimate the dissociation energy. The Varshni function was not suitable for H_2. The experimental D_e refer to the process $XY \rightarrow X + Y$ and $XH_n \rightarrow XH_{n-1} + H$. The calculated Hartree–Fock and SCF D_e were obtained from the difference between the energy of the molecule and the fragments computed either near the Hartree–Fock limit or at the same level as the force constant calculations. Since energies were in general not readily available for the dissociation fragments of the polyatomic hydride, D_e was estimated as $(1/n)(XH_n \rightarrow nH + X)$.

If the complete range of molecules is examined, it is evident that the estimated and calculated D_e's for F_2 are very much in error, and these will not be considered further. The dissociation energies of the remaining molecules seem to be represented best by the Varshni function, [8], but closer examination reveals that the reason for this is the lower error in the non-hydride molecules. If only the hydrides are considered, the Morse function is clearly superior and it is evident that D_e computed with the Morse potential, [6], are much better than either the Hartree–Fock D_e or the SCF D_e.

It has thus been found that the dissociation energies of hydride bonds can be computed satisfactorily with moderate size SCF wavefunctions. The method is superior to the direct computation of dissociation energies in terms of energy differences. Application of the procedure to the study of the dependence of bond dissociation energies on molecular conformations and the effects of substituents on bond dissociation energies is in progress.

We thank the National Research Council of Canada and the donors of the Petroleum Research Fund, administered by the American Chemical Society, for financial support of this research.

1. G. HERZBERG. Molecular spectra and molecular structure. Vol. 1. Spectra of diatomic molecules. Van Nostrand, Princeton. 1950. p. 101.
2. (*a*) R. RYDBERG. Z. Phys. **73**, 376 (1931); **80**, 514 (1933); (*b*) O. KLEIN. Z. Phys. **76**, 221 (1932); (*c*) A. L. G. REES. Proc. Phys. Soc. London. **59**, 998 (1947).
3. P. M. MORSE. Phys. Rev. **34**, 210 (1932).
4. H. B. SCHLEGEL, S. WOLFE, and F. BERNARDI. J. Chem. Phys. **63**, 3632 (1975).
5. P. PULAY. Mol. Phys. **17**, 197 (1969).
6. Y. P. VARSHNI. Rev. Mod. Phys. **29**, 664 (1957); **31**, 839 (1959).
7. D. STEELE, E. R. LIPPINCOTT, and J. T. VANDERSLICE. Rev. Mod. Phys. **34**, 239 (1962).
8. D. STEELE and E. R. LIPPINCOTT. J. Chem. Phys. **35**, 2065 (1961).
9. (*a*) G. H. AYLWARD and T. J. V. FINDLAY. SI chemical data. Wiley, Adelaide, Australia. 1971; (*b*) R. C. WEAST (*Editor*) Handbook of physics and chemistry. 55th ed. CRC Press, Cleveland. 1974.
10. W. G. RICHARDS, T. E. H. WALKER, and R. K. HINKLEY. A bibliography of *ab initio* molecular wave functions. Clarendon Press, Oxford. 1971.
11. S. ROTHENBERG, R. H. YOUNG, and H. F. SCHAEFER III. J. Am. Chem. Soc. **92**, 3243 (1970).

An ESCA Investigation of some Halogeno(methyl)-Silane and -Germane Series

JOHN E. DRAKE[1] AND CHRIS RIDDLE
Department of Chemistry, University of Windsor, Windsor, Ontario N9B 3P4
AND
L. COATSWORTH
Department of Chemistry, University of Western Ontario, London, Ontario N6A 3K7
Received May 9, 1975

JOHN E. DRAKE, CHRIS RIDDLE, and L. COATSWORTH. Can. J. Chem. **53**, 3602 (1975).

Core-level binding energies of all atoms are reported for two series of compounds; Me_nMCl_{4-n} and Me_3MX ($n = 0 \rightarrow 4$, M = Si or Ge, X = F, Cl, Br, I and (for M = Ge) CN, N_3, and NCS). Binding energy shifts are discussed using a 'whole-molecule' approach and are correlated with estimated atomic charges derived from an electronegativity-equalization procedure. Carbon 1*s* binding energies are also correlated to ^{13}C n.m.r. chemical shifts.

JOHN E. DRAKE, CHRIS RIDDLE et L. COATSWORTH. Can. J. Chem. **53**, 3602 (1975).

On rapporte les énergies de liaison au niveau du noyau de tous les atomes pour deux séries de composés; Me_nMCl_{4-n} et Me_3MX ($n = 0 \rightarrow 4$, M = Si ou Ge, X = F, Cl, Br, I et (pour M = Ge) CN, N_3 et NCS). On discute des déplacements d'énergie de liaison en utilisant l'approche de la molécule complète et l'on fait une corrélation de ces déplacements avec les charges atomiques calculées à partir d'une méthode d'égalisation des électronégativités. On fait aussi une corrélation entre les énergies de liaison du carbone 1*s* avec les déplacements chimiques en r.m.n. du ^{13}C.

[Traduit par le journal]

Introduction

Two groups of workers (1–6) have previously presented ESCA data of silicon and germanium derivatives. Van Wazer and co-workers (1, 2) have reported core-level binding energies for a number of solid compounds, chosen to cover the expected range of binding energy shifts. These shifts were compared in analogous carbon, silicon, germanium, tin, and lead series. The observed decreases in chemical shift with increasing atomic size were similar to those predicted theoretically. Perry and Jolly (3–6) have examined gaseous samples, thus eliminating effects due to charging and uncertainties in Madelung potential. Binding energies have been related to various calculated atomic charges (6, 7) using the potential model equation of Siegbahn *et al.* (8). These calculations have met with considerable success although the correlations were least successful with the tetramethyl derivatives. Similar problems have been noted for organo-tin derivatives (9).

Our approach is to take closely related series of compounds and to observe the change in binding energies of *all* the atoms throughout the series. This initial study is designed to provide a basis for individual comparisons and an indication of which trends might be most general.

Experimental

Core-electron binding energies were determined on a McPherson ESCA-36 photoelectron spectrometer using magnesium Kα X-radiation (1253.6 eV) for photoelectron excitation. Samples were introduced in the vapor phase at pressures close to 5×10^{-5} Torr. Argon gas was bled in to form 20% of the total sample. All binding energies were referenced to the argon $2p_{3/2}$ level at 248.63 eV (10). (Those of the germanium 3*d* and silicon 2*p* levels are reported relative to the neon 2*s* level at 48.47 (10).) In a selected number of runs, the effect of varying the sample-pressure was found to be minimal as was running the samples in the absence of argon gas. Nonetheless, all of the values were obtained under similar conditions. The determinations were at least duplicated; for some compounds binding energies were determined on different samples at dates ranging over a six-month period. Reproducibility of the observed binding energies was generally excellent. Thus, the carbon 1*s* level of Me_3GeF was computed as 290.16, 290.17, 290.17, 290.21, and 290.25 eV. The separation of the neon 1*s* and argon $2p_{3/2}$ levels was determined to be 621.64 eV. This compares with a published separation of 621.76 eV (10). Typically, each spectrum was scanned five times over a 10 eV range using a 111 point array and a dwell time of one second per point. The scans were accumulated. The observed spectral lines were curve-fitted using a

[1]To whom all correspondence should be addressed.

Can. J. Chem. Downloaded from www.nrcresearchpress.com by 210.87.254.5 on 09/05/12
For personal use only.

TABLE 1. Core-electron binding energies for the chloro(methyl)-silanes, -germanes, and -stannanes

	Binding energy* (eV)								
	C 1*s*		Cl $2p_{3/2}$				M = Sn†		
Compound	Si	Ge	Si	Ge	Si 2*p*	Ge 3*d*	C 1*s*	Cl $2p_{3/2}$	Sn $3d_{5/2}$
Me_4M	289.78 (289.79)‡	289.82 (289.77)	—	—	106.02 (105.99)‡	36.11 (35.81)			
Me_3SiCH_2Cl	289.88(Me) 290.83(CH_2)	—	205.79	—	106.31	—			
Me_3MCl	289.98	290.19	205.30	205.00	106.95	37.17			
Me_2MCl_2	290.40	290.75	205.93	205.63	108.09	38.23	290.60		493.39
$MeMCl_3$	290.79	291.14	206.44	206.11	109.16	39.11	291.16	205.70	494.24
MCl_4	—	—	206.90 (206.94)	206.70 (206.59)	110.17 (110.42)	40.07 (39.78)	—	206.37	495.10

*Values corrected relative to Ar $2p_{3/2}$ = 248.63 eV (10), uncertainty ±0.05 eV, except that Si 2*p* and Ge 3*d* are reported relative to Ne 2*s* at 48.47 eV (10).
†All values for the chloro(methyl)stannanes are those of Jolly, private communication.
‡Values in parentheses are those previously reported by Perry and Jolly (6).

TABLE 2. Core-electron binding energies for the monohalogenotrimethyl-silanes and -germanes and some pseudohalogenogermane derivatives

	Binding energy* (eV)					
	C 1*s*†				X‡	
Compound Me_3MX	Si	Ge	Si 2*p*	Ge 3*d*	Si	Ge
Me_3MF	290.09	290.18	107.15	37.22	691.84	690.54
Me_3MCl	289.98	290.19	106.95	37.17	205.30	205.00
Me_3MBr	290.07	290.24	106.97	37.07	75.33	75.13
Me_3MI	289.95	290.20	106.77	36.93	625.90	625.58
$(Me_3Si)_2O$	289.76	—	106.50	—	537.00	—
Me_3GeCN	—	290.47§	—	37.16	—	290.47(C)§ 404.79(N)
Me_3GeNCS	—	290.37	—	37.27	—	292.58(C) 404.35(N) 168.70(S)
Me_3GeN_3	—	290.25	—	37.00	—	407.55[N(1)] 403.44[N(2)]

*Values corrected relative to Ar $2p_{3/2}$ = 248.63 eV (10) uncertainty ±0.05 eV, except that Si 2*p* and Ge 3*d* are reported relative to Ne 2*s* at 48.47 eV (10).
†Methyl group values, —CN and —NCS group C 1*s* values appear under column X.
‡X corresponds to F 1*s*, Cl $2p_{3/2}$, Br $3d_{5/2}$, I $3d_{5/2}$, N 1*s*, S $2p_{3/2}$, and O 1*s*.
§Only one peak f.w.h.m. 1.55 eV, *ca.* 0.3 eV greater than average. Thus, the one envelope contains two unresolved peaks, each of whose positions is known only to *ca.* ±0.15 eV.

computer program (ESCAPLOT) written by one of us (L. Coatsworth) and modified to run on the Windsor IBM S/360-50 series computer. (The program obtains a weighted least-squares fit to the data by means of stepwise Gauss–Newton iterations on the parameters. Within each iteration parameters are selected for modification in a stepwise manner. The parameter selected at a given step is the one which, differentially at least, makes the greatest reduction in the error sum of squares. If it is necessary to avoid matrix singularity problems, only a subset of the parameters may be modified in a given iteration. In addition, parameters with boundary values whose modification in a given iteration would lead to boundary violations are not modified.) Mixed Gauss–Lorentz band contours were fitted on a quadratic baseline. The reproducibility of data from separate runs was such that binding energies are quoted to ±0.05 eV (Tables 1 and 2). Data, which have been reported (3, 4, 6) for Me_4M and MCl_4 (M = Si, Ge), are included in Table 1 in parentheses and referred to argon at 248.63 eV. Values for C 1*s* and Cl $2p_{3/2}$ levels agreed to within the quoted error limits. For silicon 2*p* and germanium 3*d*, our values were *ca.* 0.1 eV higher on average than those of Jolly *et al.* and the separation of binding energies $MCl_4 \rightarrow MMe_4$ were in close agreement. The experimental binding energies of the Me_3MX series are given in Table 2.

The calculations of peak positions were performed

Can. J. Chem. Downloaded from www.nrcresearchpress.com by 210.87.254.5 on 09/05/12
For personal use only.

Can. J. Chem. Downloaded from www.nrcresearchpress.com by 210.87.254.5 on 09/05/12
For personal use only.

without the introduction of constraints. Gauss fractions between 0.3 and 0.6 were normal; values outside this range generally reflected poor quality spectra and an inability to obtain a good computer fit. The argon $2p_{3/2}$ level was consistently observed at 248.2 ± 0.2 eV with a full-width at half-maximum (f.w.h.m.) of 0.96 eV (average of 33 determinations). Average f.w.h.m. values for the simple singlet peaks of C 1*s*, F 1*s*, and N 1*s* were 1.24 eV (41 determinations), 1.25 eV (4 determinations), and 1.09 eV (4 determinations), respectively. For peaks where there was a good separation of levels, I $3d_{5/2}$ and Cl $2p_{3/2}$ f.w.h.m. values were 1.26 eV (4 determinations) and 1.18 eV (15 determinations), respectively. The separation between Cl $2p_{3/2}$ and $2p_{1/2}$ levels was 1.62 ± 0.03 eV and their areas averaged to 1:0.50 (±0.1) (14 determinations). Similarly for argon the $2p_{3/2}$ to $2p_{1/2}$ ratio was determined as 1:0.48 (±0.1). The Br $3d_{5/2}$ level was separated only 1.08 eV on average from the $3d_{3/2}$ level. With an average f.w.h.m. value of 1.30 eV (7 determinations) it was not always possible to get good peak deconvolution and values are only quoted to ±0.10 eV. Sulfur similarly was not always well resolved. Peak separation was 1.17 eV and f.w.h.m. values averaged to 1.15 eV (2 determinations).

^{13}C n.m.r. spectra were recorded on a Varian XL-100 spectrometer locked on the ^{2}H resonance of the $CDCl_3$ solvent and using TMS as internal reference. Chemical shifts are reported in p.p.m. (downfield (+)) from TMS (Table 3).

Materials

Tetramethylsilane, trimethylchlorosilane, dimethyldichlorosilane, methyltrichlorosilane, tetrachlorosilane, tetramethylgermane, dimethyldichlorogermane, methyltrichlorogermane, tetrachlorogermane, and trimethylbromogermane were obtained commercially (Ventron Corporation, Alfa Products) as was Me_3SiCH_2Cl (Laramie Chem. Co.). Samples of trimethylfluorosilane, hexamethyldisiloxane, trimethylfluorogermane, trimethylcyanogermane, trimethylazidogermane, and trimethylisothiocyanatogermane were generously donated by Dr. R. T. Hemmings. Trimethylchlorogermane was prepared by treating dimethyldichlorogermane with methyllithium (11). Reaction of trimethylsilane with bromine or iodine yielded trimethylbromosilane and trimethyliodosilane (based on details given in ref. 12). Trimethyliodogermane was synthesized in the exchange reaction of hydrogen iodide and trimethylbromogermane (based on details given in ref. 13).

All samples were distilled on the vacuum line and their purity checked by infrared and n.m.r. spectroscopy and, where appropriate, by vapor pressure determination.

TABLE 3. ^{13}C n.m.r. chemical shift *vs.* C 1*s* binding energy (b.e.)

Compound	b.e.(C 1*s*) (eV)	$\delta_{^{13}C}$ (p.p.m.)
Me_4Ge	289.89	−0.660
Me_3GeBr	290.29	5.683
$\underline{Me}_3GeCN$	290.4	−1.200
$Me_3Ge\underline{C}N$	290.4	126.05
Me_2GeCl_2	290.79	10.771
$MeGeCl_3$	291.11	15.922

Charge Calculations

The mode of calculation was basically that described in detail elsewhere (14). This gives partial charges based on the Hinze–Jaffé concept of orbital electronegativity (15–17). The calculations use the value of the valence shell ionization potentials, *I*, and electron affinities, *A* (15, 17). The relationship of the orbital electronegativity of the element, χ_M, to the charge, δ_M, on the element M is given by (14)

$$\chi_M = a + b\delta_M$$

where

$$a = (I + A)/2$$

and

$$b = I - A$$

The previously reported values of *a* and *b* (14, 15, 17) are listed in the footnote of Table 4.

Charge transfer was estimated by setting the electronegativity function of one atom equal to that of the other and solving the appropriate equations. The charge calculations for the two series, Me_nGeCl_{4-n} and Me_3GeX, where $n = 0 \rightarrow 4$ and X = F, Cl, Br, I, are shown in Table 4*a*, where the methyl group was treated as a moiety (*i.e.* $\chi_C = 7.37 + 3.29\delta_C$) and the halogen atoms were assumed to utilize only *p*-orbitals. Charge calculations were also carried out (Table 4*b*) with the carbon atom treated as an 'unbonded tetrahedral carbon atom' (*i.e.* $\chi_C = 7.98 + 13.27\delta_C$). (The correlations of these charge calculations with the experimental binding energies are displayed in Figs. 3 and 4*a*.)

Further calculations were carried out to allow for the incorporation of *s*-orbital participation on the part of the halogen atoms. For this purpose plots were made of $(I + A)$ for the change from 100% *s*- to 100% *p*-character for each halogen (15) (see Fig. 1 for an example using chlorine) and a linear correlation assumed for the corresponding changes in *I*. From these plots, $(I + A)$ and *I* values can be read for any % *s*-character and the *a* and *b* values calculated. The appropriate $(I + A)$ and *I* values, transcribed from Jaffe's papers (15, 17) are listed as a footnote in Table 5 while the *a* and *b* values for various degrees of *s*-character are listed in Table 5. The calculated charges appear in Tables 6 and 7.

Sample Calculations

(i) $GeCl_4$

$\chi_{Ge} = 8.07 + 6.82\delta_{Ge}$ for tetrahedral Ge

$\chi_{Cl} = 9.38 + 11.30\delta_{Cl}$ for the *p*-orbitals of Cl

In the molecule

$$\chi_{Ge} = \chi_{Cl}$$

[1] $\therefore\ 8.07 + 6.82\delta_{Ge} = 9.38 + 11.30\delta_{Cl}$

and

[2] $$\delta_{Ge} + 4\delta_{Cl} = 0$$

Solving [1] and [2] we obtain

$$\delta_{Ge} = +0.136$$

$$\delta_{Cl} = -0.034$$

TABLE 4. Calculated partial charges, δ*

	(a)			(b)		
Compound	δ_{Ge}	δ_C	δ_X	δ_{Ge}	δ_C	δ_X
Me_4Ge	−0.092	+0.023	—	−0.009	+0.002	—
Me_3GeCl	−0.067	+0.074	−0.156	+0.030	+0.023	−0.098
Me_2GeCl_2	−0.030	+0.150	−0.134	+0.067	+0.042	−0.075
$MeGeCl_3$	+0.028	+0.270	−0.099	+0.103	+0.059	−0.054
$GeCl_4$	+0.136	—	−0.034	+0.136	—	−0.034
Me_3GeF	−0.053	+0.103	−0.258	+0.074	+0.044	−0.205
Me_3GeBr	−0.076	+0.055	−0.090	+0.005	+0.009	−0.032
Me_3GeI	−0.085	+0.037	−0.027	−0.005	+0.002	−0.001
GeF_4	+0.368	—	−0.092	+0.368	—	−0.092
$GeBr_4$	+0.036	—	−0.009	+0.036	—	−0.009

*Charges calculated assuming that germanium is using sp^3 hybrid orbitals, $\chi_{Ge} = 8.07 + 6.82\delta_{Ge}$; that the halogens are using only *p*-orbitals, $\chi_F = 12.18 + 17.36\delta_F$; $\chi_{Cl} = 9.38 + 11.30\delta_{Cl}$; $\chi_{Br} = 8.40 + 9.40\delta_{Br}$; $\chi_I = 8.10 + 9.15\delta_I$; and that the carbon atom is treated as (*a*) a methyl group moiety using $\chi_C = 7.37 + 3.99\delta_C$ as suggested by Huheey (14), or (*b*) as an 'unbonded tetrahedral carbon atom' using $\chi_C = 7.98 + 13.27\delta_C$.

(ii) $MeGeCl_3$

Assuming 10% *s*-character in Cl orbital; *i.e.* EESOP, for Cl:

From Fig. 1

$$I + A = 20.6$$

$$I = 16.0$$

$$A = 4.6$$

$$\therefore\ a = 10.3$$

$$b = 11.4$$

$$10.3 + 11.4\delta_{Cl} = 8.07 + 6.82\delta_{Ge}$$

$$[3] \qquad \delta_{Cl} = -0.196 + 0.598\delta_{Ge}$$

Also

$$7.98 + 13.27\delta_C = 8.07 + 6.82\delta_{Ge}$$

$$[4] \qquad \delta_C = 0.007 + 0.514\delta_{Ge}$$

Since

$$\delta_C + \delta_{Ge} + 3\delta_{Cl} = 0$$

$$0.007 + 0.514\delta_{Ge} + \delta_{Ge} - 0.588 + 1.794\delta_{Ge} = 0$$

$$3.308\delta_{Ge} = 0.581$$

$$\therefore\ \delta_{Ge} = +0.176$$

From [3]

$$\delta_{Cl} = -0.196 + (0.598 \times 0.176) = -0.091$$

From [4]

$$\delta_C = 0.007 + (0.514 \times 0.176) = +0.097$$

Results and Discussion

The experimentally-determined computer-fitted binding energies for two series of silicon and germanium compounds, a 'methyl–halogen' replacement series, Me_nMCl_{4-n}, and a 'halogen–halogen' replacement series, Me_3MX, are presented in Tables 1 and 2. The trends in the core-level binding energies of the former series are illustrated in Fig. 2. Clearly, there is a step-wise *increase* in *all* of the binding energies as chlorine atoms successively 'replace' methyl groups in the series Me_4M through to MCl_4 (M = Si, Ge), which may be rationalized by consideration of the inductive effect. As the more electron-

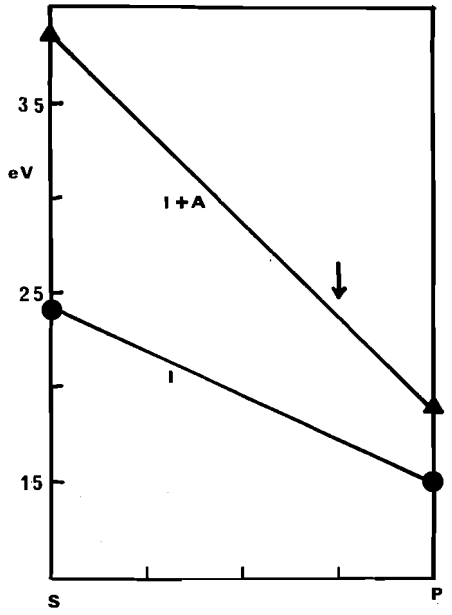

FIG. 1. $(I + A)$ values of chlorine as a function of *s*-orbital participation.

Can. J. Chem. Downloaded from www.nrcresearchpress.com by 210.87.254.5 on 09/05/12
For personal use only.

TABLE 5. Values of a and b for varying degrees of s-orbital participation*

Element	% s-character	a	b
F	0 (pure p)	12.18	17.36
	5	13.0	17.4
	10	13.93	17.15
	15	15.0	16.4
	20	15.95	16.1
	25	16.9	16.2
Cl	0	9.38	11.3
	5	9.75	11.5
	10	10.3	11.4
	15	10.78	11.45
	20	11.25	11.4
	25	11.75	11.3
Br	0	8.4	9.4
	5	8.8	9.4
	10	9.33	9.35
	15	9.85	9.2
	20	10.38	9.15
	25	10.83	9.15
I	0	8.1	9.15
	5	8.4	9.2
	10	8.8	9.0
	15	9.2	8.6
	20	9.55	8.4
	25	9.98	8.05

*Calculated using the following values of I and $(I + A)$: fluorine, $I = 20.86(p)$, $38.24(s)$; $(I + A) = 24.36(p)$, $62.61(s)$; chlorine, $I = 15.03(p)$, $24.02(s)$; $(I + A) = 18.76(p)$, $38.47(s)$; bromine, $I = 13.10(p)$, $22.07(s)$; $(I + A) = 16.80(p)$, $36.57(s)$; iodine, $I = 12.67(p)$, $18.00(s)$; $(I + A) = 16.19(p)$, $31.38(s)$; see refs. 15, 17.

withdrawing chlorine atoms are introduced so one might expect the electron density to be redistributed from the carbon atoms toward the chlorine atoms.

The observed increase in C 1s binding energies (as $n = 4 \rightarrow 1$ in the series Me_nMCl_{4-n}) is thus as expected as the carbon atoms become increasingly $\delta+$. The slope of the two lines (M = Si and M = Ge) are similar, though slightly steeper for the germanium series, suggesting that the transmission of charge is marginally more favorable with germanium than with silicon. The increases in the binding energies (silicon 2p or germanium 3d) of the central atom (as $n = 4 \rightarrow 0$ in the series Me_nMCl_{4-n}) are also as expected for the increases in the $\delta+$ character of Si and Ge. The slopes of the two series are similar and indeed the differences in the binding energies, (Δb.e.) from Me_4M to MCl_4 are not large, being 4.15 eV for M = Si and 3.96 eV for M = Ge. (By extrapolation, the change in the corresponding tin series is *ca.* 3.4 eV.) The ionic radii of silicon and germanium are close enough that a similar change in binding energy is to be expected for similar charge changes. Thus, a similar bonding model is suggested for both series.

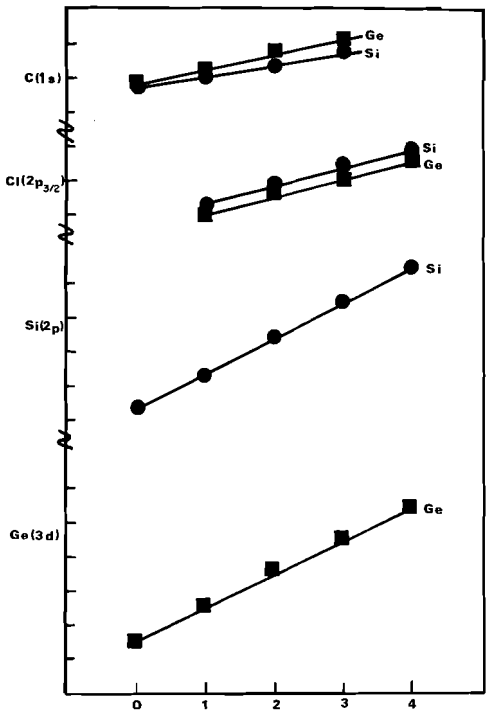

FIG. 2. Core-binding energies (eV) as a function of the number of chlorine atoms in the series Me_nMCl_{4-n} (M = Ge, Si). Ge series, ■; Si series, ●.

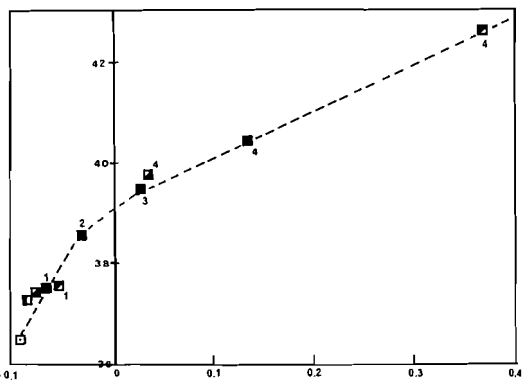

FIG. 3. Ge 3d core-level binding energies (eV) as a function of the calculated charge on germanium, δ_{Ge}. (Assuming CH_3 acts as the methyl group moiety and that the halogen atoms are using 'pure p-orbitals'.) ■: $GeCl_4$, (*4*); $MeGeCl_3$, (*3*); Me_2GeCl_2, (*2*); Me_3GeCl, (*1*). ⊡, Me_4Ge. ◩: GeF_4, (*4*); Me_3GeF, (*1*). ◪: $GeBr_4$, (*4*); Me_3GeBr, (*1*). ◧, Me_3GeI.

Can. J. Chem. Downloaded from www.nrcresearchpress.com by 210.87.254.5 on 09/05/12
For personal use only.

Can. J. Chem. Downloaded from www.nrcresearchpress.com by 210.87.254.5 on 09/05/12
For personal use only.

TABLE 6. Calculated charges of the germane series with changing *s*-orbital participation by the halogen

Compound	5% *s*			10% *s*			15% *s*			20% *s*			25% *s*		
	δ_{Ge}	δ_X	δ_C	δ_{Ge}	δ_X	δ_C	δ_{Ge}	δ_X	δ_C	δ_{Ge}	δ_X	δ_C	δ_{Ge}	δ_X	δ_C
Me_3GeCl	+0.040	−0.122	+0.028	+0.055	−0.163	+0.035	+0.069	−0.196	+0.042	+0.082	−0.230	+0.049	+0.097	−0.267	+0.057
Me_2GeCl_2	+0.086	−0.095	+0.051	+0.117	−0.126	+0.067	+0.143	−0.152	+0.081	+0.169	−0.178	+0.094	+0.197	−0.207	+0.109
$MeGeCl_3$	+0.131	−0.068	+0.074	+0.176	−0.091	+0.097	+0.213	−0.110	+0.116	+0.251	−0.129	+0.136	+0.290	−0.151	+0.163
$GeCl_4$	+0.173	−0.043	—	+0.231	−0.058	—	+0.280	−0.070	—	+0.329	−0.082	—	+0.382	−0.095	—
Me_3GeF	+0.089	−0.248	+0.053	+0.109	−0.299	+0.063	+0.136	−0.366	+0.077	+0.158	−0.422	+0.088	+0.177	−0.470	+0.098
Me_3GeBr	+0.017	−0.065	+0.016	+0.035	−0.110	+0.025	+0.053	−0.154	+0.033	+0.067	−0.192	+0.041	+0.085	−0.238	+0.051
Me_3GeI	+0.005	−0.033	+0.009	+0.018	−0.067	+0.016	+0.033	−0.105	+0.024	+0.046	−0.139	+0.031	+0.064	−0.183	+0.040
GeF_4	+0.441	−0.110	—	+0.527	−0.132	—	+0.635	−0.160	—	+0.725	−0.180	—	+0.812	−0.203	—
$GeBr_4$	+0.076	−0.019	—	+0.134	−0.034	—	+0.195	−0.049	—	+0.244	−0.061	—	+0.303	−0.076	—

TABLE 7. Calculated charges of the silane series with changing *s*-orbital participation by the halogen

Compound*	0% *s* (pure *p*)			5% *s*			10% *s*			15% *s*			20% *s*		
	δ_{Si}	δ_X	δ_C	δ_{Si}	δ_X	δ_C	δ_{Si}	δ_X	δ_C	δ_{Si}	δ_X	δ_C	δ_{Si}	δ_X	δ_C
Me_3SiCl	+0.088	−0.114	+0.009	+0.096	−0.139	+0.014	+0.109	−0.177	+0.023	+0.119	−0.210	+0.030	+0.130	−0.243	+0.038
Me_2SiCl_2	+0.119	−0.089	+0.030	+0.134	−0.108	+0.040	+0.159	−0.137	+0.057	+0.180	−0.162	+0.072	+0.201	−0.187	+0.086
$MeSiCl_3$	+0.148	−0.066	+0.049	+0.171	−0.079	+0.065	+0.207	−0.099	+0.090	+0.238	−0.116	+0.111	+0.268	−0.133	+0.132
$SiCl_4$	+0.175	−0.044	—	+0.206	−0.051	—	+0.253	−0.063	—	+0.292	−0.073	—	+0.332	−0.083	—
Me_3SiF	+0.122	−0.218	+0.032	+0.135	−0.258	+0.041	+0.151	−0.307	+0.052	+0.173	−0.374	+0.067	+0.191	−0.430	+0.079
Me_3SiBr	+0.067	−0.052	−0.005	+0.078	−0.085	+0.002	+0.092	−0.128	+0.012	+0.107	−0.172	+0.022	+0.122	−0.217	+0.032
Me_3SiI	+0.060	−0.028	−0.010	+0.068	−0.053	−0.005	+0.079	−0.088	+0.003	+0.091	−0.125	+0.011	+0.102	−0.158	+0.018
SiF_4	+0.365	−0.091	—	+0.426	−0.106	—	+0.498	−0.125	—	+0.587	−0.147	—	+0.662	−0.166	—
$SiBr_4$	+0.097	−0.024	—	+0.132	−0.033	—	+0.178	−0.045	—	+0.225	−0.056	—	+0.272	−0.068	—

*Me_4Si: $\delta_{Si} = +0.055$; $\delta_C = -0.014$.

Can. J. Chem. Downloaded from www.nrcresearchpress.com by 210.87.254.5 on 09/05/12
For personal use only.

The slopes of the two chlorine $2p_{3/2}$ plots are similar for both series. The increase in the Cl $2p_{3/2}$ binding energies (as $n = 3 \rightarrow 0$ Me_nMCl_{4-n}) suggests that the chlorine atoms are becoming *less* $\delta-$ as the redistributed charge comes from fewer methyl groups and there is increasing 'competition' from other chlorine atoms. The values of the chlorine $2p_{3/2}$ binding energies are consistently lower for the germanium series (Cl more $\delta-$ for the germanium analogs). This suggests that the inductive effect is greater for individual germanium compounds than for the silicon analogs and is in agreement with known dipole-moments (*e.g.* Me_3SiCl 2.1 D, Me_3GeCl 2.8 D; remembering that the Si—Cl and Ge—Cl bond lengths in these compounds (2.03 and 2.17 Å, respectively) are similar).

In the case of Me_3SiCH_2Cl, we find the methyl C 1*s* binding energy and the silicon 2*p* binding energy intermediate between those of Me_4Si and Me_3SiCl. The methylene carbon adjacent to chlorine is shifted 1 eV to higher binding energy than the methyl carbons. However, the chlorine $2p_{3/2}$ level is not as negative as that for Me_3SiCl but nearer to that for Me_2SiCl_2. If the chlorine in Me_3SiCl were involved in π-bonding we might have expected it to have an unduly high binding energy; clearly this is not so.

In the 'halogen–halogen' replacement series, Me_3MX (Table 2), the central atom binding energies increase only slightly across the series $F \rightarrow I$, (0.38 eV for M = Si and 0.29 eV for M = Ge). The 1*s* binding energies of the methyl carbon atoms are equal within experimental error for all the silanes. The same is true for the germanium compounds where the C 1*s* binding energies are *ca.* 0.2 eV above those for the silanes. Thus, different halogens have similar effects on binding energies although their Pauling electronegativities vary considerably. We will return to this point later.

Charge Calculations

To complement the preceding qualitative analysis of the data we determined the relationship of the binding energies to calculated charges on the individual atoms. The correlations should be linear (1–7) since aberrations due to relaxation effects should not significantly alter the general linearity. However, such correlations have not been as successful with organoderivatives as they have with the binary halides (9) or the hydrogen halides (6) of group IV. Because the *absolute* value of the calculated charge is less significant than the *relative* values based on a particular model and because it seems desirable to avoid the introduction of many arbitrary constants (7) we base our calculations of charge on those of Huheey (14) which in turn were based on the Hinze–Jaffe method (15–17).

Initially, the charges (for the methylchlorogermane series) on Ge, C, and Cl were calculated on the assumption that germanium used sp^3 hybrids and chlorine used pure *p*-orbitals in bonding while C is part of a methyl group moiety (14). The resulting plots of binding energy (b.e.) *vs.* charge lead to nonlinear plots in *all* cases (for example, Fig. 3, b.e.(Ge 3*d*) *vs.* δ_{Ge}). These plots suggest that the calculations are over-emphasizing the electron-releasing nature of the methyl group. This apparently results because no distinction can be made in the simple equalization procedure between a hydrogen atom attached to carbon or directly to germanium. Nevertheless, the plots do show the general trends previously noted, namely, that the charges on *all* of the atoms become more positive (or less negative) as an increasing number of chlorine atoms replace methyl groups, and that the binding energies of all the trimethylhalogermanes are similar.

An alternative to overemphasizing the influence of the hydrogen atoms on the partial charges of nonadjacent groups is to ignore their presence. This is reasonable as chemical shift effects are not long range. Thus, charges were calculated treating the carbon atom as an 'unbonded tetrahedral carbon'. A remarkably linear plot of b.e.(Ge 3*d*) *vs.* δ_{Ge} for the methylchlorogermane series (Fig. 4, *A*) is now obtained. However, $GeBr_4$ and GeF_4 fall well off the line and plots of b.e.(Cl $2p_{3/2}$) *vs.* δ_{Cl} for the germanium series, while linear, do not coincide with those of the silicon series, nor do the b.e.(C 1*s*) *vs.* δ_C plots for the two series. Further, the calculated charges on germanium are very much lower than those obtained by Perry and Jolly by their CHELEQ method (6). A similarity might be expected since their calculations are based on the concept of charge equalization and the orbital electronegativity values of Jaffe *et al.* (14, 16). One 'mechanism' for allowing a greater charge-transfer to halides is to assume a degree of hybridization or *s*-

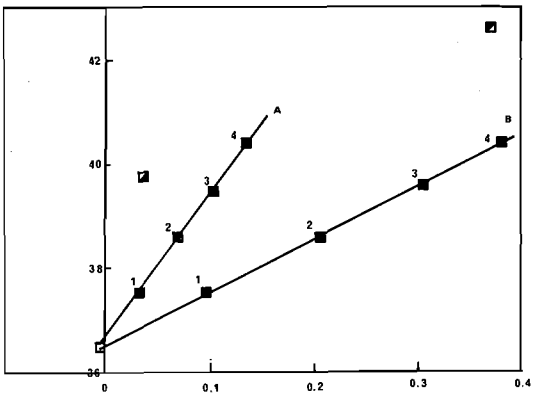

FIG. 4. Ge 3*d* core-level binding energies (eV) as a function of the calculated charge on germanium, δ_{Ge}. (Assuming an 'unbonded tetrahedral carbon' atom and that the halogen atoms are using (*A*) 'pure *p*-orbitals' and (*B*) 25% *s*-orbitals.) ■: $GeCl_4$, (*4*); $MeGeCl_3$, (*3*); Me_2GeCl_2, (*2*); Me_3GeCl, (*1*). ⊡, Me_4Ge. ◩, GeF_4 (using pure *p*). ◪, $GeBr_4$ (using pure *p*).

orbital participation. Siegbahn *et al.* suggest such an approximation in treating the data for fluoro- and bromo-methanes (ref. 8, p. 110). In Fig. 4, *B*, it can be seen that by assuming *ca.* 25% *s*-orbital participation (essentially half that possible on symmetry grounds) a linear plot is still maintained but the absolute values of the charges are significantly increased. Obviously, for all of the halides, the calculated charge can be altered merely by altering the allowance for *s*-orbital participation. It is not possible to know (*a*) how much *s*-orbital participation, if any, is most reasonable, and (*b*) how much such participation is likely to vary through the halide series. To obtain coincident plots along the series Me_4Ge, $GeBr_4$, $GeCl_4$, and GeF_4, a decreasing amount of *s*-orbital participation is required from Br through to F. Thus, it is possible to get relative values on this model, by 'fixing' fluorine as using 'pure-*p*' orbitals (not unreasonable in view of the large difference in the energy of its 2*s* and 2*p*-orbitals). The *s*-character for chlorine and bromine was then altered until a linear plot was obtained. Figure 5 displays a good correlation with 10% *s*-character on the chlorine atom. With 15% and 20% *s*-character for bromine and iodine, respectively, Me_3GeI, Me_3GeBr, and $GeBr_4$ fit the same linear plot. (We describe these calculations which assume *e*lectronegativity *e*qualization involving *s*-*o*rbital *p*articipation as EESOP calculations.)

Using these EESOP values, a plot of b.e.(C 1*s*) *vs.* δ_C is also remarkably linear and when the concept is extended to the silicon series a single linear plot can be obtained for b.e.(C 1*s*) *vs.* δ_C (Fig. 6) provided it is assumed that the *s*-character involved in the silicon series is slightly reduced (5% for Cl, 10% for Br, and 15% for I). Further, if a plot is made of b.e.(Cl $2p_{3/2}$) *vs.*

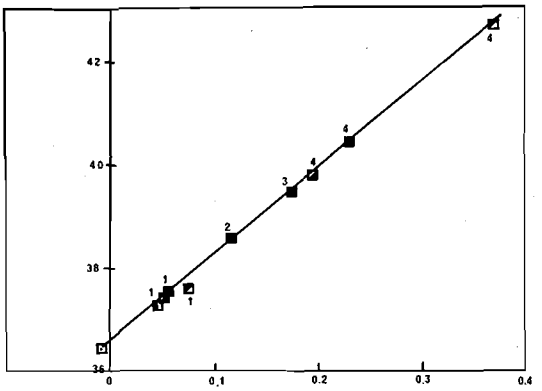

FIG. 5. Ge 3*d* core-level binding energies (eV) as a function of the calculated charge on germanium, δ_{Ge}. (Assuming an 'unbonded tetrahedral carbon' atom and that the halogen atoms are using varying degrees of *s*-orbital participation (F = 0%; Cl = 10%; Br = 15%; I = 20%).) ■: $GeCl_4$, (*4*); $MeGeCl_3$, (*3*); Me_2GeCl_2, (*2*); Me_3GeCl, (*1*). ⊡, Me_4Ge. ◩: GeF_4, (*4*); Me_3GeF, (*1*). ◪: $GeBr_4$, (*4*); Me_3GeBr, (*1*). ◧, Me_3GeI.

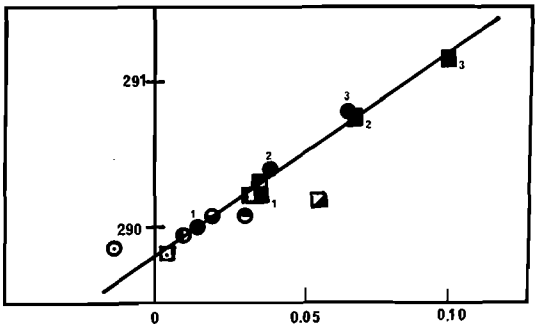

FIG. 6. C 1*s* core-level binding energies (eV) for the germanium and silicon series as a function of the calculated charge on carbon, δ_C. (Assuming an 'unbonded tetrahedral carbon' atom and that the halogen atoms are using varying degrees of *s*-orbital participation (for the germanium series, F = 0%, Cl = 10%, Br = 15%, I = 20%; for the silicon series, F = 0%, Cl = 5%, Br = 10%, I = 15%).) ■: $MeGeCl_3$, (*3*); Me_2GeCl_2, (*2*); Me_3GeCl, (*1*). ⊡, Me_4Ge. ◪, Me_3GeF. ◩, Me_3GeBr. ◧, Me_3GeI. ●: $MeSiCl_3$, (*3*); Me_2SiCl_2, (*2*); Me_3SiCl, (*1*). ⊙, Me_4Si. ◓, Me_3SiF. ◒, Me_3SiBr. ◐, Me_3SiI.

Can. J. Chem. Downloaded from www.nrcresearchpress.com by 210.87.254.5 on 09/05/12
For personal use only.

Can. J. Chem. Downloaded from www.nrcresearchpress.com by 210.87.254.5 on 09/05/12
For personal use only.

δ_{Cl} using the values for both the germanium and silicon series, another linear correlation is obtained (Fig. 7). Finally, the plot of b.e.(Si $2p$) *vs.* δ_{Si} for the various halides is linear (Fig. 8).

In summation, the features noted in the opening of the discussion can be rationalized by allowing for varying degrees of *s*-orbital participation by the halogen atoms (other than fluorine). In view of the assumptions, no claims are made of the importance of the absolute values. However, on this model the degree of *s*-orbital participation is, not unreasonably, Cl < Br < I and is marginally less for the silanes than the germanes. We can reproduce Perry and Jolly's charge calculations for the series GeF_4, $GeCl_4$, and $GeBr_4$, in which *d*-orbital participation was assumed (6) by allowing the *s*-orbital participation for fluorine to be *ca.* 12%, for chlorine *ca.* 17.5%, and for bromine *ca.* 20%. Our value of δ_{Ge} for Me_4Ge, based on the 'non-bonded tetrahedral atom' is essentially the same as that displayed in their correlation (6).

The EESOP approximation gives similar values to the 'electronegativities' of all of the halogens. Thus, the similarity in the influence of the various halogens in the series Me_3MX (X = F, Cl, Br, I) is consistent with this model. It is clear, however, that Me_3GeF and Me_3SiF do not 'fit' on the C 1*s*, the Ge 3*d*, or the Si $2p$ plots. Even with no *s*-character it is clear that the calculated charges on Ge, Si, and C need to be less positive. Obviously, one mechanism for reducing the positive charge would be (p–d) π back-donation from F to Ge or Si.

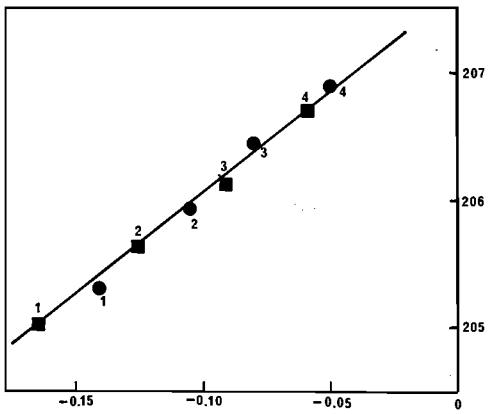

FIG. 7. Cl $2p_{3/2}$ core-level binding energies (eV) as a function of the calculated charge on chlorine δ_{Cl}. (Assuming an 'unbonded tetrahedral carbon' atom and that the chlorine atoms are using 5% *s*-character for the silicon series and 10% *s*-character for the germanium series.) ■: $GeCl_4$, (*4*); $MeGeCl_3$, (*3*); Me_2GeCl_2, (*2*); Me_3GeCl, (*1*). ●: $SiCl_4$, (*4*); $MeSiCl_3$, (*3*); Me_2SiCl_2, (*2*); Me_3SiCl, (*1*).

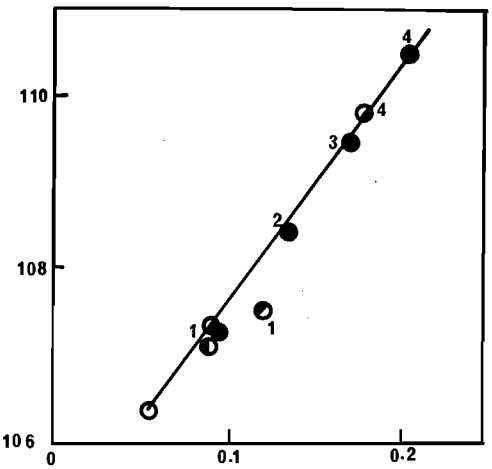

FIG. 8. Si $2p_{3/2}$ core-level binding energies (eV) as a function of calculated charge, δ_{Si}. (Assuming an 'unbonded tetrahedral carbon' atom and that the halogen atoms are using varying degrees of *s*-orbital participation (F = 0%, Cl = 5%, Br = 10%, I = 15%.) ●: $SiCl_4$, (*4*); $MeSiCl_3$, (*3*); Me_2SiCl_2, (*2*); Me_3SiCl, (*1*). ⊙, Me_4Si. ◐, Me_3SiF. ◑: $SiBr_4$, (*4*); Me_3SiBr, (*1*). ◐, Me_3SiI.

Data was collected on selected pseudohalides that contain a bond from germanium to a first row element. The binding energy of the methyl (C 1*s*) in Me_3GeN_3 is similar to the values for the halogens but in Me_3GeNCS and Me_3GeCN it increases. The germanium binding energy increases, again only slightly, as $N_3 \rightarrow CN \rightarrow NCS$, so that the azide lies between the bromide and iodide, the cyanide may be compared to the chloride and the isothiocyanate to the fluoride. Thus, charges on germanium that were associated with equal charging of the methyl groups for X = F, Cl, Br, and I now accompany varying methyl carbon charges.

Based on our EESOP calculations the binding energies (Ge 3*d* and C 1*s*) for the series $Me_3Ge—N_3$, —NCS, and —CN (Table 2) correspond to charges on germanium of 0.04, 0.055, and 0.05, respectively (Fig. 5), and on the carbon atom of the methyl-group of 0.025, 0.029, and 0.034, respectively (Fig. 6). This 'leaves' a charge of −0.115, −0.142, and −0.152 to be assigned to the $—N_3$, —NCS, and —CN groups, respectively. In $Me_3Ge—N_3$ the azido

Can. J. Chem. Downloaded from www.nrcresearchpress.com by 210.87.254.5 on 09/05/12
For personal use only.

group does not induce a large charge difference. This apparently low electronegativity is consistent with a degree of (π–d) π-bonding between Ge and the $-N_3$ group as has been suggested from the p.e. spectrum of silicon azides (18). The nitrogen 1s binding energies cannot be compared absolutely with those of the ionic azides (19) because of the phase change. However, ours are *ca.* 4.0 eV higher, which is consistent with the lower negative charge on the covalent azide. The separation of the N 1s levels is *ca.* 4.2 eV for both $Na^+N_3^-$ and $Me_3Ge—N_3$. Thus, delocalization of electron density within the N—N—N π-system apparently allows redistribution of any induced partial charge with similar results for both ionic and covalent azides. Alternatively, one can naively consider that the resonance structures $(Me_3Ge)N{=}\overset{+}{N}{=}\overset{-}{N}$ and $(Me_3Ge)\overset{-}{N}{-}\overset{+}{N}{\equiv}N$ allow the nitrogen atoms to maintain their relative charge differences. In $Me_3Ge—NCS$, the thiocyanato group apparently acts as a more electronegative group than the azide, or indeed any halogen group. The N 1s binding energy is slightly higher than that of the 'non-central' nitrogen atom in the azide. These two facts are consistent with its formulation as $(Me_3Ge)N{=}C{=}S$. There is N-bonding to germanium, the induced partial charge is spread over the whole moiety but there is no effective contribution from a resonance form that makes the nitrogen more negative. The nitrogen 1s binding energies in Me_3GeCN and Me_3GeNCS are separated by *ca.* 0.5 eV as has been observed in the potassium salts by Jolly *et al.* (19). In Me_3GeCN, the value is again slightly higher, but still much closer to, the 'non-central' nitrogen atom value. The C 1s binding energies of the Me— groups and the —CN group are so close that they form one, unresolvable peak. This is consistent with the expected C-bonded structure. Had the isocyanide form been important, then contributions from forms such as $Me_3Ge\overset{+}{N}{\equiv}\overset{-}{C}$ would surely result in the nitrogen atom having a binding energy approaching that of the 'central' nitrogen atom in an azide, while the binding energy of the carbon atom would be much lower than that of the methyl group carbon atom.

Finally, it is interesting to note that our correlations have been achieved despite the fact that no allowance has been made for relaxation energies nor has the potential term been included. The deficiencies in the assumptions may become apparent as more data are accumulated, but to date there is no reason to believe that consideration of the factors would improve the correlations.

Addendum

The N.M.R./ESCA Correlation

The idea that n.m.r. chemical shifts and ESCA core-level binding energies might be related parameters was held briefly (20). As Gelius has pointed out (21) there is some basis for such a correlation. In the n.m.r. effect the average screening constant, changes in which are called 'chemical shifts', contains paramagnetic and diamagnetic components. The paramagnetic term is the dominant one and does not depend on the molecular ground-state electron distribution. The diamagnetic term *only* is proportional to the ESCA shift. Although no general correlation can therefore be expected it has been postulated that in a closely related series the paramagnetic term might remain fairly constant. In the halomethanes CH_nX_{4-n} ($n = 0 \rightarrow 4$, X = F, Cl, Br, I) thirteen of the possible seventeen compounds have ^{13}C data reported. There is no general correlation of *all* these data, but for any one value of n all derivatives do exhibit linearity of δ_{13_C} *vs.* b.e.(C 1s) (21). Our δ_{13_C} values for a limited number of the germanium derivatives (Table 3) correspond to the analogs in the halomethane series (R_nMX_{4-n}, R = H or Me, M = C or Ge, respectively). That a plot of δ_{13_C} *vs.* b.e.(C 1s) for Me_4Ge, Me_3GeBr, Me_2GeCl_2, and $MeGeCl_3$ is linear we suggest is merely fortuitous for so was a similar plot for CH_4, CH_3Br, CH_2Cl_2, and $CHCl_3$. It is clear that neither b.e.(C 1s) *vs.* δ_{13_C} value in Me_3GeCN will fall on this same plot.

We are grateful to I. Adams, R. Lazier, and in particular to M. Bancroft, for their assistance in running the McPherson-36 and for helpful discussion. We also are indebted to M. Baillargeon for his work in modifying the computer program. We thank the National Research Council of Canada for financial support.

1. R. Nordberg, H. Brecht, R. G. Albridge, A. Fahlman, and J. R. Van Wazer. Inorg. Chem. **9**, 2469 (1970).
2. W. E. Morgan and J. R. Van Wazer. J. Phys. Chem. **77**, 964 (1973).

3. W. B. PERRY and W. L. JOLLY. Chem. Phys. Lett. **17**, 611 (1972).
4. W. B. PERRY and W. L. JOLLY. Chem. Phys. Lett. **20**, 617 (1973).
5. W. B. PERRY and W. L. JOLLY. Chem. Phys. Lett. **23**, 529 (1973).
6. W. B. PERRY and W. L. JOLLY. Inorg. Chem. **13**, 1215 (1974).
7. W. B. PERRY and W. L. JOLLY. J. Am. Chem. Soc. **95**, 5442 (1973).
8. K. SIEGBAHN, C. NORDLING, G. JOHANSSON, J. HEDMAN, P. F. HEDEN, K. HAMRIN, U. GELIUS, T. BERGMARK, L. O. WERME, R. MANNE, and Y. BAER. ESCA applied to free molecules. North-Holland, Amsterdam, and American Elsevier, New York, N.Y. 1969.
9. J. E. HUHEEY and J. C. WATTS. Inorg. Chem. **10**, 1553 (1971).
10. G. JOHANSSON, J. HEDMAN, A. BERNDTSSON, M. KLASSON, and R. NILSSON. J. Electron Spectrosc. **2**, 295 (1973).
11. M. SCHMIDT and I. RUIDISCH. Z. Anorg. Chem. **311**, 331 (1961).
12. M. G. VORONKOV and Y. I. KHUDOBIN. Izv. Akad. Nauk SSSR, Otd. Khim. Nank. 805 (1956).
13. S. CRADOCK and E. A. V. EBSWORTH. J. Chem. Soc. (A), 12 (1967).
14. J. E. HUHEEY. J. Phys. Chem. **69**, 3284 (1965).
15. J. HINZE and H. H. JAFFÉ. J. Am. Chem. Soc. **84**, 540 (1962).
16. J. HINZE, M. A. WHITEHEAD, and H. H. JAFFÉ. J. Am. Chem. Soc. **85**, 148 (1963).
17. J. HINZE and H. H. JAFFÉ. J. Phys. Chem. **67**, 1501 (1963).
18. S. CRADOCK, E. A. V. EBSWORTH, and J. D. MURDOCH. J. Chem. Soc. Faraday Trans. 2, **68**, 86 (1972).
19. D. N. HENDRICKSON, J. M. HOLLANDER, and W. L. JOLLY. Inorg. Chem. **8**, 2642 (1969).
20. (*a*) H. BASCH. Chem. Phys. Lett. **5**, 337 (1970). (*b*) V. GELIUS, G. JOHANSSON, H. SIEGBAHN, C. J. ALLAN, D. A. ALLISON, J. ALLISON, and K. SIEGBAHN. J. Electron Spectrosc. **1**, 285 (1972–73). (*c*) D. ZEROKA. Chem. Phys. Lett. **14**, 47 (1972).
21. U. GELIUS. Phys. Scr. **9**, 133 (1974).

Can. J. Chem. Downloaded from www.nrcresearchpress.com by 210.87.254.5 on 09/05/12
For personal use only.

Synthèse de l'aza-1-twistane

PIERRE DESLONGCHAMPS, LUC RUEST ET SERGE DUBÉ[1]

Laboratoire de synthèse organique, Université de Sherbrooke, Sherbrooke, Québec J1K 2R1

Reçu le 27 mars 1975

PIERRE DESLONGCHAMPS, LUC RUEST et SERGE DUBÉ. Can. J. Chem. **53**, 3613 (1975).

Nous avons réalisé une synthèse en cinq étapes de l'aza-1-twistane à partir de la benzoyl-2 octahydro-1,2,3,4,4a,7,8,8a isoquinolone-6(5) *cis* (**7**).

PIERRE DESLONGCHAMPS, LUC RUEST, and SERGE DUBÉ. Can. J. Chem. **53**, 3613 (1975).

A five-step synthesis of 1-azatwistane starting from the known *cis* 2-benzoyl-1,2,3,4,4a,7,8,8a-octahydro-6(5)-isoquinolone (**7**) is reported.

C'est à la suite de travaux réalisés dans notre laboratoire sur le twistane, **1**, (1–3) que nous avons entrepris la synthèse de l'analogue azoté, l'aza-1-twistane, **2**. D'autres groupes de recherche se sont intéressés en même temps que nous à la synthèse de l'aza-1-twistane. Perelman *et al.* (4) ont réussi à faire la synthèse de l'iodure de méthyl-1 aza-1-twistanium, **3**. Cependant il leur a été impossible d'effectuer la déméthylation du produit **3** de façon à obtenir l'aza-1-twistane. La méthode de fermeture de cycle utilisée par

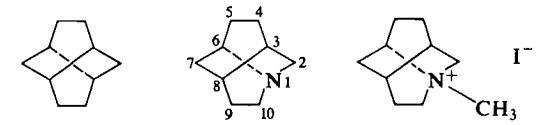

1

2

3

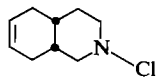

4

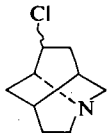

5

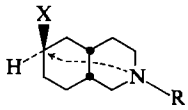

6

Perelman *et al.* est semblable à celle que nous avons utilisée dans notre synthèse de l'aza-1-twistane. Nous avions déjà utilisé cette méthode dans la synthèse du twistane. Dans sa synthèse de l'aza-1-twistane, Heusler (5) utilise comme précurseur la chloroamine **4** qu'il transforme en un mélange de deux chloro-5 aza-1-twistanes épimériques, **5**, dont il obtient par réduction l'aza-1-twistane **2**. Notre synthèse de l'aza-1-twistane a déjà fait l'objet d'une publication préliminaire (6), qui a paru en même temps que les publications préliminaires de Perelman *et al.* (4) et de Heusler (5). Nous présentons maintenant notre travail d'une manière détaillée.

Au départ, la synthèse de l'aza-1-twistane ne semblait pas présenter plus de problèmes que la synthèse du twistane, Essentiellement, il s'agissait d'utiliser comme précurseur un produit du genre de la molécule modèle **6**. Cette molécule porte sur l'atome d'azote un groupement quelconque 'R' susceptible d'être enlevé en temps opportun et, en position 6, un bon groupe partant (*e.g.* atome de chlore, groupement mésylate, groupement tosylate, etc.). On trouve, au sein même de la molécule, une base (l'atome d'azote) susceptible d'effectuer facilement la cyclisation, du moins nous l'espérions, par déplacement du groupe placé en position 6 de l'isoquinoléine. Pour que soit possible la substitution nucléophilique interne impliquée dans la cyclisation, il fallait que les hydrogènes en positions 4a et 8a soient *cis* l'un par rapport à l'autre. Il fallait en outre que le groupe partant soit du même côté de la molécule que les hydrogènes de la jonction. C'est pour satisfaire à ces exigences que nous avons choisi comme produit de départ l'isoquinolone *cis* **7**.

Augustine (7) avait déjà effectué la préparation du produit **7**. Nous avons repris sa méthode. Nous avons d'abord préparé l'isoquinolone **8** par addition de méthylvinylcétone à l'énamine de la *N*-benzoylpipéridone. Par hydrogénation catalytique dans l'éthanol, en présence d'acide chlorhydrique, l'isoquinolone **8** a conduit à un mélange des deux cétones saturées **7** et **9**, que nous avons séparées par chromatographie préparative sur plaque de silice. Le mélange contenait 65% d'un isomère, présumément le *cis*, et 35% de l'autre isomère, présumément le *trans*. Augus-

[1]Détenteur d'une bourse d'entretien du CNR 1968–1971. Adresse actuelle: Faculté des sciences, Université nationale du Rwanda, B.P. 117, Butaré, Rwanda, Afrique Centrale.

Can. J. Chem. Downloaded from www.nrcresearchpress.com by 210.87.254.6 on 09/05/12
For personal use only.

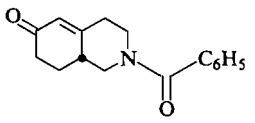

8

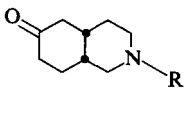

7 R = COC_6H_5
13 R = H

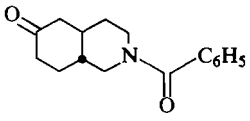

9

tine avait établi la stéréochimie des produits **7** et **9** par analogie avec la série des β-décalones et par application de la règle de von Auwers et de Skita. Nous avons utilisé une preuve chimique, plus sûre: nous avons fait une réduction de Birch sur la cétone insaturée **8**. Il est connu (8) qu'une telle réaction conduit exclusivement à l'isomère *trans*. Les résultats que nous avons obtenus confirment la stéréochimie établie par Augustine.

Dans le but de faciliter l'accès à notre produit de départ, l'isoquinolone **7**, nous avons tenté une autre synthèse de ce produit, par l'intermédiaire des cétals **10** et **11**. Par chauffage dans le benzène en présence d'éthylène glycol et d'acide *p*-toluènesulfonique, la cétone **8** a conduit au cétal **10**. L'hydrogénation du cétal **10** a conduit à un mélange des cétals **11** et **12**, comme on peut le voir par comparaison avec des échantillons authentiques préparés à partir des cétones **7** et **9**. L'analyse par chromatographie en phase

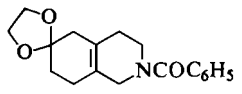

10

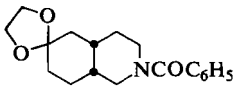

11

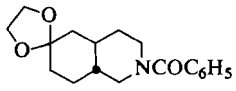

12

gazeuse du mélange des cétones **7** et **9** obtenu par hydrolyse du mélange des cétals **11** et **12** a démontré que le mélange contenant environ 55% du cétal *cis*. Nous espérions aussi par cette voie pouvoir séparer plus facilement les isomères *cis* et *trans* au niveau des cétals **11** et **12**. Cependant les cétals **11** et **12** avaient des valeurs de R_f très voisines et il nous a été impossible de les séparer. C'est pourquoi il nous a fallu revenir à notre méthode initiale, soit l'hydrogénation catalytique de la cétone **8**.

Il existait au départ plusieurs voies possibles pour passer de la cétone **7** à l'aza-1-twistane. Nous avions tout d'abord pensé travailler avec les amines secondaires **13**, **15** et **16**. Dans ce cas, il s'agissait de libérer d'abord l'amine par hydrolyse de la fonction amide du produit **7**, puis de transformer le groupement fonctionnel en position 6 en un bon nucléofuge.

Le produit **7** fut d'abord transformé en sel d'imidate correspondant **17** à l'aide du tétrafluoroborure de triéthyloxonium. L'hydrolyse du sel **17** en milieu basique aqueux a fournit la cétone-amine **13** (9, 10). Par réduction avec de

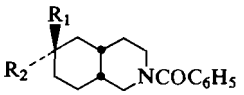

18 R_1 = OH, R_2 = H
19 R_1 = H, R_2 = OH
20 R_1 = OSO_2CH_3, R_2 = H
21 R_1 = H, R_2 = OSO_2CH_3

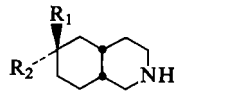

14 R_1 = H, R_2 = OH
15 R_1 = OH, R_2 = H
16 R_1 = OSO_2CH_3, R_2 = H
22 R_1 = H, R_2 = OSO_2CH_3

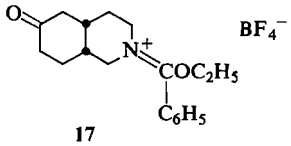

17

l'hydrure de lithium et d'aluminium, la cétone-amine **13** a conduit présumément à un mélange des alcools **14** et **15**. Les deux alcools avaient la même valeur de R_f et il a été impossible de les séparer ou de déterminer la proportion de chacun dans le mélange. De plus, à cause de l'instabilité de ces amines et de leur grande polarité, l'utilisation des techniques de chromatographie était difficile. A ce stade, nous nous sommes rendus compte qu'il serait difficile de faire la synthèse de l'aza-1-twistane, **2**, par la voie des amines secondaires (**7** → **13** → **15** → **16** → **2**).

Nous avons alors décidé de tenter de faire plutôt la synthèse de l'aza-1-twistane par la voie des amides (**7** → **18** → **20** → **16** → **2**). Comme les amides sont des produits plus stables que les amines secondaires, nous avons choisi de conserver le plus longtemps possible la fonction amide et de travailler à placer d'abord en position 6 un bon nucléofuge. Nous espérions aussi pouvoir en cours de route séparer le mélange d'épimères que nous devions nous attendre à obtenir au niveau de la position 6.

Nous avons tout d'abord réduit la cétone **7** à l'aide de borohydrure de sodium. Le produit de la réaction était présumément un mélange des

Can. J. Chem. Downloaded from www.nrcresearchpress.com by 210.87.254.6 on 09/05/12
For personal use only.

Can. J. Chem. Downloaded from www.nrcresearchpress.com by 210.87.254.6 on 09/05/12
For personal use only.

alcools **18** et **19**, mais les deux épimères avaient la même valeur de R_f et il a été impossible de les séparer. Par traitement avec du chlorure de méthanesulfonyle dans le dichlorométhane, en présence de pyridine, à $-15\,°C$, nous avons transformé le mélange des alcools **18** et **19** en un mélange des mésylates **20** et **21**. Les mésylates **20** et **21**, tout comme les alcools **18** et **19**, avaient la même valeur de R_f et il a été impossible de les séparer par chromatographie sur couche mince ou sur colonne. Nous avons fait l'hydrolyse de la fonction amide des mésylates **20** et **21** de la même façon que précédemment (**7** → **13**). Là encore les épimères, les mésylates **16** et **22**, avaient la même valeur de R_f et il a été impossible de les séparer. Rappelons que seulement l'un des deux épimères, c'est-à-dire le mésylate **16**, pouvait nous conduire à l'aza-1-twistane, **2**. Ce contretemps compromettait notre synthèse, mais nous avons quand même tenter d'effectuer la fermeture de cycle qui devait nous conduire à l'aza-1-twistane, **2**. Pour ce faire, nous avons chauffé le mélange des mésylates **16** et **22** dans le benzène pendant 30 h. Il semble sur la foi de comparaisons faites sur plaque mince avec un échantillon authentique[2] d'aza-1-twistane, **2** que nous ayons effectivement obtenu le produit désiré, en quantité si minime cependant qu'il nous a été impossible de le caractériser davantage. Le milieu réactionnel contenait en plus beaucoup d'autres produits, provenant peut-être de la décomposition de l'épimère de mauvaise configuration. Il se peut en outre que la cyclisation ait été incomplète ou bien qu'il y ait eu prépondérance du mauvais épimère **22** dans le mélange de départ.

Il était important à l'étape de la cyclisation d'avoir une réaction nette, parce que l'aza-1-twistane, **2**, une substance très polaire, est difficile à purifier par les méthodes habituelles. Nous avons alors décidé de procéder par la voie des amines tertiaires (**7** → **23** → **25** → **27** → **28** → **2**). La réduction de la cétone **7**, par traitement avec de l'hydrure de lithium et d'aluminium dans le tétrahydrofuranne, a conduit comme prévu à un mélange des alcools épimériques **23** et **24**. Même si les deux alcools avaient des valeurs de R_f très voisines, nous avons réussi à les séparer par chromatographie préparative. Le mélange

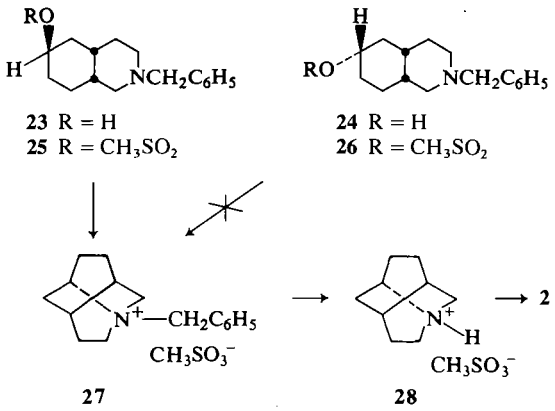

23 R = H
25 R = CH_3SO_2

24 R = H
26 R = CH_3SO_2

27 **28**

contenait environ 30% d'un épimère et environ 70% de l'autre épimère. Nous ignorions la stéréochimie de chacun des alcools au niveau de la position 6. La meilleure façon d'établir la stéréochimie des deux épimères, c'était en définitive de faire la synthèse de l'aza-1-twistane, **2**. C'est pourquoi nous avons décidé d'effectuer la même série de réactions sur les deux alcools **23** et **24**. Seul l'épimère α pouvait nous conduire à l'aza-1-twistane, **2**.

Nous avons préparé de la façon habituelle les mésylates **25** et **26** à partir des alcools **23** et **24**. L'un des deux mésylates devait nous conduire à l'aza-1-twistane, **2**. Nous avons tout d'abord chauffé à tour de rôle les deux mésylates dans le benzène pendant 48 h sans noter aucune réaction. Nous avons alors repris le mésylate de l'alcool majoritaire **27** et nous l'avons chauffé dans le toluène pendant 24 h. L'analyse sur plaque mince du produit obtenu a montré la présence de plusieurs produits de décomposition. Nous avons finalement chauffé à reflux dans le toluène pendant 20 h le mésylate de l'alcool minoritaire **25**. Nous avons obtenu de cette façon avec un rendement de 86% le sel quaternaire **27**. Ces résultats nous ont permis d'établir *a posteriori* la stéréochimie des alcools **23** et **24** et des mésylates **25** et **26**.

Il a été facile ensuite d'obtenir l'aza-1-twistane **2**. Nous avons fait sans difficulté l'hydrogénolyse du sel quaternaire **27** pour obtenir le méthanesulfonate de l'aza-1-twistane **28** quantitativement. Il suffisait ensuite de laver le sel **28** en milieu basique pour obtenir l'aza-1-twistane. Nous avons caractérisé le produit sous forme de chlorhydrate, car l'amine elle-même est instable. Les données physiques et spectrales concordent avec la nature du produit et sont identiques à celles

[2]Cet échantillon nous a été généreusement fourni par le docteur K. Heusler, de l'Institut de recherche Woodward (Bâle, Suisse) (*cf.* réf. 5).

Can. J. Chem. Downloaded from www.nrcresearchpress.com by 210.87.254.6 on 09/05/12
For personal use only.

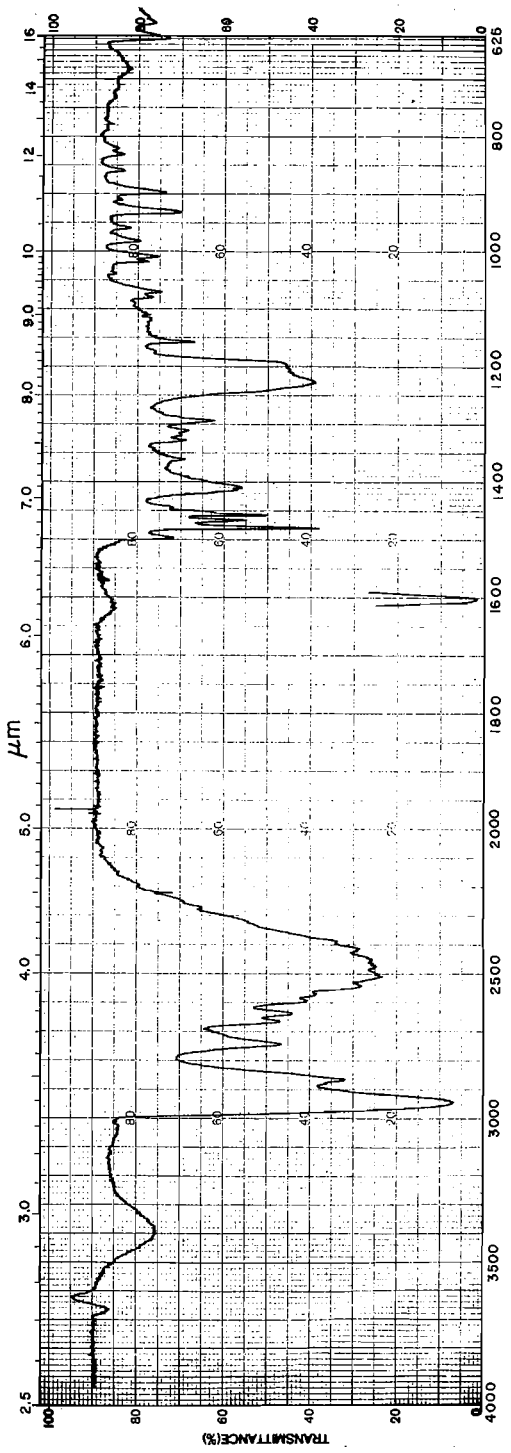

FIG. 1. Spectre infrarouge ($CHCl_3$) du chlorhydrate de l'azatwistane.

Can. J. Chem. Downloaded from www.nrcresearchpress.com by 210.87.254.6 on 09/05/12
For personal use only.

d'un échantillon authentique. L'identité des deux produits a été confirmée par chromatographie sur plaque mince et par chromatographie en phase gazeuse. Le spectre infrarouge du chlorhydrate de l'azatwistane est reproduit à la Fig. 1.

Partie expérimentale

Nous avons pris les spectres infrarouges sur deux spectrophotomètres Perkin-Elmer, modèles 137 et 257. Pour les spectres de résonance magnétique nucléaire nous avons utilisé un appareil A-60 de la compagnie Varian, le tétraméthylsilane servant de référence interne. Les spectres de masse ont été pris sur un appareil Hitachi–Perkin-Elmer, modèle RMU-6D.

Les points de fusion, déterminés au moyen d'un appareil Büchi, ne sont pas corrigés. Pour nos analyses en phase gazeuse, nous nous sommes servis d'un chromatographe Varian, modèle 90-P, utilisant l'hélium comme gaz porteur. La colonne, d'une longueur de 5 pieds et d'un diamètre de $\frac{1}{4}$ po, contenait du SE-30 5% sur Chromosorb P.

Nous avons utilisé comme desséchant du sulfate de sodium anhydre. Les plaques minces utilisées pour les chromatographies sur couche mince étaient faites de gel de silice GF 254 de Merck ou G/UV 254 de Macherey, Nagel et cie ou d'alumine GF 254 ou G/UV 254 des mêmes fournisseurs. Nous avons aussi utilisé des chromagrammes de silice (no 6060) et d'alumine (no 6063) de la compagnie Eastman. Nous avons utilisé comme révélateur un réactif au chlorure de platine pour les amines et l'iode pour les autres produits. Les chromatographies sur colonne ont été faites sur du gel de silice de Baker (60–200 M) ou de Merck (75–325 M, p*H* 7). L'éther de pétrole utilisé est la fraction de pétrole distillant entre 30 et 60 °C.

Cétone insaturée ***8***

Nous avons essentiellement suivi la méthode expérimentale rapportée par Augustine (7) pour préparer la cétone insaturée **8**. On a préparé un échantillon analytique par recristallisation du produit dans un mélange de benzène et d'éther de pétrole; p.f. 142–143 °C (litt. (7) 144–145 °C); s.m. *m/e* 255 (M^+, ion moléculaire); i.r. ν_{max} ($CHCl_3$) 1685 et 1630 cm^{-1}; r.m.n. ($CDCl_3$) 6.00 δ (1H, CCHCO).

Anal. calc. pour $C_{16}H_{17}NO_2$: C, 75.27; H, 6.71; N, 5.48. Trouvé: C, 75.36; H, 6.74; N, 5.70.

Cétones saturées ***7*** *et* ***9***

La cétone **8** (2.1 g) a été réduite selon le mode opératoire décrit par Augustine (7). On recueille une substance cristalline blanche (2.2 g, 100%) fondant à 142–146°C. La substance est constituée de deux produits, qu'on sépare par chromatographie préparative sur silice, à raison de 75 mg par plaque de 20 cm × 40 cm (éluant, solution de méthanol dans l'éther à 5%). Le mélange contient 64% (1.4 g) de la cétone **7** et 32% (800 mg) de la cétone **9**.

On prépare un échantillon analytique de la cétone **7** par recristallisation du produit dans un mélange de benzène et d'éther de pétrole; p.f. 153 °C (litt. (7) 148–149 °C); s.m. *m/e* 257 (M^+, ion moléculaire); i.r. ν_{max} ($CHCl_3$) 1750 et 1630 cm^{-1}.

Anal. calc. pour $C_{16}H_{19}NO_2$: C, 74.67; H, 7.44; N, 5.44. Trouvé: C, 74.66; H, 7.52; N, 5.69.

On prépare un échantillon analytique de la cétone **9** par recristallisation du produit dans un mélange de benzène et d'éther de pétrole; p.f. 164.5–165.5 °C (litt. (7) 159–160 °C); s.m. *m/e* 257 (M^+, ion moléculaire); i.r. ν_{max} ($CHCl_3$) 1705 et 1630 cm^{-1}.

Anal. calc. pour $C_{16}H_{19}NO_2$: C, 74.67; H, 7.44; N, 5.44. Trouvé; C, 74.78; H, 7.59; N, 5.52.

Réduction de Birch sur la cétone ***8***

A de l'ammoniac liquide préalablement distillé (250 ml), on ajoute du lithium jusqu'à persistance de la coloration bleue, puis la cétone **8** (1.03 g) en solution dans du tétrahydrofuranne (10 ml). Après avoir laissé agiter pendant 60 s, on ajoute du chlorure d'ammonium pour détruire l'excès de lithium. On laisse évaporer l'ammoniac, on ajoute de l'eau et on extrait au dichlorométhane. Après séchage et évaporation du solvant, on obtient une huile jaunâtre (800 mg), dont on tire par chromatographie sur colonne (silice) la fraction correspondant aux cétones **7**, **8** et **9** (720 mg). Le mélange obtenu était constitué uniquement du produit de départ, la cétone **8** et de la cétone **9**. On sépare les deux produits par chromatographie préparative sur silice (éluant, solution de méthanol dans l'éther à 5%). Les propriétés physiques et spectrales du produit réduit sont identiques à celles du produit **9**. Il a été impossible de trouver trace du produit **7** dans le milieu réactionnel.

Cétal ***10***

A une solution de la cétone insaturée **8** (400 mg, 1.57 mmol) dans du benzène anhydre (200 ml), on ajoute de l'éthylène glycol (900 mg, 14.5 mol) et de l'acide *p*-toluènesulfonique (5 mg). On coiffe le ballon d'un séparateur d'eau et d'un réfrigérant et on chauffe à reflux pendant 40 h. Après réduction du volume de la solution, on ajoute une solution saturée (100 ml) de carbonate de sodium et on extrait au dichlorométhane. On lave la phase organique avec une solution saturée de chlorure de sodium. L'huile obtenue après séchage et évaporation du solvant est ensuite purifiée par chromatographie préparative sur silice (éluant, solution de méthanol dans l'éther à 5%). On obtient ainsi une huile incolore (190 mg, 41%). On prépare un échantillon analytique par microdistillation sous vide; s.m. *m/e* 299 (M^+, ion moléculaire); i.r. ν_{max} (CH_2Cl_2) 1640, 1455 et 1115 cm^{-1}; r.m.n. ($CDCl_3$) 3.97 δ (4H, singulet, OCH_2CH_2O).

Anal. calc. pour $C_{18}H_{21}NO_3$: C, 72.21; H, 7.07; N, 4.68. Trouvé: C, 72.30; H, 7.07; N, 4.92.

Cétal ***11***

A une solution de la cétone **7** (200 mg, 0.78 mmol) dans du benzène anhydre (150 ml), on ajoute de l'éthylène glycol (360 mg, 5.8 mmol) et de l'acide *p*-toluènesulfonique (5 mg). On coiffe le ballon d'un séparateur d'eau et d'un réfrigérant et on chauffe à reflux pendant 24 h. Après réduction du volume de la solution, on ajoute une solution saturée (100 ml) de carbonate de sodium et on extrait au dichlorométhane. On lave la phase organique avec une solution saturée de chlorure de sodium. L'huile obtenue après séchage et évaporation du solvant est ensuite purifiée par chromatographie préparative sur silice (éluant, solution de méthanol dans l'éther à 5%). On obtient ainsi une huile incolore qu'on cristallise par

Can. J. Chem. Downloaded from www.nrcresearchpress.com by 210.87.254.6 on 09/05/12
For personal use only.

trituration dans du cyclohexane (222 mg, 100%). Un échantillon est recristallisé dans le cyclohexane pour envoi à l'analyse; p.f. 108 °C; s.m. *m/e* 301 (M^+, ion moléculaire); i.r. ν_{max} (CH_2Cl_2) 1625, 1440 et 1118 cm^{-1}; r.m.n. ($CDCl_3$) 3.92 δ (4H, singulet, OCH_2CH_2O).

Anal. calc. pour $C_{18}H_{23}NO_3$: C, 71.73; H, 7.64; N, 4.65. Trouvé: C, 71.91; H, 7.72; N, 4.72.

Cétal ***12***

A une solution de la cétone **9** (500 mg, 1.95 mmol) dans du benzène anhydre (175 ml) on ajoute de l'éthylène glycol (900 mg, 14.5 mmol) et de l'acide *p*-toluènesulfonique (25 mg). On coiffe le ballon d'un séparateur d'eau et d'un réfrigérant et on chauffe à reflux pendant 37 h. Après réduction du volume de la solution, on ajoute une solution saturée (100 ml) de carbonate de sodium et on extrait au chloroforme. On lave la phase organique avec une solution saturée de chlorure de sodium. L'huile obtenue après séchage et évaporation du solvant est cristallisée par trituration dans du cyclohexane chaud (468 mg, 80%). Un échantillon est recristallisé dans le cyclohexane pour envoi à l'analyse; p.f. 124–125 °C; s.m. *m/e* 301 (M^+, ion moléculaire); i.r. ν_{max} (CH_2Cl_2) 1628, 1442 et 1120 cm^{-1}; r.m.n. ($CDCl_3$) 3.95 δ (4H, singulet, OCH_2CH_2O).

Anal. calc. pour $C_{18}H_{23}NO_3$: C, 71.73; H, 7.85. Trouvé: C, 71.64; H, 7.85.

Hydrogénation du cétal ***10***

A une solution du cétal **10** (975 mg, 3.25 mmol) dans l'éthanol (150 ml), placée dans un ballon à hydrogénation, on ajoute de l'oxyde de platine (200 mg). Après avoir enlevé l'air, on place sous atmosphère d'hydrogène (3 atm) et on agite mécaniquement à la température de la pièce pendant 36 h. Après avoir filtré le catalyseur, on évapore l'éthanol, puis on reprend le résidu dans du dichlorométhane. Après séchage et évaporation du solvant, on recueille une huile incolore (975 mg, 100%) constituée de deux produits, les cétals **11** et **12**, qu'il a été impossible de séparer. Il a également été impossible de déterminer la proportion de chacun des produits dans le mélange; i.r. ν_{max} (CH_2Cl_2) 1632, 1450 et 1122 cm^{-1}; r.m.n. ($CDCl_3$) 3.92 δ (4H, singulet, OCH_2CH_2O).

Hydrolyse du mélange des cétals ***11*** *et* ***12***

A une solution du mélange des cétals **11** et **12** (238 mg) dans l'éther (20 ml) on ajoute de l'acide chlorhydrique 0.5 *N* (30 ml), puis on laisse agiter à la température de la pièce pendant 4 h. On sépare ensuite la phase éthérée qu'on lave avec une solution saturée de chlorure de sodium jusqu'à neutralité. Après séchage et évaporation du solvant, on recueille des cristaux blancs (185 mg, 85%). Des comparaisons faites avec des échantillons authentiques des cétones **7** et **9** par chromatographie en phase gazeuse ont permis d'établir que le mélange contient environ 45% de la cétone **9** et environ 55% de la cétone **7**.

Cétone ***13***

A une solution du réactif de Meerwein (3.0 g, 16 mmol) dans du dichlorométhane (20 ml) filtré sur alumine, on ajoute du carbonate de sodium (1.2 g, 11 mmol) et on agite vigoureusement pendant 15 min. Après addition de la cétone **7** (300 mg, 1.17 mmol) on agite pendant 75 min. Le milieu réactionnel est ensuite lavé soigneusement à deux reprises avec une solution saturée de carbonate de sodium (25 ml). Après séchage et évaporation du solvant, l'huile résiduelle est dissoute dans une solution d'acide chlorhydrique 0.1 *N* (25 ml). On lave la phase aqueuse avec du dichlorométhane pour enlever le benzoate d'éthyle formé au cours de la réaction. Après basification de la phase aqueuse, extraction au dichlorométhane, séchage et évaporation du solvant, on recueille une huile incolore (182 mg, 100%). Il a été impossible de cristalliser le chlorhydrate et le picrate de la cétone **13**. Le styphnate, recristallisé dans un mélange d'éthanol et d'éther de pétrole, fond à 174–176 °C (déc.); s.m. *m/e* 153 (M^+, ion moléculaire); i.r. ν_{max} (film liquide) 3500 et 1715 cm^{-1}; r.m.n. ($CDCl_3$) 0.7–3.1 δ (massif).

Anal. calc. pour le styphnate: C, 45.23; H, 4.55; N, 14.07. Trouvé: C, 45.21; H, 4.62; N, 13.95.

Alcools ***14*** *et* ***15***

A une suspension d'hydrure de lithium et d'aluminium (280 mg, 7.8 mmol) dans le tétrahydrofuranne anhydre (35 ml), on ajoute la cétone **13** (362 mg, 2.4 mmol) et on chauffe à reflux pendant 3 h. On laisse ensuite refroidir le milieu réactionnel, puis on ajoute de l'eau pour détruire l'excès d'hydrure. Après séchage et évaporation du solvant, on obtient une huile jaunâtre (195 mg, 54%); i.r ν_{max} (CH_2Cl_2) 3575 cm^{-1}.

Alcools ***18*** *et* ***19***

A une solution de la cétone **7** (258 mg, 1.0 mmol) dans le méthanol (10 ml), on ajoute du borohydrure de sodium (81 mg, 2.5 mmol) en solution dans l'eau (5 ml). Après avoir laissé agiter pendant 3 h, on ajoute de l'acétone (1 ml) pour détruire l'excès d'hydrure. On réduit le volume de la solution, on ajoute de l'eau et on extrait à l'éther. Après séchage et évaporation du solvant, on obtient une huile incolore très épaisse (249 mg, 96%); s.m. *m/e* 259 (M^+, ion moléculaire); i.r. ν_{max} ($CHCl_3$) 3570, 3450 et 1615 cm^{-1}.

Mésylates ***20*** *et* ***21***

A une solution des alcools **18** et **19** (258 mg, 1 mmol) dans du dichlorométhane (10 ml) distillé et filtré sur alumine on ajoute de la pyridine (2 ml) et on refroidit la solution à 0 °C. Après addition de chlorure de méthanesulfonyle (450 mg, 0.3 ml, 3.9 mmol), on conserve au congélateur pendant 48 h. On jette ensuite le milieu réactionnel dans une solution saturée de carbonate de sodium et on extrait au dichlorométhane. Le produit obtenu après séchage et évaporation du solvant est purifié par chromatographie préparative sur silice (éluant, solution de méthanol dans l'éther à 5%). On obtient une huile jaunâtre (280 mg, 83%); s.m. *m/e* 337 (M^+, ion moléculaire); i.r. ν_{max} ($CHCl_3$) 1358, 1170 et 935 cm^{-1}; r.m.n. ($CDCl_3$) 3.02 δ (3H, singulet, OSO_2CH_3).

Mésylates ***16*** *et* ***22***

A une solution du réactif de Meerwein (1.0 g, 5.3 mmol) dans du dichlorométhane (10 ml) filtré sur alumine, on ajoute du carbonate de sodium (282 mg, 2.6 mmol) et on agite vigoureusement pendant 15 min. On ajoute une solution des mésylates **20** et **21** (250 mg, 0.74 mmol) dans du dichlorométhane (3 ml), puis on laisse agiter à la température de la pièce pendant 2 h. Dilué par addition de dichlorométhane (10 ml), le milieu réactionnel est versé dans une solution saturée de carbonate de sodium (25 ml). On agite vigoureusement pendant 15 min. Après séparation de la phase organique, séchage et évaporation du solvant on obtient une huile jaunâtre

Can. J. Chem. Downloaded from www.nrcresearchpress.com by 210.87.254.6 on 09/05/12
For personal use only.

dont on tire par chromatographie préparative sur alumine (éluant, solution de méthanol dans le chloroforme à 50%) une huile incolore (170 mg, 100%); s.m. *m/e* 233 (M^+, ion moléculaire); i.r. ν_{max} ($CHCl_3$) 1340, 1165 et 925 cm^{-1}; r.m.n. ($CDCl_3$) 3.00 δ (3H, singulet, OSO_2CH_3).

Alcools 23 et 24

A une solution de la cétone **7** (258 mg, 1 mmol) dans du tétrahydrofuranne anhydre (30 ml) on ajoute de l'hydrure de lithium et d'aluminium (380 mg, 10 mmol) et on chauffe à reflux pendant 4 h. Après addition d'eau pour détruire l'excès d'hydrure, la solution est séchée et le solvant est évaporé. On recueille une huile incolore (233 mg, 91%), constituée de deux produits qu'on sépare par chromatographie préparative sur silice (éluant, solution de méthanol dans l'éther à 5%).

L'alcool **24** (R_f 0.4, 77%) est une huile incolore qui solidifie après un séjour de 6 mois au congélateur. Le picrate et le styphnate, recristallisés tous les deux dans l'éthanol absolu, fondent à 77–79 °C et 96–97 °C respectivement. Le flavianate, recristallisé dans le méthanol, a un point de fusion de 148–149 °C; s.m. *m/e* 245 (M^+, ion moléculaire); i.r. ν_{max} ($CHCl_3$) 3610 et 3450 cm^{-1}; r.m.n. ($CDCl_3$) 3.50 δ (2H, singulet NCH_2C), 3.4–3.9 δ (1H, massif, CHO) et 7.30 δ (5H, singulet, C_6H_5).

Anal. calc. pour le picrate: C, 55.69; H, 5.52. Trouvé: C, 55.59; H, 5.64.

L'alcool **23** (R_f 0.5, 23%) est une huile incolore dont le picrate, recristallisé dans l'éthanol absolu, fond à 163–164 °C; s.m. *m/e* 245 (M^+, ion moléculaire); i.r. ν_{max} ($CHCl_3$) 3600 et 3450 cm^{-1}; r.m.n. ($CDCl_3$) 3.49 δ (2H, singulet, NCH_2C), 3.5–4.1 δ (1H, massif, CHO) et 7.39 δ (5H, singulet, C_6H_5).

Anal. calc. pour le picrate: C, 55.69; H, 5.52; N, 11.81. Trouvé: C, 55.37; H, 5.48; N, 11.86.

Mésylate 26

A une solution de l'alcool **24** (224 mg, 0.91 mmol) dans du dichlorométhane anhydre (25 ml) on ajoute de la pyridine (1.8 ml) et on refroidit la solution à 0 °C. Après addition de chlorure de méthanesulfonyl (450 mg, 0.3 ml, 3.9 mmol) on place au congélateur pendant 15 h. On jette ensuite le milieu réactionnel dans une solution saturée de carbonate de sodium et on extrait au dichlorométhane. La phase organique est ensuite lavée à l'eau. Après séchage et évaporation du solvant, on obtient un solide brunâtre fondant à 75–80 °C (300 mg, 100%). Le chlorhydrate du produit **26**, recristallisé dans un mélange de chloroforme et d'éther de pétrole, fond à 128–129 °C, tandis que son picrate, recristallisé dans l'éthanol absolu, a un point de fusion de 155–156 °C; s.m. *m/e* 323 (M^+, ion moléculaire); i.r. ν_{max} (CH_2Cl_2) 1360, 1200 et 1050 cm^{-1}; r.m.n. ($CDCl_3$) 2.98 δ (3H, singulet, OSO_2CH_3).

Anal. calc. pour le picrate: C, 49.99; H, 5.10; N, 10.13. Trouvé: C, 50.30; H, 5.44; N, 9.84.

Mésylate 25

A une solution de l'alcool **23** (640 mg, 2.6 mmol) dans du dichlorométhane anhydre (30 ml) on ajoute de la pyridine (5 ml) et on refroidit la solution à 0 °C. Après addition du chlorure de méthanesulfonyle (1.36 g, 0.9 ml, 12 mmol) on place au congélateur pendant 15 h. On jette ensuite le milieu réactionnel dans une solution saturée de carbonate de sodium et on extrait au dichlorométhane. La phase organique est ensuite lavée à l'eau. Après séchage et évaporation du solvant, on recueille une huile jaunâtre, (844 mg, 100%). Le chlorhydrate du produit **25**, recristallisé dans l'acétone, fond à 166–167 °C; s.m. *m/e* 323 (M^+, ion moléculaire); i.r. ν_{max} (CH_2Cl_2) 1355, 1178 et 935 cm^{-1}; r.m.n. ($CDCl_3$) 2.98 δ (3H, singulet, OSO_2CH_3).

Anal. calc. pour le chlorhydrate: C, 55.77; H, 7.22. Trouvé: C, 55.96; H, 7.19.

Cyclisation du mésylate 25

On chauffe à reflux pendant 20 h une solution du mésylate **25** (700 mg) dans le toluène (100 ml). Par filtration on recueille un solide blanc fondant à 180–181 °C (600 mg, 86%). On prépare un échantillon analytique du sel quaternaire **27** par recristallisation dans l'acétone; p.f. 188 °C; i.r. ν_{max} (CH_2Cl_2) 1205 et 1045 cm^{-1}; r.m.n. (CDCl) 2.80 δ (3H, singulet, OSO_2CH_3), 4.72 δ (2H, singulet large, NCH_2C) et 7.2–7.7 δ (5H, massif, C_6H_5).

Anal. calc. pour $C_{17}H_2N_5O_3S$: C, 63.15; H, 7.74; N, 4.33. Trouvé: C, 63.02; H, 7.69; N, 4.58.

Aza-1-twistane, 2

A une solution du sel quaternaire **27** (321 mg, 1 mmol) dans de l'éthanol anhydre (70 ml) on ajoute du charbon palladié (400 mg, préparation commerciale à 10%). Après avoir enlevé l'air, on place sous atmosphère d'hydrogène (1 atm) et on agite mécaniquement à la température de la pièce pendant 40 h. On filtre le catalyseur. Après évaporation du solvant, on recueille une huile incolore (**28**, 237 mg, 100%); r.m.n. ($CDCl_3$) 2.37 δ (3H, singulet, CH_3). On dissout l'huile dans l'ammoniaque diluée et on extrait au dichlorométhane. Après séchage et évaporation du solvant, on obtient une huile jaunâtre (**2**, 135 mg, 100%). Le chlorhydrate, recristallisé dans un mélange de dichlorométhane et d'acétone pour envoi à l'analyse, fond à 320–323 °C (déc.); s.m. *m/e* 137 (M^+, ion moléculaire). La seule bande importante du spectre infrarouge du chlorhydrate est une bande large centrée à 2450 cm^{-1} (Fig. 1); r.m.n. ($CDCl_3$) 1.3–2.6 δ (10H), 2.8–3.6 δ (4H, $CH_2\overset{H}{\underset{|}{N}}\overset{+}{C}H_4$), 3.7–4.0 δ (1H, CH) et 9.0–10.0 δ (1H, $\overset{+}{N}H$).

Anal. calc. pour le chlorhydrate: C, 62.24; H, 9.30. Trouvé: C, 62.49; H, 9.45.

Nous remercions de leur aide le Conseil National de Recherches du Canada et le Ministère de l'Education du Québec.

1. J. GAUTHIER et P. DESLONGCHAMPS. Can. J. Chem. **45**, 297 (1967).
2. A. BÉLANGER, J. POUPART et P. DESLONGCHAMPS. Tetrahedron Lett. 2127 (1968).
3. A. BÉLANGER, Y. LAMBERT et P. DESLONGCHAMPS. Can. J. Chem. **47**, 795 (1969).
4. D. PERELMAN, S. SICSIC et Z. WELVART. Tetrahedron Lett. 103 (1970).
5. K. HEUSLER. Tetrahedron Lett. 97 (1970).
6. S. DUBÉ et P. DESLONGCHAMPS. Tetrahedron Lett. 101 (1970).
7. L. AUGUSTINE. J. Org. Chem. **33**, 1853 (1958).
8. G. STORK et S. D. DARLING. J. Am. Chem. Soc. **82**, 1512 (1960).
9. H. MUXFELDT et W. ROGALSKI. J. Am. Chem. Soc. **87**, 933 (1965).
10. P. DESLONGCHAMPS, C. LEBREUX et R. TAILLEFER. Can. J. Chem. **51**, 1665 (1973).

The Synthesis of Primary Alkyl Chlorides from Alcohols and Hydrogen Chloride in Hexamethylphosphoric Triamide[1]

RICHARD FUCHS

Department of Chemistry, University of Houston, Houston, Texas 77004

AND

LARRY L. COLE

Department of Chemistry, Prairie View A & M University, Prairie View, Texas 77445

Received July 11, 1975

RICHARD FUCHS and LARRY L. COLE. Can. J. Chem. **53**, 3620 (1975).

The reaction of hydrogen chloride with primary alcohols, which occurs slowly and in poor yields in water, has been found to give good yields of alkyl chlorides in 30–45 min at 70–85 °C in the solvent hexamethylphosphoric triamide. 2-Octanol and neopentyl alcohol required longer reaction periods. Neopentyl chloride was formed without contamination by rearrangement products.

RICHARD FUCHS et LARRY L. COLE. Can. J. Chem. **53**, 3620 (1975).

La réaction de l'acide chlorhydrique avec les alcools primaires, qui se produit lentement et avec de faibles rendements dans l'eau, conduit à des bons rendements en chlorure d'alkyle en 30–45 min, à 70–85 °C, dans le HMPT comme solvant. L'octanol-2 et l'alcool néopentylique demandent des périodes de réaction plus longues. Le chlorure de néopentyle se forme sans contamination par des produits de réarrangement.

[Traduit par le journal]

The much greater reactivity of aqueous hydriodic acid compared with hydrochloric acid toward primary alcohols is usually attributed to the greater nucleophilicity of iodide ion (*vs.* chloride). Both acids are sufficiently strong to protonate alcohols extensively, but the subsequent S_N2 displacement of water from the protonated alcohol occurs readily only with iodide. For this reason the conversion of primary alcohols to chlorides with hydrochloric acid usually requires quite high temperatures and the addition of large amounts of zinc chloride, or poor yields are the result (1).

It has occurred to us that the reaction rate could be increased by making use of the greater nucleophilicity of chloride ion in dipolar aprotic solvents compared with protonic solvents (2). We have chosen to examine hexamethylphosphoric triamide (HMPT), because it is moderately resistant to acid attack (3), and the products of such attack by hydrogen chloride are readily separated from alkyl chlorides.

The reaction is carried out at 50–85 °C using a 35–37% (by weight) solution of hydrogen chloride in HMPT. Within 30 min the alcohol is essentially undetectable by gas chromatography. Yields given in Table 1 are based on isolated products.

The reaction appears to be a convenient method giving very good yields, for the conversion of primary alcohols to the corresponding chloride. The mechanism may involve direct attack of chloride ion on a protonated alcohol:

$$RCH_2OH \overset{H^+}{\rightleftarrows} RCH_2\overset{+}{O}H_2 \overset{Cl^-}{\underset{S_N2}{\rightarrow}} RCH_2Cl + H_2O$$

but the intervention of a reagent containing a phosphorus–chloride bond (formed by the reaction of hydrogen chloride with HMPT) cannot at present be ruled out.

When optically active 2-octanol was used as substrate, the resulting 2-chlorooctane was racemized, probably by repeated displacement of chloride from the initially formed product by the chloride ion in the reaction mixture. No conclusions can therefore be drawn concerning the mechanism of hydroxyl replacement.

Experimental

The reagent is prepared by slowly passing hydrogen chloride gas from a commercial cylinder into HMPT. The mixture is allowed to warm somewhat to prevent crystal-

[1]This work was presented in part at the Southwest Regional Meeting of the American Chemical Society, Austin, Texas, December, 1968. The research was supported by the Robert A. Welch Foundation Grant E-136.

Can. J. Chem. Downloaded from www.nrcresearchpress.com by 210.87.254.6 on 09/05/12
For personal use only.

TABLE 1. Reaction of alcohols with hydrogen chloride in HMPT

Product	b.p. (°C)	i.r.(C–Cl, cm^{-1})	Reaction temperature (°C)	Yield (%)
1-Chlorohexane	130–133	650, 704	75–85	76
1-Chlorooctane	120–123 (137 Torr)	654, 790	75–85	87
2-Chlorooctane*	115 (140 Torr)	672	75–87	89
1-Chlorobutane	74–78	653, 709	70–80	74
Neopentyl chloride†	80–85	714, 900	71–80	65
m-Methoxybenzyl chloride	116 (10 Torr)‡	680	50–65	87

*When the temperature was raised to 100 °C the crude product of 2-chlorooctane showed (by g.c.) large amounts of 2-octene and unchanged 2-octanol.

†Although unchanged neopentyl alcohol was detected in the pentane extract, a g.c. analysis showed no traces of products of rearrangement. A number of other cases of neopentyl displacement in HMPT without rearrangement have recently been reported (6), although these reactions were not under acidic conditions. Neopentyl chloride has been prepared from the alcohol in two steps (53% overall yield) via neopentyl tosylate, and in unstated yield by the reaction of the alcohol with triphenylphosphine and carbon tetrachloride (6).

‡Reported (4, 5) 55 °C at 0.3 Torr, 124 °C at 13 Torr.

lization, but is maintained below 115 °C. Above this temperature an exothermic reaction occurs resulting in solvent decomposition. Gas flow is continued until the composition reaches 35–37% hydrogen chloride by weight. Smaller concentrations of hydrogen chloride lead to incomplete conversion, as do molar ratios (HCl:ROH) appreciably less than 10.

1-Chlorohexane was prepared by mixing 4.2 g (39 mmol) of 1-hexanol with 40 g of the HMPT·HCl reagent and heating on the steam bath for 45 min. The mixture was diluted with 50 ml of ice and water and was extracted twice with 40 ml of hexane. The organic layer was washed with sodium bicarbonate solution and with water, dried with magnesium sulfate, and filtered. Hexane was removed on a rotary evaporator and the residue of 1-chlorohexane was distilled at 130–133 °C (lit. (1) 131–134 °C) to give 3.59 g (76% yield). The identity of the product was confirmed by comparison of the g.c. retention time and i.r. spectrum with those of an authentic sample.

1- and 2-chlorooctanes, 1-chlorobutane, *m*-methoxybenzyl chloride, and neopentyl chloride were prepared by a procedure similar to that described for the preparation of 1-chlorohexane.

When hydrogen fluoride replaced hydrogen chloride in the reactions described above, no trace of alkyl fluoride was found.

Further studies are required before the stereochemical and mechanistic details of this reaction can be more fully understood.

1. R. H. CLARK and H. R. L. STREIGHT. Trans. R. Soc. Can. Sect. 3, **23**, 77 (1929).
2. A. J. PARKER. Chem. Rev. **69**, 1 (1969).
3. H. NORMANT. Angew. Chem. Int. Ed. Engl. **6**, 1046 (1967).
4. R. FUCHS and D. M. CARLTON. J. Am. Chem. Soc. **85**, 104 (1963).
5. R. PSCHORR. Ann. **391**, 44 (1912).
6. P. H. ANDERSON, B. STEPHENSON, and H. S. MOSHER. J. Am. Chem. Soc. **96**, 3171 (1974); B. STEPHENSON, G. SOLLADIÉ, and H. S. MOSHER. J. Am. Chem. Soc. **94**, 4184 (1974).

Can. J. Chem. Downloaded from www.nrcresearchpress.com by 210.87.254.6 on 09/05/12
For personal use only.

Separation of the Enthalpic and Entropic Contributions to Substituent Effects for the Equilibrium Constants of Aromatic Acids

T. M. KRYGOWSKI[1] AND W. R. FAWCETT

Guelph-Waterloo Centre for Graduate Studies in Chemistry (Guelph Campus), University of Guelph, Guelph, Ontario N1G 2W1

Received February 19, 1975

T. M. KRYGOWSKI and W. R. FAWCETT. Can. J. Chem. **53**, 3622 (1975).

Separation of the substituent effect $\rho\sigma$ into entropic $\rho_S\sigma_S$ and enthalpic $\rho_H\sigma_H$ contributions is presented within the framework of the general Hammett equation. Analysis of the experimental data for aromatic acids shows that, in general, entropic effects are the major contribution to the total substituent effect, the entropic reaction constant being approximately equal to the normal Hammett ρ. A comparison of the present results with those based on a separation of inductive and resonance effects shows that the entropic and inductive effects are directly related. On the other hand, strongly resonance interacting substituents were found to be enthalpy controlled. The substituent effect on enthalpy and entropy changes is discussed from a molecular point of view and related to inductive and resonance effects. A list of 16 enthalpic (σ_H) and entropic (σ_S) substituent constants are presented.

T. M. KRYGOWSKI et W. R. FAWCETT. Can. J. Chem. **53**, 3622 (1975).

On présente une séparation des effets de substituants $\rho\sigma$ en contributions entropique $\rho_S\sigma_S$ et enthalpique $\rho_H\sigma_H$ à l'intérieur de la généralisation de l'équation de Hammett. Une analyse des données expérimentales, pour des acides aromatiques, montre qu'en général les effets entropiques contribuent d'une façon majeure à l'effet total du substituant; la constante de réaction entropique est pratiquement égale à la valeur normale de ρ. Une comparaison des résultats actuels avec ceux calculés en faisant l'hypothèse qu'il existe une séparation des effets inductif et de résonance, montre que les effets entropiques et inductifs sont reliés directement. Par ailleurs, on a trouvé que les substituants interagissant d'une façon forte par résonance sont controlés par l'enthalpie. On discute de l'effet des substituants sur les changements dans l'enthalpie et dans l'entropie à partir d'un point de vue moléculaire relié aux effets inductif et de résonance. On présente une liste de 16 constantes de substituants enthalpiques (σ_H) et entropiques (σ_S).

[Traduit par le journal]

Introduction

Structure–reactivity relationships are usually discussed in physical organic chemistry within the context of linear free energy relationships (LFER) (1–4), the most popular examples being the Brønsted (5) and Hammett (6) equations. The LFER postulate states that changes in the free energy of activation $\Delta G^{\ddagger}$ within the reaction series $\{R_s\}$ in which the compounds undergo a regular variation in structure can be linearly related to the appropriate changes in standard free energy of reaction, ΔG^0 provided these changes are produced by the same kind of variation in structure. The postulate may be expressed quantitatively as follows:

$$[1] \qquad \Delta G^{\ddagger} = \alpha(\Delta G^0) + \beta$$

where α and β are constants.

In the case of the Hammett equation, ΔG^0 is replaced by the substituent constant σ which depends only on the nature of the substituent[2] and is independent of the nature of the reaction. According to Hammett (3, 6) and others (1, 8, 9) σ is defined for the so-called Hammett reaction, [2], in water in the following way:

$$[2] \quad \text{X—Ph—COOH} + \text{Ph—COO}^- \overset{K}{\rightleftharpoons} \text{X—Ph—COO}^- + \text{Ph—COOH}$$

$$[3] \qquad \log K = \rho\sigma$$

or

$$[4] \qquad \delta(\Delta G^0) = -2.303RT\,\rho\sigma$$

where ρ is the reaction constant and $\delta(\Delta G^0)$ is the variation in ΔG^0 due to changes in structure. The reaction constant is defined to be unity for

[1]Visiting professor on leave from the Department of Chemistry, University of Warsaw, Poland.

[2]This is true according to the generalized concept of substituent (7); otherwise, substituent constants also depend on their position in relation to the reaction site.

Can. J. Chem. Downloaded from www.nrcresearchpress.com by 210.87.254.5 on 09/05/12
For personal use only.

Can. J. Chem. Downloaded from www.nrcresearchpress.com by 210.87.254.5 on 09/05/12
For personal use only.

the Hammett reaction in water at 25 °C and 1 atm.

The LFER concept was developed further by Taft (10) who postulated that the separate contributions of resonance, inductive, and steric effects to the observed substituent effect could be estimated quantitatively using a modified form of [1]. Taft's postulate can be summarized as follows (11): (*i*) the effects being separated operate in the system independently, that is, by independent mechanisms; (*ii*) the LFER postulate, [1], holds separately for each of the effects. The postulate can be expressed quantitatively as follows:

$$[5] \qquad (\Delta G^{+})_j = \alpha_j(\Delta G^0)_j + \beta_j$$

where the subscript j refers to each of the independent effects, generally considered to be inductive (i), resonance (r), and steric (s). In general, the proportionality constants α_j are not equal for the various contributions ($\alpha_i \neq \alpha_r \neq \alpha_s$) and they depend on the nature of the reaction and on experimental conditions.

Application of Taft's equation has permitted the different effects of substituents at the reaction site to be analyzed. Although several other extensions of the Hammett equation, including those by Exner (12), van Bekkum *et al.* (13), and Yukawa and Tsuno (14), have been developed, they all represent extensions of the Taft postulate in different ways and on the basis of different model reactions. It should be pointed out that Hammett in his early discussion of the relation between structure and reactivity pointed out that the free energy change with substituent can be considered as a sum of three terms: an entropy change, and the changes in kinetic and potential energies. All three terms must be considered in any attempt to correlate structure with reactivity but little is usually known about the first two (4).

A recent analysis (15) of the Taft postulates has led to the following conclusions[3]: (*i*) a Hammett $\rho\sigma$ equation with constant σ values valid over a range of temperatures for a variety of reactions in different solvents holds only when either the field or the resonance interaction is negligible compared with the other; (*ii*) a simple relationship between ΔH^0 and ΔS^0 values for a given reaction series cannot be anticipated when a substantial range of substituents are considered.

[3]For a general discussion of this problem see also refs. 1, 3, 10, and 11.

The aim of the present paper is to introduce a different extension of the LFER, namely in terms of the independent enthalpic $\delta\Delta H^0$ and entropic $\delta\Delta S^0$ contributions to the structural effect normally considered, $\delta\Delta G^0$. The results of the new analysis are compared with those from the normal Hammett equation as well as those from its extension in which substituent effects are separated into inductive and resonance contributions (16). Finally, the separation of the substituent effect into enthalpic and entropic contributions is associated with the so-called compensation effect (17) and the related concepts of isokinetic (18) and isoequilibrium relationships (19).

Independence of the Enthalpic and Entropic Contributions in the LFER

It is implicitly assumed in the general LFER as well as in its extension by Taft that the enthalpic and entropic terms in ΔG are mutually colinear and vary in the same way with changes in structure, or that one or other of these terms is constant within the reaction series. Thus, the ratio $\Delta S/\Delta H$ or ΔS or ΔH should be constant, independent of the nature of the reaction which follows a LFER. It is clear from the literature that no one of these conditions is generally fulfilled (15). Thus, on the basis of a thorough statistical analysis of enthalpy–entropy relationships, Exner (18, 20) has concluded that much of the earlier evidence for linearity between ΔH and ΔS is doubtful since these quantities were normally obtained from Arrhenius or van't Hoff plots and could not be considered as statistically independent.

It is postulated here that for a series of compounds with some regular variation in structure, the effects of structure variation can be represented by a linear variation in two independent quantities, one enthalpic and the second entropic. Thus, the linear relationships used here are

$$[6] \qquad \Delta H = \alpha_H(\Delta H^0) + \beta_H$$

and

$$[7] \qquad \Delta S = \alpha_S(\Delta S^0) + \beta_S$$

ΔH and ΔS represent either standard enthalpy and entropy changes or the enthalpy and entropy of activation depending on whether equilibrium constant or rate constant data, respectively are being considered. These may be combined to

Can. J. Chem. Downloaded from www.nrcresearchpress.com by 210.87.254.5 on 09/05/12
For personal use only.

TABLE 1. A summary of σ parameters

Substituent	σ		σ_H	f_H*	σ_S	f_S*
	Hepler (9)	McDaniel and Brown (8)				
H	0.000	0.000	0.000	—	0.000	—
m-NO_2	0.744	0.710	−0.198	0.17	0.942	0.83
p-NO_2	0.780	0.788	−0.236	0.18	1.016	0.82
m-Br	0.394	0.391	−0.051	0.10	0.446	0.90
p-Br	0.224	0.232	−0.029	0.10	0.253	0.90
m-Cl	0.371	0.373	−0.066	0.13	0.437	0.87
p-Cl	0.220	0.227	−0.095	0.23	0.315	0.77
m-F	0.341	0.337	−0.081	0.16	0.422	0.84
m-I	0.350	0.350	−0.059	0.12	0.409	0.88
p-I	0.209	0.180	0.023	0.11	0.186	0.89
m-OH	0.127	0.120	−0.037	0.18	0.164	0.82
p-OH	−0.377	−0.370	−0.191	0.51	−0.186	0.49
m-CH_3	−0.048	−0.069	0.029	0.27	−0.077	0.73
p-CH_3	−0.158	−0.170	−0.103	0.65	−0.055	0.35
m-CH_3O	0.113	0.115	0.045	0.39	0.068	0.61
p-CH_3O	−0.280	−0.268	−0.359	0.81	0.079	0.19

*f_H and f_S are fractional substituent constants and are defined by [19]; when multiplied by 100 they simply express the percentage of enthalpic and entropic contribution to the total substituent effect.

obtain the following expression for the variation in free energy change:

$$[8] \quad \Delta G = \alpha_H(\Delta H^0) - \alpha_S(T\Delta S^0) + \beta_H - \beta_S T$$

When this relationship is compared with the common LFER, [1], it is apparent that the essential difference in the present approach is that the proportionality constants α_H and α_S are not assumed to be necessarily equal as they are in the usual LFER.

When the above postulate is extended to the particular case of the Hammett equation, one may rewrite [3] in the form

$$[9] \quad \log K = \rho_H\sigma_H + \rho_S\sigma_S$$

where σ_H and σ_S are independent substituent constants accounting for the enthalpic and entropic contributions, respectively and ρ_H and ρ_S, the corresponding reaction constants analogous to α_H and α_S in the general linear relations [6] and [7]. In the present paper only equilibrium constant data will be considered but, as usual, [9] may be applied to either rate or equilibrium constant data. σ_H and σ_S are defined by the relations

$$[10a] \quad \sigma_H = \frac{-\delta(\Delta H^0)}{2.303RT}$$

and

$$[10b] \quad \sigma_S = \frac{\delta(\Delta S^0)}{2.303R}$$

where $\delta(\Delta H^0)$ and $\delta(\Delta S^0)$ are the changes in the standard enthalpy and entropy of [2] with changes in substituent. These quantities may be calculated from the recently published data of Hepler and co-workers (9). In agreement with Hammett's original concept ρ_H and ρ_S are defined to be unity for [2] in water at 25 °C and 1 atm. Available values of σ_H and σ_S together with original σ values from McDaniel and Brown (8) and Hepler (9) are summarized in Table 1.

Interpretation of σ_H and σ_S

The Hammett σ constants directly reflect a shift in the position of [2] with a change in substituent. Thus, when σ is positive, [2] is shifted to the right and the substituted anion $XPhCOO^-$ acts as a weaker base than the unsubstituted anion $PhCOO^-$. Thus, substituents with positive σ's are normally classified as electron withdrawing such that they decrease the total electron charge density on the reaction site for both the acid and its anion. When σ is negative, the reverse situation holds; the sub-

Can. J. Chem. Downloaded from www.nrcresearchpress.com by 210.87.254.5 on 09/05/12
For personal use only.

stituent is assumed to be electron repelling and to increase the electron charge density at the reaction site.

The same kind of interpretation cannot be applied to σ_H and σ_S. From [2] it is apparent that changes in ΔS^0 with substituent chiefly reflect changes in the way the components of this equilibrium interact with the medium, the more important contributions being from the anions. However, although $\delta\Delta S^0$ reflects changes in solute–solvent interactions, its magnitude is governed by changes in the electron charge density distribution in the solute molecule. According to Hepler (21) changes in ΔH^0 with the substituent can be attributed to both intramolecular (internal) and intermolecular (external) changes, that is

$$[11] \qquad \delta\Delta H^0 = \delta\Delta H^0_{int} + \delta\Delta H^0_{ext}$$

The latter contribution is often assumed to be proportional to the corresponding entropy change (21):

$$[12] \qquad \delta\Delta H^0_{ext} = \beta_e \delta\Delta S^0$$

where β_e has the significance of a temperature and should be the same for all aqueous acids of the same charge type (21). From a molecular point of view the internal contribution to the change in enthalpy is composed of inductive (field) and resonance contributions:

$$[13] \qquad \delta\Delta H^0_{int} = \delta\Delta H^0_i + \delta\Delta H^0_r$$

Thus, combining [11]–[13], one obtains the following expression for $\delta\Delta G^0$:

$$[14] \quad \delta\Delta G^0 = \delta\Delta H^0_i + \delta\Delta H^0_r + (\beta_e - T)\,\delta\Delta S^0$$

Previous extensions of the original Hammett relationship have assumed that the inductive and resonance contributions to the total substituent effect are independent (16). The relationship of $\delta\Delta S^0$ to these contributions is more subtle and will be examined in more detail below. However, it is apparent that $\delta\Delta H^0$ and $\delta\Delta S^0$, and thus σ_H and σ_S are related to one another, albeit, in a complicated fashion.

On plotting σ_S against σ_H (Fig. 1), an approximate linear correlation is apparent if three of the 16 substituents listed in Table 1 (*p*-OH, *p*-OCH_3, and *p*-CH_3) are excluded. The best straight line for the remaining 13 points is

$$[15] \qquad \sigma_S = -3.6\,\sigma_H + 0.15$$

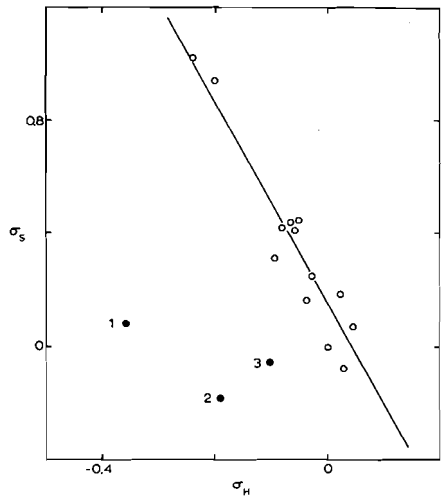

FIG. 1. Plot of the entropy substituent constant, σ_S against the enthalpy substituent constant, σ_H. The three points (●) lying outside the approximate linear relationship are (*1*) *p*-CH_3O, (*2*) *p*-OH, and (*3*) *p*-CH_3.

with a correlation coefficient $R = 0.953$. The large value of the slope is evidence for the predominant role of entropy in the substituent effect, a point which is well recognized in the literature (1).

The three substituents which deviate from the linear relationship in Fig. 1 are known to interact with the reaction site (—COOH or $—COO^-$) by resonance as electron donors. In considering the role of inductive and resonance contributions in substituent effects in more detail, two points must be emphasized: (*i*) $\delta\Delta H^0_i$ and $\delta\Delta H^0_r$ are not necessarily related to each other in any regular fashion; (*ii*) since these quantities are associated with variation in the electron charge distribution in the solute molecules, changes in ΔH^0_i and ΔH^0_r will cause changes in solvent organization around the solute and thus changes in ΔS^0. In other words, one may assume an empirical relationship between these quantities of the form

$$[16] \qquad \delta\Delta S^0 = \alpha_i \delta\Delta H^0_i + \alpha_r \delta\Delta H^0_r + \gamma$$

Inductive and resonance contributions to the substituent effect are normally estimated using the well known substituent constants σ_i and σ_r (16). If it is assumed that $\delta\Delta H^0_i$ and $\delta\Delta H^0_r$ can be related to these experimentally independent quantities by equations similar to [10], then the above relationship may be tested by planar regression. Application of standard regression

Can. J. Chem. Downloaded from www.nrcresearchpress.com by 210.87.254.5 on 09/05/12
For personal use only.

techniques to values of σ_S for *para*-substituents results in the equation

$$[17a] \quad \sigma_S(para) = (1.2 \pm 0.2)\sigma_i \pm (0.8 \pm 0.2)\sigma_r + (0 \pm 0.1)$$

for 8 points with $R = 0.946$. Keeping in mind the fact that there is no correlation between σ_i and σ_r ($R_{ir} = -0.081$), this result is good evidence that both inductive and resonance effects contribute to $\delta\Delta S^0$, the inductive contribution being predominant (67% of the explained variation in σ_S). When this analysis is applied to *meta*-substituent constants the resulting regression plane is

$$[17b] \quad \sigma_S(meta) = (1.2 \pm 0.1)\sigma_i + (0.4 \pm 0.1)\sigma_r + (0 \pm 0.1)$$

Thus, although ρ_i is independent of the position of the substituent, ρ_r increases significantly when *meta*-substituents are replaced by *para*-substituents. The first result agrees with the usual assumption that the inductive effect is approximately the same for *para*- and *meta*-substituents. In fact, a more rigorous treatment of this question has shown that the difference in inductive effects for these substituents should be the order of 10% (42) but this difference could not be detected within the precision of the present analysis. The increase in ρ_r when the substituent is moved from a *meta*-position to a *para*-position follows the generally accepted concept that resonance effects are considerably higher in the *para*-position.

As pointed out above, resonance interactions between the substituent and reaction site (COOH or COO^-) are only important for *para*-substituted electron-donating groups, the chief contribution to this interaction being generally inductive in character. This is probably the chief reason for the good correlation between σ and σ_S, namely

$$[18] \quad \sigma = 0.91\sigma_S - 0.07$$

with $R = 0.946$ for 16 points. Thus, the total substituent effect closely follows the entropic contribution. The enthalpic contribution, being relatively small and related through [14] and [16], is hidden in the statistical analysis because of the small non-inductive contribution of the reaction sites in the chosen reference reaction [2]. Thus, the generally observed validity of the original Hammett substituent constants breaks down when there is a significant increase or decrease in the enthalpic contribution for a process being compared with the reference reaction.

In order to assess more easily the relative contributions of enthalpy and entropy to the substituent effect of individual substituents, fractional substituent constants f_H and f_S defined by the following equations are included in Table 1:

$$[19a] \quad f_H = \frac{|\sigma_H|}{|\sigma_H| + |\sigma_S|}$$

$$[19b] \quad f_S = \frac{|\sigma_S|}{|\sigma_H| + |\sigma_S|}$$

where $|\sigma_H|$ and $|\sigma_S|$ are the absolute values of the enthalpic and entropic substituent constants for a given substituent. It is apparent that for most substituents considered the entropic contribution is more than 80% of the total substituent effect. Only in three cases (*p*-OH, *p*-CH_3, and *p*-OCH_3) is the enthalpic contribution greater than 50%. As argued above, this reflects the fact that resonance interactions are strong for these substituents. This point may be further clarified on the basis of the following analysis. In that interaction of *meta*-substituents is chiefly inductive in character, one may assume that $\Delta^{pm}(\Delta H^0)$ and $\Delta^{pm}(\Delta S^0)$ which are defined by the equations

$$[20a] \quad \Delta^{pm}(\Delta H^0) = \Delta H^0_{para} - \Delta H^0_{meta}$$

$$[20b] \quad \Delta^{pm}(\Delta S^0) = \Delta S^0_{para} - \Delta S^0_{meta}$$

chiefly reflect the excess in the given thermodynamic quantity due to resonance when a given substituent is *para*-substituted rather than *meta*-substituted. Then, following Hepler and coworkers (15, 19, 21), one may estimate the internal contribution to ΔH^0 due to resonance as

$$[21] \quad \Delta H_r = \Delta^{pm}(\Delta H^0) - \beta_e\Delta^{pm}(\Delta S^0)$$

where $\beta_e \simeq 300$ K (21, 22). When ΔH_r was plotted against the experimentally independent parameter σ_r, a good straight line was obtained. Although the analysis must be considered approximate because of the approximations made, and the small magnitude of ΔH_r with respect to experimental error, it clearly shows that the resonance contribution to the substituent effect for *p*-OH and *p*-OCH_3 is the largest for the substituents considered here.

Considerable insight into the relative importance of internal and environmental contributions to the substituent effect can be obtained

Can. J. Chem. Downloaded from www.nrcresearchpress.com by 210.87.254.5 on 09/05/12
For personal use only.

by examining thermodynamic data for the corresponding reaction in the gas phase. One would expect ΔH^0 for [2] in the gas phase to be negative for electron-withdrawing substituents because the energy required to break the O—H bond in the substituted acid should be less than that required for the unsubstituted acid. This trend is confirmed in experimental studies of the intrinsic acidities of organic acids in the gas phase (23). On the other hand, the environmental contribution to ΔH^0 should be positive for electron-withdrawing substituents since energy must be expended in breaking the hydrogen bonds in the structured solvent, water. If one accepts that the environmental contribution to ΔH^0 is proportional to ΔS^0, then the positive contribution should increase with increase in electron-withdrawing character. The fact that the majority of σ_H values are negative indicates that the environmental contribution to $\delta(\Delta H^0)$ is greater than the intrinsic contribution. A more extensive analysis of data for the gas phase acidities of substituted benzoic acids obtained recently by Kebarle and co-workers (41) is given in the following section.

Application to Equilibrium Data for the Ionization of Aromatic Acids

The proposal made above was tested with equilibrium constant data for reactions of substituted aromatic acids in various solvents including the ionization of anilinium cations and phenols. The latter two reaction series are known not to fit the original Hammett equation well because of resonance interaction of some substituents with the reaction site ($-NH_3^+$ or —OH). The results are compared with the parameters obtained by analyzing the same data on the basis of substituent constants for the separate inductive and resonance effects (16) and on the basis of the classical Hammett equation.

The constants ρ_H, ρ_S, ρ_i, ρ_r, and ρ in the equations

$$[22] \quad \log K_e = \log K_{eo} + \rho_H\sigma_H + \rho_S\sigma_S$$

$$[23] \quad \log K_e = \log K_{eo} + \rho_i\sigma_i + \rho_r\sigma_r$$

$$[24] \quad \log K_e = \log K_{eo} + \rho\sigma$$

were determined by standard regression techniques (24) for a plane and straight line. K_e is the equilibrium constant and K_{eo}, the value for the unsubstituted compound in the given series.[4] The results together with estimated errors and correlation coefficients are summarized in Table 2. It should be noted that the values of σ used were those obtained recently by Hepler and co-workers (9).

Since σ_H and σ_S do not vary by the same amounts for a given data set, it is not possible to determine the relative contributions of enthalpy and entropy to the explained variation in log K_e simply by examining the values of ρ_H and ρ_S obtained by the regression analysis. However, this may be achieved by calculating the partial regression coefficients (24) which are defined by the equations

$$[25a] \quad \rho_H' = |\rho_H| \left(\frac{\sum_{i=1}^{n} (\sigma_{H,i} - \bar{\sigma}_H)^2}{\sum_{i=1}^{n} (\log K_{e,i} - \overline{\log K_e})^2} \right)^{1/2}$$

and

$$[25b] \quad \rho_S' = |\rho_S| \left(\frac{\sum_{i=1}^{n} (\sigma_{S,i} - \bar{\sigma}_S)^2}{\sum_{i=1}^{n} (\log K_{e,i} - \overline{\log K_e})^2} \right)^{1/2}$$

where $\bar{\sigma}_H$, $\bar{\sigma}_S$, and $\overline{\log K_e}$ represent the average values of the quantities σ_H, σ_S, and log K_e for the given data set. For convenience ρ_H' and ρ_S' are normalized in the following way:

$$[26a] \quad \bar{\rho}_H = \frac{100\rho_H'}{\rho_H' + \rho_S'}$$

and

$$[26b] \quad \bar{\rho}_S = \frac{100\rho_S'}{\rho_H' + \rho_S'}$$

$\bar{\rho}_H$ and $\bar{\rho}_S$ may be regarded as the percentage of enthalpic and entropic contributions, respectively to the observed substituent effects. Values of $\bar{\rho}_H$ and $\bar{\rho}_S$ calculated for the data considered are also recorded in Table 2. The same kind of analysis was performed when the data for *para*-substituted compounds were analyzed on the basis of [23].

[4]Equations 3 and 9 imply that ρ, and ρ_H and ρ_S should be determined by one and two parameter fits, respectively, rather than by two and three parameter fits as indicated by [22] and [24]. Comparison of results obtained by the two methods showed no significant difference in ρ values. Thus, the results are reported for fits of [22] and [24] since [24] corresponds to the form of the Hammett equation normally used.

Can. J. Chem. Downloaded from www.nrcresearchpress.com by 210.87.254.5 on 09/05/12
For personal use only.

TABLE 2. Results of application of the enthalpy–entropy separated and normal Hammett equations to equilibrium data for the reactions of aromatic acids*

Reaction	ρ_H	ρ_S	$\bar{\rho}_H$	$\bar{\rho}_S$	$\Delta\bar{\rho}_S$	R_P	ρ	R_L	n
1. Ionization of benzoic acids in water (8)	1.00	1.00	24	76	0	1.00	1.00	1.00	15
2. Reaction 1 in 33.2% ethanol–water (25)	0.95±0.14	1.31±0.04	19	81	6±3	0.995	1.33±0.06	0.991	12
3. Reaction 1 in 52.0% ethanol–water (25)	1.0±0.2	1.42±0.07	19	81	6±4	0.990	1.44±0.08	0.985	12
4. Reaction 1 in 73.4% ethanol–water (25)	1.2±0.2	1.54±0.07	20	80	4±4	0.991	1.55±0.08	0.988	12
5. Reaction 1 in 84.5% ethanol–water (25)	1.2±0.3	1.55±0.10	20	80	4±5	0.981	1.57±0.10	0.978	12
6. Reaction 1 in ethanol (25)	1.2±0.2	1.70±0.06	19	81	5±3	0.994	1.72±0.08	0.990	12
7. Reaction 1 in methanol (25)	1.5±0.4	1.39±0.09	19	81	−1±5	0.994	1.36±0.06	0.994	9
8. Reaction 1 in *n*-butyl alcohol (27)	1.4±0.3	1.48±0.1	22	78	1±5	0.977	1.47±0.09	0.976	14
9. Reaction 1 in ethylene glycol (14)	1.3±0.2	1.24±0.06	22	75	−2±5	0.982	1.24±0.07	0.982	14
10. Reaction 1 in 26.5% dioxane–water (28)	0.9±0.1	1.22±0.03	17	83	4±2	0.997	1.22±0.04	0.994	11
11. Reaction 1 in 43.5% dioxane–water (28)	1.1±0.1	1.33±0.06	21	79	3±4	0.987	1.33±0.06	0.986	14
12. Reaction 1 in 73.5% dioxane–water (28)	0.9±0.8	1.3±0.2	17	83	6±15	0.859	1.3±0.2	0.855	14
13. Reaction 1 in dimethylsulfoxide (26)	1.4±0.9	2.4±0.2	12	88	6±8	0.977	2.48±0.20	0.973	11
14. Protonation of benzoic acid in sulfuric acid (29)	1.1±0.2	1.01±0.09	36	64	−2±5	0.986	1.03±0.07	0.986	9
15. Reaction 1 in 60% H_2SO_4 (30)	1.9±0.1	1.20±0.05	37	63	−10±2	0.994	1.26±0.08	0.974	14
16. Protonation of salicylic acid in sulfuric acid (29)	1.5±0.2	1.29±0.06	27	73	−3±3	0.992	1.30±0.06	0.990	12
17. Ionization of phenols in water (31)	1.0±0.8	2.5±0.3	12	88	13±9	0.959	2.5±0.3	0.940	12
18. Reaction 17 in dimethylsulfoxide (32)	3.9±2.3	4.9±0.7	21	79	4±12	0.937	4.9±0.7	0.935	9
19. Ionization of hydroxyazobenzenes in dimethylsulfoxide (32)	0.7±0.2	0.8±0.1	22	78	3±5	0.984	0.84±0.05	0.983	10
20. Ionization of 5-methyl-2-hydroxyazobenzenes in dimethylsulfoxide (32)	−0.1±0.2	0.81±0.07	5	95	20±8	0.984	0.86±0.14	0.917	9

Can. J. Chem. Downloaded from www.nrcresearchpress.com by 210.87.254.5 on 09/05/12
For personal use only.

TABLE 2 (*Concluded*)

Reaction	ρ_H	ρ_S	$\bar{\rho}_H$	$\bar{\rho}_S$	$\Delta\bar{\rho}_S$	R_P	ρ	R_L	n
21. Ionization of 4-phenylazo-1-naphthol in dimethylsulfoxide (32)	−1.6±0.7	1.1±0.2	31	69	7±14	0.895	1.1±0.2	0.885	9
22. Ionization of 1-phenylazo-1-naphthol in dimethylsulfoxide (32)	1.1±0.5	1.8±0.2	17	83	8±7	0.978	1.9±0.2	0.969	9
23. Ionization of phenyl phosphoric acid in water (33)	0.6±0.2	0.71±0.04	20	80	1±5	0.989	0.71±0.04	0.988	9
24. Reaction 23 in 50% ethanol–water (33)	0.6±0.2	0.98±0.05	15	85	7±5	0.988	0.98±0.05	0.987	10
25. Ionization of monohydrogen phenyl phosphate anion in water (33)	0.6±0.2	0.97±0.06	15	85	7±5	0.988	0.96±0.06	0.982	10
26. Reaction 25 in 50% ethanol–water (33)	0.5±0.2	0.97±0.06	14	86	8±5	0.988	0.96±0.07	0.980	10
27. Protonation of diphenylamines in 20% ethanol–water (34)	2.0±1.4	3.7±0.4	14	86	9±10	0.970	3.8±0.4	0.960	8
28. Dehydration of 2,2,2-trifluoro-1,1-dihydroxyethylbenzene (35)	3.1±0.2	2.1±0.1	37	63	−9±3	0.996	2.1±0.2	0.975	7
29. Ionization of benzamides in water (36)	1.3±0.1	1.27±0.04	26	74	1±2	0.995	1.27±0.04	0.995	11
30. Protonation of benzyldimethyl amines (37)	1.0±0.5	1.3±0.1	14	86	4±7	0.993	1.4±0.1	0.992	8
31. Ionization of anilinium cations in water (31)	2.3±1.0	3.4±0.3	18	82	7±8	0.965	3.47±0.33	0.958	12

*$\bar{\rho}_H$ and $\bar{\rho}_S$ are normalized partial reaction constants (see [25] and [26]) which give the percent of the explained variation in log K_e which can be attributed to enthalpic and entropic effects, respectively. $\Delta\bar{\rho}_S$ is the difference between $\bar{\rho}_S$ for the given reaction and that for the reference reaction calculated on the basis of the same set of substituents. R_P and R_L are the correlation coefficients for planar and linear regressions, respectively and n, the number of data points.

Can. J. Chem. Downloaded from www.nrcresearchpress.com by 210.87.254.5 on 09/05/12
For personal use only.

It is apparent from the data in Table 2 that ρ_S is approximately equal to the classical Hammett reaction constant ρ. This result is a direct consequence of the linear relationship between σ and σ_S pointed out above. On the other hand, ρ_H is usually less than ρ_S even though ρ_H is defined to be equal to ρ_S for the reference reaction. The data in Table 2 clearly show that the relative contributions of enthalpy and entropy to the changes in standard free energy of reaction vary with the nature of the reaction and with the medium.

Keeping in mind the analysis of the relationship between σ_H and σ_S presented above, one might expect ρ_H and ρ_S to depend somewhat on the nature of the specific substituents chosen in a given experimental study, that is, on whether enthalpy controlled substituents are included. In order to avoid misinterpretation of the data presented in Table 2, $\bar{\rho}^0{}_S$, the value of $\bar{\rho}_S$ for the reference reaction, [2], estimated for the same collection of substituents considered in a given data set was also calculated. The quantity $\Delta\bar{\rho}_S = \bar{\rho}_S - \bar{\rho}^0{}_S$ and its estimated error reported in Table 2 were used as a test of statistical reliability of $\bar{\rho}_S$. Thus, when $\Delta\bar{\rho}_S$ is non-zero and greater than its estimated error, the value of $\bar{\rho}_S$ for the given reaction was considered to be reliably different from the value obtained for the reference reaction. The same calculation was not carried out for $\bar{\rho}_H$ since this parameter is normally estimated with less precision.

From the data in Table 2, it is apparent that $\Delta\bar{\rho}_S$ is significant for 11 of the 31 cases considered; these systems will be emphasized in the following discussion. Although the entropic contribution usually accounts for approximately 80% of the explained variation in log K_e, $\bar{\rho}_S$ varies from a low of 63% for the protonation of benzoic acid in 60% sulfuric acid (29) to a high of 95% for the ionization of 5-methyl-2-hydroxyazobenzenes in dimethylsulfoxide (32).

The variation in $\bar{\rho}_S$ can be discussed both from the point of view of changes in internal interactions and changes in solute–solvent interactions, although it is clear that the two effects cannot be separated completely. Considering internal interactions first, it is useful to compare the protonation of benzoic acid, and ionization of phenol with the ionization of benzoic acid. The protonated form of benzoic acid can interact strongly by resonance with electron-donating substituents such as methoxy:

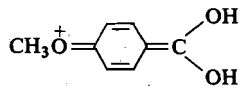

1

Since electron-donating substituents in the *para*-position are enthalpy controlled, one expects $\bar{\rho}_H$ to be significantly higher for the protonation of benzoic acid than it is for the reference reaction. In the case of ionization of phenols, the phenoxide anion can interact strongly by resonance with electron-withdrawing substituents. These substituents are entropy controlled, so that this reaction has a higher value of $\bar{\rho}_S$ than the reference reaction. Thus, in some cases, the change in $\bar{\rho}_S$ with nature of the reaction can be clearly attributed to changes in resonance interactions.

The effect of medium on reaction parameters for [2] can be seen by examining the first 13 sets of data presented in Table 2. Since internal contributions to the substituent effect will not change, the changes observed can be attributed to change in solute–solvent interactions and thus, are most conveniently discussed in terms of changes in ρ_S. Considering the fact that the charged components of [2] are anions, the most important property of the solvent is its acidity, that is its ability to solvate anions (38). If one chooses the Dimroth–Reichardt parameter E_T (39) as a measure of solvent acidity it is apparent that ρ_S decreases with an increase in solvent acidity. Thus ρ_S has its largest value in dimethylsulfoxide which in turn is the least acidic of the solvents considered (E_T = 45.0) and its lowest value in water the most acidic solvent (E_T = 63.1). This result is consistent with well known solvent effects on acid–base reactions. Thus, as solute–solvent interactions increase in strength, the differentiation in the acidity of benzoic acids due to change in substituent becomes less pronounced. The above type of analysis only considers solute–solvent interactions in terms of their acidity or basicity and ignores structure-breaking and structure-making effects which accompany solute–solvent interactions. Obviously, a complete analysis must consider all effects (38).

When the recent gas phase data for the acidity constants of benzoic acids measured by Kebarle

Can. J. Chem. Downloaded from www.nrcresearchpress.com by 210.87.254.5 on 09/05/12
For personal use only.

and co-workers (41) are analyzed according to [9], the following result is obtained.[5]

$$[27] \qquad \log K_a = 8.2\sigma_S + 2.8\sigma_H$$

with $R = 0.990$ for 12 points. The value of ρ_S is surprisingly high compared to ρ_H, the corresponding values of $\bar{\rho}_S$ and $\Delta\bar{\rho}_S$ being 90 and 15%, respectively. These results indicate that there is a very strong correlation between the standard enthalpy change for the gas phase reaction and σ_S, whereas that for σ_H is weak. No explanation can be offered for this result. However, the high values of ρ_S and ρ_H support the proposal made above that the reaction constants increase with a decrease in solute–solvent interactions, the highest value of ρ_S being that observed in the gas phase. Thus, when solute–solvent interactions are absent the differentiation n acidities of the benzoic acids increases significantly.

Values of ρ_i obtained by fitting [23] to data for *para*-substituted derivatives in the 32 reaction series listed in Table 2 have been compared with the corresponding values of ρ_S, a good linear relationship being obtained. This result is interpreted as evidence that the chief intramolecular interaction which controls solute–solvent interactions and which is quantitatively estimated for the substituent effect as ρ_S, is inductive in character. On the other hand, a purely electronic (intramolecular) interpretation of ρ_i must be considered naive because it does not account for changes in ρ_i with the nature of the solvent.

Discussion

In the same way that the LFER is an empirical relationship with no clear theoretical basis, there is no theoretical justification for a linear enthalpy–entropy relationship. However, the above analysis suggests that use of the method proposed here would result in a significant clarification of the relative importance of the inductive and resonance contributions to the observed changes in ΔG with substituent, and also of the relationship of internal interactions in the reactant molecule to external interactions with surrounding solvent molecules. The fact that there is a good correlation between the classical σ and σ_S means that addition of the parameter σ_H to the relationship describing substituent effects should result in an improved fit of the data; this is confirmed by the results summarized in Table 2. A comparison of the present analysis with that based on separation of inductive and resonance effects reveals the direct relationship between the inductive reaction constant ρ_i and the entropic one, ρ_S. However, the inductive–resonance analysis describes the total substituent effect much more poorly and thus, does not provide a clear indication of the relative importance of these two effects. As argued above, the relative contributions of entropy and enthalpy to the substituent effect, $\bar{\rho}_S$ and $\bar{\rho}_H$ provide a clear indication of the relative importance of resonance effects in comparison with the reference reaction.

Further support for the proposed analysis is obtained by analysis of the dependence of other substituent constants on σ_H and σ_S. As is well known (16, 40), several different series of substituent constants have been proposed for reaction types which do not follow the original Hammett equation and for *ortho*-substituents. Results of fitting the equation

$$[28] \qquad \sigma_j = \rho_H\sigma_H + \rho_S\sigma_S$$

where σ_j represents a particular series of substituent constants are summarized for five sets of constants in Table 3. It is immediately apparent that good fits are obtained in all cases so that all these analyses could be replaced by the analysis proposed here. Two results are of particular interest. The 'right' substituent constants (σ^0) are proposed for reactions with very low or negligible contribution from resonance interaction. On applying [28] one obtains $\bar{\rho}_S = 86\%$, that is, 10% higher than that for the reference reaction. Thus, a reaction with low resonance interactions may be described as entropy controlled. On the other hand, the parameter σ_p^+ is used when electron-donating substituents interact strongly with the reaction site by resonance (16). Then, $\bar{\rho}_S$ is decreased to 44% indicating that such reactions may be described as enthalpy controlled.

From the analysis of the data presented here it is evident that the theoretical background of the LFER must be more carefully investigated using advanced quantum mechanical calculations and

[5]The data of Kebarle and co-workers (41) are actually estimates of the standard enthalpy change for the gas phase ionization of benzoic acids and correspond to the difference between the bond dissociation energy for the O—H bond in the acid and the electron affinity of the corresponding radical, RCOO·. Assuming ΔS^0 for the reaction is negligible, $\log K_a$ is given by $-\Delta H^0/2.3RT$.

TABLE 3. Results of application of the enthalpy–entropy separated Hammett equation to various substituent constants*

Substituent constant σ_J	ρ_H	ρ_S	$\bar{\rho}_H$	$\bar{\rho}_S$	$\Delta\bar{\rho}_S$	R_P	n
1. σ^0 (or σ^n) (16)	0.45±0.16	0.87±0.05	14	86	10± 5	0.978	16
2. σ_p^+ (16)	2.3 ±0.3	1.4 ±0.3	56	44	−13± 8	0.982	7
3. σ_{ortho} (40)	1.25±0.08	1.08±0.03	30	70	− 3± 2	0.999	6
4. σ^0_{ortho} (40)	2.5 ±0.1	1.38±0.05	41	59	−13± 2	0.998	6
5. σ^-_{ortho} (40)	1.4 ±0.5	1.3 ±0.2	29	71	− 1±11	0.967	6

*For definitions of the various substituent constants see refs. 16 and 40. The various parameters tabulated are defined in Table 2. In the case of *ortho*-substituent constants (3–5), σ_S and σ_H for *para*-positions were chosen for the regression analysis.

gas phase measurements of the appropriate equilibrium constants. It should then be possible to separate intramolecular and intermolecular interactions which the above analysis has shown to contribute to both enthalpic and entropic changes in a complex way. The usefulness of the present analysis in elucidating these effects could be increased considerably if values of ΔH^0 and ΔS^0 were available for a larger variety of substituents, especially those which interact strongly by resonance. In this regard, it must be emphasized that these 'irregular' substituents should be included in any experimental study of substituent effects in order that statistically reliable results be obtained.

The data analyzed in this paper represent only a small fraction of those available. However, the data selected amply illustrate the usefulness of separately considering enthalpic and entropic contributions to the substituent effect. The present treatment could prove especially useful in the analysis of kinetic data obtained for a series of compounds at one temperature in that it provides a method of separating enthalpic and entropic effects. Thus, it could be used to obtain a better picture of the transition state and of its interactions with the environment.

Finally the approach presented in this paper is limited to the Hammett representation of the LFER. Undoubtedly, the same type of treatment could be extended to other equations based on LFER in the areas of both structure–property relationships and medium effects.

The authors would like to express their gratitude to M. Charton, L. G. Hepler, and J. Shorter for helpful comments and discussion of an original version of this paper.

The financial support of the National Research Council of Canada is gratefully acknowledged.

1. J. E. LEFFLER and E. GRUNWALD. Rates and equilibria of organic reactions. J. Wiley, New York. 1963.
2. YU. A. ZHDANOV and V. I. MINKIN. Korrelatsionnyi analiz v organicheskoi khimii. Izd. Rostovsk. Univ., Rostov. 1966.
3. L. P. HAMMETT. Physical organic chemistry. McGraw-Hill, New York. 1970.
4. H. H. JAFFE. Chem. Rev. **53**, 191 (1953).
5. J. N. BRØNSTED and K. J. PEDERSON. Z. Phys. Chem. **108**, 185 (1924).
6. L. P. HAMMETT. J. Am. Chem. Soc. **59**, 96 (1937).
7. T. M. KRYGOWSKI. Bull. Acad. Pol. Sci. Ser. Sci. Chim. **19**, 49 (1971); T. M. KRYGOWSKI. Tetrahedron, **28**, 4981 (1972).
8. D. C. MCDANIEL and H. C. BROWN. J. Org. Chem. **23**, 420 (1958).
9. T. MATSUI, HON CHUNG KO, and L. G. HEPLER. Can. J. Chem. **52**, 2906 (1974).
10. R. W. TAFT, JR. J. Am. Chem. Soc. **25**, 4534 (1953); R. W. TAFT, JR. *In* Steric effects in organic chemistry. *Edited by* M. S. Newman. J. Wiley, New York. 1956. p. 556; J. SHORTER. *In* Advances in linear free energy relationships. *Edited by* N. B. Chapman and J. Shorter. Plenum Press, New York. 1972. p. 71.
11. V. A. PALM. Osnovy kolichestvennoi teorii organicheskikh reaktsii. Izd. Khimii, Leningrad. 1967.
12. O. EXNER. Collect. Czech. Chem. Commun. **31**, 65 (1966).
13. H. VAN BEKKUM, P. E. VERKADE, and B. M. WEPSTER. Rec. Trav. Chim. Pays-Bas, **78**, 815 (1959).
14. Y. YUKAWA and Y. TSUNO. Bull. Chem. Soc. Jpn. **32**, 971 (1959).
15. L. D. HANSEN and L. G. HEPLER. Can. J. Chem. **50**, 1030 (1972).
16. O. EXNER. *In* Advances in linear free energy relationships. *Edited by* N. B. Chapman and J. Shorter. Plenum Press, New York. 1972. p. 1.
17. K. J. LAIDLER. Trans. Faraday Soc. **55**, 1725 (1959).
18. O. EXNER. Collect. Czech. Chem. Commun. **39**, 515 (1974).
19. L. G. HEPLER. Can. J. Chem. **49**, 2803 (1971).
20. O. EXNER. Collect. Czech. Chem. Commun. **37**, 1425 (1972).
21. L. G. HEPLER. J. Am. Chem. Soc. **85**, 3089 (1963).
22. P. D. BOLTON and F. M. HALL. J. Chem. Soc. B, 259 (1969).
23. R. YAMDAGNI and P. KEBARLE. J. Am. Chem. Soc.

Can. J. Chem. Downloaded from www.nrcresearchpress.com by 210.87.254.5 on 09/05/12
For personal use only.

95, 4050 (1973); K. HIRAOKA, R. YAMDAGNI, and P. KEBARLE. J. Am. Chem. Soc. **95**, 6833 (1973).
24. M. EZEKIEL and K. A. FOX. Methods of correlation and regression analysis. 3rd ed. J. Wiley, New York. 1959.
25. L. N. BYKOVA and S. I. PETROV. Usp. Khim. **39**, 1631 (1970).
26. K. KALFUS and M. VEČEŘA. Collect. Czech. Chem. Commun. **37**, 3607 (1972).
27. J. H. ELLIOT and M. KILPATRICK. J. Phys. Chem. **45**, 472 (1941).
28. J. H. ELLIOT and M. KILPATRICK. J. Phys. Chem. **45**, 485 (1941).
29. R. I. ZALEWSKI. Bull. Acad. Pol. Sci. **20**, 853 (1972).
30. R. STEWART and K. YATES. J. Am. Chem. Soc. **82**, 4059 (1960).
31. A. J. BIGGS and R. A. ROBINSON. J. Chem. Soc. 388 (1961).
32. K. KALFUS, J. SOCHA, and M. VEČEŘA. Collect. Czech. Chem. Commun. **39**, 275 (1974).
33. H. H. JAFFE, L. D. FREEDMAN, and G. O. DOACH. J. Am. Chem. Soc. **75**, 2209 (1953).
34. D. DOLMAN and R. STEWART. Can. J. Chem. **45**, 903 (1967).
35. R. STEWART and J. D. VAN DYKE. Can. J. Chem. **48**, 2961 (1970).
36. J. T. EDWARD, H. S. CHANG, K. YATES, and R. STEWART. Can. J. Chem. **38**, 1518 (1960).
37. D. G. LEE and R. SRINIVASAN. Can. J. Chem. **51**, 2542 (1973).
38. T. M. KRYGOWSKI and W. R. FAWCETT. J. Am. Chem. Soc. **97**, 2143 (1975).
39. C. REICHARDT. Losungsmittel-effekte in der organische Chemie. Verlag Chemie, Weinheim/Bergstr., Germany. 1973.
40. J. SHORTER. *In* Advances in linear free energy relationships. *Edited by* N. B. Chapman and J. Shorter. Plenum Press, New York. 1972. p. 71.
41. R. YAMDAGNI, T. B. MCMAHON, and P. KEBARLE. J. Am. Chem. Soc. **96**, 4035 (1974).

Can. J. Chem. Downloaded from www.nrcresearchpress.com by 210.87.254.5 on 09/05/12
For personal use only.

Direct Specific Heat Measurements on Solutions of Volatile Solutes by Flow Microcalorimetry: Partial Molal Heat Capacity of Benzene in Water at 25 °C

CARMEL JOLICOEUR, PATRICK PICKER, AND GÉRALD PERRON

CACTUS (Centre d'Applications en Calorimétrie et Thermodynamique de l'Université de Sherbrooke), Université de Sherbrooke, Sherbrooke, Québec J1K 2R1

Received April 11, 1975

CARMEL JOLICOEUR, PATRICK PICKER, and GÉRALD PERRON. Can. J. Chem. **53**, 3634 (1975).

The direct specific heat measurement on aqueous benzene solutions by flow microcalorimetry have been repeated to elucidate discrepancies among earlier results. Through extensive variations of experimental conditions, the origin of difficulties encountered previously has been investigated and a simple procedure has been devised to circumvent problems inherent to this particular type of measurements.

CARMEL JOLICOEUR, PATRICK PICKER et GÉRALD PERRON. Can. J. Chem. **53**, 3634 (1975).

La chaleur spécifique des solutions aqueuses de benzène a été redéterminée par microcalorimétrie dynamique dans le but de résoudre le désaccord entre différentes valeurs publiées antérieurement. Les difficultés rencontrées dans ce type de mesures ont été étudiées par des variations systématiques des conditions expérimentales et une procédure fut mise au point pour éliminer certains effets parasites décelés récemment.

Introduction

In collaboration with other workers, we recently investigated the partial molal volumes and heat capacities of various organic solutes in water and in methanol (1). As part of the latter study, direct differential specific heat measurements had been carried out on dilute aqueous solutions of benzene, using the flow microcalorimeter described by Picker *et al.* (2). From these data, the limiting apparent molal heat capacity ϕ_c^0 of benzene in water was calculated as 552 J K^{-1} mol^{-1}, in reasonable agreement with previous results derived from solubility measurements (3). However, data reported recently by other investigators (4) indicated quite clearly that the earlier ϕ_c^0 values for benzene were erroneous. This problem, and other experimental difficulties encountered with solutions containing volatile organic solutes, has prompted us to reexamine the method of direct measurements of specific heat increments, which has been found precise and useful in a variety of other systems (5). A series of systematic tests were thus performed with aqueous solutions of benzene, to identify the potential sources of problem in specific heat measurements with such volatile solutes.

Experimental

The water used for these measurements was distilled and deionized (specific conductance: <1 μmho). Fisher Spectranalyzed benzene was used either as such, or after washing with dilute aqueous sulfuric acid and sodium hydroxide and drying over molecular sieve (Davidson Chemicals, 3 Å). Benzene solutions were prepared by weight, following vacuum degassing of the water. The solution was then separated into 25 ml aliquots which were sealed under Teflon in glass bottles, leaving minimal vapor space. The vials were kept at ~ 10 °C until and during the measurement, to minimize benzene evaporation. Under these conditions, no significant variation could be detected in three consecutive runs from the same aliquot.

The differential flow microcalorimeter used in this study (2) consists of twin capillary cells which are heated at equal and constant power ($\Delta T = 1$–2 K). When the liquid flow rates are identical, any difference in volumetric specific heat creates a temperature difference between the twin cells, which is nulled by feedback action on the Joules heating in the reference cell. The ratio of the volumetric specific heats of the flowing liquids is then equal to the ratio of heating powers under steady-state thermal equilibrium. The condition of identical flow rates is achieved by simply connecting the twin cells in series. (See Fig. 2, ref. 2). A coil of capillary tubing, inserted in series between the two cells, acts as a delay line allowing different solutions to flow in each cell, for a time determined by the length of the coil and the flow rate.

Results and Discussion

The main findings of this investigation are given in Fig. 1, which illustrates actual recorder tracings obtained while flowing alternately in the microcalorimeter a solution of benzene (0.01167 *m*) and water, under a flow rate of 1.0 cm^3/min and a heating power of 112.9 mW.

Can. J. Chem. Downloaded from www.nrcresearchpress.com by 210.87.254.5 on 09/05/12
For personal use only.

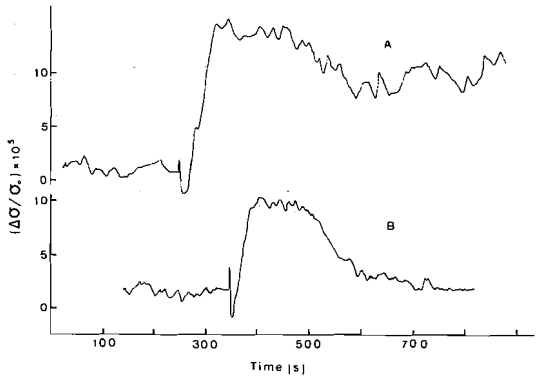

FIG. 1. Recorder tracing of differential specific heat measurement for an aqueous benzene solution (0.01167 *m*) against water; *A*: run under usual conditions; *B*: run carried out while cooling the liquids after passage in the first cell.

The initial base line corresponds to water flowing in both cells, and a steady-state increment is observed when the benzene solution flows in the working cell. As the benzene solution reaches the reference cell, symmetry is restored and the base line should again be observed, as in the case of recording B. In curve A, which was obtained under usual conditions, the last portion (benzene solution in both cells) exhibits a rather large noise, an effect previously attributed to the formation of benzene vapor bubbles as the solution flows past the heating elements. In earlier work (1), the specific heat increment was measured from the initial base line only, discarding the last part of the curve. It has been found in the present investigation that the magnitude of the base line shift (recording A) can be enhanced or reduced by respectively heating or cooling the delay coil between the two flow cells. Hence, the tracing B was recorded with the capillary tubing coil immersed in a water bath at 10 °C; under these conditions, the base line offset was suppressed, and the steady-state deviation was found significantly smaller than had been measured previously.

The above observations strongly suggest that the base line offset was related to evaporation of benzene in the flow cells, a phenomenon which could affect the measurement in two ways. The endothermic evaporation of benzene will cause a base line shift if the heat of evaporation is not symmetrically evolved in both cells. On the other hand, once benzene vapor bubbles are formed, they can remain trapped in the delay coil (this was noted to occur), thus changing the relative flow rates in the cells.

While the suggested corrective measure seems broadly valid (it has been used successfully with solutions of other volatile solutes, namely, tetrahydropyran), the explanation remains tentative. Other phenomena such as surface adsorption of benzene in the cells and delay coil, and microphase separation (demixing) in the cells could also contribute to the effects observed. We have, on the other hand, tested that the addition of ionic and non-ionic surfactants ($C < 0.01$ *M*) to both the water and the benzene solution had no significant consequence on the base line shift. Likewise, degassing of the water before preparing the solutions had no noticeable influence on the behavior of the latter. Also, changing the benzene concentration, flow rates or heating power did not affect the relative importance of the observed base line shift. We were thus left with the explanation that cooling of the solution after passage through the first cell presumably redissolves the benzene, thus restoring homogeneity and concentration symmetry.

From eight successive runs such as that shown in Fig. 1*B*, the fractional increment in volumetric specific heat (σ) of benzene solution (0.01167 *m*) relative to water was found as: $(\sigma - \sigma_0)/\sigma_0 = 0.76 \times 10^{-4}$ with a standard deviation of $\pm 0.06 \times 10^{-4}$ (σ_0 is the volumetric specific heat of water: $\sigma_0 = c_p^0 d_0$, with $d_0 = 0.997047$ g cm^{-3} (6) and $c_p^0 = 4.1793$ J K^{-1} g^{-1} (7)). The density difference between the benzene solution and water ($d - d_0$) was taken as -56 p.p.m. from measurements reported by Masterton (8) combined with our own data obtained at higher benzene concentrations. The apparent molal heat capacity of benzene was then calculated (5) as 374 ± 2 J K^{-1} mol^{-1}. Considering the difficulties involved in the measurements, this is in rather good agreement with the value of 356 ± 5 J K^{-1} mol^{-1} reported recently by Gill *et al.* (4). Though it is possible that there remains a small systematic error in our measurements, the procedure suggested here seems useful in that it enables direct measurements on volatile solutes with the same ease and precision as had been achieved with nonvolatile solutes (5).

The authors gratefully acknowledge financial support of this research by the National Research Council of

Can. J. Chem. Downloaded from www.nrcresearchpress.com by 210.87.254.5 on 09/05/12
For personal use only.

Canada. We also thank Dr. I. Wadsö for making his paper available to us before publication, and Professor J. E. Desnoyers for discussion on some of the problems.

1. C. JOLICOEUR, P. R. PHILIP, G. PERRON, P. A. LEDUC, and J. E. DESNOYERS. Can. J. Chem. **50**, 3167 (1972).
2. P. PICKER, P. A. LEDUC, P. R. PHILIP, and J. E. DESNOYERS. J. Chem. Thermodyn. **3**, 631 (1971).
3. F. FRANKS, M. GENT, and H. H. JOHNSON. J. Chem. Soc. 2716 (1963).
4. S. J. GILL, N. F. NICHOLS, and I. WADSÖ. J. Chem. Thermodyn. **7**, 175 (1975).
5. J. L. FORTIER, P. A. LEDUC, and J. E. DESNOYERS. J. Solution Chem. **3**, 323 (1974). C. JOLICOEUR and J. BOILEAU. J. Solution Chem. **3**, 889 (1974); C. JOLICOEUR and P. R. PHILIP. J. Solution Chem. **4**, 3 (1975).
6. G. S. KELL. J. Chem. Eng. Data, **12**, 66 (1967).
7. H. F. STIMSON. Am. J. Phys. **23**, 614 (1955).
8. W. L. MASTERTON. J. Chem. Phys. **22**, 1830 (1954).

Can. J. Chem. Downloaded from www.nrcresearchpress.com by 210.87.254.5 on 09/05/12
For personal use only.

Derivatives of 2-Pyrazolin-5-one. II. Catalyzed Sodium Borohydride Reduction of Some 4–(2-Nitrobenzylidene)-2-pyrazolin-5-ones. A Reappraisal[1]

RONALD T. COUTTS AND ABDEL-MONAEM EL-HAWARI

Faculty of Pharmacy and Pharmaceutical Sciences, University of Alberta, Edmonton, Alberta T6G 2H7

Received June 12, 1975

RONALD T. COUTTS and ABDEL-MONAEM EL-HAWARI. Can. J. Chem. **53**, 3637 (1975).

A reexamination of the sodium borohydride and palladium–charcoal reduction of 3-methyl-4-(*o*-nitrobenzylidene)-1-phenyl-2-pyrazolin-5-one (**3***a*) has revealed that the final product is 3-methyl-4-(*o*-aminobenzyl)-1-phenyl-2-pyrazolin-5-one (**5***a*), and not 9-hydroxy-3-methyl-3a,4,9,9a-tetrahydro-1*H*-pyrazolo[3,4-*b*]quinoline as claimed previously. Reduction of **3***a* to **5***a* proceeds via the 4-(*o*-nitrobenzyl) compound. Chemical and physical properties of **5***a* are described which support the assignment of this revised structure to the reduction product of **3***a*. Two analogs of **3***a* were also reduced in the same manner and yielded products analogous to **5***a* and not the previously claimed pyrazolo[3,4-*b*]quinolines.

RONALD T. COUTTS et ABDEL-MONAEM EL-HAWARI. Can. J. Chem. **53**, 3637 (1975).

Un réexamen de la réduction, par le borohydrure de sodium et le palladium sur charbon, de la méthyl-3 (*o*-nitrobenzylidène)-4 phényl-1 pyrazoline-2 one-5 (**3***a*) révèle que le produit final est la méthyl-3 (*o*-aminobenzyl)-4 phényl-1 pyrazoline-2 one-5 (**5***a*) et non pas l'hydroxy-9 méthyl-3 tétrahydro-3a,4,9,9a 1*H*-pyrazolo[3,4-*b*]quinoléine tel qu'il avait été prétendu antérieurement. La réduction de **3***a* en **5***a* se produit par l'intermédiaire du composé (*o*-nitrobenzyl)-4. Les propriétés chimiques et physiques de **5***a* sont en accord avec la structure revisée du produit de réduction de **3***a*. On a aussi réduit de la même manière deux analogues de **3***a*; ils conduisent aussi à des produits analogues à **5***a* et non pas aux pyrazolo[3,4-*b*]quinoléines proposées antérieurement.

[Traduit par le journal]

Narang *et al.* (1) first claimed that one product of the reduction of 3-methyl-4-(*o*-nitrobenzylidene)-1-phenyl-2-pyrazolin-5-one (**1***a*) by aluminum amalgam, zinc and acetic acid, or alcoholic hydrochloric acid, was a cyclic hydroxylamine, namely 9-hydroxy-3-methyl-3a,4,9,9a-tetrahydro-1*H*-pyrazolo[3,4-*b*]quinoline, **2***a*. The same product was the major one obtained by us (2) when **1***a* was reduced with sodium borohydride and palladium–charcoal or with cyclohexene and palladium–charcoal. We also concluded that other *N*-hydroxypyrazolo[3,4-*b*]quinolines (**2***b*–**2***e*), together with unidentified reduced products, were formed when the appropriate pyrazolones (**1***b*–**1***e*) were similarly reduced. We now report that some of our previous conclusions (2) were erroneous. A more detailed investigation of the reduction of three pyrazolones (**1***a*–**1***c*) is now described and the major products correctly identified. Structures of previously unidentified products have also been deduced. Chemical properties of the products of reduction of pyrazolones (**1***a*–**1***c*) are also described.

Initially the (*o*-nitrobenzylidene)pyrazolones (**1***a*–**1***c*) were reduced by the previously reported method (2) except that methanol was used as solvent instead of an ethanol–methanol mixture. The same products were isolated, *i.e.* the major amphoteric compounds which were claimed to be the 9-hydroxypyrazolo[3,4-*b*]quinolines (**2***a*–**2***c*), and the minor ones which had been left unidentified. However, due to some difficulties in obtaining pure analytical samples of some of these derivatives, a modification in the reduction procedure was sought. The *o*-nitrobenzylidene derivatives (**1***a*–**1***c*) were first reduced by means of sodium borohydride in dioxane solution in the absence of catalyst. This resulted in the reduction of only the benzylidene double bond and 4-(2-nitrobenzyl)-2-pyrazolin-5-ones, **3**, were isolated in excellent yields. These compounds were readily characterized by elemental analysis, i.r., and n.m.r. spectroscopy.

Once the benzylidene double bond is reduced, these pyrazolones (**3**) become soluble in dilute

[1]A previous study (2) is considered to be part I of the series.

Can. J. Chem. Downloaded from www.nrcresearchpress.com by 210.87.254.6 on 09/05/12
For personal use only.

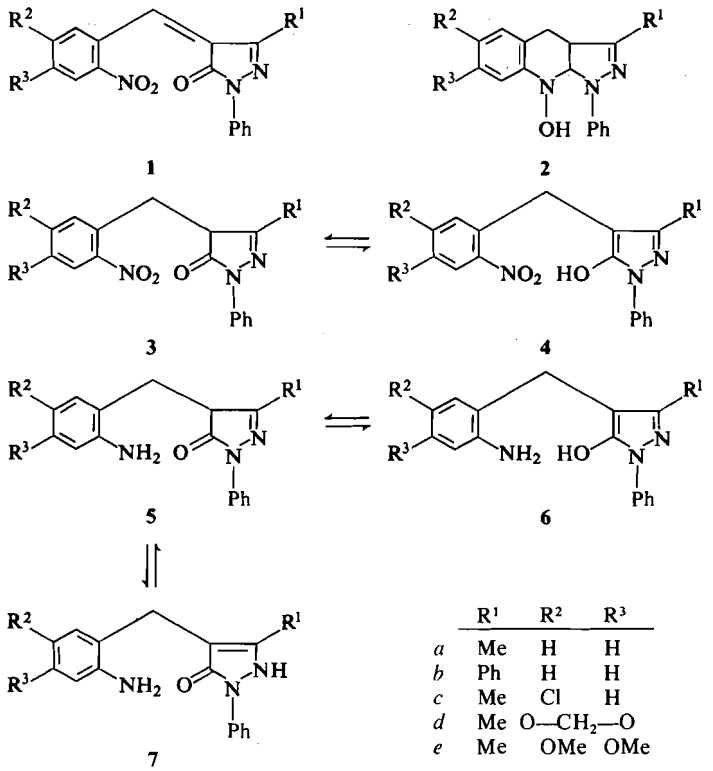

	R^1	R^2	R^3
a	Me	H	H
b	Ph	H	H
c	Me	Cl	H
d	Me	O—CH_2—O	
e	Me	OMe	OMe

alkali due to their ability to enolize (**3** ⇋ **4**). In view of this, catalytic (10% Pd–C) sodium borohydride reductions of the pyrazolones, **3**, were carried out in dilute sodium hydroxide solution. Acidification of the filtrate from the reaction with dilute acetic acid caused precipitation of the reduced products. By using this modified procedure, only one product was isolated from each reaction. Although melting points were considerably higher than those of the amphoteric products obtained by reduction in methanol, they had the same solubility characteristics and the same i.r. spectra as those reported for the compounds prepared by Coutts and Edwards (2).

Narang *et al.* (1) concluded that the 9-hydroxypyrazolo[3,4-*b*]quinoline **2***a* was the reduction product of the pyrazolone **1***a* from a correct elemental analysis, and because the product was found to be soluble in both acids and alkalis. When Coutts and Edwards (2) reduced the same compound, **1***a*, and derivatives, **1***b*–**1***e*, they concluded that in addition to the correct elemental analyses and solubility characteristics, the i.r. spectra of the reduction products were also in agreement with structure **2**. The i.r. spectra (solid) showed broad absorption in the 2100–3500 cm^{-1} range with maxima between 2850 and 3090 cm^{-1} which was attributed to the N—OH function. Also a C=O absorption band was apparently absent from these spectra. Similar spectra were obtained when the pure samples obtained in the present investigation were examined as solids (KBr or Nujol), but two additional medium intensity absorption maxima were located at ~3200 and ~3350 cm^{-1}. This observation was considered initially to be due to the ability of such compounds as **2** to tautomerize and thus display an NH absorption band in addition to that of the N—OH function. However, the plausibility of *N*-hydroxy structures being formed at all, was seriously questioned when the p.m.r. and mass spectra of these reduction products were recorded and interpreted.

The p.m.r. spectrum of the amphoteric product obtained by reduction of the pyrazolone **3***a*, displayed two signals at δ 2.10 (CH_3) and at δ 3.43 (CH_2) and an aromatic multiplet (12 protons). When the sample was shaken with deuterium oxide, three protons within the aromatic area were found to be D-exchangeable. Three D-exchangeable protons, with almost the same chemical shifts were also found in the p.m.r.

Can. J. Chem. Downloaded from www.nrcresearchpress.com by 210.87.254.6 on 09/05/12
For personal use only.

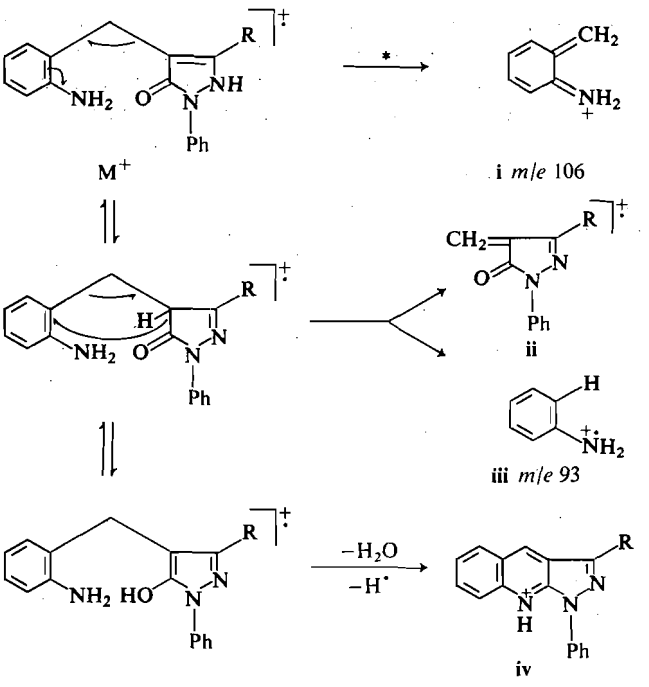

Relative Abundance of Ions (%)

	M^+	i	ii	iii	iv
5*a* (R = Me)	24	100	19	42	6
5*b* (R = Ph)	34	100	23	10	11

SCHEME 1

spectrum of the reduction product of the analogs **3***b* and **3***c*. The presence of three D-exchangeable protons in each of these spectra does not agree with the proposed structure **2** or the NH tautomer, in which only one or two such protons would be expected.

The mass spectra of the reduction products of **3***a* and **3***b* were also inconsistent with structure **2**. The mode of fragmentation of these compounds under electron impact (Scheme 1) revealed that intact pyrazolone rings (ion **ii**) were present. This, together with additional evidence from the mass spectra (Scheme 1) and the p.m.r. data, indicated that the amine structure (**5** ⇋ **6** ⇋ **7**) was more acceptable for the amphoteric reduction products. This structure better explains the solubility of the reduced products in sodium hydroxide solution. It is now questioned whether cyclic hydroxylamines of structure **2** would have acidic properties; the literature describes some related cyclic hydroxylamines which are weakly acidic (3, 4), and others which have no acidic properties (3, 5).

An examination of the i.r. spectra of amines **5***a*–**5***c* as solids revealed the presence of strong absorption bands at 1628, 1625, and 1630 cm^{-1} respectively. These bands were not considered to be due to carbonyl stretching and were initially assigned to C=N absorption (2). An additional strong peak between 1600 and 1604 cm^{-1} in each of the spectra of **5***a*–**5***c* was not explained. This apparent lack of carbonyl absorption contributed to the earlier incorrect assignment of structure **2** to the amphoteric reduction products. It is now obvious that the bands at 1600–1604 cm^{-1} are due to C=N stretching. 3-Methyl-1-phenyl-2-pyrazolin-5-ones are known (6, 7) to exist only in the 'OH-forms' (*cf.* **6**) in the solid state; we have confirmed that their i.r. spectra lack C=O absorption and the C=N absorption bands are located at 1606 and 1601 cm^{-1} respectively. Accordingly, the other strong absorption band located between 1625 and 1630 cm^{-1} in the solid spectra of **5***a*–**5***c* must be due to a bonded C=O absorption and suggests that the amines exist in the 'NH-form' (7) in the solid state. Intra- and

Can. J. Chem. Downloaded from www.nrcresearchpress.com by 210.87.254.6 on 09/05/12
For personal use only.

Can. J. Chem. Downloaded from www.nrcresearchpress.com by 210.87.254.6 on 09/05/12
For personal use only.

intermolecular hydrogen-bonding between the carbonyl group and the amine group would explain the carbonyl absorption frequencies, and the presence of the amine absorption maxima at relatively low wave numbers. Dilute solutions (2%) of the amines **5***a* and **5***b* in chloroform gave spectra with carbonyl absorption bands at 1712 and 1711 cm^{-1} respectively, indicative of the 'CH-form' (**5**) existing in solution.

The assignment of the absorption bands near 1625 cm^{-1} in the solid spectra of **5***a*–**5***c* to a C=O absorption was substantiated by examining the spectra of some derivatives of amines **5***a* and **5***b* whose syntheses are described below. The i.r. spectra of the *N*-methyl derivatives **8***a* and **8***b*, which cannot tautomerize and therefore cannot display C=N absorption bands, show carbonyl absorption at 1624 and 1630 cm^{-1} respectively. On the other hand, the dibenzoyl compound **9** and the triacetyl derivatives **10***a* and **10***b* lack a pyrazolone C=O group but possess a ring C=N function. No absorption near 1625 cm^{-1} was observed in the i.r. spectra of these compounds; all showed strong bands in the 1595–1600 cm^{-1} region attributable to C=N.

Methyl derivatives of the amines **5***a* and **5***b* were prepared by reacting them with dimethyl sulfate. *N*-methyl derivatives, **8**, were the only products obtained although theoretically, the C_4-methyl and *O*-methyl isomers were possible products. The i.r., p.m.r., and mass spectra of the methylated products were consistent with the proposed structures. The methyl signals of **8***a* and **8***b* were located at δ 2.98 and 2.91 respectively; the *N*-methyl signals of antipyrene, **11***a*, and aminopyrene, **11***b*, were found to have similar chemical shifts (δ 2.95 and 2.90). The methyl derivative **8***a* displayed a strong fragment ion (97% relative abundance) at *m/e* 56 which was shown by accurate mass to be $C_3H_6N^+$ and corresponds to $MeC\overset{+}{\equiv}NMe \leftrightarrow MeC\overset{+}{=}NMe$. This peak is also the base peak in aminopyrene, **11***b*. Similarly, the base peak in the mass spectrum of the phenyl analog **8***b* was at *m/e* 118 ($PhC\overset{+}{\equiv}NMe \leftrightarrow PhC\overset{+}{=}NMe$). These results are in agreement with previous reports that the pyrazolone ring is preferentially methylated with dimethyl sulfate at N-2 (8, 9).

The action of benzoyl chloride on the amine **5***a* produced a dibenzoyl derivative identified as **9** from its elemental analysis ($C_{31}H_{25}N_3O_3$), i.r., p.m.r., and mass spectra. This compound was insoluble in sodium hydroxide solution which indicated that the labile proton in the pyrazolone ring was replaced during benzoylation. The i.r. spectrum (solid) displayed two C=O absorption bands at 1645 cm^{-1} (NHCOPh) and at 1760 cm^{-1} (OCOPh) and an NH absorption band at 3315 cm^{-1}. The p.m.r. spectrum showed a methyl signal, a methylene signal, an appropriate aromatic multiplet, and a D-exchangeable proton at δ 8.01 (NH). The mass spectrum of **5** displayed the molecular ion at *m/e* 487 which fragmented initially by the expulsion of benzoyl (PhCO·)

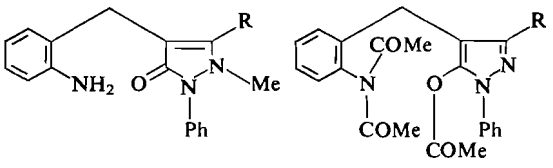

8 *a* R = Me, *b* R = Ph **10**

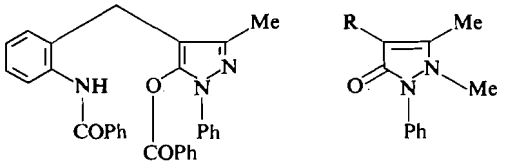

9 **11** *a* R = H, *b* R = NMe_2

and benzoyloxy (PhCOO·) radicals and a benzoic acid molecule. The presence of two strong metastable ions at *m/e* 275.1 and 273.6 suggested that the last two expulsions were direct fragmentations of the molecular ion.

Acetylation of the amine derivatives **5***a* and **5***b* by heating with acetic anhydride for 1 h gave monoacetyl derivatives. However, when heating was prolonged, triacetyl products were isolated. The monoacetylated derivatives were soluble in dilute alkali solutions and if these solutions were immediately acidified, the acetylated products reprecipitated. Due to this ability to enolize, the products were obviously *N*-acetates and not *O*-acetates. Elemental analysis, i.r. spectroscopy, and mass spectrometry all confirmed the structures of the monoacetates as being **12***a* and **12***b*. The mass spectrum of **12***a*, for example, showed a molecular ion at *m/e* 321 which fragmented initially by the expulsion of a water molecule, a ketene molecule, and a CH_3CONH radical. The triacetates are identified as 5-acetyloxy-4-(2-diacetylaminobenzyl)-1-phenyl-pyrazolones, **10***a*

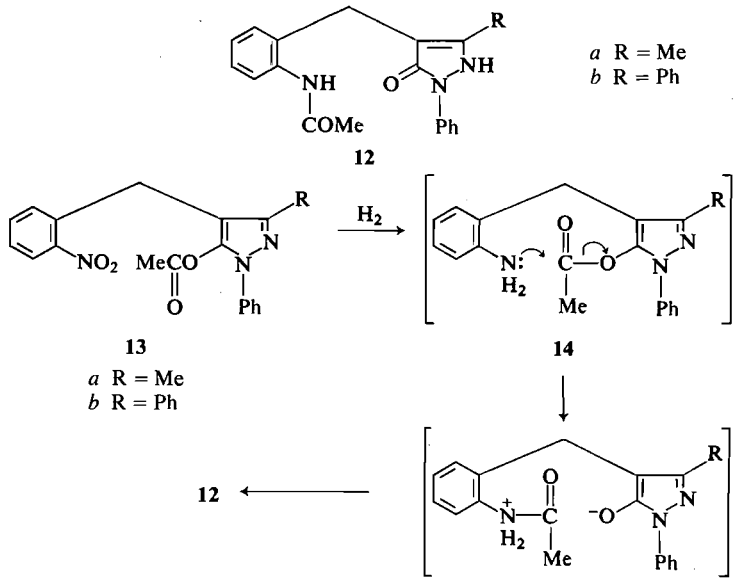

SCHEME 2

and **10***b*. Both dissolved slowly in dilute alkalis. When the alkaline solutions were acidified, they yielded the monoacetyl derivatives **12**. The elemental analyses as well as the i.r., p.m.r., and mass spectra supported the proposed structures, **10***a* and **10***b*. Both p.m.r. spectra displayed a six-proton signal for the *N*-diacetyl function, a three-proton signal for the *O*-acetyl group, a methylene signal, and an aromatic multiplet. The i.r. spectra were devoid of any NH or OH absorption bands. The methyl derivative **10***a* displayed three strong C=O bands at 1790 cm^{-1} ($OCOCH_3$), and at 1685 and 1730 cm^{-1} due to the *N*,*N*-diacetyl doublet (10). In the i.r. spectrum of the phenyl analog **10***b*, the corresponding bands appeared at 1793, 1705, and 1718 cm^{-1}. The presence of the carbonyl absorptions of an *N*,*N*-diacetyl function at a higher frequency than the carbonyl absorption bands of monoacetyl compounds has already been commented upon (11).

Attempts were made to prepare the *O*-acetyl derivatives **14**, for comparison purposes, through the reduction of the 5-acetyloxy-4-(2-nitrobenzyl)-1-phenylpyrazoles, **13**. The latter compounds were prepared by treating the appropriate nitropyrazolone, **3**, with acetic anhydride. The presence of *O*-acetyl functions in the products was confirmed by i.r. spectroscopy (ν_{max} 1781 cm^{-1} in **13***a* and 1790 cm^{-1} in **13***b*), by p.m.r. ($OCOCH_3$ protons came to resonance at δ 2.03 in **13***a* and δ 2.02 in **13***b*) and by mass spectral fragmentation (direct loss of $CH_3COO^{\bullet}$ radical from the molecular ion). When the *O*-acetyl compounds were reduced either by catalytic hydrogenation over platinum or by sodium borohydride – palladium–charcoal in dioxane, oily products were obtained. The only crystallizable compounds isolated were the *N*-acetyl derivatives, **12**, rather than the desired *O*-acetates, **14**. The isolation of such products indicated that the acetyl group, originally attached to the oxygen atom of the pyrazole ring, migrated to the amine function once the latter was formed. Migration of acyl residues from one heteroatom to another in the same molecule is well documented (12–16) but no examples comparable to the one shown in this present study between the *O*-acetyl lactam and the amine function appear to have been reported. In this instance, the amine and acetyl group seem suitably orientated to allow this migration to occur intramolecularly (Scheme 2).

Experimental

Melting points (capillary tube) are uncorrected. Infrared spectra were recorded as Nujol mulls, unless stated otherwise, on a Beckman IR-10 spectrophotometer; p.m.r. spectra were taken on a Varian A-60D spectrometer with tetramethylsilane as internal standard. Mass spectra were determined by Dr. A. M. Hogg and his associates, Department of Chemistry, University of Alberta, on an AEI MS-9 or MS-12 mass spectrometer at an ionizing potential of 70 eV using the direct probe technique. Elemental

Can. J. Chem. Downloaded from www.nrcresearchpress.com by 210.87.254.6 on 09/05/12
For personal use only.

Can. J. Chem. Downloaded from www.nrcresearchpress.com by 210.87.254.6 on 09/05/12
For personal use only.

analyses were determined in the microanalytical laboratories of the Faculty of Pharmacy and Pharmaceutical Sciences and the Department of Chemistry, University of Alberta.

3-Methyl-4-(2-nitrobenzyl)-1-phenyl-2-pyrazolin-5-one, 3a

A solution of 3-methyl-4-(2-nitrobenzylidene)-1-phenyl-2-pyrazolin-5-one (2) (**1***a*, 4.0 g) in dioxane (80 ml) was added dropwise to a stirred solution of sodium borohydride (2.0 g) in 50% aqueous dioxane (20.0 ml). After addition was completed, stirring was continued for 1 h. The reaction mixture was cooled and acidified with dilute hydrochloric acid then diluted with water. The precipitate was collected and crystallized from ethanol to give the title compound as yellow crystals (3.4 g); m.p. 168–169 °C; i.r. ν_{max} 2300–3200 (OH), 1605 (C=N), and 1530 and 1335 (NO_2) cm^{-1}; p.m.r. (DMSO-d_6) δ 2.05 (3H, s, CH_3), 3.95 (2H, s, CH_2), 7.41 (1H, br, exchanged with D_2O, OH), and 7.10–8.10 (9H, m, aromatic protons).

Anal. Calcd. for $C_{17}H_{15}N_3O_3$: C, 66.01; H, 4.88; N, 13.58. Found: C, 65.91; H, 5.00; N, 13.39.

1,3-Diphenyl-4-(2-nitrobenzyl)-2-pyrazolin-5-one, 3b

This compound (2.7 g, m.p. 185–186 °C) was obtained as yellow crystals when 1,3-diphenyl-4-(2-nitrobenzylidene)-2-pyrazolin-5-one (2) (**1***b*, 3.0 g) was reduced as described in the preparation of **3***a*; i.r. ν_{max} 2400–3200 (OH), 1604 (C=N), and 1527 and 1340 (NO_2) cm^{-1}; p.m.r. (DMSO-d_6) δ 4.20 (2H, br s, CH_2), 7.81 (1H, br s, exchanged with D_2O, OH), and 7.10–8.10 (14H, m, aromatic protons).

Anal. Calcd. for $C_{22}H_{17}N_3O_3$: C, 71.15; H, 4.61; N, 11.31. Found: C, 17.30; H, 4.41; N, 11.24.

4-(5-Chloro-2-nitrobenzyl)-3-methyl-1-phenyl-2-pyrazolin-5-one, 3c

This pale yellow solid (2.65 g, m.p. 145–146 °C) was obtained when 4-(5-chloro-2-nitrobenzylidene)-3-methyl-1-phenyl-2-pyrazolin-5-one (2) (**1***c*, 3.0 g) was reduced as described in the preparation of **3***a*; i.r. ν_{max} 2100–3300 (OH), 1606 (C=N), and 1526 and 1342 (NO_2) cm^{-1}; p.m.r. (DMSO-d_6) δ 2.12 (3H, s, CH_3), 4.03 (2H, s, CH_2), 7.10–8.31 (8H, m, aromatic protons), and 11.00–12.70 (1H, br s, exchanged with D_2O, OH).

Anal. Calcd. for $C_{17}H_{14}ClN_3O_3$: C, 59.39; H, 4.10; N, 12.22. Found: C, 59.53; H, 4.21; N, 12.47.

General Procedure for Sodium Borohydride and Palladium–Charcoal Reductions

A solution of sodium borohydride (1.0 g) in water (20 ml) was carefully added to a suspension of palladium–charcoal (0.10 g) in water (10 ml). To the resulting suspension, a solution of the nitro compound (2.0 g), dissolved in 10% aqueous sodium hydroxide (40 ml) was added dropwise over a period of 30 min. Nitrogen was bubbled through the reaction mixture during the addition of the nitro compound and for a further 15 min. The mixture was then filtered and the filtrate acidified with dilute acetic acid and diluted with ice-cold water. The precipitated product was crystallized from methanol or ethanol.

4-(2-Aminobenzyl)-3-methyl-1-phenyl-2-pyrazolin-5-one, 5a

This colorless compound (1.70 g), m.p. 153–154 °C (from ethanol) was obtained when the pyrazolone **3***a* was reduced according to the *general procedure* outlined above (lit. (1, 2) m.p. 142 °C). Infrared (Nujol) ν_{max} 1628 (bonded C=O), 1604 (C=N), and broad absorption between 2100 and 3500 with maxima at 3200 and 3345 (OH and NH_2) cm^{-1}; (chloroform, 2% solution) ν_{max} 1712 (C=O) cm^{-1}; (DMSO-d_6, 2% solution) ν_{max} 1660 (C=O) and 1603 (C=N) cm^{-1}; p.m.r. (DMSO-d_6) δ 2.10 (3H, s, CH_3), 3.43 (2H, s, CH_2), and 6.30–7.90 (12H, m, aromatic protons and 3 additional protons which exchanged with D_2O, *i.e.* NH_2 and pyrazolone proton); ($CDCl_3$) δ 6.50–8.20 (9H, m, aromatic protons) and 6.00–6.50 (3H, br, exchanged with D_2O, NH_2 and pyrazolone proton); mass spectrum (see Scheme 1) ion **ii** measured 186.0790, $C_{11}H_{10}N_2O$ requires 186.0793; ion **i** measured 106.0655, C_7H_8N requires 106.0657.

Anal. Calcd. for $C_{17}H_{17}N_3O$: C, 73.09; H, 6.13; N, 15.04. Found: C, 73.08; H, 6.08; N, 14.91.

The hydrochloride of **5***a* was obtained by bubbling dry hydrogen chloride through a solution of the title compound in tetrahydrofuran. Compound **5***a*·HCl was colorless with m.p. 254–256 °C (lit. (2) m.p. 252–254 °C).

Anal. Calcd. for $C_{17}H_{18}ClN_3O$: C, 64.65; H, 5.74; N, 13.31. Found: C, 64.71; H, 5.72; N, 13.19.

4-(2-Aminobenzyl)-1,3-diphenyl-2-pyrazolin-5-one, 5b

When pyrazolone **3***b* was reduced using the *general procedure*, the title compound (1.79 g), m.p. 151–153 °C (from ethanol) was obtained as colorless needles. Infrared (Nujol) ν_{max} 1625 (bonded C=O), 1600 (C=N), and 2200–3400 with maxima at 3170 and 3350 (OH and NH_2) cm^{-1}; (chloroform, 2% solution) ν_{max} 1711 (C=O) cm^{-1}; (DMSO-d_6, 2% solution) ν_{max} 1654 (C=O) cm^{-1}; p.m.r. (DMSO-d_6) δ 3.68 (2H, s, CH_2) and 6.30–8.00 (17H, m, aromatic protons and 3 additional protons which exchanged with D_2O, *i.e.* NH_2 and pyrazolone proton); ($CDCl_3$) δ 3.63 (2H, s, CH_2), 6.40–8.20 (14H, m, aromatic protons), and 5.00–5.60 (3H, br, exchanged with D_2O, NH_2 and pyrazolone proton). Mass spectrum (see Scheme 1) ion **i** measured 106.0661, C_7H_8N requires 106.0657; ion **ii** measured 248.0945, $C_{16}H_{12}N_2O$ requires 248.0950; ion **iii** measured 93.0584, C_6H_7N requires 93.0579.

The hydrochloride of **5***b* was a colorless solid, m.p. 211–213 °C (from methanol) (lit. (2) m.p. 182–183 °C).

Anal. Calcd. for $C_{22}H_{20}ClN_3O$: C, 69.93; H, 5.34; N, 11.12. Found: C, 69.99; H, 5.20; N, 11.08.

4-(2-Amino-5-chlorobenzyl)-3-methyl-1-phenyl-2-pyrazolin-5-one, 5c

When pyrazolone **3***c* was reduced by the *general procedure*, the title compound was obtained as a colorless solid (1.22 g), m.p. 119–121 °C (from ethanol). Infrared ν_{max} 1630 (bonded C=O), 1602 (C=N), and 2100–3420 with maxima at 3230 and 3390 (OH and NH_2) cm^{-1}; p.m.r. (DMSO-d_6) δ 2.08 (3H, s, CH_3), 3.48 (2H, s, CH_2), and 6.40–8.00 (11H, m, aromatic protons and 3 D_2O-exchangeable protons, *i.e.* NH_2 and pyrazolone proton).

Anal Calcd. for $C_{17}H_{16}ClN_3O$: C, 65.06; H, 5.14; N, 13.39. Found: C, 65.12; H, 5.21; N, 13.45.

When this compound was dissolved in aqueous sodium hydroxide, and the alkaline solution acidified with dilute hydrochloric acid, the hydrochloride of **5***c* precipitated as a pale yellow solid, m.p. 229–230 °C (from methanol) (lit. (2) m.p. 224–225 °C).

Anal. Calcd. for $C_{17}H_{17}Cl_2N_3O$: C, 58.29; H, 4.89; N, 11.99. Found: C, 58.53; H, 5.03; N, 12.21.

Can. J. Chem. Downloaded from www.nrcresearchpress.com by 210.87.254.6 on 09/05/12
For personal use only.

4-(2-Aminobenzyl)-2,3-dimethyl-1-phenyl-3-pyrazolin-5-one, 8a

To an ice-cold solution of 4-(2-aminobenzyl)-3-methyl-1-phenyl-2-pyrazolin-5-one (0.5 g) in 10% sodium hydroxide (15 ml), dimethyl sulfate (0.25 g) was added dropwise with stirring. The mixture was heated under reflux for 1 h. After cooling, the gummy precipitate formed was collected and washed with 10% sodium hydroxide, then with water. Crystallization from methanol gave the title compound as colorless needles (0.18 g); m.p. 191–192 °C. Infrared ν_{max} 1624 (bonded C=O) and 3230 and 3375 (NH_2) cm^{-1}; p.m.r. (DMSO-d_6) δ 2.20 (3H, s, C—CH_3), 2.98 (3H, s, N—CH_3), 3.35 (2H, s, CH_2), 5.16 (2H, br s, exchanged with D_2O, NH_2), and 6.30–7.60 (9H, m, aromatic protons); mass spectrum *m/e* (% relative abundance) 293 (M^+, 100), 263 (61), 56 (97).

Anal. Calcd. for $C_{18}H_{19}N_3O$: C, 73.69; H, 6.53; N, 14.32. Found: C, 73.78; H, 6.43; N, 14.12.

4-(2-Aminobenzyl)-1,3-diphenyl-3-methyl-3-pyrazolin-5-one, 8b

This compound (0.26 g) ,m.p. 195–196 °C was obtained as colorless needles when 4-(2-aminobenzyl)-1,3-diphenyl-2-pyrazolin-5-one (**5b**, 0.5 g) was treated with dimethyl sulfate in the manner described immediately above. Infrared ν_{max} 1630 (C=O) and 3235 and 3405 (NH_2) cm^{-1}; p.m.r. (DMSO-d_6) δ 2.91 (3H, s, N—CH_3), 3.44 (2H, s, CH_2), 5.17 (2H, br s, exchanged with D_2O, NH_2), and 6.30–7.90 (14H, m, aromatic protons); mass spectrum *m/e* (% relative abundance) 355 (M^+, 72), 325 (40), 118 (100); accurate mass measurements 325.1337 ($C_{22}H_{17}N_2O$ requires 325.1341), 118.0658 (C_8H_8N requires 118.0657).

Anal. Calcd. for $C_{23}H_{21}N_3O$: C, 77.72; H, 5.96; N, 11.82. Found: C, 77.40; H, 5.97; N, 12.11.

4-(2-Benzoylamino)benzyl-5-benzoyloxy-3-methyl-1-phenylpyrazole, 9

To an ice-cold solution of 4-(2-aminobenzyl)-3-methyl-1-phenyl-2-pyrazolin-5-one (0.5 g) in dilute sodium hydroxide (10 ml) was added benzoyl chloride (0.75 ml) with vigorous stirring. After 1 h, more benzoyl chloride (0.5 ml) was added and stirring continued at room temperature for a further 30 min. The reaction mixture was extracted with ether then the ethereal extract was washed successively with 10% hydrochloric acid, 10% sodium carbonate, and water. Concentration of the dried ethereal solution gave the colorless title compound (0.51 g), m.p. 137–138 °C (from chloroform); i.r. ν_{max} 1760 (OCOPh), 1645 (NHCOPh), 1600 (C=N), and 3315 (NH) cm^{-1}; p.m.r. ($CDCl_3$) δ 2.12 (3H, s, CH_3), 3.80 (2H, s, CH_2), 8.02 (1H, br s, exchanges with D_2O, NH), and 6.80–7.90 (19H, m, aromatic protons); mass spectrum *m/e* (% relative abundance) 487 (M^+, 4), 382 (3), 366 (9), 365 (30), 105 (100).

Anal. Calcd. for $C_{31}H_{25}N_3O_3$: C, 76.37; H, 5.17; N, 8.61. Found: C, 76.43; H, 5.33; N, 8.60.

Acetylation of 4-(2-Aminobenzyl)-3-methyl-1-phenyl-2-pyrazolin-5-one, 5a, and the Phenyl Analog, 5b

(*a*) A solution of the title compound (**5a**, 0.5 g) in acetic anhydride (5.0 ml) was heated under reflux for 1 h. The cooled solution was poured into 5% aqueous sodium hydroxide and stirred until homogeneous; the alkaline solution was then extracted with ether. This was dried (Na_2SO_4) and evaporated to give a yellow solid residue which crystallized from ethanol into white crystals (0.4 g), m.p. 208–209 °C, identified as *4-(2-acetylaminobenzyl)-3-methyl-1-phenyl-2-pyrazolin-5-one* (**12a**). Infrared ν_{max} 1660 (C=O) and 2500–3300 with maximum at 3180 (OH and NH) cm^{-1}; p.m.r. (DMSO-d_6) δ 2.14 (3H, s, CH_3), 2.20 (3H, s, CH_3), 3.57 (2H, s, CH_2), 7.00–7.90 (9H, m, aromatic protons), and 9.21 (1H, br s, exchanged with D_2O, NH); mass spectrum *m/e* (% relative abundance) 321 (M^+, 62), 303 (23), 278 (14), 263 (22), 186 (29).

Anal. Calcd. for $C_{19}H_{19}N_3O_2$: C, 71.01; H, 5.96; N, 13.08. Found: C, 70.87; H, 5.81; N, 13.12.

(*b*) When the above reaction was repeated and the mixture heated under reflux for 3 h, a colorless crystalline product (0.43 g), m.p. 113–114 °C, was obtained after crystallization from ethanol. This was *5-acetyloxy-4-(2-diacetylaminobenzyl)-3-methyl-1-phenylpyrazole* (**10a**). Infrared ν_{max} 1790 (ester C=O), 1730 and 1685 (diacetyl C=O), and 1600 (C=N) cm^{-1}; p.m.r. (DMSO-d_6) δ 2.02 (3H, s, CH_3,) 2.18 (3H, s, CH_3), 2.11 (6H, s, diacetyl protons), 3.48 (2H, s, CH_2), and 7.20–7.50 (9H, m, aromatic protons); mass spectrum *m/e* (% relative abundance) 405 (M^+, 2), 363 (85), 345 (6), 321 (100), 303 (41).

Anal. Calcd. for $C_{23}H_{23}N_3O_4$: C, 68.15; H, 5.68; N, 10.37. Found: C, 68.03; H, 5.71; N, 10.51.

This compound was insoluble in aqueous sodium hydroxide, but on stirring for several hours in 5% sodium hydroxide solution it dissolved. The solution was filtered and acidified with acetic acid to give a white precipitate which crystallized from ethanol, m.p. 208–210 °C. The i.r. spectrum of this product was identical with that of the monoacetyl derivative **12a**.

(*c*) Similarly, heating 4-(2-aminobenzyl)-1,3-diphenyl-2-pyrazolin-5-one (**5b**, 0.5 g) in acetic anhydride (5.0 ml) for 1 h yielded *4-(2-acetylaminobenzyl)-1,3-diphenyl-2-pyrazolin-5-one* (**12b**) as colorless crystals (0.41 g) m.p. 219–221 °C (from ethanol); i.r. ν_{max} 1662 (C=O) and 2100–3260 (NH and OH) cm^{-1}; p.m.r. (DMSO-d_6) δ 2.10 (3H, s, CH_3), 3.84 (2H, s, CH_2), 6.80–8.00 (15H, m, aromatic protons), and 9.33 (1H, br s, exchanged with D_2O, NH).

Anal. Calcd. for $C_{24}H_{21}N_3O_2$: C, 75.21; H, 5.52; N, 10.96. Found: C, 75.22; H, 5.53; N, 10.75.

(*d*) A triacetyl derivative, *5-acetyloxy-4-(2-diacetylaminobenzyl)-1,3-diphenylpyrazole* (**10b**) was isolated as colorless crystals (0.42 g), m.p. 110–111 °C (from ethanol) when the above reaction, *c*, was repeated and heating with acetic anhydride was prolonged for 4 h. Infrared ν_{max} 1793 (ester C=O), 1718 and 1705 (diacetyl C=O), and 1595 (C=N) cm^{-1}; p.m.r. (DMSO-d_6) δ 2.02 (6H, s, diacetyl protons), 2.20 (3H, s, $OCOCH_3$), 3.75 (2H, s, CH_2), and 7.05–7.70 (14H, m, aromatic protons).

Anal. Calcd. for $C_{28}H_{25}N_3O_4$: C, 71.93; H, 5.39; N, 8.98. Found: C, 72.13; H, 5.18; N, 8.85.

Hydrolysis of this compound with 5% aqueous sodium hydroxide readily gave the monoacetyl derivative **12b**.

5-Acetyloxy-3-methyl-4-(2-nitrobenzyl)-1-phenylpyrazole, 13a, and the 3-Phenyl Analog, 13b; Preparation and Reduction

(*a*) A solution of 3-methyl-4-(2-nitrobenzyl)-1-phenyl-2-pyrazolin-5-one (1.0 g) in acetic anhydride (10 ml) was heated under reflux for 1 h. After cooling, the reaction mixture was poured into ice-cold 5% sodium hydroxide solution (100 ml). Stirring precipitated a pale yellow solid (1.05 g) which crystallized from ethanol as colorless

crystals, m.p. 85–86 °C. This was the title compound, **13***a*; i.r. ν_{max} 1781 (C=O) and 1600 (C=N) cm^{-1}; p.m.r. ($CDCl_3$) δ 2.17 (3H, s, C—CH_3), 2.03 (3H, s, CO—CH_3), 4.05 (2H, s, CH_2), and 7.20–8.10 (9H, m, aromatic protons).

Anal. Calcd. for $C_{19}H_{17}N_3O_4$: C, 64.94; H, 4.88; N, 11.95. Found: C, 64.77; H, 5.15; N, 11.79.

(*b*) Acetylation of 1,3-diphenyl-4-(2-nitrobenzyl)-2-pyrazolin-5-one (1.0 g) using the above method yielded *5-acetyloxy-1,3-diphenyl-4-(2-nitrobenzyl)pyrazole* (**13***b*) (1.01 g) as a pale yellow crystalline powder, m.p. 118–119 °C (from ethanol); i.r. ν_{max} 1790 (C=O) and 1597 (C=N) cm^{-1}; p.m.r. ($CDCl_3$) δ 2.02 (3H, s, $COCH_3$), 4.28 (2H, s, CH_2), and 7.20–8.10 (14H, m, aromatic protons); mass spectrum *m/e* (% relative abundance) 413 (M^+, 12) 371 (51), 354 (14), 353 (18).

Anal. Calcd. for $C_{24}H_{19}N_3O_4$: C, 69.70; H, 4.64; N, 10.16. Found: C, 69.90; H, 5.06; N, 10.41.

(*c*) A solution of 5-acetyloxy-2-methyl-4-(2-nitrobenzyl)-1-phenylpyrazole (0.5 g) in ethanol (20 ml) was hydrogenated over platinum oxide at room temperature and atmospheric pressure. When the calculated amount of hydrogen was taken up, the solution was filtered and the filtrate evaporated to yield a yellow oil. Trituration of this oil with methanol gave a pale yellow solid (0.15 g). This was crystallized as pale yellow crystals, m.p. 205–207 °C, from the same solvent and was found (i.r. mixture m.p.) to be identical to the previously identified 4-(2-acetylaminobenzyl)-3-methyl-1-phenyl-2-pyrazolin-5-one, **12***a*.

(*d*) A solution of 5-acetyloxy-2-methyl-4-(2-nitrobenzyl)-1-phenylpyrazole (0.5 g) in dioxane (20 ml) was reduced with sodium borohydride and palladium–charcoal using the general procedure outlined earlier, except for the solvent change. After acidification of the filtered reaction mixture with acetic acid, it was extracted with ether. The ethereal extract was washed with 10% sodium carbonate, dried (Na_2SO_4), and then evaporated. Crystallization of the resulting semisolid from ethanol yielded a pale yellow solid (0.12 g), m.p. 206–207 °C identified (i.r., mixture m.p.) as 4-(2-acetylaminobenzyl)-3-methyl-1-phenyl-2-pyrazolin-5-one, **12***a*.

(*e*) Hydrogenation of 5-acetyloxy-1,3-diphenyl-4-(2-nitrobenzyl)pyrazole (0.5 g) over platinum oxide as described in *c* above gave a white crystalline compound (0.21 g), m.p. 218–219 °C (from ethanol). Comparison of its i.r. and p.m.r. spectra with those of an authentic sample indicated that it was 4-(2-acetylaminobenzyl)-1,3-diphenyl-2-pyrazolin-5-one, **12***b*.

The authors wish to thank the Medical Research Council of Canada for operating grant MA-2993 which financed this project and Mr. W. Dylke for technical assistance.

1. K. S. Narang, J. N. Ray, and A. Singh. J. Indian Chem. Soc. **11**, 427 (1934).
2. R. T. Coutts and J. B. Edwards. Can. J. Chem. **44**, 2009 (1966).
3. T. Kato and H. Yamanaka. J. Org. Chem. **30**, 910 (1965).
4. R. J. Sundberg. J. Org. Chem. **30**, 3604 (1965).
5. R. M. Acheson, R. G. Bolton, and I. Hunter. J. Chem. Soc. C, 1067 (1970).
6. W. Pelz, W. Puschel, H. Schellenberger, and K. Loffler. Angew. Chem. **72**, 967 (1960).
7. S. Refn. Spectrochim. Acta, **17**, 40 (1961).
8. R. H. Wiley and P. Wiley. Pyrazolones, pyrazolidones and derivatives. Interscience, New York. 1964.
9. K. Bodendorf and H. Raaf. Ann. **592**, 26 (1955).
10. J. F. Grove, P. W. Jeffs, and D. W. Rustidge. J. Chem. Soc. 1956 (1956).
11. R. A. Abramovitch. J. Chem. Soc. 1413 (1957).
12. B. Witkop and J. B. Patrick. J. Am. Chem. Soc. **74**, 3861 (1952).
13. L. L. Miller. Diss. Abstr. **25**, 6236 (1965).
14. Y. Akabori. Kagaku No Ryoiki. **19**, 270 (1965); Chem. Abstr. **63**, 16631a (1965).
15. L. V. Pavlova and F. Y. Rachinskii. Usp. Khim. **37**, 1369 (1968); Chem. Abstr. **69**, 105471g (1968).
16. H. Tani, N. Oguni, and T. Araki. Bull. Chem. Soc. Jpn. **37**, 1245 (1964).

Can. J. Chem. Downloaded from www.nrcresearchpress.com by 210.87.254.6 on 09/05/12
For personal use only.

Derivatives of 2-Pyrazolin-5-one. III. The Preparation and Properties of Some 1′-Phenylspiro[indoline-2,4′-[2]pyrazoline]-5′-ones[1]

RONALD T. COUTTS, ABDEL-MONAEM EL-HAWARI, AND DAVID F. BIGGS

Faculty of Pharmacy and Pharmaceutical Sciences, University of Alberta, Edmonton, Alberta T6G 2H7

Received June 12, 1975

RONALD T. COUTTS, ABDEL-MONAEM EL-HAWARI, and DAVID F. BIGGS. Can. J. Chem. **53**, 3645 (1975).

The choice of solvent has a great influence on the nature of the products obtained when suitably substituted aromatic nitro-compounds are reduced by means of sodium borohydride in the presence of palladium–charcoal. When derivatives of 4-(2-nitrobenzylidene)-1-phenyl-2-pyrazolin-5-one are reduced by this reagent in dioxane, three products are obtained. They are identified as derivatives of 1′-phenylspiro[indoline-2,4′-[2]pyrazoline]-5′-one, of 1-hydroxy-1′-phenylspiro[indoline-2,4′-[2]pyrazoline]-5′-one, and of 4-(2-aminobenzyl)-1-phenyl-2-pyrazolin-5-one. The 1-hydroxyspiro[indolinepyrazolones] are very reactive compounds. The products of their oxidation, reductions with various reagents, and reactions with chemical nucleophiles have been isolated and identified. Some preliminary pharmacological properties of four of the synthesized compounds are reported.

RONALD T. COUTTS, ABDEL-MONAEM EL-HAWARI et DAVID F. BIGGS. Can. J. Chem. **53**, 3645 (1975).

Le choix du solvant a une grande influence sur la nature des produits obtenus lors de la réduction, par $NaBH_4$ en présence de Pd–C, de composés nitro-aromatiques substitués de façon appropriée. Quand on réduit la (nitro-2 benzylidène)-4 phényl-1 pyrazoline-2 one-5 par ce réactif dans le dioxanne, on obtient trois produits: la phényl-1′ spiro[indoline-2,4′-[2]-pyrazoline]-one-5′, l'hydroxy-1 phényl-1′ spiro[indoline-2,4′-[2]-pyrazoline]-one-5′ et la (amino-2 benzyl)-4 phényl-1 pyrazoline-2 one-5. Les hydroxy-1 spiro[indolinepyrazolones] sont des composés très réactifs. On a isolé et identifié les produits de leur oxydation, de leur réduction avec divers réactifs et de leurs réactions avec des nucléophiles chimiques. On rapporte quelques propriétés pharmacologiques préliminaires pour quatre des composés synthétisés.

[Traduit par le journal]

When 3-methyl-4-(2-nitrobenzylidene)-1-phenyl-2-pyrazolin-5-one, **1***a*, and the 3-phenyl analog **1***b* were reduced by sodium borohydride in the presence of 10% palladium–charcoal and using an ethanol–methanol mixture as solvent, two products were obtained in each instance (1). The major products were concluded initially to be cyclic hydroxylamines, **2**, but are now known (2) to be the aminobenzyl compounds, **3**; the minor products were left unidentified because of difficulties in purification.

It is well known that metal hydride reductions are often influenced by the nature of the solvent used (3, 4). This fact led to a repeat of the sodium borohydride – palladium–charcoal reductions just described, in another solvent, to determine whether this might facilitate cyclization to the desired *N*-hydroxy compounds, **2**, and whether previously unidentified products could be obtained in pure form. We have found dioxane to be a suitable solvent for catalytic sodium borohydride reductions (1, 5, 6) so this solvent was selected for the present investigation.

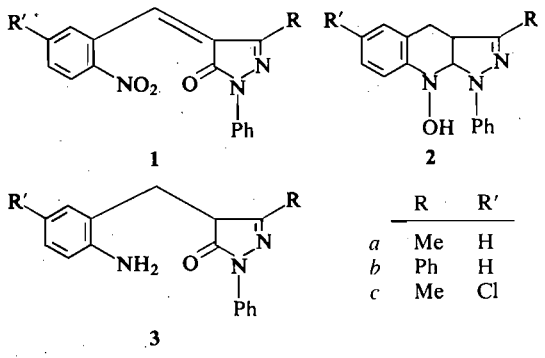

	R	R′
a	Me	H
b	Ph	H
c	Me	Cl

3-Methyl-4-(2-nitrobenzylidene)-1-phenyl-2-pyrazolin-5-one, **1***a*, therefore, was reduced with sodium borohydride and palladium–charcoal in dioxane. When hydrochloric acid was used to decompose the surplus hydride and precipitate the acidic products, a yellow impure

[1]For part II see ref. 2.

Can. J. Chem. Downloaded from www.nrcresearchpress.com by 210.87.254.42 on 09/05/12
For personal use only.

solid was obtained. Replacing hydrochloric acid with acetic acid produced a white solid which was easily separated by fractional crystallization into three compounds. The major product is identified as the cyclic *N*-hydroxy compound, 1-hydroxy-3′-methyl-1′-phenylspiro[indoline-2,4′-[2]pyrazoline]-5′-one, **4***a*. The other two products are shown to be 3′-methyl-1′-phenylspiro[indoline-2,4′-[2]pyrazoline]-5′-one, **4***b*, and the previously described amphoteric amine **3***a*.

4

	R	R^1	R^2
a	OH	Me	H
b	H	Me	H
c	OH	Ph	H
d	H	Ph	H
e	OH	Me	Cl
f	H	Me	Cl
g	H	Me	OMe
h	H	Me	OH
i	H	Me	OAc

The identity of the *N*-hydroxy compound **4***a* was first suspected from its analysis ($C_{17}H_{15}N_3O_2$; M^+ *m/e* 293) and from the observations that it reduced Tollen's reagent, and gave a purple-red color with triphenyltetrazolium chloride, a reaction which is claimed to be specific for hydroxylamine derivatives (7, 8). That the pyrazolone ring still remained intact was suspected from the i.r. spectrum which showed a C=O absorption band at 1690 cm^{-1}. This C=O is present at a lower frequency than that usually demonstrated in 5,5-disubstituted pyrazolone derivatives. However, an intramolecular hydrogen bonding with the N—OH group is possible in such a structure **5** in which the donor and the acceptor groups are in *peri* positions. Katritzky and Lagowski (9) described a similar effect in 8-hydroxyquinoline 1-oxide and its azo derivative. Support for hydrogen bonding in **4***a* is the position of the i.r. O—H stretching band which was broad and centered at 3275 cm^{-1}.

All pyrazolones which have a hydrogen atom at C-4 are soluble in dilute sodium hydroxide solution. The product, $C_{17}H_{15}N_3O_2$, obtained by reduction of **1***a*, was not soluble in aqueous alkali, which was indicative of the absence of a hydrogen atom at C-4, and consistent with the cyclic hydroxylamine structure **4***a*.

The p.m.r. spectrum of the compound suspected to be **4***a* was consistent with that structure. When recorded in DMSO-d_6, the spectrum displayed, in addition to the aromatic and methyl

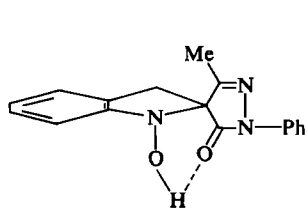

5

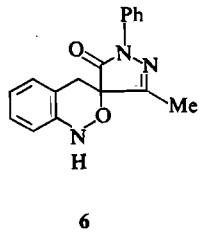

6

signals, a broad methylene signal at δ 3.28, and a one-proton signal at δ 9.67 which exchanged with deuterium. Assignment of this D-exchangeable signal to the N—OH function is consistent with the conclusions reached by other investigators of hydroxylamines (10–12). The appearance of the two methylene protons as a broad singlet was not expected since these two protons are non-equivalent. However, this appears to be only a solvent effect since the p.m.r. spectrum repeated in pyridine displayed, for these methylene protons, a doublet of doublets with a geminal coupling constant of 16 Hz. Also, in pyridine, the N—OH signal appeared further downfield as a broad peak centered at δ 12.1. Most of the data so far presented are also compatible with the reduction product, $C_{17}H_{15}N_3O_2$, being the isomeric structure **6**. This was considered, but the fact that the product isolated was neutral suggested that such a structure was not appropriate. Compound **6** would be expected to be basic since it is known that the related isoxazolidines (cyclic 5-membered-NH—O-compounds) are strong bases (13). Interpretation of the mass spectrum of the reduced product and its chemical reactivity confirmed that structure **6** was not tenable and that structure **4***a* was indeed the appropriate one. The mass spectrum contained an abundant molecular ion and diagnostic $(M-1)^+$, $(M-16)^+$ and $(M-17)^+$ ions. The last two fragments correspond to the loss of an oxygen atom and a hydroxyl radical from the molecular ion. A strong metastable ion of appropriate *m/e* value in the spectrum indicated that the transition $M^+ \rightarrow (M-17)^+$ was direct. No literature studies have been reported on the mass spectra of cyclic hydroxylamines, but these findings are consistent with our previous study (14) on aromatic hydroxylamines which were found to fragment by expelling an oxygen atom and a hydroxyl radical.

Some speculation on a possible mechanism to explain this unexpected formation of spiro-compound **4***a* by reduction of **1***a*, is warranted.

Can. J. Chem. Downloaded from www.nrcresearchpress.com by 210.87.254.42 on 09/05/12
For personal use only.

Can. J. Chem. Downloaded from www.nrcresearchpress.com by 210.87.254.42 on 09/05/12
For personal use only.

If the initial stage in the reduction of **1***a* is the hydrogenation of the benzylidene double bond to produce 3-methyl-4-(2-nitrobenzyl)-1-phenyl-2-pyrazolin-5-one, **7***a*, (*cf* 2), this intermediate might be expected to undergo base-catalyzed cyclization to the indoline **8**, which, on subsequent reduction and dehydration, would be converted to the 1-hydroxyspiro[indolinepyrazolone], **4***a*. Such a mechanism is in keeping with the one suggested to explain the formation of 1-hydroxyindoles by base-catalyzed cyclization of a variety of *o*-nitrobenzyl derivatives. A similar intermediate (**9**, in which R^1 and R^2 are electron-withdrawing groups) was proposed for that reaction (15, 16).

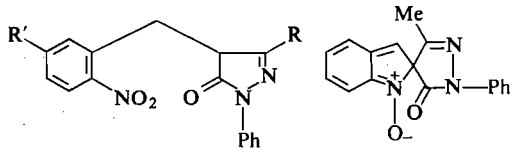

7

	R	R′
a	Me	H
b	Ph	H
c	Me	Cl

10

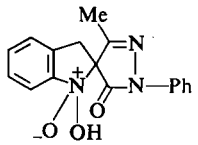

8

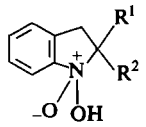

9

When the *N*-hydroxy compound **4***a* was reduced catalytically it gave an almost quantitative yield of a product, $C_{17}H_{15}N_3O$, which is identified as the previously mentioned spiroamine **4***b*. The same product was also isolated when the reduction was carried out using iron and ferrous ammonium sulfate or zinc and ammonium chloride. The base peak in the mass spectrum of this compound was the molecular ion (*m/e* 277) which fragmented initially by the expulsion of a CO molecule to a fragment ion of *m/e* 249. In the mass spectrum of the deuterated reduced compound, these two ions appeared at *m/e* 278 and 250 respectively, consistent with a compound with one D-exchangeable hydrogen atom (**4***b*, NH → ND). The i.r. and p.m.r. spectra were also consistent with structure **4***b*.

4-(2-Nitrobenzylidene)-1,3-diphenyl-2-pyrazolin-5-one, **1***b*, was then reduced with sodium borohydride and palladium–charcoal in a manner similar to that described for the methyl analog **1***a*. In this case, only two products were obtained. For reasons similar to those presented to identify the products obtained in the reduction of the methyl analog **1***a*, the major product obtained from the reduction of **1***b* is identified as 1′,3′-diphenyl-1-hydroxyspiro[indoline-2,4′-[2]pyrazoline]-5′-one, **4***c*, while the minor product was found to be the amphoteric amine **3***b* (2).

Reduction of this hydroxylamine **4***c* either catalytically or using iron and ferrous ammonium sulfate as just described for the methyl analog **4***a*, yielded a compound $C_{22}H_{17}N_3O$, which gave i.r., p.m.r., and mass spectra consistent with this compound being the phenyl analog of **4***b*, *i.e.* 1′,3′-diphenylspiro[indoline-2,4′-[2]pyrazoline]-5′-one, **4***d*. Zinc and ammonium chloride reduction of 1,3-diphenyl-4-(2-nitrobenzyl)-2-pyrazolin-5-one, **7***b*, was an alternative way of preparing the spiro(indoline)pyrazolone **4***d*. The precursor **7***b* is readily obtained by sodium borohydride reduction of the nitrobenzylidene compound **1***b* (2).

Relatively mild oxidation will convert some cyclic *N*-hydroxy compounds to the corresponding nitrones. Frequently, this is done in the absence of any catalyst by simply bubbling air through solutions of the *N*-hydroxy compound. Often, however, a catalyst is required before oxidation occurs, and copper sulfate – ammonia has been used extensively for this purpose (17, 18). It was also used in the present study to oxidize **4***a*. Crystallization of the crude product gave a dark brown solid which, despite difficulty in getting a pure sample for elemental analysis, is believed to consist mainly of the cyclic *N*-oxide **10**. The mass spectrum of this compound displayed a molecular ion at *m/e* 291 ($C_{17}H_{13}N_3O_2$). It liberated iodine from potassium iodide solution, a property common to *N*-oxides (19). Its i.r. spectrum was devoid of any amine or hydroxy absorption, and it displayed a carbonyl band at 1728 cm^{-1} which was located at a higher frequency than that of the *N*-hydroxy compound **4***a* due to the lack of any hydrogen bonding. The p.m.r. spectrum showed no D-exchangeable protons; it displayed only two signals, a methyl singlet and an aromatic 10-proton multiplet.

Various nucleophilic reagents are known to react with aromatic hydroxylamines and hydroxamic acids. Reactions in which the nucleophile is a halogen (20, 21), oxygen (22), sulfur (23, 24), nitrogen (25), or carbon (26) species have been

Can. J. Chem. Downloaded from www.nrcresearchpress.com by 210.87.254.42 on 09/05/12
For personal use only.

reported. Few of these reactions involved cyclic hydroxylamines. Therefore, in the present study, different nucleophilic species, *i.e.* chloride ion, water, methanol, and acetic acid, were reacted, in acidic media, with the *N*-hydroxy compound **4***a*. In each case, it was deduced that a 5-substituted indoline derivative (**4***f*–**4***i*) was obtained, possible by an S_NI' mechanism (Scheme 1) such as that proposed by Heller *et al.* (27) for nucleophilic attack on phenylhydroxylamine. Thus, when hydrogen chloride was bubbled through a cold solution of the *N*-hydroxy compound **4***a* in tetrahydrofuran, a black semisolid product was obtained. Chromatography of this product on a silica gel column yielded 5-chloro-3′-methyl-5′-phenylspiro[indoline-2,4′-[2]pyrazoline]-5′-one, **4***f*, as a crystalline solid. This compound was identified by its elemental analysis ($C_{17}H_{14}ClN_3O$) as well as its spectral (i.r., n.m.r.) properties. The location of the chlorine atom in the position *para* to the nitrogen atom (**4***f*) was suggested from the ample literature evidence which has revealed that when hydrochloric acid and other nucleophilic reagents react with aromatic hydroxylamines, *p*-substituted amines are the major products isolated (20, 28, 29). Confirmation of this assignment could not be obtained from the p.m.r. spectrum of the product since the aromatic signal was complex and could not be easily interpreted. Proof of the location of the chlorine atom became necessary when another isomeric chlorinated compound was obtained by the action of acetyl chloride on the hydroxylamine **4***a*. Both chloro compounds displayed very similar mass spectra but their melting points, i.r. and p.m.r. spectra were different. Therefore, it was found necessary to prepare an authentic sample of **4***f* for comparison purposes.

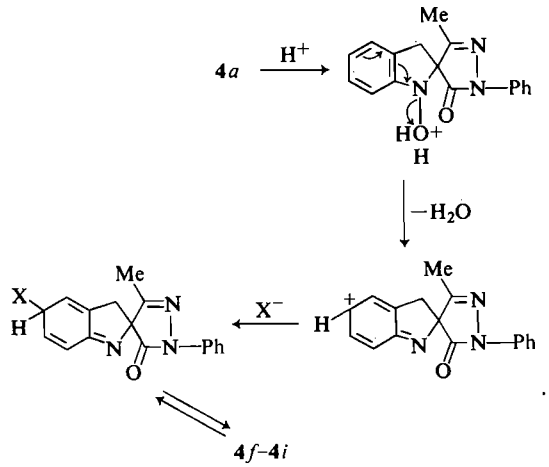

SCHEME 1

3-Chloro-6-nitrobenzaldehyde was condensed with 3-methyl-1-phenyl-2-pyrazolin-5-one and the product **1***c* (1) was reduced with sodium borohydride and palladium–charcoal in dioxane. 5-Chloro-1-hydroxy-3′-methyl-1′-phenylspiro[indoline-2,4′-[2]pyrazoline]-5′-one **4***e*, $C_{17}H_{14}ClN_3O_2$, was the main product isolated, as well as a small amount of 4-(2-amino-5-chlorobenzyl)-3-methyl-1-phenyl-2-pyrazolin-5-one, **3***c*. The major product, **4***e*, was identified from its physical and chemical properties which were similar to those of the other *N*-hydroxyindolines, **4***a* and **4***c*. Catalytic hydrogenation of **4***e* over platinum yielded the 5-chloroindoline **4***f*. Comparison of the spectral data and melting points of this compound with those of the product obtained by treating **4***a* with hydrogen chloride proved that both were identical. The 5-chloroindoline **4***f* and the *N*-hydroxy derivative **4***e* were also both obtained when 4-(5-chloro-2-nitrobenzyl)-3-methyl-1-phenyl-2-pyrazolin-5-one **7***c* (2) was reduced by means of zinc and ammonium chloride in ethanol.

Heating the *N*-hydroxy compound **4***a* with methanol in the presence of a catalytic amount of sulfuric acid, resulted in decomposition. When this reaction was repeated at 0 °C, a dark green solution was obtained from which was isolated a colorless compound which was identified as 5-methoxy-3′-methyl-1′-phenylspiro[indoline-2,4′-[2]pyrazoline]-5′-one, **4***g*, since it analyzed correctly for $C_{18}H_{17}N_3O_2$ and its mass spectrum displayed a molecular ion at *m/e* 307, and showed, with minor differences, fragmentation patterns similar to those of the 5-chloroindoline **4***f*. The i.r. and p.m.r. spectra were consistent with structure **4***g*. The complexity of the n.m.r. aromatic signal did not allow deduction of the exact location of the OCH_3 group but the pattern displayed for this signal was very similar to that in the spectrum of the 5-chloroindoline **4***f*.

A better yield of this compound was obtained when methanolic sulfuric acid was replaced with a solution of boron trifluoride in methanol. This observation was the result of an attempt to methylate the *N*-hydroxy function by the use of diazomethane in methanol, with boron trifluoride as a catalyst. Acid catalyzed nucleophilic attack

Can. J. Chem. Downloaded from www.nrcresearchpress.com by 210.87.254.42 on 09/05/12
For personal use only.

by methanol occurred rather than methylation of the *N*-hydroxy function, and the only product isolated was the 5-methoxy compound **4***g*.

When the *N*-hydroxy compound **4***a* was reacted with a mixture of dioxane and water in the presence of catalytic amounts of sulfuric acid, an alkali-soluble product, $C_{17}H_{15}N_3O_2$, was isolated. A comparison of its i.r., p.m.r., and mass spectra with those of **4***f* and **4***g* indicated that this phenolic product was 5-hydroxy-3′-methyl-1′-phenylspiro[indoline-2,4′-[2]pyrazoline]-5′-one, **4***h*.

The related 5-acetoxy derivative **4***i* was obtained by heating **4***a* with glacial acetic acid for 1 h. This compound was identified by its elemental analysis ($C_{19}H_{17}N_3O_3$), mass spectrum (M^+ at *m/e* 335), i.r., and p.m.r. spectra.

Previous studies have shown that the cyclic *N*-acetoxy carbonyl function gives rise to an i.r. absorption band in the region of 1800 cm^{-1} and the presence of this absorption band is very diagnostic (30, 31). It was desirable, therefore, to acetylate the cyclic *N*-hydroxy compounds (**4***a* and **4***c*) as a means of confirming their structures and to study the chemical behavior of these *N*-acetyloxy products. A number of conventional procedures were attempted but most of them led to the formation of rearrangement and decomposition products. The only successful method was to react the *N*-hydroxy compound in pyridine at -10 °C with excess acetic anhydride. The *N*-acetyloxy products thus obtained were stable for several weeks at 0 °C but decomposed rapidly on standing at room temperature.

The acetylated product, ($C_{19}H_{17}N_3O_3$; M^+, *m/e* 335), obtained from the *N*-hydroxy compound **4***a* was identified as 1-acetyloxy-3′-methyl-1′-phenylspiro[indoline-2,4′-[2]pyrazoline]-5′-one, **11***a*. That *O*-acetylation had occurred was confirmed by the presence of an *N*-acetyloxy C=O absorption band at 1790 cm^{-1}. In addition a lactam C=O band was located at 1723 cm^{-1} and the spectrum was devoid of any O—H or N—H bands. The p.m.r. spectrum showed two methyl signals (C—CH_3 and $OCOCH_3$), an aromatic multiplet (9 protons) and the methylene group signal as a doublet of doublets (J = 16.5 Hz). This spectrum had to be measured directly after dissolving in cold solvent because, in both solvents used, the compound decomposed and/or rearranged very rapidly; the *N*-acetyloxy signal disappeared with the appearance of some new signals and the spectrum became very complicated.

Heating the *N*-acetyloxy compound **11***a* in methanol or ethanol yielded two different crystalline products. One was identical to the 5-acetyloxy derivative **4***i* obtained earlier by the nucleophilic attack of acetic acid at C-5. The other product remains unidentified, although it is known from its elemental analysis ($C_{17}H_{13}N_3O$) and its mass spectrum (M^+, *m/e* 275) that it is a result of the loss of an acetic acid molecule from the parent *N*-acetoxy compound **11***a*. The same compound was also isolated, as described later, during attempts to methylate the *N*-hydroxy compound **4***a*.

Acetylation of the cyclic *N*-hydroxyindoline **4***c* with acetic anhydride and pyridine at -10 °C also yielded an *N*-acetoxy derivative identified as 1-acetyloxy-1′,3′-diphenylspiro[indoline-2,4′-[2]pyrazoline]-5′-one **11***b* by its elemental analysis ($C_{24}H_{19}N_3O_3$) and by similarities of its spectral data with those of the methyl analog **11***a*. It was noted that the acetyloxy derivative **11***b* was relatively stable at room temperature

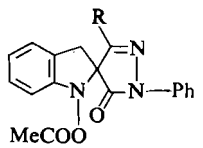

11

	R
a	Me
b	Ph

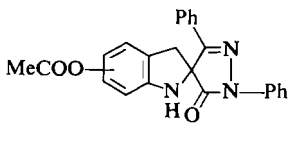

12

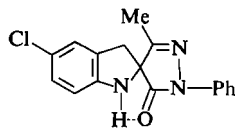

4*f*

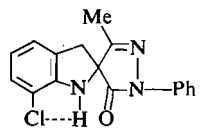

13

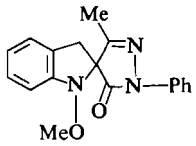

14

and in cold solvents. Rearrangement still occurred in solution but at a much slower rate than that demonstrated by the methyl analog **11***a*. Heating **11***b* in ethanol produced only one re-

Can. J. Chem. Downloaded from www.nrcresearchpress.com by 210.87.254.42 on 09/05/12
For personal use only.

arrangement product of formula $C_{24}H_{19}N_3O_3$. Infrared evidence supported the presence of an NH and two C=O groups (lactam and ester) in the molecule. The p.m.r. spectrum had signals which could be ascribed to $COCH_3$, CH_2, NH, and thirteen aromatic protons. Based on these data this compound was identified as *x*-acetyloxy-1′,3′-diphenylspiro[indoline-2,4′-[2]pyrazoline]-5′-one **12**. Although it is most likely that **12** is substituted at the 5-position as was the case with the methyl analog **4***i*, the exact position of the substituent was not determined due to the complex nature of the aromatic signal in the p.m.r. spectrum and due to the lack of an authentic sample.

When 1-hydroxy-3′-methyl-1′-phenylspiro[indoline-2,4′-[2]pyrazoline]-5′-one, **4***a*, was treated with acetyl chloride at room temperature it failed to react. When this mixture was heated in dry benzene for several hours, a reddish solution was formed which on evaporation and crystallization yielded two compounds, neither of which was the *N*-acetyloxy derivative **11***a*. The minor product $C_{19}H_{15}N_3O_3$, was dark red in color and was shown by mass spectrometry to be a monoacetate (M^+, *m/e* 333; $M-CH_2=C=O$, *m/e* 291). It readily hydrolyzed to give a phenol, $C_{17}H_{13}N_3O_2$ (M^+, *m/e* 291) which was yellow in color. Insufficient quantities of this acetate were isolated to permit identification. Its dark color, however, is indicative of a highly conjugated system.

The elemental analysis ($C_{17}H_{14}ClN_3O$) as well as the mass spectrum (M^+, *m/e* 311) of the major product confirmed the presence of a chlorine atom in its molecular formula. The possibility of this compound being the same 5-chloroindoline, **4***f*, obtained earlier was ruled out by comparing i.r. and p.m.r. spectra and by the depression of a mixture melting point. However, the similarities of the spectral data of this product and that of **4***f* suggested that they were isomeric. The p.m.r. spectrum was essentially similar to that of the 5-chloroindoline derivative **4***f* except in the aromatic area where the substitution pattern differed. Again, this pattern was complex and could not be resolved. Since the chlorine atom in isomer **4***f* was known to be located at the 5-position, it was considered likely that the other isomer was a 7-chloro derivative, **13**. These two positions are more susceptible than any other position to attack by nucleophilic reagents. Accordingly, this product is tentatively identified as 7-chloro-3′-methyl-1′-phenylspiro[indoline-2,4′-[2]pyrazoline]-5′-one, **13**. Support for this conclusion was found in its i.r. spectrum which had an NH absorption band at 3295 cm^{-1} and a C=O band at 1728 cm^{-1}. Compared to the corresponding absorption bands (3365 and 1710 cm^{-1}) in the related 5-chloroindoline, **4***f*, the N—H absorption showed a bathochromic shift of 70 cm^{-1} and the C=O a hypsochromic shift of 18 cm^{-1}. Intramolecular hydrogen bonding between the chlorine atom at C-7 and the amine hydrogen may be responsible for these shifts. In addition to the effect on the NH absorption, this also could affect the C=O absorption which is now located near the normal value ($\sim$1725 cm^{-1}) for compounds which do not display intramolecular hydrogen bonding. Hydrogen bonding between chlorine and hydrogen is now accepted (32) and the large frequency shift demonstrated here for the NH absorption may indicate that chlorine is a stronger electron donor than oxygen in this molecule.

The formation of a chlorinated product as a result of treating the *N*-hydroxy compound **4***a* with acetyl chloride was not unexpected due to the availability, in the reaction mixture, of chloride ions for nucleophilic attack. An explanation as to why a C-7 (**13**) and not a C-5 (**4***f*) chlorinated product, was obtained in the reaction with acetyl chloride is not possible although it may be due in part to the different solvents used (tetrahydrofuran for C-5 substitution and benzene for C-7 attack).

An attempt to react the 1-hydroxyindoline **4***a* with diazomethane, in the absence of any catalyst, failed to yield a methoxy derivative. When this reaction was carried out in methanol using boron trifluoride as catalyst, it produced the 5-methoxyindole **4***g*. The reaction was repeated in dioxane, and alcohol-free diazomethane and boron trifluoride-ether complex were used. This produced initially a dark-green product which was converted to a high melting pale yellow solid when treated with cold ethanol. This latter compound analyzed for $C_{17}H_{13}N_3O$ (M^+, *m/e* 275) and gave i.r. and mass spectra which were identical to the dehydrated product obtained when the *N*-acetyloxy compound **11***a* was treated with ethanol, as described earlier. A mixture melting point of both compounds showed no depression. The desired *N*-methoxyindoline, **14**, was obtained by methylating **4***a* with methyl iodide in the presence of sodium methoxide.

Can. J. Chem. Downloaded from www.nrcresearchpress.com by 210.87.254.42 on 09/05/12
For personal use only.

Identification of this compound was based on its elemental analysis ($C_{18}H_{17}N_3O_2$) as well as its i.r. (ν C=O at 1719 cm^{-1}) and p.m.r. (N—OH signal absent; N—OCH_3 at δ 3.80) spectra. The mass spectrum of this compound was also informative; it displayed a molecular ion at *m/e* 307 and strong $(M - 30)^+$ and $(M - 31)^+$ ions resulting from the expulsion of a CH_2O molecule and a CH_3O radical respectively from the molecular ion. The expulsion of a methoxy radical is not normally observed in the mass spectra of methyl ethers other than aromatic ethers where an *ortho*-effect operates (33, 34).

Pharmacology

A preliminary pharmacological screening of four of the compounds described above was undertaken. An observational technique similar to that described by Irwin (35, 36) was employed in an attempt to detect any behavioral neurological or autonomic changes after administering each compound to mice. Since the synthesized compounds possess a [2]pyrazolin-5-one nucleus and thus bear some chemical similarity to the known analgesics, antipyrine, aminopyrine, and nifenazone, selected compounds were also evaluated for their analgesic activity by means of the phenylquinone writhing test (37).

The two 1-hydroxyspiro[indolinepyrazolones] (**4***a* and **4***c*) were virtually devoid of pharmacological activity showing only a small decrease in motor activity and orientating movements when a 200 mg/kg oral dose of each was given to mice. On the other hand the spiro[indolinepyrazolones] (**4***b* and **4***d*) possessed some pharmacological activity. At an oral dose of 100 mg/kg or an intraperitoneal dose of 50 mg/kg, compound **4***b* caused a marked decrease in motor activity and orientating movements, and some muscle relaxation. Similar signs were observed with chlordiazepoxide (50 mg/kg intraperitoneally) in mice except that with this latter compound, ptosis and more marked muscle relaxation were evident.

The two spiro[indolinepyrazolones] (**4***b* and **4***d*) showed weak analgesic activity in mice. At oral doses of 200 mg/kg, these two compounds caused 45–48% protection as compared with 94% protection when the same dose of aminopyrine was administered.

Experimental

Melting points (capillary tube) are uncorrected. Infrared spectra were recorded as Nujol mulls, unless stated otherwise, using a Beckman IR-10 spectrophotometer, and p.m.r. spectra were obtained using a Varian A-60D spectrometer with DMSO-d_6 as solvent and TMS as internal standard. Mass spectra were measured on an A.E.I. MS-9 or MS-12 mass spectrometer at an ionization potential of 70 eV by Dr. A. M. Hogg and his associates, Department of Chemistry, University of Alberta, using the direct probe technique. Elemental analyses were performed by Mr. W. Dylke of our faculty. Deuterated **4***b* was prepared by repeatedly crystallizing **4***b* from dioxane–D_2O.

Reduction of 3-Methyl-4-(2-nitrobenzylidene)-1-phenyl-2-pyrazolin-5-one, 1a

(*a*) A solution of sodium borohydride (1.5 g) in water (20 ml) was added to a suspension of palladium–charcoal (10%, 0.15 g) in water (10 ml), followed by dioxane (20 ml). A solution of 3-methyl-4-(2-nitrobenzylidene)-1-phenyl-2-pyrazolin-5-one (1) (3.0 g) in dioxane (50 ml) was added dropwise to this mixture over a period of 30 min. Nitrogen was bubbled through the reaction mixture during the addition of the nitro-compound and for a further 15 min. The mixture was filtered and acidified with dilute hydrochloric acid then flooded with water (300 ml). It yielded a dark yellow precipitate (2.8 g). Attempts to purify the crude product by crystallization proved difficult. Chromatography on a silica gel column using chloroform–ether (9:1) followed by evaporation of eluate gave a yellowish crystalline compound (1.2 g), m.p. 187–188 °C dec. (ethanol) which was identified as 1-hydroxy-3′-methyl-1′-phenylspiro[indoline-2,4′-[2]pyrazoline]-5′-one, **4***a*. This compound reduced Tollen's reagent and gave, in the presence of alkali, a purple-red color with triphenyltetrazolium chloride. Infrared ν_{max} 1690 (C=O) and 3275 br (N—OH) cm^{-1}; p.m.r. δ 1.97 (3H, s, CH_3), 3.28 (2H, br, CH_2), 9.67 (1H, br, exchanged with D_2O, N—OH), and 6.70–8.10 (9H, m, aromatic protons); p.m.r. (pyridine) δ 2.10 (3H, s, CH_3), 3.44 (2H, doublet of doublets, J = 16 Hz, CH_2), 12.11 (1H, br s, D-exchangeable, N—OH), and 7.10—7.80 (9H, m, aromatic protons); mass spectrum *m/e* (% relative abundance) 293 (M^+, 70), 292 (18), 277 (55), 276 (32), 249 (35).

Anal. Calcd. for $C_{17}H_{15}N_3O_2$: C, 69.61; H, 5.16; N, 14.33. Found: C, 69.62; H, 5.07; N, 14.29.

Further elution of the column with a more polar solvent yielded only small amounts of dark brown oils which were not investigated.

(*b*) The above reaction was repeated but this time the filtrate was diluted with ice-cold water until a precipitate formed. The white solid (1.6 g) had m.p. 192–193 °C dec. (from ethanol). Infrared and p.m.r. spectra were identical to those of the *N*-hydroxyindoline **4***a* described in preparation *a*.

The filtrate remaining was acidified with glacial acetic acid to give a white precipitate (0.5 g) which was crystallized from ethanol to a small amount (0.08 g) of colorless crystals identified as 3′-methyl-1′-phenylspiro[indoline-2,4′-[2]pyrazoline]-5′-one, **4***b*, m.p. 126–127 °C. Infrared ν_{max} 1725 (C=O) and 3305 (NH) cm^{-1}; p.m.r. ($CDCl_3$) δ 2.09 (3H, s, CH_3), 3.33 (2H, d of d, J = 16.5 Hz, CH_2), 5.57 (1H, br s, D-exchangeable, NH), and 6.56–8.10 (9H, m, aromatic protons); mass spectrum *m/e* (% relative abundance) 277 (100), 276 (18), 260 (7), 249 (33).

Anal. Calcd. for $C_{17}H_{15}N_3O$: C, 73.63; H, 5.45; N, 15.15. Found: C, 73.93; H, 5.49; N, 14.94.

Can. J. Chem. Downloaded from www.nrcresearchpress.com by 210.87.254.42 on 09/05/12
For personal use only.

The mother liquor remaining after the removal of the above product was concentrated to yield a third product (0.33 g), m.p. 153–154 °C. This was 4-(2-aminobenzyl)-3-methyl-1-phenyl-2-pyrazolin-5-one, **3***a*, (lit. (2) m.p. 153–154 °C); i.r., p.m.r., and mass spectrum were identical to literature spectra (2).

Anal. Calcd. for $C_{17}H_{17}N_3O$: C, 73.09; H, 6.13; N, 15.04. Found: C, 73.18; H, 6.18; N, 14.98.

Reduction of 1,3-Diphenyl-4-(2-nitrobenzylidene)-2-pyrazolin-5-one, 1b

The title compound (1) (3.0 g) was reduced in the same manner as the analog **1***a*, using method *a*. The reaction mixture was filtered free of palladium–charcoal and acidified with dilute acetic acid (300 ml).

The precipitate formed was crystallized from ethanol to an off-white solid (1.2 g), m.p. 178–179 °C dec. which was identified as 1′,3′-diphenyl-1-hydroxyspiro[indoline-2,4′-[2]pyrazoline]-5′-one, **4***c*. This compound reduced Tollen's reagent and gave a positive test with triphenyltetrazolium chloride (7, 8) for an *N*-hydroxy compound. Infrared ν_{max} 1696 (C=O) and 3347 (N—OH) cm^{-1}; p.m.r. δ 3.47 (2H, br s, CH_2), 9.80 (1H, br s, D-exchangeable, N—OH), and 6.70–8.32 (14H, m, aromatic protons). Mass spectrum *m/e* (% relative abundance) 355 (42), 354 (4), 339 (100), 338 (24), 323 (9), 311 (50).

Anal. Calcd. for $C_{22}H_{17}N_3O_2$: C, 74.35; H, 4.79; N, 11.82. Found: C, 74.23; H, 4.87; N, 11.89.

Concentration of the mother liquors after the removal of the above product gave 0.35 g of a second compound, 4-(2-aminobenzyl)-1,3-diphenyl-2-pyrazolin-5-one, **3***b*, m.p. 151–153 °C (lit. (2) m.p. 151–153 °C). Infrared, p.m.r., and mass spectrum were identical to literature spectra (2).

Anal. Calcd. for $C_{22}H_{19}N_3O$: C, 77.40; H, 5.61; N, 12.31. Found: C, 77.46; H, 5.76; N, 12.26.

Reduction of 4-(5-Chloro-2-nitrobenzylidene)-3-methyl-1-phenyl-2-pyrazolin-5-one, 1c

The title compound (1) (2.0 g) was reduced in the same manner as the analog **1***a*, using method *a* except that the filtrate was acidified with dilute acetic acid, followed by water. This yielded a white solid (1.3 g), m.p. 143–145 °C (from ethanol) which reduced Tollen's reagent and gave a purple-red color with triphenyltetrazolium chloride, and is identified as 5-chloro-1-hydroxy-3′-methyl-1′-phenylspiro[indoline-2,4′-[2]pyrazoline]-5′-one, **4***e*. Infrared ν_{max} 1685 (C=O), 3280 br (N—OH), and 1605 (C=N) cm^{-1}; p.m.r. δ 2.20 (3H, s, CH_3), 3.46 (2H, s, CH_2), 6.90–8.10 (8H, m, aromatic protons), and 8.60 (1H, br s, D-exchangeable, N—OH); mass spectrum *m/e* (% relative abundance) 329 (12), 327 (32), 313 (44), 312 (23), 311 (76), 310 (33), 285 (14), 283 (35).

Anal. Calcd. for $C_{17}H_{14}ClN_3O_2$: C, 62.29, H, 4.30, N, 12.82. Found: C, 62.13; H, 4.48; N, 13.09.

Concentration of the mother liquors after removal of the above product gave 4-(2-amino-5-chlorobenzyl)-3-methyl-1-phenyl-2-pyrazolin-5-one, **3***c*, (0.18 g), m.p. 118–120 °C (lit. (2) m.p. 119–121 °C). Infrared, p.m.r., and mass spectra were identical to those reported (2).

Anal. Calcd. for $C_{17}H_{16}ClN_3O$: C, 65.06; H, 5.14. Found: C, 65.08; H, 5.12.

3′-Methyl-1′-phenylspiro[indoline-2,4′-[2]pyrazoline]-5′-one, 4b

(*a*) This compound was a minor product of the reduction of **1***a*, method *b*, as described above.

(*b*) A solution of 1-hydroxy-3′-methyl-1′-phenylspiro[indoline-2,4′-[2]pyrazoline]-5′-one (**4***a*, 0.5 g) in ethanol (70 ml) was hydrogenated over platinum oxide (0.05 g) at atmospheric pressure and room temperature. After the theoretical amount of hydrogen was absorbed, the catalyst was removed by filtration and the filtrate was concentrated *in vacuo*, then cooled, and a white crystalline product (0.43 g) separated. This was recrystallized from ethanol giving 3′-methyl-1′-phenylspiro[indoline-2,4′-[2]pyrazoline]-5′-one, **4***b*, as white crystals, m.p. 129–130 °C, identical to the product obtained by method *a*.

(*c*) To a heated solution of the 1-hydroxyspiro[indoline-pyrazolone] (**4***a*, 0.5 g) in ethanol (30 ml) was added reduced iron (1.0 g) followed by a solution of ferrous ammonium sulfate (0.3 g) in water (25 ml) and the mixture was heated, under reflux, for 10 h then filtered. The filtrate was evaporated to dryness and the residue was dissolved in hot ethanol and refiltered. Cooling of this filtrate yielded the spiro(indoline)pyrazolone **4***b* as white crystals (0.44 g), m.p. 128–129 °C, identical to the product obtained by method *a*.

(*d*) Ammonium chloride (0.1 g) in water (5 ml) was added to a stirred solution of the *N*-hydroxy compound (**4***a*, 0.5 g) in 60% ethanol (25 ml). Zinc powder (0.5 g) was added in small portions and the mixture was refluxed for 1 h. After removal of the excess zinc and zinc oxide, the solution was concentrated *in vacuo* and extracted with chloroform (50 ml). Evaporation of the dried ($CaCl_2$) chloroform gave a white solid (0.41 g) which crystallized from ethanol as colorless crystals of **4***b*, m.p. 127–129 °C, identical to the product obtained by method *a*.

1,3′-Diphenylspiro[indoline-2,4′-[2]pyrazoline]-5′-one, 4d

(*a*) 1-Hydroxy-1′,3′-diphenylspiro[indoline-2,4′-[2]pyrazoline]-5′-one (**4***c*, 0.5 g) was hydrogenated in a manner similar to that described for the preparation of **4***b*, method *b*. This gave the pale yellow title compound (**4***d*, 0.38 g), m.p. 193–194 °C. Infrared ν_{max} 1728 (C=O) and 3390 (NH) cm^{-1}; p.m.r. δ 3.51 (2H, br s, CH_2), 4.60 (1H, br s, D-exchangeable, NH), and 6.60–8.30 (14H, m, aromatic protons); mass spectrum *m/e* (% relative abundance) 339 (100), 338 (22), 322 (9), 311 (49).

Anal. Calcd. for $C_{22}H_{17}N_3O$: C, 77.85; H, 5.05; N, 12.38. Found: C, 77.69; H, 5.14; N, 12.41.

(*b*) Reduction of the 1-hydroxyspiro[indolinepyrazolone] (**4***c*, 0.4 g) with iron and ferrous ammonium sulfate in the manner described for the preparation of compound **4***b*, method *c*, gave the title compound (**4***d*, 0.29 g) as pale yellow crystals, m.p. 192–194 °C.

(*c*) 1,3-Diphenyl-4-(2-nitrobenzyl)-2-pyrazolin-5-one (2) (**7***b*, 1.0 g), dissolved in 50% ethanol (40 ml), was added to a solution of ammonium chloride (0.2 g) in water (10 ml). Zinc dust (0.5 g) was added and the mixture was heated under reflux for 2 h under nitrogen, then filtered. The filtrate was evaporated and the residue was recrystallized from ethanol to give the title compound (**4***d*, 0.78 g), m.p. 193–194 °C, as pale yellow crystals identical to the product obtained by method *a*.

5-Chloro-3′-methyl-1′-phenylspiro[indoline-2,4′-[2]pyrazoline]-5′-one, 4f

(*a*) A stream of hydrogen chloride was passed through a solution of 1-hydroxy-3′-methyl-1′-phenylspiro[indoline-2,4′-[2]pyrazoline]-5′-one (**4***a*, 0.5 g) in tetrahydrofuran (10 ml) for 30 s at 0 °C. The solution was left

Can. J. Chem. Downloaded from www.nrcresearchpress.com by 210.87.254.42 on 09/05/12
For personal use only.

standing at 0 °C for 12 h then evaporated *in vacuo* to dryness. The resulting black semisolid was chromatographed on a silica gel column using petroleum ether (30–60 °C, 100 ml) then benzene (100 ml) as solvent. Evaporation of the benzene eluate gave a dark yellow solid which crystallized from ethanol yielding the title compound **4***f* as white crystals (0.26 g), m.p. 153–154 °C. Infrared ν_{max} 1710 (C=O) and 3365 (N—H) cm^{-1}; p.m.r. ($CDCl_3$) δ 2.04 (3H, s, CH_3), 3.33 (2H, d of d, J = 16 Hz, CH_2), 4.00 (1H, br s, D-exchangeable, N—H), and 6.40–8.10 (8H, m, aromatic protons); mass spectrum *m/e* (% relative abundance) 313 (34), 312 (23), 311 (100), 310 (13), 294 (6), 285 (20), 283 (57).

Anal. Calcd. for $C_{17}H_{14}ClN_3O$: C, 65.49; H, 4.53; N, 13.48. Found: C, 65.06; H, 4.67; N, 13.21.

(*b*) Catalytic hydrogenation of 5-chloro-1-hydroxy-3′-methyl-1′-phenylspiro[indoline-2,4′-[2]pyrazoline]-5′-one (**4***e*, 0.35 g) in the way described for the preparation of **4***b*, method *b*, gave the title compound **4***f* (0.21 g) as colorless crystals, m.p. 152–153 °C, identical to the product obtained by method *a* immediately above.

(*c*) 4-(5-Chloro-2-nitrobenzyl)-3-methyl-1-phenyl-2-pyrazolin-5-one (2) (1.0 g) was reduced with zinc and ammonium chloride in the manner described for the preparation of the analog **4***d*, method *c*. This gave the title compound **4***f* (0.41 g) m.p. 153–154 °C with identical properties to the product obtained by method *a* immediately above.

Concentration of the mother liquors remaining after the removal of the above product yielded a second product (0.15 g), m.p. 144–145 °C which was identical (i.r., mass spectrum) to 5-chloro-1-hydroxy-3′-methyl-1′-phenylspiro[indoline-2,4′-[2]pyrazoline]-5′-one, **4***e*.

Oxidation of 1-Hydroxy-3′-methyl-1′-phenylspiro[indoline-2,4′-[2]pyrazoline]-5′-one, 4a

Air was bubbled for 3 h through a solution of the 1-hydroxyspiro[indolinepyrazolone] (**4***a*, 0.3 g) in aqueous (60%) ethanol (25 ml) containing ammonia (1 ml) and copper sulfate (5 mg). Water (50 ml) was added and the dark brown precipitate which formed was extracted into chloroform (20 ml). The dried ($CaCl_2$) chloroform solution was concentrated *in vacuo* and the residue was crystallized from aqueous ethanol as a dark brown solid (0.18 g), m.p. 121–124 °C. This compound was tentatively identified as 3′-methyl-1′-phenylspiro[[2*H*]indole-2,4′-[2]pyrazoline]-5′-one-1-oxide (**10**); i.r. ν_{max} 1728 (C=O) cm^{-1}, NH and OH absorption absent; p.m.r. ($CDCl_3$) δ 2.07 (3H, s, CH_3) and 6.70–8.20 (10H, m, aromatic protons; mass spectrum M^+ *m/e* 291 ($C_{17}H_{13}N_3O_2$).

Anal. Calcd. for $C_{17}H_{13}N_3O_2$: N, 14.42. Found: N, 14.22. (Satisfactory C, H analyses could not be obtained.)

5-Methoxy-3′-methyl-1′-phenylspiro[indoline-2,4′-[2]pyrazoline]-5′-one, 4g

(*a*) Concentrated sulfuric acid (0.5 ml) was added dropwise to a suspension of 1-hydroxy-3′-methyl-1′-phenylspiro[indoline-2,4′-[2]pyrazoline]-5′-one (**4***a*, 0.5 g) in methanol (15 ml) at 0 °C, and the mixture was left overnight at 0 °C. The solution was made alkaline with dilute sodium hydroxide then reacidified with glacial acetic acid and extracted with chloroform. The dried ($MgSO_4$) chloroform solution was evaporated to dryness to give a dark green oil which solidified when triturated with methanol. This was crystallized from ethanol as white crystals (0.37 g), m.p. 135–137 °C and is identified as the title compound **4***g*. Infrared ν_{max} 1710 (C=O) and 3310 (NH) cm^{-1}; p.m.r. ($CDCl_3$) δ 2.03 (3H, s, C—CH_3), 3.77 (3H, s, O—CH_3), 3.33 (2H, d of d, J = 16.5 Hz, CH_2), 4.28 (1H, br s, D-exchangeable, NH), and 6.50–8.40 (8H, m, aromatic protons); mass spectrum *m/e* (% relative abundance) 307 (100), 306 (34), 290 (9), 279 (26).

Anal. Calcd. for $C_{18}H_{17}N_3O_2$: C, 70.34; H, 5.58; N, 13.67. Found: C, 70.21; H, 5.49; N, 13.70.

(*b*) Excess diazomethane in ether was added to a stirred solution of 1-hydroxy-3′-methyl-1′-phenylspiro[indoline-2,4′-[2]pyrazoline]-5′-one (**4***a*, 0.8 g) in methanol (80 ml) containing a catalytic amount (2 ml) of boron trifluoride (14% solution in methanol). The resulting green solution was allowed to stand for 24 h at room temperature then evaporated under reduced pressure leaving a green solid. Crystallization of this crude product from ethanol yielded a white crystalline solid (0.68 g), m.p. 137–138 °C, which was identical (i.r., p.m.r.) to the product **4***g* obtained by method *a* immediately above.

5-Hydroxy-3′-methyl-1′-phenylspiro[indoline-2,4′-[2]pyrazoline]-5′-one, 4h

1-Hydroxy-3′-methyl-1′-phenylspiro[indoline-2,4′-[2*H*]pyrazoline]-5′-one (**4***a*, 0.5 g) was dissolved in an ice-cold mixture of dioxane (8 ml) and water (7 ml). Concentrated sulfuric acid (0.5 ml) was added dropwise and the reaction mixture was allowed to stand at room temperature for 12 h. Dilute sodium hydroxide (10 ml) was added, and the solution was reacidified with glacial acetic acid and extracted with chloroform. Evaporation of the dried ($MgSO_4$) chloroform extract yielded the title compound **4***h* as a pale brown solid which crystallized from aqueous ethanol to an off-white alkali-soluble solid (0.19 g), m.p. 114–116 °C. Infrared ν_{max} 1709 (C=O) and 3100–3500 (NH, OH) cm^{-1}; p.m.r. δ 2.10 (3H, s, CH_3), 3.29 (2H, br s, CH_2), 4.70 (1H, br s, D-exchangeable, NH) 11.10 (1H, br s, D-exchangeable, OH), and 6.70–8.35 (8H, m, aromatic protons); mass spectrum *m/e* (% relative abundance) 293 (M^+, 19), 265 (26).

Anal. Calcd. for $C_{17}H_{15}N_3O_2$: C, 69.61; H, 5.16. Found: C, 70.09; H, 4.73.

5-Acetyloxy-3′-methyl-1′-phenylspiro[indoline-2,4′-[2]pyrazoline]-5′-one, 4i

A solution of the 1-hydroxyspiro[indolinepyrazolone] (**4***a*, 0.5 g) in glacial acetic acid (10 ml) was heated under reflux for 1 h. The resulting red solution was added to cold water (100 ml) and the pale brown precipitate formed was extracted with ether. The ethereal extract was washed with a saturated solution of sodium bicarbonate then with water and dried (Na_2SO_4). Evaporation of this extract yielded a pale yellow solid (0.38 g) which crystallized from ethanol to off-white crystals of the title compound **4***i*, m.p. 120–121 °C. Infrared ν_{max} 1712 (lactam C=O), 1744 (ester C=O), and 3380 (NH) cm^{-1}; p.m.r. ($CDCl_3$) δ 2.06 (3H, s, C—CH_3), 2.23 (3H, s, $COCH_3$), 3.36 (2H, d of d, J = 15 Hz, CH_2), 4.52 (1H, br s, D-exchangeable, NH), and 6.50–8.50 (8H, m, aromatic protons); mass spectrum *m/e* (% relative abundance) 335 (59), 293 (80), 292 (25), 277 (37), 265 (33), 249 (36), 91 (100).

Anal. Calcd. for $C_{19}H_{17}N_3O_3$: C, 68.05; H, 5.11; N, 12.53. Found: C, 67.95; H, 5.17; N, 12.31.

1-Acetyloxy-3′-methyl-1′-phenylspiro[indoline-2,4′-[2]pyrazoline]-5′-one, 11a

Cold acetic anhydride (3.0 ml) was added to a solution

Can. J. Chem. Downloaded from www.nrcresearchpress.com by 210.87.254.42 on 09/05/12
For personal use only.

of the 1-hydroxyspiro[indolinepyrazolone] (**4***a*, 0.3 g) in cold pyridine (3.0 ml) and the mixture was kept for 24 h at −10 °C. The title compound **11***a* separated as a colorless crystalline solid (0.26 g), m.p. 92–93 °C. Infrared ν_{max} 1790 (*N*-acetyloxy C=O) and 1723 (lactam C=O) cm^{-1} (NH and OH absorption bands absent); p.m.r. (measured directly after dissolving in cold $CDCl_3$ or DMSO-d_6) δ 2.05 (3H, s, CH_3), 2.14 (3H, s, CH_3), 3.38 (2H, d of d, J = 16.5 Hz, CH_2), and 6.50–8.20 (9H, m, aromatic protons); mass spectrum *m/e* (% relative abundance) 335 (55), 307 (7), 293 (56), 275 (66), 265 (60).

Anal. Calcd. for $C_{19}H_{17}N_3O_3$: C, 68.05; H, 5.11; N, 12.53. Found: C, 68.31; H, 5.23; N, 12.81.

Attempts to crystallize **11***a* (0.25 g) from ethanol or methanol resulted in the formation of an off-white crystalline solid (0.09 g), m.p. 306–308 °C; i.r. ν_{max} 1640 br (C=O) and 3410 (NH) cm^{-1}; p.m.r. δ 2.63 (3H, s, CH_3), 4.00–5.10 (1H, br s, D-exchangeable), and 7.20–8.30 (9H, m, aromatic protons); mass spectrum *m/e* (% relative abundance) 275 (100), 274 (81), 260 (5), 115 (16), 77 (15).

Anal. Calcd. for $C_{17}H_{13}N_3O$: C, 74.19; H, 4.76; N, 15.27. Found: C, 74.49; H, 4.57; N, 14.98.

When the mother liquor remaining after removal of the above compound was concentrated and allowed to stand, a pale yellow solid (0.13 g), m.p. 117–118 °C deposited and was identified (i.r., p.m.r.) as 5-acetyloxy-3′-methyl-1′-phenylspiro[indoline-2,4′-[2]pyrazoline]-5′-one, **4***i*.

1-Acetyloxy-1′,3′-diphenylspiro[indoline-2,4′-[2]pyrazoline]-5′-one, 11b

When 1′,3′-diphenyl-1-hydroxyspiro[indoline-2,4′-[2]-pyrazoline]-5′-one (**4***c*, 0.3 g) was acetylated in the same manner as described above in the preparation of compound **11***a*, no product separated from the cooled solution. It was then diluted with ethanol (3 ml) and poured into ice-cold water with stirring. The title compound (**11***b*, 0.32 g) precipitated, m.p. 90–91 °C. Infrared ν_{max} 1792 (*N*-acetyloxy C=O), 1725 (lactam C=O) cm^{-1} (NH and OH absorption bands absent); p.m.r. (measured rapidly) δ 2.00 (3H, s, $OCOCH_3$), 3.61 (2H, d of d, J = 16.0 Hz, CH_2), and 6.90–9.30 (14H, m, aromatic protons); mass spectrum *m/e* (% relative abundance) 397 (24), 369 (9), 355 (22), 354 (14), 339 (13), 337 (10), 327 (38), 311 (15).

Anal. Calcd. for $C_{24}H_{19}N_3O_3$: C, 72.53; H, 4.81; N, 10.57. Found: C, 72.19; H, 4.83; N, 10.26.

Heating the above compound (**11***b*, 0.3 g) in ethanol produced a reddish solution. This was added, with stirring, to ice-cold water (100 ml) and the brown precipitate formed was collected and dried. Crystallization twice from benzene–petroleum ether (40–60 °C) gave a yellow solid (0.12 g), m.p. 115–117 °C, which is partially identified as *x*-acetyloxy-1′,3′-diphenylspiro[indoline-2,4′-[2]pyrazoline]-5′-one, **12**. Infrared ν_{max} 1723 (lactam C=O), 1750 (ester C=O), and 3340 (NH) cm^{-1}; p.m.r. ($CDCl_3$) δ 2.23 (3H, s, $COCH_3$), 3.58 (2H, d of d, J = 15.5 Hz, CH_2), 5.70 (1H, br s, D-exchangeable, NH), and 6.70–8.30 (13H, m, aromatic protons).

Anal. Calcd. for $C_{24}H_{19}N_3O_3$: C, 72.53; H, 4.81; N, 10.57. Found: C, 72.11; H, 4.99; N, 10.29.

Action of Acetyl Chloride on 1-Hydroxy-3′-methyl-1′-phenylspiro[indoline-2,4′-[2]pyrazoline]-5′-one, 4a

To a solution of the title compound (**4***a*, 0.5 g) in hot dry benzene (10 ml), acetyl chloride (1.0 ml) was added and the mixture heated under reflux for 10 h. The resulting red solution was evaporated to dryness, leaving a dark oil which was dissolved in hot ethanol. Cooling gave a small quantity (0.07 g) of a product as red needles, m.p. 209–210 °C. This compound remains unidentified (its hydrolysis is described below). Infrared ν_{max} 1688 and 1712 (C=O) cm^{-1}; p.m.r. ($CDCl_3$) δ 2.44 (3H, s, CH_3), 2.48 (3H, s, CH_3), 7.00–8.20 (8H, m, aromatic protons), and 9.80 (1H, d, J = 8 Hz, unassigned); mass spectrum *m/e* (% relative abundance) 333 (47), 291 (70), 186 (7), 158 (24), 77 (100).

Anal. Calcd. for $C_{19}H_{15}N_3O_3$: C, 68.46; H, 4.54; N, 12.61. Found: C, 68.74; H, 4.95; N, 12.75.

After the above product was collected, the filtrate was concentrated and from it pale orange crystals (0.30 g), m.p. 188–189 °C separated. This was 7-chloro-3′-methyl-1′-phenylspiro[indoline-2,4′-[2]pyrazoline]-5′-one, **13**; i.r. ν_{max} 1728 (C=O) and 3295 (NH) cm^{-1}; p.m.r. ($CDCl_3$) δ 2.10 (3H, s, CH_3), 3.46 (2H, d of d, J = 16 Hz, CH_2), 4.58 (1H, br s, D-exchangeable, NH), and 6.55–8.10 (8H, m, aromatic protons); mass spectrum *m/e* (% relative abundance) 311 (M^+, 100), 294 (9), 283 (60).

Anal. Calcd. for $C_{17}H_{14}ClN_3O$: C, 65.49; H, 4.53; N, 13.48. Found: C, 65.31; H, 4.66; N, 13.11.

A sample (60 mg) of the unidentified acetate, m.p. 209–210 °C described above was suspended in 10% aqueous sodium hydroxide (5.0 ml) and stirred for 2 h. The resulting yellow solution was filtered, acidified with dilute hydrochloric acid and extracted with ether. Evaporation of the dried (Na_2SO_4) ethereal extract yielded a yellow solid (40 mg), m.p. 179–180 °C (ethanol). Infrared ν_{max} 1637 (C=O) and 2000–3300 (OH) cm^{-1}; p.m.r. δ 2.58 (3H, s, CH_3), 4.00–5.20 (1H, br s, D-exchangeable, OH), 8.62 (1H, d, J = 8 Hz, unassigned), and 6.70–8.10 (8H, m, aromatic protons); mass spectrum *m/e* (% relative abundance) 291 (M^+, 72), 205 (8), 200 (8), 186 (10), 178 (10), 158 (59), 130 (24), 120 (100).

Anal. Calcd. for $C_{17}H_{13}N_3O_2$: C, 70.09; H, 4.50; N, 14.42. Found: C, 69.73; H, 4.51; N, 14.02.

Methylation of 1-Hydroxy-3′-methyl-1′-phenylspiro[indoline-2,4′-[2]pyrazoline]-5′-one, 4a

(*a*) See preparation of 5-methoxy-3′-methyl-1′-phenylspiro[indoline-2,4′-[2]pyrazoline]-5′-one, **4***g*, method *b*.

(*b*) Reaction *a* was repeated in dioxane (80.0 ml) using alcohol-free ethereal solution of diazomethane and boron trifluoride – ether complex (1 ml). Solvents were removed under reduced pressure leaving a green residue which was extracted with chloroform. Evaporation of the chloroform solution yielded a green solid, i.r. ν_{max} 1720 (C=O) cm^{-1}, NH and OH absorption absent, which recrystallized from ethanol as a yellow solid (0.21 g), m.p. 306–308 °C, identical to the unidentified product obtained by crystallizing **9***a* from ethanol.

(*c*) Methyl iodide (1.0 g) in methanol (5.0 ml) was added to a solution of the 1-hydroxyspiro[indolinepyrazolone] (**4***a*, 0.5 g) in methanol (15.0 ml) containing 0.2 g of sodium. The mixture was heated under reflux for 3 h during which time a yellow color developed. The solvent was evaporated and the residue extracted with ether. Evaporation of the dried (Na_2SO_4) ethereal extract gave a yellow solid which was crystallized from methanol to give 1-methoxy-3′-methyl-1′-phenylspiro[indoline-2,4′-[2]pyrazoline]-5′-one, **14**, as pale yellow crystals (0.39 g), m.p. 112–114 °C. Infrared ν_{max} 1719 (C=O) cm^{-1} (NH,

OH absorption absent); p.m.r. ($CDCl_3$) δ 1.96 (3H, s, C—CH_3), 3.80 (3H, s, O—CH_3), 3.27 (2H, d of d, J = 17 Hz, CH_2), and 6.80–8.30 (9H, m, aromatic protons); mass spectrum *m/e* (% relative abundance) 307 (80), 276 (61), 248 (28), 233 (7), 207 (7).

Anal. Calcd. for $C_{18}H_{17}N_3O_2$: C, 70.34; H, 5.58; N, 13.67. Found: C, 70.41; H, 5.38; N, 13.29.

The authors thank the Medical Research Council of Canada for operating grant MA-2993 which financed this project.

1. R. T. Coutts and J. B. Edwards. Can. J. Chem. **44**, 2009 (1966).
2. R. T. Coutts and A.-m. El-hawari. Can. J. Chem. This issue.
3. H. C. Brown. Hydroboration. Benjamin, New York. 1962. p. 242.
4. R. T. Coutts. J. Chem. Soc. C, 713 (1969).
5. R. T. Coutts and D. G. Wibberley. J. Chem. Soc. 4610 (1963).
6. R. T. Coutts and K. W. Hindmarsh. Can. J. Pharm. Sci. **1**, 11 (1966).
7. G. A. Snow. J. Chem. Soc. 2588 (1954).
8. M. A. T. Rogers. J. Chem. Soc. 769 (1955).
9. A. R. Katritzky and J. M. Lagowski. Chemistry of heterocyclic *N*-oxides. Academic Press, London. 1971. p. 153.
10. T. Kato and H. Yamanaka. J. Org. Chem. **30**, 910 (1965).
11. R. M. Acheson, R. G. Bolton, and I. Hunter. J. Chem. Soc. C, 1067 (1970).
12. E. E. Schweizer and C. M. Kopay. J. Org. Chem. **37**, 1561 (1972).
13. A. Quilico. *In* Five- and six-membered compounds with nitrogen and oxygen (excluding oxazoles). *Edited by* R. H. Wiley. Vol. 17 in the series The chemistry of heterocyclic compounds. Consulting editor A. Weissberger. Interscience, New York. 1962. p. 229.
14. R. T. Coutts and G. Mukherjee. Org. Mass Spectrom. **3**, 63 (1970).
15. J. D. Loudon and G. Tennant. Q. Rev. Chem. Soc. **18**, 389 (1964).
16. P. N. Preston and G. Tennant. Chem. Rev. **72**, 627 (1972).
17. R. F. C. Brown, V. M. Clark, M. Lamchen, and A. Todd. J. Chem. Soc. 2116 (1959).
18. R. F. C. Brown, V. M. Clark, I. O. Sutherland, and A. Todd. J. Chem. Soc. 2109 (1959).
19. A. R. Katritzky. Q. Rev. Chem. Soc. **10**, 395 (1956).
20. R. T. Coutts and N. J. Pound. Can. J. Chem. **48**, 1859 (1970).
21. G. Stöhrer and G. B. Brown. Science, **167**, 1622 (1970).
22. P. G. Gassman and G. A. Campbell. Chem. Commun. 1437 (1971).
23. E. Boyland, D. Manson, and R. Nery. J. Chem. Soc. 606 (1962).
24. J. T. Edward and J. Whiting. Can. J. Chem. **49**, 3502 (1971).
25. U. Wölcke, J. M. Birdsall, and G. B. Brown. Tetrahedron Lett. 785 (1969).
26. S. Takahashi and H. Kano. Chem. Pharm. Bull. (Tokyo), **12**, 282 (1964).
27. H. E. Heller, E. D. Hughes, and C. K. Ingold. Nature, **168**, 909 (1951).
28. E. Bamberger. Ann. **441**, 297 (1925).
29. G. R. Robertson and R. A. Evans. J. Org. Chem. **5**, 142 (1940).
30. J. P. Freeman. J. Am. Chem. Soc. **80**, 5954 (1958).
31. J. D. Loudon and I. Wellings. J. Chem. Soc. 3462 (1960); 3470 (1960).
32. S. N. Vinogradov and R. H. Linnell. Hydrogen bonding. Van Nostrand Reinhold, New York. 1971.
33. J. Cable, S. A. Kagal, and J. K. MacLeod. Org. Mass Spectrom. **6**, 301 (1972).
34. R. T. Coutts and J. L. Malicky. Org. Mass Spectrom. **7**, 985 (1973).
35. S. Irwin. Science, **136**, 123 (1962).
36. S. Irwin. *In* Animal and clinical pharmacologic techniques in drug evaluation, *Edited by* J. H. Nodine and P. E. Siegler. Year Book Med. Pubs., Chicago. 1964. p. 36.
37. E. Siegmund, R. Cadmus, and G. Lu. Proc. Soc. Exp. Biol. (N.Y.), **95**, 729 (1957).

Can. J. Chem. Downloaded from www.nrcresearchpress.com by 210.87.254.42 on 09/05/12
For personal use only.

Organic Sulfur Mechanisms. 17. A Brief Study of the Photolysis of an Unsaturated Cyclic Sulfone

J. F. KING, E. G. LEWARS, D. R. K. HARDING, AND R. M. ENANOZA
Department of Chemistry, University of Western Ontario, London, Ontario N6A 5B7

Received July 14, 1975

J. F. KING, E. G. LEWARS, D. R. K. HARDING, and R. M. ENANOZA. Can. J. Chem. **53**, 3656 (1975).

Photolysis of 3-phenyl-2*H*-thiopyran 1,1-dioxide (**3**) in methanol gives a mixture of 3-phenyl-5-methoxy-5,6-dihydro-2*H*-thiopyran 1,1-dioxide (**4**) and methyl 4-phenyl-2,4-pentadiene-1-sulfonate (**5**). Formation of **5** shows that the photochemical ring opening of cyclohexadienic sulfonyl compounds (**1**) does not require an atom bearing a free electron pair in the heterocyclic ring, and therefore argues in favor of a mechanism involving cycloreversion to the sulfene (**1** → **2**).

J. F. KING, E. G. LEWARS, D. R. K. HARDING et R. M. ENANOZA. Can. J. Chem. **53**, 3656 (1975).

La photolyse du phényl-3 2*H*-thiopyrannedioxyde-1,1 (**3**) dans le méthanol conduit à un mélange de phényl-3 méthoxy-5 dihydro-5,6 2*H*-thiopyrannedioxyde-1,1 (**4**) et de phényl-4 pentadiène-2,4 sulfonate-1 de méthyle (**5**). La formation de **5** démontre que l'ouverture photochimique du cycle des composés cyclohexadiénique sulfonyle (**1**) ne requière pas un atome portant une paire d'électrons libre dans le noyau hétérocyclique et suggère ainsi un mécanisme impliquant une cycloréversion vers le sulfène (**1** → **2**).

[Traduit par le journal]

Photolysis of unsaturated sultones (1–3), and sultams (4) derived from **1***a* and **1***b*, respectively, is known to give products formulated as arising from the sulfene **2** formed by photochemical ring opening. Doubt about the actual intermediacy of

1 *a* X = O *b* X = N—R *c* X = CH_2 **2**

the sulfene in these reactions, however, has been expressed by Charlton and de Mayo (5) as a result of flash photolysis experiments, which required any sulfene formed in these reactions to have a lifetime of less than 20 μs. In the examples which had been studied, X is an oxygen atom or an N—R group, and in **2** the oxygen or nitrogen is particularly favorably arranged for an intramolecular reaction with the sulfene portion, *e.g.* to reform the starting material. This consideration when taken with the high reactivity of sulfenes (for a review see ref. 6), led us to conclude that such a short lifetime was not inconsistent with structures **2***a* and **2***b*. Because of the smaller nucleophilicity of an olefinic carbon as compared with a carbonyl oxygen or an imine nitrogen, we hoped that **2***c*, if formed from **1***c*, might have a longer lifetime and be observable on flash photolysis. The experience of Chapman and coworkers (7, 8) with ketene analogs of these systems lends support to such a notion. Accordingly, we have looked at the photolysis of 3-phenyl-2*H*-thiopyran 1,1-dioxide, **3**, and although the original aim has not been achieved, we have made a relevant observation which we wish to record in this brief note.

Photolysis of a methanolic solution of **3** (9) gave two principal products, which were separable on thin layer chromatography (t.l.c.). Structures **4** and **5** for the respective major (43%) and minor (30%) products were deduced from their i.r. and n.m.r. spectra and were confirmed by synthesis, respectively, of (*a*) **4** by methylation of **6** (the precursor of **3**), and (*b*) **7**, the tetrahydro derivative of **5**, via a sulfo-Cope rearrangement (10) of **8** followed by hydrogenation and esterification, as shown in Scheme 1. Nuclear magnetic resonance spectra of different samples of **5** indicated the presence of varying amounts of another product consistent with the presence of a small amount of the geometric isomer (presumably *trans*) of **5**.

Compound **4** presumably arises from a photochemical Markovnikov addition of the solvent (11, 12); compare, for example, the addition of

Can. J. Chem. Downloaded from www.nrcresearchpress.com by 210.87.254.42 on 09/05/12
For personal use only.

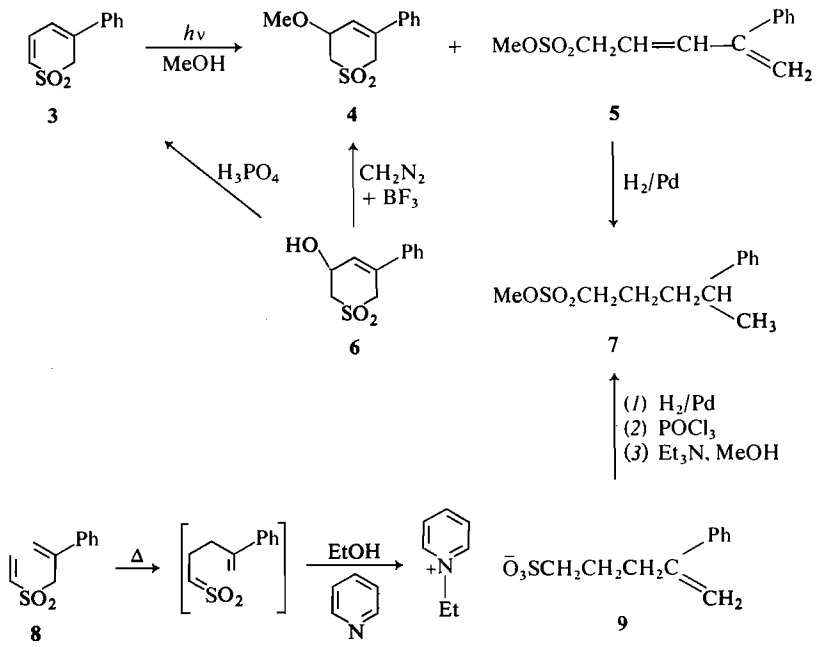

SCHEME 1

methanol to 1-phenylcyclohexene (11, 13). Of greater interest to us, however, is the formation of **5**, which is obviously consistent with the intermediacy of the 4-phenyl derivative of sulfene **2***c*. Some of the more plausible alternative mechanisms to sulfene formation in the photolyses of **1***a* or **1***b* derivatives, involve excitation of the non-bonded electrons on the ring oxygen or nitrogen atoms. No such process can be invoked in the present case (**3** → **5**), and further, since the ring opening can take place in the absence of these non-bonded electron pairs, they are clearly not required for this reaction to occur. To the extent that the proof of a reaction mechanism involves the accumulation of evidence discrediting all possible alternative routes, the observation of the reaction **3** → **5** lends further credibility to the proposal of the general sulfene-forming cycloreversion **1** → **2** originally proposed by de Mayo (1).

Hall and Smith in an independent study (14) appearing after completion of our work, have made closely related observations (Scheme 2). They suggest that the sultine (**12**) arises from the sulfene formed by ring-opening of **10**; sultine formation from cyclization of unsaturated sulfenes has been proposed previously (see ref. 6).

Photolysis of **3** in an aprotic solvent led to a mixture which included a crystalline product which appeared from its spectra to possess both formyl and sulfinyl groups, suggesting perhaps the further transformation of a cyclic sultine (akin to **12**). The nature of this reaction indicated that this system would need considerable work before it might be appropriate to attempt the

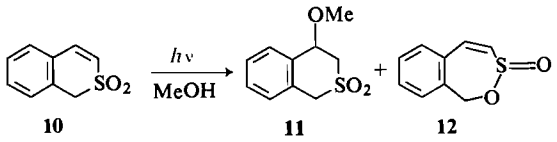

SCHEME 2

flash photolysis experiments which initially prompted this study, and work on this has been suspended for now.

Experimental

Solutions were irradiated in 1.7 × 20 cm Pyrex tubes suspended *ca.* 2 cm from the cooling jacket of a 450 W medium-pressure Hanovia mercury lamp and immersed in a water bath at *ca.* 10 °C. The progress of the photolyses was followed by observing the disappearance of the peak due to starting diene **3**, using a Varian Series 1400 gas chromatograph with a flame ionization detector, fitted with a 3% SE-30 on Varaport 30 (100–120 mesh) 5 ft × $\frac{1}{8}$ in. copper column at 180 °C, with nitrogen as the carrier gas. Control experiments showed that no reaction of **3** with methanol takes place without irradiation (even in the presence of added H_2SO_4).

Preparative t.l.c. was performed using 20 × 20 cm glass

Can. J. Chem. Downloaded from www.nrcresearchpress.com by 210.87.254.42 on 09/05/12
For personal use only.

Can. J. Chem. Downloaded from www.nrcresearchpress.com by 210.87.254.42 on 09/05/12
For personal use only.

plates bearing 20 g of silica gel, and analytical t.l.c. using microscope slides coated with thin layers of silica gel. The bands on the preparative plates were visualized by means of the ultraviolet phosphor in the silica gel, and extracted with CH_2Cl_2–MeOH (100:15 v/v). Infrared spectra were measured with a Beckman IR 20-A spectrometer, 60 MHz n.m.r. spectra were taken with a Varian T-60, and 100 MHz n.m.r. spectra with a Varian HA-100 spectrometer.

Formation of Photoadducts 4 and 5

A solution of the diene **3** (342 mg) in methanol (Fisher Spectrograde, 35 ml) was purged with nitrogen for 10 min, then irradiated for 2 h, when v.p.c. showed that little if any **3** remained. Two identical irradiations were conducted, so a total of 684 mg of **3** was irradiated. The combined solutions (clear and colorless with no sign of polymer) were evaporated at *ca.* 35 °C to give a pale brown oil (816 mg). This was subjected to preparative t.l.c. (CH_2Cl_2), giving two bands. The less mobile band (338 mg, 43%) was shown to be 3-phenyl-5-methoxyl-5,6-dihydro-2*H*-thiopyran 1,1-dioxide, **4**, by comparison of its n.m.r. and i.r. spectra with those obtained from a specimen synthesized by an independent route, whereas the more mobile band (226 mg, 30%) was identified as the sulfonate **5** by synthesis of its tetrahydro derivative (for details see below). The ester **5**, as obtained from t.l.c. appeared from its spectra to be substantially pure, but like the sulfone **4** was not obtained in a form which gave fully satisfactory analyses; molecular distillation (oil diffusion pump, 110 °C) led to decomposition.

The 100 MHz n.m.r. spectrum of **5** showed bands assigned (and confirmed by decoupling experiments) as follows: δ 3.72 (s, 3H, CH_3O), 3.84 (dd, 2H, C-1 H's, $J_{1,2}$ = 8 Hz, $J_{1,3}$ = 1.5 Hz), 5.28 (apparent t, 1H, C-5, H, $J_{gem} \sim$ 1.5 Hz, $J_{3,5} \sim$ 1.5 Hz), 5.58 (apparent d, 1H, C-5 H), 5.79 (dt, 1H, C-2 H, $J_{2,3}$ = 11 Hz), 6.50 (d of m, 1H, C-3 H), and 7.27 p.p.m. (m, 5H, Ph). In addition a peak at 3.56 p.p.m. perhaps due to the methoxyl peak of (about 5% of) the geometric isomer of **5** (*i.e.* probably *trans*) was observed. The i.r. spectrum of **5** showed strong bands at 1355, 1175, and 990 cm^{-1}.

Hydrogenation of sulfonate **5** to the hydrogenated sulfonate **7** was readily effected: sulfonate **5** (distilled; 18.8 mg) and 5% Pd/C *ca.* 20 mg) in ethyl acetate (3 ml) were hydrogenated at 25 °C and *ca.* 1 atm; hydrogen uptake was complete in 15 min, and 97% of the theoretical amount of hydrogen needed to saturate the two double bonds of **5** was absorbed. The reaction mixture was filtered through Celite and evaporated to give the hydrogenated sulfonate **7** as a colorless oil, 17 mg (90%). The i.r. and n.m.r. spectra of this material were identical to those of an authentic specimen synthesized as described below.

Synthesis of Methyl 4-Phenylpentane-1-sulfonate, 7, from 8

The *N*-ethylpyridinium salt **9** (4.5 g. 13.5 mmol), obtained by heating 2-phenyl-2-propenyl vinyl sulfone, **8**, for 2 h at 170 °C in a mixture of equal volumes of ethanol and pyridine in a sealed tube (*cf.* ref. 10), was dissolved in ethanol (70 ml) and hydrogenated for 15 h at 4 atm over platinum oxide (500 mg) on a Parr apparatus. The hydrogenation was then stopped. A further portion of catalyst (250 mg) was added and then the hydrogenation was continued for another 3 h. Removal of the catalyst and the solvent yielded, after drying *in vacuo*, 4.15 g (90%) of sticky crystalline material. The n.m.r. (HA 100) showed ($CDCl_3$) δ 0.60–2.30 (m, *ca.* 15 H), 2.35–4.10 (m, 10 H), and 6.80–7.50 p.p.m. (m, 5 H) (*i.e.* apparently the pyridine ring was reduced).

The reduced salt (4 g, 11.8 mmol) was heated with phosphorus oxychloride (20 ml) for 1 h on a steam bath. The solution was cooled and then poured onto ice. The resulting mixture was stirred for 0.25 h and then extracted with ether. The ether layer was washed several times with water until the aqueous wash remained neutral. The ether layer was dried over magnesium sulfate. Removal of the ether and subsequent drying *in vacuo* afforded 2.2 g (76%) of the sulfonyl chloride; this corresponds to a 56% yield from the starting sulfone. A small amount of this oil was distilled twice on a cold finger apparatus. The n.m.r. (HA 100) showed ($CDCl_3$) δ 1.26 (d, 3H), 1.55–2.15 (m, 4 H), 2.50–2.90 (m, 1 H), 3.40–3.65 (m, 2 H), and 7.00–7.45 p.p.m. (m, 5 H). The i.r. showed ν_{max} (film) 1365 and 1158 cm^{-1}.

Anal. Calcd. for $C_{11}H_{15}ClO_2S$: C, 53.54; H, 6.13; Cl, 14.37; S, 13.00. Found: C, 53.49; H, 6.12; Cl, 14.21; S, 12.80.

4-Phenylpentane-1-sulfonyl chloride (0.5 g, 2.04 mmol) was dissolved in dry methanol (10 ml) and treated with triethylamine (0.5 ml). The mixture was stirred for 0.5 h before the methanol was removed. The residue was partitioned between water and ether. The ether layer was washed successively with 3 *N* hydrochloric acid and saturated sodium bicarbonate solution and then dried over magnesium sulfate. Removal of the ether and drying *in vacuo* gave 0.35 g (71%) of oil. This material was distilled on a cold finger apparatus. The n.m.r. (HA 100) showed ($CDCl_3$) δ 1.24 (d, 3 H), 1.44–2.02 (m, 4 H), 2.50–2.85 (m, 1 H), 2.85–3.21 (m, 2 H), 3.77 (s, 3 H), and 7.00–7.50 p.p.m. (m, 5 H). The i.r. showed ν_{max} (CCl_4) 1365, 1345, and 1162 (SO_2) cm^{-1}.

Anal. Calcd. for $C_{12}H_{18}O_3S$: C, 59.47; H, 7.49; S, 13.23. Found: C, 59.52; H, 7.35; S, 13.02.

Synthesis of 3-Phenyl-5-methoxy-5,6-dihydro-2H-thiopyran 1,1-dioxide, 4

To a solution of 3-phenyl-5-keto-5,6-dihydro-2*H*-thiopyran-1,1-dioxide (9) (0.20 g, 0.90 mmol) in ethanol (10 ml) was added with stirring at room temperature a solution of sodium borohydride (0.042 g, 1.08 mmol) in water (2 ml). After stirring for 3 h, hydrochloric acid solution (1 *N*, 5 ml) was added and the mixture was then concentrated *in vacuo* at 50 °C to a gummy residue. Traces of water were removed by an azeotropic distillation *in vacuo* at 50 °C of a methanolic solution of the residue. The final residue was then taken up in methylene chloride (20 ml), filtered, dried over anhydrous magnesium sulfate, and evaporated to dryness to give crude 3-phenyl-5-hydroxy-5,6-dihydro-2*H*-thiopyran-1,1-dioxide (**6**). To this hydroxysulfone in methylene chloride (25 ml) over an ice-water bath was added boron trifluoride etherate (2 drops) and an ethereal solution (50 ml) of diazomethane (generated from 1 g of *N*-nitrosomethylurea). Nitrogen was immediately evolved. Boron trifluoride was destroyed by anhydrous sodium carbonate and the mixture was then filtered and evaporated to dryness leaving a mobile residue which was distilled (100–120 °C at 1 Torr) to give the desired product (0.115 g or 54%). The n.m.r. spectrum

($CDCl_3$) showed bands assigned (by first order analysis with the aid of decoupling experiments) as follows: δ 7.31 (5H, Ph), 6.25 (m, $W_{1/2}$ = 7 Hz, C-4H), 4.50 (m, $W_{1/2}$ = 23 Hz, C-5H), 4.10 (d of t, C-2eq H), 3.90 (d of m, C-2ax H), 3.60 (m, C-6eq H), 3.45 (s, OCH_3), and 3.10 p.p.m. (dd, C-6ax H). The major couplings were $J_{2a,2e}$ = 17.0 Hz, $J_{6a,6e}$ = 13.5 Hz, $J_{5,6e}$ = 5.5 Hz, $J_{5,6a}$ = 10.0 Hz; in addition small couplings (1 to 3 Hz) were observed as follows: the C-4H with 2ax, 2eq, 5, and 6eq, the C-5H also with 2ax and 2eq, and the C-2eq H with 6eq (this last being the basis for assigning the 4.10 p.p.m. signal to the equatorial hydrogen on C-2). The i.r. spectrum showed strong bands at 1328, 1129, and 1086 cm^{-1}.

We thank the National Research Council of Canada for support of this work.

1. E. HENMO, P. DE MAYO, A. B. M. A. SATTAR, and A. STOESSL. Proc. Chem. Soc. London, 238 (1961).
2. J. F. KING, P. DE MAYO, E. MORKVED, A. B. M. A. SATTAR, and A. STOESSL. Can. J. Chem. **41**, 100 (1963).
3. S. T. WEINTRAUB and B. F. PLUMMER. J. Org. Chem. **36**, 361 (1971).
4. T. DURST and J. F. KING. Can. J. Chem. **44**, 1869 (1966).
5. J. L. CHARLTON and P. DE MAYO, Can. J. Chem. **46**, 55 (1968).
6. J. F. KING. Acc. Chem. Res. **8**, 10 (1975).
7. O. L. CHAPMAN. Proc. XXIII. Int. Congr. Pure Appl. Chem. Spec. Lect. **1**, 311 (1971).
8. O. L. CHAPMAN, C. L. MCINTOSH, and J. PACANSKY. J. Am. Chem. Soc. **95**, 244 (1973).
9. G. PAGANI. Gazz. Chim. Ital. **97**, 1518 (1967).
10. J. F. KING and D. R. K. HARDING. Chem. Commun. 959 (1971); J. Am. Chem. Soc. In press.
11. P. J. KROPP. J. Am. Chem. Soc. **91**, 5783 (1969).
12. J. A. MARSHALL. Acc. Chem. Res. **2**, 33 (1969).
13. M. TADA and H. SHINOZAKI. Bull. Chem. Soc. Jpn. **43**, 1270 (1970).
14. C. R. HALL and D. J. H. SMITH. Tetrahedron Lett. 3633 (1974).

Can. J. Chem. Downloaded from www.nrcresearchpress.com by 210.87.254.42 on 09/05/12
For personal use only.

Aryne Formation from 2-Bromolaudanosine. Fate of the 5,6,12,12a-Tetrahydrodibenzo[*b*,*g*]indolizinium Ion and an Alternative Synthesis of Glaucine

IJAZ AHMAD AND MARTIN S. GIBSON

Department of Chemistry, Brock University, St. Catharines, Ontario L2S 3A1

Received May 30, 1975

IJAZ AHMAD and MARTIN S. GIBSON. Can. J. Chem. **53**, 3660 (1975).

A synthesis of 2-bromolaudanosine (**10**) is described. The aryne formed from **10** and amide ion in ammonia yields the corresponding 5,6,12,12a-tetrahydrodibenzo[*b*,*g*]indolizinium ion (**13**) by intramolecular capture, and 2-aminolaudanosine (**11**) by external addition of amide ion. Compound **13** is converted *in situ* to 5,6-dimethoxy-2-(4,5-dimethoxy-2-vinylphenyl)-1-methylindoline (**14**) and 5,6-dimethoxy-2-(4,5-dimethoxy-2-ethylphenyl)-1-methylindole (**15**). Compound **11** provides an alternative source of glaucine (**12**).

IJAZ AHMAD et MARTIN S. GIBSON. Can. J. Chem. **53**, 3660 (1975).

On décrit une synthèse de la bromo-2 laudanosine (**10**). L'aryne, qui se forme par réaction de **10** avec l'ion amidure dans l'ammoniac, conduit à l'ion correspondant tétrahydro-5,6,12,12a dibenzo[*b*,*g*] indolizinium (**13**) par capture intramoléculaire et à l'amino-2 laudanosine (**11**) par addition externe de l'ion amidure. On transforme *in situ* le composé **13** en diméthoxy-5,6 (diméthoxy-4,5 vinyl-2 phényl)-2 méthyl-1 indoline (**14**) et en diméthoxy-5,6 (diméthoxy-4,5 éthyl-2 phényl)-2 méthyl-1 indole (**15**). Le composé **11** s'avère une source de rechange pour la glaucine (**12**).

[Traduit par le journal]

The use of appropriately substituted 1-(2- or 3-halogenobenzyl)-1,2,3,4-tetrahydroisoquinolines (**1**) as sources of arynes for synthesis of modified 1-benzyl-1,2,3,4-tetrahydroisoquinoline alkaloids such as aporphines (**2**), morphinandienones (**3**), and 5,6,12,12a-tetrahydrodibenzo-[*b*,*g*]indolizinium salts (**4**)(Scheme 1) has attracted considerable attention in recent years.[1] Thus, cine-substitution via an aryne (X_1 = H, X_2 = Br → X_1 = NH_2, X_2 = H), coupled with Pschorr cyclization, has been used in synthesis of the aporphine alkaloid laureline (1), whilst direct aporphine formation from a phenolic precursor (R = H) has been achieved in a synthesis of domesticine (2). The possibility of aporphine and morphinandienone formation occurring from such a phenolic precursor (R = H) has also been explored, without success under the conditions initially employed (1*b*), but successfully at higher mole ratios (between 8 and 10 to 1) of sodamide or potassamide to halogenocompound (3, 4). Parallel routes have been used to synthesize 5,6,12,12a-tetrahydrodibenzo[*b*,*g*]-indolizinium salts, both via the corresponding tetrahydroindolizines (5, 6) and directly (4, 7).

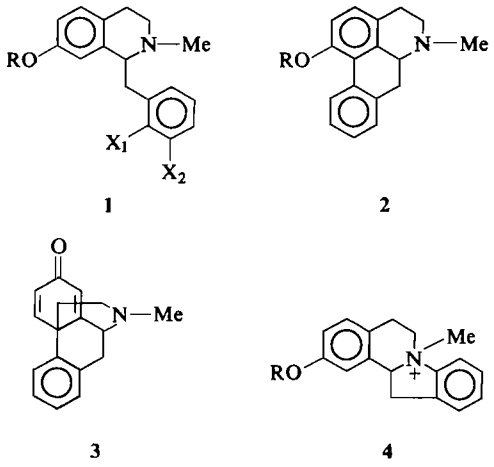

SCHEME I

An aryne route has also been used for indoline synthesis associated with *Erythrina* alkaloid studies (8).

The formation and demise of 5,6,12,12a-tetrahydrodibenzo[*b*,*g*]indolizinium ions in potassamide-ammonia is important in leading to by-products in such aporphine syntheses (1). Direct evidence for formation of such ions under these conditions was provided in due course by Kametani *et al.* (7) using a 7-hydroxyisoquinoline

[1]Other substituents are omitted for simplicity in formulae **1–4**.

Can. J. Chem. Downloaded from www.nrcresearchpress.com by 210.87.254.5 on 09/05/12
For personal use only.

Can. J. Chem. Downloaded from www.nrcresearchpress.com by 210.87.254.5 on 09/05/12
For personal use only.

precursor, the cation produced being presumably stabilized by deprotonation of the phenolic group and regenerated during work-up; no Hofmann elimination was observed. Similar results have been reported by Kessar *et al.* (4). These workers also obtained indications of Hofmann elimination (1) when using a 6-hydroxyisoquinoline precursor although this case was complicated by accompanying dehydrogenation. The original problem of the behavior of non-phenolic 5,6,12,-12a-tetrahydrodibenzo[*b*,*g*]indolizinium ions in potassamide–ammonia is considered in the present communication.

The tetramethoxy series shown (Scheme 2) was chosen for examination. Bromination of 3,4-dimethoxyphenylacetic acid gave the bromo-acid **5** which was treated with thionyl (or oxalyl) chloride, followed by the amine **6**, to give the amide **7**. After cyclization of **7** with phosphoryl chloride in benzene, isolation of the product **8** as the iminium chloride **8***a* was most conveniently effected by treatment of the reaction mixture with anhydrous methanol. Treatment of **8** with methyl iodide gave **9** which was reduced with sodium borohydride to 2-bromolaudanosine (**10**), identical with material prepared by brominating a sample of (±)-laudanosine.

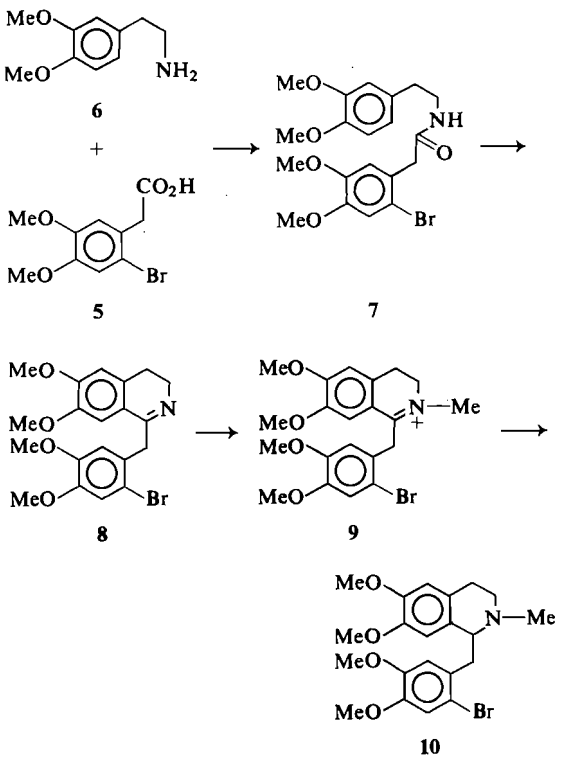

SCHEME 2

Aryne reactions of **10** were carried out both with potassamide and with sodamide in liquid ammonia and the products were isolated chromatographically. In order of elution, these were **A** ($C_{21}H_{25}NO_4$), **B** ($C_{21}H_{25}NO_4$), and **C** ($C_{21}H_{28}N_2O_4$).

Compound **C** was recognized as the diamine **11** by melting point and i.r. spectral correlations and by known conversion to (±)-glaucine, **12**, (Scheme 3) which was characterized as the methiodide (9). External addition of amide ion to the aryne had thus occurred preferentially at the carbon atom remote from the methoxy-groups as expected (1); interestingly, 4-amino-veratrole had been previously identified as the main product from reaction of 4-bromoveratrole with potassamide in ammonia.[2]

Compound **B** proved to be the indoline **14**, identity being confirmed by comparison with an authentic sample prepared from **13** by conventional Hofmann elimination (10). The mass spectrum of **14** shows the $M - 2$ fragment characteristically associated with indolines (dihydroindoles) which can undergo loss of hydrogen to give the corresponding indoles (6, 8). Contrary to earlier report, **14** forms a methiodide (10).

Compound **A**, the most interesting product, was identified as the indole **15**. This formulation is supported by the n.m.r. spectrum, which established *inter alia* the presence of an ethyl group, mass spectrum, and instantaneous positive Ehrlich reaction. Formation of **15** from **13** under analogous conditions was confirmed in a separate experiment.

It is clear that intramolecular addition of the tertiary nitrogen atom to the aryne will compete with other possible internal or external nucleophilic additions in these reactions. The likely fate of the resulting tetrahydrodibenzoindolizinium ion (unless otherwise stabilized) is Hofmann elimination to give the corresponding indoline.[3] The isomeric indole presumably arises from isomerization of the indoline, or of its conjugate base followed by reprotonation, under the reaction conditions though these mechanisms have yet to be distinguished experimentally. There is

[2]M. S. Gibson and G. W. Prenton. Unpublished results.
[3]Available data on the (impure) laureline by-product are consistent with this view.

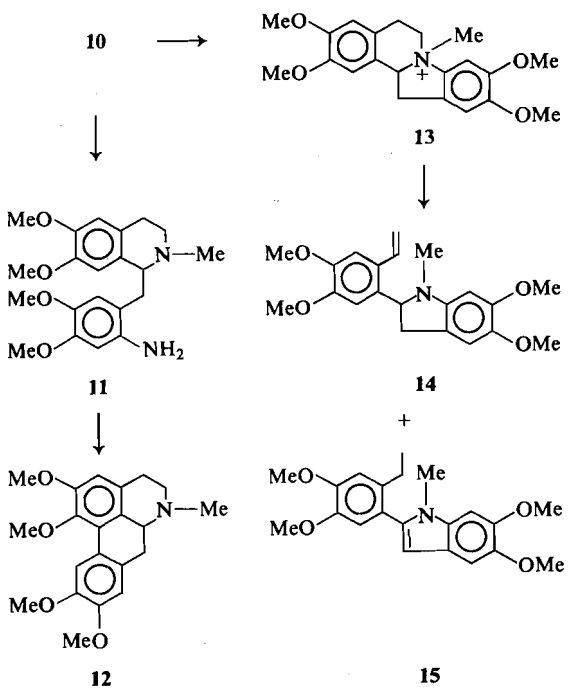

SCHEME 3

no direct evidence for alternative Hofmann elimination to give a nine-membered ring, but we subscribe to the view that any such process might pass unnoticed owing to protonation and recyclization to the indolizinium ion, *e.g.* during workup (4). Some phenolic indolizinium ions survive potassamide–ammonia treatment (*i.e.* do not undergo Hofmann elimination), as noted above (4, 7).

The indolizinium salt **13** was required during this work, necessitating a reexamination of the reaction of 2-bromotetrahydropapaverine with sodamide in ammonia. This has been reported to yield the desired 5,6,12,12a-tetrahydrodibenzo[*b*,*g*]indolizine together with its product of oxidation, the 5,6-dihydrodibenzo[*b*,*g*]indolizine (6). We were not able to isolate the former compound satisfactorily using the published procedure and have found it expedient to collect the two products together, concentrate the former, and quaternize with methyl iodide to give the indolizinium salt **13**. The relative ease of oxidation of the tetrahydro- to the dihydroindolizines (cf. oxidation of indolines to indoles) is presumably a cause of difficultly reproducible yields in these reactions and *ipso facto* of discrepancies in yields reported in syntheses of 5,6,12,12a - tetrahydrodibenzo[*b*,*g*]indolizinium alkaloids (5, 6).

Experimental

Proton magnetic resonance spectra were recorded on a Varian A-60 spectrometer using tetramethylsilane as internal standard. Mass spectra were determined with an AEI-MS30 double-beam double-focusing mass spectrometer.

Liquid ammonia was distilled from potassium chips prior to use.

2-Bromo-4,5-dimethoxyphenylacetic Acid, 5

The published method (11) was modified as follows. A solution of bromine (4.2 g) in glacial acetic acid (25 ml) was added dropwise to a stirred solution of 3,4-dimethoxyphenylacetic acid (5.0 g) in acetic acid (20 ml) with external cooling in ice water. The resulting slurry was heated at 60 °C for 20 min and then poured into ice water with stirring. The precipitate was filtered off and washed with aqueous sodium bisulfite solution and water. Crystallization from aqueous ethanol (50%) gave the bromo-acid **5** as needles (5.0 g, 71%), m.p. 117–118 °C (lit. (11) m.p. 113–114 °C).

N-(3,4-Dimethoxyphenethyl)-2-bromo-4,5-dimethoxyphenylacetamide, 7

2-Bromo-4,5-dimethoxyphenylacetic acid **5** (5.0 g) was converted to the acid chloride by reaction with $SOCl_2$ (6.5 ml) in dry benzene (20 ml). After removal of excess $SOCl_2$ and benzene *in vacuo*, the acid chloride was dissolved in ether (25 ml) and added during 15 min to a stirred solution of 3,4-dimethoxyphenethylamine **6** (4.3 ml) in ether (70 ml) and 40% (w/v) aqueous NaOH solution (4 ml). The resulting mixture was poured into water (250 ml) with stirring and the p*H* was adjusted to 8–9. The precipitate was filtered off, washed with water, and dried. Crystallization from benzene–ethanol gave the *amide* **7** as needles (6.7 g, 84%), m.p. 161–162 °C.

Anal. Calcd. for $C_{20}H_{24}BrNO_5$: C, 54.80; H, 5.52; N, 3.20 Found: C, 54.86; H, 5.43; N, 3.14.

1-(2-Bromo-4,5-dimethoxybenzyl)-3,4-dihydro-6,7-dimethoxyisoquinolinium Chloride, 8a

A solution of **7** (5.0 g) in dry benzene (11 ml) and freshly distilled $POCl_3$ (7.5 ml) was heated under reflux (steam bath) for 3.5 h under dry nitrogen. Excess $POCl_3$ was destroyed by dropwise addition of anhydrous methanol (35 ml) to the cooled solution until the vigorous reaction subsided, when more methanol (15 ml) was added to ensure completion. After 1 h, the mixture was poured into ether (400 ml) and, after chilling, the precipitate was filtered off, washed with ether, and dried. Crystallization from ether–methanol gave the *iminium chloride* **8a** (4.8 g, 92%) as a hemi-solvate, m.p. 232–234 °C; i.r. (KBr) 1655 cm^{-1} ($\diagdown C{=}\overset{+}{N}-$). Alternative attempts at crystallization resulted in yellowing of the sample.

Anal. Calcd. for $C_{20}H_{23}BrClNO_4 \cdot \frac{1}{2}CH_3OH$: C, 52.07; H, 5.32; N, 2.96. Found: C, 51.76; H, 5.10; N, 3.07.

1-(2-Bromo-4,5-dimethoxybenzyl)-3,4-dihydro-2-methyl-6,7-dimethoxyisoquinolinium Iodide, 9

The iminium chloride **8a** (2.5 g) was shaken with ammonium hydroxide (25 ml, *d* 0.88), water (10 ml), and benzene (100 ml) until the solid disappeared. The benzene layer was separated, washed with water, dried (K_2CO_3), and evaporated. The residual base was dissolved in

Can. J. Chem. Downloaded from www.nrcresearchpress.com by 210.87.254.5 on 09/05/12
For personal use only.

Can. J. Chem. Downloaded from www.nrcresearchpress.com by 210.87.254.5 on 09/05/12
For personal use only.

methanol (5 ml) and methyl iodide (7 ml) was added. After 48 h, the crystalline *iminium iodide* **9** (3.0 g, 97%) was filtered off. Crystallization from acetonitrile gave pale yellow orthorhombic crystals, m.p. 246–247 °C (dec.); i.r. (KBr) 1630 cm^{-1} ($\diagdown C{=}\overset{+}{N}{-}\diagup$).

Anal. Calcd. for $C_{21}H_{25}BrINO_4$: C, 44.86; H, 4.48; N, 2.49. Found: C, 44.67; H, 4.41; N, 2.45.

1-(2-Bromo-4,5-dimethoxybenzyl)-1,2,3,4-tetrahydro-2-methyl-6,7-dimethoxyisoquinoline [(±)-2-Bromolaudanosine], 10

To a stirred suspension of the iminium iodide **9** (2.5 g) in methanol (125 ml) and water (15 ml) was added $NaBH_4$ (2 g) in very small portions. The yellow color slowly faded. The solution was then stirred for 6 h at room temperature followed by 30 min at reflux. Solvents were evaporated and the residue was treated with water, made basic (NaOH), and extracted with ether. The ether extract was washed, dried (K_2CO_3), and evaporated to give (±)-2-bromolaudanosine **10** (1.5 g, 77%), which crystallized from ethanol as needles, m.p. 122–124 °C identical with a sample (m.p. 123–124 °C) prepared by Dr. G. W. Prenton by brominating (±)-laudanosine.

Anal. Calcd. for $C_{21}H_{26}BrNO_4$: C, 57.80; H, 5.96; Br, 18.18; N, 3.18. Found: C, 57.8; H, 6.1; Br, 18.2; N, 3.3.

Aryne Reaction of 2-Bromolaudanosine, (a), with Potassamide, (b), with Sodamide in Ammonia

(*a*) A solution of (±)-2-bromolaudanosine **10** (4.5 g) in anhydrous tetrahydrofuran (35 ml) was added slowly to a stirred solution of potassamide, prepared from potassium (14 g), in liquid ammonia (300 ml). The resulting reddish-brown mixture was stirred in refluxing ammonia for 6 h and ammonium chloride (35 g) was then added in portions. Ammonia was allowed to evaporate overnight under a stream of nitrogen and the residue was then treated with water (80 ml) and extracted with benzene (total; 800 ml). The benzene extract was washed with water, dried (K_2CO_3), and evaporated to give a dark brown oil which contained at least five components (t.l.c.).

The oil was chromatographed on neutral alumina using benzene as eluant. One component concentrated in the first eluates (totalling 900 ml). Evaporation *in vacuo* gave a pale yellow oil which was dissolved in ethanol (5 ml) and kept overnight to give colorless crystals (0.4 g, 11%) of *5,6-dimethoxy-2-(4,5-dimethoxy-2-ethylphenyl)-1-methylindole*, **15**, m.p. 132–133 °C; n.m.r. ($CDCl_3$) δ 7.11 (s, 1H, aromatic proton), 6.86 (s, 2H, aromatic protons), 6.79 (s, 1H, aromatic proton), 6.32 (s, 1H, aromatic proton), 3.96 (s, 3H, OMe), 3.91 (s, 6H, OMe), 3.82 (s, 3H, OMe), 3.46 (s, 3H, NMe), 2.49 (q, J = 8.0 Hz, 2H, CH_2CH_3), and 1.09 (t, J = 8.0 Hz, 3H, CH_2CH_3); mass spectrum *m/e* 355 (M^+), 340 ($M - CH_3$), 190 ($C_{11}H_{12}NO_2$), 177.5 (M^{2+}), and 165 ($C_{10}H_{13}O_2$); u.v. λ_{max} (methanol) 304 (log ε 4.03) and 220 nm (4.36). Compound **15** gave an immediate violet coloration when treated with a cold solution of *p*-dimethylaminobenzaldehyde in ethanol and HCl (Ehrlich's reagent), and did not form a methiodide when treated with methyl iodide.

Anal. Calcd. for $C_{21}H_{25}NO_4$: C, 70.96; H, 7.09; N, 3.94. Found: C, 71.24; H, 7.37; N, 3.74.

Further elution with benzene–ether (9:1) gave eluates (totalling 700 ml) which were evaporated *in vacuo* to yield a pale yellow oil which crystallized slowly after addition of a few drops of methanol. Recrystallization from methanol gave colorless aggregates (0.1 g, 2.7%) of 5,6-dimethoxy-2-(4,5-dimethoxy-2-vinylphenyl)-1-methylindoline, **14**, m.p. 125–127 °C, identical with a sample prepared as described below; mass spectrum *m/e* 355 (M^+), 353 ($M - 2$), 340 ($M - CH_3$), 338, 324, 312, 310, 201, 192 ($C_{11}H_{14}NO_2$), 180, 177.5 (M^{2+}), 177, 165, 162, 161, 146 and 136; u.v. λ_{max} (methanol) 306 (log ε 3.85) and 258 nm (4.20).

Elution was continued, increasing the proportion of ether in the eluting mixture to benzene–ether (2:1). Evaporation of these eluates *in vacuo* gave a yellow oil which crystallized slowly from methanol (20 ml) to give colorless needles (1.35 g, 35%), m.p. 142–144 °C, of 1-(2-amino-4,5-dimethoxybenzyl)-1,2,3,4-tetrahydro-2-methyl-6,7-dimethoxyisoquinoline, **11**, identical (mixture m.p., t.l.c., i.r. spectrum) with a sample from a previous experiment.

From a previous similar experiment using 2-bromolaudanosine (2.0 g), compound **11** was isolated according to an earlier procedure (9). The product was decolorized (charcoal) and crystallized three times from methanol to give colorless needles (0.3 g, 18%) of **11**, m.p. 144 °C (lit. (9) m.p. 144–145 °C); the i.r. spectrum corresponded with published data.

(*b*) A solution of 2-bromolaudanosine (4.0 g) in anhydrous tetrahydrofuran (35 ml) was added slowly to a stirred solution of sodamide, prepared from sodium (15 g), in liquid ammonia (375 ml). The brown mixture was stirred for 5 h and ammonium chloride (50 g) was then added in portions. The mixture was then worked up as in the foregoing experiment to give a brown oil which contained, as above, at least five components (t.l.c.).

Chromatography (Florisil–benzene) gave, from the first eluates, a pale yellow oil which crystallized slowly after addition of a few drops of ethanol to give the indole **15** (0.08 g, 2.5%), m.p. 132–133 °C, identical with the foregoing sample (mixture m.p., i.r. and u.v. spectra, t.l.c., and Ehrlich reaction).

Further elution (benzene–ether) gave a pale yellow oil which crystallized, as above, from methanol to give the indoline **14** (0.8 g, 25%), m.p. 125–127 °C, identical with a sample prepared as described below.

Next eluted was a small amount of unidentified reddish material, followed (ether as eluant) by **11** (0.3 g, 8%), m.p. 143–145 °C, identical with the foregoing sample (mixture m.p., t.l.c., i.r. spectrum).

1,2,9,10-Tetramethoxyaporphine [(±)-Glaucine], 12

Compound **11** was converted to glaucine **12** as described by Kametani and Noguchi (9) and was characterized as the methiodide (2–3% overall), m.p. 216 °C (lit. (9) m.p. 218–220 °C); mass spectrum *m/e* 370 (M^+), 369 ($M - 1$), 355 ($M - CH_3$), 354, 340, 324, 312, 165, 152, 142 (CH_3I), 128 (HI), and 127 (I). The u.v. spectrum was identical with that reported.

1-(2-Bromo-4,5-dimethoxybenzyl)-1,2,3,4-tetrahydro-6,7-dimethoxyisoquinoline [(±)-2-Bromotetrahydropapaverine]

Sodium borohydride (1.6 g) was added in small portions to a stirred solution of the iminium chloride **8***a* (2.0 g) in methanol (50 ml) and water (7 ml). After 8 h at room temperature followed by 1 h at reflux, solvents were evaporated *in vacuo* and the solid residue was

Can. J. Chem. Downloaded from www.nrcresearchpress.com by 210.87.254.5 on 09/05/12
For personal use only.

treated with water, made basic (NaOH), and the mixture was extracted with ether. The ether solution was washed, dried (K_2CO_3), and evaporated to give 2-bromotetrahydropapaverine as plates (1.7 g, 89%), m.p. 112 °C (lit. (12) m.p. 111 °C). Infrared and n.m.r. data corresponded with those reported.

Aryne Reaction of 2-Bromotetrahydropapaverine: 5,6-Dihydro-2,3,9,10-tetramethoxydibenzo[b,g]indolizine and 5,6,12,12a-Tetrahydro-2,3,9,10-tetramethoxy-7-methyldibenzo[b,g]indolizinium Iodide

(*a*) The published procedure (6) was first followed, but from the complex mixture only the dihydroindolizine (2–5%), m.p. 200–202 °C, could be isolated; none of the desired iodide was obtained when the mixture was treated with methyl iodide.

From a similar experiment with 2-bromotetrahydropapaverine (5.0 g), the crude product was chromatographed on Florisil using benzene and benzene–ether as eluants to give an oil; this was treated with methyl iodide (15 ml) in benzene (5 ml) to give the desired iodide which crystallized from acetonitrile as colorless needles (0.6 g, 10.5%), m.p. 243–245 °C (dec.), identical with the product from the following procedure.

(*b*) A solution of 2-bromotetrahydropapaverine (5.0 g) in dry tetrahydrofuran (45 ml) was added slowly to a stirred solution of potassamide, prepared from potassium (14 g) in liquid ammonia (500 ml). After 5 h, ammonium chloride (35 g) was added and the reaction products were isolated using benzene as in the cases described above. The brown oil thus obtained was chromatographed on Florisil using benzene and benzene–ether (6:1) as eluants and the 5,6-dihydro- and 5,6,12,12a-tetrahydroindolizines were collected together (volume eluted, 900 ml). Evaporation *in vacuo* and crystallization of the pale yellow residue from ethanol gave the 5,6-dihydroindolizine as colorless scales (0.92 g, 23%), m.p. 201–202 °C (lit. (6) m.p. 202–204 °C); the mass spectrum corresponded with that reported. The ethanolic mother liquor was evaporated *in vacuo* and the residue was treated with methyl iodide (15 ml) in benzene (7 ml). The 5,6,12,12*a*-tetrahydroindolizinium iodide, **13**, crystallized from acetonitrile as needles (1.4 g, 25%), m.p. 243–245 °C (dec.) (lit. (6) m.p. 243–245 °C (dec.)); identity was confirmed by mass spectral correlation.

*Formation of 5,6-Dimethoxy-2-(4,5-dimethoxy-2-ethylphenyl)-1-methylindole, **15** from the 5,6,12,12a-Tetrahydroindolizinium Iodide, **13***

Compound **13** (0.5 g) was added to a stirred solution of potassamide, prepared from potassium (2 g), in liquid ammonia (100 ml) and dry tetrahydrofuran (5 ml). After 5.5 h, ammonium chloride (10 g) was added and the mixture was worked up in the normal way to give a brown oil. Thin layer chromatography showed the presence of at least four components, resembling those obtained (with the exception of **11**) from reaction of 2-bromolaudanosine and potassamide under similar conditions. The oil was chromatographed on Florisil using benzene and benzene–ether as eluants. Fractions containing **15** (t.l.c.) were collected and evaporated. Addition of a few drops of ethanol to the pale yellow oil led to the slow crystallization of the indole **15** (20 mg, 5.5%), m.p. 132–133 °C, identical (mixture m.p., t.l.c., and mass spectrum) with the foregoing sample.

5,6-Dimethoxy-2-(4,5-dimethoxy-2-vinylphenyl)-1-methylindoline and -1,1-dimethylindolinium Iodide

The published procedure (10) was modified as follows. Potassium hydroxide (6.0 g) was added to a boiling solution of **13** (0.25 g) in water (21 ml) and the mixture was refluxed for 6 h, cooled, and extracted with ether. The ether solution was washed, dried (K_2CO_3), and evaporated *in vacuo* to give a pale yellow oil which crystallized slowly after addition of a few drops of methanol. Recrystallization from methanol gave the indoline **14** (0.16 g, 87%), m.p. 126–127.5 °C (lit. (10) m.p. 125–126 °C). The indoline produced a violet coloration slowly when heated with Ehrlich's reagent, presumably as a result of conversion to an indole derivative. Identity of the various samples of **14** was established by mixture m.p., t.l.c., and spectral correlations.

Methyl iodide (2.5 ml) was added to a solution of **14** (0.1 g) in benzene (0.75 ml). After 28h at *ca.* 40 °C, the crystalline deposit was collected and crystallized from acetonitrile to give *5,6-dimethoxy-2-(4,5-dimethoxy-2-vinylphenyl)-1,1-dimethylindolinium iodide* as colorless needles (0.13 g, 93%), m.p. 214–215 °C; the mass spectrum showed *m/e* 369 ($M^+ - 1$), 355 ($M^+ - CH_3$), 354, 353, 340, 338, and 326.

Anal. Calcd. for $C_{22}H_{28}INO_4$: C, 53.13; H, 5.67; N, 2.82. Found: C, 53.48; H, 5.57; N, 3.01.

We thank Professor A. H. Jackson (Cardiff) for helpful correspondence and for samples, and the National Research Council of Canada for financial support.

1. (*a*) M. S. Gibson and J. M. Walthew. Chem. Ind. (London), 185 (1965); (*b*) M. S. Gibson, G. W. Prenton, and J. M. Walthew. J. Chem. Soc. C, 2234 (1970).
2. S. V. Kessar, S. Batra, and S. S. Gandhi. Indian J. Chem. **8**, 468 (1970).
3. T. Kametani, S. Shibuya, K. Kigasawa, M. Hiiragi, and O. Kusama. J. Chem. Soc. C, 2712 (1971).
4. S. V. Kessar, R. Randhawa, and S. S. Gandhi. Tetrahedron Lett. 2923 (1973).
5. F. Benington and R. D. Morin. J. Org. Chem. **32**, 1050 (1967).
6. T. Kametani and K. Ogasawara. J. Chem. Soc. C, 2208 (1967).
7. T. Kametani, K. Fukumoto, and T. Nakano. Tetrahedron. **28**, 4667 (1972).
8. D. H. R. Barton, R. B. Boar, and D. A. Widdowson. J. Chem. Soc. C, 1208 (1970).
9. T. Kametani and I. Noguchi. J. Chem. Soc. C, 1440 (1967).
10. R. Robinson and S. Sugasawa. J. Chem. Soc. 789 (1932).
11. Japanese Patent No. 6668 (1964); Chem. Abs. **61**, 13251 (1964).
12. T. Kametani and M. Ihara. J. Chem. Soc. C, 530 (1967).

Crystal Structure of $Zn_3V_{0.5}P_{1.5}O_8$

K. Loralee Idler and Crispin Calvo

Department of Chemistry, McMaster University, Hamilton, Ontario L8S 4M1

Received May 26, 1975

K. Loralee Idler and Crispin Calvo. Can. J. Chem. **53**, 3665 (1975).

The stable phase in the $Zn_3(PO_4)_2$–$Zn_3(VO_4)_2$ system near 25 mol% $Zn_3(VO_4)_2$ is monoclinic with space group $C2/c$ and unit cell parameters $a = 15.941(6)$, $b = 5.314(2)$, $c = 8.265(2)$ Å, $\beta = 106.96(3)°$ and $Z = 4$. The structure was refined by full-matrix least-squares methods using 910 reflections, $R = 0.073$. The composition, $Zn_3P_{1.50}V_{0.50(4)}O_8$, was determined by site population analysis with the V and P randomly distributed. One-third of the zinc ions lie on twofold axes and these show an average Zn—O bond length of 1.955 Å while the remaining ZnO_4 group has a mean Zn—O bond length of 1.948 Å. The structure consists of sheets parallel to (100) formed of chains containing rings of corner shared $Zn(1)O_4$ and $(V,P)O_4$ tetrahedra. The $Zn(2)O_4$ groups, in turn, form chains parallel to the b axis through corner sharing.

K. Loralee Idler et Crispin Calvo. Can. J. Chem. **53**, 3665 (1975).

La phase stable dans le système $Zn_3(PO_4)_2$–$Zn_3(VO_4)_2$ près de 25 mol% en $Zn_3(VO_4)_2$ est monoclinique avec un groupe d'espace $C2/c$ et des paramètres de maille de $a = 15.941(6)$, $b = 5.314(2)$, $c = 8.265(2)$ Å, $\beta = 106.96(3)°$ et $Z = 4$. On a affiné la structure par la méthode des moindres carrés (matrice complète) utilisant 910 réflexions. $R = 0.073$. On a déterminé la composition $Zn_3P_{1.50}V_{0.50(4)}O_8$ par une analyse des populations de site avec le V et le P distribués au hazard. Un tiers des ions Zn se trouve sur un axe binaire et pour ceux-ci on trouve une longueur moyenne du lien Zn—O de 1.955 Å alors que le reste des groupes ZnO_4 a une longueur moyenne du lien Zn—O de 1.948 Å. La structure consiste de feuillets parallèles à l'axe 100 formés de chaînes contenant des cycles de tétraèdre $Zn(1)O_4$ et $(V,P)O_4$ dont les sommets sont mis en commun. Les groupes $Zn(2)O_4$ toutefois forment des chaînes parallèles à l'axe b par la mise en commun de sommets.

[Traduit par le journal]

Introduction

In their study of the $Zn_3(PO_4)_2$–$Zn_3(VO_4)_2$ join, Brown and Hummel (1) found a new phase stable between 18 and 28 mol% $Zn_3(VO_4)_2$ and below 835 °C. Below 800 °C only 2 or 3% $Zn_3(VO_4)_2$ dissolves in α-$Zn_3(PO_4)_2$, whereas above this temperature the solubility of the vanadate in the phosphate increases sharply. Previous phase studies involving $Zn_3(PO_4)_2$ and $M_3(PO_4)_2$ (2–4) have shown the intolerance of the α-$Zn_3(PO_4)_2$ structure to the substitution of divalent cations. Since all the cations are tetrahedrally coordinated in this phase (5) this instability could be a result of the octahedral site preference of the added cations. Alternately, Baur and Tillmanns (6) have indicated that the edge shared between ZnO_4 tetrahedra, in violation of Pauling's third rule, might be the source of the instability.

The substitution for the pentavalent ion has not been much investigated. A large number of unique structures, showing $M_3X_2O_8$ stoichiometry with X a tetrahedrally coordinated pentavalent ion and M a divalent ion with an ionic radius less than 1 Å, have been determined. Although isomorphism between the arsenates and vanadates is common, only one structure type, graftonite, has been found among the phosphates and either the vanadates and/or the arsenates. Thus new structure types, at least compared to the end members, would be expected in systems with mixed anions. Uniform coordination numbers for either the M ion or the anion are rare with the $M_3X_2O_8$ stoichiometry. Previous to the present investigation only α-$Zn_3(PO_4)_2$ has shown fourfold coordination for all of the M type ions.

Experiments

Small crystals of $Zn_3P_{1.5}V_{0.5}O_8$ were grown from a melt composed of 44 mol% of $Zn_3P_2O_8$ in $Zn_3V_2O_8$. The melt was slowly cooled from 900 to 750 °C as suggested by the phase diagram (1). A small, very irregularly shaped crystal with dimensions 0.04 × 0.08 × 0.10 mm was used to determine both the unit cell parameters and the diffraction intensities. Fifteen reflections with 2θ values lying between 25 and 30° were accurately centered on a Syntex $P\bar{1}$ automatic diffractometer. Graphite monochromatized MoKα radiation (0.71069 Å) was used. The crystal data at 21 °C are as follows:

Can. J. Chem. Downloaded from www.nrcresearchpress.com by 210.87.254.5 on 09/05/12
For personal use only.

TABLE 1. Atomic parameters with estimated standard deviations in parentheses*

Atom site	x	y	z	U_{11}	U_{22}	U_{33}	U_{12}	U_{13}	U_{23}
Zn(1)	0	0.0587(3)	3/4	13.1(6)	14.7(6)	19.0(7)	—	6.5(5)	—
Zn(2)	0.18558(6)	0.7929(2)	0.7137(1)	16.3(4)	98(4)	18.2(5)	2.1(4)	5.5(3)	0.7(4)
X†	0.1209(3)	0.292(1)	0.5294(6)	11(2)	10(2)	11(2)	−2(2)	3(2)	−1(2)
O(1)	0.6021(4)	0.672(1)	0.3456(8)	20(3)	19(3)	21(3)	−5(2)	8(2)	−2(2)
O(2)	0.6491(4)	0.931(1)	0.0253(7)	21(3)	16(3)	16(3)	5(2)	3(2)	2(2)
O(3)	0.4601(4)	0.747(1)	0.9089(8)	16(3)	25(3)	19(3)	−2(2)	6(2)	−7(2)
O(4)	0.2964(4)	0.638(1)	0.8495(7)	16(3)	9(2)	14(3)	2(2)	1(2)	−3(2)

*The expression for the temperature factor is $\exp[-2\pi^2 10^{-4}(U_{11}h^2b_1^2 + \ldots + 2U_{12}hk\,b_1b_2 + \ldots)]$ and the b_i's are reciprocal lattice parameters.
†X = 0.25(2)V + 0.75P.

$Zn_3P_{1.5}V_{0.5}O_8$ f.w. = 396.04

Monoclinic, $a = 15.941(6)$, $b = 5.314(2)$, $c = 8.265(2)$ Å, $\beta = 106.96(3)°$, $V = 669.59$ Å^3, $Z = 4$, $D_x = 3.92$ g cm^{-3}. Space group $C2/c$. Systematic absences: $h + k$ odd in general, $h0l$ with l odd.

The density was not measured because the sample was not uniform and a sufficient number of crystals could not be extracted. Intensity data, using a $\theta/2\theta$ scan, were collected with a sphere defined by $2\theta \leq 60°$. The background was measured at either side of the peak and used to determine the intensity measure. Those data with $I > 0$, 910 in number, were used in this refinement. All the data were corrected for Lorentz and polarization effects. Absorption corrections were applied assuming an idealized crystal shape.

A trial structure with Zn(1) on the twofold axes, was derived from the Patterson function. This model was refined by full-matrix least-squares methods. Atomic scattering factors for Zn^{2+}, V^{5+}, P, and O were obtained from Cromer and Waber (7). Anomalous-scattering corrections were applied (8).

The ratio of V-to-P was determined using the program RFINE (9) assuming the site to be fully occupied. Extinction corrections were applied as suggested by Larson (10). Weights were set equal to $(10.7 + 0.073F_o + 0.0005F_o^2 + 3500(\sigma(F_o)/F_o)^2$ with the coefficients for the observed structure factors, F_o, chosen so that the difference between the observed and calculated structure factors would be independent of the structure factor. The refinement was terminated when the calculated shifts were less than $1/4\sigma$. The R value was 0.073 and

$$R_w = \{\Sigma\omega|F_o - F_c|^2/\Sigma\omega|F_o|^2\}^{1/2} = 0.056$$

The final atomic and thermal parameters are in Table 1.[1]

Description of the Structure

All the cations are coordinated to four oxygen atoms which lie at the corners of a distorted tetrahedron. The Zn(I)O_4 and XO_4 groups are linked, each at two corners, into four-membered rings about the centers of symmetry (Fig. 1). These rings form chains generated by translational symmetry along a and the twofold axis through Zn(1). Adjacent chains are linked by Zn(2) which shares O(4) and O(4)′. The Zn(2)O_4 groups form chains with adjacent tetrahedra and are generated by the twofold screw axes. Each oxygen of this group is shared with a separate XO_4 group.

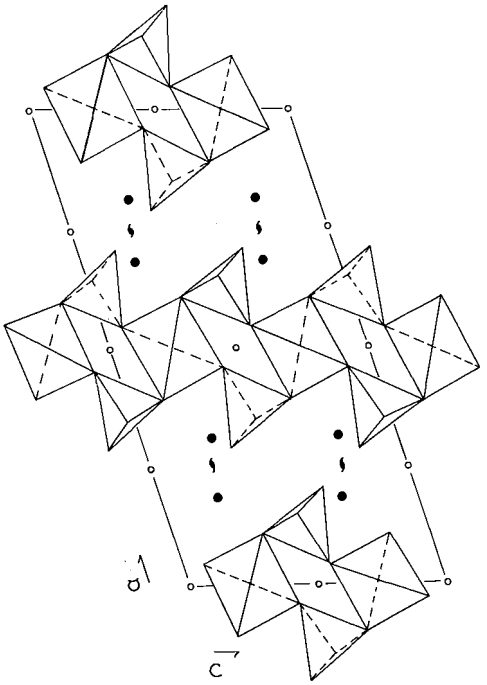

FIG. 1. The structure of $Zn_3V_{1/2}P_{3/2}O_8$ viewed down the b axis. The Zn(1)O_4 and PO_4 tetrahedra are outlined. The Zn(2) ions are indicated as filled circles.

The average X—O bond length is 1.575 Å (Table 2). If Vegard's law is assumed valid the composition weighted mean of the ⟨P—O⟩ (1.537 Å) and ⟨V—O⟩ (1.721 Å) (11) for tetrahedral coordination predicts a value of 1.583 Å for ⟨X—O⟩. The individual X—O bonds faithfully reflect the environments of the oxygen atoms. O(2) and O(3) are both shared between X and only one Zn ion and their X—O bond lengths are shorter than those involving O(1) and O(4) in which each is shared with two

[1]A table of observed and calculated structure factors is available, at a nominal charge, from the Depository of Unpublished Data, CISTI, National Research Council of Canada, Ottawa, Canada K1A 0S2.

Can. J. Chem. Downloaded from www.nrcresearchpress.com by 210.87.254.5 on 09/05/12
For personal use only.

TABLE 2. Bond lengths and angles in $Zn_3V_{1/2}P_{3/2}O_8$

Bond	Distance (Å)	Bonds	Angle (deg)	Bonds	Angle (deg)
Zn(1)—O(1)	2.007(6) 2×	O(1)—Zn(1)—O(1)′	104.6(3)	O(1)—Zn(1)—O(3)′	101.4(3)
Zn(1)—O(3)	1.902(7) 2×	—O(3)	116.5(3)	O(3)—Zn(1)—O(3)′	116.6(3)
Zn(2)—O(1)	1.960(7)	O(1)—Zn(2)—O(2)	114.7(3)	O(2)—Zn(2)—O(4)	102.2(2)
—O(2)	1.911(6)	—O(4)	111.3(3)	—O(4)′	113.6(2)
—O(4)	1.976(5)	—O(4)′	103.7(3)	O(4)—Zn(2)—O(4)′	111.6(2)
—O(4)′	1.948(6)				
X—O(1)	1.593(8)	O(1)—X—O(2)	109.6(5)	O(2)—X—O(3)	115.7(5)
—O(2)	1.541(8)	—O(3)	108.1(4)	—O(4)	107.8(4)
—O(3)	1.539(9)	—O(4)	106.2(4)	O(3)—X—O(4)	108.9(5)
—O(4)	1.626(5)				

Zn ions. Further, the average Zn—O(1) bond is longer than the average Zn—O(4) bond leading to X—O(4) > X—O(1). A parallel situation exists for O(1) and O(3) but the bond lengths involved are not significantly different. The major angular distortion of the XO_4 group involves a large O(1)—X—O(3) bond angle reflecting an enhanced repulsion between the oxygen atoms arising from the short X—O bond lengths.

Both ZnO_4 groups show a large range of O—Zn—O angles showing that the $Zn(1)O_4$ tetrahedron is distorted by a displacement of Zn ions towards the O(1)—O(1)′ edge. The O(*n*)—Zn(1)—O(*n*)′ angle is 116.6° for $n = 3$ and 104.6° for $n = 1$. The O(3)—O(3)′ and O(1)—O(1)′ edges are twisted about the twofold axis so as to subtend an angle deviating by 10° from the orthogonality required for a regular tetrahedron. The distortion of the $Zn(2)O_4$ group is smaller since the range of bond angles and the bond lengths is smaller than for the $Zn(1)O_4$ group. The mean Zn(*N*)—O bond lengths, at 1.955 and 1.948 Å for $N = 1$ and 2, respectively, are hardly significantly different, although the former cation has six neighboring cations and the latter has only five.

Discussion

The present structure has all the cations tetrahedrally coordinated as in the case in α-$Zn_3(PO_4)_2$. The unit cell parameters of the latter are $a = 8.196, b = 5.634, c = 15.007$ Å, $\beta = 105.0°$, $Z = 4$ and space group $C2/c$ (5). Its structure consists of interconnected $Zn(1)O_4$ and PO_4 groups forming sheets generated by the twofold screw axes at the 1/4,1/4 and 1/4,3/4 (Fig. 2). These $Zn(1)O_4$ groups lie on twofold axes and the $Zn(2)O_4$ groups lie in general positions but share an edge across centers of symmetry. The glide planes related adjacent sheets in α-$Zn_3(PO_4)_2$ and, in contrast, groups within a sheet in the present structure. The ⟨Zn—O⟩ distance is 1.956 Å in α-$Zn_3(PO_4)_2$ and 1.950 Å in the present case.

The role of the added cations in destabilizing the α-$Zn_3P_2O_8$ structure may lie in finding an alternative to the shared edges between the divalent cations of type 2, as has been previously suggested (6). This would be expected particularly if cation substitution increasingly generates cation pairs of different types in the sites that share this edge. The alternative structure possibilities, β-$Zn_3P_2O_8$ and γ-$Zn_3P_2O_8$, both have all the anions shared with three cations provided all bonds less than 2.55 Å are counted as being in the primary coordination sphere of the divalent cations. In α-$Zn_3P_2O_8$ and the present struc-

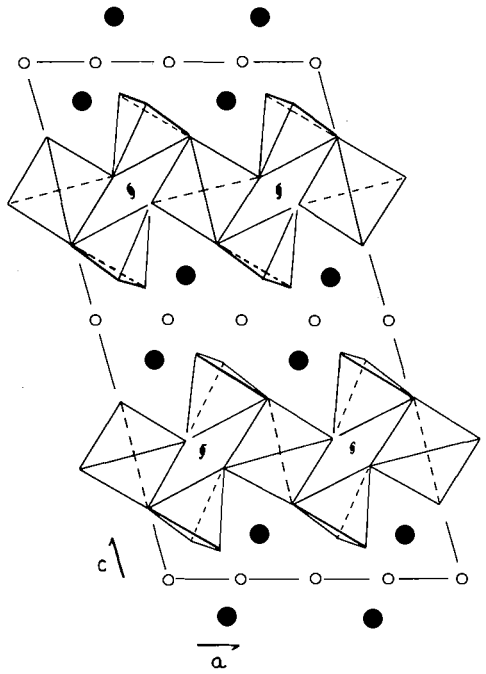

FIG. 2. The structure of α-$Zn_3P_2O_8$ viewed down the *b* axis. The $Zn(1)O_4$ and PO_4 tetrahedra are outlined. The Zn(2) ions are indicated as filled circles.

Can. J. Chem. Downloaded from www.nrcresearchpress.com by 210.87.254.5 on 09/05/12
For personal use only.

ture the average coordination number of the anion is 2.5. Thus there seems to be some preference for tetrahedral Zn at low temperatures for these compositions.

The role of the added vanadium is even less apparent and very little further can be said. The XO_4 tetrahedra in α-$Zn_3(PO_4)_2$ and the present structure show similar angular distortions from ideality. This follows if the Zn on the twofold axes and further the oxygen atoms shared by the same number of cations are considered equivalent. Thus, the angle subtended at the phosphorus atom by those oxygen atoms bonded to only one Zn and one P atom is 115.4(3)° in α-$Zn_3(PO_4)_2$ (5*b*) compared with 115.7(5)° in the present structure. However, the distortion of the zinc ion site at the twofold axis is entirely different. In α-$Zn_3P_2O_8$ the edge O(1)—O(1)′, where the oxygen atoms are threefold coordinated, subtends an O(1)—Zn(1)—O(1) angle of 102° whereas the O(4)—O(4)′ edge involving twofold coordinated oxygen atoms shows an angle of 130° at the zinc ion. The distortions are opposite in the present structure. The substitution of vanadium for phosphorus in α-$Zn_3(PO_4)_2$, assuming just a radial distortion of the XO_4, would cause the two O(*n*)—Zn—O(*n*)′, $n = 1$ and 3, to become more nearly identical, thus pushing the structure in the correct direction. However, this assumes that all the other features are maintained constant.

This research has been supported by a grant from the National Research Council of Canada.

1. J. J. BROWN and F. A. HUMMEL. Trans. British Ceramic Soc. **64**, 419 (1965).
2. F. A. HUMMEL and F. L. KATNACK. J. Electrochem. Soc. **105**, 125 (1958).
3. J. F. SARVER, F. L. KATNACK, and F. A. HUMMEL. J. Electrochem. Soc. **106**, 528 (1958).
4. J. J. BROWN and F. A. HUMMEL. J. Electrochem. Soc. **110**, 1218 (1963).
5. (*a*) C. CALVO. Can. J. Chem. **43**, 436 (1965). (*b*) C. CALVO and R. FAGGIANI. Unpublished results.
6. W. H. BAUR and E. TILLMANNS. Z. Kristallogr. **131**, 213 (1970).
7. D. T. CROMER and J. T. WABER. Acta Crystallogr. **18**, 104 (1965).
8. D. T. CROMER. Acta Cryst. **18**, 17 (1955).
9. L. FINGER. Program and Abstracts, Amer. Crystallogr. Assoc. Winter Meeting 54 (1969).
10. A. C. LARSON. Acta Cryst. **23**, 664 (1967).
11. R. GOPAL. Ph.D. Thesis. McMaster University, Hamilton, Ontario. 1972.

Can. J. Chem. Downloaded from www.nrcresearchpress.com by 210.87.254.5 on 09/05/12
For personal use only.

Reactions of Sodium Tetrahydroborate and Cyanotrihydroborate with Rhodium(I), (II), and (III) Systems in the Presence of Tertiary Phosphines

DAVID G. HOLAH, ALAN N. HUGHES, AND BENJAMIN C. HUI
Department of Chemistry, Lakehead University, Thunder Bay, Ontario P7B 5E1
Received June 6, 1975

DAVID G. HOLAH, ALAN N. HUGHES, and BENJAMIN C. HUI. Can. J. Chem. **53**, 3669 (1975).

The nitrogen atmosphere reactions of phosphine – Rh(I), Rh(II), and Rh(III) chloride systems with $NaBH_4$ and $NaBH_3CN$ and also similar reactions of $[RhCl(CO)_2]_2$ in the presence of phosphines are reported. Among the interesting products formed in the various reactions are hydrido, tetrahydroborato, hydrido–tetrahydroborato and hydrido–cyanotrihydroborato complexes such as the highly unstable Rh(I) species $Rh(BH_4)(PPh_3)_2$, the much more stable Rh(II) complex $RhH(BH_4)(o\text{-tolyl}_3P)$, the Rh(III)–5-phenyl-5*H*-dibenzophosphole (DBP) complex $RhH_2Cl(DBP)_3$, and the Rh(III) complex $RhH_2(BH_3CN)(PPh_3)_3$. Complexes of Rh(I) with BH_3CN and additional CO and N_2 ligands are also reported. These results are briefly discussed in the context of the previously proposed mechanism for the reaction of tetrahydroborate ion with Co, Ni, and Cu halides in the presence of phosphine ligands.

DAVID G. HOLAH, ALAN N. HUGHES et BENJAMIN C. HUI. Can. J. Chem. **53**, 3669 (1975).

On rapporte les réactions, sous atmosphère d'azote, des systèmes phosphine/chlorure de Rh(I), Rh(II) et Rh(III) avec $NaBH_4$ et $NaBH_3CN$ et d'autres réactions similaires du $[RhCl(CO)_2]_2$ en présence de phosphine. Parmi les produits intéressants formés dans les diverses réactions on retrouve des complexes hydrido, tétrahydroborato, hydrido tétrahydroborato et hydrido cyanotrihydroborato telle que l'espèce très instable du Rh(I), $Rh(BH_4)(PPh_3)_2$, le complexe beaucoup plus stable du Rh(II), $RhH(BH_4)(o\text{-tolyl}_3P)$, le complexe Rh(III) phényl-5 (5H) dibenzophosphole (DBP), $RhH_2Cl(DBP)_3$, et le complexe du Rh(III), $RhH_2(BH_3CN)(PPh_3)_3$. On rapporte aussi les complexes de Rh(I) avec BH_3CN et des ligands CO et N_2 additionnels. On discute de ces résultats dans le contexte du mécanisme proposé antérieurement pour la réaction de l'ion tétrahydroborate avec les halogénures de Co, Ni et Cu en présence de ligands de phosphine.

[Traduit par le journal]

Introduction

Recently we have reported (1–3) that solutions of divalent metal compounds, in the presence of stabilizing ligands, can be reduced in a stepwise manner by $NaBH_4$ to give a variety of thermodynamically stable complexes, including some with coordinated tetrahydroborate groupings. In particular, a series of univalent metal complexes such as $MClL_3$ (where M = Co or Ni, L = PPh_3), $M(BH_4)L_3$ (M = Co or Ni), $Cu(BH_4)L_2$, the related $M(BH_3CN)L_2$ (M = Ni or Cu), and $M(BH_3CN)L_4$ (M = Co; L = DBP or ½(diphos)) can be synthesized by carefully controlling reaction conditions.

In this paper we report an extension of this work to similar reactions involving rhodium(I), (II), and (III) systems. Relatively few tetrahydroborato complexes of rhodium are known. For example, the active homogeneous hydrogenation catalyst $RhCl_2(BH_4)(py)_2(dmf)$ (4) (py = pyridine, dmf = dimethylformamide), which may be prepared by the reaction of $NaBH_4$ on $RhCl_3(py)_3$ in dmf (4, 5), is interesting in that it contains neither carbonyl nor phosphine ligands, unlike all other reported rhodium (or iridium) tetrahydroborato and cyanotrihydroborato complexes. Thus, the complexes $M(BH_4)(CO)L_2$ and $M(BH_3CN)(CO)L_2$ have been prepared (6, 7) by the reaction of $NaBH_4$ or $NaBH_3CN$ on the compounds $MX(CO)L_2$ (M = Rh or Ir, X = Cl or ClO_4, and L = PPh_3, $P(C_6H_{11})_3$, $P[(CH_3)_3SiCH_2]_3$). Infrared spectra (6, 7) strongly indicate a bidentate BH_4 structure for the $M(BH_4)(CO)L_2$ complexes, while the BH_3CN in $M(BH_3CN)(CO)L_2$ is *N*-bonded to the metal, as in the case of similar Cu and Co complexes (3). The same workers (6) have also found that the nature of the product depends largely upon the metal and the phosphine ligand. For example, sometimes only hydrido complexes are obtained.

Results and Discussion

Sodium tetrahydroborate and cyanotrihydroborate react with $RhCl_3$ in the presence of phosphine ligands, with various Rh(I), (II), and (III)

Can. J. Chem. Downloaded from www.nrcresearchpress.com by 210.87.254.6 on 09/05/12
For personal use only.

Can. J. Chem. Downloaded from www.nrcresearchpress.com by 210.87.254.6 on 09/05/12
For personal use only.

TABLE 1. Complexes characterization

Compound	Color	Analyses*			Infrared spectra (cm^{-1})						
		C	H	N	δ_{B-H}	ν_{MH_2B}	ν_{B-H}	ν_{CN}	ν_{CO}	ν_{M-H}	Other
$Rh(BH_4)(PPh_3)_2$?	Yellow	66.6	4.6	—	1120w	1890	2410				
		67.3	5.3	—			2385				
$RhH_2(BH_3CN)(PPh_3)_3$	Yellow	71.1	5.9	1.4	1118s		2328s	2207s		2060s	796m(δ_{Rh-H})
		70.8	5.4	1.5			2260sh			2048s	785m
$RhH(BH_4)$(*o*-tolyl$_3$P)	Greenish-brown	59.2	5.8	—	1148s	1966m	2425s			2135w	805s(δ_{Rh-H})
		59.6	6.2	—		1850m	2380s				
$RhH_2Cl(DBP)_3$	Brown	71.0	4.8	—						1970mb	235w(ν_{Rh-Cl})
		70.4	4.5	—							
$Rh(BH_3CN)(N_2)(CO)(DBP)_3$	Yellow	69.1	4.7	3.1	1114m		2335m	2205m	1995s		2108s(ν_{N_2})
		68.6	4.3	4.3							
$RhH(CO)(DBP)_3$	Brown	71.7	4.8	—					1944s	1900w	
		72.2	4.4	—							
$Rh(BH_3CN)(CO)(DBP)_3$	Orange	69.8	4.3	1.5	1114m		2340m	2202m	1984s		2108w(ν_{N_2})
		70.6	4.4	1.5				2188sh			
$RhCl_2(BH_4)(py)_2$(dmf)†							2540				
							2440				
$Rh(BH_4)(CO)(PPh_3)_2$‡							2452		1955		
							2416				
$Rh(BH_4)(CO)[(C_6H_{11})_3P]_2$‡							2460		1931		
							2402				
$Rh(BH_4)(CO)$(diphos)$_2$§							2385		1937		
							2370				
$Rh(BH_3CN)(CO)(PPh_3)_2$‡							2360	2192	1997		

*Calculated values below found.
†Reference 4.
‡Reference 6.
§Reference 7.

Can. J. Chem. Downloaded from www.nrcresearchpress.com by 210.87.254.6 on 09/05/12
For personal use only.

phosphine complexes and with Rh(I) carbonyl complexes in the presence of phosphine ligands under an N_2 atmosphere to yield hydrido, tetrahydroborato, or cyanotrihydroborato complexes. These results are presented and discussed below.

Reactions of $RhCl_3.3H_2O$ with $NaBH_4$ and $NaBH_3CN$ in the Presence of a Ligand

The reaction of $RhCl_3.3H_2O$ in ethanol with a sixfold excess of PPh_3 and $NaBH_4$ at room temperature does not produce any tetrahydroborato complex, and only $RhH(PPh_3)_4$ (8) can be isolated. $NaBH_3CN$ also reacts readily with a mixture of $RhCl_3$ and PPh_3 to give a yellow solution, but we have been unable to isolate any characterizable product from this reaction. Other ligands such as DBP[1] and $AsPh_3$ (in 6 molar ratio) also fail to form tetrahydroborato complexes. Thus, with DBP, the known (9) homogeneous hydrogenation catalyst $RhH(DBP)_4$ forms while with $AsPh_3$, only $RhH_2Cl(AsPh_3)_2$ (10) can be isolated. Presumably the great differences in the nature of the products obtained from the DBP and $AsPh_3$ reactions are due to the fact that DBP complexes with $RhCl_3$ only slowly and it is the free $RhCl_3$ which is reacting with $NaBH_4$ whereas in the case of $AsPh_3$, complex formation is rapid and it is an Rh(III)–arsine complex which is reacting with $NaBH_4$.

Reactions of Rh(I), Rh(II), and Rh(III) Phosphine Complexes

Treatment of $RhCl(PPh_3)_3$ (11) in the presence of some free phosphine (3–6 mol) with $NaBH_4$ in EtOH again yields only the hydrido–tetrakisphosphine complex as in the reaction with $RhCl_3$ in the presence of PPh_3. However, it has been observed (7) that an excess of phosphine in the reactions involving $NaBH_4$ and phosphine–metal complexes tends to lead to the formation of hydrido complexes. Several (mainly unsuccessful) attempts have therefore been made to prepare tetrahydroborato complexes of Rh(I) (*e.g.* $Rh(BH_4)(PPh_3)_3$, the Rh(I) analog of the known Co(I) complex $Co(BH_4)(PPh_3)_3$ (3)) by using $RhCl(PPh_3)_3$ alone as starting material. For example, with no added PPh_3, in EtOH, THF/EtOH or C_6H_6/EtOH, $RhCl(PPh_3)_3$ reacts with $NaBH_4$ (1 mol or a large excess) to produce only the known (8) orange $RhH(PPh_3)_3$. However, that this reaction goes through an intermediate complex which contains a BH_4 ligand is clear since such a complex can be isolated by decreasing the reaction time although the conditions required for this appear to be critical. Thus, if after adding $NaBH_4$ to $RhCl(PPh_3)_3$ in C_6H_6/EtOH and stirring for 5 min the solution is concentrated, addition of EtOH immediately precipitates a yellow complex which analyzes very well for $Rh(BH_4)(PPh_3)_2$ (Table 1). The infrared spectrum of this compound is compatible with the proposed structure since it has bands at 2410 and 2382 cm^{-1} assignable to the stretching frequencies of the terminal B—H bonds (see ref. 3 for a discussion of the i.r. spectra of BH_4 complexes) and a band at 1890 cm^{-1} probably due to the ring breathing mode of Rh—H_2—B. However, this tetrahydroborato complex is extremely air sensitive (ignites in air) and must also be very unstable in solution since as already mentioned, prolonging the reaction time leads only to the formation of $RhH(PPh_3)_3$ even when only 1 mol of $NaBH_4$ is used. It has therefore been impossible to characterize this adduct more fully, and, indeed, it is extremely difficult to duplicate the reaction.

Turning to cyanotrihydroborate reactions with $RhCl(PPh_3)_3$, $NaBH_3CN$ reacts readily with this Rh(I) complex in 1:1 C_6H_6/EtOH solution to produce the pale yellow Rh(III) *N*-bonded complex $RhH_2(BH_3CN)(PPh_3)_3$ which presumably is formed by the oxidative addition of hydrogen to an intermediate Rh(I)–BH_3CN species. Such additions of H_2 or N_2 to Rh(I) complexes are relatively common and they occur spontaneously in solution. In this connection, we have also noted previously (3) that similar complexes of Co(I) readily form dinitrogen complexes. It is possible that these additions are dictated by steric requirements of the various ligands.

The infrared spectrum of this compound (see Table 1) shows the expected bands at 2048 and 2060 cm^{-1} corresponding to the Rh—H stretching frequencies for the *cis* dihydride structure which would be anticipated from oxidative H_2 addition. Furthermore, the cyanotrihydroborate grouping shows bands at 2260 and 2328 cm^{-1}

[1]DBP is the cyclic phosphine, 5-phenyl-5*H*-dibenzophosphole which is a somewhat more rigid, flattened version of PPh_3.

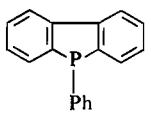

DBP

Can. J. Chem. Downloaded from www.nrcresearchpress.com by 210.87.254.6 on 09/05/12
For personal use only.

(ν_{B-H}) and at 2207 cm^{-1} ($\nu_{C\equiv N}$) indicative of an *N*-bonded BH_3CN grouping (3, 6). For comparison with this and other compounds reported in this paper, i.r. data for some of the related known Rh complexes are also listed in Table 1. Unfortunately, it was not possible to identify the Rh—H protons in the high-field n.m.r. spectrum since $RhH_2(BH_3CN)(PPh_3)_3$ decomposes immediately by eliminating a gas (presumably molecular hydrogen) on dissolving in suitable n.m.r. solvents such as benzene or chloroform. Such decompositions of Rh(III) hydrides are well known (12).

Regarding reactions of Rh(II) complexes, the paramagnetic, bluish-green, square planar Rh(II) complex of tri-*o*-tolylphosphine, $RhCl_2(o\text{-tolyl}_3P)_2$ (13), reacts with $NaBH_4$ in benzene/ethanol solution to yield a dark pyrophoric solid. The infrared spectrum of this compound shows the presence of phosphine ligands and a broad band at ~1970 cm^{-1}, indicative of a hydrido species. Reproducible chemical analyses have not so far been obtained because of the extreme oxygen sensitivity of the compound and this species is presently under further investigation. However, a stable Rh(II)–tetrahydroborato complex with tri-*o*-tolylphosphine can be obtained if the $NaBH_4$ reaction with $RhCl_2(o\text{-tolyl}_3P)_2$ described above is carried out in ethanol solution in the presence of an excess of the free ligand. Thus, addition of an excess of $NaBH_4$ to a suspension of $RhCl_2(o\text{-tolyl}_3P)_2$ and 1 mol of $o\text{-tolyl}_3P$ in ethanol precipitates a greenish-brown solid. The compound analyzed well for $RhH(BH_4)(o\text{-tolyl}_3P)$ and appears to have some degree of stability in air over short periods. If no free ligand is present in the reaction mixture only impure adduct can be obtained.

Again, the i.r. spectrum is consistent with the proposed formula as it shows bands at 2425, 2380, and 1148 cm^{-1} corresponding to the stretching and bending modes of the terminal B—H bonds. Bands at 1966 and 1850 cm^{-1} probably correspond to bonding of the type Rh—H—B, while the weak absorption at 2135 cm^{-1} is associated with the Rh—H stretch.

Although the analytical results, the method of preparation and the infrared spectrum strongly indicate that the complex is $RhH(BH_4)(o\text{-tolyl}_3P)$, they do not by themselves exclude the possibility that $RhCl_2(o\text{-tolyl}_3P)_2$ is reduced to an Rh(I) tetrahydroborato species to which oxidative addition of H_2 occurs to give the Rh(III) complex $RhH_2(BH_4)(o\text{-tolyl}_3P)$. Neither do they exclude the possibility that, in an intermediate Rh(I)–BH_4–$o\text{-tolyl}_3P$ complex, internal metalation by insertion of an Rh atom into a CH_3 group occurs to give $RhH(BH_4)[CH_2C_6H_4P(o\text{-tolyl})_2]$ in which the resulting Rh(III) atom is coordinated by phosphorus, hydride, tetrahydroborate and a methylene group and in which the hydride group is derived from one of the methyl groups.[2] If the former (H_2 addition to Rh(I)) were to occur, analytical data would remain essentially unchanged and the metal hydride peak at 2135 cm^{-1} in the i.r. spectrum of the adduct is sufficiently broad to be an unresolved doublet similar to the doublet observed for $RhH_2(BH_3CN)(PPh_3)_3$ (Table 1). If the latter (internal metalation) were to occur, again the analytical data would remain unchanged and only one metal hydride i.r. absorption would be expected. However, such reactions would be unlikely in that they would almost certainly proceed via an Rh(I) chloro species in the presence of an excess of the phosphine and, as we have seen in the preceding section, the Rh(I) chloro compound $RhCl(PPh_3)_3$ yields with $NaBH_4$ only the Rh(I) complexes $Rh(BH_4)(PPh_3)_2$, $RhH(PPh_3)_3$, or $RhH(PPh_3)_4$ depending upon the reaction conditions.

That the adduct obtained by treatment of $RhCl_2(o\text{-tolyl}_3P)_2$ is indeed the Rh(II) complex $RhH(BH_4)(o\text{-tolyl}_3P)$ is clearly confirmed by n.m.r. spectroscopic studies. For example, the spectrum in dichloromethane solution shows a single Rh—H signal as a doublet centered on 30.0 τ with a coupling constant of 27 Hz indicative of a *cis* J_{P-H} arrangement. The peaks of the doublet are slightly broadened and this is presumably due to a small unresolved coupling with the BH_4 protons and/or the Rh atom. The methyl groups appear initially in the n.m.r. spectrum as three broadened peaks of unequal area at 7.61 τ (low intensity), 7.73 τ (medium intensity), and 7.82 τ (slightly higher intensity). This suggests possibly nonequivalence of the methyl groups and perhaps some coupling with the phosphorus atom. Nonequivalence could conceivably arise from π back-donation from the rhodium atom to the phosphorus atom thereby inhibiting rotation about the Rh—P bond. Al-

[2]We are indebted to a referee for this suggestion.

Can. J. Chem. Downloaded from www.nrcresearchpress.com by 210.87.254.6 on 09/05/12
For personal use only.

ternatively, it could be simply a steric inhibition of rotation or a weak interaction of one methyl group with the rhodium atom. On the other hand, the signal multiplicity could arise from superimposed methyl and nonequivalent methylene signals of $RhH(BH_4)[CH_2C_6H_4P(o\text{-tolyl})_2]$.

No other signals occur in the range 7.80–40.00 τ. This shows that only one metal hydride grouping is present and therefore excludes the structure $RhH_2(BH_4)(o\text{-tolyl}_3P)$. If the spectrum is recorded in deuterated dichloromethane, careful integration over several samples of the aromatic and methyl regions of the spectrum shows a ratio of 12 aromatic protons to 8.9 methyl protons. This eliminates the possibility that internal metalation has occurred to give $RhH(BH_4)[CH_2C_6H_4P(o\text{-tolyl})_2]$, since this would require a ratio of 12 aromatic to 8 methyl and methylene protons.

The n.m.r. measurements must be carried out immediately on very freshly prepared solutions under a nitrogen atmosphere since fairly rapid decomposition of the adduct occurs in solution. This decomposition is reflected in the spectrum in which the Rh—H doublet broadens and becomes more complex before finally disappearing altogether after about 3 h. Also, during the decomposition, the methyl signal modifies to become a strong doublet (J = 8 Hz) at 7.61 τ and 7.75 τ with a weak doublet (J = 13 Hz) at 7.67 τ and 7.89 τ superimposed. This suggests the formation of at least two products during decomposition. The peak at 7.61 τ of this strong doublet in the decomposed solution coincides in location with the weak peak at 7.61 τ in freshly prepared solutions and indicates that even in the very fresh solutions, a small amount of decomposition had already occurred.

Magnetic measurements show that in contrast to the paramagnetic starting material, the adduct $RhH(BH_4)(o\text{-tolyl}_3P)$ is diamagnetic. It is therefore probable that $RhH(BH_4)(o\text{-tolyl}_3P)$ is dimeric with a strong Rh–Rh interaction although the solution instability precluded molecular weight measurements. This is not unexpected since although $RhCl_2(o\text{-tolyl}_3P)_2$ (13) and $RhCl_2(PBu^t{}_2R)_2$ (R = Me, Et, or Pr^n) (14) are monomeric and paramagnetic, the binuclear carboxylates $[Rh(OOCR)_2L]_2$ (L = H_2O, MeOH, or PPh_3) (15) and the Rh_2^{4+} ion (16) are dimeric and diamagnetic. This suggests that the complex $RhH(BH_4)(o\text{-tolyl}_3P)$ may have one of the following possible structures:

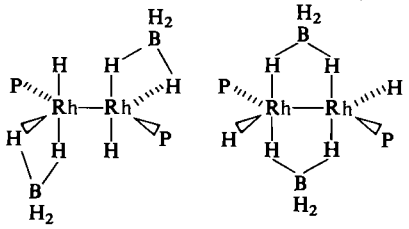

In either case, the metal hydride protons are equivalent and *cis* to the phosphine ligand as suggested by the n.m.r. spectrum although it should be noted that tetrahydroborato bridged complexes of the second type above appear not to have been previously reported.

This Rh(II) complex is interesting in that virtually all other known tetrahydroborato complexes of rhodium contain carbonyl and tertiary phosphine ligands (6, 7), except for the previously mentioned Rh(III) complex (4) which is stabilized by pyridine and the highly unstable and not fully characterized Rh(I) complex $Rh(BH_4)(PPh_3)_2$ reported in this paper. No identifiable product could be obtained from reactions of the Rh(II) complex with $NaBH_3CN$.

In reactions of Rh(III) phosphine complexes with tetrahydroborate and cyanotrihydroborate no Rh(III)–BH_4 or Rh(III)–BH_3CN complexes could be obtained. For example, the reaction of $RhCl_3(DBP)_3$ (17) with $NaBH_4$ proceeds readily in C_6H_6/ethanol and, when an excess of reducing agent is used, only $RhH_2Cl(DBP)_3$ can be obtained as a brown solid. Again the n.m.r. spectrum at high field does not show the presence of the metal hydrogen bonds since the complex shows the typical solution instability of Rh(III) hydrides and elimination of molecular hydrogen occurs on dissolution. The infrared spectrum of this compound, however, has broad bands at $\sim$1970 cm^{-1} possibly due to poor resolution of two metal–hydride stretching frequencies.

There are apparently two possible mechanisms for this reaction. Thus, a two-step replacement of two chlorine atoms on an Rh(III) atom may occur or it is possible that in this reaction, Rh(III) is reduced to Rh(I) which undergoes oxidative-addition of H_2 of the type observed in the case of the reaction of $RhCl(PPh_3)_3$ with $NaBH_3CN$. For reasons to be given later in this paper, we prefer the first of these mechanisms. On the other hand, the Rh(III) dibenzophos-

Can. J. Chem. Downloaded from www.nrcresearchpress.com by 210.87.254.6 on 09/05/12
For personal use only.

phole complex is reduced by cyanotrihydroborate in C_6H_6/EtOH, to give a compound analyzing quite well for the Rh(I) species $Rh(BH_3CN)(N_2)(CO)(DBP)_3$. The infrared spectrum of this complex is virtually identical with that of $Rh(BH_3CN)(CO)(DBP)_3$ which may be prepared from $[RhCl(CO)_2]_2$ solution (see next section), except for the intense N_2 stretching frequency which occurs at 2108 cm^{-1} in the i.r. spectrum of the complex tentatively formulated as $Rh(BH_3CN)(N_2)(CO)(DBP)_3$ and also a small ($\sim$10 cm^{-1}) shift of the CO frequency to higher wave number compatible with competition in π back-donation from the Rh atom between coordinated N_2 and CO. Again, it is probably due to the steric and electronic requirements of both DBP and BH_3CN that both abstraction of CO from ethanol and coordination of dinitrogen occur. Repetition of this reaction under argon gave a crude product which formed an oil on treatment with dry solvents and which could not be characterized.

Reactions of $[RhCl(CO)_2]_2$ with $NaBH_4$ and $NaBH_3CN$ in the Presence of DBP

Addition of DBP in a 3:1 ratio to $[RhCl(CO)_2]_2$ (18) in ethanolic solution followed by an excess of $NaBH_4$ produces the hydrido complex $RhH(CO)(DBP)_3$, which cannot be made by the general method of adding $NaBH_4$ to $RhCl(CO)_2(DBP)$ in the presence of an excess of DBP in boiling ethanol (9). The n.m.r. spectrum of this complex in benzene shows the hydrogen bound to rhodium as a sharp quartet (1:3:3:1) of doublets with J_{P-H} = 14 Hz and J_{Rh-H} = 2.5 Hz centered at 19.05 τ. This pattern can be ascribed to a trigonal bipyramidal structure with the hydride and CO in the apical positions, *i.e.* an arrangement in which the three phosphorous atoms are magnetically equivalent and which would produce coupling constants of the magnitude observed. The sharpness of the peaks in the spectrum suggests that very little dissociation of the phosphine ligands occurs and, in this respect, the complex behaves quite differently from the analogous PPh_3 compound $RhH(CO)(PPh_3)_3$. This PPh_3 complex has been reported (19) to dissociate extensively at room temperature and the n.m.r. spectrum shows a broad metal hydride band at 19.27 τ. However, on cooling a solution of $RhH(CO)(PPh_3)_3$ to -30 °C, a similar quartet of doublets can be observed at 19.69 τ (19).

A similar reaction with $NaBH_3CN$ gives the five-coordinated $Rh(BH_3CN)(CO)(DBP)_3$ which shows bands in the i.r. spectrum assignable to ν_{B-H} (2340 cm^{-1}), ν_{CN} (2188 and 2202 cm^{-1}), and ν_{CO} (1984 cm^{-1}). Undoubtedly the compound can readily pick up dinitrogen to form $Rh(BH_3CN)(N_2)(CO)(DBP)_3$ (see previous discussion) as the i.r. spectrum also shows a weak band at 2108 cm^{-1} probably due to $\nu_{N\equiv N}$. The analogous four-coordinate species $Rh(BH_3CN)(CO)(PPh_3)_2$ has been synthesized (6) and the infrared spectrum is similar to that of the five-coordinate DBP complex (Table 1).

In summary, clearly the reactions of phosphine – Rh(I) chloride complexes with $NaBH_4$ follow in broad outline the mechanism proposed earlier (3) for the later stages of the similar reduction of divalent 3*d* metal halides with $NaBH_4$ in the presence of phosphines. The resulting unstable and highly air sensitive Rh(I)–BH_4 complex is considerably less stable than the corresponding Co(I) and Ni(I) complexes. This mechanism also appears to be the case in reactions of phosphine – Rh(I) chloride complexes with $NaBH_3CN$.

Rh(II) and Rh(III) appear generally to be stabilized by a complexing phosphine ligand and this supposition is supported by similar studies on ruthenium systems to be reported in a later paper. However, there are two possible mechanisms (discussed earlier) whereby some of the Rh(III) dihydrides may be formed from Rh(III) chloride complexes although, on the basis of the results discussed in this paper and results obtained with related ruthenium systems, we feel that these dihydrides arise from direct replacement of chloro groups by hydrido groups.

If this is the case, there is one anomaly in that reduction of $RhCl_3(DBP)_3$ with the milder reducing agent $NaBH_3CN$ leads to the Rh(I) complex $Rh(BH_3CN)(N_2)(CO)(DBP)_3$. This may, however, be explained by postulating an intermediate Rh(III) dihydro species such as $RhH_2(BH_3CN)(DBP)_2$ which, because of the known instability of Rh(III) hydrides (particularly in solution) mentioned earlier and possibly also steric requirements of the ligands, undergoes exchange of dihydrogen for molecular nitrogen.

Can. J. Chem. Downloaded from www.nrcresearchpress.com by 210.87.254.6 on 09/05/12
For personal use only.

Some support for this comes from the fact that although the i.r. spectrum of $Rh(BH_3CN)(N_2)(CO)(DBP)_3$ is virtually identical (apart from the N_2 peak) with that of the nitrogen free adduct $Rh(BH_3CN)(CO)(DBP)_3$ prepared by a different method, there is an additional very small but very sharp peak at 2132 cm^{-1} indicative of the presence of small amounts of an Rh(III) hydride and this indicates (as does the N analysis) that the H_2–N_2 exchange is not quite complete.

It is therefore clear that the question of platinum group metal halide reactions in the presence of phosphines and $NaBH_4$ or $NaBH_3CN$ requires further extensive study. In particular, it would seem desirable to extend the investigation to ruthenium systems and our studies in this area will form the subject of a later paper.

Experimental

Materials

DBP (20), $RhCl(PPh_3)_3$ (11), $[RhCl(CO)_2]_2$ (18), $RhCl_3(DBP)_3$ (17), and $RhCl_2(o\text{-tolyl}_3P)_2$ (13) were prepared as described in the literature. Rhodium trichloride hydrate was obtained from Engelhard Industries and $NaBH_4$, $NaBD_4$, and $NaBH_3CN$ were obtained from the Ventron Corporation. Triphenylphosphine was recrystallized from ethanol prior to use while other compounds were of reagent grade and were used without further purification. All solvents were purified in the usual manner, degassed, and stored over molecular sieves (type 4A).

Physical Measurements

All physical measurements were carried out as previously described (21). Nuclear magnetic resonance measurements were carried out on a Varian A60-A spectrometer using benzene or dichloromethane as solvent at room temperature. Chemical shifts were determined using the solvent itself as internal reference, calibration being made using the known complex $RhH(CO)(PPh_3)_3$ (19) as standard.

Syntheses

The general procedure was as previously described (3) with all reactions being carried out under strict nitrogen atmosphere conditions. Analytical and spectral data are given in Table 1. Yields were normally in the range 50–70%.

$Rh(BH_4)(PPh_3)_2$

$RhCl(PPh_3)_3$ (~0.2 g) was suspended in 2:1 benzene/ethanol mixture (~15 ml), and an excess of $NaBH_4$ (~0.1 g) suspended in ethanol (~5 ml) was added dropwise. The solution became clear reddish-brown. After 5 min, the solvent volume was greatly decreased under reduced pressure and ethanol (~10 ml) was added. The residual yellow solid was separated by filtration. The product was then washed successively with ethanol, water, ethanol, and *n*-hexane.

$RhH_2(BH_3CN)(PPh_3)_3$

An excess of $NaBH_3CN$ (~0.1 g) in ethanol (~5 ml) was added to $RhCl(PPh_3)_3$ (~0.2 g) dissolved in the minimum amount of benzene. The solution was stirred for ~20 h and then concentrated under reduced pressure to small volume. The product was precipitated by the addition of ethanol.

$RhH(BH_4)(o\text{-tolyl}_3P)$

An excess of $NaBH_4$ suspended in ethanol was added dropwise to a mixture of $RhCl_2(o\text{-tolyl}_3P)_2$ (0.34 g) and $o\text{-tolyl}_3P$ (0.15 g) also in ethanol (~5 ml). The mixture was stirred for at least 6 h before the brown product was separated by filtration.

$RhH_2Cl(DBP)_3$ and $Rh(BH_3CN)(N_2)(CO)(DBP)_3$

$RhCl_3(DBP)_3$ (0.3 g) was dissolved in the minimum amount of benzene to which an excess of $NaBH_4$ (or $NaBH_3CN$) suspended in ethanol was then added. The mixture was left stirring for ~20 h when a clear reddish-brown solution (orange-red for the Rh(I) complex) resulted. The solution was then concentrated to small volume and the product was precipitated by addition of ethanol.

$RhH(CO)(DBP)_3$ and $Rh(BH_3CN)(CO)(DBP)_3$

$[RhCl(CO)_2]_2$ (~0.2 g) and DBP (~0.46 g) were mixed together in the minimum amount of ethanol and this was followed by the addition of either $NaBH_4$ or $NaBH_3CN$ suspended in ethanol. The mixture was stirred for about 5 h before the product was separated by filtration.

We thank the National Research Council of Canada for generous financial support of this work. We also thank the Ventron Corporation, Beverly, Massachusetts, in particular Mr. Robert Wade, for a gift of chemicals.

1. D. G. Holah, A. N. Hughes, B. C. Hui, and K. Wright. Inorg. Nucl. Chem. Lett. **9**, 835 (1973).
2. D. G. Holah, A. N. Hughes, and B. C. Hui. Inorg. Nucl. Chem. Lett. **10**, 427 (1974).
3. D. G. Holah, A. N. Hughes, B. C. Hui, and K. Wright. Can. J. Chem. **52**, 2990 (1974).
4. I. Jardine and F. J. McQuillin. Chem. Commun. 477 (1969).
5. P. Abley and F. J. McQuillin. J. Catal. **24**, 536 (1972); Chem. Commun. 477 (1969); J. Chem. Soc. A, 844 (1971); P. Abley, I. Jardine, and F. J. McQuillin. J. Chem. Soc. A, 840 (1971).
6. L. Vaska, W. V. Miller, and B. R. Flynn. Chem. Commun. 1615 (1971).
7. A. T. T. Hsieh, J. D. Ruddick, and G. Wilkinson. J. Chem. Soc. Dalton Trans. 1966 (1972).
8. J. J. Levison and S. D. Robinson. J. Chem. Soc. A, 2947 (1970).
9. D. Budd, D. G. Holah, A. N. Hughes, and B. C. Hui. Can. J. Chem. **52**, 775 (1974).
10. J. T. Mague and G. Wilkinson. J. Chem. Soc. A, 1736 (1966).
11. J. A. Osborn, F. H. Jardine, J. F. Young, and G. Wilkinson. J. Chem. Soc. A, 1711 (1966).
12. A. Sacco, R. Ugo, and A. Moles. J. Chem. Soc. A, 1670 (1966).

13. M. A. BENNETT, R. BRAMLEY, and P. A. LONGSTAFF. Chem. Commun. 806 (1966); M. A. BENNETT and P. A. LONGSTAFF. J. Am. Chem. Soc. **91**, 6267 (1969).
14. C. MASTERS and B. L. SHAW. J. Chem. Soc. A, 3679 (1971).
15. F. A. COTTON, B. G. DEBOER, M. D. LAPRADE, J. R. PIPAL, and D. A. UCKO. J. Am. Chem. Soc. **92**, 2926 (1970); T. A. STEPHENSON, S. M. MOREHOUSE, A. R. POWELL, J. P. HEFFER, and G. WILKINSON. J. Chem. Soc. 3632 (1965).
16. P. LEGZDINS, R. W. MITCHELL, G. L. REMPEL, J. D. RUDDICK, and G. WILKINSON. J. Chem. Soc. A, 3322 (1970).
17. D. G. HOLAH, A. N. HUGHES, B. C. HUI, N. KRUPA, and K. WRIGHT. Phosphorus, **5**, 145 (1975).
18. J. A. MCCLEVERTY and G. WILKINSON. Inorg. Synth. **8**, 211 (1966).
19. D. EVANS, G. YAGUPSKY, and G. WILKINSON. J. Chem. Soc. A, 2660 (1968).
20. H. HOFFMAN. Chem. Ber. **95**, 2563 (1962).
21. P. R. HECKLEY, D. G. HOLAH, and D. BROWN. Can. J. Chem. **49**, 1151 (1971).

Can. J. Chem. Downloaded from www.nrcresearchpress.com by 210.87.254.6 on 09/05/12
For personal use only.

Spectres de masse d'hydrazino-2 benzo- et naphtothiazoles et d'hydrazones des méthyl-3 benzo- et naphtothiazolinones-2

JEAN-CLAUDE RICHER ET PHILIPPE LAPOINTE

Département de Chimie, Université de Montréal, B.P. 6210, Montréal, Québec H3C 3V1

ET

MARTINE BELJEAN ET MICHEL PAYS

UER des Sciences Pharmaceutiques, 1 rue Vaubenard, 14000 Caen, France

Reçu le 9 avril 1975

JEAN-CLAUDE RICHER, PHILIPPE LAPOINTE, MARTINE BELJEAN et MICHEL PAYS. Can. J. Chem. **53**, 3677 (1975).

On rapporte les spectres de masse, sous impact électronique, des hydrazones de la méthyl-3 benzothiazolinone-2 (**1**), des chloro-4, 5, 6 et 7 méthyl-3 benzothiazolinones-2 (**2**, **3**, **4** et **5**) et de la méthyl-3 naphto[2,1-*d*]thiazolinone-2 (**6**) de même que ceux de l'hydrazino-2 benzothiazole (**7**), des chloro-4, 5, 6 et 7 hydrazino-2 benzothiazoles (**8**, **9**, **10** et **11**) et de l'hydrazino-2 naphto-[2,1-*d*]thiazole (**12**). On compare les résultats obtenus dans les deux séries. L'hydrazone-2 de la méthyl-3 benzothiazolinone-2 et ses dérivés présentent tous un pic de base équivalent à l'ion moléculaire; la fragmentation conduit principalement à des pertes successives de $H_2N\cdot$, HCN, HCN puis CS. Des chemins mineurs impliquent des pertes initiales de N_2H_2, $NH\cdot$ et NH_3. Dans le cas de l'hydrazino-2 benzothiazole et de ses dérivés, le pic de base est toujours équivalent à l'ion moléculaire; on note toutefois que les proportions relatives des divers ions de fragmentation varient suivant la position de la sonde à l'intérieur de l'appareil et l'on peut en conclure que l'on observe un spectre de masse correspondant au mélange des tautomères possibles hydrazone–hydrazine. Les principaux chemins de fragmentation impliquent la perte initiale de NH_3 (conduisant à un ion stabilisé), de $NH_2\cdot$ (probablement due à la forme hydrazone) et de N_2H_2.

JEAN-CLAUDE RICHER, PHILIPPE LAPOINTE, MARTINE BELJEAN, and MICHEL PAYS. Can. J. Chem. **53**, 3677 (1975).

Electron impact mass spectra are reported for the hydrazones of 3-methyl-2-benzothiazolinone (**1**), of 4-, 5-, 6-, and 7-chloro-3-methylbenzo-2-thiazolinones (**2**, **3**, **4**, and **5**) and of 3-methylnaphtho[2,1-*d*]-2-thiazolinone (**6**), as well as for 2-hydrazinobenzothiazole (**7**), for 4-, 5-, 6-, and 7-chloro-2-hydrazinobenzothiazoles (**8**, **9**, **10**, and **11**) and for 2-hydrazinonaphtho[2,1-*d*]thiazole (**12**). The results obtained in the two series are compared. The 2-hydrazone and 3-methylbenzo-2-thiazolinone and its derivatives all form a base peak corresponding to the molecular ion; fragmentation proceeds mainly by successive losses of $\cdot NH_2$, HCN, HCN, and then CS. Initial losses of N_2H_2, $NH\cdot$, and NH_3 are minor fragmentation routes.

In the case of 2-hydrazinobenzothiazole and its derivatives, the base peak is still that of the molecular ion; however, the relative proportions of the various fragment ions vary with the position of sampling probe inside the apparatus. Thus it is concluded that the observed mass spectrum is that of a mixture of the possible hydrazone–hydrazine tautomers. The principal fragmentations involve the initial loss of NH_3 (leading to a stabilized ion), of $NH_2\cdot$ (probably from the hydrazone form), and of N_2H_2.

[Journal translation]

Introduction

Dans le cadre de nos travaux (1) sur la synthèse et la caractérisation d'hydrazino-2 benzo- et naphtothiazoles et d'hydrazones de méthyl-3 benzo- et naphtothiazolones-2, nous avons été amenés (*a*) à examiner les modes de fragmentation de ces composés en spectrométrie de masse sous impact électronique et (*b*) à comparer nos résultats à ceux obtenus antérieurement (2) pour divers benzothiazoles. Ce sont les résultats obtenus au cours de ces études qui font l'objet de la présente communication.

Partie expérimentale

La synthèse des dérivés examinés a été rapportée antérieurement (1). On a obtenu les données relatives aux masses exactes à l'aide d'un spectromètre AEI MS-902 relié à un ordinateur PDP-8; toutes les valeurs expérimentales correspondent à ± 0.0015 unité de masse aux valeurs calculées. On a déterminé les spectres de masse à basse résolution à l'aide d'un spectromètre Hitachi RMU-

Can. J. Chem. Downloaded from www.nrcresearchpress.com by 210.87.254.6 on 09/05/12
For personal use only.

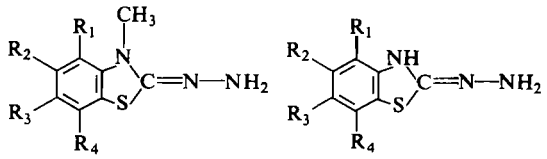

1 et **7** $R_1 = R_2 = R_3 = R_4 = H$
2 et **8** $R_1 = Cl, R_2 = R_3 = R_4 = H$
3 et **9** $R_2 = Cl, R_1 = R_3 = R_4 = H$
4 et **10** $R_3 = Cl, R_1 = R_2 = R_4 = H$
5 et **11** $R_4 = Cl, R_1 = R_2 = R_3 = H$
6 et **12** $R_1 = R_2 = H$, R_3 et $R_4 = —CH=CH—CH=CH—$

6D; l'énergie du faisceau ionisant était évaluée par une lecture directe du voltmètre puisque des mesures plus précises n'étaient pas nécessaires. On a observé des pics métastables dans ces spectres à basse résolution; quelques fois on les a obtenus en balayant la tension d'accélération avec le champ magnétique et le champ électrostatique à des valeurs constantes.

Résultats et discussion

Hydrazones des méthyl-3 benzo- et naphto[2,1-d]thiazolinones-2 (1 à 6)

Les spectres à 70 eV et à 15 eV des composés **1** à **6** présentent plusieurs caractéristiques communes. Le schéma 1 résume les divers modes de fragmentation des composés **2** à **5** qui sont à toutes fins pratiques identiques. L'ion moléculaire est le pic parent à 15 eV et à 70 eV pour tous ces composés. A 15 eV les seuls autres pics importants que l'on observe correspondent aux fragmentations $(M - H_2N\cdot)$, $(M - H_2N\cdot - HCN)$, $(M - H_2N\cdot - HCN - HCN)$ et $(M - H_2N\cdot - HCN - HCN - CS)$. On présente dans le schéma 2 une rationalisation de ce chemin principal de fragmentation. Aucune étude spéciale n'a toutefois été effectuée pour confirmer ces hypothèses; la perte de CS conduisant aux ions du type **b** est toutefois fréquente (3) pour des dérivés aromatiques.

En plus de ce chemin principal de fragmentation, on observe, à 70 eV, des chemins mineurs impliquant des pertes initiales de N_2H_2, de NH_3 et de NH. Les spectres à haute résolution ont confirmé que l'ion $(M - 15)$ correspond bien à une perte de NH et non pas à une perte de $CH_3\cdot$. Le fait que les dérivés **1** à **6** ne perdent pas de $\cdot CH_3$ est a rapproché du résultat obtenu antérieurement (2*b*) avec l'imino-2 méthyl-3 dihydro-2,3 benzothiazole (**13***c*) alors que de la même manière l'intensité de l'ion correspondant à la

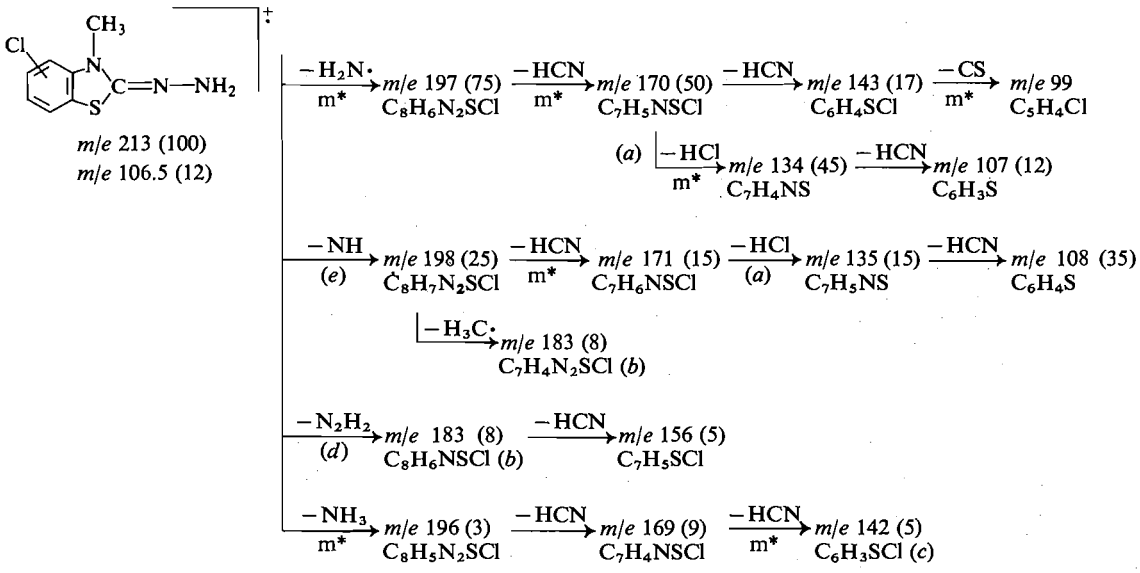

SCHÉMA 1. Fragmentations principales des composés **2** à **5**. Les compositions élémentaires résultent de mesures exactes des masses. Les valeurs entre parenthèse sont les intensités relatives à 70 eV. m* indique qu'un ion métastable a pu être observé sur le spectre à basse resolution alors que (*d*) indique qu'un ion métastable a été observé en balayant la tension d'accélération. (*a*) Ces fragmentations ne sont pas présentes dans les spectres des composés **1** et **6**. (*b*) On a pu montré que le pic à $(M - 30)$ est en fait un doublet pour lequel les ions correspondent respectivement à des pertes de N_2H_2 et CH_4N. (*c*) Dans le cas du dérivé naphtalénique **6**, on peut mettre en évidence que l'ion correspondant perd CS. (*e*) Aucun ion métastable n'a pu être observé pour cette fragmentation même en balayant la tension d'accélération.

Can. J. Chem. Downloaded from www.nrcresearchpress.com by 210.87.254.6 on 09/05/12
For personal use only.

Can. J. Chem. Downloaded from www.nrcresearchpress.com by 210.87.254.6 on 09/05/12
For personal use only.

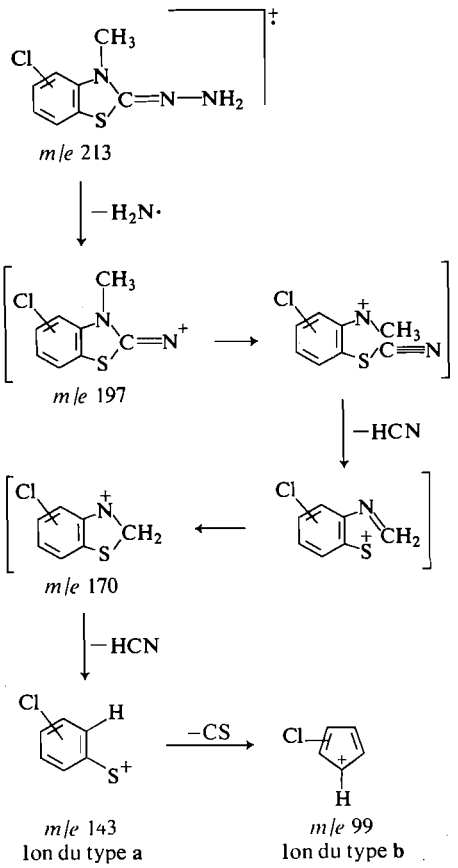

SCHÉMA 2. Rationalisation des principales fragmentations des hydrazones des méthyl-3 benzothiazolinones-2. Aucune étude spéciale n'a été effectuée pour confirmer ces hypothèses.

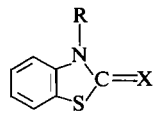

13

(*a*) R = —CH_2—$CH(CH_3)_2$, X = N—NH_2
(*b*) R = —$(CH_2)_9$—CH_3, X = N—NH_2
(*c*) R = CH_3, X = NH

perte d'un groupe méthyle est trop faible pour être mesurée. Aucun ion métastable n'a pu être observé pour la fragmentation impliquant la perte de NH; on ne peut donc pas éliminer la possibilité que la formation de l'ion (M − 15) provienne d'une autre voie comme, par exemple, une décomposition thermique dans la chambre à ionisation. Dans tous ces spectres, on n'observe pas de perte abondante de H·.

Les spectres des dérivés chlorés **2** à **5** présentent des particularités dues à la présence d'atomes de chlore qui sont expulsés sous forme de HCl. D'une façon générale, le schéma 1 peut toutefois aussi s'appliquer pour décrire les modes de fragmentation des dérivés **1** et **6**; originalement c'est d'ailleurs en se basant sur les résultats obtenus à l'aide du produit **6** qu'il a pu être mis en évidence que le pic à (M − 30) correspond à un doublet dû à la présence d'ions provenant de la perte de N_2H_2 et de CH_4N.

Hydrazino-2 benzo- et naphto[2,1-d]thiazoles (7 à 12)

Les spectres de masse, sous impact électronique, de ces dérivés présentent tous la caractéristique que les proportions relatives des divers ions de fragmentation varient suivant la position de la sonde à l'intérieur du spectromètre. Ces observations sont en accord avec le fait (4) que ces hydrazino-2 benzothiazoles existent sous forme de tautomères dont un couple est représenté par [1]; les divers spectres correspondent donc à des mélanges variables des divers tautomères. Certains composés examinés par Millard et Temple (2*a*) pouvaient présenter une telle isomérie; il ne semble pas qu'elle ait pu être détectée par spectrométrie de masse.

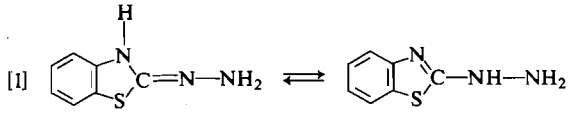

Dans les spectres de chacun de ces composés, la fragmentation principale correspond à la perte de NH_3 et à la formation d'entités du type **c** qui sont hautement stabilisées par résonance

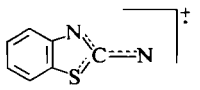

Ion radical du type **c**

et qui, à l'exception des dérivés chlorés **8** à **11** qui perdent ·Cl, ne semblent pas subir de fragmentation ultérieure à 15 eV.

On observe aussi (*a*) une perte importante de N_2H_2 conduisant à un ion radical du type **d**

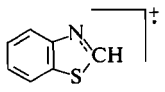

Ion radical du type **d**

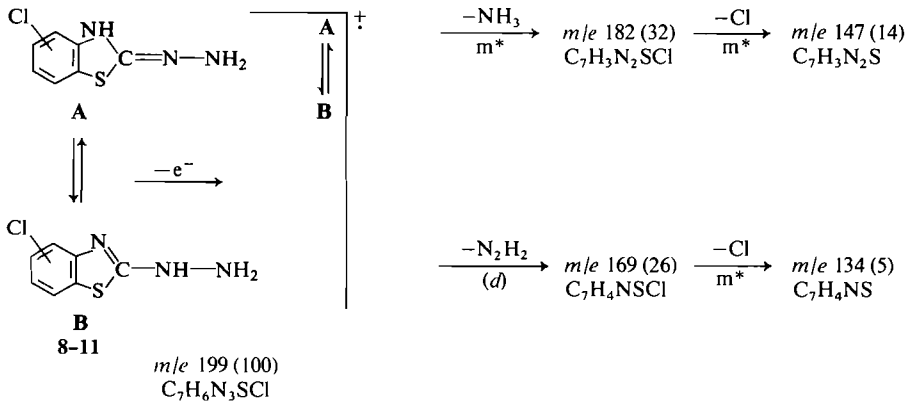

SCHÉMA 3. Fragmentations principales des composés **8** à **11**. La position de l'équilibre **A** ⇄ **B** est influencée par la position de la sonde à l'intérieur du spectromètre. Les intensités relatives des pics qui sont indiquées entre parenthèse ont été déterminées à 15 eV. Le (*d*) indique qu'un ion métastable a été observé en balayant la tension d'accélération.

dont la formation a aussi été invoqué par DeJongh et Thomson (5) lors de la fragmentation de la benzothiazolethione-2 et (*b*) une perte de $H_2N\cdot$ telle qu'observée plus haut lors de la décomposition des méthyl-3 hydrazones correspondantes; toutefois ce processus de fragmentation est maintenant mineur par rapport aux précédents. A 15 eV, les principaux pics observés peuvent être résumés par le schéma 3.

On a effectué des essais supplémentaires avec les chlorhydrates des hydrazones des (méthyl-2 propyl)-3 et décyl-3 benzothiazolinones-2 (**13***a* et **13***b*). Dans ces cas, on observe encore un ion moléculaire correspondant à l'amine libre; ce pic n'est toutefois plus le pic de base. En effet la rupture de la chaîne latérale, avec transfert d'hydrogène, semble le processus le plus efficace et dans les deux cas l'ion le plus important est l'ion radical **e**. Il est donc peu probable que des

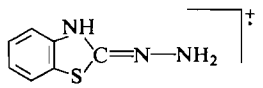

Ion radical du type **e**

hydrazones des benzothiazolinones-2 substituées par de longues chaînes en position 3 puissent s'avérer de quelque utilité que ce soit pour la caractérisation, par spectrométrie de masse sous forme d'azines, de divers composés carbonylés. Les résultats rapportés dans le présent travail suggèrent toutefois que les hydrazones de méthyl-3 benzo- ou naphtothiazolinones-2 pourraient être utiles à ces fins.

Les auteurs remercient vivement le Conseil National de Recherches du Canada et les autorités chargées d'administrer les accords culturels franco-québécois pour l'aide financière apportée sous forme d'octrois de recherches (CNR A-1295) et de frais de mission. Leur reconnaissance va aussi à Dr. A. S. Blair (Université de Montréal) pour l'aide technique fournie et au Dr. D. C. DeJongh pour des discussions utiles concernant cette publication.

1. M. PAYS et M. BELJEAN. Bull. Soc. Chim. Fr. 3044 (1973).
2. (*a*) B. J. MILLARD et A. F. TEMPLE. Org. Mass Spectrom. **1**, 285 (1968); (*b*) H. OGURA, S. SUGIMOTO et T. ITHOH. Org. Mass Spectrom. **3**, 1341 (1970).
3. H. BUDZIKIEWICZ, C. DJERASSI et D. H. WILLIAMS. Interpretation of mass spectra of organic compounds. Holden-Day Inc. 1964. pp. 163 et 167.
4. H. LARIVÉ, A. J. CHARBONNET et J. METZGER. Bull. Soc. Chim. Fr. 1675 (1963).
5. D. C. DEJONGH et M. L. THOMSON. J. Org. Chem. **38**, 1356 (1973).

Can. J. Chem. Downloaded from www.nrcresearchpress.com by 210.87.254.6 on 09/05/12
For personal use only.

Syntheses of Pentacyclic Morphinan Analogs

JAMES L. DOUGLAS AND JACQUES MEUNIER
Bristol Laboratories of Canada, Candiac, Quebec J5R 1J1

Received June 10, 1975

JAMES L. DOUGLAS and JACQUES MEUNIER. Can. J. Chem. **53**, 3681 (1975).

The synthesis of a series of morphinans with an additional aromatic or alicyclic ring fused to the 5,6 positions or an alicyclic ring fused to the 16,17 positions is described. The synthetic sequence involved elaboration of a 1,2,3,4,5,6-hexahydrobenz[*f*]isoquinoline or a quinolizidine, Grewe cyclization to a morphinan, and modification of the functional groups of the morphinan. These morphinans showed poor to moderate analgesic and narcotic antagonist activity.

JAMES L. DOUGLAS et JACQUES MEUNIER. Can. J. Chem. **53**, 3681 (1975).

La synthèse d'une série de morphinanes ayant un cycle aromatique ou alicyclique additionnel se rattachant aux positions 5,6 ou ayant un cycle alicyclique en position 16,17 est décrite. L'élaboration de cette synthèse implique la préparation de l'hexahydro 1,2,3,4,5,6-benz[*f*]isoquinoline ou d'une quinolizidine suivi d'une cyclisation de Grewe et enfin la modification des divers groupements fonctionnels du morphinane. Ces derniers démontrèrent une activité analgésique et antagonistique des stupéfiants allant de faible à moyenne.

As part of a research program directed towards the synthesis of new analgesics with a minimum of side effects, it was decided to study elaborations of the morphinan[1] system **1**. Because of the good balance of analgesic activity to side effects claimed for phenyl substituted benzomorphans such as **2** (1) and **3** (2, 3), morphinans with a ring fused at the 5,6 positions (*e.g.* compounds such as **37**, for which we have coined the term 5,6-benzomorphinans) were one of the major objectives. Furthermore, since some

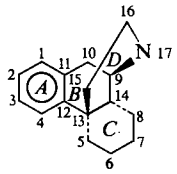

1

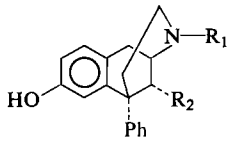

2 $R_1 = CONH_2$, $R_2 = H$
3 $R_1 = R_2 = Me$

narcotic antagonists have been found to produce analgesia with low addiction liability (for recent reviews on narcotic analgesics and antagonists see ref. 4), another objective was to synthesize morphinans with nitrogen substituents such as cyclopropylmethyl that are known to produce antagonist activity. This effect of the nitrogen substituent also inspired the synthesis of the 16,17 fused ring compound **39**.

As the basis for our synthetic scheme, we used the Grewe cyclization to form the morphinan nucleus, a reaction that has long been used for the synthesis of morphinans and benzomorphans (1, 2, 5, 6). The precursors for the Grewe cyclizations were produced by several synthetic routes.

For the first route, the dihydronaphthalene **4** (7) was condensed with formaldehyde and methylamine to give the tricyclic amine **5**.[2] Reaction of **5** with benzyl or anisyl chloride gave a quaternary salt which on treatment with phenyllithium underwent a Steven's rearrangement to the benzisoquinoline derivative **6** or **7**. The Steven's rearrangement has been used in a

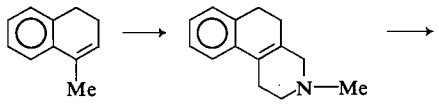

4 **5**

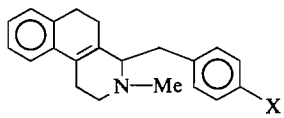

6 X = H **7** X = OMe

[1]Although the absolute configuration depicted in **1** (and following structures) is that of the natural opiates, the synthetic compounds are actually enantiomeric mixtures.

[2]Amine **5** was first synthesized by P. Rivest and M. Menard (8) of these laboratories.

Can. J. Chem. Downloaded from www.nrcresearchpress.com by 210.87.254.105 on 09/05/12
For personal use only.

Can. J. Chem. Downloaded from www.nrcresearchpress.com by 210.87.254.105 on 09/05/12
For personal use only.

similar manner for the preparation of benzomorphan precursors (1, 2, 9).

As an alternative synthesis of compounds with the skeleton of **6**, the following sequence was carried out. (It had the advantage that it was more amenable to the production of substituted derivatives of **6**.) The tetralones **8**, **9**, and **10** were treated with lithioacetonitrile (10) to give the cyano alcohols **11**, **12**, and **13**. These could be reduced, either *in situ* or as the isolated products, with lithium aluminum hydride, to the amino alcohols **14**, **15**, and **16**. The amino alcohols were readily dehydrated to the amino olefins **17**, **18**, and **19** by heating their hydro-

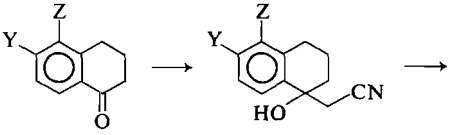

8 Y = Z = H
9 Y = OMe, Z = H
10 Y = H, Z = OMe

11 Y = Z = H
12 Y = OMe, Z = H
13 Y = H, Z = OMe

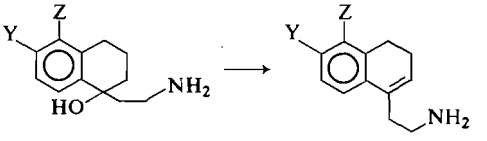

14 Y = Z = H
15 Y = OMe, Z = H
16 Y = H, Z = OMe

17 Y = Z = H
18 Y = OMe, Z = H
19 Y = H, Z = OMe

chloride salts. In fact, amino alcohol **15** dehydrated on attempted formation of its oxalate salt. The cyano alcohol **11** could be dehydrated to the exocyclic olefin **20**, but in our hands,

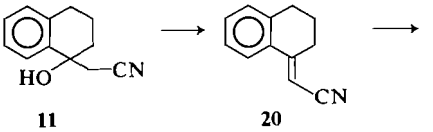

11 **20**

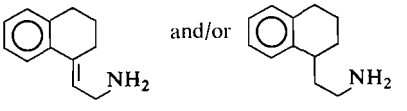

21 **22**

could only be reduced to the exocyclic olefin **21** or the fully reduced **22**, contrary to the report of Lockhart and co-workers (11), who produced endocyclic olefin **17** from **20**.

The condensation of an amine with an aldehyde (generated *in situ* from a glycidic ester) followed by acid catalyzed cyclization of the imine to an olefin to give morphinan and benzomorphan precursors has been used extensively (12). Thus the glycidic ester **23** hydrolyzed and underwent a decarboxylative rearrangement to *p*-methoxyphenylacetaldehyde under the acidic reaction conditions. The aldehyde condensed with the amine **17**, **18**, or **19** and the resulting imine cyclized to give the benzisoquinoline derivatives **24**, **25**, and **26**. The glycidic ester **23** was prepared by essentially the method of Knorr *et al.* (13).

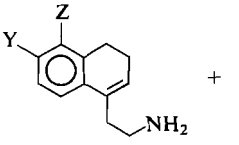

17 Y = Z = H
18 Y = OMe, Z = H
19 Y = H, Z = OMe

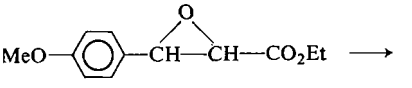

23

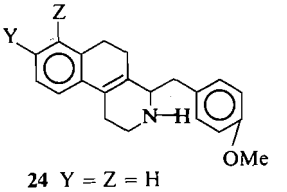

24 Y = Z = H
25 Y = OMe, Z = H
26 Y = H, Z = OMe

Because of the important effect of nitrogen substituents on the narcotic agonist–antagonist activity of morphinans, a morphinan with a ring fused to the 16,17 position was a synthetic objective. Such a compound would also be amenable to synthesis via Grewe cyclization. The pre-

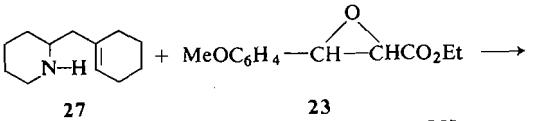

27 **23**

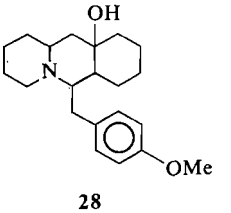

28

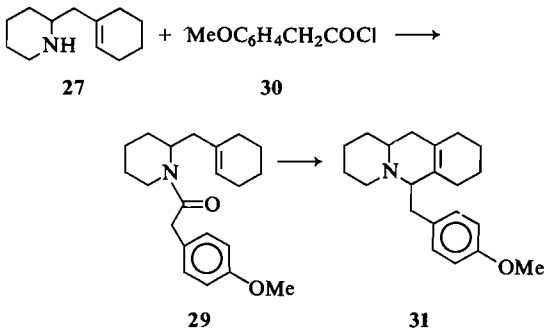

cursors were formed as follows. The piperidine **27** was prepared by the method of Prelog *et al.* (14). Picolyllithium was condensed with cyclohexanone to give a pyridine-cyclohexanol which on catalytic reduction and dehydration gave the piperidine **27**. The piperidine **27** could be converted to a suitable precursor for the Grewe cyclization by two methods. The amine–aldehyde condensation using glycidic ester **23** as the aldehyde precursor, gave the quinolizidine **28**. The yield was rather poor but this was likely due to the crystallization process used to purify **28** in which only one of its isomers was isolated. The other method used for generating a suitable quinolizidine involved a Bischler–Napieralski cyclization of an amide to an olefin. The amide **29** was prepared by acylation of amine **27** with acid chloride **30**. Treatment of amide **29** with phosphorus oxychloride (Bischler–Napieralski conditions) followed by reduction of the iminium salt with sodium borohydride gave the quinolizidine **31**.

It was found that the Grewe cyclization would not occur in the presence of a secondary amino group, so the benzisoquinolines **24**, **25**, and **26** were alkylated. Treatment of **24**, **25**, and **26** with

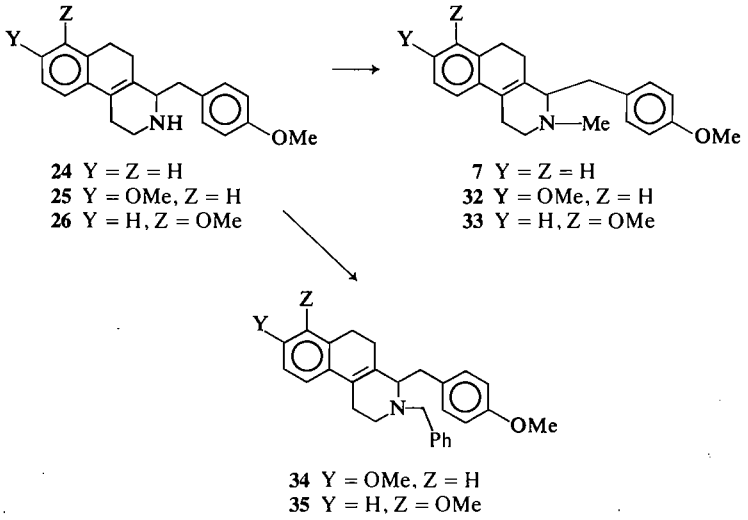

24 Y = Z = H
25 Y = OMe, Z = H
26 Y = H, Z = OMe

7 Y = Z = H
32 Y = OMe, Z = H
33 Y = H, Z = OMe

34 Y = OMe, Z = H
35 Y = H, Z = OMe

formic acid – formaldehyde (Clarke–Eschweiler conditions) gave the *N*-methyl derivatives **7**, **32**, and **33** while alkylation of **25** and **26** with benzyl bromide gave the *N*-benzyl derivatives **34** and **35**. Although *N*-cyclopropylmethyl substituted morphinans were desired, the intermediates **24**, **25**, and **26** were not alkylated with this group because of their likely instability to the strongly acidic Grewe cyclization conditions.

Several different reagents were used to carry out the Grewe cyclization. The unsubstituted morphinan **36** was synthesized by cyclization of benzisoquinoline **6** in 85% phosphoric acid (15). Strongly heating the morphinan precursors **7**, **35**, **28**, and **31** with 48% hydrobromic acid (2, 16) for 7–10 days gave the morphinans **37**, **38**, and **39**, rapid *O*-demethylation preceding the slow cyclization step. Hydrobromic acid induced *O*-demethylation was used to prepare derivatives **40** and **41** of **7** and **33**. Polyphosphoric acid cyclized the benzisoquinolines **32**, **33**, and **34** to the benzomorphinans **42**, **43**, and **44**. Attempted cyclization of **32** and **34** using hydrobromic acid failed, apparently due to instability of the inter-

Can. J. Chem. Downloaded from www.nrcresearchpress.com by 210.87.254.105 on 09/05/12
For personal use only.

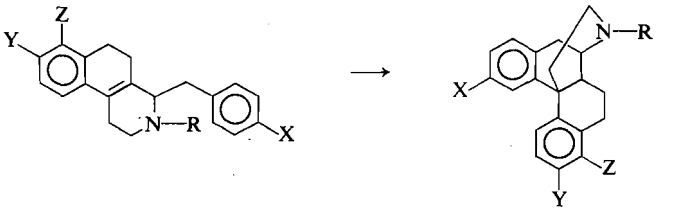

6 X = Y = Z = H, R = Me
7 X = OMe, Y = Z = H, R = Me
35 X = Z = OMe, Y = H, R = CH_2Ph
32 X = Y = OMe, Z = H, R = Me
33 X = Z = OMe, Y = H, R = Me
34 X = Y = OMe, Z = H, R = CH_2Ph
40 X = OH, Y = Z = H, R = Me
41 X = Z = OH, Y = H, R = Me

36 X = Y = H, R = Me
37 X = OH, Y = Z = H, R = Me
38 X = Z = OH, Y = H, R = CH_2Ph
42 X = Y = OMe, Z = H, R = Me
43 X = Z = OMe, Y = H, R = Me
44 X = Y = OMe, Z = H, R = CH_2Ph
45 X = Y = OH, Z = H, R = Me
46 X = Z = OH, Y = H, R = Me

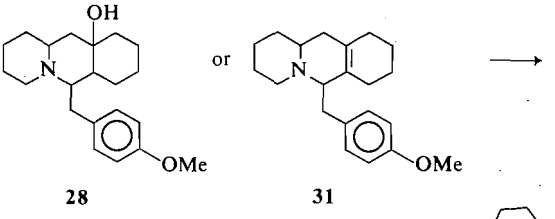

28 **31**

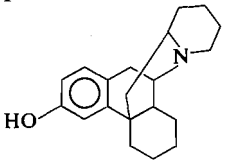

39

mediate uncyclized diphenol. Hydrobromic acid was also used to demethylate the morphinans **42** and **43** to the diphenols **45** and **46**.

In order to convert morphinan **37** into other *N*-alkyl derivatives, *N*-demethylation with cyanogen bromide (**37–49**) was carried out in the manner described by Blocke and Clarke (1) for their benzomorphan series. Secondary amine **49** was acylated with cyclopropyl or cyclobutylcarbonyl chloride to give an ester amide (*i.e.*, **50**) which was reduced with lithium aluminum hydride to the cyclopropylmethyl or cyclobutylmethyl derivatives **51** or **52**.

Rather surprisingly, we were unable to remove the *N*-benzyl groups of **44** and **38** by hydrogenolysis, despite the use of various catalysts and varying conditions of solvent and acidity. However, by analogy with *N*-dealkylations using ethyl or phenyl chloroformate (17), it was found that cyclopropylcarbonyl chloride displaced the benzyl groups to give amides **53** and **54**. The reaction was very slow and required a large excess of the acid chloride. Reduction of the amides with lithium aluminum hydride gave the cyclopropylmethyl derivatives **55** and **56**. Since hydrobromic acid would undoubtedly have cleaved the cyclopropane ring, *O*-demethylation of **55** to diphenol **57** was accomplished with boron tribromide (18).

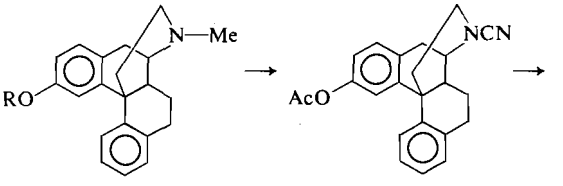

37 R = H
47 R = Ac

48

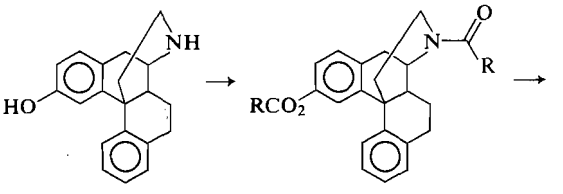

49

50*a* R = —◁
50*b* R = —◇

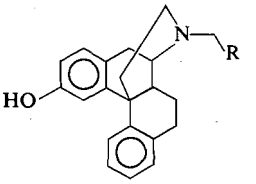

51 R = —◁
52 R = —◇

Can. J. Chem. Downloaded from www.nrcresearchpress.com by 210.87.254.105 on 09/05/12
For personal use only.

Can. J. Chem. Downloaded from www.nrcresearchpress.com by 210.87.254.105 on 09/05/12
For personal use only.

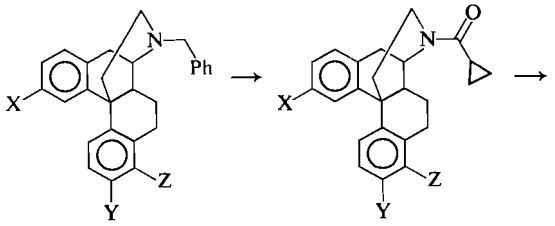

44 X = Y = OMe, Z = H
38 X = Z = OH, Y = H

53 X = Y = OMe, Z = H
54 X = Z = , Y = H

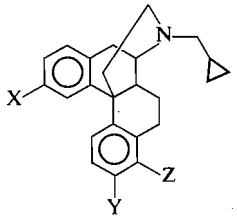

55 X = Y = OMe, Z = H
56 X = Z = OH, Y = H
57 X = Y = OH, Z = H

A modification of the benzomorphinan skeleton was accomplished by reduction of the second aromatic ring. A selective Birch reduction (19) of benzomorphinan **51** gave the diene **58**. Conditions were fairly critical: if insufficient lithium was used, (an excess being required), the reduction was incomplete, while if too large an excess was used, reduction of the phenolic ring also occurred. Catalytic hydrogenation converted **58** to **59**. It was necessary to use a pre-reduced catalyst for this step because of the tendency of the catalyst to promote disproportionation of **58** to **59** and **51**.

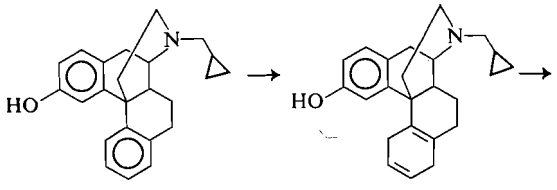

51 **58**

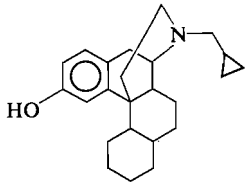

59

Structural assignments for the various new compounds follow in a straightforward manner from their mode of synthesis with confirmation provided by analyses and n.m.r. and i.r. spectra. Some trouble was had in obtaining satisfactory analyses for the phenolic morphinans. This was probably caused by difficulties in purification due to their insolubility in common solvents. The n.m.r. spectra readily indicated the success or lack of it in the Grewe cyclization by the appearance of high field methylene protons at δ 1.3–2.0 p.p.m. and the characteristic pattern due to aromatic portion **60** (see Experimental).

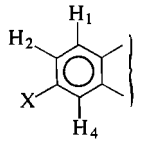

60

Although the Grewe cyclization normally gives morphinans with a *B*/*C cis* ring fusion (5, 20) it was desirable to have further proof of this for the benzomorphinans described here. Fullerton *et al.* (20) have described a method for determining the relative stereochemistry of alkyl group R_2 in a series of benzomorphans of type **61**. The quaternization of **61** with methyl iodide

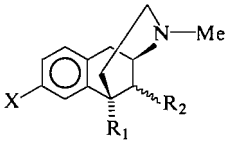

61

under carefully specified conditions was found to proceed to 85–95% of completion after 16 h for compounds with R_1/R_2 *cis* and only 5–30% for compounds with R_1/R_2 *trans*. As Table 1 shows, benzomorphinans **36** and **37** showed

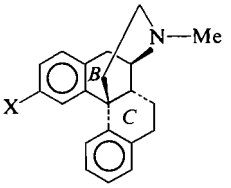

36 X = H
37 X = OH

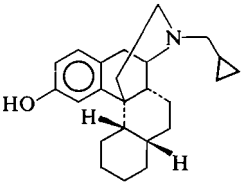

59

TABLE 1. Rate of quaternization of benzomorphinans (as % reaction)

Compound	Percentage reaction at reaction times				
	2 h	6 h	8 h	16 h	72 h
36	—	67.4	—	95.0	—
37	30.4	67.7	—	98.0	—
61*	32.5	—	75.0	91.9	—
61†	—	—	3.9	7.8	26.8

*X = OH, R_1 = *n*-propyl, R_2 = α-*n*-propyl (20).
†X = OH, R_1 = *n*-propyl, R_2 = β-*n*-propyl (20).

reaction rates comparable to R_1/R_2 *cis* of the benzomorphans when the conditions of Fullerton *et al.* (20) were followed closely, probably indicating a *B/C cis* ring junction. (Two typical examples from the work of Fullerton *et al.* (20) are included in the table.)

That the Birch reduction of **51** gave the unconjugated diene **58** is indicated by its u.v. spectrum; the spectrum (λ_{max} 282 nm, ε 1970) shows only the phenolic chromophore and no conjugated diene. The n.m.r. spectrum of **58** indicates that it is not one of the other possible unconjugated isomers. Catalytic hydrogenation of **58** probably gives the isomer shown for **59** on steric grounds but there is no proof of this.

The existence of Bohlmann bands (at 2760 cm^{-1}) in the i.r. spectra of quinolizidines **28** and **31** is evidence that they have a *trans* ring fusion (21). Although the broad phenolic absorption in the spectrum of **39** obscures the region of the Bohlmann bands, it is possible that the *trans* fusion is carried into this structure, giving the relative stereochemistry shown; rings *C*, *D*, *E* all *trans* chair conformations.

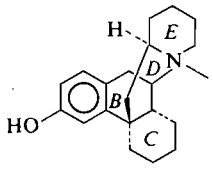

39

Table 2 shows the pharmacological activities found for the various morphinans tested. Those compounds that are active range from moderate to poor, the most interesting being **51**, which shows a balance of analgesic and antagonist activity similar to pentazocine.[3]

[3]Pentazocine is an analgesic which shows low addiction liability and which has been introduced into clinical practice in recent years.

Experimental

Melting points were determined in a Gallenkamp melting point apparatus and are not corrected. Melting points above 250 °C were determined on samples sealed in evacuated capillaries. The n.m.r. spectra were recorded with a Varian A-60A spectrometer in deuteriochloroform, or when necessary to effect solution, mixed deuteriochloroform and deuteriodimethylsulfoxide, with tetramethylsilane as internal standard. The i.r. spectra were recorded on a Unicam SP-200G spectrometer with solids as Nujol mulls. The u.v. spectra were recorded with a Unicam SP-800 spectrometer as methanol solutions. The phrase 'extracted in the usual manner' is used to indicate the following. The aqueous mixture was extracted by shaking with an equal volume of the specified solvent followed by a further extraction with half the volume of solvent. The combined organic extracts were washed with half their volume of water (and the water further extracted with a small volume of organic solvent) and in the case of ethyl acetate or ether, further washed with saturated NaCl solution. The combined organic extracts were dried over Na_2SO_4, treated with charcoal if highly colored, filtered, and the solvent evaporated under reduced pressure.

4-Benzyl- and 4-(4-Methoxybenzyl)-3-methyl-1,2,3,4,5,6-hexahydrobenz[f]isoquinoline, 6 and 7

The preparation is described for **7**; essentially the same method was used for **6**.

A solution of anisyl chloride (24) (26.7 g, 170 mmol) and amine **5** (8) (34.0 g, 170 mmol) in 100 ml of acetone was maintained at 0 °C for 1 h then at 24 °C for ½ h. The solvent was evaporated to give a foam. The powdered foam was suspended in ether (300 ml) and a solution of 220 ml of 2.2 *M* phenyllithium in 40 ml of ether and 40 ml of benzene was added with stirring at such a rate that reflux was maintained. The reaction mixture was allowed to cool to 24 °C over ½ h then cooled to 0 °C and added to ice water (550 ml). The resulting mixture was extracted with ether in the usual manner to give the crude product as an oil. The oil was mixed wih *n*-hexane (260 ml) and 3 *N* HCl (260 ml) and enough methanol added to bring the oily hydrochloride salt into solution. After separation, the aqueous layer was made basic with 25% NaOH and extracted in the usual manner with methylene chloride to give the product as an oil (57.9 g).

Amine **6** was distilled at 150–166 °C/0.05 Torr to give the product in 70% yield as a yellow oil, n.m.r. δ 1.8–3.1 (m, 11 H, methylene and methine), 2.33 (s, 3H, N—CH_3), and 6.8–7.2 (m, 9H, aromatic).

Can. J. Chem. Downloaded from www.nrcresearchpress.com by 210.87.254.105 on 09/05/12
For personal use only.

TABLE 2. Pharmacological data

	Structure					Activity ED_{50} mg/kg¶	
	R	X	Y	Z	Salt or base	Analgesic*	Antagonist†
36	CH_3	H	H	H	base	marginal	IN
37‡	CH_3	OH	H	H	base	2.5	IN
38	CH_2Ph	OH	H	OH	$2CHCl_3$	34.0	IN
42	CH_3	OCH_3	OCH_3	H	HCl	IN	IN
43	CH_3	OCH_3	H	OCH_3	HCl	IN	IN
44	CH_2Ph	OCH_3	OCH_3	H	HCl	IN	IN
45	CH_3	OH	OH	H	base	9.0	IN
46	CH_3	OH	H	OH	$\frac{1}{4}H_2O$	18.0	IN
49	H	OH	H	H	base	IN	IN
51	CH_2	OH	H	H	HCl	4.6	10.0
52	CH_2	OH	H	H	$\frac{1}{2}H_2O$	4.5	IN
55	CH_2	OCH_3	OCH_3	H	HCl	IN	IN
56	CH_2	OH	H	OH	HCl	35.0	18.5
57	CH_2	OH	OH	H	$\frac{1}{2}CH_3OH$	IN	IN
58	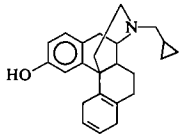				$\frac{1}{2}C_2H_5OH$	25.0	15.5
59	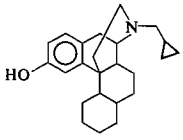				base	26.0	10.0
39§	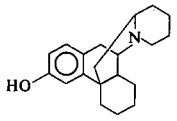				base	IN	IN
Pentazocine	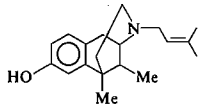				base	5.0	12.0

*Analgesic activity was measured by the 'mouse writhing' test (22).
†Antagonist activity was measured by the 'morphine antagonist (rat tail flick)' test (23).
‡Compound **37** produced tremors at 40 mg/kg.
§Compound **39** produced ataxia at 20 mg/kg.
¶IN indicates no significant analgesic or antagonist activity.

The amine **7** was purified via its picrate salt (recrystallized from acetone, m.p. 210–212 °C (dec.)) to give a yellow-brown solid (22.9 g, 42% yield). Amine **7** had n.m.r. δ 1.9–3.1 (m, 11H, methylene and methine), 2.35 (s, 3H, N—CH_3), 3.70 (s, 3H, OCH_3), and 6.6–7.2 (m, 8H, aromatic).

Heating **7** under reflux for 3 h with 48% HBr gave the phenol **40** as its hydrobromide salt. The salt was re-

Can. J. Chem. Downloaded from www.nrcresearchpress.com by 210.87.254.105 on 09/05/12
For personal use only.

Can. J. Chem. Downloaded from www.nrcresearchpress.com by 210.87.254.105 on 09/05/12
For personal use only.

crystallized from ethanol–acetonitrile, m.p. 264–265 °C (dec.), 74% yield.

Anal. Calcd. for $C_{21}H_{23}NO{\cdot}HBr$: C, 65.29; H, 6.26; N, 3.63; Br, 20.68. Found: C, 65.38; H, 6.40; N, 3.62; Br, 20.83.

*7- and 8-Methoxy-4-(2-aminoethyl)-1,2-dihydronaphthalene, **17**, **18**, and **19***

A 1.67 *M* solution of *n*-butyllithium in hexane (288 ml, 0.48 mol) was cooled to −78 °C and 240 ml of tetrahydrofuran (THF) was added. A solution of acetonitrile (24 ml, 0.46 mol) in 360 ml of THF was added over 20 min. The mixture was stirred for 1 h at −78 °C and a solution of methoxytetralone **9** or **10** (70.4 g, 0.40 mol) or tetralone **8** (58.5 g, 0.40 mol) in 400 ml of THF was added over 15 min. The cold bath was removed and stirring was continued for another 15 min. Lithium aluminum hydride (18 g, 0.48 mol) was added and the mixture was stirred at 24 °C for 3 h, then cooled to 0 °C. Water (18 ml) was added cautiously followed by 13.5 ml of 20% NaOH and 63 ml of water. The mixture was stirred at 24 °C for 15 min and the inorganic salts were filtered off. The ether solution was extracted with 10% HCl (2 × 500 + 200 ml) and the aqueous layers were made basic with 25% NaOH and extracted in the usual manner with ether (3 × 500 ml) to give a yellow oil. A benzene solution of the oil was saturated with HCl (gas) and refluxed under a water separator until water ceased to pass over. The mixture was cooled to 10 °C and the crystalline hydrochloride salt was collected in approximately 70% overall yield.

The free base **17** had n.m.r. δ 0.98 (s, 2H, NH_2), 2.0–3.0 (m, 8H, methylene), 5.85 (t, 1H, J = 4 Hz, olefin), and 7.1 (m, 4H, aromatic).

The free base **18** had n.m.r. δ 0.93 (s, 2H, NH_2), 2.0–3.0 (m, 8H, methylene), 3.79 (s, 3H, OCH_3), 5.78 (t, 1H, J = 4.5 Hz, olefin), 6.7 (m, 2H, aromatic), and 7.20 (d, 1H, J = 9.5 Hz, aromatic). The oxalate salt had m.p. 272–275 °C (dec.).

Anal. Calcd. for $C_{13}H_{13}NO{\cdot}\frac{1}{2}C_2H_2O_4$: C, 67.72; H, 7.31; N, 5.64. Found: C, 67.87; H, 7.33; N, 5.55.

The free base **19** had n.m.r. δ 1.08 (s, 2H, NH_2), 2.0–3.0 (m, 8H, methylene), 3.73 (s, 3H, OCH_3), 5.80 (t, 1H, J = 4 Hz, olefin), and 6.5–7.1 (m, 3H, aromatic). Its hydrochloride salt had m.p. 218–220 °C (dec.).

Anal. Calcd. for $C_{13}H_{17}NO{\cdot}HCl$: C, 65.14; H, 7.57; N, 5.84; Cl, 14.78. Found: C, 65.13; H, 7.44; N, 5.69; Cl, 14.61.

*Ethyl-3-(4-methoxyphenyl)-2,3-epoxypropionate, **23***

Ethanol free sodium ethoxide (prepared from 10.0 g (0.432 g atom) of sodium) was mixed with 200 ml of toluene and cooled to 0 °C. A solution of *p*-methoxybenzaldehyde (56.0 g, 0.412 mol) and ethyl chloroacetate (50.5 g, 0.412 mol) in 200 ml of toluene was added at such a rate that the temperature remained below 10 °C. The mixture was stirred at 24 °C for 16 h, washed with water (2 × 400 ml), dried (Na_2SO_4), and the solvent evaporated to give a yellow liquid of about 80% purity (81.2 g). The liquid solidified on standing at 5 °C and could be partially purified by washing with a small volume of cold ethanol to give pale yellow crystals of **23**; m.p. 40–43 °C; i.r. ν_{max} 1750 (ester) cm^{-1}; n.m.r. δ 1.28 (t, 3H, J = 7 Hz, $CO_2CH_2CH_3$), 3.33 and 3.93 (d, 1H each, J = 1.5 Hz, methines of epoxide), 3.73 (s, 3H, OCH_3), 4.20 (q, 2H, J = 7 Hz, $CO_2CH_2CH_3$), and 6.80 and 7.13 (d, 2H each, J = 8.5 Hz, aromatic).

*7- and 8-Methoxy-4-(4-methoxybenzyl)-1,2,3,4,5,6-hexahydrobenz[f]isoquinoline, **24**, **25**, and **26***

A mixture of the hydrochloride salt of **17**, **18**, or **19** (0.138 mol) in water (800 ml) was acidified to p*H* 3 by the addition of HCl (aqueous). The resulting mixture was heated under reflux (under nitrogen) and with vigorous stirring a solution of glycidic ester **23** (38.0 g, 0.172 mol) in 200 ml of ethanol was added dropwise over a period of 8 h. Reflux was maintained for 16 h, 300 ml of concentrated HCl was added and reflux was continued for a further 4 h. The mixture was allowed to cool, seeded to induce crystallization, then cooled to 0 °C. The hydrochloride salt was collected and recrystallized from methanol to give the product **25** or **26** (37.2 g, 71% yield). In the case of **24**, after the final period of reflux benzene, hexane, and methanol were added, the mixture shaken and the aqueous layer separated. The aqueous layer was made basic and extracted with methylene chloride in the usual way to give **24** (56% yield) which had n.m.r. δ 1.97 (s, 1H, NH), 2.1–3.3 (m, 11H, methylene and methine), 3.80 (s, 3H, OCH_3), and 6.8–7.4 (m, 8H, aromatic).

The free base **25** had n.m.r. δ 1.90 (s, 1H, NH), 2.2–3.3 (m, 11H, methylene and methine), 3.83 (s, 6H, OCH_3), and 6.7–7.4 (m, 7H, aromatic). The hydrochloride salt of **25** had m.p. 241–243 °C (dec.).

Anal. Calcd. for $C_{22}H_{25}NO_2{\cdot}HCl$: C, 71.05; H, 7.05; N, 3.77; Cl, 9.53. Found: C, 71.13; H, 7.14; N, 3.75; Cl, 9.75.

The free base **26** had n.m.r. δ 1.56 (s, 1H, NH), 2.1–3.3 (m, 11H, methylene and methine), 3.68 and 3.73 (s, 3H each, OCH_3), and 6.5–7.1 (m, 7H, aromatic). The hydrochloride salt of **26** had m.p. 254–256 °C (dec.).

Anal. Calcd. for $C_{22}H_{25}NO_2{\cdot}HCl$: C, 71.05; H, 7.05; N, 3.77; Cl, 9.53. Found: C, 71.06; H, 7.17; N, 3.79; Cl, 9.77.

*7- and 8-Methoxy-4-(4-methoxybenzyl)-3-methyl-1,2,3,4,5,6-hexahydrobenz[f]isoquinoline, **7**, **32**, and **33***

A solution of 85% formic acid (1.30 g) and 37% formaldehyde (2.16 g) was added slowly with cooling to 10 mmol of the secondary amine **24**, **25**, or **26** (as their free bases). The mixture was heated gently until CO_2 evolution ceased and was then heated under reflux for 5 h. The mixture was allowed to cool, 10% NaOH (20 ml) was added and the mixture was extracted in the usual way with methylene chloride to give the *N*-methyl amine **7**, **32**, or **33** as a yellow oil (90–95% yield).

Amine **32** had n.m.r. δ 1.9–3.2 (m, 11H, methylene and methine), 2.33 (s, 3H, NCH_3), 3.60 and 3.62 (s, 3H each, OCH_3), and 6.5–7.2 (m, 7H, aromatic).

Amine **33** had n.m.r. δ 1.9–3.3 (m, 11H, methylene and methine), 2.43 (s, 3H, NCH_3), 3.77 and 3.82 (s, 3H each, OCH_3), and 6.7–7.4 (m, 7H, aromatic).

Heating **33** under reflux for 3 h with 48% HBr followed by base treatment (concentrated NH_4OH) and extraction in the usual manner with ethyl acetate gave the diphenol **41**, recrystallized from acetone, m.p. 110 °C (dec.).

Anal. Calcd. for $C_{21}H_{23}NO_2{\cdot}C_3H_6O$: C, 75.96; H, 7.70; N, 3.69. Found: C, 75.99; H, 7.84; N, 3.64.

Can. J. Chem. Downloaded from www.nrcresearchpress.com by 210.87.254.105 on 09/05/12
For personal use only.

7- and 8-Methoxy-4-(4-methoxybenzyl)-3-benzyl-1,2,3,4,5,6-hexahydrobenz[f]isoquinoline, 34 and 35

A solution of benzyl bromide (1.3 ml, 11 mmol) in 10 ml of benzene was added over 1.75 h to a refluxing solution of **25** or **26** (3.35 g, 10 mmol) and triethylamine (2.0 ml, 14.6 mmol) in 33 ml of benzene. The solution was heated under reflux for another 4 h, then left at 24 °C for 16 h. The resulting mixture was washed with water (3 × 20 ml), dried, and the solvent evaporated to give the product **34** or **35** as a yellow oil (3.7 g, 85% yield). Amine **34** had n.m.r. δ 1.9–3.2 (m, 11H, methylene and methine), 3.63 (s, 2H, benzyl CH_2), 3.73 (s, 6H, OCH_3), and 6.6–7.1 (m, 12H, aromatic). Amine **35** had n.m.r. δ 1.9–3.2 (m, 11H, methylene and methine), 3.63 (s, 2H, benzyl CH_2), 3.72 and 3.75 (s, 3H each, OCH_3), and 6.5–7.1 (m, 12H, aromatic). The hydrochloride salt of **35** (recrystallized from acetone) had m.p. 201–202 °C.

Anal. Calcd. for $C_{29}H_{31}NO_2 \cdot HCl$: C, 75.39; H, 6.98; N, 3.03; Cl, 7.67. Found: C, 75.63; H, 7.03; N, 3.08; Cl, 7.78.

17-Methyl-5,6-benzomorphinan, 36

Amine **6** (10 g) was stirred with 100 ml of 85% phosphoric acid under nitrogen at 150 °C for 43 h. The cooled mixture was poured into ice water (600 ml), made basic with 50% NaOH and extracted with methylene chloride in the usual manner to give a brown oil (9.8 g). The oil was chromatographed on grade II alumina (750 g); elution with benzene–chloroform 9:1 gave the product as a pale brown solid (4.75 g, 47.5% yield). Recrystallization from hexane–cyclohexane gave **36** as cubic crystals, m.p. 95.5–97 °C; n.m.r. δ 1.5–3.1 (m, 12H, methylene and methine), 2.39 (s, 3H, N—CH_3), and 6.8–7.7 (m, 8H, aromatic).

Anal. Calcd. for $C_{21}H_{23}N$: C, 87.15; H, 8.01; N, 4.84. Found: C, 87.34; H, 8.06; N, 4.78.

3-Hydroxy-17-methyl-5,6-benzomorphinan, 37 and 3,18-dihydroxy-17-benzyl-5,6-benzomorphinan, 38

A mixture of amine **7** or **35** (10 g) was heated under nitrogen at 135–140 °C for 10 days with 48% HBr (100 ml). The cooled mixture was poured into ice water (200 ml), made basic with concentrated NH_4OH and extracted with chloroform or ethyl acetate in the usual manner to give the crude product, **37** or **38**.

Benzomorphinan **37** was recrystallized from benzene–ethanol to give crystals (4.66 g, 49%) with m.p. 243–245 °C (dec.); i.r. ν_{max} 2500–3100 (H-bonded OH) cm^{-1}; n.m.r. δ 1.5–3.0 (m, 12H, methylene and methine), 2.27 (s, 3H, NCH_3), 6.30 (d, 1H, J = 2 Hz, H_4) 6.53 (d of d, 1H, J = 8.5 and 2 Hz, H_2), 6.94 (d, 1H, J = 8.5 Hz, H_1), 7.1–7.6 (m, 4H, aromatic), and 8.96 (s, 1H, OH).

Anal. Calcd. for $C_{21}H_{23}NO$: C, 82.58; H, 7.59; N, 4.59. Found: C, 82.78; H, 7.54; N, 4.57.

Benzomorphinan **38** (10 g) was chromatographed on 2 kg of silicic acid (elution with chloroform–methanol 9:1) to give 6.0 g (64%) of colorless solid with n.m.r. δ 1.5–3.1 (m, 12H, methylene and methine), 3.73 (s, 2H, NCH_2Ph), and 6.4–7.4 (m, 13H, aromatic + OH).

18- and 19-Methoxy-17-methyl-3,6-benzomorphinan, 42 and 43 and 19-Methoxy-17-benzyl-5,6-benzomorphinan, 44

A mixture of the amine **32**, **33**, or **34** (8.0 g) and polyphosphoric acid (40 g) was heated at 100 °C with stirring for 6 h. To the cooled mixture, 50 ml of water followed by 250 ml of 25% NaOH were added cautiously. The resulting mixture was extracted in the usual manner with ethyl acetate to give an orange oil (4 to 5 g).

The benzomorphinans **42** and **43** were purified by chromatography on silica gel (1 kg, elution with chloroform–methanol 9:1) to give 2.7 to 2.9 g (34 to 36% yield) of colorless solid.

Benzomorphinan **42** had n.m.r. δ 1.5–3.1 (m, 12H, methylene and methine), 2.43 (s, 3H, NCH_3), 3.57 and 3.73 (s, 3H each, OCH_3), and 6.5–7.5 (m, 6H, aromatic).

Benzomorphinan **43** was recrystallized from ethyl acetate to give crystals with m.p. 143–145 °C, n.m.r. δ 1.5–3.1 (m, 12H, methylene and methine), 2.43 (s, 3H, NCH_3), 3.59 and 3.77 (s, 3H each, OCH_3), and 6.4–7.3 (m, 6H, aromatic).

Anal. Calcd. for $C_{23}H_{27}NO_2$: C, 79.05; H, 7.79; N, 4.01. Found: C, 79.12; H, 7.96; N, 3.81.

The crude *N*-benzylbenzomorphinan **44** was converted to its hydrochloride salt and recrystallized from acetone to give a 21% yield of moderately pure product. The free base of **44** had n.m.r. δ 1.5–3.1 (m, 12H, methylene and methine), 2.14 (s, 3H, NCH_3), 3.62 and 3.79 (s, 3H each, OCH_3), 3.73 (s, 2H, NCH_2Ph), and 6.5–7.6 (m, 11H, aromatic).

3,18- and 3,19-Dihydroxy-17-methyl-5,6-benzomorphinans, 45 and 46

A mixture of the dimethoxybenzomorphinan **42** or **43** (1.72 g) and 17 ml of 48% HBr was heated under reflux for 3 h. The solution was cooled to 0 °C and 150 ml of water followed by 150 ml of concentrated NH_4OH were added. The resulting mixture was extracted in the usual manner with ethyl acetate to give the diphenol **45** or **46** (1.5 g, 95% yield) as a brown solid. The products were recrystallized from ethyl acetate.

Diphenol **45** had m.p. 287–289 °C; n.m.r. δ 1.4–3.2 (m, 12H, methylene and methine), 2.32 (s, 3H, NCH_3), 6.3–7.4 (m, 6H, aromatic), and 8.3 (br, 2H, OH).

Anal. Calcd. for $C_{21}H_{23}NO_2$: C, 78.47; H, 7.21; N, 4.36. Found: C, 78.20; H, 7.26; N, 4.27.

Diphenol **46** had m.p. 307–309 °C; n.m.r. δ 1.4–3.2 (m, 12H, methylene and methine), 2.33 (s, 3H, NCH_3), 6.3–7.1 (m, 6H, aromatic), and 8.3 (br, 2H, OH).

Anal. Calcd. for $C_{21}H_{23}NO_2 \cdot \frac{1}{4}H_2O$: C, 77.39; H, 7.27; N, 4.30. Found: C, 77.54; H, 7.26; N, 4.20.

3-Acetoxy-17-methyl-5,6-benzomorphinan, 47

The benzomorphinan **37** was converted to its acetate **47** in virtually quantitative yield by the method of Block and Clarke (1). The product had i.r. ν_{max} 1770 (acetate) cm^{-1}; n.m.r. δ 1.5–3.1 (m, 12H, methylene and methine), 2.17 (s, 3H, CH_3CO_2), 2.47 (s, 3H, NCH_3), and 6.6–7.7 (m, 7H, aromatic).

3-Acetoxy-17-cyano-5,6-benzomorphinan, 48

The acetoxy benzomorphinan **47** was *N*-demethylated with cyanogen bromide by the method of Block and Clarke (1) to give the cyano compound **48** in quantitative yield, which had i.r. ν_{max} 2220 (N—CN), and 1770 (acetate) cm^{-1}; n.m.r. δ 1.5–3.9 (m, 12H, methylene and methine), 2.20 (s, 3H, CH_3CO_2), and 6.7–7.6 (m, 7H, aromatic).

Can. J. Chem. Downloaded from www.nrcresearchpress.com by 210.87.254.105 on 09/05/12
For personal use only.

3-Hydroxy-5,6-benzomorphinan, 49

The acetoxy-cyano compound **48** was reduced with lithium aluminum hydride by the method of Block and Clarke (1) to give the benzomorphinan **49** in high yield. The product was recrystallized from methanol to give crystals with m.p. 301–304 °C (dec.); i.r. ν_{max} 3280 (NH), and 2400–3300 (hydrogen bonded OH) cm^{-1}; n.m.r. δ 1.4–3.2 (m, 12H, methylene and methine) 4.6 (br, 1H, NH), 6.08 (d, 1H, J = 2.5 Hz, H_4), 6.25 (d of d, 1H, J = 8.5 and 2.5 Hz, H_2), 6.70 (d, 1H, J = 8.5 Hz, H_1), and 7.0–7.6 (m, 5H, aromatic and OH).

3-Hydroxy-17-cyclopropylmethyl and Cyclobutylmethyl-5,6-benzomorphinans, 51 and 52

The procedure is described for **51** but essentially the same method was used for **52**.

A solution of cyclopropylcarbonyl chloride (4.2 g, 40 mmol) in 20 ml of methylene chloride was added over 10 min to a slurry of benzomorphinan **49** (5.4 g, 18.5 mmol) and pyridine (7.0 ml, 40 mmol) in 30 ml of methylene chloride. The solution was stirred at 24 °C for 30 min and washed with water, 10% aqueous $NaHCO_3$, 10% HCl, and water. The solvent was evaporated to give the crude ester amide **50** (6.4 g) as a yellow foam. The product had i.r. ν_{max} 1760 (ester), and 1645 (amide) cm^{-1}.

A solution of the amide **50** (6.4 g, 15 mmol) in 100 ml of THF was added over 10 min to a slurry of lithium aluminum hydride (3.5 g, 92 mmol) in 30 ml of THF. The mixture was heated under reflux for 1 h, allowed to cool, and saturated NaCl (18.5 ml) was added dropwise. THF (30 ml) was added and the mixture was heated under reflux for 30 min. Inorganic salts were filtered from the cooled mixture and the solvent was evaporated to give the crude product. The product was purified by trituration with benzene–ethanol to give benzomorphinan **51** as an almost colorless powder (2.51 g, 49% yield) which had m.p. 263–265 °C; i.r. ν_{max} 2400–3100 (hydrogen bonded OH) cm^{-1}; n.m.r. δ 0–1.3 (m, 5H, cyclopropyl), 1.5–3.5 (m, 14H, methylene and methine), 6.43 (d, 1H, J = 2.5 Hz, H_4), 6.58 (d of d, 1H, J = 8 and 2.5 Hz, H_2), 6.97 (d, 1H, J = 8 Hz, H_1), and 7.1–7.7 (m, 5H, aromatic + OH).

The cyclobutylbenzomorphinan **52** was recrystallized from dioxane–water and had m.p. 224–225 °C; n.m.r. δ 1.5–3.0 (m, 21H, methylene and methine), 6.32 (d, 1H, J = 2 Hz, H_4), 6.47 (d of d, 1H, J = 8 and 2 Hz, H_2), 6.83 (d, 1H, J = 8 Hz, H_1), and 7.0–7.6 (m, 4H, aromatic).

Anal. Calcd. for $C_{25}H_{29}NO \cdot \frac{1}{2}H_2O$: C, 81.48; H, 8.21; N, 3.80. Found: C, 81.63; H, 8.27; N, 3.80.

3,19-Dimethoxy-17-cyclopropylcarbonyl-5,6-benzomorphinan, 53

A solution of the benzylamine **44** (4.0 g, 9.4 mmol) in 40 ml toluene was heated under reflux and 3 portions of cyclopropylcarbonyl chloride (1 ml each) were added at 5 h intervals. The mixture was cooled, washed with dilute NaOH, dried, then reacted further by addition of 5 portions of acid chloride (1 ml each) at 5 h intervals (except for two overnight reflux periods). The cooled mixture was washed with dilute NaOH and two times with 3 *N* HCl (aqueous) – methanol. The solvent was evaporated to give the crude amide **53** as a brown foam (2.64 g, 69% yield). The product had i.r. ν_{max} 1640 (amide) cm^{-1}; n.m.r. δ 0.5–1.1 (m, 4H, cyclopropyl), 1.5–3.2 (m, 13H, methylene and methine), 3.63 and 3.80 (s, 3H each, OCH_3), and 6.5–7.6 (m, 6H, aromatic).

3,19-Dimethoxy-17-cyclopropylmethyl-5,6-benzomorphinan, 55

Lithium aluminum hydride (600 mg, 16 mmol) was added to a solution of amide **53** (3.1 g, 7.7 mmol) in 45 ml of THF and the stirred mixture was heated under reflux for 2.25 h. The mixture was cooled to 0 °C and 0.6 ml of water followed by 0.6 ml of 25% NaOH and 2.4 ml of water was added cautiously. The mixture was stirred for 15 min, the inorganic salts were filtered off, and the solvent was evaporated. The crude product (as its hydrochloride salt) was recrystallized from methanol–chloroform to give pure amine (HCl salt) **55** (2.24 g, 68% yield) with m.p. 307–309 °C; n.m.r. (on free base) δ −0.1–1.3 (m, 5H, cyclopropyl), 1.4–3.3 (m, 14H, methylene and methine), 3.62 and 3.78 (s, 3H each, OCH_3), and 6.5–7.6 (m, 6H, aromatic).

Anal. Calcd. for $C_{26}H_{31}NO \cdot HCl$: C, 73.31; H, 7.57; N, 3.29; Cl, 8.32. Found: C, 73.19; H, 7.63; N, 3.29; Cl, 8.22.

3,19-Dihydroxy-17-cyclopropylmethyl-5,6-benzomorphinan, 57

A solution of the methoxy compound **55** (1.3 g, 3.3 mmol) in 25 ml of methylene chloride was added over 30 min to a solution of boron tribromide (0.95 ml, 2.48 g, 9.9 mmol) in 12 ml of methylene chloride under nitrogen at −78 °C. The resulting mixture was stirred at 24 °C for 3 h, then poured into ice and concentrated NH_4OH. The methylene chloride was separated and the aqueous layer was extracted with ethyl acetate – methanol in the usual manner (the methylene chloride solution was combined with the other organic extracts) to give the crude product. The product was recrystallized from methanol–acetone to give diphenol **57** (490 mg, 41% yield) with m.p. 285–287 °C (dec.); n.m.r. δ −0.2–1.1 (m, 5H, cyclopropyl), 1.4–4.0 (m, 14H, methylene and methine) 6.3–7.5 (m, 6H, aromatic), and 8.9 (br, 2H, OH).

Anal. Calcd. for $C_{24}H_{27}NO_2 \cdot \frac{1}{2}CH_4O$: C, 77.95; H, 7.74; N, 3.71. Found: C, 78.25; H, 7.66; N, 3.64.

3,18-Dihydroxy-17-cyclopropylmethyl-5,6-benzomorphinan, 56

A solution of cyclopropylcarbonyl chloride (1.84 g, 17.7 mmol) in 10 ml of chloroform was added over 15 min to a mixture of diphenol **38** (3.1 g, 7.7 mmol) and pyridine (1.44 g, 18.2 mmol) in 30 ml of chloroform. The mixture was stirred at 24 °C for 1 h, washed with water, dilute $NaHCO_3$, and water, then dried. The solvent was evaporated to give the crude diester (4.1 g) as an orange oil.

The oil was treated with repeated quantities of the acid chloride in the same manner as **53** was prepared. The resulting diester amide **54** had i.r. ν_{max} 1750 (ester), and 1630 (amide) cm^{-1}; n.m.r. δ 0.4–1.4 (m, 12H, cyclopropyl), 1.4–3.8 (m, 15H, methylene and methine), and 6.7–7.5 (m, 6H, aromatic).

The diester amide **54** was reduced with lithium aluminum hydride in the same manner as **55** to give the diphenol **56** as a brown powder which had m.p. 257–260 °C; n.m.r. δ −0.1–1.0 (m, 5H, cyclopropyl), 1.5–3.5 (m, 14H, methylene and methine), and 6.5–7.5 (m, 6H, aromatic).

Can. J. Chem. Downloaded from www.nrcresearchpress.com by 210.87.254.105 on 09/05/12
For personal use only.

3-Hydroxy-17-cyclopropylmethyl-18,21-dihydro-5,6-benzomorphinan, 58

Lithium (500 mg, 72 mmol) was added in small portions to a slurry of phenol **51** (2.51 g, 7.3 mmol) in 25 ml of dimethoxyethane and 50 ml of liquid ammonia at −78 °C. The mixture was stirred at the ammonia reflux temperature for 1 h. A solution of *tert*-butyl alcohol (7.4 g, 100 mmol) in 15 ml of dimethoxyethane was added over 15 min and the resulting mixture was stirred for 2 h while the ammonia evaporated. Ethanol (5 ml) was added and after a further 30 min stirring, dilute HCl was added until the mixture was acidic. The mixture was made basic with concentrated NH_4OH and extracted in the usual manner with chloroform to give the crude diene **58** as a brown solid (2.34 g, 93%). The product was recrystallized from ethanol–chloroform to give material with m.p. 240–243 °C (dec.); i.r. ν_{max} 2400–3200 (hydrogen bonded OH) cm^{-1}; u.v. λ_{max}^{MeOH} 282 nm (ε 1970); n.m.r. δ −0.1–1.1 (m, 5H, cyclopropyl), 1.2–3.3 (m, 18H, methylene and methine), 5.84 (m, 2H, olefin), and 6.5–7.1 (m, 3H, aromatic).

Anal. Calcd. for $C_{24}H_{29}NO \cdot \frac{1}{2}C_2H_6O$: C, 81.05; H, 8.71; N, 3.78. Found: C, 80.93; H, 8.61; N, 3.78.

3-Hydroxy-17-cyclopropylmethyl-5,6-butanomorphinan, 59

A mixture of crude diene **58** (1.14 g) and pre-hydrogenated 10% palladium-on-charcoal (1.0 g) in 100 ml of methanol was hydrogenated in a Parr shaker at 24 °C and 4 atm pressure. After the rapid uptake of hydrogen had ceased, the catalyst was filtered off and the solution concentrated. Crystalline morphinan **59** (530 mg, 46%) was collected and recrystallized from methanol to give material with m.p. 222–224 °C (dec.); n.m.r. δ −0.1–1.0 (m, 5H, cyclopropyl), 1.1–3.2 (m, 24H, methylene and methine), 6.58 (d of d, 1H, J = 8 and 2 Hz, H_2), 6.77 (d, 1H, J = 2 Hz, H_4), and 6.88 (d, 1H, J = 8 Hz, H_1).

1-(2-Piperidylmethyl)-cyclohexene, 27

The piperidine **27** was prepared in 63% overall yield from α-picoline by the method of Prelog *et al.* (14) and had i.r. ν_{max} 3200–3100 (NH) cm^{-1}; n.m.r. δ 0.9–3.2 (m, 19H, methylene and methine), 1.33 (s, 1H, NH), and 5.50 (br, 1H, olefin).

4-(4-Methoxybenzyl)-2-hydroxy-2,3-butanoquinolizidine, 28

A mixture of amine **27** (18 g, 0.10 mol) and 550 ml water was acidified to p*H* 3 by the addition of concentrated HCl. To the stirred, refluxing mixture was added a solution of the glycidic ester **23** (41 g, containing *ca.* 0.15 mol) in 180 ml ethanol over a period of 4 days. Methanol and HCl were added to the mixture and it was washed twice with benzene–hexane. The aqueous layer was made basic with 25% NaOH and extracted in the usual manner with methylene chloride to give the crude product (22 g). Since this material contained more than 50% starting material (by n.m.r.), it was dissolved in methylene chloride and treated for 30 min at 24 °C with trifluoroacetic anhydride. The resulting solution was extracted with dilute HCl containing methanol. The aqueous layers were washed with benzene–hexane, made basic with NaOH and extracted in the usual way with methylene chloride to give the amine **28** (9.5 g) as a brown oil. The amine was purified via its hydrochloride salt, crystallized from toluene (4.4 g, 12% yield) and recrystallized from ethyl acetate – methanol to give crystals with m.p. 241–243 °C (dec.). The free base **28** had i.r. ν_{max} 3350 (OH), 2800, 2760, and 2680 (w) (Bohlmann bands) cm^{-1}; n.m.r. δ 0.9–3.5 (m, 24H, aliphatic + OH), 3.74 (s, 3H, OCH_3), and 6.79 and 7.18 (d, 2H each, J = 9 Hz, aromatic).

Anal. Calcd. for $C_{21}H_{31}NO_2 \cdot HCl$: C, 68.93; H, 8.82; N, 3.83; Cl, 9.69. Found: C, 68.79; H, 8.95; N, 3.75; Cl, 9.58.

1-(1-(4-Methoxyphenylacetyl)-2-piperidylmethyl)-cyclohexene, 29

para-Methoxyphenylacetyl chloride **30** was prepared from *p*-methoxyphenylacetic acid and thionyl chloride and obtained as an unstable yellow liquid, b.p. 88–90 °C/0.2 Torr.

A solution of the acid chloride **30** (26.6 g, 0.145 mol) in 54 ml of benzene was added over 15 min to a solution of piperidine **27** (22.2 g, 0.124 mol) and triethylamine (37 ml, 0.27 mol) in 67 ml of benzene at 5 °C. The mixture was stirred at 24 °C for 30 min and then heated under reflux for 30 min. The cooled mixture was washed with 2 *N* HCl (400 + 200 ml), 10% NaOH (5 × 100 ml) and water (100 ml). The solvent was evaporated to give the amide **29** as a yellow oil (35.0 g, 74%) which had i.r. ν_{max} 1630 (amide) cm^{-1}; n.m.r. δ 1.2–3.0 (m, 19H, methylene and methine), 3.70 (s, 2H, $COCH_2Ar$), 3.84 (s, 3H, OCH_3), 5.52 (br, 1H, olefin), and 6.97 and 7.30 (d, 2H each, J = 9 Hz, aromatic).

4-(4-Methoxybenzyl)-2,3-butano-2,3-dehydroquinolizidine, 31

A solution of amide **29** (28.5 g, 87.5 mmol) and phosphorus oxychloride (28.5 ml, 47.6 g, 311 mmol) in 285 ml of toluene was heated under reflux for 5 h. The cooled solution was washed with 25% NaOH (until the washings remained basic) and with water. Evaporation of the solvent gave a brown oil. A solution of the oil in 230 ml of ethanol was acidified to p*H* 2 with concentrated HCl, cooled to 0 °C and sodium borohydride (5.7 g, 150 mmol) was added in small portions over 1 h. The mixture was stirred for 16 h at 24 °C, then concentrated to an oily residue. The residue was mixed with 2% NaOH and extracted in the usual manner with methylene chloride to give a brown oil. The oil was dissolved in benzene–hexane and extracted with 3 *N* HCl containing methanol. The aqueous layer was washed with benzene–hexane, made basic with 50% NaOH and extracted with benzene in the usual way to give the crude product as a brown oil. The product was purified by forming its picrate salt, which was recrystallized from acetone (m.p. 163–166 °C (dec.)). The free base **31** was obtained as a pale yellow oil (6.0 g, 19% overall yield from piperidine **27**) which had i.r. ν_{max} 2920, 2860, 2840, 2810, 2780, 2760, and 2680 cm^{-1}; n.m.r. δ 1.0–3.4 (m, 22H, methylene and methine), 3.83 (s, 3H, OCH_3), and 6.87 and 7.83 (d, 2H each, J = 9 Hz, aromatic).

3-Hydroxy-16,17-butanomorphinan, 39

The procedure is described for amine **31**; the same method was used to convert the hydrochloride salt of **28** to morphinan **39**.

A mixture of the amine **31** (6.0 g, 19.3 mmol), in 60 ml of 48% HBr was heated under reflux for 7 days. The cooled mixture was made basic with concentrated NH_4OH and

extracted in the usual manner with chloroform to give the crude product as a brown tar. The tar was crystallized from ethyl acetate to give the morphinan **39** (1.2 g, 21% yield) which had m.p. 195–197 °C (dec.); i.r. ν_{max} 2500–3300 (hydrogen bonded OH) cm^{-1}; n.m.r. δ 0.5–3.0 (m, 23H, aliphatic), 6.40 (d of d, 1H, J = 8 and 2 Hz, H_2), 6.58 (d, 1H, J = 2 Hz, H_4), 6.68 (d, 1H, J = 8 Hz, H_1), and 8.4 (br, 1H, OH).

Anal. Calcd. for $C_{20}H_{27}NO$: C, 80.76; H, 9.15; N, 4.71. Found: C, 80.50; H, 9.19; N, 4.45.

We thank Mr. L. Morris for the synthesis of compound **52** and Dr. A. W. Pircio of Bristol Laboratories, Syracuse, N.Y., for the pharmacological data. Thanks are also given to Dr. Y. G. Perron and Dr. M. Menard of these laboratories and Dr. B. Belleau of McGill University, Montreal, Quebec for their comments and suggestions during the course of this work.

1. F. B. Block and F. H. Clarke. J. Med. Chem. **12**, 845 (1969).
2. N. Yokoyama, F. B. Block, and F. H. Clarke. J. Med. Chem. **13**, 488 (1970).
3. D. R. Jasinski, W. R. Martin, and R. Hoeldtke. Clin. Pharmacol. Ther. **12**, 613 (1971).
4. A. F. Casey. Prog. Med. Chem. **7**, 229 (1970); J. W. Lewis, K. W. Bentley, and A. Cowan. Annu. Rev. Pharmacol. **11**, 241 (1971).
5. R. Grewe and A. Mondon. Chem. Ber. **81**, 279 (1948); O. Schnider and A. Grussner. Helv. Chim. Acta, **32**, 821 (1949).
6. J. Hellerbach *et al.* Synthetic analgesics. Part II. Pergamon Press Ltd., New York. 1966.
7. E. W. Garbisch, Jr. J. Org. Chem. **26**, 4165 (1961).
8. M. Menard, P. Rivest, L. Morris, J. Meunier, and Y. G. Perron. Can. J. Chem. **52**, 2316 (1974).
9. E. M. Fry and E. L. May. J. Org. Chem. **26**, 2592 (1961).
10. E. M. Kaiser and C. R. Hauser. J. Org. Chem. **33**, 3402 (1968).
11. P. J. Hattersly, I. M. Lockhart, and M. Wright. J. Chem. Soc. C, 217 (1969).
12. (*a*) H. Henecka. Ann. **583**, 110 (1953); (*b*) S. Sugasawa and S. Saito. Chem. Pharm. Bull. **4**, 237 (1956); (*c*) M. Sasamoto. Chem. Pharm. Bull. **8**, 324 (1960); (*d*) T. Kametani, K. Kigasawa, M. Hayasaka, K. Wakisaka, F. Satoh., T. Aoyama, and H. Ishimaru. J. Heterocycl. Chem. **8**, 769 (1971).
13. A. Knorr, E. Laage, and A. Weissenborn. Chem. Abstr. **28**, 2367 (1934).
14. V. Prelog, L. Frenkiel, and S. Szpilfogel. Helv. Chim. Acta, **29**, 484 (1946).
15. K. Kanematsu, M. Takeda, A. E. Jacobsen, and E. L. May. J. Med. Chem. **12**, 405 (1969).
16. E. L. May and E. M. Fry. J. Org. Chem. **22**, 1366 (1957).
17. G. Kraiss and K. Nador. Tetrahedron Lett. 57 (1971); J. D. Hobson and J. G. McCluskey. J. Chem. Soc. C, 2015 (1967).
18. J. F. W. McOmie, M. L. Watts, and D. E. West. Tetrahedron, **24**, 2289 (1968).
19. A. P. Krapcho and A. A. Bothner-by. J. Am. Chem. Soc. **81**, 3658 (1959).
20. S. E. Fullerton, E. L. May, and E. D. Becker. J. Org. Chem. **27**, 2144 (1962).
21. T. M. Moynehan, K. Schofield, R. A. Y. Jones, and A. R. Katritzky. J. Chem. Soc. 2637 (1962).
22. E. Siegmund, R. Cadmus, and G. Lu. Proc. Soc. Exp. Biol. Med. **95**, 729 (1957).
23. L. S. Harris and A. K. Pierson. J. Pharmacol. Exp. Ther. **143**, 141 (1964).
24. K. Rorig, J. D. Johnston, R. W. Hamilton, and T. J. Telinski. Org. Syn. Coll. Vol. **4**, 576 (1963).

Can. J. Chem. Downloaded from www.nrcresearchpress.com by 210.87.254.105 on 09/05/12
For personal use only.

Can. J. Chem. Downloaded from www.nrcresearchpress.com by 210.87.254.5 on 09/05/12
For personal use only.

A General, Selective Synthesis of Thiol Esters

SATORU MASAMUNE, SUSUMU KAMATA, JAMES DIAKUR, YOSHIKAZU SUGIHARA, AND GORDON S. BATES

Department of Chemistry, University of Alberta, Edmonton, Alberta T6G 2G2

Received August 14, 1975

SATORU MASAMUNE, SUSUMU KAMATA, JAMES DIAKUR, YOSHIKAZU SUGIHARA, and GORDON S. BATES. Can. J. Chem. **53**, 3693 (1975).

Use of diethyl phosphorochloridate and Tl(I) thiolates constitutes a general, selective synthesis of thiol esters. Primary, secondary, and tertiary alkane- and arenethiols of various carboxylic acids, including those containing hydroxy groups have been prepared under mild conditions.

SATORU MASAMUNE, SUSUMU KAMATA, JAMES DIAKUR, YOSHIKAZU SUGIHARA et GORDON S. BATES. Can. J. Chem. **53**, 3693 (1975).

L'utilisation de phosphodichloridate de diéthyle et de thiolates de Tl(I) s'avère être une méthode générale et sélective pour la synthèse de thiol esters. On a préparé, sous des conditions douces, des arène- et alkane thiols primaires, secondaires et tertiaires de divers acides carboxyliques y compris ceux contenant des groupes hydroxyles.

[Traduit par le journal]

In view of ever-increasing interest in the enzymatic synthesis of acyl-CoA (1*a*) and its involvement in fatty acid biosynthesis (acyl transfer reaction) (1*b*), it is rather surprising that there has not been developed a general, *selective* method to prepare thiol esters, applicable to sensitive, complex organic substrates (for a recent review see ref. 2). Two procedures recently reported are useful in a certain case, but both seem to be limited in scope. One employing disulfides and triphenylphosphine (3) is applicable to the preparation of pyridine-2-thiol and benzenethiol esters, but not to that of alkanethiol esters, while the other involving diphenoxy or diethyloxyphosphinyl alkanecarboxylate intermediates (4) proceeds well only with less substituted (mainly primary) alkanethiols.[1] A mechanistic examination of the latter reaction has led to the development of a versatile and effective synthesis of thiol esters as summarized below. This method also solves one of the general problems in the synthesis of macrolide antibiotics in which the 2-methylpropane-2-thiol ester has already been shown to be a superb protective group and to be readily activated for further reactions (5).

The reaction sequence that we have found to be most satisfactory is formulated below.

$$RCO_2H \xrightarrow[(C_2H_5)_3N \text{ in THF}]{(C_2H_5O)_2P(O)Cl} \underset{\mathbf{1}}{RCO_2P(OC_2H_5)_2} \xrightarrow{Tl(I)SR'} RCOSR'$$

The selection of diethyl phosphorochloridate (6) is due to the high selectivity of the chloridate towards the carboxy group with respect to hydroxy, a requirement that must be met in many cases. This selectivity,[2] as is clearly demonstrated by entries 3 and 4 in Table 1, can be favorably compared with that occurring with the methods involving triphenylphosphine and carbon tetrachloride (or conventional halogenating reagents) which react with both the carboxy (7) and hydroxy groups (8).

Near quantitative precipitation of triethyl-

[1]We have eliminated the possibility (although obviously remote) that $(C_2H_5O)_2P(O)SC_2H_5$ (I) is an intermediate in the reaction of Yamada *et al.* (4), since the reaction of (I) and cyclohexanecarboxylic acid in dimethyl formamide did not proceed even in the presence of triethylamine.

[2]Both cyclohexanol and *tert*-butyl alcohol were recovered virtually quantitatively under the present conditions using diethyl phosphorochloridate.

TABLE 1. Selected examples of the thiol ester synthesis

Entry	Product*		Yield (%)
1	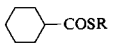	R = $C(CH_3)_3$	94
		R = $CH(CH_3)_2$	90
		R = $(CH_2)_2CH_3$	91
		R = C_6H_5	92
2	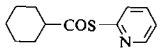		90
3	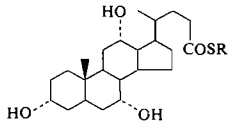	R = $C(CH_3)_3$	86
		R = $CH(CH_3)_2$	90
		R = $(CH_2)_2CH_3$	86
4	$CH_3(CH_2)_5CH(OH)(CH_2)_{10}COSC(CH_3)_3$		84
5	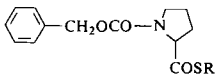	R = $C(CH_3)_3$	89
		R = $CH(CH_3)_2$	93
		R = $(CH_2)_2CH_3$	95

*Elemental analyses and spectral data of all products are consistent with those formulated in Table 1.

amine hydrochloride that is removed by filtration in the first step ensures the formation of the intermediate anhydride (**1**) and also avoids some complications that may arise with the use of other phosphorating reagents (4, 9).

Because of the thermal instability of the intermediate (**1**),[3] the ensuing last step requires an appropriate thiolate counter-ion that brings the reaction to completion with high efficiency. Among several common cations tested, such as Na^+ and K^+, Tl(I) proved to be the most satisfactory, because of the case of preparation and reasonable solubility in aprotic solvents of its crystalline thiolate salts. Thus, the yellow Tl(I) salts of primary, secondary, and tertiary (*5b*) alkanethiols have been prepared in excellent yields with the use of Tl(I) ethoxide and the thiols. In this way a high-yield synthesis of thiol esters, regardless of the nature of substitution in the alkane- and arenethiols, has now been achieved under mild conditions. This method is applicable to even a reactive thiol ester such as pyridine-2-thiol (entry 2 in Table 1) and appears in some cases to supersede those methods employed previously,[4] because of its simplicity of work-up procedure. Needless to say, in the case of a hydroxy acid, the selectivity of the present method allows one to operate on the hydroxy group of the resulting alkanethiol ester, and then to effect further conversion of the carboxy group.[5] The following experimental description illustrates the procedure summarized in Table 1.

The 2-Methylpropane-2-thiol Ester of Cholic Acid

To a solution of 817 mg (2 mmol) of cholic acid and 222 mg (2.2 mmol) of triethylamine in 10 ml of anhydrous tetrahydrofuran was added a solution of 363 mg (2.1 mmol) of diethyl phosphorochloridate in 5 ml of tetrahydrofuran dropwise at room temperature under a nitrogen

[3]The intermediate is rather labile to heat and base and prone to disproportionate (10) according to the equation: $2RCO_2P(O)(OR')_2 = (RCO)_2O + ((R'O)_2PO)_2O$.

[4]Pyridine-2-thiol esters were prepared previously either through the acid chloride or by means of dicyclohexylcarbodiimide (11) and later by Mukaiyama *et al.* (3) and by other groups, using triphenylphosphine and the corresponding disulfide. The latter procedure very often involves a tedious work-up to isolate the pure product from triphenylphosphine oxide that forms concomitantly.

[5]In cases where the acid chlorides are available, and thus the selective activation of the carboxy group is not demanded, the method previously reported (*5b*) is to be preferred. Conventional methods of preparing thiol esters often require more vigorous conditions and lead to lower yields, in particular with highly substituted thiols.

Can. J. Chem. Downloaded from www.nrcresearchpress.com by 210.87.254.5 on 09/05/12
For personal use only.

atmosphere. The mixture was stirred at room temperature for 3 h, and the precipitated triethylamine hydrochloride was removed by filtration and washed with 10 ml of tetrahydrofuran. To the combined filtrate and washings was added 650 mg (2.2 mmol) of Tl(I) 2-methyl-2-propanethiolate, and the mixture was stirred at room temperature overnight. The tetrahydrofuran was evaporated under reduced pressure, and then ethyl acetate was added to the residue. The work-up involving washings with aqueous solutions in the usual manner gave 840 mg (86%) of the crystalline thiol ester, m.p. 164–165 °C (from ether – Skelly B).

The authors are grateful to the National Research Council of Canada for financial support.

1. (*a*) J. C. LONDESBOROUGH and L. T. WEBSTER, JR. *In* The enzymes. Vol. X. 3rd ed. *Edited by* P. D. Boyer. Academic Press, New York. 1974. Chapt. 14; (*b*) P. R. VAGELOS. *In* The enzymes. Vol. VIII. 3rd ed. *Edited by* P. D. Boyer. Academic Press, New York. 1973. Chapt. 5.
2. L. FIELD. Synthesis, 106 (1972).
3. (*a*) T. MUKAIYAMA, R. MATSUEDA, and H. MARAYAMA. Bull. Chem. Soc. Jpn. **43**, 1271 (1970); (*b*) T. MUKAIYAMA. Synth. Commun. **2**, 243 (1972); (*c*) E. J. COREY and K. C. NICOLAOU. J. Am. Chem. Soc. **96**, 5614 (1974); (*d*) H. GERLACH and A. THALMANN. Helv. Chim. Acta, **57**, 2661 (1974).
4. S. YAMADA, Y. YOKOYAMA, and T. SHIOIRI. J. Org. Chem. **39**, 3302 (1974).
5. (*a*) S. MASAMUNE, H. YAMAMOTO, S. KAMATA, and A. FUKUZAWA. J. Am. Chem. Soc. **97**, 3513 (1975); (*b*) S. MASAMUNE, S. KAMATA, and W. SCHILLING. J. Am. Chem. Soc. **97**, 3515 (1975).
6. T. KOIZUMI, N. YAMAMOTO, and E. YOSHII. Chem. Pharm. Bull. Jpn. **21**, 312 (1973).
7. J. B. LEE. J. Am. Chem. Soc. **88**, 3440 (1966).
8. J. HOOZ and S. S. H. GILANI. Can. J. Chem. **46**, 86 (1968).
9. T. SHIOIRI, K. NINOMIYA, and S. YAMADA. J. Am. Chem. Soc. **94**, 6203 (1972).
10. J. C. SHEEHAN and V. S. FRANK. J. Am. Chem. Soc. **72**, 1312 (1950); F. CRAMER and K. G. GARTNER. Chem. Ber. **91**, 704 (1958).
11. K. LLOYD and G. T. YOUNG. Chem. Commun. 1400 (1968); J. Chem. Soc. C, 2890 (1971).

Can. J. Chem. Downloaded from www.nrcresearchpress.com by 210.87.254.5 on 09/05/12
For personal use only.

Canadian Journal of Chemistry

Published by
THE NATIONAL RESEARCH COUNCIL OF CANADA

Volume 53 Number 24 December 15, 1975

Journal canadien de chimie

Publié par
LE CONSEIL NATIONAL DE RECHERCHES DU CANADA

Volume 53 numéro 24 15 décembre 1975

Can. J. Chem. Downloaded from www.nrcresearchpress.com by 210.87.254.6 on 09/05/12
For personal use only.

Mechanistic Information from the Effect of Pressure on the Kinetics of Hydrolysis of Iodopentaaquochromium(III) Ion

MILTON CORNELIUS WEEKES AND THOMAS WILSON SWADDLE[1]

Department of Chemistry, The University of Calgary, Calgary, Alberta T2N 1N4

Received July 9, 1975

MILTON CORNELIUS WEEKES and THOMAS WILSON SWADDLE. Can. J. Chem. **53**, 3697 (1975).

The rate of hydrolysis of iodopentaaquochromium(III) ion has been measured as a function of pressure (0.1 to 250 MPa) and hydrogen ion concentration (0.1 to 1.0 mol kg^{-1}) at 298.2 K and ionic strength 1.0 mol kg^{-1} (aqueous $HClO_4$–$LiClO_4$). The volumes of activation for the acid independent and inversely acid dependent hydrolysis pathways are -5.4 ± 0.5 and -1.6 ± 0.3 cm^3 mol^{-1} respectively, and are not detectably pressure-dependent. Consideration of these values, together with the molar volume change of -3.3 ± 0.3 cm^3 mol^{-1} determined dilatometrically for the completed hydrolysis reaction, indicates that the mechanisms of the two pathways are associative interchange (I_a) and dissociative conjugate base (D_{cb}) respectively.

MILTON CORNELIUS WEEKES et THOMAS WILSON SWADDLE. Can. J. Chem. **53**, 3697 (1975).

On a mesuré la vitesse d'hydrolyse de l'ion iodopentaaquochrome(III) en fonction de la pression (0.1 à 250 MPa) et de la concentration des ions hydrogènes (0.1 à 1.0 mol kg^{-1}) à 298.2 K et à une force ionique de 1.0 mol kg^{-1} ($HClO_4/LiClO_4$ aqueux). Les volumes d'activation pour les hydrolyses indépendante de l'acide et dépendante inversement sur l'acide sont respectivement de -5.4 ± 0.5 et -1.6 ± 0.3 cm^3 mol^{-1} et ne sont pas dépendantes de la pression dans les limites de détection. Un examen de ces valeurs, en comparaison avec les changements volumiques molaires de -3.3 ± 0.3 cm^3 mol^{-1} déterminés d'une façon dilatométrique pour la réaction d'hydrolyse complète, indique que les mecanismes des deux voies sont respectivement un interchange associatif (I_a) et une base conjuguée dissociative (D_{cb}).

[Traduit par le journal]

Introduction

In recent articles (1, 2), we summarized evidence which we take to indicate that simple chromium(III) substitution reactions of the type

[1] $Cr(solvent)_5X^{(3-n)+} + solvent \rightleftharpoons Cr(solvent)_6^{3+} + X^{n-}$

proceed via an associative interchange (I_a) mechanism (3), except perhaps where 'induced solvolysis' (*e.g.*, of $Cr(solvent)_5N_3^{2+}$ by NO^+), *trans*-activation, or conjugate base solvolysis are involved, in which cases the mechanism is probably of the dissociative type (D or D_{cb}). For the aquation of the iodopentaaquochromium(III) ion, however, the distinction between I_a and alternative D or I_d mechanisms is less clear, since I^- is an excellent 'leaving group'.

[2] $Cr(H_2O)_5I^{2+} + H_2O \rightarrow Cr(H_2O)_5^{3+} + I^-$

King and co-workers (4, 5) have presented observations relating to the solvolysis of $Cr(H_2O)_5I^{2+}$ in acidic aqueous methanol and aqueous dimethylsulfoxide which are most readily interpreted in terms of a D mechanism, but which do not rule out an I_a process (1). We have therefore sought mechanistic information

[1]To whom correspondence should be addressed.

TABLE 1. Pressure and hydrogen ion dependence of the pseudo-first-order rate coefficients k_{obs} (s^{-1}, $\times 10^4$) for the aquation of $(H_2O)_5CrI^{2+}$ in acidic aqueous solution at 298.2 K and ionic strength 1.05 mol kg^{-1}[a]

$[H^+]$ (mol kg^{-1})	Pressure (MPa)[b]						
	0.1	10	40	100	150	200	250
1.048	1.10	1.18	1.26	1.35	1.40	1.65	1.80
0.843		1.24	1.32		1.54	1.77	1.93
0.550	1.39	1.48	1.55		1.82	1.92	
0.350				2.19			
0.219			2.59				
0.200	2.69		2.73	2.87	3.13	3.32	3.45
0.141		3.38	3.57	3.89	4.17		4.40
0.105		4.30				5.35	5.43

[a]Initial $[(H_2O)_5CrI^{2+}] \approx 1 \times 10^{-4}$ mol kg^{-1}.
[b]Accuracy ±0.4 MPa (1 MPa = 9.869 atm).

from the effects of pressure on the rates of the acid independent (aquation) and inversely acid dependent (conjugate base hydrolysis) pathways of reaction 2, which operate concurrently in aqueous solutions in which the hydrogen ion concentration is about 0.1 to 1.0 mol kg^{-1}.

Experimental

Solutions were prepared at 294 K on the basis of the molar (mol dm^{-3}) concentration scale, but the molar concentrations of solutes in the solutions used in the kinetic studies (1.000 mol dm^{-3} $HClO_4$–$LiClO_4$) were converted to the pressure-independent molal (mol kg^{-1}) scale by multiplying by 1.048.

Solutions of $Cr(H_2O)_5I^{2+}$ perchlorate in aqueous perchloric acid were prepared and characterized as previously described (6). Solid $[Cr(H_2O)_5I]SO_4 \cdot H_2O$ was made by the method of Moore and Basolo (7), and analyzed gravimetrically for I^- and SO_4^{2-} and spectrophotometrically for Cr as CrO_4^{2-} after oxidation with alkaline hydrogen peroxide solution. The spectrum of the freshly-aquated sulfate salt in aqueous $HClO_4$ showed that no significant amount of $Cr(H_2O)_5SO_4^+$ was present in the solid salt.

Anal. Calcd. for $[Cr(H_2O)_5I]SO_4 \cdot H_2O$: Cr, 13.6; I, 33.1; SO_4, 25.1. Found: Cr, 13.2; I, 32.8; SO_4, 26.0.

Kinetic Measurements

The rate of disappearance of $(H_2O)_5CrI^{2+}$ in aqueous $HClO_4$–$LiClO_4$ solutions was followed spectrophotometrically at 260 nm using a Cary 17H spectrophotometer, the solution sample being contained in the Hastelloy-C-lined pressurizable assembly described previously (8). The pressurizable optical cell was thermostated (298.2 ± 0.1 K) with a close-fitting aluminum jacket through which water circulated rapidly from an external thermostat bath.

Measurement of Volume of Reaction

Typically, a weighted sample ($\sim 2 \times 10^{-4}$ mol) of $[Cr(H_2O)_5I]SO_4 \cdot H_2O$ was dissolved rapidly in 50 cm^3 $HClO_4$ (1.00 mol dm^{-3}) which was maintained at 298.15 K, with a variation of less than 0.01 K, in an oilbath shielded from drafts. A Carlsberg-type dilatometer, also at 298.15 K, was quickly filled with the solution and replaced promptly in the bath, and the progress of reaction 2 was then followed by observing the meniscus height h_t as a function of time t (9). It was shown, using plain water, that the initial temperature perturbations associated with this procedure subsided within 20 min at most.

Results

The rate of aquation of $(H_2O)_5CrI^{2+}$ was accurately first order in $[(H_2O)_5CrI^{2+}]$ at a given $[H^+]$; the corresponding rate coefficients k_{obs} (Table 1), obtained by least-squares reduction of the spectrophotometric data, reproducible within 1%, were the same at atmospheric pressure and a given $[H^+]$ whether the reaction was carried out in the pressurizable assembly or in ordinary glass vessels, and agreed well with those reported previously (6). Graphical analysis of the data of Table 1 (supplemented with data from ref. 6, for atmospheric pressure) showed that, at any one pressure, k_{obs} was accurately a linear function of $[H^+]^{-1}$, the intercept k_a and slope k_b representing the rate coefficients of the aquation and conjugate base hydrolysis pathways respectively.

$$[3] \qquad k_{obs} = k_a + k_b[H^+]^{-1}$$

Plots of $\ln k_a$ and $\ln k_b$ against pressure P were also linear, within the experimental uncertainty, with no systematic deviations of the data points from the representative straight line. Thus, the volumes of activation ΔV_a^* and ΔV_b^* (−5.6 and −1.4 cm^3 mol^{-1} respectively, from the slopes of these plots) were independent of pressure ($0 < P \leq 250$ MPa) within the experimental error, and were therefore recalculated directly using an IBM 371/145 computer by a least-squares fit of

Can. J. Chem. Downloaded from www.nrcresearchpress.com by 210.87.254.6 on 09/05/12
For personal use only.

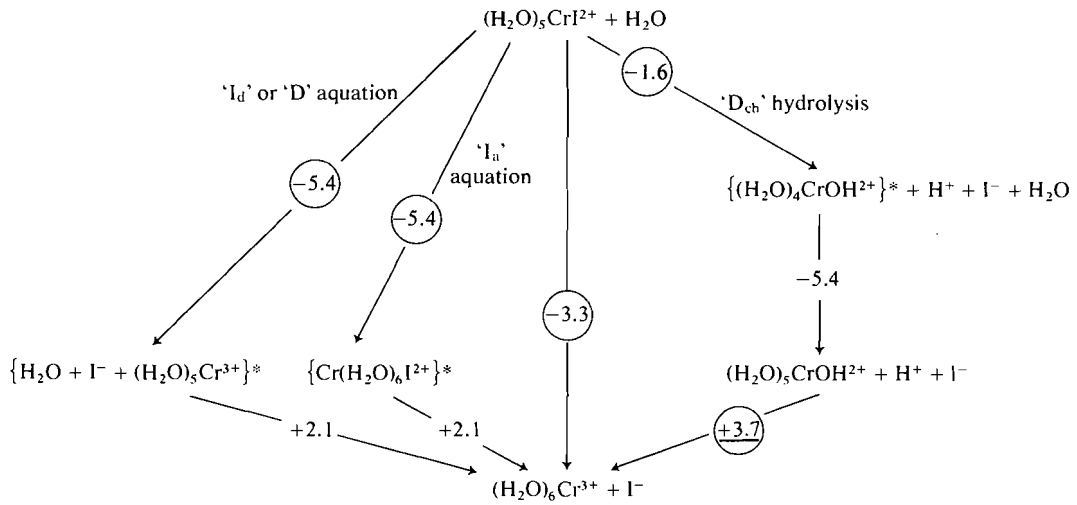

FIG. 1. Volume changes ($cm^3\ mol^{-1}$) associated with the various steps in the aquation (left hand side) and conjugate base hydrolysis (right hand side) of the iodopentaaquochromium(III) ion in aqueous perchlorate media at 298.2 K and ionic strength 1.0 mol kg^{-1}. Asterisks denote transition states. Circled data are from this study, that underlined is from ref. 8, and the remainder are obtained by difference.

k_{obs} values to the equation

$$[4]\quad k_{obs} = k_a^0 \exp(-P\Delta V_a^*/RT) + k_b^0[H^+]^{-1} \exp(-P\Delta V_b^*/RT)$$

where k_a^0 and k_b^0 represent the values of k_a and k_b at zero pressure. The values and standard errors of the parameters so calculated were

$$\Delta V_a^* = -5.4 \pm 0.5\ cm^3\ mol^{-1}$$

$$\Delta V_b^* = -1.6 \pm 0.3\ cm^3\ mol^{-1}$$

$$k_a^0 = (7.84 \pm 0.28) \times 10^{-5}\ s^{-1}$$

and

$$k_b^0 = (3.72 \pm 0.06) \times 10^{-5}\ mol\ kg^{-1}\ s^{-1}$$

for $T = 298.2$ K and ionic strength $I = 1.048$ mol kg^{-1} ($HClO_4$–$LiClO_4$).

From the dilatometric measurements, plots of $\ln(h_t - h_\infty)$ *vs.* time t were found to be linear, with slopes corresponding to k_{obs} values in satisfactory agreement with those obtained spectrophotometrically, and, by extrapolation of h_t back to the time of dissolution of the $[Cr(H_2O)_5I]SO_4 \cdot H_2O$, the molar volume change ΔV^0 for the completed reaction 2 was calculated. The mean of five such determinations gave $\Delta V^0 = -3.3 \pm 0.3\ cm^3\ mol^{-1}$ for $I = 1.05$ mol kg^{-1} at 298.15 K and 0.1 MPa.

Discussion

The volume changes associated with the various steps in the hydrolysis of $Cr(H_2O)_5I^{2+}$ are summarized in Fig. 1, in which no distinction is made between D and I_d mechanisms for aquation, the transition states for both being represented by $\{I^- + (H_2O)_5Cr^{3+}\}^*$. This simplification seems justified in the present context. There is no reason to suppose that the hypothetical D *intermediate* $(H_2O)_5Cr^{3+}$ would differ much in free energy from the *transition state* for its formation, and hence, on the basis of the Hammond principle (10), the D transition state itself may be represented approximately as $\{I^- + (H_2O)_5Cr^{3+}\}$. In an I_d process, as typified by substitution reactions of cobalt(III) ammines (1, 3, 11), the bond between the central metal atom and the departing ligand is broken and the departing ligand fully solvated, in the transition state, so that the distinction between I_d and D transition states need not be made in the present context.

The volume change $\Delta V_a^* = -5.4\ cm^3\ mol^{-1}$ on going from the initial state to the transition state of the aquation reaction is certainly consistent with an I_a mechanism, in which H_2O—Cr bond formation must involve contraction (12), but does not *in itself* rule out the possibility of a dissociative type of mechanism in which the positive contribution of Cr—I bond breaking to ΔV_a^* is more than compensated for by a large, negative contribution from solvation of the newly-created tripositive chromium(III) ion and mononegative iodide. However, when ΔV_a^* is com-

Can. J. Chem. Downloaded from www.nrcresearchpress.com by 210.87.254.6 on 09/05/12
For personal use only.

Can. J. Chem. Downloaded from www.nrcresearchpress.com by 210.87.254.6 on 09/05/12
For personal use only.

pared to the molar volume change $\Delta V^0 = -3.3$ cm^3 mol^{-1} for the completed reaction, it becomes very difficult to reconcile it with a D or I_d aquation mechanism, since these would then require that the difference in solvation between the initial and transition states be greater than between the initial and final states. This point is brought into sharper focus by consideration of the *positive* volume change that occurs on going from the transition state to the final state; it is very hard to accept that this could arise from the formation of a bond between the incoming water molecule and the $Cr(H_2O)_5^{3+}$ moiety, so that the possibility that the acid-independent aquation reaction proceeds via a D or I_d mechanism may be discounted. This observation is, however, consistent with an overall I_a aquation process whereby the iodide ligand is expelled from the transition state $\{Cr(H_2O)_6I^{2+}\}^*$ in which the modest degree of additional solvation required (see below) has been partly achieved (9), so that the bond-breaking contribution to the further volume change outweighs the solvational part. The same argument can be applied in support of an I_a mechanism for the aquations of $Cr(NH_3)_5X^{2+}$ (X = Cl, Br, I), for which ΔV_a^* is again some 2 to 3 cm^3 mol^{-1} more negative than ΔV^0 (9). By contrast, for the aquations of $Co(NH_3)_5X^{(3-n)+}$, to which an I_d mechanism is assigned, ΔV_a^* is always more *positive* than ΔV^0 by an amount which corresponds to the addition of H_2O to a transient $Co(NH_3)_5^{3+}$ species (11).

In the conjugate base hydrolysis pathway (right hand side of Fig. 1), the presumed intermediate $(H_2O)_4CrOH^{2+}$ of a D_{cb} process is identified with the transition state of the reaction. This transition state will be reached in two steps

$$[5] \quad (H_2O)_5CrI^{2+} \overset{\text{fast}}{\rightleftharpoons} (H_2O)_4Cr(OH)I^+ + H^+$$

$$[6] \quad (H_2O)_4Cr(OH)I^+ \xrightarrow{\text{rate determining}} (H_2O)_4CrOH^{2+} + I^-$$

The volume change associated with [5] is not known, but ΔV values for the analogous reactions of $Cr(H_2O)_6^{3+}$ (8), $Fe(H_2O)_6^{3+}$ (13), $Tl(H_2O)_6^{3+}$ (13), and $Co(NH_3)_5OH_2^{3+}$ (8) all lie in the range -1 to -4 cm^3 mol^{-1}, so that ΔV is likely to be about -2 cm^3 mol^{-1} for [5]. The volume change for [6] can therefore be estimated to be very close to zero, which is reasonable if the mechanism is D_{cb} and the bond-breaking and solvational changes effectively cancel each other, but not if the mechanism were of an associative type, since both the H_2O—Cr bond-making and the solvational changes would then be expected to make negative contributions to the volume change. This inferred near-cancellation of Cr—I bond-breaking and solvational contributions indicates that the solvational changes must be fairly small in the reaction under consideration, since the bond-breaking contribution is small in metal complexes, and this is confirmed by the lack of any significant pressure-dependence of ΔV_a^* or ΔV_b^* (11).

This same inferred compensation of volume changes arising from Cr—I bond stretching by the contraction due to concomitant solvation of the developing additional charges lends further support to the assignment of an I_a mechanism to the aquation reaction, as ΔV_a^* may then be largely accounted for in terms of the contraction caused by removal of the attacking water molecule from the second coordination sphere of the dipositive complex ion and its implantation in the first (12). This interpretation is, in turn, supported by the inference from Fig. 1 that ΔV_a^* is the same as the volume change (-5.4 cm^3 mol^{-1}) for the similar addition of a water molecule to $\{(H_2O)_4CrOH^{2+}\}^*$, which, despite the difference in coordination number, resembles $(H_2O)_5CrI^{2+}$ closely in that it is an aquochromium(III) complex containing a simple mononegative anion in its first coordination sphere.

ΔV_a^* for $(H_2O)_5CrI^{2+}$ is about 60% as large numerically as the corresponding quantity for aquo-exchange in $Cr(H_2O)_6^{3+}$ (12), which again seems reasonable when ΔV_a^* is ascribed in large part to the H_2O—CrI^{2+} bond-making contribution, since the second coordination sphere from which the attacking water molecule is removed is presumably more extensive and structured in the tripositive than in the dipositive complex ion.

In summary, we can say that if, as in this discussion, the mechanisms of hydrolysis of $Cr(H_2O)_5I^{2+}$ are to be represented in terms of the Langford–Gray models (3), then the mechanism of simple aquation is best described as I_a and that of conjugate base hydrolysis as D_{cb}, on the basis of the respective volumes of activation relative to the overall volume of reaction. Whatever detailed mechanistic model is proposed, it does at least seem necessary to recognize that the aquation pathway (left hand side of Fig. 1) involves a rate determining step which is mechanistically different from, and more com-

pact than, that of the conjugate base hydrolysis pathway (reaction 6). Full confirmation of this would, however, require direct measurement of the volume change associated with [5].

We thank Professor D. R. Stranks for discussions, and the National Research Council of Canada for financial assistance.

1. T. W. SWADDLE. Coord. Chem. Rev. **14**, 217 (1974).
2. D. S. T. LO and T. W. SWADDLE. Inorg. Chem. **14**, 1878 (1975).
3. C. H. LANGFORD and H. B. GRAY. Ligand substitution dynamics. W. A. Benjamin, New York, New York. 1965.
4. S. P. FERRARIS and E. L. KING. J. Am. Chem. Soc. **92**, 1215 (1970).
5. D. B. VANDERHEIDEN and E. L. KING. J. Am. Chem. Soc. **95**, 3860 (1973).
6. T. W. SWADDLE and E. L. KING. Inorg. Chem. **4**, 532 (1965).
7. P. MOORE and F. BASOLO. Inorg. Chem. **4**, 1670 (1965).
8. T. W. SWADDLE and P.-C. Kong. Can. J. Chem. **48**, 3223 (1970).
9. G. GUASTALLA and T. W. SWADDLE. Can. J. Chem. **51**, 821 (1973).
10. G. S. HAMMOND. J. Am. Chem. Soc. **77**, 334 (1955).
11. W. E. JONES, L. R. CAREY, and T. W. SWADDLE. Can. J. Chem. **50**, 2739 (1972).
12. D. R. STRANKS and T. W. SWADDLE. J. Am. Chem. Soc. **93**, 2783 (1971).
13. N. VANDERHOEK. Ph.D. Thesis, University of Adelaide. Adelaide, South Australia. 1973.

Can. J. Chem. Downloaded from www.nrcresearchpress.com by 210.87.254.6 on 09/05/12
For personal use only.

Chromic Acid Esters as Corrosion Inhibitors

EDWARD L. GHALI AND BERTRAND GIRARD

Department of Applied Science, University of Quebec at Chicoutimi, Chicoutimi, Quebec G7H 2B1

AND

JEAN-MARIE HACHEY

Department of Pure Science, University of Quebec at Chicoutimi, Chicoutimi, Quebec G7H 2B1

Received February 17, 1975[1]

EDWARD L. GHALI, BERTRAND GIRARD, and JEAN-MARIE HACHEY. Can. J. Chem. **53**, 3702 (1975).

The hydrolysis of the chromate ester, derived from 1-methylcyclohexanol, was studied by electrochemical methods. Progressive and complete hydrolysis in an open or closed system yields chromic acid and 1-methylcyclohexanol. No evidence of the presence of monoester was detected. In a closed system, where most of the hydrolyzed alcohol is retained in solution, a side reaction between chromic acid and the alcohol has been detected and followed by conductivity measurements.

Electrochemical characteristics of pure iron immersed in aqueous solutions containing hydrolyzed ester were found to be identical to those in aqueous solutions containing equivalent quantities of Cr^{VI} as CrO_3. Sulfuric acid additions to the above solutions still give comparable electrochemical characteristics; however, the anodic current in the passive region was found to be less for solutions containing hydrolyzed ester than for solutions containing equivalent quantities of Cr^{VI} as CrO_3.

EDWARD L. GHALI, BERTRAND GIRARD et JEAN-MARIE HACHEY. Can. J. Chem. **53**, 3702 (1975).

L'hydrolyse de l'ester chromique dérivé du méthyl-1 cyclohexanol fut étudiée par des méthodes électrochimiques. L'hydrolyse progressive et complète dans un système ouvert ou fermé donne l'acide chromique et le méthyl-1 cyclohexanol. Nous n'avons pas pu détecter la présence de monoester. Dans un système fermé, où presque tout l'alcool est retenu en solution, une réaction secondaire entre l'acide chromique et l'alcool a été décelée par des mesures de la conductivité.

Les caractéristiques électrochimiques du fer pur dans l'eau contenant les produits d'hydrolyse de l'ester sont identiques à celles déterminées dans des solutions aqueuses contenant des quantités équivalentes de Cr^{VI} sous forme de CrO_3. Des additions d'acide sulfurique dans ces solutions donnent toujours des caractéristiques électrochimiques comparables. Cependant, dans le cas des solutions contenant les produits d'hydrolyse de l'ester, le courant anodique dans la région de passivation était inférieur à celui mesuré pour des solutions renfermant des quantités équivalentes de Cr^{VI} sous forme de CrO_3.

Chromates and dichromates of alkaline metals, and even chromium trioxide, have long been utilized as corrosion inhibitors in aqueous media in many industrial applications; different mechanisms to explain the kinetics of inhibition have been suggested (1–3).

Chromic acid esters derived from tertiary alcohols have been synthesized and briefly described in the literature by many authors; several papers published in this field have been summarized in a review article (4). In particular, the synthesis of the chromate ester derived from 1-methylcyclohexanol has already been accomplished by Cerveny (5); however, the spectroscopic characteristics of this compound were not described. He principally carried out some studies concerning the inhibiting effect of different chromic acid esters and especially those of tertiary alcohols (5–7).

The mechanism of the action of chromic acid esters can be summarized as follows: (*a*) the ester, soluble in a nonpolar phase, diffuses to the interface of the nonpolar and polar solutions, (*b*) hydrolysis occurs, and (*c*) the liberated chromate ions may act as corrosion inhibitors. Cerveny found that the diffusion of the ester, the liberation of chromate ions by hydrolysis, and concomitant passivation occur so fast that in a real system electrochemical corrosion of metal can be stopped in the presence of an oil film containing the ester. The physico-chemical properties of mineral oils are affected slightly or not at all by the chromic acid esters. Cerveny also reported that the minimum concentration of the

[1]Revision received September 8, 1975.

Can. J. Chem. Downloaded from www.nrcresearchpress.com by 210.87.254.42 on 09/05/12
For personal use only.

Can. J. Chem. Downloaded from www.nrcresearchpress.com by 210.87.254.42 on 09/05/12
For personal use only.

chromate in aqueous solutions necessary for inhibition is 10^{-5} to 10^{-4} *M* (5, 7).

Chromate esters have the advantage of being soluble in nonpolar media; many interesting applications can then be found if they have the same inhibiting effect as inorganic inhibitors in aqueous solutions. For the system 'atmosphere – oil containing chromic acid ester – aqueous layer – metal' or other comparable systems, the process of hydrolysis is considered as one of the important stages in the inhibition by chromic acid esters since it liberates the chromates which contribute to the protection of the metal. It is also interesting to determine whether the inhibiting action of hydrolyzed esters is different or equivalent to that of the chromates. The object of this work was then to study the process of hydrolysis of chromic acid esters and to examine the products of hydrolysis as corrosion inhibitors, compared to the chromates, in distilled water and in acidic medium.

Experimental

Synthesis of Di(1-methylcyclohexyl) Chromate

This product was synthesized according to the general procedure described by Wienhaus (8) for chromate esters derived from tertiary alcohols. The infrared spectra, the proton magnetic resonance spectra and gas chromatographic analysis were taken to identify the ester and its products of hydrolysis. The infrared spectra were measured on a Unicam Spectrophotometer, Model SP-1000 as films of pure liquid and in solution in CCl_4 between NaCl plates. Proton magnetic resonance spectra were taken on a Hitachi–Perkin–Elmer spectrometer, Model R-24 at 60 MHz. Tetramethylsilane was used as the internal standard and chemical shifts on the δ scale are given. The ultraviolet spectra were recorded on a Perkin–Elmer spectrophotometer, Model Coleman 124. Gas chromatographic analyses were done on a Hewlett–Packard instrument, Model 5754B (column: Cu 3/16 in. i.d. × 6 ft, Carbowax 20 M 10% (w/w) on Chromosorb P, 60–80 mesh, oven temperature 140 °C).

Analytically pure chemicals were used for the preparation of the ester and for the electrochemical investigations. The pure iron (Ferrovac) used was prepared by Colt Industries (Canada) Ltd. and was delivered in the form of hot rolled rods of 1 in. diameter. It had the following percentage composition: C: 0.004; Mn: 0.001; P: 0.002; S: 0.005; Si: 0.008; Ni: 0.027; Cr: 0.01; Mo: 0.001; V: 0.004; W: 0.01; Co: 0.003.

The potentiostat for polarization studies was PRT 30-01 Type, Tacussel Electronique, ultra-fast. Conductivity measurements were made using CDM 2e Type Radiometer (Copenhagen). p*H* measurements were conducted employing Fisher Accumet Model 220 p*H* meter.

Preliminary experiments showed that the water/ester ratio may have an influence on the product of hydrolysis. Hydrolysis in both closed and open systems was achieved by mixing an excess of water (1 l) with a small quantity of ester (0.095 to 9.5 g). (A closed system is one in an air-tight beaker insulated from the atmosphere by a watch-glass cover sealed with paraffin. An open system is one where the solution was in direct contact with the atmosphere.)

Electrochemical characteristics of iron including polarization curves were determined in aqueous solutions with the addition of hydrolyzed chromate ester or equivalent quantities of Cr^{VI} as CrO_3. The same study was also done in acidic solutions (sulfuric acid) containing hydrolyzed esters and chromates, respectively. The rectangular surface examined had a geometrical area of 1 cm^2. The surface was mechanically polished with abrasive papers and finally with aluminum oxide suspensions of 1 μ followed by 0.05 μ. The sample was washed with distilled water, alcohol, then distilled water, and finally immersed immediately in the electrolyte. The solution used for polarization studies was deaerated by bubbling nitrogen for 12 h. Cathodic polarization was carried out for 30 min at 1200 mV/S.C.E. before plotting the potentiokinetic curve. The potential was varied in the noble direction at a uniform rate of 16.7 mV/min. The 1 l solution used was circulated (50 ml/min) and maintained at a constant temperature of 26 ± 0.5 °C. Concentration of chloride ions in solution was found to be less than 1 p.p.m.

Results and Discussion

Identification of Di(1-methylcyclohexyl) Chromate

The infrared spectra of the chromate ester show the following characteristics: (1) disappearance of all —OH bands; (2) presence of Cr—O bands at 968 and 990 cm^{-1}. These results agree well with those of Zeiss and Matthews (9) who observed Cr—O bands at 971 and 990 cm^{-1} for di(2,4-dimethyl-4-hexyl) chromate.

Characteristics of the p.m.r. spectrum in CCl_4 of the synthesized chromic acid ester are given in Table 1. A comparison is made with those of 1-methylcyclohexanol. It can be observed that the methyl group of the chromate ester appears at a lower field (~1.5 p.p.m.) in comparison to the methyl group of the alcohol (~1.2 p.p.m.). The protons of the ring are also deshielded but to a less degree (6 Hz). Similar observations have previously been noted (10) in the case of other tertiary alicyclic alcohols methylated in the α position.

The ultraviolet spectrum in hexane (reagent grade) shows a maximum absorbance at 375 nm ($\log \varepsilon = 1.7$) and at 285 nm ($\log \varepsilon = 3.9$). Zeiss and Zwanzig (11) noted two absorption bands for the chromate ester derived from 2-methylfenchol: one at 287 and the other at 393 nm. However, these authors gave no values for the extinction coefficient.

The quantity of chromium determined by

TABLE 1. Proton magnetic resonance spectra determined in CCl_4

Compound	Chemical shift	Multiplicity	Type of protons
1-Methylcyclohexanol	1.18±0.02	Singlet	CH_3
	1.48±0.02	Broad singlet	$(CH_2)_5$
	3.10±0.02	Singlet	OH
Di(1-methylcyclohexyl) chromate	1.50±0.02	Singlet	CH_3
	1.57±0.02	Broad singlet	$(CH_2)_5$

chemical analysis (12) was in good agreement with stoichiometric composition of di(1-methylcyclohexyl) chromate.

Hydrolysis of Di(1-methylcyclohexyl) Chromate

The p*H* values were measured at different times during the hydrolysis of di(1-methylcyclohexyl) chromate in a closed system (~9.5 g of ester in 1 l water).

In the first 10 min, the p*H* value decreased rapidly (Fig. 1). Further decrease was much slower, and the p*H* value remained practically constant (within the limits of the sensitivity of the p*H* meter and other experimental errors) even after one week. The first rapid decrease obviously corresponded to the progressive hydrolysis of the chromate ester into chromic acid and 1-methylcyclohexanol. This period was followed by a very slight gradual increase in p*H*, but this could not be characterized clearly because of the limit of sensitivity of the method employed.

Assuming that one of the products of hydrolysis is a good electrolyte (chromic acid) as compared to the ester, measurement of conductivity should indicate the rate of hydrolysis of the ester. Preliminary measurements showed a variation of conductivity of an 'ester + water' solution as a function of time, and also the variation depended on whether the system was open or closed. Results are given in Fig. 2.

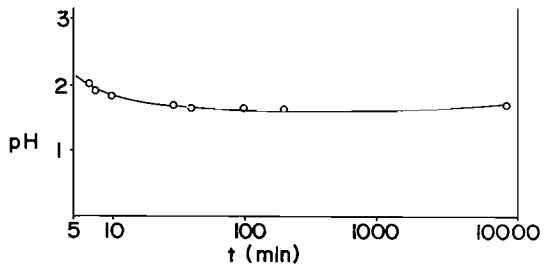

FIG. 1. Hydrolysis of chromic acid ester; p*H* as a function of time.

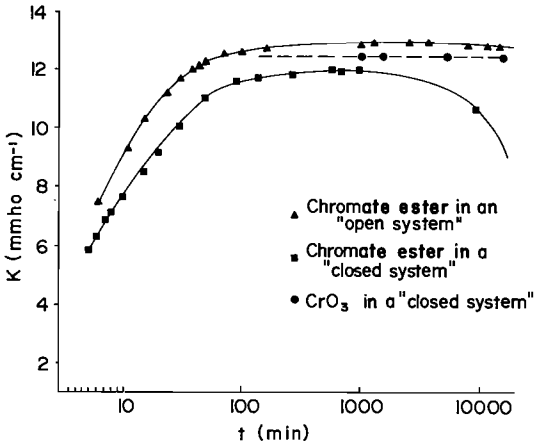

FIG. 2. Hydrolysis of chromic acid ester; specific conductivity as a function of time.

Hydrolysis of a closed system led to three distinct regions of conductivity as a function of time. (*1*) A region where conductivity increased rapidly and continuously for the first 2 h. (*2*) A region where conductivity was a maximum and could be considered constant for a period of 20 h. (*3*) A region where conductivity first decreased rapidly, then slowly; and the slow drift was observed even after 25 days.

In an open system conductivity first increased as in (*1*) until the maximum was reached. It then remained constant even after 25 days.

Conductivity of an inorganic chromate in a closed system is also given in Fig. 2. The final conductivity of the hydrolyzed ester in an open system is equal to the conductivity of a chromate solution containing the same amount of Cr^{VI}. Hydrolysis of the ester was completed after 1000 min.

Electrochemical Characteristics of Pure Iron in Solutions Containing Hydrolyzed Chromic Acid Ester

Aqueous Solutions

The dissolution or corrosion potential of iron immersed in a solution with hydrolysis products

Can. J. Chem. Downloaded from www.nrcresearchpress.com by 210.87.254.42 on 09/05/12
For personal use only.

Can. J. Chem. Downloaded from www.nrcresearchpress.com by 210.87.254.42 on 09/05/12
For personal use only.

of chromate ester of 1-methylcyclohexanol is the same as that of iron immersed in a solution containing CrO_3 with the equivalent quantity of Cr^{VI} and with the same pH. This result has been confirmed for different concentrations and different values of pH (Fig. 3). The linear relation between potential and the logarithm of the concentration is found to be the same for CrO_3 and for hydrolyzed ester. Figure 4 gives the polarization curves for iron immersed in a solution with hydrolysis products of chromate ester and with CrO_3 containing the equivalent quantity of Cr^{VI}. The cathodic curves of iron in the two solutions were found to be almost the same. This is also valid for anodic curves. However, it can be noted that the anodic current in the passivation region is somewhat more important in the case of CrO_3 than in the presence of hydrolysis products of chromate ester.

The electrochemical characteristics (corrosion current, cathodic exchange current, and hydrogen overvoltage) are determined for iron in different concentrations of CrO_3 and hydrolyzed chromate ester. The results are given in Figs. 5 and 6, which show that for the concentrations and pH used, the electrochemical parameters are almost the same as those determined previously.

Aqueous Solutions Containing Sulfuric Acid

Figure 7 shows polarization curves of iron in the two solutions containing sulfuric acid (5×10^{-4} M): one with CrO_3 and the other with hydrolyzed chromic acid ester with the equivalent quantity for Cr^{VI}. The curves are almost identical, indicating that the electrochemical

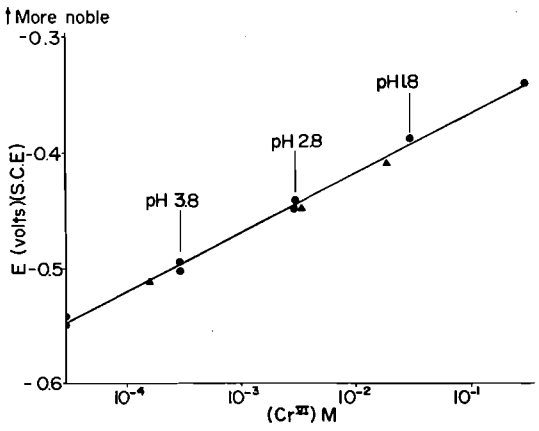

FIG. 3. Dissolution potential of an iron electrode as a function of pH and Cr^{VI} content (mol l^{-1}) in CrO_3 solution (●) and hydrolyzed chromate ester (▲).

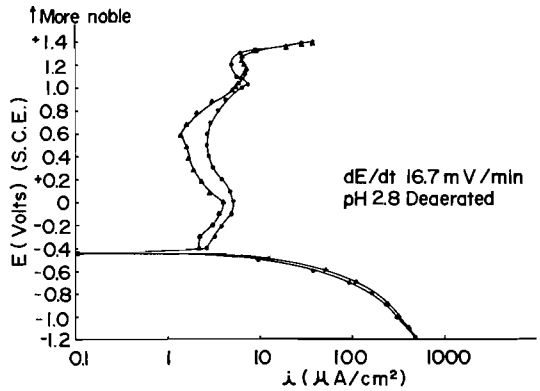

FIG. 4. Polarization curves of CrO_3 in water (●) and hydrolyzed chromate ester (▲). $[Cr^{VI}] = 3 \times 10^{-3}$ M; pH = 2.8.

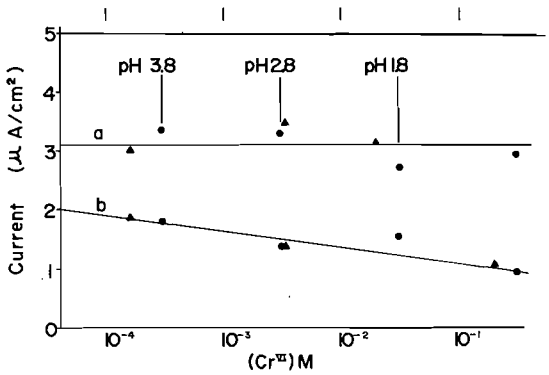

FIG. 5. Corrosion currents (*a*) and cathodic exchange currents (*b*) as a function of pH and Cr^{VI} content of hydrolyzed chromate ester (▲) and CrO_3 in water (●).

parameters are not different. It can also be observed that the anodic current during passivation is more important in the case of CrO_3 than that of hydrolyzed ester.

We can also mention that for a low concentration of hydrolyzed ester, below that required to produce an effective inhibition, we found that there is no important variation of electrochemical characteristics of iron if compared with that of iron in the same solution but with equivalent quantity of Cr^{VI} in a CrO_3 solution.

Interpretations

The results of hydrolysis (Fig. 2) suggest the following explanations in the case of large excess of water and small quantities of ester. In the closed system, the first step where the conduct-

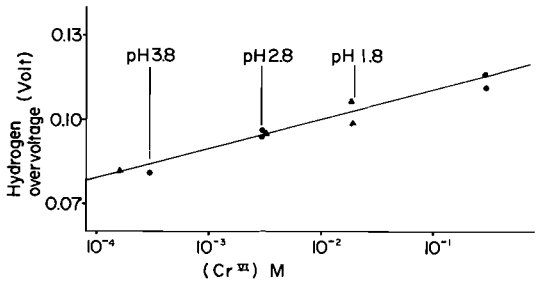

FIG. 6. Hydrogen overvoltage (in V) at $i = 10\ \mu A$ as a function of pH and Cr^{VI} content of hydrolyzed chromate ester (▲) and CrO_3 in water (●).

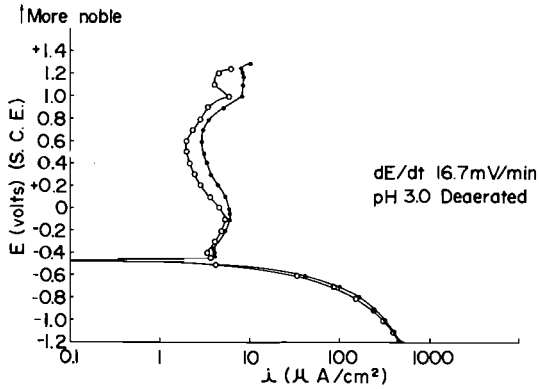

FIG. 7. Polarization curves of iron in $5 \times 10^{-4}\ M$ H_2SO_4 solutions containing CrO_3 (●) or hydrolyzed chromate ester (○). $[Cr^{VI}] = 1 \times 10^{-2}\ M$; p$H$ = 3.0.

ivity is continuously increasing agrees with the progressive hydrolysis of the chromic acid ester.

The region of maximum conductivity would correspond to complete hydrolysis, *i.e.*, the reaction mixture then contains 1-methylcyclohexanol and chromic acid

$$ROCrO_2OR \xrightarrow{\text{excess } H_2O} 2ROH + H_2CrO_4$$

Finally, the region showing a drift in conductivity after the maximum would correspond to the reaction of a strong acid (chromic acid) with a weak base (1-methylcyclohexanol). Indeed, the behavior of 1-methylcyclohexanol in the presence of chromic acid is a consequence of the basic character of the alcohols (13, 14) which act as Lewis bases, capable of accepting a proton dissociated from the chromic acid. This reaction is obviously impossible if one permits evaporation of the alcohol in an open system (Fig. 2). This hypothesis has been verified by preparing a solution with a mixture of 1-methylcyclohexanol and chromic acid similar to that expected from complete hydrolysis of the chromic ester; a similar curve for the region showing a drift in the conductivity was obtained.

This explanation is also supported by the following results: the extraction of the hydrolysis products derived from di(1-methylcyclohexyl) chromate gives more than 80% of the expected amount of 1-methylcyclohexanol; it is the single organic product obtained from the mixture. In view of these results, one must conclude that there is no oxidation–reduction reaction during the hydrolysis. Moreover, during the extraction, the organic layer remains colorless, indicating the absence of chromate ester, which is soluble in the organic solvents used (ether, hexane). In order to extract all traces of organic compounds possibly present, extractions have also been performed after saturation of the aqueous layer with NaCl; these extractions gave the same results as those obtained in the untreated aqueous layer. Similar results were observed after the extraction of the aqueous layer previously neutralized with a solution of 10% NaOH.

Furthermore, we mixed 1-methylcyclohexanol and an aqueous solution of chromic acid under the same conditions as the hydrolysis of di(1-methylcyclohexyl) chromate. We extracted the mixture with hexane and observed that the hexane fraction always remained colorless. The absence of chromic ester was verified by p.m.r. analysis; the hydrolyzed chromate ester gave (Table 2) the same characteristics as those observed for the mixture '1-methylcyclohexanol + CrO_3 + H_2O'. These results also show the disappearance of the —OH signal, which is fused with the H_2O signal.

In order to evaluate the stability of CrO_3 in water, we studied the behavior of an aqueous solution of CrO_3 under the same conditions as those existing during the hydrolysis (*i.e.* closed system, continuous agitation, constant temperature). Conductivity of such a solution remained constant (Fig. 2), thus indicating the stability of the chromates.

The maximum conductivity of completely hydrolyzed chromate ester in either an open or closed system corresponds to the conductivity of an equivalent quantity of Cr^{VI} present as H_2CrO_4. Figure 8 shows a linear relation between the concentration of Cr^{VI} (in p.p.m.) contained in H_2CrO_4 and log K (in $\mu mho\ cm^{-1}$). The calculated quantities of Cr^{VI} as H_2CrO_4,

Can. J. Chem. Downloaded from www.nrcresearchpress.com by 210.87.254.42 on 09/05/12
For personal use only.

TABLE 2. Proton magnetic resonance spectra determined in distilled water

Compound or mixture	Chemical shift	Multiplicity	Type of protons
1-Methylcyclohexanol	1.18±0.02	Singlet	CH_3
	1.20±0.05	Singlet	OH
	1.50±0.02	Broad singlet	$(CH_2)_5$
1-Methylcyclohexanol $+CrO_3 + H_2O$	~1.2	Singlet	CH_3
	~1.5	Broad singlet	$(CH_2)_5$

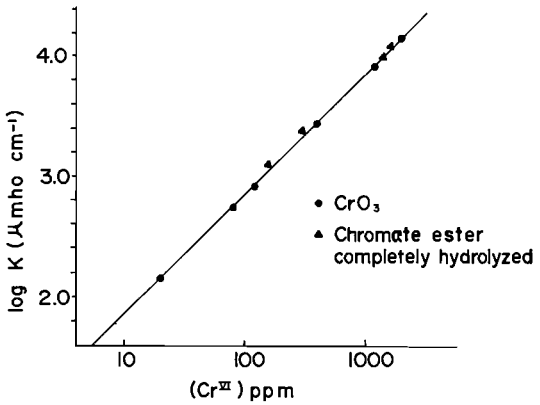

FIG. 8. Logarithm of specific conductivity as a function of Cr^{VI} content of CrO_3 in water (●) and hydrolyzed chromic acid ester (▲).

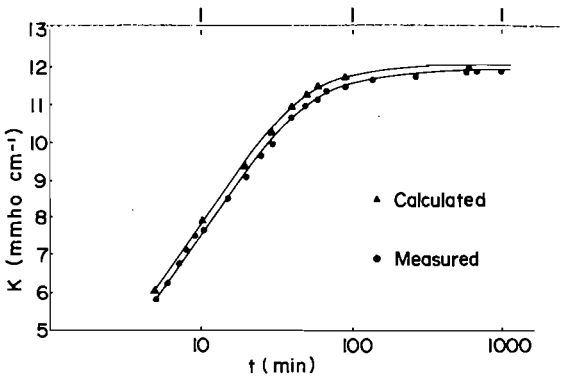

FIG. 9. Hydrolysis of chromate ester: ●: experimental curve, ▲: calculated curve considering that hydrolysis is complete.

assuming complete hydrolysis of ester in chromate, show the same linear relation with respect to log K. This observation is confirmed for four different concentrations of hydrolyzed esters. We can therefore conclude that complete dissociation gives chromic acid as a final product along with the alcohol.

It is interesting to consider the stable ions formed during hydrolysis. We consider that maximum conductivity in an open or closed system corresponds to complete dissociation. The progressively increasing conductivities from the beginning of dissociation until the maximum permits an estimate of the rate of dissociation. The fraction of ester hydrolyzed at any time of the hydrolysis can thus be determined. By using a calibration curve of conductivity *vs.* $[CrO_3]$ (Fig. 8), and by assuming that the chromate ester hydrolysis products are completely dissociated, it is possible to construct calculated curves of conductivity *vs.* time during the hydrolysis of chromic acid ester. Close agreement between the calculated and experimental curves (Fig. 9) support the assumption that the chromic acid ions are the ones responsible for the conductivity values obtained. There may be some formation of monoester but this intermediate cannot be detected.

The presence of alcohol as a product of hydrolysis of chromate ester does not affect the inhibiting power of chromates in an aqueous solution, with or without the presence of sulfuric acid. This is the case at least when water is present in large excess, certainly corresponds to most of the practical conditions. This assumption may not hold when the amount of alcohol is comparable to the amount of water present. It may be noted from Figs. 4 and 7 that the current density during passivation is slightly lower for iron in solutions containing hydrolyzed chromate ester than for solutions containing CrO_3 and this may contribute to a slightly higher protective power of chromate ester employed as inhibitors.

In a closed system, a side reaction occurs between the protons of the chromic acid and the alcohol. This may shift the pH towards higher values. If this shift is very significant, it will affect the electrochemical characteristics of iron and consequently improve the inhibiting power of hydrolyzed esters.

Can. J. Chem. Downloaded from www.nrcresearchpress.com by 210.87.254.42 on 09/05/12
For personal use only.

Conclusions

The hydrolyzed chromate ester of 1-methylcyclohexanol is as effective as chromium trioxide for protecting metallic surfaces in a polar medium. The complete and progressive hydrolysis of chromate ester gives chromic acid and the alcohol. The monoester, if present, is assumed to be very unstable. If the hydrolysis is done in a closed system, a side reaction of the chromic acid with alcohol may occur. It has been shown that conductivity measurement is suitable to study the rate of hydrolysis of organometallic compounds.

The authors wish to thank the Minister of Education of Quebec for the research grant (Programme de Formation de Chercheurs et d'Action Concertée). We are grateful to Miss Raymonde Caron for experimental assistance.

1. G. H. CARTLEDGE. Br. Corros. J. **1**, 293 (1966).
2. T. P. HOAR and U. R. EVANS. J. Chem. Soc. 2476 (1932).
3. D. M. BRASHER, J. G. BEYNON, K. S. RAJAGOPALAN, and J. G. N. THOMAS. Br. Corros. J. **5**, 264 (1970).
4. W. TREIBS. Chem. Ztg. Chem. Apparatur, **24**, 953 (1967).
5. L. CERVENY. Ann. Univ. Ferrara, Sez, 5, Suppl. **4(2)**, 701 (1966).
6. L. CERVENY. Werkst. Korros. **9**, 543 (1958).
7. L. CERVENY. Ann. Univ. Ferrara, Sez, 5, 1970 (Pub. 1971) (Suppl. 5) p. 699.
8. H. WIENHAUS. Ber. **47**, 322 (1914).
9. H. H. ZEISS and C. N. MATTHEWS. J. Am. Chem. Soc. **78**, 1694 (1956).
10. J. M. HACHEY. Ph.D. Thesis, Université de Montréal, Montréal, Québec. 1972.
11. H. H. ZEISS and F. R. ZWANZIG. J. Am. Chem. Soc. **79**, 1733 (1957).
12. A. I. VOGEL. A text book of quantitative inorganic analysis. Longmans, London. 1961. p. 311.
13. E. S. GOULD. Mechanism and structure in organic chemistry. Holt, Reinhard and Winston, New York, 1959. Chapt. 4.
14. J. B. HENDRICKSON, D. J. CRAM, and G. S. HAMMOND. Organic chemistry. McGraw-Hill. 1970. Chapt. 8.

Can. J. Chem. Downloaded from www.nrcresearchpress.com by 210.87.254.42 on 09/05/12
For personal use only.

Kinetics and Mechanism of the Oxidation of Benzyl Alcohol and Benzaldehyde by Aqueous Sodium Dichromate

DONALD G. LEE AND UDO A. SPITZER

The Department of Chemistry, University of Regina, Regina, Saskatchewan S4S 0A2

Received May 6, 1975

DONALD G. LEE and UDO A. SPITZER. Can. J. Chem. **53**, 3709 (1975).

A kinetic study of the oxidation of a series of substituted benzyl alcohols and benzaldehydes by neutral aqueous sodium dichromate has been completed. The aldehydes are more resistant to oxidation because the reaction mechanism presumably involves hydration prior to oxidation, and under the conditions employed the extent of this hydration is suppressed. These conclusions are consistent with the activation parameters which indicate that the difference in oxidation rate is due to a more negative entropy of activation for the aldehydes.

DONALD G. LEE et UDO A. SPITZER. Can. J. Chem. **53**, 3709 (1975).

On a complété une étude cinétique de l'oxydation d'une série d'alcools benzyliques substitués et de benzaldéhydes par du dichromate de sodium aqueux en milieu neutre. Les aldéhydes sont plus résistants à l'oxydation dû au fait que le mécanisme de réaction implique probablement une hydratation avant l'oxydation et dans les conditions utilisées l'hydratation est supprimée. Ces conclusions sont en accord avec les paramètres d'activation qui indiquent que les différences entre les vitesses de réaction sont dûes à une entropie qui est plus négative pour l'activation des aldéhydes.

[Traduit par le journal]

Introduction

The oxidation of aromatic alcohols to the corresponding aldehydes by aqueous sodium dichromate at elevated temperatures (~100 °C) is a reaction that may be used for synthetic preparations that are difficult to accomplish using other oxidants (1). For example, Wakselman *et al.* have recently described the preparation of 7-coumarincarbaldehyde in 84% yield by treatment of the corresponding alcohol with aqueous sodium dichromate at reflux temperature (2). The reaction is of particular interest because it is known that under acidic conditions (which are usually employed for chromic acid oxidations) primary alcohols are oxidized by chromium(VI) to give substantial amounts of carboxylic acids or esters (3, 4) unless the aldehyde can be distilled from the reaction mixture as it forms (5, 6). However, neutral chromium(VI) solutions do not oxidize aromatic aldehydes at an appreciable rate until considerably higher temperatures (150–200 °C) are attained (1).

In the present work we have attempted to increase our quantitative understanding of these reactions by studying the kinetics of the oxidation of several substituted benzyl alcohols and benzaldehydes by aqueous sodium dichromate.

Experimental

The kinetic analyses were performed using a pseudo first-order approach where the substrate concentrations were in excess and the chromium(VI) concentration was monitored spectrophotometrically. In all cases good pseudo first-order kinetics were maintained for more than two half-lives of the reaction (Fig. 1).

The rate data were obtained in the following manner. The required amount of alcohol was weighed into a flask, 20 ml of phosphate buffer was added, and the flask was stoppered and placed in a thermostated bath. Then 1.00 ml of 0.1 *M* chromium(VI) solution was added and the timer started after the solution had been thoroughly mixed. One ml aliquots were withdrawn at intervals, quenched by dilution with cold water to 10.0 ml, centrifuged, and analyzed spectrophotometrically for chromium(VI).

Since the oxidation of the aldehydes could only be studied at temperatures above 150 °C it was necessary to use a sealed reactor for these experiments. The reaction vessel, which has previously been described (7), was charged with the reactants at room temperature, sealed, purged with nitrogen, and brought to a pressure of 320 p.s.i. of N_2. The reactor was then heated to and stabilized at the desired temperature. This required about 1 h of heating; however, since the reactions were always pseudo first-order the rates could be followed by withdrawing samples when the temperature had stabilized and taking the time of the first sample as zero.

The pseudo first-order rate constants were obtained from the slopes of plots of the logarithm of the concentration of $HCrO_4^-$ against time, and then converted to second-order rate constants through division by the concentration of the substrate.

Can. J. Chem. Downloaded from www.nrcresearchpress.com by 210.87.254.40 on 09/05/12
For personal use only.

Can. J. Chem. Downloaded from www.nrcresearchpress.com by 210.87.254.40 on 09/05/12
For personal use only.

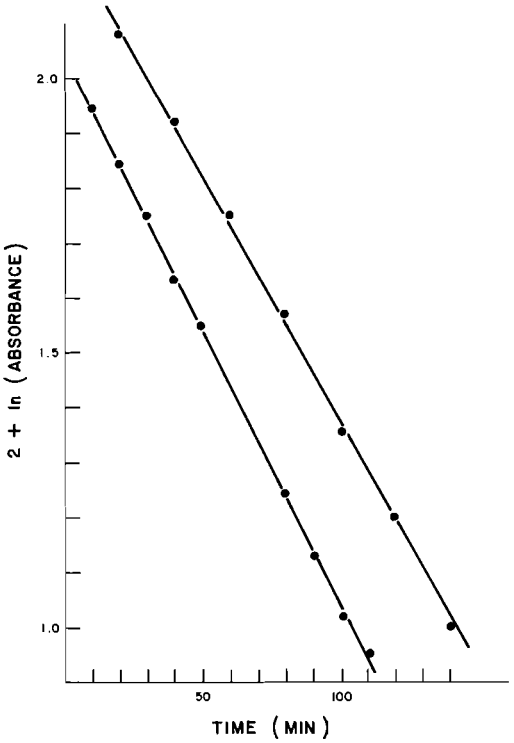

FIG. 1. Pseudo first-order rate plots for the oxidation of benzyl alcohol at 95.9 °C (upper) and the oxidation of benzaldehyde at 170 °C (lower).

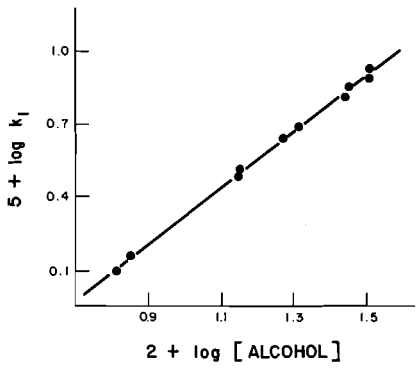

FIG. 2. Dependence of rate constants upon benzyl alcohol concentration. Slope = 1.09, r = 0.997.

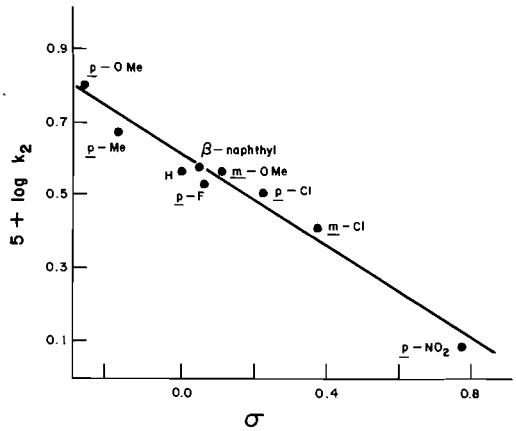

FIG. 3. Hammett plot for the aqueous dichromate oxidation of benzyl alcohols. Slope = −0.61, r = 0.972.

The substituted benzyl alcohols and benzaldehydes were all obtained commercially and purified prior to use. Benzyl alcohol α,α-d_2 was prepared by the lithium aluminum deuteride reduction of benzoic acid (8).

Results and Discussions

Oxidation of Benzyl Alcohol

The aqueous dichromate oxidation of benzyl alcohol appears to be similar in several respects to chromic acid oxidations (9). Some of the common features are: the reaction is first-order in oxidant (Fig. 1) and in benzyl alcohol (Fig. 2); a primary isotope effect is observed when the α-hydrogens are replaced by deuterium (Table 1); a negative Hammett ρ value is obtained (Fig. 3); and similar activation parameters ($\Delta H^{\ddagger}$ = 17.9 ± 0.4 kcal/mole and $\Delta S^{\ddagger}$ = 25 ± 2 e.u.) are obtained (10). Furthermore, chromic acid oxidations of alcohols are known to exhibit rate increases when non-polar organic co-solvents are used (11). These increases, caused by the decrease in solvent polarity, have been attributed to an equilibrium shift favoring the formation of chromate esters. A similar effect was noted in the aqueous sodium dichromate oxidations when various mixtures of dioxane and water were used.

Because of these several similarities it is not unlikely that parallel mechanisms prevail for the two reactions. Consequently we have assumed, in analogy with chromic acid oxidations, that chromium(VI) esters are also involved as intermediates in the oxidation of alcohols by aqueous sodium dichromate. (See Scheme 1).

[1] $HCrO_4^- + \phi CH_2OH \rightleftharpoons \phi CH_2OCrO_3^- + H_2O$

[2] $\phi CH_2OCrO_3^- \rightarrow \phi CHO + HCrO_3^-$

SCHEME 1

The unfavorable entropy of activation may, at least partially, be due to formation of a cyclic transition state such as **1**.

TABLE 1. Isotope effects on the oxidation of benzyl alcohol by aqueous sodium dichromate*

Substrate	[Alcohol] (M)	$k_2 \times 10^4$ ($M^{-1}s^{-1}$)†	k_H/k_D
Benzyl alcohol	0.0744	7.8	
Benzyl alcohol	0.0964	7.3	
			9.4±0.9
Benzyl alcohol α,α-d_2	0.0907	0.76	
Benzyl alcohol α,α-d_2	0.108	0.85	

*[Cr(VI)] = 5.8×10^{-3} M, T = 96.4 °C. The pH was adjusted to 5.52 at 25 °C, [$H_2PO_4^-$] = 0.750 M, [HPO_4^{2-}] = 0.138 M.
†The second-order rate constants were obtained by division of the pseudo first-order constants with the concentration of alcohol present.

TABLE 2. Rate constants for the oxidation of benzyl alcohol*

pH†	[$H_2PO_4^-$] (M)	[HPO_4^{2-}] (M)	$k_1 \times 10^5$ (s^{-1})‡	log k_2§
7.50	0.0494	0.380	1.73	−4.53
7.02	0.126	0.350	2.74	−4.31
6.63	0.260	0.300	3.44	−4.21
6.09	0.500	0.225	4.39	−4.09
5.41	0.748	0.130	6.11	−4.04

*[Cr(VI)] = 5.18×10^{-3} M, [alcohol] = 0.06 − 0.07 M, T = 96 °C.
†pH was measured at 25 °C.
‡k_1 is a pseudo first-order rate constant.
§$k_2 = k_1$/[alcohol].

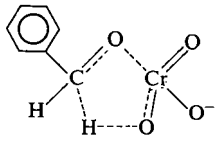

1

The negative Hammett ρ value (−0.6) is probably a consequence of the fact that the slow step involves development of a carbonyl which would be destabilized by electron-withdrawing substituents. The magnitude of the ρ value is less than that observed for the corresponding chromic acid oxidations, thus suggesting that the carbonyl is less fully developed under neutral conditions.

The slight increase in rate that is observed as the pH is decreased (Table 2) is difficult to account for quantitatively and may, in fact, be due to experimental uncertainties since the pH was measured at 25 °C while the reactions were actually carried out at 96 °C (7).

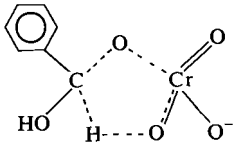

2

The Oxidation of Benzaldehyde

The rate of the oxidation of benzaldehyde shows a first-order dependence upon both the oxidant (Fig. 1) and the substrate (Fig. 4), but requires a much higher temperature than the oxidation of benzyl alcohol (Table 3).

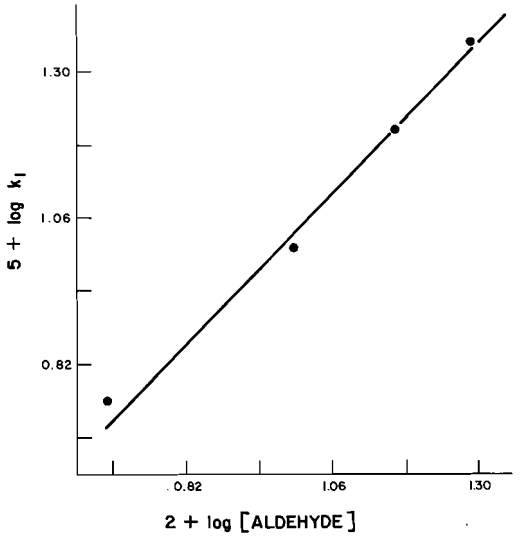

FIG. 4. Dependence of rate upon benzaldehyde concentration. Slope = 0.9 ± 0.1, r = 0.989.

Can. J. Chem. Downloaded from www.nrcresearchpress.com by 210.87.254.40 on 09/05/12
For personal use only.

TABLE 3. Rate constants for the oxidation of benzaldehyde*

pH†	$[H_2PO_4^-]$ (M)	$[HPO_4^{2-}]$ (M)	$k_1 \times 10^4$ (s^{-1})	log k_2‡
7.02	0.126	0.350	2.54	−2.57
6.56	0.264	0.300	1.53	−2.79
6.03	0.500	0.220	1.20	−2.90
5.46	0.750	0.133	1.11	−2.93

*[Cr(VI)] = 5.45×10^{-3} M, [benzaldehyde] = 0.0946, T = 170 °C.
†pH was measured at 25 °C.
‡$k_2 = k_1$/[benzaldehyde].

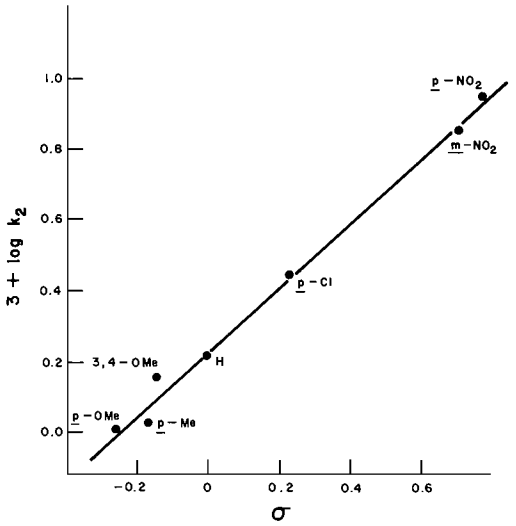

FIG. 5. Hammett plot for the aqueous dichromate oxidation of benzaldehyde. Slope = 1.1, r = 0.983.

The Hammett ρ value is positive for the oxidation of substituted benzaldehydes (Fig. 5) in contrast to the negative ρ value observed for the oxidation of the corresponding benzyl alcohols. A similar observation for the oxidation of aldehydes by chromic acid (12) has been shown to be due to a pre-oxidative hydration step [3]. The suppression of such a hydration step at high temperatures (13) offers an explanation as to why aldehydes are more resistant to oxidation under the conditions required for oxidation by aqueous

$$[3] \qquad RCHO + H_2O \overset{K}{\rightleftharpoons} RCH(OH)_2$$

sodium dichromate. Because $HCrO_4^-$ is not a vigorous oxidant, high temperatures must be used to obtain a reasonable reaction rate; however, independent studies have shown that the extent of carbonyl hydration decreases as temperature increases (13, 14). Consequently the expected increase in the rate of [6] (Scheme 2)

$$[4] \qquad \phi CHO + H_2O \overset{K_4}{\rightleftharpoons} \phi CH(OH)_2$$

$$[5] \qquad \phi CH(OH)_2 + HCrO_4^- \rightleftharpoons \phi \overset{OH}{\overset{|}{C}}HOCrO_3^- + H_2O$$

$$[6] \qquad \phi \overset{OH}{\overset{|}{C}}HOCrO_3^- \rightarrow \phi CO_2H + HCrO_3^-$$

SCHEME 2

with temperature would be partly nulified by a concurrent decrease in K_4, and it is thus necessary to use higher temperatures for aldehyde oxidations than for alcohol oxidations. It is for this reason that aqueous sodium dichromate is particularly useful for the oxidation of alcohols to aldehydes (1).

When the response of the rate of reaction to temperature changes was studied the activation parameters were found to be $\Delta H^{\ddagger} = 13.2 \pm 0.4$ kcal/mole and $\Delta S^{\ddagger} = -30 \pm 4$ e.u. This highly unfavorable entropy of activation is probably due to a combination of three factors: (*i*) the transition state is likely cyclic as in **2**, (*ii*) the formation of an aldehyde hydrate which precedes the rate determining step would have a negative entropy (14), and (*iii*) it is likely that the esterification step would also exhibit a negative entropy (15).

A further interesting fact that emerges from a consideration of the activation parameters is that the difference in the rates of oxidation of benzyl alcohol and benzaldehyde is due mainly to a difference in the entropy of activation, which is in turn likely related to the additional hydration step that occurs only in the aldehyde oxidation mechanism.

The authors are grateful to the National Research Council of Canada and the Saskatchewan Research Council for financial assistance.

Can. J. Chem. Downloaded from www.nrcresearchpress.com by 210.87.254.40 on 09/05/12
For personal use only.

1. D. G. LEE and U. A. SPITZER. J. Org. Chem. **35**, 3589 (1970).
2. M. WAKSELMAN, J. F. HAMON, and M. VILKAS. Tetrahedron, **30**, 4069 (1974).
3. W. A. MOSHER and D. M. PREISS. J. Am. Chem. Soc. **75**, 5605 (1953).
4. G. R. ROBERTSON. *In* Organic synthesis. Coll. Vol. I. Wiley, New York. 1941. p. 138.
5. E. WERTHEIM. J. Am. Chem. Soc. **44**, 2658 (1922).
6. A. L. HENNE, R. L. PELLEY, and R. M. ALM. J. Am. Chem. Soc. **72**, 3370 (1950).
7. D. G. LEE and U. A. SPITZER. Can. J. Chem. **49**, 2763 (1971).
8. H. O. HOUSE. Modern synthetic reactions. Benjamin, New York. 1965.
9. R. STEWART. Oxidation mechanisms. Benjamin, New York. 1964. pp. 37–45.
10. D. G. LEE and D. T. JOHNSON. Can. J. Chem. **43**, 1952 (1965).
11. F. H. WESTHEIMER. Chem. Rev. **45**, 419 (1949).
12. J. ROCEK and C. S. NG. J. Org. Chem. **38**, 3348 (1973).
13. J. L. KURZ. J. Am. Chem. Soc. **89**, 3524 (1967).
14. R. P. BELL. Adv. Phys. Org. Chem. **4**, 1 (1966).
15. H. A. SMITH. J. Am. Chem. Soc. **61**, 254 (1939); E. K. EURANTO. The chemistry of carboxylic acids and esters. *Edited by* S. Patai. Interscience, Toronto. 1969. p. 505–588.

Can. J. Chem. Downloaded from www.nrcresearchpress.com by 210.87.254.40 on 09/05/12
For personal use only.

4-Methylene-1,2,3-benzotriazines

HANDRICK FONG AND KEITH VAUGHAN

Department of Chemistry, Saint Mary's University, Halifax, Nova Scotia B3H 3C3

Received June 3, 1975

HANDRICK FONG and KEITH VAUGHAN. Can. J. Chem. **53,** 3714 (1975).

Diazotization of 2′-aminoacetophenone, followed by coupling with primary aliphatic amines, affords unstable triazenes which readily undergo cyclodehydration over neutral alumina to give 3-alkyl-4-methylene-1,2,3-benzotriazines (**5***a–d*). 3-Aryl-4-methylene-1,2,3-benzotriazines (**8***a–c*) are likewise obtained by cyclodehydration of the stable 1-(*ortho*-acetylphenyl)-3-aryltriazenes (**7***a–c*). Attempted synthesis of the unsubstituted 4-methylene-1,2,3-benzotriazine (**5***e*), by the same method, did not succeed. 4-Hydroxy-1,2,3-benzotriazines (**4**) are postulated as intermediates in the cyclodehydration; this hypothesis is supported by the isolation of the stable 4-hydroxy-1,2,3-benzotriazine (**12**) from the coupling reaction of methylamine with the diazonium salt derived from *ortho*-aminobenzophenone. An account of a preliminary study of the thermolysis of 3-methyl-4-methylene-1,2,3-benzotriazine (**5***a*) is included.

HANDRICK FONG et KEITH VAUGHAN. Can. J. Chem. **53,** 3714 (1975).

La diazotation de l'amino-2′ acétophénone suivie par un couplage avec des amines aliphatiques primaires conduit aux triazènes instables qui subissent facilement une cyclodéshydratation en présence d'alumine neutre pour donner les alkyl-3 méthylène-4 benzotriazines-1,2,3 (**5***a–d*). De la même manière on peut obtenir les aryl-3 méthylène-4 benzotriazines-1,2,3,(**8***a–c*) par cyclodéshydratation des(*ortho*-acétylphényl-1) aryl-3 triazènes (**7***a–c*) stables. On n'a pas réussi à synthétiser par cette méthode le méthylène-4 benzotriazine-1,2,3 (**5***e*) non-substitué. On fait l'hypothèse que les hydroxy-4 benzotriazines-1,2,3 (**4**) sont des intermédiaires dans la cyclodéshydratation; cette hypothèse se base sur le fait que l'on peut isoler l'hydroxy-4 benzotriazine-1,2,3 (**12**) stable à partir de la réaction de couplage de la méthylamine avec le sel de diazonium dérivé de l'*ortho*-aminobenzophénone. On inclut un rapport préliminaire sur l'étude de la thermolyse du méthyl-3 méthylène-4 benzotriazine-1,2,3 (**5***a*).

[Traduit par le journal]

Introduction

In the series of 1,2,3-benzotriazines represented by **1**, the 4-oxo (**1***a*), 4-thio (**1***b*), and 4-imino (**1***c*) derivatives are well known and have been extensively studied (1).

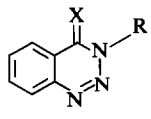

1 *a* X = O; *b* X = S; *c* X = NR′; *d* X = CH_2

Several methods are available for the synthesis of the 4-oxo derivatives; for example, the diazotization of substituted anthranilamides has long been known to give 1,2,3-benzotriazinones (2). In a similar manner, diazotization of *ortho*-aminothiobenzamide gives rise to 4-mercapto-1,2,3-benzotriazine, the tautomer of **1***b* (R = H) (3). Early work (4) on the diazotization of *ortho*-aminobenzamidines, which affords the 4-imino-1,2,3-benzotriazines (**1***c*), has been extended by Stevens and co-workers (5) to cover a wide variety of *N*-alkyl and *N*-aryl substituents. In contrast to the extent of knowledge of the derivatives **1***a*, **1***b*, and **1***c*, no example of a 4-methylene derivative (**1***d*) has previously been reported.[1]

In a previous report (6), the formation of triazenes, **2**, in the coupling reaction of aryl diazonium salts with primary aliphatic amines was shown to be strongly influenced by the nature of the substituent X [1].

[1] 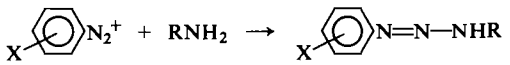

2

Maximum yields of triazene are obtained when X is a strongly electron-withdrawing group (*i.e.* —NO_2, —COMe, —CO_2Me, —CN), preferably in the *para*-position. However, reaction of *ortho*-substituted diazonium salts with alkylamines frequently afforded unstable triazenes, sometimes giving rise to anomalous products. For example, 1-(*ortho*-carbalkoxyphenyl)-3-alkyltriazenes, **9**,

[1]4-Methyl-1,2,3-benzotriazine, which has been reported recently (ref. 12), could be regarded as the 'tautomer' of the unsubstituted 4-methylene-1,2,3-benzotriazine (**1***d*, R = H).

Can. J. Chem. Downloaded from www.nrcresearchpress.com by 210.87.254.40 on 09/05/12
For personal use only.

Can. J. Chem. Downloaded from www.nrcresearchpress.com by 210.87.254.40 on 09/05/12
For personal use only.

have previously been shown (7) to undergo facile cyclization to 4-oxo-1,2,3-benzotriazines, **1***a*, and the *ortho*-nitrophenyltriazene (**2**, X = *ortho*-NO_2, R = Me) decomposes in the solid state or in solution (6). In the present work, we describe a study of the coupling reaction of the diazonium salts derived from *ortho*-aminophenyl ketones with primary amines; the triazenes obtained therefrom are the precursors of 4-methylene-1,2,3-benzotriazines (**1***d*), reported here for the first time.

Discussion

Treatment of an aqueous solution of the diazonium salt derived from *ortho*-aminoacetophenone with an excess of methylamine afforded an unstable orange-red solid **A**. Stirring the solid **A** in chloroform solution over neutral alumina gave a high yield of 3-methyl-4-methylene-1,2,3-benzotriazine (**5***a*, R = Me), the expected product of cyclodehydration of the *ortho*-acetylphenyltriazene, **3** (Scheme 1); no other product

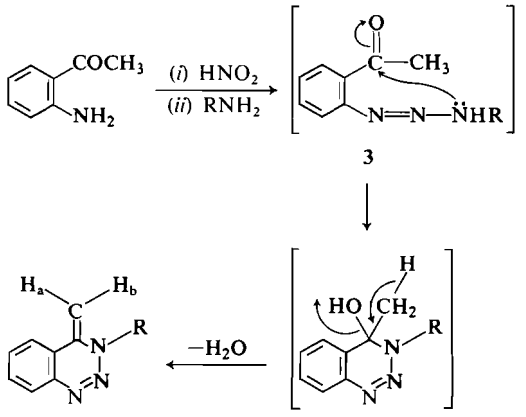

5 *a* R = Me
b R = Et
c R = *n*-Pr
d R = $PhCH_2$
e R = H

SCHEME 1

was obtained from the alumina catalyzed reaction. The n.m.r. spectrum of the orange-red solid **A** suggests the presence of the open-chain triazene **3**, as well as the 4-methylenetriazine **5***a*, and at least one other component, which may be the hydroxytriazine intermediate, **4**. The presence of the open-chain triazene **3** is inferred from comparison with the n.m.r. spectrum of the previously reported isomer, 1-(*para*-acetylphenyl)-3-methyltriazene (6). Attempted purification of the orange-red solid **A** by column chromatography on alumina, with CCl_4 as eluent, resulted only in formation of the 4-methylenetriazine **5***a*. Apparently the cyclodehydration of the triazene **3** occurs incompletely during the coupling reaction and is catalyzed by adsorption on alumina during chromatography or in the slurry. Attempted recrystallization of the orange-red solid **A** was unsuccessful, being accompanied by considerable decomposition.

3-Methyl-4-methylene-1,2,3-benzotriazine, **5***a*, is a yellow crystalline solid, which displays the expected spectral characteristics. Carbonyl absorption is absent in the infrared spectrum; the only prominent absorption in the i.r. is at 1620 cm^{-1}, assigned to the exocyclic C=C ethylenic group (8). The most characteristic features of the n.m.r. spectrum of **5***a* are the doublets at 4.40 and 3.83 p.p.m., arising from geminal coupling of the non-equivalent vinylic protons of the 4-methylene-group, H_A and H_B; the observed coupling constant (2.4 Hz) is typical of geminal, vinylic systems (ref. 8, p. 128). The assignment of the resonances at 4.40 and 3.83 p.p.m. to the vinylic protons H_A and H_B respectively is based on consideration of the deshielding effect of the benzene ring; proton H_A is in closer proximity to the π-electron system of the benzene ring and should therefore resonate at lower field. The AB pattern exhibited by **5***a* is typical of all 4-methylene-triazines described here.

The mass spectrum of **5***a*, surprisingly, does not exhibit a fragment corresponding to direct loss of N_2, which is characteristic of 1,2,3-benzotriazines (9). The initial fragmentation, as indicated by the base peak at *m/e* 130, involves the loss of CH_3N from the molecular ion. The most likely explanation for this unusual mode of fragmentation is that the molecular ion rearranges to give the more stable methylaminocinnoline ion (Scheme 2), which would then readily lose the methylamino group as CH_3N to give the parent cinnoline ion at *m/e* 130. The strong peak at *m/e* 103 in the mass spectrum of **5***a* is invariably observed in the mass spectra of benzodiazines (10), arising in this case by loss of HCN from the cinnoline fragment. An alternative mode of fragmentation of the molecular ion, indicated by a less abundant fragment at *m/e* 116, probably involves loss of the CH_3N_2 grouping from the unrearranged molecular ion.

The formation of 3-alkyl-4-methylene-1,2,3-benzotriazines by the method described above

TABLE 1. Spectral data for 3-alkyl-4-methylene-1,2,3-benzotriazines (5)

	R	$\nu_{max}(cm^{-1})$	δ (p.p.m.) Aromatic	H_a	H_b	R
5*a*	Me	1620	7.1–7.6 (m)	4.4 (d)*	3.83 (d)*	3.55 (3H, s, N—Me)
5*b*	Et	1620	7.1–7.7 (m)	4.4 (d)*	3.85 (d)*	3.95 (2H, q, CH_2)‡ 1.35 (3H, t, CH_3)‡
5*c*	*n*-Pr	1620	7.2–7.8 (m)	4.4 (d)*	— †	3.7–4.1 (3H, m, H_b+CH_2) 1.8 (2H, m, CH_2) 1.0 (3H, t, CH_3)‡
5*d*	$PhCH_2$	1620	6.9–7.9 (m)	4.4 (d)*	3.80 (d)*	5.2 (2H, s, benzylic CH_2)

*J = 2.4 Hz.
†H_b doublet is masked by the triplet of the N—CH_2 group.
‡J = 7 Hz.

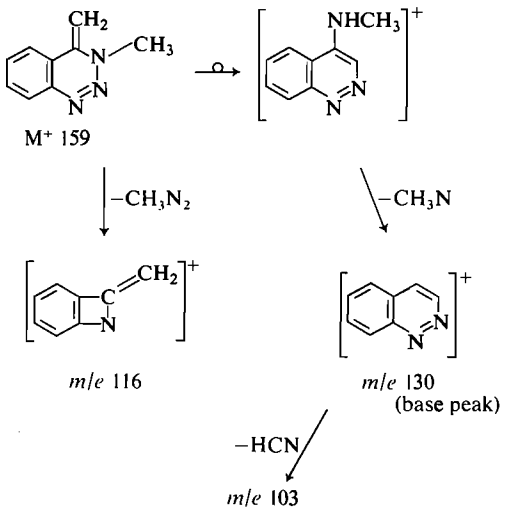

SCHEME 2

has been extended to the 3-ethyl- (**5***b*), 3-*n*-propyl- (**5***c*), and 3-benzyl- (**5***d*) 4-methylene-1,2,3-benzotriazines, which exhibit spectral characteristics analogous to those of 3-methyl-4-methylene-1,2,3-benzotriazine (Table 1). The 3-ethyl- and 3-*n*-propyl derivatives are both oils, with a strong orange color, whereas the 3-benzyl-derivative is, like the 3-methyl analog, a yellow solid. Attempted synthesis of the unsubstituted 4-methylene-1,2,3-benzotriazine, **5***e*, by the same method did not succeed; treatment of the diazonium salt from *ortho*-aminoacetophenone with aqueous ammonia afforded only *ortho*-aminoacetophenone, presumably by formation and fragmentation of the 1-aryltriazene (**6**, R = Me) [2]. Similar treatment of *ortho*-aminobenzophenone likewise resulted in regeneration of starting material.

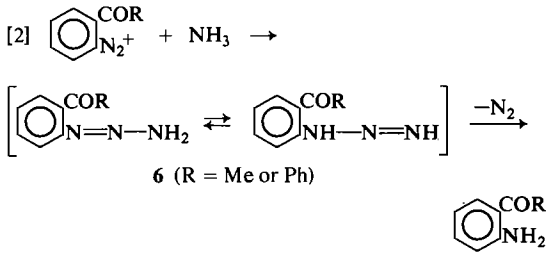

3-Aryl-4-methylene-1,2,3-benzotriazines, **8**, should, by analogy, be available from the cyclization of 1,3-diaryltriazenes, Ar—N=N—NH-Ar′, with an *ortho*-acetyl substituent in one aryl group. A search of the literature determined that no such diaryltriazene had previously been reported. Accordingly, *ortho*-aminoacetophenone was diazotized and coupled, in turn, with aniline, *para*-anisidine, *para*-aminoacetophenone, and methyl *para*-aminobenzoate, affording the 3-aryl-1-(*ortho*-acetylphenyl)-triazenes **7***a* (X = H), **7***b* (X = —OMe), **7***c* (X = —COMe), and **7***d* (X = —CO_2Me) respectively. Unlike the 3-alkyl-1-(*ortho*-acetylphenyl)-triazenes, these diaryltriazenes are stable crystalline solids, which exhibit the expected spectral characteristics (Table 2).

Some difficulty was encountered when cyclization of 3-phenyl-1-(*ortho*-acetylphenyl)-triazene, **7***a*, was attempted over alumina. Experiments carried out with acidic, basic, and neutral alumina, in turn, led to the conclusion that, as in the case of the 3-alkyl analogs, the best catalyst for the cyclization is neutral alumina. Various times for the reaction over neutral alumina were employed; surprisingly, a reaction time of only 2.5 h was necessary to effect complete cyclization. Longer reaction times resulted in a change in the nature of the product, but the exact course

Can. J. Chem. Downloaded from www.nrcresearchpress.com by 210.87.254.40 on 09/05/12
For personal use only.

TABLE 2. Spectral data for 1-(*ortho*-acetylphenyl)-3-aryltriazenes (7)

	X	$\nu_{max}(cm^{-1})$	δ (p.p.m.) Aromatic	*ortho*-CH_3CO—	X
7*a*	H	3200 (NH) 1645 (C=O)	6.7–8.0 (m)	2.55 (s)	—
7*b*	CH_3O—	3200 (NH) 1645 (C=O)	6.7–8.0 (m)	2.60 (s)	3.80 (s, O—CH_3)
7*c*	CH_3CO—	3200 (NH) 1680 (C=O, *para*) 1645 (C=O, *ortho*)	7.0–8.2 (m)	2.60 (s)	2.67 (s, *para*-CH_3CO—)
7*d*	CH_3OCO—	3200 (NH) 1730 (C=O, ester) 1645 (C=O, ketone)	7.0–8.2 (m)	2.65 (s)	3.95 (s, CH_3OCO—)

of this apparent decomposition has not been determined. The product of the 2.5 h treatment of 7*a* over neutral alumina is a red oil, which resisted attempts at crystallization and appeared

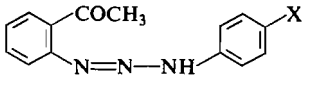

7 *a* X = H
b X = OMe
c X = COMe
d X = CO_2Me

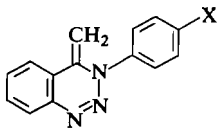

8 *a* X = H
b X = OMe
c X = COMe

to decompose during column chromatography. In spite of these difficulties, the spectral characteristics of the red oil demonstrate unequivocally that it is 3-phenyl-4-methylene-1,2,3-benzotriazine, 8*a*. The carbonyl absorption at 1645 cm^{-1} in the i.r. spectrum of 7*a* is completely absent in the i.r. spectrum of 8*a*. The conversion 7*a* → 8*a* is also accompanied by a characteristic change in the n.m.r. spectrum; the methyl singlet at 2.55 p.p.m. in the n.m.r. spectrum of 7*a* is absent in the n.m.r. spectrum of 8*a*, being replaced by the twin doublets of the vinylic protons, H_A and H_B, at 4.40 and 3.85 p.p.m. respectively.

Likewise, 3-(*para*-methoxyphenyl)-4-methylene-1,2,3-benzotriazine, 8*b*, was obtained as an oil from the corresponding triazene, 7*b*; on the other hand, 3-(*para*-acetylphenyl)-4-methylene-1,2,3-benzotriazine, 8*c*, was obtained as a crystalline solid. Both compounds display spectral characteristics analogous to those of the 3-phenyl derivative (Table 3). However, attempts to cyclize the ester 7*d* by this method did not succeed.

The facile cyclization of the *ortho*-acetylphenyltriazenes, 3, is somewhat different from the previously reported behavior of the unstable 1-(*ortho*-carbalkoxyphenyl)-3-alkyltriazenes, 9,

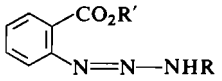

9

which readily undergo cyclization to the benzotriazinones (1*a*, R = alkyl) (7). The cyclization of the esters is a straight forward example of nucleophilic substitution at the carbonyl group, but analogous cyclization of the ketone 3 (Scheme 1) would afford the 4-hydroxytriazine intermediate 4 which is precluded from formation of an oxo derivative by the nature of the leaving group (*i.e.* CH_3—). Instead elimination of water from the 4-hydroxytriazine, involving the α-hydrogen of the original keto group, can take place, affording the 4-methylenetriazine 5.

Thus, the formation of the 4-methylenetriazines 5 necessitates the presence of α-hydrogen in the acyl group of the *ortho*-aminophenyl ketone used as starting material; absence of an α-hydrogen might well be the condition required for the formation of a stable 4-hydroxytriazine analogous to 4. Accordingly, *ortho*-aminobenzophenone, 10, was diazotized and the resulting diazonium salt solution was treated with an excess of methylamine, whereupon a white solid precipitated immediately. The white solid is quite stable, but does not exhibit the spectral characteristics of the expected triazene 11. Although

Can. J. Chem. Downloaded from www.nrcresearchpress.com by 210.87.254.40 on 09/05/12
For personal use only.

TABLE 3. Spectral data for 3-aryl-4-methylene-1,2,3-benzotriazines (**8**)

	X	$\nu_{max}(cm^{-1})$	δ (p.p.m.) Aromatic	H_a	H_b	X
8*a*	H	1600	7.1–7.9 (m)	4.4 (d)*	3.85 (d)*	—
8*b*	CH_3O—	1610	6.8–7.9 (m)	4.4 (d)*	3.80 (d)*	3.85 (s, O—CH_3)
8*c*	CH_3CO—	1680 (C=O, ketone) 1600	7.1–8.2 (m)	4.5 (d)*	4.05 (d)*	2.67 (s, *para*-CH_3CO—)

*J = 2.4 Hz.

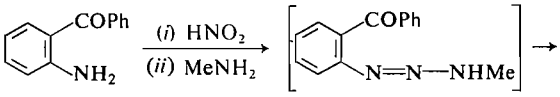

10 **11**

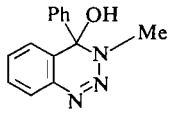

12

the molecular weight of 239, determined by mass spectrometry, correlated with formula **11**, the i.r. spectrum of the white solid does not display a band in the carbonyl region. There is, however, a strong, broad band at 2600–3300 cm^{-1}, indicating the presence of a hydroxyl group. The mass and i.r. spectral evidence clearly show that the white solid is the 4-hydroxy-1,2,3-benzotriazine, **12**; the n.m.r. spectrum of the white solid is also consistent with structure **12**. The 4-hydroxytriazine, **12**, represents the first reported example of a triazine derivative of this type.

Due to the interest in the thermolysis of 1,2,3-benzotriazines reflected in the recent literature (11), the thermal properties of the 4-methylenetriazines **5**, seem to be of potential significance. However, the results obtained so far from thermolysis experiments with the 3-methyl derivative **5***a* are disappointing. Little or no change was observed after refluxing **5***a* in ethanol, benzene, or *para*-xylene. Decomposition did take place when **5***a* was refluxed in diglyme, but this reaction afforded only intractable tar. The 3-methyl derivative **5***a* does decompose in the cold when stored for long periods; the yellow crystalline solid darkens in color and becomes gummy in texture. The exact nature of this decomposition is under further investigation.

Experimental

Melting points were obtained on a hot-stage apparatus and are uncorrected. Infrared spectra were recorded with liquid paraffin mulls on a Perkin-Elmer Model 467 grating spectrophotometer, and u.v. spectra on a Perkin-Elmer Model 402 ultraviolet and visible spectrophotometer. Nuclear magnetic resonance spectra were recorded in deuteriochloroform as solvent, using tetramethylsilane as internal standard, with a Varian EM360 60 MHz spectrometer. Mass spectral data were obtained with a Dupont–C.E.C. Model 21-491 spectrometer.

3-Methyl-4-methylene-1,2,3-benzotriazine, 5a

ortho-Aminoacetophenone (0.85 g, 0.0063 mol) was dissolved in 15 ml of 2 *M* hydrochloric acid and diluted with 15 ml of water. The resulting solution was cooled to 0–5 °C, diazotized by the dropwise addition of an aqueous solution of sodium nitrite (0.45 g, 0.0065 mol), and left stirring for 15 min. Aqueous methylamine (2.8 ml of 40%, 0.036 mol) was then added to the cold diazonium salt solution in one portion. After stirring for a further 10 min, filtration of the resulting mixture afforded a bright orange-red solid (yield 0.91 g, m.p. 59–62 °C).

After drying under suction, the orange-red solid (0.91 g) was dissolved in chloroform (50 ml) and neutral alumina (28 g) was added. The resulting slurry was stirred at room temperature for 4.5 h, after which the alumina was removed by filtration and washed several times with small portions of chloroform. The combined chloroform extract and washings were evaporated to dryness affording 3-methyl-4-methylene-1,2,3-benzotriazine, **5***a*, (0.785 g, 0.0049 mol, 78.5%) m.p. 64–66 °C, as yellow needles; ν_{max} 1620 cm^{-1} (exocyclic C=C); λ_{max} (cyclohexane) 210 (ε 36 500), 268 (ε 14 300), 277 (ε 14 100), 333 (ε 4300), 348 (ε 3500), 375 (ε 1800), and 394 (ε 1800) nm; M^+ 159 ($C_9H_9N_3$), *m/e* 130 ($M - NCH_3$, base), 116 ($M - N_2CH_3$), 103, 89.[2]

The above procedure was repeated with ethylamine, *n*-propylamine, or benzylamine in place of methylamine to afford the 3-alkyl-4-methylene-1,2,3-benzotriazines: **5***b*, R = Et, b.p. 103 °C (2.0 Torr), 60% yield; **5***c*, R = *n*-Pr, b.p. 97 °C (dec.) (1.5 Torr), 90% yield; **5***d*, R = $PhCH_2$, m.p. 80 °C (dec.), 67% yield. Spectral data of these compounds are given in Table 1.

1-(ortho-Acetylphenyl)-3-aryltriazenes, 7

ortho-Aminoacetophenone (0.02 mol) was dissolved in 2 *M* hydrochloric acid (30 ml), and diluted with water (20 ml). The solution was cooled to 0–5 °C, diazotized with sodium nitrite (0.02 mol) in water and stirred for 20 min. A solution of the aromatic amine (0.025 mol) in 2 *M*

[2]Elemental analysis was not attempted, due to the unstable nature of the compound which could only be stored under refrigeration.

Can. J. Chem. Downloaded from www.nrcresearchpress.com by 210.87.254.40 on 09/05/12
For personal use only.

Can. J. Chem. Downloaded from www.nrcresearchpress.com by 210.87.254.40 on 09/05/12
For personal use only.

hydrochloric acid (30 ml) was added slowly to the diazonium salt solution, and, after stirring for a further 15 min, the resulting mixture was neutralized with an excess of sodium acetate trihydrate (~50 g). The resulting yellow precipitate was filtered and recrystallized from ethanol affording the 1-(*ortho*-acetylphenyl)-3-aryltriazene as follows (aromatic amine, X, % yield, m.p.): **7***a*, aniline, X = H, 63% yield, m.p. 102–104 °C; **7***b*, *p*-anisidine, X = OCH_3, 81% yield, m.p. 136–138 °C; **7***c*, *p*-aminoacetophenone, X = $COCH_3$, 94% yield, m.p. 175–177 °C; **7***d*, methyl *p*-aminobenzoate, X = CO_2CH_3, 51% yield, m.p. 126–128 °C. Spectral data of these compounds are given in Table 2.

3-Aryl-4-methylene-1,2,3-benzotriazines, 8

The 1-(*ortho*-acetylphenyl)-3-aryltriazene **7** (0.003 mol) was dissolved in chloroform (50 ml) and stirred over neutral alumina (25 g) for 2.5–5.0 h. Filtration of the slurry, followed by washing of the alumina with chloroform, and evaporation of the combined chloroform washings afforded the 3-aryl-4-methylene-1,2,3-benzotriazines as follows: **8***a*, X = H, red oil, 70% yield (reaction time 2.5 h); **8***b*, X = OCH_3, red oil, 57% yield (reaction time 4.5 h); **8***c*, X = $COCH_3$, m.p. 121–123 °C ($CHCl_3$), 48% yield (reaction time 5.0 h). Spectral data of these compounds are given in Table 3.

4-Hydroxy-3-methyl-4-phenyl-1,2,3-benzotriazine, 12

ortho-Aminobenzophenone (5.08 g) was suspended in 2 *M* hydrochloric acid (60 ml) and the mixture heated to boiling. Concentrated hydrochloric acid (4.0 ml) was added to bring the amine into solution, which was then diluted with water (80 ml) and cooled to 0–5 °C. At this point, the hydrochloride salt precipitated. The cold slurry was diazotized with sodium nitrite (1.8 g) in a minimum volume of water over a period of 1 h, after which time a clear solution was obtained. Aqueous methylamine (40%, 11.2 ml) was added in one portion, and the resulting white precipitate was filtered, suction dried, and recrystallized from ethanol, affording 4-hydroxy-3-methyl-4-phenyl-1,2,3-benzotriazine, **12** (4.6 g, 76%), m.p. 142–144 °C (EtOH), ν_{max} 2600–3300 cm^{-1} (broad, OH); δ 6.9–7.8 (9H, m, aromatic), 3.6 (1H, s, broad, OH), and 3.3 (3H, s, N—CH_3) p.p.m.; M^+ 239.

Anal. Calcd. for $C_{14}H_{13}N_3O$: C, 70.28; H, 5.48; N, 17.56. Found: C, 70.08; H, 5.37; N, 17.33.

Attempted Synthesis of 1-ortho-Acetylphenyltriazene, 3 (R = H)

ortho-Aminoacetophenone (1.71 g) was dissolved in 2 *M* hydrochloric acid (20 ml), diluted with water (40 ml) and diazotized at 0 °C with sodium nitrite (0.90 g). Concentrated ammonia was added dropwise to the diazonium salt solution until slightly basic and the resulting mixture extracted with chloroform. Evaporation of the dried chloroform extracts afforded *ortho*-aminoacetophenone (quantitative recovery), identical in all respects with the starting material.

Likewise, diazotization of *ortho*-aminobenzophenone followed by neutralization of the diazonium salt solution with ammonia, afforded the starting material, recovery 82%.

Thermolysis of 3-Methyl-4-methylene-1,2,3-benzotriazine, 5a

(*a*) The 4-methylenetriazine (0.67 g) was heated dry over a steam bath for 1.0 h. The residue, although considerably darkened in color, crystallized on cooling and was found to be identical with the starting material.

(*b*) The 4-methylenetriazine (0.53 g) was recovered unchanged after refluxing in absolute ethanol (50 ml) for 3 h.

(*c*) The 4-methylenetriazine (0.94 g) was refluxed in benzene (50 ml) for 24 h and, after evaporation of the solvent, was recovered unchanged (87% recovery).

(*d*) The 4-methylenetriazine (0.74 g) was refluxed in *p*-xylene (25 ml) for 2 h; evaporation afforded unchanged starting material (93%).

(*e*) The 4-methylenetriazine (0.785 g) was refluxed in anhydrous diglyme for 6.5 h; evaporation under vacuum at 100 °C afforded a black oil, which was purified by column chromatography on neutral alumina with chloroform eluent affording unchanged starting material (83% recovery).

(*f*) The 4-methylenetriazine (0.9 g) was refluxed in diglyme for 18 h; the residue, after evaporation, was a black tar, which remained intractable to purification. This residue did not appear to contain starting material.

The financial assistance of the National Research Council of Canada is gratefully acknowledged as is that of the Saint Mary's University Senate Research Committee which supported the completion of this project.

1. J. G. ERICKSON, P. F. WILEY, and V. P. WYSTRACH. The chemistry of heterocyclic compounds. Vol. 10. Interscience Publishers Inc., New York. 1956. pp. 13–27.
2. A. WEDDIGE and H. FINGER. J. Prakt. Chem. **35**, 262 (1887).
3. A. REISSERT and F. GRUBE. Chem. Ber. **42**, 3710 (1909).
4. R. C. SHAH. J. Ind. Inst. Sci. **7**, 205 (1924).
5. M. W. PARTRIDGE and M. F. G. STEVENS. J. Chem. Soc. 3663 (1964); H. N. E. STEVENS and M. F. G. STEVENS. J. Chem. Soc. C, 765 (1970).
6. T. P. AHERN and K. VAUGHAN. J. Chem. Soc. Chem. Commun. 701 (1973).
7. R. J. LEBLANC and K. VAUGHAN. Can. J. Chem. **50**, 2544 (1972).
8. D. H. WILLIAMS and I. FLEMING. Spectroscopic methods in organic chemistry. McGraw-Hill Publishing Co. Ltd., London. 1966. p. 61.
9. R. A. W. JOHNSTONE, D. W. PAULING, P. N. PRESTON, H. N. E. STEVENS, and M. F. G. STEVENS. J. Chem. Soc. C, 1238 (1970).
10. 8 Peak index of mass spectra. I.C.I. Ltd. and the Mass Spectrometry Data Centre (AWRE, Aldermaston), U.K. p. 75; (CRC Atlas of spectral data. CRC Press. 1973. pp. B-868, B-883).
11. D. H. HEY, C. W. REES, and A. R. TODD. J. Chem. Soc. C, 1028 (1968); H. E. CRABTREE, R. K. SMALLEY, and H. SUSCHITZKY. J. Chem. Soc. C, 2730 (1968); A. W. MURRAY, and K. VAUGHAN. J. Chem. Soc. C, 2070 (1970); J. G. ARCHER, A. J. BARKER, and R. K. SMALLEY. J. Chem. Soc. Perkin Trans. 1, 1169 (1973); N. BASHIR and T. L. GILCHRIST. J. Chem. Soc. Perkin Trans. 1, 868 (1973); M. S. S. SIDDIQUHI and M. F. G. STEVENS. J. Chem. Soc. Perkin Trans. 1, 2482 (1974).
12. B. M. ADGER, S. BRADBURY, M. KEATING, C. W. REES, R. C. STORR, and M. T. WILLIAMS. J. Chem. Soc. Perkin Trans. 1, 31 (1975).

Preparation and Properties of Carboxylic, Monothiocarboxylic, Dithiocarboxylic, and Sulfinic Acid Derivatives of Trithiane, Tetrathiocane, and Pentathiecane

MICHAEL E. PEACH,[1] MAX SCHMIDT, AND ECKHARD WEISSFLOG

Institut für Anorganische Chemie der Universität Würzburg, 87 Würzburg, Am Hubland, West Germany

Received July 14, 1975

MICHAEL E. PEACH, MAX SCHMIDT, and ECKHARD WEISSFLOG. Can. J. Chem. **53**, 3720 (1975).

The monoacids derived from trithiane, tetrathiocane, and pentathiecane, $C_3H_5S_3X$ (X = CO_2H, COSH, CS_2H), $C_4H_7S_4X$ (X = CO_2H, CS_2H), and $C_5H_9S_5X$ (X = CO_2H, CS_2H) and the lithium salts $C_3H_5S_3SO_2Li$, $C_4H_7S_4SO_2Li$, and $C_5H_9S_5SO_2Li$ have been prepared and their reactions studied. The corresponding esters $C_3H_5S_3CO_2R$ (R = CH_3, C_2H_5, *n*-C_3H_7, *i*-C_3H_7, *n*-C_4H_9, *n*-C_5H_{11}), $C_3H_5S_3COSCH_3$, $C_4H_7S_4CO_2R$ (R = CH_3, C_2H_5) and the ammonium salts, $C_3H_5S_3CO_2NH_4$, $C_3H_5S_3CS_2NH_4$, $C_3H_5S_3CS_2N(n\text{-}Bu)_4$, $C_4H_7S_4CO_2NH_4$, $(C_4H_7S_4CO_2)_2(Me_2NHCH_2)_2$, and $C_5H_9S_5CO_2NH_4$ have been isolated. The reactions of the acid anion with various metal ions have been investigated. Nuclear magnetic resonance, mass, and infrared spectroscopic data of some of the products are reported.

MICHAEL E. PEACH, MAX SCHMIDT et ECKHARD WEISSFLOG. Can. J. Chem. **53**, 3720 (1975).

On a préparé et étudié les réactions des monoacides dérivés du trithiane, tétrathiocane et pentathiécane, $C_3H_5S_3X$ (X = CO_2H, COSH, CS_2H), $C_4H_7S_4X$ (X = CO_2H, CS_2H) et $C_5H_9S_5X$ (X = CO_2H, CS_2H) et les sels de lithium $C_3H_5S_3SO_2Li$, $C_4H_7S_4SO_2Li$ et $C_5H_9S_5SO_2Li$. Les esters correspondants $C_3H_5S_3CO_2R$ (R = CH_3, C_2H_5, *n*-C_3H_7, *i*-C_3H_7, *n*-C_4H_9, *n*-C_5H_{11}), $C_3H_5S_3COSCH_3$, $C_4H_7S_4CO_2R$ (R = CH_3, C_2H_5) et les sels d'ammonium $C_3H_5S_3CO_2NH_4$, $C_3H_5S_3CS_2NH_4$, $C_3H_5S_3CS_2N(n\text{-}Bu)_4$, $C_4H_7S_4CO_2NH_4$, $(C_4H_7S_4CO_2)_2$-$(Me_2NHCH_2)_2$ et $C_5H_9S_5CO_2NH_4$ ont été isolés. On a examiné les réactions de l'anion acide avec divers ions métalliques. On rapporte les spectres r.m.n., de masse et les propriétés spectroscopiques infrarouges de quelques-uns des composés.

[Traduit par le journal]

Introduction

The methylene protons in *s*-trithiane (1,3,5-trithiocyclohexane abbreviated as TrH) and 2-monosubstituted as well as 2,4,6-trisubstituted trithianes are slightly acidic and monolithium and trilithium derivatives respectively were obtained on treatment with *n*-butyllithium in THF. The lithium derivatives reacted with various electrophiles to form more highly substituted trithianes (1, 2). Analogous lithium derivatives of tetrathiocane (TtH 1,3,5,7-tetrathiocyclooctane) have been prepared and their substitution reactions studied (3). This paper describes the addition of carbon dioxide, carbonyl sulfide, carbon disulfide, and sulfur dioxide to various lithium derivatives of *s*-trithiane, tetrathiocane, and pentathiecane (PeH 1,3,5,7,9-pentathiocyclodecane) and the properties and reactions of the products isolated.

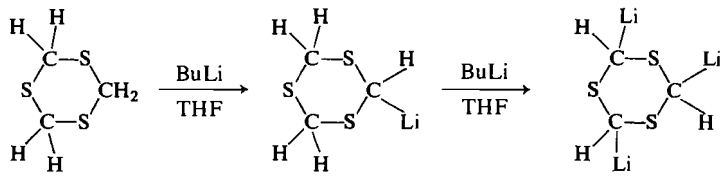

(TrH) (TrLi)

Results and Discussion

Acids

Carbon dioxide, carbonyl sulfide, and carbon disulfide can be added to organolithium compounds to give the lithium salts of the corresponding carboxylic, monothiocarboxylic and

[1]On leave from Acadia University, Wolfville, Nova Scotia B0P 1X0 (1974–1975) and to whom correspondence should be addressed at Acadia University.

Can. J. Chem. Downloaded from www.nrcresearchpress.com by 210.87.254.105 on 09/05/12
For personal use only.

Can. J. Chem. Downloaded from www.nrcresearchpress.com by 210.87.254.105 on 09/05/12
For personal use only.

dithiocarboxylic acids respectively (4). The monolithium derivatives of *s*-trithiane reacted similarly:

$$\mathrm{TrLi} + \mathrm{CO_2} \rightarrow \mathrm{TrCO_2Li} \xrightarrow{\mathrm{H^+}} \mathrm{TrCO_2H}$$

$$\mathrm{TrLi} + \mathrm{COS} \rightarrow \mathrm{TrCOSLi} \xrightarrow{\mathrm{H^+}} \mathrm{TrCOSH}$$

$$\mathrm{TrLi} + \mathrm{CS_2} \rightarrow \mathrm{TrCS_2Li} \xrightarrow{\mathrm{H^+}} \mathrm{TrCS_2H}$$

The free acids precipitated upon acidification of an aqueous solution of the lithium salt. The crystalline acids $\mathrm{TtCO_2H}$ and $\mathrm{PeCO_2H}$ were prepared analogously from carbon dioxide addition to TtLi and PeLi respectively. The acids $\mathrm{TtCS_2H}$ and $\mathrm{PeCS_2H}$ were non-crystalline. Attempts to purify TtCOSH always resulted in partial hydrolysis to $\mathrm{TtCO_2H}$. The carboxylic acid $\mathrm{TtCO_2H}$ was isolated when the impure TtCOSH was dissolved in aqueous ammonia (from which $\mathrm{TtCO_2NH_4}$ could be isolated) and the mixture acidified with hydrochloric acid.

It should be possible to prepare the sulfinic acids ($\mathrm{RSO_2H}$) by addition of sulfur dioxide to a lithium derivative (RLi) followed by acidification (4). The free sulfinic acids of monosubstituted *s*-trithiane, tetrathiocane, and pentathiecane could not be isolated from aqueous solution, but decomposed with liberation of sulfur dioxide. Slightly impure lithium sulfinates precipitated from the THF solutions at room temperature. If an aqueous solution of $\mathrm{TrSO_2H}$ was allowed to stand at room temperature for 2–3 days, the yellow sulfone $\mathrm{Tr_2SO_2}$ precipitated.

Attempts to prepare the trifunctional acids from trithiane, $(\mathrm{CH(CO_2H)S})_3$ and $(\mathrm{CH(CS_2H)S})_3$, gave unidentified oily products which could not be purified by distillation, extraction etc. and appeared to decompose at room temperature. Similar products were obtained when gaseous carbon dioxide was blown through a THF solution of TrLi at −20 °C. This may be due to preferential formation of a lithium derivative with the carboxylate.

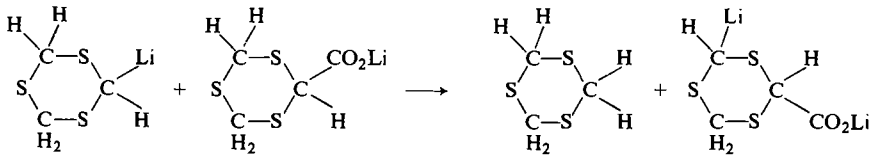

The possibility of partial formation of a ketone cannot be excluded (4):

$$\mathrm{TrLi} + \mathrm{TrCO_2Li} \xrightarrow{\mathrm{H_2O}} \mathrm{Tr_2CO} + 2\mathrm{LiOH}$$

The monoacids were obtained by effectively reacting all the lithium derivative TrLi immediately. This was achieved by pouring the THF solution of TrLi onto an excess of solid $\mathrm{CO_2}$ or by adding an excess of liquid $\mathrm{CS_2}$, $\mathrm{SO_2}$, or a THF solution of COS to the TrLi solution at or below −10 °C.

Esters

The methyl ester of $\mathrm{TrCO_2Me}$ was prepared by the reaction of a methanol solution of the free acid with diazomethane at 0 °C:

$$\mathrm{TrCO_2H} + \mathrm{CH_2N_2} \rightarrow \mathrm{TrCO_2CH_3} + \mathrm{N_2}\uparrow$$

Impure TrCOSMe and $\mathrm{TrCS_2Me}$ could be prepared analogously using a methanol suspension of the free acids TrCOSH or $\mathrm{TrCS_2H}$. Attempts to prepare the methyl esters by reaction of the lithium salt $\mathrm{TrCS_2Li}$, as prepared in THF solution, or a suspension of $\mathrm{Pb(S_2CTr)_2}$ or $\mathrm{AgS_2CTr}$ in carbon tetrachloride with methyl iodide failed. The carboxylic esters were obtained by various other methods, either acid catalyzed reaction of the free acid with an alcohol;

$$\mathrm{TrCO_2H} + \mathrm{ROH} \xrightarrow{\mathrm{H^+}} \mathrm{TrCO_2R} + \mathrm{H_2O} \qquad \mathrm{R} = \mathrm{Me, Et, }n\text{-Pr, }i\text{-Pr, }n\text{-Bu}$$

$$\mathrm{TtCO_2H} + \mathrm{ROH} \xrightarrow{\mathrm{H^+}} \mathrm{TtCO_2R} + \mathrm{H_2O} \qquad \mathrm{R} = \mathrm{Me, Et}$$

or via the intermediate formation of an acid chloride (not isolated), which also reacted with methanethiol;

$$\mathrm{TrCO_2H} + \mathrm{SOCl_2} \rightarrow \mathrm{TrCOCl} \begin{cases} \xrightarrow{\mathrm{EtOH}} \mathrm{TrCO_2Et} + \mathrm{HCl} \\ \xrightarrow{\mathrm{MeSH}} \mathrm{TrCOSMe} + \mathrm{HCl} \end{cases}$$

or by alcoholysis; *e.g.*

$$\mathrm{TrCO_2Me} + \mathrm{ROH} \rightarrow \mathrm{TrCO_2R} + \mathrm{MeOH} \qquad \mathrm{R} = n\text{-Bu, amyl}$$

Can. J. Chem. Downloaded from www.nrcresearchpress.com by 210.87.254.105 on 09/05/12
For personal use only.

The ethyl ester, $TrCO_2Et$, has previously been prepared from the lithium derivative TrLi and ethyl chloroformate, $ClCO_2Et$ (1).

Salts

The ammonium salts of the carboxylic, monothiocarboxylic and dithiocarboxylic acids, $TrCO_2NH_4$, $TrCOSNH_4$, $TrCS_2NH_4$, $TtCO_2NH_4$, and $PeCO_2NH_4$ were readily obtained by dissolving the acid in a slight excess of aqueous ammonia and subsequent removal of the solvent. The tetra-*n*-butylammonium salt $(n\text{-}Bu)_4NS_2CTr$ precipitated on adding an aqueous solution of tetra-*n*-butylammonium iodide to a solution of the lithium salt, $TrCS_2Li$. The tetra-*n*-butylammonium salts $(n\text{-}Bu)_4NSOCTr$ and $(n\text{-}Bu)_4NO_2CTr$ did not precipitate from aqueous solution. The lithium salts $TrCO_2Li$ and $TrCS_2Li$ could not be isolated. The salts of $TrCS_2H$ decomposed to a tar on storage for over a week at room temperature. A tar was formed immediately in the reaction of a benzene solution of $TrCS_2H$ with piperidine and an impure pyridinium salt precipitated with pyridine. Piperidine salts of dithiocarboxylic acids are stable and have been used to prepare the compounds CH_3CS_2X ($X = CH_3$, Me_3Si, Me_3Ge, Me_3Sn, and Et_3Pb) (5). The analogous derivatives $TrCS_2SiMe_3$ and $TrCS_2SnMe_3$ could not be obtained by the reaction of a THF solution of $TrCS_2Li$ with Me_3SiCl or Me_3SnI. The salt $(TtCO_2)_2(Me_2NHCH_2)_2$ precipitated from an aqueous solution of $TtCO_2Li$ on addition of tetramethylethylenediamine, followed by acidification.

Metal Derivatives

Trithiane has a chair structure and can act as a mono-, di-, or tridentate ligand. Complexes have been formed with some metal ions Ag(I) (6), Hg(II) (6), Cu(I) (7), and various metal carbonyls (8). Pentathiecane can be purified via its silver complex (9). Carboxylic acids (10), monothiocarboxylic acids (11), and dithiocarboxylic acids (12) can also form derivatives with various metal ions. The acids $TrCO_2H$, TrCOSH, and $TrCS_2H$ have two functional groups, the trithiane ring and the acidic group, either or both of which could react with metal ions.

Precipitates formed on mixing solutions of the lithium or ammonium salts with solutions of various metal ions. Qualitative tests showed that the anions $TrCO_2^-$, $TrCOS^-$, $TrCS_2^-$, $TrSO_2^-$, $TtCO_2^-$, $TtCS_2^-$, $TtSO_2^-$, $PeCO_2^-$, $PeCS_2^-$, and $PeSO_2^-$ formed white-brown, green-brown, and brown precipitates with Ag^+, Cu^{2+}, and Fe^{3+} ions respectively. Precipitates were also formed on mixing aqueous solutions of $TrCS_2^-$ or $TrCOS^-$ anions with Pb^{2+}, Ni^{2+}, Co^{2+}, or Zn^{2+} cations. Most of these products were not analytically pure, and probably hydrated (see Table 1). The infrared spectra showed water to be present in most cases.

Attempts to prepare the derivatives of $TrCS_2H$ with the cations Tl^+, Pd^{2+}, and Hg^{2+} by shaking an aqueous acidic solution of the cation with a benzene solution of the acid only gave a pure product with Pd^{2+}.

The derivatives were insoluble in most common solvents. It is not clear what their structures are, but the extreme insolubility may be caused by complexing with the sulfur in the ring and the acidic group of the molecule. Most of the metal derivatives were relatively thermally unstable and could not be purified by Soxhlet extraction.

Oxidation

Dithiocarboxylic acids can readily be oxidized even in air to the corresponding disulfide RC(S)SSC(S)R (11). Trithiane forms adducts with iodine (13) and bromine causes fracture of the C—S bond.[2] An unidentified product, the mass spectrum of which showed it to contain iodine, was obtained by the addition of a DMSO–I_2 – KI solution to a solution of $TrCS_2H$ in DMSO, or a similar reaction in aqueous solution using $TrCS_2Li$. Only traces of a product were obtained when oxygen was blown through a solution of $TrCS_2H$ in aqueous ammonia. It is also noteworthy that metal derivatives of the oxidizing anions Cu(II) and Fe(III) could be isolated; these cations usually oxidize thiols to disulfides, being reduced to Cu(I) and Fe(II) respectively (14).

Infrared

The structures of the products were deduced from their i.r., n.m.r. and mass spectra. The i.r. spectra were characteristic of the functional groups present. The monothio acid, TrCOSH, could contain a —C(=O)SH or a —C(=S)OH group. A recent microwave study of monothioformic acid, HCOSH, has confirmed earlier observations that the structure is HC(=O)SH,

[2]E. Weissflog, private communication.

TABLE 1. Metal derivatives isolated

Compound	Color	Decomposition temperature (°C)	Found (%)			Calculated (%)		
			C	H	S	C	H	S
$TrCO_2Ag$	white	>165	16.2	1.6	31.3	16.6	1.7	33.2
$(TrCO_2)_2Cu{\cdot}2H_2O$	green	>140	20.2	3.0	40.6	20.8	3.0	41.6
$(TrCO_2)_3Fe{\cdot}3H_2O$	brown	>200	21.5	2.1	43.7	22.1	3.2	44.1
$(TtCO_2)_2Cu{\cdot}3H_2O$	green	>118	21.1	3.1	46.1	21.0	3.5	44.8
$(TtCO_2)_3Fe{\cdot}3H_2O$	brown	>200	22.9	2.8	49.6	22.8	3.4	48.6
$PeCO_2Ag{\cdot}H_2O$	white	>110	18.0	3.2	41.5	18.0	2.8	40.2
$(PeCO_2)_2Cu{\cdot}12H_2O$	green	>115	17.3	3.8	36.6	17.4	5.1	38.8
$(PeCO_2)_2Fe{\cdot}4H_2O$	brown	>130	22.6	4.7	52.1	22.8	3.7	50.7
TrCOSAg	black	> 53	15.3	1.9	—	15.7	1.7	—
$(TrCOS)_2Pb{\cdot}4H_2O$	brown	> 53	14.0	1.7	—	14.3	2.7	—
$(TrCOS)_2Zn{\cdot}4H_2O$	yellow	> 80	17.6	2.8	—	18.1	3.4	—
$(TrCOS)_2Cu$	green	>140	21.6	2.6	—	21.0	2.2	—
$TrCS_2Ag{\cdot}2H_2O$	brown	>120	13.2	1.3	—	13.4	2.5	—
$(TrCS_2)_2Ni$	black	>100	20.0	2.1	—	19.8	2.1	—
$(TrCS_2)_2Fe{\cdot}2H_2O$	brown	> 75	18.6	2.0	—	18.5	2.7	—
$(TrCS_2)_2Pb{\cdot}4H_2O$	brown	> 84	13.4	1.3	—	13.6	2.6	—
$(TrCS_2)_2Zn$	black	>120	19.3	2.1	—	19.5	2.1	—
$(TrCS_2)_2Cu$	black	>110	20.2	2.4	—	19.6	2.1	—
$(TrCS_2)_3Fe$	black	> 63	20.6	2.2	—	20.7	2.2	—
$(TrCS_2)_2Pd$	brown	>145	18.2	2.0	—	18.0	1.9	—

TABLE 2. Summary of ^1H n.m.r. data[a]

Compound[b]	δ_1(p.p.m.)	δ_2(p.p.m.)	$\Delta\delta$(p.p.m.)	J(Hz)	Single proton δ(p.p.m.)	
$TrCO_2H(D)$	4.45	4.23	0.22	15.0	5.12	
$TrCO_2H(D_2O)$	4.60	4.20	0.40	14.6	5.10	
$TrCO_2NH_4(D)$	4.30	4.15	0.16	15.1	4.84	
$TrCO_2NH_4(D_2O)$	4.64	4.37	0.27	14.7	5.30	
$TrCO_2CH_3(C)$	5.13	3.55	1.58	15.8	4.33	3.87 (Me)
$TrCO_2C_2H_5(C)$	5.00	3.66	1.34	14.5	4.45	Ref. 1
TrCOSH(D)	4.54	4.28	0.27	15.7	5.14	
$TrCOSNH_4(D_2O)$	4.54	4.26	0.28	14.8	5.38	
$TrCOSNH_4(D)$	4.35	4.12	0.23	14.0	5.06	
$TrCOSCH_3(C)$	5.31	3.86	1.45	14.0	4.28	2.42 (Me)
$TrCS_2NH_4(D_2O)$	4.58	4.04	0.53	14.5	5.70	
$TrCS_2NH_4(D)$	4.54	4.00	0.55	15.0	5.58	
$TrCS_2Py(D)$	4.52	4.00	0.53	14.4	5.60	

[a]Corrected to TMS as internal standard.
[b]Solvents B = $CDCl_3$, C = CCl_4(TMS), D = DMSO-d_6, D_2O = D_2O(External TMS).

and shown that this can exist in *cis* and *trans* forms (15). The i.r. spectra showed that the structure was TrC(=O)SH, with S—H and C=O bands observed at 2498 and 2542, and 1675 cm^{-1} respectively.

Nuclear Magnetic Resonance Spectra

The n.m.r. spectra of monosubstituted *s*-trithiane derivatives should be an AB system for the methylene groups at positions C-4 and C-6. A single line should be observed for the proton remaining at position C-2, unless it can couple with the other substituent on C-2. Such spectra have been observed previously for a number of monosubstituted *s*-trithiane derivatives (1, 2). The acids $TrCO_2H$, TrCOSH, and $TrCS_2H$ are insufficiently soluble in normal organic solvents to allow their ^1H n.m.r. spectra to be measured. The spectra can be obtained using DMSO-d_6 as solvent or for $TrCO_2H$, D_2O. The acidic protons cannot be observed due to exchange with the deuterated solvent. The acid $TrCS_2H$ decom-

Can. J. Chem. Downloaded from www.nrcresearchpress.com by 210.87.254.105 on 09/05/12
For personal use only.

Can. J. Chem. Downloaded from www.nrcresearchpress.com by 210.87.254.105 on 09/05/12
For personal use only.

TABLE 3. Analytical data and physical properties of new compounds

Compounds	m.p. (°C)	Decomposition temperature (°C)	Color	Yield (%)	Found (%)				Calculated (%)			
					C	H	S	N	C	H	S	N
$TrCO_2H$	185–186	>210	white	70	26.82	3.56	53.30	—	26.40	3.30	52.70	—
$TrCO_2NH_4$	—	>207	white	100	23.66	4.52	48.61	6.75	24.10	4.52	48.20	7.03
$TrCO_2Me$	100–101	>210	white	34	30.26	4.34	48.46	—	30.60	4.60	49.00	—
$TrCO_2Et$	102–103	—	white	69	33.73	4.71	45.27	—	34.28	4.76	45.71	—
$TrCO_2(n\text{-Pr})$	86–87	—	white	71	37.16	5.23	42.94	—	37.50	5.36	42.86	—
$TrCO_2(n\text{-Bu})$	59–60	—	white	30	40.11	5.56	40.25	—	40.33	5.88	40.33	—
$TrCO_2(i\text{-Pr})$	48–50	—	white	50	36.98	5.31	42.64	—	37.50	5.36	42.86	—
$TrCO_2(n\text{-}C_5H_{11})$	44–45	—	white	46	42.51	6.43	37.63	—	42.86	6.35	38.10	—
$TtCO_2H$	149–151	>150	white	70	26.23	3.61	56.20	—	26.30	3.51	56.20	—
$TtCO_2NH_4$	145–150	—	white	100	23.91	3.72	51.83	5.40	24.50	4.39	52.20	5.71
$(TtCO_2)_2(Me_2HNCH_2)_2$	155–156	—	white	53	33.50	5.77	44.85	4.63	33.50	5.58	44.80	4.89
$TtCO_2Me$	24–25	—	white	26	29.57	4.20	52.11	—	29.75	4.13	52.89	—
$TtCO_2Et$	20–25	—	white	23	32.51	4.75	49.87	—	32.81	4.69	50.00	—
$PeCO_2H$	160–162	—	white	85	25.85	3.86	57.95	—	26.25	3.65	58.30	—
$PeCO_2NH_4$	115–120	—	white	100	24.58	4.57	54.32	4.40	24.70	4.46	54.90	4.81
TrCOSH	89–91	> 75	white	60	24.63	2.93	65.3	—	24.22	3.05	64.7	—
$TrCOSNH_4$	143–144	>150	white	52	22.45	4.16	—	6.17	22.31	4.21	—	6.50
TrCOSMe	163–164	>240	white	40	28.15	3.53	—	—	28.28	3.80	—	—
$TrCS_2H$	82–84	> 90	orange	80	21.82	2.34	74.01	—	22.40	2.80	74.80	—
$TrCS_2NH_4$	94–95	>190	orange	100	20.34	3.92	—	5.62	20.78	3.90	—	6.06
$TrCS_2N(n\text{-Bu})_4$	80–82	>100	red	64	54.02	9.12	—	3.00	53.91	8.83	—	2.99
$TtCS_2H$	—	> 80	orange-red	95	23.40	3.32	73.40	—	23.10	3.07	73.90	—
$PeCS_2H$	—	> 60	orange-red	29	24.88	3.74	72.51	—	23.53	3.27	73.25	—
$TrSO_2Tr$	141–143	>143	white	40	22.15	3.12	66.10	—	21.30	2.96	66.30	—

Can. J. Chem. Downloaded from www.nrcresearchpress.com by 210.87.254.105 on 09/05/12
For personal use only.

posed relatively rapidly in DMSO and the spectrum of a freshly prepared solution was not consistent with that of a monosubstituted derivative of *s*-trithiane. Details of some of the spectra are shown in Table 2.

The chemical shift of the methyl group in $TrCO_2Me$, 3.87 p.p.m., is similar to that observed in methyl formate, 3.77 p.p.m. (16), while that in TrCOSMe, 2.42 p.p.m., is considerably different. The presence of a —SMe group in TrCOSMe was indicated. The chemical shift was somewhat similar to that observed for the —SMe group in MeSEt, namely 2.10 p.p.m. (16).

Mass Spectra

The 70 eV mass spectra of the various acids and, where possible, the methyl esters have been examined. In all cases the molecular ion was observed, confirming the molecular structure. In the various trithiane derivatives a relatively intense peak was observed at *m/e* 137, corresponding to reactions such as

$$C_3H_5S_3COSH^{\ddagger} \rightarrow C_3H_5S_3^{+} + COSH\cdot$$

The spectra below *m/e* 137 were somewhat similar to that of *s*-trithiane, except that the ions CHS^{+} (*m/e* 45) and $C_2H_3S_2^{+}$ (*m/e* 91) were more intense than the ions $CH_2S^{\ddagger}$ (*m/e* 46) and $C_2H_4S_2^{\ddagger}$ (*m/e* 92) whereas the reverse was observed in the mass spectrum of *s*-trithiane (17). Only one metastable peak was observed, and this corresponded to the reaction

$$C_3H_5S_3CO_2CH_3^{\ddagger} \xrightarrow{*} C_2H_5SCO_2CH_3^{\ddagger} + CS_2$$

An analogous reaction involving loss of CS_2 from the molecular ion is observed in the spectrum of trithiane (17).

Thermal Stability

Trithiane and pentathiecane are stable up to at least 250 °C, and trithiane sublimes before reaching its melting point, 215–218 °C (18). Tetrathiacane is not as thermally stable and decomposed above its melting point, 51–52 °C (19). The acids prepared were not very thermally stable and decomposition occurred above their melting points, see Table 3. The metal derivatives of $TrCO_2H$, TrCOSH, $TrCS_2H$ were considerably less thermally stable, making their purification by Soxhlet extraction virtually impossible.

Experimental

The starting materials trithiane, tetrathiocane, and pentathiecane were prepared by literature methods (18, 19). The physical properties and analyses of the new compounds are shown in Table 3.

Microanalyses (C, H, and N) were performed by combustion (Frau Ullrich, Universität Würzburg). The sulfur was estimated by microcombustion, according to Schöninger. Infrared spectra were recorded as KBr discs or mulls with Nujol on a Perkin-Elmer 457. The proton n.m.r. spectra were recorded on a Varian T60. Mass spectra were obtained using a Varian MAT-CH7 and DTA on a DuPont Thermal Analyser 990.

Preparation of Acids

Solutions of approximately 10 mmol of the monolithium derivatives TrLi, TtLi, or PeLi were prepared by literature methods (2, 3). Trithiane (1.38 g, 10 mmol) in 100 ml dry THF was refluxed in a nitrogen atmosphere until it had dissolved. The solution was cooled rapidly to −10 °C and the trithiane precipitated as fine crystals. The suspension was well stirred and kept at −10 – −20 °C during the drop by drop addition of 10 mmol of *n*-BuLi in hexane. The precipitate dissolved, forming a colorless solution. After 0.5 h at −10 – −20 °C the solution at −20 °C was poured onto an excess of Dry Ice under nitrogen and allowed to warm to room temperature. Water (100 ml) was added and the organic solvent removed under vacuum. The unreacted trithiane was filtered off. The free acid precipitated from the aqueous solution at 0 °C on acidification with HCl to p*H* 1. Further product was obtained by reducing the volume of the solution. The product was purified by dissolving in alkali and reprecipitation with acid or recrystallization from water. It was dried in a vacuum desiccator.

The same procedure was used to prepare the monothio- and dithiocarboxylic acids and sulfinic acids except that a THF solution of COS (prepared by bubbling a brisk stream of COS through 50 ml of THF at −50 to −60 °C) or 10 ml of CS_2 or liquid SO_2 (10 ml) was added to the solution of the lithium derivative, instead of pouring onto solid CO_2. The free sulfinic acids could not be isolated, probably due to decomposition *in vacuo* of RSO_2H with loss of SO_2.

Preparation of Ammonium Salts

The free acid was dissolved in the minimum quantity of aqueous ammonia. The solvent and excess ammonia were removed under vacuum. The salt $(Me_2HNCH_2CH_2NHMe_2)^{2+}$ $(TtCO_2^{-})_2$ precipitated on adding excess tetramethylethylenediamine to the $TtCO_2^{-}Li^{+}$ solution, followed by acidification. Addition of a saturated aqueous solution of Bu_4NI to $TrCS_2Li$ precipitated the salt Bu_4NS_2CTr. No precipitate formed with Bu_4NI and $TrCO_2Li$ or TrCOSLi. The impure pyridinium salt, $PyHS_2CTr$, precipitated on adding pyridine to a benzene solution of $TrCS_2H$. A tar formed using piperidine instead of pyridine.

Preparation of Esters

The ester $TrCO_2Me$ precipitated when approximately 10 mmol of CH_2N_2 in ether was added to 1 mmol of $TrCO_2H$ in 20 ml MeOH (0 °C). The esters $TrCO_2R$

(R = Me, Et, *n*-Pr, *i*-Pr, *n*-Bu) and $TtCO_2R$ (R = Me, Et) were prepared by the acid catalyzed reaction of $TrCO_2H$ or $TtCO_2H$ (5 mmol) with 20 ml of ROH and 0.5 ml concentrated H_2SO_4 catalyst. This mixture was refluxed for 1 h and the ester precipitated on cooling. The product was purified by refluxing in ROH, and further washing. $TrCO_2$(*n*-Bu) was prepared by alcoholysis of $TrCO_2Me$ (5 mmol) with 20 ml *n*-BuOH and 1 ml concentrated H_2SO_4. The mixture was refluxed for 15 h and the product precipitated on cooling. The *n*-amylester was prepared similarly from $TrCO_2Me$ and amyl alcohol. $TrCO_2Et$ and TrCOSMe were prepared from the acid chloride, TrCOCl, which was not isolated, and EtOH or MeSH. $TrCO_2H$ (5 mmol) was dissolved in 20 ml $SOCl_2$ (40 °C); after completion of the reaction the excess $SOCl_2$ was removed under vacuum, leaving an oily liquid. Absolute EtOH (5 ml) or 25 ml of a benzene solution of MeSH were added and the product precipitated.

Metal Derivatives

Approximately 2 mmol of either the freshly prepared solution of the lithium salt, or of the corresponding ammonium salt was added to a slight excess of an aqueous solution of the metal ion. The precipitate was filtered off and dried *in vacuo*. The compound $(TrCS_2)_2Pd$ was prepared by shaking an aqueous acidic solution of $PdCl_2$ with a benzene solution of $TrCS_2H$. Similar attempts to prepare $TrCS_2Tl$ and $(TrCS_2)_2Hg$ gave impure products.

This work was supported by Fonds der Chemischen Industrie. One of the authors (M.E.P.) wishes to thank the Alexander von Humboldt Foundation for the award of a fellowship while on leave from Acadia University, Wolfville, Nova Scotia. Mr. Alfred Kreiner is thanked for help with some of the experimental work.

1. D. SEEBACH, E. J. COREY, and A. K. BECK. Chem. Ber. **107**, 367 (1974).
2. M. SCHMIDT and E. WEISSFLOG. Z. Anorg. Allg. Chem. In press.
3. M. SCHMIDT and E. WEISSFLOG. To be published.
4. H. SCHÖLLKOPF. *In* Houben-Weyl Methoden der Organischen Chemie. Band XIII/1. Georg Thieme Verlag, Stuttgart. 1970. p. 87.
5. S. KATO, A. HORI, H. SHIOTANI, M. MIZUTA, N. HAYASHI, and T. TAKATUWA. J. Organometal. Chem. **82**, 223 (1974).
6. J. A. W. DALZIEL and T. G. HEWITT. J. Chem. Soc. A, 233 (1966).
7. A. DOMENICANO, R. SPAGNA, and A. VICIAGO. Chem. Commun. 1291 (1968).
8. W. D. SCHENK and M. SCHMIDT. J. Organometal. Chem. In press.
9. M. SCHMIDT and E. WEISSFLOG. Z. Anorg. Allg. Chem. **406**, 271 (1974).
10. C. OLDHAM. Prog. Inorg. Chem. **10**, 223 (1968); W. LINDELL and F. HUBER. Z. Anorg. Allg. Chem. **408**, 167 (1974).
11. E. E. REID. Organic chemistry of bivalent sulfur. Vol. IV. Chemical Publishing Co. Inc., New York. 1962. p. 11.
12. R. EISENBERG. Prog. Inorg. Chem. **12**, 295 (1970); O. PIOVESANA and G. CAPPUCCILLI. Inorg. Chem. **11**, 1543 (1974).
13. E. FROMM and C. SHILTIS. Ber. **56**, 941 (1923).
14. M. E. PEACH. Can. J. Chem. **46**, 2699 (1968).
15. W. H. HOCKING and G. WINNEWISSER. J. Chem. Soc. Chem. Commun. 63 (1975).
16. NMR spectra catalog. Vol. 1. Varian Associates, Palo Alto, California. 1962.
17. M. E. PEACH, E. WEISSFLOG, and N. PELZ. Org. Mass Spectrom. In press.
18. E. BAUMANN. Ber. **23**, 67 (1890); Organic synthesis. Vol. 16. *Edited by* J. R. Johnson. J. Wiley and Sons Inc., New York. 1936. p. 81.
19. M. SCHMIDT, K. BLAETTNER, P. KOCHENDÖRFER, and H. RUF. Z. Naturforsch. Teil B, **21**, 622 (1966).

Can. J. Chem. Downloaded from www.nrcresearchpress.com by 210.87.254.105 on 09/05/12
For personal use only.

Preparation and Properties of some Trimethylgermyl and Trimethylplumbyl Esters of Dimethylcarbamic and Dimethylthiocarbamic Acids

A. E. LEMIRE AND J. C. THOMPSON

University of Toronto, Department of Chemistry, Toronto, Ontario M5S 1A1

Received March 21, 1975

A. E. LEMIRE and J. C. THOMPSON. Can. J. Chem. **53**, 3727 (1975).

The preparation of the trimethylgermyl esters of *N,N*-dimethylcarbamic, *N,N*-dimethylmonothiocarbamic, and *N,N*-dimethyldithiocarbamic acids and the trimethylplumbyl ester of *N,N*-dimethylmonothiocarbamic acid is reported. Some of these esters exhibit temperature dependent n.m.r. spectra. Infrared and u.v. spectra for these and related compounds are also described.

A. E. LEMIRE et J. C. THOMPSON. Can. J. Chem. **53**, 3727 (1975).

On rapporte la préparation des esters triméthylgermylés des acides *N,N* diméthylcarbamique, *N,N*-diméthylmonothiocarbamique et *N,N*-diméthyldithiocarbamique et la préparation de l'ester triméthylplumbyle de l'acide *N,N*-diméthylmonothiocarbamique. Dans quelques uns de ces esters, le spectre r.m.n. varie en fonction de la température. On décrit aussi les spectres i.r. et u.v. de ces composés et d'autres qui leur sont reliés.

[Traduit par le journal]

Can. J. Chem. Downloaded from www.nrcresearchpress.com by 210.87.254.6 on 09/05/12
For personal use only.

While many reports of the stannyl esters of dialkyldithiocarbamic acid may be found in the literature (1, 2), there is comparatively little information on germyl and plumbyl esters. Satgé *et al.* (3) have reported the preparation of a few esters of diethyldithiocarbamic acid and diethylcarbamic acid. The trimethylplumbyl ester of dimethyldithiocarbamic has also been prepared (4).

As part of a systematic n.m.r. study (5–7) of hindered rotation in such esters we had occasion to synthesize the trimethylgermyl and trimethylplumbyl esters of dimethylcarbamic and dimethylthiocarbamic acids and in this paper report upon their synthesis and properties.

Generally the synthesis of such compounds has been carried out by reacting aminosilanes, germanes, or stannanes with CO_2, CS_2, or COS (1, 3), although the dithiocarbamates have sometimes been prepared by reacting the trialkyl group IV halide with sodium dialkyldithiocarbamate. We have found that the monothiocarbamates and carbamates may also be conveniently prepared by the reaction between the group IV halide and an acid salt; this procedure obviates the necessity of working directly with the aminosilanes etc., which are often quite moisture sensitive.

Experimental

Synthesis

The following general procedure was followed for all of the compounds except $Me_2NC(S)SPbMe_3$ (4).

A solution of the trimethylgermyl halide or trimethylplumbyl acetate in hexane was added to a slurry of the stoichiometric amount of $Me_2NC(X)YH{\cdot}HNMe_2$ (8, 9) (X = O, S; Y = O, S) in hexane under a nitrogen atmosphere. The reaction mixture was stirred for 2 h, then filtered under nitrogen and the solvent was evaporated under vacuum to yield an oil. The oil was distilled under vacuum with warming and condensed in a Dry Ice trap. Results of analyses are listed in Table 1.

The compound $Me_2NC(O)SGeMe_3$ appears to be somewhat air sensitive; it also decomposes after standing several months in a sealed tube (under vacuum). It may also be prepared by the direct reaction of Me_3GeNMe_2 and COS.

An attempt to prepare $Me_2NC(S)OGeMe_3$ by the reaction of $Me_2NC(S)Cl$ and Me_3GeOLi was made but only starting materials were recovered.

Solutions of $Me_2NC(S)SPbMe_3$ are unstable; a white precipitate forms if the solution is allowed to stand for a few hours.

$Me_2NC(O)SPbMe_3$ decomposes (turns grey) on standing several weeks in a sealed tube.

Spectra

Nuclear magnetic resonance spectra were obtained on a Varian A56-60D n.m.r. spectrometer. Details of sample preparation have been described previously (5–7).

Infrared spectra were run on a Perkin-Elmer 180 i.r. spectrometer. Demountable cells with NaCl windows and a 1 mm path length were used. Solutions of ~10 mol% concentration in CCl_4 and $CHCl_3$ were used. The spectrometer was calibrated using the standard polystyrene film.

Ultraviolet spectra were run on a Unicam SP 800 spectrometer over the range 210–450 nm. Solutions were made up to cover the concentration range 0.05–0.00005 mol l^{-1}.

Results and Discussion

Nuclear Magnetic Resonance

The ^1H chemical shifts for the compounds described herein are listed in Table 2. As would

Can. J. Chem. Downloaded from www.nrcresearchpress.com by 210.87.254.6 on 09/05/12
For personal use only.

TABLE 1. Analytical data

Compound	Melting point (°C)	Analysis									
		C		H		N		S		O	
		Calcd.	Found	Calcd.	Found	Calcd.	Found	Calcd.	Found	Calcd.	Found
$Me_2NC(O)OGeMe_3$	Colorless liquid	35.02	34.94	7.35	7.43	6.81	6.93	—	—	15.55	15.79
$Me_2NC(O)SGeMe_3$	28–30	32.48	32.49	6.82	6.78	6.31	6.35	14.45	14.81	7.21	7.25
$Me_2NC(S)SGeMe_3$	25–26	30.29	30.34	6.36	6.83	5.89	5.93	26.95	26.52	—	—
$Me_2NC(S)SPbMe_3$		19.35	19.53	4.07	4.19	3.77	3.72				
$Me_2NC(S)OPbMe_3$	58–60	20.25	20.51	4.24	4.79	3.93	3.91	8.99	8.72	4.49	4.59

TABLE 2. ^1H chemical shifts

Compound	Chemical shifts δ*		$J(^{207}Pb—C—^1H)$ (Hz)
	NMe_2	Ester grouping	
$Me_3GeOC(O)NMe_2$	2.84	0.53	
$Me_3GeSC(O)NMe_2$	3.01	0.61	
$Me_3GeSC(S)NMe_2$	3.26	0.66	
$Me_3PbSC(O)NMe_2$	2.96 3.08	1.35	66.4
$Me_3PbSC(S)NMe_2$	3.45	1.40	64.7

*In 10 mol% solution in CCl_4 at the ambient temperature of the probe.

be expected, the chemical shifts of the protons of the ester group —Y—MMe_3 follow the same pattern as that observed in the tetramethyl compounds Me_4M (10).

The carbamate and dithiocarbamate esters exhibit a single resonance for the *N*-methyl protons at room temperature.

When the temperature is lowered the *N*-methyl resonance of trimethylgermyl *N,N*-dimethyldithiocarbamate (in $CHCl_3$ solution) splits into a doublet of separation ~1.3 Hz below 250 K. However, no splitting of the resonance was observed in hexane solutions at temperatures as low as 214 K. The trimethylplumbyl ester of *N,N*-dimethyldithiocarbamic acid showed no splitting of the *N*-methyl resonance at 211 K in either chloroform or *n*-hexane solutions.

Similarly trimethylgermyl dimethylcarbamate showed no splitting of the *N*-methyl peak at 214 K in *n*-hexane and chloroform solution. In chloroform solution, however, the *N*-methyl peak was broad at room temperatures and sharpened at lower temperatures.

The *N*-methyl resonance of the trimethylgermyl monothiocarbamate splits into a doublet just below room temperature in both chloroform and *n*-hexane solution.

In chloroform solution the two *N*-methyl peaks were asymmetric at low temperatures with the low field peak being broader than the high field one. At temperatures just below the coalescence temperature, however, they appeared to have the same widths. In *n*-hexane solution the two peaks had the same widths at low temperatures.

The trimethylplumbyl monothiocarbamate showed a splitting of the *N*-methyl resonance in both *n*-hexane and chloroform solutions at room temperature. In both solutions at low temperatures the low field *N*-methyl peak was slightly broader.

The splitting of the *N*-methyl resonance in these compounds is due to hindered rotation about the C—N bond which causes the two *N*-methyl groups to reside in slightly different magnetic environments; the situation is exactly analogous to that in amides. Activation parameters for the hindered rotation in these and similar compounds have been determined (27).

The unequal line widths of the two *N*-methyl resonances in the monothiocarbamates are somewhat unusual. We have also observed unequal *N*-methyl line widths in solutions of trimethylstannyl dimethylmonothiocarbamate (7). A similar broadening was reported in the compound $(CH_3)_2CClSn(SSeCNC(CH_3)_2)_2$ and attributed to unequal coupling with the ^{77}Se isotope (11). In light of the results of our work, it appears that the effect is more general and is not due to selenium coupling.[1] We have previously suggested that the broadening may be due to the formation of dimeric or higher polymeric species at low temperatures (7).

Infrared Spectra

Normal coordinate analysis of the dimethyldithiocarbamate anion (12) and dimethylamides and thioamides (13) suggest that a high degree of coupling of i.r. modes takes place and hence few of the bands can be described as 'pure'. Thus a detailed analysis of the i.r. spectra would prove quite difficult.

However, a few major bands may be identified.

The dithiocarbamates have a strong band at ~1489 cm^{-1} which may be identified as the 'thioureide' band which Chatt *et al.* (14) have

[1]A referee has suggested that the unequal broadening may be due to unequal quadrupole broadening as part of unresolved $J(^1H–^{14}N)$ coupling. If this were indeed the case, however, it is rather strange that analogous broadening is not observed in the spectra of all the compounds studied.

Can. J. Chem. Downloaded from www.nrcresearchpress.com by 210.87.254.6 on 09/05/12
For personal use only.

Can. J. Chem. Downloaded from www.nrcresearchpress.com by 210.87.254.6 on 09/05/12
For personal use only.

suggested arises from a polar $\overset{+}{N}$—C—$\bar{S}$ vibration.

Trimethylgermyl dimethylcarbamate has a strong band at 1662 cm^{-1} in (10% CCl_4 solutions) which may be identified as the carbonyl stretch. The band position shifts 20 cm^{-1} to lower wave numbers in chloroform solution. This is consistent with an H-bonding interaction between the carbamate and the chloroform which tends to weaken the carbon–oxygen bond.

The monothiocarbamates also have a strong band in the carbonyl stretching region (1630 cm^{-1}, $Me_2NC(O)SGeMe_3$; 1609 cm^{-1} $Me_2NC(O)SPbMe_3$) and the monothiocarbamates may thus be established as being the *S*-esters rather than the *O*-esters.

Ultraviolet Spectra

The u.v. spectra of these and related compounds are listed in Table 3.

The u.v. spectra of dithiocarbamates have been fairly extensively studied (15–23) and four types of bands may be distinguished which have been assigned as follows: (*a*) Type I, $n \rightarrow \pi^*$ (280–360 nm); (*b*) Type II, $\pi \rightarrow \pi$ (280 nm); (*c*) Type III, $\pi \rightarrow \pi^*$ (240–250 nm); (*d*) Type IV, unassigned (220 nm).

In the trimethylsilyl and trimethylgermyl dithiocarbamates, bands I and II shift to longer wavelengths relative to the analogous *tert*-butyl ester while band III shifts to shorter wavelengths. The shift of the $n \rightarrow \pi^*$ (band I) transition in these esters suggests that the extent of conjugation at the ester sulfur with the thiocarbonyl group is being reduced (15, 16, 24). This might arise if the trimethylsilyl and trimethylgermyl groups were acting as π acceptors (Si > Ge). The trimethylplumbyl dithiocarbamate has a u.v. spectrum very similar to the methyl and *tert*-butyl esters and thus shows little evidence of conjugation. The u.v. spectra of the trimethylstannyl dithiocarbamate is considerably different from the silyl and germyl derivatives. This may reflect some internal coordination in the tin structure in solution; some internal coordination in the solid state has been demonstrated in its crystal structure (25).

The trimethylgermyl and plumbyl monothiocarbamates have only an $n \rightarrow \pi^*$ transition in the region above 220 nm; the $\pi \rightarrow \pi^*$ transitions are presumably shifted to lower wavelengths. Once again the shift of the $n \rightarrow \pi^*$ transition in the germyl ester suggests that the —$GeMe_3$ group is acting as a π acceptor. The position of the $n \rightarrow \pi^*$ transition in the trimethylplumbyl monothiocarbamate is obscured by strong end absorption which has a broad tail and presumably arises from the expected $\pi \rightarrow \pi^*$ transition below 220 nm.

The carbamates showed no u.v. absorption above 220 nm.

It must be noted that for all the compounds studied the shifts of the u.v. bands were slight and hence interpretation of the reason for these shifts is somewhat speculative. Nonetheless the trend of the shifts appear to be real in that in a recent paper (26) quite similar shifts were reported for group IV esters of several dithioacids.

TABLE 3. Ultraviolet spectral data

Compound	λ (nm)	log ε
Dithiocarbamates		
$Me_2NC(S)SMe$	226.4	4.08
	248.0	3.88
	278.5	3.98
	344.0	1.69
$Me_2NC(S)SCMe_3$	226.5	3.99
	249.0	3.92
	282.0	3.96
	350.0	1.63
$Me_2NC(S)SSiMe_3$*	233.0	
	243.0	
	282.0	
	359.0	
$Me_2NC(S)SGeMe_3$	232.0 (shoulder)	3.88
	246.0	4.02
	283.5	3.93
	356.5	1.62
$Me_2NC(S)SSnMe_3$	248.5	4.03
	286.5	3.82
	348.0	1.70
$Me_2NC(S)SPbMe_3$*	248.5	
	279.5 (shoulder)	
	345.0 (shoulder)	
Monothiocarbamates		
O-Esters		
$Me_2NC(S)OMe$	249.5	4.16
	290.0	1.94
$Me_2NC(S)OSiMe_3$	252.0	4.03
	295.0	1.87
S-Esters		
$Me_2NC(O)SMe$	277	0.82
$Me_2NC(O)SCMe_3$	End absorption	
$Me_2NC(O)SGeMe_3$	End absorption	
	283	0.98
$Me_2NC(O)SSnMe_3$	283.5	0.71
$Me_2NC(O)SPbMe_3$	End absorption	
Carbamates		
No u.v. absorption was found in solutions of any of the carbamate esters.		

*Extinction coefficients could not be determined accurately because of the instability of the solutions.

1. T. A. GEORGE, K. JONES, and M. F. LAPPERT. J. Chem. Soc. A, 2157 (1965).
2. F. BONATI and R. UGO. J. Organomet. Chem. **10**, 257 (1967).
3. J. SATGÉ, M. LESBRE, and M. BAUDET. C. R. **259**, 4733 (1964).
4. H. SHAPIRO and F. W. FREY. The organic compounds of lead. Interscience Publishers, New York. 1968. p. 249.
5. A. E. LEMIRE and J. C. THOMPSON. Can. J. Chem. **48**, 842 (1970).
6. A. E. LEMIRE and J. C. THOMPSON. J. Am. Chem. Soc. **93**, 1163 (1971).
7. A. E. LEMIRE and J. C. THOMPSON. Can. J. Chem. **50**, 1386 (1972).
8. J. PARROD. C. R. **234**, 1062 (1952).
9. H. TILLES. J. Am. Chem. Soc. **81**, 714 (1959).
10. A. ALLRED and E. ROCHOW. J. Am. Chem. Soc. **79**, 5361 (1957).
11. T. KAMITANI and T. TANAKA. Inorg. Nucl. Chem. Lett. **6**, 91 (1970).
12. K. A. JENSEN, B. M. DAHL, P. H. NIELSEN, and G. BORCH. Acta Chem. Scand. **25**, 2029 (1971).
13. G. DURGAPRASAD, D. SATHYANARAYANA, and C. PATEL. Bull. Chem. Soc. Jpn. **44**, 316 (1971).
14. J. CHATT, L. A. DUNCANSON, and L. M. VENANZI. Nature, **177**, 1042 (1956).
15. M. J. JANSSEN. Recl. Trav. Chim. Pays.-Bas, **79**, 454 (1960).
16. M. J. JANSSEN. Recl. Trav. Chim. Pays.-Bas, **79**, 464 (1960).
17. M. L. SHANKARANARAYANA and C. C. PATEL. Acta Chem. Scand. **19**, 1113 (1965).
18. J. SANDSTRÖM. Acta Chem. Scand. **16**, 1616 (1962).
19. G. ISAKSSON and J. SANDSTRÖM. Acta Chem. Scand. **21**, 1605 (1967).
20. H. P. KOCH. J. Chem. Soc. 401 (1949).
21. J. FABIAN. Theor. Chim. Acta, **12**, 200 (1968).
22. G. ST. NIKOLOV and N. TYUTYULKOV. Inorg. Nucl. Chem. Lett. **7**, 1209 (1971).
23. G. ST. NIKOLOV, N. JORDANOV, and I. HAVEZOV. J. Inorg. Nucl. Chem. **33**, 1059 (1971).
24. S. NAGAKURA. Bull. Chem. Soc. Jpn. **25**, 164 (1952).
25. G. M. SHELDRICK and W. D. SHELDRICK. J. Chem. Soc. A, 490 (1970).
26. S. KATO, M. MIZUTA, and Y. ISHII. J. Organomet. Chem. **55**, 121 (1973).
27. A. E. LEMIRE and J. C. THOMPSON. Can. J. Chem. This issue.

Can. J. Chem. Downloaded from www.nrcresearchpress.com by 210.87.254.6 on 09/05/12
For personal use only.

Studies of Hindered Rotation in Some Group IV Esters of Dimethylcarbamic and Dimethylthiocarbamic Acids

A. E. LEMIRE AND J. C. THOMPSON

Department of Chemistry, University of Toronto, Toronto, Ontario M5S 1A1

Received March 24, 1975

A. E. LEMIRE and J. C. THOMPSON. Can. J. Chem. **53,** 3732 (1975).

Activation parameters for hindered rotation about the C—N bond have been obtained for some trimethylgermyl, trimethylplumbyl, and *tert*-butyl esters of *N,N*-dimethylcarbamic, *N,N*-dimethylmonothiocarbamic, and *N,N*-dimethyldithiocarbamic acids. These are compared with previous results for some group IV esters and general considerations as to factors influencing barriers to rotation are discussed. It was found that the degeneracy of the *N*-methyl resonances observed in the room or low temperature ^1H spectra appeared also to extend to the room temperature ^{13}C spectra. A 'steric' effect was noted on the carbonyl and thiocarbonyl resonances.

A. E. LEMIRE et J. C. THOMPSON. Can. J. Chem. **53,** 3732 (1975).

On a obtenu les paramètres d'activation pour la rotation empêchée autour du lien C—N des quelques esters *N,N*-diméthylcarbamates, *N,N*-diméthylmonothiocarbamates et *N,N*-diméthyldithiocarbamates de triméthylgermyle, de triméthylplumbyle et de *tert*-butyle. On compare ces données avec des résultats antérieurs pour quelques esters du groupe IV; on discute aussi, sous forme de considérations générales, des facteurs influençant les barrières à la rotation. On a trouvé que la dégénérescence des résonances de *N*-méthyles, qui est observée dans les spectres du proton à température de la pièce ou a basse température, semble s'étendre aussi aux spectres du ^{13}C à température de la pièce. On note un effet 'stérique' sur les résonances du carbonyle et du thiocarbonyle.

[Traduit par le journal]

Can. J. Chem. Downloaded from www.nrcresearchpress.com by 210.87.254.105 on 09/05/12
For personal use only.

As part of a systematic study of factors influencing the barrier to rotation about the C—N bond in amide-like systems, we have previously reported activation parameters for hindered rotation for methyl (1), trimethylsilyl (2), and trimethylstannyl (3) esters of *N,N*-dimethylthiocarbamic acids. In this paper we complete the study by reporting on the results obtained for the trimethylgermyl, trimethylplumbyl, and *tert*-butyl esters.

Although, after the advent of total line shape methods, many compounds were studied by variable temperature n.m.r., systematic studies are still rare. However, for some systems, primarily amides and thioamides, some correlations have been made between structural features and activation parameters (4, 5). One of the most comprehensive studies is a recent series of papers by Reeves and co-workers (6–8) in which they discussed factors influencing rates of rotation in amides and thioamides with halide and pseudo-halide substituents.

Some difficulties arose in interpreting the results obtained when the *N*-methyl resonances exhibited no splitting at low temperatures, as in such cases it is impossible to decide whether the barrier to rotation is so low that exchange cannot be frozen out or whether the two *N*-methyl resonances are instead degenerate. As the *N*-methyl ^{13}C splitting in dimethylamides is at least an order of magnitude greater than the ^1H splitting (9), we felt ^{13}C studies of the esters might resolve this difficulty and we thus present the results of some preliminary investigations.

Experimental

Preparation of Compounds

The synthesis of most of the compounds used in this study have been described previously (1–3, 10–12). However, the preparation of $Me_2NC(S)SCMe_3$ does not appear to have been reported in the literature and is therefore described herein.

$Me_2NC(S)SCMe_3$

Me_3CSH (4.5 g, 0.05 mol) dissolved in 10 ml of pentane was added dropwise with stirring to 40 ml of a 1.26 *M* solution of $(CH_3)_3CLi$ in a 3-necked flask equipped with an N_2 inlet, a dropping funnel, and a condenser. The reaction was very vigorous and it was necessary to cool the reaction flask in a Dry Ice bath throughout the period of addition. A white precipitate formed halfway through the addition.

$Me_2NC(S)Cl$ (6.1 g, 0.05 mol) dissolved in 25 ml of dry ether was then added while cooling the reaction flask in a Dry Ice bath. When the addition was complete, the reaction mixture was allowed to warm gradually to room

TABLE 1. Activation parameters for hindered rotation[a]

Compound	Solvent	E_a (kcal/mol)	$\Delta H^{\ddagger}_{298.2}$ (kcal/mol)	$\Delta G^{\ddagger}_{298.2}$ (kcal/mol)	$\Delta S^{\ddagger}_{298.2}$ (e.u.)
$Me_2NC(S)SMe$	*n*-Hexane	13.0±0.3	12.5±0.3	14.7±0.3	−7.4±1
	$CHCl_3$	17.7±0.9	17.1±0.9	15.9±0.9	4.2±3
$Me_2NC(S)OMe$	Cyclohexane	14.2±0.4	13.6±0.4	17.1±0.4	−11.7±1
	Neat	14.5±0.2	13.9±0.2	17.4±0.2	−11.7±0.5
	$CHCl_3$	18.7±0.4	18.1±0.4	17.9±0.4	0.7±1
$Me_2NC(O)OMe$	*n*-Hexane		No splitting		
	$CHCl_3$	12.3±0.6	11.7±0.6	15.7±0.6	−13.2±2
$Me_2NC(O)SMe$	*n*-Hexane		No splitting		
	$CHCl_3$	13.0±1.0	12.4±1.0	15.0±1.0	−8.8±4
$Me_2NC(S)SCMe_3$	*n*-Hexane	11.7±1.6	11.1±0.6	14.4±0.6	−10.9±2
	$CHCl_3$	14.9±0.9	14.2±0.9	14.8±0.9	−1.8±4
$Me_2NC(O)SCMe_3$	*n*-Hexane		No splitting		
	$CHCl_3$	12.5±1.0	11.9±1.0	14.2±1.0	−7.8±4
$Me_2NC(O)OCMe_3$	*n*-Hexane		No splitting		
	$CHCl_3$			12.2±2.0[b]	
$Me_2NC(S)SSiMe_3$	*n*-Hexane		No splitting		
	$CHCl_3$	12.4±0.7	11.8±0.7	14.9±0.7	−10.2±3
$Me_2NC(S)OSiMe_3$	Neat	20.8±0.4	20.2±0.4	19.7±0.4	1.7±1
	n-Hexane	19.5±0.2	18.9±0.2	19.3±0.2	−1.3±1
	$CHCl_3$	13.4±0.3	12.8±0.3	18.2±0.3	−18.0±1
$Me_2NC(O)OSiMe_3$	*n*-Hexane	15.0±0.4	14.4±0.4	16.1±0.4	−5.7±1
	$CHCl_3$		No splitting		
$Me_2NC(S)SGeMe_3$	*n*-Hexane		No splitting		
	$CHCl_3$	13.2±0.9	12.6±0.9	14.8±0.9	−7.5±3
$Me_2NC(O)OGeMe_3$	*n*-Hexane		No splitting		
	$CHCl_3$		No splitting		
$Me_2NC(O)SGeMe_3$	*n*-Hexane	15.3±0.3	14.8±0.3	15.9±0.3	−3.7±1
	$CHCl_3$	15.0±0.6	14.4±0.6	16.0±0.6	−5.6±2
$Me_2NC(S)SSnMe_3$	*n*-Hexane		No splitting		
	$CHCl_3$		No splitting		
$Me_2NC(O)OSnMe_3$	*n*-Hexane		No splitting		
	$CHCl_3$		No splitting		
$Me_2NC(O)SSnMe_3$	*n*-Hexane	17.0±0.2	16.4±0.2	16.4±0.2	0.2±1
	$CHCl_3$	19.9±0.3	19.3±0.3	16.3±0.3	9.1±1
$Me_2NC(S)SPbMe_3$	*n*-Hexane		No splitting		
	$CHCl_3$		No splitting		
$Me_2NC(O)SPbMe_3$	*n*-Hexane	15.6±0.8	15.0±0.8	15.9±0.8	−3.0±3
	$CHCl_3$	16.1±0.6	15.5±0.6	15.9±0.6	−1.2±2

[a]The error limits quoted are those obtained from the statistical treatment of the least squares line but, as has been pointed out by several workers, may not be indicative of the true error situation (30, 31).
[b]At coalescence temperature.

temperature. At this time the reaction mixture consisted of a colorless solution with a white precipitate. The reaction mixture was then stirred for 2 h at room temperature during which time the solution turned yellow. The solution was filtered and the solvent evaporated off using a water pump to yield a yellow oil.

The oil was fractionally distilled and a 10% yield of a yellow viscous liquid boiling at 40 °C at 5 Torr was obtained.

Anal. Calcd. for $Me_2NC(S)SCMe_3$: C, 47.41; H, 8.53; N, 7.90; S, 36.17. Found: C, 47.40; H, 8.54; N, 7.96; S, 36.16.

Methods

The techniques for obtaining and analyzing n.m.r. spectra have been described previously (1–3). ^1H spectra were obtained on a Varian A56-60D n.m.r. spectrometer. ^{13}C spectra were run on a Varian XL-100 n.m.r. spectrometer.

Results

A summary of activation parameters obtained from the ^1H spectra for hindered rotation in the compounds $Me_2NC(X)YMMe_3$ (X = O, S; Y = O, S; M = C → Pb) is found in Table 1. We have previously reported values for the methyl (1), trimethylsilyl (2), and trimethylstannyl (3) esters and these are included here to facilitate comparisons.

The trimethylgermyl, trimethylplumbyl, and *tert*-butyl (except $Me_2NC(O)OCMe_3$) have not

Can. J. Chem. Downloaded from www.nrcresearchpress.com by 210.87.254.105 on 09/05/12
For personal use only.

Can. J. Chem. Downloaded from www.nrcresearchpress.com by 210.87.254.105 on 09/05/12
For personal use only.

been studied previously and hence are discussed in some detail here.

$Me_2NC(O)OCMe_3$

A 10 mol% solution of the ester in *n*-hexane showed no splitting of the *N*-methyl resonance at 210 K. A very small splitting (*ca.* 0.5 Hz) was observed in a 10 mol% solution in chloroform at 210 K. The nonexchanging chemical shift exhibited a marked temperature dependence. Previously Lustig *et al.* (10) had observed a broadening of the *N*-methyl peak at 233 K but no splitting.

Activation parameters were not calculated because, with such a small *N*-methyl splitting, the exchange region covers only 2–3 K. Moreover, when the peak separation and the line widths are of the same order of magnitude the line shape equation becomes very insensitive. However, the free energy of activation $\Delta G^{\ddagger}$ may be estimated as 12 ± 2 kcal/mol from an analysis of the coalescence temperature spectrum.

$Me_2NC(O)SCMe_3$

A 10 mol% solution of the ester in hexane showed no splitting of the *N*-methyl resonance at 205.9 K. A splitting was observed in a 10 mol% solution in chloroform at low temperatures. The nonexchanging chemical shift was small (*ca.* 1.1 Hz) and exhibited a marked temperature dependence.

$Me_2NC(S)SCMe_3$

A 10 mol% solution in hexane exhibited no splitting of the *N*-methyl resonance at room temperature but a splitting of 6.03 Hz was observed at low temperatures. The limited solubility of the compound precluded an extensive study of the temperature dependence of the nonexchanging chemical shifts.

In a 10 mol% solution in chloroform, a splitting of 8.10 Hz was observed at low temperatures. The nonexchanging chemical shift showed a negligible temperature dependence outside the exchange region.

$Me_2NC(O)OGeMe_3$

No splitting of the *N*-methyl peak was observed in an *n*-hexane solution (10 mol%) at 213.9 K nor in a chloroform solution (10 mol%) at 213.0 K.

$Me_2NC(O)SGeMe_3$

Splitting of the *N*-methyl resonance just below room temperature was observed in both chloroform (10 mol%) and *n*-hexane (10 mol%). In chloroform solution, at low temperatures below the exchange region, the low field *N*-methyl peak was slightly broader than the high field one.

$Me_2NC(O)SPbMe_3$

A splitting of the *N*-methyl resonance was observed at room temperature in *n*-hexane ($\delta\nu_\infty$ = 14.5 Hz) and in chloroform ($\delta\nu_\infty$ = 14.0 Hz) solution. At low temperatures, the two *N*-methyl peaks had slightly different widths.

$Me_2NC(S)SPbMe_3$

No splitting of the *N*-methyl resonance was observed at 211.2 K in dilute solutions in chloroform and *n*-hexane.

Discussion

Proton Chemical Shifts

The proton chemical shifts are listed in Table 2. The chemical shifts of the protons of the ester grouping, $—MMe_3$, follow the same

TABLE 2. ^1H chemical shifts

Compound	Chemical shifts, δ[a]	
	NMe_2	Ester grouping
$Me_2NC(O)OMe$	2.87	3.60
$Me_2NC(O)SMe$	2.97	2.26
$Me_2NC(S)SMe$	3.44	2.56
$Me_2NC(S)OMe$	3.34 3.11	3.94
$Me_2NC(O)OCMe_3$	2.84	1.42
$Me_2NC(O)SCMe_3$	3.12	1.56
$Me_2NC(S)SCMe_3$	3.60	1.72
$Me_2NC(O)OSiMe_3$	2.90	0.23
$Me_2NC(S)SSiMe_3$	3.63	0.53
$Me_2NC(S)OSiMe_3$	3.34 3.16	0.39
$Me_2NC(O)OGeMe_3$	2.84	0.53
$Me_2NC(O)SGeMe_3$	3.01	0.61
$Me_2NC(S)SGeMe_3$	3.26	0.66
$Me_2NC(O)OSnMe_3$	2.93	0.51
$Me_2NC(O)SSnMe_3$	3.12 2.95	0.51
$Me_2NC(S)SSnMe_3$	3.50	0.59
$Me_2NC(O)SPbMe_3$	2.96 3.08	1.35
$Me_2NC(S)SPbMe_3$	3.45	1.40

[a]In 10 mol% solution in CCl_4 at the ambient temperature of the probe.

TABLE 3. ^{13}C chemical shifts

Compound	δ (in p.p.m. from TMS)[a] —M($\overset{*}{C}H_3$)$_3$	—N($\overset{*}{C}H_3$)$_2$	$\overset{*}{C}$=X	Y$\overset{*}{C}$(CH$_3$)$_3$ or Y$\overset{*}{C}$H$_3$
$(CH_3)_2NC(O)OCH_3$		36.2_2	157.2_5	52.5_6
$(CH_3)_2NC(O)OC(CH_3)_3$	28.4_6	35.9_9	155.9_8	79.0_7
$(CH_3)_2NC(O)OSi(CH_3)_3$	1.9_2	35.9_9	155.5_7	
		36.5_3		
$(CH_3)_2NC(O)OGe(CH_3)_3$	3.4_8	36.4_1	158.7_3	
$(CH_3)_2NC(O)OSn(CH_3)_3$	-2.0_2	36.8_2	161.3_1	
$(CH_3)_2NC(O)SCH_3$		36.6_1	168.7_3	13.0_6
$(CH_3)_2NC(O)SC(CH_3)_2$	30.4_8	36.3_1	168.3_9	47.1_8
$(CH_3)_2NC(O)SGe(CH_3)_3$	2.4_6	36.1_5	168.4_3	
		39.3_4		
$(CH_3)_2NC(O)SSn(CH_3)_3$	-3.2_3	36.5_1	170.7_7	
		40.7_3		
$(CH_3)_2NC(O)SPb(CH_3)_3$	10.1_7	36.4_6	172.2_2	
		40.6_5		
$(CH_3)_2NC(S)OCH_3$		37.7_9	189.1_5	58.1_4
		42.8_3		
$(CH_3)_2NC(S)OSi(CH_3)_3$	0.8_1	38.1_8	185.9_8	
		42.1_8		
$(CH_3)_2NC(S)SCH_3$		41.5_9	198.4_0	20.6_4
		45.5_0		
$(CH_3)_2NC(S)SC(CH_3)_3$	29.4_7	43.1_1 (broad)	196.1_6	51.2_7
$(CH_3)_2NC(S)SSi(CH_3)_3$	1.5_2	44.0_3	194.8_3	
$(CH_3)_2NC(S)SGe(CH_3)_3$	3.0_9	44.2_9	196.4_4	
$(CH_3)_2NC(S)SSn(CH_3)_3$	-0.6_6	45.6_0	198.8_4	
$(CH_3)_2NC(S)SPb(CH_3)_3$	13.5_9	45.5_1	201.4_3	

[a]In $CDCl_3$ solution.

pattern that was observed in the tetramethyl compounds by Allred and Rochow (13).

In dithiocarbamate systems, Nikolov (14) has suggested that the position of the *N*-methyl resonance might be taken as a measure of the C—N bond order, but we have found little correlation between the *N*-methyl chemical shift and barriers to rotation (1–8).

It has also been suggested that *N*-methyl resonances at 3.4 δ are indicative of chelated dithiocarbamate ligands (15), but our results for the methyl ester, $Me_2NC(S)SMe$, suggest that this correlation is unlikely.

It appears, however, that correlations of ^{15}N chemical shifts with bond order may well exist (16).[1]

^{13}C Chemical Shifts

The ^{13}C chemical shifts obtained in this study are listed in Table 3. While spectra were run in both $CDCl_3$ and C_6D_{12} solutions, only the $CDCl_3$ results are listed for the sake of simplicity, as there were no significant differences observed. While solvent effects on the position of the carbonyl resonance have previously been noted (17), Maciel and Natterstad (18) have found that substituents (capable of conjugation) in a position adjacent to the carbonyl group tended to reduce the sensitivity of its shielding to solvent changes; this also appeared to be the case in the systems we have studied. Downfield shifts of carbonyl carbons relative to olefin carbons have been explained as being due to the polarization, $\overset{+}{C}—\overset{-}{O}$, of the carbonyl bond (ref. 19, p. 102). Adjacent heteroatoms with unshared electrons offset this effect as conjugation between the heteroatom and carbon can result in higher electron density at the carbonyl carbon than in an isolated carbonyl bond (ref. 19, p. 280, 20).

Such an effect is demonstrated by the compounds studied in this work. The carbonyl resonance in the carbamate and thiocarbamate

[1]L. W. Reeves, private communication.

Can. J. Chem. Downloaded from www.nrcresearchpress.com by 210.87.254.105 on 09/05/12
For personal use only.

Can. J. Chem. Downloaded from www.nrcresearchpress.com by 210.87.254.105 on 09/05/12
For personal use only.

esters was shifted upfield relative to the carbonyl resonance in ketones.

Such an effect also makes correlation of the ^{13}C chemical shift of the carbonyl carbon with barriers to rotation seem unlikely as conjugation involving either the nitrogen or the ester lone pair would put extra charge density upon the carbon but would affect the barriers to rotation about the C—N bond in opposite directions.

This expectation was borne out in our studies. For example, there is little change in the ^{13}C chemical shift of $Me_2NC(O)SCMe_3$ and $Me_2NC(O)SGeMe_3$ while there is a considerable difference in the barriers to rotation.

As was expected, in those cases where the *N*-methyl resonance is split, the splitting is generally greater than that observed in the proton spectra. The larger splitting is probably due to a steric shift to lower field of the *N*-methyl carbon *cis* to the C=X chromophore (21).

In spite of the expected larger splittings, however, a splitting of the *N*-methyl ^{13}C resonance was observed only for those compounds for which a splitting was also observed at room temperature or lower in the proton spectra.

Those compounds which showed no splitting (*i.e.*, $Me_2NC(O)OMMe_3$, M = Ge → Sn; $Me_2NC(S)SMMe_3$, M = Sn, Pb) or a small splitting of the order of 1 Hz (*i.e.*, $Me_2NC(O)OMMe_3$, M = C, Si; $Me_2NC(S)SMMe_3$, M = Si, Ge; $Me_2NC(O)OMe$; $Me_2NC(O)SMe$; $Me_2NC(O)SCMe_3$) also showed no splitting in the room temperature ^{13}C spectra.

The ^{13}C spectra also show some unusual effects arising from the presence of the group IV atoms.

For a given series of esters, the resonances of the trimethyl grouping follow the order C > Pb > Ge > Si > Sn. This may be contrasted with the order C > Si > Ge > Pb > Sn obtained for the tetramethyl compounds (22).

Even in the alkyl compounds the shifts are rather unusual for they do not parallel those observed for the ^1H chemical shifts and hence electronegativities derived from ^{13}C and ^1H chemical shifts are not consistent with each other (13). However, in the case of the tetramethyl derivatives, it has been suggested that the ^{13}C chemical shifts are considerably dependent upon diamagnetic contributions, σ_d, as well as paramagnetic contributions, σ_p (23). Both σ_d and σ_p vary with atomic number; however they do not vary at the same rate and for heavier elements, σ_d takes on an increasing importance. This interplay has been used to rationalize the shifts observed in the tetramethyl derivatives (23).

That the order in the carbamate and thiocarbamate esters is different from that in the tetraalkyl derivatives is not wholly unexpected as the bonding between the ester sulfur or oxygen and the central metal is expected to be different from that between carbon and the metal and hence may lead to different magnetic anisotropy contributions. What is unusual, is that the trends are the same whether M is bonded to oxygen or sulfur; whereas in the case of silicon, for example, it is generally felt that the bonding between silicon and oxygen involves a greater *d–p* π overlap than does the bond between silicon and sulfur (24).

Another interesting feature of the spectra of both the thiocarbamates and carbamates is the shift of the carbonyl or thiocarbonyl resonance to lower fields in the heavier members of the series. This may be contrasted with the upfield shifts observed by Grishin *et al.* (25) in the ^{13}C spectra of organometallic ketones.

A similar downfield shift was noted in the C_2 phenyl chemical shift of some phenyl organometallics by Doddrell *et al.* (26) and attributed by them to a decrease in the γ-effects of the methyls due to less steric compression about C_2 as the C—M bond length increases.

It appears likely that the shift observed in the carbamate and thiocarbamate esters is due to a similar steric effect rather than being indicative of any variation in bonding of the group IV element and the ester sulfur or oxygen.

Barriers to Rotation

As has been noted previously, a general lowering of barriers is seen on going from amides or thioamides to carbamates or thiocarbamates due to the possibility of competitive delocalization occurring in the latter two cases (Scheme 1, **1c**) (1–3, 27).

With group IV esters of carbamic and thiocarbamic acids, two further interactions (**1***d* and **1***e*) are possible and would be expected to modify barriers to rotation.

In **1***d* the —MMe_3 group acts as an electron-withdrawing group and tends to raise barriers to rotation by decreasing the importance of resonance form **1***c*. In **1***e*, the group IV element

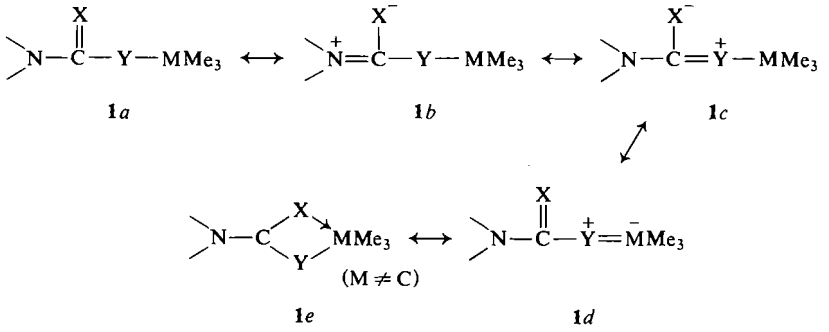

SCHEME 1

achieves five-coordination and a raising of the barrier would be expected because donation of the lone pair on nitrogen into the N—C—X system would be facilitated.

In the cases of the monothiocarbamates studied in this work, there appears to be a general raising of barriers to rotation relative to the analogous methyl esters. There also appears to be a raising of barriers relative to the *tert*-butyl ester $Me_2NC(O)SCMe_3$, but because of the small $\delta\nu_\infty$ observed in this system, the measured barrier is probably not sufficiently accurate to justify any conclusions.

We believe the raising of barriers in the monothiocarbamates to be largely due to the presence of contributions such as **1***d*. The i.r. evidence is more consistent with a unidentate mode of bonding of the monothiocarbamate group (**1***d*) than with a bidentate mode (**1***e*) (12).

However if the $—MMe_3$ group is acting as an electron-withdrawing group as in **1***d*, then one would expect the order to be Ge > Sn > Pb, C as germanium is generally believed to be much more likely to take part in (*p–d*) π interactions than is tin (28). The actual ordering however is Sn > Ge, Pb > C. This suggests that the actual situation may involve contributions from both **1***d* and **1***e* with the contribution of **1***e* becoming more important in the tin ester because of the greater tendency of tin to higher coordination.

It must also be noted that the raising of the barriers relative to the *tert*-butyl esters is small (*ca.* 2 kcal). This is not entirely unexpected as contributing structures such as **1***d* and **1***e* would only have a second order effect and also the increasing size of the substituent $—MMe_3$ (M = C → Pb) would be expected to act to counteract any raising of the barriers.

The reason for the small *N*-methyl splittings or lack of any splitting observed in the dithiocarbamates and the carbamates is somewhat more ambiguous.

In the case of no splitting at all, three possible explanations come to mind: (*a*) formation of a cyclic structure **1***e*, (*b*) intramolecular exchange (Scheme 2), or (*c*) the —MMe group acting as an electron-releasing group and hence lowering barriers to rotation (but this would be an opposite role to that observed in monothiocarbamates).

Intramolecular exchange may be ruled out in the case of the monothiocarbamates as one would expect to see separate resonances for both species **2***a* and **2***b*, but only one set of signals is observed.

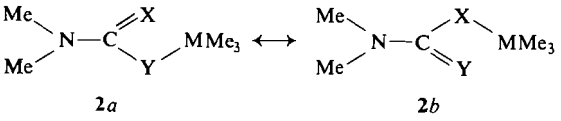

SCHEME 2

Such a process cannot be ruled out *a priori* in the case of the dithiocarbamates or the carbamates. However the process does not explain why the magnitude of the *N*-methyl splitting should be so much smaller in the trimethylsilyl and trimethylgermyl dithiocarbamates relative to the methyl and *tert*-butyl esters.

Nonetheless small *N*-methyl splittings have been observed for some cases where symmetric structures are highly unlikely (6–8) and the question of what factors determine the anisotropy that gives rise to two nonequivalent *N*-methyl positions is an interesting but not completely resolved one. Reeves and co-workers (29) have suggested that competitive delocalization (**1***c*) may cause the charge distributions in both the C—X and C—Y bonds to become similar.

Can. J. Chem. Downloaded from www.nrcresearchpress.com by 210.87.254.105 on 09/05/12
For personal use only.

However as even the maximum $\delta\nu_\infty$ observed are relatively small (maximum $\sim$14 Hz) and exhibit marked solvent effects, any explanation for lack of splitting being observed can only be speculative.

In our studies we have also noted a dependence of activation parameters on solvent. In general there appears to be a slight raising of barriers in going from hexane to chloroform solutions.

Finally in all studies of hindered rotation the question of the actual meaning of the activation entropies obtained is a problem. Theoretical considerations suggest $\Delta S^\ddagger$ should lie within the limits $0 \rightarrow 1.4$ e.u. (29) and Reeves has recently suggested that experimentally determined values assuming realistic error limits would probably fall in the range -4 to $+4$ e.u.[1]

In a few cases the entropies we obtained lay outside these limits. While solvation effects would be expected to alter $\Delta S^\ddagger$ and might cause it to lie outside these limits, it seems a highly dubious procedure to ascribe large ΔS values to solvation effects. It is much more likely that the ΔS values arise from systematic errors occurring because of difficulties in determining what the true $\delta\nu_\infty$ is when $\delta\nu_\infty$ exhibits a temperature dependence outside the exchange region. The extreme sensitivity of E_a and $\Delta S^\ddagger$ to errors in input parameters has been pointed out by several workers (30, 31). Thus $\Delta G^\ddagger$ seems still to be the safest parameter to use in making comparisons.

1. A. E. LEMIRE and J. C. THOMPSON. Can. J. Chem. **48**, 824 (1970).
2. A. E. LEMIRE and J. C. THOMPSON. J. Am. Chem. Soc. **93**, 1163 (1971).
3. A. E. LEMIRE and J. C. THOMPSON. Can. J. Chem. **50**, 1386 (1972).
4. W. E. STEWART and T. H. SIDDALL III. Chem. Rev. **70**, 517 (1970).
5. L. L. GRAHAM and R. E. DIEL. J. Phys. Chem. **73**, 2696 (1969).
6. L. W. REEVES, R. C. SHADDICK, and K. N. SHAW. Can J. Chem. **49**, 3683 (1971).
7. E. A. ALLAN, R. F. HOBSON, L. W. REEVES, and K. N. SHAW. J. Am. Chem. Soc. **94**, 6604 (1972).
8. L. W. REEVES and K. N. SHAW. Can. J. Chem. **49**, 3671 (1971).
9. Y. GISHIN, N. SERGEYEV, O. SUBBOTIN, and Y. USTYNYOK. Mol. Phys. **25**, 297 (1973).
10. E. LUSTIG, W. R. BENSON, and N. DUY. J. Org. Chem. **32**, 851 (1967).
11. H. TILLES. J. Am. Chem. Soc. **81**, 714 (1959).
12. A. E. LEMIRE. Ph. D. Thesis, University of Toronto, Toronto, Ontario. 1974.
13. A. ALLRED and E. ROCHOW. J. Am. Chem. Soc. **79**, 5361 (1957).
14. G. S. NIKOLOV. Inorg. Nucl. Chem. Lett. **7**, 1213 (1971).
15. J. C. MAY, D. PETRIDIS, and C. CURRAN. Inorg. Chem. Acta, **5**, 511 (1971).
16. P. HAMPSON and A. MATHIAS. Mol. Phys. **11**, 541 (1966).
17. G. E. MACIEL and G. C. RUBEN. J. Am. Chem. Soc. **85**, 3903 (1963).
18. G. E. MACIEL and J. J. NATTERSTAD. J. Chem. Phys. **42**, 2752 (1965).
19. J. B. STOTHERS. Carbon-13 n.m.r. spectroscopy. Academic Press, New York. 1972. p. 102.
20. G. C. LEVY and G. L. NELSON. Carbon-13 nuclear magnetic resonance for organic chemists. Wiley, New York. 1972. p. 120.
21. G. C. LEVY and G. L. NELSON. J. Am. Chem. Soc. **94**, 4897 (1972).
22. H. SPIESECKE and W. G. SCHNEIDER. J. Chem. Phys. **35**, 722 (1961).
23. J. MASON. J. Chem. Soc. A, 1038 (1971).
24. C. J. ATTRIDGE. Organomet. Chem. Rev. **A5**, 323 (1970).
25. Y. K. GRISHIN, S. V. PONOMAREV, S. A. LOBEDEV. Zh. Org. Khim. **10**, 404 (1974).
26. D. DODDRELL, K. G. LEWIS, C. E. MULGUINEY, W. ADCOCK, W. KITCHING, and M. BULLPIT. Aust. J. Chem. **27**, 417 (1974).
27. R. L. MIDDAUGH, R. S. DRAGO, and N. J. NIEDZIELSKI. J. Am. Chem. Soc. **86**, 388 (1964).
28. E. A. V. EBSWORTH. Organometallic compounds of the group IV elements. Vol. I. Marcel Dekker, New York. 1968.
29. R. F. HOBSON, L. W. REEVES, and K. N. SHAW. J. Phys. Chem. **77**, 1228 (1973).
30. R. R. SHOUP, E. D. BECKER, and M. L. MCNELL. J. Phys. Chem. **76**, 71 (1972).
31. S. VAN DER WERF and J. B. F. N. ENGBERTS. Recl. Trav. Chim. Pays-Bas, **40**, 663 (1971).

Can. J. Chem. Downloaded from www.nrcresearchpress.com by 210.87.254.105 on 09/05/12
For personal use only.

A Relationship between the Sizes and Energies of Atomic Orbitals

R. DAUDEL AND P. G. MEZEY
Centre de Mécanique Ondulatoire Appliquée, C.N.R.S., Paris, France
AND
J. D. GODDARD AND I. G. CSIZMADIA
Department of Chemistry, University of Toronto, Toronto, Ontario M5S 1A1

Received May 9, 1975

R. DAUDEL, P. G. MEZEY, J. D. GODDARD, and I. G. CSIZMADIA. Can. J. Chem. **53**, 3739 (1975).

An approximate relationship of the form

$$\bar{E}^{1.5}V = \text{constant}$$

where $\bar{E}$ is the mean potential acting upon and V the mean volume of an electron in a closed shell of an atom has previously been proposed. This concept of a simple relationship between the sizes and energies of atomic orbitals which is predicted by simple quantum mechanical arguments has been further examined in this present work. The potential energy for a series of two electron atoms and ions has been replaced by the total electronic energy as these two quantities are simply connected by the virial theorem. For polyelectronic atoms, a quantity per electron pair which sums to the total electronic energy has been used. The volume of the ith atomic orbital

$$V_i = \frac{4\pi}{3}\langle r_i^2\rangle^{3/2}$$

has been calculated from its size as previously defined in terms of the spherical quadratic operator evaluated at the orbital centroid of charge. A relationship of the above form between the sizes and energies of atomic orbitals holds well for core orbitals but gradually deteriorates on going from the innermost (core) to outermost (valence) shell.

R. DAUDEL, P. G. MEZEY, J. D. GODDARD et I. G. CSIZMADIA. Can. J. Chem. **53**, 3739 (1975).

On a proposé antérieurement une relation approchée de la forme

$$\bar{E}^{1.5}V = \text{constante}$$

où $\bar{E}$ est le potentiel moyen agissant sur et V le volume moyen d'un électron dans la sphère fermée d'un atome. Ce concept d'une relation simple entre les grosseurs et les énergies des orbitales atomiques, qui est prédit par des arguments simples de mécanique quantique, est examiné à nouveau dans le présent travail. On a remplacé l'énergie potentielle pour une série d'atomes et d'ions à deux électrons par une énergie électronique totale puisque ces deux quantités sont reliées d'une façon simple par le théorème viriel. Pour des atomes polyélectroniques, on a utilisé une quantité par paire d'électrons qui correspond à la somme de l'énergie électronique totale. Le volume de la $i$eme orbitale atomique

$$V_i = \frac{4\pi}{3}\langle r_i^2\rangle^{3/2}$$

est calculé à partir de sa grosseur telle que définie antérieurement en termes de l'opérateur quadratique sphérique évalué au centroïde de charge de l'orbitale. Une relation de la forme mentionnée plus haut entre les grosseurs et les énergies des orbitales atomiques est valable pour les orbitales du noyau mais se détériore graduellement lorsque l'on passe des couches de l'intérieur (noyau) vers celles de l'extérieur (valance).

[Traduit par le journal]

Introduction

An earlier investigation (1) of atomic electronic distributions revealed that

$$[1] \qquad \bar{E}_i^{1.5}\, V_i = \text{constant}$$

where $\bar{E}_i$ is the mean Hartree potential experienced by and V_i the mean volume associated with an electron when it visits the ith loge. The deviations from [1] were small, *i.e.* never greater than a factor of two while $\bar{E}_i$ and V_i varied by 10^4 and 10^5, respectively. The results of ref. 1 were later analyzed (2) in terms of the Thomas–Fermi statistical model for atomic electronic structure and it was shown that the Thomas–Fermi model predicts a relationship of the form of [1]. In addition, the analysis showed that such a relationship should hold better when $\bar{E}$ is

Can. J. Chem. Downloaded from www.nrcresearchpress.com by 210.87.254.5 on 09/05/12
For personal use only.

greatest, *i.e.* better for inner orbitals as compared to outer orbitals.

An even simpler quantum mechanical model, namely, the particle-in-a-box also predicts that a relationship like [1] should hold (3). For a particle in a one-dimensional box or in a sphere the energy is given by

$$[2] \qquad E_0 = -n^2 \frac{\pi^2 \hbar^2}{2ml^2}$$

where n is a quantum number and l is the linear dimension of a volume $1/N$ times the confining volume, where N is the number of identical particles including consideration of the electron spin, *i.e.*

$$[3] \qquad l = \left(\frac{V}{N}\right)^{1/3}$$

Substituting [3] into [2] and rearranging gives

$$[4a] \qquad E_0 V^{2/3} = -n^2 \frac{\pi^2 \hbar^2}{2m} \left(\frac{1}{N}\right)^{-2/3}$$

or

$$[4b] \qquad {E_0}^{3/2} V = \text{constant}$$

which is equivalent to the empirically observed relation [1]. Rearrangement and conversion from c.g.s. to atomic units of [4*a*] yields

$$[4c] \qquad \frac{1}{E_0} = -\frac{2}{n^2\pi^2} \left(\frac{1}{N}\right)^{2/3} V^{2/3}$$

The volume may be rewritten in terms of $\langle r^2 \rangle$ as

$$[5a] \qquad V = \frac{4\pi}{3} \langle r^2 \rangle^{3/2}$$

and substituted into [4*c*] to give

$$[4d] \qquad \frac{1}{E_0} = -\frac{2}{\pi^2} \frac{1}{n^2} \left(\frac{4\pi}{3}\right)^{2/3} \left(\frac{1}{N}\right)^{2/3} \langle r^2 \rangle$$

which with evaluation of the numerical constant yields

$$[4e] \qquad \frac{1}{E_0} \approx -0.53 \frac{1}{n^2} \left(\frac{1}{N}\right)^{2/3} \langle r^2 \rangle$$

as the predicted energy–size relationship on the basis of a particle-in-a-box model. Therefore it is plausible that a relationship between the size or volume of an atomic orbital and its energy may indeed exist. In the present work, the basic concepts of refs. 1 and 4 have been retained. The energies were obtained from Hartree–Fock–Roothaan SCF calculations on four sets of systems corresponding to four different electronic configurations (helium, beryllium, neon, and magnesium) of closed shell atoms and ions. The volumes of the atomic orbitals were calculated in terms of their sizes (5) as given by the expectation value of r^2 evaluated at the centroid of charge of the atomic orbital, *i.e.* at the nucleus. The volume of the ith atomic orbital may be written as

$$[5b] \qquad V_i = \frac{4\pi}{3} \langle r_i^2 \rangle^{3/2}$$

and rewriting [1] with a redefinition of the constant term yields [6] where e_i is an energy quantity for the ith atomic orbital

$$[6] \qquad e_i \langle r_i^2 \rangle = \text{constant}$$

However, it should be noted that there exists a degree of arbitrariness in the definitions of both the energy and the size or volume terms. A more flexible functional form

$$[7] \qquad e_i \langle r_i^2 \rangle^{\gamma} = C$$

where γ is a positive parameter and C a constant was also considered.

Method of Calculation

Hartree–Fock–Roothaan SCF calculations were performed on the closed shell atomic species given in Table 1. The SCF atomic orbitals were expanded in terms of an extensive set of uncontracted gaussian type functions with the exponents from the work of Huzinaga *et al.* (6, 7). For Al^+, Al^{3+}, Si^{2+}, and P^{3+} the final sets of four p-type gaussians specified by Huzinaga were not included in the basis set since such functions are primarily introduced to describe the 3p orbitals which is unnecessary for the cations considered in which the outermost filled orbital is 3s. The calculated total atomic energies for all the species studied are compared to the Hartree–Fock values (8, 9) in Table 2. The total atomic energies are all close to the Hartree–Fock limit. Previous studies (10) have indicated that $\langle r^2 \rangle$ and hence size is not strongly basis set dependent. It may be concluded that both the values for the energies and for the sizes are of near Hartree–Fock quality. All calculations were performed on the IBM 370/165 of the Centre Interregionale des Calculs Electroniques (CIRCE) Orsay, France, employing the the IBMOL-IV program system (11).

For the two-electron species the total electronic energy was employed as E in [6] or [7]. It was a

Can. J. Chem. Downloaded from www.nrcresearchpress.com by 210.87.254.5 on 09/05/12
For personal use only.

TABLE 1. Atomic species studied and basis sets employed*

System	Electronic configuration	Species	Basis	PGTF
Helium	$1s^2$	H^-, He	10s	10
		Li^+, Be^{2+}, B^{3+}	13s	13
Beryllium	$1s^22s^2$	Li^-, Be, B^+, C^{2+}, N^{3+}	13s	13
Neon	$1s^22s^22p^6$	F^-, Ne	13s7p	34
		Na^+, Mg^{2+}, Al^{3+}	17s8p	41
Magnesium	$1s^22s^22p^63s^2$	Na^-, Mg, Al^+, Si^{2+}, P^{3+}	17s8p	41

*For H and He, see ref. 6; for all others, see ref. 7. For Al, Si, and P, see text regarding truncation of the basis set.

TABLE 2. Total energies*

System	Species	Total energies (a. u.) This work	Hartree–Fock
Helium	H^-	−0.4877120	−0.4878
	He	−2.8616696	−2.8616799
	Li^+	−7.2362055	−7.2364140
	Be^{2+}	−13.611110	−13.611256
	B^{3+}	−21.985948	−21.986189
Beryllium	Li^-	−7.4278398	−7.42823
	Be	−14.572800	−14.573021
	B^+	−24.237208	−24.237564
	C^{2+}	−36.408017	−36.408484
	N^{3+}	−51.081279	−51.08231
Neon	F^-	−99.455201	−99.45936
	Ne	−128.54467	−128.54705
	Na^+	−161.67377	−161.67691
	Mg^{2+}	−198.82711	−198.83051
	Al^{3+}	−239.99492	−240.00001
Magnesium	Na^-	−161.85066	−161.85464
	Mg	−199.61095	−199.61461
	Al^+	−241.66923	−241.67433
	Si^{2+}	−287.98851	−287.99561
	P^{3+}	−338.55317	−338.56263

*For H^-, see ref. 9. For neutral species, see ref. 8*a*. For monopositive species, see ref. 8*b*. For mononegative and di- and tri-positive species, see ref. 8*c*.

matter of choice to use the total energy as either component could equally well have been employed since the virial theorem relates all three quantities.

[8] total $E = -\text{kinetic } E = \frac{1}{2}$ potential E

For atomic SCF calculations employing large gaussian basis sets, any deviations from [8] are small. For many electron atoms an analogous quantity was used

[9] $$e_i = 2h_i + \sum_j^{\text{all pairs}} g_{ij}$$

where h_i is the one-electron and g_{ij} the two-electron parts of the atomic hamiltonian. The quantity e_i includes on the average all interactions experienced by a given atomic orbital. The choice of e_i is consistent with the two electron case since these terms sum to the total atomic energy.

[10] $$E = \sum_i^{\text{all pairs}} e_i$$

The volume term was obtained from the size as discussed previously (*cf.* [5]). The $\langle r_i^2 \rangle$ was computed using the one-electron properties package available as part of the POLYATOM system (12). Calculation of the size then involves a simple coordinate transformation (5). The integrals from the SCF calculations were trans-

Can. J. Chem. Downloaded from www.nrcresearchpress.com by 210.87.254.5 on 09/05/12
For personal use only.

TABLE 3. Energies and sizes of electron pairs $1s^2$

System	Species	Energy (hartree)	Size (bohr^2)
Helium	H^-	−0.4877120	8.83061
	He	−2.8616696	1.18484
	Li^+	−7.2362055	0.44535
	Be^{2+}	−13.611110	0.23183
	B^{3+}	−21.985948	0.14189
Beryllium	Li^-	−6.763504	0.44640
	Be	−12.67480	0.23296
	B^+	−20.62712	0.14269
	C^{2+}	−30.59080	0.09626
	N^{3+}	−42.55910	0.06927
Neon	F^-	−66.23648	0.04163
	Ne	−82.68392	0.03347
	Na^+	−101.1638	0.02748
	Mg^{2+}	−121.6672	0.02296
	Al^{3+}	−144.1830	0.01946
Magnesium	Na^-	−100.7259	0.02748
	Mg	−120.9298	0.02296
	Al^+	−143.1907	0.01945
	Si^{2+}	−167.5086	0.01670
	P^{3+}	−193.8291	0.01448

formed to integrals over the final self-consistent atomic orbitals to compute the energetic quantities.

The data for the various systems were used to determine the optimal parameters for the linear equation

$$[11a] \qquad \left(\frac{1}{e_i}\right) = m\langle r_i^2\rangle + \left(\frac{1}{e_i}\right)_0$$

which is a simple rearrangement of [6] with allowance made for the possibility of an intercept. Parameter optimization involved a standard linear least squares analysis. Rearrangement of [7] yields, allowing for an intercept,

$$[12] \qquad \left(\frac{1}{e_i}\right) = m\langle r_i^2\rangle^\gamma + \left(\frac{1}{e_i}\right)_0$$

where the parameters were obtained from a conjugate gradient minimization procedure.

Results and Discussion

The results for the energies and sizes for the helium-, beryllium-, neon-, and magnesium-like systems are collected according to atomic orbital type in Tables 3 to 6. Although the results for the energies and sizes for the mononegative ions are presented the data for the negatively charged species were not used in obtaining the parameters in the case of the outermost orbital (*e.g.* for the 1s orbital H^- was excluded, for the 2s orbital Li^-, etc). Attempted fittings verified that the sizes and energies for the outermost orbital of negative ions were not given properly by the SCF calculations.

The two electron helium-like systems (He, Li^+, Be^{2+}, B^{3+}) are unique in that the K shell is the valence shell. A linear relationship is adequate to fit the four data points as evidenced by the optimum exponent for the nonlinear fit (see Fig. 6) being close to unity. Figure 1 illustrates the linear fit for the neutral and cationic species of this series.

The K shells of the other atomic species studied may be considered to be core orbitals. In agreement with the predictions of (2) as judged by the deviations of the fits the series of heavier atoms or ions where E or e_i is greater are better described by a relationship of the form of [1] than is the beryllium-like system. A simple linear form is again adequate as evidenced by the optimal γ values (Fig. 6) close to unity. All 1s data can be fit to a single linear equation but there appears a distinction between inner and outer 1s orbitals as the systems are best described if treated separately.

Similar results were obtained for the 2s orbitals. It is clear from considering the parameters for both the linear and nonlinear equations that the outer 2s orbital (beryllium system) is best

Can. J. Chem. Downloaded from www.nrcresearchpress.com by 210.87.254.5 on 09/05/12
For personal use only.

TABLE 4. Energies and sizes of electron pairs $2s^2$

System	Species	Energy (hartree)	Size (bohr^2)
Beryllium	Li^-	−0.664338	40.68362
	Be	−1.897988	8.42672
	B^+	−3.61010	3.82571
	C^{2+}	−5.81710	2.21461
	N^{3+}	−8.52220	1.45094
Neon	F^-	−9.87932	1.32118
	Ne	−13.04200	0.96707
	Na^+	−16.77074	0.73143
	Mg^{2+}	−21.02835	0.57079
	Al^{3+}	−25.80969	0.45762
Magnesium	Na^-	−16.33898	0.73126
	Mg	−20.31783	0.57110
	Al^+	−24.87611	0.45812
	Si^{2+}	−29.96641	0.37554
	P^{3+}	−35.57501	0.31340

TABLE 5. Energies and sizes of electron pairs $2p^2$

System	Species	Energy (hartree)	Size (bohr^2)
Neon	F^-	−7.779814	2.11883
	Ne	−10.939486	1.22930
	Na^+	−14.579730	0.81605
	Mg^{2+}	−18.710012	0.58852
	Al^{3+}	−23.334018	0.44689
Magnesium	Na^-	−14.130558	0.82256
	Mg	−17.950978	0.59770
	Al^+	−22.335380	0.45502
	Si^{2+}	−27.243352	0.35842
	P^{3+}	−32.680932	0.28991

TABLE 6. Energies and sizes of electron pairs $3s^2$

System	Species	Energy (hartree)	Size (bohr^2)
Magnesium	Na^-	−2.393974	40.21533
	Mg	−4.510224	12.41209
	Al^+	−6.583994	6.79748
	Si^{2+}	−8.783222	4.50878
	P^{3+}	−11.160560	3.27524

treated separately from the 2s inner systems (neon and magnesium systems). The optimized nonlinear m values decrease from the m value of the linear case and smaller deviations suggest that a nonlinear equation is preferable for describing the energy–size relationship. The data for the heavier atoms and inner shells are more consistent with the existence of an energy–size relationship than are the data for the light atoms and outer orbitals. Since the m values for 1s and 2s orbital series are quite different no relationship as general as [6] or [7] holds, since the parameters show a marked dependence on the principal quantum number.

For the 3s orbital the m value has changed from the 1s and 2s results and the optimized exponent value has also further decreased. Since the 3s orbitals are valence in character previous results for the 1s and 2s valence series suggest that any fit should not be as good. Relative to

Can. J. Chem. Downloaded from www.nrcresearchpress.com by 210.87.254.5 on 09/05/12
For personal use only.

Can. J. Chem. Downloaded from www.nrcresearchpress.com by 210.87.254.5 on 09/05/12
For personal use only.

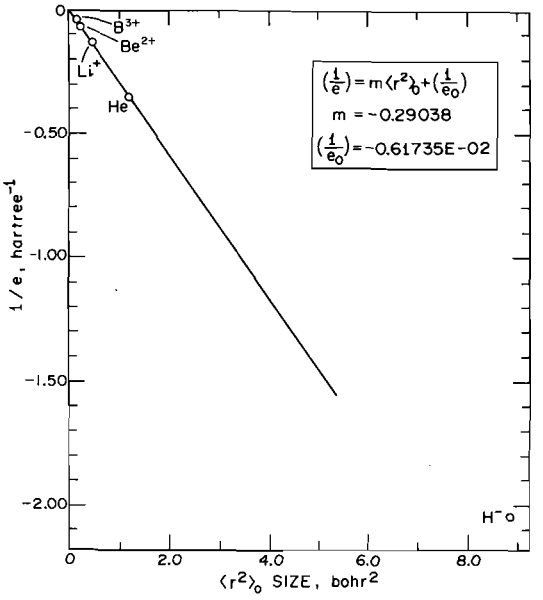

FIG. 1. Linear fit for the helium-like system: $1s^2$.

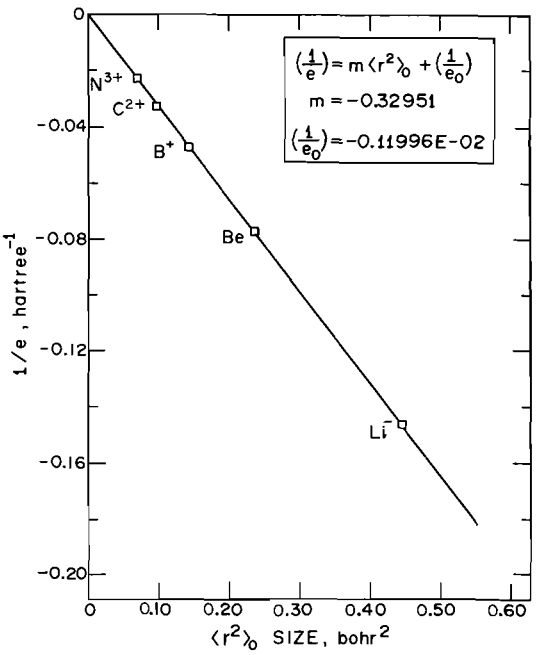

FIG. 2. Linear fit for the beryllium-like system: $1s^2$.

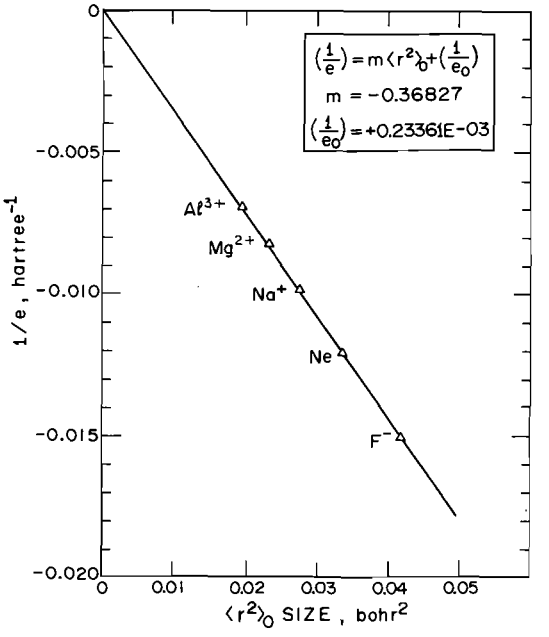

FIG. 3. Linear fit for the neon-like system: $1s^2$.

the inner shell 2s results the quality of the fit for the 3s orbitals has decreased by several powers of ten (standard deviations).

The same general comments may be made concerning the 2p orbitals, *i.e.* the valence and inner 2p orbitals are best treated separately and a nonlinear equation provides a better description. The m and γ values are different from the 2s results indicating dependence on the angular quantum number.

Linear fits for the various sets of 1s core orbitals are illustrated in Figs. 1 to 5. Judging from these plots the linear form is quite adequate to represent an energy–size relationship for core orbitals. The simultaneous linear fit for all 1s core orbitals is also adequate. For other orbitals the linear fits were not sufficient. The nonlinear plots for all orbitals are presented in Figs. 6 and 7. A dependence on the value of the principal quantum number is evident as is a distinction between core and valence orbitals. It is interesting that the most satisfactory energy–size relationship is obtained for the core orbitals which are essentially localized and close to the correct loge representation of electron pairs.

It might be anticipated that if individual electron pairs obey an energy–size relationship then so also should the total energies and total sizes.

$$[11b] \qquad \frac{1}{E} = m\langle r^2\rangle + \frac{1}{E_0}$$

For the energy quantity, such an extension is of particular interest since for the electron pairs the energy per pair (eq. 9) is somewhat arbitrarily defined as compared to the total energy. A linear plot for the total energy – total size relationship

Can. J. Chem. Downloaded from www.nrcresearchpress.com by 210.87.254.5 on 09/05/12
For personal use only.

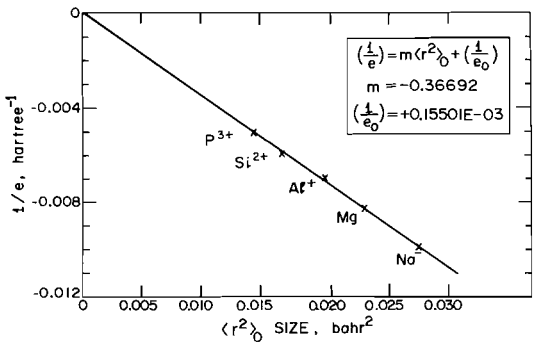

FIG. 4. Linear fit for the magnesium-like system: $1s^2$.

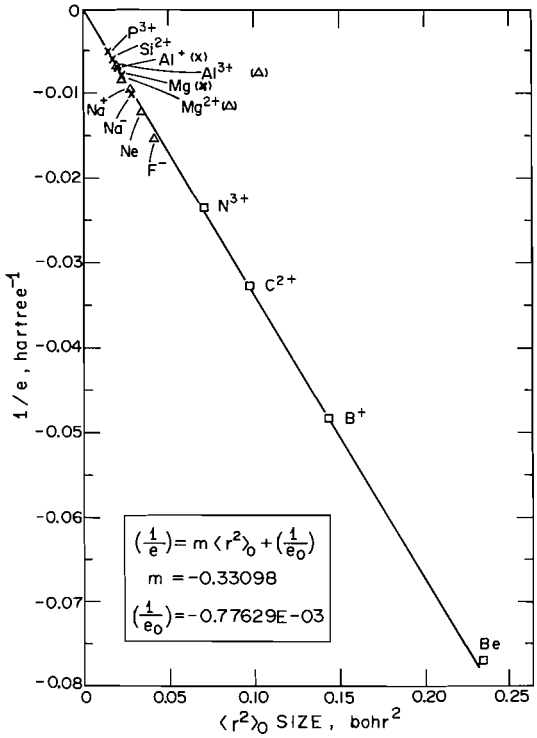

FIG. 5. Linear fit for all $1s^2$ core electrons.

is shown in Fig. 8. The fits are not in general as good as those for the individual orbitals and in particular not as good as the fits for the core orbitals. However, it appears that the relationship for the size and energy for individual orbitals is at least as valid for total atomic systems.

The association of a simple model with the nonlinear parameter (γ) in [7] requires noting the pattern in the variation of γ. The closer an orbital is to the nucleus the closer γ is to unity.

$$[13] \qquad \gamma_{3s} < \gamma_{2p} < \gamma_{2s} < \gamma_{1s} \approx 1$$

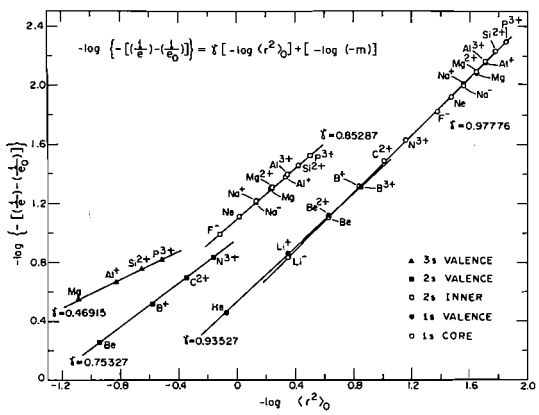

FIG. 6. Nonlinear fits for s electron pairs.

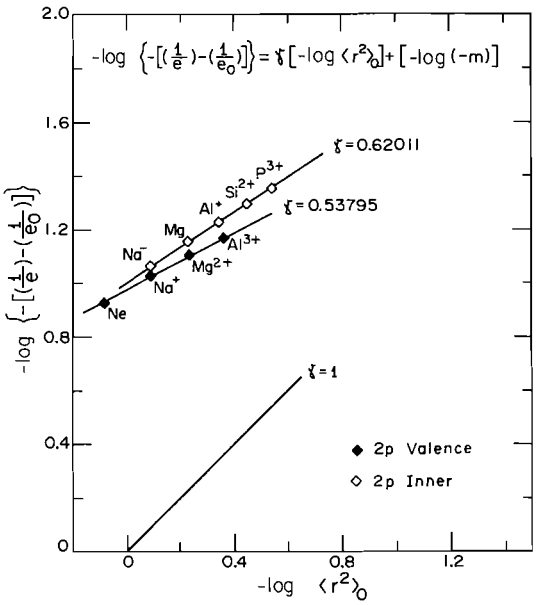

FIG. 7. Nonlinear fits for p electron pairs.

γ also varies with the saturation of a shell

$$[14] \qquad \gamma_{2s}^{Be} < \gamma_{2s}^{Ne} < 1$$

and

$$[15] \qquad \gamma_{2p}^{Ne} < \gamma_{2p}^{Mg} < 1$$

It appears that the presence of an outer orbital leads to an increase in the γ values of the inner orbitals towards unity.

A comparison of the calculated slopes for the linear energy–size relationship (eq. 11*a*) with the predicted quantities from the simple particle-in-a-box model proves of interest. Table 7 collects

TABLE 7. Comparison of particle-in-a-box predictions and calculated values (linear fits) for the slope (m) of the energy–size relationship

	Predicted m	Calculated m				
n	Particle-in-a-box	Electron	He	Be	Ne	Mg
1	−0.53	1s	−0.29	−0.32	−0.37	−0.37
2	−0.13	2s		−0.058	−0.072	−0.079
3	−0.059	3s				−0.014

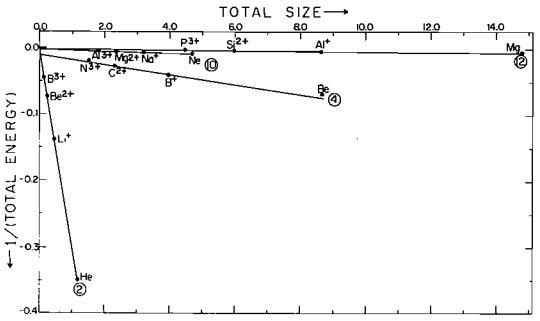

FIG. 8. Linear fits for total energy–total size.

the relevant data. In all cases the particle-in-a-box predicts a larger absolute value for the slope. Thus, the particle-in-a-box model for a certain energy value predicts a smaller size than calculated results for the same energy. Such a result is due to the uniform potential assumed by the particle in a box while the potential calculated for atomic systems is not uniform.

Conclusions

In agreement with the predictions of the particle-in-a-box and Thomas–Fermi models a simple relationship between the energies and sizes of core atomic SCF orbitals was found, namely

$$[16] \qquad \left\{\left(\frac{1}{e_i}\right) - \left(\frac{1}{e_{i0}}\right)\right\} = m\langle r_i^2\rangle_0$$

It was possible to successfully fit a more flexible nonlinear equation

$$[17] \qquad \left\{\left(\frac{1}{e_i}\right) - \left(\frac{1}{e_{i0}}\right)\right\} = m\langle r_i^2\rangle_0^{\gamma}$$

for all computed sets of atomic orbitals. Also of interest is the possibility of the existence of different energy–size relationships holding for different atomic and molecular states. Excited atomic states should, according to the particle-in-a-box model, show a dependence on the quantum number n. Calculations on atomic excited states are also planned. Extensions of similar energy–size relations to the core and valence localized molecular orbitals of simple molecules may prove of interest and work in this area is in progress.

Two of us (J.D.G., I.G.C.) wish to express their thanks to Professor Daudel and the staff of the Centre de Mecanique Ondulatoire Appliquee (Paris) for the hospitality extended to us. Valuable discussions with Dr. M. E. Stephens are acknowledged.

The authors thank the Conseil National de la Recherche Scientifique (France) and the National Research Council of Canada for financial support.

1. S. ODIOT and R. DAUDEL. C.R. Acad. Sci. t.**238**, 1384 (1954).
2. C. A. COULSON. C.R. Acad. Sci. t.**239**, 868 (1954).
3. V. F. WEISSKOPF. Science, **187**, 605 (1975).
4. R. DAUDEL. *In* Wave mechanics: the first fifty years. *Edited by* W. C. Price, S. C. Chissick, and T. Ravensdale. Butterworths, London. 1973.
5. M. A. ROBB, W. J. HAINES, and I. G. CSIZMADIA. J. Am. Chem. Soc. **95**, 42 (1973).
6. S. HUZINAGA. J. Chem. Phys. **42**, 1293 (1965).
7. S. HUZINAGA and Y. SAKAI. J. Chem. Phys. **50**, 1371 (1969).
8. (*a*) C. ROETTI and E. CLEMENTI. J. Chem. Phys. **60**, 3342 (1974). (*b*) C. ROETTI and E. CLEMENTI. J. Chem. Phys. **61**, 2062 (1974). (*c*) E. CLEMENTI. IBM J. Res. Develop. Supp. **9**, 2 (1965).
9. A. W. WEISS. Phys. Rev. **122**, 1826 (1961).
10. J. D. GODDARD. M.Sc. Thesis. University of Toronto, Toronto, Ontario. 1974.
11. A. VEILLARD. IBMOL: Computations of wave functions for molecules of general geometry, Version 4. IBM Research Laboratory, San Jose. 1968.
12. D. B. NEUMANN *et al.* POLYATOM (Version 2) Quantum Chemistry Program Exchange Pgm. No. 199. Department of Chemistry, Indiana University, Bloomington, Indiana.

Can. J. Chem. Downloaded from www.nrcresearchpress.com by 210.87.254.5 on 09/05/12
For personal use only.

A Systematic *ab initio* LCAO–MO–SCF Study of the Ionization Potentials, Electron, Proton, Hydrogen, and Hydride Affinities of SH_n Molecules and Ions

ROY E. KARI

Department of Chemistry, Laurentian University, Sudbury, Ontario P3E 2C6

AND

IMRE G. CSIZMADIA

Department of Chemistry, University of Toronto, Toronto, Ontario M5S 1A1

Received June 3, 1975

ROY E. KARI and IMRE G. CSIZMADIA. Can. J. Chem. **53**, 3747 (1975).

Equilibrium geometries and energies are obtained for SH_n (n = 0, 1, 2, 3) neutral and charged species by the Roothaan LCAO–MO–SCF method. A large gaussian basis set including d and p polarization functions was employed. The calculated ionization potentials, electron, proton, hydrogen, and hydride affinities are discussed as well as compared with similar previously calculated properties for OH_n (n = 0, 1, 2, 3) species.

ROY E. KARI et IMRE G. CSIZMADIA. Can. J. Chem. **53**, 3747 (1975).

Utilisant la méthode LCAO–MO–SCF de Roothaan, on obtient les géométries et les énergies d'équilibre des espèces neutres et chargées SH_n (n = 0, 1, 2, 3). On a utilisé une base gaussiène large incluant des fonctions de polarisation d et p. On discute des potentiels d'ionisation calculés, des affinités des électrons, des protons, de l'hydrogène et de l'hydrure et on les compare avec les propriétés semblables calculées antérieurement pour les espèces OH_n (n = 0, 1, 2, 3).
[Traduit par le journal]

Can. J. Chem. Downloaded from www.nrcresearchpress.com by 210.87.254.5 on 09/05/12
For personal use only.

Introduction

The application of LCAO–MO–SCF single determinantal theory to determine molecular properties dependant on energy differences has not been altogether successful. The reason for this lack of success is evident when the total electronic energy (E_{el}) is written as

$$E_{el} = E_{SCF} + (E_{HF} - E_{SCF}) + E_C + E_R$$

where E_{HF} is the Hartree–Fock or lower limit of the single-determinantal (E_{SCF}) energy, E_C is the correlation energy, and E_R is the relativistic energy. In this scheme, the determination of energy differences (ΔE_{el}) is thus limited by the magnitude of the differences in the last three terms of the above equation. Neglecting the term E_R does not lead to large errors since the largest contributions to the relativistic energy are made by core electrons which are least disturbed in chemical reactions. Neglecting either of the other two remaining terms will often result in both appreciable and systematic errors.

Although numerous *ab initio* LCAO–MO–SCF calculations have been previously performed (1–11) to predict energetic properties of sulfur hydrides, the different basis sets used cause large variations in the $(E_{HF} - E_{SCF})$ term and hence are not suitable for making comparisons either within the set of sulfur hydrides or between sulfur and other atom hydrides. To alleviate this difficulty, the present study employed a uniform basis set, including d and p gaussian polarization functions, on a comprehensive selection of both charged and neutral sulfur atom and monosulfur hydride species as listed below.[1]

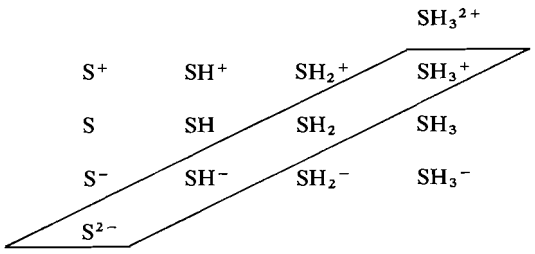

Since the same gaussian basis set was used to describe both charged and neutral species, some variation of the term $(E_{HF} - E_{SCF})$ still occurs. However, due to the systematic nature of this variation, it is possible to estimate both the magnitude and sign of this term. Then, in conjunction with known experimental values for

[1]Eighteen electron closed-shell species are enclosed in the box.

properties such as ionization potentials, electron and proton affinities, it is possible to estimate the changes in correlation energy. When sufficiently accurate experimental measurements are not available, an attempt is made to extrapolate these known correlation energy changes to obtain an estimate of the corresponding experimental values.

Method

For all singlet states, the normal Roothaan (12) closed-shell molecular orbital method was used. For states of higher multiplicity, the restricted single determinant open-shell molecular orbital method (13) was used. Although the open-shell method sometimes leads to energy convergence difficulties, no such difficulties were encountered here or in a previous study (14) of oxygen hydrides.

In a preliminary study (15) of the effects of polarization functions on calculated energy differences, it was found that unless these functions were used on both the sulfur and hydrogen atoms, less confidence could be placed on the relative as well as the absolute magnitudes of the calculated energy differences. This is caused by the varying effect that a given polarization function will have on the $(E_{HF} - E_{SCF})$ energy term of each molecular species. In addition, since the neutral species basis sets were not here modified for ionic species, polarization functions appear to have an added importance in describing the diffuse additional electron in the negatively charged hydrides.

The actual gaussian basis sets used in these calculations included a $(12^s, 9^p, 2^d)$ basis set on sulfur contracted to a $[6^s, 4^p, 2^d]$ basis set. The hydrogen atom was described by a $(4^s, 1^p)$ basis set contracted to a $[2^s, 1^p]$ basis set. The sulfur s and p exponents and contraction coefficients were those given by Veillard (16) and the hydrogen s exponents and contraction coefficients were those suggested by Basch *et al.* (17). The sulfur d exponents (0.25 and 1.3225) were estimated as being the most suitable for descriptions of the electron densities both near the nucleus and in the bonding regions. The hydrogen p exponent (0.9) was obtained from previous CI results given by Csizmadia *et al.* (18).

For the species investigated, the above basis sets represented the following basis set sizes: S, (51)–[30]; SH, (58)–[35]; SH_2, (65)–[40]; SH_3, (72)–[45]. No distinction was made in the basis sets for ionic or neutral species.

The potential surfaces $E(r,\phi)$, generated by variation of the S—H bond length (r) and the H—S—H bond angle (ϕ), were calculated for all of the hydrides listed in the introduction. For economic reasons, these variations were restricted to the following symmetries: SH, $C_{\infty v}$; SH_2, $D_{\infty h}$ and C_{2v}; SH_3, D_{3h} and C_{3v}. No equilibrium symmetries other than those presently investigated have been previously proposed. It is conceivable that SH_3, neutral or ionic, might exist in a pentagonal bipyramid form with the lone pairs forming two corners of a triangle. However, this geometry was not investigated.

Results and Discussion

Total Energies

The calculated total energies for all of the points on the potential surface considered are listed in Table 1 for atoms, Table 2 for diatomic hydrides, Table 3 for triatomic hydrides, and Table 4 for quaternatomic hydrides. In order to economize on the amount of computer time required to compute an energy surface for each species, the increments in both bond-angle and bond-length variations were deliberately chosen quite large.

TABLE 1. Computed total atomic energies

Atomic species	State	Total energy (hartree)		
		Present	Hartree–Fock	Experimental
H^-	^1S	−0.405271	−0.4878[a]	−0.5245[a]
H	^2S	−0.497639	−0.5	−0.5
S^+	^4S	−397.1372	−397.1729[b]	−398.762[c]
S	^3P	−397.4823	−397.5048[b]	−399.144[c]
S^-	^2P	−397.4834	−397.5382[b]	−399.222[b]
S^{2-}	^1S	−397.1532	−397.2079	—

[a]Reference 24.
[b]Reference 25.
[c]Reference 1*b*.

Can. J. Chem. Downloaded from www.nrcresearchpress.com by 210.87.254.5 on 09/05/12
For personal use only.

TABLE 2. Computed total energies (hartree) of sulfur–hydride diatomics

Species	State	Total energy for bond length (bohr) = 2.4	2.45	2.5	2.6	2.8
SH^+	$^3\Sigma$	−397.726090	−397.728140	−397.729309	*−397.729437*	−397.723252
SH	$^2\Pi$	−398.074473	−398.075947	*−398.076538*	−398.075503	−398.066962
SH^-	$^1\Sigma$	−398.089225	−398.090790	*−398.091500*	−398.090789	−398.083272

TABLE 3. Computed total energies (hartree) for SH_2^- ($^2\Sigma_g$ and $^2A_1$), SH_2 ($^1\Sigma_g$ and $^1A_1$), SH_2^+ ($^2\Pi$ and $^2B_1$)

Bond angle (deg)	Species	Total energy for bond length (bohr) = 2.3	2.4	2.6	2.8
180.000000	SH_2^-	−398.481247	−398.507445	−398.537221	−398.547014
	SH_2	−398.544482	−398.553452	−398.549563	−398.527557
	SH_2^+	−398.200658	−398.214782	−398.221605	−398.210579
124.392864	SH_2^-	−398.468299	−398.497134	−398.532347	*−398.547250*
	SH_2	−398.646920	−398.658323	−398.659232	−398.641713
	SH_2^+	−398.294337	−398.308364	−398.314367	−398.301647
109.471202	SH_2^-	−398.463630	−398.487535	—	−398.532224
	SH_2	−398.666462	−398.677927	—	−398.660597
	SH_2^+	−398.313047	−398.326821	—	−398.318512
89.326260	SH_2^-	−398.460667	−398.479952	−398.502445	−398.511982
	SH_2	−398.671740	−398.683834	*−398.685532*	−398.667985
	SH_2^+	−398.317416	−398.331568	*−398.337412*	−398.324021
82.952420	SH_2^-	−398.456274	−398.475460	−398.497242	−398.506085
	SH_2	−398.667714	−398.680184	−398.682572	−398.665601
	SH_2^+	−398.313024	−398.327526	−398.334015	−398.321173

TABLE 4. Computed total energies (hartree) for SH_3^- ($^1A_1$), SH_3 ($^2A_1$), SH_3^+ ($^1A_1$), and SH_3^{2+} ($^2A_1$)

Bond angle (deg)	Species	Total energy for bond length (bohr) = 2.2	2.4	2.5	2.6	2.8
120.0	SH_3^-	−398.747999	−398.872159	—	−398.950619	*−398.996160*
	SH_3	−398.945363	−399.036034	—	−399.076436	*−399.085592*
	SH_3^+	−398.857122	−398.907383	−398.912727	−398.909015	−398.883071
	SH_3^{2+}	−398.161395	−398.228079	—	−398.247117	−398.239284
115.0	SH_3^-	−398.747719	−398.856512	—	−398.927447	−398.970200
	SH_3	−398.944206	−399.033744	—	−399.074616	−399.084684
	SH_3^+	−398.875058	−398.927224	—	−398.830623	−398.906222
	SH_3^{2+}	−398.163879	−398.230447	—	*−398.249591*	−398.241451
110.0	SH_3^-	−398.750952	−398.847731	—	−398.909567	−398.947615
	SH_3	−398.944533	−399.028883	—	−399.068444	−399.078790
	SH_3^+	−398.887796	−398.941276	−398.948092	−398.945743	−398.922053
	SH_3^{2+}	−398.159913	−398.226673	—	−398.245470	−398.237238
100.0	SH_3^-	−398.754593	—	—	−398.884616	−398.912404
	SH_3	−398.945961	—	—	−399.053274	−399.061227
	SH_3^+	−398.899227	—	*−398.962557*	−398.960968	−398.938375
	SH_3^{2+}	−398.138254	—	—	−398.227244	−398.220268
85.0	SH_3^-	−398.738053	−398.816747	—	−398.856161	−398.875772
	SH_3	−398.929306	−399.000858	—	−399.029513	−399.034411
	SH_3^+	−398.884646	−398.943983	—	−398.953439	−398.933485
	SH_3^{2+}	−398.074577	−398.147104	—	−398.171774	−398.167978

Can. J. Chem. Downloaded from www.nrcresearchpress.com by 210.87.254.5 on 09/05/12
For personal use only.

Can. J. Chem. Downloaded from www.nrcresearchpress.com by 210.87.254.5 on 09/05/12
For personal use only.

TABLE 5. Equilibrium SCF energies for sulfur hydrides as determined by least-squares polynomial fitting

Species	State	SCF energies (hartree)			
		Present	Best MO[a]	Hartree–Fock[b]	Experimental[c]
SH^+	$^3\Sigma$	−397.7299	−397.7590[d]	−397.766	−399.398
SH	$^2\Pi$	−398.0789	−398.1017[d]	−398.102[d]	−399.780
SH^-	$^1\Sigma$	−398.0933	−398.1461[e]	−398.146[e]	−399.865
SH_2^+	$^2B_1$	−398.3391	—	−398.375	—
SH_2	$^1A_1$	−398.6883	−398.6862[f]	−398.712[f]	−400.409[h]
SH_2^-	$^2A_1$	−398.5472[g]	—	—	—
SH_3^{2+}	$^2A_1$	−398.2497	—	−398.285	—
SH_3^+	$^1A_1$	−398.9622	—	−398.998	—
SH_3	$^2A_1$	−398.0856[g]	—	—	—
SH_3^-	$^1A_1$	−398.9962[g]	—	—	—

[a]No entry is made here if the present results are the best.
[b]Hartree–Fock energies are estimated from either best MO or present results.
[c]Unless stated otherwise, experimental parameters are as given in ref. 1*b*.
[d]Reference 1*b*.
[e]Reference 2.
[f]A value of −398.726 in ref. 9 appears to be too low.
[g]No equilibrium geometries were found for these species. The energies quoted correspond to the bond lengths and angles listed in Tables 3 and 4.
[h]Assuming $E(SH_2) = E(SH) + E(H) - E_{zp} - D_0^o(H - SH)$ where $E_{zp} = 0.015$ and $D_0^o(H - SH) = 0.120$.

TABLE 6. Equilibrium bond lengths

Species	r_e (bohr)		
	Theoretical		
	Present	Best MO	Experimental
SH^+	2.555	—	—
SH	2.519	2.513[a]	2.551[a]
SH^-	2.528	2.516[b]	2.55[b]
SH_2^+	2.54	—	2.57[c]
SH_2	2.51	—	2.53[d]
SH_2^-	2.8	—	—
SH_3^{2+}	2.62	—	—
SH_3^+	2.57	—	—
SH_3	2.8	—	—
SH_3^-	2.8	—	—

[a]Reference 1.
[b]Reference 2.
[c]Reference 26.
[d]Reference 27.

The equilibrium energies and geometries listed in Tables 5 to 7 were obtained by a least-squares fitting of the energy surface points to a polynomial of the form

$$E(r,\phi) = \sum_{i,j=0} a_{ij} r^i \phi^j$$

Generally, the coefficient a_{ij} was found to be significant only for i equal to 0, 2, and 4 with j varying from 0 to 4. By comparing the results of this fitting with an alternative third order spline function fit, it was found that although the equilibrium bond angles could not be reproduced by both methods to more than 1 or 2°, both the equilibrium bond lengths and energies were reproduced to the significance quoted in Tables 5 to 7.

The Hartree–Fock energies listed in Tables 1 and 5 are either abstracted from previous estimates or based on best MO or present calculations. Those based on the present calculations were estimated by calculating $(E_{HF} - E_{SCF})$ as a percentage of E_{SCF} for species where E_{HF} was previously estimated and then decreasing the present calculated SCF energies by the same percentage. Generally, different percentages were

TABLE 7. Equilibrium bond angles and inversion barriers

Species	ϕ (deg)		Barrier (kcal/mol)	
	Present	Experimental	Present	Experimental
SH_2^+	96.0	92.9[a]	73.4	13.2[a]
SH_2	96.0	92.2[b]	84.8	36.1[c]
SH_2^-	124.4	—	—	—
SH_3^{2+}	116.0	—	1.7	—
SH_3^+	98.7	—	30.4	—
SH_3	120	—	—	—
SH_3^-	120	—	—	—

[a]Reference 26.
[b]Reference 27.
[c]Reference 28.

TABLE 8. Ionization potentials and electron affinities of sulfur and some of its hydrides

Species	Ionization potential (eV)		Electron affinity (eV)	
	Calculated	Experimental	Calculated	Experimental
S^+	—	—	−9.4	−10.4
S	9.4	10.4	−0.03	−2.07[a]
S^-	0.03	—	+9.0	—
S^{2-}	−9.0	—	—	—
SH^+	—	—	−9.5	−10.4[b]
SH	9.5	10.4[b]	−0.4	−2.3[a]
SH^-	0.4	—	—	—
SH_2^+	—	—	−9.5	−10.5[c]
SH_2	9.5	10.5[c]	<3.8	—
SH_2^-	>−3.8	—	—	—
SH_3^{2+}	—	—	−19.4	—
SH_3^+	19.4	—	—	—

[a]Reference 29.
[b]Reference 30.
[c]Reference 31.

calculated for cations, anions, and neutral species.

Ionization Potentials and Electron Affinities

For all ionization potentials (IP) and electron affinities (EA) listed in Table 8, it was assumed that in the course of electron capture, the incoming electron occupied the lowest available empty orbital and the ionized electron was removed from the highest occupied orbital. As a consequence of these definitions, the EA of a species (M) is the negative, in the arithmetic sense, of the IP of the corresponding species having a charge smaller by +1 (*i.e.* M^-). For example, the EA of S is calculated to be −0.03 eV while the IP of S^- is calculated to be +0.03 eV.

As in the previous publication dealing with OH_n oxygen hydrides (14), the thermodynamic convention (endothermic processes show positive energy differences and exothermic processes show negative energy differences) will be used to specify energy differences. Thus, in any chemical reaction, the energy differences between products and reactants may be written as

$$\Delta E_T^M = \Delta E_{HF}^M(Re) + \Delta E_C^M(Re) + \Delta E_R^M(Re) + \Delta E_{ZP}^M(Re)$$

where $\Delta E_{HF}^M(Re)$ is the difference in Hartree–Fock energies between the products and the reactants in their respective equilibrium geometries and the other terms refer to similar correlation, relativistic, and zero-point energy differences. Hence, $IP(M) = \Delta E_T^M$ for the reaction $M \rightleftharpoons M^+ + e^-$ and $EA(M) = \Delta E_T^M$ for the reaction $M + e^- \rightleftharpoons M^-$.

Since one of the purposes of this work was to show that there are no fundamental differences between corresponding oxygen and sulfur hydrides, it is necessary to determine whether or

Can. J. Chem. Downloaded from www.nrcresearchpress.com by 210.87.254.5 on 09/05/12
For personal use only.

TABLE 9. Theoretical estimates of the proton affinity components of O^- and S^-

Species	Component	Proton affinity (hartree)	Energies (hartree)[g] $E^{(A-H)}$	$E^{(A^-)}$
O^-	Experimental[a]	−0.616	−75.780	−75.164
	Zero-point[b]	0.008	0.008	0.0
	Hartree–Fock[a]	−0.632	−75.422	−74.790
	Calculated[a]	−0.651	−75.400	−74.749
	Correlation (u.a.)[c]	0.009	−0.316	−0.325
	Correlation (s.a.)[d]	0.071	−0.254	−0.325
S^-	Experimental[e]	−0.558	−399.780	−399.222
	Zero-point[f]	0.006	0.006	0.0
	Hartree–Fock[e]	−0.564	−398.102	−397.538
	Calculated[e]	−0.596	−398.079	−397.483
	Correlation (u.a.)[c]	−0.034	−0.667	−0.633
	Correlation (s.a.)[d]	+0.038	−0.595	−0.633

[a]From ref. 14. Values not corrected for zero-point energy differences.
[b]Reference 32.
[c]United atom correlation energies (F, ^2P) and (Cl, ^2P) (33); (O^-, ^2P) and (S^-, ^2P) (34).
[d]Separated atom correlation energies (O, ^3P) and (S, ^3P) (33).
[e]From Tables 1 and 5.
[f]Reference 1*b*.
[g]1 hartree = 27.21165 eV.

not the proof of this statement lies within the current SCF approximation and does not rely too heavily on correlation energy differences.

In previously dealing with oxygen hydrides (14), an estimate of $\Delta E_C{}^M(\mathrm{Re})$ was attempted for all energy difference properties. This was made possible by the wealth of previously published experimental and theoretical data describing oxygen hydrides. Due to the lack of similar data for sulfur hydrides, an estimate of $\Delta E_C{}^M(\mathrm{Re})$ here is not possible for any but the atomic and diatomic species. $\Delta E_C{}^M$ for the ionization potentials of O and S are estimated to be 1.8 (19) and 1.3 (20) eV respectively and illustrates a general trend (19–21) that $\Delta E_C{}^M$ is smaller in magnitude for second row atoms. However, the difference $(\Delta E_C{}^O - \Delta E_C{}^S)$ is only 0.5 eV whereas the corresponding calculated, estimated Hartree–Fock, and experimental energy differences are 2.5, 2.7, and 3.2 eV indicating that the calculated IP are entirely adequate to show qualitative differences between sulfur and oxygen hydrides.

Unfortunately, without the use of separately optimized exponents, the LCAO–MO–SCF method is not able to describe anions with the same consistency that it describes neutral and cationic species. For example, the IP of neutral (or EA of cations) and cationic sulfur or sulfur hydrides uniformly deviates from the experimental value by approximately 1.0 eV. This difference is well within the correlation energy correction. However, the EA of neutral (IP of anions) sulfur and sulfur hydrides differs from the experimental value by approximately 2.0 eV which can only be explained by assuming that the quantity $(E_{HF} - E_{SCF})$ is different for the anion and neutral species. Previously calculated EA of neutral oxygen and oxygen hydrides (14) differed from the experimental values by approximately 2.8 eV. Since the change in correlation energy contributes −1.03 and −1.93 eV to EA's of S and O (see Table 9 for details) respectively, the difference in the term $(E_{HF} - E_{SCF})$ must account for 0.97 and 0.87 eV of the discrepancy between calculated and experimental EA's of sulfur and oxygen atoms and hydrides. Although the calculated EA's of neutral sulfur and oxygen hydrides will differ considerably from those calculated with Hartree–Fock wavefunctions, they do so equally in the term $(E_{HF} - E_{SCF})$. Thus, the comparisons shown in Fig. 1 are relatively and qualitatively correct.

Proton, Hydrogen, and Hydride Affinities

The proton (A_{H^+}), hydrogen (A_H), and hydride (A_{H^-}) affinities for the reactions

$$M + H^+ \xrightarrow{A_{H^+}} MH^+$$

$$M + H \xrightarrow{A_H} MH$$

$$M + H^- \xrightarrow{A_{H^-}} MH^-$$

Can. J. Chem. Downloaded from www.nrcresearchpress.com by 210.87.254.5 on 09/05/12
For personal use only.

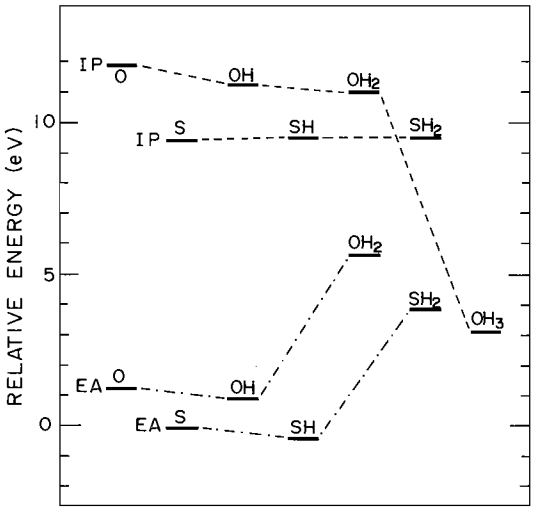

FIG. 1. Electron affinities and ionization potentials of some neutral oxygen and sulfur hydrides. The oxygen values are from ref. 14.

may be defined in theoretical terms as the sum of Hartree–Fock, correlation, relativistic, and zero-point energy component differences. To obtain an estimate of the accuracy of the presently calculated affinities, it is necessary to estimate the magnitudes of the energy components which are not accounted for in a single-determinantal SCF calculation of affinities. Because the majority of relativistic energy is accounted for by electrons near the core of the heavy atom nucleus and because the core is generally least disturbed in the formation of a chemical bond, it has become customary to ignore relativistic energy differences and to assume that these differences are negligible for all affinities. A similar assumption cannot be made for the differences between the remaining energy components.

Since the electronic energy of a bare proton is zero by definition, the proton affinity is equal to the difference in energy between the protonated species and the parent molecule and is thus the simplest affinity to examine in detail. Although a reasonably accurate estimate can be made for the Hartree–Fock energy from SCF calculations, the estimation of correlation energy components requires an experimental knowledge of both the proton affinity and the zero-point energies of the species involved. Unfortunately, only the proton affinity of SH_2 (22, 23) has been determined to any reasonable accuracy but, in this case, the zero-point energy of SH_3^+ is not available. Thus, the only recourse is to estimate experimental proton affinities from strictly theoretical considerations which in turn limits these considerations to the simplest system possible.

Theoretical estimates of the proton affinity components of O^- and S^- in the reactions

$$O^- + H^+ \rightarrow OH$$

$$S^- + H^+ \rightarrow SH$$

are summarized in Table 9. From this table, three methods may be used to estimate the experimental proton affinity. First, independently estimated experimental energies may be used; second, independently estimated Hartree–Fock energies may be coupled with united atom (u.a.) correlation energies and finally with separated atom (s.a.) correlation energies. Generally (1*a*), it has been noted that there is more correlation energy in a diatomic hydride (A—H) than in the s.a. estimate and less than that in the u.a. estimate. Thus, the correlation energy component in the u.a. approximation will form a lower bound while the s.a. approximation will form an upper bound. If it is assumed that the true proton affinities of O^- and S^- are -0.608 and -0.552 and the respective H—F A_{H^+} are -0.632 and -0.564, then zero-point energy corrections will tend to increase these latter values by approximately 0.008 and 0.006 hartree. The correlation energy component will also increase the H—F A_{H^+} value by 0.016 and 0.006 for O^- and S^- respectively. The positive correlation component implies that the magnitude of the correlation energy decreases in an isoelectronic series of the form

$$|E_C^{AH_2^+}| < |E_C^{AH}| < |E_C^{A^-}|$$

or

$$|E_C^{AH_3^+}| < |E_C^{AH}| < |E_C^{AH^-}|$$

Looking next at the term $(E_{HF} - E_{SCF})$ for the calculated proton affinities of O^- and S^-, it may be noted from Table 10 that the calculated values are both more negative than the Hartree–Fock values. This again is caused by the less adequate representation by the gaussian basis set of the negatively charged atom and results from the fact that gaussian exponents are generally optimized for neutral atoms and as such produce better representations of neutral rather than charged species. An unfortunate specific example of this behavior can be illustrated by the presently used hydrogen and hydride ion exponents. Uncontracted, these exponents yield an energy of

Can. J. Chem. Downloaded from www.nrcresearchpress.com by 210.87.254.5 on 09/05/12
For personal use only.

TABLE 10. Proton (A_{H^+}), hydrogen (A_H), and hydride (A_{H^-}) affinities (kcal/mol) of sulfur and sulfur hydride species

Species		Theoretical		Experimental or best estimate
		Calculated	Hartree–Fock	
S^+	A_H	−59.7	−58.4	−81.6[a]
	A_{H^-}	−337	−254	—
S	A_{H^+}	−155	−164	−154
	A_H	−62.1	−61.0	−81.6
	A_{H^-}	−129	−73	—
S^-	A_{H^+}	−374	−354	−346
	A_H	−70.5	−67.7	−86.0
S^{2-}	A_{H^+}	−590	−589	—
SH^+	A_H	−70.0	−68.4	—
	A_{H^-}	−347	−288	—
SH	A_{H^+}	−163	−171	—
	A_H	−70.2	−69.0	−75.3
SH^-	A_{H^+}	−373	−355	−336
SH_2^+	A_{H^+}	56	—	—
	A_H	−78.8	−77.2	—
SH_2	A_{H^+}	−172	−179	−169 ± 2[b]

[a]For all estimates, it is assumed that the zero-point energy of $SH^+ = SH = SH^- = 3.77$ kcal/mol.
[b]Reference 23.

−0.499 a.u. for the hydrogen atom and −0.4122075 for the hydride ion. With a partial reoptimization (exponents 18.9496, 2.9687, 0.46834, 0.074865) this energy is reduced to −0.4794386 a.u. for the hydride ion. Further examination of all of the proton affinities in Table 10 will show that, in general, the calculated affinity of a negative species will be more negative whereas the calculated affinity of a neutral species will be less negative than the corresponding Hartree–Fock affinities.

In summary, because the calculated A_{H^+} for neutral species represents an upper bound to the H—F A_{H^+} which in turn represents a lower bound to the experimental A_{H^+}, it is possible, for neutral species, to calculate A_{H^+} values which through fortuitous cancellations are very accurate. For negative ions, both correlation energy and the term $(E_{HF} - E_{SCF})$ reinforce each other resulting in a larger discrepancy between the experimental and calculated A_{H^+}. Thus, the calculated A_{H^+} represents only a lower bound to the true A_{H^+} and may differ from the true value by as much as 30 kcal/mol. In a previous study (15) of the effect of polarization functions on calculated proton affinities, it was noted that the difference between the calculated and H—F proton affinities decreased as the size of the species increased. This can be seen as well from Table 10 where the calculated A_{H^+} for S differs from the H—F value by 9 kcal/mol whereas the same difference for SH_2 is only −1 kcal/mol. Thus, the larger the species, then the greater the confidence that may be attached to the calculated A_{H^+}.

An analysis similar to the above could be done for both hydrogen and hydride affinities. Considering the sizeable error introduced by the poor representation of the hydride ion in the present calculations, such an exercise would not be productive for hydride affinities. For hydrogen affinities, since the bare hydrogen atom possesses no correlation energy, the only additional error not accounted for in the discussion of proton affinities is the term $(E_{HF} - E_{SCF})$ for the hydrogen atom. This term then accounts for 1.5 kcal/mol in the discrepancy between calculated and Hartree–Fock hydrogen affinities. Also, because the addition of a hydrogen atom does not change the charge on the species, the previous discussion concerning the basis set artifacts introduced in calculating energy differences between charged and neutral species is no longer relevant. Thus, provided that the calculated SCF energies of the parent and hydrogenated species are equally accurate relative to their respective

Can. J. Chem. Downloaded from www.nrcresearchpress.com by 210.87.254.5 on 09/05/12
For personal use only.

TABLE 11. Affinity differences[a] (kcal/mol) between oxygen and sulfur species

Component		Affinity difference for species							
		A^+	A	A^-	AH^+	AH	AH^-	AH_2^+	AH_2
Calculated	A_{H+}	—	36	−35	—	14	−50	8	−5
	A_H	−21	−7	−6	−29	−20	—	−39	—
	A_{H-}	−64	24	−63	—	—	—	—	—
Hartree–Fock	A_{H+}	—	44	−43	—	17	−53	—	2
	A_H	−22	−10	−13	−36	−23	—	−38	—
	A_{H-}	−98	−3.0	−91	—	—	—	—	—
Experimental	A_{H+}	—	47	−38	—	—	−59	—	3
	A_H	−33	−19	−29	—	−43	—	—	—

[a]Difference = [affinity(oxygen) − affinity(sulfur)] where affinity(oxygen) is from ref. 14, Table XI.

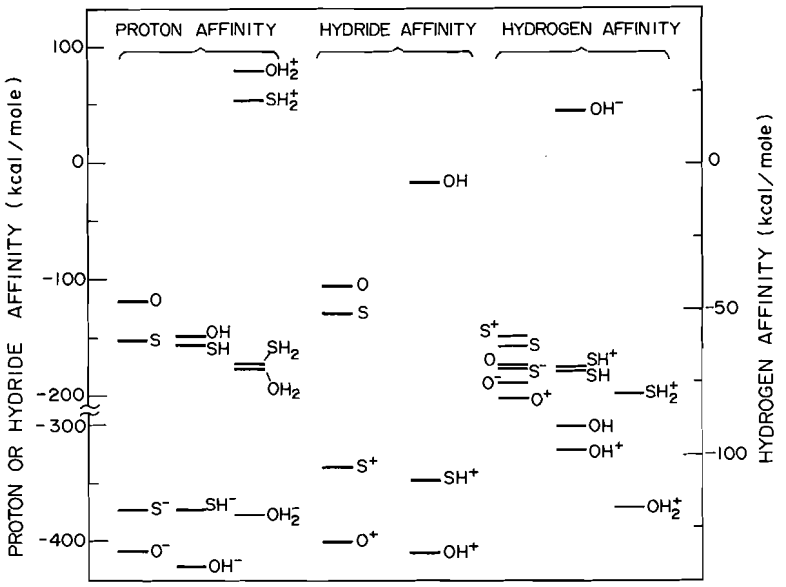

FIG. 2. Proton, hydrogen, and hydride affinities of some oxygen and sulfur hydrides. The oxygen values are from ref. 14.

Hartree–Fock energies, the discrepancy between calculated and Hartree–Fock hydrogen affinities should be in the neighborhood of 1.5 kcal/mol. As can be seen from Table 10, this is indeed true for all species.

Conclusions

The ionization potentials of neutral sulfur hydrides are shown in Fig. 1 to be smaller in magnitude than the corresponding ionization potentials of neutral oxygen hydrides. But, the electron affinities of the same oxygen hydrides are considerably larger than the corresponding sulfur hydrides. Since the valence electrons of sulfur compounds are more readily available, the neutral sulfur compounds can be considered to be more basic, whereas for negatively charged species, the oxygen analogs are more basic. Also from Fig. 1, it may be noted that all of the sulfur values have a smaller spread. This indicates that the hydrogen adjacent to the heteroatom creates a smaller perturbation on the electronic structure of the S atom than on that of the O atom.

A previous study (1) on first and second row monohydrides showed that the IP's in this case did not correlate well with corresponding united atom ionization potentials. This same trend is shown in Fig. 1 for A, AH, and AH_2 where the IP's show a decrease whereas the united atom IP's show increases from O to Ne or S to Ar.

Can. J. Chem. Downloaded from www.nrcresearchpress.com by 210.87.254.5 on 09/05/12
For personal use only.

However, the IP of OH_3 does show a marked decrease which is consistent in the decrease in IP when comparing Ne and Na. Although no equilibrium structure was found for SH_3 in a C_{3v} symmetry, it is expected that should some other equilibrium structure for SH_3 exist, its IP would also show a marked decrease from that of SH_2.

The differences in affinities between similar oxygen and sulfur species are illustrated in Fig. 2 and listed in Table 11. The general trends which may be noted from this figure and table are as follows: (*a*) Proton affinities of the sulfur atom and neutral hydrides are less than analogous oxygen hydrides and this difference decreases as the number of attached hydrogen atoms increases. (*b*) Proton affinities of the sulfur anion and negatively charged hydrides are greater than analogous oxygen hydrides and this difference tends to increase as the number of attached hydrogen atoms increases. (*c*) Hydrogen affinities for all sulfur hydrides are greater than analogous oxygen hydrides and this difference tends to increase as the number of attached hydrogen atoms increases.

It was previously noted that the calculated proton affinities of neutral species tended to be more accurate in an absolute sense. This statement will no longer apply to the differences listed in Table 11 since basis set artifacts operate in a similar manner for both oxygen and sulfur hydrides. As can be seen from the small deviation of the calculated from Hartree–Fock affinities, the basis sets used to describe oxygen hydrides and sulfur hydrides are relatively equally good. In addition to the cancellation of these errors, the neglect of correlation energy is also cancelled insofar as the correlation energy changes are similar for both oxygen and sulfur hydrides. Thus, the calculated differences listed in Table 11 represent good estimates in both an absolute and relative sense.

The technical assistance of Dr. P. Mezey and Dr. M. A. Robb as well as the continued financial assistance by the National Research Council of Canada are gratefully acknowledged.

1. (*a*) P. E. CADE and W. M. HUO. J. Chem. Phys. **47**, 614 (1967); (*b*) J. Chem. Phys. **47**, 649 (1967).
2. P. E. CADE. J. Chem Phys. **47**, 2390 (1967).
3. P. E. CADE. Can. J. Phys. **46**, 1989 (1968).
4. F. P. BOER and W. N. LIPSCOMB. J. Chem. Phys. **50**, 989 (1969).
5. D. B. COOK, A. HINCHLIFFE, and P. PALMIERI. Chem. Phys. Lett. **3**, 223 (1969).
6. D. B. COOK and P. PALMIERI. Chem. Phys. Lett. **3**, 219 (1969).
7. B. ROOS and P. SIEGBAHN. Theor. Chim. Acta, **17**, 199 (1970).
8. B. ROOS and P. SIEGBAHN. Theor. Chim. Acta, **21**, 368 (1971).
9. S. ROTHENBERG, R. Y. YOUNG, and H. F. SCHAEFER. J. Am. Chem. Soc. **92**, 3243 (1970).
10. H. SAKAI, S. YAMABE, T. YAMABE, K. FUKUI, and H. KATO. Chem. Phys. Lett. **25**, 541 (1974).
11. T. YAMABE, T. AOYAGI, S. NAGATA, H. SAKAI, and K. FUKUI. Chem. Phys. Lett. **28**, 182 (1974).
12. C. C. J. ROOTHAAN. Rev. Mod. Phys. **23**, 69 (1951).
13. C. C. J. ROOTHAAN. Rev. Mod. Phys. **32**, 179 (1960).
14. R. E. KARI and I. G. CSIZMADIA. J. Am. Chem. Soc. In press.
15. R. E. KARI and I. G. CSIZMADIA. To be published.
16. A. VEILLARD. Theor. Chim. Acta, **12**, 405 (1968).
17. H. BASCH, N. B. ROBIN, and N. A. KUEBLER. J. Chem. Phys. **47**, 1201 (1967).
18. I. G. CSIZMADIA, R. E. KARI, J. C. POLANYI, A. C. ROACH, and M. A. ROBB. J. Chem. Phys. **52**, 6205 (1970).
19. E. CLEMENTI. J. Chem. Phys. **39**, 175 (1963).
20. E. CLEMENTI. J. Chem. Phys. **38**, 2248 (1963).
21. E. CLEMENTI, A. D. MCLEAN, D. L. RAIMONDI, and M. YOSHIMINE. Phys. Rev. **133**, A1274 (1964).
22. M. A. HANEY and J. L. FRANKLIN. J. Phys. Chem. **73**, 4328 (1969).
23. J. M. HOPKINS and L. I. BONE. J. Chem. Phys. **58**, 1473 (1973).
24. A. W. WEISS. Phys. Rev. **122**, 1826 (1961).
25. E. CLEMENTI, A. D. MCLEAN, D. L. RAIMONDI, and M. YOSHIMINE. Phys. Rev. **133**, A1276 (1964).
26. R. N. DIXON, G. DUXBURY, M. HORANI, and J. ROSTAS. Mol. Phys. **22**, 977 (1971).
27. T. H. EDWARDS, N. K. MONCUR, and L. E. SNYDER. J. Chem. Phys. **46**, 2139 (1967).
28. F. B. BROWN. J. Chem. Phys. **58**, 827 (1973).
29. R. S. BERRY. Chem. Rev. **69**, 533 (1969).
30. B. A. MORROW. Can. J. Phys. **44**, 2447 (1966).
31. W. C. PRICE. J. Chem. Phys. **4**, 147 (1936).
32. G. HERZBERG. Spectra of diatomic molecules. D. Van Nostrand, Toronto. 1950. p. 560.
33. A. VEILLARD and E. CLEMENTI. J. Chem. Phys. **49**, 2415 (1968).
34. P. E. CADE. Proc. Phys. Soc. **91**, 842 (1967).

Can. J. Chem. Downloaded from www.nrcresearchpress.com by 210.87.254.5 on 09/05/12
For personal use only.

The Redox Behavior of 9,10-Anthraquinone-2-sulfonate in Acidic Aqueous Solution

ARTHUR D. BROADBENT AND RONALD J. MELANSON

Department of Chemistry, Mount Allison University, Sackville, New Brunswick E0A 3C0

Received August 1, 1975

ARTHUR D. BROADBENT and RONALD J. MELANSON. Can. J. Chem. **53**, 3757 (1975).

A green intermediate, observed during reduction of 9,10-anthraquinone-2-sulfonate (A) to the corresponding anthrahydroquinone (AH_2) in acidic aqueous solution, has been identified as a quinhydrone-like charge-transfer complex of A and AH_2. Spectrophotometric and potentiometric measurements have shown that changes in the slope of the potentiometric titration curves with varying initial [A] are caused only by this complex ($A\cdot\cdot\cdot AH_2$) and not by any semiquinone radical ($AH\cdot$) or radical anion ($A\cdot^-$) intermediate. The very low semiquinone formation constant in acidic solution indicates that the pK_a of $AH\cdot < 7.0$. Electrochemically determined pK_a values for similar radicals in the range 8.5–10.5 are invalid because of interference by charge-transfer complexes of this type.

ARTHUR D. BROADBENT et RONALD J. MELANSON. Can. J. Chem. **53**, 3757 (1975).

On identifie l'intermédiaire vert, observé durant la réduction de l'anthraquinone-9,10 sulfonate-2 (A) en anthrahydroquinone (AH_2) correspondante en solution acide aqueuse, comme étant un complexe de transfert de charge de type quinhydrone dérivé de A et AH_2. Des mesures spectrophotométriques et potentiométriques ont permis de montrer que les changements dans la pente des courbes de titrations potentiométriques, lorsque l'on fait varier les [A] initiales, sont uniquement causés par ce complexe ($A\cdot\cdot\cdot AH_2$) et non pas par le radical semiquinone ($AH\cdot$) ou le radical anion ($A\cdot^-$) intermédiaire. La très basse constante de formation de la semiquinone en solution acide indique que le pK_a de $AH\cdot < 7.0$. Les valeurs de pK_a de 8.5 à 10.5 déterminées électrochimiquement pour des radicaux similaires sont invalides à cause de l'interférence des complexes de transfert de charge de ce type.

[Traduit par le journal]

Can. J. Chem. Downloaded from www.nrcresearchpress.com by 210.87.254.105 on 09/05/12
For personal use only.

Introduction

Flash photolysis of 9,10-anthraquinone-2-sulfonate (A) in aqueous solution causes reduction to the corresponding anthrasemiquinone radical ($AH\cdot$) or radical anion ($A\cdot^-$). Variations in the yields of these radicals with changing pH indicate that the pK_a of $AH\cdot$ is 3.25 (1), in agreement with values for related radicals generated by pulse radiolysis or flash photolysis (2, 3). However, Gill and Stonehill (4) have reported a polarographically determined pK_a of 9.02 for $AH\cdot$, and a full evaluation of the data of Burstein and Davidson (5) gives a value of 8.4 (see Fig. 1). This discrepancy in the reported pK_a values for $AH\cdot$ prompted a reexamination of the redox behavior of A in acidic solution.

The redox potential (E) in the reversible reduction of a quinone to a hydroquinone, involving a semiquinone radical intermediate, is given by the Nernst equations

$$[1] \qquad E = E_m + \frac{RT}{2F}\ln\frac{a_A}{a_{A^{2-}}} = E_2 + \frac{RT}{F}\ln\frac{a_A}{a_{A\cdot^-}} = E_1 + \frac{RT}{F}\ln\frac{a_{A\cdot^-}}{a_{A^{2-}}}$$

where E_m, E_1, and E_2 are the respective midpoint potentials for the two-electron ($A^{2-} \rightleftarrows A + 2e^-$) and single electron ($A^{2-} \rightleftarrows A\cdot^- + e^-$, $A\cdot^- \rightleftarrows A + e^-$) redox systems, and a is the activity of the species indicated. Equations 1 give

$$[2] \qquad E_m = \tfrac{1}{2}(E_1 + E_2)$$

$$[3] \qquad E_2 - E_1 = \frac{RT}{F}\ln K_s$$

where K_s, the semiquinone formation constant, is the equilibrium constant for

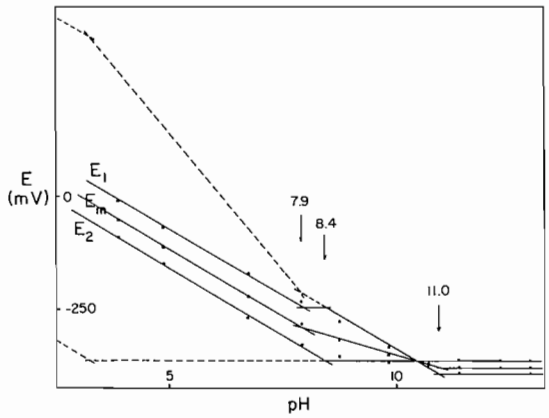

FIG. 1. Redox potentials E_m, E_1, and E_2 as a function of pH for A (E *vs.* n.h.e.).

$$[4] \qquad A + A^{2-} \rightleftarrows 2\,A\cdot^{-}$$

and can be determined from the slope of potentiometric titration curves using the Michaelis index potential, E_i (6). This is given by

$$[5] \quad E_i = E_{0.50} - E_{0.25} = E_{0.75} - E_{0.50} \qquad E_{0.50} = E_m$$

where the subscripts represent the fractional degree of oxidation of A^{2-} to A (α). E_m, E_1, and E_2, and therefore K_s, are pH-dependent because of acid–base equilibria of A^{2-} (conjugate acids AH^- and AH_2) and $A\cdot^-$ (conjugate acid AH·). Variations in these mid-point potentials with changing pH allows evaluation of pK_a values of species in the reversible redox system (7).

Figure 1 gives the fully evaluated data from the paper by Burstein and Davidson (5), clearly showing pK_a values of 7.9 and 11.0 for AH_2 and AH^-, respectively, and of 8.4 for AH·. The dependence of E_m on pH agrees with that of Conant *et al.* (8). The dotted lines represent the variations of E_1 and E_2 expected for a pK_a of 3.25 for AH·. A distinction between the pK_a values of 8.4 and 3.25 for AH· is thus possible, because of the large difference in the expected values of $E_2 - E_1$ and K_s in acidic solution.

Results

Changes in the visible spectrum of solutions of AH_2 with variation in pH allowed spectrophotometric titration as a means of pK_a measurement, and gave values of 7.97 and 11.08 for AH_2 and AH^-, respectively, in agreement with the potentiometrically determined values (5, 8).

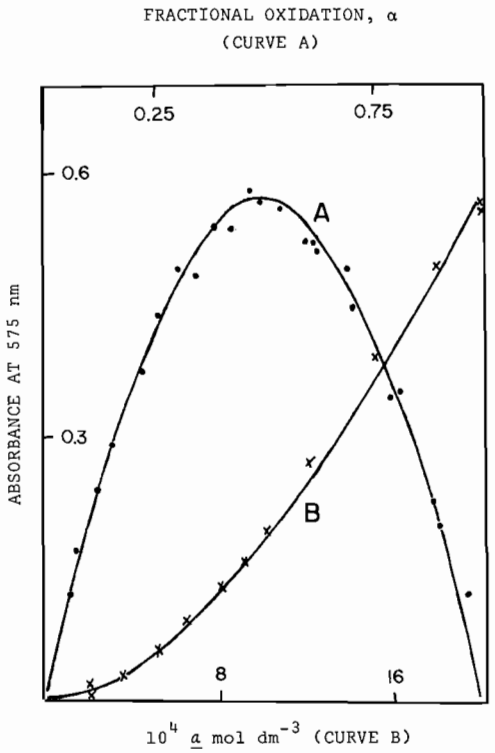

FIG. 2. Curve A: absorbance at 575 nm as a function of α ($a = 2 \times 10^{-3}$ mol dm^{-3}). Curve B: maximum absorbance at 575 nm (at $\alpha = 0.50$) as a function of a.

Reduction of A to AH_2 in acidic solution changes the almost colorless solution to greenish-yellow, but, at [A] $> 1 \times 10^{-3}$ mol dm^{-3}, an intense green intermediate (λ_{max} 575 nm) is clearly recognisable during the reduction. Figure 2 illustrates the variation of absorbance at 575 nm with change in the fractional oxidation of AH_2 (α), and also the variation of the maximum absorbance at 575 nm (at $\alpha = 0.50$) with change in the initial [A].

TABLE 1. Variation of the Michaelis index potential (E_i) with change in the initial [A]

[A] × 10^3 (mol dm^{-3})		E_i (mV)	
Initial	Actual*	Observed	Calculated
19.8	16.9	30.3	29.2
10.0	8.62	23.5	24.2
4.99	4.41	20.0	20.6
2.00	1.67	17.4	17.2
0.86	0.68	15.9	15.5
0.40	0.35	15.7	14.9
0.20	0.17	14.8	14.5

*Mean [A] during oxidative titration.

Can. J. Chem. Downloaded from www.nrcresearchpress.com by 210.87.254.105 on 09/05/12
For personal use only.

Can. J. Chem. Downloaded from www.nrcresearchpress.com by 210.87.254.105 on 09/05/12
For personal use only.

Oxidative potentiometric titrations of AH_2 in acetate buffer solution gave redox potential-titration curves which were perfectly symmetrical about the constant mid-point potential (E_m = −330 mV *vs.* s.c.e.), but for which E_i depended upon the initial [A] (Table 1).

Discussion

The experimental results indicate that the green intermediate, observed on reduction of A to AH_2 in acidic solution, is of the type described by Michaelis and Fetcher (9) for partially reduced phenanthraquinone-3-sulfonate in acidic solution, which they established (10) is a diamagnetic, quinhydrone-like complex which is now considered to be a charge-transfer complex of the quinone and hydroquinone, rather than a dimer of the semiquinone radical.

The variation of E_i with initial [A] demonstrates that the green intermediate is not AH· or $A^{\cdot -}$, neither of which exhibit pronounced absorption at 575 nm (1). The potentiometric E_i values decrease with decreasing initial [A] to values lower than reported by Burstein and Davidson (5). In fact, the results indicate that the observed E_i values can be accounted for solely by the formation of a quinhydrone-like complex ($A\cdots AH_2$), and that E_i would decrease to close to the limiting value of 14.1 mV at 25 °C, corresponding to a two-electron redox system with no intermediate, if the [A] were decreased below 2×10^{-4} mol dm^{-3}. Thus, in acidic solution, K_s is very small indeed, in agreement with a pK_a of 3.25 for AH·, which requires that $E_2 - E_1 \approx -550$ mV at pH 4.6, corresponding to $K_s \approx 10^{-9}$. Actually, because $K_s < 10^{-4}$ cannot be determined experimentally, the results only show that the pK_a of AH· < 7. The stability of $A^{\cdot -}$ in aqueous solutions is therefore determined exclusively by the acid–base behavior of the anthrahydroquinone.

It is probable that electrochemically determined pK_a values for other anthrasemiquinone radicals are also in error (4, 11) because of interference by quinhydrone complexes of the type described, which exist in acidic, neutral, and, to a lesser extent, in alkaline solutions of partially reduced quinones (9–12). Their presence leads to exaggerated E_i values, which are not indicative of semiquinone formation alone. In fact, the formation of soluble quinhydrones in organic redox systems has largely been ignored.

The symmetry of curve A in Fig. 2, and the symmetry of the potentiometric titration curves, indicate that charge-transfer complexes of A with AH· or $A^{\cdot -}$ are negligible at equilibrium, in accord with the low value of K_s, although there is evidence that $A\cdots AH_2$ and $A\cdots AH\cdot$ are kinetically significant (13). Ehrenberg (14) has demonstrated that solutions of partially reduced isoalloxazines contain a variety of bimolecular complexes of this type.

Assuming that for A, $K_s = 0$, the only complication in the reversible redox sequence is the reaction

$$[6] \qquad A + AH_2 \rightleftarrows A\cdots AH_2$$

Elimination of [A] and [AH_2] from equations

$$[7] \quad K_c = [A\cdots AH_2]/[A]\cdot[AH_2]$$

$$[8] \quad a = 2\,[A\cdots AH_2] + [A] + [AH_2]$$

$$[9] \quad \alpha = ([A\cdots AH_2] + [A])/a$$

yields the equation

$$[10] \quad [A\cdots AH_2] = \frac{(K_c a + 1) \pm [(2K_c a + 1) - K_c{}^2 a^2 (1 - 2\alpha)^2]^{1/2}}{2K_c}$$

which has the appropriate form since $[A\cdots AH_2] = 0$ when $\alpha = 0$ or 1, and $[A\cdots AH_2] = [A\cdots AH_2]_{max}$ when $\alpha = 0.50$.

Rearrangement of the Nernst equation gives

$$[11] \quad [A] = [AH_2]10^{\gamma} \text{ where } \gamma = \frac{(E - E_m)2F}{2.303RT}$$

Substitutions from [8], [9], and [11] into [7] and rearrangement gives

$$[12] \quad K_c = \frac{\alpha(10^{-\gamma} - 10^{\gamma}) + (10^{\gamma} - 1)}{a(1 - 2\alpha)^2}$$

Equation 12 is similar to but simpler than equations for the calculation of K_c developed by Michaelis (6, 9). It allows calculation of K_c from any point on the potentiometric titration curve. A large number of calculations based on various values of a and α resulted in a mean value of $K_c = 350 \pm 50$. Some typical results are shown in Table 2. The mean deviation is unavoidably large because the value of K_c from [12] is extremely sensitive to very small changes in the values of $E - E_m$ (*e.g.* ±0.1 mV) and α (*e.g.* ±0.005). The curves A and B in Fig. 2 and E_i values in Table 1 were all calculated from the

TABLE 2. Typical data for calculation of K_c from potentiometric titrations

$a \times 10^3$ (mol dm^{-3})*	α	$E - E_m$ (mV)	K_c
17.5	0.10	−50.0	349
17.4	0.20	−36.2	381
17.3	0.25	−30.5	405
17.2	0.30	−24.0	381
17.0	0.40	−12.0	372
16.7	0.60	11.0	294
16.4	0.70	23.2	358
16.3	0.75	30.0	405
16.2	0.80	37.0	446
16.1	0.90	53.5	527
4.54	0.25	−19.6	275
4.51	0.30	−15.5	293
4.46	0.40	−7.6	306
4.37	0.60	7.9	367
4.33	0.70	16.0	350
4.32	0.75	20.4	348

*Corrected for dilution during titration.

above equations assuming $K_c = 350$ and ε (575 nm) = 540 dm^3 mol^{-1} cm^{-1} for A$\cdots$AH$_2$.

Experimental

The spectrophotometric and potentiometric studies were performed on solutions of A containing 0.100 mol dm^{-3} acetic acid and sodium acetate at 24–25 °C (p*H* 4.65).

Absorbance measurements, using a Shimadzu QV500 spectrophotometer, were obtained at 575 nm using a 5.00 cm optical cell attached to a polarographic unit. After partial reduction of A with a small volume of weakly alkaline $Na_2S_2O_4$ solution, α was determined polarographically (Sargent Model XVI Recording Polarograph) from the limiting diffusion currents of A and AH$_2$, assuming equal diffusion coefficients, before the solution was admitted to the optical cell. All operations were conducted in a N_2 atmosphere.

For potentiometric titrations, A was reduced with a weakly alkaline solution of $Na_2S_2O_4$, or with hydrogen and colloidal palladium, and the resulting AH$_2$ was then titrated in a N_2 atmosphere with buffered $K_3Fe(CN)_6$ solution, the potentials established at two bright Pt electrodes being measured with respect to a saturated calomel electrode using a Leeds and Northrup Students' Potentiometer, calibrated with a Weston Standard Cell. No problems were encountered when using $Na_2S_2O_4$ to reduce A in the acidic buffer, provided that excess $Na_2S_2O_4$ was avoided.

The authors gratefully acknowledge financial support from the National Research Council of Canada.

1. B. E. HULME, E. J. LAND, and G. O. PHILLIPS. J. Chem. Soc. Faraday Trans. 1, **68**, 1992 (1972).
2. R. L. WILLSON. J. Chem. Soc. Chem. Commun. 1249 (1971).
3. V. A. KUZ'MIN and A. K. CHIBISOV. J. Chem. Soc. Chem. Commun. 1559 (1971).
4. R. GILL and H. I. STONEHILL. J. Chem. Soc. 1845 (1952).
5. E. BURSTEIN and A. W. DAVIDSON. Trans. Electrochem. Soc. **80**, 175 (1941).
6. L. MICHAELIS. Chem. Rev. **16**, 243 (1935). L. MICHAELIS and M. P. SCHUBERT. Chem. Rev. **22**, 437 (1938).
7. W. M. CLARK. Oxidation–reduction potentials of organic systems. Williams and Wilkins Co., Baltimore. 1960.
8. J. B. CONANT, H. M. KAHN, L. F. FIESER, and S. S. KURTZ. J. Am. Chem. Soc. **44**, 1382 (1922).
9. L. MICHAELIS and E. S. FETCHER. J. Am. Chem. Soc. **59**, 2460 (1937).
10. L. MICHAELIS, R. K. REBER, and J. A. KUCK. J. Am. Chem. Soc. **60**, 214 (1938).
11. A. D. BROADBENT and H. ZOLLINGER. Helv. Chim. Acta, **49**, 1729 (1966).
12. M. W. CHEUNG and J. H. SWINEHART. J. Phys. Chem. **76**, 1875 (1972).
13. C. E. JOHNSON and S. WINSTEIN. J. Am. Chem. Soc. **74**, 3105 (1955).
14. A. EHRENBERG. Electronic aspects of biochemistry. *Edited by* B. Pullman. Academic Press, New York. 1964.

Can. J. Chem. Downloaded from www.nrcresearchpress.com by 210.87.254.105 on 09/05/12
For personal use only.

The 1,3,5-Trinitrobenzene–Phenoxide σ-Complex. Ambident Phenoxide Ion in SNAr Systems[1]

ERWIN BUNCEL, ANDRZEJ JOŃCZYK,[2] AND JOHN G. K. WEBB
Department of Chemistry, Queen's University, Kingston, Ontario K7L 3N6
Received July 14, 1975

ERWIN BUNCEL, ANDRZEJ JOŃCZYK, and JOHN G. K. WEBB. Can. J. Chem. **53**, 3761 (1975).

1,3,5-Trinitrobenzene reacts with potassium phenoxide in dimethyl sulfoxide solution to yield a σ-complex in which bonding has occurred between the *para* carbon of the phenoxy moiety and an unsubstituted carbon of the nitroaromatic substrate. A minor proportion of *ortho* adduct is also obtained. When the reaction is performed in DMSO–MeOH (80:20, v/v) one obtains initially the methoxide adduct of TNB which is then smoothly transformed into the phenoxide adduct. The latter is stable to dilute mineral acid, unlike the former; formation of a σ-complex involving bonding between the phenoxy oxygen and a carbon of TNB is thereby excluded. The reaction represents the first instance of phenoxide ion acting as an ambident nucleophile towards aromatic carbon. The implication of this finding on the course of related SNAr reactions is discussed on the basis of kinetic and thermodynamic control of product formation.

ERWIN BUNCEL, ANDRZEJ JOŃCZYK et JOHN G. K. WEBB. Can. J. Chem. **53**, 3761 (1975).

Le trinitro-1,3,5 benzène (TNB) réagit avec le phénolate de potassium dans le DMSO pour conduire à un complexe-σ dans lequel un lien s'établit entre la position-*para* d'un phénolate et un carbone non substitué du substrat nitroaromatique. On obtient aussi des quantités plus faibles d'adduit *ortho*. Quand on effectue la réaction dans le DMSO–MeOH (80:20 v/v) on obtient au début le produit d'addition du méthylate sur le TNB qui se transforme par la suite en adduit du phénolate. Ce dernier est stable en milieu acide dilué ce qui n'est pas le cas du premier; la formation d'un complexe-σ impliquant un lien entre l'oxygène du phénolate et un carbone du TNB est exclue sur cette base. La réaction correspond au premier cas où l'ion phénolate agit comme nucléophile ambident vis-à-vis un carbone aromatique. On discute de l'implication de ce résultat sur l'orientation des réactions SNAr; cette discussion est faite en se basant sur le contrôle cinétique et thermodynamique de la formation du produit.

[Traduit par le journal]

Whereas alkoxide ion σ-complexes of nitroaromatic compounds have been extensively investigated (1–4) and their structures fully established (*e.g.* **1**) (5, 6), corresponding aryloxide ion complexes have so far received only scant attention (7–10). Moreover, little agreement exists at present concerning the structures of such aryloxide complexes. Bond formation between the phenoxy oxygen and the nitrogen center of a nitro group was proposed by Tronov and co-workers (7, 8), on the basis of colorimetric studies, for the reaction of phenoxide ion with dinitrobenzene. A more conventional structure, **2**, involving bonding between phenoxy oxygen and an unsubstituted carbon of the nitroaromatic was advanced by Shein and Byval'kevich (9), on the basis of n.m.r. and u.v.–visible spectroscopy, for the phenoxide ion reaction with 1,3,5-trinitrobenzene (TNB). In contrast, we have reported evidence in a preliminary communication (10) for a structure involving bond formation between the *para* carbon of phenoxide and an unsubstituted carbon of the nitroaromatic, as given by **3**.

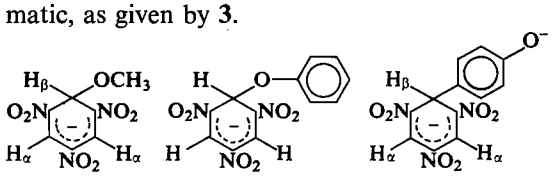

1 **2** **3**

Since **3** represents apparently the first case illustrating the ability of phenoxide ion to act as an ambident nucleophile towards aromatic carbon, we wish to present further evidence in order to reinforce our interpretation and also to discuss the implications of this unusual finding.

[1]Presented in part at the 58th Annual Canadian Chemical Conference of the Chemical Institute of Canada, Toronto, Ontario, May, 1975.

[2]Permanent address: Institute of Organic Chemistry and Technology, Politechnika, Warsaw, Poland.

Can. J. Chem. Downloaded from www.nrcresearchpress.com by 210.87.254.40 on 09/05/12
For personal use only.

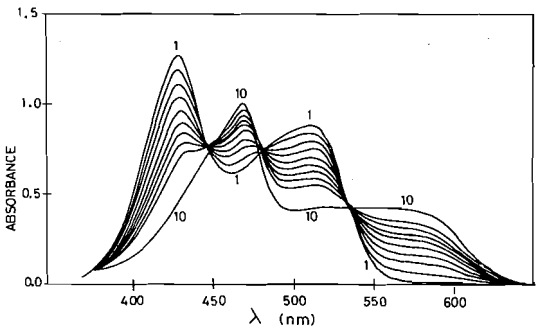

FIG. 1. Visible absorption spectra as a function of time demonstrating transformation of the trinitrobenzene–methoxide σ-complex to the trinitrobenzene phenoxide σ-complex.

Results and Discussion

Interaction Between TNB and Potassium Phenoxide in DMSO–Methanol

An instantaneous deep red color appears on mixing solutions of TNB (0.4 *M*) and PhOK (0.8 *M*) in DMSO–methanol (80:20, v/v). This color, however, is due to the TNB–methoxide adduct **1**, not a phenoxide adduct. Thus the u.v.–visible spectrum (following 100 fold dilution of the reaction solution and recording the spectrum in a 0.1 mm cell) taken 1 min after mixing is fully characteristic of complex **1** (spectrum 1 in Fig. 1). Periodic monitoring of the reaction solution in this way reveals certain spectral changes occurring with time, namely a decrease in the absorption maxima at 428 and 510 nm due to **1** and the appearance of new absorptions at 468 and 570 (broad) nm. The spectral changes are complete in about 6 h at 45 °C. An experiment performed using the authentic, separately prepared, TNB–methoxide complex (**1**) as the starting material showed identical spectral changes.

Evidence that the new complex is not the result of C—O bonding was obtained by acidification of the reaction solution. In Fig. 2*a* are shown selected spectra in a typical run, taken as described above, while in Fig. 2*b* are shown the spectra of the corresponding acidified reaction solutions. It is evident from these spectra that whereas the initially formed species is destroyed by acid the species responsible for the final spectrum is stable under acidic conditions. Alkoxide complexes of nitroaromatics are known to be decomposed by acid, regenerating the starting nitro compound (11). However aryl complexes

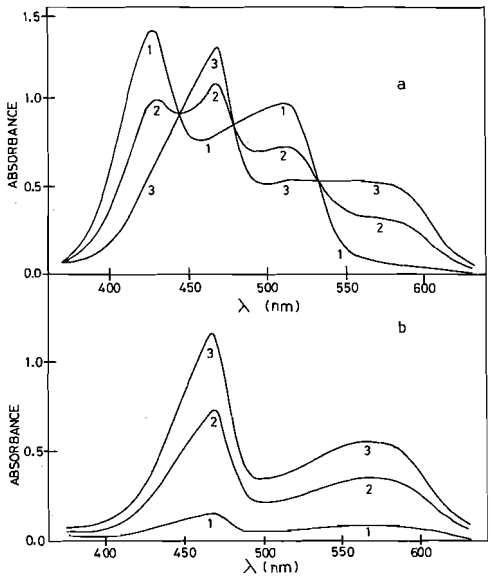

FIG. 2. (*a*) Selected spectra in the conversion of the TNB–methoxide complex to the TNB–phenoxide complex. (*b*) Spectra of the acidified reaction solutions.

are expected to be stable, in line with the much poorer leaving group ability of a phenyl moiety compared with methoxy (12, 13).

Confirmation of the postulated bonding type in the complex was afforded by n.m.r. spectroscopy. It was readily established that the initially formed spectrum in the interaction of TNB (0.4 *M*) and PhOK (0.8 *M*) in DMSO–MeOH (80:20, v/v) is due to the methoxide complex. On mixing the reactants the absorption at 9.25 p.p.m. due to TNB disappears while new absorptions characteristic of **1** arise. The H_α absorption occurs at 8.69 p.p.m. (doublet, $J = 1.2$ Hz) while H_β occurs at 6.37 p.p.m. (poorly resolved triplet). In time, as the reaction proceeds, these absorptions gradually disappear and new signals appear at 8.54 and 5.72 p.p.m. In the reaction mixture containing excess potassium phenoxide, or phenol, the phenoxy protons of the complex are difficult to resolve. The overall n.m.r. spectral characteristics are nevertheless suggestive of structure **3**.[3] In particular it can be noted that H_β in **3** is further upfield than the corresponding proton in **1**. The chemical shift dif-

[3]More precise characterization of the complex was obtained in further work using a Bruker 60 MHz instrument and is given in the section entitled 'Interaction between TNB and phenoxide in DMSO'. Evidence for formation of an *ortho* adduct will also be presented in that section.

Can. J. Chem. Downloaded from www.nrcresearchpress.com by 210.87.254.40 on 09/05/12
For personal use only.

Can. J. Chem. Downloaded from www.nrcresearchpress.com by 210.87.254.40 on 09/05/12
For personal use only.

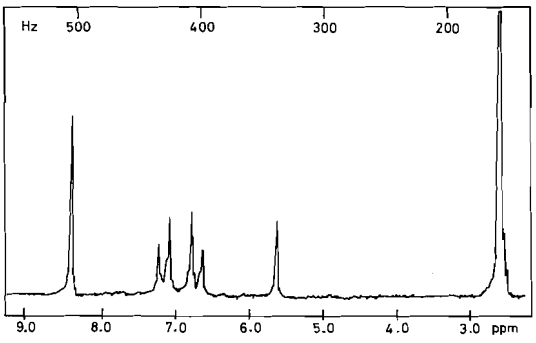

FIG. 3. Nuclear magnetic resonance spectrum of the isolated trinitrobenzene-phenoxide σ-complex in DMSO-d_6.

ference between H_α and H_β is 2.32 p.p.m. in the initial complex **1**, but 2.82 p.p.m. in the product. This is in accord with bonding at C_1 by an atom of lesser electronegativity than oxygen. Isolation of the reaction product on acidification (see Experimental) yielded a compound which showed, in addition to the above mentioned signals at 8.54 and 5.72 p.p.m. (integral height ratios 2.1 : 1.0), characteristic absorptions for the phenoxy moiety (integral 4.2). A quartet centered at 6.9 p.p.m. is characteristic of an A_2B_2 spin system for *para* disubstituted benzene derivatives. These features of the n.m.r. spectrum are completely in accord with structure **3**. The spectrum is reproduced in Fig. 3.[3]

Reaction Schemes

Several possible pathways may be proposed for formation of **3** in this system, as shown in Scheme 1. In this scheme, complex **1** is first generated via the solvolytic equilibrium $PhO^- + MeOH \rightleftarrows PhOH + MeO^-$ as a result of the highly favorable kinetic and thermodynamic factors in formation of **1** from TNB and MeO^- (14, 15). Proceeding from **1** as the effective starting material, paths *a*, *b*, and *c* represent displacement mechanisms by phenoxide ion. These displacements could occur directly by S_N2 type processes at the sp^3 center of the Meisenheimer complex or indirectly by S_N2' type displacement. Alternatively, prior dissociation of **1** to yield a small equilibrium concentration of free TNB would occur via *e*. Reaction of TNB with PhO^- could then proceed via *d* to give **2** and via *f* and *g* to give **3**. Since there seem to be no definitive cases known of S_N2 or S_N2' displacement processes on Meisenheimer complexes, we give preference to the dissociative mechanism, namely that **3** is formed from **1** via the route *e*, *f*, and *g*.

Interaction Between TNB and Phenoxide in DMSO; State of Ionization of the TNB–Phenoxide Adduct

In order to obtain an independent confirmation of our conclusions, experiments were carried out with trinitrobenzene and potassium phenoxide using pure DMSO as the medium, rather than DMSO–MeOH as described above. In summary, the work showed that the complex **3** can be obtained directly without the intervention of **1**. The evidence was obtained by u.v.–visible and n.m.r. spectroscopy on the complex formed *in situ* as well as on the isolated reaction product (see Experimental). The fact that one could obtain **3** directly in this manner supports the dissociative mechanism given at the end of the last

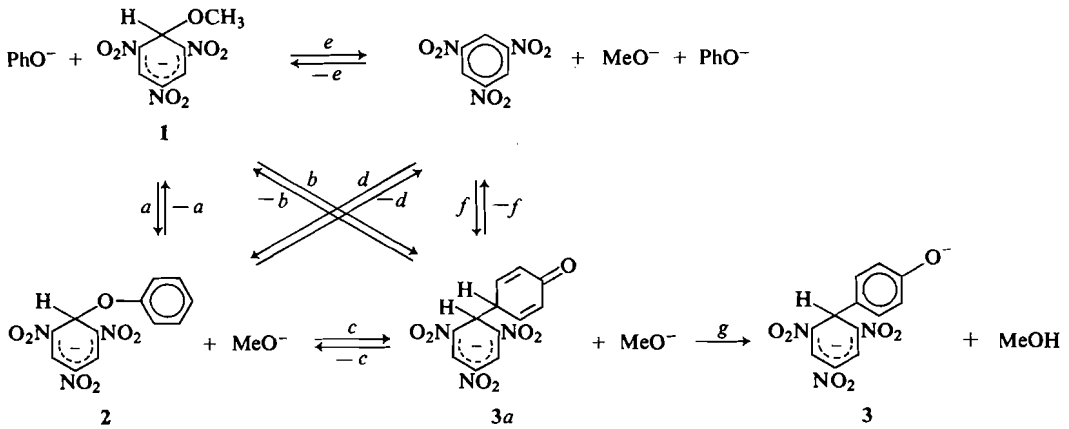

SCHEME 1

Can. J. Chem. Downloaded from www.nrcresearchpress.com by 210.87.254.40 on 09/05/12
For personal use only.

section as the most probable pathway for formation of **3** in that system.

A noteworthy aspect revealed as a result of further investigation was evidence for the *ortho* phenoxy adduct, **4**, formed by bonding between

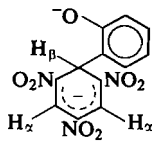

4

an *ortho* carbon of phenoxide ion and an unsubstituted carbon of TNB. Formation of another complex, apart from **3**, was indicated by the presence in a number of the n.m.r. spectra of a signal at 5.88 p.p.m., downfield of the 5.54 p.p.m. signal due to H_β of the *para* phenoxide adduct of TNB. That this new complex did not result from bonding via the oxygen of phenoxide was indicated by the fact that the 5.88 p.p.m. signal was observed both *in situ* in the reaction solutions and also in the product isolated on acidification. Generally the 5.88 p.p.m. signal was small relative to the 5.54 p.p.m. signal, though on one occasion it reached about a third of that magnitude. In that case a signal due to H_α of **4** was also seen at 8.35 p.p.m. (J = 0.3 Hz), slightly downfield of the H_α signal at 8.34 p.p.m. (J = 0.5 Hz) due to the *para* adduct. The H_β signal, however, appeared as a broadened singlet for both adducts. Moreover, the phenoxy protons of **4** could not be clearly distinguished but due to extensive overlap resulted in a diffuse pattern in the quartet arising from the phenoxy protons of the *para* adduct.

Information has also been obtained on the state(s) of ionization of the TNB–phenoxide adduct. In the first place the question arises whether aromatization of **3***a* leads to the dianionic complex **3** or a monoanionic species **3***h*. One would expect that if reaction of TNB with phenoxide is performed with at least a 2:1 molar ratio of PhOK–TNB, then **3** should be formed directly from **3***a* on proton abstraction by the base. On the other hand, if one uses a 1:1 molar ratio PhOK–TNB, then **3***h* should be obtained. In this case the tautomerization **3***a* → **3***h* would be effected by way of a solvent molecule, in an inter- or intramolecular fashion (12). In practice this series of experiments was generally performed using a PhOK–TNB ratio of 1.4:1 so

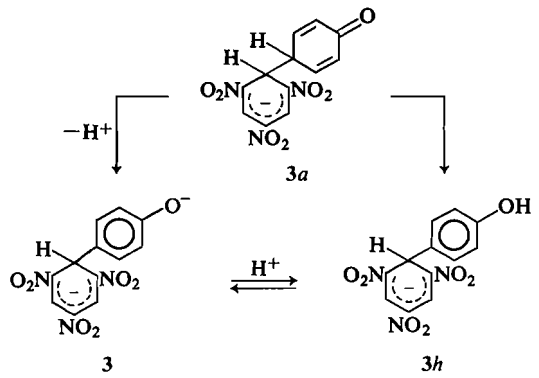

3*a* **3** **3***h*

that formation of a mixture of **3** and **3***h* would be expected. However when the conditions of a 1:1 and 2:1 ratio of PhOK–TNB were employed, some minor differences in the signal positions due to **3***h* and **3** could be observed. Thus the H_α and H_β signals of **3***h* (PhOK:TNB 1:1) are found at 8.34 and 5.54 p.p.m. respectively, while those of **3** (PhOK:TNB 2:1) occur at 8.30 and 5.40 p.p.m. The shift in signals corresponding to the change **3***h* → **3** was also seen on addition of KOMe–MeOH to a reaction mixture obtained from a 1:1 ratio PhOK–TNB. In that case one could also observe a shift of the center of the quartet due to the phenoxy ring hydrogens in the complex from 6.84 p.p.m. to 6.43 p.p.m. In solutions containing mixtures of **3***h* and **3** there is presumably rapid proton exchange between these species, accounting for the observation of a single peak. During isolation of the adduct the work-up procedure used involved acidification with a slight excess of sulfuric acid or with acetic acid (see Experimental). Under these conditions one expects to obtain the monoanion **3***h* and indeed the n.m.r. spectral characteristics as well as the elemental analysis of the isolated material corresponded to this species.

The possibility of observing a second protonation equilibrium arises in these systems, namely protonation of a nitro group of the adduct. The protonation of anion **3***h* to yield the nitronic acid derivative **3***h*$_2$ was in fact observed in the

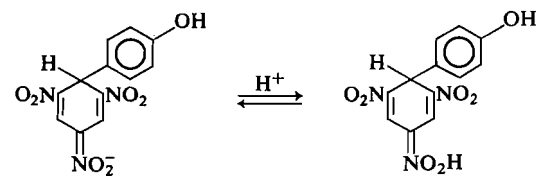

3*h* **3***h*$_2$

Can. J. Chem. Downloaded from www.nrcresearchpress.com by 210.87.254.40 on 09/05/12
For personal use only.

presence of moderately concentrated acid by u.v.-visible spectroscopy. Thus on treatment of a solution of **3***h* in DMSO–MeOH with concentrated sulfuric acid in increasing amounts the absorption maxima at 468 and 570 nm due to **3***h* diminished and eventually disappeared, while a new absorption at 372 nm increased in intensity. The spectrum in acid solution can be ascribed to species $\mathbf{3}h_2$, by analogy with literature data on nitronic acids derived from trinitrobenzene derivatives (16). Thus all three ionization states (3, **3***h*, $\mathbf{3}h_2$) have been realized in this work.

The Ambident Nature of Phenoxide Ion in SNAr Systems. Kinetic and Thermodynamic Control

Formation of complex **3** from TNB and phenoxide ion, rather than of complex **2** (Scheme 1), is accounted for on the basis of the ability of the phenoxide ion to act as an ambident nucleophile (17), coupled with considerations of kinetic and thermodynamic control. Thus whereas **2** would be expected to be the kinetically preferred product, literature data (15) indicate that the equilibrium constant for its formation should be small, several orders of magnitude less than for formation of **1**. This is in line with the much smaller basicity of PhO^- compared with MeO^-. Formation of **3***a* from TNB via path *f* is probably less facile kinetically than formation of **2** via *d*. However, whereas both *d* and *f* are reversible processes, *g*, proton loss from the *para* carbon of the quinoid intermediate **3***a* with concomitant rearomatization, is effectively irreversible. Therefore the overall process in which phenoxide ion acts as a carbon nucleophile leads to the product of thermodynamic control. It should be pointed out, however, that this discussion is not consistent with the findings of Shein and Byval'kevich (9) who report that TNB and phenoxide ion react in DMSO to give adduct **2**.

The ability of phenoxide ion to act as an ambident nucleophile in aliphatic systems is well established (17). This is in contrast with nucleophilic substitution at aromatic carbon (SNAr) where phenoxide appears to act only as an oxygen nucleophile. For example, picryl chloride reacts with phenoxide ion to yield picryl phenyl ether (18), which appears to be a general reaction of nitro-activated aryl halides (19, 20).

The interaction of phenoxide ion with nitro-activated aryl halides and other derivatives can be discussed according to Scheme 2. In this scheme σ-complexes are shown as reaction intermediates in accord with current views of the mechanism of nucleophilic aromatic substitution (19–25). Normally attack by oxygen of PhO^- (route *h*) is kinetically preferred and expulsion of X^- from intermediate **5** leads to the observed product **6**. In juxtaposition, route *j* is apparently disfavored in the typical reaction systems. Nevertheless, this route could in principle compete under certain conditions. This could occur, for example, if X were a poor leaving group so that step *i* would be relatively unfavorable, allowing competition from route *j*. Under such circumstances complex **8** might be observable as well as the final substitution product **9**.

Thus the possibility of phenoxide ion acting as a carbon nucleophile might be realized in certain activated aromatic derivatives. If one could observe such a process in suitably designed sys-

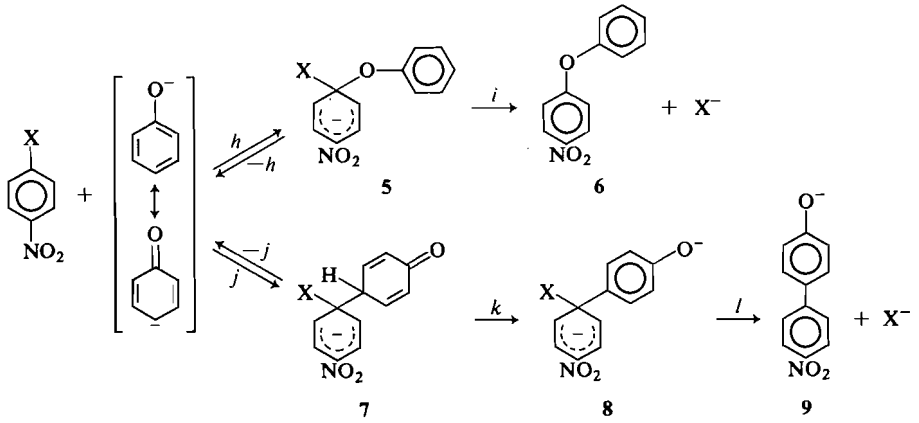

SCHEME 2

Can. J. Chem. Downloaded from www.nrcresearchpress.com by 210.87.254.40 on 09/05/12
For personal use only.

tems this would establish the validity of our discussion as well as provide a ready synthesis of diphenyl derivatives by a novel reaction. Investigation of reaction systems of these types is under active consideration.

Experimental

Materials and Methods

Dimethyl sulfoxide was distilled either from barium oxide or from calcium hydride under nitrogen. Methanol was distilled from magnesium metal. Acetonitrile was dried over molecular sieves and distilled under nitrogen. The deuterated solvents were dried over molecular sieves. 1,3,5-Trinitrobenzene (TNB) was recrystallized from ethanol, m.p. 123 °C. Anhydrous potassium phenoxide was prepared by the method of Kornblum and Lurie (26). Methanolic potassium phenoxide was obtained by neutralizing phenol with MeOK–MeOH. Solutions of potassium phenoxide in DMSO were obtained by using the anhydrous PhOK, or from the methanolic solution by addition of DMSO and distilling off the methanol under reduced pressure. Potassium 1-methoxy-2,4,6-trinitrocyclohexadienate, **1**, was prepared as described previously (27). Manipulation of air/moisture sensitive materials was carried out in a dry box under nitrogen.

Nuclear magnetic resonance measurements were carried out on a Varian T60 instrument or on a Bruker 60 MHz HFX-60, the preliminary work (10) being done largely on the former instrument. Visible spectra were recorded on a Unicam SP800 spectrophotometer.

Reaction of TNB with Potassium Phenoxide in DMSO–MeOH (80:20, v/v)

Reaction solutions were prepared by mixing solutions of TNB in DMSO and PhOK in MeOH, such that the final solvent composition was 80:20 v/v DMSO:MeOH and reagent concentrations of the order TNB 0.4 *M*, PhOK 0.4–0.9 *M*. In some experiments excess phenol (up to 0.5 *M*) was present; the signal due to the H_β proton in **3** tended to be partly obscured by the solvent OH absorption and addition of phenol caused a low-field shift of the combined phenol–methanol OH signal, lessening the interference with the H_β signal. Most of the reactions were carried out at 45 °C by immersing the reaction vessel (usually a 10 ml volumetric flask) in a constant temperature bath. Samples for n.m.r. observation were removed at appropriate times and kept cold until analyzed. For visible spectral analysis 0.1 ml aliquots were removed, diluted to 10 ml with 80:20 DMSO–MeOH, and spectra recorded in a 0.1 mm cell. When testing for acid reversibility of complex formation, 0.1 ml of 1 *N* H_2SO_4 was added to the flasks containing the diluted solutions whose visible spectra had previously been recorded, and the spectra taken once more.

For isolation of the TNB–phenoxide complex, reaction was performed as described above but on a larger scale, using 0.042 mol of TNB, 0.085 mol PhOK, and 0.080 mol PhOH in 100 ml of 80:20 DMSO–MeOH (v/v). On completion of reaction, as shown by n.m.r. and u.v.–visible spectroscopy, the reaction mixture was cooled to 10 °C in a 250 ml round bottom flask and 4.25 ml 10 *N* H_2SO_4 slowly added while stirring. The dark red solution was added to 1.5 l chloroform which caused a tarry red material as well as a granular precipitate of K_2SO_4 to separate. The flask was shaken for 2 days during which time the chloroform was decanted several times and replaced with fresh solvent. Three successive extractions resulted in the tarry material becoming crystalline. After the final decantation of chloroform, acetonitrile was added to dissolve the red solid, and the inorganic material was filtered off. The acetonitrile solution was dried ($MgSO_4$), the solvent removed on a rotary evaporator, and the dark crystalline solid dried *in vacuo* (11.7 g). Attempts to crystallize the product were unsuccessful. Experimental analysis results (Schwartzkopf Laboratories): C, 40.55; H, 2.68; N, 11.04; S, 5.02; K, 8.85. The sulfur content is due to solvated DMSO, which is also shown by the n.m.r. spectrum, and corresponds to 0.60 mol of DMSO of solvation. Analysis calculated for $(C_{12}H_8N_3O_7K)\cdot 0.60(C_2H_6SO)$: C, 40.38; H, 3.02; N, 10.67; S, 5.02; K, 9.94. Thus the product is identified as the potassium salt of **3***h*.

Reaction of TNB with Potassium Phenoxide in DMSO

In this portion of the work anhydrous PhOK was usually used as the reagent. In a typical reaction, solutions of TNB and PhOK in DMSO were mixed so as to yield final concentrations of reagents 0.5 *M* and 0.7 *M* respectively. For n.m.r. observation the reaction solution was prepared in a sample tube and followed at the ambient temperature of the spectrophotometer. Monitoring by u.v.–visible absorption was performed by 100 fold dilution and use of 0.1 mm cells as previously.

Isolation of complex in this phase of the work was performed by a modified method. Following completion of the reaction, the DMSO solution was added to a stirred solution of chloroform containing acetic acid in slight excess. The treatment yielded at this stage the σ-complex as a solid material, rather than as the tarry oil obtained in the previous method. After several more extractions with chloroform the solid was dissolved in acetonitrile. Removal of solvent yielded a material in which DMSO of solvation was largely replaced by CH_3CN of solvation. The latter could be replaced by benzene after several treatments with this solvent, and drying *in vacuo* yielded the complex practically free of solvent of crystallization. The isolated TNB–phenoxide complex has absorptions at 468 nm (ε 31 800) and at 572 nm (ε 14 800).

Formation of Side Products

In a number of experiments formation of side products was indicated by the appearance of additional signals in the n.m.r. spectra as the reaction proceeded. Absorptions occurring at 8.10 p.p.m. (d, J = 2 Hz) and at 8.56 p.p.m. (t, J = 2 Hz) may be due to substitution of a nitro group by phenoxy. These absorptions increased in proportion when TNB was present in excess of PhOK (a condition which was avoided in the routine experiments).

Continuing financial support of this research by the National Research Council of Canada is gratefully acknowledged, as is a helpful discussion with Professor N. Kornblum.

1. M. J. STRAUSS. Chem. Rev. **70**, 667 (1970).
2. M. R. CRAMPTON. Adv. Phys. Org. Chem. **7**, 211 (1969).
3. E. BUNCEL, A. R. NORRIS, and K. E. RUSSELL. Q. Rev. Chem. Soc. **22**, 123 (1968).
4. R. FOSTER and C. A. FYFE. Rev. Pure Appl. Chem. **16**, 16 (1966).
5. M. R. CRAMPTON and V. GOLD. J. Chem. Soc. 4293 (1964).
6. K. L. SERVIS. J. Am. Chem. Soc. **89**, 1508 (1967).
7. B. V. TRONOV and V. M. MOROZOVA. Izv. Vyssh. Uchebn. Zaved., Khim. Khim. Tekhnol. **6**, 39 (1958); Chem. Abstr. **53**, 14985 (1959).
8. A. B. TRONOV. Org. Kompleks. Soedin. **99**, 103 (1965); Chem. Abstr. **66**, 85369 (1967).
9. S. M. SHEIN and O. G. BYVAL'KEVICH. Zh. Org. Khim. **8**, 328 (1972).
10. E. BUNCEL and J. G. K. WEBB. J. Am. Chem. Soc. **95**, 8470 (1973).
11. O. WENNERSTRÖM. Acta Chem. Scand. **25**, 2341 (1971).
12. D. J. CRAM. Fundamentals of carbanion chemistry. Academic Press, New York. 1965.
13. E. BUNCEL. Carbanions. Mechanistic and isotopic aspects. Elsevier, Amsterdam. 1975.
14. C. F. BERNASCONI. J. Am. Chem. Soc. **92**, 4682 (1970).
15. M. R. CRAMPTON. J. Chem. Soc. B, 1208 (1968).
16. C. MOBERG and O. WENNERSTRÖM. Acta Chem. Scand. **25**, 2871 (1971).
17. N. KORNBLUM, P. J. BERRIGAN, and W. J. LE NOBLE. J. Am. Chem. Soc. **85**, 1141 (1963).
18. R. C. FARMER. J. Chem. Soc. 3425 (1959); 3430 (1959); 3433 (1959).
19. J. F. BUNNETT and R. E. ZAHLER. Chem. Rev. **49**, 273 (1951).
20. J. MILLER. Aromatic nucleophilic substitution. Elsevier, Amsterdam. 1968.
21. J. A. ORVIK and J. F. BUNNETT. J. Am. Chem. Soc. **92**, 2417 (1970).
22. J. H. FENDLER, E. J. FENDLER, and L. M. CASILIO. J. Org. Chem. **36**, 1749 (1971).
23. F. TERRIER, F. MILLOT, and R. SCHAAL. J. Chem. Soc. Perkin Trans. 2, 1192 (1972).
24. C. F. BERNASCONI and C. L. GEHRIGER. J. Am. Chem. Soc. **96**, 1092 (1974).
25. S. D. Ross. *In* Comprehensive Chemical Kinetics. Vol. 13. *Edited by* C. H. Bamford and C. F. H. Tipper. Elsevier, Amsterdam. 1972.
26. N. KORNBLUM and A. P. LURIE. J. Am. Chem. Soc. **81**, 2705 (1959).
27. E. BUNCEL and J. G. K. WEBB. Can. J. Chem. **52**, 630 (1974).

Can. J. Chem. Downloaded from www.nrcresearchpress.com by 210.87.254.40 on 09/05/12
For personal use only.

Stereodynamic Investigation of Dibenzo-1,5-cyclooctadiene and 5,6,11,12-tetrahydrodibenzo[*b*,*f*][1,4]diazocine Derivatives

FRANÇOISE SAURIOL-LORD AND MAURICE ST-JACQUES

Département de chimie, Université de Montréal, Montréal, Québec H3C 3V1

Received July 14, 1975

FRANÇOISE SAURIOL-LORD and MAURICE ST-JACQUES. Can. J. Chem. **53**, 3768 (1975).

A dynamic n.m.r. study of a deuterated derivative of dibenzo-1,5-cyclooctadiene (**2**-d_4), *N*,*N*′-dimethyl-1,4-diazocine **3**, and *N*,*N*′-diacetyl-1,4-diazocine (**4**) is reported. Two spectral changes of different origin are observed for **2**-d_4, one for **3** and three for **4**. The results reveal the presence of a mixture of chair and twist-boat conformations for **2**-d_4 and **4**, while the single spectral change observed for **3** is interpreted in terms of a single twist-boat form. Interconversion pathways are suggested to explain the characteristic behavior of each compound investigated.

FRANÇOISE SAURIOL-LORD et MAURICE ST-JACQUES. Can. J. Chem. **53**, 3768 (1975).

L'étude par r.m.n. dynamique d'un dérivé deutérié du dibenzo cyclooctadiène-1,5 (**2**-d_4), ainsi que de la *N*,*N*′-diméthyl diazocine-1,4 (**3**) et de la *N*,*N*′-diacétyl-1,4 diazocine (**4**) est présentée dans cet article. Deux modifications spectrales d'origine différente ont été observées pour **2**-d_4, un pour **3** et trois pour **4**. Les résultats ont révèlé la présence d'un mélange de conformations chaise et bateau-croisé pour **2**-d_4 et **4**, alors que le seul changement d'allure spectral observé pour le composé **3** est interprété uniquement en terme d'un bateau-croisé. Des chemins d'interconversion conformationnelle sont proposés pour expliquer le comportement dynamique de chaque composé examiné.

[Traduit par le journal]

Important aspects of conformational analysis involve the assessment of the nature of the most stable conformation and of the rates of various types of stereomutations characterizing different classes of molecules.

Recently, dynamic nuclear magnetic resonance (d.n.m.r.) spectroscopy (1) has been used to study 1,5-cyclooctadiene (2), dibenzo-1,5-cyclooctadiene (3), *syn*-3,7-dibromo-*cis*,*cis*-1,5-cyclooctadiene (4), as well as derivatives of 5,6,11,12-tetrahydrodibenzo[*b*,*f*][1,4]diazocine (5–8) and has revealed the complexity of the stereodynamic properties of this fundamental ring system.

Specifically, the conformational properties of 1,5-cyclooctadiene (**1**) are significantly different from that of dibenzo-1,5-cyclooctadiene (**2**). The stable conformation of **1** has been reported to be a twist boat which can undergo two dynamic processes (2) while **2** exists as a mixture of chair and boat conformations of varying proportion depending on the nature of the solvent (3). For this latter molecule, owing to spectral complexities and solubility problems, only one of the possible dynamic processes has been identified for the boat form. In order to define more precisely the stereodynamic properties of **2**, the deuterated derivative **2**-d_4 was prepared and studied by the d.n.m.r. method.

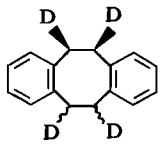

2-d_4

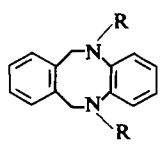

3 R = CH_3

4 R = $COCH_3$

Several investigations (5–8) have shown that heteroatoms in the ring modify significantly its conformational properties and an examination of the literature has led us to anticipate a markedly different behavior for *N*,*N*′-dimethyldiazocine (**3**) and *N*,*N*′-diacetyldiazocine (**4**) because no spectral change was reported for compounds analogous to **3** (*e.g.* R = $CH_2C_6H_5$) whereas two spectral changes were observed for **4** but none was attributed to hindered amide bond rotation. Because of the basic importance of **3** and the apparently incomplete study of **4** it appeared that a detailed comparative study of **3** and **4** was necessary.

We now wish to report the results of our study of **2**-d_4, our observation of a spectral change for **3** and another spectral change for **4** which apparently has escaped earlier detection. These observations and their interpretation contribute significantly to our understanding of the conformational properties of such cyclic systems.

Can. J. Chem. Downloaded from www.nrcresearchpress.com by 210.87.254.6 on 09/05/12
For personal use only.

Can. J. Chem. Downloaded from www.nrcresearchpress.com by 210.87.254.6 on 09/05/12
For personal use only.

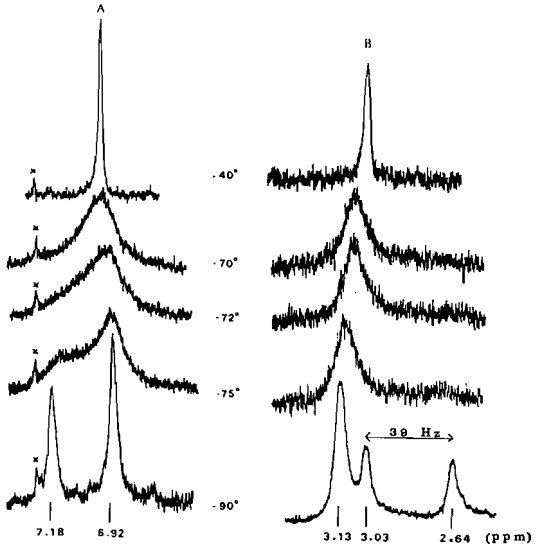

FIG. 1. Proton magnetic resonance spectra (100 MHz) of **2**-d_4 in $CDCl_3$–CS_2 (2:3) at several temperatures. (A) Aromatic region (* = $CHCl_3$ trace in the solvent). (B) Aliphatic (CHD) region.

Results

The 100 MHz deuterium decoupled p.m.r. spectrum of **2**-d_4 was recorded at several temperatures in two representative solvent systems: a mixture of $CDCl_3$–CS_2 (2:3 by volume) and a mixture of CD_2Cl_2–C_3H_6 (2:1). Firstly, Fig. 1 shows several spectra of **2**-d_4 in $CDCl_3$–CS_2. At temperatures above −40 °C both the aromatic (A) and the aliphatic (B) signals appear as singlets (δ 6.98 and δ 3.01 respectively) which broaden and change below −70 °C such that at −90 °C the aromatic region contains two peaks (δ 6.92 and δ 7.18) in the proportion 60:40, while the CHD region contains three peaks (δ 2.64, δ 3.03, and δ 3.13). Integration is less accurate in this region because of the overlap of the signals at δ 3.03 and δ 3.13.

Assuming an exchange between two equally populated sites and using a coalescence temperature (T_c) of −72 °C, a free energy of activation $\Delta G^{\ddagger} = 10.0 \pm 0.5$ kcal/mol is calculated from the change in the aromatic signal. The data are summarized with other information in Table 1 where the more intense lines are assigned to a conformation labelled B and the lesser intense lines are assigned to a conformation C.

Figure 2 shows the behavior of the CHD signal of **2**-d_4 dissolved in CD_2Cl_2–C_3H_6 (2:1) at several temperatures. The spectrum at −110 °C is similar to that observed in Fig. 1B with the exception that the signals of C are less intense. Below this temperature the tall signal broadens and splits up such that four lines are observed at −136 °C (δ 2.64 and 3.07; δ 2.90 and 3.40). Limited solubility made it difficult to obtain good spectra at lower temperatures. The value of $\Delta G^{\ddagger} = 7.8 \pm 0.3$ kcal/mol at −115 °C (T_c) is calculated from the splitting of the tall line. The aromatic region is the same as that published in a preliminary communication for **2** and the results are reported in Table 1.

Figure 3 illustrates the spectral change observed for the methylene protons of **3** in $CHFCl_2$ at low temperatures. The high temperature singlet (δ 4.23) broadens and below −95 °C (T_c) splits up into an AB quartet characterized by $\Delta\nu = 1.27$ p.p.m. and $J = -16.2$ Hz. The *N*-methyl signal (δ 2.85) remained unchanged down to −150 °C, the lowest temperature reached.

Figure 4 shows the spectral change observed for the methyl signal of the *N*-acetyl groups of **4** dissolved in pyridine. At +13 °C three signals are clearly visible, the most intense (δ 1.84) accounting for about 75% of the total intensity and the two others (δ 2.03 and δ 2.20) accounting equally for the rest. At higher temperatures these three signals merge together to give a

TABLE 1. Observations for **2**-d_4 in two solvent systems

			Conformation B[a]		Conformation C[a]	
	$\Delta G^{\ddagger}$ (kcal/mol)	T_c (°C)	%	T_c (°C)	%	T_c (°C)
Aromatic region						
$CDCl_3$ + CS_2 (2:3)	10.0±0.5	−72	60	−90	40	−90
CD_2Cl_2 + propene (2:1)	10.0±0.5	−72	87	−100	13	−100
Aliphatic (CHD) region						
$CDCl_3$ + CS_2 (2:3)	9.9±0.5	−70	67[b]	−90	33[b]	−90
CD_2Cl_2 + propene (2:1)	7.8±0.3	−115	89	−128	11	−128

[a]The letters B and C symbolize different conformations which will be identified later.
[b]Integration is less precise for the aliphatic than for the aromatic protons at −90 °C because of line overlap for the former.

Can. J. Chem. Downloaded from www.nrcresearchpress.com by 210.87.254.6 on 09/05/12
For personal use only.

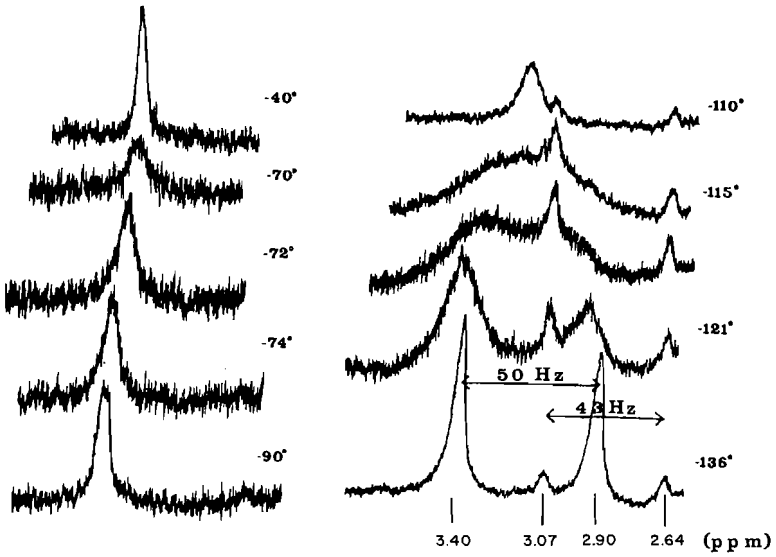

FIG. 2. Proton magnetic resonance spectra (100 MHz) of the aliphatic (CHD) protons of **2**-d_4 in CD_2Cl_2–C_3H_6 (2:1) at several temperatures.

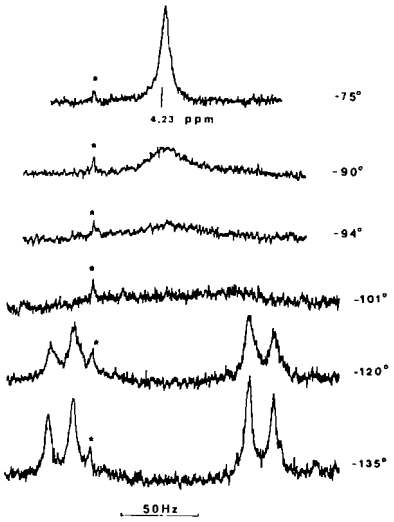

FIG. 3. Proton magnetic resonance spectra (100 MHz) of the methylene protons of *N,N'*-dimethyldiazocine, **3**, at several temperatures (* = impurity).

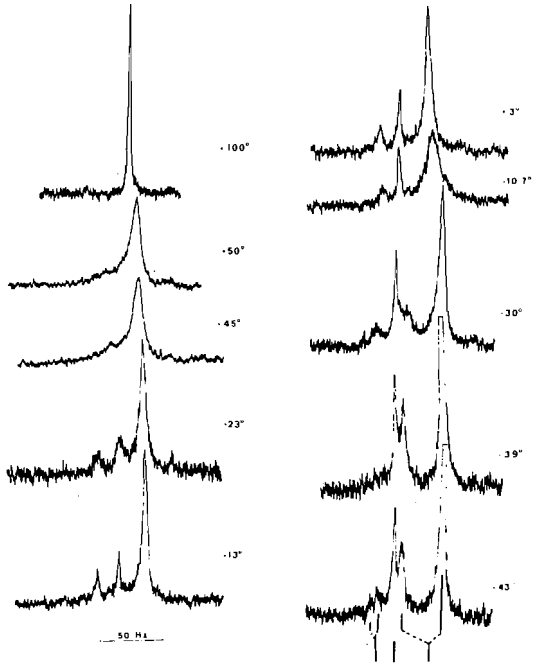

FIG. 4. Proton magnetic resonance spectra (100 MHz) of the methyl protons of *N,N'*-diacetyldiazocine, **4**, at several temperatures. The stick diagram under the spectrum at −43 °C illustrates the splitting pattern observed at low temperatures.

narrow singlet at 100 °C whereas at lower temperatures the high and low field lines split into doublets with components of unequal intensity as shown for the spectrum at −43 °C. These two spectral changes are characterized by $\Delta G^{\ddagger}$ values of 16.6 ± 0.5 and 13.0 ± 0.5 kcal/mol.

The temperature effect on the methylene proton signal of **4** was observed to be similar to that published (5, 6). The spectrum consists of a singlet at +110 °C, appears as an AB quartet at +25 °C, and consists of two AB quartets of unequal intensity at −50 °C. The $\Delta G^{\ddagger}$ values characterizing these two spectral changes are 16.9 and 12.9 kcal/mol (6). Careful recording of

Can. J. Chem. Downloaded from www.nrcresearchpress.com by 210.87.254.6 on 09/05/12
For personal use only.

the spectrum at +25 °C has however revealed the presence of additional very small peaks in this region which could be ascribed to a minor conformation.

Discussion

Dibenzo-1,5-cyclooctadiene

Compound **2**-d_4 actually exists as a mixture of *syn* and *anti* isomers and for all practical purposes both sides of the molecule can be considered independent (9) as far as n.m.r. is concerned. The p.m.r. spectrum of the CHD region (Fig. 1B) can easily be interpreted in terms of a mixture of chair (C) and a member of the boat family whereby the doublet is assigned to the axial and equatorial protons of C and the intense line is assigned to the boat form whose proton environments are still averaged out by rapid inversion. Since 1,5-cyclooctadiene exists in a twist-boat (TB) form (2), it is very likely that **2**-d_4 should also exist as a TB (10). The spectrum of **2**-d_4 at −136 °C (Fig. 2) contains two intense lines characteristic of this TB form in addition to two less intense signals belonging to C. It is clear that the inversion process has been slowed down on the n.m.r. time scale but the observation of only two intense signals is compatible with either a symmetrical boat (B) or two rapidly equilibrating TB forms with average symmetry equivalent to B. In fact the spectrum of **2**-d_4 in a TB conformation should exhibit two AB patterns (eight lines) or four lines if the coupling constants were not resolved, unless the chemical shift differences for protons on the nonidentical carbons of TB are too small to be resolved. The spectrum of **2**-d_4 is therefore compatible with the existence of a major TB conformation and a minor C conformation in agreement with earlier suggestions for **2** (3, 6).

Consequently the spectral changes observed for **2**-d_4 identify and characterize the following processes: (*1*) chair-to-boat interconversion with $\Delta G^{\ddagger}$ = 10.0 kcal/mol and (*2*) boat inversion with $\Delta G^{\ddagger}$ = 7.8 kcal/mol as illustrated with structures **5**, **6***e*, and **6***i*.

The chair form **5** possesses two nonequivalent protons (namely the equatorial H_1 and the axial H_2 where the numbers are labels) and theoretically its low temperature spectrum should consist of an AB quartet. Instead a doublet is observed, suggesting that the coupling constant between H_1 and H_2 is not resolved at −90 °C (Fig. 1B) or −136 °C (Fig. 2) owing to line broadening through long range coupling with the aromatic

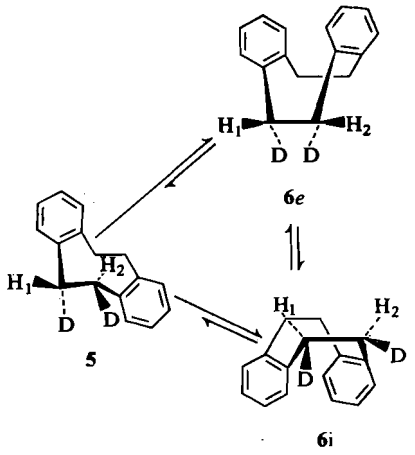

protons and a dihedral angle in the range 110 ± 10° as suggested from Dreiding models.

The averaged TB conformations represented by **6***e* and **6***i* then each account for a tall line in the spectrum of **2**-d_4 at −136 °C (Fig. 2) because H_1 and H_2 are both at equivalent exterior positions in **6***e* and both at equivalent interior positions in **6***i*.

An increase in temperature from −136 °C increases the rate of boat inversion (**6***e* ⇌ **6***i*) which exchanges exterior and interior proton environments and consequently produces a singlet above −115 °C. At still higher temperatures the chair-to-boat interconversion (**5** ⇌ **6***e* and **5** ⇌ **6***i*) becomes rapid on the p.m.r. time scale and all the aliphatic signals coalesce. Only this last process produces a change in the aromatic signal as shown in Fig. 1A.

Figure 5 illustrates possible pathways for the chair-to-boat interconversion whereby the E-conformations which contain six coplanar carbon atoms are of high energy (10). They can be reached from either B or C by a 'wagging' of a benzo group. Such a conformational modification interestingly requires an energy similar to that required for the inversion of benzocycloheptene (11) which has been shown to proceed via a benzo wag involving a $\Delta G^{\ddagger}$ = 10.7 kcal/mol. Furthermore the difference between $\Delta G^{\ddagger}$ for **1** and **2** ($\Delta\Delta G^{\ddagger}$ = 5.1 kcal/mol) is very similar to the $\Delta\Delta G^{\ddagger}$ = 5.7 kcal/mol observed for benzocycloheptene and cycloheptene (11).

Figure 6 illustrates the possible pathways for boat inversion which is shown to occur when the molecule passes through skew (S) forms. A possible transition state for this process could consist of a conformation intermediate between

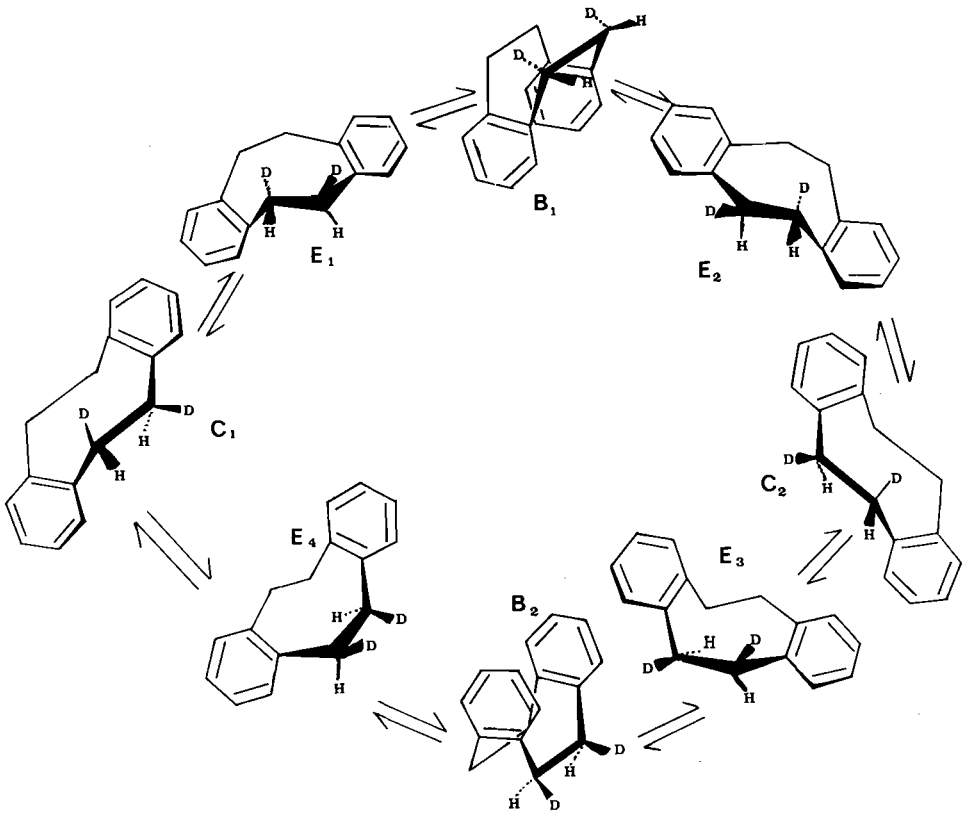

FIG. 5. Pathways for the boat-to-chair interconversion of **2**-d_4.

TB and S possessing two groups of five coplanar carbon atoms and called a folded boat (FB) by other workers (6), but recent calculations (10) suggest that S is of higher energy than FB. Consequently boat inversion through S has a lower $\Delta G^{\ddagger}$ (7.8 kcal/mol) than that characterizing a 'wagging' to E ($\Delta G^{\ddagger}$ = 10.0 kcal/mol). Furthermore it is clear that the partial averaging of two twist-boat forms (*e.g.* $TB_1 \rightleftharpoons B_1 \rightleftharpoons TB_4$) results in the average symmetry of B_1 and does not lead to an exchange of interior and exterior aliphatic protons in the boat family. Such an exchange of environment can only occur when the molecule goes through the S forms.

Finally, it is interesting to contrast the above conclusion that **2** exists as a mixture of chair and boat forms (the latter predominating) with the observation that this compound in the crystalline state exists in a centro-symmetrical form, presumably the chair (12).

N,N'-Dimethyldiazocine, **3**

The $\Delta G^{\ddagger}$ value of 8.2 kcal/mol calculated from the only spectral change observed for **3** provides a clue as to the nature of its stable conformation in solution and its inversion pathway. Results from studies of derivatives of cyclohexane (Ref. 1, p. 584) suggest that the replacement in **2**-d_4 of two CHD groups in a 1,4-relationship by two N—CH_3 groups might increase only slightly the activation energies for boat inversion and chair-to-boat interconversion. Since the value of 8.2 kcal/mol is rather close to that of 7.8 kcal/mol determined for boat inversion in **2**-d_4, it seems highly probable that the spectral change observed for **3** is due to a boat inversion and that its stable conformation is undoubtedly also a TB form. A mixture of B and C is ruled out because it is incompatible with the spectrum at −150 °C. A stable chair conformation with chair inversion responsible for the spectral change appears very unlikely since it would involve a $C \rightleftharpoons B$ step which is expected to have a $\Delta G^{\ddagger}$ near or slightly above 10.0 kcal/mol.

Thus only the TB form has been detected by n.m.r. for **3** and its inversion pathway is analo-

Can. J. Chem. Downloaded from www.nrcresearchpress.com by 210.87.254.6 on 09/05/12
For personal use only.

Can. J. Chem. Downloaded from www.nrcresearchpress.com by 210.87.254.6 on 09/05/12
For personal use only.

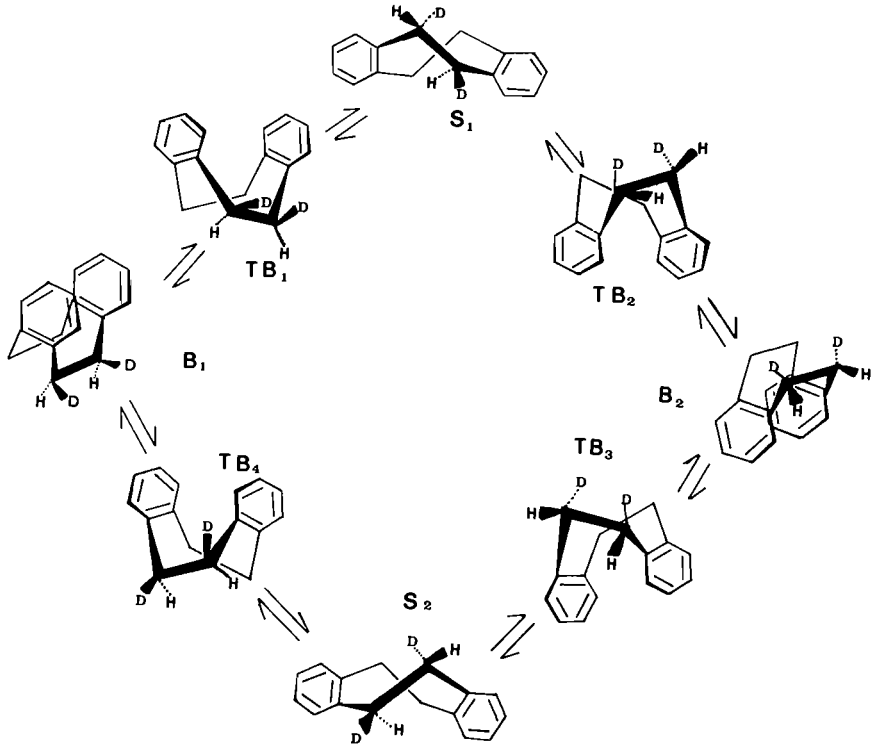

FIG. 6 Pathways for the boat inversion of **2**-d_4.

gous to that described in Fig. 6 keeping in mind that two 1,4-CHD are replaced by two N—CH_3 groups. As for **2**-d_4 the partial averaging TB ⇌ B ⇌ TB is still rapid at −150 °C for **3**. Furthermore it is logical to suggest that the failure to observe a spectral change for compounds analogous to **3** (*e.g.* R = alkyl) (6) can be interpreted in terms of a rapid boat inversion at the relatively high temperatures investigated.

N,N'-Diacetyldiazocine, 4

Our study of the acetyl methyl region of the spectrum of **4** has revealed two spectral changes: one near +50 °C ($\Delta G^{\ddagger}$ = 16.6 kcal/mol) which was apparently not detected by other workers (5, 6) and another near −11 °C ($\Delta G^{\ddagger}$ = 13.0 kcal/mol) which has previously been reported (5, 6). These activation energies are equal within experimental error to the values of 16.9 and 12.9 kcal/mol previously determined (6) from the two spectral changes observed for the methylene proton signal although the origin of the spectral changes with similar $\Delta G^{\ddagger}$ need not necessarily be the same.

Interpretation of the spectral behavior of the methylene protons has shown that at +13 °C the ring conformation is an average of chair and boat forms (6). The spectrum at +13 °C in Fig. 4 which consists of three lines of unequal intensity is also compatible with an averaged ring conformation for which the methyl lines reveal the existence of more than one rotational conformer for which methyl groups in different environments show characteristic chemical shifts which average out at higher temperature when rotation of the amide bond becomes rapid on the p.m.r. time scale.

Amide rotation barriers for the typical molecules **7** and **8** are 16.7 and 16.6 kcal/mol respectively (13). These values illustrate clearly that the value of 16.6 kcal/mol determined for **4** is of the correct magnitude.

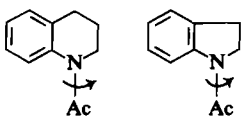

7 **8**

Can. J. Chem. Downloaded from www.nrcresearchpress.com by 210.87.254.6 on 09/05/12
For personal use only.

A study (14) of the p.m.r. spectrum of *N*-methylacetanilide has shown that the *exo* conformer **9** is more stable than the *endo* conformer **10** and furthermore that the acetyl methyl absorbs at higher field in the *exo* form. Consequently a singlet, a doublet, and a singlet are expected for the methyl groups in structures **11**, **12**, and **13** respectively. Since both methyl groups are *exo* in **11**, the methyl signal is expected to appear at higher field than that of the *endo* methyls of **13**.

Accordingly the intense methyl line (δ 1.83) in the spectrum of **4** at +13 °C belongs to **11** while the less intense doublet (δ 2.03 and δ 2.20) must be associated with **12** for which methyl *a* is expected to be at higher field than *b*. Conformation **13** is apparently present in a negligible amount. Table 2 shows the relative proportions of *exo* and *endo* conformers for model amides. It is seen that structural factors have a very pronounced effect on the observed populations and the result obtained for **4** is indeed not abnormal.

It is important to explain at this point that only the methylene signals of the *exo–exo* chair and boat forms are sufficiently intense to be detected clearly for d.n.m.r. analysis (6).

Thus three dynamic processes have been identified for 4: (*1*) boat-to-chair interconversion with $\Delta G^{\ddagger}$ = 12.9 kcal/mol (6), (*2*) boat inversion with $\Delta G^{\ddagger}$ = 16.9 kcal/mol (6), and (*3*) hindered amide rotation with $\Delta G^{\ddagger}$ = 16.6 kcal/mol. The equality within experimental errors of the two last barriers suggests that boat inversion and amide rotation proceed through a common transition state. Accordingly detailed conformational transformation pathways are analyzed next for each process.

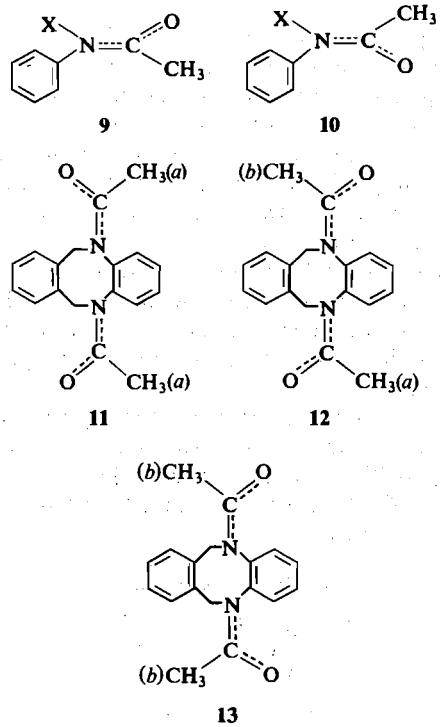

TABLE 2. Relative population of *exo* and *endo* conformers of a few amides

Compound	Conformation		Reference
	Exo (%)	*Endo* (%)	
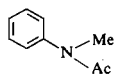	99.5	0.5	15
	11	89	15
	96	4	15
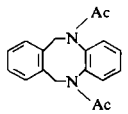	**11**, 75% (2 *exo*) **12**, 25% (1 *endo* and 1 *exo*) **13**, 0% (2 *endo*)		This work

Firstly, let us consider the B ⇌ C transformation which effectively averages the two unequal methylene AB systems at low temperatures into an average AB near 25 °C. This process can be depicted in terms of Fig. 5 where two 1,4-CHD are replaced by two N—Ac groups. Accordingly one of the E forms becomes **14** which can be reached from B or C by 'wagging' of the carbon substituted benzo group while **15** requires the 'wagging' of the nitrogen substituted benzo group.

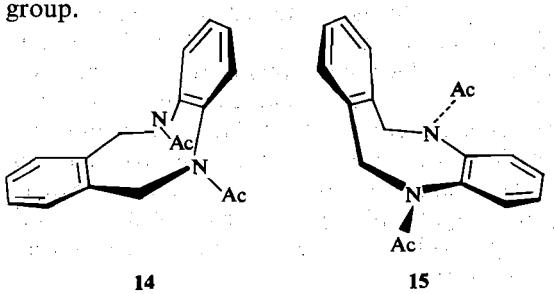

Can. J. Chem. Downloaded from www.nrcresearchpress.com by 210.87.254.6 on 09/05/12
For personal use only.

A comparison of the barrier to Ar–C rotation in *o*-xylene (**16**) (1.5–2.0 kcal/mol) (16) and the Ar–N rotation in **17** (19.3 kcal/mol) (17) suggests that **14** should be of lower energy than **15** and hence the B $\rightleftharpoons$ C transformation should involve preferentially a wagging of the carbon end of the molecule (called *C*-wag compared to *N*-wag for the other end of the molecule). When *C*-wag is rapid on the n.m.r. time scale, the methylene protons are not completely averaged out in accord with the AB observed at +25 °C. Only when B inversion (or *N*-wag) becomes rapid will the methylene proton signal average to a singlet.

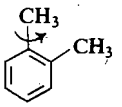

16

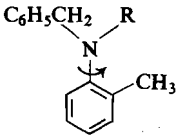

17; R = CH_3CO—
18; R = C_6H_5CO—
19; R = *p*-CH_3—C_6H_4—SO_2—
20; R = CH_3—

Comparison of the $\Delta G^{\ddagger}$ barrier of 12.9 kcal/mol of **4** with that of 10.0 kcal/mol for **2** suggests that structural factors other than Ar–C rotation are also responsible for the difference.

Boat inversion can easily be visualized with the aid of Fig. 6 after replacement of two CHD groups by N—Ac groups. The transition state for this process is either an FB form (6) which contains two sets of five coplanar ring atoms such as in **21** or the S form as calculated (10) for **2**. The N—Ac groups are in different positions for both conformations.

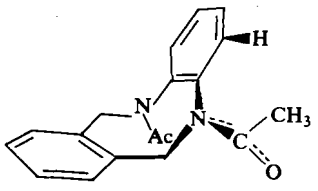

21

Since S and FB are close on the pseudorotation cycle of the boat family (10), it is not obvious which one will be more energetic for **4**. It is however significant that both forms must be overcome during boat inversion. The steric interaction between the methyl group and the *ortho* proton present in FB and shown in **21** may indeed make the energy of FB very close to that of S. This steric interaction may be the determining factor inducing amide rotation and consequently explain why amide rotation and boat inversion have essentially identical energy barriers.

Torsional interactions were found (10) to be important in determining the boat inversion barrier of **2**, and consequently the appreciable rotation about the Ar—N bonds required to go through conformations FB and S suggests that boat inversion should also be influenced by factors which determine the activation energy for this type of rotation. For example, the free energies of activation for boat inversion of **4** (16.9 kcal/mol), *N*,*N*′-dibenzoyl-1,4-diazocine (10.1 kcal/mol) (6), *N*,*N*′-di-*p*-tolylsulfonyl-1,4-diazocine (10.1 kcal/mol) (6), and **3** (8.2 kcal/mol) follow a trend parallel to the rotation barriers of analogous *o*-toluidine derivatives (17, 18): **17** (19.3 kcal/mol), **18** (18.1 kcal/mol), **19** (15.3 kcal/mol), and **20** (6.2 kcal/mol). Thus it is reasonable to conclude that Ar–N rotation accounts for a large part of $\Delta G^{\ddagger}$ observed for the boat inversion of **4**.

Our observations for **2**-d_4, **3**, and **4** thus prove to be essential to a complete understanding of the complex stereodynamic problem on hand. In fact, the comparable $\Delta G^{\ddagger}$ values for boat inversion in **2**-d_4 and **3** suggest that the transannular interactions invoked earlier (6) should not dominate the explanation of the trend reported earlier for derivatives of 1,4-diazocine (6) and that arguments involving Ar–N rotation presented above are more satisfying. Consequently the observation for **4** that boat inversion has a higher $\Delta G^{\ddagger}$ than the B $\rightleftharpoons$ C process (contrary to the order found for the parent compound **2**-d_4) can be explained by invoking a greater energy demand for the appreciable Ar–N rotation required to reach the transition state of boat inversion than for the *C*-wag involved in the B $\rightleftharpoons$ C process which requires little Ar–N rotation.

Experimental

The v.p.c. analyses and separations were carried out on a Varian-aerograph A90-P3 instrument using ¼ in. SE-30 columns and helium as carrier gas. Mass spectral analyses were performed on an Hitachi–Perkin–Elmer model RMU-6D instrument operating at 70 and 10 eV.

Routine analytical p.m.r. spectra were recorded on a JEOL C-60H spectrometer operating at 60 MHz in the external lock mode. The low temperature p.m.r. spectra were obtained at 100 MHz using a JEOL JNM-4H-100 spectrometer. Solutions containing a small quantity of

TMS were degassed and sealed. Deuterium decoupling, when required, was effected by means of the JEOL Hetero Spin Decoupler model JNM-SD-HC.

Temperatures were monitored by means of a JEOL temperature control unit model JES-VT-3 and determined accurately with a calibrated thermocouple placed inside a solvent-containing dummy n.m.r. tube.

Dibenzo-1,5-cyclooctadiene-d_4, 2-d_4

This compound was prepared by catalytic reduction of dibenzocyclooctatetraene (0.051 g) with deuterium gas and 0.14 g of palladium-on-carbon (5%) in 10 ml of ethyl acetate using an apparatus previously described (9). The crude product which showed no olefinic proton signal in the p.m.r. spectrum was purified by v.p.c. and identified by its p.m.r. spectrum in $CDCl_3$ (singlet at δ 7.0 (8H) and singlet at 3.0 p.p.m. (4H)) and had a retention time in analytical v.p.c. identical to the hydrogenated product.

The isotopic composition obtained from a mass spectrum at 10 eV is: $d_5 = 9.5\%$, $d_4 = 74.8\%$, $d_3 = 13.8\%$ and $d_2 = 1.9\%$.

The low temperature spectra were recorded for concentrations of 16–20 mg ml^{-1} of solution.

N,N'-Dimethyldiazocine, 3, and N,N'-Diacetyldiazocine, 4

These known compounds were prepared according to published procedures (19–21) and characterized by their melting points and p.m.r. spectra which agreed with those published.

The low temperature spectra were taken for an 8% solution of **3** in $CHFCl_2$ and a 10% solution of **4** in pyridine.

We wish to acknowledge the assistance of Mr. Robert Mayer with the recording of the p.m.r. spectra at low temperature and we express our gratitude to the National Research Council of Canada for financial assistance.

1. L. M. JACKMAN and F. A. COTTON. Dynamic nuclear magnetic resonance spectroscopy. Academic Press, New York, San Francisco, London. 1975.
2. F. A. L. ANET and L. KOZERSKI. J. Am. Chem. Soc. **95**, 3707 (1973).
3. D. MONTECALVO, M. ST-JACQUES, and R. WASYLISHEN. J. Am. Chem. Soc. **95**, 2023 (1973).
4. R. K. MACKENZIE, D. D. MACNICOL, H. H. MILLS, R. A. RAPHAEL, F. B. WILSON, and J. A. ZABKIEWICZ. J. Chem. Soc. Perkin Trans. 2, 1632 (1972).
5. A. SAUNDERS and J. M. SPARKE. J. Chem. Soc. Perkin Trans. 2, 1660 (1972).
6. R. CROSSLEY, A. P. DOWNING, M. NOGRADI, A. BRAGA de OLIVEIRA, W. D. OLLIS, and I. O. SUTHERLAND. J. Chem. Soc. Perkin Trans. 2, 205 (1973).
7. W. D. OLLIS, J. F. STODDART, and I. O. SUTHERLAND. Tetrahedron, **30**, 1903 (1974).
8. M. S. PUAR, H. L. YALE, and A. I. COHEN. Org. Magn. Reson. **6**, 106 (1974).
9. M. ST-JACQUES and C. VAZIRI. Org. Magn. Reson. **4**, 77 (1972); L. CANUEL and M. ST-JACQUES. Can. J. Chem. **52**, 3581 (1974).
10. N. L. ALLINGER and J. T. SPRAGUE. Tetrahedron, **31**, 21 (1975).
11. M. ST-JACQUES and C. VAZIRI. Can. J. Chem. **51**, 1192 (1973); N. L. ALLINGER and J. T. SPRAGUE. J. Am. Chem. Soc. **94**, 5734 (1972).
12. W. BAKER, R. BANKS, D. R. LYON, and F. G. MANN. J. Chem. Soc. 27 (1945).
13. G. V. GARNER, O. METH-COHN, and SUSCHITZKY. J. Chem. Soc. C, 1234 (1971).
14. W. E. STEWART and T. H. SIDDALL. Chem. Rev. **70**, 517 (1970); A. J. R. BOURN, D. G. GILLIES, and E. W. RANDALL. Tetrahedron, **20**, 1811 (1969).
15. C. C. COSTAIN and J. M. DOWLING. J. Chem. Phys. **32**, 158 (1960).
16. R. C. LIVINGSTON, D. M. GRANT, R. J. PUGMIRE, K. A. STRONG, and M. ROBERT. J. Chem. Phys. **58**, 1438 (1973); E. E. BURNELL and P. DIEHL. Mol. Phys. **24**, 489 (1972); H. D. RUDOLPH, K. WALZER, and I. KRUTZIK. J. Mol. Spectrosc. **47**, 34 (1973).
17. B. J. PRICE, J. A. EGGLESTON, and I. O. SUTHERLAND. J. Chem. Soc. B, 922 (1967).
18. S. BROWNSTEIN, E. C. HORSWILL, and K. U. INGOLD. J. Am. Chem. Soc. **92**, 7217 (1970).
19. R. C. ELDERFIELD and V. MEYER. J. Am. Chem. Soc. **76**, 1887 (1954).
20. G. W. H. CHEESEMAN. J. Chem. Soc. **3**, 3308 (1955).
21. N. J. HARPER and J. M. SPRAKE. J. Chem. Soc. C, 882 (1969).

Can. J. Chem. Downloaded from www.nrcresearchpress.com by 210.87.254.6 on 09/05/12
For personal use only.

SCF MO Study of Benzo[*d*]aceheptylene

ARCHANA DASGUPTA AND NANDA K. DASGUPTA[1]

Department of Chemistry, The University of Alberta, Edmonton, Alberta T6G 2E1

Received March 24, 1975

ARCHANA DASGUPTA and NANDA K. DASGUPTA. Can. J. Chem. **53**, 3777 (1975).

The molecule benzo[*d*]aceheptylene has been studied using the method of Dewar and Harget, and Yamaguchi *et al.* Heats of atomization, bond energies, reactivity, bond length, and $\pi^* \leftarrow \pi$ transitions are reported and aromaticity of the molecule is discussed.

ARCHANA DASGUPTA et NANDA K. DASGUPTA. Can. J. Chem. **53**, 3777 (1975).

On a étudié la molécule benzo[*d*]aceheptylène à l'aide de la méthode de Dewar et d'Harget et de Yamaguchi *et al.* On rapporte les chaleurs d'atomisation, les énergies de liaison, la réactivité, les longueurs de liaison et les transitions $\pi^* \leftarrow \pi$ et on discute de l'aromaticité de la molécule.

[Traduit par le journal]

Introduction

Recently 8,5,10-trimethyl benzo[*d*]aceheptylene was isolated along with the synthesis of its isomer 2,4,11-trimethyl azuleno[8,8*a*,1,2-*def*]heptalene (1). The properties of the former compound have not been reported (2) but its structure (3) has been determined by X-ray analysis and found to have small but significant deviation from planar structure. Since the parent hydrocarbon, benzo[*d*]aceheptylene contains five-, six-, and seven-membered rings fused together, it would be interesting to predict the properties of the molecule (Fig. 1) using π-electron approximation in the context of the 'β-variable' method. Both the molecules, benzo[*d*]aceheptylene (molecule **1**) and azuleno[*def*]heptalene (molecule **2**), are iso-π-electronic containing 18π electrons. Since they obey Hückel's $4n + 2$ rule they might be aromatic. But it was observed that the molecule azuleno[*def*]heptalene (4) is not aromatic. Hence it would also be interesting to see whether the molecule benzo[*d*]aceheptylene behaves similarly as molecule **2** so far as aromaticity is concerned. Moreover the Pariser–Parr–Pople (PPP) theory was developed for the study of planar conjugated systems. But the molecule **1** has small deviation from planarity. Hence, how far it is justified to apply the PPP theory on such a molecule is questionable. However, we studied molecule **1** using a planar model with 1.4 Å as bond lengths to see how the predicted results are in agreement with the experimental ones. The difficulty is that only a few of the experimental results are available in the literature.

[1]Permanent address: Department of Chemistry, Visva-Bharati University, Santiniketan, West Bengal, India.

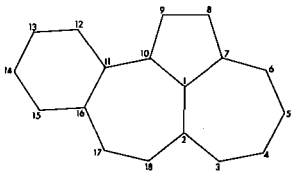

FIG. 1. Structure of benzo[*d*]aceheptylene.

Method and Parameters

The simple Hückel calculations were done. The SCF method used here is well known and has been described by Dewar and Harget (5) and Yamaguchi *et al.* (6). In a recent paper (7) we have applied this 'β-variable' technique proposed by Dewar and Harget (5) (designated as SCF(*a*)) and Yamaguchi *et al.* (6) (designated as SCF(*b*)) successfully on some nonbenzenoid hydrocarbons in predicting their properties. Spectral transitions have also been predicted using configuration interactions. The final vectors and integrals obtained from the SCF(*b*) method were used in the calculation of CI.

The pertinent integrals are calculated as follows:

(*i*) The one center, two electron repulsion integrals γ_{ss} (11.134 eV) were estimated from the relation

$$\gamma_{ss} = I_s - A_s$$

where I_s and A_s are the sp^2 valence state ionization energy (11.16 eV) (8) and electron affinity, respectively, of the carbon atom.

(*ii*) For the Dewar and Harget method, two center, two electron repulsion integrals were estimated using Ohno's formula (9) and for the other method we used Mataga–Nishimoto formula (10). In both SCF(*a*) and SCF(*b*) methods,

Can. J. Chem. Downloaded from www.nrcresearchpress.com by 210.87.254.42 on 09/05/12
For personal use only.

the γ_{st} for non-neighboring centers were calculated from the initial geometry of the molecule and they are not varied during interaction. For bonded atoms, γ_{st} and the resonance integrals β_{st} were calculated after each iteration on the basis of bond length – bond order relations. For SCF(*a*) method the relations are

$$[1] \qquad r_{st}\,(\text{Å}) = 1.512 - 0.174\,p_{st}$$

and

$$[2] \qquad \beta_{st} = -6.927\,S_{st}$$

where p_{st} is the π-bond order and S_{st} is the overlap integral between two π_{2p} orbitals with orbital exponent 1.59.

For the SCF(*b*) method the relations are

$$[3] \qquad r_{st}\,(\text{Å}) = 1.520 - 0.186\,p_{st}$$

and

$$[4] \qquad \beta_{st} = \beta_0 \exp\,[a(r_0 - r_{st})]$$

where r_0 is equal to 1.397 (Å), a is equal to 1.7 Å^{-1}, and β_0 has been taken to be equal to −2.15 eV (7). In both SCF methods β_{st} for non-bonded atoms were taken to be equal to zero.

In the HMO method bond length has been calculated using [3].

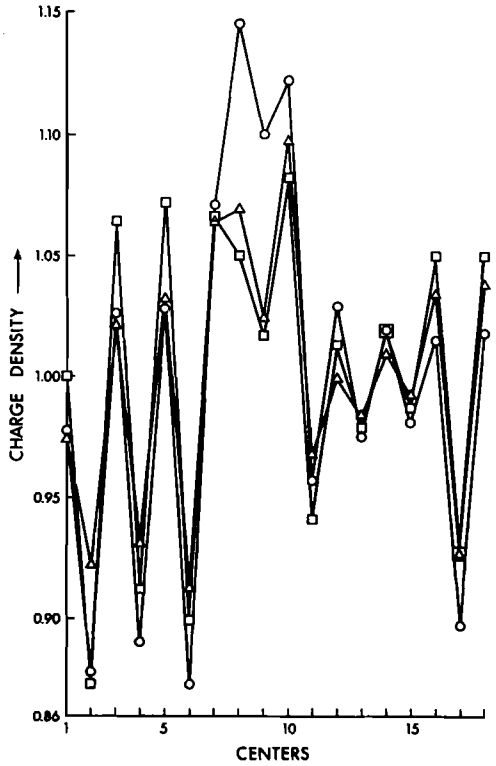

FIG. 2. Variation of charge density; Hückel, ○; SCF(*a*), □; SCF(*b*), △.

Results and Discussion

(a) Reactivity

Figure 2 represents the variation of charge densities. It is clear from the figure that the SCF(*b*) method has evened out the charge densities in the different centers. The wide variation in the π-dipole moment in the HMO (5.39 D), SCF (*a*) (1.65 D), and SCF (*b*) (2.31 D) methods can be expected from the calculated charge densities. In this type of compound HMO method predicts π-dipole moment too high compared to the SCF methods. This is also seen in this case. The large π-dipole moment predicts that there might be charge separation in the molecule rendering it reactive. The π-electron density of the five-membered ring is increased at the cost of seven-membered rings only as in azulene with a tendency to form a local sextet in all the five- and seven-membered rings and it is clear from Fig. 2 that the benzene ring retains its sextet.

According to HMO method the highest charge density is at C_8 suggesting that the electrophilic attack will be at this position. This is also in agreement with SCF(*b*) method though C_8 center has the second highest charge density. The highest charge density calculated by the SCF(*b*) method is at C_{10} but the position is not suitable for electrophilic attack. But SCF(*a*) method suggests that the center C_5 is the most favorable position for electrophilic attack as the calculated charge density is the second highest at this center, the highest being at C_{10}. The lowest charge density calculated by the HMO and SCF(*b*) method is at C_6 indicating that the nucleophilic attack takes place at this center. Although the lowest charge density calculated by the SCF(*a*) method is at C_2, the center is unfavorable for this reaction and the next favorable position is C_6. Thus it is seen that so far as prediction of position of nucleophilic attack the three methods agree whereas the SCF(*a*) method disagrees with the other two methods as regards the position of electrophilic attack.

All the three methods agree that the 17–18 bond of this molecule is the most suitable for dienophilic activity because it has the highest

Can. J. Chem. Downloaded from www.nrcresearchpress.com by 210.87.254.42 on 09/05/12
For personal use only.

TABLE 1. $\pi^* \leftarrow \pi$ transitions and oscillator strengths

Experiment*		CI		SCF (*a*)		SCF (*b*)	
eV	log ε	eV	*f*	eV	*f*	eV	*f*
		1.48	0.029			1.79	0.13
		2.66	0.026	2.37	0.21		
3.12		3.19	0.162	3.35	0.41	3.22	0.28
{3.77	4.47	{3.85	0.644	{4.05	0.39	{3.95	0.45
{3.99	4.54	{4.02	0.451	{4.22	0.32	{4.09	0.40
		4.40	0.376				
4.64	4.66	4.70	1.046	{4.43	0.28	{4.50	0.57
				{4.86	0.29	{4.63	0.36
5.19	4.34	{4.96	0.455	5.20	0.27	{4.95	0.25
		{5.11	0.013			{5.06	0.24

*Private communication with Professor K. Hafner.

bond order (Hückel 0.777, SCF(*a*) 0.891, and SCF(*b*) 0.861).

(b) Bond Lengths

Bond lengths have been calculated according to the bond order – bond length relations shown earlier. Figure 3 shows the comparison between the bond lengths calculated by the three methods and experimental value. As expected with similar compounds the agreement of any set of theoretical bond lengths with the experimental is somewhat erratic. As in azulene, the bond common to the five- and seven-membered rings has a single bond character.

An interesting feature is that all bonds in the six-membered ring except C_{11}–C_{16} predicted by the three methods are equal and have a value lying between 1.39 and 1.41 Å which is the bond length of an aromatic hydrocarbon. Even the bond C_{11}–C_{16} has the value 1.404, 1.410, and 1.420 Å calculated by the SCF(*a*), SCF(*b*), and HMO methods, respectively. It seems that the π electrons are delocalized in this region. A similar situation is also observed in the periphery of the five-membered ring. In the other part of the molecule π-electrons are localized. Thus in the peripheries of the molecule it is seen that there are two regions, one aromatic and the other polyolefinic in nature.

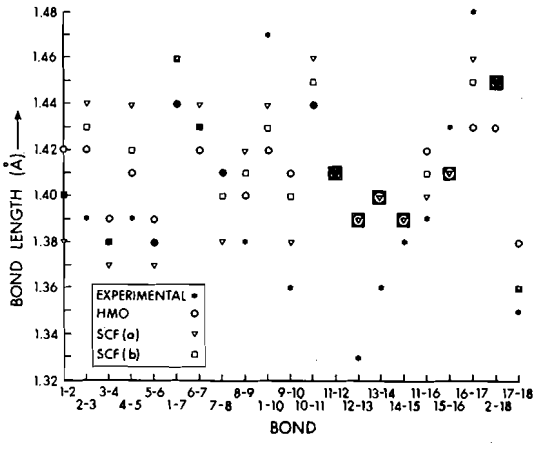

FIG. 3. Comparison of bond lengths.

(c) Spectra, Ionization Energy and Electron Affinity

The highest occupied orbital energy and lowest unoccupied orbital energy are respectively −8.12 and −3.15 eV. The ionization potential calculated by the formula of Kunii and Kuroda (11) is 7.06 eV. Table 1 contains the calculated $\pi^* \leftarrow \pi$ singlet–singlet transitions along with the oscillator strengths and experimental values. We attempted point-to-point correlation between the observed spectra and theoretical transitions. It is seen from Table 1 and Fig. 4 that the agreement between the theoretical results and the experimental value is good, specially very good with CI results.

(d) Aromaticity

It is well known that for the same number of π-electrons and the same number of rings delocalization energy per π-electron (DE/e) decreases as the number of benzene rings are replaced by five- and seven-membered rings. Thus the DE/e decreases in the order of chrysene (0.400) > benzo[*d*]aceheptylene (0.374) > azuleno[*def*]heptalene (0.356). However, DE/e is not useful in the prediction of aromaticity because many molecules which are not aromatic such as pentalene or heptalene have reasonably

Can. J. Chem. Downloaded from www.nrcresearchpress.com by 210.87.254.42 on 09/05/12
For personal use only.

TABLE 2. Resonance energy E_R, E_R/C—C, and E_R/e for various molecules

Molecule	Resonance energy (E_R) Dewar and Harget (eV)	Hess and Schaad (in β)	E_R/C—C	E_R/e
Benzo[*d*]aceheptylene	1.414	0.502	0.067	0.028
Aceheptylene			0.037*	0.016†
Azuleno[*def*]heptalene			0.033*	0.009†
Acenaphthylene			0.105*	0.039‡
Pleiadiene			0.091*	0.033†
Acepleiadylene			0.080*	0.034‡
Cyclohept[*bc*]acenaphthylene			0.081*	0.032†
Naphth[*cde*]azulene			0.082*	0.033†
Benzopleiadiene			0.075*	0.030†
Dipleiadadiene			0.069*	0.017†

*Reference 13.
†Reference 4.
‡Reference 12.

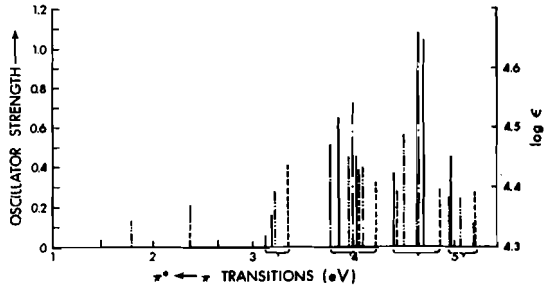

FIG. 4. Comparison of $\pi^* \leftarrow \pi$ transition energy and oscillator strengths (CI, —; SCF(*a*), ---; SCF(*b*) ·····; experimental, -·-·-), log ε value against transition 3.12 eV has been shown arbitrarily.

high DE/e. Hence in order to predict aromaticity of the molecule we have calculated the resonance energy and resonance energy per C—C bond (E_R/C—C) using the method of Dewar and Harget (5) and resonance energy per π-electron (E_R/e) by the method of Hess and Schaad (12). Table 2 contains these results along with the resonance energy per C—C bond and resonance energy per π electron for some similar molecules. The heat of atomization, π- and σ-bond energies calculated by the method of Dewar and Harget (5) are respectively 156.479, 25.229, and 78.000 eV. Dewar and Harget have shown that calculated heat of atomization by this method is in good agreement with the experimental value for many conjugated systems. Semibenzenoid (4) nature of the molecule is exhibited by its E_R/C—C value which falls in between the benzenoid (0.111 to 0.163) and nonbenzenoid (0.032 to 0.048) (13) systems. If the E_R/C—C of the molecule is compared with that of other semibenzenoid compounds (13) it would be clear that E_R/C—C of the molecule is less than acenaphthylene (0.105), pleiadiene (0.091), acepleiadylene (0.080), cyclohept[*be*]acenaphthylene (0.081), and naphth[*cde*]azulene (0.082) which are aromatic. However, the E_R/C—C for this molecule is comparable to that of benzopleiadiene (0.075) and dipleiadadiene (0.069), both of which have not yet been synthesized. The same conclusion can be drawn by comparing the value of E_R/e calculated by Hess and Schaad's method for this molecule with that of other similar molecules (Table 2). Hence we can conclude that the molecule is not aromatic like its isomer azuleno[*def*]heptalene.

The authors take the opportunity to express their gratitude to Professor F. W. Birss for many stimulating discussions, helpful comments, and financial support. They are also thankful to the Computing Services, University of Alberta, for computational facilities. They are also thankful to Professor K. Hafner for supplying the spectral data.

1. K. HAFNER, G. HAFNER-SCHNEIDER, and F. BAUR. Angew. Chem. Int. Ed. 7, 808 (1968).
2. K. HAFNER, G. HAFNER-SCHNEIDER, W. G. FRIEBE, and F. BAUR. Unpublished results.
3. H. J. LINDNER. Tetrahedron Lett. **32**, 3013 (1971).
4. A. DASGUPTA and N. K. DASGUPTA. Tetrahedron, **28**, 3587 (1972).

Can. J. Chem. Downloaded from www.nrcresearchpress.com by 210.87.254.42 on 09/05/12
For personal use only.

5. M. J. S. DEWAR and A. J. HARGET. Proc. R. Soc. London, A**315**, 443 (1970) and references therein.
6. H. YAMAGUCHI, T. NAKAJIMA, and T. L. KUNII. Theoret. Chim. Acta, **12**, 349 (1968).
7. ARCHANA DASGUPTA and NANDA K. DASGUPTA. Can. J. Chem. **52**, 155 (1974); Can. J. Chem. **53**, 915 (1975).
8. J. HINZE and H. H. JAFFE. J. Am. Chem. Soc. **84**, 540 (1962).
9. K. OHNO. Theor. Chim. Acta, **2**, 219 (1964).
10. N. MATAGA and K. NISHIMOTO. Z. Phys. Chem. **13**, 140 (1957).
11. T. L. KUNII and H. KURODA. Theor. Chim. Acta, **11**, 97 (1968).
12. B. A. HESS, JR. and L. J. SCHAAD. J. Am. Chem. Soc. **93**, 305 (1971).
13. ARCHANA DASGUPTA and N. K. DASGUPTA. Theor. Chim. Acta, **33**, 177 (1974).

Can. J. Chem. Downloaded from www.nrcresearchpress.com by 210.87.254.42 on 09/05/12
For personal use only.

Further Synthetic Applications of Functionalized 1,3-Dipoles

J. WILLIAM LOWN AND B. ERIK LANDBERG
Department of Chemistry, University of Alberta, Edmonton, Alberta T6G 2G2

Received July 8, 1975

J. WILLIAM LOWN and B. ERIK LANDBERG. Can. J. Chem. **53**, 3782 (1975).

Reactions of nitrile imines, azomethine imines, and ethyl diazoacetate (as representatives of functionalized 1,3-dipoles) with reactive olefins lead to a series of novel fused heterocycles after suitable ring closure. The influence of the nature of the heterocyclic leaving group and the substituents in the phenacyl residue in a group of phenacylimidazolium salts on the course of their reaction to produce 1,2-dihydrofurans and perhydropyrazolopyrroles is investigated.

J. WILLIAM LOWN et B. ERIK LANDBERG. Can. J. Chem. **53**, 3782 (1975).

Les réactions de nitrile-imines, azométhine-imines et diazoacétate d'éthyle (représentant des dipoles-1,3 fonctionnalisés) avec des alcènes réactifs conduisent, après une cyclisation appropriée, à une série de nouveaux hétérocycles fusionnés. On a étudié l'influence de la nature de l'hétérocycle nucléofuge et des substituants du résidu phénacyle dans le groupe des sels de phénacylimidazolium sur l'évolution de leur réaction pour conduire à des dihydro-1,2 furannes et des perhydropyrazolopyrroles.

[Traduit par le journal]

In preceding papers we have described a synthetic approach to a wide variety of fused heterocyclic systems employing cycloadditions with 1,3-dipoles bearing an additional functionality (*i.e.* besides their basic 4π electron reactive system) with subsequent ring closures (1–4) (see Eq. 1).

[1] 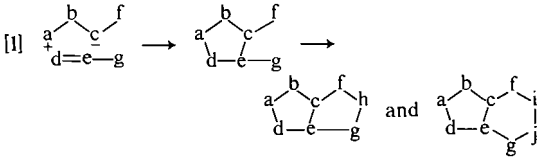

Azomethine ylides were found to be especially suited for the study of stereo and regiochemistry which are important if subsequent elaboration of cycloadducts to fused systems was to be successful. This general scheme allowed the synthesis of 5–5, 5–6, 5–5–5, 6–5–6, 6–6–5, 6–6–5–5, 6–6–6–5, and 6–6–5–6 fused systems. This synthetic scheme is now extended into other 1,3-dipolar systems; nitrile and azomethine imines and ethyl diazoacetate to provide fused pyrazoles. Also in order to investigate the competition between Michael addition to form dihydrofurans (2) and 1,3-dipolar additions to activated alkenes, some reactions of azomethine ylides derived from phenacylimidazolium salts are described.

Nitrile imines can be generated by the thermal decomposition of pyridinium betaines (5). Phenylazophenacylpyridinium betaine **1***a* prepared by the method of Krollpfeiffer and Braun (6*a*) liberates the nitrile imine and pyridine in refluxing benzene [2]. The benzoylnitrile imine under-

[2] 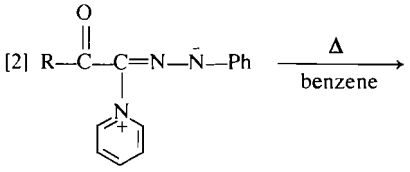

1
a R = Ph
b R = *p*-ClC$_6$H$_4$

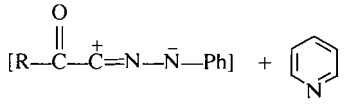

went cycloaddition to *trans*-dibenzoylethylene to give 1-phenyl-3,4,5-tribenzoyl-Δ^2-pyrazoline, **2***a*, and the corresponding pyrazole **3***a* in 37 and 48% yields respectively. Treatment of the pyra-

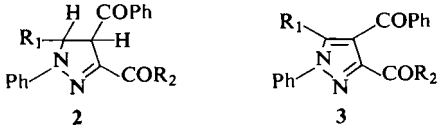

2 **3**
a R_1 = COPh, R_2 = Ph
b R_1 = COPh, R_2 = C_6H_4Cl
c R_1 = Ph, R_2 = Ph

zole **3***a* with hydrazine in refluxing ethanol afforded a product assigned the structure of 3-benzoyl-2,4,7-triphenylpyrazolo[3,4-*d*]pyridazine, **4***a*, in 69% yield. In order to confirm the di-

Can. J. Chem. Downloaded from www.nrcresearchpress.com by 210.87.254.6 on 09/05/12
For personal use only.

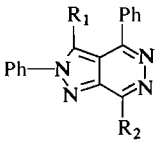

a R_1 = COPh, R_2 = Ph
b R_1 = COPh, R_2 = C_6H_4Cl
c R_1 = Ph, R_2 = Ph

4

rection of condensation across the available carbonyl positions the chlorine labelled betaine **1***b* was employed in a similar experiment. The pyrazoline **2***b* and the pyrazole **3***b* were obtained in 38 and 57% yields respectively. The pyrazole **3***b* afforded upon reaction with hydrazine, 7-benzoyl-1,6-diphenyl-3-(4-chlorophenyl)-pyrazolo-[3,4-*d*]pyridazine, **4***b* in 68% yield. A peak in the mass spectrum at *m/e* 111 (C_6H_4Cl) but not at *m/e* 139 (ClC_6H_4CO) (both prominent peaks in the starting material), indicated that the condensation had proceeded as shown. The nitrile imine generated from **1***a* was found to be reactive toward *N*-phenylmaleimide. In this case (as well as the preceding reactions) the reaction conditions were found to be important in controlling yields. For example when 10 mmol amounts of **1***a* and *N*-phenylmaleimide were present in 50 ml of refluxing benzene, the yield of adduct **5** was 21% while the dipole dimer **6** was obtained in 54%

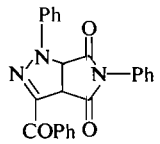

5

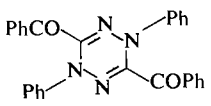

6

yield. Although originally described by Krollpfeiffer and Braun (6*a*) the correct structure of **6** was assigned by Huisgen and co-workers (6*b*). When a benzene solution of the betaine was slowly added to a refluxing solution of the dipolarophile, the yield of cycloadduct increased to 53% and the yield of dimer decreased to 12%. Huisgen has also shown that nitrile imine undergoes (3 + 3) self addition which is rare for 1,3-dipoles (6*c*). Reaction of betaine **1***a* under similar conditions with dimethyl fumarate afforded pyrazoline **7** and the pyrazole **8** in 19 and 39% yields respectively, the latter also being available from **7** by dehydrogenation with chloranil. Two equivalents of hydrazine reacted with **8** to give the pyrazolo[3,4-*d*]pyridazine derivative **9** in 35% yield.

Reaction of the nitrile imine from betaine **1**

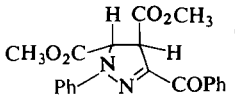

7

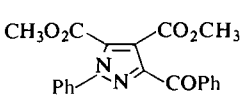

8

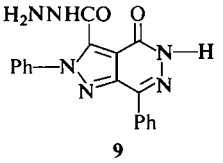

9

with phenylbenzoylacetylene occurred regiospecifically to give **3***c* directly in 28% yield. The direction of addition was proven by the quantitative conversion of the latter to give 1,4,6,7-tetraphenylpyrazolo[3,4-*d*]pyridazine, **4***c*. In general the nitrile imines were unreactive towards chalcones and only slightly reactive towards *cis*-dibenzoylethylene. A small amount of pyrazole **3***a* was isolated from the latter reaction.

Pyrazolines have also been generated employing azomethine imine cycloadditions to alkynes. Oppolzer's method of preparation allows the introduction of a functional group on the nitrogen end of the dipolar species, whereas nitrile imines are necessarily available only with the functional group on the carbon end (12). Two azomethine imines, derived from hydrazides and formaldehyde were investigated, [3]. The dipolar species

[3] $R_1CONHNHR_2 + H_2CO \longrightarrow$

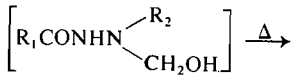

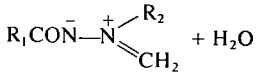

10*a* R_1 = CH_3, R_2 = Ph
10*b* R_1 = Ph, R_2 = CH_3

10*a* was found to be unreactive toward dibenzoylethylene or dibenzoylacetylene but did react with *N*-phenylmaleimide to give cycloadduct **11**. However the functionalized azomethine imine **10***b* did react with dibenzoylethylene to afford pyrazolidine **12** in 63% yield. The latter compound was resistant to chloranil dehydrogenation in refluxing toluene. Reaction of dibenzoylacetylene with **10***b* gave the desired pyrazoline **13** in 63% yield. Condensation of the latter with hydrazine proceeded smoothly across

Can. J. Chem. Downloaded from www.nrcresearchpress.com by 210.87.254.6 on 09/05/12
For personal use only.

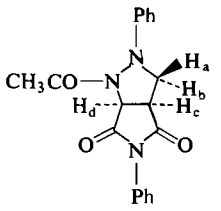

11

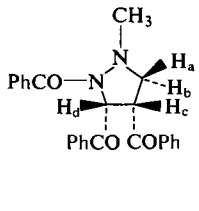

12

the *N*-benzoyl and 5-benzoyl moieties (rather than the 4,5 benzoyl groups) to give 3-benzoyl-4,7-diphenyl-1-methylpyrazolo[1,5-*d*]-as-triazine **14**. Two peaks in the mass spectrum of **14** at

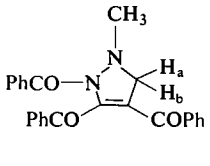

13

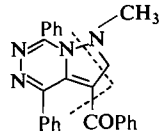

14

m/e 287 (*M* − COPh) and 244 (*M* − COPh − CH_3—N—CH_2) support the proposed structure and rule out the isomer corresponding to condensation across the 4,5-benzoyl groups of **13**.

Pyrazolines have long been available by the cycloadditions of ethyl diazoacetate to olefins (5, 7, 8). The ester function now allows development of the fused ring. Upon reaction of ethyl diazoacetate with *trans*-dibenzoylethylene the pyrazoline **15** and the pyrazole **16** were formed in 23 and 8% yields respectively. The tautomeric

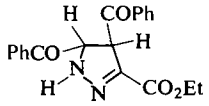

15

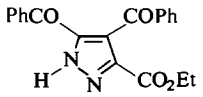

16

form **15** predominates for the pyrazoline as shown by i.r. and n.m.r. The i.r. spectrum of the pyrazole **16** shows N—H absorption and there is no evidence for methine in the n.m.r. Reaction of ethyl diazoacetate with benzoylacetylene afforded **16** in 64% yield. Similarly **17** formed by reaction with dimethyl acetylenedicarboxylate **14**, reacted with hydrazine to give the pyrazolopyridazine **18** in 99% yield.

Pyridinium, and isoquinolinium phenacylides undergo cycloadditions to reactive dipolarophiles to give, for example, indolizines and 1,3-diazapentalenes (2, 9–11). We have shown that although isoquinolinium phenacylide reacts as expected with *cis*- or *trans*-dibenzoylethylene to form cycloadducts (2) pyridinium phenacylides in contrast give 1,2-dihydrofurans **19** presumably

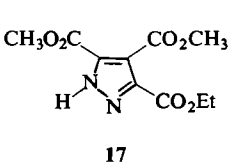

17

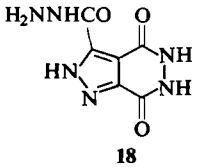

18

[4] 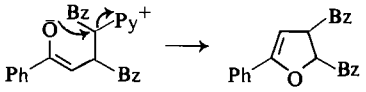

19

via Michael addition followed by ring closure and elimination of pyridine [4]. Since the 1,2-dihydrofurans were valuable as a source of pyridazino[4,5-*c*]pyridazines via a novel ring transformation and the cycloadducts could be further developed synthetically, the distribution of these two types of product was examined as a function of the nature of the group leaving to form **19**.

3-Methylimidazolium phenacylide, generated from the chloride or bromide salt with triethylamine in pyridine at 50 °C afforded both the dihydrofuran **19** and a cycloadduct **20***a* in 23 and 12% yields respectively. The experiment was repeated with different substituents in the *para*-position of the phenacyl group.

It is apparent that as the substituent X becomes more electronegative the reaction favors

[5] 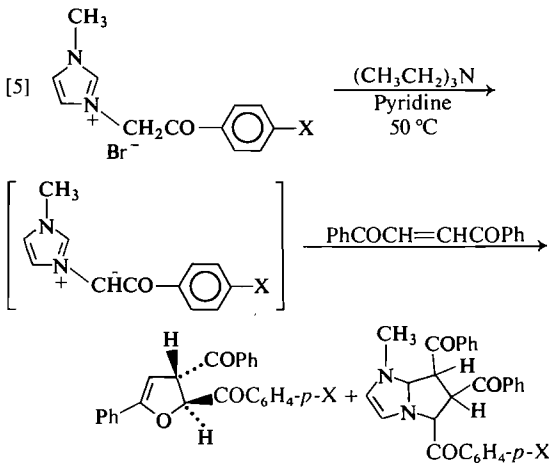

19 20

	% (19)	% (20)
a X = H	23	12
b X = CH_3	12	19
c X = Cl	49	0
d X = NO_2	65.5	0
e X = OCH_3	No reaction	No reaction

Can. J. Chem. Downloaded from www.nrcresearchpress.com by 210.87.254.6 on 09/05/12
For personal use only.

Can. J. Chem. Downloaded from www.nrcresearchpress.com by 210.87.254.6 on 09/05/12
For personal use only.

ring closure rather than cycloaddition. The i.r. and n.m.r. spectra of **20***a* and **20***b* indicated the presence of a concentration independent enolic OH. It is likely that it is the 5-aroyl group which is enolised since it then conjugates with the bridgehead nitrogen. Comparison of the n.m.r. spectra of **20***a* and **20***b* shows they are virtually identical except for the OH proton which appears at 5.90 δ in **20***a* and 6.14 δ in **20***b* as expected if this proton is adjacent to the aryl residue bearing the different substituents. A model shows that the OH group could be conveniently chelated to the 6-benzoyl group. 3-Methylbenzimidazolium phenacylide reacted with *trans*-dibenzoylethylene under these conditions to give the tricyclic structure **21** in 18% yield and no dihydrofuran while 3-methylbenzimidazolium 4′-nitrophenacylide yielded only dihydrofuran **19***d* in 45% yield.

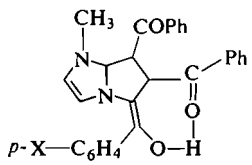

20*a* X = H
20*b* X = CH_3

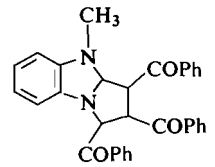

21

Compound **19***d* like **19***a* and **19***c* reported in a previous paper (2) underwent a ring transformation when treated with hydrazine to afford 3,5-diphenyl-8-(4′-nitrophenyl)-3,5,7-dihydropyridazino[4,5-*c*]pyridazine **22** in 30% yield. An attempt to force the isoquinolinium system to behave in a similar fashion (*i.e.* to eliminate isoquinoline) and form a dihydrofuran as in [5] failed in that only cycloadduct **23** was obtained in 55% yield analogous to products previously reported (2). The explanation for the sensitivity of the reaction's course to substituent effects in the case of the imidazole system seems to be twofold. First, as the X substituent becomes more electronegative, the enolate intermediate can more readily undergo ring closure owing to the increased partial positive charge adjacent to the heterocycle. Second, the degree of resonance energy in the imidazole system that must be overcome if cycloaddition is to occur is not as great as in the more aromatic pyridine but greater than in the isoquinoline system. The two effects, resonance energy and ease of elimination, are more nearly balanced in the imidazole system.

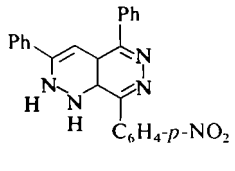

22

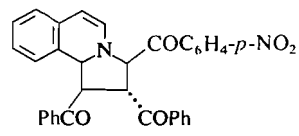

23

Although ring closure of functionalized 1,3-dipole adducts with hydrazine has proven to be a useful route to many fused heterocycles, attempts at the analogous Paal–Knorr condensations have in general met with only limited success (1–3). For example condensation of the carbonyl groups in **20***a* and **20***b* with isopropylamine was deemed plausible due to the ready formation of the enol and facile loss of water in the mass spectrum of the substrate. In the event, the amine reacted with only one carbonyl group (with loss of one molecule of H_2O) to give imines the structure of which (**24***a*, **24***b*) were determined by analysis of the mass spectrum. Detection of the fragments (*m/e* 199, $C_{12}H_{11}N_2O$), (*m/e* 185, $C_{11}H_9N_2O$), (*m/e* 290, $C_{20}H_{20}NO$), (*m/e* 272 $C_{17}H_{18}NO$), and (*m/e* 119, COC_6H_4-*p*-CH_3) rule out the two other possible isomers of **24**. In contrast to **20***a* and **20***b* the i.r. and n.m.r. spectra showed no trace of enolic OH. A space-filling model indicates that an enolic OH on the 5-aroyl group could not chelate to the imine nitrogen due to the steric hindrance of the isopropylmethine group. Compounds **24***a* and **24***b* are stable in refluxing toluene and show no tendency to complete the condensation.

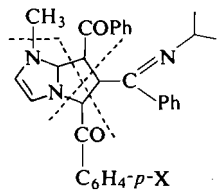

24*a* X = H
24*b* X = CH_3

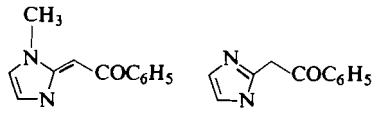

m/e 199 *m/e* 185

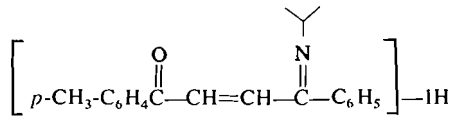

m/e 290

Can. J. Chem. Downloaded from www.nrcresearchpress.com by 210.87.254.6 on 09/05/12
For personal use only.

Experimental

Melting points were determined on a Fisher-Johns apparatus and are uncorrected. The i.r. spectra were recorded on a Perkin-Elmer 421 spectrophotometer. The n.m.r. spectra were recorded on Varian A-60, and A-100 spectrometers employing 10–15% solutions in $CDCl_3$ with tetramethylsilane as an internal standard. DMSO-d_6 was used for less soluble samples. Mass spectra were determined on Associated Electrical Industries MS-2 and MS-9 spectrometers. Peak measurements were made by comparison with perfluorotributylamine at a resolving power of 15 000. Microanalyses were carried out by Mrs. D. Mahlow of this department.

Materials

Phenylazophenacylpyridinium Betaine, 1a

This and the analogous *p*-chlorophenyl compound **1***b* were prepared by reacting the phenacylpyridinium bromides with benzenediazonium chloride according to the method of Krollpfeiffer and Braun (6*a*) in 35% yield, m.p. 120–121 °C (lit. (6) m.p. 122–123 °C).

3-Methyl-1-phenacylimidazolium Chloride

This and analogous salts were prepared by mixing equivalent amounts of the phenacyl chloride or bromide and 1-methylimidazole in tetrahydrofuran with continuous stirring for 12 h, followed by precipitation of the salt by addition of ether.

N-Benzoyl-N′-methylhydrazine

This compound was prepared in 6% yield from methylhydrazine and methyl benzoate, with the reflux period being 18 h, instead of 2 h as described by Hinman and Fulton (13). *N*-Acetyl-*N*′-phenylhydrazine was commercially available (Aldrich).

Cycloaddition Reactions with Azomethine Imines

Oppolzer's general procedure 'A' was employed in the synthesis of compounds **11**, **12**, and **13** (12). The preparation of **12** is described. To a solution of 3 g (12.7 mmol) of *trans*-dibenzoylethylene in 100 ml of toluene was added 1.5 g (10 mmol) of *N*-benzoyl-*N*′-methylhydrazine (13) and 0.4 g (13 mmol) of paraformaldehyde. The solution was refluxed 3 h through a Soxhlet thimble with molecular sieve, concentrated and the residue chromatographed on 100 g of Florisil with benzene to give 2.5 g (63% yield) of 1,4,5-tribenzoyl-2-methylpyrazolidine **12** as a yellow oil. Pyrazoline **13** was isolated in a similar manner and **11** precipitated from solution. The analytical and spectral data are summarized in Tables 1 and 2. Additional supportive data for the structures is provided by double irradiation experiments on pyrazolidines **11** and **12**.

Reaction of 1,4,5-Tribenzoyl-2-methyl-Δ^4-pyrazoline with Hydrazine

The pyrazoline **13** (1.8 g, 4.5 mmol) was dissolved in 20 ml of methanol, hydrazine (2 ml) was added, and the solution refluxed for 2 h. Removal of the solvent and excess hydrazine *in vacuo* and trituration with benzene – petroleum ether gave 1.6 g (90% yield) of 3-benzoyl-4,7-diphenyl-1-methylpyrazolo[1,5-*d*]-as-triazine **14** as a yellow oil. The mass spectrum contained major peaks at *m/e* 392 (molecular ion), 287 ($M - COC_6H_5$), 244 ($M - COC_6H_5 - CH_3 - N - CH_2$), 105 ($COC_6H_5$), and 77 ($C_6H_5$).

Cycloaddition Reactions with Nitrile Imines

This general procedure was developed for the synthesis of compounds **2***a*–**2***c*, **3***a*–**3***c*, **5**, **7**, and **8**. The representative preparation of **2***a* is described. To a solution of 2.36 g (10 mmol) of *trans*-dibenzoylethylene in 100 ml of benzene at reflux with stirring was added dropwise during 15 min a solution of 2.9 g (9.6 mmol) of phenylazophenacylpyridinium betaine in 60 ml of benzene. After a further 30 min at reflux the excess solvent was removed *in vacuo* and the residue subjected to column chromatography on 100 g of Florisil with 1:1 benzene – light petroleum as eluant. The first band to be eluted contained some dipole dimer (0.15 g), the second, eluted with 500 ml of benzene afforded 1.7 g (37% yield) of 1-phenyl-3,4,5-tribenzoyl-Δ^2-pyrazoline **2***a* as yellow powdery crystals m.p. 157–160 °C. The third dark band eluted with chloroform and 5% ethanol gave 2.2 g (48% yield) of 1-phenyl-3,4,5-tribenzoylpyrazole **3***a* as a red oil. Analytical and spectral data are summarized in Tables 1 and 2. The corresponding pyrazoles could be obtained from the pyrazolines by refluxing with one equivalent of *p*-chloranil in benzene as previously described (1).

Reactions of 1,4-Dicarbonyl Compounds with Hydrazine

Pyridazines **4***a*–**4***c*, **9**, and **18** were prepared in the following manner. 1-Phenyl-3,4,5-tribenzoylpyrrole (2 g, 4.4 mmol) was dissolved in 20 ml of 90% ethanol. Hydrazine (2 ml, 94%, 60 mmol) was added and the solution heated under reflux for 18 h. The pyridazine **4***a* was obtained upon trituration of the ethanolic solution with water in 69% yield (1.35 g). Spectral and analytical data are tabulated.

Compound	Proton irradiated	Decoupling frequency (Hz)	Lines collapsed		Measured remaining coupling
			Original form	Final form	
11	H_d	555	t, 3.88 (H_c)	d	$J_{ac} = 7.8$
	H_b	447	q, 3.61 (H_a)	d	$J_{ac} = 7.8$
	H_c	388	d, 5.55 (H_d)	s	—
	H_a	361	d, 4.97 (H_b)	s	—
12	H_d	650	q, 4.75 (H_c)	t	$J_{ac} = 8.0$, $J_{bc} = 7.0$
	H_c	475	d, 6.50 (H_d)	s	
	H_c	475	m, 3.4–6 (H_aH_b)	d,d	
	H_aH_b	341	q, 4.75 (H_c)	d	$J_{cd} = 7.0$

Can. J. Chem. Downloaded from www.nrcresearchpress.com by 210.87.254.6 on 09/05/12
For personal use only.

TABLE 1. Analytical data on new heterocycles

Compound		Melting point (°C)	Yield (%)	Calculated				Found			
				C	H	N	Molecular ion[a]	C	H	N	Molecular ion[a]
2*a*	$C_{30}H_{22}N_2O_3$	157–160[b]	37	78.54	4.83	6.11	458.1630	78.40	4.93	6.07	458.1639
3	$C_{30}H_{20}N_2O_3$	oil	48	—	—	—	456.1475	—	—	—	456.1488
4	$C_{30}H_{20}N_4O$	135–138[b]	69	—	—	—	452.1637	—	—	—	452.1625
2*b*	$C_{30}H_{21}N_2O_3Cl$[e]	155–158[b]	38	73.09	4.29	5.68	492.1240	75.84	4.27	4.40	492.1248
3*b*	$C_{30}H_{19}N_2O_3Cl$	oil	57	—	—	—	490.1092	—	—	—	490.1098
3*c*	$C_{29}H_{20}N_2O_2$	oil	28	—	—	—	428.1525	—	—	—	428.1514
4*b*	$C_{30}H_{19}N_4OCl$	oil	68	—	—	—	486.1248	—	—	—	486.1252
4*c*	$C_{29}H_{20}N_4$	oil	100	—	—	—	424.1688	—	—	—	424.1679
4*d*	$C_{30}H_{19}N_4OCl$	oil	68	—	—	—	486.1248	—	—	—	486.1252
5	$C_{24}H_{17}N_3O_3$	225–227[b]	53	—	—	—	395.1270	—	—	—	395.1279
7	$C_{20}H_{18}N_2O_5$	oil	19	—	—	—	366.1216	—	—	—	366.1207
8	$C_{20}H_{16}N_2O_5$	oil	39	—	—	—	364.1060	—	—	—	364.1068
9	$C_{18}H_{14}N_6O_2$	300–301	35	62.40	4.08	24.25	346.1178	61.48	4.32	23.36	346.1171
11	$C_{19}H_{17}N_3O_3$	200–202	5	—	—	—	335.1270	—	—	—	335.1280
12	$C_{25}H_{22}N_2O_3$	oil	63	—	—	—	398.1629	—	—	—	398.1632
13	$C_{25}H_{20}N_2O_3$	oil	63	—	—	—	396.1473	—	—	—	396.1478
14	$C_{25}H_{24}N_4O$	oil	90	—	—	—	392.1627	—	—	—	392.1628
15	$C_{20}H_{18}N_2O_4$	oil	23	—	—	—	350.1266				350.1260
16	$C_{20}H_{16}N_2O_4$	180–181	64	68.98	4.63	8.05	348.1110	69.14	4.63	8.24	348.1107
17	$C_{10}H_{12}N_2O_6$	oil	60	—	—	—	256.0694	—	—	—	256.0707
18	$C_6H_6N_6O_3$	>320[c]	90	—	—	40.01	210.0501	—	—	42.32	210.0504
19*b*	$C_{25}H_{20}O_3$	oil[d]	12	—	—	—	368.1413	—	—	—	368.1426
19*d*	$C_{24}H_{17}NO_5$	172–175	65.5	72.17	4.29	3.51	399.1106	72.15	4.41	3.58	399.1050
20*a*	$C_{28}H_{24}N_2O_3$	180–181	12	—	—	—	436.1787	—	—	—	436.1771
20*b*	$C_{29}H_{26}N_2O_3$	186–188	19	77.30	5.82	6.22	450.1943	77.46	5.93	6.22	450.1930
21	$C_{32}H_{26}N_2O_3$	oil	18	—	—	—	486.1939	—	—	—	486.1935
22	$C_{24}H_{19}N_5O_2$	159–160	30	67.42	4.95	16.39	409.1539	67.05	4.91	16.29	409.1531
23	$C_{33}H_{24}N_2O_5$	193–195	55				528.1688				528.1668
24*a*	$C_{31}H_{31}N_3O_2$	oil	18	—	—	—	477.2416	—	—	—	477.2428
24*b*	$C_{32}H_{33}N_3O_2$	oil	55	—	—	—	491.2573	—	—	—	491.2250

[a]Mass spectrum.
[b]Readily dehydrogenates, difficult to purify.
[c]Does not melt at temperatures ≤ 320 °C.
[d]**19***a* and **19***c* are reported in previous papers (1, 2).
[e]Anal. calcd. for Cl, 7.19; found Cl, 7.32.

Can. J. Chem. Downloaded from www.nrcresearchpress.com by 210.87.254.6 on 09/05/12
For personal use only.

TABLE 2. Spectral data

Compound	Infrared spectra (cm^{-1})	Nuclear magnetic resonance spectra (δ relative to TMS)		
		Ar—H	NH—OH	R—H
2*a*	1685 (C═O)[a]	7–8.2, m, 20H[c]	—	6.10, 5.45, ABq, 2H, J = 7.5 Hz (H_4, H_5)
3	1680 (C═O)[a]	7–8.2, m[c]	—	—
3*c*	1680 (C═O)[a]	7.2–8.0, m, 20H[c]	—	—
4	1680 (C═O)[a]	7–7.8, m[c]	—	—
2*b*	1685 (C═O)[a]	7–8, m, 19H[c]	—	6.11, 5.42, ABq, 2H, J = 7.5 Hz (H_4, H_5)
3*b*	1680 (C═O)[a]	7–8, m[c]	—	—
4*b*	1680 (C═O)[a]	7–8, m[c]	—	—
5	1720, 1620 (C═O)[a]	7–8, m, 10H[c]	—	5.34, 5.52, ABq, 2H, J = 6.0 Hz, (H_4, H_5)
7	1745 (C═O)[a]	7–8.3, m, 10H[c]	—	5.20, 4.64, ABq, 2H, J = 6.0 Hz; 3.74, s, 3H, (OCH_3)
8	1750 (C═O)[a]	7–8.3, m, 10H[c]	—	3.90, s, 3H (OCH_3)
9	1670 (C═O), 3180, 3300 (NH)[b]	7.4–8.3, m, 10H[d]	4–6, s, b, (4NH)	—
11	1685, 1725 (C═O)[a]	6.4–7.5, m, 10H[d]	—	5.55, d, 1H, J_{cd} = 7.8 Hz (H_d); 4.47, d, 1H, J_{ab} = 12 Hz (H_b); 3.88 t, 1H, J_{cd} = 7.8, J_{ac} = 7.8 (H_c); 3.61, q, 1H, J_{ab} = 12 Hz, J_{ac} = 7.8 Hz, (H_a); 2.10, s, 3H, (CH_3)
12	1680 (C═O)[a]	7–8.2, m, 15H[c]	—	6.50 d, 1H, J_{cd} = 8 Hz (H_d); 4.75 q, 1H, J_{cd} = 7, J_{ac} = 8 Hz (H_c); 3.5 m, 2H, (H_aH_b); 2.69 s, 3H (CH_3)
13	1675 (C═O)[a]	7–8, m, 15H[c]	—	5.18 s, 2H (H_a, H_b); 3.14 s, 3H (CH_3)
14	1675 (C═O)[a]	7–8.2 m, 15H[c]	—	4.50, s, 2H (H_a, H_5); 2.71, s, 3H (CH_3)
15	1740, 1680 (C═O) 3400 (NH)[a]	7–8, m, 10H[c]	—[g]	5.70, 4.68, ABq, 2H, J = 8.0 Hz; 4.28, q, 2H, J = 8.0 Hz (OCH_2CH_3); 1.30, t, 3H, J = 8.0 Hz (CH_3)
16	1670, 1720 (C═O)[a] 3400, 3250 (NH)	7.2–8.2, m, 10H[c]	—[g]	4.20, q, 2H, J = 8.0 Hz (OCH_2CH_3); 1.02, t, 3H, J = 8.0 Hz (CH_3)

Can. J. Chem. Downloaded from www.nrcresearchpress.com by 210.87.254.6 on 09/05/12
For personal use only.

TABLE 2 (*Concluded*)

Compound	Infrared spectra (cm^{-1})	Nuclear magnetic resonance spectra (δ relative to TMS)		
		Ar—H	NH—OH	R—H
17	3400, 3250 (NH) 1730 (C=O)[a]	—[c]	3.8, s, b, ($\frac{2}{3}$NH)	7.33, s, $\frac{1}{3}$H (H_3); 4.38, q, 2H, J = 8.0 Hz, (OCH_2-CH_3); 3.9, 3.92, s, s, 6H (OCH_3); 1.33, t, 3H, J = 8.0, (CH_3)
18	3250, 3150 (NH)[b]	—[d]	6.1, s, b, (NH)	—
19*b*	1680 (C=O)[a]	7–8, m, 19H[d]	—	2.38, s, 3H, (CH_3)
19*d*	1630 (C=O) 1340, 1535 (NO_2)[b]	7–8, m[d]	—	—
20*a*	3370 (OH)[e] 1680 (C=O)[a]	7.2–8, m, 17H[c]	5.90, s, b, (OH)	7.04, 6.83, ABq, 2H, J = 1.2 Hz (H_5H_6); 6.66, s, (H_{6a}); 3.32, s, 3H (CH_3)
20*b*	3370 (OH)[e] 1680 (C=O)[a]	7.2–8, m, 16H[c]	6.14, s, b, (OH)	7.06, 6.86, ABq, 2H, J = 1.2 Hz (H_5, H_6); 6.68, s, (H_{6a}); 3.34, s, 3H (CH_3); 2.38, s, 3H (Ar—CH_3)
21	3350 (OH) 1680 (C=O)[a]	7–8 m, 23H[c]	—	3.52, s, 3H (CH_3)
22	1350, 1535 (NO_2)[b,f]	7.2–8.2, m, 17H[d]	—[h]	2.02, 2.08 ABq, J = 4.5 Hz (H_{4a}, H_{8a})
23	1680 (C=O) 1350, 1520 (NO_2)[b,f]	—		—
24*a*	1650 (C=O)[a]	6.6–8.5, m, 20H[c]	—	4.03, s, N—CH_3; 3.3, m, 1H ($CH(CH_3)_2$); 1.2, m, 6H (CH_3)
24*b*	1648 (C=O)[a]	6.6–8.5, m, 19H[c]	—	4.03, s, N—CH_3; 3.3, m, 1H ($CH(CH_3)_2$); 1.2, m, 6H, (CH_3); 2.36, s, 3H (CH_3)

[a]In $CHCl_3$.
[b]As a Nujol mull.
[c]In $CDCl_3$.
[d]In DMSO-d_6.
[e]No concentration dependence.
[f]Insufficiently soluble for n.m.r. The spectra of similar cycloadducts are reported in a previous paper.
[g]No NH evident in n.m.r.
[h]OH and methines obscured by Ar—H.

Can. J. Chem. Downloaded from www.nrcresearchpress.com by 210.87.254.6 on 09/05/12
For personal use only.

Cycloaddition Reactions of Ethyl Diazoacetate

Reaction with trans-Dibenzoylethylene

Ethyl diazoacetate (2.28 g, 20 mmol) and 4.72 g (20 mmol) of *trans*-dibenzoylethylene were heated in 50 ml of benzene at 50 °C for 18 h. Chromatography on 100 g of Florisil with benzene afforded in successive fractions, 1 g of *trans*-dibenzoylethylene, 1.35 g of the pyrazoline **15** (23% yield) as an orange oil and 0.5 g of the pyrazole **16** (8% yield), m.p. 180–181 °C in the third fraction eluted with chloroform and 5% ethanol.

Reaction with Dibenzoylacetylene and Dimethyl Acetylenedicarboxylate

Ethyl diazoacetate and dibenzoylacetylene (10 mmol each) were warmed in 50 ml of benzene at 40 °C for 2 h. After 1 h the product began to precipitate out. The precipitation was completed by adding an equal volume of hexane to give **16** in 64% yield. Reaction with dimethyl acetylenedicarboxylate afforded in the same manner a 60% yield of **17** as an orange oil after purification by chromatography (Florisil–benzene).

Reaction of Imidazolium Phenacylides with trans-Dibenzoylethylene

1-Phenacyl-3-methylimidazolium chloride (2.36 g, 10 mmol) and 2.36 g (10 mmol) of *trans*-dibenzoylethylene were stirred in 100 ml of pyridine at 40 °C when 3 ml (25 mmol) of triethylamine was added. The solution darkened and was stirred for 2 h at 50 °C. The solvent was removed *in vacuo* and the solution filtered to remove triethylamine hydrochloride. The remaining pyridine was evaporated, 10 ml of benzene was added to the residue and this solution subjected to chromatography on 100 g of Florisil with benzene as eluant. The first band gave 0.55 g of 4,5-dihydro-2-phenyl-4,5-dibenzoylfuran, **19***a* (16% yield), m.p. 119–121 °C (lit. (2) m.p. 116–119 °C). The second band, eluted with chloroform and 2% ethanol gave 4,5,6,6a-tetrahydro-1-methyl-4,5,6-tribenzoyl-1,3a-diazapentalene **20***a* as tan crystals from benzene (0.5 g, 12% yield) m.p. 180–181 °C. Compounds **19***b* and **20***b* were prepared and isolated in the same fashion in 12 and 19% yields respectively. The mass spectrum of **20***b* contained major peaks at *m/e* 450 (molecular ion), 432 ($M - H_2O$), 415, 399 ($M - 51$), 373 ($M - C_6H_5$), 345 ($M - COC_6H_5$), 331 ($M - COC_6H_4 - CH_3$), 313, 296, 264 ($M - 186$), 199 ($C_{12}H_{11}N_2O$), 185 ($C_{11}H_9N_2O$), 157, 199 ($COC_6H_4CH_3$), 105 (COC_6H_5), 91 ($C_6H_4CH_3$), 77 (C_6H_5).

Mass measurements. Calcd. for $C_{29}H_{26}N_2O_3$: 450.1943; found: 450.1930. Calcd. for $C_{12}H_{11}N_2O$: 199.0870; found: 199.0855. Calcd. for $C_{11}H_9N_2O$: 185.0714; found: 185.0715.

Reaction of Isoquinolinium p-Nitrophenacylide with trans-Dibenzoylethylene

p-Nitrophenacylisoquinolinium bromide (3.73 g, 10 mmol) and 2.36 g (10 mmol) of dibenzoylethylene in 100 ml of pyridine were heated to 50 °C and 3 ml (25 mmol) of triethylamine was added. The mixture turned dark and was stirred for 2 h at 50 °C, cooled and concentrated to half volume, filtered and then further concentrated. The residue was crystallized from benzene–hexane to give **23**, 2.8 g (52% yield), m.p. 182–183 °C. A further 0.15 g (3%) could be obtained by chromatography of the mother liquor on 100 g of Florisil with benzene as eluant. Spectral and analytical data of **23** are in Tables 1 and 2. The compound was insufficiently soluble in DMSO-d_6 to afford an n.m.r. spectrum.

Attempted Paal–Knorr Condensations

(*a*) Compound **20***b* (1 g, 2.2 mmol) in 20 ml of methanol was stirred 3 days at 40 °C with 5 ml (65 mmol) of isopropylamine in a stoppered flask. The solvent was removed *in vacuo* and the residue subjected to Florisil chromatography employing as the eluant a solution of chloroform and 2% ethanol affording **24***b*, 0.6 g of an orange oil (55% yield). The mass spectrum contained the following major peaks *m/e* 491 (M), 448 ($M - C_3H_7$), 434 ($M - N - C_3H_7$), 361, 330 ($435 - C_6H_5CO$), 303, 290 ($C_{20}H_{20}NO$), 276 ($C_{19}H_{18}NO$), 199 ($C_{12}H_{11}N_2O$), 157, 119 ($COC_6H_4CH_3$), 105 (COC_6H_5), 91 ($C_6H_4CH_3$), 77 (C_6H_5), 51, 43 (C_3H_7).

Mass measurements. Calcd. for $C_{32}H_{33}N_3O_2$: 491.2573; found: 491.2250. Calcd. for $C_{20}H_{20}NO$: 290.1545; found: 290.1532. Calcd. for $C_{19}H_{18}NO$: 276.1388; found: 276.1356. Calcd. for $C_{11}H_9N_2O$: 185.0714; found: 185.0722. Calcd. for $C_{12}H_{11}N_2O$: 199.0870; found: 199.0860.

(*b*) Compound **20***a* (1 g, 20 mmol) was subjected to similar reaction conditions to afford the imine **24***a*, 0.2 g (18% yield). Both imines are subject to hydrolysis on the column to afford some starting material. Neither imine reacted further in refluxing toluene.

This research was supported by the National Research Council of Canada and the Chemistry Department of the University of Alberta.

1. J. W. LOWN and B. E. LANDBERG. Can. J. Chem. **52**, 798 (1974).
2. B. E. LANDBERG and J. W. LOWN. J. Chem. Soc. Perkin Trans. 1, 1326 (1975).
3. J. W. LOWN and M. H. AKHTAR. Can. J. Chem. **50**, 2236 (1972).
4. J. W. LOWN and M. H. AKHTAR. J. Chem. Soc. Perkin Trans. 1, 1459 (1972).
5. R. HUISGEN. Angew. Chem. Int. Ed. Engl. **2**, 565 (1963).
6. (*a*) F. KROLLPFEIFFER and E. BRAUN. Chem. Ber. **70**, 89 (1937); (*b*) R. HUISGEN, E. AUFDERHAAR, and G. WALLBILLICH. Chem. Ber. **98**, 1476 (1965); (*c*) R. HUISGEN, K. ADELSBERGER, E. AUFDERHAAR, H. KNUPFER, and G. WALLBILLICH. Monatsch. Chem. **98**, 1618 (1967).
7. E. BUCHNER. Chem. Ber. **21**, 2637 (1888).
8. T. L. JACOBS. *In* Heterocyclic compounds. Vol. 5. *Edited by* R. C. Elderfield. Wiley, New York. 1957. p. 72.
9. O. METH-COHN. Tetrahedron Lett. 413 (1975).
10. C. STUCKWISCH. Synthesis, 469 (1973).
11. T. SASAKI, K. KANEMATSU, and Y. YAKIMOTO. J. Chem. Soc. C, 481 (1970).
12. W. OPPOLZER. Tetrahedron Lett. 2199 (1970).
13. R. HINMAN and J. FULTON. J. Am. Chem. Soc. **80**, 1895 (1958).
14. E. BUCHNER. Ber. Dtsch. Chem. Ges. **22**, 842 (1889).

Single Crystal Electron Spin Resonance of Low Spin Co(II) and of Cu(II) Schiff Base Complexes

V. MALATESTA AND B. R. MCGARVEY

Department of Chemistry, University of Windsor, Windsor, Ontario N9B 3P4

Received June 9, 1975

V. MALATESTA and B. R. MCGARVEY. Can. J. Chem. **53**, 3791 (1975).

Single crystal e.s.r. studies have been done on *N,N'*-ethylenebis(*o*-aminobenzylideniminato)-nickel(II) and *N,N'*-ethylenebis(benzoylacetoniminato)nickel(II) doped with the corresponding Co(II) and Cu(II) complexes. It is shown for the cobalt(II) complexes that the unpaired electron is in a d_{yz} orbital and that the d orbitals are arranged (d_{xz}), ($d_{x^2-y^2}$), (d_{z^2}), (d_{yz}), (d_{xy}) in order of increasing energy with the $d_{x^2-y^2}$, d_{z^2}, and d_{yz} orbitals being close together. The large energy separation between the d_{xz} and d_{yz} orbitals which is found in the cobalt(II) complexes is not observed in the corresponding copper(II) complexes. ^{14}N hyperfine constants were measured for both copper(II) complexes.

V. MALATESTA et B. R. MCGARVEY. Can. J. Chem. **53**, 3791 (1975).

On a fait des études r.p.e. de cristaux uniques du *N,N'*-éthylène bis(*o*-aminobenzylidèniminato) nickel(II) et du *N,N'*-éthylène bis(benzoylacétoniminato) nickel(II) dopés avec les complexes correspondants du Co(II) et du Cu(II). On a montré, dans le cas des complexes du Co(II), que l'électron non pairé occupé l'orbitale d_{yz} et que les orbitales d sont arrangées par ordre croissant d'énergie (d_{xz}) < ($d_{x^2-y^2}$) < (d_{z^2}) < (d_{yz}) < (d_{xy}) et que les trois orbitales centrales sont près les unes des autres. La grande séparation d'énergie qui est trouvée entre les orbitales d_{xz} et d_{yz} des complexes du cobalt(II) ne se retrouve pas dans les complexes correspondants du cuivre(II). On a mesuré les constantes hyperfines du ^{14}N pour les deux complexes du cuivre.

[Traduit par le journal]

Introduction

Many e.s.r. studies of four and five coordinate Schiff base complexes of low spin Co(II) have been reported in the past few years (1–10). The aim of many of these studies was to determine the ground state by comparing the spin Hamiltonian parameters predicted by theory for different ground states to the experimental parameters. Two difficulties associated with most of these studies have prevented a definitive determination of the ground states. First, with one exception (1), all of the work has been done on frozen solutions and powders in which it is not possible to assign the three g and A values in the spin Hamiltonian to specific molecular axes. Two studies (2, 5) have used frozen nematic solutions in an attempt to identify the axes but they disagreed as to which molecular axis will be the aligning axis in the liquid crystal. Second, the theory used to predict spin Hamiltonian parameters did not properly account for the large distortions from axial symmetry found in these complexes and the contribution of low lying excited quartet states to the g and A values.

Recently, the theory for the spin Hamiltonian of low spin d^7 complexes was reinvestigated (11) and the contribution of low lying quartet states was examined. Also, the effect of possible configuration interaction between d_{z^2} and $d_{x^2-y^2}$ orbitals in the $^2A_1$ state was considered for low symmetry complexes. For the low spin symmetry complexes studied here, it was found that an unambiguous assignment of ground states on the basis of g and ^{59}Co hyperfine splitting values alone is difficult in most cases due to the large number of variable parameters and is certainly impossible if the correct assignment to molecular axes is not known. The complexes considered here are four coordinate square planar complexes and the z direction is taken to be normal to the plane of the complex. In all cases the symmetry of the complex requires that the x and y axes bisect two cobalt ligand bonds. For this type of complex only two ground states need be considered, both of which have the d_{xy} orbitals unoccupied. One state is the $^2B_2$ state in which the unpaired electron occupies a d_{yz} orbital. The $^2B_1$ state in which the unpaired electron occupies a d_{xz} orbital is identical to the $^2B_2$ if one interchanges the x and y labels for the axes. The second state is the $^2A_1$ state in which the unpaired electron is in the ($ad_{z^2} + bd_{x^2-y^2}$) orbital

Can. J. Chem. Downloaded from www.nrcresearchpress.com by 210.87.254.40 on 09/05/12
For personal use only.

Can. J. Chem. Downloaded from www.nrcresearchpress.com by 210.87.254.40 on 09/05/12
For personal use only.

and b can vary from zero to unity in the low symmetry complexes and is a parameter to be fitted against experimental results. It was shown (11) that the relative values of g_y and g_z seem to provide a good indicator of which state is the correct one with $g_z > g_y$ for the $^2B_2$ state and $g_y > g_z$ for the $^2A_1$ state. Thus, it has become clear that only single crystal e.s.r. studies, in which the orientation of at least the z molecular axis is known, are essential if one hopes to determine the ground state.

Five single crystal studies of low spin Co(II) complexes are known to the authors (1, 12–15) and only two (1, 15) are of complexes having oxygen and nitrogen bonding to the cobalt ion. Zelewsky and Fierz (1) in their study of *N,N'*-ethylenebis(salicylideneiminato)cobalt(II), [Co(salen)], claimed that only a $^2B_2$ ground state would explain their results but they provided no details. Chacko and Manoharan (15) also claimed a $^2B_2$ ground state for bis[1-methyl-3-(2-chloro-6-methyl)phenyltriazine-1-oxide]cobalt(II), [Co(BPT)], but the crystal structure of their host lattice Ni(BPT) is unknown so that they could not be certain about their assignment of molecular axes.

We have succeeded in growing crystals of *N,N'*-ethylenebis(*o*-aminobenzylideniminato)nickel(II), [Ni(amben)], and *N,N'*-ethylenebis(benzoylacetoniminato)nickel(II), Ni[(benacacen)], into which the corresponding complexes of Co(II) and Cu(II) have been doped. The e.s.r. study of the copper complexes was undertaken primarily to determine the orientation of the complexes in the crystal since the crystal structure of both systems has not yet been done. The copper resonances for these complexes are always nearly axial with the axis perpendicular to the molecular plane. As will be seen, the results on ^{14}N hyperfine interactions in the copper complexes will be useful in interpreting the results for the cobalt complexes. In Fig. 1 is given the molecular structure for both complexes and the location of the x and y axes.

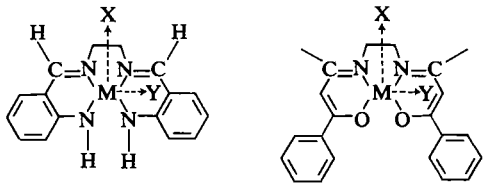

a *b*

FIG. 1. (*a*) Structure of M(amben); (*b*) Structure of M(benacacen). M = Co, Cu.

Experimental

Preparation of Complexes

All solvents were carefully dried and stored under nitrogen. Particular care was taken with *N,N'*-dimethylformamide which was distilled *in vacuo* and stored over molecular sieves (4-A) in a nitrogen atmosphere. The reagents, 1-benzoylacetone, ethylenediamine, cobalt(II), nickel(II), copper(II) acetates were obtained commercially and used without further purification. *Ortho*-aminobenzaldehyde was prepared by the method described by Smith and Opie (16). Preparation and manipulation of cobalt complexes were carried out under an atmosphere of prepurified nitrogen to prevent formation of cobalt(II)-O_2-peroxycobalt(II) species.

Ni(amben), Co(amben), and Cu(amben) were prepared by the method of Green and Tasker (17). The complexes of Ni(benacacen), Co(benacacen), and Cu(benacacen) were prepared according to Everett and Holm (18).

Growth of Crystals

Ni(amben) crystals doped with approximately 2% Co(II) or 1% Cu(II) were prepared by slow evaporation of degassed dimethylformamide solutions. Dark red flat hexagonal crystals (Fig. 2) were obtained after several days. Dark red crystals of Ni(benacacen) doped with Co(II) and Cu(II) were grown from dichloromethane solutions. Dichloromethane was deaerated with a stream of nitrogen gas at room temperature for 1 h before solutes were added. Growth of crystals took place under an atmosphere of prepurified nitrogen. Hexagonal crystals in the shape depicted in Fig. 2 were obtained.

Electron Spin Resonance

Electron spin resonance spectra were taken with a Varian E-12 spectrometer having a rotating cylindrical cavity and a rotating magnet. Single crystals were mounted on a quartz rod along the axes labelled 1, 2, and 3 in Fig. 2 and spectra taken every 15° for a rotation of the magnetic field in the plane perpendicular to the mounting axis. A speck of DPPH was used to calibrate the klystron frequency. The magnetic field was calibrated by a proton n.m.r. spectrometer. All spectra were taken at room temperature with the exception of that for (Ni, Co)(benacacen) which were taken at liquid nitrogen temperature because

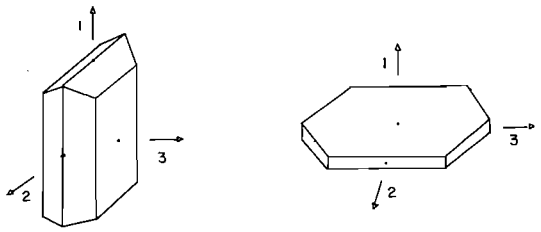

a b

FIG. 2. (*a*) Crystal habit of Ni(benacacen) and location of three rotation axes. (*b*) Crystal habit of Ni(amben) and location of three rotation axes.

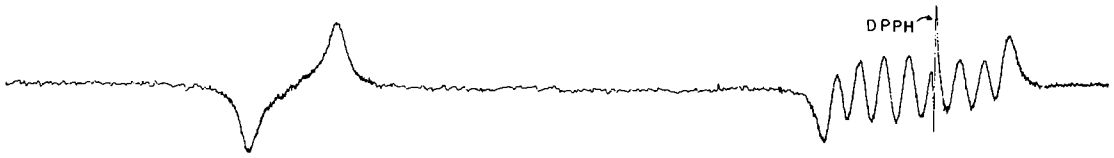

FIG. 3. Electron spin resonance spectrum of (Ni, Co)(amben).

Can. J. Chem. Downloaded from www.nrcresearchpress.com by 210.87.254.40 on 09/05/12
For personal use only.

spin–lattice relaxation times for this Co(II) complex were too short at room temperature to give narrow lines in the spectra.

Results

The e.s.r. results have been fitted to the spin Hamiltonian

$$[1]\quad \mathcal{H} = \beta[g_xH_xS_x + g_yH_yS_y + g_zH_zS_z] + A_xS_xI_x + A_yS_yI_y + A_zS_zI_z + \sum_i [{}^{N}A_iS_zI_{zi} + {}^{N}B_i(S_xI_{xi} + S_yI_{yi})]$$

where A_x, A_y, and A_z are the hyperfine terms for the central metal nucleus and ${}^{N}A$ and ${}^{N}B$ are the nitrogen nuclear hyperfine terms which were resolved in the case of the copper complexes. In this study, the principal axes for the g and A tensors were found to be the same within experimental error for all complexes. For the nitrogen hyperfine terms the z direction for each nucleus is along the copper nitrogen bond.

M(amben)

For this system a pair of resonances from magnetically inequivalent complexes was observed only in the 23 planes, the two resonances becoming equivalent in the 12 and 13 planes. Further, one principal axis was along the 1 axis for both pairs. From the work of Weil *et al.* (19) we learn that this behavior indicates that the crystal is orthorhombic. Both the copper and cobalt crystals were studied at room temperature as it was found that the e.s.r. spectra for the Co(II) crystal did not display any appreciable line narrowing at liquid nitrogen temperatures. Representative spectra for Co(II) and Cu(II) doped crystals are given in Figs. 3 and 4. The copper resonance consisted of four sets of nine lines due to the hyperfine interaction of one copper nucleus ($I = \frac{3}{2}$) and four nearly equivalent nitrogen nuclei ($I = 1$). The hyperfine interaction of ^{65}Cu was not resolved from that of ^{63}Cu.

The spin Hamiltonian parameters for both Co(II) and Cu(II) complexes are given in Table 1. The orientation of the principal axes for g and A tensors is given by the two polar angles θ and ϕ where θ is the angle between the axis and crystal axis 1 and ϕ is the angle which the projection in the 23 plane makes with axis 2 of the crystal. The axis normal to the molecular plane or z axis is taken to be that axis with the large g value and A value in the copper system and is found to be in the 23 plane of the crystal. The x axis has been assigned by an analogy with similar Co(II) complexes (1, 13, 14) in which the large g value is always associated with the x axis. The growth habits of this crystal also support this assignment, since growth of the crystal along the long axis or y axis of molecule would be poor, which is the case for the 1 axis of the crystal.

The Co(II) results agree as well as can be expected with the powder results of Engelhardt *et al.* (10) but their assignment of g_z is in error. The assignment of xyz axes does agree with that of Urbach *et al.* (5), who studied related Co(II) complexes in frozen nematic solutions.

M(benacacen)

For this system a pair of resonances from magnetically inequivalent complexes was observed in both the 12 and 13 planes with both resonances becoming equivalent in the 23 plane. Since all three tensor components are different and have different orientations for the inequivalent pairs we deduce from Weil *et al.* (19) that the host crystal is monoclinic. The copper crystal was studied at room temperature, but it was necessary to study the Co(II) crystal at liquid nitrogen temperatures to obtain narrow lines in the spectrum. Representative spectra are given in Figs. 5 and 6. The copper resonance has four sets of five lines due to hyperfine interaction of one copper nucleus and two equivalent nitrogen nuclei. In Fig. 6 the outside copper

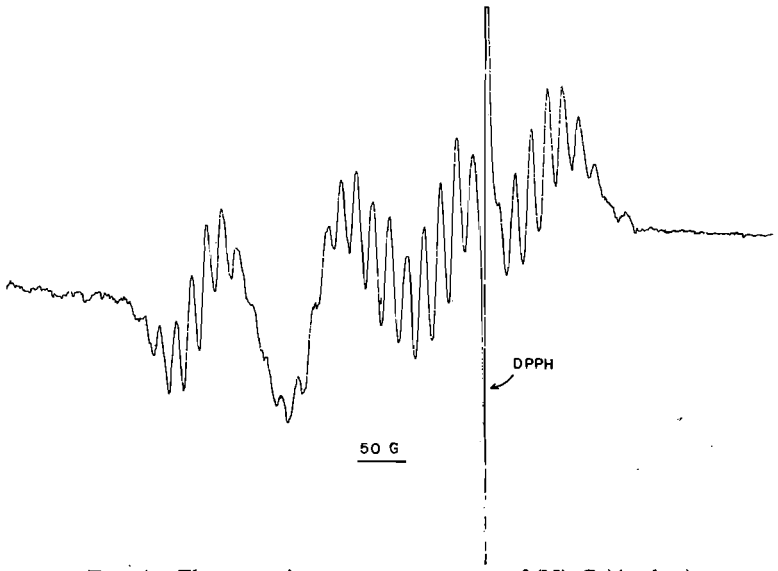

FIG. 4. Electron spin resonance spectrum of (Ni, Cu)(amben).

TABLE 1. Spin Hamiltonian parameters for Co(II) and Cu(II) complexes doped into corresponding Ni(II) crystals

Parameter	Value			
	Co(amben)	Co(benacacen)	Cu(amben)	Cu(benacacen)
g_x	2.6586 ± 0.0006	3.372 ± 0.002	2.038 ± 0.002	2.040 ± 0.001
g_y	1.9814 ± 0.0007	1.882 ± 0.001	2.038 ± 0.001	2.033 ± 0.001
g_z	2.0068 ± 0.0010	1.954 ± 0.006	2.1489 ± 0.0005	2.1857 ± 0.0005
$A_x(10^{-4}\ cm^{-1})$	3.5 ± 0.2	165.6 ± 0.2	57 ± 7	30.4 ± 0.4
$A_y(10^{-4}\ cm^{-1})$	29.5 ± 0.1	37 ± 5	48.1 ± 0.2	43.7 ± 0.4
$A_z(10^{-4}\ cm^{-1})$	24.0 ± 0.1	47 ± 5	205.4 ± 0.1	200.1 ± 0.1[a]
$^{N}A(10^{-4}\ cm^{-1})$	—	—	18.6 ± 0.5	17.5 ± 0.4[a]
$^{N}B(10^{-4}\ cm^{-1})$	—	—	14.9 ± 0.5	13.1 ± 0.4[a]
θ_x	90°	106 ± 1°	90°	89 ± 20°
ϕ_x	114 ± 2°	105 ± 1°	116 ± 2°	141 ± 30°
θ_y	0°	55 ± 5°	0°	66 ± 20°
ϕ_y	—	184 ± 5°	—	232 ± 30°
θ_z	90°	38 ± 5°	90°	24 ± 2°
ϕ_z	24 ± 2°	37 ± 5°	26 ± 2°	48 ± 2°

[a]For ^{63}Cu isotope.

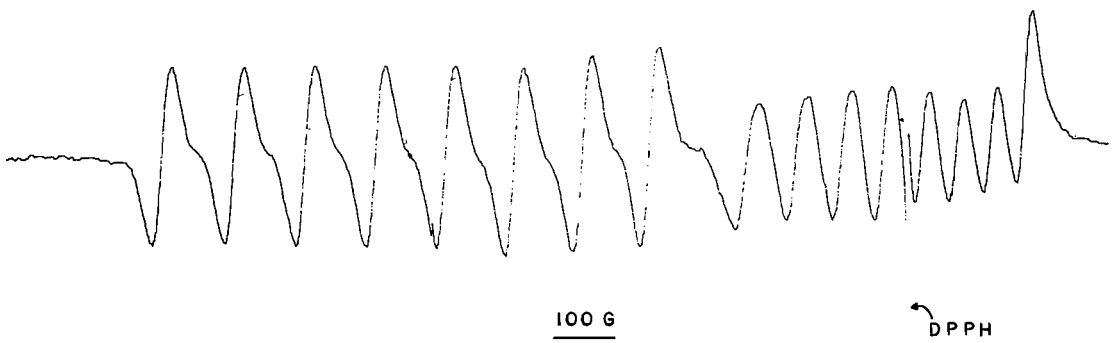

FIG. 5. Electron spin resonance spectrum of (Ni, Co)(benacacen).

Can. J. Chem. Downloaded from www.nrcresearchpress.com by 210.87.254.40 on 09/05/12
For personal use only.

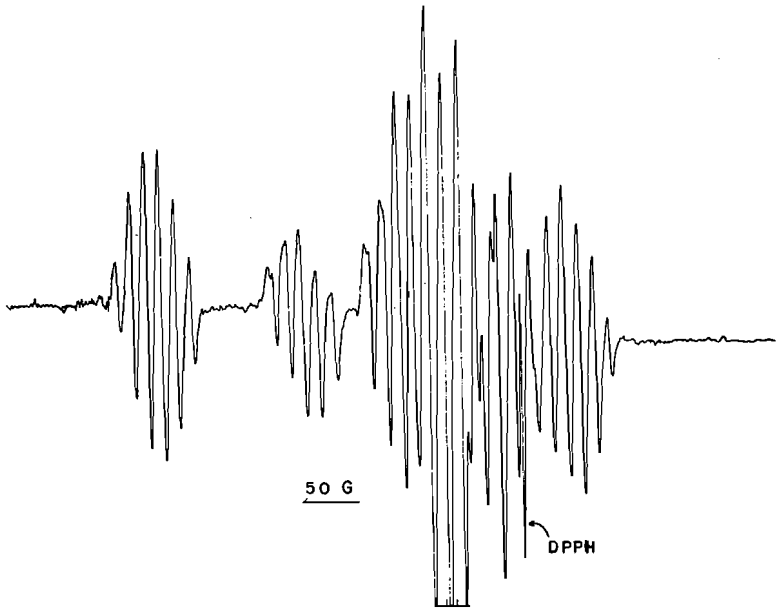

FIG. 6. Electron spin resonance spectrum of (Ni, Cu)(benacacen).

hyperfine lines are seen to consist of six lines due to partial resolution of ^{65}Cu hyperfine lines from those due to ^{63}Cu. We analyzed only the ^{63}Cu lines.

The spin Hamiltonian parameters for both Co(II) and Cu(II) complexes are given in Table 1. The x, y, and z axes have been assigned in a similar fashion to that used for M(amben). In this case, only the direction of the x axis in Co(II)(benacacen) and the z axis in Cu(II)(benacacen) are determined with any accuracy due to the near axial character of both resonances. These two axes are 92° from each other, so it appears reasonable to assume both complexes are oriented similarly in the host crystal. Due to the better resolution in this copper complex, it was possible to find the principal axes of the ^{14}N hyperfine. It was found that the z axis is perpendicular to the Cu z axis and 38 $\pm$ 10° from the Co x axis. Thus, as expected, we have confirmation that the x and y axes of the g and A tensors bisect the metal ligand bonds in the plane of the complex.

The Co(II) results agree rather poorly with the values found by Hoffman *et al.* (2) for a frozen nematic solution. They reported values of: $g_x = 3.084$, $g_y = 1.937$, $g_z = 2.01$, $A_x = 149.9 \times 10^{-4}$ cm^{-1}, $A_y = 28.9 \times 10^{-4}$ cm^{-1}, and $A_z = 30.8 \times 10^{-4}$ cm^{-1}. The considerable differences between these values and ours are very likely due to solvent interactions.

Discussion

The spin Hamiltonian parameters for other similar Co(II) complexes are compared to those determined in this study in Table 2. Co(amben), Co(benacacen), and Co(salen) all have $g_z > g_y$ which suggests that the $^2B_2$ state would be the better choice for all three complexes. In the case of Co(amben) there is additional evidence from ^{14}N hyperfine data which argues strongly against the ground state being $^2A_1$ with a small value for the b parameter.

If the unpaired electron were in an a_1 orbital, symmetry would allow direct admixture of 2s and $2p_\sigma$ orbitals from the nitrogen atom which would lead to a ^{14}N hyperfine splitting. We can estimate the extent of such a splitting for the case of a d_{z^2} orbital. The d_{z^2} orbital can be written as

$$[2] \qquad d_{z^2} = \frac{1}{\sqrt{3}}(d_{z^2-y^2} + d_{z^2-x^2})$$

where for our discussion the x and y axes are directed at the ligand atoms. The $d_{z^2-y^2}$ and $d_{z^2-x^2}$ orbitals are similar to the $d_{x^2-y^2}$ orbital occupied by the unpaired electron in copper complexes in that one of the lobes points towards a nitrogen atom. Thus, if we assume a similar

Can. J. Chem. Downloaded from www.nrcresearchpress.com by 210.87.254.40 on 09/05/12
For personal use only.

TABLE 2. Spin Hamiltonian parameters for low spin Co(II) complexes from single crystal studies

Complex	g_x	g_y	g_z	A_x^a	A_y^a	A_z^a	Reference
Co(amben)	2.6586	1.9814	2.0068	3.5	29.5	24.0	This work
Co(benacacen)	3.372	1.882	1.954	165.4	37	47	This work
Co(salen)	3.805	1.66	1.74	291	52	30	1
$Co[(CN)_2C_2S_2]_2^{2-}$	2.798	2.025	1.977	50	28	28	13
$Co(sacsac)_2$	3.280	1.904	1.899	105	35	35	14

[a]Values $\times 10^{-4}$ cm^{-1}.

covalency in Co(II) and Cu(II) complexes we can estimate the hyperfine constant for a ^{14}N atom in the plane of a cobalt complex to be one-third that observed in the corresponding copper complex. In Co(amben) where the ^{14}N hyperfine splitting is not resolved we might expect a contribution of $\sim 5^{N}A$ to the line width. For Co(amben) the line width of resonance lines is 10×10^{-4} cm^{-1} when the magnetic field is along the z principal axis while the expected line width for a d_{z^2} electron due to ^{14}N hyperfine is 25×10^{-4} cm^{-1}. When the magnetic field is along the y principal axis the experimental line width is 17×10^{-4} cm^{-1} and the expected ^{14}N width would be 29×10^{-4} cm^{-1}. This would suggest the electron is either in a d_{yz} or d_{xz} orbital or an a_1 orbital in which the b parameter is large so that it is basically a $d_{x^2-y^2}$ or $d_{3y^2-r^2}$ orbital. A similar analysis of the Co(benacacen) spectra does not lead to any definite conclusions because the expected contribution to the line width in this case is only $\sim 2^{N}A$ and this predicts line widths comparable to those observed.

We have attempted to fit the spin Hamiltonian parameters to the theoretical equations for the $^2A_1$ state (11) when the b parameter is large and have found that it is possible, but the values of the various parameters are not very satisfactory. For the $^2B_2$ state theory gives for the spin Hamiltonian parameter the following equations (11):

$$[3]\quad g_z = 2.0023 + \frac{2}{3}\eta_5^2 - 3\eta_3^2 - \frac{2}{3}\eta_2\eta_5 - 3\eta_2\eta_3 + 2\eta_2$$

$$[4]\quad g_x = 2.0023 - 2\eta_2^2 - 3\eta_2\eta_3 + 6\eta_3 + 2\eta_4$$

$$[5]\quad g_y = 2.0023 + \frac{2}{3}\eta_5^2 - 3\eta_3^2 - 2\eta_1$$

$$[6]\quad A_z = K + P\left\{\frac{2}{7}(1 - \eta_5 + \eta_5') + \frac{3}{7}(\eta_3 - \eta_4 + \eta_1) + 2\eta_2 - \frac{2}{21}\eta_5^2 - \frac{9}{14}\eta_3^2 - \frac{8}{21}\eta_5\eta_2 - \frac{45}{14}\eta_3\eta_2\right\}$$

$$[7]\quad A_x = K + P\left\{-\frac{4}{7} + 6\eta_3 + 2\eta_4 + \frac{3}{7}(\eta_2 - \eta_1) + \frac{4}{21}\eta_5^2 + \frac{3}{14}\eta_3^2 - \frac{2}{21}\eta_5\eta_6 + \frac{4}{7}\eta_3\eta_6 - \frac{6}{7}\eta_2\eta_3 - \frac{2}{7}\eta_2\eta_5\right\}$$

$$[8]\quad A_y = K + P\left\{\frac{2}{7}(1 + \eta_5 - \eta_5') - \frac{3}{7}(\eta_2 + \eta_3 - \eta_4) - 2\eta_1 - \frac{2}{21}\eta_5^2 - \frac{8}{21}\eta_5\eta_6 + \frac{2}{7}\eta_3\eta_6 + \frac{1}{7}\eta_2\eta_5 + \frac{3}{14}\eta_2\eta_3\right\}$$

$$[9]\quad \begin{aligned} \eta_1 &= \xi/\Delta[^2A_2(yz \rightarrow xy)] \\ \eta_2 &= \xi/\Delta[^2B_1(xz \rightarrow yz)] \\ \eta_3 &= \xi/\Delta[^2A_1(z^2 \rightarrow yz)] \\ \eta_4 &= \xi/\Delta[^2A_1(x^2 - y^2 \rightarrow yz)] \\ \eta_5 &= \xi/\Delta[^4A_1(xz \rightarrow xy)] \\ \eta_6 &= \xi/\Delta[^4B_1(z^2 \rightarrow xy)] \\ \eta_5' &= \xi/\Delta[^2A_1(xz \rightarrow xy)] \end{aligned}$$

where K is the Fermi contact interaction, $P = 2.0023 g_N \beta_e \beta_N \langle r^{-3} \rangle$, ξ is the spin orbit interaction parameter for a single d electron, and $\Delta[^2A_2(yz \rightarrow xy)]$ is the energy difference between the excited $^2A_2$ state, produced by promoting an electron from the d_{yz} orbital to the d_{xy} orbital, and the ground state. The preceding equations were derived from the full determinental wave

Can. J. Chem. Downloaded from www.nrcresearchpress.com by 210.87.254.40 on 09/05/12
For personal use only.

Can. J. Chem. Downloaded from www.nrcresearchpress.com by 210.87.254.40 on 09/05/12
For personal use only.

functions and therefore all η_i parameters must have positive values.

There are nine adjustable parameters in eqs. 3–8 and only six equations. We must therefore make reasonable assumptions concerning the values of three parameters to obtain values for the other six. It can be shown that $\Delta[^2A_1(xz \rightarrow xy)]$ is $\sim 15\,000\ cm^{-1}$ larger than $\Delta[^4A_1(xz \rightarrow xy)]$ so that if we assume $\xi \sim 400\ cm^{-1}$ we can estimate η_5' from η_5 using the equation:

$$\eta_5' = \frac{2\eta_5}{2 + 75\eta_5}$$

$\Delta[^4B_1(z^2 \rightarrow xy)]$ should be smaller than $\Delta[^4A_1(xz \rightarrow xy)]$ so that $\eta_6 \geq \eta_5$. We have assumed $\eta_6 = \eta_5$ for convenience because the value chosen for η_6 has little influence on the values of the other parameters since it only appears in the small terms $\eta_5\eta_6$ and $\eta_3\eta_6$ and these two terms partially cancel each other out. We have shown that assuming $\eta_6 = 0$ changes none of the other parameters by more than a few percent. This assumption about η_6 might not be justified if both η_6 and η_3 or η_5 were very large but eqs. 3–8 are not valid when this occurs.

Unfortunately, there are no other approximations that appear intuitively reasonable. We have therefore solved eqs. 3–8 for different assumed values of η_1 to determine the possible range of values for the other η_i parameters plus P and K. A plot of the η_i's obtained is given in Figs. 7 and 8. For Co(amben) these were obtained assuming A_x is negative and A_y, A_z were positive because this choice of sign gave the most reasonable value for P. Similarly, the best choice for Co(benacacen) is to take A_x, A_y, and A_z as positive.

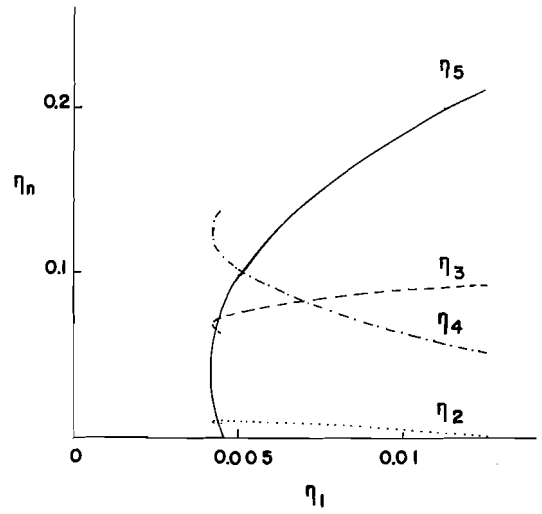

FIG. 7. Plot of η_i (as defined in text) for assumed values of η_1 for Co(amben).

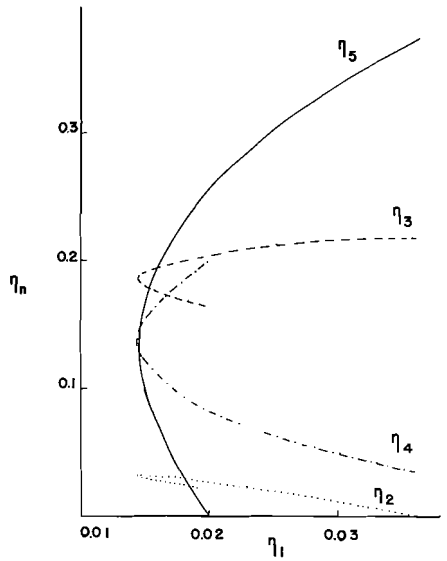

FIG. 8. Plot of η_i (as defined in text) for assumed values of η_1 for Co(benacacen).

For Co(amben) no solutions exist for $\eta_1 < 0.0042$, from 0.0042 to 0.0045 two solutions are found and from 0.0045 to 0.0125 one solution is found. Above 0.0125, η_2 becomes negative and therefore no physically meaningful solution is possible for $\eta_1 > 0.0125$. We note from Fig. 7 that η_2 and η_3 change slowly over the allowed range of η_1 and therefore approximate values for these parameters are obtained. The same is true for P and K with P ranging from 148 to 154 $\times 10^{-4}\ cm^{-1}$ and K from -16 to $-15 \times 10^{-4}\ cm^{-1}$.

For Co(benacacen) the results are similar except for scale. Allowed solutions occur only in the range of 0.0144 to 0.036 for η_1. Both η_3 and η_2 are larger than for Co(amben). It is this larger value of η_3 that makes both g_x and A_x much larger in magnitude for Co(benacacen) than for Co(amben). The value of $6\eta_3$ for Co(benacacen) in [7] is much larger in magnitude than the Fermi contact term K and the normal dipolar term of $\frac{4}{7}P$ and makes A_x large and positive. In Co(amben) η_3 is small enough that it just cancels out the negative Fermi and dipolar terms giving rise to an

Can. J. Chem. Downloaded from www.nrcresearchpress.com by 210.87.254.40 on 09/05/12
For personal use only.

A_x of very small magnitude. P for Co(benacacen) varies from 250 to 238 $\times 10^{-4}$ cm^{-1}.

The P value for Co(benacacen) is normal for a Co(II) complex (11) but that for Co(amben) is appreciably smaller, indicating considerable delocalization of the unpaired electron into the π system of the ligand if our ground state assignment is correct. The K values are smaller in magnitude than normal (20) but this might be due to some small direct admixture of the 4s orbital with the d_{yz} orbital which is allowed in these complexes since the true site symmetry can be no better than C_2, with the symmetry axis aligned with the molecular x axis.

A simple crystal field analysis would indicate that $\Delta[^2B_1(xz \rightarrow yz)] + \Delta[^2A_2(yz \rightarrow xy)] \cong \Delta[^4A_1(xz \rightarrow xy)] + 15\,000$ cm^{-1}. Using reasonable values of ξ plus η_1 and η_2 shows that values of $\eta_5 > 0.05$ for Co(benacacen) and 0.01 for Co(amben) would be inconsistent with our model. For this range of values of η_5, $\eta_3 \sim \eta_4$, and $\eta_2 \sim \eta_1$ with (η_3, η_4) being approximately an order of magnitude larger than (η_2, η_1) for both cobalt(II) complexes. It is therefore clear that $\Delta[^2A_1(z^2 \rightarrow yz)]$ and $\Delta[^2A_1(x^2 - y^2 \rightarrow yz)]$ are smaller than $\Delta[^2A_2(yz \rightarrow xy)]$ and $\Delta[^2B_1(xz \rightarrow yz)]$ and this should be useful in assigning bands in the optical spectra of these complexes.

Optical studies on Co(benacacen), Co(amben), and related complexes have been carried out by several workers (5, 7, 17, 21–23). In general for CoN_2O_2 complexes two d–d bands are found, one between 4000 and 5000 cm^{-1} and a second between 8000 and 9000 cm^{-1}. Both bands appear to have structure but it is not clear whether this is due to vibronic couplings or to the presence of two or more separate transitions. In CoN_4 complexes the two bands are found in the regions of 5000–7000 cm^{-1} and 11 000–12 000 cm^{-1}. Circular dichroism studies (5, 7, 22) have revealed the possible presence of several more d–d bands between 16 000 and 21 000 cm^{-1} for CoN_2O_2 complexes and between 13 000 and 20 000 cm^{-1} for CoN_4 complexes.

No agreement concerning assignments of these transitions exists in the literature. Hipp and Baker (22) assumed in their assignments that the ground state had the unpaired electron in a $d_{x^2-y^2}$ orbital while most other workers assumed the unpaired electron to be in the d_{z^2} orbital. Busetto *et al.* (7, 21) and Urbach *et al.* (5) both tried to assign bands using e.s.r. results and crystal field theory but arrived at very different assignments assuming the same ground state. The assignment of Urbach *et al.* (5) is internally inconsistent because the crystal field parameters they used would predict the $(xy)(z^2)(yz)$ quartet state to be 5200 cm^{-1} below the doublet state they assumed as the ground state.

It is dangerous to base too much of an optical assignment on ΔE's estimated from e.s.r. parameters η_i, as has been done for these complexes (5, 7), because this requires a good estimate of ξ. It is well known (24) that the effective value of ξ can be less than 50% of the free ion value when there is strong covalency in both the ground state and the excited state coupled by the spin–orbit operator. In the Co(II) complexes studied here we can expect this might be the case for parameters η_1 and η_2 but not for the parameters η_3 and η_4 because these last two parameters involve excited states that have d orbitals that are not expected to have strong covalent interactions with ligand orbitals. Thus, although η_1 and η_2 are 10-fold smaller than η_3 and η_4 we cannot expect the respective values of ΔE's for η_1 and η_2 to be 10-fold larger than those for η_3 and η_4. It does seem reasonable, though, to assume that the lower frequency d–d band will be associated with $\Delta E[^2A_1(z^2 \rightarrow yz)]$ and $\Delta E[^2A_1(x^2 - y^2 \rightarrow yz)]$ while the second band is associated with $\Delta[^2A_2(yz \rightarrow xy)]$ or $\Delta[^2B_1(xz \rightarrow yz)]$ or perhaps with both.

These assignments are, of course, correct only if we are correct in our assumption as to the ground state. It does seem clear, however, from the behavior of the spectral bands and the e.s.r. parameters, that both complexes have the same ground state and that amben generates a stronger crystal field than benacacen. The smaller values of η_i in Co(amben) go along with the shift to higher frequencies of the optical bands.

A more comprehensive crystal field analysis of the e.s.r. and optical studies seems unwarranted at this time, but our results do indicate that orbital energies in increasing order are d_{xz}, ($d_{x^2-y^2}$, d_{z^2}, d_{yz}), d_{xy} with $d_{x^2-y^2}$, d_{z^2}, and d_{yz} being clustered closely together in undetermined order. This ordering suggests large configurational mixing of $d_{x^2-y^2}$ and d_{z^2}.

If we use standard methods (25) for estimating repulsion energies we find that $\Delta[^2B_1(xz \rightarrow yz)]$ is a direct measure of the difference in orbital energies of d_{xz} and d_{yz}. The small value of η_2 in both complexes studied indicates that this difference is large ($\geq$8000 cm^{-1} for Co(benaca-

Can. J. Chem. Downloaded from www.nrcresearchpress.com by 210.87.254.40 on 09/05/12
For personal use only.

cen) and $\geq 11\,000\ cm^{-1}$ for Co(amben)). The near axial g values for the copper complexes indicates that d_{xz} and d_{yz} are nearly degenerate in these complexes. This apparent large splitting of d_{xz} and d_{yz} is not an artifact of our choice of ground state since any attempt to analyze the e.s.r. results in terms of a $^2A_1$ ground state also requires this same large splitting. Analysis of e.s.r. results on Co(sacsac) and $Co(mnt)_2^{2-}$ (11) in terms of a $^2A_1$ ground state also required the d_{yz} orbital to be much higher in energy than the d_{xz} orbital. It appears to be generally true that Co(II) complexes involving two chelate ligands have a large splitting of the d_{xz} and d_{yz} orbitals while the corresponding Cu(II) complexes have nearly degenerate d_{xz} and d_{yz} orbitals. We have no explanation for this but feel it is somehow connected to the fact that symmetry requires the d_{xz} and d_{yz} orbitals to interact with different π orbitals in the ligands.

It has been suggested that the large value of $\Delta[^2B_1(xz \rightarrow yz)]$ is not due to a difference in orbital energies but due to a difference in the repulsive coulombic and exchange integrals for d_{xz} and d_{yz}. Although this may be true, it does not really answer the question because if we accept the proposition that the coulombic and exchange integrals for d_{xz} and d_{yz} with the other d orbitals are very different; then the 'hole formalism' method of treating d^7 and d^9 configurations breaks down and we must conclude that all d–d transitions in both Co(II) and Cu(II) complexes involve nonzero repulsive energy differences. Following this reasoning further, we find we must now ask why the coulombic and exchange integrals for d_{xz} and d_{yz} are the same for Cu(II) complexes and very different for Co(II) complexes and therefore have not really solved the problem at all.

Analysis of the copper results yields little that is new or different from that found for other copper nitrogen complexes. The copper hyperfine terms in axial symmetry can be expressed (20) as

$$[10]\quad A_{\parallel} = K + P\left[-\frac{4}{7} + (g_{\parallel} - 2.0023) + \frac{3}{7}(g_{\perp} - 2.0023)\right]$$

$$[11]\quad A_{\perp} = K + P\left[\frac{2}{7} + \frac{11}{14}(g_{\perp} - 2.0023)\right]$$

These equations give $P = 217.5 \times 10^{-4}\ cm^{-1}$ and $K = -116.3 \times 10^{-4}\ cm^{-1}$ for Cu(amben) and $P = 237.6 \times 10^{-4}\ cm^{-1}$ and $K = -111.4 \times 10^{-4}\ cm^{-1}$ for Cu(benacacen). The values of K and P are consistent with the values found for other copper complexes (20). The smaller value of P for Cu(amben) would indicate slightly more σ bonding in this system consistent with a higher ligand field interaction for this ligand (5, 9).

Since very few reliable values of ^NA and ^NB are found in the literature, it is of interest to compare our values with those found for other complexes. Theory gives for ^NA and ^NB the approximate equations (24).

$$[12]\quad {}^NA = C_s^2A_{2s} + 2C_p^2A_{2p} + g_{\perp}P_M(1 - 4C_p^2)$$

$$[13]\quad {}^NB = C_s^2A_{2s} - C_p^2A_{2p} - \frac{1}{2}g_{\parallel}P_M(1 - 4C_p^2)$$

$$[14]\quad A_{2s} = \frac{4}{3}g_e g_N \beta_e \beta_N |\phi_{2s}(0)|^2$$

$$[15]\quad A_{2p} = \frac{2}{5}g_e g_N \beta_e \beta_N \langle r^{-3}\rangle_{2p}$$

$$[16]\quad P_M = g_e g_N \beta_e \beta_N / R^3$$

where g_e and g_N are electronic and nuclear g factors, β_e and β_N are electronic and nuclear magnetons, $|\phi_{2s}(0)|^2$ is the probability of a nitrogen 2s orbital at the nitrogen nucleus, $\langle r^{-3}\rangle_{2p}$ is average value of r^{-3} for a nitrogen 2p orbital, and R is the distance between a copper and nitrogen atom. From Morton (26) we obtain the values of $A_{2s} = 513 \times 10^{-4}\ cm^{-1}$ and $A_{2p} = 15.9 \times 10^{-4}\ cm^{-1}$. Assuming $R = 1.95$ Å gives $P_M = 0.26 \times 10^{-4}\ cm^{-1}$. C_p and C_s are MO mixing coefficients for a nitrogen atom 2p and 2s orbital in the MO containing the unpaired electron. The p orbital is σ in character. Values of C_s^2 and C_p^2 obtained from eqs. 12–16 are given in Table 3 for a series of copper complexes, including those studied here. In the case of Cu(amben) and Cu(benacacen) the errors in C_s^2 are $\sim \pm 0.001$ while those in C_p^2 are $\sim \pm 0.02$. Presumably similar errors apply to values from the literature.

It is seen from the data in Table 3 that in general C_p^2 is two to three times that of C_s^2 indicating that σ bonding to nitrogen occurs through an sp^2 to sp^3 hybrid. The main variation appears to be in C_s^2 which becomes larger for those ligands giving rise to the larger ligand

TABLE 3. Comparison of nitrogen hyperfine constants for copper(II) complexes

Complex	$^{N}A^{a}$	$^{N}B^{a}$	C_s^2	C_p^2	Reference
Cu(amben)	18.6	14.9	0.031	0.07	This work
Cu(benacacen)	17.5	13.1	0.029	0.09	This work
Cu(N mesal)$_2$	15.0	11.5	0.025	0.06	27
CuPc	18.6	15.5	0.033	0.05	28, 29
CuTPP	16.1	14.6	0.029	0.02	30
Cu(picolinate)	14.5	9.9	0.022	0.08	31
Cu($NH_2CH_2CO_2$)$_2$	11.4	7.4	0.017	0.07	32

[a]Values $\times 10^{-4}$ cm^{-1}.

fields. No significant difference is observed for the two ligands amben and benacacen.

This work was supported by a grant from the National Research Council of Canada.

1. O. VON ZELEWSKY and H. FIERZ. Helv. Chim. Acta, **56**, 977 (1973).
2. B. M. HOFFMAN, F. BASOLO, and D. L. DIEMENTE. J. Am. Chem. Soc. **95**, 6497 (1973).
3. D. DIEMENTE, B. M. HOFFMAN, and F. BASOLO. Chem. Commun. 467 (1970).
4. B. M. HOFFMAN, D. DIEMENTE, and F. BASOLO. J. Am. Chem. Soc. **92**, 61 (1970).
5. F. L. URBACH, R. D. BEREMAN, J. A. TOPICH, M. HARIHARAN, and B. J. KALBACHER. J. Am. Chem. Soc. **96**, 5063 (1974).
6. E. I. OCHIAI. J. Chem. Soc. Chem. Commun. 489 (1972); J. Inorg. Chem. **35**, 1727 (1973).
7. C. BUSETTO, F. CARIATI, A. FUSI, M. GULLOTI, F. MORAZZONI, A. PASINI, R. UGO, and V. VALENTI. J. Chem. Soc. Dalton Trans. 754 (1973).
8. C. BUSETTO, F. CARIATI, P. C. FANTUCCI, D. GALIZZIOLI, and F. MORAZZONI. Inorg. Nucl. Chem. Lett. **9**, 313 (1973).
9. L. M. ENGELHARDT and M. GREEN. J. Chem. Soc. Dalton Trans. 724 (1972).
10. L. M. ENGELHARDT, J. D. DUNCAN, and M. GREEN. Inorg. Nucl. Chem. Lett. **8**, 725 (1972).
11. B. R. MCGARVEY. Can. J. Chem. **53**, 2498 (1975).
12. R. B. BENTLEY, E. E. MABBS, W. R. SMAIL, M. GERLOCH, and J. LEWIS. J. Chem. Soc. A, 3003 (1970).
13. A. H. MAKI, N. EDELSTEIN, A. DAVIDSON, and R. H. HOLM. J. Am. Chem. Soc. **86**, 4580 (1964).
14. A. K. GREGSON, R. L. MARTIN, and S. MITRA. Chem. Phys. Lett. **5**, 310 (1970).
15. V. P. CHACKO and P. T. MANOHARAN. J. Magn. Reson. **16**, 75 (1974).
16. D. E. SMITH and J. W. OPIE. Org. Synth. Coll. Vol. 111, 56 (1955).
17. M. GREEN and P. A. TASKER. J. Chem. Soc. A, 2531 (1970); 3105 (1970).
18. G. W. EVERETT and R. H. HOLM. J. Am. Chem. Soc. **88**, 2442 (1966).
19. J. A. WEIL, T. BUCH, and J. E. CLAPP. Advances in magnetic resonance. Vol. 6. Academic Press, New York. 1973, pp. 183–257.
20. B. R. MCGARVEY. J. Phys. Chem. **71**, 51 (1967).
21. C. BUSETTO, F. CARIATI, P. FANTUCCI, D. GALIZZIOLI, F. MORAZZONI, and V. VALENTI. Gazz. Chim. Ital. **102**, 1040 (1972).
22. C. J. HIPP and W. A. BAKER. J. Am. Chem. Soc. **92**, 792 (1970).
23. Y. NISHIDA and S. KIDA. Bull. Chem. Soc. Jpn. **45**, 461 (1972).
24. B. R. MCGARVEY. Transition metal chemistry. Vol. 3. *Edited by* R. L. Carlin. Marcel Dekker, New York. 1966. p. 90–201.
25. C. J. BALLHAUSEN. Introduction to ligand field theory. McGraw-Hill Co., New York. 1962.
26. J. R. MORTON. Chem. Rev. **64**, 453 (1964).
27. B. W. MOORES and R. L. BELFORD. Electron spin resonance of metal complexes. *Edited by* T. F. Yen. Plenum Press, New York. 1969. p. 13.
28. S. E. HARRISON and J. M. ASSOUR. J. Chem. Phys. **40**, 365 (1964).
29. C. M. GUZY, J. B. RAYNOR, and M. C. R. SYMONS. J. Chem. Soc. A, 2299 (1969).
30. P. T. MANOHARAN and M. T. ROGERS. Electron spin resonance of metal complexes. *Edited by* T. F. Yen. Plenum Press, New York. 1969. p. 143.
31. G. H. RIST and J. S. HYDE. J. Chem. Phys. **52**, 4633 (1970).
32. J. STANKOWSKI and A. WIECKOWSKI. J. Magn. Reson. **15**, 498 (1974).

Can. J. Chem. Downloaded from www.nrcresearchpress.com by 210.87.254.40 on 09/05/12
For personal use only.

The Distribution of Oxidation States of Iodine Isotopes in the Fission by Protons of Natural Uranium[1,2]

M. DIKŠIĆ AND L. YAFFE

Department of Chemistry, McGill University, Montreal, Quebec H3C 3G1

Received June 27, 1975

M. DIKŠIĆ and L. YAFFE. Can. J. Chem. **53**, 3801 (1975).

Oxidation states of iodine, produced in the fission of uranium by protons of energies 30 and 80 MeV in solid matrices of $UO_2(NO_3)_2.6H_2O$ and $UO_2SO_4.3H_2O$, have been studied. No proton energy dependence was found. The percentage distribution of I^{7+} as $(IO_4)^-$ is independent of the matrix. However I^{5+} (as IO_3^-) is enriched at the expense of the reduced state ($I_2^0 + I^-$) due to oxidation by the $(NO_3)^-$ formed by the radiation decomposition of $UO_2(NO_3)_2.6H_2O$. Formation of the nuclide by isomeric decay does not perturb the distribution. The result of β^- decay is to increase the I^{7+} component. Iodine isotopes formed independently in fission have the same distribution of oxidation states, but not unique enough to serve as a measure of this mode of formation.

M. DIKŠIĆ et L. YAFFE. Can. J. Chem. **53**, 3801 (1975).

On a étudié les états d'oxydation de l'iode produit par la fission de l'uranium par des protons d'énergies 30 et 80 MeV dans des matrices solides du $UO_2(NO_3)_2 \cdot 6H_2O$ et $UO_2SO_4 \cdot 3H_2O$. On n'a pas trouvé de dépendance sur l'énergie des protons. La distribution des pourcentages de I^{7+} sous forme de $(IO_4)^-$ est indépendante de la matrice. Toutefois I^{5+} sous forme de (IO_3^-) est enrichi au dépens de l'état réduit ($I_2^0 + I^-$) dû à l'oxydation par $(NO_3)^-$ formé par la décomposition sous radiation de $UO_2(NO_3)_2 \cdot 6H_2O$. La formation de nuclides par décomposition isomérique ne perturbe pas la distribution. Le résultat d'une décomposition β^- est d'augmenter le composant I^{7+}. Les isotopes de l'iode formés indépendament dans la fission ont la même distribution d'état d'oxydation; cette distribution n'est toutefois pas suffisamment spécifique pour servir de mesure pour ce mode de formation.

[Traduit par le journal]

Introduction

Theoretical calculations (1–13) have shown that fission fragments should initially have a large positive charge. The linear velocity of the fragment following fission is very large compared to the slower-moving electrons, which will be left behind, and Perfilov (4), *e.g.*, has suggested an average initial charge of the fragments of ~20. These fragments will be very unstable chemically, and thus would abstract electrons from the matrix, leading to a dependence of the distribution of chemically stable oxidation states on the matrix (5, 6). The final distribution will also depend on the mode of disintegration, *e.g.* isomeric transition, short-lived isobaric precursor, etc. Changes in chemical states as a result of isomeric transitions have been studied for a variety of radionuclides (7–12).

The chemically stable oxidation states of iodine in solution are -1, 0, $1+$, $5+$, and $7+$. The chemical behavior of these oxidation states in solution is quite complex and not yet completely understood. The behavior of iodine in tracer quantities often differs from that of the element in macro concentrations (13, 14). Exchange between different chemical states is not likely in a solid matrix (15) on the tracer level, but might readily occur in solution. Burgus and Davies (14) have studied exchange reactions between different oxidation states of iodine as a function of concentration, time, and p*H*. The exchange between I^-–(IO_3^-) has been reported to be slow (16–19) at room temperature.

Brown and Wahl (20) suggested that the dependence of oxidation state on mode of formation of the fragment might be put to practical advantage. If the oxidation states were all the same for species formed independently in fission, these might be distinguished from those formed by isobaric decay of a precursor. Erdal *et al.* (21) determined the dependence of oxidation states of tin isotopes as a function of the β-decay process.

[1]This research was supported by the National Research Council of Canada.

[2]This paper is dedicated to Professor C. A. Winkler of McGill University on the occasion of his sixty-fifth birthday by one of his colleagues (L. Yaffe).

Can. J. Chem. Downloaded from www.nrcresearchpress.com by 210.87.254.5 on 09/05/12
For personal use only.

Can. J. Chem. Downloaded from www.nrcresearchpress.com by 210.87.254.5 on 09/05/12
For personal use only.

Differences in the oxidation states of iodine isotopes formed in fission have been reported by several groups (6, 22–27) and qualitative relationships have been proposed to explain the distribution of oxidation states as a function of the mode of formation of the isotopes. However, many of these appear as a combination of an isomeric transition and the result of a β-decay. Moreover, some of these isomeric transitions have only recently (28) been found, *e.g.* ^{134m}I, and thus were not taken into account. In addition, in previous work, separation of the fission-produced iodine commenced only after a time long enough to allow tellurium precursors to decay to iodine, thus introducing a product resulting from the combination of isomeric transition, direct formation, and β-decay.

No data are available for oxidation states of iodine produced by the proton-induced fission of uranium. This is the basis of the work presented in this paper. Separations were made as quickly as possible after irradiation. The nuclide ^{128}I is shielded from β-decay and was used at 80 MeV as an internal standard, presumably indicative of the distribution of oxidation states for a primary fragment. Cross sections at 30 MeV were too small to enable this to be used. No metastable state of ^{128}I has yet been reported, even though other odd–odd iodine isotopes in this mass region have such known states, *e.g.* ^{130}I, ^{132}I, ^{134}I, ^{136}I.

Experimental

(a) Exchange Experiments

Experiments were initially made to check the exchange of oxidation states under identical conditions used in the present investigations. Tracer ^{131}I was used in the form of I^- and IO_3^- to perform those experiments.

A mixture of ^{131}I in KI was oxidized to I_2^0 with NO_2^- in acid solution and I_2^0 was extracted with CCl_4. A stock solution of IO_3^- was prepared by oxidizing the I_2^0 with HNO_3. The $*I^-$ solutions (* refers to the tracer label) were prepared by reducing the I_2^0 with aqueous bisulfite solutions, and 6 *M* HNO_3 was added to the solution to destroy the bisulfite ion. The solution of labelled I^- was used the same day for the exchange experiments.

Experiments to determine whether exchange occurred between $*IO_3^-$ and IO_4^-, I_2^0 and $*IO_3^-$, $*I_2^0$ and IO_4^-, $*I^-$ and IO_3^-, $*I^-$ and IO_4^-, and $*IO_3^-$ and IO_4^-, both in 0.1 *M* HNO_3 and in the presence of uranyl nitrate and uranyl sulfate. Procedures used were similar to those of Willard and Thompson (22) and Burgus and Davies (14).

The fractions were separated approximately at the same time as in the post-irradiation studies. The I^- activity in the IO_4^- fraction was found to be just under 2%. No other exchange was observed in any of the other systems.

(b) Oxidation Distribution Studies

Samples of either uranyl nitrate or uranyl sulfate were placed in thin-walled aluminum tubes and irradiated in the internal circulating beam of the McGill proton synchrocyclotron. The targets after irradiation were dissolved in distilled H_2O (about 15 min after the end of the irradiation), made 0.1 *M* in HNO_3 and (typically 2 min after dissolution) $\sim 7 \times 10^{-4}$ mol IO_4^-, $\sim 7 \times 10^{-4}$ mol IO_3^-, and 7×10^{-5} mol I^- were added. The addition of the I^- resulted in its oxidation to I_2^0 by the IO_4^-. The *I_2^0 fraction* (representing the initial I^- and I_2^0 fractions), was extracted into CCl_4. The *IO_3^- fraction* was precipitated at *pH* = 3 by a 25-fold excess of Ba^{2+} ion. After separation, this fraction was reduced with hydroxylamine and the I_2^0 extracted into CCl_4. The *IO_4^- fraction* was precipitated with Bi^{3+} from 1 *M* HNO_3, reduced with $NH_2OH.HCl$ solution and I_2 extracted into CCl_4.

In each case for further purification, the iodine was re-extracted into HSO_3^- solution, oxidized with NO_2^-, and again reduced with HSO_3^-. The samples were finally precipitated as AgI, dried at 110 °C, and chemical yields determined by weighing.

The timing of the separation of each fraction was typically as follows. ($I^- + I_2^0$): about 2 min after the oxidation of I^- to I_2^0, IO_3^- and IO_4^- about 10 and 20 min respectively after the above oxidation. The I_2^0 was in contact with other oxidation states for a maximum period of 2 min.

The γ-radiation was measured by a 30-cc Ge(Li) detector, with a resolution at full-width at half-maximum of ~2.8 keV at 1.33 MeV, connected to a 4096-channel pulse-height analyzer. Full-peak areas were computed by subtracting a straight-line background using a computer code. The activities were determined and extrapolated to the end of irradiation by the CLSQ least-squares computer code (29).

Results and Discussion

The distribution of iodine isotopes found in different oxidation states is given in Tables 1–3. The first two tables contain results obtained from the fission of naturally-occurring uranium induced by protons of energies 30 and 80 MeV re-

TABLE 1. Distribution of oxidation states (%) of iodine isotopes in the fission of uranium (as $UO_2SO_4.3H_2O$) by protons of energy 80 MeV

Isotope	Relative amount		
	$I^- + I^0$	IO_3^-	IO_4^-
^{128}I	56±8	30±8	14±5
^{130}I	59±3	24±2	17±1
^{131}I	42±3	29±3	29±3
^{132m}I	59±5	24±2	17±2
$^{132m+g}$I	55±1	23±1	22±1
^{133}I	45±2	29±1	26±1
^{134}I	48±3	26±1	26±1
^{135}I	58±2	25±1	17±1

Can. J. Chem. Downloaded from www.nrcresearchpress.com by 210.87.254.5 on 09/05/12
For personal use only.

TABLE 2. Distribution of oxidation states (%) of iodine isotopes in the fission of uranium (as $UO_2SO_4.3H_2O$) by protons of energy 30 MeV

Isotope	Relative amount		
	$I^- + I^0$	IO_3^-	IO_4^-
^{130}I	54±3	29±2	17±2
^{131}I	45±3	28±3	27±2
^{132m}I	52±2	30±3	19±3
$^{132m+g}I$	50±3	33±2	17±1
^{133}I	45±2	32±2	28±1
^{134}I	47±2	33±1	21±1
^{135}I	53±3	30±1	17±1

TABLE 3. Distribution of oxidation states (%) of iodine isotopes in the fission of uranium (as $UO_2(NO_3)_2.6H_2O$) by protons of energy 80 MeV

Isotope	Relative amount		
	$I^- + I^0$	IO_3^-	IO_4^-
^{128}I	32±6	46±9	22±8
^{130}I	23±1	63±4	14±1
^{131}I	26±4	45±5	29±3
^{132m}I	31±4	51±5	18±3
$^{132m+g}I$	27±2	54±2	18±2
^{133}I	22±2	50±3	28±2
^{134}I	31±2	44±2	25±4
^{135}I	36±4	47±4	17±2

spectively in a matrix of $UO_2SO_4.3H_2O$. Table 3 shows the distribution obtained in a matrix of $UO_2(NO_3)_2.6H_2O$ with protons of 80-MeV energy. A comparison of Tables 1 and 2 shows no apparent energy dependence for the same matrix. The kinetic energy of the fragments does not differ significantly for fission induced by 30- and 80-MeV protons (30), so from this point of view an energy difference would have been surprising. Dehmer and Wahl (31), at any rate, showed that a recoil energy of ~100 eV was all that was needed for the reduction of higher oxidation states of tin to Sn^{2+} (an amount infinitesimally small compared to the recoil energies occurring in fission).

However, as the bombarding energy increases, Z_p, the most probable nuclear charge in fission will shift (32) towards Z_A, the most stable charge for mass A. Thus the ratios of nuclei formed directly in fission to those formed by the β-decay of a precursor or from an isomeric state will be quite different for 30 and 80 MeV bombarding energies. This would be expected to have a large influence on the distribution of oxidation states (see later discussion).

The percentage distribution of IO_4^- shows very little influence of the matrix on the oxidation states (*cf.* Tables 1 and 3). However, in the case of the other two oxidation states, I^{5+} (as IO_3^-) is enriched in the nitrate matrix directly at the expense of the reduced states ($I^- + I^0$) as shown in Table 4. This can readily be accounted for by the irradiation decomposition of uranyl nitrate. The standard oxidation–reduction potential for reducing NO_3^- to its reduced form is 1.3 V, sufficient to oxidize I_2 to IO_3^- (1.2 V), but not sufficient to oxidize IO_3^- to IO_4^- (1.7 V) (33). Thus the 'primeval' distribution should be that found in the sulfate matrix. One would expect, if this were the only mechanism occurring, to find the same percentage change for all the iodine isotopes. This within the limits of experimental error is true, with the exception of ^{130}I, ^{131}I, and ^{134}I. Some other mechanism, as yet unexplained, contributes to this difference.

The difference in distributions among the iodine isotopes themselves can be better understood if one understands their genetic origin. These are shown in Table 5 which lists the mode of production and calculates the percentage formed independently, taking into account cross sections for independent formation of the iodine isotopes and their precursors (34–36), and the contribution from the precursor during the irradiation (2 min) and from the end of irradiation till chemical separation (20 min) using known half-lives (37) and standard growth and decay equations.

The data in Table 1 show that ^{128}I (which has large error bars because of its low formation

TABLE 4. Differences in distributions of oxidation states of iodine isotopes formed in the fission of uranium by protons of energy 80 MeV as a function of matrix
[N = $UO_2(NO_3)_2.6H_2O$, S = $UO_2SO_4.3H_2O$]

Isotope	$\Delta_{IO_3^-}$ (N − S)	$\Delta_{I^-+I^0}$ (N − S)
^{128}I	16±12	−24±10
^{130}I	37±4	−36±3
^{131}I	16±6	−16±5
^{132m}I	27±5	−28±6
$^{132m+g}I$	31±2	−28±2
^{133}I	21±3	−23±3
^{134}I	18±2	−17±4
^{135}I	22±4	−22±4

TABLE 5. Production of iodine isotopes studied

Isotope	Mode of production	% Independent formation
^{128}I	Independent	100
^{130}I	Independent + isomer	97
^{131}I	Independent + ^{131}Te decay	58
^{132m}I	Independent	100
$^{132m+g}I$	Independent + isomer	70
^{133}I	Independent + ^{133}Te decay	69
^{134}I	Independent + isomer + ^{134}Te decay	34
^{135}I	Independent + ^{135}Te decay	91

cross sections at these energies), and ^{132m}I, each formed 100% independently have virtually similar distributions. However, the distribution is not unique enough to enable this to be a measure of independent formation (20). Distributions similar to these are also found in ^{130}I and $^{132m+g}I$, indicating that formation by isomeric decay does not perturb the distribution. The same conclusion has been reached by Jones (39), who studied the chemical effects of internal conversions (IT) of ^{80}Br in $NaBrO_3$ crystals, and Jones and Warren (41) who investigated the chemical effects of IT in ^{131}Te and the results of the β^- decay of ^{132}Te in telluric acid crystals. The study most closely related to the present one is the work of Hall and Walton (26) who studied the distribution of oxidation states of iodine isotopes produced in the thermal-neutron fission of uranium in $UO_2(IO_3)_2.H_2O$ crystals as a function of neutron dose and decay time. In their studies ^{135}I, which is mainly formed directly in the fission process at low excitation energies, behaved differently from the other iodine isotopes. Fragments formed directly in the fission process are stripped of approximately 20 electrons and thus one would expect those isobars closest in atomic number to the original fragments to be found in the highest oxidized state. The data reported in this paper, however, show that those products which are formed mainly independently, *e.g.* ^{132m}I, ^{128}I, and ^{130}I are the least oxidized. This is evidence for the fact that the initial electronic charge has no major effect on the final distribution in solid matrices. Similar conclusions were indeed reached by Hall and Walton (26) for their fissioning system.

It is very difficult to compare these conclusions with the data from other previous work. For example, Gordon (38) studied the distribution resulting from the decay of ^{132}Te and suggested a major role for Auger electrons in the break-up of the tellurate molecule. However, the study, unlike the present, was done in aqueous solution. Hillman and Weiss (7) studied the effect of the isomeric transition in ^{127}Te and ^{129}Te. Contrary to Gordon, they found no difference in yields of products resulting from decay of the monomeric and polymeric forms of tellurium, but found higher yields of Te(IV) resulting from the IT decay of a Te(IV) parent. However, again in aqueous solution vacancies could very quickly be occupied by electrons from the solvent and thus molecular disruption may not occur.

Bulbulian and Maddock (40) in the thermal annealing of telluric acid crystals studied the influence of isomeric transitions from ^{121}Te, ^{127}Te, and ^{129}Te. From their results one can derive the conclusion that the greater the percentage of isomeric transition in the decay (*cf.* ^{121}Te and ^{129}Te), the greater the retention of Te(VI). However, one should remember that the environment in their solid matrix has undergone less radiation damage than that in the present case.

In the case of the solid matrix used in this study the fission fragment will be thermalized and brought to rest in a region which has received very great radiation damage: a very 'hot' spot. Here one would have very little influence by the Auger electrons released during the isomeric transition, since the area would contain large numbers of free electrons.

Our results, *cf.* ^{131}I, ^{133}I, and ^{134}I, would indicate that in the solid matrix, the influence of β^--decay is to increase the I^{7+} component. Similar increases of the oxidized forms of iodine formed in β^- decay were reported by Hall and Walton (26). ^{135}I, which is produced mainly independently in this study, conforms to the independent distribution with a slight β-decay contribution.

If one examines Table 3, bearing in mind the oxidation effect due to matrix decomposition discussed earlier, the same trends are apparent.

The authors wish to record their appreciation once more to Professor S. K. T. Mark, Director, Foster Radiation Laboratory, for his cooperation.

The authors are also pleased to acknowledge with thanks valuable discussions with Dr. A. G. Maddock.

1. N. BOHR. Phys. Rev. **59**, 270 (1941); **58**, 654 (1940).
2. W. E. LAMB. Phys. Rev. **58**, 696 (1940).

Can. J. Chem. Downloaded from www.nrcresearchpress.com by 210.87.254.5 on 09/05/12
For personal use only.

3. J. H. M. BRUNINGS, J. K. KNIPP, and E. TALLER. Phys. Rev. **60**, 657 (1941).
4. N. A. PERFILOV. Compt. Rend. Acad. Sci. URSS, **28**, 426 (1940).
5. A. W. CASTLEMAN, JR., I. N. TANG, and H. R. MUNKELWITZ. J. Inorg. Nucl. Chem. **30**, 5 (1968).
6. S. SPIRIDON and A. CALUSARU. J. Inorg. Nucl. Chem. **35**, 713 (1973).
7. M. HILLMAN and A. J. WEISS. Radiochem. Acta, **15**, 79 (1971).
8. E. SEGRÈ, R. S. HALFORD, and G. T. SEABORG. Phys. Rev. **55**, 321 (1939).
9. D. DEVAULT and W. F. LIBBY. Phys. Rev. **55**, 322 (1939).
10. G. T. SEABORG, G. FRIEDLANDER, and J. W. KENNEDY. J. Am. Chem. Soc. **62**, 1309 (1940).
11. R. L. HAHN. J. Chem. Phys. **39**, 3482 (1963); **41**, 1968 (1964).
12. M. BERTET and R. MUXART. Proceedings of Symposium on Chemical Effect Associated with Nuclear Transformations, Dec. 7–11, 1964, IAEA Proceedings Series STI/PUB/91, Vienna, **2**, 13 (1965).
13. M. KAHN and A. C. WAHL. J. Chem. Phys. **21**, 1185 (1963).
14. W. H. BURGUS and T. H. DAVIES. *In* Radiochemical studies: the fission products. Vol. 1. McGraw-Hill, New York. 1951.
15. S. KAUČIĆ and M. VLATKOVIĆ. Croat. Chem. Acta, **35**, 305 (1963).
16. O. E. MYERS and J. W. KENNEDY. J. Am. Chem. Soc. **72**, 897 (1950).
17. D. HULL, C. SHIFTETT, and S. LIND. J. Am. Chem. Soc. **58**, 535 (1936).
18. A. POLESITSKY. Compt. Rend. Acad. Sci., URSS, **24**, 540 (1939).
19. M. COTTIN and M. HAISSINSKY. Compt. Rend. **224**, 1536 (1947).
20. L. C. BROWN and A. C. WAHL. J. Inorg. Nucl. Chem. **29**, 2133 (1967).
21. B. R. ERDAL, A. C. WAHL, and R. L. FERGUSON. J. Inorg. Nucl. Chem. **33**, 2763 (1971).
22. H. H. WILLARD and J. J. THOMPSON. J. Am. Chem. Soc. **56**, 1827 (1934).
23. W. H. BURGUS, T. H. DAVIES, R. R. EDWARDS, H. GEST, C. W. STANLEY, R. R. WILLIAMS, and C. D. CORYELL. J. Chem. Phys. **45**, 165 (1948).
24. Y. PAISS and S. AMIEL. J. Am. Chem. Soc. **86**, 2332 (1964).
25. F. H. FROHNER. Z. Phys. **170**, 62 (1962).
26. D. HALL and G. N. WALTON. J. Inorg. Nucl. Chem. **19**, 16 (1961).
27. H. O. DENSCHLAG, N. HENZEL, and G. HERRMANN. Radiochim. Acta, **1**, 172 (1963).
28. H. N. ERTEN, C. D. CORYELL, and W. B. WALTERS. Bull. Am. Phys. Soc. **14**, 1225 (1969). C. D. CORYELL, H. N. ERTEN, P. K. HOPKE, W. B. WALTERS, R. DAMS, and H. C. GRIFFIN. Nucl. Phys. A**179**, 689 (1972).
29. J. B. CUMMING. Application of computers to nuclear and radiochemistry. National Academy of Sciences, National Research Council Nuclear Science Series No. NAS-NS3107, 1962. p. 25.
30. V. E. VIOLA, JR. Nuclear data A**1**, 391 (No. 5) (1966).
31. J. L. DEHMER and A. C. WAHL. J. Inorg. Nucl. Chem. **31**, 562 (1969).
32. L. YAFFE. Proc. Symp. on Physics and Chemistry of Fission. Paper SM-122/3, IAEA, Vienna. 1969. p. 701.
33. Handbook of Chemistry and Physics. Chemical Rubber Co., Cleveland, Ohio. 1971. p. D-112.
34. M. DIKŠIĆ, D. K. MCMILLAN, and L. YAFFE. J. Inorg. Nucl. Chem. **36**, 7 (1974).
35. M. DIKŠIĆ and L. YAFFE. Can. J. Chem. **53**, 3116 (1975).
36. M. DIKŠIĆ, L. YAFFE, and D. G. SARANTITES. Phys. Rev. **10**C 1172 (1974).
37. C. M. LEDERER, J. M. HOLLANDER, and I. PERLMAN. Table of isotopes. 6th ed. John Wiley and Sons Inc., New York, N.Y., 1967.
38. R. M. GORDON. J. Inorg. Nucl. Chem. **29**, 287 (1967).
39. C. H. W. JONES. Radiochem. Acta, **14**, 1 (1970).
40. S. BULBULIAN and A. G. MADDOCK. J. Chem. Soc. (A), 2810 (1971).
41. C. H. W. JONES and J. L. WARREN. J. Inorg. Nucl. Chem. **30**, 2289 (1968); **32**, 2119 (1970).

Can. J. Chem. Downloaded from www.nrcresearchpress.com by 210.87.254.5 on 09/05/12
For personal use only.

The Temperature Dependence of Raman Band Parameters for Aquated Mg(II) and Zn(II)

J. TIMOTHY BULMER, DONALD E. IRISH,[1] AND LARS ÖDBERG[2]

Guelph-Waterloo Centre for Graduate Work in Chemistry, Waterloo, Ontario N2L 3G1

Received July 3, 1975

J. TIMOTHY BULMER, DONALD E. IRISH, and LARS ÖDBERG. Can. J. Chem. **53**, 3806 (1975).

The weak polarized Raman bands, previously assigned to the ν_1 mode of the octahedral species $Mg(H_2O)_6^{2+}$ and $Zn(H_2O)_6^{2+}$, have been studied over the temperature ranges -32 to 99 °C and -29 to 80 °C respectively. The signal-to-noise ratio has been enhanced by multiscan averaging with a spectrometer interfaced to a PDP/11 computer. The digitized band profiles have been examined analytically to extract these parameters: position of maximum, position of centroid, full width at half height (f.w.h.h.), and intensity. The dependence on concentration and acidity has also been measured. Whereas the 390 cm^{-1} line of aquated zinc(II) shifts only 3 cm^{-1} to lower frequencies and broadens by about 16 cm^{-1} for a 110 °C temperature increase, the 362 cm^{-1} band of aquated magnesium(II) shifts down by 15 cm^{-1} but broadens to the same extent for a 130 °C temperature increase. The results are interpreted in terms of the difference in the magnitude of forces between these cations and hydrated water molecules.

J. TIMOTHY BULMER, DONALD E. IRISH et LARS ÖDBERG. Can. J. Chem. **53**, 3806 (1975).

On a étudié les bandes Raman faibles polarisées assignées antérieurement au mode ν_1, des espèces octaédriques $Mg(H_2O)_6^{2+}$ et $Zn(H_2O)_6^{2+}$, à des températures respectives allant de -32 à 99 °C et -29 à 80 °C. Le rapport signal à bruit a été augmenté en moyennant, à l'aide d'un balayage répétitif, avec un spectromètre relié avec un ordinateur PDP/11. Les profils des bandes digitalées ont été examinés d'une façon analytique pour en extraire ces paramètres: position du maximum, position du centroide, largeur complète à demi hauteur et intensité. On a aussi mesuré la dépendance sur la concentration et sur l'acidité. Alors que la ligne à 390 cm^{-1} du zinc(II) aqueux se déplace de 3 cm^{-1} vers les fréquences les plus basses et s'élargit par environ 16 cm^{-1} lorsque la température est augmenté de 110 °C, la bande à 362 cm^{-1} du magnésium(II) aqueux se déplace vers les bas champ par 15 cm^{-1} mais s'élargit par la même quantité pour une augmentation de température de 130 °C. On interprète les résultats en termes d'une différence dans l'amplitude des forces entre ces cations et les molécules d'eau hydratées.

[Traduit par le journal]

Introduction

Many physicochemical properties of electrolyte solutions have been rationalized by considering ions to bind water molecules to themselves sufficiently strongly that discrete species are formed. Especially for polyvalent cations, the species have been described as aquated cations or aquocomplex ions. In accordance with the model of Frank and Wen (1) a specific number of water molecules, the hydration number, occupy the peripheral solvation sphere and assume a reasonably well-defined spatial arrangement. For some cations, possibly Be^{2+}, a secondary layer of water molecules may be bound relatively strongly to the first but more often the secondary solvation sheath is conceived as consisting of a region occupied by disordered molecules interposed between the hydrogen-bonded structure of bulk water and the ion-imposed structure of the aquated cation (1). Hydration numbers have been estimated by a large number of methods, often yielding discordant results, but for many ions there is a growing confidence that reasonable values have been obtained (2, 3).

One of the more direct manifestations of aquated cations is the observation of low-frequency vibrational bands. These bands have been observed for both crystalline hydrates (4–8) and aqueous solutions (4, 9–12). For the latter, the Raman bands are weak and diffuse, and there is some disagreement in the literature as to the existence of certain bands (8, 11). The observation of Raman intensity implies some covalence in the interaction and it is thus not surprising

[1]To whom correspondence should be addressed.

[2]Present address: Department of Physical Chemistry, Royal Institute of Technology (KTH), S-100 44 Stockholm, Sweden.

Can. J. Chem. Downloaded from www.nrcresearchpress.com by 210.87.254.40 on 09/05/12
For personal use only.

Can. J. Chem. Downloaded from www.nrcresearchpress.com by 210.87.254.40 on 09/05/12
For personal use only.

that signals are strongest from those cations which are most electronegative (12); indeed lines have not yet been detected for ions of family 1A, or the heavier atoms of families 1B and 2A. The only characteristics reported have been frequencies and some estimated depolarization ratios.

In this study the potential of a laser Raman spectrometer interfaced to a PDP 11/20 computer has been exploited to obtain quality spectra of the ν_1 totally symmetric stretch of hexaquomagnesium(II) and hexaquozinc(II) ions. Frequencies, line widths (f.w.h.h.), intensities, and asymmetries have been studied over the temperature range −32 to 99 °C. Dependence on p*H* and concentration have also been examined. Accuracy and sensitivity was enhanced by multiple-scan averaging and spectral analyses were performed by digital computer methods.

Experimental

Fisher reagent grade magnesium nitrate and zinc nitrate were used without further purification. Solutions were prepared by weight and filtered before use through 0.6 μm Millipore filters. Raman spectra were excited by the 514.5 nm line of a Spectra-Physics 165 argon ion laser operating at 1.4 W and were recorded on a Jarrell-Ash 25-100 spectrophotometer equipped with SSR model 1105/1120 photon counting equipment, interfaced to a PDP 11/20 computer. Details are published elsewhere (13). Typical accumulation times were 8 h for Mg^{2+} and 4 h for Zn^{2+}. A spectral slit width of 6 cm^{-1} was used throughout the experiments. Depolarization ratios were obtained using a Polaroid analyzer and a Karl Lambrecht polarization scrambler mounted in the Jarrell-Ash accessory. Single spectra of the perpendicular and parallel components were recorded for this purpose.

Samples contained in sealed melting point tubes were placed in a specially constructed, variable temperature housing (Fig. 1). An evacuated chamber provided insulation from the surroundings and insured frost-free windows. The inner wall (H) of this jacket was a cylindrical Pyrex glass finger (17 mm i.d.) terminating in a graded glass-to-metal seal (N). The outer metal wall (B), contained an inlet window (A) and an outlet window (D) for the laser beam, a 25 mm window (C) for detection of the 90° scattered Raman signal, and a viewing window (G). The melting point tube was positioned in a recess (J) in a central copper block (I); a copper–constantan thermocouple (O) was mounted into this block. Temperature was controlled by the passage of nitrogen gas through the inner compartment; the gas came from liquid nitrogen boil off for low temperatures or from an electrical heater for high temperatures. The assembly was positioned on the Jarrell-Ash tripod, equipped with a translation stage for alignment. The laser beam passed down through the entrance window, glass wall, sample tube, glass wall, and exit window to focus on an alignment spot. Temperature was monitored with a Hewlett Packard 3420A differential voltmeter. The temperature stability was within ±1 °C.

The computer data analysis commenced with the summation of the individual scans. The curved background arising from the Rayleigh wing was then removed by the subtraction of an exponential–quadratic baseline. The advantages of this baseline function have recently been described in detail (13). The FORTRAN program for background removal also applies a trapezoidal area calculation to evaluate the intensity of the baseline-corrected spectrum and permits smoothing. Band statistics such as half-band width, peak maximum, and centroid of the baseline-corrected spectra were determined using a modified version of the program PC 134 developed by Jones *et al.* (14). Estimated errors in the band parameters are: $\bar{\nu}_{max}$, ±1 cm^{-1}; f.w.h.h., ±2 cm^{-1}; centroid, ±2 cm^{-1}; relative intensities, ±5%. A linear baseline correction and trapezoidal area calculation were applied to the 1050 cm^{-1} band of nitrate ion, recorded as an internal intensity reference. Band fitting was performed with an adaptation of the Murphy and Bernstein modification (15) of the program developed by Pitha and Jones (16).

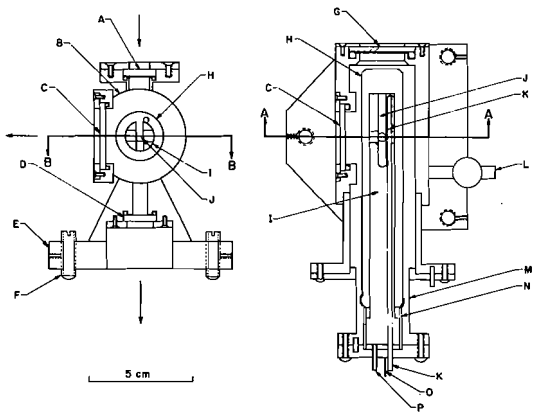

FIG. 1. Cross sections of sample thermostat. AA (end view): A, entrance window; B, outer metal jacket; C, window for collection of scattered light; D, exit window; E, base plate; F, levelling screw. BB (top view): G, viewing window; H, Pyrex inner jacket; I, copper sample holder; J, recess for melting point tube; K, perforated gas inlet tube; L, pump port and valve; M, thin walled stainless steel thermal disconnect; N, Kovar metal end of inner jacket H; O, thermocouple from J; P, gas outlet tube.

Results

Zinc Nitrate

The Raman spectrum of 3.36 *m* zinc nitrate solution at 80 °C is shown in Fig. 2. The baseline obtained as described in the experimental section is also shown. The band parameters are given in Table 1. The intensity is expressed as a percentage of one-half the integrated intensity of the 1050 cm^{-1} line from the nitrate ion present; it is thus based on equal populations of the two species. In Fig. 3 the baseline-corrected spectra of samples held at the different temperatures are presented.

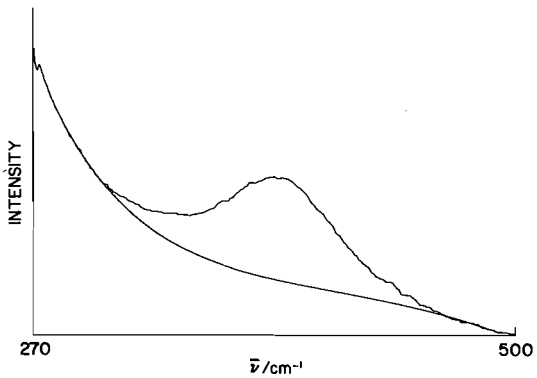

FIG. 2. Raman spectra of a 3.36 mol kg^{-1} $Zn(NO_3)_2$ solution at 80 °C. Accumulation time, 4.2 h. The exponential-quadratic baseline is also shown.

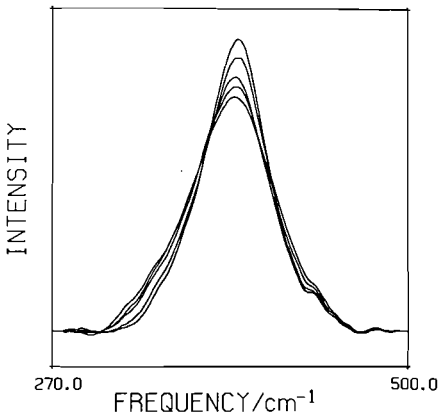

FIG. 3. Baseline-corrected, smoothed spectra of the 3.36 mol kg^{-1} $Zn(NO_3)_2$ solution at temperatures −29, −2, 24, 51, and 80 °C, in order of decreasing amplitudes.

The observed band is highly polarized. The depolarization ratio at −30 °C is 0.05 ± 0.02, and it decreases with increasing temperature. At temperatures above 25 °C we could no longer detect a perpendicular component, which implies $\rho < 0.02$.

Magnesium Nitrate

In Fig. 4, baseline-corrected Raman spectra for a 3.06 *m* magnesium nitrate solution recorded at different temperatures are plotted. The band parameters are given in Table 2. We have also investigated the dependence of the magnesium band parameters on concentration at 25 °C. The results are given in Table 3. To some samples concentrated HNO_3 was added. No changes in the spectra could be detected. Polarization studies revealed no perpendicular component of the band which implies $\rho < 0.05$; the band possesses only an isotropic component.

Discussion

If one accepts the view that the magnesium and zinc cations exist in solution as octahedral hexaquocations (2, 3) the representation of the normal modes and their activities are $A_{1g}(R) + E_g(R) + 2F_{1u}(i.r.) + F_{2g}(R) + F_{2u}(i.a.)$, neglecting the hydrogen atoms of water. From vibrational spectra of crystals (5, 6) and normal coordinate calculations (7) the Raman frequencies are 370, 205, 253 cm^{-1} for $Mg(H_2O)_6^{2+}$ and 393, 200, 296 cm^{-1} for $Zn(H_2O)_6^{2+}$. In aqueous solutions, vibrations at 357–365 and 240 cm^{-1}, and 385–400 and 230 cm^{-1}, have been reported for magnesium and zinc respectively (9–12). Da Silveira *et al.* (9) report a vibration at 315 cm^{-1} for concentrated magnesium solutions and at 335 cm^{-1} for concentrated zinc solutions. These two vibrations are within the spectral regions investigated by us. We found no evidence of these bands and doubt that they arise from the hexaquocations (8). Ananthanarayanan (6, 7) also reports no such lines. The vibrations at 360 and 390 cm^{-1} are the only ones with sufficient intensity for a quantitative study. The high polarization of these two bands strongly supports

TABLE 1. Band parameters for the totally symmetric vibration of the hydrated zinc ion in 3.36 *m* $Zn(NO_3)_2$

Temperature (°C)	Half width (cm^{-1})	Intensity $\frac{I_{390}}{\frac{1}{2}I_{1050}}$ (%)	$\bar{\nu}_{max}$ (cm^{-1})	Centroid (cm^{-1})
−29	48.2	7.22	390.2	388.0
−2	51.5	7.18	391.0	387.4
24	56.4	7.16	387.5	384.9
51	61.0	7.34	388.4	385.1
80	64.0	7.40	387.0	385.1

Can. J. Chem. Downloaded from www.nrcresearchpress.com by 210.87.254.40 on 09/05/12
For personal use only.

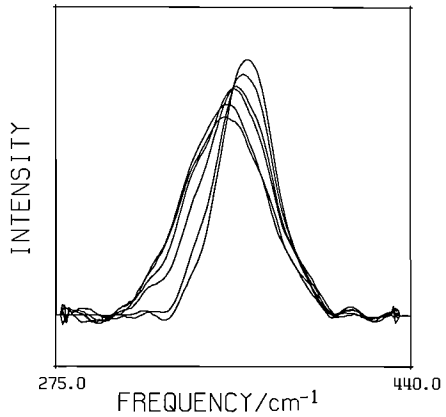

FIG. 4. Baseline-corrected, smoothed spectra of the 3.06 mol kg^{-1} $Mg(NO_3)_2$ solution at temperatures −32, −4, 26, 52, 80, and 99 °C, in order of decreasing amplitudes.

the assignment to the A_{1g} symmetric vibration.

From the results in Table 1 and Fig. 3 it can be seen that the band parameters for zinc, except the line width, stay virtually constant. This suggests that the hydrated zinc ion is a well-defined stable complex in the temperature interval investigated. The relatively high intensity of the vibration implies a substantial degree of covalent character of the metal–oxygen bond (17), and supports the assumption of a well-defined aquozinc complex.

For low frequency vibrations the excitation of 'hot bands' must be considered. At the lowest temperatures investigated 10% of the molecules occupy the $v = 1$ level and this fraction increases to about 20% over the temperature range. Thus transitions $2 \leftarrow 1$ must contribute to the observed contour. The small 3 cm^{-1} shift to low frequencies of both the band maximum and the centroid may arise from these transitions, but if so the anharmonicity of the potential surface cannot be large.

The broadening of the band with temperature increase is probably attributable to increased collisional frequency and vibrational energy transfer. The processes

$$2M(v = 1) \rightarrow M(v = 0) + M(v = 2)$$

and

$$M'(v = 1) + M(v = 0) \rightarrow M'(v = 0) + M(v = 1)$$

would decrease the lifetime in the excited state, τ, and increase the linewidth, $\bar{\nu}_{1/2}$; these are related by $\bar{\nu}_{1/2} = (\pi c \tau)^{-1}$ (18). The isotropic part of the scattered light is independent of reorientational changes and thus for the strongly polarized bands studied in this work contributions to the line shape from such motions can be

TABLE 2. Band parameters for the totally symmetric vibration of the hydrated magnesium ion in 3.06 *m* $Mg(NO_3)_2$

Temperature (°C)	Half width (cm^{-1})	Intensity $\frac{I_{360}}{\frac{1}{2}I_{1050}}$ (%)	$\bar{\nu}_{max}$ (cm^{-1})	Centroid (cm^{-1})
−32	29.7	1.84	362.5	364.5
−4	31.4	1.94	361.4	363.2
26	39.1	2.12	358.7	358.0
52	42.7	2.26	357.2	356.3
79	43.3	2.14	355.1	353.6
80	43.2	2.14	355.3	354.5
99	45.5	2.08	354.9	354.1

TABLE 3. Band parameters for the totally symmetric vibration of the hydrated magnesium ion at 25 °C

Concentration (mol kg^{-1})	Half width (cm^{-1})	Intensity $\frac{I_{360}}{\frac{1}{2}I_{1050}}$ (%)	$\bar{\nu}_{max}$ (cm^{-1})	Centroid (cm^{-1})
1.02	36.5	1.78	358.8	358.2
3.06	39.1	2.12	358.7	358.0
4.36	36.8	2.04	358.3	356.5

Can. J. Chem. Downloaded from www.nrcresearchpress.com by 210.87.254.40 on 09/05/12
For personal use only.

Can. J. Chem. Downloaded from www.nrcresearchpress.com by 210.87.254.40 on 09/05/12
For personal use only.

neglected. Such processes may make a small contribution to the line shape of the band from $Zn(H_2O)_6^{2+}$ at the lowest temperatures, where a slightly larger value of ρ was observed, but vibrational motions must be the greatest contributor to the line shape.

Another process which may contribute to line broadening is the exchange of water between the hydration sphere and the bulk solvent. From n.m.r. (19, 20) and ultrasonic studies (21) a rate of the order of 10^6 s^{-1} at room temperature and an activation energy of 12–14 kcal mol^{-1} have been inferred. Although presence of acid or nitrate ion may enhance this rate (22), this process is about five orders of magnitude too slow to broaden a Raman line (23). The observed line was also unaltered by addition of acid. For these reasons we believe this process need not be considered.

For the magnesium ion there is a significant decrease in the vibration frequency and the line shape changes as temperature increases. The potential surface for aquated magnesium is not likely to differ significantly from that of aquated zinc and thus 'hot bands' are not considered to be responsible for these differences. We will explore the plausibility of explanations which involve changes in the solvation number or the solvation geometry.

From examination of Fig. 4 one might infer that increase in temperature causes a lower frequency band to increase in intensity at the expense of the 362 cm^{-1} band. In order to evaluate appropriateness of a two-line model the contours were resolved into two Cauchy–Gauss product functions (15, 16). The effect of constraining the shape function, the positions and/or f.w.h.h.'s for the series was explored. Two bands at 362 and 343 cm^{-1} do fit the contours reasonably well. Two lines could imply a two species equilibrium

$$Mg(H_2O)_6^{2+} + (x - 6)H_2O \rightleftharpoons Mg(H_2O)_x^{2+}$$

In general when an additional halide ion binds to a metal ion the symmetric stretch of the resulting complex occurs at lower frequency (12). The series of complexes $TlCl_x^{(3-x)}$ provides one example of this trend: ν_1 shifts from 327 to 305 in about 7 cm^{-1} steps as x increases from 1 to 4 (24). A new line at 343 cm^{-1} could thus result from the addition of water to the solvation sphere of magnesium for temperatures ≥ -4 °C. From compressibilities and ionic vibration potentials Bockris and Saluja (25) obtained a solvation number of ten for Mg^{2+} which decreased to about five with increasing concentration. The Raman band profile exhibited no significant change in shape for a concentration increase from 1.02 to 4.36 *m*. The dilute solution value of Bockris and Saluja is not consistent with the value six obtained by n.m.r. experiments at low temperatures (22, 26, 27). Although the temperature increase would weaken the water–cation binding and thus permit entry of more water molecules, an increase of four seems unlikely; a closest-packed structure would be implied.

An alternative model which could require two lines but does not require equilibria between variously hydrated forms is heat-induced distortion of the octahedral symmetry. Weakening (and thus lengthening) of two water–cation bonds would lower the symmetry to D_{4h}. The E_g degeneracy would be lifted giving A_{1g} and B_{1g} modes. Two symmetric stretching modes would then occur; one arises from the stretch of the axial bonds and the other from the stretch of the equatorial bonds. Assignment of the two polarized bands at 362 and 343 cm^{-1} to these modes is analogous to a suggestion by Lundeen and Tobias (28) to explain two bands from $Ag(NH_3)_6^{+}$ for the $AgNO_3/NH_3$ system.

Yet another consideration is the possibility that the hydration sphere is perturbed by the introduction of the nitrate ion at higher temperatures. This is unlikely. No diagnostic splitting or asymmetry of the ν_4 band of nitrate ion was observed at any temperature (*cf.* ref. 11). The position of the maximum of the band from $Mg(H_2O)_6^{2+}$ occurs at 355 cm^{-1} and above whereas when nitrate is contacting Mg^{2+}, due to reduced water content, the line occurs at 345 cm^{-1} and lower (11).

Although it is impossible to exclude the above explanations completely, and some contribution to the line shape may come from these sources, the two-line model is not convincing on other grounds. The correlation coefficients from the band fitting program suggest a lack of uniqueness in the results. This is further indicated by failure to converge on the same fit for two spectra at 79 and 80 °C, and by some inconsistency in trends of f.w.h.h. and the ratio of the two band areas. It should also be noted that the spectra fail to display an isosbestic point (Fig. 4).

An alternative model which requires only a

single band, slightly skewed by the hot band, is attractive. As the temperature rises the entire array of ions and water molecules will move apart. The water–cation bonds would be uniformly weakened and the vibration would monotonically shift to lower frequencies. The fact that this effect is observed for Mg^{2+} and not for Zn^{2+} is consistent with the notion that water molecules are more strongly and symmetrically bound to the latter because of the intrinsic covalence endowed by the 'softer' zinc cation (29). The interpretation appears consistent with X-ray studies of aqueous $Mg(NO_3)_2$ solutions (30).

This work was supported by the National Research Council of Canada. The authors also express their gratitude to the Wallenberg Foundation and to the Swedish Natural Sciences Research Council for support for L. Ödberg, to Mr. T. Jarv for preparation of Fig. 1, and to J. Selwood and C. Gendron of the Science Workshop for cell construction.

1. H. S. FRANK and W.-Y. WEN. Discuss. Faraday Soc. **24**, 133 (1957).
2. J. F. HINTON and E. S. AMIS. Chem. Rev. **71**, 627 (1971).
3. S. F. LINCOLN. Coord. Chem. Rev. **6**, 309 (1971).
4. J. P. MATHIEU. C. R. **231**, 896 (1950).
5. R. L. LAFONT. C. R. **244**, 1481 (1957).
6. V. ANANTHANARAYANAN. Z. Phys. **163**, 144 (1961).
7. V. ANANTHANARAYANAN. J. Chem. Phys. **52**, 3844 (1970).
8. T. G. CHANG and D. E. IRISH. Can. J. Chem. **51**, 118 (1973).
9. A. DA SILVEIRA, M. A. MARQUES, and N. M. MARQUES. Mol. Phys. **9**, 271 (1965).
10. R. E. HESTER and R. A. PLANE. Inorg. Chem. **3**, 768 (1964).
11. T. G. CHANG and D. E. IRISH. J. Phys. Chem. **77**, 52 (1973).
12. D. E. IRISH. *In* Ionic interactions. Vol. II. *Edited by* S. Petrucci. Academic Press, New York. 1971. p. 220.
13. J. T. BULMER, D. E. IRISH, F. W. GROSSMAN, G. HERRIOT, M. TSENG, and A. J. WEERHEIM. Appl. Spectrosc. In press.
14. R. N. JONES, T. E. BACH, H. FUHRER, V. B. KARTHA, J. PITHA, K. S. SESHADRI, R. VENKATARAGHAVAN, and R. P. YOUNG. Computer programs for absorption spectrophotometry, N.R.C.C. Bulletin No. 11. National Research Council of Canada, Ottawa. 1968. p. 115.
15. W. F. MURPHY and H. J. BERNSTEIN. J. Phys. Chem. **76**, 1147 (1972).
16. J. PITHA and R. N. JONES. Optimization methods for fitting curves to infrared band envelopes, N.R.C.C. Bulletin No. 12. National Research Council of Canada, Ottawa. 1968. p. 9.
17. J. H. B. GEORGE, J. A. ROLFE, and L. A. WOODWARD. Trans. Faraday Soc. **49**, 375 (1953).
18. J. E. GRIFFITHS, M. CLERC, and P. M. RENTZEPIS. J. Chem. Phys. **60**, 3824 (1974).
19. R. G. WAWRO and T. J. SWIFT. J. Am. Chem. Soc. **90**, 2792 (1968).
20. A. FRATIELLO, V. KUBO, S. PEAK, B. SANCHEZ, and R. E. SCHUSTER. Inorg. Chem. **10**, 2552 (1971).
21. M. EIGEN and L. DEMAYER. *In* Techniques of organic chemistry. Vol. VIII. 2nd ed. *Edited by* A. Weissberger. Interscience Publishers, Inc., New York. 1963.
22. R. D. GREEN and N. SHEPPARD. J. Chem. Soc. Faraday II, **68**, 821 (1972).
23. H. CHEN and D. E. IRISH. J. Phys. Chem. **75**, 2672 (1971).
24. T. G. SPIRO. Inorg. Chem. **4**, 731 (1965).
25. J. O'M. BOCKRIS and P. P. S. SALUJA. J. Phys. Chem. **76**, 2140 (1972).
26. N. A. MATWIYOFF and H. TAUBE. J. Am. Chem. Soc. **90**, 2796 (1968).
27. A. FRATIELLO, R. E. LEE, V. M. NISHIDA, and R. E. SCHUSTER. J. Chem. Phys. **48**, 3705 (1968).
28. J. W. LUNDEEN and R. S. TOBIAS. J. Chem. Phys. **63**, 924 (1975).
29. R. G. PEARSON. J. Am. Chem. Soc. **85**, 3533 (1963); J. Chem. Educ. **45**, 581 (1968); **45**, 643 (1968).
30. M. A. MARQUES and M. I. DEB. MARQUES. Proc. K. Ned. Akad. Wet. B**77**, 286 (1974).

Can. J. Chem. Downloaded from www.nrcresearchpress.com by 210.87.254.40 on 09/05/12
For personal use only.

Magnetic and Spectral Studies on Cobalt(II) and Copper(II) Salts of Methylsulfuric, Trifluoromethylsulfuric, and Paratolylsulfuric Acids

ANITA L. ARDUINI, MAUREEN GARNETT, ROBERT C. THOMPSON, AND TONY C. T. WONG

Department of Chemistry, The University of British Columbia, Vancouver, British Columbia V6T 1W5

Received July 4, 1975

ANITA L. ARDUINI, MAUREEN GARNETT, ROBERT C. THOMPSON, and TONY C. T. WONG. Can. J. Chem. **53**, 3812 (1975).

The compounds $Co(CF_3SO_3)_2$, $Cu(CF_3SO_3)_2$, $Co(CH_3SO_3)_2$, $Cu(CH_3SO_3)_2$, $Co(p\text{-}CH_3C_6H_4SO_3)_2$, and $Cu(p\text{-}CH_3C_6H_4SO_3)_2$ have been prepared and infrared spectra, electronic spectra, and magnetic susceptibility studies are reported. Electronic spectral and magnetic studies have also been made on $Cu(FSO_3)_2$ and previously published data on $Co(FSO_3)_2$ are reexamined here. The studies indicate that in all salts the metal ions are hexacoordinated by oxygen atoms provided by anions acting as tridentate bridging ligands. The MO_6 skeleton is significantly distorted from regular octahedral geometry for all salts with the possible exceptions of $Co(FSO_3)_2$, $Co(p\text{-}CH_3C_6H_4SO_3)_2$, and $Co(CH_3SO_3)_2$. Values of the spin–orbit coupling constants for the salts, as estimated from the magnetic studies, decrease with increasing anion basicity, suggesting a correlation between basicity and the degree of covalent character in the metal–anion bonds. In the case of the cobalt salts the interelectron repulsion parameter B also seems to decrease with increasing anion basicity.

ANITA L. ARDUINI, MAUREEN GARNETT, ROBERT C. THOMPSON et TONY C. T. WONG. Can. J. Chem. **53**, 3812 (1975).

On a préparé les composés $Co(CF_3SO_3)_2$, $Cu(CF_3SO_3)_2$, $Co(CH_3SO_3)_2$, $Cu(CH_3SO_3)_2$, $Co(p\text{-}CH_3C_6H_4SO_3)_2$ et $Cu(p\text{-}CH_3C_6H_4SO_3)_2$ et on rapporte les spectres infrarouges, les spectres électroniques et les études de susceptibilité magnétique. On a aussi déterminé les spectres électroniques et effectué des études magnétiques sur le $Cu(FSO_3)_2$ et on réexamine ici les données publiées antérieurement sur le $Co(FSO_3)_2$. Ces études indiquent que dans tous ces sels les ions métalliques sont hexacoordonnés par des atomes d'oxygène qui leur sont fournis par les anions qui agissent comme ligands tridentates pontés. Le squelette MO_6 est assez déformé de la géométrie octaédrique régulière pour tous les sels à l'exception possiblement de $Co(FSO_3)_2$, $Co(p\text{-}CH_3C_6H_4SO_3)_2$ et $Co(CH_3SO_3)_2$. Les valeurs des constantes de couplage spin–orbite pour les sels, telles que déterminées par les études magnétiques, diminuent avec une augmentation de la basicité de l'anion suggérant une corrélation entre la basicité et le degré du caractère covalent des liens métal–anion. Dans le cas des sels de cobalt, le paramètre B de répulsion interélectronique semble aussi diminuer à mesure que la basicité de l'anion augmente.
[Traduit par le journal]

Introduction

Earlier studies on cobalt(II) and copper(II) salts of fluorosulfuric acid indicated polymeric structures for these compounds with FSO_3^- anions acting as tridentate ligands and metal ions in an environment of six oxygen atoms (1, 2). A structural model was proposed involving a layer type of structure in which each fluorosulfate group acts, via its three oxygen atoms, as a bridge between three different metal ions (2). On the basis of vibrational and electronic spectral studies and magnetic susceptibility measurements $Co(FSO_3)_2$ was shown to have octahedral coordination of cobalt ions with a CoO_6 skeleton not significantly distorted from O_h symmetry. In addition, a relatively high degree of ionic character in the metal–anion bonds was suggested for this salt, consistent with the fact that the fluorosulfate ion is the anion of a very strong acid (3, 4).

The work described here has involved the preparation of a related series of salts: cobalt(II) and copper(II) methylsulfate, trifluoromethylsulfate, and paratolylsulfate. Infrared spectra, electronic spectra, and magnetic susceptibility studies are recorded for these compounds along with the electronic spectrum and magnetic properties of the previously studied salt, $Cu(FSO_3)_2$.

The anions involved here are structurally similar, XSO_3^-, all having the potential to act as tridentate bridging ligands through the three oxygen atoms bonded to sulfur. Indeed, the

Can. J. Chem. Downloaded from www.nrcresearchpress.com by 210.87.254.105 on 09/05/12
For personal use only.

Can. J. Chem. Downloaded from www.nrcresearchpress.com by 210.87.254.105 on 09/05/12
For personal use only.

studies to be presented here indicate that the salts all have similar basic structures and that the general structural model proposed previously for transition metal fluorosulfates (2) is equally plausible for all of the salts under consideration. While the anions are structurally similar their electronic properties are different. From studies on the relative acidities of the parent acids (5, 6) the base strengths of the anions may be considered to increase in the order

$$FSO_3^- \approx CF_3SO_3^- < CH_3SO_3^- \approx p\text{-}CH_3C_6H_4SO_3^-$$

The present work examines, in particular, the effect of such anion differences on details of the molecular and electronic structures of the salts.

Experimental

All solvents and starting materials were reagent grade and used without further purification unless otherwise stated. All of the anhydrous salts were found to be very hygroscopic and required handling in a nitrogen atmosphere dry box. The preparation of $Cu(FSO_3)_2$ has been described previously (7). Analyses were obtained in the A. Bernhardt microanalytical laboratories.

Preparations

Copper(II) Methylsulfate, $Cu(CH_3SO_3)_2$

This salt was prepared by the reaction of copper(II) benzoate with methylsulfuric acid in a procedure analogous to that used previously to prepare copper(II) fluorosulfate (7). Methylsulfuric acid was freshly distilled at approximately 120 °C and 1 Torr into a reaction flask containing copper(II) benzoate. Rapid reaction occurred and the insoluble, white, copper(II) methylsulfate was vacuum filtered, washed several times with diethyl ether, and dried under vacuum at room temperature.

Anal. Calcd. for $CuC_2H_6S_2O_6$: Cu, 25.0; S, 25.3; C, 9.46; H 2.38. Found: Cu, 25.2; S, 25.4; C, 9.63; H, 2.56.

Copper(II) Trifluoromethylsulfate, $Cu(CF_3SO_3)_2$

Trifluoromethylsulfuric acid was freshly distilled at about 70 °C and 20 Torr into a reaction flask containing copper(II) benzoate. The white, insoluble, salt was filtered, washed with freshly distilled trifluoromethylsulfuric acid, and dried under vacuum at 60 °C.

Anal. Calcd. for $CuC_2F_6S_2O_6$: Cu, 17.6; C, 6.64; F, 31.5; S, 17.7. Found: Cu, 17.7; C, 6.71; F, 31.5; S, 17.4.

Copper(II) Paratolysulfate, $Cu(p\text{-}CH_3C_6H_4SO_3)_2$

This compound was prepared by the reaction of aqueous solutions of silver(I) paratolysulfate and copper(II) chloride dihydrate in stoichiometric proportions. After removal of precipitated silver(I) chloride from the solution, the filtrate was evaporated to dryness yielding a pale blue solid. Dehydration of this solid by heating to 70 °C under vacuum gave the pale green anhydrous salt.

Anal. Calcd. for $CuC_{14}H_{14}S_2O_6$: Cu, 15.7; C, 41.4; H, 3.48; S, 15.8. Found: Cu, 16.0; C, 41.2; H, 3.72; S, 16.0.

Cobalt(II) Methylsulfate, $Co(CH_3SO_3)_2$

Barium methylsulfate, prepared as described previously (8) and cobalt(II) sulfate heptahydrate were reacted in stoichiometric proportions in aqueous solution. After removal of precipitated barium sulfate, the solution was evaporated to dryness and heating the product at 100 °C under vacuum gave the pale purple anhydrous salt.

Anal. Calcd. for $CoC_2H_6S_2O_6$: C, 9.63; H, 2.43; S, 25.7; Co, 23.7. Found: C, 9.51; H, 2.55; S, 25.5; Co, 23.8.

Cobalt(II) Trifluoromethylsulfate, $Co(CF_3SO_3)_2$

Using a procedure analogous to that described previously for the preparation of cobalt(II) fluorosulfate (2), excess trifluoromethylsulfuric acid was freshly distilled at 8 Torr and 56 °C into a reaction flask containing finely powdered anhydrous cobalt(II) metabromobenzoate. A pink precipitate of cobalt(II) trifluoromethylsulfate formed immediately in the exothermic reaction; the reaction mixture was left stirring for 48 h to ensure completion of the reaction. The solid product was filtered and dried under vacuum at 65 °C.

Anal. Calcd. for $CoC_2F_6S_2O_6$: C, 6.73; F, 31.9; S, 18.0; Co, 16.5. Found: C, 6.91; F, 31.7; S, 17.7; Co, 16.5.

Cobalt(II) Paratolysulfate, $Co(p\text{-}CH_3C_6H_4SO_3)_2$

This salt was prepared by the reaction of aqueous solutions of silver(I) paratolylsulfate and cobalt(II) chloride hexahydrate in stoichiometric proportions. After removal of precipitated silver chloride by filtration, the solution was evaporated to dryness. Heating the product at 120 °C under vacuum gave the pale blue anhydrous salt.

Anal. Calcd. for $CoC_{14}H_{14}S_2O_6$; C, 41.9; H, 3.52; S, 16.0; Co, 14.7. Found: C, 41.9; H, 3.63; S, 15.7; Co, 14.9.

Physical Methods

Infrared spectra were obtained on samples mulled in Nujol and contained between KRS-5 (Harshaw Chemical Co.) plates on a Perkin–Elmer model 457 spectrophotometer. Spectra were calibrated using polystyrene film and frequencies are considered accurate to ± 4 cm^{-1}.

Electronic spectra were obtained on powdered samples (diffuse reflectance) over the range 13.5–28.5 kK using a Bausch and Lomb Spectronic 600 spectrophotometer and on samples mulled in hexachlorobutadiene and Nujol over the range 5–33 kK using a Cary model 14 spectrophotometer. The mull spectra were corrected for background due to light scattering from the sample (2).

Magnetic susceptibilities were determined at field strengths of approximately 4500 and 7000 G using the Guoy equipment and calibration procedure described previously (2). None of the samples gave evidence for dependence of magnetic susceptibilities on field strength. The diamagnetic susceptibilities used to correct molar magnetic susceptibility values for the diamagnetic contributions of ligands and metal ions are: 11×10^{-6} for copper, 13×10^{-6} for cobalt, 40×10^{-6} for FSO_3^-, 46×10^{-6} for $CF_3SO_3^-$, 35×10^{-6} for $CH_3SO_3^-$, and 89×10^{-6} for $CH_3C_6H_4SO_3^-$ (all values in units of cm^3 mol^{-1}).

Results and Discussion

Infrared Spectra

The infrared spectra (over the frequency range 250 to 1400 cm^{-1}) are given in Table 1 together with data previously reported (7) on $Cu(FSO_3)_2$ and $Co(FSO_3)_2$. Previous studies on the vibra-

Can. J. Chem. Downloaded from www.nrcresearchpress.com by 210.87.254.105 on 09/05/12
For personal use only.

TABLE 1. Infrared spectra[a]

C_{3v} assignment for XSO_3 part	Infrared frequencies (cm^{-1})							
	$Cu(FSO_3)_2$[b]	$Cu(CF_3SO_3)_2$	$Cu(CH_3SO_3)_2$	$Cu(p\text{-}CH_3C_6H_4SO_3)_2$	$Co(FSO_3)_2$[b]	$Co(CF_3SO_3)_2$	$Co(CH_3SO_3)_2$	$Co(p\text{-}CH_3C_6H_4SO_3)_2$
$\nu_4(E)SO_3$ as. stretch	1306 vs	1280 s	1283 m	1275 s	1266 vs	1235 s	1233 s	1200 s
	1223 vs	1225 s	1187 s	1266 sh			1170 s	
			1141 s	1240 sh				
				1160 s				
$\nu_1(A_1)SO_3$ sym. stretch	1115 s	1058 s	1086 m	1130 s	1114 s	1042 s	1070 s	1143 m
			1074 m	1110 s				
$\nu_2(A_1)SX$ stretch	861 s		786 m	680 s	858 s		787 s	673 m
$\nu_5(E)SO_3$ as. defn.	630 m	640 s	574 m	588 m	614 s	630 s	590 m	570 m
	604 m		561 m	575 m			530 m	
			550 sh	560 m				
$\nu_3(A_1)SO_3$ sym. defn.	564 m	530 m	517 w	490 w	568 m	525 m	512 m	488 w
			510 w					
$\nu_6(E)SX$ defn. $+CH_3$, CF_3 and $CH_3C_6H_4$ internal vibrations	428 m	1183 m	1352 w	1080 m	422 m	1197 m	1330 w	1105 vw
	416 m	608 w	1336 w	1056 m		945 w	970 w	1063 m
	300 m	592 w	1246 w	1042 m		610 sh	385 w	1045 vw
		388 w	1256 w	1013 m		595 w	373 w	1015 m
		372 w	1110 vw	950 vw		358 m	350 w	950 vw
		340 w	980 w	815 m		350 m		815 m
			398 w	705 w				703 w
				635 vw				635 vw
				425 w				398 w
				380 w				370 w
				365 sh				335 w

[a]v = very, s = strong, m = medium, w = weak, sh = shoulder, as. = asymmetric, sym. = symmetric, defn. = deformation.
[b]Data from ref. 7.

Can. J. Chem. Downloaded from www.nrcresearchpress.com by 210.87.254.105 on 09/05/12
For personal use only.

tional spectra of fluorosulfates (1, 7, 9) methylsulfates (10, 11) and trifluoromethylsulfates (11–14) have provided a considerable amount of information in regard to the fundamental modes of vibration of these anions and, in the present work, have made possible the identification of those bands arising primarily from SO_3 stretching, SC stretching, and SO_3 deformation vibrations of the CSO_3 parts of the anions. This is done in Table 1 where C_{3v} nomenclature is used in band assignment. The $\nu_6(E)$ mode which occurs at 422 cm^{-1} in the spectrum of $Co(FSO_3)_2$ and appears as a split band at 428 and 416 cm^{-1} in $Cu(FSO_3)_2$ is not identified in the spectra of the other salts.

In addition, we were not able to identify with certainty the $\nu_2(A_1)$ mode described as an SC stretch in the spectra of $Cu(CF_3SO_3)_2$ and $Co(CF_3SO_3)_2$. A very weak peak is observed at 775 cm^{-1} in the spectra of both salts and this may be the ν_2 vibration. No attempt is made here at a detailed assignment of the internal vibrations of the CF_3, CH_3, and $CH_3C_6H_4$ parts of the anions. We do note, however, that bands at 1183 and 592 cm^{-1} in $Cu(CF_3SO_3)_2$ and at 1197 and 595 cm^{-1} in $Co(CF_3SO_3)_2$ may be assigned to CF_3 stretching and bending modes respectively. Other bands due to CF_3 vibrations in these salts are obscured by the relatively more intense SO_3 vibrations.

The vibrational spectra of $Co(CF_3SO)_2$ and $Co(p\text{-}CH_3C_6H_4SO_3)_2$ indicate C_{3v} symmetry for the CSO_3 groups in these salts. Within the limitation of resolution of the instrument used ($\sim$3 cm^{-1}) there is no evidence for splitting of either the $\nu_4(E)$ or $\nu_5(E)$ modes which would result from a lowering of symmetry below C_{3v}. We interpret this result as indicating that the anions are acting as tridentate bridging ligands in which the three oxygens are involved in coordination in an equivalent manner to cobalt ions. This form of anion coordination was proposed earlier for a number of metal bisfluorosulfates including $Co(FSO_3)_2$ (2, 7). The CSO_3 groups in $Co(CH_3SO_3)_2$ and $Cu(CF_3SO_3)_2$ have symmetries reduced below C_{3v} as evidenced by a splitting of ν_4 in the case of the copper salt and a splitting of both ν_4 and ν_5 in the case of the cobalt salt. This reduction in symmetry may result from a form of coordination in which two oxygen atoms of each anion are more strongly bonded to the metal ion than the third as described previously for $Cu(FSO_3)_2$ (1, 2).

The infrared spectra of $Cu(CH_3SO_3)_2$ and $Cu(p\text{-}CH_3C_6H_4SO_3)_2$ are relatively more complex than those described above. Whereas a maximum of three bands are expected in each of the SO_3 stretching and deformation regions, four to six bands are observed in these salts indicating the presence of more than one type of anion in the lattice. The postulate of non-equivalent fluorosulfate ions in $Sr(FSO_3)_2$, $Sn(FSO_3)_2$, $Pb(FSO_3)_2$, and $Sn(FSO_3)_4$ was made previously to account for similar complexities in their vibrational spectra (7, 15).

Electronic Spectra and Magnetism of Copper Salts

The electronic spectra of all four copper salts (including $Cu(FSO_3)_2$, the spectrum of which has not been reported previously) consist of absorption in the near-infrared region over the range of about 8.0 to 14.0 kK. $Cu(FSO_3)_2$, $Cu(CF_3SO_3)_2$, and $Cu(p\text{-}CH_3C_6H_4SO_3)_2$ exhibit single, broad, asymmetrical bands with band maxima at 10.4, 10.4, and 11.2 kK respectively. The absorption spectrum of $Cu(CH_3SO_3)_2$ is centered at about 10.8 kK and consists of a principal band with a maximum at 11.6 kK and a strong shoulder at about 9.5 kK. These ligand field bands are at 1 to 2 kK lower in energy than oberved for aqueous copper(II) consistent with hexacoordination of copper by ligands slightly lower than H_2O in the spectrochemical series.

Assuming an elongated tetragonal CuO_6 octahedron (D_{4h} symmetry), as was suggested previously for $Cu(FSO_3)_2$ (1, 2) three electronic transitions are expected, corresponding to transitions from a ground $^2B_{1g}$ state to excited $^2A_{1g}$, $^2B_{2g}$, and ^2E_g states. The absorption bands observed here likely contain all three transitions (or four if the symmetry is lower), only partly resolved in the case of $Cu(CH_3SO_3)_2$ and unresolved for the other three salts. Band energies in the electronic spectra of copper(II) species are determined, not only by the ligand field strengths of the ligands involved, but also by the degree of distortion from O_h symmetry. It has been shown, for example, that in ethylenediamine complexes of copper(II), band energies increase with increasing degree of tetragonal distortion (16) a consequence, largely, of a shift in the $^2B_{1g} \rightarrow {}^2E_g$ component to higher energies (17). The relatively low band energies observed for $Cu(FSO_3)_2$ and $Cu(CF_3SO_3)_2$ compared to the

TABLE 2. Magnetic moment data for copper salts[a,b]

$Cu(FSO_3)_2$ (t.i.p. = 100×10^{-6})		$Cu(CF_3SO_3)_2$ (t.i.p. = 100×10^{-6})		$Cu(CH_3SO_3)_2$ (t.i.p. = 90×10^{-6})		$Cu(p\text{-}CH_3C_6H_4SO_3)_2$ (t.i.p. = 93×10^{-6})	
T (K)	μ_{eff}	T (K)	μ_{eff}	T (K)	μ_{eff}	T (K)	μ_{eff}
312	2.08	311	1.87	306	1.88	311	1.91
300	2.08	301	1.87	289	1.87	301	1.92
287	2.07	289	1.87	273	1.88	290	1.93
272	2.08	271	1.87	245	1.88	265	1.92
240	2.08	240	1.86	214	1.88	234	1.93
211	2.08	212	1.85	185	1.87	214	1.92
181	2.07	181	1.85	156	1.86	177	1.94
152	2.07	153	1.84	136	1.85	145	1.93
123	2.07	127	1.82	122	1.87	132	1.93
100	2.07			95	1.82	96	1.93

[a]t.i.p. = $4N\beta^2/\Delta$ (18). The Δ values, obtained from the electronic spectra, were 10.4, 10.4, 11.6, and 11.2 kK for $Cu(FSO_3)_2$, $Cu(CF_3SO_3)_2$, $Cu(CH_3SO_3)_2$, and $Cu(p\text{-}CH_3C_6H_4SO_3)_2$ respectively. t.i.p. values are in units of $cm^3\ mol^{-1}$.
[b]$\mu_{eff} = 2.828\ [(\chi_M - \text{t.i.p.})T]^{1/2}$ B.M., where χ_M is the molar magnetic susceptibility corrected for the diamagnetism of all atoms and t.i.p. is the temperature independent paramagnetism.

other two salts may reflect both a smaller degree of tetragonal distortion in the salts and a weaker ligand field strength associated with the FSO_3^- and $CF_3SO_3^-$ anions.

Magnetic susceptibility data, obtained over the temperature range 312–95 K for the copper salts, are given in Table 2. Magnetic moment data for $Cu(FSO_3)_2$ were reported previously by Goubeau and Milne (1) and our results are in good agreement with the earlier study. The magnetic moments observed for all four salts are essentially temperature independent and of a magnitude normally observed for hexacoordinated copper(II) (18).

For a copper(II) ion a tetragonally elongated octahedral environment the magnetic susceptibility is anisotropic (19) and the average magnetic moment is given by the expression

$$\bar{\mu} = \left[\left(1 - \frac{4k_{\parallel}\lambda}{\Delta_2}\right)^2 + 2\left(1 - \frac{k_{\perp}\lambda}{\Delta_3}\right)^2\right]^{1/2}$$

where $k_{\parallel}$ and $k_{\perp}$ are orbital reduction factors, λ is the spin–orbit coupling constant, and Δ_2 and Δ_3 are the energy separations between the ground $^2B_{1g}$ state and the excited $^2B_{2g}$ and ^2E_g states respectively. Setting Δ_2 and Δ_3 at values ranging from 10.4 kK to 11.6 kK, as appropriate for the salts under consideration here, and $k_{\parallel}\lambda$ and $k_{\perp}\lambda$ at $-830\ cm^{-1}$ (free-ion value), the calculated values of $\bar{\mu}$ range from 1.99 to 2.02 B.M. The magnetic moments observed for three of the salts under investigation are significantly lower than these calculated values consistent with, as is commonly observed, a reduction in $k\lambda$ values below the free ion value. The relatively high magnetic moment observed for $Cu(FSO_3)_2$ indicates higher $k\lambda$ values for this salt compared to the other three. This, in turn, may reflect a relatively high degree of ionic character in the metal–anion bonds implying that, compared to the other three anions, FSO_3^- is a significantly weaker base towards copper ion.

Electronic Spectra and Magnetism of Cobalt Salts

The electronic spectra of $Co(CF_3SO_3)_2$, $Co(CH_3SO_3)_2$, and $Co(p\text{-}CH_3C_6H_4SO_3)_2$, with band assignments assuming a ligand environment of O_h symmetry about cobalt(II), are given in Table 3. The shoulder at 20.6 kK appears also in the spectrum of $Co(FSO_3)_2$ and has been assigned to an enhanced spin-forbidden transition (2). It is not possible to say for certain whether the additional structure which appears on the visible bands of $Co(CH_3SO_3)_2$ and $Co(p\text{-}CH_3C_6H_4SO_3)_2$ is due to spin–orbit coupling, low-symmetry splitting of the $^4T_{1g}(P)$ level or enhanced spin-forbidden transitions to doublet states. It has been pointed out (20) that in such cases the last possibility is likely in view of the presence of a number of doublet states near the $^4T_{1g}(P)$ state (21).

The ligand field parameters Dq and B were calculated as before (2) using the $^4T_{1g}(F) \rightarrow {}^4T_{2g}(F)$ transition energies given in Table 3 and the values 18.4, 17.9, and 17.6 kK (the latter value estimated from the center of the visible band) for the $^4T_{1g}(F) \rightarrow {}^4T_{1g}(P)$ transitions observed in the diffuse reflectance spectra of

Can. J. Chem. Downloaded from www.nrcresearchpress.com by 210.87.254.105 on 09/05/12
For personal use only.

TABLE 3. Electronic spectra of cobalt salts

Energies of band maxima (kK)*						
$Co(CF_3SO_3)_2$		$Co(CH_3SO_3)_2$		$Co(p\text{-}CH_3C_6H_4SO_3)_2$		
(a)	(b)	(a)	(b)	(a)	(b)	Assignment
20.6 sh	20.6 sh	20.6 sh	20.6 sh	20.4 sh	20.6 sh	—
18.4	18.6	17.9	18.3	18.3	18.5	$^4T_{1g}(F) \rightarrow {}^4T_{1g}(P)$
				16.9	17.1	
		16.0 sh	16.1 sh	16.0 sh	16.1 sh	
	13.8					$\rightarrow {}^4A_{2g}(F)$
	6.80		6.67		6.80	$\rightarrow {}^4T_{2g}(F)$

*(a) Diffuse reflectance spectra, (b) mull spectra.

TABLE 4. Parameters Dq, B, λ, v, and k for cobalt salts

	Value			
Parameter	$Co(FSO_3)_2$[a]	$Co(CF_3SO_3)_2$	$Co(CH_3SO_3)_2$	$Co(p\text{-}CH_3C_6H_4SO_3)_2$
$Dq(cm^{-1})$	765	780	765	780
$B(cm^{-1})$	860	840	815	790
$-\lambda(cm^{-1})$	170	170	150	130
v	0	−3	0	0
k	1	0.9	1	1

[a]Data taken from ref. 2.

$Co(CF_3SO_3)_2$, $Co(CH_3SO_3)_2$, and $Co(p\text{-}CH_3C_6H_4SO_3)_2$ respectively. Values of Dq and B are given in Table 4 and, because of uncertainties in transition energies due to the broad nature of the ligand field bands, the parameters are considered accurate only to about $\pm 20\ cm^{-1}$. Thus, within experimental uncertainties, there is no difference in Dq values for the different salts and the variation in B is just significant. The B parameter is significantly lower than the free-ion value of 971 cm^{-1} in all salts.

The magnetic susceptibilities of $Co(CF_3SO_3)_2$, $Co(CH_3SO_3)_2$, and $Co(p\text{-}CH_3C_6H_4SO_3)_2$ were measured over the temperature range 310–85 K and the data are given in Table 5. All three salts exhibit magnetic moments which are in excess of the spin-only value and which are temperature dependent as expected for hexacoordinated cobalt(II).

The effects of electron delocalization and low symmetry ligand fields on the magnetic properties of complexes with $^4T_{1g}$ ground terms have been examined by Figgis *et al.* (22). These authors have calculated theoretical magnetic moments from expressions involving four parameters: λ, spin–orbit coupling constant; k, the orbital reduction factor which allows for a reduction in the orbital contribution to the magnetic moment due to electron delocalization; v, the distortion parameter which is equal to Δ/λ where Δ is the magnitude of splitting of the $^4T_{1g}(F)$ term by fields of axial symmetry, and A, which allows for the admixture of the higher lying $^4T_{1g}(P)$ term into the ground $^4T_{1g}(F)$ term by the primary cubic field. The experimental magnetic moment values for salts studied here were compared to the theoretical data tabulated by Figgis *et al.* and reasonable fits were obtained with $A = 1.43$ for all three salts and with the values of λ, k, and v listed in Table 4. The magnetic moment values given by the theory for each set of parameter values are given in Table 5 to enable a direct comparison between experiment and theory. The accuracy to which the parameters are determined is considered to be about $\pm 5\%$ in the case of k and λ and, because of the relative intensitivity of the calculated magnetic moments to small distortions, ± 2 in the case of v.

The analysis of the magnetic data for $Co(CF_3SO_3)_2$ gives $v = -3$, implying a splitting of the ground $^4T_{1g}(F)$ term by about 500 cm^{-1}. We note that the effect of this low symmetry field is not sufficiently large to give an observable splitting of the bands in the electronic spectrum

Can. J. Chem. Downloaded from www.nrcresearchpress.com by 210.87.254.105 on 09/05/12
For personal use only.

TABLE 5. Magnetic moment data for cobalt salts

$Co(CF_3SO_3)_2$			$Co(CH_3SO_3)_2$			$Co(p\text{-}CH_3C_6H_4SO_3)_2$		
	μ_{eff}			μ_{eff}			μ_{eff}	
T (K)	Exp.[a]	Theory[b]	T (K)	Exp.[a]	Theory[b]	T (K)	Exp.[a]	Theory[b]
310	4.87	4.85	307	5.18	5.14	310	5.19	5.13
300	4.86	4.85	286	5.16	5.14	300	5.18	5.14
299	4.86	4.85	275	5.16	5.14	290	5.17	5.14
288	4.85	4.84	245	5.14	5.13	257	5.16	5.14
263	4.83	4.83	222	5.11	5.11	230	5.14	5.14
234	4.81	4.80	218	5.10	5.10	200	5.09	5.12
206	4.78	4.77	185	5.04	5.05	170	5.06	5.07
174	4.72	4.72	174	5.02	5.03	140	4.96	4.99
145	4.64	4.64	159	4.97	4.98	115	4.92	4.87
125	4.58	4.57	139	4.89	4.90	100	4.82	4.78
107	4.56	4.49	133	4.89	4.88	95	4.75	4.74
95	4.43	4.43	123	4.84	4.82	85	4.68	4.67
84	4.36	4.36	111	4.76	4.75			
			99	4.66	4.67			

[a]$\mu_{eff} = 2.828\,(\chi_M T)^{1/2}$ where χ_M is the experimentally determined molar magnetic susceptibility corrected for the diamagnetism of all atoms.
[b]Data obtained from ref. 22 for $A = 1.43$ and λ, v, and k values given in Table 4.

of this salt. In addition, the observation of an infrared spectrum which shows C_{3v} symmetry for the CSO_3 part of the anion suggests the distortion of the CoO_6 skeleton is of a trigonal nature in which all of the metal–oxygen interactions remain equivalent and in which the C_{3v} symmetry of the anion is retained. The fact that $v = 0$ for the other salts implies less distortion of the CoO_6 skeleton in these salts; although, because of the relative insensitivity of the calculated magnetic moments to small distortions it is possible that distortions giving rise to splitting of ground terms by as much as 300 cm^{-1} could go undetected by the magnetic moment results.

The variation in λ values for the four cobalt salts under discussion correlates quite well with the variation in anion basicities given in the introduction. As the base strength of the anion increases the value of λ for the salt decreases; if λ reflects the degree of covalent bonding, there is a correlation between basicity and the degree of covalent character in the metal–anion bonds. The interelectron repulsion parameter, B, also provides a measure of covalent character in metal–ligand bonds and a similar reduction in B on going from $Co(FSO_3)_2$ and $Co(CF_3SO_3)_2$ to $Co(p\text{-}CH_3C_6H_4SO_3)_2$ is indicated by the analysis of the spectral data as discussed above. The values of k obtained for the four cobalt salts are all relatively high and the lack of correlation with λ is, according to Figgis *et al.* (22), not unexpected. These authors point out that the k values do not, in fact, provide a good measure of the degree of covalent bonding.

Financial support provided by a grant from the National Research Council of Canada is gratefully acknowledged.

1. J. GOUBEAU and J. B. MILNE. Can. J. Chem. **45**, 2321 (1967).
2. J. M. TAYLOR and R. C. THOMPSON. Can. J. Chem. **49**, 511 (1971).
3. R. J. GILLESPIE. Acc. Chem. Res. **1**, 202 (1968).
4. R. C. THOMPSON. *In* Inorganic sulphur chemistry. *Edited by* G. Nickless. Elsevier. Amsterdam. 1968. p. 587.
5. J. BARR, R. J. GILLESPIE, and E. A. ROBINSON. Can. J. Chem. **39**, 1266 (1961).
6. A. ENGELBRECHT and B. M. RODE. Monatsh. Chem. **103**, 1315 (1972).
7. C. S. ALLEYNE, K. O'SULLIVAN MAILER, and R. C. THOMPSON. Can. J. Chem. **52**, 336 (1974).
8. T. GRAMSTAD and R. N. HASZELDINE. J. Chem. Soc. 173 (1956).
9. A. RUOFF, J. B. MILNE, G. KAUFMANN, and M. LEROY. Z. Anorg. Allg. Chem. **372**, 119 (1970).
10. R. J. GILLESPIE and E. A. ROBINSON. Can. J. Chem. **40**, 644 (1962).
11. H. BURGER, K. BURCZYK, and A. BLASCHETTE. Monatsh. Chem. **101**, 102 (1970).
12. F. A. SCHRÖDER, B. GÄNSWEIN, and G. BRAUER. Z. Anorg. Allg. Chem. **391**, 295 (1972).
13. P. A. YEATS, J. R. SAMS, and F. AUBKE. Inorg. Chem. **10**, 1877 (1971).
14. J. R. DALZIEL, R. D. KLETT, P. A. YEATS, and F. AUBKE. Can. J. Chem. **52**, 231 (1974).

Can. J. Chem. Downloaded from www.nrcresearchpress.com by 210.87.254.105 on 09/05/12
For personal use only.

15. P. A. YEATS, B. L. POH, B. F. E. FORD, J. R. SAMS, and F. AUBKE. J. Chem. Soc. (A), 2188 (1970).
16. A. B. P. LEVER and E. MANTOVANI. Inorg. Chem. **10**, 817 (1971).
17. B. J. HATHAWAY, D. E. BILLINGS, P. NICHOLLS, and I. M. PROCTOR. J. Chem. Soc. A, 319 (1969).
18. B. N. FIGGIS and J. LEWIS. *In* Progress in inorganic chemistry. Vol. 6. *Edited by* F. A. Cotton. Interscience, New York. 1965. p. 37.
19. F. E. MABBS and D. J. MACHIN. Magnetism and transition metal complexes. Chapman and Hall, London. 1973.
20. A. B. P. LEVER. Inorganic electronic spectroscopy. Elsevier Publ. Co., Inc., Amsterdam. 1968.
21. J. FERGUSON, D. WOOD, and K. KNOX. J. Chem. Phys. **39**, 881 (1963).
22. B. N. FIGGIS, M. GERLOCH, J. LEWIS, F. E. MABBS, and G. A. WEBB. J. Chem. Soc. A, 2086 (1968).

Can. J. Chem. Downloaded from www.nrcresearchpress.com by 210.87.254.105 on 09/05/12
For personal use only.

Studies on the Syntheses of Heterocyclic Compounds. Part DCXXXVI.[1] An Alternative Synthesis of Pentazocine

TETSUJI KAMETANI, TOSHIO HONDA, SHYH-PYNG HUANG, AND KEIICHIRO FUKUMOTO

Pharmaceutical Institute, Tohoku University, Aobayama, Sendai, Japan

Received June 10, 1975

TETSUJI KAMETANI, TOSHIO HONDA, SHYH-PYNG HUANG, and KEIICHIRO FUKUMOTO. Can. J. Chem. **53**, 3820–3823 (1975).

The important starting material in a synthesis of pentazocine (**1**) was easily prepared by treating gaseous formaldehyde with 2-lithio-2-butene. Both *E*- and *Z*-2-bromo-2-butenes (**2**, **3**) gave the same *Z*-type of alcohol (**4**) which was converted into pentazocine.

TETSUJI KAMETANI, TOSHIO HONDA, SHYH-PYNG HUANG et KEIICHIRO FUKUMOTO. Can. J. Chem. **53**, 3820–3823 (1975).

On a préparé, par réaction de la formaldehyde à l'état gazeux avec le lithio-2 butène-2, le composé important pour la synthèse de la pentazocine (**1**). Les deux bromo-2 butènes-3 *E* et *Z* (**2**, **3**) conduisent au même alcool de type *Z* (**4**) qui peut être transformé en pentazocine.

[Traduit par le journal]

Previously, we reported two simple syntheses of pentazocine (**1**) (1, 2), an analgesic agent having no addiction liability (3–7), by Pictet–Spengler type reaction and Bischler–Napieralski type reaction. In both cases, the starting material is a mixture of two isomers, 1-cyano-2-methyl-1-

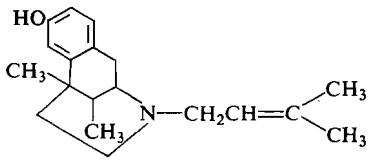

1

butene (**14**) and 1-cyano-2-methyl-2-butene (**13**), obtained by condensation of ethyl methyl ketone with cyanoacetic acid, and the stereochemistry of both compounds (**13** and **14**) is unknown. In order to clarify these points we have investigated the selective synthesis of 1-cyano-2-methyl-2-butene (**6**) whose stereochemistry was also determined easily, and here we wish to report a novel synthesis of *Z*-type 1-cyano-2-methyl-2-butene and the conversion of **6** into pentazocine (**1**).

The lithium derivatives (8) of *E*- and *Z*-2-bromo-2-butenes were prepared at −10 to −20 °C by reaction with lithium metal, and these were treated with formaldehyde gas separately to give the same *Z*-type alcohol (**4**) in 63% yield. The structure was easily determined by n.m.r. spectral analysis which showed a methylene proton at δ 3.96 as a singlet, indicating a *Z*-type olefin, while the corresponding signal in the *E*-isomer (11) should appear at higher field (δ 3.75–3.80). It has been reported by Lenox and Katzenellenbogen (11) that both the *E*- and *Z*-isomer were separable by gas chroma-

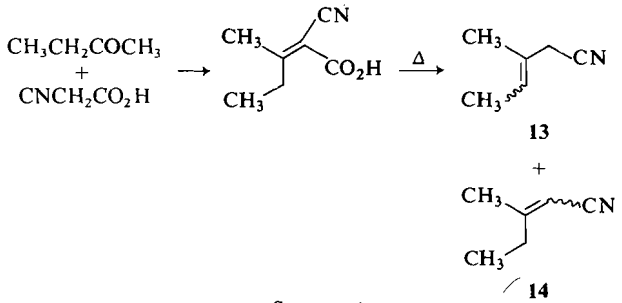

SCHEME 1

[1]For part DCXXXV, see ref. 12.

Can. J. Chem. Downloaded from www.nrcresearchpress.com by 210.87.254.42 on 09/05/12
For personal use only.

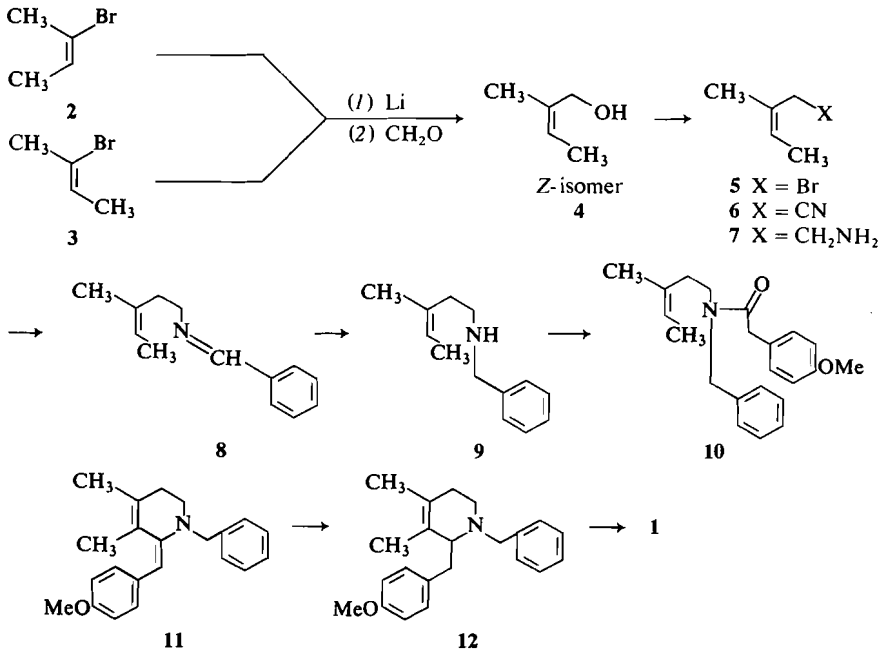

SCHEME 2

tography. However, our product (**4**) showed only one peak in the gas chromatogram in a condition described in the experimental part, indicating that it was not a mixture of the *E*- and *Z*-isomer. Although it has been reported (8, 9) that the reaction products of 2-lithio-2-butene with various electrophiles retained the configuration of the starting material, we obtained only the *Z*-type of alcohol from both the *Z*- and *E*-2-lithio-2-butenes, but the mechanism was not clear in this reaction. On the other hand, the *E*- and *Z*-type of alcohols have previously been prepared by two groups (10, 11). A convenient method using easily available starting materials has just been developed in our laboratory.

Treatment of the alcohol (**4**) with phosphorus tribromide gave the allylic bromide (**5**) which was converted into the corresponding cyanide (**6**) in 55% yield without the migration of the double bond by cuprous cyanide. Hydrogenation of the nitrile (**6**) in the presence of Raney cobalt in methanol, followed by condensation with benzaldehyde, afforded the Schiff base (**8**) which was treated with sodium borohydride to give in 56% yield the secondary amine (**9**). Schotten–Baumann reaction of the amine (**9**) with 4-methoxyphenylacetic acid chloride gave the tertiary amide (**10**) in 94% yield. Bischler–Napieralski reaction of the amide (**10**), followed by reduction with sodium borohydride, gave in 43% yield the 1-benzyl-1,2,5,6-tetrahydro-2-(4-methoxybenzyl)-3,4-dimethylpyridine (**12**), which was identical with the authentic sample.[2] The tetrahydropyridine derivative (**12**) was already converted into pentazocine. Thus, we were able to carry out satisfactorily the synthesis of pentazocine by using a facile method.

Experimental

Melting points are uncorrected. The i.r. spectra were taken in $CHCl_3$ solution with a Hitachi EPI-S2 spectrometer. Nuclear magnetic resonance spectra were measured on a JEOL JNM-PMX 60 in CCl_4 solution using TMS as an internal standard. The apparatus used for gas chromatography was a Shimazu GC 6A equipped with a hydrogen flame ionization detector and a 'silanized' spiral glass column (1 m × 3 mm i.d.). The column was packed with 10% Carbowax 6000 or 10% DEGS. Column temperature was 130 °C. Both the detector and flash heater were maintained at 150 °C. Nitrogen was used as a carrier gas at a flow-rate of 21 ml/min.

2-Methyl-2-butene-1-ol (4)

Lithium (2.3 g) was cut into small pieces and placed in a three-necked flask containing ether (200 ml), to which *E*-2-bromo-2-butene (20 g) was added with stirring at −10 to −20 °C. The addition requires about 1 h, and the

[2]The authentic sample was given by Dr. K. Kigasawa, Grelan Pharmaceutical Company.

Can. J. Chem. Downloaded from www.nrcresearchpress.com by 210.87.254.42 on 09/05/12
For personal use only.

Can. J. Chem. Downloaded from www.nrcresearchpress.com by 210.87.254.42 on 09/05/12
For personal use only.

mixture was then stirred for a further 30 min at −10 °C. Formaldehyde gas, prepared by heating paraformaldehyde, was then distilled into the stirred reaction mixture at −10 °C. The reaction mixture was stirred at room temperature for 3 h and then treated with a saturated aqueous ammonium chloride solution. The ethereal layer was separated and the aqueous phase was extracted with ether. The combined extracts were washed with water and dried over Na_2SO_4. Evaporation of the solvent gave an oil which was distilled to afford the alcohol (**4**) (8 g) (63%) as a colorless oil; b.p. 58–60 °C/11 Torr; ν_{max} 3600 and 3450 (OH); n.m.r. δ 1.58 ($CH_3CH{=}C$<, 3H, d, J = 8 Hz), 1.68 (CH_3C=<, 3H, s), 3.96 (CH_2OH, 2H, s), and 5.22 (olefinic proton, 1H, q, J = 8 Hz).

Anal. Calcd. for $C_5H_{10}O$: C, 69.72; H, 11.70. Found: C, 69.24; H, 11.30.

The reaction of the *Z*-2-bromo-2-butene with lithium metal was carried out in the same manner as in the case of the *E*-isomer to give the lithium derivative, which was then treated with formaldehyde gas to afford the allylic alcohol (**4**). The alcohol was identical with that obtained from the *E*-2-bromo-2-butene by n.m.r. spectral and gas chromatographic comparisons.

*1-Cyano-2-methyl-2-butene (**6**)*

To a solution of the alcohol (**4**) (10 g) in methylene chloride (50 ml) was added dropwise phosphorus tribromide (10 g) at 0 °C with stirring. After stirring for an additional 1 h at the same temperature, the solution was washed with water and dried over Na_2SO_4. Evaporation of the solvent gave the allylic bromide (**5**) which was used in the next reaction without purification. A mixture of the bromide (**5**), cuprous cyanide (10 g), and dimethylformamide (50 ml) was stirred at room temperature for 5 h. The reaction mixture was poured into an excess of water and extracted with ether. The ethereal solution was washed with water, dried over Na_2SO_4, and evaporated. Vacuum distillation of the residue gave the nitrile (**6**) (6 g) as a colorless oil; b.p. 52–54 °C/14 Torr; ν_{max} 2250 (C≡N); n.m.r. 1.62 ($CH_3CH{=}C$<, 3H, d, J = 8 Hz), 1.68 (CH_3C=<, 3H, s), 2.92 (CH_2CN, 2H, s), and 5.50 (olefinic proton, 1H, q, J = 8 Hz).

Anal. Calcd. for C_6H_9N: C, 75.73; H, 9.54. Found: C, 75.78; H, 9.42.

*1-Amino-3-methyl-2-pentene (**7**)*

A solution of 1-cyano-2-methyl-2-butene (**6**) (3 g) in methanol (50 ml) was hydrogenated in the presence of Raney cobalt (1.5 g) at 80 °C under 100 atm of hydrogen until hydrogen uptake ceased (*ca.* 4 h). The mixture was filtered and the filtrate was used in the following reaction without isolation.

*5-Benzylamino-3-methyl-2-pentene (**9**)*

A mixture of the above amine (**7**) and benzaldehyde (2.2 g) in methanol (100 ml) was refluxed for 2 h. After the reaction mixture had been cooled at room temperature, sodium borohydride (1.5 g) was added in small portions to this solution with stirring. The stirring was continued for an additional 1 h. Evaporation of the solvent gave a pale yellowish oil, which was distilled *in vacuo* to give the benzylamine derivative (**9**) as a colorless oil (3.2 g); b.p. 114–116 °C/3 Torr; n.m.r. δ 1.58 (CH_3-CH=C<, 3H, d, J = 7 Hz), 1.63 (CH_3C=<, 3H, s), 2.22 (CH_2CH_2NH, 2H, t, J = 7 Hz), 2.60 (CH_2CH_2-NH, 2H, t, J = 7 Hz), 3.68 ($NHCH_2Ph$, 2H, s), 5.30 (olefinic proton, 1H, distorted q, J = 7 Hz), and 7.18 (C_6H_5, 5H, s). The oxalate of **9** was recrystallized from ethanol to afford colorless needles; m.p. 196–197 °C.

Anal. Calcd. for $C_{15}H_{21}O_4N$: C, 64.49; H, 7.58; N, 5.01. Found: C, 64.99; H, 7.66; N, 5.12.

*N-Benzyl-N-(3-methyl-2-pentenyl)-4-methoxyphenylacetamide (**10**)*

To a cooled and stirred solution of **9** (1 g) in ether (10 ml) was added dropwise a solution of the acid chloride, which was prepared by the usual method from 4-methoxyphenylacetic acid (1.2 g) in ether (20 ml). The reaction mixture was kept alkaline by simultaneous addition of saturated aqueous $NaHCO_3$ solution within 30 min. After the stirring had been continued at room temperature for 1 h, the reaction mixture was extracted with ether. The extract was washed successively with water, 5% HCl solution, and water, dried over Na_2SO_4, and evaporated to give the amide (1.6 g) as a colorless viscous syrup; ν_{max} 1650 (C=O); n.m.r. δ 1.42–1.68 (2 × CH_3, 6H), 2.33–2.66 (CH_2CH_2N, 4H, m), 3.43 ($COCH_2Ph$, 2H, s), 3.75 (OCH_3, 3H, s), 4.33 (NCH_2Ph, 2H, s), 5.16 (olefinic proton, 1H, broad s), 6.70 (aromatic protons, 2H, d, J = 8 Hz), 7.00 (aromatic protons, 2H, d, J = 8 Hz), and 7.15 (aromatic protons, 5H, s).

*1-Benzyl-1,2,5,6-tetrahydro-2-(4-methoxybenzyl)-3,4-dimethylpyridine (**12**)*

A solution of the amide (**10**) (1 g) and $POCl_3$ (1 ml) in dry benzene (20 ml) was heated at 70 °C for 2 h. After cooling, the reaction mixture was poured into an excess of *n*-hexane. The precipitated hydrochloride was separated by decantation and then dissolved in methanol. To this solution was added in small portions sodium borohydride (0.4 g) with stirring. After removal of the solvent, the residue was decomposed with water and then extracted with chloroform. The organic layer was washed with water and dried over Na_2SO_4. Evaporation of the solvent gave a pale yellowish oil (0.4 g), which was characterized as oxalate; m.p. 158–160 °C (lit. (*4a*) m.p. 158–160 °C, mixture m.p. 158–160 °C). The i.r. and n.m.r. spectra were identical with those of an authentic sample, which was given by Dr. K. Kigasawa, Grelan Pharmaceutical Co. Ltd.

We thank R. Kato, R. Suenaga, E. Nagaoka, A. Satoh, C. Koyanagi, and K. Kawamura, Pharmaceutical Institute, Tohoku University, for microanalyses and spectral measurements.

1. T. Kametani, K. Kigasawa, M. Hiiragi, T. Hayasaka, K. Wakisaka, F. Satoh, T. Aoyama, and H. Ishimaru. J. Heterocyclic Chem. **8**, 769 (1971).

2. T. KAMETANI, K. KIGASAWA, M. HIIRAGI, F. SATOH, H. SUGI, and T. URYU. J. Heterocyclic Chem. **9**, 1065 (1972).
3. S. ARCHER, N. F. ALBERTSON, L. S. HAUIS, A. K. PIERSON, and J. G. BIRD. J. Med. Chem. **7**, 123 (1964).
4. (*a*) T. KAMETANI, K. KIGASAWA, M. HIIRAGI, T. HAYASAKA, N. WAGATSUMA, and K. WAKISAKA. J. Heterocyclic Chem. **6**, 43 (1969); (*b*) N. F. ALBERTSON and W. F. WETTERAU. J. Med. Chem. **13**, 302 (1970).
5. T. ATSUMI, K. KOBAYASHI, T. TAKEBAYASHI, and H. YAMAMOTO. Sumitomokagaku Deutsche Offenlegungsschrift, **192**, 7724 (1970).
6. K. TAMAOKI, F. FUJII, S. YATA, and S. KUDO. *In* Abstract of symposium on organic synthetic chemistry. The Society of Synthetic Organic Chemistry, Tokyo. 1972. p. 16.
7. T. KAMETANI, S.-P. HUANG, M. IHARA, and K. FUKUMOTO. Chem. Pharm. Bull. (Tokyo), **23**, 2011 (1975).
8. F. G. BORDWELL and P. S. LANDIS. J. Am. Chem. Soc. **79**, 1593 (1957).
9. D. Y. GURTIN, H. W. JOHNSON, JR., and E. G. STEINER. J. Am. Chem. Soc. **77**, 4566 (1955).
10. P. A. GRIECO. Chem. Commun. 702 (1972).
11. R. S. LENOX and J. A. KATZENELLENBOGEN. J. Am. Chem. Soc. **95**, 957 (1973).
12. T. KAMETANI, K. FUKUMOTO, M. IHARA, M. TAKEMURA, H. MATSUMOTO, B. R. PAI, K. NAGARAJAN, M. S. PREMILA, and H. SUGUNA. Heterocycles, **3**, 811 (1975).

Can. J. Chem. Downloaded from www.nrcresearchpress.com by 210.87.254.42 on 09/05/12
For personal use only.

Studies on the Syntheses of Heterocyclic Compounds. Part DCXXXVIII.[1] Simple Synthesis of Benz[*d*]indeno[1,2-*b*]azepine from 1-Benzoyl-3,4-dihydroisoquinoline

TETSUJI KAMETANI, MANAKKAL SIVARAMAN PREMILA, SHOJI HIRATA, HIDEHARU SETO, HIDEO NEMOTO, AND KEIICHIRO FUKUMOTO

Pharmaceutical Institute, Tohoku University, Aobayama, Sendai, Japan

Received June 10, 1975

TETSUJI KAMETANI, MANAKKAL SIVARAMAN PREMILA, SHOJI HIRATA, HIDEHARU SETO, HIDEO NEMOTO, and KEIICHIRO FUKUMOTO. Can. J. Chem. **53**, 3824 (1975).

1-Benzoyl-3,4-dihydroisoquinoline methiodides (**13**, **14**, **15**) were converted into 5-benzoyl-2,3-dihydro-1*H*-3-benzazepines (**18**, **19**, **20**), respectively, cyclization and reduction of which gave benz[*d*]indeno[1,2-*b*]azepines (**27**, **28**, **29**).

TETSUJI KAMETANI, MANAKKAL SIVARAMAN PREMILA, SHOJI HIRATA, HIDEHARU SETO, HIDEO NEMOTO et KEIICHIRO FUKUMOTO. Can. J. Chem. **53**, 3824 (1975).

On a transformé respectivement les méthiodures (**13**, **14**, **15**) de benzoyl-1 dihydro-3,4 isoquinoléines en benzoyl-5 dihydro-2,3 1*H*-benzazépines-3 (**18**, **19**, **20**); la cyclisation et la réduction de ces derniers composés conduit aux benz[*d*] indéno[1,2-*b*]azépines (**27**, **28**, **29**).

[Traduit par le journal]

The 3-benzazepine skeleton is found in the rhoeadine, isopavine, and cephalotaxine type alkaloids (1, 2). The rhoeadine alkaloids have been synthesized by Irie *et al.* (3) through the benzindenoazepine (**1**), and by Brossi and co-workers (4) from the phthalide alkaloid, bicuculline. Recently, Manske and co-workers (5) reported the second conversion of the benzindenoazepine (**2**) into the rhoeadine ring system.

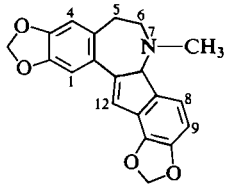

1

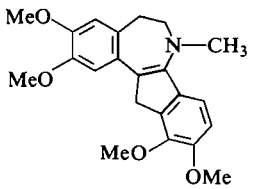

2

We have been investigating the synthesis of benzazepine and benzindenoazepine type compounds from 1-benzylisoquinolines and have reported the conversion of β-hydroxylaudanosine (**3**) into 2,3-dihydro-5-phenyl-1*H*-3-benzazepine (**4**) by rearrangement (6). We have also reported the conversion of the spiro-isoquinoline (**5**) into the benzindanoazepines (**6**, **7**) (7) and the total synthesis of reframidine (**9**), an isopavine alkaloid, by ring expansion of the 3,4-dihydroisoquinoline (**8**) with diazomethane (8). We are interested in this type of reaction and examined whether this ring expansion could provide the key step for the construction of the rhoeadine framework (9). We wish to report the synthesis of various substituted 5-benzoyl-2,3-dihydro-3-methyl-1*H*-3-benzazepines from the corresponding 1-benzoyl-3,4-dihydroisoquinoline methiodides by ring expansion and their conversion into 5,6,7,12-tetrahydro-7-methylbenz[*d*]indeno[1,2-*b*]azepines, which have the same framework as the key precursor (**2**) for the *cis*-alpigenine synthesis of Manske (5).

A methanol solution of 3,4-dihydro-6,7-dimethoxy-1-(3,4-methylenedioxybenzoyl)isoquinoline methiodide (**13**), prepared from 1-benzoyl-3,4-dihydroisoquinoline (**10**) (10) by reaction with methyl iodide in warm benzene, was treated with an excess of ethereal diazomethane at 0 °C to give in good yield a mixture of 5-benzoyl-2,3-dihydro-3-methyl-1*H*-3-benzazepine (**18**), m.p. 179–181 °C, and the isomeric 4-benzoylazepine (**21**), m.p. 125.5–126.5 °C, in the ratio of 5.5:1. The structure of **18** was assigned on the basis of spectral data. The molecular formula, $C_{21}H_{21}NO_5$, obtained by microanalysis and mass spectrum measurements (M^+, *m/e* 367) showed the introduction of one carbon atom, and the i.r.

[1]For part DCXXXVII, see ref. 17.

Can. J. Chem. Downloaded from www.nrcresearchpress.com by 210.87.254.40 on 09/05/12
For personal use only.

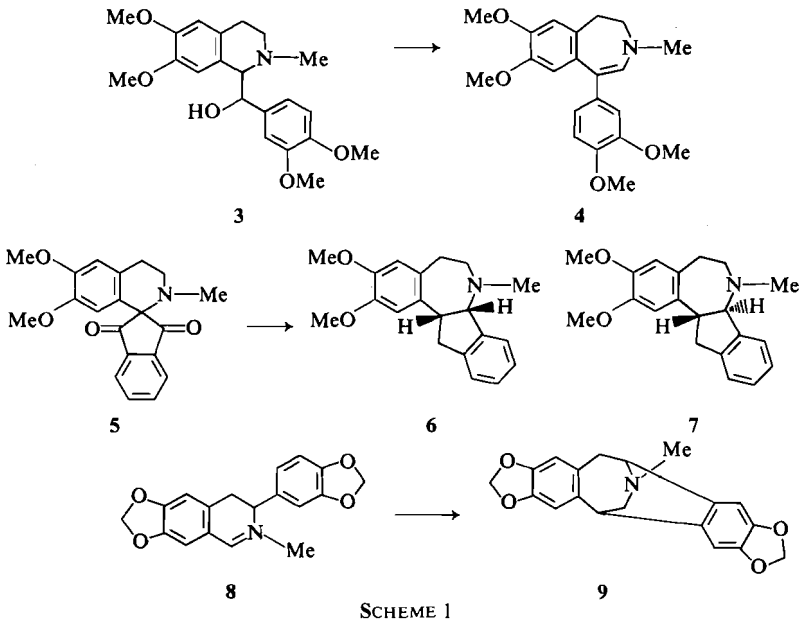

SCHEME 1

Can. J. Chem. Downloaded from www.nrcresearchpress.com by 210.87.254.40 on 09/05/12
For personal use only.

spectrum (ν_{max} ($CHCl_3$) 1637 cm^{-1}) indicated the presence of a conjugated carbonyl group. The u.v. spectrum revealed that λ_{max} (MeOH) 297 nm shifted to 287 nm on addition of concentrated hydrochloric acid. This shift indicated the presence of a conjugated enamine system (6), which was also supported by the n.m.r. spectrum which showed the *N*-methyl at δ 3.06. Moreover, the n.m.r. spectrum suggested the presence of a benzoyl group at the β-position of the enamine system as the chemical shifts of an aromatic proton (δ 6.55 or 6.61) and that of a methoxyl group (δ 3.6) resonated at unusually high field. The structure of the second benzazepine (**21**) was also determined by microanalysis, mass (M^+ *m/e* 307, $C_{21}H_{21}NO_5$), i.r. (ν_{max} ($CHCl_3$) 1640 cm^{-1}), u.v., and n.m.r. spectra. The n.m.r. spectrum showed the *N*-methyl group at δ 2.63 and the olefinic proton at δ 5.93 in addition to the normal chemical shift positions of the two methoxyls, the methylenedioxy, and five aromatic protons, indicating the presence of the benzoyl group at the α-position in the enamine system.

It is interesting that when chloroform is used as solvent instead of methanol, reaction of (**13**) with ethereal diazomethane afforded the 5-benzoylazepine (**18**) and a trace of the 4-isomer (**21**). This shows that in a more polar solvent such as methanol there is enhanced formation of carbonium ion (**17**) which has two paths, shown by arrows *a* and *b* in Scheme 2, for rearrangement whereas in a nonpolar solvent, chloroform, there is more likelihood for direct displacement of nitrogen by anchimeric assistance by path *a* (11) through intermediate formation of an aziridinium salt.

The attempted conversion of the 5-benzoylazepine (**18**) into the benz[*d*]indeno[1,2-*b*]azepine system by several methods, including treatment with a mineral acid, photolytic and thermolytic methods (12) along an electrocyclic reaction mechanism (13), gave only negative results. However, cyclization with phosphorus oxychloride in boiling toluene was successful and 12-chloro-5,6,7,7a-tetrahydro-7-methylbenz-[*d*]indeno[1,2-*b*]azepine (**22**) was formed in moderate yield. Its structure was supported by its mass (M^+, *m/e* 385 and 387 (isotope ion), 350 (M^+ − Cl)), i.r., and n.m.r. spectra. Thus, the absence of a carbonyl group in the i.r. spectrum, and the presence of four aromatic protons in the n.m.r. spectrum showed that cyclization had taken place. The chemical shifts of the methine protons (δ 4.90) and the *N*-methyl group (δ 2.15) were found at abnormally high field, and hence the olefinic linkage must be located between C-12 and C-12a.

Hydrogenolysis of the chlorine atom could be achieved by treatment of (**22**) with sodium

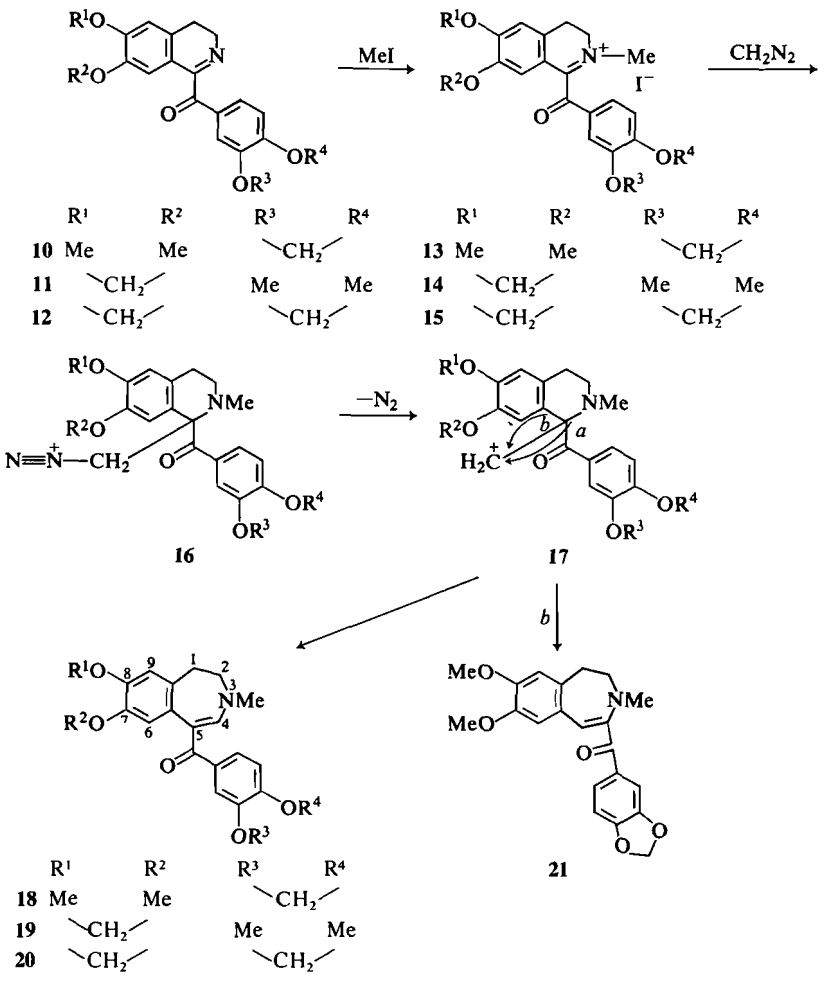

SCHEME 2

borohydride in methanol followed by addition of sodium hydroxide to give 5,6,7,12-tetrahydro-7-methylbenz[*d*]indeno[1,2-*b*]azepine (**27**), in moderate yield, which could also be obtained in poor yield by reduction of (**22**) using zinc and sodium hydroxide. The structure (**27**) of this product was easily determined by its mass (M^+; *m/e* 351) and n.m.r. spectrum which showed a methylene group (situated between the phenyl and olefinic carbon atoms) at δ 3.70 as a singlet, but lacked an olefinic proton. Moreover, the chemical shift of the *N*-methyl group at δ 2.93 indicated that this group formed part of an enamine system. Enamine formation by sodium borohydride reduction of König's salts is reported by Grewe and von Bonin (14).

Treatment of **22** with sodium borohydride in the absence of sodium hydroxide resulted in the recovery of the starting material, and the reaction of **22** with methanolic sodium hydroxide gave the unstable 5,6,7,7a-tetrahydro-12-methoxy-7-methylbenz[*d*]indeno[1,2-*b*]azepine (**30**) (δ ($CDCl_3$) 3.00 (>CH—OCH_3) and 5.47 (>C*H*—OCH_3)). Therefore, reduction must proceed through the enamine (**25**) and the α,β-unsaturated imminium salt (**26**) as shown in Scheme 3. The presence of sodium borohydride afforded compound **27** by attack of the hydride, but in the absence of a reducing agent gave **30** by attack of the solvent.

Similarly, the two other benz[*d*]indeno[1,2-*b*]azepines (**28, 29**) were synthesized from 3,4-

Can. J. Chem. Downloaded from www.nrcresearchpress.com by 210.87.254.40 on 09/05/12
For personal use only.

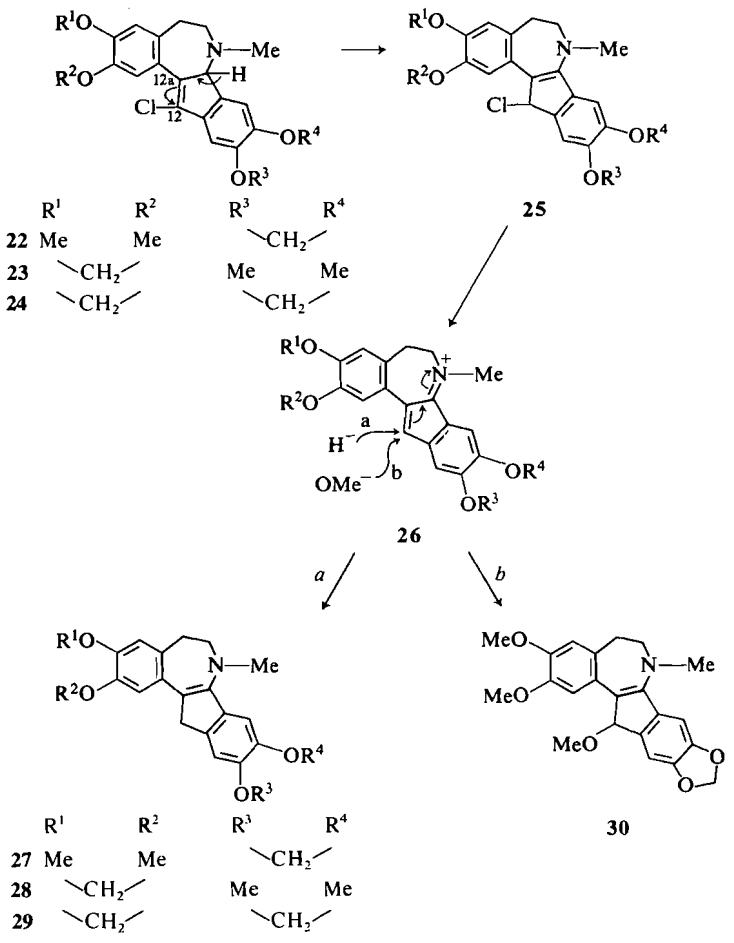

	R¹	R²	R³	R⁴
22	Me	Me		CH_2
23		CH_2	Me	Me
24		CH_2		CH_2

	R¹	R²	R³	R⁴
27	Me	Me		CH_2
28		CH_2	Me	Me
29		CH_2		CH_2

SCHEME 3

dihydro-1-(3,4-dimethoxybenzoyl)-(**11**) (15) and 3,4-dihydro-6,7-methylenedioxy-1-(3,4-methylenedioxybenzoyl)isoquinoline (**12**) (16), respectively. Thus, the 1-benzoyl-3,4-dihydroisoquinolines (**11**, **12**) were treated with methyl iodide to give the corresponding methiodides (**14**, **15**) which were subjected to ring expansion with an excess of ethereal diazomethane at 0 °C in chloroform to afford the 3-benzazepines (**19**, **20**). Heating the 3-benzazepines with phosphorus oxychloride in dry toluene furnished the 12-chloro - 5,6,7,7a - tetrahydrobenz[*d*]indeno[1,2 - *b*]azepines (**23**, **24**), which were reduced with sodium borohydride in methanol in the presence of sodium hydroxide to give the expected 5,6,7,12-tetrahydrobenz[*d*]indeno[1,2-*b*]azepines (**28**, **29**).

Thus, we have accomplished a convenient synthesis of 5,6,7,12-tetrahydrobenz[*d*]indeno-[1,2-*b*]azepines, which have the same framework as the key intermediate (**2**) for the total synthesis of *cis*-alpigenine by Manske, from 1-benzoyl-3,4-dihydroisoquinoline methiodides in three steps by an application of the ring expansion reaction with diazomethane.

Experimental

Melting points are not corrected and were measured with a Yanagimoto micro melting point apparatus (MP-S2). Infrared and u.v. spectra were measured with a Hitachi 215 grating spectrophotometer and with a Hitachi 124 spectrophotometer, respectively, n.m.r. spectra with a JEOL JNM-PMX 60 spectrometer with tetramethylsilane as internal standard, and mass spectra with a Hitachi RMU-7 spectrometer.

Can. J. Chem. Downloaded from www.nrcresearchpress.com by 210.87.254.40 on 09/05/12
For personal use only.

Can. J. Chem. Downloaded from www.nrcresearchpress.com by 210.87.254.40 on 09/05/12
For personal use only.

3,4-Dihydro-6,7-dimethoxy-2-methyl-1-(3,4-methylenedioxybenzoyl)isoquinolinium Iodide (13)

A mixture of 3,4-dihydro-6,7-dimethoxy-1-(3,4-methylenedioxybenzoyl)isoquinoline (**10**) (5.2 g), benzene (30 ml), and methyl iodide (11 ml) was gently refluxed for 2 h. The methiodide separated out after a short while. After allowing the mixture to cool, the methiodide was filtered off and washed with ether to obtain a yellow solid (7.2 g) which was recrystallized from MeOH to give yellow crystals (4.6 g), m.p. 190–192 °C.

Anal. Calcd. for $C_{20}H_{20}NO_5I \cdot \frac{1}{2}H_2O$: C, 48.99; H, 4.32; N, 2.86. Found: C, 49.20; H, 4.27; N, 2.91.

3,4-Dihydro-2-methyl-6,7-methylenedioxy-1-(3,4-methylenedioxybenzoyl)isoquinolinium Iodide (15)

A mixture of 3,4-dihydro-6,7-methylenedioxy-1-(3,4-methylenedioxybenzoyl)isoquinoline (**12**) (5.0 g), methyl iodide (28.0 ml), MeOH (150 ml), and acetone (150 ml) was refluxed for 3 h and then worked up as before to give the methiodide as orange needles (6.5 g) from MeOH; m.p. 221–222 °C; i.r. ($CHCl_3$) 1640 cm^{-1} (CO).

Anal. Calcd. for $C_{19}H_{16}NO_5I$: C, 49.05; H, 3.47; N, 3.01. Found: C, 48.88; H, 3.77; N, 2.99.

2,3-Dihydro-7,8-dimethoxy-3-methyl-5-(3,4-methylenedioxybenzoyl)-1H-3-benzazepine (18)

An excess of ethereal diazomethane was added to a solution of the methiodide (**13**) (4.3 g) in MeOH (500 ml) at 0 °C. After leaving it overnight in the refrigerator, the solvent was evaporated to leave a syrup which was dissolved in chloroform. The solution was then washed with 10% NH_4OH and water, dried (Na_2SO_4), and distilled to leave a syrup (4.2 g) which was chromatographed on silica gel (150 g). Elution with chloroform gave 2,3-dihydro-7,8-dimethoxy-3-methyl-4-(3,4-methylenedioxybenzoyl)-1*H*-3-benzazepine (**21**) (350 mg) which was crystallized from MeOH to give yellow crystals; m.p. 125.5–126.5 °C; i.r. ($CHCl_3$) 1640 cm^{-1} (CO); n.m.r. ($CDCl_3$) δ 2.63 (3H, s, NCH_3), 2.8–3.1 (2H, m, $ArCH_2CH_2N$), 3.15–3.4 (2H, m, $ArCH_2CH_2N$), 3.83 (3H, s, OCH_3), 3.88 (3H, s, OCH_3), 5.93 (1H, s, 5-H), 6.05 (2H, s, OCH_2O), 6.70 (2H, s, 6-H and 9-H), 6.83 (1H, d, J = 8 Hz, 5′-H), 7.46 (1H, d, J = 2 Hz. 2′-H), and 7.65 (1H, dd, J = 2 and 8 Hz, 6′-H); m.s. *m/e* 367 (M^+); u.v. (MeOH) 287 nm and u.v. (MeOH–HCl) 257, 317, and 363 nm.

Anal. Calcd. for $C_{21}H_{21}NO_5$: C, 68.65; H, 5.76; N, 3.81. Found: C, 68,58; H, 5.72; N, 3.85.

Further elution with chloroform gave the required 2,3-dihydro-7,8-dimethoxy-3-methyl-5-(3,4-methylenedioxybenzoyl)-1*H*-3-benzazepine (**18**) (2.3 g) which was recrystallized from MeOH to give yellow crystals (1.9 g); m.p. 179–181 °C; i.r. ($CHCl_3$) 1637 cm^{-1} (CO); n.m.r. ($CDCl_3$) δ 3.06 (3H, s, NCH_3), 2.9–3.2 (2H, m, $ArCH_2CH_2N$), 3.4–3.7 (2H, m, $ArCH_2CH_2N$), 3.6 (3H, s, 7-OCH_3), 3.85 (3H, s, 8-OCH_3), 5.96 (2H, s, OCH_2O), 6.56, 6.61, 6.80 (3H, each s, =CH and ArH), 7.06 (2H, s, ArH), and 7.13 (1H, dd, J = 2 and 7 Hz, 6′-H); m.s. *m/e* 367 (M^+); u.v. (MeOH) 297 and 350 nm and u.v. (MeOH–HCl) 266, 287, and 363 nm.

Anal. Calcd. for $C_{21}H_{21}NO_5$: C, 68,65; H, 5.76; N, 3.81. Found: C, 68.25; H, 5.92; N, 3.60.

2,3-Dihydro-5-(3,4-dimethoxybenzoyl)-3-methyl-7,8-methylenedioxy-1H-3-benzazepine (19)

An excess of ethereal diazomethane was added to a stirred solution of the methiodide (**14**) (15) (4 g) in chloroform (700 ml) at 0 °C. Stirring was continued for 1–1.5 h. The solvent was then removed *in vacuo* and the residue dissolved in chloroform. The chloroform extract was washed with 10% ammonia and water, dried (Na_2SO_4) and evaporated to leave a gum (4.1 g) which was purified by crystallization from benzene. Further recrystallization from MeOH gave yellow crystals; m.p. 204–205 °C; i.r. ($CHCl_3$) 1640 cm^{-1} (CO); n.m.r. ($CDCl_3$) δ 3.01 (3H, s, NCH_3), 2.85–3.15 (2H, m, $ArCH_2CH_2N$), 3.35–3.7 (2H, m, $ArCH_2CH_2N$), 3.81 (3H, s, OCH_3), 3.87 (3H, s, OCH_3), 5.81 (2H, s, OCH_2O), and 6.53–7.33 (5H, m, =CH— and ArH); m.s. *m/e* 367 (M^+); u.v. (MeOH) 303 and 347 nm and u.v. (MeOH–HCl) 265, 297, and 360 nm.

Anal. Calcd. for $C_{21}H_{21}NO_5$: C, 68.65; H, 5.75; N, 3.81. Found: C, 68.54; H, 5.93; N, 3.59.

2,3-Dihydro-3-methyl-7,8-methylenedioxy-5-(3,4-methylenedioxybenzoyl)-1H-3-benzazepine (20)

The methiodide (**15**) (5 g) in chloroform (400 ml) was treated with an excess of ethereal diazomethane at 0 °C for 5 h. After evaporation of chloroform, the residue was dissolved in chloroform and to this solution was added triethylamine (1.1 g), and the solvent was removed by distillation to leave a gum, which was subjected to alumina chromatography using benzene as a solvent to give the benzazepine (**20**) as yellow needles (3.5 g) from benzene; m.p. 165 °C; i.r. ($CHCl_3$) 1638 (CO) and 1570 cm^{-1} (C=C); n.m.r. ($CDCl_3$) 2.99 (3H, s, NCH_3), 2.8–3.1 (2H, m, $ArCH_2CH_2N$), 3.3–3.6 (2H, m, $ArCH_2CH_2N$), 5.78 (2H, s, OCH_2O), 5.91 (2H, s, OCH_2O), 6.46 (1H, s, 4-H), 6.58 (1H, s, 1-H), 6.73 (1H, s, 8-H), and 6.98–7.50 (3H, m, ArH); u.v. (MeOH) 300 and 233 nm and u.v. (MeOH–HCl) 330, 289, and 238.

Anal. Calcd. for $C_{20}H_{17}NO_5$: C, 68.37; H, 4.88; N, 3.99. Found: C, 68.10; H, 4.88; N, 3.91.

12-Chloro-5,6,7,7a-tetrahydro-2,3-dimethoxy-7-methyl-9,10-methylenedioxybenz[d]indeno[1,2-b]azepine (22)

A mixture of the dihydrobenzazepine (**18**) (200 mg), phosphorus oxychloride (0.4 ml), and toluene (50 ml) was refluxed for 1 h. The excess solvent and reagent were removed *in vacuo*, the residual syrup cooled and treated with MeOH when yellow crystals of the hydrochloride separated out. Collection by filtration gave the hydrochloride, whose suspension in chloroform was washed with 10% ammonia and water. The organic layer was dried (Na_2SO_4) and distilled to leave a syrup which on trituration with MeOH readily crystallized to give the indenobenzazepine (**22**) (100 mg); m.p. 156 °C (dec.) (sublime and darken); n.m.r. ($CDCl_3$) δ 2.15 (3H, s, NCH_3), 3.90 (6H, s, 2 × OCH_3), 4.90 (1H, s, 7a-H), 6.01 (2H, s, OCH_2O), 6.65, 6.93, 7.10, and 7.31 (4H, each s, ArH); m.s. *m/e* 385 and 387 (M^+), 350 (M^+ − Cl).

Anal. Calcd. for $C_{21}H_{20}NO_4Cl$: C, 65.36; H, 5.23; N, 3.63. Found: C, 65.19; H, 5.36; N, 3.78.

12-Chloro-5,6,7,7a-tetrahydro-9,10-dimethoxy-7-methyl-2,3-methylenedioxybenz[d]indeno[1,2-b]azepine (23)

A mixture of the dihydrobenzazepine (**19**) (0.2 g),

Can. J. Chem. Downloaded from www.nrcresearchpress.com by 210.87.254.40 on 09/05/12
For personal use only.

toluene (70 ml), and phosphorus oxychloride (0.4 ml) was refluxed for 0.5 h. It was worked up as before to give a residue which on crystallization from MeOH gave pale yellow crystals (105 mg); m.p. 158 °C (dec.); n.m.r. ($CDCl_3$) δ 2.08 (3H, s, NCH_3), 3.88 (3H, s, OCH_3), 3.93 (3H, s, OCH_3), 4.53 (1H, s, 7a-H), 5.92 (2H, s, OCH_2O), 6.59, 6.92, 7.05, and 7.15 (4H, each s, ArH); m.s. *m/e* 385 and 387 (M^+); u.v. (MeOH) 285 nm.

Anal. Calcd. for $C_{20}H_{20}NO_4Cl$: C, 65.36; H, 5.23; N, 3.63. Found: C, 64.92; H, 5.20; N, 3.51.

12-Chloro-5,6,7,7a-tetrahydro-7-methyl-2,3;9,10-bismethylenedioxybenz[d]indeno[1,2-b]azepine (24)

A mixture of the dihydrobenzazepine (**20**) (0.2 g), phosphorus oxychloride (0.2 g), and dry toluene (70 ml) was refluxed for 0.5 h. The reaction mixture was washed with 10% ammonia and water, dried (Na_2SO_4), and evaporated to afford a colorless syrup, which was purified with silica gel (5 g) chromatography by elution with chloroform to afford the indenoazepine (**24**) (200 mg); n.m.r. ($CDCl_3$) 2.07 (3H, s, NCH_3), 4.45 (1H, s, 7a-H), 5.90 (2H, s, OCH_2O), 5.95 (2H, s, OCH_2O), 6.53, 6.93, and 7.15 (each 1H, s, ArH). The hydrochloride of **4** gave colorless prisms from MeOH, m.p. 217–219 °C.

Anal. Calcd. for $C_{20}H_{16}NO_4Cl \cdot HCl \cdot \frac{1}{4}H_2O$: C, 58.47; H, 4.29. Found: C, 58.45; H, 4.28.

5,6,7,12-Tetrahydro-2,3-dimethoxy-7-methyl-9,10-methylenedioxybenz[d]indeno[1,2-b]azepine (27)

Sodium borohydride (100 mg) was added in portions to a stirred solution of the above chloroindenobenzazepine (**22**) (100 mg) in MeOH (70 ml). After addition, the mixture was stirred for 1–2 min and NaOH (1 pellet) was added and the stirring continued for 5 h. The solvent was removed, the residue was treated with water and extracted with chloroform. The chloroform extract was washed with water, dried (Na_2SO_4) and evaporated to leave a solid, which was crystallized from EtOH to give pale pink crystals (55 mg); m.p. 175–177 °C; n.m.r. ($CDCl_3$,) δ 2.93 (3H, s, NCH_3), 2.8–3.1 (2H, m, $ArCH_2CH_2N$), 3.1–3.4 (2H, m, $ArCH_2CH_2N$), 3.70 (2H, s, CH_2), 3.87, 3.90 (6H, each s, 2 × OCH_3), 5.93 (2H, s, OCH_2O), 6.65 (1H, s, ArH), 6.87 (1H, s, ArH), and 6.97 (2H, s, ArH); m.s. *m/e* 351 (M^+); u.v. (MeOH) 258 and 347 nm and u.v. (MeOH–HCl) 243, 293, and 355 nm.

Anal. Calcd. for $C_{21}H_{21}NO_4$: C, 71.78: H, 6.02; N, 3.95. Found: C, 71.55; H, 6.14; N, 4.04.

5,6,7,7a-Tetrahydro-2,3,12-trimethoxy-7-methyl-9,10-methylenedioxybenz[d]indeno[1,2-b]azepine (30)

Sodium hydroxide (1 pellet) was added to the chloroindenobenzazepine (**22**) (50 mg) in MeOH (30 ml) and the mixture left overnight at room temperature. The solvent was then removed *in vacuo* and the residue worked up as usual to give a brown syrup (53 mg) which on trituration with MeOH gave yellow crystals (20 mg); m.p. 145–147 °C; n.m.r. ($CDCl_3$) δ 2.83 (3H, s, NCH_3), 3.00 (3H, s, 12-OCH_3), 3.87, 3.93 (6H, each s, 2 × OCH_3), 5.47 (1H, s, 12-H), 5.97 (2H, s, OCH_2O), 6.63, 6.90, 6.95, and 7.62 (4H, each s, ArH); m.s. *m/e* 381 (M^+), which was so unstable that it darkened during purification.

5,6,7,12-Tetrahydro-9-10-dimethoxy-7-methyl-2,3-methylenedioxybenz[d]indeno[1,2-b]azepine (28)

Sodium borohydride (100 mg) was added in portions to a stirred solution of the above chloroindenobenzazepine (**23**) (100 mg) in MeOH (30.0 ml). After addition, the mixture was stirred for 3–4 min and sodium hydroxide (1 pellet) was added and the stirring continued for 5.5 h. It was worked up as before and crystallization from EtOH gave yellow crystals (56 mg); m.p. 189–191 °C; n.m.r. ($CDCl_3$) δ 2.97 (3H, s, NCH_3), 2.8–3.07 (2H, m, $ArCH_2CH_2N$), 3.1–3.37 (2H, m, $ArCH_2CH_2N$), 3.67 (2H, s, CH_2Ar), 3.88 (6H, s, 2 × OCH_3), 5.88 (2H, s, OCH_2O), 6.62 (1H, s, ArH), and 6.95 and 7.00 (3H, 2 × s, ArH); m.s. *m/e* 351 (M^+); u.v. (MeOH) 253 (sh), 273 (sh) and 347 nm and u.v. (MeOH–HCl) 243, 297, and 350 nm.

Anal. Calcd. for $C_{21}H_{21}NO_4$: C, 71.78; H, 6.02; N, 3.99. Found: C, 71.54; H, 5.98; N, 4.03.

5,6,7,12-Tetrahydro-7-methyl-2,3;9,10-bismethylenedioxybenz[d]indeno[1,2-b]azepine (29)

To a mixture of the chloroindenobenzazepine (**24**) (90 mg) and sodium borohydride (70 mg) in MeOH (30 ml) was added sodium hydroxide (70 mg), and this solution was stirred at room temperature for 2 h. The usual work up gave **8** (70 mg) as orange prisms from MeOH; m.p. 166–167 °C; n.m.r. ($CDCl_3$) δ 2.92 (3H, s, NCH_3), 2.7–3.05 (2H, m, $ArCH_2CH_2N$), 3.05–3.35 (2H, m, $ArCH_2CH_2N$), 3.62 (2H, s, $ArCH_2$), 5.87 (2H, s, OCH_2O), 5.92 (2H, s, OCH_2O), 6.60 (1H, s, ArH), 6.84 (1H, s, ArH), and 6.93 (2H, s, ArH).

Anal. Calcd. for $C_{20}H_{17}NO_4$: C, 71.63; H, 5.11; N, 4.18. Found: C, 71.90; H, 4.94; N, 4.50.

We thank A. Sato, C. Koyanagi, K. Kawamura, R. Kato, R. Suenaga, and E. Nagaoka, Pharmaceutical Institute, Tohoku University, for microanalyses and spectral measurements, and Dr. K. Okui, Research Laboratories, Chugai Pharmaceutical Co. Ltd., for microanalyses.

1. T. KAMETANI. The chemistry of the isoquinoline alkaloids. Hirokawa Publishing Company, Inc., Tokyo, and Elsevier Publishing Company, Amsterdam. 1968; T. KAMETANI. The chemistry of the isoquinoline alkaloids, Vol. 2. The Sendai Institute of Heterocyclic Chemistry, Sendai, Japan. 1974.
2. M. SHAMMA. The isoquinoline alkaloids. Academic Press, New York. 1972.
3. H. IRIE, S. TANI, and H. YAMANE. Chem. Commun. 1713 (1970); J. Chem. Soc. Perkin Trans. 1, 2986 (1972).
4. W. KLÖTZER, S. TEITEL, and A. BROSSI. Helv. Chim. Acta, **55**, 2228 (1972).
5. K. ORITO, R. H. MANSKE, and R. RODRIGO. J. Am. Chem. Soc. **96**, 1944 (1974).
6. T. KAMETANI, S. HIRATA, S. SHIBUYA, and K. FUKUMOTO. J. Chem. Soc. C, 1927 (1971).
7. T. KAMETANI, S. HIRATA, S. HIBINO, H. NEMOTO, M. IHARA, and K. FUKUMOTO. Heterocycles, **3**, 151 (1975).
8. T. KAMETANI, S. HIRATA, and K. OGASAWARA. J. Chem. Soc. Perkin Trans. 1, 1466 (1973).
9. T. KAMETANI, S. HIRATA, F. SATOH, and K. FUKUMOTO. J. Chem. Soc. Perkin Trans. 1, 2509 (1974).
10. J. S. BUCK, W. H. PERKIN, JR., and T. S. STEVENS. J. Chem. Soc. **127**, 675 (1925).

11. C. K. INGOLD. Structure and mechanism in organic chemistry. Cornell University Press, Ithaca and London. 1969. pp. 457–471.
12. R. F. CHILDS, M. SAKAI, and S. WINSTEIN. J. Am. Chem. Soc. **90**, 7144 (1968); R. F. CHILDS and S. WINSTEIN. J. Am. Chem. Soc. **90**, 7146 (1968).
13. R. B. WOODWARD and R. HOFFMANN. The conservation of orbital symmetry. Academic Press Inc. 1970.
14. R. GREWE and W. VON BONIN. Ber. **94**, 234 (1961).
15. R. H. HAWORTH, W. H. PERKIN, JR., and J. RANKIN. J. Chem. Soc. **127**, 2020 (1925).
16. J. S. BUCK, W. H. PERKIN, JR., and T. S. STEVENS. J. Chem. Soc. **127**, 1470 (1925).
17. T. KAMETANI, R. NITADORI, H. TERASAWA, K. TAKAHASHI, and M. IHARA. Heterocycles, **3**, 821 (1975).

Can. J. Chem. Downloaded from www.nrcresearchpress.com by 210.87.254.40 on 09/05/12
For personal use only.

Molecular Rearrangements. Part VI. Aryl(alkyl)amines (II) Thermal Rearrangement of *N*-Benzylaniline

M. Z. A. BADR[1] AND H. A. H. EL-SHERIEF

Chemistry Department, Faculty of Science, Assiut University, Assiut, Egypt, E.A.R.

Received February 19, 1974[2]

M. Z. A. BADR and H. A. H. EL-SHERIEF. Can. J. Chem. **53**, 3831 (1975).

Heating *N*-benzylaniline resulted in migration of the benzyl group to the *ortho*- and *para*-positions of the aniline nucleus. Ammonia, toluene, biphenyl, diphenylmethane, dibenzyl, *trans*-stilbene, aniline, together with 9-phenylacridine, and 2,3-diphenylindole, were also formed.

When phenol, quinoline, or isoquinoline were used as solvents, the normal rearrangement products were accompanied by 2- and 4-benzylphenols, 3-benzylquinoline, 2- and 4-(aminophenyl)quinoline, 4-benzylisoquinoline, and 1-(aminophenyl)isoquinolines.

It is concluded that the pyrolysis of the secondary amine depends on its homolytic fission to benzyl and phenylamine free radicals. Homolysis of some initially separated products was also observed.

M. Z. A. BADR et H. A. H. EL-SHERIEF. Can. J. Chem. **53**, 3831 (1975).

Par chauffage, le groupe benzyle de la *N*-benzylaniline se transpose aux positions *ortho* et *para* du noyau aniline. On obtient aussi de l'ammoniac, du toluène, du biphényle, du diphénylméthane, du dibenzyle, du *trans*-stilbène, de l'aniline ainsi que du phényle-9 acridine et du diphényl-2,3 indole.

Quand on utilise le phénol, la quinoléine ou l'isoquinoléine comme solvants, on obtient les produits de réarrangement normaux ainsi que les benzyl-2 et -4 phénols, du benzyl-3 quinoléine, les (aminophényl)-2 et -4 quinoléine, le benzyl-4 isoquinoléine et l'(aminophényl)-1 isoquinoléine.

La pyrolyse de l'amine secondaire dépend de sa rupture homolytique en radicaux libres benzyle et phénylamine. On observe aussi l'homolyse de quelques produits préalablement isolés.

[Traduit par le journal]

The present paper describes a novel rearrangement of *N*-monoalkylaniline involving an alkyl–N bond fission to ring alkylated anilines, when heated at elevated temperature in absence of any promoter, either alone or in the presence of aromatic solvents where their ring alkylation was also observed. Thus *N*-benzylaniline reacted on heating in a sealed tube in nitrogen atmosphere at about 315 °C. Ammonia was produced together with aniline, toluene, biphenyl, diphenylmethane, dibenzyl, *trans*-stilbene, *o*- and *p*-aminodiphenylmethanes, 9-phenylacridine,and 2,3-diphenylindole in relatively high yield, together with high boiling products not yet resolved. When heated at its boiling point under reflux for 100 h, the amine gave about the same products but in lower yields, with the difference that some benzaldehyde was isolated, with stilbene, diphenyl, and 9-phenylacridine not easily identified.

The products of this thermal rearrangement are quite different from those of the proton catalyzed rearrangement.

The presence of toluene, aniline, biphenyl, diphenylmethane, and dibenzyl in the products strongly suggests that the change depends on a free radical mechanism. This suggestion was further confirmed through the study of the rearrangement in high boiling solvents and scavengers under nitrogen atmosphere. In phenol, the normal products of rearrangement were obtained together with 2- and 4-benzylphenols. However, in anisole, the solvent molecules underwent molecular rearrangement to the expected products of the alkyl–aryl ether reaction, namely, *o*- and *p*-cresol together with phenol and its benzylated products. The products of anisole rearrangement were also isolated when it was heated alone under the conditions of the amine rearrangement.

The thermal rearrangement of *N*-benzylaniline in quinoline gave the normal rearrangement

[1]Author to whom correspondence should be addressed.

[2]Revision received May 15, 1975.

Can. J. Chem. Downloaded from www.nrcresearchpress.com by 210.87.254.5 on 09/05/12
For personal use only.

Can. J. Chem. Downloaded from www.nrcresearchpress.com by 210.87.254.5 on 09/05/12
For personal use only.

TABLE 1. Products of pyrolysis of *N*-benzylaniline

(*a*) Experimental conditions

Experiment number	Solvent		Reaction temperature (°C)	Reaction time (days)	Amine used (g)
	Type	Amount (g)			
1	—	—	Reflux[b]	4.2	40
2[a]	—	—	315	12	40
3[a]	Phenol	12	315	12	40
4[a]	Anisole	11	315	12	40
5[a]	Quinoline	20	315	12	60
6[a]	Isoquinoline	—	315	12	60

(*b*) Experimental results

Product	Boiling point of fraction (°C/Torr)	Experiment number 1		2		3		3		5		6	
		Amount (g)	%	Amount (g)	%	Amount (g)	%	Amount (g)	%	Amount (g)	%	Amount (g)	%
Ammonia	—	'Evolved'	—	'Evolved'	—	'Evolved'	—	'Evolved'	—	'Evolved'	—	'Evolved'	—
Toluene	110/760	1	4	6	16.3	2.4	6	2.4	7.7	9.6	19.8	10.5	25
Dibenzyl[i]	125–135/10	0.55	2.4	0.7	1.9	0.4	1	0.5	1.6	0.57	1.2	0.6	1.4
Diphenylmethane[i]	125–135/10	0.95	4.1	1.2	3.2	6.2	15.6	0.95	2	0.44	0.9	0.4	1
Biphenyl	—	—	—	0.005	0.02	0.01	0.03	0.001	0.002	0.008	0.02	0.004	0.01
Stilbene	160–180/10	—	—	0.08	0.2	0.6	1.5	0.32	1	0.08	0.2	0.004	0.01
Aniline	184/160	5	21.7	11.5	31.8	10.1	25.4	8.5	27.2	12.3	25.4	12.5	29.8
o- and *p*-Aminodiphenyl methane[j]	165–170/4	6	26.1	6.5	17.8	13.5	34.2	11.7	37.5	20.0	41.2	13	31
9-Phenylacridine	220–240/2	—	—	3.5	9.5	3.0	7.3	2.8	9	—	—	—	—
2,3-Diphenylindole	220–240/5	—	—	3.5	9.5	4	10.1	4	12.8	5.5	11.3	5	12
Benzyl isomers of solvent used[g]	—	—	—	—	—	5.1[c]	—	—[d]	—	5[e]	—	5[f]	—
Non-volatile residue	Non-volatile	3.2	—	4.0	—	2.6	—	3.7[h]	—	4.2	—	6	—

[a]In nitrogen atmosphere.
[b]Benzaldehyde (1.8 g), n_D^{20} 1.5450, DNP derivative m.p. 236 °C.
[c]Fractions 70–120 °C/10 Torr contain benzylphenols in the ratio of 94.3% *o*- and 5.7% *p*-isomer identified by paper chromatography of their azodyes with diazotised sulfanilic acid, R_f (*o*-isomer) 0.61, R_f (*p*-isomer) 0.74, solvent butanol, water and ethyl alcohol in the ratio 5:5:1.7.
[d]It was separated into (2.2 g) of phenol (69%) and cresols (31%) in the ratio, *o*-isomer (95.5%), *p*-isomer (4.5%) benzylphenols (1.1 g) in the ratio *o*-isomer (97.3%) and *p*-isomer (2.7%) as found by g.l.c.
[e]The only isomer separated at 207–210 °C/7 Torr was 3-benzylquinoline (5 g) together with three different isomeric 2- and 4-(aminophenyl)quinolines (11 g) separated by trituration with petroleum ether (40–60) identified by i.r., mass spectra and u.v. (*cf.* Table 2).
[f]The only isomer separated at 185–196 °C/8 Torr was 4-benzylisoquinoline together with isomeric 1-(2-aminophenyl)isoquinoline (5 g) and the 1-(4-) isomer (3.5 g) identified by i.r., mass spectra, u.v. (*cf.* Table 3) from fraction 215–218 °C/8 Torr.
[g]Neutral and amine products.
[h]Together with phenolic products.
[i]Identified by g.l.c.
[j]Separated by column chromatography on silica gel (100–150 mesh) using benzene as eluant.

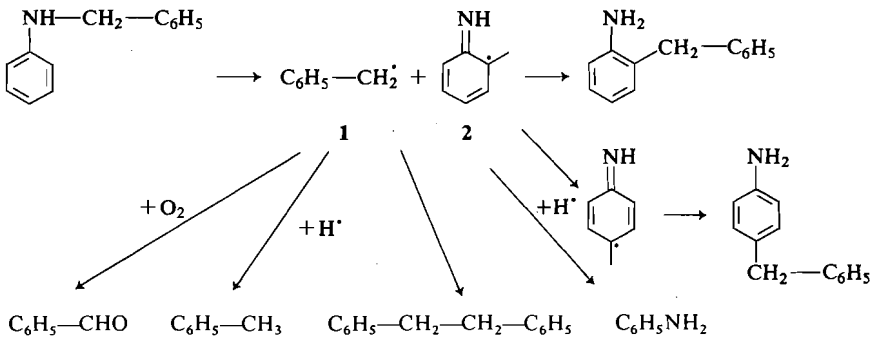

SCHEME 1

products together with 3-benzylquinoline, 2-(4-aminophenyl)quinoline, 4-(4-aminophenyl)-quinoline and an isomeric product which was identified as 4-(2-aminophenyl)quinoline.

With isoquinoline, the normal rearrangement products were accompanied by 4-benzylisoquinoline, 1-(4-aminophenyl)isoquinoline and the isomeric 1-(2-aminophenyl)isoquinoline as summarized in Table 1.

The rearrangement mechanism may take place according to Scheme 1.

Diphenylmethane may be produced through deamination of both isomeric *o*- and *p*-aminodiphenylmethane (route *a*) according to Scheme 2, however, heating the two isomers alone in a sealed tube under the conditions of the amine rearrangement produced neither ammonia nor diphenylmethane. On the other hand, heating aniline alone in a sealed tube at about 315 °C for 10 days resulted in the formation of ammonia (route *b*), which was collected in a concentrated HCl trap and identified as the hydrochloride and other derivatives. Consequently, diphenylmethane was most favorably produced through coupling of one phenyl free radical, which resulted from homolysis of the aniline byproduct, with the benzyl free radical (route *c*).

Combination of two phenyl radicals produced biphenyl (route *d*). The formation of biphenyl or diphenylmethane and ammonia may take place according to Scheme 2. The production of ammonia was assumed to partially proceed through intermediate formation of the amino free radical (route *b*). Such amino free radicals have been shown to exist (1).

9-Phenylacridine can reasonably be assumed to be formed from 2-aminodiphenylmethane as is shown in Scheme 3.

The formation of 2,3-diphenylindole can be explained according to Scheme 4.

Trans-stilbene could result from abstraction of the methylene hydrogens (β-scission) from dibenzyl under the influence of the free radicals present in the reaction medium in a procedure described previously (2).

Substitution by the benzyl radical on phenol gave the expected products. Production of *o*- and *p*-benzylphenols instead of isomeric benzylanisoles during the amine rearrangement insures that anisole rearrangement under such condi-

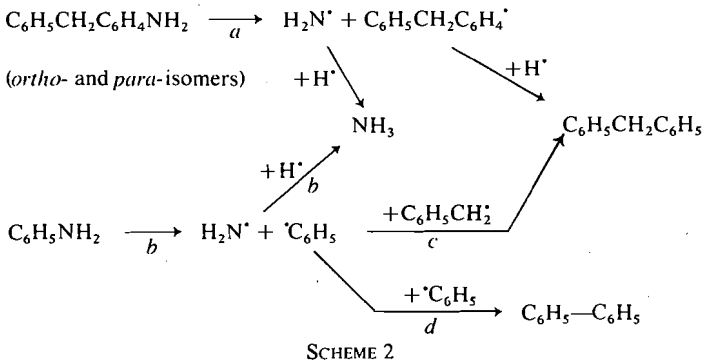

SCHEME 2

Can. J. Chem. Downloaded from www.nrcresearchpress.com by 210.87.254.5 on 09/05/12
For personal use only.

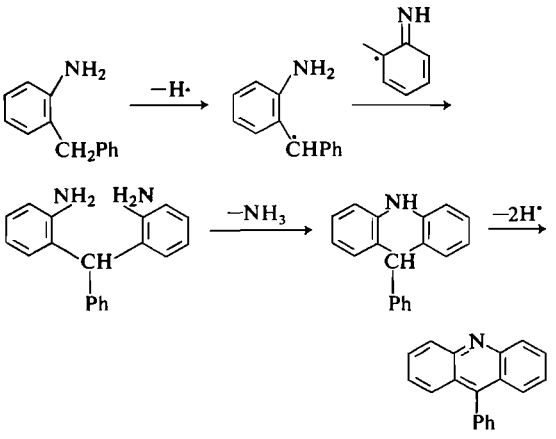

SCHEME 3

tions precedes the substitution step by benzyl radical, itself a product of the amine pyrolysis. However, absence of any other methyl derivatives among the products in an anisole solvent and the higher yield of *o*-cresol, strongly favor the assumption that the methyl group of anisole did not migrate as a separate free radical but possibly through an intramolecular route. However, the formation of *p*-cresol partially through an intermolecular migration of the methyl group within a solvent cage (3) was not excluded.

Thermal rearrangement of the amine in quinoline gave the expected products together with 3-benzylquinoline and three isomeric 2- and 4-(aminophenyl)quinolines. Free radical substitution at the 3-position of the quinoline nucleus was also observed by other workers (4, 5). Substitution by the benzyl radical at the 3-position of quinoline during the amine pyrolysis instead of at the 2- or 4-positions as observed in benzyl naphthyl ether pyrolysis in a quinoline solvent (6), could not be attributed to the difference in thermodynamic instability (7) of different isomeric benzylquinolines under such high thermal conditions. When both 2- and 4-benzylquinolines were heated under the conditions of the amine rearrangement, neither of the isomers were isomerized to their respective 3-benzylquinolines. On the other hand, the benzyl radical has less basic character (lower electron density) when compared with the aniline free radical (which has higher electron density). Since the increase of the nucleophilic character of a radical reflects an increase in its selectivity (8), consequently, in such radical competition the benzyl radical with its lower nucleophilic character will substitute selectively at the 3-position of quinoline which has a higher electron density than the 2- and 4-positions which will be attacked selectively and at a faster rate (9) by the anilino free radical with its higher nucleophilic character, producing the three isomeric 2- and 4-(aminophenyl)quinolines isolated.

Similarly, pyrolysis of the amine in isoquinoline gave the normal products together with 4-benzylisoquinoline and two isomeric 1-(2- and 4-aminophenyl)isoquinolines. On the same basis as above, during such radical competition, the less nucleophilic benzyl radical substitutes at the 4-position of isoquinoline with its higher electron density, while the anilino radical substitutes selectively and at a faster rate at the 1-position with its lower electron density.

The absence of biquinolyl or bi-isoquinolyl during such types of rearrangement strongly suggests that reactions with either quinoline or isoquinoline are based mainly on homolytic substitution steps rather than homolytic dehydrogenation processes yielding quinolyl or isoquinolyl radicals followed by coupling processes such as observed before (6).

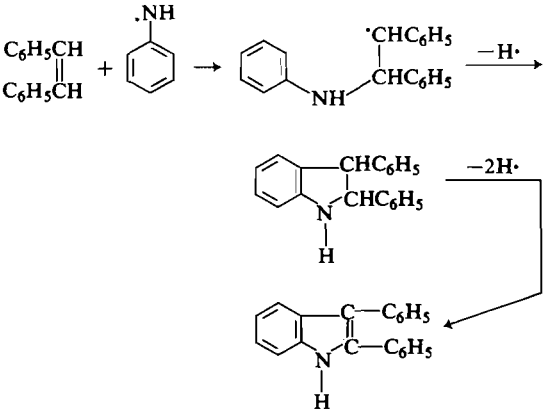

SCHEME 4

Experimental

Analysis

Infrared spectroscopic analysis was carried out on a Pye-Unicam i.r. spectrophotometer, model SP 200G. The u.v. absorptions were carried out on a Pye-Unicam u.v. spectrophotometer, model SP8000. Gas-liquid chromatography analysis was carried out on a Pye-Unicam gas chromatograph, series 104, with a dual flame ionization detector, temperature programed, model 24. The column used was 20% SE30 on Chromosorb W (35–80) mesh. Thin layer chromatographic analysis was carried out on silica gel (25–40 mesh) using the solvents benzene–cyclo-

Can. J. Chem. Downloaded from www.nrcresearchpress.com by 210.87.254.5 on 09/05/12
For personal use only.

TABLE 2. Ultraviolet absorptions of isomeric aminophenyl quinolines

Isomer	λ_{max}(nm)	ε_{max}	λ_{max}(nm)	ε_{max}
4-(2-Aminophenyl)quinoline	230	18 555	285	8 555
4-(4-Aminophenyl)quinoline	230	12 220	285	4 888
2-(4-Aminophenyl)quinoline	255	32 999	285	7 940

TABLE 3. Ultraviolet absorption of isomeric aminophenyl isoquinolines

Isomer	λ_{max}(nm)	ε_{max}	λ_{max}(nm)	ε_{max}
1-(2-Aminophenyl)isoquinoline	235	14 200	285	3 100
1-(4-Aminophenyl)isoquinoline	235	8 500	285	2 000

hexane (3:1 by volume) and *n*-hexane – ethyl acetate (7:3 by volume); the spots were visualized by iodine vapor. Paper chromatographic analysis was carried out using C. Schleicher and Schull paper No. 2316. In phenol analysis, the paper was sprayed before use to the point of saturation with 4% aqueous Na_2CO_3 solution and dried in air at room temperature. Molecular ion determinations were recorded on a UNC-CH Hitachi mass spectrometer at 70 eV.

Pyrolysis of N-Benzylaniline

N-Benzylaniline was heated alone or with phenol, anisole, quinoline, or isoquinoline in a nitrogen atmosphere and the reaction products were distilled first under atmospheric pressure where ammonia was evolved and trapped as its hydrochloride, and toluene collected. The higher boiling products were separated into neutral and amine ones by treatment with concentrated HCl and extraction with ether.

Phenolic products are separated by means of Claisen's solution. The results are summarized in Table 1.

Thermal Rearrangement of Anisole

Redistilled anisole (6 g) was heated in a sealed tube at about 315 °C for 12 days. Fractionation of the products gave together with recovered anisole, rearranged phenolic products (0.4 g; 6.7%) which were found by g.l.c. to consist of phenol (67.8%) and cresols (32.2%), a mixture of *o*-cresol (70.2%) and *p*-cresol (29.8%).

Preparation of Reference Compounds

N-Benzylaniline (10): b.p. 148–149 °C/3 Torr; m.p. 36 °C; picrate m.p. 48 °C.

Diphenylmethane (11): b.p. 261–262 °C/760 Torr; m.p. 26 °C; n_D^{27} 1.5788.

o-Aminodiphenylmethane (12): crystallized from petroleum ether (40–60 °C), m.p. 52 °C; *N*-acetyl derivative, m.p. 135 °C; *N*-benzoyl derivative, m.p. 116 °C.

p-Aminodiphenylmethane (13): b.p. 165–167 °C/2 Torr; crystallized from petroleum ether (40–60 °C), m.p. 34–36 °C; picrate, m.p. 179 °C.

9-Phenylacridine (14): Yellow prisms, m.p. 182–183 °C.

o-Benzylphenol (15): b.p. 172–180 °C/15 Torr; phenyl urethane derivative, m.p. 117 °C.

p-Benzylphenol (16): b.p. 170–190 °C/14 Torr; crystallized from petroleum ether (60–80 °C) as hairy white needles, m.p. 84 °C; benzoate m.p. 87 °C.

o-Benzylanisole (17): Crystallized from ethanol as white crystals, m.p. 27–28 °C.

p-Benzylanisole (18): b.p. 152–155 °C/7 Torr; n_D^{20} 1.5781.

2-Benzylquinoline (19): crystallized from methanol as yellow orange needles, m.p. 156–157 °C.

3-Benzylquinoline (20): b.p. 170–190 °C; crystallized from petroleum ether (60–80 °C), m.p. 67–68 °C; picrate m.p. 180–182 °C.

4-Benzylquinoline (21): b.p. 230 °C/14 Torr; picrate m.p. 179 °C.

4-Benzylisoquinoline (22): crystallized from petroleum ether (60–80 °C) as colorless crystals, m.p. 119–120 °C; picrate m.p. 195–196 °C, methiodide m.p. 196–197 °C.

2-(4-Aminophenyl)quinoline (23): yellow crystals m.p. 134 °C; picrate, m.p. 194 °C.

1-(4-Aminophenyl)isoquinoline (24): b.p. 200–215 °C/0.1 Torr, crystallized from benzene, m.p. 190–191 °C.

2,3-Diphenylindole (25): crystallized from petroleum ether (60–80 °C), m.p. 123–124 °C.

We thank Dr. M. M. Bursey for his assistance with the mass spectral measurements.

1. N. J. FRISWELL and B. G. GOWENLOCK. *In* Advances in free radical chemistry, Vol. 11 *edited by* G. H. Williams. 1967. pp. 1–5.
2. C. HORREX and S. E. MILES. Discuss. Faraday Soc. **10**, 187 (1951).
3. Y. OGATA and K. TAKAGI. J. Org. Chem. **35**, 1944 (1970).
4. R. BRESLOW and L. N. LUKENS. J. Biol. Chem. **235**, 292 (1960); B. B. BRODIE, J. AXELROD, P. A. SHORE, and S. UNEFRIEND. J. Biol. Chem. **208**, 74 (1954); R. O. C. NORMAN and G. K. RADDA. Proc. Chem. Soc. London, 138 (1962).
5. H. F. JANSEN and J. P. WIBAUT. Recl. Trav. Chim. Pays-Bas, **56**, 699 (1939).
6. M. Z. A. BADR and M. M. ALY. Tetrahedron, **28**, 3401 (1972); M. Z. A. BADR and H. A. H. EL-SHERIEF. Can. J. Chem. **50**, 259 (1972).

Can. J. Chem. Downloaded from www.nrcresearchpress.com by 210.87.254.5 on 09/05/12
For personal use only.

7. J. W. ENGELSMA and E. C. KROOGMAN. Proc. Chem. Soc. London, 258 (1958).
8. M. SZWARC and J. H. BINKS. Theoretical organic chemistry. Special Publication 12, The Chemical Society. Butterworths, London. 1959. p. 262.
9. C. A. COULSON. J. Chem. Soc. London, 1435, (1955); C. W. WHELAND. J. Am. Chem. Soc. **64**, 900 (1942).
10. A. I. VOGEL. Practical organic chemistry. Longmans, 1956. p. 572.
11. A. I. VOGEL. Practical organic chemistry. Longmans, 1956. p. 315.
12. C. L. HEWETT, L. J. LERMIT, H. T. OPENSHAW, A. R. TODD, A. H. WILLIAMS, and F. N. WOODWARD. J. Chem. Soc. London, 292 (1948).
13. W. J. HICKINBOTTOM. J. Chem. Soc. London, 1119 (1937).
14. A. BERNTHESEN. Ann., **224**, 13 (1884).
15. F. M. ELKOBAISI and W. J. HICKINBOTTOM. J. Chem. Soc. London, 1873 (1959).
16. R. C. HUSTON. J. Am. Chem. Soc. **46**, 2775 (1924).
17. B. M. DUBININ. J. Gen. Chem. USSR **19**, 696 (1949); Chem. Abst. **44**, 1060 (1950).
18. L. N. PETROVA and O. V. SCHVARTS. J. Gen. Chem. USSR **20**, 1681 (1950).
19. H. DECKER and R. POSCHORR. Chem. Ber. **37**, 3400 (1904).
20. M. AVRAMOFF and Y. SPRINZAK, J. Am. Chem. Soc. **58**, 4090 (1936).
21. 1. P. RABE and R. PASTERNACK. Chem. Ber. **46**, 1026 (1913).
22. L. RUGHEIMER and B. FRILING. Ann. **326**, 265 (1903).
23. H. JOHN and H. OTTAWA. J. Prakt. Chem. **133**, 13 (1932); H. GILMAN and G. C. GAINER. J. Am. Chem. Soc. **69**, 877 (1947).
24. H. GILMAN and G. C. GAINER. J. Am. Chem. Soc. **69**, 1946 (1947).
25. M. J. KAMLET and J. C. DACONS. J. Org. Chem. **26**, 220 (1961); C. F. H. ALLEN and J. A. VAN ALLEN. J. Am. Chem. Soc. **73**, 5850 (1951).

Can. J. Chem. Downloaded from www.nrcresearchpress.com by 210.87.254.5 on 09/05/12
For personal use only.

Fermi-Resonance Minima in the Vibrational Spectrum of Water in Crystalline Hydrates[1]

DAVID A. OTHEN AND OSVALD KNOP
Department of Chemistry, Dalhousie University, Halifax, Nova Scotia B3H 4J3
AND
MICHAEL FALK
Atlantic Regional Laboratory, National Research Council of Canada, Halifax, Nova Scotia B3H 3Z1
Received July 21, 1975

DAVID A. OTHEN, OSVALD KNOP, and MICHAEL FALK. Can. J. Chem. **53**, 3837 (1975).

The infrared absorption and Raman spectra of polycrystalline tetrachlorocuprate(II) dihydrates $M_2CuCl_4.2H_2O$ (M = K, Rb, Cs, NH_4) contain minima in the OH stretching region which sharpen at low temperature. These minima are shown to be 'Evans holes', or negative absorption features, caused by Fermi resonance between the broad and intense H_2O stretching fundamental ν_1 and a relatively narrow band due to the overtone of the H_2O bending vibration $2\nu_2$. Our findings confirm that Fermi resonance can lead to unusual spectral features, which must be taken into account in the analysis of the stretching region of the spectra of H_2O and D_2O in condensed phases, as has been done by Scherer *et al.* for the spectrum of liquid water.

DAVID A. OTHEN, OSVALD KNOP et MICHAEL FALK. Can. J. Chem. **53**, 3837 (1975).

La région des vibrations de valence OH dans les absorptions infrarouge et les spectres Raman des dihydrates de tétrachlorocuprate(II) cristallins, $M_2CuCl_4.2H_2O$ (M = K, Rb, Cs, NH_4), contient des minima qui se sont révélés "trous de Evans", c'est-à-dire caractéristiques d'absorption négative. Ces minima, qui deviennent plus étroits à basse température, sont causés par une résonance de Fermi entre la vibration fondamental ν_1 large et intense de l'eau et une bande relativement étroite due à la vibration harmonique $2\nu_2(H_2O)$ de déformation. Nos résultats confirment que la résonance de Fermi peut conduire, dans la région de vibration de valance, à des caractéristiques spectrales peu communes dont on doit tenir compte en analysant les spectres de H_2O et de D_2O dans des phases condensées, tel qu'il a été fait par Scherer *et al.* pour le spectre de l'eau liquide.

In the course of our recent study (1, 2) of the tetrachlorocuprates(II) $M_2CuCl_4.2H_2O$ (M = K, Rb, Cs, NH_4) unusual features were observed in the i.r. spectra of these compounds. They were recognized as 'Evans holes', or 'negative absorptions', arising from Fermi-resonance interactions. Their appearance was so striking as to merit a detailed discussion, especially in view of the importance of Evans holes to the interpretation of the OH stretching profiles in the spectrum of liquid water and hence to the problem of its structure (3, 4).

Evans (5) has shown that whenever a sharp vibrational transition of low inherent intensity, *e.g.* an overtone, falls within the energy range of a much broader and more intense transition of the same symmetry species, Fermi-resonance interaction may occur resulting in the spectral phenomena schematically illustrated in Fig. 1. When the sharp feature is located sufficiently close to the center of the broad absorption band, a transmittance window may form at the frequency of the sharp band. The 'missing' band intensity is redistributed by resonance repulsion into the absorption region on both sides of the transmittance window. Such transmittance windows, which have been detected in a wide variety of hydrogen-bonded systems exhibiting broad bands (6–10), are the Evans holes.

Recently Scherer *et al.* (11) have analyzed the stretching regions of their Raman spectra of liquid water and of water–$(CH_3)_2SO$ mixtures assuming the presence of an Evans hole, but the spectral feature corresponding to the transmittance window is not evident in the spectra. A clear demonstration that Evans holes do occur in the spectra of H_2O is therefore desirable. Spectra of crystalline hydrates afford a good opportunity for this, for many of them contain broad OH stretching bands but relatively narrow ν_2 and $2\nu_2$ bands.

Maximum effect, corresponding to case *c* in

[1]NRCC No. 14944.

Can. J. Chem. Downloaded from www.nrcresearchpress.com by 210.87.254.42 on 09/05/12
For personal use only.

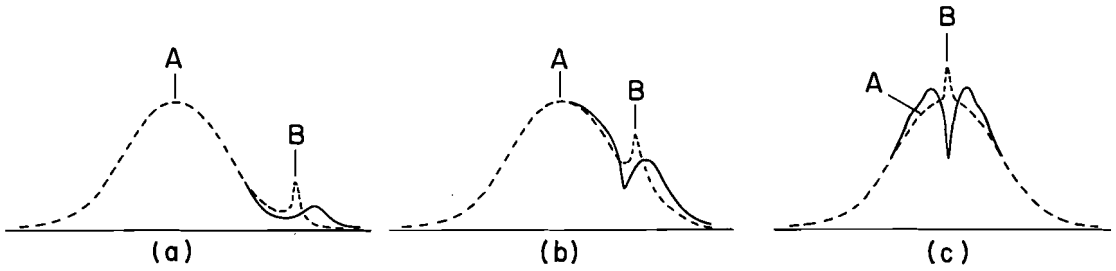

FIG. 1. Spectral phenomena resulting from Fermi resonance between an intense and broad vibrational transition *A* and a weak and relatively sharp vibrational transition *B* (schematic). Cases *a*, *b*, and *c* correspond to decreasing distances between band centers. Dashed line, resonance absent; full line, resonance taking place. After Evans (5) and Claydon and Sheppard (8).

Fig. 1, should arise in hydrates which are sufficiently strongly hydrogen-bonded for the values of OH stretching frequencies to be lowered into the 3200 cm^{-1} region where $2\nu_2$ normally occurs. This is the situation in the tetrachlorocuprates dihydrates, and so their spectra are particularly suited for a study of the phenomenon.

Experimental

The preparation and authentication of the samples and the preparation of specimens have been described elsewhere (1, 2). Sample powders were dispersed in KCl, RbCl, or CsCl pellets, or they were studied as Fluorolube mulls supported on KBr windows. A Perkin–Elmer model 521, and later a model 180, spectrophotometer was used in this work. A Cryo-Tip (Air Products and Chemicals, Inc.) low-temperature sample holder was used to cool samples below liquid-nitrogen temperature; it was capable of reaching about 23 K.

Results

Figure 2 shows the i.r. spectra of $K_2CuCl_4.2H_2O$ and $Rb_2CuCl_4.2H_2O$ in the region of the H_2O bending fundamental and in the OH stretching region.[2] The feature of interest (vertical arrow) is the absorbance minimum near 3200 cm^{-1}, which sharpens and intensifies on cooling. The minimum is present, with minor frequency shifts, in the spectra of all four dihydrates studied.

The following analysis shows that the minimum is not merely an accidentally narrow region of high transmittance between absorption bands but an Evans hole resulting from Fermi resonance between the broad, intense fundamental

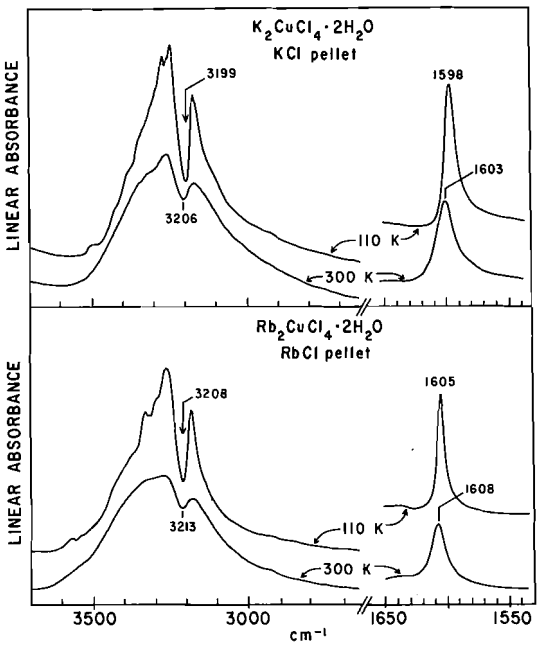

FIG. 2. Infrared spectra of $K_2CuCl_4.2H_2O$ and $Rb_2CuCl_4.2H_2O$ at 300 K and 110 K in the regions of the stretching and bending fundamentals of H_2O. Cooling to 23 K produced very little further change.

ν_1 and a relatively narrow combination band $\nu_2(i) + \nu_2(j)$ produced by different factor-group components i and j of ν_2.

(i) Frequency of the Minimum in the I.R. Spectrum

Analysis of the OH stretching frequencies of HDO and H_2O (1, 2) shows that the center of the ν_1 band of the tetrachlorocuprates dihydrates should occur near 3200 cm^{-1} and thus in the region of the minimum. The H_2O bending fundamental ν_2 in $M_2CuCl_4.2H_2O$ gives rise to four factor-group components, A_{1g}, B_{1g}, A_{2u}, and

[2]Spectral data for the corresponding Cs compound are listed in Table 2, but they are not as accurate as those for K and Rb. The i.r. spectrum of the ammonium compound has been studied in considerable detail but is not suitable for inclusion in this paper because of complications due to NH_4^+ bands; it will be described elsewhere (2).

Can. J. Chem. Downloaded from www.nrcresearchpress.com by 210.87.254.42 on 09/05/12
For personal use only.

TABLE 1. Observed and calculated frequencies (cm^{-1}) of $\nu_2(i) + \nu_2(j)$ in $K_2CuCl_4.2H_2O$ and $Rb_2CuCl_4.2H_2O$ at room temperature

Description	Frequency	
	K	Rb
Components of ν_2		
A_{2u}	1603(1)[a]	1608(1)[b]
B_{2u}	1603(5)[c]	1607(5)[c]
A_{1g}	1628(3)[d]	1631(3)[d]
B_{1g}	1630(3)[d]	1636(3)[d]
Isotopically isolated	1616(1)[a]	1620(1)[b]
Minimum in the i.r. spectrum		
Calculated[e]		
$\nu_2(A_{1g}) + \nu_2(A_{2u}) + 2x_{22}$	3202(3)	3210(3)
$\nu_2(B_{1g}) + \nu_2(B_{2u}) + 2x_{22}$	3204(4)	3214(6)
Mean of doublet	3203(5)	3212(5)
Observed	3206(4)[b]	3213(2)[b]
Minima in the Raman A_{1g} *spectrum*		
Calculated[e]		
$2\nu_2(A_{2u}) + 2x_{22}$	3175(2)	3187(2)
$2\nu_2(B_{2u}) + 2x_{22}$	3179(7)	3185(7)
Mean of doublet	3177(6)	3186(7)
Observed	3195(10)[f]	3299(10)[f]
Calculated[e]		
$2\nu_2(A_{1g}) + 2x_{22}$	3227(4)	3233(4)
$2\nu_2(B_{1g}) + 2x_{22}$	3231(4)	3243(4)
Mean of doublet	3229(4)	3238(4)
Observed	3247(10)[f]	3250(10)[f]

[a]Reference 1.
[b]This work.
[c]Inactive component. Frequency calculated on the assumption that the mean frequency of the four factor-group components equals the isotopically isolated frequency.
[d]Reference 12.
[e]The anharmonicity $2x_{22} = -29\ cm^{-1}$ has been assumed throughout (*cf.* ref. 2).
[f]Frequency estimated from Fig. 4 of ref. 12.

B_{2u}. For the K and Rb compounds all four frequencies are known (1, 2). From them one may calculate the expected frequencies of the two binary combinations of symmetry species A_{2u} that may enter into Fermi resonance with the i.r.-active A_{2u} component of ν_1. The calculation (Table 1) assumes an anharmonicity of $-2x_{22} = 29\ cm^{-1}$ (*cf.* ref. 2). The calculated frequencies of the two combination bands lie within a few cm^{-1} of each other and would not be expected to be resolved. The *mean* frequencies of these calculated doublets are in good agreement with the observed frequencies of the minimum in the i.r. spectra of the K and Rb compounds if allowance is made for the uncertainties in the frequencies of the i.r. and Raman components of ν_2 and for a small uncertainty in the anharmonicity.

(ii) Effect of Temperature

The shift of the frequency of the minimum with temperature is in the same direction for the K, Rb, and Cs compounds. Within experimental error it is twice the magnitude of the corresponding shifts of the i.r. active A_{2u} component of ν_2 (Table 2).

(iii) Effect of the Cation

In the series K, Rb, Cs the effect of the cation on the frequency of the minimum is in the same direction and, within experimental error, of twice the magnitude of the effect of the cation on the ν_2 band (Table 2).

(iv) Effect of Deuteration

A corresponding minimum is observed in the OD stretching region of the i.r. spectrum of each of the deuterated compounds. The frequency dependence on temperature and the cation (Table 2) is similar to that in the undeuterated compounds.

(v) Line Width

The half-width of the minimum in the spectra

Can. J. Chem. Downloaded from www.nrcresearchpress.com by 210.87.254.42 on 09/05/12
For personal use only.

TABLE 2. Effects of temperature, cation, and deuteration on the i.r. frequency of ν_2 and of the minimum in the OH stretching region

	Frequency (cm^{-1})			
	ν_2		Minimum	
Compound	300 K	115 K	300 K	115 K
$K_2CuCl_4.2H_2O$	1603(1)	1598(1)	3206(2)	3199(1)
$Rb_2CuCl_4.2H_2O$	1608(1)	1605(1)	3213(2)	3208(1)
$Cs_2CuCl_4.2H_2O$	1612(1)*	1609(1)	3226(3)*	3223(2)
$K_2CuCl_4.2D_2O$	1185(1)	1184(1)	2370(3)	2366(2)
$Rb_2CuCl_4.2D_2O$	1190(1)	1188(1)	2384(3)	2382(2)

*At 280 K.

of both the undeuterated and the deuterated compounds decreases on cooling (Fig. 2). An accidental region of low absorptivity between two absorption bands would be expected to widen at lower temperatures as the bands on both sides tend to become narrower.

(vi) Frequency of the Minimum in the Raman Spectrum

The four possible first overtones of the factor-group components of ν_2, *i.e.* the binary combinations $2\nu_2(i)$ where $i = A_{1g}$, B_{1g}, A_{2u}, or B_{2u}, have the symmetry species A_{1g} and can enter into Fermi resonance with the intense Raman-active A_{1g} component of ν_1. The calculated frequencies of these four components (Table 1) fall into two sets of closely-spaced doublets. As in the i.r. spectrum, each of these doublets may be expected to remain unresolved. The Raman spectra of the K and Rb compounds have been recorded by Mathieu and Couture-Mathieu (12); their Fig. 4 shows clearly two sharp minima in the OH stretching region. The separation of the two observed Raman minima is 53 cm^{-1} for the K and 49 cm^{-1} for the Rb compound; the separations of the mean frequencies of the calculated doublets are 52 and 50 cm^{-1} respectively, in very good agreement. The actual frequencies of the observed minima lie somewhat above the calculated frequencies of the unresolved doublets (Table 1). This is expected, as in the Raman spectrum the frequencies of the overtones occur *on the side* of the ν_1 band. The situation thus corresponds to case *b* in Fig. 1, while the situation in the i.r. spectrum appears to correspond to case *c*, with the frequency of the overtone very near to the center of the ν_1 band.

Conclusion

The occurrence of Fermi resonance between the vibrational levels ν_1 and $2\nu_2$ in $M_2CuCl_4.2H_2O$ and in other crystalline hydrates has been recognized before (1, 12). The present observations demonstrate that, in addition, an Evans hole is present, characterized by the close similarity of the spectral *minimum* in the i.r. spectrum and the frequency corresponding to $2\nu_2$.

Our findings confirm that Fermi resonance can lead to unusual spectral features, which must be taken into account in the analysis of the stretching region of the spectra of H_2O and D_2O in condensed phases, as has been done by Scherer *et al.* (11) for the spectrum of liquid water.

We wish to thank Mr. P. F. Seto and M. Denis Bégin for their assistance in obtaining some of the spectra. A grant-in-aid of research from the National Research Council of Canada to one of us (O.K.) is acknowledged.

1. G. H. THOMAS, M. FALK, and O. KNOP. Can. J. Chem. **52**, 1029 (1974).
2. D. A. OTHEN, O. KNOP, and M. FALK. To be published.
3. D. EISENBERG and W. KAUZMANN. The structure and properties of water. Oxford University Press. 1969.
4. M. FALK. Proc. Electrochem. Soc., Symp. on Chemistry and Physics of Aqueous Solutions. Toronto, 1975. p. 19.
5. J. C. EVANS. Spectrochim. Acta, **16**, 994 (1960).
6. J. C. EVANS and N. WRIGHT. Spectrochim. Acta, **16**, 352 (1960).
7. J. C. EVANS. Spectrochim. Acta, **16**, 1382 (1960); **17**, 129 (1961); **18**, 507 (1962).
8. M. F. CLAYDON and N. SHEPPARD. Chem. Commun. 1431 (1969).
9. D. P. C. THACKERAY and B. C. STACE. Spectrochim. Acta, **30A**, 1961 (1974).
10. R. L. DEAN, F. N. MASRI, and J. L. WOOD. Spectrochim. Acta, **31A**, 79 (1975).
11. J. R. SCHERER, M. K. GO, and S. KINT. J. Phys. Chem. **77**, 2108 (1973); **78**, 1304 (1974).
12. J.-P. MATHIEU and L. COUTURE-MATHIEU. J. Chim. Phys. **50**, 573 (1953).

Can. J. Chem. Downloaded from www.nrcresearchpress.com by 210.87.254.42 on 09/05/12
For personal use only.

Zinc Hydroxide: Solubility Product and Hydroxy-complex Stability Constants from 12.5–75 °C

RANDY A. REICHLE, KEITH G. MCCURDY, AND LOREN G. HEPLER
Department of Chemistry, University of Lethbridge, Lethbridge, Alberta T1K 3M4

Received June 30, 1975

RANDY A. REICHLE, KEITH G. MCCURDY, and LOREN G. HEPLER. Can. J. Chem. **53**, 3841 (1975).

We have made atomic absorption measurements leading to the solubility of zinc hydroxide at 12.5, 25.0, 50.0, and 75.0 °C from pH = 6.7 to pH = 13.8. Results have been used for evaluation of the solubility product and stepwise constants for association of Zn^{2+}(aq) with OH^-(aq) to form solute species of type $Zn(OH)_i^{2-i}$(aq) with i = 1–4. Evidence is presented to support the reliability of the various equilibrium constants. Uncertainties in derived enthalpies are assessed.

RANDY A. REICHLE, KEITH G. MCCURDY et LOREN G. HEPLER. Can. J. Chem. **53**, 3841 (1975).

On a fait des mesures d'absorption atomique conduisant à la solubilité de l'hydroxyde de zinc à 12.5, 25.0, 50.0 et 75.0 °C, à des pH = 6.7 à 13.8. On a utilisé les résultats pour évaluer le produit de solubilité et les constantes successives pour l'association de Zn^{2+}(aq) avec OH^-(aq) pour former des espèces solutées du type $Zn(OH)_i^{2-i}$(aq) avec i = 1–4. On présente des données pour supporter la fiabilité de diverses constantes d'équilibre. On établit les incertitudes dans les enthalpies qui en dérivent.

[Traduit par le journal]

Introduction

It is well established that zinc hydroxide is slightly soluble in water, becoming more soluble as the pH is either lowered or raised. There are, however, substantial differences between solubilities at 25 °C reported by various investigators and we know of no solubility measurements that have covered a substantial range of temperature. As a result of these limitations on the available solubility data there are related uncertainties in the equilibrium constants for association of Zn^{2+}(aq) with OH^-(aq) and in the solubility product of zinc hydroxide. We have therefore measured (by atomic absorption spectrophotometry) the solubility of zinc hydroxide at 12.5, 25.0, 50.0, and 75.0 °C from pH = 6.7 to pH = 13.8. Results have been used for evaluation of the solubility product and stepwise equilibrium constants for association of Zn^{2+}(aq) with OH^-(aq).

Experimental

Zinc hydroxide was first precipitated from aqueous zinc sulfate solution by NH_3(aq), washed thoroughly to remove all sulfate, and then dissolved in a small excess of NH_3(aq) as described by Dietrich and Johnston (1). The resulting solution was then transferred to a polyethylene container (to avoid contamination of the product with silica) and placed in a vacuum oven maintained at 60 °C; crystals of zinc hydroxide were soon formed. This procedure leads to the orthorhombic form of $Zn(OH)_2$(c), sometimes called the ε phase.

Solubility determinations began by adding zinc hydroxide and either HCl(aq) or NaOH(aq) to polyethylene test tubes with care taken to exclude CO_2. The stoppered test tubes (containing N_2) were then shaken gently in constant temperature baths controlled to within ±0.1° at 12.5 and 75 °C and to within ±0.05° at 25 and 50 °C. Additional HCl(aq) or NaOH(aq) was added to many of the tubes after they had been in the baths for a few days. Samples of solution in contact with solid zinc hydroxide were removed periodically for analysis. It was found that the concentration of zinc in these solutions usually approached constancy in about 10 days. Solutions were then allowed to stand (without agitation) in the baths for 3 days, which permitted zinc hydroxide to settle, thus facilitating removal of supernatant liquid for analysis.

Zinc analyses were done with a Model 500 Jarrell Ash Atomic Absorption Spectrophotometer. Six standard solutions for calibration were prepared by weight, ranging from 0.01533 to 7.05×10^{-5} m zinc sulfate. Further solutions for calibration were prepared by dilution of some of the original standard solutions, with final concentrations down to 1.41×10^{-6} m.

The pH of each solution (at the temperature of solubility measurement) was measured immediately after the supernatant liquid was removed for analysis for zinc. A Radiometer (Model 26) pH Meter with Corning multipurpose glass electrode and saturated KCl calomel reference electrode was used for these measurements. The system was calibrated with standard buffers described by Bower and Bates (2).

The first solubility measurements were made at 50 °C. The same solid samples were then successively equilibrated at 25 and 12.5 °C. A new set of samples was made up and equilibrated at 75 °C. Subsequent measurements were made by equilibrating separately prepared samples at each temperature. Uncertainties in our experimental solubilities (Table 1) are ~5%.

Can. J. Chem. Downloaded from www.nrcresearchpress.com by 210.87.254.105 on 09/05/12
For personal use only.

Can. J. Chem. Downloaded from www.nrcresearchpress.com by 210.87.254.105 on 09/05/12
For personal use only.

TABLE 1. Solubility* of zinc hydroxide

12.5 °C		25.0 °C		50.0 °C		75.0°C	
pH	$S(\times 10^5)$	pH	$S(\times 10^5)$	pH	$S(\times 10^5)$	pH	$S(\times 10^5)$
13.80	327	13.19	178	12.50	261	12.22	1029
13.71	216	12.97	67.3	12.24	88.7	11.95	319
13.51	91.8	12.77	28.3	11.99	33.7	11.68	104
13.34	45.1	12.52	11.2	11.76	14.8	11.35	29.1
13.18	25.2	12.29	5.74	11.55	8.03	11.14	12.6
12.85	6.12	11.05	0.54	11.25	2.92	10.85	5.27
12.21	1.68	10.84	0.46	10.99	2.14	10.54	3.06
11.51	0.50	10.14	0.31	10.75	1.38	10.22	2.14
11.50	0.31	9.43	0.38	10.25	0.92	10.01	2.06
11.10	0.24	9.18	0.54	10.02	0.84	9.71	1.84
9.83	0.23	8.97	0.61	9.55	0.76	9.54	1.76
9.49	0.23	8.91	0.92	9.08	0.87	8.93	1.68
9.27	0.31	8.72	0.84	8.77	0.99	8.55	1.84
9.14	0.38	8.67	1.22	8.52	1.15	8.38	2.06
8.99	0.46	8.41	1.30	8.27	1.45	8.08	2.06
8.55	1.33	7.90	4.74	8.04	1.84	7.89	1.99
7.96	13.2	7.63	17.2	7.82	2.43	7.65	2.37
7.70	48.3	7.44	32.1	7.54	4.97	7.18	7.22
7.32	265	7.31	49.7	7.26	10.7	6.94	13.1
7.22	415	7.00	204	7.05	19.6		
7.06	844			6.75	53.4		

*S represents the solubility expressed in mol of zinc per kg of water.

Results and Calculations

Results of our solubility determinations are summarized in Table 1, where S represents the total molality of dissolved zinc. Earlier investigations have been cited by Sillén and Martell (3, 4) and Schindler (5). Our results at 25 °C generally agree with those of earlier investigators, although there are significant differences, particularly near the high and low ends of the pH range. There are no earlier solubility data available for higher temperatures to compare with our results.

We begin by interpreting our solubility results in terms of $Zn(OH)_2(c)$ in equilibrium with saturated solution that can contain species that we represent by $Zn^{2+}(aq)$, $Zn(OH)^+(aq)$, $Zn(OH)_2(aq)$, $Zn(OH)_3^-(aq)$, and $Zn(OH)_4^{2-}(aq)$. It is convenient to relate these species to one another and to our solubility data by way of the following equilibria and corresponding equilibrium constants:

$$[1a] \quad Zn(OH)_2(c) \rightleftharpoons Zn(OH)^+(aq) + OH^-(aq)$$

$$[1b] \quad K_1 = [Zn(OH)^+][OH^-]$$

$$[2a] \quad Zn(OH)_2(c) \rightleftharpoons Zn(OH)_2(aq)$$

$$[2b] \quad K_2 = [Zn(OH)_2]$$

$$[3a] \quad Zn(OH)_2(c) + OH^-(aq) \rightleftharpoons Zn(OH)_3^-(aq)$$

$$[3b] \quad K_3 = [Zn(OH)_3^-]/[OH^-]$$

$$[4a] \quad Zn(OH)_2(c) + 2OH^-(aq) \rightleftharpoons Zn(OH)_4^{2-}(aq)$$

$$[4b] \quad K_4 = [Zn(OH)_4^{2-}]/[OH^-]^2$$

$$[5a] \quad Zn(OH)_2(c) \rightleftharpoons Zn^{2+}(aq) + 2OH^-(aq)$$

$$[5b] \quad K_{sp} = [Zn^{2+}][OH^-]^2$$

The square brackets above 'should' indicate thermodynamic activities of the enclosed species, but we have used molalities instead, which means that the equilibrium constants we have evaluated might better be called equilibrium quotients. Consequences of the approximation $a \cong m$ are discussed later in this paper.

The total solubility S can be represented as the sum of molalities of all zinc-containing solute species

$$[6] \quad S = [Zn^{2+}] + [Zn(OH)^+] + [Zn(OH)_2] + [Zn(OH)_3^-] + [Zn(OH)_4^{2-}]$$

Substitution of [1b], [2b], [3b], [4b], and [5b] in [6] leads to

$$[7] \quad S = \frac{K_{sp}}{[OH^-]^2} + \frac{K_1}{[OH^-]} + K_2 + K_3[OH^-] + K_4[OH^-]^2$$

TABLE 2. Equilibrium constants derived from solubilities

t(°C)	K_{sp}(× 10^{17})	K_1(× 10^{11})	K_2(× 10^6)	K_3(× 10^3)	K_4(× 10^2)
12.5	1.42	1.13	1.66	1.12	5.70
25.0	1.74	2.54	2.62	1.32	6.47
50.0	2.34	7.70	7.02	2.56	7.92
75.0	3.16	20.2	15.0	2.74	8.99

Now there are several ways to proceed with evaluation of the various equilibrium constants in [7]. One way is to begin with consideration of our solubilities at relatively low pH where Zn^{2+}(aq) and $Zn(OH)^+$(aq) are likely to be the only important solute species so that we need use only the first two terms on the right hand side of [7]. We thus obtain

$$[8] \qquad S[OH^-] = (K_{sp}/[OH^-]) + K_1$$

that is suitable for graphical evaluation of K_{sp} and K_1. Using pK_w = 14.44, 14.00, 13.28, and 12.71 from Olofsson and Hepler (6) for t = 12.5, 25.0, 50.0, and 75.0 °C to obtain $[OH^-]$ values from our pH values (Table 1), we have constructed graphs of $S[OH^-]$ *vs.* $1/[OH^-]$ and derived the values of K_{sp} and K_1 that are listed in Table 2.

Next we have limited our attention to solubilities at high pH where only $Zn(OH)^-$(aq) and $Zn(OH)_4^{2-}$(aq) are likely to be important solute species. Taking only the last two terms on the right hand side of [7], we obtain

$$[9] \qquad S/[OH^-] = K_3 + K_4[OH^-]$$

and from graphs of $S/[OH^-]$ *vs.* $[OH^-]$ we find the values of K_3 and K_4 that are listed in Table 2.

Now we solve [7] for K_2 in terms of S, $[OH^-]$, and various K values already obtained by way of [8] and [9]. Because $Zn(OH)_2$(aq) is relatively most important at the minimum in solubility, we use the minimum solubility at each temperature with the corresponding pH and other equilibrium constants (Table 2) to obtain the K_2 values that are listed in Table 2.

It should be recognized that the evaluation procedure we have used effectively concentrates most of the uncertainties in all of our work in the reported values of K_2 rather than the other K values.

We have used K values in Table 2 to calculate the fraction f of Zn(II) that exists as Zn^{2+}(aq), $Zn(OH)^+$(aq), $Zn(OH)_2$(aq), $Zn(OH)_3^-$(aq), and $Zn(OH)_4^{2-}$(aq) as pH is varied. Results for 25 °C

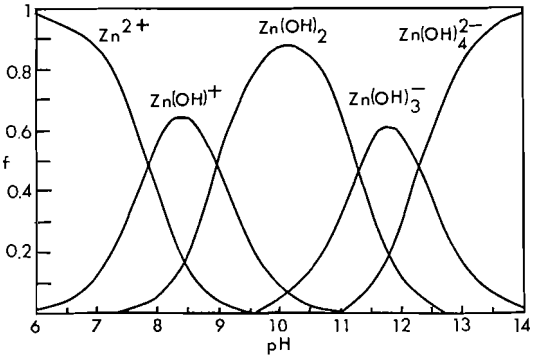

FIG. 1. Graph of fraction f of Zn(II) existing as Zn^{2+}(aq), $Zn(OH)^-$(aq), $Zn(OH)_2$(aq), $Zn(OH)_3^-$, and $Zn(OH)_4^{2-}$(aq) over a range of pH at 25 °C.

are displayed in Fig. 1. Ranges of satisfactory validity of [8] and [9] can be deduced from Fig. 1, or by using data in Table 1 for making appropriate graphs of $S/[OH^-]$ *vs.* $1/[OH^-]$ and $[OH^-]$.

Another approach has been to use all of our solubility–pH data at each temperature for computer calculations leading to overall 'best' fits of [7] and hence the desired K values. Different weighting procedures lead to slightly different K values, but all of the K values obtained in this way are in good agreement with those already listed in Table 2. For some further calculations and comparisons with results of earlier investigators, we will take the values listed in Table 2 to be the best ones that can be derived from our solubilities in combination with our neglect of activity coefficients.

Whether our K values do or do not have the significance we ascribe to them, use of these K values in [7] does lead to calculated solubilities that agree well with the experimental values in Table 1 over the whole range of temperature and pH. In this sense, our K values have uncertainties of a few percent.

Our measurements and calculations have led to $K_{sp} = 1.74 \times 10^{-17}$ at 25 °C. Because this K_{sp} was evaluated from our solubilities in solu-

Can. J. Chem. Downloaded from www.nrcresearchpress.com by 210.87.254.105 on 09/05/12
For personal use only.

Can. J. Chem. Downloaded from www.nrcresearchpress.com by 210.87.254.105 on 09/05/12
For personal use only.

tions of relatively low pH, all of which were quite dilute, it is appropriate to take this value to be nearly equal to the thermodynamic solubility product in spite of our neglect of activity coefficients. This value can be compared with results of previous investigators as follows.

Reported solubility products at or near 25 °C range from 10^{-13} to 10^{-21}. Here we consider only a few of what appear to be the best of these earlier investigations. Fulton and Swinehart (7) have found $K_{sp} = 0.7 \times 10^{-17}$. Schindler *et al.* (8) have reported $K_{sp} = 3.39 \times 10^{-17}$. Davies and Staveley (9) have reported $K_{sp} = 3.80 \times 10^{-17}$. Each of these thermodynamic (activity coefficients have been considered) solubility products applies to the orthorhombic (ε) modification of zinc hydroxide and can therefore be compared with our value. Our assessment of all of these investigations leads us to suggest that $K_{sp} = 3.5 \times 10^{-17}$ is the 'best' value. The discrepancy between this 'best' value and our result corresponds to a difference of 0.4 kcal mol^{-1} in ΔG^0 for [5*a*].

Application of $d \ln K_{sp}/dT = \Delta H^0/RT^2$ to our results leads to $\Delta H^0 = 2.5$ kcal mol^{-1} for the reaction represented by [5*a*]. We know of no published K_{sp} values at several temperatures that permit calculation of a ΔH^0 value to compare with our result above, but calorimetric measurements have led to ΔH_f^0 values listed in ref. 10 that correspond to $\Delta H^0 = 7.02$ kcal mol^{-1} for [5*a*]. More recently, Davies and Stavely (9) have made new calorimetric measurements that lead to $\Delta H^0 = 7.92$ kcal mol^{-1} for this same reaction. It is nearly certain that this last ΔH^0 is the best one available for this reaction.

The difference between our ΔH^0 and the calorimetric value (10) is much larger than can be accounted for on the basis of statistical analysis of 'reasonable' uncertainties in the various experimental results. It seems to us most likely that the source of the discrepancy lies in the interpretation of our solubilities in terms of [1*a*], [2*a*], [3*a*], [4*a*], and [5*a*] and/or the assumption that the solid phase remains pure $Zn(OH)_2$(c,ε) at temperatures above 25 °C.

Sillén and Martell (3, 4) have reviewed some evidence for dinuclear species in the Zn^{2+}–OH^- system and much evidence for a variety of di- and polynuclear species in other M^{2+}–OH^- systems. Experience with other systems (3, 4) suggests that neglect of small concentrations of these species would lead to only small errors in our K_{sp} values, but to substantially greater errors in the ΔH^0 obtained by differentiation and thence magnification of all experimental and interpretive errors.

The work of Schindler *et al.* (8) has shown that $Zn(OH)_2$(c,ε) is unstable with respect to ZnO(c) and H_2O(liq) and also with respect to $Zn(OH)_2$(amorph), with further evidence that conversion between the various forms of $Zn(OH)_2$ and ZnO is often slow. Since these conversions might be expected to proceed faster at higher temperatures, it is possible that the solid phase in apparent equilibrium with our saturated solutions above 25 °C was some phase other than $Zn(OH)_2$ (c,ε) or was a mixture of phases, which might also account for the error in our calculated ΔH^0 for [5*a*].

We have represented formation of $Zn(OH)^+$(aq) by [1*a*] and have obtained $K_1 = 2.54 \times 10^{-11}$ at 25 °C for this reaction. By combining our K_1 with our K_{sp} we also obtain the equilibrium constant for the reaction

$$[10] \quad Zn^{2+}(aq) + OH^-(aq) \rightleftharpoons Zn(OH)^+(aq)$$

that we report as $\beta_1 = 1.46 \times 10^6$. Further combination of this β_1 with K_w leads to the equilibrium constant for the 'hydrolysis' or 'acid ionization' reaction that we represent by

$$[11] \quad Zn^{2+}(aq) + H_2O(liq) \rightleftharpoons Zn(OH)^+(aq) + H^+(aq)$$

and $K_h = 1.46 \times 10^{-8}$. Because all of these values are based on solubilities in very dilute solutions, all are close to the thermodynamic constants in spite of our neglect of activity coefficients.

Sillén and Martell (3, 4) have reviewed many earlier investigations that have led to a wide range (10^{-3} to 10^3 times our values) of values for K_1, β_1, or K_h. We call particular attention to the $K_h = 1.10 \times 10^{-9}$ reported by Perrin (11) and the $\beta_1 = 2.04 \times 10^6$ reported by Gubeli and Ste-Marie (12) for 1.0 *M* $NaClO_4$ solution as the 'best' previous values for comparison with our results. It is seen that our K_h value is about 10 times that of Perrin (11) while our β_1 value is nearly the same as that of Gubeli and Ste-Marie (12).

Perrin's (11) K_h values at several temperatures from 15 to 42 °C have led him to $\Delta H^0 = 13.4$ kcal mol^{-1} (quoted as probably correct to within about 1 kcal mol^{-1}) for [11]. Combination of our $\Delta H^0 = 2.5$ kcal mol^{-1} for [5*a*] with our $\Delta H^0 = 8.9$ kcal mol^{-1} for [1*a*] (obtained from

d ln K_1/dT) and $\Delta H^0 = 13.3$ kcal mol^{-1} for ionization of water (6) leads to $\Delta H^0 = 19.7$ kcal mol^{-1} for [11]. Or we can combine our ΔH^0 for [1*a*] with ΔH^0 from Davies and Staveley (9) and ΔH^0 of ionization of water (6) to obtain $\Delta H^0 = 14.3$ kcal mol^{-1} for [11]. The former value is in poor agreement with Perrin (11), while the latter value is in good agreement with his results.

Formation constants for $Zn(OH)_i^{2-i}(aq)$ species as in

[12] $Zn^{2+}(aq) + iOH^-(aq) \rightleftharpoons Zn(OH)_i^{2-i}(aq)$

calculated from $\beta_1 = K_i/K_{sp}$ are as follows for 25 °C: $\beta_2 = 1.51 \times 10^{11}$, $\beta_3 = 7.59 \times 10^{13}$, and $\beta_4 = 3.72 \times 10^{15}$.

It is possible to calculate ΔH^0 values for reactions represented by [2*b*], [3*b*], and [4*b*] and thence for reactions of type [12] (i = 2–4) by way of d ln K/dT, but we decline to list the values so obtained. We have already discussed reasons for lack of confidence in related ΔH^0 values for [1*a*], [5*a*], [10], and [11]. Similar uncertainties apply to reactions of type [12] (i = 2–4). For these latter reactions and [2*a*], [3*a*], and [4*a*] there is also the increasingly significant error introduced by our neglect of activity coefficients.

Conclusions

The experimental work and subsequent calculations described here show that it is possible to use atomic absorption spectrophotometry to obtain reliable solubilities of sparingly soluble substances and then to derive reliable equilibrium constants (solubility products and stability constants) from these solubilities. Unfortunately, it also appears that the combination of experimental and interpretive uncertainties is sufficiently great that it is not possible to obtain entirely reliable enthalpies and entropies of reaction by way of d ln K/dT in this way.

We are grateful to the Alberta Department of the Environment for support of this research, and to the STEP program for support of some preliminary investigations that partly led to the work described here.

1. H. G. Dietrich and J. Johnston. J. Am. Chem. Soc. **49**, 1419 (1927).
2. V. E. Bower and R. G. Bates. J. Res. Natl. Bur. Stand. **59**, 261 (1957).
3. L. G. Sillén and A. E. Martell. Stability constants of metal-ion complexes. Special Publication No. 17. The Chemical Society, London. 1964.
4. L. G. Sillén and A. E. Martell. Stability constants of metal-ion complexes, Supplement No. 1. Special Publication No. 25. The Chemical Society, London. 1971.
5. P. W. Schindler. *In* Equilibrium concepts in natural water systems. Advances in Chemistry Series 67. American Chemical Society, Washington, D.C. 1967.
6. G. Olofsson and L. G. Hepler. J. Solution Chem. **4**, 127 (1975).
7. J. W. Fulton and D. F. Swinehart. J. Am. Chem. Soc. **76**, 864 (1954).
8. P. Schindler, H. Althaus, and W. Feitknecht. Helv. Chim. Acta, **47**, 982 (1964).
9. A. Davies and L. A. K. Staveley. J. Chem. Thermodyn. **4**, 267 (1972).
10. D. D. Wagman, W. H. Evans, V. B. Parker, I. Halow, S. M. Bailey, and R. H. Schumm. National Bureau of Standards Technical Note 270-3, U.S. Government Printing Office, Washington, D.C. 1968.
11. D. D. Perrin. J. Chem. Soc. 4500 (1962).
12. A. O. Gubeli and J. Ste-Marie. Can. J. Chem. **45**, 827 (1967).

Can. J. Chem. Downloaded from www.nrcresearchpress.com by 210.87.254.105 on 09/05/12
For personal use only.